BULLETIN OF THE CHEMICAL SOCIETY OF JAPAN VOL. 43 1—8 (1970)

A Study of the Decomposition Reaction of Cumene Hydroperoxide in the Presence of Triphenylsulfonium Chloride

Katsutoshi OHKUBO, Tokio YAMABE and Kenichi FUKUI

Faculty of Engineering, Kyoto University, Sakyo-ku, Kyoto

(Received March 29, 1969)

The homogeneous decomposition reaction of cumene hydroperoxide in cumene was studied by the use of triphenylsulfonium chloride over a low-temperature range (30—80°C). The hydroperoxide was decomposed remarkably in the presence of the sulfonium catalyst, whereas in the absence of the catalyst it was decomposed only a little. Among the homolytic decomposition products, acetophenone and dicumyl peroxide were found to be the main products, while α-cumyl alcohol was formed in only a small amount. Moreover, methyl alcohol was found in appreciable amounts. Traces of heterolytic reaction products, such as phenol and acetone, were also detected. After discussing the reaction mechanism and the nature of catalytic action, it is concluded that the partially-occupied *d* orbital of the sulfonium cation may play a role in breaking the oxygen-oxygen bond of the hydroperoxide homolytically. The counter chloride anion seems to take part in the heterolytic reaction to some extent.

The thermal decomposition of cumene hydroperoxide (CHP) above 100°C in various kinds of solvents has been studied by several authors.[1-7] Most of these studies have been based on kinetic methods. However, there are some discrepancies in their results,[2,3] particularly in the kinetic order of decomposition reaction. These discrepancies may be attributed to the distribution of the decomposition products which depends on the polarity of the solvents, the reaction temperature, and the presence or absence of catalysts.

CHP itself is thermally stable in hydrocarbons up to 130—140°C,[3] but by catalysts such as ferrous salt[4] and peroxides[4] it is decomposed even below 80°C. We found that sulfonium salts also decompose CHP at low temperatures (below 80°C), even though the character of the catalytic action is different from that of the above catalysts.

In the low-temperature decomposition of CHP by the use of triphenylsulfonium chloride, the main decomposition products are homolytic products: acetophenone (AP), dicumyl peroxide (DCP), and α-cumyl alcohol (CA). It is noticeable that the sulfonium salt catalyses the formation of methyl alcohol, which is scarcely at all found in the usual thermal decomposition of CHP in cumene.[1-3] This decomposition reaction is of a heterolytic nature because of the formation of phenol and acetone. Such processes of a heterolytic nature may be caused by an action of the counter chloride anion of the sulfonium catalyst. A presumption is made that the partially-occupied *d* orbitals[8] of the sulfonium cation might play an important role in the decomposition of CHP.

Experimental

Reagents. Commercial cumene hydroperoxide (CHP) (purity below 70%) was distilled in order to collect a fraction, 60°C/0.1 mmHg. In order to free it from traces of impurities, the fraction was extracted with sodium bicarbonate, filtered chromatographically through activated alumina (200—300 mesh), and stored in a nitrogen atmosphere at 0°C. The cumene was purified as has previously been described.[8,9] The sample of α-cumyl alcohol (CA) used (free from acetophenone) was recrystallized several times from ligroin. The dicumyl peroxide (DCP) and hydroquinone employed were of a commercially pure grade. The triphenylsulfonium chloride was prepared by the method described in a previous report.[10]

1) J. W. Forgham and H. L. Williams, *Can. J. Res.*, **B27**, 943 (1949).
2) V. Stannett and R. B. Mesrobian, *J. Amer. Chem. Soc.*, **72**, 4125 (1950).
3) M. S. Kharasch, A. Fono and W. Nudenberg, *J. Org. Chem.*, **16**, 113 (1951).
4) M. S. Kharasch, A. Fono and W. Nudenberg *ibid.*, **15**, 753, 763 (1950).
5) M. S. Kharasch, F. S. Arimoto and W. Nudenberg, *ibid.*, **16**, 1556 (1951).
6) D. H. Johnson and A. V. Tobolsky, *J. Amer. Chem. Soc.*, **74**, 938 (1952).
7) B. Baysal and A. V. Tobolsky, *J. Polym. Sci.*, **8**, 529 (1952).
8) K. Fukui, K. Ohkubo and T. Yamabe, This Bulletin, **42**, 312 (1969).
9) K. Ohkubo, T. Yamabe and K. Fukui, *ibid.*, **42**, 2220 (1969).
10) K. Fukui, K. Kanai, T. Takezono and H. Kitano, *Kogyo Kagaku Zasshi*, **67**, 1131 (1964).

Analysis of Reaction Products. The CHP, DCP, AP, and CA were determined in a way previously described.[9] The gaseous reaction products were collected by condensation at −76°C and were determined by gas chromatography as well as by an Orsat apparatus. For oxygen absorption, Fieser's solution[11] and a pyrogallol solution were used. The determination of the products obtained in trace amounts was also performed. The phenol was converted to tribromophenol.[12] The acetone was estimated on the basis of the iodoform equivalent.[13]

Reaction Procedure. The decomposition reaction of CHP in the presence of triphenylsulfonium chloride was carried out as follows. Triphenylsulfonium chloride was introduced into a reaction vessel containing CHP (22.5 mmol) and cumene (20 m*l*). The homogeneous reaction mixture was stirred with a magnetic stirrer at the desired temperature. The evolved gas was then collected at −76°C by a gas trap attached to an Orsat apparatus. The decomposition of CHP in cumene was followed by iodometric titration.

Results and Discussion

It is worthy of emphasis that CHP in cumene decomposes appreciably in the presence of sulfonium salts at relatively low temperatures (below 80°C), even though CHP is thermally so stable that little decomposition takes places in 48 hr at 100°C.[14] These phenomena are indicated in Fig. 1, where the thermal decomposition is very little, while the catalytic reaction is accelerated with the increase in the amount of the sulfonium catalyst and in the reaction temperature. The decrease in catalytic ability for CHP decomposition with the reaction time, especially at 80°C, may be connected with the masking action[9] of the products and of

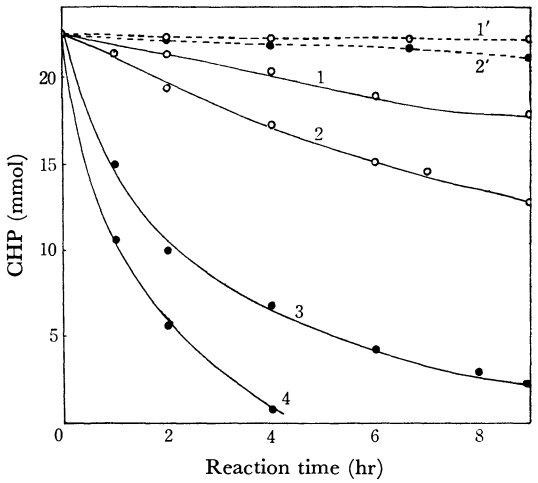

Fig. 1. The decomposition of CHP in the presence of $(C_6H_5)_3SCl$.
—○—: at 65°C, 1. 0.27 mmol 2. 0.35 mmol
—●—: at 80°C, 3. 0.27 mmol 4. 2.12 mmol
---○---: at 65°C, 1′. None
---●---: at 80°C, 2′. None

CHP itself, since the kinetic order of the reaction rate to the amount of the catalyst gradually decreases with the reaction time considering a first-order cleavage of CHP[3,6,7] (from the 0.55th order at the initial step to the 0.51st order and 0.47th order at 2.0 hr and 3.0 hr respectively). Table 1 indicates the distribution of reaction products with the reaction time. The formation of AP, DCP, and CA suggests that the catalytic decomposition of CHP is homolytic, while the small quantities of

TABLE 1. THE DECOMPOSION OF CHP (22.4 mmol) BY $(C_6H_5)_3SCl$ (0.37 mmol) AT 65°C

Reaction time (hr)	CHP decomposed (mmol)	Products[c] AP (%)	DCP[a] (%)	CA (%)	C_6H_5OH (%)	CH_3COCH_3 (%)	Gas[b] (%)
1.0	0.9	48.3	45.5	1.1	trace	trace	30.3
2.0	3.2	45.4	46.6	1.8	0.6	0.3	37.2
4.0	5.1 (0.05)*	42.0	40.8	5.9	—	—	—
7.0	7.8 (0.10)*	44.3	39.6	7.4	1.0	0.9	—
10.3	12.5 (0.50)*	41.2 (63.8)*	38.4 (21.4)*	9.6 (5.2)*	1.2 (0.0)*	1.1 (0.0)*	33.4 —

* Thermal decomposition of CHP.
a) Mol% was calculated from 2× DCP formed(mol)/ CHP decomposed(mol).
b) The gas evolved in this experiment was not thoroughly analyzed, but contains mainly methane. Oxygen was not detected in appreciable amounts.
c) Products were presented by mol% on the basis of CHP decomposed.

11) L. F. Fieser, *J. Amer. Chem. Soc.*, **46**, 2639 (1924).
12) R. L. Shriner, R. C. Fuson and D. Y. Curtin, "The Systematic Identification of Organic Compounds," John Wiley & Sons, New York (1956), p. 264.
13) R. L. Shriner, R. C. Fuson and D. Y. Curtin, *ibid.*, John Wiley & Sons, New York (1956), p. 156.
14) M. S. Kharasch, A. Fono and A. C. Poshkus, *J. Org. Chem.*, **15**, 775 (1950).

TABLE 2. THE EFFECT OF THE AMOUNT OF $(C_6H_5)_3SCl$ UPON THE DECOMPOSITION OF CHP (22.5 mmol)

$(C_6H_5)_3SCl$ (mmol)	Reaction temp. (°C)	Reaction time (hr)	CHP decomposed (mmol)	Products[a] AP (%)	DCP (%)	CA (%)	CH_3OH[b] (%)	C_6H_5OH (%)	CH_4[c] (%)	O_2 (%)
0.27	65	9.0	4.50	50.6	37.4	11.1	12.1	—	30.4	0.0
0.27	65	13.0	7.2	57.8	30.2	9.2	18.2	1.7	—	0.0
0.37	65	9.0	10.1	52.6	30.3	8.0	12.8	—	32.0	0.0
0.50	65	13.0	12.40	58.8	21.1	10.1	17.4	2.0	—	—
0.27	80	9.0	20.47	51.4	32.8	14.5	—	—	32.1	—
2.12	80	5.0	22.39	59.3	24.7	15.6	11.7	1.2	—	—
7.03	80	4.0	21.80	48.8	38.2	8.8	13.2	1.5	—	0.0

a) Products were presented by mol% on the basis of CHP decomposed. But DCP (%) was calculated from 2×DCP formed(mol)/CHP decomposed(mol).
b) This amount of methyl alcohol was determined from that of CH_3OH in the gas trap and its amount in the reaction mixture was negleted.
c) Gaseous products were not analyzed but tentatively assumed as methane.

phenol and acetone produced imply that this reaction might include the heterolytic cleavage of CHP. Moreover, as is shown in Table 2, one of the products of this reaction is an appreciable amount of methyl alcohol, which is hardly ever found in a usual homolytic thermal decomposition reaction in such non-polar solvents as cumene. From these results, the mechanism of this low-temperature reaction may be discussed.

$$\mathrm{ROOH} + (C_6H_5)_3SCl \longrightarrow \left[\begin{array}{c} H \\ \overset{\alpha}{O}\text{–}\overset{\beta}{O}\cdots\overset{+}{S}(C_6H_5)_3\cdots Cl^- \\ R \end{array}\right] \longrightarrow \mathrm{RO}\cdot + \cdot\mathrm{OH} + (C_6H_5)_3SCl \quad (1)$$

$$(R = C_6H_5(CH_3)_2C\text{–})$$

In the first step of this reaction, sulfonium salt may cleave the oxygen-oxygen bond of CHP into two parts, α-cumyloxy and hydroxy radicals. In all the bonds of CHP, the oxygen-oxygen bond is the weakest in the sense that the dissociation energy of this bond is considerably smaller than those of the other bonds. Following a molecular orbital calculation by Fukui *et al.*,[15] the lowest vacant orbitals of hydroperoxides are the $p\sigma$-type anti-bonding orbitals of the O–O bond. In the catalytic process, the electron of the partially-occupied *d* orbital[8] of the central sulfur atom of the sulfonium cation may be transferred to this lowest vacant orbital. The interaction of this orbital with electron-donor molecules would take place in the direction of the bond axis from the β-oxygen side, since the partial population of the β-oxygen of this vacant orbital is larger than that of the α-oxygen.[15] The charge transferred from the sulfonium moiety to the oxygen-oxygen bond may increase the antibonding character of the bond and promote the scission. This circumstance is portrayed in Fig. 2. In this figure, the structure of the triphenylsulfonium ion is assumed to be a propeller-like D_3 symmetry, like the triphenylcarbonium cation.[16] In this connection the mode of the interaction between the $p\sigma$-orbital of the O–O bond and the "partially occupied" *d*-orbital[8] on the sulfonium sulfur atom comes into question. From both energetic and steric points of view, the d_{z^2}-orbital seems to the most probable *d*-orbital interacting with CHP. Several reasons for this can be mentioned: (1) d_{xy} and $d_{x^2-y^2}$ orbitals in the field of the sp^2-hybridized S atom[8] are energetically unstable because of the interaction with three sulfur-phenyl bonds; (2) the interaction of the *d*-orbitals (d_{xy} and $d_{x^2-y^2}$) with CHP will be sterically hindered by phenyl groups; (3) d_{xy} and d_{yz} orbitals become somewhat unstable by the interaction, through d-π-type conjugation, with π-orbitals of phenyl groups,[17-19] while phenyl rings also sterically hinder the interaction with CHP to some extent (see Fig. 2), and (4) the d_{z^2}-orbital is most acceptable because it has no conjugation with the π orbitals of phenyl groups and because it has only a small interaction with sulfur-phenyl bonds.

In the transition state shown in the scheme of reaction (1), the hydroxyl group may bear a somewhat ionic character in view of the large electron affinity of the HO radical (~136 kcal).[20] At this stage, the partially-ionic hydroxyl group would exhibit a counter-anion like behavior.*1 In conformity with the liberation of the OH radical, the

15) T. Yonezawa, O. Yamamoto, H. Kato and K. Fukui, *Nippon Kagaku Zasshi*, **87**, 26 (1966).

16) D. W. A. Sharp and N. Sheppard, *J. Chem. Soc.*, **1957**, 674.

17) L. Goodman and R. W. Taft, *J. Amer. Chem. Soc.*, **87**, 4385 (1965).

18) R. W. Taft and J. W. Rokshys, Jr., *ibid.*, **87**, 4387 (1965).

19) C. C. Price and S. Oae, "Sulfur Bonding," The Ronald Press, New York (1962), p. 152.

20) N. Uri, *Chem. Rev.*, **50**, 375 (1952).

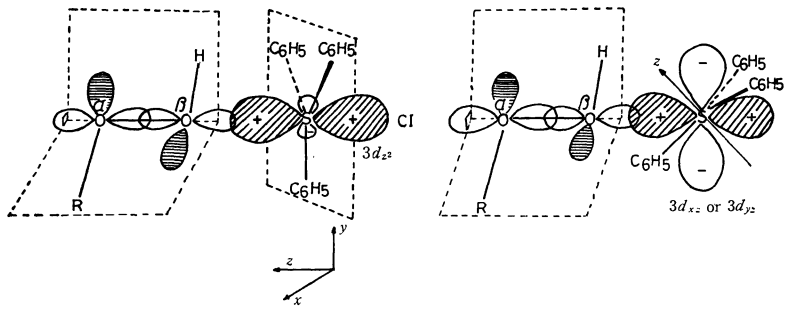

Fig. 2. Assumed mode of reaction between ROOH and $(C_6H_5)_3SCl$.

electron migration would take place, again through the central sulfur, to an opposite-side-lying chlorine atom, thus regenerating the triphenylsulfonium chloride. Actually, triphenylsulfonium hydroxide is never formed in the final system. The α-cumyloxy radicals primarily formed are then readily converted to the major reaction products (presented in Table 1) through reactions (2a), (2b), and (2c).

$$\mathrm{RO}\cdot \xrightarrow{\beta\text{-scission}} \mathrm{AP} + \mathrm{CH_3}\cdot \quad (2a)$$

$$\mathrm{RO}\cdot \xrightarrow[\mathrm{RO}\cdot]{\text{coupling}} \mathrm{DCP} \quad (2b)$$

$$\mathrm{RO}\cdot \xrightarrow[\mathrm{RH}]{\text{hydrogen abstraction}} \mathrm{ROH} + \mathrm{R}\cdot \quad (2c)$$

(R = α-cumyl)

The reaction of the RO radical with ROOH is not presented because the reaction does not seem essential; the concentration of ROOH is much lower than that of RH.

Among the above products, DCP and AP are formed predominantly. The formation of such large amounts of the former may be attributed to its thermal stability in this temperature range. However, an accumulation of DCP causes gradual decomposition as the reaction proceeds, because DCP is decomposed by the sulfonium catalyst[9] to some extent. The results are shown in Table 1. The remarkable formation of AP may be attributed to the ease of the β-scission of a carbon-methyl bond in the α-cumyloxy radical. After the α-cumyloxy radical is formed from the cleavage of the O–O bond of CHP, the odd electron may conjugate with the sigma electrons of a $C–CH_3$ bond through π-type orbital overlapping. This is a pi-participation of the oxygen *p*-electron in the β-methyl fission.

Interestingly, CA is formed only in small amounts. No such result was observed in the thermal decomposition at higher temperatures,[3,4] where both CA and AP are produced in comparable amounts. The CA formation may be depressed at lower reaction temperatures by the steric hindrance of both bulky reactants (α-cumyloxy radical and cumene). The small quantity of CA formation will be discussed below.

On the other hand, the hydroxy radical primarily formed from CHP readily undergoes conversion to CH_3OH and H_2O through hydrogen abstraction or through coupling with the methyl radical.

$$\cdot\mathrm{OH} \xrightarrow[\mathrm{RH}]{} \mathrm{H_2O} + \mathrm{R}\cdot \quad (3a)$$

$$\cdot\mathrm{OH} \xrightarrow[\mathrm{ROOH}]{} \mathrm{H_2O} + \mathrm{RO_2}\cdot \quad (3b)$$

$$\cdot\mathrm{OH} \xrightarrow[\cdot\mathrm{CH_3}]{} \mathrm{CH_3OH} \quad (3c)$$

Reactions (3a) and (3c) are probable because water*2 and methyl alcohol are found in the products in appreciable amounts (see Tables 2 and 3). Reaction (3b) seems not very likely to occur since the oxygen evolution expected from the recombination of the cumylperoxy radical*3 was not observed. Kharasch[3] also argued the difficulty of reaction (3b) from the kinetic point of view. The coupling and disproportionation of the OH radical must also be mentioned.

$$\cdot\mathrm{OH} + \cdot\mathrm{OH} \rightleftharpoons \mathrm{H_2O_2} \quad (3d)$$

$$\cdot\mathrm{OH} + \cdot\mathrm{OH} \longrightarrow \mathrm{H_2O} + \cdot\mathrm{O}\cdot \quad (3e)$$

However, these reactions are obviously much less important than (3a) and (3c). In reaction (3d), the reverse reaction is dominant in the present case. Reaction (3e) may be difficult energetically; actually, no evolution of gaseous oxygen was observed.

*1 This is expected from the fact that triphenylsulfonium chloride is actually very hygroscopic and that an air-polluted sample shows an appreciable OH peak in the infrared region. It should here be stressed, however, that in spite of such a strong affinity to OH groups, triphenylsulfonium salt does not decompose easily in polar sovents containing OH groups, such as water, hydroperoxides and various kinds of alcohols, and can even be recrystallized from them. It should further be emphasized that no products formed by the coupling of R· or CH_3· with the chlorine atom, such as α-cumyl chloride and methyl chloride, result from this decomposition reaction.

*2 The quantitative determination of the amount of water was not performed in our experiments.

*3 Cumylperoxy radicals (RO_2·) easily combine with each other to evolve gaseous oxygen: $2RO_2\cdot \rightarrow [RO_4R] \rightarrow 2RO\cdot + O_2$

Radicals produced secondarily by dismutation or by reaction with the solvent (RH) may take part in the decomposition of CHP.[1,2] In the first place, the methyl radical formed mainly from the β-scission of the α-cumyloxy radical contributes to the formation of methyl alcohol reaction (4a) as well as to the formation of gaseous products through reactions (4b) and (4c):

$$\bullet CH_3 \xrightarrow{ROOH} CH_3OH + RO\bullet \quad (4a)$$

$$\bullet CH_3 \xrightarrow{RH} CH_4 + \bullet R \quad (4b)$$

$$\bullet CH_3 \xrightarrow{RO\bullet} C_2H_6 + AP \quad (4c)$$

Reaction (4a) may be promoted by the sulfonium catalyst for the same reasons as is the decomposition of CHP (see reaction (1)). Reactions (4b) and (4c) appear to take place more readily than (4a), since gaseous products are actually formed in larger amounts than methyl alcohol*4 (see Tables 2 and 3).

In the second place, the slight CA formation, compared with that of AP, would be explained by the behavior of the α-cumyloxy radicals (RO$\bullet$) formed in the primary step (1) and in the secondary step (4a). The possible reactions of CA formation may be reactions (2c), (5a), and (5b):

$$RO\bullet \xrightarrow{RH} ROH + R\bullet \quad (2c)$$

$$RO\bullet \xrightarrow{ROOH} ROH + RO_2\bullet \quad (5a)$$

$$RO\bullet \xrightarrow{H_2O} ROH + HO\bullet \quad (5b)$$

If the ease of the hydrogen abstraction of the RO radical depends mainly on the bond-dissociation energy in hydrogen donors, reactions (2c) and (5a) will be more predominant than (5b), because the dissociation energies of R–H ($\sim$85 kcal) and ROO–H ($\sim$89.5 kcal)*5 are considerably lower than HO–H ($\sim$120 kcal[10]). However, reaction (5a) is unlikely, like (3b), because of the low concentration of ROOH compared with RH; the absence of reaction (5a) can be ascertained from the lack of any evolution of oxygen, even though ROOH is as good a hydrogen donor as RH. Hence, it may be reasonable to conclude that CA is formed predominantly through the reaction path (2c). At any rate, the small amount of CA may be attributed to the prevalence of the intramolecular reaction (2a) over the intermolecular one (2c).

In the third place, it should be noted that the coupling product of α-cumyl radicals (R$\bullet$), namely, bi-α-cumyl (R–R), is not found in any appreciable amount. From the facts that the R radicals formed tend to be easily deactivated by the trapping of the RH solvent or of other solvents (ROOH and H_2O), and that the amount of active R radicals may be small, the chance of coupling may be small.

In the thermal decomposition of CHP in cumene at the temperatures of 128°C and 158°C, Kharasch and his co-workers[3] confirmed the negligible amount of bi-α-cumyl in spite of the remarkable formation of R radicals. They attributed this result to the reaction of the R radical with ROOH, which contributes to the CA formation through the following path:

$$ROOH + R\bullet \rightleftarrows \text{Complex A}$$

$$\text{Complex A} + RH \longrightarrow 2ROH + R\bullet$$

However, such a complex was not confirmed. As for the explanation of the negligible formation of bi-α-cumyl, the difficulty of R–R formation must first of all be mentioned, especially in the low-temperature reaction of our experiments.

The homolytic nature of the low-temperature decomposition by the sulfonium chloride may have been clarified in the above discussions. However, the reaction seems to involve a somewhat heterolytic part. The formations of phenol and acetone in measurable amounts (as is shown in Tables 1 and 2) should be regarded as the result of heterolytic decomposition. In this connection, the role of the chloride anion of sulfonium salt should be noticed. It may be reasonable to presume, as was indicated in the works by Barb and his co-workers,[23,24] by Kolthoff and Medals,[25,26] by Taube and Bray,[27] and by Allen,[28] that the chloride anion is converted to the chlorine atom through charge-transfer to the hydroxy radical:

$$Cl^- + \bullet OH \longrightarrow Cl\bullet + OH^- \quad (6a)$$

$$Cl\bullet + RH \longrightarrow HCl + R\bullet \quad (6b)$$

(or ROOH) (or RO_2)

$$C_6H_5C(CH_3)_2O_2H \xrightarrow{H^+(HCl)} C_6H_5OH + (CH_3)_2CO + H^+(HCl) \quad (6c)$$

The possibility of (6a) is also supported by the fact that reaction (6a) has the very small activation energy of 3 kcal.[20] The chlorine atom thus formed

*4 The methane formation should be ascribed to the hydrogen abstraction of $CH_3\cdot$. The activation energy of the reaction $CH_3\cdot + ROOH$ (R=*t*-butyl) $\rightarrow CH_4 + RO_2\cdot$ is 8.1 kcal, while that of $CH_3\cdot + RH$(*n*-hexane) $\rightarrow CH_4 + R\cdot$ is 11.7 kcal.[21]

21) A. F. Trotman-Dickenson, "Gas Kinetics," Butterworth Scientific Publications, London (1955).

*5 The dissociation energy of ROO–H is assumed to be the same as that of HOO–H (89.5 kcal).[22]

22) S. W. Benson, *J. Amer. Chem. Soc.*, **86**, 3922 (1964).

23) W.G. Barb, J.H.P. Baxendale, P. George and K.R. Hargrave, *Trans. Faraday Soc.*, **47**, 462 (1951).

24) W.G. Barb, J.H.P. Baxendale, P. George and K.R. Hargrave, *ibid.*, **47**, 591 (1951).

25) I. M. Kolthoff and A. I. Medala, *J. Amer. Chem. Soc.*, **71**, 377 (1949).

26) I. M. Kolthoff and A. I. Medala, *ibid.*, **71**, 3784 (1949).

27) H. Taube and W. C. Bray, *ibid.*, **62**, 3357 (1940).

28) A. O. Allen, *J. Phy. & Colloid Chem.*, **52**, 479 (1948).

TABLE 3. TEMPERATURE EFFECT UPON THE DECOMPOSITION OF CHP (22.5 mmol) BY TRIPHENYLSULFONIUM CHLORIDE

$(C_6H_5)_3SCl$ (mmol)	Reaction temp. (°C)	Reaction time (hr)	CHP decomposed (mmol)	Products[a] AP (%)	DCP (%)	CA (%)	CH_3OH (%)	CH_4[b] (%)	O_2 (%)
none	80	9.0	1.20	42.9	40.0	9.65	trace	33.0	0.0
0.27	80	9.0	20.47	51.4	32.8	14.5	—	32.1	0.0
0.27	65	9.0	10.1	52.6	37.3	8.0	12.8	35.0	0.0
3.35	55	4.0	5.50	41.6	41.3	8.2	9.8	—	—
2.12	30	4.0	0.00						

a) Products were presented by mol% on the basis of CHP decomposed.
But DCP (%) was calculated from 2× DCP formed(mol)/CHP decomposed(mol).
b) The gase evolved in this experiment was not fully analyzed, but contained mainly methane.

will react with RH or ROOH to produce HCl, which behaves as a catalyst for reaction (6c). However, in the sulfonium chloride, the supply of free Cl^- can not be expected because of the appreciable covalent nature[8] of the bond between the sulfonium cation and the counter-anion. Actually, more than 70% of the triphenylsulfonium chloride can be recovered from the reaction mixture, even after a 13-hr reaction. Hence, the contribution of the chloride anion is limited, even if it takes part in the heterolytic decomposition. This is reflected in the very small amounts of phenol and acetone formed.

Another possibility for the heterolytic decomposition of CHP has been postulated by Kharasch and his co-workers[3] in the following self-decomposition of CHP ((7) and (8)):

$$C_6H_5(CH_3)_2COOH \xrightarrow{\text{heterolytic cleavage}} C_6H_5(CH_3)_2CO^+ + OH^- \quad (7)$$

$$C_6H_5(CH_3)_2CO^+ \xrightarrow{\text{rearrangement}} C_6H_5O(CH_3)_2C^+ \quad (8)$$

The cation formed is capable of further conversion to give phenol and acetone. However, it seems difficult for reaction (7) to occur without traces of acidic impurities; therfore, the small amounts of phenol and acetone formed may be ascribed to the contribution of the chloride anion.

The temperature effect on the catalytic decomposition of CHP is shown in Table 3. As the table shows, the homolytic decomposition proceeds even at 55°C, but it disappears at 30°C. The increase in the temperature depresses the DCP formation, implying the thermal decomposition of DCP, whereas AP and CA increase to some extent.

It is necessary to investigate the effect of the decomposition products on the reaction in order to clarify the mechanism. Table 4 indicates the additive effect of CA, DCP, and hydroquinone. Hydroquinone is employed as an additive of the hydrogen donor. At first, the reaction system initially containing CA as an additive evolves gaseous oxygen, which is undetectable in the absence of the alcohol. This phenomenon may be attributed to the heterolytic decomposition of CHP, as was first pointed out by Kharasch and his co-workers.[3],*6 It is obvious that the catalytic decomposition is markedly prevented by the addition of CA. This fact may be directly connected with the masking action[9] of the additive. Such a masking action of CA depresses the catalytic activity on the homolytic decomposition of CHP, leading to the heterolytic decomposition.

Secondary, the effect of DCP addition is apparently confirmed in the remarkable formation of AP and CH_3OH. This result suggests that the growth of the RO· concentration caused by the DCP decomposition promotes reaction (2a) and subsequently (4a).

Thirdly, it is well known that hydroquinone is a good hydrogen donor as well as a radical scavenger. The remarkable effect of its addition appears to be the reaction with RO radicals to give ROH. Furthermore, hydroquinone depresses the catalytic activity through the masking action caused by the hydrogen bonds of hydroquinone molecules and disturbs the dismutation or recombination of RO radicals by the exclusive formation of ROH.

In connection with the CHP decomposition by triphenylsulfonium chloride, the reactions of CHP with such other sulfur compounds as sulfide and thiophene were also carried out. Diphenyl sulfide produced CA mainly, while thiophene formed AP predominantly, as is shown in Table 5. The sulfides have no electron in *d*-orbitals, but have lone-pair

*6 They have suggested the following mechanism of the oxygen evolution:

$$ROOH + ROH \rightleftharpoons ROO^- + ROH_2^+$$
(conjugate base) (conjugate acid)

$$ROO^- + ROOH \longrightarrow ROH + O_2 + RO^-$$

$$RO^- + ROH_2^+ \longrightarrow 2ROH$$

(R=α-cumyl)

Table 4. The effect of additives upon the decomposition of CHP (22.5 mmol) by triphenylsulfonium chloride (0.37 mmol) at 80°C for 9.0 hr

Additive (mol% on basis of CHP)	CHP decomposed (mmol)	Products[a] AP (%)	DCP (%)	CA (%)	CH_3OH (%)	C_6H_5OH (%)	CH_3COCH_3 (%)	CH_4[b] (%)	O_2 (%)
None	21.38	40.2	36.5	12.3	11.7	1.5	1.3	32.4	0.0
α-Cumyl alcohol (5.0%)	17.4	46.7	30.7	16.8	13.6	2.8	2.2	—	4.0
Dicumyl peroxide (5.0%)	22.5	54.9	—	9.4	19.3	—	—	—	0.0
Hydroquinone (10%)	14.0	32.6	25.0	35.5	15.8	3.0	2.5	—	0.0

a) Products were presented by mol% on the of basis of CHP decomposed. But DCP (%) was calculaed from 2× DCP formed(mol)/CHP decomposed(mol).
b) Gaseous products were not analyzed and assumed as methane because ethane may be produced only in negligibly small amounts.

Table 5. The decomposition products of CHP by the use of sulfur compounds (initial amount of CHP: 22.5 mmol, reaction temperature: 80°C)

Compound	The amount of the compound (mmol)	Reaction time (hr)	The amount of CHP decomposed (mmol)	Products AP (mmol)	DCP (mmol)	CA (mmol)
$(C_6H_5)_2S$	2.84	3.0	6.0	0.72	1.0	3.0
$(C_6H_5)_2S$	7.40	4.0	20.0	1.64	2.2	13.8
$(C_6H_5)_2S$	10.8	4.0[a]	trace			
$(C_6H_5)_2S{=}O$	23.4	3.0	trace			
$CH(CH)_3S$	6.0	3.0	4.6	4.0		
$CH(CH)_3S$	23.8	4.0[b]	15.6	13.6		

a) The reaction temperature was 25°C.
b) The reaction temperature was 65°C.

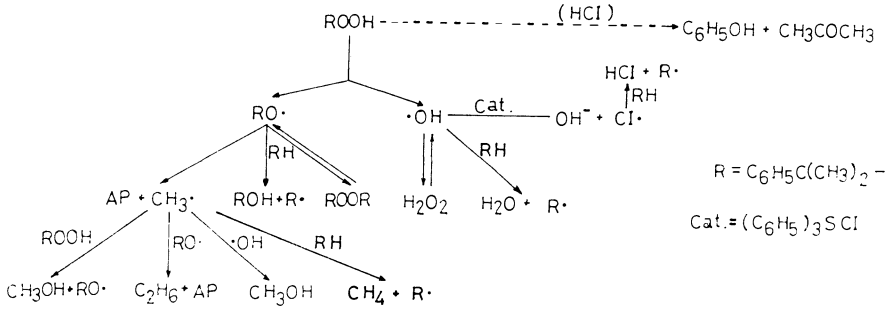

Fig. 3. A scheme for the mechanism of CHP decomposition by $(C_6H_5)_3SCl$.

electrons in the *p*-orbitals. They may act on CHP as nucleophiles and come to be sulfoxides themselves, which means that the hydrogen atom of CHP might migrate to the RO radical to form ROH in the transition state of the reaction. Detailed discussions will not be undertaken here, however, since the mechanism of the reaction of sulfides with hydroperoxide has been extensively discussed by many authors.[29-33]

29) L. Bateman and K. R. Hargraue, *Proc. Roy. Soc.*, **A 224**, 389, 399 (1954).
30) L. Bateman and J. Cunneen, *J. Chem. Sec.*, **1955**, 1596.
31) L. Bateman and F. W. Sibley, *ibid.*, **1955**, 1996.
32) D. Barnard, *ibid.*, **1956**, 489.
33) K. R. Hargraves, *Proc. Roy. Soc.*, **A 225**, 55 (1956).

In conclusion, the decomposition mechanism of cumene hydroperoxide by triphenylsulfonium chloride is schematically illustrated in Fig. 3.

The features of the present experiments may be summarized thus:

a) In the low-temperature range (55—80°C), triphenylsulfonium chloride decomposes CHP remarkably. The partially-occupied $3d_{z^2}$ orbital of the central sulfur atom of the sulfonium salt may participate in the cleavage of the O–O bond of CHP.

b) The chloride anion of the sulfonium catalyst seems to be connected with the heterolytic decomposition of CHP.

c) Among the decomposition products, AP and DCP are mainly formed, while CA is found only in small quantities.

d) Methyl alcohol is formed in appreciable amounts. The catalyst is likely to aid its formation.

e) The hydroxy radicals primarily formed are consumed to produce H_2O and CH_3OH.

BULLETIN OF THE CHEMICAL SOCIETY OF JAPAN VOL. 43 8—12 (1970)

Absorption Spectra of ^2E States of Some Chromium(III) Complexes Revealed by Flash Method

Takeshi OHNO and Shunji KATO

Institute of Chemistry, College of General Education, Osaka University, Toyonaka, Osaka

(Received April 9, 1969)

Excited states of some chromium(III) complexes were studied by a flash technique at −196°C. Transient species with strong absorption bands in visible and near UV regions were observed to decay at the same rate as their phosphorescence for $Cr^{III}(acac)_3$, $K_3[Cr^{III}(NCS)_6]$, $NH_4[Cr^{III}(NCS)_4(NH_3)_2]$, and $Cr^{III}(exan)_3$. They are therefore ^2E states (phosphorescent states). A strong absorption band for $Cr^{III}(acac)_3$ is assigned to a charge transfer transition from ^2E state based on the intensity and energy of the transition. A transition to localized excited states in ligand with a small extinction coefficient was observed in near infrared region for $Cr^{III}(acac)_3$.

It is known that triplet excited states of organic compounds play important roles in photochemical reactions.[1] Triplet excited states have often been confirmed in rigid media at low temperature by their phosphorescence and ESR signals.[2] However, they are scarcely observed in fluid media at room temperature, at which photochemical reactions usually take place. Absorption spectra of triplet excited states are observed with less difficulty by means of flash technique even in a condition where neither phosphorescence nor ESR signals were detected.[3]

Among coordination compounds of transition metals, many chromium(III) complexes are known to emit phosphorescence in rigid solvents[4]; the most prominent example is ruby laser.[5] The phosphorescent state has been assigned to ^2E state.[6] Although no phosphorescence has been observed for the complexes in fluid media at room temperature, ^2E states are believed to have a significant part in photoreactions.[7] Direct observation of these states is desirable for a precise discussion of the mechanism of the photochemical reactions of the complexes. These states are expected to be detected as absorption spectra in fluid media by means of flash technique.

For this purpose, it is desirable to examine favorable complexes which have high extinction coefficients in the excited states. Absorption bands due to *d–d* transition from ^2E state will be weak since such transitions are all parity-forbidden. It is hard

1) T. Ohno, S. Kato and M. Koizumi, This Bulletin, **39**, 232, (1966).

2) J. G. Calvert and J. N. Pitts, Jr., "Photochemistry," John Wiley & Sons, Inc., New York (1966).

3) G. Porter and M. W. Windsor, *Discuss. Faraday Soc.*, **17**, 178 (1954).

4) G. B. Porter and H. L. Schläfer, *Ber. Bunsenges. Phys. Chem.*, **68**, 316 (1964).

5) T. H. Maiman, R. H. Hoskins, I. J. D'Haenens, C. K. Asawa and V. Eutuhov, *Phys. Rev.*, **123**, 1151 (1961).

6) G. B. Porter and H. L. Schläfer, *Z. Physik. Chem., N. F.*, **40**, 280 (1964).

7) H. L. Schläfer, *Z. Physik. Chem.* (Frankfurt), **11**, 65 (1957). M. R. Edelson and R. A. Plane, *Inorg. Chem.*, **3**, 231 (1964).

to analyze such weak bands because the measurements will be seriously interferred by the absorption of the ground state unchanged after flash irradiation. For this reason $NH_4[Cr^{III}(NCS)_4(NH_3)_2]$, $K_3[Cr^{III}(NCS)_6]$, $Cr^{III}(acac)_3$,*1 and $Cr^{III}(exan)_3$,*2 were examined, the ^2E states of which were expected to show intense charge transfer absorptions in visble or near UV regions. In the present investigation, identification of transient absorption bands for these complexes was made, and the decay of the absorption bands was compared with that of their phosphorescence.

Experimental

Chromium(III) Complexes. They were prepared by the usual methods. Preparation of $NH_4[Cr^{III}(NCS)_4(NH_3)_2]\cdot 3/2H_2O$, $K_3[Cr^{III}(NCS)_6]\cdot 4H_2O$, $Cr^{III}(acac)_3$, and $Cr^{III}(exan)_3$ was based on the method by Dakin, Repsler, Cooperstein, and Dubsky respectively.[8]

Solvents. Ethanol was dried over calcium oxide, followed by refluxing with silver nitrate and distillation. Ether was dried over calcium chloride and distilled over metallic sodium. Isopentane was distilled over metallic sodium.

Polymer Rods doped with Chromium(III) Complexes. Methyl methacrylate monomer solution of a chromium(III) complex was polymerized in a glass tube at 40°C for three days using azobis-butyronitrile. The polymer rod thus prepared was cut in a length of 10 cm and polished at the ends with a fine emery. The polymer rods were clear and had no serious stria.

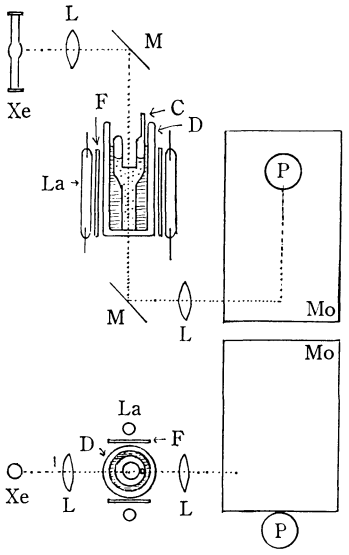

Fig. 1. Schematic diagram of the optical system of the flash apparatus.
Xe: 150 W xenon lamp (Ushio UXL-150), L: lenz, M: mirror, C: quartz cell, D: Dewar's vessel, F: cut-off filter (Toshiba Co), La: flash lamp, P: photomultiplier (1P-28 or 7102), Mo: monochrometer (Nalumi RM-23)

*1 acac: acetylacetonate ion.

*2 exan: ethylxanthogenate ion.

8) Y. Shimura, "Jikken Kagaku Koza," Vol. 11, Maruzen, Tokyo (1957), pp. 58—60.

Measurements. A schematic diagram of the optical system is shown in Fig. 1. The output of the photomultiplier was recorded by a Hitachi synchroscope V-116. Two flash lamps were connected in series to a 4μF capacitor and fired at 10 kV. Cut-off filter transmitted light of wave numbers lower than 27 kK. A photomultiplier IP-28 (Hamamatsu TV Co.) was used for higher wave numbers, and a photomultiplier 7102 (Hamamatsu TV Co.) for lower wave numbers than 16 kK.

A quartz cell, 8 mm in inner diameter and 10 cm in optical path, was placed in a quartz Dewar vessel filled with liquid nitrogen. The polymer rod was placed in a coolant without cover.

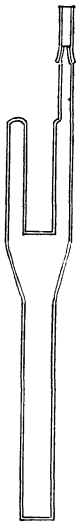

Fig. 2. Cross section of the quartz cell.

Results

When $Cr^{III}(acac)_3$, $NH_4[Cr^{III}(NCS)_4(NH_3)_2]$, $K_3[Cr^{III}(NCS)_6]$, and $Cr^{III}(exan)_3$ were irradiated with flash light in EPA or rigid polymethyl methacrylate at −196°C, transient absorption spectra were observed without any permanent change. The spectra shown in Fig. 3 were constructed from the absorbances measured on the oscillograms obtained for different wave numbers of monitoring light, 20 μsec after the triggering of the photolysis flash. A typical oscillogram is shown in Fig. 4.

In Fig. 3, ΔA in the ordinate is the transient increase in absorbance caused by flash irradiation. ΔA is expressed as follows,

$$\Delta A = (\varepsilon_T C_T + \varepsilon_G \Delta C_G) l \qquad (1)$$

where ε_T and ε_G represent the molar extinction coefficients of the transient species and the complex in the ground state, respectively, C_T the concentration of the transient species, ΔC_G the transient decrease in the concentration of the ground state and l the optical path length. In order to obtain the

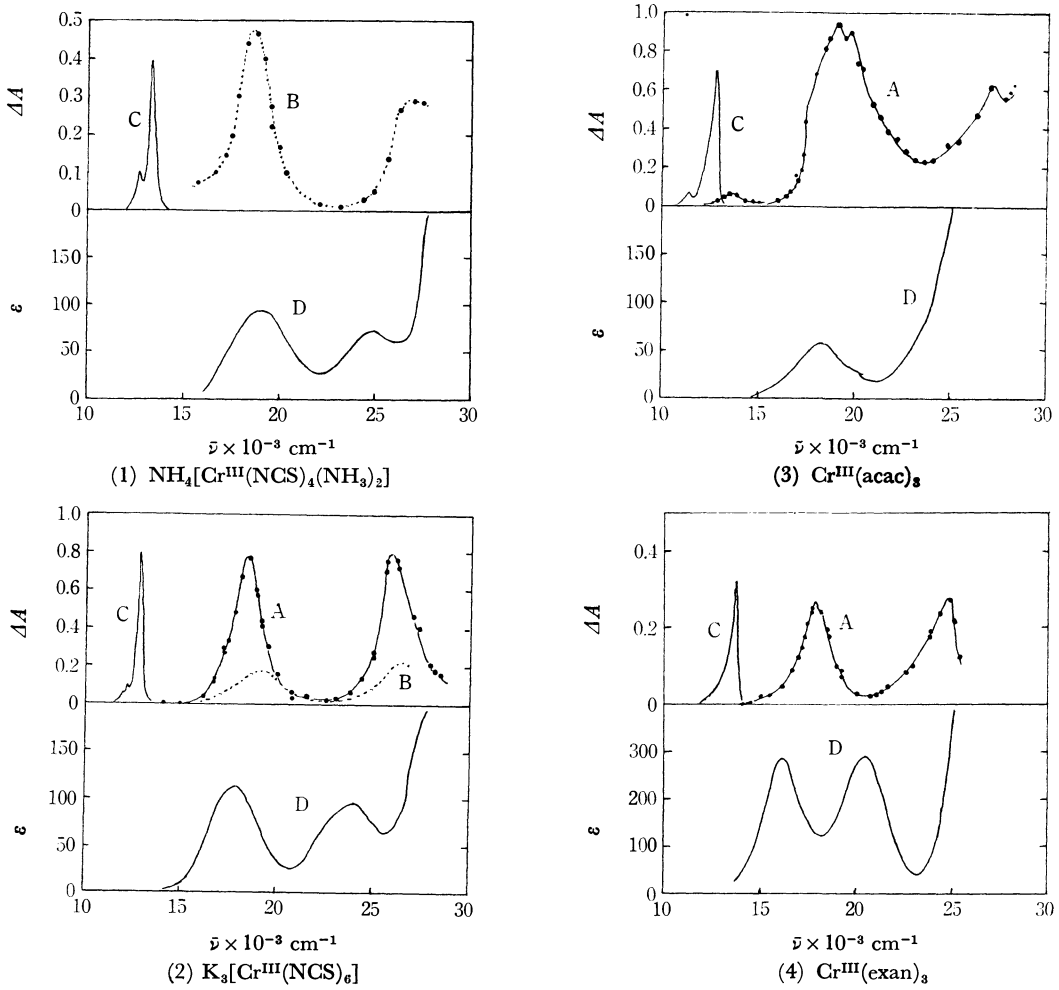

Fig. 3. Absorption spectra of the transient species and the ground states and phosphorescence spectra. A: absorption spectrum of the transient in EPA, B: absorption spectrum of the transient in polymethyl methacrylate, C: phosphorescence spectrum, D: absorption spectrum of the ground state in ethanol.

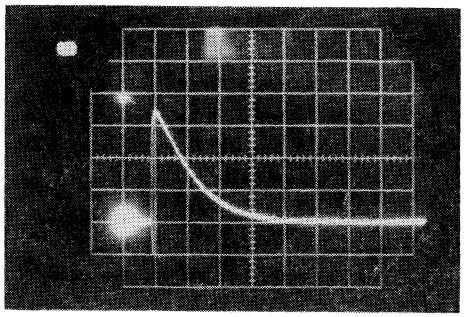

Fig. 4. A typical oscillogram of the decay curve of transient absorption.
$Cr^{III}(acac)_3$: 5×10^{-4}M in EPA. Point upper left is 0% transmission, straight line at bottom 100% transmission, and one division 5 msec. Monitoring light is 18.5 kK.

true absorption spectrum of the transient species, a correction must be made for the term $\varepsilon_G \Delta C_G$. Although the number of molecules in the ground state transiently consumed by light absorption is difficult to estimate, it cannot exceed the number of photons absorbed by the sample. The number was measured by using the aqueous solution of the same complex as an actinometer, the quantum yield of which is known to be 0.28. The highest value of $-\Delta C_G$ thus obtained was 4.3×10^{-5} mol/l for $NH_4[Cr^{III}(NCS)_4(NH_3)_2]$ in polymer. It follows that the correction to obtain true absorbance of the transient species is estimated to be 0.04 in the *d–d* bands at the largest. In the region of wave numbers lower than 15 kK, there is practically no absorption of the ground state to be corrected.

For the same concentrated solutions of $Cr^{III}(acac)_3$ and $K_3[Cr^{III}(NCS)_6]$ with that of $NH_4[Cr^{III}(NCS)_4(NH_3)_2]$, the highest values of $-\Delta C_G$ are similar to that of the last, because both solutions of the complexes have very similar absorption spectra to that of the last in visible regions. Over

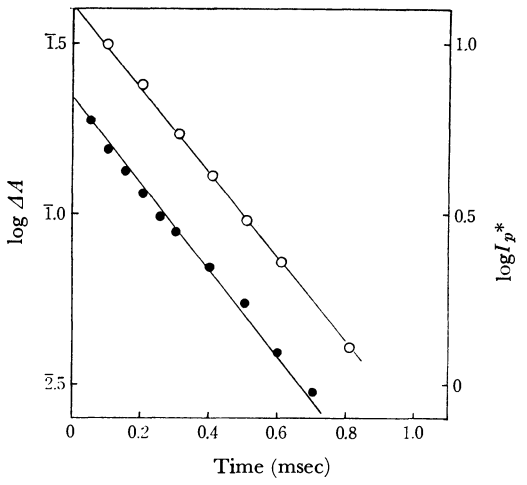

Fig. 5. Decays of the transient absorption and the phosphorescence of 5×10^{-4}M $Cr^{III}(acac)_3$ in EPA at −196°C.
—○—: transient absorption at 21.3 kK
—●—: phosphorescence at 12.8 kK
* I_p=intensity of phosphorescence

27 kK in the case of $Cr^{III}(acac)_3$, the largest correction (0.14) appears. Even this largest possible value is less than one fifth of the observed absorbance change. Thus the ΔA spectra in Fig. 3 can be regarded as the spectra of the transient species without correction.

The general features of transient spectra resemble each other, although peaks in UV regions for some complexes are obscure on account of the interference of the intense charge transfer absorption of the ground states. A weak absorption band appears in near IR regions only for $Cr^{III}(acac)_3$. For other complexes, no such band was detected even in the conditions of higher flash energy.

Table 1. Life-time of the trasient species at −196°C

Complex	Solvent	Life-time (msec) Absorption	Phosphorescence	
$Cr^{III}(acac)_3$	EPA	0.33	0.36	0.42*
$Cr^{III}(acac)_3$	polymer	0.44	0.44	
$Cr^{III}(exan)_3$	EPA	0.28	0.31	
$K_3[Cr^{III}(NCS)_6]$	EPA	10.1	9.6	2.38*
$K_3[Cr^{III}(NCS)_6]$	polymer	3.1	2.6	
$NH_4[Cr^{III}(NCS)_4(NH_3)_2]$	polymer	0.16	0.16	0.31*

* measured by L. S. Forster at −140——150°C in ethylene glycol and water (2 : 1) except for $Cr^{III}(acac)_3$ in EPA at −188°C.[9]

9) K. K. Chatterjee and L. S. Forster, *Spectrochim. Acta*, **20**, 1603 (1964); D. C. Bhatnagar and L. S. Forster, *ibid.*, **21**, 1803, (1965); K. DeArmond and L. S. Forster, *ibid.*, **19**, 1687, (1963).

The transient absorption decayed in a first order process (Fig. 5), and the decay constant for each complex was independent of the monitoring wave number. This result proves that the whole spectrum is due to a single transient species.

Phosphorescence also decayed in a first order process (Fig. 5). The rate constants are represented in Table 1 with those for the transient absorptions. The coincidence between the life-time of the transient absorption and that of the phosphorescence for each complex indicates that both measurements were made for the same species in different ways.

Molar extinction coefficients of the transient species can be calculated from the absorbances and the numbers of photon absorbed, if the quantum yields of the species are known.

The values ε' in Table 2 are calculated on a tentative assumption that the quantum yields are equal to unity. A discussion for ε will be given.

Table 2. Life-time of the transient species at −196°C

Complex	Solvent	Peak kK (cm^{-1})	ε'	ε
			10^3 l/mol·cm	
$NH_4[Cr^{III}(NCS)_4(NH_3)_2]$	polymer	18.6	1.1	3.8
		27	0.8	2.8
$K_3[Cr^{III}(NCS)_6]$	EPA	18.6	1.8	3.8
		26	1.9	4.0
$Cr^{III}(acac)_3$	EPA	13.5	0.2	0.3
		18.5	2.2	3.3
		27	1.4	2.1

Discussion

1) Origin on the Transient Spectra. It is established that the phosphorescence states of trivalent chromium complexes in rigid media are ^2E states. The good agreement of the life-time of the transient spectrum with that of the phosphorescence for each complex may lead to the conclusion that the spectrum is due to the ^2E state. The life-time obtained in the present investigation is comparable with the values measured by Forster at −140——150°C as seen in Table 1.

2) Assignments of the Transient Absorption Bands. The extinction coefficients of the transient species ^2E estimated by assuming that the quantum yields Φ_E of the doublet states are unity, are the lowest possible values. These values are high to attribute the transient absorption bands to the *d–d* transition from ^2E state because they are parity-forbidden. The most probable assignments are charge transfer transitions as expected at the beginning.

Forster *et al.* reported the phosphorescence quantum yields (Φ_P), the natural life-times (τ_0), and the actual life-times (τ) of some chromium complexes. Employing these values, Φ_Es of NH_4-

$[Cr^{III}(NCS)_4(NH_3)_2]$, $Cr^{III}(acac)_3$, and $K_3[Cr^{III}(NCS)_6]$ are calculated by the following equation to be 0.29, 0.67, and 0.47, respectively.

$$\Phi_E = \frac{\tau_0}{\tau} \times \Phi_P \qquad (2)$$

The extinction coefficients corrected on the basis of these values are given in the last column of Table 1.

Barrunum assigned the electronic spectrum of $Cr^{III}(acac)_3$ by comparing it with many acetylacetonate complexes.[10] Hanazaki and Nagakura calculated completely the energy levels of the same complexes, using "composite molecule method" and obtained assigments similar to Barrunum's[10]. In Fig. 6 solid lines show the energy levels observed in the absorption spectrum of the complex and assigned by Hanazaki and Nagakura. The levels of doublet states represented by broken lines are calculated by the method presented by Tanabe and Sugano[12] using parameters, $Dq=1.78$, $B=0.57$, and $C=4\times B=2.28$ kK.

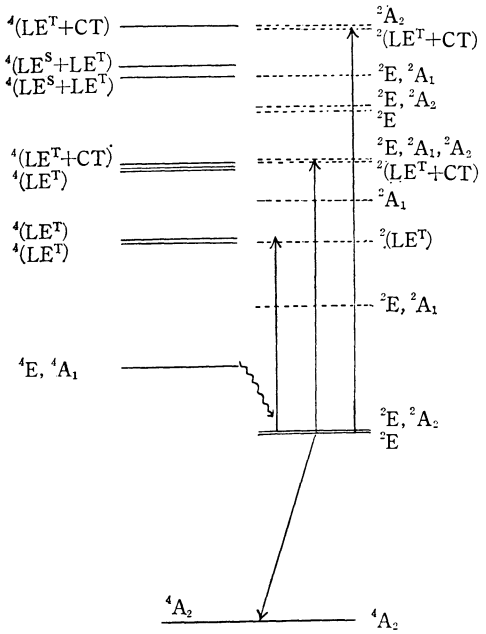

Fig. 6. Energy levels of $Cr^{III}(acac)_3$.
Solid line shows energy level of the quartet state, broken line a calculated energy level of the doublet state, and solid arrow the transition observed in this work.
LE^T: triplet state on localized excitation in ligand
LE^S: singlet state on localized excitation in ligand
CT: charge transfer excited state

Quartet charge transfer states are located 30.1 and 39.2 kK above the ground $^4A_2$ state. The energy levels of the doublet charge transfer states may not be much apart from that of the corresponding quartet state. Since ^2E state is 12.8 kK higher than the ground state, the energy differences between the doublet charge transfer states and ^2E state are 17.3 and 26.3 kK, which agree with the wave numbers of the peaks of the transient absorption spectrum.

The weak band at 13 kK for $Cr^{III}(acac)_3$ might be due to a d–d transition from ^2E state considered from the magnitude of the extinction coefficient. The energy level of $^2A_1$ state is calculated to be 14.95 kK above ^2E state, which is only 1.5 kK greater than the observed value. However, it is difficult to explain why similar bands in near IR regions were not observed for other compounds.

Another possible assignment of this band is the charge transfer transition to $^2(LE^T)$ state, which is inferred to be located 13 kK higher than ^2E state as seen in Fig. 6. This assignment is more plausible because the transition to $^4(LE^T)$ state appears in the spectrum of the ground state only for $Cr^{III}(acac)_3$ among all compounds examined.

The authors are grateful to Dr. Ichiro Hanazaki for his help to assign the transitions from ^2E state of $Cr^{III}(acac)_3$. A financial support from Fuji Photo Film Co., Ltd. is acknowledged.

10) D. W. Barrunum, *J. Inorg. Nucl. Chem.*, **21**, 221 (1961).

11) I. Hanazaki and S. Nagakura, to be published in *J. Chem. Phys.*

12) Y. Tanabe and S. Sugano, *J. Phys. Soc. Jap.*, **9**, 753 (1954).

BULLETIN OF THE CHEMICAL SOCIETY OF JAPAN VOL. 43 13—19 (1970)

Temperature Dependence of Fluorescence Spectra and Fluorescence Polarization of Some Organic Compounds in Polar Solvents. The Franck-Condon Excited States

Hiroaki BABA and Chie MUGIYA*1

Division of Chemistry, Research Institute of Applied Electricity, Hokkaido University, Sapporo

(Received May 30, 1969)

Fluorescence and absorption spectra and fluorescence polarization were measured at different temperatures, ranging from room temperature to 77°K, for 9,10-diazaphenanthrene, 2-naphthol and 2,3-naphthalenediol in polar solvents. At about 120°K, the fluorescence spectra shifted rapidly to the blue as the temperature was lowered. This observation is quantitatively interpreted on the basis of a kinetic scheme involving competitive rate processes, *viz.*, radiative transition from the Franck-Condon excited state, as defined for the dipole orientation of the solvent, and relaxation of the Franck-Condon state into the equilibrium excited state. The Franck-Condon destabilization energies are evaluated from the observed blue shifts. Along with the fluorescence blues hifts, the degrees of polarization increased rapidly, but at a somewhat higher temperature of about 140°K. This phenomenon is related to the rotational relaxation of the solute molecule, and is discussed in comparison with the fluorescence blue shift.

It is generally accepted that, in organic compounds in solution, absorption and emission transitions occur according to the Franck-Condon principle.[1-4] The effect of this principle on the electronic spectra is of especial importance when both solute and solvent molecules are polar, and there is a difference in the dipole moment between the ground and excited states of the solute. At the instant of the formation of its excited state, the solute molecule is considered to be surrounded by the solvent molecules whose orientation is appropriate to the ground state of the solute. Such a situation is referred to as the Franck-Condon excited state. This state may pass into the equilibrium excited state, where the solvent orientation is appropriate to the excited state, through a process of relaxation. Thus the fluorescence transition originates usually from the equilibrium excited state.

A few attempts have been made to obtain experimental evidence for the participation of the Franck-Condon principle in the solvent effect on the electronic spectra of aromatic compounds.[2-4] These investigations are based on the idea that the relaxation process mentioned above should be inhibited if the solvent has such a high viscosity that the relaxation time is longer than the fluorescence lifetime.

In addition to the relaxation of the solvent orientation from the Franck-Condon into the equilibrium excited state, rotational relaxation of the solute molecule may occur during the fluorescence lifetime, which leads to the depolarization of the fluorescence.[5-7] The two relaxation processes would be correlated with each other through the viscosity and hence the temperature of the solvent.

The purpose of the present study is to obtain detailed and definite information as to the Franck-Condon excited state by dealing quantitatively with these relaxation phenomena. Thus, absorption and fluorescence spectra along with degrees of fluorescence polarization were measured in a wide range of temperature with 9,10-diazaphenanthrene, 2-naphthol and 2,3-naphthalenediol as polar solutes. It has been reported[8] that for the diazaphenanthrene the dipole momet is smaller in the fluorescent

*1 Submitted to Hokkaido University, in partial fulfillment of the requirements for the degree of Doctor of Science. Present address: Department of Chemical Engineering, Faculty of Engineering Science, Osaka University, Toyonaka, Osaka.

1) N. S. Bayliss and E. G. McRae, *J. Phys. Chem.*, **58**, 1002 (1954).

2) E. Lippert, W. Lüder and F. Moll, *Spectrochim. Acta*, **10**, 858 (1959).

3) D. M. Hercules and L. B. Rogers, *J. Phys. Chem.*, **64**, 397 (1960).

4) M. L. Bhaumik and R. Hardwick, *J. Chem. Phys.*, **39**, 1595 (1963).

5) P. Pringsheim, "Fluorescence and Phosphorescence," Interscience Publishers, Inc., New York (1949), pp. 370—379.

6) F. Perrin, *Ann. Phys.*, **12**, 169 (1929).

7) J. R. Lombardi, J. W. Raymonda and A. C. Albrecht, *J. Chem. Phys.*, **40**, 1148 (1964).

8) C. Mugiya and H. Baba, This Bulletin, **40**, 2201 (1967).

excited state, which is of an (n,π^*) type,[9] than in the ground state.

Experimental

Materials. 9,10-Diazaphenanthrene (Aldrich Chemical Co., U.S.A.) was purified either by the method described in a previous paper[8] or by zone melting. 2-Naphthol and 2,3-naphthalenediol were recrystallized from ligroin and from water, and were further purified by vacuum sublimation.

Mixtures of isopentane and *n*-butyl chloride (volume ratio, 6.5 : 3.5) and of ethyl ether, isopentane and ethanol (volume ratio, 8 : 3 : 5) were used as polar solvents; these mixtures, abbreviated to PB and EPA respectively, give good rigid glasses at 77°K. Isopentane was passed through a freshly activated silica-gel column, and the other solvents were purified by methods described in "Organic Solvents."[10]

Apparatus and Procedure. Absorption spectra were obtained with a Hitachi EPS-3 spectrophotometer, and fluorescence spectra and their polarizations were measured with an apparatus constructed in our laboratory.[11] All these measurements were made on sample solutions in a 1-cm square quartz cell which was placed in a glass Dewar with quartz windows. For cooling the sample cell, nitrogen gas was passed through liquid nitrogen, and then led to the Dewar. The cell could be maintained at any desired temperature between 280 and 77°K by controlling the flow velocity of the nitrogen gas. The errors in the temperature were estimated to be ±1°K. The degrees of polarization, P,[11] were measured by the method of photoselection, and were corrected for instrumental factors in the usual manner.[11]

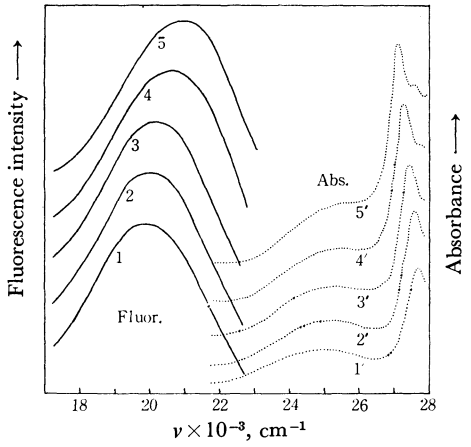

Fig. 1. Fluorescence and absorption spectra at different temperatures for 9,10-diazaphenanthrene in PB.
1, 24°; 2, −78°; 3, −150°; 4, −168°; 5, −196°; 1′, 23°; 2′, −53°; 3′, −118°; 4′, −156°; 5′, −196°C

9) E. Lippert and W. Voss, *Z. Physik. Chem., N. F.*, **31**, 321 (1962).

10) A. Weissberger, E. S. Proskauer, J. A. Riddick and E. E. Toops, Jr., "Organic Solvents," 2nd ed., Interscience Publishers, Inc., New York (1955).

11) T. Takemura and H. Baba, This Bulletin, **42**, 2756 (1969).

Results

The fluorescence and absorption spectra of 9,10-diazaphenanthrene, 2-naphthol and 2,3-naphthalenediol observed at different temperatures are shown in Figs. 1—3. To avoid confusion the spectral curves are moved upward successively. The position of the fluorescence maximum or peak is plotted against temperature in Figs. 4—6.

The P values for the fluorescence with respect to excitation into the lowest singlet excited state were determined at different temperatures. The results are shown in Figs. 4—6.

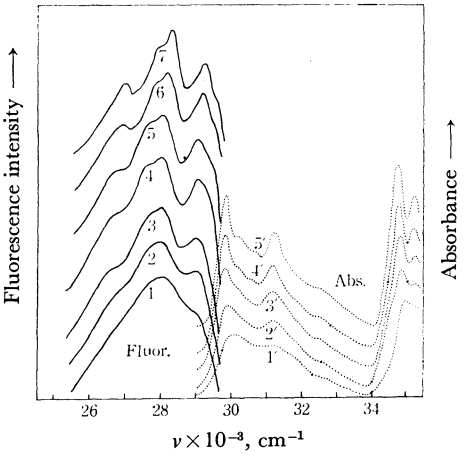

Fig. 2. Fluorescence and absorption spectra at different temperatures for 2-naphthol in EPA.
1, 24°; 2, −53°; 3, −117°; 4, −134°; 5, −152°; 6, −171°; 7, −196°; 1′, 24°; 2′, −69°; 3′, −135°; 4′, −161°; 5′, −196°C

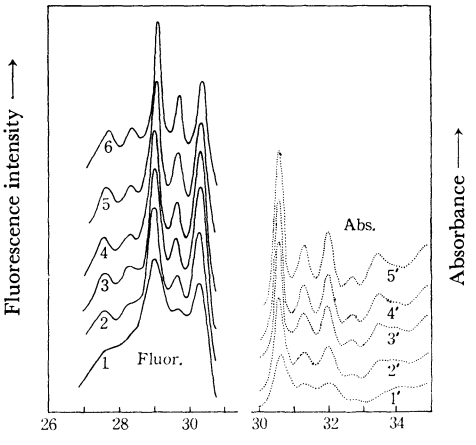

Fig. 3. Fluorescence and absorption spectra at different temperatures for 2,3-naphthalenediol in EPA.
1, 22°; 2, −57°; 3, −109°; 4, −136°; 5, −167°; 6, −196°; 1′, 23°; 2′, −59°; 3′, −109°; 4′, −148°; 5′, −196°C.

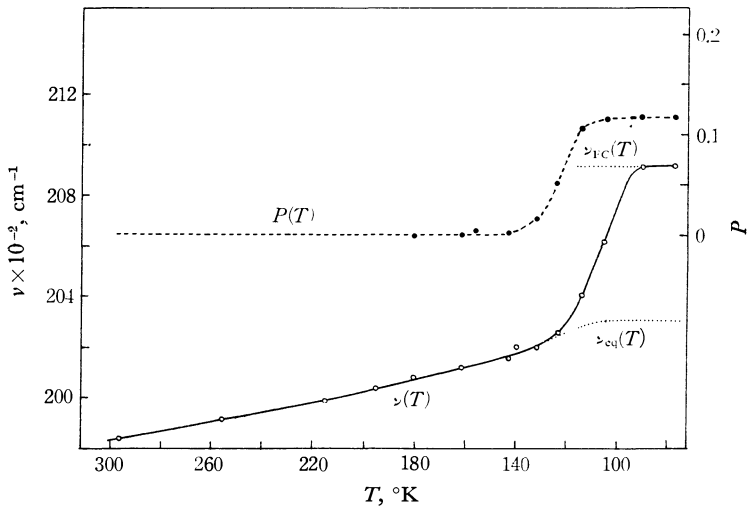

Fig. 4. Plots of ν and P *vs.* T for 9,10-diazaphenanthrene in PB.
ν represents the frequency of the fluorescence maximum.

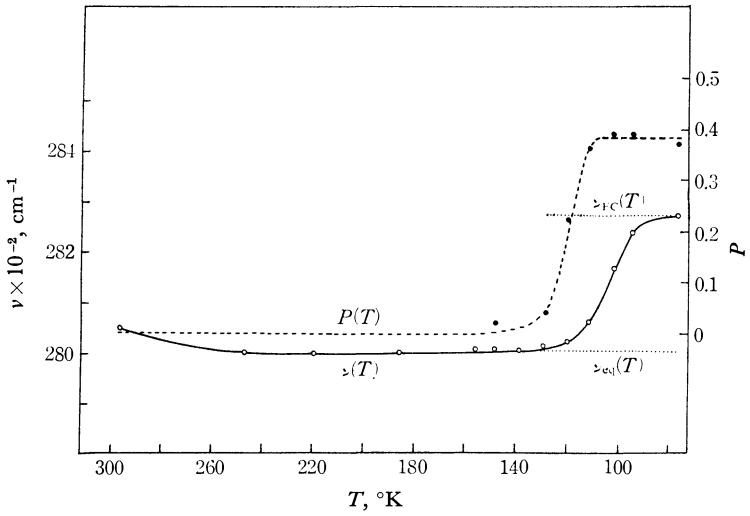

Fig. 5. Plots of ν and P *vs.* T for 2-naphthol in EPA.
ν represents the frequency of the fluorescence peak at about 28000 cm^{-1}.

Discussion

Since polar substances were employed as solutes and solvents in this study, the solute dipole-solvent dipole interaction is expected to play a major role in understanding the behavior of the observed electronic spectra. The ground state of a solute molecule will hereafter be denoted by g, and the lowest singlet excited state in which we are interested will be denoted by e. Thus, the dipole moments in the g and e states are expressed as μ_g and μ_e, respectively.

For 9,10-diazaphenanthrene, $\mu_g = 3.9$D;[12] the e state is known to be of an (n,π^*) type,[9] and the value of μ_e was determined to be 1.15D from the solvent effect on the absorption and fluorescence spectra.[8] Thus the electronic transition $g \rightarrow e$ is accompanied by a marked decrease in the dipole moment. For 2-naphthol, $\mu_g = 1.4$D;[12] the e state is the $L_b(\pi,\pi^*)$, and the dipole moment increases by 0.5—1D on going from the g to the e state.[13] As regards 2,3-naphthalenediol no pertinent data are available for μ_g and μ_e values, but the situation is probably similar to that in 2-naphthol.

Franck-Condon Blue Shift. An absorption transition occurs in general from the equilibrium ground state to the Franck-Condon excited state.

12) A. L. McClellan, "Tables of Experimental Dipole Moments," W. H. Freeman and Company, San Francisco (1963).

13) N. Mataga, Y. Kaifu and M. Koizumi, This Bulletin, **29**, 465 (1956).

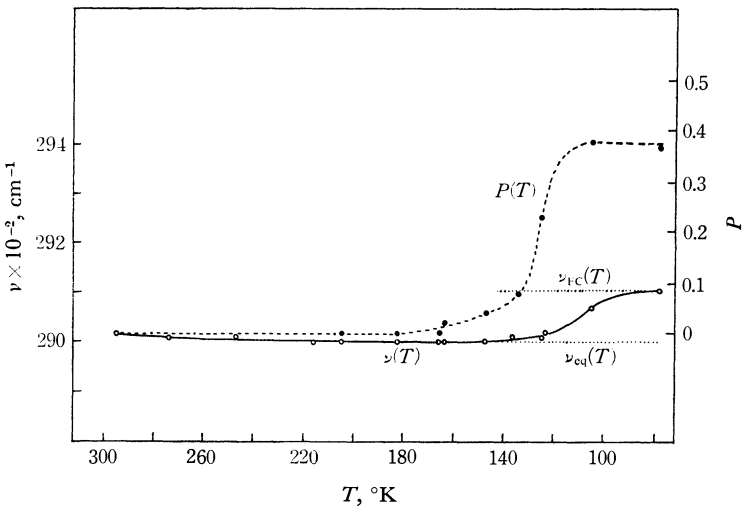

Fig. 6. Plots of ν and P *vs.* T for 2,3-naphthalenediol in EPA.
ν represents the frequency of the fluorescence peak at about 29000 cm^{-1}.

If it is assumed that there is complete reorientation of the solvent dipoles in the excited state, the fluorescence transition will start from the equilibrium excited state for the Franck-Condon ground state where the solvent orientation is appropriate to the excited state.

Dielectric constants (D) and refractive indices (n) of solvents will increase with a decrease of the temperature. On the above assumption, we expect from the theory of the solvent effect[13,14] that as the temperature decreases both the absorption (corresponding to $g \rightarrow e$) and fluorescence (corresponding to $e \rightarrow g$) spectra are gradually displaced to the blue for 9,10-diazaphenanthrene in which $\mu_e < \mu_g$, and to the red for 2-naphthol and 2,3-naphthalenediol in which $\mu_e > \mu_g$. This expectation is fulfilled in the case of the absorption spectra (*cf.* Figs. 1—3). The fluorescence spectra show similar behaviors at temperatures higher than 120°K.

With all the solute compounds studied, the fluorescence spectrum shifts rapidly to the blue as the temperature is lowered below 120°K. At such low temperatures the solvent becomes rigid, and the reorientation of the solvent dipoles will be inhibited partly or completely, depending on the viscosity of the solvent. The blue shift is therefore attributable to the fact that the fluorescence transition occurs also from the Franck-Condon excited state. The blue shift of this kind will be called a "Franck-Condon blue shift." In the light of the foregoing discussions, it can readily be understood that such a blue shift does not take place in the case of the absorption transition.

In Figs. 4—6, $\nu(T)$ represents the frequency in wavenumbers of the fluorescence maximum or peak which was actually observed as a function of temperature. Let $\nu_{eq}(T)$ and $\nu_{FC}(T)$ represent the corresponding frequencies which would be observed if the fluorescence were to originate exclusively in the equilibrium excitated state and the Franck-Condon excited state, respectively. At high temperatures $\nu_{eq}(T)$ will agree with $\nu(T)$, whereas in the low-temperature region where the Franck-Condon blue shift takes place, $\nu_{eq}(T)$ must deviate from $\nu(T)$. For the latter region, $\nu_{eq}(T)$ curve was obtained by extrapolation from the $\nu(T)$ curve at higher temperatures. (See the dotted lines in Figs. 4—6.)

On the other hand, $\nu_{FC}(T)$ is considered to agree with the observed $\nu(T)$ at temperatures near 77°K. The $\nu_{FC}(T)$ curve for the higher temperatures was obtained again by extrapolation.

Now, let $\nu_{eq}(T)$ and $\nu_{FC}(T)$ at 77°K be written as ν^0_{eq} and ν^0_{FC}. Then, the difference

$$\delta\nu^0_{FC} = \nu^0_{FC} - \nu^0_{eq} \ (= E^0_{FC}/\boldsymbol{hc}) \qquad (1)$$

corresponds to the sum of the Franck-Condon destabilization energies, denoted by E^0_{FC}, for the

Table 1. Constants related to temperature dependence of fluorescence spectra and fluorescence polarization

	9,10-Diazaphenanthrene in PB	2-Naphthol in EPA	2,3-Naphthalenediol in EPA
$\delta\nu^0_{FC}$ (cm^{-1})	610	265	100
E^0_{FC} (kcal/mol)	1.75	0.76	0.29
c_1	1.20×10^8	5.89×10^7	4.78×10^7
c_2 (deg)	1.96×10^3	1.87×10^3	1.95×10^3
$E_{a,r}$ (kcal/mol)	3.9	3.7	3.9
$E_{a,r'}$ (kcal/mol)	6.5	8.3	7.0

14) E. G. McRae, *J. Phys. Chem.*, **61**, 562 (1957).

excited and ground states at 77°K. In Eq. (1), h is the Planck constant, and c is the volocity of light. The values of $\delta\nu^0_{FC}$ and E^0_{FC} are given in Table 1.

In general, absorption and fluorescence bands of a polar solute molecule will undergo frequency shifts on changing the solvent from a nonpolar to a polar substance. Their respective frequency shifts will be designated as $\Delta\nu_a$ and $\Delta\nu_f$. If, at a given temperature, the viscosity of the solvent is so low that the fluorescence is observed only from the equilibrium excited state, $\Delta\nu_a-\Delta\nu_f$ corresponds to the sum of the Franck-Condon destabilization energies, denoted by E_{FC}, at that temperature. According to McRae,[14] $\Delta\nu_a-\Delta\nu_f$ $(=E_{FC}/hc)$ is approximately given as*2

$$\Delta\nu_a-\Delta\nu_f=\frac{E_{FC}}{hc}\simeq\frac{2}{hc}\frac{(\mu_g-\mu_e)^2}{a^3}\left[\frac{D-1}{D+2}-\frac{n_D^2-1}{n_D^2+2}\right] \quad (2)$$

where a is the cavity radius, and n_D and D are the refractive index for the sodium D line and dielectric constant of the polar solvent. Equation (2) shows that E_{FC} should be large when dipole moments differ greatly between the ground and excited states and the solvent has a large orientation polarization.

For 9,10-diazaphenanthrene in PB, $\delta\nu^0_{FC}$ amounted to 610 cm^{-1}, while $\Delta\nu_a-\Delta\nu_f$ at 23°C was found to be 250 cm^{-1} with n-pentane as the nonpolar reference solvent; that is, the E_{FC} value is much larger at 77°K than at room temperature. This observation is in agreement with the expectation that when the temperature is lowered the D value of the solvent will increase to a far greater extent than its n_D value.

It is seen in Table 1 that E^0_{FC} for 9,10-diazaphenanthrene is considerably large as compared with E^0_{FC} for the naphthalene derivatives. This might be interpreted as due to the fact that $(\mu_g-\mu_e)^2$ is of much higher value for the diazaphenanthrene.

Relaxation from the Franck-Condon Excited State into the Equilibrium Excited State. Let $\delta\nu(T)$ denote the difference between $\nu(T)$ and $\nu_{eq}(T)$:

$$\delta\nu(T)=\nu(T)-\nu_{eq}(T) \quad (3)$$

The experimental results shown in Figs. 4—6 were found to be reproduced very well by empirical relations of the following type:

$$\delta\nu^0_{FC}/\delta\nu(T)=1+c_1\exp(-c_2/T) \quad (4)$$

where c_1 and c_2 are constants inherent to each of the solute-solvent systems. In Fig. 7 are shown the $\delta\nu(T)$ curves as obtained from Eq. (4) with the constants c_1 and c_2 given in Table 1. In the same figure are also given the experimental points, which

*2 The meaning of the symbol $\Delta\nu$ used in this paper is different from that of the same symbol in McRae's paper. It can be shown, however, that in either case $\Delta\nu_a-\Delta\nu_f$ is expressed in the same form.

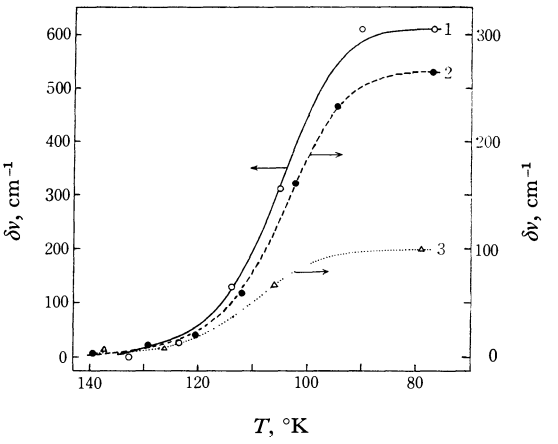

Fig. 7. Calculated $\delta\nu(T)$ curves and experimental points.
1, 9,10-diazaphenanthrene; 2, 2-naphthol; 3, 2,3-naphthalenediol.
The ordinate to be used is indicated by an arrow.

are seen to fall on the $\delta\nu(T)$ curves.

The relaxation process in which the solvent molecules surrounding the excited solute molecule reorient themselves from the Franck-Condon to the equilibrium state is assumed to be of the first order with respect to the solute. The deactivation processes of the solute molecule can then be represented by a kinetic scheme shown in Fig. 8, with the rate constants denoted by k's. Here the asterisk refers to the excited state, f and q mean fluorescent and nonfluorescent transitions, respectively, and the subscript r indicates the relaxation process mentioned above. Among the various rate constants, k_r is considered to be particularly sensitive to temperature; hence it is written as $k_r(T)$, the other constants being regarded as independent of temperature.

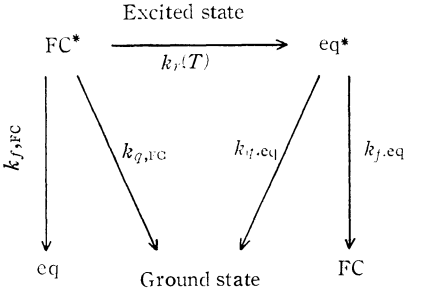

Fig. 8. Kinetic scheme of deactivation processes.

Let $\phi_{FC}(T)$ and $\phi_{eq}(T)$ denote the quantum yields of the fluorescence emissions from the Franck-Condon and equilibrium excited states, respectively. Then it follows from the scheme of Fig. 8 that

$$\phi_{FC}(T)=\frac{k_{f,FC}}{k_r(T)+k_{f,FC}+k_{q,FC}} \quad (5)$$

$$\phi_{eq}(T) = \frac{k_r(T)}{k_r(T) + k_{f,FC} + k_{q,FC}} \times \frac{k_{f,eq}}{k_{f,eq} + k_{q,eq}} \quad (6)$$

It is to be expected that, if both $\phi_{FC}(T)$ and $\phi_{eq}(T)$ are of finite values, there appear simultaneously two kinds of fluorescence spectra associated with FC*→eq and eq*→FC transitions. Actually this is not the case, as is seen from Figs. 1—3, so that the two spectra in question are assumed to coalesce into a single spectrum. It is further assumed that the frequency of the fluorescence maximum or peak is expressed as

$$\nu(T) = \frac{\phi_{FC}(T)}{\phi_{FC}(T) + \phi_{eq}(T)}\nu_{FC}(T) + \frac{\phi_{eq}(T)}{\phi_{FC}(T) + \phi_{eq}(T)}\nu_{eq}(T) \quad (7)$$

A combination of Eqs. (3) and (5)—(7) leads to the following equation:

$$\delta\nu^0_{FC}/\delta\nu(T) = 1 + \tau_f k_r(T) \quad (8)$$

where τ_f is the lifetime of the fluorescence from the equilibrium excited state, *i. e.*,

$$\tau_f = 1/(k_{f,eq} + k_{q,eq})$$

In the derivation of Eq. (8), assumptions have been made that

$$k_{f,FC} \simeq k_{f,eq}$$

and

$$\nu_{FC}(T) - \nu_{eq}(T) = \delta\nu_{FC}(T) \simeq \delta\nu^0_{FC}$$

The latter relation is to be reasonable in the limited range of T under consideration.

Let us express $k_r(T)$ by an equation of the Arrhenius type, that is

$$k_r(T) = A\exp(-E_{a,r}/RT) \quad (9)$$

and put

$$\tau_f A = c_1 \quad (10)$$

$$E_{a,r}/R = c_2 \quad (11)$$

Then Eq. (8) becomes identical in form with Eq. (4). In other words, in the empirical relation of Eq. (4), c_1 is related to the fluorescence lifetime τ_f, and c_2 to the activation energy $E_{a,r}$ of the relaxation process. It may be noted in this connection that the natural lifetimes, τ°_f, of 9,10-diazaphenanthrene, 2-naphthol and 2,3-naphthalenediol as obtained from the absorption intensities are 5.0×10^{-7}, 5.7×10^{-8} and 4.5×10^{-8} sec, respectively. From these τ°_f values and a knowledge of the fluorescence quantum yields, the actual lifetime, τ_f, was estimated to be about 5×10^{-8} sec for 9,10-diazaphenanthrene and about 1×10^{-8} sec for the two naphthalene derivatives. The values of $E_{a,f}$ obtained from the c_2 values are given in Table 1.

The relaxation time for the process FC*→eq* (Fig. 8) will be denoted by $\tau_r(T)$. Since $\tau_r(T) = 1/k_r(T)$, it follows from Eq. (8) that

$$\frac{\delta\nu^0_{FC}}{\delta\nu(T)} = 1 + \frac{\tau_f}{\tau_r(T)} \quad (12)$$

It is seen that, at the temperature where $\delta\nu(T) = (1/2)\,\delta\nu^0_{FC}$, $\tau_r(T)$ is equal to τ_f; that is, the relaxation time is of the order of 10^{-8} sec.

In the foregoing argument the fluorescence lifetime τ_f was defined with respect to the equilibrium excited state. It would not be unreasonable to presume that

$$k_{q,FC} \simeq k_{q,eq}$$

Then, if $k_r(T)\to0$, the lifetime of the Franck-Condon excited state becomes equal to τ_f. With finite values of $k_r(T)$, the former lifetime will be shorter than τ_f. Even in such cases, however, the mean lifetime of the excited solute molecules as a whole, which include the molecules belonging to the Franck-Condon excited state and to the equilibrium excited state, is found to be given by τ_f.*3 Thus, in the following discussion, τ_f will be used as the fluorescence lifetime regardless of the vlaues of $k_r(T)$.

Temperature Dependence of Fluorescence Polarization and Rotational Relaxation. As is seen in Figs. 4—6, the fluorescence P values increase rapidly as the temperature is lowered below 140°K; this temperature is somewhat higher than the temperature where the fluorescence blue shifts begin.

The temperature dependecnce of the fluorescence polarization is obviously related to the rotational relaxation of the solute molecule. At 77°K, the viscosity of the solvent must be too high for the solute molecule to rotate within the fluorescence lifetime τ_f. The value of P at this temperature, denoted by P_0, will therefore be regarded as its value in the absence of rotational relaxation. At higher temperatures the rotational depolarization of fluorescence may take place, and the P value will be given by [6,7]

$$\frac{1/P(T) - 1/3}{1/P_0 - 1/3} = 1 + \frac{\tau_f}{\tau_{r'}(T)} \quad (13)$$

where $\tau_{r'}(T)$ stands for the relaxation time for rotation of the solute molecule. It should be noted that Eq. (13) is analogous to Eq. (12).

Since $k_r(T) = 1/\tau_r(T)$, it follows from Eq. (9) that

$$1/\tau_r(T) = A\exp(-E_{a,r}/RT) \quad (14)$$

Similarly, $1/\tau_{r'}(T)$ is expressed as

*3 This statement is based on the following considerations. According to the kinetic scheme of Fig. 8

$$dN^*_{eq}/dt = -[k_r(T) + k_{f,FC} + k_{q,FC}]N^*_{FC}$$

$$dN^*_{eq}/dt = k_r(T)N^*_{FC} - (k_{f,eq} + k_{q,eq})N^*_{eq}$$

where N^*_{FC} and N^*_{eq} are the numbers of molecules belonging to the FC* and eq* states, respectively. Combining these equations on the assumption that $k_{f,FC} \simeq k_{f,eq}$ and $k_{q,FC} \simeq k_{q,eq}$, we obtain

$$d(N^*_{FC} + N^*_{eq})/dt = -(k_{f,eq} + k_{q,eq})(N^*_{FC} + N^*_{eq})$$

$$1/\tau_{r'}(T) = A' \exp(-E_{a,r'}/RT) \quad (15)$$

The $P(T)$ curves shown in Figs. 4—6 were found to be satisfactorily represented by Eq. (13) with $\tau_{r'}(T)$ in the form of Eq. (15). Thus, the activation energies $E_{a,r'}$ were determined from the analysis of the $P(T)$ curves, with the results listed in Table 1.

Comparison of the Two Relaxation Processes. We are concerned with two relaxation processes; one is associated with the passage from the Franck-Condon to the equilibrium excited state, and the other is the rotational relaxation of the solute. These relaxation processes will hereafter be represented by R and R′, respectively.

The relation between the relaxation R′ and fluorescence depolarization is generally established, and is represented by Eq. (13). The temperature dependence of ν, on the whole, is similar to that of P, and the observed $\nu(T)$ curve at low temperatures can be explained by the kinetic scheme of Fig. 8, which leads to Eq. (8) or (12). As has been pointed out, Eq. (12) is analogous to Eq. (13). Both equations are of the same form, and involve one and the same fluorescence lifetime, τ_f. Furthermore, τ_r and $\tau_{r'}$ are dependent on a common factor, *i. e.*, the viscosity of the solvent. Thus, we might conclude that the rapid blue shift of the fluorescence spectra at low temperatures is due to prohibition of the relaxation process R.

Let us turn to discussion of the difference between the two relaxation phenomena. It was experimentally found that, in every case, the ratio of the left-hand side of Eq. (12) to that of Eq. (13) was larger than unity in the temperature region of interest (*cf.* Figs. 4—6). This along with the expressions of Eqs. (12) and (13) means that $\tau_r(T) < \tau_{r'}(T)$; further, it is seen in Table 1 that $E_{a,r} < E_{a,r'}$

The above observations may be rationalized by considering the difference between the detailed mechanisms of the two relaxation processes. In the relaxation R, the solvent dipoles in the vicinity of the solute molecule reorient themselves to a configuration which is energetically favorable in relation to the charge distribution of the excited state of the solute. On the other hand, in the relaxation R′ the excited solute molecule must rotate with reference to laboratory-fixed coordinate axes, and such a rotational motion is presumably hindered by attraction between solute and solvent molecules, produced by dipole-dipole interaction or hydrogen bonding. Therfore, one may expect that the relaxation R occurs more easily than the relaxation R′, and that $\tau_r(T) < \tau_{r'}(T)$ and $E_{a,r} < E_{a,r'}$.

Other Related Problems. For 2-naphthol and 2,3-naphthalenediol, EPA was used as the solvent; accordingly, a hydrogen-bonded complex was probably formed between the solutes and the solvent. In general, the Franck-Condon principle should be taken into account also with respect to hydrogen bonding.[15] It is inferred, however, that in the case of the hydrogen-bonded complex in question the relaxation from the Franck-Condon to the equilibrium excited state of the complex is completed within the fluorescence lifetime, even at 77°K.[16] For this reason, in the discussion of the fluorescence blue shift, no consideration has been given to the relaxation process involving hydrogen bonding.

It has been recognized that often the Arrhenius equation is not applicable to the temperature dependence of dielectric and other relaxation processes in liquids at low temperatures where the liquid substances show glassy behavior.[17] As has been stated, however, the present experimental results were satisfactorily analyzed with the relaxation times $\tau_r(T)$ and $\tau_{r'}(T)$ expressed in the forms of Eqs. (14) and (15) which are based on the Arrhenius equation.

In Figs. 1—3 are shown in part the second electronic absorption bands. In 9,10-diazaphenanthrene the second absorption band corresponds to the $g \rightarrow L_b$ transition, and in the naphthalene derivatives it corresponds to the $g \rightarrow L_a$. On lowering the temperature, each of these absorption bands is gradually displaced to the red as may be expected.

The authors wish to express their thanks to Dr. Satoshi Suzuki for his help in carrying out the polarization measurements.

15) G. C. Pimentel, *J. Amer. Chem. Soc.*, **79**, 3323 (1957).

16) N. Mataga, Y. Kaifu and M. Koizumi, This Bulletin, **29**, 115 (1956).

17) R. H. Cole, *Ann. Rev. Phys. Chem.*, **11**, 149 (1960).

BULLETIN OF THE CHEMICAL SOCIETY OF JAPAN VOL. 43 20—23 (1970)

Steric Structure of L-Proline Oligopeptides. III. Calculated Absorption Spectra of L-Proline Oligopetides

Hirofumi OKABAYASHI and Toshizo ISEMURA

Physical Chemistry, Institute for Protein Research, Osaka University, Kita-ku, Osaka

(Received June 2, 1969)

The electronic excited states in L-proline oligopeptides were derived from molecular-exciton theory. The dipole-dipole approximation was used in the calculation of transition energies. The calculated absorption spectra related to the conformation of L-proline oligopeptides were compared with observed ones. A satisfactory agreement between the calculated and observed results was obtained.

In previous papers[1,2] the ultraviolet absorption spectra of *N*-tertiary amyloxy carbonyl-L-prolyl oligopeptides synthesized in a stepwise manner were reported. The red shifts of the absorption maxima were related to the conformation. By means of ORD[1] and CD[1] spectra, it was established that the appearance of the helical conformation commences at the tetramer, while the pentamer, hexamer and octamer have the poly-L-proline II-like conformation. Band splitting of the absorption spectra of the dimer was observed. The very broad absorption spectrum of the trimer might be due to three absorption maxima with almost the same intensities. It was also found that the absorption maxima on the longest-wavelength side of the tetramer, pentamer, hexamer and octamer are identical with the shoulder around 200 mμ found in the dimer, but with an increased intensity. Consequently, the absorption band with perpendicular polarization is expected to appear as a shoulder at about 185 mμ (Table 1[1,2] and Fig. 1[1,2]).

According to these results, the absorption maximum around 203 mμ of poly-L-proline II has been identified as the shoulder with an increased intensity around 200 mμ found in the spectra of the dimer.[1,2]

Some investigators[3] have tried to observed band

TABLE 1. WAVELENGTHS OF UV ABSORPTION MAXIMA OF L-PROLINE OLIGOPEPTIDES

	In water (mμ)	In acetonitrile (mμ)
Monomer	—	183
Dimer	—	185 198
Trimer	198	185—198*
Tetramer	201	198—200
Pentamer	203	200—201
Hexamer	203	201
Octamer	203	—
Poly-L-Proline II	203	—
Poly-L-Proline I	208	—

* The trimer has a very broad absorption spectrum in the region 185—198 mμ.

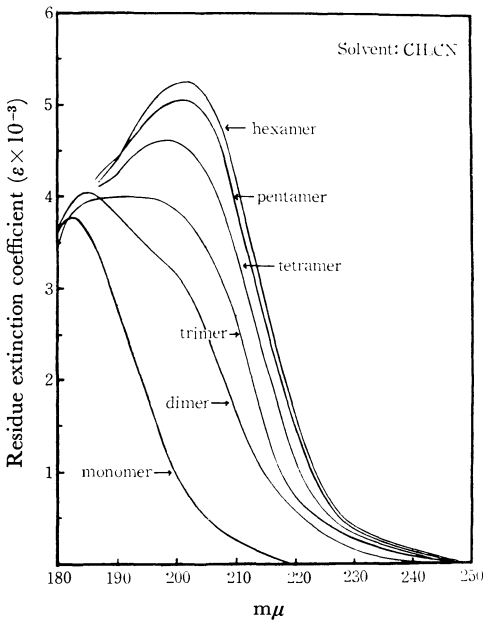

Fig. 1. The ultraviolet absorption spectra of L-proline oligopeptides (see Refs. 1, 2).

*1 Presented at Symposium on Molecular Structures of the Chemical Society of Japan (October, 1967).

*2 Present Address: Department of Industrial Chemistry, Nagoya Institute of Technology, Gokise, Showa-ku, Nagoya.

1) H. Okabayashi, T. Isemura and S. Sakakibara, *Biopolymers*, **6**, 323 (1968).

2) H. Okabayashi and T. Isemura, Abstract for Symposium on Molecular Structures (October, 1967), p. 17.

3) W. B. Gratzer, W. Rhodes and G. D. Fasman, *Biopolymers*, **1**, 319 (1963).

splitting of the absorption spectra of poly-L-proline I and II without success.

In this study the calculations of the absorption spectra of L-proline oligopeptides were attempted by Tinoco's method[4-6] and compared with the observed absorption spectra. Good agreement between the calculated and the observed absorption spectra was found.

Optical properties of the α-helix and the 3_{10}-helix of polypeptides have been calculated by Tinoco and Woody[5] and the chainlength dependence of the absorbance was thoroughly discussed. Tinoco and Woody[5] have also found that there was satisfactory agreement between experimental absorption spectra and the calculated results. However, the calculated absorption spectra of oligopeptides have not yet been compared with experimental results.

Theory

Following the general expressions used by Tinoco *et al.*;[5,6] the ground state wave function of a oligomer is represented by

$$\Psi = \phi_1\phi_2\phi_3 \cdots \phi_N \tag{1}$$

and a singly excited state, localized at molecule i, by

$$\Psi'_i = \phi_1\phi_2\phi_3 \cdots \phi'_i \cdots \phi_N \tag{2}$$

where ϕ_i and $\phi_{i'}$ are the residue ground- and singly excited state wave functions, respectively, and N is the number of residue.

The perturbed, singly excited states of the oligopeptides are written as follows:

$$\Psi'_K = \sum_{i=1}^{N} C_{iK}\Psi'_i \qquad K = 1, 2, 3, \cdots N \tag{3}$$

The Hamiltonian of the oligomer is represented by

$$\boldsymbol{H} = \sum_{i}^{N} H_i + \sum_{i<j}^{N} \boldsymbol{V}_{ij} \tag{4}$$

where $\boldsymbol{V}_{ij}$ is the interaction operator between residue i and j.

The coefficients, C_{ik}, and the eigenvalues, E_k, are obtained by solving the secular equation

$$D_N = |\, V_{ij} - \delta_{ij}E \,| = 0 \tag{5}$$

The secular determinant D_H has the form,

$$D_N = \begin{vmatrix} V_{11}-E & V_{12} & V_{13} & \cdots & V_{1N} \\ V_{21} & V_{22}-E & V_{23} & \cdots & V_{2N} \\ V_{31} & V_{32} & V_{33}-E & \cdots & V_{3N} \\ V_{41} & V_{42} & V_{43} & \cdots & V_{4N} \\ \vdots & \vdots & \vdots & & \vdots \\ V_{N1} & V_{N2} & V_{N3} & \cdots & V_{NN}-E \end{vmatrix} \tag{6}$$

where $V_{ij} = \langle \phi_i | \boldsymbol{H} | \phi'_i \rangle$ $(i \neq j)$ and $V_{ij} = \langle \phi_i | \boldsymbol{H} | \phi'_i \rangle$

Calculation and Results

Figure 2 shows the coorodinate system[7] for the calculation of the absorption spectra of L-proline oligopeptides. The three fold axis of the oligopeptides is identical with the z axis perpendicular to the plane of the paper. Each residue of the oligomers is located around the three fold axis on the assumption that the tetramer, pentamer, hexamer and octamer exist entirely in a poly-L-proline II-like structure and the dimer and trimer assume the same conformation as found in the helical structure of poly-L-proline II.

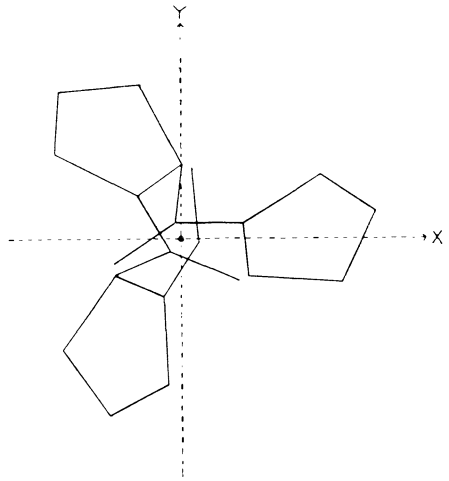

Fig. 2. Schematic representation of the poly-L-proline II-like structures of L-proline oligopeptides. Cowan and McGavin's coordinate system[7] is used.

It is assumed that the magnitude and direction of the π–π^* transition moment μ in the peptide groups of L-proline oligomers are the same as those of π–π^* transition moment (μ=3.05D) for the absorption at 190 mμ in myristamide.[8] This assumption seems to be the most reasonable approximation at the present time. In the calculations the

4) I. Tinoco, Jr., *J. Chem. Phys.*, **33**, 1332 (1960).
5) I. Tinoco, Jr., and R. W. Woody, *ibid.*, **38**, 1317 (1963).
6) D. F. Bradley, I. Tinoco, Jr., and R. W. Woody, *Biopolymers*, **1**, 239 (1963).
7) P. Cowan and S. McGavin, *Nature*, **176**, 501 (1955).
8) D. L. Peterson and W. T. Simpson, *J. Amer. Chem. Soc.*, **79**, 2375 (1957).

dipole-dipole approximation for the interaction potential was used:

$$V_{ij} = \frac{(\mu_i \cdot \mu_j)}{R_{ij}^3} - 3\frac{(\mu_i \cdot \boldsymbol{R}_{ij})(\mu_i \cdot \boldsymbol{R}_{ij})}{R_{ij}^5} \qquad (7)$$

where μ_i is the π-π^* transition dipole moment of the ith peptide group with $\mu_i = \mu$ and R_{ij} the distance between the $\pi = \pi^*$ transition dipole moment of the ith peptide group and that of the jth peptide group, and moreover the nearest neighbor interaction and all neighboring interaction were considered.

The calculated values of the absorption maxima and the dipole strengths of L-proline oligopeptides are shown in Fig. 3.

The absorption band maxima with parallel polarization at the longest-wavelength side apparently are displaced to red with increasing chain length. Moreover, the calculated absorption maxima also are convergent as are the observed ones. Naturally the perpendicular band maxima should converge. In these calculations the maxima of the calculated perpendicular bands tend to converge at about 186 mμ.

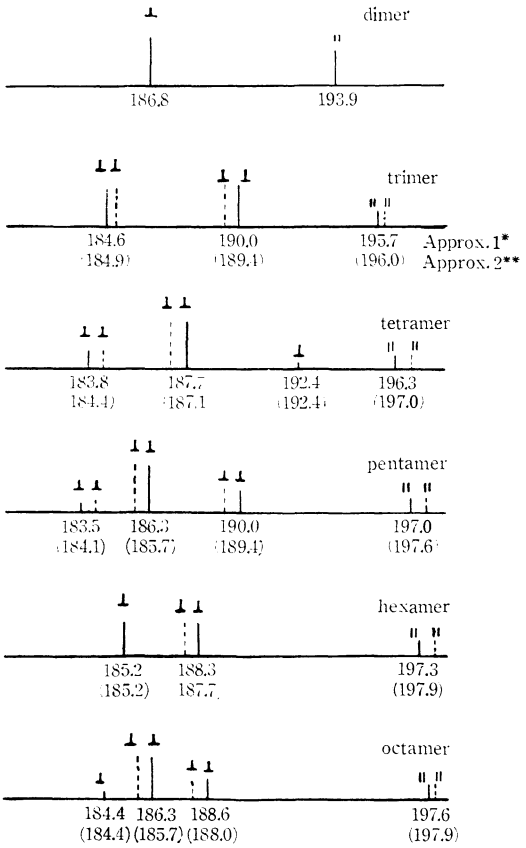

Fig. 3. Calculated absorption spectra and calculated dipole strengths of L-proline oligopeptides. The values and the direction of μ are chosen to coincide with those of the 1900 A transition in myristamide.

* The calculations were carried out by the nearest neighbor approximation.

** All neighboring interactions were considered in this approximation.

The solid lines are obtained by approximation 1 and the broken lines by approximation 2.

The change in the intensity of the observed absorption spectra and the calculated values of the dipole strengths of L-proline oligopeptides should be compared.

In the dimer the calculated dipole strengths are in good accord with the observed intensity of the peak and the shoulder of the dimer.

The present calculations indicate that the absorption spectra of the trimer should have two perpendicular bands and a parallel band. This result should be regarded as the theoretical prediction for the broadening which was observed in the asborption spectra of the trimer.

There is a noteworthy change in the intensity of the band maxima at about 200 mμ of the tetramer, pentamer and hexamer. In particualr, the change of the intensity between the trimer and other three oligomers (tetramer, pentamer and hexamer) is notable and seems to be associated with the helical structure of the oligomers.

However, the present calculations for the change of dipole strengths with increasing chain length do not agree with that of the observed intensities. That is, the calculated dipole strengths of four oligomers (trimer, tetramer, pentamer and hexamer) are almost the same, and moreover there is no increase in the dipole strengths between the trimer and the tetramer.

Disagreement between the calculated dipole

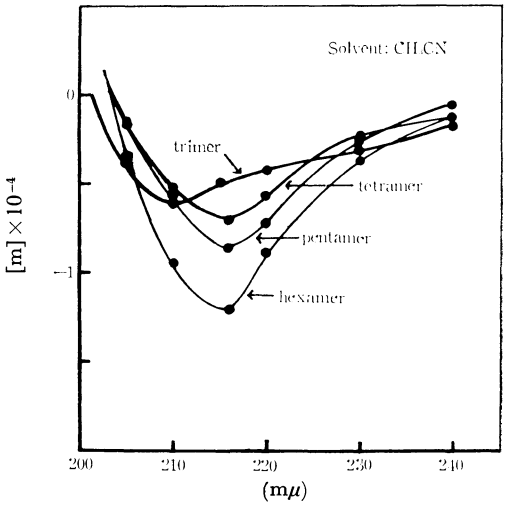

Fig. 4. The ORD curves of L-proline oligopeptides in acetonitrile.
Trimer, concn. = 1.590 mg/20 m*l* of CH_3CN
Tetramer, concn. = 1.65 mg/20 m*l* of CH_3CN
Pentamer, concn. = 1.61 mg/20 m*l* of CH_3CN
Hexamer, concn. = 1.64 mg/20 m*l* of CH_3CN
Quartz cells of 1 mm path length were employed.

strengths and the observed intensity of these oligomers may depend upon the calculation in which zero-order exciton wave functions were used. For a satisfactory explanation of the intensity the use of first-order exciton[9] wave functions or other developed methods[10,11] may be required.

The ORD curves of the trimer, tetramer, pentamer and hexamer were obtained. The measurements were carried out on a Jasco Model ORD/UV-5 Spectropolarimeter.

The position of the minimum and cross-over point in the ORD curve of the trimer is at about 210 mμ and 201 mμ.

The ORD curves of the three oligomer (tetramer, pentamer and hexamer exhibit the same minimum and cross-over points[2] as does poly-L-proline II (see Fig. 4).

These facts clearly indicate that the helical structure of the poly-L-proline II type as measured by absorption spectra appears at the tetrapeptide and that the pentamer and hexamer have complete poly-L-proline II-like structures. These observations were in aqueous solutions and in methyl alcohol as well as in acetonitrile. Although the absorption spectra of the dimer and trimer differ from that found for the poly-L-proline II-like structure, the calculated and observed results agree sufficiently well to ascertain that these oligomers likewise assume a poly-L-proline II-like conformation.

9) I. Tinoco, Jr., *J. Amer. Chem. Soc.*, **82**, 4785 (1960).
10) W. Rhodes, *ibid.*, **83**, 3609 (1961).
11) S. Yomosa and H. Nakano, *J. Phys. Soc. Jap.*, **21**, 1369 (1966).

The authors wish to thank Professor G. D. Fasman for discussions concerning the calculated and experimental results.

BULLETIN OF THE CHEMICAL SOCIETY OF JAPAN VOL. 43 23—30 (1970)

Isotopic Exchange between Hydrogen Sulfide and Deuterium on the Surface of Cuprous Sulfide

Kazuo FUEKI, Hideaki INABA and Takashi MUKAIBO

Department of Industrial Chemistry, Faculty of Engineering, The University of Tokyo, Hongo, Bunkyo-ku, Tokyo

(Received June 5, 1969)

The isotopic exchange between H_2S and D_2 has been followed in the temperature range 425—525°C on a cuprous sulfide specimen. At high sulfur activities of Cu_2S, the predominant reaction is $H_2S+D_2=H_2+D_2S$, and at moderate sulfur activities the same reaction is predominant in the initial period. Analysis of kinetic data shows that the exchange reaction is first order. From the first-order rate constant, k_i, the rate constant of sulfidation of Cu_2S by "hydrogen sulfide"* and k_i', the rate constant of reduction of Cu_2S by "hydrogen"* are determined. It is shown that k_i is inversely proportional to the sulfur activity of Cu_2S and that k_i' is independent of it. Dependence of k_i and k_i' on sulfur activity is interpreted on the basis of a theory proposed by Kobayashi and Wagner. The formation of HD becomes remarkable as the sulfur activity of Cu_2S decreases. This finding shows that the reaction, $H_2S+D_2=HD+HDS$, becomes appreciable with the decrease in sulfur activity.

Oxidation and sulfidation of metals and reduction of oxides and sulfides at high temperatures implies the reaction at the gas-solid interface as an elementary step. Since not only gaseous reactants but also species in the solid phase take part in the reaction at the gas-solid interface, it is necessary to determine the reaction rate as a function of the activity of reactants in the solid phase as well as the partial pressure of reactant gases in order to discuss the reaction mechanism.

Kobayashi and Wagner[1] have constructed solid-state electrochemical cells, such as $Ag|AgI|Ag_2S|Pt$ and $Cu|CuI|Cu_2S|Pt$, and determined the rate of reduction of Cu_2S and Ag_2S by H_2 as a function of the sulfur activity, using the coulometric titration technique. They have proposed a new theory for interpreting the dependence of reaction rate on the

*1 Terms such as "hydrogen" and "hydrogen sulfide" are used in a generic sense, irrespective of isotopic species.

1) H. Kobayashi and C. Wagner, *J. Chem. Phys.*, **26**, 1609 (1957).

sulfur activity of sulfides and discussed the reaction mechanism.

On the basis of the theory proposed by Kobayashi and Wagner, several kinetic studies[2-5] have been carried out on the reaction at the gas-solid interface. As to experimental technique, the isotopic exchange method and the chemical relaxation method have been developed in addition to the coulometric titration technique.

In the present work, the isotopic exchange between H_2S and D_2 on the surface of Cu_2S is studied, and the rate of sulfidation of Cu_2S by H_2S and the rate of reduction of the sulfide by H_2 are determined as a function of the sulfur activity of Cu_2S.

From the result, the mechanism of reaction on the surface of Cu_2S is discussed.

Experimental

Apparatus. The apparatus is shown in Fig. 1. A is a Cu_2S specimen placed in a reaction vessel B, which is heated by an electric furnace C. A magnetic pump D and valves E are used for circulating the gas mixture in the reaction system in the direction indicated by arrows. M is a mercury manometer. F is used to collect a small portion of gas. G is a U-shaped glass trap for the separation of "hydrogen sulfide" from "hydrogen". H is a bulb to transfer samples of gas to a mass spectrometer. I, J, and K are reservoirs for purified D_2, H_2S, and H_2, respectively, and L a reservoir for gas mixtures of H_2S and D_2.

Materials. *a) Purification of* H_2. Hydrogen of commercial grade was passed through paradium-asbestos catalyser heated at 450°C to convert the trace of oxygen into water vapor. The gas was then dried by means of a tube filled with desiccating agent $Mg(ClO_4)_2$ and stored in a gas reservoir.

b) Purification of D_2. Heavy water supplied by the Showa Denko Co. was electrolysed in a U-shaped electrolytic cell equipped with a diaphragm of sintered glass. Impurity oxygen was removed in the same way as in the purification of H_2. A typical composition of deuterium gas was 96% D_2, 3.1% HD and 0.9% H_2.

c) Purification of H_2S. Hydrogen sulfide gas, 99.9% pure, was passed through a desiccating tube of $Mg(ClO_4)_2$ and condensed in a trap cooled by liquid nitrogen. The trap then was evacuated to remove uncondensed gaseous impurities and the condensed hydrogen sulfide was evaporated by removing liquid nitrogen.

d) Preparation of Cu_2S *Specimen.* A copper specimen, 9.0 cm long and 4.2 cm wide, was taken from a high purity copper sheet with thickness 0.22 mm. After being polished with a 1000-emery paper, the specimen was cleaned by petroleum ether and stored in a desiccator. The finished copper specimen was then folded and placed in a pyrex tube. High purity sulfur with an amount 5% more than that necessary for the formation of stoichiometric cuprous sulfide was added to the tube. After evacuation, the tube was sealed and placed in a furnace heated at 400°C to let copper react with sulfur to form Cu_2S. After the completion of sulfidation, the specimen was annealed in a H_2S-H_2 gas mixture.

Experimental Procedure. Prior to the isotopic exchange reaction, a H_2S-H_2 gas mixture, the sulfur activity of which was the same as that of a H_2S-D_2 gas mixture to be used in the isotopic exchange reaction, was admitted to the reaction vessel and the Cu_2S specimen was kept in the atmosphere for a period until equilibrium was attained between the Cu_2S specimen and the H_2S-H_2 gas mixture. The H_2S-H_2 gas mixture

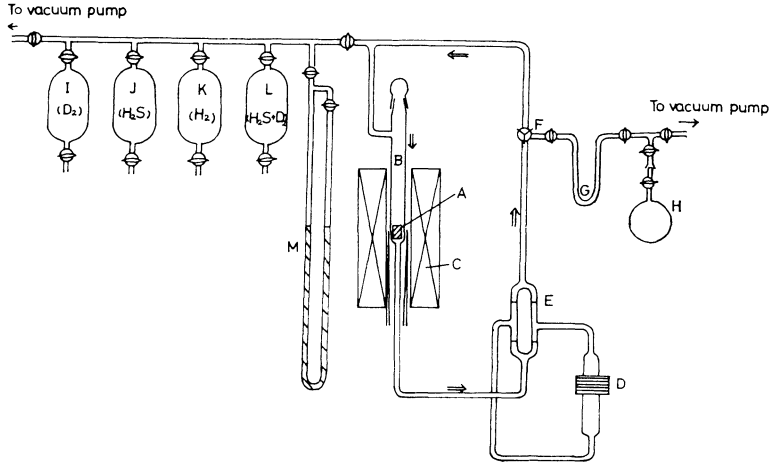

Fig. 1. Apparatus for the isotopic exchange experiment
A Cu_2S specimen, B reaction vessel, C furnace, D magnetic pump, E valves, F sampling tube, G U-shaped trap, H sampling bulb for mass-spectroscopic analysis, I—L gas reservoirs, M mercury manometer

2) H. J. Grabke, *Ber. Bunsenges. Physik. Chem.*, **69**, 48 (1965).
3) H. J. Grabke, *ibid.*, **70**, 664 (1966).
4) S. Stotz, *ibid.*, **70**, 37 (1966).
5) E. Bechtold, *ibid.*, **69**, 328 (1965).

was removed and a H_2S-D_2 gas mixture was introduced into the reaction system and circulated by a circulation pump.

Small portions of the mixture were collected in F, and then expanded to G. After "hydrogen sulfide" in the U-shaped tube G was frozen out with liquid nitrogen around the trap, "hydrogen" was transferred to the bulb H to be analyzed by means of a mass-spectrometer.

Results and Discussion

Blank Experiment. In order to investigate whether or not the isotopic exchange reaction between D_2 and H_2S occurs in the absence of Cu_2S, a blank experiment has been carried out at various temperatures. No exchange was observed below 525°C, and about 5% of the initial amount of D_2 was found to have exchanged after 3 hr of reaction at 575°C. Thus the experiment was carried out below 525°C.

Change in Mole Fractions of H_2, HD and D_2 with Time. From the data of mass-spectroscopic analysis, mole fractions of H_2, HD and D_2 were calculated, where the mole fraction is the number of moles of a specific kind of hydrogen divided by the total number of moles of "hydrogen." The mole fractions are denoted by x_{H_2}, x_{HD} and x_{D_2}.

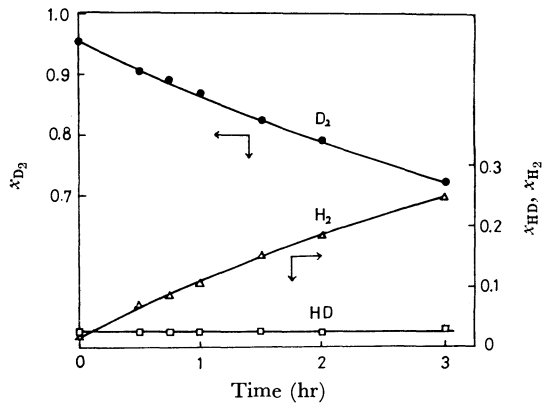

Fig. 2. Change in x_{D_2}, x_{HD} and x_{H_2} with time. (478°C, $P^\circ_{H_2S}$=160 mmHg, $P^\circ_{D_2}$=20 mmHg, a_S=4)

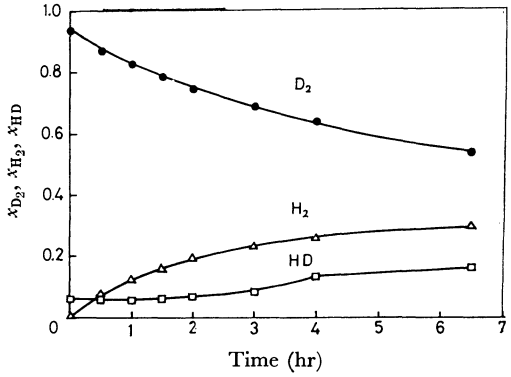

Fig. 3. Change in x_{D_2}, x_{DH} and x_{H_2} with time. (478°C, $P^\circ_{H_2S}$=20 mmHg, $P^\circ_{D_2}$=20 mmHg, a_S=1)

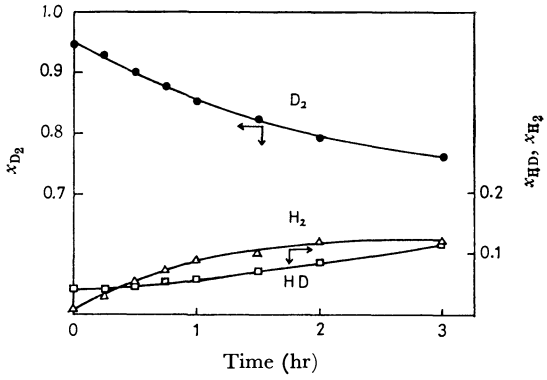

Fig. 4. Change in x_{D_2}, x_{HD} and x_{H_2} with time. (478°C, $P^\circ_{H_2S}$=40 mmHg, $P^\circ_{D_2}$=160 mmHg, a_S=1/4)

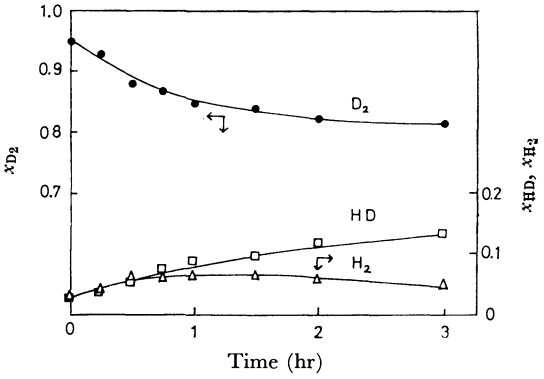

Fig. 5. Change in x_{D_2}, x_{HD} and x_{H_2} with time. (478°C, $P^\circ_{H_2S}$=40 mmHg, $P^\circ_{D_2}$=400 mmHg, a_S=1/10)

Figures 2 to 5 give the plots of x_{H_2}, x_{HD} and x_{D_2} against time at different sulfur activities. The sulfur activity, a_S, was defined as the pressure ratio of "hydrogen sulfide" to "hydrogen." Figure 2 shows the change in x_{H_2}, x_{HD} and x_{D_2} with time in the case where a_S is 4. As seen from the figure, x_{HD} remains unchanged, whereas x_{H_2} increases and x_{D_2} decreases. Thus, the predominant exchange reaction is

$$H_2S + D_2 = D_2S + H_2 \quad (1)$$

This reaction proceeds *via* the sulfidation of Cu_2S by H_2S and the reduction by H_2 as follows:

$$H_2S = H_2 + \text{"S(a)"} \quad (2)$$

$$D_2 + \text{"S(a)"} = D_2S \quad (3)$$

where "S(a)" denotes sulfur atoms or ions on the surface of Cu_2S. Accordingly, the rate of sulfidation of Cu_2S by H_2S can be obtained from the kinetic of reaction (1).

The change in mole fractions of H_2, HD, and D_2 at $a_S=1$ is given in Fig. 3. x_{HD} is constant during the initial period of reaction and then increases with time. As seen in Fig. 4, the change in mole fractions with time at $a_S=1/4$ is similar to that at $a_S=1$, but the initial period where x_{HD} is constant is shorter. At $a_S=1/10$, the formation of HD is remarkable. HD would be formed by the reaction

$$H_2S + D_2 = HDS + HD \quad (4)$$

Reaction (4) probably proceeds *via* steps,

$$H_2S = H(a) + HS(a) \quad (5)$$

$$D_2 = 2D(a) \quad (6)$$

$$H(a) + D(a) = HD \quad (7)$$

$$HS(a) + D(a) = HDS$$

where H(a), D(a), HS(a) represent H, D and HS adsorbed on the surface of Cu_2S.

It is noteworthy that the mechanism of reaction at the gas-solid interface changes with the activity of reactants in the solid phase.

Order of Reaction and Rate Constants of Sulfidation and Reduction. According to McKay's law,[6] the rate of isotopic exchange is first order regardless of the individual forward or reverse reactions. If only reaction (1) occurs and the reaction obeys McKay's law, the rate of exchange per unit area of Cu_2S specimen is given by the equation

$$\frac{\dot{n}_{D_2}}{A} = k_i P_{D_2S} - k_i' P_{D_2} \quad (9)$$

or

$$\frac{\dot{n}_{H_2}}{A} = k_i P_{H_2S} - k_i' P_{H_2} \quad (10)$$

where A is the apparent surface area of Cu_2S specimen, n_{H2} and n_{D2} are, respectively, numbers of moles of H_2 and D_2 in the reaction system at the time of t, k_i is the rate constant of sulfidation of Cu_2S by "hydrogen sulfide" and k_i' is the rate constant of reduction of Cu_2S by "hydrogen."

Let us solve Eq. (9). The equation is rewritten as

$$\frac{\dot{n}_{D_2}}{A} = \frac{RT}{V}(k_i n_{D_2S} - k_i' n_{D_2}) \quad (11)$$

where V is the dead volume of the reaction system. Since only reaction (1) is assumed to occur, $n^\circ_{D_2}$, the number of moles of D_2 at the beginning of reaction, is equal to the sum of n_{D_2} and n_{D_2S} at the time of t, thus

$$n^\circ_{D_2} = n_{D_2} + n_{D_2S} \quad (12)$$

Insertion of Eq. (12) into Eq. (11) yields

$$\frac{\dot{n}_{D_2}}{A} = \frac{RT}{V}\{k_i n^\circ_{D_2} - (k_i + k_i')n_{D_2}\} \quad (13)$$

At equilibrium $n_{D_2}=0$, accordingly,

$$\frac{n^e_{D_2}}{n^\circ_{D_2}} = \frac{k_i}{k_i + k_i'} \quad (14)$$

where $n^e_{D_2}$ represents the number of moles of D_2 at equilibrium. Inserting Eq. (14) into Eq. (13), we obtain

$$\dot{n}_{D_2} = -\frac{ART}{V}(k_i + k_i')(n_{D_2} - n^e_{D_2}) \quad (15)$$

Integration of Eq. (15) yields

$$-\log \frac{n_{D_2} - n^e_{D_2}}{n^\circ_{D_2} - n^e_{D_2}} = \frac{ART(k_i + k_i')}{2.303V}t \quad (16)$$

By replacing n_{D_2}, $n^\circ_{D_2}$ and $n^e_{D_2}$ by x_{D_2}, $x^\circ_{D_2}$ and $x^e_{D_2}$, respectively, Eq. (16) is rewritten as

$$-\log \frac{x_{D_2} - x^e_{D_2}}{x^\circ_{D_2} - x^e_{D_2}} = \frac{ART(k_i + k_i')}{2.303V}t \quad (17)$$

If we denote the slope of the polt of $-\log\{x_{D_2} - x^e_{D_2})/(x^\circ_{D_2} - x^e_{D_2}\}$- against t by α, we have

$$\alpha = \frac{ART(k_i + k_i')}{2.303V} \quad (18)$$

k_i and k_i' are represented by the following equations.

$$k_i = \frac{2.303\alpha V}{ART}\frac{x^e_{D_2}}{x^\circ_{D_2}} \quad (19)$$

and

$$k_i' = \frac{2.303\alpha V}{ART}\left(1 - \frac{x^e_{D_2}}{x^\circ_{D_2}}\right) \quad (20)$$

Therefore, if α is determined experimentally, k_i and k_i' can be calculated by Eqs. (19) and (20).

The solution of Eq. (10) has a form

$$-\log \frac{x^e_{H_2} - x_{H_2}}{x^e_{H_2} - x^\circ_{H_2}} = \frac{ART(k_i + k_i')}{2.303V}t \quad (21)$$

The slope of the plot of $\log\{(x^e_{H_2} - x_{H_2})/(x^e_{H_2} - x^\circ_{H_2})\}$ *vs.* t. is the same that of the plot of $\log\{(x_{D_2} - x^e_{D_2})/(x^\circ_{D_2} - x^e_{D_2})\}$ *vs.* t. Therefore, it is also possible to calculate the values of k_i and k_i' from the data for H_2.

The plot of $\log\{(x_{D_2} - x^e_{D_2})/(x^\circ_{D_2} - x^e_{D_2})\}$ *vs.* t for the data given in Fig. 2 is shown in Fig. 6. In this figure the plot of $\log\{(x^e_{H_2} - x_{H_2})/(x^e_{H_2} - x^\circ_{H_2})\}$ *vs.* t

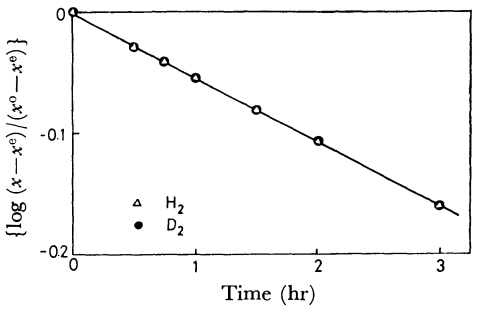

Fig. 6. Plot of $\log\{(x-x^e)/(x^\circ-x^e)\}$ *vs.* t for the data given in Fig. 2.
(478°C, $P^\circ_{H_2S}=160$ mmHg, $P^\circ_{D_2}=40$ mmHg, $a_S=1/4$)

6) H. A. C. McKay, *Nature*, **142**, 997 (1938).

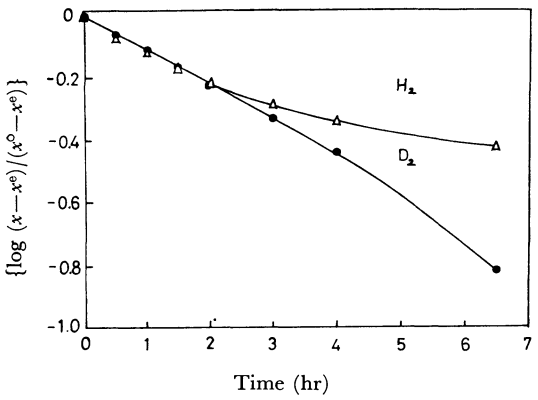

Fig. 7. Plot of $\log\{(x-x^e)/(x^o-x^e)\}$ *vs.* t for the data given in Fig. 3.
(478°C, $P^o_{H_2S}$=20mmHg, $P^o_{D_2}$ =20 mmHg, a_S=1)

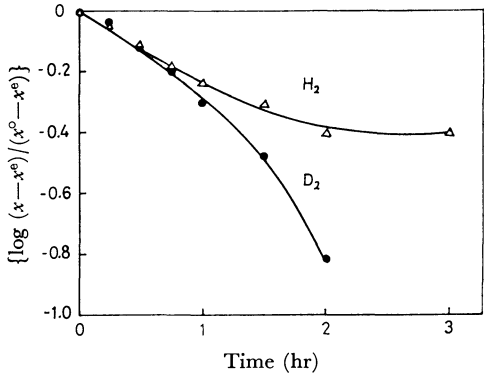

Fig. 8. Plot of $\log\{(x-x^e)/(x^o-x^e)\}$ *vs.* t for the data given in Fig. 4.
(478°C, $P^o_{H_2S}$=40 mmHg, $P^o_{D_2}$ =160 mmHg, a_S= 1/4)

TABLE 1. VALUES OF k_i AND k_i'

Temp. (°C)	$P^o_{H_2S}$ (mmHg)	$P^o_{D_2}$ (mmHg)	a_S	observed $k_i\times10^9$ mol/atm cm²·sec	observed $k_i'\times10^9$ mol/atm cm²·sec	mean $k_i\times10^9$ mol/atm cm²·sec	mean $k_i'\times10^9$ mol/atm cm²·sec
525	20	20	1	5.40	4.89	5.82 ±0.34	5.33 ±0.31
	40	40	1	5.82	5.50		
	80	80	1	6.42	5.59		
500	80	80	1	4.02	3.94		
478	160	40	4	0.591	2.31	0.655±0.064	2.52 ±0.21
	320	80	4	0.719	2.73		
	40	20	2	1.18	2.32	1.24 ±0.08	2.46 ±0.16
	80	40	2	1.20	2.36		
	133	66	2	1.36	2.69		
	20	20	1	3.01	2.92	2.57 ±0.27	2.53 ±0.24
	20	20	1	2.71	2.64		
	33	33	1	2.41	2.37		
	40	40	1	2.76	2.71		
	80	80	1	2.30	2.26		
	80	80	1	2.25	2.29		
	20	41	1/2	5.08	2.76	5.92 ±0.21	2.93 ±0.31
	27	54	1/2	5.70	2.67		
	90	180	1/2	6.20	3.36		
	21	82	1/4	13.0	2.97		
450	40	40	1	0.836	0.868	0.919±0.058	0.929±0.043
	80	80	1	1.000	0.990		
425	40	40	1	0.538	0.521	0.507±0.014	0.523±0.015
	73	73	1	0.507	0.493		

is also given. $x^e_{D_2}$ and $x^e_{H_2}$ are calculated by the equations

$$x^e_{D_2} + x^e_{H_2} = 1 \tag{22}$$

$$\frac{x^e_{D_2}}{x^e_{H_2}} = \frac{P^o_{D_2}}{P^o_{H_2S}} \tag{23}$$

where $P^o_{D_2}$ and $P^o_{H_2S}$ are the partial pressures of D_2 and H_2S at the beginning of reaction, respectively.

Both plots are straight and coincide well with each other.

Similar plots for the data given in Fig. 3 and

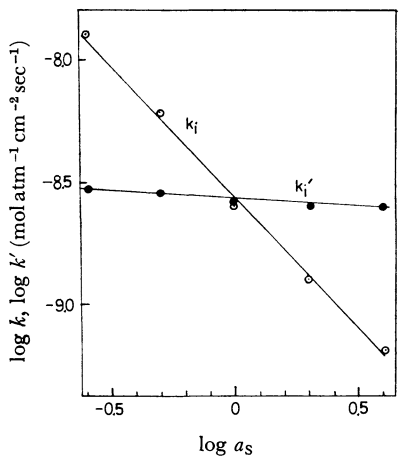

Fig. 9. Plots of log k_i and log k_i' against log a_S.

Fig. 4 are shown in Fig. 7 and Fig. 8, respectively. McKay's law holds in the initial period where x_{HD} remains constant, and the straight line portion for D_2 well agrees with that for H_2.

The values of k_i and $k_{i'}$ calculated by Eqs. (19) and (20) are listed in Table 1. It is seen from the table that the value of k_i is the same irrespective of the total pressure, if the values of a_S is the same.

Dependence of k_i and $k_{i'}$ on a_S. Figure 9 gives the plot of log k_i *vs.* log a_S and that of log $k_{i'}$ *vs.* log a_S. Both plots are linear. The slope for the former plot is -1.07 and that for the latter is -0.07. Such dependence of k_i and $k_{i'}$ on a_s is explained on the basis of the theory by Kobayashi and Wagner as follows.

The reaction between H_2S and H_2 on the surface of Cu_2S proceeds by the following parallel reactions

$$H_2S \rightleftarrows H_2 + S \quad (24\text{ A})$$

$$H_2S + e^- \rightleftarrows H_2 + S^- \quad (24\text{ B})$$

$$H_2S + 2e^- \rightleftarrows H_2 + S^{2-} \quad (24\text{ C})$$

where e^- denotes electrons in Cu_2S, and S, S^- and S^{2-} are adsorbed sulfur atoms, monovalent sulfur ions and divalent sulfur ions, respectively.

Assuming that adsorbed sulfur atoms and sulfur ions are in equilibrium with those in bulk of cuprous sulfide, we obtain the following rate equations:

$$\left(\frac{\dot{n}_{H_2}}{A}\right)_A = k_1 P_{H_2S} - k_1' P_{H_2} a_S \quad (25\text{ A})$$

$$\left(\frac{\dot{n}_{H_2}}{A}\right)_B = k_2 P_{H_2S} a_e - k_2' P_{H_2} a_{S^-} \quad (25\text{ B})$$

$$\left(\frac{\dot{n}_{H_2}}{A}\right)_C = k_3 P_{H_2S} (a_e)^2 - k_3' P_{H_2} a_{S^{2-}} \quad (25\text{ C})$$

where a_S, a_S^-, a_S^{2-} and a_e represent the activities of respective species. The first terms on the right side are the rate of sulfidation of Cu_2S and the second ones are the rate of reduction.

There are also several equilibrium relationships in solid phase. They are:

$$S^- \rightleftarrows S + e^-$$

$$\frac{a_S a_e}{a_{S^-}} = K_1 \quad (26)$$

$$S^{2-} \rightleftarrows S + 2e^-$$

$$\frac{a_S (a_e)^2}{a_{S^{2-}}} = K_2 \quad (27)$$

Moreover, for cuprous sulfide, we have

$$(a_{Cu})^2 a_S = K_3 \quad (28)$$

According to Wagner and Wagner[7] the activity of cuprous ions in cuprous sulfide is independent of the composition of Cu_2S. Hence

$$a_{Cu} = K_4' a_{Cu^+} a_e = K_4 a_e \quad (29)$$

From Eqs. (28) and (29), we obtain

$$a_e = K_5 (a_S)^{-1/2} \quad (30)$$

Combination of Eqs. (26), (27) and (30) yields

$$a_{S^-} = K_6 (a_S)^{1/2} \quad (31)$$

$$a_{S^{2-}} = K_7 \quad (32)$$

Inserting Eqs. (30), (31) and (32) into Eqs. (25 A), (25 B) and (25 C), we obtain

$$\left(\frac{\dot{n}_{H_2}}{A}\right)_A = k_1 P_{H_2S} - k_1' P_{H_2} a_S \quad (33\text{ A})$$

$$\left(\frac{\dot{n}_{H_2}}{A}\right)_B = k_2 K_5 P_{H_2S} (a_S)^{-1/2} - k_2' K_6 P_{H_2} (a_S)^{1/2} \quad (33\text{ B})$$

$$\left(\frac{\dot{n}_{H_2}}{A}\right)_C = k_3 K_5^2 P_{H_2S} (a_S)^{-1} - k_3' K_7 P_{H_2} \quad (33\text{ C})$$

These equations are summarized into a generalized formula

$$\frac{\dot{n}_{H_2}}{A} = v_{ox} - v_{red} = k P_{H_2S} (a_S)^{-m/2} - k' P_{H_2} (a_S)^{n/2} \quad (34)$$

or

$$\frac{\dot{n}_{H_2}}{A} = k P_{H_2S} (a_e)^m - k' P_{H_2} (a_e)^{-n} \quad (35)$$

where m and n are constants characteristic of reaction mechanism, namely,

$m=0$, $n=2$ for mechanism (24 A)

$m=1$, $n=1$ for mechanism (24 B)

$m=2$, $n=0$ for mechanism (24 C)

From a comparison of Eq. (34) with Eq. (9) or (10) we obtain

$$k_i = k (a_S)^{-m/2} \quad (36)$$

$$k_i' = k' (a_S)^{n/2} \quad (37)$$

As mentioned already, the slope of the plot of log k_i *vs.* log a_S is -1.07 and that of the plot of log $k_{i'}$ *vs.* log a_S is -0.07. It is thus concluded that m is 2 and n is 0. This result shows that mechanism (24 C) prevails in this case.

7) J. B. Wagner and C. Wagner, *J. Chem. Phys.*, **26**, 1597 (1957).

TABLE 2. COMPARISON OF DATA OF ISOTOPIC EXCHANGE WITH THAT OF COPPER SULFIDATION

Temp. (°C)	k_L° mol / atm cm^2·sec	a_S^e	$k_i(1)$ mol / atm cm^2·sec	$k_i(a_S^e)$ mol / atm cm^2·sec
500	5.93×10^{-7}	1.78×10^{-4}	3.94×10^{-9}	2.21×10^{-5}
450	2.22×10^{-7}	1.12×10^{-4}	0.919×10^{-9}	8.21×10^{-6}

Comparison of the Data of the Isotopic Exchange with That of Copper Sulfidation. The authors[8] have studied the sulfidation of Cu by H_2S and H_2S-H_2 gas mixtures and found that; (1) the reaction obeys the linear rate law, (2) the linear rate constant is proportional to the partial pressure of H_2S, and (3) the linear rate constant is nearly independent of the partial pressure of hydrogen. The findings show that the sulfidation of Cu by H_2S is mainly controlled by the reaction at the gas sulfide interface. k_L°, the linear rate constant at 1 atm of H_2S, is listed in the second column of Table 2.

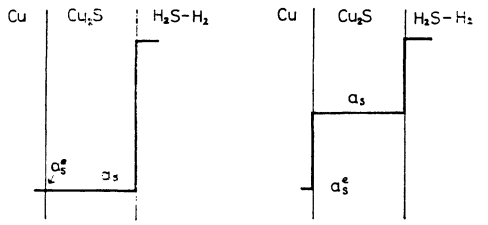

Fig. 10. Schematic representations of distribution of sulfur activity during the sulfidation of copper.

If the reaction at the gas-sulfide interface is much slower than the reaction at the metal-sulfide interface and the diffusion of materials across the sulfide, the sulfur activity would drop at the gas-sulfide interface appreciably, because a large driving force is needed at the interface to advance the reaction. In an ideal case, the sulfur activity at the gas-sulfide interface is equal to the sulfur activity in coexistence of Cu and Cu_2S, as schematically shown in Fig. 10(a). In this case, the rate of sulfidation of Cu by H_2S should be equal to k_i at a_S^e. The fifth column in Table 2 gives the estimated k_i values at a_S^e, assuming that the relationship between k_i and a_S found in the present work holds down to a_S^e. The calculated k_i value at a_S^e is about two orders higher than the observed linear rate constant k_L° in magnitude.

A possible explanation for this discrepancy is as follows. If the reaction at the metal-sulfide interface is as slow as the reaction at the gas-sulfide interface, the sulfur activity also drops at the metal-sulfide interface as shown in Fig. 10(b). Accordingly, a_S, the sulfur activity of Cu_2S at the gas-sulfide interface, is higher than a_S^e, and the k_i value at a_S is smaller than that at a_S^e. Further experiment is needed to elucidate the cause of the discrepancy.

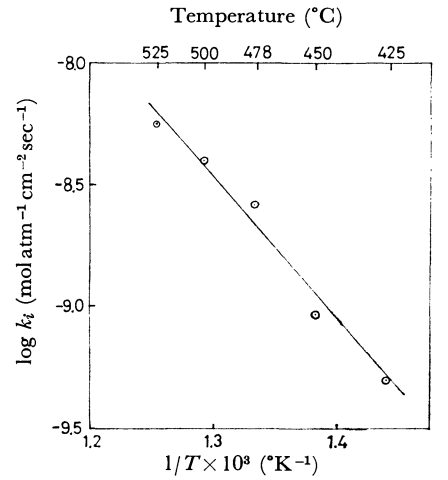

Fig. 11. Arrhenius plot for k_i at $a_S=1$.

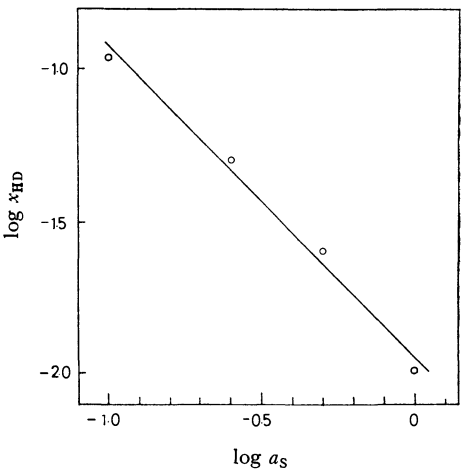

Fig. 12. Relationship between x_{HD} and a_S at 15% conversion of D_2. (478°C)

The Arrhenius plot of k_i at $a_S=1$ is given in Fig. 11. Activation energy determined from the slope is 27.8 kcal/mol. On the other hand, the activation energy of sulfidation of Cu in H_2S is 21.3 kcal/mol. In the latter case, the sulfur activity of Cu_2S surface would change with tempera-

8) M. Takeda, K. Fueki and T. Mukaibo, *J. Electrochem. Soc. Jap.*, **36**, 95 (1968).

ture. The difference in the activation energy might be due to the difference in the temperature dependence of sulfur activity on Cu_2S surface.

Formation of HD. As already mentioned, the formation of HD becomes remarkable as the sulfur activity of Cu_2S decreases. Figure 12 shows the relationship between the sulfur activity of Cu_2S and the mole fraction of HD at the time where 15% of the initial amount of D_2 has been exchanged. Correlation between the formation of HD and the sulfur activity is evident. However, because of the lack of adequate kinetic data, detailed discussion on the mechanism of formation of HD is difficult for the time being.

Summary

(1) The isotopic exchange between H_2S and D_2 on Cu_2S was investigated as a function of temperature and a_S, the sulfur activity of Cu_2S.

(2) It was found that when a_S is high the exchange reaction $H_2S+D_2=H_2+D_2S$ is predominant and the formation of HD is small. It was also found that when a_S is low the formation of HD proceeds after an initial period of reaction.

(3) The rate of exchange reaction $H_2S+D_2=H_2+D_2S$ was found to obey McKay's law, and the first-order rate constants were obtained. k_i, the rate constant of sulfidation of Cu_2S by H_2S, and k_i', the rate constant of reduction of Cu_2S by H_2 were calculated from the first-order rate constants.

(4) Both plots of $\log k_i$ *vs.* $\log a_S$ and $\log k_i'$ *vs.* $\log a_S$ were linear. The slope of the former plot was -1.07 whereas that of the latter was -0.07.

(5) Based on the theory proposed by Kobayashi and Wagner, the predominant reaction mechanism for the reaction $H_2S+D_2=H_2+D_2S$ was discussed.

(6) Activation energy was found to be 27.8 kcal/mol.

The authors wish to express their sincere thanks to Dr. M. Tsuchiya of the Faculty of Engineering, University of Tokyo, for his help in carrying out mass-spectroscopic analysis.

BULLETIN OF THE CHEMICAL SOCIETY OF JAPAN VOL. 43 30—33 (1970)

Measurement of Contact Potential Difference for Organic Crystals. Work Function of Violanthrene

Masahiro KOTANI and Hideo AKAMATU

Department of Chemistry, Faculty of Science, The University of Tokyo, Hongo, Bunkyo-ku, Tokyo

(Received June 6, 1969)

A vibrating-reed type cell for measuring contact potential difference was constructed and successfully applied for organic crystals. From the observed contact potential difference for violanthrene against graphite, the work function has been estimated as 4.50 ± 0.1 eV. In association with the activation energy for electrical conductivity, 0.8—0.9 eV, the electronic energy diagram for violanthrene has been illustrated, which revealed the extrinsic nature of semiconduction and the energy gap, 2.3—2.5 eV, being comparable with the first excited singlet state of violanthrene molecule.

The electrical properties of organic compounds in crystalline state, made of conjugated π-electron systems, have been extensively investigated and their semiconductive characters are now widely accepted.[1] Such a molecular crystal may be approximated to be an assembly of neutral molecules, the interactions between them being relatively weak. In contrast to covalent semiconductors such as silicon or germanium, there are no dangling bonds on the surface of molecular crystals which may give rise to unfilled energy levels in the forbidden gap. The electrical properties of molecular crystals may thus be expected to be relatively simple with respect to surface conditions. However, a number of cases have been reported where the electrical properties of such crystals are influenced by the surface conditions. In spite of its potential significance relatively few studies have been made on the surface properties of molecular crystals. This may be attributed partly to the lack of appropriate methods for investigation. Conductivity measurements are sometimes unsatisfactory with respect to reproducibility and the effect of impurity doping has not been well understood for this calss

1) F. Gutmann and L. E. Lyons, "Organic Semiconductors," John Wiley & Sons, New York, N. Y. (1967).

of crystals.

Measurements of work function can be used as an efficient means for surface studies. The work function is a quantity which depends on the surface as well as on the bulk properties. When data are obtained for clean surfaces they can be used in discussing how surface and bulk properties are related to each other. Further, gas adsorption experiments may yield information about interactions between the adsorbed molecules and the crystal surface.

Measurements of contact potential differences of organic crystals were reported by several authors. However, numerical data published on work function are still very scarce. From the experiments on photoemission the threshold energy can be obtained. This quantity corresponds to the energy of the filled band, whereas the work function gives the location of the Fermi level. Nelson has reported measurements of contact potential differences[2] using the electron beam retardation technique. His data are mainly on organic dyes deposited on inorganic semiconductors such as cadmium sulfide. The same technique was applied to the measurements of the contact potential differences of several organic compounds.[3] The vibrating condensor method was applied to the photovoltage measurements.[4] Irradiation with light produced change in contact potential difference. This was attributed to the difference of diffusion of mobile electrons and holes, *i. e.*, the Dember photovoltage. Analogous information was obtained by Putzeiko[5] using a related technique, Bergmann's condensor method. The surface under test and a transparent conducting plate, a mica plate made half transparent by vacuum evaporation of platinum, constituted the capacitor. The surface was irradiated an by intermittent light through the transparent electrode. This gave rise to an alternating photovoltage. Harada *et al.*[6] have published the results of several experiments on photoemission. They include contact potential differences obtained from current-voltage characteristics for several aromatic compounds, from which the work functions for the organic crystals can be evaluated.

The present paper describes the determination of the work function for organic crystals through measurements of contact potential differences using the vibrating condensor method. Compared to other methods such as thermionic or photoelectric emission which are employed in surface studies, this method is advantageous in that it allows measurements without introducing distubances on the surface; it requires a sample to be neither heated nor irradiated. Further, it does not require vacuum; it allows measurements in various gases at wide range of pressure. The electronic structure of crystalline violanthrene will be discussed on the basis of the work function observed.

Experiment

A vibrating-reed type cell, made of Pyrex glass, was constructed for measuring contact potential differences (Fig. 1). A copper disc (1) with an area of about 1.5 cm^2) coated with gold by vacuum evaporation served as a substrate. It was set over an oven (3) where the sample was sublimed onto the surface. The disc covered with a layer of the sample was then transferred to the centre of the cell by an iron wire pulled by turning a ground joint (4). It constituted a parallel plate capacitor coupled with a reference electrode (2). The two electrodes were about 1 mm apart. The reference electrode was a film of colloidal graphite (Aquadag) which was painted on a thin Pyrex plate and treated in air at 500°C for an hour. The reference electrode was held by a glass rod. A piece of iron was attached to the glass rod which brought the reference electrode into resonant vibration by means of an electromagnet, which was driven by an audio range oscillator coupled with a power amplifier. The frequency of vibrations ranged from 50 to 70 Hz. The glass rod was covered with conductive silver paint and served as a lead.

The inner wall of the spherical part of the cell was coated with gold by vacuum evaporation and grounded in order to avoid disturbances due to charging. The coating served also as a shielding against electric fields outside.

A gold film was used also as an auxiliary standard electrode, which was formed by vacuum evaporation onto a Pyrex plate. The contact potential difference between the freshly evaporated gold film and a standard graphite surface showed a large drift immediately after

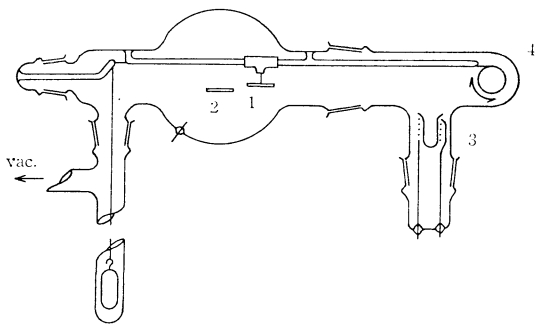

Fig. 1. The cell.
1. Sample, 2. Reference electrode, 3. Oven, 4. Ground joint. The signal is fed from the sample electrode. The reference electrode is connected with the potentiometer.

2) R. C. Nelson, *J. Opt. Soc. Am.*, **46**, 1016 (1956).
3) Ref. 1, p. 796.
4) I. A. Akimov, *Doklady Akad. Nauk SSSR*, **128**, 691 (1959).
5) E. K. Putzeiko, *ibid.*, **129**, 303 (1959).
6) Y. Harada and H. Inokuchi, This Bulletin, **39**, 1443 (1966); M. Kochi, Y. Harada and H. Inokuchi, *ibid.*, **40**, 531 (1967).

evaporation, but after several hours of exposure to the air it attained a stationary value which was found to be fairly reproducible. The work function of this "aged" surface was determined to be 5.1 eV from the contact potential difference against the graphite surface.

A potentiometer made of a mercury battery and a Helipot, a precision variohm, supplied potential for the reference electrode. The signal from the sample electrode was amplified with a preamplifier with imput resistance of 10^{12} ohm and was put into an oscilloscope. The cell and the preamplifier were placed in a shielding cage. The null indication procedure was employed in which the potentiometer was adjusted to give a minimum magnitude of the signal. In order to minimize the hum noize of commercial frequency (50 Hz), the lead connecting the sample and the preamplifier should be as short as possible. The cell was not quite satisfactory as the lead was designed to serve also as a cable to carry the sample electrode. To maintain steady vibrations of the reference electrode and to avoid vibrations in other parts of the cell, care must be taken to prevent mechanical disturbances.

The sensitivity of the apparatus was ± 1 mV for a uniform metal surface. When the surface was covered by an organic film, it exhibited a higher noise level and gave a lower sensitivity. The sensitivity of measurements for organic films was generally 20 to 30 mV. The reproducibility of the surface is a factor which must be considered. It was the principal factor for the experimental error in the case of violanthrene.

Measurements were carried out in a vacuum of 10^{-5} Torr, but the cell was designed for measurements in various ambient gases. Sublimation of organic compounds was performed in the cell in order to measure uncontaminated films. Ground joints and grease were used.

Conductivity measurements were made with a vibrating reed electrometer. A surface type arrangement was employed, with Aquadag electrodes.

Violanthrene was prepared from violanthrone, a commercial product, by reduction with powdered zinc metal. After it was treated by usual chemical methods, the final purification was made by successive sublimation in vacuum.

Results and Discussion

The work function of an electrical conductor can be evaluated by the relation

$$\Phi = \Phi_0 - \Delta$$

where Φ denotes the work function of the sample, Φ_0 that of the references material and Δ the contact potential difference. For this relation to be valid the thermal equilibrium of electrons between the sample and the reference material must be attained. If the equilibrium is not attained, the observed contact potential difference depends not only on the sample but also on the substrate materials employed. The preliminary experiments were made for violanthrene film deposited on several kinds of metals. The results are summarized in Table 1. For Φ_0, the value of 4.74 ± 0.1 eV for graphite was adopted after Apker *et al.*[7] In evaluating from the observed contact potential differences, it is essential that the work function of the reference surface be constant throughout the measurements. We did not measure the work fuction of the graphite films used. However, the contact potential difference measurements revealed that the constancy of the work function of the graphite film made by the procedure described above was kept within the range of ±0.05 eV. The work function of the sample thus evaluated shows a good constancy within the experimental error irrespective of the substrate metal and indicates that the above relation is valid.

TABLE 1. THE EFFECT OF THE SUBSTRATE MATERIAL ON THE OBSERVED WORK FUNCTION OF VIOLANTHRENE

Substrate	Reference	Φ (eV)
Pt	Aquadag	4.5
Cu	Aquadag	4.4
Brass	Aquadag	4.5
Au	Aquadag	4.5
Au	Au	4.5
Ni	Au	4.5

Having thus verified that the observed contact potential difference does not depend on the choice of the substrate metal, we employed gold as the substrate. As an auxiliary standard a gold film evaported on a Pyrex plate was also used. Its work function was determined to be 5.1 eV using graphite as the primary standard, Table 2 shows the results of the measurements. For both reference materials the same value of 4.50 ± 0.1 eV was obtained for the work function of violanthrene.

TABLE 2. THE WORK FUNCTION OF VIOLANTHRENE

Reference	CPD (eV)	Φ (eV)
Au	0.5	4.6
Au	0.63	4.47
Au	0.70	4.40
Au	0.6	4.5
Aquadag	0.2	4.5
Aquadag	0.24	4.50
	mean	4.50 ± 0.1

The temperature dependence for the electrical conductivity of violanthrene was measured with a surface type arrangement. It is well expressed by the relation

$$j = j_0 \exp(-E/kT)$$

within the temperature range of 53 to 191°C, where

7) L. Apker, E. Taft and J. Dickey, *Phys. Rev.*, **74**, 1462 (1948).

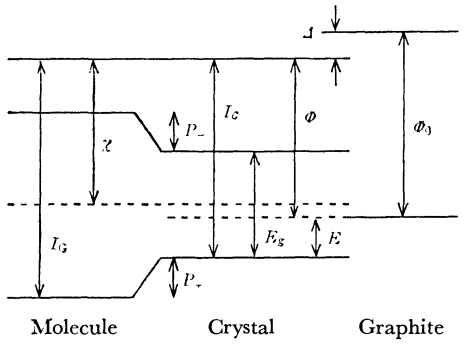

Fig. 2. The energy diagram for violanthrene in the isolated and in the crystalline state.
I_G, I_C, Ionization energy; P_+, P_-, polarization energy; Φ, work function; E_g, band gap; Δ, contact potential difference; E, activation energy for electrical conduction.

j is the observed current. The activation energy E was found to be 0.8—0.9 eV.

A tentative electronic energy diagram can be constructed, as shown in Fig. 2, using experimental and theoretical data available. Figure 2 represents energy levels of violanthrene for gaseous and crystalline states. The ionization energy of gaseous violanthrene is estimated to be 6.84 eV.[8] For alternant hydrocarbons Mulliken's electronegativity, $\chi=(I+A)/2$, can be approximated by the mean value of the energy of the highest occupied orbital and the energy of the lowest vacant orbital, where I and A denote the ionization energy and the electron affinity respectively. This quantity has been estimated from experimental data for alternant hydrocarbons to be 4.15 eV.[9]

In Fig. 2 are also shown the energy levels of graphite which stands in the electrical equilibrium with crystalline violanthrene. The contact potential difference between violanthrene and graphite was observed to be 0.24 eV.

When an electron is emitted from a neutral crystal it leaves behind a positive charge which polarizes the medium surrounding it. This stabilizes the electric charge in a dielectric atmosphere compared to the isolated charge in the vacuum. The polarization energy corresponds to the difference in ionization energies of gaseous and crystalline states. An analogous discussion leads to the conclusion that the electron affinity of a molecule must be larger for the crystalline state than for the gaseous state. The energy difference, the polarization energy due to a negative charge in a crystal, seems to be the same as that for positive charge in the crystal. As the Fermi level must be located half way between the top of the filled levels and the lowest conducting level in an intrinsic semiconductor, we conclude that the work function of crystalline alternant hydrocarbons is equal to the molecular electronegativity χ. Energy levels are illustrated in Fig. 2, in which 0.8—0.9 eV, obtained as the activation energy for dark conduction, is assigned as the energy difference between the top of the filled band and the Fermi energy. Thus the ionization energy and the band gap are evaluated to be 5.3 to 5.4 eV and 2.3 to to 2.5 eV, respectively.

The ionization energy of 5.20 eV for crystalline violanthrene was obtained form the threshold energy for photoelectric emission.[10] Kearns and Calvin have reported measurements of photoelectric emission for several crystalline compounds including violanthrene.[11] Their values for crystal ionization energy are generally lower than those obtained by other investigators by 0.5 to 0.6 eV, as in pentacene and metal-free phthalocyanine.

In conclusion, the Fermi level does not lie midway between the valence band and the conduction band. The origin of its extrinsic nature, whether it comes from the presence of some chemical or structural impurities in the bulk or from some surface conditions such as gas adsorption, remains to be explored. It is worth noteing that the band gap is comparable with the energy for the first excited singlet state of violanthrene molecule, *i.e.*, 2.5 eV.

The authors thank Dr. Haruo Kuroda for his valuable discussions.

8) H. Kuroda, *Nature*, **201**, 1214 (1964).
9) R. S. Becker and E. Chen, *J. Chem. Phys.*, **45**, 2403 (1966).
10) T. Hirooka, M. Kochi, H. Inokuchi and Y. Harada, This Bulletin, **42**, 1481 (1969).
11) D. Kearns and M. Calvin, *J. Chem. Phys.*, **34**, 2026 (1961).

BULLETIN OF THE CHEMICAL SOCIETY OF JAPAN VOL. 43 34—38 (1970)

Electrical Conductivity of Graphite Bromine Lamellar Compounds

Tadashi SASA, Yoichi TAKAHASHI and Takashi MUKAIBO

Department of Nuclear Engineering, The University of Tokyo, Hongo, Bunkyo-ku, Tokyo

(Received June 12, 1969)

Polycrystalline graphite was allowed to react with bromine vapor, and the change of its electrical conductivity during the course of bromination and debromination was studied. The graphite was found to behave in two different ways depending on the process of bromination. When the vapor pressure of bromine was changed stepwise, following the equilibrium line of bromine absorption of graphite, the electrical conductivity showed a reversible change. On the other hand, when a graphite sample was brominated with the saturated vapor, an increase of the electrical conductivity steeper than that of the former case was observed. These results were discussed in relation to the structural analysis of the brominated graphite. A metastable phase of graphite bromide, the electrical conductivity of which remained unchanged in spite of a considerable increase of absorbed bromine, was found. The electrical conductivity of the residue compounds was also investigated, and a steep decrease was observed at high concentrations of bromine.

Graphite reacts with bromine at room temperature to form a lamellar compound. The saturated composition of the graphite bromine lamellar compound is C_8Br, and its structure was clarified by Rüdorff[1] as the second stage structure, where the bromine atoms are intercalated in every other layer spacing of graphite. The mechanism of bromine absorption of graphite has been investigated by several workers. Mukaibo and Takahashi[2] measured the rate of bromination of graphite, and obtained an apparent activation energy of the reaction of 5—7 kcal/mol. Saunders *et al.*[3] measured the dimensional change of pyrolytic graphite by bromine absorption, and observed a metastable structure which has a practically full expansion along the direction of *c*-axis by only about one-third of the limiting uptake. Hooley *et al.*[4,5] also investigated the rate of absorption and the dimensional change, and proposed a mechanism in which all layers are open to the intercalation at a relatively initial stage. The authors[6] measured the change of X-ray diffraction pattern of graphite during the course of bromination, and confirmed that the second stage structure of the lamellar compound appeared in the initial stage of the reaction.

Knowledge of electrical properties of the compounds gives valuable information about the electronic state of the species intercalated in graphite. Hennig[7] reported that the electrical resistance of polycrystalline graphite decreases with bromine uptake, and suggested that one-seventh of the intercalated bromine atoms would be ionized. Blackman *et al.*[8] measured the electrical resistance of pyrolytic graphite reacting with bromine vapor in the direction of both the *a*-axis, and the *c*-axis, and observed an initial steep decrease of the resistance in the *a*-axis direction.

We have investigated changes of the electrical conductivity of graphite with bromine absorption in two different processes, *i.e.*, the stepwise bromination and the rapid bromination. In the former case, the vapor pressure of bromine was increased stepwise, and the relation between the electrical conductivity and the equilibrium concentration of the absorbed bromine at every step has been investigated. In the latter, the change of the electrical conductivity of the graphite sample during the course of the reaction with saturated bromine vapor has been measured.

Experimental

Materials. The following three graphite samples have been used

1) High purity artificial graphite, heat-treated at

1) W. Rüdorff, *Z. Anorg. Allg. Chem.*, **245**, 383 (1941).

2) T. Mukaibo and Y. Takahashi, This Bulletin, **36**, 625 (1963).

3) G. A. Saunders, A. R. Ubbelohde and D. A. Young, *Proc. Roy. Soc., Ser. A*, **271**, 499 (1963).

4) J. G. Hooley and J. L. Smee, *Carbon*, **2**, 135 (1964).

5) J. G. Hooley, W. P. Garby and J. Valentin, *ibid.*, **3**, 7 (1965).

6) Y. Takahashi, T. Sasa and T. Mukaibo, *Tanso*, **1969** (No. 52), 199.

7) G. R. Hennig, *J. Chem. Phys.*, **20**, 1443 (1952).

8) L. C. F. Blackman, J. F. Mathews and A. R. Ubbelohde, *Proc. Roy. Soc., Ser. A*, **256**, 15 (1960).

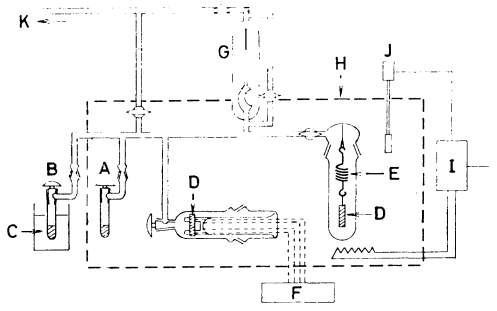

Fig. 1. Apparatus for the measurement of the electrical conductivity and the bromine content of graphite bromide.
A. Bromine container which provides saturated vapor of bromine.
B. Bromine container which provides bromine vapor of lower pressures.
C. Alcohol bath cooled by solid carbon dioxide.
D. Graphite specimen.
E. Quartz spring balance.
F. System for the measurement of electrical conductivity.
G. Glass spoon gauge for pressure measurement.
H. Water bath.
I. Temperature controller.
J. Photo-transistor detector.
K. To vacuum line.

2400°C, $c_0=3.364\pm0.001$ Å, specific resistivity 1.7×10^{-3} Ω·cm (type A).

2) Similar artificial graphite, heat-treated at 3000°C, $c_0=3.361\pm0.001$ Å, specific resistivity 1.4×10^{-3} Ω·cm (type B).

3) Natural graphite with pitch-binder, heat-treated at 3000°C, $c_0=3.356\pm0.002$ Å, specific resistivity 1.1×10^{-3} Ω·cm (type C).

The samples were cut in small specimen of 1.5 mm × 2 mm × 20 mm for measurements of the electrical conductivity and the weight gain.

GR-grade bromine was distilled and forced to pass through concentrated sulfuric acid before use.

Apparatus. The apparatus is shown in Fig. 1. It was difficult to measure both the electrical conductivity and the weight gain with the same specimen. Two graphite specimens cut from a homogeneous block were used for the measurements. The electrical conductivity was measured with one of the specimens by means of a four cantact potentiometric method, with a current of 60—80 mA and a detected potential of 0.3—3 mV. The specimen and the four platinum contacts are shown enlarged in Fig. 2. The other specimen was suspended by a quartz spring balance (sensitivity 20 mm/g), and the concentration of absorbed bromine was measured by means of a running microscope. The reaction temperature was in the range of 20—30°C, and was controlled to ±0.01°C by a controller connected with a photo-transistor detector. The bromine container A, in Fig. 1, provided the vapor of saturation pressure. The container B was controlled at desired temperatures by means of a water bath or an alcohol bath cooled by solid carbon dioxide. Thus the vapor pressure of bromine was controlled at desired values.

The whole system was evacuated before the run, and the bromine vapor was allowed to enter into the reaction tubes by the stop-cock A or B. On debromination, the container B was cooled so as to trap the bromine vapor. After the bromine vapor was completely pumped out, the electrical conductivity of the bromine residue compound was measured.

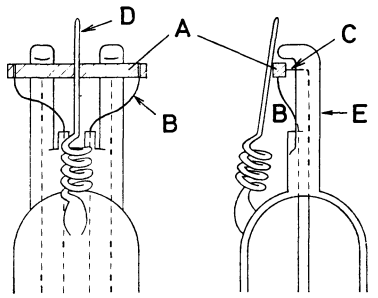

Fig. 2. Graphite specimen and electrodes for the measurement of electrical conductivity.
A. Graphite specimen, 1.5×2×20(mm).
B. Current electrode of platinum wire (0.2 mm).
C. Potential probe of platinum.
D. Glass spring to hold the sample.
E. Glass rod.

Results

Stepwise Bromination. Figure 3 shows the relation between the relative vapor pressure of bromine and the bromine uptake by graphite of the type C at 20.6°C. Open circles represent the equilibrium state of bromine absorption while the bromine vapor pressure was increased stepwise, and solid circles represent that while the vapor pressure was decreased. There existed a threshold pressure of bromine absorption, over which two stages of bromine absorption process was observed. It is consistent with the result obtained by Maire and Mering.[9] The electrical conductivity *vs.* bromine

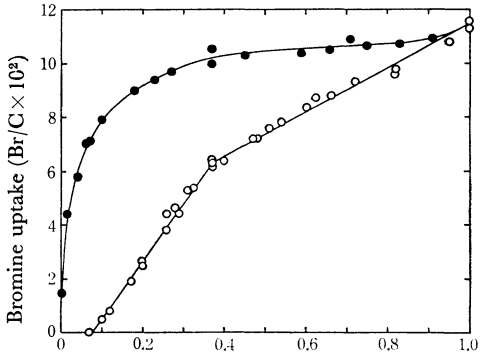

Fig. 3. Bromine vapor pressure and bromine absorption of graphite (type C) at 20.6°C.
○ on bromination
● on debromination

9) J. Maire and J. Mering, Proc. 3rd Conf. Carbon, 337 (1959).

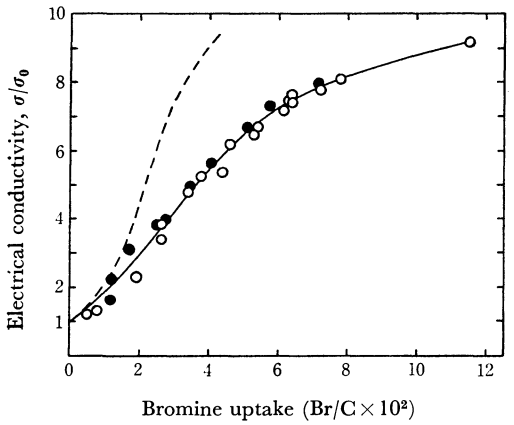

Fig. 4. Electrical conductivity of stepwise brominated graphite.
○ on bromination
● on debromination
dashed line: after Hennig

uptake curve corresponding to Fig. 3 is shown in Fig. 4. Here, σ represents the conductivity of the graphite bromide, and σ_0 that of the virgin graphite. The change was found to be almost completely reversible on bromination and debromination. The dashed line represents Hennig's work[7] on polycrystalline graphite. Similar results have been obtained also with graphite of types A and B.

Rapid Bromination. The solid line in Fig. 5 shows the change of the electrical conductivity of type C graphite reacting with bromine vapor of saturation pressure. The dashed line represents the case of the stepwise bromination of Fig. 4. The electrical conductivity increased more steeply in the rapid bromination, and reached the final value on bromine uptake of only about one-third of the limiting value.

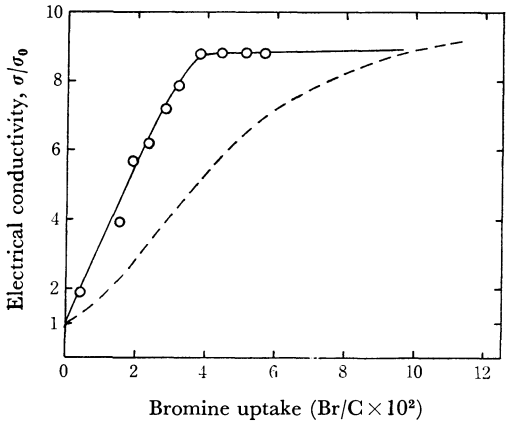

Fig. 5. Change of electrical conductivity of graphite (type C) by rapid bromination. (20.6°C)
Solid line: rapid bromination.
Dashed line: stepwise bromination

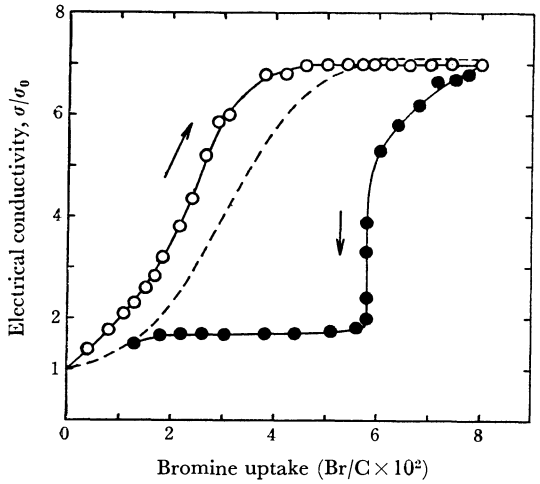

Fig. 6. Change of electrical conductivity of graphite (type B) by rapid bromination. (22°C)
○ on bromination
● on debromination
dashed line: stepwise bromination

Similar results have been obtained on graphite of types A and B. The latter case is shown in Fig. 6. A remarkable hysteresis has been observed. Moreover, an anomalous discontinuous change of electrical conductivity has been observed on debromination.

The residue compound thus formed was again allowed to absorb bromine by stepwise bromination. The curve of electrical conductivity *vs.* bromine content is shown in Fig. 7. In the earlier stage of this rebromination, the electrical conductivity of residue compound showed little change, while the

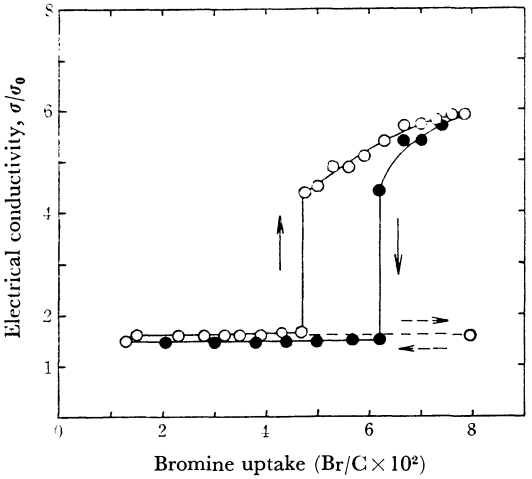

Fig. 7. Effect of stepwise bromination on electrical conductivity of the residue compound formed by the rapid bromination.
○ on bromination (stepwise)
● on debromination

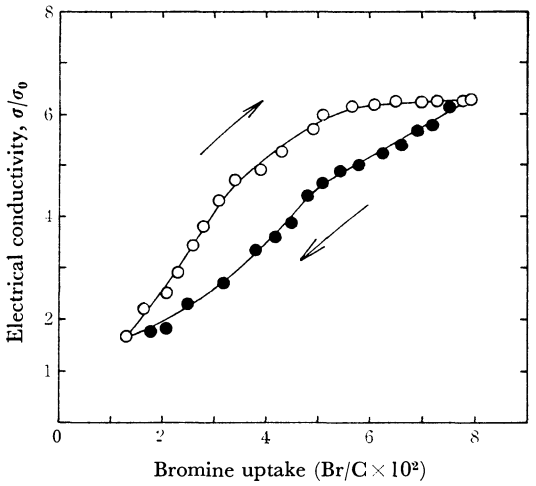

Fig. 8. Effect of rapid bromination on electrical conductivity of the residue compound formed by the stepwise bromination.
○ on bromination (rapid)
● on debromination

progress of bromine absorption was observed by weight gain. By a careful increase, a little at a time, of the reacting bromine vapor pressure, the graphite could absorb bromine almost to the saturated concentration without any change in electrical conductivity (dashed line). However, if the sample, during the course of rebromination of this type, was left to contact with bromine vapor of a constant pressure for a sufficient length of time such as 24 hr, the electrical conductivity increased to the value of the equilibrium state of the same bromine concentration (solid line). It should be noted that no bromine absorption or desorption was accompanied during the transition in electrical conductivity. The curve on debromination showed again a discontinuous change of conductivity.

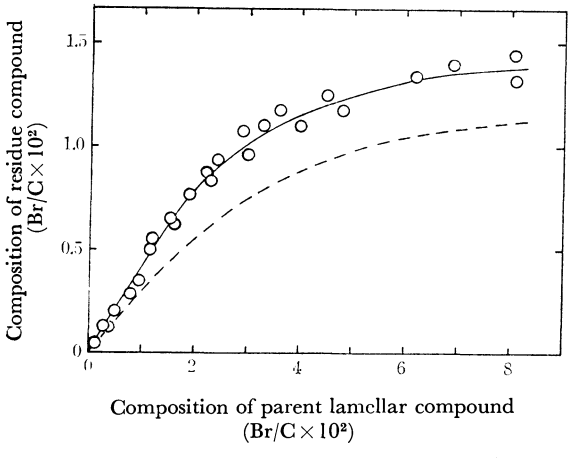

Fig. 9. Dependence of the composition of residue compound on the composition of parent lamellar compound. (dashed line: after Hennig)

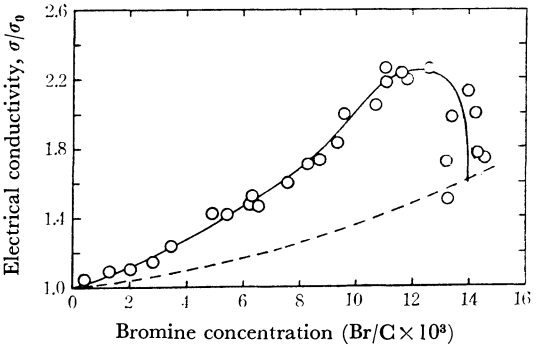

Fig. 10. Electrical conductivity of graphite bromine residue compound.
Solid line: residue compound
Dashed line: lamellar compound

The residue compound, on the other hand, formed by the stepwise bromination of the virgin graphite, followed by debromination, was later forced to absorb bromine by rapid bromination. Figure 8 shows the result of the reaction. The change was reversible, and such a discontinuous change of electrical conductivity as in Fig. 7 was not observed.

Residue Compounds. Figure 9 gives the dependence of the composition of the residue compound on the composition of the parent lamellar compound. The result coincides with Hennig's work[10] qualitatively. The electrical conductivity of the residue compound is plotted against the bromine content by the solid line in Fig. 10. The electrical conductivity increased with the bromine content over the range up to about Br/C$=1.2\times 10^{-2}$. Beyond this concentration the conductivity decreased rather steeply.

The dashed line in Fig. 10 represents the electrical conductivity of the lamellar compound. The residue compound has a larger conductivity than the lamellar compound of the same bromine concentration. The results presented above are consistent with the works by Hennig[10] and Kosai[11].

Discussion

1) Electrical Conductivity of Graphite Bromide in Equilibrium. A single relation could be found between the electrical conductivity and the bromine concentration of the compound in equilibrium state of absorption.

Figure 3, which illustrates the relation between the vapor pressure and the bromine uptake, suggests that the bromine absorption of graphite can be divided into two stages at about half the saturated concentration of absorbed bromine. The curve of electrical conductivity *vs.* bromine content, however, did not show such a break. The single relation could be applied both during the course of bromina-

10) G. R. Hennig, *J. Chem. Phys.*, **20**, 1438 (1952).
11) A. Kosai, *Oyobutsuri*, **30**, 402 (1961).

tion and debromination.

The curve in Fig. 4 shows a discrepancy from Hennig's result. It may be attributed to the differences in the type and the degree of crystallization of the graphite samples used.

2) The Mechanism of Bromine Absorption of Graphite. A steeper increase of the electrical conductivity was observed on the rapid bromination of graphite than in the case of the stepwise bromination for the same bromine concentration. It may be related to the difference in the structure between the rapidly brominated graphite bromide and the graphite bromide brominated stepwise.

The authors have reported[6] the change of the layer structure of graphite in the rapid bromination. As the reaction proceeded, distinct double peaks were observed in the X-ray diffraction pattern. These peaks were attributed respectively to the virgin graphite remaining and the second stage structure of the graphite bromine lamellar compound. No other phase could be found through the reaction. It is consistent with the result which Saunders *et al.*[3] reported on the measurement of the dimensional change of pyrolytic graphite with bromine absorption. The results suggest that the bromine intercalation into graphite layers would proceed as follows. At the first stage of the reaction, when the bromine vapor of saturation pressure contacts graphite, bromine begins to invade every other layer spacing of graphite. After a while, the absorbed bromine may be distributed dilutely in the crystallite and the second stage is formed.

It was also reported[6] that when the vapor pressure of the reacting bromine was increased stepwise, the (00l) peaks in the X-ray diffraction pattern of graphite showed gradual and continuous shifts to the lower diffraction angles, and finally reached that of the second stage structure of the saturated graphite bromide. Thus, bromine appears to be distributed rather orderly in the graphite lattice in the course of the stepwise bromination. The number of layer spacings occupied by bromine is dependent on the relative vapor pressure of bromine, and the bromine layer intercalated between the carbon layers seems to have a relatively high density. In the case of the above mentioned stepwise bromination, it may be probable that a certain fraction of the intercalated bromine is ionized as suggested by Hennig.[7] On the other hand, the more dilute distribution of bromine in the transient condition of the rapid bromination is supposed to increase the fraction of ionized bromine. It explains why the electrical conductivity of the rapidly brominated graphite for the same bromine concentration was higher than that of the sample brominated stepwise.

3) Metastable Phase of Graphite Bromide. In Figs. 6 and 7, a strange phase of graphite bromide is found, which contains a sufficient quantity of bromine, but the electrical conductivity of which remains unchanged. The phase was apparently not a stable one, and appeared only during the course of bromination and debromination. Only the normal phase is stable, the electrical conductivity of which increases with bromine concentration. The transition between the metastable phase and the normal phase was observed as a discontinuous change of electrical conductivity. The structural analysis of the metastable phase by X-ray diffraction was attempted, but adequate conditions for the appearance of the metastable phase could not be established.

The metastable phase was found only in rapidly brominated graphite, and the method of the first bromination process of virgin graphite is supposed to determine its succeeding behavior. Once a virgin graphite sample has been rapidly brominated, the memory strongly remains in it, and the residue compound also forms the metastable phase in any condition of bromination. No satisfactory explanation is found for the phenomena at present. The role of the bromine in the metastable phase of graphite bromide is interesting.

4) Residue Compounds. Figure 9 shows the retention of bromine in the graphite lattice. About half of the bromine absorbed by graphite was retained in the dilute region. The fraction of the retained bromine is higher than Hennig's result, which may be attributed to the difference of the type of the graphite sample.

The steep decrease of the electrical conductivity of the bromine residue compound at the higher bromine concentration was also observed by Hennig[7] and Kosai.[11] They explained this phenomenon to be the result of the mechanical disintegration of graphite crystal by a considerable dimensional change with bromination. This is plausible in a way. The reproducibility of the data was fairly good, and the point of the saturated residue compound coincided with the line of lamellar compound. It may be possible to consider the decrease of the electrical conductivity as a transition from the electronic state of the residue compound to that of the lamellar compound.

BULLETIN OF THE CHEMICAL SOCIETY OF JAPAN VOL. 43 39—41 (1970)

Far Infrared Spectra of Potassium Oxalate Monohydrate and Its Deutero Analog

Kunio FUKUSHIMA

Department of Chemistry, Faculty of Science, Shizuoka University, Oya, Sizuoka

(Received June 12, 1969)

The far infrared spectra of potassium oxalate monohydrate and its deutero analog in their crystalline state were measured. Assignment of the infrared absorption bands was made on the basis of frequency shift associated with deuterium substitution of hydrogen atoms in water of crystallization and also on the basis of comparison of neutron scattering spectra of the compounds with the infrared spectra.

Molecules of the water of crystallization form various types of bondings with surrounding atoms and ions through hydrogen bond and lone-pair coordination. Chidambaram *et al.* classified molecules of the water of crystallization on the basis of their coordination to ions and electron accepter groups.[1] In the present study, potassium oxalate monohydrate (p.o.m.), which belongs to type A,[1] was chosen as a representative of crystals containing molecules of the water of crystallization whose lone pairs are not specifically directed to any of the surrounding atoms and ions. A spectroscopic investigation in the region of 4000—60 cm^{-1} was carried out. The IR spectra of p.o.m. and its deutero analog (*d*-p.o.m.) have been observed by several investigators.[2-4] In the lower frequency region, measurement of Raman spectra of metal oxalate in aqueous solution was made.[5] However, no measurement of far IR spectra has been reported so far. In the present investigation, far IR spectra of p.o.m. and *d*-p.o.m. were measured in order to obtain optically active lattice vibration frequencies and to assign several IR absorption bands.

Experimental

The far IR spectra of p.o.m. in Nujol mull were measured in the region of 400—60 cm^{-1} with a Hitachi FIS-3 Far IR Spectrometer. Sample for the measurement was obtained by recrystallization of a special grade reagent p.o.m. of Koso Chemical Co., Ltd. from aqueous solution. The measurement was made for the sample in Nujol mull, sealed in a thin polyethylene sack. *d*-p.o.m. was prepared by vacuum distillation of p.o.m.-heavy water solution and vacuum drying of the residue. The far IR spectra of the Nujol mull were measured. The far IR spectra are shown in Figs. 1 and 2. IR spectra of the same samples in the region of 4000—400 cm^{-1} were measured with a Perkin-Elmer 521 Spectrophotometer and a Hitachi EPI-L Spectrophotometer. The spectra are shown in Figs. 3 and 4.

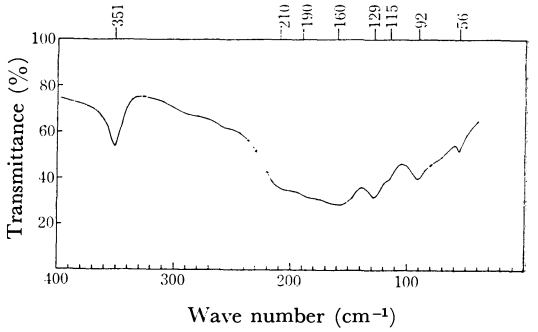

Fig. 1. Far infrared spectra of potassium oxalate monohydrate crystal in Nujol mull.

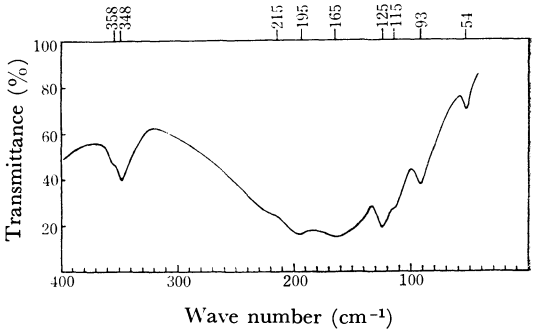

Fig. 2. Far infrared spectra of deuterated potassium oxalate monohydrate crystal in Nujol mull.

1) R. Chidambaram, A. Sequeira and S. K. Sikka, *J. Chem. Phys.*, **41**, 3616 (1964); B. F. Pedersen, *Acta Chem. Scand.*, **18**, 1635 (1964).

2) J. P. Collman and H. F. Holtzclaw, Jr., *J. Amer. Chem. Soc.*, **80**, 2054 (1958).

3) M. J. Schmelz, T. Miyazawa, S. Mizushima, T. J. Lane and J. V. Quagliano, *Spectrochim. Acta*, **9**, 51 (1958).

4) B. F. Pedersen, *Acta Chem. Scand.*, **21**, 801 (1967).

5) E. C. Gruen and R. A. Plane, *Inorg. Chem.*, **6**, 1123 (1967).

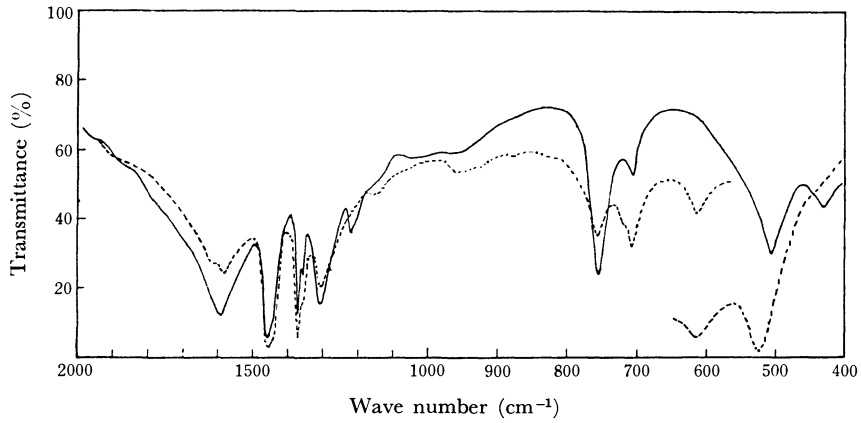

Fig. 3. Infrared spectra of deuterated potassium oxalate monohydrate crystal in Nujol mull (solid line) and potassium oxalate monohydrate crystal in Nujol mull (dotted line).

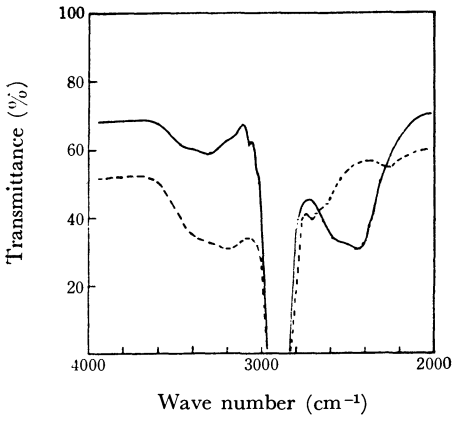

Fig. 4. Infrared spectra of deuterated potassium oxalate monohydrate crystal in Nujol mull (solid line) and potassium oxalate monohydrate crystal in Nujol mull (dotted line).

Assignment of IR Absorption Bands

Assignment of IR absorption bands in the region of 4000—300 cm^{-1} has been discussed by Schmelz *et al.*[3] and also by Pedersen.[4] However, several new experimental facts found in the present study suggest the following assignment of some IR absorption bands.

As the relative intensities of O–H and O–D stretching bands of the residue show that deuteration was carried out almost perfectly, IR spectra of the residue may be interpreted as those of deuterate. (see Figs. 2, 3 and 4).

Schmelz *et al.* and Pedersen did not point out the presence of a shoulder band at the higher frequency side of the strong band at 1580 cm^{-1} of p.o.m.[3,4] In their studies, IR spectra were recorded with a spectrometer equipped with prism optics. In the present study, IR spectra were obtained with grating spectrometers having higher resolving power. From the result the presence of a shoulder band at 1608 cm^{-1} and the shift of shoulder band to lower frequency on deuteration were confirmed. A band corresponding to the shoulder band appears at 1225 cm^{-1} in the spectra of *d*-p.o.m. Therefore, the two bands at 1608 cm^{-1} and 1225 cm^{-1} are assigned to H_2O bending and D_2O bending vibration, respectively. Schmelz *et al.* and Pedersen found a shift of frequency of the band at 710 cm^{-1} associated with deuteration.[3,4] In accordance with their results, the band of p.o.m. at 718 cm^{-1} shifts to lower frequency on deuteration as shown in Fig. 3, and the corresponding band appears at 505 cm^{-1} for *d*-p.o.m. It was also found that the band of p.o.m. at 614 cm^{-1} shifts to lower frequency on deuteration and two bands appear at 432 cm^{-1} and 358 cm^{-1} for *d*-p.o.m. as shown in Figs. 2 and 3. The results along with the observed neutron scattering peaks, 700 cm^{-1}, 605 cm^{-1}, 500 cm^{-1} (p.o.m.) and 505 cm^{-1}, 450

TABLE 1. OBSERVED FREQUENCIES (cm^{-1})

IR		Neutron scattering*	
$K_2C_2O_4 \cdot H_2O$	$K_2C_2O_4 \cdot D_2O$	$K_2C_2O_4 \cdot H_2O$	$K_2C_2O_4 \cdot D_2O$
718	505	700	505
614	432	605	450
524	358	500	370
351	348		
210	215		
190	195	195	190
160	165		
129	125		136
115	115	110	
92	93	95	94
56	54		

* Taken from Ref. 6

cm^{-1}, 370 cm^{-1} (*d*-p.o.m.),[6] confirm assignment of the IR absorption bands at 718 cm^{-1}, 614 cm^{-1}, 524 cm^{-1} (p.o.m.) and the bands at 505 cm^{-1}, 432 cm^{-1}, 358 cm^{-1} (*d*-p.o.m.) to the rotational lattice vibrations primarily associated with molecules of the water of crystallization and with those of the heavy water of crystallization, respectively. This assignment is consistent with the fact that the IR absorption bands due to molecules of the water of crystallization and of the heavy water of crystallization molecules were observed in the region of 900—300 cm^{-1} in the case of aquo complexes.[7] No shift of frequency of the band at 524 cm^{-1} (p.o.m.) on deuteration may be explained by overlapping of CO_2 wagging band. The band at 710 cm^{-1} (p.o.m. and *d*-p.o.m.) is considered to be due to Nujol.

Far IR absorption bands in the region of 250—60 cm^{-1} (Figs. 1 and 2) may be due to translational lattice vibrations. Assignment of these bands will have to be discussed on the basis of calculation of lattice vibrations and other experimental data. In this paper, only the correspondence of frequencies of IR absorption bands with those of neutron scattering peaks[6] is pointed out for the bands at 190 cm^{-1}, 115 cm^{-1}, 92 cm^{-1} (p.o.m.) and 195 cm^{-1}, 125 cm^{-1}, 115 cm^{-1}, 93 cm^{-1} (*d*-p.o.m.) as shown in Table 1.

The author wishes to thank Professor T. Miyazawa of Osaka University for kindly allowing him use of the Hitachi FIS-3 Far Infrared Spectrometer, Perkin-Elmer 521 Spectrophotometer and Hitachi EPI-L Spectrophotometer. Thanks are also due to Dr. T. Kitagawa and Miss M. Tsuchida for their kind assistance during the course of measurements.

6) H. J. Prask and H. Boutin, *J. Chem. Phys.*, **45**, 699 (1966).

7) I. Nakagawa and T. Shimanouchi, *Spectrochim. Acta*, **20**, 429 (1964).

BULLETIN OF THE CHEMICAL SOCIETY OF JAPAN VOL. 43 41—46 (1970)

The Phosphorescence Processes in Pyrimidine and 2-Chloropymidine

Nobuyuki NISHI, Ryoichi SHIMADA and Yoshiya KANDA

Department of Chemistry, Faculty of Science, Kyushu University, Hakozaki, Fukuoka

(Received June 14, 1969)

The phosphorescence spectra of pyrimidine and 2-chloropyrimidine have been observed at 4.2°K. A detailed vibrational analysis of the pyrimidine spectrum suggests that the emission arises from two components of the emitting triplet state. The phosphorescence lifetimes of pyrimidine and 2-chloropyrimidine have been measured for the 0–0 band and the strongest "vibronic band" (the phosphorescence maximum), which involves various modes of vibrations, at different temperatures between 77 and 1.5°K. The decay curve observed for the 0–0 band has been resolved into two exponential components, and that for the vibronic band, into three exponential components, where the third component was extremely weak in intensity at a very low temperature. From the comparison of the observed and calculated lifetimes of the individual phosphorescence components and their relative intensities, it was deduced that: (1) the 0–0 band involves emissions arising from the B_2 and A_1 components of the $^3B_1(n,\pi^*)$ state, while the vibronic band involves an additional, third emission which very likely arises from the A_2 component; (2) the $^1A_2(n,\pi^*)$ state is located below the $^1B_1(n,\pi^*)$ state; (3) the $^3A_1(\pi,\pi^*)$ state is located below the $^1A_2(n,\pi^*)$ state, and (4) the major intersystem crossing takes place from both the $^1A_2(n,\pi^*)$ and $^1B_1(n,\pi^*)$ states to the $^3A_1(\pi,\pi^*)$ state in pyrimidine and 2-chloropyrimidine.

The phosphorescence spectrum of pyrimidine has been studied by Shimada[1] and by Krishna and Goodman,[2] who assigned the emitting triplet state to a $^3B_1(n,\pi^*)$ state on the basis of vibrational analysis and the solvent effects. Their assignment agreed with the result calculated by Goodman and Harrell.[3] Krishna and Goodman[4] confirmed this assignment by polarization measurements. Furthermore, they[5] calculated the transition probability of the triplet-singlet transition and concluded that

1) R. Shimada, *Spectrochim. Acta*, **17**, 30 (1961).

2) V. G. Krishna and L. Goodman, *J. Amer. Chem. Soc.*, **83**, 2042 (1961).

3) L. Goodman and R. W. Harrell, *J. Chem. Phys.*, **30**, 1131 (1959).

4) V. G. Krishna and L. Goodman, *ibid.*, **36**, 2217 (1962).

5) L. Goodman and V. G. Krishna, *Rev. Mod. Phys.*, **35**, 541 (1963).

two components can radiatively combine with the ground state in the lowest triplet state of pyrimidine. The same conclusion has, very recently, been obtained by Yonezawa, Katô and Kato.[6] Cohen and Goodman[7] measured the quantum yields of the phosphorescence, fluorescence, internal conversion, and intersystem crossing in pyrimidine and determined the rate constants for these radiative and non-radiative processes. They concluded that the phosphorescence process in pyrimidine is $^1B_1(n,\pi^*) \rightsquigarrow {}^1A_2(n,\pi^*) \rightsquigarrow T(n,\pi^*) \rightarrow {}^1A_1$.*1

de Groot, Hesselmann, Schmidt and van der Waals[8] and Hall, Armstrong, Moomaw and El-Sayed[9] studied the phosphorescence decays of quinoxaline and pyrazine respectively and showed that the decay curves of these compounds were non-exponential at very low temperatures ($\sim$1.5°K). The different phosphorescence components, which were analyzed from the decay curves, were ascribed to the transitions from the different sublevels of the lowest triplet state to the ground state. Very recently, Azumi and Nakano[10] measured the phosphorescence lifetime of quinoxaline at various temperatures and estimated the rate constants of the radiative and non-radiative processes from three sublevels of the lowest triplet state to the ground state.

It should be interesting to study the phosphorescence decay of pyrimidine, because the phosphorescence is emitted from two sublevels of the lowest triplet state through first-order perturbation in pyrimidine, while in quinoxaline or pyrazine the phosphorescence is emitted from only one sublevel, and the phosphorescence emitted from two sublevels can provide more information about the phosphorescence processes. This study was undertaken in order to investigate the phosphorescence processes of pyrimidine and 2-chloropyrimidine in more detail through careful analyses of the phosphorescence spectra and decay curves.

Experimental

The pyrimidine was obtained through the reductive dechlorination of trichloropyrimidine with Pd-charcoal.[11] The 2-chloropyrimidine was synthesized with 2-aminopyrimidine, $NaNO_2$, and HCl by means of a diazo reaction.[12] The samples were purified by repeated vacuum distillation just before the experiments.

The phosphorescence spectrum was observed in a methylcyclohexane matrix at 4.2°K with a Hilger spectrograph, type E2. The optical setup and the other apparatus used in this work were the same as those described previously,[13] except that quartz dewars and a thin pyrex sample-cell were used in this case. The 3131 Å Hg-line which was isolated from a 1-kW high-pressure mercury arc lamp, type Orc-CHM-612, with a filter combination of a saturated $NiSO_4$ aqueous solution and a Corning 7-54 glass filter,[14] was used for the excitation of the sample. The necessary exposure time was 24 hr with a slit-width of 25 μ and an Eastman Kodak 103a-O plate. The concentration of the sample was 10^{-4}M.

The lifetime measurement was carried out for each of the 0–0 bands and for one of the vibronic(phosphorescence maximum) bands of the phosphorescence spectrum obtained in methylcyclohexane and benzene matrices at different temperatures between 77 and 1.5°K. The exciting and phosphorescence beams were chopped off with a shutter device designed particularly for this study. The sample was placed between two shutters which were connected with strings and pulleys. First the excitation path was opened and the emission path was closed by a rear shutter so that the excitation could be saturated. Immediately after the excitation path was closed by a front shutter, which was operated by a trigger, the emission path was opened. The two shutters worked so quickly that a short lifetime such as $\sim$5 msec could be determined quite precisely. The lifetime was analyzed with a Bausch & Lomb 500-mm grating monochromator, fixed at a constant wavelength (*e.g.*, the wavelength of the phosphorescence 0–0 band), and with an Iwasaki synchroscope, type SS-5004. The slit-width of the monochromator ranged from 0.5 to 2.5 mm depending on the phosphorescence intensity.

Results

Pyrimidine and 2-chloropyrimidine emit blue phosphorescences in methylcyclohexane and benzene matrices at 4.2°K. The spectra observed at 4.2°K consist of very sharp and highly-resolved bands compared with those observed at 90°K.[1] Their spectral data and microphotometer tracings are given in Table 1 and Fig. 1 respectively.

The decay curves of the phosphorescence lifetimes of pyrimidine and 2-chloropyrimidine, measured for the 0–0 and vibronic bands obtained in methylcyclohexane and benzene matrices at 1.5°K, are shown in Fig. 2. These curves are non-exponential. The curves for the 0–0 bands can be resolved into two components, which give lifetimes of 15 and 58 msec in methylcyclohexane and of 13 and 150 msec in benzene for pyrimidine, and lifetimes of 14

6) T. Yonezawa, H. Katô and H. Kato, *Theoret. Chim. Acta*, **13**, 125 (1969).

7) B. J. Cohen and L. Goodman, *J. Chem. Phys.*, **46**, 713 (1967).

*1 $\rightarrow$ and $\rightsquigarrow$ denote radiative and non-radiative processes respectively.

8) M. S. de Groot, I. A. M. Hesselmann and J. H. van der Waals, *Mol. Phys.*, **12**, 259 (1967); M. S. de Groot, I. A. M. Hesselmann, J. Schmidt and J. H. van der Waals, *ibid.*, **15**, 17 (1968).

9) L. Hall, A. Armstrong, W. Moomaw and M. A. El-Sayed, *J. Chem. Phys.*, **48**, 1395 (1968).

10) T. Azumi and Y. Nakano, *ibid.*, **50**, 539 (1969).

11) N. Whittaker, *J. Chem. Soc.*, 1646 (1953).

12) "Organic Synthesis," Coll. Vol. IV (1963), p. 182.

13) A. Nakahara, M. Koyanagi and Y. Kanda, *J. Chem. Phys.*, **50**, 552 (1969).

14) M. Kasha, *J. Opt. Soc. Amer.*, **38**, 929 (1948).

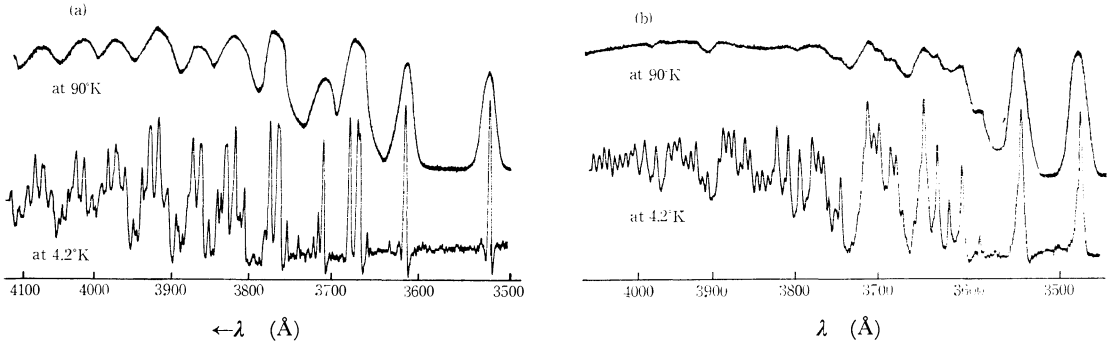

Fig. 1. The phosphorescence spectra of (a) pyrimidine and (b) 2-chloropyrimidine observed in methylcyclohexane at 90 and 4.2°K.

TABLE 1. VIBRATIONAL ANALYSIS OF THE PHOSPHORESCENCE SPECTRUM OF PYRIMIDINE IN METHYLCYCLOHEXANE AT 4.2°K

ν (cm^{-1})	$\Delta\nu$ (cm^{-1})	Assignment		Symmetry species
28214 vs	0	0, 0		
27816 vw	398	0, 394		a_2
27535 vs	679	0, 677		a_1
27498 vw	716	0, 719		b_1
27412 vw	802	0, 804		b_1
27225 w	989	0, 993		a_1
27161 s	1053	0, 344+719	Fermi-resonance	a_1
27143 s	1071	0, 1068		a_1
27082 s	1132	0, 1138		a_1
26862 s	1352	0, 677×2		a_1
26812 m	1402	0, 1402		a_1
26771 w	1443	0, 719×2		a_1
26727 vw	1486	0, 677+804		b_1
26643 w	1571	0, 1570		a_1
26539 m	1675	0, 677+993		a_1
26475 s	1738	0, 677+(344+719)	F.r.	a_1
26463 s	1751	0, 677+1068		a_1
26397 s	1817	0, 677+1138		a_1
26356 vw	1858	0, 719+1138		b_1
26175 m	2039	0, 677×3		a_1
26135 w	2079	0, 677+1402		a_1
26087 s	2127	0, 1068×2		a_1
26068 vw	2146	0, 1075×2		a_1
26018 s	2196	0, (344+719)+1138	F.r.	a_1
26006 s	2208	0, 1068+1138		a_1
25970 m	2244	0, 677+1570		a_1
25938 m	2276	0, 1138×2		a_1

s: strong, m: medium, w: weak, v: very.

and 56 msec in methylcyclohexane and of 30 and 178 msec in benzene for 2-chloropyrimidine. The decay curves for the vibronic bands contain a third, very weak component in addition to the above two. This gives a lifetime of 160 msec in methylcyclohexane and one of 200 msec in benzene for pyrimidine. The intensity of this third component was too weak for it to be analyzed for 2-chloropyrimidine.

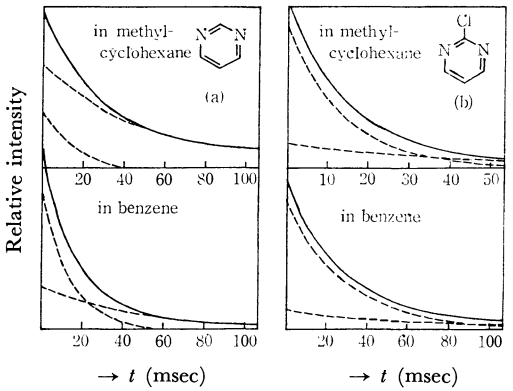

Fig. 2. The phosphorescence decay curves of (a) pyrimidine and (b) 2-chloropyrimidine observed in methylcyclohexane and benzene at 1.5°K —, and analyzed exponential decay curves ----.

We will hereafter call these three lifetime components "short-", "medium-" and "long-lifetime components".

In pyrimidine, the phosphorescence intensity of the medium-lifetime component, which was estimated through the extrapolation of the analyzed exponential curve to $t=0$, is stronger than that of the short-lifetime component in methylcyclohexane, while the former is slightly weaker than the latter in benzene at 1.5°K. In 2-chloropyrimidine, the intensity of the short-lifetime component is stronger than that of the medium-lifetime component in both matrices at 1.5°K. The long lifetime component is very weak in intensity in both matrices. The short-lifetime components increase their intensities with an increase in the temperature for both molecules.

The medium-lifetime component shows a characteristic temperature dependence. The lifetime remains almost constant at temperatures ranging from 1.5 to about 4.2°K. Above 4.2°K, the lifetime begins to decrease with an increase in the temperature, and then it again comes to show a constant value from about 30°K. The values of the lifetime measured in methylcyclohexane at various tempera-

tures are given in Table 2.

The phosphorescence decay curves of the 0–0 and vibronic bands observed at 77°K for both molecules were practically exponential in both matrices. The lifetimes were found to be 27 and 26msec in methylcyclohexane and 29 and 93msec in benzene for pyrimidine and 2-chloropyrimidine respectively. These values are the same as those of the medium-lifetime components measured at 30°K.

TABLE 2. THE LIFETIMES OF THE MEDIUM COMPONENTS OF THE PHOSPHORESCENCES OF PYRIMIDINE AND 2-CHLOROPYRIMIDINE MEASURED IN METHYLCYCLOHEXANE AT VARIOUS TEMPERATURES

	T (°K)	1.5	4.2	7	9	15	27	35	77
τ (msec)	Pyrimidine	58	58	40	37	33	31	27	27
	2-Choloro-pyrimidine	56	56	—	35	32	—	28	26

Discussion

Vibrational Analysis of the Phosphorescenc Spectrum of Pyrimidine.

The Raman and infrared spectra of pyrimidine have been studied by many workers,[15-18] but the assignments they have given for the fundamental vibrational frequencies do not entirely agree with each other. We will use here the fundamental frequencies given by Sbrana, Adembri, and Califano[17] because their assignments seem to be the most reliable. We will use the same coordinate orientation as that used by Lord, Marston, and Miller;[15] that is, the x axis is perpendicular to the plane of the molecule, and the z axis, along the C_2 axis.

The vibrational analysis of the phosphorescence spectrum observed at 4.2°K is essentially the same as that observed at 90°K,[1] except that the highly-resolved fine structure obtained at 4.2°K enables us to carry out the vibrational analysis in much more detail.

A band at 24214 cm^{-1}, highest in wave number and strongest in intensity, was taken to be the 0–0 band of the spectrum. The very strong bands, which are separated by 679, 1053, 1071 and 1132 cm^{-1} from the 0–0 band, were assigned to the totally symmetric vibrations ν_{6a}, $\nu_{16b}+\nu_{10b}$, ν_{12}, and ν_{9a}*2 respectively. The splitting of the ν_{12} band and the $\nu_{16b}+\nu_{10b}$ band, which is intensified by the Fermi-resonance, is quite remarkable. The rather weak bands separated by 989, 1402, and 1571 cm^{-1} from the 0–0 band were assigned to the ν_1, ν_{19a}, and ν_{8a} totally symmetric vibrations respectively. All the other prominent bands were assigned to combinations and overtones of these totally symmetric vibrations.

Several extremely weak bands, separated by 398, 716, and 802 cm^{-1} from the 0–0 band, were observed between the 0–0 and 1132 bands. These frequencies may be assigned to three nontotally symmetric vibrations, ν_{16a}, ν_{10b}, and ν_{11} respectively, on the basis of their intensities and frequencies. The first belongs to the a_2 species, and the latter two, to the b_1 species. These vibrations also appear as overtones and combinations with the ν_{6a} and ν_{9a} vibrations in the longer-wavelength region. The detailes of the vibrational analysis are summarized in Table 1.

The degrees of the polarization of the $^3B_1(n,\pi^*)\rightarrow {}^1A_1$ phosphorescence relative to excitation into the $^1B_1(n,\pi^*)$ and $^1B_2(\pi,\pi^*)$ states were observed by Krishna and Goodman to be -0.25 and $+0.15$ respectively.[4] These values are about 75 and 30% of the expected values of -0.33 and $+0.5$ for the angles of $\theta=90°$*3 and 0° respectively. Although their values were not at the ideal limits, these results clearly indicate that the transition moment of the $^3B_1\rightarrow {}^1A_1$ phosphorescence is not completly along the y axis, but partially along the z axis.

Our vibrational analysis of the phosphorescence spectrum also supports this finding. The observation of the a_2 and b_1 vibrations suggests that there are at least two emitting components in the $^3B_1(n,\pi^*)$ state. The transitions to the a_2 and b_1 vibrational levels in the ground state can proceed from the B_2 and A_1 components of the $^3B_1(n,\pi^*)$ state respectively by borrowing intensities from the electronically-allowed $^1B_1(n,\pi^*)$–$^1A_1$ transition through second-order spin-orbit-vibronic interaction. The emission from the A_2 component is negligibly weak because of the vanishingly small matrix element of the spin-orbit interaction between the $^1A_2(n,\pi^*)$ and $^3B_1(n,\pi^*)$ states.

The absorption and phosphorescence spectra of 2-chloropyrimidine very closely resemble those of pyrimidine. Polarization measurements of the phosphorescence relative to the absorptions indicate that these two molecules have quite similar electronic structures.[19] Some nontotally symmetric vibrations were also observed in the phosphorescence spectrum of 2-chloropyrimidine. A detailed vibrational analysis of this molecule will be published soon.

Lifetime of the Phosphorescence. The decay

15) R. C. Lord, A. L. Marston and F. A. Miller, *Spectrochim. Acta*, **9**, 113 (1957).

16) V. I. Berezin and S. K. Potapov, *Opt. Spectry.*, **18**, 22 (1965).

17) G. Sbrana, G. Adembri and S. Califano, *Spectrochim. Acta*, **22**, 1831 (1966).

18) K. K. Innes, J. P. Byrne and I. G. Ross, *J. Mol. Spectry.*, **22**, 125 (1967).

*2 The notations given for the fundamental modes are the same as those used by Lord, Marston and Miller.[15]

*3 θ is the angle between the transition moments of absorption and emission.

19) N. Nishi, R. Shimada and Y. Kanda, Preprints for the 21st Annual Meeting of the Chemical Society of Japan (April, 1968), I, p. 244.

curve of the 0–0 band of the phosphorescence observed below 4.2°K consists of two exponential components. Above 4.2°K the lifetime of the medium component shortens with an increase in the temperature. This may indicate that below 4.2°K the spin-lattice relaxation process between the triplet state multiplets is slower than both the triplet→triplet internal conversion process and the triplet→ground state radiative process. Hence spin-polarization is nearly preserved, while above 4.2°K the spin-lattice relaxation takes place and the deactivation of the triplet-state-energy *via* a triplet component, from which the phosphorescence is emitted with a short lifetime, gradually increases. This also explains the increase in the intensity of the short-lifetime component with an increase in the temperature. When the temperature goes up above 30°K, the spin-lattice relaxation process fully exceeds other processes and the deactivation of the triplet-state-energy comes approximately to obey the following expression,

$$\tau \approx \frac{3}{k_{qx}+k_{py}+k_{qy}+k_{pz}+k_{qz}} \approx \frac{3}{k_{py}+k_{pz}} = \frac{3}{\frac{1}{\tau_{py}}+\frac{1}{\tau_{pz}}}$$

where k_p and k_q are radiative and non-radiative rate constants respectively, and where x, y, and z are the indices of the three components of the triplet state.

If the lifetime values of pyrimidine and 2-chloropyrimidine observed in benzene at 1.5°K are substituted into this expression, one obtains 36 and 75 msec respectively. These values approximately agree with those observed at 77°K within the limit of experimental error. If the values observed in methylcyclohexane are substituted into it, however, the agreement becomes rather poor. This may be mainly due to the fact that the ratio of the lifetime values of the medium component to those of the short component is not sufficiently large in this matrix. Therefore, the short-lifetime component was analyzed to be slightly longer in lifetime than the real one.

The transition probability of the $^3B_1(n,\pi^*)$–$^1A_1$ transition of pyrimidine has been calculated by Goodman and Krishna[5] and by Yonezawa, Katô, and Kato.[6] They have shown that: (1) the $^3B_1$–$^1A_1$ transition borrows its intensity from the electronically-allowed S–S and T–T transitions through the first-order spin-orbit interaction; (2) the transition moment is mainly along the y axis, but partially along the z axis also; (3) the $^3B_1\rightarrow{}^1A_1$ phosphorescence polarized along the y axis originates from the B_2 component of the $^3B_1(n,\pi^*)$ state and has a lifetime of about 4 msec,[5] and (4) the $^3B_1\rightarrow{}^1A_1$ phosphorescence along the z axis originates from the A_1 component and has a lifetime of about 70 msec.[5]

These considerations lead to the conclusion that the short-lifetime component should be ascribed to the $^3B_1(n,\pi^*)B_2\rightarrow{}^1A_1$*[4] transition, and the medium-lifetime component, to the $^3B_1(n,\pi^*)A_1\rightarrow{}^1A_1$ transition.

The long-lifetime component with an extremely weak intensity that has been observed only in the vibronic bands can perhaps be ascribed to the $^3B_1(n,\pi^*)A_2\rightarrow{}^1A_1$ transition, but there is no positive evidence in support of this assignment.

Phosphorescence Process. The splitting of two (n,π^*) states of A_2 and B_1 symmetry species in pyrimidine has been calculated to be 1590 and 275 cm^{-1} in the singlet and triplet states respectively, with the A_2 state below the B_1 state in the singlet and with the opposite order in the triplet state.[20] The $^3A_1(\pi,\pi^*)$ state was calculated to be located lower in energy than the $^1B_1(n,\pi^*)$ state by about 1.4 eV.[21] On the other hand, the $^3B_2(\pi,\pi^*)$ state may be expected by analogy with the low-lying triplet states of benzene to lie above the $^1B_1(n,\pi^*)$ state.[21]

Cohen and Goodman[7] have indicated, on the basis of the quantum yields of the radiative and non-radiative processes, that: (1) the rate constants of the $^1B_1(n,\pi^*)\rightarrow{}^1A_1$, $T_1(n,\pi^*)\rightarrow{}^1A_1$, $^1B_1(n,\pi^*)\rightsquigarrow{}^1A_2(n,\pi^*)$ and $^1B_1$ or $^1A_2(n,\pi^*)\rightsquigarrow T$ are 5×10^6, ~50, 9.1×10^8 and 1.2×10^8 sec^{-1} respectively; (2) the intersystem crossing proceeds from the $^1A_2(n,\pi^*)$ state because the internal conversion has the fastest rate constant, hence, the phosphorescence process in pyrimidine is $^1B_1(n,\pi^*)\rightsquigarrow{}^1A_2(n,\pi^*)\rightsquigarrow{}^3B_1(n,\pi^*)\rightarrow{}^1A_1$, and (3) the intersystem crossing rates are largely dependent on factors other than the matrix element of the first-order spin-orbit interaction. Their considerations are based on the assumption that the $^3A_1(\pi,\pi^*)$ state is located above the $^1A_2(n,\pi^*)$ state.

The intersystem crossing which proceeds from the $^1A_2(n,\pi^*)$ state to the A_2 component of the $^3B_1(n,\pi^*)$ state must take place through the first-order spin-orbit interaction, and that to the B_2 or A_1 component, through the second-order spin-orbit-vibronic interaction. The first-order intersystem crossing between the $^1A_2(n,\pi^*)$ and $^3B_1(n,\pi^*)$ states must be extremely inefficient because of the vanishingly small values of one- and two-center integrals of the matrix element of the spin-orbit interaction and because of the very small Franck-Condon factor, as has been pointed out by El-Sayed.[22] The second-order intersystem crossing between the $^1A_2(n,\pi^*)$ and $^3B_1(n,\pi^*)$ states through the intermediate (π,π^*) states is expected to be much less efficient than the first-order intersystem crossing between the $S(\pi,\pi^*)$

*4 $^3B_1(n,\pi^*)B_2$ denotes the B_2 component of the $^3B_1(n,\pi^*)$ state.

20) M. A. El-Sayed and G. W. Robinson, *J. Chem. Phys.*, **35**, 1896 (1961).

21) R. McWeeny and T. E. Peacock, *Proc. Phys. Soc.*, **A70**, 41 (1957).

22) M. A. El-Sayed, *J. Chem. Phys.*, **36**, 573 (1962).

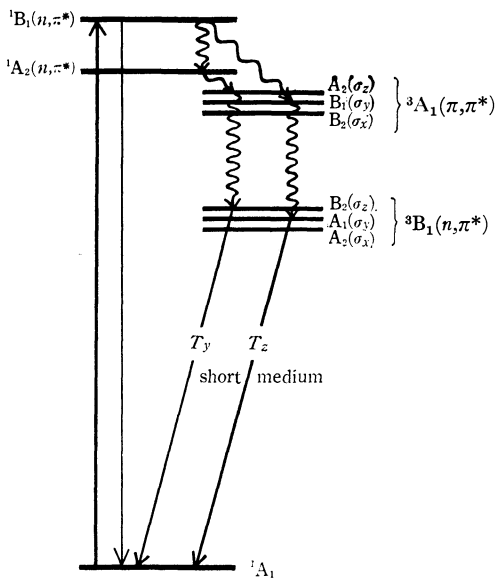

Fig. 3. Phosphorescence processes in pyrimidine and 2-chloropyrimidine.

state of the B_2 or A_1 symmetry and the $^3B_1(n,\pi^*)$ states. In pyrazine, the intersystem crossing proceeds from the $S(n,\pi^*)$ state to the $T(\pi,\pi^*)$ state through the first-order spin-orbit interaction,[7,22] this leads to the strong phosphorescence. Therfore, if Cohen and Goodman's conclusions were correct, pyrimidine should phosphoresce considerably less efficiently than pyrazine. This is, however, contrary to the results of their quantum yield measurements, which show that the rate constant of the intersystem crossing in pyrimidine is smaller than that in pyrazine by a factor of only two.

The observed rather high phosphorescence yield of pyrimidine indicates that the phosphorescence must arise from a non-radiative process, either (1) $^1B_1(n,\pi^*)\rightsquigarrow{}^3A_1(\pi,\pi^*)\rightsquigarrow{}^3B_1(n,\pi^*)$ or (2) $^1A_2(n,\pi^*)\rightsquigarrow{}^3A_1(\pi,\pi^*)\rightsquigarrow{}^3B_1(n,\pi^*)$. The former process requires that the intersystem crossing proceed from the second excited singlet state, while the latter requires that the $^3A_1(\pi,\pi^*)$ state lie below the $^1A_2(n,\pi^*)$ state.

The fact that the 0–0 band of the phophorescence spectrum involves two types of emissions, those due to the $^3B_1(n,\pi^*)A_1\rightarrow{}^1A_1$ and $^3B_1(n,\pi^*)B_2\rightarrow{}^1A_1$ transitions, at 1.5°K indicates that both the above two requirements are satisfied in pyrimidine, because these emissions must originate from the non-radiative paths of $^1B_1(n,\pi^*)\rightsquigarrow{}^3A_1(\pi,\pi^*)B_1\rightsquigarrow{}^3B_1(n,\pi^*)A_1$ and $^1B_1(n,\pi^*)\rightsquigarrow{}^1A_2(n,\pi^*)\rightsquigarrow{}^3A_1(\pi,\pi^*)A_2\rightsquigarrow{}^3B_1(n,\pi^*)B_2$ respectively. The internal conversion processes between triplet states comply with the requirement of the preservation of spin-polarization (see Fig. 3).

The fluorescence spectrum of pyrimidine was first observed by Börresen[23] and by Cohen, Baba and Goodman.[24] It was assigned to the $^1B_1(n,\pi^*)\rightarrow{}^1A_1$ transition by Cohen and Goodman.[7] This assignment was confirmed by the experimental findings[25] that: (1) the 0–0 band of the fluorescence spectrum exactly coincides with the 0–0 band of the $^1B_1(n,\pi^*)\leftarrow{}^1A_1$ absorption spectrum, and (2) the spectral structure of the fluorescence agrees exactly with the hot bands of the absorption. Neither the absorption nor the fluorescence due to the $^1A_2(n,\pi^*)-{}^1A_1$ transition has been observed. The fact that the fluorescence comes from the second excited singlet state supports the idea that the intersystem crossing can proceed from the $^1B_1(n,\pi^*)$ state.

Halosubstitution induces a blue shift for (n,π^*) states and a red shift for (π,π^*) states. An increase in the energy difference between the $^1B_1(n,\pi^*)$ and $^3A_1(\pi,\pi^*)$ states in 2-chloropyrimidine decreases the rate constant of the intersystem crossing between these two states and hence increases the rate constant of the competing internal conversion between the $^1B_1(n,\pi^*)$ and $^1A_2(n,\pi^*)$ states. This results in an increase in the relative intensity of the short-lifetime component in 2-chloropyrimidine, although its overall phosphorescence intensity is weaker in intensity than that of pyrimidine.

In conclusion, our experimental results support the generally-accepted assumption that the $^1A_2(n,\pi^*)$ state is located below the $^1B_1(n,\pi^*)$ state. Further work is now being undertaken to obtain conclusive evidence regarding the order of these two (n,π^*) states.

The authors are grateful to Dr. Hiroko Shimada for her helpful discussions throughout this work.

23) H. C. Börresen, *Acta Chem. Scand.*, **17**, 921 (1963).
24) B. J. Cohen, H. Baba and L. Goodman, *J. Chem. Phys.*, **43**, 2902 (1965).
25) M. Hirai, N. Nishi, R. Shimada and Y. Kanda, Preprints for the 22nd Annual Meeting of the Chemical Society of Japan (April, 1969), I. p. 101.

BULLETIN OF THE CHEMICAL SOCIETY OF JAPAN VOL. 43 47—52 (1970)

Initial Rate and Aging Effect of Ethylene Polymerization with Ziegler-Natta Catalysts. III

Tsuneo MATSUDA,* Takashi FURUKAWA,** Shigeyasu TOGO*** and Toyosuke TANAKA*

* *Faculty of Science and Engineering, Saitama University, Shimo-ohkubo, Urawa-shi, Saitama*
** *Toyo Ink Co., Aoto, Katsushika-ku, Tokyo*
*** *Nihon Yushi Co., Taketoyo, Chita-Gun, Aichi*

(Received June 16, 1969)

The initial rate and the aging effect of ethylene polymerization with $TiCl_4$- and $TiCl_3$-$AlEt_3$ catalyst were investigated. The initial rate, r, was expressed by the equation; $r=k_1P_E+k_2P_E^2$, where p_E is the ethylene partial pressure and where k_1 and k_2 are constants. The explanation of the equation is as follows:

$$\text{(active site)} + M \xrightarrow{k_1} \text{(polymerization site)}, \text{ rate, } k_1P_E$$

$$\text{(polymerization site)} + M^* \xrightarrow{k_2} \text{(propagation)}, \text{ rate, } k_2P_E^2$$

M shows the ethylene monomer which is liberated by the catalyst formation or which is introduced into the system. M* is the monomer which is introduced into the system. The initial rate decreased in the $TiCl_4$-$AlEt_3$ system with the aging-time interval; on the other hand, in the $TiCl_3$-$AlEt_3$ system the rate showed its maximum at about half an hour's aging. The optimum aging temperature was found to be 20°C. The decrease in the rates between the two systems may be ascribed to the reduction of the Ti atom in the initial valence state of the reaction to the lower valence.

In a preceding paper,[1] the kinetics in the stastionary state of ethylene polymerization and the effect of hydrogen on the rate in connection with the $TiCl_3$-$AlEt_3$ catalyst system were described. This paper will be concerned with the initial rate and the aging effect of ethylene polymerization by the $TiCl_4$- and $TiCl_3$-$AlEt_3$ systems. It is well known that the catalyst systems of the Ziegler-Natta type consist of the reaction products resulting from titanium halides in conjugation with alkylaluminum compounds. We have confirmed that the active sites of the catalyst result from the reaction of titanium halides ($TiCl_4$ or $TiCl_3$) and alkylaluminum, while the polymerization sites result from the addition of monomer molecules to the active sites.

When triethylaluminum as alkylaluminum is employed, the liberation of ethylene and other saturated hydrocarbons has been verified by different authors.[2-7] By the addition to the active sites of ethylene liberated in the reaction of titanium halides with triethylaluminum, some polymerization sites will be formed prior to the introduction of the ethylene monomer into the reaction system. A considerable number of active sites will also exist on the catalyst surface. If the polymerization starts at the active sites, the initial rate will be second-order with respect to the monomer concentration, but if it starts at the polymerization sites, the order will be first. This is bacause a molecule of ethylene reacts with an active site to produce a polymerization site; then another molecule affects the polymerization site and the propagation proceeds.

In order to verify this, we studied the initial rate of ethylene polymerization with the $TiCl_4$- and $TiCl_3$-$AlEt_3$ catalyst systems.

The aging effects of the catalysts on the initial rate are still controversial. Very few studies have been made of the aging effect in the $TiCl_4$- and $TiCl_3$-

1) T. Matsuda, T. Keii, A. Kojima and T. Ishida, *Kogyo Kagaku Zasshi*, **71**, 1124, 1128 (1968).
2) A. Malatesta, *Can. J. Chem.*, **37**, 1176 (1959).
3) E. J. Arlman and J. R. de Jong, *Rec. Trav. Chim. Pays-Bas*, **79**, 910, 1319 (1960).
4) R. Havinga and Y. Y. Tan, *ibid.*, **79**, 56 (1960).
5) L. Rodriguez and J. Gabant, *J. Polym. Sci.*, **57**, 881 (1962).
6) L. Rodriguez, H. Looy and J. Gabant, *J. Polym. Sci., Part A-1*, **4**, 1905, 1917 (1966).
7) M. L. Cooper and J. B. Rose, *J. Chem. Soc.*, **1959**, 795.

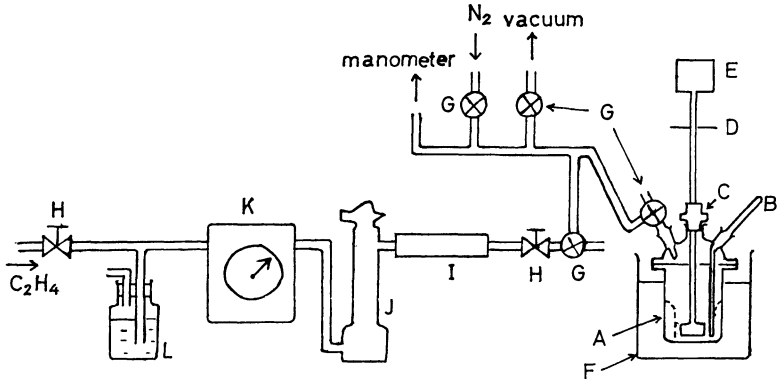

Fig. 1. Diagram of the apparatus of ethylene polymerization.
A, Reactor (esparable flask); B, Thermometer; C, Vacuum Stirrer; D, Stroboscope; E, Motor; F, Water bath; G, Valves; H, Needle valves; I, P_2O_5; J, NaOH pellet; K, Wet gas meter; L, Monostat

$AlEt_3$ catalyst systems.[8-11] Simon and Gyhmes[8] investigated the aging effect on the polymerization rate of ethylene in the $TiCl_4$-$AlEt_3$ catalyst system, and indicated that the effect did not appear at a particular temperature. Kodama and his co-workers[9] found that the activity of such a catalyst decreased considerably with time at 60°C, although the catalyst activity did not change much at 30°C for up to 4 hr. Hoeg and Liebman[10] studied the aging effect on the propylene polymerization, using $TiCl_3$ and $Al(iso\text{-}Bu)_3$, and found that these catalysts were thermally unstable. Schnecko and his co-workers[11] examined the difference in the aging effect by monomers upon the ethylene, propylene, and butene-1 polymerization rates by the $TiCl_3$-$AlEt_3$ and $TiCl_3$-$AlEt_2Cl$ systems. Thus, the different aging effects reported by various authors may be ascribed to the formation of lower valence states of titanium, which presumably are less stable and less efficient as catalysts, or to the coagulation of catalyst particles, whereby the available surface is decreased.

We examined the time and temperature effect of aging on the initial rate and attempted to analyze the valence state of titanium in the course of aging, which presumably causes the rate decrease.

Experimental

Reagents. The titanium tetrachloride was purified by distillating it several times with Cu powder until the distillate lacked color and by then diluting it to 10 wt% solution with *n*-heptane. The *δ*-Type of titanium trichloride supplied by the Toho Titanium Co. was used without any purification. The triethylaluminum was employed as 10 wt% *n*-heptane solution given by the Mitsubishi petrochemical Co. The toluene was purified by rectification in the presence of metallic sodium. The ethylene and nitrogen were dried under NaOH pellets and P_2O_5.

Polymerization Apparatus and Technique. The apparatus is shown in Fig. 1. Polymerization was carried out in a 500-m*l* separable flask provided with three depressed sides. Agitation was kept at 1000 rpm

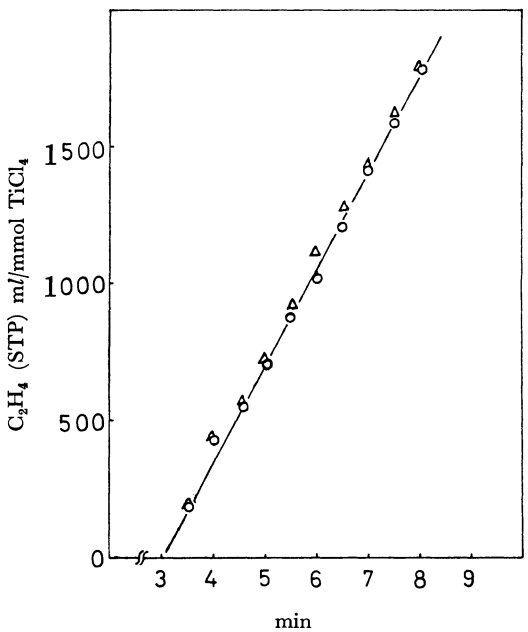

Fig. 2. The effect of nitrogen on the rate of ethylene consumption.
○, Without nitrogen; △, In addition of nitrogen P_E=40 cmHg; Polymerization temperature 20°C

8) A. Simon and G. Gyhmes, *J. Polym. Sci.*, **53**, 327 (1961).
9) S. Kodama, T. Kagiya, S. Machi, T. Shimizu, S. Yuasa and K. Fukui, *J. Appl. Polym. Sci.*, **3**, 20 (1960).
10) D. F. Hoeg and S. Liebman, *Ind. Eng. Chem., Process Des. Develop.*, **1**, 120 (1962).
11) H. Schnecko, M. Reinmöller, W. Lintz, K. Weirauch and W. Kern, *Makromol. Chem.*, **84**, 156 (1959).

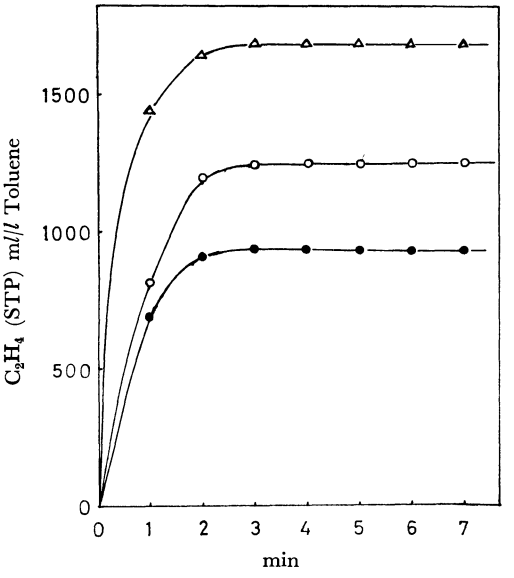

Fig. 3. The dissolution rate of ethylene in toluene.
● P_E=15 cmHg at 40°C, ○ P_E=15 cmHg at 0°C, △ P_E=74 cmHg at 20°C

sufficient to obtain non-diffusion controlled conditions regarding the polymerization rate.

In a 500-ml flask replaced with nitrogen, 200 ml of toluene and the required amounts of $TiCl_4$ or $TiCl_3$ and $AlEt_3$ were in this order intorduced by syringes under a nitrogen atmosphere. Stirring at a constant speed was accomplished, and the flask was immersed in a water bath which was adjusted to keep the fluctuation of the temperature within 0.1°C.

The rather excessive mole ratio of $AlEt_3$ to titanium halides was chosen so that the $AlEt_3$ reacted enough with titanium halides and so that the rate of polymerization was independent of the $AlEt_3$ concentration;[12] *i.e.*, the Al/Ti ratio in the catalyst system was chosen to be 4, while the concentration of titanium halides was 1 mmol.

After the evacuation of the reaction apparatus, ethylene was fed through a needle valve; the time of polymerization was recorded immediately. The rate of ethylene consumption in polymerization was measured by a wet-flow meter.

Analysis of Titanium. The valence state of titanium was analysed by the method described by Martin and Stedefeder.[13] In a three-necked, 300-ml flask equipped with a stirrer and containing a catalyst solution, 30 ml of alcohol and 10 ml of 2N HCl solution, both of which had already been cooled, are added under nitrogen at −50——70°C; the solution is then titrated with a 0.1M $FeCl_3$ solution, using methyleneblue as the indicator. No effect of nitrogen on the rate of ethylene consumption was observed, as is shown in Fig. 2. Even at the low partial pressure of ethylene of 10 cmHg, with or without nitrogen, and even on the introduction of nitrogen during polymerization, the rate of ethylene consumption did not alter. Therefore, all the polymerizations at low ethylene partial pressures were carried out with the addition of nitrogen, keeping the total reaction pressure at the atmospheric level.

As may be shown in Fig. 3, ethylene, when dissovled, reaches the saturated state within a few minutes after the introduction of ethylene at rather high partial pressures, but at pressures of ethylene lower than 10 cmHg, satulation was reached after at least 10 min. During this interval, the polymerization and the dissolution of ethylene will take place at the same time; therefore, we chose the polymerization at ethylene partial pressures higher than 10 cmHg. Meaningful flowmeter readings began only after 3 min due to the filling-up of the reaction flask.

Results and Discussion

Initial Rate of Polymerization. The ethylene consumption *versus* the time had a linear relationship for about 10 min. Some representative results are shown in Figs. 4 and 5. The initial rate of polymerization, r, was defined in terms of the decline of the straight lines dotted for an interval from 3 min to 10 min. About the relation of initial rates to the partial pressure of ethylene, P_E, we found that r/P_E was proportional to P_E (Figs. 6 and 7). Therefore, r is expressed by the following equation:

$$r = k_1 P_E + k_2 P_E^2 \quad (1)$$

In this equation k_1 and k_2 are constants. The values of the constants, k_1 and k_2 are shown in Table 1; the activation energies calculated using

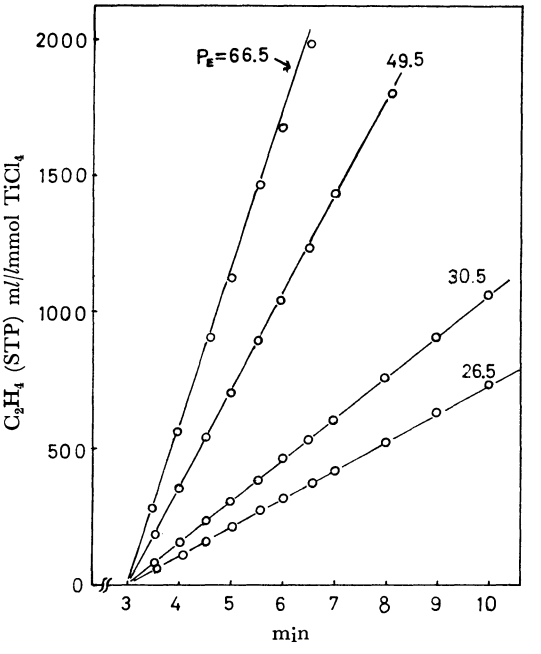

Fig. 4. The amount of ethylene consumed *vs.* time at $TiCl_4$-$AlEt_3$.
Polymerization temperature 20°C

12) T. Keii, T. Takagi, M. Taira, K. Soga, N. Saiki and Y. Murayama, *Shokubai*, **5**, 243 (1963).
13) H. Martin and J. Stedfeder, *Ann.*, **618**, 17 (1958).

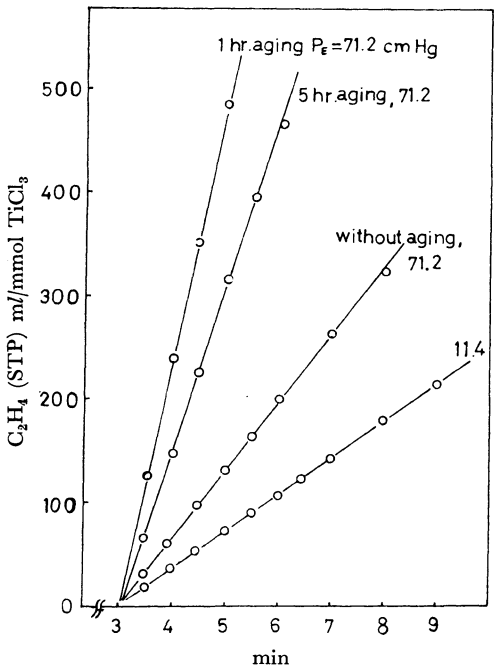

Fig. 5. The amount of ethylene consumed *vs.* time at $TiCl_3$-$AlEt_3$.
Polymerization temperature 20°C

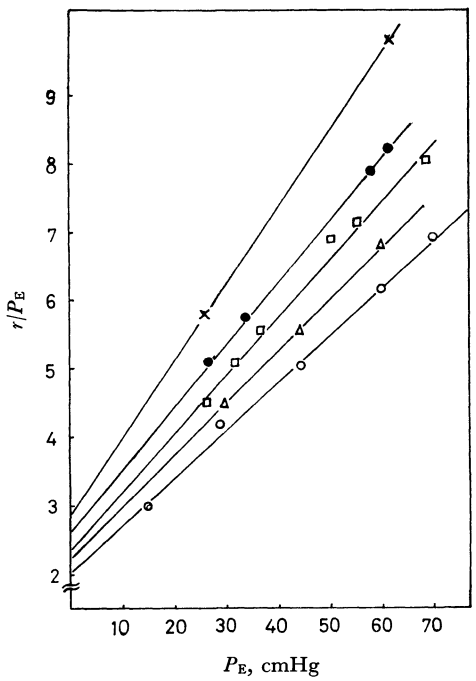

Fig. 6. The relationship between r and P_E at $TiCl_4$-$AlEt_3$.
Unit of ordinate; C_2H_4(STP) ml/mmol $TiCl_4$·min
○ 6°C, △ 12.5°C, □ 20°C, ● 30°C, × 43.5°C

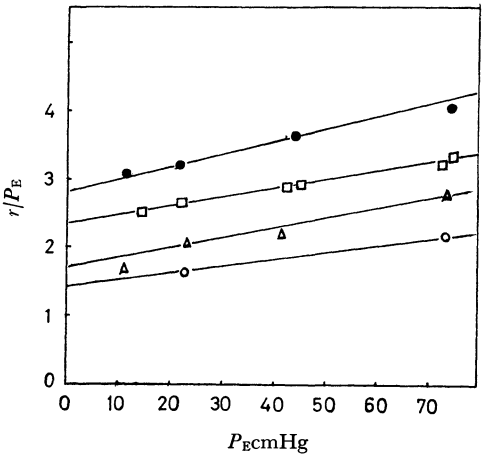

Fig. 7. The relationship between r and P_E at $TiCl_3$-$AlEt_3$.
Unit of ordinate; C_2H_4 (STP) ml/mmol $TiCl_3$·min
○ 6°C, △ 10°C, □ 20°C, ● 30°C

k_1 and k_2 are listed in the last column of the table. The first term, k_1P_E, refers to the initial rate starting from the polymerization sites resulting in a catalyst complex formation, while the second term, k_2P_E, refers to the rate starting from the polymerization sites built up by the reaction of the active sites and ethylene molecules introduced.

The activation energies in the $TiCl_3$-$AlEt_3$ system are larger than those in the $TiCl_4$-$AlEt_3$ system. Consequently, the polymerization sites in the two catalyst systems will be different. The difference in the activation energies calculated by k_1 and k_2 will be the energy required for the formation of the active sites.

Schindler[14] described the rate equation in ethylene polymerization by the $TiCl_4$-Al(iso-Bu)$_2$ system as:

$$R_p = \frac{KP_E^2}{1 + K'P_E} \qquad (2)$$

TABLE 1. THE RATE CONSTANTS AND ACTIVATION ENERGIES OF ETHYLENE POLYMERIZATION

Temperature °C	$TiCl_4$-$AlEt_3$		$TiCl_3$-$AlEt_3$	
	k_1	k_2	k_1	k_2
2	—	—	1.50	1.00×10^{-2}
6	2.10	6.65×10^{-2}	—	—
10	—	—	1.75	1.60
12.5	2.40	7.67	—	—
20	2.50	8.67	2.40	1.63
30	2.65	9.67	2.75	2.67
43.5	2.90	11.0	—	—
A.E.*	1.0	3.5	2.6	5.7

* Activation energy (kcal/mol)

14) A. Schindler, *J. Polym. Sci., Part C*, **4**, 81 (1963).

Here R_p is the rate of the polymerization, and K and K' are constants. The equation expresses the second-order kinetics with respect to the ethylene partial pressure as long as the pressure remains low enough in order to make $K'P_E$ small compared to unity. The values of k_1 in Eq. (1) are not as small as the k_2 values, which can be neglected, as may be seen in Table 1.

At a low pressure the rate will be first-order with respect to P_E, judging from our data. Keii and his co-workers[15] reported that the rate of the initial state in propylene polymerization was second-order with respect to the propylene partial pressure. In this case, the rate starting from the polymerization sites which were already formed during the catalyst complex formation will be neglected in the propylene polymerization; *i. e.*, the first term in Eq. (1) will be neglected in comparison with the second term. Consequently, the polymerization sites constructed in the reaction of the active sites with the propylene monomers introduced will be more active than the other polymerization sites already present as a result of the catalyst formation. Though the activation energies almost agree with those obtained by Fukui, Kagiya and their co-workers,[16] the energies seem to be rather small in comparison with those reported by other authors.[17-18] Our lower values are difficult to ascribe to the diffusion control of ethylene into the solvent, so it seems that our values are attributable to the ethylene polymerization in the initial stage.

Aging Effect

The relation of the aging time to the initial rate in the $TiCl_4$ and $TiCl_3$-$AlEt_3$ systems at 20°C is shown in Fig. 8. The initial rate decreases with the aging interval in the $TiCl_4$-$AlEt_3$ system, and in the $TiCl_3$-$AlEt_3$ system the rate attains its maximum value after about half an hour of aging. The maximum in $TiCl_3$-$AlEt_3$ may be due to an increase in the concentration of the active sites, followed by an increase in the effective surface area by the collapse of $TiCl_3$ particles. On the other hand, the decrease in r may be ascribed to the

Table 2. Analytical results on titanium valences

Aging time (hr)	0	3	5	Catalyst system
Ti^{2+} (%)	23	0	0	$TiCl_4$-$AlEt_3$
Ti^{3+} (%)	77	0	0	

Aging time (hr)	0	0.75	4.5	
Ti^{2+} (%)	32	36	94.5	$TiCl_3$-$AlEt_3$
Ti^{3+} (%)	63.4	40	0	

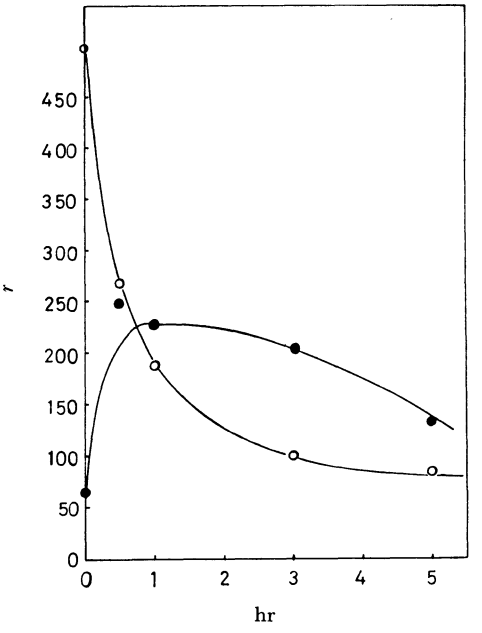

Fig. 8. The relationship between r and aging time.
Aging temperature, 20°C
Unit of ordinate; C_2H_4 (STP) ml/mmol $TiCl_4$- or $TiCl_3$·min
○ $TiCl_4$-$AlEt_3$, ● $TiCl_3$-$AlEt_3$

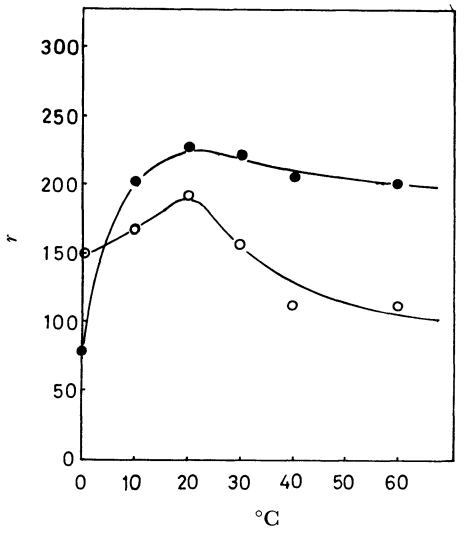

Fig. 9. The relationship between r and aging temperature.
Aging interval: an hour
Unit of ordinate: same as in Fig. 8
○ $TiCl_4$-$AlEt_3$, ● $TiCl_3$-$AlEt_3$

15) T. Keii, K. Soga and N. Saiki, Preprint for the International Symposium on Makromolecular Chemistry (Prague, 1965), p. 190.
16) K. Fukuki, T. Kagiya, S. Machi, T. Shimizu and S. Yuasa, This Bulletin, **35**, 303, 396 (1962).
17) M. N. Berger and M. B. Grieveson, *Makromol. Chem.*, **83**, 80 (1965).
18) H. Schnecko, M. Reinmöller, K. Weirauch, V. Bednjagin and W. Kern, *ibid.*, **73**, 154 (1964).

reduction of titanium to the state of the lower valences of titanium in the $TiCl_4$- and $TiCl_3$-$AlEt_3$ systems.

The results of the analysis are shown in Table 2. The titanium ion is reduced to the lower valence state with the aging time. Especially, $TiCl_4$ is more easily reduced than $TiCl_3$. After an aging time of more than 3 hr, $TiCl_4$ is almost completely reduced, but the activity of ethylene polymerization remains. Some of the Ti^{3+} or Ti^{4+} remains, for the active sites of polymerization will be titanium ions with the valences higher than two.[19-21] Even if the active species are di- or tri-valent titanium, they may be changed through oxidation or disproportionation to mono- or tetra-valent titanium by the hydrochloric acid added in analysis.

The decrease in the initial rate with the aging time may be ascribed to reduction into the lower-valence state of titanium. The fact that the sum of the Ti^{2+} and the Ti^{3+} present in the $TiCl_3$-$AlEt_3$ system is not 100 per cent may come from the titanium of the valence state lower than two, or tetravalent titanium may be present. The relation between the initial rate and the aging temperature after an hour's aging is shown in Fig. 9. The optimum aging temperature is found to be 20°C. The initial rate in $TiCl_3$-$AlEt_3$ was not much affected by the temperature, but in $TiCl_4$-$AlEt_3$ it was affected remarkably. The decrease in the rate caused by the aging temperature may also be ascribed to the reduction of the titanium atoms.

A more accurate determination of the cause of the aging effect will have to await another analytical method, because not all the valence states of titanium can be detected by the method of Martin and Stedefeder.[13] We are still in the process of developing a better analytical method to detect all the valence states of titanium.

19) E. J. Arlman and P. Cossee, *J. Catal.*, **3**, 99 (1964).
20) C. J. Brnning, W. R. Wszolek and F. X. Weber, *J. Polym. Sci., Part A-1*, **6**, 755 (1968).
21) A. Schindler, *Makromol. Chem.*, **118**, 1 (1968).

BULLETIN OF THE CHEMICAL SOCIETY OF JAPAN VOL. 43 52—56 (1970)

Chemical Reactivity of Adamantane and Related Compounds

Hiroshi FUJIMOTO, Yoshihiko KITAGAWA,*1 Hideyuki HAO*1 and Kenichi FUKUI

Faculty of Engineering, Kyoto University, Sakyo-ku, Kyoto

(Received June 17, 1969)

The chemical reactivity of hydrogens in adamantane and substituted adamantanes has been calculated. The results of calculation have shown that the bridgehead hydrogens are most reactive toward electrophilic reagents or radicals. The chemical reactivity of hydrogens in diamantane, triamantane, and tetramantane has also been predicted. A discussion has been made of the stable configuration of the 1-adamantyl cation, radical, and anion and of the nature of the back-side conjugation between the two tertiary carbons in these species. A mode of the electrocyclic polymerization of *p*-quinodimethane to form polyamantane has been predicted on the basis of the symmetry properties of the frontier orbitals in the pi and sigma parts of *p*-quinodimethane.

Recently the chemistry of adamantane and its homologues has been developed in connection with the chemical reactivity of the bridgehead hydrogen atoms. Stetter and Wulff have shown that the ionic bromination of adamantane occurred exclusively at the bridgehead.[1] The homolytic abstraction of hydrogen of adamantane and substituted adamantanes has also been reported, demonstrating the occurrence of the predominant removal of the bridgehead hydrogen atoms.[2,3] It has been shown that one of the theoretical reactivity indices, delocalizability, can be a good measure of the reactivity of hydrogens in aliphatic systems.[4,5] Here we will present the results of

*1 Present address: Ōe Works, Sumitomo Chemical Co., Ltd., Ehime.

1) H. Stetter and C. Wulff, *Chem. Ber.*, **93**, 1366 (1960).

2) I. Tabushi, J. Hamuro and R. Oda, *J. Amer. Chem. Soc.*, **89**, 7127 (1967).

3) P. H. Owens, G. J. Gleicher and L. M. Smith, Jr., *ibid.*, **90**, 4127 (1968).

4) K. Fukui, "Molecular Orbitals in Chemistry, Physics and Biology," ed. by P.-O. Löwdin and B. Pullman, Academic Press, New York (1964), p. 513, and the references cited therein.

5) K. Fukui, "Modern Quantum Chemistry," Vol. 1, ed. by O. Sinanoglu, Academic Press, New York (1965), p. 49, and the references cited therein.

calculations on adamantane and related compounds undertaken in order to test the validity of the theoretical reactivity indices for such compounds with bridgehead atoms. Calculations have also been carried out on three adamantane homologues, diamantane, triamantane and tetramantane, in an effort to predict the favorable course of the homolytic abstraction of hydrogens. In addition, the potentiality of an ingenious method for the preparation of polyamantane will be suggested.

The Chemical Reactivity of Adamantane and Substituted Adamantanes. It is well known that the quantum-mechanical theory of chemical reactivity has been successfully applied to organic molecules. Of the various chemical reactivity theories thus far presented, the delocalization approach is unique in that this method can be applied to both saturated and unsaturated molecules in a unified manner. The delocalization approach has also achieved a fair success in explaining or predicting the favorable steric course of electrocyclic processes.[6,7] By an application of the molecular orbital (MO) perturbation theory to the chemical reaction, the chemical reactivity indices, superdelocalizability (S_r) and delocalizability (D_r), have been derived.[8,9] Of these, the former is used for unsaturated molecules, and the latter, for saturated molecules. The index D_r is a reliable measure of the reactivity of hydrogens in paraffin hydrocarbons and their derivatives toward abstraction reactions.

The values of delocalizability for electrophilic attack, $D_r^{(E)}$, are shown in Table 1 with respect to adamantane and several 1-substituted adamantanes. Calculation was made by the simple LCAO MO method for saturated compounds which had previously been employed for paraffin hydrocarbons.[9] We can see that bridgehead hydrogens have the largest chemical reactivity toward attacking electrophiles.

The values of delocalizability for radical attack, $D_r^{(R)}$, are given in Table 2. The experimental findings that the bridgehead hydrogens are most readily removed can be successfully interpreted in terms of $D_r^{(R)}$.[2] Owens *et al.* showed that the relative rate of the homolytic abstraction of bridgehead hydrogen in adamantane and in substituted adamantanes decreased in the order:[3]

$$-CH_3 > -H > -OCH_3 > -COOCH_3 > -CN$$

Because of the rough setting of parameters for oxygen hybrids, we can not make a sharp comparison between the results of calculation given in

Table 1. The delocalizability at hydrogen atoms for electrophilic abstraction

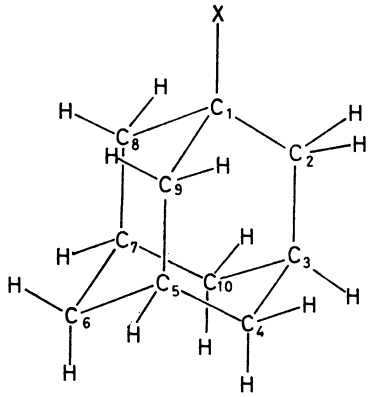

X	Position of attack		
	2	3	4
H	1.0387	1.0407	1.0387
CH_3	1.0388	1.0407	1.0387
OCH_3	1.0383	1.0406	1.0387
$COOCH_3$	1.0380	1.0406	1.0387
CN*	1.0387	1.0406	1.0387

Parameters used are as follows:

Coulomb integrals

$C(sp^3)$	: α
$C(sp^2)$	: $\alpha+0.1\beta$
H	: $\alpha-0.2\beta$
O	: $\alpha+0.3\beta$

Resonance integrals

between hybrids belonging to adjacent atoms

$C(sp^3)$–$C(sp^3)$	: β
$C(sp^3)$–$C(sp^2)$	: β
C–H	: 1.1β
C=O	: 1.2β
C–O	: 0.6β

between hybrids belonging to the same atom

$C(sp^3)$	: 0.34β
$C(sp^2)$	: 0.40β
O	: 0.30β

* The parameters were tentatively put equal to those of carbonyl group.

Table 2. The delocalizability at hydrogen atoms for homolytic abstraction

X	Position of attack		
	2	3	4
H	1.0195	1.0316	1.0195
CH_3	1.0207	1.0318	1.0195
OCH_3	1.0284	1.0329	1.0195
$COOCH_3$	1.0233	1.0322	1.0197
CN	1.0215	1.0319	1.0196

Numbering is the same as Table 1.

6) K. Fukui, This Bulletin, **39**, 498 (1966).
7) K. Fukui and H. Fujimoto, *ibid.*, **39**, 2116 (1966).
8) K. Fukui, T. Yonezawa and C. Nagata, *J. Chem. Phys.*, **32**, 1743 (1960).
9) K. Fukui, H. Kato and T. Yonezawa, This Bulletin, **34**, 1111 (1961).

Table 2 and the experimental order of reactivity. However, it should be noted that the calculation gave a correct order with respect to adamantane and 1-methyl adamantane, and also with respect to methoxy, carbomethoxy, and cyano deirvatives.

The $D_T^{(B)}$ values of hydrogens in diamantane, triamantane, and tetramantane are shown in Fig. 1. It can be predicted that, in all of these adamantane homologues, the bridgehead hydrogens can most readily be removed by a radical.

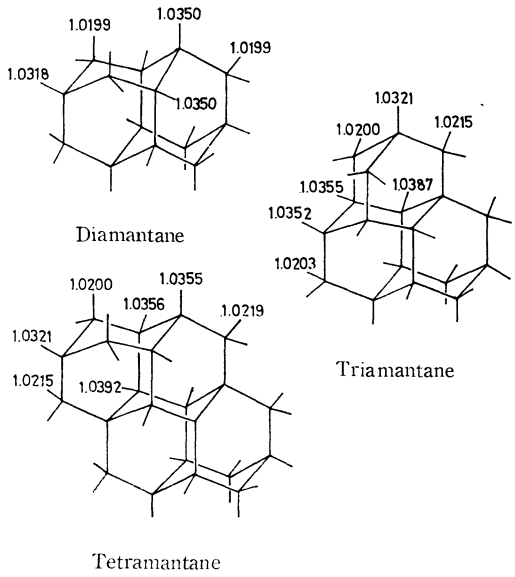

Fig. 1. The delocalizability at hydrogen atoms for homolytic abstraction.

The Electronic Structure of Adamantane, the Adamantyl Radical and Ions. The atom populations and atom-bond populations of adamantane and 1-chloroadamantane, as calculated by the extended Hückel MO method,[10] are shown in Fig. 2. The underlined values indicate the atom populations, while those in parenthesis are those obtained by a SCF MO method for valence electrons with an approximation of the zero-differential overlaps.[11] It can be seen that bridgehead hydrogen have larger electron populations than as secondary hydrogens. The effect of the substituent at the bridgehead carbon, namely, the change in populations, is transmitted in opposite fashions to the adjacent secondary carbons and to the other bridgehead carbons. A similar relation also holds with respect to hydrogens attached to the secondary and tertiary carbons.

The results of the calculations by the extended Hückel MO method on the stable configurations of the 1-adamantyl cation, radical and anion are shown in Fig. 3. In these calculations, only the position of the carbon atom 1 was changed upwards or downwards along the C_3 symmetry axis from its normal position; the positions of the other atoms were unchanged. Here, it should be noted that the most stable position of the carbon 1 in the radical is found to be almost the same as in the parent

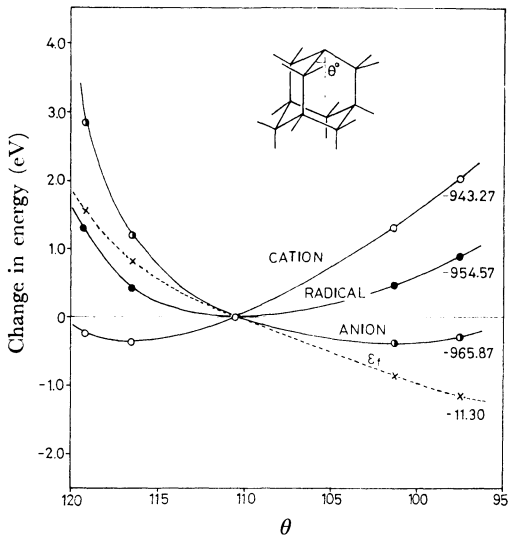

Fig. 3. Energy diagram of 1-adamantyl cation, radical and anion.

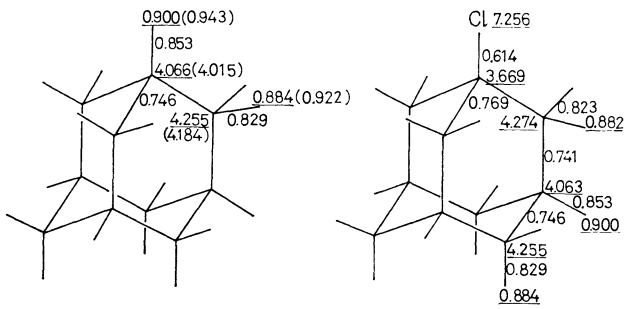

Fig. 2. Atom populations and atom bond populations in adamantane and 1-chloroadamantane.

10) R. Hoffmann, *J. Chem. Phys.*, **39**, 1397 (1963); **40**, 2047, 2474, 2480, 2745 (1964).

11) H. Fujimoto and K. Fukui, unpublished.

compound. The cation becomes more stable as the angle θ increases up to about 117°, while the anion is most stable at about $\theta=101°$. The broken line in Fig. 3 indicates the change in the energy of the orbital, ε_f, housing an electron in radical; this we may term the "frontier orbital." As we employ a one-electron approximation in the extended Hückel MO method, we can see that the stable configuration of the radical and the anion largely depends on the change in the energy of this particular orbital along with the configuration change.

It has been pointed out that the back-side interaction between the hybrids at the carbons 1 and 3 has a significant influence upon the physical properties of the adamantly cation.[12] Here, let us discuss the nature of the stabilization and unstabilization due to the back-side conjugation in the 1-adamantyl cation, radical and anion. The conjugation energy between the two hybrids, χ_1 and χ_3 (see the figure in Table 3), at the carbons 1 and 3 is given by:

$$E_{\chi_1\chi_3} = 2\sum_i v_i C_{\chi_1}^{(i)} C_{\chi_3}^{(i)} h_{\chi_1\chi_3},$$

where v_i is the occupation number of the ith MO (0, 1 or 2), $C_{\chi_1}^{(i)}$ is the coefficient of χ_1 in the ith MO, $h_{\chi_1\chi_3}$ is the resonance integral between the hybrids χ_1 and χ_3, and $\sum$ implies the summation over all the MO's. We tentatively take the sp^3 hybrid as χ_3, while the hybrid χ_1 is determined by the relation between the hybridized state and the bond angle,[13] corresponding to the most stable configuration of each species shown in Fig. 3. The results of calculation are given in Table 3. It may be seen that the stabilization due to the back-side conjugation between the hybrids χ_1 and χ_3 is larger in the cation than in the radical or anion. The partial conjugation energy arising from the frontier orbital,

$$E_{\chi_1\chi_3}^{(f)} = 2C_{\chi_1}^{(f)} C_{\chi_3}^{(f)} h_{\chi_1\chi_3},$$

is +0.0124 eV (contributing to unstabilization) with regard to the most stable configuration of the radical.

The partial valence-inactive population[14] of the hybrid, χ_1, in the half-occupied MO is found to be 0.7154, which is important in the event of chemical interaction with other chemical systems. This result makes us suppose that the unpaired electron in the half-occupied level might be somewhat delocalized over the other constituent atoms. The sum of the one-electron energies of the 2-adamantyl radical with the sp^2 hybridized state at the carbon 2 was found in the extended Hückel MO calculation to be lower than that of 2-adamantyl with the sp^3 state at the carbon 2 by the amount of ~0.6 eV.

Table 3. Conjugation stabilization due to a pair of hybrids in 1-adamantyl radical, cation and anion

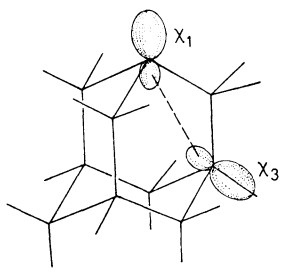

Species	$E_{\chi_1\chi_3}$ (eV)
Radical	−0.0057
Cation	−0.0541
Anion	−0.0010

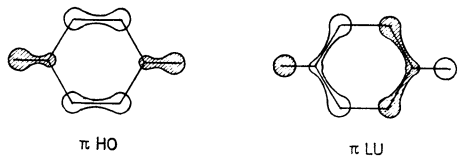

Fig. 4. The nodal property of HO and LU in the pi-electronic part of *p*-quinodimethane.
The shaded and unshaded areas correspond to the positive and negative regions of the wave functions, respectively

A Potential Route to Polyamantane. Now let us present a proposition regarding the potentiality of the preparative method of polyamantane. When we concentrate on the larger homologues of adamantane, we can find that an elemental unit of the repeated sequence has the same constituents as *p*-quinodimethane. Therefore, polyamantane might be produced by the electrocyclic polymerization of *p*-quinodimethane, as long as the methods of the initiation and termination are successfully devised in order to arrange that both chain-end rings have the normal valency. The nodal properties of the highest occuped (HO) MO and one of the lowest unoccupied (LU) MO in the pi-electronic part are shown in Fig. 4. The charge-transfer interaction due to the transfer of one electron from the HO of one molecule into the LU of another molecule favors such an eight-centric cyclic interaction as is shown in Fig. 5, leading to the formation of a polyamantane chain with the adamantane sequence of the form **I.**

We must here make a reservation that the consideration of sigma-pi interaction[7] predicts the

12) P. von R. Schleyer, R. C. Fort, Jr., W. E. Watts, M. B. Comisarow and G. A. Olah, *J. Amer. Chem. Soc.*, **86**, 4195 (1964).

13) C. A. Coulson, "Valence," Clarendon Press, Oxford (1953), p. 193.

14) K. Ruedenberg, *Rev. Mod. Phys.*, **34**, 326 (1962).

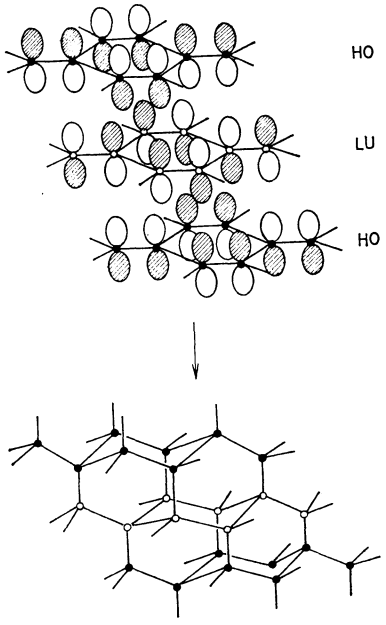

I

Fig. 5. A schematic representation of the mode of the intermolecular pi-pi overlap interaction in *p*-quinodimethane.

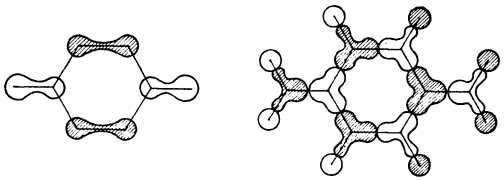

Fig. 6. The nodal property of pi-HO and sigma-LU of *p*-quinodimethane.

formation of a somewhat different sequence. In the chemical interaction of planar conjugated systems in which hybridization change takes place, it has been pointed out,[7] the interaction between the pi part and the sigma part can not be neglected. The interaction between the HO of the pi-electronic part and the LU of the sigma part is usually most

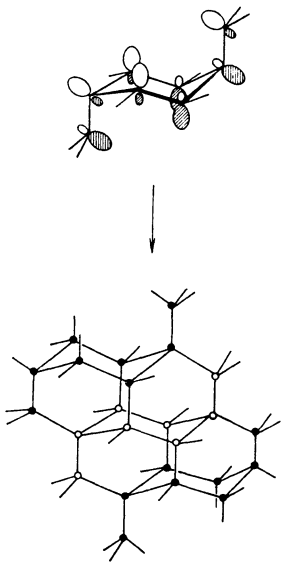

II

Fig. 7. A schematic representation of the mode of the intramolecular sigma-pi overlap interaction in *p*-quinodimethane.

important. The nodal properties of these MO's are given in Fig. 6. Therefore, the sigma-pi interaction favors such configuration change a way as is shown in Fig. 7; this may cause the predominant formation of polyamantane of the form II. However, in usual multi-centric interaction between two conjugated molecules, the stereo-controlling effect due to the intramolecular sigma-pi interaction is rather weak and is overcome by that due to the intermolecular pi-pi interaction between two reactants. This point would be clarified if the preparation of polyamantane by the thermally-induced polymerization of *p*-quinodimethane should be achieved.

The calculations were carried out partly on the HITAC 5020E computer at the Computer Center of the University of Tokyo and partly on the FACOM 230.60 at the Computer Center of Kyoto University.

BULLETIN OF THE CHEMICAL SOCIETY OF JAPAN VOL. 43 57—63 (1970)

The Effect of Pressure on the Electronic Absorpion Spectra of TCNQ Ion Radical Salts

Nobuko SAKAI, Ichimin SHIROTANI and Shigeru MINOMURA

The Institute for Solid State Physics, The University of Tokyo, Roppongi, Minato-ku, Tokyo

(Received June 20, 1969)

The effect of pressure up to 7 kbar on the electronic absorption spectra of the crystalline TCNQ anion radical salts and Li(TCNQ) in PVA has been studied. For simple TCNQ salts such as Li(TCNQ), a blue shift with an increase in the pressure has been observed in the absorption band associated with the intramolecular transition. The magnitude of the blue shift is between 45 and 86 cm^{-1}/kbar. The observed shift has been discussed in terms of the crystal-field effect of the cations. For *N*-MePhe(TCNQ) and $M(TCNQ)_2$, composed of the formally-neutral TCNQ and its anion radical such as $TEA(TCNQ)_2$, a pressure-induced absorption band has been observed at around 20 kK; it may be assigned to the charge-transfer band between the anion radicals.

The electronic absorption spectra of most organic compounds exhibit a red shift with an increase in the pressure.[1-3] However, the absorption band at 18.5 kK of the quaterrylene ($C_{40}H_{20}$) evaporated film is less affected by the pressure,[4] and in the cases of azulene, ferrocene, and the *trans*-stilbene-2,3-dichloro-5,6-dicyano-*p*-benzoquinone complex, a small blue shift is observed at high pressures.[5] In a previous paper,[6] a large blue shift with the pressure has been reported in several ion radical salts which possess an ionic structure in the ground state.

The electrical conductivity of the anion-radical salts of 7,7,8,8-tetracyanoquinodimethane (TCNQ) depends greatly on the nature of the cation.[7] The salts with metal cations generally show low to intermediate conductivity (10^{-5}—10^{-2} $\Omega^{-1}cm^{-1}$), while the salts with cations of planar aromatic heterocyclic molecules show high conductivity ($\sim 10^{2}$ $\Omega^{-1}cm^{-1}$). The conductivity of these solids arises from the motion of the odd π electron among the TCNQ sites. Their conduction mechanism has been discussed by several authors.[8-10]

Recently, the crystalline electronic spectra of TCNQ salts have been studied at room temperature.[10-12] The crystalline spectra are quite different from that of the TCNQ anion radical monomer and depend greatly on the nature of the cations. Boyd and Phillips have reported the absorption spectra of the monomer [$(TCNQ^{-})$] and the dimer [$(TCNQ^{-})_2$] in an aqueous solution of Li(TCNQ).[13] The crystalline spectrum of Li(TCNQ) is similar to that of the dimer in an aqueous solution.

We have studied the absorption spectra of several TCNQ salts in the visible region at high pressures and have found spectral blue and red shifts with the pressure in the low-conductive salts and a pressure-induced absorption band in the high-conductive compounds. In this paper these results will be discussed.

Experimental

The samples used in this experiment were all TCNQ salts, including lithium [Li(TCNQ)], potassium [K-(TCNQ)], *N*-methylphenazinium [*N*-MePhe(TCNQ)],

1) S. Wiederhorn and H. G. Drickamer, *J. Phys. Chem. Solids*, **9**, 330 (1959).

2) J. R. Gott and W. G. Maisch, *J. Chem. Phys.*, **39**, 2229 (1963); H. W. Offen, *ibid.*, **42**, 430 (1965).

3) H. Ohigashi, I. Shirotani, H. Inokuchi and S. Minomura, *J. Phys. Soc. Jap.*, **19**, 1996 (1964); *J. Chem. Phys.*, **43**, 314 (1965); *Molecular Crystals*, **1**, 463 (1966).

4) I. Shirotani, H. Inokuchi and S. Akimoto, This Bulletin, **40**, 2277 (1967).

5) R. B. Aust, W. H. Bentley and H. G. Drickamer, *J. Chem. Phys.*, **41**, 1856 (1964); J. C. Zahner and H. G. Drickamer, *ibid.*, **35**, 375 (1961); H. W. Offen and T. T. Nakashima, *ibid.*, **47**, 4446 (1967).

6) I. Shirotani, N. Sakai, H. Inokuchi and S. Minomura, This Bulletin, **42**, 2087 (1969).

7) L. M. Melby, R. J. Harder, W. R. Hertler, W. Mahler, R. E. Benson and W. E. Mochel, *J. Amer. Chem. Soc.*, **84**, 3374 (1962); W. J. Siemons, P. E. Bierstedt and R. G. Kepler, *J. Chem. Phys.*, **39**, 3523 (1963); L. R. Melby, *Can. J. Chem.*, **43**, 1448 (1965).

8) E. Menefee and Y. H. Pao, *J. Chem. Phys.*, **36**, 3472 (1962).

9) O. H. LeBlanc, Jr., *ibid.*, **42**, 4307 (1965).

10) T. Kondow, K. Siratori and H. Inokuchi, *J. Phys. Soc. Jap.*, **23**, 98 (1967).

11) H. Kuroda, S. Hiroma and H. Akamatu, This Bulletin, **41**, 2855 (1968).

12) Y. Iida, *ibid.*, **42**, 71, 637 (1969).

13) R. H. Boyd and W. D. Phillips, *J. Chem. Phys.*, **43**, 2927 (1965).

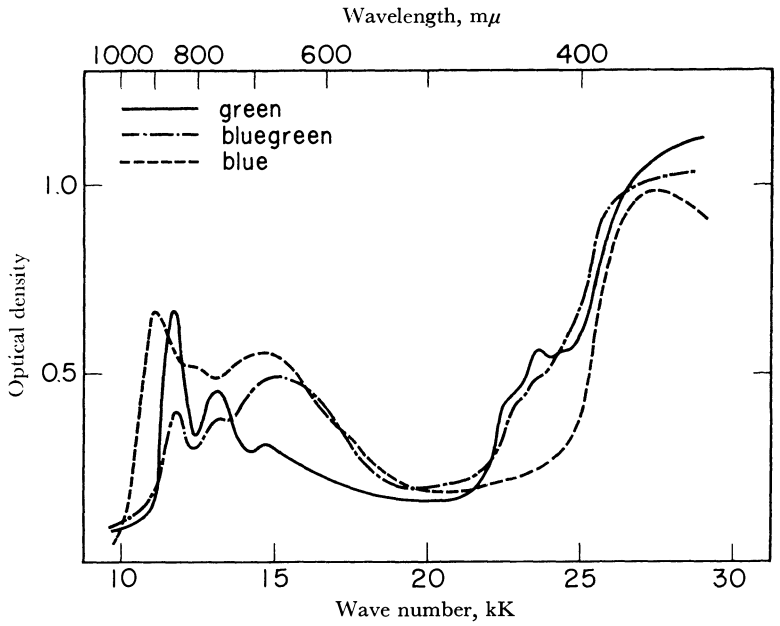

Fig. 1. The absorption spectra of Li(TCNQ) PVA films of three different concentrations; ——— the green, -·-·-· the blue green, and ·-·-·-·- the blue PVA film.

quinolinium [Q(TCNQ)$_2$], bipyridinium [BiP(TCNQ)$_2$], 4-amino-2,3,5,6-tetramethylanilinium [DAD(TCNQ)$_2$], triethylammonium [TEA(TCNQ)$_2$] and cobalticinium [CoC(TCNQ)$_2$]. These compounds were provided by Kondow, who has previously reported their preparations in detail.[10] Li(TCNQ)-polyvinylalcohol (PAV) film was prepared by drying a 10 wt% warm aqueous slurry of PVA in which Li(TCNQ) was dissolved. A uniformly-colored plastic film was formed after the evaporation of the solvent. The absorption spectra were measured on powdered samples rubbed on a quartz glass plate and on PVA film at room temperature by using a Shimazu SV-50A spectrophotometer. The high-pressure optical cell has been described elsewhere.[4] A hydrostatic pressure up to 7 kbar was applied by means of a pressure-transmitting medium (kerosene or white gasoline) through a pressure-intensifier. The pressure was determined by a Harwood manganine resistance gauge and a Heise Bourdon tube gauge.

Results and Discussion

Figure 1 shows the absorption spectra of Li(TCNQ) PVA film of three different concentrations at 1 bar. In the green PVA film, the absorption peaks almost agree with that in acetonitril. Therefore, Li(TCNQ) seems to be in a monomer state in the green film. The absorption spectrum of the blue PVA film is similar to that of the dimer of the TCNQ anion radical in an aqueous solution, and it has a new absorption peak at 11.0 kK which does not exist in the monomer state. In the blue green PVA film, the dimer and the monomer may be supposed to coexist. The absorption peak at 11.0 kK in the dimer state revealed a small red shift (-18 cm^{-1}/kbar) with an increase in the pressure, while the other absorption peaks of these PVA film were insensitive to the pressure up to 7 kbar.

Figure 2 shows the effect of the pressure on the absorption spectra of the crystalline K(TCNQ). The crystalline spectra of K(TCNQ) exhibited absorption bands located at 8.3, 16.1, and 27.5 kK. The two peaks in the visible region showed a large blue shift with an increase in the pressure ($+45$ and $+58$ cm^{-1}/kbar for the 16.1 and 27.5 kK peaks respectively). Similar results on Li(TCNQ) have been reported in a previous paper.[6] The rates

TABLE 1. SPECTRAL DATA FOR TCNQ ANION RADICAL SALTS, NEUTRAL TCNQ, AND THREE ORGANIC COMPOUNDS

Compound	Absorption peak (kK)	Pressure shift (cm^{-1}/kbar)
Li (TCNQ)	26.5	+86
	16.0	+51
	7.7	—
in PVA film	11.0	−18
K (TCNQ)	27.5	+58
	16.1	+45
	8.3	—
TCNQ	22.3	−84
Azulene	14.4	+ 6[a]
Ferrocene	23.3	+20[a]
trans-Stilbene-DDQ	16.0	+ 5[a]

a) Ref. 5.

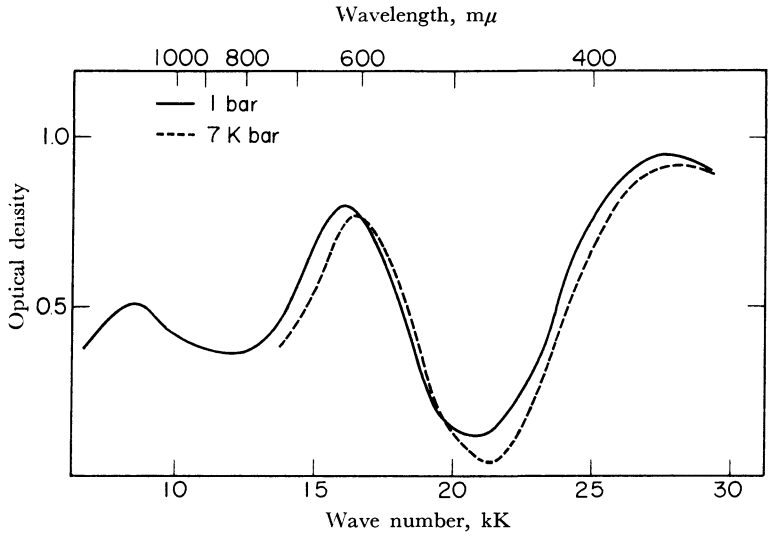

Fig. 2. The pressure dependence of the absorption spectra of the crystalline K(TCNQ).

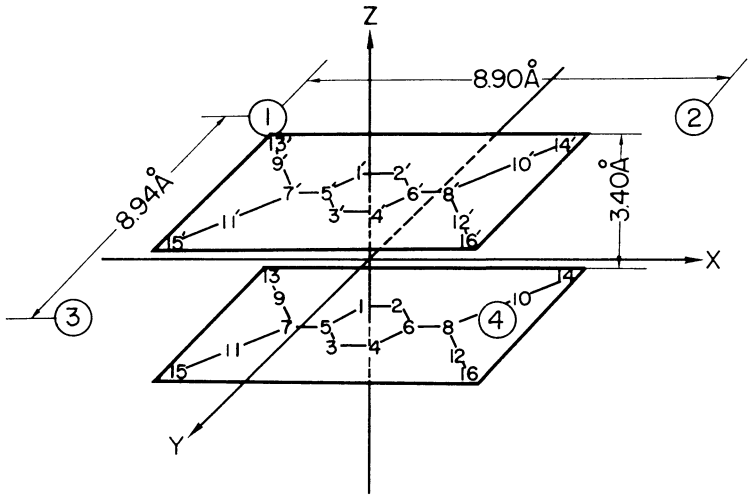

Fig. 3. The assumed crystal field for K(TCNQ).

of the pressure shift of several TCNQ salts are given in Table 1. The energy shifts are approximately proportional to the applied pressure.

The absorption spectra of crystalline Li(TCNQ) and K(TCNQ) are similar to that of the dimer in an aqueous solution. The spectroscopic evidence supports a bimolecular association of the TCNQ ion radicals in the solid. As has been stated earier, the absorption bands of the dimer observed in the PVA film were insensitive to the pressure. Therefore, it seems that the major contribution to the blue shift arises from the crystal field*1 of metal-positive ions.

In accordance with Menefee and Pao,[8] the pressure dependence on the splitting of energy levels brought about by a model crystal field of the cations was tentatively calculated to explain the large blue shift. The crystal field was assumed on the basis of the crystal structure of K(TCNQ)[14] which is shown in Fig. 3; two molecules of $TCNQ^-$ are stacked face to face with a spacing of 3.4 Å, and four positive nuclei with a point charge of $+e/4$ are put on the corners of the rectangle (8.94×8.90 Å) formed in the middle between two molecules and the parallel to the $TCNQ^-$ molecular plane. Since this cluster belongs to the D_{2h} symmetry group, the new molecular orbitals are given by:

$$\Phi_{n-} = A_{n-}(\psi_n - \psi_{n'}),\ \Phi_{n+} = A_{n+}(\psi_n + \psi_{n'}),$$

*1 "Crystal field" means the electrostatic field by ions in the crystal.

14) G. R. Anderson and C. J. Fritchie, Jr., Paper for Second National Meeting of the Society for Applied Spectroscopy, San Diego (1963), p. 111.

where ϕ_n and $\phi_{n'}$ are the nth molecular orbitals centered on the first and second $TCNQ^-$ radical ions respectively, and where A is the normalization coefficient. For $\phi_{n'}$, the results of the open-shell SCF-LCAO-MO calculations by Lowitz[15] were used here;

$$\begin{aligned}\phi_8(b_{1u}) = &-0.22901(\phi_1+\phi_2+\phi_3+\phi_4)\\ &+0.18931(\phi_5+\phi_6)+0.50263(\phi_7+\phi_8)\\ &+0.01933(\phi_9+\phi_{10}+\phi_{11}+\phi_{12})\\ &-0.23007(\phi_{13}+\phi_{14}+\phi_{15}+\phi_{16}),\\ &(E=1.92061\text{ eV}),\ (n=8)\\ \phi_9(b_{2g}) = &-0.25063(\phi_1-\phi_2+\phi_3-\phi_4)\\ &-0.26414(\phi_5-\phi_6)+0.45618(\phi_7-\phi_8)\\ &+0.08375(\phi_9-\phi_{10}+\phi_{11}-\phi_{12})\\ &-0.20304(\phi_{13}-\phi_{14}+\phi_{15}-\phi_{16})\\ &(E=4.4249\text{ eV}),\ (n=9,\text{ highest occupied level})\\ \phi_{10}(b_{1u}) = &-0.19752(\phi_1+\phi_2+\phi_3+\phi_4)\\ &+0.51425(\phi_5+\phi_6)-0.19426(\phi_7+\phi_8)\\ &-0.16327(\phi_9+\phi_{10}+\phi_{11}+\phi_{12})\\ &+0.18226(\phi_{13}+\phi_{14}+\phi_{15}+\phi_{16}),\\ &(E=8.89412\text{ eV}),\ (n=10,\text{ lowestvacant level})\end{aligned}$$

where ϕ_i is the atomic orbital for the ith atom and where E is the eigenvalue. The stabilization energy by the crystal field is given by;

$$\begin{aligned}\Delta E &= \int \Phi_n V \Phi_n d\tau\\ &= (-e^2/4)\int \Phi_n(1/r_1+1/r_2+1/r_3+1/r_4)\Phi_n d\tau,\end{aligned}$$

where r_a is the distance from each atom of $TCNQ^-$ to the nucleus, a, which was obtained from the bond lengths shown in Table 2 and from the bond angles (assumed to be 120 or 180°). The calculated values of ΔE (for $n=8,9,10$) and the splitting energy by the assumed crystal field at the atmospheric pressure and at 10 kbar are shown in Table 3.*2 It was assumed that, at 10 kbar, $TCNQ^-$ salts were isotropically compressed in volume to 90.5%*3 without a change in the $TCNQ^-$ molecular structure. The stabilization energy and the splitting energy by the crystal field were larger on the low-energy level than on the high energy level, and both increased with an increase in the pressure. Table 3(b) gives the pressure-induced shift of some of the transitions considered; this shift was calculated according to the results shown in Table 3(a). A considerable blue shift was obtained. On the basis of the calculated results, it seems reasonable to conclude that the large blue shift of the electronic

Table 2. Bond lengths in $K(TCNQ)$[a]

C(1)-C(2)	1.37 Å
C(2)-C(6)	1.42
C(6)-C(8)	1.40
C(8)-C(10)	1.41
C(10)-N(14)	1.13

a) Ref. 14.

Table 3. The stabilization energy and the splitting energy by the crystal field at the atmospheric pressure and at 10 kbar (a), and the pressure shift of several transitions (b)

(a)

Molecular orbital	ΔE (eV) 1 bar		ΔE (eV) 10 kbar	
$\Phi_{8-}(a_g)=N_{8-}(\psi_8-\psi_{8'})$	−2.732	>0.568	−2.935	>0.759
$\Phi_{8+}(b_{1u})=N_{8+}(\psi_8+\psi_{8'})$	−2.164		−2.176	
$\Phi_{9-}(b_{3u})=N_{9-}(\psi_9-\psi_{9'})$	−2.532	>0.508	−2.698	>0.656
$\Phi_{9+}(b_{2g})=N_{9+}(\psi_9+\psi_{9'})$	−2.024		−2.042	
$\Phi_{10-}(a_g)=N_{10-}(\psi_{10}-\psi_{10'})$	−2.024	>0.399	−2.159	>0.515
$\Phi_{10+}(b_{1u})=N_{10+}(\psi_{10}+\psi_{10'})$	−1.625		−1.644	

(b)

Transition energy at 1 bar (eV)	Transition	Pressure-induced shift (cm^{-1}/kbar)
0.508	$B_{1u}\leftarrow A_g$	+120
2.644	$B_{2u}\leftarrow A_g$	− 4
3.721	$B_{3u}\leftarrow A_g$	+269
4.978	$B_{3u}\leftarrow A_g$	+ 24
5.857	$B_{1u}\leftarrow A_g$	+144

15) D. A. Lowitz, *J. Chem. Phys.*, **46**, 4698 (1967).

*2 In the calculation of ΔE, as usual, terms coming from nonadjacent atoms were ignored, and for the integrals in terms of atomic orbitals, the following approximations were made;

$$\int \phi_i^2/r_a d\tau \simeq 1/r_{a'},\ \int \phi_i\phi_j/r_a d\tau \simeq \tfrac{1}{2}(1/r_{ai}+1/r_{aj})S_{ij},$$
$$\int \phi_i\phi_{i'}r_a d\tau \simeq 1/r_a\delta_{ii'}$$

where r_{ai} is the separation of the positive nucleus, a, and the i atom, where S_{ij} is the overlap integral, and where $\delta_{ii'}$ is the overlap integral which refers to the same kind of atoms located on two $TCNQ^-$ molecules. For $S_{CC'}$, S_{CN} and $\delta_{CC'}$ (or $\delta_{NN'}$), the approximate expressions which Roothaan [*J. Chem. Phys.*, **19**, 1445 (1951)] has given for three two-center integrals, ($2p\pi_C$-$2p\pi_C$), ($2p\pi_C$-$2p\pi_N$), and ($2p\sigma_C$-$2p\sigma_C$) respectively, were used.

*3 This value is the volume change with the pressure for general crystals of aromatic molecules, as extrapolated from Bridgman's data [Samara and Drickamer, *J. Chem. Phys.*, **37**, 474 (1962)]. The compressibility of ion radical salts has not been measured, but it is probably less than that of ordinary hydrocarbon solids.

transition observed in Li(TCNQ) and K(TCNQ) arises from the crystal field of metal cations.

Li(TCNQ) and K(TCNQ) have the absorption band in the near-infrared region. The effect of the pressure on these peaks has not yet been studied becasue of interference by the absorption of water contained in the pressure-transmitting medium. This band can be assigned to the charge-transfer band between the anion radicals.[12] It is well-known that the charge-transfer band of molecular complexes shows a red shift at high pressures.[2] A similar effect may be expected for $TCNQ^-$ ion radical salts.*4 The electrical resistance of Li(TCNQ) drops rapidly in the low-pressure region and levels off at high pressures. The values of the activation energy decreases from 0.32 eV at 1 bar to 0.07 eV at 169 kbar.[16] Since the near-infrared band is located in the energy region of twice the activation energy for electrical conductivity, the study of the pressure effect on this band is important. The new absorption band at 11.0 kK in the blue PVA film of Li(TCNQ) can be assigned to the charge-tranfer band between TCNQ-anion radicals which corresponds to the crystalline absorption band in the near-infrared region, for this band does not exist in the monomer state and the spectral red shift was observed at high pressures.

Figure 4 shows several isobars of the absorption spectra for *N*-MePhe(TCNQ). The pressure effect on the bands at 11.5 and 17.0 kK is not clear, for these bands are appreciably weak and diffused. The pressure shift of the band at 26.0 kK was not observed, at least up to 7 kbar. However, a remarkable pressure effect was observed; that is, the pressure-induced absorption band was found at around 20 kK at high pressures. The absorption intensity of this band increased with an increase in the pressure. This bahaviour was reversible with a decrease in the pressure. *N*-MePhe(TCNQ) shows an unusually high conductivity ($1.4\times10^2\Omega^{-1}\cdot cm^{-1}$) in spite of a simple salt of the M(TCNQ) type.[7] According to the crystal structure analysis by Fritchie,[17] $TCNQ^-$ molecules pack face to face to form a regular linear chain column with an interplanar spacing of 3.26 Å. This interplanar spacing is much shorter than the van der Waals distance. Therefore, the strong charge-transfer interaction may be expected to have been induced by compression. The absorption intensity increased remarkably with the pressure. As has been expected from Mulliken's charge-transfer theory,[18] the absorption intensity of the charge-transfer band increases with the pressure[2]. Thus, the pressure-induced absorption band at 20 kK may be ascribed to a new charge-transfer absorption band.

Figures 5 and 6 show several isobars of the absorption spectra for $TEA(TCNQ)_2$ and $Q(TCNQ)_2$. The pressure-induced absorption band was found at around 20 kK at high pressures. The absorption intensity of this band increased with an increase in the pressure. On the other hand, the absorption intensity of the weak peak at 17 kK, the nature of

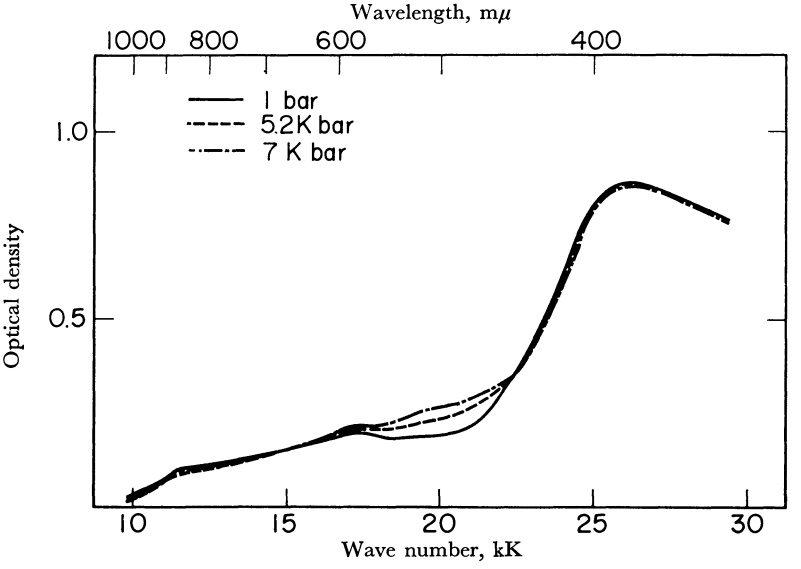

Fig. 4. The pressure dependence of the absorption spectra of the crystalline *N*-MePhe(TCNQ).

*4 In the case of Na(chloranil) salt, the inter-radical charge-transfer band has shown a red shift with an increase in the pressure.[6]

16) I. Shirotani, T. Kajiwara, H. Inokuchi and S. Akimoto, This Bulletin, **42**, 366 (1969).
17) C. J. Fritche, Jr., *Acta Cryst.*, **20**, 892 (1966).
18) R. S. Mulliken, *J. Amer. Chem. Soc.*, **74**, 811 (1952), *J. Phys. Chem.*, **56**, 801 (1952).

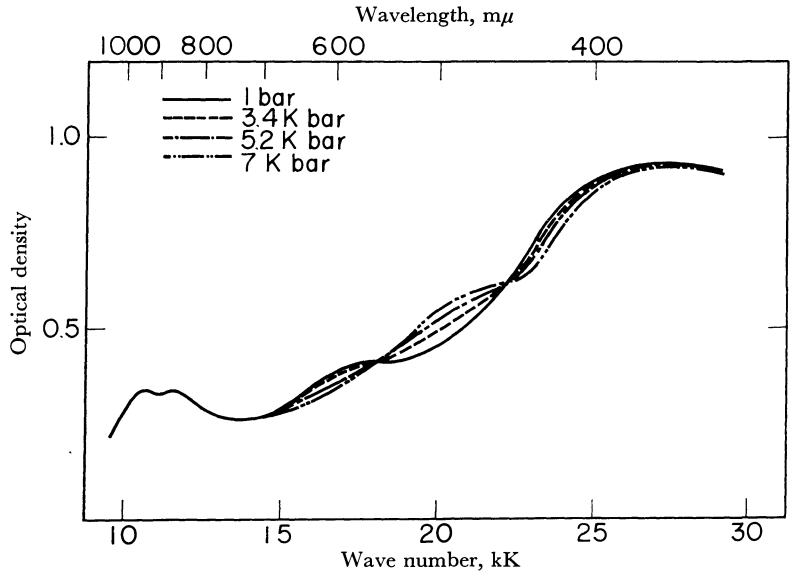

Fig. 5. The pressure dependence of the absorption spectra of the crystalline TEA(TCNQ)$_2$.

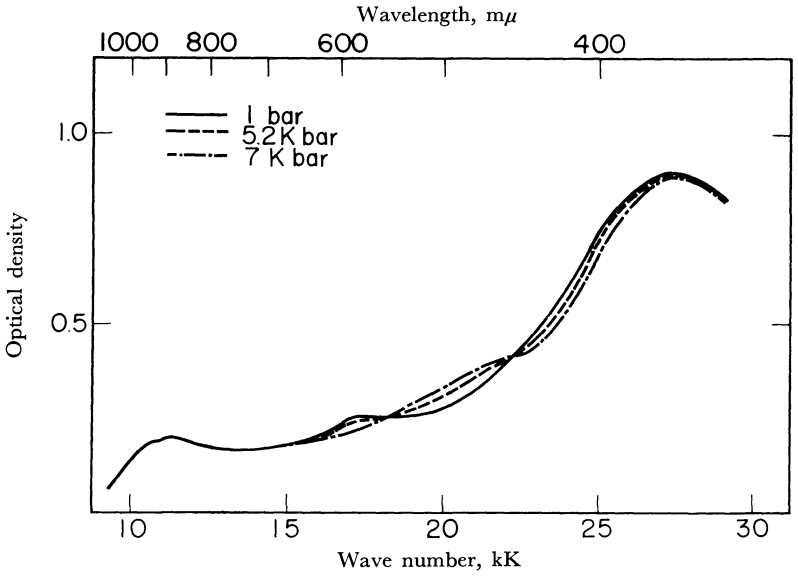

Fig. 6. The pressure dependence of the absorption spectra of the crystalline Q(TCNQ)$_2$.

which was not clear, decreased with an increase in the pressure. These pressure effects were reversible with a decrease in the pressure. Similar results were also obtained for BiP(TCNQ)$_2$, CoC(TCNQ)$_2$, and DAD(TCNQ)$_2$.

The TCNQ salts of the M(TCNQ)$_2$ type show a high conductivity and a small activation energy.[7] The crystalline structure has been analysed for TEA(TCNQ)$_2$ and Q(TCNQ)$_2$.[19] TCNQ$^-$ molecules pack face to face with an interplanar spacing of 3.21—3.32Å. The strong charge-transfer interaction may be expected to be induced by compression in these TCNQ anion radical salts, also. Thus, the pressure-induced absorption band may be ascribed to a new charge-transfer absorption band.

The pressure shift of the bands at 11 and 27 kK associated with the intramolecular transition was not obaserved, at least up to 7 kbar. The energy shift with the pressure may arise from the characteristic crystalline structure of TCNQ salts. Further, in the case of the M(TCNQ)$_2$ type, the crystal-field effect is considered to be weakened by the

19) H. Kobayashi, private communication.

presence of the neutral TCNQ molecules.

The authors would like to thank Professor H. Inokuchi for his useful suggestions and Drs. T. Kondow and T. Maekawa for supplying the samples used in this experiment. Their thanks are also due to Drs. T. Kajiwara, T. Sakata and H. Kobayashi for their useful discussion.

BULLETIN OF THE CHEMICAL SOCIETY OF JAPAN VOL. 43 63—67 (1970)

Comparison of the Recoil Reactions in the ^{80m}Br-CH_4 and ^{82m}Br-CH_4 Systems

Enzo Tachikawa

Division of Chemistry, Japan Atomic Energy Research Institute, Tokai-Mura, Ibaraki

(Received June 24, 1969)

The reactions of ^{80}Br and ^{82}Br excited by the isomeric transition processes with CH_4 have been compared with each other. Similar reaction processes; energetic and thermal ionic, are involved in both cases. However, the isotope effect appears in the energetic process to form CH_3Br, but not in the thermal ionic process to form CH_3Br and CH_2Br_2. The difference in the γ-transitions of ^{80m}Br and ^{82m}Br to the ground states is responsible for the above results. It is concluded that at least a part of the recoil Br atoms enter chemical combinations with surrounding molecules within 10^{-8}sec, the life-time of the excited ^{80}Br atom. Furthermore, the yield of $CH_3{}^{80}Br$, lower than that of $CH_3{}^{82}Br$, is discussed on the basis of the different kinetic energies achieved on the Br atoms.

The atom or ion formed as result of nuclear transformation loses its energy or its charge, or both, in collisions with other molecules of the medium until most of the charges have been lost and its energy reduced to tens or *ev.* or even below, at which time it may enter a permanent stable combination if an appropriate reaction path is available.[1]

The investigations of such processes in the gas phase have now been extended by many workers to studied of the nature of the reactive species in the reaction of Br formed by the (I. T.) process with methane. Using additives, it has been concluded that CH_3 ^{82}Br in gaseous methane must, principally, result from an atom with excess kinetic energy, and CH_2 ^{82}BrBr, from the thermal ionic Br atom.[2,3]

Other experiments[4] strongly indicate that the reaction of the ^{80}Br from the ^{79}Br(n,γ)^{80}Br process with CH_4 is probably not dependent upon the charge. This remarkable difference in reactive species must result from the characteristics of the Br atoms activated by the different nuclear reactions; the (n, γ) process is strictly a high-energy recoil phenomenon, while on the other hand, the (I.T.) process involves little recoil and a high positive charge, ranging from $+1$ to $+14$.[5,6]

It was though interesting to see if differences in the product distribution could also be found between the ^{80}Br and the ^{82}Br formed by (I. T.) processes in the reactions with CH_4, since the γ-transitions involved are somewhat different in the two species. The γ-transition of ^{82m}Br to the ground state is performed in a single transition, whereas that of ^{80m}Br is attained in two steps.[7]

Nicholas and Rack[8] dealt with a comparison of the total organic yields from ^{80m}Br-CH_4 and ^{82m}Br-CH_4. The difference found between them does not exceed the experimental uncertainties. However, this does not provide any comparisons of the individual reaction processes, the energetic and thermal ionic processes.

In the present paper, we will deal in more detailed investigations of the reactions in these systems; particular, we look for a possible isotope effect between them in order to obtain some information on the time scale of the reactons of the recoil Br atom.

1) J. E. Willard, "Chemical Effects of Nuclear Transformation," Vol. I, IAEA, Vienna (1961), p. 215.
2) J. Okamoto and E. Tachikawa, This Bulletin, **42**, 1504 (1969).
3) E. Tachikawa, *ibid.*, **42**, 2404 (1969).
4) E. P. Rack and A. A. Gordus, *J. Phys. Chem.*, **65**, 944 (1961).
5) A. R. Kazanjian and W. F. Libby, *ibid.*, **42**, 2779 (1965).
6) S. Wexler and G. Anderson, *ibid.*, **33**, 850 (1960).
7) C. M. Lederer, J. M. Hollander and I. Perlman, "Table of Isotopes," John Willey & Sons. Inc., New York (1968), pp. 215, 217.

Experimental

The general experimental techniques are quite similar to those used in earlier bromine experiments.[2] The ^{80m}BrBr was formed by irradiating gaseous Br_2, sealed in a thin-wall quartz capillary, with thermal neutrons for one minute; it was used in the I.T. experiments 2—3 hr after irradiation. As a neutron source, the JRR-4 reactor in the JAERI was used.

Under these conditions, the percentage of ^{82}Br activity for which correction had to made was less than one per cent. The ^{80m}BrBr reaction mixture was allowed to stand more than 2 hr to permit a ^{80m}Br-^{80}Br parent-daughter equilibrium to be established. The sample were then analyzed by a radio-gas-chromatograph equipped with a G-M counter. The total activity was also measured by a G-M counter and corrected for ^{82}Br activity. The results obtained were expressed in per cent yields by applying decay corrections. In the experiments on the ^{82m}Br-CH_4 system, the neutron-irradiated bromine was mixed with CH_4 before the decaying-out of ^{82m}Br. The products were analyzed 48 hr later. The radioactive assays in a radio-gas-chromatograph and the total activity measurements were performed by a scintillation counter (2″×2″ well-type NaI(Tl) scintillator). A correction for ^{80}Br was not required in these procedures.

The experiments were carried out a total pressure of 51±2 cmHg. The ratio of Br_2 as a scavenger to CH_4 was kept constant. In some experiments, however, a constant amount of Br_2 was used.

Materials. The methane was obtained from the Takachiho Chemical Co., had a listed purity of 99.5%. The bromine used was the highest grade available. Xenon and argon, supplied by the Takachiho Chemical Co. and the Nihon Sanso Co., were used without additional purification (the listed purities are 99.995% and 99.994% respectively).

Result

CH_3Br and CH_2Br_2 are the only products from the reactions of ^{80}Br or ^{82}Br with gaseous methane; this is consistent with the finding in the early observations.[3]

The moderator effects on these products have been studied under a constant pressure of 5 cmHg Br_2 in both systems, ^{80m}Br-CH_4 and ^{82m}Br-CH_4. The results obtained using Xe are summarized in Table 1. A significant difference between the two systems is seen in the yields of CH_3Br; $CH_3{}^{82}Br$ is higher than $CH_3{}^{80}Br$ over the entire range of mole fractions of Xe. However, both could be extrapolated to 0.0±0.3% at 1.0 m.f. of Xe. Contrarily, both $CH_2{}^{80}BrBr$ and $CH_2{}^{82}BrBr$ decrease from 1.1±0.2% to 0.5±0.3% upon the addition of Xe.

As was the case in Table 1, the presence of a constant amount of Br_2 alters the reaction conditions so that the amount of Br_2 relative to CH_4 varies with the mole fraction of the moderator. Accordingly, the probability of the reactive collision of the energetic or thermal ionic Br atom with Br_2, relative to that with CH_4, rapidly increases with the amount of the moderator. In a highly-moderated system, thus, the Br-flux available to the reaction with CH_4 is very much reduced.

The most suitable conditions for studying the moderator effect specifically on these products is, thus, to keep the value of Br_2/CH_4 constant over the entire range of mole fractions of the moderator. Table 2 shows the results obtained with the addition of Br_2/CH_4=0.11±0.01, using Ar as a moderator.

Table 1. Moderator effects on CH_3Br and CH_2Br_2 from the ^{80m}Br-CH_4 and ^{82m}Br-CH_4 systems (Br_2 is 5.0 cmHg)

Gas pressure added Xe (cmHg)	CH_4 (cmHg)	m.f. of Xe	CH_3Br (%)	CH_2Br_2 (%)
^{80m}Br-CH_4 system				
0.0	46.4	0.0	3.5±0.3	1.3±0.1
5.6	40.4	0.111	2.3±0.2	0.9±0.1
21.5	25.2	0.416	1.2±0.1	0.6±0.1
28.3	18.3	0.548	0.8±0.1	0.7±0.1
42.1	4.3	0.819	0.2±0.1	0.6±0.1
^{82m}Br-CH_4				
0.0	45.9	0.0	5.0±0.5	1.1±0.1
3.4	43.8	0.064	3.6±0.3	0.8±0.1
5.5	41.8	0.104	4.0±0.4	1.1±0.1
11.1	35.8	0.214	3.1±0.3	0.8±0.1
14.4	32.6	0.276	3.0±0.3	1.0±0.1
16.3	30.9	0.311	2.3±0.2	0.7±0.1
17.8	28.9	0.344	1.9±0.2	0.9±0.1
20.7	25.8	0.402	1.6±0.1	0.9±0.1
33.6	12.5	0.658	0.7±0.1	0.9±0.1
38.8	8.9	0.736	0.5±0.1	0.6±0.1

Table 2. Moderator effect on CH_3Br and CH_2Br_2 from the ^{80m}Br-CH_4 and ^{82m}Br-CH_4 systems (Br_2/CH_4=0.11±0.01)

Gas pressure added Br_2 (cmHg)	Ar (cmHg)	CH_4 (cmHg)	m.f. of Ar	CH_3Br (%)	CH_2Br_2 (%)
^{80m}Br-CH_4					
5.0	0.0	46.2	0.0	3.5±0.3	1.2±0.1
4.0	10.7	36.7	0.209	2.3±0.2	1.1±0.1
3.0	20.5	27.4	0.404	1.6±0.2	1.0±0.1
2.5	25.9	22.8	0.506	1.4±0.1	1.1±0.1
2.0	31.0	18.4	0.608	1.0±0.1	1.1±0.1
1.5	36.1	14.5	0.697	0.8±0.1	1.1±0.1
1.0	40.0	9.4	0.798	0.6±0.1	1.2±0.1
0.5	45.8	5.3	0.888	0.5±0.1	1.2±0.1
^{82m}Br-CH_4					
5.0	0.0	45.9	0.0	5.0±0.5	1.0±0.1
4.0	9.9	37.4	0.193	4.0±0.4	0.9±0.1
3.0	21.2	27.1	0.413	2.6±0.2	1.2±0.1
2.0	30.6	18.1	0.603	1.6±0.2	1.1±0.1
1.0	41.1	9.6	0.795	1.0±0.1	1.1±0.1

$CH_3{}^{80}Br$ and $CH_3{}^{82}Br$ are moderator-sensitive, and both are extrapolated to $0.5\pm0.3\%$ at 1.0 mol fraction of Ar. On the other hand, both $CH_2{}^{80}BrBr$ and $CH_2{}^{82}BrBr$ are constant within range of experimental uncertainty over the whole range of mole fractions of Ar.

Discussions

Reaction of Br with CH_4. The most convenient way to differentiate the energetic reaction from the kinetic enregy-independent (thermal ionic) reactions is through the addition of inert gas as an energy sink of the energetic Br atom. Judging from the ionization potentials of the inert gas and the Br atom, the charge transfer from the Br^{+1} atom to the inert gas molecule seems not to be important.

Thus, if a product is formed *via* the kinetic energy process, its yield should be reduced by the addition of inert gas. The conclusion drawn from the results shown in Table 2 is that $3.5\%-0.5\%=3.0\%$ for $CH_3{}^{80}Br$ and $5.0\%-0.5\%=4.5\%$ for $CH_3{}^{82}Br$ are moderator-sensitive and formed *via* an energetic process, probably through the direct substitution reaction of hydrogen by energetic ^{80}Br and ^{82}Br, neutral or ionic.[2] One-half per cent of $CH_3{}^{80}Br$ and $CH_3{}^{82}Br$ and 1.1% of $CH_2{}^{80}BrBr$ and $CH_2{}^{82}BrBr$ are formed *via* thermal ionic processes.

Nicholas and Rack have discussed the nature of the thermal ionic reaction and suggested the following equation:[8]

$$CH_4 + Br^{+1} \longrightarrow CH_3Br^{+1} + H \qquad (1)$$

However, the formation of CH_2Br_2 can hardly be explained by this equation. Instead, we suggest the formation of CH_4Br^{+1*} through the ion-molecule reaction of thermal Br^{+1}:

$$CH_4 + Br^{+1} \longrightarrow CH_4Br^{+1*} \qquad (2)$$

Such a reaction is very favored energetically and more probable for the CH_2Br_2 formation.[9,10]

Comparison of the Reactions of ^{80}Br and ^{82}Br. The finding that similar reaction mechanisms are involved in the two systems is rather to be expected, since the orginal physical properties of ^{80}Br and ^{82}Br are similar. However, the importance of a careful inspection of the results is that there is an isotope effect between ^{80}Br and ^{82}Br on the energetic reaction (1.5 ± 0.2), but not on the thermal inoic reactions.

Nicholas and Rack[8] measured the total organic yield from the recation of ^{82}Br with CH_4 and compared it with the value found by Spicer and Gordus[11] in the ^{80m}Br-CH_4 system. They attemped to conclude the same organic yield from the reaction of the (I.T.)-induced ^{80}Br and ^{82}Br with CH_4, based upon the value (1.1 ± 0.1) for the ratio. A possible explanation for the discrepancy between the present results and the reported results is that the ratio of the total organic yields ($CH_3Br+CH_2Br_2$) from the present systems turns out to be 1.3 ± 0.2, instead. This indicates that the comparison of the total organic yields makes the difference between them less significant. Furthermore, under the conditions adopted by Spicer and Gordus, containing a smaller amount of Br_2 as a scavenger, the yield increases[8,12] considerable and the ratio between them is closer to unity. In addition, the differences in the experimental procedure might be at least partly responsible for this discrepancy.

The same yields for the thermal ionic process in both systems are consistent with the previous conclusion[2,3] that the ionization potential of the reactant relative to that of Br is the most important controlling factor in the thermal ionic process.

Among the explanations for the isotope effect in the energetic reaction which must be considered is that CH_4 shows a different efficiency in the energy degradation for ^{80}Br and ^{82}Br.[13,14] Thus, the spectrum of the Br atom in the energetic reaction range could be different in ^{80m}Br-CH_4 and in ^{82m}Br-CH_4. Under the present conditions, no precise information concerning the encrgy degradation of the Br atom is available. As a crude evaluation, however,[14] the average logarithmic energy loss, α, of ^{80}Br and ^{82}Br in collision with CH_4 can be calculated using the atom-molecule elastic collision model. The value of 1.03 has been obtained for the $\alpha^{80}{}_{Br-CH_4}/\alpha^{82}{}_{Br-CH_4}$ ratio.

It is well known that the actual collisions of the recoil atom are generally of a highly inelastic nature,[15] with a strong bond coupling of the atoms in the molecule attacked. Thus, the above gives only qualitative information concerning the difference in the energy degradation between the two systems. It is very unlikely, therfore, to explain the observed isotope effect.

Here it will be very interesting to check the decay schemes[7] of ^{80m}Br and ^{82m}Br precisely (see Fig. 1). The γ-transition of ^{82m}Br to the ground

8) J. Nicholas and E. P. Rack, *J. Chem. Phys.*, **48**, 4085 (1968).

9) Neutralization[10] of the CH_4Br^{+1*} probably takes place *via* the charge transfer and results in decomposition to fragments, such as CH_3Br, CH_2Br, and so on. The formed CH_2Br radical could be scavenged by Br_2 to form CH_2Br_2.

10) E. P. Rack and A. A. Gordus, *J. Chem. Phys.*, **34**, 1855 (1961).

11) L. D. Spicer and A. A. Gordus, "Chemical Effects of Nuclear Transformation," Vol. I, IAEA, Vienna (1965), p. 185.

12) J. A. Merrigan, W. K. Ellgren, Jr., and E. P. Rack, *J. Chem. Phys.*, **44**, 174 (1966).

13) E. K. C. Lee, G. Miller and F. S. Rowland, *J. Amer. Chem. Soc.*, **87**, 190 (1965).

14) R. Wolfgang, *Progr. Reaction Kinetics*, **3**, 97 (1965).

15) J. W. Root and F. S. Rowland, *J. Chem. Phys.*, **46**, 4299 (1967).

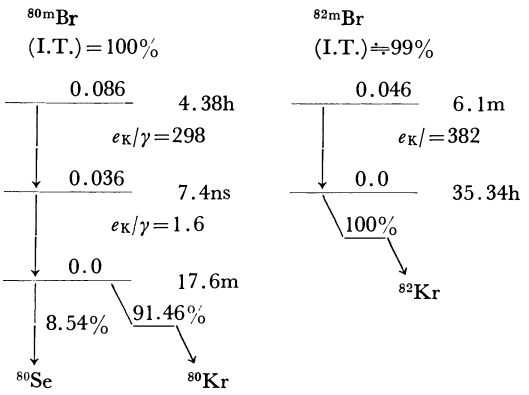

Fig. 1

state is attained in a single transition, the internal conversion ratio of which is 382. This means that 99.7% of the ^{82m}BrBr explodes,[16] to result in the highly-charged ^{82}Br atom with excess kinetic energy. On the other hand, ^{80m}Br is converted to the gronud state by two successive γ-transitions. The first transition (49 keV) is fully converted, while the second transition (37 keV) is partly converted (62%). The time required for the completion of the charging process initiated by nuclear internal conversion ranges from 10^{-15} to 10^{-16} sec.[17]

The charge and kinetic energy distributions on the excited ^{80}Br resulting from the molecular explosion of ^{80m}BrBr will be identical with those on ^{82}Br. However, the excited ^{80}Br has a successive transition to the ground state with a hilf-life of 7.4×10^{-9} sec. Thus, there are two possibilities, depending upon the length of the lifetime in the excited state relative compared to the time required for the atom to have a chemical reaction with the surrounding molecules: 1) the lifetime is too short for the atom to have a chemical reaction prior to the transition to the ground state or 2) the lifetime is long enough for the atom to react chemically with its environment during that period.

In Case 1, the following internal conversion leads to an additional build-up of the charge on the free atom, but it does not affect the kinetic energy of the atom. Most of the freshly built charges are also neutralized in the subsequent collisions with the environment.[5] The chemical consequences of the atom will, thus, be essentially the same as if the atom had not undergone the second internal conversion. As a result, if this is the case, it is probable that no isotope effect appears between ^{80}Br and ^{82}Br.

In Case 2, the kinetic energy achieved on the ^{80}Br atom in the chemical combination as a result of the γ-emission is of an order of a few-hundredths eV;[5,18] this energy is not sufficient to break any bond in the molecule, only to produce a little excitation of it. On the other hand, the ^{80}Br ion freed *via* the molecular explosion following the internal conversion has a kinetic energy which is very much dependent on the remainder of the molecule containing the Br atom.[16] If the excited ^{80}Br atom is in a chemical combination with surrounding atoms other than ^{80}BrBr*, then it is probable that the kinetic energy achieved on the ^{80}Br in the molecular explosion is different from that on the ^{82}Br freed from ^{82m}BrBr and that an isotope effect between them might appear on the energetic reaction, whereas the thermal ionic yields are more or less the same in both systems as long as the reaction occurs with the thremal Br^{+1} atom.

Most of the physicochemical stage, such as the energy-transfer, dissociation and ion-molecule reactions, terminated before 10^{-9} to 10^{-10} sec.[19] This also suggests that at least a part of the ^{80}Br in the excited state reacts chemically with the surrounding molecules. Thus, alternatively, the present results might be understood to indicate that the time scale of the reaction of the recoil Br atom is less than the order of 10^{-8} sec, the life-time of the excited ^{80}Br atom.

It is tempting to ascribe the yield of $CH_3{}^{80}Br$, which is lower than that of $CH_3{}^{82}Br$, to these differences in kinetic energy. Gordus and Willard[20] measured the total organic yields from the reaction of ^{80}Br in different parent compounds with CH_4. They showed that the yield increases with an increase in the mass of the residue to which ^{80m}Br is orginaly attached, that is, in the following order: $HBr < CH_3Br < C_2H_5Br < Br_2 < CCl_3Br < CHBr_3$. Qualitatively, this is in the same order as the increasing kinetic energy achieved on ^{80}Br in the molecular explosion.

Generally the reaction schemes[21,22] of the recoil halogen atom are very similar to those of the recoil tritium atom as far as the energetic reactions are concerned. One of the most important reactions of the recoil tritium is well known to be a hydrogen abstraction reaction to form HT.[23] As the present results show, the total organic yield in the reaction

16) T. A. Carlson and R. M. White, "Chemical Effects of Nuclear Transformation," Vol. I, IAEA, Vienna (1965), p. 23.
17) S. Wexler, *ibid.*, Vol. I (1961), p. 115.
18) C. Hsiung and A. A. Gordus, *ibid.*, Vol. II (1965), p. 461.
19) J. W. T. Spinks and R. J. Woods, "An Introduction to Radiation Chemistry," John Willey & Sons, Inc., New York (1964), p. 252.
20) A. A. Gordus and J. E. Willard, *J. Amer. Chem. Soc.*, **79**, 4609 (1957).
21) C. M. Wai and F. S. Rowland, *ibid.*, **90**, 3638 (1968).
22) Yi-N. Tang, T. Smail and F. S. Rowland, *ibid.*, **91**, 2130 (1969).
23) E. Tachikawa and F. S. Rowland, *ibid.*, **90**, 4767 (1968).

of the Br atom with CH_4 is less than 10%. It can reasonably assumed that the hydrogen abstraction reaction of the excited ^{80}Br freed from the molecular explosion of the $^{80m}BrBr$ is very popular. The kinetic energy achieved on the Br atom as a result of the explosion of the $H^{80}Br^*$ will be in the range of a few electron volts, which will already be in the range for the energetic reaction. On the other hand, the initial kinetic energy of the Br atom, resulting from the explosion of Br_2, as in the ^{82m}Br-CH_4 system, could be of the order of 100 eV. The atom having such a high kinetic energy shows a complete spectrum over the entire range of the energetic reaction. This implies that the average number of possible collisions of atom in the reaction range is smaller for the ^{80}Br atom than for the ^{82}Br atom; that is, the flux of the ^{80}Br atom in the energetic reaction range is greately reduced compared to that of the ^{82}Br atom.

The author is very grateful to Mr. T. Ohkubo for his assistance throughout this work. He is also indebted to Drs. K. Motojima and M. Koike for their encouragement during the Course of the work.

BULLETIN OF THE CHEMICAL SOCIETY OF JAPAN VOL. 43 67—74 (1970)

The Photochemical Rearrangements of *N*-Acetyl Diphenylamine and *N*-Acetyl Carbazole

Haruo SHIZUKA, Motonobu KATO, Toshio OCHIAI, Kohji MATSUI and Toshifumi MORITA

Department of Chemistry, Gunma University, Tenjin-cho, Kiryu

(Received June 30, 1969)

The photochemical reactions of *N*-acetyl diphenylamine and *N*-acetyl carbazole in solution have been studied. *N*-Acetyl diphenylamine and *N*-acetyl carbazole undergo the photo-Fries-rearrangement by means of 2537Å irradiation. The reaction products consist of the *ortho*- and *para*-isomers, plus corresponding amines transformed through the deacetylation of the original compounds. The quantum yields in the early stages of the rearrangement were measured under various conditions by spectrophotometry. The reaction mechanism has been discussed on the basis of the relation between the rate constants of the rearrangement and the odd π electron densities obtained from simple Hückel MO calculations.

Recently, the photo-Fries-rearrangements have been extensively stidied.[1-18] There are two mechanisms which have been proposed for the photo-Fries-rearrangement. One is a molecular pathway, involving a bridged intermediate proposed by

1) J. C. Anderson and C. B. Reese, *Proc. Chem. Soc.*, **1960**, 217.
2) J. C. Anderson and C. B. Reese, *J. Chem. Soc.*, **1963**, 1781.
3) H. Kobsa, *J. Org. Chem.* ,**27**, 2293 (1962).
4) D. Elad, *Tetrahedron Lett.*, **1963**, 873.
5) D. Elad, D. V. Rao and V. I. Stenberg, *J. Org. Chem.*, **30**, 3252 (1965).
6) W. M. Horspool and P. L. Parson, *J. Chem. Soc.*, **1965**, 5162.
7) R. A. Finnegan and A. W. Hagen, *Tetrahedron Lett.*, **1963**, 365.
8) R. A. Finnegan and J. J. Matice, *Tetrahedron*, **21**, 1015 (1965).
9) R. A. Finnegan and D. Knutson, *J. Amer. Chem. Soc.*, **89**, 1970 (1967).
10) D. Bellus, P. Hrdlovic and Z. Manasek, *J. Polym. Sci., Part B*, **4**, 1 (1966).
11) D. Bellus and P. Hrdlovic, *Chem. Rev.*, **67**, 599 (1967).
12) G. M. Coppinger and E. R. Bell, *J. Phys. Chem.*, **70**, 3479 (1966).
13) H. Shizuka and I. Tanaka, This Bulletin, **41**, 2343 (1968).
14) H. Shizuka, *ibid.*, **42**, 52 (1969).
15) H. Shizuka, *ibid.*, **42**, 57 (1969).
16) H. Shizuka and I. Tanaka, *ibid.*, **42**, 909 (1969).
17) H. Shizuka, T. Morita, Y. Mori and I. Tanaka, *ibid.*, **42**, 1831 (1969).
18) M. R. Sandner, E. Hedaya and D. J. Trecker, *J. Amer. Chem. Soc.*, **90**, 7249 (1968).

Anderson and Reese[2] or a concerted, symmetry-allowed process proposed by Sander *et al.*[18] The other is a radical mechanism, as has been proposed by Kobsa,[3] by Finnegan *et al.*,[7-9] and by Shizuka *et al.*[13-17]

In the study of the photochemical reactions of acetanilide and phenyl acetate, it has been shown that, in the liquid phase, the photo-Fries-rearrangement occurs *via* the predissociation by the intersystem crossing $^3\sigma_0(\text{N–C}) \leftarrow S_1(\pi\pi^*)$, forming pair radicals which recombine efficiently in a solvent cage into the original substance, *o*- and *p*-isomers.[13-15,17]

The photochemical reactions of acetanilide have been exmained in the vapor phase at 120°C and in a rigid matrix at −196°C, but no photochemical rearrangement was observed in either case.[16] Bellus *et al.* have reported that the radiolysis of phenyl esters in solution yielded the same products as those of the photo-Fries-rearrangement and involved the radical mechanism due to homolytic fission.[19]

On the other hand, the photocyclization of diphenylamine to carbazole has been reported.[20-24] Therefore, the photochemical reaction of *N*-Acetyl diphenylamine may be expected to be either a photo-Fries-rearrangement or a photocyclization.

In the case of *N*-Acetyl carbazole, it has also been predicted that its photochemical reaction may occur through the photo-Fires-rearrangement or though a photochemical isomerization such as *N*-acetyl pyrrole,[25] since *N*-acetyl carbazole has a *N*-$COCH_3$ group like acetanilide and since the nitrogen atom is present in such a five-membered ring as that of *N*-acetyl pyrrole. It has been shown that *N*-acetyl pyrrole upon 2537 Å irradiation in both the liquid and vapor phases, converts to an intermediate *via* the lowest excited singlet state and is subsequently changed to 2-acetyl pyrrole or to the ground state of the original substance; its isomerization mechanism involves a molecular pathway.[25] For these reasons, it seemed that it would be interesting to ivestigate the photochemical reactions of *N*-acetyl diphenylamine and *N*-acetyl carbazole. This paper will report on the photochemical reactions of these compounds at 2537 Å in the liquid phase, and will also include a discussion of the photo-Fries-rearrangement.

Experimental

The experimental procedure and solvents were almost the same as those previously described.[13-17] *N*-Acetyl diphenylamine and *N*-acetyl carbazole were prepared by treating the corresponding amines with acetic anhydride and were purified by repeated recrystallizations from ligroin.

A low-pressure mercury lamp with a Vycor glass filter was used as the 2537 Å radiation source, while a mercury xenon lamp with a diffraction grating was used as the 2800 Å range radiation source. Actinometry was carried out in a reaction cell (quartz) using a ferric oxalate actinometer solution.[26] The light intensity at 2537 Å and at 2800 Å were 4.9×10^{14} photon·sec^{-1}·ml^{-1} and 2.4×10^{14} photon·sec^{-1}·ml^{-1} respectively.

The mixture of the photo-products after a long irradiation at 2537 Å was condensed by an evaporator, separated by column chromatography (silica gel), and purified by repeated recrystallizations from ligroin. The components of the photoproducts were determined by thin-layer chromatography. The reaction products were identified by means of UV, IR, mp, and elementary analysis. The quantum yields in the early stages of the photochemical reaction were determined spectrophotometrically.

Results and Discussion

Reaction Products. *a) N-Acetyl Diphenylamine (N-Ace DA).* Figure 1-1 shows the sepctral change of the cyclohexane solution of *N*-Ace DA. The absorption band (246 mμ) of *N*-Ace DA decreased, and new bands with maxima at 227, 288, 320, and 381 mμ appeared as the irradiation time increased; the spectrum had two isosbestic points, at 238 and at 265 mμ.

The reaction products were separated from *N*-Ace DA by column chromatography and were crystallized after a long irradiation at 2537 Å on a highly-concentrated solution of *N*-Ace DA. It was comfirmed by thin-layer chromatography that the photoproducts comprised three compounds; 2-acetyl diphenylamine (2-Ace DA), 4-acetyl diphenylamine (4-Ace DA), and diphenylamine (DA). They were identified by means of UV, IR, mp, and elementary analysis in comparison with authentic samples. Neither *N*-acetyl carbazole (*N*-Ace CA) not any carbazole derivative was obtained from the irradiated solution. Therefore, it can be said that a photocyclization of *N*-Ace DA such as that of DA did not occur, but that the photo-Fries-rearrangement did occur. Figure 1-2 shows the absorption spectra of 2-Ace DA, 4-Ace DA,

19) D. Bellus, K. Schaffner, and J. Hoigne, *Helv. Chim. Acta*, **51**, 1980 (1968).
20) C. A. Parker and W. J. Barnes, *Analyst*, **82**, 606 (1957).
21) E. J. Bowen and J. H. Eland, *Proc. Chem. Soc.*, **1963**, 202.
22) K. H. Grellmann, G. H. Shermann, and H. Linschitz, *J. Amer. Chem. Soc.*, **85**, 1881 (1963).
23) H. Linschitz and K. H. Grellmann, *ibid.*, **86**, 303 (1964).
24) H. Stegemeyer, *Naturwissenschaften*, **53**, 582 (1966).
25) H. Shizuka, E. Okutsu, Y. Mori and I. Tanaka, *Molecular Photochem.*, **1**, 135 (1969).
26) C. A. Parker, *Proc. Roy. Soc.* (London), **220A**, 104 (1953).

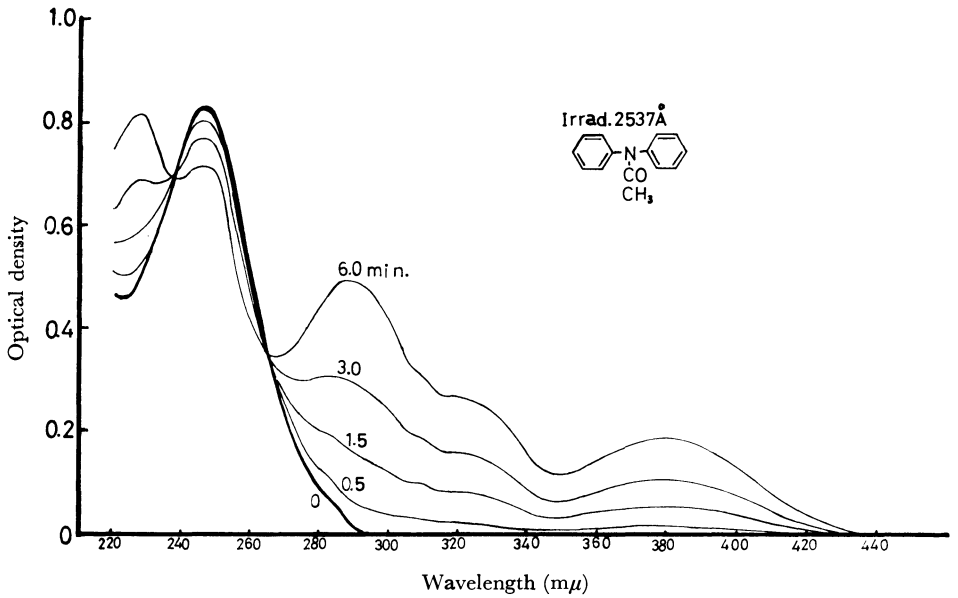

Fig. 1-1. Spectral change of cyclohexane solution of *N*-Ace DA with lapse of irradiation time at 2537 Å. Numbers refer to time in minutes.

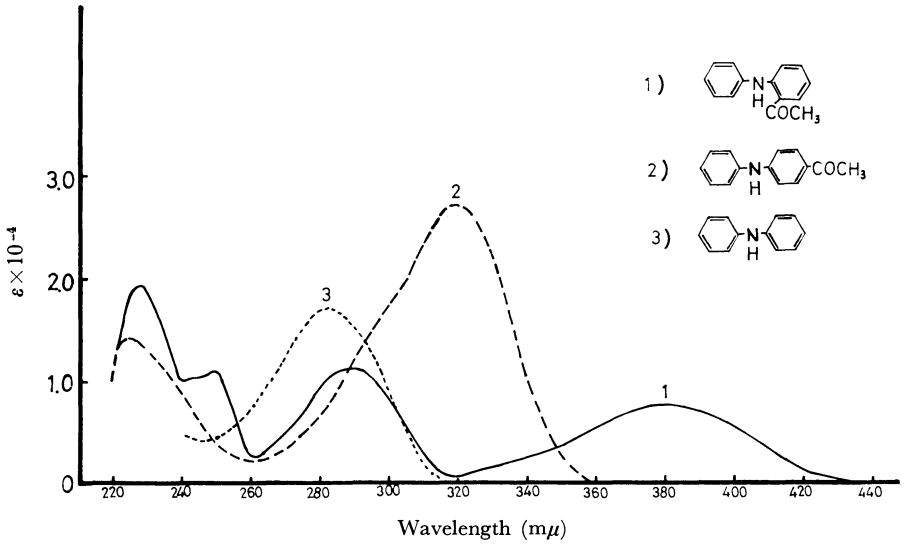

Fig. 1-2. Absorption spectra of the photo-products from *N*-Ace DA: 1) 2-Ace DA, 2) 4-Ace DA, and 3) DA.

and DA respectively in a cyclohexane solution.

b) N-Acetyl Carbazole (N-Ace CA). The spectrum of the cyclohexane solution of *N*-Ace CA changed by 2537 Å irradiation is shown in Fig. 2-1.

The reaction products of *N*-Ace CA at 2537 Å were identified by the same procedure as was used for *N*-Ace DA. The photochemical reaction of *N*-Ace CA yielded 1-acetyl carbazole (1-Ace CA), 3-acetyl carbazole (3-Ace CA), and carbazole (CA). Figure 2-2 shows the absorption spectra of these products. In view of the above facts, the photochemical rearrangement of *N*-Ace CA seems to be a photo-Fries-reaction and not to be analogous to the photochemical isomerization of *N*-acetyl pyrrole, which gives only the product (2-acetyl pyrrole).[25]

The quantum yields for the formation of these photoproducts were measured spectrophotometrically. The molar extinction coefficients of the original compounds and the photoproducts are summarized in Table 1.

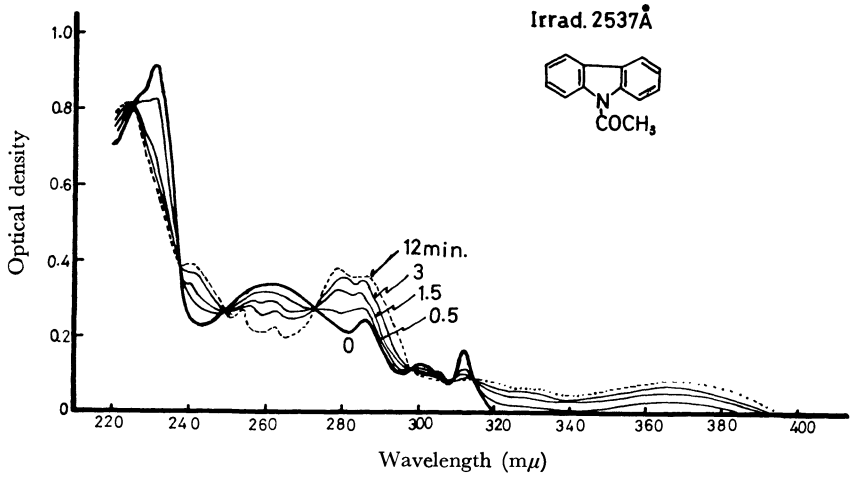

Fig. 2-1. Spectral change of cyclohexane solution of *N*-Ace DA at 2537 Å.

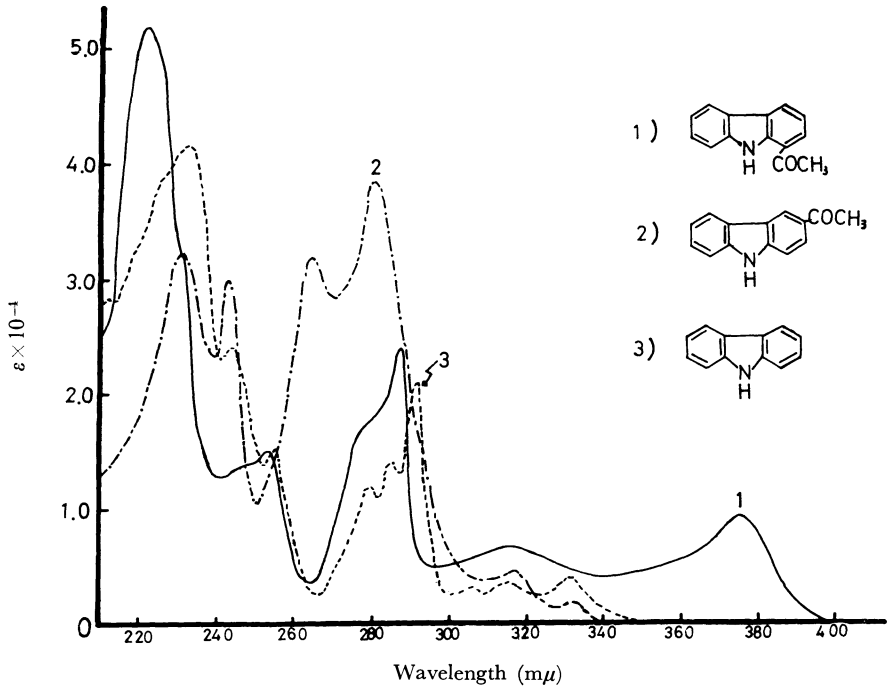

Fig. 2-2. Absorption spectra of the photo-products from *N*-Ace CA: 1) 1-Ace CA, 2) 3-Ace CA, and 3) CA.

Effect of Irradiation Time, Concentration, and Triplet Quencher on Quantum Yields. The quantum yields were measured under various condition; the results are shown in Fig. 3 and in Table 2.

The quantum yield for 2-Ace DA formation from *N*-Ace DA at 2537 Å did not change with the variation in the *N*-Ace DA concentration ($<\sim 10^{-3}$ mol/*l*), as is shown in Fig. 3. The photo-Fries-rearrangement of *N*-Ace DA is an intramolecular reaction, as has been proposed by several workers.[1,2,13,15,17] The addition of piperylene as a triplet quencher (E_T=2.48 eV)[13,17,27-29] did not affect the quantum yield for this isomerization in the concentration range from 10^{-4} to 5×10^{-2} mol/*l*, as is shown in Fig. 3(c). Dissolved oxygen had scarcely any effect on the quantum yields. Similar results were obtained regarding the quantum yields

27) A. A. Lamola and G. S. Hammond, *J. Chem. Phys.*, **43**, 2129 (1965).
28) P. E. Eaton and W. S. Hurt, *J. Amer. Chem. Soc.*, **88**, 5038 (1966).
29) E. Y. Y. Lam, D. Valentine and G. S. Hammond, *ibid.*, **89**, 3482 (1967).

Table 1. Molar extinction coefficients

Substance	Solvent	λ (mμ)	ε ($\times 10^{-4}$)
N-Ace DA	CH	246	1.18
	EtOH	237	1.05
2-Ace DA	CH	288	1.13
		381	0.78
	EtOH	287	1.06
		383	0.75
4-Ace DA	CH	320	2.71
	EtOH	342	2.87
DA	CH	282	1.74
	EtOH	285	2.03
N-Ace CA	CH	263	1.62
		313	0.88
	EtOH	262	1.69
		312	0.66
1-Ace CA	CH	287	2.39
		374	0.94
	EtOH	287	1.91
		372	0.84
3-Ace CA	CH	280	3.87
		332	0.19
	EtOH	286	2.98
		350	0.22
CA	CH	291	2.17
		331	0.42
	EtOH	293	1.61
		336	0.32

CH: cyclohexane EtOH: ethanol

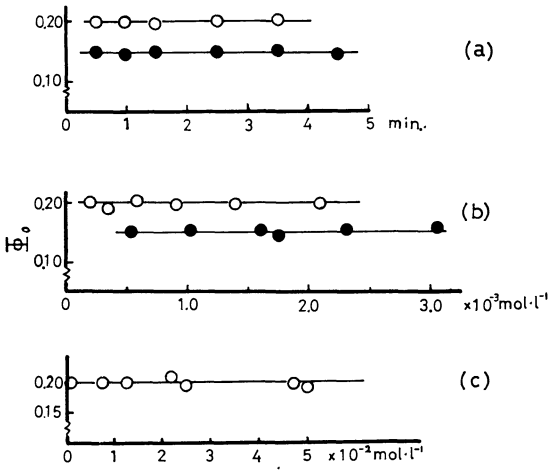

Fig. 3. Dependence of the quantum yield for the formation of 2-Ace DA at 2537 A.
(a) on irradiation time.
(b) on the concentration of *N*-Ace DA.
(c) on the concentration of piperylene as a triplet quencher.
○: in cyclohexane
●: in ethanol

Table 2. Quantum yields for the product formations of *N*-Ace DA at 2537 Å and 20°C

Substance	Solvent	Φ_O	Φ_P	Φ_{NH}	Φ_Σ
N-Ace DA	CH	0.20	0.096	0.048	0.344
	EtOH	0.15	0.064	0.045	0.259
N-Ace CA	CH	0.10	0.09	0.06	0.25
	EtOH	0.07	0.05	0.05	0.17

Φ_O, Φ_P, and Φ_{NH} are the quantum yields for the formations of 2-Ace DA, 4-Ace DA, and DA, and those for the formations of 7-Ace CA, 3-Ace CA, and CA, respectively.

$$\Phi_\Sigma = \Phi_O + \Phi_P + \Phi_{NH}$$

for the product formations from *N*-Ace CA at 2537 Å. The quantum yields decreased in a polar solvent, as is shown in Table 2. However, the variation in the rearrangement quantum yields with the solvent was smaller than that of acetanilide.[14] The dependences of the quantum yields of *N*-Ace DA and *N*-Ace CA on the solvent resemble those of phenyl acetate and *p*-substituted phenyl acetates.[17] As was described in a previous paper,[17] they may be due to the fact that *N*-Ace DA and *N*-Ace CA have no hydrogen atom to form hydrogen bonds with a proton acceptor. In the photo-Fries-rearrangement of acetanilide, a hydrogen-bond formation between the lowest excited singlet state in acetanilide and ethanol causes the decrease in the rearrangement quantum yields of acetanilide.[14] Sandner *et al.* have reported that the quantum yield of the photo-Fries product from any given ester did not vary with the solvent.[18] Their finding differs from ours. These differences might be caused by the experimental conditions; Sandner *et al.* performed the photochemical rearrangement of *p*-tolyl acetate in a very high concentration (0.556 mol/*l*) and with a very long irradiation (28—136 hr).

The primary process of the photo-Fries-rearrangement occurs from the lowest excited singlet state, as has been shown by Shizuka and Tanaka.[13] In the cases of *N*-Ace DA and *N*-Ace CA, their primary processes are the same as those described before, because these is no dependence of the rearrangement quantum yields on piperylene and dissolved oxygen, which are triplet quenchers, and no effect of the excitation wavelengths from 2537 to 2800 Å on the quantum yields.

The photo-Fries-rearrangements of *N*-Ace DA and *N*-Ace CA are similar to those of acetanilide[13-15] and phenyl acetate.[17] It may be assumed that their reaction mechanism involves the predissociation forming pair radicals and a subsequent recombination reaction between the pair radicals in a solvent cage.

Relations between the Rearrangement Quantum Yields and the Odd π Electron Densities. The recombination reaction between the pair

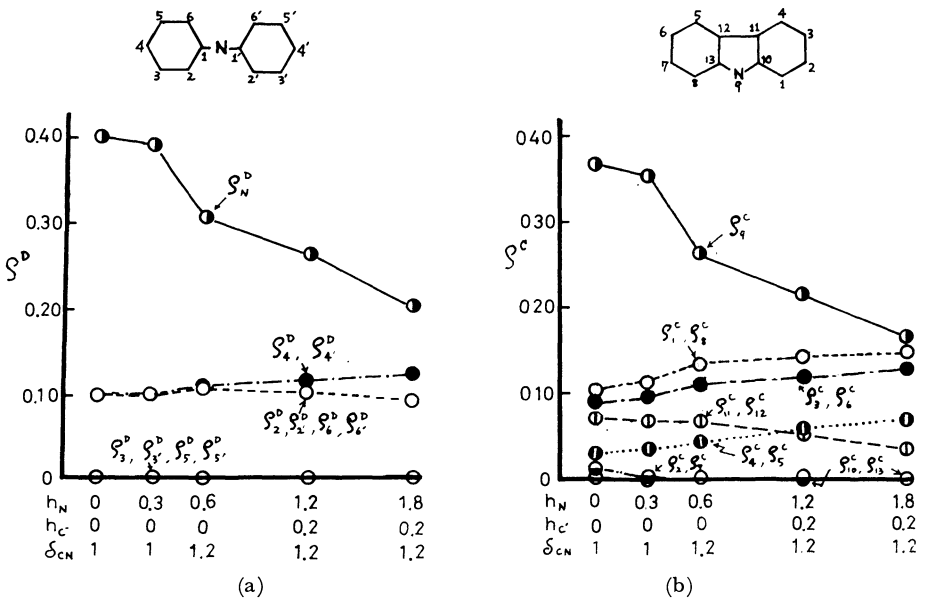

Fig. 4. Odd π electron densities of diphenyl amino (a) and carbazolyl (b) radicals as functions of h_N, $h_{C'}$, and δ_{CN}.
See the foot note.*2

radicals consists of a back reaction and of *o*- and *p*-rearrangements in a solvent cage. It has been shown that the rates of this recombination reaction in a solvent cage are proportional to the odd π electron densities of the anilino or phenoxy radical.[15,17]

The approximate odd π electron densities (ρ) of diphenyl amino and carbazolyl radicals were obtained from a simple Hückel MO calculation using the various values of Coulomb integrals (α) and resonance integrals (β). Figure 4 (a) and (b) show the odd π electron densities*1 of the diphenyl amino and carbazolyl radicals respectively.

The h_N parameter, which is equal to 0.6, is an appropriate value in the valency state of a nitrogen atom such as that of the pyridine molecule.[30-32] It is assumed that the valency state of the nitrogen atom in the case of the diphenyl amino or carbazolyl radical is nearly the same as that of pyridine, since the odd π electron on the nitrogen atom is considered to migrate to the benzene ring of their radicals. Therefore, we took the h_N value (0.6) in the present estimation. The relation between the quantum yields (Φ) and the odd π electron densities (ρ) is as follows:

N-Ace DA:

$$k_O^D : k_P^D = \frac{1}{4}\Phi_2^D : \frac{1}{2}\Phi_4^D \quad (1)$$

$$= 1 : 0.96$$

$$\rho_2^D : \rho_4^D = 0.11037 : 0.11438 \quad (2)$$

$$= 1 : 1.04$$

$$k_O^D : k_P^D \approx \rho_2^D : \rho_4^D \quad (3)$$

N-Ace CA:

$$k_O^C : k_P^D = \frac{1}{2}\Phi_1^C : \frac{1}{2}\Phi_3^C \quad (4)$$

$$= 1 : 0.9$$

$$\rho_1^C : \rho_3^C = 0.13498 : 0.11243 \quad (5)$$

$$= 1 : 0.83$$

$$k_O^D : k_P^C \approx \rho_1^C : \rho_3^C \quad (6)$$

where k_O and k_P are the rate constants of the *ortho*- and *para*-rearrangements respectively.

The rate constants (k) of the *o*- and *p*-rearrangements were proportional to the odd π electron densities on the radicals, as are shown in Eqs. (3) and (6). These results lend some support to the radical mechanism for the secondary processes in the photo-Fries-rearrangement as has been tentatively suggested by Kobsa[3] and has been shown by Shizuka *et al.*[15,17] On the other hand, Sandner

*1 The odd π electron densities were obtained from the square of the coefficient of the atomic orbital in the highest-occupied molecular orbital, ϕ_7.

*2 $\alpha_N = \alpha_C + h_N\beta_{CC}$, $\alpha_{C'} = \alpha_C + h_{C'}\beta_C$, $\beta_{CCN} = \delta_{CN}\beta_{CC}$
where α_C: Carbon atom Coulomb integral, α_N: Nitrogen atom Coulomb integral. $\alpha_{C'}$: Coulomb integral of the carbon atom next to the nitrogen atom, β_{CC}: carbon-carbon resonance integral, β_{CN}: carbon-nitrogen resonance integral, h_N, $h_{C'}$, and, δ_{CN}: parameters of α_N, $\alpha_{C'}$, and, β_{CN} respectively.

30) C. A. Coulson and J. Jacobs, *J. Chem. Soc.*, **1949**, 1983.
31) S. F. Mason, *ibid.*, **1958**, 674.
32) R. D. Brown, *ibid.*, **1959**, 3451.

et al. have proposed that the photo-Fries-rearrangement originates from an upper singlet state and proceeds to the products by a molecular pathway that is independent of its reaction environment.[18] Considering Sandner *et al.*'s formulation, which involves a concerted, symmetry-allowed process, it may be predicted that the quantum yield for the product formations in the photo-Fries-rearrangement is medium-independent and the *ortho*/*para* ratio is wavelength-dependent. However, the quantum yields for the product formations in the early stages of the photochemical reaction are medium-dependent[14,17] and are also dependent on the reaction phase.[16],*3

If the photo-Fries-rearrangement had occurred through a molecular pathway, the rearrangement products would be obtained in the vapor phase, since the photoisomerization of benzene[33-38] or *N*-acetyl pyrrole,[25] which involves a molecular pathway, yields the corresponding isomers even in the vapor phase. On the basis of the study of the benzene photosensitization of acetanilide,[13] the solvent effect on the rearrangement quantum yields,[14] and the effect of the excitation wavelength on the yields,[14] it is not reasonable that the photo-Fries-rearrangement originated from the upper excited singlet state, as has been proposed by Sandner *et al.*[18] The results obtained in the present work are consistent with the mechanism of the photo-Fries-rearrangement proposed by Shizuka *et al.*[13-17]

The estimations of the dissociation and the back reaction quantum yields of *N*-Ace DA and *N*-Ace CA were carried out as is described below. It is reasonable to consider that the rate constant of the back reaction, k_B, is also proportional to the odd π electron density at the position of the nitrogen atom, because the recombination rate constants, k_O, k_P, and k_B, are parallel to the odd π electron densities, ρ_O, ρ_P, and ρ_N respectively.[15,17]

N-Ace DA:

$$\frac{k_B^D}{k_0^D} = \frac{\Phi_B^D}{(1/4)\Phi_0^D} = \frac{\rho_N^D}{\rho_2^D} = \frac{0.30747}{0.11035} \approx 2.8 \qquad (7)$$

$$\Phi_B^D \approx 0.14$$

N-Ace CA:

$$\frac{k_B^C}{k_0^C} = \frac{\Phi_B^C}{(1/2)\Phi_0^C} = \frac{\rho_N^C}{\rho_1^C} = \frac{0.26368}{0.13498} \approx 2.0 \qquad (8)$$

$$\Phi_B^C \approx 0.10$$

The dissociation quantum yields (Φ_{dis}) are given by:

$$\Phi_{dis}^D = \Phi_\Sigma^D + \Phi_B^D \approx 0.48 \qquad (9)$$

$$\Phi_{dis}^C = \Phi_\Sigma^C + \Phi_B^C \approx 0.35 \qquad (10)$$

The recombination ratios (γ) between the pair radicals are quite high, just as in the cases of acetanilide[15] and phenyl acetate.[17]

$$\left.\begin{aligned} \gamma^D &= \frac{\Phi_O^D + \Phi_P^D + \Phi_B^D}{\Phi_{dis}^D} = 0.91 \\ \gamma^C &= \frac{\Phi_O^C + \Phi_P^C + \Phi_B^C}{\Phi_{dis}^C} = 0.81 \end{aligned}\right\} \qquad (11)$$

These results indicate that the recombination reaction between the pair radicals occurs efficiently in a solvent cage. From these results, it can be said that the photochemical rearrangement of *N*-Ace DA and *N*-Ace CA can be explained by a mechanism similar to those of acetanilide and phenyl acetate described in previous papers.[13-17]

In general, the quantum yields for the product formations in the photo-Fries-rearrangement are parallel to the odd π electron densities described above. There are some exceptions in the case of *N*-Ace CA. The values of ρ^C_{11}, ρ^C_{12}, ρ^C_4, and ρ^C_5 on the carbazolyl radical (see Fig. 4(b)) are not very small. However, no shift of the acetyl group to their positions by UV light could be observed. The non-occurrence of the shift to the positions 11 and 12 may be understood from the fact that their positions are blocked by phenyl groups. It is well known that the photo-Fries-rearrangements of *p*-substituted phenyl acetate[3,17] and *p*-substituted acetanilide[15] do not take place at the *p*-positions on their molecules, but at the *o*-positions. For both the 4 and 5 positions, it may be assumed that a transient complex formed in the recombination reaction between pair radicals has an unstable structure because of the lack of resonance energy compared with that of the *o*- or *p*-position. Finally, the reaction schemes of *N*-Ace DA and *N*-Ace CA at 2537 Å in the liquid phase are as follows:

$$S_0 + h\nu \longrightarrow S_1(\pi\pi^*) \qquad (12)$$

$$S_1(\pi\pi^*) \xrightarrow{k_s} S_0 \qquad (13)$$

$$S_1(\pi\pi^*) \xrightarrow{k_f} S_0 + h\nu' \qquad (14)$$

$$S_1(\pi\pi^*) \xrightarrow{k_c} T_1(\pi\pi^*) \qquad (15)$$

$$S_1(\pi\pi^*) \xrightarrow{k_{dis}} \text{ 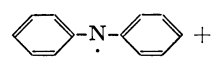 } + \cdot CCH_3 \quad (\text{or}) \qquad (16)$$

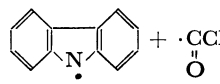

*3 We examined the photochemical reaction of phenyl acetate in the gas phase at 2537 Å and at room temperature. The rearrangement products were not observed.

33) K. Shindo and S. Lipsky, *J. Chem. Phys.*, **45**, 2292 (1966).
34) F. Mellows and S. Lipsky, *J. Phys. Chem.*, **70**, 4076 (1966).
35) H. R. Ward, J. S. Wishnok and P. D. Sherman, Jr., *J. Amer. Chem. Soc.*, **89**, 162 (1967).
36) L. Kaplan and K. F. Wilzback, *ibid.*, **89**, 1030 (1967).
37) K. E. Wilzback, A. L. Harkness and L. Kaplan, *ibid.*, **90**, 1116 (1968).
38) See the review on *Photochemical Reactions of Benzene and its Derivative.* which was described in *Denkikagaku*, **36**, 628 (1968) by I. Tanaka and H. Shizuka.

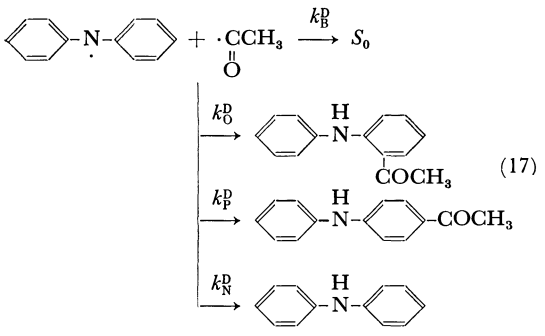

(17)

or

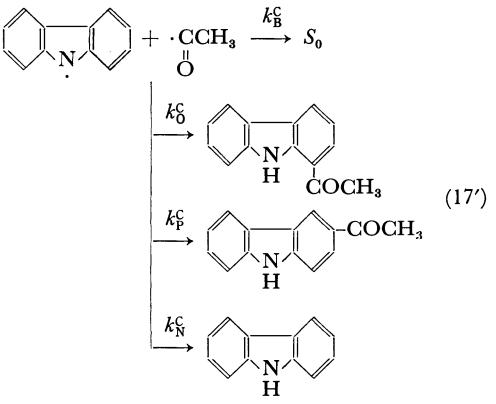

(17′)

BULLETIN OF THE CHEMICAL SOCIETY OF JAPAN VOL. 43 74—80 (1970)

Calculation of the Hyperfine Coupling Constants of Some σ Electron Radicals

Teijiro YONEZAWA, Takashi KAWAMURA and Hiroshi KATO

Department of Hydrocarbon Chemistry, Faculty of Engineering, Kyoto University, Yoshida, Sakyo-ku, Kyoto

(Received August 4, 1969)

The isotropic hyperfine coupling constants of cyclopropyl, vinyl, formaldiminoxy, formyl, and hydrogen cyanide anion radicals are calculated by a method which corresponds to the extension of the McLachlan procedure. These hyperfine coupling constants are then studied, and the contributions from the spin delocalization and spin polarization mechanisms are estimated. The role of one-center exchange integrals in the estimation of these hyperfine coupling constants is also studied; it is shown to be important in the claculation of the hyperfine coupling constants of the nuclei of the radical-center atom and of the atoms bonded to it.

Recently the hyperfine coupling constants of σ-electron radicals have attracted much theoretical interest; many authors have calculated them with the hyperconjugation method,[1] with the extended Hückel method,[2,3] and with the semiempirical or *ab initio* unrestricted SCF methods.[4-7]

In this work, we will calculate the isotropic hyperfine coupling constants of some σ-electron radicals containing hydrogen, carbon, nitrogen, or oxygen atoms by a method[8] which is an extension of the McLachlan procedure.[9] The results of the present calculations will then be compared with the results obtained by other methods, and the effects of the spin polarization will be shown to be important even in the case of σ-electron radicals.

Method and Parameters

The differences between Fock's operators for α and β spin electrons in the unrestricted SCF method can be treated as a perturbation. Taking the first-order approximation with respect to exchange

1) W. T. Dixon, *Mol. Phys.*, **9**, 201 (1965).
2) G. A. Petersson and A. D. McLachlan, *J. Chem. Phys.*, **45**, 628 (1966).
3) a) R. S. Drago and H. Petersen, Jr., *J. Amer. Chem. Soc.*, **89**, 3978 (1967); b) R. S. Drato and H. Petersen, Jr., *ibid.*, **89**, 5774 (1967); c) R. E. Cramer and R. S. Drago, *ibid.*, **90**, 4790 (1968).
4) T. Yonezawa, H. Nakatsuji, T. Kawamura and K. Kato, This Bulletin, **40**, 2211 (1967).
5) N. M. Atherton and A. Hinchliffe, *Mol. Phys.*, **12**, 349 (1967).
6) J. A. Pople, D. L. Beveridge and P. A. Dobosh, *J. Amer. Chem. Soc.*, **90**, 4201 (1968).
7) A. Hinchliffe and D. B. Cook, *Chem. Phys. Lett.*, **1**, 217 (1967).
8) T. Yonezawa, T. Kawamura and H. Kato, *J. Chem. Phys.*, **50**, 3482 (1969).
9) A. D. McLchlan, *Mol. Phys.*, **3**, 233 (1960).

interaction, the elements of the spin-density matrix can be written as:[8]

$$\rho_{vw} = p^0_{vw} - \frac{1}{4}\sum_r\sum_s(\pi^{\alpha}_{vw,rs}+\pi^{\beta}_{vw,rs})\sum_t\sum_u p^0_{tu}(rt|us), \quad (1)$$

where the electron repulsion integral is denoted as:

$$(rt|us) = \iint \chi_r(1)\chi_t(1)(e^2/r_{12})\chi_u(2)\chi_s(2)\,dv_1dv_2$$

and where $\pi^{\alpha}_{vw,rs}$ and $\pi^{\beta}_{vw,rs}$ are mutual polarizabilities defined as:

$$\pi^{\alpha}_{vw,rs} = 2\sum_{j<0}\sum_{i\geqq 0}(C_{iv}C_{jw}+C_{jv}C_{iw})C_{ir}C_{js}/(\varepsilon_i-\varepsilon_j)$$

$$\pi^{\beta}_{vw,rs} = 2\sum_{j\leqq 0}\sum_{i>0}(C_{iv}C_{jw}+C_{jv}C_{iw})C_{ir}C_{js}/(\varepsilon_i-\varepsilon_j). \quad (2)$$

The molecular orbitals (MO), obtained by an extended Hückel MO method, are denoted by i and j; a positive number represents a doubly-occupied MO, zero is for the singly occupied MO, and vacant MO's are expressed by negative numbers. The coefficient of the rth atomic orbital (AO), χ_r, in the ith MO and its orbital energy are denoted as C_{ir} and ε_i respectively, while p^0_{tu} represents the "odd-electron" density matrix element, $C_{0t}C_{0u}$.

When multicenter integrals for the Dirac delta function are neglected, the isotropic hyperfine coupling constant of the nucleus Y, a^Y, becomes:

$$a^Y = \frac{8\pi}{3}g_Y\beta_N\sum_v^{\text{on}}\sum_w^{Y}\rho_{vw}\langle\chi_v|\delta(r_Y)|\chi_w\rangle \text{ gauss}, \quad (3)$$

where $\delta(r_Y)$ is the Dirac delta function and where g_Y and β_N have their usual meanings. As to the AO's χ_v and χ_w in Eq. (3), the valence-shell and inner-shell AO's are taken into consideration, while the effects of outer-shell AO's are neglected. Inner-shell electrons are assumed to be localized in one inner-shell AO in a zero-order approximation to exchange interaction.

Under these approximations, a^Y can be divided into three terms according to their mechanisms; the spin-delocalization term, a^Y_D: the spin-polarization term due to valence-shell electrons, a^Y_{PV}, and the spin-polarization term concerning inner-shell electrons, a^Y_{PI}, as:

$$a^Y = a^Y_D + a^Y_{PV} + a^Y_{PI}. \quad (4)$$

The contribution to a^Y from the term due to the spin-delocalization mechanism, a^Y_D, can be given from Eq. (3) and the first term of Eq. (1) as:

$$a^Y_D = A^Y_V P^0_{vv} \quad (5)$$

$$A^Y_V = \frac{8}{3}\pi g_Y\beta_N\langle\chi_v|\delta(r_Y)|\chi_v\rangle, \quad (6)$$

where χ_v is the valence-shell s AO of the atom Y. The values of A^Y_V adopted in this work for ^{1}H, ^{13}C, ^{14}N, and ^{17}O are listed in Table 1.

The valence-electron spin-polarization term, a^Y_{PV}, comes from the second term of Eq. (1) and is given by:

$$a^Y_{PV} = -\frac{1}{4}A^Y_V\sum_r\sum_s(\pi^{\alpha}_{vv,rs}+\pi^{\beta}_{vv,rs})\sum_t\sum_u p^0_{tu}(rt|us), \quad (7)$$

where the suffix v denotes the valence-shell s AO of the atom Y. In the estimation of the multicenter electron erpulsion integrals, the zero-differential-overlap approximation is adopted. One-center exchange integrals, which are expected to play an important role in the calculation of hyperfine coupling constants, are taken into account. The one-center Coulomb integral, $(rr|rr)$, is estimated by Pariser approxiamtion[10] by using the valence-state ionization potentials and electron affinities tabulated by Pritchard and Skinner.[11] The one-center exchange integrals are estimated from the table of Hinze and Jaffe.[12] To assure rotational invariance, the one-center Coulomb integral between p_π AO and p_σ AO is evaluated as:

$$(\sigma\sigma|\pi\pi) = (\sigma\sigma|\sigma\sigma) - 2(\sigma\pi|\pi\sigma).$$

The other Coulomb integrals are estimated by means of the Ohno approximation.[13]

The inner-shell-electron spin-polarzation term, a^Y_{PI},s come from the second term of Eq. (1):

$$a^Y_{PI} = -\frac{1}{4}A^Y_I\sum_r\sum_s(\pi^{\alpha}_{vw,rs}+\pi^{\beta}_{vw,rs}+\pi^{\alpha}_{wv,rs}+\pi^{\beta}_{wv,rs}) \times\sum_t\sum_u p^0_{tu}(rt|us), \quad (8)$$

Table 1. Values of A^Y_V, A^Y_I, and one-center electron repulsion integrals including inner-shell AO's

Nucleus Y	A^Y_V[a] (gauss)	A^Y_I[a] (gauss)	$(1s2p\|2p2s)$[a] (eV)	$(1s2s\|2s2s)$ (eV)	$(1s2s\|2p2p)$ (eV)
^{1}H	877	—	—	—	—
^{13}C	1210	−5340	0.6373	−0.3167	−0.1689
^{14}N	604	−2580	0.7924	−0.4095	−0.2195
^{17}O	−1810	7540	0.9481	−0.5036	−0.2708

a) Ref. 8.

10) R. Pariser, *J. Chem. Phys.*, **21**, 568 (1953).
11) H. O. Pritchard and H. A. Skinner, *Chem. Rev.*, **55**, 745 (1955).
12) J. Hinze and H. H. Jaffe, *J. Chem. Phys.*, **38**, 1834 (1963).
13) K. Ohno, *Theor. Chem. Acta*, **2**, 219 (1964).

where v and w denote the valence-shell $2s$ and the inner-shell $1s$ AO's respectively, and where A_I^Y is given by:

$$A_I^Y = \frac{8}{3}\pi g_Y \beta_N \langle \chi_v | \delta(r_Y) | \chi_w \rangle, \quad (9)$$

the values of which are listed in Table 1. The multicenter electron repulsion integrals in Eq. (8), including the inner-shell AO's, may be ignored because the differential overaps between the inner-shell AO and the AO's centered on the other atoms are negligible. The energy differences between the inner-shell orbitals and the valence-shell vacant MO's are approximated as the negative values of the inner-shell-electron X-ray term values listed by Slater.[14] Therefore, we obtain:

$$a_{PI}^Y = \frac{A_I^Y}{2E_w}\left(\sum_{f<0} + \sum_{f\leqq 0}\right)\left[\sum_{r}^{\text{VAO's on Y}} \sum_{t} \sum_{u} C_{fv} C_{fr} p_{tu}^0 (rt|uw)\right], \quad (10)$$

where E_w is the X-ray term value of the inner-shell $1s$ AO of the atom Y (χ_w), where r, t, and u denote valence-shell AO's on the atom Y, and where v represents the valence-shell $2s$ AO of the atom Y. For the computation of a one-center electron repulsion integral including both inner-shell $1s$ AO and valence-shell $2s$ AO, $1s$ and $2p$ Slater AO's[15] and the following orthogonalized $2s$ AO function are adopted:

$$\chi'_{2s} = (1-S^2)^{-1/2}(\chi_{2s} - S\chi_{1s}),$$

where S is the overlap integral between Slater AO's χ_{1s}-χ_{2s}. The estimated values of the integrals are listed in Table 1. The evaluated values of $(1s\ 2p|2p\ 2s)$ are reliable when compared with the other estimation,[8] but the estimation of the other electron-repulsion integrals concerning inner-shell $1s$ AO's seems to be less reliable.

The zero-order MO's are calculated with an exended Hückel MO method by solving a secular equation:

$$|H_{rs} - \delta_{rs}\varepsilon| = 0$$

where r and s cover all the valence-shell AO's of the radical. The diagonal element of the Hamiltonian, H_{rr}, is approximated as the negative value of Mulliken's orbital electronegativity, as tabulated by Pritchard and Skinner.[11] The off-diagonal elements of the Hamiltonian are estimated as:

$$H_{rs} = \begin{cases} (K/2)S_{rs}(H_{rr}+H_{ss}) & \text{(for nearest neighbors)} \\ 0 & \text{(for non-nearest neighbors)}, \end{cases} \quad (11)$$

where S_{rs} is the χ_r-χ_s overlap integral: the Wolfsberg-Helmholz[16] parameter, K, will be fixed

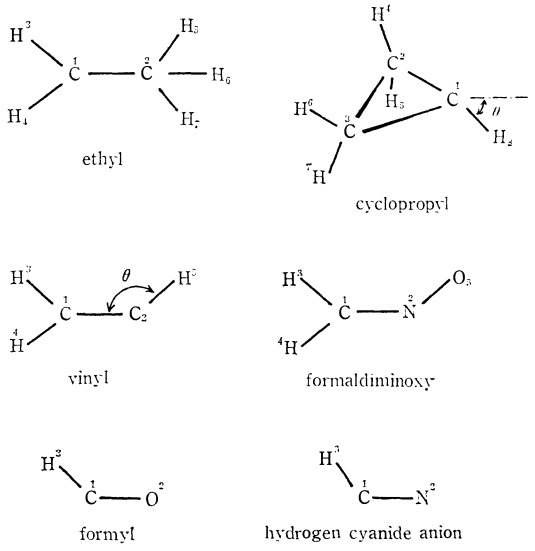

Fig. 1. Numbering of atoms of calculated radicals.

TABLE 2. DEPENDENCE OF CALCULATED HYPERFINE COUPLING CONSTANTS OF METHYL AND ETHYL RADICALS ON WOLFSBERG-HELMHOLZ PARAMETER K

Radical	Nucleus Y	a^Y (gauss) Value of K 0.6	0.7	0.8	Exp.
Methyl	H	−27.09	−24.41	−21.66	(−) 23.04[a]
	C	41.18	35.40	30.58	(+) 38.34[b]
Ethyl	3H, 4H	−25.28	−22.20	−19.74	(−) 22.38[a]
	βH[c]	27.37	26.75	26.27	(+) 26.87[a]
	1C	38.54	33.15	28.65	(+) 39.07[b]
	2C	−5.64	−5.24	−4.84	(−) 13.57[b]

a) Ref. 18.
b) R. W. Fessenden, *J. Phys. Chem.*, **71**, 74 (1967).
c) The mean value of hyperfine coupling constants of 5H, 6H, and 7H.

14) J. C. Slater, "Quantum Theory of Atomic Structure," Vol. I, McGraw-Hill Book Co., New York (1960), p. 206.
15) J. C. Slater, *Phys. Rev.*, **36**, 57 (1930).
16) M. Wolfsberg and L. Helmholz, *J. Chem. Phys.*, **20**, 837 (1952).

to fit selected experimental values of hyperfine coupling constants in the following section. We use Slater 2*s* and 2*p* AO's for first-row elements and the Slater-type 1*s* AO with the orbital exponent of 1.2 for hydrogen.

Results and Discussion

The numberings of the atoms and the conformational parameters of the calculated radicals are shown in Fig. 1.

Wolfsberg-Helmholz Parameter, *K*, and Calculated Coupling Constants. To obtain the appropriate value of the parameter, *K*, of Eq. (11), the ^{1}H and ^{13}C hyperfine coupling constants of methyl and ethyl radicals are calculated by changing the value of *K*.

The hyperfine coupling constants of the protons of the methyl radical and the α protons (3H and 4H) of the ethyl radical arise mainly through the valence-electron spin-polarization mechanism. The spin densities which appear through valence-and inner-shell-electron spin-polarization determine the ^{13}C coupling constants of the methyl and ethyl radicals. On the other hand, the hyperfine coupling constant of the β protons (5H, 6H, and 7H) of the ethyl radical are determined mainly by the spin delocalization. Therefore, the contributions of the spin delocalization, the valence-shell-electron spin-polarization, and the inner-shell-electron spin-polarization mechanism to the hyperfine coupling constants will be estimated with the set of parameters which gives good calculated values of the hyperfine coupling constants of these radicals.

Table 3. Calculated hyperfine coupling constants of cyclopropyl radical (gauss)

θ	0°	20°	40°	60°	Exp.
a^{4H}	35.6	33.7	26.1	18.1	(+) 23.42[a,b]
a_D^{4H}	34.6	33.2	26.3	19.4	
a_{PV}^{4H}	1.0	0.5	−0.2	−1.3	
a^{5H}	35.6	32.6	27.2	17.6	(+) 23.42[a,b]
a_D^{5H}	34.6	32.0	27.9	20.1	
a_{PV}^{5H}	1.0	0.6	−0.7	−2.5	
a^{8H}	−22.9	−21.0	−16.7	−12.2	±6.51[a]
a_D^{8H}	0.0	0.5	1.6	2.4	
a_{PV}^{8H}	−22.9	−21.5	−18.3	−14.6	
a^{1C}	34.0	43.0	65.2	91.0	——
a_D^{1C}	0.0	8.5	30.1	56.0	
a_{PV}^{1C}	41.6	41.7	41.3	39.8	
a_{PI}^{1C}	−7.6	−7.2	−6.2	−4.8	
a^{2C}	−5.3	−4.7	−2.9	−0.35	——
a_D^{2C}	0.0	0.1	0.5	0.94	
a_{PV}^{2C}	−5.3	−4.7	−3.0	−0.55	
a_{PI}^{2C}	~0.0	−0.1	−0.4	−0.7	

a) Ref. 18.
b) The average of a^{4H} and a^{5H} was observed.

The calculated values of the hyperfine coupling constants of the methyl and ethyl radicals are listed in Table 2, together with the values of *K* used. The best results are obtained for $K=0.7$, so we will use this value in the following calculations.

Cyclopropyl Radical. The geometry of this radical is assumed to be the same as that of cyclopropane[17] except for the angle between the 1C–8H bond and the carbon plane. This angle, θ, varies in the calculations. The calculated hyperfine coupling constants are listed in Table 3, together with the contributions from the spin-delocalization, the valence-electron spin-polarization, and the inner-shell-electron spin-polarization mechanisms. These results show that the spin-polarization mechanism is important in the estimation of the hyperfine coupling constants of the nuclei of the radical-center atom and of the atoms bonded to it. Dixon[1] successfully calculated the hyperfine coupling constants of the β protons of this radical with the assumed geometry of $\theta=54.75°$. Drago and Petersen[2b] calculated the hyperfine coupling constants of the protons of this radical by the extended Hückel method. They obtained 7.56, 22.00, and 18.96 gauss for 8H, 5H, and 4H respectively, when $\theta=20°$. These results agree with the experimental values[18]; they predicted that the angle would be approximately 20°. The present results show that the spin-polarization mechanism contributes about −14 gauss to the hyperfine coupling constant of 8H, even when $\theta=60°$. The extended Hückel calculation presents only the spin density due to the spin-delocalization mechanism. When the present results and their extended Hückel calculations are compared, the angle is predicted to be large than 20°. The sign of the hyperfine coupling constant of 8H can not be fixed, because the present estimation of the positive contribution of the spin-delocalization mechanism to the 8H coupling constant (+2.4 gauss, $\theta=60°$) appears too small when compared with the results of other calculations.[2,3] The present calculation predicts that, when θ increases, the constant of 1C will steeply increase, mainly because of the increase in the *s*-nature of the odd-electron orbital on 1C. As is shown in Table 3, the hyperfine coupling constants of β protons (4H and 5H) arise dominantly from spin-delocalization. Therefore, the hyperfine coupling constants of β protons can be estimated directly by Roothaan's restricted open-shell SCF MO method[19] or by a simple MO

17) "Tables of Interatomic Distances and Configuration in Molecules and Ions," ed. by L. E. Sutton, Special Publ. Nos. 11 and 18, The Chemical Society, London (1958 and 1965).
18) R. W. Fessenden and R. H. Schuler, *J. Chem. Phys.*, **39**, 2147 (1963).
19) C. C. J. Roothaan, *Rev. Mod. Phys.*, **32**, 179 (1960).

TABLE 4. CALCULATED HYPERFINE COUPLING CONSTANTS OF VINYL RADICAL (GAUSS)

θ	120°	130°	140°	150°	180°	Exp.
a^{1C}	−6.0	−7.0	−7.8	−8.7	−9.9	(−) 8.55[a]
a_D^{1C}	1.7	1.3	1.0	0.6	0.0	
a_{PV}^{1C}	−7.7	−8.2	−8.4	−9.2	−9.9	
a_{PI}^{1C}	−0.1	−0.1	−0.1	−0.1	~0.0	
a^{2C}	106.0	87.7	70.3	55.6	38.0	(+) 107.57[a]
a_D^{2C}	68.6	50.8	34.2	20.2	0.0	
a_{PV}^{2C}	42.4	42.4	42.1	41.8	40.8	
a_{PI}^{2C}	−5.0	−5.5	−6.0	−6.4	−7.0	
a^{3H}	73.6	75.8	76.6	76.0	64.4	(+) 68[b]
a_D^{3H}	73.0	74.5	74.7	73.6	61.8	
a_{PV}^{3H}	0.6	1.3	1.9	2.4	2.6	
a^{4H}	19.3	26.3	33.9	42.0	64.4	(+) 34[b]
a_D^{4H}	19.0	25.7	33.0	40.7	61.8	
a_{PV}^{4H}	0.3	0.6	0.9	1.3	2.6	
a^{5H}	−8.3	−11.5	−14.9	−18.1	−23.2	±13.39[c]
a_D^{5H}	11.2	8.5	5.9	3.5	0.0	
a_{PV}^{5H}	−19.5	−20.0	−20.8	−21.6	−23.2	

a) R. W. Fessenden, *J. Phys. Chem.*, **71**, 74 (1967).
b) E. L. Conchlan, F. J. Adrian and V. A. Bowers, *J. Chem. Phys.*, **40**, 213 (1964).
c) Ref. 18.

method such as the extended Hückel method.

Vinyl Radical. The geometry of the vinyl radical is assumed to be planar, with a 1.34 Å CC bond, 1.08 A CH bonds, and a 120° H–C–H bond angle. The bond angle of 1C–2C–5H, θ, varies in the calculations. Table 4 shows the calculated hyperfine coupling constants of the vinyl radical and the contributions of the spin-delocalization, the valence-electron spin-polarization, and the inner-shell-electron spin-polarization mechanisms. The comparison between the calculated and the experimental ratios of $|a^{3H}/a^{4H}|$ and $|a^{1C}/a^{2C}|$ shows that the angle θ may be in the $130° < \theta < 150°$ range. The results in Table 4 show that only the hyperfine coupling constants of β protons (3H and 4H) can be directly calculated with a restricted MO method, because the spin-polarization mechanism makes a minor contribution to them. The present calculation predicts that the 1C and 5H hyperfine coupling constants will be negative; the prediction for the former coincides with that of the unrestricted SCF calculation done with the INDO approximation of Pople, Beveridge and Dobosh.[6] The sign of the calculated 5H coupling constant agrees with our semiempirical unrestricted SCF calculation.[4] The present calculation shows that the odd-electron density on 2C attracts, through exchange interaction, electrons with the same spin as the odd electron, resulting in negative spin densities at the nuclei of 1C and 5H.

Formaldiminoxy Radical. Although the electron-spin-resonance spectrum of the formaldiminoxy radical has, so far as we know, not been reported, the hyperfine coupling constants of this radical have been calculated and compared with those of the aldiminoxy radicals. The geometry of this radical is assumed to be planar, with bond lenghts of $r(CH) = 1.08$Å, $r(CN) = 1.28$Å, and $r(NO) = 1.24$Å, and with bond angles of $\angle HCH = 120°$ and $\angle CNO = 125°$. The calculated values are summarized in Table 5. The calculated hyperfine coupling constant of ^{14}N agrees with the experimental values of the acetaldiminoxy and benzaldiminoxy radicals. The proton *trans* to the odd-electron orbital on the nitrogen has a larger coupling constant than that of the *cis* proton, as in the case of the vinyl radical. The ^{17}O coupling constant

TABLE 5. CALCULATED HYPERFINE COUPLING CONSTANTS OF FORMALDIMINOXY RADICAL (IN UNIT OF GAUSS)

Nucleus Y	a_D^Y	a_{PV}^Y	a_{PI}^Y	a^Y	Exp.[a]
^{14}N	22.9	16.3	−1.7	37.5	(+) 30—33
^{13}C	2.41	−6.43	−0.23	−4.30	—
^{17}O	−0.02	−8.71	0.78	−7.95	—
3H	62.8	−1.7	—	61.6	(+) 27.0
4H	11.0	−0.8	—	10.2	(+) 5.2, 6.5

a) Data for *syn*-acetoaldiminoxy and *syn*- and *anti*-benzaldiminoxy radicals. J. R. Thomas, *J. Amer. Chem. Soc.*, **86**, 1446 (1964); B. C. Gilbert and R. O. C. Norman, *J. Chem. Soc., B*, **1966**, 727. The identification of Tohomas for *syn*- and *anti*-isomers are not proper.

Table 6. Calculated hyperfine coupling constants of formyl and hydrogn cyanide anion radicals (gauss)

Radical	Nucleus Y	a_D^Y	a_{PV}^Y	a_{PI}^Y	a^Y	Exp.
HCO	^{1}H	57.5	−13.3	——	44.2	(+) 137[a]
	^{13}C	119	33.3	−3.4	149	(+) 134.7[b]
	^{17}O	−0.12	−5.13	0.77	−4.48	——
HCN^-	^{1}H	48.8	−10.1	——	38.7	(+) 137[c]
	^{13}C	81.2	25.5	−2.9	103.8	(+) 74 [c]
	^{14}N	0.40	4.82	−0.65	4.57	(+) 6.5[c]

a) Ref. 21. b) Ref. 22. c) Ref. 23.

of the iminoxy radical can be predicted to be about −8 gauss.

Formyl and Hydrogen Cyanide Anion Radicals. The formyl and hydrogen cyanide anion (HCN^-) radicals are isoelectronic, and both radicals are predicted to have essentially the same conformation and electronic configuration from Walsh's scheme for the molecular orbitals of HAB molecules.[20] The formyl radical has been prepared by Adrian *et al.*;[21] the isotropic proton hyperfine coupling has the extremely large value of 137 gauss, and the ^{13}C coupling is 134.7 gauss.[22] The electron-spin-resonance spectrum of the HCN^- radical was studied by Symons and his co-workers,[23] who reported that the hyperfine coupling constants of ^{1}H, ^{13}C, and ^{14}N are 137, 74, and 6.5 gauss respectively. The isotropic hyperfine coupling constants of the formyl radical have been calculated by the extended Hückel method,[2] the unrestricted SCF method with CNDO/2 approximations,[5] and the *ab initio* unrestricted SCF MO method.[7]

The geometry of the formyl radical used in the present calculation has a 1.09Å CH bond, a 1.198Å CO bond, and a bond angle of 119.5°. The structure of the hydrogen cyanide anion radical is assumed to have $r(CH)=1.09$Å, $r(CN)=1.26$Å, and $\angle HCN=120°$. The calculated hyperfine coupling constants of these radicals are listed in Table 6. The calculated proton coupling constants for HCO and HCN^- are too small when compared with the experimental values, as when calculated with the extended Hückel method.[2] The results for the ^{13}C constants are passable. Inner-shell electrons make minor contributions to these ^{13}C coupling constants. It is interesting to point out that the spin-polarization of valence-electrons gives about 1/4 of the coupling constant of the nucleus of the radical-center atom of these σ electron radicals.

The present calculation predicts that the ^{17}O coupling constant will be small and negative; this prediction coincides with the calculation by the *ab initio* unrestricted SCF MO method.[7] The calculated value of the ^{14}N coupling constant of HCN^- agrees fairly well with the experimental value. The present calculation show that a positive spin density arises at the position of the oxygen or the nitrogen nucleus of the HCO or HCN^- radical.

Table 7. Contributions to a_{PV}^Y from one-center exchange integrals between atomic orbitals centered on the radical-center atom (in unit of gauss)

Radical	Nucleus Y[a]	a^Y [b]	a_{PV}^Y [b]	Condtribution[c]
Cyclopropyl	1C	65.2	41.3	42.7
$\theta=40°$	2C	−2.9	−3.0	−0.81
	8H	−16.7	−18.3	−14.4
Vinyl	2C	87.7	42.4	43.8
$\theta=130°$	1C	−7.0	−8.2	−3.3
	5H	−11.5	−20.0	−20.0
Formald-	N	37.6	16.3	18.1
iminoxy	C	−4.3	−6.4	−1.83
	O	−8.0	−8.7	−0.97
HCO	C	149	33.3	42.1
	O	4.48	−5.13	3.10
	H	44.2	−13.3	−13.3
HCN^-	C	103.8	25.5	32.0
	N	4.57	4.82	−0.65
	H	38.7	−10.1	−8.78

a) Numbering of atoms are shown in Fig. 1.
b) Calculated value listed in Tables 3—6.
c) The contribution to the hyperfine coupling constant of nucleus Y from one-center exchange integrals between AO's centered on the radical-center atom. Estimated as $-(1/4)A_V^Y\sum'_{r,s,t,u}(\pi^\alpha_{vv,rs}+\pi^\beta_{vv,rs})p^0_{tu}(rt|us)$, where $\sum'$ denote the summation over one-center exchange integrals between AO's on the radical center atom and v expresses the valence shell s AO atom Y.

20) A. D. Walsh, *J. Chem. Soc.*, **1953**, 2288.
21) F. J. Adrian, E. L. Cochran and V. A. Bowers, *J. Chem. Phys.*, **36**, 1661 (1962).
22) F. J. Adrian, E. L. Cochran and V. A. Bowers, *ibid.*, **44**, 4626 (1966).
23) K. D. J. Root, M. C. R. Symons and B. C. Weatherley, *Mol. Phys.*, **11**, 161 (1966).

The mechanism of these spin densities is as follows: the spin density on the 2*s* AO of the oxygen or the nitrogen atom arises from the valence-electron spin-polarization contribution, a^{O}_{FV} or a^{N}_{FV}. The main part (about 120%) of a^{O}_{FV} or a^{N}_{FV} comes from terms containing odd-electron density matrix elements, p^{o}_{lu}, between the AO's of the oxygen atom or of the nitrogen atom. That is, the odd electron in the in-plane orbital on the radical-center carbon atom delocalizes into the in-plane lone-pair orbital on the oxygen or the nitrogen atom, which in turn induces a positive spin density on the 2*s* AO of the oxygen or the nitrogen atom of the HCO or HCN^{-} radical through the exchange interaction, as in the case of π-electron radicals. This situation is also observed in the case of the ^{17}O coupling constant of the formaldiminoxy radical.

Role of One-center Exchange Integrals. For the calculation of the hyperfine coupling constants of σ electron radicals with a semiempirical unrestricted SCF MO method, Atherton and Hincliffe[5] adopted CNDO/2 approximations, whereas Pople, Beveridge and Dobosh[6] used INDO approximations. In the former method, one-center exchange integrals are neglected, while in the latter they are included. Although it is well established that one-center exchange integrals are essential in the calculation of the hyperfine coupling constants of π electron radicals,[24,25] the role of these integrals in the calculation of the hyperfine coupling constants of the σ electron radicals has not yet been sufficiently studied. The present method can give the contribution from each electron repulsion integral to the hyperfine coupling constants.

Table 7 shows the contributions through one-center exchange integrals between valence-shell AO's centered on the radical-center atom to the hyperfine coupling constants of the calculated σ electron radicals. Except for the ^{17}O coupling constants of HCO and the formaldiminoxy radical, and the ^{14}N coupling constant of HCN^{-}, the one-center exchange integral contributions listed in Table 7 approximately determine the value of a^{X}_{FV}, the hyperfine coupling which arises through the valence-electron spin-polarization, of the nuclei of the radical-center atoms and of the atoms bonded to them. As has been mentioned in the preceding section, the hyperfine coupling constants of the ^{17}O of HCO and H_2CNO or of the ^{14}N of HCN^{-} arise through the odd-electron density delocalized into the in-plane lone-pair orbital on the oxygen atom or on the nitrogen atom, and the contribution listed in Table 7 is not important.

The results listed in Tables 3—7 show that, in the case of σ-electron radicals, spin-polarization make contributions to the hyperfine coupling constants of the nuclei of radical-center atoms and the atoms bonded to them that cannot be neglected, and that, in estimating these contributions, one-center exchange integrals should be included in the calculations.

The calculations were carried out on the HITAC 5020E electronic computer of the University of Tokyo and on the FACOM 230 computer of Kyoto University. The authors wish to acknowledge the help of the staff of each computer.

24) H. McConnell and D. B. Chesnut, *J. Chem. Phys.*, **28**, 107 (1958).
25) M. Karplus and G. K. Fraenkel, *ibid.*, **35**, 1312 (1961).

BULLETIN OF THE CHEMICAL SOCIETY OF JAPAN VOL. 43 81—84 (1970)

Benzyl Bromide-Amine Reaction in Nitrobenzene-Ethanol Mixtures

P. S. RADHAKRISHNAMURTI and G. P. PANIGRAHI

Department of Chemistry, Khallikote College, Berhampur (Gm), Orissa, India

(Received September 11, 1968)

The reactions between benzyl bromide and various bases as well as *p*-nitrobenzyl bromide and various bases have been studied in nitrobenzene-ethanol mixtures (80 : 20 v/v). The reaction is total second order as stated earlier. Comparison is made with the previous work on the same reaction with benzyl chloride and *p*-nitrobenzyl chloride.

In our earlier communications[1,2] we reported the kinetics of reaction of benzyl chloride as well as of *p*-nitrobenzyl chloride with bases in nitrobenzene-ethanol mixtures. We report here the kinetics of reaction of benzyl bromide as well as of *p*-nitrobenzyl bromide with bases in nitrobenzene-ethanol mixtures (80 : 20 v/v).

Experimental

Materials. All substances are of AnalaR grade. Nitrobenzene is also of AnalaR grade.

Rate Measurements. The reactions were followed as per the procedure stated earlier.[1,2] Solvolysis correction was also done with benzyl bromide reaction.

TABLE 1

Solvent: Nitrobenzene-Ethanol (80 : 20 v/v)
Substrate: Benzyl bromide

Base	$10^2 \times k\ l\ mol^{-1}min^{-1}$ 80°C	70°C	pK_a*
Aniline	47.20	29.90	4.25
N-Methylaniline	95.70	63.60	4.85
β-Naphthylamine	36.00	23.40	4.11
p-Toluidine	85.60	59.90	5.07
m-Toluidine	56.90	38.00	4.67
o-Toluidine	25.70	15.90	4.38
p-Chloroaniline	24.60	14.10	3.81
m-Chloroaniline	15.50	8.80	3.32
n-Butylamine	436.00	308.00	10.61†
Benzylamine	284.00	—	9.34†
Diethylamine	526.00	375.00	11.10†

* Braude and Nachod, "Determination of Organic Structures by Physical Methods," Vol. 1 (1955).
† Lange, "Handbook of Chemistry" (1961).

1) P. S. Radhakrishnamurti and G. P. Panigrahi, *J. Indian Chem. Soc.*, **45**, 323 (1968).
2) P. S. Radhakrishnamurti and G. P. Panigrahi, *Israel J. Chem.*, **6**, 137 (1968).

Discussion

The second order rate constants for benzyl bromide and bases are given in Table 1. A glance at the table indicates that all the aliphatic amines react much faster than the aromatic amines. All the compounds react in consonance with their basicity except for a few where other factors seem to operate, such as the *ortho* effect. A plot of log *k* *vs.* pK_a showed linearity.

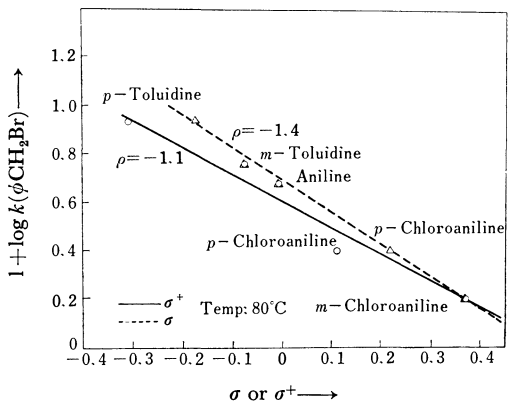

Fig. 1

Where ever σ and σ^+ are different σ and σ^+ points are indicated by △ and ○ respectively.

To analyze the data a correlation was made with Hammett's substituent constants for aromatic amines. A plot of log *k* *vs.* σ and σ^+ showed linearity (Fig. 1). The slopes were −1.4 and −1.1 respectively. All these establish that the attack by amine on the benzyl bromide is facilitated by electron releasing groups in the base and retarded by electron attracting groups in the substrates.

p-Nitrobenzyl bromide was also subjected to react with all these bases. The reactions were uniformly slower compared to benzyl bromide. This establishes that electron withdrawing groups

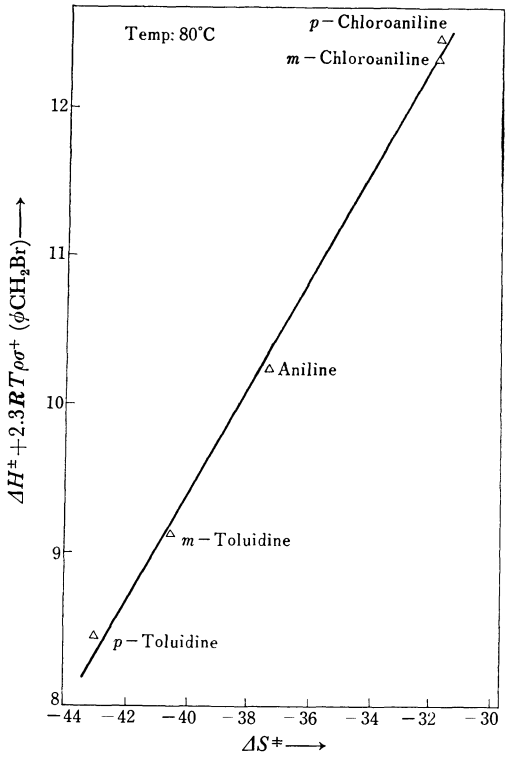

Fig. 2

either in the substrate or in the attacking base retard the process. The important features in these reactions are: (1) Anionisation of the halogen, (2) the coordination of the basic nitrogen atom with the adjacent methylene group by means of the unshared electron pair. These two are affected in turn by electron withdrawing substituents and hence retardation. The rate constants are given in Table 2.

log k *vs.* pK_a as well as log k *vs.* σ and σ^+ showed linearity. The ρ values are −1.75 and −1.4

TABLE 2

Solvent: Nitrobenzene-Ethanol (80:20 v/v)
Substrate: *p*-Nitrobenzyl bromide

Base	$10^2 \times k$ $l\,mol^{-1}min^{-1}$	
	80°C	70°C
Aniline	25.50	16.60
N-Methylaniline	40.00	26.70
β-Naphthylamine	18.90	12.40
p-Toluidine	41.50	27.60
m-Toluidine	30.70	19.00
o-Toluidine	10.80	6.89
p-Chloroaniline	9.41	5.11
m-Chloroaniline	6.11	3.28
n-Butylamine	276.00	196.00
Benzylamine	135.00	93.00
Diethylamine	390.00	290.00

TABLE 3

Solvent: Nitrobenzene-Ethanol (80 : 20 v/v)
Temperature: 80°C
Base: Aniline

Substrate	$10^2 \times k$ $l\,mol^{-1}min^{-1}$
Benzyl chloride	0.755
Benzyl bromide	47.20
p-Nitrobenzyl chloride	0.356
p-Nitrobenzyl bromide	25.50

respectively. The most reactive base is diethylamine. The two aliphatic primary amines react quite in consonance with their electron availability.

In the aromatic series, *N*-methylaniline certainly reacts faster than aniline as the pK_a values indicate. All toluidines react faster than the corresponding chloro compounds. Similar reasoning explains the reactivity of these bases with *p*-nitrobenzyl bromide.

Comparison of the Reactivity of Benzyl Chloride and Benzyl Bromide. It is interesting to note that bromide derivative reacts faster than the chloride derivative (Table 3). This is quite in accord with the well known theories of substituent effects.[3]

Mechanism of the Process. It was postulated that it is possible to rationalize the inactivity of benzyl chloride with primary aromatic amines in pure nitrobenzene on the basis of a four centered transition state. It was also suggested that alternatively the abnormality could be due to specific solvent influences. The present work with benzyl bromide and *p*-nitrobenzyl bromide rules out the possibility of a likely four centered transition state. All these reactions, in general, are through a three centered transition state. Any inactivity or abnormality is to be traced to solvation phenomena.

Our arguments are based on the following facts: (1) Benzyl chloride and *p*-nitrobenzyl chloride are unreactive in pure nitrobenzene medium but reactive in nitrobenzene-ethanol mixture, nitrobenzene-dimethylformamide mixture, nitrobenzene-dimethylsulfoxide mixture and nitrobenzene-acetic acid mixture. This reaction did not occur in nitrobenzene-benzene, nitrobenzene-chlorobenzene, nitrobenzene-dioxane and nitrobenzene-acetonitrile mixtures. The relative reactivity in the solvent mixtures is nitrobenzene-DMSO (80 : 20 v/v)> nitrobenzene-ethanol (80 : 20 v/v)> nitrobenzene-acetic acid (80 : 20 v/v)> nitrobenzene-DMF (80 : 20 v/v).

(2) Benzyl bromide and *p*-nitrobenzyl bromide did react in pure nitrobenzene medium but crystallization occured at a very early stage of the reaction.

3) E. S. Gould, "Mechanism and Structure in Organic Chemistry" (1965), pp. 260—261.

Hence the kinetics of these derivatives were studied in nitrobenzene-ethanol mixtures. A complete analysis of solvent influence on bromide derivatives will be dealt with in a separate communication.

These two facts put together mean that the abnormal inactivity noticed with benzyl chloride and *p*-nitrobenzyl chloride is due to greater ground state solvation. The bromide derivatives react in nitrobenzene indicating greater transition state solvation though crystallization occurs.

A plot of log k of benzyl chloride *vs.* log k of benzyl bromide is perfectly linear indicating a similar process in both chlorides and bromides. The mechanism as mentioned earlier is a three centered transition state as follows:

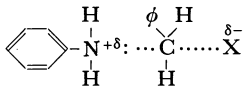

(Three centered transition state)

X=Cl, Br, *etc.*

The reaction is an S_N2 reaction having a dominant S_N1 character.

Thermodynamic Parameters. The values of activation energies, frequency factor and other derived thermodynamic constants for benzyl bromide-amine reaction are collected in Tables 4 and 5. Both the parameters E and $\log_{10} PZ$ tend to increase together. Linearity is obtained by plotting $\log_{10} PZ$ against $1/\sqrt{E}$ as it should be on the basis of thermodynamic considerations[4] (Fairclough-Hinshelwood relationship) if both the Arrhenius parameters are the controlling factors of the rate.

The small frequency factors would mean that standard entropy of activation $\Delta S^{\pm}$ has a relatively larger negative value or that the transmission coefficient is small.

Enthalpy-Entropy Relationship. It was of interest to examine the relationship between activation enthalpy and entropy. The possibility of correlation between $\Delta S^{\pm}$ and $\Delta H^{\pm}$ was investigated by a conventional isokinetic plot. It appears that the plot showed a tendency of scatter which is discriminating and characteristic of the nature and position of the groups. This observation together with ideas put forward by Hepler[5a,b,c] and others suggested that if the enthalpy and entropy changes are resolved into external and internal components a relationship may exist between the external parameters. In this treatment external contributions to enthalpy and entropy are associated with solvent interactions, and the internal contributions arise from differences in enthalpy and entropy within the reactant molecules and the transition state. If the reasonable assumption is made that the internal motions of the substituents do not contribute to the free energy, *viz.*, internal entropy changes are zero, the following equation[6a,b] may be used as a test of external entropy and enthalpy relationship.

$$(\delta\Delta H^{\pm}+2.303\boldsymbol{R}T\rho\sigma^{+}) = b\delta\Delta S^{\pm}$$

where δ and Δ operator symbols represent the effect of the substituents and of chemical reaction on the activation enthalpy and entropy, σ^{+} is the electrophilic substituent constant of Brown and Okamoto, ρ is the Hammett reaction constant which is -1.1 at 80°C for benzyl bromide-amine reaction; b is a constant characteristic of the reaction and can be obtained from the slope of a plot of $\delta\Delta H^{\pm}+2.303\boldsymbol{R}T\rho\sigma^{+}$ against $\delta\Delta S^{\pm}$. The plot

Table 4

Solvent: Nitrobenzene-ethanol (80:20 v/v)
Temperature: 80°C
Substrate: Benzyl bromide

Base	E kcal/mol	$\log_{10} PZ$	$-\Delta S^{\pm}$	$\Delta H^{\pm}$ kcal/mol
Aniline	10.95	4.67	37.42	10.25
N-Methylaniline	9.82	4.28	39.35	9.12
β-Naphthylamine	10.33	4.17	39.80	9.63
p-Toluidine	8.60	3.48	42.98	7.90
m-Toluidine	9.72	3.99	40.61	9.02
o-Toluidine	11.22	4.57	37.96	10.52
p-Chloroaniline	13.40	5.90	31.86	12.70
m-Chloroaniline	13.70	5.89	31.93	13.00
n-Butylamine	9.44	4.73	37.25	8.74
Diethylamine	8.13	3.98	40.88	7.43

Table 5

Solvent: Nitrobenzene-ethanol (80:20 v/v)
Temperature: 80°C
Substrate: *p*-Nitrobenzyl bromide

Base	E kcal/mol	$\log_{10} PZ$	$-\Delta S^{\pm}$	$\Delta H^{\pm}$ kcal/mol
Aniline	10.32	4.02	40.51	9.62
N-Methylaniline	9.56	3.74	41.78	8.86
β-Naphthylamine	10.16	3.79	41.57	9.45
p-Toluidine	9.82	3.92	40.97	9.12
m-Toluidine	11.60	4.90	36.52	10.90
o-Toluidine	10.74	3.90	41.04	10.04
p-Chloroaniline	14.60	6.23	30.37	13.90
m-Chloroaniline	14.95	6.26	30.24	14.25
n-Butylamine	8.24	3.76	41.67	7.54
Benzylamine	8.93	3.88	41.12	8.23
Diethylamine	7.14	3.23	44.11	6.43

4) R. A. Fairclough and C. N. Hinshelwood, *J. Chem. Soc.*, **1937**, 538.

5) a) L. G. Hepler, *J. Amer. Chem. Soc.*, **85**, 3089 (1963). b) K. J. Laidler, *Trans. Faraday Soc.*, **55**, 1725 (1959). c) C. D. Ritchie and W. F. Sager, *Progr. Phys. Org. Chem.*, **2**, 323 (1964).

6) a) I. Lee, *J. Korean Chem. Soc.*, **7**, 211, 238 (1963). b) I. Lee, *Chem. Abstr.*, **61**, 5015e, 7770e (1964).

shows perfect linearity (Fig. 2). The right hand side of the equation represents external entropy change. Since $\delta\Delta S^{\pm}=\delta\Delta S(\text{internal})+\delta\Delta S(\text{external})$, then for $\delta\Delta S(\text{internal})=0$, $\delta\Delta S^{\pm}=\delta\Delta S(\text{external})$. Similarly the left hand side of the equation represents the external enthalpy changes due to the substituents, provided that the term "$2.303\,\boldsymbol{R}\boldsymbol{T}\rho\sigma^{+}$" may be identified with $\delta\Delta H$ (internal). This assumption is consistent with Hammett's original concept in which substituent constants represent changes in the potential energy of the system.

It is pertinent to refer to the work of Campbell and Hogg[7] wherein they found, in their reactions of electrophilic additions to alkenes, that there is no alteration of the reaction mechanism with changes in solvent polarity.

7) D. S. Campbell and D. R. Hogg, *J. Chem. Soc.*, *B*, **1967**, 889.

BULLETIN OF THE CHEMICAL SOCIETY OF JAPAN VOL. 43 84—89 (1970)

Thermal Decomposition of Uranyl Dihydrogen Orthophosphate Trihydrate

Mutsukazu KAMO*1 and Shigeru OHASHI

Department of Chemistry, Faculty of Science, Kyushu University, Fukuoka

(Received April 21, 1969)

The thermal decomposition of uranyl dihydrogen orthophosphate trihydrate was studied by means of paper chromatography, X-ray diffractometry, differential thermal analysis, thermogravimetric analysis, infrared spectroscopy and chemical analysis. From these studies, it was revealed that in the thermal decomposition of the uranyl salt the following reactions take place. 1) The formation of condensed phosphates with relatively small polymerization degrees such as di- and triphosphates takes place below 300°C, accompanied by the elimination of water. 2) A uranyl salt of long-chain metaphosphate, $[UO_2(PO_3)_2]_n$ is produced bewteen 300 and 840°C. 3) The metaphosphate is melted at about 900°C, while uranium(VI) is reduced to uranium(IV) at the same time. 4) As a result of the reduction, the formation of uranium(IV) diphosphate, UP_2O_7, starts. 5) Finally, almost pure uranium(IV) diphosphate is produced at 1200°C.

Condensed phosphates of uranium prepared hitherto are di- and triphosphates of uranium(VI), di- and metaphosphates of uranium(IV) and diphosphates of uranium(IV and VI).[1-3] It has not been decided whether uranium(IV) metaphosphate is a cyclic or linear phosphate. Uranyl diphosphate is only one condensed phosphate of uranium(VI) which has so far been prepared by dehydration condensation. It appears that uranyl ion is not stable against heating. When uranyl salts are heated with orthophosphoric acid or phosphorus pentoxide, uranium(VI) is reduced to uranium(IV).[3] Uranyl diphosphate, $(UO_2)_2P_2O_7$ is also reduced to diuranium(IV and VI) trioxide diphosphate, $U_2O_3P_2O_7$ at 1020°C.[4] The purpose of the present investigation is to determine what chemical reactions take place and what kinds of condensed phosphates of uranium are produced during the process of the thermal decomposition of uranyl dihydrogen orthophosphate trihydrate (UDOT).

When dihydrogen orthophosphate of a certain metal ion with a charge n, M^{n+} is heated until all water of constitution is lost, metaphosphate, $[M(PO_3)_n]_x$ is produced by the reaction

$$x\cdot M(H_2PO_4)_n \longrightarrow [M(PO_3)_n]_x + x\cdot n\cdot H_2O \quad (1)$$

Metaphosphates are usually divided into two groups, cyclic and linear metaphosphates. Cyclic metaphosphates have ring structures, and their molecular weights are usually not very high. Linear metaphosphates have open-chain structures, and their molecular weights are considerably high.

Thilo and Grunze have found a certain relation between the structure of metaphosphate and the

*1 Present address: National Institute for Researches in Inorganic Materials.

1) "Gmelins Handbuch der anorganischen Chemie," 8 Auflage, System-Nummer **55**, Verlag Chemie, Berlin (1936), s. 181.

2) Y. Shibata, "Mukikagakuzensho," XVII-1, Maruzen Co., Ltd., Tokyo (1953), p. 263.

3) Y. Baskin, *J. Inorg. Nucl. Chem.*, **29**, 383 (1967).

4) V. Pekárek and V. Vesely, *ibid.*, **27**, 1151 (1965).

size and charge of metal ion. If metal ions with the same charge are considered, metaphosphates of the metal ions with medium sizes are the cyclic ones, while those of the metal ions with smaller or larger sizes are the linear ones.[5,6]

It is of principal interest to determine which kind of metaphosphate of uranium(VI) will be produced when UDOT is heated. According to the rule mentioned above, the formation of a linear metaphosphate is expected for the uranyl salt because of the big size of uranyl ions. The present studies were carried out by means of paper chromatography, X-ray diffractometry, differential thermal analysis, thermogravimetric analysis, infrared spectroscopy and chemical analysis.

Experimental

Preparation of Uranyl Dihydrogen Orthophosphate Trihydrate (UDOT), $UO_2(H_2PO_4)_2 \cdot 3H_2O$.[7] Before the preparation of UDOT, uranyl monohydrogen orthophosphate tetrahydrate was first prepared from uranyl nitrate hexahydrate and orthophosphoric acid by the usual method.[8] UDOT was prepared by shaking a mixture of 10 g of the uranyl monohydrogen orthophosphate tetrahydrate and 35 m*l* of 85% orthophosphoric acid for 2—3 weeks at 20°C and then by filtering the resulting solid with a glassfilter (yield 3.5 g). By addition of another 10 g of the uranyl monohydrogen orthophosphate tetrahydrate to the filtrate UDOT was prepared with yield higher than that of the first procedure (yield 12.7 g). The wet solid was washed with acetone and then carbon tetrachloride and dried in a vacuume desiccator over calcium chloride for 12 hr. Analytical results of the UDOT thus prepared are as follows.

Found: UO_3, 55.2%; P_2O_5, 28.0%; H_2O, 16.8% (by difference). Calcd for $UO_2(H_2PO_4)_2 \cdot 3H_2O$: UO_3, 55.22%; P_2O_5, 27.40%; H_2O, 17.38%.

The X-ray diffraction pattern (Fig. 4) was identical with the one reported by Dunn.[9]

Analysis of Uranium. A volumetric method with dichromate[10] was used for the analysis of uranium in uranium phosphate samples obtained by heating the UDOT. A sample was dissolved in a mixed solution of sulfuric acid and orthophosphoric acid. Uranium(VI) in the solution was then reduced to uranium(IV) with Jone's reductor. After the addition of iron(III) chloride solution, the resulting iron(II) was titrated with a standard solution of potassium dichromate.

Analysis of Phosphorus. A pH titration method was used for the determination of phosphorus in the uranium phosphate samples. Since uranium disturbs the determination of phosphorus by this method, uranium should be removed from a sample solution before titration.

A sample was dissolved in a 1M hydrochloric acid solution. The solution was passed through a cation-exchange resin column of Dowex 50W-X 8 of hydrogen form. The column was then washed with water until the washings were neutral to litmus. After condensed phosphates in the effluent mixed with the washings were completely hydrolyzed, the resulting orthophosphate was titrated with a standard solution of sodium hydroxide with a Hirama automatic recording titrator.

Preparation of Sample Solutions for Paper Chromatography. Paper chromatography was used to determine the distribution of condensed phosphate species in the uranium phosphate samples. Thus, the samples must be dissolved in a nearly neutral solution without heating in order to prevent condensed phosphates from hydrolysis. Since uranium interferes with the normal behavior of condensed phosphates in paper chromatography, it must be removed from sample solutions. It was found that the following method is suitable for this purpose.

For the dissolution of a sample containing approximately 0.1 mmol of uranium, about 10 m*l* of a 0.6M sodium hydrogen carbonate solution was used. Three 15 m*l* portions of a mixed benzene solution of TTA (thenoyltrifluoroacetone) and TBP (tributyl phosphate), with concentrations 0.2M and 0.1M, respectively, were used to extract uranium from the solution. When the extraction of uranium was performed, no phosphate species were extracted into the organic phase.

The samples heated in the temperature range between 100 and 750°C were dissolved by the simultaneous use of the aqueous solution of sodium hydrogen carbonate and the benzene solution of TTA and TBP. However, the samples heated at higher temperature than 750°C were not dissolved by this procedure. Thus, these samples were first dissolved in the aqueous solution of sodium hydrogen carbonate, and then the extraction of uranium was carried out with the benzene solution of TTA and TBP. For the most insoluble samples which were produced by heating the UDOT at 1000, 1100 and 1200°C, it took about a month to dissolve them in the sodium hydrogen carbonate solution.

Paper Chromatographic Separation and Determination of Phosphates. For one-dimensional paper chromatography fifter paper of Toyo Roshi No. 51A, 20×18 cm was used. A developing solvent was prepared by mixing 250 m*l* of a 20% trichloroacetic acid solution (100 g of trichloroacetic acid and 7 m*l* of 28% aqueous ammonia per 500 m*l* of the solution), 100 m*l* of water and 650 m*l* of acetone.[11] Development was performed at 20°C for about 4 hr by the ascending method.

An acidic molybdate solution was sprayed to detect phosphates on the filter paper. The paper was then dried and placed under ultraviolet rays until blue spots of phosphates appeared.[12]

Determination of phosphate species on the paper chromatogram was performed by a colorimetric meth-

5) E. Thilo and I. Grunze, *Z. Anorg. Allg. Chem.*, **290**, 209 (1957).

6) E. Thilo and I. Grunze, *ibid.*, **290**, 223 (1957).

7) J. M. Schreyer and C. F. Baes, Jr., *J. Amer. Chem. Soc.*, **76**, 354 (1954).

8) T. Moeller, "Inorganic Syntheses," V. McGraw-Hill Book Co., Inc., New York (1957), p. 150.

9) H. W. Dunn, "X-ray Diffraction Data for Some Uranium Compounds," ORNL-2092, (1956), p. 13.

10) J. M. Schreyer and C. F. Baes, Jr., *Anal. Chem.*, **25**, 644 (1953).

11) D. N. Bernhart and W. B. Chess, *ibid.*, **31**, 1026 (1959).

12) C. S. Hanes and F. A. Isherwood, *Nature*, **164**, 1107 (1949).

od.[13] Each phosphate species on the paper was leached with an aqueous ammonia and treated with a Mo(V)–Mo(VI) reagent.[14] The absorbance of the sample solution was measured at 830 mμ.

Two-dimensional paper chromatography[15] was carried out to identify phosphate species which were contained in oily substances derived from the heating products of the UDOT between 800 and 940°C. Filter paper of Toyo Roshi No. 51A, 40×40 cm was used. The first development was carried out at 5°C for 40 hr with the basic solvent[15] which was a mixture of 20 m*l* of 2-propanol, 20 m*l* of *N*,*N*-dimethylformamide, 20 m*l* of methyl ethyl ketone and 1 m*l* of 28% aqueous ammonia. After developing with the basic solvent and then drying, the second development was performed at 5°C for 16 hr at a right angle to the direction of the first development with the acidic solvent[15] which was prepared by mixing 60 m*l* of methanol, 10.3 m*l* of a trichloroacetic acid solution (20 g of trichloroacetic acid and 4.6 m*l* of 28% aqueous ammonia in 100 m*l* of water), 5 m*l* of acetic acid and 10 m*l* of water.

Instruments. X-Ray diffraction patterns for powder samples were obtained with a Rigaku-denki X-ray diffractometer Model D-3F, nickel-filtered Cu*K*α radiation being used.

Thermal analyses were carried out at a heating rate of 12°C/min in static air with a Shimazu thermoanalyzer DT-2A. As a reference material, α-alumina was used. Samples were not diluted.

Infrared spectra were measured with a Hitachi EPI-S2 spectrophotometer by the usual KBr-disk method.

Results and Discussion

A thermogravimetric analysis (TGA) curve and differential thermal analysis (DTA) curves for the UDOT are given in Figs. 1 and 2, respectively. From the TGA curve, it seems that the first two water molecules are eliminated up to 120°C, the additional two water molecules are eliminated between 120 and 200°C and the last one is gradually eliminated between 200 and 700°C. An explanation for the weight loss observed at nearly 900°C will be mentioned later.

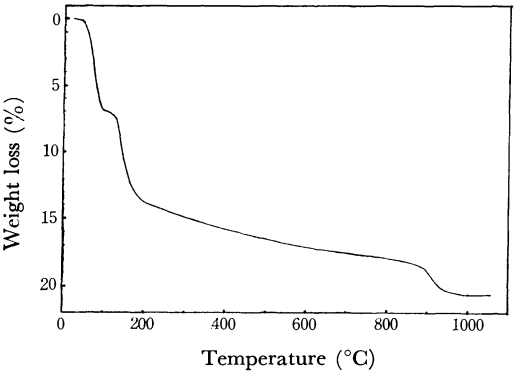

Fig. 1. Thermogravimetric analysis of $UO_2(H_2PO_4)_2 \cdot 3H_2O$.

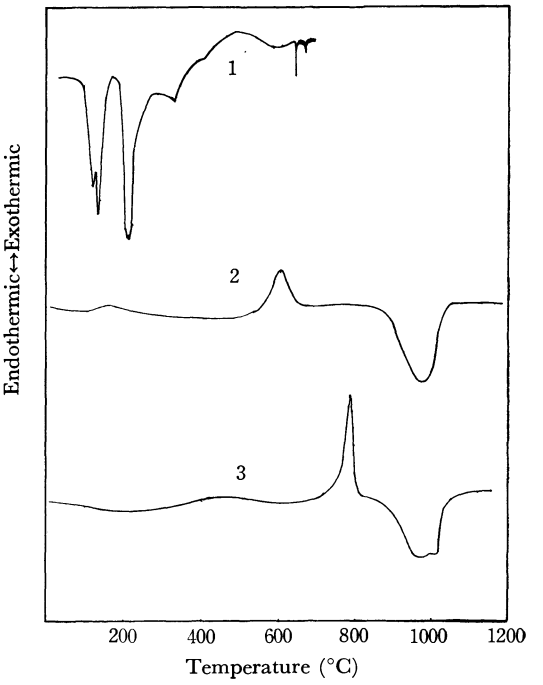

Fig. 2. Differential thermal analysis.
1) $UO_2(H_2PO_4)_2 \cdot 3H_2O$
2) The sample produced by heating $UO_2(H_2PO_4)_2 \cdot 3H_2O$ at 600°C
3) The sample produced by heating $UO_2(H_2PO_4)_2 \cdot 3H_2O$ at 800°C

When the UDOT was heated in a cell for the DTA measurement, the sample fused and overflowed the cell at about 650°C. Thus two samples which had been heated at 600 and 800°C in an electric furnace were used for the observation of the behavior in DTA at temperatures higher than 600°C.

The two endothermic peaks in the temperature range lower than 300°C in curve 1 of Fig. 2 correspond to the two-step change of the weight loss in the temperature range in the TGA curve of Fig. 1. Thus, they are due to the evaporation of water. There is no sufficient data to discuss thoroughly the exothermic peaks at 600 and 800°C in curves 2 and 3 of Fig. 2, respectively. However, these exothermic peaks seem to be due to the transformation of amorphous substances from an unequilibrium state to an equilibrium state and/or the crystallizaton of amorphous substances. The endothermic peaks observed at about 1000°C will be discussed later.

From these curves, fifteen points of heating temperature were selected in order to investigate the distribution change of phosphate species during the process of the thermal decomposition; they were

13) M. J. Smith, *Anal. Chem.*, **31**, 1023 (1959).
14) F. Lucena-Conde and L. Prat, *Anal. Chim. Acta*, **16**, 473 (1957).
15) E. Thilo and U. Schülke, *Z. Anorg. Allg. Chem.*, **341**, 293 (1965).
16) E. Steger and G. Leukroth, *ibid.*, **303**, 169 (1960).

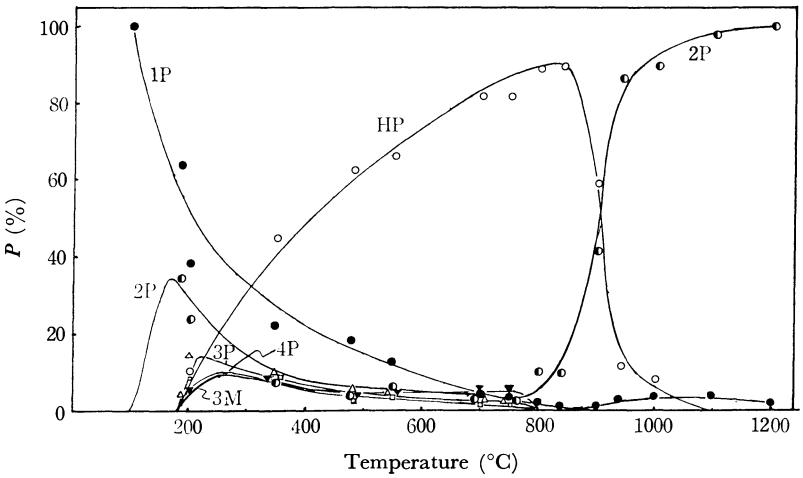

Fig. 3. Distribution of condensed phosphate species in heating products of $UO_2(H_2PO_4)_2 \cdot 3H_2O$. 1P(●): Orthophosphate, 2P(◐): Diphosphate, 3P(△): Triphosphate, 4P(□): Tetraphosphate, HP(○): Highpolyphosphate, 3M(▲): Trimetaphosphate

100, 180, 205, 350, 480, 550, 700, 750, 800, 840, 900, 940, 1000, 1100 and 1200°C. Phosphate species in the samples heated in air at these temperatures were analyzed by the dissolution procedure and paper chromatography. The distribution of the phosphate species thus obtained are given in Fig. 3, where the "high polyphosphate" means both the linear phosphates longer than tetraphosphate and the cyclic phosphates larger than trimetaphosphate.

In the case of samples heated at 800, 840, 900 and 940°C, when extraction was carried out, oily substances resulted at the bottom of the aqueous solutions. The oily substances were separated from the aqueous and benzene solutions and dissolved in water. The phosphate species in these aqueous solutions were proved to be highly polymerized phosphate (probably metaphosphate with a long-chain structure) by two-dimensional paper chromatography. The P% values of the high polyphosphate in Fig. 3 represent the amount of phosphorus in the oily substances.

Figure 3 shows that di-, tri-, tetra- and trimetaphosphates are formed in the temperature range between 180 and 350°C. At temperatures higher than 350°C, the amount of orthophosphate and these condensed phosphates except for diphosphate decreases with temperature and approaches nearly zero at 840°C. On the other hand, the amount of high polyphosphate increases with temperature and reaches about 90% at 840°C. At nearly 900°C, an abrupt change takes place, *i.e.*, the high polyphosphate undergoes decomposition, while diphosphate is formed again. At 1200°C the amount of diphosphate become almost 100%. Since the dissolution of the samples heated at a higher temperature than 900°C took a long time, the hydrolytic degradation of the samples during the dissolution must be taken into consideration. However, it can be concluded that the extent of this hydrolytic degradation was not large, because only small

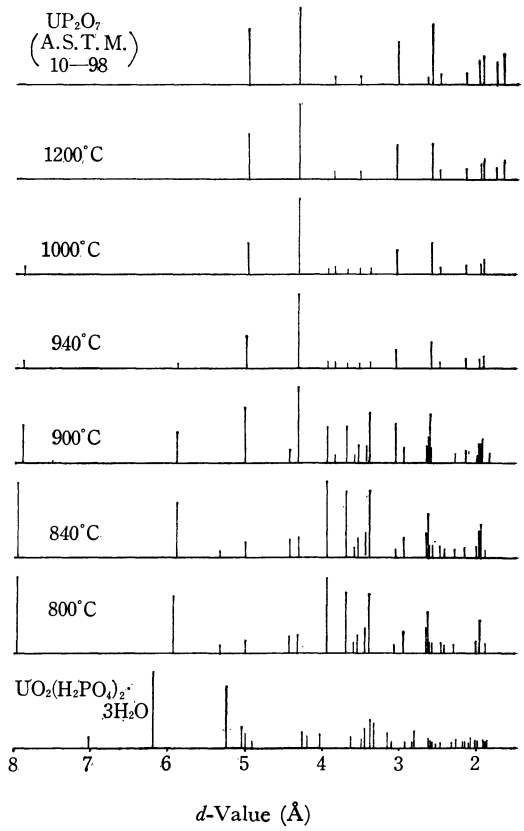

Fig. 4. X-Ray diffraction patterns of $UO_2(H_2PO_4)_2 \cdot 3H_2O$ and its heating products.

amounts of orthophosphate were observed in the solutions of the samples in question.

The results of the X-ray diffractometric analysis are given in Fig. 4. The uranium phosphate samples heated at temperatures higher than 750°C are crystalline, while those obtained in the temperature range between 100 and 750°C are amorphous. The diffraction pattern for the sample heated at 1200°C is in good agreement with that of uranium(IV) diphosphate, UP_2O_7, which is described in an A.S.T.M. card 10—98. The diffraction pattern for the sample heated at 800°C, which was confirmed to be the uranyl salt of long-chain metaphosphate by the paper chromatographic analysis, has not so far been reported.

The X-ray diffraction patterns for the samples producted in the temperature range between 800 and 1200°C show the gradual increase of the content of the uranium(IV) diphosphate and the gradual decrease of that of the uranyl salt of long-chain metaphosphate with temperature. This fact essentially agrees with the results of paper chromatographic analysis.

An infrared spectrum for the sample heated at 1200°C is similar to that for silicon, tin, titanium and zirconium diphosphates.[16] The composition of the sample heated at 1200°C is as follows.

Found; UO_2, 67.0; P_2O_5, 34.6%. Calcd for UP_2O_7; UO_2, 65.55; P_2O_5, 34.45%.

These data also indicate that the sample in question is uranium(IV) diphosphate.

We see that the most reasonable reactions which take place in the process of the thermal decomposition of the UDOT are as follows.

In the temperature range between room temperature and 100°C the reaction

$$UO_2(H_2PO_4)_2\cdot 3H_2O \longrightarrow UO_2(H_2PO_4)_2\cdot H_2O + 2H_2O \quad (2)$$

is expected to take place, because no condenced phosphates appear in the products, and the TGA curve indicates the elimination of two water molecules.

In the temperature range between 100 and 180°C, one more molecule of crystallization water may be eliminated.

$$UO_2(H_2PO_4)_2\cdot H_2O \longrightarrow UO_2(H_2PO_4)_2 + H_2O \quad (3)$$

However, the formation of diphosphate was confirmed by means of paper chromatography. Thus, the reaction

$$UO_2(H_2PO_4)_2 \longrightarrow UO_2H_2P_2O_7 + H_2O \quad (4)$$

also occurs. In the temperature range between 180 and 200°C, further dehydration reaction takes place. Until the temperature reaches 200°C, four water molecules were eliminated as a whole. Thus, if reactions (2), (3) and (4) are completed, there might be no orthophosphate in the product. However, a considerable amount of orthophosphate was observed in the sample heated at 200°C by means of paper chromatography. Thus in addition to reactions (3) and (4), condensation reactions may take place in the temperature range between 100 and 200°C:

$$UO_2H_2P_2O_7 + UO_2(H_2PO_4)_2 \longrightarrow$$

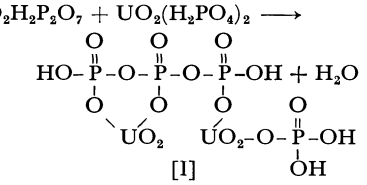

$$+ H_2O \quad (5)$$

[I]

$$n\cdot UO_2H_2P_2O_7 \longrightarrow (UO_2)_nH_2P_{2n}O_{6n+1} + (n-1)H_2O \quad (6)$$

Here n is relatively small in this temperature range.

At nearly 300°C, the contents of tri-, tetra- and trimetaphosphates reach their maxima. When the temperature rises from 300 to 800°C, the contents of ortho-, di-, tri-, tetra- and trimetaphosphates decrease, while the content of the high polyphosphate still increases. Accordingly, in this temperature range the condensation reactions such as reactions (5) and (6) mainly occur, and the intermediates such as product [I] in reaction (5) seem to be the sources of ortho-, di-, triphosphate, *etc.* in the sample solutions.

At 800°C the condensation reactions are over, and the main component of the sample is the uranyl salt of long-chain metaphosphate, *i.e.*, uranyl metaphosphate, $[UO_2(PO_3)_2]_n$.

$$(UO_2)_nH_2P_{2n}O_{6n+1} \longrightarrow [UO_2(PO_3)_2]_n + H_2O \quad (7)$$

It was confirmed by visual observation that the melting of the sample occurs at about 900°C, and the product swells at the same time. The wide endothermic peak at 900—1000°C in the DTA curve might be due to the melting of the sample and the reduction of uranium(VI) to uranium(IV) accompanied by the formation of oxygen gas. The reduction of uranium(VI) to uranium(IV) was ascertained by the titration of the sample solutions with dichromate. This titration did not give quantitative data for uranium(IV) because a part of it was oxidized during the dissolution of the samples. Owing to the reduction of uranyl ions, UO_2^{2+} to uranium(IV) ions, U^{4+}, the positive charge of the cations increases from 2 to 4. Since the balance between the positive charge of the uranium(IV) cations and the negative charge of the phosphate anions should be kept, the degradation of the long-chain metaphosphates occurs to form finally uranium(IV) diphosphate.

$$[UO_2(PO_3)_2]_n \longrightarrow n\cdot UP_2O_7 + n/2\cdot O_2 \quad (8)$$

However, it must be noted that the thermal decomposition of reaction (8) occurred in air. Thus, the weight loss at about 900°C on the TGA curve is due to the escape of oxygen gas from the sample. The total weight loss of the UDOT exactly coincides

16) E. Stege and G. Leukroth, *ibid.*, **303**, 169 (1960).

with the calculated value, 20.6% which is derived on the assumption that the UDOT, $UO_2(H_2PO_4)_2 \cdot 3H_2O$ is completely changed into uranium(IV) diphosphate, UP_2O_7.

The authors wish to express their thanks to the staff of the Government Industrial Research Institute, Kyushu for the thermal analysis. This work was supported in part by grant-in-aids from the Ministry of Education and Asahi Press.

BULLETIN OF THE CHEMICAL SOCIETY OF JAPAN VOL. 43 89—94 (1970)

The Chemistry of Americium. I. A Study of the Preparation of Am(V) and Its Behavior by Means of TTA Extraction

Mitsuo HARA

The Research Institute for Iron, Steel and Other Metals, Tohoku University, Katahira-cho, Sendai

(Received May 8, 1969)

The method for preparing Am(V) in various solutions was investigated by utilizing the difference in extractability between Am(V) and Am(III) in an TTA-isobutanol extraction system; Am(III) was quantitatively extracted with 0.1 M TTA in isobutanol from a 1 M acetate buffer solution at a pH greater than 3, while the percentage of Am(V) extracted into the organic phase was increased substantially with an increase in the pH from 3 to 5. When the organic phase containing Am(V) was shaken with an aqueous phase having a proper pH value and composition, Am(V) was selectively stripped into the aqueous phase. The stability of the valency state of Am(V) in the perchlorate, the acetate, and the sulfate solutions was then studied by examining the variation in the percentage of americium extracted as a function of the standing time. The rate of change in the valency state in the acetate and the perchlorate media is very slow, while it is rather rapid in the sulfate medium. This difference may be attributable to the faster rate of the disproportionation reaction of Am(V) in the last medium than in the former two. By applying the above results, the chemical behavior of Am(V) in the aqueous solution was investigated by TTA extraction; it was found that Am(V) would be in the form of AmO_2^+ in the absence of a complexing reagent. By the addition of acetate ions, the step-by-step formation of the acetate complex of Am(V) was observed. The stability constants of $[AmO_2Ac]$ and $[AmO_2Ac_2]^-$ were determined to be (25.0 ± 3.1) $(mol/l)^{-1}$ and (12.8 ± 1.2) $(mol/l)^{-2}$ respectively.

Although many papers on the chemical behavior of Am(III), which is the most stable oxidation state of americium in aqueous solutions, have been published, the knowledge concerning that of americium in higher oxidation states in rather poor, especially when a tracer concentration is involved. Investigations of americium in higher oxidation states have been limited to work on the absorption spectra of Am(V) and Am(VI) in various solutions,[1-5] the disproportionation reaction of Am(V),[1-3,6-9] and the self-reductions of both Am(V) and Am(VI).[1-3,6,10,11] The backwardness in this study is primarily due to the technical difficulty involved in the experimentation and does not reflect any lack of importance in these valency states. Americium is the heaviest of the actinide elements which are known to have pentavalent and hexavalent

1) G. R. Hall and P. D. Herniman, *J. Chem. Soc.*, **1954**, 2214.
2) G. R. Hall and T. L. Markin, *J. Inorg. Nucl. Chem.*, **4**, 296 (1957).
3) G. N. Yakovlev and V. N. Kosyakov, Proc. Intern. Conf. Peaceful Uses of Atomic Energy, **7**, 363 (1956).
4) S. E. Stepanou, J. P. Nigon and R. A. Penneman, *J. Chem. Phys.*, **21**, 42 (1953).
5) S. R. Gunn, UCRL-2541 (1954).
6) S. R. Gunn and B. B. Cunningham, *J. Amer. Chem. Soc.*, **79**, 1563 (1957).
7) J. S. Coleman, *Inorg. Chem.*, **2**, 53 (1963).
8) A. A. Zaitsev, V. N. Kosyakov, A. G. Rykov, Yu. D. Sobolev, and G. N. Yakovlev, *Radiokhimiya*, **2**, 339 (1960).
9) S. E. Stepanou, L. B. Asprey and R. A. Penneman, AECU-925 (1950).
10) L. B. Asprey, S. E. Stepanou, and R. A. Penneman, *J. Amer. Chem. Soc.*, **73**, 5715 (1951).
11) L. B. Asprey and S. E. Stepanou, AECU-924 (1950).

oxidation states. In contrast to americium, the chemical properties of uranium, neptunium, and plutonium at higher oxidation states have been established comparatively well; therefore, a complete understanding of the properties of Am(V) or of Am(VI) is especially important for us if we are to understand the properties of the actinide series as a whole. Furthermore, for the separation and recovery of americium it is very effective to utilize the chemical properties of the higher oxidation states of americium.

It is well known that lanthanide(III,IV) and actinide(III,IV,V) ions coprecipitate with lanthanum fluoride under selected conditions.[12] However, Moore found that Am(VI) did not coprecipitate with lanthanum fluoride; he used this unique property of Am(VI) toward coprecipitation in separating and purifying americium.[13] Stokely and Moore developed a method for the purification of americium based on TTA-xylene extraction.[14] They suggested that Am(VI) was readily reduced to Am(V) when the pH was adjusted to 4—5 by the addition of an acetate buffer to Am(VI) solutions. In this pH range lanthanide(III,IV) and actinide(III,IV,VI) ions had been known to be extracted into a 0.5M solution of TTA,[15] but they found that Am(V) remained in the aqueous phase and was efficiently separated from the other metal ions. In order to study the chemistry of Am(V), it is necessary to establish a simple method for the preparation of a Am(V) solution and to find the conditions in which the oxidation state will continue as long as possible. Stokely and Moore's method is helpful for the preparation of Am(V). By their method, however, Am(V) is obtained only in an acetate buffer solution which contains many foreign materials, such as the peroxysulfate and sulfate ions; therefore, their method is not sufficient for general use.

The purpose of the present investigation is to establish a method for the production of Am(V) in various solutions and to get some idea of the stability of the valency state in these media. Furthermore, the usefulness of the method has been confirmed by showing its practical application to the determination of the stability constant of the acetate complex of Am(V), although the accuracy is limited because of the technical difficulty involved in the experiment due to the instability of Am(V).

12) E. K. Hyde, "Radiochemical Separations of the Actinide Elements," in "The Actinide Elements," National Nuclear Energy Series, Division IV, Vol. 14A, ed. by G. T. Seaborg and J. J. Katz, McGraw-Hill Book Co., Inc., New York (1954), Chap. 15.

13) F. L. Moore, *Anal. Chem.*, **35**, 715 (1963).

14) J. R. Stokely, Jr., and F. L. Moore, *ibid.*, **39**, 994 (1967).

15) S. C. Foti and E. C. Freiling, *Talanta*, **11**, 385 (1964).

Experimental

Reagents. $^{241}AmO_2$ which had been obtained from the Oak Ridge National Laboratory was dissolved in conc. nitric acid. The solution was then evaporated to dryness, and the residue was dissolved with 2N nitric acid and diluted to 1N in a nitric acid concentration. This solution served as the stock solution of americium. Before use, an aliquot of the stock solution was diluted to about 10^{-6}M with respect to americium with a nitric acid solution of a suitable concentration, thus making the acidity 0.1N. The radiochemical purity of ^{241}Am was confirmed by α- and γ-ray spectrometry. The xylene and isobutanol were purified by distillation, and the other chemicals, such as 2-thenoyltrifluoroacetone (TTA), ammonium persulfate and silver nitrate, were of the highest purity.

Apparatus. In order to check the radiochemical purity, the γ-ray spectra were measured with a $1\frac{3}{4}'' \times 1''$ NaI(Tl) detector coupled with a Kobe-Kogyo 100-channel pulse-height analyzer, Model AN-100, while the α-ray spectra were measured with an Osaka-Denpa gridded ionization chamber coupled with a TMC-400 channel pulse-height analyzer. For the determination of the distribution ratio, the γ-activity was counted with the above-mentioned scintillator coupled with a Kobe-Kogyo scaler, Model SA-250. For the solvent extraction, an Iwaki universal mechanical shaker, Model V-S, was used. A Toa-Denpa-Kogyo pH-meter, Model PE-2, was used for the pH measurements.

Procedure. The experiments were carried out by the following procedure except as otherwise noted.

Procedure for the Preparation of an Am(V) Solution. To 20 m*l* of a sample solution of americium in a beaker, 5 m*l* of a 0.5M ammonium persulfate solution and 1 m*l* of a 0.2% silver nitrate solution were added. The mixture was heated for 10 min in a water bath at 90—95°C. Then 1 m*l* more of the ammonium persulfate solution was added and the solution was heated for a few more minutes. Immediately after its removal from the hot water bath, the beaker was placed in an ice bath and left standing for at least 10 min. Then 5 m*l* of a 1M ammonium acetate solution which had previously been cooled was added, and the combination was mixed completely. The solution was transferred into a separatory funnel and 25 m*l* of a 0.1M TTA solution of isobutanol were added. The separatory funnel was mechanically shaken for 5 min, and the aqueous phase discarded. Then, Am(V) was back-extracted into the aqueous phase of a suitable composition, leaving Am(III) and Am(VI) in the organic phase. This solution was used as an aqueous phase for the following solvent extraction experiments.

Procedure for the Extraction. The solvent extraction was carried out by bringing in contact 10-m*l* portions of an organic phase and of an aqueous phase for 3 min at room temperature. After shaking, a suitable aliquot of each phase was placed in a polyethylene test tube and its γ-activity was counted with an accuracy of $\pm 2\%$. The rest of the aqueous phase was used for the measurement of the pH.

The distribution ratio (D) and the percentage extracted ($E\%$) were calculated by means of the usual relationship:

$$D = \frac{\gamma\text{-activity per ml of the organic phase}}{\gamma\text{-activity per ml of the aqueous phase}}$$

$$E\% = \frac{100 \cdot D}{D + V_{aq}/V_{org}}$$

where V_{aq} and V_{org} are the volumes of the aqueous and organic phases respectively.

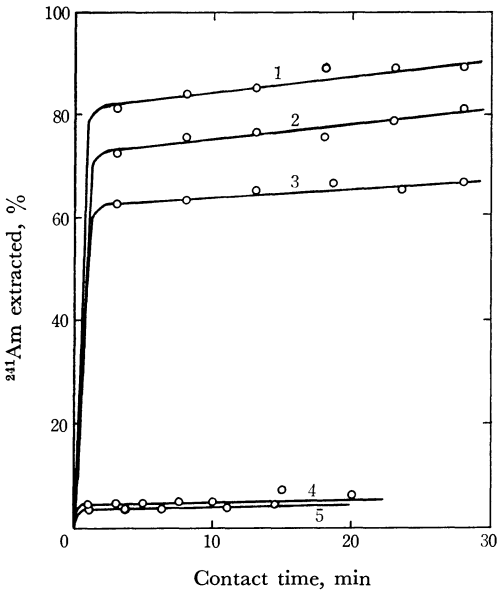

Fig. 1. The effect of the contact time on the TTA extraction of Am(V).
0.1M TTA-isobutanol: 1. pH=5.5, 2. pH=5.3, 3. pH=5.1
0.5M TTA-xylene: 4. pH=5.1, 5. pH=3.9

Results and Discussion

The Effect of the Contact Time on the TTA Extraction of Am(V). The effects of the contact time on the extraction of Am(V) with TTA solutions were investigated. A freshly-prepared Am(V) solution in 0.1M acetic acid-ammonium acetate was mixed with either 0.5M TTA in xylene or 0.1M TTA in isobutanol. The percentage of americium extracted is shown in Fig. 1 as a function of the contact time. As is clearly shown in Fig. 1, the percentage of americium extracted instantly reaches a nearly constant value and gradually increases afterward. This tendency holds irrespective of the kind of diluent and the pH value of the aqueous phase.

The gradual increase in the percentage of americium extracted may be attributable to the reduction of Am(V) to Am(III) in both phases during extraction, because Am(III) is much more extractable than Am(V). Am(V) is probably reduced either by the organic substances or by the radiolysis products produced in the solution by the absorption of alpha rays of ^{241}Am. In the TTA-xylene system the latter mechanism is more probable than the former, since the rate of the reduction of Am(V) is estimated from Fig. 1 to be several per cents/hr, a value which nearly agrees with the rate of self-reduction reported by Hall and Markin.[2] However, a portion of Am(V) is probably reduced isobutanol because the percentage of americium extracted in the isobutanol system increases at a rate which can not be explained simply by the self-reduction reaction of Am(V). In order to minimize the contribution of Am(III) to the distribution ratio of Am(V), it is desirable to select as short a contact time as possible. In view of both this and the rate of extraction, it has been decided to bring the two phases into contact for 3 min.

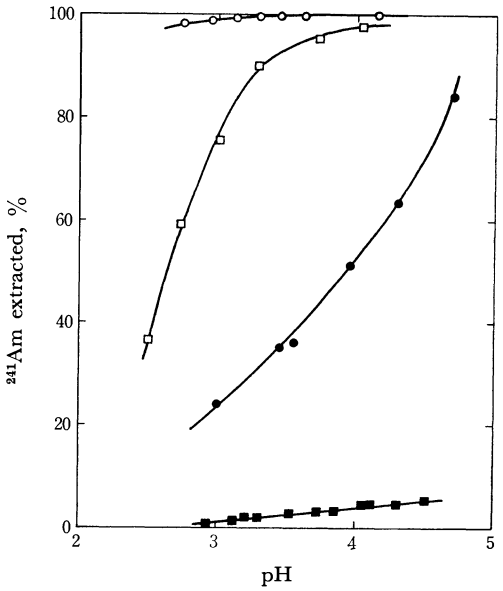

Fig. 2. The effect of pH on the extraction of Am(V) and Am(III) with TTA.
0.1M TTA-isobutanol: ○ Am(III), ● Am(V)
0.5M TTA-xylene: □ Am(III), ■ Am(V)

The Effect of the pH on the TTA Extraction of Am(V). Fig. 2 shows the effect of the pH of the aqueous phase on the extraction of Am(V) and Am(III). Am(III) is quantitatively extracted by the 0.1M TTA solution of isobutanol from 1M acetate buffer solutions when the pH of the solution is higher than 3. On the other hand, only 25% of Am(V) is extracted at pH 3, 40% at pH 4, and nearly 100% at pH 5. These results suggest the possibility of the preparation of Am(V) solutions; that is, when the aqueous solution which contains Am(III) and Am(V) is in contact with a 0.1M TTA solution of isobutanol, Am(III) and Am(V) will be extracted into the organic phase. When the organic phase is mixed with a new aqueous phase with a proper pH value, Am(V) will be selectively stripped into the aqueous phase, while

all the Am(III) will remain in the organic phase. It is this fact that is used in the present study for the preparation of aqueous solutions of Am(V).

The dependence of the percentage of Am(V) and of Am(III) extracted on the pH in a 1.0M acetate buffer-0.5M TTA solution of the xylene system is shown in Fig. 2. Am(III) is also quantitatively extracted at pH above 4, while Am(V) is only partially extracted (10% at most). Besides xylene, chloroform, carbon tetrachloride, benzene and cyclohexane all failed to extract Am(V). Cyclohexanone and hexone extracted the Am(V) complex, but less readily than isobutanol did.

The influence and the role of the solvent in the extraction of chelate compounds have been discussed from various points of view, such as the polarity of the solvent, the solubility of the chelate compounds in the organic solvent, and the coordination of the solvent with or the addition of the solvent to the central atoms in chelate compounds, but no final conclusions have yet been reached. Alimarin and Zolotov, however, discussed the solvent effect from the point of view of the coordination number of the central atom in chelates;[16] their conclusion seems to be capable of explaining the results obtained in the present work. The molecules of a polar solvent displace the water molecules which occupy the free coordination positions of the central atom, making the chelate more organophilic; thus such polar solvents as isobutanol, cyclohexanone, and hexone extract the Am(V)-TTA chelate better than non-active solvents do.

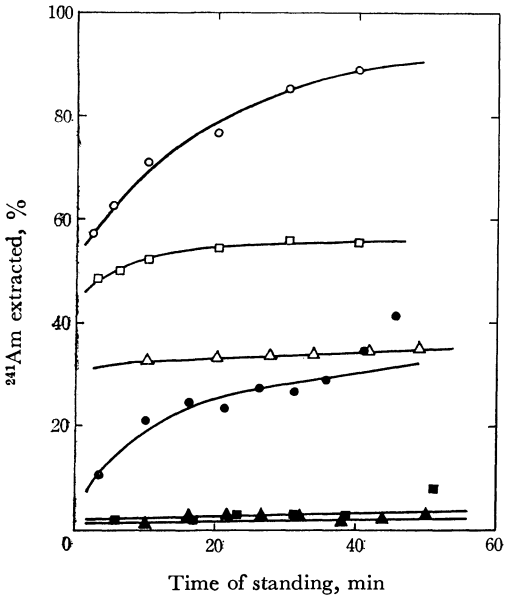

Fig. 3. Effect of time of standing in the TTA extraction of Am(V).
○ 0.1M TTA-isobutanol/0.1M sulfate (pH=4.4)
□ 0.1M TTA-isobutanol/0.1M acetate (pH=5.0)
△ 0.1M TTA-isobutanol/0.1M perchlorate (pH=4.5)
● 0.5M TTA-xylene/1.0M sulfate (pH=4.1)
■ 0.5M TTA-xylene/1.0M acetate (pH=3.4)
▲ 0.5M TTA-xylene/1.0M perchlorate (pH=4.5)

The Stability of the Valency State of Am(V) in Various Aqueous Solutions. The perchlorate, acetate, and sulfate solutions of Am(V) were stored at 0°C. Suitable aliquots of the solutions were subjected to TTA extraction after a definite time of standing. The variation in the percentage of americium is shown in Fig. 3 as a function of the time. In the cases of the acetate and perchlorate solutions, the variation in the percentage of americium extracted is about 3%/hr, which may be due to the reduction of Am(V) to Am(III), as has been discussed before. Thus, Am(V) is not very stable in either perchlorate or acetate solutions, but the contribution of Am(III) to the distribution ratio is negligible within about 10 min after the preparation of the Am(V) solutions. As Am(III) is gradually generated during storage, it is necessary before use to remove Am(III) by extraction with a 0.5M TTA solution of xylene at a pH value above 4. On the other hand, the tendency of the percentage of americium extracted in the sulfate system to increase with the standing time is faster than in the perchlorate and the acetate systems; that is, Am(V) seems to be less stable in sulfate solutions. The cause of the instability of Am(V) in sulfate media is not clear, but Coleman's observation[7] seems to suggest one reason; he

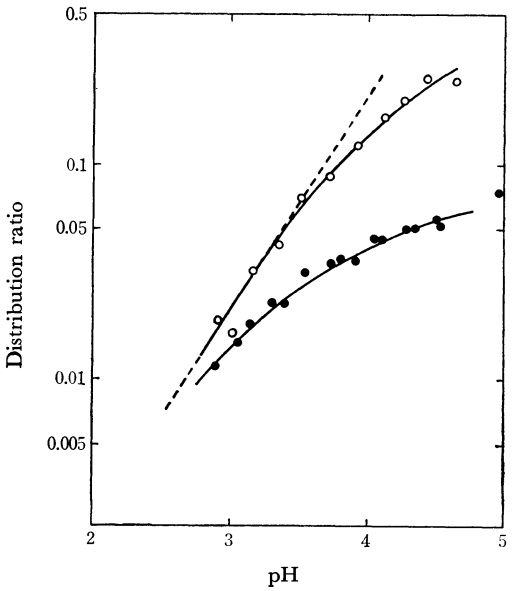

Fig. 4. The pH dependence of the distribution ratio of Am(V) in the TTA-xylene extraction.
○ 0.1M acetate solution
● 1.0M acetate solution

16) I. P. Alimarin and Yu. A. Zolotov, *ibid.*, **9**, 891 (1962).

studied the rate of the disproportionation of Am(V) in various acid media and found that the rate constant in a sulfuric acid medium was many times greater than that in other acids, such as nitric and hydrochloric acids. In any case, the dependence of the rate of the decrease of Am(V) on the nature of the coexisting anion deserves further study. Attempts to prevent Am(V) from reduction using such holding oxidants as $(NH_4)_2S_2O_8$–Ag^+ and ozone failed; what is worse, a part of the TTA was decomposed by such strong oxidizing reagents.

The Determination of the Stability Constant of the Acetate Complex of Am(V). The pH dependence of the distribution ratio of Am(V) between a 0.5M TTA solution of xylene and a 1.0 or 0.1M acetate solution is shown in Fig. 4. The distribution ratios in the 0.1M acetate system are larger than those in the 1.0M acetate system at the same pH value; this observation suggests the formation of acetate complexes of Am(V). The curves in the figure in both systems approach a straight line with a slope of about one with the decrease in the pH. Irving and Edgington extracted Np(V) in a 0.05M HNO_3 solution with 0.05M TTA in cyclohexane, and demonstrated the first-order dependency of the distribution ratio on pH.[17]

As the chemical properties of Am(V) are expected to be similar to those of Np(V), the deviation of the distribution ratio from the straight line (the dotted line in Fig. 4) can be understood in terms of the formation of the acetate complexes of Am(V). It is apparent from the following equation that the acetate ion concentration, [Ac$^-$], increases with an increase in the pH at a constant total acetic acid concentration, $[HAc]_i$:

$$\log \frac{[HAc]_i - [Ac^-]}{[Ac^-]} = pK_a - pH$$

where pK_a is the acid constant of acetic acid. The dependency of the distribution ratio on the TTA concentration in xylene is found to be second-order as is shown in Fig. 5; the same tendency holds in the case of Np(V).[17] Considering these results, it may be assumed, by analogy with Np(V), that Am(V) would be found in the form of AmO_2^+ in an aqueous solution containing no complex-forming reagent. This assumption is also warranted by the results of infrared spectroscopy by Jones and Penneman.[18] In the presence of acetate ions, AmO_2^+ forms acetate complexes. The species extracted in the organic phase are the neutral chelate compounds of AmO_2^+ and TTA. Therefore, the equilibria concerned in the extraction and in the acetate complex formation of Am(V) can be written as:

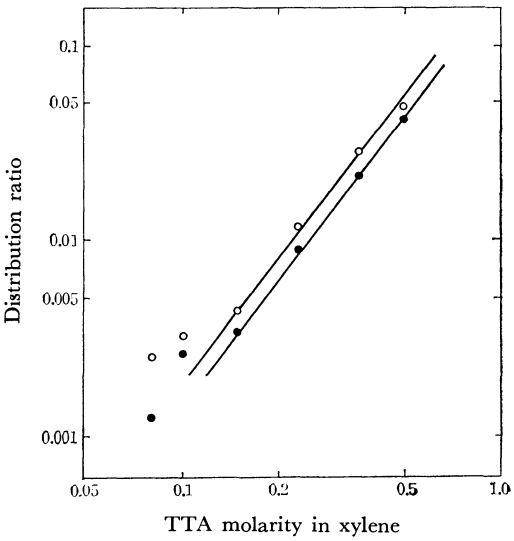

Fig. 5. Relationship between the distribution ratio and the concentration of TTA in xylene in the extraction of Am(V) from 0.1M acetate solution.
○ pH=4.6 ● pH=3.6

$$AmO_2^+ + 2HA_{org} \rightleftharpoons AmO_2HA_{2,org} + H^+ \quad (1)$$

$$AmO_2^+ + Ac^- \rightleftharpoons AmO_2Ac \quad (2)$$

$$AmO_2Ac + Ac^- \rightleftharpoons AmO_2Ac_2^- \quad (3)$$

where HA and Ac$^-$ indicate the TTA molecule and the acetate ion respectively. The subscript "org" indicates the organic phase, while the unsubscripted species refer to the aqueous phase. The formation of a complex higher than $AmO_2Ac_2^-$ may be neglect-

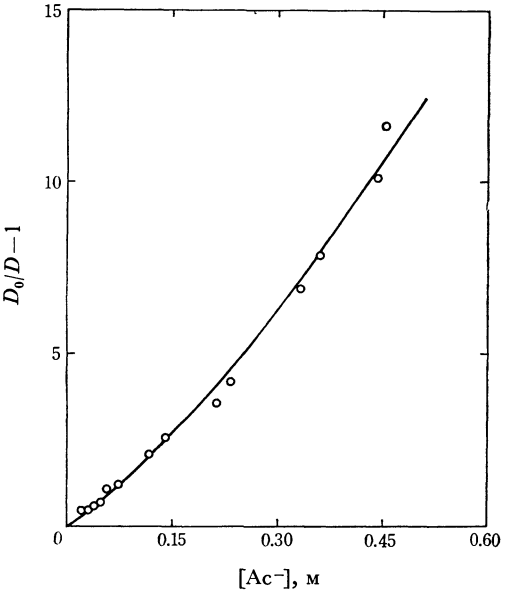

Fig. 6. Relationship between $(D_0/D-1)$ and acetate ion concentration.

17) H. Irving and D. N. Edgington, *J. Inorg. Nucl. Chem.*, **20**, 314 (1961).

18) L. H. Jones and R. A. Penneman, *J. Chem. Phys.*, **21**, 542 (1953).

ed in the range of acetate-ion concentrations investigated. The distribution ratio of Am(V), D, can then be defined as:

$$D = \frac{[\mathrm{Am(V)}]_{org}}{[\mathrm{Am(V)}]_{aq}} = \frac{[\mathrm{AmO_2HA_2}]_{org}}{[\mathrm{AmO_2^+}]+[\mathrm{AmO_2Ac}]+[\mathrm{AmO_2Ac_2^-}]} \quad (4)$$

If one uses K_0 for the equilibrium constant of Reaction (1) and β_1 and β_2 for the stability constants of AmO_2Ac and $AmO_2Ac_2^-$ respectively, Eq. (4) is reduced to:

$$D = \frac{K_0[\mathrm{HA}]_{org}^2}{[\mathrm{H^+}](1+\beta_1[\mathrm{Ac^-}]+\beta_2[\mathrm{Ac^-}]^2)} \quad (4')$$

where $[HA]_{org}$ is the concentration of TTA in the organic phase and while $[H^+]$ and $[Ac^-]$ are the concentrations of hydrogen ions and acetate ions respectively in the aqueous phase. One can then rewrite Eq. (4') as:

$$D = D_0(1+\beta_1[\mathrm{Ac^-}]+\beta_2[\mathrm{Ac^-}]^2)^{-1} \quad (5)$$

where D_0 is the distribution ratio when the acetate ion is absent and is defined as the inclination of the dotted line in Fig. 4. Using the experimental values of D and the corresponding values of D_0 read from the dotted line, the magnitudes of $(D_0/D-1)$ are calculated. The relation between $(D_0/D-1)$ and $[Ac^-]$ is shown in Fig. 6. Using the method of least squares, the best-fit values for β_1 and β_2 were founds to be $(25.0\pm3.1)(\mathrm{mol}/l)^{-1}$ and $(12.8\pm1.2)(\mathrm{mol}/l)^{-2}$ respectively.

This author wishes to thank Professor Shin Suzuko and Dr. Yasushi Inoue for their kind and valuable advice throughout this study. A part of the expence has been defrayed by a grant-in-aid from the Ministry of Eduction.

BULLETIN OF THE CHEMICAL SOCIETY OF JAPAN VOL. 43 94—96 (1970)

Activity Coefficient of Sodium in Dilute Sodium and Gold Alloy at 1400°K

Kazushi HIROTA and Takashi KATSURA

Department of Chemistry, Tokyo Institute of Technology, Ookayama, Meguro-ku, Tokyo

(Received May 12, 1969)

The equilibria between the molten Na_2CO_3 and the Au-Na alloys were determined at 1400°K under $CO+CO_2$ gaseous mixtures. The activity coefficient of Na in the Au-Na alloys was constantly 0.0392 ± 0.0028 at concentrations ranging from 0.2 to 0.02 wt% Na.

In the thermodynamic study of ionic solutions, the electromotive force measurement between the solution and a pure metal has generally proved very useful when the pure liquid or solid metal is stable at a desired temperature. However, if the vapor pressure of the pure metal is high, it is not practical to construct the cell. This is just the case with the liquid metallic sodium at a high temperature. At 1400°K, for example, the vapor pressure of sodium is about 6.2 atm.[1] To avoid such difficulty, an attempt was made to determine precisely the activity coefficients of sodium in the gold-sodium alloys, especially at low sodium concentrations.

Experimental

The quenching method was adopted to obtain the equilibrium concentration of sodium in the alloy. About 2 g of purified gold, or a sodium-gold alloy, and about 10 g of pure sodium carbonate were put into an alumina crucible (Nippon Kagaku Togyo Co., SSA-H-010). The crucible was then heated in a vertical-type tube furnace at 1400°K, through which there had previously been passed a desired gaseous mixture, $CO+CO_2$, until equilibrium was attained between the condensed and the gas phases. A small-size alumina tube (Degussa, AL-23) was dipped into the liquid sodium carbonate phase to bubble in the same gaseous mixture as that of the inside of the furnace. The crucible was then quenched as quickly as possible after equilibrium was attained between the condensed and gas phases.

Pure gold was obtained as follows: Commercially-pure gold was first dissolved in aqua regia, and then treated with hydrochloric acid to expel the nitric acid. The gold complex was then extracted by diethyl ether. The gold metal was precipitated from the hydrochloric acid solution by sulfur dioxide gas.

The temperature was calibrated against the gold and diopside points; the fluctuation of the temperature was within ±2°K throughout the study. The gases, CO_2 (99.95% purity or more) and CO (99.5% or more),

1) M. M. Makansi, C. H. Muendel and W. A. Selke, *J. Phys. Chem.*, **59**, 40 (1955).

were mixed by an apparatus previously described[2]; the fluctuation in mixing ratio, CO_2/CO, was estimated to be within $\pm 0.5\%$.

Analytical Method for Determining Na in Na-Au Alloy. A flame-photometric method was mainly adopted. About 0.2 to 3 g of the alloy sample was dissolved on a hot plate by the use of 20 m*l* of aqua regia in a quartz glass beaker; after almost dried, exactly 5 m*l* of concentrated sulfuric acid was added to expel the remaining nitric acid. The residual mass was treated by hot water, and then sulfur dioxide was passed through this hot solution for about 20 min in order to effect the complete precipitation of the gold.

After filtration, the solution was evaporated almost to dryness in order to expel the excess sulfuric acid. The residue was dissolved in water to make the solution up to 100 m*l*. The solution almost free from sulfuric acid was determined for sodium by the flame photometer (EPU-2A, H-2, Hitachi Co.). The concentration of sodium in the 100 m*l* solution was kept around 10 ppm Na by adjusting the sample weight of the alloy. The effect of the sulfuric acid in the sample solution was negligible in such a low concentration of sulfuric acid. The contamination from reagents was determined to be constantly 0.03 ± 0.01 mg Na. Some duplicated analyses showed the deviation of ± 0.003 wt% Na at a high Na content and that of ± 0.002 wt% Na at a low content.

Criteria for Equilibrium. Two methods were applied to criticize the attainment of equilibrium; one was based on the both-side reactions (b.s.r. in Table 1), and the other, on the electromotive force measurement (emf in Table 1). The former is the reaction of gold-sodium alloy, comprising an arbitrary concentration of sodium, with sodium carbonate under a desired $CO+CO_2$ gaseous mixture; it finally obtains the equilibrium concentration value in between the concentrations of the starting alloys. The other method adopted was the electromotive force measurement of the following cell:

Na-Au alloy $|Na_2CO_3$ melt $|CO+CO_2$ mixed gas

The apparatus for this purpose is shown in Fig. 1. The electromotive force of this cell was corrected for the thermoelectromotive force of the lead wire in the cell. The system was assumed to be in equilibrium when the corrected electromotive force was observed to be zero. Iridium and Pt-Rh wires do not react with liquid gold and liquid sodium carbonate respectively.

Table 1. Sodium concentration in Au–Na alloy in equilibrium with Na_2CO_3 melt and $CO+CO_2$ gas mixture at 1400°K

Partial pressure of CO_2 in gas mixture (in atm)	wt% Na in alloy at equilibrium	wt% Na in starting alloy	Method and reaction time (hour)	$\Delta G^\circ(1)/4.606RT+\log(P_{Na}/N_{Na})$
0.194	0.203	—	emf*	2.435
0.200	0.190	0.08	b.s.r.** (3.5)	2.431
0.200	0.208	0.58	b.s.r. (4.0)	2.401
0.260	0.140	—	emf	2.440
0.316	0.113	—	emf	2.438
0.409	0.079	—	emf	2.444
0.500	0.064	—	emf	2.411
0.500	0.058	0.06	b.s.r. (3.0)	2.461
0.500	0.056	0.00	b.s.r. (5.0)	2.471
0.667	0.036	—	emf	2.447
0.727	0.029	—	emf	2.457
0.800	0.024	0.00	b.s.r. (5.5)	2.437
0.800	0.025	0.18	b.s.r. (5.0)	2.417
0.800	0.023	—	emf	2.457
			average	2.439 ± 0.03

* electromotive force measurement
** both side reaction method

2) L. S. Darken and R. W. Gurry, *J. Amer. Chem. Soc.*, **67**, 1398 (1945).

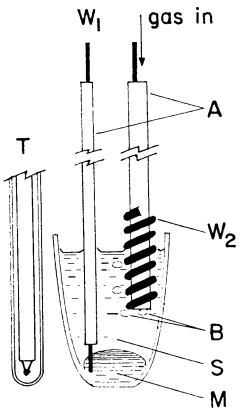

Fig. 1. Construction of the cell, $Na+Au|Na_2CO_3|CO_2+CO$.
A: alumina tube, B: bubble of the $CO+CO_2$ gas mixture, M: Na+Au metal phase, S: sodium carbonate melt, T: thermocouple, W_1: Iridium wire, W_2: Pt wire.

Results and Discussion

The results are summarized in Table 1. Liquid sodium carbonate was practically pure under the equilibrium condition. After quenching, the sodium carbonate mass was immediately dissolved in water; no evolution of gas was ascertained. This means that the amount of metallic sodium in the carbonate phase is negligible under the present experimental conditions. The dissolution of the alumina crucible and alumina tube into sodium carbonate increases with a decrease in the CO_2 partial pressure; at most, 0.03 wt% Al_2O_3 was found in sodium carbonate after 22 hr heating when the CO_2 partial pressure was 0.05 atm. The dissolution of gold into liquid sodium carbonate was found to be 0.05 wt% as Au, for example, when the composition of the gaseous mixture was 20% CO_2 and 80% CO. The dissolution of gold seems to be a function of the CO partial pressure in the gaseous mixture.

In the present experiment, the following reactions may be expected in the system:

$$CO(g) + Na_2CO_3(1) = 2Na(g) + 2CO_2(g) \quad (1)$$

$$Na_2CO_3(1) = Na_2O(1) + CO_2(g) \quad (2)$$

The standard free energy of the reaction (2) can be calculated to be 33.094 kcal/mol at 1400°K.[3] Then,

$$\log (a_{Na_2CO_3}/a_{Na_2O} \cdot P_{CO_2}) = 5.166 \quad (3)$$

where P_{CO_2} is the partial pressure of CO_2 in atm. $a_{Na_2CO_3}$ and a_{Na_2O} are the activities of Na_2CO_3 and of Na_2O respectively, referred to the liquid state. Therefore, the decomposition of the sodium carbonate melt into the sodium oxide and carbon dioxide gas is negligible under the present experimental conditions. The similar decomposition reactions of sodium carbonate into NaO, Na_2O_2, *etc.* are also negligible. Judging from these results, it may be concluded, within the present limits of experimental error, that the partial pressure of the CO and CO_2 of the gaseous mixture are unaffected by being brought into contact with the sodium carbonate melt.

At the equilibrium of the system, the partial pressure of monatomic sodium, P_{Na}, may be represented by:

$$-\ln P_{Na} = \Delta G^\circ(1)/2\boldsymbol{R}T + \ln P_{CO_2} - (1/2)\ln P_{CO} - (1/2)\ln a_{Na_2CO_3} \quad (4)$$

where $\Delta G^\circ(1)$ is the standard free energy of the reaction (1) at 1400°K, $\boldsymbol{R}$ is gas constant, T is the absolute temperature, and P_{CO_2} and P_{CO} are the partial pressures of CO_2 and CO in the gas mixture respectively. $a_{Na_2CO_3}$ is the activity of Na_2CO_3 referred to the liquid state. At the equilibrium of the system, the partial pressures of monatomic sodium, calculated from Eq. (4), were ranged from 2 mmHg to 0.2 mmHg.

From Eq. (4) and the fact that the carbonate phase was essentially pure, that is to say, assuming the activity of sodium carbonate to be unity, we obtain:

$$\Delta G^\circ(1)/4.606\boldsymbol{R}T + \log (P_{Na}/N_{Na}) = (1/2)\log P_{CO} - \log P_{CO_2} - \log N_{Na} \quad (5)$$

where N_{Na} is the atom fraction of Na in the alloy. By the use of the right hand side of Eq. (5), the left hand side was calculated; the results are given in the last column of Table 1. It may be concluded from these results that the P_{Na}/N_{Na} is almost constant within the limits of experimental error in the concentration range of the present investigation, about 0.02 to 0.2 wt% Na. We obtain the following result:

$$\Delta G^\circ(1)/4.606\boldsymbol{R}T + \log (P_{Na}/N_{Na}) = 2.44 \pm 0.03 \quad (6)$$

The $\Delta G^\circ(1)$ can be calculated from the values of the standard free energies of the formations of CO(g), CO_2(g), and Na_2CO_3 (1) at 1400°K. The standard free energies of the formation of CO and CO_2 gases are known to be highly reliable, and are taken from the literature.[3] Also a recent compilation by "JANAF"[3] gives the standard free enery of the formation of Na_2CO_3 (1) to be -173.627 kcal/mol. Thus, if we use these values, $\Delta G^\circ(1)$ can be calculated to be $+40.557$ kcal/mol. By substituting proper values into Eq. (6), we obtain the following result at concentrations ranging from 0.2 to 0.02 wt% Na:

$$P_{Na}/N_{Na} = 0.188 \pm 0.013 \text{ (atom)} \quad (7)$$

at 1400°K.

When we choose the pure liquid standard state for the activity of sodium, a_{Na}, the activity coefficient, $\gamma_{Na} = a_{Na}/N_{Na}$, can be calculated from (7) as follows:

$$\gamma_{Na} = 0.0392 \pm 0.0028 \quad (8)$$

where the values of the standard free energy change of the condensation of monatomic sodium gas to the pure liquid sodium used in the calculation were $+4.373$ kcal/mol.[3]

3) "JANAF" Thermochemical Tables, PB-168-370, U. S. Department of Commerce/National Bureau of Standards, 1965.

BULLETIN OF THE CHEMICAL SOCIETY OF JAPAN VOL. 43 97—99 (1970)

Cobalt(II, III), Nickel(II) and Copper(II) Complexes with Tetra- and Hexamethylenediaminetetraacetate

Hiroshi OGINO, Shigeru KOBAYASHI and Nobuyuki TANAKA

Department of Chemistry, Faculty of Science, Tohoku University, Katahira-cho, Sendai

(Received May 28, 1969)

Synthesis of new complexes of cobalt(II), cobalt(III), nickel(II) and copper(II), $[Co_2hdta]\cdot 6.5H_2O$, $K[Co\ tdta]\cdot 3H_2O$, $[Ni_2\ hdta]\cdot 6.5H_2O$, $Na_2[Cu\ tdta]\cdot 6H_2O$, $[Cu_2\ tdta]\cdot 1.5H_2O$ and $[Cu_2\ hdta]\cdot 6.5H_2O$, has been carried out, where tdta and hdta represent $(OOCCH_2)_2N(CH_2)_4N(CH_2COO)_2^{4-}$ and $(OOCCH_2)_2N(CH_2)_6N(CH_2COO)_2^{4-}$, respectively. The infrared, nuclear magnetic resonance and visible and ultraviolet absorption spectra were measured. The infrared and the NMR spectra of the Co(III) complex with tdta indicate that a quadrivalent tdta anion behaves as a hexadentate in this complex.

The preparation and properties of the cobalt(II), cobalt(III), nickel(II) and copper(II) complexes with ethylenediaminetetraacetate (edta) have been extensively investigated. The stability constants of complexes with higher homologues of EDTA have also been reported.[1-3] This paper presents the synthesis and properties of cobalt(II), cobalt(III), nickel(II) and copper(II) complexes with tetramethylenediaminetetraacetate ($(^-OOCCH_2)_2N(CH_2)_4N(CH_2COO^-)_2$) and hexamethylenediaminetetraacetate ($(^-OOCCH_2)_2N(CH_2)_6N(CH_2COO^-)_2$).

Experimental

Preparation. H_4tdta[1] and H_4hdta[2] have been prepared by Schwarzenbach and Ackermann and by Müller and Bersin, respectively, where tdta and hdta represent quadrivalent anions of tetra- and hexamethylenediaminetetraacetate, respectively. In this study, however, these compounds were prepared with procedures similar to that applied to the synthesis of trimethylenediaminetetraacetic acid by Tanaka and Ogino.[4]

Tetramethylenediaminetetraacetic Acid: Monochloroacetic acid (170 g; 1.8 mol) was dissolved in 50 m*l* of water, to which 144 g (3.6 mol) of sodium hydroxide dissolved in 100 m*l* of water was added drop by drop with stirring at about 10°C, followed by the addition of 28 g (0.3 mol) of tetramethylenediamine. The resulting solution was heated at 100°C for 1 hr and was left standing overnight. The pH of the solution was adjusted to 2.3 with concentrated hydrochloric acid. The solution was evaporated on a water-bath, and the white powder containing sodium chloride was collected. This mixture was washed with water to remove as much sodium chloride as possible. The compound was recrystallized from hot water, when the hydrate was obtained. Recrystallization was repeated five times. Found: C, 40.22; H, 6.85; N, 7.76%. Calcd for $C_{12}H_{20}N_2O_8\cdot 2H_2O$: C, 40.45; H, 6.74; N, 7.87%.

Hexamethylenediaminetetraacetic Acid: Hexamethylenediaminetetraacetic acid was prepared with the same procedure as for tetramethylenediaminetetraacetic acid, except that 35 g (0.3 mol) of hexamethylenediamine was added instead of 28 g (0.3 mol) of tetramethylenediamine. The compound was recrystallized from hot water. Found: C, 47.98; H, 7.22; N, 7.89%. Calcd for $C_{14}H_{24}N_2O_8$: C, 48.28; H, 6.90; N, 8.05%.

$Na_2[Cu\ tdta]\cdot 6H_2O$: Copper(II) chloride dihydrate (3.4 g; 0.02 mol) was dissolved into 50 m*l* of water. Tetramethylenediaminetetraacetic acid (7.1 g; 0.02 mol) suspended in 50 m*l* of water was dissolved by adding 2.12 g (0.02 mol) of sodium carbonate. This solution was added to the copper(II) solution. The pH of the mixture was adjusted to about 7 with sodium bicarbonate. The resulting solution was evaporated on a water-bath to a volume of 20 m*l* and cooled in an ice-bath. A light blue crystalline compound appeared, which was collected and washed with water, alcohol and ether. The compound was recrystallized from hot water. Found: C, 26.83; H, 5.67; N, 5.31; H_2O, 21%. Calcd for $Na_2[CuC_{12}H_{16}N_2O_8]\cdot 6H_2O$: C, 26.99; H, 5.25; N, 5.25; H_2O, 20.2%.

$[Cu_2tdta]\cdot 1.5H_2O$: Copper(II) chloride dihydrate (6.8 g; 0.04 mol) was dissolved in 50 m*l* of water. Tetramethylenediaminetetraacetic acid (7.1 g; 0.02 mol) suspended in 50 m*l* of water was dissolved by adding 2.12 g (0.02 mol) of sodium carbonate. This solution was added to the copper(II) solution. The pH of the mixture was adjusted to about 6 with sodium bicarbonate. A dark blue crystalline compound was crystallized immediately. The compound was collected and washed with water, alcohol and ether. Since it was not sufficiently soluble in water, it was purified in the following way: The compound was dissolved into dilute nitric acid solution and filtered. The pH of the solution was

1) G. Schwarzenbach and H. Ackermann, *Helv. Chim. Acta*, **31**, 1029 (1948).
2) A. Müller and T. Bersin, *ibid.*, **38**, 1708 (1955).
3) G. Anderegg, *ibid.*, **47**, 1801 (1964).
4) N. Tanaka and H. Ogino, This Bulletin, **37**, 877 (1964).

adjusted to 6 with sodium carbonate, and the compound deposited was collected. Found: C, 30.52; H, 4.57; N, 6.13; H_2O, 6%. Calcd for $[Cu_2C_{12}H_{16}N_2O_8]\cdot 1.5H_2O$: C, 30.64; H, 4.04; N, 5.96; H_2O, 5.7%.

$[Co_2hdta]\cdot 6.5H_2O$: Cobalt(II) chloride hexahydrate (9.5 g; 0.04 mol) was dissolved in 50 m*l* of water. Hexamethylenediaminetetraacetic acid (7.0 g; 0.02 mol) suspended in 50 m*l* of water was dissolved by adding 2.12 g (0.02 mol) of sodium carbonate. The solution was added to cobalt(II) solution. The resulting solution was left standing overnight. Pink powder was collected and washed with water, alcohol and ether. Since the compound was not sufficiently soluble in water, it was purified in the same way as for $[Cu_2tdta]\cdot 1.5H_2O$. Found: C, 29.22; H, 6.03; N, 5.06; H_2O, 19%. Calcd for $[Co_2C_{14}H_{20}N_2O_8]\cdot 6.5H_2O$: C, 29.03; H, 5.70; N, 4.84; H_2O, 20.2%.

$[Ni_2hdta]\cdot 6.5H_2O$: This compound was prepared in the same way as for $[Co_2hdta]\cdot 6.5H_2O$. Found: C, 28.88; H, 5.99; N, 5.08; H_2O, 19.5%. Calcd for $[Ni_2C_{14}H_{20}N_2O_8]6.5H_2O$: C, 29.05; H, 5.71; N, 4.84; H_2O, 20.2%.

$[Cu_2hdta]\cdot 6.5H_2O$: This compound was prepared in the same way as for $[Co_2hdta]\cdot 6.5H_2O$. Found: C, 28.38; H, 5.89; N, 4.65; H_2O, 20%. Calcd for $[Cu_2C_{14}H_{20}N_2O_8]\cdot 6.5H_2O$: C, 28.57; H, 5.61; N, 4.76; H_2O, 19.9%.

K[Co tdta]$\cdot 3H_2O$: H_4tdta (7.1 g; 0.02 mol), potassium acetate (12.0 g; 0.12 mol) and cobalt(II) acetate tetrahydrate (5.0 g; 0.02 mol) were dissolved into 100 m*l* of water, to which 2.85 g of lead dioxide was added. The pink solution turned to dark blue immediately. The solution was filtered and the filtrate was evaporated under reduced pressure to 50 m*l* at about 50°C. After the solution was cooled to 0°C, alcohol was added drop by drop, when dark blue crystals were deposited, which were collected and washed with cold water, alcohol and ether. The compound was recrystallized from water of about 50°C by the addition of alcohol. The crystals decompose at about 100°C. Found: C, 31.05; H, 4.93; N, 5.97; H_2O, 11%. Calcd for $K[CoC_{12}H_{16}N_2O_8]\cdot 3H_2O$: C, 30.77; H, 4.70; N, 5.98; H_2O, 11.5%. It should be noted that the preparation of cobalt(III)-HDTA complexes was not successful because no suitable oxidizing agent was found to oxidize cobalt(II)-HDTA complexes to the cobalt(III) state.

Measurement. The crystalline water of the complexes was determined by a Shimadzu RT-2 recording thermobalance. The infrared spectra were obtained with a Hitachi EPI-2G recording infrared spectrophotometer by the potassium bromide disk method. The proton NMR spectra were obtained with a Varian A-60 high resolution nuclear magnetic resonance spectrometer, and the visible and ultraviolet absorption spectra, with a Hitachi EPS-3 spectrophotometer.

Result and Discussion

Infrared Absorption Spectra. In Table 1 are given the frequencies of the absorption bands of H_4edta, H_4tdta$\cdot 2H_2O$, H_4hdta, $Na_2[Cu\ tdta]\cdot 6H_2O$, $[Cu_2tdta]\cdot 1.5H_2O$, $[Co_2hdta]\cdot 6.5H_2O$, $[Ni_2hdta]\cdot 6.5H_2O$, $[Cu_2hdta]\cdot 6.5H_2O$, Na[Co edta]$\cdot 4H_2O$ and K[Co tdta]$\cdot 3H_2O$. The values obtained for H_4hdta almost agree with those in literature.[4]

Table 1. Infrared absorption of H_4edta, H_4tdta$\cdot 2H_2O$ and H_4hdta and their complexes (cm^{-1})

Compound	COOH	COO⁻ or COO⁻···M	COO⁻···M
H_4edta[4]	1634, 1704		
H_4tdta$\cdot 2H_2O$	1682		
H_4hdta	1682, 1709		
H_4hdta[4]	1686, 1709		
$Na_2[Cu\ tdta]\cdot 6H_2O$		1597	
$[Cu_2\ tdta]\cdot 1.5H_2O$		1577, 1613	
$[Co_2\ hdta]\cdot 6.5H_2O$		1595, 1626	
$[Ni_2\ hdta]\cdot 6.5H_2O$		1582, 1600	
$[Cu_2\ hdta]\cdot 6.5H_2O$		1585, 1634	
Na[Co edta]$\cdot 4H_2O$			1639
K[Co tdta]$\cdot 3H_2O$			1619, 1639

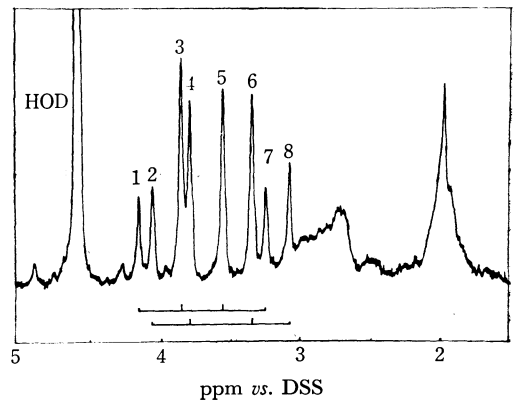

Fig. 1. Proton NMR spectra of K[Co tdta]$\cdot 3H_2O$ in D_2O. (DSS: Sodium 3-(trimethylsilyl)-1-propanesulfonate)

Table 2. Chemical shift (ppm *vs.* DSS) and coupling constants (cps) of tdta and hdta anion and K[Co tdta]$\cdot 3H_2O$

Compound	Chemical shift* H_c	H_b	H_a**	Coupling constant
edta[5]	—	2.70	3.22	
tdta	1.38	2.44	3.06	
hdta	1.28	2.48	3.10	
Co^{III}edta[6]			3.75 (0.33)	16.5
			3.92 (0.15)	18.5
Co^{III}tdta	1.97	2.71	3.57 (0.66)	16.2
			3.71 (0.51)	18.4

* $^-OOCCH_2$ CH_2COO^-
$N-CH_2-(CH_2)_n-CH_2-N$
$^-OOCCH_2$ CH_2COO^-
H_a H_b H_c

$n = 0$ (edta), 2 (tdta) and 4 (hdta)

** Relative chemical shifts of two AB protons are given in parentheses.

5) J. L. Sudmeier and C. N. Reilley, *Anal. Chem.*, **36**, 1698 (1964).

6) J. B. Terill and C. N. Reilley, *Inorg. Chem.*, **5**, 1988 (1966).

It has been reported that in the case of such divalent metal complexes as dealt with in this study, coordinated and free carboxyl ions cannot be distiguished from each other by their infrared absorption spectra.[7] The cobalt(III) complex with tdta gave a strong carboxylate band at higher frequencies than those of the absorption band due to free COO^-. Although the carboxylate band of $K[Co\ tdta]\cdot 3H_2O$ splits into two absorption peaks at 1639 cm^{-1} and 1619 (sh) cm^{-1}, both peaks are considered to be associated with the coordinated carboxyl groups. This suggests that a quadrivalent tdta anion in the cobalt(III) complex behaves as a hexadentate.

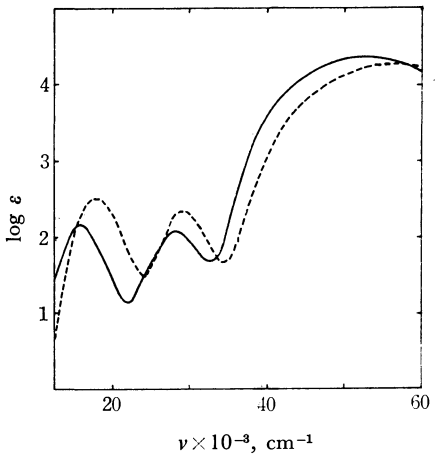

Fig. 2. Visible and ultraviolet absorption spectra of $K[Co\ tdta]\cdot 3H_2O$ (full line) and $Na[Co\ edta]\cdot 4H_2O$ (broken line).

Nuclear Magnetic Resonance Spectra. Proton NMR spectra of tdta and hdta anions were measured in 0.2M aqueous sodium hydroxide solution and those of cobalt(III) complex with tdta, in D_2O. The latter is shown in Fig. 1. In Table 2 are given the chemical shifts of proton NMR spectra of these compounds.

$K[Co\ tdta]\cdot 3H_2O$: Spectrum of the acetate protons splits into eight peaks in a region from 3.0 ppm to 4.2 ppm, indicating two AB patterns. The coupling constants are also given in Table 2. The two AB patterns show that four acetates are divided into two groups; the acetates of one group are of the out-of-plane type while those of the other group are of the in-plane type, when the plane involving two nitrogen atoms and a central metal ion is considered.

Table 3. Frequencies and log ε of visible and ultraviolet absorption maxima for Co(III) complexes with edta and tdta

Compound	I band		II band		Specific band	
	$\bar{\nu}\times 10^{-3}$ cm^{-1}	log ε	$\bar{\nu}\times 10^{-3}$ cm^{-1}	log ε	$\bar{\nu}\times 10^{-3}$ cm^{-1}	log ε
$Na[Co\ edta]\cdot 4H_2O$[8]	18.6	2.51	26.0	2.36	44.3	4.33
$K[Co\ tdta]\cdot 3H_2O$	17.2	2.13	25.4	2.08	42.0	4.37

Visible and Ultraviolet Absorption Spectra. The visible and ultraviolet absorption spectra of cobalt(III) complexes with edta and tdta are shown in Fig. 2, and wave numbers and log ε of absorption maxima for cobalt(III) complexes with edta and tdta are given in Table 3. The first and the second absorption bands of the cobalt(III) complex with tdta give a red shift as compared with edta, indicating that the spectrochemical series is in the order of edta > tdta.

7) Y. Shimura, *Kagaku*, **15**, 331 (1959).

8) J. Hidaka, Y. Shimura and R. Tsuchida, This Bulletin, **33**, 847 (1960).

BULLETIN OF THE CHEMICAL SOCIETY OF JAPAN VOL. 43 100—104 (1970)

The Solvent Extraction of Metal Ions from Sulfuric Acid Solutions with a Mixed Extractant — Long-chain Primary Amine and Di-2-ethylhexylphosphoric Acid

Hiroto WATANABE

Department of Industrial Chemistry, Muroran Institute of Technology, Muroran, Hokkaido

(Received May 31, 1969)

The distribution of metal ions between phases of dilute sulfuric acid and carbon tetrachloride containing long-chain primary amine (Primene JM) and di-2-ethylhexylphosphoric acid (D2EHPA) has been investigated. The degree of the extraction of bi- and tervalent metal ions, such as zinc, iron(III), indium, lanthanum, and cerium(III), is found to be the lowest when the organic phase contains 5 g/*l* of Primene JM and 7—8 g/*l* of D2EHPA, while a minimum extraction of thorium occurs at a different composition of the organic phase. Thus, thorium can be quantitatively separated from most other metals by extraction from a 0.1 N sulfuric acid medium with carbon tetrachloride containing 5 g/*l* of Primene JM and 7—8 g/*l* of D2EHPA. Under these extraction conditions, a single extraction is sufficient for the quantitative separation of thorium from high concentrations of lanthanide metals. Contrary to the usual method of extraction using long-chain amines, which involves a tedious multiple extraction, the mixed-extractant technique described is simple and will find many uses in the determinations of thorium in a variety of samples.

Solutions of long-chain amines in water-immiscible solvents have been found capable of extracting a wide variety of metal ions from acid solutions.[1] In particular, it has generally been accepted that ter- and quadrivalent metal ions can be readily extracted from a sulfuric acid solution by long-chain primary amines.[2-5] In this aspect, the present author has investigated the extraction of indium and iron(III) from dilute sulfuric acid solutions with Primene JM dissolved in carbon tetrachloride.[6] Such long-chain amines have frequently been called the "liquid anion exchangers." In contrast to the amines, there is another group of extractants that have been named the "liquid cation exchangers." Di-2-ethylhexylphosphoric acid, which is representative of the acidic organophosphorus compounds, has been used as a cationic extractant for a large number of aqueous cations.[7,8]

For both types of extractants, a synergistic effect has been demonstrated.[1,9-11] As in the case of uranium(VI) extraction, the addition of neutral organophosphorus compounds to D2EHPA enhances the distribution ratio of uranium(VI) by a factor of from ten to hundreds. The synergistic effect for the acidic organophosphorus compounds has been investigated extensively and used for the separation of metals. Although there have been a number of studies of the synergism in the extraction of metals, both with β-diketones, particularly thenoyl trifluoroacetone, and with bases,[12-16] little attention has been paid to the influence of certain acidic extractants on the metal extraction

1) D. F. Peppard, "Advanced Inorganic and Radiochemistry," Vol. 9, ed. by H. J. Emeleus and A. G. Sharpe, Academic Press, London and New York (1966), p. 49.

2) T. Ishimori, E. Akatsu, W. Cheng, K. Tsukuechi and T. Osakabe, *JAERI Report*-1062 (1964).

3) D. J. Crouse, Jr., and K. B. Brown, *Ind. Eng. Chem.*, **51**, 1461 (1959).

4) C. F. Coleman, K. B. Brown, J. G. Moore and D. J. Crouse, *Ind. Eng. Chem.*, **50**, 1756 (1958).

5) K. Kawamura and T. Takeuchi, *J. At. Energ. Soc. Jap.*, **4**, 774 (1962).

6) H. Watanabe and K. Akatsuka, *Nippon Kagaku Zasshi*, **89**, 280 (1968).

7) C. A. Blake, Jr., C. F. Base, Jr., and K. B. Brown, *Ind. Eng. Chem.*, **50**, 1763 (1958).

8) H. Green, *Talanta*, **11**, 1561 (1964).

9) C. Deptula, *J. Inorg. Nucl. Chem.*, **29**, 1097 (1967).

10) Y. Marcus, *Chem. Rev.*, **63**, 139 (1963).

11) D. F. Peppard, G. W. Mason and C. M. Andrejasich, *J. Inorg. Nucl. Chem.*, **25**, 1175 (1963).

12) L. Newman and P. Klotz, *J. Phys. Chem.*, **65**, 796 (1961); *ibid.*, **67**, 205 (1963).

13) L. Newman and P. Klotz, *Inorg. Chem.*, **5**, 461 (1966).

14) H. M. N. H. Irving and N. S. Al-Niami, *J. Inorg. Nucl. Chem.*, **27**, 717, 1671 (1965).

15) R. J. Casly, J. J. M. Fardy and W. R. Walker, *ibid.*, **29**, 1139 (1967).

16) T. Shigematsu, M. Tabushi, M. Matsui and T. Honjyo, This Bulletin, **39**, 165 (1966).

with high-molecular-weight amines. Deptula[9,17] has examined the extraction behavior of such compounds as H_2PtCl_6, $H_2Cr_2O_7$, and UO_2SO_4 from sulfuric acid solutions by a mixture of long-chain tertiary amines and dialkylphosphoric acids in benzene. He found that the extent of extraction was increased or decreased depending on the sulfuric acid concentrations, suggesting a synergistic or an antagonistic effect of the amine with the alkylphosphoric acid. However, no further attempt has been made at formulating a quantitative explanation of the extraction mechanism applicable to the mutual separation of metal ions.

A similar effect can be expected for the extraction of other metal ions. By a combination of long-chain amines and alkylphosphoric acids, it will be possible to change the selectivity of long-chain amines or alkylphosphoric acids to the metal ions. In this respect the present attempt was made to extract zinc, iron(III), indium, lanthanum, cerium(III), and thorium from sulfuric acid solutions with a mixture of Primene JM and D2EHPA in carbon tetrachloride. The results of the present experiment establish that thorium can be quantitatively separated from large amounts of bivalent and tervalent ions without multiple extraction or scrubbing.

Experimental

Apparatus. An Iwaki-V-S Shaking Unit was used for equilibration.

Reagents. The purification of D2EHPA[18] in carbon tetrachloride involves the scrubbing of the sodium monoalkylphosphate with an equal volume of a 10% sodium carbonate solution,[19] followed by acidification with an equal volume of a 1N sulfuric acid solution.

Primene JM,[20] trialkylmethylamine, a homologous mixture of C_{18-24} amines, was converted into the sulfate form by washing the amine solution in carbon tetrachloride with an equal volume of a 1N sodium hydroxide solution and by then equilibrating it twice with an equal volume of a 1N sulfuric acid solution. The concentration of the D2EHPA solution was determined by potentiometric titration with a standard sodium hydroxide solution in an ethanol medium.

Organic solutions of mixed extractants are prepared as follows. A constant portion of a purified amine solution and of various volumes of a purified D2EHPA solution are mixed together in a 100-ml volumetric flask, and the mixture is diluted to the mark with purified carbon tetrachloride. Then, these solutions are equilibrated with an equal volume of a 0.1N sulfuric acid solution. After the phases have separated, the organic phase was filtered through paper to remove the entrained aqueous phase.

The aqueous solutions used for the extraction of iron(III), zinc, lanthanum, indium, and thorium were prepared by the precipitation of the metal hydroxides and by the subsequent dissolution in a sulfuric acid solution of an appropriate concentration. The solution of cerium(III) was obtained by dissolving cerium(IV) sulfate into a sulfuric acid solution of an appropriate concentration and by subsequent reduction to cerium(III) with a suitable amount of hydrogen peroxide.

Procedure. For all the operations, 15-ml portions of the aqueous and the organic solutions were mixed together in a 100-ml glass separatory funnel and the mixture was equilibrated at room temperature. A fifteen-minutes shaking period at a rate of 200 strokes per minute was more than adequate. Then, the aqueous phase was filtered through paper to remove the entrained organic phase. The metal content in the aqueous phase was determined either spectrophotometrically or complexometrically.[21-23] The analytical procedures used are summarized in Table 1. The amount of metals in the organic phase was calculated by means of a material balance.

Table 1. The analytical methods used

Metals	Spectrophotometric	Complexometric
Th	Xylenol Orange	EDTA, Xylenol Orange
Fe	*o*-Phenanthroline	EDTA, Variamine Blue B HCl
In	Xylenol Orange	EDTA, Xylenol Orange
La, Ce		EDTA, Xylenol Orange
Zn		EDTA, BT

Results

The effect of the D2EHPA concentration on the iron(III) extraction was examined at fixed concentrations of Primene JM and iron(III), and at various fixed concentrations of sulfuric acid. It follows from Fig. 1 that the degree of iron(III) extraction passes through a minimum and then increases with an increase in the D2EHPA concentrations. The composition of the organic phase at which an appreciable decrease in the iron(III) extraction occurs depends on the sulfuric acid concentration.

Similar behavior is observed with the extraction of indium and lanthanum from a 0.1N sulfuric acid solution as can be seen in Fig. 2. The degree of extraction decreases with the increase in the initial concentration of iron(III) because of the fixed amount of extractant in the organic phase, but the concentration ratio of Primene JM to D2EHPA at which minimum extraction is observed does not

17) C. Deptula and S. Minc, *Chem. Abstr.*, **60**, 3543b (1964).

18) The D2EHPA was kindly supplied by the Kao Soap Co., Ltd.

19) C. A. Blake, K. B. Brown and C. F. Coleman, *USAEC ORNL*-1903 (1955).

20) The Primene JM was obtained from the Japan Organo Co., Ltd.

21) M. Otomo, *Bunseki Kagaku*, **14**, 229 (1965).

22) N. Ishiwatari, S. Nagai and Y. Higuchi, *ibid.*, **12**, 603 (1963).

23) K. Ueno, "Kireito Tekiteiho (Complexometric Titrations)," Nankodo, Tokyo (1966).

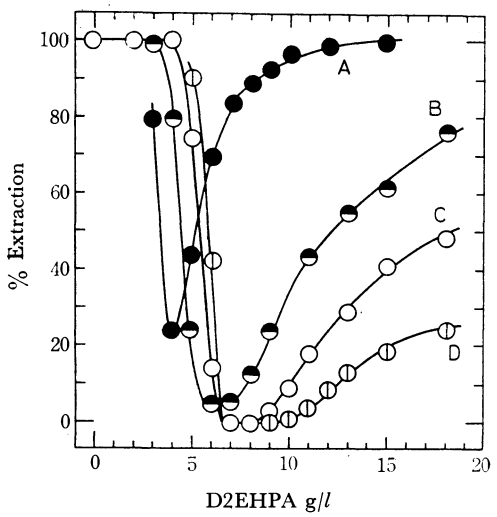

Fig. 1. The influence of D2EHPA on Fe^{3+} extraction with Primene JM (5 g/l) in CCl_4; 1.7×10^{-4}M total iron(III).
(A) 0.010N H_2SO_4 in aqueous phase, (B) 0.050N, (C) 0.10N, (D) 0.20N

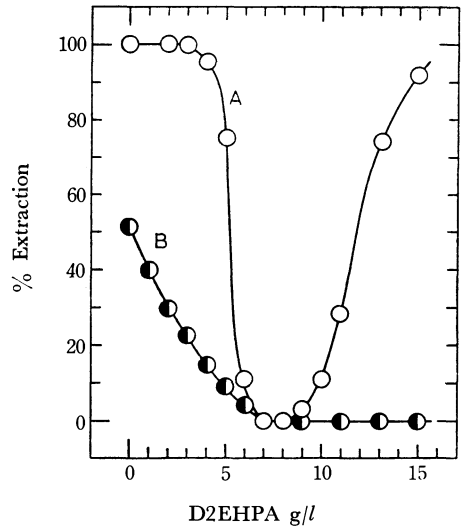

Fig. 2. The influence of D2EHPA on In^{3+} and La^{3+} extraction from 0.10N H_2SO_4 with Primene JM(5 g/l); (A) 3.48×10^{-5}M total indium, (B) 2.29×10^{-3}M total lanthanum.

change appreciably with the initial concentration of iron(III), as is shown in Fig. 3. In order to examine the extraction behavior of bivalent cations, zinc was extracted from a 0.1N sulfuric acid solution. As is shown in Fig. 3, no extraction of zinc was obtained when iron is not extracted. On the contrary, thorium was found to be extractable when bi- and tervalent ions are not extracted, the minimum extraction occurring in the higher D2EHPA-concentration range. This is demonstrated in

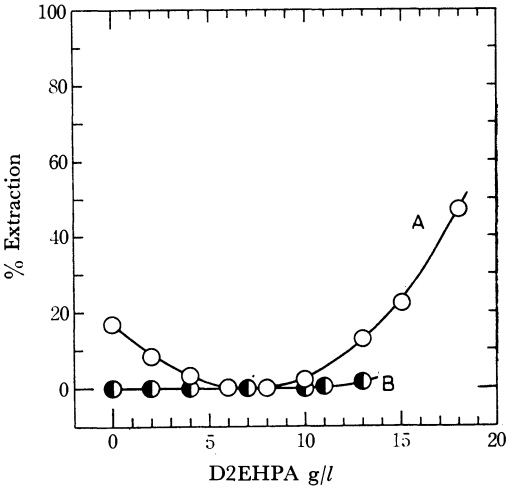

Fig. 3. The influence of D2EHPA on Fe^{3+} and Zn^{2+} extraction from 0.10N H_2SO_4 with Primene JM(5 g/l); (A) 8.40×10^{-3}M total iron(III), (B) 2.15×10^{-3}M total zinc.

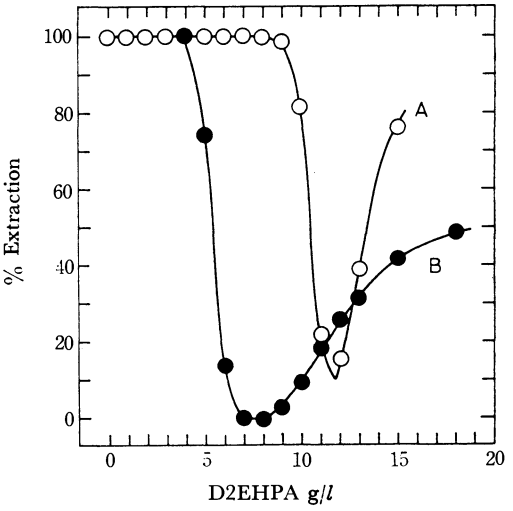

Fig. 4. The influence of D2EHPA on Th^{4+} and Fe^{3+} extraction from 0.10N H_2SO_4 with Primene JM(5 g/l); (A) 1.08×10^{-5}M total thorium, (B) 1.70×10^{-4}M total iron(III).

Fig. 4 for the case where the initial concentration of thorium is 1.08×10^{-5}M. In this figure, the extraction curve of iron(III) from the 0.1N sulfuric acid solution is shown for the sake of comparison with that of thorium. When the initial concentration of thorium is higher, the extractant concentration should be increased to achieve the complete recovery of thorium in the aqueous phase. For a high concentration of Primene JM, say 50 g/l,[24] thorium was completely extracted throughout the D2EHPA-concentration range studied. This

24) Tributyl phosphate was used to avoid any third-phase formation; the TBP concentration was 100 g/l.

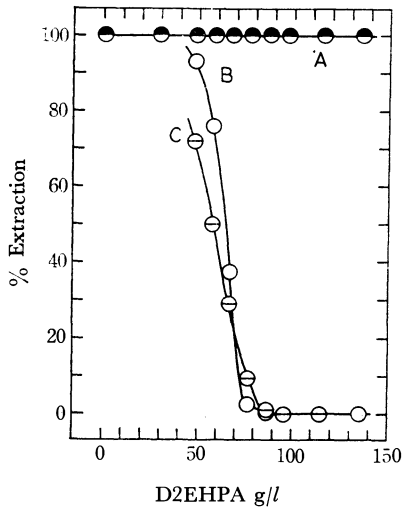

Fig. 5. The influence of D2EHPA on Th^{4+}, La^{3+} and Ce^{3+} extraction with Primene JM(50 g/*l*).
(A) $(0.212-1.09)\times10^{-2}$M total thorium, 0.01—0.5N H_2SO_4 in aqueous phase
(B) 5.32×10^{-3}M total lanthanum in 0.1N H_2SO_4
(C) 8.25×10^{-3}M total cerium(III) in 0.1N H_2SO_4

extraction behavior of thorium is quite different from that of lanthanum and cerium(III), as can be seen in Fig. 5.

Discussion

As is shown in Fig. 1, the extraction curve for iron(III) shows a minimum at a certain D2EHPA concentration. This can be explained, as has been done by Deptula,[9] on the basis of the interaction between amine sulfate and dialkylphosphoric acid in the organic phase. It is well known that iron(III) is extractable by either Primene JM or D2EHPA from dilute sulfuric acid solutions.[4,5] The appearance of a minimum in Fig. 1 may be due to the formation of an extremely stable complex by means of Eq. (1), which reduces the free concentration of both extractants participating in the extraction reactions and, hence, the degree of extraction.

$$(RNH_3)_2SO_4 + (HR)_2 = ((RNH_3)_2SO_4)(HR)_2 \quad (1)$$

Note that HR, $(RNH_3)_2SO_4$, and R are D2EHPA, amine sulfate, and an alkyl chain respectively. Equations (2) and (3) are the simplest generalized expressions for the iron(III) extraction.[25,26]

$$Fe^{3+} + 3(HR)_2 = Fe(HR_2)_3 + 3H^+ \quad (2)$$

$$Fe^{3+} + OH^- + SO_4^{2-} + (RNH_3)_2SO_4 = (RNH_3)_2FeOH(SO_4)_2 \quad (3)$$

In Fig. 1, the descending portion of the extraction curve corresponds to the decrease in the free concentration of amine sulfate, and the increase in the extent of extraction beyond the minimum is due to the increase in the free concentration of D2EHPA.

As can be seen in Fig. 1, the extraction curves depend on the sulfuric acid concentration. This is attributable to the strong affinity of the protonated amine for D2EHPA in the organic phase. The formation reaction of protonated amine is shown by Eq. (4):

$$2RNH_2 + 2H^+ + SO_4^{2-} = (RNH_3)_2SO_4 \quad (4)$$

For a decrease in the sulfuric acid concentration in the aqueous phase and, hence, for a small concentration of amine sulfate in the organic phase, a small amount of D2EHPA may be sufficient to complete the formation of $((RNH_3)_2SO_4)(HR)_2$, thereby resulting in the shift of the minimum in the extraction curve to the left. The concentration range of D2EHPA depressing the iron(III) extraction is broadened by increasing the sulfuric acid concentration. This trend may be caused by the competitive reaction of the hydrogen ion and the iron(III) ion against D2EHPA, as is represented by Eq. (2). If the equilibrium constant for the formation of $Fe(HR_2)_3$ or $(RNH_3)_2FeOH(SO_4)_2$ is comparable to that for the formation of $((RNH_3)_2SO_4)(HR)_2$, the minimum of the extraction curve will be found in the higher D2EHPA-concentration range. This is the case for thorium, as can be seen in Fig. 4. Thorium can be quantitatively extracted in the region in which no iron(III) is extracted. For high concentrations of Primene JM, say 50 g/*l*, thorium is quantitatively extractable over the whole range of D2EHPA studied (Fig. 5). This different extraction behavior from that indicated in Fig. 4 may be due to the higher concentration of Primene JM. As the concentration of Primene JM increases, the shape of the extraction curve at the minimum point tends to become sharp and the minimum point moves towards higher concentration ranges of D2EHPA. This can be explained by the concept that the equilibrium constant for the formation of extractable thorium species is comparable to that for the formation of $((RNH_3)_2SO_4)(HR)_2$.

The above treatment is not very accurate, however, since no account is taken of the presence of bisulfate species. In other words, Eqs. (1), (3) and (4) should have contained the terms of the bisulfate species.[27] However, the explanation using simple Eqs. (1)—(4) appeared to be satisfactory enough since the object of this investigation was to find the conditions which would enhance the selectivity

25) D. F. Peppard, G. W. Mason, C. Maler and W. J. Driscoll, *J. Inorg. Nucl. Chem.*, **4**, 334 (1957).
26) R. W. Cattrall and B. O. West, *ibid.*, **28**, 3035 (1966).
27) K. A. Allen, *J. Phys. Chem.*, **60**, 239, 943 (1956).

of extraction with high-molecular-weight amines.

It was found that the separation of thorium by extraction from many other metals can be carried out very easily using the present mixed-extractant system. That is, thorium can be completely extracted in the region in which no iron(III) is extracted (Fig. 4); tervalent indium, lanthanum, cerium, and also bivalent zinc behave analogously to iron(III), as can be seen Figs. 3 and 5.[28] As Figs. 2, 3, and 5 show, the initial concentrations of bi- and tervalent ions seem to have no appreciable influence on the thorium extraction. Thus, for the extraction of thorium these results may provide an improved method, one with a number of advantages over the previous methods using Primene JM as a single extractant.[5] A dilute solution of sulfuric acid can be used as the aqueous phase, and the complete separation of thorium can be achieved from large amounts of bi- and tervalent metals without multiple extraction and scrubbing. Further, there is the additional advantage that the separation of the two phases is very rapid compared to the case when single extractant is used. It was ascertained that thirty seconds are more than adequate for the complete separation.

From these experiments it is apparent that the degree of the extraction of bi- and tervalent metals can be successfully controlled by the combination of Primene JM with D2EHPA. This suggests that, with a proper combination, the selectivity of metal extraction with the high-molecular-weight amines and, presumably, with other extractants such as D2EHPA will be enhanced to an appreciable extent. Thus, there is good a possibility of developing a highly selective method of extraction for a certain metal ion on the basis of these findings.

The author wishes to express his sincere appreciation to Professor Masayo Murozumi of Muroran Institute of Technology, Professor Masaichi Nagayama and Dr. Katsumi Goto of Hokkaido University for their valuable discussions and for criticizing the manuscript.

28) Lanthanide metals show a different extraction behavior from that of iron(III), indium and zinc; above a certain D2EHPA concentration, the extraction remains completely depressed.

BULLETIN OF THE CHEMICAL SOCIETY OF JAPAN VOL. 43 104—108 (1970)

Volumetric Determinations of Cyanide, Thiocyanate, and Iodide Ions with Mercury(II) Ethylenediaminetetraacetate Using These Mixed-ligand Complexes as Indicators

Toshiaki NOMURA

Department of Chemistry, Faculty of Science, Shinshu University, Asahi, Matsumoto

(Received June 2, 1969)

Mercury(II) complexes of EDTA, methylthymolblue, or cresolphthaleincomplexone form mixed-ligand complexes with cyanide, thiocyanate, or iodide ions. These anions can be determined with mercury(II) ethylenediaminetetraacetate, using the other mercury(II) complexes as indicators, because of the difference between the stability constant of the mixed-ligand complex of EDTA and that of the other complexes. The previously reported methods, however, require a calibration curve. The determination was simplified by Titer methods, using these mixed-ligand complexes as indicators. To the anion-sample solutions adjusted to a given pH value with a buffer solution, 5 m*l* portions of 1×10^{-4}M mercury(II), an organic reagent, and anion solutions were added, these mixtures were then titrated with a 1×10^{-2}M standard mercury(II) ethylenediaminetetraacetate solution. These solutions change in color from pale pink (PC) or yellow (MTB) to red-violet (PC) or blue (MTB) by the end point. The Titer values were determined by the use known of standard anion solutions.

Mercury(II) reacts with ethylenediaminetetraacetate (EDTA) to form mercury(II) ethylenediaminetetraacetate (Hg-EDTA). This colorless complex was found to react with cyanide, thiocyanate, iodide, bromide, *etc.* to form colorless mixed-ligand complexes.[1] The cyano complex among these mixed-ligand complexes reacts with an

1) S. Komatsu and T. Nomura, *Nippon Kagaku Zasshi*, **87**, 841 (1966); **87**, 845 (1966); **88**, 63 (1967).

excess cyanide to form mercury(II) cyanide and EDTA.[2]

Cresolphthaleincomplexone (PC, pale pink) reacts with mercury(II) to form mercury(II)-cresolphthaleincomplexone (Hg-PC),[3] which is red-violet in color and which reacts with cyanide[4] or iodide. The solutions containing the mixed-ligand complex produced with Hg-PC and cyanide or iodide ions are pale pink.

Mercury(II)-methylthymolblue (Hg-MTB, yellow or yellowish green)[5] reacts with cyanide, thiocyanate,[6] iodide, bromide, or chloride[7] to form these mixed-ligand complexes, which are blue in color. The cyano or iodo mixed-ligand complexes among these complexes react with excess cyanide or iodide to form mercury(II) cyanide or iodide and MTB.

Some of these mixed-ligand complexes have low stability constants, and dissociate to mercury(II) anion complexes and organic reagents in the presence of an excess amount of anions. Therefore, the volumetric determination of anions can be achieved with a standard Hg-EDTA solution using the mercury(II)-organic reagent complex as indicator,[8-10] in just the same fashion as in the volumetric determination of metal ions with EDTA using metal indicators.[11] In these methods, the required volume (equivalent weight) of the standard Hg-EDTA solution is not equal to the equivalent weight of anions in the sample solution, because the color change of the solution at the end point is caused by the appearance of the color of the mixed-ligand complex of the mercury(II)-organic reagent-anion, *i. e.*, the required volume of the standard Hg-EDTA solution corresponds to the equivalent weight of anions minus the equivalent weight of the mixed-ligand complex formed in the sample solution. Therefore, the usual Titer method, in which the anions are determined by multiplying the required volume of the standard solution by the weight of anions necessary to titrate one m*l* of the standard Hg-EDTA solution, can not be applied to this procedure; the calibration curves are necessary for the determination. However, if one uses a mixed-ligand complex as an indicator, the Titer method can be used for the determination of these anions. This paper will describe this method, in which the anions can be determined with a good reproducibility. The proposed methods are especially suitable for anion concentrations of the order of 0.01 M and are satisfactorily simple and reproducible. The interfering anions will also be discussed.

Experimental

Reagents. All the reagents were analytical grade and were used without further purification.

1×10^{-4} M Cresolphthaleincomplexone (PC) Solution. The stock solution of 1×10^{-3} M was prepared by dissolving 320 mg of Dotite PC and by then diluting to 500 m*l* with methyl alcohol. This solution was stored in a brown glass bottle. The working solution of 1×10^{-4} M was prepared by dilution with water.

1×10^{-4} M Methylthymolblue (MTB) and 1×10^{-2} M Standard Thiocyanate-ion Solution. These solutions were prepared as in a preceding experiment.[9]

1×10^{-2} M Standard Cyanide-ion Solution. This solution was prepared as in a preceding experiment.[8]

1×10^{-2} M Standard Iodide-ion and Standard Hg-EDTA Solutions. These solutions were prepared as in a preceding experiment.[10]

1×10^{-4} M Hg-SCN, Hg-CN, and Hg-I Solutions. These solutions were prepared by the addition of 10 m*l* portions of mercury(II) nitrate and the corresponding standard anion solutions of 1×10^{-2} M and by subsequent dilution to 1 *l* with water.

Buffer Solutions. Buffer solutions having a given pH value were prepared by properly mixing the following solutions; pH<8, 0.1 M potassium dihydrogen phosphate and 0.1 M disodium hydrogen phosphate solutions; between pH 8 and 9, 0.1 M potassium dihydrogen phosphate and 0.05 M borax solutions; pH>9, 0.1 M sodium carbonate and 0.1 M sodium hydrogen carbonate solutions or 0.1 M disodium hydrogen phosphate and 0.1 M sodium hydroxide solutions.

Apparatus. The titrations of anion solutions were carried out with a 1/20 graduated microburette. A Hitachi-Horiba M-4-type pH meter was used for the measurement of the pH values.

Procedure. The pH values of the anion sample solutions were adjusted to an appropriate value with a buffer solution, to which 5 m*l* portions of organic-reagent (MTB for SCN^- or I^-, PC for CN^- or I^-) and Hg-X (X=anion=SCN^-, CN^- or I^-) solutions of 1×10^{-4} M were added. Then the solutions were diluted to about 50 m*l* with water. The solutions were titrated with a standard 1×10^{-2} M Hg-EDTA solution until the solutions changed in color from yellow or a greenish-yellow (MTB) or pale pink (PC) to blue (MTB) or red-violet (PC) with respect to the blank solution, which had been prepared by the same procedure as has been described above, except for the addition of the anion sample solution. The amount of the anion in the sample solution was calculated by multipling the required vol-

2) S. Komatsu and T. Nomura, *ibid.*, **87**, 1060 (1966).
3) S. Komatsu and T. Nomura, *ibid.*, **88**, 542 (1967).
4) T. Nomura, *ibid.*, **88**, 635 (1967).
5) N. Iritani and T. Miyahara, *Bunseki Kagaku*, **12**, 1183 (1963).
6) T. Nomura, This Bulletin, **41**, 1619 (1968); *Nippon Kagaku Zasshi*, **88**, 961 (1967).
7) T. Nomura and S. Komatsu, *ibid.*, **90**, 168 (1969).
8) T. Nomura, K. Takeuchi and S. Komatsu, *ibid.*, **89**, 291 (1968).
9) T. Nomura and S. Komatsu, *Bunseki Kagaku*, **17**, 1406 (1968).
10) T. Nomura, This Bulletin, **42**, 952 (1969).
11) K. Ueno, "Kireito Tekiteiho," Nankodo, Tokyo (1960).

ume of the standard Hg-EDTA solution (*titer*) by the Titer which was determined on a solution with a known concentration.

Results and Discussion

Determination of the Thiocyanate Ion Using the Hg-MTB-SCN Complex as an Indicator. In the volumetric determination of the thiocyanate ion using the Hg-MTB complex as an indicator,[9] the optimum pH range being 6.3—6.8. A sample solution containing up to 11.0 mg of thiocyanate ion was titrated by the standard procedure at pH 6.7 in the presence of MTB and Hg-SCN. The color change by the end point was from yellow to blue. The Titer was calculated from the volume of the standard Hg-EDTA solution required to titrate 2.745 mg of the thiocyanate ion:

$$1\ ml \text{ of a } 1\times10^{-2}\text{M standard Hg-EDTA solution} = 0.5434\ \text{mg of } SCN^- \quad (1)$$

The results are shown in Table 1. The *titer* value was an average of two titrations. In the determination of a small amount of the thiocyanate ion, the relative error was large, while in the determination of a larger amount of the thiocyanate ion (above 11 mg), the color change at the end point became indistinct, resulting in an even greater error.

Table 1. Determination of the thiocyanate ion by means of the Titer method

Taken (mg)	*Titer* (ml)	Found (mg)	Error (mg)	Error (%)
0.137	0.25	0.136	−0.001	0.73
0.274	0.50	0.272	−0.002	0.73
0.549	1.02	0.554	+0.005	0.91
1.098	2.02	1.098	0	0
2.745	5.05	2.744	−0.001	0.04
5.489	10.08	5.477	−0.012	0.22
8.234	15.10	8.205	−0.029	0.35
10.98	20.12	10.93	−0.05	0.41

1 m*l* of a 1×10^{-2}M standard Hg-EDTA solution = 0.5434 mg of SCN^-

In the previous method,[9] the end point was determined visually by the color change from yellow to blue, without any standard color reference, so there was a relatively large error. In addition to this, a preliminary test for the existence of an excess of the thiocyanate ion was necessary. In the present method, however, the color at the end point is compared with that of the reference blank solution. Therefore, the individual error is smaller than that in the previous method. In addition to this advantage, no preliminary test is necessary. When the thiocyanate ion is not present in the sample, the color of the solution before the titration is blue, while when the thiocyanate ion is present, the color is yellow, as is shown in Eq. (2):

$$\underset{\text{blue}}{\text{Hg-MTB-SCN}} + SCN^- \rightleftharpoons \text{Hg}(SCN)_2 + \underset{\text{yellow}}{\text{MTB}} \quad (2)$$

The blue color at the end point, however, gradually changes to green upon the addition of an excess of the Hg-EDTA solution because the Hg-EDTA-SCN complex is more stable than the Hg-MTB-SCN complex. That is, at the end point:

$$\text{Hg}(SCN)_2 + \text{MTB} + \text{Hg-EDTA} \rightleftharpoons \text{Hg-EDTA-SCN} + \underset{\text{blue}}{\text{Hg-MTB-SCN}} \quad (3)$$

and after the addition of an excess amount of the standard solution:

$$\text{Hg-MTB-SCN} + \text{Hg-EDTA} \rightleftharpoons \text{Hg-EDTA-SCN} + \underset{\text{green}}{\text{Hg-MTB}} \quad (4)$$

However, this color change does not disturb the end-point determination.

Determination of the Iodide Ion Using the Hg-MTB-I Complex as an Indicator. The method used here was virtually identical with that described in a previous paper,[10] but here the Hg-MTB-I complex was used as an indicator.

A sample solution containing up to 31 mg of the iodide ion was titrated at pH 7.5 in the presence of MTB and Hg-I. The color change at the end point was form greenish yellow to blue. The Titer was calculated from the volume of the standard Hg-EDTA solution required to titrate 6.225 mg of the iodide ion:

$$1\ ml \text{ of a } 1\times10^{-2}\text{M standard Hg-EDTA solution} = 1.186\ \text{mg of } I^- \quad (5)$$

The results are shown in Table 2. The *titer* value was an average of two titrations. This method had the same advantages as in the case of the determination of thiocyanate described above.

The blue color appearing after the end point did not change upon the addition of the *titer*, for the stability of Hg-MTB-I is greater than that of Hg-EDTA-I. When an excess of iodide existed in the solution, the color was greenish yellow, as is shown in Eq. (6):

$$\text{Hg-MTB-I} + 2I^- + \text{Hg-EDTA} \rightleftharpoons \text{Hg-EDTA-I} + \text{HgI}_2 + \underset{\text{greenish yellow}}{\text{MTB}} \quad (6)$$

Hg-MTB-I dissociated to mercury(II) iodide and MTB with an excess of iodide, but Hg-EDTA-I did not.

Interfering anions, such as sulfide, cyanide, and thiocyanate,[10] could be removed the hydrogen peroxide method, which will be described in the section concerned with the determination of iodide.

Table 2. Determination of the iodide ion by means of the Titer method

Taken (mg)	*Titer* (ml)	Found (mg)	Error (mg)	Error (%)
0.311	0.26	0.308	−0.003	0.96
0.623	0.52	0.617	−0.006	0.96
1.245	1.04	1.233	−0.012	0.96
2.490	2.10	2.491	+0.001	0.04
6.225	5.25	6.227	+0.002	0.03
12.45	10.52	12.48	+0.03	0.24
18.68	15.77	18.70	+0.02	0.11
24.90	21.13	25.06	+0.16	0.64
31.13	26.31	31.20	+0.07	0.22

1 ml of a 1×10^{-2}M standard Hg-EDTA solution = 1.186 mg of I^-

Bromide could not, however, be removed by this method.

Determination of Cyanide Using the Hg-PC-CN Complex as an Indicator. The method used here was virtually identical with that described in a previous paper,[8] but the Hg-PC-I complex was used as an indicator.

A cyanide-sample solution (up to 6.2 mg) was titrated at pH 11.2 in the presence of PC and Hg-CN. The color change at the end point was from a pale pink to red-violet. The Titer was calculated from the volume of the standard Hg-EDTA solution required for 1.241 mg of cyanide. The results are shown in Table 3.

1 ml of a 1×10^{-2}M standard Hg-EDTA solution = 0.2434 mg of CN^- (7)

Table 3. Determination of the cyanide ion by means of the Titer method

Taken (mg)	*Titer* (ml)	Found (mg)	Error (mg)	Error (%)
0.062	0.25	0.061	−0.001	1.61
0.124	0.50	0.122	−0.002	1.61
0.248	1.02	0.248	0	0
0.496	2.05	0.499	+0.003	0.60
1.241	5.10	1.241	0	0
2.482	10.22	2.488	+0.006	0.24
3.723	15.30	3.724	+0.001	0.03
4.964	20.36	4.956	−0.008	0.16
6.205	25.40	6.182	−0.023	0.37

1 ml of a 1×10^{-2}M standard Hg-EDTA solution = 0.2434 mg of CN^-

Determination of Iodide Using the Hg-PC-I Complex as an Indicator. Iodide could also be determined using the Hg-PC-I complex as an indicator.

Hg-PC-I Complex. The iodide ion reacts with Hg-PC (red-violet) to form a mixed-ligand complex. The color of this complex was a pale pink. The molar ratio of Hg-PC to iodide in the mixed-ligand complex was found to be 1 : 1 by the molar ratio method and by the continuous variation method. The mixed-ligand complex does not dissociate to mercury(II) iodide and PC in the presence of the excess iodide.

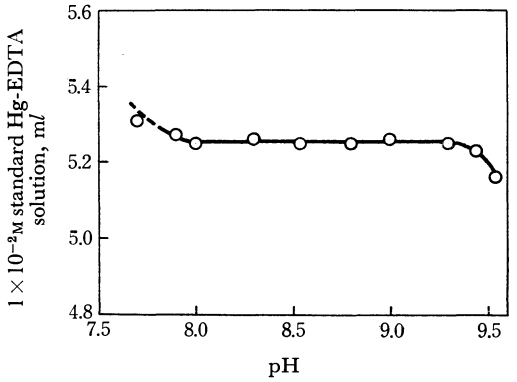

Fig. 1. Effect of pH.
Each 5 ml of PC and Hg-I solutions of 1×10^{-4}M, 6.225 mg of iodide ion.

Effect of pH. The effect of the pH on the titration of iodide was investigated by the same method as in the case of cyanide. The sample solution containing 6.225 mg of iodide was adjusted to an appropriate pH value with a buffer solution, to which 5 ml portions of PC and 1×10^{-4}M Hg-I solutions were added. The results are shown in Fig. 1.

At pH values below 7.9 it was difficult to distinguish the end point. At pH values above 9.5, however, the solution gradually changed from a pale pink to violet at the beginning of the end point. Between pH 8.0 and 9.3, the color of the solution at the end point changed from pink to red-violet.

Table 4. Determination of the iodide ion by means of the Titer method

Taken (mg)	*Titer* (ml)	Found (mg)	Error (mg)	Error (%)
0.311	0.27	0.320	+0.009	2.89
0.623	0.53	0.629	+0.006	0.96
1.245	1.04	1.233	−0.012	0.96
2.490	2.10	2.491	+0.001	0.04
6.225	5.25	6.227	+0.002	0.03
12.45	10.48	12.43	−0.02	0.16
18.68	15.69	18.61	−0.07	0.37
24.90	21.01	24.92	+0.02	0.08
31.13	26.25	31.13	0	0

1 ml of a 1×10^{-2}M standard Hg-EDTA solution = 1.186 mg of I^-

Titer Method. Iodide was determined by titration at pH values between 8.0 and 9.3 in the presence of PC and Hg-I. The color change at the end point was from a pale pink to red-violet. The Titer was calculated from the volume of the standard Hg-EDTA solution required for 6.225 mg of iodide.

$$1\,ml \text{ of a } 1\times10^{-2}\text{M standard Hg-EDTA solution} = 1.186 \text{ mg of } I^- \quad (8)$$

The results are shown in Table 4.

Diverse Ions. In this method, various cations interfered, as in the case reported in a previous paper.[10] Some anions, such as sulfide, cyanide, and thiosulfate, interfered in minute amounts. Bromide, chloride, fluoride, thiocyanate, sulfate, nitrate, and perchlorate, however, did not interfere at all. The interfering anions could be removed by the following procedure.

TABLE 5. REMOVAL OF INTERFERING ANIONS

Iodide ion taken in (mg)	Interfering anions added			Iodide ion found (mg)
	S^{2-} (mg)	CN^- (mg)	$S_2O_3^{2-}$ (mg)	
2.490	—	—	—	2.491
2.490	0.32	0.52	0.56	2.467
6.225	—	—	—	6.227
6.225	0.32	0.52	0.56	6.215

To an iodide-ion sample solution (pH 8.0—9.3), 2 m*l* of 3% hydrogen peroxide were added. This solution was then boiled until large bubbles appeared, it was then cooled to room temperature, and 5 m*l* portions of PC and Hg-I soultion of 1×10^{-4}M were added, and the solution was treated in the usual way.

Some representative results of this method are shown in Table 5. Excess hydrogen peroxide did not interfere.

TABLE 6. SIMULTANEOUS DETERMINATION OF CYANIDE AND IODIDE IONS

Taken		Found	
CN^- (mg)	I^- (mg)	CN^- (mg)	I^- (mg)
0.238	1.245	0.241	1.242
0.238	6.225	0.239	6.224
1.191	1.245	1.193	1.240
1.191	6.225	1.198	6.219

1 m*l* of a 1×10^{-2}M standard Hg-EDTA solution = 0.2434 mg of CN^- = 1.186 mg of I^-

Simultaneous Determination of Cyanide and Iodide Ions. When cyanide and iodide ions were both present in the same sample, the simultaneous determination of these ions was performed with a standard Hg-EDTA solution, using the Hg-PC-I complex as an indicator. However, when iodide ions did not exist in the sample solution, cyanide could not be determined by this method.

An aliquot of a sample solution containing cyanide and iodide was titrated with the standard Hg-EDTA solution using the Hg-PC-I complex according to the procedure of iodide determination (*titer* A). Another, identical aliquot was treated according to the procedure described in the Diverse Ions section for the determination of iodide ion, also using the Hg-PC-I complex (*titer* B). The volume of the standard Hg-EDTA solution required for cyanide is given by, (A—B) and the volume for iodide, B. These results are shown in Table 6.

The author wishes to thank Professor S. Komatsu for his many helpful discussions and suggestions during this work.

BULLETIN OF THE CHEMICAL SOCIETY OF JAPAN VOL. 43 109—113 (1970)

The Hydrolysis of the Beryllium Ion in Heavy Water*1,*2

Hidetake KAKIHANA and Masunobu MAEDA

Research Laboratory of Nuclear Reactor, Tokyo Institute of Technology, Ookayama, Meguro-ku, Tokyo

(Received June 26, 1969)

The hydrolysis of Be^{2+} ion in heavy water containing 3M $NaClO_4$ as an ionic medium was investigated at 25°C by potentiometric titrations, employing a technique of constant-current coulometry. The deuterium-ion concentrations was measured by the use of a commercial glass electrode. The emf data in the range of the total beryllium concentration from 2.5 to 10 mM can be explained on the basis of the following complex formation: $Be_2(OD)^{3+}$, $-\log\beta_{1,2}=3.28\pm0.04$; $Be_3(OD)_3{}^{3+}$, $-\log\beta_{3,3}=9.399\pm0.007$; $Be(OD)_2$, $-\log\beta_{2,1}=11.89\pm0.07$. The composition of the species formed in heavy water is the same as that in light water, but the values of the stability constants are smaller in heavy water than in light water.

Since the discovery of deuterium oxide, many investigations of the chemical reactions in heavy water have been made; these investigations played important roles in the investigation of the mechanisms of chemical reactions.

As for the hydrolytic reactions of metal ions, several investigations have been made in heavy water.[1-4] However, as far as we know, the investigations made so far have been only of the mononuclear hydrolysis species; there have been none of the polynuclear species in heavy water.

The present work was carried out in order to ascertain the differences in the hydrolytic reactions of metal ions in heavy water and in light water.

The hydrolysis of the beryllium ion was chosen as the first of a series of studies of the hydrolysis in heavy water. The hydrolysis of the beryllium ion in light water has been investigated by several researchers,[5-12] and it has been confirmed that $Be_3(OH)_3{}^{3+}$ is the main hydrolysis species. The hydrolysis of the beryllium ion in H_2O-D_2O mixed solvents has previously been studied by the present authors;[13] we found that the composition of the main hydrolysis product is the same as that in light water and that the value of the stability constant of the main species decreases gradually with an increase in the deuterium-atom fraction.

Symbols

B total concentration of Be
b concentration of free Be^{2+}
D total excess concentration of the deuterium ion
d concentration of the free deuteriun ion
Z average number of deuterium ions split off per beryllium$=(d-D)/B$
$\beta_{p,q}$ stability constant of the following reaction:

$$qBe^{2+} + pD_2O = Be_q(OD)_q^{(2q-p)} + pD^+$$

p number of OD groups in hydrolyzed species
q number of beryllium atoms in hydrolyzed species
$\bar{p}$ and $\bar{q}$ average numbers of p and q respectively

Experimental

Reagents and Analysis. *Reagents Used.* These were, unless otherwise stated, prepared and analyzed as has been described in Ref. 5 and Ref. 13.

Beryllium Perchlorate in Heavy Water. This was prepared by the repeated evaporation of beryllium perchlorate in light water (which had itself been prepared and

*1 Ionic Equilibria in Heavy Water. II.

*2 Part I: H. Kakihana and M. Maeda, This Bulletin, **42**, 1458 (1969).

1) J. Hudis and R. W. Dodson, *J. Amer. Chem. Soc.*, **78**, 911 (1956).
2) J. C. Sullivan and J. C. Hindman, *J. Phys. Chem.*, **63**, 1332 (1959).
3) S. W. Rabideau and R. J. Kline, *ibid.*, **64**, 680 (1960).
4) T. E. Rogers and G. M. Waind, *Trans. Faraday Soc.*, **57**, 1360 (1961).
5) H. Kakihana and L. G. Sillén, *Acta Chem. Scand.*, **10**, 985 (1956).
6) B. Carell and Å. Olin, *ibid.*, **15**, 1875 (1961).
7) P. Schindler and A. B. Garret, *Helv. Chim. Acta*, **43**, 2176 (1960).
8) E. Matijević, *J. Colloid Sci.*, **20**, 322 (1965).
6) F. Bertin, G. Thomas and J. C. Merlin, *Compt. Rend.*, **260**, 1670 (1965).
10) H. Ohtaki, *Inorg. Chem.*, **6**, 808 (1967).
11) H. Ohtaki and H. Kato, *ibid.*, **6**, 1935 (1967).
12) R. E. Mesmer and C. F. Baes, Jr., *ibid.*, **6**, 1951 (1967).
13) H. Kakihana and M. Maeda, This Bulletin, **42**, 1458 (1969).

analyzed as has been described in Ref. 10 under an infrared lamp, while adding heavy water. The beryllium content of the stock solution was determined by the method described in Ref. 5.

Sodium Perchlorate. This was prepared by neutralizing a $HClO_4$ solution with recrystallized Na_2CO_3. The sodium perchlorate was dried at about 120°C and stored in a glass bottle.

Sodium Chloride of Analytical Grade. This was heated for a few hours at 360°C in an electric oven and then stored in a glass bottle.

Apparatus. *Apparatus Used.* These were, unless otherwise stated, the same as those described in Ref. 13.

The Titration Cell. This consisted of a Wilhelm-type half cell[14] for emf measurements and a modified one for constant-current coulometry.

Coulometric Analyzer. Such an analyzer (Leeds & Northrup Co., Philadelphia) was used as a constant-current power source.

Experimental Procedures. All the measurements were carried out in a paraffin-oil thermostat kept at 25.00 ± 0.01°C and placed in a room thermostated at 25 ± 1°C.

The hydrolysis of the Be^{2+} ion in heavy water was followed by measurements of the deuterium-ion concentration.

$NaClO_4$ was added to all the test solutions so that they contained 3M ClO_4^- as an ionic medium; the total Be(II) concentration was kept constant in each series of experiments.

The deuterium-ion concentration of a test solution was measured by means of this cell;

$$\text{Ref}\,|\,B\text{M Be}^{2+},\ D\text{M D}^+,\ (3-D-2B)\text{M Na}^+,\ 3\text{M ClO}_4^-|\text{GE}, \qquad \text{(A)}$$

where GE denotes a glass electrode, and Ref, the reference half-cell;

$$|3\text{M NaClO}_4 \text{ in heavy water}|2.99\text{M NaClO}_4 \text{ and } 0.01\text{M AgClO}_4 \text{ in light water}|\text{AgCl-Ag}.$$

The emf of the cell(A) can be denoted as follows:[15]

$$E = E_0 + 59.15\log d + E_j, \qquad (1)$$

where E_0 is a constant and E_j, a liquid junction potential at the junction, test solution | 3M $NaClO_4$ in heavy water. E_j was disregarded since the concentration of the deuterium ion was maintained at less than 0.01M in the present work.[15] Therefore, the emf of the cell (A) can be denoted as follows:

$$E = E_0 + 59.15\log d. \qquad (2)$$

The total beryllium concentration in a test solution was maintained in the 2.5—10 mM range. The concentration of the deuterium ion in the cell (A) was varied by generating D^+ ions or OD^- ions by means of constant-current coulometry, using the same cell assembly as that described by Biedermann and Ciavatta.[16–18]

As an inert salt in the salt bridge, "3M $NaClO_4$ in heavy water" was used. A constant current of 6.43 mA was passed in small steps (a few microfaradays). The potentiometric titrations were conducted in both directions. First, the "forward titration" was carried out by generating OD^- ions, and then the "back titration" was performed to reacidify the hydrolyzed beryllium solution by generating D^+ ions. A steady emf was usually attained within fifteen minutes for $Z\lesssim0.8$, while in solution with $Z>0.8$ a steady emf was obtained within two or three hours. During the measurements, a test solution was stirred by a vigorous stream of nitrogen which had been purified by leading it through heavy water and 3M $NaClO_4$ in heavy water.

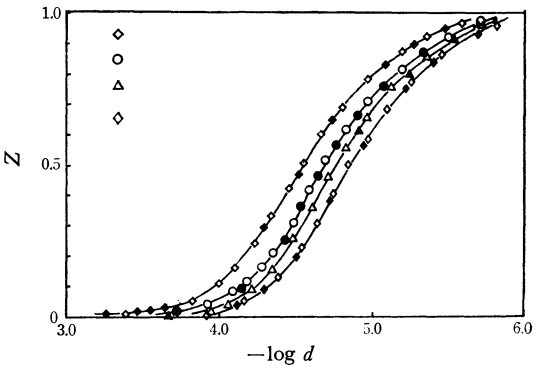

Fig. 1. Average number, Z, of OD bound per Be, as a function of $-\log d$.
Open symbols denote points from forward titrations and filled symbols from back titrations. Drawn curves were calculated with the stability constants given in Table 3.
◇ 0.008358M ○ 0.004969M
△ 0.004000M ◇ 0.002704M

Results and Calculations

The $Z(\log d)_B$ data, which were calculated from the potentiometric measurements by the use of Eq. (2), are shown graphically in Fig. 1.

The experimental data were analyzed by graphical methods and by computer calculations. The hydrolysis data were first submitted to graphical analysis in order to obtain preliminary information on the composition of the hydrolytic species formed; then, on the basis of the information obtained, computer analysis was made to evaluate the most probable hydrolysis scheme and the stability constants of the species formed.

(1) The Evaluation of the Composition of the Hydrolysis Products by Graphical Analysis. The average compositions of the hydrolysis products, $\bar{p}$ and $\bar{q}$, were calculated by the integration method described by Sillén.[19]

The average composition calculated thereby is plotted in Fig. 2 in the form of $\bar{q}$ *vs.* $(2\bar{q}-\bar{p})$.[20]

14) W. Forsling, S. Hietanen and L. G. Sillén, *Acta Chem. Scand.*, **6**, 901 (1952).
15) H. Kakihana, M. Maeda and T. Amaya, This Bulletin, to be published.
16) L. Ciavatta, *Ark. Kemi*, **20**, 417 (1962).
17) G. Biedermann and L. Ciavatta, *ibid.*, **22**, 253 (1964).
18) G. Biedermann and L. Ciavatta, *ibid.*, **22**, 303 (1964).
19) L. G. Sillén, *Acta Chem. Scand.*, **15**, 1981 (1961).
20) H. S. Dunsmore, S. Hietanen and L. G. Sillén, *ibid.*, **17**, 2644 (1963).

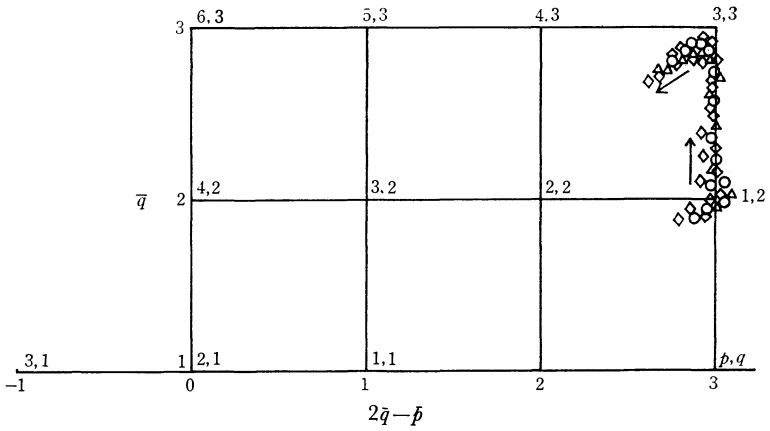

Fig. 2. Average composition of the complexes $\bar{q}(2\bar{q}-\bar{p})$. Direction of an arrow carresponds to the increase in Z. All the points are shown using the same symbols as in Fig. 1.

From this figure, some qualitative information may be obtained on the composition of the hydrolytic species. From Fig. 2, it may be seen that the (1,2) species may be present at low Z and that the (3,3) species is predominant in the main region of Z; moreover, some other minor species may be present at high Z, the composition of which would be either (2,2), (3,2), (2,1) or (3,1), judging from the directions of the plots.

(2) The Evaluation of the Composition and the Stability Constants of the Hydrolysis Products by Computer Analysis. On the basis of the restrictions suggested above, and with the help of an electronic computer (HITAC 5020) the generalized least-squares method was used to determine the most probable hydrolysis scheme containing the lowest number of species which would suffice to account for the experimental data and for the stability constants of the species formed.

The least-squares calculations on the electronic computer were carried out in order to make the error square sum $U=\sum(Z-Z_{calcd})^2$ minimum for the set of stability constants. Z_{calcd} denotes the $Z_{calcd}=\sum\sum p\beta_{p,q}b^q d^{-p}/B$ for a particular set of stability constants.

(2-1) Hydrolysis Scheme in the Lower Region of Z (When Z is less than 0.5). On the basis of the restrictions described in the section of the graphical analysis, we chose the two-species scheme of (1,2)—(3,3). The values for the stability constants of the species calculated by the generalized least-squares method are listed in Table 1, together with the error square sum. In addition, apart from the suggestion made by the graphical analysis and based upon the assumption that the minor species at low Z is less polymerized than the main species, $Be_3(OD)_3^{3+}$, we chose seven different minor species, each of which was paired with $Be_3(OD)_3^{3+}$. The results calculated are also collected in Table 1.

From the results shown in Table 1 and from the fact that the (1,2)—(3,3) scheme gives an excellent fit with the experimental data, it is evident that, at low Z, $Be_2(OD)^{3+}$ is the most probable of the minor species chosen.

(2-2) Hydrolysis Scheme in the Higher Region of Z (when Z is more than 0.5). Based on the information obtained by the graphical analysis, we chose four species, (2,2), (3,2), (2,1), and (3,1); each of them was combined with the (1,2)-(3,3) scheme, which is significant in the $Z<0.5$ region.

Table 1. The error square sums and values of the stability constants for the schemes of $Be_q(OD)_q^{(2q-p)+}-Be_3(OD)_3^{3+}$, where $Z\lesssim 0.5$

(p,q)	$\beta_{p,q}$	$\beta_{3,3}$	U
(1,2)	5.33×10^{-4}	4.00×10^{-10}	1.40×10^{-3}
(1,1)	6.33×10^{-3}	3.99×10^{-10}	9.90×10^{-3}
(1,3)	8.12×10^{-2}	4.32×10^{-10}	3.30×10^{-3}
(2,1)	1.09×10^{-14}	4.01×10^{-10}	9.90×10^{-3}
(2,2)	1.21×10^{-10}	4.01×10^{-10}	9.85×10^{-3}
(2,3)	8.29×10^{-6}	3.41×10^{-10}	7.36×10^{-3}
(3,1)	1.22×10^{-8}	3.99×10^{-10}	9.93×10^{-3}
(3,2)	2.27×10^{-17}	4.00×10^{-10}	9.90×10^{-3}

Table 2. The error square sums and the values of the stability constants for the schemes of $Be_2(OD)^{3+}-Be_3(OD)_3^{3+}-Be_q(OD)_q^{(2q-p)}$, where the values of the stability constants of $Be_2(OD)^{3+}$ and $Be_3(OD)_3^{3+}$ respectively are allowed to vary

(p,q)	$\beta_{1,2}\times10^4$	$\beta_{3,3}\times10^{10}$	$\beta_{p,q}$	U
(2,2)	4.70	4.13	3.71×10^{-10}	7.90×10^{-3}
(3,2)	5.57	3.98	9.98×10^{-15}	2.46×10^{-3}
(2,1)	5.30	3.98	1.28×10^{-12}	2.40×10^{-3}
(3,1)	4.69	4.07	1.04×10^{-18}	3.31×10^{-3}

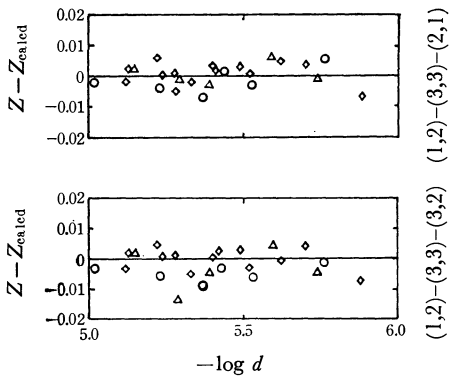

Fig. 3. $(Z-Z_{calcd})$ as a function of $-\log d$ for $Z>0.7$. Symbols are the same as those in Fig. 1.

The values of the stability constants for each set of the three-species schemes were allowed to vary, and the corresponding error-square sums were calculated over the whole range of Z.

The results calculated thereby are listed in Table 2, together with the stability constants of the species. Table 2 shows that the scheme containing the (2,1) species gives rise to the least-error square sum of the schemes chosen, and that the scheme containing the (3,2) species gives rise to the second least-error square sum. Figure 3 shows that the systematic deviations from the experimental data for $Z>0.7$ are slightly less for the scheme containing the (2,1) species than for the scheme containing the (3,2) species.

From the above evidence, it seems reasonable

TABLE 3. THE VALUES FOR THE STABILITY CONSTANTS OF THE HYDROLYSIS SPECIES OF BERYLLIUM ION IN HEAVY WATER AND IN LIGHT WATER CONTAINING 3M $NaClO_4$ AS AN IONIC MEDIUM*

	in heavy water	in light water
$-\log \beta_{1,2}$	3.28 ±0.04	3.16 ±0.05
$-\log \beta_{3,3}$	9.399±0.007	8.662±0.007
$-\log \beta_{2,1}$	11.89 ±0.07	11.16 ±0.06

* The uncertainties of the constants were estimated by multiplying by three the standard deviations.

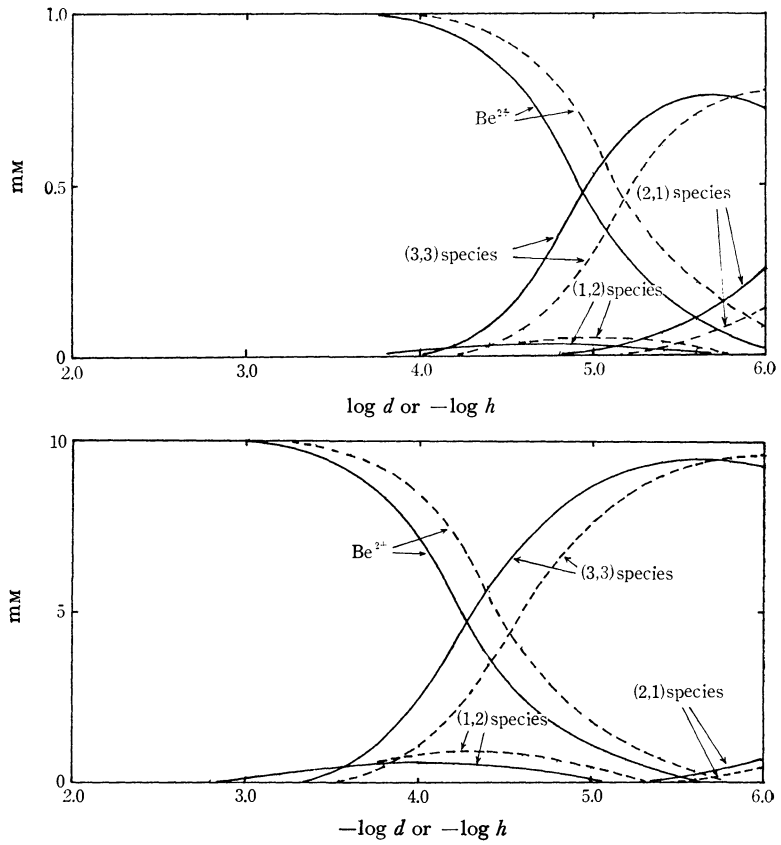

Fig. 4. The calculated distribution of the hydrolytic species in heavy water and in light water at total beryllium concentrations and 1 and 10 mM. Dashed curves represent the distribution of the species in heavy water and full curves the distribution of the species in light water.

to prefer $Be(OD)_2$ as the third species that exists at higher Z values.

The above considerations lead to the conclusion that the data in heavy water can be explained on the basis of the $Be_2(OD)^{3+}$-$Be_3(OD)_3{}^{3+}$-$Be(OD)_2$ scheme within the limits of accuracy of the present experiments.

The final values for the stability constants are tabulated in Table 3, together with the results we have obtained in light water employing the same method as that used for the heavy-water system.

(3) Distribution of the Species. The distribution of the hydrolytic species in heavy water and in light water, calculated at the total beryllium concentrations of 1 mM and 10 mM, and assuming the values of the stability constants in Table 3, are represented in Fig. 4. There is a general tendency for the species to be less hydrolyzed in heavy water than in light water at a given pH. The dominance of the (3,3) species in the accessible pH region is apparent both in heavy water and in light water. The amount of the (1,2) species increases and the amount of the (2,1) species decreases with an increase in the total concentration of beryllium.

Conclusion

In the present work, it has been found that the compositions of the species formed in heavy water, *i. e.*, $Be_2(OD)^{3+}$, $Be_3(OD)_3{}^{3+}$, and $Be(OD)_2$, are the same as those in light water, while the values of the stability constants of the hydrolysis products in heavy water are smaller than those in light water.

The fact that the values for the stability constants of the hydrolysis products of the beryllium ion, which can be regarded as a weak acid, are smaller in heavy water than in light water has been seen to be consistent with the results for the dissociation of the weak acids[21] and with those for the mononuclear hydrolytic reactions of the metal ions.[1-3]

The authors wish to express their gratitude to Dr. Hitoshi Ohtaki, Nagoya University, for his valuable advice and discussions.

21) L. L. Schaleger, P. Salomaa and F. A. Long, "Chemical Physics of Ionic Solutions," ed. by B. E. Conway and R. G. Barradas, John Wiley & Sons, Inc., New York (1966), p. 237.

BULLETIN OF THE CHEMICAL SOCIETY OF JAPAN VOL. 43 114—118 (1970)

Selectivity in the Metal-Complex-Catalyzed Decarboxylation of Oxaloacetic Acid and a Role of Metal Ion in an Enzyme System

Megumu MUNAKATA, Masakazu MATSUI, Masayuki TABUSHI and Tsunenobu SHIGEMATSU

Institute for Chemical Research, Kyoto University, Uji

(Received July 9, 1969)

The catalytic action of metal ions in the presence of various coordinating agents and a role of metal ions for the activations of an enzyme in a decarboxylation reaction were investigated. Many of the ligands studied decreased the catalytic activity of metal ions. However, α,α'-dipyridyl selectively enhanced the catalytic activities of divalent metal ions, except Cu^{2+}. The activity of Cu^{2+} was specifically enhanced only with histidine and its derivatives. Histidine destroyed Ni^{2+} and Co^{2+} catalysis. The specific enhancement may be due to the increase in the electronegativities of the metal ions with $d\pi$(metal)–$p\pi$(ligand) back donation and to the stereo-configuration of the metal complexes. The catalytic behavior in these metal ion coordinating agent systems was different from that in the metal-enzyme systems. It was assumed that the activation of enzyme resulted from the change in the configuration of enzyme by the coordination of metal ions, and not from the catalytic action of metal ions enhanced by the coordination of enzyme. This was supported by the fact that the catalysis of compounds containing amino groups, active sites of enzyme, remarkably depended on the stereo-configuration. In the enzyme-model system, Mn^{2+} was generally preferable to Cu^{2+} and Ni^{2+}. The catalytic actions of Cu^{2+} and Ni^{2+} were lowered by the complex formation with the active sites. This may solve the question why, in enzymatic reactions, Mn^{2+} having small complex-forming ability is more selective and effective than Cu^{2+} and Ni^{2+} with large complex-forming abilities.

It is well known that metal ions paly an important part in enzymatic reactions, and interesting reports have been published by many authors.[1] Though the role of metal ions is very complicated, it must be noted that a metal ion is specific for the activation of an enzyme, and this specificity should offer a key to the question on the role of metal ion in an enzymatic reaction.

From the concept that the interaction between metal ions and the residual groups of an enzyme is an important factor for enzyme activity, Steinberger and Westheimer[2] have investigated the effect of various coordinating ligands upon copper ion catalysis in the decarboxylation of dimethyloxaloacetic acid, and stated that negative ions, such as citrate and acetate, diminished the catalytic activity of cupric ion, while complexing agents, which did not destroy the charge of the copper ion, did not destroy its catalytic ability. Rund and Plane[3] reported that catalytic activities of manganous and nickel ions for the decaboxylation of dimethyloxaloacetic acid were enhanced in the presence of *o*-phenanthroline, and the enhancement rate was completely comparable to those in the presence of the enzyme.

The present authors also found that α,α'-dipyridyl increased the catalytic activities of divalent cations, such as manganous, cobaltous, nickel and zinc ions, for the decarboxylation of oxaloacetic acid, but both of α,α'-dipyridyl and *o*-phenanthroline selectively destroyed the catalytic ability of cupric ion. Cupric ion catalysis was enhanced only with histidine and its derivatives. The specific enhancement of catalytic activities of metal ions in the presence of such ligands was discussed from a view point of the stereo-configuration of metal complexes and the back donation of the $d\pi$(metal ion)–$p\pi$-(ligand) bonding. The effect of these ligands on the metal ions catalysis appears different from that in the metal-enzyme system, and therefore it seemed unreasonable that the metal-α,α'-dipyridyl or *o*-phenanthroline system was an enzyme-like model.

Many of the works on the role of metal ion in the enzymatic decarboxylation have been carried out mainly from a view-point of catalytic abilities of metal ions, but little attention has been paid

1) See, for example, a) S. Granick, *Chem. Rev.*, **38**, 379 (1946); b) H. S. Mason, *Advan. Enzymol.*, **19**, 79 (1957).

2) R. Steinberger and F. H. Westheimer, *J. Amer. Chem. Soc.*, **73**, 429 (1951).

3) a) J. V. Rund and R. A. Plane, *ibid.*, **86**, 367 (1964); b) J. V. Rund and K. G. Claus, *ibid.*, **89**, 2256 (1967).

to the activation of the enzyme with metal ions. In this paper, a brief discussion on the role of metal ions in the enzymatic reaction was also made from the results obtained in various metal-ligand systems and in some amino compound systems, and an idea that metal ions acted as an enzyme activator, was proposed.

Experimental

Material. A reagent grade oxaloacetic acid was obtained from the Tokyo Kasei Co., Ltd. The aqueous solution was freshly prepared before use. Solutions of metal ions were made up by dissolving the reagent grade chloride salts and the concentrations were gravimetrically determined. Reagent grade coordinating agents were used without further purification, but ethylenediamine, diethylenetriamine and triethylenetetramine were purified by distillation. Buffer solutions were prepared from sodium hydroxide solution and acetic acid or monochloroacetic acid.

Experimental Procedure. The rate of decarboxylation of oxaloacetic acid was determined by measuring the pressure of carbon dioxide gas evolved in Walburg flasks. A freshly prepared solution of oxaloacetic acid was introduced into the main room of a reaction vessel and a solution of a catalyst was put into the sub-chamber of the vessel. All test solutions contained 4×10^{-3}M oxaloacetic acid, 2×10^{-4}M cupric ion or 4×10^{-4}M other divalent metal ions, and 4×10^{-2}M acetic acid or monochloroacetic acid (buffer), in the final concentration. The vessel was immersed in a water bath held at 30.00 ± 0.01°C, and after about five minutes, the catalyst was transferred to the main room and then the solution was stirred. Pressure readings were made at regular intervals. Since decarboxylation reactions follow first order kinetics with respect to the concentration of oxaloacetic acid, the data were treated in the usual manner to determine the observed first-order rate constants.

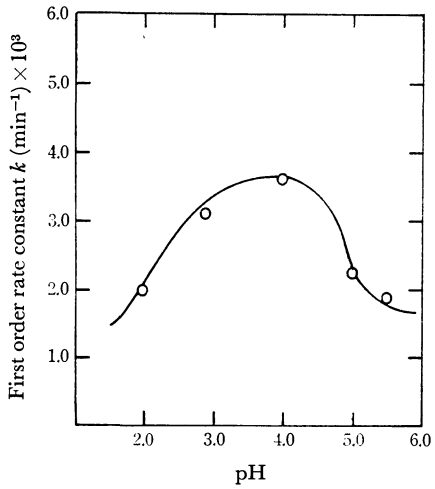

Fig. 1. Effect of pH on the uncatalyzed decorboxylation of oxaloacetic acid.
Oxaloacetic acid: 4×10^{-3}M

Results and Discussion

Effect of pH. As shown in Fig. 1, the first order rate constant of uncatalyzed decarboxylation of oxa-

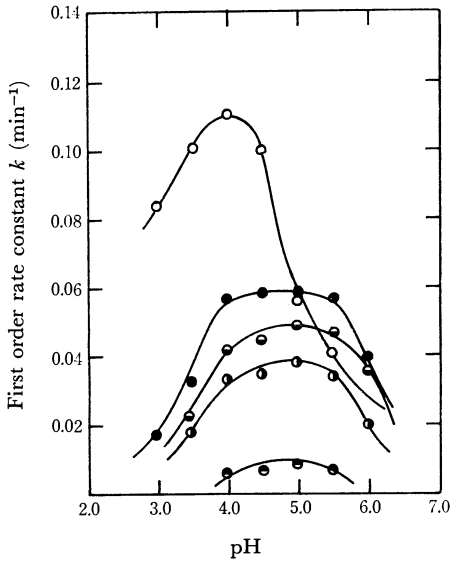

Fig. 2. Effect of pH of the metal-ion-catalyzed decorboxylation of oxaloacetic acid.
○: Cu (2×10^{-4}M); ●: Ni (4×10^{-4}M)
◒: Zn (4×10^{-4}M); ◑: Co (4×10^{-4}M)
◓: Mn (4×10^{-4}M); oxaloacetic acid: 4×10^{-3}M

Table 1. Effect of ligand on catalytic activity of metal ion

Metal ion	Moles of ligand (per mole of metal)	k min^{-1} $\times10^2$	k_0 min^{-1} $\times10^2$ (no ligand)	Relative rate
Ni^{2+}	1 gly	5.84	5.96	0.98
	1 cys	5.95	5.96	~1
	2 cys	5.90	5.96	~1
	1 AA	5.66	5.96	0.95
	2 AA	5.36	5.96	0.90
	2 imid	5.42	5.96	0.91
	2 CN^-	4.41	5.96	0.74
	1 trien	3.53	5.96	0.59
Cu^{2+}	1 gly	5.66	5.78	0.98
	1 cys	5.26	5.78	0.91
	1 AA	5.20	5.78	0.90
	2 AA	4.79	5.78	0.86
	2 imid	5.32	5.78	0.92
	1 en	4.28	5.78	0.74
	1 dien	1.56	5.78	0.27
	1 trien	1.04	5.78	0.18

pH: 5.00; Ni^{2+}: 4×10^{-4}M; Cu^{2+}: 2×10^{-4}M; oxaloacetic acid: 4×10^{-3}M; gly: glycine; cys: cystein; AA: acetylacetone; imid: imidazole; en: ethylenediamine; dien: diethylenetriamine; trien: triethylenetetramine.

TABLE 2. ENHANCEMENT OF THE CATALYTIC ACTIVITY OF METAL ION WITH LIGAND

Moles of ligand (per mole of metal)	Mn^{2+} pH=5.00	Co^{2+} pH=5.00	Ni^{2+} pH=5.00	Cu^{2+} pH=5.00	Cu^{2+} pH=4.00	Zn^{2+} pH=5.00
no ligand	0.815*	3.83	5.96	5.78	11.1	4.90
1 phen	1.10 (1.35)**	6.05 (1.58)	14.4 (2.41)	4.60 (0.80)	8.15 (0.73)	6.66 (1.36)
2 phen	<1.10***	5.29 (1.38)	17.3 (2.90)	2.05 (0.35)	3.69 (0.33)	6.17 (1.26)
3 phen	<1.10***	1.00 (0.26)	1.49 (0.25)	—	—	2.16 (0.44)
1 dipy	1.01 (1.24)	6.01 (1.57)	10.7 (1.80)	5.79 (~1.0)	11.0 (1.0)	7.11 (1.45)
2 dipy	1.07 (1.31)	6.00 (1.57)	13.4 (2.08)	4.90 (0.85)	8.40 (0.76)	7.69 (1.57)
3 dipy	1.07 (1.31)	3.41 (0.89)	1.85 (0.31)	—	—	6.22 (1.27)
1 tpy	—	3.81 (~1.0)	4.11 (0.69)	—	6.66 (6.66)	4.36 (0.89)
1 hid	0.830 (~1.0)	3.64 (0.95)	5.24 (0.88)	9.77 (1.69)	—	5.00 (~1.0)
1 trien	8.90 (10.9)	3.41 (0.89)	3.49 (0.59)	2.11 (0.18)	—	9.09 (1.95)

* (first order rate constant) $\times 10^2$ min^{-1}

** enhancement rate

*** not obey to the first order reaction; metal ion (except of Cu): 4×10^{-4}M; Cu: 2×10^{-4}M; oxaloacetic acid: 4×10^{-4}M; phen: *o*-phenanthroline; dipy: α,α'-dipyridyl; typy: α,α',α''-terpyridyl; hid: histidine.

loacetic acid depends largely upon the pH value. This dependency can be caused by the fact that the rate depends on the concentration of oxaloacetic acid anions.[2] The first order rate constants of metal-ion-catalyzed decarboxylation of oxaloacetic acid also depend on pH (Fig. 2). Catalysis with manganous, cobaltous, nickel and zinc ions give maximum near pH 5.00 and that cupric ion, at pH 4.00. The decrease in the catalytic activity above the optimum pH may be due to the formation of metal hydroxide, besides decrease in hydrogen ion concentration. Because copper hydroxide is more stable than the other metal hydroxides, the decrease of the catalysis begins in a lower pH region. The catalytic activities of these metal ions are related to the electronegativities of the metal or the stabilities of the metal-oxaloacetic acid chelates.[4] The order at pH 4.00 is $Mn \ll Co < Ni < Cu > Zn$.

Effect of ligands. The effect of various coordinating agents on the nickel and cupric ion catalysis in decarboxylation of oxaloacetic acid was studied at pH 5.00, and the results are summarized in Table 1. The catalytic activities of nickel and cupric ions are somewhat reduced glycine, cystein and acetylacetone, and strongly hindered with ethylenediamine (en), diethylenetriamine (dien), triethylenetetramine (trien) and cyanide. The phenomena can be explained by the fact that the latter chelates are more stable than the former. Steinberger and Westheimer[2] have reported that the ligands, which do not destroy the charge on the cupric ion, do not destory the catalytic activity. However, in the present experiment, even neutral ligands, such as en, dien, trien and imidazole, destroy the catalytic activities of metal ions. The decrease in the catalytic activities may result from the fact that the electronegativities of metal ions are decreased by the coordination of complexing agents, and the stability of the metal-substrate compounds is lowered with competition with the complexing agents.

Specific Enhancement of Metal Ions with α,α'-Dipyridyl and *o*-Phenanthroline. In contrast to the above complexing agents, there are special cases where the catalytic activities of metal ions are enhanced by the coordination of ligands. Rund and Plane[3] showed that *o*-phenanthroline enhanced the catalytic activities of manganous, nickel and zinc ions. We also found that α,α'-dipyridyl enhanced the catalysis with divalent ions, but both the complexing agents selectively destroyed the cupric ion catalysis. As seen in Table 2, the catalytic activities of the metal ions, except cupric ion, are enhanced in the presence of two moles or less of these agents per mole of the metal ion, and the enhancement is also related to the electronegativity of the metal ion: The order is $Mn < Co < Ni > Zn$. But the addition of three moles of *o*-phenanthroline decreases the activities of cobaltous, nickel and zinc ions, and the addition of three moles of α,α'-dipyridyl decreases the activities of cobaltous and nickel ions. The decrease may be caused by the fact that all the coordination sites of the metal ions are occupied with the ligands to form the 1 : 3 chelates. In the case of manganous ion with *o*-phenanthroline and α,α'-dipyridyl, and zinc ion with α,α'-dipyridyl, where the decrease in the activity is not observed, the 1 : 3 chelates are not formed even in the presence of three moles of the agents, because of the low stability of the chelates. Generally, the catalysis of metal chelate compounds is stereo-specific, and the characteristics of the atomic orbital (symmetry, orientation, *etc.*) of the metal ions controls the coordination with substrate. Activation of metal ions with α,α'-dipyridyl and *o*-phenanthroline may be due to the specific configuration of the metal chelates

4) J. F. Speck, *J. Biol. Chem.*, **178**, 315 (1949).

and to the increasing electronegativities of the metal ion coordinated with the ligands. From the fact that the catalysis of metal ions is enhanced even in the 1 : 2 chelates, the metal ions must be six-coordinate and octahedral, in order to bind to a substrate which acts as a bidentate ligand, as follows:[2]

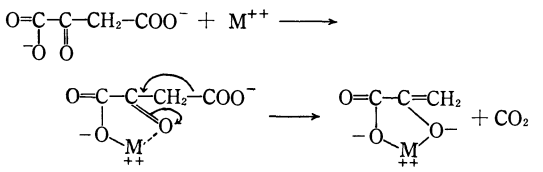

Complex (I) Complex (II)

The selective loss of the activity of cupric ion by the chelation can be subsequently explained by the square-planer configuration (dsp^2) of copper complexes.

As described above, the substrate (oxaloacetic acid) more easily combines to metal ion of octahedral configuration, when the metal ion is coordinated with α,α'-dipyridyl or *o*-phenanthroline molecules. However, basides these ligands, many other complexing agents form the octahedral chelate compounds. The specific enhancement with α,α'-dipyridyl and *o*-phenanthroline must, therefore, result from the change in the electronegativities of metal ions, in addition to the stereo-configuration effect. The electronegativities of metal ions coordinated with these ligands are probably increased by the back donation from an occupied $d\pi$ orbital of the metals to an empty $p\pi$ orbital of nitrogen atoms of the ligands. The increasing electronegativity promotes the decomposition of complex (I) to complex (II), as well as the formation of complex (I), in the mechanism described above, and thus enhances the decarboxylation rate. In copper complexes, the effect of the back donation is overcome by the stereo-configuration effect.

Specific Enhancement of Catalytic Activity of Cupric Ion with Histidine and Its Derivatives. The catalytic activity of cupric ion is selectively enhanced with histidine (hid), histidine methyl ester (ϕ-me) and histamine (him), while the activities of manganous and zinc ions are not affected, and the activities of cobaltous and nickel ions are decreased by them. As shown in Table 3, the increasing order of cupric ion catalysis is as follows: ϕ-me $>$ hid $>$ him $>$ *N*-ace-ϕ $\simeq$ H_2O $\simeq$ Bu-NH_2 $\geq$ imid $\geq$ DBA $\gg$ gly-ϕ, where *N*-ace-ϕ is *N*-acetylhistidine; Bu-NH_2: butylamine; imd: imidazole; DBA: diamino-butyric acid; and gly-ϕ: glycylhistidine. Histidine is less effective than histidine methyl ester. This may be attributed to the coordination of carboxyl group of the former. The presence of two moles of histidine or histidine methyl ester per mole of copper ion becomes less effective, but this tendency is not observed even in the presence of three moles of histamine. This indicates that histamine complex is less stable, and explains the fact that histamine is less effective than histidine and histidine methyl ester. Diaminobutyric acid, in which imidazol ring of histidine is replaced by amino group, and *N*-acetylhistidine, in which amino group of histidine is blocked, does not influence the activity. The activity is enhanced neither with imidazole nor normal amine. The results indicate that the catalytic activity of cupric ion is enhanced with ligands containing imidazole ring and amino group, but not with ligands containing only imidazole or only amino group. The fact suggests that the stereo-configuration of copper chelate compound is important for the enhancement of the catalysis. It may be considered that the configuration distorted by the Jahn-Taller effect is favorable to be coordinated with substrate. Imidazole ring is indispensable also to the back donation from a $d\pi$ orbital of copper ion to a $p\pi$ orbital of imidazole nitrogen.

Table 3. Enhancement of catalytic activity of copper ion with ligand

Moles of ligand (per mole of metal)	k min^{-1} $\times 10^2$	k_0 min^{-1} $\times 10^2$ (no ligand)	Relative rate
1 hid-me	10.7	5.78	1.85
2 hid-me	8.44	5.78	1.46
1 hid	9.77	5.78	1.69
2 hid	7.69	5.78	1.33
3 hid	7.05	5.78	1.22
1 him	6.13	5.78	1.06
2 him	6.65	5.78	1.15
3 him	6.65	5.78	1.15
1 *N*-acet-hid	5.66	5.78	0.98
2 *N*-acet-hid	5.54	5.78	0.96
2 Bu-NH_2	5.66	5.78	0.98
2 imid	5.32	5.78	0.92
1 DBA	5.43	5.78	0.94
1 gly-hid	3.12	5.78	0.54

pH: 5.00; oxaloacetic acid: 4×10^{-3}M; Cu: 2×10^{-4}M; hid-me: histidine methyl ester; hid: histidine; him: histamine; *N*-acetyl-hid: *N*-acetyl-histidine; Bu-NH_2: butylamine; imid: imidazol; DBA: diaminobutyric acid; gly-hid: glycyl-histidine.

In contrast to the case of α,α'-dipyridyl and *o*-phenanthroline chelate compounds, the catalytic activities of cobaltous and nickel histidine chelate compounds are lower than those of the metal aquo-ions. The reason for this is not yet evident, but it probably results from the difference in the configuration and/or from the weak back donation in the latter chelate compounds.

Consideration on the Role of Metal Ions as Enzyme Activator. It is interesting to reveal the role of metal ions in the enzyme-catalyzed decarboxylation of oxaloacetic acid. Speck[4] has reported

that enzyme of the decarboxylation of oxaloacetic acid required metal ions to have full activity, and in most cases, manganous ion was more effective, while cupric and nickel ions were less effective. The order was Mn>Co>Ni>Cu<Zn. Rund and Plane[3] have described that manganous ion catalysis was enhanced sixteen times or more by the coordination with *o*-phenanthroline, but nickel ion catalysis showed only two-told increase, and they concluded that this activation behavior was almost the same as in the metal-enzyme systems.

In this research, however, the enhancement of manganous ion catalysis is the smallest among metal ions studied in either case of α,α'-dipyridyl or of *o*-phenanthroline (*cf.* Table 2), and the situation is not the same as in the enzyme system. The difference between Rund and Plane's result and the present result might be due to experimental conditions, especially to the metal ion concentration and accordingly, the ligand concentration. They carried out their experiments with 5.78×10^{-2}M manganous ion and with 8.5×10^{-5} or 2.64×10^{-3}M nickel ion, but we kept the metal ion concentration constant, 4×10^{-4}M, because α,α'-dipyridyl and *o*-phenanthroline acted as catalyst, when the concentration exceeded 10^{-3}M. Rund and Plane did not consider the catalysis of the ligands and so they might have overestimated the enhancement of manganous ion catalysis.

As described above, the enhancement of metal-ligand systems and metal-enzyme systems appears different, that is, manganous ion is not as effective in the former system, but very available in the latter. This may lead to the idea that in enzyme system, metal ions are enzyme activator rather than catalyst and may change the configuration of enzyme protein favorable to interact with substrate.

In order to examine whether enzyme activity is correlated with the configuration or not, the catalysis of some compounds containing amino groups considered to be an active site of enzyme,[5] was studied. Table 4 shows the first-order rate constant of decarboxylation reaction in the absence of any metal ions. As seen in the table, the catalysis is not always positively related with the number of amino groups, but the catalytic activity of diamino compounds remarkably depends upon the apparent distance between two amino groups. Ethylenediamine is most active; urea, in which two amino radicals combine the same carbon atom, and trimethylenediamine and pentamethylenediamine, in which three or five carbon atoms keep away two amino radicals, are less effective. This strongly suggests that catalytic activity is very sensitive to the setero-configuration of enzyme, or to the configuration of active sites.

TABLE 4. CATALYTIC ACTIVITY OF THE COMPOUND CONTAINING AMINE GROUPS

Compound (4×10^{-4}M)		k min^{-1} $\times10^{2}$
urea	$H_2N-\overset{\overset{O}{\|}}{C}-NH_2$	0.29
PDA	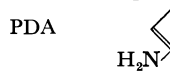	1.58
en	$H_2H-CH_2-CH_2-NH_2$	3.44
TMDA	$H_2N-CH_2-CH_2-CH_2-NH_2$	0.44
PMDA	$H_2N-(CH_2)_5-NH_2$	0.35
Bu-NH_2	$CH_3-(CH_2)_3-NH_2$	0.30
dien	$H_2N-(CH_2)_2-NH-(CH_2)_2-NH_2$	1.56
trien	$(H_2N-(CH_2)_2-NH-CH_2)_2-$	8.66

Oxaloacetic acid: 4×10^{-3}M
pH: 5.00

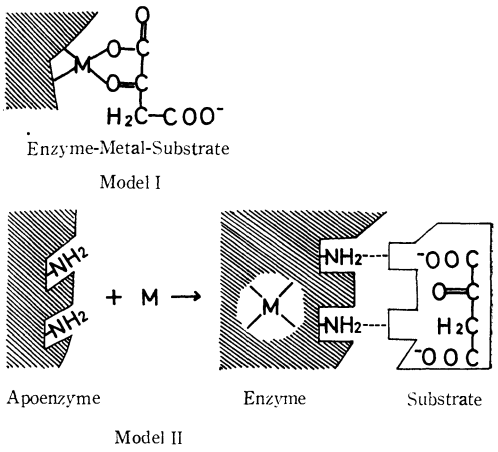

Fig. 3. Models for the activation of an enzyme with a metal ion.

From the above results, it seems reasonable to assume that enzyme activation results from the change in the configuration of enzyme caused by the coordination of metal ions (model II in Fig.3), but not from the increase in the metal ion catalysis caused by the coordination of enzyme (model I in Fig. 3). It is not true that electronegativity of manganous ion increases much in the presence of enzyme and becomes greater than that of nickel or cupric ions.

Although model II is no more than imagination at the present time, it is expected to elucidate the role of metal ions in enzymatic reaction.

5) S. Warren, B. Zerner, F. H. Westheimer, *Biochimia*, **5**, 817 (1966).

BULLETIN OF THE CHEMICAL SOCIETY OF JAPAN VOL. 43 119—124 (1970)

Mechanism of Isotopic Exchange of Trisacetylacetonatoaluminum with Acetylacetone-^{14}C in Organic Solvents

Kazuo SAITO and Kazuyo MASUDA

Chemistry Department, Faculty of Science, Tohoku University, Katahira-cho, Sendai

(Received July 19, 1969)

The kinetic study concerning isotopic exchange of acetylacetone (acacH) and trisacetylacetonatoaluminum [Al(acac)$_3$] (*Bull. Chem. Soc. Jap.*, **41**, 384 (1968)) has been extended to solutions in various organic solvents. Similar catalytic actions of water and acid were observed, and the concentration of acacH did not affect the rate, so that the kinetic formula is expressed by

$$R = [\text{complex}](k_1+k_2[H_2O]+k_1'[\text{acid}]+k_2'[\text{acid}][H_2O])$$

The rate constants and activation parameters are listed in Table 1. The k_1 values are zero in non-polar solvents such as toluene and xylenes, whereas the k_2 values are greater in these solvents than in polar solvents such as tetrahydrofuran and ethylacetate. The activation enthalpy is practically constant in these solvents, regardless of the participation of catalysts. The third and the fourth term seem to represent acid-catalysed reaction paths involving different proton carriers. The whole result appears to support our previous tentative conclusions that the exchange proceeds *via* an intermediate in which one of the acetylacetonate ligands is present as unidentate, and that the ease with which the free end recombines with the aluminum ion is responsible in determining the reaction rates.

In a previous paper we reported the isotopic exchange kinetics of trisacetylacetonatoaluminum [Al(acac)$_3$] and acetylacetone-^{14}C in tetrahydrofuran and postulated a plausible mechanism.[1] One of the three acetylacetonate ligands seemed to be present as unidentate with considerably long life time, and break of the remaining bond appeared to be the rate determining step. The catalytic effect of water and some acids was understood to retard the recombination of free end of the unidentate ligand by occupying the vacant coordination site of aluminum ion and the free end of unidentate acetylacetonate, respectively.

We have extended the study in other organic solvents, ethylacetate, toluene, *o*-, *m*- and *p*-xylene, in order to make clear the exchange mechanism. The exchange rate has been measured in solutions containing varying amounts of the complex, free acetylacetone (acacH), water and acids at various temperatures, and the rate formulae, rate constants and activation parameters have been discussed.

Experimental

Materials. Acetylacetone-^{14}C and trisacetylacetonatoaluminum were synthesized by the same method described previously.[1] The specific activity of the acacH was *ca.* 0.02 mCi per mg, and it contained water of the order of 10^{-1}M.

Extra pure grade ethylacetate was shaken with an aqueous solution of sodium hydrogen sulfite, water, aqueous solution of sodium carbonate and a saturated calcium chloride solution, dried with calcium chloride, distilled, further dried with phosphorus pentoxide and distilled. Toluene and xylenes were shaken with concentrated sulfuric acid, water, sodium hydroxide solution and water, dried with calcium chloride, refluxed with sodium and distilled.

m-Toluic acid and phenol were sublimed at 5 mmHg. Reagents for the scintillation counting, anisole, *p*-terphenyl and *p*-di-(5-phenyl-2-oxazolyl)-benzene (POPOP) were purified as mentioned previously.

Experimental Procedure. The method is essentially the same as that used previously.[1] Trisacetylacetonatoaluminum was precipitated crystalline within 6 hr by pouring an aliquot of the reaction mixture (*e. g.* 1 m*l*) into chilled petroleum ether (−20°C, 20 m*l*). The exchange reaction stopped instantaneously and no zero time exchange was observed.

Since the solvents and the free ligand acacH contained a significant amount of water, the water content of the reaction mixtures was determined by Karl-Fischer titration in a mixture of pyridine and ethyleneglycol (5+1). Little change in water content was observed within a given kinetic run. Five or six aliquots were withdrawn during one kinetic run, and altogether about two hundred kinetic runs were carried out.

The absorption spectra of the reaction mixtures were identical with the sum of those of [Al(acac)$_3$] and acacH in all the solvents, and no reaction other than isotopic exchange took place, regardless of the presence of water and the acids.

Measurements. Coincidence liquid scintillation counting was employed.[1] The counting rate at the

1) K. Saito and K. Masuda, This Bulletin, **41**, 384 (1968).

end of the exchange reaction (infinite time) was calculated from that of acacH-^{14}C and the used amounts of [Al(acac)$_3$] and acacH. The absorption spectra in the visible and ultraviolet region were measured with a Hitachi EPU-2A spectrometer.

Results

The experimental results were treated with McKay's formula

$$R = -2.3\frac{3ab}{3a+b}\cdot\frac{\log(1-F)}{t}, \qquad (1)$$

where a and b denote the concentrations of the complex with three exchangable ligands and that of the free ligand, respectively. F is the fraction of reaction and t the lapse of time in minutes. Good linear relationship was observed between $\log(1-F)$ and t in each run, and between R and a in all the solvents used. (diagram similar to Fig. 1 of Ref. 1). Hence the rate is expressed by $R=k_0a$.

Figure 1 shows the relationship between k_0 and the concentration of water in ethylacetate solutions at various temperatures. Figure 2 gives similar relationships in toluene at various temperatures, and Fig. 3 those in *o*-, *m*- and *p*-xylene at 25°C. The full and the open circles in Fig. 2 denote k_0 values obtained in the presence of different amounts of free ligand. Since acacH-^{14}C contained a small amount of water, change in b brought about the change in water concentration, and the influence of b was not examined individually. However, the fact that the full and the open circles are on the same line at a given temperature clearly indicates that k_0 is independent of b. The straight lines are expressed by

$$k_0 = k_1 + k_2[H_2O]. \qquad (2)$$

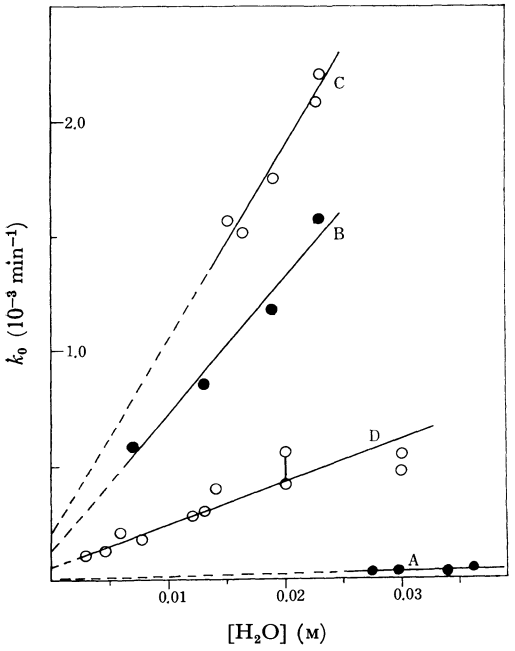

Fig. 1. Relationship between k_0 and the concentration of water in ethylacetate.
A (0°C), B (30°C), C (35°C) in ethylacetate; D (25°C) in tetrahydrofuran. (b=0.070M)

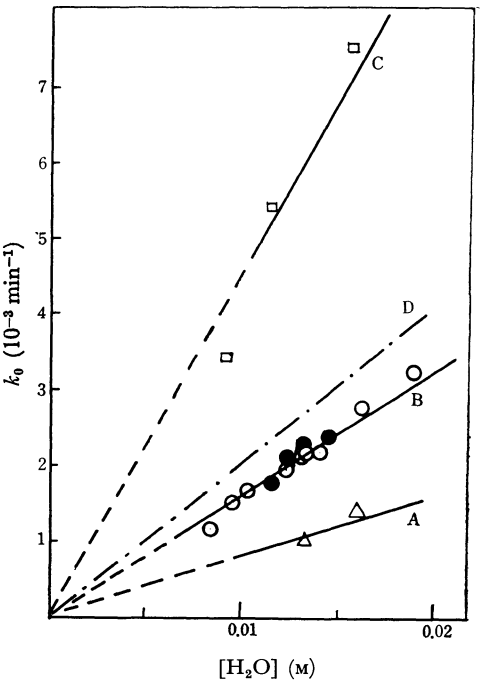

Fig. 2. Relationship between k_0 and the concentration of water in toluene.
A (0°C), B (25°C), C (35°C) in toluene; D (25°C) in xylenes (see Fig. 3).
△□○ b=0.070M ● b varying

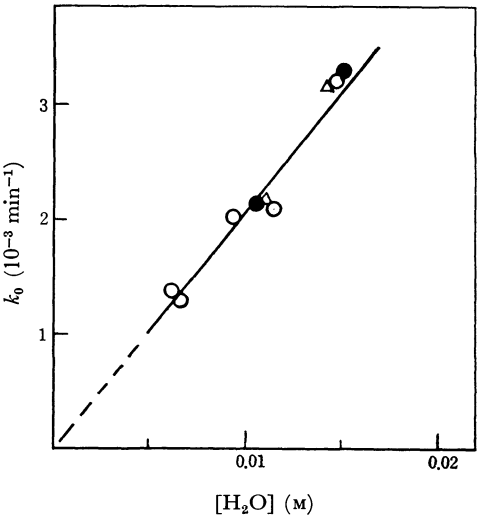

Fig. 3. Relationship between k_0 and the concentration of water in xylene isomers.
25°C, b=0.070M ○ ortho, ● meta, △ para

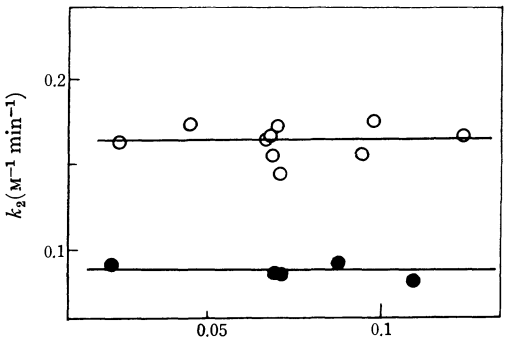

Fig. 4. Influence of the concentration of acetylacetone on the k_2 values.
○ 25°C in toluene, ● 35°C in ethylacetate

The slope and the intercept of Figs. 1, 2 and 3 correspond to k_2 and k_1, respectively, under the given conditions. The lines in Figs. 2 and 3 pass the zero point, to indicate that k_1 is almost zero in toluene and xylenes. No difference in rate constant was observed in the three isomers of xylene.

Figure 4 shows the influence of b upon k_2 in ethylacetate and in toluene. It further demostrates that k_2 is independent of b.

The exchange reaction is catalysed by acids. When m-toluic acid and phenol were used, the relationship between k_0 and acid concentration was similar to that in Fig. 3 of Ref. 1 in less than 0.021M acid in the solvents. Hence the catalytic effect increases linearly with the increase in acid concentration. Figure 5 shows the influence of water concentration upon the exchange rate in the presence of a given amount of m-toluic acid at various temperatures in ethylacetate and at 25°C in toluene.

Similar diagrams were obtained by use of phenol in place of m-toluic acid in ethylacetate. It appears as if the acid catalysis operates in two ways with and without the aid of water. The overall relationship is thus expressed by

$$k_0 = k_1 + k_2[H_2O] + k_1'[\text{acid}] + k_2'[\text{acid}][H_2O]. \quad (3)$$

The intercept and the slope of lines in Fig. 5 correspond to k_1' and k_2' of Eq. (3), respectively at a given temperature. The third and the last term of Eq. (3) express the acid catalysis operating with and without the aid of water, respectively.

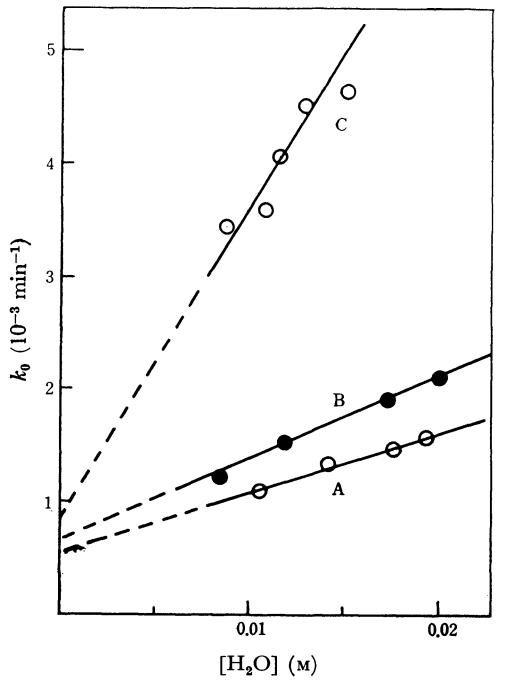

Fig. 5. Influence of the concentration of water upon the k_0 values in the presence of a given amount of m-toluic acid.
A: 25°C in ethylacetate, B: 30°C in ethylacetate, C: 25°C in toluene.
(b=0.070M, [m-toluic acid])=0.090M)

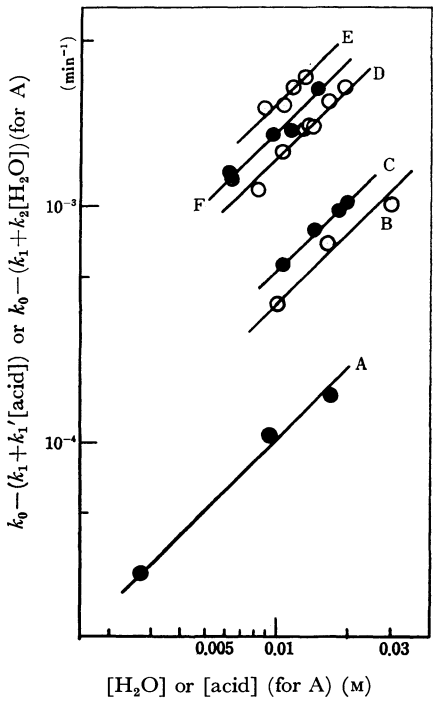

Fig. 6. Logarithmic plots indicating the influence of water in the presence of a given amount of m-toluic acid, and that of m-toluic acid in the presence of a given amount of water.
A: 25°C in tetrahydrofuran, [H$_2$O], 0.027M, [acid] varying;
B: 25°C in tetrahydrofuran, [H$_2$O] varying, [acid], 0.015M;
C: 25°C in ethylacetate, [H$_2$O] varying, [acid], 0.009M;
D: 25°C in toluene, [H$_2$O] vaying, [acid] none;
E: 25°C in toluene, [H$_2$O] varying, [acid], 0.004M;
F: 25°C in o-xylene, [H$_2$O] varying, [acid] none.

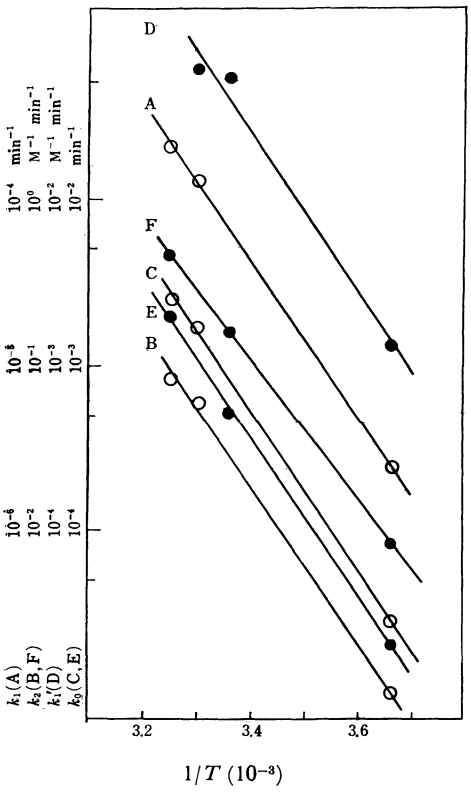

Fig. 7. Arrhenius plots of the rate constants of Eq. (3) in various solvents.
A: k_1 in ethylacetate; B: k_2 in ethylacetate;
C: k_0 in ethylacetate ([H_2O]=0.027M, [acid] none);
D: k_1' in ethylacetate;
E: k_0 in tetrahydrofuran ([H_2O]=0.027M, see the text);
F: k_2 in toluene.

Figure 6 is the log-log plots indicating the influence of water in the presence of a given amount of acid, and that of *m*-toluic acid in the presence of a given amount of water. The k_1 and the k_2 values were obtained in the absence of acid, and the k_1' values from the intercept of Fig. 5. These diagrams with a slope 45° demonstrate that Eq. (3) is quite appropriate in the present systems.

Figure 7 gives the Arrhenius plots of k_1, k_2, k_1' and k_0 in the solvents. The k_1 and k_1' values were obtained by extrapolation on Fig. 1 and Fig. 5, respectively, and their accuracy cannot be high enough. However, it is noteworthy that the values in tetrahydrofuran and ethylacetate are practically the same and that in toluene does not differ much. In tetrahydrofuran the Arrhenius activation energies were not obtained individually for k_1 and k_2. The E_a values were, however, obtained in the presence of varying amounts of water, and they were all found to be equal to 22 kcal per mole. Hence it is clear that both k_1 and k_2 have the same E_a values.

Table 1 summarizes the kinetic constants obtained in various solvents, together with the dielectric constants and dipole moments and the activation parameters in the solvents. The values for the acid-catalyzed paths do not seem very accurate, because they were obtained on the basis of extrapolated values and their approximate values are given in the footnote.

Discussion

Dissociation Mechanism. Since the exchange rate is independent of the concentration of acetylacetone, regardless of the presence of catalyst such as water and acid, the reaction must proceed through

Table 1. Rate constants and activation parameters at 25°C

Solvents		Tetrahydrofuran	Ethylacetate	Toluene	Xylenes
k_0 10^{-4} min^{-1} [a]		2.5	4.75	23.8	31.0
k_1 10^{-4} min^{-1}		0.6	0.64	0	0
k_2 10^{-2} M^{-1}min^{-1}		2.0	2.75	16	21
k_1' 10^{-2} M^{-1}min^{-1} [b]		0.93	5.4	9.5	
k_2' M^{-2}min^{-1} [b]		(1.2)	(3.0)	(13)	
Dielectric const.		7.39	6.03	2.38	2.57 (*o*-)[c]
Dipole moment (Debye)		1.70	1.87	0.39	0.62 (*o*-)[d]
$\Delta H^{\neq}$ [f] (kcal/mole)	k_0[a]	21.4[e]	21.4	19.2	
	k_1	[21.4][e]	21.4		
	k_2	[21.4][e]	21.4	19.2	
$\Delta S^{\neq}$ [g] (e.u.)	k_0[a]	−7.8	−8.0	−12.2	
	k_1		−12.2		
	k_2		0.04	−3.8	

a) [H_2O], 0.015M; [acid], none. b) acid, *m*-toluic c) at 20°C; *m*- 2.37; *p*- 2.27.
d) *o*-, 0.62 Debye; *p*-, non-polar. e) See text. Anticipated values in square brackets.
f) $\Delta H^{\neq}$ values in ethylacetate for k_1' and k_2' are both 21.4 kcal/mol.
g) $\Delta S^{\neq}$ values for k_1' and k_2' in ethylacetate are +1.4 and +9.5 e.u. respectively.

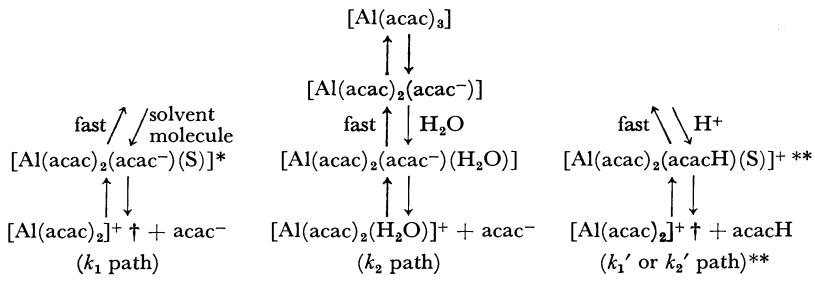

* S: solvent molecule ** In k_2' path, (H_2O) in place of S
† Presumably with coordinated solvent molecule (or with H_2O for the k_2' path).

Fig. 8. Plausible reaction mechanism.
(acac$^-$) denotes unidentate acetylacetonato ligand.

the dissociation mechanism, in which the break of metal-ligand bond is responsible for determining the rate. Whenever a bidentate chelate ligand undergoes isotopic exchange, two reaction mechanisms can be considered: (i) The break of one of the metal-ligand bonds is the rate-determining step, and the remaining bond breaks rapidly. The catalytic effect is understood by considering that water molecule or acid proton approaches the coordinated oxygen atom to assist the bond rupture. (ii) The ligand can be present as unidentate with considerably long life time, and break of the remaining bond is the rate-determining step. Catalytic actions can be interpreted by assuming that water molecule and the acid proton occupy the vacant coordination site of aluminum ion and the negatively charged free end of unidentate ligand, respectively, and retard recombination of the free end.

From the experimental results, we tend to conclude that mechanism (ii) is more plausible (Fig. 8). The activation enthalpies in tetrahydrofuran and ethylacetate are the same, regardless of the presence of catalysts, and that in toluene does not differ much. If (i) were operating, the ease of break of one of the metal-ligand bonds would be affected by the catalysts, and the $\Delta H^{\neq}$ values for k_1, k_2, *etc.* should have different values. Whenever (ii) operates, on the other hand, the rate constants are dependent on the ease with which the free end of unidentate ligand recombines with the metal ion. The transition state would involve elongation of the remaining bond of unidentate ligand, and be affected little by the protonation at the free end of the same ligand or by the occupation of coordination site on the aluminum ion by water molecule.

The k_1 Path. The fact that k_1 value is zero in toluene and xylenes, whereas it is greater in tetrahydrofuran and ethylacetate, seems to be related to the dipole moment and the dielectric constant of the solvents. We believe that activation entropy is responsible for such a difference. Polar solvents can occupy the free end of unidentate ligand or the vacant coordination site of metal ions to retard the recombination and leave more chance for the remaining bond to be broken.

Comparison of activation enthalpy, however, could also account for the difference. Since the present metal-ligand bond is regarded rather ionic, coordination of polar solvent molecule on the vacant coordination site would decrease the effective charge of the aluminum ion to make the remaining metal-ligand bond weaker, and to decrease the $\Delta H^{\neq}$ value. Such an interpretation is alternatively expressed as the small dielectric constants of the aromatic hydrocarbons being unfavorable for the break of aluminum-oxygen bond. These two contributions cannot be distinguished, unfortunately, because the k_1 value is zero.

The k_2 Path. The greater k_2 values in aromatic hydrocarbons than in polar solvents might be correlated with the ease with which water molecules coordinate the vacant site of the metal ion. The affinity between water and solvent molecules would be greater in tetrahydrofuran and ethylacetate than in toluene and xylenes.

In the latters, water molecules would have more chance to be present near the complex molecules and to creep in the coordination site whenever one of the aluminum-oxygen bond is broken, so that the recombination of unidentate ligand is retarded to a greater extent. Further, in these solvents, the coordination of water molecules to the vacant coordination site would decrease the effective charge of the cation and make the ionic metal-ligand bond weaker. Thus the activation enthalpy for the k_2 path could become smaller than that for the k_1 path, although the actual value for the latter cannot be known.

In polar solvents, on the other hand, the k_2 term is regarded to represent a reaction path in which water molecule occupies the vacant coordination site in place of the solvent molecule. Hence the difference in the rate constants k_1 and k_2 would not be so remarkable as in the non-polar solvents.

Acid Catalysis. The acid catalyzed reaction path operates in two ways. The k_1' path represents a reaction mechanism in which the acid acts as a

proton source without cooperation with water, whereas the k_2' path that operating with the aid of water. So far as the role of acid is to provide protons to the free end of unidentate ligand, the difference between the two paths consists in the kind of proton carrier. Hydroxonium ions must be the carrier for the k_2' path, while the acid molecule itself or the solvent molecule would be the proton carrier in the k_1' path.

As seen in Table 1, acid catalysis is more marked in toluene than in ethylacetate or tetrahydrofuran. Since protons have less affinity with the solvent molecule in toluene than in the polar solvents, acid molecules themselves would be the more plausible proton carrier in the former solvent. They would have greater possibility to be present near the complex molecule, to be ready to transfer protons to the free end of unidentate ligand, and retard the recombination to a greater extent. It would be also possible that the acid anion occupies the vacant coordination site as water molecule does in the k_2 path, whenever proton transfer takes place. Such a cooperative effect cannot be expected when the solvent molecule carries proton in the polar solvents. A similar trend is observed with the k_2' values. When hydroxonium ions carry protons, proton transfer to the free end of unidentate ligand can be accompanied by the addition of water molecule to the vacant coordination site of aluminum ion, and a cooperative effect is expected with a greater probability in toluene than in the polar solvents. The relative figure of the k_1' and the k_2' values would be related to the competition between water and the acid anion or the solvent molecule as proton carrier. Such a competition would be ruled by various factors including acid strength in the non-aqueous media and also affinity of water with the solvent molecule.

Importance of the Unidentate Complex as Intermediate. Aluminum complexes are generally regarded as substitution labile,[2] except for a few cases.[1,3] Rapid establishment of ligand interchange equilibria and racemization was demonstrated by Fortman and Sievers on the basis of p.m.r. coalescence measurement with acetylacetonato, hexafluoroacetylacetonato and hexamethylacetylacetonato complexes of aluminum.[4] They postulated several possible intramolecular reaction mechanisms, but gave no conclusion as to which of them is most plausible. We have pointed out the importance of an intermediate state involving a unidentate ligand, but our result is not enough for choosing the most appropriate one. We are essentially dealing with slow reactions, and our "rapid reaction" could be slower than their reaction by several orders. Whenever the free end of unidentate ligand recombines with the aluminum ion without undergoing isotopic exchange reaction, the life time of intermediate must be long enough to allow some kinds of steric change which can bring about the inversion of individual tris complex molecules.

Although our experiment cannot provide useful information concerning the "twist mechanism," it clearly rules out any kind of intermolecular mechanism and seems to establish the importance of unidentate intermediate in considering the reaction mechanism of ligand substitution in chelate compounds.

We wish to express sincere thanks to Nishina Memorial Foundation for grant-in-aid. We are also indebted to Mr. Hiroaki Kido for useful discussion, and to Miss Mizue Tachikawa for help in experiments.

2) M. Eigen, *Pure Appl. Chem.*, **6**, 105 (1963).
3) K. Saito, M. Takahashi, Y. Miyakawa and K. Masuda, This Bulletin, **41**, 1139 (1968).
4) J. J. Fortman and R. E. Sievers, *Inorg. Chem.*, **6**, 2022 (1967).

BULLETIN OF THE CHEMICAL SOCIETY OF JAPAN VOL. 43 125—129 (1970)

Studies on Dithiocarbamates. XII. Kinetic Studies on the Hydrolysis of Mesoionic 4,5-Diphenyl-1,3,4-thiadiazole

P. B. TALUKDAR, S. BANERJEE and A. CHAKRABORTY

Research and Development Division, East India Pharmaceutical Works, Calcutta-61, India

(Received March 28, 1969)

Kinetic studies of the compound given in the title were conducted in aqueous alcohols over a wide range of pH. The observed rate constants are dependent on the hydroxide-ion concentration as well as polarity of the medium. Hydrolytic decomposition is characterised by a small magnitude of entropy (ΔS^*) and negative salt-effect. Mechanism consistent with these facts has been suggested.

We had been interested for some time in the physicochemical properties of heterocyclic systems containing –NCS fragment as an essential part of their structure.[1-4] In continuation of this work, we recently reported[5] the synthesis and spectral characteristics of a series of mesoionic 1,3,4-thiadiazoles (I). This provided us with an opportunity to examine the hydrolytic behaviour of a typical compound (II) as a representative member of the series.

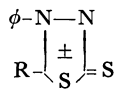

I

II, R=ϕ

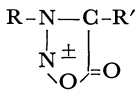

III

Quite apart from their structural peculiarities,[6,7] mesoionic compounds (I and III) were also reported to have interesting pharmacological properties.[6,7] Consequently, fairly extensive kinetic[8-10] data are now available on more readily accessible sydnone derivatives (III), which show sensitivity to both acid and alkali. Comparative data on mesoionic thiadiazoles (I) are highly desirable as it is anticipated that any intrinsic difference in properties between these two systems is bound to have profound reflection on the observed data. With this objective in view, our studies are mainly concerned with effects of pH, temperature, solvent composition and ionic strength on the rate constants. These results, in conjunction with the isolation of a derivative of the product of hydrolysis in alkaline condition provide sufficient evidence on the probable course of degradation of II under alkaline condition.

Experimental

Materials. Mesoionic 4,5-diphenyl-1,3,4-thiadiazole (II) has been previously described.[5,7] AR-grade solvents were fractionated over metallic sodium and mid-fractions were stored in amber-coloured bottles

TABLE 1. THE APPARENT FIRST ORDER RATE CONSTANTS UNDER VARIOUS EXPERIMENTAL CONDITIONS AT 25°C

No.	Solv. comp. % solv. (v/v)	Experimental pH	Ionic str. μ	Rate const $10^4 \times k_{ob}$ in sec^{-1}	Calcd second order rate const. k in l/mol/sec
1	50-EtOH	7.80	0.05	0.006489	1.028
2	50-EtOH	8.30	0.05	0.02079	1.042
3	50-EtOH	8.70	0.05	0.09137	1.854
4	50-EtOH	9.60	0.05	0.561	1.409
5	50-EtOH	10.10	0.05	1.381	1.097
6	50-EtOH	10.50	0.05	4.606	1.456
7	50-EtOH	10.70	0.05	7.170	1.431
8	50-MeOH	9.55	0.05	1.421	4.005
9	50-*i*-PrOH	10.55	0.05	4.103	1.156
10	50-EtOH	10.55	0.25	3.070	0.865
11	50-EtOH	10.55	0.50	2.457	0.692
12	40-EtOH	10.30	0.05	3.141	1.574
13	30-EtOH	10.10	0.05	2.214	1.759
14	30-EtOH	10.10	0.25	1.706	1.355
15	30-EtOH	10.10	0.50	0.959	0.762

1) P. B. Talukdar, *J. Indian Chem. Soc.*, **44**, 17 (1967).
2) P. B. Talukdar and S. Banerjee, *ibid.*, **44**, 1060 (1967).
3) P. B. Talukdar and S. K. Sen Gupta, *ibid.*, **45**, 291 (1968).
4) P. B. Talukdar, S. Banerjee and A. Chakraborty, *ibid.*, **45**, 775 (1968).
5) P. B. Talukdar and S. K. Sen Gupta, *ibid.*, in press; *ibid.*, **45**, 356 (1968), for short communication.
6) L. B. Kier and E. B. Roche, *J. Pharm. Sci.*, **56**, 149 (1967).
7) T. G. Stewart and L. B. Kier, *ibid.*, **54**, 731 (1965).
8) E. R. Garrett, *ibid.*, **53**, 42 (1964).
9) E. R. Garrett and P. J. Mehta, *ibid.*, **56**, 1468 (1967).
10) S. A. Zotova and V. G. Yashunskii, *Zh. Org. Khim.*, **3**, 942 (1967).

prior to their uses, and calibrated by checking their specific-gravities against literature values. Conductivity water was prepared in an all-glass apparatus from distilled water over potassium permanganate.

Acetate buffers were used for studies under acidic conditions, but phosphate and borate buffers were used under alkaline conditions; ionic strength (μ) was maintained at around 0.1 with requisite amount of KCl and the pH values were checked in a standard Cambridge pH-meter. The pH values recorded in Table 1 refer to those observed under the actual experimental condition (after 24 hr) after mixing the required amount of solvents and stock buffers. Higher ionic strength was achieved through addition of extra amount of KCl to the required quantity of buffer.

Spectrophotometric measurements were carried out with a Hilger UVISPEK spectrophotometer in 1 cm cells.

Kinetic Measurements. Initial experiments have shown that the characteristic long wavelength band[5,7] of the mesoionic thiadiazole appears at 382—383 mμ under the projected experimental condition, and the band position remains practically unchanged with change in pH; hence all kinetic runs were followed by measuring the loss of intensity of this band at 382 mμ.

A fairly concentrated solution of the substrate was first prepared in an appropriate solvent so that the observed optical density is around unity. After the thermal equilibration of the stock solutions, aliquots were mixed and the fall in intensity was followed until at least 80% of the substrate reacted. Other details were the same as before.[2,4]

Constancy of the thermostatic bath was within ± 0.2°C and the accuracy of the data was better than 3% by agreement between duplicate experiments.

Product Study. 200 mg of the compound was first dissolved by warming in about 30 m*l* of ethanol; it was cooled to 25°C and diluted with an equal volume of water. To the yellow solution, aqueous NaOH (10%) was added dropwise with stirring at 25°C maintaining the pH at 9—10. When there was no more fading away of colour (about 30 min), pH was adjusted at 5—6 with drops of acetic acid and gently warmed on a steam bath for about 5 min. A solution of *p*-nitrobenzaldehyde (120 mg) in minimum quantity of alcohol was added with swirling to the above solution and the mixture was heated on a steam bath for another 10 min. On cooling down to room temperature, a yellow precipitate was obtained; this was collected, washed with a few drops of ethanol.

Two crystallisations from ethanol yielded 85 mg (50%) of pale yellow needles, mp 149.5—150°C, with immediate solidification and remelts at 169—170°C; λ_{max}^{EtOH} 226 mμ (ε, 18750) and 325 mμ (ε, 20060). IR (Nujol): 1660 (–CO, amide) and 1640 (–C=N) cm^{-1}. Found: N, 12.28%. Calcd for $C_{20}H_{15}N_3O_3$: C, 12.17%.

Identity of the product was established by comparison with an authentic sample of *p*-nitrobenzylidene derivative (IX) of *N*-benzoyl-*N*-phenylhydrazine synthesized by the following method:

A solution of phenylhydrazone of *p*-nitrobenzaldehyde (200 mg; mp 159—160°C) in 30 m*l* of dry benzene was refluxed with equimolar amounts of benzoyl chloride and pyridine for 10 hr. After working up in the usual way, the residue was crystallised from ethanol to give pale yellow needles, mp 169—170°C, with similar characteristics and identical absorption bands as the above compound.

Results and Discussion

Effects of pH and Temperature. The apparent first order rate-constants at various pH in 50% aqueous ethanol are shown in Table 1. Data clearly show appreciable acceleration of rate with rise in pH so much so that it is extremely difficult to measure the rate at a higher pH (>10.5). On the other hand, the reaction is extremely sluggish between pH 7—8 and there was practically no change in optical density in acidic buffers (4.90 and 3.65) over a week.

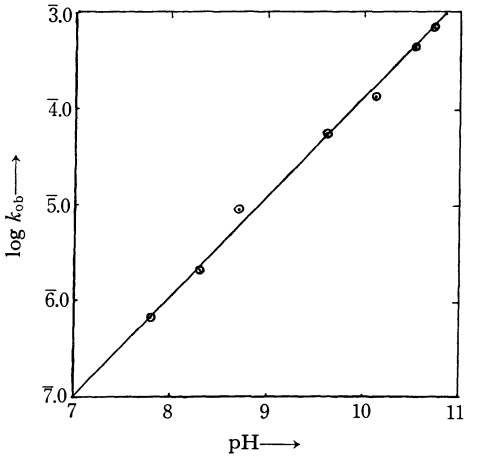

Fig. 1. pH-rate profile in 50% aqueous ethanol at 25°C and μ=0.05.

The observed behaviour of II in the acidic region is quite a surprise when one recalls the facile degradation of sydnones under a similar condition to yield the appropriate hydrazines.[10,11] However, the significance of the data becomes readily comprehensible from the pH-rate profile (Fig. 1) where the slope is almost equal to unity suggesting specific hydroxide-ion catalysed reaction at the rate-limiting step. Presumably, the reaction is first-order with respect to hydroxide ion concentration. Similar specific hydroxide-ion catalysed hydrolysis has been observed with some sydnone derivatives.[9]

That the observed reaction is also first-order with respect to the substrate is shown not only by the excellent first-order plots (log o.d. *vs.* time), but also by the constancy of half-lives ($t_{1/2}$=24—25 min) at five different initial concentrations (0.8 to 2.0×10^{-3}M) of the substrate in 50% ethanol at 25°C for pH=10.5 and μ=0.05. Evidently, the overall reaction is a clean second-order one. Hence, the rate law for the observed reaction is

11) R. A. Eade and J. C. Earl, *J. Chem. Soc.*, **1946**, 591.

$$-\frac{dA}{dt} = k[A][OH]^-$$

$$= k_{ob}[A], \text{ for a given pH.}$$

Thus $k_{ob}=k[OH]^-$, hence the bimolecular rate-constants for the hydroxide-ion catalysed reaction could be obtained from k_{ob}; these are shown in Table 1 and are reasonably constant under identical conditions (No. 1—7).

Table 2. Temperature dependency of rate constants in 50% aqueous ethanol at pH=10.50 and μ=0.05

Temp. °C	10^4 k_{ob} in sec^{-1}	Kinetic parameters
15	1.379	E_A=20.19 kcal/mol
20	2.239	ΔH^*=19.60 kcal/mol
25	4.606	ΔG^*=22.02 kcal/mol (at 25°)
30	7.932	ΔS^*=−8.13 e.u.

Data on the temperature dependency of rate-constants are shown in Table 2. The derived activation parameters are quite comparable to those reported[9] for the base-catalysed decomposition of sydnones and to other bimolecular reactions. Although the absolute value of ΔS^* could not be emphasized, the small negative value is highly significant. It is now recognised that, for a unimolecular reaction, the magnitude of ΔS^* is usually very small and tends to be zero.[12] Interpretation of such data is extremely difficult,[13] but in the given instance it undoubtedly reflects the small difference between the reactant and the transition-state with respect to their imposed constraints. The situation could be resolved by assuming the formation of an initial transition complex through the rate-determining attack of the hydroxide ion followed by smooth and rapid rearrangement to another intermediate prior to its decomposition.

The Effect of Variation in Solvent Composition. The influence of the variation in solvent composition on the rate-constant is also included in Table 1. Although the same quantity of buffer was used in each case, and the ionic strength was maintained at the same level, the observed pH of the medium, as anticipated, shows considerable variation with change in the nature of the co-solvent. The impact of solvent composition on the rate-constants is, therefore, apparently submerged in the apparent first-order rate-constants due to inherent difference in pH of the medium. Assuming that there is no significant difference in the ionisation of water for the solvents under consideration, the calculated second-order rate-constants clearly demonstrate the expected order of solvent effect where the rate-constants increase with increasing polarity of the medium. This apparently indicates ionic character of the transition state. But no attempt is made here to correlate the rate-constants with any known[14] parameter of the solvent, because microscopic polarity in the cybotactic[15] region of the reacting species is extremely difficult to be adequately expressed by known parameters of the solvent.

Parker[16] has already discussed the mode of solvation in a protic solvent where hydrogen-bonding is considered to play a vital role. It has already been observed by us[5] that λ_{max} of the thiadiazole (II) is quite sensitive to the protic character of the solvent. In the given instance, then, it might be true that the increased population of a specific dipolar form[6,7] of II (which is stabilised through hydrogen-bonding) makes an effective contribution in increasing the rate in a more polar solvent. At the same time, solvation to the transition-state, which is largely anionic in character, appears to be favoured in more polar medium suggesting appreciable charge dispersion[17] at the transition state. This ought to be viewed against the small magnitude of ΔS^* as noted earlier. Although no attempt has been made to find out the changes in ΔS^* by changing the solvent composition, it is probably the difference in the solvation of the reactant[18] rather than the transition-state that appears to be important here; however, possibility of the changes in ΔH^* can not be altogether discarded and the origin of the solvation effect is still a matter of debate.[19]

From all accounts, it appears reasonable to exclude water as a direct participant and its role is essentially associated with solvation phenomenon. Thus, kinetic data in solvents of similar composition (50% aqueous methanol, ethanol and 2-propanol, Table 1) tend to confirm this, but comparatively higher rate in 50% methanol may be due to some other specific interactions. Alternatively, hydroxide-

12) L. L. Schaleger and F. A. Long, *Advan. Phys. Org. Chem.*, **1**, 1 (1963).

13) C. A. Bunton and V. J. Schiner, *J. Amer. Chem. Soc.*, **83**, 3207 (1961).

14) C. C. Reichardt, *Angew. Chem. Int. Ed. Engl.*, **4**, 29 (1965).

15) E. M. Kosowar, "An Introduction to Physical Organic Chemistry," John Wiley & Sons, New York (1968), p. 262.

16) A. J. Parker, *Advan. Phys. Org. Chem.*, **5**, 173 (1967).

17) J. E. Leffler and E. Grunwald, "Rates and Equilibria of Organic Reactions," John Wiley & Sons, New York (1963), p. 267.

18) Y. C. Mac, W. A. Millen, A. J. Parker and W. D. Watts, *J. Chem. Soc., B*, **1967**, 525; R. Alexander, K. C. F. Ko, A. J. Parker and T. J. Broxton, *J. Amer. Chem. Soc.*, **90**, 5049 (1968).

19) J. E. Crooks, *Annual Reports, The Chemical Society* (London), **64**, 37 (1967).

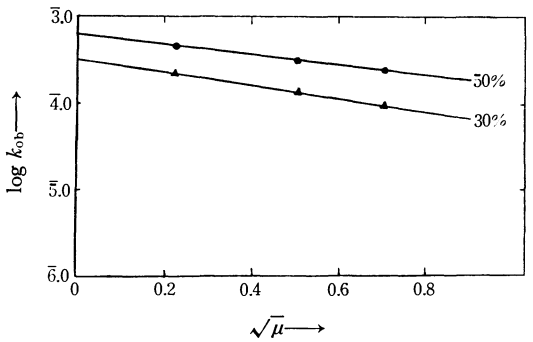

Fig. 2. Effect of electrolyte on the rate.

ion is known to be a structure-maker[20] and with a suitable orientation may lower the activation energy in the formation of the tetrahedral intermediate (see below).

Salt-effect on the Rate Constants. Data for the effect of the ionic strength (μ) in the reaction medium are presented in Table 1 for three different alcohol-water compositions. In all cases rate retardation is observed for increased values of μ. Qualitatively, this is consistent with the salt-effect upon ion-molecule reaction;[21] for example, fairly large electrolyte effect is observed for the attack of hydroxide-ion on *p*-nitrodiphenylphosphate in water.[22] Actually, the plots of log k_{ob} against $\sqrt{\mu}$ is linear (Fig. 2), the lower the proportion of alcohol, the larger the slope (−0.6 and −0.75 at 50% and 30% ethanol respectively). Again, from the plot of the slope against % water, the intercept yields a value almost equal to unity. Thus the predicted salt-effect in absence of alcohol (*i. e.*, in 100% water) has got the value as required by limiting Deybe-Hückel equation for reaction between two oppositely charged species, each carrying a unit charge.

However, our results could not be directly compared with those reported[9] for sydnones where the effect of electrolyte on the acid-catalysed reaction was examined. But it is still more difficult to account for such salt-effects as pointed out recently by Bunton and Robinson.[29] According to them it is highly unlikely that ion-pairing is important in aqueous alcohol. Further, possibility of changing the lyate ion from OH^- to more nucleophilic alkoxide-ion[23] with increase in alcohol content could not be a significant factor under the experimental set up. It has also been suggested[20] that for anion-molecule reaction in polar hydroxylic solvent, the transition state is stabilised relative to the nucleophilic anion by cations of low charge density (*e. g.* K^+) and this is apparently consistent with our observation.

Alternatively, the negative salt-effect may be attributed to preferential solvation of K^+ and Cl^- by water so that less water is available as solvating species.[24] The magnitude of salt-effect should, in that case, be more pronounced in a less polar medium; but this is contrary to our experience. Consequently, the observed electrolyte effect could be reasonably attributed to its interaction at the transition-state.

Product Isolation and Mechanism of Degradation. Any mechanistic interpretation on the alkaline decomposition of II must, therefore, satisfy the following facts: (1) first-order dependence on hydroxide-ion concentration, (2) rate increases with increased polarity of the medium, (3) small magnitude of ΔS^*, and (4) the negative salt-effect. In accordance with these facts the following scheme is suggested:

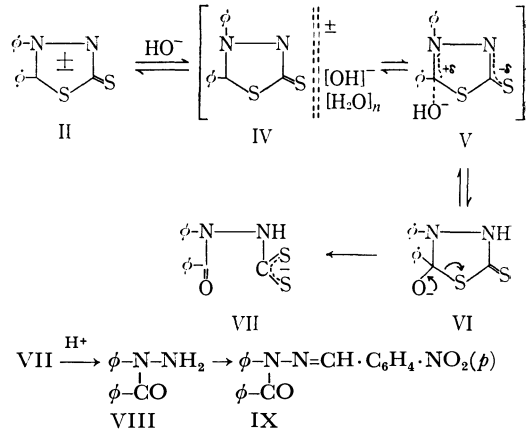

The most difficult step in the proposed scheme is to locate the site of the attack of hydroxide-ion. The same difficulty was encountered in explaining the base-catalysed decomposition of sydnones and consequently, two alternative mechanisms, involving positions 2 and 5 were proposed.[8,25] It is difficult to comprehend a situation where the attack of hydroxide-ion occurs on the carbon atom bearing the exocyclic sulphur atom with a large formal negative charge. In this respect we are in agreement with the views of Garrett[8] on sydnone derivatives.

What is intended here is to show that the solvated thiadiazole (II) becomes highly polarised by the approach of the hydrated hydroxide-ion so as to form a complex (IV) in a rate determining step.

20) C. A. Bunton and L. Robinson, *J. Amer. Chem. Soc.*, **90**, 5965 (1968).
21) C. K. Ingold, "Structure and Mechanism in Organic Chemistry," Cornell University Press, Ithaca, New York (1953), Chap. VII.
22) C. A. Bunton, S. Farber and E. J. Fendler, *J. Org. Chem.*, **33**, 29 (1968).
23) R. G. Burns and B. D. England, *Tetrahedron Lett.*, **1960**, 1.
24) N. B. Chapman, E. Ehsan, J. Shorter and K. J. Toyane, *J. Chem. Soc., B*, **1968**, 178.
25) E. B. Roche and L. B. Kier, *Tetrahedron*, **24**, 1672 (1968).

This rapidly rearranges, possibly involving OH^- transfer through water clusters,[26] to give the tetrahedral intermediate (VI). The intermediate, in turn, collapses in a fast step to yield the dithiocarbazinate (VII) under the alkaline condition. In support of the main sequence of the reaction, we have already isolated *N*-benzoyl-*N*-phenylhydrazine (VIII) as *p*-nitrobenzylidene derivative (IX) in fair yield. Isolation of the same compound in a poorer yield has been recently claimed[27] but no data were provided. We plan to continue our studies in order to resolve the details of the proposed mechanism.

We thank Mr. P. Bagchi, Research Director, for his keen interest and Dr. S. K. Das Gupta for IR spectra.

26) Ref. 15, p. 287.

27) R. Grashey, M. Bauman and W. D. Lubos, *Tetrahedron Lett.*, **1968**, 5881.

BULLETIN OF THE CHEMICAL SOCIETY OF JAPAN VOL. 43 129—134 (1970)

Mass Spectra of Diaryl Disulfides, Diaryl Thiolsulfinates and Diaryl Thiolsulfonates

Seizi KOZUKA, Hideo TAKAHASHI and Shigeru OAE

Department of Applied Chemistry, Faculty of Engineering, Osaka City University, Sumiyoshi-ku, Osaka

(Received April 30, 1969)

The mass spectra of diaryl disulfides, diaryl thiolsulfinates and diaryl thiolsulfonates have been studied by analyzing metastable peaks and mass numbers. The main fragmentation observed for the disulfides was the cleavage of the S–S bond while the fragmentation of thiolsulfinates was similar to that of disulfides after elimination of oxygen. In the case of thiosulfonates, however, no such deoxygenation was observed, formation of sulfonium ion and one oxygen migration from the sulfone sulfur to the thiol sulfur were observed. Formation of thiabenzonium ion was observed in the mass spectra of sulfinates and sulfonates.

The mass spectra of organic sulfur compounds have been investigated considerably in recent years, and those of alkyl and diaryl sulfides,[1-4] sulfoxides[2,5,6] and sulfones[5-7] have been well understood.

However, the mass spectra of the aromatic compounds containing S–S bond, *i.e.*, disulfides (I), thiolsulfinates (II), and thiolsulfonates (III) have received rather scant attention except for diphenyl disulfide.[4]

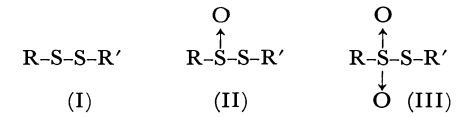

(R, R′=aryl)

This paper describes a detailed study on the electron impact fragmentation of these three types of sulfur compounds where R and R′ are aryl groups. The following compounds were subjected to mass spectrometric analysis.

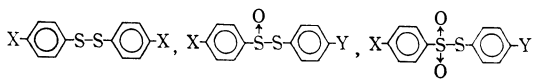

Ia X=H, b X=CH_3, c X=Cl, d X=OCH_3, e X=NO_2

IIa X=H, Y=H, b X=H, Y=CH_3, c X=CH_3, Y=CH_3, d X=H, Y=OCH_3

IIIa X=H, Y=H, b X=CH_3, Y=CH_3, c X=H, Y=NO_2, d X=H, Y=Cl

1) P. Natalis and J. L. Franklin, *J. Phys. Chem.*, **69**, 2943 (1965).
2) R. G. Gills and J. L. Occolowits, *Tetrahedron Lett.*, **1966**, 1997.
3) J. H. Bowie, S.-O. Lawesson, J. O. Madsen, C. Nolde, G. Schroll and D. H. Williams, *J. Chem. Soc., B*, **1966**, 946.
4) J. H. Bowie, S.-O. Lawesson, J. O. Madsen, C. Nolde and D. H. Williams, *ibid., B*, **1966**, 951.
5) J. O. Madsen, C. Nolde, S.-O. Lawesson, G. Schroll, J. H. Bowie and D. H. Williams, *Tetrahedron Lett.*, **1965**, 4377.
6) J. H. Bowie, D. H. Williams, S.-O. Lawesson, J. O. Madsen, C. Nolde and G. Schroll, *Tetrahedron*, **22**, 3515 (1966).
7) S. Meyerson, H. Drews and E. K. Fields, *Anal. Chem.*, **36**, 1294 (1964).

Results and Discussion

Diaryl Disulfides. Of first group of compounds (Ia—Ie), the mass spectrum of only the unsubstituted compound (Ia)[4] has been reported. The substituent effect on the fragmentation has not been investigated. The main spectra of these compounds are summarized in Table 1.

TABLE 1. RELATIVE ABUNDANCE OF MAJOR PEAKS AND METASTABLE PEAKS OF DIARYL DISULFIDES

Compd. / Ion	Relative Abundance Ia	Ib	Ic	Id	Ie
M	86	75.8	42	38.6	100
M-(S)	4.7	1.9	0.1	0.2	9.4
M-(SH)	14.1	3.2	0.2	trace	trace
M-(S_2)	20	7.7	2.3	0.3	0.3
M-(S-C$_6$H$_4$-X)	100	100	100	100	5.7
M-(C_6H_4X)	4.1	1.3	1.0	0.6	1.5
C_6H_4X	15.1	12.8	1.8	0.3	1.0
M-(X)	—	trace	0.4	0.2	3.1
C_6H_4S	—	5.1	44.4	1.6	45
Metastable peak					
M→M-(SH)	present	present	—	—	—
M→M-(S_2)	present	present	—	—	present

A few characteristic features of these spectra may be summarized as follows.

1) All the compounds give prominent parent peaks.

2) The largest peaks for the compounds are fragment peaks formed by cleavage of the S–S bond except in the case of the nitro compound. The anomaly of the nitro compound may be due to the facile decomposition of the ion formed by cleavage of the S–S bond. In this case, three distinctive peaks observed (*i.e.*, *m/e*, 138, 124 and 108) suggest the succeeding decomposition of the daughter ions.

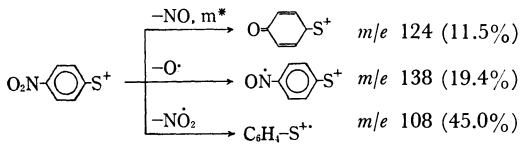

Scheme 1

3) Elimination of S or S_2 from the parent ions was observed, although the process was minor.

4) The relatively high intensity of the fragment having mass number 108 is to be noted. This ion is probably formed by the subsequent cleavage of the X–C bond of the X-C$_6$H$_4$-S$^+$ ion. The intensities of these ions are apparently affected by the substituent X and decrease in the order $-NO_2 > -Cl > -CH_3 > -OCH_3$. This order is consistent with the relative stability of the precursor ions. These observations suggest the fragmentation scheme of of these diaryl disulfides as shown below:

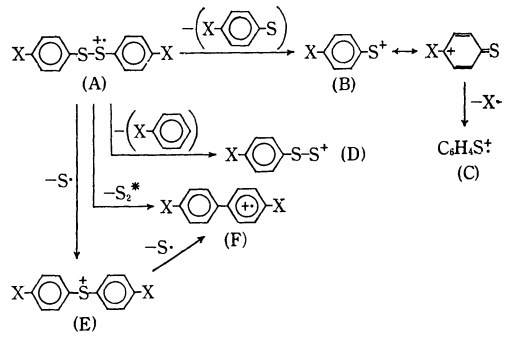

Scheme 2

The main fragmentation process for these compounds is (A)→(B)→(C) and a small portion of the parent ion undergoes decomposition through other pathways.

Ion (F) may be formed either by the direct desulfurization of the parent ion or through ion (E). The direct process is confirmed by the aid of the metastable peak. However, the pathway giving (F) from (E) is also not unreasonable in view of the similar fragmentation of diarylsulfides.[6]

Diaryl Thiol Sulfinates. The mass spectra of diaryl sulfides were investigated by Natalis *et al.*[1,4,5] and the main fragment peaks reported corresponded to those of the diaryl cation and the sulfenium ion formed by the loss of one aryl group. On the other hand, diaryl sulfoxides are known to give the following fragmentation.

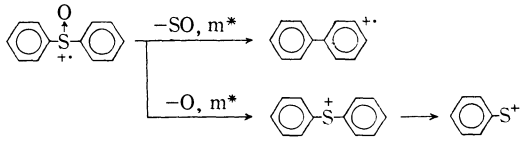

These results suggest that the oxidation of sulfur atom of diaryl sulfides does not give rise to any distinctive difference in mass spectra of these compounds. Thus, it is interesting to compare the mass spectra of diaryl thiolsulfinates with those of the corresponding disulfides.

The main spectra of the sulfinates are summarized in Table 2.

As was expected, all the sulfinates give no parent peak or a very small one and the spectra are similar to those of disulfides, hence the general fragmentation patterns for these compounds are initial elimination of oxygen followed by cleavage of the S–S bond or the elimination of sulfur, similar to the fragmentation of the disulfides.

A question arises as to whether the spectra were simply from the sulfinates, since the thiolsulfinates are known to undergo thermal disproportionation to

Table 2. Relative abundane of major peaks and metastable peaks of diaryl thiolsulfinates

Compd. / Ion	Relative abundance IIa	IIb	IIc	IId
M	—	5	trace	trace
M-(O)	89	42	66	12
M-(SO)	7.0	2.8	2.7	2.4
M-(S_2O)	4.7	5	8.1	3.6
X-⟨⟩-SO	22.6	14.2	8.1	9.7
Y-⟨⟩-SO		14.2		6.1
X-⟨⟩-S	100	100	100	23.2
Y-⟨⟩-S		34		100
m/e 97 ⟨⟩S	4.6	4.0	5	6.1
X-⟨⟩S			0.7	—
Y-⟨⟩S		3.4		—
Metastable peak				
M-(O)→ M-(SOH)	present	present	present	—
M-(O)→ M-(SO)	present	present	present	—
M-(O)→ M-(ϕ-SO)	present	—	present	—
M-(O)→ M-(ϕ-S_2O)	present	—	present	—

give the corresponding thiolsulfonates and disulfides.[8]

In the present study, only small peaks corresponding to thiolsulfonates were observed.

The peaks are, however, too small to be expected from disproportionation and moreover the whole pattern of the spectra is quite different from the combined spectra of the equimolar mixture of the thiolsulfonate and the corresponding disulfide. Therefore it should be assumed that the spectra show just the fragmentation of thiolsulfinates.

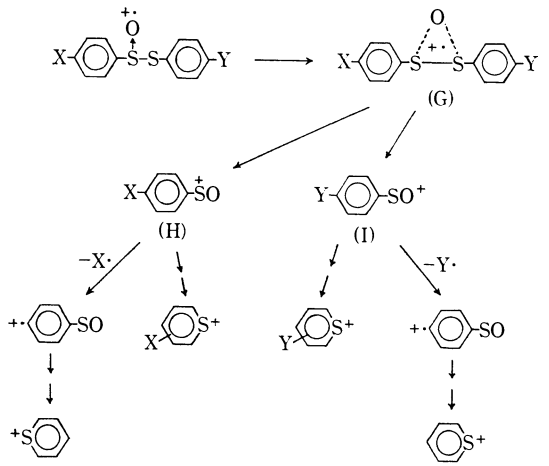

Scheme 3

In addition to these processes, a fragmentation giving thiabenzonium ion was observed as in the case of diaryl sulfoxides,[6] shown in Scheme 3.

The path giving the thiabenzonium ion from diphenylsulfoxide was confirmed by the presence of the metastable peak and the component of the ion was also determined by means of high resolution mass spectrometry.[6] On the other hand, the ion of the mass number 97 in this work seems to be formed in a somewhat different way since these peaks appear at the same mass number even in methyl-substituted compounds, although there were also small peaks corresponding to the substituted thiabenzonium ion. Thus the process giving the thiabenzonium ion must include the elimination process of the substituent and hence is considered as a rearrangement ion.

Comparing these spectra with those of diaryl sulfoxides, a minor but noticeable difference is observed in deoxygenation. Although similar deoxygenation is observable in the case of diaryl sulfoxides the parent peaks are always observed quite clearly, unlike the case of the thiolsulfinates which undergo deoxygenation almost exclusively. The

Table 3. Relative abundance and metastable peaks of diaryl thiolsulfonates

Compd. / Ion	Relative abundance IIIa	IIIb	IIIc	IIId
M	39	33	7.8	40
M-(S)	1.2	1.5	0.8	2.7
M-(SO_2)	5.1	7.8	19.4	39.1
X-⟨⟩-SO_2	33	30	65	63.3
X-⟨⟩-SO	82	100	8.5	63.7
Y-⟨⟩-S			0.2	46.9
X-⟨⟩-S	48	37	—	13.1
Y-⟨⟩-S			1.2	68.3
⟨⟩S	12.2	2.6	3.4	9.1
X-⟨⟩S		3		
Y-⟨⟩S			—	2.2
X-C_6H_4	trace	46	trace	trace
Y-C_6H_4			trace	80.5
H-C_6H_4	100	18.2	100	100
Metastable peak				
M → X-⟨⟩-SO	present	present	—	present
X-⟨⟩-SO_2 → XC_6H_4	present	present	present	present
M → X-⟨⟩-SO_2	—	—	present	present

8) D. Barnard, *J. Chem. Soc.*, **1957**, 4675.

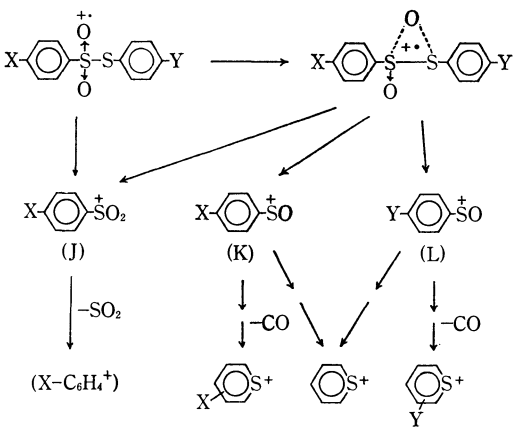

Scheme 4

observation that thiolsulfinates undergo more facile deoxygenation than the sulfoxides seems to conflict with the strength of the S–O bonds of these compounds obtained from IR spectra.[9] The facile deoxygenation in diaryl thiolsulfinates, however, may be rationalized in terms of resonance stabilization of the daughter ions. Namely, although the S–O bond of thiolsulfinate is stronger than that of sulfoxide, the deoxygenation of the former gives disulfide ions which is undoubtedly much more stable than sulfide ions formed by the deoxygenation of sulfoxides. The initial ionization to introduce a positive charge on the oxygen atom of the S–O bond would be easier with thiolsulfinate than with sulfoxide since the positive charge on the sulfur atom can be delocalized to a greater extent more with the former than the latter. This resonance stabilization perhaps outweighs the small difference in the bond strength resulting in the more facile deoxygenation with thiolsulfinate than sulfoxide.

Diaryl Thiolsulfonates. Mass spectrometric analyses were also carried out with the sulfur compounds containing one more oxygen atom around the S–S bond *i. e.*, diaryl thiolsulfonates. The common spectral features of these compounds are summarized in Table 3. As the mass spectra of these thiolsulfonates give the matastable peaks corresponding to the path from the parent ions to the fragments (J), (K) and (L), an intermediate with three-membered ring containing oxygen may be postulated. The main fragmentation scheme for these sulfonates can be depicted as shown in Scheme 4. This includes the cleavage of the S–S bond before or after the migration of one oxygen atom from the sulfone sulfur to the thiol sulfur.

The oxygen migration at the two sulfur atoms appears to be an important process in the fragmentation of diaryl thiolsulfonates. This oxygen migration is also observed in the mass spectra of diaryl thiolsulfinates but minor since the initial elimination of the oxygen is the major process in the fragmentation of thiolsulfinates. On the other hand, the elimination of oxygen atom from the sulfonate linkage is not observed. This difference between the sulfonates and the sulfinates is in good accordance with the difference in the bond strength of the S–O bonds.[9] Similar observations have also been made for the mass spectra of diphenyl sulfoxide in which deoxygenation was found to be minor but no such process was found in that of diphenyl sulfone.[6]

Formation of the thiabenzonium ion is also found in these cases. It is suggested that the formation of the thiabenzonium ion is a common phenomenon with sulfur compounds having an S–O bond adjacent to phenyl group.

The common pattern of the cleavage for these sulfur compounds *i. e.*, disulfides, thiolsulfinates and thiolsulfonates is the cleavage of the S–S bond. Cleavage involving one oxygen migration is also a common process for the sulfinates and the sulfonates.

Experimental

The spectra were recorded with a Hitachi RMU-6E single focus mass spectrometer using 80 eV at the emission

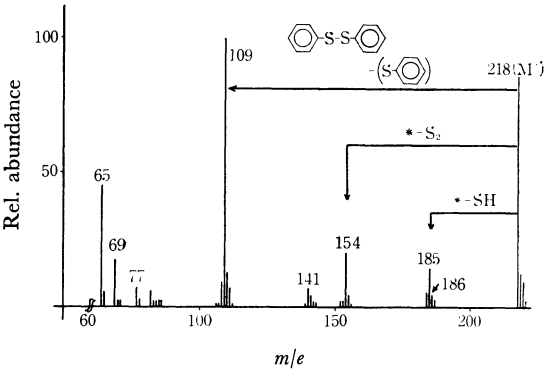

Fig. 1. The mass spectra of .

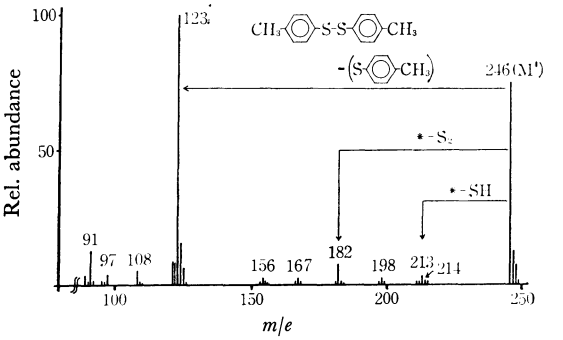

Fig. 2. The mass spectra of .

9) S. Ghesretti and G. Modena, *Ann. Chim.* (Rome), **53**, 1083 (1963).

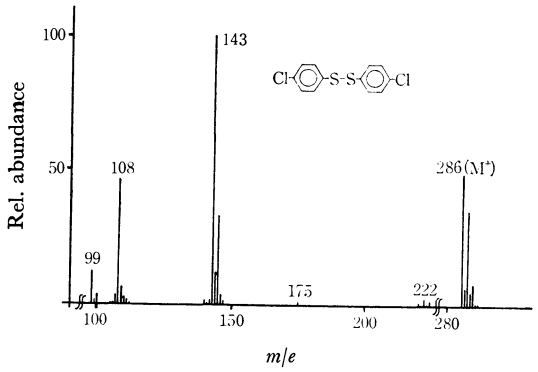

Fig. 3. The mass spectra of Cl-S-S-Cl.

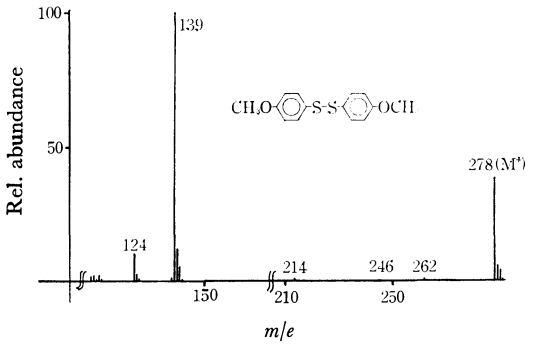

Fig. 4. The mass spectra of CH_3O-S-S-OCH_3.

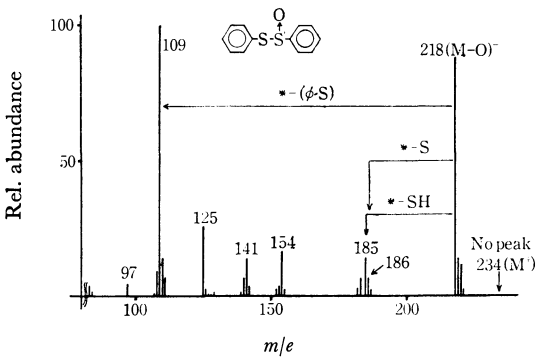

Fig. 5. The mass spectra of O-S-S-.

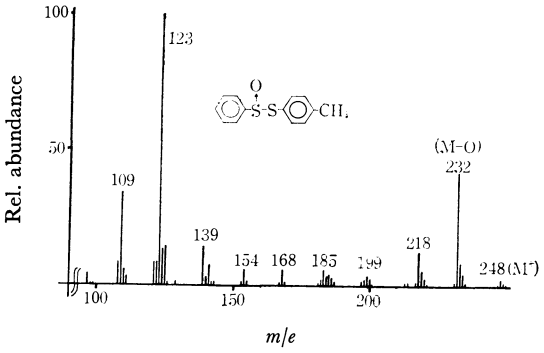

Fig. 6. The mass spectra of O-S-S-CH_3.

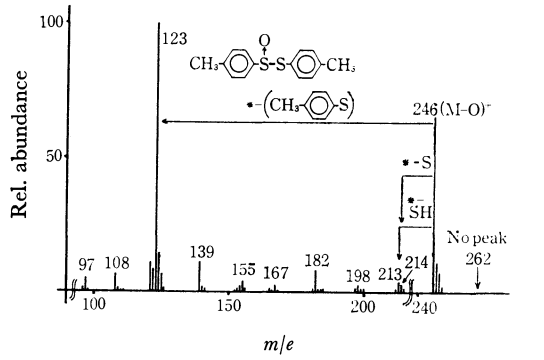

Fig. 7. The mass spectra of CH_3-S-S-CH_3.

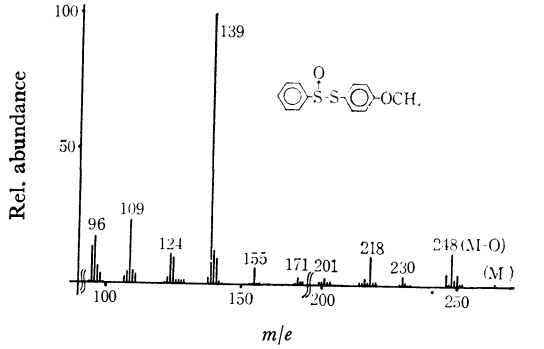

Fig. 8. The mass spectra of O-S-S-OCH_3.

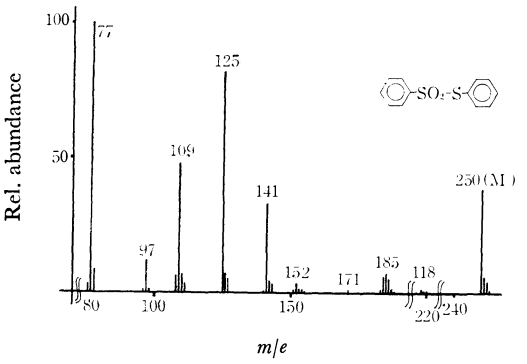

Fig. 9. The mass spectra of 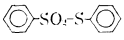 .

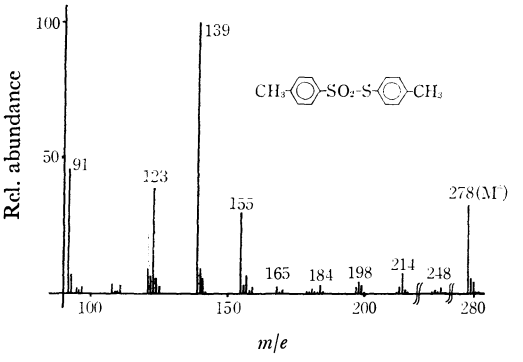

Fig. 10. The mass spectra of .

current of 110 μA. Samples were introduced into the ionization chamber through an all glass inlet system (141-B) heated up to approx. 200°C. These spectra are shown in Figs. 1—12.

Disulfides (Ia—e) were prepared by the iodine oxidation of the corresponding thiophenol.[10] Thiolsulfinates

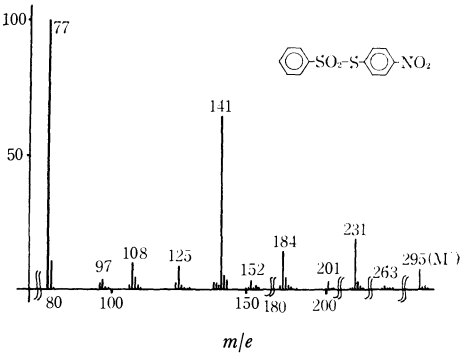

Fig. 11. The mass spectra of 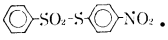 .

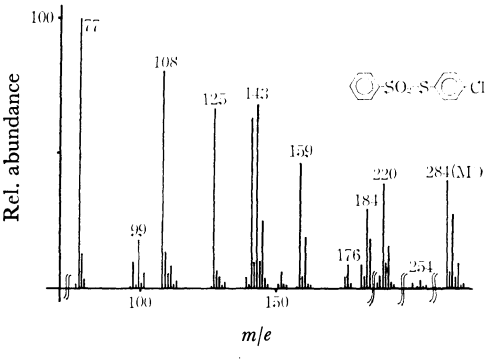

Fig. 12. The mass spectra of 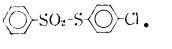 .

(IIa—d) were obtained by the reaction of thio phenol and sulfinyl chloride.[11] Thiolsulfonates (IIIa—d) were prepared from benzenesulfonyl chloride and benzenesulfinic acid.[12]

10) P. Klason, J. Carlson, *Ber.*, **39**, 738 (1906).

11) D. Barnard and E. J. Peray, *J. Chem. Soc.*, **1962**, 1669.

12) H. H. Gilman, L. H. Smith and H. H. Parker, *J. Amer. Chem. Soc.*, **47**, 851 (1925).

BULLETIN OF THE CHEMICAL SOCIETY OF JAPAN VOL. 43 135—138 (1970)

Syntheses of Benzo[e]-1,3,4-triazepine Derivatives from 2-Aminobenzophenones[1)]

Takumi ISHIWAKA, Mitsuru SANO, Kakuzo ISAGAWA and Yasaburo FUSHIZAKI

Department of Applied Chemistry, Faculty of Engineering, University of Osaka Prefecture, Sakai, Osaka

(Received May 15, 1969)

2-Aminobenzophenone semicarbazones (II) or 2-aminobenzophenone phenylhydrazones (III) were cyclized to 3,7-disubstituted 5-phenyl-2,3-dihydro-1*H*-benzo[*e*]-1,3,4-triazepines (IV) by treating them with paraformaldehyde. On the other hand, 3,7-disubstituted 2-oxo-5-phenyl-2,3-dihydro-1*H*-benzo[*e*]-1,3,4-triazepines (V) were prepared by the fusion of II at 190—195°C or by the treatment of III with phosgene. In the latter reactions, 1-carboxy derivatives (VI) of V were obtained by using two equimolar amounts of phosgene. Vf was treated with sodium ethoxide to give a ring-cleavage product, 5-chloro-2-ethoxycarbonylaminobenzophenone phenylhydrazone (VIIIf), which was then fused to afford 6-chloro-1,2-dihydro-2-oxo-4-phenylquinazoline (VIIb).

Although some 7-substituted 2-oxo-5-phenyl-2,3-dihydro-1*H*-benzo[*e*]-1,3,4-triazepines have been prepared by Sulkowski and Childress[2,3)] in recent years, the syntheses of 3,7-disubstituted benzo[*e*]-1,3,4-triazepines and 2-oxo-benzo[*e*]-1,3,4-triazepines have never been reported. Now, this paper will report the syntheses of several new benzo[*e*]-1,3,4-triazepines and 2-oxo-benzo[*e*]-1,3,4-triazepines from 2-aminobenzophenones (I), and will describe their properties.

Compounds Ia and Ib[4,5)] were treated in the customary way with semicarbazide hydrochloride

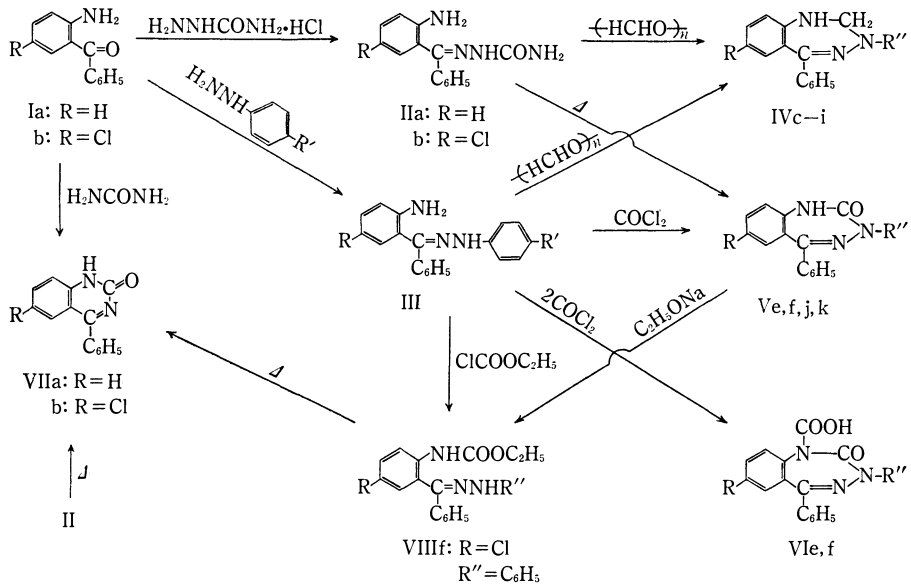

c-k: R and R'' are shown in Table 1

Scheme 1

1) Part VII of "*o*-Aminobenzophenone Derivatives." This paper was presented at the 21st Annual Meeting of the Chemical Society of Japan, Osaka, April, 1968. Part VI: Y. Toi, K. Isagawa and Y. Fushizaki, *Nippon Kagaku Zasshi*, **90**, 1047 (1969).

2) T. S. Sulkowski and S. J. Childress, *J. Med. Chem.*, **7**, 386 (1964).

3) T. S. Sulkowski and S. J. Childress, U. S. 3176008; *Chem. Abstr.*, **62**, 16284 (1965).

4) L. H. Sternbach, E. Reeder, O. Keller and W. Metlesics, *J. Org. Chem.*, **26**, 4488 (1961).

5) H. J. Scheifele, Jr., and D. F. DeTar, "Organic Syntheses," Coll. Vol. IV, p. 34 (1962).

or phenylhydrazines to give semicarbazones (IIa and IIb) or phenylhydrazones (III). 3,7-Disubstituted 5-phenyl-2,3-dihydro-1*H*-benzo[*e*]-1,3,4-triazepines and 3,7-disubstituted 2-oxo-5-phenyl-2,3-dihydro-1*H*-benzo[*e*]-1,3,4-triazepines were prepared according to the methods outlined below (Scheme 1).

The first method employed was the condensation of II or III with paraformaldehyde in refluxing xylene. The compounds IV shown in Table 1 were obtained by this method.

The second method was the intramolecular condensation. IIa and IIb gave 2-oxo-benzo[*e*]-1,3,4-triazepines (Vj and Vk respectively) on fusion at 190—195°C. The fusion of IIa and IIb at 230—240°C, however, did not give the 2-oxo-benzo[*e*]-1,3,4-triazepines, but instead produced the corresponding 1,2-dihydro-2-oxo-4-phenylquinazolines (VIIa) and (VIIb), which were identified by their preparation from Ia or Ib and urea.[6]

The third convenient approach was the treatment of III (R=R′=H, or R=Cl, R′=H) with phosgene according to the method of Sulkowski.[2] In this reaction, it was found that a small amount of 1-carboxy-3,5-diphenyl-2-oxo-2,3-dihydro-1*H*-benzo[*e*]-1,3,4-triazepine (VIe) along with a desired 2-oxo-benzo[*e*]-1,3,4-triazepine Ve, and the 1-carboxy-7-chloro derivative (VIf), along with Vf, were formed. By using two equimolar amounts of phosgene, the yields of VIe and VIf were increased to 16% and 30% respectively.

Several new compounds prepared in the course of this work, are summarized in Table 1.

Vf brought about a ring-cleavage reaction in the presence of sodium ethoxide to afford 5-chloro-2-ethoxycarbonylaminobenzophenone phen-

Table 1. Benzo[*e*]-1,3,4-triazepines and 2-oxo-benzo[*e*]-1,3,4-triazepines

		Compound R	Compound R″	Yield (%)	Mp (°C)	Elementary analysis (%) Calcd C	Calcd H	Calcd N	Found C	Found H	Found N
IV	c	H	$CONH_2$	15	209—210	67.65	5.30	21.04	67.65	5.39	20.86
	d	Cl	$CONH_2$	13	217—218	59.91	4.36	18.63	60.20	4.51	18.36
	e	H	C_6H_5	27	180—181	80.24	5.72	14.04	80.15	5.64	14.03
	f	Cl	C_6H_5	24	168—169	71.96	4.83	12.59	72.27	4.79	12.72
	g	Cl	*p*-$CH_3C_6H_4$	22	141—142	72.51	5.22	12.08	72.77	5.34	11.82
	h	Cl	*p*-ClC_6H_4	34	137—138	65.23	4.11	11.41	64.99	4.22	11.19
	i	Cl	*p*-$COOC_2H_5C_6H_4$	23	181—182	68.06	4.97	10.35	67.78	4.88	10.19
V	e	H	C_6H_5	14	207—208	76.66	4.83	13.41	76.36	4.80	13.13
	f	Cl	C_6H_5	40	243—244	69.07	4.06	12.08	69.00	4.08	12.03
	j	H	H	20	230—231[a]	70.87	4.67	17.71	70.60	4.80	17.52
	k	Cl	H	25	235—237[b]	61.89	3.71	15.47	61.99	3.90	15.74
VI	e	H	C_6H_5	16	141—142	70.58	4.23	11.76	70.47	4.21	11.63
	f	Cl	C_6H_5	30	172—173	64.38	3.60	10.72	64.66	3.79	10.42

a) Lit,[2] mp 238°C.
b) Lit,[2] mp 246—248°C.

Table 2. Spectroscopic data for 2-oxo-benzo[*e*]-1,3,4-triazepines

Compounds		UV[a] (mμ) λ_{max} ($\varepsilon \times 10^{-4}$)			IR[b] (cm^{-1}) C=O	IR[b] (cm^{-1}) C=O	NMR[c] δ (ppm) NH	NMR[c] δ (ppm) COOH	NMR[c] δ (ppm) Arom H
V	e	224[s](2.54)	246[s](1.99)	300 (0.39)	1680	—	9.52[b]	—	7.10—7.72[m]
	f	227 (3.51)	248[s](2.06)	309 (0.42)	1690	—	9.72[b]	—	7.05—7.83[m]
	j	222[s](3.10)	247[s](1.58)	294 (0.71)	1700	—	9.02[b]	—	6.94—7.86[m]
	k	224 (4.45)	250[s](2.42)	302 (0.90)	1700	—	9.10[b]	—	6.91—7.79[m]
VI	e	250 (3.21)	356 (0.61)		1650	1785	—	11.22[b]	7.10—8.46[m]
	f	250 (3.68)	371 (0.56)		1650	1785	—	11.06[b]	7.28—8.48[m]

a) Measured in 99% EtOH. s: shoulder
b) Measured in $CHCl_3$ (0.002 mol/*l*) for Ve, Vj, Vk, VIe and VIf: measured in KBr disk for Vf.
c) Measured in $CDCl_3$-DMSO-d_6 (1:2) for Ve, Vf, Vj and Vk: measured in $CDCl_3$ for VIe and VIf, using tetramethylsilane as the internal standard. b: broad, m: multiplet.

6) T. S. Sulkowski and S. J. Childress, *J. Org. Chem.*, **27**, 4424 (1962).

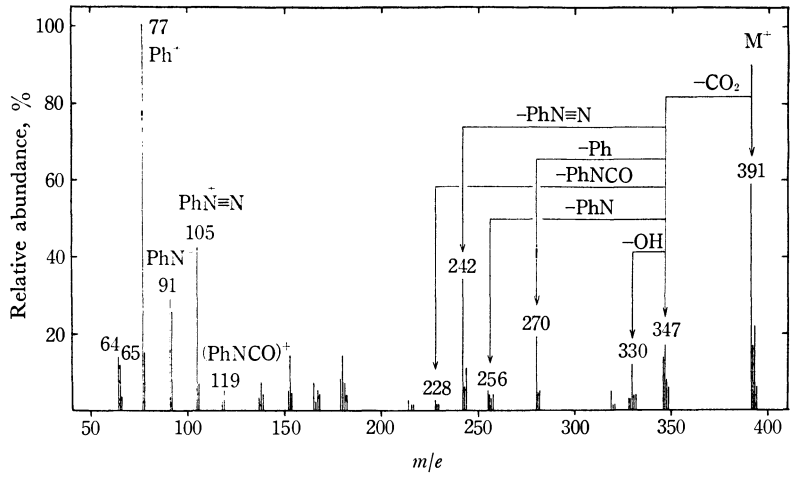

Fig. 1. Mass spectrum of VIf.

ylhydrazone (VIIIf), which was also prepared by the reaction of III (R=Cl, R'=H) with ethyl chlorocarbonate. VIIIf was heated at 170—175°C to give VIIb.

The UV, IR, and NMR data for the 2-oxo-benzo[e]-1,3,4-triazepine derivatives are shown in Table 2. By comparing the UV spectra of Ve and Vf with those of VIe and VIf, it is found that the absorption bands of VIe and VIf are situated in a region of wavelength longer than those of the corresponding Ve and Vf. The IR spectra (chloroform) of VIe and VIf showed the bands at 1785 cm^{-1} and 1650 cm^{-1} due to two carbonyl groups; the lower-frequency band can be assigned to the carbonyl group of lactam. The facts that the lactam C=O groups of both VIe and VIf appear at a lower frequency than those of Ve and Vf (KBr disk), and that the carboxylic C=O groups of VIe and VIf exist in a region of higher frequency,*1 suggest the presence of strong intramolecular hydrogen bonds in VIe and VIf. The mass spectrum of VIf is shown in Fig. 1, where the molecular ion peak is observed at *m/e* 391 (relative isotope ratio, 35.7%) and where the fragment at *m/e* 347 (relative isotop ratio, 33.7%), which corresponds to 7-chloro-2-oxo-benzo[e]-1,3,4-triazepine Vf or 7-chloro-3,5-diphenyl-2-hydroxy-benzo[e]-1,3,4-triazepine, is formed by the loss of CO_2 from the molecular ion. Furthermore, the relative abundance of the molecular ion peak is quite strong, so the molecular ion is probably more stable.

*1 Mori and his co-workers[7] discussed the intramolecular hydrogen bonds of α-hydroxy carboxylic and *o*-hydroxy benzoic acids by measuring their infrared carbonyl stretching absorption spectra. They reported that *trans*-carbonyl C=O groups of salicylic and mandelic acids could be expected at 1750 cm^{-1} and 1785 cm^{-1} respectively.

7) N. Mori, Y. Asano, T. Irie and Y. Tsuzuki, This Bulletin, **42**, 482 (1969).

Experimental

All the melting points are uncorrected. The infrared spectra were recorded with a Hitachi EPI-S2 infrared spectrophotometer. The ultraviolet spectra were obtained using a Hitachi EPS-2U recording spectrophotometer. The NMR spectra were determined on a Hitachi R-20 spectrometer, while the mass spectrum was determined with a Hitachi Model RMU-6D spectrometer.

General Method for the Preparation of Benzo-[e]-1,3,4-triazepines (IV). *i*) A solution of equimolar amounts of II and paraformaldehyde (5 mmol each) in 50 m*l* of dry xylene was refluxed for 6 hr. The reaction mixture was concentrated *in vacuo*. The residual oil was taken up in 50 m*l* of ether, the insoluble material was removed by filtration, the filtrate was evaporated to dryness *in vacuo*, and the residue was purified by recrystallization.

3-Carbamoyl-5-phenyl-2,3-dihydro-1H-benzo[e]-1,3,4-triazepine (IVc). Pale yellow needles. UV λ_{max}^{EtOH} mμ ($\varepsilon\times10^{-4}$): 229 (3.24), 299(0.88); IR(KBr): 3490, 3350, 1705 cm^{-1}.

3-Carbamoyl-7-chloro-5-phenyl-2,3-dihydro-1H-benzo[e]-1,3,4-triazepine (IVd). Pale yellow needles. UV λ_{max}^{EtOH} mμ ($\varepsilon\times10^{-4}$): 235 (2.89), 292(1.06); IR(KBr): 3430, 3280, 1695 cm^{-1}.

ii) A solution of equimolar amounts of III and paraformaldehyde (5 mmol each) in 50 m*l* of dry xylene was refluxed for 6 hr. After the solvent had then been removed, the residue was dissolved in benzene and chromatographed on silica gel with the same solvent. The first eluate (about 70 m*l*) was concentrated *in vacuo*, the residual oil was solidified by adding *n*-hexane, and the resulting crystals were purified by recrystallization.

3,5-Diphenyl-2,3-dihydro-1H-benzo[e]-1,3,4-triazepine (IVe). Yellow needles. UV λ_{max}^{EtOH} mμ ($\varepsilon\times10^{-4}$): 230(3.41), 331(1.05); IR(KBr): 3430 cm^{-1}: NMR ($CDCl_3$): δ 6.62—7.60 (m, 14H, aromatic protons), δ 5.14(s, 1H, NH), δ 4.97 ppm(s, 2H, CH_2).

7-Chloro-3,5-diphenyl-2,3-dihydro-1H-benzo[e]-1,3,4-triazepine (IVf). Yellow prisms. UV λ_{max}^{EtOH} mμ ($\varepsilon\times10^{-4}$): 233(2.95), 256^{s}(2.34), 333(0.95); IR(KBr): 3410, 1600

cm^{-1}; NMR($CDCl_3$): δ 6.70—7.69(m, 13H, aromatic protons), δ 5.05(b, 1H, NH), δ 4.92 ppm (s, 2H, CH_2).

7-Chloro-5-phenyl-3-(4-tolyl)-2,3-dihydro-1H-benzo[e]-1,3,4-triazepine (IVg). Yellow needles. UV λ_{max}^{EtOH} mμ ($\varepsilon\times10^{-4}$): 234(2.54), 255^{s}(2.21), 338(0.77); IR(KBr): 3400, 1610 cm^{-1}; NMR($CDCl_3$): δ 6.68—7.72(m, 12H, aromatic protons), δ 4.95(b, 1H, NH), δ 4.92(s, 2H, CH_2), δ 2.31 ppm (s, 3H, CH_3).

7-Chloro-3-(4-chlorophenyl)-5-phenyl-2,3-dihydro-1H-benzo-[e]-1,3,4-triazepine (IVh). Yellow needles. UV λ_{max}^{EtOH} mμ ($\varepsilon\times10^{-4}$): 232(2.06), 265(1.77), 335(0.69); IR (KBr): 3400, 1590 cm^{-1}; NMR ($CDCl_3$): δ 6.70—7.76 (m, 12H, aromatic protons), δ 5.03(b, 1H, NH), δ 4.87 ppm (s, 2H, CH_2).

7-Chloro-3-(4-ethoxycarbonylphenyl)-5-phenyl-2,3-dihydro-1H-benzo[e]-1,3,4-triazepine (IVi). Yellow needles. UV λ_{max}^{EtOH} mμ ($\varepsilon\times10^{-4}$): 236.5(1.72), 269(1.01), 336.5(1.21); IR(KBr): 3390, 1690, 1610 cm^{-1}; NMR($CDCl_3$): δ 6.72—8.12(m, 12H, aromatic protons), δ 5.13(b, 1H, NH), δ 4.99(s, 2H, CH_2), δ 4.35(q, 2H, CH_2), δ 1.38 ppm (t, 3H, CH_3).

3,5-Diphenyl-2-oxo-2,3-dihydro-1*H*-benzo[*e*]-1,3,4-triazepine (Ve). To a solution of 1.44 g (5 mmol) of III (R=R'=H) and 2 m*l* of triethylamine in 20 m*l* of benzene, a solution of 20 m*l* of benzene containing 0.50 g of phosgene (5 mmol) was stirred in, drop by drop, at 5—10°C. After having been stirred at room temperature for 2 hr, the reaction mixture was poured into water to remove the triethylamine hydrochloride. The crude product was collected by filtration; subsequent recrystallization from acetone afforded 0.20 g of Ve as yellow prisms.

A small amount of the 1-carboxy derivative (VIe) was obtained from the benzene solution by the same manner as was used in the preparation of VIe (described below).

7-Chloro-3,5-diphenyl-2-oxo-2,3-dihydro-1*H*-benzo[*e*]-1,3,4-triazepine (Vf). This compound was prepared by the same procedure as has been described for the preparation of Ve. 1.61 g (5 mmol) of III (R=Cl, R'=H) and 0.50 g of phosgene gave 0.69 g of Vf as yellow needles.

2-Oxo-5-phenyl-2,3-dihydro-1*H*-benzo[*e*]-1,3,4-triazepine (Vj). IIa (1.27 g, 5 mmol) was heated to 190—195°C for 1 hr. After cooling to room temperature, the resulting dark solid was shaken with 50 m*l* of ethanol, the insoluble material was removed, and the filtrate was taken to dryness *in vacuo*. The residue was washed with 30 m*l* of methylene chloride and recrystallized from ethanol to afford 0.24 g of Vj as pale yellow needles.

7-Chloro-2-oxo-5-phenyl-2,3-dihydro-1*H*-benzo-[*e*]-1,3,4-triazepine (Vk). IIb (1.44 g, 5 mmol) was worked up according to the procedure described for the preparation of Vj. Recrystallization from ethanol afforded 0.34 g of Vk as yellow needles.

1-Carboxy-3,5-diphenyl-2-oxo-2,3-dihydro-1*H*-benzo[*e*]-1,3,4-triazepine (VIe). To a solution of 1.44 g (5 mmol) of III (R=R'=H) in 12 m*l* of benzene containing 2 m*l* of triethylamine, 1.00 g (10 mmol) of phosgene in 20 m*l* of benzene was stirred in, drop by drop, at 5—10°C, and then the resulting solution was stirred at room temperature for an additional 2 hr. After the reaction mixture had then been washed with water and dried over anhydrous magnesium sulfate, the benzene was removed and the residue was recrystallized from a mixture of ethanol and benzene to afford 0.28 g of VIe as yellow needles.

1-Carboxy-7-chloro-2-oxo-5-phenyl-2,3-dihydro-1*H*-benzo[*e*]-1,3,4-triazepine (VIf). This compound was prepared by the same procedure as has been described for the preparation of VIe. 1.61 g (5 mmol) of III (R=Cl, R'=H) and 1.00 g (10 mmol) of phosgene gave 0.59 g of VIf as yellow needles.

1,2-Dihydro-2-oxo-4-phenylquinazoline (VIIa). IIa (0.76 g, 3 mmol) was fused at 230—240°C for 3 hr. After cooling to room temperature, the resulting solid was shaken with 50 m*l* of warm ethanol, the insoluble part was removed by filtration, and the yellow solid obtained by the evaporation of the solvent from the filtrate was recrystallized from a mixture of ethyl acetate and ethanol to afford 0.37 g of VIIa as pale yellow prisms; mp 243—245°C; yield 55%.

Found: C, 75.48; H, 4.67; N, 12.83%.

The product was identified by means of mixed-melting-point measurements and by a comparison of its UV and IR spectra with those of the sample obtained from the reaction of Ia with urea.[6]

6-Chloro-1,2-dihydro-2-oxo-4-phenylquinazoline (VIIb). 3-mmol portions of IIb and VIIIf were fused at 230—240°C and 170—175°C respectively. The resulting solid was worked up as has been described above for VIIa and recrystallized from a mixture of ethyl acetate and ethanol to afford VIIb as colorless needles; mp 256—258°C; yields, 0.28 g (36%) and 0.24 g (31%) respectively.

These products were identified by means of mixed-melting-point measurements and by a comparison of their UV and IR spectra with those of the sample obtained from the reaction of Ib with urea.

5-Chloro-2-ethoxycarbonylaminobenzophenone Phenylhydrazone (VIIIf). *i) From Vf.* Into a solution of 0.70 g (2 mmol) of Vf in 150 m*l* of ethanol, a solution of 10 m*l* of ethanol containing 50 mg (22 mmol) of sodium metal was added. After the solution had then been refluxed for 6 hr, the solvent was removed; the residual oil was solidified by adding a small amount of ethanol. The crude crystals were recrystallized from ethanol to afford 0.49 g (62%) of VIIIf as pale yellow needles; mp 174—175°C. UV λ_{max}^{EtOH} mμ ($\varepsilon\times10^{-4}$): 238(2.10), 300(0.87); IR(KBr): 3300, 3410, 1735, 1600 cm^{-1}; NMR ($CDCl_3$): δ 6.69—8.53(m, 13H, aromatic protons), δ 11.62(s, 1H, NH), δ 4.28(q, 2H, CH_2), δ 1.45 ppm(t, 3H, CH_3).

Found: C, 67.08; H, 5.13; N, 10.58%. Calcd for $C_{22}H_{20}N_3O_2Cl$: C, 67.09; H, 5.12; N, 10.67%.

ii) From III (R=Cl, R'=H). Into a solution of 1.61 g (5 mmol) of III (R=Cl, R'=H) in 30 m*l* of dry benzene containing 1 m*l* of triethylamine, a solution of 0.54 g (5 mmol) of ethyl chlorocarbonate in 20 m*l* of dry benzene was stirred in, drop by drop, at room temperature over a 30-min period. After the solution had been refluxed for 6 hr and cooled at room temperature, a benzene-insoluble solid was removed by filtration. The brownish-yellow oil which was obtained by the evaporation of the solvent from the filtrate was solidified by adding a small amount of ethanol. The crude crystals were recrystallized from ethanol to afford 1.16 g (59%) of VIIIf as pale yellow needles; mp 170—172°C.

The product was identified by means of mixed-melting-point measurements and by a comparison of its IR and NMR spectra with those of the above sample.

BULLETIN OF THE CHEMICAL SOCIETY OF JAPAN VOL. 43 139—142 (1970)

Studies on the Baudisch Reaction. II. The Copper(II)-Hydroxylamine Complex[1)]

Iwao TANIMOTO

Faculty of Home Economics, Kyoto Women's University, Higashiyama-ku, Kyoto

(Received May 16, 1969)

Kinetic investigation of the Baudisch reaction indicates that the reaction follows first-order kinetics, and the isokinetic temperature lies at −11°C. Both kinetic studies and product studies require the formation of a phenol-copper-hydroxylamine-hydrogen peroxide complex during the course of the reaction. It was found that the yield of *o*-nitrosophenol which is the main product of the Baudisch reaction is counterbalanced by that of catechol according to the pH of the reaction system. Maximum yield of *o*-nitrosophenol is attained in the lower pH region (pH=2.5—3.5). Catechol which is the main product in the higher pH region (pH>4) seems to be produced through the same complex.

Several tentative mechanisms on the Baudisch reaction—the conversion of aromatic hydrocarbons or phenols to *o*-nitrosophenol by hydrogen peroxide, hydroxylamine hydrochloride, and copper(II) ion—were submitted by several investigators,[2-4)] but they could hardly explain our findings.[1,5)] We pointed out that the marked steric effect of a methyl group occupying a position meta to the phenolic hydroxy group and the exclusive production of the ortho isomer might be the reflection of the formation of a bulky copper complex as an intermediate. In this paper, it is shown that this consideration has been further confirmed by spectroscopic and kinetic studies.

Results and Discussion

Copper(II)-Hydroxylamine Hydrochloride Complex in the Reaction Medium. In order to investigate the nature of the complex which might be produced during the course of the reaction, several experiments were undertaken. In methanol, the mixture of anhydrous copper(II) salt and hydroxylamine hydrochloride showed a characteristic absorption spectrum. The absorption maxima were at 230 and 273 mμ (Fig. 1).

A study by the molar ratio method showed that

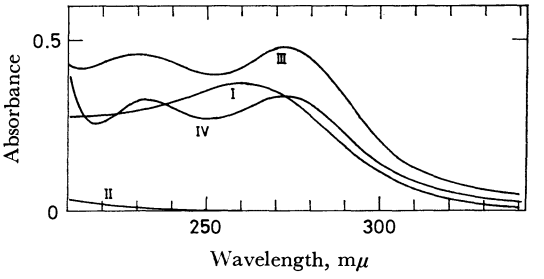

Fig. 1. Absorption spectrum of a copper-hydroxylamine hydrochloride complex in methanolic medium: I, $CuSO_4$ anhyd. (2×10^{-3}M); II, $NH_2OH\cdot HCl$ (4×10^{-3}M); III, $CuSO_4$-$NH_2OH\cdot HCl$ (1 : 2); IV, $Cu(OH)_2$-$NH_2OH\cdot HCl$ (1 : 2).

hydroxylamine hydrochloride combined with copper(II) ion in the mole ratio of 2 : 1 to form a complex species.[6)] Since a mixture of this methanolic complex solution and phenol solely produced *o*-nitrosophenol when it was treated with hydrogen peroxide, the species observed by spectroscopy seems to be a precursor of the actual complex which is produced during the course of the Baudisch reaction. The copper(II)-hydroxylamine hydrochloride complex could also be detected in aqueous medium by spectroscopy.

Kinetic Studies. Kinetic measurements for the formation of *o*-nitrosophenols from phenols were

1) Part I: K. Maruyama, I. Tanimoto and R. Gotō, *J. Org. Chem.*, **32**, 2516 (1967).

2) a) O. Baudisch, *Naturwissenschaften*, **27**, 768 (1939). b) O. Baudisch and S. H. Smith, *ibid.*, **27**, 769 (1939). c) O. Baudisch, *J. Amer. Chem. Soc.*, **63**, 622 (1941).

3) G. Cronheim, *J. Org. Chem.*, **12**, 1 (1947).

4) J. O. Konecny, *J. Amer. Chem. Soc.*, **77**, 5748 (1955).

5) K. Maruyama, I. Tanimoto and R. Goto, *Tetrahedron Lett.*, **1966**, 5889.

6) A copper(II)-hydroxylamine complex $CuSO_4$-$2NH_2OH$ reported by M. Adams and E. Overman (*J. Amer. Chem. Soc.*, **31**, 637 (1909)) is insoluble in methanol and different from the complex described here. However, the insoluble complex also reacted with phenol and hydrogen peroxide in the acidic medium to give *o*-nitrosophenol. It seems likely that the active complex involved in the Baudisch reaction is a protonated species.

TABLE 1. KINETIC DATA FOR THE BAUDISCH REACTION[a)]

	$k\times10^5$, sec^{-1}				E	$\Delta S^{\neq}$[b)]
	0.0°C	10.0°C	20.0°C	30.0°C	kcal·mol^{-1}	e.u.
m-Chlorophenol	1.02	4.36	14.8	53.5	21.6±0.2	− 4.1
o-Chlorophenol	0.441[c)]	1.91	6.38	16.6	20.4±0.7	− 9.2
p-Chlorophenol	1.65	4.22	12.6	42.1	18.2±0.8	−16.2
m-Cresol	1.36	5.35	12.3	36.2	17.6±0.6	−17.8
Phenol	2.39	3.56	14.0	29.8	14.9±1.5	−28.2
o-Cresol	0.301	1.11	2.92	4.10	14.7±1.5	−32.2
p-Cresol	0.856	2.19[d)]	4.17	6.31	11.9±0.9	−39.7
2,5-Xylenol	0.138	0.244	0.583	0.710	9.5±0.9	−52.6
3,5-Xylenol	0.800	1.87	2.54	3.05	7.2±1.1	−56.6

a) All reactions were conducted under nitrogen atmosphere. Phenol (1×10^{-2} mol), copper (II) nitrate (1×10^{-2} mol) and hydroxylamine hydro chloride (2×10^{-2} mol) were stirred in 198 m*l* of a Walpole buffer (pH 2.50) after the addition of a hydrogen peroxide solution (30%) (2 m*l*). The temperature was controlled within ±0.1°C.
b) The entropy of activation was calculated at 10.0°C.
c) The reaction was conducted at 0.4°C.
d) The reaction was conducted at 10.3°C.

carried out. Phenol, *o*-, *m*- and *p*-cresols, *o*-, *m*- and *p*-chlorophenols, 2,5- and 3,5-xylenols were studied. The concentration of phenol at any time was assumed to be given by the difference between its initial concentration and the concentration of the product. The experimental kinetic plots gave first-order kinetics in the phenols in spite of the fact that other reactants, *i. e.* copper(II) salt, hydroxylamine hydrochloride and hydrogen peroxide, were not contained in a very large excess over the phenols in the reaction system; a logarithmic plot of the data gave a straight line from 15 min to 90 min after the reaction started. Therefore, the following reaction steps are compatible with the kinetics if we assume that steps 1 and 2 proceed fast enough to produce complex I and the conversion of complex I in step 3 is a slow rate-determining

$$Cu^{2+} + \text{Phenol} \xrightarrow{\text{fast}} \text{Cu-Phenolate} \quad (1)$$

$$\text{Cu-Phenolate} + x\text{NH}_2\text{OH} + \text{H}_2\text{O}_2 \xrightarrow{\text{fast}} \text{Complex I} \quad (2)$$

$$\text{Complex I} \xrightarrow{\text{solw}} \cdots \longrightarrow o\text{-Nitrosophenol} \quad (3)$$

step, because in such a case the limiting factor in determining the concentration of complex I is the amount of phenol. At present, the details of the reaction steps from complex I to *o*-nitrosophenol are not known, but the thermodynamic quantities for the reactions seem to give an important clue to this point.

In Table 1, first-order rate constants have been tabulated together with the thermodynamic quantities of the reactions. The negative values of $\Delta S^{\neq}$ for all of the reactions studied suggest that the reactions require a highly ordered arrangement of atoms in the transition state. In fact, the large negative value of $\Delta S^{\neq}$ for the reaction of phenol may be explained if one assumes the ring-closure process to form cyclic complex II or III from a

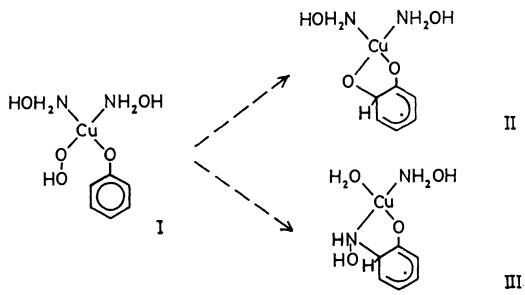

copper-hydroxylamine-phenolate complex I. The reaction pathway from complex I to complex II or III is not known as yet, but radical nature of attack may be assumed[7)] in spite of the fact that the activation energies suggest somewhat electrophilic attack on the aromatic ring (see Table 1). However, as can be seen from Table 1, the reactions are predominantly controlled by entropy

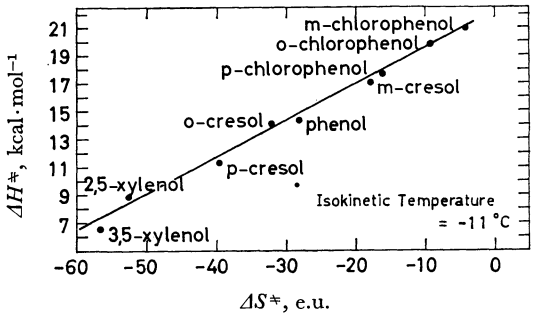

Fig.2. Isokinetic plot for the Baudisch reaction of phenols in aqueous medium. The enthalpy of activation was calculated from energy of activation by subtracting 0.6 kcal·mol^{-1}.

7) J. K. Kochi, *J. Amer. Chem. Soc.*, **84**, 774 (1962); *ibid.*, **85**, 1958 (1963).

factor, *viz.*, the reaction of highest energy of activation has the highest rate of reaction. A plot between enthalpy of activation and entropy of activation is sufficiently linear (Fig. 2). The existence of the linear relationship indicates a constant mechanism for the related series of reactions. The isokinetic temperature calculated by the method of least squares was -11°C. Thus, near room temperature, the Baudisch reaction is conducted in the region in which the entropy of activation is a commanding factor.

The Catechol Production. From preliminary experiments, it was found that the yield of *o*-nitrosophenol is seriously affected by pH values of the system. Therefore, the identification of other reaction products was attempted and the effect of pH on the yield of the products was investigated. In 1955, Brackman and Havinga investigated the oxidation of phenol under conditions identical with the Baudisch conditions, but they failed to find *o*-nitrosophenol and catechol.[8] However, even in the Baudisch system, phenol was converted predominantly to catechol in the pH region higher than 4.0 (Fig. 3). On the other hand, neither catechol nor hydroquinone were found under the optimum conditions for *o*-nitrosophenol formation (pH=2.5—3.5). Catechol and hydroquinone were found in the molar ratio of 1.8 at pH 5.5 where no *o*-nitrosophenol was produced. The absence of resorcinol in the reaction products was confirmed by thin layer chromatography. Since the selective formation of ortho isomer is not generally observed when a free hydroxy radical is responsible for the hydroxylation of phenol,[9,10] the predominant formation of catechol under the Baudisch conditions will be due to a copper(II)-hydroxylamine-hydrogen peroxide-phenol complex I. Furthermore, yield of catechol much higher than that formed by the reaction of phenol with simple copper(II) ion and hydrogen peroxide was observed under the Baudisch conditions (Fig. 3). This fact indicates that the production of catechol from phenol was much promoted by the formation of complex I.

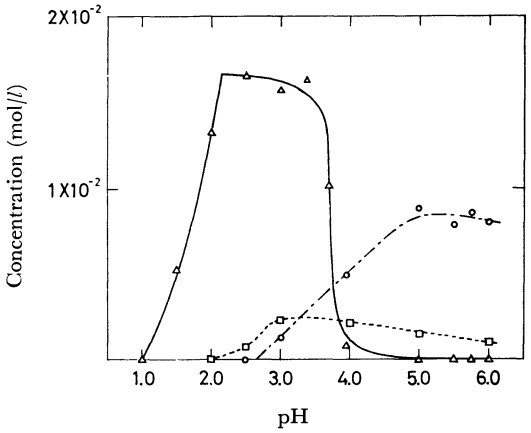

Fig. 3. pH dependence of the formation of *o*-nitrosophenol and catechol from phenol: (—△—) *o*-nitrosophenol; (---○---) catechol, under the Baudisch conditions; (—□—) catechol, by copper(II) nitrate and hydrogen peroxide. All of the reactions were conducted at 30°C for 30 min under a nitrogen atmosphere. The maximum concentration of catechol produced the Baudisch reaction may be comparable with that of *o*-nitrosophenol, because our estimation of catechol may be slightly low owing to the limited extraction of catechol.

At pH 5.5, coppper(II) nitrate was reduced to a brownish white precipitate in the aqueous mixture of phenol and hydroxylamine hydrochloride and had no ability to achieve *o*-nitrosation. However, the mixture retained the ability for catechol production. Even if the pH of the mixture was brought again to pH 2.5, the ability to achieve *o*-nitrosation was not restored. The results indicate that a reduced form of the copper complex has no ability to achieve *o*-nitrosation of phenol, but is responsible for *o*-hydroxylation.

It seems most likely that the complex which is responsible for the formation of catechol is essentially the same as that responsible for the formation of *o*-nitrosophenol. However, in the higher pH region, the copper in the complex is reduced and catalyzes *o*-hydroxylation only. In the lower pH region, the reducing power of hydroxylamine is probably suppressed by the protonation and copper(II)—indispensable for the *o*-nitrosation of phenol—is retained in the reaction system.

Experimental

Materials. *m*- and *p*-Cresols were purified according to the method of Brückner,[11] the boiling point of *m*-cresol was 202°C (lit, 202.2°C) and that of *p*-cresol was 201°C (lit, 202.5°C). *m*- and *p*-Chlorophenols were purified *via* their benzoates, as in the case of phenol.[12] The benzoate of *m*-chlorophenol (mp 69—70.5°C, lit, 71°C) and the benzoate of *p*-chlorophenol (mp 85—86°C, lit, 87—88°C) were hydrolyzed to the phenols, and the phenols were used after distillation. Copper(II) hydroxide was prepared according to literature.[13] Reagent grade 30% hydrogen peroxide solution was obtained from Mitsubishi Chemical Co. and iodometric titration showed that the concentration was 10.2 M. Other

8) W. Brackman and E. Havinga, *Rec. Trav. Chim., Pays-Bas*, **74**, 937, 1021, 1070, 1100, 1107 (1955).

9) G. Stein and J. Weiss, *J. Chem. Soc.*, **1951**, 3265.

10) G. A. Hamilton, J. W. Hanifin, Jr., and J. P. Friedman, *J. Amer. Chem. Soc.*, **88**, 5269 (1966).

11) H. Brückner, *Z. Anal. Chem.*, **75**, 289 (1928).

12) E. Berliner, F. Berliner and I. Nelidow, *J. Amer. Chem. Soc.*, **76**, 507 (1954).

13) G. Brauer, "Handbuch der Präparativen Anorganische Chemie," Part 1, F. Enke Verlag, Stuttgart (1954), p. 756.

reagents were reagent grade and, if necessary, were used after further purification. Silica gel G (Merck, according to Stahl) was used as an absorbent in thin layer chromatography.

Spectrophotometry. The ultraviolet spectrum of copper(II) sulfate solution (2×10^{-3}M) or hydroxylamine hydrochloride solution (4×10^{-3}M) was determined using 1 mm quartz cell with a recording spectrophotometer.

To prepare stock copper(II)-hydroxylamine hydrochloride complex solution, anhydrous copper(II) sulfate (0.160 g, 1×10^{-3} mol) or copper(II) hydroxide (0.0976 g, 1×10^{-3} mol) was dissolved in a small amount of concentrated methanolic solution containing 0.138 g (2×10^{-3} mol) of hydroxylamine hydrochloride and the resulting mixture was diluted to 10 m*l* with methanol. After the stock solution was diluted 50-fold determination of its ultraviolet spectrum was carried out.

Determination of *o*-Nitrosophenol. General procedures for the Baudisch reaction and the determination of *o*-nitrosophenol produced were described previously.[1]

Kinetic Studies. The general procedure for the Baudisch reaction described previously[1] was used under conditions controlled by a Walpole buffer (pH 2.5). Determination of *o*-nitrosophenols was carried out at intervals of 20 min.

Determination of Catechol. Copper(II) nitrate trihydrate (1.208 g, 5×10^{-3} mol) and phenol (0.471 g, 5×10^{-3} mol) were dissolved in 100 m*l* of a suitable Walpole buffer or an acetic acid-sodium acetate buffer. After the mixture was stirred with 1 m*l* of 30% hydrogen peroxide solution for 30 min at 30°C under nitrogen atmosphere, 20 m*l* of the reaction mixture was pipetted out and acidified with 2 m*l* of concentrated hydrochloric acid. The acidified solution was extracted with 20 m*l* of ether and the twice each with 5 m*l* of the same solvent. After being washed with water, all of the extract was extracted with 10 m*l* of aqueous 5% sodium hydroxide and then with 5 m*l* of the solution. The aqueous extracts were brought together and acidified with 1N hydrochloric acid and diluted to 100 m*l*. Catechol was determined spectroscopically according to the method of Willard and Wooten.[14] In the reactions under the conditions of the Baudisch reaction, hydroxylamine hydrochloride (0.695 g, 1×10^{-2} mol) was added to the above reaction mixture just before the addition of hydrogen peroxide.

Ratio of Catechol to Hydroquinone. The ethereal extract (50 m*l*) from 50 m*l* of the reaction mixture was evaporated to about 10 m*l* and submitted to thin layer chromatography. The unidimensional ascending technique was employed in a benzene-methyl ethyl ketone-2% aqueous formic acid (90 : 10 : 10) system. When the solvent front was allowed to ascend about 15 cm, the plate was dried and run in the same solvent again. After the plate was dried, Folin-Ciocalteu reagent[15] was sprayed on it and the blue spots due to catechol and hydroquinone were scraped separately into small beakers. To each of the beakers 2.5% potassium dihydrogen phosphate solution (2 m*l*) was added[9] and then 1 m*l* of Folin-Ciocalteu reagent. The dark green solution was filtered using sintered glassfilters and each of the filtrates, together with washings, was diluted to 10 m*l* with water. The intensity was then measured at 520 mμ after the sample solution was kept at 35°C for 30 min.

The work was supported in part by a Research Grant from Kyoto Women's University. The author wishes to express his gratitude to Professor Kazuhiro Maruyama, Kyoto University, for his stimulating suggestions and discussions. The continued kind encouragement of Professor Ryōzō Gotō of Kyoto University is gratefully acknowledged.

14) H. H. Willard and A. L. Wooten, *Anal. Chem.*, **22**, 670 (1950).

15) F. D. Snell and C. T. Snell, "Colorimetric Method of Analysis," D. Van Nostrand Company, Inc., New York, N. Y. (1953), p. 116.

BULLETIN OF THE CHEMICAL SOCIETY OF JAPAN VOL. 43 143—147 (1970)

Studies on Interactions of Isocyanides with Transition Metal Complexes. IV.*1 Dicarbonyl(isocyanide)-π-cyclopentadienylacylmolybdenum*2

Yasuhiro YAMAMOTO and Hiroshi YAMAZAKI

The Institute of Physical and Chemical Research, Yamato-machi, Saitama

(Received May 23, 1969)

Isocyanides were treated with π-$C_5H_5Mo(CO)_3R$ (R=CH_3, CH_2Ph) in benzene at room temperature to give π-$C_5H_5Mo(CO)_2$(isocyanide)COR (A), which exist as a *trans*-isomer in the solid state and as a mixture of *trans*- and *cis*-isomers in solutions, based on the NMR spectra. The structures of the compounds (A) are discussed on the basis of the spectroscopic studies. Studies on *trans* to *cis* isomerization were also carried out kinetically.

In the previous paper, we have reported that isocyanides insert into the alkylnickel sigma bonds of triphenylphosphine-π-cyclopentadienylalkylnickel to give π-cyclopentadienyl(isocyanide) alkylalkyliminomethylnickel.[1] In the course of our studies on this series,[2,3] we obtained dicarbonyl(isocyanide)-π-cyclopentadienylacylmolybdenum as a mixture of *cis*- and *trans*- isomers in solutions by the reactions of isocyanides with tricarbonyl-π-cyclopentadienylalkylmolybdenum.

Reactions of tricarbonyl-π-cyclopentadienylalkylmolybdenum with phosphorus ligands have been studied under a variety of conditions to give dicarbonyl(phosphorus ligand)-π-cyclopentadienylacylmolybdenum.[4,5] These monosubstituted compounds, π-$C_5H_5Mo(CO)_2(PR_3)COR$, can be expected to exist as *cis*- and *trans*- isomers. However, the structures of the resultant complexes have consisted solely of the *trans*-isomer, and existence of a *cis*-isomer has not been known as yet.

We wish to report the isomerism between *cis*- and *trans*-dicarbonyl (isocyanide)-π-cyclopentadienylacylmolybdenum, and their temperature- and time-dependent phenomena.

*1 Part I: Y. Yamamoto and N. Hagihara, This Bulletin, **39**, 1085 (1966). Part II: Y. Yamamoto and N. Hagihara, *ibid.*, **42**, 2077 (1969). Part III: Y. Yamamoto, H. Yamazaki and N. Hagihara, *J. Organometal. Chem.*, **18**, 189 (1969).

*2 Presented at the 22nd Annual Meeting of the Chemical Society of Japan, Tokyo, April, 1969.

1) Y. Yamamoto, H. Yamazaki and N. Hagihara, This Bulletin, **41**, 532 (1968); *J. Organometal. Chem.*, **18**, 189 (1969).

2) Y. Yamamoto and N. Hagihara, This Bulletin, **39**, 1085 (1966).

3) Y. Yamamoto and N. Hagihara, *ibid.*, **42**, 2077 (1969).

4) K. W. Barnett and P. M. Treichel, *Inorg. Chem.*, **6**, 294 (1967).

5) P. J. Craig and M. Green, *J. Chem. Soc., A*, **1968**, 1978; *ibid.*, **1969**, 157.

Results and Discussion

Preparation and Identification of π-$C_5H_5Mo(CO)_2(CNR')COR$. Treatment of *t*-butyl isocyanide with tricarbonyl-π-cyclopentadienylmethylmolybdenum, π-$C_5H_5Mo(CO)_3CH_3$, in benzene at room temperature gave yellow crystals **1**, which were soluble in most organic solvents and stable to air in the solid state. Compound **1** was formulated as π-$C_5H_5Mo(CO)_3(CNC(CH_3)_3)CH_3$, based on the elementary analysis. The structure was characterized by spectroscopic study and chemical reaction. The infrared spectrum showed four bands at 2140, 1962, 1880 and 1615 cm^{-1}; the first band was attributable to a terminal isocyanide group, the last band to a ketonic carbonyl group and the other two bands to the terminal carbonyl groups. The reaction of *t*-butyl isocyanide with π-$C_5H_5Mo(CO)_2(PPh_3)COCH_3$ also gave compound **1**. It was concluded from the results that compound **1** was π-$C_5H_5Mo(CO)_2(CNC(CH_3)_3)COCH_3$. The NMR spectrum showed two signals for each of cyclopentadienyl, isocyanide and acyl protons, suggesting the existence of two isomers, *cis*- and *trans*-isomers, which were depicted as follows.

The reaction with 2,6-dimethylphenyl isocyanide gave a similar complex, π-$C_5H_5Mo(CO)_2(C_9H_9N)COCH_3$ **2**. π-$C_5H_5Mo(CO)_3CH_2Ph$ was allowed to react with *t*-butyl isocyanide to give π-$C_5H_5Mo(CO)_2(CNC(CH_3)_3)COCH_2Ph$ **3** which were shown to exist as a mixture of *cis*- and *trans*-isomers in solutions by NMR spectrum. The complexes prepared here are summarized in Tables 1 and 2.

It should be noted that the benzylic methylene

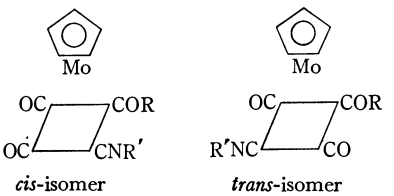

cis-isomer *trans*-isomer

TABLE 1. PRODUCTS OF THE REACTIONS OF TRICARBONYL-π-CYCLOPENTADIENYLALKYLMOLYBDENUM WITH ISOCYANIDES: π-$C_5H_5Mo(CO)_2(CNR')COR$

R	R′	Mp (°C)	Yield (%)	Analyses Found (Calcd) C	H	N	IR (cm^{-1})*3 N≡C	C≡O	>C=O
CH_2Ph	$C(CH_3)_3$	115.5—116.5	73	60.14	5.23	3.54	2140	1958	1615
				(60.16)	(5.30)	(3.54)		1880	
CH_3	$C(CH_3)_3$	104—105	56	49.07	4.88	4.12	2140	1962	1615
				(48.91)	(4.99)	(4.06)		1880	
CH_3	C_8H_9*2	91.5—92.5	42	57.44	4.78	3.58	2119	1948	1623
				(57.61)	(4.57)	(3.73)		1878	

*1 All melting points were measured in the nitrogen filled capillaries.
*2 2,6-dimethylphenyl.
*3 KBr disk.

TABLE 2. NMR SPECTRA OF π-$C_5H_5Mo(CO)_2(CNR')COR$

R	R′	Solvent		(τ) $(CH_3)_3$	$COCH_3$	$COCH_2$	C_5H_5	C_6H_5 *2
CH_2Ph	$C(CH_3)_3$	C_6D_6	*cis*	9.1*2		5.70, 5.63	5.02	2.55—3.05
			trans			5.43	5.10	
		CS_2	*cis*	8.62		6.09*3	4.87	2.7 —3.2
			trans	8.54		5.93	5.01	
		$CDCl_3$	*cis*	8.52*2		5.85, 5.92	4.75	2.6 —3.2
			trans			5.76	4.88	
CH_3	$C(CH_3)_3$	CS_2	*cis*	8.53	7.73		4.85	
			trans	8.50	7.65		4.99	
		$CDCl_3$	*cis*	8.50	7.54		4.66	
			trans	8.48	7.43		4.81	
CH_3	C_8H_9*1	CS_2	*cis*		7.58		4.72	3.85—3.0
			trans		7.53		4.83	8.66*4

*1 1,2-Dimethylphenyl.
*2 The chemical shift difference between *cis*- and *trans*-isomer was too small to be analyzed.
*3 This signal was broad.
*4 This signal was attributable to *ortho*- and *meta*-methyl groups.

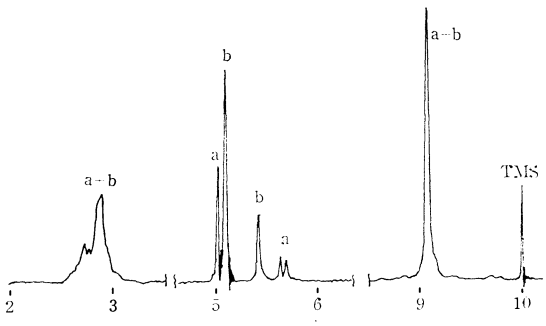

Fig. 1. NMR spectrum of π-$C_5H_5Mo(CO)_2(CNC(CH_3)_3)COCH_2Ph$ in C_6D_6 at 23°C.

protons of the isomer (a) in C_6D_6, as shown in Fig. 1, consist of two relatively sharp resonances of equal intensity separated by 4.2 cps, suggesting the magnetic nonequivalence of methylene protons of the isomer (a).

The origin of the magnetic nonequivalence has been the subject of several investigations.[6,7] Two reasons may be generally considered for the origin of magnetic nonequivalence of the methylene protons: (1) the restricted rotation of the methylene and (2) the existence of an asymmetric moiety adjacent to the methylene. In both cases, the protons of a methylene group display AB-type nuclear magnetic resonance spectra.[6]

Thus, if the phenylacetyl group is in *cis* position to a *t*-butyl isocyanide ligand in the complex **3**, the *cis*-isomer will be more sterically inhibited than the *trans*-isomer. Furthermore, there is no plane of symmetry in the *cis*-isomer.

It is reasonable to conclude that the isomer (a) is assigned to a *cis*-isomer and the isomer (b) to a *trans*-isomer.

The only two central peaks of the AB quartet were

6) For example, E. I. Snyder, *J. Amer. Chem. Soc.*, **85**, 2624 (1963).
7) H. S. Gutowsky, *J. Chem. Phys.*, **37**, 2196 (1962); H. S. Gutowsky, G. G. Beiford and P. E. McMahon, *ibid.*, **36**, 3353 (1962).

TABLE 3. *cis*- AND *trans*-ISOMER RATIO OF π-C_5H_5-$Mo(CO)_2(CNR')COR$ IN A VARIETY OF SOLVENTS AT 23°C

R	R'	Solvent	Dielectric constant*1	*trans* (%)	*cis* (%)
CH_2Ph	$C(CH_3)_3$	C_6D_6	2.24	64	36
		CS_2	2.59	73	27
		$CDCl_3$	3.73	66	34
		CH_3COCH_3	19.6	63	37
CH_3	$C(CH_3)_3$	CS_2	2.59	69	31
		$CDCl_3$	3.73	64	39
CH_3	C_8H_9*2	$CDCl_3$	3.73	67	33

*1 R. J. Angelici and F. Basolo, *J. Amer. Chem. Soc.*, **84**, 2495 (1962). C_6D_6=value of C_6H_6. $CDCl_3$= Value of $CHCl_3$.

*2 2,6-Dimethylphenyl.

TABLE 4. TEMPERATURE-DEPENDENCE OF THE ISOMER RATIO OF π-$C_5H_5Mo(CO)_2(CNC(CH_3)_3)COR$ IN $CDCl_3$

Temp. (°C)	R=CH_2Ph		R=CH_3	
	trans (%)	*cis* (%)	*trans* (%)	*cis* (%)
23	66	34	64	36
− 3	75	25	67	33
−10	77	23	68	32

observed in the NMR spectrum of the benzyl protons of the *cis*-isomer, because of large $J_{AB}/\delta_B-\delta_A$ value and also of low concentration of the *cis*-isomer. In this assignment the cyclopentadienyl proton resonance of a *cis*-isomer exists in the lower field than that of a *trans*-isomer.

In an attempt to examine the structures of the complexes **1**, **2**, and **3** in the solid state, the crystalline samples of the complexes are dissolved in deuteriochloroform at −50°C and NMR spectra were recorded at this temperature. Only the *trans*-isomer was present in the solutions. When the solutions were allowed to reach room temperature, the growth of the cyclopentadienyl resonance due to the *cis*-isomer could be observed. It seems reasonable to assume that in the crystalline state these complexes exist only as the *trans*-isomer.

Trans-structures of the complexes **1**, **2**, and **3** in the solid state were also supported by infrared spectra. It is known that stereochemistry of the monosubstituted compounds π-$C_5H_5Mo(CO)_2LX$ (L=phosphorus ligands, X=alkyl, acyl, halogen) is assigned from the optical densities, D_a and D_s, of the asymmetric and symmetric CO stretching vibrations.[8,9] The application of this rule to the complexes **1**, **2**, and **3** suggests that they are *trans*-forms.

Temperature- and Time-dependent Phenomena in the Isomerism of Dicarbonyl(isocyanide)-π-cyclopentadienylacylmolybdenum. The compounds **1**, **2**, and **3** were found to exist as the *trans*-isomer in the solid state, and as a mixture of *cis*- and *trans*-isomers in solutions. The final equilibrium position scarcely depends on solvents, and the equiliblium mixtures of *cis*- and *trans*-π-$C_5H_5Mo(CO)_2(CNR')COR$ in a variety of solvents contained *ca.* 65% of the *trans*-isomer, as shown in Table 3.

The temperature-dependence of equilibrium positions was also observed. Thus, the concentration of the *trans*-isomer increased with lowering temperature, as shown in Table 4.

The *trans* to *cis* isomerization was briefly studied kinetically and found to proceed at a conveniently measurable rate of −3—−10°C in $CDCl_3$, although it was impossible to measure the isomerization rate at room temperature.

Kinetic study showed that the reactions were first-order in the *trans*-isomer, because there was a very small change in the rate constant accompanying an almost fivefold change in concentration, as shown in Table 5. Added *t*-butyl isocyanide did not depress the rate, and this may suggest that isomerization was not responsible for the dissociative mechanism, such as had been observed in the *cis* to *trans* isomerization of $Mn(CO)_3(P(OPh)_3)_2Br$.[10] Detailed kinetic studies will be reported later.

TABLE 5. RATES OF ISOMERIZATION OF *trans* TO *cis*-π-$C_5H_5Mo(CO)_2(CNC(CH_3)_3)COR$ IN $CDCl_3$

R	°C	mol/ml(10^4)	$k(10^3)$
CH_2Ph	−3	1.67	37.7
CH_2Ph	−10	1.70	15.0
CH_3	−3	1.97	40.6
CH_3	−3	9.30	39.8
CH_3	−10	1.49	16.9
CH_3	−10	7.47	16.7

Origin of Magnetic Nonequivalence of Methylene Protons in π-$C_5H_5Mo(CO)_2(CNC(CH_3)_3)COCH_2Ph$. In an attempt to resolve whether the restricted rotation or the existence of a molecular asymmetric center is responsible for the magnetic nonequivalence of the methylene protons in the *cis*-isomer, studies on the temperature dependence of complex **3** were carried out in various solvents.

At 23°C the *cis*-isomer has a relatively broad peak at 6.09τ in the proton NMR spectrum in CS_2, which is attributable to the methylene protons. On lowering of temperature this became a little broad band and was split into doublet at −9°C. When the solution was chilled to −50°C, the absorption

8) W. Beck, A. Melnikoff and R. Stahl, *Chem. Ber.*, **99**, 3721 (1966).

9) A. R. Manning, *J. Chem. Soc., A*, **1967**, 1984.

10) R. J. Angelici, F. Basolo and A. J. Poe, *J. Amer. Chem. Soc.*, **85**, 2215 (1963).

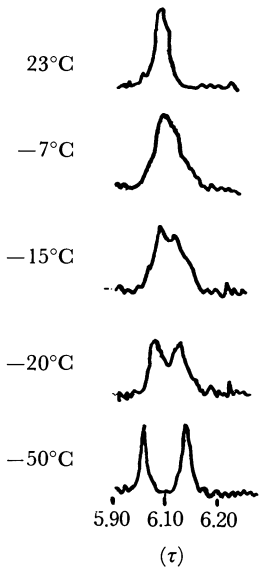

Fig. 2. Temperature dependence of the methylene protons of *cis*-π-$C_5H_5Mo(CO)_2(CNC(CH_3)_3)COCH_2Ph$ in CS_2.

at 6.09τ was split into two relatively sharp signals at 6.06 and 6.14τ, in an approximate relative intensity 1:1, as shown in Fig. 2.

The average position of two new peaks at −50°C is found quite near the original peak at 23°C.

In the proton NMR spectrum in C_6D_6, the methylene proton resonance of the *cis*-isomer at room temperature appeared as two peaks at 5.70 and 5.62τ. They became relatively broad with rise of temperature, and at 65°C the spectrum consisted of one single broad peak, as shown in Fig. 3. An attempt to measure the spectra at higher temperatures was unsuccessful, because of decomposition

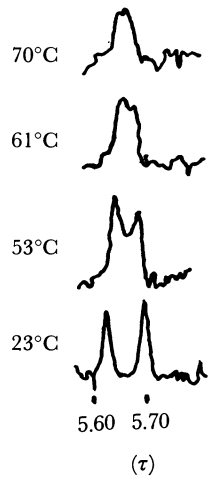

Fig. 3. Temperature dependence of the methylene protons of *cis*-π-$C_5H_5Mo(CO)_2(CNC(CH_3)_3)COCH_2Ph$ in C_6D_6.

of complex **3**. Accordingly, we could not observe a sharp singlet resonance which might be derived from rapid rotation of the phenyl acetyl group.

Although we cannot rule out response for the magnetic nonequivalence arising from the existence of the asymmetric center, it seems more reasonable to assume that the steric inhibition of free rotation of the phenyl acetyl group causes the methylene group to be magnetically nonequivalent.

Decarbonylation of π-$C_5H_5Mo(CO)_2(CNC(CH_3)_3)COCH_2Ph$ (3). Decarbonylation of complex **3** was briefly studied. With ultraviolet irradiation in benzene, evolution of carbon monoxide occurred to give complex **4**, π-$C_5H_5Mo(CO)_2(CNC(CH_3)_3)CH_2Ph$ characterized by the absence of an acyl carbonyl band from the infrared spectrum. Contrary to expectation, there was no evidence for the existence of the isomers. Thus, the NMR spectrum in CS_2 showed four signals at 8.51 (singlet, 9H, $(CH_3)_3C$) 7.16 (singlet, 2H, CH_2), 4.91 (singlet, 5H, C_5H_5) and 3.00τ (singlet, 5H, C_6H_5).

In an attempt to confirm the structure of complex **4**, the NMR spectrum in lower temperatures was studied.

The spectrum at −60°C gave rise to only a minor change as compared to the room-temperature spectrum. Difference in each chemical shift was observed.

If complex **4** is a *cis*-isomer, the benzylic methylene protons are expected to be magnetically nonequivalent as has been observed in complex **3**. No line splitting suggests that **4** is a *trans*-isomer. The relative intensities of the terminal carbonyl bands in the infrared spectrum also suggests *trans*-forms for **4**.

In the decarbonylation mechanism of acylmanganese carbonyl derivatives, it is known that the acyl CO becomes coordinated and a coordinated CO is eliminated.[11] If decarbonylation reaction of π-$C_5H_5Mo(CO)_2(CNC(CH_3)_3)COCH_2Ph$ proceeds through a similar mechanism, decarbonylation from the *cis*-isomer will preferentially proceed. However, there is no evidence that the *cis*-isomer is the first decarbonylation product, and since it is not isomerized subsequently to the *trans*-isomer, its mechanism remains undecided at present.

Experimental

Reactions were carried out under a nitrogen atmosphere. All melting points are uncorrected. The infrared spectra were obtained by a Perkin-Elmer 521 spectrometer. The NMR spectra were recorded by a Varian Model A-60 instrument, using tetramethylsilane as an internal standard.

Materials. Various isocyanides[12] and tricarbonyl-

11) For example: R. J. Mawby, F. Basolo and R. G. Pearson, *J. Amer. Chem. Soc.*, **86**, 5043 (1964).

12) I. Ugi and R. Meyer, *Chem. Ber.*, **93**, 239 (1960).

π-cyclopentadienylalkylmolybdenum[13] were prepared according to the procedures in literatures.

Reaction of Tricarbonyl-π-cyclopentadienylbenzylmolybdenum with *t*-Butyl Isocyanide. *t*-Butyl isocyanide (0.26 g) in benzene (5 m*l*) was added dropwise to a stirred solution of tricarbonyl-π-cyclopentadienylbenzylmolybdenum (1.0 g) in benzene (15 m*l*). After 9 hr at room temperature, the reaction mixture was evaporated to about 5 m*l* under reduced pressure and chromatographed on alumina, benzene being used as eluant. The orange yellow fraction was collected, and the solvent was evaporated almost to dryness. Recrystallization from THF-*n*-hexane gave π-$C_5H_5Mo(CO)_2$-$(CNC(CH_3)_3)COCH_2Ph$ (0.69 g, 57.5%).

The reactions of tricarbonyl-π-cyclopentadienylalkylmolybdenum with isocyanides were also carried out by the same procedures described above to give the corresponding dicarbonyl-π-cyclopentadienyl(isocyanide)acylmolybdenum.

Reaction of Dicarbonyl-π-cyclopentadienyl(triphenylphosphine)acetylmolybdenum with *t*-Butyl Isocyanide. *t*-Butyl isocyanide (0.3 g) in benzene (5 m*l*) was added dropwise to a solution of π-C_5H_5Mo-$(CO)_2(PPh_3)COCH_3$ (0.52 g) in benzene (15 m*l*). After 9 hr, the reaction mixture was evaporated to about 5 m*l* under reduced pressure and chromatographed on alumina, benzene being used as eluant. The yellow fraction was collected and solvent was evaporated almost to dryness. Recrystallization from benzene - *n*-hexane gave π-$C_5H_5Mo(CO)_2(CNC(CH_3)_3)COCH_3$ (0.16 g 48%).

Decarbonylation of π-$C_5H_5Mo(CO)_2(CNC(CH_3)_3)$-$COCH_2Ph$(3). Compound **1**(1.6 g) in THF (25 m*l*) was irradiated with ultraviolet light at room temperature. After 30 hr, the reaction mixture was evaporated to about 10 m*l* under reduced pressure and chromatographed on alumina, using benzene as eluant. Evaporation of the yellow fraction and recrystallization of the residue from *n*-hexane - benzene gave π-$C_5H_5Mo(CO)_2$-$(CNC(CH_3)_3)CH_2Ph$ (0.43 g, 25%, mp 68—72°C). Found: C, 58.46; H, 5.56; N, 3.85%. Calcd for $C_{19}H_{21}NO_2Mo$: C, 58.32; H, 5.54; N, 3.58%.

Determination of Rates of Isomerization. *trans* to *cis* isomerization was determined by following the appearance of cyclopentadienyl protons resonance of the *cis*-isomer. For rate studies of the isomerization of *trans*-π-$C_5H_5Mo(CO)_2$(isocyanide)COR, the solid complex was dissolved in $CDCl_3$ at −50°C and its rate of isomerization was followed in the desired temperature. Approximately 2 min was allowed for the system to attain the measured temperature. Typical changes in spectra with time are shown in Fig. 4. The spectrum at $t=0$ min is that of *trans*-π-$C_5H_5Mo(CO)_2$(isocyanide)-COR, and at $t=\infty$ that of the equilibrium position. First-order rate constants were obtained from the slope of plots of $\ln(A-A_\infty)$ *vs.* t, time, where A is a magnitude of the *trans*-complex at time t. A_∞ is *trans*-content in the equilibrium position.

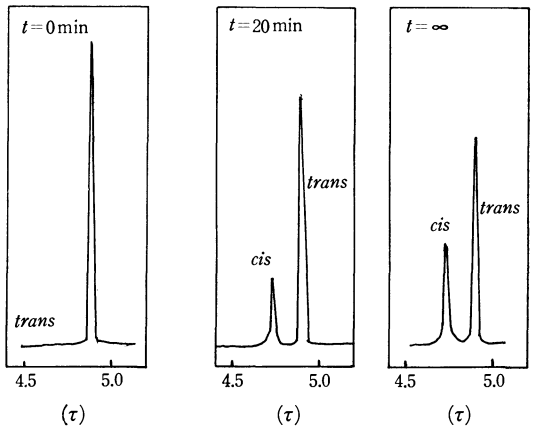

Fig. 4. NMR spectra during the isomerization of *trans*-π-$C_5H_5Mo(CO)_2(CNC(CH_3)_3)COCH_2Ph$ in $CDCl_3$ at −10°C.

13) P. J. Craig and M. Green, *Chem. Commun.*, **1967** 1246.

BULLETIN OF THE CHEMICAL SOCIETY OF JAPAN VOL. 43 148—151 (1970)

Anionic Copolymerization of Butadiene and 1,1-Diphenylethylene

Heimei Yuki and Yoshio Okamoto

Department of Chemistry, Faculty of Engineering Science, Osaka University, Toyonaka, Osaka

(Received June 6, 1969)

The anionic copolymerization of butadiene (M_1) and 1,1-diphenylethylene was investigated in tetrahydrofuran (THF) and benzene, using *n*-butyllithium (*n*-BuLi), Na-naphthalene, and Na- and K-dispersions as initiators. An alternating copolymer was formed in THF, where the reaction proceeded without termination and chain-transfer reactions. The monomer reactivity ratios, r_1, were 0.13 (Li^+), 0.09 (Na^+), and 0.09 (K^+) in THF at 0°C. The r_1 values in benzene at 40°C were 54 (Li^+), 0.71 (Na^+), and 0.10 (K^+). The order of rate constants in THF was $k_{12}>k_{11}>k_{21}$; the last of these was $0.27 M^{-1} sec^{-1}$, with *n*-BuLi at 0°C.

In a preceeding paper,[1] the anionic copolymerization of isoprene (M_1) and 1,1-diphenylethylene (M_2) was reported. In the present work, the anionic copolymerization of butadiene (M_1) and 1,1-diphenylethylene (M_2) was investigated. The results obtained were similar to those of the copolymerization reported in the preceeding paper.

Experimental

Materials. Butadiene (Phillips, polymerization grade) which had been dried over Molecular Sieves was mixed with solvent-free *n*-BuLi just before use; it was then redistilled into a glass ampoule *in vacuo*.

The methods of preparing and purifying the other materials, such as 1,1-diphenylethylene, THF, benzene, and *n*-BuLi, were described in the preceeding paper.[1] The Na- and K-dispersions were prepared in *n*-heptane.

Polymerization. The purified butadiene was first transferred into a known amount of a solvent on a vacuum line, and then the mixture kept under a vacuum was weighed to determine the amount of the monomer transferred. All the mixture was then distilled under a high vacuum into a large amount of the solvent. The solution thus obtained was transferred to glass ampoules with a hypodermic syringe under dry argon. To the ampoules, 1,1-diphenylethylene and initiator were added with syringes. After a given reaction period, the polymerization was terminated by adding a small portion of methanol. The polymer was precipitated in methanol and then filtrated, dried, and weighed. The mother liquor of the polymer precipitation was evaporated at a reduced pressure; the unchanged 1,1-diphenylethylene was thus recovered as a residue. The refractive index and the infrared spectrum of the residue were very similar to those of 1,1-diphenylethylene, indicating that the residue contained a small amount of a compound of a low molecular weight, a compound which was formed by a side reaction.

Electronic Spectrum. The electronic spectrum was taken with a Hitachi 124 Spectrophotometer.

NMR Spectrum. The spectrum of the polymer was measured on a JNM-4H-100 Spectrometer at 100 MHz in a carbon tetrachloride solution at 60°C, using tetramethylsilane as the internal standard.

Molecular Weight. The molecular weight of the polymer was measured in benzene at 37°C with a Mechrolab Vapor Pressure Osmometer, Model 301A.

Viscosity. The solution viscosity of the polymer was taken in toluene at 30.0°C, the concentration of the polymer being 0.5 g/dl.

Results

The rate of the copolymerization of butadiene (M_1) and 1,1-diphenylethylene (M_2) was investigated in THF at 0°C with *n*-BuLi. Figure 1 shows the results. The reaction was completed in 60 min, by which time almost all the butadiene had been consumed. The yield for the alternating copolymerization, which forms a copolymer, $-(M_1M_2)_n-$, is also shown in Fig. 1. This yield reached nearly 100%, indicating that an alternating copolymer was formed.[1] A linear relationship was obtained between the polymer yield (curve B in Fig. 1) and the molecular weight of the polymer, as is shown in Fig. 2. The molecular weight measured nearly agreed with the one calculated for the living polymer system, which proceeds alternatingly. There was also a good linearity between log yield and $\log[\eta]$. The relationship between the average molecular weight and intrinsic viscosity was $[\eta]=4.0\times10^{-4}M^{0.60}$ (in toluene at 30°C).

The copolymerizations in THF and in benzene were carried out by using *n*-BuLi, Na-naphthalene, Na- and K-dispersions. All of the copolymers were powders with a softening point of *ca.* 130°C, except for the viscous copolymer obtained in benzene by *n*-BuLi. The copolymer composition, $[m_1]/[m_2]$, was calculated from the polymer yield, as the butadiene was completely incorporated into the copolymer. Some of the results are shown in Table 1. The composition was checked by

1) H. Yuki and Y. Okamoto, This Bulletin, **42**, 1644 (1969).

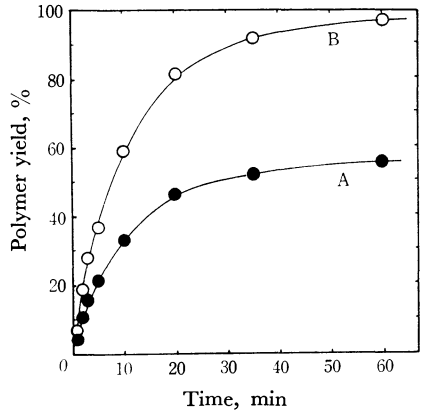

Fig. 1. Anionic copolymerization of butadiene (M_1) and 1,1-diphenylethylene (M_2)——Time *vs.* polymer yield.
A: Polymer yield based on total monomers.
B: Polymer yield based on an alternating copolymerization.
$[M_1]_0$=5.74 mmol; $[M_2]_0$=11.39 mmol; [*n*-BuLi]=0.11 mmol; THF=15.0 m*l*; temp., 0°C

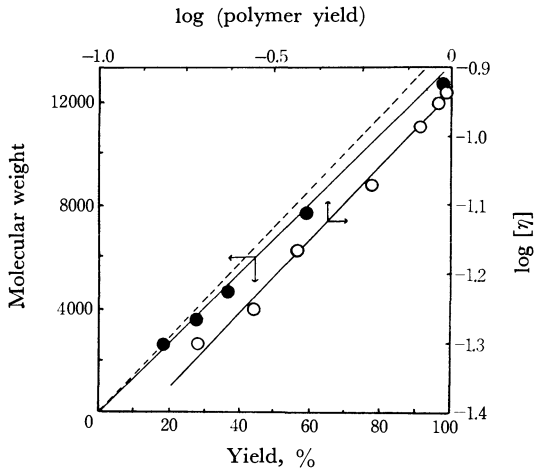

Fig. 2. Anionic copolymerization of butadiene (M_1) and 1,1-diphenylethylene (M_2).
Relationships between polymer yield and molecular weight, and between polymer yield and intrinsic viscosity.
Dotted line: Molecular weight calculated for living polymerization.
Reaction conditions are shown in Fig. 1.

Table 1. Anionic copolymerization of butadiene (M_1) and 1,1-diphenylethylene (M_2)—Material balance

M_1, 0.302 g; initiator, *n*-BuLi 0.11 mmol; temp., 0°C in THF; 40°C in benzene

Solvent 15.0 m*l*	Time hr	M_2 g	$[M_1]_0/[M_2]_0$ mol/mol	Polymer g	Unchanged[a] M_2, g	$[m_1]/[m_2]$[b] mol/mol
THF	24	0.949	1.07	1.182	0.064	1.15
THF	48	1.009	1.00	1.226	0.096	1.09
THF	48	1.328	0.758	1.254	0.382	1.06
Benzene	96	0.596	1.68	0.344	0.534	23.2
Benzene	120	0.924	1.08	0.372	0.826	14.2
Benzene	96	1.348	0.744	0.394	1.242	10.8

a) Contained *ca.* 7 mg of lithium compounds.
b) Copolymer composition.

elementary analysis and NMR spectroscopy. The results are listed in Table 2. The data supported the composition shown in Table 1. The monomer reactivity ratio, r_1, was calculated by means of the integrated Mayo-Lewis copolymer composition equation.[2] The r_1 values are shown in Tables 3 and 4. In THF at 0°C, the values were almost constant, regardless of the initiators used. Although it has been shown that $NaB(Ph)_4$ depresses the dissociation of an ion to free ions,[3] the r_1 value was not affected by the presence of $NaB(Ph)_4$ in the copolymerization initiated by Na-naphthalene in THF. In benzene at 40°C, however, the values were 54, 0.71, and 0.10 with *n*-BuLi, Na-, and K-dispersions respectively. The copolymerization carried out in benzene without an initiator gave

Table 2. Anionic copolymerization of butadiene (M_1) and 1,1-diphenylethylene (M_2)—Copolymer composition

Solvent 15 m*l*	Initiator	$[m_1]/[m_2]$[a]	Elementary analysis Calcd[b] C,%	Calcd[b] H,%	Found C,%	Found H,%	NMR $[m_1]/[m_2]$
THF	*n*-BuLi	1.00	92.26	7.74	92.00	7.70	0.97
Benzene	K-dispersion	1.08	92.20	7.80	92.03	7.69	1.05
Benzene	Na-dispersion	1.50	91.98	8.02	91.75	7.85	1.40
Benzene	*n*-BuLi	10.8	89.80	10.20	89.60	9.82	9.50

a) Copolymer composition calculated from polymer yield.
b) Based on the copolymer composition.
c) Copolymer composition obtained from NMR spectrum.

2) H. Yuki, J. Hotta, Y. Okamoto and S. Murahashi, *ibid.*, **40**, 2659 (1967).
3) D. N. Bhattacharyya, C. L. Lee, J. Smid and M. Szwarc, *J. Phys. Chem.*, **69**, 612 (1965); H. Hostalka and G. V. Schulz, *J. Polym. Sci.*, **B3**, 175 (1965).

TABLE 3. ANIONIC COPOLYMERIZATION OF BUTADIENE (M_1) AND 1,1-DIPHENYLETHYLENE (M_2)—MONOMER REACTIVITY RATIO, r_1, DETERMINED WITH *n*-BuLi IN THF AT 0°C (A) AND WITH Na-DISPERSION IN BENZENE AT 4 C (B)[a)]

Run No.	$[M_1]_0/[M_2]_0$	Time hr	Yield mol%	$[m_1]/[m_2]$[b)]	η_{sp}/C	r_1
A	1.065	24	96.4	1.15	—	0.17
A	1.000	48	94.1	1.09	—	0.17
A	0.833	24	88.7	1.05	—	0.10
A	0.758	48	83.9	1.06	—	0.12
A	0.731	24	82.3	1.05	—	0.11
A	0.508	18	66.1	1.04	—	0.10
					Average	0.13
B	1.046	187	85.2	1.50	0.50	0.79
B	0.961	187	83.3	1.42	0.52	0.70
B	0.929	187	83.2	1.38	0.74	0.71
B	0.814	187	78.2	1.35	0.42	0.75
B	0.724	187	75.7	1.25	0.68	0.61
					Average	0.71
B[c)]	0.976	187	0	—	—	—

a) $[M_1]_0$, 5.6 mmol; solvent, 15 m*l*; *n*-BuLi, 0.11 mmol; Na-dispersion, *ca.* 0.5×10^{-3} atom; temp, 0°C
b) Copolymer composition
c) Without initiator

TABLE 4. ANIONIC COPOLYMERIZATION OF BUTADIENE (M_1) AND 1,1-DIPHENYLETHYLENE (M_2)—MONOMER REACTIVITY RATIO, r_1

Solvent	Initiator	Temp. °C	Run of experiment	r_1
THF	*n*-BuLi	0	6	0.13
THF	Na-naph.	0	6	0.09
THF	K-dispersion	0	5	0.09
Benzene	*n*-BuLi	40	5	54
Benzene	Na-dispersion	40	5	0.71
Benzene	K-dispersion	40	5	0.10

no polymer, even after 187 hr at 40°C (Table 3). With Li^+ as a counter ion, the r_1 value was strongly influenced by the solvent; with Na^+ and K^+, less influence of the solvent was observed (Table 4).

The microstructures of butadiene in the homopolymer and in the alternating copolymer were investigated by NMR spectroscopy. Figure 3 shows the spectrum of the alternating copolymer obtained with *n*-BuLi in THF. The polybutadiene obtained by *n*-BuLi in THF had 82% 1,2- and 18% 1,4-structures, while the alternating copolymer had 30% 1,2- and 70% 1,4-structures.

The copolymerization in THF at 0°C was followed spectrophotometrically. As soon as *n*-BuLi was added to a monomer solution at $[M_1]_0/[M_2]_0=0.53$, an absorption maximum due to a diphenylethylene anion appeared at 496 mμ. Its optical density had been almost constant for 5 hr,

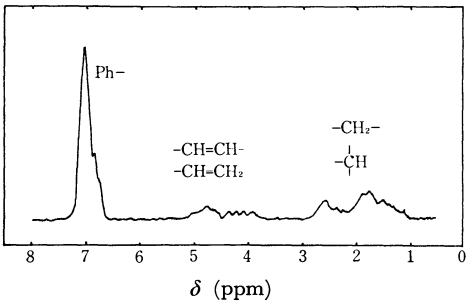

Fig. 3. NMR spectrum of the alternating copolymer of butadiene and 1,1-diphenylethylene. (in CCl_4 at 60°C)

in which time the polymerization had been completed. The molar extinction coefficient was 1.7×10^4; this agrees the value found in the copolymerization of isoprene and 1,1-diphenylethylene.[1)] These results suggest that almost all of the living ends in the system were 1,1-diphenylethylene anions.

Discussion

The results of the copolymerization investigated in this work were very similar to those found in the copolymerization of isoprene and 1,1-diphenylethylene.[1)] Both the copolymerizations in THF proceeded in living systems to give alternating copolymers, and all the r_1 values determined under the same reaction conditions were very similar. The rate of the consumption of butadiene was first-order with respect to its own concentration, as is shown in Fig. 4; this figure was obtained by analyzing the results in Fig. 1. This means that the reverse reaction between the 1,1-diphenylethylene anion and butadiene can be disregarded.[1)]

$$\sim\sim M_2^- + M_1 \underset{k_{-21}}{\overset{k_{21}}{\rightleftarrows}} \sim\sim M_1^-$$

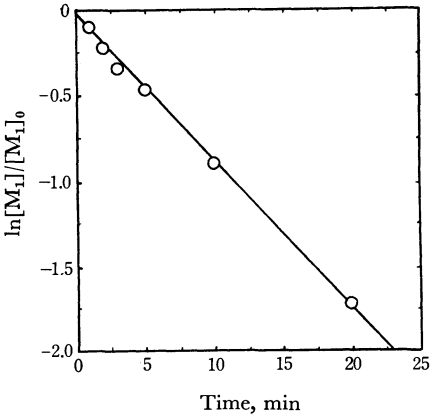

Fig. 4. Anionic copolymerization of butadiene (M_1) and 1,1-diphenylethylene (M_2)—First order plot. Reaction conditions are shown in Fig. 1.

From Fig. 4, we can get $k_{21}=0.27\text{M}^{-1}\text{ sec}^{-1}$. Various rate constants determined in the copolymerizations in THF employing methyl derivatives of butadiene as a component are collected in Table 5. The reactivities (k_{21}) of the dienes decreased with an increase in the methyl group. The retarding effect of the group, however, was different for two living ends, the styryl anion and the diphenylethylene anion, indicating that the steric effect also affects the reactivities of the dienes. As to the reactivity of the anion (k_{12}), the isoprenyl anion should be more reactive as a result of the electron-donating effect of the methyl group. However, the butadienyl anion was more reactive to 1,1-diphenylethylene than the isoprenyl anion. This must also be caused by the steric factor. Similar results were reported in the addition reactions of styrene to styryl and α-methylstyryl anions, in which the styryl anion was more reactive.[9]

Table 5. Rate constant in THF

Diene	k_{11} $\text{M}^{-1}\text{sec}^{-1}$	k_{21}, $\text{M}^{-1}\text{sec}^{-1}$		k_{12}[e] $\text{M}^{-1}\cdot\text{sec}^{-1}$
		M_2=DPE	M_2=Styrene	
Butadiene	0.59[a]	0.27[b]	3.27×10[d]	4.5
Isoprene	3.8×10^{-2} [a]	2.6×10^{-3} [b]	1.7×10[d]	0.35
2,3-Dimethyl-butadiene	1.4×10^{-3} [c]	1.6×10^{-3} [c]	4.8×10^{-1} [d]	—

a) Li, 0°C, Refs. 7 and 8.
b) Li, 0°C, this work and Ref. 1.
c) Li, 22°C, Ref. 4.
d) Na, 25°C, Ref. 6.
e) This was obtained from r_1 in Table 6 and k_{11}.

The monomer reactivity ratios, r_1, obtained in the copolymerizations of 1,1-diphenylethylene (M_2) and conjugated dienes (M_1) by means of *n*-BuLi are summarized in Table 6. In THF, 1,1-diphenylethylene is more reactive to the M_1 anion than the corresponding M_1 monomer. In benzene, however, isoprene and butadiene are more reactive than 1,1-diphenylethylene. The effects of the solvent and initiator in Tables 4 and 6 suggest that the r_1 value may increase with a decrease in the polarity of the carbon-metal bond.

Table 6. Monomer reactivity ratio, r_1, in the copolymerizations of 1,1-diphenylethylene (M_2) and dienes (M_1) by *n*-BuLi

M_1	THF[a]	Benzene[b]	Ref.
Butadiene	0.13	54	This work
Isoprene	0.11	37	1
2,3-Dimethylbutadiene	~0[c]	0.23	4,5

a) at 0°C b) at 40°C c) at 22°C

The microstructures of butadiene, isoprene, and 2,3-dimethylbutadiene in the homopolymers and in the alternating copolymers with 1,1-diphenylethylene are summarized in Table 7; all of the polymers were formed in THF by means of *n*-BuLi. The 1,4-structure was greater in the alternating copolymer than in the homopolymers, and the order of the content of the 1,4-structure was 2,3-dimethylbutadiene>isoprene>butadiene. In the alternating copolymer of 2,3-dimethylbutadiene and 1,1-diphenylethylene, no 1,2-structure was present because of its big steric hindrance. However, in the case of the butadiene-diphenylethylene alternating copolymer, the 1,2-structure existed because of its lower steric hindrance. These results suggest that the microstructure of the dienes in the alternating copolymer is controlled strongly by the steric effect. In orther words, the effect must affect the rate constant, k_{12}, as has been described above.

Table 7. Microstructures of the dienes in the homopolymers and the alternating copolymers obtained in the polymerization by *n*-BuLi in THF

Diene	Homopolymer, %			Alternating copolymer, %		
	1,2-	1,4-	3,4-	1,2-	1,4-	3,4-
Butadiene	82	18	—	30	70	—
Isoprene	29	~0	71	~0	83	17
2,3-Dimethylbutadiene	49	51	—	0	100	—

4) H. Yuki, K. Hatada and T. Inoue, *J. Polym. Sci. Part A-1*, **6**, 3333 (1968).
5) H. Yuki, Y. Okamoto and K. Sadamoto, This Bulletin, **42**, 1754 (1969).
6) M. Shima, J. Smid and M. Szwarc, *J. Polym. Sci.*, **B2**, 735 (1964).
7) M. Morton, E. E. Bostick, R. A. Livigni and L. J. Fetters, *ibid.*, **A1**, 1735 (1963).
8) M. Morton and L. J. Fetters, *ibid.*, **A2**, 3311 (1964).
9) M. Shima, D. N. Bhattacharyya, J. Smid and M. Szwarc, *J. Amer. Chem. Soc.*, **85**, 1306 (1963).

BULLETIN OF THE CHEMICAL SOCIETY OF JAPAN VOL. 43 152—155 (1970)

Studies of Phenylxanthyl and Its Analogues by Electron Spin Resonance

Kazuhiro MARUYAMA, Masaharu YOSHIDA and Katsuya MURAKAMI

Department of Chemistry, Faculty of Science, Kyoto University, Yochida, Sakyo-ku, Kyoto

(Received June 7, 1969)

Phenylxanthyl, phenylthioxanthyl, phenylselenoxanthyl, 9-phenylfluorenyl, dioxadehydrocoranthryl, and their derivatives were studied by the electron spin resonance (ESR) technique, and the odd-electron distribution in the radicals was examined. From the results, the angle between the plane of the phenyl group and the plane of the rest of the molecule was estimated at about 63°. Since these radicals are in equilibria with their dimers, heat of reaction in the system was also determined on two of them. Some discussion of the correlation between the heat of reaction and the molecular shape was undertaken.

The distribution of the odd-electron in a molecule can be determined directly by the ESR technique. In this study, phenylxanthyl and its analogues, I—XI, were examined by this method. Since, in their structural features, these radicals have a form in which two or three phenyl groups of triphenylmethyl are bridged, the investigation of these radicals is interesting, especially in the correlation between the structure and the odd-electron distribution.

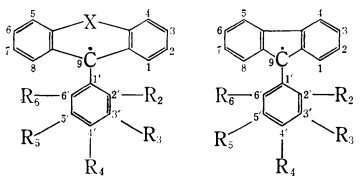

I—VIII IX—X XI

I, X=O, $R_2=R_3=R_4=R_5=R_6=H$
II, X=O, $R_2=R_3=R_5=R_6=H$, $R_4=OCH_3$
III, X=O, $R_3=R_4=R_5=R_6=H$, $R_2=OCH_3$
IV, X=S, $R_2=R_3=R_4=R_5=R_6=H$
V, X=S, $R_2=R_3=R_5=R_6=H$, $R_4=OCH_3$
VI, X=SO_2, $R_2=R_3=R_4=R_5=R_6=H$
VII, X=Se, $R_2=R_3=R_4=R_5=R_6=H$
VIII, X=O, $R_2=R_3=R_4=R_5=R_6=D$
IX, $R_2=R_3=R_4=R_5=R_6=H$
X, $R_2=R_3=H$, $R_2=R_4=R_6=CH_3$

Results and Discussion

All the radicals examined here were produced in a vacuum-sealed sample tube by treating the corresponding chlorides dissolved in a suitable solvent with amalgamated silver. The ESR measurements were made at room temperature in solutions, using THF as the solvent except in the cases of compounds IX and X. Since these compounds are scarcely dissociated to the radical form at room temperature, their ESR measurements were conducted at an elevated temperature (80°C) using xylene as the solvent.

The proton hyperfine coupling constants obtained by the analyses of the ESR spectra are tabulated in Table 1. The coupling constant due to the proton was assigned tentatively by comparison with the spectra obtained from the measurements of non-substituted phenylxanthyl and the substituted phenylxanthyl derivatives, with reference to the results of the HMO calculations. Finally, such assignments were substantiated by comparison with the ESR spectrum of d_5-phenylxanthyl. Since phenylthio- and phenylseleno-xanthyl have shown spectra quite similar to that of phenylxanthyl, as can be seen in Fig. 1, the assignments of the corresponding protons to the respective coupling constants were straightforward. As to the other compounds (IX, X, and XI), the analyses of the spectra

TABLE 1. PROTON HYPERFINE COUPLING CONSTANTS OF RADICALS (gauss)

a_H position / Radical	1,8	2,7	3,6	4,5	2′,6′	3′,5′	4′
I	2.65	0.60	2.60	0.64	0.55	0.91	0.55
II	2.86	0.64	2.86	0.64	0.64	0.20	
III	3.76		3.76				
IV	3.28	0.47	3.10	0.47	0.95		1.16
V	4.15	0.57	4.15	0.57	1.13		
VI	3.63	0.48	3.55	0.48	0.96		1.25
VII	3.70	0.59	3.70	0.59	1.17		1.17
VIII	2.65	0.60	2.60	0.64			
IX	3.28	0.58	3.47	0.97	1.95	0.39	1.95
X	3.77		3.77				

a_H position / Radical	1,13	2,12	3,11	4,10	6,8	7
XI	2.77	0.84	2.97	0.84	0.65	2.97

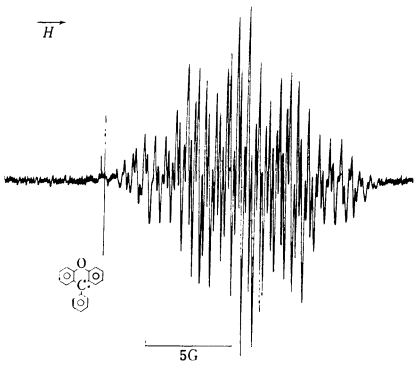

(a) ESR spectrum of I

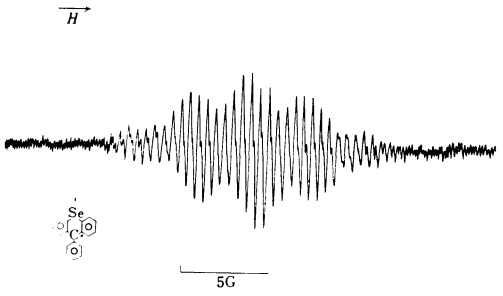

(b) ESR spectrum of III

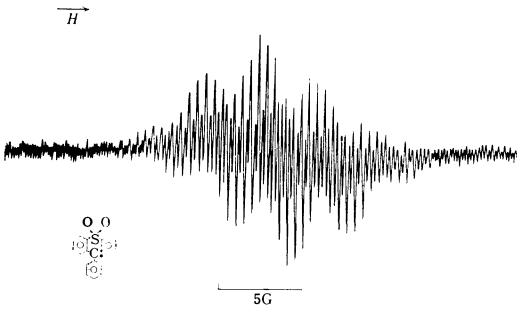

(c) ESR spectrum of VI

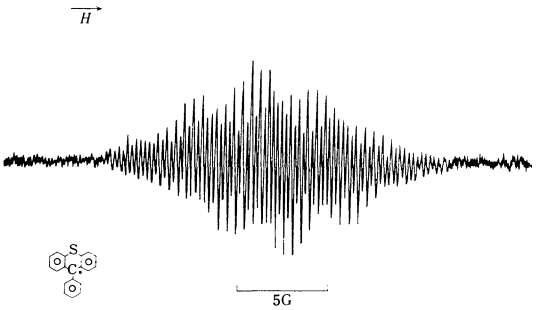

(d) ESR spectrum of VII

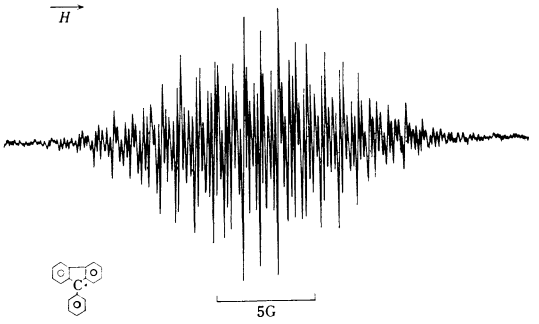

(e) ESR spectrum of IX

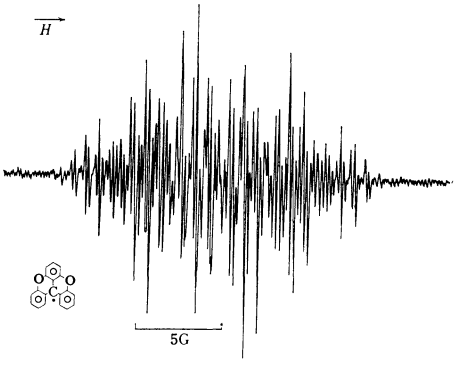

(f) ESR spectrum of XI

Fig. 1. ESR spectra of phenylxanthyl and its analogues.

and the assignments of the proton coupling constants were made quite analogously. The coupling constants obtained from the analyses of the spectra were reconfirmed by simulation with a computer.

It is interesting to compare the proton hyperfine coupling constants of these phenylxanthyl derivatives with that of triphenylmethyl, in which there is no bridge connecting the two phenyl groups. The proton hyperfine coupling constants of triphenylmethyl have been measured by several investigators. The values of the coupling constants for the respective protons reported by Ayscough and his co-workers[1] are $a_{\mathrm{H_{ortho}}}$: 2.55 gauss, $a_{\mathrm{H_{para}}}$: 2.78 gauss and $a_{\mathrm{H_{meta}}}$: 1.11 gauss. Although the value of the coupling constant can be slightly affected by the species of solvent used, those of the phenyl protons of phenylxanthyl as well as of the thio- or seleno-derivatives are outstandingly reduced compared with those of the corresponding protons of triphenylmethyl. This indicates the smaller delocalization of the odd-electron on the phenyl group. This may be due to the $C_{1'}$–C_9 bond twist of phenylxanthyl and its analogues. In view of the molecular model, the $C_{1'}$–C_9 bond of phenylxanthyl can be said to be forced to twist strongly because of the repulsion which might operate among C_1–H, C_8–H, $C_{2'}$–H, and $C_{6'}$–H. The results of HMO calculations performed under the consideration of the $C_{1'}$–C_9 bond twist are

1) P. Ayscough, A. McCann and R. Wilson, *Proc. Chem. Soc.*, **1961**, 16; D. Chesnut and G. Sloan, *J. Chem. Phys.*, **33**, 637 (1960).

TABLE 2. HMO CALCULATION OF ODD ELECTRON DENSITY OF PHENYLXANTHYL*

Angle of deviation** (in degree)	0	10	20	30	40	50	60	70	80	90
c_1***	.07371	.07426	.07585	.07846	.08191	.08602	.09036	.09419	.09691	.09791
c_3	.06632	.06729	.06864	.07086	.07382	.07728	.08094	.08422	.08649	.08732
c_9	.27100	.27280	.27820	.28680	.29820	.31150	.32540	.33760	.34620	.34930
$c_{4'}$	.07629	.07458	.06943	.06116	.05009	.03717	.02369	.01160	.00308	.00000

* The values; α_O: $\alpha+1.3\beta$, β_{C-O}: 1.5β are used for the calculation.
** Angle of deviation from the co-planar position.
*** c_1, c_3, c_9 and $c_{4'}$ are coefficients of the corresponding atomic orbitals in a molecular orbital where odd electron is found.

shown in Table 2.

The variation in the value of $(c_{4'}/c_1)^2$ with the value of the twisted angle is figured in Fig. 2, where $(c_1)^2$ and $(c_{4'})^2$ represent the odd-electron density on the respective carbon atoms (C_1 and $C_{4'}$).

By a comparison of the ratio of the coupling constants ($a_{H4'}/a_{H_1}$) experimentally obtained with the value in Fig. 2, the angle of twist of the $C_{1'}$–C_9 bond can be estimated to be about 63° for phenylxanthyl. Therefore, it may be assumed that there is a comparable order of $C_{1'}$–C_9 bond twist for thio- or selenoxanthyl derivatives, too. Such a situation is partly reflected in the equilibrium between a radical and the dimer. The relative stability of phenylxanthyl and of 9-phenylfluorenyl in comparison with that of the dimers was determined by the ESR technique (see Fig. 3). The values obtained are tabulated in Table 3, along with those of other compounds.

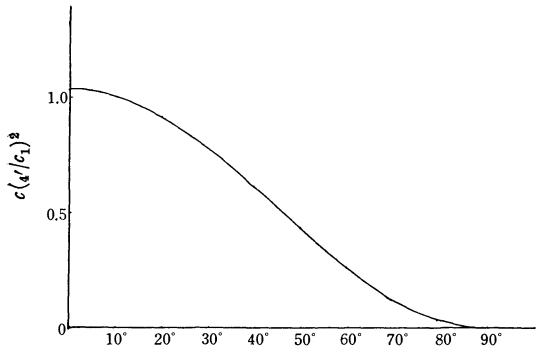

Fig. 2. Relation between $(c_4'/c_1)^2$ and angle of deviation from the co-planar position.

Since the degree of dissociation of a dimer to the radical is determined simply by the relative stability between the dimer and the resulting radical, the degree of dissociation must be controlled by two main factors. One is the stabilization of the radical due to the delocalization of the odd-electron, while the other is the steric repulsion around the bond-forming center (the central carbon atom) to

TABLE 3. HEAT OF REACTION (ΔH) IN THE SYSTEM OF EQUILIBRIUM BETWEEN RADICAL AND THE DIMER

Compound	ΔH (kcal/mol)
Phenylxanthyl dimer	8.4
9-Phenylfluorenyl dimer	26.6
Hexaphenylethane*	18.2
Pentaphenylethane*	27.0

* J. Leffler, "The Reactive Intermediate of Oragnic Chemistry," Florida University Press (1956).

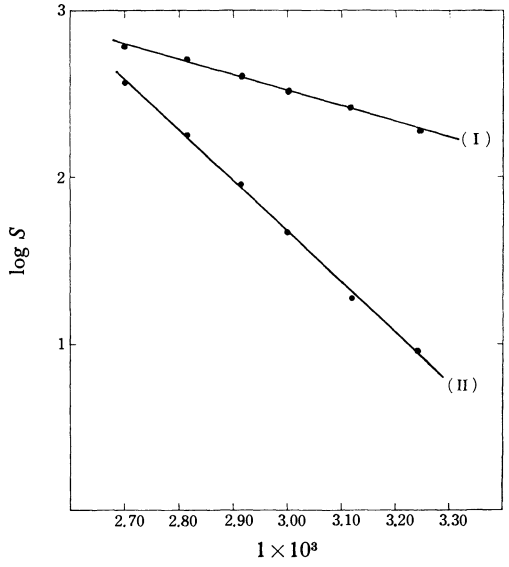

Fig. 3. Temperature dependence of radical concentration (S: signal intensity).
(I) phenylxanthyl (II) 9-phenylfluorenyl

dimerize. The former causes the potential energy of radical to be lower, while the latter causes that of its dimer to be higher. The latter is the predominant factor in the dissociation of hexaphenylethane derivatives to triphenylmethyls.[2] Therefore, the lower heat of reaction in the system

2) W. Theilacker, H. Schultz, U. Baumgarte, H.-G. Prossler, W. Rohde, F. Thater and H. Uffmann, *Angew. Chem.*, **69**, 322 (1957).

of the equilibrium between phenylxanthyl and its dimer compared with that in the cases of triphenylmethyl and 9-phenylfluorenyl can be reasonably concluded to be the result of the larger steric repulsion around the central carbon atom due to the phenyl group being situated nearly perpendicular to the rest of the molecule. The larger value of the coupling constants (1.95 gauss) due to 2′,4′,6′-protons of 9-phenylfluorenyl compared with the value of the coupling constants (0.55 gauss) of the 2′,4′,6′-protons of phenylxanthyl may be considered to be a direct reflection of the more favorable situation for the co-planarity of phenyl and fluorenyl groups in IX because of the less repulsive force between C_1–H, C_8–H, $C_{2'}$–H, and $C_{6'}$–H. Moreover, it is consistent with the higher heat of reaction in the system. The larger coupling constant (2.97 gauss) of the 3,7,11-protons of dioxadehydrocoranthryl (XI), in which three phenyl groups are forced to be co-planar, supports the above discussion.

Experimental

Materials. All the free radicals examined were made *in situ* by shaking their chlorides with amalgamated silver in a vacuum cell, and the ESR spectra were immediately observed. The chlorides were prepared from the corresponding alcohols by treatment with gaseous hydrogen chloride in ether. The method of synthesizing chlorides and their physical constants are shown in Table 4.

The ESR spectra were measured by means of a 3BX-type spectrometer manufactured by the Japan Electron Optics Lab.

Determination of the Heat of Reaction. A known amount of chloride was dissolved into a known amount of tetrahydrofuran in a cell suitable for ESR measurements, and then it was evacuated and treated with amalgamated silver which had previously been prepared in the cell. The signal intensity was measured at various temperatures according to the usual way (magnetic field modulation: 5 gauss). The $\ln S$(S: signal intensity) *vs.* $1/T$ plot gave directly the heat of reaction in the system of equilibrium. A DPPH solution dissolved in THF of a known concentration was used as the standard solution.

Table 4. Synthetic methods of chlorides and their physical constants

Precursor of*	Synthetic method	Melting point of alcohol (°C)	Melting point of chloride (°C)	Ref.
I	Xanthone $+C_6H_5MgBr$	158	106*	3
II	Xanthone $+p$-$CH_3OC_6H_4MgBr$	121	96**	4
III	Xanthone $+o$-$CH_3OC_6H_4MgBr$	oil	75—80**	
IV	Thioxanthone $+C_6H_5MgBr$	106	115**	5
V	Thioxanthone $+p$-$CH_3OC_6H_4MgBr$	135	87—90**	
VI	Sulfonylxanthone $+C_6H_5MgBr$	68	80—83**	
VII	Selenoxanthone $+C_6H_5MgBr$	115	134—136**	
VIII	Xanthone $+C_6D_5MgBr$	97	106—107**	
IX	Fluorenone $+C_6H_5MgBr$	107	78—80	6
X	Fluorenone $+2,4,6$-$(CH_3)_3C_6H_2Li$	oil	106—107	
XI	1-Hydroxyxanthone $+o$-$CH_3OC_6H_4MgBr$	180	243*)	7

* Precursors of radicals described in the column.
** Melting point of hydrolchloride of the corresponding chloride is shown.

The simulation of the ESR spectra was done by the Japan Electron Optics Lab., to the members of which our thanks are due.

BULLETIN OF THE CHEMICAL SOCIETY OF JAPAN VOL. 43 156—162 (1970)

Tri(hetero)substituted Carbonium Ions. I. Neighboring-Group Participation of the *N,N*-Dimethyldithiocarbamate Function Involving the Intermediacy of 2-Dimethylamino-1,3-dithiolanylium Ion*1

Takeshi NAKAI, Yoshio UENO and Makoto OKAWARA

Research Laboratory of Resources Utilization, Tokyo Institute of Technology, Ookayama, Meguro-ku, Tokyo

(Received June 10, 1969)

The equimolar reaction of 1,2-dichloroethane with sodium *N,N*-dimethyldithiocarbamate was studied in various solvents. As major products, ethylene bis(*N,N*-dimethyldithiocarbamate) and 2-dimethylamino-1,3-dithiolanylium salt (the perchlorate or the tetraphenylborate) were obtained in yields, largely varying with the solvent used. On the basis of the solvent effect on the product ratio, and kinetic experiments it has been verified that neighboring-group participation of the *N,N*-dimethyldithiocarbamate function would be involved through the intermediacy of the isolated anchimeric carbonium ion, and that such participation is more predominant in nonpolar aprotic solvents such as dioxane and tetrahydrofuran. The mechanism of the reaction between 2-dimethylamino-1,3-dithiolanylium ion and the dithiocarbamate anion was established.

In previous papers[1-4] we reported that polymers containing the dithiocarbamate function ($-SCSNR_2$) are effective as a photosensitive resin. They were conveniently prepared by polymer reactions since no monomer with the function was readily available. We undertook to prepare *S*-vinyl *N,N*-dialkyldithiocarbamate by dehydrochlorination of *β*-chloroethyl dithiocarbamate. However, *β*-chloroethyl dithiocarbamate could not be isolated from the equimolar reaction of 1,2-dichloroethane with *N,N*-dialkyldithiocarbamate anion, but some unexpected observations described below were made. It was found that the vacuum pyrolysis of ethylene bis(*N,N*-dialkyldithiocarbamates) afforded *S*-vinyl *N,N*-dialkyldithiocarbamates in good yields, and their radical polymerizabilities were compared with those of the oxygen analogs.[5]

The observations obtained in the equimolar reaction between 1,2-dichloroethane (I) and sodium *N,N*-dimethyldithiocarbamate hydrate (II) are as follows: (i) the expected monosubstituted product, *β*-chloroethyl *N,N*-dimethyldithiocarbamate (III) could not be obtained at all; (ii) as major products, the disubstituted ethylene bis(*N,N*-dimethyldithiocarbamate) (IV) and 2-dimethylamino-1,3-dithiolanylium ion*2 (V) (as the perchlorate) were isolated in yields varying with the solvent. The results led us to study the mechanism of this equimolar reaction.

In the present paper we describe neighboring-group participation of the *N,N*-disubstituted dithiocarbamate function involving the intermediacy of the isolatable anchimeric cation*3 (V) in the reaction of 1,2-dichloroethane with the dithiocarbamate anion, mainly on the basis of the solvent effect on the product ratio and kinetic experiments.

Results and Discussion

The Solvent Effect on the Product Ratio. The equimolar reactions of 1,2-dichloroethane (I) with sodium *N,N*-dimethyldithiocarbamate (II) were undertaken at 60°C for 6 hr in various solvents. The dithiocarbamate anion completely disappeared during reaction under this condition. Ethylene bis(*N,N*-dimethyldithiocarbamate) (IV) and 2-

*1 Part of this work has been published. T. Nakai, Y. Ueno and M. Okawara, *Tetrahedron Lett.*, **1967**, 3831.

1) M. Okawara, H. Yamashina, K. Ishiyama and E. Imoto, *Kogyo Kagaku Zasshi*, **66**, 1383 (1963).

2) M. Okawara, K. Morishita and E. Imoto, *ibid.*, **69**, 761 (1966).

3) M. Okawara, M. Ori, T. Nakai and E. Imoto, *ibid.*, **69**, 766 (1966).

4) M. Okawara and T. Nakai, *Bull. Tokyo Inst. Technol.*, **78**, 1 (1967).

5) T. Nakai, K. Shioya and M. Okawara, *Makromol. Chem.*, **108**, 95 (1967).

*2 Carbonium ion is more precisely expressed as 2-dimethylamino-1,3-dithiolan-2-ylium ion. In our papers "1,3-dithiolanylium ion" means "1,3-dithiolan-2-ylium ion."

*3 The term "anchimeric cation" refers to cyclic carbonium ion formed *via* intramolecular S_N reaction involving a neighboring group, such as V and VII.

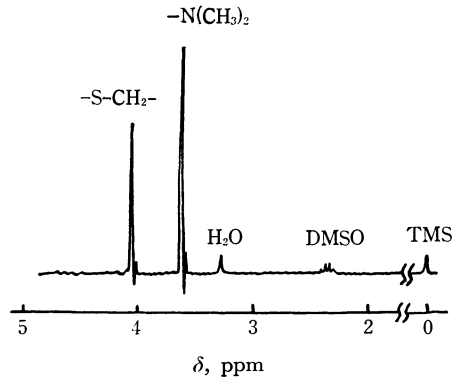

Fig. 1. The NMR spectrum of 2-dimethylamino-1,3-dithiolanylium perchlorate (Vb) in DMSO-d_6.

dimethylamino-1,3-dithiolanylium salt (V) were obtained as major products. Ethylene bis(dithiocarbamate) was identified by comparisons of both spectral data with that of authentic sample and the mixed mp determination.

The dithiolanylium salt (V) was isolated as perchlorate by treatment of an aqueous layer of the reaction mixture with sodium perchlorate. The structure of the perchlorate Vb was confirmed by elemental analysis and an independent preparation according to the reported method.[6] The NMR spectrum (Fig. 1) of the perchlorate was superimposable, exhibiting two singlet signals at δ 4.08 ($-CH_2-S-$) and 3.62 ppm (CH_3-N). Dithiolanylium ion was also isolated as the tetraphenylborate (Vc) in higher yields than the perchlorate Vb, but not quantitatively because Vc dissolved in water. The formation of dithiolanylium ion can be explained by the intramolecular nucleophilic substitution (S_Ni) reaction of β-chloroethyl dithiocarabamate (III) formed.

The reaction of I with II in ethanol afforded ethyl thioncarbamate (VI) and β-mercaptoethyl thiolcarbamate (VII) as well as major products described above. The thioncarbamate (VI) was identified by comparison of physical properties and spectral data of the authentic sample. The thiolcarbamate (VII) exhibits a strong absorption band at 1650 cm^{-1} due to $\nu_{C=O}$ for $-S-CO-N<$ and was treated with lead acetate to give a precipitate of the lead mercaptide. The formation of VI was not observed with reactions in other solvents than ethanol. Separate experiments suggested that these by-products were formed through ethanolysis and hydrolysis of 2-dimethylamino-1,3-dithiolanylium ion (V), respectively.[7]

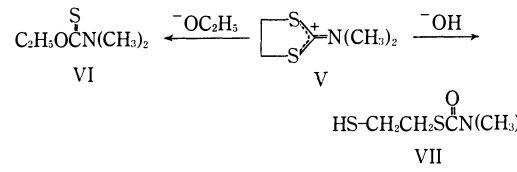

The product compositions for the equimolar reactions in various solvents are given in Table 1. The results indicate that the product ratio is largely dependent on the nature of the solvent. From the effect on the product ratio, solvents may be classified into three groups; dipolar protic (EtOH, EGOH), dipolar aprotic (DMF, DMSO, CH_3CN) and nonpolar aprotic (dioxane, THF). The yield of IV increases in the order: nonpolar>dipolar aprotic>dipolar protic. It may be noted that, especially in dioxane and THF, the disubstituted product (IV) was more favorably formed under the equimolar condition. The fact cannot be

Table 1. Products from the equimolar reactions of I with II
Reaction temp.: 60°C; time, 6 hr

Solvent	Composition (% based on II)		Others
	Ethylene bis-dithiocarbamate (IV)	2-Dimethylamino-1,3-dithiolanylium salt (Vc)[a]	
Ethanol (EtOH)	8.4	61.4	5.5,[b] 3.9[c]
Ethylene glycol (EGOH)	trace	59.6	trace[c]
Dimethylformamide (DMF)	23.0±0.5[d]	57.3±2.0	trace
Dimethylsulfoxide (DMSO)	13.4	51.5	trace
Acetonitrile (CH_3CN)	11.2	67.0	trace
Dioxane	56.9±0.1	29.0±1.0	trace
Tetrahydrofuran (THF)	67.5±2.0	21.4±2.0	trace

a) 2-Dimethylamino-1,3-dithiolanylium chloride (Va) formed could not be quantitatively isolated as the tetraphenylborate Vc (see the text).
b) *O*-Ethyl *N,N*-dimethylthioncarbamate (VI).
c) β-Mercaptoethyl *N,N*-dimethylthiolcarbamate (VIII).
d) Average and deviation of values obtained by two experiments.

6) C. Kennard and J. A. VanAllan, *J. Org. Chem.*, **24**, 470 (1959).

7) T. Nakai and M. Okawara, *Tetrahedron Lett.*, **1967**, 3835.

explained by two successive simple S_N2 reactions, I→III→IV, but suggests that the dithiocarbamate function in III somewhat participates in the second substitution process, III→IV.

The Reaction of the Dithiolanylium Ion (V) with the Dithiocarbamate Anion (II). Winstein and co-workers have reported that the acetolysis of *trans*-2-acetoxycyclohexyl brosylate was about 630 times faster than that of the *cis*-isomer. This was interpreted by anchimeric assistance of the neighboring acetoxy group through the presumed acetoxonium ion.[8] Later the cation was isolated as the tetrafluoroborate *via* another route.[9] The dithiolanylium ion (V) isolated in the present work corresponds to the anchimeric acetoxonium ion. Thus, the reaction of the dithiolanylium perchlorate (Vb) with the dithiocarbamate anion was carried out first.

The perchlorate Vb was allowed to react with the dithiocarbamate salt (II) at 50°C in DMF to result in the quantitative formation of ethylene bis(dithiocarbamate) (IV). Possible mechanism for the formation of IV may be considered as follows:

Mechanism A

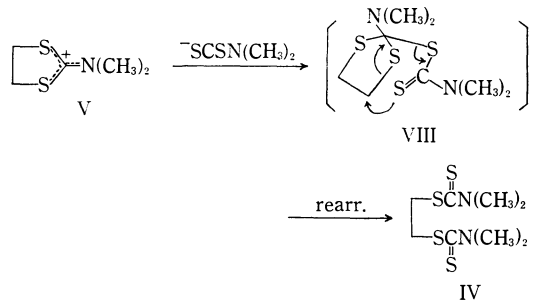

Mechanism B

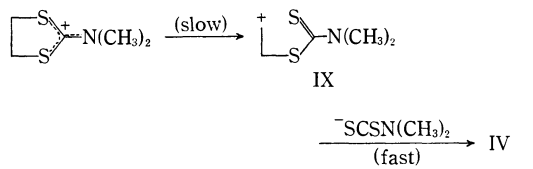

Mechanism C

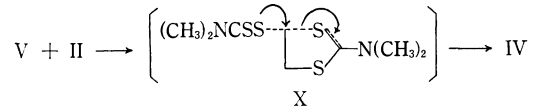

Mechanism A involves initial addition of the anion at the position of lowest electron density, *i. e.*, the centered carbon (sp^2) atom of V to afford the adduct VIII followed by rearrangement to the product IV. Mechanism B consists of initial conversion of the stabilized carbonium ion V into the unstable ion IX which rapidly reacts with the anion to give IV (S_N1 type), while mechanism C involves attack of the anion at the neutral carbon (sp^3) atom of the position 4 in V through the transition state X (S_N2 type).

Firstly mechanism A can be eliminated by our observation that the perchlorate Vc also reacts with mercaptides incapable of rearrangement to result in the formation of β-mercaptoethyl dithiocarbamates (XI).

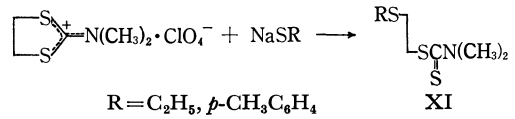

R=C_2H_5, *p*-$CH_3C_6H_4$ XI

Kinetic experiments indicate that the reaction of Vc with II fits in a second-order rate equation with respect to both reactants. The fact excludes mechanism B which should fit in a first-order rate equation. In conclusion, the dithiocarbamate anion attacks the C-4 atom to give IV through a concerted S_N2 type mechanism (mechanism C). The Arrehnius plots for the reaction in DMF is shown in Fig. 2. Activation parameters, $\Delta H^{\neq}$ and $\Delta S^{\neq}$, were 23.0 kcal/mol and +3.7 *e.u.*, respectively.

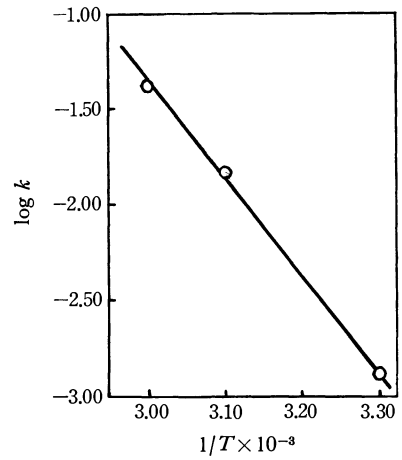

Fig. 2. The Arrehnius plot for the reaction of Vb with II in DMF.

Reaction Scheme. From results obtained, the formation of IV can be interpreted by the following scheme involving the intermediacy of the isolated anchimeric cation V.

Dichloride I reacts with II initially to give the monosubstituted III followed by rapid cyclization to the stable carbonium ion V. The carbonium ion further reacts with II to afford the disubstituted product (IV). The alternative formation of IV arising from the direct reaction of III with II not

8) For example, a) S. Winstein and R. E. Buckles, *J. Amer. Chem. Soc.*, **64**, 2780 (1942); b) S. Winstein, E. Grunwald and R. E. Buckles, *ibid.*, **70**, 816 (1948); c) S. Winstein, E. Grunwald and L. L. Ingraham, *ibid.*, **70**, 821 (1948).

9) C. B. Anderson, E. C. Friedrich and S. Winstein, *Tetrahedron Lett.*, **1963**, 2037.

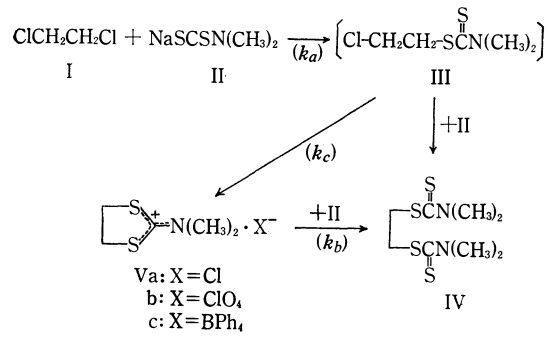

via Va might be neglected since the cyclization was rapid ($k_c \gg k_a$). In short, steps kinetically determining the product ratio are the process I→III (k_a) and Va→VI (k_b). It is expected that the rate of each product-determining process will be differently affected by the nature of the solvent used, and that the solvent effects on each process will be reflected in the product ratio.

The Neighboring-group Participation of the Dithiocarbamate Function. The rates (k_a) of the reaction I→III were obtained from those of reactions of *n*-butyl chloride with the dithiocarbamate ion. The rates (k_b) of the reaction Va (unisolatable)→IV were obtained from those for the reaction Vb→IV. The reactions were followed by determining the amount of the unreacted dithiocarbamate anion after given intervals. Kinetic experiments were carried out at 60°C in ethanol, DMF and dioxane, which represent dipolar protic dipolar aprotic and nonpolar aprotic solvent, respectively.

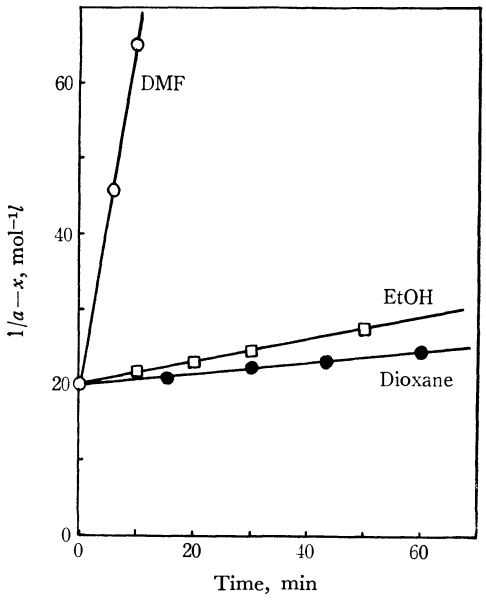

Fig. 3. The second-order rate plots for the reactions of *n*-butyl chloride with sodium *N,N*-dimethyldithiocarbamate:
The initial concn.=0.050 mol/*l*

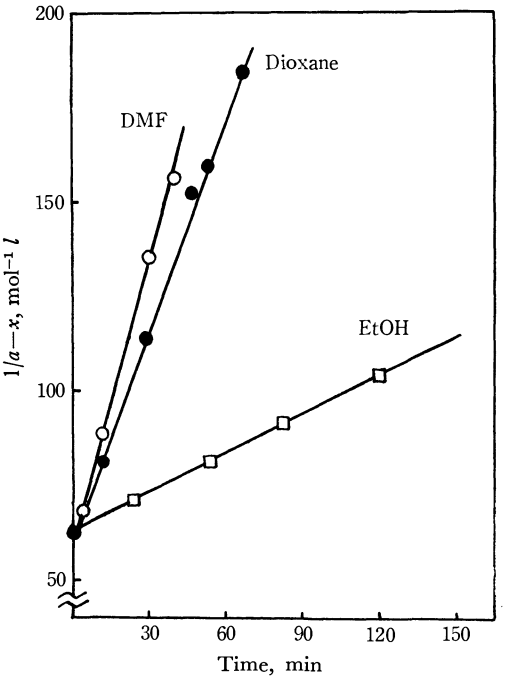

Fig. 4. The second-order rate plots for the reactions of Vb with sodium *N,N*-dimethyldithiocarbamate.
The initial concn.=0.0162 mol/*l*

Second-order rate plots for the equimolar reactions with II of *n*-butyl chloride and 2-dimethylamino-1,3-dithiolanylium perchlorate (Vb) in various solvents are shown in Figs. 3 and 4, respectively. Rate constants obtained for both reactions are summarized in Table 2.

Table 2. Rate constants for equimolar reaction with II of *n*-butyl chloride (k_a') and the perchlorate Vb (k_b') (60°C)

Solvent (Dielectric constant)	$10^3 k_a'$ (l mol^{-1}sec^{-1})	$10^3 k_b'$ (l mol^{-1}sec^{-1})	k_b'/k_a'	Product ratio* IV/V
EtOH (24.3)	0.4	7.34	18.4	0.092
DMF (36.7)	70.8	40.9	0.58	0.30
Dioxane (2.2)	0.3	34.0	113	1.32

* A more accurate product ratio for the equimolar reaction of I with II could be calculated from IV%/(100-IV%) in Table 1 as it is difficult to isolate Va quantitatively.

In conclusion, the rate of the first process (k'_a) was in the order: dioxane≈EtOH≪DMF, while that of the second (k'_b) was in the order: EtOH≪ dioxane<DMF. It is interesting to note that k'_a for DMF is very large, and that k'_b/k'_a for dioxane is significantly large, compared with those for EtOH and DMF. The unusual rate enhancement in DMF for the reaction of *n*-butyl chloride with II can be attributed to two major factors;

(i) the enhanced nucleophilicity of the dithiocarbamate anion with DMF, which is in agreement with many other observations for the S_N reactions in dipolar aprotic media[10] and (ii) the enhanced electrophilicity of the alkyl chloride due to the complex formation between the alkyl chloride and DMF molecules.[11] The rate enhancement in dioxane for the reaction of carbonium ion V with the anion can be explained by the consideration that the rate of the reaction between a cation and an anion increases with the decrease of the ionization power of the solvent since activation in such reaction requires partial neutralization of charge.[12]

Most important is the fact that in dioxane the second displacement reaction V→IV is about one hundred times faster than the first I→III, which might account for the more favorable formation of the disubstituted product (IV) in the equimolar reaction of I with II. This also led to the conclusion that participation of the neighboring dithiocarbamate function in III may be involved in the second substitution process III→IV, together with the solvent effect on the product ratio described above. In other words, dichloride I reacts with anion II to form the monosubstituted intermediate (III), which further reacts with II more readily to result in the favorable formation of the disubstituted product (IV) through the intermediacy of the isolated anchimeric cation V.

Neighboring-group participation*4 ($k'_b/k'_a>1$) was also observed in the reaction in ethanol, but less predominant than in dioxane. In DMF, the participation was not kinetically observed ($k'_b/k'_a<1$). Consequently IV may be also formed from the direct reaction of III with II not *via* V.

From the results, the relationship between rate data for each product-determining steps and the product ratio is summarized with respect to the nature of the solvent in Table 3.

Table 3. Rate data and the product ratio

Solvent	Rate of the process			Product ratio
	I→III		V→IV	IV/V
Dipolar protic	slow	<	slow	small
Dipolar aprotic	fast	>	fast	medium
Nonpolar aprotic	slow	≪	fast	large

In dipolar protic and aprotic solvents, rate difference between two kinetically product-determing steps was not so large. In nonpolar aprotic solvents, the rate difference is significantly large and consequently neighboring-group participation of the dithiocarbamate function is more predominant. This is reflected in the favorable formation of the disubstituted product (IV) in the equimolar reaction of I with II.

Such participation of the dithiocarbamate function can account for the observation that, in equimolar reactions of α,ω-dichloroalkanes with the dithiocarbamate anion (II) in ethanol, the yield of the corresponding alkylene bis(dithiocarbamate) increases in the order: 1,4-dichlorobutane>1, 3-dichloropropane>1, 2-dichloroethane, indicating that such participation increases in the same order.[13] This fact also suggests that the rate of reaction of the corresponding anchimeric carbonium ion with II increases in the same order, which has been verified.[14] Furthermore, kinetical evidence that neighboring-group participation of this function is involved in the polymer reaction of poly(vinyl chloride) with sodium *N,N*-diethyldithiocarbamate in DMF and THF has been obtained.[15]

Experimental*5

Equimolar Reactions of 1,2-Dichloroethane (I) with Sodium *N,N*-Dimethyldithiocarbamate (II) in Various Solvents. Into a solution of I (19.8 g, 0.20 mol) in 80 m*l* of the solvent was added a solution of sodium *N,N*-dimethyldithiocarbamate hydrate (II)*6

10) For reviews on the subject, see A. J. Parker, *Quart. Rev.* (London), **16**, 163 (1962); "Advances in Physical Organic Chemistry," Vol. 5, ed. by V. Gold, Academic Press Inc., New York (1967), p. 173.

11) a) S. Yoneda, I. Morishima, K. Fukui and Z. Yoshida, *Kogyo Kagaku Zasshi*, **68**, 1074 (1965); b) S. Yoneda, Z. Yoshida, I. Morishima and K. Fukui, *ibid.*, **68**, 1077 (1965).

12) E. S. Gould, "Mechanism and Structure in Organic Chemistry," Henry Holt Co., Inc., New York (1959), p. 259.

*4 Neighboring-group participation in the present work might be considered to be essentially the same as the "anchimeric assistance" proposed by Winstein[8] for solvolytic (S_N1) reactions. The phenomenon in which the cyclic compound is formed by participation of the neighboring group is called "anchimerism,"[13] and was used in a preliminary communication of this work.*1 However, this term is not appropriate for our present observation since it does not mean rate enhancement by a neighboring group.

13) a) F. L. Scott and D. F. Fenton, *Tetrahedron Lett.*, **1964**, 1681; b) F. L. Scott and E. Flynn, *ibid.*, **1964**, 1675.

14) T. Nakai, Y. Ueno and M. Okawara, Abstracts of papers presented at the 18th Symposium on Organic Reaction Mechanisms, Kyoto, October, 1967, p. 77.

15) T. Nakai, H. Kawaoka and M. Okawara, This Bulletin, **42**, 508 (1969).

*5 All melting and boiling points were uncorrected. Infrared and ultraviolet spectra were recorded on Hitachi infrared EPI-S2 and recording EPS-2 spectrophotometers, respectively. The NMR spectrum was obtained with a Varian Associates Model A-60 spectrometer in a dimethylsulfoxide-d_6 solution using tetramethylsilane as an internal standard.

*6 The dithiocarbamate salt contains two molecules of the coordinated water: T. Nakai and M. Okawara, This Bulletin, **41**, 707 (1968).

(36.0 g, 0.20 mol) in 120 ml of the solvent. The reaction mixture was stirred at 60°C for 6 hr in nitrogen atmosphere. Sodium chloride formed was filtered off and the filtrate was concentrated in reduced pressure. The mixture was poured into 300 ml of cold water to give a white precipitate, ethylene bis(*N,N*-dimethyldithiocarbamate) (IV), which was filtered, dried *in vacuo* and weighed; mp 187—189°C (lit,[16] 189°C); IR (KBr): $\nu_{C=N(thiourelde)}$[17] 1495 cm^{-1}; UV: λ_{max}^{EtOH} 250, 277 mμ.

A portion of the filtrate was treated with an excess of an aqueous solution of nickel chloride to produce no precipitate of the nickel salt, indicating that the dithiocarbamate anion completely disappeared during reaction. The filtrate was extracted with ether. A given volume of the aqueous layer was treated with an excess of an aqueous solution of sodium perchlorate to give a white precipitate, 2-dimethylamino-1,3-dithiolanylium perchlorate (Vb), which was then filtered, dried *in vacuo* and weighed; mp 179—181°C (recrystalized from acetone); UV: $\lambda_{max}^{H_2O}$ 249 mμ (ε=13000). The NMR spectrum shows two singlet signals at δ 4.08(2H) and 3.62 ppm (3H) (Fig. 1).

Found: C, 24.48; H, 4.18; N, 5.58%. Calcd for $C_5H_{10}ClNO_4S_2$: C, 24.24; H, 4.08; N, 5.66%.

A given volume of the aqueous layer was treated with an excess of an aqueous solution of sodium tetraphenylborate to afford a white precipitate, the dithiolanylium tetraphenylborate (Vc), which was filtered, dried *in vacuo* and then weighed; mp 134—136°C (recrystallized from acetonitrile).

Found: C, 74.81; H, 6.50; N, 3.22%. Calcd for $C_{29}H_{40}BNS_2$: C, 74.51; H, 6.47; N, 3.00%.

Authentic 2-dimethylamino-1,3-dithiolanylium salts were prepared by treating β-hydroxyethyl *N,N*-dimethyldithiocarbamate with *p*-toluenesulfonyl chloride in DMF[6] followed by sodium perchlorate or sodium tetraphenylborate.

The ethereal layer was dried over anhydrous sodium sulfate and the solvent was removed *in vacuo* to give a small amount of yellow oily residue. The infrared spectrum (liq. film) showed a strong absorption band at 1650 cm^{-1} due to -S-CO-N<. In the case of the reaction in ethanol, the oily residue was distilled in the reduced pressure to give ethyl *N,N*-dimethylthioncarbamate (VI) and β-mercaptoethyl *N,N*-dimethylthiolcarbamate (VII) in 5.5% and 3.9% yield, respectively. Physical properties of product VI are as follows: bp 81—82°C/10 mmHg (lit,[18] 82.6°C/10 mmHg); $n_D^{25°C}$ 1.5082 (lit,[19] $n_D^{20°C}$ 1.5075); UV: λ_{max}^{EtOH} 250.5, 285 mμ (lit,[20] 250.5, 285 mμ). Thioncarbamate (VI) was transformed with ethyl bromide into thiolcarbamate,[21] which was identified by means of spectral and physical data with the authentic compound. The physical data for thiolcarbamate (VII) are as follows: bp 112—117°C/4 mmHg; $n_D^{25°C}$ 1.5840; IR (neat): 1650, 1495 cm^{-1} (-S-CO-N<). The product was treated with a mercuric chloride solution to give a precipitate of the mercury mercaptide: mp 122—128°C; IR (KBr): $\nu_{C=O}$ 1635 cm^{-1}, and was oxidized to disulfide: mp 83—84°C (recrystallized from cyclohexane); IR (KBr): $\nu_{C=O}$ 1640 cm^{-1}.

Found: N, 8.10%. Calcd for $C_{10}H_{20}N_2O_4S_4$: N, 8.54%.

Product compositions obtained from the equimolar reactions in various solvents are shown in Table 1.

Reaction of 2-Dimethylamino-1,3-dithiolanylium Perchlorate (Vb) with Sodium *N,N*-Dimethyldithiocarbamate (II). A mixture of 2.5 g (0.01 mol) of perchlorate and 2.0 g (0.01 mol) of sodium salt in 20 ml of DMF was stirred at 60°C for 4 hr. The mixture was poured into a large amount of cold water to produce 2.6 g (98%) of a white precipitate: mp 187—189°C (recrystallized from DMF). The precipitate showed no depression upon a mixed mp determination with the authentic ethylene bis(*N,N*-dimethyldithiocarbamate) (IV), and its infrared spectrum was in complete agreement with that of the authentic sample.

Kinetic Runs. The rates of both reactions of *n*-butyl chloride and 2-dimethylamino-1,3-dithiolanylium perchlorate (Vb) with sodium *N,N*-dimethyldithiocarbamate were followed by measuring quantities of the unreacted dithiocarbamate anion after given intervals. The dithiocarbamate anion was gravimetrically determined from the quantity of the nickel chelate precipitated by treating an aqueous layer of the sample with an excess of an aqueous solution of nickel chloride. An exampe of the calibration curve is shown in Fig. 5. All reactions were carried out at 60°C under equimolar conditions.

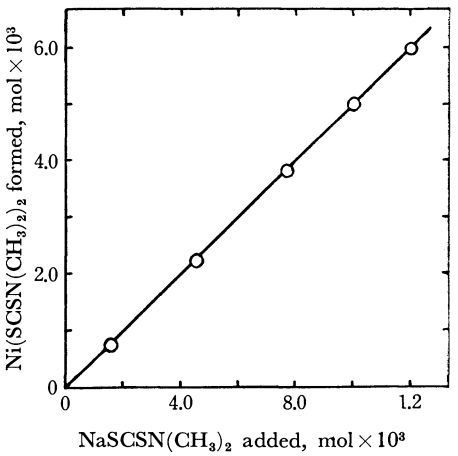

Fig. 5. The calibration curve for the determination of the dithiocarbamate anion.

Table 4. Reactions of *n*-butyl chloride with II in ethanol

Time, min	Ni-saklt formed, g	$1/a-x$, $mol^{-1}l$
10	0.2755	21.7
20	0.2717	22.0
30	0.2608	22.9
50	0.2630	22.7

16) A. W. Campbell and P. F. Tryan, *Ind. Eng. Chem.*, **45**, 125 (1953).

17) H. M. Randall, R. G. Fowler, N. Fuson and J. Dangl, "Infra-red Determination of Organic Structure," Van Nostrand, New York (1949).

18) O. Biffeter, *Ber.*, **43**, 1853 (1910).

19) B. Holmberg, *Svensk. Kem. Tids.*, **41**, 249 (1929).

20) M. J. Janssen, *Rec. Trav. Chim. Pays-Bas*, **79**, 454, 464 (1960).

21) A. F. Schöberl and A. Wagner, "Houben-Wyle: Methoden der Organischen Chemie," Vol. IX, George Thieme Verlag, Stuttgart (1955), p. 837.

Initial concentrations for reactions of *n*-butyl chloride and the dithiolanylium perchlorate were 0.050 and 0.016 mol/*l*, respectively.

n-Butyl chloride (0.5785 g) was dissolved in a solution of 1.1650 g of sodium *N,N*-dimethyldithiocarbamate in 125 m*l* of the solvent placed in a constant-temperature bath at 60±0.2°C. At various intervals a 25.0-m*l* aliquot of the yellow solution was removed and poured into cold water (*ca.* 50 m*l*). The sample solution was immediately extracted with ether, then the aqueous solution was treated with an excess of an aqueous solution of nickel chloride giving green precipitates of nickel chelate. The nickel chelate was collected in a glass filter which had been weighed. The glass filter was dried *in vacuo*. An example of results is given in Table 4. All plots of $1/a-x$ against time showed straight lines (Fig. 3).

2-Dimethylamino-1,3-dithiolanylium perchlorate (Vb) (1.000 g) was dissolved in a solution of 0.725 g of sodium *N,N*-dimethyldithiocarbamate in 150 m*l* of the solvent. At various intervals a 50.0-m*l* aliquot was removed and poured into cold water (*ca.* 100 m*l*) giving white precipitates of ethylene bis(*N,N*-dimethyldithiocarbamate) (IV). The precipitates were filtered off and the aqueous layer was treated with an excess of an aqueous solution of nickel chloride giving green precipitates of the nickel chelate. The quantity of the nickel chelate was measured as in the case of the reaction of *n*-butyl chloride with II. An example of results is shown in Table 5. All plots of $1/a-x$ against time showed straight lines (Fig. 4).

Table 5. Reactions of Vb with II in DMF

Time, min	Ni-salt formed, g	$1/a-x$, $mol^{-1}l$
5	0.1135	66.4
12	0.0840	88.9
30	0.0550	136
40	0.0445	157

BULLETIN OF THE CHEMICAL SOCIETY OF JAPAN VOL. 43 162—167 (1970)

2-Substituted Imino-1,3-dithiolanes. Their Thermal Ring-isomerizations and Reactions with Epoxides*1

Yoshio UENO, Takeshi NAKAI and Makoto OKAWARA

Research Laboratory of Resources Utilization, Tokyo Institute of Technology, Ookayama, Meguro-ku, Tokyo

(Received June 10, 1969)

Thermal ring-isomerization and reactions with epoxides of 2-substituted imino-1,3-dithiolanes (I) were studied. The methylimino (Ia) and ethylimino derivatives (Ib) were found to be ring-isomerized to the corresponding 3-alkyl-1,3-thiazolidine-2-thione (V) at about 200°C, while the phenylimino compound (Ic) was not isomerized even under more drastic conditions. The influence of various additives including Lewis acids was also examined. In contrast to the oxygen analog of I, these imino compounds were not polymerized with Lewis acids, and catalysis of any additives on isomerization was not observed. The possibility that I thermally dissociated into methyl isothiocyanate and ethylene sulfide followed by their recombination to V would be excluded by the observation that the reaction of alkyl isothiocyanate with ethylene sulfide at 150°C afforded I in good yield. Reactions of I with epoxides were carried out regarding the isomerization mechanism. All these imino compounds reacted with epoxides to give the 2-oxazolidone derivatives (III) in good yield. Mechanisms of the ring-isomerization and formation of III have been suggested, and the difference in reactivity between I and its oxygen analog has been discussed.

In a previous paper[1] we reported that 1,2-dichloroethane reacted with sodium *N,N*-dialkyldithiocarbamate to result in the formation of 2-dialkylamino-1,3-dithiolanylium ions involving participation of the dithiocarbamate function as an internal nucleophile. In a similar way, 2-alkylimino-1,3-dithiolanes were obained by the reaction of 1,2-dichloroethane with sodium *N*-monoalkyldithiocarbamate in the presence of base. We were prompted to investigate the reactivities of 2-substituted imino-1,3-dithiolanes (I) in view of the following. (1) On the addition of acid catalysts (A) such as Lewis acids, the imino compounds are expected to form complex II, the structure of which resembles that of dithiolanylium ion III. The type of carbonium ions have been demonstrated to be the interesting reactive species.[2]

*1 Presented at the 21st Annual Meeting of the Chemical Society of Japan, Osaka, April, 1968.

1) T. Nakai, Y. Ueno and M. Okawara, *Tetrahedron Lett.*, **1967**, 3831; This Bulletin, **43**, 156 (1970).

2) T. Nakai and M. Okawara, *Tetrahedron Lett.*, **1967**, 3835.

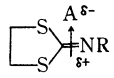

II

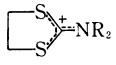

III

(2) Ring-isomerization[3] and ring-opening polymerization[4] of the oxygen analogs of I, *i. e.*, 2-substituted imino-1,3-dioxolanes (IV), have been reported. However, no information has been available on the imino-dithiolanes. Burkhardt has suggested that 2-benzoylimino-1,3-dithiolane considerably resists ring-isomerization as compared with oxygen analog.[5]

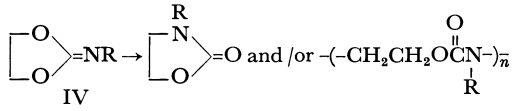

IV

In the present work we studied the possibility of ring-isomerization or ring-opening polymerization of imino-dithiolanes (I) and their reactions with epoxides.

Results

Preparation of Imino-dithiolanes (I). 2-Methylimino- (Ia) and 2-ethylimino-1,3-dithiolane (Ib) were obtained in yields of 67 and 26%, respectively, by the reaction of 1,2-dichloroethane with the corresponding sodium *N*-alkyldithiocarbamate at 60°C in the presence of potassium carbonate. 2-Phenylimino-1,3-dithiolane (Ic) was obtained in 73% yield by the reaction of 2-dimethylamino-1,3-dithiolanylium perchlorate with aniline.[2]

The infrared spectra of these imino compounds showed a strong absorption band around 1600 cm^{-1} due to the C=N group (Fig. 1). The NMR spectrum of Ia displayed a three-proton signlet at δ3.10 (*N*-methyl) and a four-proton multiplet in the region of 3.20—3.70 ppm (ring-methylene). (Fig. 2a). It is of interest that the ring-methylene protons of Ic appeared at 3.32 ppm as a singlet form.

Thermal Ring-isomerization. Ring-isomerization of these imino-dithiolanes was undertaken by heating in a sealed tube in the presence or absence of an additives listed in Table 1. Among additives employed, $AlCl_3$, BF_3OEt_2, H_3PO_4 and $FeCl_3$ have been reported to be effective as catalysts for the ring-isomerization or the ring-opening polymerization of the oxygen-analogs IV.[3,4] It was found that Ia was ring-isomerized above 200°C into 3-methyl-1,3-thiazolidine-2-thione (Va) in 48% yield in the absence of an additive. The results are summarized in Table 1. Results indicate that any additives used neither increase the yield of Va nor lower the isomerization temperature. Ring-opening polymerization was not observed. These observations are in direct contrast to those of oxygen analogs IV. The infrared spectrum of the isomerized product Va showed no absorption band at 1600 cm^{-1} and a new band at 1500 cm^{-1} due to the –S–CS–N< structure (Fig. 1). The NMR spectrum of Va confirmed the structure (Fig. 2b).

Table 1. Thermal ring-isomerization of 2-methylimimino-1,3-dithiolane (Ia) into 3-methyl-1,3-thiazolididine-2-thione (Va) in the presence of various additives

Reaction temp.: 200°C; time: 3 hr

Additive	Yield ,%
None	48
$AlCl_3$	47
$AlCl_3$*	0
BF_3OEt_2	41
H_3PO_4	46
H_2SO_4	23
$FeCl_3$	23
LiCl**	56
NEt_3	15

* 170—180°C; 60 min
** 230—240°C; 7 min

Similarly, the ethylimino derivative Ib was ring-isomerized to 3-ethyl thiazolidine-2-thione (Vb) in 66% yield in the absence of an additive. The structure was confirmed by elemental analysis

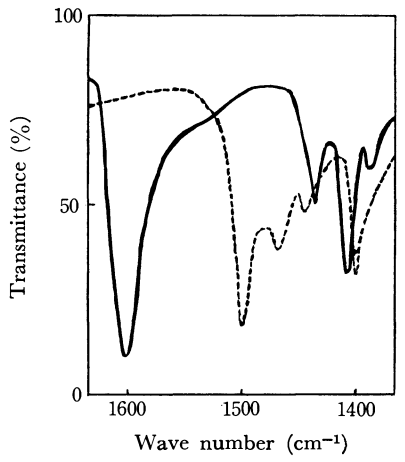

Fig. 1. The IR spectra.
——: 2-methylimino-1,3-dithiolane (Ia) (neat).
------: 3-methyl-1,3-thiazolidine-2-thione (Va) (KBr)

3) K. Gulbis, M. Roth and N. Hamann, *Angew. Chem.*, **73**, 434 (1961).

4) T. Mukaiyama, T. Fujisawa, H. Nohira and T. Hyugji, *J. Org. Chem.*, **27**, 3337 (1962); T. Fujisawa, Y. Tamura, and T. Mukaiyama, This Bulletin, **37**, 797 (1964).

5) J. Burkhardt, R. Feinauer, K. Gulbis and K. Hamann, *Chem. Ber.*, **99**, 1912 (1966).

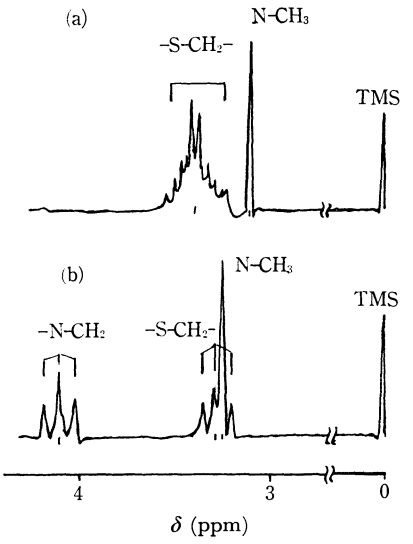

Fig. 2. The NMR spectra.
(a): 2-methylimino-1,3-dithiolane (Ia) (CCl_4)
(b): 3-methyf-1,3-thiazolidine-2-thione (Va) (CCl_4+$CDCl_3$)

and spectroscopic methods.

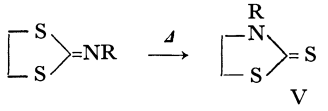

Ia: R=CH_3
b: R=C_2H_5

The phenylimino derivative (Ic), however, did not ring-isomerize and only the starting material was recovered almost quantitatively after heating at 200 or 250°C.

Reactions of Isothiocyanates with Ethylene Sulfide. Isolation of a small amount of methyl isothiocyanate during the distillation of Ia suggests that Ia may thermally dissociate into the isothiocyanante and ethylene sulfide. In order to examine the possibility that V might be formed through recombination of these dissociated fragments, the reaction of isothiocyanate with ethylene sulfide were carried out in the presence of triethylamine at 120—140°C in a sealed tube. Methyl isothiocyanate reacted with ethylene sulfide to give Ia (not Va) in 40% yield. When the reaction temperature was raised to 200—220°C, Va was formed probably *via* the ring-isomerization of Ia formed. Similarly phenyl isothiocyanate afforded Ic in 83% yield.

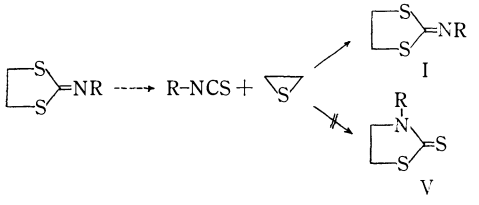

These observations indicate that the isomerized product V is not formed directly from the isothiocyanate and ethylene sulfide.

This fact is in agreement with the observation that isocyanate reacts with epoxides to give 2-imino-1,3-dioxolanes (IV), in some instances followed by the subsequent ring-isomerization to the 2-oxazolidones.[6]

Reactions of the Imino-dithiolanes with Epoxides. Recently Russian chemists have reported that the 2-phenylimino-1,3-dithiolane (Ic) reacted with epoxides at 80—90°C to afford the 2-oxazolidone derivatives (VI),[7] the details of which have not been accessible. The fact that the phenylimino derivative, which did not ring-isomerize, reacted with epoxides under the mild condition leads us to a further study on the reaction of other imino-dithiolanes with epoxides.

2-Methylimino-1,3-dithiolane (Ia) reacted with propylene oxide and epichlorohydrin at 90°C in the presence of triethylamine to produce 5-methyl- (VIa) and 5-chloromethyl-2-oxazolidone (VIb), respectively, in yields of 64% and 67%. The structure of product VI was determined by elemental analysis and spectral data (IR and NMR). The infrared spectra of VIa and VIb showed the characteristic band of the oxazolidone-carbonyl group at

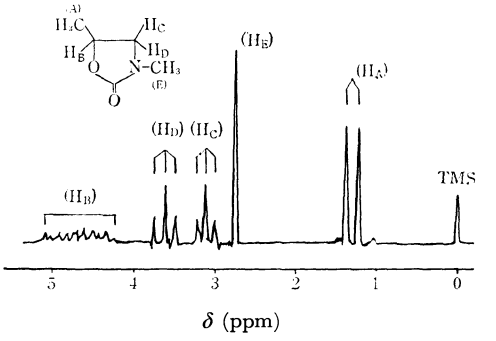

Fig. 3. The NMR spectrum of 3,5-dimethyl-2-oxazolidone (CCl_4).

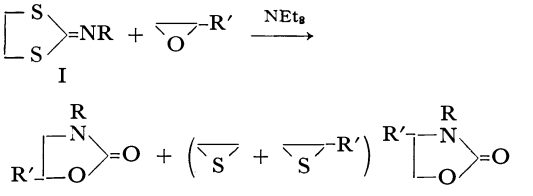

VIa: R=CH_3; R′=CH_3
b: R=CH_3; R′=CH_2Cl
c: R=C_6H_5; R′=H

6) K. Gulbis, G. Benzig, R. Maysenholder and K. Hamann, *Chem. Ber.*, **93**, 1975 (1960).
7) V. S. Etilis, A. P. Sineokov and G. A. Razuvaev, *Zh. Obshch. Kim.*, **34**, 4018 (1964); *Chem. Abstr.*, **62**, 9132 (1965).

1700 cm^{-1}. The NMR spectrum of VIa completely supports the oxazolidone structure (Fig. 3). The possibility of structure VII could be eliminated based upon the results of systematic NMR studies of oxazolidone derivatives.[8]

Discussion

On the Mechanism of Ring-isomerization. Experimental results described above of the ring-isomerization of the imino-dithiolanes (I) are summarized as follows, comparing them with oxygen analogs IV;

(1) 2-Alkylimino-1,3-dithiolanes were ring-isomerized to the thiazolidine-2-thione (V) under a severer condition than that for the oxygen analogs.

(2) Both the phenylimino- and the benzoylimino-dithiolane failed to be ring-isomerized, whereas their oxygen analogs with the same substituents isomerized more readily at lower temperatures.

(3) Acid additives were ineffective or they resulted in lower yields of the isomerized products. This is significantly different from the case of the oxygen analogs.

(4) In all cases, polymeric materials were not obtained with any Lewis acids. This fact is in direct contrast with that of the oxygen analogs.

These fact substantially exclude the following mechanism involving carbonium ion VIII which has been accepted for both the ring-isomerization[3] and the ring-opening polymerization[4] of the oxygen analogs.

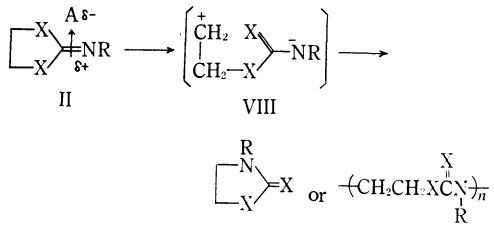

II VIII

Thus we propose another possible mechanism for the ring-isomerization concerned, which involves concerted attack of the nonbonded electron pair of the nitrogen atom on the carbon atom of the ring-methylene through the S_N-2-like transition state.

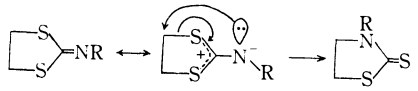

I I′ V

Structure I′ is more favorable than that of the ordinary imino compounds since the positive charge is more stabilized by the electron-donating character of the sulfur atoms. This fact is in agreement with the observation that 2-dialkylamino-1,3-dithiolanylium ions are considerably stable.[2] Although this unimolecular mechanism is sterically unfavorable and has not been completely established, this may explain the four experimental results described above. The electron density on the nitrogen atom is lowered either by the complex formation between the acidic additive and the imino compound (see (3)) or by electron delocalization to the other part of the molecule for 2-phenylimino-1,3-dithiolane (Ic) and the benzoylimino derivative shown below (see (2)).

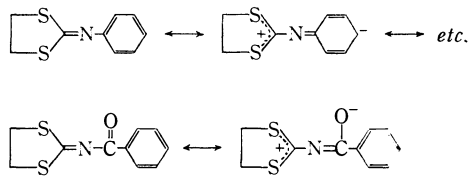

In conclusion, the difference in mechanism for ring-isomerization between the imino-dithiolanes and the imino-dioxolanes might be ascribed to the difference in stability between carbonium-ion like species IX and X. It has been accepted that the carbon-oxygen bonds in dialkoxycarbonium ions cleave more readily into the alkyl cation and the ester than the carbon-sulfur bonds in dialkoxythiocarbonium ions.[9]

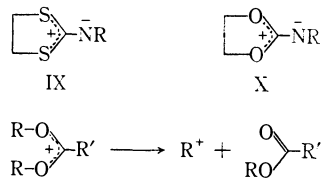

IX X

This fact may be supported by the observation that the thioncarbamate XI reacts readily with alkyl halides to form triheterosubstituted carbonium ion XII followed by exclusive transformation into thiolcarbamate XIII.[9]

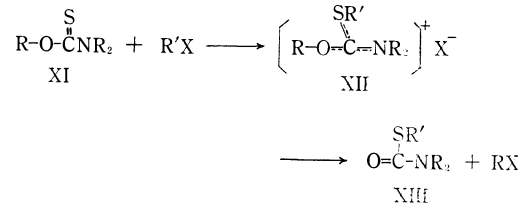

XI XII XIII

On the Mechanism for the Formation of 2-Oxazolidone Derivatives from Imino-dithiolanes and Epoxides. There are two possible mechanisms for the formation of the 2-oxazolidone

8) J. E. Herweh, T. A. Fogjia and D. Swern, *J. Org. Chem.*, **33**, 4029 (1968).

9) A. F. Schoberl and A. Waguer, "Houben-Wyle: Methoden der Organishen Chemie," Vol IX, George Thieme Verlag, Stuttgart (1955), p. 837.

derivative in the reaction of imino-dithiolane with epoxide.

Firstly scheme A involves initial thermal dissociation of I into isothiocyanate and episulfide followed by a known subsequent reaction of isothiocyanate with epoxide giving 2-imino-oxothiolane. The imino-oxothiolane formed dissociates into isocyanate and episulfide followed by the reaction of isocyanate with epoxide to afford 2-imino-dioxolane, which, in turn, ring-isomerizes leading to the formation of VI.

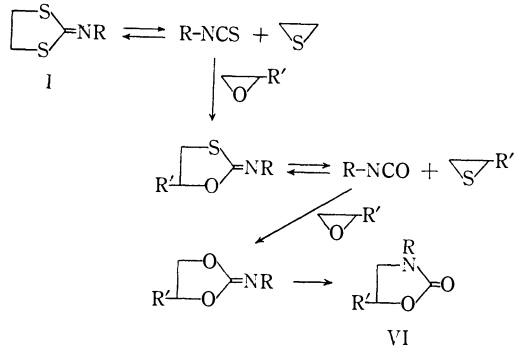

Scheme A

However, it is doubtful whether the dissociation of imino-dithiolane occurs at low temperatures such as 90°C. The fact that the formation of thioureas was not observed on treatment of Ia in the presence of excess aniline at 150°C, considerably reduces the possibility of occurrence.

The other mechanism, Scheme B, involves initial cycloaddition of epoxide to imino compound (I) followed by elimination of episulfide from the resulting spirocyclic compound (XIV), and then by further cycloaddition of epoxide to the thiocarbonyl group in oxazolidine-2-thione (XV) formed to yield another spirocyclic compound XVI. This, in turn, eliminates episulfide leading to the formation of VI.

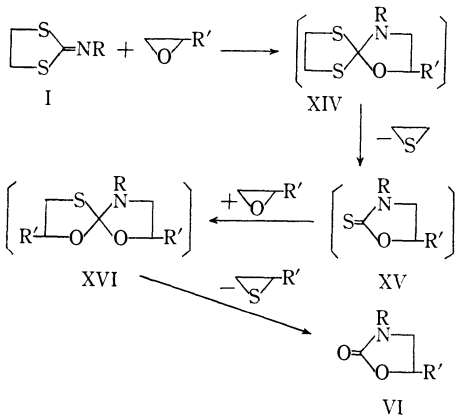

Scheme B

In support of the processes, I to XIV and XIV to XV, the following examples have been reported by Feinauer;[10] thia(or oxa)zolines (XVII) reacts with epoxide to yield the bicyclic compound XVIII *via* cycloaddition of epoxide to the *endo* C=N group, and in the case of X=S, loss of episulfide is followed leading to the formation of 2-oxazoline (XIX).

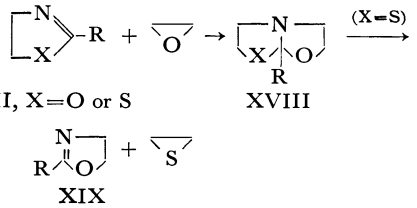

Little information on the reaction of the thiocarbonyl group with epoxides has been available in literature. In order to demonstrate the process XV→XVI→VI, we carried out the reaction of various thiocarbonyl compounds including oxazolidine-2-thione (XV) with epoxides. It was found that the thiocarbonyl group was readily converted to the corresponding carbonyl group in good yields presumably *via* spirocyclic adduct XXI as shown below. A detailed report on this type of reaction will be presented in a subsequent paper.[11]

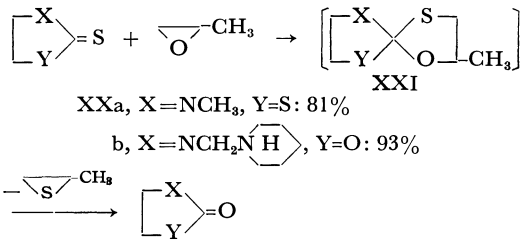

We assume that the mechanism given in Scheme B is considered more likely for the reaction of imino-dithiolanes with epoxides.

Experimental

General. All melting and boiling points are uncorrected. The IR spectra were recorded with a Hitachi EPI-S2 spectrometer. The NMR spectra were determined with a Japan Electron Optics C-100 spectrometer. Chemical shifts are reported in parts per million (ppm) from tetramethylsilane as an internal standard.

Materials. Sodium *N*-monoalkyldithiocarbamates were prepared by the reaction of the aqueous solution of alkylamine with carbon disulfide in the presence of sodium hydroxide. 2-Dimethylamino-1,3-dithiolanylium perchlorate was obtained by a method reported.[1] Methyl isothiocyanate and ethylene sulfide were prepared by standard methods. Other reagents and solvents were commercial products and used after purification by standard methods.

2-Methylimino-1,3-dithiolane (Ia). To a suspension

10) R. Feinauer, *Angew. Chem. Int. Ed. Engl.*, **5**, 894 (1964).

11) Y. Ueno, T. Nakai and M. Okawara, This Bulletin, **43**, 168 (1970).

of sodium methyldithiocarbamate (25.8 g, 0.20 mol) in absolute ethanol (200 ml), 1,2-dichloroethane (50 g, 0.50 mol) was added, and the mixture was then heated at 60°C for 1 hr. After cooling, a suspension of anhydrous potassium carbonate (27.6 g, 0.20 mol) in absolute ethanol (50 ml) was added, the reaction mixture was stirred at 60°C for further 4.5 hr, and the mixture was cooled followed by extraction with ether. The ethereal solution was dried over anhydrous sodium sulfate and the solvent was removed in reduced pressure. The residue was distilled giving a yellowish liquid (9.2 g, 35%); bp 79—81°C/0.45 mmHg; n_D (22°C) 1.6032. The IR and NMR spectra of Ia are given in Figs. 1 and 2a, respectively.

Found: C, 36.06; H, 5.30; N, 10.51%. Calcd for $C_4H_7NS_2$: C, 35.64; H, 5.39; N, 10.23%.

A higher boiling-point distillate obtained as a by-product was separated into 3-methylthiazolidine-2-thione (Va) and ethylene trithiocarbonate on column chromatography of active alumina.

The methylimino compound was also prepared by another method starting from methylamine and carbon disulfide. To a solution of carbon disulfide in ethanol, aq. methylamine solution was added drop by drop with vigorous stirring and cooling in an ice bath, where the temperature was kept below 30°C. The resulting clear orange-colored solution was added to 1,2-dichloroethane, and the mixture was stirred at 60°C for 1 hr. The yellowish solution was treated with concd. hydrochloric acid and the organic impurities were extracted with ether. An aqueous solution of potassium carbonate was added to neutralize the aqueous layer, and extracted with ether. The ethereal solution was dried over anhydrous sodium sulfate and the solvent evaporated. Work-up gave the imino compound (Ia) in 67% yield.

2-Ethylimino-1,3-dithiolane (Ib) was prepared in 26% yield as in the case of Ia; bp 85—87°C/0.30 mmHg; n_D (27°C) 1.5839; IR (neat): 1595 cm^{-1} (C=N).

Found: C, 40.19; H, 6.09; N, 9.34%. Calcd for $C_5H_9NS_2$: C, 40.81; H, 6.17; N, 9.52%.

2-Phenylimino-1,3-dithiolane (Ic) was prepared by the reaction of 2-dimethylamino-1,3-dithiolanylium perchlorate with aniline in 73% yield according to the procedure reported;[2] mp 47—48°C (lit,[2] 47—48°C); IR (KBr disk): 1570 cm^{-1} (C=N); NMR (CCl_4): δ 3.32 (s, CH_2S), 6.55—7.10 ppm (m, aromatic protons).

Ring-isomerization of Imino-dithiolane (I). Many attempts to isomerize Ia were made under various conditions as shown in Table 1. In the presence of aluminum chloride, imino-dithiolane Ia (1.3 g, 0.01 mol) and a small amount (*ca.* 0.1 g) of aluminum chloride were sealed in a tube. The tube was heated at 200°C for 3 hr in an oil-bath. After cooling, the tube was carefully opened and the reaction mixture was extracted several times with ether. The ethereal solution was evaporated *in vacuo*. Recrystallization of the residue from ether yielded 0.61 g (47%) of 3-methylthiazolidine-2-thione (Va); mp 68—69°C (lit,[12] 68—69°C); UV: λ_{max} (H_2O) 265 mμ (lit,[13] 265 mμ). The IR and NMR spectra of Va are given in Figs. 1 and 2b, respectively.

Found: C, 36.06; H, 5.30; N, 10.51%. Calcd for $C_4H_7NS_2$: C, 36.15; H, 5.31; N, 10.65%.

As in the case of Ia imino compound Ib was isomerized to 3-ethylthiazolidine-2-thione (Vb) in 67% yield in the absence of any additive; bp 155—157°C/2.5 mmHg; n_D (22°C) 1.625.

Found: C, 40.84; H, 6.34%. Calcd for $C_5H_9NS_2$: C, 40.81; H, 6.17%.

Ring-isomerization of Ic failed both under same conditions and at higher temperature (250°C), and only the starting material (Ic) was recovered.

Reactions of Isothiocyanates with Ethylene Sulfide. Methyl isothiocyanate (4.0 g, 0.055 mol), ethylene sulfide (3.0 g, 0.030 mol), and triethylamine (3.0 g, 0.03 mol) were heated in a sealed tube at 120—140°C for 3 hr. After cooling the tube was carefully opened. Distillation of the resulting mixture in the reduced pressure gave 2.7 g (41%) of 2-methylimino 1,3-dithiolane (Ia). The IR spectrum, the boiling point and the refractive index of this distillate were identical with those of the authentic sample.

In a similar fashion the reaction of phenyl isothiocyanate with ethylene sulfide gave 2-phenylimino-1,3-dithiolane (Ic) in 83% yield.

Reaction of Imino-dithiolane Ia with Epoxides. Imino-dithiolane Ia (2.0 g, 0.015 mol), propylene oxide (2.0 g, 0.034 mol) and triethylamine (0.1 g) were sealed in a tube. The tube was heated at 140—150°C for 7 hr in an oil-bath. After cooling the tube was carefully opened. Distillation of the reaction mixture gave 3,5-dimethyl-2-oxazolidone (VIa) in 64% yield: bp 90—95°C/1 mmHg (lit,[14] 92°C/1.5 mmHg); IR (neat): 1700 cm^{-1} (C=O).

The reaction of Ia with epichlorohydrin was carried out at 90°C for 27 hr as in the case of propylene oxide, to give 3-methyl-5-chloromethyl-2-oxazolidone (VIb) in 67% yield; bp 94—96°C/0.3 mmHg; IR (neat): 1700 cm^{-1} (C=O).

Found: N, 9.36%. Calcd for $C_5H_8ClNO_2$: N, 9.14%.

12) J. W. Batty, *J. Chem. Soc.*, **1949**, 786.
13) J. L. Grardway, *ibid.*, **1966**, 92.
14) A. B. Steele, U. S. 28668801 (1959).

BULLETIN OF THE CHEMICAL SOCIETY OF JAPAN VOL. 43 168—172 (1970)

Reactions of Various Thione-compounds with Epoxides. A New Method for the Transformation of the C=S Bond into the C=O*1

Yoshio UENO, Takeshi NAKAI and Makoto OKAWARA

Research Laboratory of Resources Utilization, Tokyo Institute of Technology, Ookayama, Meguro-ku, Tokyo

(Received June 10, 1969)

The reactions of propylene oxide (PO) with various thione-compounds containing two α-hetero atoms including dithiocarbamates, thioncarbamates, trithiocarbonates and thioureas, and their cyclic analogs were studied in the presence of triethylamine or boron trifluoride etherate as a catalyst. It was found that most of these thione-compounds reacted with PO at 170—180°C to afford the corresponding one-compounds in good yields. This type of reaction may provide a new method for the transformation of the C=S bonds in thione-compounds into the C=O bonds. Boron trifluoride etherate appeared to be more effective than triethylamine as the catalyst. The mechanism which involves initial cycloaddition of PO to the C=S bond followed by elimination of propylene sulfide was proposed for the transformation. The reactivities of these thione-compounds were significantly affected by whether they are cyclic or open-chain and by the nature of the α-hetero atoms: the cyclic thione-compounds were more reactive then the open-chain analogs except for a pair of thioureas and the enhancement by the α-hetero atoms was in the order: N,O≈N,N>N,S>S,S. Both observations may be interpreted in terms of basicity of the thione-compounds. These results also support the proposed mechanism for the formation of 2-oxazolidones from 2-substituted imino-1,3-dithiolanes with epoxides in our preceding paper.

In the preceding paper[1] we have reported that 2-substituted imino-1,3-dithiolane (I) reacted with epoxides giving the oxazolidone derivatives (II). The mechanism for the formation of II has been assumed to involve the cycloaddition of epoxide to the C=S bond of the intermediate 1,3-oxazolidine-2-thione (III) followed by elimination of episulfide, as illustrated below.

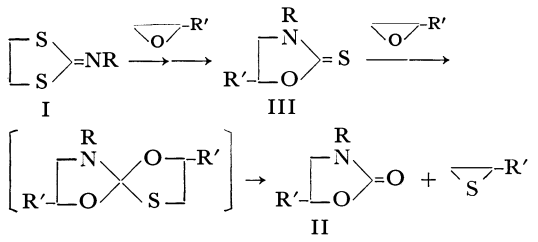

The transformation, however, of the thione-compound into the one-compound with epoxide is not found in literature. The purpose of the present study is to ascertain the proposed mechanism for the formation of II and to extend this type of reaction to a method for the transformation of the C=S bonds in various thione-compounds into the C=O bonds. Thus, the reactions of a variety of thione-compounds including the oxazolidine-2-thione (III) with epoxides were studied. This paper describes a new method for the transformation of the C=S bond in the thione-compound into the C=O bond and clarifies the scope and limitation of this method.

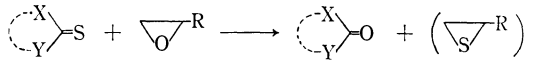

Results

We investigated open-chain and cyclic thione-compounds containing two α-hetero atoms including *S*-methyl *N*,*N*-dimethyldithiocarbamate (IV) and a cyclic analog, *N*-methyl-1,3-thiazolidine-2-thione (V) [X, Y = N and S], *O*-methyl *N*,*N*-dimethylthioncarbamate (VI) and a cyclic analog, *N*-piperidinomethyl-1,3-oxazolidine-2-thione (VII) [X, Y=N and O], dimethyl trithiocarbonate (VIII) and a cyclic analog, 1,3-dithiolane-2-thione (IX) [X, Y=S], and tetramethylthiourea (X) and a cyclic analog, *N*,*N'*-dimethyl-1,3-imidazolidine-2-thione (XI) [X, Y=N].

Oxazolidine-2-thione (VII) was prepared in 88% yield by the reaction of oxazolidine-2-thione with formaldehyde and piperidine. Other thione-compounds were either commerically-available materials or prepared by previously-reported methods.

The reaction of the thione-compound with propylene oxide (PO) was carried out in the presence of

*1 Presented at the 22nd Annual Meeting of the Chemical Society of Japan, Tokyo, April, 1969.

1) Y. Ueno, T. Nakai and M. Okawara, This Bulletin, **43**, 162 (1970).

Table 1. Reactions of thione-compounds with PO[a]

	pK_a [b]	Catalyst[c]	Product	Yield, %	$\nu_{C=O}$, cm^{-1}
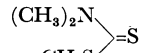 (IV)	−3.3	A	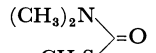	30	1650
		B		53	
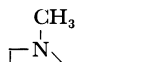 (V)	−1.6[d]	A	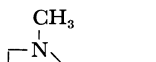	81	1665
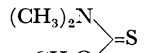 (VI)		A	e)	0	
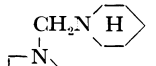 (VII)		A	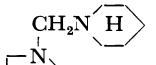	93[f]	1750
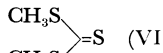 (VIII)	−5.3	A	e)	0	
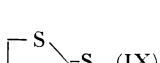 (IX)		A	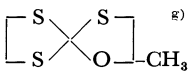 [g]	35	
		B	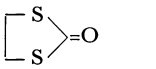	94	1660
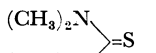 (X)	−1.0	A	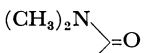	91[h]	1630
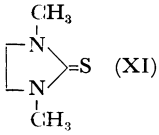 (XI)	−2.4	A	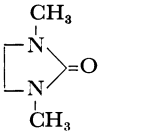	60[h,i]	1680

a) The reaction temperature: 170—180°C; time: 6.5 hr.
b) The acidities of the conjugate acids of the thione-compounds reported by M. J. Janssen (see Ref. 4).
c) A=NEt_3; B=BF_3OEt_2.
d) The present work (see Experimental section).
e) The starting material was recovered in 92% and 64% yield for VI and VIII, respectively.
f) The reaction conditions; 130—140°C, 5 hr; based on the picrate.
g) The distillate was contaminated with a small amount of triethylamine and unidentified one-compouunds were also obtained (see the text).
h) The reaction conditions: 150°C, 6.5 hr.
i) The starting material was also recovered in 28% yield.

a small amount of triethylamine or boron trifluoride etherate at 170—180°C in a sealed tube. Products obtained were identified by elemental analyses, spectrometric methods (IR and NMR) and comparison of their physical properties with those of the authentic samples. Results obtained are summarized in Table 1.

In the case of 1,3-dithiolane-2-thione (IX) a great difference in product between BF_3OEt_2 and NEt_3 was observed; the reaction in the presence of BF_3-OEt_2 gave the expected product, 1,3-dithiolane-2-one (XII) in 94% yield, whereas the reaction in the presence of NEt_3 afforded a spirocyclic compound XIII as a major product along with one-

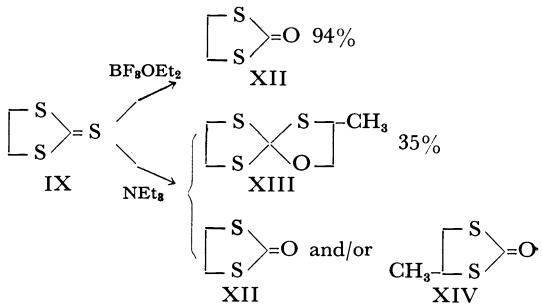

compounds XII and/or XIV.

The spirocyclic compound was identified by

(A) H_2C–S, S–CH_2(B); H_2C–S, O–C–CH_3(D); H(C)

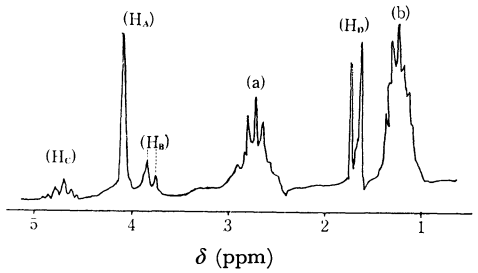

Fig. 1. The NMR spectrum of the spirocyclic compound XIII (CCl_4).
The signals (a) and (b) are due to the protons of the contaminating triethylamine (see the text).

NMR spectrum (Fig. 1) which shows a singlet at δ 4.01 ppm (4H, –S–C$\underline{H}_2$–C$\underline{H}_2$–S–), two doublets at 1.67 (3H, –CH–C$\underline{H}_3$) and 3.75 ppm (2H, –C$\underline{H}_2$–CH–), a multiplet centered at 4.55 ppm (1H, –CH_2–C$\underline{H}$–) and other signals assigned to the protons of the contaminated triethylamine at 1.3 (–CH_2–C$\underline{H}_3$) and 2.8 ppm (–C$\underline{H}_2$–CH_3) (the ratio of 3 : 2). The contamination of triethylamine was also observed in the elemental analysis (Found: N, 0.89%). The spirocyclic compound (XIII) is not very stable. After standing at room temperature for three weeks redistillation of XIII gave one-compounds.

In all cases the episulfide eliminated was detected in the distillation trap tube.

Discussion

Examination of structures of products reveals that the thione-compound is converted into the corresponding one-compound. The fact that the oxazolidine-2-thione (VII) can be easily transformed into the 2-oxazolidone supports a possibility of the proposed mecahnism for the formation of the oxazolidone (II) from the reaction of 2-substituted imino-1,3-dithiolane (I) with epoxides.[1] The results suggest that this type of reaction provides a new method for the transformation of the C=S bonds in thione-compounds into the C=O bonds.

Isolation of the spirocyclic intermediate in the case of IX suggests the cycloaddition-elimination mechanism for the transformation, as illustrated below.

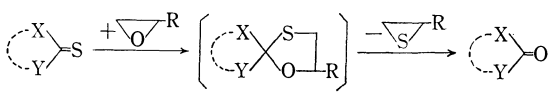

XV

Information on the elimination of episulfide from sulfur containing five-membered heterocycles is available.[2]

Catalytic Effect. As shown in the cases of IV and IX, boron trifluoride etherate appears to be more effective than triethylamine as a catalyst. It should be noted that in the case of IX the one-compound was obtained in the presence of BF_3OEt_2 whereas the spirocyclic intermediate was isolated in the presence of NEt_3. The results may be explained by the fact that BF_3OEt_2 enhances the elimination of episulfide from the oxothiolane (XV) by interaction with the hetero atoms in the ring (XVI) as well as the cycloaddition by interaction with both substrates (XVII and XVIII) while NEt_3 would activate only substrates but not the intermediate.

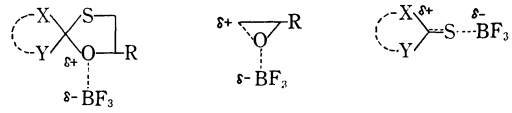

XVI XVII XVIII

Structural Effects on Reactivities. Examination of yields of products (Table 1), which might be regarded as an approximate measure of the reactivity, indicates that the reactivities of the thione-compounds studied might be significantly affected by whether these compounds are cyclic or open-chain and by the nature of the α-hetero atoms (X and Y); the cyclic thione-compounds are more reactive than the open-chain analogs except for a pair of thioureas and the enhancement by the α-hetero atoms is in the order: N,O≈N,N>N,S>S,S.

It should be noted that the yield of the one-compound appears to be parallel with the basicity (pK_a) of the thione-compound for both an open-chain and cyclic series (Table 1); the correlation was nearly linear. The fact may account for the two structural effects on the reactivities of the thione-compounds described above. The basicity of the thiocarbonyl group would be more enhanced both by the replacement of the α-hetero group (X and Y) with the stronger electron-donating group and the ring-structure. This would be due to the greater delocalization of the positive charge in structure XIX by the greater supply of electron from the α-hetero atoms.

XIX

The fact that the positive charge is more delocalized by ring-closing is in line with our observation

2) R. Feinauer, *Angew. Chem. Int. Ed. Engl*, **5**, 894 (1966).

that 2-dimethylamino-1,3-dithiolanylium ion (XX) is more stabilized than an open-chain analog XXI. This might be explained by the more developed 1,3-overlap in the ring system based upon spectral and kinetical observations.[3]

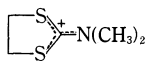

XX

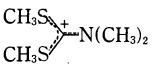

XXI

In comparison with other thione-compounds, it is remarkable that cyclic thiourea XI has lower basicity and less reactivity than the open-chain X. These observations might be explained by steric hindrance to the protonation at the thione-sulfur atom by the N-methyl group arising from the severely restricted rotation around the (S=) C–N bond.[4] Accordingly this effect appears to be very operative in lowering the reactivity of XI toward epoxide.

The results suggest the limitation that only thione-compounds of which pK_a is at least over -5.0 may be transformed into the corresponding one-compounds with epoxides.

Experimental

Melting and boiling points are uncorrected. Infrared and ultraviolet spectra were recorded with Hitachi EPI-S2 and recording EPS-2 spectrometers, respectively. NMR spectra were obtained with a Japan Electron Optics C-100 spectrometer. Chemical shifts are reported in part per million (ppm) from tetramethylsilane as an internal standard.*2

Materials. Propylene oxide (PO) was dried over calcium hydride and then distilled: bp 35°C. Triethylamine was dried over calcium hydride and then distilled: bp 88—89°C. Commercial boron trifluoride etherate was used without purification.

Thione-compounds. The following thione-compounds were either commercially available materials or prepared. *S*-Methyl *N,N*-dimethyldithiocarbamate (IV), mp 46—47°C; dimethyl trithiocarbonate (VIII), bp 85—88°C/5 mmHg; 1,3-dithiolane-2-thione (IX), mp 35—36°C; tetramethylthiourea (X), mp 77—78°C; *N,N'*-dimethyl-1,3-thiazolidine-2-thione (XI), mp 110—112°C.

N-Methylthiazolidine-2-thione(V) was obtained by the thermal ring-isomerization of 2-methylimino-1,3-dithiolane[1]: mp 68—69°C. *O*-Methyl *N,N*-dimethylthioncarbamate (VI) was prepared by the reaction of 2-dimethylamino-1,3-dithiolanylium perchlorate (XX) with sodium methoxide[5]: bp 81—82°C/10 mmHg.

N-Piperidinomethyl-oxazolidine-2-thione (VII) was prepared as follows. Into a stirred solution of 4.4 g (0.05 mol) of oxazolidine-2-thione in 20 m*l* of ethanol was added 7.5 m*l* of 30% formalin. 5 m*l* of piperidine was added drop by drop to the mixture below 10°C. The mixture was stirred at room temperature for 30 min, then at 40—60°C for an additional 30 min. The mixture was cooled in an ice box giving 8.2 g (88%) of precipitates of VII: mp 58—59°C (ethanol).

Found: C, 53.98; H, 8.06; N, 13.99%. Calcd for $C_9H_{16}N_2OS$: C, 53.55; H, 8.07; N, 13.71%.

A General Method for the Reactions of Thione-compounds with Propylene Oxide. The thione-compound (*ca.* 5 g), a slight molar excess of propylene oxide and a small amount of the catalyst were sealed in a hard-glass tube, and heated at 170—180°C for 6.5 hr. After cooling and carefully opening the tube the volatile materials were removed *in vacuo*. Distillation in the reduced pressure or recrystallization from an appropriate solvent of the residue gave the corresponding one-compound.

Reactions of 1,3-Dithiolane-2-thione (IX) with PO. *Triethylamine Catalyst.* 1,3-Dithiolane-2-thione (5.4 g) and PO (3.5 g, 0.05 mol) was heated at 170—180°C for 6.5 hr in the presence of triethylamine (1 m*l*). Distillation of the residue gave two distillates; bp 90—110°C/7 mmHg and bp 132—138°C/4 mmHg (2.7 g). The former showed a carbonyl band at 1650 cm^{-1}, however the latter did not show any absorption bands in the carbonyl region. The latter was a reddish liquid with an unpleasant odor, and was distilled after standing for three weeks giving a small amount of a low-boiling distillate spectrometrically identical with the former. The NMR spectrum (Fig. 1) of the latter confirms the structure and indicates that the distillate was contaminated with triethylamine used as a catalyst.

Found: S, 50.59; N, 0.86%. Calcd for $C_6H_{10}OS$: S, 49.44; N, 0%.

Boron Trifluoride Etherate Catalyst. In the presence of a few drops of BF_3OEt_2 the reaction was carried out under the same conditions. Distillation of the residue gave one distillate of 1,3-dithiolane-2-one (XII) in 94% yield: bp 82—90°C/0.23 mmHg. The distillate was solidified by standing at room temperature: mp 31—32°C (lit,[6] 31°C). The IR spectrum of the product was identical with that of the authentic sample.

Identifications of Products. Products obtained are summarized in Table 1 along with yields and infrared carbonyl bands. Products were identified by elemental analyses, the spectrophotometric methods and comparison of their physical properties with those of the authentic samples as follows.

S-Methyl N,N-dimethylthiolcarbamate: bp 87—89°C/30 mmHg; n_D 1.4938 (21°C) (lit,[7] bp 115—116°C/89 mmHg; n_D 1.4932 (30°C)). This compound was identical with the authentic sample prepared by the reaction of *O*-methyl *N,N*-dimethylthioncarbamate with methyl iodide[8] or by the hydrolysis of bis(methylthio)-dimethylaminocarbonium perchlorate (XXI).[9]

N-Methylthiazolidine-2-one. Bp 85—87°C/0.3 mmHg

3) T. Nakai, Y. Ueno and M. Okawara, Abstracts of papers presented at the 18th Symposium on Organic Reaction Mechanisms, Kyoto, October, 1967, p. 77.

4) M. J. Janssen, *Rec. Trav. Chim. Bays-Bas*, **81**, 650 (1962).

*2 Microanalysis was carried out by Mr. T. Saito.

5) T. Nakai and M. Okawara, *Tetrahedron Lett.*, **1967**, 3835.

6) H. Husemann, *Ann.*, **126**, 269 (1863).

7) H. Tilles, *J. Amer. Chem. Soc.*, **81**, 714 (1959).

8) A. F. Schöberl and A. Wagner, "Houben-Wyle: Methoden der Organischen Chemie," Vol. IX, George Thieme Verlag, Stuttgart (1955), p. 837.

9) T. Nakai, Y. Ueno and M. Okawara, Abstracts of papers presented at the 20th Annual Meeting of the Chemical Society of Japan, April, 1967, p. III-27.

(lit,[10] 84—85°C/0.2 mmHg).

Found: C, 40.66; H, 6.40%. Calcd for C_4H_7NOS: C, 41.02; H, 6.03%.

N-Piperidinomethyl-oxazolidine-2-one. The reaction of VII with PO was carried out at 130—140°C for 5 hr. An oily residue obtained was treated with picric acid giving precipitates of the picrate in 93% yield: mp 154—156°C (ethanol).

Found: C, 43.71; H, 4.79; N, 16.34%. Calcd for $C_{15}H_{19}N_5O_7S$: C, 43.58; H, 4.63; N, 16.94%.

Tetramethylurea. Bp 71—74°C/21 mmHg; n_D 1.4538 (21°C) (lit,[11] bp 63—64°C/12 mmHg; n_D 1.4495 (25°C)).

N,N'-Dimethyl-thiazolidine-2-one. Bp 80—82°C/2 mmHg (lit,[12] 106—108°C/20 mmHg); n_D 1.4770 (18°C).

pK_a Measurement. The value of pK_a of the thione-compound was obtained by the method by Janssen.[4] The molar extinction coefficients (ε) in the UV spectra of *N*-methyl-thiazolidine-2-thione (V) were measured in 98% and 15% sulfuric acid and water. The value of pK_a was calculated from the equation

$$pK_a = H_0 + \log [(\varepsilon_M - \varepsilon_B)/(\varepsilon_{BH} - \varepsilon_M)],$$

where H_0 denotes Hammett's acidity function($H_0 = -0.66$ for 15% sulfuric acid[13]) and ε_B, ε_M and ε_{BH} represent the molar extinction coefficients in water, and 15% and 98% sulfuric acid, respectively. The experimental data for V are shown in Table 2.

Table 2. Measurement of pK_a of V

Wavelength mμ	ε_B	ε_M	ε_{BH}	pK_a
235	3400	3800	9200	−1.8
237	3900	4400	9300	−1.7
240	4700	5400	8800	−1.4
			Aver.	−1.6

10) H. Eilingsfeld and L. Möbius, *Chem. Ber.*, **98**, 1293 (1965).

11) J. K. Lawson, Jr., and J. A. Croom, *J. Org. Chem.*, **28**, 232 (1963).

12) A. B. Jansen and D. J. Stokes, *J. Chem. Soc.*, **1962**, 4909 (1962).

13) M. J. Jorgenson and D. R. Hartter, *J. Amer. Chem. Soc.*, **85**, 878 (1963).

BULLETIN OF THE CHEMICAL SOCIETY OF JAPAN VOL. 43 172—177 (1970)

Effects of Alkyl Halides on the γ-Ray Induced Polymerization of Ethylene in Liquid Carbon Dioxide

Miyuki HAGIWARA, Hidemasa OKAMOTO and Tsutomu KAGIYA

Japan Atomic Energy Research Institute, Takasaki Radiation Chemistry Research Establishment, Takasaki, Gumma

(Received June 13, 1969)

The ^{60}Co γ-ray induced polymerization of ethylene in a liquid carbon dioxide solvent was carried out under a pressure of 400 kg/cm^2 at 30°C in the presence of such alkyl halides as CH_2Cl_2, $CHCl_3$, CCl_4, C_2H_5Cl, C_2H_5Br, C_2H_5I, $C_2H_4Cl_2$, $C_2H_2Cl_4$, C_2Cl_6, C_2F_6, C_2F_5Cl, $C_2F_4Cl_2$, $C_2H_3Cl_3$, and $C_2F_2Cl_4$, and their effects on the polymerization rate and the molecular weight of the polymer formed were investigated. Both the rate and the molecular weight were increased by adding $C_2F_4Cl_2$, C_2F_5Cl, and C_2F_6. A study of the radiolysis of these three fluorocarbons by mass spectrometric analysis showed that bond scissions of these substances took place mainly at the C–C bond. When other halogen compounds besides the three fluorocarbons were added to the reaction mixture, the rate and the molecular weight were decreased and C–X (X: halogen) bond scission was predominant in those substances. On the basis of these results, the role of the additives in the polymerization was discussed in relation to their radiolysis reactions.

In previous papers,[1-3] liquid carbon dioxide was found to be a useful solvent for the γ-ray induced polymerization of ethylene. It was shown from a kinetic study of the polymerization that the rate of initiation increased with an increase in the concentration of the carbon dioxide solvent. The role of the solvent in the initiation has been ascribed to the fact that the absorption step of radiation energy depends on the electron density of the reaction mixture. Further, the radiolysis products of the solvent were found to have some effects on the termination reaction of the polymerization.

1) M. Hagiwara, H. Mitsui, S. Machi and T. Kagiya, *J. Polym. Sci., Part A-1*, **6**, 603 (1968).
2) M. Hagiwara, H. Mitsui, S. Machi and T. Kagiya, *ibid., Part A-1*, **6**, 609 (1968).
3) M. Hagiwara, H. Mitsui, S. Machi and T. Kagiya, *ibid., Part A-1*, **6**, 721 (1968).

In consideration to their high electron density and high chemical reactivity, alkyl halides are expected to have various radiation-induced effects on the polymerization. In this paper, the effects of various alkyl halides on the polymerization of ethylene in liquid carbon dioxide will be investigated, and the role of the additives will be discussed in relation to their radiolysis reactions.

Experimental

The reaction vessel was a stainless-steel autoclave with a capacity of 100 m*l*. The ethylene used was 99.9% pure (free of CO and H_2S) and contained less than 5 ppm of O_2. The carbon dioxide was 99.99% pure; its major impurities were H_2O (37 ppm), CH_4 (20 ppm), and O_2 (2 ppm). The alkyl halides were all reagent-grade and were refined in a usual way. Both liquid carbon dioxide and alkyl halide were first charged into the vessel (liquid CO_2, 20 g; alkyl halide, 5 g). Ethylene was then fed in to about 400 kg/cm² at 30°C. The density of the reaction system could thus be kept almost constant in all experiments. The reaction temperature was controlled within ±0.5°C by using an automatic controller during the course of the reaction. The irradiation of ^{60}Co γ-rays was carried out for 3 hr at a dose rate of 2.5×10^4 rad/hr. The amount of polymer formed was determined by direct weighing. The number-average molecular weight of the polymer thus formed was obtained from the intrinsic viscosity measurements using Tung's formula.[4] Infrared absorption spectra were recorded for film samples in the range of 4000—400 cm^{-1}. Mass spectra for several kinds of alkyl halides were taken on a Hitachi mass spectrometer, Model RMU-6, under a pressure of 10^{-3} mmHg.

Results and Discussion

Polymerization in the Presence of Various Alkyl Halides. The polymer yield and the number-average molecular weight of the polymer formed in the presence of various alkyl halides are summarized in Table 1. The number of moles of the polymer chain, defind as the ratio of the polymer yield to the molecular weight, $M_p/\bar{M}_n$, is also listed in the last column of the table. The polymer yield and the polymer's molecular weight were found to decrease in many cases when alkyl halides were added to the reaction mixture. However, when some fluorocarbons, such as C_2F_6, C_2F_5Cl and CF_2ClCF_2Cl, were added, both the rate and the molecular weight increased. In the series of polymerizations in the presence of C_2H_5Cl, C_2H_5Br, or C_2H_5I, ethyl chloride or bromide gave about the same yields and molecular weights, though they were much lower than those without additives. On the other hand, ethyl iodide gave an extremely low yield. Polychlorinated hydrocarbons, such as CH_2Cl_2, $CHCl_3$, CCl_4, CH_2ClCH_2Cl, $CHCl_2$-$CHCl_2$, and C_2Cl_6, did not show any change in the yield. On the other hand, the molecular weight decreased markedly with an increase in the number of chlorine atoms in the molecule of the additives. This relation between the molecular weight and the number of chlorine atoms was also observed with the use of fluorocarbons.

Table 1. Effects of alkyl halides on polymer yield, molecular weight and number of moles of polymer chain

Alkyl halide	Polymer yiled M_p, g	Molecular weight $\bar{M}_n\times10^{-4}$	Number of moles of polymer chain $N_p\times10^4$ mol/*l*
——	0.816	13.9	0.59
CH_2Cl_2	0.472	3.8	1.42
$CHCl_3$	0.260	< 1	—
CCl_4	0.435	< 1	—
C_2H_5Cl	0.473	2.16	2.20
C_2H_5Br	0.512	3.1	1.65
C_2H_5I	0.013	—	—
CH_2ClCH_2Cl	0.522	1.8	2.91
$CHCl_2CHCl_2$	0.289	< 1	—
C_2Cl_6	0.420	0.1	42
C_2F_6	0.860	19.4	0.44
C_2F_5Cl	1.063	15.1	0.70
CF_2ClCF_2Cl	1.229	13.2	0.93
$CFCl_2CF_2Cl$	0.458	3.35	1.38
$CFCl_2CFCl_2$	0.359	0.85	4.70

Reaction conditions: pressure, 400 kg/cm²; temperature, 30°C; dose rate, 2.5×10^4 rad/hr; time, 3 hr; carbon dioxide, 20 g; alkyl halide, 5 g; reactor volume, 100 m*l*.

On the other hand, the infrared spectrum of a low-molecular-weight polymer obtained in the presence of $CHCl_3$ showed the characteristic C–Cl bands at 583 cm^{-1} (C–Cl axial), 695 cm^{-1} (C–Cl stertching), and 777 cm^{-1} (C–Cl stretching in CCl_3),

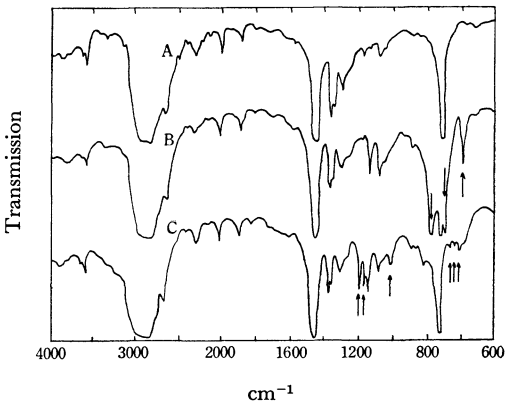

Fig. 1. Infrared spectra of polymers formed in various alkyl halides: (A) free; (B) $CHCl_3$; (C) $CFCl_2CFCl_2$. Reaction pressure, 400 kg/cm²; temperature, 30°C; dose rate, 2.5×10^4 rad/hr; time, 3 hr; carbon dioxide, 20 g; alkyl halide, 5 g.

4) L. H. Tung, *ibid.*, **24**, 333 (1957).

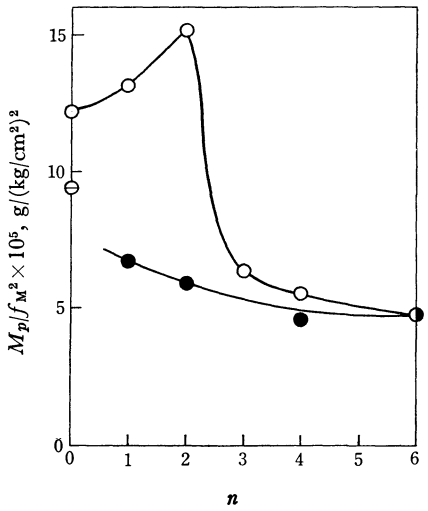

Fig. 2. The amount of polymer formed *vs.* the number of chlorine substitution of halogenated ethane derivatives: (⊖) free; (●) $C_2H_{6-n}Cl_n$; (○) $C_2F_{6-n}Cl_n$. Reaction pressure, 400 kg/cm²; temperature, 30°C; dose rate, 2.5×10^4 rad/hr; time, 3 hr; carbon dioxide, 20 g; halogenated ethane derivative, 5 g.

as is given in Fig. 1. In the case of $CFCl_2CFCl_2$, both C–Cl stretching bands (603, 633, 658 cm^{-1}) and C–F stretching bands (1000, 1156, 1190 cm^{-1}) were observed. The role of the additives and their radiolysis products in the polymerization and the step of their introduction into the polymer chain will be discussed below.

Polymerization in the Presence of Halogenated Ethane Derivatives. Using the results listed in Table 1, the polymer yields are plotted in Fig. 2 against the number of the chlorine substitution for two series of halogenated ethane derivatives, *i.e.*, $C_2H_{6-n}Cl_n$ and $C_2F_{6-n}Cl_n$, where n stands for the number of the chlorine substitution.

The fugacity of ethylene of the reaction system is inevitably changed depending on the nature of the additives. Several authors have previously reported that the polymerization rate and the polymer molecular weight are proportional to the square of ethylene fugacity.[2] Hence, the polymer yields in Fig. 2 are divided by the square of ethylene fugacity to normalize them to a unit of fugacity.

It can be seen that the yield under a unit of fugacity is much smaller in the presence of chlorinated hydrocarbons than that of the blank experiment without additives, and that it decreases gradually with the increase in the number of the chlorine substitution. On the other hand, in the case of fluorcarbons, it increases with the number of the chlorine substitution and passes through a maximum at $n=2$; thereafter it decreases with an increase in the number of the substitution. Thus, CF_2ClCF_2Cl gives a maximum yield which is about 1.5 times as large as that of the blank experiment. However, in the cases of $CF_2ClCFCl_2$ and $CFCl_2CFCl_2$ the yield becomes almost the same as that of the corresponding chlorinated hydrocarbons.

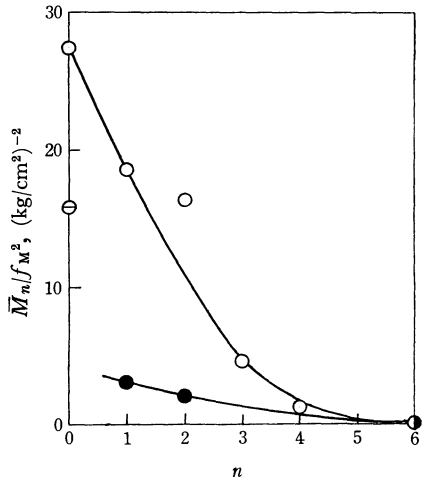

Fig. 3. Molecular weight *vs.* the number of chlorine substitution of halogenated ethane derivatives. Reaction conditions and notes are the same as Fig. 2.

Figure 3 shows the relation between the molecular weight of the polymer (normalized to a unit of ethylene fugacity) and the number of the chlorine substitution. In the series of chlorinated ethanes, the molecular weight under a unit of fugacity is markedly reduced by additives and decreases with the number of the chlorine. The decrease in the molecular weight with the chlorine content is also observed in the case of fluorocarbons. However, in the latter case, the molecular weight is larger than that in the case of no additives in the lower region of the chlorine substitution (less than $n=2$).

Futher, in Fig. 4, the number of moles of the

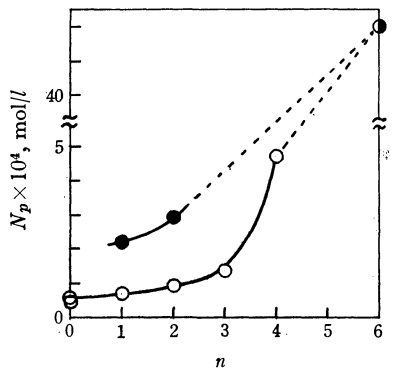

Fig. 4. Number of polymer chains *vs.* the number of chlorine substitution of halogenated ethane derivatives.
Reaction conditions and notes are the same as Fig. 2.

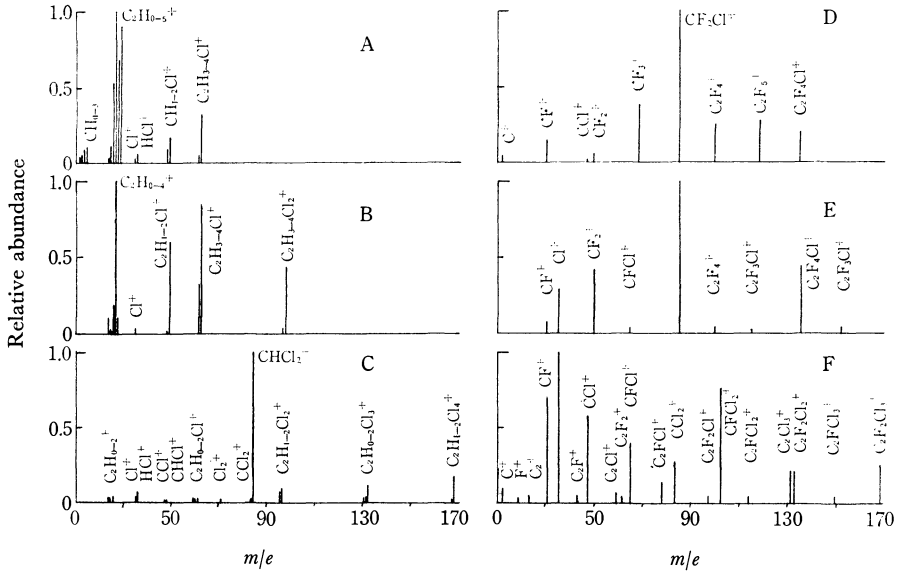

Fig. 5. Mass spectra of halogenated ethane derivatives: (A) C_2H_5Cl; (B) CH_2ClCH_2Cl; (2) $CHCl_2CHCl_2$; (D) C_2F_5Cl; (E) CF_2ClCF_2Cl; (F) $CFCl_2CFCl_2$.

polymer chain is also plotted against the number of chlorine substitution. The number of the polymer chain is shown to increase with the chlorine substitution in both hydro- and fluorocarbons.

From the results presented above, the increase in the polymer yield in the order of $C_2F_6 < C_2F_5Cl < CF_2ClCF_2Cl$, which is reported in Fig. 2, may be ascribed to the increase in the rate of initiation. The promoting effects of these fluorocarbons on the propagation reaction should also be considered in terms of the following results, obtained in the presence of C_2F_6. Thus, as is shown in Figs. 2 and 3, both the yield and the molecular weight increase upon the addition of C_2F_6. On the other hand, the number of the polymer chain is shown in Fig. 4 to be almost the same as that of the blank experiment. In contrast to the cases of C_2F_6, C_2F_5Cl, and CF_2ClCF_2Cl, the yield and the molecular weight are depressed by the addition of other fluorocarbons, such as $CF_2ClCFCl_2$ and $CFCl_2CFCl_2$, and all the chlorinated hydrocarbons employed. This means that these additives contribute mainly to promoting the termination reaction. Further, the decrease in the moleculr weight and the increase in the number of the polymer chain with the chlorine substitution suggest that the chlorine atom in these compounds plays an important role in the chain-transfer reaction.

Thus, from the point of view of their characteristic roles, the halogenated ethanes may be classified into two different groups. One group, such as C_2F_6, C_2F_5Cl, and CF_2ClCF_2Cl, promotes the polymerization, while the other group, such as $CF_2ClCFCl_2$, $CFCl_2CFCl_2$, C_2H_5Cl, CH_2ClCH_2Cl, $CHCl_2CHCl_2$ and C_2Cl_6, retards it.

Free Radicals from the Radiolysis of the Additives and Their Role in the Polymerization. In Fig. 5, the relative abundance of the ions detected by the mass spectrometer is plotted against the *m/e* for several halogenated ethane derivatives. The large relative abundance of the $C_2H_{0-5}^+$ ions in C_2H_5Cl and that of the $C_2H_{0-4}^+$, and $C_2H_{3-4}^+$ ions in CH_2ClCH_2Cl indicates that the bond cleavage by radiation occurs mainly at C–Cl and C–H in these compounds. On the other hand, C_2F_5Cl and CF_2ClCF_2Cl are shown to cleave mainly at the C–C bond, since CF_2Cl^+ and CF_3^+ in C_2F_5Cl, and CF_2Cl^+ in CF_2ClCF_2Cl, are observed to be predominant in their spectra. Moreover, the figure shows that the cleavage in highly-chlorinated ethane derivatives occurs at the C–C and C–Cl bonds about equally.

These mass spectrometric data suggest that such radicals as $CF_3\cdot$ and $CF_2Cl\cdot$ are mainly produced by the C–C bond dissociations of C_2F_5Cl and CF_2ClCF_2Cl, which promote the polymerization. Further, several kinds of hydrocarbon radicals, chlorine atoms, and highly-chlorinated radicals, such as $CHCl_2\cdot$ and $CFCl_2\cdot$, are produced by the use of C_2H_5Cl, CH_2ClCH_2Cl, $CHCl_2CHCl_2$, and $CFCl_2CFCl_2$, which retard the polymerization.

From this information on the effect of halogenated compounds on the polymerization and on the structure of their radiolysis products, it might be said that CF_3 or CF_2Cl radicals act as initiators of the polymerization. However, hydrocarbon radicals, chlorine atoms, or highly-chlorinated radicals act mostly in the termination rather than in the initiation reaction of the polymerization.

In view of the fact that the rate of cross combina-

tion is faster than that of the combination of the radical with the same structure, a cross termination reaction between the growing chain radical and the radical generated from the added halogen compounds is considered to be important. The relative fraction of the cross termination can be expressed in terms of the rate constants, $k_{AR}/(k_{AA}k_{RR})^{0.5}$, for the following reactions:

$$A\cdot + A\cdot \rightarrow A_2 \qquad k_{AA} \qquad (1)$$
$$R\cdot + R\cdot \rightarrow R_2 \qquad k_{RR} \qquad (2)$$
$$A\cdot + R\cdot \rightarrow AR \qquad k_{AR} \qquad (3)$$

where A· represents a halogen-containing radical, and R·, a growing radical.

Many data have recently been accumulated on the cross combination reactions of low-molecular-weight alkyl radicals with or without halogen atoms.[5-9] The values of $k_{AR}/(k_{AA}k_{RR})^{0.5}$ for $R=CH_3$ and C_2H_5 do not differ from each other; both lie between 1.5—2.6. Hence, the difference in the effects of the additives on the ethylene polymerization may be ascribed to the difference in the reactivities of the radicals formed by the radiolysis to the ethylene monomer rather than that to the growing radicals.

The relative reactivity of CF_3, CH_3, and CCl_3 radicals to the ethylene monomer can be evaluated in terms of their activation energies, E_a, in the following addition reactions:

$$CF_3\cdot + CH_2{=}CH_2 \rightarrow CF_3{-}CH_2CH_2\cdot \qquad E_{aCF_3} \qquad (4)$$
$$CH_3\cdot + CH_2{=}CH_2 \rightarrow CH_3{-}CH_2CH_2\cdot \qquad E_{aCH_3} \qquad (5)$$
$$CCl_3\cdot + CH_2{=}CH_2 \rightarrow CCl_3{-}CH_2CH_2\cdot \qquad E_{aCCl_3} \qquad (6)$$

Recently, a two-constant approximate formula (7) was proposed for the evaluation of the activation energy of the radical substitution reaction in the gaseous phase:[10]

$$E_a = D_i - \alpha D_f(1+\beta D_i) \qquad (7)$$

In this formula, D_i is the dissociation energy of the initial system, and D_f, that in the final system, while α and β are constants. In estimating the activation energies of the above addition reactions, (4), (5), and (6), D_i corresponds to D_π, the π-dissociation energy of ethylene. Hence,

$$E_a = D_\pi - \gamma D_f \qquad (8)$$

where γ is equal to $\alpha(1+\beta D_\pi)$. Since the D_π is constant in the reactions (4), (5), and (6), Eq. (8) shows that the activation energy depends solely upon the dissociation energy of the bond formed in the final system, D_f, and that it decreases with an increase in D_f. The C–C bond dissociation energies for CF_3–CH_3 and CH_3–CH_3 are 90[11]—117[12] and 83[13] kcal respectively, while that for CCl_3–CH_3 is estimated by thermodynamic calculation to be 77.7 kcal.[14,15] Since the order of the C–C bond dissociation energies for CF_3–CH_2CH_2·, CH_3–CH_2CH_2·, and CCl_3–HC_2CH_2· is the same as that for the corresponding compounds, such as CF_3–CH_3, CH_3–CH_3, and CCl_3–CH_3, the order of the activation energies of the reactions (4), (5), and (6) may be considered to be: $E_{aCF_3} < E_{aCH_3} < E_{aCCl_3}$.

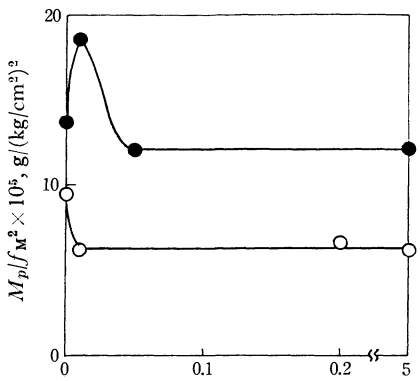

Fig. 6. The amount of polymer formed *vs.* the amount of C_2Cl_6 added. Reaction pressure, 400 kg/cm²; temperature, 30°C; dose rate, 2.5×10^4 rad/hr; time, 3 hr; carbon dioxide, 20 g; C_2F_6, 5 g; C_2F_4, (○) free, (●) 1 mol% to C_2H_4.

Figure 6 shows the results of the polymerization carried out in the presence of the mixture of C_2Cl_6 and C_2F_6. In the polymerization in the C_2F_6 solvent, the polymer yield under a unit of ethylene fugacity is markedly depressed by the addition of a very small amount of C_2Cl_6. Moreover, when a small amount of C_2F_4 (1 mol% to C_2H_4) was added to the mixed solvent of C_2Cl_6 and C_2F_6, the yield increases in the low-concentration range of C_2Cl_6, but declines to a constant value as the amount of C_2Cl_6 increases. The decrease in the yield, however, is shown to become less pronounced than in the case without C_2F_4. These facts suggest that the chlorine-

5) P. Ausloos and E. W. R. Steacie, *Can. J. Chem.*, **33**, 1062 (1955).
6) C. A. Heller, *J. Chem. Phys.*, **28**, 1255 (1955).
7) B. C. Roquitte and M. H. J. Wijnen, *J. Amer. Chem. Soc.*, **85**, 2053 (1963).
8) R. D. Giles and E. Whittle, *Trans. Faraday Soc.*, **61**, 1425 (1965).
9) R. A. Sieger and J. G. Calvert, *J. Amer. Chem. Soc.*, **76**, 5197 (1954).
10) T. Kagiya, Y. Sumida, T. Inoue and F. S. Dyachikovskii, This Bulletin, in press.
11) J. B. Farmer, I. H. S. Henderson, F. P. Lossing and D. G. H. Marsden, *J. Chem. Phys.*, **24**, 348 (1956).
12) V. H. Dibeler, R. M. Reese and F. L. Mohler, *ibid.*, **20**, 761 (1952).
13) M. Szwarc, *Chem. Rev.*, **47**, 75 (1950).
14) N. N. Semenov, "Some Problems in Chemical Kinetics and Reactivity," Vol. I, Princeton University Press, Princeton, New Jergey (1958), p. 23.
15) S. W. Benson and J. H. Buss, *J. Chem. Phys.*, **29**, 546 (1958).

containing radicals produced by the radiolysis of C_2Cl_6, which will act as a terminating agent of the growing radicals, are effectively scavenged by C_2F_4, and that they are changed into highly-fluorinated radicals which contribute mainly to the initiation reaction. The decrease in the polymer yield at high concentrations of C_2Cl_6 may be ascribed to the reaction between the growing radicals and the radicals from C_2Cl_6, which are not scavenged by C_2F_4.

BULLETIN OF THE CHEMICAL SOCIETY OF JAPAN VOL. 43 177—181 (1970)

Amino Acids and Peptides. I. Syntheses of *p*-Methoxybenzyl *p*-Nitrophenyl Carbonate, *p*-Methoxybenzyl Carbazate, and *p*-Methoxybenzyloxycarbonyl Amino Acids[1] with *p*-Methoxybenzyl Chloroformate

Shōsuke Sōfuku, Mitsuo Mizumura and Akira Hagitani

Department of Chemistry, Faculty of Science, Rikkyo (St. Paul's) University, Toshima-ku, Tokyo

(Received June 16, 1969)

A new method for the syntheses of *p*-methoxybenzyl *p*-nitrophenyl carbonate, *p*-methoxybenzyl carbazate, and *p*-methoxybenzyloxycarbonyl amino acids has been devised. These compounds were obtained in satisfactory yield from sodium *p*-nitrophenolate, 85% hydrazine hydrate, and several amino acids with *p*-methoxybenzyl chloroformate prepared from anisyl alcohol and phosgene in the presence of dimethylaniline in dry ether at −5—−10°C. This direct *p*-methoxybenzyloxycarbonylation of amino acid with the chloroformate is more convenient than the usual Weygand method.

The *p*-methoxybenzyloxycarbonyl [Z(OMe)][2] group has been widely used as a blocking substituent of the amino moiety of amino acids in peptide synthesis.[3,4] This group allows an easier removal by trifluoroacetic acid than the parent group (carbobenzoxy)[5] without the methoxy substituent. *p*-Methoxybenzyloxycarbonyl amino acids[6] were obtained for the first time by the reaction of isocyanocarboxylic acid esters with anisyl alcohol and subsequent hydrolysis. Later Weygand and Hunger[7] prepared these compounds in a synthesis analogous to that of the *t*-butyloxycarbonyl amino acids.[8] The Z(OMe) group was introduced with the use of *p*-methoxybenzyl *p*-nitrophenyl carbonate (II) or *p*-methoxybenzyloxycarbonyl azide prepared by the reaction of *p*-methoxybenzyl carbazate (III) with nitrous acid. Their method has been used in many cases, but the synthesis of II and III involves many steps, and the yields are not so high.

Recently, Schnabel *et al.*[9,10] reported the syntheses of *p*-methoxybenzyloxycarbonyl amino acids with *p*-methoxybenzyl fluoroformate. Jones and Young[11,12] described a method for synthesizing *p*-methoxybenzyl-1-piperidyl carbonate by the use of *p*-methoxybenzyl chloroformate (I). In this method I was prepared from anisyl alcohol and phosgene in dry ether at 20°C, and was coupled with 1-hydroxypiperidine in dry ether at 0°C. For the preparation of *p*-methoxybenzyloxycarbonyl

1) S. Sōfuku, M. Mizumura and A. Hagitani, This Bulletin, **42**, 278 (1969).

2) Abbreviated designation by IUPAC-IUB comission on biochemical nomenclature; *Biochem. J.*, **102**, 203 (1967).

3) M. Bodansky and M. A. Ondetti, "Peptide Synthesis," John Wiley & Sons, Inc., New York (1966), p. 31.

4) E. Schröder and K. Lübke, "The Peptide," Vol. 1, Academic Press, New York (1965), p. 34.

5) M. Bergmann and L. Zervas, *Ber.*, **65**, 1192 (1932).

6) F. C. Mckay and N. F. Albertson, *J. Amer. Chem. Soc.*, **79**, 4686 (1957).

7) F. Weygand and K. Hunger, *Chem. Ber.*, **95**, 1 (1962).

8) G. W. Anderson and A. C. McGregor, *J. Amer. Chem. Soc.*, **79**, 6180 (1957).

9) E. Schnabel, H. Herzog, P. Hofmann, E. Klauke and I. Ugi, *Angew. Chem.*, **80**, 396 (1968).

10) E. Schnabel, H. Herzog, P. Hoffmann, E. Klauke and I. Ugi, *Ann. Chem.*, **716**, 175 (1968).

11) J. H. Jones and G. T. Young, *Chem. Ind.* (London), **1966**, 1722.

12) J. H. Jones and G. T. Young, *J. Chem. Soc., C*, **1968**, 53.

amino acid, *p*-methoxybenzyl-1-piperidyl carbonate and amino acid ester hydrochloride were stirred with sodium acetate in dioxane at 20°C for 24 hr. After the publication of our short communication[1] Honda *et al.*[13] reported a convenient method of synthesis of *p*-methoxybenzyloxycarbonyl amino acids and *p*-methoxybenzyl carbazate with the use of *p*-methoxybenzyl chloroformate.

In the present investigation, I could be prepared readily from anisyl alcohol (1 eq.) and phosgene (3 eq.) in the presence of dimethylaniline (1 eq.) in dry ether at below 0°C. This reagent was very useful for the preparation of *p*-methoxybenzyl *p*-nitrophenyl carbonate (II)[14] and *p*-methoxybenzyl carbazate (III).[15]

p-Methoxybenzyloxycarbonyl amino acids could be prepared directly from a number of amino acids and I under the conditions of the Schotten-Baumann reaction without any accompanying racemization.

Results and Discussion

Reagent I was prepared by the following reaction:

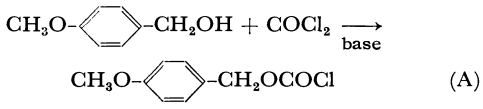

(I) (A)

Though reaction (A) could take place without a base, its addition was better for the removal of hydrogen chloride from the reaction solution. Because of the instability of I, the amount of phosgene required and the effectiveness of the base used for the preparation of I were examined by comparing the yields of II in combination with the reactions (A) and (B). Among the hydrochlorides of the bases, the one of dimethylaniline was most easily filtered off.

Addition of three equivalents of phosgene to anisyl alcohol in the presence of one equivalent of dimethylaniline gave the best yield of product II, as shown in Table 1.

After the completion of reaction (A), it was necessary to remove the salt completely by filtration and excess phosgene by evaporation under a reduced pressure at below 0°C. I was immediately dissolved in a suitable solvent, and used for succeeding reactions. The temperature of the reaction mixture was maintained as low as possible to prevent the degradation of I. For the preparation of II, sodium

Table 1. Results of the preparation of *p*-methoxybenzyl *p*-nitrophenyl carbonate in xylene

Base used in the preparation of *p*-methoxybenzyl chloroformate*2	Equiv. of phosgene to anisyl alcohol	Yield %
Pyridine	2	19
Quinoline	2	34
Dimethylaniline	2	40
Dimethylaniline	3	66
Dimethylaniline	3	44*1
——	3	48*2

*1 Ether used as solvent

*2 Reaction temperature: 20°C

p-nitrophenolate dried by azeotropic dehydration with xylene was used.

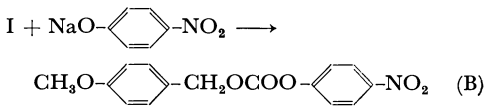

(II) (B)

In the preparation of III, it was not necessary to use anhydrous hydrazine. It could be obtained with 85% hydrazine hydrate[16] in a satisfactory yield.

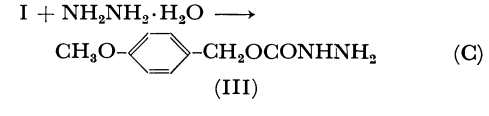

(III) (C)

Preparation of *p*-methoxybenzyloxycarbonyl amino acids was carried out with two equivalents of I and four equivalents of sodium hydroxide for an amino acid in a mixture of water and tetrahydrofuran (5 : 1).

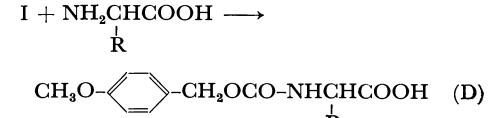

(D)

In the case of L-serine, carbobenzoxylation of the amino group has been devised,[17] and one equivalent of I was added. The crude product contained only a small amount of *N,O*-di-Z(OMe)-L-serine, which was detected by thin layer chromatography (solvent; chloroform : methanol : acetic acid=95 : 5 : 3)[18];

13) I. Honda, M. Naruse, M. Kaneoka and S. Sakakibara, the 6th Symposium on Peptide Chemistry of Japan, Fukuoka (November, 1968).

14) S. Sōfuku, M. Mizumura and A. Hagitani, the 21st Annual Meeting of the Chem. Soc. of Japan, Osaka (April, 1968).

15) S. Sōfuku, M. Mizumura and A. Hagitani, reported in a short communication to *Nippon Kagaku Zasshi*, **89**, 721 (1968).

16) "Organikum. Organisch-chemisches Grundpraktikum," Veb Deutscher Verlag der Wissenschaften, Berlin (1965), p. 625.

17) J. A. Moore, J. R. Dice, E. D. Nicolaides, R. D. Westland and E. L. Wittle, *J. Amer. Chem. Soc.*, **76**, 2884 (1954).

18) By a private letter from Dr. S. Sakakibara (Inst. for Protein Research, Osaka Univ.). The R_f values refer to the thin layer chromatography with Wakogel B-O. Compounds were detected by spraying them with *ca.* 47% hydrobromic acid and then ninhydrin.

Table 2. Results of the preparation of *p*-methoxybenzyloxycarbonyl amino acids

Compound	Yield %	Mp °C	$[\alpha]_D$	Solvent (c 2.0)	Temp. °C
Z(OMe)-glycine	80.0	95—98			
		95—98*3			
Z(OMe)-L-alanine	65.4	78—81	−11.5	acetic acid	22
		74—75*1	−11.9*1		
Z(OMe)-L-aspartic acid	40.9	125—127.5	+10.3	acetic acid	18
		122.5—124*1	+ 7.1*1		
Z(OMe)-L-glutamic acid	46.1	109—112	− 5.6	acetic acid	22
		109—111*1	− 7.44*1		
Z(OMe)-L-serine	53.3	94—96.5	+ 6.5	acetic acid	20
		97—98*1	+ 7.1*1		
		92—94*2	+ 5.8*2		
Z(OMe)-L-valine DCHA	79.2	162—165	+ 3.3	methanol	20
		162—166*4	+ 2.8*4		
Z(OMe)-L-leucine DCHA	88.7	159—162	− 6.0	methanol	21
		162*1	− 6.67*1		
Z(OMe)-L-phenylalanine DCHA	75.1	159—162	+22.7	methanol	21
		157—159*1	+22.6*1		
Z(OMe)-L-proline DCHA	82.6	145—147	−23.1	methanol	20
		147.5—149*1	−25.1*1		
Z(OMe)-L-methionine DCHA	87.9	150—153	+ 6.0	methanol	21
		152—153*1	+ 3.35*1		
α-*N*-Z(OMe)-δ-*N*-Z-L-ornithine DCHA	33.4	133—135	+ 6.3	methanol	19
		121—122*5	− 4.0*5		

Values, *1 from Ref. 7, *2 from Ref. 10; [α] value at 578 mμ, *3 from Ref. 11, *4 from Ref. 12 and *5 from Ref. 22.
DCHA: dicyclohexylammonium salt, Z(OMe): *p*-methoxybenzyloxycarbonyl, Z: benzyloxycarbonyl.
All melting points are uncorrected.

N-Z(OMe)-L-serine was purified by recrystallization. As shown in Table 2, some products were obtained as the salts of dicyclohexylamine.[19] The *p*-methoxybenzyloxycarbonyl amino acids were recrystallized from ethyl acetate - petroleum ether, and the dicyclohexylammonium salts from ethanol - petroleum ether.

Each derivative gave one spot in thin layer chromatography[18] and was examined by infrared spectrum for –O–CO–N group.[20,21]

Experimental[23]

***p*-Methoxybenzyl Chloroformate (I).** Phosgene (21 m*l*, 0.3 mol) was measured into a glass trap which had been cooled in a dry ice-acetone jar, and poured into a 500-m*l* two-necked conical flask containing 100 m*l* of dry ether, and cooled in an ice-salt bath. A solution of 12.4 m*l* of anisyl alcohol (0.1 mol) in 100 m*l* of dry ether was added in portions to the above solution over a period of 10 min. Then a solution of 12.7 m*l* of dimethylaniline (0.1 mol) in 100 m*l* of dry ether was added dropwise over a period of 1 hr, and the mixture was stirred for 2 hr at −5——10°C. After filtration of the dimethylaniline hydrochloride formed in the reaction, the filtrate was evaporated under reduced pressure at below 0°C. Twice more 100 m*l* of dry ether was added to the oily residue and evaporation was repeated to remove excess phosgene completely. The residue was immediately dissolved in a suitable solvent and the solution was used for the following reactions.

***p*-Methoxybenzyl *p*-Nitrophenyl Carbonate (II).** To a solution of 0.1 mol of I in 300 m*l* of dry xylene, 17.7 g of powdered dry sodium *p*-nitrophenolate (0.11 mol) was added in portions over a period of 10 min with vigorous stirring at 0——5°C. After 3 hr at this temperature, it was stirred overnight at room temperature and for 1 hr at 30°C. Excess sodium *p*-nitrophenolate and sodium chloride were filtered off, and the filtrate was washed successively with 0.5N hydrochloric acid, N sodium carbonate, and water, and then dried over anhydrous sodium sulfate. The filtered solution was evaporated *in vacuo*. Recrystallization of the residue from ethanol gave the pure product. Yield, 20.0 g (66.0%); mp, 104.5—105.5°C (lit,[7] 96—97°C). IR spectrum (KBr): 1760 cm^{-1}.

19) E. Klieger, E. Shröder and H. Gibian, *Ann. Chem.*, **640**, 157 (1961).
20) K. Nakanishi, "Infrared Absorption Spectra: Qualitative Analysis," Nanko-do, Tokyo (1960).
21) L. J. Bellamy, "The Infra-red Spectra of Complex molecules," Chapter 12, Methuen & Co., London (1958).
22) M. Waki and N. Izumiya, This Bulletin, **41**, 1909 (1968).
23) The infrared spectra were recorded on a Shimadzu Model IR 27-B Spectrophotometer.

Found: C, 59.52; H, 4.43; N, 4.73%. Calcd for $C_{15}H_{13}NO_6$: C, 59.41; H, 4.32; N, 4.62%.

p-Methoxybenzyl Carbazate (III). A solution of 0.1 mol of I in 100 m*l* of dry ether was added in portions over a period of 10 min to a mixture of 29.4 g of 85% hydrazine hydrate (0.5 mol) and 50 m*l* of ether with vigorous stirring at −30—−60°C. A white precipitate was immediately formed. After 30 min, 300 m*l* of water was added and the mixture was filtered. The precipitate was thoroughly washed with water. The amount of this precipitate was two-thirds of the total product, and the other one-third was isolated from the ether layer. The combined product was recrystallized from ethyl acetate-petroelum ether. Yield, 15.0 g (76.5%); mp, 74—75°C (lit,[7] 71—74°C). IR spectrum (KBr): 1690, 3330 cm^{-1}.

Found: C, 55.36; H, 6.31; N, 14.32%. Calcd for $C_9H_{12}N_2O_3$: C, 55.09; H, 6.16; N, 14.28%.

p-Methoxybenzyloxycarbonylglycine. A solution of 0.1 mol of I in 70 m*l* of tetrahydrofuran was added in portions over a period 10 min to a solution of 3.75 g of glycine (0.05 mol) in 200 m*l* of N sodium hydroxide containing 40 m*l* of tetrahydrofuran with vigorous stirring at 0—5°C. After 2 hr under these conditions, the reaction mixture was washed with 100 m*l* of ether, and acidified with 21 g of citric acid (0.1 mol) at 0—5°C, and the product was extracted with 500 m*l* of ethyl acetate. The organic layer was washed with water, dried over anhydrous sodium sulfate, and concentrated *in vacuo*. The resulting residue was crystallized from ethyl acetate and petroleum ether as fine crystalline plates; yield, 9.57 g. IR spectrum (KBr): 1695 cm^{-1}.

Found: C, 55.14; H, 5.52; N, 6.00%. Calcd for $C_{11}H_{13}NO_5$: C, 55.24; H, 5.48; N, 5.86%.

p-Methoxybenzyloxycarbonyl-L-alanine. By the same method as for Z(OMe)-glycine, 8.32 g of rod crystals of pure product was obtained from 4.45 g of L-alanine (0.05 mol) and 0.1 mol of I. IR spectrum (KBr): 1690 cm^{-1}.

Found: C, 56.94; H, 5.83; N, 5.70%. Calcd for $C_{21}H_{15}NO_5$: C, 56.90; H, 5.98; N, 5.54%.

p-Methoxybenzyloxycarbonyl-L-aspartic Acid. To a solution of 6.65 g of L-aspartic acid (0.05 mol) in 1.5N sodium hydroxide (200 m*l*) containing tetrahydrofuran (40 m*l*), 0.1 mol of I in tetrahydrofuran (70 m*l*) was added in portions over a period of 10 min at 0—5°C. The mixture was stirred for 2 hr at this temperature, then washed with ether (100 m*l*), and acidified with 35 g of citric acid; the product was extracted with ethyl acetate (500 m*l*). The organic layer was washed with water and dried over anhydrous sodium sulfate. The solution was concentrated under reduced pressure, and recrystallization of the residue from ethyl acetate-petroleum ether gave a pure granular product. Yield, 6.07 g. IR spectrum (KBr): 1710 cm^{-1}.

Found: C, 52.54; H, 5.25; N, 4.84%. Calcd for $C_{13}H_{15}NO_7$: C, 52.34; H, 5.41; N, 4.70%.

p-Methoxybenzyloxycarbonyl-L-glutamic Acid. By the same method as for Z(OMe)-L-aspartic acid, the crude product was obtained from 7.36 g of L-glutamic acid (0.05 mol) and 0.1 mol of I, and crystallized as pure granules (7.20 g) from ethyl acetate and petroleum ether. IR spectrum (KBr): 1710 cm^{-1}.

Found: C, 53.76; H, 5.22; N, 4.58%. Calcd for $C_{14}H_{17}NO_7$: C, 54.00; H, 5.50; N, 4.50%.

p-Methoxybenzyloxycarbonyl-L-serine (A). To a solution of 10.5 g of L-serine (0.1 mol) in a mixture of N sodium hydroxide (200 m*l*) and 40 m*l* of tetrahydrofuran, a solution of 0.1 mol of I in 70 m*l* of tetrahydrofuran was added in portions over a period of 10 min with vigorous stirring at 0—5°C. The reaction mixture was stirred at this temperature for 2 hr, and then washed with 100 m*l* of ether, and acidified with 21 g of citric acid at 0—5°C. An oily product was extracted with ethyl acetate. The solution was washed with water, dried over anhydrous sodium sulfate, and then concentrated under reduced pressure to dryness.

Reacrystallization of the residue from ethyl acetate and petroleum ether gave 12.8 g of the crude product (mp 87—96°C). This was again crystallized from the same solvents and 7.84 g of the pure product A was obtained. Concentration and cooling of the mother liquor gave 3.8 g of the mixture of A and *O,N*-di-Z(OMe)-L-serine (B). After recrysatllization was repeated twice from ethanol, 1.07 g of B was obtained. From the mother liquor 1.16 g of A was recovered.

Compound A, total yield, 9.0 g. IR spectrum (KBr): 1685 cm^{-1}. TLC (Wakogel B-O): R_f,[18] 0.2.

Found: C, 53.74; H, 5.70; N, 5.18%. Calcd for $C_{12}H_{15}NO_6$: C, 53.53; H, 5.62; N, 5.21%.

Compound B, mp 115—116.5°C (dec). $[\alpha]_D^{17}$ +16.67 (*c* 3, acetic acid). IR spectrum (KBr): 1765, 1650 cm^{-1}. TLC (Wakogel B-O): R_f,[18] 0.6.

Found: C, 58.28; H, 5.41; N, 3.29%. Calcd for $C_{21}H_{23}NO_9$: C, 58.19; H, 5.35; N, 3.23%.

p-Methoxybenzyloxycarbonyl-L-valine Dicyclohexylammonium Salt. Z(OMe)-L-valine was prepared by the same procedure as was used for the Z(OMe)-glycine, *viz.*, an oily residue was obtained from 5.85 g of L-valine (0.05 mol) and 0.1 mol of I. This residue was dissolved in 100 m*l* of ether, and 9.96 m*l* of dicyclohexylamine (0.05 mol) was added at 0—5°C. The white precipitate was filtered and washed with ether. Pure needle crystals were obtained by recrystallization from ethanol and petroleum ether; yield, 9.15 g. IR spectrum (KBr): 1710, 1630 cm^{-1}.

Found: C, 67.26; H, 9.23; N, 6.32%. Calcd for $C_{26}H_{42}N_2O_5$: C, 67.50; H, 9.15: N, 6.05%.

p-Methoxybenzyloxycarbonyl-L-leucine Dicyclohexylammonium Salt. This was synthesized by the same method as was used for the Z(OMe)-L-valine from 6.55 g of L-leucine. Pure dicyclohexylamine salt (21.15 g) was obtained as needle crystals after recrystallization from ethanol and petroleum ether. IR spectrum (KBr): 1710, 1630 cm^{-1}.

Found: C, 68.04; H, 9.07; N, 6.01%. Calcd for $C_{27}H_{44}N_2O_5$: C, 68.03; H, 9.31; N, 5.88%.

p-Methoxybenzyloxycarbonyl-L-phenylalanine Dicyclohexylammonium Salt. This was prepared from 8.25 g of L-phenylalanine by the same method as mentioned above. Pure white needle crystals (19.18 g) were obtained after recrystallization from ethanol and petroleum ether. IR spectrum (KBr): 1700, 1635 cm^{-1}.

Found: C, 70.76; H, 8.35; N, 5.83%. Calcd for $C_{30}H_{42}N_2O_5$: C, 70.55; H, 8.29; N, 5.49%.

p-Methoxybenzyloxycarbonyl-L-proline Dicyclohexylammonium Salt. From 5.75 g of L-proline (0.05 mol), this salt was prepared by the same method as described for Z(OMe)-L-valine dicyclohexylammonium salt. Recrystallization from ethanol and petroleum ether gave 19.02 g of pure minute crystalline plates.

IR spectrum (KBr): 1700, 1635 cm^{-1}.

Found: C, 68.02; H, 8.90; N, 6.20%. Calcd for $C_{26}H_{40}N_2O_5$: C, 67.79; H, 8.76; N, 6.08%.

***p*-Methoxybenzyloxycarbonyl-L-methionine Dicyclohexylammonium Salt.** This *p*-methoxybenzyloxycarbonyl amino acid was prepared from 7.46 g of L-methionine (0.05 mol) and 0.1 mol of I by a procedure similar to the synthesis of L-valine derivative. Its dicyclohexylamine salt was obtained as a white precipitate. Recrystallization of the salt from ethanol and petroleum ether gave pure needle crystals; yield, 21.76 g. IR spectrum (KBr): 1705, 1635 cm^{-1}.

Found: C, 63.14; H, 8.86; N, 5.76%. Calcd for $C_{26}H_{12}N_2O_5S$: C, 63.12; H, 8.56; N, 5.66%.

***α*-*N*-*p*-Methoxybenzyloxycarbonyl-*δ*-*N*-benzyloxycarbonyl-L-ornithine Dicyclohexylammonium Salt.** α-*N*-*p*-Methoxybenzyloxycarbonyl-*δ*-*N*-benzyloxycarbonyl-L-ornithine, an oily compound, was prepared from 13.3 g of *δ*-*N*-benzyloxycarbonyl-L-ornithine[24] (0.05 mol) by the same procedure as for Z(OMe)-glycine.

It was dissolved in ether (100 m*l*), and 9.96 m*l* of dicyclohexylamine (0.05 mol) was added at 0—5°C. The white precipitate formed was filtered and washed with ether (14.34 g, mp 129—135°C). This was recrystallized from ethanol and petroleum ether. Yield, 10.2 g of pure product. IR spectrum (KBr): 1695, 1630 cm^{-1}.

Found: C, 66.91; H, 7.91; N, 6.94%. Calcd for $C_{34}H_{49}N_3O_7$: C, 66.75; H, 8.07; N, 6.87%.

The authors wish to express their thanks to the staff of the Research Laboratory of the Chugai Pharmaceutical Co., Ltd., for their elemental analyses.

24) B. C. Barrass and D. T. Elmore, *J. Chem. Soc.*, **1957**, 3134.

BULLETIN OF THE CHEMICAL SOCIETY OF JAPAN VOL. 43 181—187 (1970)

Study on the Binding Nature of Acridine Orange to DNA by Means of Flow Dichroism

Hiroko TAKESADA (née YAMAGAMI), Etsuko SAITO (née MORIGUCHI), Hitoshi FUJITA, Kenshi SUZUKI and Akiyoshi WADA*1

Chemistry Division, National Institute of Radiological Sciences, Chiba

(Received June 19, 1969)

The binding nature of acridine orange to DNA was studied by means of equilibrium dialysis and flow dichroism with spectrophotometric analysis. The adsorption isotherm of the acridine orange-DNA system was obtained by means of equilibrium dialysis. From the experiment, the binding constant (K) and the fractional amount of the binding site to the total number of nucleotides (f) were estimated for native- and heat-denatured DNA. Under a shear gradient, the acridine orange-DNA complex showed a negative dichroism in visible region as well as in the ultraviolet region. This implies that acridine orange is oriented on DNA rather perpendicularly to its main axis, like base pairs. The magnitude of the dichroism of the complex at 500 mμ, near the visible absorption peak of acridine orange, was larger than each value of the complex and that of the DNA itself (260 mμ). The transition moment corresponding to the absorption at 500 mμ may be oriented in a more orderly manner and/or more nearly perpendicularly to the main axis of DNA than that corresponding to 260 mμ.

It was found that acridine orange (AO) acted as a sensitizer in the photodynamic inactivation of transforming DNA extracted from *Diplococcus pneumoniae* and that the inactivation was mediated by the dye bound to the DNA.[1] The damage to DNA accompanying the inactivation must resulted from an energy migration system involving the bound dye. In order to clarify the mechanism of the photodynamic action of DNA at a molecular level, physico-chemical studies of the binding of the dye to DNA are required.

The primary interest should be in the binding amount of the dye and the mode of binding. The nature of the acridine dye-DNA complex has been

*1 Visiting Researcher from Department of Physics, Faculty of Science, The University of Tokyo, Hongo, Bunkyo-ku, Tokyo.

1) H. Fujita, H. Yamagami, E. Moriguchi, K. Suzuki and A. Wada, presented at the 17th Annual Meeting of The Chemical Society of Japan, 1964.

reported on by many investigators.[2-8] Lerman[5] proposed an intercalation model; *i.e.*, acridine is inserted into the space between adjacent base pairs of DNA. He also[6] measured the polarized fluorescence and the dichroism of a flowing quinacrine-DNA solution and emphasized the former, which was considered to be strong evidence for his model. This model is supported by some other evidences also, *i.e.*, the reactivities of an acridine and amino groups of bases,[7] the mass per unit length,[9] the sensitized fluorescence,[10] the delayed fluorescence,[11] and the autoradiography.[12] The differential flow dichroism is one of the most sensitive techniques for demonstrating the arrangement of dye on DNA as well as the base-arrangement in a DNA molecule.[13] Nagata *et al.*[14] studied the interaction of polynuclear aromatic hydrocarbons, 4-nitroquinoline 1-oxides, and various dyes with DNA by applying the flow dichroism method developed by Wada and Kozawa.[15] In the present study, we measured the differential flow dichroism of the AO-DNA complex with the absorption spectra in order to obtain basic data for the interpretation of the photodynamic action. In addition to this, the binding constant and the fractional amount of the binding site to the total number of nucleotides were determined from the results of quantitative equilibrium dialysis.

Experimental

DNA. Pneumococcal DNA (R/Sm) was used throughout the present work in relation to the study of bacterial transformation. It was prepared by Marmur's method.[16] Bacteriophage T_2-DNA extracted by the method of Mandel and Hershey[17] was also used in the flow dichroism measurements. Denatured DNA was prepared by heating native DNA in a boiling-water bath for 15 min and by then rapidly chilling it in ice water.[18] Partially-denatured DNA was made by placing a solution of native DNA in a 0.001M phosphate buffer containing 0.0001M EDTA and 0.0025M NaCl (pH 7.0) at temperatures near but below the 'melting' temperature, *i. e.*, 62.5 and 64°C, for 15 min, followed by rapid chilling. The concentration of the DNA was determined from its optical density ($\varepsilon_{258}=6600$).

Dye. AO (Tokyo Chemical Industry) was purified in the following way.[19] It was dissolved in a mixture of water and ethanol (1 : 1), and 0.1N NaOH was added to precipitate it in the form of a free base. The dried precipitate was recrystallized twice from a mixture of water and ethanol (1 : 9). Finally the crystal was dried in a vacuum over P_2O_5. The purified AO base was identified by its melting point. A stock solution was prepared by dissolving a purified AO-base in water and by then neutralizing it with HCl.

Buffer Solution. The buffer solutions used were 0.15M NaCl+0.015M sodium citrate (pH 7.3) and a 0.001M phosphate buffer containing 0.0001M EDTA and 0.0025M NaCl (pH 7.0). The former, called the standard saline-citrate solution (abbreviated as SSC), was used in the study of equilibrium dialysis. The latter, with a low ionic strength, was used in the measurements of the flow dichroism in order to minimize the amount of unbound dye.

AO-DNA Complex. The mixture of AO and DNA was shaken vigorously in a test tube with a stopper and then stored in the dark for several hours to allow it to attain equilibrium. The composition of the mixture or the complex was expressed as the molar ratio of the nucleotide to the added dye, P/D, or of the nucleotide to the bound dye, P/D_b.

Absorption Spectrum. Measurements of the absorption spectra in the visible- and ultraviolet regions were made at room temperature by a Cary-14 spectrophotometer or by a Shimadzu spectrophotometer (Model QR-50). Silica cuvettes with a 1-cm light path were used. For diluted solutions, cuvettes with a 5-cm light path were used, while for concentrated ones a 0.8-cm silica spacer was used to make the light path 0.2 cm.

Equilibrium Dialysis. A Visking cellophane tube (23 A, 20/32) was used. The cellophane tube was washed with distilled water and conditioned by being immersed in SSC for more than 12 hr before use. Dialysis was performed with Erlenmeyer flasks in the dark. The cellophane bag containing 4 m*l* of the DNA solution was immersed in 20 m*l* of a dye solution. Equilibrium was attained after 16 to 20 hr of mechanical shaking at 30°C in a water bath. The measurements of the optical density of the inner- and outer solutions were made at room temperature. The adsorption of the dye to the cellophane membrane was estimated to be 15 to 20% of the total amount of dye, but it was presumed

2) R. F. Steiner and R. F. Beers, Jr., "Polynucleotides," Elsevier Pub. Co., Amsterdam (1961), p. 301.
3) D. F. Bradley and M. K. Wolf, *Proc. Nat. Acad. Sci. U. S.*, **45**, 944 (1959).
4) D. F. Bradley and G. Felsenfeld, *Nature*, **184**, 1920 (1959).
5) L. S. Lerman, *J. Mol. Biol.*, **3**, 18 (1961).
6) L. S. Lerman, *Proc. Nat. Acad. Sci. U. S.*, **49**, 94 (1963).
7) L. S. Lerman, *J. Mol. Biol.*, **10**, 367 (1964).
8) D. M. Neville, Jr., and D. R. Davies, *ibid.*, **17**, 57 (1966).
9) V. Luzzati, F. Masson and L. S. Lerman, *ibid.*, **3**, 634 (1961).
10) G. Weill and M. Calvin, *Biopolymers*, **1**, 401 (1963).
11) I. Isenberg, R. B. Leslie, S. L. Baird, R. Rosenbluth and R. Bersohn, *Proc. Nat. Acad. Sci. U. S.*, **52**, 379 (1964).
12) J. Cairns, *Cold Spr. Harb. Symp. Quant. Biol.*, **27**, 311 (1962).
13) A. Wada, *Biopolymers*, **2**, 361 (1964).
14) C. Nagata, M. Kodama, Y. Tagashira and A. Imamura, *ibid.*, **4**, 409 (1966).
15) A. Wada and S. Kozawa, *J. Polym. Sci.*, **A2**, 853 (1964).
16) J. Marmur, *J. Mol. Biol.*, **3**, 208 (1961).
17) J. D. Mandel and A. D. Hershey, *Anal. Biochem.*, **1**, 66 (1960).
18) J. Marmur and D. Lane, *Proc. Nat. Acad. Sci. U. S.*, **46**, 453 (1960).
19) A. L. Stone and D. F. Bradley, *J. Amer. Chem. Soc.*, **83**, 3627 (1961).

that such adsorption did not affect the equilibrium between the inner- and outer solutions.

Flow Dichroism. The details of the theory and the apparatus for the measurement of the flow dichroism were reported by Wada and Kozawa.[15]

(a) Apparatus. Measurements were made by a Shimadzu spectrophotometer equipped with an attachment. A transparent rotating cell of fused silica and a polarizer of calcite are included in this attachment. The gap between the outer- and the inner coaxial cylinders is 0.5 mm; therefore, the light-path length is 1.0 mm. The rotation speed of the inner cylinder was measured by a tachometer. The direction of the electric vector of the plane-polarized light chosen was either perpendicular or parallel to the flow axis.

(b) Measurements. The reduced flow dichroism is defined as:

$$\Delta\varepsilon/\varepsilon = \frac{\varepsilon_{//}-\varepsilon_{\perp}}{\varepsilon} = \frac{(-\log I_{//}/I_{\perp})-(-\log I_{//0}/I_{\perp 0})}{(-\log I/I_0)} \times A$$

where $I_{\perp 0}$ and $I_{//0}$ are the intensities of incident polarized lights with the electric vector perpendicular to and parallel to the flow axis respectively, where $I_{\perp}$ and $I_{//}$ are the intensities of transmitted polarized lights with the electric vector perpendicular to and parallel to the flow axis respectively, and where A is a factor depending on the concentration of the solution and on the light path of the cell.

In the present study two sorts of measurements were made: (1) measurements of $\Delta\varepsilon/\varepsilon$ over a range of wavelengths (λ) at a constant velocity gradient (3090 sec^{-1}), and (2) measurements of $\Delta\varepsilon/\varepsilon$ at 260 and 500 mμ at various velocity gradients (G). The extent of the flow dichroism is a measure of the orientation both of a macromolecule itself to the flow axis and of the chromophore in the macromolecule to the molecular axis. The reduced flow dichroism at a perfect orientation, $B(\alpha)$, was estimated from the following relation:

$$\Delta\varepsilon/\varepsilon = A(G/\Theta)\cdot B(\alpha)$$

supposing that DNA is a rigid ellipsoid of evolution.[13] In this equation, G is the velocity gradient, Θ is the rotary diffusion constant, and α is the angle between the long axis of the macromolecule and the plane of the chromophore. Theoretically, $-B(\alpha)$ takes a value from -3.0 to 1.5, with α from 0 to 90 degrees.[15]

Experimental Results

Absorption Spectra. Figures 1 (A) and (B) show two series of absorption spectra; they were obtained by adding native and denatured DNA solutions respectively of various concentrations to an AO solution of a given concentration (0.9×10^{-5}M). It can be seen in Fig. 1(A) that the absorption maximum shifts from 492 to 500 mμ and that the molar extinction coefficient at the wavelength corresponding to the maximum absorption increases with an increase in the concentration of native DNA. In this series, an isosbestic point is observed at 490 mμ. The quantitative estimation of the bound dye in the equilibrium dialysis was made at this wavelength. At low P/D ratios, the shoulder at about 470 mμ is remarkably higher for denatured DNA (Fig. 1 (B)) than for the native DNA. It is gradually lowered, however, with an increase in the P/D ratio, finally attaining the same level as that for native DNA. In the case of denatured DNA, it appears that an isosbestic point is present at 485 mμ, but, contrary to the case for native DNA, the absorption curve of free AO does

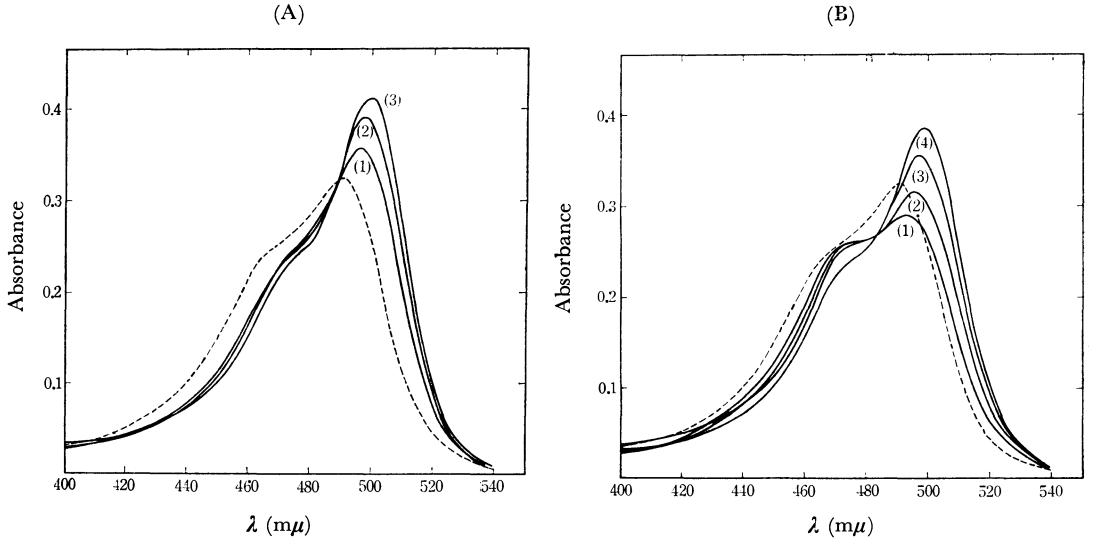

Fig. 1. The change of the absorption spectrum of AO solution by the addition of DNA (*Diplococcus pneumoniae*). The concentration of AO in SSC was 0.9×10^{-5}M. (A) Native DNA: ------, without DNA. ——, (1), (2) and (3) are the spectra in which P/D ratios are 10, 20 and 50, respectively. (B) Denatured DNA: ------, without DNA. ——, (1), (2), (3) and (4) are the spectra in which P/D ratios are 5, 10, 20 and 50, respectively.

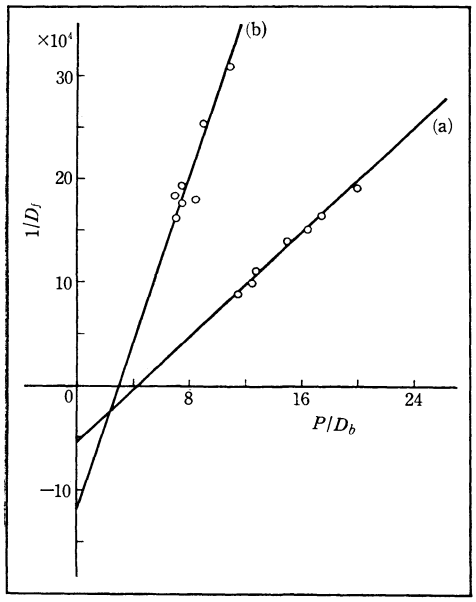

Fig. 2. Adsorption isotherm of AO to DNA in SSC at 30°C. The concentration of DNA (*D. pneumoniae*) was 20 μg/ml or 40 μg/ml (6 or 9×10^{-5}M$_p$).
(a) native DNA; (b) denatured DNA

not pass over this point, as can be seen in Fig. 1 (B). However, since it was shown by equilibrium dialysis that more than 80% of the dye cations were bound to the DNA even at ratios as low as 5, for convenience the extinction coefficient at 485 mμ was used to determine the amount of bound dye.

Equilibrium Dialysis. The adsorption isotherm was obtained in the following way. The binding constant (K) of one AO cation to a site on DNA was assumed not to be variable even if neighboring sites had been occupied by other AO cations. Then, if the fraction (f) to the total amount of nucleotides (P) in DNA is involved in forming a complex with AO, K must be given by $K=D_b/(Pf-D_b)\cdot(D_f)$. In this equation, D_f and D_b are the amounts of the unbound free dye and of the bound dye respectively. They were calculated from the optical density of the outer solution and from the difference in the optical densities of the inner- and outer solutions. P was obtained from the optical density at 258 mμ of the DNA solution. If $1/D_f$ is plotted against P/D_b, the intercept on the ordinate must give K, and that on the abscissa, $1/f$ (see Fig. 2). The values obtained at 30°C are, for the native DNA, $K=5.5\times10^4$ l/mol and $1/f=4.3$, and for the denatured DNA, $K=1.2\times10^5$ l/mol and $1/f=3.0$. Both K and f were larger for denatured DNA than for native DNA. Since the molar concentration of DNA was taken to be sufficiently lower than that of the buffer itself, the difference in the concentration of electrolytes between the inner- and outer solutions was considered to be negligible.

Flow Dichroism of the Complex. The AO-DNA complex showed a negative flow dichroism

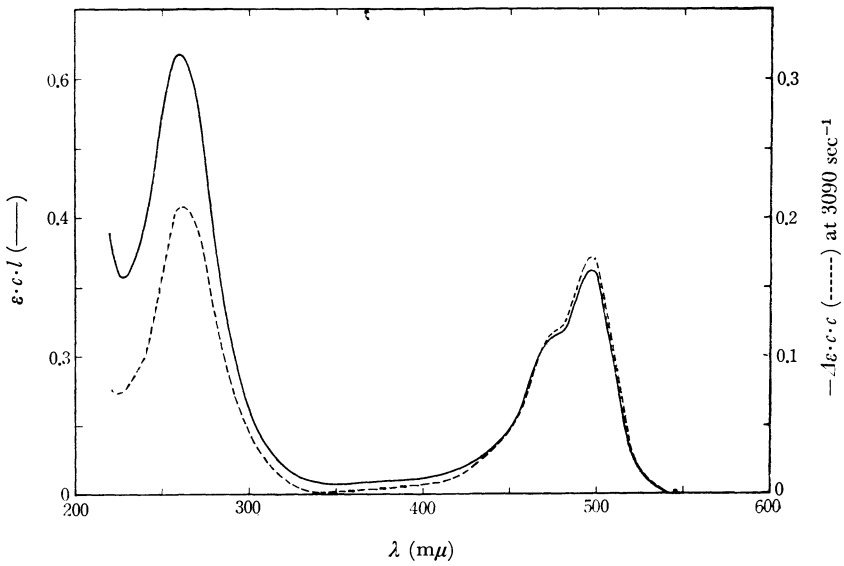

Fig. 3. Absorption spectrum (——) and differential flow dichroic spectrum (------)of AO-DNAcomplex. The concentrations of DNA and AO were 1.5×10^{-3}M$_p$ and 1.87×10^{-4}M, respectively. DNA and AO were dissolved in 0.001M phosphate buffer containing 0.0001M EDTA and 0.0025M NaCl (pH 7.0). Under this condition, more than 99.6% of AO cations are bound to DNA and the ratio of nucleotide to bound dye (P/D_b) is about 8.

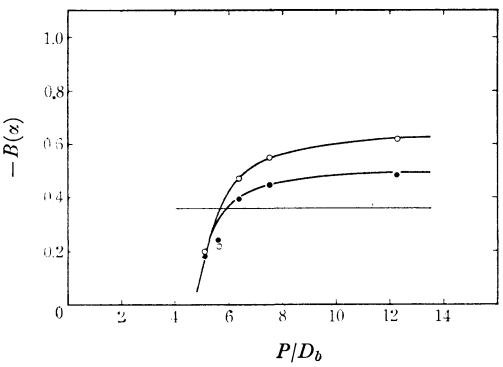

Fig. 4. The differential flow dichroism at varying P/D_b ratios of the complex of AO and native DNA. The concentration of DNA was 4.0×10^{-4} to 1.58×10^{-3}M$_p$ in 0.001M phosphate buffer containing EDTA and NaCl (see the legend of Fig. 3). The complex was prepared through the equilibrium dialysis at 30°C. —○—, complex at 500 mμ; —●—, complex at 260 mμ; ———, DNA (4.9×10^{-4}M$_p$) at 260 mμ.

in the visible region as well as in the ultraviolet region. Figure 3 shows the results of the differential flow dichroism of the complex at a P/D_b ratio of 8 over a range of wavelengths at a constant velocity gradient (3090 sec^{-1}). The dichroism of the complex measured with varying P/D_b ratios at 260 mμ and 500 mμ is shown in Fig. 4. The value of $-B(\alpha)$ of pneumococcal DNA at 260 mμ was 0.36. This is smaller than that of the complex at 260 or 500 mμ above a P/D_b of 6. At a P/D_b of 12, the value at 500 mμ of the complex was 1.7 times that of the DNA at 260 mμ. The lower values of $-B(\alpha)$ in the region of P/D_b below 6 may be due to the formation of intermolecular aggregates of the complex. Contrary to the case of pneumococcal DNA, the value of $-B(\alpha)$ at 260 mμ of the bacteriophage T_2 DNA-AO complex was nearly equal to the value at 500 mμ and also to the value of DNA itself (Preliminary experiment).

The value of $-B(\alpha)$ for DNA is very sensitive to its molecular conformation. For example, the value was diminished by partial denaturation depending on the temperature at which the DNA had been treated. The preparations of partially denatured DNA with different values of $-B(\alpha)$ at 260 mμ were equilibrated with AO at 20°C by dialysis and the flow dichroism of the complexes was measured. As is shown in Table 1, the values of the complexes at 260 mμ were decreased by elevating the treated temperature, as were those of the DNA. The value at 500 mμ of the complex, the DNA of which had been treated at 62.5°C, was larger than that of the corresponding DNA; the same tendency was seen in the complex with the native DNA.

Table 1. The effect of partial denaturation of DNA on the values of $-B(\alpha)$ of DNA (*D. pneumoniae*) and its complex with AO*

	Complex with AO		DNA
	at 500 mμ	at 260 mμ	at 260 mμ
Native DNA	0.66	0.46	0.41
Heated at 62.5°C	0.46	0.27	0.24
Heated at 64.0°C	0.15	0.15	0.15

* The concentration of DNA is 1.18×10^{-3}M$_p$. P/D_b=10.5 to 13.1
The buffer solution is the same as described in the legend of Fig. 3.

Discussion

For the analysis of the equilibrium dialysis and the flow dichroism, the amount of dye bound to DNA should be determined as accurately as possible. However, the concentration of the dye can not be simply determined from the optical density, since the observed spectrum of AO in the presence of DNA is composed of the spectra corresponding to the free monomer, the bound monomer, the free aggregate and the bound aggregate of the dye; that is, it changes depending on the P/D ratio. When various amounts of native- or denatured DNA were added to the AO solution, a series of spectra were obtained. The clear isosbestic point was observed for the native DNA-AO system. For the denatured system, the real isosbestic point was not observed, but the absorption curves passed over one point in the P/D-ratio range from 5 to 50. The extinction coefficients at these wavelengths were used for the calculation of the concentration of AO.

As may be seen in Fig. 1, the absorption spectra of the AO-denatured DNA mixture are very similar to that of the AO-native DNA mixture in the region of high P/D ratios, but it is rather different at low ratios. It is likely that, in a mixture with an extremely high P/D ratio, the dye cations bound to DNA must keep a large distance between them and so there should be very little dye-dye interaction. Therefore, the conformational change of DNA does not produce any spectral modification at such high P/D ratios. On the contray, an interaction between bound dye cations can be expected at low P/D ratios. Actually, this sort of interaction appears to occur more strongly on the denatured DNA-AO complex, since the shoulder band at about 470 mμ in the absorption spectrum is higher for the denatured DNA than for the native DNA, when the spectra for these complexes are measured at the same P/D ratio.

From the f value obtained by the adsorption isotherm, it appears that AO cations can bind to native DNA up to the ratio of 1 to 4.3 nucleotides at most. On the other hand, the ratio was 1 to 3 in the case of denatured DNA. The binding constant, K, for the denatured DNA was about twice as large

as that for the native DNA. Thus it was concluded that a large amount of AO can bind to the denatured DNA than to the native DNA. This suggests that the bases may provide further binding sites since they must come to be exposed to an outer medium by the denaturation, or that the denaturation facilitates, in some way, the adsorption of dye-aggregates to DNA, while the total number of binding sites does not increase.

The f value for the native DNA is in agreement with the saturation value of the "strong binding" obtained for the proflavine-herring sperm DNA system at an ionic strength of 0.1 at 20°C by Peacocke and Skerret.[20] Chambron *et al.*[21] investigated the thermodynamics of the interaction of proflavine and calf thymus DNA. They obtained values of $\log K=5.30$ ($K=2.0\times10^5$) and $1/f=6.1$ at 35°C, and values of $\log K=5.50$ ($K=3.2\times10^5$) and $1/f=4.4$ at 20°C, for the complex with the native DNA at an ionic strength of 0.1. The K values for their system are 4 to 5 times as large as that for the present system, while the f values for their system seem to be a little smaller than that of the present system. This discrepancy may be due to the differences in the experimental conditions and in the methods of estimating the values. They introduced the interaction energy between two bound dye-cations into their calculation, whereas we neglected it.

The principle of the ultraviolet flow dichroism of DNA must also be applicable to AO cations firmly bound to DNA. Since the oscillator dipoles of the π–π^* transition of bases and dye are known to be in the plane of these aromatic molecules, the magnitude of $-B(\alpha)$ gives an index of the orientation of the bases or dye to the long axis of the DNA molecule. The experimental results on the AO-DNA complex may be summarized as follows: (1) The AO-DNA complex gave a negative flow dichroism in the visible as well as in the ultraviolet region.

(2) The complex of pneumococcal DNA and AO gave a larger $-B(\alpha)$ value at 500 mμ than at 260 mμ, while both values are over that of DNA itself.

(3) A reduced dichroism, $(\Delta\varepsilon/\varepsilon)$, was almost constant throughout any visible region at the velocity gradient of 3090 sec^{-1}.

The theoretical value of $-B(\alpha)$ is 1.5 at 90 degrees of α,[15] but the observed values are much smaller. This may be attributed to the coexistence of random coiling parts in the DNA and small fragments, which were made during the extraction process, and/or of a folding structure of DNA like a hairpin with residual proteins.

The dichroism at 500 mμ of the complex must be due to the AO cations bound to DNA, since it was not observed in the absence of DNA. The (1) evidence suggests that the plane of the bound AO is nearly parallel to the plane of the bases in DNA. If AO cations are inserted into the spaces between base pairs parallel to them, the dichroism shown by bound dye could not be over the value for the DNA. However, the experimental result presented in (2) is not consistent with this view. According to the viscosity measurements,[5] DNA becomes longer and straighter by the binding of acridine dyes in solution. Considering that a longer molecule can be oriented more easily and gives a higher value of $-B(\alpha)$,[13] the present result that the $-B(\alpha)$ at 260 mμ of the complex is larger than that of DNA itself is reasonable. One model to explain the $-B(\alpha)_{500\,m\mu} > -B(\alpha)_{260\,m\mu}$ relation in the complex is that AO cations bind selectively to ordered parts rather than to disordered parts of DNA. However, this model is inconsistent with the results of equilibrium dialysis. Another model is as follows: On some loose structure of DNA, the transition moment corresponding to the absorption at 500 mμ may be oriented in a more orderly manner and/or nearly perpendicularly to the main axis of the DNA compared with that corresponding to 260 mμ. If the transition moments of 500 and 260 mμ were in the directions parallel to the long and short axes of AO respectively, the transition moment along the long axis could be oriented more in parallel to the plane of bases, but the other moment would be slightly declined. Actually, in the case of bacteriophage T_2-DNA which is believed to be more intact and to have better chain regularity,[13] the $-B(\alpha)$ at 500 mμ of the complex was nearly equal to the values at 260 mμ of the complex and of the DNA itself.

It can be seen in Fig. 3 that the dichroic spectrum is almost identical with the absorption spectrum. The shoulder band at about 470 mμ is also observed in the dichroic spectrum, and $\Delta\varepsilon/\varepsilon$ is almost constant over the range of wavelengths in the visible region. If the shoulder band in an absorption spectrum is attributed to dye-aggregates, the shoulder in a dichroism at the same wavelength might be also due to the dye-aggregates. However, it would be impossible to insert the dye-aggregates, even if they are dimers, into the spaces between base pairs in the sense of the intercalation model. Thus, the observed shoulder at about 470 mμ in the dichroic spectrum at the P/D_b ratio of 8 may be attributed to the characteristic of the AO monomer, as has been suggested by Zanker.[22]

As has been mentioned earlier, the intercalation model is supported by several pieces of evidence.

20) A. R. Peacocke and J. N. H. Skerrett, *Trans. Faraday Soc.*, **52**, 261 (1956).

21) J. Chambron, M. Daune and Ch. Sadron, *Biochim. Biophys. Acta*, **123**, 306 (1966); *ibid.*, **123**, 319 (1966).

22) V. Zanker, *Z. Physik. Chem.*, **199**, 225 (1952).

On the other hand, Peacocke *et al.*[23,24] proposed a modified intercalation model based on their spectrophotometric analysis. In this model, when acridine cations are bound by the "process 1" (defined by them), the acridine lies between successive nucleotide bases on the same polynucleotide chain, in a plane approximately parallel to the base planes, in which the cationic-ring nitrogen is as close as possible to a phosphate group of DNA and in which the edges of the acridine rings (positions 1—4 or 6—9) partially overlap the base ring(s) of DNA. The present dichroic measurements show that the plane of the acridine dye is oriented parallel to that of the bases rather than perpendicular. However, by this method we can not distinguish between the intercalation model and the modified one. Although the nature of binding site is still obscure, it is very likely that phosphate groups and the spaces between adjacent base pairs of DNA act as sites of binding with acridine dye.

23) D. S. Drummond, V. F. W. Simpson-Gildemeister and A. R. Peacocke, *Biopolymers*, **3**, 135 (1965).

24) N. J. Pritchard, A. Blake and A. R. Peacocke, *Nature*, **212**, 1360 (1966).

BULLETIN OF THE CHEMICAL SOCIETY OF JAPAN VOL. 43 187—191 (1970)

Study on Oxazolopyrimidines. I. Synthesis and Spectroscopic Properties of 7-Aminooxazolo[5,4-*d*]pyrimidines

Yozo Ohtsuka

Sagami Chemical Research Center, Ohnuma, Sagamihara

(Received June 19, 1969)

Several 2- and 5-substituted oxazolo[5,4-*d*]pyrimidines have been prepared from 5-amino-4-cyanooxazole derivatives *via* *N*-ethoxymethylene intermediates in order to compare them with purine derivatives. Spectroscopic data and some chemical properties of these compounds were examined. A convenient method for the preparation of a starting material was described.

Oxazolo[5,4-*d*]pyrimidines, whose chemical structure is similar to that of natural purines, are of interest as antimetabolites.[1] These compounds may also serve as models for 9-substituted purine skeletons and as synthetic intermediates for several biologically important materials. Although several of them have been prepared mainly from pyrimidine derivatives,[1,2] relatively little attention has been paid to oxazolopyrimidines, because probably none of these compounds has been found in natural products or their biological activities are indistinct. The object of the present study is twofold: one is to compare the physico-chemical data of oxazolopyrimidine and purine derivatives and the other is to find new reactions from these compounds to purine derivatives.

7-Aminooxazolo[5,4-*d*]pyrimidine may be considered the 9-0-analog of adenine. In this paper, the synthesis and spectroscopic properties of a number of 7-aminooxazolo[5,4-*d*]pyrimidine derivatives are described.

Results and Discussion

5-Amino-4-cyanooxazoles (I). Several 2-substituted 5-amino-4-cyanooxazoles were prepared by the known method.[3] For the 2-unsubstituted derivative (Ia), new and convenient method of preparation were found. One of them, the reduction of phenylazomalononitrile by zinc and formic acid afforded the compound (Ia) with a fairly good yield.

1) a) G. H. Hitchings, F. B. Elion, H. Van der Werff and E. A. Falco, *J. Biol. Chem.*, **174**, 765 (1948). b) G. H. Hitchings, G. B. Elion, E. A. Falco, P. B. Russel, M. B. Sherwood and H. Van der Werff, *ibid.*, **183**, 1 (1950), *ibid.*, **192**, 525 (1951). c) E. A. Falco, G. B. Elion and G. H. Hitchings, U. S. 2807616 (1957).

2) a) T. Johnson, *Amer. Chem. J.*, **34**, 191 (1905). b) H. Biltz and K. Strufe, *Ann.*, **404**, 170 (1914). c) E. A. Falco, G. B. Elion, E. Burgi and G. H. Hitchings, *J. Amer. Chem. Soc.*, **74**, 4897 (1952). d) K. Shirakawa, *Yakugaku Zasshi*, **73**, 643 (1953). e) G. P. Hager and C. Kaiser, *J. Amer. Pharm. Assoc.*, **44**, 193 (1955). f) M. Ishidate and H. Yuki, *Chem. Pharm. Bull.* (Tokyo), **8**, 137 (1962). g) T. Nishiwaki, *Nature*, **211**, 737 (1966). h) H. Bredereck, F. Effenberger and E. H. Schweizer, *Chem. Ber.*, **95**, 956 (1962).

3) J. P. Ferris and L. E. Orgel, *J. Amer. Chem. Soc.*, **88**, 3829 (1966).

Table 1. *N*-Ethoxymethylene derivatives of 5-amino-4-cyanooxazole

Compound			Yield (%)	A*	Mp, °C (bp, °C/mmHg)	Elemental analysis					
	R	R′				Calcd			Found		
						C(%)	H(%)	N(%)	C(%)	H(%)	N(%)
IIa	H	H	89	Dist., Et_2O	27—28 (94/0.06)	50.90	4.28	25.45	50.52	4.17	25.19
IIb	H	CH_3	70	Dist.	(89—90/0.06)	53.62	5.06	23.45	53.41	5.09	23.33
IIc	CH_3	H	84	MeC_6H_{11}	57—58	53.62	5.06	23.45	53.51	5.11	23.40
IId	CH_3	CH_3	64	Dist., MeC_6H_{11}	45—47 (95—97/0.11)	55.95	5.74	21.75	56.23	5.71	21.87
IIe	H	C_2H_5	98	Dist.	(85—86/0.4)	55.95	5.74	21.75	55.42	5.37	21.34
IIf	C_2H_5	H	83	Dist.	(105—107/0.2)	55.95	5.74	21.75	55.86	5.69	21.65
IIg	H	C_6H_5	39	MeC_6H_{11}	85—88 (155—156/0.8)	64.72	4.60	17.42	64.88	4.59	17.49
IIh	C_6H_5	H	50	MeC_6H_{11}	101—102	64.72	4.60	17.42	64.55	4.45	17.63
IIi	H	OC_2H_5	98	Et_2O-Petroleum ether	41—42 (136—137/0.2)	51.67	5.30	20.09	51.35	5.21	19.97

* Method of purification or solvent of recrystallization

Table 2. Spectroscopic properties of *N*-ethoxymethylene derivatives

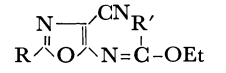

	NMR*			IR** -C≡N	UV***	
	R	R′	OC_2H_5			
IIa	7.61(1)	8.33(1)	4.38(2) 1.42(3)	2237	226 (6560)	271(10700)
IIb	7.60(1)	2.22(3)	4.33(2) 1.37(3)	2232	222 (8340)	273(10000)
IIc	2.41(3)	8.24(1)	4.39(2) 1.40(3)	2225	221 (5840)	277(12200)
IId	2.40(3)	2.19(3)	4.28(2) 1.36(3)	2230	221 (7360)	277 (8820)
IIe	7.64(1)	2.52(2) 1.21(3)	4.36(2) 1.38(3)	2233	242 (8900)	274 (8490)
IIf	2.72(2) 1.34(3)	8.25(1)	4.41(2) 1.40(3)	2227	223 (6590)	277(11400)
IIg	7.43(1)	7.38(5)	5.00(2) 1.47(3)	2236	231(15600)	287 (4300)
IIh	7.91(2) 7.23(3)	8.37(1)	4.44(2) 1.42(3)	2231	213(12200)	305(18300)
IIi	7.33(1)	4.33(4) 1.38(6)		2234	225 (4660)	267(16300)

* δ-Value in ppm, $CDCl_3$ solution with TMS (relative integrated intensity).
** NaCl liquid film (a, e, d, f, g and i) or KBr pellet (b, d, c and h), in cm^{-1}.
*** MeOH solution, in mμ (ε).

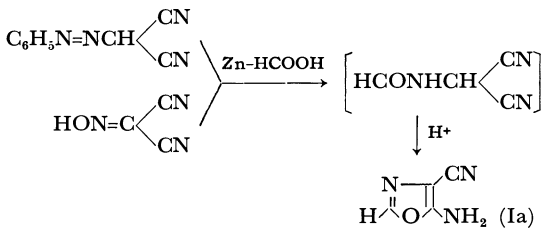

The resulting formamidomalononitrile seems to cyclize readily to the oxazole compound under acidic conditions. Hence, the product obtained by the reduction of isonitrosomalononitrile under a similar condition was also confirmed to be compound (Ia). No detectable difference was observed by the addition of acid anhydride in the system. Under the latter condition, the formation of acylaminomalononitrile has been cited in a patent.[4]

The chemical property of compound (Ia) was examined briefly. An attempt to obtain the *N*-acetyl derivative was unsuccessful. On being warmed with alkali, it decomposed to water soluble fragments. With acid it was hydrolyzed to formamidocyanoacetamide, and with hydrogen peroxide

4) K. Tanaka, T. Sugawa and S. Kimata, Japan. 424280 (1963).

TABLE 3. 7-AMINOOXAZOLO[5,4-*d*]PYRIMIDINE DERIVATIVES

Compound R	Compound R′	Yield* (%)	Solvent of recryst	Mp, °C	Elemental analysis Calcd C(%)	Calcd H(%)	Calcd N(%)	Found C(%)	Found H(%)	Found N(%)
IIIa	H	78	EtOH, H_2O	245—247	44.12	2.96	41.17	44.16	2.89	40.88
IIIb	H	CH_3 60	EtOH	191—193	48.00	4.03	37.32	47.94	4.10	37.33
IIIc	CH_3	H 84	EtOH	251—252	48.00	4.03	37.32	47.74	4.16	37.40
IIId	CH_3	CH_3 64	EtOH	211—212	51.21	4.91	34.13	51.11	4.89	34.14
IIIe	H	C_2H_5 98	H_2O	146—147	51.21	4.91	34.13	51.17	4.49	34.35
IIIf	C_2H_5	H 83	H_2O	186—187	51.21	4.91	34.13	50.82	4.91	33.96
IIIg	H	Ph 39	EtOH	214—215	62.25	3.80	26.40	61.67	3.75	26.44
IIIh	Ph	H 50	EtOH	300—301	62.25	3.80	26.40	61.83	3.73	26.46
IIIi	H	OC_2H_5 98	EtOH	211—212	46.66	4.48	31.10	46.42	4.56	31.07

* Based on II's.

TABLE 4. SPECTROSCOPIC PROPERTIES OF 7-AMINOOXAZOLO[5,4-*d*]PYRIMIDINE DERIVATIVES

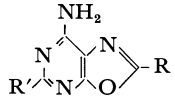

Compd	NMR* R	NMR* R′	NMR* NH_2	IR**					UV***	
IIIa	8.65(1)	8.31(1)	7.72(2)	3286 3107	1680 1120	1612 1587	1051	796	205.0(17600)	252.4(14600)
IIIb	8.51(1)	2.44(3)	7.56(2)	3370 3190	1675 1116	1609 1588	1067	791	207.4(20060)	254.7(13900)
IIIc	2.56(3)	8.14(1)	7.47(2)	3323 3159	1666 1118	1622 1598	1021	801	205.8(16100)	252.8(16100)
IIId	2.54(3)	2.40(3)	7.33(2)	3292 3131	1675 1127	1610 1598	1020	794	206.1(22300)	254.8(16600)
IIIe	8.51(1)	2.71(2) 1.24(3)	7.54(2)	3289 3072	1670 1113	1611 1602	1042	800 809	208.5(22000)	254.1(14200)
IIIf	2.91(2) 1.34(3)	8.17(1)	7.48(2)	3209 3063	1663 1110	1626 1590	1032	807	208.2(19100)	254.2(17200)
IIIg	8.65(1)	7.9 (5)	7.75(2)	3320 3200	1642 1115	1602 1587	1041	780	211.6(25000)	245.8(23300) 265.6(15600)
IIIh	7.9 (5)	8.42(1)	7.61(2)	3266 3098	1673 1137	1623 1593	1044	795	208.1(22000) 266 (8800)	235.6(18800) 302.8(22600)
IIIi	8.40(1)	4.28(2) 1.32(1)	7.61(2)	3308 3155	1677 1117	1622 1590	1056	791	211.1(22500)	261.5(14300)

* δ-Value in ppm, DMSO-d_6 solution with TMS (relative intensity)
** KBr pellet, in cm^{-1}
*** MeOH solution, in mμ (ε)

in alkaline solution, hydrolysis proceeded further to form oxamide.

7-Aminooxazolo[5,4-d]pyrimidine Derivatives (IIIa—i). Direct condensation of 5-amino-4-cyanooxazole (Ia) with formamidine to yield 7-aminooxazolopyrimidine (IIIa) has been reported to give a low yield.[3] However, it was found that the yield and the method of purification were improved by the application of Taylor's method of

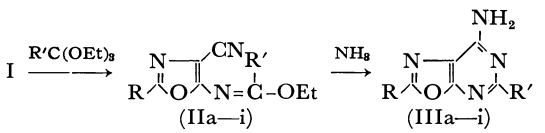

(IIa—i) (IIIa—i)

a) R=R′=H
b) R=H, R′=CH_3
c) R=CH_3, R′=H
d) R=R′=CH_3
e) R=H, R′=Et
f) R=Et, R′=H
g) R=H, R′=Ph
h) R=Ph, R′=H
i) R=H, R′=OEt

pyrimidine synthesis[5] on this system. Several 5-substituted derivatives can be obtained conveniently by this method.

5) E. C. Taylor, A. McKillop and R. N. Warrener, *Tetrahedron*, **23**, 891 (1967) and references cited therein.

N-Ethoxymethylene intermediates (II) (Tables 1 and 2) react readily with aqueous ammonia to 7-aminooxazolopyrimidines (Table 3).

Spectroscopic Properties of 7-Aminooxazolopyrimidines. *a) NMRS pectra.* The spectra for 7-aminooxazolopyrimidines in DMSO-d_6 solution, together with the assignments, are presented in Table 4. The chemical structures of these compounds are well supported by the spectra. The chemical shift of the C–H proton on the pyrimidine ring, δ_{H-5} (corresponding to the H-2 for purines), approaches the value for 9-substituted purines, such as adenosine and inosine,[6] as expected from the chemical structure. It seems to indicate the total aromatic system of the molecules in which the effect of 5-substitution on δ_{H-2} is nearly equal to that of 2-substitution on δ_{H-5}. Such a correlation of the chemical shifts with reactivity parameter of the substituents has been established in purine derivatives.[7] On the other hand, the 2-substituents have a greater influence on the chemical shifts of the N–H proton at 7-position than the 5-substituents. Geometrical proximity of the former substituent may be responsible for it.

b) IR Spectra. Existence of 7-NH_2 group in those molecules are expressed in the spectra in 3000 cm^{-1} region and near 1670 cm^{-1}. The latter band seems to correspond to that of adenine at 1672 cm^{-1}.[8] The bands attributed to the NH_2 group are removed by deuteration. The broad band in the 2900—2400 cm^{-1} region in the spectra of purine derivatives[8] disappears in the spectra of oxazolopyrimidines. This is in accordance with the previous assignment that the band is aroused from the interaction between the imidazole proton and the external group, $-NH_2$ or $-OH$, of purine bases. The bands in 1620—1500 cm^{-1} region are common to pyrimidine derivatives.[9] The band near 1050 cm^{-1} is attributed to the C–O–C deformation vibration of oxazole ring, but it is not characteristic enough for analysis.

c) UV Spectra. The total absorption curve of IIIa is similar to those of adenine, 9-methyladenine and related compounds.[10,11] As shown in Table 4, the oxazolopyrimidines have two absorption bands between 200 and 260 mμ region which are presumably due to π–π^* transitions. The band at around 250 mμ corresponds to the 260 mμ band of adenine which has been correlated with the $A_{1g}\rightarrow B_{2u}$ transition of benzene.[12] Such a blue shift of the band in going from adenine to oxazolopyrimidines can be seen in a comparison of analogous pairs; benzoxazole[13] and benzimidazole,[12] $\Delta\lambda=4$ mμ, and hypoxanthine (pH$<$9) and adenine, $\Delta\lambda=11$ mμ.[10]

This may be explained by the difference in the conjugation of the heteroatoms with the aromatic systems. The spectra did not change substantially in the aqueous solution in the pH-range of 4—9.

d) Mass Spectra. The characteristic peaks of some oxazolopyrimidines are shown in Table 5. These data indicate the principal fragmentation process of 7-aminooxazolopyrimidine ring system. The most intense peak of the compounds is that of the molecular ion. The primary fragments occur

Table 5. Characteristic peaks of mass specsra of 7-aminooxazolo[5,4-*d*]pyrimidines*

Compd.	*m/e*		Metastable peak	Relative abundance
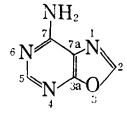 (IIIa)	136	M^+		1.00
	109	$[M-27]^+$	87.4*	0.41
	81	$[(M-27)-28]^+$	60.1*	0.11
	54	$[(M-55)-27]^+$	36.0*	0.32
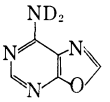 (IIIa′)	138	M^+		1.00
	111	$[M-27]^+$	89.2*	0.46
	83	$[(M-27)-28]^+$	62.0*	0.19
	56	$[(M-55)-27]^+$	37.8*	0.52
	55	$[(M-55)-28]^+$	36.5*	0.33
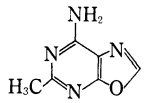 (IIIb)	150	M^+		1.00
	109	$[M-41]^+$	79.0*	0.28
	81	$[(M-41)-28]^+$	60.2*	0.12
	54	$[(M-69)-27]^+$	36.0*	0.22
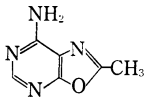 (IIIc)	150	M^+		1.00
	123	$[M-27]^+$	100.9*	0.54
	95	$[(M-27)-28]^+$	73.4*	0.13
	54	$[(M-55)-41]^+$	36.6*	0.34
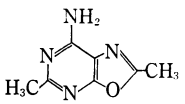 (IIId)	164	M^+		1.00
	123	$[M-41]^+$	92.3*	0.62
	95	$[(M-41)-28]^+$	73.4*	0.21
	54	$[(M-55)-41]^+$		0.14

* Conditions of measurement: 70 eV, 200—100°C (Direct)

6) F. J. Bullock and O. Jardetzky, *J. Org. Chem.*, **29**, 1988 (1964).

7) W. C. Coburn, Jr., M. C. Thorpe, J. A. Montogomery and K. Hewson, *ibid.*, **30**, 1110, 1114 (1965).

8) A. R. Katritzky and A. P. Ambler, "Physical Method in Heterocyclic Chemistry," Vol. 2, Academic Press, New York (1963) p. 302.

9) C. H. Willits, J. C. Decius, K. L. Dille and B. E. Christensene, *J. Amer. Chem. Soc.*, **77**, 2569 (1955).

10) G. H. Beaven, E. R. Holiday and E. A. Johnson, "The Nucleic Acids," Vol. 1, Academic Press, New York (1955), p. 498.

11) R. F. Stewart and N. Davidson, *J. Chem. Phys.*, **39**, 254 (1963).

12) L. B. Clark and I. Tinoco, Jr., *J. Amer. Chem. Soc.*, **87**, 11 (1965).

13) D. D. M. Casoni, A. Mangini, R. Passerini and C. Zoni, *Gazz. Chim. Ital.*, **88**, 977 (1958).

at M−27, due to loss of HCN, and in the case of 5-methyl derivatives at M−41, due to loss of CH_3CN. This fact and subsequent fragmentation show that the initial expulsion of HCN fragment originated uniquely from C-5–N-4. This process is followed by the expulsion of CO fragment which is observed in the spectra of all the compounds in the table as the peak at M′−28 (M′=M−28 or M−41). The CO fragment must have originated from C-3a–O-3. The third process produces the peak *m/e* 55 due to the expulsion of HCN, or in the case of 2-methyl derivatives, the expulsion of CH_3CN. It is inferred to involve N-1–C-2. It is very probable that the ND_2 compound (IIIa′) produces the DCN fragment which suggests the amino group participation in the process. Another minor process of the step is the expulsion of NH(ND) instead of HCN(DCN).

The characteristic fragmentation pattern of purine bases has shown the succesive expulsion of three molecules of HCN.[14] The fragments do not originate exclusively from the same site of the molecules (in the case of adenine or hypoxanthine),[15] while the ring expulsion of thiazolo[5,4-*d*]pyrimidine has been reported to occur from the fixed site of the molecule.[16] The result of oxazolopyrimidine is parallel to that of thiazolopyrimidine. In both cases, the primary process is the pyrimidine ring rupture and subsequent process is determined by the nature of five-membered rings.[17]

From these spectroscopic properties, the following conclusion can be drawn. The molecule of 7-aminooxazolopyrimidines constitutes a totally aromatic system and some of their properties are similar to those of 9-substituted adenines. However, the nature of the individual ring seems to be kept to some extent. This is caused probably by the decreased contribution of the lone-pair electron of heteroatom with the conjugated system.

Experimental

Synthesis of 5-Amino-4-cyanooxazole (Ia). *Method A.* A mixture of 45 g of zinc powder and 300 m*l* of 99% formic acid was warmed to 40°C under nitrogen with gentle stirring. To the suspension, 30 g of pulverized phenylazomalononitrile[18] was added portionwise until the reaction became self-sustaining, at which point the bath was removed to maintain the temperature at 40—50°C. After the addition, the reaction mixture was stirred for 30 min. The solid was filtered off and washed thoroughly with formic acid. The combined solution of the washings and filtrate was concentrated to nearly dryness under reduced pressure keeping the bath temperature below 40°C. Adding about 50 m*l* of water to the residue, evaporation was repeated. The final residue was allowed to stand overnight in a refrigerator. Resulting crystals were washed with a small quantity of water and taken up in 100 m*l* of water in which the residual acid was neutralized with ammonia. Recrystallization from water gave the product, 9.0 g (47%). This product was confirmed to be identical with the authentic 5-amino-4-cyanooxazole[3] from the mixed melting point determination, IR and NMR spectra.

About 3 g of colorless crystals were also obtained from the mother liquid of the recrystallization. This compound, mp 157—158°C, was identified as formamidocyanoacetamide, from its IR spectra (C≡N; 2160 cm^{-1}, amide; 1710 and 1670 cm^{-1}) and from the fact that the prolonged heating of the material in formic acid afforded formamidomalonodiamide.[19]

Method B. Analogous reduction was conducted using the ether solution of isonitrosomalononitrile[20] instead of phenylazomalononitrile. The product was identical with that produced by method A, but the yield was considerably lower. No difference was observed by the reduction in the presence of acetic anhydride.

Reaction of 5-Amino-4-cyanooxazole (Ia). Alkaline oxidation by hydrogen peroxide and acid hydrolysis of Ia were examined.

a) To an ice-cooled mixture of 1.0 g of Ia and 0.56 g of KOH in 20 m*l* of ethanol, 20 ml of hydrogen peroxide (30%) was added with stirring. After 1 hr, colorless crystals were obtained (0.6 g), which were identified as formamidocyanoacetamide (see method A). After standing for 2 days at room temperature, the precipitate was filtered off (0.4 g). Its analysis and IR spectra agreed with those of oxamide.

b) A solution of 1.0 g of Ia in 30 m*l* of formic acid (85%) was heated under reflux for 2 hr. After cooling, the solution was evaporated, and the residue was recrystallized from a small quantity of water. This product was confirmed to be formamidocyanoacetamide.

Preparation of *N*-Ethoxymethylene Intermediates. Compound I (5 g), 30 m*l* of acetic anhydride and 30 m*l* of orthoesters (including tetraethyl orthocarbonate) were heated under reflux for 7 hr. After concentrating the reaction mixture, the residue was distilled under reduced pressure. Yields and analytical data are summarized in Table 1 and structures confirmed from spectroscopic data are shown in Table 2.

Preparation of 7-Aminooxazolo[5,4-d]pyrimidines. *N*-Ethoxymethylene intermediates and a little excess of 14% ammonia water were stirred at room temperature for 30 min. Oxazolopyrimidines were separated as colorless crystals. Yields and analytical data are listed in Table 3.

Determination of Physical Properties. Melting points were measured on a hot-stage apparatus and were not corrected. The IR, Mass, NMR and UV spectra were determined with a Perkin-Elmer 337, Hitachi RMU-6E, Varian HA-100 and Carry-14 spectrometer respectively. Conditions of these measurements are cited in each table.

14) T. Goto, A. Tatematsu and S. Matsuura, *J. Org. Chem.*, **30**, 1844 (1965).

15) J. M. Rice and G. O. Dudek, *J. Amer. Chem. Soc.*, **89**, 2719 (1967).

16) T. Tatematsu, S. Inoue, S. Sugiura and T. Goto, *Nippon Kagaku Zasshi*, **87**, 66 (1966).

17) H. Budzikiewicz, C. Djerassi and D. H. Williams, "Mass Spectrometry of Organic Compounds," Holden-Day Inc., San Francisco, Cal. (1967) p. 637.

18) A. Hantzsche and K. J. Thompson, *Ber.*, **38**, 2266 (1905).

19) M. Conrad and A. Schultze, *ibid.*, **42**, 733 (1909).

20) G. Ponzio, *Gazz. Chim. Ital.*, **61**, 575 (1931).

BULLETIN OF THE CHEMICAL SOCIETY OF JAPAN VOL. 43 192—195 (1970)

Cyanoethylation of Copper, Nickel, and Palladium Glycinates*1

Toshiyuki SHONO, Yuko YAMASHOJI and Koichiro SHINRA

Department of Chemical Technology, Faculty of Engineering, Osaka University, Yamada-kami, Suita

(Received June 20, 1969)

The present authors attempted the cyanoethylation of the methylene group in glycine by means of the reaction between acrylonitrile and copper, nickel, and palladium glycinates. The cyanoethylation of *N*-salicylideneglycinato-aquo copper (II) was also carried out. Four kinds of cyanoethylated complexes were obtained by changing the reaction conditions in the case of copper glycinate. In general, acrylonitrile reacted only with the hydrogen atoms of the amino group. In the case of *N*-salicylidene-glycinato-aquo copper (II), which has no hydrogen atom on the nitrogen atom, however, two methylene hydrogens were cyanoethylated with acrylonitrile.

Masking by coordination has been found to be useful in many of the synthetic reactions of α-amino acid molecules.[1] The general procedure involves coordination with a copper(II) ion to tie up the carboxyl and the α-amino group, leaving the other functional groups free to react with a reagent.

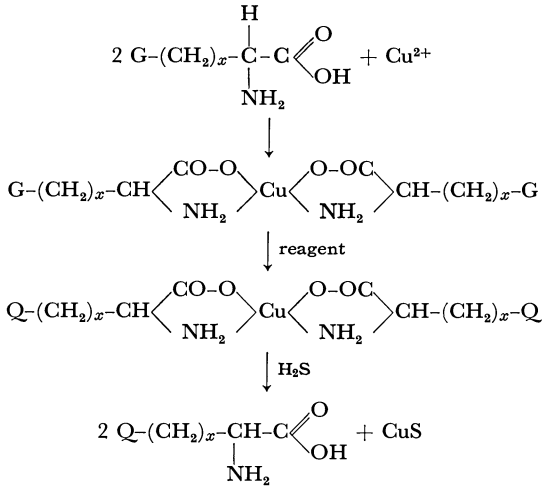

In 1956, Akabori and his co-workers synthesized threonine from copper(II) glycinate and acetaldehyde.[2] In doing so they utilized ligand polarization in addition to masking by coordination. The methylene group in copper glycinate may be more active than in free glycine, and the amino group in the copper chelates may be protected from side reactions by the coordination effect.

Recently Harada and Oh-hashi[3] have synthesized various β-hydroxy-α-amino acids using *N*-salicylideneglycinato-aquo copper(II), while Nakahara *et al.*[4] has prepared several amino acids by the reaction of this complex with various halides. In 1950, Mckinney *et al.*[5] reported the treatment of an aqueous solution of alkali metal salts of glycine with acrylonitrile. This reaction, however, have only a mono-*N*-cyanoethyl compound. In view of the masking effect and ligand polarization mentioned above, the present authors attempted the cyanoethylation of the methylene group in glycine by reactions between acrylonitrile and copper, nickel, and palladium glycinates. For the same reason, the cyanoethylation of *N*-salicylidene-glycinato-aquo copper(II) was carried out.

Experimental

The Cyanoethylation of Copper(II) Glycinate. Copper(II) glycinate was prepared according to the method described by Akabori *et al.*[2] 0.02M of copper glycinate was dissolved in 200 m*l* of aqueous pyridine composed of 150 m*l* of water and 50 m*l* of pyridine. Into this solution, acrylonitrile was stirred drop by drop. After refluxing the mixture, the dark-blue solution was evaporated to precipitate a blue complex, which was then recrystallized from water. Four kinds of cyanoethylated complexes were obtained by changing the reaction conditions, as Tables 1 and 2 show.

Regeneration of the Ligand. The cyanoethylated complex was dissolved in hot water and neutralized with hydrochloric acid. Hydrogen sulfide gas was bubbled through the solution until the blue color had disappeared, and then the precipitated cupric sulfide

*1 Presented at the 18th Meeting on Coordination Chemistry of Japan, Kyoto, September, 1968.

1) M. M. Jones "Ligand Reactivity and Catalysis," Academic Press, New York and London (1968).

2) M. Sato, K. Okawa and S. Akabori, This Bulletin, **30**, 937 (1957).

3) K. Harada and J. Oh-hashi, *J. Org. Chem.*, **32**, 1103 (1967).

4) A. Nakahara, S. Nishikawa and J. Mitani, This Bulletin, **40**, 2212 (1967).

5) L. L. Mckinney, E. H. Uhing, E. A. Setzkorn and J. C. Cowan, *J. Amer. Chem. Soc.*, **72**, 2599 (1950).

Table 1. The cyanoethylation of copper(II) glycinate

Code	Reaction conditions: Temp. (°C)	Time (hr)	Mole ratio (glycinate/AN)	Appearance of compound	Yield (%)	Infrared absorption max. of ν C≡N(cm⁻¹)
1	80	4	1/2	Blue-violet needles	50	2250
2	110	4	1/2	Dark blue needles	50	(disappeared)
3	80	4	1/20	Blue plates	60	2245 and 2265
4	80 110	4 4	1/20	Light blue needles	40	2250

was filtered. The solution was neutralized with aqueous sodium carbonate and evaporated to dryness. The white residue obtained was recrystallized from water.

The Cyanoethylation of Palladium Glycinate. Palladium glycinate was prepared according to the method described by Pinkard *et al.*[6]

0.02M of palladium glycinate was dissolved in 80 m*l* of aqueous pyridine composed of 40 m*l* of pyridine and 40 m*l* of water. To this solution, 0.08M acrylonitrile was added, drop by drop. Then the temperature was gradually raised and the reaction was continued for 4—5 hr at the boiling point. After an insoluble matter had been filtered out, the solution was evaporated to obtain a brownish porous material (yield 40%). The product was recrystallized from water.

The infrared spectrum of this complex is shown in Fig. 1, where it is compared with palladium(II) *N*-cyanoethylglycinate. The infrared spectrum of palladium(II) *N*-cyanoethylglycinate shows one NH stretching band at 3230 cm^{-1}, while this complex has no absorption band in this region.

The results of the elementary analysis of the complex (tetracyanoethylglycinate) were as follows:

Found: C, 39.75; H, 4.47; N, 17.66%. Calcd for $C_{16}H_{20}N_6O_4Pd\cdot H_2O$: C, 39.75; H, 4.55; N, 17.36%.

The NMR spectra of this complex were compared with *N*-cyanoethylglycine (CH_2 at τ=7.70 in DMSO-d_6) and palladium(II) *N*-cyanoethylglycinate (CH_2 at τ=6.67 in DMSO-d_6). The signal centered at τ=6.40 in DMSO-d_6 was considered to be due to the methylene group of the glycine part.

The Cyanoethylation of Nickel Glycinate. Nickel glycinate was prepared according to the method described by Sen *et al.*[7]

The cyanoethylation was carried out under the same conditions as was the cyanoethylation of palladium glycinate. As this complex could not be recrystallized, it was repeatedly reprecipitated from an ethanol-water system to produce a light blue powder in an 80% yield. The infrared spectrum agreed with that of the authentic nickel *N*-cyanoethylglycinate prepared from cyanoethylglycine and basic nickel carbonate.

The Cyanoethylation of *N*-Salicylideneglycinato-aquo Copper(II): [SAGCu(II)H_2O]. SAGCu(II)H_2O was prepared by the method of Nakahara.[8] 0.02M of SAGCu(II)H_2O was dissolved in 50 m*l* of hot pyridine. Into this solution, 0.04M of acrylonitrile was stirred, drop by drop. The temperature was gradually raised to the boiling point of the solvent, after which the reaction was continued for 3—4 hr. After the reaction had been completed, the solution was evaporated to precipitate a dark green complex; this complex was then recrystallized from water to obtain deep green needles in a yield of 35%. The cyanoethylated complex of the *N*-salicylideneglycinato copper(II) coordinated with pyridine was dark brown, while the hydrate was dark green. Slow recrystallization from water yielded deep green needles forming a hexa-hydrate complex. This hexa-hydrated complex lost water to the mono-hydrated complex when dried under reduced pressure

Table 2. The elementary analyses of copper(II) cyanoethyl glycinates

Code	Proposed structures	Elementary analyses
1	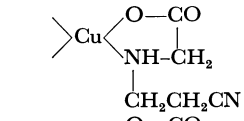	Calcd for $C_{10}H_{14}N_4O_4Cu.H_2O$: C, 35.77; H, 4.80; N, 16.69; Cu, 18.92%. Found: C, 35.93; H, 4.83; N, 16.98; Cu, 19.13%.
2	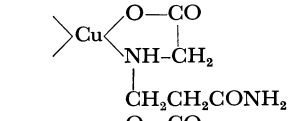	Calcd for $C_5H_{10}N_2O_3$:* C, 41.10; H, 6.85; N, 19.18%. Found: C, 40.99; H, 6.97; N, 19.65%.
3	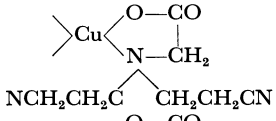	Calcd for $C_{16}H_{20}N_6O_4Cu.H_2O$: C, 43.49; H, 4.98; N, 19.02; Cu, 14.38%. Found: C, 43.24; H, 5.08; N, 18.87; Cu, 14.50%.
4	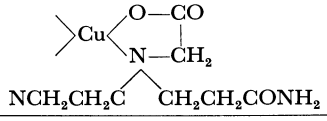	Calcd for $C_{16}H_{24}N_6O_6Cu.H_2O$: C, 42.09; H, 5.44; N, 17.59; Cu, 13.30%. Found: C, 41.89; H, 5.46; N, 17.40; Cu, 13.20%.

* Organic ligand only.

6) F. W. Pinkard, E. Sharratt, W. Wardlaw and E. G. Cox, *J. Chem. Soc.*, **1934**, 1012.

7) D. N. Sen, S. Mizushima, C. Curran and J. U. Quagliano, *J. Amer. Chem. Soc.*, **77**, 211 (1955).

8) A. Nakahara, This Bulletin, **32**, 1195 (1959).

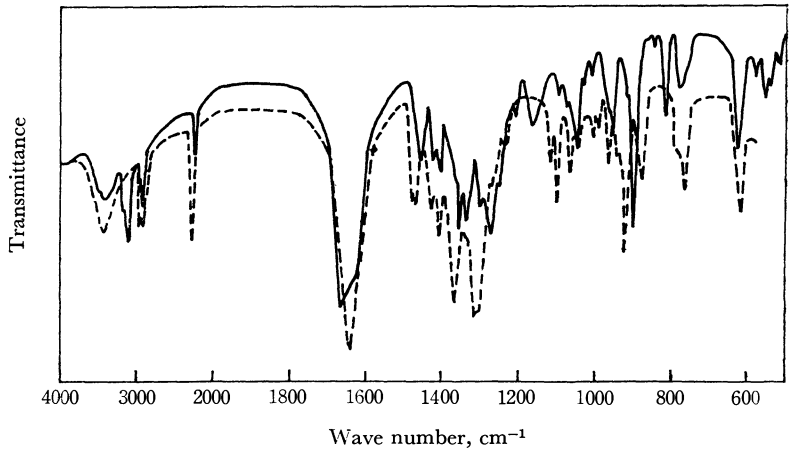

Fig. 1. The IR spectra of palladium(II) cyanoethylglycinates.
—— Paladium(II) *N*-cyanoethylglycinate
------ Palladium(II) tetracyanoethylglycinate

at 80—90°C for 5 hr.

The elementary analysis of the mono-hydrate form gave the following results:

Found: C, 49.38; H, 4.20; N, 11.44; Cu, 17.32%. Calcd for $C_{15}H_{15}N_3O_4Cu$: C, 49.38; H, 4.14; N, 11.52; Cu, 17.42%.

The Synthesis of *N*-Cyanoethylglycine. *N*-Cyanoethylglycine was prepared according to the method of Mckinney *et al.*[5]

Copper *N*-Cyanoethylglycinate. *N*-Cyanoethylglycine was dissolved in hot water, and then basic copper carbonate was added to precipitate *N*-cyanoethylglycine copper. The product was recrystallized from water to produce blue violet needles.

Palladium *N*-Cyanoethylglycinate. *N*-Cyanoethylglycine was dissolved in water, and then $K_2(PdCl_4)$ was added. After standing for 24 hr, the solution was neutralized with aqueous sodium hydroxide. The separated yellow solid was recrystallized from water to produce yellow needles.

Nickel *N*-Cyanoethylglycinate. The basic nickel carbonate was added in small portions to a hot aqueous solution of *N*-cyanoethylglycine to produce nickel *N*-cyanoethylglycinate. As the complex could not be recrystallized, purification was carried out by repeated reprecipitation from an ethanol-water system until a light blue, deliquescent powder was obtained.

Results and Discussion

The infrared spectrum (Fig. 2) of the (code 1) complex is in good agreement with the spectrum of the copper *N*-cyanoethylglycinate.

In the (code 2) complex the cyano group is hydrolyzed to the acid amide form (NH stretching at 3400 cm^{-1}, NH_2 deformation at 1620 cm^{-1}). The

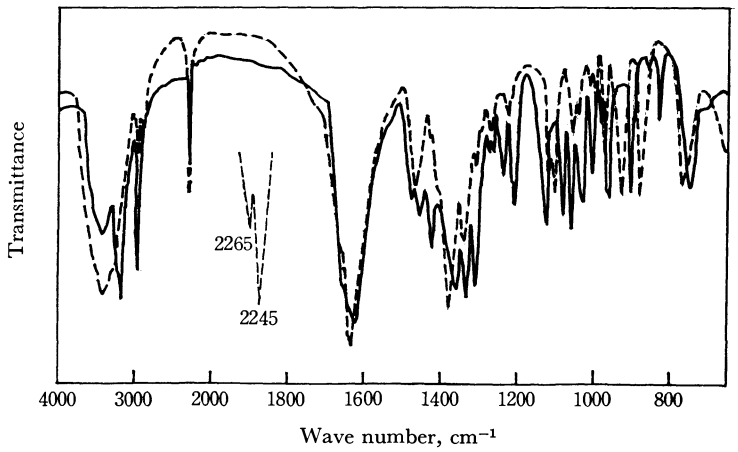

Fig. 2. The IR spectra of copper(II) cyanoethylglycinates.
—— Copper(II) *N*-cyanoethylglycinate (code 1)
------ Copper(II) tetracyanoethylglycinate (code 3)

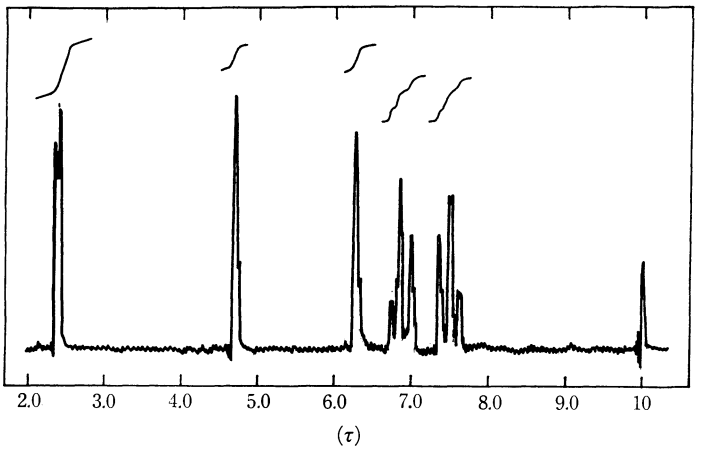

Fig. 3. The NMR spectrum of *N,N*-bis(cyanoethyl)glycine *p*-bromophenacyl ester (60 Mc, in $CDCl_3$)

appearance of two absorption bands due to CN stretching vibrations near 2250 cm^{-1} and the disappearance of the NH stretching vibration at 3200 cm^{-1} of the complex (code 3) suggest that two cyanoethyl groups were introduced to the amino nitrogen atom. From the results of the elementary analysis, the complex may be considered to be hydrate. As it was difficult to purify the complex, the copper was precipitated as copper sulfide and the organic ligand was isolated as the *p*-bromophenacyl derivative (light yellow needles, mp 63°C). The NMR spectrum of the *p*-bromophenacyl ester (see Fig. 3), obtained using chloroform-d as the solvent, that the acid part of the ester is *N,N*-bis(cyanoethyl)-glycine (CN stretching at 2250 cm^{-1}, CO stretching at 1733 and 1697 cm^{-1}).

The (code 4) complex was obtained by raising the reaction temperature to 110°C. On the basis of a comparison of the infrared spectra, it may be supposed that one of the cyanoethyl groups introduced at first was hydrolyzed to the amide group (one CN streching band and a new NH stretching band appeared).

As the SAGCu(II)·H_2O had no active hydrogen atom on the nitrogen atom, the two active hydrogen atoms of the glycine methylene group were cyanoethylated with acrylonitrile.

In the case of copper, palladium, and nickel glycinate, the amino group was supposed to be protected by coordination and cyanoethylation should have occurred at the methylene group of the glycine part. However, acrylonitrile reacted with the hydrogen atoms of the amino group. From the copper glycinate, a tetracyanoethyl complex was obtained by the additonal cyanoethylation of the dicyanoethylated compound, but no higher cyanoethylation occurred. The results for the nickel glycinate were the same as for the cyanoethylation of glycine itself, metal complexing had no effect.

In comparison to nickel glycinate, the palladium glycinate was easily cyanoethylated to the tetracyanoethyl compound. In this case, the cyanoethyl group was stable and was not hydrolyzed by alkali. As we would expect two cyanoethyl groups to be replaced on the free glycine, the reaction was repeatedly attempted by changing the amount of alkali and acrylonitrile. However, only the mono-*N*-cyanoethyl compound was obtained.

It is of interest that though only one of the amino hydrogens in free glycine was cyanoethylated in alkali, the two hydrogen atoms were replaced when coordinating with a transition metal ion (Cu^{2+}, Pd^{2+}, but not Ni^{2+}).

BULLETIN OF THE CHEMICAL SOCIETY OF JAPAN VOL. 43 196—200 (1970)

Synthesis of Corticotropin Peptides. IX. Synthesis of [1-Glycine]-ACTH(1—18)-Octadecapeptide Amide

Hideo Otsuka, Masaru Shin, Yasuhiko Kinomura and Ken Inouye

Biochemistry Division, Shionogi Research Laboratory, Shionogi & Co., Ltd., Fukushima-ku, Osaka

(Received June 20, 1969)

The synthesis is decribed of an octadecapeptide, glycyl-tyrosyl-seryl-methionyl-glutamyl-histidyl-phenyl-alanyl-arginyl-tryptophyl-glycyl-lysyl-prolyl-valyl-glycyl-lysyl-lysyl-arginyl-arginine amide, corresponding to the first eighteen amino acid residues of corticotropin except for the amino end which has been replaced by a glycine for the serine in the native hormone. The protected end product was obtained by two different coupling procedures, the active ester and the catalyzed carbodiimide, from the amino-terminal decapeptide and the octapeptide of carboxyl end. The over-all yields of the peptide, for the final coupling, deblocking and purification steps, in the active ester and the carbodiimide procedures were approximately forty and thirty per cent, respectively. The synthetic octadecapeptide amide has been shown to possess a high adrenal corticotropic activity, which is comparable to that of the corresponding l-serine octadecapeptide amide, and a lipolytic activity which is significantly lower than that of the l-serine analog.

In a previous communication we reported the synthesis of a corticotropin peptide, ACTH(1—18)-amide (I), which was shown to possess a high steroidogenic potency.[1] In 1963 Lebovitz and Engel reported that the amino-terminal serine of porcine corticotropin could be converted into a glycine without loss of corticotropic activity.[2] This implies that the hydroxymethyl group of amino-terminal serine is not essential for the activity in case of the native hormone. In connection with this finding, the synthesis of a peptide, corresponding to the first eighteen amino acid residues of adrenocorticotropin (ACTH) except for the amino end which was substituted by a glycine for the serine in the parent peptide I, was undertaken as an attempt to prepare analogs of corticotropin peptides. Here will be described the synthesis of the octadecapeptide amide, glycyl-tyrosyl-seryl-methionyl-glutamyl-histidyl-phenylalanyl-arginyl-tryptophyl-glycyl-lysyl-prolyl-valyl-glycyl-lysyl-lysyl-arginyl-arginine amide (II), which may be designated as [Gly[1]]-ACTH(1—18)-NH_2 for abbreviation.[3]

In the final reaction leading to the protected end product, the fragment corresponding to the first ten amino acid residues was coupled with the one corresponding to the rest of the molecule by two different procedures, the *N*-hydroxysuccinimide-catalyzed carbodiimide method[4] and the active ester method.[5] The syntheses of both fragments as intermediates have been already reported.[6]

A protected decapeptide Boc-Gly-Tyr-Ser-Met-Glu(OBu^t)-His-Phe-Arg-Trp-Gly-OH (III)[6a] and a partially protected octapeptide H-Lys(Boc)-Pro-Val-Gly-Lys(Boc)-Lys(Boc)-Arg-Arg-NH_2 (IV),[6b] which had been converted into the hydrochloride, were coupled with *N*,*N*′-dicyclohexylcarbodiimide (DCC) in the presence of *N*-hydroxysuccinimide as a catalyst to lead to the formation of a protected octadecapeptide Boc-Gly-Tyr-Ser-Met-Glu(OBu^t)-His-Phe-Arg-Trp-Gly-Lys(Boc)-Pro-Val-Gly-Lys(Boc)-Lys(Boc)-Arg-Arg-NH_2 (V). The crude product was submitted for purification to chromatography on a column of carboxymethyl cellulose (CMC) in the 50% *t*-butanol - 2M ammonium acetate (pH 5.70) system (Fig. 1). The purified V was obtained in a yield of 50% and was found to be homogeneous in thin-layer chromatography. The protecting groups of V were then removed by treatment with 90% trifluoroacetic acid to liberate the octadecapeptide II. The crude product was, after having been converted into the acetate by treatment with an anion-exchange resin (acetate form), purified on

1) H. Otsuka, K. Inouye, F. Shinozaki and M. Kanayama, *J. Biochem.* (Tokyo), **58**, 512 (1965).

2) H. E. Lebovitz and F. L. Engel, *Endocrinol.*, **73**, 573 (1963).

3) All amino acid residues are of the L-configuration. The abbreviated designation of amino acids, peptides and their derivatives accords with the proposal of the IUPAC-IUB Commission on Biochemical Nomenclature.

4) E. Wünsch and F. Drees, *Chem. Ber.*, **99**, 110 (1966).

5) G. W. Anderson, J. E. Zimmerman and F. M. Callahan, *J. Amer. Chem. Soc.*, **86**, 1839 (1964); *ibid.*, **85**, 3039 (1963).

6) a) H. Otsuka, K. Inouye, F. Shinozaki and M. Kanayama, This Bulletin, **39**, 1171 (1966); b) H. Otsuka, K. Inouye, M. Kanayama and F. Shinozaki, *ibid.*, **39**, 882 (1966).

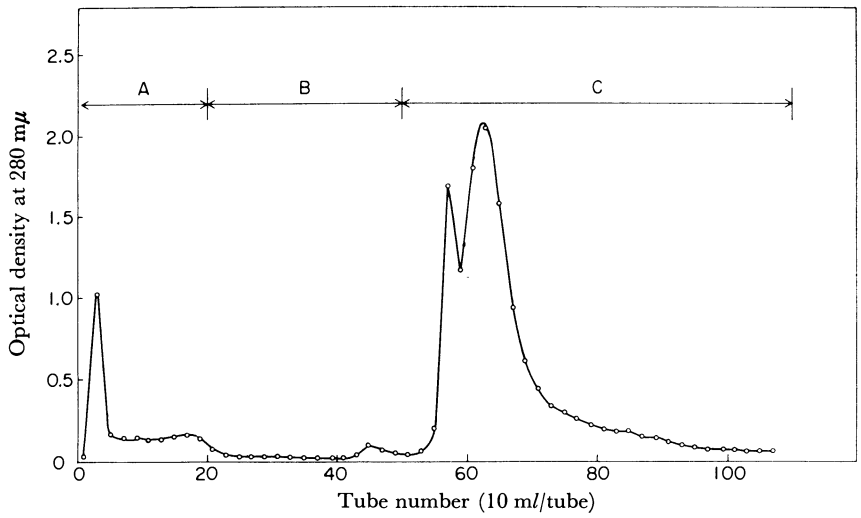

Fig. 1. Chromatography of protected octadecapeptide amide (V) on a carboxymethyl cellulose column. Material: crude product, 0.139 g. Column: carboxymethyl cellulose (Serva, 0.44 meq/g), 1.6×9 cm. Solvent: A, 50% *t*-butanol; B, 50% *t*-butanol - 2M ammonium acetate, pH 5.70 (99 : 1, 150 m*l*) through a mixing chamber containing 50% *t*-butanol (150 m*l*); C, 50% *t*-butanol - 2M ammonium acetate, pH 5.70 (98: 2, 300 m*l*) through a mixing chamber containing 50% *t*-butanol - 2M ammonium acetate, pH 5.70 (99 : 1, 300 m*l*).

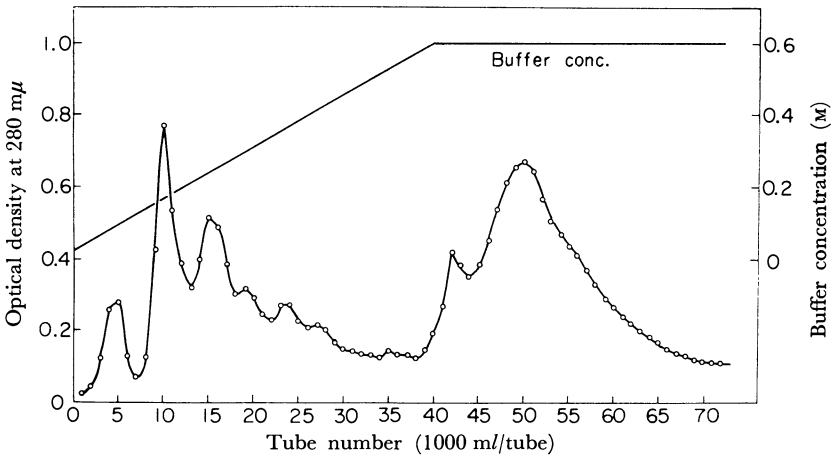

Fig. 2. Chromatography of octadecapeptide amide (II) on a carboxymethyl cellulose column.[7] Material: product obtained from crude protected octadecapeptide amide (V, 11.8 g). Column: carboxymethyl cellulose (Brown, 0.78 meq/g), 6.9×78 cm. Solvent: ammonium acetate buffer (pH 6.5).

a CMC column in the ammonium acetate buffers with successive concentration and pH gradients. The purified material was recovered from the main peak in a yield of 59%.

In an alternative procedure to obtain peptide II, decapeptide III was first esterified with *N*-hydroxysuccinimide by the DCC method[5] and the resulting active ester isolated was coupled with the acetate of octapeptide IV in the presence of triethylamine. The product was, without further purification, treated with 90% trifluoroacetic acid to remove the protecting groups. The crude octadecapeptide trifluoroacetate was converted by treatment with Amberlite IRA-400 (acetate form) into the acetate,

7) The data were taken from part of an experiment performed by Dr. Ikuo Kikkawa and staff of this Laboratory under the supervision of one of us (H.O.). We thank Dr. Kikkawa for permission to include this synthesis in the present communication.

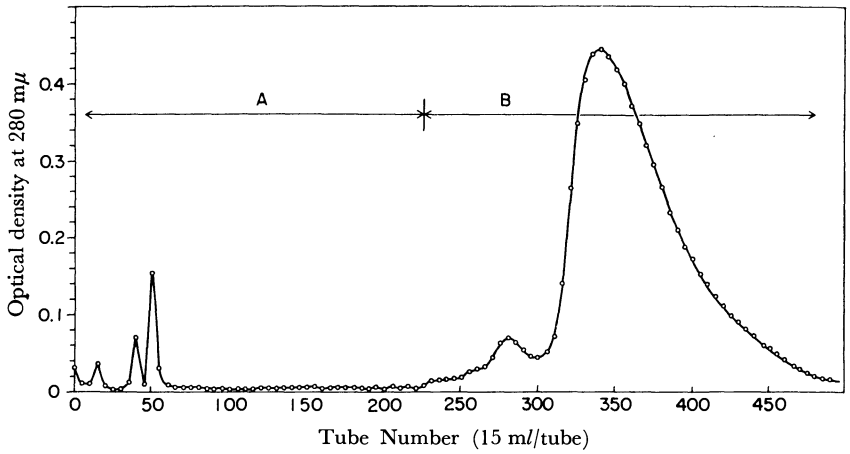

Fig. 3. Rechromatography of octadecapeptide amide (II) on a carboxymethyl cellulose column.[7] Material: partially purified II, 0.300 g. Column: carboxymethyl cellolose (Brown, 0.78 meq/g), 3.8×28 cm. Solvent: A, ammonium acetate (pH 6.5) with a linear concentration gradient of 0.025—0.6M, 3300 ml; B, 0.6M ammonium acetate (pH 6.8).

which was, after having been incubated with mercaptoethanol, submitted to chromatography on a CMC column using the ammonium acetate buffer (pH6.5) with a linear concentration gradient (Fig. 2). The octadecapeptide II was thus obtained in an over-all yield of 50% for the final coupling step. Further purification was carried out on a CMC column in the same manner as above in a recovery of 80% (Fig. 3).

In both cases peptide II obtained was found to be homogeneous to ninhydrin, Pauly, Ehrlich, Sakaguchi and methionine (PtI_6'') reagents in paper chromatography. Quantitative amino acid analysis[8] showed that an acid hydrolysate of the product contained the individual amino acids in the ratios expected by theory with the exception of tryptophan. The tryptophan-tyrosine ratio was determined spectrophotometrically to be unity.[9]

The biological properties of the octadecapeptide II are compared in Table 1 with those of the parent peptide I;[10] the latter has been reported.[1] The lipolytic activity of the Gly^1-analog (II) was found to be significantly lower than that of the Ser^1-peptide (I) and is on the same order of magnitude as that of a native corticotropin when assayed in the rat.[13] The adrenal stimulating activity of peptide II was assayed by three different procedures for the comparison with peptide I. A slightly higher activity was obtained with peptide II as compared with peptide I, when assayed by both *in vivo*[11] and *in vitro*[12] steroidogenesis procedures, whereas peptide II was found to be slightly less active than peptide I when assayed by the adrenal ascorbic acid depletion method. The synthesis of ACTH(1—23)-NH_2

Table 1. Biological activities of the synthetic octadecapeptides[10]

Peptide	Adrenal corticotropic[a] (USP units/mg)			Lipolytic[13] (Minimal effective dose, μg)	
	In vivo[b]	*In vivo*[11]	*In vitro*[12]	Rabbit	Rat
ACTH(1—18)-NH_2 (I)	45.4	62—173	10.6	0.000004	0.003
[Gly^1]-ACTH(1—18)-NH_2 (II)	21.8	161	14.9—20.2	0.00035	0.012

a) Potencies are represented in terms of the third USP Corticotropin Unit.
b) According to USP, XVII, 147 (1965).

8) D. H. Spackman, W. H. Stein and S. Moore, *Anal. Chem.*, **30**, 1190 (1958).
9) D. H. Beaven and E. R. Holiday, *Adv. Protein Chem.*, **7**, 319 (1952); T. W. Goodwin and R. A. Morton, *Biochem. J.*, **40**, 628 (1946).
10) The authors are much indebted to Dr. Akira Tanaka of this Laboratory for these biological assays: A. Tanaka, *Saishin Igaku* (Tokyo), **23**, 911 (1968).
11) A modification of Lipscomb and Nelson (H. S. Lipscomb and D. H. Nelson, *Endocrinol.*, **71**, 13 (1962)): A. Tanaka and C. H. Li, *Endocrinol. Japonica*, **13**, 180 (1966).
12) M. A. Saffran and A. V. Schally, *Endocrinol.*, **56**, 523 (1955).
13) A. Tanaka, B. T. Pickering and C. H. Li, *Arch. Biochem. Biophys.*, **99**, 294 (1962).

and the corresponding Gly[1]-analog was recently reported by Geiger *et al.*[14] They gave the latter a little higher value of activity as compared with that of the former, using the adrenal ascorbic acid depletion method.

Experimental

Glycyl-tyrosyl-seryl-methionyl-glutamyl-histidyl-phenylalanyl-arginyl-tryptophyl-glycyl-lysyl-prolyl-valyl-glycyl-lysyl-lysyl-arginyl-arginine Amide (II). *a) By the N-Hydroxysuccinimide-catalyzed Carbodiimide Method.* The partially protected octapeptide, H-Lys(Boc)-Pro-Val-Gly-Lys(Boc)-Lys (Boc)-Arg-Arg-$NH_2 \cdot 3CH_3COOH$,[6b] (IV, 0.074 g, 0.05 mmol) was dissolved in 3 m*l* of ice-cold 0.05N hydrochloric acid and the solution was immediately lyophilyzed to give the corresponding trihydrochloride. The protected decapeptide, Boc-Gly-Tyr-Ser-Met-Glu (OBu^t)-His-Phe-Arg-Trp-Gly-OH,[6a] (III, 0.080 g, 0.055 mmol) was dissolved in 1.5 m*l* of dimethylformamide together with the octapeptide hydrochloride obtained above, and to this solution were added *N*-hydroxysuccinimide (0.013 g, 0.11 mmol) and *N,N'*-dicyclohexylcarbodiimide (DCC, 0.014 g, 0.07 mmol) at 0°C. The reaction mixture was stirred at 0°C for one hour and at room temperature for 48 hr. *N,N'*-Dicyclohexylurea (DCU) which formed was filterred off and the filtrate was introduced into ice-cold ethyl acetate (100 m*l*). The precipitates which separated were filtered off, washed with cold ethyl acetate, and dried over phosphorus pentoxide *in vacuo* to afford 0.139 g of the crude product. This crude material (0.139 g) was dissolved in 5 m*l* of 50% *t*-butanol and to this was added Amberlite CG-4B (acetate form, 1.1 cc), and the mixture was shaken for 30 min. After removal of the resin, M mercaptoethanol (0.5 m*l*) was added to the filtrate. The mixture was, after having been incubated at 37°C overnight, subjected to chromatography on a column (1.6×9 cm) of carboxymethyl cellulose (Serva, 0.44 meq/g), using successively the following solvent systems: 50% *t*-butanol (200 m*l*); the one with a linear gradient obtained from 50% *t*-butanol (150 m*l*) and 50% *t*-butanol-2M ammonium acetate, pH 5.70 (99 : 1, 150 m*l*); the one with a linear gradient obtained from 50% *t*-butanol-2M ammonium acetate, pH 5.70 (99 : 1, 300 m*l*) and 50% *t*-butanol-2M ammonium acetate, pH 5.70 (98 : 2, 300 m*l*). The results of chromatography are shown in Fig. 1. Fractions corresponding to the main peak (tubes 55—70) were pooled and the bulk of the solvent was removed *in vacuo*. The residue was lyophilized to give the protected octadecapeptide (V); yield 0.105 g (50% on the weight basis). The material was found to be unreactive to ninhydrin and it behaved as a single component to Pauly and Sakaguchi reagents in thin-layer chromatography (Silica gel G, *n*-butanol-acetic acid-water=4 : 1 : 2 by volume as solvent).

To remove the protecting groups the purified peptide V (0.140 g) was treated with 90% trifluoroacetic acid (2 m*l*) at room temperature for 60 min. After the solvent had been removed *in vacuo* over potassium hydroxide pellets, the residue was dissolved in water, (5 m*l*). The aqueous solution was shaken with Amberlite CG-4B (acetate form, 2.5 cc) for one hour, and then the resin was removed by filtration. To the filtrate M mercaptoethanol (1 m*l*) was added and the mixture was, after having been kept at 37°C overnight, subjected to chromatography on a column (1.6×11 cm) of carboxymethyl cellulose (Serva, 0.44 meq/g), using successively the following ammonium acetate buffers: the one with a linear gradient obtained from 0.075M, pH 5.80 (400 m*l*) and 0.25M, pH 7.00 (400 m*l*); the one with a linear gradient obtained from 0.25M, pH 7.00 (450 m*l*) and 0.40M, pH 8.60 (450 m*l*); 0.40M, pH 8.60 (450 m*l*). Fractions (10 m*l*/tube) corresponding to the main peak (tubes 70—120) were combined and the bulk of the solvent was removed *in vacuo*. The residue was lyophilized repeatedly to constant weight and dried over phosphorus pentoxide *in vacuo* at 60°C to give the pure octadecapeptide (II); yield 0.070 g (59% for the deblocking step, as determined spectrophotometrically),[15] homogeneous (R_f=0.09) to ninhydrin, Pauly, Ehrlich, Sakaguchi and methionine (PtI_6'') reagents in paper chromatography (*n*-butanol-acetic acid-water=4 : 1 : 2 by volume as solvent). $[\alpha]_D^{23.5}$ −51.4±1.9° (*c* 0.472, 0.1N acetic acid). $\lambda_{max}^{0.1N\ NaOH}$=281 mμ (ε 6750), 288 mμ (ε 6490). Amino acid ratios in acid hydrolysate:[8] Ser 0.93, Glu 0.96, Pro 0.98, Gly 3.25, Val 1.00, Met 1.00, Tyr 1.05, Phe 1.00, Lys 3.23, His 1.07, NH_3 1.39, Arg 2.95, Trp 0.46 (decomposed partially with acid). The Trp/Tyr ratio in intact II was determined spectrophotometrically to be 0.91 : 1.[9]

b) By the Active Ester Method.[7] To a solution of Boc-Gly-Tyr-Ser-Met-Glu(OBu^t)-His-Phe-Arg-Trp-Gly-OH[6a] (III, 8.04 g, 5.2 mmol) in 240 m*l* of dimethylformamide were successively added N hydrochloric acid (5.2 m*l*), *N*-hydroxysuccinimide (2.4 g, 20.8 mmol) and DCC (4.3 g, 20.8 mmol) at an ice-salt bath temperature. The mixture was stirred at 4°C for 20 hr. Additional quantities of the succinimide (2.4 g) and DCC (4.3 g) were added and the stirring was continued for 5 hr. After removal of DCU by filtration the filtrate was introduced into 2000 m*l* of ethyl acetate-ether (1 : 1 by volume). The resulting precipitates were filtered off, washed with ethyl acetate-ether and dried *in vacuo* to yield the protected decapeptide active ester hydrochloride; 9.38 g.

H-Lys(Boc)-Pro-Val-Gly-Lys(Boc)-Lys(Boc)-Arg-Arg-$NH_2 \cdot 3CH_3COOH$[6b] (IV, 4.73 g, 3.1 mmol) and triethylamine (4.8 m*l*) were dissolved in dimethylformamide (150 m*l*) and to this solution was added the decapeptide active ester obtained above (9.38 g) at 0°C. The mixture was stirred at 4°C for 4 days, and was then poured into ice-cold ethyl acetate to separate the crude protected octadecapeptide (V), which was filtered off, washed with cold ethyl acetate and dried *in vacuo*; yield 13.11 g.

To this crude product (11.8 g) was added 90% trifluoroacetic acid (120 m*l*) and the mixture was stirred at 0°C for 15 min and at room temperature for 75 min. After the solvent had been removed *in vacuo*, the residue was dried over potassium hydroxide pellets *in vacuo* and was then dissolved in water (*ca.* 50 m*l*). The solution was applied to a column (4.4×30 cm) of Amberlite IRA-400 (acetate form) and the column was washed with water. The effluents were combined and concentrated

14) R. Geiger, K. Sturm, G. Vogel and W. Siedel, *Z. Naturforsch.*, **19b**, 858 (1964).

15) The over-all yield of peptide, calculated on the basis of the amine component used for the final coupling step, is therefore 29.5%.

in vacuo to about 400 m*l*, and to this was added 25 m*l* of M mercaptoethanol. The mixture was, after incubation at 37°C overnight, submitted to a column (6.9×78 cm) of carboxymethyl cellulose (Brown, 0.78 meq/g). The column was eluted with an ammonium acetate buffer (pH 6.5) having a linear concentration gradient of 0.025—0.6M to collect 40 *l* of fractions and then with 0.6M ammonium acetate buffer (pH 6.5) until the desired peptide totally emerged (Fig. 2). Fractions corresponding to the main peak (tubes 44—72) were combined and the bulk of the solvent was removed *in vacuo*. Repeated lyophilization of the residue gave the octadecapeptide (II) as fluffy powder. The material was dried over phosphorus pentoxide at 55°C *in vacuo* to yield 3.17 g (50.2% on the basis of the amine component used for the coupling step, as determined spectrophotometrically); homogeneous to ninhydrin, Pauly and Sakaguchi reagents in paper chromatography (*n*-butanol-acetic acid-pyridine-water=30 : 6 : 20 : 24 by volume (BAPW) as solvent). $[\alpha]_D^{28}$ $-53.6\pm1.9°$ (*c* 0.494, 0.1N acetic acid). Amino acid ratios in acid hydrolysate:[8] Ser 0.96, Glu 0.98, Pro 1.04, Gly 3.00, Val 0.99, Met 0.99, Tyr 0.99, Phe 1.02, Lys 3.00, His 0.99, Arg 3.06.

A 0.3 g-portion of the peptide obtained above was submitted, for further purification, to a column (3.8× 28 cm) of carboxymethyl cellulose (Brown, 0.78 meq/g), using the ammonium acetate buffer (pH 6.5) with a linear concentration gradient of 0.025—0.6M (3300 m*l*) followed by 0.6M ammonium acetate (pH 6.8). The results of this rechromatography are shown in Fig. 3. Fractions corresponding to the main peak (tubes 310—480) were pooled, concentrated and lyophilyzed to obtain the pure peptide II; 0.24 g, $[\alpha]_D^{23}$ $-55.3\pm1.9°$ (*c* 0.510, 0.1N acetic acid). Homogeneous to ninhydrin, Pauly, Ehrlich, Sakaguchi and methionine (PtI_6'') reagents in paper chromatography (BAPW) and in paper electrophoresis (600 V/36 cm, in 2N acetic acid). Amino acid ratios in acid hydrolysate:[8] Ser 0.94, Glu 1.01, Pro 0.99, Gly 3.00, Val 1.00, Met 0.98, Tyr 0.98, Phe 0.97, Lys 2.90, His 0.97, Arg 2.97.

Grateful acknowledgement is made to Mr. Kunio Watanabe and Miss Motoko Nakazawa for able technical assistance, to Dr. Mitsuo Ebata and staff for amino acid analysis, and to Dr. Kaoru Kuriyama and staff for optical rotation measurements.

BULLETIN OF THE CHEMICAL SOCIETY OF JAPAN VOL. 43 200—207 (1970)

Base-catalyzed 1–3 Prototropic Isomerization of Cycloheptatrienes[1]

Kazuko TAKAHASHI, Hiroshi YAMAMOTO[2] and Tetsuo NOZOE[3]

Department of Chemistry, Faculty of Science, Tohoku University, Katahira-cho, Sendai

(Received June 20, 1969)

The base-catalyzed proton migration (from the 7- to 2-position) and proton exchange (at the 7-position) of cycloheptatrienes carrying an electron-withdrawing group were studied in a medium of aqueous sodium hydroxide or alcoholic potassium hydroxide. The order of the effect of the various substituents upon the relative rates is approximately: $CN > CONH_2 > COO^-$, Ph. The base-catalyzed prototropic isomerization proceeds through: i) the abstraction of a proton of the 7-position by the base, ii) the migration of the resulting carbanion to the allylic position (the rate-determining step), and iii) the recovery of a proton from the solvent. The kinetic study of the isomerization of 7-carboxycycloheptatriene (Ia) discloses the rate of the isomerization (k[the cycloheptatriene][base]) and the parameters ($E_a = 22.6$ kcal/mol, $\Delta H^{\neq} = 22.0$ kcal/mol, $\Delta S^{\neq} = -15.4$ e.u. at 60°). The structure of the cycloheptatrienyl anions formed as intermediates is discussed.

With reference to the migration of the double bonds in cycloheptatrienes, ter Borg *et al.*[4] first described the thermal 1–5 hydrogen shift mechanism, and Chapman, Borden and other groups[5] have recently reported the photochemical 1–7 hydrogen shift shown in Schemes 1 and 2. We have also

1) Presented at the 18th Annual Meeting of the Chemical Society of Japan, Osaka, March, 1965.

2) Present Address: Department of Chemistry, Faculty of Science, Okayama University, Okayama.

3) Present Address: No. 811, 2-5-1, Kamiyoga, Setagaya-ku, Tokyo.

4) A. P. ter Borg, H. Kloosterziel and N. van Meurs, *Rec. Trav. Chim. Pays-Bas*, **82**, 717 (1963).

5) a) O. L. Chapman and G. W. Borden, *Proc. Chem. Soc.*, 221 (1963); b) A. P. ter Borg and H. Kloosterziel, *Rec. Trav. Chim. Pays-Bas*, **84**, 241 (1965); c) R. W. Murray and M. L. Kaplan, *J. Amer. Chem. Soc.*, **88**, 3527 (1966); d) G. W. Borden, O. L. Chapman, R. Swindell and T. Tezuka, *J. Amer. Chem. Soc.*, **89**, 2979 (1967); e) A. P. ter Borg, E. Razenberg and H. Kloosterziel, *Chem. Commun.*, **1967**, 1210.

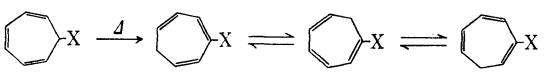

Scheme 1. 1-5 H Shift

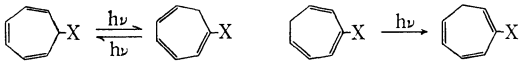

Scheme 2. 1-7 H Shift

previously recognized the same mode of the thermal isomerization reaction on various cycloheptatrienes.[6] Now, however, we have found a new type of isomerization catalyzed by the base; this isomerization will be explained herein.

The proton migration in a basic medium was first observed by Buchner and his coworkers,[7] when 7-ethoxycarbonylcycloheptatriene was converted to 2-carboxycycloheptatriene (IIIa) on being refluxed with 10% alcoholic potassium hydroxide, although they did not mention the reaction mechanism. We ourselves have examined the behavior of carboxy-,[8] cyano-, carbamoil-, and phenyl-cycloheptatriene in basic media with the view of clarifying the mechanism of the base-catalyzed isomerization.

Upon heating the 7-substituted cycloheptatrienes mentioned above, the 3-, 1- and 2-substituted isomers were successively formed according to the 1–5 hydrogen shift mechanism; the chemical shifts and the couping constants of the hydrogen atom at the 7-position [H(7)] of each substance, shown in Table 1, were used for purposes of identification throughout the present work. As will be shown below, kinetic study proved that the base-catalyzed isomerization of cycloheptatrienes in dilute alkali generally took place much faster than the thermal 1–5 hydrogen shift.

The complete disappearance of the triplet signal at τ 7.52 due to H(7) in the NMR spectrum of 7-carboxycycloheptatriene (Ia), when the mixture was set aside in 2N sodium deuteroxide for 41 hr at room temperature indicated the proton exchange at the 7-position, while no deuterium exchange was observed when Ia was kept in a neutral medium

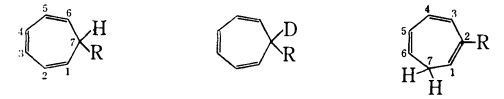

I: a: R=COOH, b: R=CN, c: R=$CONH_2$, d: R=Ph

II: a: R=COOH, b: R=CN

III: a: R=COOH, b: R=CN, c: R=$CONH_2$, d: R=Ph

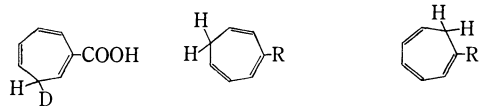

IV

V: a: R=COOH, b: R=CN, c: R=Ph

VI: a: R=COOH, b: R=Ph

such as deuterium oxide-dioxane (1 : 1) for 73 hr at the same temperature. The 7-*d*-7-carboxycycloheptatriene (IIa) thus formed was shown, on the evidence of the NMR (*i. e.* alterations of the signals due to H(7), (1), and (6)], to be isomerized to 7-*d*-2-carboxycycloheptatriene (IV) when warmed at 90°C for 10 hr in the same solvent (2N NaOD). The treatment of Ia with 2.5N sodium hydroxide at 110°C for 4 hr caused an isomerization affording 2-carboxycycloheptatriene (IIIa) in an 80% yield. The rate of the isomerization reaction of Ia to IIIa appears, from the results shown in Table 2, to depend upon the concentration of the base used (this was confirmed by the kinetic study; see below). The secondary isomerization (*i. e.*, IIIa to the other isomers, Va and VIa) was found to be considerably slower than the first-step isomerization under the same conditions, for the compound IIIa or Va remained almost unchanged when kept in 2N sodium hydroxide, even at a higher temperature such as 130°C. An enhancement of the rate of the secondary and subsequent-step isomerization of the carboxycycloheptatriene was, however, observed in a stronger base, as is shown in Tables 3 and 4; the data suggested that IIIa was successively converted to Va and the 1-substituted isomer (VIa). This was confirmed by examining the ratio of the products when IIIa or Va was treated with a concentrated base; these results are shown in Tables 5 and 6. Accordingly, the base-catalyzed proton transfer in the cycloheptatriene was considered to proceed by the step-by-step mechanism illustrated by Scheme 3; the last three compounds (IIIa, Va, and VIa) are at equilibrium.

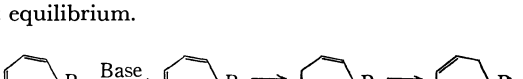

Ia IIIa Va VIa

Scheme 3 1-3 H^+ Shift

6) a) T. Nozoe and K. Takahashi, This Bulletin, **38**, 665 (1965); b) T. Nozoe, K. Takahashi and H. Yamamoto, *ibid.*, **42**, 3277 (1969).

7) a) E. Buchner, *Ber.*, **29**, 106 (1896); b) *ibid.*, **30**, 632 (1897); c) *ibid.*, **31**, 2241 (1898); d) E. Buchner and F. Lingg, *Ber.*, **31**, 2447 (1898); e) W. Braun and E. Buchner, *ibid.*, **34**, 982 (1901).

8) Structures of carboxycycloheptatrienes (norcaradienecarboxylic acid), tentatively assigned by Buchner (Ref. 7), have been revised by a) C. Grundmann and G. Ottmann, *Ann. Chem.*, **582**, 163 (1953); b) W. von Doering, G. Laber, R. Vonderwahl, N. F. Chamberlain and R. B. Williams, *J. Amer. Chem. Soc.*, **78**, 5448 (1956); c) H. Jungen and K. Rust, *Ann. Chem.*, **602**, 94 (1957).

TABLE 1. NMR SPECTRA OF CYCLOHEPTATRIENES

Compound	τ-Values for protons[a]							
	H(7)	H(1)	H(2)	H(3)	H(4)	H(5)	H(6)	Substituents
Ia	7.52 tt *J* 5.5, 1.1	4.69 ddt *J* 8.0, 5.5, 1.0	3.75m	3.40m	3.40m	3.75m	4.69 ddt	−1.24 s
Ib	7.13 tt *J* 6.0, 0.8	4.67 ddt *J* 9.0, 6.0, 0.8	3.72m	3.32 tt *J* 3, 0.7	3.32 tt	3.72m	4.67 ddt	—
Ic	7.43 tbr *J* 6.0, 0.9	4.55 ddt *J* 9.3, 6.0, 1.3	3.68m	3.33m	3.33m	3.68m	4.55 ddt	3.0—4.0m
Id	7.33 tbr *J* 5.5	*						
IIa	—	4.70 dbr *J* 8.7	3.74m	3.39m	3.39m	3.74m	4.70 dbr	−1.60 s
IIb	—	4.63 dbr *J* 9.5	3.70m	3.27 tt *J* 3, 0.7	3.27 tt	3.70m	4.63 dbr	—
IIIa	7.65 t *J* 7.0	3.42 t *J* 7.0	—	2.85 dd *J* 11.5, 0.7	3.35 dd *J* 11.5, 5.3	3.80 dd *J* 9.0, 5.3	4.64 dt *J* 9.0, 7.0	−2.40 s
IIIb	7.62 t *J* 7.0	3.97 t *J* 7.0	—	3.46 dm *J* 11.2, >1	3.20 ddt *J* 11.2, 5.0, 0.3	3.74 ddd *J* 9.3, 5.0, 0.3	4.58 dt *J* 9.3, 7.0	—
IIIc	7.70 t *J* 6.8		—					
IIId	7.75 t *J* 6.9		—					
IV	7.67 dt *J* 6.7, 3.0	3.40 d *J* 6.7	—	2.82 dd *J* 11.0, 1.0	3.31 dd *J* 11.0, 5.5	3.78 dd *J* 9.0, 5.5	4.63 dd *J* 9.0, 6.7	−1.26 s
Va	7.72 t *J* 6.8	4.40 dt *J* 9.3, 6.8	3.31 d *J* 9.3	—	2.30 d *J* 6.0	3.72 dd *J* 9.3, 6.0	4.63 dt *J* 9.3, 6.8	−2.05 s
Vb	7.67 t *J* 6.8	4.49 d *J* 9.8, 6.8	3.77 d *J* 9.8	—	2.83 d *J* 5.5	3.72 dd *J* 9.8, 5.5	4.38 dt *J* 9.8, 6.8	—
Vc	7.77 t *J* 6.8			—				
VIa	7.37 d *J* 6.7	—						
VIb	7.34 d *J* 7.0	—						

a) In carbon tetrachloride as solvent, except compounds Ic and IIIc (deuteriochloroform).
br, broad; s, singlet; d, doublet; dd, double doublet; ddd, double doublet of doublets; t, triplet; dt, double triplet; ddt, double doublet of triplets; m, multiplet; dm, doublet of multiplets; *J* in Hz.
* The spectrum is too complicated to determine the accurate chemical shift remained blank.

TABLE 2. THE ACTION OF AQ. NaOH ON Ia AT 90°C FOR 3 hr

Basicity (N)	Yield (%)			
	Ia	IIIa	Va	VIa
0.2	90	5		
1	40	40		
4	20	68		
10	15	60	10	5

TABLE 3. THE ACTION OF 20% ALC. KOH ON Ia AT 90°C

Reaction Time (hr)	Yield (%)		
	IIIa	Va	VIa
2	86	14	trace
8	58	34	8

TABLE 4. THE ACTION OF 45% ALC. KOH ON Ia AT 130°C

Reaction time (hr)	Yield (%)		
	IIIa	Va	VIa
1.5	25	31	44
14	22	28	50
37	20	26	53

TABLE 5. THE ACTION OF 28% AQ. NaOH ON IIIa AT 90°C

Reaction time (hr)	Yield (%)		
	IIIa	Va	VIa
1	93	7	
3	85	15	trace
7	78	18	4
19	70	21	9
27	56	24	20

Table 6. The action of 20% alc. KOH on Va at 90°C

Reaction time (hr)	Yield (%)		
	IIIa	Va	VIa
3	22	76	1.5
8	36	61	3

The effect of the substituents upon the relative rate of the isomerization was studied using other cycloheptatriene derivatives. The enhanced rates of the proton exhange and the isomerization resulted, to a great extent, in a cyano group. Upon the treatment of 7-cyanocycloheptatriene (Ib) with 4% sodium methoxide (in deuterium oxide) for 12 hr at room temperature, the proton exhange at the 7-position similarly took place to afford the deuterated compound (IIb) [no deuterium exchange occurred in deuterium oxide-dioxane (1 : 1)]. The 7-cyano compound (Ib) was readily converted to the 2-substituted isomer (IIIb) with 0.5% alcoholic potassium hydroxide (53% after three days at room temperature) or with 1.3% aqueous potassium hydroxide (80% after 2 hr at 45°C with stirring). Among the above reaction mixtures, a trace of 3-cyanocycloheptatriene (Vb), the secondary isomerization product, was detected (NMR). The rate of the initial isomerization was, however, much faster than those of the secondary or the subsequent isomerization, as was observed in the carboxycycloheptatriene system. It was found in the case of cyanocycloheptatriene that the hydrolysis of the cyano group took precedence over the secondary or tertiary isomerization in 2N aqueous sodium hydroxide; thus, the procedure is applicable to the preparation of IIIa and Va from the corresponding cyanocycloheptatrienes (see the Experimental section).

7-Carbamoilycycloheptatriene (Ic), when kept in 2.5N sodium hydroxide at 75°C for 10 min, gave a mixture consisting of the recovered Ic, the isomer (IIIc), Ia, and IIIa in a ratio of 13 : 14 : 68 : 5 (from NMR). Because Ia was confirmed not to isomerize to IIIa under the above conditions (*i. e.*, IIIa was derived from IIIc), the above ratio of the products suggested that the hydrolysis of the carbamoil group of Ic took place approximately 3.5 times faster than the isomerization of Ic to IIIc.[9]

Table 7. The action of 10% alc. KOH on Id at 84°C

Reaction time (hr)	Yield (%)			
	Id	IIId	Vc	VIb
0.7	40	33	11	11
1.5	16	50	17	16
4		59	21	20

Among the isomerized products of 7-phenylcycloheptatriene[10] (Id), as is shown in Table 7, a small amount of the secondary and the tertiary isomers, Vc and VIb, was present, besides the main product, IIId, on treatment even with a dilute base. The conjugative effect of the aryl group could make the subsequent isomerization easier. The effect of the various substituents upon the relative rates of the isomerization was thus considered to be, by comparison with the semi-quantitative results mentioned above: $CN > CONH_2 > COO^-$, Ph (the rates of the last two appeared to be very similar).

Cycloheptatriene itself, when treated with a mixture of 10N sodium deuteroxide and dioxane (1 : 1) at 90°C for 8 hr, remained completely unchanged. Nor was any deuterium exchange (nor isomerization) observed when 7-methoxycycloheptatriene was refluxed with 9% alcoholic potassium hydroxide for 4 hr. These results showed that a hydrogen atom of a cycloheptatriene should be replaced by an electron-withdrawing group as a requirement for the base-catalyzed proton exchange followed by the isomerization; the isomerization and the exchange rates are in proportion to the acidity of the hydrogen atom of the 7-position of cycloheptatriene.

To clarify the reaction mechanism, a kinetic study of the isomerization of 7-carboxycycloheptatriene (Ia) in a base was carried out. The disappear-

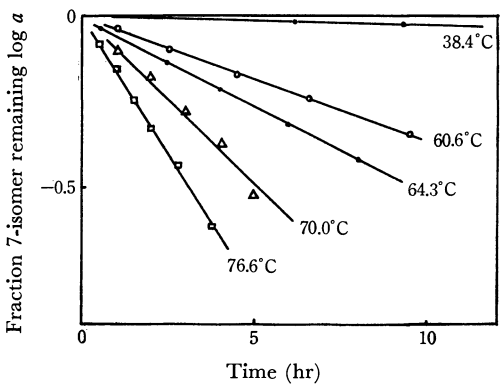

Fig. 1. Plots of the logarithm of the fraction of 7-isomer present *vs.* time at several temperatures.

9) Alkaline hydrolysis of Ic has been reported to afford IIIa but not Ia (Ref. 8a). Present experiment showed that the reaction would competitively undergo through: Ic→Ia→IIIa and Ic→IIIc→IIIa. Successful preparation of Ia from Ic was carried out by treatment with acid (see Experimental part).

10) T. Nozoe, T. Mukai, T. Tezuka and K. Osaka, *Nippon Kagaku Zasshi*, **84**, 662 (1963). They reported that 7-phenylcycloheptatriene (Id), when refluxed with 10% ethanolic sodium hydroxide for 15 hr, gave an isomer which showed a triplet signal (τ 7.76, J=7.0 Hz) due to a methylene group of a phenylcycloheptatriene.

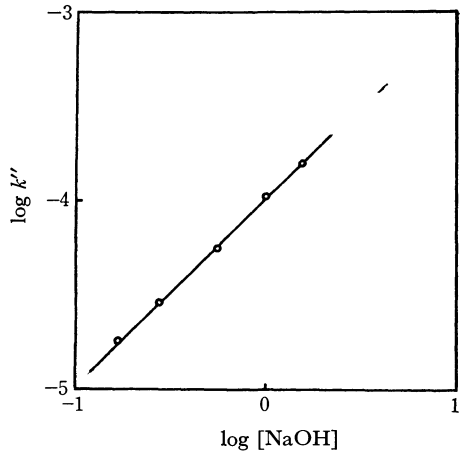

Fig. 2. Rate constants for the isomerization against a function of the base concentration.

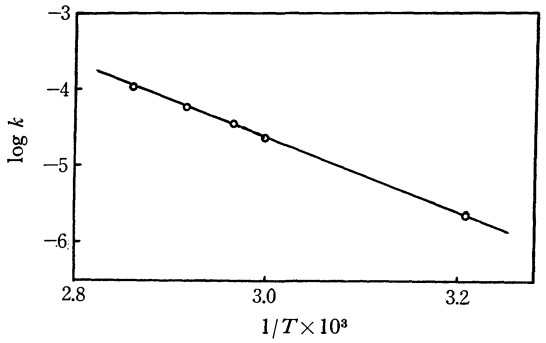

Fig. 3. Rate constants for the isomerization against a function of temperature.

TABLE 8. OBSERVED AND TRUE RATE CONSTANTS (k' AND k) FOR THE ISOMERIZATION OF Ia TO IIIa IN AQ. NaOH

Temp. (°C)	k'(sec^{-1})[a]	k(l/mol·sec)[b]
76.6±0.1	1.07×10^{-4}	1.07×10^{-4}
70.0±.10	6.0×10^{-5}	6.0×10^{-5}
64.3±0.05	3.45×10^{-5}	3.46×10^{-5}
60.6±0.1	2.30×10^{-5}	2.31×10^{-5}
38.4±0.2	2.15×10^{-6}	2.16×10^{-6}

a) In 0.996N NaOH
b) Calculated from the equation k[Ia][NaOH]

TABLE 9. RATE CONSTANTS (k'') FOR THE ISOMERIZATION OF Ia IN AQ. NaOH AT 76.1±0.1°C

Basicity (N)	k'' (sec^{-1})
1.53	1.60×10^{-4}
0.996	1.05×10^{-4}
0.547	5.56×10^{-5}
0.275	2.81×10^{-5}

TABLE 10. TRANSITION STATE PARAMETERS[a] FOR THE BASE-CATALYZED ISOMERIZATION OF Ia TO IIIa

E_a kcal/mol	log A sec^{-1}	$\Delta F^{\ddagger}$ kcal/mol	$\Delta H^{\ddagger}$ kcal/mol	$\Delta S^{\ddagger}$ e.u.
22.6	9.91	27.1	22.0	−15.4

a) The transition state parameters are reported at 60°C.

ance of Ia in 0.996N sodium hydroxide, measured spectrophotometrically, exhibited good first-order kinetics over the temperature range of 38—77°C (see Fig. 1); the observed rate constants, k', are shown in Table 8. The variation in the rates as a function of the concentration of the base was also studied at 76.0±0.1°C, the results being shown in Table 9. Assuming the observed first-order rate constants, k'', to be k[NaOH]^n, the slope of the straight line (Fig. 2), obtained by plotting log k'' against log [NaOH], indicated that n equals 1.0; thus, the rate of the isomerization may be expressed in terms of the following equation:

$$v = k\,[\text{the cycloheptatriene}]\,[\text{base}]$$

The rate constants, k, for the isomerization at the various temperatures in the unit concentration of sodium hydroxide were calculated to be as is shown in Table 8. A plot of the k values against $1/T$ was found to be linear (*cf.* Fig. 3), giving values for the transition-state quantities, $\Delta F^{\ddagger}$, $\Delta H^{\ddagger}$, and $\Delta S^{\ddagger}$ (from Eyring formulation). The results of these calculations are summarized in Table 10.

It can be postulated from the foregoing results that the base-catalyzed isomerization of cycloheptatrienes involved the carbanion formation (Step 1), the migration of the carbanion charge to the allylic position (Step 2), and finally the reformation of the isomerized cycloheptatriene by picking up a proton from the solvent (Step 3), as is illustrated by Scheme

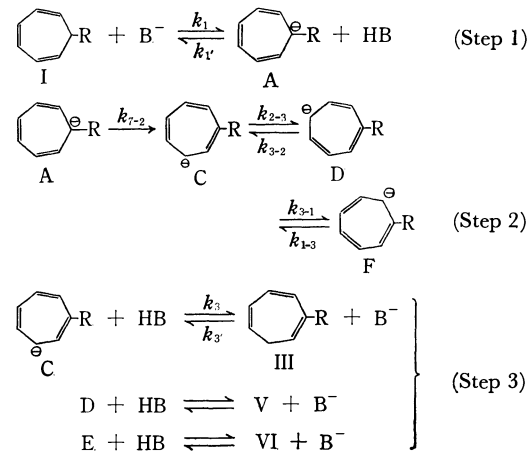

Scheme 4

4. According to the reaction pathways shown here, the rates of the formation of three substances, A, C, and III, can be expressed as follows:

$$\frac{d[A]}{dt} = k_1[I][B^-] - k_1'[A][HB] - k_{7-2}[A] \quad (1)$$

$$\frac{d[C]}{dt} = k_{7-2}[A] + k_{3-2}[D] - k_{2-3}[C] - k_3[C][HB] \quad (2)$$

$$\frac{d[III]}{dt} = k_3[C][HB] - k_{3'}[III][B^-] \quad (3)$$

where k_1, k_1', k_{7-2}, k_{2-3}, k_3, and k_3' are the rate constants of the reactions (Scheme 4); where [I], [A], [C], [D], and [III] are the concentrations (mol/l) of the corresponding substances in Scheme 4 and where B^- and HB are, respectively, the anion of the base and the protonated anion (the solvent).

Although complete deuterium exchange was observed at the 7-position of Ia when it was dissolved in 2N sodium deuteroxide at room temperature, the heating of the solution at a higher temperature was required to cause the isomerization to give IV (as a single product; see above), indicating that Step 2 was the rate-determining process in the isomerization of IIa to IV (*i. e.*, k_1, k_1', $k_3 \gg k_{7-2} \gg k_3'$, k_{2-3}). Upon the treatment of IIIa with 4N sodium deuteroxide at 100°C for 7 hr, the intensities of the methylene signal (τ 7.65) decreased to 0.75 H and the signals due to H(1) (τ 3.42, t) and H(6) (τ 4.64, dt) broadened in the NMR spectrum of the product, showing the formation of a mixture of IV and 7,7-d_2-2-carboxycycloheptatriene. This demonstrated that the proton exchange (with the solvent) at the 7-position preceded the isomerization reaction not only in 7-substituted cycloheptatrienes, but also in the 2-isomers (probably in the other isomers also), although the rates of both the exchange and the isomerization of the latter compounds were considerably slower than those of the former. Besides, the results in Table 5 and 6, as explained above, show that the compounds IIIa, Va and VIa were at equilibrium in stronger bases. Thus, the following relationship can be establisehd: k_3, $k_3' \gg k_{2-3}$, k_{3-2}, k_{3-1}, k_{1-3}.

Consequently, Eqs. (1)—(3) may be simplified as follows:

$$\frac{d[A]}{dt} = k_1[I][B^-] - k_1'[A][HB] \quad (1')$$

$$\frac{d[C]}{dt} = k_{7-2}[A] - k_3[C][HB] \quad (2')$$

$$\frac{d[III]}{dt} = k_3[C][HB] \quad (3')$$

The formation of the intermediates, A and C, in dilute aqueous sodium hydroxide is considered to be a steady-state reaction; thus, $d[A]/dt \simeq O$, and $d[C]/dt \simeq O$. Therefore,

$$\frac{d[III]}{dt} = k_{7-2}[A] = k_{7-2}\frac{k_1[I][B^-]}{k_1'[HB]} = k[I][B^-]$$

where $k = k_1 \cdot k_{7-2}/k_1'[HB] = \text{const.}$

This equation, which is in agreement with our expermental results presented above, would seem to verify the assumption of the three-step isomerization mechanism shown in Scheme 4.

Similarly, when V is formed from III, the rate of the isomerization may be calculated as follows:

$$\frac{d[V]}{dt} = k'[III][B^-]$$

where; $k' = k_{3'} \cdot k_{2-3}/k_3[HB]$

Although k' is probably much smaller than the k shown above, the higher concentration of the base would facilitate the secondary isomerization reaction. This is also in accordance with our experimental results, which show that Va was formed from IIIa only in strong alkali (see above). The equilibrium relationship among the compounds III, V, and VI could be explained similarly. The determination of the equilibrium constants of each reaction in Scheme 4 would be of interest in connection with the relationship to the pk_a values of H(7) of the compounds I, III, V, and VI.

Concerning the base-catalyzed allylic proton transfer, intramolecularity has been observed in various organic solvents and bases, as is explained in Scheme 5, where the isotopic exchange is much slower than the isomerization.[11] Scheme 5

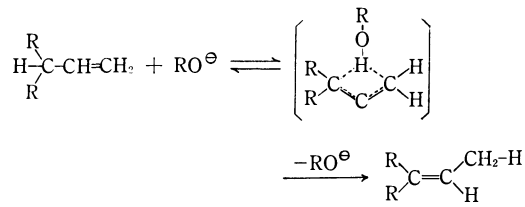

Scheme 5

In our system, however, the rate of proton exchange was much faster than that of the isomerization (*i.e.*, $k_1, k_1' \gg k_{7-2}; k_3, k_3' \gg k_{2-3}$), and no clear evidence of intramolecularity was detected.

The rate-determining step of the isomerization (Step 2 in Scheme 4) involves p-π bond rehybrization to form an allylic carbanion, the structure of which will now be discussed. According to the

11) D. J. Cram, "Fundamentals of Carbanion Chemistry," Academic Press, New York (1965), p. 175; S. Bank, C. A. Rowe, Jr., and A. Schriesheim, *J. Amer. Chem. Soc.*, **85**, 2115 (1963); G. Bergson and A. M. Weidler, *Acta Chem. Scand.*, **17**, 862, 1798, 2691, 2724 (1963); R. B. Bates, R. H. Carnighan and C. E. Staples, *J. Amer. Chem. Soc.*, **85**, 3032 (1963); V. A. Mironov, E. V. Sobolev and A. N. Elizarova, *Tetrahedron*, **19**, 1939 (1963); W. R. Roth, *Tetrahedron Lett.*, **1964**, 1009; S. McLean and P. Haynes, *ibid.*, **1964**, 2385; Y. Kitahara, I. Murata and T. Muroi, This Bulletin, **38**, 1195 (1965).

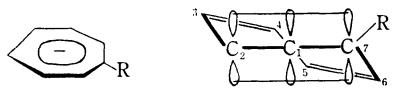

F G

molecular orbital theory, a cycloheptatrienyl anion which possesses eight electrons should exist as a triplet diradical in the ground state. The heptaphenylcycloheptatrienyl anion[12] has been reported to be a singlet because of the distortion by the phenyl groups. Dauben,[13] Doering,[14] and their co-workers have reported that they detected the D_{7h} symmetrical (coplanar) cycloheptatrienyl anion by the deuterium exhcange, which occurred randomly on each carbon atom of the seven-membered ring. Under our circumstances, the migration of the anionic charge took place only to the allyclic position (*cf.* Scheme 4); this suggests that the rehybrization is limited within the three carbon atoms concerned, eliminating the possibility of a coplanar cycloheptatrienyl anion (F) as the structure of the intermediate anion. Thus, such a three-carbon coplanar anionic structure as is shown in the formula G seems most probable.

Experimental

The NMR measurements were made at 25°C with a 60 Mc/sec Varian A-60 spectrometer.

7-Carboxycycloheptatriene (Ia). A mixture of 4.35 g of Ic (see below) and 110 m*l* of 2N sulfuric acid was heated at 120°C (bath) for 1 hr. The cooled mixture was brought to pH2 with 6N sodium hydroxide at 0°C, and then extracted with ethyl acetate. The dried extract (over $MgSO_4$) was evaporated and the residue was distilled, giving 3.65 g of Ia as a pale yellow oil, bp 98—100°C/2.5 mmHg λ_{max}^{MeOH} mμ (log ε): 260 (3.52). ν_{max}^{neat} 3300—3020 mbr, 3026 m, 2910 m, 2700 w, 2600 w, 1710 s, 1600 m, 1417 m, 1392 w, 1300 m, 1220 m, 1202 m, 998 w, 930 w, 743 m and 705 s cm^{-1}.

7-Cyanocycloheptatriene (Ib). Although Doering and Knox[15] prepared Ib from tropylium bromide and potassium cyanide in a 87% yield, a slightly modified procedure was used. A mixture of 31.4 g of 7-ethoxycycloheptatriene[6a] and 120 m*l* of 2N hydrochloric acid was stirred at 0°C for 30 min, and then 26.0 g (1.7 equiv.) of potassium cyanide dissolved in 100 m*l* of cold water were slowly stirred in at 0°C (1 hr). After stirring for further 2 hr at room temperature, the mixture was extracted with ether; the dried extract (over $MgSO_4$) was freed from the solvent and distilled, giving 24.7 g of Ib as a colorless oil (92% yield) bp 105°C/27 mmHg. λ_{max}^{MeOH} mμ (log ε): 259(3.70). ν_{max}^{neat} 3030 m, 2220 m, 1684 w, 1592 w, 1429 w, 1381 m, 1269 w, 1193 w, 1104 w, 1010 m, 975 w, 943 w, 802 w, 791 w, 745 s, 702 s and 685 s cm^{-1}.

(Found: C, 81.30; H, 6.08; N, 11.95%).

7-Carbamoilcycloheptatriene (Ic). The procedure followed that of Doering and Knox,[15] and Ic was obtained from Ib as colorless needles in a 47% yield (from ether), mp 140°C (lit,[7b,8a] 141°C). However, benzamide was also present (14%) as a by-product. ν_{max}^{KBr} 3390 s, 3205 s, 3012 m, 1661 s, 1639 sh, 1605 sh, 1429 s, 1387 m, 1269 m, 1209 w, 1140 w, 979 w, 735 s and 698 s cm^{-1}.

The Action of the Base on Ic. A mixture of 100 mg of Ic and 1.2 m*l* of 2.5N sodium hydroxide was heated while being stirred at 70°C for 10 min. The cooled mixture was extracted with ethyl acetate; the organic layer was then washed with 0.5N sodium hydroxide, dried over $MgSO_4$, and evaporated to give 23 mg of colorless needles, which were found (from NMR) to be a mixture of Ic and IIIc (1 : 1.1). The above aqueous layer, combined with the washing, was brought to pH 2 with cold 2N sulfuric acid and extracted with ethyl acetate. The dried extract (over $MgSO_4$) was evaporated to give 61 mg of a yellow oil consisting of Ia and IIIa (15 : 1, from NMR).

7-*d*-7-Carboxycycloheptatriene (IIa). A solution of 136 mg of Ia dissolved in 1 m*l* of 2N sodium deuteroxide was set aside at room temperature for 41 hr and then stirred into 1.4 m*l* of cold 2N sulfuric acid at 0°C. The contents were, after having been stirred for 5 min, extracted with ethyl acetate; the dried extract was then evaporated *in vacuo*, giving 120 mg (88%) of IIa as a yellow oil (on the evidence of NMR).

7-*d*-7-Cyanocycloheptatriene (IIb). To a solution of 40 mg of sodium methoxide dissolved in 1.0 g of deuterium oxide, 50 mg of Ib were added. After having been set aside for 12 hr at room temperature with occasional shaking, the mixture was poured into 3 m*l* of cold 1N sulfuric acid and extracted with benzene. The evaporation of the extract *in vacuo* give 38 mg of IIb as a yellow oil (from NMR).

2-Carboxycycloheptatriene (IIIa). *a)* A mixture of 3.0 g of IIIb (see below) and 24 m*l* of 2.5N sodium hydroxide was refluxed for 3 hr with stirring. A small amount of a black tar formed was removed by decantation from the cooled mixture, which was then taken to pH2 with 6N sulfuric acid at 0°C and extracted with ether. The organic layer was extracted with cold 2N sodium hydroxide. After the acidification (pH 2) of the alkaline solution, the contents were extracted with ethyl acetate. The dried extract (over $MgSO_4$) was evaporated *in vacuo* and distilled at 103°C/3 mmHg, giving 1.27 g (43%) of IIIa as colorless needles. Sublimation at 80°C(bath)/0.1 mmHg gave the pure material, mp 71—72°C (lit[7c,8b] 71.5°C). λ_{max}^{MeOH} mμ (log ε): 261(3.31). ν_{max}^{KBr} 3200—3100 mbr, 3012 m, 2976 sh, 2874 m, 2841 sh, 2653 m, 2545 m, 1692 sh, 1675 s, 1603 m, 1456 w, 1416 m, 1377 w, 1333 m, 1312 s, 1295 s, 1214 w, 1098 w, 925 w, 906 w, 882 w, 804 w, 760 m and 717 s cm^{-1}.

b) A mixture of 1.42 g of Ic and 8 m*l* of 2.5N sodium hydroxide was kept at 120°C (bath) for 1.5 hr, it was brought, after cooling, to pH 2 with cold 6N sulfuric acid, and then extracted with ether. The extract was twice shaken with cold 2N sodium hydroxide. The combined aqueous layer was taken to pH 2 with cold

12) R. Breslow and H. W. Chang, *J. Amer. Chem. Soc.*, **84**, 1484 (1962).

13) H. J. Dauben, Jr., and M. R. Rifi, *ibid.*, **85**, 3041 (1963).

14) W. von E. Doering and P. P. Gasper, *ibid.*, **85**, 3043 (1963).

15) W. von E. Doering and L. H. Knox, *ibid.*, **79**, 352 (1957).

6N sulfuric acid and extracted with ethyl acetate. The evaporation of the organic layer *in vacuo* left a brown viscous tar which recrystallized from water, giving 0.68 g, (48%) of IIIa (from IR), mp 69—70°C.

c) A solution of 100 mg of Ia in 1 m*l* of 2.5N sodium hydroxide was heated at 120°C (bath); the cooled mixture was acidified (pH 2) with 2N sulfuric acid. The precipitate was filtered off and recrystallized from water, giving 80 mg of IIIa (from IR) as colorless plates mp 71—72°C.

2-Cyanocycloheptatriene (IIIb). The material Ib (1.00 g) in 50 m*l* of 0.5% alc. potassium hydroxide was set aside at room temperature for 3 days. After the addition of 100 m*l* of water, the mixture was extracted with ether. The dried extract (over $MgSO_4$) was evaporated at 20°C under reduced pressure and distilled, giving 0.53 g of IIIb as a colorless oil bp 105—108°C/23 mmHg. The NMR data are shown in Table 1.

7-*d*-2-Carboxycycloheptatriene (IV). *a)* A solution of 136 mg of Ia in 1 m*l* of 2N sodium deuteroxide was gently refluxed for 2 hr and then, after cooling, brought to pH 2 with cold 2N sulfuric acid. The precipitate was collected and sublimed at 80°C/0.1 mmHg, giving 90 mg of colorless plates, mp 48—50°C, which were shown to be IV (from NMR; *cf.* Table 1). ν_{max}^{KBr} 3200—3100 mbr, 3003 m, 2950 sh, 2841 m, 2646 m, 2525 m, 1686 sh, 1672 s, 1597 m, 1447 m, 1412 s, 1374 s, 1332 s, 1305 sh, 1292 s, 1209 w, 920 m, 904 w, 894 w, 880 w, 801 w, 758 m and 715 s cm^{-1}.

b) A mixture of 109 mg of IIIa and 1 m*l* of 4N sodium deuteroxide was heated at 100°C(bath) for 7 hr and then treated much as above, giving 97 mg of pale yellow plates, mp 51—55°C. The product was found to be a mixture of IV and 7,7-d_2-2-carboxycycloheptatriene on the evidence of the NMR spectrum (see the main text).

3-Carboxycycloheptatriene (Va). A mixture of 10.0 g of Vb (see below) and 80 m*l* of 2.5N sodium hydroxide was stirred at 20°C for 5 hr, then at 90°C(bath) for 1 hr, and finally at 130°C(bath) for 2 hr. The cooled mixture was brought to pH 2 the careful addition of 2N sulfuric acid and extracted with ethyl acetate. The dried extract (over $MgSO_4$) was freed from the solvent and distilled, giving 7.47 g of colorless needles (70% yield), bp 106—107°C/0.2 mmHg, which sublimed at 80°C(bath)/0.1 mmHg and afforded Va as colorless needles, mp 56—57°C (lit,[7c,8b] 59.5°C). λ_{max}^{MeOH} mμ (log ε): 279(3.79). ν_{max}^{KBr} 3200—3100 mbr, 3030 m, 2967 m, 2865 m, 2825 m, 2660 m, 2545 m, 1675 s, 1610 m, 1536 m, 1435 s, 1408 w, 1395 w, 1340 m, 1294 s, 1236 w, 1200 w, 1190 sh, 1100 w, 968 w, 951 sh, 939 w, 800 w, 770 w and 740 s cm^{-1}.

3-Cyanocycloheptatriene (Vb). The compound Ib (146 g) was heated at 155°C(bath) for 2 hr under a nitrogen atmosphere (1 atm) in a flask stopped with a nitrogen balloon. (This method is frequently used because of convenience and safety in large-scale experiments on thermal isomerization). The distillation of the product gave 130 g of a pale yellow liquid (94%) bp 53°C/0.4 mmHg. This consisted of Vb (more than 90%) and 1-cyanocycloheptatriene (less than 10%), togethe with a trace of the unreacted Ib. (The percentage was derived from the NMR integration.)

Thermal Isomerization of Carboxycycloheptatrienes. When 110 mg of Ia was heated in a sealed tube at 150°C for 3 hr, the NMR spectrum showed the presence of Ia and Va in the ratio of 1 : 1, plus a trace of VIa. The compound IIIa gave a mixture of IIIa and VIa (4 : 1) when heated at 150°C for 5 hr. Similarly, Va afforded a mixture of Va and VIa (*ca.* 1 : 3) when heated at 180°C for 4 hr.

Reaction Rate Measurements. *a) The Base-catalyzed Isomerization of Ia to IIIa in 0.996N Sodium Hydroxide.* An aqueous solution of Ia (*ca.* 1×10^{-2} mol/*l*) in 0.996N sodium hydroxide was prepared. About 1.2 m*l* of the solution in a sealed tube was kept in the vapour of carbon tetrachloride (76.6±0.1°C), methanol (64.3±0.05°C), chloroform (60.6±0.1°C), and dichloromethane (38.4±0.2°C), and in an oil bath equipped with a thermostat (70±1°C). The tubes were taken out at regular intervals, and 1 m*l* of the solution was added to 10 m*l* of a mixture of 1.5N hydrochloric acid and methanol (1 : 9 v/v.). Then 1 m*l* of the dilute solution was added to 10 m*l* of methanol. The reference solution was prepared in a similar manner. The fraction of the 7-substituted cycloheptatriene remaining was calculated from:

$$a = \frac{E_\infty - E}{E_\infty - E_0}$$

where E_0, E_∞, and E are the extinctions of Ia, IIIa and the reaction mixture respectively, at 230 mμ (measured with Hitachi recording spectrophotometer, Model EPS-3). The rate constant, k', was determined from a plot of log a *vs.* the time (Fig. 1).

b) The Base-catalyzed Isomerization of Ia to IIIa in Various Strengths of the Basicity at 76.1±0.1°C. A solution (2×10^{-3} mol/*l*) of Ia in a given concentration of sodium hydroxide was heated in a sealed tube at 76.1±0.1°C (in a carbon tetrachloride vapour bath). Measurements were carried out much as in the foregoing experiment except that 1 m*l* of the reactant was diluted with 9 m*l* of methanol and 1 m*l* with hydrochloric acid strong enough to make the mixture slightly acidic (pH 2). The results are shown in Table 9.

c) Thermal Isomerization of Ia to Va. A solution of 5.839 mg of Ia dissolved in 50 m*l* of isooctane was prepared. About 1.1 m*l* of the solution sealed in a tube were heated at 99.9±0.1°C (water vapor bath). The tube was taken out at regular intervals, 1 m*l* of the solution was diluted with 10 m*l* of isooctane, and the extinction was measured at 280 mμ. The rate constant ($k=1.5\times10^{-6}$ sec^{-1}), calculated much as above, was sought in order to compare it with that of the base-catalyzed isomerization of Ia in 1N sodium hydroxide at the same temperature, the latter being obtainable from Fig. 3 ($k=8.53\times10^{-4}$ *l*/mol·sec). The base-catalyzed isomerization was, therefore, found to be 5—6×10^2 times the thermal reaction under the above conditions. This tendency could generally be the case for the isomerization of cycloheptatrienes with electron-withdrawing substituents. Accordingly, it was concluded that the thermal 1—5 hydrogen shift did not interfere with the measurement of the reaction rate of the base-catalyzed isomerization.

We wish to express our gratitude to the Sankyo Co. for its donation of a research fund which covered a part of the expenses for this work.

BULLETIN OF THE CHEMICAL SOCIETY OF JAPAN VOL. 43 208—211 (1970)

The Copolymerization of Alkylene Glycol Nitrate Acrylates and Methacrylates

Masafumi MORIYA and Tadataka YAMASHITA

Department of Applied Chemistry, Faculty of Engineering, Toyo University, Kawagoe-shi, Saitama

(Received June 23, 1969)

The copolymerization of alkylene glycol nitrate acrylates (ANA) and methacrylates (ANMA) [M_2] with styrene [M_1] has been carried out at 60°C. The alkylene glycol mononitrates used were ethylene, propylene, and butylene glycol mononitrates, abbreviated as EGN, PGN, and BGN respectively. For their acrylates and methacrylates, the following abridged notations are used: ENA and ENMA, PNA and PNMA, and BNA and BNMA respectively. The monomer reactivity ratios, r_1 and r_2, and the Alfrey-Price Q_2 and e_2 values for ANA and ANMA were evaluated as follows: $r_1=0.48$, $r_2=0.08$, $Q_2=0.49$, and $e_2=1.00$ for ENA; $r_1=0.41$, $r_2=0.20$, $Q_2=0.69$, and $e_2=0.78$ for BNA; $r_1=0.35$, $r_2=0.49$, $Q_2=0.99$, and $e_2=0.53$ for ENMA; $r_1=0.36$, $r_2=0.50$, $Q_2=0.98$, and $e_2=0.51$ for PNMA and $r_1=0.37$, $r_2=0.40$, $Q_2=0.90$, and $e_2=0.58$ for BNMA. The polar and steric effects of the ester side chain containing the nitrate group were discussed. ANA was copolymerized with some other divinyl monomers, and the resulting crosslinked copolymer were subjected to the swelling test.

In a previous paper,[1] the preparation and the radical polymerization of alkylene glycol nitrate acrylates (ANA) and methacrylates (ANMA) have been reported, and the activation energy of the overall polymerization of each monomers has been evaluated. However, no articles on the copolymerization of ANA and ANMA with other reactive monomers have been known to us. This paper will be concerned with the copolymerization of ANA and ANMA with styrene and some other divinyl monomers.

Experimental

Materials. ANA and ANMA were prepared by the same method as has been described in the previous paper[1] and were redistilled before use. The physical constants of the monomers are shown in Table 1.

The alkylene glycol mononitrates used are ethylene, propylene, and butylene glycol mononitrates, abbreviated as EGN, PGN, and BGN respectively. For their acrylates and methacrylates, the following abridged notations are used: ENA and ENMA, PNA and PNMA, and BNA and BNMA respectively. PGN and BGN are mixtures of primary and secondary alcohols. Since the isomer ratio of PGN was determined as 4 (primary) : 1 (secondary) by Pujo and Boileau,[2] that of BGN may reasonably be assumed to be nearly 4 : 1, also. The styrene used as a reference in the copolymerization was purified by the usual method and was redistilled before use. 2-Methyl-2-nitro-1,3-propylene diacrylate was prepared according to the method recently reported by Strumza and Altschular.[3] Triethylene glycol dimethacrylate was prepared according to the literature.[4]

TABLE 1. PHYSICAL CONSTANTS OF MONOMERS

Monomer	Bp (°C/mmHg)	n_D^{20}	d_4^{20}
ENA	74—76/4	1.4490	1.252
PNA	81—82/4.5	1.4420	—
BNA	72—75/2.5	1.4440	1.152
ENMA	70—72/2	1.4495	1.203
PNMA	72—74/3	1.4443	1.150
BNMA	76—78/3	1.4458	1.126

Diallyl phthalate and diallyl maleate of the G.R. grade were used after purification by the usual method. 2,2′-Azobisisobutyronitrile (AIBN) of the G.R. grade was used after two recrystallizations from ethanol. Benzoyl peroxide (BPO) of the G.R. grade was used after two reprecipitations from chloroform-methanol. The acetone, methanol, and other solvents used were purified by the usual technique.

Copolymerization Procedure. The copolymerization of ANA and ANMA with styrene was carried out in a sealed glass tube in the presence of 6.1×10^{-3} mol/l of AIBN at 60°C. The resulting copolymers were precipitated by adding a large amount of methanol and were then reprecipitated from acetone-methanol. Most runs were stopped before the copolymerization proceeded to 5% conversion. The composition of the copolymers was determined by nitrogen analysis. The

1) M. Moriya and T. Yamashita, *Kobunshi Kagaku*, in press.

2) A. M. Pujo and J. Boileau, *Mem. Poudres*, **37**, 35 (1955).

3) J. Strumza and S. Altschular, *Israel J. Chem.*, **1**, 106 (1963).

4) A. Ya. Drinberg, *Zh. Prinkl. Khim.*, **27**, 613 (1954).

monomer reactivity ratios, r_1 and r_2, were calculated by the method of Fineman and Ross.[5]

Copolymerization of ANA with Divinyl Monomers. The copolymerization of ANA with divinyl monomers (0.5—10.0 wt% on ANA) was conducted using 0.5 wt% BPO (on total monomers) in a sealed glass tube at 65°C for 40 hr. The equilibrium of the swelling was measured with disks of the resulting copolymers, 10 mm in diameter and 1 mm thick, placed in acetone at 20°C for 48 hr. The swelling ratio at equilibrium, Q_m, is given as follows:

$$Q_m = [W/0.7995 + W_0(1/\rho + 1/0.7995)]/(W_0/\rho)$$

where ρ is the density of the polymer, W_0 the weight of the polymer, W the weight of the copolymer after swelling, and 0.7995, the density of acetone at 20°C.

Results and Discussion

Copolymerization of ANA and ANMA with Styrene. The resulting copolymers were fluffy white masses. The decomposition temperature of the copolymers was determined to be 205—210°C by differential thermal analysis.

The results of the copolymerization of ANA and ANMA with styrene are summarized in Table 2. As the figures in Table 2 indicate, the rate of copolymerization increases with the concentration of ANA and ANMA in the monomer mixture.

The monomer reactivity ratios, r_1 and r_2, and the Alfrey-Price Q_2 and e_2 values of ANA and ANMA, together with the known values for unsubstituted alkyl acrylates and methacrylates, are shown in Table 3. The monomer-copolymer composition curves for ANA and ANMA, based on the data in Table 2, are shown in Figs. 1 and 2 respectively. From the figures (r_1r_2) in Table 3 and the curves in Figs. 1 and 2, it can be seen that the copolymers

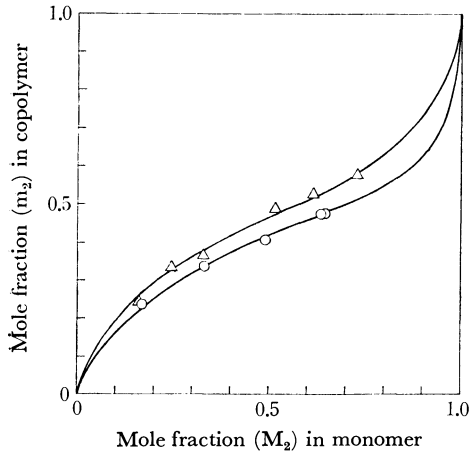

Fig. 1. Monomer-copolymer composition curves for the copolymerization of ANA with styrene.
○ (ENA), △ (BNA): found, ——: calculated

5) M. Fineman and S. D. Ross, *J. Polym. Sci.*, **5**, 269 (1950).

Table 2. The results of copolymerization of ANA and ANMA (M_2) with styrene (M_1) at 60°C

	$[M_2]$ in comonomer mol fraction	Time (min)	Conversion (%)	N (%) in copolymer	$[m_2]$ in copolymer mole fraction
ANA monomer					
ENA	0.169	300	2.5	2.79	0.234
	0.332	240	9.4	3.82	0.336
	0.491	260	5.0	4.47	0.406
	0.637	960	12.9	5.04	0.472
	0.645	1050	0.7	5.05	0.473
BNA	0.161	140	3.8	2.70	0.240
	0.247	125	3.5	3.45	0.333
	0.329	110	2.5	3.80	0.366
	0.518	55	1.5	4.68	0.484
	0.615	40	4.5	4.94	0.524
	0.730	40	7.1	5.26	0.573
ANMA monomer					
ENMA	0.098	70	0.7	2.32	0.195
	0.170	70	1.0	3.17	0.280
	0.357	70	1.4	4.60	0.445
	0.758	20	0.6	6.36	0.696
PNMA	0.123	135	2.0	2.56	0.225
	0.273	135	2.6	3.90	0.379
	0.414	70	1.9	4.63	0.478
	0.574	60	2.4	5.41	0.598
	0.652	55	3.3	5.66	0.640
	0.768	50	5.8	6.06	0.711
BNMA	0.147	90	1.9	2.79	0.258
	0.257	90	2.4	3.59	0.357
	0.384	85	3.3	4.12	0.431
	0.564	85	5.7	4.67	0.517
	0.615	60	4.8	4.99	0.572
	0.730	60	6.7	5.37	0.642

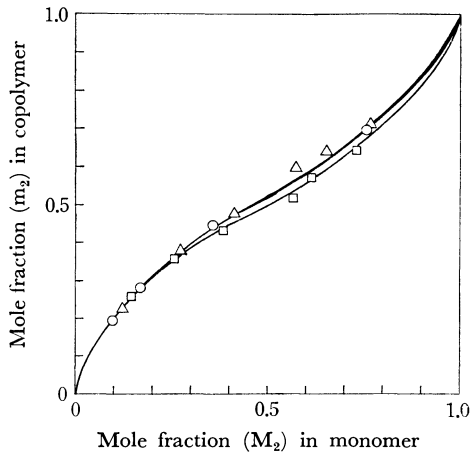

Fig. 2. Monomer-copolymer composition curves for the copolymerization of ANMA with styrene.
○ (ENMA), △ (PNMA), □ (BNMA): found
——: calculated

Table 3. Monomer reactivity ratios and Q_2 and e_2 values of ANA and ANMA at 60°C and these values of unsubstituted alkyl acrylates and methacrylates as references

M_2	r_1	r_2	$1/r_1$	r_1r_2	Q_2	e_2
ANA and ANMA						
ENA	0.48	0.08	2.08	0.038	0.49	1.00
BNA	0.41	0.20	2.44	0.082	0.69	0.78
ENMA	0.35	0.49	2.87	0.172	0.99	0.53
PNMA	0.36	0.50	2.78	0.180	0.98	0.51
BNMA	0.37	0.40	2.70	0.148	0.90	0.58
Unsubstituted alkyl acrylates and methacrylates						
MA (1)	0.75	0.18	1.34		0.42	0.60
EA (2)	0.77	0.17	1.30		0.42	0.62
n-BA (3)	0.82	0.21	1.22		0.43	0.53
IPA (4)	0.76	0.26	1.32		0.48	0.45
MMA (5)	0.52±0.02	0.46±0.02	1.92		0.74	0.40
EMA (6)	0.53±0.03	0.41±0.03	1.89		0.70	0.44
n-PMA (7)	0.57±0.01	0.38±0.04	1.76		0.65	0.44
IBMA (8)	0.55±0.02	0.40±0.05	1.82		0.68	0.43
n-BMA (9)	0.56±0.03	0.40±0.03	1.79		0.67	0.43

(1) CH_3; (2) C_2H_5; (3) *n*-C_4H_9; (4) *i*-C_3H_7 acrylates
(5) CH_3; (6) C_2H_5; (7) *n*-C_3H_7; (8) *i*-C_4H_9; (9) *n*-C_4H_9 methacrylates
(1) from Ref. 6, (2) and (4) from Ref. 8, (3) from Ref. 7, (5)—(9) from Ref. 9.

of ANA show a greater alternating tendency than a those of ANMA.

From Table 3, it may be seen that the relative reactivities, $1/r_1$, of ANA and ANMA to the attack of the polystyryl radical are larger than those of unsubstituted alkyl acrylates and methacrylates. Otsu *et al.*[8,9] have recently reported that the relative reactivities of alkyl acrylates and methacrylates to a polystyryl radical are correlated only with the polar substituent constant, σ^*, of the alkyl group in acrylates and methacrylates, and not with their steric substituent constant, E_s, in Taft's equation. The larger relative reactivities of ANA and ANMA in our experiments may also be ascribed to a strong polar effect of the alkyl group containing the nitrate group.

Taking it into consideration that the Q_2 and e_2 values for alkyl acrylates and methacrylates increase as a function of the electron-attracting nature of alkyl substituents,[8,9] the fact that these values for ANA and ANMA are larger than those of unsubstituted alkyl acrylates and methacrylates is readily explicable because of the strong electron-attracting nature of the nitrate group (see Table 4).

Table 4. Infrared spectroscopic data of acrylate and methacrylate monomers

	σ^* of alkyl group	$\nu_{C=O}$	ν_{C-O}	$1/r_1$	Q_2	e_2
Acrylate monomer						
EA (1)	−0.100	1726	1197	1.30	0.42	0.62
CLEA (2)	0.385	1727	1185	2.33	0.58	0.93
CNEA (3)	0.46	1728	1186	2.50	0.63	0.92
ENA		1728	1186	2.08	0.49	1.00
BNA		1726	1185	2.44	0.69	0.78
Methacrylate monomer						
EMA (4)	−0.100	1708	1177	1.89	0.68	0.43
BzMA (5)	0.215	1710	1165	2.27	0.86	0.42
CLEMA (6)	0.385	1717	1165	3.03	1.01	0.57
PhMA (7)	0.600	1730	1136	3.33	1.17	0.51
ENMA		1724	1165	2.87	0.99	0.53
PNMA		1715	1163	2.78	0.98	0.51
BNMA		1721	1166	2.70	0.90	0.58

(1) C_2H_5; (2) $CLCH_2CH_2$; (3) $CNCH_2CH_2$; (4) C_2H_5;
(5) $C_6H_5CH_2$; (6) $CLCH_2CH_2$; (7) C_6H_5
(1)—(3) from Ref. 8, (4)—(7) from Ref. 9.

Determined with a Hitachi EPI-2 infrared spectrophotometer. Acrylate monomers were measured in liquid film and methacrylate monomers in solution of $C_2H_4Cl_2$.

The data of the infrared spectra for ANA and ANMA in Table 4 are consistent with the increased Q_2 values for these monomers, as Otsu *et al.*[8,9] have reported that the carbonyl-stretching frequencies in acrylates and methacrylates are shifted to a

6) L. J. Young, *J. Polym. Sci.*, **54**, 411(1961).
7) "Encyclopedia of Polymer Science and Technology," Vol. 1, Interscience, New York (1964), p. 246.
8) T. Otsu, T. Ito, T. Fukumizu and M. Imoto, This Bulletin, **39**, 2257 (1966).
9) T. Otsu, T. Ito and M. Imoto, *Kogyo Kagaku Zasshi*, **69**, 986 (1966).

higher wave number as the electron-attracting character of alkyl substituents increases.

As compared with both ANA and ANMA, the $1/r_1$ and Q_2 values of ANA are smaller than those of ANMA, while the e_2 values of ANA are larger. This feature can presumably be attributed to the effect of the hyperconjugation and to the electron-releasing nature caused by the presence of the α-methyl group in ANMA.

Thus, the $1/r_1$, Q_2, and e_2 values of ANA and ANMA are larger than those of unsubstituted alkyl acrylates and methacrylates because of the polar effect of the alkyl group containing the nitrate group.

Copolymerization of ANA with Divinyl Monomers. The homopolymers of ANA reported in the previous paper are too soft and tacky to be utilized as elastomers in solid rocket propellants.[1] According to Matsuda *et al.*,[10] useful elastomers with good toughness properties have been produced by the copolymerization of nitrobutyl acrylate (nitro-BA) with some polyglycol dimethacrylates. Therefore, crosslinked polymers obtained by copolymerization with a small amount of divinyl monomers have been studied in this paper. The divinyl monomers used were diallyl phthalate (DAP), diallyl maleate (DAM), triethylene glycol dimethacrylate (TEDM), and 2-methyl-2-nitro-1,3-propylene diacrylate (MNPDA). The molecular weights of chains between crosslinking along main chains, M_c, were evaluated by the same calculation method as was used by Tanaka *et al.*[11] for the copolymers of nitro-BA with some divinyl monomers.

The relationship between the M_c value of the copolymers and the content of divinyl monomers in the monomer mixtures is plotted in Fig. 3, in which also some date for nitro-BA copolymers are given for the sake of comparison. It is found that the M_c value decreases with an increase in the content of crosslinking agents in the monomer mixtures. The M_c values of copolymers of BNA with TEDM are in the same order as those of the corresponding copolymers of nitro-BA. It may be noted that the copolymerization behavior of BNA with TEDM is similar to that of nitro-BA with TEDM.

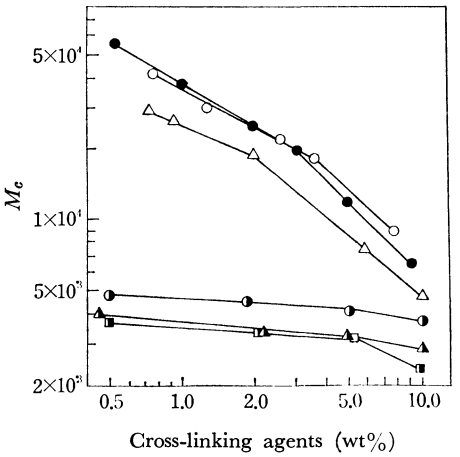

Fig. 3. Plot of M_c *vs.* divinyl monomer content
●: nitro-BA-TEDM, ○: BNA-TEDM,
△: BNA-MNPDA, ◑: BNA-DAP,
◭: BNA-DAM, ◨: ENA-DAM, ●: from Ref. 11

Generally speaking, the M_c values are highest for TEDM copolymers, medium for MNPDA copolymers, and lowest for diallyl ester copolymers. As Tanaka *et al.*[11] have reported, with regard to nitro-BA copolymers, that the tensile strength and the hardness of the copolymers increase and the elongation values decrease with an increase in the crosslinking densities, the elongation values of the copolymers of BNA with diallyl esters appear to decrease with an increase in the crosslinking densities.

10) Y. Matsuda, A. Tanaka, K. Sasaki, R. Kawai, K. Matsumoto, N. Yoshida and Y. Matsui, Papers presented at the 2nd International Symposium on Rockets and Astronautics, Tokyo, Japan (1960), p. 1.

11) A. Tanaka, K. Sasaki, Y. Hozumi and O. Hashimoto, *J. Appl. Polym. Sci.*, **8**, 1787 (1964).

BULLETIN OF THE CHEMICAL SOCIETY OF JAPAN VOL. 43 212—215 (1970)

Oxidative Coupling Reaction of Phenols with Dichromate

Hiroo TANAKA, Isao SAKATA and Ryoichi SENJU

Faculty of Agriculture, Kyushu University, Hakozaki, Fukuoka

(Received June 23, 1969)

On treatment in an aqueous solution with dichromate, *p*-cresol and creosol readily undergo nuclear oxidative coupling. The yields of dimeric and trimeric cresols and of dimeric ketone are of the same order as the yields of the previously-recorded preparations by one-electron-transfer oxidants. When manganese sulfate is added, these yields are tripled. The probable mechanism of the coupling reaction of phenols with dichromate is discussed.

During the course of an investigation of the mechanism for the gelling reaction of lignin with dichromate,[1,2] it became desirable to examine the coupling reaction of phenols with dichromate.

It has been well known that phenols react with one-electron-transfer oxidants, *e.g.*, persulfate, alkaline ferricyanide or Fenton's reagent, to produce phenoxy-radicals, which then give dimeric or trimeric products by coupling reaction.[3] This oxidation mechanism has been confirmed by the identification of the oxidation products, by the detection of an intermediate phenoxy radical by the ESR technique, and so on. However, the great majority of works on the oxidation of phenols with dichromate have dealt with the preparation of quinone[4]; the only example concerning coupling products was recorded in the case of highly alkylated phenols in 50% acetic acid and 20% sulfuric acid at 50—55°C.[5] Accordingly, it has not yet been established whether the oxidative coupling readily occurs by means of the reaction between phenols and dichromate in an aqueous solution. The present investigation was, therefore, undertaken in order to clarify this problem. In addition, the catalytic effect of the manganese ion upon this reaction will be discussed.

Results and Discussion

The oxidation of phenols by one-electron-transfer oxidants has been reported by a number of workers. In all cases, the initial step has been described as the removal of hydrogen from the phenols by a radical or multivalent metal ion; the further coupling reaction of the resulting aryloxy-radical has also been discussed. For example, the coupling reaction scheme for *p*-cresol is as follows:

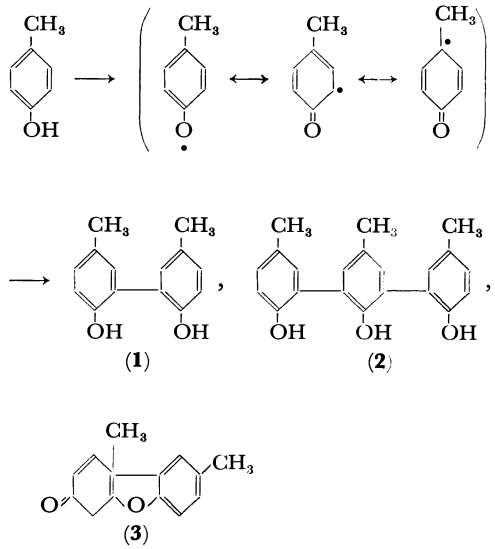

In the present experiments, on treatment with the aqueous dichromate, *p*-cresol gave a crystalline fraction (15%) consisting of *ortho*-linked dimeric (**1**) and trimeric (**2**) cresols and the dimeric ketone (**3**) (Table 1); on the other hand, creosol furnished only *ortho*-linked dimeric creosol (7—9%) as a crystalline product (Table 2). Homocatechol, meanwhile, yielded only resinous products. When manganese sulfate was added as a catalyst, the yields of crystalline products from *p*-cresol or creosol were tripled. The total yields of the oxidation products from *p*-cresol were 1.5 times as much as the best yields among the previously-recorded

1) H. Tanaka, H. Abe and R. Senju, *Kogyo Kagaku Zasshi*, **69**, 1968 (1966).

2) H. Tanaka, I. Sakata and R. Senju, *ibid.*, **71**, 404 (1968).

3) W. A. Waters, "Progress in Organic Chemistry," Vol. 5, ed. by J. W. Cook and W. Carruthers, Butterworths, London (1961), p. 1.

4) J. Cason, "Organic Reaction," Vol. 4, ed. by R. Adams, John Miller & Sons. Inc., New York (1948), p. 305.

5) H. E. Albert, *J. Amer. Chem. Soc.*, **76**, 4983 (1954).

Table 1. Dichromate oxidation products of *p*-cresol

$MnSO_4$	Total prods. (ppt.) (%)	Ether-insol. prods. (%)	Ether-sol. prods.					Total coupling prods. of (1), (2) and (3) (%)
			Neutral prods.		Alkali-sol. prods.			
			Total crude (%)	Ketone (3) (%)	Total crude (%)	Dimer (1) (%)	Trimer (2) (%)	
None	66	19	20	12	27	2	1	15
8.0 g/*l* (0.053 mol)	74	5	27	17	43	8	6	31
80.0 g/*l* (0.53 mol)	82	2	33	21	47	13	7	41

Table 2. Dichromate oxidation products of creosol

$MnSO_4$	$K_2Cr_2O_7$ mol/*l*	Total prods. (ppt.) (%)	Ether-insol. prods. (%)	Ether-sol. prods.	
				Total crude (%)	Dimer (%)
None	0.047	53	17	36	9.0
None	0.012	58	15	43	7.2
80.0 g/*l* (0.53 mol)	0.012	71	9	62	22.5

preparations;[6-13] in other words, half of the starting material was recovered as crystalline oligomers (Table 3).

When larger quantities of dichromate were employed in the oxidation of creosol, greater quantities of the dimer were obtained. In considering the reaction mechanism described below, this result seems to be due to the fact that comparatively more hexavalent chromium exists than tetra- and pentavalent species. An analysis of the residual resinous products showed that demethylation and further oxygenation occurred.

On the dichromate oxidation of homocatechol, unlike the cases of *p*-cresol and creosol, a major part of the precipitate (60%) was an ether-insoluble fraction; this was an alcohol-soluble complicated resin possibly oxygenated. Also precipitates were traces of unidentified polyphenols and carboxylic acid, detected by the paper chromatography of the ether-soluble fraction. It may be thought that the crystalline oligomer is not obtained, for the resulting products are further oxidized, too.

As is shown in Fig. 1, the velocity of the oxidation reaction increases in the following order: homocatechol>creosol>*p*-cresol. This order is proportional to the electron density of the phenolic hydroxyl group. It seems probable that the initial step in these reactions is an abstraction of one electron. Furthermore, it was detected that the addition of

Table 3. Oxidation products of *p*-cresol weth various oxidants

Oxidants	Dimer (**1**) (%)	Trimer (**2**) (%)	Ketone (**3**) (%)	Total of **1**, **2** and **3** (%)	Ref.
$K_2Cr_2O_7$	2	1	12	15	This pap.
$K_2Cr_2O_7$+$MnSO_4$ (8 g/*l*)	8	6	17	31	This pap.
$K_2Cr_2O_7$+$MnSO_4$ (80 g/*l*)	13	7	21	41	This pap.
$Na_2S_2O_8$+Ag^+, Fe^{2+}, Fe^{3+}	7	7	15	29	6
Electrolytic oxidn.	11	7		18	7
Alkaline $K_3Fe(CN)_6$	1 2	2	13	16 17	8
H_2O_2+Peroxidase	2	7	13	22	9
H_2O_2+Fe^{2+}	6		4	10	10
Solid $FeCl_3$	10 11	6 9		16 20	11
Aq. $FeCl_3$	5		1	6	11
Cl_2 or SO_2Cl_2+$ZnCl_2$	12 16	3 8		15 24	12
Nickel peroxide	small	small	small	small	13

6) R. G. R. Bacon, R. Grime and D. J. Munro, *J. Chem. Soc.*, **1954**, 2275.
7) F. Fichter and F. Ackermann, *Helv. Chim. Acta*, **2**, 583 (1919).
8) R. Pummerer, D. Melamed and H. Puttfarcken, *Ber.*, **55**, 3116 (1922); R. Pummerer, H. Puttfarcken and P. Schopflocker, *ibid.*, **58**, 1808 (1925).
9) W. W. Westerfeld and C. Lowe, *J. Biol. Chem.*, **145**, 463 (1942).
10) S. L. Cosgrove and W. A. Waters, *J. Chem. Soc.*, **1951**, 1726.
11) K. Bowden and C. H. Reece, *ibid.*, **1950**, 2249.
12) K. Bowden and C. H. Reece, *ibid.*, **1950**, 1686.
13) J. Sugita, *Nippon Kagaku Zasshi*, **87**, 603 (1966).

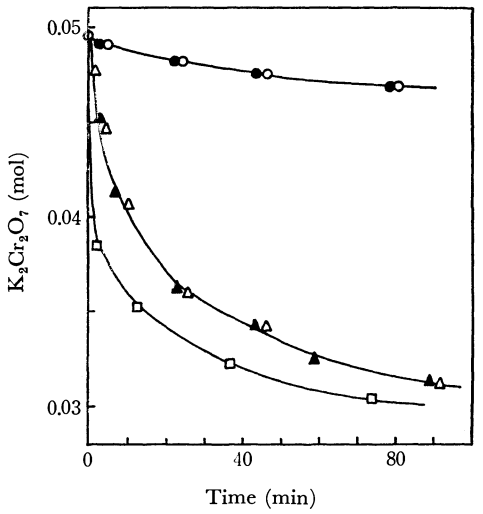

Fig. 1. Dichromate concentration-time curves for oxidation reaction of various phenols.
○●, *p*-cresol; △▲, creosol; □, homocatechol substrates: 0.05 mol, CH_3COOH: 0.2 mol $MnSO_4$; ●▲, 0.5 mol; ○△□, none, 25°C

the manganese ion is independent of the velocity change.

The catalytic effect of the manganese ion in chromium oxidation is of peculiar interest. This effect has been described in the case of alcohols,[14] but not in that of phenols. It is known that divalent manganese (Mn^{2+}) is oxidized to trivalent species (Mn^{3+}) with tetra- and pentavalent chromiums, but not with hexavalent species.[15] It is also known that trivalent manganese reacts with phenols to produce a phenoxy radical, which in turn affords a high yield of oxidative coupling products.[16] As Tables 1 and 2 show the yields of the coupling products of phenols with dichromate about triple when a large amount of the manganese ion is added.

From these facts, when the manganese ion is not present, it may be thought that one mole of chromic acid (CrO_4^{2-}) acts as one equivalent to produce the phenoxy radical; that is, only hexavalent chromium may be effective in producing the phenoxy radical, as is shown in Eq. (1), while the tetra- and pentavalent species may be ineffective. On the other hand, in the case of the presence of a large amount of the manganese ion, one mole of chromic acid has the ability of three equivalents because the trivalent manganese ion, which is produced by the reaction between the divalent manganese ion and penta- or tetravalent chromium, may also be effective in producing the phenoxy radical, as is shown in Eqs. (3) and (4). In conclusion, the mechanism for the coupling reaction of phenols with dichromate in the presence of manganese sulfate may be proposed to be as follows:

$$PhOH + Cr(VI) \longrightarrow PhO\cdot + Cr(V) \quad (1)$$

$$PhOH \text{ or } PhO\cdot + Cr(V) \text{ or } Cr(IV) \longrightarrow \text{Complicated products} \quad (2)$$

$$Mn^{2+} + Cr(V) \text{ or } Cr(IV) \longrightarrow Mn^{3+} + Cr(IV) \text{ or } Cr(III) \quad (3)$$

$$PhOH + Mn^{3+} \longrightarrow PhO\cdot + Mn^{2+} \quad (4)$$

$$PhO\cdot + PhO\cdot \longrightarrow Dimer \longrightarrow Trimer \quad (5)$$

In the absence of manganese sulfate, the reaction mechanism may be expressed by Eqs. (1), (2) and (5).

Experimental

Materials and Procedure. The phenols employed in this study were *p*-cresol, creosol, and homocatechol. The phenols and other reagents were of an analytical reagent grade. The oxidation reactions of the phenols with dichromate were carried out in an aqueous solution containing 1.2% acetic acid under gentle stirring, at a constant temperature, and in air. The consumption of dichromate was measured by the iodometry method.

In these oxidations, turbidity appeared within a few minutes after mixing; the product was eventually isolated quantitatively as a precipitate from a brown solution. In order to remove a small amount of inorganic substances, the product was treated with ether. The ether-soluble product was then separated, by 2N sodium hydroxide, into a neutral fraction and an alkali-soluble polyphenol fraction. The oxidation products were identified by a comparison of their melting points and of the results of elemental analyses of them and their derivatives with those of authentic samples. The melting points were measured with Yanagimoto's micromelting-point apparatus, while the elemental analyses were performed in the Analytical Center of Kyushu University.

Oxidation of *p*-Cresol. *(a) Products of Non-catalyzed Oxidation.* An aqueous solution (1 *l*) containing *p*-cresol (10.8 g, 0.1 mol), potassium dichromate (15 g, 0.05 mol), and acetic acid (12 g, 0.2 mol) was allowed to stand for 92 hr at 25°C. The dry weight of the precipitate was 6.3 g (66% of the weight of the oxidation products), of which the ether-insoluble and alcohol-soluble portion; an amorphous brown powder, composed 1.8 g (19%). The ether-soluble fraction gave a pale yellow, crystalline, neutral material (1.9 g, 20%) and a brown, resinous, alkali-soluble polycresol (2.5 g, 26%). The ether extraction of the aqueous filtrate from the oxidation products yielded a trace of an oily material and unchanged *p*-cresol (1.2 g, 13%).

After crystallization from methanol, the neutral fraction yielded Pummerer's ketone as colorless leaflets (1.1 g, 12%); mp 123.5°C (lit,[6-12] mp 122—128°C) (Found: C, 77.90; H, 6.57%). The alkali-soluble polycresols were distilled *in vacuo* to yield two resinous fractions, (A) (bp 150—190°C/1 mmHg; 0.4 g, 4%) and

14) K. Umeda and K. Tarama, *Nippon Kagaku Zasshi*, **83**, 1210, 1221 (1962).
15) W. Watanabe and F. H. Westheimer, *J. Chem. Phys.*, **17**, 61 (1949).
16) T. Shono, K. Yamanoi, T. Matsushita and K. Shinra, *Kogyo Kagaku Zasshi*, **70**, 2062 (1967).

(B) (bp 210—260°C/1 mmHg; 0.5 g, 5%). The fraction (A) was crystallized from benzene to give 2,2′-dihydroxy-5,5′-dimethyldiphenyl (0.2 g, 2%) as colorless prisms; mp 154—155°C (lit,[6] 153—154°C) (Found: C, 78.03; H, 6.47%). This was characterized as the diacetate; mp 87.5°C (lit,[6] 87—88°C) (Found: C, 72.37; H, 6.14%). When the (A) fraction was treated with bromine (2 molar equiv. per mol) in glacial acetic acid, 3,3′-dibromo-2,2′-dihydroxy-5,5′-dimethyldiphenyl was obtained as colorless prisms, mp 141—142°C (lit,[6] 141—142°C) after recrystallization from aqueous ethanol.

The fraction (B), crystallized from benzene, gave colorless 2,2′,2″-trihydroxy-5,5′,5″-trimethyl-*m*-terphenyl (0.1 g, 1%); mp 196.5—197°C (lit,[6] 194—197°C) (Found: C, 78.62; H, 6.16%). When the fraction (B) was treated at room temperature with bromine (2 molar equiv. per mol) in glacial acetic acid, 3,3′-dibromo-2,2′,2″-trihydroxy-5,5′,5″-trimethyl-*m*-terphenyl was obtained; mp 286—288°C (lit,[6] 284—286°C) (Found: C, 52.76; H, 3.95%).

(b) Oxidation Products Catalyzed with Manganese Ion. A mixture like that in (*a*) was stirred for 92 hr at 25°C with manganese sulfate (0.053 or 0.53 mol respectively). Fractionation and the identification of the oxidation products were performed as above. The results are summarized in Table 1.

Oxidation of Creosol. *(a) Products of Non-catalyzed Oxidation.* The following is a typical preparation carried out on a 0.036 molar scale at 25°C. An aqueous solution (1 *l*) containing creosol (5.0 g, 0.036 mol; insoluble above this value), potassium dichromate (3.6 g, 0.012 mol), and glacial acetic acid (12 g, 0.2 mol) was allowed to stand for 20 hr. The dry weight of the precipitate was 2.84 g (57%), of which the ether-insoluble, amorphous brown powder was 0.74 g (15%). The ether-soluble products were distilled *in vacuo* to yield a resinous material; bp 180—260°C/0.7 mmHg (1.1 g, 22%). This fraction was crystallized from benzene to give 2,2′-dihydroxy-3,3′-dimethoxy-5,5′-dimethyldiphenyl (0.36 g, 7.2%) as colorless needles; mp 130.5—131°C (lit,[17] 130°C) (Found: C, 70.65; H, 6.62%). The diacetate, after recrystallization from alcohol, had a mp of 163°C (lit,[17] 162—163°C) (Found: C, 67.18; H, 6.21%). The oily material other than the above crystalline material had a methoxyl content of 19.9%. The ether-insoluble fraction (soluble in alcohol) did not melt below 300°C, and its methoxyl content was 15.8%, which was less than that of the starting material (22.6%). (Found, after correction for inorganic materials: C, 63.35; H, 5.55%. Calcd for creosol; $C_8H_{10}O_2$: C, 69.54; H, 7.29%). When the proportion of dichromate was higher than in the above experiment, the yield of dimer increased from 7.2% to 9.0% (Table 2).

(b) Oxidation Products Catalyzed with Manganese Ion. A mixture like that in (*a*) was stirred for 20 hr at 25°C with manganese sulfate (0.53 mol). The fractionation and identification of oxidation products were performed by the same method as above. The results are summarized in Table 2.

Oxidation of Homocatechol. An aqueous solution (1 *l*) containing homocatechol (4.5 g, 0.036 mol), potassium dichromate (3.6 g, 0.012 mol), and glacial acetic acid (12 g, 0.2 mol) underwent rapid oxidation at 25°C. A rapid darkening and deposit of particles of a brown, amorphous solid occurred. However, the mixture was left for 5 hr. The crude product (2.7 g, 60% of the weight of homocatechol) yielded a large amount of an ether-insoluble fraction as a brown powder which was thought to be polyphenol. The ether-insoluble fraction, subjected to paper chromatography, appeared to consist of alkali-soluble polyphenols and a small amount of carboxylic acid.

17) H. Richtzenhain, *Chem. Ber.*, **82**, 447 (1949).

BULLETIN OF THE CHEMICAL SOCIETY OF JAPAN VOL. 43 215—219 (1970)

Cationic Arylation. I. Phenylation of Substituted Benzenes with Benzenediazonium Tetrafluoroborate in Homogeneous Solution

Michio KOBAYASHI, Hiroshi MINATO, Eiichi YAMADA and Nobumasa KOBORI

Department of Chemistry, Tokyo Metropolitan University, Fukazawa, Setagaya-ku, Tokyo

(Received June 27, 1969)

Substituted benzenes were phenylated with benzenediazonium tetrafluoroborate in homogeneous solutions with DMSO or acetonitrile. The distribution of substituted biphenyls and the partial rate factors indicated that this phenylation was an electrophilic substitution, but the selectivity was much smaller than those of nitration or sulfonylation. Experiments with chlorobenzene-4*d*, anisole-4*d* and chlorobenzene-d_5 showed that both the orientation and partial rate factors did not change with deuterated compounds. Therefore, it was established that the rate-determining step was the addition of phenyl cation to an aromatic nucleus, and not the abstraction of proton from the phenylated intermediate.

Abramovitch and Saha[1] studied the arylation of aromatic compounds with benzenediazonium tetrafluoroborate, and on the basis of the isomer ratios and the apparent total rate ratios they suggested that the phenyl cation initially formed isomerized to a diradical cation.

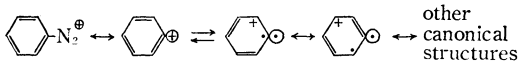

[I] [IIa] [IIb]

However, the reaction was carried out in heterogeneous media and there was no kinetic control in the reaction conditions. An investigation of this reaction in homogeneous media seemed desirable.

Recently Abramovitch and Gadallah[2] reported the results of the phenylation in mixtures of substituted benzenes and acetonitrile or sulpholan. This prompted us to report on our findings in the phenylation in homogeneous solutions consisting of aromatic solvents and dimethyl sulfoxide (DMSO) or acetonitrile. On the basis of the partial rate factors of substituted benzenes and substituted deuterated benzenes in homogeneous solution the mechanism of the phenylation with benzenediazonium tetrafluoroborate will be discussed.

Experimental

Materials. Dimethyl sulfoxide and acetonitrile were purified according to the methods described in a previous paper.[3] Benzene, toluene, ethylbenzene and chrolobenzene were washed with concentrated sulfuric acid and water successively, dried over calcium chloride, and distilled. Boiling points were 80°C, 110°C, 135.7°C and 131°C, respectively. Anisole was washed with an aqueous sodium hydroxide solution and water, dried over calcium chloride, and distilled; bp 153°C. Methyl benzoate was prepared from benzoic acids and methanol, washed with water, dried over magnesium sulfate, and then fractionally distilled; bp 110°C/50 mmHg. Nitrobenzene was washed repeatedly with a potassium dichromate solution, dried over calcium chloride, and distilled; bp 95.5°C/18 mmHg.

Benzenediazonium tetrafluoroborate was prepared according to the method decribed previously.[3]

Isomeric methylbiphenyls, ethylbiphenyls, methoxybiphenyls, chlorobiphenyls, methoxycarbonylbiphenyls and nitrobiphenyls were prepared as the reference compounds by the methods described in literature.[4] They were purified by elution chromatography, distillation or recrystallization, and their melting points and boiling points agreed with the values in literature. Dibenzyl and β-methoxynaphthalene were purified by recrystallization.

Anisole-4*d* was prepared by the hydrolysis of *p*-methoxyphenylmagnesium bromide in D_2O (isotopic purity, 99.75%, supplied by E. Merck AG, Darmstadt); bp 58°C/15 mmHg. Its isotopic purity was determined to be 92% by mass spectrometry using Hitachi RMU-6B. Chlorobenzene-4d was prepared by the same method from *p*-bromochlorobenzene; bp 131°C. Its isotopic purity was found to be 90%.

Chlorobenzene-d_5 of CIBA Limited was used without further purification. Guaranteed isotopic purity was 99.6%.

Decomposition of Benzenediazonium Tetrafluoroborate. In 20.0 g of dimethyl sulfoxide (DMSO) or acetonitrile 2.0 g of benzenediazonium tetrafluoroborate was dissolved, and the solution was diluted with substituted benzenes (the molar ratio of substituted benzene *versus* the diazonium salts was 50). The homogeneous solution was placed in a bath at 40±0.1°C, and the decomposition was followed by measuring the rate of evolution of nitrogen. After the evolution of nitrogen ceased, the reaction mixture was washed with water to remove the polar solvent, washed with a 5% sodium hydroxide solution to remove acidic products, washed with water, dried over magnesium sulfate, and then the amounts of substituted biphenyl isomers were determined by a Hitachi Gas Chromatograph K-53.

Since the presence of a large quantity of substituted benzenes made the gas chromatographic determination of substituted biphenyls unreliable because of tailing, the determination was carried out after about 80% of substituted benzenes had been evaporated. Chlorobenzene was chosen as the standard for competitive experiments since non-substituted biphenyl easily sublimes. The biphenyl isomers were identified by comparison of their retention times with those of authentic samples, and their amounts were determined by use of calibration curves. Columns used were packed with Apiezon L (10%) on Chromosorb W, and their lengths varied from 1 m to 6 m depending on the ease of separation of isomers.

Results and Discussion

Decomposition of benzenediazonium tetrafluoroborate in homogeneous mixtures of substituted

TABLE 1. FIRST ORDER RATE CONSTANTS FOR THE DECOMPOSITION OF PhN_2BF_4 IN HOMOGENEOUS SOLUTION AT 40°C

Solvents	$10^4 k_1$ (sec^{-1})
DMSO-PhH-PhCl	3.82
DMSO-PhH-$PhCH_3$	3.81
DMSO-PhCl-$PhOCH_3$	3.82
DMSO-PhCl-$PhNO_2$	3.62
DMSO-PhH-PhC_2H_5	3.84
DMSO-PhH-$PhCO_2CH_3$	4.06*
DMSO only	3.89
CH_3CN-PhH-PhC_2H_5	3.25
CH_3CN-PhH-PhCl	3.10
CH_3CN-PhCl-$PhOCH_3$	3.48
CH_3CN-PhCl-$PhNO_2$	3.44
CH_3CN-PhH-$PhCO_2CH_3$	3.19
CH_3CN only	3.15**

* at 40.2°C, ** at 39.8°C

1) R. A. Abramovitch and J. G. Saha, *Can. J. Chem.*, **43**, 3269 (1965).

2) R. A. Abramovitch and F. F. Gadallah, *J. Chem. Soc., B*, **1968**, 497.

3) R. Adams, "Organic Reactions," Vol. II, John Wiley and Sons, Inc., London (1957); P. E. Fanta, *Chem. Rev.*, **64**, 613 (1964); M. Kobayashi, E. Yamada, M. Matsui and N. Kobori, *Organic Preparations and Procedures*, in press.

benzenes-DMSO and substituted benzenes-acetonitrile was of first order, and the rate constants are shown in Table 1. The average value of first-order rate constants in DMSO-C_6H_5X was 3.84×10^{-4} (sec^{-1}) and that in CH_3CN-C_6H_5X was 3.27×10^{-4} (sec^{-1}), which were approximately the same as those in pure DMSO and in pure acetonitrile. This shows that benzenediazonium tetrafluoroborate decomposes in these solvent systems to produce phenyl cation and nitrogen gas under the same mechanism.

As products other than substituted biphenyls, 1,3-benzoxathiane (about 8 mol%) was obtained from the reactions in DMSO-C_6H_5X, and acetanilide (about 50 mol%) was obtained from the reactions in CH_3CN-C_6H_5X. Products of dimerization or disproportionation were not found. Apparently the electron-rich oxygen atom of DMSO and nitrogen atom of acetonitrile compete with the aromatic nucleus in reaction with the electrophilic phenyl cation as follows.

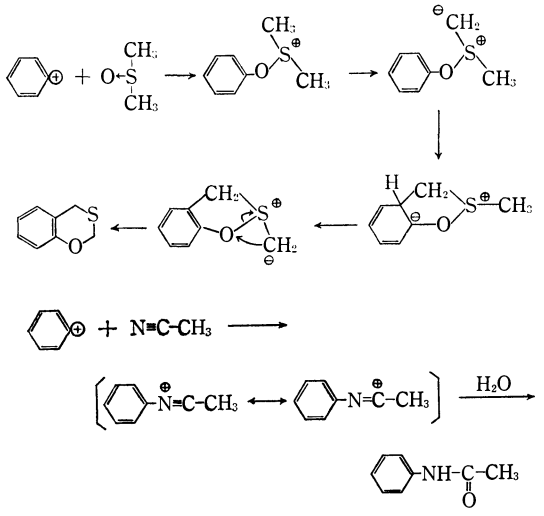

Because of these reactions, yields of biphenyls are not so high; 7% in $PhNO_2$-DMSO, 12.4% in PhCl-DMSO, and 20.8% in PhOMe-DMSO.

Orientation for phenylation with benzenediazonium tetrafluoroborate in PhX-DMSO and in PhX-CH_3CN is summarized in Table 2. Benzenes substituted with methoxy, methyl, ethyl and chloro groups are *o,p*-directors, and benzenes substituted with methoxycarbonyl and nitro groups are *m*-directors. This indicates that the reactions are of electrophilic nature. Except for nitrobenzene, more *ortho* and *para* isomers were produced in CH_3CN-PhX than in DMSO-PhX, and especially the amounts of *ortho* isomers were greater. These results are in contrast with the findings that greater amounts of *ortho* isomers were produced in DMSO-PhX than in CH_3CN-PhX by free radical phenylation with phenylazotriphenylmethane.[4]

Table 2. Orientation (%) for the phenylation of PhX with PhN_2BF_4 in homogeneous solution at 40°C

PhX	In DMSO			In CH_3CN		
	o-	*m*-	*p*-	*o*-	*m*-	*p*-
OCH_3	56.4	12.2	31.4	64.0	8.5	27.5
	56.0	12.2	31.8	65.6	8.2	26.2
CH_3	47.3	21.1	31.6			
	47.1	20.9	32.0			
C_2H_5	46.2	29.3	24.6	50.4	25.8	23.8
	42.9	29.8	27.3	49.3	25.2	25.5
Cl	48.2	24.0	27.8	61.5	15.7	22.8
	49.8	22.8	27.4	61.5	14.3	23.8
	44.1*	26.1*	29.8*			
CO_2CH_3	43.1	43.5	13.4	53.4	36.5	10.1
	46.1	42.1	11.8	52.5	37.5	10.0
NO_2	38.1	48.4	13.5	29.5	48.2	22.3
	36.4	50.3	13.3	31.8	52.0	16.2

* reaction carried out in oxygen atmosphere

Table 3. Partial rate factors for the phenylation of PhX with PhN_2BF_4 in homogeneous solution at 40°C

PhX	In DMSO			In CH_3CN		
	k_o/k	k_m/k	k_p/k	k_o/k	k_m/k	k_p/k
OCH_3	3.14	0.68	3.50	1.74	0.23	1.49
	3.14	0.68	3.57	1.80	0.22	1.44
CH_3	1.32	0.61	1.84			
	1.35	0.60	1.84			
C_2H_5	1.31	0.83	1.40	1.51	0.77	1.43
	1.31	0.91	1.67	1.39	0.71	1.44
Cl	1.02	0.51	1.17	0.67	0.17	0.49
	1.03	0.47	1.13	0.67	0.16	0.62
	1.01*	0.60*	1.37*			
CO_2CH_3	0.40	0.40	0.25	0.54	0.37	0.20
	0.44	0.40	0.22	0.57	0.41	0.22
NO_2	0.29	0.37	0.21	0.10	0.16	0.15
	0.29	0.40	0.21	0.09	0.14	0.09

* reaction carried out in oxygen atmosphere

Table 3 shows the partial rate factors calculated on the assumption that the step of σ-complex formation is rate-determining. Differences between the values in DMSO-PhX and those in CH_3CN-PhX may be ascribed to the difference in the solvation of the transition states and aryl cations. Variations in the partial rate factors in Table 3 are consistent with the electrophilic nature of the reactions except that the selectivity is very small

4) M. Kobayashi, H. Minato, N. Watanabe and N. Kobori, This Bulletin, **43**, 258 (1970).

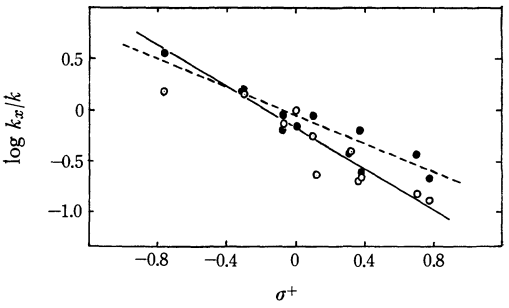

Fig. 1. The Hammett plots for the phenylation of PhX with PhN_2BF_4.
—○—: in CH_3CN, $\rho=-0.82$, $r=0.91$
---●---: in DMSO, $\rho=-0.74$, $r=0.93$

compared with that in nitration[5] or sulfonylation[6] of aromatic compounds. However, the selectivity or the partial rate factors for phenylation with phenyl cation are quite different from those of phenylation with phenyl radical.

log k_m/k or log k_p/k is better correlated with σ^+ of Brown-Okamoto than σ values Hammett, as shown in Fig. 1. However, the correlation is not so good, and the correlation coefficient is 0.93 in DMSO-PhX and 0.91 in CH_3CN-PhX. The reaction constant, ρ, is small compared with that in ordinary ionic reactions (−0.74 in DMSO-PhX and −0.82 in CH_3CN-PhX), but the fact that it is negative indicates that these reactions are electrophilic and are different from phenylation with phenyl radical.[7,8] Various features of phenylation with phenyl cation are best explained on the assumption that the phenyl cation initially formed isomerizes to a diradical cation [II] with concerted uncoupling of a pair of π-electrons, one of which falls into the vacant sp^2 σ-orbital.[1,9]

Under an oxygen atmosphere yields of phenylation with phenyl radical greatly decrease, whereas those with phenyl cation do not change, as shown by the data with chlorobenzene in Tables 2 and 3. This finding is not inconsistent with the biradical nature of phenyl cation, since the non-reactivity is ascribable to the repulsion between the strongly electrophilic oxygen and the strongly electrophilic phenyl cation.

Abramovitch and Gadallah[2] did not attempt to correlate the partial rate factors with σ^+ or σ. If their values are plotted *versus* σ^+, ρ is −0.66 at 65°C with the correlation coefficient of 0.96. This ρ value is consistent with the value reported in this paper if the difference in the temperatures is taken into consideration.

The correlation in the Hammett plots of our data as well as the data of Abramovitch and Gadallah[2] is much worse than that of ordinary ionic reactions. In an attempt to explain the apparent slight deactivation of the *meta*-position in toluene towards phenylation in CH_3CN-PhMe at 65°C ($k_m/k=0.85$), Abramovitch and Gadallah[2] suggested that the rate-determining step in these reactions was not the formation of σ-complex [III] *via* Scheme 1, but the addition of IIa to a benzene double bond to form the various possible spirocyclopropane phenonium ions [IV], followed by ring-opening to give the three substituted σ-complexes in a product-, but not rate-, determining step.

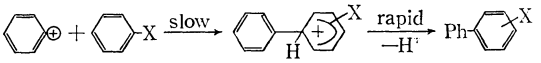

Scheme 1

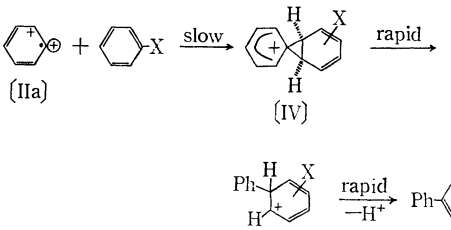

Scheme 2

Our data show considerable deactivation of the *meta* position in toluene ($k_m/k=0.60$ in DMSO-PhMe) and in ethylbenzene ($k_m/k=0.74$ in CH_3CN-PhEt and 0.87 in DMSO-PhEt), and these values are in line with their suggestion.

In an attempt to elucidate the mechanism of this phenylation further, isotope effects were examined by use of anisole-4*d*, chlorobenzene-4*d* and chlorobenzene-d_5. The results are shown in Table 4. When anisole-4*d* or chlorobenzene-4*d* was phenylated with benzenediazonium tetrafluoroborate in a mixture with DMSO, the distributions of isomeric biphenyls were approximately the same as those with anisole or chlorobenzene. When

TABLE 4. PHENYLATION OF DEUTERATED PhX WITH PhN_2BF_4 IN DMSO AT 40°C

PhX	Orientation (%)			Partial rate factors		
	o-	*m*-	*p*-	k_o/k	k_m/k	k_p/k
$PhOCH_3$-4*d*	54.8	13.5	31.7			
($PhOCH_3$)	56.2	12.2	31.6			
PhCl-4*d*	44.0	23.9	32.1			
(PhCl)	45.7	21.6	32.7	1.02	0.49	1.15
PhCl-d_5	43.8	25.3	30.9	0.89	0.52	1.26

5) L. M. Stock and H. C. Brown, *J. Amer. Chem. Soc.*, **81**, 3323 (1959).
6) F. R. Jensen and H. C. Brown, *ibid.*, **80**, 4046 (1958).
7) G. H. Williams, "Homolytic Aromatic Substitution," Pergamon Press, London (1960).
8) R. Ito, T. Migita, N. Morikawa and O. Simamura, *Tetrahedron*, **21**, 955 (1965).
9) R. W. Taft, *J. Amer. Chem. Soc.*, **83**, 3350 (1961).

a mixture of chlorobenzene-d_5 and benzene was phenylated and the partial rate factors were calculated, the values of k_H/k_D for *ortho*, *meta* and *para* were approximately 1 within experimental error of gas chromatography. These findings show that in phenylation with phenyl cation there is no isotope effect as in the cases of nitration and free radical arylation[10] of aromatic compounds.

So far there is no conclusive evidence which enables us to choose Scheme 1 or Scheme 2 as the mechanism of the phenylation with phenyl cation. However, it has been established that the rate-determining step is the addition of the phenyl cation to an aromatic nucleus, and not the abstraction of proton from the phenylated intermediate.

10) E. L. Eliel, S. Meyerson, Z. Welvart and S. H. Wilen, *ibid.*, **82**, 2936 (1960).

BULLETIN OF THE CHEMICAL SOCIETY OF JAPAN VOL. 43 219—223 (1970)

Cationic Arylation. II. Phenylation of Substituted Benzenes with Phenylazo-*p*-tolylsulfone in Acidic Solutions

Michio KOBAYASHI, Hiroshi MINATO and Nobumasa KOBORI

Department of Chemistry, Faculty of Science, Tokyo Metropolitan University, Fukazawa, Setagaya-ku, Tokyo

(Received June 27, 1969)

The acid-catalyzed decomposition of phenylazo-*p*-tolylsulfone was studied in PhX, PhX-CH_3CN and PhX-DMSO (X=OCH_3, C_2H_5, CH_3, Cl, CO_2CH_3, NO_2). The decomposition was of first order but was faster with greater concentration of trifluoroacetic acid. The orientation and the partial rate factors for the phenylation of substituted benzenes were quite different from those for the radical phenylation but quite similar to those for the phenylation with phenyl cation generated from $PhN_2^+BF_4^-$. Experiments with deuterated compounds indicated that the abstraction of proton from the phenylated complex was not rate-determining. A mechanism involving phenyl cation was proposed for the acid-catalyzed decomposition of azosulfone.

Phenylazo-*p*-tolylsulfone [I] is produced when an aqueous benzenediazonium chloride solution is mixed with an aqueous sodium *p*-toluenesulfinate solution. It is not an ionic compound, and is soluble in organic solvents and insoluble in water. When heated in a solution, it decomposes with evolution of nitrogen.

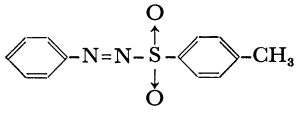

[I]

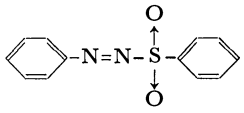

[II]

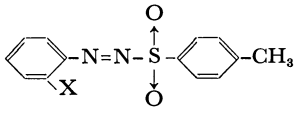

[III] X=Cl, Br

Overberger and Rosenthal[1] studied the kinetics of the decomposition of phenylazophenylsulfone [II] in neutral solutions, and found that its spontaneous decomposition was a free radical decomposition. Bunnett and Happer[2] investigated the decomposition of *o*-halophenylazophenylsulfone [III] in the presence of sodium methoxide, and found that in very dilute sodium methoxide solution the decomposition was homolytic, whereas in concentrated sodium methoxide solution the decomposition proceeded *via* *o*-halophenyl anion as the intermediate.

It seemed of great interest to investigate the decomposition of azosulfones in acidic solutions. The decomposition of phenylazo-*p*-tolylsulfone [I] in the presence of trifluoroacetic acid in substituted benzenes has been investigated, and the results are described in this paper.

Experimental

Materials. Dimethyl sulfoxide, acetonitrile and substituted benzenes were purified according to the methods described in a previous paper.[3]

1) C. G. Overberger and A. J. Rosenthal, *J. Amer. Chem. Soc.*, **82**, 108, 117 (1960).

2) J. F. Bunnett and D. A. R. Happer, *J. Org. Chem.*, **32**, 2701 (1967).

3) M. Kobayashi, H. Minato, E. Yamada and N. Kobori, This Bulletin, **43**, 215 (1970).

Sodium *p*-toluenesulfinate was prepared by the reduction of *p*-toluenesulfonyl chloride with zinc.[4]

Phenylazo-*p*-tolylsulfone was prepared by mixing an aqueous benzenediazonium chloride solution with an aqueous sodium *p*-toluenesulfinate solution at 5°C,[5] and was recrystallized from methanol. Mp 91—92°C.

Kinetic Measurements. To a solution consisting of 2.6 g (0.01 mol) of phenylazo-*p*-tolylsulfone and 39 g (0.5 mol) of benzene, some trifluoroacetic acid was added, and the solution was placed in a constant temperature bath. The rate of nitrogen evolution was measured by a gas burette.

Analyses of Phenylation Products. Phenylazo-*p*-tolylsulfone (2.6 g) was dissolved in a substituted benzene, and trifluoroacetic acid was added; the mixture consisted of 50 mol of a substituted benzene and 5.89 mol of trifluoroacetic acid per mole of phenylazo-*p*-tolylsulfone. The mixture was decomposed in a constant temperature bath at 40.0±0.1°C. In order to examine the effect of polar solvents, 20 g of dimethyl sulfoxide or acetonitrile was added to the above mixture, and these mixtures containing polar solvents were decomposed in a similar manner.

After the decomposition was over, the reaction mixture was washed successively with water, a 5% sodium hydroxide solution and water, and was then dried over anhydrous magnesium sulfate.

The amounts of substituted biphenyls produced were determined by a Hitachi Gas Chromatograph K-53 on a column packed with 10% Apiezon L on Chromosorb W, on the basis of the comparison with authentic samples.

Results and Discussion

Figure 1 shows that the rate of decomposition of phenylazo-*p*-tolylsulfone is of first order. However, the rate is dependent on the amount of trifluoroacetic acid added. Table 1 lists the first order rate constants in benzene at various temperatures in the presence of 5.89 mol or 2.95 mol of trifluoroacetic acid per mole of the azosulfone. These values are much greater than the rate constant obtained by Overberger and Rosenthal[1] for the homolytic decomposition of phenylazophenylsulfone in benzene with calcium oxide suspended ($k_1=2.2\times10^{-5}$ sec^{-1} at 70°C). This great difference cannot be ascribed to the effect of *p*-methyl substituent in phenylazo-*p*-tolylsulfone. These findings suggest that the mechanism of the decomposition in acidic solutions is different from that in neutral solutions.

Table 1. First order rate constants for the decomposition of *p*-TsN_2Ph in benzene-CF_3CO_2H

(*p*-TsN_2Ph/CF_3CO_2H =5.89 mol/mol)		(*p*-TsN_2Ph/CF_3CO_2H =2.95 mol/mol)	
Temp. (°C)	$10^4\,k_1$ (sec^{-1})	Temp. (°C)	$10^4\,k_1$ (sec^{-1})
40.5	5.39	45.6	6.24
34.9	2.34	40.7	2.94
30.0	1.11	35.5	1.19
25.5	0.53		
E_a=28.7 kcal/mol		E_a=32.3 kcal/mol	
$\Delta S^{\neq}$=16.0 e.u./mol (25°C)		$\Delta S^{\neq}$=26.1 e.u./mol (25°C)	

Figure 2 is the Arrhenius plots of the rate constants shown in Table 1, and the values of the activation energies and the activation entropies were calculated from Fig. 2. These activation parameters fit surprisingly well the isokinetic relationship established for the decomposition of benzenediazonium tetrafluoroborate in various aprotic polar solvents,[6] as shown in Fig. 3. On the basis of these

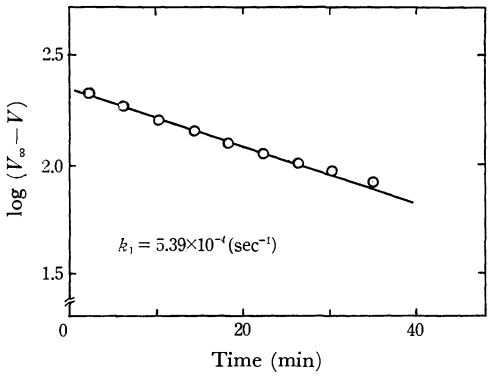

Fig. 1. First order rate plots for the decomposition of *p*-TsN_2Ph in benzene-CF_3CO_2H at 40.5°C. (*p*-TsN_2Ph/CF_3CO_2H=5.89 mol/mol)

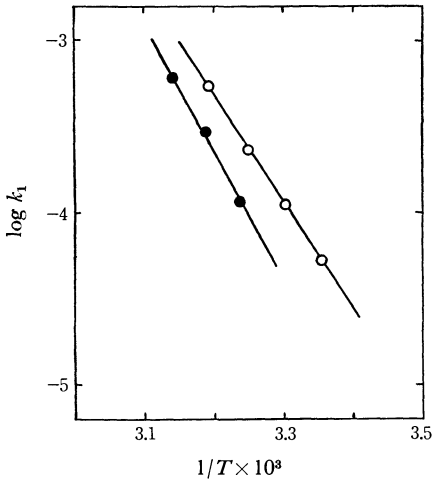

Fig. 2. The Arrhenius plots for the decomposition of *p*-TsN_2Ph in benzene-CF_3CO_2H.
○: *p*-TsN_2Ph/CF_3CO_2H=5.89 mol/mol
●: *p*-TsN_2Ph/CF_3CO_2H=2.95 mol/mol

4) A. H. Blatt, Editor, "Organic Syntheses," Coll. Vol. I, p. 492 (1941).

5) A. Hantzsch and M. Singer, *Ber.*, **30**, 312 (1897); **31**, 641 (1898).

6) K. Ishida, N. Kobori, M. Kobayashi and H. Minato, This Bulletin, **43**, 285 (1970).

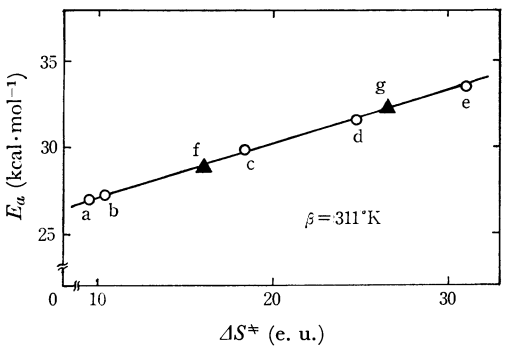

Fig. 3. Isokinetic relationship for the decomposition of PhN_2BF_4 and *p*-TsN_2Ph in various solvents
○: Decomposition of PhN_2BF_4 in aprotic polar solvents.
(a: $(CH_3)_2C=O$, b: DMSO, c: CH_3CN, d: DMF, e: CH_3NO_2)
●: Decomposition of *p*-TsN_2Ph in benzene-CF_3CO_2H
(f: *p*-TsN_2Ph/CF_3CO_2H=5.89 mol/mol, g: *p*-TsN_2Ph/CF_3CO_2H=2.95 mol/mol)

findings, the following mechanism is proposed, in which the generation of phenyl cation from benzenediazonium ion is the rate-determining step.

When trifluoroacetic acid was added to a benzene solution of the azosulfone, a new absorption corresponding to Ar–N$^+$≡N was observed at 2280 cm^{-1}, which gradually disappeared with evolution of nitrogen. This finding is consistent with the above mechanism.

Tables 2 and 3 show the orientation and the partial rate factors for the phenylation of substituted benzenes with the azosulfone in the presence of trifluoroacetic acid. *p*-Toluenesulfinic acid was not

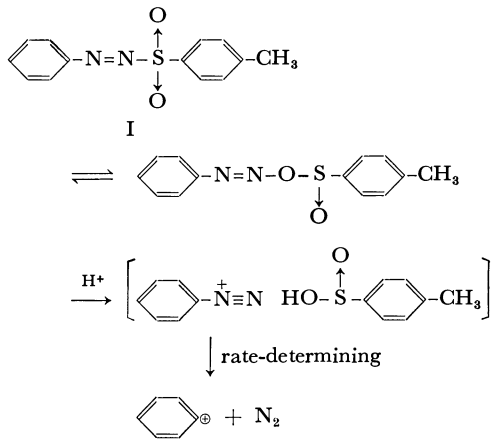

isolated, but *p*-toluenesulfonic acid and phenyl *p*-toluenesulfonate were found. *p*-Toluenesulfonic acid is ascribable to the disproportionation of *p*-toluenesulfinic acid, which Kice and his co-workers reported.[7] Products other than the phenylation products will be discussed in a forthcoming paper. When acetonitrile or DMSO was present, acetanilide or 1,3-benzoxathian was formed, as reported in a previous paper.[3]

When the substituent was $-CO_2Me$ or $-NO_2$, in a substituted benzene alone or in a mixture of a substituted benzene and acetonitrile *meta* derivatives predominate and the partial rate factors were much smaller than unity, whereas in a mixture of a substituted benzene and DMSO *o,p*-derivatives predominate. This abnormality in DMSO-PhX can be ascribed to the ocurrence of both the homolytic and heterolytic decomposition of the azosulfone in this medium, since less protons are available for protonation of the azosulfone owing to the protona-

Table 2. Orientation (%) for the phenylation of PhX with *p*-TsN_2Ph in acidic solutions at 40°C

X in PhX	Solvents								
	PhX only			CH_3CN-PhX			DMSO-PhX		
	o-	*m*-	*p*-	*o*-	*m*-	*p*-	*o*-	*m*-	*p*-
OCH_3	73.5	5.1	21.4	58.9	11.0	30.1	56.9	20.3	22.8
	76.0	4.8	19.2	59.9	10.2	29.9			
C_2H_5	54.1	21.9	24.0	52.6	25.8	21.6	49.2	27.8	23.0
	53.5	21.5	25.0	48.5	25.6	25.9			
Cl	72.8	6.6	20.6	49.6	19.3	31.1	55.4	17.7	26.9
	70.3	9.4	20.3	52.6	17.8	29.6			
CO_2CH_3	48.8	41.4	9.8	37.0	54.1	8.9	54.2	28.5	17.3
	48.6	42.2	9.2	41.3	48.7	10.0			
NO_2	24.8	70.1	5.1	22.2	48.3	29.5	68.1	17.4	14.5
	27.2	67.8	5.0	21.5	50.0	28.5			

7) J. L. Kice and K. W. Bowers, *J. Amer. Chem. Soc.*, **84**, 605 (1962); J. L. Kice and G. Guaraldi, *ibid.*, **88**, 5236 (1966); J. L. Kice and G. Guaraldi, *Tetrahedron Lett.*, **1966**, 501.

Table 3. Partial rate factors for the phenylation of PhX with p-TsN_2Ph in acidic solutions at 40°C

X in PhX	Solvents: PhX only			CH_3CN-PhX			DMSO-PhX		
	k_0/k	k_m/k	k_p/k	k_0/k	k_m/k	k_p/k	k_0/k	k_m/k	k_p/k
OCH_3	2.66	0.18	1.55	1.64	0.31	1.68	1.99	0.71	1.59
	2.66	0.17	1.34	1.79	0.30	1.79			
C_2H_5	1.32	0.59	1.17	1.60	0.78	1.31	1.49	0.79	1.30
	1.32	0.53	1.23	1.53	0.81	1.63			
Cl	0.61	0.07	0.35	0.57	0.22	0.72	0.96	0.31	0.94
	0.56	0.08	0.33	0.62	0.21	0.70			
CO_2CH_3	0.48	0.41	0.19	0.59	0.86	0.28	0.96	0.50	0.61
	0.43	0.37	0.16	0.58	0.68	0.28			
NO_2	0.07	0.21	0.03	0.08	0.17	0.21	1.33	0.34	0.57
	0.08	0.19	0.03	0.09	0.21	0.24			

tion of DMSO. Decompositions in a substituted benzene alone or in CH_3CN-PhX will be discussed further in detail.

The orientation and the partial rate factors in PhX or in CH_3CN-PhX are quite different from those for the radical phenylation of substituted benzenes[8] and quite similar to those for phenylation with phenyl cation generated from benzenediazonium tetrafluoroborate.[3,9] The partial rate factors for *meta* and *para* positions in Table 3 are better correlated with σ values of Brown-Okamoto rather than those of Hammett. However, as Fig. 4 shows,

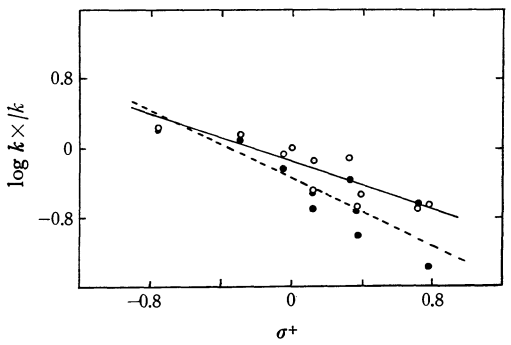

Fig. 4. The Hammett plots for the phenylation with p-TsN_2Ph in acidic solutions at 40°C.
—○—: PhX-CH_3CN, $\rho=-0.69$
—●—: PhX only, $\rho=-1.0$

the correlation coefficient is rather small, and the reaction constant ρ is very small compared with the ρ values of common electrophilic reactions (in PhX, $\rho=-1.0$, $r=0.84$; in CH_3CN-PhX, $\rho=-0.69$, $r=0.87$). These findings indicate that phenyl cation is highly reactive and unselective, and they are consistent with the suggestions made by Abramovitch and Gadallah[9] and by us,[3] which describe phenyl cation as a diradical cation produced by the transfer of one π-electron to the vacant sp^2 orbital.

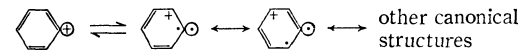

IV IVa IVb

However, at present there is no further evidence available which can determine whether the phenylation proceeds *via* an ordinary σ-complex shown in Scheme 1 or it proceeds *via* a spiro cation shown in Scheme 2.

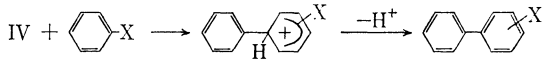

Scheme 1

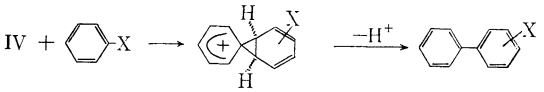

Scheme 2

In order to determine whether or not the abstraction of proton from the complex is the rate-determining step, some experiments were performed with deuterated compounds, and the results are shown

Table 4. Phenylation of deuterated PhX with p-TsN_2Ph in acidic solutions at 40°C

PhX	Orientation (%)			Partial rate factors		
	o-	*m*-	*p*-	k_0/k	k_m/k	k_p/k
$PhOCH_3$-4d	61.9	9.2	28.9			
($PhOCH_3$)	73.5	5.1	21.4			
PhCl-4d	66.1	13.1	20.8			
(PhCl)	70.3	9.4	20.3	0.56	0.08	0.33
PhCl-d_5	63.2	13.4	23.4	0.82	0.17	0.60

8) G. H. Williams, "Homolytic Aromatic Substitution," Pergamon Press, London (1960); R. Ito, T. Migita, N. Morikawa and O. Simamura, *Tetrahedron*, **21**, 955 (1965).

9) R. A. Abramovitch and F. F. Gadallah, *J. Chem. Soc., B*, **1968**, 497.

in Table 4. No significant difference in the orientation was found between chlorobenzene-4d and chlorobenzene or between anisole-4d and anisole. The partial rate factors for the phenylation of pentadeuteriochlorobenzene were calculated from a competitive reaction with benzene. The values of k_H/k_D are somewhat smaller than unity, but when experimental errors are taken into consideration, these values are regarded as indicating that there is no isotope effect in phenylation with azosulfone. Therefore, the rate of formation of the complex either in Scheme 1 or Scheme 2 must be much (slower) than the rate of the abstraction of proton from the complex. In the case of spontaneous decomposition of benzenediazonium tetrafluoroborate, the proton-abstracting species is probably DMSO or acetonitrile, whereas in the acid-catalyzed decomposition of the azosulfone the proton abstracting species is probably trifluoroacetate ion. The results of our investigations with benzenediazonium tetrafluoroborate[3] and with phenylazo-*p*-tolylsulfone indicate that regardless of the proton-abstracting species, the abstraction of a proton from the complex must occur very rapidly.

The results of this investigation together with those of Overberger and Rosenthal[1] and those of Bunnet and Happer[2] have established the very interesting features of the decomposition of arylazoarylsulfone, which are summarized as follows. It is of interest to compare the decomposition of the azosulfone with the decomposition of benzenediazonium salts, which yields phenyl radical in an alkaline medium and phenyl cation in an acidic medium.

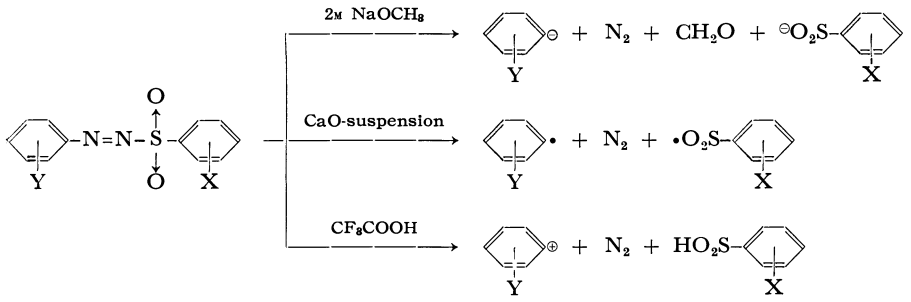

BULLETIN OF THE CHEMICAL SOCIETY OF JAPAN VOL. 43 223—225 (1970)

Cationic Arylation. III. Comparison of Phenylation of Naphthalene with Phenyl Cation and Phenyl Radical

Nobumasa KOBORI, Michio KOBAYASHI and Hiroshi MINATO

Department of Chemistry, Faculty of Science, Tokyo Metropolitan University, Fukazawa, Setagaya-ku, Tokyo

(Received June 27, 1969)

Naphthalene was phenylated with phenyl cation (from PhN_2BF_4) or phenyl radical (from $PhN_2BF_4+NaNO_2$) in dimethyl sulfoxide. Partial rate factors for phenyl radical were somewhat larger than those reported with the phenyl radical generated from *N*-nitrosoacetanilide. Partial rate factors for phenylation with phenyl cation were smaller than those for free radical phenylation and those for common electrophilic substitution reactions. These small partial rate factors for phenyl cation were not compatible with the reaction scheme involving an ordinary σ-complex, and a mechanism involving a spiro cation appeared to be plausible.

In previous papers,[1,2] we reported that phenyl cation was formed from benzenediazonium tetrafluoroborate or phenylazo-*p*-tolylsulfone. The orientation and the partial rate factors for this phenylation appeared to support the hypothesis that the phenyl cation [I] initially formed isomerized to a diradical cation [II] with concerted uncoupling of a pair of π-electrons. However, the mechanism

1) M. Kobayashi, H. Minato, E. Yamada and N. Kobori, This Bulletin, **43**, 215 (1970).

2) M. Kobayashi, H. Minato and N. Kobori, *ibid.*, **43**, 219 (1970).

of the substitution was not completely clear, especially as to whether or not a spiro cation [IV] was the intermediate.

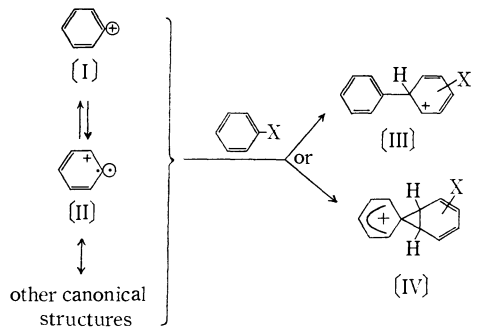

In order to clarify the nature of the phenyl cation and the mechanism of the phenylation, the electrophilic substitution with phenyl cation has been investigated with naphthalene as the substrate, and the results are described in this paper.

Since the isomerization of phenyl cation to a diradical has been postulated, it is of great interest to compare phenylation by phenyl cation with that by phenyl radical. Therefore, the phenylation of naphthalene by the phenyl radical produced from benzenediazonium tetrafluoroborate and sodium nitrate[3] has been investigated, and the results will be compared with those obtained with phenyl cation.

Experimental

Materials. Preparation of benzenediazonium tetrafluoroborate and purification of dimethyl sulfoxide (DMSO) and anisole were previously reported.[1] Naphthalene, extra pure grade of Kanto Chemicals, was used without further purification. α-Phenylnaphthalene, bp 167°C/8 mmHg (lit,[4] 180°C/10 mmHg) and β-phenylnaphthalene, mp 102°C (lit,[4] 103—104°C) were prepared according to the methods described in literature.[4]

Phenylation of Naphthalene with Benzenediazonium Tetrafluoroborate in DMSO. In 20 g of DMSO 2.0 g of benzenediazonium tetrafluoroborate was dissolved and the solution was added to an anisole-naphthalene mixture (the molar ratio of aromatic compounds *versus* the diazonium salts was 50). The homogeneous solution obtained was decomposed in a bath at 40±0.1°C. After the evolution of nitrogen gas ceased, ether was added to the reaction mixture. This mixture was washed with water to remove DMSO, with a 5% sodium hydroxide solution to remove acidic products and then with water. After it was dried over magnesium sulfate, ether, anisole and naphthalene in this mixture were removed in a vacuum. After about 70% of anisole and naphthalene was removed, the residual oil containing arylated products was analyzed by a Hitachi Gas Chromatograph K-53.

Phenylation of Naphthalene with Benzenediazonium Tetrafluoroborate and Sodium Nitrite in DMSO. Anisole (37.056 g, 0.3427 mol), naphthalene (9.748 g, 0.0761 mol) and sodium nitrite (1.736 g, 0.0253 mol) were dissolved in 100 g of DMSO, and this homogeneous solution was stirred vigorously with a mechanical stirrer. Under a nitrogen atmosphere, a solution of 1.467 g of benzenediazonium tetrafluoroborate in 10 g of DMSO was added dropwise into the above solution. Nitrogen gas was evolved immediately and the reaction was complete as soon as the diazonium salt solution was added. The reaction mixture was treated in a manner similar to that described above for the case in the absence of sodium nitrite.

Quantitative Analyses. Methoxybiphenyl isomers and phenylnaphthalene isomers were identified by comparison of their retention times with those of authentic samples, and their amounts were determined by use of calibration curves on a 2 m column packed with Apiezon L (10%) on Chromosorb W at 200°C with a gas-flow of 30 ml/min.

Results and Discussion

Anisole, instead of benzene, was used for competitive phenylation, since non-substituted biphenyls is lost by sublimation during the concentration of the reaction mixture prior to gas-chromatographic analyses. The attack of both phenyl cation and phenyl radical on the aromatic hydrocarbons

TABLE 1. ORIENTATION AND PARTIAL RATE FACTORS FOR PHENYLATION OF NAPHTHALENE

Run	[PhOCH$_3$]/ 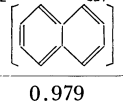	Orientation (%)		Partial rate factors	
		α-	β-	α-	β-
1[a]	0.979	73.0	27.0	3.36	1.24
2[a]	2.964	76.6	23.4	2.95	0.90
3[a]	5.774	78.7	21.3	2.92	0.74
4[b]	4.38	80.6	19.4	16.48	3.98
5[b]	4.50	77.5	22.5	13.13	3.81
6[c]				11.29	1.10
7[c]				13.71	1.34
8[d]				470	50
9[e]				2.1×10^5	2.1×10^3
10[f]				178	23.4

a) Phenylation with PhN_2BF_4 in DMSO at 40°C (Phenylation with phenyl cation)
b) Phenylation with PhN_2BF_4 and $NaNO_2$ in DMSO (Phenylation with phenyl radical)
c) Phenylation with *N*-nitrosoacetanilide, D. I. Davies, D. H. Hey and G. H. Williams, *J. Chem. Soc.*, **1961**, 3112.
d) Nitration, R. O. C. Norman and R. Taylor, "Electrophilic Substitution in Benzenoid Compounds," Elsevier Publ. Co., Amsterdam, London, New York (1965), p. 88.
e) Bromination in aq. AcOH, *ibid.*, p. 150
f) Deuteration, *ibid.*, p. 220

3) M. Kobayashi, H. Minato, E. Yamada and N. Kobori, This Bulletin, to be published
4) R. Adams, Ed. "Organic Reactions," Vol. II, p. 258 (1960).

resulted in the formation of methoxybiphenyl isomers and phenylnaphthalene isomers, but the compositions of these phenylated products were quite different from each other.

As products other than methoxybiphenyls and phenylnaphthalenes, 1,3-benzoxathian was obtained from the decomposition of benzenediazonium tetrafluoroborate in the absence of sodium nitrite, but not in the presence of sodium nitrite.

The orientation and partial rate factors for phenylation with phenyl cation and with phenyl radical are compared with other related data in Table 1. The orientation and the partial rate factors for phenylation with phenyl cation change to some extent with the molar ratio of naphthalene *versus* anisole.

The partial rate factors for phenylation with the phenyl radical generated from benzenediazonium tetrafluoroborate and sodium nitrite are a little larger than those obtained by Davies, Hey and Williams with the phenyl radical generated from *N*-nitrosoacetanilide as shown in Table 1. It is not easy to determine what is responsible for this difference in the partial rate factors. One could ascribe it to the effect of the polar solvent (DMSO) present in our medium, or to the difference in the hydrogen-abstracting species. However, we recently found that the partial rate factors for the phenylation with the phenyl free radical generated from phenylazotriphenylmethane were not influenced to any appreciable extent by the presence of the polar solvent DMSO.[5] Therefore, it does not seem to be possible to attribute this difference to the effect of solvents.

As for the hydrogen abstracting species, both NO_2 and PhN=NO· are conceivable as the hydrogen-abstracting species in a reaction mixture of benzenediazonium tetrafluoroborate and sodium nitrite as shown in Schemes 1 and 2.

$$PhN_2BF_4 + NaNO_2 \longrightarrow PhN{=}N{-}O{-}NO + NaBF_4$$

Scheme 1

$$PhN{=}N{-}O{-}NO \longrightarrow Ph\cdot + N_2 + NO_2$$

Scheme 2

$$2\,PhN{=}N{-}O{-}NO \longrightarrow PhN{=}N{-}O{-}N{=}N{-}Ph + N_2O_3$$

$$PhN{=}N{-}O{-}N{=}N{-}Ph \longrightarrow Ph\cdot + N_2 + PhN{=}N{-}O\cdot$$

In order to clarify the difference in the partial rate factors due to the origin of the phenyl radicals, the hydrogen-abstracting species in the mixture of benzenediazonium tetrafluoroborate and sodium nitrite must be identified. Such an investigation is being carried out.

As shown in Table 1, the partial rate factors for phenylation with phenyl cation are much smaller than those for nitration, bromination and deuteration, which are typical electrophilic substitution reactions. These data appear to support the hypothesis that the phenyl cation is not an ordinary cation [I] but a diradical cation [II]. If the phenyl cation is an electrophilic radical possessing the properties of both a cation and a radical, it is expected that the values of the partial rate factors for the phenylation with the phenyl cation come between those with electrophilic reagents and those with phenyl radical. However, on the contrary to such expectation, the partial rate factors with phenyl cation were smaller than both of these. A mechanism with which one could explain these findings is the following one, involving the spiro cations [V] and [VI] as the intermediates.

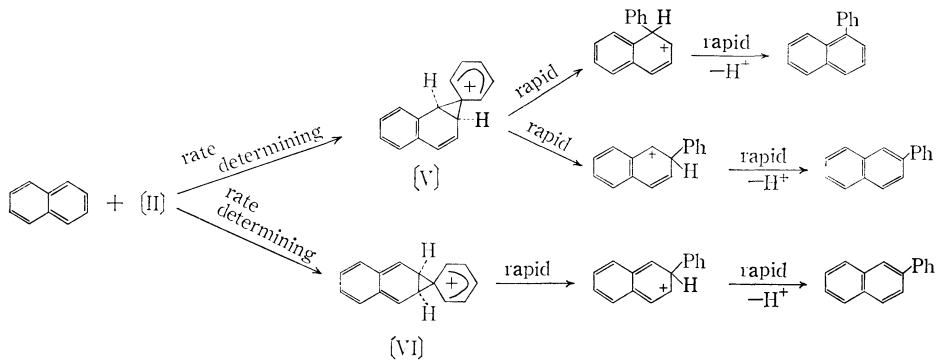

5) M. Kobayshi, H. Minato, N. Watanabe and N. Kobori, This Bulletin, **43**, 258 (1970).

BULLETIN OF THE CHEMICAL SOCIETY OF JAPAN VOL. 43 226—231 (1970)

Reaction of Salicylamine with α-Dicarbonyl Compounds. II. Formation of 2,2′-Bibenz-1,3-oxazines

Hajime KANATOMI and Ichiro MURASE

College of General Education, Kyushu University, Fukuoka

(Received June 27, 1969)

The compounds of a new type, 2,2′-bibenz-1,3-oxazine and its derivatives have been synthesized by the reactions of salicylamines with glyoxal or α-diketones in methanol at a temperature lower than 20°C. The oxazine structures were confirmed by infrared spectroscopy in solid state and by NMR spectroscopy in CCl_4, $CDCl_3$ and chlorobenzene. An oxazine-Schiff base equilibrium was observed in pyridine and in hot chlorobenzene by NMR spectra. It was found that hydrolytic decomposition of 2,2′-dimethyl-2,2′-bibenzoxazine leads to the formation of salicylidenesalicylamine through transamination. The mechanisms were investigated spectrophotometrically.

It has been reported in a previous paper[1] that the reaction of *o*-hydroxybenzylamine (salicylamine) with α-diketones, α-ketoaldehydes, and with α-keto acid ester in hot methanol gave rise to the formation of salicylidenesalicylamine in all cases. It was further found that the reactions proceeded with transamination followed by *trans*-Schiffization between salicylamine and the dicarbonyl compounds, where the former was converted into salicylaldehyde through corresponding Schiff base of the latter, and the Schiff bases were subjected to an exchange reaction at the amine moiety with unreacted salicylamine to yield salicylidenesalicylamine.

Since the initial subject of our investigation had been to obtain condensation products of salicylamine with α-dicarbonyl compounds, for which a bibenzoxazine A or a Schiff base B structure was proposed, the reactions were further examined under different conditions.

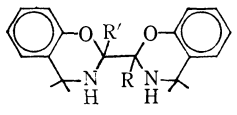

A

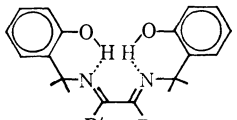

B

The possibility of forming A or B type compound is suggested from the fact that primary γ-amino alcohols condense with aldehydes or ketones to yield either oxazines or open-chain Schiff base or a tautomeric mixture of them.[2] In our previous experiments, it was found that the reactions did not terminate at the first condensation stage owing to the subsequent reactions. Therefore, it was considered that the reactions at a low temperature might be favorable for the prevent ion of subsequent reactions. Thus, two moles of salicylamine were allowed to react with α-dicarbonyl compounds at a temperature lower than 20°C in methanol, and the condensation products were obtained as expected in fairly good yields. The compounds isolated in this way are listed in Table 1.

McDonagh and Smith[3] have extensively studied a ring-chain tautomerism between oxazines and Schiff bases by means of infrared and NMR spectroscopy for the condensation products of salicylamine with aromatic or aliphatic aldehydes and ketones, and concluded that the products from aliphatic aldehydes and ketones were oxazines in the solid state exhibiting NH absorptions in infrared spectra, and even in solution they existed exclusively as oxazines, because the NMR peaks of the ring methylene protons appeared around at 6.0 τ as an AB pattern with a coupling constant of 17 Hz, and those of imino protons appeared around at 7 τ as weak several peaks.

In the present case, infrared and NMR spectroscopy were also employed for the structure determination.

The infrared spectrum of III in solid state (KBr disk) is shown as an example in Fig. 1. In the high frequency region, there is a sharp absorption at 3340 cm^{-1} and this could be due to an OH or NH group. From the shape of the band it is more

1) H. Kanatomi and I. Murase, This Bulletin, **42**, 1329 (1969).

2) a) A. C. Cope and E. M. Hancock, *J. Amer. Chem. Soc.*, **64**, 1503 (1942). b) E. D. Bergmann, E. Zimkin and S. Pinchas, *Rec. Trav. Chim. Pays-Bas* **71**, 168 (1952). c) E. D. Bergmann, E. Gil-Av and S. Pinchas, *J. Amer. Chem. Soc.*, **76**, 358 (1953). d) E. D. Bergmann, *Chem. Rev.*, **53**, 309 (1953). e) E. D. Bergmann and A. Kaluszyner, *Rec. Trav. Chim. Pays-Bas* **78**, 315 (1959). f) F. W. Holly and A. C. Cope, *J. Amer. Chem. Soc.*, **66**, 1875 (1944).

3) A. F. McDonagh and H. E. Smith, *J. Org. Chem.*, **33**, 1 (1968).

TABLE 1. CONDENSATION PRODUCTS OF SALICYLAMINES WITH α-DICARBONYL COMPOUNDS

Compound No.	Reactants: Salicylamine	Reactants: α-Dicarbonyl	Formula	Mp, °C	Recryst. solvent	Yield %
I	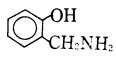	CHO-CHO	$C_{16}H_{16}N_2O_2$	139—140	—	80
II	〃	$CHO-COCH_3$	$C_{17}H_{18}N_2O_2$	155—157	acetone	85
III	〃	$CH_3COCOCH_3$	$C_{18}H_{20}N_2O_2$	99—100	petrol. benzine	85
IV	〃		$C_{20}H_{22}N_2O_2$	130—133.5	*n*-hexane	85
V	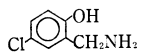	〃	$C_{20}H_{20}N_2O_2Cl_2$	142—144	CCl_4-methanol	25
VI	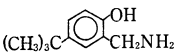	〃	$C_{28}H_{38}N_2O_2$	134—136	petrol. ether	75
VII	〃	$CH_3COCOCH_3$	$C_{26}H_{36}N_2O_2$	149—152	petrol. benzine	85

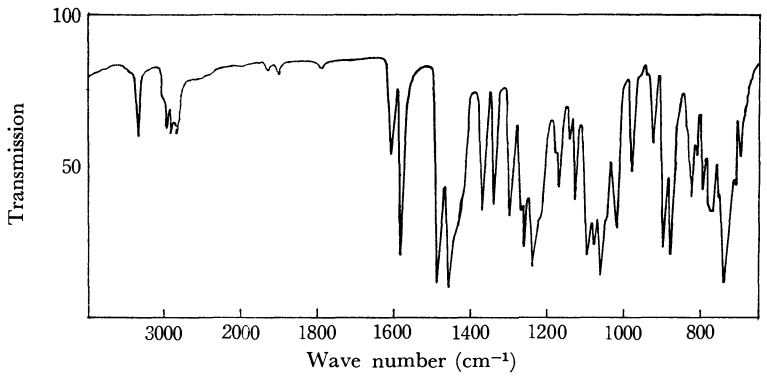

Fig. 1. IR spectrum of III (KBr).

TABLE 2. ANALYTICAL DATA AND NH STRETCHING VIBRATIONS OF 2,2′-BIBENZOXAZINE

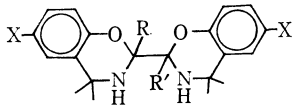

Compound No.	R	R′	X	Formula	Found, % C	Found, % H	Found, % N	Calcd, % C	Calcd, % H	Calcd, % N	NH Frequency (cm^{-1})
I	H	H	H	$C_{16}H_{16}N_2O_2$	71.39	5.75	10.10	71.62	5.98	10.42	3245
II	CH_3	H	H	$C_{17}H_{18}N_2O_2$	72.50	6.40	9.84	72.33	6.42	9.93	3330
III	CH_3	CH_3	H	$C_{18}H_{20}N_2O_2$	72.71	6.76	9.39	72.94	6.76	9.45	3340
IV	spilocyclohexyl		H	$C_{20}H_{22}N_2O_2$	74.53	6.92	8.69	74.50	6.87	8.68	3320, 3350
V	spilocyclohexyl		Cl	$C_{20}H_{20}N_2O_2Cl_2$	61.30	5.17	7.03	61.38	5.15	7.15	3360
VI	spilocyclohexyl		$(CH_3)_3C$	$C_{28}H_{38}N_2O_2$	77.52	8.83	6.30	77.37	8.82	6.44	3370
VII	CH_3	CH_3	$(CH_3)_3C$	$C_{26}H_{36}N_2O_2$	76.43	8.88	6.69	76.43	8.88	6.85	3340

likely due to NH, hydrogen bonded in the crystals. In the double bond region, one can find no absorptions around 1620—1650 cm^{-1} which are in general due to a C=N group of a Schiff base.

From these evidences, the oxazine structure A could be assigned to this compound. Other compounds showed infrared absorption patterns similar to III, exhibiting sharp NH absorptions and no C=N absorptions. The NH frequency of each compound is listed in Table 2 together with analytical data.

It is therefore concluded from the infrared diagnosis that the condensation products of salicylamine with α-dicarbonyl compounds have the bibenzoxazine structure of the type A in solid state.

The NMR spectra of III in various solvents are

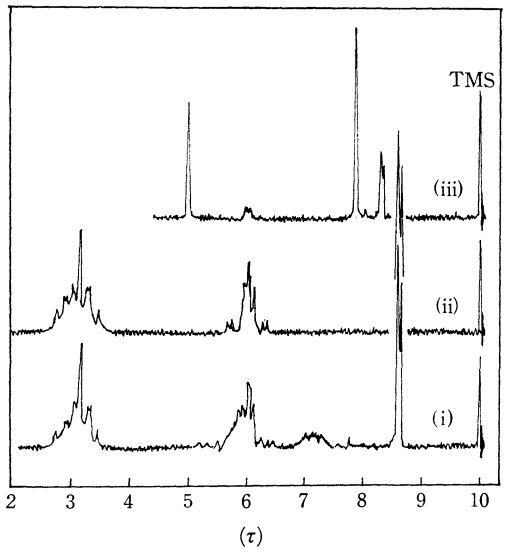

Fig. 2. NMR spectra of III, in CCl_4 (i), in CCl_4+ D_2O (ii), in pyridine (iii).

shown in Fig. 2. In CCl_4, a broad signal centred at 7.2 τ and several complex peaks around 6 τ might be due to the imino and the methylene protons of the oxazine rings corresponding to A structure. On deuteration, the coupling of the methylene protons with the imino protons was excluded and the methylene proton resonance appeared as seven peaks as seen in Fig. 2, (ii).

Assuming that III is a mixture of stereo-isomers of bibenzoxazine for which a *d,l-* and a *meso*-configuration is possible, the NMR spectra will exhibit two kinds of patterns corresponding to each isomer, since the magnetic environment of protons especially in the oxazine rings will be different from each other and this will cause a different chemical shift. It is likely that the seven peaks are an overlapping of the two kinds of AB patterns corresponding to the methylene protons of each isomer. The coupling constants are both 17 Hz and the calculated chemical shifts are 5.97 τ, 6.18 τ and 5.80 τ, 6.04 τ respectively. The spliting of the methyl proton resonance at 8.50 τ and 8.45 τ might also be due to the configurational difference of *d,l-* and the *meso*-isomer.

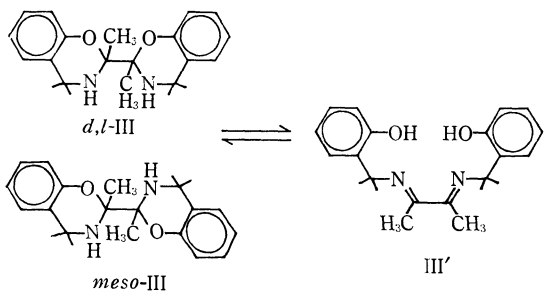

In pyridine, two singlet peaks appeared at 7.75 τ and at 5.02 τ in addition to the bibenzoxazine proton signals as seen in Fig. 2, (iii). These new peaks suggest the formation of another species in the solution. The isomeric Schiff base (III′) is proposed, in which the methyl and the methylene proton peaks appear in a field lower than that of oxazine, because these protons are less shielded. The higher one (7.75 τ) can therefore be assigned to the methyl and the lower one (5.02 τ) to the methylene protons of the Schiff base (III′). Thus, it is seen that the compound exists as an equilibrium mixture of the oxazine (III) and the Schiff base (III′) in pyridine, and the ratio calculated from the intensities of each methyl proton peak will be about 1 : 4.

In chlorobenzene, III exists as a mixture of two isomeric bibenzoxazines at 40°C as seen in Fig. 3, (ii). At 120°C, an equilibrium of oxazine-Schiff

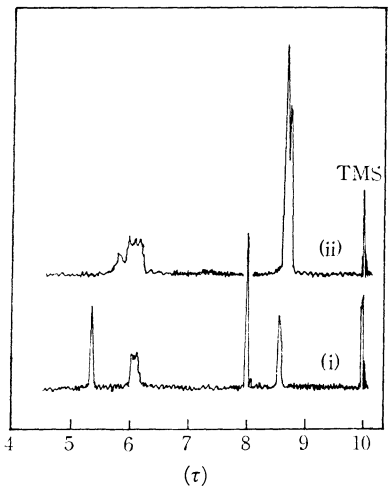

Fig. 3. NMR spectra of III in chlorobenzene, at 120°C (i), at 40°C (ii).

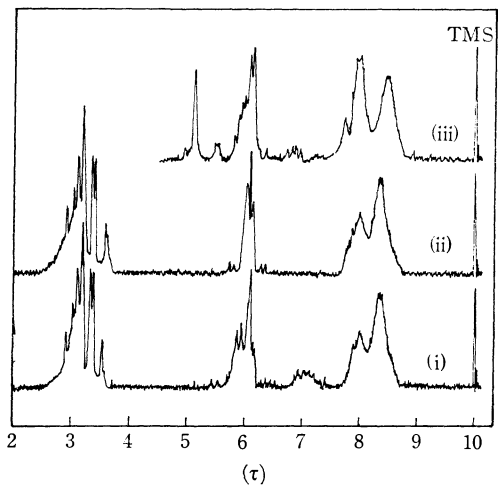

Fig. 4. NMR spectra of IV, in CCl_4 (i), in CCl_4+ D_2O (ii), in pyridine (iii).

base was observed (i). Proton signals of oxazine rings decreased in intensity and new singlet peaks appeared at 8.05 τ and at 5.30 τ which due to the methyl and the methylene protons of the isomeric Schiff base, respectively. On cooling, these peaks disappeared and the spectrum gave rise to the original pattern. It is interesting to note that an oxazine-Schiff base equilibrium exists even in such a solvent less polar than pyridine.

For compound IV, the oxazine structure in CCl_4 was confirmed. In Fig. 4, (i), several peaks around 8 τ and weak multiplet centred at 7.2 τ are due to the eight protons of the cyclohexane ring and the imino protons respectively. The resonance of the ring methylene protons appeared on deuteration as partially overlapped two AB quartets centred at 6.11 τ and 6.05 τ with coupling constants of both 17 Hz. Each corresponds to those of the *d,l*- and the *meso*-isomer, and the calculated chemical shifts are 6.01 τ, 6.21 τ and 5.95 τ, 6.15 τ, respectively.

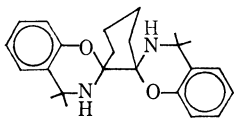

d,l-IV

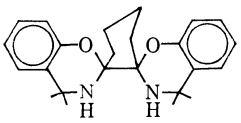

meso-IV

In pyridine, a new singlet appeared at 5.07 τ in addition to similar peaks to those observed in CCl_4. This peak can be assigned to the methylene protons of the isomeric Schiff base for the same reason as the case of III and an equilibrium between the oxazine is evidenced in the solution. The ratio of the oxazine-Schiff base is approximately 2 : 1 from the intensities of the corresponding methylene peaks. In chlorobenzene, similar oxazine-Schiff base equilibrium was observed at elevated temperature (120°C), exhibiting a new singlet peak at 5.53 τ which is due to the methylene protons of the Schiff base.

For compound I, well defined NMR spectra in various solvents could not be observed because of low solubility and of instability in solutions. The integrated spectrum in $CDCl_3$, however, shows an AB like pattern centred at 5.86 τ with a coupling constant of about 17 Hz corresponding to four protons of the methylene groups of the oxazine rings. The methine protons attached to the asymmetric carbon atoms are observed as two peaks at 4.91 τ and 4.97 τ. This suggests that I is also a mixture of the *d,l*- and *meso*-2,2′-bibenzoxazine for the same reason as given above.

Although the NMR spectrum was not measured for other compounds listed in Table 1, the oxazine structure can be confirmed by the similarity of their ultraviolet absorption spectra to those investigated above.

Higher homologues of α-diketone such as acetylpropionyl, dipropionyl, and acetylisobutylyl have beeen examined with salicylamine in the same manner as described above. However, the reactions failed to yield the corresponding oxazines, and salicylidenesalicylamine was obtained. It is clear that the transamination took place predominantly even at low temperatures in these cases. 5-Chlorosalicylamine did not react with α-diketones other than 1,2-cyclohexanedione. However, 5-*t*-butylderivative reacted with diacetyl and 1,2-cyclohexanedione to afford the corresponding oxazines. Slightly high acidity of the phenol group or low basicity of the amino group by chloro-substitution may reduce the reactivity. It is seen from these experiments that the formation of bibenzoxazines is limited when salicylamines having appropriate basicities react with α-dicarbonyl compounds which exhibit no steric hindrance.

Although bibenzoxazines have been isolated in well defined crystals, they are never stable in hot solutions, therefore, recrystallization seriously reduced the yield. In the case of III, salicylidenesalicylamine and tetramethylpyrazine were isolated from the 95% methanol solution on prolonged heating. It was found also that such decomposition scarcely occurred in absolute methanol with recovery of III. Assuming the presence of the oxazine-Schiff base equilibrium in methanol as well as in pyridine, the decomposition mechanism is given as shown in Scheme I, where the Schiff base (III′) is subjected to hydrolysis to give the ketimine (IV) and salicylamine. The ketimine (IV) undergoes transamination, and then *trans*-Schiffization between the salicylamine and affords salicylidenesalicylamine. The reaction mechanisms of the latter half have already been discussed.[1)]

A problem which arises from the above evidence

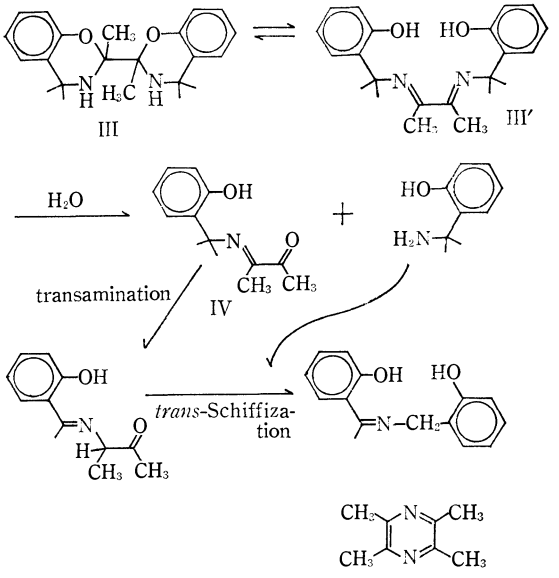

Scheme I

is that the formation of salicylidenesalicylamine may always proceed through the oxazine formation even at elevated temperatures. To elucidate this, the rate of formation of salicylidenesalicylamine from III was measured spectrophotometrically and compared with that from the mixture of salicylamine and diacetyl. For this purpose, the increasing rate of absorbance at 400 mμ was measured, since only salicylidenesalicylamine among the reactants and the products has strong absorption in this region as seen in Fig. 5 and the absorbance is proportional to the concentration of this compound.

In Fig. 6, it is seen that the rate of formation of salicylidenesalicylamine from III in 95% methanol is greater than that in absolute methanol. This clearly indicates that hydrolysis takes part in the reaction as proposed in Scheme I. Further, the rate of formation from the mixture of salicylamine and diacetyl is much greater at the initial period of the reaction than that of hydrolytic decomposition of III. It is therefore obvious that the reaction of salicylamine and diacetyl to form salicylidenesalicylamine at elevated temperature (over 20°C) does not proceed through the initial formation of bibenzoxazine (III), but the Schiff base (III′) is the first product which undergoes further reactions. It should be noted that the formation of bibenzoxazines will take another route and it is only possible in cold.

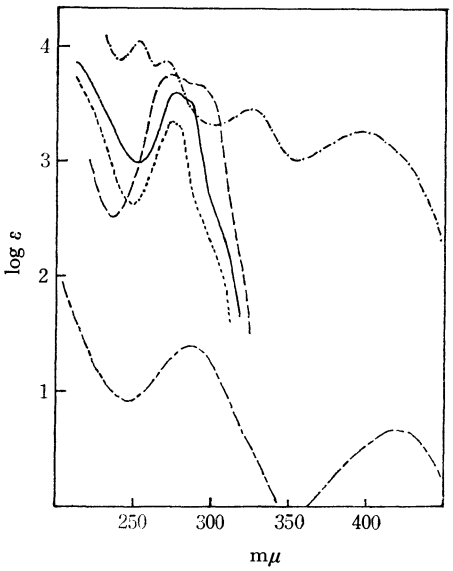

Fig. 5. Absorption spectra in methanol, III (——); salicylamine (------); diacetyl (-----); salicylidenesalicylamine (·—·—·); tetramethylprazine (-----).

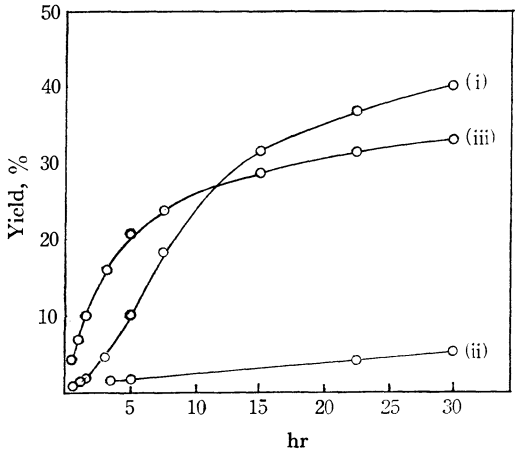

Fig. 6. Rate of formation of salicylidenesalicylamine (25°), (i) from III in methanol (*ca.* 95%), (ii) from III in absolute methanol, (iii) from salicylamine (2 mol)+diacetyl (1 mol) in absolute methanol.

Experimental

Salicylamine. Concerning the preparation of this compound, reduction of salicylaldoxime with sodium amalgam,[4] with aluminum amalgam[5] or catalytic reduction of salicylaldazine with Pd-$BaSO_4$ as a catalyst[6] have been reported. It was found, however, that catalytic reduction of salicylaldoxime by Pd-charcoal in acidic solution best proceeds conveniently in higher yield.

To a solution of salicylaldoxime (40 g) in 650 m*l* of methanol, 5% Pd-charcoal (5 g) and 36 m*l* of concentrated hydrochloric acid were added, and the hydrogenation was carried out at room temperature under atmospheric pressure with vigorous stirring. Exothermic hydrogen uptake ceased after four hours. The catalyst was filtered and the filtrate was evaporated under reduced pressure and the residue was dissolved in 250 m*l* of water. The pH of the solution was brought to 7 by the addition of concentrated ammonia and the undissolved precipitates (2—3 g) were filtered. The filtrate was made alkaline by further addition of ammonia and the resulting colorless crystals were filtered and washed with water. The crude salicylamine was dried over calcium chloride in a vacuum and recrystallized from CCl_4. Yield, 27 g (75%), mp 126°C.

General Procedure for the Preparation of 2,2′-Bibenz-1,3-oxazines. To a suspension of freshly purified salicylamine or its derivative (1 mol) in methanol was added a slight excess of calculated amount (0.5 mol) of α-diketone or aqueous 40% glyoxal, and the mixture was stirred for thirty minutes at a temperature below 20°C. Salicylamine was once dissolved into solution and colorless crystals then gradually separated out. After stirring for additional thrity minutes, the crystals were filtered and washed with cold methanol. Purification of each oxazine except I was carried out by recrystallization from the solvent listed in Table 1. In the case of the acetyl, the reaction was carried out in ice-cold methanol to avoid otherwise inevitable transamintion. The yield of each oxazine is described in Table 1.

4) D. B. Witkop and T. W. Beiler, *J. Amer. Chem. Soc.*, **76**, 5596 (1954).

5) M. Yamaguchi, *Nippon Kagaku Zasshi*, **73**, 393 (1952).

6) K. W. Rosenmund and E. Phankuch, *Ber.*, **56**, 2258 (1923).

Decomposition of 2,2′-Dimethyl-2,2′-bibenzoxazine (III): Formation of Salicylidenesalicylamine. A solution of III (0.9 g, 0.003 mol) in 30 m*l* of 95% methanol was gently refluxed in a nitrogen stream for four hours. The solution turned yellow and it was concentrated to about 5 m*l* under vacuum and kept in a refrigerator overnight. The resulting yellow crystals were filtered and recrystallized from methanol. A pure sample of salicylidenesalicylamine, mp 183—184°C was obtained in 50% yield.

The filtrate from which salicylidenesalicylamine was separated was evaporated to dryness in a vacuum and the residue was colloected. It was sublimed at 80°C in a vacuum (30 mmHg) and colorless crystals, mp 85°C were obtained. The compound was identified as tetramethylpyrazine by infrared spectra and by mixed melting point determination.

The authors express their sincere thanks to Professor Yo Ueda of Faculty of Pharmaceutical Science and Professor Taku Matsuo of Faculty of Engineering of Kyushu University for their kind help in taking NMR spectra and for their valuable discussions. This work was partly supported by a grant from the Ministry of Education.

BULLETIN OF THE CHEMICAL SOCIETY OF JAPAN VOL. 43 231—234 (1970)

Preparation of 1,4-Cycloalkanediones by Hypoiodite Oxidation of Cycloalkanols

Takasi Mori, Kiyohide Matsui and Hitosi Nozaki

Department of Industrial Chemistry, Kyoto University, Yoshida, Sakyo-ku, Kyoto

(Received June 27, 1969)

Lead tetraacetate oxidation of 11, 12 and 13-membered cycloalkanols gives improved yields of 2,5-polymethylenetetrahydrofurans II in the presence of iodine. Oxidative cleavage of II furnishes 1,4-cycloalkanediones VII.

Synthesis of [8](2,5)heterocyclophanes recently recorded involves the Paal-Knorr reaction of 1,4-cyclododecanedione (VIIb).[1] A new route has been found for an effective method of preparing homologous 1,4-diketones.*1 This consists of oxidative ring closure of cycloalkanols I to 2,5-polymethylenetetrahydrofurans II and oxidative ring reopening of II into diketones VII.

While this work was in progress, Mihailovic *et al.*[6] reported lead tetraacetate oxidation of 6, 7, 8, 10, 12 and 16-membered cycloalkanols, which yielded cycloalkanones III and cycloalkyl acetates IV as main products. Bicyclic ethers of unknown structures were obtained in the oxidation of large ring alcohols. Tetrahydrofurans II are obtained in improved yields by the synergism of iodine (hypoiodite oxidation[7]). In the absence of iodine the main products were III and IV as recorded by

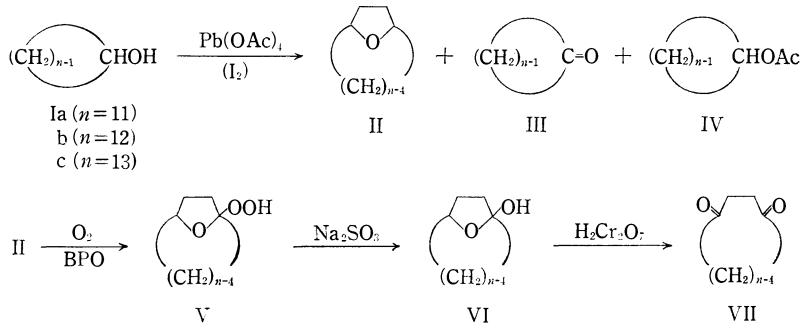

*1 Simple 1,4-cycloalkanediones hitherto recorded are 6,[2] 7,[3] 8,[4] and 12[5]-membered ones.

1) H. Nozaki, T. Koyama, T. Mori and R. Noyori, *Tetrahedron Lett.*, **1968**, 2128.

2) W. von Doering and A. A. R. Sayigh, *J. Org. Chem.*, **26**, 1365 (1961).

3) J. Rigaudy and P. Courtot, *C. R. Acad. Sci., Paris, Ser. C*, **248**, 3016 (1959).

4) A. C. Cope, S. W. Fenton and C. F. Spencer, *J. Amer. Chem. Soc.*, **74**, 5884 (1952).

5) B. Camerino and B. Patelli, *Experientia*, **20**, 260 (1964).

6) M. Lj. Mihailovic, Z. Cekovic, V. Andrevic, R. Matic and D. Jerevic, *Tetrahedron*, **24**, 4947 (1968).

7) K. Heusler and J. Kalvoda, *Angew. Chem. Int. Ed., Engl.*, **3**, 525 (1964).

Table 1. Reaction conditions and product yields in oxidation of cycloalkanols Ia—c

Substrate	Oxidant(s)	I : Oxidant(s) mole ratio	Solvent	Recovery of I (%)	Yield of product (%)[a]		
					II	III	IV
Ib	$Pb(OAc)_4$	1 : 1.2	PhH	8	8[b]	16	32[c]
Ib	$Pb(OAc)_4$, I_2	1 : 2.0 : 0.7	PhH	0	12	9	0
Ib	$Pb(OAc)_4$, I_2	1 : 2.0 : 0.5	C_6H_{12}[d]	34	18	2	0
Ib	$Pb(OAc)_4$, I_2	1 : 2.0 : 0.9	C_6H_{12}	0	27	3	0
Ib	$Pb(OAc)_4$, I_2	1 : 2.0 : 0.7	C_6H_{12}	2	37	8	0
Ia	$Pb(OAc)_4$	1 : 1.2	PhH	24	2	26	15[c]
Ia	$Pb(OAc)_4$, I_2	1 : 2.0 : 0.7	C_6H_{12}	1	23[e]	14	0[f]
Ic	$Pb(OAc)_4$	1 : 1.2	PhH	11	21	10	trace[c]
Ic	$Pb(OAc)_4$, I_2	1 : 2.0 : 0.7	C_6H_{12}	0	38[e]	2	0

a) The yields were determined from peak areas of GLC. In all experiments unidentified products were detected to the amount of 1—5% of all volatile products.
b) TLC of IIb showed one main and two minor spots.
c) A trace of cycloalkene was detected.
d) C_6H_{12} refers to cyclohexane.
e) TLC of IIa and IIc showed single spot.
f) 2,6-Hexamethylenetetrahydropyran was formed in an 11% yield.

Mihailovic.[6] The results are summarized in Table 1.

The yields were determined by gas liquid chromatography (GLC) and separation was effected by column chromatography. The best yields of II were obtained by hypoiodite oxidation conducted in cyclohexane at reflux temperature with lead tetraacetate and iodine in a mole ratio of 1 (alcohol) : 2.0 : 0.7. Although some workers successfully performed hypoiodite oxidation in benzene solution,[8] the present substrates failed to afford satisfactory results in benzene solvent. On careful thin layer chromatographic (TLC) analyses, ethers IIa and IIc showed single spot but IIb three spots as indicated. Following oxidative ring opening established them to be *cis* and/or *trans* tetrahydrofurans (mainly in the case of IIb). Each component was not characterized. The by-products III and IV were identified by comparison with authentic samples. Oxidation of Ia gave low yields of IIa, the byproduct being probably tetrahydropyran derivative (see experimental) formed in an 11% yield.

The effect of iodine is thus characterized by the increase of II at the expense of III and IV. This can be explained by assuming fast decomposition of the intermediate, $>CHOPb(OAc)_3$,[9] otherwise leading to III or IV, and/or by the consumption of lead tetraacetate through reaction with iodine.[10]

The cleavage of ether bond of II was attempted in several ways. Bromine in acetate-buffer, a reagent for oxidative cleavage of ethers recently reported,[11] did not react possibly due to the sparing solubility of II. *p*-Toluenesulfonyl acetate[12] or boron trifluoride in acetic anhydride[13] failed to give satisfactory results due to the formation of olefinic products. Hydroiodic acid afforded the desired 1,4-diiodocyclododecane, but transformation into 1,4-diketone proceeded sluggishly and the formation of olefinic products was again observed.

Finally the cleavage was carried out with success by means of autoxidation. The resulting hydroperoxides V were reduced to hemiketals VI. Chromic acid oxidation of VI afforded 1,4-diketones VII in 45—51% overall yields based on II. Among the 1,4-diketones, the 12-membered VIIb was identified by comparison with authentic sample.[5] The structures of other diketones were ascertained by elemental analyses, IR spectra and most convincingly by NMR spectra. The NMR spectra of VII showed a singlet (4H) at δ 2.62—2.65 (two methylenes between two carbonyl groups) and a diffused triplet (4H) at δ 2.35—2.40 (other α-methylenes).

The hypoiodite oxidation was applied to VIII in order to prepare a 1,4-diketone having one carbonyl group in side chain. The main product was, however, cycloundecyl acetate arising from so called "β-fragmentation,"[14] and tetrahydrafuran

8) J. F. Bagli, P. F. Morand and R. Gaudry, *J. Org. Chem.*, **28**, 1207 (1963).
9) M. Lj. Mihailovic, Z. Cekovic, Z. Macsimovic, D. Jeremic, A. Milovanovic and Lj. Lorenc, *Tetrahedron*, **21**, 1395 (1965).
10) C. Meystre, K. Heusler, J. Kalvoda, P. Wieland, G. Anner and A. Wettstein, *Helv. Chim. Acta*, **45**, 1317 (1962).
11) N. C. Deno and N. H. Potter, *J. Amer. Chem. Soc.*, **89**, 3550 (1967).
12) M. H. Karger and Y. Mazur, *ibid.*, **90**, 3878 (1968).
13) W. H. W. Lunn, W. D. Podmore and S. S. Szinai, *J. Chem. Soc., C*, **1968**, 1657.
14) M. Lj. Mihailovic, M. Jakovljevic, V. Trifumovic, R. Vukov and Z. Cekovic, *Tetrahedron*, **24**, 6959 (1968).

IX was not obtained.

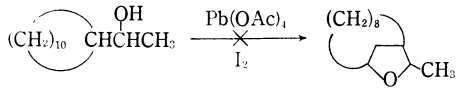

VIII IX

Experimental

All temperatures are uncorrected. NMR spectra were obtained on a JEOL C-60-H spectrometer in CCl_4 solutions with tetramethylsilane as an internal reference. Chemical shifts are given in ppm from this reference with the multiplicity of signals indicated in an abbreviated form. Mass spectra (MS) were measured on a Hitachi RMU 6C spectrometer at electrode voltage 70 eV. GLC was performed on HVSG or SE 30 on Chromosorb W with hydrogen as a carrier gas. TLC was conducted on Silica-gel G with *n*-hexane or benzene as a developing solvent.

Lead Tetraacetate Oxidation of Cycloalkanols (Ia—c). A mixture of $Pb(OAc)_4$ (6.2 g, 14 mmol), $CaCO_3$ (1.6 g, 16 mmol) and anhydrous benzene (40 m*l*) was heated at reflux for 15 min with stirring under nitrogen atmosphere. After cooling, cycloalkanol (I) (12 mmol) was added to the mixture and the whole was heated at reflux for 20 hr with vigorous stirring. The reaction mixture was cooled and inorganic substances were separated by filtration and washed with benzene. The filtrate and washings were combined, washed with aqueous KI, aqueous $Na_2S_2O_3$ and then with water, dried (Na_2SO_4) and concentrated *in vacuo*. The residual oil was subjected to TLC and GLC analyses. Products III and IV were identified by comparison of their R_f values and retention times with those of authentic samples. The yields were determined from peak areas of GLC as summarized in Table 1. Isolation of bicyclic ethers II was difficult due to their low yields and was performed in the hypoiodite oxidation experiments.

Hypoiodite Oxidation of Cycloalkanols (Ia—c). A mixture of $Pb(OAc)_4$ (26.6 g, 60 mmol), $CaCO_3$ (9.0 g, 90 mmol) and cyclohexane (450 m*l*) was heated at reflux for 15 min with stirring under nitrogen atmosphere, cooled and added with cycloalkanol (I) (30 mmol) and I_2 (5.3 g, 21 mmol). Heating and stirring were continued for 2 hr. After cooling, the inorganic substances were filtered and washed with cyclohexane. The combined cyclohexane solution was washed with aqueous $Na_2S_2O_3$ and then with water, dried (Na_2SO_4), and concentrated *in vacuo*. The residual oil was subjected to TLC and GLC, and the yields were calculated from peak areas of GLC (see Table 1). Oxidation of Ia gave a mixture of bicyclic ethers, whose separation was effected by column chromatography on alumina with *n*-hexane as an eluant. Work up of less adsorbed fractions afforded 12-oxabicyclo[7.2.1]dodecane (IIa), which formed a colorless oil, bp 93—96°C/4 mmHg. IR (cm^{-1}, neat): 1090, 1042 (C–O–C). NMR (δ): 4.25—3.80 (m, 2H), 2.20—1.15 (m, 18H). Found: C, 78.7; H, 11.9%. Calcd for $C_{11}H_{20}O$: C, 78.5; H, 12.0%. MS: parent peak at *m/e* 168.

Work up of more adsorbed fractions afforded a colorless oil, bp 93—95°C/3 mmHg. IR (cm^{-1}, neat): 1100, 1048 (C–O–C). NMR (δ): 3.98—3.50 (m,2H), 2.33—0.75 (m, 18H). Found: C, 78.7; H, 11.9%. Calcd for $C_{11}H_{20}O$: C, 78.5; H, 12.0%. MS: parent peak at *m/e* 168. Oxidative cleavage of this bicyclic ether conducted similarly as mentioned below for the preparation of 1,4-diketones from II gave an oily diketone, bp 100—105°C/2 mmHg. IR (cm^{-1}, neat): 1705 (C=O). NMR (δ); 2.70—2.00 (m, 8H), 2.00—0.90 (m, 10H). Found: C, 72.3; H, 9.9%. Calcd for $C_{11}H_{18}O_2$: C, 72.5; H, 10.0%. These data indicate that this ether is not epoxide, oxetane or tetrahydrofuran. The most likely structure should be a tetrahydropyran or 12-oxabicyclo[6.3.1]dodecane. Further information was not obtained due to lack of material.

Oxidation of Ib and work up gave IIb as a colorless oil, bp 97—100°C/3 mmHg. IR (cm^{-1}, neat): 1091, 1055 (C–O–C). NMR (δ): 4.20—3.70 (m, 2H), 2.10—0.75 (m, 20H). Found: C, 79.6; H, 12.2%. Calcd for $C_{12}H_{22}O$: C, 79.1; H, 12.2%. MS: parent peak at *m/e* 182.

Oxidation of Ic and work up gave IIc as a colorless oil, bp 110—114°C/5 mmHg. IR (cm^{-1}, neat): 1085, 1060 (C–O–C). NMR (δ): 4.00—3.50 (m, 2H), 2.05—0.85 (m, 22H). Found: C, 79.7; H, 12.5%. Calcd for $C_{13}H_{24}O$: C, 79.5; H, 12.3%. MS: parent peak at *m/e* 196.

Oxidative Cleavage of Bicyclic Ethers (IIa—c). Oxygen was bubbled at a rate of *ca.* 10 m*l*/min for 20 hr into a mixture of II (8.8 mmol) and benzoyl peroxide (20 mg) heated at 85—90°C. The resulting highly viscous oil was taken up in ether (100 m*l*), washed with aqueous Na_2SO_3 and then with water, and concentrated into about 20 m*l*. This ethereal solution was added with a mixture of $Na_2Cr_2O_7 \cdot 2H_2O$ (2.0 g, 6.7 mmol), concd. H_2SO_4 (2.5 m*l*) and water (10 m*l*), and the whole was stirred for 15 hr at room temperature. The ethereal layer was washed with aqueous $NaHCO_3$ and then with water, dried (Na_2SO_4) and concentrated *in vacuo*. Purification of the residual oil by silica-gel column chromatography with benzene as an eluant afforded the desired diketone VII as a colorless solid or oil.

Oxidation of IIa gave 1,4-cycloundecanedione (VIIa) as a colorless solid, mp 64—65°C (from *n*-hexane), in a 45% yield. IR (cm^{-1}, Nujol): 1703 (C=O). NMR (δ): 2.63 (s, 4H), 2.35 (diffused t, 4H), 1.90—1.05 (m, 10H). Found: C, 72.4; H, 10.0%. Calcd for $C_{11}H_{18}O_2$: C, 72.5; H, 10.0%.

Oxidation of IIb gave 1,4-cyclododecanedione (VIIb) as a colorless solid, mp and mixed mp 78—79°C (from petroleum ether), in a 49% yield. IR spectrum was superimposable with that of authentic specimen.[5] NMR (δ): 2.65 (s, 4H), 2.38 (diffused t, 4H), 1.85—0.95 (m, 12H).

Oxidation of IIc gave 1,4-cyclotridecanedione (VIIc) as a colorless oil, bp 110—113°C/2 mmHg, in a 51% yield. IR (cm^{-1}, neat): 1705 (C=O). NMR (δ): 2.26 (s, 4H), 2.40 (diffused t, 4H), 1.85—0.95 (m, 14H). Found: C, 74.4; H, 10.6%. Calcd for $C_{13}H_{22}O_2$: C, 74.2; H, 10.5%.

Cycloundecylmethylcarbinol (VIII). This alcohol was prepared from cycloundecanecarboxylic acid[15] through MeLi treatment[16] and $LiAlH_4$ reduction in a

15) W. Ziegenbein, *Chem. Ber.*, **94**, 2989 (1961).

16) C. H. DePuy, G. M. Dappen, K. L. Eilers and R. A. Klein, *J. Org. Chem.*, **29**, 2813 (1964).

66% yield. The product formed an oil, bp 132—133°C/7 mmHg. IR (cm^{-1}, neat): 3370 (OH), 1370 (CH_3). NMR (δ): 3.70—3.27 (m, 1H), 2.37 (broad s, 1H), 1.80—1.20 (m, 21H), 1.09 (d, 3H). Found: C, 78.5; H, 13.5%. Calcd for $C_{13}H_{26}O$: C, 78.7; H, 13.2%.

Hypoiodite Oxidation of VIII. Oxidation was performed in a similar way as mentioned above and the resulting mixture was subjected to TLC and GLC analyses. The main product was cycloundecyl acetate (IVa) isolated in a 29% yield, which was identified by comparison with authentic sample. A trace of unidentified product was detected. No evidence was obtained in support of formation of tetrahydrofuran IX.

The authors are grateful to Professor K. Sisido for his generous help and to Mr. H. Takaya, Nagoya University, for measurement of mass spectra.

BULLETIN OF THE CHEMICAL SOCIETY OF JAPAN VOL. 43 234—239 (1970)

Aromatic Sulfonylation. I. Kinetics and Kinetic Isotope Effects in the Sulfonylation*1

Michio KOBAYASHI, Hiroshi MINATO and Yoshio KOHARA

Department of Chemistry, Tokyo Metropolitan University, Fukazawa, Setagaya-ku, Tokyo

(Received July 3, 1969)

p-Toluenesulfonylation of toluene, chlorobenzene and bromobenzene in the presence of aluminum chloride was investigated in methylene chloride at 0—20°C. The rate was equal to k_3[TsCl][$AlCl_3$][ArH]. Kinetic hydrogen isotope effects were found for *p*-deuteriotoluene (k_H/k_D= 2.8) and *p*-deuteriochlorobenzene (k_H/k_D=1.98). Infrared studies indicated that not a sulfonyl cation but TsCl-$AlCl_3$ complex was present in the medium. Substitution took place exclusively at *para* positions for halobenzenes, but 13.4% *ortho* and 86.6% *para* isomers were obtained for toluene. Partial rate factors for *para* positions were 52.5($PhCH_3$), 0.224(PhCl) and 0.164(PhBr). A plausible reaction mechanism was proposed, in which the abstraction of proton from the σ-complex was rate-determining.

It is generally understood that electrophilic substitution on an aromatic nucleus involves two steps, *i. e.* formation of a σ-complex and abstraction of proton from the complex.

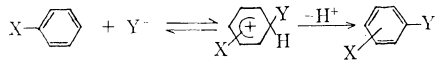

Kinetic isotope effect has been observed in a few reactions,[1] and for sulfonation the values of k_H/k_D=1.4—2.1[2,3] and 1.14—1.34[4] have been reported. Jensen and Brown[5] and Cerfontain[4] studied sulfonylation, which also involves the attack of a positively charged sulfur on an aromatic nucleus. Both groups found no primary isotope effect, and concluded that removal of proton from the intermediate was not the rate-determining step. Jensen and Brown made a through kinetic study of Friedel-Crafts sulfonylation of aromatics with aluminum chloride by using nitrobenzene or benzenesulfonyl chloride as solvent, and estimated that either sulfonyl cation $ArSO_2^+$ or ion-pair $ArSO_2^+AlCl_4^-$ was the species attacking aromatics.[6-8] However, their results are rather complicated, and both the reaction order and the mechanism vary with the solvent and the aromatics.

In order to clarify the mechanism of sulfonylation, kinetics and isotope effect of the sulfonylation with

*1 Organic Sulfur Compounds. Part XVI.

1) L. Melander, "Isotope Effects on Reaction Rate," Ronald Press, New York (1960); H. Zollinger, "Advances in Physical Organic Chemistry," Vol. II, Academic Press, London and New York (1964), p. 163.

2) L. Melander, *Ark. Kemi*, **2**, 211 (1950).

3) U. Berglund-Larsson and L. Melander, *ibid.*, **6**, 219 (1953); U. Berglund-Larsson, *ibid.*, **10**, 549 (1957).

4) a) H. Cerfontain, H. J. Hofman and A. Teldert *Rec. Trav. Chim.*, **83**, 493 (1964); b) H. Cerfontain and A. Telder, *ibid.*, **84**, 1613 (1965); c) J. K. Bosscher and H. Cerfontain, *ibid.*, **87**, 873 (1968); d) J. K. Bosscher and H. Cerfontain, *J. Chem. Soc., B*, **1968**, 1524.

5) F. R. Jensen and H. C. Brown, *J. Amer. Chem. Soc.*, **80**, 4044, Foot-note 15 (1958).

6) F. R. Jensen and H. C. Brown, *ibid.*, **80**, 4038 (1958).

7) F. R. Jensen and H. C. Brown, *ibid.*, **80**, 4042 (1958).

8) F. R. Jensen and H. C. Brown, *ibid.*, **80**, 4046 (1958).

p-toluenesulfonyl chloride and aluminum chloride have been investigated. Methylene chloride has been used as the solvent. Though it is a solvent of smaller polarity, it dissolves the TsCl-$AlCl_3$ complex well,[9] and thus it enables us to study the sulfonylation in a homogeneous medium under mild conditions. The results of this investigation will be described in this paper.

Experimental

Materials. *p*-Toluenesulfonyl chloride was recrystallized twice from *n*-hexane; mp 69°C. Toluene and chlorobenzene were shaken with concentrated sulfuric acid, dried over calcium chloride and then distilled. Bromobenzene was dried over calcium chloride and then distilled. Methylene chloride was dried over calcium chloride and over phosphorus pentoxide, and then distilled. Anhydrous aluminum chloride of first grade was used without further purification.

p-Deuteriochlorobenzene was prepared by hydrolysis of *p*-chlorophenylmagnesium bromide in heavy water (Merck, 99.75%); $n_D^{26.4}$ 1.5201; isotopic purity, 89.7 atom %D (by mass spectrometry). *p*-Deuteriotoluene was prepared by hydrolysis of *p*-tolylmagnesium bromide in heavy water (Asahi Chemicals, 99.80%); bp 110°C; isotopic purity, 80.2 atom %D (by mass spectrometry).

Kinetic Measurements. *p*-Toluenesulfonyl chloride and excess aluminum chloride were stirred in 50 m*l* of methylene chloride for 30 min at room temperature. Excess aluminum chloride undissolved was removed by filtration from the solution of TsCl-$AlCl_3$ complex, which was diluted with methylene chloride to 100 m*l*. This solution and 100 m*l* of a methylene chloride solution of an aromatic compound were placed separately in a constant temperature bath, and the reaction was started by mixing these two solutions after 30 min. For less reactive halobenzenes, 10 m*l* each of the mixed solution was sealed in an ampoule, and then these ampoules were placed in a bath. The time of mixing was regarded as the beginning of the reaction. Samples were taken out after suitable intervals, and the complex was decomposed by dilute hydrochloric acid. The methylene chloride solution was dried over magnesium sulfate, and the amount of aryl *p*-tolyl sulfone produced was determined by means of the absorption at 1320 cm^{-1} (ditolyl sulfone) or at 1325 cm^{-1} (halophenyl tolyl sulfone) by a Hitachi infrared spectrophotometer EPI-G_2. The initial concentration of aluminum chloride was determined gravimetrically by treating a portion of the solution with dilute hydrochloric acid, precipitating aluminum hydroxide with ammonia and then converting into aluminum oxide in a platinum crucible.

Sulfonylation of Toluene. The absence of 860 cm^{-1} band showed the absence of *p*-tolyl *m*-tolyl sulfone in the products. The sulfone mixture was found to contain 13.4% *p*-tolyl *o*-tolyl sulfone and 86.6% di-*p*-tolyl sulfone by gas-chromatographic analysis on a 2 m column packed with Chromosorb-SE30 at 230°C (retention time: *p*-tolyl *o*-tolyl sulfone, 19.9 min, *p*-tolyl *m*-tolyl sulfone, 23.5 min, di-*p*-tolyl sulfone, 24.5 min).

9) G. Holt and B. Pagdin, *J. Chem. Soc.*, **1960**, 2508; E. C. Dart, G. Holt and K. D. Jeffreys, *ibid.*, **1964**, 5663.

Table 1. Typical data for the sulfonylation of toluene at 5.0°C

Time (sec)	Di-(*p*-tolyl) sulfone ($mol \cdot l^{-1}$)	Rate const. ($l^2 \cdot mol^{-2} \cdot sec^{-1}$)
0.660×10^3	0.0346	1.09×10^{-3}
1.140	0.0577	1.26
1.620	0.0742	1.20
2.040	0.0869	1.22
2.460	0.0930	1.14
2.970	0.1057	1.18
3.360	0.1101	1.16
3.780	0.1193	1.19
4.320	0.1269	1.20
4.830	0.1271	1.24
5.430	0.1378	1.16
	mean	1.19×10^{-3}

Initial concentration: $[TsCl]_0$, 0.2036; $[PhCH_3]_0$, 0.9848; $[AlCl_3]_0$, 0.2887 $mol \cdot l^{-1}$.

The rate of reaction was proportional to the concentration of each of three reactants, and the third order rate constant was nearly constant as illustrated by a typical run in Table 1.

Table 2. Typical data for the sulfonylation of chlorobenzene at 15.0°C

Time (sec)	*p*-Tolyl *p*-chlorophenyl sulfone ($mol \cdot l^{-1}$)	Rate const. ($l^2 \cdot mol^{-2} \cdot sec^{-1}$)
2.23×10^4	0.0148	1.36×10^{-5}
4.73	0.0233	1.06
6.84	0.0329	1.10
11.40	0.0538	1.26
16.67	0.0666	1.16
25.44	0.0943	1.29
27.78	0.0974	1.30
36.24	0.1135	1.31
	mean	1.23×10^{-5}

Initial concentration: $[TsCl]_0$, 0.2005; $[PhCl]_0$, 1.0004; $[AlCl_3]_0$, 0.2594 $mol \cdot l^{-1}$.

Table 3. Typical data for the sulfonylation of bromobenzene at 15.0°C

Time (sec)	*p*-Tolyl *p*-bromophenyl sulfone ($mol \cdot l^{-1}$)	Rate const. ($l^2 \cdot mol^{-2} \cdot sec^{-1}$)
4.14×10^4	0.0148	1.12×10^{-5}
8.01	0.0254	1.05
12.87	0.0336	1.00
16.55	0.0404	0.88
21.36	0.0516	0.94
25.32	0.0584	0.94
59.76	0.1083	1.09
	mean	1.00×10^{-5}

Initial concentration: $[TsCl]_0$, 0.1996; $[PhBr]_0$: 0.5998; $[AlCl_3]_0$, 0.2898 $mol \cdot l^{-1}$.

TABLE 4. RATE CONSTANTS OF SULFONYLATION OF SUBSTITUTED BENZENES

X in PhX	Temp. (°C)	Initial concentrations ($mol \cdot l^{-1}$)			k_3 ($l^2 \cdot mol^{-2} \cdot sec^{-1}$)	E_a ($kcal \cdot mol^{-1}$)	$\Delta S^{\neq}$ at 0°C (e.u.)
		$[TsCl]_0$	$[PhX]_0$	$[AlCl_3]_0$			
CH_3	1.0	0.1996	0.6031	0.2158	$0.994^* \times 10^{-3}$	14.8	−20.2
	5.0	0.1994	0.3504	0.2068	1.37		
	5.0	0.2022	0.6013	0.2315	1.26*		
	5.0	0.2036	0.9848	0.2887	1.19		
	7.5	0.2004	0.6052	0.2409	1.74*		
	10.0	0.2016	0.6315	0.2425	2.35*		
H**	0.0	0.3003	0.1905	0.4332	1.16×10^{-4}	11.9	−34.6
	0.0	0.2935	0.4484	0.4449	1.07		
	0.0	0.2988	0.6261	0.4544	1.19		
	0.0	0.2370	1.1502	0.4304	1.28		
	7.0	0.2952	0.3254	0.4209	1.92		
	15.5	0.2933	0.4323	0.4721	4.02		
Cl	0.0	0.2004	0.3994	0.2603	0.532×10^{-5}	11.0	−42.5
	0.0	0.2005	0.5986	0.2603	0.453		
	0.0	0.2004	1.0000	0.2747	0.425*		
	7.0	0.2007	1.0014	0.2715	0.717*		
	15.0	0.2005	1.0004	0.2594	1.23*		
	20.0	0.1993	0.5993	0.4022	2.01		
	20.0	0.2005	0.9992	0.2354	1.70*		
Br	0.0	0.1993	0.6002	0.2821	0.283×10^{-5}	12.1	−41.5
	7.0	0.1995	0.5988	0.2613	0.524		
	15.0	0.1996	0.5998	0.2898	1.00		
	20.0	0.1997	0.6000	0.2704	1.39		

* E_a and $\Delta S^{\neq}$ were calculated on the basis of these values.
** Ref. 10.

Sulfonylation of Halobenzenes. Recrystallization of the product of tosylation of chlorobenzene yielded *p*-tolyl *p*-chlorophenyl sulfone (mp 121°C) and a mother liquor, which was found by elution chromatography to be almost completely *p*-tolyl *p*-chlorophenyl sulfone. Thus it was shown that more than 98% of *p*-toluenesulfonyl chloride reacted at *p*-position of chlorobenzene. Similarly it was found that tosylation of bromobenzene took place almost exclusively at *p*-position.

The reactions were of third order, and the third order rate constants calculated were nearly constant till about 50% reaction as illustrated by typical runs in Tables 2 and 3.

Results and Discussion

Results of kinctic studies of tosylation are summarized in Table 4. Rate constants are larger for the runs with lower concentrations of a substituted benzene. This can be ascribed to the solvent effect due to the decrease of the less polar substance in the medium. Therefore, the activation parameters were obtained on the basis of the runs with similar compositions.

In Fig. 1 values of activation enthalpy were plotted *versus* values of activation entropy, and it was shown that an isokinetic relationship holds with

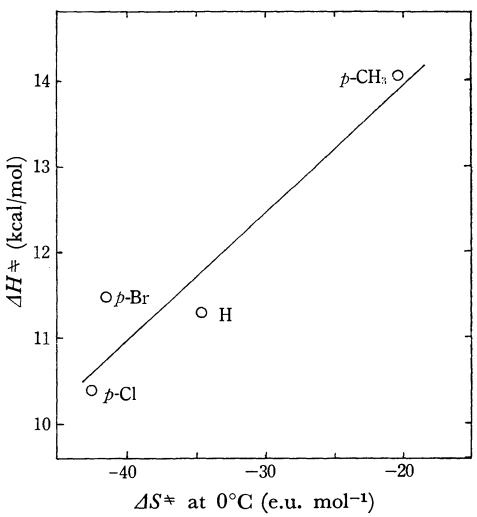

Fig. 1. Isokinetic relationship for the sulfonylation (β=152°K).

r=0.95. The isokinetic temperature, β, was 152°K.

The partial rate factors of *para* positions at 7.0°C were calculated. They were 52.5 for *p*-CH_3, 0.224 for *p*-Cl and 0.164 for *p*-Br. Figure 2 shows

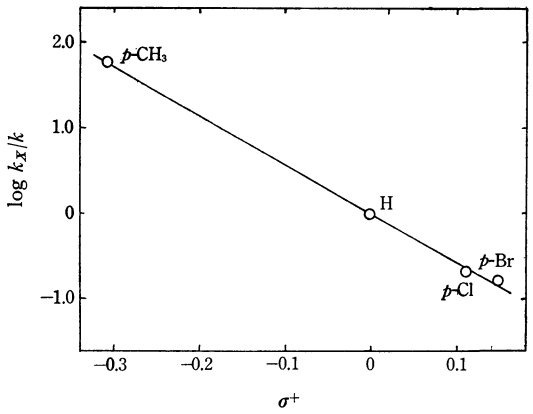

Fig. 2. Hammett plots for the sulfonylation at 7.0°C ($\rho=-5.6$).

that a good linear relationship holds between these values and σ^+ ($\rho=-5.6$).

Since the rate was proportional to the concentration of each of TsCl, $AlCl_3$ and PhX, the following mechainsm appeared plausible.

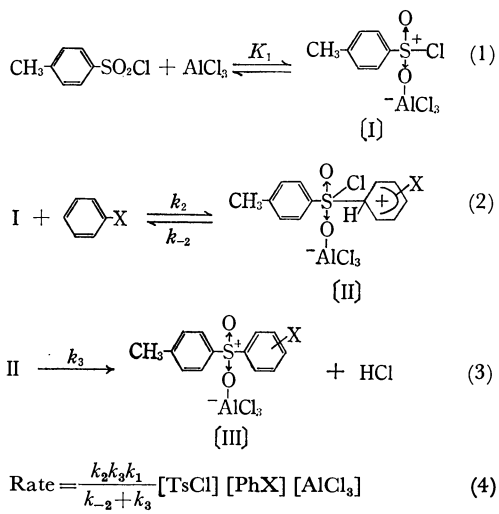

$$\text{Rate}=\frac{k_2k_3k_1}{k_{-2}+k_3}[\text{TsCl}]\,[\text{PhX}]\,[\text{AlCl}_3] \qquad (4)$$

Since the reaction was of third order, either step (2) or step (3) is the rate-determining step. In order to clarify the step which controls the rate, kinetic experiments were carried out with deuterated compounds. For *p*-deuteriotoluene $k_3=4.4\times10^{-4}$ $M^{-2}\cdot sec^{-1}$ at 5.0°C and $k_H/k_D=2.8$. For *p*-deuteriochlorobenzene $k_3=8.58\times10^{-6}M^{-2}\cdot sec^{-1}$ at 20.0°C and $k_H/k_D=1.98\pm0.3$. The values previously given were $k_H/k_D=2.0$ for hexadeuteriobenzene and $k_H/k_D=1.77\pm0.2$ for *p*-deuteriobromobenzene.[10] These data clearly confirmed that the hydrogen-abstraction step was the rate-determining step.

This conclusion is in contrast with the finding of Jensen and Brown that in benzenesulfonyl chloride as the solvent there was no kinetic isotope effect.[5] Bosscher and Cerfontain reported a very small isotope effect ($k_H/k_D=1.1$) for the sulfonylation occurring as a side reaction in the sulfonation of benzene with sulfur trioxide in trichlorofluoromethane at −35°C.[4d]

The formation of $TsCl\cdot AlCl_3$ complex and $Ts\cdot Ar\cdot AlCl_3$ complex was checked by means of infrared spctroscopy. The absorptions of asymmetric and symmetric stretching vibrations of the SO_2 group of *p*-toluenesulfonyl chloride in methylene chloride were observed at 1375 and 1175 cm^{-1}, whereas they appeared at 1365 and 1175 cm^{-1} when aluminum chloride was present in the medium. The absorptions due to the SO_2 group in *p*-tolyl *p*-chlorophenyl sulfone in methylene chloride were observed at 1325 and 1160 cm^{-1}, whereas these absorptions shifted to 1305 and 1105 cm^{-1} when aluminum chloride was added to the medium. Lindner and Weber reported that *p*-dimethylaminobenzenesulfonyl chloride absorbed at 1367 and 1160 cm^{-1} and its sulfonyl cation absorbed at 1418 and 1195 cm^{-1}. These facts indicate that not a sulfonyl cation but complexes such as shown in structure I and II are present in the reaction medium and the sulfone produced is also present as the complex III.

Since the rate of sulfonylation of toluene was greater faster than those of halobenzenes, it was expected that the rate of sulfonylation of anisole would be much greater. However, it was found that the rate was extremely solw with anisole. When a methylene chloride solution of anisole, aluminum chloride and *p*-toluenesulfonyl chloride was viewed in infrared, no shift in the sulfonyl absorption was observed, indicating the absence of $TsCl\text{-}AlCl_3$ complex. Formation of $PhOCH_3\text{-}AlCl_3$ complex was suspected, and a solution of anisole and aluminum chloride was compared with a solution of anisole alone by infrared, ultraviolet and nuclear magnetic resonance spectroscopy. The results are shown in Table 5. These spectroscopic observations are consistent with the formation of $PhOCH_3\text{-}AlCl_3$ complex. Apparently the following equilibrium exists, and the $PhOCH_3\text{-}AlCl_3$ complex predominates.

$$TsCl + PhOCH_3\text{-}AlCl_3 \rightleftharpoons PhOCH_3 + TsCl\text{-}AlCl_3$$

Table 5. Spectra of anisole-aluminum chloride-complex in CH_2Cl_2

	$PhOCH_3$	$PhOCH_3\text{-}AlCl_3$
UV λ_{max}	280 mμ	410 mμ
		497 mμ
NMR OCH_3	6.22 τ (s)	5.55 τ (s)
aromatic -H	3 τ (m)	2.65 τ (s)
IR =C-O-CH_3	1240 cm^{-1}	1135 cm^{-1}

10) M. Kobayashi, K. Honda and A. Yamaguchi, *Tetrahedron Lett.*, **1968**, 487.

11) E. Lindner and H. Weber, *Chem. Ber.*, **101**, 2832 (1968).

TABLE 6. COMPARISON OF SULFONYLATIONS IN DIFFERENT SOLVENTS

Reactant	Solvent	Rate	Reaction step*	Orientation	Partial rate factor	k_H/k_D
$PhSO_2Cl$, $AlCl_3$, Mesitylene	$PhNO_2$	k_2 [$PhSO_2Cl$][$AlCl_3$]	(5), (6), (7)			
$PhSO_2Cl$, $AlCl_3$, $PhCH_3$	$PhNO_2$	k_3 [$PhSO_2Cl$][$AlCl_3$][$PhCH_3$]	(5), (6), (7)			
$PhSO_2Cl$, $AlCl_3$, PhCl	$PhNO_2$	k_3 [$PhSO_2Cl$][$AlCl_3$][PhCl]	(5), (6), (7)			
$PhSO_2Cl$, $AlCl_3$, $PhCH_3$	$PhSO_2Cl$	k_2 [$PhSO_2Cl$-$AlCl_3$][$PhCH_3$]	(6), (7)	o=28.4% m= 8.7 p=62.9	o_f= 6.8 m_f= 2.1 p_f=30.2	1
$PhSO_2Cl$, $AlCl_3$, PhCl	$PhSO_2Cl$	$k_{3/2}$ [$PhSO_2Cl$-$AlCl_3$]$^{-1/2}$[PhCl]	(6), (8)			
TsCl, $AlCl_3$, $PhCH_3$	CH_2Cl_2	k_3 [TsCl][$AlCl_3$][$PhCH_3$]	(1), (2), (3)	o=13.4% m= 0 p=86.6	 p_f=52.5	2.8
TsCl, $AlCl_3$, PhH	CH_2Cl_2	k_3 [TsCl][$AlCl_3$][PhH]	(1), (2), (3)			2.0
TsCl, $AlCl_3$, PhCl	CH_2Cl_2	k_3 [TsCl][$AlCl_3$][PhCl]	(1), (2), (3)		p_f=0.224	1.98
TsCl, $AlCl_3$, PhBr	CH_2Cl_2	k_3 [TsCl][$AlCl_3$][PhBr]	(1), (2), (3)		p_f=0.164	1.77

* Rate-determining step proposed were underlined.

The findings of this investigation must be compared with those of the thorough study made by Jensen and Brown. They found that in nitrobenzene the rate was equal to k_2[$PhSO_2Cl$][$AlCl_3$] for reactive aromatics whereas the rate was equal to k_3[ArH][$PhSO_2Cl$][$AlCl_3$] for less reactive aromatics. The following reaction sequence was proposed, in which step (6) is rate-determining for more reactive aromatics and step (7) is rate-determining for less reactive aromatics.[6]

$$PhSO_2Cl + PhNO_2 \cdot AlCl_3 \rightleftharpoons PhSO_2Cl \cdot AlCl_3 + PhNO_2 \quad (5)$$

$$PhSO_2Cl \cdot AlCl_3 \rightleftharpoons PhSO_2^+AlCl_4^- \quad (6)$$

$$ArH + PhSO_2^+AlCl_4^- \longrightarrow ArSO_2Ph \cdot AlCl_3 + HCl \quad (7)$$

Jensen and Brown reported that in benzenesulfonyl chloride the rate was equal to k_2[$PhSO_2Cl \cdot AlCl_3$]-[$PhCH_3$] with toluene and the attacking species was $ArSO_2^+AlCl_4^-$, whereas with chlorobenzene the rate was equal to $k_{3/2}$[$PhSO_2Cl \cdot AlCl_3$]$^{1/2}$[PhCl] and the attacking species was $ArSO_2^+$ cation.[7]

$$PhSO_2^+AlCl_4^- \rightleftharpoons PhSO_2^+ + AlCl_4^- \quad (8)$$

The findings of Jensen and Brown are compared with the findings of this investigtaion in Table 6.

A comparison of the orientation and the partial rate factors in Table 6 indicates that both intra- and intermolecular selectivity are greater with TsCl-$AlCl_3$-ArH-CH_2Cl_2 than with $PhSO_2Cl$-$AlCl_3$-ArH. The ρ value in CH_2Cl_2 was -5.6, whereas the ρ value calculated from the data in $PhSO_2Cl$ was -4.8. It is reasonable that in solvents of greater polarity such as nitrobenzene (dielectric constant, 34.092 at 25°C) and benzenesulfonyl chloride the reaction intermediates formed are ion pair $ArSO_2^+$ $AlCl_4^-$ or free cation, which are more reactive and less selective than complex II formed in

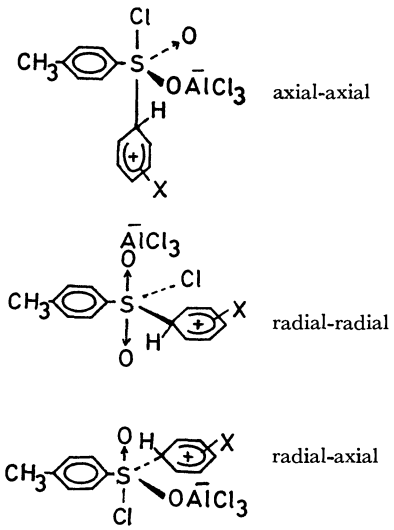

Fig. 4. Transition state of the sulfonylation.

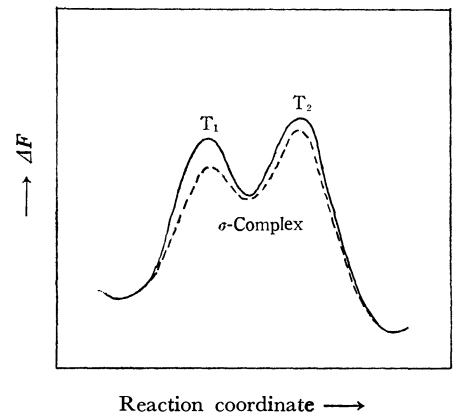

Fig. 3. Energy profile for the sulfonylation.
——: halobenzene ------: toluene

methylene chloride (dielectric constants, 9.08 at 20°C).

The isotope effect found for toluene was greater than that for benzene, chlorobenzene or bromobenzene. This finding may be explained by the energy profile shown in Fig. 3.

It is plausible that the presence of electron-releasing methyl group lowers the transition state T_1 considerably but affects the transition state T_2 very little. If so, k_{-2} as well as k_2 will be greater and k_{-2}/k_3 will be greater with toluene than with halobenzenes, and consequently the isotope effect with toluene is expected to be greater than that with halobenzenes.

It should be pointed out that three different structures are possible for the transition state from complex I to complex II, as shown in Fig. 4. However, at present it is not possible to determine which structure is more advantageous for the addition-elimination reaction discussed here.

On the basis of the reaction rate, reaction orders, activation parameters, orientations, partial rate factors, Hammett's plot, spectroscopic observations and kinetic hydrogen isotope effects, it was concluded that the reaction sequence (1), (2) and (3) best represent the reactions taking place in mixtures of *p*-toluenesulfonyl chloride, aluminum chloride and aromatic compounds in methylene chloride.

BULLETIN OF THE CHEMICAL SOCIETY OF JAPAN VOL. 43 239—245 (1970)

Association of a Reduced Riboflavin Derivative with Purines, Pyrimidines and Nicotinamide

Byung Sul Yu and Yoshimasa Kyogoku

Faculty of Pharmaceutical Sciences, The University of Tokyo, Hongo, Bunkyo-ku, Tokyo

(Received July 7, 1969)

Hydrogen bonding of a reduced riboflavin derivative in chloroform has been studied by infrared spectra measurements. The self-association of the reduced form of riboflavin tetraacetate is much stronger than that of the oxidized form. The reduced form can also form hydrogen bonded complexes with some aminopurines, aminopyrimidines, aminopyridines and nicotinamide derivatives. In the bonding with aminopyridines the contribution of a proton transfer must be predominant. At partial reduction states the formation of radicals, semiquinone forms, was detected with the aid of the electron spin resonance. The concentration of free radicals, however, is about 1 per cent of dissolved riboflavin tetraacetate. The infrared spectra at various stage of reduction can be interpreted by the sum of the two individual spectra of the fully reduced and oxidized forms.

In previous papers selective formation of hydrogen bonding between the oxidized forms of riboflavin derivatives and adenine compounds has been reported.[1-3] The association of oxidized riboflavin is thought to be relevant to the intra- and intermolecular interaction of flavin adenine dinucleotide[4-10] and to have an important role in keeping the structure of FAD.[10] The isoalloxazine ring of riboflavin takes hydrogenated and dehydrogenated forms and hence it can be an electron carrier in a respiratory chain. The present work will show the effect of hydrogenation on the association of a riboflavin derivative with other compounds such as purines, pyrimidines and nicotinamide. The results might help to interpret the nature of previously reported complexes like FMN-$FMNH_2$ and NAD^+-$FMNH_2$.[11-15],*1

1) Y. Kyogoku and B. S. Yu, This Bulletin, **41**, 1742 (1968).
2) Y. Kyogoku and B. S. Yu, *ibid.*, **42**, 1387 (1969).
3) K. Uehara, T. Mizoguchi, S. Hosomi, T. Fujiwara and K. Tomita, *J. Biochem.*, **64**, 589 (1968).
4) G. Weber, *Biochem. J.*, **47**, 114 (1950).
5) L. G. Whitby, *ibid.*, **54**, 437 (1953).
6) J. C. M. Tsibris, D. B. McCormick and L. D. Wright, *Biochemistry*, **4**, 504 (1965).
7) I. Listowsky, S. England, J. J. Betheil and S. Seifter, *ibid.*, **5**, 2548 (1966).
8) D. W. Miles and D. W. Urry, *ibid.*, **7**, 2791 (1968).
9) R. H. Sarma, P. Dannies and N. O. Kaplan, *ibid.*, **7**, 4359 (1968).
10) Y. Kyogoku and B. S. Yu, *Biochim. Biophys. Acta*, to be published.
11) I. Isenberg and A. Szent-Gyorgyi, *Proc. Nat. Acad. Sci. U. S.*, **44**, 857 (1958).
12) H. Beinert, *J. Amer. Chem. Soc.*, **78**, 5323 (1956).
13) Q. H. Gibson, V. Massey and N. M. Atherton, *Biochem. J.*, **85**, 369 (1962).
14) V. Massey and G. Palmer, *J. Biol. Chem.*, **237**, 2347 (1962).
15) E. M. Kosower, "Flavins and Flavoproteins," ed. by M. K. Slater, Elsevier, Amsterdam (1964), p. 1.

Experimental

Materials. Riboflavin-2′,3′,4′,5′-tetraacetate and 3-*N*-methylriboflavin-2′,3′,4′,5′-tetraacetate were prepared by the method described previously.[2] 9-Ethyl adenine, 1-cyclohexyluracil, 2′3′-benzylidine-5′-tritylguanosine, 2′,3′-benzylidine-5′-tritylcytidine and 4-aminopyrimidine were purchased from Cyclo Chemical Co., Los Angeles. The other chemicals were obtained from Tokyo Kasei Co. Some of them were used after recrystallization from proper solvents and the others were used without further purification. Chloroform and chloroform-d (Showa Denko Co., Kawasaki) were employed as solvents for the infrared measurements. Chloroform was dried with phosphorous pentoxide and purified by distillation. Chloroform-d was dried by passing through an alumina gel column.

The chloroform solutions of reduced riboflavin derivatives were prepared by shaking the solutions of the oxidized forms with an aqueous solution saturated with hydrosulfite. The solutions were then dried with calcium chloride. Completion of reduction was checked by visible-ultraviolet spectra, disappearance of absorptions at 450 and 350 mμ and appearance of a strong band at 300 mμ. Partial oxidation of the reduced form was done by bubbling oxygen gas in the solution of the reduced form or by mixing it with the solution of the oxidized form. Reduced *N*-methylnicotinamide was prepared from *N*-methylnicotinamide chloride by the method of Rafter and Colowick.[16] Hydrogenation at the 4-C position was confirmed by NMR measurement.

Procedures. Infrared spectra were measured with a Perkin-Elmer 621 spectrophotometer for chloroform solutions in fused quartz cells ranging from 1 to 25 mm in thickness. The spectra in the region 1800—1500 cm^{-1} were obtained by the use of potassium bromide cells with variable thickness. To avoid oxidation by atmospheric oxygen the solutions of the reduced samples were prepared in a dry box filled with nitrogen gas.

Electron spin resonance spectra were taken with a JEOL P-10 spectrometer. The concentration of free radicals was determined by comparison of the integrated area of signals with that of a standard solution of diphenyl picryl hydrazyl (Nakarai Chemical Co., Kyoto). Standard 0.01M solution was made up in chloroform. The visible-ultraviolet spectra were recorded with a Hitachi 124 spectrophotometer.

Determination of Association Constants. The self-association constant of RH was calculated from concentration dependence of a monomer band based on the theory described previously.[17] Eight spectra were recorded at different concentrations between 10^{-2} and 10^{-4}M.

Association constants between A and B can be estimated from the optical density change of the association or nonbonded band of A plotted against the mole ratio of mixing. The tangent lines (Fig. 4) show the optical density change which would occur when all of A bond to B. From the location of the cross point of the two lines, the numbers of moles, m and n, in the following equilibrium can be determined.

$$mA + nB \rightleftarrows A_mB_n$$

The association constant K in the equilibrium may be written as

$$K = \frac{C_{AB}}{C_A{}^m C_B{}^n} \tag{1}$$

where C_A, C_B and C_{AB} are the concentrations of monomer A, monomer B and the complex respectively. The length of L from the cross point to the base line is proportional to C_{0A}, the initial concentration of A, and the height l of the observed curve is proportional to mC_{AB}, the concentration of A which is used for the complex formation. Thus the following relations hold

$$\frac{C_{0A}}{L} = \frac{C_A}{L-l} = \frac{mC_{AB}}{l} \tag{2}$$

Similar relations are written for the component B

$$\frac{C_{0B}}{L} = \frac{C_B}{L-l} = \frac{nC_{AB}}{l} \tag{3}$$

The initial concentration C_{0A} and C_{0B} are related to the total concentration C_0 as follows.

$$C_{0A} = \frac{m}{m+n}C_0, \quad C_{0B} = \frac{n}{m+n}C_0 \tag{4}$$

From the relations (1), (2), (3) and (4) it follows that

$$K = \frac{(m+n)^{m+n-1}\dfrac{l}{L}}{m^m n^n \left(1-\dfrac{l}{L}\right)^{m+n} C_0{}^{m+n-1}} \tag{5}$$

The association constants determined by the above method are only reliable within the order of magnitude.

Results and Discussion

Self - association of Reduced Riboflavin Tetraacetate. *Fully Reduced Form.* The infrared spectra of RH and MeRH are given in Fig. 1. The spectrum of fully reduced RH shows very broad strong bands in the 3 μ region contradicting with the sharp N_3–H stretching band of the oxidized form R. MeRH whose oxidized form does not show any absorption in the 3 μ region also gives a broad band around 3400 cm^{-1}. These evidences indicate that the broad bands come from the hydrogenated NH groups at the N_1 and N_5 positions of the reduced isoalloxazine ring. The carbonyl

*1 The abbreviations used are; FMN and $FMNH_2$, the oxidized and reduced forms of flavin mononucleotide; NAD^+ and NADH, the oxidized and reduced froms of nicotinamide adenine dinucleotide; R and RH, the oxidized and reduced forms of riboflavin-2′,3′,4′,5′-tetraacetate; MeR and MeRH, the oxidized and reduced forms of 3-*N*-methylriboflavin-2′,3′,4′,5′-tetraacetate; FAD, flavin adenine dinucleotide; NA, nicotinamide; A, 9-ethyladenine; U, 1-cyclohexyluracil; G, 2′,3′-benzylidine-5′-tritylguanosine; C, 2′,3′-benzylidine-5′-tritylcytidine; NMR, nuclear magnetic resonance; ESR, electron spin resonance; DPPH, diphenyl picryl hydrazyl.

16) G. W. Rafter and S. P. Colowick, *J. Biol. Chem.*, **206**, 773 (1954).

17) Y. Kyogoku, R. C. Lord and A. Rich, *J. Amer. Chem. Soc.*, **89**, 496 (1967).

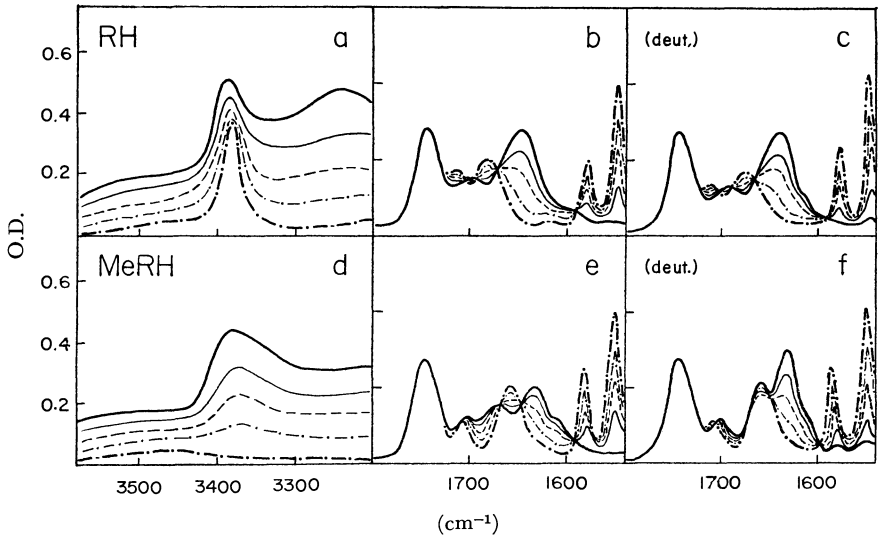

Fig. 1. Infrared spectra of the chloroform solutions of riboflavin tetraacetate (a, b, c) and *N*-methylriboflavin tetraacetate (d, e, f) in the reduced and oxidized forms. The concentration of the solution is 4×10^{-3}M, and the path length is 5 mm for the 3500—3200 cm^{-1} region and 0.5 mm for the 1800—1500 cm^{-1} region. Bold solid line, fully reduced state; bold broken line, fully oxidized state; other three fine lines, partially reduced and oxidized states.

stretching bands at 1715 and 1685 cm^{-1} of R move to lower frequency and the ring stretching bands at 1585 and 1550 cm^{-1} disappear by hydrogenation. The spectral feature of the 6 μ region shows a remarkable change in the conjugated system of the isoalloxazine ring.

The broad strong bands in the 3 μ and 6 μ regions indicate the strong self-association of RH. The fully reduced isoalloxazine ring has three NH and two carbonyl groups and thus four sites can be used for cyclic hydrogen bonds with another RH molecule. Therefore the self-association constant must be at least four times, *i. e.* about $600M^{-1}$, as big as that of R which has two sites for the cyclic dimer formation. From the concentration dependence of the 3400 cm^{-1} band of RH the self-association constant was roughly estimated to be $10^3-10^4M^{-1}$. The ability of the formation of hydrogen bonds of the N_1H and N_5H sites are much stronger than that of the N_3H group. This is understandable because the p*K* values of the N_1 and N_5 protons are around 6.5 whereas that of N_3 is 10.[8] The reduced form is a weak acid. The lower frequency shift of the carbonyl stretching band shows the increase of single bond nature in the associated reduced form. The contribution of the proton transfer form (II) may not be so small.

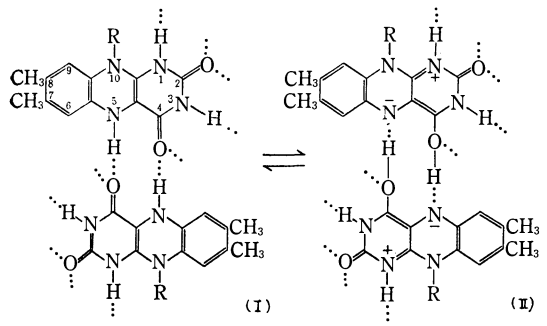

Partially Reduced State. From the potentiometric, spectral and magnetic resonance observations several investigators concluded that riboflavin is reduced and oxidized in two one electron steps and pass through a semiquinoid state.[12,13,18,19] The infrared spectra of RH and MeRH at successive oxidation states from full reduction to full oxidation are given in Fig. 1. The strong NH band of RH gradually decreases in intensity as the per cent of oxidation is increased. Gradual shifts and intensity changes of absorption bands are also observed in the 1800—1500 cm^{-1} region and isosbestic points are seen at 1670 and 1590 cm^{-1}. It is clear from the results that the infrared spectra at intermediate oxidation are explained by the sum of the spectra of two states, fully oxidized and reduced states, and any new band due to transient intermediate could not be observed. In the visible-near infrared spectrum of the FMN-$FMNH_2$ mixture in aqueous solution two bands were reported in addition to the bands due to FMN and $FMNH_2$, one with

18) R. Kuhn and T. Wagner-Jauregg, *Ber.*, **67**, 361 (1934).

19) L. Michaeris, M. P. Schubert and C. V. Smythe, *J. Biol. Chem.*, **116**, 587 (1936).

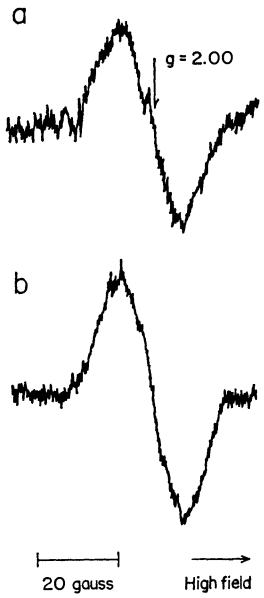

Fig. 2. Electron spin resonance spectra at 50% reduction of 1×10^{-2}M riboflavin tetraacetate in chloroform (a), plus 1×10^{-2}M 9-ethyladenine (b). The spectra were taken at the same instrument setting. Field modulation, 100 kc.

a maximum absorption near 570 mμ and another with a peak at 900 mμ.[12,13] The 570 mμ band was thought to be due to semiquinone, since it increases in intensity to a maximum at about half oxidation together with the increase of the signal intensity of ESR. The 900 mμ band was assigned to the dimer of semiquinone[12] or to the charge transfer complex of FMN-$FMNH_2$.[13] In the present investigation, however, no absorption could be seen in the wavelength region longer than 500 mμ even for the 0.01M solution of RH at 50% oxidation in 1 cm cell. The visible-near infrared spectra of the partially oxidized state did not show the presence of a intermediate species.

ESR was measured for the 0.01M solution of R at 50% reduction and a signal was observed (Fig. 2). From a comparison of the integrated area of the signal with that of DPPH, the concentration of free radicals was calculated to be 1×10^{-4}M, 1% of dissolved R. The signal amplitude did not change one hour after the preparation of the solution. Oxidation of RH by molecular oxygen or by mixing it with R produces radicals, semi-

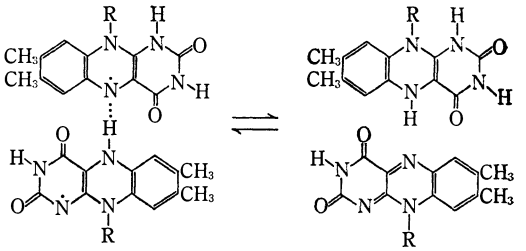

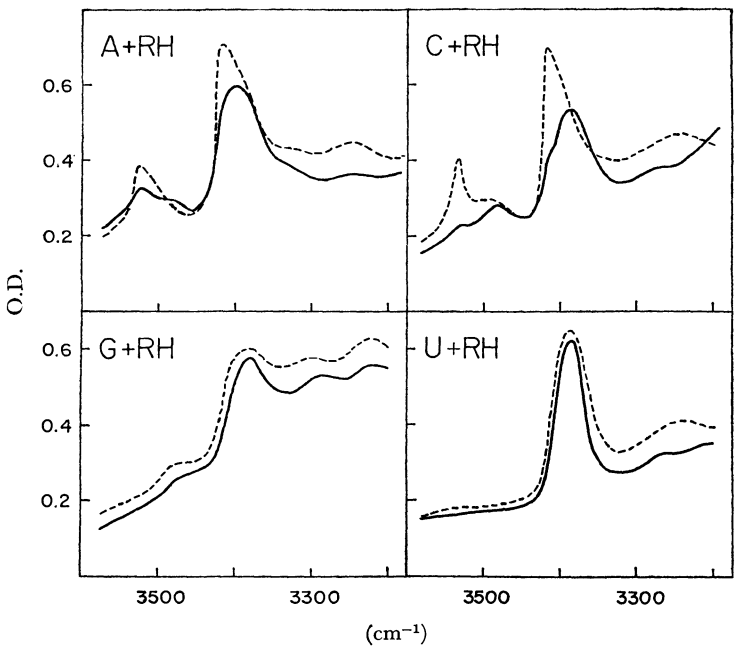

Fig. 3. Infrared spectra of the equimolar mixture solution of reduced riboflavin tetraacetate and one of the A, U, G and C compounds in chloroform. The total concentration is 8×10^{-3}M and the path length is 5 mm. Solid line, observed spectrum; dotted line, calculated sum of the individual spectrum of components.

quinone, which interact to give the fully reduced and oxidized forms as shown above.

Association with Purines, Pyrimidines and Other Related Compounds. *Interaction with 9-Ethyladenine.* Riboflavin tetraacetate formed a hydrogen bonded complex with adenine more strongly than with themselves.[1,2] The infrared spectra of the 1 : 1 mixture of RH and A also show us strong binding of A with RH (Fig. 3). The symmetric and antisymmetric stretching bands of the non-bonded amino group at 3415 and 3525 cm^{-1} become weaker than the calculated sum of the individual spectrum which would be realized if there is no interaction between them. An association band is visible at 3470 cm^{-1}, which is due to the stretching vibration of the partially bonded amino group. The intensity of the non-bonded and association bands changes as a function of the mole ratio of mixing. They reach a maximum or a minimum in the 1 (RH) : 3 (A) region (Fig. 4). RH and A form a complex which consists of three A and one RH molecules in average. The ratio is not unreasonable because RH has four sites to which A can bond with cyclic hydrogen bonds. By an application of the procedure described in the preceding section the association constant of the complex formation was estimated to be 10^7 $(l/mol)^3$ with an assumption $m=1$ and $n=3$.

The intensity of absorption bands also changes as a function of the extent of reduction. The broad band of RH gradually decreases in intensity and the band due to the free N_3H group of R at 3380 cm^{-1} becomes sharp as the extent of oxidation increases (Fig. 5). However, the intensity change of the bands of A at 3415 and 3525 cm^{-1} are not parallel with that of the N_3H group of R. This might be explained by the fact that a RH molecule can bond with three A molecules. Contribution of the intermediate state to the RH-A binding does not seem to be important, since an additional band due to the semiquinone-A complex could not be observed. In fact the concentration of radicals was determined by ESR measurement to be 1 per cent of the dissolved RH at 50% reduction and is not affected by the presence of A.

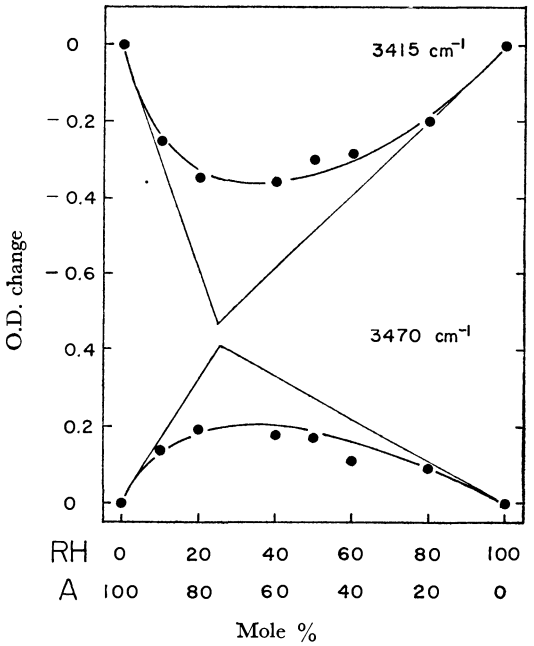

Fig. 4. Change in the optical density of the association band at 3470 cm^{-1} and the non-bonded band at 3415 cm^{-1} as a function of the mole ratio of fully reduced riboflavin tetraacetate and ethyladenine. The optical density of the pure solution is adjusted to zero.

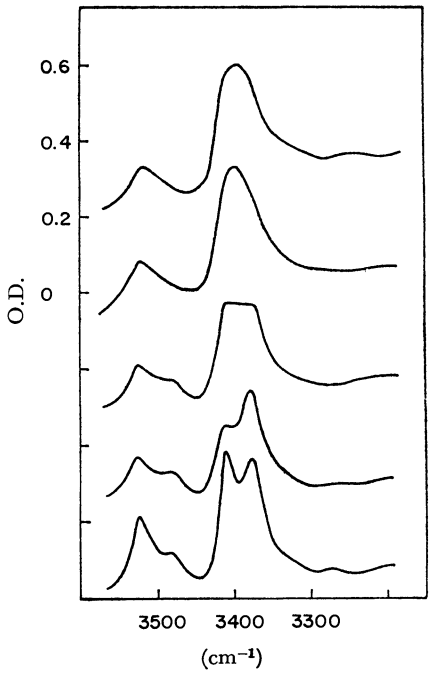

Fig. 5. Infrared spectra of the equimolar mixture solutions of riboflavin tetraacetate and ethyladenine at successive reduction states. Bottom spectrum, fully oxidized state; top spectrum, fully reduced state. The total concentration is 8×10^{-3}M and the path length is 5 mm.

Interaction with Other Compounds. Riboflavin tetraacetate selectively bonded to A and did not interact with other nucleic acid purine and pyrimidine derivatives.[1,2] Whether such specificity still holds for the association of RH was examined. The infrared spectra of the mixtures with G and U show almost the same spectra as the calculated sum of each individual (Fig. 3). A remarkable change, however, is observed in the spectrum of the mixture with C. The symmetric and antisymmetric stretching bands of the free amino group of C at 3415 and 3525 cm^{-1} almost disappear on the addition of RH. The selective binding found

for the oxidized form cannot be observed in the association of the reduced form. To find necessary conditions for the association with RH, several compounds listed in Table 1 were examined for their ability of binding with RH. Association constants were roughly estimated by the variation method described previously. A two + sign in the table shows that the compound interacts with RH as strongly as with A at an association constant in the order of 10^7 (l/mol).[3] A three + sign means stronger complex formation with a constant bigger than 10^8. Weaker bonding than that of A is shown by a one + sign. For all of the associations m and n were assumed 1 and 3 respectively.

From the table it can be concluded that both the amino group and the nitrogen atom in the heterocyclic ring are necessary but are not enough for the association. Acidity or basicisity of the donor and acceptor sites of proton may be associated with the interaction. The pK_a of 4-aminopyrimidine is 5.71, whereas that of 2-aminopyrimidine is 3.54.[20] The latter must be harder to be protonated than the former. This accounts for the fact that 2-aminopyrimidine does not associate with RH. 2-Amino-, 3-amino-, 4-aminopyridines have the pK_a's of 6.86, 5.98 and 9.14 respectively.[20] On the other hand the protons at the N_1 and N_5 positions of RH dissociate around 6.5.[21] RH is a weak acid. Therefore the contribution of proton transfer is expected in the bonding between RH and 2- or 4-aminopyridine. In fact the ring stretching mode at 1600 cm^{-1} of deuterated 2-aminopyridine completely disappears on the addition of RH. A remarkable change in the ring of 2-aminopyridine was shown. On the other hand the ring stretching band of deuterated A at 1610 cm^{-1} still remains in the mixture solution with RH (Fig. 6). In the association of A with RH the ring system is not so affected by hydrogen bonding to the ring nitrogen atoms.

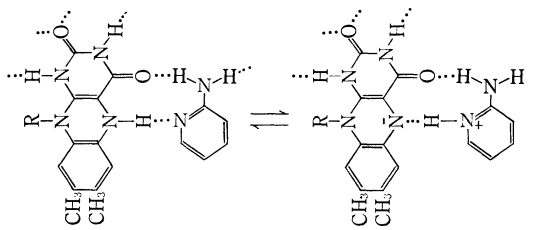

Association with Nicotinamide. As shown in Table 1 and Fig. 7 nicotinamide strongly interacts with RH. The symmetric and antisymmetric stretching bands of the amino group of NA at

Table 1. Association of reduced riboflavin tetraacetate with several compounds

Compound		Compound	
A	++	Aniline	—
G	—	Pyridine	—
C	++	Nicotinamide	+
U	—	Isonicotinamide	+
2-Aminopyridine	+++	1-Methyl-4-hydronicotinamide	+
3-Aminopyridine	+	Benzamide	—
4-Aminopyridine	++	*o*-Hydroxybenzamide	—
2-Aminopyrimidine	—	1-Phenylurea	—
4-Aminopyrimidine	+	Urethane	—

The + signs denote the strength of interaction of RH with association constants bigger than 10^8 (l/mol)^3 (+++), around 10^7 (++) and smaller than 10^7 (+).

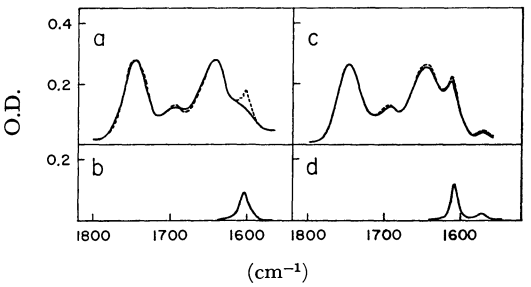

Fig. 6. Infrared spectra of the equimolar mixture solutions of RH and 2-aminopyridine (a), 2-aminopyridine (b), the equimolar mixture of RH and ethyladenine (c) and ethyladenine (d). The compounds are deuterated. The total concentration is 8×10^{-3}M and the path length is 0.5 mm.

3525 and 3410 cm^{-1} decrease in intensity. Although the amino group of NA is used for the association with RH, the scheme shown in the case of the RH-aminopyridine complex is not applicable. The ring nitrogen atom of aminopyridine is the acceptor site of proton in the RH-aminopyridine complex. Reduced *N*-methylnicotinamide whose nitrogen atom is blocked with a methyl group is expected not to interact with RH. However it shows an interaction with RH. Moreover the nitrogen atom of a nicotinic acid derivative is a weaker base than that of pyridine by 1—2 pK units (*ca.* pK_a 2—3).[22] The spectrum of NA in the 1800—1500 cm^{-1} region shows the carbonyl stretching band at 1680 cm^{-1}, which becomes strong and shifts to lower frequency when RH is added to the solution (Fig. 7). It is clear that a hydrogen bond is formed at the carbonyl group of an amide and the following structure can be proposed for the association.

20) A. Albert, R. Goldacre and J. Phillips, *J. Chem. Soc.*, **1948**, 2240.

21) P. Hemmerich and J. Spence, "Flavins and Flavoproteins," ed. by M. K. Slater, Elsevier, Amsterdam (1964), p. 82.

22) R. W. Green and H. K. Tong, *J. Amer. Chem. Soc.*, **78**, 4896 (1956).

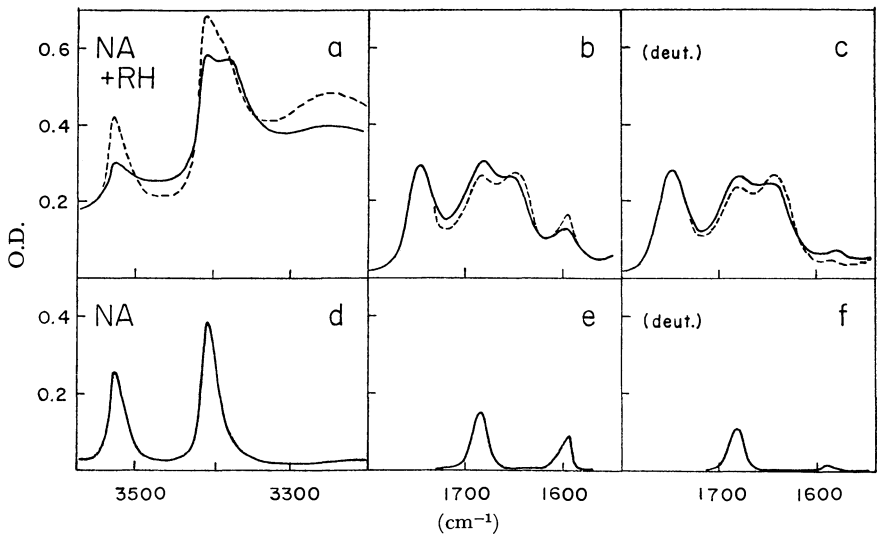

Fig. 7. Infrared spectra of nicotinamide (d, e, f) and the equimolar mixture solutions with reduced riboflavin tetraacetate (a,b,c). Solid line, observed spectra; dotted line, calculated sum of the individual spectrum. The concentration of each solute is 4×10^{-3}M and the path length is 5 mm for the 3500—3200 cm^{-1} region and 0.5 mm for the 1800—1550 cm^{-1} region.

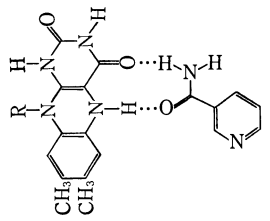

The amide group is almost planar, and there is resonance between the nitrogen and the carbonyl group which may be represented as $N-C=O \rightleftharpoons N^{+}=C-O^{-}$. In fact, infrared studies of nicotinamide-metal ion complexes suggest strongly that the oxygen atom in amides acts as a donor toward electron acceptors.[23,24] The pyridine ring increases the electron density at the oxygen atom of the amide group by inductive and resonance effects. Therefore the acceptor strength for proton at the oxygen atom of NA is expected to be greater than those of urea derivatives. This might be the reason why NA derivatives interact with RH and aliphatic urea derivatives do not.

Nicotinamide adenine dinucleotide in the oxidized form is thought to form a charge transfer complex with $FMNH_2$.[11,14] The visible spectrum of the mixture showed a broad band at 700 mμ which has been thought to be a charge transfer band. An additional absorption at 520 mμ of the mixture of $FMNH_2$ - *N*-methylnicotinamide iodide is also thought to be due to a charge transfer complex.[14] Any absorption, however, could not be detected in the longer wavelength region than 500 mμ in the chloroform system. It is doubtful whether the association found in the present experiment corresponds to the charge transfer complex of NAD^{+}-$FMNH_2$ or not.

Any interaction could not be detected between reduced *N*-methylnicotinamide and R. Radda and Calvin have also failed to observe the association between NADH and FMN which might occur under the catalysis of enzyme.[25] Although RH was found to be able to form strong hydrogen bonds with several compounds, the association of RH is probably of no physiological importance.

The authors wish to express their sincere thanks to Dr. M. Sedaka for the measurement of ESR spectra. Thanks are also due to Professor M. Tsuboi for his encouragement and advice. This work was partly supported by a grant from the U. S. Public Health Service GM10024-05.

23) K. Nagano, H. Kinoshita and A. Hirakawa, *Chem. Pharm. Bull.* (Tokyo), **12**, 1198 (1964).

24) F. R. Nordmeyer and H. Taube, *J. Amer. Chem. Soc.*, **88**, 4295 (1966).

25) G. K. Radda and M. Calvin, *Biochemistry*, **3**, 384 (1964).

BULLETIN OF THE CHEMICAL SOCIETY OF JAPAN VOL. 43 246—252 (1970)

Synthesis of Cyclic α-Amino Acids. IV. Syntheses of Adenine Nucleosides of 3-Amino-3-*C*-carboxy-3-deoxy-D-ribofuranose and 3-Amino-3-*C*-carboxy-3-deoxy-D-ribopyranose*1

Hiroaki YANAGISAWA, Mitsuhiro KINOSHITA, Saburo NAKADA and Sumio UMEZAWA

Department of Applied Chemistry, Faculty of Engineering, Keio University, Koganei-shi, Tokyo

(Received July 18, 1969)

9-(3′-Amino-3′-*C*-carboxy-3′-deoxy-β-D-ribofuranosyl)adenine (I) and 9-(3′-amino-3′-*C*-carboxy-3′-deoxy-β-D-ribopyranosyl)adenine (II) have been synthesized. They are the first examples of nucleoside-derivatives which have an α-amino acid structure in their furanose or pyranose ring. A masked derivative (VII) of α-D-*erythro*-pentofuranos-3-ulose was converted into a hydantoin derivative (IX), which was acetolyzed and then treated with dry hydrogen chloride to give an acylglycosyl chloride (XI). Condensation of this derivative with chloromercuri-6-benzamidopurine followed by hydrolysis afforded I. Treatment of the hydantoin derivative (IX) with methanolic hydrogen chloride followed by hydrolysis gave methyl 3-amino-3-*C*-carboxy-3-deoxy-α-D-ribopyranoside (XVII), which has been found to be identical with one of the isomers of methyl 3-amino-3-*C*-carboxy-3-deoxy-α-D-pentopyranoside previously reported. The 1-*O*-acetyl-3-*N*-benzoyl-2,4-di-*O*-benzoyl derivative of ethyl ester of this acid (XVII) was fused with 6-benzamidopurine in the presence of *p*-toluenesulfonic acid and followed by hydrolysis to afford II. Structural proofs for the new nucleoside-derivatives were obtained from their ultraviolet, infrared and nuclear magnetic resonance spectra.

In a previous paper[1] we described the synthesis of a new kind of monosaccharide-derivatives which have an α-amino acid structure in a pyranose. Synthesis of nucleoside-related compounds[2] is in progress in this laboratoy. Interest in nucleoside chemistry has led us to synthesize new derivatives of nucleosides which have an α-amino acid structure in their carbohydrate moiety. Puromycin (III), an antibiotic purine derivative, exhibits carcinostatic and trypanocidal activities. As a biologically active moiety of puromycin, 9-(3′-amino-3′-deoxy-β-D-ribofuranosyl)-6-dimethylaminopurine (IV) was demonstrated by Baker *et al.*[3] 3′-Amino-3′-deoxyadenosine[4] (V) was also found to be about twenty times as active as IV against the transplanted mammary adenocarcinoma of a C_3H mouse. Fukatsu and Umezawa[2] synthesized an adenosine nucleoside of 3-amino-3-deoxy-D-glucose and found it to have a weak anti-HeLa cell activity. As a result, we became interested in the synthesis of aminonucleoside-derivatives which have an α-amino acid structure in the ribofuranose or ribopyranose moiety. The present paper will present the synthesis of adenine nucleosides (I and II) of 3-amino-3-*C*-carboxy-3-deoxy-D-ribofuranose and of its pyranose-form.

The course of synthesis is summarized in Scheme 1.

Synthesis of 9-(3′-Amino-3′-*C*-carboxy-3′-deoxy-β-D-ribofuranosyl)adenine (I). The starting material, 5-*O*-benzoyl-1,2-*O*-isopropylidene-α-D-*erythro*-pentos-3-ulose (VII) was prepared from 5-*O*-benzoyl-1,2-*O*-isopropylidene-α-D-xylofuranose[5] (VI) by oxidation with Pfitzner-Moffatt reagent[6] in a good yield.

According to the Bucherer hydantoin synthesis, as reported by Hoyer,[7] VII was allowed to react with a mixture of potassium cyanide and ammonium carbonate under carbon dioxide atmosphere in an autoclave to afford 5-*O*-benzoyl-3-deoxy-1,2-*O*-isopropylidene-3-*C*-(spiro-5′-hydantoin)-α-D-pentofuranose (IX) as a major product, accompanied by the formation of 5-*O*-benzoyl-1,2-*O*-isopropylidene-

*1 A part of this paper was presented at the 22nd Annual Meeting of the Chemical Society of Japan, Tokyo, April 4, 1969.

1) H. Yanagisawa, M. Kinoshita and S. Umezawa, This Bulletin, **42**, 1719 (1969).

2) S. Fukatsu and S. Umezawa, *ibid.*, **38**, 1443 (1965).

3) B. R. Baker, J. P. Joseph and J. H. William, *J. Amer. Chem. Soc.*, **77**, 1 (1955).

4) B. R. Baker, R. E. Schaub and H. M. Kissman, *ibid.*, **77**, 5911 (1955).

5) P. A. Levene and A. L. Raymond, *J. Biol. Chem.*, **102**, 317 (1933).

6) K. E. Pfitzner and J. G. Moffatt, *J. Amer. Chem. Soc.*, **85**, 3027 (1963); J. S. Brimacombe, J. G. H. Bryan, A. Husain, M. Stacey and M. S. Tolley, *Carbohyd. Res.*, **3**, 318 (1967).

7) H. L. Hoyer, *Chem. Ber.*, **83**, 491 (1950).

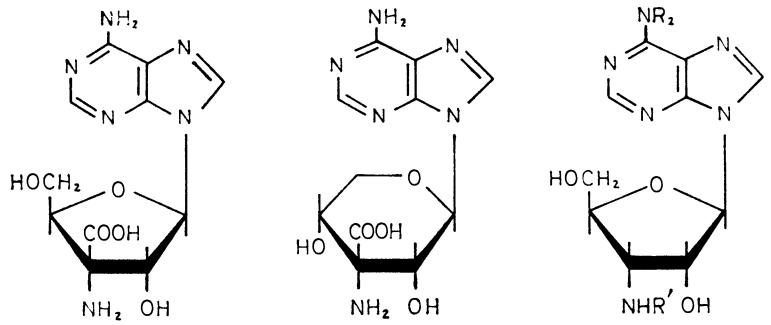

I II III (Puromycin): R = CH_3
R′ = CO·CH(NH_2) CH_2·C_6H_4·OCH_3-p
IV: R = CH_3, R′ = H
V: R = R′ = H

Chart 1

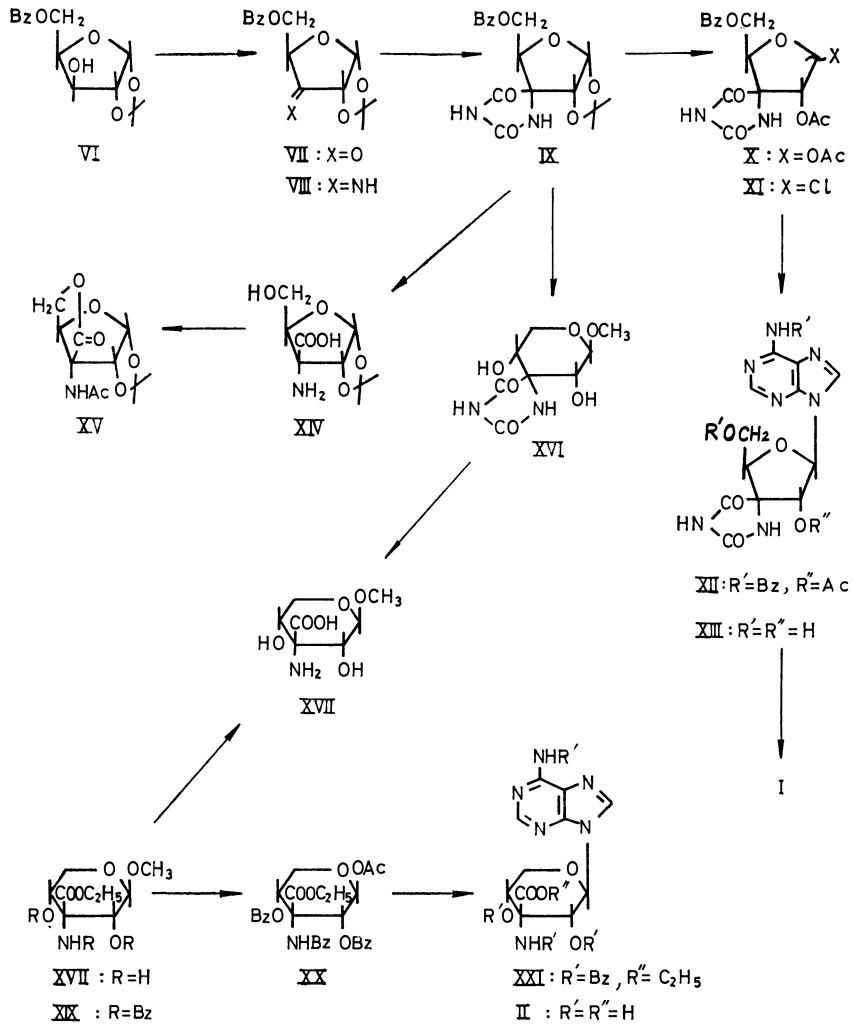

XVII: R = H
XIX: R = Bz
XX
XXI: R′ = Bz, R″ = C_2H_5
II: R′ = R″ = H

Scheme 1

α-D-*erythro*-pent-3-ulose imine (VIII). It is noteworthy that imine (VIII) was obtained as the main product by the usual Bucherer hydantoin synthesis which was carried out under atmospheric pressure without using carbon dioxide.

Hydrolysis of IX with barium hydroxide gave 3-amino-3-*C*-carboxy-3-deoxy-1,2-*O*-isopropylidene-α-D-ribofuranose (XIV), which, on *N*-acetylation with acetic anhydride in methanol, afforded a γ-lactone (XV) showing an infrared absorption band at 1780 cm^{-1}. This lactone-formation indicates that XIV has a structure of 3-*C*-carboxy derivative of 3-amino-3-deoxy-D-ribose and XV is 3-acetamido-3-*C*-carboxy-3-deoxy-1,2-*O*-isopropylidene-α-D-ribofuranose-γ-lactone.

Acetolysis of the hydantoin derivative (IX) with a mixture of acetic anhydride and acetic acid in the presence of concentrated sulfuric acid gave a glassy product of 1,2-di-*O*-acetyl-5-*O*-benzoyl-3-deoxy-3-*C*-(spiro-5′-hydantoin)-D-pentofuranose (X). Its NMR spectrum showed it to be predominantly α-anomer. The pure α-anomer was obtained by crystallization in hot acetone-diisopropyl ether. Assignment of the α-configuration to the product was based on the coupling constant ($J_{1,2}$=4.1 Hz) shown in its NMR spectrum.

Treatment of X with hydrogen chloride in ether gave a syrupy product of 2-*O*-acetyl-5-*O*-benzoyl-1-chloro-1,3-dideoxy-3-*C*-(spiro-5′-hydantoin)-D-pentofuranose (XI). The coupling constant ($J_{1,2}$=4.2 Hz) observed in the NMR spectrum of XI showed that the glycosyl chloride was again α-anomer.

Reaction of the glycosyl chloride (XI) with chloromercuri-6-benzamidopurine produced a masked nucleoside, *i.e.* 9-[2′-*O*-acetyl-5′-*O*-benzoyl-3′-deoxy-3′-*C*-(spiro-5′-hydantoin)-β-D-pentofuranosyl]-6-benzamidopurine (XII). Hydrolysis of XII with 1.5 mol of methanolic barium hydroxide at room temperature gave the deacylated hydantoin-nucleoside, 9-[3′-deoxy-3′-*C*-(spiro-5′-hydantoin)-β-D-pentofuranosyl]adenine (XIII). Further treatment of XIII with excess amount of methanolic barium hydroxide under reflux afforded the desired nucleoside, 9-(3′-amino-3′-*C*-carboxy-3′-deoxy-β-D-ribofuranosyl)adenine (I).

The structures of I and XIII were indicated by their elemental analyses, negative rotations and ultraviolet spectra which showed the characteristic maximum of 9-substituted adenine at 259 mμ. The β-configuration of the products could be interpreted adequately in terms of Tipson's "*trans* rule"[8] as extended by Baker and his co-workers.[9]

The resonance for the anomeric proton of XIII at τ 4.00 appears as a doublet with a coupling constant ($J_{1',2'}$=7.3 Hz) unusually larger than a value of ≦2 Hz[10] which is expected for a β(*trans*) anomeric configuration. However, a similar observation was recently made with 3′-*C*-methyladenosine ($J_{1',2'}$=8.2 Hz) and adenosine ($J_{1',2'}$=6.0 Hz), and discussed by Nutt *et al.*[11] It may be attributed to the deformation of the furanose ring from its usual conformation by the increase in bulky group eclipsing interaction in the nucleosides.

Synthesis of 9-(3′-Amino-3′-*C*-carboxy-3′-deoxy-β-D-ribopyranosyl)adenine (II). In a previous paper,[1] the synthesis of four diastereomers of methyl (−)-3-amino-3-deoxy-3-*C*-ethoxycarbonyl-pentopyranoside from methyl β-D-xylopyranoside has been reported. An isomer (XVIII), which showed the largest R_f-value among the four isomers on thin-layer chromatography (TLC), was hydrolyzed to afford methyl (−)-3-amino-3-*C*-carboxy-3-deoxypentopyranoside, and its partial structure was deduced from NMR spectroscopy and chemical results.

Hydantoin derivative (IX) was treated with methanolic hydrogen chloride to give methyl 3-deoxy-3-*C*-(spiro-5′-hydantoin)-β-D-pentopyranoside (XVI). The coupling constant ($J_{1,2}$=8.5 Hz) in its NMR spectrum indicated that it is a β-anomer. Hydrolysis of XVI with barium hydroxide gave methyl 3-amino-3-*C*-carboxy-3-deoxy-β-D-riboside (XVII). It has been found that this riboside was identical with the methyl (−)-3-amino-3-*C*-carboxy-3-deoxypentopyranoside, their infrared spectra, optical rotations and R_f-values on paper chromatography being identical and mixed melting point showing no depression. Consequently, the structure of isomer (XVIII) was established as methyl 3-amino-3-deoxy-3-*C*-ethoxycarbonyl-β-D-ribopyranoside.

Benzoylation of XVIII yielded methyl 3-benzamido-2,4-di-*O*-benzoyl-3-deoxy-3-*C*-ethoxycarbonyl-β-D-ribopyranoside (XIX), which, on acetolysis, gave the desired product, 1-*O*-acetyl-3-benzamido-2,4-di-*O*-benzoyl-3-deoxy-3-*C*-ethoxycarbonyl-β-D-ribopyranose (XX). Since, in the NMR spectra of XIX and XX, the small coupling constants of $J_{1,2}$=1.6—2.0 Hz and $J_{4,5a}$=1.6—2.0 Hz and a long range coupling constants of $J_{2,4}$=1.2—1.5 Hz were observed, both XIX and XX seem to exist in a 1C conformation.

Attempts to convert XX into an acylglycosyl halide with hydrogen chloride in ether and with hydrogen bromide in acetic acid were unsuccessful. However, when the condensation reaction of XX and benzamidopurine was carried out by the fusion

8) R. S. Tipson, *J. Biol. Chem.*, **130**, 55 (1939); B. R. Baker, J. P. Joseph, R. E. Schaub and J. H. Williams, *J. Org. Chem.*, **19**, 1780 (1954); J. J. Fox and I. Wempen, *Advan. in Carbohyd. Chem.*, **14**, 283 (1959); J. A. Montgomery and H. J. Thomas, *ibid.*, **17**, 315 (1962).

9) B. R. Baker, Ciba Foundation Symposium, Chem. Biol. of Purines, p. 120 (1957).

10) R. U. Lemieux and D. R. Lineback, *Ann. Rev. Biochem.*, **32**, 155 (1963).

11) R. F. Nutt, M. J. Dickinson, F. W. Holly and E. Walton, *J. Org. Chem.*, **33**, 1789 (1968).

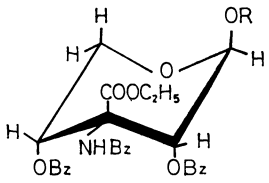

1C Conformer

XIX : R=CH_3

XX : R=Ac

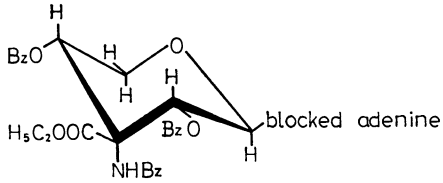

C1 Conformer

XXI

Chart 2

procedure as reported by Sato *et al.*,[12] using *p*-toluenesulfonic acid as a catalyst, and subjecting the product to chromatography on silica gel, 9-(3′-benzamido-2′,4′-di-*O*-benzoyl-3′-deoxy-3′-*C*-ethoxycarbonyl-β-D-ribopyranosyl)-6-benzamidopurine (XXI) was obtained in a 16.6% yield.

The structure of XXI was indicated by elemental analysis, ultraviolet spectrum, negative rotation and the coupling constant ($J_{1',2'}$=9.0 Hz) in NMR spectrum. The coupling constant ($J_{4',5'}$=9.0 Hz) and the absence of a long range coupling between H-2 and H-4 protons showed that XXI may exist in a Cl conformation. The conversion of conformation between XIX (or XX) and XXI may be due to the change of bulkiness of the aglycones.

Hydrolysis of XXI with barium hydroxide in aqueous methanol followed by purification through an ion-exchange column gave a crystalline nucleoside, 9-(3′-amino-3′-*C*-carboxy-3′-deoxy-β-D-ribopyranosyl)adenine (II) in a 32.7% yield.

Experimental

Thin layer chromatography (TLC) was conducted by the use of silica gel (Daiichi Pure Chemicals Co., Inc.). The prepared plates were activated at 110°C. The spray reagents used were 10% sulfuric acid and 0.5% pyridine solution of ninhydrin. NMR spectra were taken with a Varian A-60D spectrometer at the frequency of 60 MHz in deuteriochloroform and deuteriodimethyl sulfoxide (DMSO-d_6) with tetramethylsilane as an internal standard. Melting point determinations for the samples showing higher melting points than 200°C were carried out on a micro hot stage. Unless noted otherwise, all concentrations were carried out in a rotary evaporator at reduced pressure under 40°C.

5-*O*-Benzoyl-1,2-*O*-isopropylidene-α-D-*erythro*-pentos-3-ulose (VII). To a solution of 5-*O*-benzoyl-1,2-*O*-isopropylidene-α-D-xylofuranose (VI)[5] (10.5 g, 0.0357 mol) in dimethyl sulfoxide (10.5 m*l*) and dry benzene (100 m*l*) containing pyridine (1 m*l*) and trifluoroacetic acid (0.5 m*l*), dicyclohexylcarbodiimide (10.5 g, 0.0509 mol) was added under cooling, and the solution was stirred for 18 hr at room temperature. Ether (100 m*l*) was then added and insoluble matter was filtered off. The organic layer was washed with water (20 m*l*×5) and dried over sodium sulfate. Removal of the solvent yielded a brown syrup containing crystals of dicyclohexylurea. Crystallization from boiling ether afforded a crystalline 5-*O*-benzoyl-1,2-*O*-isopropylidene-α-D-*erythro*-pentos-3-ulose (VII); yield 6.44 g (61.8%), mp 96—97°C, $[\alpha]_D^{23}$ +135° (*c* 3.2, chloroform) [lit,[11] mp 98—99°C, $[\alpha]_D$ +136° (*c* 1, chloroform)].

5-*O*-Benzoyl-1,2-*O*-isopropylidene-α-D-*erythro*-pentos-3-ulose Imine (VIII). A solution of potassium cyanide (100 mg) and ammonium carbonate (350 mg) in water (1 m*l*) was added to a solution of VII (200 mg) in ethanol (1 m*l*) and the mixture was stirred at 50°C for one hour. Evaporation of ethanol from the reaction mixture afforded VIII as needles; yield 120 mg (60.3%). An analytical sample was obtained by recrystallization from diisopropyl ether; mp 162°C, $[\alpha]_D^{20}$ +36° (*c* 0.8, ethanol), ν_{max}^{Nujol} 3400, 1735, 1697 (C=N) cm^{-1}; τ^{CDCl_3} 4.03 (d, C-1H, $J_{1,2}$=3.4 Hz), 8.43, 8.65 [s,s, >$C(CH_3)_2$].

Found: C, 61.54; H, 5.67; N, 5.18%. Calcd for $C_{15}H_{17}NO_5$: C, 61.85; H, 5.88; N, 4.81%.

5-*O*-Benzoyl-3-deoxy-1,2-*O*-isopropylidene-3-*C*-(spiro-5′-hydantoin)-α-D-pentofuranose (IX). A suspension of VII (5.00 g), potassium cyanide (4.45 g) and ammonium carbonate (8.25 g) in methanol (40 m*l*) was stirred under an initial carbon dioxide pressure of 50 kg/cm^2 for 5 hr at room temperature and for additional 5 hr at 55—60°C in an autoclave. The content was evaporated to remove methanol and water (30 m*l*) was added to the residue. The mixture was acidified (pH 1—2) with 3N hydrochloric acid (24 m*l*) and extracted with four 40-m*l* portions of ethyl acetate. Evaporation of the ethyl acetate layer afforded a yellow syrup (5.77 g). TLC (diisopropyl ether) of the syrup showed a main spot (R_f 0.22). Chromatography on silica gel (80 g) in diisopropyl ether-butanone (10 : 1) gave fractions containing a total yield of 2.41 g of crude IX; R_f 0.22. Recrystallization from hot ethyl acetate (15 m*l*) plus diisopropyl ether (15 m*l*) gave the pure hydantoin derivative IX (1.64 g) melting at 195—196°C. From the mother liquor a second crop (0.39 g) melting at 194—195°C was obtained: total yield 32.7%, $[\alpha]_D^{20}$ +34° (*c* 1.02, ethanol), ν_{max}^{KBr} 3345, 3275, 1787, 1739, and 1695 cm^{-1}: τ^{CDCl_3} 0.91 [s, N(3)-H], 3.57 [s, N(1)-H], 3.96 (d, C-1H, $J_{1,2}$=3.7 Hz), 8.44, and 8.64 [s,s >$C(CH_3)_2$].

Found: C, 56.07; H, 5.38; N, 7.47%. Calcd for $C_{17}H_{18}N_2O_7$: C, 56.35; H, 5.01; N, 7.73%.

12) T. Sato, T. Shimadachi and Y. Ishido, *Nippon Kagaku Zasshi*, **81**, 1440 (1960).

Other fractions of R_f 0.49 were collected and evaporated. The residue was crystallized from diisopropyl ether to afford imine (VIII); yield 1.02 g (13.4%), mp 162°C.

3-Acetamido-3-*C*-carboxy-3-deoxy-1,2-*O*-isopropylidene-α-D-ribofuranose-γ-lactone (XV). A mixture of the hydantoin derivative (IX) (362 mg), barium hydroxide octahydrate (3.15 g) and water (24 ml) was stirred at 125°C for 12 hr. The reaction mixture was heated with ammonium carbonate (1.92 g) for 10 min at 110°C and followed by additional heating for 20 min with 1.23 g of ammonium carbonate. The resulting mixture was filtered to remove barium carbonate and the filtrate was washed with ether. The aqueous layer was evaporated to afford a colorless powder of crude 3-amino-3-*C*-carboxy-3-deoxy-1,2-*O*-isopropylidene-α-D-ribofuranose (XIV). A suspension of the crude XIV (430 mg) in methanol (5 ml) was treated with acetic anhydride (1 ml) for 3 hr at room temperature, after which the reaction mixture was evaporated. The residue was purified through a silica gel (10 g) column. Elution with ethyl acetate-benzene (1 : 1) afforded compound XV as prisms; yield 126 mg (50%). Recrystallization from acetone-diisopropyl ether; mp 147—148°C, $[\alpha]_D^{12.5}$ −59° (*c* 1.09, ethanol), ν_{max}^{KBr} 3265, 1780 (γ-lactone), 1657 and 1530 cm^{-1}; τ^{CDCl_3} 3.38 [s, N(1)–H], 4.00 (d, C–1H, $J_{1,2}$=4.0 Hz), 7.96 (s, CO–CH_3), 8.43 and 8.59 [s,s, >$CH(CH_3)_2$].

Found: C, 51.50; H, 5.79; N, 5.38%. Calcd for $C_{11}H_{15}NO_6$: C, 51.36; H, 5.88; N, 5.45%.

1,2-Di-*O*-acetyl-5-*O*-benzoyl-3-deoxy-3-*C*-(spiro-5′-hydantoin)-D-pentofuranose (X). To an ice-cooled solution of the hydantoin derivative (IX) (1.0 g) in acetic acid (7.5 ml) and acetic anhydride (7.5 ml) was added concentrated sulfuric acid (0.8 ml) dropwise and the solution was kept at room temperature for 22 hr. The reaction mixture was shaken with a mixture of 7% aqueous sodium acetate solution (40 ml), ice (10 g) and chloroform (20 ml) in a separating funnel. The aqueous layer was further extracted with three 10-ml portions of chloroform. The combined chloroform layers were dried over sodium sulfate and evaporated to give crude X (1.04 g, 92.7%) as a glassy solid, whose TLC (diisopropyl ether-butanone 3 : 1) showed a single spot having R_f-value of 0.43. A sample (490 mg) of the crude X was crystallized from hot diisopropyl ether-acetone to afford α-anomer of X (101 mg) as needles; mp 137—139°C; $[\alpha]_D^{20}$ +20° (*c* 0.88, ethanol); ν_{max}^{KBr} 3220, 1786, and 1725 cm^{-1}; τ^{CDCl_3} 3.39 (d, C–1H, $J_{1,2}$=4.1 Hz), 3.86 [s, N(1)–H], 4.71 (d, C-2H), 7.83 and 7.89 (s,s, $OCOCH_3$).

Found: C, 53.35; H, 4.63; N, 6.79%. Calcd for $C_{18}H_{18}N_2O_9$: C, 53.20; H, 4.47; N, 6.89%.

The NMR spectrum of the crude X showed that X existed mainly as an α-anomer.

2-*O*-Acetyl-5-*O*-benzoyl-1-chloro-1,3-dideoxy-3-*C*-(spiro-5′-hydantoin)-D-pentofuranose (XI). A mixture of X (500 mg), dry ether (19 ml) and acetyl chloride (0.3 ml) was saturated with dry hydrogen chloride under ice-salt cooling and allowed to stand for 38 hr in a refrigerator. The reaction mixture was evaporated at 30°C and the residual syrup was then dissolved in a small amount of absolute ether and again evaporated. This procedure was repeated three times to afford a syrup which was shown to consist of XI (R_f 0.40) by TLC using diisopropyl ether-butanone (3 : 1). The NMR signals for XI were observed at τ^{CDCl_3} 1.40 [s, N(3)–H], 3.39 (d, C–1H, $J_{1,2}$=4.2 Hz), 3.60 [s, N(1)–H], 4.72 (d, C–2H), and 7.84 (s, $OCOCH_3$).

6-Benzamido-9-[2′-*O*-acetyl-5′-*O*-benzoyl-3′-deoxy-3′-*C*-(spiro-5′-hydantoin)-β-D-pentofuranosyl]adenine (XII). A solution of XI (from 955 mg of X) in dry acetonitrile (35 ml) was stirred with chloromercuri-6-benzamidopurine (1.12 g) at 100—105°C for 2.5 hr. The reaction mixture was filtered while hot and insoluble matter was washed with acetonitrile (3×7 ml). The filtrate and washings were evaporated and the residue was chromatographed on silica gel (25 g). Elution with ethyl acetate-isopropyl alcohol (20 : 1) afforded the condensation product XII as a colorless powder, yield 442 mg (28.6%); $[\alpha]_D^{12.5}$ −32° (*c* 0.9, ethanol); λ_{max}^{MeOH} 230 and 280 mμ; ν_{max}^{KBr} 3280, and 1727 cm^{-1}.

9-[3′-Deoxy-3′-*C*-(spiro-5′-hydantoin)-β-D-pentofuranosyl]-adenine (XIII). To a solution of XII (2.22 g) in methanol (20 ml) was added 0.22N aqueous barium hydroxide solution (52 ml) and the solution was stirred for 24 hr at room temperature. Carbon dioxide gas was passed through the reaction mixture. The precipitate was filtered off and the filtrate evaporated. The residual colorless powder (2.16 g) was crystallized from water to yield crude XIII as pale-brown crytals; yield 472 mg (37%). A sample (300 mg) of the product was dissolved in hot water (10 ml). After removal of a small amount of insoluble matter by filtration, the filtrate was purified through an Amberlite IR-45 (OH^- type) column (1×18 cm). The fractions having an absorption peak at 260 mμ of UV-light were collected and concentrated. The resulting product (145 mg) was recrystallized from hot water to afford an analytical sample of XIII as colorless fine needles; mp 315—320°C (colored at 295°C), $[\alpha]_D^{25}$ −36° (*c* 0.77, dimethyl sufoxide), ν_{max}^{KBr} 1770, and 1725 cm^{-1}, $\lambda_{max}^{H_2O}$ 258.5 mμ (ε 20700), $\lambda_{max}^{0.1N\ HCl}$ 257 mμ (ε 20700) and $\lambda_{max}^{0.1N\ NaOH}$ 259.5 mμ (ε 19900); τ^{DMSO} 4.00 (d, C–1′H, $J_{1',2'}$=7.3 Hz), and 5.07 (d, C–2′H).

Found: C, 42.88; H, 4.54; N, 28.98%. Calcd for $C_{12}H_{13}N_7O_5$; C, 42.98; H, 3.91; N, 29.25%.

9-(3′-Amino-3′-*C*-carboxy-3′-deoxy-β-D-ribofuranosyl)-adenine (I). A mixture of XII (442 mg), methanol (5 ml), barium hydroxide octahydrate (1.24 g) and water (20 ml) was refluxed under stirring for 6.5 hr, after which ammonium carbonate (2.3 g) was added in portions and the mixture was heated for 30 min at 120°C. Barium carbonate was removed by filtration and washed with hot water. The filtrate and washings were collected and evaporated. The residual powder was purified through an Amberlite CG-50 column (pyridine type 1.2×20 cm) using buffer solutions, acetic acid-pyridine-water (2 : 3 : 1000 and 1 : 5 : 500). Fractions containing the product were pooled and concentrated. The residue (55 mg) was recrystallized from water to give an analytically pure sample of IV; mp 202—205°C (decomp.), $[\alpha]_D^{12.5}$ −30° (*c* 0.4, water), ν_{max}^{KBr} 3400, 3140, 1642, and 1600 cm^{-1}, $\lambda_{max}^{H_2O}$ 259 mμ (ε 14900), $\lambda_{max}^{0.1N\ HCl}$ 257 mμ (ε 14800), $\lambda_{max}^{0.1N\ NaOH}$ 260 mμ (ε 15600).

Found:[13] C, 42.71; H, 4.65; N, 27.34%. Calcd for $C_{11}H_{14}N_6O_5$: C, 42.58; H, 4.55; N, 27.09%.

Methyl 3-Deoxy-3-*C*-(spiro-5′-hydantoin)-β-D-pen-

13) The sample was dried over phosphorus pentoxide at 150°C/3 mmHg.

topyranoside (XVI). A suspension of the hydantoin derivative (IX) (640 mg) in 1N methanolic hydrogen chloride (25 ml) was refluxed for 35 hr, after which the reaction mixture was neutralized with basic lead carbonate and filtered. The filtrate was evaporated and the residue (510 mg) was recrystallized from methanol-ethyl acetate to afford XVI as colorless fine crystals; yield 130 mg(31%). An analytically pure sample was obtained by recrystallization from the same solvent as mentioned above; mp 288°C (decomp.), $[\alpha]_D^{12.5}$ −34° (*c* 2.48, water), ν_{max}^{KBr} 1755 (sh.), 1730, and 1717 cm^{-1}, τ^{D_2O} 5.56 (d, C-1H or C-2H, $J_{1,2}$=8.5 Hz), 6.29 (d, C-1H or C-2H) and 6.41 (s, OCH_3).

Found: C, 41.43; H, 5.28; N, 12.08%. Calcd for $C_8H_{12}N_2O_6$: C, 41.38; H, 5.21; N, 12.07%.

Methyl 3-Amino-3-*C*-carboxy-3-deoxy-β-D-ribopyranoside (XVII). A mixture of XVI (130 mg), barium hydroxide octahydrate (707 mg) and water (5 ml) was heated at 65—70°C for 20 hr, after which carbon dioxide gas was passed through the resulting mixture. The precipitate was removed by filtration and the filtrate evaporated. The residue (125 mg) was recrystallized from aqueous acetone to yield XVII as needles; yield 34 mg (29.4%), mp 250°C (decomp.), $[\alpha]_D^{15}$ −43° (*c* 1.0, water), R_f 0.13 (paper chromatography with *n*-butanol-acetic acid-water 4 : 1 : 1).

Methyl 3-Amino-3-deoxy-3-*C*-ethoxycarbonyl-β-D-ribopyranoside (XVIII). As reported in a previous paper,[1] periodate oxidation of methyl β-D-xylopyranoside followed by cyclization with ethyl nitroacetate and successive hydrogenation afforded a diastereomeric mixture of methyl (−)-3-amino-3-deoxy-3-*C*-ethoxycarbonylpentopyranoside, from which, an isomer (XVIII) of a R_f-value 0.73 on TLC could be obtained by column chromatography using ethyl acetate-ethanol (6 : 1). The amino acid which was obtained from XVIII by hydrolysis could also be described. Its partial structure could be described but a definite assignment of the configuration of the amino and carboxyl groups at C-3 could not be made. This amino acid[14] was now found to be identical with the above-mentioned amino acid XVII obtained from XVI by comparison of their melting points, infrared spectra and optical rotations.

Methyl 3-Benzamido-2,4-di-*O*-benzoyl-3-deoxy-3-ethoxycarbonyl-β-D-ribopyranoside (XIX). To a solution of XVIII (3.45 g) in dry pyridine (94 ml) was added benzoyl chloride (8.7 ml) under ice-cooling and kept for 18 hr at room temperature. The reaction mixture was poured into ice-water and extracted with four 50-ml portions of chloroform. The organic layer was washed with saturated aqueous potassium hydrogen sulfate and potassium hydrogencarbonate and evaporated to give a brown syrup. Purification through a silica gel column (200 g, 3.8×40 cm), eluting with *n*-hexane-butanone (5 : 1, 4 : 1 and 3 : 1) gave XIX (3.76 g, 46.4%) as a yellow syrup, which was crystallized by treatment with diisopropyl ether. Recrystallization from diisopropyl ether afforded an analytical sample; mp 135—136°C, $[\alpha]_D^{21}$ −64.3° (*c* 1.32, chloroform), ν_{max}^{KBr} 3415, 1745, 1724, 1673 cm^{-1}; τ^{CDCl_3} 2.98 (s, N-H), 3.72 (m, C-4H), 4.40 (d,d, C-2H, $J_{1,2}$=1.6 Hz, $J_{2,4}$= 1.5 Hz), 5.00 (d, C-1H), 5.39 (d,d, C-5H, $J_{4,5}$=2.0 Hz, $J_{5a,5e}$=12.9 Hz), 5.61 (q, ester CH_2, J=7.3 Hz), 5.90 (d,d, C-5H, $J_{4,5}$=1.7 Hz), 6.56 (s, OCH_3) and 8.66 (t, ester CH_3).

Found: C, 66.06; H, 5.37; N, 2.80%. Calcd for $C_{30}H_{29}NO_9$: C, 65.80; H, 5.39; N, 2.56%.

1-*O*-Acetyl-3-benzamido-2,4-di-*O*-benzoyl-3-deoxy-3-*C*-ethoxycarbonyl-β-D-ribopyranose (XX). A mixture of XIX (500 mg), acetic acid (11 ml), acetic anhydride (11 ml) and concentrated sulfuric acid (0.7 ml) was stirred until the solid was dissolved completely. After standing for 2 days at room temperature, the resulting solution was treated with sodium acetate (3 g) under stirring for 30 min and evaporated. To the residue was added water (15 ml) and ether (15 ml) and the mixture was shaken. The separated ether-layer was washed with a 10% sodium hydrogencarbonate solution, dried over sodium sulfate and evaporated. The residual yellow syrup (585 mg), which was a mixture of two products of R_f-value 0.62 and 0.29 on TLC (*n*-hexane-butanone 3 : 1), was chromatographed on silica gel (20 g). Elution with the same solvent system gave two kinds of pale-yellow syrups; A 168 mg (R_f (0.62) and B 261 mg (R_f 0.29). Treatment of B with diisopropyl ether afforded XX as colorless needles; yield 186 mg (35.4%), mp 155—157°C, $[\alpha]_D^{21}$ −59° (*c* 1.16, chloroform), τ^{CDCl_3} 2.96 (s, N-H), 3.63 (d, C-1H, $J_{1,2}$=2.0 Hz), 3.72 (m, C-4H), 4.38 (d,d, C-2H, $J_{2,4}$=1.2 Hz), 5.25 (d,d, C-5H, $J_{4,5}$=2.0 Hz, $J_{5a,5e}$= 13.1 Hz), 5.60 (q, ester CH_2, J=7.3 Hz), 5.81 (d,d, C-5H, $J_{4,5}$= 1.6 Hz), 7.85 (s, $COCH_3$) and 8.61 (t, ester CH_3).

Found: C, 65.12; H, 5.42; N, 2.62%. Calcd for $C_{31}H_{29}NO_{10}$: C, 64.69; H, 5.08; N, 2.43%.

An additional amount of XX (73 mg) was obtained from the syrup A by treatment with acetic anhydride, acetic acid and sulfuric acid as described above; total yield 49.2%.

6-Benzamido-9-(3′-benzamido-2′,4′-di-*O*-benzoyl-3′-deoxy-3′-*C*-ethoxycarbonyl-β-D-ribopyranosyl)-purine (XXI). A mixture of XX (362 mg) and 6-benzamidopurine (181 mg) was heated to cause it to melt in an oil bath (*ca.* 155°C). *p*-Toluenesulfonic acid (15 mg) was added to the melt and the mixture was heated for 30 min under reduced pressure (5 mmHg). After cooling, the solid mass was pulverized and extracted with ethanol. Evaporation of ethanol gave a glassy product (483 mg), which was then purified through a silica gel column (15 g, 1.2×29.5 cm) with chloroform-ethyl acetate mixtures (10 : 1, 8 : 1 and 3 : 1) to afford XXI as a colorless powder; yield 79 mg (16.6%). Since the product contained a small amount of insoluble matter in ethanol, the product was again treated with ethanol, filtered and the filtrate was concentrated to afford an analytically pure sample; mp 145—148°C, $[\alpha]_D^{8}$ −103°(*c* 0.46, ethanol), λ_{max}^{MeOH} 279 mμ (ε 20700), 230 mμ (ε 41300), τ^{CDCl_3} 2.86 (d, C-1′H or C-2′H, $J_{1',2'}$=9.1 Hz), 3.38 (d, C-1′H or C-2′H), 3.81 (d,d, C-4′H, $J_{4',5'_e}$=6.0 Hz, $J_{4',5'_a}$=9.0 Hz), 5.62 (q, ester CH_2, J=7.2 Hz), and 8.70 (t, ester CH_3).

Found: C, 64.55; H, 4.87; N, 10.38%. Calcd for $C_{41}H_{34}N_6O_9 \cdot C_2H_5OH$: C, 64.57; H, 4.91; N, 10.51%.

9-(3′-Amino-3′-*C*-carboxy-3′-deoxy-β-D-ribopyranosyl)adenine (II). To a solution of XXI (400 mg) in methanol (2.5 ml) was added 0.36N barium hydroxide solution (8.2 ml) and the mixture was kept for 2 days at 37°C. After evaporation of methanol, the residue was diluted with water and carbon dioxide gas was

14) Compound VIA-1 in Table 2 in the previous paper (Ref. 1).

passed through the solution for 30 min. Barium carbonnate was filtered off and the filtrate was washed with four 10-m*l* portions of ether. The aqueous layer was evaporated to afford a colorless powder (558 mg), which was purified through an Amberlite CG-50 pyridine type column (1×15 cm) by using buffer solutions, pyridine-acetic acid-water (1.5 : 1.0 : 1000 and 10 : 2.0 : 1000). Fractions containing the nucleoside was concentrated and the residue (249 mg) was recrystallized from water to yield colorless prisms of II (53 mg, 32.7%); mp 247°C (decomp.). $[\alpha]_D^{18}$ −20° (*c* 0.22, 0.1N HCl), $\lambda_{max}^{H_2O}$ 260 mμ (ε 15700), $\lambda_{max}^{0.1N\ HCl}$ 257 mμ (ε 14400) and $\lambda_{max}^{0.1N\ NaOH}$ 261 mμ (ε 13400).

Found:[13] C, 42.21; H, 4.75; N, 26.74%. Calcd for $C_{11}H_{14}N_6O_5$: C, 42.58; H, 4.55; N, 27.09%.

BULLETIN OF THE CHEMICAL SOCIETY OF JAPAN VOL. 43 252—257 (1970)

Studies of the Thiocarbonyl Compounds. I. Syntheses and Thermal Rearrangement of *O,S*-Diaryl Dithiocarbonates*1

Yoshiaki ARAKI

Department of Chemistry, Faculty of Science, Kyoto University, Sakyo-ku, Kyoto

(Received July 22, 1969)

Various *O,S*-diaryl dithiocarbonates with the general formula of *p*-X-C_6H_4-S-C(=S)-O-C_6H_4-Y-*p* (I) were prepared. When these substances were kept at an elevated temperature, they rearranged smoothly to *S,S*-diaryl dithiocarbonates of this general formula: *p*-X-C_6H_4-S-C(=O)-S-C_6H_4-Y-*p* (II). Kinetic studies showed that the rearrangement followed fairly good first-order kinetics. The rate constants in diphenyl ether at 200°C increased in the order: $Y=OCH_3<CH_3<H<Cl<COCH_3<CN<NO_2$. The entropies of activation were negative, and no crossover products were obtained. A four-membered cyclic structure can be suggested as the transition state for this rearrangement.

It is well known that the reaction mechanism of the formation of olefins by the pyrolysis of xanthate esters which have a β-hydrogen atom in the alcohol moiety, commonly called the Chugaev reaction, is an intramolecular *cis* elimination through a cyclic transition state.[1] On the other hand, xanthate esters which have no β-hydrogen atom, such as methyl benzyl xanthate, rearrange on pyrolysis to give dithiolcarbonates.[2] However, it has been thought that this reaction is unusual, and no mechanistic work has yet been made. It seemed that it would be interesting to investigate whether *O,S*-diaryl dithiocarbonates (I) also rearrange to *S,S*-diaryl dithiocarbonates (II) at elevated temperatures.

$$\underset{\text{(I)}}{\text{Ar-S-C(=S)-O-Ar'}} \xrightarrow{\Delta} \underset{\text{(II)}}{\text{Ar-S-C(=O)-S-Ar'}}$$

The present author synthesized twelve compounds I (I-1—I-12), all of them were new compounds except the diphenyl ester (I-3);[3] he also studied the kinetics of their thermal rearrangements in order to establish the reaction mechanism.

Results and Discussion

Syntheses of *O,S*-Diaryl Dithiocarbonates (I). The compounds I were synthesized by the

Method A: $\text{Ar-S-C(=S)-Cl} + \text{KO-Ar'} \longrightarrow \text{I} + \text{KCl}$

Method B: $\text{Ar-S-C(=S)-Cl} + \text{HO-Ar'} + \text{pyridine} \longrightarrow \text{I} + \text{pyridine}\cdot\text{HCl}$

Method C: $\frac{1}{2}(\text{Ar-S})_2\text{Pb} + \text{Cl-C(=S)-O-Ar'} \longrightarrow \text{I} + \frac{1}{2}\text{PbCl}_2$

*1 Presented at the 21st Annual Meeting of the Chemical Society of Japan, Osaka, April, 1968.

1) H. R. Nace, "Organic Reactions," Vol. 12, p. 57 (1962).

2) a) P. V. Laakso, *Suomen Kemistilehti*, **13B**, 8 (1940); *Chem. Abstr.*, **34**, 5059 (1940); b) P. V. Laakso, *Suomen Kemistilehti*, **16B**, 19 (1943); *Chem. Abstr.*, **40**, 4687 (1946); c) G. Bulmer and F. G. Mann, *J. Chem. Soc.*, **1945**, 666.

3) a) G. Daccomo, *Annali di Chimica e di Farmacologia*, **13**, 273; *Chem. Zentr.*, **1891II**, 532; b) G. Daccomo, *Annali di Chimica e di Farmacologia*, **16**, 129; *Chem. Zentr.*, **1892II**, 827; c) M. H. Rivier, *Bull. Soc. Chim. Fr.*, [3] **35**, 837 (1906); d) M.H. Rivier, *ibid.*, [4] **1**, 733 (1907).

TABLE 1. *O,S*-DIARYL DITHIOCARBONATES

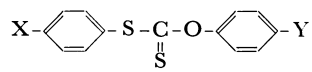

Compd. No.	X	Y	Appearance	Mp[a] °C	Method	Yield %	$\lambda_{max}^{CHCl_3}$ (mμ) ($\varepsilon \times 10^{-4}$)	Formula	Analysis (%) Found (Calcd) C	H	S
I-1	H	OCH_3	pale yellow prisms[b]	48.5—49.5	A	89	286 (1.28)	$C_{11}H_{12}O_2S_2$	61.08 (60.84)	4.36 (4.38)	22.92 (23.20)
I-2	H	CH_3	pale yellow plates[b]	59.5—60.5	A	85	289 (1.08)	$C_{11}H_{12}OS_2$	64.40 (64.58)	4.48 (4.65)	24.56 (24.63)
I-3	H	H	pale yellow plates[b]	42.5—43.0[c]	A C	100 63	289.5 (1.05)	$C_{13}H_{10}OS_2$	63.14 (63.38)	4.02 (4.09)	25.66 (26.03)
I-4	H	Cl	pale yellow needles[b]	68.0—69.0	A	97	289 (1.06)	$C_{13}H_9ClOS_2$	55.71 (55.61)	3.16 (3.23)	22.61 (22.84)
I-5	H	$COCH_3$	pale yellow plates[b]	93.0—94.0	A	93	286 (1.24)	$C_{15}H_{12}O_2S_2$	62.65 (62.47)	4.24 (4.19)	22.06 (22.24)
I-6	H	CN	pale yellow plates[b]	108.0—109.0	A	96	290 (1.06)	$C_{14}H_9NOS_2$	61.68 (61.97)	3.17 (3.34)	23.43 (23.63)
I-7	H	NO_2	pale yellow plates[b]	111.0—111.5	A	91	287.5 (1.75)	$C_{13}H_9NO_3S_2$	53.39 (53.59)	3.01 (3.11)	21.80 (22.01)
I-8	OCH_3	NO_2	pale yellow plates[b]	102.5—103.5	A	95	282.5 (1.79)	$C_{14}H_{11}NO_4S_2$	52.25 (52.32)	3.33 (3.45)	19.75 (19.95)
I-9	CH_3	NO_2	pale yellow prisms[b]	103.0—103.5	A	96	288.5 (1.75)	$C_{14}H_{11}NO_3S_2$	54.81 (55.07)	3.44 (3.36)	20.85 (21.00)
I-10	Cl	NO_2	pale yellow needles[b]	105.5—106.5	A	91	287 (1.79)	$C_{13}H_8ClNO_3S_2$	48.03 (47.93)	2.72 (2.48)	19.80 (19.68)
I-11	NO_2	NO_2	orange prisms[d]	170.0—171.0	B	95	272 (2.36)	$C_{13}H_8N_2O_5S_2$	46.13 (46.42)	2.49 (2.40)	19.13 (19.07)
I-12	NO_2	Cl	pale yellow needles[b]	109.0—110.0	B	90	272 (1.60)	$C_{13}H_8ClNO_3S_2$	48.08 (47.93)	2.73 (2.48)	19.43 (19.68)

a) All melting points are uncorrected. b) Recrystallized from ethanol.
c) Ref. 3c and Ref. 3d; mp 51°C. d) Recrystallized from acetone-ethanol.

reaction of a substituted phenol with an aryl chlorodithioformate (Methods A and B). In order to establish the structure of the compounds I, another method (Method C) was also used; in this aryl chlorothionoformates were treated with lead thiophenolates, giving the compounds I. By these three methods, the various compounds I were obtained in good yields. The data are shown in Table 1.

Thermal Rearrangement. In order to examine the possibility of the thermal rearrangement, the compounds I were kept at 200°C without any solvent under a nitrogen atmosphere; the reaction mixture was then analyzed by thin-layer chromatography on silica gel. It was found that the compounds I were gradually converted to other compounds. The elemental analysis showed that the composition of the products was identical with that of original compounds I. The infrared spectra of the products showed peaks at *ca.* 1720 cm^{-1} ($\nu_{C=O}$). These data suggest that the products are *S,S*-diaryl dithiocarbonates (II).

Identification of the Thermal Rearrangement Products. In order to identify the thermal rearrangement products, the compounds II were synthesized by Methods D and E. The results are shown in Table 2. The compounds which

Method D: $\mathrm{Ar\text{-}S\text{-}\overset{\overset{O}{\|}}{C}\text{-}Cl} + \frac{1}{2}\mathrm{Pb(S\text{-}Ar')_2} \longrightarrow$ II $+ \frac{1}{2}\mathrm{PbCl_2}$

Method E: $\mathrm{Ar\text{-}S\text{-}\overset{\overset{O}{\|}}{C}\text{-}Cl} + \mathrm{HS\text{-}Ar'} +$ $\longrightarrow$ II + $\cdot$HCl

were produced by heating the compounds I at 200°C were identified with the compounds II by mixed-melting-point tests and by a comparison of the IR spectra.

Kinetics of the Rearrangement. In order to clarify the influence of the substituents upon the rearrangement rates, the kinetics of the rearrangement were investigated in a diphenyl ether solution. The rates were followed by the ampoule technique and were determined by measuring the amounts of the remaining reactants, I, and of the products, II, by UV spectrophotometry. It was found that the rearrangement followed fairly good first-order kinetics. A typical run is shown in Table 3 and Fig. 1. The first-order rate constants

Table 2. *S,S*-Diaryl dithiocarbonates

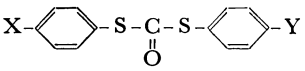

Compd. No.	X	Y	Appearance	Mp[a] °C	Method	Yield %	$\lambda_{max}^{CHCl_3}$ (mμ) ($\varepsilon \times 10^{-4}$)	Analysis[b] (%) C Found	H Found	S Found
II-1	H	OCH_3	colorless prisms[c]	65.5—66.0	E	98	—[d]	60.94	4.38	22.92
II-2	H	CH_3	colorless needles[c]	69.5—73.5	E	98	—[d]	64.83	4.71	24.42
II-3	H	H	colorless prisms[c]	41.5—42.0[e]	D	91	—[d]	63.12	4.37	25.78
II-4	H	Cl	colorless prisms[c]	61.5—62.0	E	100	—[d]	55.67	3.24	22.72
II-5	H	$COCH_3$	colorless plates[c]	34.0—35.0	E	100	277 (1.56)	62.54	4.34	22.07
II-6	H	CN	colorless needles[c]	69.0—70.0	E	100	276 (1.50)	62.18	3.26	23.76
II-7	H	NO_2	colorless plates[c]	68.7—69.2	D E	100 100	297.5(1.28)	53.85	3.37	21.84
II-8	OCH_3	NO_2	colorless needles[c]	108.0—109.0	E	97	298 (1.50)	52.05	3.27	19.82
II-9	CH_3	NO_2	colorless needles[c]	95.0—95.5	E	98	298 (1.35)	54.81	3.36	20.90
II-10	Cl	NO_2	colorless needles[f]	128.0—129.0	E	99	294.5(1.40)	48.16	2.48	19.69
II-11	NO_2	NO_2	pale yellow needles[g]	191.5—192.5[h]	E	100	297 (2.25)	46.12	2.41	18.78

a) All melting points are uncorrected.
b) In each compound, the molecular formula and the theoretical values for the elemental analysis are equal to those of the corresponding I in Table 1.
c) Recrystallized from ethanol.
d) No absorption maximum within the measurable range.
e) Ref. 3c; mp 41°C, Ref. 4; mp 43°C, Ref. 5; mp 41—43°C.
f) Recrystallized from acetic acid.
g) Recrystallized from benzene.
h) Ref. 5; mp 183.5—184.5°C.

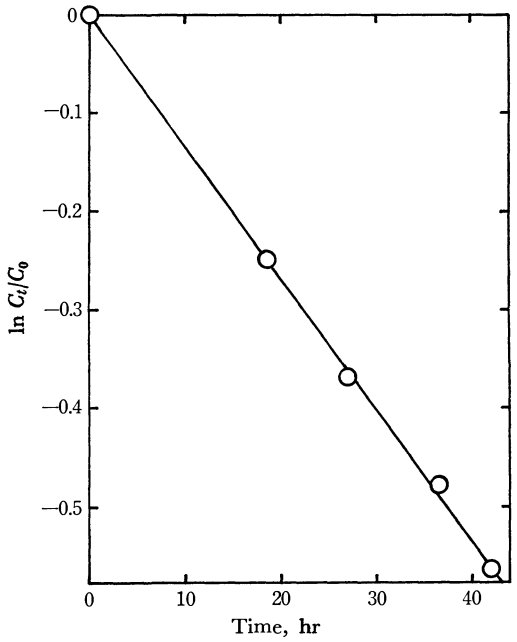

Fig. 1. Rate plot for the rearrangement of *O,S*-diphenyl dithiocarbonate at 200.5—0.1°C.

Table 3. Rearrangement of *O,S*-diphenyl dithiocarbonate (I-3) at 200.5±0.1°C

Time (sec)	% of I-3 remaining	$k \times 10^6$ (sec^{-1})
0	100	
666000	78.0	3.73
972000	69.3	3.78
1314000	62.1	3.63
1512000	57.1	3.71

Table 4. First-order rate constants of the rearrangement at 200.5±0.1°C

Compd. No.	$k \times 10^6$ (sec^{-1})	Relative rates
I-1	0.830	0.224
I-2	1.97	0.531
I-3	3.71	1.00
I-4	3.89	1.05
I-5	25.5	6.87
I-6	51.4	13.6
I-7	106	28.6

were derived from the slopes of the straight lines obtained by plotting $\ln C_t/C_0$ against the time, where C_t and C_0 are the concentrations of I at time t and time 0 respectively. The data are summarized in Tables 4, 5, and 6. From these data,

4) J. E. Purvis, H. O. Jones and H. S. Tasker, *J. Chem. Soc.*, **97**, 2287 (1910).
5) J. R. Cox, Jr., C. L. Gladys, L. Field and D. E. Pearson, *J. Org. Chem.*, **25**, 1083 (1960).

Table 5. First-order rate constants of the rearrangement at 170.0±0.1°C

Compd. No.	$k\times10^6$ (sec^{-1})	Relative rates
I-8	8.87	1.07
I-9	8.89	1.07
I-7	8.27	1.00
I-10	6.05	0.732
I-11	3.54	0.428

Table 6. Activation parameters and rate constants of the rearrangement

Compd. No.	$k\times10^6$ (sec^{-1}) at 230.0±0.1°C	E_a (kcal/mol)	$\Delta S^{\neq}$ (e.u.)
I-1	9.57	39.2	−6.5
I-3	40.5	38.3	−5.4
I-7	—	34.7	−5.3

the energies and entropies of activation were calculated for some of the compounds I. The values are given in Table 6.

In Table 4 it can be observed that electron-withdrawing substituents attached to the migrating group accelerate the rearrangement. The logarithms of the rate constants in Table 4 were plotted against Hammett's σ values (Fig. 2). By means of the method of least-squares, the best straight line was obtained ($\rho=1.87$).

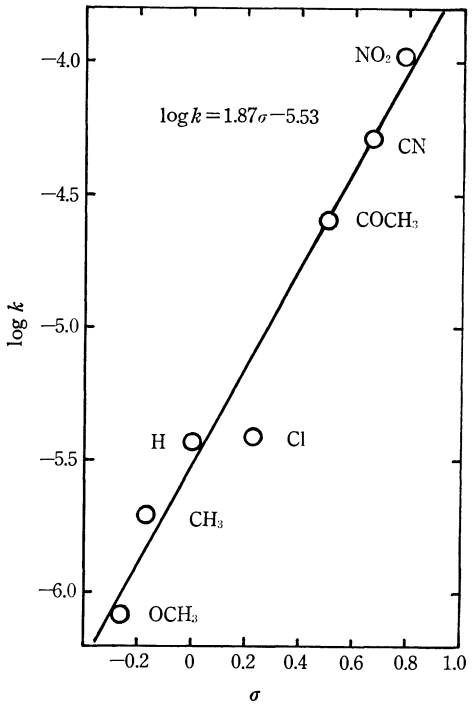

Fig. 2. Hammett plot for rate of rearrangement of 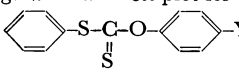 at 200.5±0.1°C.

On the other hand, the data in Table 5 show that electron-donating substituents attached to the phenylthio moiety accelerate the reaction. Figure 3 shows a Hammett plot of log k in Table 5 against the σ values ($\rho=-0.41$).

In order to establish the mechanism of the rearrangement of the compounds I, it was necessary to determine whether the mechanism of the rearrangement is intermolecular or intramolecular. A crossover reaction was performed with two compounds of I. That is, an equimolar mixture of I-3 and I-12*[2] was heated without any solvent at 230°C under a nitrogen atmosphere. If the rearrangement is intermolecular, such crossover products as II-4 and/or II-7 should be detected in the crossover reaction mixture in addition to II-3 and II-10. In order to confirm this, the crossover reaction mixture obtained was analyzed by thin-layer chromatography on silica gel. The chromatograms of that reaction mixture, however, showed no detectable amounts of II-4 and/or II-7. This finding suggests that the rearrangement is intramolecular.

Furthermore, if the rearrangement proceeds through an intimate ion-pair,[6] such as in Scheme 1, the order of the rate constants should be the inverse of the experimental results shown in Table 4, because the stability of the aryl cation, which contributes to the reaction rate, should decrease in

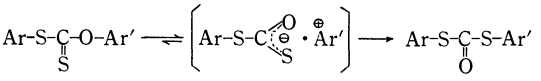

Scheme 1

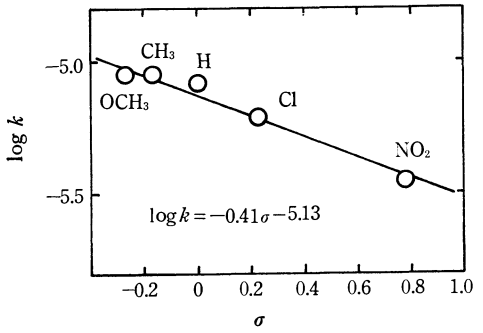

Fig. 3. Hammett plot for rate of rearrangement of 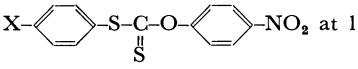 at 170.0±0.1°C.

*[2] I-3 and I-12 were chosen because of their similar rate constants (rate constant of I-12 is 3.39×10^{-5} sec^{-1} at 230.0°C).

6) a) T. Taguchi and M. Nakao, *Tetrahedron*, **18**, 245 (1962); b) T. Taguchi, Y. Kawazoe and M. Nakao, *Tetrahedron Lett.*, **1963**, 131; c) T. Taguchi, Y. Kawazoe, K. Yoshihira, H. Kanayama, M. Mori, K. Tabata and K. Harano, *ibid.*, **1965**, 2717.

the order: $Y=OCH_3>CH_3>H>Cl>COCH_3>CN>NO_2$.

When these results are taken into consideration, it seems reasonable to conclude that the rearrangement of the compounds I take place through an intramolecular four-membered cyclic transition state, as in Scheme 2:

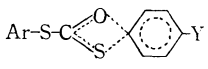

Scheme 2

Moreover, since the formation of the four-membered cyclic transition state requires a restriction of the rotation, the entropy should decrease in going from the reactants to the transition state. In fact, as is shown in Table 6, the entropies of activation are negative. These data are in agreement with this conclusion. Furthermore, the entropies of activation obtained for the rearrangements of arylimino ethers,[7] diaryl thionocarbonates,[8] and aryl *N,N*-dialkylthionocarbamates,[8e,9] all of which are regarded as having four-membered cyclic transition states, are in the same range as these data. This fact also supports this conclusion.

Consequently, a four-membered cyclic structure (Scheme 2) formed by a nucleophilic attack of the thiocarbonyl sulfur atom on the migrating aromatic ring can be considered to be the transition state in the rearrangement of the compounds I.

This conclusion is also supported by the kinetic data. That is, the positive slope of the straight line in Fig. 2 shows that this rearrangement is a nucleophilic reaction. The increased reactivity in Table 4 can be explained as follows: Since electron-withdrawing substituents decrease the electron density on the reaction center, these substituents facilitate a nucleophilic attack of the thiocarbonyl sulfur atom. On the other hand, electron-donating groups attached to the phenylthio moiety make the electrons on the thiocarbonyl sulfur atom more available for a nucleophilic attack, so these groups accelerate the rearrangement (Table 5).

Investigations of similar rearrangement reactions involving cyclic transition states are now in progress. These results will be reported elsewhere later.

7) a) K. B. Wiberg and B. I. Rowland, *J. Amer. Chem. Soc.*, **77**, 2205 (1955); b) J. W. Schulenberg and S. Archer, "Organic Reactions," Vol. 14, p. 1 (1965).

8) a) A. Schönberg and L. Vargha, *Ber.*, **63**, 178 (1930); b) A. Schönberg, L. Vargha and W. Paul, *Ann.*, **483**, 107 (1930); c) H. R. Al-Kazimi, D. S. Tarbell and D. Plant, *J. Amer. Chem. Soc.*, **77**, 2479 (1955); d) D. H. Powers and D. S. Tarbell, *ibid.*, **78**, 70 (1956); e) H. Kwart and E. R. Evans, *J. Org. Chem.*, **31**, 410 (1966).

9) a) J. D. Edwards and M. Pianka, *J. Chem. Soc.*, **1965**, 7338; b) M. S. Newman and H. A. Karnes, *J. Org. Chem.*, **31**, 3980 (1966); c) K. Miyazaki, *Tetrahedron Lett.*, **1968**, 2793; d) H. M. Relles and G. Pizzolato, *J. Org. Chem.*, **33**, 2249 (1968).

Experimental*3

Materials. The aryl chlorodithioformates were synthesized by the reaction of a corresponding thiophenol, thiophosgene, and sodium hydroxide according to a known method:[3d] *p*-methoxyphenyl-, orange red oil, bp 126—129°C/0.95 mmHg; *p*-methylphenyl-, orange red oil, bp 112—113°C/0.8 mmHg (lit,[10] bp 102—104°C/1.0 mmHg); phenyl-, orange red oil, bp 143—144°C/22 mmHg (lit,[3d] bp 135°C/15 mmHg); *p*-chlorophenyl-, orange red oil, bp 102—103°C/0.8 mmHg; *p*-nitrophenyl-, orange crystals, bp 144—145°C/0.8 mmHg, mp 45.0—46.0°C.

The aryl chlorothionoformates were also prepared by a known method:[3c] phenyl-, colorless oil, bp 74.0°C/5 mmHg (lit,[3c] bp 91°C/10 mmHg); *p*-nitrophenyl-, colorless plates (from *n*-hexane), mp 59.0—60.0°C (lit,[11] mp 59.0—60.0°C).

The aryl chlorothiolformates were prepared as follows: To a solution of 1 mol of phosgene and 1 mol of thiophenol in 600 m*l* of dry toluene, 1 mol of dry pyridine was added gradually under vigorous agitation. The temperature was kept at 20—30°C during the reaction period of 2 hr. Then, the reaction mixture was filtered and the solvent was removed under reduced pressure.*4 The residue was fractionated, and the product was obtained in a high yield: phenyl-, colorless oil, bp 110°C/21 mmHg (lit,[3d] bp 104°C/13 mmHg, bp 150°C/22 mmHg, bp 225—227°C/724 mmHg); *p*-nitrophenyl-, colorless needles (from *n*-hexane), mp 60.0—62.0°C.

***O,S*-Diaryl Dithiocarbonates (I).** The compounds I were prepared by three methods, A, B, and C. Method A was used most often. The results are listed in Table 1.

Method A. Example 1. *O*-(*p*-Nitrophenyl) *S*-(*p*-Methylphenyl) Dithiocarbonate (I-9). To a suspension of 3.54 g (0.02 mol) of potassium *p*-nitrophenolate in 25 m*l* of dry acetone at 0°C in an ice-water bath, there was added, all at once, 3.93 g (0.02 mol) of *p*-methylphenyl chlorodithioformate in 20 m*l* of dry acetone. The resulting mixture was then stirred for 1 hr, with the temperature kept at 5—10°C. Then the cooling bath was removed, and the reaction mixture was stirred for 2 hr at room temperature and poured into *ca.* 500 m*l* of cold water. In this way 5.85 g (96%) of pale yellow crystals with mp 97—99°C was obtained. Recrystallization from ethanol gave 4.40 g (72%) of pale yellow prisms with mp 103.0—103.5°C.

Example 2. *O,S*-Diphenyl Dithiocarbonate (I-3). To 50 m*l* of cooled absolute ethanol, there was added, in small portions, 3.9 g (0.1 mol) of potassium. After hydrogen evolution had ceased, 9.4 g (0.1 mol) of phenol was added. The resulting solution was then added gradually with continuous stirring to a cooled solution of 18.9 g (0.1 mol) of phenyl chlorodithioformate in 50 m*l* of absolute ethanol in an ice-water bath, with the temperature kept at 5—10°C. After the addition had been completed, stirring was continued an additional hour at a temperature below 10°C. The reaction mixture

*3 All boiling and melting points are uncorrected.

10) H. C. Godt, Jr., and R. E. Wann, *J. Org. Chem.*, **26**, 4047 (1961).

11) A. F. McKay, D. L. Garmaise, G. Y. Paris, S. Gelblum and R. J. Ranz, *Can. J. Chem.*, **38**, 2042 (1960).

*4 At this step, *p*-nitrophenyl chlorothiolformate was solidified.

was then poured into *ca.* 1000 m*l* of cold water; orange crystals with mp 39.0—40.5°C were thus afforded quantitatively. Recrystallization from ethanol gave 17.7 g (72%) of pale yellow plates with mp 42.5—43.0°C.

In this method, when phenyl chlorodithioformate was added to a solution of potassium phenolate in ethanol, diphenyl trithiocarbonate and diphenyl thionocarbonate were obtained, but the compound I-3 was not obtained.

Method B. This method worked well with phenols bearing electron-withdrawing substituents.

Example. *O,S*-Bis(*p*-nitrophenyl) Dithiocarbonate (I-11). To a cooled solution of 1.39 g (0.01 mol) of *p*-nitrophenol and 2.34 g (0.01 mol) of *p*-nitrophenyl chlorodithioformate dissolved in 20 m*l* of dry acetone in an ice-water bath, there was added, all at once, 0.79 g (0.01 mol) of dry pyridine with vigorous agitation. The cooling bath was then removed, and stirring was continued for two more hours at room temperature. The reaction mixture was poured into *ca.* 500 m*l* of cold water; 3.20 g (95%) of orange crystals with mp 160—164°C were thus obtained. Recrystallization from acetone-ethanol gave 2.12 g (63%) of orange prisms with mp 170.0—171.0°C.

Method C. Example. *O,S*-Diphenyl Dithiocarbonate (I-3). A mixture of 7.8 g (0.045 mol) of phenyl chlorothionoformate and 9.7 g (0.023 mol) of lead thiophenolate in 80 m*l* of dry benzene was heated under reflux for 6 hr. After cooling to room temperature, the reaction mixture was filtered and the solvent was removed under reduced pressure to give pale yellow crystals. Recrystallization from ethanol gave pale yellow plates with mp 42.5—43.0°C.

The synthesis of the compound I-11 by this method was attempted. As a result, it was found that, besides I-11, bis(*p*-nitrophenyl) trithiocarbonate and bis(*p*-nitrophenyl) thionocarbonate were formed in large quantities.

***S,S*-Diaryl Dithiocarbonates (II).** The compounds II were prepared by two methods, D and E. Method E was used most often because of its convenience. The data are shown in Table 2.

Method D. Example. *S,S*-Diphenyl Dithiocarbonate (II-3). A mixture of 0.86 g (0.005 mol) of phenyl chlorothiolformate and 1.1 g (0.0026 mol) of lead thiophenolate in 10 m*l* of dry benzene was heated under reflux for 24 hr. After it had then been cooled to room temperature, a white solid was removed by filtration; the filtrate was concentrated to dryness to yield 1.12 g (91%) of white crystals with mp 38—40°C. Recrystallization from ethanol gave white prisms with mp 41.5—42.0°C.

Method E. Example. *S,S*-Bis(*p*-nitrophenyl) Dithiocarbonate (II-11). Into a cooled solution of 1.55 g (0.01 mol) of *p*-nitrothiophenol and 2.18 g (0.01 mol) of *p*-nitrophenyl chlorothiolformate dissolved in 20 m*l* of dry acetone in an ice-water bath, there was added, all at once, 0.79 g (0.01 mol) of dry pyridine with vigorous agitation. The cooling bath was then removed and stirring was continued for two more hours. The reaction mixture was poured into *ca.* 500 m*l* of cold water; 3.36 g (100%) of yellow crystals with mp 188—189°C was thus obtained. Recrystallization from benzene gave pale yellow needles with mp 191.5—192.5°C.

Thermal Rearrangement of I. The rearrangement of I was carried out at 200°C in a test tube without any solvent. That is, *ca.* 500 mg of I was placed in a test tube and heated to 200.5±0.1°C in a constant-temperature bath under a slow stream of nitrogen. On thin-layer chromatography on silica gel, it was shown that the compound I gradually underwent a change to another compound. When the compound I had changed completely, the reaction mixture was chromatographed on a silica gel column using a solvent mixture of benzene and *n*-hexane in order to isolate the product. After the solvent had been removed under reduced pressure, the product was recrystallized and identified by means of its IR spectrum and by a determination of melting-point and of a mixed-melting-point with an authentic sample.

Crossover Reaction. An equimolar mixture of I-3 and I-12 was heated in a test tube without any solvent at 230°C for 1 hr under a slow stream of nitrogen. The resulting mixture was then analyzed by thin-layer chromatography on silica gel with a solvent mixture of benzene-*n*-hexane (1 : 1). The chromatograms showed that II-3 and II-10 were produced. However, neither II-4 nor II-7 was detected.

Kinetic Measurements. The rates were followed by the ampoule technique. That is, approximately 30 mg of I was dissolved in diphenyl ether giving a final volume of 5 m*l*. This corresponds to about a 0.02M solution. About 1 m*l* of this solution was then transferred to each of four ampoules. These ampoules were flushed with nitrogen, sealed, and then immersed in a constant-temperature bath controlled to ±0.1°C. Ampoules were taken out from the bath at appropriate intervals and cooled immediately by immersion in cold water. From each run thus obtained, I and II were separated by thin-layer chromatography on silica gel with a solvent mixture of benzene and *n*-hexane and extracted with chloroform. The absorbance at the wavelength of the maximum absorption (Tables 1 and 2) was measured*5 for the compounds thus isolated in order to determine the relative amounts of I and II. In all cases, a plot of the logarithm of C_t/C_0 against the time in sec, where C_t and C_0 are the concentrations of I at time t and time 0 respectively, gave a straight line, indicating the reaction to be of first-order (Fig. 1). The results of a typical kinetic run are illustrated in Table 3. From these data, the rate constants were calculated (Tables 4, 5, and 6).

The author wishes to express his thanks to Professor Aritsune Kaji for his helpful discussions and encouragement throughout the course of this work. He also wishes to thank Dr. Jun-ichi Hayami for his continuing interest and helpful advice.

*5 A Hitachi Perkin-Elmer 139 UV-VIS spectrophotometer was used for the ultraviolet spectrophotometric measurements.

BULLETIN OF THE CHEMICAL SOCIETY OF JAPAN VOL. 43 258—259 (1970)

Phenylation with Phenyl Radical Generated from Phenylazotriphenylmethane

Michio KOBAYASHI, Hiroshi MINATO, Nobuko WATANABE and Nobumasa KOBORI

Department of Chemistry, Tokyo Metropolitan University, Fukazawa, Setagaya, Tokyo

(Received July 25, 1969)

Phenylazotriphenylmethane was decomposed in substituted benzenes, and orientations and partial rate factors for phenylation were determined.

Phenylazotriphenylmethane (PAT) decomposes on heating with evolution of nitrogen to yield phenyl radical and triphenylmethyl radical.[1] Though many investigations have been performed on the reactions of phenyl radicals produced from PAT,[2] no systematic ones on the orientations and the partial rate factors for phenylation by means of PAT have been reported except for a few reports involving limited numbers of substrates.[3] It has long been known that substituted biphenyls are produced when phenyl radical is generated in substituted benzenes,[4] but the details of the mechanism of this homolytic substitution have not been completely clarified yet. Although the absence of kinetic hydrogen isotope effect has been reported for phenylation with *N*-nitrosoacetanilide in contrast with the phenylation by benzoyl peroxide, it has recently been found that kinetic hydrogen isotope effect is observable in the phenylation with phenyl radical produced from benzenediazonium tetrafluoroborate-sodium nitrite, and the importance of the role of a hydrogen abstractor has been pointed out.[5] In view of these findings, it seemed highly desirable to carry out a systematic investigation on phenylation with PAT and to determine whether or not orientations and partial rate factors are different from those of other phenyl radical sources due to the difference in hydrogen abstractors. Such investigation has been performed, and the results will be described in this paper.

$$Ph\text{-}N{=}N\text{-}CPh_3 \rightarrow Ph\cdot + N_2 + \cdot CPh_3$$

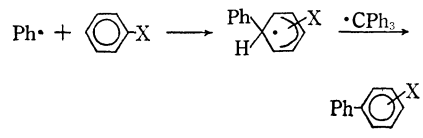

Experimental

Benzene and substituted benzenes were purified by the methods described in a previous paper.[6] Ethylbenzene was purified by distillation, bp 131—134°C. The purity of all the aromatic solvents were checked by a Hitachi Gas Chromatograph K53.

Phenylazotriphenylmethane was prepared by the bromine-water oxidation of phenylhydrazotriphenylmethane,[7] which was synthesized from the reaction between phenylhydrazine and triphenylmethyl chloride[8] in ether. Crude PAT was recrystallized from benzene-ethanol, mp 111—112°C (decomp.).

Authentic samples of substituted biphenyls were prepared by the methods described previously.[6]

Results and Discussion

Phenylazotriphenylmethane (PAT) was dissolved in a large excess of a substituted benzene ($PhNO_2$, PhCN, PhCl, PhEt and PhOMe), and the PAT solution was allowed to decompose at 60°C under nitrogen atmosphere. Evolution of nitrogen was almost quantitative and followed a first-order rate equation. The rate constants were about 4.2×10^{-4} sec at 60°C.

Formation of triphenylmethane was almost quantitative, and the total yields of substituted biphenyl isomers were about 50%. The amounts of substituted biphenyl isomers were determined by a Hitachi Gas Chromatograph K53 by use of calibration curves. The orientations and the partial rate factors for phenylation of substituted benzenes by PAT are summarized in Table 1. The partial

1) H. Wieland, E. Popper and H. Seefried, *Ber.*, **55**, 1816 (1922).

2) W. A. Pryor, J. T. Echols, Jr., and K. Smith, *J. Amer. Chem. Soc.*, **88**, 1189 (1966); M. Harada, R. Ito, T. Migita and O. Simamura, *Kogyo Kagaku Zasshi*, **69**, **607**, 962 (1966).

3) Chlorobiphenyls (*o*, 58%; *m*, 28%; *p*, 14%) were obtained from the decomposition of PAT in chlorobenzene at 45°C. R. Huisgen and R. Grashey, *Ann. Chem.*, 46 (1957).

4) D. H. Hey, *J. Chem. Soc.*, **1934**, 1966.

5) M. Kobayashi, H. Minato, N. Kobori and E. Yamada, submitted to this Bulletin.

6) M. Kobayashi, H. Minato, E. Yamada and N. Kobori, This Bulletin, **43**, 215 (1970).

7) M. Gomberg and H. W. Berger, *Ber.*, **36**, 1088 (1903).

8) C. R. Hauser and B. E. Hudson, Jr., "Organic Syntheses," Coll. Vol. 3, p. 842 (1955).

Table 1. Orientations and partial rate factors for phenylation at 60°C

PhX	Orientations (%)			Partial rate factors			
	o-	*m*-	*p*-	k_o/k	k_m/k	k_p/k	k_x/k_H
PhOMe	69	21	10	4.2	1.4	2.6	2.3
PhEt	49	35	16	1.7	1.5	1.3	1.4
PhCl	59	24	17	3.8	1.5	2.2	2.1
PhCN	69	9	22	6.9	1.0	4.6	3.4
$PhNO_2$	79	7	14	9.2	1.1	6.0	4.4

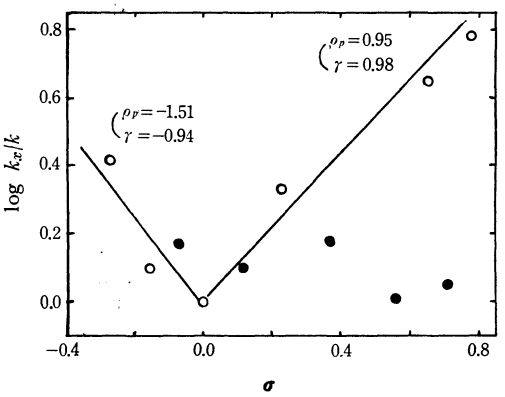

Fig. 1. Hammett plots for phenylation.
—●—: log k_m/k —○—: log k_p/k

rate factors were determined by means of competitive phenylation in a mixture of a substituted benzene and benzene or chlorobenzene as the standard according to the following equation.

$$Ph\cdot + PhH \xrightarrow{k_H} PhPh$$

$$Ph\cdot + PhX \xrightarrow{k_x} Ph\text{-}C_6H_4\text{-}X$$

$$\frac{1}{k_x}\cdot\frac{[PhC_6H_4X]}{[PhX]_0} = \frac{1}{k_H}\cdot\frac{[PhPh]}{[PhH]_0}$$

where $k_H = 6k$

$k_x = 2k_o + 2k_m + k_p$

$[PhX]_0$ and $[PhH]_0$ are the initial concentrations of the aromatic solvents.

When the partial rate factors of meta or para positions were plotted *versus* Hammett's σ values, two straight lines of V-shape were obtained as shown in Fig. 1. The ρ value was −1.51 (correlation coefficient, $\gamma=0.94$) for *p*-substituents of negative σ values and 0.95 ($\gamma=0.98$) for *p*-substituents of positive σ values. Similar V-shape lines were obtained when the partial rate factors of para positions for phenylations with benzoyl peroxide (80°C)[9] or *N*-nitrosoacetanilide (20°C)[10] were plotted *versus* σ values. The ρ_p values obtained for *p*-substituents of negative and positive σ values were −1.42 and 1.14 for benzoyl peroxide at 80°C and −0.39 and 1.27 for *N*-nitrosoacetanilide at 20°C, respectively. The ρ values for PAT and benzoyl peroxide are in fairly good agreement, but the ρ values for *N*-nitrosoacetanilide are quite different from those for PAT and benzoyl peroxide especially with respect to the electron-releasing *p*-substituents. Such difference in the ρ values is probably not ascribable to the difference in temperature. The difference in hydrogen abstractors, the difference in solvents and some other factors are probably responsible for such difference in the partial rate factors. This interesting problem has been currently investigated in our laboratories.

9) G. H. Williams "Homolytic Aromatic Substitution," Pergamon Press, Oxford (1960), pp. 68, 73; The value for OMe was taken from C. S. Rondestvedt, Jr., and H. S. Blanchard, *J. Org. Chem.*, **21**, 229 (1956).

10) R. Ito, T. Migita, N. Morikawa and O. Simamura, *Tetrahedron*, **21**, 955 (1965). The value for Me was used instead of the value for Et.

BULLETIN OF THE CHEMICAL SOCIETY OF JAPAN VOL. 43 260—262 (1970)

Alkylation of Sodium Dithionite*1

Kuniko Matsuo, Michio Kobayashi and Hiroshi Minato

Department of Chemistry, Tokyo Metropolitan University, Fukazawa, Setagaya-ku, Tokyo

(Received July 29, 1969)

Reaction between sodium dithionite and triethyloxonium fluoborate under nitrogen yielded an unstable oil capable of absorbing oxygen. When it was washed and distilled under reduced pressure, ethyl ethanesulfinate was obtained. The reaction between sodium dithionite and alkyl iodides in water or in DMSO yielded dialkyl sulfone. The reaction between sodium ethanesulfinate and triethyloxonium fluoborate in dichloromethane yielded an oily mixture which was 89% ethyl ethanesulfinate and 11% diethyl sulfone. The reaction of alkyl iodides with an excess of sodium dithionite yielded, besides a sulfone, sodium alkanesulfonate, not sodium alkanesulfinate. Mechanisms of these reactions were discussed.

Sodium dithionite (sodium hydrosulfite) is a powerful reducing agent, and its aqueous solution reduces oxygen efficiently at room temperature. Though it is a readily available compound, its ester has not been reported in literature. Since dithionite anion is an ambident anion like sulfinate anion, alkylation of sodium dithionite may result in the formation of both *S*-alkylated and *O*-alkylated products. Therefore, alkylation of sodium dithionite has been investigated by use of several alkylating agents in various solvents, and results will be described in this paper.

Experimental

Reaction between Sodium Dithionite and Triethyloxonium Fluoborate. Nitrogen was bubbled through 40 m*l* of dichloromethane, and then 2.204 g (0.0127 mol) of anhydrous sodium dithionite was suspended in the dichloromethane. Under nitrogen atmosphere 4.784 g (0.0252 mol) of triethyloxonium fluoborate was added to the suspension, and the mixture was stirred for 4.5 hr at room temperature. Inorganic salts were filtered, and the filtrate was washed with 100 m*l* of water and dried over anhydrous magnesium sulfate. Dichloromethane was removed by distillation, and ethyl ethanesulfinate was obtained by distillation of the residue at 66°C/30 mmHg. The yield was 0.284 g (0.18 mol per mol $Na_2S_2O_4$ initially present and 0.42 mol per mol $Na_2S_2O_4$ consumed; see below). It was identified by comparison of its infrared and nuclear magnetic resonance spectra with those of the authentic sample.

As a separate experiment a similar mixture of sodium dithionite and triethyloxonium fluoborate was stirred under the same conditions for 4.5 hr, and the inorganic residue was analyzed for sodium dithionite. It was found that 56% of sodium dithionite remained unreacted.

Reaction between Sodium Dithionite and Methyl Iodide. In 25 m*l* of deaerated water 5.046 g (0.0284 mol) of sodium dithionite and 12 g of methyl iodide (0.080 mol) were dissolved, and the mixture was stirred and refluxed (40—50°C) for 105 min under nitrogen atmosphere. The organic components were extracted with dichloromethane, and the dichloromethane solution was dried over magnesium sulfate. Evaporation of the solvent yielded crystals of dimethyl sulfone; 0.24 g (9%), mp 105.5—106.0°C.

Reaction between Sodium Ethanesulfinate and Triethyloxonium Fluoborate. Pure sodium ethanesulfinate was prepared by alkaline hydrolysis of ethyl ethanesulfinate, which was synthesized from ethanesulfinyl chloride and ethanol.[1] It was dried in vacuum at 120°C.

To 3.130 g (0.0270 mol) of dried sodium ethanesulfinate, 30 m*l* of a dichloromethane solution containing 5.48 g (0.0290 mol) of triethyloxonium fluoborate was added, and the mixture was stirred for 5 hr at room temperature. Inorganic solids were filtered, and the filtrate was washed with water and then dried over magnesium sulfate. Evaporation of dichloromethane yielded an oil which was identified by its infrared spectrum to be a mixture of ethyl ethanesulfinate and diethyl sulfone. The yield was 2.35 g (0.70 mol per mol of sodium ethanesulfinate). The amounts of the two components were determined by use of the absorption at 890 cm^{-1} for the ester (ε=222) and the absorption at 1320 cm^{-1} for the sulfone (ε=748). The molar ratio of the ester and the sulfone was found to be 88.7 : 11.3.

Results and Discussion

When sodium dithionite and triethyloxonium fluoborate were stirred in dichloromethane at room temperature for 4.5 hr and then the solvent was removed, an oily residue was obtained, which was capable of absorbing oxygen. Attempts to crystallize the residue failed, and distillation under reduced

*1 Part XVIII of Organic Sulfur Compounds.

1) E. J. Corey and T. Durst, *J. Amer. Chem. Soc.*, **90**, 5550 (1968); I. B. Douglass, *J. Org. Chem.*, **30**, 634 (1965).

pressure did not yield identifiable products. However, when the oil was washed with water and then distilled under reduced pressure, ethyl ethanesulfinate was obtained in 42% yield (on the basis of the sodium dithionite consumed). Thus, this reaction is regarded as a one-step synthesis of ethyl ethanesulfinate.

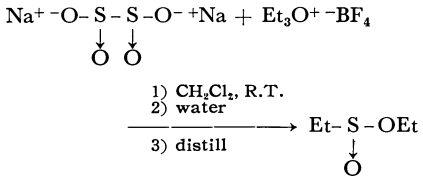

When methyl iodide was refluxed with sodium dithionite in water or in 20% methanol-water or in dimethyl sulfoxide, dimethyl sulfone was the only product. From ethyl iodide diethyl sulfone was obtained under similar conditions. When trimethylsulfoxonium iodide was stirred with sodium dithionite in dimethyl sulfoxide at 60°C, dimethyl sulfone was obtained.

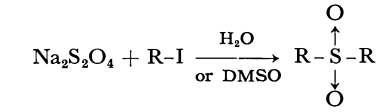

(R = Me or Et)

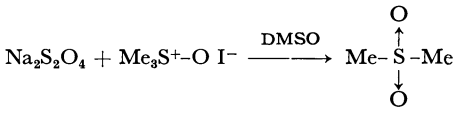

The findings that a powerful alkylating agent ($Et_3O^+-BF_4$) can attack oxygen atoms while weaker alkylating agents (RI, $Me_3S^+O\ I^-$) can react only with sulfur atoms are in line with the results obtained for alkylation of sodium *p*-toluenesulfinate.[2]

It should be mentioned that anhydrous sodium dithionite is extraordinarily insoluble in organic solvents. It is insoluble not only in non-polar organic solvents but also in such polar solvents as acetonitrile, dimethyl sulfoxide, *N,N*-dimethylformamide, hexamethylphosphoramide, nitromethane, acetone and alcohols.

It was previously reported that *O*-alkylation takes place exclusively when sodium *p*-toluenesulfinate was treated with triethyloxonium fluoborate in dichloromethane.[3] However, there have been no reports describing a similar reaction with sodium alkanesulfinate. When sodium ethanesulfinate was stirred with triethyloxonium fluoborate in dichloromethane for 5 hr and then the solvent was evaporated, the residual oil was found to be composed of 89% ethyl ethanesulfinate and 11% diethyl sulfone. This difference in the reactivities of arenesulfinate

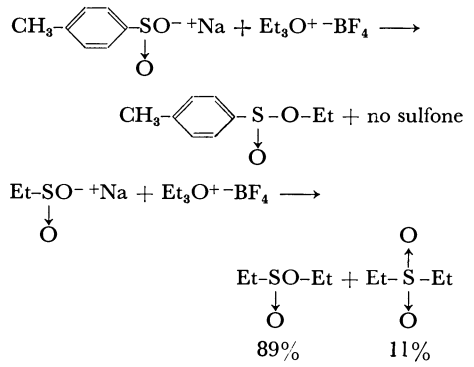

anion and alkanesulfinate anion may be ascribable to the delocalization of the lone pair on sulfur due to the resonance involving benzene ring in the case of arenesulfinate anion and to the lack of such delocalization in the case of alkanesulfinate anion.

No quantitative determinations have been reported as to the absorption of oxygen by a sodium dithionite solution. When sodium dithionite was dissolved in deaerated water and then a measured amount of oxygen was introduced, it was found that half a mole of oxygen was absorbed per mole of sodium dithionite. The reaction is probably expressed as follows.

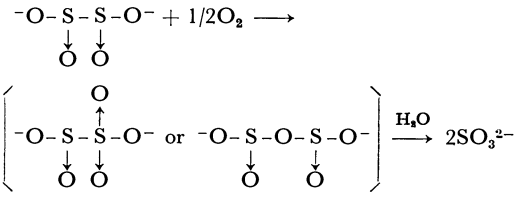

When sodium dithionite and triethyloxonium fluoborate were stirred in dichloromethane and then the solvent was evaporated, the oily residue obtained was capable of absorbing oxygen. It is possible that this mixture contained diethyl dithionite, though attempts for its characterization did not succeed.

As for the mechanism of the reaction between sodium dithionite and triethyloxonium fluoborate, various routes are possible such 1) *O*-alkylation twice, 2) *O*-alkylation followed by *S*-alkylation, 3) the reverse of 2), 4) *S*-alkylation twice, *etc.* Since no sulfone was found as a product and diethyl sulfone was a product from the reaction between the triethyloxonium salt and ethanesulfinate anion, the mechanisms involving ethanesulfinate anion as a chief intermediate can be excluded. Since no α-disulfone was found and the hydrolysis of an α-disulfone yields ethanesulfinate anion,[4] the possibility 4) can be excluded. Possibilities 2) and 3) would yield ethyl ethoxysulfinyl sulfone, which does not appear to be capable of absorbing oxygen,

2) J. S. Meek and J. S. Fowler, *J. Org. Chem.*, **33**, 3422 (1968).

3) M. Kobayashi, This Bulletin, **39**, 1296 (1966).

4) P. Allen, Jr., and P. J. Conway, *Can. J. Chem.*, **47**, 873 (1969).

nor to yield ethyl ethanesulfinate upon further reaction. On the basis of various findings and considerations, the following mechanism appears to be most plausible.

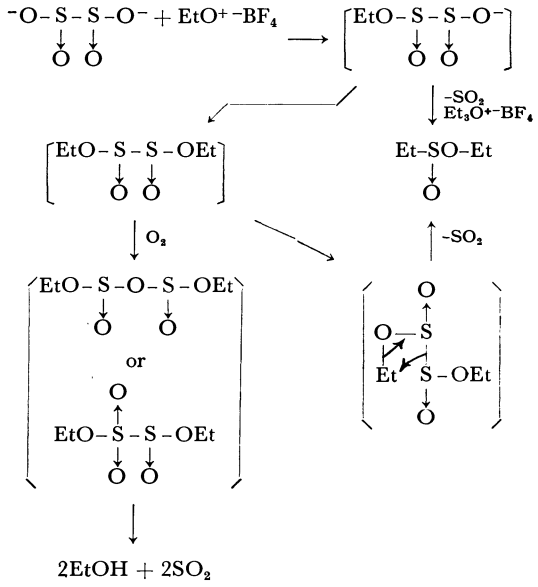

The reaction between sodium dithionite and alkyl iodides probably involves alkanesulfonylsulfinate anion as an intermediate. In order to check whether or not an alkanesulfinate anion is formed as an intermediate, 5 mol of sodium dithionite were treated with a mole of ethyl iodide in water under nitrogen. Evaporation of water and extraction with ethanol yielded sodium ethanesulfonate, and no soidum ethanesulfinate. In several experiments with sodium dithionite and alkyl iodides, yields of sulfones were always low and usually less than 9%. The formation of sodium alkanesulfonate and the low yields of sulfones may be explained by the following scheme.

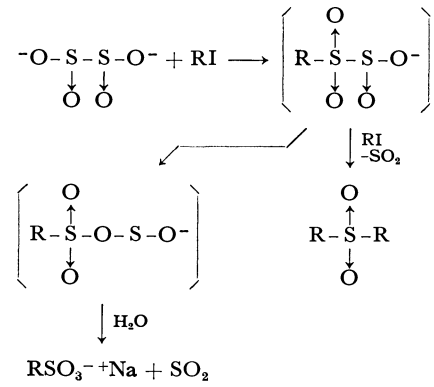

The intermediate alkanesulfonylsulfinate resembles alkyl alkanesulfinyl sulfone studied by Kice and his co-workers, who established that a sulfinylsulfone homolytically decomposes and the combination of the radicals formed yields sulfonyl sulfenyl anhydride.[5]

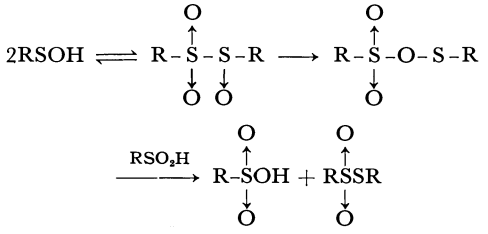

Grateful acknowledgement is made to the donors of the Petroleum Research Fund, administered by the American Chemical Society, for support of this research.

5) J. L. Kice and N. E. Pawlowski, *J. Amer. Chem. Soc.*, **86**, 4898 (1964); J. L. Kice, G. Guaraldi and C. G. Venier, *J. Org. Chem.*, **31**, 3561 (1966).

NOTES

BULLETIN OF THE CHEMICAL SOCIETY OF JAPAN VOL. 43 263 (1970)

Ultrasonic Study of Molecular Compounds of Oxalic Acid with Urea, Thio-urea and Allyl-thiourea

Sheo PRAKASH, Om PRAKASH and C. V. CHATURVEDI

Chemical Laboratories, University of Allahabad, Allahabad-2, India

(Received March 13, 1969)

Urea is known to form an inclusion compound with a few dicarboxylic acids, such as oxalic acid. The work has been extended to ascertain the formation of such compounds with thiourea and allyl thiourea by measuring the ultrasound velocity in the aqueous medium and the present note deals with such study.

A suitable optical glass-cell[1] was designed for keeping the solution and with the help of the filter, the light of wavelength 3656.71 Å from a mercury vapour lamp was allowed to fall at right angles to the path of ultrasound waves. As shown by Debye and Sears[2] ultrasound waves traversing a liquid set up a periodical inhomogeneity which acts as an optical grating. The diffraction pattern was photographed on orthochromatic AGFA plates and the distance between fringes was measured by a comparator.

The source of ultrasonic power was a generator having a gold plated circular quartz crystal 1″ in diameter as transducer. The 0.1M solution of oxalic acid, urea, thiourea and allyl thiourea were prepared in double distilled water. All reagents were A. R. grade. Mixtures of various composition were prepared by adding to fixed volume of oxalic acid, different volumes of urea, thiourea and allyl thiourea solution and then the total volume was raised to 50 m*l*. In each case photographs for the diffraction pattern of the solutions were taken at 25° ± 0.1°C. The density of each mixture was measured just after the velocity measurement with the help of density bottle. Adiabatic compressibility of each mixture was calculated using the equation $\beta=1/V^2\rho$ where V is the ultrasonic velocity and ρ the density of the solution. Compressibility lowering values of mixtures were obtained by subtracting the compressibility of mixtures from the compressibility of water which is 44.04 $cm^2/dyne \times 10^{12}$. The probable errors involved in the measurement of the ultrasonic velocity and compressibility are 0.15 and 0.4 per cent respectively.

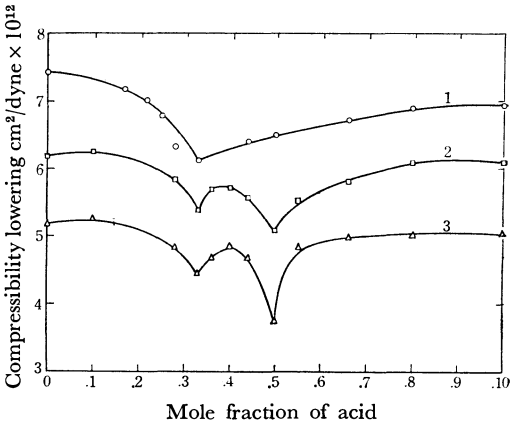

Fig. 1. Variation of compressibility lowering with composition at fixed temperature mixtures are equi-molar (0.1M).
1. Urea+Oxalic acid, 2. Allyl thiourea+Oxalic acid 3. Thio-urea+Oxalic acid

From the figure, it is observed that in each case the sound velocity and compressibility lowering decreases at first with increase in mole fraction of oxalic acid, it passes through a minimum and then increases. In case of urea a break is obtained at 1-oxalic acid - 2- urea composition in conformity with the result of Radell and Brodman,[3] while in the other two there are two breaks, one corresponding to 1 : 1 and the other to 1 : 2. The minima in the curves indicate the stoichiometry in which the reactant interact and thus they exhibit the composition of the compounds formed.

1) S. P. Srivastava, Sheo Prakash and S. Prakash, *Z. Physik. Chem.*, **50, 3/4,** (1966).

2) P. Debye and F. W. Sears, *Proc. Nat. Acad Sci. U. S. A.*, **18**, 410 (1932).

3) J. Radell, B. W. Brodman and J. J. Domanski, *J. Phys. Chem.*, **71**, 1556 (1967).

BULLETIN OF THE CHEMICAL SOCIETY OF JAPAN VOL. 43 264—265 (1970)

Study of Raman Spectra of Complex Halide Anions of Mercury(II) in Solution

J. R. SARAF, R. C. AGGARWAL and J. PRASAD

Lucknow University, Lucknow, India

(Received April 2, 1969)

From a study of Raman spectra, Delwaulle[1-3] obtained evidence for the existence of mixed halide complex anions $[HgI_nCl_{4-n}]^{2-}$ and $[HgI_nBr_{4-n}]^{2-}$, but she failed to get definite evidence for the corresponding complex anions containing bromide and chloride. Woodward and co-workers[4] confirmed the formation of complex anions $[HgI_nBr_{4-n}]^{2-}$. Aggarwal[5] estalbished the existence of the complex anion $[HgCl_2Br_2]^{2-}$ from physico-chemical studies of the system $HgCl_2$-KBr-H_2O.

The aim of the present work is to investigate the formation of mixed halide (Cl^- and Br^-) complex anions of mercury(II) with the help of Raman spectra.

TABLE 1. $[HgCl_2:KCl=1:2]$-KBr-H_2O SYSTEM

Solution No.	Relative concentration			$\Delta\nu$ cm^{-1}	Intensity (visual)
	$[Hg^{II}]$	$[Cl^-]$	$[Br^-]$		
1	1	4	0	270	s
2	¼	4	0	272	s
3	¼	3⅞	⅛	270	s
4	¼	3¾	¼	255	m
5	¼	3½	½	191	w
				256	w
6	¼	3	1	190	m
7	¼	2½	1½	191	m
8	¼	2	2	191	s
9	¼	1¾	2¼	191	s
10	¼	1½	2½	188	s
11	¼	1¼	2¾	183	s
12	¼	1	3	182	s
13	1	0	4	170	s

The solutions corresponding to Table 1 were prepared by dissolving different amounts of KBr in solutions containing $HgCl_2$ and KCl always in the molar ratio $\geqslant 0.5$. The Hg^{II}/(Halide) ratio was kept constant at 1/16 in all the solutions except solution Nos. 1 and 15. This ratio was selected to enable us to observe the changes in the Raman shifts due to successive replacement of Cl^- by Br^- from the complex $[HgCl_4]^{2-}$ on the progressive addition of KBr.

From the table it is seen that with a gradual increase in the ratio Br^-/Cl^-, hereinafter to be represented by x, the shift due to $[HgCl_4]^{2-}$ ($x=0$), is lowered in value. These results may be explained by assuming that Br^- ions take part in the formation of mixed halide species and thus the shift in the position of maximum intensity to a lower value is, presumably, due to the successive replacement of chloride ions by bromide ions.

The solutions corresponding to Table 2 were prepared by dissolving varying quantities of KBr

TABLE 2. $[HgCl_2:KCl=1:1]$-KBr-H_2O SYSTEM

Solution No.	Relative concentration			$\Delta\nu$ cm^{-1}	Intensity (visual)
	$[Hg^{II}]$	$[Cl^-]$	$[Br^-]$		
1	1	3	0	295	s
				320	m
2	1	3	1/9	295	s
				320	m
3	1	3	1/6	293	m
				320	w
4	1	3	⅓	292	w
				320	w
5	1	3	1	256	m
6	1	3	1½	255	m
7	1	3	2	192	m
				256	w
8	1	3	3	190	s
9	1	3	4	188	s
10	1	3	6	183	s
11	1	3	9	180	s
12	1	3	12	176	s
13	1	3	21	175	s
14	1	0	4	170	s
15	1	0	3	183	s

s, strong m, medium w, weak

1) M. L. Delwaulle (Fac. Sci. Lille), *Bull. Soc. Chim. Fr.*, **1955**, 1294.

2) M. L. Delwaulle, *C. R. Congr. Soc. Sevantes Paris Dept., Secti. Sci.*, **41**, (1955).

3) M. L. Delwaulle, *C. R. Acad. Sci., Paris*, **206**, 1108 (1938).

4) T. A. Ralfe, D. E. Sheppard and A. Woodward, *Trans. Faraday Soc.*, **50**, 1275 (1954).

5) R. C. Aggarwal, unpublished work (1958).

6) M. R. Nayer and J. R. Saraf, Jr., *Indian Chem. Soc.*, **20**, 312 (1943).

in solutions containing $HgCl_2$ and KCL always in 1 : 1 molar ratio. In a solution No. 1, with $x=0$, two lines are observed corresponding to $[HgCl_3]^-$ and $HgCl_2$ in agreement with the observations of earlier workers.[6] The intensity of these lines decreases with increasing value of x (soln. 1 to 4). With further increase in the value of x, Raman shifts are obtained at lower $\Delta\nu$ values which are more or less similar to those observed in the solutions of Table 1 containing Hg^{2+}, Br^- and Cl^- ions. The similarity of the Raman shifts observed in solutions of Tables 1 and 2 suggests the formation of similar mixed halide anions in the two different series of solutions.

A comparison of the results of Tables 1 and 2 further shows that the position of maximum intensity falls to a minimum value of 183 cm^{-1} in Table 1 as against 175 cm^{-1} in Table 2. This suggests that the Cl^- ions are more labile in the complex anion $[HgCl_3]^-$ as compared to $[HgCl_4]^{2-}$. The greater lability of $[HgCl_3]^-$ enables the formation of mixed halide complexes of Hg^{II} in which the number of the Br^- ions appears to be greater than those formed from $[HgCl_4]^{2-}$.

Another series of solutions was prepared by dissolving varying amounts of KCl in solutions containing $HgBr_2$ and KBr always in 1 : 1 molar ratio. When $x=0$ a line 183 cm^{-1} corresponding to the complex anion[7] $[HgBr_3]^-$ is obtained. With the addition of Cl^- ions this line shifts gradually to a minimum value 175 cm^{-1} when $x=1/7$. Since the bromo complexes of Hg^{2+} are more stable than the corresponding chloro complexes, the replacement of Br^- ions by Cl^- ions is not favoured and hence the observed shifts to lower $\Delta\nu$ side produced on addition of Cl^- ions to $[HgBr_3]^-$ ions can only be due to formation of a four-coordinated complex of Hg^{2+} *viz.* $[HgBr_3Cl]^{2-}$.

The fourth series of solutions was prepared by dissolving $HgCl_2$ and KBr in different molar proportions *viz.* 1 : 2, 1 : 3, 1 : 4 and 1 : 6. In 1 : 2 solution two strong lines at $\Delta\nu$ 191 and 270 cm^{-1} are observed. The shifts at 270 may be attributed to the anion $[HgCl_4]^{2-}$ while the other at 191 cm^{-1} is, in all probability, due to the mixed halide complex anion formed in solutions.

It is interesting to note that in all the series of solutions except that in Table 1 the minimum shift is almost the same indicating the existence of similar species in these solutions at some state.

Our observations compare favourably with those made by Delwaulle and Woodward from a study of mixed halide complex anions of mercury(II). We find that the shifts, in each series, lie between the $\Delta\nu$ values of $[HgCl_4]^{2-}$ and $[HgBr_4]^{2-}$ suggesting the formation of mixed halide complex anions as shown below:

	$[HgCl_4]^{2-}$	increasing Br^-/Cl^-	$[HgBr_4]^{2-}$
$\Delta\nu$ (cm^{-1})	270	255 ⟶ 176	170

With the increasing Br^-/Cl^- ratio anions likely to be formed are $[HgCl_4]^{2-}$, $[HgCl_3Br]^{2-}$, $[HgCl_2Br_2]^{2-}$, $[HgClBr_3]^{2-}$ and $[HgBr_4]^{2-}$— the shifts decreasing in the order given. Broadness of the lines in many cases suggests the simultaneous existence of more than one complex anion in solution. The position of maximum intensity corresponds to the species present in relatively greater concentration.

The authors wish to express their grateful thanks to Dr. B. G. Gokhale, Professor and Head of the Physics Department, Lucknow University for providing all possible facilities and for his keen interest in the progress of the work.

7) S. L. Short, D. N. Waters and D. F. Morris, *J. Inorg. Nucl. Chem.*, **26**, 902 (1964).

BULLETIN OF THE CHEMICAL SOCIETY OF JAPAN VOL. 43 266—268 (1970)

Action of Pyridine upon Organotin Compounds of the R_2SnO–SnR'_2X_2 Mixed Type

Taichi HARADA*1

The Institute of Physical and Chemical Research, Yamato-machi, Saitama

(Received April 7, 1969)

In a previous paper, the author[1] reported various new organotin complexes of the mixed type R_2SnO–SnR'_2X_2. The position of halogens have not been determined and the problem whether these complexes are monomeric or polymeric in the solid state remains to be solved. The present investigation was performed in order to obtain further information regarding the chemical structure.

Experimental

$(Me_2SnO)_2$–$SnMe_2Cl_2$, by adding pyridine in water, gave Me_2SnO and pyridine hydrochloride. The same products were obtained from Me_2SnO–$SnMe_2Cl_2$ in aqueous and alcoholic solutions. Et_2SnO–$SnMe_2Cl_2$ gave a mixture of Et_2SnO, Me_2SnO and pyridine hydrochloride.

However, Me_2SnO–$SnMe_2Cl_2$,[3] Et_2SnO–$SnMe_2Cl_2$[1] and n-Bu_2SnO–$SnMe_2Cl_2$,[1] in benzene or petroleum ether, gave the pyridine complex. This compound was identical with Me_2SnCl_2–$2NC_5H_5$ obtained from Me_2SnCl_2 and pyridine in benzene, which was confirmed by comparison of both infrared spectra shown in Fig. 1 and the melting point (163°C).[4,5,6b] Et_2SnO–$SnEt_2Cl_2$ reacted with pyridine giving mainly Et_2SnCl_2–$2NC_5H_5$ (1.0 g of the sample gave 0.55 g of crystals, mp 135°C), which was identical with that obtained from Et_2SnCl_2 and two moles of pyridine. This was confirmed by infrared spectrum shown in Fig. 2 and the melting point (135°C).[5] In the case of n-Bu_2SnO–Sn n-Pr_2Cl_2, n-Pr_2SnCl_2–$2NC_5H_5$ (mp 114°C)[5] was obtained, on the contrary $H(Et_2SnO)_3OH$–$SnEt_2Cl_2$ was not reacted with pyridine.

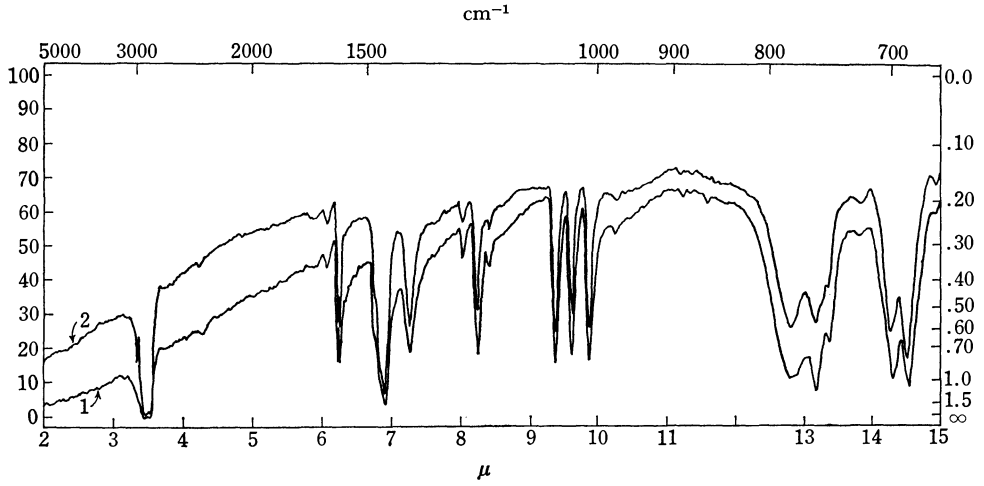

Fig. 1. Infrared spectra of Me_2SnCl_2–$2NC_5H_5$.
1. Obtained from Me_2SnCl_2 and pyridine
2. Obtained from Et_2SnO–$SnMe_2Cl_2$ and pyridine

*1 Present address: No. 8-10, 3-Chome, Funabashi, Setagaya-ku, Tokyo

1) T. Harada, This Bulletin, **41**, 737 (1968).
2) T. Harada, *Sci. Pap. Inst. Phys. Chem. Res.* (Tokyo), **35**, 290 (1939); *ibid.*, **38**, 146 (1940).
3) M. P. Brown, R. Okawara and E. G. Rochow, *Spectrochim. Acta*, **16**, 595 (1960).
4) K. A. Kocheshkov, *Usheuic Zupiski (Wiss. Ber. Moskau Staats Univ.)*, **3**, 297 (1934); *Chem. Abstr.*, **30**, 8184 (1936).
5) R. K. Ingham, S. D. Rosenberg and H. Gilman, *Chem. Rev.*, **60**, 459 (1960).
6) a) P. Pfeiffer and O. Brach, *Z. Anorg. Chem.*, **87**, 229 (1914). b) P. Pfeiffer, *ibid.*, **133**, 91 (1924).

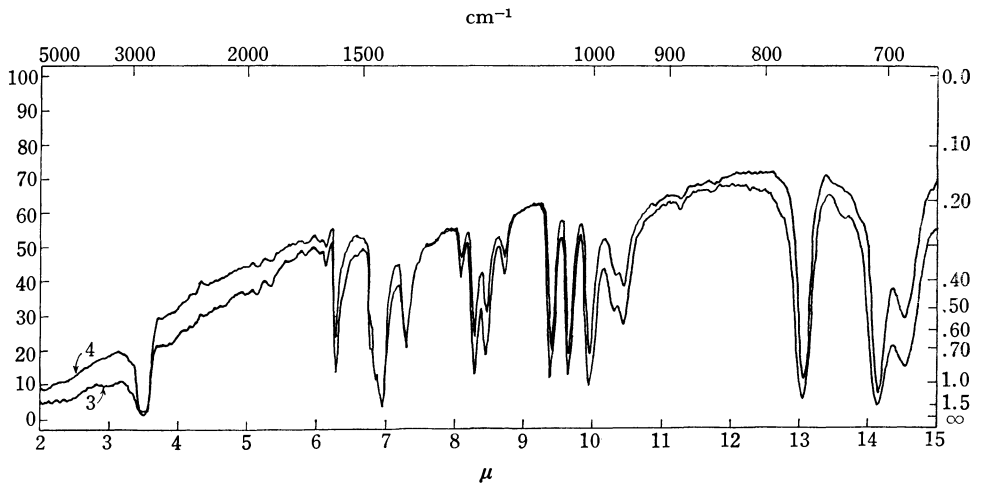

Fig. 2. Infrared spectra of Et_2SnCl_2–$2NC_5H_5$.
3. Obtained from Et_2SnCl_2 and pyridine
4. Obtained from Et_2SnO–$SnEt_2Cl_2$ and pyridine

Results and Discussion

From the results it is concluded that the complex $R'_2SnX_2 \cdot 2NC_5H_5$ is formed according to the following reaction.

$$R_2SnO \cdot SnR'_2X_2 + 2NC_5H_5 = R'_2SnX_2 \cdot 2NC_5H_5 + R_2SnO.$$

This reaction is very important for the investigation of the positions of halogens. The erroneous structure for Et_2SnO–$SnEt_2Cl_2$ in question is a linear structure, $ClEt_2Sn$–O–$SnEt_2Cl$, proposed by Pfeiffer and Brach,[6a] or a dimeric form, proposed by Brown, Okawara and Rochow,[3] and by Okawara and Wada.[7] The former structure should take up two moles of pyridine to form $ClEt_2Sn\cdots O\cdots SnEt_2Cl$, or should not take up any
$\quad\quad\quad

Thus the question has not been settled only by means of molecular weight determination. If the formation of the compounds $R_2SnO\text{-}SnR'_2X_2$[1,13] and $R_2SnO\text{-}SnR_2X_2$ is considered as a result of the pyridine complex formation, the structure of the compound in question should take $Et_2SnO\cdot SnEt_2X_2$ linking (or less probably its polymer), rather than $XEt_2Sn\text{-}O\text{-}SnEt_2X$ (or its polymer). On the other hand, the compound $R°(R_2SnO)_3\text{-}OR°\text{-}SnR'_2X_2$ ($R°$ = alkyl of solvent alcohol or H of water)[1] takes the form $R°OR_2Sn\text{-}O\langle{}^{SnR_2}_{SnR'_2X_2}\rangle O\text{-}SnR_2OR°$ at first, and then gradually turns to a stable form $R°OR_2Sn-O\langle{}^{SnR_2X}_{SnR_2'X}\rangle O-SnR_2OR°$ by the migration of one of the halogens, since this type compound does not yield the pyridine complex but indicates free OH stretching band[14] in the case ($R°=H$).

The author wishes to thank Dr. Yonezo Morino, Emeritus Professor, the University of Tokyo, for his interest and encouragement throughout this work. Thanks are also due to members of the Second organic chemistry laboratory, the Institute of Physical and Chemical Research, for the measurements of infrared spectra.

13) T. Harada, *Sci. Pap. Inst. Phys. Chem. Res.* (Tokyo), **43**, 176 (1947).

14) R. Okawara, *Nippon Kagaku Zasshi*, **86**, 543 (1965).

BULLETIN OF THE CHEMICAL SOCIETY OF JAPAN VOL. 43 268—271 (1970)

An Electron Spin Resonance Study of the Anion Radicals of 2,1,3-Benzoselenadiazole and Related Compounds

Mamoru KAMIYA and Yukio AKAHORI

Shizuoka College of Pharmacy, Oshika, Shizuoka

(Received April 10, 1969)

In the course of several recent ESR studies[1,2] of the aromatic anion radicals containing selenadiazole- or thiadiazole-ring little has been established about the effects of the preparation conditions on the spin distribution or about the electronic situation of the selenium atom. In the present work the titled anion radicals have been prepared first by metal reductions in several solvents at low temperatures. The solvent effect on the nitrogen hyperfine splitting constants is discussed in terms of a meso-ionic structure associated with the present compounds. Also, a few remarks are given about the possibilities of *p*- and *d*-orbital models for the selenium atom using information about the experimental hydrogen hyperfine splitting constants.

Experimental

The ESR measurements were done with a JES-3BS-X-type spectrometer with 100 kc/sec field modulation at −60—+20°C. The line separations were checked by referring to the spectra of an aqueous solution of peroxylamine disulfonate. The *g*-values were determined with a sample marker of Mn^{2+} in MgO. The anion radicals were prepared by a standard technique of metal reduction. Solvents used (THF, DME, DMF, THP, and Me-THP) were all obtained from the Merck Co. and were carefully dried by the usual methods. The 2,1,3-benzothiadiazole[3] and -benzoselenadiazole[4] were synthesized by reactions of *o*-phenylenediamine with thionyl chloride and selenium dioxide respectively. The 2-methyl-2,1,3-benzotriazole was obtained by the reaction of benzotriazole with diazomethane.[5] The compounds were purified by repeated sublimations under a high vacuum.

Results and Discussion

The instabilities of the former two anion radicals are predicted by the active metalation reactions as has been reported previously.[6] In fact, the hyperfine spectra of benzothiadiazole and benzoselenadiazole anion radicals could be observed only below a temperature of −40°C; at room temperature the sample solutions allowed to come in contact with a metal mirror readily yielded intensely-coloured solutions (purple in the former

1) G. A. Russell, E. G. Janzen and E. T. Strom, *J. Amer. Chem. Soc.*, **86**, 1807 (1964).

2) E. T. Strom and G. A. Russell, *ibid.*, **87**, 3326 (1965).

3) A. M. Khaletskii and V. G. Pesin, *Chem. Abstr.*, **46**, 106 (1952).

4) E. Sawicki and F. E. Ray, *J. Org. Chem.*, **19**, 1903 (1954).

5) N. O. Cappel and W. C. Fernelius, *ibid.*, **5**, 40 (1940).

6) M. Ziegler and O. Glemser, *Chem. Ber.*, **91**, 2889 (1958).

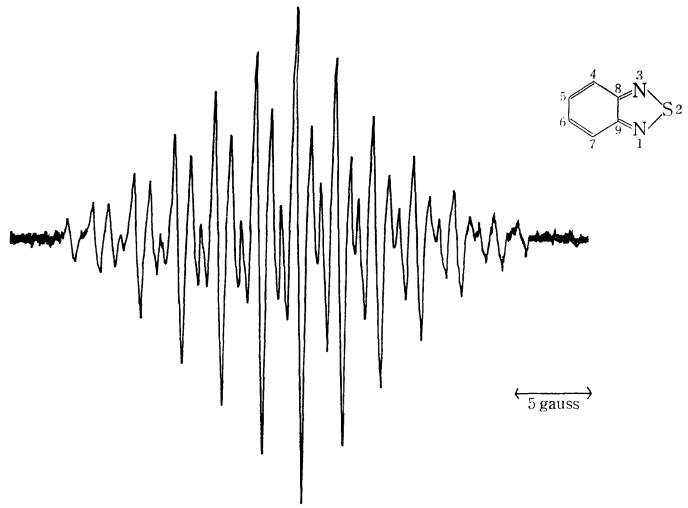

Fig. 1(a). The spectrum of 2,1,3-benzothiadiazole anion radical in THF at −40°C produced by potassium reduction.

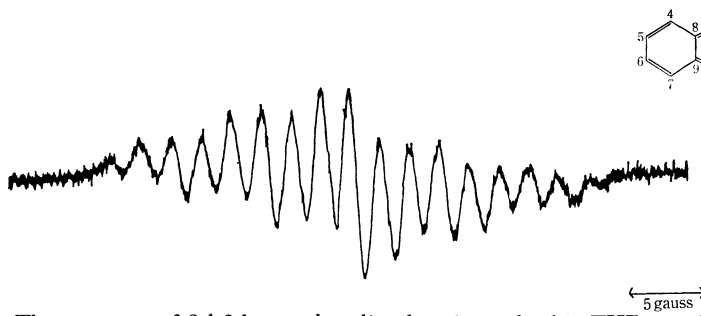

Fig. 1(b). The spectrum of 2,1,3-benzoselenadiazole anion radical in THF at −40°C produced by potassium reduction.

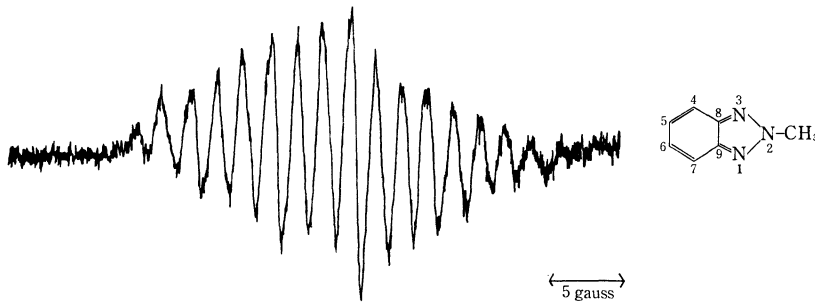

Fig. 1(c). The spectrum of 2-methyl-2,1,3-benzotriazole anion radical in THF at −40°C produced by potassium reduction.

and yellow in the latter) which showed rather asymmetric singlets with $g=2.004_0$—2.004_5 and $\Delta Hmsl=15$—20 gauss. This suggests the existence of more than one radical species although the existence of only one mono-negative radical species has been suggested from a study of the absorption spectrum of the metal-reduced benzoselenadiazole solution in THF.[7] 2,1,3-Benzoxadiazole produced no ESR signals in metal reduction; it simply showed a colour-change to dark green.

Some of the spectra are illustrated in Fig. 1, while the hyperfine splitting constants determined from the spectra are summarized in Table 1. The results indicate the noticiable facts that, as for benzothiadiazole and benzoselenadiazole, a decrease in a^N and a concurrent increase in the sum of a^H take place in the sequence of; DMF$<$THF$\approx$DMF$<$THP$\approx$Me-THP, although both a^N and a^H are not much affected by the cation species and no metal splittings are detected in any case.

7) J. Fajer, *J. Phys. Chem.*, **69**, 1773 (1965).

8) W. Baker, W. D. Ollis and V. D. Poole, *J. Chem. Soc.*, **1950**, 1546; E. S. Lane and C. Williams, *ibid.*, **1955**, 1468.

TABLE 1. THE HYPERFINE SPLITTING CONSTANTS (a^H AND a^N) OBTAINED IN METAL REDUCTIONS AT −40°C

		DMF	DME	THF	THP	Me-THP
2,1,3-Benzothiadiazole	$a^N_{1,3}$	5.47	5.33	5.36(5.30)	5.09(5.05)	5.10
	$a^H_{4,7}$	2.59	2.65	2.68(2.72)	2.75(2.81)	2.75
	$a^H_{5,6}$	1.55	1.64	1.62(1.65)	1.68(1.65)	1.71
2,1,3-Benzoselenadiazole	$a^N_{1,3}$	5.72	5.67	5.64(5.64)	5.32(5.30)	5.35
	$a^H_{4,7}$	1.85	1.88	1.88(1.85)	1.95(1.92)	1.92
	$a^H_{5,6}$	1.85	1.88	1.88(1.85)	1.95(1.92)	1.92
2-Methyl-2,1,3-benzotriazole	$a^N_{1,3}$	5.40	5.22	5.25	5.28	5.30
	$a^H_{4,7}$	1.68	1.74	1.75	1.79	1.75
	$a^H_{5,6}$	1.68	1.74	1.75	1.79	1.75

An initial value of the h.f.s.c. (in gauss) shows the one (a mean value of several recordings) obtained in K-reduction and a value in parenthesis shows the one obtained in Na-reduction.

TABLE 2. SPIN DENSITIES IN ANION RADICAL AND ELECTRON DENSITIES IN NEUTRAL MOLECULE CALCULATED FOR 2,1,3-BENZOSELENADIAZOLE WITH A FEW OPTIMUM PARAMETERS ASSIGNED TO Se WITH A *p*-ORBITAL MODEL

			Se	$N_{1,3}$	$C_{4,7}$	$C_{5,6}$	$C_{8,9}$
$h^{\cdot\cdot}_{Se}=1.0$	$k_{NSe}=0.2$						
	HMO	q	1.915	1.188	1.002	0.959	0.894
	HMO	ρ	0.041	0.279	0.073	0.067	0.061
	McLachlan	ρ	0.041	0.322	0.054	0.054	0.049
$h^{\cdot\cdot}_{Se}=1.1$	$k_{NSe}=0.2$						
	HMO	q	1.928	1.185	1.002	0.957	0.892
	HMO	ρ	0.034	0.280	0.073	0.067	0.062
	McLachlan	ρ	0.035	0.324	0.054	0.054	0.050
$h^{\cdot\cdot}_{Se}=1.2$	$k_{NSe}=0.2$						
	HMO	q	1.939	1.183	1.001	0.956	0.890
	HMO	ρ	0.029	0.281	0.073	0.068	0.063
	McLachlan	ρ	0.030	0.325	0.054	0.055	0.051

Accordingly, it may be assumed that there exists a specific solvent effect giving rise to a decrease in the nitrogen spin density followed by an increase in the nitrogen electronegativity. A probable explanation of the current effect is that, because of the meso-ionic structure associated with these compounds, the above tendency is more promoted in a solvent with less ability at solvating cations according to the resonance structures of the anion radicals which enable a selective electrostatic interaction between the nitrogen and the metal cation as shown below.

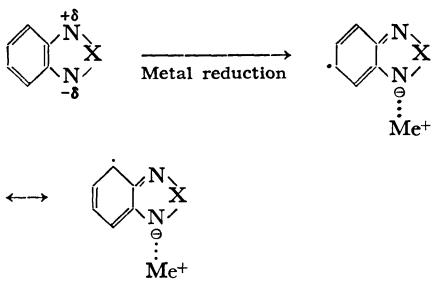

The effects of temperatures on the hyperfine splitting constants appeared to be somewhat complex as a result of the variations in the line-width.

Meanwhile, we found that the spectrum of the benzoselenadiazole anion radical has a pattern very similar to that of 2-methyl-2,1,3-benzotriazole, as is illustrated in Fig. 1 (b) and (c). This indicates that the replacement of the selenium atom with the *N*-methyl group has little effect on the spin distribution. Hückel- and McLachlan-calculations of spin densities based upon a *p*-orbital model for the selenium atom yielded the values of $h^{\cdot\cdot}_{Se}=1.0$—1.1 and $k_{SeN}=0.2$—0.3 as the optimum parameters for reproducing an equal spin density of the four ring carbons. It should be noted here that these parameters do not reflect the solvent effect on the nitrogen hyperfine splitting constant since the equality of the four a^H values holds in various solvents. (In the McLachlan calculation the λ-value involved in a corrected Coulomb integral, $\alpha_r(\alpha_r=\alpha^\circ_r+2\lambda\rho^\circ_r\beta)$, was taken to be 1.2, while $h^{\cdot}_N$ and k_{CN} were fixed as the well-accepted values of $h^{\cdot}_N=0.5$ and $k_{CN}=1.0$.) The spin- and electron-densities calculated with the optimum parameters are given in Table 2.

By comparing the current results with those for benzothiadiazole,[2] we can conclude that the conjugation of the nitrogen atom with an adjacent carbon atom is greater in benzoselenadiazole; this conclusion indicates that, as has previously been mentioned, if a major contribution to the hybrid

structure contains a meso-ionic form with oppositely-charged nitrogens, this form should be more associated with benzoselenadiazole because the exchange of the nitrogen charges is essentially intermediated by the C–C conjugated bonds between the two nitrogens. This assumption is in harmony with the observed reactivities in mono-nitrogen quarternisation[9] (benzoselenadiazole>benzothiadiazole), which can be activated by the presence of negatively-charged nitrogen.

A *d*-orbital model accepted for the sulfur atom[2] was also tested; the optimum parameters were found to be $h_{Se}=0.1-02.$, $k_{NSe}=0.05-0.07$, and $k_{SeSe}'=1.0$. However, this model seems to be unreasonable, as has been indicated in dibenzoselenophene,[10] in part at least because of a too small k_{NSe} value as compared with k_{NS} (=0.8) in benzothiadiazole.[2]

9) A. J. Nunn and J. T. Raiph, *J. Chem. Soc.*, **1965**, 6769; *ibid.*, **1966**, 1568.

10) R. Gerdil and E. A. C. Lucken, *J. Amer. Chem. Soc.*, **87**, 213 (1965).

BULLETIN OF THE CHEMICAL SOCIETY OF JAPAN VOL. 43 271—273 (1970)

Coordination Chemistry of Lanthanide Elements. I. Complexes of Trivalent Lanthanide Halides with Trimorpholino Phosphine Oxide

J. T. DONOGHUE and E. FERNANDEZ[1)]

Department of Chemistry, University of Arkansas, Fayetteville, Arkansas, U. S. A.

(Received May 10, 1969)

In previous papers we have reported on complexes of lanthanides[2,3)] and transition metals[4)] with phosphoryl donors. The ligand hexamethyl phosphoramide $O=P[N(CH_3)_2]_3$ has been found to form two series of lanthanide complexes: $LnCl_3 \cdot 3HMPA$ and $Ln(ClO_4)_3 \cdot 6HMPA$ in which the coordination number was found to be six. This coordination number, although not unique for lanthanides, is sufficiently unusual to be of interest. For hexamethyl phosphoramide complexes, it was concluded that the steric requirements of the amide molecule were of prime importance in directing the coordination number of six for the lanthanides. The steric requirements of the amide are such as to obscure the natural tendency for coordination number to decrease from left to right in the lanthanide series. In this paper we report complexes of lanthanide halides with trimorpholino phosphine oxide.

Experimental

Preparation of Compounds. 0.001 mol of anhydrous lanthanide halide was dissolved in 25 m*l* of hot absolute alcohol. A solution of 0.003 mol of trimorpholino phosphine oxide in 25 m*l* of hot absolute ethanol was prepared. These solutions were mixed together and allowed to stir until cool. All reactions were carried out in a nitrogen atmosphere. After cooling, 75 m*l* of absolute ether were added to the solutions to complete precipitation. The solids were filtered under nitrogen and washed five times with 10 m*l* portions of cold, absolute ether. The dried solids were stored *in vacuo* over H_2SO_4. Analytical data for the ligand and its complexes are reported in Table 1.

Conductivity Measurements. Conductivities of nitromethane solutions of the complexes were obtained using an Industrial Instruments Inc. conductivity bridge which had been previously calibrated with 0.01N KCl solution. The results are summarized in Table 1.

Spectral Measurements. Infrared spectra for the free ligand and its complexes were obtained using a Perkin-Elmer 337 spectrophotometer. The results for the phosphoryl stretching frequency $\nu_{P=O}$ of trimorpholino phosphine oxide and its complexes are reported in Table 1.

Reagents. Trimorpholino phosphine oxide was obtained from Aldrich Chemical Co. and was used without further purification. Analytical data are given in Table 1.

Lanthanide halides were obtained from American Potash and Chemical Corporation and were 99.9+% pure and were used without further purification.

All other chemicals used in this study were reagent grade.

Results. Analytical, conductivity, and infrared spectral data are summarized in Table 1.

1) National Science Foundation Undergraduate Research Participant; Present address: St. Mary College, Xavier, Kansas.

2) J. T. Donoghue and D. A. Peters, *J. Inorg. Nucl. Chem.*, **31**, 467 (1969).

3) J. T. Donoghue, E. Fernandez, J. A. McMillan and D. A. Peters, *ibid.*, in press.

4) J. T. Donoghue, E. Fernandez and D. A. Peters, *Inorg. Chem.*, in press.

TABLE 1. PROPERTIES OF TRIMORPHOLINO PHOSPHINE OXIDE-LANTHANIDE COMPLEXES

$MCl_3 \cdot 3L$*4 M=	Analytical results*1 Carbon Calcd	Carbon Found	Hydrogen Calcd	Hydrogen Found	Nitrogen Calcd	Nitrogen Found	Metal Calcd	Metal Found	$\nu_{P=O}$,*2 cm^{-1}	Conductivity*3 mol at 25°C
L	46.2	46.5	8.0	7.9	13.8	13.9			1205	
Sc	40.5	40.1	6.8	7.0	11.8	11.5	4.2	4.6	1191	4.5
Y	38.8	38.7	6.5	6.8	11.4	11.5	8.0	8.0	1190	3.2
La	37.2	37.2	6.3	6.6	10.8	10.9	12.0	11.5	1191	2.2
Ce	37.1	37.1	6.3	6.6	10.8	10.7	12.1	11.7	1191	2.5
Pr	37.0	36.7	6.3	6.6	10.8	10.7	12.4	11.9	1191	2.0
Nd	36.9	37.2	6.3	6.3	10.8	10.7	12.6	12.3	1191	1.7
Pm	36.7	37.0	6.3	6.5	10.8	10.9	12.8	12.8	1195	2.0
Sm	36.7	37.0	6.2	6.5	10.7	10.9	13.0	13.2	1193	1.1
Eu	36.6	36.6	6.2	6.5	10.7	10.7	13.3	13.0	1195	2.5
Gd	36.6	36.4	6.2	6.2	10.7	10.7	13.5	13.0	1191	1.8
Tb	36.5	36.7	6.2	6.2	10.7	10.9	13.7	13.3	1191	1.9
Dy	36.5	36.6	6.1	6.1	10.6	10.4	13.9	14.1	1192	2.3
Ho	36.4	26.5	6.1	6.1	10.6	10.4	14.0	13.7	1191	2.3
Er	36.3	36.2	6.1	6.3	10.6	10.6	14.1	14.1	1191	2.5
Tm	36.2	36.2	6.1	6.3	10.6	10.3	14.3	14.0	1191	1.7
Yb	36.1	36.2	6.1	6.3	10.5	10.5	14.5	14.0	1191	1.9
Lu	36.0	36.2	6.1	6.3	10.5	10.5	14.7	14.0	1192	

*1 Analytical work performed by A. Bernhardt, W. Germany.
*2 Phosphoryl frequencies reported were obtained on Nujol mulls of ligand and complexes.
*3 Conductivities of 1×10^{-4}M solutions were obtained at 25°C.
*4 L denotes trimorpholino phoshine oxide $(\overset{O}{\underset{}{\frown}}\overset{N}{\underset{}{\smile}})_3PO$.

Discussion

All of the complexes studied were found to be quite hygroscopic and it was necessary to perform most operations with the exclusion of air. No attempts were made to record melting points for these complexes. The colors of the complexes were found to be essentially the same as those of the anhydrous chlorides.

The analytical data (Table 1) suggest that the complexes may be formulated as $LnCl_3 \cdot 3L$ (L=trimorpholino phosphine oxide, O=P- $[N\langle^{CH_2CH_2}_{CH_2CH_2}\rangle O]_3$). No tendency to reduction of coordination number in progressing across the lanthanide series with decreasing crystal radius of the lanthanide ions was exhibited.

Infrared spectra of mulls of the ligand and its complexes were obtained and interpreted in terms of the location of the phosphoryl stretching frequency, $\nu_{P=O}$, of the ligand. The phosphoryl frequency (Table 1) was found to decrease on coordination in every case. Reductions are on the order of 15—20 cm^{-1}. This is taken as evidence that the site of coordination in the ligand is at the phosphoryl oxygen of the ligand. These shifts, though not as large as those noted for transition metal complexes,[4] are in the same direction as those noted for transition metal complexes.

Conductivities of the complexes in nitromethane solutions suggest that the species are non-electrolytes in nitromethane and accordingly must contain coordinated halide ion. The species may be thus formulated as $[LnCl_3L_3]$ species.

The data presented may be collectively interpreted to infer that in these lanthanide complexes of trimorpholino phosphine oxide, the coordination number of the lanthanides is six for all cases studied. This is in agreement with results obtained when the ligand is hexamethyl phosphoramide[2,3] or diphenyl sulfoxide.[5]

The most common coordination numbers exhibited by lanthanides in complexes containing monodentate ligands are eight and seven.[6-8] With hexamethyl phosphoramide as ligand, in the

5) S. K. Ramalingam and S. Soundararajan, *Z. Anorg. Allg. Chem.*, **353**, 216 (1967); S. K. Ramalingam and S. Soundararajan, *J. Inorg. Nucl. Chem.*, **20**, 1963 (1967); V. Krishnamurthy and S. Soundararajan, *Can. J. Chem.*, **45**, 189 (1967).
6) D. R. Cousins and F. A. Hart, *Chem. Ind.* (London), **1965**, 1259.
7) J. R. Ferraro and C. Cristallini, *J. Inorg. Nucl. Chem.*, **29**, 139 (1967).
8) T. Meoller and G. Vincenti, *ibid.*, **27**, 1477 (1965).

complexes $LnCl_3 \cdot 3HMPA$ and $Ln(ClO_4)_3 \cdot 6HMPA$, it was possible to interpret the failure of the lanthanides to achieve apparent maximum coordination numbers higher than six, as due to the steric requirements of the ligand itself.[2,3] However, for trimorpholino phosphine oxide the situation may involve other factors. In complexes of triphenylphosphine oxide, whose steric requirements are similar to those of trimorpholino phosphine oxide, coordination numbers higher than six have been found in derivatives of the type $LnX_3 \cdot xL$. It might be expected that trimorpholino phosphine oxide would exhibit similar behavior, but it does not. Clearly some factor other than ligand steric requirement is involved in determination of coordination number in lanthanide complexes of trimorpholino phosphine oxide.

We would like to acknowledge the aid of the Donors of the Petroleum Research Found of the American Chemical Society through Grant No. 1108-G3.

BULLETIN OF THE CHEMICAL SOCIETY OF JAPAN VOL. 43 273—275 (1970)

The Preparation of Niobium Stannide by the Iodide Process

Takeshi KAWAI and Shiro IWATA

Research Reactor Institute, Kyoto University, Kumatori-cho, Sennan-gun, Osaka

(Received May 31, 1969)

Nb_3Sn has been prepared by various methods[1,2] because of its good characteristics as a superconductor. This paper will describe the applicability of the iodide process, one of the chemical transport reactions, to the preparation of Nb_3Sn.

Experimental

A Sintered Source Material. About 10 g of a blend of a stoichiometric mixture of Nb and Sn powder*1 was divided into 10 parts; pellets (6 mmϕ × 8 mm) were then made under a pressure of 3×10^3 kg/cm^2. These pellets were sintered at 1000°C for 10 hr in a flow of Ar gas at a flow rate of 2 *l*/min.

The Iodide Process. To carry out the closed-tube transport experiment, fused silica tube (0.8 cm in int. diam., 0.015 cm in wall thickness, and 20 cm in length) containing the source material and a known amount of the transport agent, iodine,*2 was sealed off after evacuating and out-gassing treatment.

This reaction tube was placed in a horizontal tube furnace, which was so designed that the reaction region (5 cm) of this closed system could be uniformly heated at 900°C, and the deposition region (5 cm), at 1000°C. The transport region (10 cm) between the reaction and deposition regions had a linear temperature gradient.

We obtained a thin layer of Nb_3Sn deposited on the silica tube wall at a rate of 0.3 mg/hr.

The chemical compositions of the Nb_3Sn was determined by X-ray fluorescence spectrometric and chemical analytic methods.[1] In the chemical method, the niobium was determined as niobium pentoxide, Nb_2O_5; after volatilizing the tin as its bromide, the tin was determined iodometrically. In the X-ray spectrometric method, a ratio method was employed in which the net intensities of the X-ray spectral lines of niobium and tin were measured and their ratio calculated. The purity of Nb_3Sn was 70.0±0.2 wt% Nb, 29.6±0.3 wt% Sn (Calcd, Nb, 70.13 wt% Sn, 29.87 wt%).

The X-ray powder diffraction pattern yielded a lattice constant of 5.3 Å for vapor-deposited niobium stannide with a β-tungsten structure.

Results and Discussion

(1) Effects of the Stoichiometry of the Sintered Source Material. The weight ratio of Nb to Sn in the source materials influences the stoichiometry of the deposits. The composition of deposits as a function of the weight ratio of Nb to Sn in the materials is shown in Fig. 1. As a general tendency, the ratio of Nb to Sn in deposits increases with an increase in this ratio in the materials.

These results may be attributed to the fact that the free-energy changes of Nb and Sn iodides are different; also, Nb and Sn show different reactivities for I_2 molecules because of their differences in intermolecular forces between the gaseous iodine molecules and each atom of the material.*3

The dispersion of data results from the following

1) R. S. Holmes, *RCA Rev.*, **25** (1964).

2) T. L. Chu and J. R. Gavaler, *J. Electrochem. Soc.*, **113**, 1289 (1966). Von H. J. Bode, R. G. Maier and G. Wilhelm, *Z. Naturforsch.*, **19a**, 804 (1964).

*1 Nb and Sn powder were obtained from Mitsuwa Pure Chemicals, Ltd., and Wako Pure Chemicals, Ltd., respectively, and their purity were 99.5% as given by producer.

*2 The iodine was vacuum distilled from the capsule into the reaction tube.

*3 T. Kawai (to be published).

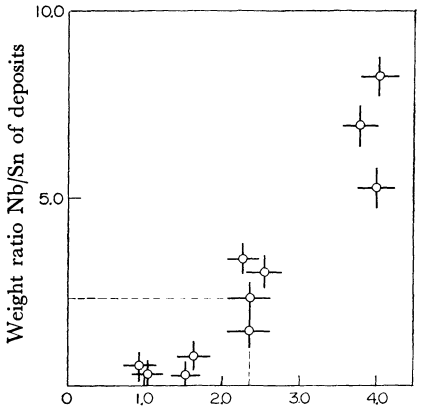

Fig. 1. Effects of the stoichiometry of the sintered source material.

reasons: 1) a small amount of Sn on the surface of these pellets evaporated for sintering because of its volatility, and 2) the mixture was not blended uniformly.

This problem should be resolved by pulverizing these sintered pellets again and using this powder as a source material. However, it is evident that, to obtain a stoichiometric Nb_3Sn, it is necessary to maintain a Nb/Sn ratio of approximately 2.4 in the source materials.

(2) Effects of the Initial Amount of a Transport Agent.[3] The dependence of the transport rate upon the initial amount of the agent, I_2, is depicted in Fig. 2.

In the small-amount range of I_2, the transport rate is approximately proportional to the square root of the concentration.*3 In this range, it may be supposed that the heterogeneous chemical reaction in the reaction region is the rate-determining step.

Above 1.5×10^{-5} mol/cm^3, the transport rate is very litttle dependent on the amount of I_2, because the diffusion rate of gaseous iodides determines the total kinetic rate of the iodide process. We are, therefore, able to obtain the glossy Nb_3Sn deposited on a silica tube wall in this range.

Above 5×10^{-5} mol/cm^3, the natural convection of gaseous iodides may be attributed to the transport rate, and the quantity deposited increases rapidly, but the deposit is a powder and does not have uniform properties.

(3) Other Important Problems. When we apply the iodide process or, in general, the chemical transport reaction to the deposition of the Nb_3Sn film on various substrates, there are other important problems besides the two effects pointed out previously.

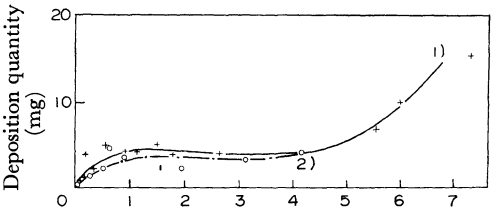

Fig. 2. Effects of the initial amount of a transport agent.

	the temp. of the react. region. °K	the temp. of the deposit. region. °K	a transport length. cm
1) (+)	1173	1273	10
2) (○)	1173	1223	7

The preparing conditions of the pellets.

	pressure kg/cm^2	sintering times hr	sintering temp. °C
1)	$1-3\times10^3$	9—10	1000
2)	3×10^3	10	1000

We must understand how to choose the temperature in the reaction and in the deposition region. In this experiment, we have fixed the temperatures of the reaction and the deposition region at 900 and 1000°C respectively, basing these values on the thermodynamic analysis of Zr and V iodides and on the results of the spoon-gauge experiment.*4

If we had the thermodynamic data of Nb iodides, we could solve the above problems, but these data have not yet been obtained.

In an attempt to solve these problems, we should have further information in addition to the thermodynamic data of Nb iodides, that is, information 1) the chemical form of iodides which contribute to the transport of Nb_3Sn; 2) the heterogeneous reaction rate between gaseous iodines and Nb-Sn surface atoms, and 3) the thermal decomposition rate of gaseous iodides or the deposition rate of Nb_3Sn from the vapor phase.

As to the first point, we have done investigations with the spoon-gauge and the DTA instrument.*5 From this information and from the data of the NbI_5-Nb phase diagram reported by Seabaugh and Corbett,[4] it follows that NbI_3 and NbI_4 contribute more to the transport than does Nb_3I_8. For Sn, it can be deduced from the thermodynamic analysis that SnI_2 is more favorable than SnI_4.

3) T. Hashino and T. Kawai, *Trans. Faraday Soc.*, **63**, 3088 (1967).

*4 T. Kawai and S. Iwata (to be published). The spoon-gauge has been made by Nishiyama Seisakusho Ltd, Osaka, and has the sensitivity of 0.1 mmHg as a result of the improvement of a spoon-form.

*5 A length of 3 cm fused-silica tube containing samples was sealed off and used as a DTA sample container. T. Kawai and S. Iwata (to be published).

4) P. W. Seabaugh and J. D. Corbett, *Inorg. Chem.*, **4**, 176 (1965).

As for the second and third points, we are going to investigate them experimentally and theoretically.

The authors wish to express their deep gratitude to Mr. Hiroo Katsuya, Sumitomo Denko Co., Kumatori-cho, Sennan-gun, Osaka, for his preparation of the sintered pellets, and to Mr. Mitsuru Tsuyama, Shimadzu Seisakusho Ltd., Kyoto, for his measurement of the DTA data.

BULLETIN OF THE CHEMICAL SOCIETY OF JAPAN VOL. 43 275—276 (1970)

Reactions of Nitrogen Oxides with Isocyanide

Takeo SAEGUSA, Shiro KOBAYASHI and Yoshihiko ITO

Department of Synthetic Chemistry, Faculty of Engineering, Kyoto University, Yoshida, Sakyo-ku, Kyoto

(Received June 6, 1969)

Various types of oxidizing agents, such as metal oxides,[1] ozone,[2] peracid,[3] *etc.*, are known for the oxidation of isocyanide to isocyanate. We wish to report the reduction of nitrogen oxide and dinitrogen oxide with isocyanide. Nitrogen oxides are reduced to elementary nitrogen and the isocyanide is oxidized to isocyanate.

Nitrogen oxide is reduced more readily than dinitrogen oxide. The results are shown in Table 1 (Exp. No. 1—4). The main gaseous product was nitrogen, whose amount roughly satisfies the stoichiometric relation:

$$RNC + NO \longrightarrow RNCO + \tfrac{1}{2} N_2$$

Small amounts of dinitrogen oxide (yield = about 10%; based upon nitrogen oxide) and carbon dioxide (less than a few percent) were formed as by-products. The production of carbon dioxide may be attributed to the hydrolysis of the product isocyanate with water which is present as impurity. The amine from the isocyanate hydrolysis may have been converted into the corresponding urea by the second molecule of isocyanate. In fact, a small amount of urea was isolated from the reaction mixture.

The nitrogen oxide-isocyanide reaction proceeded even at atmospheric pressure. Nitrogen oxide gas was passed at rate of 1.5 *l*/hr through a mixture of 50 mmol of cyclohexyl isocyanide and 10 m*l* of toluene (solvent) at 95°C for 10 hr. Cyclohexyl isocyanate was produced in 56% yield.

Dinitrogen oxide also oxidized isocyanide into isocyanate. Only 22% of cyclohexyl isocyanide was converted into isocyanate even after the reaction at 120—130°C for 16 hr (Exp. No. 5).

$$RNC + N_2O \rightarrow RNCO + N_2$$

From the reaction conditions and the conversion rate, we see that the oxidizing reactivity of dinitrogen oxide is much lower than that of nitrogen oxide. This finding does not support a mechanism of

Table 1. Reaction of nitrogen oxides with isocyanide

Exp. No.	RNC	(mmol)	Solvent	(m*l*)	Nitrogen Oxide	Reaction Temp. (°C)	Reaction Time (hr)	Yield of RNCO[a] (%)	N_2 (mmol)
1	-NC	10	C_6H_6	3	NO	80	5	77	3.3
2	*t*-C_4H_9NC	20	$(C_2H_5)_2O$	5	NO	120	8	50	—
3	*n*-$C_6H_{13}NC$	10	C_6H_6	3	NO	100	8	62	—
4	-NC	10	C_2H_5OH	5	NO	110	8	80[b]	—
5	-NC	13	C_6H_6	3	N_2O	120—130	16	22	—

a) Based on the isocyanide initially charged.
b) Isolated as ethyl *N*-cyclohexylurethane which is the reaction product of *N*-cyclohexyl isocyanate and ethanol (solvent).

1) A. Gautier, *Ann. Chim.* (Paris) [4], **17**, 229 (1869).
2) H. Feuer, H. Rubinstein and A. T. Nielsen, *J. Org. Chem.*, **23**, 1107 (1958).
3) T. Shono, M. Kimura, Y. Ito, K. Nishida and R. Oda, This Bulletin, **37**, 635 (1964).

stepwise reduction of nitrogen oxide to nitrogen through the intermediate stage of dinitrogen oxide.

It is interesting to compare the reaction of phosphite with nitrogen oxide with that of isocyanide. It has been reported that nitrogen oxide reacts with triethyl phosphite to produce triethyl phosphate and dinitrogen oxide in liquid phase at room temperature, and that dinitrogen oxide has no tendency to oxidize triethyl phosphite under the same reaction conditions.[4]

$$(EtO)_3P + 2NO \rightarrow (EtO)_3PO + N_2O$$

However, we found that dinitrogen oxide also has the capacity of oxidizing triethyl phosphite to triethyl phosphate at higher temperatures and pressures. Thus, triethyl phosphate was obtained in more than 80% yield by the triethyl phosphite-dinitrogen oxide reaction under the same reaction conditions as described in the cyclohexyl isocyanide-dinitrogen oxide reaction.

$$(EtO)_3P + N_2O \rightarrow (EtO)_3PO + N_2$$

4) L. P. Kuhn, J. O. Doali and C. Wellman, *J. Amer. Chem. Soc.*, **82**, 4792 (1960).

Experimental

General Procedure. A mixture of isocyanide and solvent was placed in a 50 m*l* stainless-steel pressure tube, to which nitrogen oxide (or dinitrogen oxide) was compressed to 20 kg/cm^2 at room temperature. The pressure tube was closed and the content was heated without shaking or stirring. After the reaction, the gases were trapped and analyzed by glpc with a column of silica gel (column temp. -78°C for nitrogen and nitrogen oxide and 40°C for dinitrogen oxide and carbon dioxide). Isocyanide and isocyanate were analyzed also by glpc with columns of silicone DC 550 and PEG 6000.

BULLETIN OF THE CHEMICAL SOCIETY OF JAPAN VOL. 43 276—277 (1970)

Reaction between Anilines and Excess of Methyl Vinyl Ketone*1

Atsushi KAWASAKI and Yoshiro OGATA

Department of Applied Chemistry, Faculty of Engineering, Nagoya University, Chikusa-ku, Nagoya

(Received June 13, 1969)

Substituted anilines add to methyl vinyl ketone forming 4-anilino-2-butanone derivatives,[1-3] *i. e.*, 1 : 1 adducts. Since the adducts are secondary amines, their addition to methyl vinyl ketone is also expected. Many reports are concerned with 4-anilino-2-butanone,[1-3] but there has been no report on the formation of *N,N*-bis(3-oxobutyl)-anilines. The authors found that excess of methyl vinyl ketone can give *N,N*-bis(3-oxobutyl)anilines in a phosphate buffer of dioxane.

$$ArNH_2 + CH_2{=}CHCOCH_3 \rightarrow ArNHCH_2CH_2COCH_3$$

$$ArNHCH_2CH_2COCH_3 + CH_2{=}CHCOCH_3 \rightarrow ArN(CH_2CH_2COCH_3)_2$$

Mono- and dibasic phosphate ions were found to be effective catalysts for the addition of aniline to methyl vinyl ketone to form 4-anilino-2-butanone.[1] This reaction was effectively carried out in 0.025M phosphate buffer of dioxane-water (50 : 50 or 60 : 40 in volume%). Formation of 1 : 2 adducts requires an excess (more than 2 mol equiv.) of methyl vinyl ketone and a longer reaction time because of the lower reactivity of the sterically hindered secondary amines.

The structure of the products was determined by elemental analysis, IR and NMR spectra as shown in Tables 1 and 2.

The melting points of these compounds are higher than those of 1 : 1 adducts, and the NH absorption bands are absent. Both aniline derivatives having an electron-withdrawing and an electron-releasing substituent afford 1 : 2 adducts. The yields of 1 : 2 adducts lower than those of the corresponding 1 : 1 adducts may be explained by the contamination of 1 : 1 adducts having a lower nucleophilicity than that of parent anilines. The contaminating 1 : 1 adducts are removed completely by recrystallization from petroleum ether (*p*-methyl and unsubstituted derivatives) or chloroform (*p*-nitro derivative). NMR spectra were assigned as shown in Table 2. It is interesting to note that *p*-substituents affect the chemical shifts

*1 Contribution No. 122.

1) Y. Ogata, A. Kawasaki and I. Kishi, *J. Chem. Soc., B*, **1968**, 703.

2) S. Tamura and M. Yamasaki, *J. Pharm. Soc. Jap.*, **76**, 915 (1956).

3) N. Murata, H. Arai and Y. Tashima, *Kogyo Kagaku Zasshi*, **56**, 709 (1953).

TABLE 1. *N,N*-BIS(3-OXOBUTYL)ANILINES

p-Substituent (X)	Yield (%)	Mp (°C)	$\nu_{C=O}$ (cm^{-1})	Analysis (%) C Found	C Calcd	H Found	H Calcd	N Found	N Calcd
H	59	54— 56	1715	71.54	72.07	8.33	8.21	6.12	6.00
Me	38	61— 62	1710	72.26	72.84	8.61	8.56	5.52	5.66
NO_2	34	156—158	1715	60.10	60.42	6.46	6.52	10.01	10.07

TABLE 2. THE NMR SPECTRA (τ-VALUE IN CCl_4 OR $CDCl_3$)

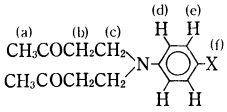

(X=H, CH_3, NO_2)

p-Substituent (X)	Proton a	b	c	d	e	f	Coupling constant (Hz) J_{bc}	J_{de}	J_{ef}
H	7.96(S)	7.40(T)	6.52(T)	3.48(D)	2.93(T)	3.48(S)	8	7	8
Me	7.97(S)	7.44(T)	6.58(T)	3.54(D)	3.12(D)	7.81(S)	7	9	—
NO_2	7.84(S)	7.23(T)	6.30(T)	3.47(D)	1.97(D)	—	7	9	—

S: singlet, D: doublet, T: triplet

of the acetyl (a) or methylene (b,c) protons which are remote from them.

The reaction path may involve the phosphate ion-catalyzed addition of the resulting 4-anilino-2-butanone to methyl vinyl ketone as in the addition of aniline to methyl vinyl ketone.[1)]

Experimental

IR and NMR spectra were determined by a Perkin-Elmer grating IR spectrophotometer Model 337 and a Varian HA-100 apparatus, respectively.

Materials. Methyl vinyl ketone and substituted anilines were purified as reported previously.[1)]

***N,N*-Bis(3-oxobutyl)-*p*-toluidine.** *p*-Toluidine (1.07 g, 0.01 mol) and methyl vinyl ketone (1.68 g, 0.024 mol) were dissolved in a mixture of 8 m*l* of dioxane and 8 m*l* of 0.025M phosphate buffer. The solution was kept standing at room temperature with occasional stirring for 15 hr. After addition of a saturated sodium chloride solution (10 m*l*), the reaction mixture was extracted twice with ether (each 10 m*l*). The ethereal extract was washed with water, dried with anhydrous sodium sulfate, and the solvent was removed *in vacuo*. The residue (1.75 g) was recrystallized from petroleum ether, giving 0.94 g (38%) of colorless crystals of *N,N*-bis(3-oxobutyl)-*p*-toluidine, mp 61—62°C. The residue contains 4-(*p*-toluidino)-2-butanone.

Other products were obtained by a similar procedure.

The authors wish to thank Toray Co. for the measurement of NMR spectra, members of Professor Sasaki's laboratory for the elemental analysis and Mr. T. Nakamura for his assistance.

BULLETIN OF THE CHEMICAL SOCIETY OF JAPAN VOL. 43 278—279 (1970)

On the Nature of the First Ionization Potential of Tropolone

Pill-Soon SONG and Michael A. LATINO

Department of Chemistry, Texas Technological University, Lubbock, Texas 79409, U. S. A.

(Received June 6, 1969)

Information concerning ionization potentials of molecules provides an important clue to their electronic states. An interesting question as to the nature of the first ionization potential of tropolone is whether the first ionization potential represents energy to remove an electron from the non-bonding orbital on oxygen or from a π-molecular orbital. Higasi *et al.* measured the first ionization potentials of tropolone and related molecules.[1] They measured the ionization potential (vertical) of tropolone mass spectrometrically using two different methods of evaluation; namely, 9.86 eV by the critical slope method and 9.83 eV by the linear extrapolation method. The ionization has been interpreted to originate from the nonbonding electron orbital on the carbonyl oxygen. Higasi *et al.* concluded that the higher ionization potential of tropolone than tropone is then, due to the intramolecular hydrogen bonding in the former. On the other hand, the lower ionization potential (9.43 eV) of 2-amino tropone than tropolone is interpreted as being due to weaker hydrogen bonding. However, they have not ruled out a possibility of the π-electron ionization potential being the lowest. This Note is concerned with that last point.

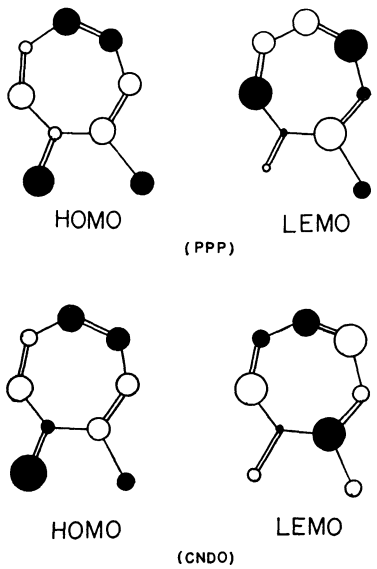

Fig. 1. Wavefunctions of the highest occupied (HOMO) and lowest empty (LEMO) molecular orbitals of tropolone calculated by the PPP and CNDO methods. The dark and open circles represent plus and minus signs, respectively, and the radius indicates an approximate magnitude of the LCAO coefficients.

The symmetry of the highest occupied (HOMO) and lowest empty (LEMO) MOs is of interest to characterize excitation and ionization processes in the molecule. Figure 1 shows HOMO and LEMO obtained from PPP SCF MO[2,3] and CNDO/2 SCF MO[4] computations.[2-4] It turns out that both HOMO and LEMO are of π-orbital origin. The HOMOs from PPP and CNDO appear to be in close agreement. Our calculations using both methods, therefore, suggest that the lowest ionization potential is due to the ionization of π-electron. If we apply Koopmans' theorem, we obtain the first ionization potentials of 8.75 eV (π, PPP) and 9.93 eV (π, CNDO) for tropolone. Furthermore, the molecular orbital of non-bonding character (63% of the MO is made up of the carbonyl oxygen nonbonding orbitals) is predicted to have an energy significantly lower (by 2.4 eV) than the HOMO shown in Fig. 1. This would qualitatively mean that the second ionization potential may be of the nonbonding origin. Numerical agreement between the CNDO-calculated and experimental ionization potentials of tropolone may be fortuitous since Koopmans' theorem ionization potentials are frequently higher than observed values. Furthermore, CNDO tends to yield poor eigenvalues.[5] Nevertheless, relative ordering of the π- and σ-HOMOs with an energy gap of 2.4 eV appears to be sufficiently large to warrant further experimental investigations of ionization potentials of tropolone and substituted tropolone series. It has been observed that CNDO correclty predicted the first ionization potential of pyridine being of σ-type, although the same method failed to predict the

1) K. Higasi, T. Nozoe and I. Omura, This Bulletin, **30**, 408 (1957).

2) R. Pariser and R. G. Parr, *J. Chem. Phys.*, **21**, 466, 767 (1953).

3) J. A. Pople, *Trans. Faraday Soc.*, **49**, 1375 (1953).

4) J. A. Pople and G. A. Segal, *J. Chem. Soc.*, **1966**, 3289.

5) J. E. Bloor and D. L. Breen, *J. Amer. Chem. Soc.*, **89**, 6835 (1967).

observed ordering of the two types of ionization potentials for pyrazine in which the energy difference is rather small.[5] In the present case, the energy spacing of 2.4 eV is sufficiently large.

In connection with our prediction discussed above, it is useful to describe ionization potentials of related molecules. Tropilidene(cycloheptatriene) has an ionization potential of 8.55 eV.[6] Obviously, the ionization potential here is π-type. It is therefore an interesting question whether the carbonyl group in tropone lowers the π-HOMO energy of the seven-membered ring system sufficiently to place it below the nonbonding level. The interpretation given by Higasi *et al.*[1] implies such a situation. The ionization potential of 2-amino tropone is lower than that of tropone and tropolone.[1] Higasi *et al.* interpret this trend to be due to weaker intramolecular hydrogen bonding in 2-amino tropone than in tropolone. However, since substituent effects on ionization potential of non-bonding electron are relatively small,[7] there exists a possibility that the lowering of the ionization potential of tropone by 2-amino substitution reflects the π-electron ionization process. Further experimental and theoretical investigations are certainly warranted to establish the nature of the ionization process in tropolone series.

This work (Electronic Structures and Spectra of Some Natural Products of Theoretical Interest. II.) was supported by the National Science Foundation) (Grant No. GB-8055) and the Robert A. Welch Foundation (Grant No. D-182). One of the authors(MAL) would like to thank NASA for a predoctoral fellowship (1966—1968). The computational assistance by the staff of the Texas Technological University computer center is greatly appreciated.

6) A. G. Harrison, L. R. Honnen, J. J. Dauben, Jr., and F. P. Lossing, *J. Amer. Chem. Soc.*, **82**, 5593 (1960).

7) K. Higasi, I. Omura and H. Baba, *J. Chem. Phys.*, **24**, 623 (1956).

BULLETIN OF THE CHEMICAL SOCIETY OF JAPAN VOL. 43 279—281 (1970)

Dipole Moment of the Triethylamine-Iodine Complex

Akinobu FUNATSU*1 and Koichi TOYODA

Department of Chemistry, Faculty of Science, Kumamoto University, Kurokami-machi, Kumamoto

(Received June 23, 1969)

One of the present authors[1] has recently reported that his experimental measurements of the dipole moment of the triethylamine-iodine (Et_3N-I_2) complex have confirmed the value previously reported by Tsubomura and Nagakura[2] in a dioxane solution. The very large value, 12D, for the experimental dipole moment of this complex in a dioxane solution, combined with the ultraviolet spectra, suggests very strongly that the predominant species in this solution is an ion pair such as triethylamine hydroiodide ($Et_3N \cdot HI$). Kobinata and Nagakura[3] measured the dipole moment of the $EtNH_2$-I_2 and Et_2NH-I_2 complexes and obtained the following results: 6.2—6.5 and 6.2D in benzene, and 7.0D for the Et_2NH-I_2 complex in dioxane. We believe these experimental results support the foregoing suggestion. Subsequently, Boule[4] has been able to measure the dipole moment of this complex in *n*-heptane and has found a much lower value, 5.5—5.7D. We have reinvestigated the dipole moment of the Et_3N-I_2 complex in cyclohexane and in benzene, whose importance as a typical example is so great that extra efforts to obtain accurate data are justified.

Experimental

The Et_3N and cyclohexane were purified by the procedure given by Nagakura and Gouterman.[5] They were stored under an N_2 atmosphere in a desicator before use. The iodine was resublimed and stored in a dark bottle until use. The benzene for "Chromatographic Purposes" was used after having been dried over sodium and distilled under a N_2 atmosphere. The dielectric constants of the solutions were measured with a home-

*1 Present address: The Chemo-Sero-Therapeutic Research Institute, Kumamoto.

1) K. Toyoda and W. B. Person, *J. Amer. Chem. Soc.*, **88**, 1629 (1966).

2) H. Tsubomura and S. Nagakura, *J. Chem. Phys.*, **27**, 819 (1957).

3) S. Kobinata and S. Nagakura, *J. Amer. Chem. Soc.*, **88**, 3905 (1966).

4) P. Boule, *ibid.*, **90**, 517 (1968).

5) S. Nagakura and M. Gouterman, *J. Chem. Phys.*, **26**, 881 (1957).

made resonance-method apparatus which used the electric circuit reported by Nakagawa.[6] A dielectric-constant-measurement cell with cylindrical platinum electrodes was used. The densities of the solutions were measured by the use of a pycnometer[7] for volatile liquids. The temperature was kept constant within 25.00 ± 0.05°C during the series of measurements. The dipole moment of nitrobenzene obtained by means of this apparatus was 4.12D in a benzene solution at 25°C. In each series of measurements, benzene or cyclohexane solutions containing a fixed concentration of Et_3N and various concentrations of iodine were used. The latter concentrations ranged from 0 to 3×10^{-3} mol/*l* in benzene solutions and from 0 to 7.2×10^{-4} mol/*l* in cyclohexane solutions; they never exceeded a 15th of that of amine in the solution. The dipole moments of the complex increased with an increase in the amine concentration in a mixed solvent containing benzene or cyclohexane and an amine. The dipole moments of the complexes were obtained by the use of the Kobinata-Nagakura method[3] modified by the ordinary Halverstadt-Kumler method.[8] Nagakura[9] noticed that a white precipitate appears at sufficiently high concentrations when there is a large excess of amine. These white crystals have been identified as $Et_3N\cdot HI$ by means of a comparison between the infrared spectrum of the white crystals and that of a synthetic salt.

Results and Discussion

We found that the present complex is unstable in a benzene solution as well as in a dioxane solution. As is shown in Fig. 1, the dielectric

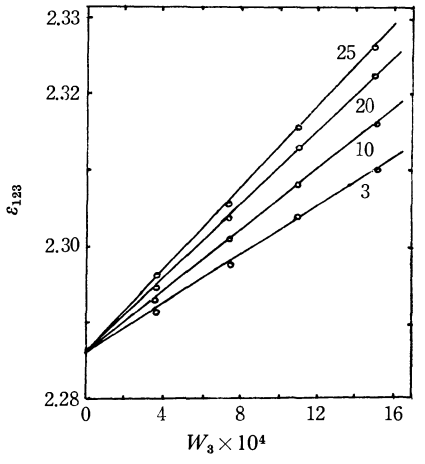

Fig. 1. The relation between the dielectric constant of the solutions (ε_{123}) and the weight fraction of complexes (W_3) in benzene. The Arabic numerals in the figure show the times passed in minutes starting from mixing the solutions.

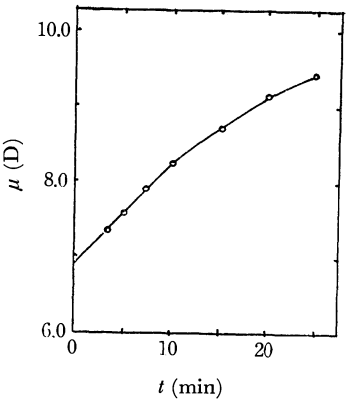

Fig. 2. The relation between the dipole moment (μ) and the time (t) in benzene.

constants of the benzene solutions increase with the time minutes after the two solutions are mixed. Furthermore, each time, the relationship between the weight fractions of the complex and the dielectric constants or the densities of the solutions is linear. These linearities seem to show that, under the present experimental conditions, the dipole-dipole interaction between the complexes or ions is negligibly small. The dipole moments of the complex were calculated from the slopes of these straight lines on each run by the use of only the first term of the Kobinata-Nagakura equation,[3] for the residual terms were negligibly small compared with the first term. Figure 2 shows the relation between the time and the dipole moments of the present complex obtained in this way. In a benzene solution, the values of the dipole moment of the complex obtained by extrapolating the results to zero time are 6.55, 6.85, and 6.94D. We were not able to find that the dielectric constants and the densities of the solutions change with the time in cyclohexane within 30 min

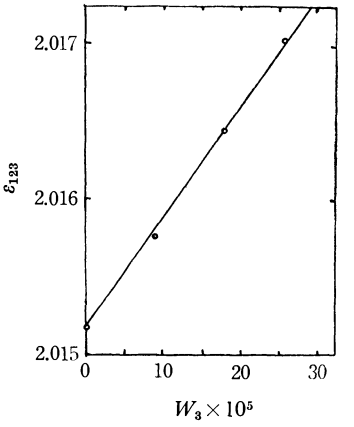

Fig. 3. The relation between ε_{123} and W_3 in cyclohexane. This straight line is able to express $\varepsilon_{123}=2.01516+7.467W_3$.

6) I. Nakagawa, *Nippon Kagaku Zasshi*, **79**, 1353 (1958).
7) M. R. Lipkin, J. A. Davison, W. T. Harvey and S. S. Kurtz, Jr., *Anal. Chem.*, **16**, 55 (1944).
8) I. F. Halverstadt and W. D. Kumler, *J. Amer. Chem. Soc.*, **64**, 2988 (1942).
9) S. Nagakura, *ibid.*, **80**, 520 (1958).

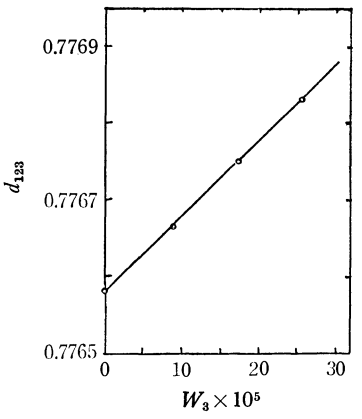

Fig. 4. The relation between the density of the solutions (d_{123}) and the weight fraction of the complexes (W_3) in cyclohexane. This straight line is able to express

$$d_{123}=0.77658+1.020W_3.$$

after the two solutions were mixed. In cyclohexane solutions, the relations between the observed dielectric constants or the densities of the solutions and the weight fraction of the complexes for a series of measurements within 30 min after the mixing of the two solutions are shown in Figs. 3 and 4. The experimental values of the dipole moment of the complex thus obtained in a cyclohexane solution are 5.23, 5.60, and 5.65D. These values are in good agreement with the Boule values.[4]

From the dipole moment thus obtained, the contribution of the dative structure in the present complex can be estimated at 30%, assuming that it takes a geometrical configuration of the trimethylamine-iodine complex[10] and that the negative charge in the dative structure is on the center of the iodine molecule.

10) K. O. Strømme, *Acta Chem. Scand.*, **13**, 268 (1959).

BULLETIN OF THE CHEMICAL SOCIETY OF JAPAN VOL. 43 281—282 (1970)

Oxidation of 2,4-Diphenyl-1,5-benzodiazepine with Peracetic Acid

Masakatsu MATSUMOTO, Akira IIO and Teijiro YONEZAWA

Department of Hydrocarbon Chemistry, Faculty of Engineering, Kyoto University, Yoshida, Sakyo-ku, Kyoto

(Received June 27, 1969)

It has been reported that two 1,5-benzodiazepines, (I-a: R,R′=CH_3) and (I-b: R=CH_3, R′=Ph), undergo oxidative ring-contraction with peracetic acid or monopersulfuric acid.[1] In a recent publication,[2] we have also reported the photooxidation of the dimethyl- (I-a) and the diphenylbenzodiazepine (I-c: R,R′=Ph) in benzene; the diphenylbenzodiazepine (I-c) is oxidized photochemically at the 3-CH_2 group, as in the oxidation of the benzodiazepines (I-a) and (I-b). In the present paper, we will report the oxidation of the diphenylbenzodiazepine (I-c) with peracetic acid.

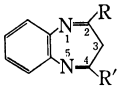

(I)

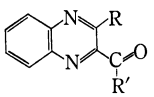

(II)

When the diphenylbenzodiazepine (I-c) was oxidized with peracetic acid, the corresponding ring-contraction product, 2-benzoyl-3-phenylquinoxaline (II-c), was not obtained; rather, Compound A, mp 154—156°C, was obtained as the main product, together with 2-phenylbenziminazole (IV), *N*-benzoyl-*o*-nitroaniline (V), and *N*,*N*′-dibenzoyl-*o*-phenylenediamine (VI). The NMR spectrum of Compound A in hexadeuteriodimethylsulfoxide showed two doublets (at τ=4.92(J=4.0 Hz, 1H) and τ=3.35 (J=4.0 Hz, 1H)), three multiplets (centered at τ=2.75 (5H), τ=2.40 (5H), and τ=2.15 (4H)), and two singlets (at τ=0.35 (1H) and τ=−0.10 (1H)). The doublet at τ=3.35 and the two singlets disappeared upon the addition of of D_2O. The infrared spectrum appeared in KBr $\nu_{C=O}$ at 1645 cm^{-1} and in ν_{N-H} and ν_{O-H} at 3370 −3220 cm^{-1}. The mass spectrum showed a parent peak at *m/e* 346. On the basis of these results, Compound A was identified as an amine (III).

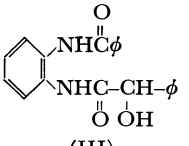

(III)

From the facts that, in the oxidation with peracetic acid, the diphenylbenzodiazepine (I-c) gave

1) J. A. Barltrop, C. G. Richards, D. M. Russell and G. Ryback, *J. Chem. Soc.*, **1959**, 1132.

2) T. Yonezawa, M. Matsumoto and H. Kato, This Bulletin, **41**, 2543 (1968).

the amide (III), while the dimethyl- (I-a) and the methylphenylbenzodiazepine (I-b) gave acetylquinoxalines (II: R′=CH_3, a: R=CH_3, b: R=Ph), it is thought that, in the mechanism of the oxidative ring-contraction shown by Barltrop *et al.*,[1] there may be a subsequent, reversible reaction between the intermediates an alcohol (VII) and a quinoxaline (VIII), which plays important roles.*1

In the case of the diphenylbenzodiazepine (I-c), the alcohol (VII) formed at first might undergo ring-contraction to form the quinoxaline (VIII), which they might suffer further oxidation to give the amide (III), while in the case of the dimethyl- (I-a) and the methylphenylbenzodiazepine (I-b), the alcohol (VII) might form a 3,6-diaza-4,5-benzotropone (IX) by succesive oxidation and the 6-oxo intermediate (IX) is thought to be rearranged.

Experimental

2,4-Diphenyl-1,5-benzodiazepine (I-c). This was prepared by the condensation of dibenzoylmethane with *o*-phenylenediamine catalysed by *p*-toluenesulfonic acid in xylene;[1] colourless needles, mp 140.0°C, crystallized from methanol.

Oxidation of I-c with Peracetic Acid. A mixture of the diazepine (I-c) (0.5 g) and hydrogen peroxide (0.90 m*l* of a 30% aqueous solution) in 30% aqueous acetic acid (30 m*l*) with a slight amount of H_2SO_4 was set aside for two days. As the reaction proceeded, the violet reaction mixture turned dark brown. The reaction mixture was basified and filtered, and then the solid part was crystallized from hot water, giving pale brown crystals melting at 154—156°C, which were identified at the amide (III) described previously, in a yield of 44%.

Found: C, 72.91; H, 5.21; N, 8.20%. Calcd for $C_{21}H_{18}O_3N_2$: C, 72.82; H, 5.24; N, 8.09%.

The filtrate was extracted with methylene chloride, the extracts were condensed, and the residue was chromatographed in methylene chloride on silica gel. Then *N*-benzoyl-*o*-nitroaniline (V) mp 92°C from aqueous methanol, 2-phenylbenziminazole (IV) mp 313°C from methanol, and *N*,*N*′-dibenzoyl-*o*-phenylenediamine (VI) mp 324°C from ethanol*2 were obtained successively in yields of 8, 9, and 3% respectively. The three products, IV, V, and VI, were identified by comparing the IR spectra with those of authentic materials.

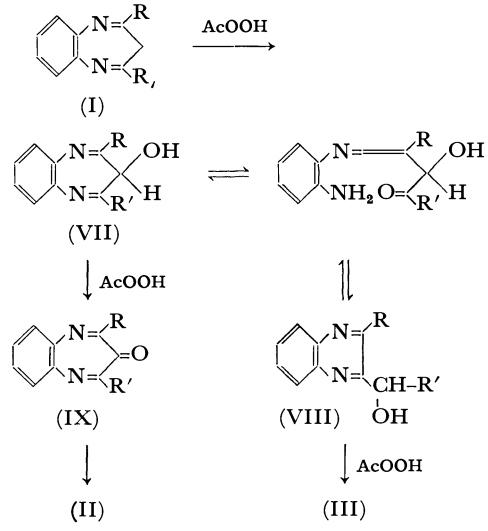

*1 As the intermediates VII and VIII, some other forms can be considered.

*2 Many articles have given 300—303°C as the mp of compound VI.

BULLETIN OF THE CHEMICAL SOCIETY OF JAPAN VOL. 43 282—284 (1970)

The Oxidation State of ^{126}I Arising from the (n,2n) Reaction in Inorganic Iodine Compounds

Nobufusa SAITO and Fumitoshi AMBE

The Institute of Physical and Chemical Research, Yamato-machi, Saitama

(Received June 27, 1969)

A comparison of the chemical effects of the (n,γ) and (n,2n) reactions has been thought to present a basis for deciding whether or not the final state of recoil atoms is dependent on the initial recoil energy, since the (n,2n) reactions are estimated to impart a far larger recoil energy to the atoms than the (n,γ) reactions induced by thermal neutrons. In an earlier paper, we reported that ^{78}Br arising from the (n,2n) reaction gave nearly the same retention as ^{80m}Br from the (n,γ) reaction in $NaBrO_3$.[1,2] However, almost concurrently, Aten and his co-

1) N. Saito, F. Ambe and H. Sano, *Nature*, **205**, 688 (1965).

2) F. Ambe, H. Sano and N. Saito, *Radiochim. Acta*, **9**, 116 (1968).

workers reported that ^{126}I arising from the (n,2n) reaction showed a considerably lower retention than ^{128}I from the (n,γ) reaction in KIO_3.[3] Recently, Dupetit and Aten have reported similar experiments on $CsIO_3$[4] and $CsIO_4$.[5] The present work was undertaken in order to see if this difference found between the behavior of ^{126}I and ^{128}I is a general phenomenon in inorganic iodine compounds of different types.

KIO_3, $KH(IO_3)_2$, I_2O_5, and $NaIO_4$ were irradiated with fast neutrons obtained from the 66 cm cyclotron of this Institute, and the distribution of the ^{126}I produced by the $^{127}I(n,2n)^{126}I$ reaction among various oxidation states was determined. The results were compared with data found in literature on the ^{128}I from the $^{127}I(n,\gamma)^{128}I$ reaction.

Experimental

The samples were commercially-available reagents of a high purity. They were irradiated for 3 hr with fast neutrons obtained by bombarding a metallic lithium target with 3.5 MeV deuterons accelerated in the cyclotron. The temperature of the samples during the neutron irradiation was slightly higher than room temperature. The neutron flux was 10^6—10^7 neutrons/cm^2·sec. The irradiated samples were subjected to the following chemical separation procedure within a few hours after neutron irradiation. The irradiated KIO_3 and $NaIO_4$ were dissolved in water, while the $KH(IO_3)_2$ and I_2O_5 were dissolved in aqueous solutions containing a large excess of KOH. The alkaline solutions were then carefully neutralized with dilute nitric acid. ^{126}I atoms in different oxidation states were separated by the following chemical procedures after an appropriate amount of a carrier (I^-, IO_3^- or IO_4^-) had been added: (1) Iodine atoms in the lower oxidation states (I^-, I_2 and IO^-) were precipitated as AgI. (2) Iodine atoms in the lower oxidation states were separated by exchange extraction with I_2 dissolved in CCl_4. (3) IO_3^- ions were precipitated as $Ba(IO_3)_2 \cdot H_2O$. (4) IO_3^- and IO_4^- ions were separated from iodine atoms in the lower oxidation states by an anion-exchange procedure.[6] (5) IO_4^- ions were precipitated as KIO_4. The radioactivity of ^{126}I was measured by means of a NaI scintillation counter after the short-lived nuclides had decayed. The data were reproducible with allowable deviations, and the results obtained by the different procedures were in good agreement.

Results

The results obtained are shown in Table 1. Storage for several hours at room temperature was found to cause no detectable change in the chemical distribution of ^{126}I in the irradiated materials. In I(V) compounds a slight increase in the parent form was observed after storage exceeding 24 hr at room temperature. In Table 2 the data on the (n,γ) reaction reported by previous workers are summarized. A comparison of Tables 1 and 2 indicates that for both I(V) and I(VII) compounds the distribution of radioactive recoil iodine atoms is considerably different for the (n,γ) and (n,2n) reactions. It may thus be concluded that, for all the I(V) compounds studied, the retention of ^{126}I is lower than that of ^{128}I; this conclusion is in accordance with the previous report on KIO_3 and $CsIO_3$.[3,4] Since we found no significant difference between the behavior of the recoil bromine arising from the $^{79}Br(n,\gamma)^{80m}Br$ and $^{79}Br(n,2n)^{78}Br$ reactions in $NaBrO_3$,[1,2] it is unlikely that the difference observed in the iodine compounds stems from the difference in recoil energy accompanying each nuclear reaction. We also reported previously that the ^{80m}Br and ^{82}Br arising from the (n,γ) reactions showed slightly different retention values in various bromates, and interpreted the difference as resulting from the highly-converted isomeric transition of ^{82m}Br to ^{82}Br after the (n,γ) reaction.[7,8]

Table 1. Oxidation state of ^{126}I arising from the (n,2n) reaction (the present work)

Compound	I^-+I_2 (%)	IO_3^- (%)	IO_4^- (%)
KIO_3	44±1	56±1	<1
$KH(IO_3)_2$	60±1	40±1	<1
I_2O_5	44±1	56±1	<1
KIO_4	4±1	94±2	2±1

Table 2. Oxidation state of ^{128}I arising from the (n,γ) reaction (a summary of data of previous workers)

Compound	I^-+I_2 (%)	IO_3^- (%)	IO_4^- (%)	Reference
KIO_3	33	67	0	a)
$KH(IO_3)_2$	47	53	0	a)
I_2O_5	31	69	0	b)
KIO_4	10	86	4	c)

a) R. E. Cleary, W. H. Hamill and R. R. Williams, Jr., *J. Amer. Chem. Soc.*, **74**, 4675 (1952).
b) M. Vlatković and A. H. W. Aten, Jr., "Chemical Effects of Nuclear Transformations (Proc. Symp. Prague)," Vol. I, p. 551, IAEA, Vienna (1961).
c) A. H. W. Aten, Jr., G. K. Koch, G. A. Wesselink and A. M. de Roos, *J. Amer. Chem. Soc.*, **79**, 63 (1957).

3) A. H. W. Aten, Jr., M. Lindner-Groen and L. Lindner, "Chemical Effects of Nuclear Transformations (Proc. Symp. Vienna)," Vol. II, p. 125, IAEA, Vienna, 1965.
4) G. A. Dupetit and A. H. W. Aten, Jr., *Radiochim. Acta*, **7**, 165 (1967).
5) G. A. Dupetit, *ibid.*, **7**, 167 (1967).
6) M. L. Good, M. B. Purdy and T. Hoering, *J. Inorg. Nucl. Chem.*, **6**, 73 (1958).
7) N. Saito, F. Ambe and H. Sano, *Nature*, **206**, 505 (1965).
8) N. Saito, F. Ambe and H. Sano, *Radiochim. Acta*, **7**, 131 (1967).

Thus, it may be possible that the difference observed in the retention of ^{126}I and ^{128}I is also a result of an internal conversion process of the excited ^{126}I or ^{128}I.

We are grateful to Mr. A. Shimamura for his technical assistance in the neutron irradiations.

BULLETIN OF THE CHEMICAL SOCIETY OF JAPAN VOL. 43 284—285 (1970)

Recoil Reactions of Fluorine-18 in Hexa- and Pentammine Cobalt(III) Salts

Nobufusa SAITO, Fumitoshi AMBE, Shizuko AMBE and Akira SHIMAMURA

The Institute of Physical and Chemical Research, Yamato-machi, Saitama

(Received June 27, 1969)

Several investigations have been reported on the recoil reactions of chlorine,[1] and bromine[2-7] in cobalt complex salts. However, no report has been made on the recoil reactions of fluorine in similar compounds. In this note we wish to report on the chemical fate of the ^{18}F recoil atoms produced by three types of nuclear reactions in hexa- and pentamminecobalt(III) salts.

The samples were prepared by traditional methods and identified by means of absorption spectra of the aqueous solutions in visible region. Analytical results of the cobalt, nitrogen, and fluorine content were satisfactory for the present purpose.

The $^{19}F(n,2n)^{18}F$ Reaction. Recoil reactions of ^{18}F following the $^{19}F(n,2n)^{18}F$ reaction were studied in $[Co(NH_3)_6]F_3$ and $[Co(NH_3)_5F](NO_3)_2 \cdot H_2O$. The samples were irradiated with fast neutrons at an ambient temperature for 1—3 hr. The fast neutrons were obtained by bombarding a metallic lithium target with 3.5 MeV deuterons accelerated in the 66 cm cyclotron of this Institute. The neutron flux was 10^6—10^7 neutrons/cm^2·sec.

The irradiated sample was dissolved in a slightly alkaline solution containing the carriers. The solution was shaken with a 1% oxine-chloroform solution in order to eliminate 2.5 hr ^{56}Mn produced by the (n,α) reaction from ^{59}Co. The aqueous phase was washed with chloroform and passed through a column of a cation-exchange resin, Diaion SK#1 in the sodium form. The resin was then washed with a sufficient amount of water which had been made slightly alkaline with ammonia. ^{18}F atoms in the form of fluoride ions passed through the column, while those in the ligand of cobalt complex cations were adsorbed on the resin. A tracer experiment confirmed that there occurred no appreciable isotope exchange reaction of fluorine atoms between fluoride and $[Co(NH_3)_5F]^{2+}$ ions during the course of separation procedure.

The annihilation γ-rays of the positron emitted by the 111 min ^{18}F were measured by means of a single-channel γ-ray spectrometer equipped with a NaI scintillation detector.

The ligand yield (the fraction of the recoil atoms found as the ligands of the complex ions[2]) was $5.3 \pm 0.1\%$ for $[Co(NH_3)_6]F_3$ and $17.8 \pm 0.3\%$ for $[Co(NH_3)_5F](NO_3)_2 \cdot H_2O$.

The $^{17}O(d,n)^{18}F$ Reaction. $[Co(NH_3)_6](NO_3)_3$ and $[Co(NH_3)_5F](NO_3)_2 \cdot H_2O$ were bombarded with 3 MeV deuterons for 5 min. The beam current was 0.05—0.5 A/cm^2. Although the target assembly was cooled with water, the temperature of the samples during bombardment might have been higher than room temperature. The samples were considerably decomposed by the heat and by the radiation (about 10^9 rad) to which the samples were exposed during irradiation. The chemical distribution of the ^{18}F produced by the $^{17}O(d,n)^{18}F$ reaction was determined by a procedure similar to that employed in the case of the (n,2n) reaction. As was expected from the inconstancy of the conditions of irradiation, the reproducibility of the results was low. The ligand yield was 2—7% for $[Co(NH_3)_6](NO_3)_3$ and 5—17% for $[Co(HN_3)_5F](NO_3)_2 \cdot H_2O$.

The $^{16}O(t,n)^{18}F$ Reaction. $[Co(HN_3)_6](NO_3)_3$ or $[Co(NH_3)_5F](NO_3)_2 \cdot H_2O$ was mixed with lithium carbonate in the gram-formula weight ratio of 1 to 2. The mixture was irradiated with

1) N. Ikeda, K. Yoshihara and S. Yamagishi, This Bulletin, **34**, 140 (1961).
2) N. Saito, H. Sano and T. Tominaga, *ibid.*, **33**, 20 (1960).
3) N. Saito, T. Tominaga and H. Sano, *ibid.*, **35**, 63 (1962).
4) K. Yoshihara and G. Harbottle, *Radiochim. Acta*, **1**, 68 (1963).
5) G. B. Schmidt and W. Herr, *Z. Naturforsch.*, **18A**, 505 (1963).
6) N. Saito, S. Ito and T. Tominaga, This Bulletin, **38**, 504 (1965).
7) N. Saito, M. Takeda and T. Tominaga, *ibid.*, **40**, 690 (1967).

neutrons for 5 min at the temperature of dry ice in the rotary specimen rack of the TRIGA Mark II reactor of Rikkyo University. The neutron flux was about 5×10^{11} neutrons/cm^2·se. The ligand yields of ^{18}F produced by the ^{16}O(t,n)^{18}F reaction (which was induced by the tritons from the ^{6}Li(n,α)T reaction) were determined to be $5\pm1\%$ for $[Co(NH_3)_6](NO_3)_3$ and $4\pm1\%$ for $[Co(NH_3)_5F](NO_3)_2\cdot H_2O$.

From the observations described above, it can be concluded that some of the ^{18}F atoms, produced by the (n,2n), (d,n), and (t,n) reactions, form ^{18}F-labeled cobalt complex ions as has been reported for radioactive chlorine and bromine atoms following various nuclear reactions in similar compounds.[1-7]

BULLETIN OF THE CHEMICAL SOCIETY OF JAPAN VOL. 43 285—286 (1970)

Decomposition of Benzenediazonium Tetrafluoroborate in Aprotic Polar Solvents

Kazuhiro ISHIDA, Nobumasa KOBORI, Michio KOBAYASHI and Hiroshi MINATO

Department of Chemistry, Tokyo Metropolitan University, Fukazawa, Setagaya, Tokyo

(Received June 27, 1969)

The decomposition of aryldiazonium tetrafluoroborate has been investigated in dimethyl sulfoxide, acetonitrile, nitromethane, dimethylformamide and acetone.

Experimental

Materials. Dimethyl sulfoxide was dried with calcium hydride and distilled at 86°C/25 mmHg. Acetonitrile was refluxed with phosphorus pentoxide, and then distilled at 81°C. Nitromethane was dried with calcium chloride and then distilled at 101°C. Dimethylformamide was distilled at 153°C. Acetone was treated according to the method of Hudson and Wardill,[1] and distilled at 56.5°C. Benzenediazonium tetrafluoroborate was prepared by the addition of an aqueous hydrogen tetrafluoroborate solution to a benzenediazonium chloride solution obtained from the aniline purified by distillation at 109°C/30 mmHg. The crystals were filtered, washed successively with cold water, ethanol and ether, and then they were dried *in vacuo*.

Kinetic Measurements. The diazonium salt was decomposed in a water bath, the temperature of which was regulated within ±0.1°C. The rate of decomposition was followed by measuring the evolution of nitrogen gas by use of a gas burette.

Results and Discussion

The decomposition of benzenediazonium tetrafluoroborate in these solvents were of first order. The first-order rate constants in these five solvents are shown in Table 1. Figure 1 shows the plots of $\log k$ *versus* $1/T$, and the activation parameters obtained from Fig. 1 are shown in Table 2. Figure 2 shows that the values of activation energies and activation entropies fit an isokinetic relationship very well. The activation entropy was small in a solvent with a small activation energy, and *vice versa*. The isokinetic temperature was 311°K.

It was found that the decomposition of benzenediazonium tetrafluoroborate in DMSO yielded

TABLE 1. FIRST ORDER RATE CONSTANTS FOR THE DECOMPOSITION OF PhN_2BF_4

in DMSO		in CH_3CN		in DMF		in CH_3NO_2		in $(CH_3)_2CO$	
Temp. (°C)	$k_1\times10^4$ (sec^{-1})	Temp. (°C)	$k_1\times10^4$ (sec^{-1})	Temp. (°C)	$k_1\times10^4$ (sec^{-1})	Temp. (°C)	$k_1\times10^4$ (sec^{-1})	Temp. (°C)	$k_1\times10^4$ (sec^{-1})
24.0	0.388	30.2	0.685	30.2	0.778	25.1	0.294	35.0	1.34
30.0	1.000	35.0	1.68	35.0	1.792	30.1	0.711	39.8	2.87
34.0	1.82	39.8	2.84	39.8	3.17	35.5	1.87	44.3	4.84
40.3	3.84	44.8	6.91	44.8	9.27	40.1	4.39		
45.7	8.61								

1) R. F. Hudson and J. E. Wardill, *J. Chem. Soc.*, **1950**, 1731.

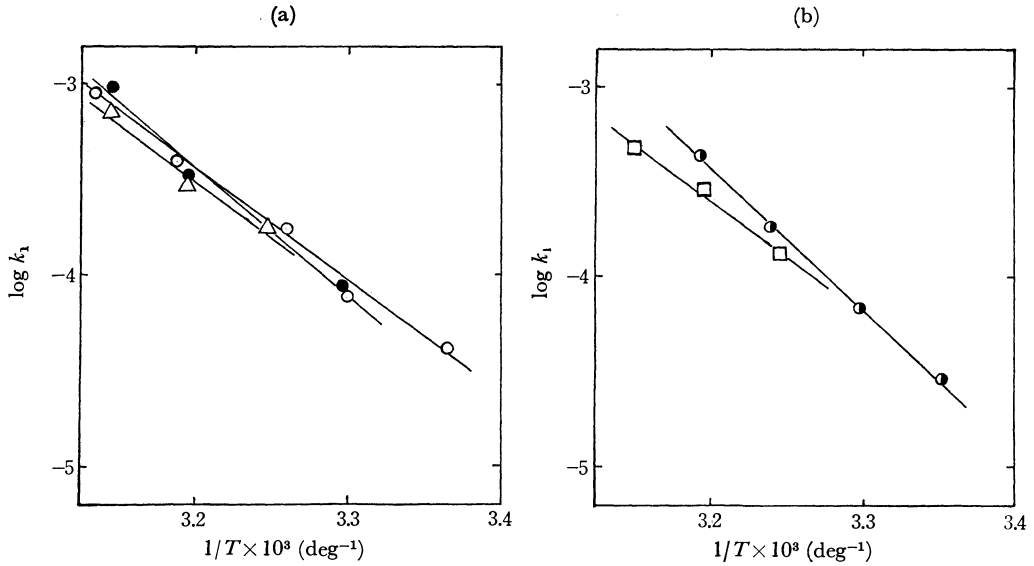

Fig. 1. Arrhenius plots for the decomposition of PhN_2BF_4.
○: in DMSO, △: in CH_3CN, ●: in DMF,
◑: in CH_3NO_2, □: in $(CH_3)_2CO$

Table 2. Activation parameters for the decomposition of PhN_2BF_4

Solvent	E_a (kcal/mol)	$\Delta S^{\neq}_{25°C}$ (e.u.)
$(CH_3)_2CO$	26.9	9.2
DMSO	27.1	10.4
CH_3CN	29.7	18.3
DMF	31.6	24.7
CH_3NO_2	33.5	30.9

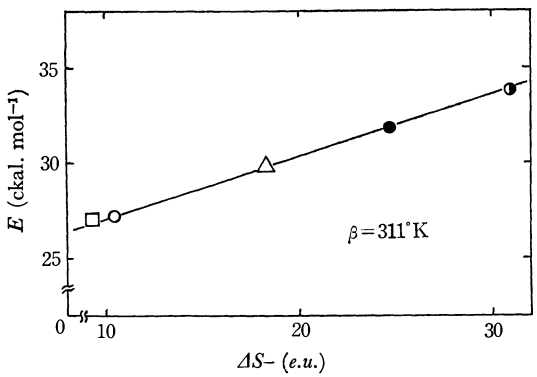

Fig. 2. Isokinetic relationship for the decomposition of PhN_2BF_4.
□: in $(CH_3)_2CO$, ○: in DMSO, △: in CH_3CN,
●: in DMF, ◑: in CH_3NO_2

7.8% of 1,3-benzoxathian, 25.0% of phenol and 32.5% of *o*-hydroxybenzyl methyl sulfide. The results of both kinetic studies and product studies are best explained by the monomolecular decomposition of the diazonium ion to phenyl cation and nitrogen.

Thus, the decomposition in these aprotic polar solvents is in quite a contrast with the decomposition in methanol[2] or in pyridine,[3] in which the decomposition was homolytic and phenyl radical was the intermediate. Methanol and pyridine are rather strong nucleophiles, and attack the diazonium cation to yield a diazoether or a triazene, which undergoes homolyses. The nucleophilicity of the solvents used in this investigation was not strong enough to cause the combination with the diazonium ion. However, the polarity of these solvents is apparently large enough to assist the formation of phenyl cation stabilized by solvation.

It was found that the rate of decomposition of benzenediazonium tetrafluoroborate in an aqueous DMSO solution was approximately the same as that in pure DMSO. This indicates that the mechanism of decomposition in an aprotic polar solvent is similar to the mechanism reported for decomposition in water.[4a,4b]

2) D. F. DeTar and M. N. Turetzky, *J. Amer. Chem. Soc.*, **77**, 1945 (1955); **78**, 3925 (1956).

3) R. A. Abramovitch and J. G. Saha, *Tetrahedron*, **21**, 3297 (1965).

4) a) M. L. Crossley, R. H. Kiene and C. H. Benbrook, *J. Amer. Chem. Soc.*, **62**, 1400 (1940); E. S. Lewis and E. B. Miller, *ibid.*, **75**, 429 (1953); D. F. DeTar and A. R. Ballentine, *ibid.*, **78**, 3916 (1956); D. Schule-Frohlindo and H. Blume, *Z. Phys. Chem. Neue Folge*, **59**, 299 (1968).

BULLETIN OF THE CHEMICAL SOCIETY OF JAPAN VOL. 43 287—288 (1970)

Addition Compounds of Boron Nitride with Alkali Metals and Their Catalytic Activity

Chie MUGIYA, Noriko OHIGASHI, Yoshihiro MORI and Hiroo INOKUCHI

The Institute for Solid State Physics, The University of Tokyo, Roppongi, Minato-ku, Tokyo

(Received July 11, 1969)

Boron nitride consists of parallel-layer planes, in each of which boron and nitrogen atoms occupy alternate sites on regular hexagonal lattice. Therefore, the structure of boron nitride (BN) bears a relation to graphite; the distance between the planes (3.30 Å) is almost the same as in graphite (3.345 Å), and their interatomic distances in the hexagonal plane are close, 1.45 Å (for boron nitride) and 1.42 Å (for graphite). However, because of the greater electronegativity of nitrogen as compared with that of boron, there is an uneven distribution of the electrons, giving a partly ionic character to the lattice. The nuclear magnetic resonance study of the bonding has led to the conclusion that boron nitride has a 45% double-bond resonating configuration.[1]

It is well known that graphite reacts with striking readiness with the molten alkali metals, potassium, rubidium and cesium, or their vapours, to form alkali metal-graphite lamellar compounds.

Recently, a strong chemisorption was found on these lamellar compounds of graphite by the methods of hydrogen-deuterium exchange reaction and ortho-parahydrogen conversion.[2]

The similarity of the structures of graphite and boron nitride led Croft and Rudorff to attempt the preparation of boron nitride intercalation compounds.[3,4] However, because of the difficulty of preparing and identifying them, there remains some ambiguity.

In this paper, we will discuss the preparation of boron nitride alkali metal compounds and their catalytic activity.

Experimental Procedures

Boron nitride, a white powder provided by Borax Consolidated, Ltd., and the Showa Denko Co., was used to prepare its alkali metal complexes.

Among the alkali metals, commercial-grade sodium and potassium metals were employed, while the rubidium and cesium were obtained by the reduction of their chlorides by calcium metal. The purified alkali metal was admitted into a vacuum reaction vessel, in which a degassed boron nitride powder was kept, by distillation. By further heating at 200°C for two or three days in an electric furnace, the reaction between alkali metal and boron nitride was completed. The Cs-BN complex was deep blue.

The principle of the kinetic studies of parahydrogen-orthohydrogen conversion and of hydrogen-deuterium equilibration over these complexes has already been reported.[2] These studies were carried out at room temperature and at 77°K in a constant-volume reaction system which was protected from grease and other condensable gases by traps cooled in liquid nitrogen.

For electrical conductivity measurements, a small piece of boron nitride (3.7 mm in diameter, 1.5 mm thick) was fused at around 3000°C in an arc-imaging furnace to make a fused specimen. The thin aluminum films evaporated onto both sides of the fused specimen were used as electrodes.

Results and Discussion

Boron nitride is a typical electric insulator, its observed electrical conductivity at 15°C and apparent activation energy being 10^{-17}—10^{-22} Ω^{-1} cm^{-1} and $\sim$1 eV respectively. The ionization potential, estimated from its photoemission in a vacuum ultra-violet region, was about 5.6 eV.*1 The details of the experimental procedure have already been reported.[6]

No catalytic activity was found on the powder specimen of boron nitride at all. However, the complexes between BN and alkali metals revealed a marked catalytic activity for such reactions as para-orthohydrogen conversion and hydrogen-deuterium equilibration. Table 1 summarizes their kinetic data. It can be seen form Table 1 that

1) A. H. Silver and P. J. Bray, *J. Chem. Phys.*, **32**, 288 (1960).

2) H. Inokuchi, N. Wakayama, T. Kondow and Y. Mori, *ibid.*, **46**, 837 (1967).

3) R. C. Croft, *Austral. J. Chem.*, **9**, 206 (1956).

4) W. Rudorff and E. Stumpp, *Z. Naturforsch.*, **13b**, 459 (1958).

*1 Taylor and Coulson have calculated an electronic structure of boron nitride with a tight-binding approximation. They reported that the electrons of the BN crystal cocupy one band, approximately 2.4 eV in width, separated from the next-higher band by a gap of about 4.6 eV.[5]

5) R. Taylor and C. A. Coulson, *Proc. Phys. Soc.*, **A65**, 834 (1952).

6) Y. Harada and H. Inokuchi, This Bulletin, **39**, 1443 (1966); M. Kochi, Y. Harada and H. Inokuchi, This Bulletin, **40**, 531 (1967).

Table 1. The conversion and the exchange of hydrogen with boron nitride-alkali metals system

Complex	Reaction	Temperature (°K)	$min^{-1}g^{-1}$*
BN-K	$H_2+D_2\rightleftharpoons 2HD$	295	0.8×10^{-2}
		77	non-detectable
	$pH_2\rightleftharpoons oH_2$	295	1.3×10^{-2}
		77	1.2×10^{-3}
BN-Rb	$H_2+D_2\rightleftharpoons 2HD$	295	1.0×10^{-2}
		77	non-detectable
	$pH_2\rightleftharpoons oH_2$	295	1.0×10^{-2}
		77	1.3×10^{-3}
BN-Cs	$H_2+D_2\rightleftharpoons 2HD$	295	1.4×10^{-2}
		77	non-detectable
	$pH_2\rightleftharpoons oH_2$	295	4.2×10^{-2}
		77	1.4×10^{-3}

* $k=\frac{2.303}{t}\log\left(\frac{C_0-C_e}{C_t-C_0}\right)$; where C_0, C_e and C_t are concentrations of para-H_2 at the initial point, in equilibrium at the given temperature, and after t min, respectively. For D_2, the similar calculation is applied.

the rate constants have about the same magnitude for both the reactions at room temperature, and that only para-$H_2\rightleftharpoons$ortho-H_2 conversion can be catalyzed at 77°K, implying that at higher temperatures the reactions occur by the chemical mechanism, and at lower temperatures, by the physical one.

We have already reported that graphite makes lamellar complexes with alkali metals, which are very active in the above catalytic reactions.[2] Though a quantitative comparison of catalytic activity can not be made between BN- and graphite-alkali metals complexes since the surface area has not yet been measured, it seems that boron nitride complexes have an activity comparable with graphite.

What is the cause of this activity over the BN-complexes? The promotion may take place by means of an electron transfer from the alkali metal to a partner molecule: ($nM^+\cdot BN^{n-}$). The excess charge on the B–N hexagonal skeleton may give a predominant mechanism of catalytic activity. However, we could not find any detectable change in the crystal structure of boron nitride upon the addition of alkali metals.

A more detailed and systematic study will be required to establish the structures of these complexes and the nature of the catalytic active sites.

BULLETIN OF THE CHEMICAL SOCIETY OF JAPAN VOL. 43 288—290 (1970)

The Preparation of Some Trialkylstannylferrocenes*1

Toshihiro Dodo,*2 Hideo Suzuki and Toshio Takiguchi

Department of Synthetic Chemistry, Kiryu College of Technology, Gunma University, Tenjin-cho, Kiryu

(Received July 17, 1969)

During the last decade, several papers dealing with triorganosilyl-,[1-5] triorganogermyl-[6] and diorganophosphyl[7]-substituted ferrocenes have appeared. However, there has been an entire absence of descriptions of the triorganostannyl-substituted ferrocenes. The present authors wish to report herewith on the preparation of a series of mono- and 1,1′-bis(trialkylstannyl)substituted ferrocenes, as shown in Table 1, by the reaction of lithioferrocenes with the corresponding trialkyltin chlorides. The NMR and IR data of the products well characterized their chemical structure; they are given in Table 2.

Experimental

Trialkylstannylferrocenes. The lithiation of ferrocenes was performed by the use of *n*-butyllithium

*1 Taken from the thesis of one of us, T. D., submitted in partial fulfilment of the requirement for the Tech. degree, 1969.

*2 Present address: Mitsui-Toatsu Chem. Ind. Co., Ōtake, Hiroshima.

1) R. A. Benkeser, D. Goggin and G. Schroll, *J. Amer. Chem. Soc.*, **76**, 4025 (1954).

2) M. Rausch, M. Vogel and H. Rosenberg, *J. Org. Chem.*, **22**, 900 (1957).

3) M. Kumada, H. Tsunemi and S. Iwasaki, *J. Organometal. Chem.*, **10**, 111 (1967).

4) G. P. Sollott and W. R. Peterson, Jr., *J. Amer. Chem. Soc.*, **89**, 5054 (1967).

5) R. L. Schaaf, P. T. Kan, C. T. Lenk and E. V. Deck, *J. Org. Chem.*, **25**, 1986 (1960).

6) D. Seyferth, H. P. Hofmann, R. Burton and J. F. Hehing, *Inorg. Chem.*, **1**, 227 (1962).

7) G. P. Sollott, H. E. Mertwoy, S. Portnoy and T. L. Snead, *J. Org. Chem.*, **28**, 1090 (1963).

TABLE 1. TRIALKYLSTANNYLFERROCENES

Compd.	Yield (%)	Bp(°C/mmHg) n_D^{25}	Formula	Analysis (%) Found / Calcd C	H	Sn[a]	Fe[b]	Mol wt[c]
$CpFeC_5H_4SnEt_3$	10.7	135—140/1.0 1.5860	$C_{16}H_{24}SnFe$	47.07 46.60	6.04 6.14	30.87 30.40	14.55 14.30	388 391
$Fe(C_5H_4SnEt_3)_2$	19.4	160—164/1.0 1.5761	$C_{22}H_{38}Sn_2Fe$	44.45 44.35	6.39 6.38	40.11 39.88	9.63 9.38	595 597
$CpFeC_5H_4SnPr_3$	11.5	122—125/0.5 1.5689	$C_{19}H_{30}SnFe$	53.36 52.71	7.27 6.93	28.10 27.44	13.13 12.91	440 433
$Fe(C_5H_4SnPr_3)_2$	20.8	187—193/0.5 1.5571	$C_{28}H_{50}Sn_2Fe$	49.96 49.46	7.49 7.36	35.22 34.96	8.45 8.22	670 679
$CpFeC_5H_4SnBu_3$	9.7	140—146/0.5 1.5540	$C_{22}H_{36}SnFe$	55.67 55.63	7.62 7.58	25.78 25.01	12.10 11.67	481 475
$Fe(C_5H_4SnBu_3)_2$	20.4	170—173/0.17 1.5437	$C_{234}H_{62}Sn_2Fe$	53.43 53.45	7.30 7.12	31.55 31.10	7.52 7.31	758 763

a) Determined volumetrically with EDTA and Zz^{2+}. b) Determined colorimetrically with thiocyanate.
c) Determined cryoscoipically in benzene.

TABLE 2. NMR AND IR DATA OF TRIALKYLSTANNYLFERROCENES

NMR CCl_4 (τ value)

Compound	$H_{u.r}$	$H_{\alpha,\beta}$		H_b
$CpFeC_5H_4SnEt_3$	5.92[s] (5.0)	5.76[t] (2.3)	6.08[t] (2.2)	7.98—9.52[m] (18.5)
$Fe(C_5H_4SnEt_3)_2$		5.82[t] (4.0)	6.11[t] (4.0)	7.99—9.50[m] (29.4)
$CpFeC_5H_4SnPr_3$	6.01[s] (5.0)	5.77[t] (2.0)	6.09[t] (1.9)	7.83—9.54[m] (23.0)
$Fe(C_5H_4SnPr_3)_2$		5.86[t] (4.0)	6.14[t] (4.0)	7.82—9.55[m] (42.6)
$CpFeC_5H_4SnBu_3$	6.01[s] (5.0)	5.76[t] (2.1)	6.09[t] (2.1)	7.82—9.60[m] (30.0)
$Fe(C_5H_4SnBu_3)_2$		5.84[t] (4.0)	6.12[t] (4.0)	7.82—9.60[m] (53.6)

$H_{u.r}$: unsubstituted ring protons, $H_{\alpha,\beta}$: alpha and beta protons on stannyl substituted rings,
H_b: protons of alkyl groups, s: singlet, t: triplet, m: multiplet

IR data

Compound	Wave number (cm^{-1})								
$CpFeC_5H_4SnEt_3$	3061m	2928vs	2896vs	2851 s	1462m	1417m	1377m	1136 s	1106 s
	1023 s	998 s	957w	943w	814 s				
$Fe(C_5H_4SnEt_3)_2$	3063m	2930vs	2904vs	2859 s	1464 s	1419m	1378m	1297w	1233w
	1178m	1139 s	1052 s	1025 s	958m	943m	823 s		
$CpFeC_5H_4SnPr_3$	3060m	2936vs	2916vs	2844 s	1462m	1412m	1377m	1300m	1274w
	1181w	1136m	1106 s	1060 s	1023 s	998m	814 s	793m	
$Fe(C_5H_4SnPr_3)_2$	3058m	2940vs	2916vs	2846 s	1452m	1414m	1376m	1330m	1296w
	1274w	1180w	1137m	1060 s	1024 s	986m	822 s	793m	
$CpFeC_5H_4SnBu_3$	3063m	2947vs	2913vs	2844 s	1456 s	1413m	1376 s	1355w	1337m
	1289m	1248w	1181m	1136 s	1105 s	1069 s	1047 s	1022m	995m
	959m	873m	863m	805 s					
$Fe(C_5H_4SnBu_3)_2$	3065m	2950vs	2914vs	2844 s	1457 s	1414m	1376 s	1357w	1338m
	1291m	1248w	1180m	1136 s	1070 s	1049m	1023 s	998m	873m
	863m	820 s	808m						

according to a method previously reported;[1] the metalation was confirmed in advance of the reaction with trialkyltinchloride by carbonation to give the mixed mono- and dicarboxyferrocenes. As an example, the preparation of the triethylstannylferrocenes will be described.

Triethylstanylferrocenes. A 20.0 g (0.11 mol) sample of ferrocene in 300 m*l* of anhydrous tetrahydrofuran was lithiated by the use of 300 m*l* of a 0.41 molar solution of *n*-butyllithium in anhydrous ether. A solution of triethyltin chloride (132.7 g 0.6 mol) in 180 m*l* of ether was added to the above orange-

yellow lithiated ferrocene suspension over a period of 4 hr at below −60°C. After the addition, the mixture was stirred at −30°C for 15 hr, and then at room temperature for a further 30 hr, during which period the colored precipitate seemed to be dissolved to give a dark red solution. The whole mixture was then concentrated on a steam bath to about 500 m*l*, and the concentrate was repeatedly washed with water to neutrality and dried over calcium chloride. The complete removal of unreacted ferrocene was effected by repeated freezing out in a dry ice-acetone mixture followed by sublimation at 3 mmHg. The remaining liquid was fractionated through a packed column to give triethylstannylferrocene (4.7 g 10.7%) and 1,1′-bis-(triethylstannyl)-ferrocene (12.5 g, 19.4%), both being high-boiling mobile liquids with a distinct brown color.

Procedures analogous to those used for the triethyl-derivatives gave the tributyl- and tripropyl-derivatives, as is shown in Table 1.

The authors' thanks are due to Dr. H. Watanabe for his kind discussion on the various phases of this work and to the Hitachi Chem. Ind. Co. for the supply of dicyclopentadiene used herein.

SHORT COMMUNICATIONS

Oxidation of Propylene Adsorbed on Oxide Catalysts

Yutaka KUBOKAWA, Takehiko ONO, Takeshi TOMINO and Norio YANO

Department of Applied Chemistry, University of Osaka Prefecture, Sakai, Osaka

(Received October 15, 1969)

Although the oxidation of olefins on oxide catalysts has been investigated by many workers, the nature of the adsorption complex during the oxidation reaction still remains to be unclarified.[1] In the present work, the interaction of oxygen with propylene adsorbed on various oxides was investigated. On the catalyst[2] which had already adsorbed propylene it was found that the amount of oxygen adsorbed increased markedly compared to that on the cleaned catalyst. In the case of Co_3O_4, the increase in the amount of oxygen adsorbed was proportional to the amount of propylene previously adsorbed as seen in Fig. 1. On ZnO the amount of oxygen adsorbed on propylene-covered surface was very small at 0°C. After the measurement at 0°C the temperature of the catalyst was raised in oxygen. It was found that an appreciable adsorption of oxygen occurred above 80°C. The amount of oxygen adsorbed at 80°C after contact for 3 hr was also proportional to the amount of propylene adsorbed.

After the oxygen adsorption experiment, the oxygen remaining in the gas phase was removed by Töpler pump and desorption experiments were carried out. It was found that the desorbtion of oxygen as well as of propylene decreased markedly compared to the desorption in the case where only oxygen or propylene had been adsorbed. This suggests that enhancement of the oxygen adsorption results from the interaction of oxygen with propylene adsorbed with the formation of an adsorption complex.

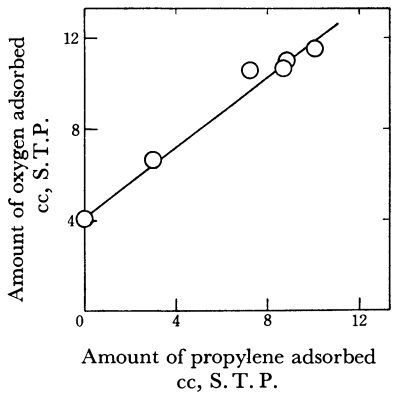

Fig. 1. Enhancement of oxygen adsorption on Co_3O_4 (8.55 g; 100 m²).

After formation of the propylene-oxygen complex, the temperature of the catalyst was raised in steps in oxygen. It was found that the complex was oxidized to carbon dioxide and water. The result obtained with ZnO is shown in Fig. 2. It is seen that the amount of oxygen reacted at each stage passes through two maxima, one corresponding to the uptake at 80°C with the formation of complex, and the other corresponding to the reaction at 350°C with the formation of carbon dioxide. This suggests that the oxidation of propylene adsorbed on ZnO proceeds in the two consecutive steps, *i.e.*, the complex formation with a low activation energy, and the oxidation of the complex to carbon dioxide and water with a high activation energy. It was found that such a two step mechanism could be applied in the catalytic oxidation of propylene on oxides as well as the oxidation of propylene adsorbed. Details will be published in a forthcoming paper.

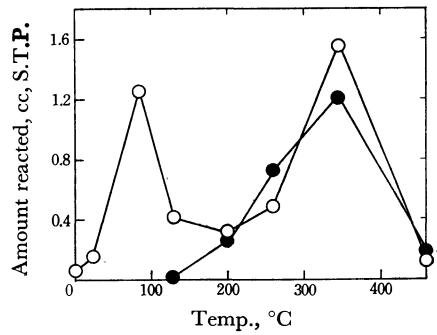

Fig. 2. Interaction of oxygen with propylene adsorbed on ZnO (5 g; 15.3 m²), —○—, O_2 reacted; —●—, CO_2 formed.

1) H. H. Voge and C. R. Adams, "Advances in Catalysis," Vol. 17, Academic Press, N.Y. (1967), p. 151.

2) Prior to the experiment the catalyst was evacuated at 450°C. The time of evacuation was 24 hr on Co_3O_4 and 10 hr on ZnO.

The Structure of an Antibiotic, B-58941

Takashi SUZUKI

Research and Development Division, Takeda Chemical Ind., Ltd., Higashiyodogawa-ku, Osaka

(Received October 7, 1969)

Streptomyces fradiae var. acinicolor B-58941 produced a basic macrolide[1] (I), $C_{37}H_{59}O_{12}N$, *m/e* 709 (M^+), mp 229°C, $[\alpha]_D^{22}$ −88.4° (*c* 1, $CHCl_3$), UV: 240 mμ (log ε: 4.21), IR: 2705, 1738, 1730, 1715, 1682, 1615 cm^{-1}, NMR*[1]: 9.71 (1H, COH), 6.54 (1H, d, 16Hz), 6.34 (1H, d, 16Hz), 2.52 (6H, $-NMe_2$), 1.40 (3H, –C–Me), 1.3—1.0 (15H, 5 *s*-Me), 0.87 (3H, t), similar to acumycin[2] and cirramycin B.[3]

I gave the diacetate (II), $C_{41}H_{63}O_{14}N$, mp 121°C, which lacked a free OH, and a monothiosemicarbazone which showed a new signal at 7.52 ppm (1H, t, $-N{=}CH{-}CH_2-$) in its NMR spectrum.

The mild hydrolysis of I afforded a neutral sugar (III), $C_6H_{10}O_3$, *m/e* 130 (M^+), UV: 280 mμ (log ε: 1.27), IR: 3420, 1720 cm^{-1}, NMR: 5.7—5.0 (1H, O–CH), 4.6—3.8 (1H, Me–CH), 2.3—1.8 (4H), 1.5—1.1 (3H, *s*-Me), positive to Fehling's reagent and iodoform reaction, and a basic substance (IV, B-58941-B), $C_{31}H_{51}O_{10}N$, mp 123°C, UV: 240 mμ (log ε: 4.11), IR: 2725, 1740—1710, 1687, 1620 cm^{-1}, which appeared to be very similar to cirramycin A_1 (CMA_1) in its physicochemical and biochemical properties. The periodate oxidation of III yielded one mole each of acetaldehyde and succinaldehydic acid. III was concluded to be 2,3,6-trideoxyhexopyranos-4-ulose.

From the hydrolysate of IV mycaminose[5] (V), $C_8H_{17}O_4N$, was obtained. The catalytic reduction of I gave a tetrahydro product which lacked an absorption maximum at 240 mμ and showed the presence of a new signal due to *s*-Me and the loss of the *t*-Me. The treatment of IV with KI-AcOH afforded a compound, UV: 281 mμ (log ε: 4.09), which showed a new signal at 1.78 ppm (3H, (s), C=C–Me).

The structure of CMA_1 has been proposed by Kawaguchi *et al.*,[4] but the position of the attachment of the macrolactone moiety ot V has not been established. The author has undertaken NMR spin-decoupling studies of II. As Fig. 1 shows, all the protons in II were unambiguously assigned, and the structure of IV was shown to be in good agreement with that of CMA_1. The signal due to H_3, which was coupled to H_2 and H_4, showed a downfield shift upon acetylation, whereas the signal due to H_5 (doublet-like) did not shift. This certainly establishes that the anomeric hydroxyl of V is combined with the C_5–OH of II. Since the anomeric H'_1 is coupled to H'_2, which shifts downfield upon acetylation, III should be bonding at the C'_4–OH of V. In conclusion, the structure I may be proposed for B-58941.

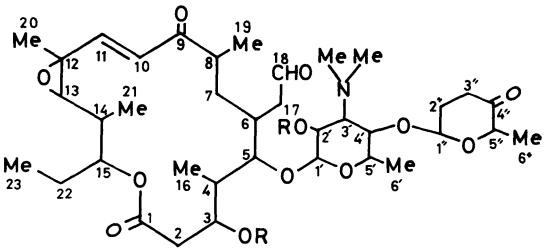

I R=H II R=Ac

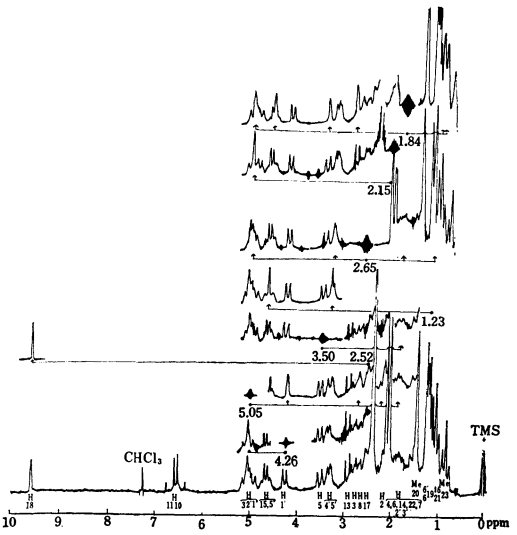

1) T. Kusaka, T. Suzuki and H. Yamamoto, *Ann. Rept. Takeda Res. Lab.* (in press).

*1 Measured in $CDCl_3$, δ (ppm), 100 Mc.

2) B. Bickel, E. Gäuman, R. Hütter, W. Sackmann, E. Vischer, W. Vaser, A. Wettstein and H. Zahner, *Helv. Chim. Acta*, **45**, 1396 (1962).

3) H. Kawaguchi, H. Koshiyama and M. Okunishi, U. S. 3159549 (1964); H. Koshiyama, M. Okanishi, T. Ohmori, T. Miyake, H. Tsukiura, M. Matsuzaki and H. Kawaguchi, *J. Antibiot., Ser. A*, **16**, 59 (1963).

4) H. Tsukiura, M. Konishi, M. Saka, T. Naito and H. Kawaguchi, *ibid.*, **22**, 61, 89 (1969).

5) F. A. Hochstein and P. P. Regna, *J. Amer. Chem. Soc.*, **77**, 3353 (1955).

Hydroxylation of Toluene and Xylenes with *t*-Butyl Hydroperoxide-Aluminum Chloride

Shizunobu HASHIMOTO and Wataro KOIKE

Department of Applied Chemistry, Doshisha University, Karasuma-imadegawa, Kamikyo-ku, Kyoto

(Received July 18, 1969)

Although extensive studies of the oxidation reactions of various organic compounds with hydroperoxides have been carried out, the oxidation of an unactivated aromatic nucleus by hydroperoxides has been neglected. Hamilton *et al.*[1] have, however, reported on the hydroxylation of aromatic compounds by hydrogen peroxide in the presence of ferric ion and catecol. They showed that the use of alkyl hydroperoxides, such as ethyl and *t*-butyl hydroperoxides, instead of hydrogen peroxide was ineffective in the hydroxylation in the catalytic system. We wish to report here our preliminary results of a synthetically-useful method for introducing a hydroxy group directly into the aromatic nucleus of simple methylbenzenes, using *t*-butyl hydroperoxide in the presence of aluminum chloride.

In a typical experiment, a solution of 0.05 mol of the peroxide in 30 m*l* of toluene was added to a stirred mixture of 0.1 mol of aluminum chloride and 90 m*l* of toluene at −20°C over a half hour period. After having been stirred for an aditional 2 hr at this temperature, the reaction mixture was poured into ice cold hydrochloric acid. After the usual working-up, cresols (*o*- : *m*- : *p*-=56 : 8 : 36) were obtained in a 76 mol% yield, accompanied by *t*-butyltoluenes (*m*- : *p*-=65 : 35) in a 78 mol% yield.

An electrophilic mechanism for this hydroxylation is predicted by the cresol-isomer distribution and by the necessity that aluminum chloride be present.[2] The rates of this hydroxylation of methylbenzenes relative to benzene obtained by the competitive method[3] were *m*-xylene : *p*-xylene : *o*-xylene : toluene : benzene=136.6 : 63.5 : 62.1 : 13.8 : 1.0. The relative rates in our system with methylbenzenes were somewhat higher than those from electrophilic oxygenation with diiospropyl peroxydicarbonate - aluminum chloride[4] ($K_{toluene}/K_{benzene}$ =9.6), and with di-*t*-butyl peroxide-aluminum chloride[5] ($K_{toluene}/K_{benzene}$=10.4). Our results suggest, therefore, that the oxidizing agent is an electrophile which exhibits a high substrate selectivity.

Information was obtained concerning the nature of the oxidizing species by carrying out the reaction of *n*-butyl hydroperoxide with toluene in the presence of aluminum chloride at −20°C for 2 hr. In this case, the oxygenation products were obtained not as phenolic metarials but as alkyl aryl ethers, namely, *n*-butyl tolyl ethers (10 mol%). This indicates that the oxidizing agent is not the hydroxy group but the alkoxy group.

On the basis of the experimental findings, the following electrophilic substitution process may be proposed for the title reaction, where the *t*-butyl oxonium ion (I) is the oxidizing agent. Since *t*-butyl hydroperoxide is prone to dissociate essentially in the form of $t\text{-BuOO}^{\delta-}\text{–H}^{\delta+}$, alumium chloride may initially co-ordinate with the peroxide at the oxygen ($\delta-$) to cause the heterolytic fission of the O–O bond. I attacks the aromatic substrate to form, presumably, a *t*-butyl aryl ether (II). The free phenol should arise from the subsequent dealkylation of II under the present reaction conditions,[6] followed by treatment with hydrochloric acid:

$$t\text{-BuOOH} + AlCl_3 \longrightarrow \underset{(I)}{t\text{-BuO}^+} + [AlCl_3(OH)]^-$$

$$I + ArH \longrightarrow \underset{(II)}{ArOBu\text{-}t} + H^+$$

$$II + ArH + AlCl_3 \longrightarrow ArOAlCl_2 + ArBu\text{-}t + HCl$$

$$ArOAlCl_2 \xrightarrow[H^+]{H_2O} ArOH + HOAlCl_2$$

1) G. A. Hamilton, J. W. Hanifin, Jr., and J. P. Friedman, *J. Amer. Chem. Soc.*, **88**, 5269 (1966).

2) The yield of phenols was dependent on the ratio of aluminum chloride to peroxide, at least a 2 : 1 molar ratio being required for good results.

3) a) The relative rates were determined by gas-liquid chromatography. b) The relative rates of xylene *vs.* toluene were *m*-xylene : *p*-xylene : *o*-xylene=9.9 : 4.6 : 4.5.

4) P. Kovacic and S. T. Morneweck, *J. Amer. Chem. Soc.*, **87**, 1566(1965).

5) S. Hashimoto, W. Koike and T. Murachi, *Kogyo Kagaku Zasshi*, **72**, 2015 (1969).

6) *t*-Butyl phenyl ether underwent rapid decomposition in toluene at −20°C in the presence of aluminum chloride. The essentially quantitative dealkylation yielded phenol and *t*-butyltoluenes. However, *n*-butyl phenyl ether did not decompose under the condition.

Dose-rate Dependency of the Radiation-induced Polymerization of Ethylene in an Aqueous Solution of *tert*-Butyl Alcohol

Shiro SENRUI, Hirondo KURIHARA and Masaaki TAKEHISA

Takasaki Radiation Chemistry Research Establishment, Japan Atomic Energy Research Institute, Takasaki, Gumma

(Received October 20, 1969)

Recently, Suganuma *et al.*[1,2] have reported the kinetics of the radiation-induced polymerization of ethylene in the presence of *t*-butyl alcohol. Judging from the dose-rate dependency of STY (polymerization rate, mole ethylene/*l*/hr), they concluded that the monomolecular termination process played an important role.

We wish to report an attempt to elucidate the effect of the dose rate on the polymerization of ethylene in the presence of *t*-butyl alcohol and water.

The rate of the polymerization of ethylene was determined by measuring the yield in a 100-cc (internal volume) autoclave in which the pressure was held constant at 400 kg/cm^2 during the polymerization. The differential STY increased with an increase in time at an initial stage of the polymerization, while in the succeeding stage it became constant and was independent of the time. In this region, the reaction seems to be stationary on the concentration of active species. As is shown in Fig. 1, the differential STY in the latter stage was proportional to the square root of the dose rate. This suggests that the active species are mutually terminated.

As has been described above, the bi-molecular termination is assumed for this polymerization. The correlation between the active species concentration, [R·], and the reaction time, t, is given as:

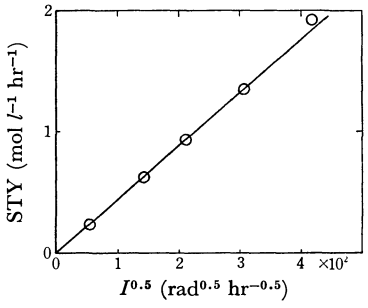

Fig. 1. Dose rate dependency of differential STY in the stationary state.

$$[\mathrm{R}\cdot] = \frac{\sqrt{K_i I}\{\exp(2\sqrt{K_i I k_t}t)-1\}}{\sqrt{k_t}\{\exp(2\sqrt{K_i I k_t}t)+1\}} \quad (1)$$

From the long-chain approximation, the overall polymerization rate, R, is given as:

$$R = R_p = K_p[\mathrm{R}\cdot] \quad (2)$$

By introducing Eq. (1) into Eq. (2) and integrating it, the polymer yield, M_p, is given as:

$$M_p = \frac{K_p}{k_t}[\ln\{1+\exp(2\sqrt{K_i I k_t}t)\}-\ln 2-\sqrt{K_i I k_t}t] \quad (3)$$

This equation indicates that the differential STY in the latter stage is proportional to the square root of the dose rate, as is shown in Fig. 1. The relationship between M_p and 2 $(K_i I k_t)^{0.5}t$ should be shown as a normalized curve, regardless of the dose rate and the reaction time.

If it is assumed that M_p is proportional to I^α, the dose-rate exponent, α, can be calculated by the use of Eq. (3). As is shown in Fig. 2, α varies with the dose rate and with the reaction time in the range from 0.5 to 1.0. This shows that the type of termination reaction can not be decided simply from the value of α, for this relation is calculated by assuming bi-molecular termination.

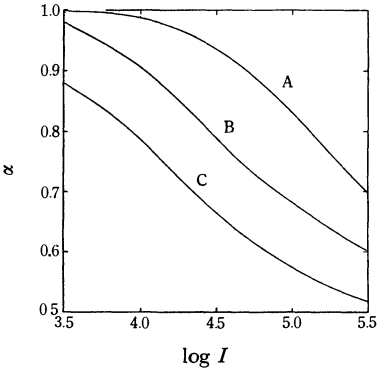

Fig. 2. Dose rate dependency of α.
A: 0.5 hr B: 1.0 hr C: 2.0 hr

The dose-rate exponent, α, shown in Fig. 2, is in good agreement with the experimental results. This fact can not be explained by the monomolecular termination mechanism alone, indicating that the bi-molecular termination process plays an important role.

Precise investigations of reaction mechanism are now under way and will be reported elsewhere.

1) F. Suganuma, S. Machi, H. Mitsui, M. Hagiwara and T. Kagiya, *J. Polym. Sci., Part A-1*, **6**, 2069 (1968).
2) F. Suganuma, H. Mitsui, S. Machi, M. Hagiwara and T. Kagiya, *ibid.*, **6**, 3127 (1968).

The Asymmetrically-selective Oxidation Reaction of 3,4-Dihydroxyphenylalanine Catalyzed by the Poly-L-lysine-copper(II) Complex

Masahiro HATANO, Tsunenori NOZAWA and Michio YONEYAMA

The Chemical Research Institute of Non-aqueous Solutions, Tohoku University, Katahira-cho, Sendai

(Received November 8, 1969)

Many polymer-metal complexes[1,2] have been found to exhibit high catalytic efficiencies in comparison with the low molecular analogs. However, no polymer-metal complex showing an asymmetrically selective catalysis has been reported. In this communication we wish to report that the oxidation reaction of 3,4-dihydroxyphenylalanine (DOPA) can be catalyzed by the poly-L-lysine-copper(II) complex (PLL-Cu(II)) with an appreciable asymmetric selectivity. This is the first example of a synthetic polymer-metal complex used to catalyze a reaction with an asymmetric selectivity. Most of the experimental details have been reported elsewhere.[1] At several temperatures from 25 to 10°C, the circular dichroism of the catalyst and the rate of the oxidation reaction were measured. These kinetic and circular dichroism results are collected in Table 1, which indicates that the initial oxidation rate of D-DOPA (V_D) is greater than that of L-DOPA (V_L) and that the ratio of the rate of D-DOPA to that of L-DOPA (V_D/V_L) increases with a decrease in the reaction temperature measured, reaching 1.5 at 10°C. These observations seem to be of great interest by analogy with the catalytic behavior of enzymes. It has been reported that the asymmetric induction in the oxidation reaction may be attributed to the selective formation of the substrate-catalyst complex.[1] It is evident from Table 1 that, at a constant T_{Cu}/T_N*1 (0.13), the asymmetric selectivity ratio in the reaction increased with an increase in the α-helix content in the catalyst. However, when the T_{Cu}/T_N was varied, the selectivity did not increase with the α-helix content. That is, the catalyst prepared at $T_{Cu}/T_N=0.05$ exhibited almost no selectivity, though it had a much higher α-helix content than the catalyst prepared at $T_{Cu}/T_N=0.13$. These results mean that the α-helix structure in the catalyst may be necessary, but may not be sufficient to show an appreciable selectivity. The chief difference, other than the α-helix content, between the catalyst prepared at $T_{Cu}/T_N=0.05$ and that prepared at $T_{Cu}/T_N=0.13$ may be the distances between the cupric complex units along the polymer chain,*2 because the asymmetric structure in a cupric complex unit did not differ very much, judging from the fact that the molar ellipticity in the wave length of 240—650 mμ changed little with the variation in the T_{Cu}/T_N ratio.[1] Therefore, the selectivity in the catalysis can not be correlated with the separated cupric complex unit only, but two or more cupric complex units may act cooperatively in the selective catalysis. Consequently, it seems that the results can be explained by the assumption that the helix structure in the catalyst serves to hold the two or more cupric complex units in a special steric configuration, thus forming a site which can bind D-DOPA selectively.

TABLE 1. OXIDATION RATE OF DOPA CATALYZED BY PLL-Cu(II)[a]

T_{Cu}/T_N	Temp. (°C)	V_D	V_L	V_D/V_L	α-Helix content (%)
		$\times 10^{-5}$ mol/l min			
0.13	25	2.9_3	2.7_4	1.0_7	15.6
0.13	20	2.2_0	1.9_0	1.1_6	17.2
0.13	15	1.8_5	1.3_0	1.4_2	24.0
0.13	10	1.4_3	0.9_3	1.5_3	27.6
0.15	20	2.8_2	2.7_9	1.0_2	6.3
0.13	20	3.5_0	2.7_9	1.2_5	17.2
0.10	20	2.9_5	2.7_6	1.0_7	25.6
0.05	20	2.7_7	2.6_8	1.0_3	57.6

a) The kinetic experiments were carried out at pH 10.5 at the condition of $T_{Cu}=2.0\times10^{-4}$M. The initial concentration of DOPA was 1.0×10^{-4}M in the upper four runs and 2.1×10^{-4}M in the lower four runs.

1) M. Hatano, T. Nozawa, S. Ikeda and T. Yamamoto, *Kogyo Kagaku Zasshi*, **72**, 474 (1969); *Makromol. Chem.*, to be published.

2) H. Sigel, *Angew. Chem.*, **81**, 161 (1969).

*1 T_{Cu} and T_N represent the total analytical concentration of the cupric ion and that of lysine residue of PLL in the solution, respectively.

*2 From the results of various experiments, it may be considered that a cupric complex unit is made of a cupric ion coordinated by four amino nitrogens in a plane and one peptide nitrogen at the apical position and that PLL-Cu(II), as a whole, takes a certain helical structure in all T_{Cu}/T_N of 0.05—0.15. These results will be reported elsewhere.

On the Photochemical Decomposition of Bismercuracycloalkanes

Tsutomu SAKAKIBARA, Shigeatsu KURATA and Yoshinobu ODAIRA

Department of Chemical Technology, Faculty of Engineering, Osaka University, Yamadakami, Suita, Osaka,

(Received October 9, 1969)

In previous papers,[1,2] new information on the photochemical reactions of inorgano- and organomercury compounds has been given. In this communication, an abnormal behavior of alkyl radical in the photolysis of bismercuracycloalkanes will be described.

In a typical experiment, 1.0 g of 1,6-bismercuracyclodecane (I) (n=4) was irradiated in 230 m*l* of benzene for 29 hr at room temperature in carbon dioxide atmosphere with a 120 W low pressure mercury lamp. 83 m*l* of gaseous products was evolved and its glc analysis showed the presence of n-butane (42.0%), butene-1 (42.0%), cyclobutane (5.4%) and lower hydrocarbons (10.5%), which consisted of methane (5.5%), ethane and ethylene (4.2%), and propane and propylene (0.8%). Neither n-octane nor cyclooctane was detected. The results of photolysis of I (n=4) in various solvents are shown in Table 1.

The formation of n-butane, butenes and cyclobutane obviously shows the photochemically homolytic fission of C–Hg bond of I (n=4). Though the formation of cyclobutane seems to take place directly through subsequent C–Hg bond fission of a radical II formed by the photolysis of I (n=4), an alternative path through the intramolecular metathesis of II cannot be eliminated.[3]

It is of interest that the yield of n-butane was almost independent of the hydrogen-donating ability of the solvent (Table 1). Even in the systems without suitable hydrogen-donating agents such as tetrachloroethylene or the solid phase, the formation of n-butane was notable. It is noteworthy that the formation of lower hydrocarbons, such as methane, ethane or ethylene, was significant in all cases. Similar results were found in the photochemical reaction of 1,7-bismercuracyclododecane (I) (n=5) in benzene, *viz.*, in addition to pentenes and cyclopentane, the products contained a considerable amount of n-pentane and lower hydrocarbons.

In order to clarify the results, detection of the radical species formed during the photochemical reaction of I (n=5) was made by ESR studies. Though no diradical intermediate could be detected, a spectrum assinged to a cyclic alkyl radical I-a or I-b was obtained. Characteristics of the hyperfine structure of this radical were as follows; g-factor (2.0022), hyperfine coupling constant (in Gauss) ($A^{H}_{\alpha}=A^{H}_{\beta 1}=22.5$, $A^{H}_{\beta 2}=2A^{H}_{\beta 1}$).[4]

From the ESR result, it may be concluded that the radical I-a or I-b, generated from I (n=5) through the hydrogen-abstraction by other radicals such as II (n=5), must lead to the formation of lower hydrocarbons *via* further decomposition of C–Hg bonds.

A mechanism involving an inter- or intramolecular hydrogen-abstraction by the photochemically formed radical intermediate II should be given for the photochemical decomposition of I.

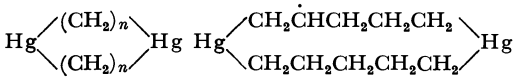

(I) (n=4, 5)

(I-a)

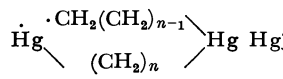

(II) (n=4, 5)

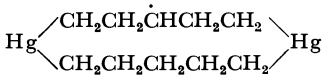

(I-b)

TABLE 1. PHOTOLYSIS OF I (n=4) IN VARIOUS SOLVENTS

Reaction condition[a]			Gaseous products				
Solvent (m*l*)		Irradiation (hr)	Evolved gas (m*l*)	Composition (%)[b]			
				n-Butane	Butenes	Cyclobutane	Lower H. C.
	(800)	4.5	140	58.8	13.5	0.02	27.6
THF	(220)	5.0	87.5	52.2	8.4	0.3	39.1
	(230)	29	83.0	42.0	42.0	5.4	10.5
$CCl_2=CCl_2$	(170)	25	19.0	28.9	13.8	0.8	53.7
None[c]		15	54.7	69.3	0.9	4.2	25.6

a) 1.0 g of I (n=4) was photolyzed in various solvents.
b) The evolved gas was analyzed by gas-liquid chromatography using Goley column (U-90).
c) I (n=4) was photolyzed in solid phase in carbon dioxide atmosphere.

1) Y. Odaira, H. Matsuo, T. Sakakibara and S. Tsutsumi, *Nippon Kagaku Zasshi*, **88**, 39 (1967).
2) T. Sakakibara, Y. Odaira and S. Tsutsumi, *Tetrahedron Lett.*, **1968**, 503.
3) *Cf.* R. E. Rebbert and P. Ausloos, *J. Amer. Chem. Soc.*, **86**, 2068 (1964).
4) *Cf.* K. Kuwata and K. Inada, *Tetrahedron Lett.*, **1967**, 11.

BULLETIN OF THE CHEMICAL SOCIETY OF JAPAN VOL. 43 297—300 (1970)

Kinetic Studies of the Pulse Radiolysis of *trans*-Stilbene in Several Solvents*[1]

Hisashi UEDA*[2]

The Department of Chemistry, The Ohio State University, Columbus, Ohio 43210, U. S. A.

(Received June, 10, 1969)

The kinetics of the transient species of *trans*-stilbene in several solvents were studied using single pulsed electron beam (0.5 μsec × 300 mA) and the spectroscopic method. The species existing immediately (0—20 μsec) after a pulse is found to disappear according to a sum of two first-order decay-rate equations. The temperature dependence of the formation and decay of this species shows that there are two different *trans*-stilbene cations, R_s and R_f, which have almost identical absorption spectra but different formation and decay rates. The rate constants for R_s were not affected by the temperature, however, those for R_f were strongly affected. R_f is not found in the solution of *trans*-stilbene in 1,2-dichloroethane if a small amount of CCl_4 is added. Some effects of the dielectric constant were observed on the decay-rate constant of R_f. From these facts, it can be concluded that R_f is formed by an ordinary transfer of a hole from the solvent cation to the solute molecule. As R_s seems to be formed by a mechanism other than that of R_f, a possible scheme for it has been discussed.

The decay kinetics of the ionic species in solution have already been studied by the electrochemical method.[1,2] It was found that the solvation or the dielectric properties of the solvent greatly affect the decay kinetics of the ions. In the present work, therefore, the effect of the dielectric constant on the decay kinetics of the ionic transient species formed by ionizing radiation was investigated.

The kinetic data for the formation and the decay of the cation of *trans*-stilbene in alkyl-halides have already been included in a previous paper, together with the spectroscopic data.[3] The kinetic analyses in the previous paper, however, were carried out only for the time period of 0—9 μsec after a pulse; this method has, the present author believes, led to the right conclusion. Nevertheless, it is expected that some more information can be obtained by including the variation of the optical densities due to the ions still left 10—20 μsec after a pulse. Therefore, some further analyses of the rate curves are another purpose of the present study.

Experimental

The experimental procedures are the same as those reported in the previous paper.[3] The acetonitrile (AN) was purified by passing it through a vacuum-dried layer (30 cm) of alumina in a vacuum and by successive distillations in a vacuum. The solvents used were AN, carbon tetrachloride (possessing the two extreme values of dielectric constants, 35.99 and 2.25, at 25°C), *n*-butylchloride (BuCl), 1,1-dichloroethane (11DCE), 1,2-dichloroethane (12DCE), 1,1,2-trichloroethane (TCE), 1,1,2,2-tetrachloroethane (TECE), and 2-methyl tetrahydrofuran (MTHF) whose dielectric constants are between those two extremes.

Results

Figure 1 shows that the attempts to analyse the kinetic data with second-order rate curves were unsuccessful. For this reason, analyses with first-order rate curves were attempted; however, here the results were not successful, either. However, Fig. 2 shows that the decay rate of the transient species of *trans*-stilbene in AN consists of two processes with two different first-order rate constants, k_s and k_f, where the suffix f signifies that the rate is faster than that with s at 25°C. It will be seen that the decay curve, C, of the total light absorption can be interpreted as the sum of the two rate curves, S and F, the faster and the slower decays at 25°C. The rate curves obtained with 11DCE, CCl_4 MTHF, and all the other solvents have exactly the same shape, each consisting of two first-order rate curves, S and F. The kinetic constants for the S and F curves obtained with various solvents are listed in Table 1. In Fig. 3, the values of A_f and A_s (the relative values of the initial amount of the

*1 Supported by the U. S. Atomic Energy Commission.

*2 Present address: Tokyo Kogyo Shikenjo, Mita, Meguro-ku, Tokyo.

1) F. Accasina, S. Petrucci and R. N. Fuoss, *J. Amer. Chem. Soc.*, **81**, 1301 (1954).
2) E. Grunwald, *Anal. Chem.*, **26**, 1696 (1954).
3) H. Ueda, This Bulletin, **41**, 2578 (1968).
4) M. Burton, M. Dillon and R. Rein, *J. Chem. Phys.*, **41**, 2228 (1964).
5) H. Hase, *J. Phys. Soc. Jap.*, **24**, 589 (1968).
6) T. Higashimura, private communication.

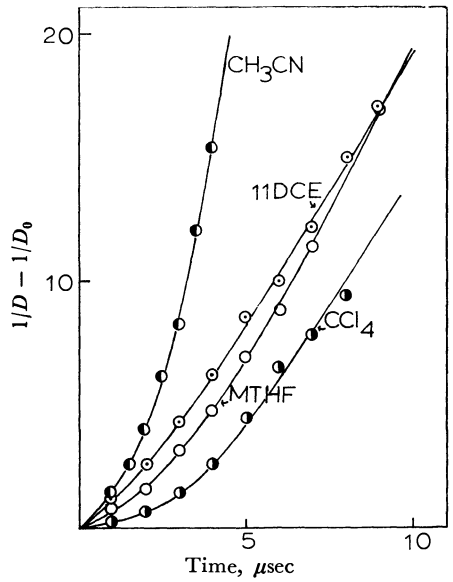

Fig. 1. Analyses of the results with second order rate equations. The ordinate indicates the difference of the inverse of the optical densities, $1/D$ and $1/D_0$, where D_0 signifies the optical density at the end of a pulsed irradiation and at 25°C. The abscissa indicates the time after a pulse.

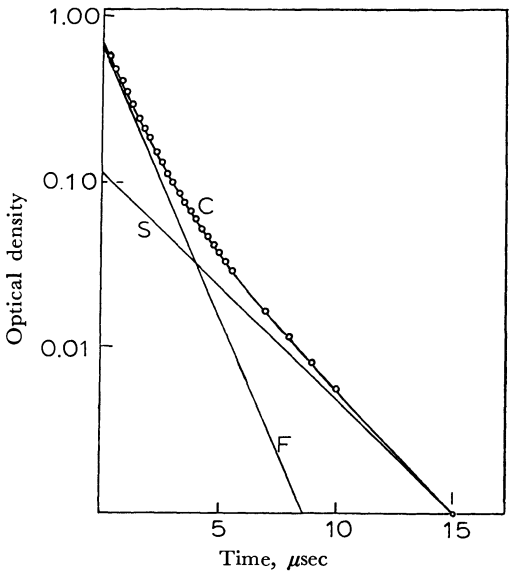

Fig. 2. Analyses of the results with first order decay rates. The ordinate shows the optical density, at 25°C, of the sample cell on a log scale and the abscissa shows the time after a pulse, in μsec.
Solvent: CH_3CN
trans-Stilbene: 1.76×10^{-2} mol/*l*

transient species decaying with k_f and k_s) expressed in the scale of optical density are plotted against the temperature. The solvent used for this experiment was 11DCE because that substance has the lowest

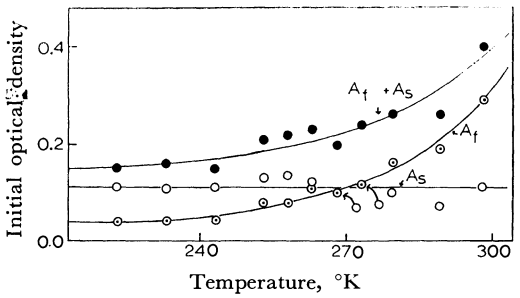

Fig. 3. The temperature dependence of the initial optical density, at 490 mμ, of the solution of *trans*-stilbene in 11DCE at the concentration of 1.40×10^{-2} mol/*l*. Explanations of A_f and A_s are in text.

melting point (−98°C) among the solvents used. It was found that A_s is constant in the temperature region studied and that it is 0.11. It was also found that k_s is constant in the same temperature region and is 3.70×10^4 sec^{-1}. In Table 1, the A_f, A_s, k_f, and k_s values are shown for various solvents and mixed solvents of BuCl and 11DCE. In Table 2 the effects of the solute concentration on the k_f, A_f, and A_s values are shown.

Discussion

A second-order rate has been observed for a recombination process of free radicals; for this reason, a second-order rate has been expected for the decay of ions in a solution. In the present study, however, second-order rates can not be used for the analyses of the results. All are precisely interpreted by the sums of first-order rate equations. Similar types of decay rates have also been observed for the decay of trapped electrons in rigid glass matrices.[4] In these cases, however, the analyses of the rate curves were qualitative and the components were selected rather arbitrarily. Recent work[5,6] has indicated (I) that the ratio of the two (though in some papers three components have been postulated[4]) components is affected by the temperautre, the wavelength of the bleaching light, *etc.*, and (II) that the addition of a scavenger affects only the component with the slower decay rate.

In the present case, the consideration of a pseudo-first-order reaction might be necessary. In Table 2, the values of k_f slightly depends on that of A_f, but the values of the k_f/A_f ratio is not constant. The value of k_s does not depend on that of A_s and can ont be interpreted by a pseudo-first-order reaction. Another possibility is that the cation disintegrates spontaneously: $(RH^+) \rightarrow R\cdot + H^+$. This, however, would leave a free radical R· which should have some light absorption in the near UV region. No such formation has been found in the solutions studied. Therefore, some other type of charge neutralization with a first-order rate must be considered.

TABLE 1. THE RATE CONSTANTS AND THE INITIAL OPTICAL DENSITIES FOR VARIOUS SOLUTIONS OF *trans*-STILBENE AT 25°C

Solvents	Concn.	A_f[a]	A_s[a]	A_f/A_s	k_f[b]	k_s[c]
n-Butylchloride	5.75[d]	0.30	0.11	2.7	4.15	6.94
75% BuCl[e] + 25% 11DCE[f]	1.92	0.29	0.10	2.9	2.86	4.23
50% BuCl + 50% 11DCE	2.13	0.32	0.10	3.2	2.69	4.17
25% BuCl + 75% 11DCE	2.12	0.29	0.11	2.6	2.15	3.66
1,1-Dichloroethane	1.73	0.29	0.11	2.9	2.17	3.70
1,2-Dichloroethane	2.22	0.43	0.28	1.5	2.17	5.38
1,2-Dichloroethane with 25 vol% CCl_4	1.60	—	0.09	—	—	4.53
1,1,2-Trichloroethane	1.87	0.73	0.38	1.9	2.67	5.30
1,1,2-Trichloroethane with 0.19 mol/*l* of C_2Cl_6	1.21	0.32	0.20	1.6	1.67	3.45
1,1,2,2-Tetrachloroethane	2.10	0.60	0.14	4.2	0.86	1.60
Carbon Tetrachloride[g]	2.99	12.1	0.14	86	3.34	1.78
Acetonitrile[h]	1.76	0.65	0.11	5.9	3.36	13.8
2-Methyltetrahydrofuran[i]	5.41	0.42	0.12	3.5	2.05	4.50

a) all except g—i were observed at 490 mμ. b) $\times 10^5$ sec^{-1} c) $\times 10^4$ sec^{-1} d) $\times 10^{-2}$ mol/*l*
e) *n*-Butylchloride f) 1,1-Dichloroethane g) at 380 mμ h) at 495 mμ i) at 500 mμ

TABLE 2. EFFECTS OF *trans*-STILBENE CONCENTRATION ON THE KINETIC CONSTANTS AT 25°C

Concentration	A_f	A_s[a]	k_f $\times 10^5$ sec^{-1}	k_f/A_f
2.70×10^{-4}[b]	0.13	0.044	1.34	1.06×10^6
1.16×10^{-3}	0.18	0.060	1.62	0.90
1.70×10^{-3}	0.24	0.081	1.72	0.72
3.19×10^{-3}	0.26	0.088	2.02	0.78
1.30×10^{-2}	0.29	0.099	2.16	0.75
1.73×10^{-2}	0.30	0.099	2.14	0.72
3.48×10^{-2}	0.30	0.102	2.08	0.69
8.97×10^{-2}	0.31	0.103	2.00	0.65

a) k_s is constant and is 3.70×10^4 sec^{-1}.
b) mol/*l*.

In the previous paper it was established that the cation of *trans*-stilbene is formed in the solvents typically represented by 11DCE. Also, an anion can be assigned to the spectrum from a solution in MTHF.[3,7] In CCl_4 the spectrum[3] is almost completely different from that of the cation reported to be formed in polycrystalline CCl_4 by Shida and Hamill.[7] This fact might lead to the conclusion that the transient species formed in CCl_4 in the liquid phase is not an ionic species. However, the addition of a small amount of NH_3 destroyed the optical density due to the transient species observed in CCl_4 almost completely.[3] This indicates that the transient species observed in CCl_4 is also of cationic origin. In AN it is uncertain if the existing species is either one of the ions or both. The shape of the decay curve obtained with AN, shown in Figs. 1 and 2, is identical with those in the other solvents used in this study. Therefore, it is highly probable that the transient species observed have ionic natures in all the cases studied.

In Table 1, it will be seen that the number of C-Cl bonds in a unit volume of the solvent determines A_f. If CCl_4 or C_2Cl_6 exists in the solution, A_f decreases or disappears. The addition of a small amount of CCl_4 or C_2Cl_6 may result in a small decrease in the overall dielectric constant of the solution. The real effect of these compounds, however, will not be through the dielectric constant, but by a means similar to the one by which CCl_3CH_3 and CCl_3CHCl_2, when used as solvents, did not give the solute cations.[3] The absorption spectra of the transient species obtained by CCl_4 are entirely different from those obtained by other solvents, *e.g.*, 12DCE; therefore, the extinction constant at 380 mμ may be considerably larger than that of the pure stilbene cation, at 490 mμ. This would make it possible to interpret the large A_f and A_f/A_s values for CCl_4.

The k_f values for BuCl, 11DCE, and TECE decrease in that order. As the dielectric constant is also expected to increase in that order, it seems that the larger the dielectric constant of the solvent, the smaller the k_f. Such a tendency has also been found for the mixtures of BuCl and 11DCE.

Let the species with the k_f rate constant be named R_f, and that with k_s, R_s. The facts that the temperature strongly affects the formation of R_f, and that the decay rate of R_f, *i.e.*, k_f, is affected by the dielectric constant of the solvent, lead to the conclusion that the normal charge-transfer mechanism from the solvent cation to the solute molecule yields R_f. The effect of CCl_4, which acts as if it were a scavenger to the solute cation, R_f, in 12DCE can also be well explained by this mechanism. The charge transfer between 12DCE is intercepted by one of the added CCl_4 molecules during the

7) T. Shida and W. H. Hamill, *J. Chem. Phys.*, **44**, 2375 (1966).

charge transportation to a solute molecule; then, some chemical reaction at this CCl_4 molecule is started. At any rate, CCl_4^+, if once formed in the liquid phase, should not be good for the production of the solute cation.

It is hard to say if A_s is affected by the dielectric constant of the solvent, as is shown in Table 1. The difference between R_s and R_f is that A_s is little affected by either the temperature or the added CCl_4. The A_s value for MTHF, in which the *trans*-stilbene anion has been obtained, is also similar to those obtained by several of the alkyl halides used.

The k_s values, it seems, do not depend on the dielectric constant of the solvent. The large value for acetonitrile is puzzling, but it is possible to say that the large dielectric constant of acetonitrile does not contribute to the stability of the R_s.

As the R_s is not affected by the temperature or the added CCl_4, the formation of R_s should be different from that of R_f. As the absorption spectra for R_f and R_s are identical,[3] they must be identical species with different routes of formation and decay.

The main purpose of this work, to establish the effect of the dielectric constant of the solvent on the formation and decay kinetics of the solute ions, has not been achieved conclusively, on the other hand, our knowledge of the values of the dielectric constants of the solvent compounds used in this study, especially those values under the influence of a strong electrostatic field, is very little. If these values were known exactly, the present data could perhaps be interpreted in a different way.

The formation and the decay of the solute cation include many steps such as: (A) the excitation of the solvent molecule to form S*′; (B) the partial stabilization of S*′ to form S*; (C) excitation transportation to a solute molecule; (D) excitation transfer to the solute molecule to form R*′ (E) the partial stabilization of R*′ to form R*; (F) the transportation of the excitation or the counterexcitation, and (G) recombination. Here "excitation" is taken in a wide sense and can include both ionization and simple excitation. The rate-determining steps for the formation and the decay processes will be only a few of them. Therefore, a direct determination of the entire process based on the observed reaction rate, which is determined by the rate-determining steps only, will be imperfect. The decay process of the solute cation includes at least the (E), (F), and (G) steps. Even when only the rate-determining step is temperature-independent and proceeds by a first-order rate, while the remaining two steps are not temperature-independent and do not so proceed, the overall result to be observed can be temperature-independent and can proceed with a first-order rate. On the other hand if any one of these steps is destroyed by the scavenger like CCl_4, all the steps seem to be destroyed by the scavenger. For these reasons, it would not be safe to say that the temperature independent kinetic data-obtained for R_s allow us to exclude the possibility of any thermal movements of charged species leading to the formation and decay of R_s.

However, the formation of R_s should be somehow different form that of R_f. As it has been concluded that R_f is formed by a normal charge transfer from a solvent cation to the solute molecule, some other mechanism should be found for R_s. A tentative scheme for R_s may be the following excitation transfer leading to an ion-pair formation:

$$\text{Solvent}_a \rightsquigarrow \text{Solvent}_a^*$$

$$\text{Solvent}_a^* + \text{Solvent}_b \rightarrow \text{Solvent}_a + \text{Solvent}_b^*$$

$$\text{Solvent}_p^* + \textit{trans}\text{-stilbene} \rightarrow \text{Solvent}_p^- + R_s^{(+)}$$

$$R_s^{(+)} + \text{Solvent}_p^- \rightarrow \textit{trans}\text{-stilbene} + \text{Solvent}_p,$$

where the asterisk signifies a non-ionic excited state. The suffix letters are for the identification of each solvent molecule. The plus sign in the parentheses indicates that this R_s species has a net positive charge. As no charge transfer is involved in these schemes, a temperature-independent rate can be expected. Since no transportation of a positive or a negative charge is involved in the decay process of the solute cation, it can proceed with a first-order rate.

The determination of the *G*-value for the formation of the cation of *trans*-stilbene has not been attempted in this work. The determination of the *G*-value is essentially the determination of the extinction constant of the light abosrption by the cation of *trnas*-stilbene. This naturally includes the preparation of a solution of the cation of *trans*-stilbene with a known concentration, and such a preparation can not be done easily. For this reason, the *G*-value determination was reserved for future experiments.

The author wishes to thank Mr. Jerome Brandon for his cooperation in the experiments involved in this study.

BULLETIN OF THE CHEMICAL SOCIETY OF JAPAN VOL. 43 301—305 (1970)

Studies on Nylon Monolayers. I. Pressure-Area Curves for Nylon Monolayers on Water

Toshiko SEIMIYA

Department of Chemistry, Faculty of Science, Tokyo Metropolitan University, Setagaya-ku, Tokyo

(Received April 21, 1969)

The conditions under which nylon monolayer spread on water exhibits a reproducible and well-defined *F-A* curve favorable for detailed investigation of the surface chemical properties of nylon were studied. For this purpose monolayers of Nylons 6 and 8 were spread from such solvents as methyl alcohol, methyl alcohol saturated with calcium chloride, aqueous solution of 90% formic acid and the mixture of phenol and benzene in 1 : 3 volume ratio. The effects of the nature of these solvents, the volume of spreading solution, surface aging and substrate pH on the properties of spread film were studied. It was found that the monolayers can be classified into two different types of film, A and B, according to the behavior of *F-A* curve against compression. The type A film appeared usually at the first compression of the spread film. *F-A* curve of A film varied according to the nature of the spreading solvent and the film was unstable. It readily underwent change to type B by being allowed to stand after the film was compressed to a certain extent, by increasing the volume of the spreading solution or merely by compressing film A to a sufficiently high surface pressure. *F-A* curve of type B film obtained was almost independent of the nature of the spreading solvent and repetition of compression and expansion of the film.

The surface pressure-area curve (*F-A* curve) of nylon monolayer on distilled water has been studied by many investigators[1-6] since the study by Crisp.[7] Recently studies on monolayers of nylon homologues having from three to twelve CH_2 groups in a monomer chain have been reported.[8] However, in most of these studies, various spreading solvents were used without confirming the reproducibility of *F-A* curves of the monolayers, *viz.*, most of the *F-A* curves were obtained only by a single compression of the film. Thus, it is very difficult to draw any conclusion as to whether or not the *F-A* curves are reversible, film substance changes its state, loss of the film substance occurs, and aging or hysteresis appears upon compression and expansion of the film. It is rather unexpected that such fundamental studies have not yet been well established although these troublesome phenomena frequently occur upon careful observation. Accordingly, the present author felt it necessary to examine first of all a well defined condition under which reproducible measurements of nylon monolayer are possible.

The present study deals with the effect of the nature of the spreading solvent, amount of spreading solution, aging and substrate pH upon the nature of monolayers of Nylons 6 and 8.

Experimental

Materials. The samples used in the present study were Nylon 6 of Toyo Rayon Co. and Nylon 8 of Nippon Rayon Co. For the purification,[8] the flakes of Nylon 6 were dissolved in the aqueous solution of formic acid and those of Nylon 8 in methyl alcohol, and both samples were precipitated by adding water to these solutions. The precipitates were extracted with ethyl ether for about 20 hr, using Soxhlet apparatus and the extract was evaporated to dryness *in vacuo*. The spreading solvents used were methyl alcohol saturated with calcium chloride (CM), methyl alcohol (MA), aqueous solution of 90% formic acid (FA) and the mixture of phenol and benzene in volume ratio of 1 : 3 (BP). Surface active contaminants were removed from the solvent by ordinary methods to the extent that the solvents, when spread on water, evaporated and compressed, showed the surface pressure being less than 0.1 dyn/cm which was the sensitivity of the surface balance. The concentration of nylon in the solutions was 0.3 mg/m*l*. Water was obtained by refluxing first an aqueous solution of acidic, then alkaline potassium permanganate, followed by repeated distillations. The substrate solution used was distilled water or dilute hydrochloric acid.

Methods. The surface pressure was measured by Wilhelmy type surface balance of ± 0.1 dyn/cm accuracy. The trough and barrier made of polymethyl methacrylate were crylate a coated with purified paraffin. The size of the trough was $200 \times 60 \times 10$ mm. The hanging-plate

1) C. W. N. Cumper and A. E. Alexander, *Trans. Faraday Soc.*, **46**, 235 (1950).
2) T. Isemura and K. Hamaguchi, This Bulletin, **25**, 40 (1951); **27**, 125 (1954).
3) H. Hotta, *ibid.*, **27**, 80 (1954).
4) H. Hotta, *J. Colloid Sci.*, **9**, 504 (1954).
5) K. Inokuchi, This Bulletin, **29**, 490 (1956).
6) G. E. Hibbered and A. E. Alexander, *Proc. 3rd Int. Cong. Surface Activity*, **2**, 144 (1960).
7) D. J. Crisp, *J. Colloid Sci.*, **1**, 161 (1946).
8) T. Yamashita, This Bulletin, **38**, 430 (1960).

was made from microscope cover glass of 11.0×7.5×0.13 mm in size. The spreading solution of nylon was slowly applied by a micro-syringe onto the surface. Unless otherwise stated, an aliquot of 15 μl of sample solution was spread on water surface of 120 cm^2 in area, and the compression of the film was started 20 min after the spreading. This was found sufficient for the film to attain a steady state. This film was compressed at the rate of 8 mm/min by a mortor driven barrier. The rate is conventionally chosen but is the one usually adopted in such measurements.[5] The trough was enclosed in a glass cabinet and the evaporation of water from and the dissolution of carbon dioxide into the substrate water were avoided by passing a current of humid nitrogen free from carbon dioxide slowly and continuously. The measurements were carried out in an air thermostat held at 25±0.5°C.

Results and Discussion

The Effect of the Nature of Spreading Solvent. The *F-A* curves for Nylons 6 and 8 monolayers spread from CM, MA, FA and BP are shown in Figs. 1a, 1b, 2a, 2b and 2c. The first compression curves of *F-A* are denoted by A. After the first compression to a sufficiently high surface pressure, the films were expanded to the initial area, and the second compression was started after allowing them to stand for about an hour. The *F-A* curves thus obtained are denoted by B.

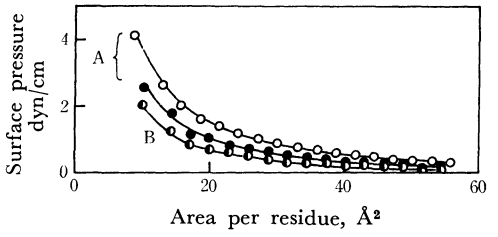

Fig. 1a. *F-A* curves of Nylon 6 monolayer spread from CM.
●: First compression, on distilled water (film A)
○: First compression, on hydrochloric acid (pH 1.6) (film A)
◐: Second compression of above two films (film B)

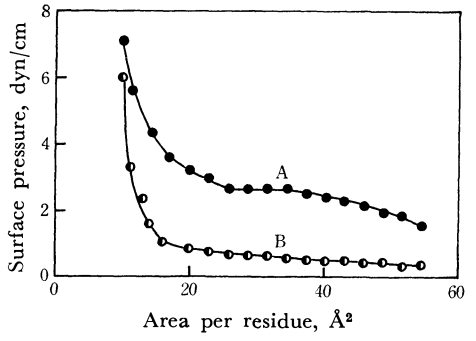

Fig. 1b. *F-A* curves of Nylon 6 monolayer spread from BP on distilled water.
●: First compression (film A)
◐: Second compression (film B)

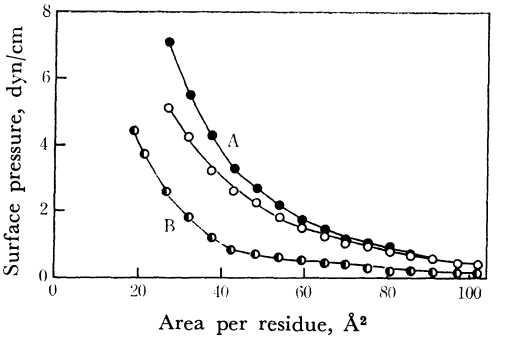

Fig. 2a. *F-A* curves of Nylon 8 monolayer spread from MA.
●: First compression, on pH 6.1—2.0 (film A)
○: First compression, on pH 1.1 (film A)
◐: Second compression of above two films (film B)

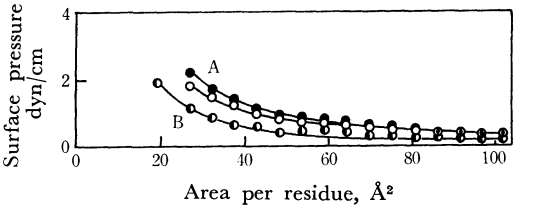

Fig. 2b. *F-A* curves of Nylon 8 monolayer spread from FA.
○: First compression, on distilled water (film A)
●: First compression, on hydrochloric acid (pH 1.1) (film A)
◐: Second compression of above two films (film B)

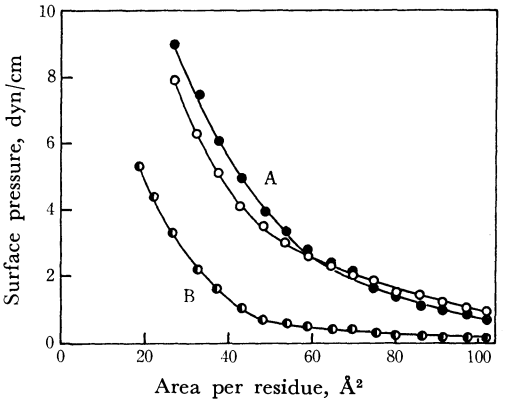

Fig. 2c. *F-A* curves of Nylon 8 monolayer on distilled water.
●: First compression, spreading solvent; BP (film A)
○: First compression, spreading solvent; CM (film A)
◐: Second compression of above two films (film B)

In some cases expansion and compression were repeated but the results gave the same *F-A* curve as that of B. It was shown that two types of film A and B are obtained in all cases, namely the film appearing at the first compression and the film at the second and further compressions. The film of the type A obtained by the first compression varies in the shape of *F-A* curve according to the nature of the spreading solvent, while the type B film is more condensed and the differences in *F-A* curve due to the nature of solvent and the repetition of the compression are far smaller than the type A film. From these facts together with the fact that the *F-A* curve of the type B film is fairly reproducible, the present author considers it best to measure the B film for the study of nylon monolayer under a well defined condition. Independence of type B film of the rate of compression is likely to hold since the shape of *F-A* curve of this film is independent of the effective rate of compression (the rate referred to the fractional area) which actually changes when an apparent rate is held constant at 8 mm/min. Type B film is also independent of the aging as mentioned later. The present study has been made also under such conditions.

In this connection, it is noted that most studies on nylon monolayers reported up to the present were made for the film corresponding to that of type A of our experiments, and discussion based upon such measurements inevitably becomes ambiguous and unreliable. For the film of the type B, we further examined the loss, if any, of the film substance due to its dissolution into the substrate. For this purpose, the spreading solution was applied with and without the aid of a specially prepared glass applicator having a small hollow at its top as shown in Fig. 3. The applicator was immersed

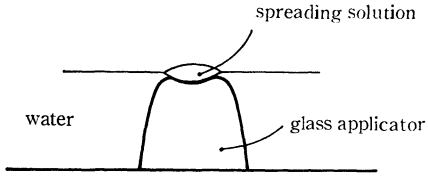

Fig. 3. Schematic representation of glass applicator.

just beneath the water surface and the spreading solution was slowly applied at the top of the applicator. Hardly any difference was observed between the *F-A* curves of monolayers spread with and without the aid of the applicator for both Nylons 6 and 8 dissolved in BP, CM, and MA except for the monolayer of Nylon 8 spread from FA, where the monolayers spread without using the applicator exhibit lower *F-A* curves both for A and B films as shown in Fig. 4. The difference in the case of FA solvent may be due to its insufficient nature as a spreading solvent. As shown in Table 1, it is evident that FA is larger in density and surface

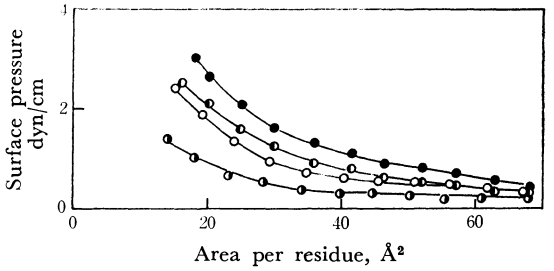

Fig. 4. *F-A* curves of Nylon 8 monolayer spread from FA on distilled water.
With glass applicator
●: First compression
◐: Second compression
Without glass applicator
○: First compression
◐: Second compression

Table 1. Physical properties of solvent

Solvent	Density (d_4^{20})	Surface tension (γ^{20})
FA	1.220	37.6 dyn/cm
MA	0.7915	22.6
CM	0.9264	22.9
BP	0.9766	30.4

tension than other solvents. These differences in properties suggest the less spreadability and the larger tendency to draw the solute into the substrate solution in the case of FA. Thus, the use of FA without the applicator is not favorable for spreading Nylon 8, while the coincidence as a whole of *F-A* curves of B type for the other different solvents may be taken as an indication of the film free from the loss of the substance during spreading. As to the film dissolution into the substrate solution during or after spreading the film, we further note that *F-A* curve of film B is reproducible under repeated compressions during which the possibility of the rapid reversible dissolution and redeposition of the film substance were confirmed not to occur except for the case in Fig. 4. This rapid dissolution and redeposition, if they happen, might produce pressure increase on the clean side of the water surface of Langmuir trough, but they could not be detected actually even after a long aging of the film under a high surface pressure. These facts lead to the conclusion that the dissolution of nylon into the subsolution is considered negligible for the monolayers except for the Nylon 8 monolayer spread from FA without using the applicator. The glass applicator was herefore used hereafter only in the case of FA as a spreading solvent.

Aging of Film before Compression. The effect of aging of the spread film on the *F-A* curve was measured for both Nylons 6 and 8 monolayers. After the monolayer was spread from the solution it was left to stand for from 20 min to 20 hr before

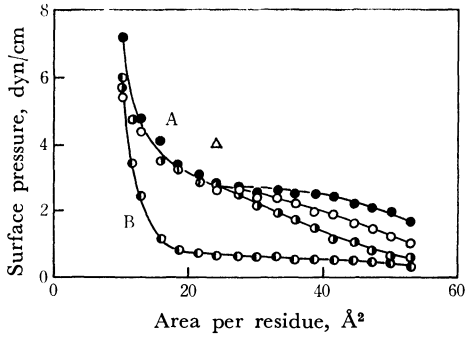

Fig. 5. Nylon 6 dissolved in BP on distilled water.
●: First compression after 20 min aging (film A)
○: First compression after 3½ hr aging (film A)
◑: First compression after 18 hr aging (film A)
◐: Second compression of above three films (film B)
△: Surface pressure under a rapid compression

the compression was started. There was no appreciable difference in the *F-A* curves for the films spread from CM and MA, but the *F-A* curve for Nylon 6 spread from BP (Fig. 5) which was more expanded than the one spread from CM showed a tendency of aging. In Fig. 5 pressure decreased during a prolonged aging of about 18 hr and the *F-A* curve of type A gradually shifted towards type B. When the original film of type A was compressed 20 min after spreading up to the molecular area of about 24 Å²/residue, at relatively high speed (about 10 times the ordinary rate, 8 mm/min) the surface pressure increased to the point indicated by the open triangle in Fig. 5 which is higher than the corresponding point on curve A obtained under the ordinary rate of compression (solid circle). Thus type A film of Nylon 6 spread from BP apparently exhibited a more expanded behavior than that from the other solvent when it was compressed immediately after the spreading. However this state seemed unstable and the film showed a tendency to condense even when it was left to stand at a lower surface pressure without compression. The plateau region described in an other report[5] was also observed in *F-A* curve for Nylon 6 (Fig. 1b) obtained by compressing the film 20 min after the spreading. This may be explained as a result of mutually opposite actions of pressure increase by compression and decrease by the above mentioned tendency of film condensation presumably becoming distinct at higher pressure.

Effect of the Volume of Spreading Solution. In order to examine the effects of the volume of spreading solution and the initial amount of film substance on the surface pressure, *F-A* curve of Nylon 6 film spread from 15 μl (standard volume)

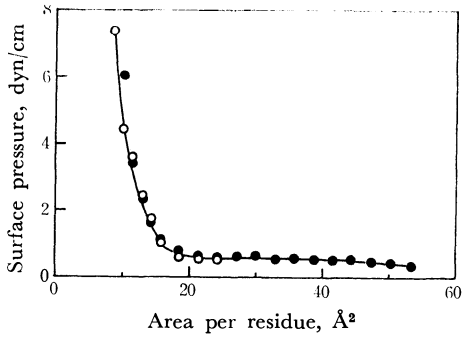

Fig. 6. *F-A* curves of Nylon 6 monolayer spread from BP on distilled water.
●: 15 μl spreading solution; second compression
○: 30 μl spreading solution; first compression

and 30 μl of the BP solutions on the aqueous surface of the same area (120 cm²) were compared (Fig. 6). When the film was spread from twice the standard volume of spreading solution, the *F-A* curve of type B appeared at the first compression and no change occured on further repetition of expansion and compression as shown by open circles in Fig. 6. This is markedly different from the FA curve for the film spread from 15 μl solution shown in Fig. 1b and also in Fig. 6.

The Nylon 8 monolayers which were spread from 5, 10, 15 and 20 μl of MA solutions showed, under repeated compresion, transition in type of *F-A* curves from A to B for all films except for the one spread from 5 μl solution which showed only one type of film A. The last case is expected to occur since the extent of compression of the film as expressed in area per residue is apparently insufficient to change A film to B.

As can be seen in Fig. 2a, film B is condensed to about one half of film A. Therefore, it may be presumed that a reaction like condensation of nylon monomer residues has occurred in this case in the monolayer of type B as a whole. This is probably due to the tendency of film contraction particularly increasing at high compression of film A. Types of the film, spread and compressed under varying amounts of spreading solution are shown in Table 2.

TABLE 2. THE TYPE OF FILM UNDER VARIOUS CONDITIONS

Spreading solution	Spreading volume	First compression	Further compression
Nylon 6 in BP	15 μl	A	B
	30	B	B
Nylon 8 in MA	5	A	A
	10	A	B
	15	A	B
	20	A	B

Concentration of spreading solution, 0.3 mg/ml
Initial spreading area, 120 cm²

A general tendency can be seen that the type A film appears at first compression and type B film at second and further compressions. Type A film obtained by spreading monolayer of Nylon 6 from BP solution is unstable and shows a tendency to undergo transition into type B by merely being kept at the initial spreading state of fairly large area, or by immediate compression of the film after being spread from twice the standard volume of the solution of the specified concentration. In the case of Nylon 8 film spread from MA, it is observed that the surface pressure of the type A film drops rapidly and the type B film finally appears when it is compressed and kept at certain small area. These fats also indicate the importance of the ratio, R, of the amount of film substance to the initial area of spreading for the study of nylon monolayer. It is likely that the appearance of the type A film only, A and B films, and B film only is dependent respectively on the value R being below, within, and beyond a certain range proper to the substance.

Effect of Substrate pH. The effect of acid in the substrate water on nylon film has mostly been studied with sulfuric acid having concentration greater than 1 N, where the *F-A* curve is more expanded than that on distilled water.[1,3,7,8] However, useful information can also be obtained from measurements of the film on acid substrate of concentration below 0.1 N, since nylon exhibits an amphoteric nature in this region.[9] Measurements were made for the *F-A* curve of the nylon monolayer on hydrochloric acid of concentration ranging from zero to 0.1 N. Measurement of the type A film on the acid substrate gave the result that both the *F-A* curves of Nylon 6 monolayer spread from CM solution and Nylon 8 monolayer from FA solution showed the film of more expanded type on acid than on distilled water (Figs. 1a and 2b) while Nylon 8 film from MA solution gave a curve almost independent of pH ranging from 2.0 to neutral (Fig. 2a). The film was more expanded than for the former two films, but contrary to the former films the area decreased below pH 1.1 (Figs. 1a and 2a).

It is known that the nylon molecules are usually in the extended state in acid solution where the molecules bear positive charges due to the addition of H^+ ion to the amide group.[8] A similar state of affairs may prevail in the case of monolayers shown in Figs. 1a and 2b, but this effect cannot explain the condensation of monolayer of Nylon 8 at pH 1.1 shown in Fig. 2a. The type B film of Nylon 8 obtained from MA also gave films independent of pH. Thus we have found fairly stable nylon monolayers of type B and in some cases type A which are obtained by spreading MA solution of Nylon 8 on acid and neutral water substrate.

In conclusion it should be emphasized that for the study of the monolayer of nylon on water, it is important to establish the conditions of monolayer preparation and of *F-A* curve measurement. Thus, it is necessary to specify clearly the nature of solvent, the concentration and the amount of spreading solution, pH of the substrate, the method of application of the spreading solution, the manners of compression and expansion of the monolayer with regard to the reproducibility of *F-A* curves and the aging of the monolayer. A check of the preservation of the substance in the monolayer during the spreading and compression is also important, although it is not carried out because of the difficulty of practice.

The author wishes to express her thanks to Professor T. Sasaki of Tokyo Metropolitan University for his guidance throughout this experiment. The author also thanks Assistant Professor M. Muramatsu for his advice. The cost of this research was defrayed from the Scientific Research Grant of the Ministry of Education.

9) A. R. Mathieson, C. S. Whewell and P. E. Williams, *J. Appl. Polym. Sci.*, **8**, 2009 (1964).

BULLETIN OF THE CHEMICAL SOCIETY OF JAPAN VOL. 43 306—309 (1970)

Studies of Nylon Monolayers. II. Compression Characteristics of the Nylon 8 Monolayer on Water

Toshiko SEIMIYA

Department of Chemistry, Faculty of Science, Tokyo Metropolitan University, Setagaya-ku, Tokyo

(Received June 20, 1969)

It was reported in the preceding paper that two types of film, A and B, can be distinguished in *F-A* curves for monolyers of Nylons 6 and 8 on the basis of the difference in behavior in relation to compression and expansion. In the present experiment, the compression and expansion were repeated for the monolayers of Nylon 8 spread from methyl alcohol in order to study the *F-A* characteristics of these films in detail. It was found that, during the process of first compression, the pressure drops rapidly and the transition of film A to film B occurs beyond a certain degree of compression of the monolayer. The transition was interpreted as the condensation of the monomer residue of the nylon molecule. The equations of the state for the expanded film were found to apply better than Singer's equation for both types of film, A and B. Further, the effect of the concentrated sulfuric acid solution (3 and 6 N) as a substrate on the *F-A* curve was examined. There were little difference in the behavior of the monolayers on 3 N sulfuric acid irrespective of the spreading solvent used, but the difference was marked on dilute hydrochloric acid.

In the preceding paper,[1] two types of film, A and B, were distinguished in *F-A* curves for the monolayers of Nylons 6 and 8 on the basis of the difference in behavior of the film in relation to compression and expansion.

In the present paper we will study these films in detail. Nylon 8 spread from methyl alcohol (MA) was used for the study of the *F-A* curve, because MA gives the most stable film on a neutral substrate, thus facilitating the measurement. Singer's approximate formula for polymer film and the equation of expanded film were applied to these data, and their applicability was checked. The effect of the concentrated sulfuric acid solution as a substrate on the *F-A* curve of Nylon 8 was also studied.

Experimental

The sample of Nylon 8 used was purified by dissolving it in MA and then by precipitating on addition of water. The precipitates were treated with ethyl ether in order to remove any impurities and were then dried *in vacuo*. MA was used mainly as a spreading solvent, but in some special cases formic acid (FA) and benzene-phenol mixture (BP) were also used. The concentration of nylon in the spreading solution was 0.3 mg/m*l*. The distilled water was prepared by refluxing an aqueous solution of acidic potassium permanganate and by distilling it three times, first with the addition of excess alkali. Aqueous solutions of 3 and 6 N sulfuric acid were used as substrates. The surface pressure was measured by a Wilhelmy balance using a glass hanging-plate. Special care was taken to withdraw the sufficiently-dipped plate just prior to the measurement in order to keep the receding angle at zero. The surface pressure-area curves (*F-A* curves) were plotted under various experimental conditions, as has been described in the preceding paper.[1]

1) T. Seimiya, This Bulletin **43**, 301 (1970).

Results and Discussion

Repetition of Compression and Expansion. A typical *F-A* curve for Nylon 8 is shown in Fig. 1. In this figure, the monolayer spread from the MA solution on the aqueous surface of a large area at pH 6 was first compressed, then expanded, and finally again compressed. The compression of the film was started from the point 0 to the point 1, as is shown in Fig. 1; then, after 15 min's rest at the point

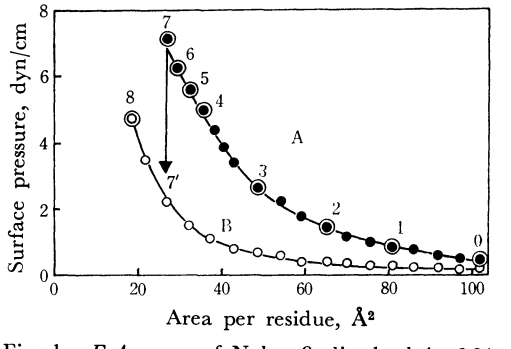

Fig. 1. *F-A* curve of Nylon 8 dissolved in MA on distilled water.
●: Film A
○: Film B

1 and the confirmation of no change in the surface pressure, the film was expanded again to the point 0 and finally compressed further to the point 2. Thus, the compression and expansion to the point 0 were repeated till the point 7 was reached along the curve A. An abrupt and irreversible change occurred at the point 7 where the surface pressure fell to the point 7′ simply on standing, as is indicated in Fig. 1. Such a change occurred rather suddenly and rapidly when the surface film was compressed to a 24—27 Å²/residue. Further compression proceeded along the curve B and the point 8 was reached. The full curve of the film B was realized when the film A, after the compression to the point 7, was expanded to the initial area of the 0 point and the second series of compression was started. The point 8 was again reached at the end of such compression. A further series of expansions and compressions of the film resulted in the same curve B.

The above behavior has been proved to occur for the monolayer spread from the solution which had been aged for from 0 to 50 days after preparation. It has been reported that the surface pressure depression occurs when the spreading solution is kept for a long time after preparation; this has been ascribed to the hydrolysis of nylon by sulfuric acid in the spreading solvent.[2] However, no such effect was found in the present experiment.

In order to examine the dissolution of nylon film into the substrate water, we have made two experiments. In the first experiment, each solvent, MA and FA, was dropped on the monolayer surface at the points of compression of 2, 3, 7′, and 8, but no change could be observed in the surface pressure after the dissolution of these solvents. In the second experiment, the surface pressure of the clean side of the substrate surface coexisting with the monolayer on the opposite side was measured. It was found that the pressure remained zero for about 1 to 2 hr after the spreading of the monolayer, even under a high compression of the film at the point 7′. These two facts, together with the reproducibility of the *F-A* curve mentioned above, confirm that the film substance is not lost from the monolayer either by a drag of the solvent as it spreads and dissolves in water or by a direct dissolution from the monolayer after it has been spread on the water.

Equation of State. First, an approximate form of Singer's equation[3] for the monolayers of polymers:

$$FA = kT(1+A_0/A)/x \qquad (1)$$

was tested for its applicability. Here, A_0 denotes the co-area of a residue in a molecule, and x, the degree of polymerization. The plot of FA against $1/A$ is shown in Fig. 2. As is shown in this figure, a linear relation is obtained for the film B; this

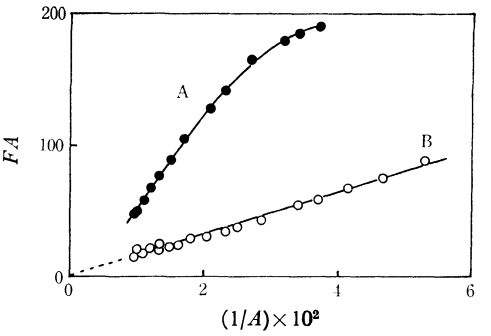

Fig. 2. Examination of Singer's approximate equation.
●: Film A
○: Film B

suggests a fairly good applicability of the above equation, but for the film A the plots largely deviates from linearity. Next, the applicability of the equation of the state for an expanded film:[4]

$$(F-F_0)(A-A_0) = kT \qquad (2)$$

was examined. Here, F_0 denotes a constant, independent of F and A. By means of a trial-and-error method, values of F_0 and A_0 were found which gave the best linearity when $F-F_0$ was plotted against $1/(A-A_0)$. As is shown in Fig. 3, the plots

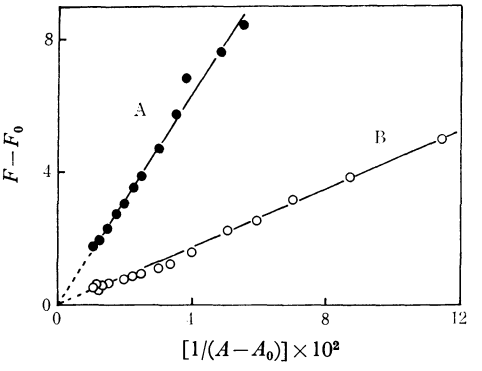

Fig. 3. Examination of equation of state for expanded film.
●: Film A
○: Film B

are on straight lines passing through the point of origin both for the A and B films. Here, $F_0=-1.35$ (dyn/cm), and $A_0=9$ (Å²/residue) for the film A, and $F_0=-0.35$, and $A_0=10$ for the film B. The values of $F_0=-1.30$, and $A_0=10$ can also be used to show a good linear plot for the film A. Thus, it is evidnet that, as a whole, Eq. (2) expresses the behavior of both the A and B films better than Eq. (1). Further, the constant of the right-hand side of Eq. (2) was calculated from the inclination of the two straight lines, A and B, in Fig. 3. The values

2) H. Hotta, This Bulletin, **27**, 80 (1954).
3) S. J. Singer, *J. Chem. Phys.*, **16**, 872 (1948).
4) I. Langmuir, *ibid.*, **1**, 756 (1933).

are about 1/3 kT and 1/10 kT for the A and B films respectively, instead of the kT shown in Eq. (2). This indicates that the equation:

$$(F-F_0)(A-A_0) = ikT$$

is applicable for both films, with $i=1/3$ for the film A and $i=1/10$ for the film B. Thus, two equations:

$$(F-F_0)(3A-3A_0) = kT$$

and $$(F-F_0')(10A-10A_0) = kT$$

are obtained for the A and B films. This means that the actual co-areas of the nylon residue are about three times and ten times as large as the co-area of the apparent residue. Thus, the groups of residues of these sizes seem to behave as a kinetic unit in the films A and B, and the condensation of the film may be understood as the formation of such clusters of residues in a polymer molecule.

Behavior of Nylon Monolayers on the Concentrated Acid Substrate. In the previous work,[1] the effect of acid on the nylon monolayer was studied by measuring the *F-A* curve on a dilute acid solution (concentration below 1/10 N), but in the present experiment concentrated sulfuric acid which is commonly used for studies of the nylon monolayer, was used as the substrate solution.[5-8] The *F-A* curve obtained for the monolayers on 3 and 6 N sulfuric acid solution are shown in Fig. 4. For the substrate of the 3 N sulfuric acid solution, the film A shows nearly the same *F-A* curve as on distilled water, but it tends to flatten when the compression proceeds beyond the area of about 35 Å²/residue. The film B exhibits the same curve as that of the monolayer spread on distilled water and no flattening is observed. When the 6 N sulfuric acid solution is used as the substrate, the expansion of the film is more marked than that of the film on distilled water for both the films A and B, as is shown in Fig. 4. As has been described before,[1] the film of Nylon 8 gives type-A curves of varying degrees of condensation on the dilute acid substrate; however, it expands again when the substrate becomes strongly acidic. These expansions of film on a strong acid substrate can be explained in terms of interaction between the monolayer and the hydrogen ion, interaction which results in repulsion among the molecules in the charged monolayer. As has been mentioned above, the *F-A* curve obtained on the strong acid substrate shows a tendency to flatten in the high-pressure region. However, it is not proper to explain this as a property of the equilibrium state, as is generally done:[2,5-9] it is better explained as a non-equilibrium state of the transition of the film from A to B, as has been noted.

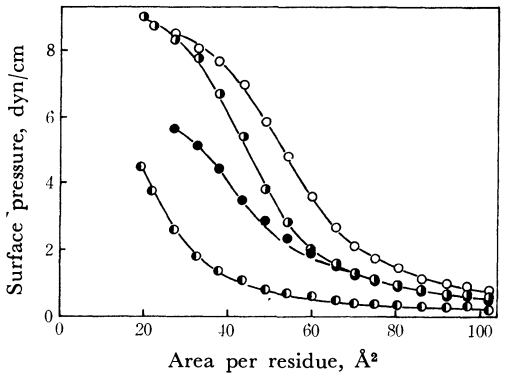

Fig. 4. *F-A* curves of Nylon 8 monolayer spread from MA on sulfuric acid.
●: 3 N, film A ○: 6 N, film A
◐: 3 N, film B ◑: 6 N, film B

In the preceding paper,[1] it has been reported that the *F-A* curves on distilled water differ according to the solvents used, as is shown in Fig. 5. However, for the films spread on the 3 N sulfuric

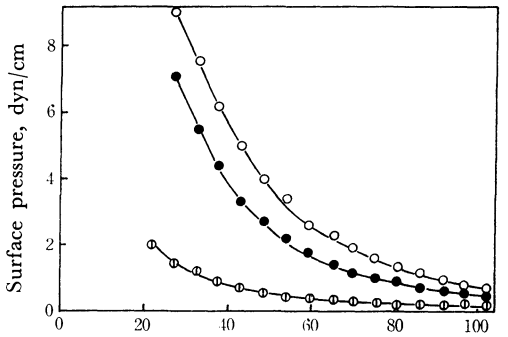

Fig. 5. *F-A* curves of Nylon 8 monolayer on distilled water.
●: Spread from MA
○: Spread from BP } film A
◑: Spread from FA

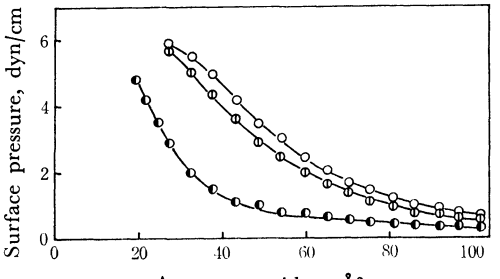

Fig. 6. *F-A* curves of Nylon 8 monolayer on 3 N sulfuric acid.
○: Spread from BP } film A
◑: Spread from FA
◐: Spread from BP and FA, film B

5) D. J. Crisp, *J. Colloid Sci.*, **1**, 161 (1946).
6) C. W. N. Cumper and A. E. Alexander, *Trans. Faraday Soc.*, **45**, 235 (1950).
7) G. E. Hibbered and A. E. Alexander, *Pro. 3rd Int. Congr. Surface Activity*, **2**, 145 (1960).
8) T. Yamashita, This Bulletin, **38**, 430 (1965).
9) K. Inokuchi, *ibid.*, **29**, 490 (1956).

acid substrate, only a little difference could be noted for the films spread from MA, FA, and BP solvents, as Figs. 4 and 6 show. The *F-A* curves of the nylon monolayer on an acid substrate of the 3 N sulfuric acid solution are often reported to show a tendency to expand more than that on the substrate of a neutral pH because of the absorption of the hydrogen ion.[5-8] However, for Nylon 8 no such phenomena are found, at least not for the solvents of MA and BP.

The author wishes to express her thanks to Professor Tsunetaka Sasaki of Tokyo Metropolitan University for his helpful guidance throughout this experiment. She also wishes to thank Assistant Professor Mitsuo Muramatsu for his useful advice. The cost of this research was defrayed by a Scientific Research Grant of the Ministry of Education.

BULLETIN OF THE CHEMICAL SOCIETY OF JAPAN VOL. 43 309—314 (1970)

Studies of the Nylon Monolayer. III. The Interaction between the Nylon Monolayer and Acid Dye

Toshiko SEIMIYA

Department of Chemistry, Faculty of Science, Tokyo Metropolitan University, Setagaya-ku, Tokyo

(Received July 15, 1969)

The interaction of the monolayers of the Nylons 6 and 8 with the acid dye Orange II was studied by measuring the surface pressure of the nylon monolayers with and without Orange II in the substrate water. No change in the surface tension with the time was observed for the aqueous solution of Orange II in the concentration and pH ranges studied. The interaction between the nylon monolayers (film B) and Orange II was examined by observing the change in the *F-A* curve of the nylon monolayer due to the addition of Orange II to the substrate and the spreading of the solution. The presence of dye in a spreading solution has little effect, while the pH's of the both the spreading solution and the substrate exhibit a marked effect on *F-A* curves. The observed interaction is compared with the behavior of practical dyeing in bulk of the solution.

The interaction between monolayer and dye has been studied by several investigators[1-5] as a simple model of actual dyeing phenomena. It is evident that pressure-area (*F-A*) measurement does not offer reliable information about the interaction between dye and monolayer unless the measurement is conducted for a monolayer of exactly-defined conditions, conditions which produce a sufficiently reproducible *F-A* curve characteristic of the monolayer. The published reports are not satisfactory[6,7] from this point of view. In our previous paper,[8] the conditions of the formation of a reproducible monolayer characteristic of the Nylons 6 and 8 were reported. The present paper will describe our study of the interaction between the monolayers of the Nylons 6 and 8 prepared under such conditions and Orange II, which is commonly used for dyeing nylon.

Experimental

Materials. For the preparation of Orange II, 3.5 g of sulfanilic acid were reacted with 1.2 m*l* of hydrochloric acid and 1.4 g of sodium nitrate. The diazo compound thus obtained was slowly added to a dilute aqueous sodium hydroxide solution containing 3 g of *β*-naphthol. After coupling had been completed, the product was precipitated by adding 8 g of sodium chloride to the solution. The Orange II thus obtained was purified by repeated recrystallization from ethyl alcohol, followed by a Soxhlet extraction with ethyl ether to remove the residual impurities. The product was finally dried *in vacuo*. The Nylons 6 and 8 were purified by dissolving them in an aqueous solution of formic acid and in one of methyl alcohol respectively, and by then precipitating them by adding water to these solutions. The precipitates were extracted with ethyl ether and dried *in vacuo*.

1) C. H. Giles and E. L. Neustädter, *J. Chem. Soc.*, **1952**, 918, 1864, 3806.
2) C. H. Giles, E. L. Neustädter and M. M. Allingham, *Discuss. Faraday Soc.*, **16**, 92 (1954).
3) C. H. Giles and A. Cameron, *J. Chem. Soc.*, **1957**, 3140.
4) C. H. Giles, A. Cameron and MacEwan, *ibid.*, **1957**, 4304; **1958**, 1224.
5) C. H. Giles and MacEwan, *ibid.*, **1959**, 1791.
6) M. Hayashi, T. Tachibana and A. Yabe, *Kogyo Kagaku Zasshi*, **63**, 1545 (1960).
7) M. Hayashi, T. Tachibana and A. Yabe, *ibid.*, **64**, 170 (1961).
8) T. Seimiya, This Bulletin, **43**, 301 (1970).

Water was obtained by refluxing an aqueous solution of acidic potassium permanganate and by subsequent distilling, first with the addition of excess alkali, and then without the addition.

Methods. The surface tension and surface pressure were measured by means of a Wilhelmy torsion balance. The pH of the substrate water for the nylon monolayer was controlled with hydrochloric acid to about unity (called acid) or without any special control (pH≃6; called "neutral"). The change in the pH between before and after the *F-A* measurements was less than 0.1. The spreading solution was prepared by dissolving the Nylon 6 in methyl alcohol saturated with calcium chloride (CM), and the Nylon 8 in methyl alcohol (MA) or an aqueous solution of formic acid (FA). The concentrations of the spreading solutions were 0.3 mg/m*l*. The details of the experimental procedures were the same as those presented in a former report.[8]

Results and Discussion

Surface Tension of an Aqueous Orange II Solution. It has been reported that the surface tension of an aqueous Orange II solution gradually decreases with the time as a result of the adsorption of Orange II at the air-water interface.[6] It is of interest whether or not the Orange II is really surface-active and how long it takes the surface tension of its aqueous solution to attain its equilibrium. For this purpose, we measured the change in the surface tension of an aqueous Orange II solution with the change in the concentration with the time. No change with the time was observed for any concentration or pH of the solutions studied. The surface tension *vs.* the concentration of the aqueous Orange II solution is shown in Fig. 1. It is confirmed that the surface tension of water is not affected by the addition of Orange II up to a concentration of 1×10^{-3} mol/*l*, while beyond that point it gradually decreases. The adsorption of Orange II is, therefore, considered to be zero for solutions with concentrations of less than 1×10^{-3} mol/*l*. Figure 2 shows the pH dependence of the surface tension of an aqueous solution of 2.57×10^{-4} mol/*l* Orange II. A considerable decrease in the surface tension can be seen in the strongly acid region. It may be noted in this connection that an appreciable decrease in surface tension extending over a period of 20 hr has been reported for an aqueous Orange II solution.[6] In the present experiment, however, the change in the surface tension with time was not observed during a period of 180 min for the ranges of the concentration of

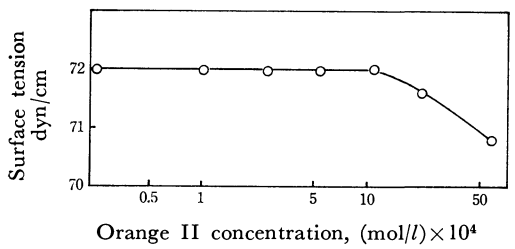

Fig. 1. Surface tension *vs.* concentration of aqueous Orange II solution.
Solution: neutral

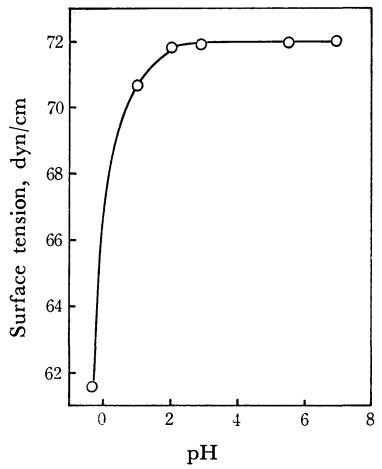

Fig. 2. Surface tension *vs.* pH of aqueous Orange II solution.
Dye concentration: 2.57×10^{-4} mol/*l*

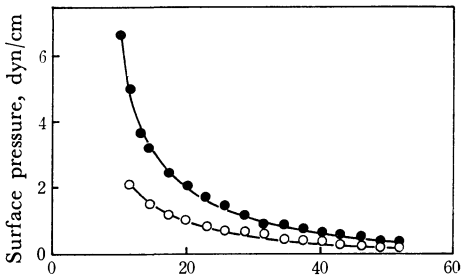

Fig. 3a. *F-A* curves of Nylon 6 dissolved in CM spread on 5.73×10^{-4} mol/*l* aqueous Orange II solution (●) and on blank substrate (○).
pH: 6.4, film A

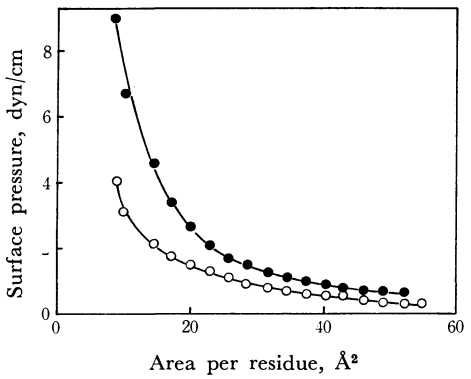

Fig. 3b. *F-A* curves of Nylon 6 dissolved in CM spread on 5.73×10^{-4} mol/*l* aqueous Orange II solution (●) and on blank substrate (○).
pH: 1.6, film A

Orange II and the pH of the substrate studied. Here, it may be suggested that the trace of an impurity present in distilled water sharply influences the results obtained.

***F-A* Curves of Nylons 6 and 8 on an Aqueous Orange II Solution.** The *F-A* curves for the Nylon 6 spread from CM on 5.73×10^{-4} mol/*l* Orange II solutions of pH 6.4 and 1.6 are shown in Fig. 3. Here, and in all of the following experiments, the surface pressure is expressed as the difference between the surface tension of water or an aqueous Orange II solution with and without a monolayer. The *F-A* curves measured on an aqueous Orange II solution for both neutral and acid substrates show those of a more expanded type than the blank *F-A* curve on the substrate containing no dye. This behavior is in good agreement with results reported in the literature.[6]

The *F-A* curves of the Nylon 8 spread from neutral MA on both neutral and acid substrates containing Orange II are shown in Fig. 4. Here, the two types of monolayers, A (expanded type) and B

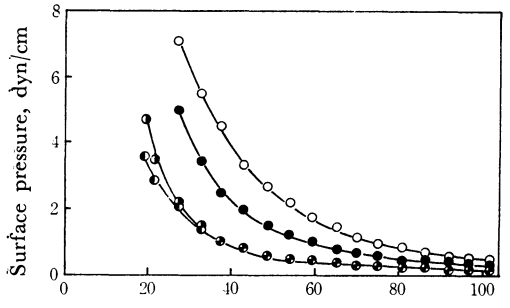

Fig. 4a. *F-A* curves of Nylon 8 dissolved in MA.
Substrate pH: 6.3
2.60×10^{-4} mol/*l* Orange II
●: Film A ◐: Film B
Blank substrate
○: Film A ◑: Film B

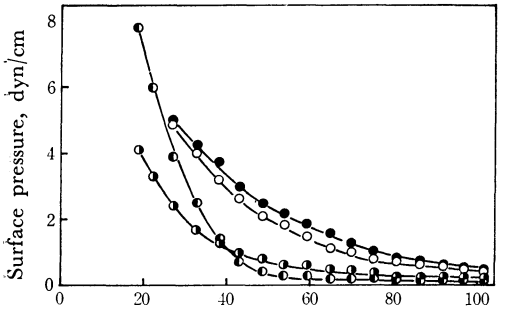

Fig. 4b. *F-A* curves of Nylon 8 dissolved in MA.
Substrate pH: 1.2
2.60×10^{-4} mol/*l* Orange II
●: Film A ◐: Film B
Blank substrate
○: Film A ◑: Film B

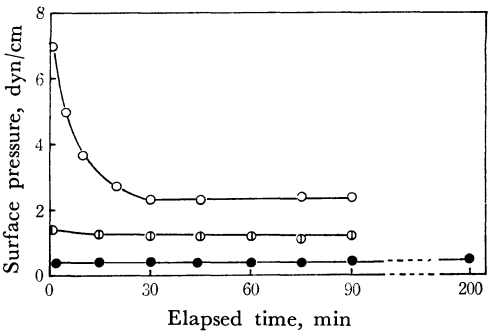

Fig. 5. Surface aging of Nylon 8 film on aqueous Orange II solution.
Dye concentration: 2.60×10^{-4} mol/*l*
Substrate pH: 6.3
○: 26.9 Å/residue
◫: 53.9 Å/residue
●: 102.5 Å/residue

(condensed type), were distinguished, as is shown in Fig. 5, by the gradual change in surface pressure beyond a certain compression, much as in former reports.[8,9] This decrease in the surface pressure of the nylon monolayer spread on the Orange II substrate appearing at a high compression is opposite to what has been previously reported.[6] The monolayers of both A and B film on the acid substrate undergo expansion as a result of the presence of Orange II; the expansion is especially remarkable for the film B (Fig. 4b). In the case of the neutral substrate, the A film rather condenses on the Orange II substrate, while the B film is not affected by the presence of the dye (Fig. 4a). The surface pressure was further measured for the nylon monolayer prepared by adding Orange II to both the substrate and the spreading solution. The *F-A* curves obtained are shown in Fig. 6 for a neutral spreading solution and in Fig. 7 for an acidic one.

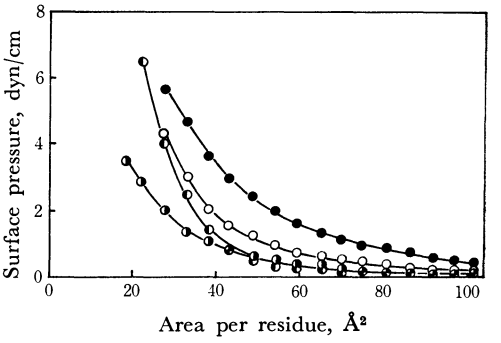

Fig. 6. *F-A* curves of Nylon 8 dissolved in MA with dye spread on 2.61×10^{-4} mol/*l* aqueous Orange II solution.
Substrate pH 1.8
●: Film A ◐: Film B
Substrate pH 6.5
○: Film A ◑: Film B

9) T. Seimiya, This Bulletin, **43**, 306 (1970).

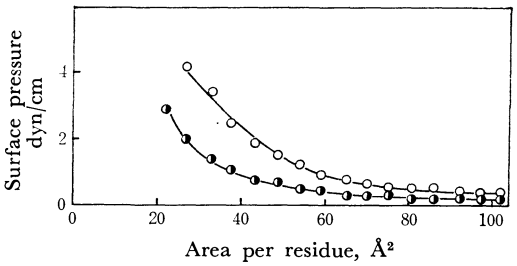

Fig. 7. *F-A* curves of Nylon 8 dissolved in MA with dye spread on 2.62×10^{-4} mol/*l* aqueous Orange II solution.
Spreading solution: acid
Substrate pH: 1.1
○: Film A ◑: Film B

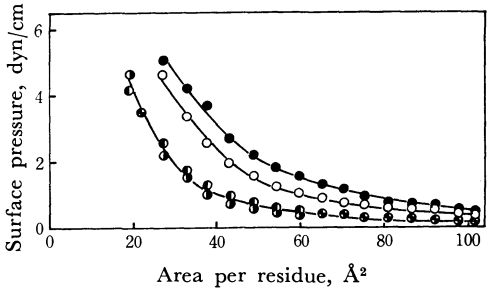

Fig. 8. *F-A* curves of Nylon 8 dissolved in MA with dye.
Spreading solution: acid
On distilled water,
○: Film A ◑: Film B
On 0.1 N HCl,
●: Film A ◐: Film B

We further plotted *F-A* curves for the monolayer spread from the mixed solution of Nylon 8 and Orange II in MA on distilled water and on a 0.1 N hydrochloric acid solution (Fig. 8), and those for monolayers spread from the solution of Nylon 8 dissolved in FA (with and without the dye) on the

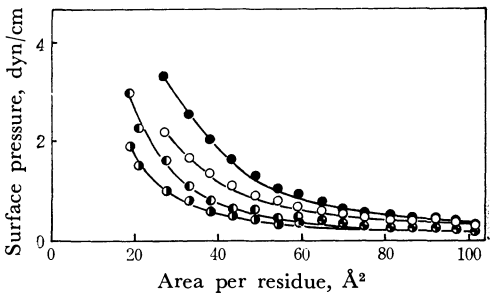

Fig. 9a. *F-A* curves of Nylon 8 dissolved in FA.
Spreading solution: acid
Substrate pH: 1.2
On 2.59×10^{-4} mol/*l* Orange II
●: Film A ◐: Film B
On blank substrate
○: Film A ◑: Film B

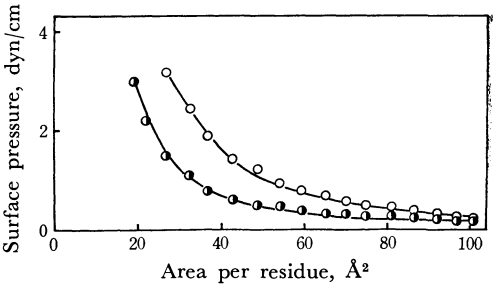

Fig. 9b. *F-A* curves of Nylon 8 dissolved in FA with dye spread on 2.59×10^{-4} mol/*l* aqueous Orange II solution.
Spreading solution: acid
Substrate pH 1.7
○: Film A ◑: Film B

TABLE 1. MUTUAL INTERACTION BETWEEN NYLON 8 MONOLAYER AND ORANGE II

System No.	Spreading solution		Substrate		Mutual interaction		Fig. cited
	Solute	Acidity	Solute	Acidity	film A	film B	
	MA as spreading solvent						
1	Nylon	Neutral	Dye	Neutral	0	0	4a
2	Nylon	Neutral	None	Neutral	—	—	4a
3	Nylon	Neutral	Dye	Acid	0	+	4b
4	Nylon	Neutral	None	Acid	—	—	4b
5	Nylon+Dye	Neutral	Dye	Neutral	0	0	6
6	Nylon+Dye	Neutral	Dye	Acid	0	+	6
7	Nylon+Dye	Acid	Dye	Acid	0	0	7
8	Nylon+Dye	Acid	None	Neutral	0	0	8
9	Nylon+Dye	Acid	None	Acid	0	0	8
	FA as spreading solvent						
10	Nylon	Acid	Dye	Acid	+	+	9a
11	Nylon	Acid	None	Acid	—	—	9a
12	Nylon+Dye	Acid	Dye	Acid	+	+	9b

+: distinct
0: imperceptible } interaction between Nylon 8 and dye
—: control system

same substrate (Figs. 9a and 9b).

The results mentioned above are summarized in Table 1. In this table we can see differences in the behavior of monolayers, particularly the interactions between the dye and the Nylon 8 in the states of monolayers spread under different conditions. Several remarks can be made:

(1) The A-type film spread on the substrate without Orange II is sensitive to the pH, while the B-type film is not (Nos. 2 and 4).

(2) The difference is hardly observable between the *F-A* curves of monolayers spread from the solutions containing and not containing the dye, if the rest of the conditions are the same (Nos. 1 and 5, 3 and 6, 7 and 10).

(3) The change in pH markedly influences the *F-A* curves. The surface pressure of B-type films compared at a high compression of $A=20$ Å^2/residue showed the largest film pressure for the neutral spreading solution on the acid substrate (Nos. 3 and 6), but in other cases the film pressure was fairly low (Nos. 1, 2, 4, 5, 7, 8, and 9). If the interaction between dye and nylon is expressed as an increase at a certain pressure of the area of the nylon monolayer due to the introduction of a dye in the substrate water, the B-type film spread from a neutral solvent on an acid substrate containing dye shows the largest interaction in the case of MA (Nos. 3 and 6). However, under the same conditions the interaction is rather ambiguous for the A-type film (Nos. 3 and 6). This is because of the unstable nature of the A film, as has been stated in the former report. Thus, because of its reproducible nature, the B film proved to be useful for the study of interactions of this kind.

(4) However, when FA was used as a spreading solvent, the interaction between dye and nylon has been confirmed for the monolayer spread from an acidic solution on an acidic substrate, judging from the expansion of the monolayer (Nos. 10 and 12).

(5) As will be shown in a later section, the Nylon 8 becomes insoluble in MA when treated with hydrochloric acid, but the solubility in FA is not affected by such treatment. These facts are considered to be closely related to the reactivity of the dye with the nylon spread from FA even under acidic conditions. While the H^+ ion in the substrate helps the expansion of the Nylon 8 and dyeing with Orange II, the above effect of the H^+ ion on the solubility of nylon in a spreading solvent proved to play an important role. Thus, the results of the present study confirm the view that, for the monolayer dyeing, the state of the monolayer and the dye should be taken into account; the overall conditions for optimum deying correspond to the systems Nos. 3 and 6 for MA, and Nos. 10 and 12 for FA.

(6) It should be noted that, as has been mentioned above, the interaction between monolayer and dye inferred in the present paper is marked in the smaller-area region (Nos. 3 and 6). However, a reverse case of monolayer interactions has also been reported, a case in which the increase in surface area is marked at a smaller surface pressure and vanishes at a larger surface pressure of the monolayer.[10] Such a difference in behavior might be closely related to the nature of the interaction in the monolayer, the interaction presumably being stronger in the present experiment, where it appears at a high compression.

(7) In the case of bulk dyeing, that is, the usual dyeing of nylon fibers in a dyeing solution, the spreadability of molecules has no significance, and the diffusion of dye into the nylon fiber is the rate-determining step for dyeing, so a relatively long time (more than a day) is required for dyeing. On the other hand, in the case of monolayer dyeing the process of dyeing is sensitive to the spreading conditions, but the rate itself is very fast. Thus, the monolayer dyeing can offer some useful knowledge for the study of the mechanism of dyeing, apart from the rate problem.

(8) As has already been stated, we made an experiment in which the spreading solution contained both Orange II and the Nylon 8, but the results were not appreciably different from the monolayer spread from the solvent containing the Nylon 8 alone, as may be seen by comparing, for instance, Experiments Nos. 1 and 5, 3 and 6, or 10 and 12.

Further Experiments Concerning the Interaction between the Nylon and Dye in the Bulk of the Solution. *(1) Bulk Dyeing.* The amount of Orange II taken up in the dyeing process was measured by colorimetry for 100 mg of the Nylon 8 in a 2.61×10^{-4} mol/*l* solution of Orange II. The amounts of equilibrium dyeing measured after about 24 hr were 3.28×10^{-5} mol/g Nylon 8 for the neutral solution, and 4.70×10^{-4} mol/g for the acid solution of pH unity. The amount of the end amino group of the Nylon 8, as determined by potentiometric titration,[11] was 3.50×10^{-5} equivalent/g nylon; this value was in agreement with the amount of Orange II dyed from the neutral solution, while the amount dyed from the acid solution was far more than the amount expected from the amino content. This is essentially in agreement with the general trend of the dyeing mechanism of nylons with acid dyes.[12]

(2) Paper Chromatography. A drop of aqueous Orange II was placed as a spot on filter paper (Toyo Roshi, No. 50) previously soaked with a 1% nylon-methanol solution. After the paper had been dried, the spot was eluted with water of 6 and 1 pHs. The distance of the spot eluted was then

10) T. Sasaki, R. Matuura and N. Fujimoto, This Bulletin, **24**, 203 (1951).

11) J. E. Waltz and G. B. Taylor, *Anal. Chem.*, **19**, 448 (1947).

12) T. Vickerstaff, "The Physical Chemistry of Dyeing," Oliver and Boyed, London (1954).

Table 2. Movement of Orange II on filter paper

pH of eluent	Treatment of filter paper	Movement of dye spot
6	Treated with nylon	4.65cm
	Untreated	4.65
1	Treated with nylon	0.75
	Untreated	1.75

compared with that obtained for untreated filter paper. The results are shown in Table 2. With an eluent of pH 6 no difference was found in the distance travelled by the spot on the filter papers treated and not treated with a nylon solution. However with an eluent of pH 1, the distance travelled on the treated paper was less than half the length travelled on the untreated filter paper; this may be interpreted as an indication of a distinct interaction at pH 1.

(3) Solubility. The solubilities of the dyed Nylon 8 in MA and FA were also measured: they are qualitatively listed in Table 3. As can be seen in this table, the insoluble nature of the Nylon 8 in MA is not due to dyeing, but is caused merely by the treatment with hydrochloric acid. MA does not dissolve the treated Nylon 8, even at an elevated temperature, while FA is a good solvent for the Nylon 8 at room temperature under any conditions. Such a difference in solubility probably influences the spreadability of the nylon monolayer when these solvents are used, and this in turn probably influences the processes of monolayer dyeing, as has been mentioned already.

Table 3. Solubility of Nylon 8

Solvent	Undyed	Treated with HCL	Neutral dyeing	Acid dyeing
HCOOH	Soluble	Soluble	Soluble	Soluble
CH_3OH	Soluble	Insoluble	Soluble	Insoluble

The author wishes to expresses her thanks to Professor T. Sasaki of Tokyo Metropolitan University for his helpful guidance throughout this experiment. The author also wishes to thank Assistant Professor M. Muramatsu for his useful advice. The cost of this research was defrayed by a Scientific Research Grant of the Ministry of Education.

BULLETIN OF THE CHEMICAL SOCIETY OF JAPAN VOL. 43 314—318 (1970)

Stochastic Model for Chemical Relaxation

Kenji ISHIDA

Department of Applied Chemistry, Ibaraki University, Hitachi

(Received June 25, 1969)

The stochastic formulation of chemical rate equations requires that the process of chemical relaxation should be accompanied with the fluctuation of chemical composition. It is shown that the factor Γ, which Eigen and de Maeyer introduced in the thermodynamic analyses of chemical relaxations, may be interpreted as the fluctuation of chemical composition.

For chemical phenomena, in general, the concept of fluctuation is almost out of question. According to the stochastic theory of chemical kinetics,[1] the fluctuation of chemical composition in an ordinary reaction system is negligibly small compared with the mean value derived from the deterministic theory.[2] There is, however, a chemical phenomenon for which the fluctuation of chemical composition may become an important factor to the description of chemical rate process. It is chemical relaxation. The chemical relaxation we treat in this paper is the process of equilibriation to a constant stationary state after a stepwise perturbation due to the change of a state variable (*e.g.*, temperature jump). If such a chemical relaxation is stochastically treated the fluctuation of chemical composition is explicitly included in the integrated relaxation equation through the relation to equilibrium constant. It is of significance that the stochastic theory of chemical kinetics makes it possible to relate the fluctuation of chemical composition to equilibrium constant.

One-step Reaction

As an introduction to the stochastic model for

1) For an extensive review of this work, see D. A McQuarrie, "Stochastic Approach to Chemical Kinetics," Methuen, London (1967).

2) It has been recently discussed by Oppenheim *et al.* that the stochastic formulation must be reduced to the deterministic formulation in the thermodynamic limit: $N\to\infty$, $V\to\infty$, N/V is constant, where N is the total number of molecules in the system with volume V (I. Oppenheim, K. E. Shuler and G. H. Weiss, *J. Chem. Phys.*, **50**, 460 (1969)).

chemical relaxation, we consider the case of one-step reaction A⇌B taking place in a closed system.

Let $P_{n_A,n_B}(t)$ be the probability that the number of A and B molecules found in the reacting system at time t are n_A and n_B, respectively. According to the stochastic theory of chemical kinetics, then, it follows that the probability distribution $P_{n_A^{(0)},n_B^{(0)}}(0)$ for the system in the initial chemical equilibrium is given by

$$P_{n_A^{(0)},n_B^{(0)}}(0) = \frac{N!}{n_A^{(0)}!\,n_B^{(0)}!}\left(\frac{k_{-1}^{(0)}}{k_1^{(0)}+k_{-1}^{(0)}}\right)^{n_A^{(0)}} \times\left(\frac{k_1^{(0)}}{k_1^{(0)}+k_{-1}^{(0)}}\right)^{n_B^{(0)}} \quad (1)$$

where $N=n_A^{(0)}+n_B^{(0)}$ is the total number of molecules in the system and $k_1^{(0)}$ and $k_{-1}^{(0)}$ denote the transition probabilities per one molecule and per unit time for the reactions A→B and B→A, respectively.[3] If the system governed by the equilibrium probability distribution (1) is disturbed by changing one of the external state variables, which define the thermodynamic equilibrium for the system, it approaches its new stable equilibrium in the manner described by the equation

$$\begin{aligned} dP_{n_A,n_B}(t)/dt = {} & k_1(n_A+1)P_{n_A+1,n_B-1}(t) \\ & -(k_1 n_A + k_{-1}n_B)P_{n_A,n_B}(t) \\ & +k_{-1}(n_B+1)P_{n_A-1,n_B+1}(t) \\ & (0 \leqq n_A, n_B \leqq N) \end{aligned} \quad (2)$$

on the basis of the idea that chemical reaction is Markov process homogeneous in time. In this equation, k_1 and k_{-1} are the transition probabilities in the relaxing system and $P_{N+1,-1}(t)=P_{-1,N+1}(t)=0$ is assumed. Solving Eq. (2) under the initial condition (1), we obtain the binomial distribution

$$P_{n_A,n_B}(t) = \frac{N!}{n_A!\,n_B!}\{p_A(t)\}^{n_A}\{p_B(t)\}^{n_B} \quad (3)$$

where

$$p_A(t) = \frac{k_{-1}}{k_1+k_{-1}} + \frac{\dfrac{k_{-1}^{(0)}}{k_1^{(0)}+k_{-1}^{(0)}}k_1 - \dfrac{k_1^{(0)}}{k_1^{(0)}+k_{-1}^{(0)}}k_{-1}}{k_1+k_{-1}}\,e^{-(k_1+k_{-1})t}$$

and

$$p_B(t) = 1 - p_A(t)$$

Equation (3) represents the probability distribution in the course of the relaxation process under consideration. The expected value of the number of A molecules, $\langle n_A\rangle$, is given by $\langle n_A\rangle = Np_A(t)$. Since the expected value $\langle n_A^{(0)}\rangle$ in the initial equilibrium state is $\langle n_A^{(0)}\rangle = Np_A(0) = Nk_{-1}^{(0)}/(k_1^{(0)}+k_{-1}^{(0)})$, the change of the number of A molecules due to the perturbation, $\Delta\langle n_A\rangle = \langle n_A^{(0)}\rangle - \langle n_A\rangle$, can be written as

$$\Delta\langle n_A\rangle = N\left(\frac{k_{-1}^{(0)}}{k_1^{(0)}+k_{-1}^{(0)}} - \frac{k_{-1}}{k_1+k_{-1}}\right)(1-e^{-(k_1+k_{-1})t}) \quad (4)$$

or

$$\Delta\langle n_A\rangle = N\left(\frac{1}{K_1^{(0)}+1} - \frac{1}{K_1+1}\right)(1-e^{-t/\tau_1}) \quad (5)$$

where we have introduced the equilibrium constant $K_1^{(0)}=k_1^{(0)}/k_{-1}^{(0)}$ and $K_1=k_1/k_{-1}$ and the relaxation time $\tau_1=(k_1+k_{-1})^{-1}$.

When the change δZ of an external state variable Z is applied to the system in the initial chemical equilibrium, the equilibrium constant for the relaxing system can be expressed by

$$K_1 = K_1^{(0)}\{1 + (\partial \ln K_1/\partial Z)_0 \delta Z\} \quad (6)$$

where the subscript 0 denotes the initial state. Substituting Eq. (6) into Eq. (5), we obtain

$$\Delta\langle n_A\rangle = N\frac{K_1^{(0)}}{(K_1^{(0)}+1)^2}\left(\frac{\partial \ln K_1}{\partial Z}\right)_0 \delta Z(1-e^{-t/\tau_1}) \quad (7)$$

The initial probability distribution (1), however, has the variance

$$\begin{aligned} \sigma^2(0) &= \langle (n_A^{(0)} - \langle n_A^{(0)}\rangle)^2\rangle \\ &= Nk_1^{(0)}k_{-1}^{(0)}/(k_1^{(0)}+k_{-1}^{(0)})^2 \end{aligned} \quad (8)$$

We now give an elementary discussion of this equation. The factor $k_1^{(0)}/(k_1^{(0)}+k_{-1}^{(0)})$ represents the transition probability per one molecule and per unit time for A→B under the condition that either forward or reverse reaction occurs and similarly the factor $k_{-1}^{(0)}/(k_1^{(0)}+k_{-1}^{(0)})$ the conditional transition probability for B→A. Since, however, the forward and reverse reactions in the reacting system in chemical equilibrium are considered to occur almost

---

3) If Eq. (2) for the reacting system before perturbation is solved with the initial condition $P_{N,0}(0)=1$, Eq. (1) is obtained as the equilibrium probability distribution which is independent of the initial condition.

This probability distribution can be also derived by the statistical-mechanical procedure as follows. In the ideal gas phase reaction, the equilibrium probability distribution for each component is given by the Poisson distribution

$$p(n_\gamma^{(0)}) = e^{-\lambda_\gamma(p.f.)_\gamma}\{\lambda_\gamma(p.f.)_\gamma\}^{n_\gamma^{(0)}}/n_\gamma^{(0)}! \quad (\gamma = A, B)$$

where λ_γ is the absolute activity of γ-component and $(p.f.)_\gamma$ the partition function. However, as the convolution of Poisson distributions is also the Poisson distribution, the probability distribution for the total number of molecules, $n_A^{(0)}+n_B^{(0)}=N$, is

$$p(N) = e^{-\{\lambda_A(p.f.)_A+\lambda_B(p.f.)_B\}} \times\{\lambda_A(p.f.)_A+\lambda_B(p.f.)_B\}^N/N!$$

It follows that the conditional probability distribution for an arbitrarily fixed N, $p(n_A^{(0)}, n_B^{(0)}\,|\,N)$, is given by the binomial distribution,

$$\begin{aligned} p(n_A^{(0)}, n_B^{(0)}|N) &= p(n_A^{(0)})p(n_B^{(0)})/p(N) \\ &= \frac{N!}{n_A^{(0)}!\,n_B^{(0)}!}\left\{\frac{(p.f.)_A}{(p.f.)_A+(p.f.)_B}\right\}^{n_A^{(0)}} \times \left\{\frac{(p.f.)_B}{(p.f.)_A+(p.f.)_B}\right\}^{n_B^{(0)}} \end{aligned}$$

where the thermodynamic condition of chemical equilibrium, $\lambda_A=\lambda_B$, is used. This is equivalent to Eq. (1) because of $(p.f.)_B/(p.f.)_A=\langle n_B^{(0)}\rangle/\langle n_A^{(0)}\rangle=k_1^{(0)}/k_{-1}^{(0)}=K_1^{(0)}$.

simultaneously with various reaction probabilities, the chemical compositions must be more or less fluctuating about the expected values. The fluctuation $\sigma^2(0)$ may therefore be regarded as the expected value of such an event. We then have in place of Eq. (8)

$$\sigma^2(0) = NK_1^{(0)}/(K_1^{(0)} + 1)^2 \tag{9}$$

which tells us the relation of fluctuation to equilibrium constant. On applying Eq. (9) to Eq. (7), we find that

$$\Delta\langle n_A\rangle = \sigma^2(0)\left(\frac{\partial \ln K_1}{\partial Z}\right)_0 \delta Z(1 - e^{-t/\tau_1}) \tag{10}$$

To the same approximation, this can be also written as

$$\Delta\langle n_A\rangle = \sigma^2(\infty)\left(\frac{\partial \ln K_1}{\partial Z}\right)_0 \delta Z(1-e^{-t/\tau_1}) \tag{11}$$

because the relation between $\sigma^2(0)$ and the fluctuation $\sigma^2(\infty)$ in the new chemical equilibrium is given by

$$\begin{aligned}\sigma^2(\infty) &= NK_1/(K_1 + 1)^2 \\ &\simeq \sigma^2(0)\left\{1 - \frac{K_1^{(0)} - 1}{K_1^{(0)} + 1}\left(\frac{\partial \ln K_1}{\partial Z}\right)_0 \delta Z\right\}\end{aligned} \tag{12}$$

where Eqs. (6) and (9) have been used and $|(K_1^{(0)}-1)/(K_1^{(0)}+1)|<1$ holds for all possible values of $K_1^{(0)}$.

It is instructive to compare such a stochastic analysis with the theory of Eigen and de Maeyer. We transform the fluctuation $\sigma^2(\infty)$ as follows:

$$\begin{aligned}\sigma^2(\infty) &= Np_A(\infty)\{1 - p_A(\infty)\} \\ &= \langle n_A\rangle_\infty\langle n_B\rangle_\infty/N \\ &= (1/\langle n_A\rangle_\infty + 1/\langle n_B\rangle_\infty)^{-1}\end{aligned} \tag{13}$$

where $\langle n_A\rangle_\infty = Np_A(\infty)$ and $\langle n_B\rangle_\infty = Np_B(\infty)$ are the mean numbers of A and B molecules in the new chemical equilibrium, respectively. The last expression of Eq. (12) is in form in agreement with the factor Γ that Eigen and de Maeyer have introduced through the thermodynamic considerations of chemical relaxations.[4]

According to the stochastic nonequilibrium thermodynamics of chemical reactions,[5] the fluctuation $\sigma^2(\infty)$ can be closely correlated to the chemical affinity A by

$$\sigma^2(\infty) = \left\{-\frac{1}{\boldsymbol{k}T}\left(\frac{\partial A}{\partial \xi}\right)_\infty\right\}^{-1} \tag{14}$$

where $\boldsymbol{k}$ is Boltzmann's constant, T the temperature of the relaxing system in chemical equilibrium and ξ the degree of advancement. Since the chemical affinity is expressed in the form

$$A = \boldsymbol{k}T\{\ln(\langle n_A\rangle/\langle n_A\rangle_\infty) - \ln(\langle n_B\rangle/\langle n_B\rangle_\infty)\}$$

it can be easily shown that Eq. (14) is equivalent to Eq. (13). From the stochastic point of view, therefore, the factor Γ of Eigen and de Maeyer is to be interpreted as the fluctuation of chemical composition.

To test this theory for other chemical relaxations, we take a second-order reaction $A+B\rightleftarrows C$ as an example. The stochastic process for this reaction is described by

$$\begin{aligned}dP_{n_C}(t)/dt = {} & k_2\{n_A^{(0)} - (n_C - 1 - n_C^{(0)})\} \\ & \times \{n_B^{(0)} - (n_C - 1 - n_C^{(0)})\}P_{n_C-1}(t) \\ & -[k_2\{n_A^{(0)} - (n_C - n_C^{(0)})\} \\ & \times \{n_B^{(0)} - (n_C - n_C^{(0)})\} + k_{-2}n_C]P_{n_C}(t) \\ & +k_{-2}(n_C + 1)P_{n_C+1}(t)\end{aligned} \tag{15}$$

where $P_{n_C}(t)$ denotes the probability that the number of molecules of chemical species C existing in the relaxing system at time t is n_C, $n_A^{(0)}$, $n_B^{(0)}$ ($\geq n_A^{(0)}$) and $n_C^{(0)}$ are the numbers of A, B and C molecules in the initial chemical equilibrium and k_2 and k_{-2} the transition probabilities per molecule and per unit time for the forward and reverse reactions, respectively. Since the difference between $\sigma^2(0)$ and $\sigma^2(\infty)$ is not so large, as is clear from Eq. (12), it has been assumed that the numbers of A, B and C molecules in the initial chemical equilibrium are given by $n_A^{(0)}$, $n_B^{(0)}$ are $n_C^{(0)}$ in the probabilistic mean of $P_{n_A^{(0)},\, n_B^{(0)},\, n_C^{(0)}}(0)=1$. If the inequality $n_C - n_C^{(0)} \ll n_A^{(0)}, n_B^{(0)}$, which corresponds to the linear approximation in the usual analysis of chemical relaxation, holds during the relaxation process, Eq. (15) is reduced to

$$\begin{aligned}dP_{n_C}(t)/dt = {} & k_2\{(n_A^{(0)}n_B^{(0)} + n_B^{(0)}n_C^{(0)} + n_C^{(0)}n_A^{(0)}) \\ & -(n_A^{(0)} + n_B^{(0)})(n_C - 1)\}P_{n_C-1}(t) \\ & -[k_2\{(n_A^{(0)}n_B^{(0)} + n_B^{(0)}n_C^{(0)} + n_C^{(0)}n_A^{(0)}) \\ & -(n_A^{(0)} + n_B^{(0)})n_C\} + k_{-2}n_C]P_{n_C}(t) \\ & +k_{-2}(n_C + 1)P_{n_C+1}(t)\end{aligned} \tag{15'}$$

Solving this differential-difference equation by the use of the generating function of $P_{n_C}(t)$,

$$G(\theta, t) = \sum_{n_C=0}^{\infty} \theta^{n_C}P_{n_C}(t), \qquad |\theta| \leqq 1$$

we obtain, as the solution subject to the initial condition

4) M. Eigen and L. de Maeyer, "Technique of Organic Chemistry," 2nd Ed., Vol. VIII, part 2, ed. by S. L. Fries, E. S. Lewis and A. Weissberger, Interscience Publishers, Inc., New York, N. Y. (1963), p. 934. In deriving the thermodynamic relation of the change of concentration to that of equilibrium constant, they have defined the factor $\Gamma_m = 1/(\sum_i \nu_i^2/\bar{m}_i)$, where ν_i is the stoichiometric coefficient and $\bar{m}_i$ the molality in chemical equilibrium state. The index of Γ, however, changes with the kind of concentration variable. Whatever concentration variables may be used, the factor Γ is correlated to the fluctuation of chemical composition. For example, the factor Γ for the chemical relaxation of $A\rightleftarrows B$ has been given by $\Gamma_\alpha = 1/(1/\bar{\alpha}+1/(1-\bar{\alpha})) = \bar{\alpha}(1-\bar{\alpha}) = K_0/(1+K_0)^2$, where $\bar{\alpha}$ is the mole fraction of chemical species A and $K_0=(1-\bar{\alpha})/\bar{\alpha}$ the equilibrium constant. The factor Γ_α is consistent with $\sigma^2(\infty)/N = p_A(\infty)\{1-p_A(\infty)\}$, if it is assumed that $p_A(\infty)=\bar{\alpha}$.

5) K. Ishida, *J. Phys. Chem.*, **70**, 3806 (1966); **72**, 92 (1968).

$$P_{n_C^{(0)}}(0) = 1,\ i.e.,\ G(\theta, 0) = \theta^{n_C^{(0)}},$$

$$G(\theta, t) = \{k_2(n_A^{(0)} + n_B^{(0)}) + k_{-2}\}^{-\frac{n_A^{(0)} n_B^{(0)}}{n_A^{(0)} + n_B^{(0)}} - n_C^{(0)}} \times \{k_{-2} + k_2(n_A^{(0)} + n_B^{(0)})e^{-t/\tau_2} + k_2(n_A^{(0)} + n_B^{(0)})(1 - e^{-t/\tau_2})\theta\}^{\frac{n_A^{(0)} n_B^{(0)}}{n_A^{(0)} + n_B^{(0)}}} \times \{k_{-2}(1 - e^{-t/\tau_2}) + [k_2(n_A^{(0)} + n_B^{(0)}) + k_{-2}e^{-t/\tau_2}]\theta\}^{n_C^{(0)}} \quad (16)$$

where $\tau_2 = \{k_2(n_A^{(0)} + n_B^{(0)}) + k_{-2}\}^{-1}$ is the relaxation time. Since, then, the mean number of C molecules, $\langle n_C \rangle$, is given by $\theta \partial G/\partial\theta \,|_{\theta=1} = \langle n_C \rangle$, we have as the deviation from the initial value, $\Delta\langle n_C \rangle = \langle n_C \rangle - n_C^{(0)}$,

$$\Delta\langle n_C \rangle = \frac{k_2 n_A^{(0)} n_B^{(0)} - k_{-2} n_C^{(0)}}{k_2(n_A^{(0)} + n_B^{(0)}) + k_{-2}}(1 - e^{-t/\tau_2}) \quad (17)$$

By the procedure given in Appendix I, we can transform Eq. (17) into the equation involving the fluctuation of chemical species C

$$\Delta\langle n_C \rangle = \sigma_C^2(\infty)\left(\frac{\partial \ln K_2}{\partial Z}\right)_0 \delta Z(1 - e^{-t/\tau_2}) \quad (18)$$

which is of the same form as Eq. (11). In Eq. (18), $K_2 = k_2/k_{-2}$ is the equilibrium constant and the fluctuation for chemical species C is given by

$$\sigma_C^2(\infty) = \frac{(n_A^{(0)} n_B^{(0)} + n_B^{(0)} n_C^{(0)} + n_C^{(0)} n_A^{(0)})K_2}{\{1 - (n_A^{(0)} + n_B^{(0)})K_2\}^2} \quad (19)$$

which has been calculated by the formula

$$\sigma_C^2(t) = (\theta^2 \partial^2 G/\partial\theta^2 + \theta \partial G/\partial\theta)|_{\theta=1} - (\theta \partial G/\partial\theta\,|_{\theta=1})^2$$

When, however, it is taken into consideration that the approximation $\langle n_C \rangle^2_\infty - n_C^{(0)2} \ll n_A^{(0)} n_B^{(0)} + n_B^{(0)} n_C^{(0)} + n_C^{(0)} n_A^{(0)}$ holds for the chemical relaxation we are concerned with, Eq. (19) can be transformed into the form of the factor Γ of Eigen - de Maeyer,

$$\sigma_C^2(\infty) = (1/\langle n_A \rangle_\infty + 1/\langle n_B \rangle_\infty + 1/\langle n_C \rangle_\infty)^{-1} \quad (20)$$

where $\langle n_A \rangle_\infty = n_A^{(0)} - (\langle n_C \rangle_\infty - n_C^{(0)})$ and $\langle n_B \rangle_\infty = n_B^{(0)} - (\langle n_C \rangle_\infty - n_C^{(0)})$. We thus see from Eqs. (11) and (18) that the stochastic theory of chemical relaxation may make it possible to evaluate the fluctuation of chemical composition.

Two-step Reaction

Up to the present, we have stochastically discussed only the chemical relaxations of one-step reactions, but we must also investigate along the same line as in the preceding section how the fluctuation of chemical composition appears in the chemical relaxation of multiple-step reaction. For instance, we can take up a two-step reaction $A \rightleftarrows B \rightleftarrows C$. For practical purposes, however, we are interested in the reaction such as $A + B \rightleftarrows C \rightleftarrows D$.

It is necessary to write down the equation describing the stochastic process for the chemical relaxation of this reaction. Let us denote by $n_A^{(0)}$, $n_B^{(0)}$, $n_C^{(0)}$ and $n_D^{(0)}$ the numbers of A, B, C and D molecules present in the initial equilibrium system, respectively. If the changes of the numbers of A (and B), C and D molecules from the equilibrium values due to the change of an external state variable Z are chosen as the random variables, which assume the realized values x, y and z at time t, the joint probability distribution $P_{x,y,z}(t)$ satisfies the linear equation similar to Eq. (15′)

$$\begin{aligned} dP_{x,y,z}(t)/dt = {} & \kappa_1\{n_A^{(0)} n_B^{(0)} + (n_A^{(0)} + n_B^{(0)})(x+1)\}P_{x+1,y-1,z}(t) \\ & + \kappa_{-1}(n_C^{(0)} + y + 1)P_{x-1,y+1,z}(t) \\ & - \{\kappa_1(n_A^{(0)} n_B^{(0)} + (n_A^{(0)} + n_B^{(0)})x) \\ & + (\kappa_{-1} + \kappa_2)(n_C^{(0)} + y) + \kappa_{-2}(n_D^{(0)} + z)\}P_{x,y,z}(t) \\ & + \kappa_2(n_C^{(0)} + y + 1)P_{x,y+1,z-1}(t) \\ & + \kappa_{-2}(n_D^{(0)} + z + 1)P_{x,y-1,z+1}(t) \end{aligned} \quad (21)$$

where κ_1 and κ_{-1} are the transition probabilities for the forward and reverse reactions of $A + B \rightleftarrows C$ and similarly κ_2 and κ_{-2} the transition probabilities for $C \rightleftarrows D$. Defining the generating function $P_{x,y,z}(t)$ by

$$G(\theta_1, \theta_2, \theta_3; t) = \sum_{x,y,z=0}^{\infty} \theta_1^x \theta_2^y \theta_3^z P_{x,y,z}(t)$$

we obtain, from Eq. (21),

$$\begin{aligned} \frac{\partial G}{\partial t} = {} & -\kappa_1(n_A^{(0)} + n_B^{(0)})(\theta_1 - \theta_2)\frac{\partial G}{\partial \theta_1} \\ & + \{\kappa_{-1}\theta_1 - (\kappa_{-1} + \kappa_2)\theta_2 + \kappa_2\theta_3\} \\ & \times \frac{\partial G}{\partial \theta_2} + \kappa_{-2}(\theta_2 - \theta_3)\frac{\partial G}{\partial \theta_3} \\ & - \{\kappa_1 n_A^{(0)} n_B^{(0)}(1 - \theta_2/\theta_1) + \kappa_{-1} n_C^{(0)}(1 - \theta_1/\theta_2) \\ & + \kappa_2 n_C^{(0)}(1 - \theta_3/\theta_2) + \kappa_{-2} n_D^{(0)}(1 - \theta_2/\theta_3)\}G \end{aligned}$$

This partial differential equation is to be solved with the initial condition $G(\theta_1, \theta_2, \theta_3; 0) = 1$, which means that $P_{0,0,0}(0) = 1$. The solution can be written in the form

$$\begin{aligned} G(\theta_1, \theta_2, \theta_3; t) = {} & \theta_1^{-\frac{n_A^{(0)} n_B^{(0)}}{n_A^{(0)} + n_B^{(0)}}} \theta_2^{-n_C^{(0)}} \theta_3^{-n_D^{(0)}} \\ & \times \left\{\sum_{i=1}^{3} p_i(t)\theta_i\right\}^{\frac{n_A^{(0)} n_B^{(0)}}{n_A^{(0)} + n_B^{(0)}}} \left\{\sum_{i=1}^{3} q_i(t)\theta_i\right\}^{n_C^{(0)}} \\ & \times \left\{\sum_{i=1}^{3} r_i(t)\theta_i\right\}^{n_D^{(0)}} \end{aligned} \quad (22)$$

where $p_i(t)$, $q_i(t)$ and $r_i(t)$ will be given in Appendix II.

For the sake of simplicity, we restrict ourselves to investigate how the change of the number of D molecules in the relaxing system can be related to the fluctuation. From Eq. (22), we obtain as the expected value

$$\langle z \rangle = \frac{n_A^{(0)} n_B^{(0)}}{n_A^{(0)} + n_B^{(0)}} p_3(t) + n_C^{(0)} q_3(t) + n_D^{(0)}\{r_3(t) - 1\} \quad (23)$$

where we have used $(\theta_3 \partial G/\partial\theta_3)\,|_{\theta_1=\theta_2=\theta_3=1} = \langle z \rangle$. If the equilibriation in the first stage is much faster than in the second, it follows that $\kappa_1(n_A^{(0)} + n_B^{(0)})$ and

κ_{-1} are sufficiently large compared with κ_2 and κ_{-2}. We then have the inequality $\alpha \gg \beta$ and the approximations

$$\alpha = \kappa_1(n_A^{(0)} + n_B^{(0)}) + \kappa_{-1}$$

and

$$\beta = \frac{\kappa_1(n_A^{(0)} + n_B^{(0)}))\kappa_2}{\kappa_1(n_A^{(0)} + n_B^{(0)}) + \kappa_{-1}} + \kappa_{-2}$$

In such a case, Eq. (23) may be written as

$$\langle z\rangle = \left\{\frac{n_A^{(0)}n_B^{(0)}}{n_A^{(0)}+n_B^{(0)}} + n_C^{(0)} - n_D^{(0)}\frac{\kappa_{-2}\alpha}{\kappa_1(n_A^{(0)} + n_B^{(0)})\kappa_2}\right\} \times \frac{\kappa_1(n_A^{(0)} + n_B^{(0)})\kappa_2}{\alpha\beta}(1 - e^{-t/\tau_2}) \quad (24)$$

where $\tau_2=\beta^{-1}$ denotes the relaxation time. If, however, we introduce the equilibrium constants $\kappa_1/\kappa_{-1}=K_1$, $\kappa_2/\kappa_{-2}=K_2$, $n_C^{(0)}/n_A^{(0)}n_B^{(0)}=K_1^{(0)}$ and $n_D^{(0)}/n_C^{(0)}=K_2^{(0)}$, we obtain, by the same procedure as in the transformation from Eq. (17) to Eq. (18)

$$\langle z\rangle = \sigma_D^2(\infty)\left\{1 + \frac{n_A^{(0)}n_B^{(0)}}{n_A^{(0)}n_B^{(0)} + n_B^{(0)}n_C^{(0)} + n_C^{(0)}n_A^{(0)}} \times \frac{(\partial \ln K_1/\partial Z)_0}{(\partial \ln K_2/\partial Z)_0}\right\}(\partial \ln K_2/\partial Z)_0\delta Z(1 - e^{-t/\tau_2}) \quad (25)$$

where the fluctuation $\sigma_D^2(\infty)$ for chemical species D in the new chemical equilibrium state is given by

$$\sigma_D^2(\infty) = \left\{\frac{n_A^{(0)}n_B^{(0)}}{n_A^{(0)}+n_B^{(0)}} + n_C^{(0)} + n_D^{(0)}\right\} \times \frac{\kappa_1(n_A^{(0)} + n_B^{(0)})\kappa_2}{\alpha\beta}\left\{1 - \frac{\kappa_1(n_A^{(0)} + n_B^{(0)})\kappa_2}{\alpha\beta}\right\}$$

Since the first stage of the reaction is considered to be in stationary state, it may be expected that

$$|(\partial \ln K_1/\partial Z)_0/(\partial \ln K_2/\partial Z)_0| = |n_D^{(0)}/(n_C^{(0)} + n_D^{(0)})|$$

It is then concluded that Eq. (25) is reduced to

$$\langle z\rangle = \sigma_D^2(\infty)(\partial \ln K_2/\partial Z)_0\delta Z(1 - e^{-t/\tau_2}) \quad (26)$$

which is of the same form as Eqs. (11) and (18).

We can in general say that chemical relaxation should be accompanied with the fluctuation of chemical composition.

Appendix I

The first member on the right-hand side of Eq. (17) can be written in the form

$$\frac{k_2n_A^{(0)}n_B^{(0)} - k_{-2}n_C^{(0)}}{k_2(n_A^{(0)} + n_B^{(0)}) + k_{-2}} = \sigma_C^2(\infty)(K_2 - K_2^{(0)}) \times \frac{n_A^{(0)}n_B^{(0)}\{(n_A^{(0)} + n_B^{(0)})K_2 + 1\}}{(n_A^{(0)}n_B^{(0)} + n_B^{(0)}n_C^{(0)} + n_C^{(0)}n_A^{(0)})K_2} \quad (A.1)$$

where the fluctuation (19) and the equilibrium constants $n_C^{(0)}/n_A^{(0)}n_B^{(0)}=K_1^{(0)}$ and $k_2/k_{-2}=K_2$ have been used. If we apply $K_2=K_2^{(0)}\{1+(\partial \ln K_2/\partial Z)_0\delta Z\}$ to Eq. (A.1), we have, by neglecting the terms of higher order than the first of δZ,

$$\frac{k_2n_A^{(0)}n_B^{(0)} - k_{-2}n_C^{(0)}}{k_2(n_A^{(0)} + n_B^{(0)}) + k_{-2}} = \sigma_C^2(\infty)\left(\frac{\partial \ln K_2}{\partial Z}\right)_0\delta Z \times \left\{1 - \frac{n_A^{(0)}n_B^{(0)}}{n_A^{(0)}n_B^{(0)} + n_B^{(0)}n_C^{(0)} + n_C^{(0)}n_A^{(0)}}\left(\frac{\partial \ln K_2}{\partial Z}\right)_0\delta Z\right\} \simeq \sigma_C^2(\infty)\left(\frac{\partial \ln K_2}{\partial Z}\right)_0\delta Z \quad (A.2)$$

since it is necessary that $1 \gg |(\partial \ln K_2/\partial Z)_0\delta Z| > 0$ for the linearization such as Eq. (15′).[6] We thus obtain Eq. (18) from Eq. (17).

Appendix II

In Eq. (22), $p_i(t)$, $q_i(t)$ and $r_i(t)$ $(i=1, 2, 3)$ have the following expressions:

$$p_1(t) = \frac{\kappa_{-1}\kappa_{-2}}{\alpha\beta} - \frac{\kappa_1(n_A^{(0)} + n_B^{(0)})(\kappa_2 + \kappa_{-2}-\alpha)}{\alpha(\alpha-\beta)}e^{-\alpha t} + \frac{\kappa_1(n_A^{(0)} + n_B^{(0)})(\kappa_2 + \kappa_{-2}-\beta)}{\beta(\alpha-\beta)}e^{-\beta t}$$

$$p_2(t) = \frac{\kappa_1(n_A^{(0)} + n_B^{(0)})\kappa_{-2}}{\alpha\beta} + \frac{\kappa_1(n_A^{(0)} + n_B^{(0)})(\kappa_{-2}-\alpha)}{\alpha(\alpha-\beta)}e^{-\alpha t} - \frac{\kappa_1(n_A^{(0)} + n_B^{(0)})(\kappa_{-2}-\beta)}{\beta(\alpha-\beta)}e^{-\beta t}$$

$$p_3(t) = \frac{\kappa_1(n_A^{(0)} + n_B^{(0)})\kappa_2}{\alpha\beta} + \frac{\kappa_1(n_A^{(0)} + n_B^{(0)})\kappa_2}{\alpha(\alpha-\beta)}e^{-\alpha t} - \frac{\kappa_1(n_A^{(0)} + n_B^{(0)})\kappa_2}{\beta(\alpha-\beta)}e^{-\beta t}$$

$$q_1(t) = \frac{\kappa_{-1}\kappa_{-2}}{\alpha\beta} + \frac{\kappa_{-1}(\kappa_{-2} - \alpha)}{\alpha(\alpha - \beta)}e^{-\alpha t} - \frac{\kappa_{-1}(\kappa_{-2} - \beta)}{\beta(\alpha - \beta)}e^{-\beta t}$$

$$q_2(t) = \frac{k_1(n_A^{(0)} + n_B^{(0)})\kappa_{-2}}{\alpha\beta} - \frac{\kappa_1(n_A^{(0)} + n_B^{(0)})\kappa_2 + \kappa_{-1}\kappa_{-2} - (\kappa_{-1} + \kappa_2)\alpha}{\alpha(\alpha - \beta)}e^{-\alpha t} + \frac{\kappa_1(n_A^{(0)} + n_B^{(0)})\kappa_2 + \kappa_{-1}\kappa_{-2} - (\kappa_{-1} + \kappa_2)\beta}{\beta(\alpha - \beta)}e^{-\beta t}$$

$$q_3(t) = \frac{\kappa_1(n_A^{(0)} + n_B^{(0)})\kappa_2}{\alpha\beta} + \frac{\kappa_2(\kappa_1(n_A^{(0)} + n_B^{(0)}) - \alpha)}{\alpha(\alpha - \beta)}e^{-\alpha t} - \frac{\kappa_2(\kappa_1(n_A^{(0)} + n_B^{(0)}) - \beta)}{\beta(\alpha-\beta)}e^{-\beta t}$$

and

$$r_1(t) = \frac{\kappa_{-1}\kappa_{-2}}{\alpha\beta} + \frac{\kappa_{-1}\kappa_{-2}}{\alpha(\alpha-\beta)}e^{-\alpha t} - \frac{\kappa_{-1}\kappa_{-2}}{\beta(\alpha-\beta)}e^{-\beta t}$$

$$r_2(t) = \frac{\kappa_1(n_A^{(0)} + n_B^{(0)})\kappa_{-2}}{\alpha\beta} + \frac{\kappa_{-2}(\kappa_1(n_A^{(0)} + n_B^{(0)})-\alpha)}{\alpha(\alpha - \beta)}e^{-\alpha t} - \frac{\kappa_{-2}(\kappa_1(n_A^{(0)} + n_B^{(0)}) - \beta)}{\beta(\alpha - \beta)}e^{-\beta t}$$

$$r_3(t) = \frac{\kappa_1(n_A^{(0)} + n_B^{(0)})\kappa_2}{\alpha\beta} + \frac{\kappa_{-2}(\kappa_2 + \kappa_{-2} - \beta)}{\alpha(\alpha - \beta)}e^{-\alpha t} - \frac{\kappa_{-2}(\kappa_2 + \kappa_{-2} - \alpha)}{\beta(\alpha - \beta)}e^{-\beta t}$$

where α and β $(\alpha>\beta>0)$ are the roots of the equation

$$\eta^2 - \{\kappa_1(n_A^{(0)} + n_B^{(0)}) + \kappa_{-1} + \kappa_2 + \kappa_{-2}\}\eta + \kappa_1(n_A^{(0)} + n_B^{(0)})(\kappa_2 + \kappa_{-2}) + \kappa_{-1}\kappa_{-2} = 0$$

and $\sum_{i=1}^{3} p_i(t) = \sum_{i=1}^{3} q_i(t) = \sum_{i=1}^{3} r_i(t) = 1$ and $p_i(\infty)=q_i(\infty)=r_i(\infty)$ are satisfied.

6) G. H. Czerlinski, "Chemical Relaxation," Marcel Dekker Inc., New York, N. Y. (1966), p. 27.

BULLETIN OF THE CHEMICAL SOCIETY OF JAPAN VOL. 43 319—325 (1970)

The Paramagnetic Species Formed on the Surfaces of Various Oxides by Naphthalene Derivatives

Hisashi UEDA

Government Chemical Industrial Research Institute, Tokyo, Meguro-ku, Tokyo

(Received July 1, 1969)

The ESR intensities from the paramagnetic species formed by mixing a naphthalene derivative with an oxide powder were studied after the mixture had been heated at various temperatures. The measurements were made at 20°C. As additives 1-nitronaphthalene, 1-naphthol, 1,4-naphthoquinone, naphthalic acid, 1-naphthylamine, 1-nitroso-2-naphthol, naphthalene, triphenylene, and anthracene were used. As oxides, alumina, Al_2O_3-MoO_3, silicagel, TiO_2, MgO, MoO_3, CuO, and $ZnCrO_4$ were used. The ESR intensities obtained by the first six oxides depended only on the ionization potential of the additives, while those obtained by CuO and $ZnCrO_4$ did not. The ESR intensities obtained when 1-naphthol was mixed with alumina samples with various surface areas were exactly proportional to the surface areas of the alumina specimens used. It was concluded that, in the first six oxides, the additives are chemisorbed by the oxides at the active-oxygen anion sites on the surface. The introduction of either NH_3 or N_2O onto the adsorbed species formed on Al_2O_3-MoO_3 particles decreased (in the case of NH_3) or increased (in the case of N_2O) the ESR intensities. From these facts, it is concluded that a cationic complex, (naphthalene derivative$^+$-O^{2-}), is formed on the surface of these six oxides. In the case of CuO, the presence of (Cu^+-naphthylamine$^+$) is concluded.

The effects of various additives on the ESR intensities of zinc oxide were previously studied by the present author;[1] it was found that the surface ionization of the aromatic additive on the particle of zinc oxide, $Ar+ZnO \rightarrow Ar^+ + (ZnO)^-$, is in an equilibrium with the transfer of the hole from Ar^+ to Zni (interstitial zinc atom), $Ar^+ + Zni \rightarrow Ar + Zni^+$. Though the surface ionization of the aromatic compound on silica-alumina has long been established using perylene, diphenylethylene, and diphenylamine as additives,[2,3] the detailed mechanism has not yet been made clear. In some recent studies, the formation of a negative ion is claimed for the system consisting of an oxide and nitrobenzene.[4-6] Therefore, some criterion is strongly desired with which it is possible to predict the type of paramagnetic species to be formed on the surface from an additive compound with a particular type of molecular structure or functional group. Hoping to obtain a generalized solution for this problem, we have tested systems consisting of various oxides and naphthalene derivatives with various substituted functional groups together with anthracene and triphenylene, which it is also possible to consider as naphthalene derivatives. Naphthalene derivatives have been selected because (1) their ionization potentials are lower than those of the benzene derivatives with the same functional groups; (2) the desired substituted compounds are easier to acquire than those of anthracene or other, larger condensed-ring compounds, and (3) the ionization energies may be calculated as a problem of the variation in h and k by a proper molecular orbital theory.

Experimental

The additive compounds were used after recrystallization. Benzene, the solvent for the additive solution (0.2 mmol of a solute in 2.0 m*l* of the solvent), was used after having been shaken with concentrated sulfuric acid and by subsequent distillations. Special reagent-grade oxides, shown in Table 3, were used without further purification. The additive solution (2.0 m*l*) was poured on the oxide (1.0 g) and the solvent was evaporated in air. After the evaporation of the benzene, the mixture was placed in an ESR sample tube and was then evacuated to at least 10^{-2} mmHg (or to the vapor pressure of the additive). The sample thus prepared was examined first at room temperature. After the measurement, the tube was placed in a copper block with a hole to fit the diameter and the length of the sample tube, heated to 50°C for three minutes, and then cooled to 20°C. Then the measurement was made. Identical operations were repeated at different heating

1) H. Ueda, *Can. J. Chem.*, **46**, 891 (1968).
2) D. M. Brower, *Chem. Ind.*, (London) **1961**, 177.
3) J. J. Rooney and R. C. Pink, *Proc. Chem. Soc.*, **1961**, 70.
4) V. V. S. Rao, R. D. Iyenger and A. C. Zettlemoyer, *J. Catal.*, **12**, 278 (1968).
5) R. D. Flockhart, I. R. Leith and R. C. Pink, *Chem. Commun.*, **1966**, 885.
6) A. J. Trench and R. L. Nelson, *Trans. Faraday Soc.*, **63**, 2254 (1967).

temperatures, 100, 150, 200, and 250°C. The ESR intensity measurements were made using the same microwave power and at the same crystal current. Carbon powder ground with alumina and sealed in a vacuum was used as the intensity standard by measuring it between each ten measurements of the additive-oxide samples.

Results

In Table 1 the relative values of the ESR intensities obtained from Al_2O_3-MoO_3 (10%) containing various additives, after the sample had been heated at 250°C, x_1, x_2, x_3, u_1, u_2, and u_3, are shown. In the table, x denotes the intensity of the line with $g=2.004\pm0.001$ and with δH_{msl} smaller than 10 gauss, and u denotes the intensity of the line with $g=1.9328$. Both x and u are relative values, and so they are shown on different scales. The suffix 1 denotes the value for the sample in vacuum, 2 that for the sample in N_2O (350 mmHg), and 3 that for sample in NH_3 (300 mmHg). In Fig. 1, the x_1 values of Table 1 and the corresponding values for different oxides, *i.e.*, Al_2O_3, MoO_3, MgO, TiO_2 and silicagel, are plotted against the light absorption wave number in kilo Kaiser of the additve. The wave number value used here is equal to $10^7/\lambda_{max}$, where λ_{max} denotes the maximum peak wavelength in mμ of the absorption peaks observed below 500 mμ.*1 Figure 2 shows the spin concentration obtained by γ-alumina with 1-naphthol at room temperature *versus* the surface area of the alumina sample, which was measured by the helium-nitrogen BET method. The results show that unpaired electrons are formed on the surface and that the concentration is 3.3×10^{11} spins/cm^2, which may be compared with the value reported by Rooney and Pink, 2×10^{11} spins/cm^2 for perylene-silica-alumina. Table 2 shows the line-width at the maximum slope of the singlet ESR absorption, with $g=$

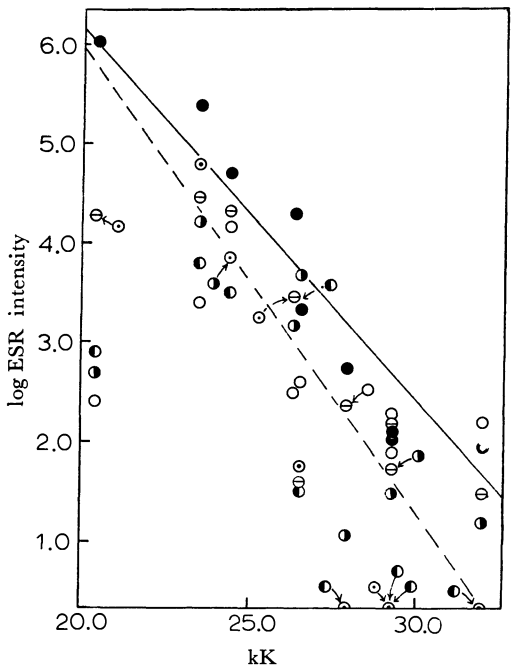

Fig. 1. Relative ESR intensities of Al_2O_3-MoO_3 *vs.* absorption wave number of additives.
● Al_2O_3-MoO_3, ⊖ Al_2O_3, ○ MoO, ⊙ MgO, ◐ TiO_2, ◐ Silicagel

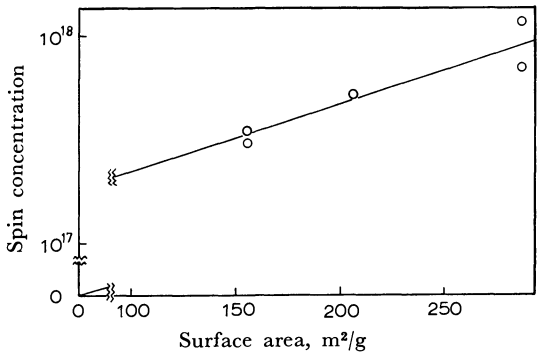

Fig. 2. Spin concentration (per gram) *vs.* surface area. Oxide: γ-Alumina. Additive: 1-Naphthol.

TABLE 1. RELATIVE ESR INTENSITIES OBSERVED

Additive	x_1	x_2	x_3	u_1	u_2	u_3
1-Naphthol	1.11×10^6	2.20×10^6	2.60×10^4	1.49×10^3	1.57×10^3	1.41×10^3
1,4-Naphthoquinone	2.48×10^5	8.10×10^5	4.95×10^4	3.90×10^3	4.80×10^3	3.10×10^3
1-Nitroso-2-naphthol	6.55×10^4	2.46×10^5	4.50×10^4	1.15×10^3	9.35×10^2	1.38×10^3
1-Nitronaphthalene	2.00×10^4	2.25×10^5	2.27×10^3	3.92×10^2	3.50×10^2	4.33×10^2
Anthracene	2.32×10^3	6.25×10^4	2.65×10^2	1.50×10^3	5.65×10^3	7.40×10^2
1-Naphthylamine	5.80×10^2	2.67×10^5	2.20×10^2	2.00×10^3	8.87×10^3	1.18×10^3
Triphenylene	1.24×10^2	4.10×10^2	2.45×10^2	8.12×10^2	1.30×10^3	3.23×10^2
1,8-Naphthalene-dicarboxylic acid	1.20×10^2	1.20×10^2	1.20×10^2	5.26×10^2	7.75×10^2	2.78×10^2
Naphthalene	92	1.50×10^2	95	4.39×10^2	5.90×10^2	2.88×10^2

*1 Some of the additives absorb in the near IR region; this phenomenon must be due to a different type of transition and so was ignored.

2.004 ± 0.001, for the species formed by various additives. It can be seen that both the δH_{msl} and g values depend upon the additives. In Table 3 the same quantities as in Table 2 are shown for various oxides mixed with 1-nitroso-2-naphthol as the additive. The results show that the oxides also slightly affect the spectroscopic constants. In the case of perylene-silica-alumina, the hyperfine splitting was partly resolved in the spectrum. In the present study only 1-nitroso-2-naphthol gave a

Table 2. The line widths at maximum slope of the ESR absorption spectra from the species on Al_2O_3-MoO_3

Additive	δH_{msl}, gauss	δg, $\times10^{-4}$
1,4-Naphthoquinone	7.3	+0.6
1-Nitronaphthalene	8.8	+3.6
1,8-Naphthalene-dicarboxylic acid	8.7	−2.4
1-Naphthylamine	8.8	−4.2
1-Naphthol	8.0	0.0
1-Nitroso-2-naphthol	8.4	0.0
Naphthalene	7.3	−4.2
Triphenylene	5.5	−9.0
Anthracene	6.5	−9.0

Table 3. The line widths at maximum slope of the ESR absorption spectra from the species formed by 1-nitroso-2-naphthol and various oxides

Oxide	δH_{msl}	δg, $\times10^{-4}$
Al_2O_3-MoO_3	8.4	0.0
Al_2O_3	7.3	+6.6
TiO_2	6.6	0.0
Silicagel	5.5	+6.6
MoO_3	6.2	0.0
MgO	5.5	−6.6
CuO	5.5	−3.5
$ZnCrO_4$	8.8	+5.4

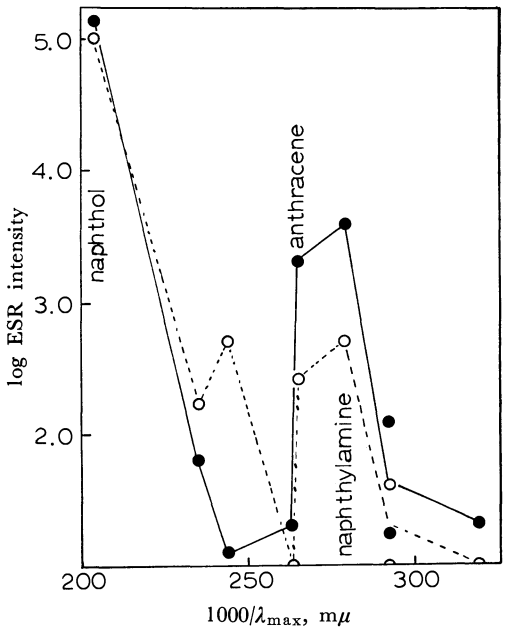

Fig. 3. Relative ESR intensities of CuO and $ZnCrO_4$ *vs.* $1000/\lambda_{max}$ of additives.
○ $ZnCrO_4$, ● CuO

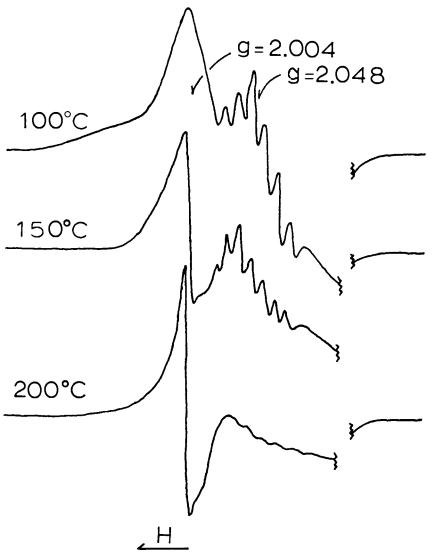

Fig. 4. First derivatives of the ESR spectra from CuO - 1-naphtylamine.

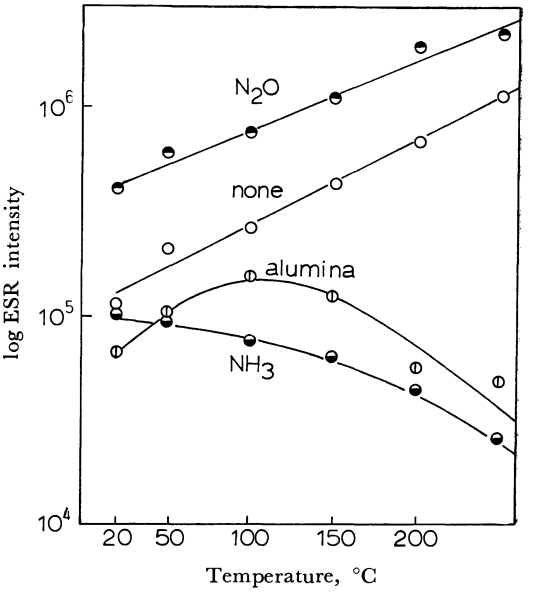

Fig. 5. Temperature dependence of the ESR intensities of Al_2O_3 and Al_2O_3-MoO_3 containing 1-naphthol with and without N_2O or NH_3.
○ Al_2O_3-MoO_3 in vacuum, ◐ Al_2O_3 in vacuum, ◓ Al_2O_3-MoO_3 in N_2O, ◒ Al_2O_3-MoO_3 in NH_3

hyperfine structure in the spectrum (three lines), but this structure disappeared when the specimen was heated at higher temperatures. Figure 3 shows the same quantities as those in Fig. 1 except for CuO (filled circles) and $ZnCrO_4$ (white circles). In this figure, the ESR intensities are stronger only for the additives which have either –OH or a $-NH_2$ group, or which are Lewis bases. Figure 4 shows the dependence of the relative ESR intensities for the sample consisting of CuO and 1-naphthylamine on the temperature of the heat treatment at 100, 150 and 200°C. The vertical amplitude of the spectrum at 200°C is six times as strong as that at 100 or 150°C. In Fig. 5 the temperature dependence of the relative (all on the same scale) ESR intensities for alumina and Al_2O_3-MoO_3, with 1-naphthol as the additive and with or without N_2O or NH_3 are shown. It can be seen that when both N_2O and Mo^{6+} exist on the surface they give the same type of activity to the surface of alumina, while NH_3 gives the opposite activity.

Discussion

The determination of the sign of the electric charge on an organic ionic species is often difficult[7,8] if the available information is limited to the spectroscopic data. Such difficulty increases if the spectroscopic measurement is made for a solid sample. In the case of zinc oxide[1] the presence of the electron donor, Zni, which gave the line with $g=1.96$ and which could easily be identified, has already been established. By using this fact, the sign of the aromatic ionic species on zinc oxice was determined. In some studies, the criterion that the electronegativity of the functional group attached to the aromatic ring determines the sign of the ionic species to be formed by that compound, has been used. However, it seems that this criterion is not as good as the one stating that the type of environment, in which the ionization occurs, determines the sign of the ionic species. This latter criterion can be written, alternatively, as stating that the atmosphere, the solvent, the matrix or the nature of the surface where the ionization occurs determines the type of the ionic species to be formed, rather than the intrinsic nature of the additive or the solute. Generally speaking, an aromatic compound with a low ionization potential, typically represented by perylene, also has a large electron affinity. In other words, it is equally easy to form an anion and a cation. The results obtained by radiation chemical studies of rigid glass solid solutions of aromatic compounds in solvents of various chemical structures have indicated that the matrix determines the sign of the electric charge of the ionic species to be formed.[9] In the present work, the additives with lower ionization potentials gave stronger ESR intensities, as is shownin Fig. 1. It cannot directly be concluded, for the foregoing reason, that cations were giving the ESR signals. However, the facts in Fig. 1 at least indicate that ionic species are formed.

Recently many studies have been made of ionic intermediates in radiation chemistry. Probably the most reliable method for the discrimination of ions in condensed phases has been the addition of N_2O or NH_3 to observe its effects on the formation of ionic intermediates. If an aromatic hydrocarbon is dissolved in an aliphatic ether and if this solution is irradiated, the electron primarily formed by ionizing radiation is captured by the solute molecule to form its negative ion. This formation of the negative ion can be effectively prevented by adding a small amount of N_2O to the solution, since N_2O scavenges the electron primarily formed.[10] If N_2O is added to a system in which a cation is to be formed, it increases the amount of the cation.[8] On the other hand, if NH_3 is added, it scavenges the positively-charged molecular species.[8] The results in Table 1 show that, for all the additives studied, the ESR intensities are partly cancelled by NH_3 and increased by N_2O. It seems that Table 1 provides enough evidence to establish the formation of a cation or a cation-like species in these systems. The results in Fig. 2 show that the phenomenon is a surface process.

In the case of the silica-alumina-perylene system, a carefully-created anaerobic environment was needed for the formation of the cation. This also indicates that the ionization is a surface process. The ESR data in Tables 2 and 3 show that the molecular orbital for the unpaired electron is made by an admixture of the wave functions of both the oxide and the additive orbitals. In other words, the unpaired spin is both on the oxide and the additive sides. Therefore, the additive is adsorbed by the oxide particles by chemisorption. The fact that the positive ions of the oxides shown in Fig. 1 (for example, the Mg^{2+} of MgO) do not affect the spectrum indicates that the chemisorption takes place at the O^{2-} site of the surface by an overlapping of its $2p$ orbital and the π-orbital of the aromatic additive molecule. If the cation of the oxide, *e.g.*, Mg^{2+}, accepts the electron directly from the additive molecule, what determines the ESR intensity will be both the electron affinity of the cation of the oxide and the ionization potential of the additive molecule. The results in Fig. 1 indicate that only the ionization potential of the additive determines the ESR intensity. The difference in the total intensities of the

7) For example, H. Ueda, *J. Phys. Chem.*, **68**, 1304 (1964).

8) H. Ueda, This Bulletin, **41**, 2578 (1968).

9) T. Shida and W. H. Hamill, *J. Chem. Phys.*, **44**, 2375, 4372 (1966).

10) G. Scholes and M. Simic, *Nature*, **202**, 895 (1964); S. Sato, T. Terao, M. Kono and S. Shida, This Bulletin, **40**, 1818 (1967).

ESR signal for different oxides indicates that the ionization which follows the chemisorption takes place on those O^{2-} ions which are in or which occupy certain active sites on the surface, probably somehow extruding above the surface. This assumed O^{2-} is written as O^{*2-} in this paper. Therefore, the nature of the surface-active sites at which the chemisorption occurs may be concluded to be quite similar for all the oxides shown in Fig. 1, while their relative concentrations are different for different oxides.

In the case of CuO and $ZnCrO_4$, the ESR intensities are strong only for the additives which have either $-NH_2$ or -OH groups. This is probably due to the fact that, in these oxides, the bond between the metal cation and oxygen is weak; as a result, there are few active O^{*2-} ions on the surface because the O^{*2-} ions can escape from the surface more easily than O^{2-} ions. Incidentally, it is assumed that a chemical bond is formed between the lone pair of the $-NH_2$ or -OH group and the metal cation of the oxide, *e.g.*, Cu^{2+}. A good piece of evidence to support this speculation is the spectrum shown in Fig. 4. At room tmeperature (CuO-1-naphthylamine) gives a broad ESR spectrum with $g=2.050$. When the sample is subjected to heat treatment at 100°C, a hyperfine splitting consisting of seven lines with an approximate intensity ratio of 1 : 2 : 2 : 2 : 2 : 2 : 1 appears, with its absorption center at $g=2.050$. If the splitting factor due to the amino-nitrogen is twice as large as that of amino hydrogen, these seven lines can most reasonably be interpreted by $a_H=14.6$ gauss and $a_N=29.2$ gauss. The large *s*-character or isotropy of this unpaired spin shows that one of the sigma lone-pair electrons is donated to the 3*d* orbital of Cu^{2+}. Between 100°C and 150°C, naphthylamine approaches Cu^{2+}; directing its $-NH_2$ group toward the Cu^{2+} ion. The (Cu^{2+}-naphthylamine) weak complex thus formed becomes a more strongly-combined charge-transfer complex (Cu^{+}-naphthylamine^{+}) at 200°C, giving rise to the strong ESR absorption at $g=2.004$; this indicates that the unpaired electron is mostly on the (naphthylamine^{+}) side.

In the past literature, the formation of the positively-charged species has been handled as a hole transfer from an active site or acid center to the adsorbed (it is not certain if a chemisorption or a van der Waals adsorption has been assumed) aromatic molecule. This theory does not, however, work well when the following two facts are to be interpreted. Firstly, if there are such holes (naturally having unpaired electrons), they and their counterparts (electrons or anions) should be observed even when no additives are added, provided that the electrons are not in the conduction band. Secondly, by such a mechanism the increment in the signal intensity in the presence of N_2O cannot be interpreted. If the active site consists of a proton, the counter anion should be O^{2-} or OH^{-}. For such systems, the effect of N_2O on the ESR intensity cannot be expected. The fact that the quenching of the ESR intensity by NH_3 is not done thoroughly also indicates that such a hole transfer is not true. If the active site consists of a proton, it should be very effectively scavenged by NH_3. These facts suggest that the formation of the positively-charged species is governed by several equilibrium reactions among O^{*2-}, trapped electrons (T^{-}), the aromatic additive (Ar), N_2O, and NH_3 (if these are added).

The existence of some electron traps can be concluded from Fig. 5. In the naphthol-alumina sample, the ESR intensity begins to decrease if the temperature of the heat treatment is above 100°C. This is not due to the thermal decomposition of the positively-charged species, for in the naphthol-Al_2O_3-MoO_3 system no such decrease in intensity is found as far as to a heat treatment temperature of 250°C. In the latter sample, a signal due to Mo^{5+} ($g=1.9328$) appears together with the line $g=2.004$. By these facts, the decrease in the ESR intensity in alumina is concluded to be caused by a recombination of the trapped electron and the cation complex formed. If Mo^{6+} is present, the electron is also trapped by Mo^{6+} to form Mo^{5+}; therefore, the recombination between the trapped electron and the cation complex, though it is probably still taking place, is far slower than that in the alumina-naphthol sample.

The following equilibrium equations describe the surface reactions leading to the cation complex:

$$ArO^{*2-} \rightleftarrows Ar^{+}O^{*2-} + e^{-};\ K_i \qquad (1)$$

$$e^{-} + T \rightleftarrows T^{-};\ K_t \qquad (2)$$

$$T^{-} + Ar^{+}O^{*2-} \rightleftarrows T + ArO^{*2-};\ K_r \qquad (3)$$

Ar denotes an additive, T denotes an electron trap such as Mo^{6+} and T^{-} denotes the trapped state, *e.g.*, Mo^{5+}. Only two of (1), (2) and (3) are independent; therefore, (1′) and (3′) are used for the analysis of the data. In (1′) and (3′), x denotes $[Ar^{+}O^{*2-}]$, u denotes $[T^{-}]$, and t denotes [T].

$$[ArO^{*2-}]\cdot K_i = x\cdot[e^{-}] \qquad (1')$$

$$u\cdot x\cdot K_r = t\cdot[ArO^{*2-}] \qquad (3')$$

As the total concentration of the positively-charged species is equal to that of the negatively-charged species (the suffixes used are those in Table 1):

$$x_1 = u_1 + [e^{-}] \qquad (4)$$

From (1′), (3′) and (4), we obtain:

$$x_1^2 = [ArO^{*2-}]\cdot K_i + t_1\cdot[ArO^{*2-}]/K_r$$

is derived. As K_r is large, and as $t_1/K_r\cdot K_t$ can be neglected,

$$x_1 = \sqrt{[ArO^{*2-}]\cdot K_i}$$

$$t_1 = u_1\cdot x_1\cdot K_r/[ArO^{*2-}]$$

are obtained. If N_2O is added to this system,

$$N_2O + T^{-} \rightleftarrows N_2O^{-} + T;\ K_s \qquad (5)$$

is expected in addition to (1), (2) and (3).*2 Then,

$$u_2 \cdot [N_2O] \cdot K_s = t_2 \cdot [N_2O^-]$$

is derived. In this case, (4) should be altered:

$$x_2 = u_2 + [e^-] + [N_2O^-] \quad (6)$$

Together with (1') and (3'), and neglecting $t/K_r \cdot K_i$, (6) gives:

$$x_2 = \sqrt{[ArO^{*2-}] \cdot (K_i + [N_2O] \cdot K_s/K_r)}$$

Therefore,

$$(x_2/x_1)^2 - 1 = [N_2O] \cdot K_s/K_i \cdot K_r \equiv Y_{21}$$

$$1/Y_{21} \cdot x_1^2 = K_r/[N_2O] \cdot [ArO^{*2-}] \cdot K_s$$

are obtained. As $[ArO^{*2-}] \cdot [N_2O]$ will be equal for all the additives used, the value on the left side gives the relative value of K_r. t_2 is shown in the same way as t_1:

$$t_2 = u_2 \cdot x_2 \cdot K_r/[ArO^{*2-}]$$

If NH_3 is added,

$$Ar^+O^{*2-} + NH_3 \rightleftarrows ArO^{*2-} + NH_3^+ \; ; \; K_c$$

$$x_3 \cdot [NH_3] \cdot K_c = [ArO^{*2-}] \cdot [NH_3] \quad (7)$$

take place instead of (3). The equation corresponding to (4) or (6) is:

$$x_3 + [NH_3^+] = u + [e^-] \quad (8)$$

From (7), (8), (1'), and (3'), and neglecting $t/K_r \cdot K_i$,

$$x_3^2 = [ArO^{*2-}] \cdot K_i/(1 + [NH_3] \cdot K_c/[ArO^{*2-}])$$

$$(x_1/x_3)^2 - 1 = [NH_3] \cdot K_c/[ArO^{*2-}] \equiv Y_{13}$$

are obtained. Since $K_c/[ArO^{*2-}]$ should be equal for all the additives, Y_{13} gives the relative value of K_c. The relative values of $[ArO^{*2-}] \cdot K_i$, t_2, $K_r/[ArO^{*2-}] \cdot [N_2O] \cdot K_s$, and $[NH_3] \cdot K_c/[ArO^{*2-}]$ are shown in Table 4.

It is well-known that the $-NO_2$ group in an aromatic nitro compound deaccelerates a nucleophillic substitution reaction, while an amino group on an aromatic amine accelerates it. These facts show that these groups greatly change the electron densities on some particular carbon atoms of the aromatic ring. The drawing of a direct analogy between such facts and the criterion for the determination of the sign of the electric charge in an ionic species on the oxide surface seems to be wrong for the following reasons. It is not the free cation, Ar^+, but the chemisorbed species, Ar^+O^{*2-}, that is formed by the charge transfer from Ar to T. The cation complex, Ar^+O^{*2-}, can also be written as $(ArO^*)^-$, which it is possible to describe as an anion. This view may also be related to the fact that a strictly anaerobic condition was needed for the observation of the "perylene cation" on silica-alumina. The rate constants of O_2 and N_2O when reacting with a hydrated electron are comparable and are very large. Therefore, O_2 has a strong ability to destroy an anion, but not a cation. On the other hand, the cation of perylene has been observed in a mixture of O_2 and anhydrous HF.[11] Therefore, the "perylene cation" previously reported might not have been the free cation. Perylene$^+O^{*2-}$ or $(perylene\text{-}O^*)^-$ might be a more proper form to describe the paramagnetic species observed. Therefore, to use the electron density distribution function of "Ar" and not that of "ArO^{*2-}" to predict the formation of either a cation or an anion on an oxide surface is not right.

As is shown in Table 4, the activities of Mo^{6+}, *i.e.*, t_2, are not the same for different additives, though its chemical concentrations are all the same.

TABLE 4. RELATIVE VALUES OF SURFACE REACTION CONSTANTS FOR Al_2O_3-MoO_3

Additive	For ArO^{*2-}		For Ar^+O^{*2-}	
	$[ArO^{*2-}] \cdot K_i$	t_2	$\frac{K_r}{[ArO^{\circ 2-}] \cdot [N_2O] \cdot K_s}$	$\frac{[NH_3] \cdot K_c}{[ArO^{*2-}]}$
1-Naphthol	3.02×10^{3}	1.23×10^{-3}	2.89×10^{-5}	2.4×10
1,4-Naphthoquinone	1.54×10^{2}	8.40×10^{-3}	1.73×10^{-4}	3.2×10^{-1}
1-Nitroso-2-naphthol	1.05×10	5.25×10^{-3}	1.85×10^{-3}	1.4×10^{-2}
1-Nitronaphthalene*	1.00	1.00	1.00	1.00
Anthracene	1.35×10^{-2}	1.39×10^{2}	3.16	1.00
1-Naphthylamine	8.35×10^{-4}	4.50×10^{-2}	1.46×10^{-3}	7.9×10^{-2}
Triphenylene	3.80×10^{-5}	4.61	6.95×10^{2}	$\simeq0$
1,8-Naphthalenedicarboxylic acid	3.52×10^{-5}		7.39×10^{2}	$\simeq0$
Naphthalene	2.10×10^{-5}	8.44	7.50×10^{3}	$\simeq0$

* The values for this compound are put to be the standard values.

*2 It may be more proper to use the chemical equations, $N_2O+e^- \rightleftarrows N_2+O^-$, and so on, instead of (5). Though the negative-charge transfer to N_2O itself has been established, the behavior and fate of N_2O on the solid surfaces investigated in this study have not yet been made clear. Therefore, further discussion or theoretical treatment, beyond (5), of the fate of N_2O after scavenging an electron or an anion has been omitted in the present report.

11) W. Ij. Aalbersberg, G. J. Hoijtink, E. L. Mackor and W. P. Weijland, *J. Chem. Soc.*, **1959**, 3049.

This is partly due to the fact that the system studied is not a homogeneous solution; therefore, the equilibria in (2), (3) and (5) are more involved than those to be found with a homogeneous system like an equeous solution of Mo^{6+}. From (5) and (3),

$$N_2O + ArO^{*2-} \rightleftarrows Ar^+O^{*2-} + N_2O^-;\ K_s/K_r$$

is derived. In this reaction, Mo^{6+}-Mo^{5+} functions as a catalyst. The different activities of Mo^{6+} for different kinds of Ar mean that the catalytic activities of Mo^{6+}-Mo^{5+} are different for different kinds of Ar. This is due to the heterogeneous nature of the system.

In my previous paper,[1] no rule was found for the relation between the physical properties of the additives and the ESR intensities obtained by use of them. This is partly due to the fact that the compounds used in the previous paper consisted of rather varied types of substances. Such complexity has been avoided in the present work by using naphthalene derivatives.

The measurement of the active sites in a catalyst by means of the "additive-ESR-method" cannot be done so simply as has been thought possible. The selection of a proper additive with known equilibrium constants, a proper temperature, and a proper atmosphere to "develop" the paramagnetic species seems to be important.

The author wishes to thank Dr. N. Todo and Mrs. M. Yamadaya of his Institute for their helpful suggestions.

BULLETIN OF THE CHEMICAL SOCIETY OF JAPAN VOL. 43 325—330 (1970)

Radiative Lifetime Measuements of Some Excited States of N_2^+ and CH

Tsuguo SAWADA and Hitoshi KAMADA

Faculty of Engineering, The University of Tokyo, Hongo, Bunkyo-ku, Tokyo

(Received July 2, 1969)

Time-sampling technique has been applied to radiative lifetime measurements. The time resolution of the apparatus was about 10 nsec. The excited molecules were produced by electron bombardment of N_2 and CH_4. The measured lifetimes of $N_2^+(B^2\sum_u^+)$, $CH(A^2\Delta)$ and $CH(B^2\sum^-)$ are $(6.5\pm0.5)\times10^{-8}$ sec, $(4.3\pm0.2)\times10^{-7}$ sec and $(7.6\pm0.4)\times10^{-7}$ sec, respectively. Band oscillator strengths have been computed on the assumption that the electronic transition moment is constant in the range in which the transition takes place.

For the study of unstable chemical species such as ions and free radicals, the knowledge of radiative lifetime is indispensable. As a matter of principle transition probabilities and oscillater strengths can be determined by measuring absorption coefficients. Some investigations[1,2] on OH and CN molecules along this line have been reported. However, there are difficulties in the determination of absorption coefficients of unstable chemical species. Experimental data on the measurements of the concentration of the molecules excited to upper states are not always available.

On the other hand, it is possible to calculate reliable transition probabilities and oscillator strengths from the measurements of the radiative lifetime. The lifetime measurements for a number of well known molecule transitions have recently been reported. The following two methods have been reported on the measurements of the lifetime.

(a) Direct measurement of decay time[3,4]
(b) Phase shift method[5,6]

The radiative lifetimes fall in the range 10^{-9} to 10^{-6} sec for allowed transitions. In (a), the lifetime is obtained from the decay time of the emitted light. Thus a good time resolution is required in the apparatus.

In this paper, the results of the lifetime measurements of $N_2^+(B^2\sum_u^+)$, $CH(A^2\Delta)$ and $CH(B^2\sum^-)$ by means of the time sampling method are reported. These excited molecules are produced by pulsed beam electron impact below 300 eV.

Absorption oscillator strengths of the $N_2^+(B^2\sum_u^+ X^2\sum_g^+)$, the $CH(A^2\Delta-X^2\Pi)$ and the CH $(B^2\sum^- -X^2\Pi)$ are calculated on the assumption that the

1) O. Oldenberg and F. F. Rieke, *J. Chem. Phys.*, **6**, 439, 779 (1938).
2) P. J. Dyne, *ibid.*, **28**, 999 (1958).
3) R. G. Bennet and F. W. Dalby, *ibid.*, **31**, 434 (1959).
4) M. Jeunehomme, *ibid.*, **44**, 2672 (1966).
5) E. H. Fink and K. H. Welge, *Z. Naturforsch.*, **19a**, 1193 (1964).
6) G. M. Lawrence, *J. Quant. Spectrosc. Radiat. Transfer*, **5**, 359 (1965).

electronic transition moment is constant in the range in which the transition takes place.

Theory

The radiative lifetime $\tau_{v'}$ of the upper vibrational level in an electronic transition can be expressed by summing over fine structures due to rotational and electron spin

$$1/\tau_{v'} = A_{v'} = \sum_{v''} A_{v'v''} \quad (1)$$

where $A_{v'v''}$ is the Einstein coefficient. The oscillator strength $f_{v'v''}$ is defined as

$$f_{v'v''} = 1.51 \cdot (G'/G'') \cdot A_{v'v''} \cdot \lambda^2_{v'v''} \quad (2)$$

where λ is the wavelength in cm, $A_{v'v''}$ in sec^{-1} and G'/G'' is equal to the ratio of the upper to lower electronic statistical weights as defined by Mulliken.[7]

The band intensity is related to the Franck-Condon factor $q_{v'v''}$[8] as

$$I_{v'v''} = K \cdot N_{v'} \cdot \lambda^{-4}{}_{v'v''} \cdot R_e^2 \cdot q_{v'v''} \quad (3)$$

where K is a constant, $N_{v'}$ is the population of the upper vibrational level v'. R_e is an electronic transition moment. On the assumption that R_e is not a slowly varying function of the internuclear distance but a constant for all v'-v'' transitions in a given band system, the ratio $A_{v'v''}/A_{v'}$ is expressed as

$$A_{v'v''}/A_{v'} = q_{v'v''} \cdot \lambda^{-3}{}_{v'v''} / \sum_{v''} q_{v'v''} \cdot \lambda^{-3}{}_{v'v''} \quad (4)$$

$A_{v'v''}$ can be expressed by the product of $A_{v'}$ and the Franck-Condon factor to a good approximation.

$$A_{v'v''} = A_{v'} \cdot q_{v'v''} \quad (5)$$

In order to calculate the oscillator strengths for individual bands, the theoretical computations of the Franck-Condon factors must be available.

Experimental

An electron gun was used for the formation and excitation of unstable molecules from sample gases. Figure 1 shows a schematic diagram of the electron gun. The emitter is an indirectly-heated oxide-coated cathode which emits at a temperature below 1000°K. However, it can be poisoned easily by organic or other vapors with loss of emission and discoloration. The electron energy can be varied from 30 to 300 eV, and a current about 3 mA can be produced. The first grid is a control grid which is biased by a potential of −50 V.

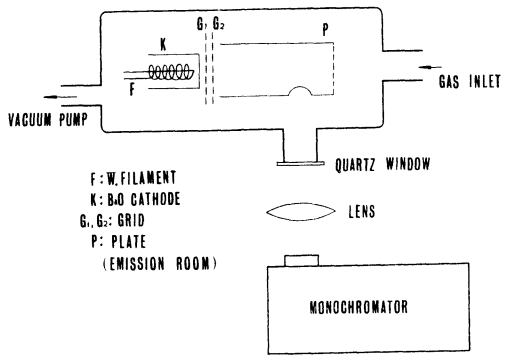

Fig. 1. Schematic diagram of the electron gun.

The pulse applied to the control grid is 50 V in amplitude and is controllable in duration up to 1.0 μsec. The rise and fall time of this pulse is 4.0×10^{-9} sec (4 nsec) and 6.0×10^{-9} sec (6 nsec), respectively. The excitation room is a cylindrical plate, 8 mm in diameter and 20 mm in length. The emitted light can be taken out from the hole, 6 mm in diameter, as shown in Fig. 1. The emitted light is made monochromatic with a small Nippon-Jarrel Ash grating monochromator.

A good time resolution is required for the measurements of lifetimes. In order to measure periodic faint

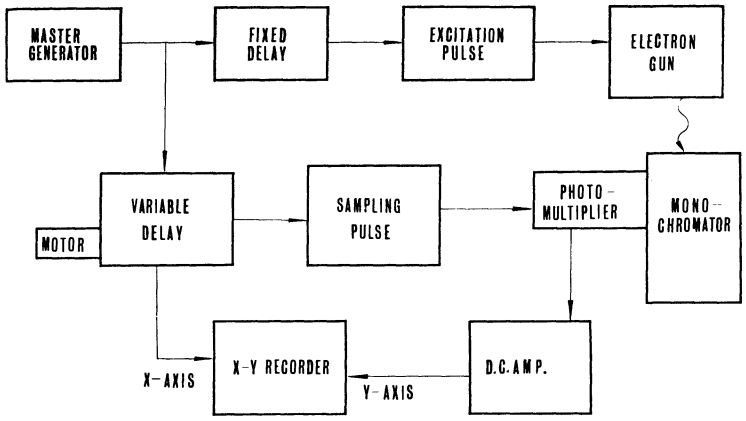

Fig. 2. Block diagram of the apparatus.

7) R. S. Mulliken, *J. Chem. Phys.*, **7**, 14 (1939).
8) G. Herzberg, "Molecular Spectra and Molecular Structure I: Spectra of Diatomic Molecules," CD Van Nostland CO., Inc., Princeton, N. J. (1950)

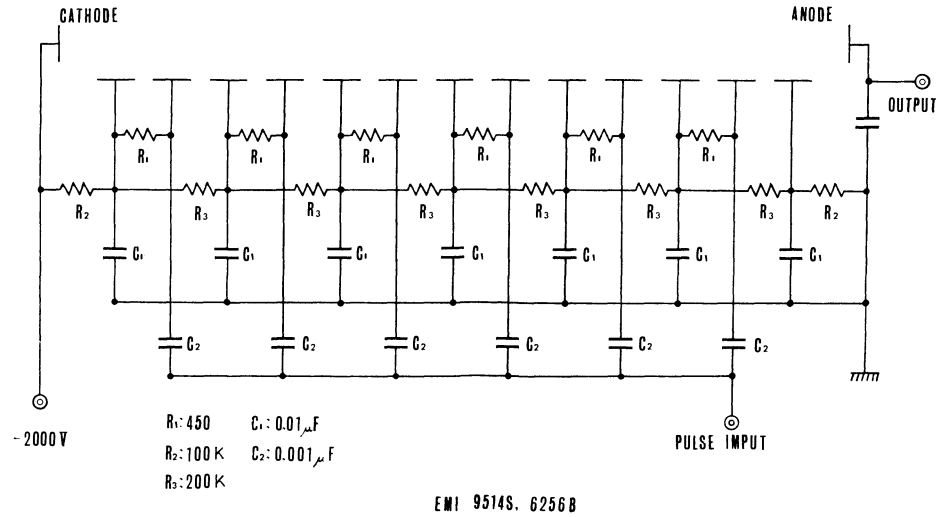

Fig. 3. Circuit of the pulsed photomultiplier.

light intensity, the photomultiplier sampling technique[9] can be utilized. Thus, the pulsed photomultiplier samples the output of periodically emitted light, and this sampling pulse is phased slowly by means of the variable delay circuit. The emitted light is then recorded as a function of time on a X-Y recorder. The advantage of this method is that the output current inside the phototube can be combined to the high-input impedance vacuum-tube voltmeter to detect very faint light. This sampling technique is applicable to time-resolved spectroscopy at a fixed phase of a periodic light. The block diagram of the apparatus is shown in Fig. 2. The master generator produces two equal pluses at a repetition rate variable from 1 to 10 k Hz. One pulse is fed to the Control grid of the electron gun after a fixed delay circuit, and the other initiates the sampling pulse. Th delay time of this pulse increases slowly and continuously by a motor-driven 50 kΩ variable resistance. The variable delay network consists of a phantastron circuit and a cathode follower. The delay time can be moved to 10 μsec in six steps. The pulse applied to photomultiplier is 100 V in amplitude. The 3C-2V coaxial cable is used as a pulse-forming network, and its length determines the pulse duration. The minimum pulse duration obtained is about 20 nsec. The sampled phototube signal is integrated with a simple RC network by which the time constant of the recording system is determined. The output of the voltmeter is recorded on the X-Y recorder, and the delay time is scanned at a rate determined by the speed of the motor and the grear ratio.

Figure 3 indicates a schematic diagram of the pulsed photomultiplier circuit. The method which has been most widely used is that in which the high voltage pulse is applied directly to the cathode and the dynodes.[9] However, it is difficult technically to produce an extremely stabilized high-voltage pulse, which is needed to reduce fluctuations of the phototube gain. The dynodecontrolled technique is therefore used in the present measurements.[10] The gating pulse is applied to the alternate dynodes throught the load resistance, the potentials of which are the same as those of the adjacent dynodes during the closed-gate period. EMI 9514S and 6256B as the head-on type photomultiplier and in some cases 931A and 1P21 as the side-window type are used for detection of light.

Since the actual gated period is equal to the sampling pulse duration minus the transit time of the electron in the photomultiplier, the time resolution is ultimately determined by the transit time spread.[11] In the dynode-controlled technique, the background current during the closed gate period must also be controlled to a lower value in order to obtain better time resolution.

Results and Discussion

Lifetime Measurements. a) *He Lines.* Measurements of the radiative lifetime of three excited states are summarized in Table 1. Our data agree well with those of other investigators within the range of experimental errors. Measurements were made at an electron energy of 80 eV.

Table 1. Lifetimes of He terms[a]

	4^3S-2^3P 3188 Å	3^3P-2^3S 3889 Å	3^1P-2^1S 5016 Å
Heron *et al.*[12]	6.75±0.1	11.5±0.5	7.4±0.1
Bennet and Dalby[3]	7.75±0.4	10.6±0.5	≦1.5
Lawrence[6]	—	10.5±0.5	—
This work	7.3±0.3	10.4±0.6	3.0±0.5[b]

a) Unit: 10^{-8} sec
b) This value was measured at a gas pressure of 11 μ.

9) C. F. Hendee and W. B. Brown, *Philips. Tech. Rev.*, **19**, 50 (1958).

10) H. M. Crosswhite, D. W. Steinhaus and G. H. Dieke, *J. Opt. Soc. Amer.*, **41**, 299 (1951).

11) S. Minami and K. Nishikawa, *Applied Opts.*, **5**, 173 (1968).

Variations of the lifetime with the gas pressure were examined. However, except for that of 3^1P level no significant dependence was recognized within the range of the gas pressure from 1.0 μ to 10 μ. It is well known that the 3^1P-2^1S transition is affected by the trapping of resonance radiation because of 3^1P level corresponding to the upper level of the 537A resonance line.[12] Our data for the 3^1P level

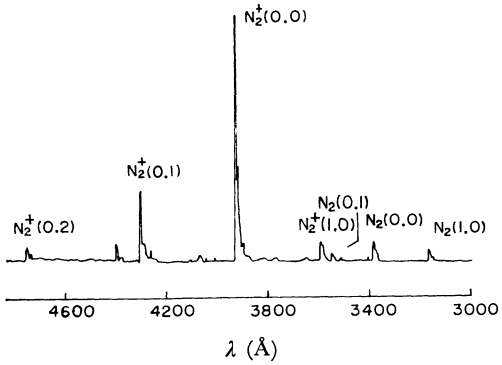

Fig. 4. Emission spectrum obtained from nitrogen (gas pressure 5 μ) excited by 120 eV electrons.

shown in Table 1 were obtained at a gas pressure of 11 μ. Because of the decrease of the trapped resonance radiation, the lifetime measured at a lower pressure can be considered to be a measure of the resolving time of the apparatus. The minimum resolving time obtained was about 10 nsec.

b) $B^2\Sigma_u^+$ *State of* N_2^+. Figure 4 shows the emission spectrum obtained from the bombardment of N_2 gas at an electron beam of 120 eV. The measurement was made at a pressure of 5 μ. The spectrum consists of the $B^2\Sigma_u^+$-$X^2\Sigma_g^+$ system of N_2^+ and the $C^3\Pi_u$-$B^3\Pi_g$ system of N_2. The result agrees well with those of other measurements.[3,5] The radiative lifetime was measured by use of 0.5 m grating monochromator (about 15Å bandwidth) in order to separate various emission bands. The dependence of the lifetime for the (0,0) band of N_2^+ upon the electron energy is shown in Fig. 5. The apparent lifetime increases slowly up to an electron energy of 100 eV, and remains constant beyond it. A similar tendency has been reported by Bennet and Dalby,[3] who assumed that this was due to a mixing of other bands, since they used interference filters of about 100Å bandwidth instead of a monochromator. The fact that our experiments with a monochromator showed a similar tendency indicates that their interpretation is not correct. This cannot be ascribed to the cascade population of the $N_2^+(B^2\Sigma_u^+)$, because no higher electronic states are known from which the transitions to this level are allowed. It is highly desirable to investigate the lifetime down to the excitation threshold.[13] However, the measurements near the threshold were unreliable because of the low signal level compared with the noise level. The value obtained above 100 eV was taken as the lifetime of the N_2^+ $(B^2\Sigma_u^+)$. A lifetime

$$(6.5\pm0.5)\times10^{-8}\ \text{sec}$$

was obtained. The variation of the lifetime with gas pressure was not recognized within the range of our experiments from 1 μ to 5 μ. It can be considered that neither the collision quenching effect nor the trapped resonance radiation has significant influence on the lifetime in the range of the gas pressure below 5 μ.[4] The decay curve

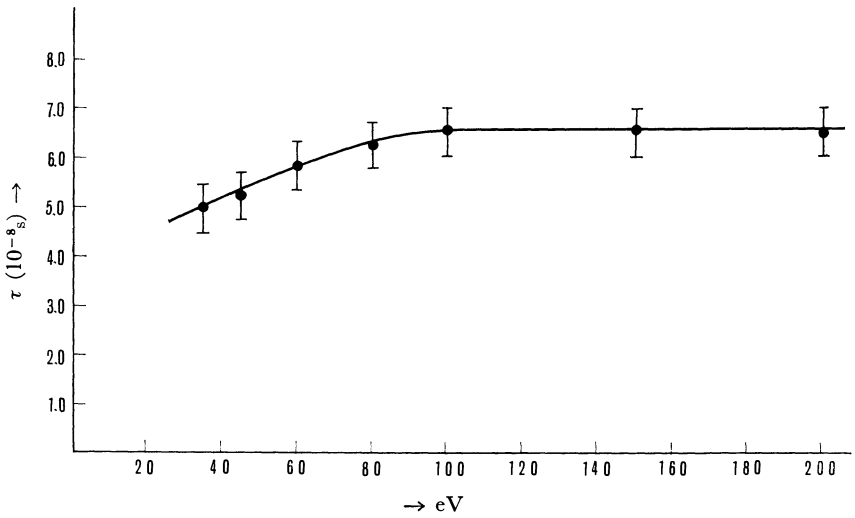

Fig. 5. The dependancy of the lifetime of the $N_2^+(B^2\Sigma_u^+)$ level upon electron energy.

12) S. Heron, R. W. P. Mcwhirter and E. H. Rhoderick, *Proc. Roy. Soc., Ser. A*, **234**, 565 (1956).

13) R. E. Fox, *J. Chem. Phys.*, **35**, 1379 (1961).

was plotted as a function of time on semilogarith mic graph paper to determine the mean lifetimes. The observed decay was closely exponential.

c) $A^2\Delta$ and $B^2\sum^-$ States of CH. Figure 6 shows the spectrum obtained when CH_4 was bombarded with 100 eV electrons. The spectrum was taken with a small grating monochromator (15 Å bandwidth). The emission bands of the CH($A^2\Delta$-$X^2\Pi$) and the CH($B^2\sum^-$-$X^2\Pi$) are observed together with several atomic lines such as H_β, H_γ and H_δ. There are some other emission bands which seem to be those of CO^+. The formation of CO^+ is perhaps due to the reactons between the excited carbons and the oxide coated cathode. Similar

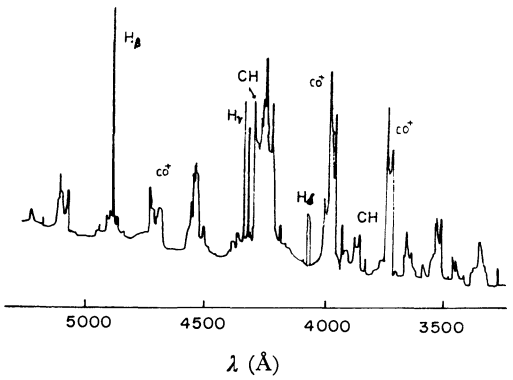

Fig. 6. Spectrum observed when methane (gas pressure of 5 μ) was bombarded with 100 eV electrons. The monochromator (15 Å bandwidth) was used.

results were also obtained from the bombardment of C_2H_4 and C_2H_6. The strong band observed at 4300 Å is the (0,0) band of the ($A^2\Delta$-$X^2\Pi$) system of CH. The (0,0) band of the ($B^2\sum^-$-$X^2\Pi$) system of CH is observed near 3900 Å though its intensity is small.[14,15] The radiative lifetimes were measured by use of a small monochromator in order to separate interfering bands. The dependence of the apparent lifetime of the CH($A^2\Delta$) state upon the electron energy is shown in Fig. 7. The lifetime is almost constant within the range of the electron energy from 40 eV to 150 eV. Below 40 eV, the emitted light intensity decreases so markedly that no accurate measurements can be done. The lifetime of the CH($A^2\Delta$) state was independent of the pressure in the range from 1 μ to 10 μ. Similar results have been reported.[16,17] It seems that both the collision quenching and the trapped resonance radiation do not occur. The duration of the pulsed electron beam was 1.0 μsec. The sampling pulse width was varied up to 0.3 μsec, but the change of lifetime was negligible. We conclude the lifetime for the CH($A^2\Delta$) level as

$$(4.3\pm0.2)\times10^{-7}\,\text{sec}$$

This value is a little lower than those of Bennet and Dalby,[16] and Fink and Welge.[17] Bennet and Dalby used interference filters with the 100 Å bandwidth for the lifetime measurements. Fink and Welge measured τ using the phase shift method with the 20 Å bandwidth monochromator. The bandwidth in our experiment was the same as that of Fink and Welge. The lifetime for the CH($B^2\sum^-$) level

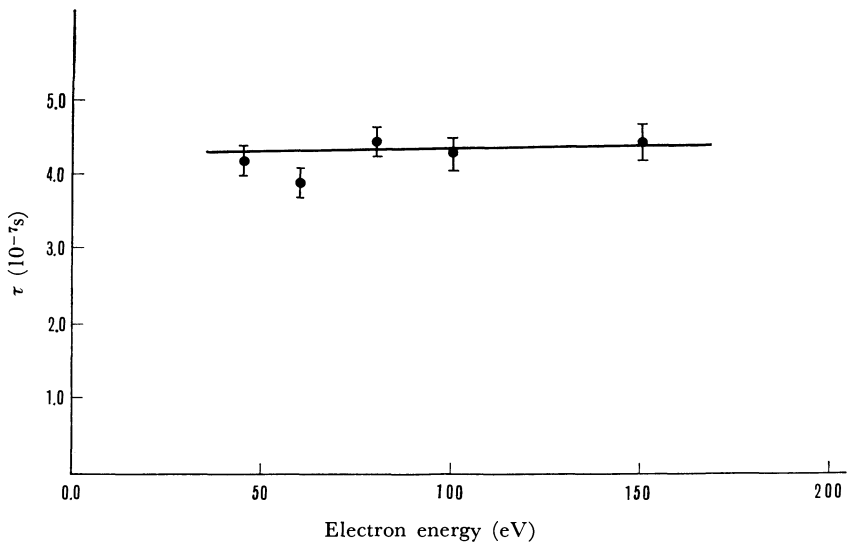

Fig. 7. The dependancy of the lifetime of the CH($A^2\Delta$) level upon electron energy.

14) L. Wallace, *Astrophys. J.*, **68**, 164 (1962).
15) R. W. B. Pearce and A. G. Gaydon, "The Identification of Molecular Spectra," Chapman & Hall Ltd., London (1950).
16) R. G. Bernnet and F. W. Dalby, *J. Chem. Phys.*, **32**, 1716 (1960).
17) E. H. Fink and K. H. Welge, *ibid.*, **46**, 4315 (1967).

at an electron energy of 100 eV was

$$(7.6\pm0.4)\times10^{-7}\ \text{sec}$$

No variation of lifetime with the gas pressure was observed within the range from 5 μ to 10 μ. Precise investigations below 100 eV could not be done for the CH($B^2\sum^-$) state because the intensity of the emitted light was too small.

It should be examined whether cascading effects from higher electronic states occur. However, higher electronic states allowed to combine with $A^2\Delta$ and $B^2\sum^-$ are not yet known. Therefore, it may be assumed that the possibility of cascading effects is ruled out.

Oscillator Strength. Oscillator strengths $f_{v'v''}$ for individual bands can be calculated from Eq. (2), using the lifetimes of the upper level v'. It is necessary to know the theoretical calculations of the Frannck-Condon factors $q_{v'v''}$. Nicholls[18] has computed them numerically for the various band systems of N_2 and N_2^+. The oscillator strengths for the (0,0) band of the ($B^2\sum_u^+$–$X^2\sum_g^+$) of N_2^+ is evaluated using q_{00} value of Nicholls to be

$$f_{00}=(2.3\pm0.2)\times10^{-2},$$

where the wavelength used is 3914 A. G'/G'' is equal to unity. This value agrees very well with the results of Jeunehomme, $(2.47\pm0.18)\times10^{-2}$. Similar calculations were made for the (0.0) bands of CH($A^2\Delta$–$X^2\Pi$) and CH($B^2\sum^-$–$X^2\Pi$) respectively. Recently, Huo[19] has computed the Franck-Condon factor q_{00} for the ($A^2\Delta$–$X^2\Pi$) transition of CH. By use of Huo's value ($q_{00}=0.9905$), for the (0,0) band of CH($A^2\Delta$–$X^2\Pi$),

$$f_{00}=(6.5\pm0.3)\times10^{-3}$$

was obtained. The wavelength used is 4313 Å. For the CH($B^2\sum^-$—$X^2\Pi$),

$$f_{00}/q_{00}=(1.5\pm0.1)\times10^{-3}$$

was obtained. No theoretical calculation of the Franck-Condon factor for the above electronic transition has been reported. Hence, f_{00}/q_{00} was calculated insted of f_{00}. The wavelength used is 3880 Å. The results of this work are summarized in Table 2.

TABLE 2.

Molecule	Transition	Lifetime (10^{-8} sec)	Oscillator strength
N_2^+	$B^2\sum_u^+$–$X^2\sum_g^+$	6.5±0.5	0.023±0.002[a]
CH	$A^2\Delta$–$X^2\Pi$	43±2.0	0.0065±0.0003
CH	$B^2\sum^-$–$X^2\Pi$	76±4.0	0.0015±0.0001[b]

a) The calculated Franck-Condon factor is that of Nicholls.[18]
b) This value is f_{00}/q_{00} instead of f_{00}.

In the calculation of the oscillator strengths, as described previously, we assumed that electronic transition moment is independent of the internuclear separations.

The authors are indebted to Mr. Hiroshi Yamamoto of Toshiba Co., Ltd., for his assistance in designing and constructing the electron gun.

18) R. W. Nicholls, *J. Res. Nat. Bur. Stand. A*, **65**, 451 (1961).

19) W. M. Huo, *J. Chem. Phys.*, **49**, 1482 (1968).

BULLETIN OF THE CHEMICAL SOCIETY OF JAPAN VOL. 43 331—334 (1970)

Radiative Lifetime Measurements of $N_2(C^3\Pi_u)$, $NH(A^3\Pi)$ and $NH(c^1\Pi)$

Tsuguo SAWADA and Hitoshi KAMADA

Faculty of Engineering, The University of Tokyo, Hongo, Bunkyo-ku, Tokyo

(Received July 25, 1969)

The radiative lifetimes of $N_2(C^3\Pi_u)$, $NH(A^3\Pi)$, and $NH(c^1\Pi)$ states were measured by the use of the time-sampling technique. The excited molecules were produced by the electron bombardment of N_2 and NH_3 gas. The lifetimes obtained in this experiment for $N_2(C^3\pi\Pi)$, $NH(A^3\Pi)$, and $NH(c^1\Pi)$ were $(4.8\pm0.3)\times10^{-8}$ sec, $(4.1\pm0.2)\times10^{-7}$ sec, and $(4.3\pm0.2)\times10^{-7}$ sec respectively. The oscillator strengths of the respective transitions were also calculated.

Th radiative lifetimes of several unstable chemical species, such as ions or free radicals, have been measured by several investigators.[1-4] Knowledge of lifetimes is very important in the field of astrophysics and spectroscopy. Particularly, oscillator strengths and dipole transition probabilities can be obtained from the lifetimes provided that the theoretical or experimental Franck-Condon factors are known.

We wish to report here on one radiative-lifetime measurements of $N_2(C^3\Pi_u)$, $NH(A^3\Pi)$, and $NH(c^1\Pi)$. These excited molecules are produced by electron impact below 200 eV, and the lifetimes are obtained by determining the fluorescence decay directly. Lifetime measurements of the $N_2(C^3\Pi_u)$ level have been performed previously,[1,2,5,6] but there have been different interpretations of the collision quenching and cascading effect. In this paper, new evidence will be reported. In the case of NH, Bennet and Dalby[7] measured $NH(A^3\Pi)$, and Fink and Welge[2] measured $NH(A^3\Pi)$ and $NH(c^1\Pi)$, using the phase shift method. We studied these lifetimes in more detail and obtained slightly different results.

The approximate absorption oscillator strengths of the $(C^3\Pi_u-B^3\Pi_g)$ system of N_2 and the $(A^3\Pi-X^3\Sigma)$ system and the $(c^1\Pi-a^1\Delta)$ system of NH were calculated on the assumption that the electronic dipole strengths are constant for each v''-progression.

Experimental

The excited molecules are formed by the bombardment of pulsed low-energy electrons (15—200 eV) at a repetition rate of 5 Hz. The emitted light from excited molecules is dispersed with a small Nippon-Jarrel Ash grating monochromator and detected by a photomultiplier. The photomultiplier (EMI 6256S, 9514S) detects light only during the pulsed period. The gate pulse is fed into the alternate dynodes of the photomultiplier through the load resistance. The potentials of the alternate dynodes are the same as those of the adjacent dynodes during the closed-gate period. This pulse is phased slowly by means of a variable-delay network. Then, the emitted light intensity is recorded as a function of the time on a recorder. This method is called the time-sampling technique. The time-resolution used in this experiment was about 10 nsec. The details of the apparatus will be published elsewhere.[8]

Results and Disussion

Lifetime Measurement of $N_2(C^3\Pi_u)$. When N_2 gas at a pressure of 1 μ is bombarded with electrons below 200 eV, the emission of the $(C^3\Pi_u-B^3\Pi_g)$ system of N_2 appears very readily. The peak at 3371 Å is the (0,0) band. The peaks at 3577 Å and 3805 Å are the (0,1) band and the (0,2) band respectively. The radiative lifetime was measured

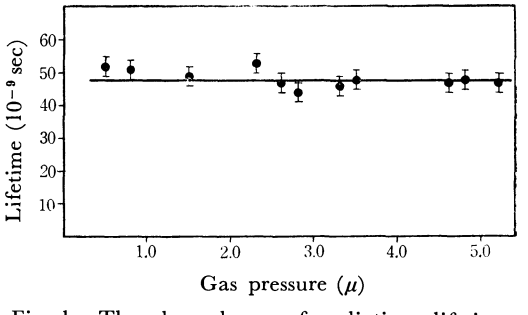

Fig. 1. The dependence of radiative lifetime of N_2 $(C^3\Pi_u)$ level upon gas pressure.

1) R. G. Bennet and F. W. Dalby, *J. Chem. Phys.*, **31**, 434 (1959); **32**, 1111 (1960); **33**, 179 (1960); **36** 399 (1962); **40**, 1414 (1964).

2) E. H. Fink and K. H. Welge, *Z. Naturforsch.*, **19a**, 1193 (1964); *J. Chem. Phys.*, **46**, 4315 (1967).

3) M. Jeunehomme and A. B. F. Duncan, *J. Chem. Phys.*, **41**, 1962 (1964); M. Jeunehomme and R. P. Schwenker, *ibid.*, **42**, 2406 (1965).

4) G. M. Lawrence, *J. Quant. Spectrosc. Radiat. Transfer*, **5**, 359 (1965).

5) M. Jeunehomme, *J. Chem. Phys.*, **44**, 2672 (1966).

6) J. E. Hesser, *ibid.*, **48**, 2518 (1968).

7) R. G. Bennet and F. W. Dalby, *ibid.*, **32**, 1716 (1960).

8) T. Sawada and H. Kamada, This Bulletin, **43**, 325 (1970).

for the (0,0) band of N_2 by the use of a 0.5 m grating monochromator (about 15 Å bandwidth) in order to separate the other emission bands. τ was measured as a function of the gas pressure in order to investigate the collision quenching effect. This is shown in Fig. 1. No such strong dependence of τ upon the pressure was observed in the region below 5 μ. Fink and Welge[2] reported a slow decrease in τ with a decrease in the gas pressure. This dependence was in the wrong direction to be explained by collision quenching, and so they spoke of the possibility of some chemical reactions. However, Jeunehomme[5] indicated a marked increase in τ at pressures lower than 70 μ. He explained this dependence on the basis of the presence of a recombination process between slow electrons and molecular ions. Our results indicate that both possibilities, that of chemical reactions and that of the presence of a recombination process, can be ruled out at pressures below 5 μ.

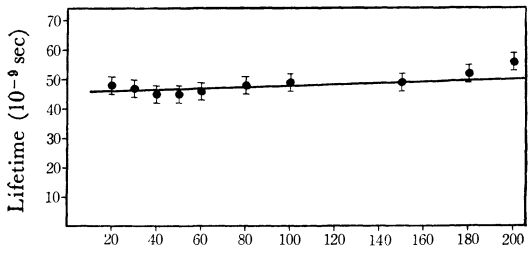

Fig. 2. The dependence of radiative lifetime of $N_2(C^3\Pi_u)$ level upon electron energy.

Figure 2 shows the energy dependence of τ. There appears a slight decrease with a diminishing in the electron energy. This indicates the existence of some cascading states. Similar tendencies have been reported by Bennet and Dalby[1] and by Fink and Welge.[2] However, their results show a more marked decrease in τ than do ours. In order to check the cascading effect in detail, the width of the excitation electron-pulse was varied within a wide range (0.02 μsec—0.3 μsec) at a constant electron energy. If there are some long-lived cascading states, the measured lifetime should be affected by the excitation electron-pulse duration. Thus, if the lifetimes of the initial states in the cascades are different from that of the $N_2(C^3\pi\Pi)$ state, the relative excitation of these states may depend upon the electron pulse duration. The radiative lifetime decreased slightly (17% from 0.02 μsec to 0.3 μsec) when the electron-pulse duration was shortened. These results indicate strongly the presence of some long-lived cascading states. Extrapolating to the excitation threshold and zero pulse duration, we obtained:

$$(4.8\pm0.3)\times10^{-8}\ \text{sec}$$

as the radiative lifetime of the $N_2(C^3\Pi_u)$ level. Our result agrees very well with Jeunehomme's extrapolated value, $(4.9\pm0.5)\times10^{-8}$ sec.

Lifetime Measurement of NH($A^3\Pi$) and NH($c^1\Pi$). When NH_3 is bombarded Eith 100 eV electrons, the ($A^3\Pi$–$X^3\Sigma$)system and the ($c^1\Pi$–$a^1\Delta$) system of NH appear within the wavelength region of 3240—3400 Å. Th emission spectrum is shown in Fig. 3. The peak at 3360 Å is the (0,0) band of the NH($A^3\Pi$–$X^3\Sigma$) system, while the wide-spread emission from 3240 Å to 3400 Å is the (0,0) band of the NH($c^1\Pi$–$a^1\Delta$) system.

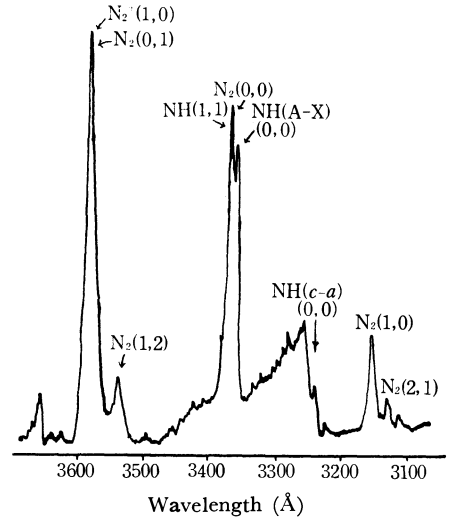

Fig. 3. The emission spectrum obtained when NH_3 gas was bombarded with 100 V electrons at a gas pressure of 0.5 μ.

The apparent lifetime of the NH($A^3\Pi$) level was measured as a function of the electron energy in order to investigate the cascading effect and the trapped resonance radiation. The (0,0) band of the $N_2(C$–$B)$ system appears near the (0,0) band of the NH(A–X) system. Therefore, the grating monochromator (10 Å bandwidth) was used to separate the interfering bands.

The bands at 3370 Å consist of the (1,1) band of the NH(A–X) system and the (0,0) band of the $N_2(C$–$B)$ system, as is shown in Fig. 3. The energy dependence of τ at a constant wavelength of 3365 Å is shown in Fig. 4 (b), and at one of 3358 Å, in Fig. 4 (a). In Fig. 4 (a), the lifetime is constant within the range from 60 V to 200 V, but τ decreases with a diminishing in the electron energy at 3365 Å. This effect can be explained as the mixing effect of the N_2 (0,0) band rather than the cascading from the higher electronic states. The time-resolved spectrum within the wavelength region from 3000 to 3600 Å at a fixed delay-time of 0.1 μsec after the cut-off of the excitation electrons[9] showed that the (0,0) band of the $N_2(C$–$B)$

9) T. Sawada and H. Kamada, unpublished data.

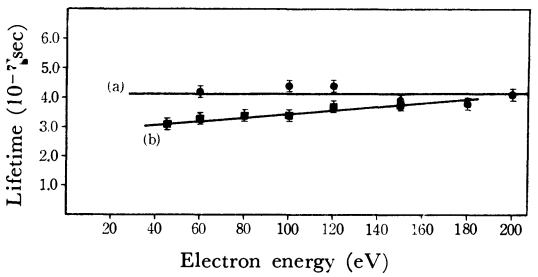

Fig. 4. The dependence of radiative lifetime of $NH(A^3\Pi)$ level upon electron energy.
The fixed wavelength, (a) 3358 Å, (b) 3365 Å

system is superimposed upon the (1,1) band of NH with an intensity of about 55% at an energy of 200 eV. It can be assumed that the effect of the interfering band is considerably eliminated in the lifetime measurement at 3358 Å. No significant pressure-dependence was observed in the range from 1 μ to 5 μ. A lifetime of

$$(4.1\pm0.2)\times10^{-7}\ \text{sec}$$

was obtained. This value agrees within the limits of experimental error with that of Fink and Welge,[2] $(4.6\pm0.8)\times10^{-7}$ sec, measured by the phase shift method. Bennet and Dalby[1] obtained $(4.25\pm0.6)\times10^{-7}$ sec using an interference filter with a 100 Å bandwidth. Figure 5 shows the emission decay of the $NH(A^3\Pi)$ level plotted on the semilogarithmic graph.

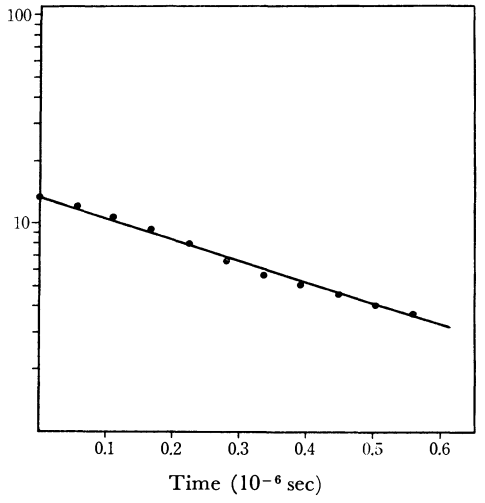

Fig. 5. Semilogarithmic plot of the emission decay associated with the $(A\text{-}X)$ system of NH.

The radiative lifetime of the $NH(c^1\Pi)$ level was measured at a fixed wavelength of 3240 Å. The energy dependence of τ within the range from 45 eV to 150 eV was investigated. However, no significant effect was observed. Consequently, the possibility of the cascading effect from the higher electronic states should be investigated in detail. The $NH(d^1\Sigma)$ level can be allowed to combine with the $NH(c^1\Pi)$ level,[10] but it can be assumed that the cascading from the level is negligibly small. No variation in τ with the gas pressure was observed within the range of our experiment, from 1 μ to 5 μ. A lifetime of

$$(4.3\pm0.2)\times10^{-7}\ \text{sec}$$

was obtained. This value agrees with Fink and Welge's value $(4.3\pm0.4)\times10^{-7}$ sec. The exponential decay of the $NH(c^1\Pi)$ level is plotted in Fig. 6.

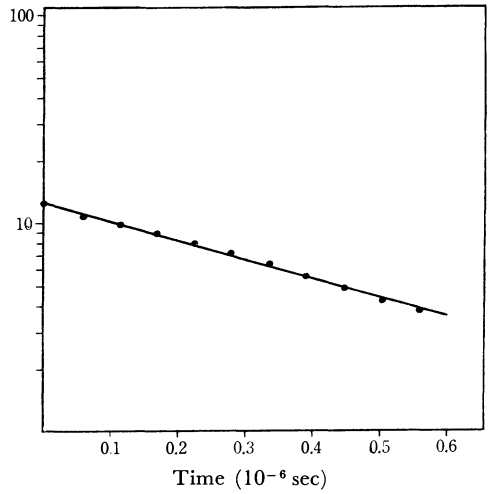

Fig. 6. Semilogarithmic plot of the emission decay associated with the $(c\text{-}a)$ system of NH.

Oscillator Strength. The radiative lifetime, $\tau_{v'}$, of the upper vibrational level in an electronic transition can be expressed by summing over the fine structure due to rotational and electron spin;

$$1/\tau_{v'} = A_{v'} = \sum_{v''} A_{v'v''}$$

where $A_{v'v''}$ is the Einstein coefficient. On the assumption that the mean-square electronic transition moment, $R_e^2(v')$, is constant for all v''-progressions, approximate absorption oscillator strengths can be obtained from this equation:

$$f_{v'v''} = 1.51\cdot(G'/G'')\cdot q_{v'v''}\cdot\lambda^2_{v'v''}/\tau_{v'}$$

where G'/G'' is the ratio of the upper electronic statistical weight to the lower, as defined by Mulliken,[11] where $q_{v'v''}$ is the Franck-Condon factor, and where $\lambda_{v'v''}$ is the wavelength in cm.

In calculating oscillator strengths, it is necessary to use the theoretical calculations of the Franck-Condon factors. The oscillator strengths for the (0,0) band of the $(C^3\Pi_u\text{-}B^3\Pi_g)$ system of N_2 is evaluated by use of the q_{00} value of Nicholls as:

$$f_{00} = (1.6\pm0.1)\times10^{-2}.$$

10) R. W. B. Pearce and A. G. Gaydon, "The Identification of Molecular Spectra," Chapman & Hall Ltd., London (1950).
11) R. S. Mulliken, *J. Chem. Phys.*, **7**, 14 (1939).

The wavelength used here is 3371 Å. G'/G'' is equal to one.

Similar calculations were carried out for the (0,0) band of the NH($A^3\Pi$–$X^3\sum$) and the (0,0) band of the NH($c^1\Pi$–$a^1\Delta$). However, no theoretical calculations of the Franck-Condon factors for the above electronic transitions have been reported. Hence, f_{00}/q_{00} was calculated instead of f_{00}. Thus, for the (0,0) band of NH($A^3\Pi$–$X^3\sum$) we obtained:

$$f_{00}/q_{00} = (8.3\pm0.4) \times 10^{-3}$$

and for the (0,0) band of NH($c^1\Pi$–$a^1\Delta$) we obtained:

$$f_{00}/q_{00} = (3.9\pm0.2)\times10^{-3}$$

where the wavelengths were 3360 Å and 3350 Å. It may be assumed that the Franck-Condon factors for the (0,0) bands of NH(A–X) and NH(c–a) are almost equal to one.

The authors are indebted to Mr. Yasuhisa Saito of the Toshiba Co., Ltd., for his assistance in constructing the electron gun.

12) R. W. Nicholls, *J. Res. Nat. Bur. Stand.*, *A*, **65**, 451 (1961).

BULLETIN OF THE CHEMICAL SOCIETY OF JAPAN VOL. 43 334—339 (1970)

Alternating Copolymerization of β-Cyanoacrolein with α-Methylstyrene

Ichiro TAKEMURA and Hiroshi SUMITOMO

Faculty of Agriculture, Nagoya University, Chikusa-ku, Nagoya

(Received July 4, 1969)

Alternating copolymer was obtained in the system of β-cyanoacrolein (CAL) and α-methylstyrene (α-MeSt). In the presence of air copolymerization proceeds even without any radical initiator at room temperature. In the radical initiated copolymerization of α-MeSt (M_1) and CAL (M_2), the values of monomer reactivity ratios $r_1=0.033$ and $r_2=0$ were obtained. Neither the rate of copolymerization nor viscosity number of the copolymer formed were influenced by the presence of air in the reaction system. The result of copolymerization in the ternary system involving methyl acrylate (MA) could not be entirely explained by the copolymerization equation given by Alfrey and Goldfinger for the three component system. It was found that the composition of the copolymer formed changed with the solvent dilution. Formation of 1 : 1 molecular complex between the monomers was evidenced by the application of the continuous variation method to α-MeSt-CAL system. It was concluded that the molecular complex due to some donor-acceptor type interaction between CAL and α-MeSt plays an important role in the copolymerization.

In the radical copolymerization of β-cyanoacrolein (CAL) with styrene (St), the monomer reactivity ratios were determined and the result was discussed with consideration of penultimate effect.[1] The radical copolymerization of CAL with acrylonitrile was also investigated, compared with that in CAL-St system.[2] It was reported that CAL induced the polymerization of *N*-vinylcarbazole (VCZ) which was cationic polymerization induced by the donor-acceptor type interaction between CAL and VCZ.[3]

The present study is concerned with the alternating copolymerization of CAL with α-methylstyrene (α-MeSt).

1) H. Sumitomo and K. Azuma, *J. Polym. Sci. B*, **4**, 883 (1966).

2) I. Takemura and H. Sumitomo, This Bulletin, **42**, 634 (1969).

3) H. Sumitomo and I. Takemura, *ibid.*, **42**, 631 (1969).

Experimental

Materials. CAL was synthesized from β-cyanopropionaldehyde.[1] α-MeSt was washed successively with 5% aqueous solution of sodium thiosulfate, water, an aqueous solution of sodium hydroxide and water, and dried on anhydrous sodium sulfate. Methyl acrylate (MA) was purified by distillation. Benzoylperoxide (Bz_2O_2) was purified by reprecipitation in chloroform (solvent) methanol - (precipitant) system. Dioxane was distilled after refluxing with sodium. Tetrahydrofuran (THF) was also purified in the same way. Benzene was purified in the usual way.

Copolymerization. Copolymerization of CAL with α-MeSt was carried out in dioxane in an evacuated sealed tube at 80°C using Bz_2O_2 as an initiator. Copolymerization in the systems of CAL-MA, α-MeSt-MA and CAL-α-MeSt-MA were also conducted by the same method. The resulting copolymer was precipitated into a large excess of methanol. The copolymer thus isolated was purified by the precipitation from the system of tetrahydrofuran (solvent) - methanol (precipitant).

Table 1. α-MeSt - CAL copolymerization. Effects of solvent, radical initiator and air

Expt. No.	Monomer			Wt. ratio of dioxane monomer	Bz_2O_2 mol% to monomer	Atmosphere[a]	Temp. °C	Time hr	Convn. %	η_{sp}/c[b]	Mole fraction of α-MeSt in copolymer
	α-MeSt g	CAL g	Mole fraction of α-MeSt								
52	3.54	—	—	—	—	A	80	5	0	—	—
53	3.54	—	—	—	—	V	80	5	0	—	—
54	3.54	—	—	—	0.5	A	80	5	0	—	—
55	3.54	—	—	—	0.5	V	80	5	0	—	—
56	3.54	—	—	—	—	A	21—22	8	0	—	—
57	3.54	—	—	—	—	V	21—22	8	0	—	—
29	2.36	1.62	0.5	—	—	A	80	5	3.8	0.18	0.512
30	2.36	1.62	0.5	—	—	V	80	7	4.2	0.18	0.539
42	2.36	1.62	0.5	2	—	A	80	5	1.2	—	0.538
43	2.36	1.62	0.5	2	—	V	80	9	1.6	—	0.532
44	2.36	1.62	0.5	2	0.5	A	80	3	11.6	0.08	0.512
45	2.36	1.62	0.5	2	0.5	V	80	3	11.6	0.08[c]	0.508
58	2.36	1.62	0.5	—	—	A	21—22	8	0.3	—	—
59	2.36	1.62	0.5	—	—	V	21—22	8	0.2	—	—

a) A, air; V, vacuum.
b) THF, $c = 0.2$ g/100 ml, 25°C.
c) M_n(VPO) = 2380.

Determination of Polymer Composition. The compositions of the copolymers obtained in the systems of CAL - α-MeSt and CAL-MA were determined from nitrogen analysis by the Kjeldahl method. Those for α-MeSt - MA and α-MeSt - CAL - MA systems were determined by elemental analysis.

Measurement of Solution Viscosity. Viscosity number, η_{sp}/c, of a copolymer was measured at the concentration of 0.2g/100 ml in THF at 25°C with use of an Ostwald viscometer.

Nuclear Magnetic Resonance Spectrum. Nuclear magnetic resonance (NMR) spectrum was measured in carbon tetrachloride and carbon tetrachloride-methylene chloride mixture at 60°C with a Japan Electron Optics JNM-4H-100 spectrometer.

Continuous Variation Method. Continuous variation method applied to α-MeSt - CAL system was carried out in benzene using a quartz cell with a path length of 1 mm.

Results and Discussion

The results of the preliminary experiment of the copolymerization of CAL with α-MeSt are summarized in Table 1.

Although no homopolymerization of both CAL and α-MeSt takes place under the present conditions, copolymerization between them proceeds at room temperature in the presence of air even without any initiator.

The results of infrared analysis and the contents of α-MeSt in the products suggest the formation of 1 : 1 alternating copolymer of CAL with α-MeSt. The rate of copolymerization and the viscosity number of copolymer obtained are independent of the presence of air in the reaction system. This is curious from the view point of conventional free radical polymerization. In Figs. 1 and 2 are shown the results of copolymerization carried out in dioxane with benzoyl peroxide (Bz_2O_2) as an initiator at 80°C, with varying composition of monomer feed in the system of α-MeSt (M_1) and CAL (M_2).

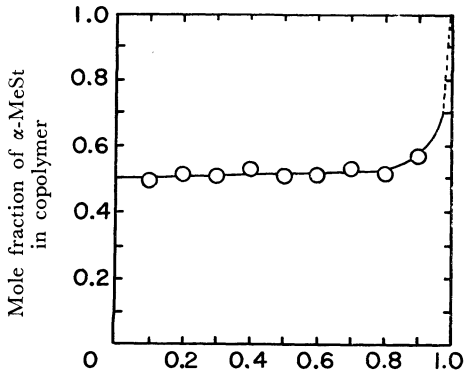

Fig. 1. Composition of copolymer as a function of monomer composition in α-MeSt (M_1) - CAL (M_2) system.
Solv., dioxane; initiator, Bz_2O_2; at 80°C.
○, Experimental value; —, Calculated from $r_1=0.033$ and $r_2=0$.

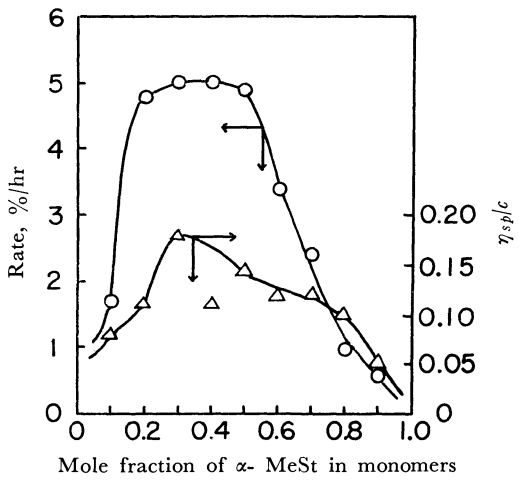

Fig. 2. Influence of monomer composition on the rate of copolymerization and on η_{sp}/c of copolymer in α-MeSt-CAL system.

As shown in Fig. 1, α-MeSt contents of the copolymer are 50 mol% within experimental error throughout the range of the monomer composition. There is a remarkable agreement between the experimental values and the curve calculated from the values of monomer reactivity ratios, $r_1=0.033$ and $r_2=0$. r_1 has a very small value and $r_2=0$, and the product r_1r_2 is nearly equal to zero. This means that both monomers have a very large alternating tendency.

The fact that the viscosity number of the copolymer has a maximum at the mole fraction of α-MeSt of about 0.40 indicates that there may be some interaction between CAL and α-MeSt as shown in Fig. 2. Q and e values obtained for the monomers are given in Table 2.

TABLE 2. Q-e VALUES

Monomer	Q	e
α-MeSt[a)]	0.98	−1.27
CAL[b)]	0.53	2.07

a) Ref. 4.
b) Obtained from copolymerization in CAL-St and CAL-AN systems.

Both monomers have large e values of the opposite sign. Thus some donor-acceptor type interaction is expected to take place between the monomers. In Table 3 is given the comparison of the monomer reactivity ratios between the observed values and those calculated from Q and e values.

Figure 3 shows the NMR spectra of poly α-MeSt (P α-MeSt) and the copolymer. In the spectrum

4) "Copolymerization," ed. by G. E. Ham, Interscience Publishers, New York (1964), p. 845.

Table 3. Parameters in α-MeSt (M_1) - CAL (M_2) system

	r_1	r_2	r_1r_2
Obsd	0.033	0	0
Calcd[a)]	0.026	0.0005	≅0

a) From Q-e value.

of P α-MeSt, the phenyl proton signal appears at the value 2.95—3.20, whereas the signal is seen as a singlet at 2.90 in the copolymer. The difference may be explained as follows. In P α-MeSt, the phenyl proton signal shifts to the higher field with splitting due to the shielding effect of the benzene ring in the sequence of α-MeSt unit. However, in the copolymer the shift is attributed to the alternation of CAL and α-MeSt units.

In the IR spectra of acrolein homopolymer and its copolymer with CAL, a weak C=O absorption band appears and there exist strong C–O–C absorption bands due to the substituted tetrahydropyrane ring formed between adjacent pendant aldehyde groups. On the other hand, the spectrum of the copolymer of CAL and α-MeSt indicates that aldehyde group remains free.[5)]

From these facts it seems that some interaction between CAL and α-MeSt plays an important role

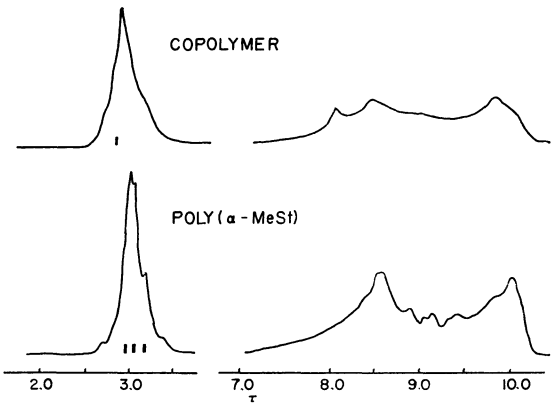

Fig. 3. NMR spectra of copolymer and poly-(α-methylstyrene).

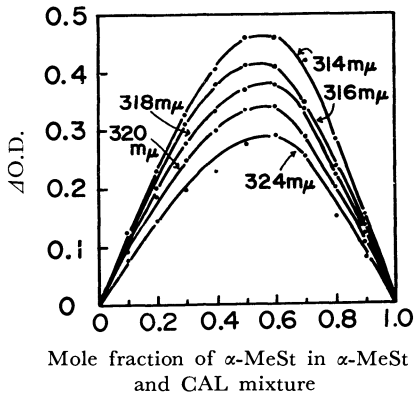

Fig. 4. Continuous variation method in α-MeSt and CAL system.
[CAL]=[α-MeSt]=0.5 mol/l; [CAL]+[α-MeSt] =0.5 mol/l; in benzene; path length, 0.1 cm.

Table 4. α-MeSt (M_1) - CAL(M_2) - MA (M_3) terpolymerization
Solv.: dioxane,[a)] Initiator: Bz_2O_2,[b)] Temp.: 80°C

Expt. No.	Monomer composition mole fraction			Time hr	Convn. %	Elemental analysis			Terpolymer composition mole fraction		
	α-MeSt	CAL	MA			C%	H%	N%	α-MeSt	CAL	MA
T-1	0.15	0.15	0.70	2	6.3	73.41	7.40	3.33	0.339	0.198	0.463
T-2	0.20	0.20	0.60	1	2.9	75.51	7.31	3.44	0.447	0.244	0.309
T-3	0.25	0.25	0.50	2	7.1	75.80	6.93	3.95	0.451	0.279	0.270
T-4	0.30	0.30	0.40	2	8.1	76.79	6.80	4.64	0.474	0.330	0.196
T-5	0.05	0.05	0.90	0.5	7.7	63.87	7.33	1.17	0.169	0.076	0.755
T-7	0.35	0.35	0.30	1	4.1	77.76	6.68	5.03	0.498	0.360	0.142
T-8	0.40	0.40	0.20	1	4.7	78.23	6.31	5.33	0.512	0.382	0.106
T-9	0.45	0.45	0.10	1	6.1	79.18	6.43	5.93	0.529	0.427	0.044
B-4	0.50	0.20	0.30	0.8	2.6	76.20	6.92	4.09	0.461	0.290	0.249
B-5	0.20	0.50	0.30	0.8	4.2	74.33	6.48	5.29	0.434	0.367	0.199
B-6	0.10	0.80	0.10	0.8	3.1	73.83	6.62	6.07	0.384	0.417	0.199
B-7	0.80	0.10	0.10	1.3	1.8	79.06	7.16	3.64	0.549	0.266	0.185
B-8	0.10	0.40	0.50	0.7	2.9	72.72	6.95	4.47	0.366	0.307	0.327
B-9	0.40	0.10	0.50	1	3.5	76.68	7.13	2.69	0.489	0.193	0.318
B-10	0.10	0.10	0.80	0.5	3.2	66.24	6.97	1.63	0.222	0.108	0.670

a) Dioxane/monomer = 2 (wt).
b) 0.5 mol%/Monomer.

5) Unpublished data.

in the alternating copolynerization in the system of CAL and α-MeSt. Although coloring was not observed when CAL was mixed with α-MeSt, an absorption maximum by the continuous variation method appeared at the molar ratio of CAL to α-MeSt of around one as shown in Fig. 4. This means that some molecular complex due to a donor-acceptor type interaction between CAL and α-MeSt was formed.

In Table 4 and Fig. 5 are summarized the results of terpolymerization including CAL, α-MeSt and methyl acrylate (MA).

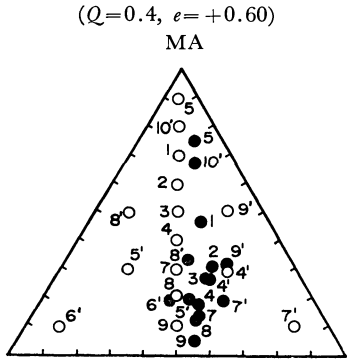

Fig. 5. Terpolymerization in α-MeSt - CAL - MA system.
Solv., dioxane; initiator, Bz_2O_2; at 80°C.
○, Composition in monomers;
●, Composition in terpolymer.

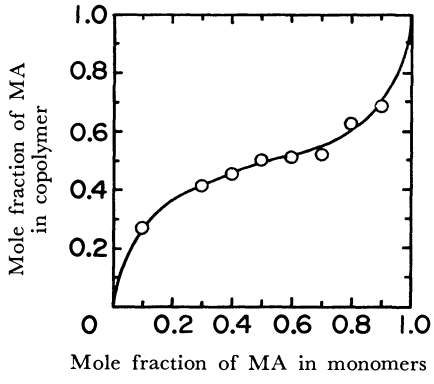

Fig. 6. Composition of copolymer as a function of monomer composition in MA (M_1)-α-MeSt (M_2) system.
Solv., dioxane; initiator, Bz_2O_2; at 80°C.
○, Experimental value; —, Calculated from $r_1=0.13$ and $r_2=0.21$

Deviation of the composition of terpolymer from the assumed copolymerization of 1:1 molecular complex of CAL and α-MeSt with MA, suggests that some interaction α-MeSt and MA may also take place other than that between α-

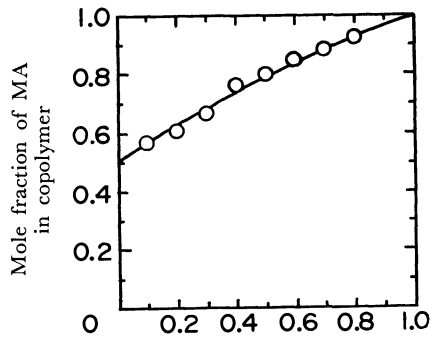

Fig. 7. Composition of copolymer as a function of monomer composition in MA (M_1)-CAL (M_2) system.
Solv., dioxane; intiator, Bz_2O_2; at 80°C.
○, Experimental value; —, Calculated from $r_1=2.73$ and $r_2=0$

MeSt and CAL. The following monomer reactivity ratios were determined in α-MeSt - MA and MA-CAL systems. The composition curve in these copolymerization systems are shown in Figs. 6 and 7.

MA (M_1) - α-MeSt (M_2), $r_1=0.13$ and $r_2=0.21$;
MA (M_1) - CAL (M_2), $r_1=2.73$ and $r_2=0$.

The Alfrey-Goldfinger's equation[6] was used for the anlaysis of the results in the ternary system. If k_{22} equals zero, since no homopolymerization of CAL occurs, the composition relationship in the ternary system is given as follows.

$$\frac{m_1}{m_2}=\frac{M_1}{M_2}\times\frac{(M_1+M_2/r_{12}+M_3/r_{13})(M_1/r_{31}+M_2/r_{32}+M_3/r_{31}R)}{(M_1+M_3/R)(M_1/r_{31}r_{12}+M_2/r_{32}r_{12}+M_3/r_{13}r_{32})}$$

$$\frac{m_1}{m_3}=\frac{M_1}{M_3}\times\frac{(M_1+M_2/r_{12}+M_3/r_{13})(M_1/r_{31}+M_2/r_{32}+M_3/r_{31}R)}{(M_1/r_{13}+M_2/r_{32}+M_3)(M_1/r_{13}+M_2/r_{12}R+M_3/r_{13}R)}$$

The value of R was determined from Q-e values, but not experimentally. Copolymerization parameters thus obtained are listed in Table 5.

Calculation of R using the results of terpolymerization and the binary copolymerization parameters gives $R\leqq 0$, except for B-6 and B-10. R calculated from the Q-e values is about 112 as shown in Table 5. If $R\cong 0$, it follows that $k_{21}\cong 0$ or $k_{21}\ll k_{23}$. Thus the relation $R=0$ should be discorded because it is inconsistent with the large alternating tendencies of CAL and α-MeSt, the reactivity of each monomer deduced from Q and e values and the existence of a donor-acceptor type interaction between CAL and α-MeSt. With respect to M_1 (mole fraction of

6) T. Alfrey, Jr., and G. Goldfinger, *J. Chem. Phys.*, **12**, 332 (1944).

Table 5. Copolymerization parameters in α-MeSt (M_1) - CAL (M_2) - MA (M_3) system

	r_{12}	r_{21}	r_{13}	r_{31}	r_{23}	r_{32}	$R=k_{21}/k_{23}$
Obsd	0.033	0	0.21	0.13	0	2.70	—
Calcd[a)]	0.026	0.0005	0.215	0.14	0.06	1.93	112

a) Calcd from the following Q-e values.
α-MeSt $Q=0.98$ $e=-1.28$
CAL $Q=0.53$ $e=2.07$
MA $Q=0.42$ $e=0.60$

α-MeSt in monomers) above 0.3, we have $R\cong 0$. If M_1 becomes smaller R tends to deviate gradually from zero. Deviation is very remarkable as to T-5 and B-8 where M_1 is very small. This shows that R changes with monomer composition. It is concluded that the equation proposed by Alfrey and Goldfinger can not be applied to the present ternary system.

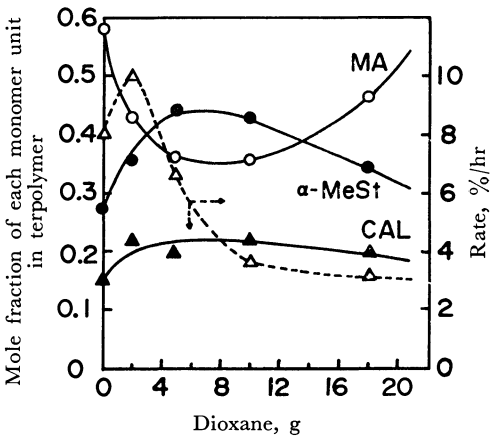

Fig. 8. Effect of solvent dilution on α-MeSt-CAL-MA terpolymerization.
Monomer composition, α-MeSt : CAL : MA = 1.5 : 1.5 : 7
Total amount of monomers, 8.02 g

The effect of solvent dilution on terpolymerization was investigated. The composition of the terpolymer varies with the amount of dioxane added as seen in Fig. 8. It should also be noted that a maximum of the rate appears with the addition of a small amount of the solvent.

This behavior is very different from that of general radical copolymerization, and can not be explained by the Alfrey-Goldfinger equation. Iwatsuki and Yamashita[7)] have discussed similar behaviors found in the systems of chloroethylvinylether-maleic anhydride-acrylonitrile and *p*-dioxene-maleic anhydride-acrylonitrile.

The change in the composition of terpolymer and the rate of copolymerisation seems to be much larger than the estimated values from the simple solvation effect of dioxane. Hence it appears that the interaction between each monomer would change with the addition of solvent and that species with different reactivities are formed in the system. The results show that the interaction between CAL and α- MeSt is very strong even in the terpolymerization. It is concluded that the complex formation between CAL and α-MeSt due to some donor-acceptor type interaction plays a very important role in the copolymerization system of CAL and α-MeSt.

7) S. Iwatsuki and Y. Yamashita, *J. Polym. Sci. A-1*, **5**, 1753 (1967).

BULLETIN OF THE CHEMICAL SOCIETY OF JAPAN VOL. 43 340—344 (1970)

Mechanism of Hydrogen Formation in the Vapor Phase Radiolysis of Methanol

Tatsuo YAMAMOTO

Tokyo Metropolitan Isotope Research Center, Setagaya-ku, Tokyo

(Received July 19, 1969)

The yields of isotopic hydrogen in the vapor phase radiolysis of deuterated methanol(CH_3OD) were found to be $G(H_2)=6.1$, $G(HD)=5.3$ and $G(D_2)=0.2$. The molecular yields of isotopic hydrogen were also determined by adding propylene as a radical scavenger, $G_M(H_2)=1.5$, $G_M(HD)=0.6$ and $G_M(D_2)\sim 0$. In order to estimate the contribution of ionic species for the formation of hydrogen, the ion-molecule reaction of CH_3OD has also been investigated by using a mass spectrometer of the differential pumping type. The product ions, such as $(CH_3OCH_3CH_3OD)D^+$ or $(CH_3OD)_3D^+$, which were considered to be formed by the higher order ion-molecule reactions were observed. The mechanism of hydrogen formation was discussed on the basis of the ionic, the molecular and the radical mechanisms.

Although extensive studies of the radiolysis of methanol have been carried out in the liquid phase, little attention has been paid to vapor phase radiolysis.[1-4]

Baxendale *et al.*[1] calculated the yields of radiolysis products of CH_3OD from mass spectral data, considering the ion-molecule reactions. In the ion-molecule reactions of CH_3OD^+ and CH_2OD^+ with CH_3OD, they assumed that only H^+ transfer from CH_3OD^+ or CH_2OD^+ occurred to form CH_3ODH^+. However this is not true, because recent studies[5-7] on ion-molecule reactions of CH_3OD indicate that D^+ transfer also occurs from OD as well as H^+ transfer from CH_3 and CH_2.

Prasil[8] also calculated the relative yields of products using the quasi-equilibrium theory in semi-classical approximation, considering direct excitation as well as ionization. However, the molecular yield of hydrogen thus obtained seemed to be larger compared with the experimental values.

In order to obtain information on the vapor phase radiolysis of methanol, the ion-molecule reaction of methanol was also studied by a conventional mass spectrometer.[5] However, it is very doubtful that the mechanism of ion-molecule reactions thus obtained can be applied to the mechanism of vapor phase radiolysis of methanol, since radiolysis is usually made at considerably higher pressure compared with that in the mass spectrometer.

The present investigation has been undertaken in order to elucidate the mechanism of hydrogen formation in the vapor phase radiolysis of CH_3OD.

The following experiments were carried out.

(1) The isotopic composition of hydrogen formed by γ-radiolysis was determined by mass spectrometric analysis, and the molecular yields of isotopic hydrogen were also estimated by adding propylene as a radical scavenger.

(2) The ion-molecule reaction of CH_3OD was studied in the pressure range of $6\times10^{-3}-1\times10^{-1}$ mmHg with a mass spectrometer of the differential pumping type.

Experimental

Materials. Deuterated methanol, CH_3OD, from Showa Denko Co. (99%) was used without further purification. Before irradiation, the sample was thoroughly degassed by the freezethaw method. Propylene and nitrous oxide from Takachiho Chem. Indust. Co. were used after purification by distillation.

Irradiation and Analysis. A glass reaction vessel of about 700 m*l* with a break-seal was used. Before introducing the sample into the reaction vessel, both the sample preparation system and the reaction vessel were flamed out several times in a vacuum. Deuterated methanol vapor of about 60 mmHg was irradiated at room temperature with a ^{60}Co source of 3000 Ci. The molecular yield of hydrogen was determined by

1) J. H. Baxendale and R. D. Sedgwick, *Trans. Faraday Soc.*, **57**, 2157 (1961).

2) E. Lindholm and P. Wilmenius, *Arkiv Kemi*, **20**, 255 (1962).

3) M. Meaburn and F. W. Mellows, *Trans. Faraday Soc.*, **61**, 1701 (1965).

4) T. Ohma and H. Sakurai, This Bulletin, **40**, 1368 (1968).

5) T. Yamamoto, Y. Shinozaki and G. Meshitsuka, *Mass Spectroscopy*, **12**, 93 (1964).

6) P. Wilmenius and E. Lindholm, *Arkiv Physik*, **21**, 97 (1962).

7) D. J. Hyatt, E. A. Dodman and M. J. Henchman, "Ion-Molecule Reactions in the Gas Phase," ed. by R. F. Gould, American Chemical Society Publications, Washington D. C. (1966), p. 131.

8) Z. Prasil, *Collect. Czech. Chem. Commun.*, **31**, 3252 (1966).

adding a few percent propylene as a hydrogen atom scavenger. Dose rate was determined with nitrous oxide of 200 mmHg on the basis of $G(N_2)=10.0$.[9] Energy absorbed by methanol was calculated from the electron densities. The dose rate was approximately 3.3×10^{18} eV·g^{-1}·hr^{-1} and the total dose was $\sim10^{20}$ eV·g^{-1}.

After irradiation, the amount and composition of products volatile at liquid nitrogen temperature were determined by gas burette and mass spectrometric analysis.

Ion-Molecule Reaction. In order to investigate the ion-molecule reaction in the higher pressure range, a Hitachi mass spectrometer, Model RMU-5, was rearranged and equipped with an ion source of the differential pumping type. The relevant dimensions of the ion soruce are: electron beam hole 0.02 cm; ion exit slit 0.02×0.5 cm^2; repeller electrode-ion exit slit 0.31cm and center of electron beam-ion exit slit 0.25 cm. Electron bombardment was carried out at 70 eV. Pressure of the ionization chamber could not be measured directly, but was estimated from the pressure of the sample reservoir by the conventional method[10] using methane. The revised ion source made it possible to carry out experiment at the pressure of ionization chamber up to about 0.14 mmHg.

Results

Gamma Radiolysis. The G value of each isotopic hydrogen obtained with and without propylene in the system is shown in Table 1. The total yield of isotopic hydrogen G_{total}(hydrogen), is found to be 11.6. This value is somewhat higher than that obtained by Baxendale.[1] In contrast with the results in the liquid phase radiolysis, the yield of H_2 is higher than that of HD. The yield of D_2 is very small as shown in Table 1.

Table 1. Observed yields of isotopic hydrogen

	$G(H_2)$	$G(HD)$	$G(D_2)$	G(Total)
Total yield	6.1	5.3	0.2	11.6
Molecular yield	1.5	0.6	~0	2.1

Addition of propylene as a hydrogen atom scavenger reduces the total hydrogen yield from G_{total}(hydrogen)=11.6 to G_{total}(hydrogen)=2.1, which corresponds to the molecular yield of isotopic hydrogen. The molecular yield of H_2 is about 2.5 times greater than that of HD, and the molecular yield of D_2 is negligibly small.

Ion-Molecule Reaction. In the pressure range of 0.006–0.02 mmHg, the relation between the ionization chamber pressure and the ion current fraction of each ion, $(i_j/\sum i_j)$, where i_j is the ion current for jth ion and $\sum i_j$ the total ion current, is

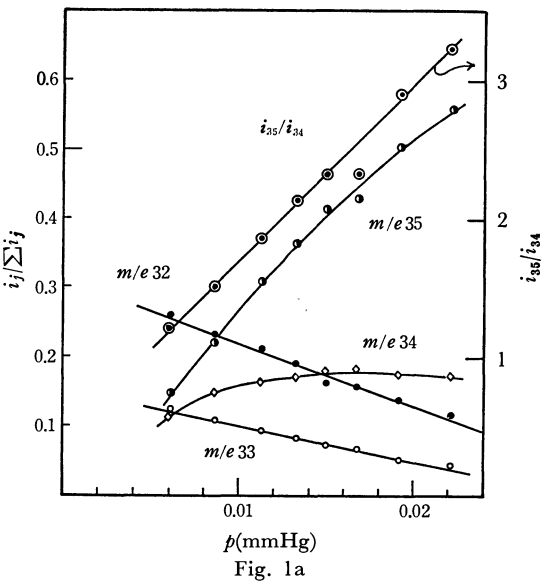

Fig. 1a

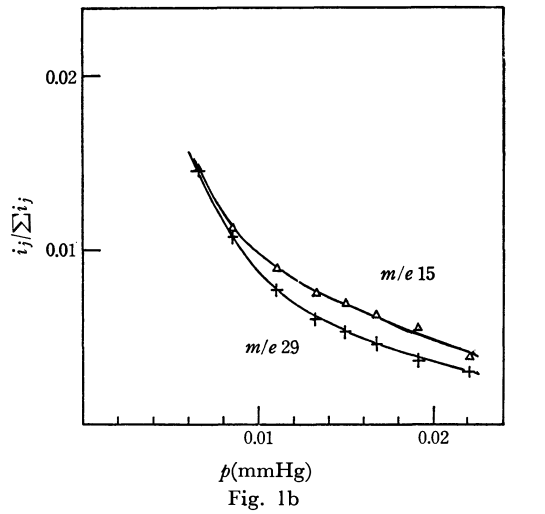

Fig. 1b

Fig. 1a, b. Relation between ionization chamber pressure and $i_j/\sum i_j$ or i_{35}/i_{34}.

shown in Fig. 1. We see that all primary ions decrease as the ionization chamber pressure increases. These primary ions are considered to decrease by either one of the ion-molecule reactions, such as proton or deuteron transfer, hydride ion transfer or charge transfer. On the other hand, as reported by Hyatt *et. al.*[7], $i_{CH_3OD_2^+}/i_{CH_3ODH^+}$ increases with the increase in the ionization chamber pressure. Table 2 shows the results obtained at the higher pressures up to 0.14 mmHg. At 0.14 mmHg, only a trace of CH_2OD^+, which is the most abundant primary ion at low pressure, is observed and the ratio $i_{CH_3OD_2^+}/i_{CH_3ODH^+}$ exceeds 10. We see that the primary ions and the lower order product ions decrease and the higher order product ions increase with the increase in pressure. The results

9) F. T. Jones and T. J. Sworski, *J. Phys. Chem.*, **70**, 1546 (1966).

10) C. E. Melton, "Mass Spectrometry of Organic Ions," ed. by F. W. McLafferty, Academic Press, New York and London, (1963) p. 80.

indicate that the ion-molecule reactions occur successively to form the higher order product ions at a higher pressure. It is also clear that the deuteronated ions formed by the higher order ion-molecule reactions are much greater than the protonated ions. Munson[11] also observed the higher order product ions using CH_3OH and presented the mechanism of their formation.

Discussion

Ionic Mechanism. Primary processes in radiation chemistry are mostly caused by secondary electrons with energies less than 100 eV. A number of discussions for the ionic mechanism of radiolysis have been made on the basis of the results obtained by mass spectrometer at low pressure. As shown in Table 2, the higher order product ions, which do not appear in mass spectrum at low pressure, are observed remarkably at higher pressure, indicating that the contribution of these higher order product ions must be considered in the ionic mechanism of radiolysis. It can be assumed that fragment ions are formed from parent ion by the unimolecular decomposition in a much shorter time than collision time of parent ion with neutral molecule at the pressure employed in radiolysis experiments. Thus the abundance of ions formed primarily by the irradiation of ^{60}Co γ-rays should be the same as that in the usual mass spectrum. Table 3 shows the fragmentation processes and abundance of various ions in the mass spectrum of CH_3OD and the possible types of ion-molecule reactions. According to the types of ion-molecule reactions, these primary ions react with neighboring CH_3OD molecules to form the secondary ions, CH_3ODH^+ and $CH_3OD_2^+$. As the pressure increases, these secondary ions react further with CH_3OD molecules by the reactions such as.

$$CH_3ODH^+ + CH_3OD \rightarrow CH_3OD + CH_3ODH^+ \quad (1a)$$

$$\rightarrow CH_3OH + CH_3OD_2^+ \quad (1b)$$

$$CH_3OD_2^+ + CH_3OD \rightarrow CH_3OD + CH_3OD_2^+ \quad (2)$$

Secondary ion CH_3ODH^+ can transfer either a proton or a deuteron by reaction (1a) or (1b). Secondary ion $CH_3OD_2^+$ will not change its identity by reaction (2) since only a deuteron can be transferred. Therefore, the ratio $i_{CH_3OD_2^+}/i_{CH_3ODH^+}$ increases with the increase in the ionization chamber pressure. The ions, such as $(CH_3OCH_3)D^+$, $(CH_3OD)_2H^+$ and $(CH_3OD)_2D^+$, are formed by the following reactions.

$$CH_3ODH^+ + CH_3OD \rightarrow (CH_3OCH_3)D^+ + HDO \quad (3)$$

$$CH_3OD_2^+ + CH_3OD \rightarrow (CH_3OCH_3)D^+ + D_2O \quad (4)$$

$$CH_3ODH^+ + CH_3OD \rightarrow (CH_3OD)_2H^+ \text{ or } (CH_3ODCH_3OH)D^+ \quad (5)$$

$$CH_3OD_2^+ + CH_3OD \rightarrow (CH_3OD)_2D^+ \quad (6)$$

Table 2. Variation of relative ion current with ionization chamber pressure

m/e	Ion	Relative ion current(%) Pressure (mmHg) 0.07	0.10	0.14
32	CH_2OD^+	4.1	0.7	0.2
34	CH_3ODH^+	9.4	5.5	3.2
35	$CH_3OD_2^+$	65.4	51.9	34.1
48	$(CHOCH_3)D^+$	9.6	11.9	9.7
67	$(CH_3OD)_2H^+$	1.0	1.6	3.3
68	$(CH_3OD)_2D^+$	10.1	26.2	36.1
81	$(CH_3OCH_3CH_3OD)D^+$	0.3	1.3	4.6
101	$(CH_3OD)_3D^+$	0.1	0.9	8.7

Table 3. Fragmentation process and abundance in the mass spectrum of CH_3OD and possible type of ion-molecule reaction

Fragmentation process[1]	Abundance[5] (%)	Type of ion-molecule reaction[5,9]
$CH_3OD + e \rightarrow CH_3OD^+ + 2e$	24.8	P, D
$\rightarrow CH_2OD^+ + H + 2e$	37.7	P, D
$\rightarrow CH_3O^+ + D + 2e$	2.9	P
$\rightarrow HCOD^+ + H_2 + 2e$	2.4	C
$\rightarrow COD^+ + H_2 + H + 2e$	4.5	D, H, d
$\rightarrow HCO^+ + H_2 + D + 2e$	16.1	P, H, d
$\rightarrow CO^+ + H_2 + HD + 2e$	1.6	H
$\rightarrow CH_3^+ + OD + 2e$	10.0	H

P: Proton transfer
D: Deuteron transfer
H: Hydride ion transfer
C: Charge transfer
d: Dissociative charge transfer

11) M. S. B. Munson, *J. Amer. Chem. Soc.*, **87**, 5313 (1965).

From the fact that the higher order product ions, $(CH_3OCH_3CH_3OD)D^+$ and $(CH_3OD)_3D^+$, were also observed, it is reasonable to assume that the primary ions formed in the radiolysis are ultimately converted to deuteronated ions by successive ion-molecule reactions. These product ions recombine with electrons, and dissociate into D atoms, not H atoms, and products.

$$(CH_3OCH_3CH_3OD)D^+ + e \rightarrow D + \text{Products} \quad (7)$$

$$(CH_3OD)_3D^+ + e \rightarrow D + \text{Products} \quad (8)$$

D atom formed by reaction (7) or (8) reacts with CH_3OD and abstracts H atom from the methyl group of CH_3OD to give HD.

$$D + CH_3OD \rightarrow HD + CH_2OD \quad (9)$$

$$D + CH_3OD \rightarrow D_2 + CH_3O \quad (9')$$

The direct formation of molecular hydrogen (D_2) by neutralization reactions and the formation of D_2 by reaction, (9'), if any, are negligibly small, because of the very small observed value of $G(D_2)$. Furthermore it can not be considered that molecular hydrogen HD is formed preferentially by neutralization reactions.

Baxendale and Sedgwick[1] explained that a part of molecular hydrogen is produced from excited methanol molecule which is formed by the neutralization reaction of secondary ion, CH_3ODH^+,with electron. As shown in Table 2, higher order ions are produced by successive ion-molecule reactions. It may be reasonable to consider that hydrogen is not formed molecularly from the excited molecules by the neutralization reactions of these higher order ions with electrons. Therefore, hydrogen formed through ion-molecule reactions followed neutralization is considered to be only HD by the reactions (7), (8) and (9).

As shown in Table 3, the primary ions are also accompanied with atomic or molecular hydrogen.

Table 4. Yield of isotopic hydrogen calculated from data in Table 3

	H_2	HD	D_2
M_i/N	0.67	1.21	0
M_{i-m}/N	0.24_6	0.01_6	0
G_i	2.6	4.7	0
G_{i-m}	1.0	0.1	0

N: number of ion pair produced
M_i: number of isotopic hydrogen produced through the ionization of CH_3OD
M_{i-m}: number of isotopic hydrogen produced molecularly by the fragmentation of CH_3OD^+
G_i: G-value of isotopic hydrogen produced through the ionization of CH_3OD
G_{i-m}: G-value of isotopic hydrogen produced molecularly by the fragmentation of CH_3OD^+
G-values are calculated by the following equation using $W=25.9$ eV.

$$G = \frac{100}{W} \times \frac{M}{N}$$

The yields (M_i/N) of isotopic hydrogen are shown in Table 4, where M_i is the number of molecules produced through ionization of CH_3OD and N is the number of ion pairs induced by irradiation. From these data, the total yield of isotopic hydrogen through ionization is estimated to be $M_i/N(H_2)=0.67$ and $M_i/N(HD)=1.21$. By the saturation current method, Ohma and Sakurai[4] obtained $M/N(H_2)=3.00$ for the ionic yield of hydrogen from CH_3OH, where M is the number of hydrogen molecules produced. Combining $M/N(H_2)=3.00$ with the observed $G_{total}(\text{hydrogen})=11.6$, the energy to produce an ion pair from methanol (W) is calculated to be 25.9 eV. Baxendale and Sedgwick obtained $W=27.7$ eV on the assumption that molecular hydrogen was also produced by the decomposition of excited methanol molecule formed by the neutralization of $CH_3OH_2^+$ with electron. The yield of isotopic hydrogen through ionization, G_i, can then be estimated from the relation, $G_i(\text{hydrogen})=100/W\times[M_i/N(\text{hydrogen})]$, and $G_i(H_2)=2.6$ and $G_i(HD)=4.7$ were obtained.

Molecular Mechanism. The observed molecular yields of hydrogen are $G_M(H_2)=1.5$ and $G_M(HD)=0.6$. On the other hand, as shown in Table 4, molecular yields by the fragmentation of CH_3OD^+ are $G_{i-m}(H_2)=1.0$ and $G_{i-m}(HD)=0.1$.

The fact that the value of W=25.9 eV is more than twice the ionization potential(10.85 eV) suggests that directly excited CH_3OD molecule may well be formed by reaction (10) and that the excited molecule thus formed may give hydrogen by the molecular mechanism, reaction (11).

$$CH_3OD \rightsquigarrow CH_3OD^* \quad (10)$$

$$CH_3OD^* \rightarrow H_2, HD + \text{Formaldehyde} \quad (11)$$

The molecular yields of hydrogen formed by the dissociation of CH_3OD^*, $G_m(H_2)$ and $G_m(HD)$, can be estimated as

$$G_m(H_2) = \underset{1.5}{G_M(H_2)} - \underset{1.0}{G_{i-m}(H_2)} = 0.5$$

$$G_m(HD) = \underset{0.6}{G_M(HD)} - \underset{\mathbf{0.1}}{G_{i-m}(HD)} = 0.5\,.$$

Porter and Noyes[12] investigated the photolysis ($\lambda<200$ mμ) of CD_3OH vapor and obtained 80% HD and 20% H_2 as unscavengeable hydrogen. A similar result was also obtained by Hagege *et al.*[13] ($\lambda=124$ and 185 mμ). If one considers that the excited molecules formed by radiolysis are the same as those formed by photolysis, the ratio of $\Phi(H_2)$ to $\Phi(HD)$ in the photolysis of CD_3OH must correspond to the ratio of $G_m(D_2)$ to $G_m(HD)$ in the radiolysis of CH_3OD. In the present investigation, $G_M(D_2)$ was found to be negligibly small, indicating that $G_m(D_2)$ is also negligible. There-

12) R. P. Porter and W. A. Noyes, Jr., *ibid.*, **81**, 2307 (1959).
13) J. Hagege, S. Leach and C. Vermeil, *J. Chim. Phys.*, **62**, 736 (1965).

fore, it is clear that radiolysis and photolysis are quite different in the mechanism of hydrogen formation.

There is also some possibility that hot hydrogen atom may be a source of unscavengeable hydrogen, but at present no definite information concerning quantitative estimation has been achieved. However, the fact that $G_M(D_2)$ is negligibly small indicates that the contribution of hot hydrogen atom may not be so large.

Radical Mechanism. The observed total hydrogen yield, G_{total}(hydrogen)=11.6, can not be explained only by ionic and molecular mechanisms, because the sum of the yields by the two mechanisms, G(hydrogen)=8.3, is much smaller than the observed value. The difference can only be explained by assuming that hydrogen atoms formed by the dissociation of CH_3OD^* are also the precursors of hydrogen molecules. The calculated yields by the radical mechanism, $G_r(H_2)$ and G_r(HD), are found to be 3.0 and 0.1 which indicates that reaction (11a) is more important than reaction (11b).

$$CH_3OD^* \rightarrow H + CH_2OD \quad (11a)$$

$$CH_3OD^* \rightarrow D + CH_3O \quad (11b)$$

The results obtained by direct photolysis[12,13] and by the mercury-photosensitized decomposition of methanol vapor[14] show that reaction(11b) is more important than reaction(11a). The difference between radiolysis and photolysis can be explained as follows. In the photolysis data, the energy of light applied was lower than the ionization potential of methanol molecule, but enough to excite methanol molecule electronically. The absorption band of methanol vapor is observed in the vacuum ultraviolet region λ_{max} 174 mμ, and attributed to the (n-σ^*) transition which corresponds to the excitation of the non-bonding electron of oxygen atom in methanol.[15] Therefore, the formation of hydrogen atom by the scission of O–H bond in the primary process is explained by the assumption that the excitation of methanol molecule by the absorption of ultraviolet light is limited to the oxygen atom of methanol molecule, and thus causes the scission of O–H bond of methanol molecule. In radiolysis, it is well known that most of the excited molecules are formed by the interaction of electrons. Thus, it is reasonable to consider that the induced excitation energy is not localized but distributed at random among methanol molecule. Therefore, the scission of C–H bond occurs more easily than that of O–H bond, because the bond energy of C–H is lower by about 10 kcal/mol than that of O–H.

TABLE 5. CALCULATED YIELDS OF ISOTOPIC HYDROGEN ON THE BASIS OF IONIC, MOLECULAR AND RADICAL MECHANISMS

	$G(H_2)$	G(HD)	$G(D_2)$
Ionic	2.6	4.7	—
Molecular	0.5	0.5	—
Radical	3.0	0.1	—
Observed	6.1	5.3	0.2

The yields are defined as follows :
Ionic : yields of isotopic hydrogen, formed molecularly as well as radically, through the ionization of CH_3OD
Molecular : yields of isotopic hydrogen formed molecularly by the dissociation of directly excited methanol molecule (CH_3OD^*)
Radical: yields of isotopic hydrogen formed radically by the dissociation of directly excited methanol molecule (CH_3OD^*)

The calculated yields of isotopic hydrogen in each radiolysis mechanism are summarized in Table 5.

The author wishes to thank Dr. Gisuke Meshitsuka and Dr. Yoshiharu Shinozaki for their useful discussions. The author is also indebted to Mr. Yukio Inokoshi for his assistance in the experimental works.

14) R. F. Pottie, A. G. Harrison and F. P. Lossing, *Can. J. Chem.*, **39**, 102 (1961).
A. R. Knight and H. E. Gunning, *ibid.*, **39**, 1231 (1961).

15) H. Tsubomura, K. Kimura, K. Kaya, J. Tanaka and S. Nagakura, This Bulletin, **37**, 417 (1964).

BULLETIN OF THE CHEMICAL SOCIETY OF JAPAN VOL. 43 345—349 (1970)

Electronic States of *p*-Chloranil and Its Anion-Radical as Revealed by Their Infrared Spectra

Yôichi IIDA

Department of Chemistry, Faculty of Science, Hokkaido University, Sapporo, Hokkaido

(Received July 31, 1969)

The infrared spectra (650—4000 cm^{-1}) of *p*-chloranil and its anion-radical were measured. Appreciable frequency differences between their corresponding bands were noted. The fundamental frequencies were assigned, and the simple UBFF's were determined for both the neutral and anion-radical molecules. Their stretching force constants for the bonds in the conjugated systems are related to the bond orders. The values of the bond orders thus obtained for *p*-chloranil and its anion-radical were in good agreement with those evaluated by the molecular-orbital calculation, except for the C=O bond in the anion-radical. In view of these results, it was concluded that the difference in the infrared spectra between these two molecules was almost entirely attributable to the difference in their electronic structures caused by an odd electron on the *p*-chloranil anion-radical. The bond lengths were also estimated on the basis of the bond orders. It was shown that the application of this method might bring valuable knowledge on the molecular and electronic structures of ion-radicals as well as of neutral molecules in general.

It has been noticed that the infrared spectrum of a neutral molecule is appreciably different from that of its ion-radical molecule.[1-5] Obviously, the difference in spectra may be attributed to the difference in their intramolecular force fields. Up to now, however, there has been no attempt to explain the spectrum difference by the use of normal coordinate analysis.

The present paper will describe the infrared spectra of *p*-chloranil and its anion-radical (*i.e.*, the semiquinone ion). The *p*-chloranil molecule is a well-known electron acceptor, and its anion-radical (see Fig. 1) is quite stable. The purpose of this paper is to make a normal coordinate analysis for these molecules and to discuss their molecular and electronic structures on the basis of their intramolecular force fields. In this respect, it is interesting to investigate the effect of an extra electron upon the *p*-chloranil anion-radical.

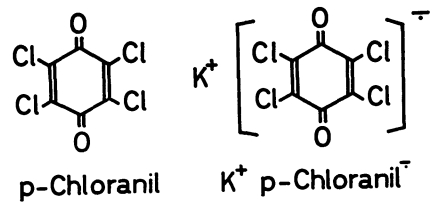

Fig. 1. *p*-Chloranil and its anion-radical salt with potassium cation.

Experimental

Commercially-available *p*-chloranil was purified by recrystallization from benzene and then by sublimation *in vacuo*. Its anion-radical salt with the potassium cation (K^+ *p*-Chloranil$^-$) was synthesized according to the method of Torrey and Hunter.[6] The infrared spectra of these solid compounds were measured as Nujol mulls in the range from 650 to 4000 cm^{-1} using a HITACHI EPI-S2 infrared spectrophotometer. Alternative

TABLE 1. OBSERVED AND CALCULATED FREQUENCIES (cm^{-1}) IN THE INFRARED SPECTRA OF *p*-CHLORANIL AND ITS ANION-RADICAL

p-Chloranil			*p*-Chloranil$^-$		
Obsd	Calcd	Symmetry	Obsd	Calcd	Symmetry
1686(s)	1685	B_{2u}	1524(s)	1520	B_{2u}
1678(sh)					
1571(s)	1569	B_{3u}	1540(s)	1539	B_{3u}
1260(m)	1238	B_{3u}	1176(w)	1288	B_{3u}
1235(m)				(?)	
1115(s)	1116	B_{2u}	1147(s)	1141	B_{2u}
908(m)	916	B_{2u}	918(s)	910	B_{2u}
752(s)	736	B_{3u}	725(s)	736	B_{3u}
715(s)			694(m)		

1) Y. Matsunaga, *Can. J. Chem.*, **38**, 1172 (1960).
2) Y. Matsunaga, *Helv. Phys. Acta*, **36**, 800 (1963).
3) Y. Matsunaga, *J. Chem. Phys.*, **41**, 1609 (1964).
4) M. Kinoshita and H. Akamatu, *Nature*, **207**, 291 (1965).
5) J. Stanley, D. Smith, B. Latimer and J. P. Devlin, *J. Phys. Chem.*, **70**, 2011 (1966).
6) H. A. Torrey and W. H. Hunter, *J. Amer. Chem. Soc.*, **34**, 702 (1912).

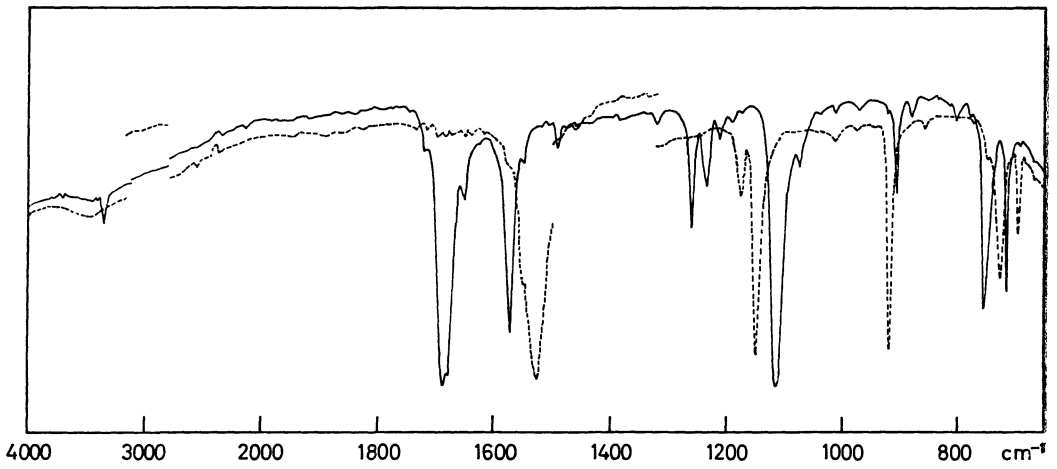

——*p*-Chloranil, ----K^+*p*-Chloranil$^-$

Fig. 2. Infrared spectra of *p*-chloranil and K^+ *p*-chloranil$^-$.

measurements in the regions where the absorption due to Nujol appears were made using hexachlorobutadiene mulls. The spectra for these compounds are reproduced in Fig. 2. Since the counter cation of the salt is a simple metal cation, the observed spectrum of the salt in the region from 650 to 4000 cm^{-1} should be solely due to that of the anion-radical itself. The values of the absorption peaks observed for *p*-chloranil and its anion-radical are listed in Table 1.

Normal Coordinate Treatment for In-plane Vibrations

The molecular and crystal structures of *p*-chloranil were determined by Chu, Jeffrey and Sakurai.[7] Since the molecular and crystal structures of K^+ *p*-Chloranil$^-$ have not yet been ascertained, it was assumed that the molecular structure of the anion-radical was almost identical with that of *p*-chloranil. This assumption means that the ***G*** matrix calculated for *p*-chloranil was also used for the anion-radical (see below). Since only the intramolecular vibrations are expected to appear in the region from 650 to 4000 cm^{-1}, the vibrational spectra of the crystalline compounds can be approximately treated under the molecular point group D_{2h}. Generally, the effect of crystal fields on vibrational frequencies is small. Therefore, as the first approximation, its contribution to the spectra of *p*-chloranil and of the anion-radical was ignored in our treatment. Hence, thirty normal modes of vibrations for *p*-chloranil or its anion-radical were reduced to the symmetry species:

$$\Gamma = 6A_g + 5B_{1g} + 5B_{2u} + 5B_{3u} + 1B_{2g} + 3B_{3g} + 2A_u + 3B_{1u}\,, \qquad (1)$$

where the first four are the in-plane vibrations, and the rest, the out-of-plane vibrations.[8] We calculated only the in-plane vibrations, because no out-of-plane vibration is expected to appear in the region now under consideration.

Wilson's ***GF*** matrix method was used in this work. The representation of each type of internal coordinate for in-plane fundamental vibrations is given in Fig. 3. A simple Urey-Bradley force field was employed as the potential function. Therefore, four bond-stretching (K(C=O), K(C=C), K(C-C) and K(C-Cl)), five angle-bending (H(O=C-C), H(C-C-Cl), H(C=C-Cl), H(C-C-C), and H(C=C-C)), and five non-bonded repulsion force constants (F(O=C-C), F(C-C-Cl), F(C=C-Cl), F(C-C-C), and F(C=C-C)) were necessary. At

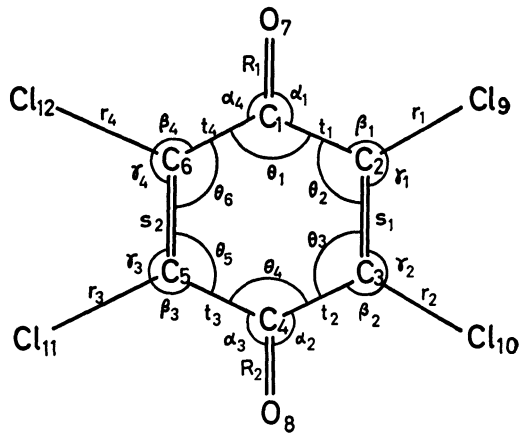

Fig. 3. Internal coordinates for *p*-chloranil or its anion-radical.

7) S. Chu, G. A. Jeffrey and T. Sakurai, *Acta Cryst.*, **15**, 661 (1962).

8) F. E. Prichard, *Spectrochim. Acta*, **20**, 127 (1964).

Table 2. Force constants for *p*-chloranil and its anion-radical (md/Å)

Force constant	*p*-Chloranil	Its anion-radical
K(C=O)	9.7	7.3
K(C=C)	6.6	6.1
K(C–C)	3.0	3.5
K(C–Cl)	2.67	2.67
H(O=C–C)	0.32	
H(C–C–Cl)	0.08	
H(C=C–Cl)	0.08	
H(C–C–C)	0.229	
H(C–C=C)	0.25	
F(O=C–C)	0.80	
F(C–C–Cl)	0.928	
F(C=C–Cl)	0.928	
F(C–C–C)	0.30	
F(C–C=C)	0.37	

$F' = -0.1F$.

this time, it was assumed that the stretching force constants of *p*-chloranil were different from those of the anion-radical, while the other force constants of *p*-chloranil were almost the same as the corresponding ones of the anion-radical. The initial values of the force constants were transferred from the values for benzene and its chloro-derivatives.[9,10] Refinements of the force constants were then carried out by the trial-and-error method*1 making use of the Jacobian matrices. The final sets of force constants thus obtained for these molecules are shown in Table 2. In both of these molecules, the calculated values of the fundamental vibrations (see Table 1) agreed well with the observed values, except for the following two points, which remain to be elucidated:

(1) Two absorption peaks were observed, at 752 and 715 cm^{-1} for the neutral molecule or at 725 and 694 cm^{-1} for the anion-radical, while only one fundamental in-plane vibration was expected to appear around this region.*2 To assign one of them to an out-of-plane vibration is improbable, because such a vibration should appear in the region below 650 cm^{-1}.

(2) The calculated 1288 cm^{-1} band in the anion-radical cannot be assigned to any of the observed bands, presumably because of its weak intensity.

Since a total of 14 force constants were evaluated from an experimental assignment of 6 frequencies, we suspect that these values of the force constants are not the best ones for each of these compounds. However, the stretching force constants are still meaningful, because the observed fundamental frequencies are almost all due to the stretching modes. In the discussion below, we will discuss only the difference in the stretching force constants between *p*-chloranil and its anion-radical.

As is shown in Table 2, appreciable differences in the force constants were found in K(C=C), K(C–C), and K(C=O)—namely, K(C=C) = 6.6 md/Å, K(C–C) = 3.0, and K(C=O) = 9.7 for *p*-chloranil, while K(C=C) = 6.1, K(C–C) = 3.5, and K(C=O) = 7.3 for the anion-radical. From these results, we can see that the stretching force constants for the bonds in the conjugated systems are strongly affected. It is expected that the extra electron on the anion-radical is the essential factor causing the decrease in the values of K(C–C) and K(C–O) and the increase in the value of K(C–C), compared to the values of *p*-chloranil.

Discussion

According to Coulson and Longuet-Higgins,[11] the stretching force constant of a bond (12) in a conjugated system can be expressed by:

$$K(12) = \{(1-p(12))K_s + p(12)K_d\} + \left[\left\{\frac{K_sK_d(s-d)}{K_s(1-p(12))+K_dp(12)}\right\}^2 \frac{\pi(1212)}{2}\right], \quad (2)$$

where K_s and K_d are the force constants associated with pure single and double bonds respectively; where $p(12)$ is the bond order, and $\pi(1212)$, the self-polarizability, of the bond (12), and where s and d are the bond lengths of pure single and double bonds respectively.

Carbon-Carbon Bonds. In a homopolar carbon-carbon bond, the second term, involving the self-polarizability, may be small.[12] In this case, the stretching force constant, $K(12)$, is predominantly determined by the bond order, $p(12)$. The lower part of Fig. 4 shows the empirical relation of $K(12)$ to $p(12)$, in which several standard points indicated by the open circles are connected smoothly. They were determined on the basis of the values of $K(12)$ and $p(12)$ for the carbon-carbon bonds in the ethylene, benzene, and butadiene molecules.[9,13] Little contribution of $\pi(1212)$ to $K(12)$ is best shown

9) Y. Kakiuchi, *Nippon Kagaku Zasshi*, **75**, 143 (1954).
10) J. R. Scherer, *Spectrochim. Acta*, **20**, 345 (1964).
*1 The calculations were carried out on a HITAC 5020E at the Computer Center, The University of Tokyo.
*2 In *p*-bromanil, the corresponding bands were found at 705 and 650 cm^{-1}, and in its anion-radical, at 684 and 618 cm^{-1}. The bands at 752 and 725 cm^{-1} in *p*-chloranil and its anion-radical shifted to 650 and 618 cm^{-1} in *p*-bromanil and its anion-radical respectively, whereas the speculation of a similar shifts is not adequate to the cases of the other bands. For this reason, the bands at 752 and 725 cm^{-1} in *p*-chloranil and its anion-radical were assigned to the fundamental vibrations of the C-Cl stretching mode.
11) C. A. Coulson and H. C. Longuet-Higgins, *Proc. Roy. Soc.*, **A193**, 456 (1948).
12) A. Streitwieser, Jr., "Molecular Orbital Theory," John Wiley & Sons, New York and London (1961).
13) K. Ito and T. Shimanouchi, private communication.

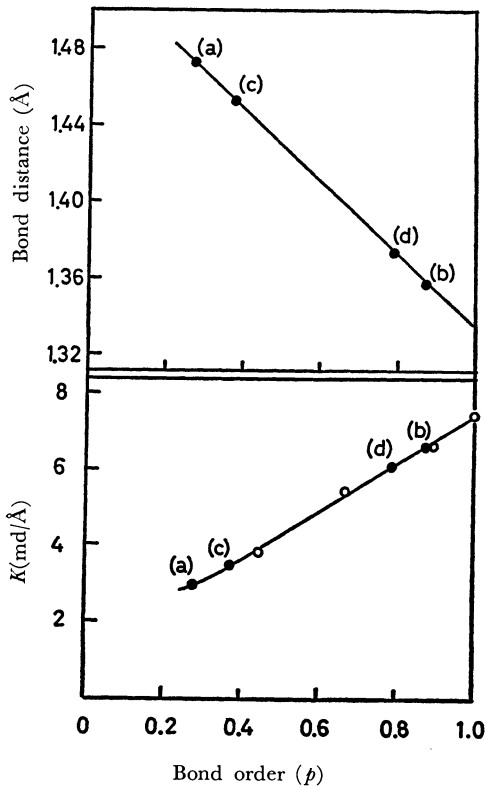

Fig. 4. The lower part illustrates the empirical relation between $K(12)$ and $p(12)$ of a carbon-carbon bond, and the upper part, the relation of $l(12)$ to $p(12)$. (a) and (b) show the values due to C–C and C=C bonds for *p*-chloranil, and (c) and (d), those for its anion-radical, respectively. Open circles indicate the standard points based on the values of $K(12)$ and $p(12)$ in the ethylene, benzene and butadiene molecules.

by the approximate linearity between the $K(12)$ and $p(12)$ values. We cannot adopt the K(C–C) value of ethane as K_s, because the value of K_s should not be that due to the C_{sp^3}–C_{sp^3} bond of ethane, but that due to the C_{sp^2}–C_{sp^2} bond, with $p(12)=0$.

TABLE 3. THE VALUES OF THE BOND ORDERS OF p(C–C), p(C=C) AND p(C=O) FOR *p*-CHLORANIL AND ITS ANION-RADICAL

Bond	*p*-Chloranil		*p*-Chloranil⁻	
	IR[a]	MO[b]	IR[a]	MO[b]
C–C	0.27	0.20	0.37	0.32
C=C	0.87	0.96	0.79	0.83
C=O	0.82	0.91	0.40	0.79

a) The values obtained from the stretch force constants.
b) The values calculated from the molecular orbitals.

By the use of this empirical formula, we can evaluate the bond orders of the C=C and C–C bonds for *p*-chloranil and its anion-radical. From the values of K(C=C) and K(C–C) in their infrared spectra, the p(C=C) and p(C–C) values for these molecules were estimated to be as shown in Table 3. It seems that the extra electron on the anion-radical leads to a decrease in p(C=C) of 0.08 and to an increase in p(C–C) of 0.10, compared to the values of the neutral *p*-chloranil. In order to confirm this result, we further calculated the p(C=C) and p(C–C) values of these molecules by the use of their molecular orbitals. For simplicity, the SCF molecular orbitals of *p*-benzoquinone were used,[14] because the electronic state of the π-conjugated system in *p*-chloranil can be regarded as very similar to that in *p*-benzoquinone. We also assumed that the extra electron enters into the lowest-vacant orbital of *p*-benzoquinone. This orbital has the irreducible representation of the symmetry, b_{3g}, where the coefficients of the O_7, C_1, C_2, and C_3 atomic orbitals were assumed to be represented by -0.3564, $+0.3315$, $+0.3627$, and -0.3627 respectively.[14] With these assumptions, we calculated the values of p(C=C) and p(C–C) for these molecules from their molecular orbitals, as is shown in Table 3. This calculation suggests that the extra electron causes a decrease in p(C=C) of 0.13 and an increase in p(C–C) of 0.12, compared to the values of *p*-chloranil. These results are in good agreement with those evaluated from the infrared spectra.

There is a well-known relation between the bond order and the bond length, l, of a carbon-carbon bond.[12] This was illustrated in the upper part of Fig. 4. In this relation, p(C=C) and p(C–C) derived from the infrared spectra give l(C=C) and l(C–C) respectively. These values of l(C=C) and l(C–C) for *p*-chloranil and its anion-radical are collected in Table 4. The estimated l(C=C) and l(C–C) values of *p*-chloranil are in good agreement with the results of the X-ray study.[7] Table 4 shows that the unpaired electron on the anion-radical may cause an increase of 0.01 Å in l(C=C) and a decrease of 0.02 Å in l(C–C), compared to the values of *p*-chloranil. However, no observation of the molecular structure of the anion-radical has yet been made.

Carbon-Oxygen Bond. If we take $K_s=5.0$ md/Å and $K_d=10.7$ for C=O bond, values proposed by Bratoz and Besnainou,[14] and neglect the contribution of the self-polarizability to the stretching force constant, those force constants for *p*-chloranil and its anion-radical give the values of p(C=O) as 0.82 and 0.40 respectively. These values should be compared with those of 0.91 and 0.79 respectively calculated from their molecular orbitals. In *p*-chloranil, the agreement is rather satisfactory.

14) S. Bratoz and M. S. Besnainou, *J. Chem. Phys.*, **34**, 1142 (1961).

Table 4. The values of the bond lengths of l(C=C) and l(C-C) for *p*-chloranil and its anion-radical
(in unit of Å)

Bond	*p*-Chloranil		*p*-Chloranil$^-$	
	IR[a]	Obsd[b]	IR[a]	Obsd[c]
C-C	1.47	1.477	1.45	(1.44)
C=C	1.36	1.342	1.37	(1.38)

a) The values estimated from the bond orders, which were derived from the stretching force constants in the infrared spectra.
b) The observed values by the X-ray study; see Ref. 7.
c) The values estimated in the *p*-benzoquinone anion-radical from its molecular orbitals; see O. Kikuchi and K. Someno, This Bulletin, **40**, 2972 (1967).

Although there is a definite trend towards less bond order, no quantitative agreement is obtained for the anion-radical. One reason for this might be the neglect of the self-polarizability.

As for the relation between the force constant and the bond length of a C=O bond, Badger proposed the following equation:[15]

$$K(\mathrm{C{=}O}) = 1.86/\{l(\mathrm{C{=}O}) - 0.68\}^3, \qquad (3)$$

where K and l are in md/Å and Å units respectively. For *p*-chloranil and its anion-radical, the values of l(C=O) derived from their force constants by Eq. (3) were 1.26 Å and 1.31 Å respectively. The former value is rather larger than the observed value of 1.195 Å.[7] Although the agreement is not satisfactory, we may expect than the C=O bond length of the anion-radical is longer than that of *p*-chloranil by 0.05 Å; however, no experimental result is available at present.

15) R. M. Badger, *J. Chem. Phys.*, **3**, 710 (1935); see also J. A. Ladd, W. J. Orville-Thomas and B. C. Cox, *Spectrochim. Acta*, **20**, 1771 (1964).

Concluding Remarks. The present investigation clearly shows that the predominant factor in the frequency differences between *p*-chloranil and its anion-radical is the difference in their electronic structures. Nevertheless, we noticed some disagreements between the C=O bond orders obtained from their infrared spectra and those obtained from their molecular orbitals. We consider that these disagreements may be caused by the frequency shifts due to the crystal-field effect as well as by the neglect of the self-polarizability. The crystal-field effect may be more important for the ion-radical salts than for neutral molecular crystals.

Rigorously speaking, the $\boldsymbol{G}$ matrix for the anion-radical is not identical with that for *p*-chloranil, since the bond lengths of the anion-radical estimated from the bond orders were found to be slightly different from those of *p*-chloranil. The difference in their $\boldsymbol{G}$ matrices may make some contribution to the frequency difference. However, this contribution is negligibly small for the bands due to the stretching modes.

The set of force constants presented in Table 2 cannot be regarded as a unique solution. In this sense, it is important to note the couplings between the stretching force constants and the other force constants. However, our primary interest exists in studying the difference in the force constants between *p*-chloranil and its anion-radical. We consider that the set of force constants presented here is reliable enough for this purpose.

In conclusion, the application of the infrared spectra of a neutral molecule and its ion-radical can bring about valuable knowledge as to their molecular and electronic structures, such as bond lengths and bond orders. It is interesting to see that their frequency differences give some information concerning the nature of the half-filled orbital in the ion-radical molecular orbitals.

The author would like to express his appreciation to Professor Yoshio Matsunaga and Dr. Takao Iijima for their kind advice regarding this work.

BULLETIN OF THE CHEMICAL SOCIETY OF JAPAN VOL. 43 350—354 (1970)

Electrochemical Properties of α-Ferric Oxide in Sulfuric Acid Solutions

Hiroshi YONEYAMA and Hideo TAMURA

Department of Chemical Technology, Faculty of Engineering, Osaka University, Suita, Osaka

(Received August 4, 1969)

I-V curves of the α-Fe_2O_3 electrode containing different amounts of Ti were obtained potentiostatically in H_2SO_4 solutions. The anodic current, indicating the dissolution reaction, was almost constant and was not affected by the a_{H^+} of the electrolyte in the potential range 0.4—1.0V *vs.* SCE, but it was dependent on the conductivity of the electrode. It was suggested that the dissolution reaction of this electrode is governed by the electron-transfer mechanism, much as is that of the heavily-doped N-type Ge. The flat-band potential of the α-Fe_2O_3 electrode was estimated on the basis of the capacity measurement. This potential changed with the a_{H^+} of the electrolyte.

The mechanism of electric conduction in 3*d* transition metal oxides[1] deviating a little from stoichiometry have been considered to be different from that in the usual semiconductors, such as Ge and ZnO. In a previous paper[2] we studied redox reactions on lithiated NiO showing P-type conduction and made it clear that the electrical property of the electrode determined the electro chemical reactions on it. A study of the electrochemical reactions of N-type 3*d* transition metal oxide is a useful course of study in elucidating the effect of the electrical property of the electrode on the reactions. α-Fe_2O_3 containing Ti is a typical N-type semiconductor among 3*d* transition metal oxides.[3,4] Therefore, we planned to study the electrochemical properties of α-Fe_2O_3 as a step in the study of the reactions on this electrode. In this paper the polarization behavior and the differential capacity of this electrode will be discussed.

Experimental

Electrode. High-purity Fe power (99.99% up) was dissolved in hot H_2SO_4 solution, and then the hot solution was filtered. $FeSO_4$ was precipitated from the filtrate on cooling it. The precipitate was washed by decantation, filtrated, and washed with deionized water and then with CH_3OH. After having been dried, the $FeSO_4$ was decomposed to Fe_2O_3 in the air at 450°C. The Fe_2O_3 prepared in this way was mixed with 0.2—1.0 atom % Ti in the form of high purity TiO_2 (99.9% up) and ground in an agate mortar. The mixture was pressed into a tablet at 2.25 t/cm² (15 mm dia and 3—4 mm thick). This tablet was fired in the air for 4.5 hr at 1200°C and for 5 hr at 1300°C. The tablets shrank to a diameter of about 10 mm during sinterring, though they still had an apparent porosity of about 20%. Platinum contacts on the end faces of the tablet were made by firing platinum powder pasted on them at 1250°C as a contact material for soldering a lead wire. As the electrical lead was needed for mechanical strength, the vapor-deposition technique was not adopted for making the contact on α-Fe_2O_3. The conduction type of the sample was checked by thermo-electromotive force measurements and was found to be of the N-type, as had already been reported by Morin[3] and by Verway and his co-workers.[4] This sample was fabricated into a electrode in the same way as was used in the study of the lithiated NiO electrode,[5] after the apparent resistivity of the sample had been estimated by the voltage-drop method. Silver and indium were also used to make the electrical contact to α-Fe_2O_3. Ag contact was made by firing Ag powder pasted on an end face of the tablet of α-Fe_2O_3 at 900°C. Indium contact was made by soldering the indium, though the soldering was often unsuccessful. In the case of indium contact, the contact area was restricted to a part of an end face of the tablet of α-Fe_2O_3, since impregnation of a benzene solution of polystyrene was necessary after mounting a specimen in glass tube. The sample used in this study had the Ti content and contact material shown in Table 1. The electrode area was estimated by the method described previously.[5] In this estimation the ac resistance measured in 2 N H_2SO_4 was chosen as the resistance of the electrode. After all the measurements described below, the α-Fe_2O_3 specimen was taken out of the glass tube and its surface was erased with emery paper. The specific resistivity of the α-Fe_2O_3 used in this study was then estimated by the four-probe method.[6] This value is shown in Fig. 1 as a function of the Ti content.

Cell Equipment. The cell equipment has been described previously.[2] The counter electrode was a platinized platinum net (2×4 cm). The test electrode was conditioned by pre-electrolysis in 0.1 N H_2SO_4 at 1.2V and 0.2V *vs.* SCE each 20—30 min.

Electrolyte. 0.1, 0.2, 0.5, and 1.0 N H_2SO_4 were

1) F. J. Morin, *Bell System Tech. J.* **37**, 1047 (1958).
2) H. Yoneyama and H. Tamura, This Bulletin, to be published.
3) F. J. Morin, *Phys. Rev.* **83**, 1005 (1951), *ibid.*, **93**, 1195 (1954).
4) E. J. W. Verway, P. W. Haaijman and F. C. Romeijn, *Chem. Weckblad*, **44**, 705 (1948).
5) H. Yoneyama and H. Tamura, This Bulletin, **42**, 1795 (1969).
6) L. B. Valdes, *Proc. IRE*, **42**, 420 (1954).

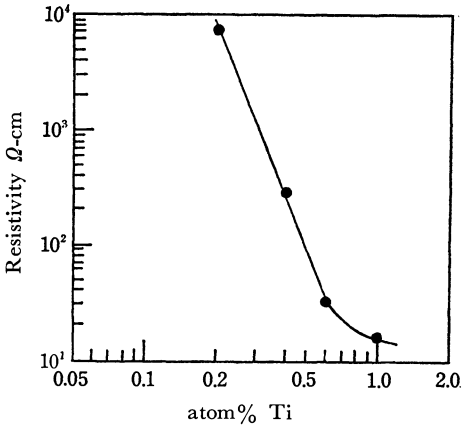

Fig. 1. Resistivity of αFe_2O_3 as a function of Ti content.

prepared using analytical-grade H_2SO_4.

Bridge. The bridge was constructed after the model of Toshima and Uchida.[7] The arrangement is shown in Fig. 2. The ac input voltage into the bridge circuit was set in 3 mV. 2.5, 5, and 10 kc were chosen as the ac frequencies. The null point was detected by a tunned-null detector with a 70 db gain.

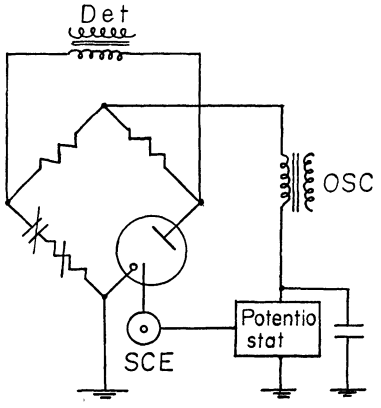

Fig. 2. Bridge arrangement with a potentiostat for superposition of AC with DC voltage.

Results and Discussion

When the electrode was polarized potentiostatically, the current flow was suppressed in the 0.4—1.0 V potential region. Typical I-V curves are shown in Fig. 3. The current attained a stationary value within 5 min—2 hr[8] after the potential setting. I-V curves was usually obtained with a potential raising, but if it was done with a potential lowering from 1.5 V the steady-state current was somewhat smaller. The I-V curves can be separated into three regions, as is indicated in Fig. 3. In the

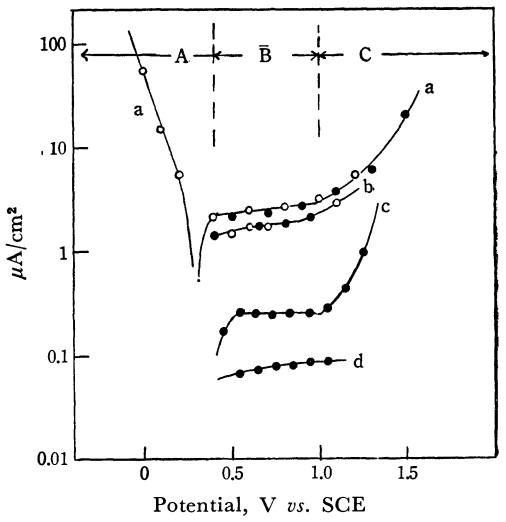

Fig. 3. I—V curves of α-Fe_2O_3 in H_2SO_4 solutions. Electrode had the following Ti content. (atom%). a; 1.0, b; 0.6, c; 0.4, and d; 0.2 electrolyte: —○— 1 N —●— 0.1 N

region A, the I-V curve refers to the hydrogen evolution reaction or the reduction reaction of the electrode, while oxygen evolution possibly occurs in the region C. In the region B the current was not affected by the stirring of the electrolyte or by the concentration of sulfuric acid, as Fig. 3 shows. According to the potential-pH diagram,[9] Fe_2O_3 is not stable in the region B. In order to clarify the nature of the current in the region B, the quantity of Fe dissolved into the electrolyte was determined by colorimetric method after the electrode C had been polarized potentiostatically at 0.9 V for a known period and then compared with the quantity of electricity passed through during the polarization. As a result, 16 μA·H produced 32.5 μg Fe; *i.e.*, one faraday amounts to 54.5 g Fe. From this result, the current in the region B can be said to refer to the anodic dissolution reaction of the electrode.

When a N-type semiconductor comes in contact with a metal having a large work function, a potential barrier is formed on the contact face depending on the difference between their work functions, and then a space-charge layer is created in the interface. As platinum has a large work function, 5.10 eV,[10] a potential barrier should have been formed on the interface between Pt and α-Fe_2O_3. Such a potential barrier occasionally controls the current flow. However, the Pt-α-Fe_2O_3 contact did not control the electrochemical reactions even if the potential barrier existed at the contact face, for generally a current flow is hindered cathodically by this barrier

7) S. Toshima and I. Uchida, *Denki Kagaku*, **34**, 624 (1966).

8) Nearly 2 hr was required at 0.5 V with the potential raising measurement.

9) M. Pourbaix, "Atlas of the Electrochemical Equilibria in Aqueous Solution," Pergamon Press, Oxford, London (1966), p. 307.

10) "Landolt-Börnstein," 6 Aufl., Bd./6, Springer-Verlag, Berlin, Gottingen, Heidelberg (1959), p. 913.

if the electrochemical reactions are controlled by this barrier, but a distinct current appeared in the region A. Moreover, a distinct cathodic current showing the reduction of Fe^{3+} was observed in the potential comparable to the region B.[11] The suppression of the anodic current flow in the region B does not, therefore, stem from Pt-α-Fe_2O_3 contact.

In the anodic dissolution reaction of the common semiconductors, a saturation current is usually observed in N-type semiconductors.[12-14] The holes are connected with this current flow. As a hole probably exists in α-Fe_2O_3,[15] hole-connected mechanism cannot be simply denied. In order to clarify this point, an I-V curve was obtained in the electrolyte containing Ce^{4+}. If hole is connected with the anodic dissolution reaction, the current should increase in the electrolyte containing Ce^{4+} compared with the case when only H_2SO_4 is present because the holes injected from the reduction of Ce^{4+} would participate in the dissolution reaction.[16] Of cource, this method may not be complete for determining the kind of charge carrier involved in the reaction, since some particular effects, such as the Hall effect and carrier injection, which can be observed in common semiconductors have not been observed in 3*d* transition metal oxides.[1] The I-V curves obtained in each electrolyte are shown in Fig. 4. The current decreased slightly in the electrolyte containing Ce^{4+}. The mechanism of hole transfer is, therefore, doubtful. In addition, Fig. 1 shows that the current in the region B was the larger for the electrode with a smaller resistivity.

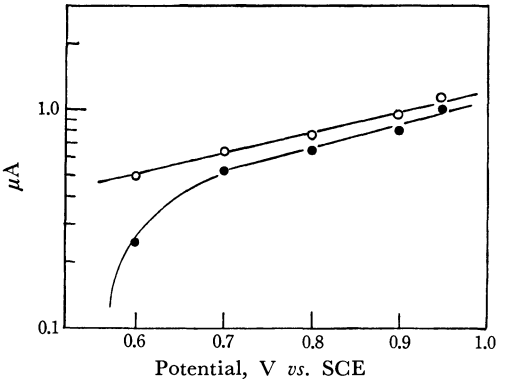

Fig. 4. I—V curves of α-Fe_2O_3 in the electrolyte of —○— 1 N H_2SO_4 and —●— 0.01 M Ce^{4+}/1 N H_2SO_4. Measurement was carried out with potential decreasing direction at the B electrode.

If it is assumed that the resistivity of α-Fe_2O_3 is almost completely determined by the electron density and its mobility,[15] these results lead to the conclusion that the electron in the electrode is connected with the current in the region B. The situation in which the dissolution reaction of the α-Fe_2O_3 electrode proceeds by means of electron transfer is similar to the one observed in the dissolution reaction of heavily-doped N-type Ge.[17] The nearly constant current observed in the region B conceivably appears as a result of the formation of a potential barrier in the electrode surface region or as a result of so-called "passivation" which occurs at the iron electrode in the potential comparable to the region B.[18] The former mechanism is obeyed in the following hypothesis. The energy band of α-Fe_2O_3 will be bent upwards at the electrode in the potential comparable to the region B, since the flat-band potential of α-Fe_2O_3 is quite low as will be presented below. If the electron in the intermediate of the dissolution reaction must jump over this energy barrier in order to flow into the electrode during the process of the dissolution reaction, the current flow would naturally be hindered by this barrier,

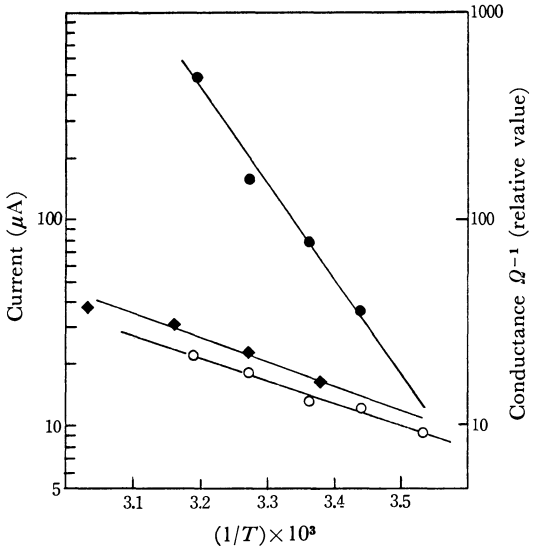

Fig. 5. Temperature dependence of electrode reactions and electrical transference in the electrode, electrode B
◆ conductance estimated from Pt-α-Fe_2O_3-Pt system
● cathodic reaction at 0 V *vs.* SCE
○ anodic reaction at 0.7 V

11) H. Yoneyama, S. Hamamatsu and H. Tamura, This Bulletin, to be published.
12) D. R. Turner, *J. Electrochem. Soc.*, **103**, 252 (1956).
13) F. Beck and H. Gerisher, *Z. Elektrochem.* **63**, 500 (1959).
14) F. Lohmann, *Ber. Bunsenges. Physik. Chem.* **70**, 87 (1966).
15) R. F. G. Gardner, F. Sweet and D. W. Tanner, *J. Phys. Chem. Solid* **24**, 1175 (1963); *ibid.*, **1183** (1963). conductivity δ is related with density n_e, n_p and mobility μ_e μ_p, in the form $\delta=n_eq\mu_e+n_pa\mu_p$, where e and p represent electron and hole, respecrively. μ_e of α-Fe_2O_3 is a order of 10^{-2} cm^2V^{-1} sec^{-1} and $\mu_p 10^{-9}$ cm^2V^{-1} sec^{-1} for α-Fe_2O_3 containing 1 atom % Ti.
16) F. Beck and H. Gerisher, *Z. Elektrochem.* **63**, 943 (1959).
17) R. Greth and M. E. Cowher, *J. Electrochem Soc.* **115**, 645 (1968).
18) K. Bohnhoffer, *Z. Metalkunde*, **44**, 77 (1953).

though its intermediate and its energy state are not clear at present. The finding that the activation energy of the reaction indicated by the current in the region B, 4.8 kcal/mol, was almost equal to that of the electrical transference of α-Fe_2O_3 estimated from the Pt-α-Fe_2O_3-Pt system, 5.0 kcal/mol, may support this mechanism.

The capacitance *C*-electrode potential *V* curves of the B electrode are shown in Fig. 6. *C* monotonously decreases with an increase in the electrode

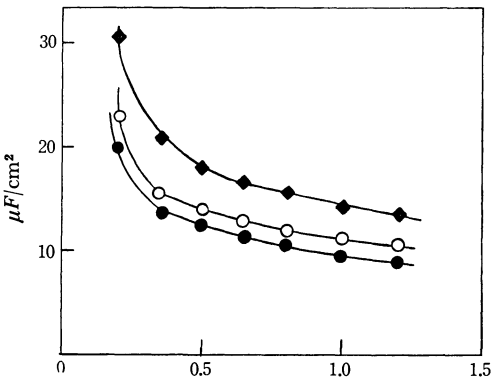

Fig. 6. Differential capacity of α-Fe_2O_3 containing Ti (1.0 atom%) in 0.1 N H_2SO_4. Contact material; Pt —◆— 2.5 kc —○— 5 kc —●— 10 kc

potential. The *C*-*V* curves of the A, C and D electrodes are similar to that of the B. *C* was of an order of 10 μf/cm², as Fig. 6 shows. This is comparable to the double-layer capacity, as has often been pointed out,[19,20] and the measured *C* value normally refers to the space charge in the semiconductor surface region. Similarly, capacitance may be fixed in the passivation film when the passivated film exists on the electrode.[21] Therefore, if it is assumed that the measured *C* value refers to the space-charge capacity induced in the electrode surface, an abnormally large value of *C* may indicate that the estimation of the surface area was incorrect. Unfortunately, the correct estimation of the true surface area of the electrode of a sintered body is very difficult, especially on the oxide electrode. If the measured *C* value can be ascribed to the space-charge capacity in the electrode surface, then the flat-band potential can be estimated from the Mott-Schottky relation.[19-21] The discrepancies in the *C* values measured at various frequencies shown in

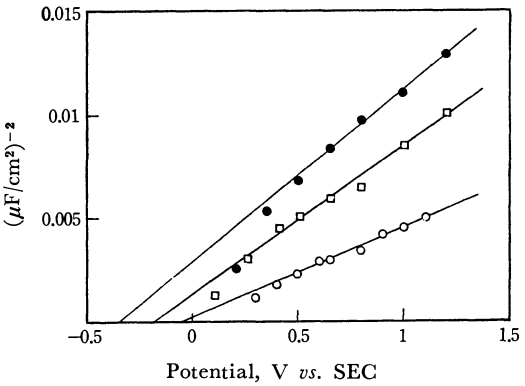

Fig. 7. Mott-Schottky plot for αFe_2O_3 electrode having platinum contact under exhaustion condition. electrode B —●— 0.1 N H_2SO_4 —□— 0.5 N H_2SO_4 —○— 1 N H_2SO_4

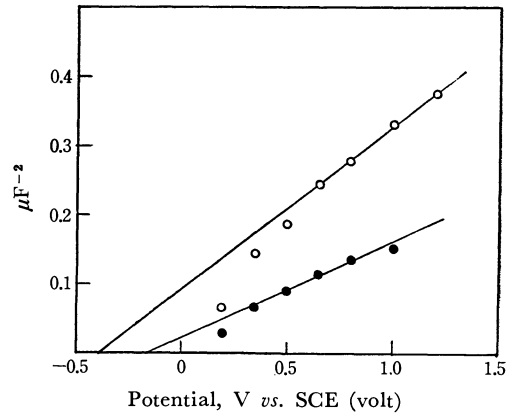

Fig. 8. Mott-Schottoky plot for αFe_2O_3 electrode having indium contact under exhaustion condition. —○— 0.1 N H_2SO_4 —●— 1 N H_2SO_4.

Fig. 6 are due to the Faradic process or to the slow surface state on the electrode surface.[22] As the measured *C* values are more confused by these effects the lower the frequencies adopted, $1/C^2$-*V* curves were obtained on the basis of the *C* value at 10 kc; they are shown in Figs. 7 and 8 for the A and B electrodes respectively. The finding that the $1/C^2$-*V* curves show a linear relation above 0.5 V indicates that the space-charge layer was fixed in the electrode surface region above 0.5 V, since the *C* connected with the space-charge layer on the interface between α-Fe_2O_3 and the contact metal would be diminished with an increase in the electrode potential even if it did exist. The coincidence of the flat-band potential of the A electrode with that of the B indicates that a energy barrier on the interface between the contact metal and α-Fe_2O_3 did not have any serious effect on the *C*-*V* curves, for the energy-barrier height which may be formed on

19) F. Dewald, *Bell System Tech. J.*, **39**, 615 (1960).
20) T. O. Rose and J. L. Wininger, *J. Electrochem. Soc.*, **113**, 184 (1966).
21) S. Toshima, *Denki Kagaku*, **34**, 565 (1966).
22) H. Gerisher, "Advance in Electrochemistry and Electrochemical Engineering," Vol. 1, ed. by P. Delahey and C. W. Tobias, Interscience Publishers, New York (1961), p. 163.
23) A. Kondo and Y. Takahashi, *Kogyo kagaku Zasshi*, **71**, 1949 (1968).

TABLE 1. FLAT-BAND POTENTIAL FROM MOTT-SCHOTTKY PLOT

	Electrode		Flat-band potential V			
	atom% Ti	metal	0.1 N	0.2 N	0.5 N	1 N
A	1.0	In	−0.32	−0.24	−0.16	−0.16
B	1.0	Pt	−0.33	−0.24	−0.16	−0.13
				−0.22		−0.07
				−0.29		
				−0.31		
				−0.26		
C	0.6	Pt	−0.26			
D	0.6	Ag	−0.32			
F	0.4	Pt				
G	0.2	Pt				
Average (*vs.* SCE)			−0.31	−0.275	−0.16	−0.10
After junction potential corrected (NHE)			−0.07	−0.03	+0.09	+0.16
a_{H^+}			0.032	0.0486	0.0895	0.146

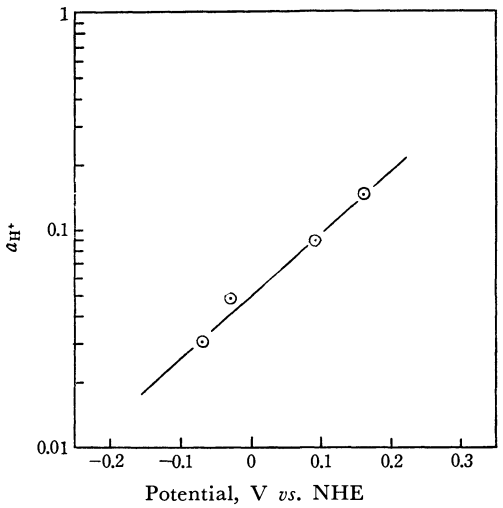

Fig. 9. Flat-band potential of αFe_2O_3 electrode as a function of a_{H^+}.

the interface between Pt and α-Fe_2O_3 will be different from the one on the contact face between In and α-Fe_2O_3. Pt has a larger work function, 5.10 eV,[10] than In because In makes an ohmic contact with ZnO, which has the lower work function of 4.3 eV.[23]

The estimated flat-band potentials in the electrolytes having different activities a_{H^+} of the proton are collected in Table 1. After the acid concentration of the electrolyte had been analytically determined and the liquid junction potential between the electrolyte and saturated KCl solution had been corrected according to Henderson's equation, the average values of the flat-band potential shown in Table 1 were plotted against a_{H^+}. They are presented in Fig. 9. The dependence of the flat-band potential on a_{H^+} may be attributed to the specific adsorption of the proton on the surface of the electrode, as has been observed at the lithiated NiO electrode.[20] The flat-band potential, E, of the α-Fe_2O_3 electrode in the acid electrolyte was changed with a_{H^+} according to the following experimental equation estimated by the least-squares methode,

$$E(\text{NHE}) = 0.45 + 0.35 \log a_{H^+}$$

The authors wish to thank Shinnichi Hamamatsu for preparing the electrode.

BULLETIN OF THE CHEMICAL SOCIETY OF JAPAN VOL. 43 355—358 (1970)

Charge-Transfer Interaction and Chemical Reaction. II. Interaction of s-Triaminobenzene with Several Electron Acceptors

Tsuguo YAMAOKA*1 and Saburo NAGAKURA

The Institute for Solid State Physics, The University of Tokyo, Roppongi, Minato-ku, Tokyo

(Received August 5, 1969)

The charge-transfer interaction was studied for systems including s-triaminobenzene as electron donor. The formation of 1 : 1 stable outer (π,π) complexes at room temperature was observed for the systems including s-trinitrobenzene, trininitrotoluene and tetracyanobenzene as electron acceptors. From the analysis of the observed absorption intensities and peak positions of charge-transfer bands, the equilibrium constants of these complexes were determined and the ionization potential of s-triaminobenzene was estimated to be 7.3—7.4 eV. Chloranil was found to form a stable outer (π,π) complex with s-triaminobenzene only at low temperature, and to be led to a substitution reaction by raising the temperature. The spectrum of the reaction intermediate, the inner (σ) complex of s-triaminobenzene with chloranil, was observed at ~500 mμ. A tentative reaction mechanism was proposed.

Aromatic amines are known to act as electron donors and to form charge-transfer (abbreviated hereafter to CT) complexes with a number of electron acceptors.[1,2] Several workers have reported that some aromatic amines are led to chemical reactions with strong electron acceptors through CT complexes.[3-5] In the preceding paper[6] we gave electronic absorption spectra for solutions containing aniline and chloranil in the mixed solvent of ether-isopropyl alcohol (3 : 1) at various temperatures ranging from 36°K to room temperature. We found that these two molecules form a stable outer (π,π) complex at low temperatures below 200°K but with raising temperature they react with each other yielding 2,5-dichloro-3,6-dianilino-*p*-benzoquinone.

s-Triaminobenzene (abbreviated hereafter to TAB) is known to exhibit a characteristic feature in the fact that protonation occurs more easily on the ring carbon atom than on the nitrogen atom at room temperature and the triaminobenzenium ion is formed.[7] In this connection, we undertook to make a further study on the electron-donating property of TAB, paying special attention to the relation between the CT interaction and chemical reaction. Trinitrotoluene (TNT), s-trinitrobenzene (TNB), tetracyanobenzene (TCNB) and chloranil were used as electron acceptors.

Experimental

Materials. TAB was synthesized and purified by the method described previously.[7] Aniline and dimethylaniline were distilled under reduced pressure just before use. *p*-Phenylenediamine was purified by repeated recrystallizations from ethyl ether.

TNT and TNB were recrystallized twice from ethanol and thereafter once from ethyl ether. Chloranil was recrystallized three times from acetone. TCNB[8] was purified by recrystallization from ethanol: mp 258°C in a sealed tube in agreement with the value in literature.[9]

Chloroform was purified by distillation after washing with water. Methylene chloride was dried over calcium chloride and distilled. Ethyl ether was treated with sodium metal and distilled.

Measurements. Electronic absorption spectra were measured with a Cary recording spectrophotometer Model 14M. The spectra at low temperatures were measured by immersing cells in a quartz Dewar vessel containing liquid nitrogen or dry ice-acetone as a refrigerant. Infrared spectra were measured with a Hitachi EPI 2 spectrophotometer, Nujol mulls being used.

*1 Present address: Department of Printing, Faculty of Engineering, The University of Chiba, Yayoi-cho, Chiba.

1) A. Zweig, J. E. Lancaster, M. T. Neglia and W. H. Jura, *J. Amer. Chem. Soc.*, **86**, 4130 (1964).

2) S. Iwata, J. Tanaka and S. Nagakura, *ibid.*, **88**, 894 (1966).

3) W. Liptay and N. Tamberg, *Z. Elektrochem.*, **66**, 59 (1962).

4) J. W. Eastman, G. Engelsma and M. Calvin, *J. Amer. Chem. Soc.*, **84**, 1339 (1962).

5) Z. Rappoport, *J. Chem. Soc.*, **1963**, 4498.

6) T. Nogami, K. Yoshihara and S. Nagakura, *J. Phys. Chem.*, **73**, 2670 (1969).

7) T. Yamaoka, H. Hosoya and S. Nagakura, *Tetrahedron*, **24**, 6203 (1968).

8) TCNB was prepared in our laboratory by Dr. A. Ishitani who is now at the General Research Institute, Toyo Rayon Co., Ltd.

9) E. A. Lawton and D. D. McRichie, *J. Org. Chem.*, **24**, 26 (1959).

Results and Discussion

Outer (π,π) Complex Formation of TAB with TNT, TNB and TCNB. We measured absorption spectra for various solutions containing TAB as an electron donor and TNT, TNB and TCNB as electron acceptors. Chloroform, ethyl ether and methylene chloride were used as solvents. The results show that TAB interacts with electron acceptors such as TNT, TNB and TCNB to give new absorption bands due to neither electron donor nor acceptor in near ultraviolet and visible regions. Some of the observed bands are shown in Fig. 1. The maximum appears at 440 mμ (in chloroform) and 460 mμ (in ethyl ether) for the TAB-TNT complex; at 460 mμ (in chloroform) and 493 mμ (in ethyl ether) for the TAB-TNB complex; at 420 mμ and 530 mμ for the TAB-TCNB complex in methylene chloride. The peak positions (in eV) of the bands are plotted against those of the CT bands for the hexamethylbenzene (abbreviated hereafter to HMB) complexes with the corresponding acceptors.[2,10] The result given in Fig. 2 shows that the points lie on a straight line. This supports the view that the new bands are interpreted as the CT absorption.

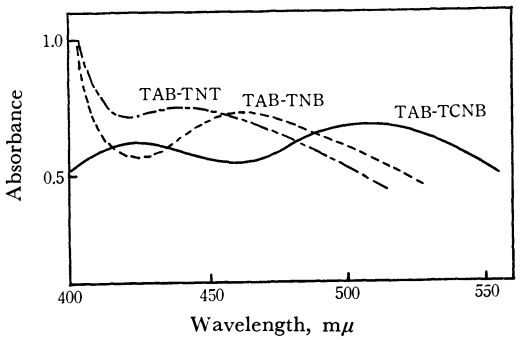

Fig. 1. Spectra of the TAB complexes with TCNB (——) in methylene chloride, and with TNB (- - -) and TNT (— - —) in chloroform.

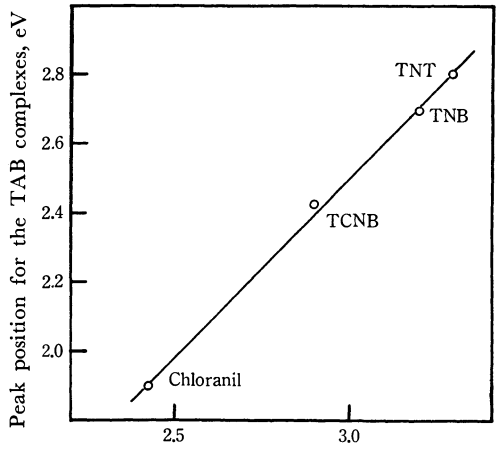

Fig. 2. Plots of the peak positions (in eV) of the new bands observed for the TAB complexes with several electron acceptors in ethyl ether against those of the CT bands for the HMB complexes with corresponding electron acceptors in cyclohexane.

Figure 3 shows that plots of the CT band positions observed for the TNT or TNB complexes with aniline, TAB, dimethylaniline and *p*-phenylenediamine in chloroform against the ionization potentials of the donors except for TAB.[11] From this figure, the electron donating ability of TAB is found to be stronger than that of aniline and weaker than that of dimethylaniline, and its ionization potential can be estimated to be 7.3—7.4 eV.

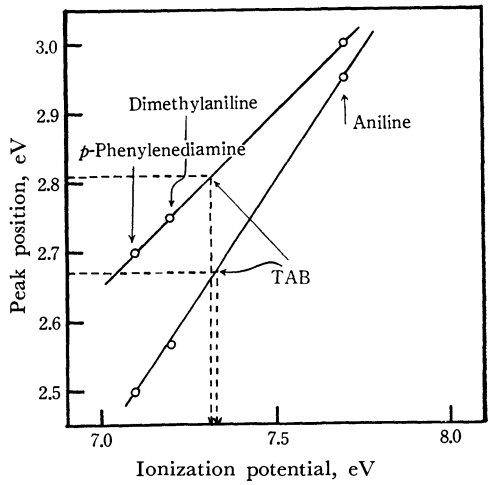

Fig. 3. Plots of the peak positions (in eV) of the CT bands observed for the TNT and TNB complexes against the ionization potentials of aromatic amines as electron donors.

Benesi-Hildebrand plots[12] were carried out for the system containing TAB-TNT and TAB-TNB in chloroform, the well-known straight-line relationship being obtained.[13] This means that 1 : 1 complexes are formed for these systems. The equilibrium constants (K) and the molar extinction coefficients at 25°C were obtained. The results are summarized in Table 1.

10) R. Foster and T. J. Thomson, *Trans. Faraday Soc.*, **59**, 296 (1963).

11) G. Briegleb, "Elektronen-Donator-Acceptor-Komplexe," Springer-Verlag, Berlin (1961).

12) H. A. Benesi and J. H. Hildebrand, *J. Amer. Chem. Soc.*, **71**, 2703 (1949).

13) The concentrations of electron donor C_D and acceptor C_A used for the Benesi-Hildebrand plots are as follows: For TAB-TNT complex, $C_D=2.96\times10^{-3}$ mol/*l*, $C_A=4.04\times10^{-2}$, 2.45×10^{-2}, 1.70×10^{-2} and 1.15×10^{-2} mol/*l*; for TAB-TNB complex, $C_D=2.81\times10^{-4}$ mol/*l*, $C_A=5.56\times10^{-2}$, 2.50×10^{-2}, 1.61×10^{-2} and 1.21×10^{-2} mol/*l*.

Table 1. Equilibrium constant (K) and molar extinction coefficients of CT bands for the TAB-TNT and TAB-TNB system

Complex	K(mol^{-1} l)	ε_{max}
TAB-TNT	15	500
TAB-TNB	20	600

According to Fig. 1, the two CT bands are clearly observed at 420 and 503 mμ for the TCNB-TAB complex in methylene chloride. The frequency difference $\Delta\nu$ between the two peaks is 3920 cm^{-1}. Iwata *et al.*[2] first found that the CT complexes of TCNB with some electron donors show the two CT bands with $\Delta\nu$ values of 5400—6700 cm^{-1}, and these values correspond to the theoretically evaluated energy difference between the two lowest vacant orbitals of TCNB. This means that the two closely located vacant orbitals of the acceptor play an important role in the appearance of the two CT bands for the TCNB complexes. The energy difference (3920 cm^{-1}) is considerably smaller for the TAB-TCNB complex than for the other TCNB complexes. This seems to be related with the fact that the TCNB complex with mesitylene which has the same symmetry as TAB shows a smaller $\Delta\nu$ value than the TCNB complexes with benzene, toluene, durene and hexamethylbenzene.

Outer or Inner Complex Formation and the Reaction of TAB with Chloranil. As mentioned above, TAB forms the stable 1 : 1 outer (π,π) complexes with TNT, TNB and TCNB at room temperature. However, when it interacts with chloranil, the situation seems to be more complex. A blue color formation was observed when TAB was mixed with chloranil in mixed solvent of ether-isopropyl alcohol (3 : 1) at the liquid nitrogen temperature.[14] The color of the solution rapidly turned red immediately after the rigid solution was melted with raising temperature and finally became yellow. However, when the solvent is ethyl ether, the blue color is considerably stable below dry ice-acetone temperature.

The absorption spectra of the TAB-chloranil complex under various conditions are shown in Fig. 4. Curve 1 measured at the liquid nitrogen temperature shows the absorption peak at 660 mμ. This band may be regarded as a CT band. This is supported by the fact that the transition energy of this absorption band fits well into the straight line representing the relation between the CT transition energies of the TAB and hexamethylbenzene complexes with the respective electron acceptors, as is shown in Fig. 2. The blue color of the solution became weaker with rising temperature and this

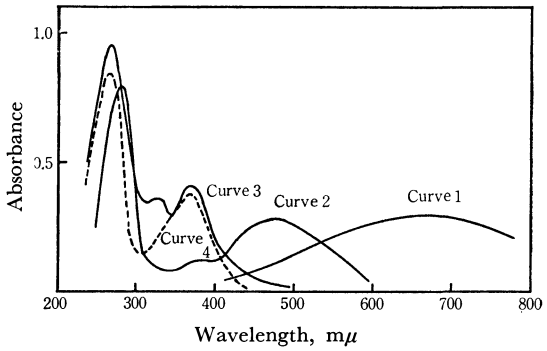

Fig. 4. Time dependence of the spectra for the solution containing 10^{-3} mol/l chloranil and a large excess amount of TAB in 1 : 3 mixed solvent of isopropyl alcohol and ethyl ether. Curve 1, the outer (π, π) complex; curve 2, the inner (σ) complex; curve 3, the adduct of the both components; curve 4, the spectrum of the ring protonated TAB.

color change was found to be reversible for the temperature change near −170°C.

As mentioned above, the blue solution containing TAB and chloranil in mixed solvent of ether-isopropyl alcohol turns red in the intermediate state and finally yellow with increasing temperature. The spectral change is shown in Fig. 4. By raising the temperature, curve 1 due to the outer (π,π) complex changes into curve 2 with the absorption peaks at 500 and 370 mμ, and finally we can obtain curve 3, the absorption spectrum of the product which shows the peaks at 220, 272, 320 and 370 mμ.

It is worth noting that curve 2 of Fig. 4 is similar to the absorption spectra observed[15] with the chloranil-methylamine and chloranil-methoxide ion systems which produce the inner complex shown in Figs. 5(a) and 5(b). A similar spectrum was also observed when *N*,*N*-dimethyl-*m*-phenylenediamine, *m*-phenylenediamine or *m*-aminophenol is mixed with chloranil in the etheral solution. We conclude that the spectrum originates from the inner complex[16] shown in Fig. 5(c). This structure was also supported by the molecular orbital calculation.[17]

Let us consider the absorption spectrum given by curve 3 in Fig. 4. The spectrum, except for the

14) Actual mixing was carried out by iterating a process of adding only a small amount of the donor solution of room temperature to a large amount of the acceptor solution at liquid nitrogen temperature.

15) The chloranil-methylamine (in ether and water mixed solvent) and chloranil-methoxide ion (in methanol) systems show the absorption peak at 505 and 475 mμ, respectively. Although these peak wavelengths are somewhat dependent upon the solvent, they, particularly the latter correspond to the 475 mμ peak of curve 2.

16) Any attempt to isolate the inner complex was unsuccessful, because it easily decomposes on filteration from solutions and on vaporization of solvents.

17) T. Nogami, K. Yoshihara, T. Yamaoka and S. Nagakura, to be published.

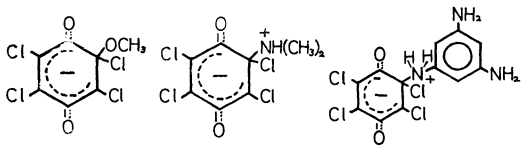

(a) (b) (c)

Fig. 5. Structures of intermediate σ complexes.

peak at 320 mμ, agrees well with that of 1,3,5-triaminobenzenium ion.[7,18] The existence of this ion in the system was also demonstrated by the fact that the infrared spectrum measured for the precipitate (in Nujol mulls) produced in the presence of an excess amount of TAB is the same as that of the triaminobenzenium ion.[7]

The peak at 320 mμ seems to be due to another product. This view is supported by the fact that the relative intensity of the 320 mμ band to the bands changes with the conditions.[19] A fairly pure product with the band at 320 mμ is obtained as a precipitate[20] when an excess amount of chloranil is mixed with TAB in acetone. By an analogy with the products of similar reactions of chloranil with aromatic or aliphatic amines,[6,21,22] the precipitate is expected to be 2,5,6-trichloro-3-triaminobenzo-*p*-benzoquinone or/and 2,5-dichloro-3,6-bis(triaminobenzo)*p*-benzoquinone. Elementary analysis shows that the main part of the precipitate in the presence of an excess amount of chloranil is the former.

Found: C, 41.73; H, 4.13; N, 12.9; Cl, 27.37%. Calcd for the former ($C_{12}H_8N_3Cl_3O_2$): C, 43.24; H, 2.40; N, 12.64; Cl, 31.98%. The discrepancy of elementary analysis from the calculated is due to the difficulty in the separation of the triaminobenzenium ion from the precipitate[23] and also to its hygroscopic property. The elementary analysis data can be expalined by taking account of the mixing of small amounts of the triaminobenzenium ion and water. At least it may be concluded that the main product is not 2,5-dichloro-3,6-bis (triaminobenzo)*p*-benzoquinone. The NMR spectrum measured for the deuterated DMSO solution of the precipitate is consistent with the above-mentioned structure of the main product.[24]

From the above-mentioned results on the structures of the reaction intermediates and products, a possible mechanism of the reaction is proposed as follows:

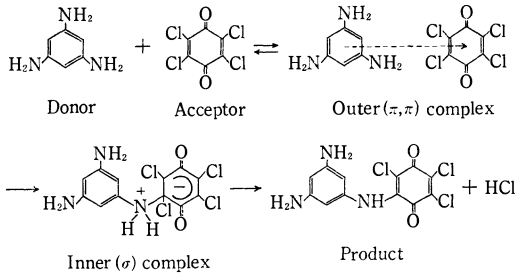

Hydrogen chloride produced in the above reaction attacks TAB to yield the triaminobenzenium ion.[7] For this reason we can observe its absorption spectrum for reaction products.

Increasing the concentration of TAB in solution, we can expect to produce 2,5-dichloro-3,6-bis-(triaminobenzo)*p*-benzoquinone together with 2,5,6-trichloro-3-triaminobenzo-*p*-benzoquinone and the triaminobenzenium ion. Actually, elementary analysis of the product shows that the mixture of the above compounds is precipitated. A similar tendency was also observed by Kumanotani *et al.*[21] for the toluquinone-*n*-butylamine system.

The above-mentioned mechanism with the outer (π,π) and inner (σ) complexes as intermediates was demonstrated to be correct by analyzing the results of the temperature dependence of the decay curve of the inner (σ) complex.[17] The details of this analysis together with a kinetic study on the other systems will be published.

The authors wish to express their gratitude to Professor Takahiro Tsunoda, the University of Chiba, for his continuous encouragement throughout the course of this research. They are also greatly indebted to Dr. Keitaro Yoshihara and Mr. Takashi Nogami for their helpful discussion.

18) H. Köhler and G. Scheibe, *Z. Anorg. Allg. Chem.*, **385**, 221 (1956).

19) For example, the 320 mμ band becomes relatively stronger for the product obtained from the dilute solution containing a great excess amount of chloranil.

20) The precipitate exhibits no infrared band due to the 1,3,5-triaminobenzenium ion. However, it is shown to include a small amount of the ion from visible and ultraviolet absorption measurement.

21) J. Kumanotani, F. Kagawa, A. Hikosaka and K. Sugita, This Bulletin, **41**, 2118 (1968).

22) D. Buckley, H. B. Henbest and P. Slade, *J. Chem. Soc.*, **1957**, 4891.

23) We tried to separate each product by chromatography and other methods, but we were not successful mainly because of the very small solubility of the precipitate.

24) The NMR spectrum of the precipitate in deuterated DMSO solution shows three peaks at τ=6.40, 4.30 and 2.80 which are assigned to the proton signals of NH_2, ring and NH from their τ values and intensities. For the purpose of comparison, the NMR spectra of triaminobenzene and diphenylamine were also measured with the results: τ=7.20 (NH_2 proton), 4.60 (ring proton) for triaminobenzene; τ=1.89 (NH proton) for diphenylamine.

BULLETIN OF THE CHEMICAL SOCIETY OF JAPAN VOL. 43 359—361 (1970)

Steric Structure of L-Proline Oligopeptides. IV. Proton Magnetic Resonance Studies of L-Proline Oligopeptides*[1]

Hirofumi OKABAYASHI*[2] and Toshizo ISEMURA

Division of Physical Chemistry, Institute for Protein Research, Osaka University, Kita-ku, Osaka

(Received August 16, 1969)

The NMR spectra of *t*-amyloxycarbonyl-L-proline oligopeptides were measured and compared with those of two poly-L-prolines, I and II. The α-CH resonance peaks of the oligopeptides were observed at sheilding values of 5.2 and 5.4 ppm, values which were in accord with those of the α-CH resonance peaks of the poly-L-prolines I and II, respectively. The behavior of the α-CH peaks was related to the conformation of the L-proline oligopeptides. Moreover, the contribution of the two terminal L-proline residues to the α-CH resonance peaks was discussed.

In our preceding papers,[1,2] we have made configurational studies of L-proline oligopeptides by such methods as infrared absorption spectra, far-ultraviolet absorption spectra, optical rotatory dispersion, and circular dichroic spectra. The results have led to the conclusions presented below.

In *t*-amyloxycarbonyl-L-proline oligopeptides, the helical structures of the poly-L-proline II-type begin to appear at the tetramer, and the molecules of the pentamer, hexamer, and octamer have a helical structure similar to that of the poly-L-proline II.

The structures of the poly-L-prolines I and II have already been established by the X-ray diffraction method.[3,4] The I form has a right-handed helical structure with a residue translation of 1.85 A, in which the peptide bonds are in the *cis* configuration, while the formII is left-handed with a residue translation of 3.12 A and with the peptide bonds *trans*.

In this work, high-resolution proton magnetic resonance spectroscopy was used for the study of the steric structure of *t*-amyloxycarbonyl-L-proline oligopeptides; the configuration of the peptide groups of the oligomers will be discussed by comparing the NMR spectra of these oligomers with those of the poly-L-prolines I and II. Especially, the differences between the configurations of the two terminal L-prolyl residues and those of the other L-prolyl residues will be described.

Sakai, Okabayashi and Isemura[5-7] have already observed a marked difference in the magnetic shielding values of the α-CH peaks of the poly-L-prolines I and II.

Experimental

The L-proline oligopeptides used in the present investigation were as follows: *t*-amyloxycarbonyl-L-proline (monomer), *t*-amyloxycarbonyl-L-prolylproline (dimer), *t*-amyloxycarbonyl-L-prolylprolylproline (trimer), *t*-amyloxycarbonyl-L-prolylprolylprolylproline (tetramer), *t*-amyloxycarbonyl-L-prolylprolylprolylprolylproline (pentamer), *t*-amyloxycarbonyl-L-prolylprolylprolylprolylprolylproline (hexamer), and *t*-amyloxycarbonyl-L-prolylprolylprolylprolylprolylprolylprolylproline (octamer).

These oligopeptides were synthesized by Dr. S. Sakakibara (Peptide Center, Institute For Protein Research, Osaka University, Osaka) and one of the present authors (H. Okabayashi).

The poly-L-proline I was synthesized by the polymerization of L-proline-*N*-carboxyanhydride in acetonitrile. The molecular weight was *ca.* 6000. The poly-L-proline II was prepared by transforming the poly-L-proline I into the form II in an acetic acid solution.

The deuterochloroform (isotopic purity: 99%), tetradeuteroacetic acid (isotopic purity: 99%), tetradeuteromethanol (isotopic purity: 99%), and tetramethylsilane used for spectroscopy were manufactured

*1 Parts of this paper were presented at the 21th Annual Meeting of the Chemical Society of Japan, April, 1968, and at the 17th Symposium on High Polymer of the Chemical Society of Japan, October, 1968.

*2 Present Address: Department of Industrial Chemistry, Nagoya Institute of Technology, Gokiso, Showa-ku, Nagoya.

1) T. Isemura, H. Okabayashi and S. Sakakibara, *Biopolymers*, **6**, 307 (1968).

2) H. Okabayashi, T. Isemura and S. Sakakibara, *ibid.*, **6**, 323 (1968).

3) W. Traub and U. Shmueli, in "Aspects of Protein Structure," ed. by G. N. Ramachandran, Academic Press, New York (1963), p. 81.

4) P. M. Cowan and S. McGavin, *Nature*, **176**, 501 (1955).

5) H. Okabayashi, R. Sakai and T. Isemura, Preprint of the 21th Annual Meeting of the Chemical Society of Japan, IV (April, 1968), p. 2685.

6) H. Okabayashi, R. Sakai and T. Isemura, Abstract, at the symposium on High Polymers of the Chemical Society of Japan (October, 1968), p. 721.

7) R. Sakai, H. Okabayashi and T. Isemura, This Bulletin, **42**, 3028 (1969).

by E. Merck Aktiengesellschaft, Darmstedt, Germany. These solvents were used without further purification. Tetramethylsilane (TMS) was used as an internal reference for all the resonance peaks. All the proton magnetic resonance spectra were obtained on a Japan Electron Optics Laboratory (Jeolco) model JNM-4H-100 NMR spectrometer at a frequency of 100 MHz. The spectra of L-proline oligomers at a temperature of 26 ± 2°C were accumulated thirty-two times, using a spectrum accumulator (Jeolco model JPA).

Results and Discussion

According to the NMR studies which have been made by Sakai, Okabayashi, and Isemura,[5-7] the magnetic shielding value of the α-CH peak of the poly-L-proline I was different from that of the form II. The α-CH peaks of the form I appeared at the shielding value of 5.5_{ppm} in a mixed solvent (deuterochloroform : tetradeuteroacetic acid = 8 : 1), and that of the poly-L-proline II, at 5.2 ppm in tetradeuteroacetic acid.

This difference might be due to the different configurations of the peptide groups of the two poly-L-prolines.

Figure 1 show the NMR spectra of the pyrrolidine rings of *t*-amyloxycarbonyl-L-proline and of poly-L-prolines in CD_3COOD. The peak assignments are also included in Fig. 1. The NMR spectrum of the poly-L-proline I in tetradeuteroacetic acid was obtained by measuring it rapidly, as soon as the sample had been completely dissolved. In tetradueteroacetic acid the α-CH peak of the poly-L-proline I has a shielding value of 5.4_{ppm}, and that of *t*-amyloxycarbonyl-L-proline, one of 5.7_{ppm}.

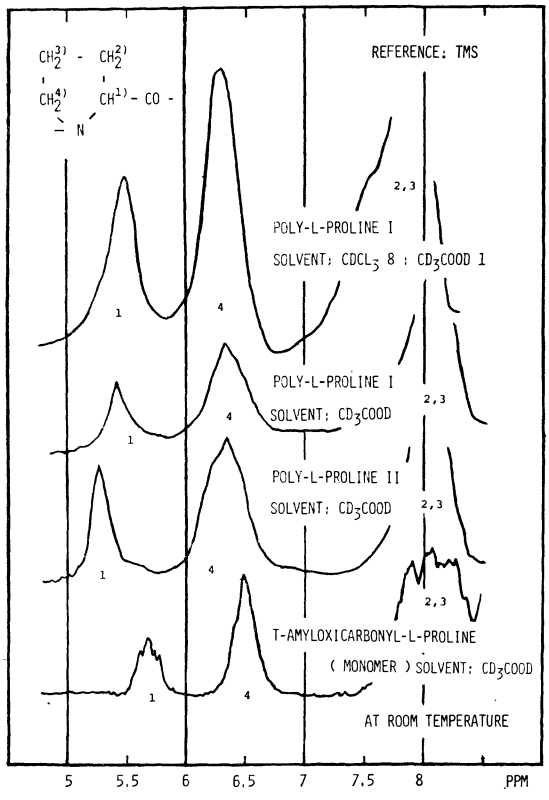

Fig. 1. NMR spectra of *t*-amyloxycarbonyl-L-proline, poly-L-prolines I and II at 26°C.

Figure 2 gives the NMR spectra of *t*-amyloxycarbonyl-L-proline oligopeptides in comparison with those of the poly-L-prolines I and II. The spectra of the oligomers were accumulated thirty-two times by means of the spectrum accumulator.

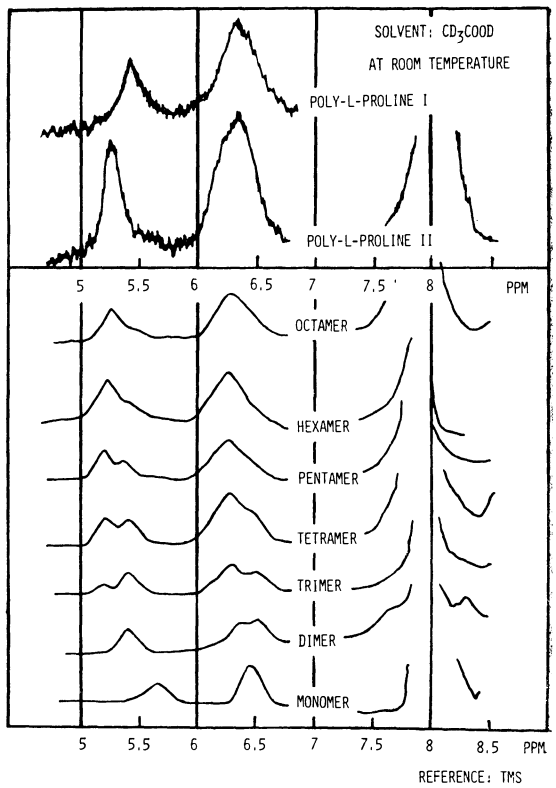

Fig. 2. NMR spectra of *t*-amyloxycarbonyl-L-proline oligopeptides, poly-L-prolines I and II at 26°C.

In the NMR spectra of the dimer, the resonance peak of 5.4_{ppm} is assigned to the two α-CH protons of the dimer. Since the shielding value of the α-CH resonance peak of the dimer is in agreement with that of the poly-L-proline I, it seems that the coincidence suggests the configuration of the dimer. However, it does not always follow that the α-CH resonance peak of the dimer corresponds to the *cis* configuration of the peptide groups of the poly-L-proline I. For the two L-proline residues of the dimer can be regarded as the terminal residues. It is unreasonable to identify the two terminal residues of the dimer with the two residues of the poly-L-proline I. Although there is a probability that the dimer has the *cis* configuration of the peptide group,

TABLE 1. THE RATIOS OF THE AREAS OF THE α-CH PEAKS AT 5.2_{ppm} TO THOSE OF THE OTHER α-CH PEAKS AT 5.4_{ppm}

Oligomers	Trimer	Tetramer	Pentamer	Hexamer	Octamer
Experimental values* (B/A)	2.01 ± 0.03	1.08 ± 0.02	0.66 ± 0.02	0.51 ± 0.02	0.35 ± 0.01
Theoretical values (B/A)	2	1	$2/3\fallingdotseq0.67$	0.5	$1/3\fallingdotseq0.33$

A = Area of the peak at 5.2_{ppm}. B = Area of the peak at 5.4_{ppm}.
* These experimental values were calculated from the NMR spectra of L-proline oligopeptides accumulated for thirty-two times by spectrum accumulator.

the NMR measurement at 100 MHz does not a resolution sufficient to make clear the configuration of the dimer. The NMR spectra at 220 MHz will give the configuration of the two L-proline residues of the dimer.

In the NMR spectra of the trimer, tetramer, pentamer, hexamer, and octamer, two α-CH peaks were observed. The magnetic shielding values of the two peaks in the five oligomers are 5.2 and 5.4_{ppm}. The resonance position of the α-CH peak at 5.2_{ppm} is the same as the α-CH resonance spectrum of the II poly-L-proline gives. Furthermore, as L-prolyl residues increase, the α-CH resonance peak of 5.2_{ppm} increases in intensity, whereas that of 5.4_{ppm} decreases in intensity, as can be well seen in Fig. 2. The behavior of the α-CH resonance peak of 5.2_{ppm} indicates that the peptide groups of the oligomers assume a *trans* configuration with an increase in the chain length.

The fact that the oligopeptides larger than the tetramer assume the conformation of the poly-L-proline II (peptide bonds: *trans*) was established by various methods, as has already been mentioned. Nevertheless, the peak attributable to the conformation of the poly-L-proline I (peptide bonds: *cis*) appears fairly clearly in the NMR spectra of the oligopeptide. If we assume that the α-CH peaks of terminal residues appear around the same position as that for the *cis* configuration, the α-CH peaks of terminal residues may be expected to decrease very regularly with the function of the length of the peptide chain. This inference was clearly suggested by the experimental findings.

In order to discuss the effect of the terminations, it is convenient to assume that, in the α-CH resonance peaks of L-proline oligopeptides, all the α-CH peaks at the magnetic shielding value of 5.4_{ppm} in tetradeuteroacetic acid are to be attributed to the α-CH protons of the two terminal L-proline residues. As has already been mentioned, one of the α-CH peaks at 5.2_{ppm} may be ascribed to the trans configuration of the peptide bonds in the oligopeptides. On the basis of the above assumptions, the ratios of the intensities of the two terminal α-resonance peaks to those of the other α-CH peaks can easily be calculated.

The experimental values of the ratios are obtained from the ratios of the areas of the α-CH resonance peaks at 5.2_{ppm} to those of the other α-CH peaks at 5.4_{ppm}. These experimental ratios are summarized in Table 1, along with the theoretical values.

The experimental values are compared with the theoretical values in Table 1. The agreement of the experimental values with the theoretical values is satisfactory. These facts show that the previous inference is plausible. That is, it may be concluded that the *L*-proline residues placed between the two terminal residues have a poly-L-proline II-like configuration.

In the NMR spectra of the oligopeptides, the change in the δ-CH_2 resonance peaks should be noteworthy. These δ-CH_2 resonance peaks might be related to the conformation of the oligomers. However, it is difficult to obtain information about the configuration of these oligopeptides from the δ-CH_2 resonance peak.

Further information about the effect of the terminal residues on the α-CH resonance peaks and the δ-CH_2 resonance peaks of L-proline oligopeptides can be obtained from the NMR spectra of L-proline oligopeptides, including the deuterized L-prolines.

The authors are grateful to Mr. O. Masuda for recording the NMR spectra.

BULLETIN OF THE CHEMICAL SOCIETY OF JAPAN VOL. 43 362—367 (1970)

Crystal and Molecular Structure of Di-μ-chloro-bis(π-1-ethoxycarbonyl-2-hydroxyallyl)dipalladium(II)

Kunio ODA, Noritake YASUOKA, Tatzuo UEKI,*1 Nobutami KASAI*2 and Masao KAKUDO

Department of Applied Chemistry, Faculty of Engineering, Osaka University, Yamadakami, Suita, Osaka

(Received August 25, 1969)

The crystal and molecular structures of di-μ-chloro-bis-(π-1-ethoxycarbonyl-2-hydroxyallyl)-dipalladium, $(C_6H_9O_3PdCl)_2$ have been determined from the three-dimensional data. The crystals are triclinic; space group $P\bar{1}$; with one dimeric molecule per unit-cell; $a=4.80$, $b=10.31$, $c=10.64$ Å, $\alpha=117.4$, $\beta=102.3$, and $\gamma=84.1°$. The final discrepancy index is 14.0% for 1208 reflections. The two palladium atoms are joined by two chlorine bridges to form a square planar arrangement. The molecule possesses a center of symmetry which coincides with a crystallographic center of symmetry in the crystal; the overall coordination scheme of the palladium atom is similar to that established for the π-allyl palladium chloride dimer. The dihedral angle between the plane of four atoms [Pd, Pd', Cl, and Cl'] and the π-allyl plane is 108. There are intermolecular hydrogen-bonds between the enolic hydroxyl group of one molecule and the carbonyl-group of the other molecule related by the center of symmetry.

A number of π-allylic complexes have been synthesized from palladium(II) chloride and various mono-olefins or conjugated di-olefins.[1] However, few complexes have been synthesized from unsaturated ketones and esters.

The ethanolysis of diketene is accelerated by the addition of sodium tetrachloropalladate(II).[2] The yellow crystals separated at the end of this reaction were identified as di-μ-chloro-bis-(π-1-ethoxycarbonyl-2-hydroxyallyl)dipalladium(II) on the basis of the analytical data, the molecular weight, and the infrared spectrum. The same complex was also prepared directly by the reaction of palladium(II) chloride with ethyl acetoacetate in water.

The IR data reveal that, instead of the usual chelate structure, the complex may have a π-allylic linkage. The stretching absorption bands of O–H and C=O groups are both shifted to lower frequency, indicating the existence of intra- or intermolecular hydrogen-bonding.

Proton magnetic resonance spectra are frequently utilized as one of the most powerful tools in the structural study of π-allylic metal complexes. Unfortunately, however, no suitable inert solvents are available for the present complex. Thus, the three-dimensional X-ray analysis of this complex was carried out in order to determine the exact structure; a preliminary report has already been reported.[3]

Experimental

Di-μ-chloro-bis-(π-1-ethoxycarbonyl-2-hydroxyallyl)-dipalladium, $(C_6H_9O_3PdCl)_2$, was recrystallized as yellow needles in a dark place from a benzene solution. The complex is easily decomposed by the irradiation of the benzene solution by visible light.

By the use of Cu$K\alpha$ radiation, the unit-cell dimensions were determined from (*hk*0), (*h*0*l*), and (0*kl*) Weissenberg photographs, on which the powder patterns of tungsten ($a=3.16535$ Å) were superposed for the calibration. In the least-squares refinement of the cell dimensions, 26 high angle reflections were used.

$$a = 4.80\pm0.01\text{ Å}, \quad \alpha = 117.4\pm0.2°,$$
$$b = 10.31\pm0.06\text{ Å}, \quad \beta = 102.3\pm0.1°,$$
$$c = 10.64\pm0.06\text{ Å}, \quad \gamma = 84.1\pm0.3°.$$

The volume of the unit cell, U, is 457 Å^3; $D_m=1.96$ (by flotation in an aqueous solution of $ZnBr_2$); with $Z=1$ (as a dimeric molecule $(C_6H_9O_3PdCl)_2$; $M=542.0$) $D_c=1.97$ g·cm^{-3}. There was no symmetry in the X-ray photographs except that imposed by the Friedel condition, and the space group is either $P1$ or $P\bar{1}$.

Nickel-filtered Cu$K\alpha$ radiation was used to collect equi-inclination Weissenberg data for the layers from

*1 Present address: Institute for Protein Research, Osaka University, Joan-cho, Kita-ku, Osaka.

*2 To whom any correspondence should be addressed.

1) For example, M. L. H. Green and P. L. I. Nagy, "Advances in Organometallic Chemistry," Vol. 2. ed. by F. G. A. Stone and R. West, Academic Press, New York (1964), p. 325.

2) Y. Tezuka, T. Ogura and S. Kawaguchi, This Bulletin, **42**, 443 (1969).

3) K. Oda, N. Yasuoka, T. Ueki, N. Kasai, M. Kakudo, Y. Tezuka, T. Ogura and S. Kawaguchi, *Chem. Commun.*, **1968**, 989.

$(0kl)$ through $(3kl)$ and from $(hk0)$ through $(hk4)$ by the multiple-film technique. In all, 1323 independent reflections were obtained, but the refinement was carried out by using 1208 reflections with 2θ less than 120°. The relative intensities were estimated visually, and then corrected for Lorentz and polarization factors. As the dimensions of the crystal used in the experiment were about $0.05\times0.08\times0.10$ mm, the absorption correction was ignored ($\mu=98$ cm^{-1}).

Determination and Refinement of the Structure

In the three-dimensionsl Patterson function, the vectors of Pd-Pd′, Pd-Cl, and Pd-Cl′ lie on the same plane, and a centro-symmetrical arrangement of two palladium and two chlorine atoms was easily derived. Therefore, the space group was assumed to be $P\bar{1}$, the structure has been determined satisfactorily in this space group. The other non-hydrogen atoms were found on the three-dimensional electron density map based on the positions of the palladium and chlorine atoms. The positional and isotropic thermal parameters were then refined by a block-diagonal least-squares procedure. After four cycles, the residual, R, was reduced to 0.167 for 1068 non-zero reflections. The isotropic thermal parameters for palladium and chlorine atoms were then expressed in their anisotropic form, using the expression:

$$T = \exp\{-(\beta_{11}h^2 + \beta_{22}k^2 + \beta_{33}l^2 + \beta_{12}hk + \beta_{23}kl + \beta_{13}hl)\},$$

and the least-squares refinement was continued. After a further five cycles of refinement, R was 0.140 ($R=0.170$ for all reflections). At this stage, the refinement was assumed to be finished, since the maximum shift of coordinates was less than 1% of the estimated standard deviation. Hydrogen atoms could not be located on the three-dimensional difference-synthesis, and their contributions to the calculated structure factors have not been estimated.

Throughout the refinement, the neutral atomic scattering factors were taken from those given by Hanson *et al.*[4] The Patterson function was calculated on a NEAC-2200 computer of this university, with the program written by one of the present authors (N.Y.). The least-squares refinement and other calculations were carried out on a HITAC-5020E computer at the University of Tokyo, with programs written by Dr. Tamaichi Ashida.

The final atomic positional parameters, along

Table 1. Final atomic coordinates with their estimated standard deviations ($\times10^2$Å) in parentheses

	x	y	z
Pd	0.2359(0.3)	0.1370(0.3)	0.1142(0.3)
Cl	−0.0120(1.2)	−0.0402(1.1)	0.1361(1.0)
C (1)	0.5072(4.6)	0.2942(4.6)	0.1377(5.1)
C (2)	0.4002(4.4)	0.3516(4.4)	0.2680(4.9)
C (3)	0.4780(3.9)	0.2554(3.9)	0.3216(4.4)
C (4)	0.3278(4.1)	0.2749(4.1)	0.4477(4.5)
C (5)	0.2472(4.5)	0.1693(4.5)	0.5994(4.9)
C (6)	0.4465(8.6)	0.2694(8.6)	0.7497(9.6)
O (1)	0.2262(2.5)	0.4717(2.5)	0.3145(2.8)
O (2)	0.1276(2.6)	0.3636(2.6)	0.4857(2.9)
O (3)	0.4186(3.0)	0.1748(3.0)	0.4976(3.3)

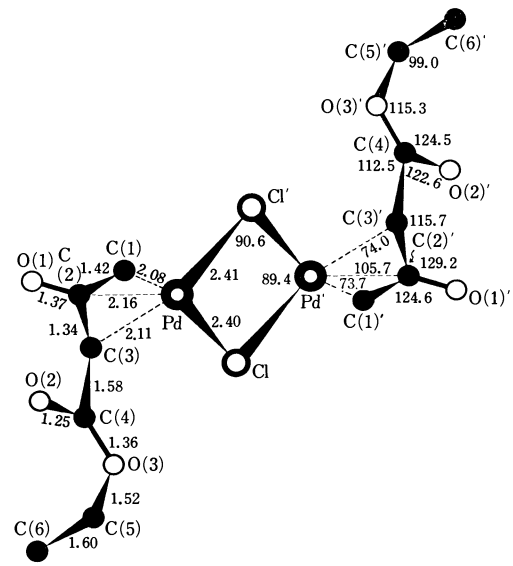

Fig. 1. Plan of the molecule with bond lengths (Å) and bond angles (°).

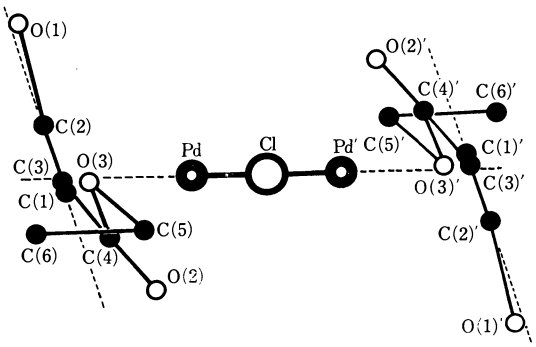

Fig. 2. The molecule viewed along the Cl-Cl′ vector.
Δ_I: Deviations from the plane of four atoms (Pd, Pd′, Cl & Cl′) (Å).
Δ_{II}: Deviations from the allyl plane (Å).

	Δ_I	Δ_{II}		Δ_I	Δ_{II}
C (1)	0.14	0.00	O (1)	2.05	0.13
C (2)	0.72	0.00	O (2)	2.07	0.69
C (3)	0.01	0.00	O (3)	0.01	0.29
C (4)	0.81	0.32			
C (5)	0.73	0.83			
C (6)	0.71	0.56			

4) H. P. Hanson, F. Herman, J. D. Lea and S. S. Skillman, *Acta Crystallogr.*, **17**, 1040 (1964).

TABLE 2.

(a) FINAL ANISOTROPIC THERMAL PARAMETERS ($\times 10^4$) WITH THEIR ESTIMATED STANDARD DEVIATIONS ($\times 10^4$) IN PARENTHESES

	β_{11}	β_{22}	β_{33}	β_{12}	β_{23}	β_{13}
Pd	682(16)	78(3)	69(3)	9(11)	22(5)	60(11)
Cl	1003(76)	135(13)	76(11)	97(49)	81(19)	77(44)

(b) FINAL ISOTROPIC THERMAL PARAMETERS WITH THEIR ESTIMATED STANDARD DEVIATIONS

	B		B		B
C(1)	6.54(0.97)	C(2)	6.08(0.91)	C(3)	5.16(0.78)
C(4)	5.43(0.82)	C(5)	6.17(0.92)	C(6)	14.04(2.42)
O(1)	5.15(0.51)	O(2)	5.50(0.54)	O(3)	6.56(0.63)

TABLE 3. THE OBSERVED AND CALCULATED STRUCTURE FACTORS

L FO FC	L FO FC	L FO FC	L FO FC	L FO FC	L FO FC	L FO FC	L FO FC
H,K= 0 0	H,K= 0 5	-3 21 22	7 14 -25	-9 22 -19	-5 20 18	8 0 8	3 8 6
-9 23 27	-11 14 -19	-2 8 13	8 9 -15	-8 20 -21	-4 0 0	9 11 12	4 23 -23
-8 35 37	-10 16 -22	-1 11 -4	H,K= 1 4	-7 14 -15	-3 29 -25	H,K= 1-10	5 30 -34
-7 26 24	-9 29 -31	0 11 -18	-11 29 -23	-6 7 7	-2 50 -45	0 6 7	6 24 -26
-6 0 -4	-8 8 6	H,K= 0 11	-10 18 -18	-5 27 26	-1 19 -18	1 13 18	H,K= 2 4
-5 86 -78	-7 35 32	-8 13 -13	-9 16 -13	-4 23 28	0 28 -28	2 11 12	-11 9 -1
-4 79 -68	-6 56 56	-7 0 -6	-8 25 21	-3 7 17	1 20 14	3 10 7	-10 10 8
-3 81 -71	-5 41 38	-6 0 7	-7 50 51	-2 0 1	2 38 38	4 10 -5	-9 24 18
-2 12 0	-4 23 18	-5 15 15	-6 55 52	-1 14 -20	3 31 32	5 14 -12	-8 26 22
H,K= 0 1	-3 47 -42	-4 25 21	-5 26 23	0 21 -27	4 29 26	6 14 -17	-7 17 15
-10 14 18	-2 68 -69	-3 17 10	-4 43 -31	1 16 -18	5 15 13	H,K= 1-11	-6 20 -16
-9 19 22	-1 65 -60	-2 0 -2	-3 63 -60	H,K= 1 10	6 23 -18	4 10 9	-5 28 -30
-8 0 12	0 22 -20	H,K= 1 0	-2 83 -89	-10 8 -10	7 25 -26	5 10 -3	-4 35 -36
-7 0 -3	1 21 18	-10 13 15	-1 43 -36	-9 13 -15	8 21 -22	6 0 -9	-3 32 -35
-6 58 -55	2 67 62	-9 12 7	0 24 16	-8 0 -11	9 0 -8	H,K= 2 0	-2 0 -4
-5 51 -45	3 40 38	-8 10 -10	1 71 58	-7 0 2	10 0 0	-10 11 -14	-1 42 44
-4 59 -51	4 17 19	-7 17 -20	2 74 62	-6 0 18	H,K= 1 -5	-9 14 -22	0 45 46
-3 3 -5	5 0 -5	-6 49 -48	3 41 34	-5 10 21	-5 23 23	-8 21 -18	1 31 35
-2 79 71	6 23 -23	-5 27 -23	4 0 -6	-4 7 17	-4 19 20	-7 0 -6	2 0 0
-1 93 125	7 20 -26	-4 6 -3	5 22 -27	-3 7 3	-3 20 16	-6 23 17	3 11 -12
0 74 63	H,K= 0 6	-3 36 32	6 19 -33	-2 0 -17	-2 15 -13	-5 34 24	4 34 -38
1 18 12	-11 16 -16	-2 67 74	H,K= 1 5	-1 23 -26	-1 34 -31	-4 40 40	5 21 -23
2 43 -35	-10 8 -15	-1 88 92	-11 12 -11	0 8 -15	0 39 -41	-3 17 14	H,K= 2 5
3 104 -94	-9 0 -3	1 37 -36	-10 0 -5	H,K= 1 11	1 21 -19	-2 0 -2	-11 11 11
4 91 -75	-8 25 23	2 53 -51	-9 16 11	-3 9 -12	2 21 -16	-1 24 -21	-10 17 14
5 17 -15	-7 34 31	3 75 -66	-8 41 37	H,K= 1 -1	3 31 29	0 27 -37	-9 15 12
6 35 27	-6 41 40	4 51 -43	-7 28 25	-10 15 18	4 36 38	1 23 -25	-8 9 -8
7 32 37	-5 14 12	5 14 11	-6 21 18	-9 22 26	5 41 39	2 17 -18	-7 13 -15
8 37 41	-4 28 -24	6 45 46	-5 10 -10	-8 22 20	6 11 13	3 6 1	-6 21 -19
9 14 14	-3 57 -64	7 32 34	-4 48 -47	-7 0 -1	7 11 -10	4 30 27	-5 28 -26
H,K= 0 2	-2 48 -46	8 22 25	-3 76 -77	-6 41 -38	8 27 -29	5 26 27	-4 8 -7
-10 6 10	-1 36 -32	H,K= 1 1	-2 24 -19	-5 64 -62	9 20 -22	6 19 19	-3 11 8
-9 0 -3	0 36 27	-10 10 -6	-1 11 3	-4 56 -52	10 17 -14	7 0 0	-2 31 35
-8 22 -21	1 64 46	-9 12 -14	0 65 52	-3 13 -8	11 12 3	8 0 -8	-1 20 20
-7 30 -30	2 49 48	-8 34 -29	1 72 58	-2 61 60	H,K= 1 -6	H,K= 2 1	0 24 23
-6 26 -22	3 24 21	-7 30 -25	2 38 32	-1 58 76	-5 12 10	-10 16 -24	1 0 0
-5 21 -17	4 11 -5	-6 0 -4	3 0 -1	0 72 122	-4 31 29	-9 18 -21	2 15 -14
-4 8 8	5 28 -29	-5 31 31	4 12 -27	1 19 18	-3 29 27	-8 9 -4	3 26 -26
-3 53 55	6 25 -29	-4 14 13	H,K= 1 6	2 57 -54	-2 28 23	-7 23 19	4 20 -19
-2 63 63	H,K= 0 7	-3 50 57	-10 10 11	3 85 -84	-1 7 -4	-6 52 45	5 0 -8
-1 46 45	-9 8 15	-2 29 26	-9 25 25	4 71 -64	0 37 -34	-5 34 28	H,K= 2 6
0 30 -26	-8 15 18	-1 20 15	-8 0 1	5 30 -23	1 54 -49	-4 35 28	-11 14 17
1 7 -2	-7 20 20	0 71 -71	-7 11 10	6 15 12	2 36 -35	-3 15 -13	-10 6 6
2 88 -80	-6 0 -1	1 24 10	-6 25 -20	7 38 42	3 0 3	-2 40 -54	-9 14 -12
3 41 -41	-5 15 -14	2 100 -83	-5 32 -31	8 32 35	4 23 21	-1 58 -53	-8 25 -22
4 27 -26	-4 32 -36	3 11 -12	-4 39 -36	9 14 15	5 41 43	0 9 -12	-7 19 -19
5 24 19	-3 43 -39	4 12 7	-3 7 -5	H,K= 1 -2	6 35 34	1 11 -10	-6 19 -19
6 31 35	-2 13 -11	5 43 36	-2 0 5	-9 24 24	7 0 8	2 24 23	-5 8 4
7 34 37	-1 21 17	6 32 27	-1 41 34	-8 31 33	8 12 -13	3 40 37	-4 24 24
8 13 17	0 37 34	7 31 26	0 46 41	-7 25 26	9 25 -25	4 26 27	-3 26 27
H,K= 0 3	1 41 37	H,K= 1 2	1 20 24	-6 9 -4	10 18 -20	5 9 6	-2 14 15
-10 15 -15	2 19 18	-10 25 -23	2 0 -4	-5 52 -48	H,K= 1 -7	6 12 -6	-1 13 13
-9 21 -26	3 0 -3	-9 32 -34	3 11 -17	-4 71 -66	-3 31 33	7 12 -12	0 15 -13
-8 29 -29	4 28 -26	-8 20 -20	4 28 -32	-3 58 -54	-2 29 34	8 16 -17	1 19 -18
-7 22 -19	5 19 -25	H,K= 1 7	H,K= 1 7	-2 15 -10	-1 20 19	H,K= 2 2	2 15 -18
-6 0 4	H,K= 0 8	-7 0 1	-11 10 18	-1 53 58	0 7 -6	-11 15 -20	3 14 -13
-5 46 40	-9 8 14	-6 46 42	-10 7 14	0 80 114	1 33 -30	-10 15 -20	4 0 0
-4 60 61	-8 0 0	-5 33 27	-9 10 2	1 55 62	2 44 -52	-9 12 -13	H,K= 2 7
-3 15 15	-7 0 -8	-4 74 73	-8 12 -12	2 25 19	3 26 -23	-8 23 20	-11 9 5
-2 7 5	-6 16 -17	-3 0 -1	-7 21 -19	3 40 -39	4 9 3	-7 40 37	-10 6 -7
-1 5 -10	-5 24 -25	-2 48 -45	-6 32 -30	4 73 -74	5 23 24	-6 52 45	-9 20 -22
0 43 -45	-4 20 -16	-1 44 -49	-5 15 -11	5 44 -44	6 31 31	-5 30 29	-8 21 -18
1 40 -40	-3 8 5	0 13 -14	-4 10 4	6 19 -16	7 25 26	-4 16 -14	-7 27 -27
2 37 -31	-2 22 17	1 64 -51	-3 28 22	7 15 11	8 0 2	-3 65 -71	-6 0 13
3 0 -3	-1 18 20	2 6 -1	-2 25 24	8 27 27	9 14 -14	-2 37 -50	-5 25 23
4 24 22	0 30 24	3 47 30	-1 23 27	9 20 24	10 16 -15	-1 33 -41	-4 33 32
5 28 30	1 8 10	4 41 33	0 0 2	H,K= 1 -3	H,K= 1 -8	0 3 2	-3 22 19
6 21 24	2 19 -19	5 24 22	1 10 -3	-8 32 30	-3 10 8	1 32 30	-2 11 6
7 10 13	H,K= 0 9	6 19 14	2 24 -20	-7 20 26	-2 25 28	2 74 77	-1 20 -19
H,K= 0 4	7 0 -4	7 14 -18	3 22 -22	-6 29 28	-1 29 29	3 21 17	0 28 -25
-11 5 -9	-9 0 0	H,K= 1 3	4 6 -13	-5 13 -9	0 14 16	4 6 5	1 22 -20
-10 26 -29	-8 17 -15	-11 20 -19	H,K= 1 8	-4 42 -43	1 14 -10	5 16 -18	2 6 -8
-9 23 -26	-7 15 -18	-10 33 -32	-11 11 14	-3 57 -61	2 17 -16	6 20 -24	3 0 5
-8 30 -28	-6 18 -23	-9 29 -26	-10 0 4	-2 27 -27	3 41 -41	7 21 -21	H,K= 2 8
-7 13 11	-5 0 -5	-8 0 0	-9 14 -14	-1 18 -14	4 12 -17	H,K= 2 3	-11 8 -1
-6 44 44	-4 10 12	-7 32 28	-8 25 -22	0 47 46	5 10 2	-11 13 -15	-10 9 -12
-5 61 63	-3 25 22	-6 61 60	-7 30 -30	1 50 53	6 16 17	-10 10 -9	-9 20 -20
-4 26 22	-2 14 16	-5 54 57	-6 0 -5	2 57 62	7 14 16	-9 14 12	-8 14 -18
-3 30 26	-1 23 19	-4 16 10	-5 0 6	3 0 3	8 20 18	-8 28 26	-7 0 0
-2 57 -62	0 11 -3	-3 39 -39	-4 36 31	4 0 1	H,K= 1 -9	-7 45 41	-6 20 20
-1 60 -56	1 8 -13	-2 59 -58	-3 27 26	5 54 -54	-1 11 16	-6 27 23	-5 27 26
0 43 -47	2 9 -17	-1 71 -80	-2 14 17	6 24 -26	0 27 24	-5 4 1	-4 27 26
1 16 -13	H,K= 0 10	0 40 -28	-1 7 0	7 17 -15	1 12 9	-4 67 -71	-3 13 5
2 11 10	-9 7 -10	1 11 6	0 14 -15	8 0 0	2 17 1	-3 42 -43	-2 17 -17
3 44 41	-8 16 -18	2 84 69	1 25 -24	9 0 7	3 10 -12	-2 43 -52	-1 31 -29
4 33 34	-7 21 -21	3 40 31	2 14 -17	10 20 19	4 14 -19	-1 0 1	0 24 -21
5 16 17	-6 0 -4	4 41 33	3 7 -6	H,K= 1 -4	5 12 -18	0 42 44	1 11 -10
6 0 0	-5 6 11	5 10 -2	H,K= 1 9	-7 25 23	6 0 -4	1 63 71	2 14 10
7 0 -11	-4 19 20	6 7 -16	-10 11 -8	-6 18 23	7 0 6	2 30 26	

TABLE 3. THE OBSERVED AND CALCULATED STRUCTURE FACTORS (Continued)

L	FO	FC
H,K= 2 9		
-10	14	-13
-9	11	-9
-8	9	-3
-7	15	15
-6	17	16
-5	21	22
-4	10	2
-3	7	-8
-2	26	-25
-1	22	-20
0	7	-8
H,K= 2 10		
-8	11	9
-7	13	12
-6	13	8
-5	8	1
-4	10	-8
-3	17	-17
-2	16	-14
-1	8	-3
H,K= 2 -1		
-9	9	-5
-8	12	-18
-7	25	-25
-6	14	-11
-5	0	0
-4	21	18
-3	39	37
-2	48	44
-1	11	14
0	16	-18
1	34	-34
2	45	-50
3	30	-22
4	8	0
5	21	18
6	38	37
7	21	22
8	12	3
9	11	-11
H,K= 2 -2		
-7	10	-13
-6	47	-44
-5	24	-20
-4	20	-15
-3	28	24
-2	44	49
-1	62	67
0	13	7
1	9	-5
2	54	-54
3	54	-49
4	37	-36
5	17	15
6	23	19
7	31	34
8	28	19
9	9	1
H,K= 2 -3		
-8	9	15
-7	9	4
-6	24	-21
-5	47	-45
-4	40	-37
-3	9	-6
-2	28	23
-1	49	49
0	63	71
1	16	13
2	24	-22
3	47	-44
4	54	-48
5	22	-18
6	9	8
7	22	21
8	24	23
9	9	13
H,K= 2 -4		
-6	10	3
-5	21	-22
-4	41	-38
-3	41	-37
-2	0	-4
-1	21	22
0	44	44
1	39	39
2	25	22
3	20	-16
4	33	-29
5	36	-31
6	13	-15
7	0	2
8	10	12
9	11	13
H,K= 2 -5		
-5	9	1
-4	18	-17
-3	25	-23
-2	37	-31
-1	10	-7
0	13	11
1	27	23
2	30	28
3	18	18
4	10	6
5	19	-20
6	16	-17
7	15	-15
8	6	-7
9	9	2
H,K= 2 -6		
-5	11	14
-4	9	7
-3	12	-10
-2	15	-13
-1	30	-27
0	19	-18
1	0	0
2	19	20
3	15	13
4	32	29
5	11	10
6	9	-6
7	15	-19
8	12	-15
9	9	-11
H,K= 2 -7		
-3	9	11
-2	10	-3
-1	12	-13
0	29	-26
1	27	-22
2	13	-9
3	23	21
4	17	15
5	28	26
6	14	11
7	10	-5
8	13	-18
9	10	-13
H,K= 2 -8		
-3	20	22
-2	13	13
-1	6	0
0	22	-18
1	26	-21
2	28	-26
3	10	-1
4	12	13
5	24	21
6	18	16
7	11	8
8	9	-5
H,K= 2 -9		
-1	16	12
0	6	0
1	17	-16
2	19	-17
3	20	-18
4	9	-2
5	9	9
6	16	16
7	11	10
H,K= 2-10		
2	12	-8
3	19	-14
4	12	-11
5	0	-3
H,K= 3 0		
-7	24	22
-6	26	23
-5	23	25
-4	7	-9
-3	24	-26
-2	25	-36
-1	24	-23
0	5	-9
1	18	20
2	31	30
3	22	19
4	10	9
5	11	-5
6	14	-16
7	12	-10
H,K= 3 1		
-8	21	19
-7	34	29
-6	22	19
-5	0	2
-4	30	-38
-3	30	-36
-2	37	-36
-1	0	0
0	18	23
1	38	38
2	33	30
3	0	8
4	17	-15
5	21	-20
6	15	-17
7	10	-6
H,K= 3 2		
-10	0	3
-9	18	14
-8	24	22
-7	18	14
-6	0	-2
-5	23	-21
-4	37	-41
-3	20	-26
-2	0	-3
-1	16	19
0	37	40
1	33	35
2	0	3
3	14	-13
4	24	-23
5	22	-21
6	8	-9
H,K= 3 3		
-10	12	11
-9	14	13
-8	9	1
-7	0	-1
-6	21	-20
-5	26	-27
-4	13	-10
-3	5	0
-2	9	12
-1	29	33
0	25	25
1	0	5
2	16	-13
3	14	-14
4	24	-25
5	9	-8
H,K= 3 4		
-11	14	11
-10	11	7
-9	9	-4
-8	14	-9
-7	22	-21
-6	13	-11
-5	8	-5
-4	12	13
-3	11	6
-2	28	33
-1	8	7
0	5	-1
1	11	-11
2	12	-11
3	18	-20
4	9	-4
5	8	4
H,K= 3 5		
-11	8	7
-10	9	-4
-9	17	-15
-8	20	-20
-7	13	-14
-6	8	3
-5	15	12
-4	24	23
-3	22	23
-2	5	3
-1	11	-8
0	17	-13
1	22	-18
2	11	-11
3	12	-1
4	9	10
H,K= 3 6		
-10	14	-13
-9	18	-18
-8	13	-13
-7	0	-5
-6	14	14
-5	33	29
-4	23	19
-3	8	9
-2	13	-14
-1	23	-17
0	27	-25
1	9	-8
2	0	2
3	19	14
H,K= 3 7		
-10	14	-11
-9	14	-13
-8	0	-6
-7	13	11
-6	24	23
-5	19	18
-4	11	9
-3	9	-7
-2	25	-22
-1	29	-25
0	6	-8
1	0	2
2	21	15
H,K= 3 8		
-10	10	-8
-9	11	-2
-8	9	6
-7	14	17
-6	6	7
-5	11	10
-4	0	-7
-3	20	-17
-2	20	-18
-1	8	-8
0	7	2
H,K= 3 9		
-9	10	8
-8	0	8
-7	9	4
-6	6	1
-5	0	-6
-4	13	-12
-3	11	-10
-2	0	-3
-1	9	3
H,K= 3 10		
-5	15	-12
-4	10	-3
H,K= 3 -1		
-9	11	-16
-8	0	-5
-7	0	6
-6	25	23
-5	14	10
-4	24	28
-3	6	-5
-2	17	-18
-1	20	-27
0	10	-12
1	15	-19
2	13	11
3	18	14
4	19	20
5	11	10
6	6	4
7	11	-10
H,K= 3 -2		
-8	8	-13
-7	13	-12
-6	6	5
-5	13	12
-4	17	16
-3	22	19
-2	11	12
-1	11	-9
0	23	-23
1	19	-17
2	20	-22
3	0	0
4	14	14
5	19	16
6	18	17
7	6	5
8	0	-5
H,K= 3 -3		
-7	6	-13
-6	21	-19
-5	0	-2
-4	10	9
-3	24	21
-2	28	25
-1	20	18
0	8	-5
1	25	-25
2	29	-27
3	22	-18
4	0	-2
5	15	12
6	22	21
7	14	14
8	11	5
H,K= 3 -4		
-6	14	-18
-5	24	-21
-4	9	-9
-3	9	9
-2	33	30
-1	29	23
0	22	19
1	8	-3
2	28	-25
3	33	-29
4	21	-16
5	0	3
6	11	9
7	19	18
8	11	11
H,K= 3 -5		
-5	12	-18
-4	22	-20
-3	9	-7
-2	11	4
-1	33	30
0	24	21
1	17	14
2	10	-4
3	16	-13
4	30	-29
5	9	-7
6	9	-1
7	9	8
8	10	10
H,K= 3 -6		
-4	13	-17
-3	12	-14
-2	11	-10
-1	0	3
0	20	19
1	20	18
2	12	10
3	6	0
4	0	-4
5	18	-19
6	9	-8
7	0	-2
H,K= 3 -7		
-3	11	-13
-2	8	-11
-1	14	-11
0	9	0
1	9	7
2	20	17
3	7	7
4	11	8
5	9	-3
6	11	-9
7	11	-11
H,K= 3 -8		
-1	14	-12
0	12	-12
1	10	-3
2	9	4
3	14	13
4	8	11
5	8	7
6	10	-1
H,K= 4 0		
-4	23	-28
-3	15	-9
-2	0	-8
-1	0	10
0	17	20
1	22	21
2	0	3
3	0	-2
4	15	-13
H,K= 4 1		
-4	12	-7
-3	11	-8
-2	0	10
-1	19	18
0	17	20
1	0	5
2	9	-4
3	12	-12
4	15	-14
H,K= 4 2		
-4	5	3
-3	11	4
-2	19	19
-1	14	9
0	0	6
1	9	-5
2	11	-10
3	14	-12
4	8	-6
H,K= 4 3		
-4	10	10
-3	15	12
-2	0	8
-1	0	1
0	7	-10
1	0	-9
2	0	-8
3	8	-5
H,K= 4 4		
-4	15	12
-3	11	11
-2	9	-5
-1	14	-13
0	12	-11
1	0	-8
2	8	-2
3	7	5
H,K= 4 5		
-4	9	8
-3	11	-2
-2	18	-18
-1	14	-11
0	9	-11
1	7	0
2	10	9
H,K= 4 6		
-2	15	-13
-1	8	-11
0	0	0
1	7	10
H,K= 4 7		
-4	5	-7
-3	12	-12
-2	10	-5
H,K= 4 8		
-4	8	-8
H,K= 4 -1		
-4	12	-13
-3	24	-21
-2	19	-15
-1	0	-3
0	6	7
1	15	15
2	23	19
3	9	4
H,K= 4 -2		
-4	7	3
-3	12	-7
-2	16	-16
-1	12	-14
0	0	-5
1	0	4
2	0	9
3	13	12
H,K= 4 -3		
-3	9	4
-2	8	-4
-1	8	-6
0	12	-17
1	0	-6
2	0	0
3	0	6
4	12	9
H,K= 4 -4		
-3	10	11
-2	0	8
-1	0	-3
0	0	-4
1	15	-16
2	11	-10
3	0	-2
4	10	7
H,K= 4 -5		
-2	14	16
-1	0	6
0	0	0
1	8	-7
2	15	-13
3	12	-11
4	10	-1
H,K= 4 -6		
-1	0	14
0	7	7
1	0	0
2	11	-8
3	10	-9
4	14	-10
H,K= 5 0		
-4	4	0
-3	0	2
-2	0	6
-1	8	8
0	6	4
1	9	-1
H,K= 5 1		
-4	10	5
-3	0	3
-2	8	10
H,K= 5 2		
-4	7	4
-3	0	9
-2	8	-2
-1	0	-3
0	5	-6
H,K= 5 3		
0	6	-7
H,K= 5 -1		
-4	8	-9
-3	0	-2
-2	0	4
-1	8	7
0	6	9
H,K= 5 -2		
-3	0	-8
-2	0	-3
-1	0	2
0	8	10
1	7	5

with their estimated standard deviations, are given in Table 1, while the thermal parameters are shown in Table 2. The observed and calculated structure factors are given in Table 3.

Results and Discussion

A plan of the molecule is shown in Fig. 1. The bond distances and angles, along with their estimated standard deviations are listed in Table 4. Figure 2 shows the molecule viewed parallel to the plane containing the chlorine bridge along the Cl-Cl′ line. The refinement is not enough to make a detailed discussion of the bond distances and angles, which may be due to a strong thermal vibration or disorder in the ligand group. Nevertheless, some conclusions can be drawn.

The most important conclusion drawn from the present structure determination is that the π-allyl coordination of the ethyl acetoacetate group to the palladium atom is established for this complex. The coordination configuration resembles those found in the dimeric π-allylpalladium chloride.[5]

Four heavier atoms, palladium and chlorine and their centrosymmetric equivalents, lie on the same plane. This plane of the four atoms fits the equation:

$$-0.765X + 0.595Y + 0.247Z = 0\,.$$

where the orthogonal axes, X, Y, and Z, refer to the triclinic axes by the following transformation:

$$X = ax\cdot\sin\gamma + cz(\cos\beta - \cos\alpha\cdot\cos\gamma)/\sin\gamma$$

$$Y = by + ax\cdot\cos\gamma + cz\cdot\cos\alpha$$

$$Z = cz\{(1 - \cos^2\alpha - \cos^2\beta - \cos^2\gamma + 2\cos\alpha\cdot\cos\beta\cdot\cos\gamma)/\sin^2\gamma\}^{1/2}\,.$$

5) A. E. Smith, *Acta Crystallogr.*, **18**, 331 (1965).

TABLE 4. BOND DISTANCES (Å) AND BOND ANGLES (°) WITH THEIR RESPECTIVE ESTIMATED STANDARD DEVIATIONS IN PARENTHESES

Pd-Cl	2.40(0.01)	Cl-Pd-Cl′	89.4(0.4)
Pd-Cl′	2.41(0.01)	Cl-Pd-C(3)	104.3(1.2)
Pd-C(1)	2.08(0.05)	C(1)-Pd-Cl′	102.7(1.5)
Pp-C(2)	2.16(0.05)	Pd-C(1)-C(2)	73.7(2.9)
Pd-C(3)	2.11(0.04)	Pd-C(3)-C(2)	74.0(2.8)
C(1)-C(2)	1.42(0.07)	Pd-C(2)-O(1)	122.1(3.2)
C(2)-C(3)	1.34(0.07)	C(1)-C(2)-C(3)	105.7(4.3)
C(3)-C(4)	1.58(0.06)	C(1)-C(2)-O(1)	124.6(4.3)
C(5)-C(6)	1.60(0.10)	C(3)-C(2)-O(1)	129.2(4.3)
C(2)-O(1)	1.37(0.06)	C(2)-C(3)-C(4)	115.7(4.0)
C(4)-O(2)	1.25(0.05)	C(3)-C(4)-O(2)	122.6(3.9)
C(4)-O(3)	1.36(0.06)	C(3)-C(4)-O(3)	112.5(3.6)
C(5)-O(3)	1.52(0.06)	O(2)-C(4)-O(3)	124.5(4.0)
		C(4)-O(3)-C(5)	115.3(3.5)
		O(3)-C(5)-C(6)	99.0(4.6)

INTERMOLECULAR HYDROGEN-BOND DISTANCE (Å)

O(1)-O(2)″	2.81(0.04)

DIHEDRAL ANGLES (°)

Pd, Pd′, Cl, Cl′/C(1), C(2), C(3)	108.4
Pd, C(1), C(3)/C(1), C(2), C(3)	106.1

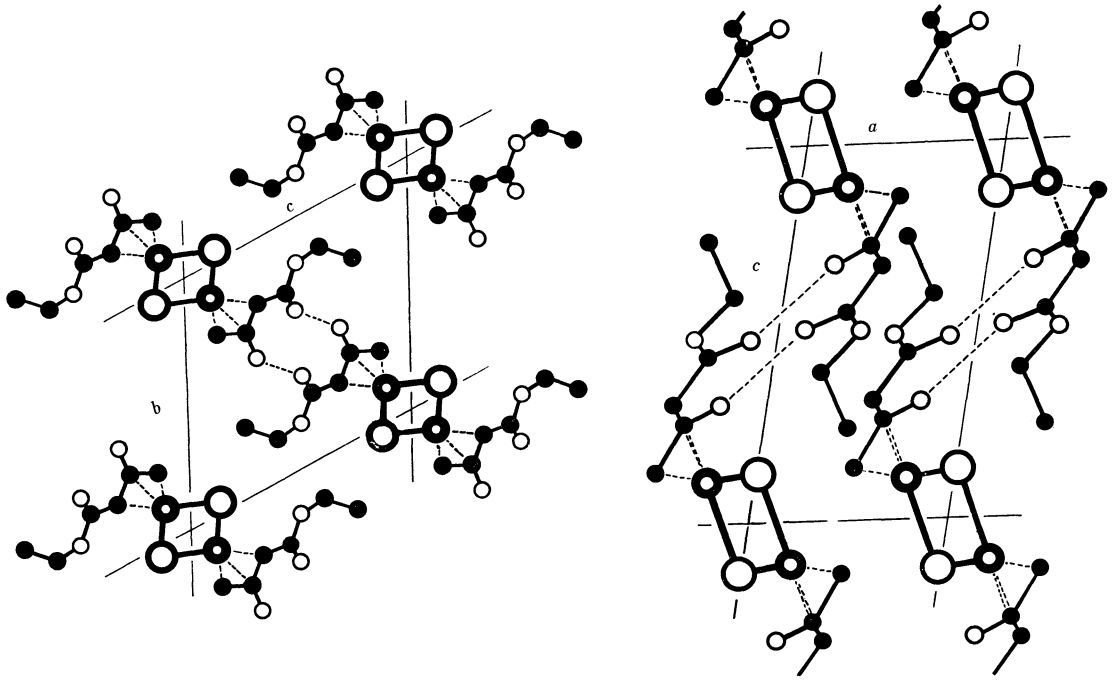

Fig. 3(a) Fig. 3(b)

Fig. 3. Crystal structure.
(a) Projected down along the *a* axis, and (b) Projected down along the *b* axis.

The π-allyl fragment, which must be planar, makes an angle of 108° with this plane of four atoms (Fig. 2) and an angle of 106° with the plane containing the palladium and two carbon atoms, C(1) and C(3). These two values are very similar to those found in other allyl complexes.[6-8] The two carbon atoms of the π-allyl fragment, C(1) and C(3) are 0.13 and 0.10 Å respectively below the plane of the four atoms, while the C(2) atom is 0.72 Å above the plane.

The distance of Pd-Pd′ is 3.418±0.006 Å, which with the values which have previously appeared in the literature;[5,6] this Pd-Pd distance indicates that there is no metal-metal interaction. The average palladium-chlorine distance of 2.41±0.01 Å is identical, within the range of experimental error, with that in dimeric π-allylpalladium chloride, 2.413±0.002 Å.[5] The angle of Cl-Pd-Cl′ is 89.4±0.4°, which is very close to the expected square planar value of 90°. The three palladium-carbon distances are also equal, with a mean of 2.12±0.05 Å, which corresponds to that of 2.117±0.008 Å found in dimeric π-allylpalladium chloride.[5] Recently, it was pointed out that the bonding of the metal to the allyl group is not always symmetrical.[6] A typical example of the symmetrical bonding is π-allylpalladium chloride, while a representative unsymemtrical one is triphenylphosphine-2-methylallylpalladium chloride.[9] In the present complex, however, the symmetrical bonding is again observed.

The C(4) atom bonded to C(3) is 0.32 Å out of the plane of the π-allyl fragment, bent towards the palladium, as can be seen in Fig. 2. The hydroxyl group, a part of the ligand which is attached to the central carbon atom of the π-allyl fragment, does not lie on the π-allyl plane; O(1) is 0.13 Å out of the plane, bent towards the palladium. This value is smaller than that in the triphenylphosphine-2-methylallylpalladium chloride[9] and other π-allylpalladium complexes.[6,7] The shift from the plane may result from the interaction of hydrogen bonds discussed below and from the σ-π electron mixing in the ligand with the metal atom in a way which has been discussed for metal-cyclic ligand bonds by Kettle.[10]

The crystal structure is shown in Fig. 3. The intermolecular atomic contacts less than 4.5 Å were calculated for this complex. None of them, however, is short enough to suggest any significant deviations from normal van der Waals interactions except for the hydrogen bonds.

The hydrogen bonding, between the enolic hydroxyl group of one molecule and the carbonyl group of the other molecules related by the center of symmetry, forms endless sheets of molecules extended along the *c* axis. This hydrogen bond distance is 2.81±0.04 Å.

The authors wish to express their deep thanks to Professor Shinichi Kawaguchi and his co-workers of the Osaka City Univesity for their kindness in supplying crystals and in engaging in helpful discussions. The authors are also indebted to Dr. Tamaichi Ashida for his computer programs.

6) R. Mason and A. G. Wheeler, *J. Chem. Soc., A*, 2549 (1968).

7) R. Uttech and H. Dietrich, *Z. Kristallogr.*, **122**, 60 (1965).

8) M. McPartlin and R. Mason, *Chem. Commun.*, 16 (1967).

9) R. Mason and D. R. Russell, *ibid.*, 26 (1966).

10) S. F. A. Kettle, *Inorg. Chim. Acta*, **1**, 303 (1967).

BULLETIN OF THE CHEMICAL SOCIETY OF JAPAN VOL. 43 368—371 (1970)

Microwave Spectrum of Ethylene Episulfone

Yuji NAKANO, Shuji SAITO and Yonezo MORINO

Sagami Chemical Research Center, Sagamihara-shi, Kanagawa

(Received August 29, 1969)

Microwave spectra of normal, ^{13}C-, and ^{34}S-isotopic species of ethylene episulfone have been investigated. Analysis of the spectra shows that the molecule has the C_{2v} symmetry. The structural parameters obtained from the spectral data for the normal and ^{13}C-ethylene episulfone are: $r(C\text{–}C)=1.590\pm0.011$ Å, $r(C\text{–}S)=1.731\pm0.006$ Å, $r(S\text{–}O)=1.439\pm0.006$ Å, $\angle CSC=54°40'\pm15'$, and $\angle OSO=121°26'\pm30'$, on the assumption that the C–H distances and the $\angle HCH$ and $\angle H_2CC$ angles are the same as those of ethylene sulfide. Stark-effect measurements have yielded a value of 4.41 ± 0.05 D for the dipole moment along the *a* axis. The structure obtained has been compared with those of other related molecules.

Molecules containing the sulfur atom have recently acquired great importance in the field of organic chemistry because they exhibit specific behavior in their chemical reactions. One of the best ways to understand the characteristics of the sulfur-containing compounds is to consider them from the point of view of the molecular structure.

Fundamental molecules which contain sulfur atoms in various oxidation states have been studied by microwave spectroscopy. The r_s structure of dimethyl sulfide was determined by Pierce and Hayashi[1] and by Dreizler and Rudolph,[2] while that of dimethyl sulfoxide was determined by Feder *et al.*[3] As for the structure of three-membered ring compounds, Cunningham *et al.*[4] obtained the r_0 structure of ethylene episulfide, and Saito,[5] that of ethylene episulfoxide. Alkyl sulfones have not been subjected to study by microwave spectroscopy, though there have been a number of investigations by means of X-ray crystallography.[6–8] Desiderato and Sass reported an unusually long distance (1.60 Å) for the ring carbon-carbon bond and a rather short distance (1.73 Å) for the carbon-sulfur bond for *cis*-2-butene episulfone.[8] They pointed out that the anomalies could be explained by a model in which the charge and/or bonds were highly delocalized. Pochan *et al.*[9] determined the three-membered ring stucture of cyclopropanone by microwave spectroscopy; their finding was somewhat similar to that of *cis*-2-butene episulfone in the point of the long carbon-carbon bond.

We have studied the microwave spectrum of ethylene episulfone with the aim of determining its molecular structure accurately. The results obtained settle the controversy regarding the carbon-carbon bonds of episulfone compounds in a convincing way, and, when combined with earlier microwave spectroscopic studies of the simplest and fundamental sulfides and sulfoxides, they provide further insight into the properties of alkyl sulfone compounds.

Experimental

The spectra were observed with a conventional 110 kHz square- or sinusoidal wave Stark modulated spectrometer. Frequencies were reproducible to ±0.1 MHz or better. The sample of ethylene episulfone used in this study was prepared by passing the sulfur dioxide gas through an ether solution of diazomethane cooled at about $-20°C$ according to the method of Hesse and Majmudar[10] and then stored at $-10°C$. Measurements were made at room temperature at a pressure of about 0.01 mmHg. The intensity of the lines decreased slowly in a few hours because of the decomposition or adsorption of the sample in the absorption cell. For the measurement of the ^{13}C-isotopic species, the sample was allowed to flow through the cell in order to maintain the signal-to-noise ratio as high as possible.

Results

A. Microwave Spectrum. The spectrum of the normal isotopic ethylene episulfone was observed

1) L. Pierce and M. Hayashi, *J. Chem. Phys.*, **35**, 479 (1961).
2) H. Dreizler and H. D. Rudolph, *Z. Naturforsch.*, *A*, **17**, 712 (1962).
3) W. Feder, H. Dreizler, H. D. Rudolph and V. Typke, *ibid.*, *A*, **24**, 266 (1969).
4) G. L. Cunningham, Jr., A. W. Boyd, R. J. Myers and W. D. Gwinn, *J. Chem. Phys.*, **19**, 676 (1951).
5) S. Saito, This Bulletin, **42**, 663 (1969).
6) G. A. Jeffrey, *Acta Crystallogr.*, **4**, 58 (1951).
7) D. E. Sands, *Z. Kristallogr.*, **119**, 245 (1963).
8) R. Desiderato and R. L. Sass, *Acta Crystallogr.*, **23**, 430 (1967).
9) J. M. Pochan, J. E. Baldwin and W. H. Flygare, *J. Amer. Chem. Soc.*, **91**, 1896 (1969); **90**, 1072 (1968).
10) G. Hesse and S. Majmudar, *Chem. Ber.*, **93**, 1129 (1960); G. Hesse, E. Reichold and S. Majmudar, *ibid.*, **90**, 2106 (1957).

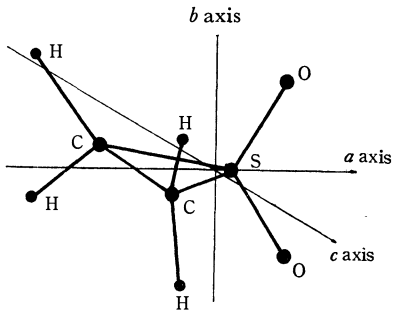

Fig. 1. Principal axes in ethylene episulfone.

by using an oscilloscope. All the *a*-type *R*-branch transitions of $J=2\leftarrow1$ and $3\leftarrow2$ were assigned by means of their well-resolved Stark patterns. Several *Q*-branch transitions were measured by means of a recorder. It was found that the intensities of the transitions depended upon the parity of the limiting prolate quantum number, K_{-1}; the ratios of the intensities of the transitions with even values of K_{-1} to those of the transitions with odd values were about ten to six. This fact suggests that the ethylene episulfone molecule has a C_2 symmetry along the *a* axis, and that there are two sets of two hydrogen atoms interchangeable by rotation about the C_2 axis.[11] Hence, it can be concluded that ethylene episulfone has the C_{2v} molecular symmetry, as shown in Fig. 1. The frequencies of the observed transitions are given in Table 1. The *R*-branch transitions of the ^{34}S-isotopic species in natural abundance were easily identified by means of their Stark effects and by their locations relative to the lines of the normal species. Since the ^{13}C-isotopic species has two equivalent carbon positions, the spectral lines will exhibit half the intensity of the lines for the ^{34}S-isotopic species. It was, however, difficult to assign the transitions of the ^{13}C-isotopic species in natural abundance, because their S/N ratios were about 20 and they were apt to be masked or disturbed by other strong lines. Since the vapor pressure of ethylene episulfone is low below 0°C, it was impossible to increase the intensity of the ground-state lines by cooling the absorption cell. Among the nine *R*-branch transitions of $J=1\leftarrow0$, $2\leftarrow1$, and $3\leftarrow2$, only five transitions were observed and assigned. The observed transitions for ^{13}C- and ^{34}S-isotopic species are listed in Table 2.

Table 1. Observed microwave transition frequencies of normal ethylene episulfone (MHz)

Transition	ν_{obsd}[a]	$\nu_{obsd}-\nu_{calcd}$
$1_{01}\leftarrow0_{00}$	8684.43	0.00
$2_{02}\leftarrow1_{01}$	16951.80	−0.26
$2_{12}\leftarrow1_{11}$	16204.49	−0.24
$2_{11}\leftarrow1_{10}$	18532.84	−0.15
$3_{03}\leftarrow2_{02}$	24648.25	−0.19
$3_{13}\leftarrow2_{12}$	24079.99	−0.17
$3_{12}\leftarrow2_{11}$	27471.37	−0.46
$3_{22}\leftarrow2_{21}$	26052.83	−0.46
$3_{21}\leftarrow2_{20}$	27457.41	−0.73
$4_{04}\leftarrow3_{03}$	32073.25[b]	−0.72
$4_{14}\leftarrow3_{13}$	31793.60[b]	−0.41
$3_{22}\leftarrow3_{03}$	11159.11[c]	0.00
$4_{13}\leftarrow4_{14}$	10995.50[c]	0.01
$4_{23}\leftarrow4_{04}$	13488.11[c]	−0.10
$5_{23}\leftarrow5_{24}$	8230.87[c]	0.01

a) Accuracy, ±0.1 MHz, unless otherwise indicated. b) ±0.2 MHz. c) ±0.3 MHz.

11) C. H. Townes and A. L. Schawlow, "Microwave Spectroscopy," McGraw-Hill, New York (1955), p. 104.

Table 2. Observed microwave transition frequencies of ^{34}S- and ^{13}C-isotopic species (MHz)

Transition	ν_{obsd}[a]	$\nu_{obsd}-\nu_{calcd}$
^{34}S-Species		
$2_{02}\leftarrow1_{01}$	16937.96	0.00
$2_{11}\leftarrow1_{10}$	18513.55	0.00
$3_{03}\leftarrow2_{02}$	24629.87[b]	−0.61
$3_{13}\leftarrow2_{12}$	24059.79	−0.52
$3_{21}\leftarrow2_{20}$	27426.90	0.00
^{13}C-Species		
$2_{12}\leftarrow1_{11}$	15957.48	0.00
$2_{11}\leftarrow1_{10}$	18161.58	0.00
$3_{12}\leftarrow2_{11}$	26955.56	0.54
$3_{22}\leftarrow2_{21}$	25589.54	0.23
$3_{21}\leftarrow2_{20}$	26862.16	0.00
$4_{14}\leftarrow3_{13}$	31356.00[b]	−1.59

a) Accuracy, ±0.1 MHz, unless otherwise indicated. b) ±0.2 MHz.

B. Rotational Constants. The rotational constants of the normal species were determined in the rigid-rotor approximation by using the frequency of the $1_{01}\leftarrow0_{00}$ transition and the values of $(A-C)/2$ and κ obtained from $(A-C)/2$ *versus* κ plots of the *Q*-branch transitions. The results thus obtained are shown in Table 3. The rotational constants for the ^{13}C- and ^{34}S-isotopic species were calculated from three low-J transitions; they are also listed in Table 3. Large errors associated with the A rotational constants for the ^{13}C- and ^{34}S-isotopic species arose from the lack of observed

Table 3. Rotational constants (MHz) and moments of inertia (amu·Å²)[a] for ethylene episulfone

	Normal species	^{34}S-Species	^{13}C-Species
A	6676.58±0.2	6673.87±2.0	6623.35±2.0
B	4924.28±0.1	4918.66±0.1	4815.91±0.1
C	3760.15±0.1	3757.57±0.1	3713.86±0.1
I_a	75.717	75.748	76.326
I_b	102.661	102.778	104.971
I_c	134.444	134.537	136.120

a) Conversion factor is 5.05531×10^5 MHz·amu·Å².

Q-branch lines. Using the rotational constants shown in Table 3, the transition frequencies were calculated; the differences between the calculated and the observed frequencies are given in Tables 1 and 2. The discrepancies seem to be primarily due to the neglect of the centrifugal distortion effects.

C. Dipole Moment. The Stark-effect coefficients were measured for the $M=0$, $1_{01}\leftarrow 0_{00}$ transition and for the $M=0$ and 1 components of the $2_{02}\leftarrow 1_{01}$ transition. The effective electrode spacing was determined from the measurements of the Stark effect of the $1\leftarrow 0$ transition of OCS, using its dipole moment of 0.71521 D obtained by Muenter.[12] The observed values of the Stark coefficients are shown in Table 4. The dipole moment was determined to be 4.41 ± 0.05 D along the a axis.

TABLE 4. STARK COEFFICIENTS[a] AND DIPOLE MOMENTS OF ETHYLENE EPISULFONE

Transition		$\Delta\nu/E^2_{obsd}$	Dipole moment
$1_{01}\leftarrow 0_{00}$	$M=0$	2.980×10^{-4}	4.380D
$2_{02}\leftarrow 1_{01}$	$M=0$	-0.884×10^{-4}	4.417D
	$M=1$	0.671×10^{-4}	4.425D
$\mu=\mu_a=4.41\pm0.05$D			

a) Values in MHz·(V/cm)$^{-2}$.

D. Molecular Structure. As has been described above, the microwave data are strongly indicative of the C_{2v} symmetry for ethylene episulfone; hence, the structural calculations have been carried out on this basis. Since no studies have been made of the deuterated species of ethylene episulfone, scarcely no structural information about the methylene groups was obtained from the moments of inertia for the normal, ^{13}C-, and ^{34}S-isotopic species. We assume that the structural parameters related to the methylene groups are the same as those of ethylene sulfide, that is, r(C–H) = 1.078Å, ∠HCH = 116°0′, and ∠H_2CC = 151°43′,[4] as were assumed for ethylene episulfoxide.[5] Moreover, the moments of inertia for the ^{34}S-isotopic species cannot be used to obtain the molecular structure, for the sulfur atom is located only 0.24 Å from the center of gravity. Four structural parameters between heavy atoms, the S–O and C–S distances and the ∠OSO and ∠CSC angles, were calculated from the moments of inertia for the normal and ^{13}C-isotopic species. First, we used all the moments of inertia simultaneously, but this led to an unreasonable structure, because the I_a and I_c of the normal species and the corresponding moments of inertia for the ^{13}C-species had an almost parallel dependence on the structural parameters to be determined. Therefore, the structure of ethylene episulfone was determined from three moments of inertia for the normal species and the I_b of the ^{13}C-species. The results are given in Table 5. The errors quoted were estimated from the uncertainties of the rotational constants.

Discussion

Two distinct features of the structure of ethylene episulfone are the long C–C bond and the rather short C–S bond. Though the C–C and C–S bond distances obtained above deviate from the corresponding normal single-bond distances by amounts considerably larger than the estimated errors, it is valuable to consider the accuracies of the structure determined in this study. Besides the errors associated with the uncertainties of the rotational constants, there are uncertainties which originate in the assumption made with regard to the methylene groups. It might be expected that the C–H bond distances of ethylene episulfone are different from those of episulfides and episulfoxides, for α hydrogen atoms are highly activated by the introduction of a sulfone group.[13] To estimate the uncertainties due to the unestablished C–H bond distances, a trial calculation was done on an assumption that the C–H distances are longer by 0.01 Å than the value cited in Table 5. The calculated results show that the changes of the distances are −0.002 Å for the C–C bond and +0.001 Å for the C–S bonds; both values are within the estimated uncertainties listed in Table 5. Thus, an unusually long C–C bond and short C–S bonds have been established for ethylene episulfone in spite of the tentatively-assumed C–H distances.

TABLE 5. r_0 STRUCTURE OF ETHYLENE EPISULFONE

r(S–O)	1.439±0.006 Å
r(C–S)	1.731±0.006 Å
r(C–C)[a]	1.590±0.011 Å
∠OSO	121°26′±30′
∠CSC	54°40′±15′
Assumed parameters	
r(C–H)	1.078 Å
∠CHC	116° 0′
∠H_2CC	151°43′

a) C–C distance is not independent of the other parameters listed above.

In order to make the remarkable properties of ethylene episulfone clear, it would be helpful to compare the C–C and C–S bond distances and the ∠CSC and ∠OSO bond angles of related compounds. Table 6 indicates that the three-membered-ring structure of ethylene episulfone is very similar to that of *cis*-2-butene episulfone, although the structure of the former was determined by gas-phase microwave spectroscopy, and that of the

12) J. S. Muenter, *J. Chem. Phys.*, **48**, 4544 (1968).

13) S. Oae, "Chemistry of Organic Sulfur Compounds," Vol. II, Kagakudojin, Kyoto (1969), p. 315.

Table 6. C-S, C-C and S-O bond distances (Å), and ∠CSC and ∠OSO angles in various compounds

Molecule		r(C-S)	r(C-C)	r(S-O)	∠CSC	∠OSO
$(CH_2)_2SO_2$[a]	r_0	1.731	1.590	1.439	54°40′	121°26′
$(CH_2)_2SO$[b]	r_0	1.822	1.504	1.483	48°46′	—
$(CH_2)_2S$[c]	r_0	1.819	1.492	—	48°25′	—
$(CH_3)_2SO_2$[d]	X[n]	1.78	—	1.44	103°	117.9°
$(CH_3)_2SO$[e]	r_s	1.799	—	1.485	96°34′	—
$(CH_3)_2S$[f]	r_s	1.802	—	—	98°52′	—
$(CH_3CH)_2SO_2$[g]	X[n]	1.73_0[o]	1.60[p]	1.42_5[r]	55.4°	120.4°
Thiophene[h]	r_s	1.71_4	—	—	92°10′	—
CS[i]	r_e	1.5349	—	—	—	—
$(CH_2)_2CO$[j]	r_s	—	1.575[q]	—	—	—
$(CH_2)_2NH$[k]	r_0	1.480	—	—	—	—
$(CH_2)_2PH$[l]	r_s	—	1.502	—	—	—
$(CH_2)_2O$[c]	r_0	—	1.472	—	—	—
SO_2[m]	r_e	—	—	1.4307_6	—	119°19.8′

a) This work. b) Ref. 5. c) Ref. 4. d) Ref. 7. e) Ref. 3. f) Ref. 1. g) Ref. 8. h) Ref. 14. i) R. C. Mockler and G. R. Bird, *Phys. Rev.*, **98**, 1837 (1955). j) Ref. 9. k) Ref. 15. l) Ref. 16. m) Ref. 17. n) X-Ray crystallography. o) The mean value of 1.72Å and 1.74Å. p) Ring carbon-carbon bond. q) The C-C bond perpendicular to the CO bond. r) The mean value of 1.41Å and 1.44Å.

latter, by X-ray crystallography.[8] The C–S bond distances of dimethyl sulfide[1] and dimethyl sulfoxide[3] are nearly equal, and those of ethylene episulfide[4] and ethylene sulfoxide[5] are also almost identical. The C–S distance is 0.02 Å longer for alkyl episulfone than for dialkyl sulfone. This difference may be attributable to the ring strain. In accord with the fact that the C–S distance of dimethyl sulfone is shorter than those of dimethyl sulfide and dimethyl sulfoxide, the C–S distance of ethylene episulfone is also shorter than those of ethylene episulfide and ethylene episulfoxide. The decrease is, however, remarkable for the latter; it amounts to 0.09 Å, and, in fact, the C–S distance is almost equal to that of thiophene.[14] Thus, it can be concluded that the C–S bond of ethylene episulfone has a considerable double-bond character.

Contrary to the well-known fact that the C–C bonds of usual three-membered-ring compounds, such as ethylene oxide,[4] ethylene episulfide,[4] ethylene episulfoxide,[5] ethylenimine,[15] and phosphirane,[16] are shorter than the normal C–C single bond, the C–C bond of ethylene episulfone is longer than the normal C–C single bond by the unusually long distance of 0.05 Å. The C–C distance obtained by the present study seems to be the longest among those of the three-membered-ring molecules studied so far by microwave spectroscopy or by other spectroscopic methods. According to the recent study of cyclopropanone by Pochan *et al.*, the length of the C–C bond perpendicular to the CO bond is unusually long (1.575 Å), while that of the C–C bond adjacent to the CO bond is considerably short (1.475 Å).[9] They stated that the 1.575 Å C–C bond was the longest, but in actuality the C–C bond in ethylene episulfone is longer by 0.015 Å.

It is most likely that the unusually long C–C bond distance is strongly correlated with the short C–S bond distance; for instance, the migration of electrons from the C–C bond to the C–S bonds would bring about the increase in the double-bond nature of the latter and the loosening of the former bond. At any rate, the above findings will be interesting in connection with the molecular orbital calculations and will be important and suggestive for the consideration of the reaction mechanisms involving these molecules. Furthermore, the similarity between the structures of ethylene episulfone and cyclopropanone gives interesting support to the similarities between the chemistry of carbonyl and sulfone compounds.

The structures of the SO_2 group of ethylene episulfone, dimethyl sulfone, and *cis*-2-butene episulfone are approximately the same as that of sulfur dioxide.[17] It must be added that the observed value of the dipole moment of ethylene episulfone is close to the sum of the bond moment of the C–S bond for ethylene sulfide[4] and that of the S–O bond for ethylene episulfoxide.[5]

14) B. Bak, D. Christensen, L. Hansen-Nygaard and J. Rastrup-Andersen, *J. Mol. Spectrosc.*, **7**, 58 (1961).
15) T. E. Turner, V. C. Fiora and W. M. Kendrick, *J. Chem. Phys.*, **23**, 1966 (1955).
16) M. T. Bowers, R. A. Beaudet, H. Goldwhite and R. Tang, *J. Amer. Chem. Soc.*, **91**, 17 (1969).
17) S. Saito, *J. Mol. Spectrosc.*, **30**, 1 (1969); Y. Morino, Y. Kikuchi, S. Saito and E. Hirota, *ibid.*, **13**, 95 (1964).

BULLETIN OF THE CHEMICAL SOCIETY OF JAPAN VOL. 43 372—379 (1970)

Frequency Distribution, Specific Heat, and Young's Moduli of Orthorhombic Polyethylene with Skeletal Approximation

Teizo KITAGAWA and Tatsuo MIYAZAWA

Institute for Protein Research, Osaka University Joan-cho, Kita-ku, Osaka

(Received September 2, 1969)

In preliminary studies on the frequency distribution, specific heat and Young's moduli of the orthorhombic polyethylene crystal, methylene groups were treated as single dynamic units. Inter-methylene force constants were estimated from the intermolecular potential function of methane and from deBoer's potential function. Dynamical matrices of acoustic vibrations were constructed. A practical method was worked out for deriving the frequency distribution of acoustic vibrations from the volume enclosed in constant-frequency surfaces in a three-dimensional phase-difference space. With reference to specific heat in the lowest temperature region, inter-methylene force constants were adjusted. An efficient method was used for calculating the frequency distribution of crystal vibrations of chain-polymers. The frequency distribution of orthorhombic polyethylene crystal and specific heats in low temperature region were calculated in agreement with experimental results. A simple approximate method was used for treating Young's moduli of orthorhombic chain-polymer crystals. Applicability of the skeletal approximation is discussed.

Experimental specific heat[1-4] of polyethylene with various degree of crystallinity was extrapolated to 100% crystallinity and specific heat of the crystalline region and amorphous region was obtained by Wunderlich.[5] Stockmeyer and Hecht[6] treated the lattice dynamics of a model crystal with anisotropic force field in a tetragonal lattice. Tarasov[7] treated a chain-polymer crystal model as elastic rods with weak inter-rod interactions. These over-simplified models might be useful in studying temperature dependence of specific heat. However, these models are not applicable for analysing spectroscopic data including infrared and Raman frequencies.

For polymer-chain crystals, the specific heat of the crystalline region is proportional to the third power of absolute temperature in the lowest temperature region, but is nearly proportional to temperature at intermediate temperatures below 70°K. Thus, experimental specific heat may be reproduced[5] by adjusting characteristic frequencies (ν_{D3} and ν_{D1}) of a combination of the three-dimensional and one-dimensional Debye models. However, if the frequency distribution of the combined Debye models is quite different from the actual distribution, the physical meaning of characteristic frequencies (especially ν_{D1}) is not clear.

Specific heat of crystalline material is due to the frequency distribution of crystal vibrations which depend upon the force field. The intramolecular force field of polyethylene[8] and hydrocarbon molecules[9-11] were studied and a general theory of polymer-chain vibrations was derived.[12-14] However, for the purpose of studying frequency distribution, specific heat or neutron-scattering cross sections theoretically, normal vibrations of acoustic branches and optical branches of the three-dimensional crystal need be treated.

A general method of group-theoretical analysis of crystal vibrations was reported previously[15] for orthorhombic crystals. Furthermore, general matrix methods were derived for studying molecular crystals and chain-polymer crystals and for

1) I. V. Sochara, *Dokl. Akad. Nauk SSSR*, **130**, 126 (1960).
2) F. S. Daiton, D. M. Evans, F. E. Hoare and T. P. Melia, *Polymer*, **3**, 277 (1962).
3) L. L. Isaacs and C. W. Garland, *J. Phys. Chem. Solids.*, **23**, 311 (1962).
4) B. Wunderlich, *J. Chem. Phys.*, **37**, 1207 (1962).
5) B. Wunderlich, *ibid.*, **37**, 1221 (1962); *J. Polym. Sci., Part C*, **1**, 41 (1963).
6) W. H. Stockmeyer and C. E. Hecht, *J. Chem. Phys.*, **21**, 1954 (1953).
7) V. V. Tarasov, *J. Chem. Phys.* (USSR), **24**, 111 (1950); *J. Amer. Chem. Soc.*, **80**, 5052 (1958).
8) M. Tasumi, T. Shimanouchi and T. Miyazawa, *J. Mol. Spectrosc.*, **9**, 261 (1962); **11**, 422 (1963).
9) T. Shimanouchi, *Pure Appl. Chem.*, **7**, 261 (1962).
10) J. H. Schachtschneider and R. G. Snyder, *Spectrochim. Acta*, **19**, 117 (1963).
11) H. Takahashi, T. Shimanouchi, K. Fukushima and T. Miyazawa, *J. Mol. Spectrosc.*, **13**, 43 (1964).
12) P. Higgs, *Proc. Roy. Soc.* (London), **220**, 472 (1953).
13) T. Miyazawa, *J. Chem. Phys.*, **35**, 693 (1961).
14) H. Sugeta and T. Miyazawa, *ibid.*, **47**, 2034 (1967).
15) T. Kitagawa and T. Miyazawa, This Bulletin, **42**, 3437 (1969).

approximately calculating the frequency distribution of low frequency lattice vibrations. In the present study, a practical method of calculating frequency distributions of chain-polymer crystals was developed and frequency distribution, specific heat and Young's moduli of polyethylene crystal were treated. Methylene groups were approximately regarded as single dynamic units since internal vibrations of methylene groups lie above 700 cm^{-1} and thus contribute little to specific heat below 150°K. The present study has been reported in a short communication.[16]

Force Field of Polyethylene Crystal

Crystal Structure. The X-ray diffraction of the orthorhombic polyethylene crystal (P_{nam}) was analysed by Bunn.[17] Two molecular chains pass through a unit cell along the c axis and there are four methylene groups per unit cell. Lattice constants at room temperature are $a_0=7.40$, $b_0=4.93$ and $c_0=2.54$ Å, with the bond length of 1.53 Å (C–C) and the bond angle of 112°(C–C–C). The setting angle of the main-chain plane (angle α in Fig. 1) is 48.7°.

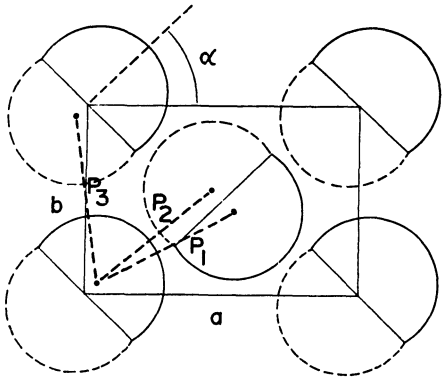

Fig. 1. Interchain potential of polyethylene crystal (skeletal approximation).

Intrachain Force Field. For normal vibration treatment, the force field of the polyethylene crystal was expressed as the sum of the intrachain terms and interchain terms.

$$V(\text{crystal}) = V(\text{intrachain}) + V(\text{interchain}) \quad (1)$$

The intrachain force field used was the Urey-Bradley force field,[9]

$$V(\text{intrachain}) = \frac{1}{2}\sum[K_r(\Delta r)^2 + K_\phi(\Delta\phi)^2 + K_q(\Delta q)^2 + K_t(\Delta t)^2] \quad (2)$$

where K_r, K_ϕ, K_q and K_t are force constants associated with the bond-stretching (Δr), angle-bending ($\Delta\phi$), repulsion (Δq) and internal-rotation coordinates (Δt). The values of intrachain force constants were adjusted (Table 1) so as to reproduce the frequency-dispersion curves of the isolated polyethylene chain.[8] The number of each type of terms per unit cell is listed in Table 1.

Table 1. Force constants and equilibrium distances

	N	d(Å)	Force constant
K_r	4	1.53	4.0 md/Å
K_q	4	2.5	0.35 md/Å
P_1	4	4.12	0.025 md/Å
P_2	8	4.18	
P_3	4	4.51	0.003 md/Å
K_t	4		0.047 md·Å
K_ϕ	4		0.59 md·Å

N; number of potential terms per unit cell.

Interchain Force Field. There are three types of close contacts (p_1, p_2 and p_3 in Fig. 1) between methylene groups of neighboring chains. Accordingly, the interchain force field was expressed as

$$V(\text{interchain}) = \frac{1}{2}\sum[P_1(\Delta p_1)^2 + P_2(\Delta p_2)^2 + P_3(\Delta p_3)^2] \quad (3)$$

where P_1, P_2, and P_3 are the force constants associated with the intermethylene stretching coordinates Δp_1, Δp_2 and Δp_3. These force constants were adjusted with reference to the experimental specific heat[18] at temperatures below 10°K where P_1 and P_2 were taken equal (intermethylene distances are nearly equal).

Acoustic Branches and Specific Heat

Normal Vibration Treatments. For an orthorhombic crystal, normal modes are specified with phase-difference vector $\boldsymbol{\delta}(\delta_a,\delta_b,\delta_c)$, whose components are phase differences of atomic displacements between adjacent unit cells along the a, b, and c axes. A group-theoretical method for constructing symmetry coordinates of orthorhombic crystals was described previously.[15]

For orthorhombic polyethylene, there are four methylene groups per unit cell. If methylene groups are treated as single dynamic units, there are twelve vibrational modes for any given phase-difference vector. Twelve Cartesian symmetry coordinates were described.[15] In the present study, dynamical matrices were diagonalized with a NEAC 2201 electronic computer.

16) T. Miyazawa and T. Kitagawa, *J. Polym. Sci., Part B*, **2**, 395 (1964).
17) C. W. Bunn, *Trans. Faraday Soc.*, **35**, 482 (1939).
18) W. Reese and J. E. Tucker, *J. Chem. Phys.*, **43**, 105 (1965).

Acoustic Branches. Specific heat of a crystal in the lowest temperature region is due to acoustic vibrations of lowest frequencies. Since the frequency distribution of these acoustic vibrations is proportional to the second power of frequency, the specific heat is proportional to the third power of absolute temperature. For a chain-polymer crystal, the coefficient may be derived as a function of interchain force constants.

For an orthorhombic crystal, three acoustic vibrations are reduced, in the limit of $\boldsymbol{\delta}\to 0$, to translations (B_{1u}, B_{2u}, B_{3u}) along the a, b, and c axes. Actually, however, three frequencies are degenerate and accordingly the eigenvector matrix ($\boldsymbol{L}_S$) of the dynamical matrix ($\boldsymbol{D}_S$) is not uniquely determined. The eigenvector matrix $\boldsymbol{L}_S(0)$ may be obtained approximately after diagonalization of $\boldsymbol{L}_S(\boldsymbol{\delta}_0)$ for a very small $\boldsymbol{\delta}_0$.

The eigenvector matrix $\boldsymbol{L}_S(0)$ may be used in deriving the dynamical matrix $\boldsymbol{H}(\boldsymbol{\delta})$ of acoustic vibrations. Thus, elements of the dynamical matrix $\boldsymbol{D}_S(\boldsymbol{\delta})$ [12×12] are expanded up to second power of δ_a, δ_b and δ_c and subsequently are subjected to the orthogonal transformation with $\boldsymbol{L}_S(0)$. In the transformed matrix, cross terms for overall-rotational modes (about the chain axis) and translatory acoustic modes are proportional to the first power of δ_a, δ_b and δ_c. Thus, the second-order perturbation treatment is applied for obtaining the dynamical matrix $\boldsymbol{H}(\boldsymbol{\delta})$ of translatory acoustic modes along the a, b and c axes, respectively,

$$\left.\begin{aligned} H_{11} &= A_1\delta_a^2 + B_1\delta_b^2 + C_1\delta_c^2 \\ H_{22} &= A_2\delta_a^2 + B_2\delta_b^2 + C_2\delta_c^2 \\ H_{33} &= A_3\delta_a^2 + B_3\delta_b^2 + C_3\delta_c^2 \\ H_{23} &= D_1\delta_b\delta_c \\ H_{13} &= D_2\delta_a\delta_c \\ H_{12} &= D_3\delta_a\delta_b \end{aligned}\right\} \quad (4)$$

For the orthorhombic crystal of polyethylene, the coefficients A, B, C and D were obtained as functions of interchain force constants (Table 2). The diagonal element H_{33} is associated with the translatory mode along the c axis and accordingly is independent of P_1 since the contact line (p_1) is perpendicular to the axis. Also, the translatory mode along the c axis involves intrachain distortions and accordingly C_3 is a sum of interchain terms (P_2 and P_3), and a constant intrachain term of 0.0620. It may be mentioned also that C_1, C_2 and C_3 are independent of P_1 because the contact p_1 is between adjacent chains in the ab plane (perpendicular to the c axis). Similarly, A_1, A_2 and A_3 are independent of P_3 because the contact p_3 is between adjacent chains along the b axis (perpendicular the to a axis).

TABLE 2. THE COEFFICIENTS (A, B, C AND D) OF DYNAMICAL MATRIX ELEMENTS FOR ACOUSTIC MODES

H_{11}	A_1	$= 0.0143P_1 + 0.0201P_2$
	B_1	$= 0.0143P_1 + 0.0201P_2 + 0.0110P_3$
	C_1	$= 0.0201P_2 + 0.0003P_3$
H_{22}	A_2	$= 0.0035P_1 + 0.0124P_2$
	B_2	$= 0.0035P_1 + 0.0124P_2 + 0.0646P_3$
	C_2	$= 0.0124P_2 + 0.0161P_3$
H_{33}	A_3	$= 0.0033P_2$
	B_3	$= 0.0033P_2 + 0.0056P_3$
	C_3	$= 0.0033P_2 + 0.0014P_3 + 0.0620$
H_{23}	D_1	$= 0.0127P_2 + 0.0191P_3$
H_{13}	D_2	$= 0.0162P_2$
H_{12}	D_3	$= 0.0142P_1 + 0.0315P_2$

Constant-frequency Surfaces. Frequencies [$\nu_i(\boldsymbol{\delta})$] of three acoustic vibrations may be obtained from eigenvalues [$\lambda_i(\boldsymbol{\delta})$] of a dynamical matrix $\boldsymbol{D}(\boldsymbol{\delta})$,

$$\lambda_i(\boldsymbol{\delta}) = [2\pi c\nu_i(\boldsymbol{\delta})]^2 \quad (5)$$

If off-diagonal terms are negligible as compared with diagonal terms, then eigenvalues (λ_i) approximate to diagonal elements (H_{ii}) and constant-frequency surfaces of acoustic vibrations are ellipsoids in the phase-difference space. The sum of volumes enclosed in three constant-frequency surfaces is given as

$$v(\nu) = (4\pi/3)\times 8\pi^3c^3\nu^3\sum_{i=1}^{3}(A_iB_iC_i)^{-1/2} \quad (6)$$

Actually, however, off-diagonal elements of dynamical matrices are not negligible as compared with diagonal elements, and accordingly diagonalization of dynamical matrices is required. In practical treatments, it may be recalled that all elements of dynamical matrices Eq. (4) are given as quadratic forms of components (δ_a, δ_b, δ_c) of phase-difference vector ($\boldsymbol{\delta}$). Accordingly with the use of spherical polar coordinates[19] in $\boldsymbol{\delta}$ space, phase-differences are now written as

$$\left.\begin{aligned} \delta_a &= |\boldsymbol{\delta}|\cdot\sin\theta\cos\phi \\ \delta_b &= |\boldsymbol{\delta}|\cdot\sin\theta\sin\phi \\ \delta_c &= |\boldsymbol{\delta}|\cdot\cos\theta \end{aligned}\right\} \quad (7)$$

where $|\boldsymbol{\delta}|$ is the length of a phase-difference vector $\boldsymbol{\delta}$. Substituting Eq. (7) into Eq. (4), it may be seen that frequencies (ν_i) of acoustic vibrations are proportional to $|\boldsymbol{\delta}|$ and ratios

$$\rho_i(\theta,\ \phi) = |\boldsymbol{\delta}|/\nu_i(\boldsymbol{\delta}) \quad (8)$$

depend upon the angles θ and ϕ in $\boldsymbol{\delta}$ space. Accordingly, dynamical matrices are now expressed as $\boldsymbol{H}(|\boldsymbol{\delta}|, \theta, \phi)$ and are diagonalized for a given $|\boldsymbol{\delta}|$ but for many samples of θ and ϕ. Then for the ith acoustic branch, the constant-frequency (ν) surfaces may be obtained by numerical calculation of ratios $\rho_i(\theta,\phi)$ as functions of θ and ϕ. The volume enclosed in a constant-frequency (ν) surface of the ith branch is given as

$$v_i(\nu) = (8\nu^3/3)\int_0^{\pi/2}\int_0^{\pi/2}[\rho_i(\theta,\ \phi)]^3\sin\theta\,d\theta\,d\phi \quad (9)$$

19) W. V. Houston, *Rev. Mod. Phys.*, **20**, 161 (1948).

since, for orthorhombic crystals, the irreducible zone of the $\boldsymbol{\delta}$ space is one-eighth of the first Brillouin zone.[15] In practical calculation, numerical integration is carried out with divisions of $\Delta\theta=\pi/90$ and $\Delta\phi=\pi/36$ (confirmed to be sufficiently fine). The sum of volumes enclosed in constant-frequency surfaces of three acoustic vibrations is given as

$$v(\nu) = (8\nu^3/3)\sum_{i=1}^{3}\sum_{\phi}\sum_{\theta}[\rho_i(\theta,\ \phi)]^3 \sin\theta\cdot\Delta\theta\Delta\phi \qquad (10)$$

$$\theta = \pi/180,\ 3\pi/180,\cdots,\ 89\pi/180$$

$$\phi = \pi/72,\ 3\pi/72,\cdots,\ 35\pi/72$$

Frequency Distribution. Under the cyclic boundary condition, allowed phase-difference vectors are distributed uniformly in the first Brillouin zone. Accordingly the number (per unit cell) of acoustic vibrations lying below a given frequency (ν) is given as $v(\nu)/8\pi^3$ since the total volume of the first Brillouin zone is $8\pi^3$. For an orthorhombic crystal containing n equivalent groups (or molecules), the normalized fraction of the number of acoustic vibrations lying between ν and $\nu+d\nu$ is given as $g(\nu)d\nu$, where $g(\nu)$ is obtained by differentiation.

$$g(\nu) = d[v(\nu)/8\pi^3 n]/d\nu = \gamma\nu^2 \qquad (11)$$

$$\gamma = \{\sum_{i=1}^{3}\sum_{\phi}\sum_{\theta}[\rho_i(\theta,\ \phi)]^3 \sin\theta\}\times(\Delta\theta\Delta\phi/n\pi^3) \qquad (12)$$

For the orthorhombic crystal of polyethylene, the number of methylene groups per unit cell is $n=4$.

Specific Heat. The specific heat of a crystal is given as the sum of terms due to crystal vibrations,

$$C_v/R = \sum_{\nu} G(\nu)u^2\exp(-u)[1-\exp(-u)]^{-2} \qquad (13)$$

$$u = hc\nu/kT \qquad (14)$$

where $G(\nu)$ is the normalized distribution (histogram at ν) of vibrational frequencies. In the lowest temperature region, the specific heat is primarily due to the frequency distribution of acoustic vibrations [Eq. (11)]. Accordingly, $G(\nu)$ in Eq. (13) is replaced with $g(\nu)d\nu$ and the integration is carried out yielding

$$C_v/R = \gamma(k/hc)^3T^3\int_0^{\infty} u^4\exp(-u)[1-\exp(-u)]^{-2}du$$

$$= 25.98\,\gamma\,(k/hc)^3T^3 \qquad (15)$$

The value of C_v/RT^3 is therefore proportional to γ which depends upon interchain force constants.

For orthorhombic polyethylene, inter-methylene force constants may be estimated from the intermolecular potential function of methane or from deBoer's potential function (to be discussed later). If estimated values of three constants (P_1, P_2 and P_3) are adjusted under fixed relative ratios, the value of γ is nearly proportional to $P^{-3/2}$. For polyethylene, the value of $10^5C_v/RT^3$ is experimentally obtained as 1.9 (by Isaacs[3]) or as 1.68 (by Tucker and Reese[18]). In the present study, intermethylene force constants were adjusted to $P_1=P_2=0.025$ and $P_3=0.003$ md/Å so that $10^5C_v/RT^3$ is calculated as 1.86.

Frequency Distribution and Specific Heat

Factor-group Modes. For the orthorhombic crystal of polyethylene, there are five lattice modes with $\boldsymbol{\delta}=0$ (factor-group modes, Fig. 2). The B_{2u}, B_{1u} and A_u modes are antiparallel translatory modes along a, b and c axes and A_g and B_{3g} are rotatory modes around the chain axis.[20] These frequencies were calculated as 153, 104 and 47 cm^{-1} and 97 and 100 cm^{-1} with the intermethylene force constants (Table 1).

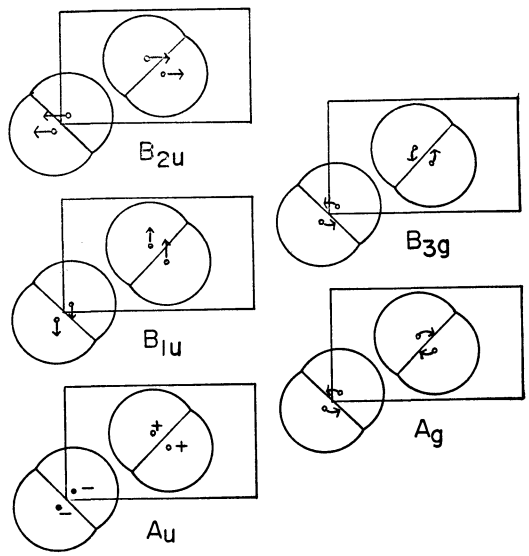

Fig. 2. Lattice vibrations ($\boldsymbol{\delta}=0$) of orthorhombic polyethylene.

Dispersion Curves. For any given phase-difference vector $\boldsymbol{\delta}$, there are eight vibrations of polyethylene below 700 cm^{-1}. Frequencies of these vibrations vary with $\boldsymbol{\delta}$. As an example, the dispersion curves are shown in Fig. 3 for $\boldsymbol{\delta}=(0,0,0)\rightarrow(0,0,\pi)$. It may be noted that, as $\boldsymbol{\delta}\rightarrow 0$, five optical branches become the factor-group modes (Fig. 2) and three acoustic branches are reduced to overall translations along the a, b and c axes. Symmetry assignments (Δ_1—Δ_4) of dispersion curves were made by a group-theoretical treatment.[15] Dispersion curves of the same symmetry species do not intersect one another.

Sampling of Phase-difference Vectors. The frequency distribution of a crystal may be calculated after normal-coordinate treatments of crystal vibrations with all possible phase-difference vectors. Under the cyclic boundary condition, phase-difference components along the a, b or c axis are

20) S. Krimm, C. Y. Liang and G. B. B. M. Sutherland, *J. Chem. Phys.*, **25**, 549 (1956).

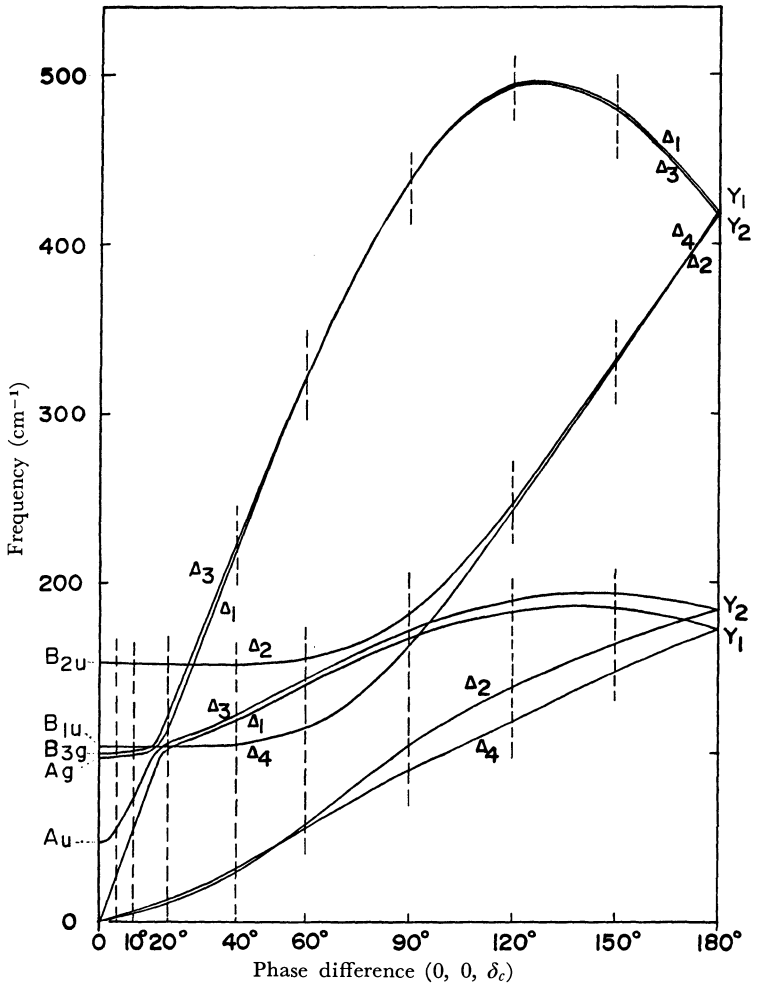

Fig. 3. Dispersion curves [$\boldsymbol{\delta}=(0, 0, 0)\rightarrow(0, 0, \pi)$] of vibrational frequencies of orthorhombic polyethylene (skeletal approximation).

uniformly distributed in the region $-\pi<\delta\leqq\pi$. For an orthorhombic crystal, however, the irreducible volume in $\boldsymbol{\delta}$ space is one eighth ($0\leq\delta\leq\pi$) of the first Brillouin zone.[15]

Vibrational frequencies of chain-polymer crystals change little with δ_a or δ_b, because the interchain force field is much weaker than the intrachain force field. On the other hand, vibrational frequencies change sensitively with δ_c and accordingly it is advisable to take many more values of δ_c than of δ_a or δ_b.

In the present study on polyethylene, the phase-differences of δ_a or δ_b were given nine values (10, 30, 50, ..., 150, and 170°) at an interval of 20°. On the other hand, the phase-difference of δ_c were given 540 values (1/6, 3/6, 5/6, 7/6,..., 1077/6, and 1079°/6 at an interval of 1°/3, yielding a total of 43,740 δ vecotrs in the irreducible volume. However, computation of vibrational frequencies for these many δ vectors is not practical and accordingly it was desirable to use an interpolation method. Thus, for every set of δ_a and δ_b, dynamical matrices were diagonalized to yield vibrational frequencies only for each of ten values of δ_c (0, 5, 10, 20, 40, 60, 90, 120, 150, and 180°). These δ_c values were selected nonuniformly so as to reproduce low-frequencies satisfactorily for small δ_c values (Fig. 3).

Interpolation. For frequency-interpolation, a cubic equation was constructed as

$$\nu(\delta_c) = \mathrm{d}_0 + \mathrm{d}_1\delta_c + \mathrm{d}_2\delta_c^2 + \mathrm{d}_3\delta_c^3 \qquad (16)$$

which satisfies frequencies (ν_1, ν_2, ν_3, and ν_4) for successively selected values of $\delta_c=\delta_1$, δ_2, δ_3 and δ_4. Equation (12) may be used for $\delta_2<\delta_c<\delta_3$ and is applicable to δ_c values of 5—150°. However, the equation for $\delta_1=90°$, $\delta_2=120°$, $\delta_3=150°$ and $\delta_4=180°$ was also used for δ_c values of 150—180°. In practical computation, Eq. (16) was rewritten as

$$\nu(\delta_c) = (\nu_1\ \nu_2\ \nu_3\ \nu_4)\cdot\boldsymbol{w}_\delta \qquad (17)$$

$$\boldsymbol{w}_\delta = \begin{bmatrix} 1 & 1 & 1 & 1 \\ \delta_1 & \delta_2 & \delta_3 & \delta_4 \\ \delta_1^2 & \delta_2^2 & \delta_3^2 & \delta_4^2 \\ \delta_1^3 & \delta_2^3 & \delta_3^3 & \delta_4^3 \end{bmatrix}^{-1} \begin{bmatrix} 1 \\ \delta_c \\ \delta_c^2 \\ \delta_c^3 \end{bmatrix} \tag{18}$$

and the $\boldsymbol{w}_\delta$ vector was used commonly for any set of δ_a and δ_b. For the δ_c values of 0—5°, a quartic equation was constructed as

$$\nu(\delta_c) = d_0' + d_2'\delta_c^2 + d_4'\delta_c^4 \tag{19}$$

which satisfies frequencies for $\delta_c = 0$, 5 and 10°. Vibrational frequencies thus calculated with the interpolation method were confirmed to agree, better than ± 0.7 cm^{-1}, with those calculated with diagonalization of dynamical matrices. Thus, the computation time consumed in frequency calculations for 43740 $\boldsymbol{\delta}$ vectors was drastically reduced.

Frequency Distribution. The frequencies of a total of 349920 vibrations of orthorhombic polyethylene were collected. The frequency distribution was constructed with the frequency interval of 1 cm^{-1} and was then normalized to the vibrational degree of freedom of a methylene group below 700 cm^{-1},

$$\sum_\nu G(\nu) = 2 \tag{20}$$

The frequency distribution histogram of polyethylene crystal (skeletal approximation) is shown in Fig. 4 with a frequency interval of 5 cm^{-1}. Two peaks appear at about 500 and 200 cm^{-1}, as expected previously from dispersion curves of an isolated chain of polyethylene.[8] Existence of these peaks was confirmed by scattering experiments of thermal neutron from crystalline polyethylene.[21,22]

Specific Heat. The normalized frequency distribution $G(\nu)$ [Eq.(20)] was substituted into

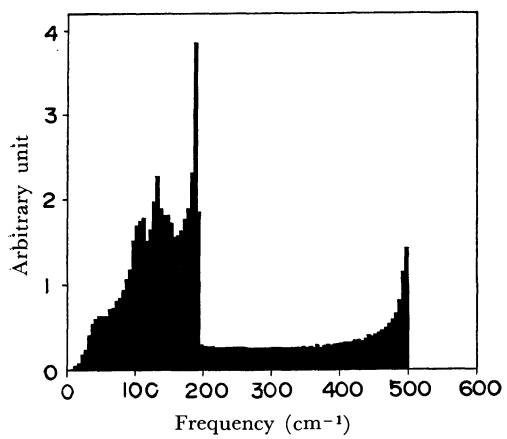

Fig. 4. The frequency distribution histogram of orthorhombic polyethylene crystal (skeletal approximation).

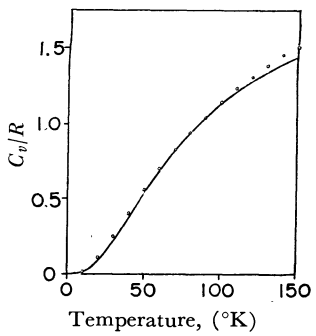

Fig. 5. Specific heat (C_v/R) of orthorhombic polyethylene crystal; open circles: experimental,[5] solid line: calculated with the skeletal approximation.

Eq. (13) and the specific heat at constant volume was obtained as shown in Fig. 5. At temperatures above ~15°K, calculated values of C_v/R gradually deviate from the T^3 law and then become nearly proportional to T, in good agreement with experimental values.[5] The specific heat (C_v/R) due to internal modes of methylene groups was estimated as small as 0.002 at 100°K and as 0.038 at 150°K.

Young's Moduli

Chain-polymer Crystal. For chain-polymer crystals, Young's modulus along the chain direction (c axis) depends primarily upon the intrachain force field whereas Young's moduli along the a or b axes depend primarily upon the interchain force field. Comparison of the calculated and experimental values of Young's moduli (a or b axes) serves as a check on calculated force constants of the interchain force field.

Intrachain forces of chain-polymer crystals are much stronger than interchain forces. Accordingly, in treating Young's moduli along the a or b axes, intrachain displacements (Δc) may well be neglected. Under homogeneous deformation, the potential energy of orthorhombic chain-polymer crystals may be written with two external-deformation coordinates (Δa and Δb) and an internal-deformation coordinate ($\Delta\alpha$) [Fig. 1],

$$V = \frac{1}{2}\tilde{\boldsymbol{\beta}}\boldsymbol{C}\boldsymbol{\beta} \tag{21}$$

$$\tilde{\boldsymbol{\beta}} = (\Delta a\ \Delta b\ \Delta\alpha) \tag{22}$$

where $\boldsymbol{C}$ is the elastic stiffness constant matrix. Then, in equilibrium, the tension (f_a) along the a axis is balanced with $-\partial V/\partial \Delta a$ and the tension (f_b) along the b axis is balanced with $-\partial V/\partial \Delta b$, but the internal tension (f_α) is always equal to zero so that $\partial V/\partial \Delta\alpha = 0$. Under homogeneous deformation, therefore,

$$\boldsymbol{\beta} = \begin{bmatrix} S_{11} & S_{12} & S_{13} \\ S_{21} & S_{22} & S_{23} \\ S_{31} & S_{32} & S_{33} \end{bmatrix} \begin{bmatrix} f_a \\ f_b \\ 0 \end{bmatrix} \tag{23}$$

21) H. R. Danner, G. J. Safford, H. Boutin and M. Berger, *J. Chem. Phys.*, **40**, 1417 (1964).
22) W. R. Myers, J. L. Donovan and J. S. King, *ibid.*, **42**, 4299 (1965).

where $\boldsymbol{S}(=\boldsymbol{C}^{-1})$ is the elastic compliance matrix. From Eq. (23) Young's moduli along the a and b axes are derived as

$$\left.\begin{aligned} E_a &= a_0/b_0c_0S_{11} \\ E_b &= b_0/a_0c_0S_{22} \end{aligned}\right\} \quad (23)$$

Relative ratio of external and internal deformations $[(\Delta a/a_0) : (\Delta b/b_0) : \Delta\alpha]$ is equal to $[(S_{11}/a_0) : (S_{21}/b_0) : S_{31}]$ under the tension of f_a, but is equal to $[(S_{12}/a_0) : (S_{22}/b_0) : S_{32}]$ under the tension f_b.

Polyethylene. Young's moduli (in unit of 10^{11} dyne/cm^2) of orthorhombic polyethylene crystal were calculated as $E_a=0.9$ and $E_b=0.3$, from the interchain force constants at lowest temperatures. In comparison, experimental values[23] at room temperature are $E_a=0.4$ and $E_b=0.3$.

Discussions

Intermethylene Force Constants. Effective force constants of $CH_2\cdots CH_2$ contacts (p) are useful for studying crystal vibrations and solid state properties of hydrocarbon polymers. Intermethylene force constants may be transferred from the second derivative (kcal/Å^2) of intermolecular potential (V) of methane,[24]

$$d^2V/dp^2 = 2.008\times 10^9/p^{14} - 1.630\times 10^5/p^8 \quad (25)$$

Thus for intermethylene contacts of $p_1=4.12$, $p_2=4.18$ and $p_3=4.51$ Å, intermethylene force constants at room temperature were calculated as $P_1=0.018$, $P_2=0.015$ and $P_3=0.002$ md/Å, respectively. If these intermethylene constants at room temperature are used, the specific heats at temperatures below 10°K are calculated slightly larger than the experimental data, indicating that intermethylene constants at <10°K should be larger than those at room temperature. In fact, at lower temperatures, intermethylene contacts become shorter and intermethylene force constants are expected to become larger than those at room temperature.

In treating elastic constants of polyethylene crystal, interchain force constants were derived by Odajima and Maeda[25] from deBoer's repulsive potential function[26] for H$\cdots$H contacts (x). Force constants (in unit of md/Å) are given as

$$d^2V/dx^2 = 150\cdot\exp(-3.53x) \quad (26)$$

In the present study, Eq.(26) was transferred to the case of intermethylene force constants. Actual intermethylene contacts (p) were converted to corresponding H$\cdots$H contacts (x),

$$x = (r_H/r_{CH_2})p \quad (27)$$

where r_H and r_{CH_2}, are van der Waals' radii[27] of hydrogen (1.2Å) and methylene group (2.0Å). Thus, from intermethylene contacts, force constants of orthorhombic polyethylene crystal were estimated as $P_1=0.024$, $P_2=0.022$, and $P_3=0.003$ md/Å. With reference to experimental specific heats at temperatures below 10°K, these values of force constants were only slightly adjusted to yield the final set of force constants as listed in Table 1. Equations (26) and (27) were also used for estimating effective interchain force constants of orthorhombic polyoxymethylene crystal.[28]

Constant-frequency Surfaces. In the dynamical matrices of acoustic vibrations of polyethylene crystal, off-diagonal elements may not be neglected as compared with diagonal elements. Accordingly, constant-frequency surfaces of polyethylene are much distorted from ellipsoidal surfaces. However, if off-diagonal elements are neglected, constant-frequency surfaces become ellipsoidal, and the specific heat ($10^5C_v/RT^3$) in the lowest temperature region is calculated as 1.02, that is much smaller than the theoretically correct value of 1.86. Accordingly, off-diagonal elements of dynamical matrices can not be neglected, and the volume enclosed in constant-frequency surfaces need be numerically integrated with Eqs. (7)—(10).

Frequency Distribution. The prominent peaks of the frequency distribution (Fig. 4) at 500 and 200 cm^{-1} correspond to the maximum frequencies of the dispersion curves of the C–C–C bending branches and C–C internal-rotation branches around δ_c values of 120—150° (Fig. 3). In the region 450—200 cm^{-1}, four dispersion curves of the C–C–C bending branches are almost straight and depend little upon δ_a or δ_b. Accordingly, the frequency distribution is nearly constant in the region 450—200 cm^{-1}, as expected similarly for Debye's one-dimensional elastic continuum.[29]

In the frequency distribution of polyethylene (Fig. 4), there is a peak at the high-frequency cut-off of 500 cm^{-1} but, with Tarasov's model, no peak is expected to appear at the one-dimensional characteristic frequency (ν_{D1}). With the three-dimensional Debye model, a peak is expected to appear at the cut-off frequency (ν_{D3}) below which the frequency distribution is proportional to ν^2. In the frequency distribution of polyethylene (Fig. 4), a ν_{D3} peak can not be identified uniquely among several peaks due to low-frequency optical modes. The characteristic frequencies were adjusted[5] to $\nu_{D1}=375$ cm^{-1} and $\nu_{D3}=85$ cm^{-1} so as to reproduce experimental specific heat. However, these can not be identified uniquely in the frequency

23) I. Sakurada, T. Ito and K. Nakamae, *J. Polym. Sci., Part C*, **15**, 75 (1966).
24) I. Miyagawa, *Nippon Kagaku Zasshi*, **75**, 1169, 1173, 1177 (1954).
25) A. Odajima and T. Maeda, *J. Polym. Sci., Part C*, **15**, 55 (1966).
26) J. deBoer, *Physica*, **1**, 363 (1942).
27) L. Pauling, "The Nature of Chemical Bonds," Cornell University Press, Ithaca, New York (1960).
28) T. Kitagawa and T. Miyazawa, *Rept. Progr. Polym. Phys. Jap.*, **9**, 175 (1966); Int. Sym. Macromol. Chem., Tokyo (paper 2.5.04) (1966).
29) P. Debye, *Ann. Phys.*, **39**, 789 (1912).

distribution of polyethylene (Fig. 4).

Skeletal Approximation. In the normal vibration treatment of orthorhombic polyethylene crystal by Tasumi and Shimanouchi,[30] hydrogen atoms as well as carbon atoms were treated as single dynamic units and the factor group frequencies were calculated as 134(A_g), 109(B_{3g}), 99(B_{2u}), 71(B_{1u}), and 55 cm^{-1}(A_u). It may be remarked that the requencies of the rotatory modes (A_g and B_{3g}) are higher than the frequencies of the translatory modes (B_{2u} and B_{1u}). In the present study, the lattice dynamics of polyethylene was studied where methylene groups were treated as single dynamic units at sites of carbon atoms. With this skeletal approximation, the frequencies of the rotatory modes are lower than the frequencies of the translatory modes.

30) M. Tasumi and T. Shimanouchi, *J. Chem. Phys.*, **43**, 1245 (1965).

In the rotatory modes of polyethylene chain about the axis, displacements of carbon atoms are much smaller than those of hydrogen atoms. Accordingly, changes in intermethylene contacts are much smaller than in inter-hydrogen contacts. Therefore, the rotatory frequencies calculated with the skeletal approximation are lower than those calculated by Tasumi.[30]

On the other hand, in the translatory modes of polyethylene chain, displacements of carbon atoms are equal to displacements of hydrogen atoms. Accordingly, changes in intermethylene contacts do not differ much from changes in inter-hydrogen contacts and the skeletal approximation is fairly applicable. In fact, intermethylene force constants estimated from deBoer's potential function were only slightly adjusted so as to reproduce experimental specific heat in the lowest temperature region.

BULLETIN OF THE CHEMICAL SOCIETY OF JAPAN VOL. 43 379—387 (1970)

Nuclear Magnetic Resonance in Paramagnetic Solution. Proton Magnetic Resonance Studies of Some Substituted Aniline Derivatives in the Presence of Paramagnetic Ni(II) and Co(II) Acetylacetonates

Teijiro YONEZAWA, Isao MORISHIMA, Yoshinori AKANA and Kazuhiko FUKUTA

Department of Hydrocarbon Chemistry, Faculty of Engineering, Kyoto University, Sakyo-ku, Kyoto

(Received September 9, 1969)

To study the geometrical and electronic structures of molecules, the paramagnetic shifts of substituted aniline proton resonances due to complexing with nickel or cobalt acetylacetonates, $M(AA)_2$ (M=Ni or Co), were observed. The NMR spectra of solutions containing an excess of aniline derivatives and $M(AA)_2$ show contact (for $Ni(AA)_2$) and pseudocontact (for $Co(AA)_2$) shift ratios for various ligand protons. The contact shift ratios for N–H and $N–CH_3$ protons reveal that the NH_2 or NHR group of aniline derivatives is not coplanar with the aromatic ring for the coordinated molecules. This was confirmed by pseudo-contact shift studies.

Recently we have been interested in the NMR spectra of solutions containing ligand molecules and the paramagnetic metal chelate.[1] The paramagnetic ("contact") shifts and the dipolar ("pseudo-contact") shifts have been pointed out as being useful in the elucidation of the structure of the complex, the nature of metal-ligand bonding, and the mechanism of the odd-electron distribution.[1] From a simple observation of the relative contact shift of different protons in a ligand molecule with the oriented nitrogen lone pairs available for bonding with the metal, the electron-spin distribution occurring through the σ or π bond framework of a ligand molecule is made clear.[1d]

In the present work the paramagnetic contact and pseudocontact shifts of substituted aniline proton resonances due to complexing with nickel or cobalt acetylacetonate, $M(AA)_2$, were studied.

Previously Kluiber and Horrocks reported similar observations and discussed spin delocalization through a π-orbital in relation to a metal-ligand interaction.[2] In the present investigation, we have studied the configuration of such metal complexes from different points of view. We have indicated

1) a) D. R. Eaton and W. D. Phillips, *Advan. Magnetic Resonance*, **1**, 103 (1965). b) J. A. Hakpe and R. L. Ward, *J. Chem. Phys.*, **39**, 1211 (1963). c) W. D. Horrocks, Jr., R. C. Taylor and G. N. LaMar, *J. Amer. Chem. Soc.*, **86**, 3031 (1964). d) T. Yonezawa, I. Morishima and Y. Ohmori, *ibid.*, **92** (1970), in press.

2) R. W. Kluiber and W. D. Horrocks, Jr., *Inorg. Chem.*, **6**, 431 (1967).

that the amino group coordinated to metal acetylacetonate is non-planar and has the hybridized nitrogen lone-pair orbital available for bonding with the metal.

Aniline may be considered to be a molecule of the general type of NH_2X, in which X is an unsaturated system which may act as an electron reservoir. A recent microwave study[3] has shown that the amino-nitrogen atoms in these types of molecules (aniline; X=C_6H_5; formamide, X=CHO; cyanamide, X=CN; nitramide, X=NO_2) retain, to a greater or lesser extent, pyramidal configurations.

In the present investigation we have examined the orientation of nitrogen lone-pair electrons of aniline by a study of the paramagnetic proton shifts. For this study we have selected a series of substituted aniline derivatives (1—11) and examined the structures of complexes to determine whether they take a planar (I) or a non-planar structure (II).

Planar Non-Planar

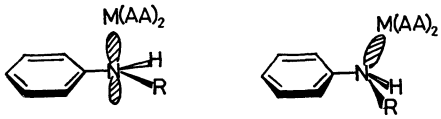

(I) (II)

N-Phenyl aziridine (11) was used as the molecule with a typical non-planar structure (II) at the nitrogen atom.

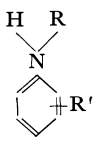

	R	R'
1.	H	H
2.	H	*o*-CH_3
3.	H	*m*-CH_3
4.	H	*p*-CH_3
5.	CH_3	H
6.	CH_3	*m*-CH_3
7.	H	*o*-C_2H_5
8.	H	*p*-C_2H_5
9.	C_2H_5	H
10.	H	*o*-di(CH_3)$_2$

11. 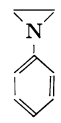

The NMR spectra of solutions containing an excess of aniline derivatives and $M(AA)_2$ (M=Ni or Co) provide isotropic contact and pseudocontact shifts.[1b,c] The contact shift reflects the mode of the odd-electron distribution in which σ and/or π orbital are concerned, while the pseudocontact shift depends on the geometric structure of the complexed molecules.

It has been well established that induced paramagnetic shifts of protons of ligand complexed with $Ni(AA)_2$ come predominantly from isotropic contact interaction, while the corresponding shift for $Co(AA)_2$-complex system involves the shift due to both contact and pseudocontact interactions.[1] The contact interaction shift is described by Eq. (1):

$$\left(\frac{\Delta\nu}{\nu}\right)_i = \left(\frac{\Delta H}{H}\right)_i = -A_i \frac{\gamma_e}{\gamma_H} \frac{g\beta S(S+1)}{3kT} \qquad (1)$$

where A_i is the isotropic hyperfine contact interaction constant for the ith proton and where the other symbols have their usual meaning.[1] A_i is a measure of the amount of unpaired spin density at the ith proton. The other isotropic mechanism, the pseudocontact interaction (spin dipole-dipole interaction), may be important if there is an anisotropy in the g-tensor of the paramagnetic complex. The shift due to this cause is described by Eq. (2) for axially-symmetric molecules:[1]

$$\left(\frac{\Delta\nu}{\nu}\right)_i = \left(\frac{\Delta H}{H}\right)_i = -\frac{\beta^2 S(s+1)}{27kT}(g_{//} + 2g_\perp) \times (g_{//} - g_\perp)\frac{3\cos^2\theta_i - 1}{r_i} \qquad (2)$$

Here, θ_i is the angle between the ligand-field axis of the complex and the radius vector, r_i, from the metal atom to the ith proton, and $g_{//}$ and $g_\perp$ are g-factors parallel and perpendicular to the ligand-field axis respectively. In the present study, the metal-nitrogen bond serves to define the ligand-field axis.

For mono-N-substituted anilines, the relative contact shift of N–H and N–methyl protons was found to be nearly the same at that for alkyl amines. This is an evidence of a pyramidal structure of the amino-nitrogen atom of aniline derivatives. The preference for non-planar configuration of complexed anilines was further confirmed by pseudocontact-shift studies. The location of metal coordinated at the nitrogen atom was determined from the pseudocontact shift for the $Co(AA)_2$ system.

Experimental

All the chemicals except for the No. 11 compound were obtained from a standard commercial source (Tokyo Kasei Co.). The *N*-phenylaziridine was given kindly by Mr. Kondo of our department. Commercially-available $Ni(AA)_2$ and $Co(AA)_2$ were dried *in vacuo* over 24 hr at 55°C.

The proton spectra were obtained at 60 MHz for $CDCl_3$ solutions containing various amounts of ligand and $Ni(AA)_2$ or $Co(AA)_2$. A typical spectrum is shown in Fig. 1 from $CDCl_3$ solutions of $Ni(AA)_2$ and $Co(AA)_2$ containing excess *N*-methyl-*m*-methyl aniline. The paramagnetic shifts of benzene-ring and N-CH_3 protons were observed at 0.8 M ligand and 0.3 M $Ni(AA)_2$ (0.1 M $Ni(AA)_2$ for N-H protons) concentrations in deuterochloroform at room temperature, using tetramethylsilane as the internal standard.

Results and Discussion

The proton-resonance positions in a paramagnetic solution were shifted from a diamagnetic position to a higher or lower field by an amount proportional to the concentration of $Ni(AA)_2$ or $Co(AA)_2$. The large isotropic resonance shifts allow us to observe proton spin-spin splitting in the simplest, first-order spectra of aniline derivatives in the presence of $Co(AA)_2$ (see Fig. 1-c).

3) D. G. Lister and T. K. Tyler, *Chem. Commun.*, **1966**, 152.

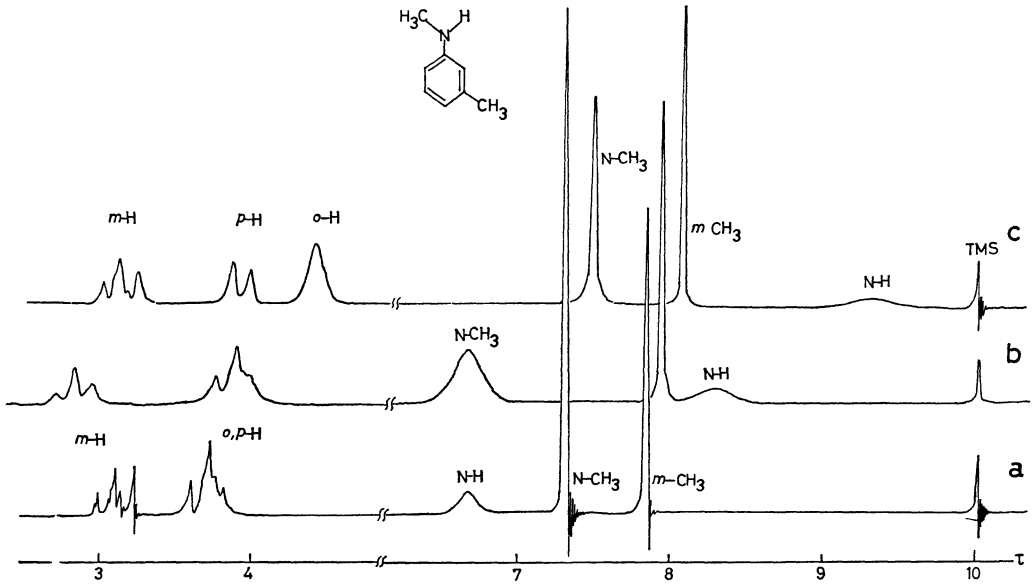

Fig. 1. Proton spectrum of *N*-methyl-*m*-methyl aniline alone and in the presence of $Ni(AA)_2$ or $Co(AA)_2$ in $CDCl_3$ solution.

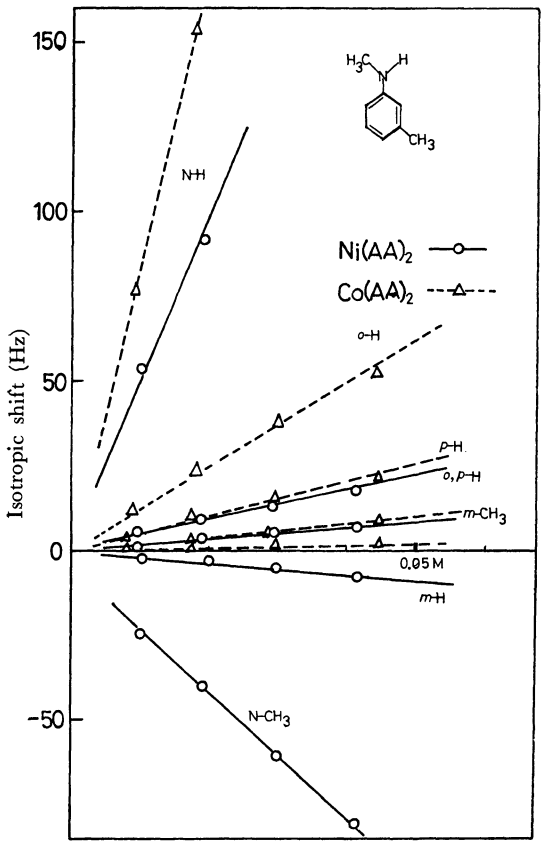

Fig. 2. Plots of the isotropic paramagnetic shifts *vs.* concentration of $Ni(AA)_2$ or $Co(AA)_2$ in $CDCl_3$ solution.

The observed coupling constants of *ortho-meta* and *meta-para* couplings for aniline are 7.5 Hz and 7.1 Hz respectively, for example. The observed isotropic shifts for ring and *N*-substituent protons are plotted against the amount of added $M(AA)_2$. A representative linear plot is given for *N*-methyl-*m*-methylaniline in Fig. 2. The concentration employed here ranges from 0 to 0.82 mol/*l* for ligand molecules and from 0 to 0.05 mol/*l* for $M(AA)_2$. The relative paramagnetic shifts for each proton are equal to the relative values of the slope of the linear plots for each proton. These values are given in Tables 1 and 2, taking the shift of the *ortho* proton in each molecule as 10.00. A positive or negative sign stands for an upfield or a downfield paramagnetic shift respectively. The N-H proton signal became broad and shifted strongly upfield for both nickel and cobalt systems. Phenyl-ring protons exhibit alternating upfield and downfield shifts with no attenuation, characteristic of π-orbital spin delocalization.[1c] The similar magnitudes but opposite signs for the contact shifts of a methyl group and a phenyl proton of the same position in aniline derivatives are also characteristic of the π-delocalization predicted by the theory of McConnell.[4] For the $Co(AA)_2$ system the corresponding proton resonance shifts are all upfield except for that of the *para*-methyl group. Unequal for *ortho* and *para* ring protons were observed, unlike as in the $Ni(AA)_2$ system. For both systems, mono- and di-*N*-alkyl anilines coordinate much less effectively

4) H. M. McConnell, *J. Chem. Phys.*, **24**, 764 (1956); *ibid.*, **28**, 1188 (1958).

TABLE 1. RELATIVE ISOTROPIC SHIFTS IN ANILINES COMPLEXED WITH $Ni(AA)_2$

	R	R'	Absolute[a] shift	Relative shfts							
				Ring proton			Aryl CH_3 or CH_2			NH	N-CH_3 or CH_2
				o	*m*	*p*	*o*	*m*	*p*		
1	H	H'	48.0	10.0[b]	−4.17	10.0[b]					
2	H	*o*-CH_3	30.4	10.0	−4.05	10.0	−6.80				
3	H	*m*-CH_3	44.0	10.0	−4.09	10.0		3.75			
4	H	*p*-CH_3	32.4	10.0	−4.44				−10.9		
5	CH_3	H	13.2	10.0	−4.75	10.0					−53.0
6	CH_3	*m*-CH_3	21.0	10.0	−4.28			4.14		119	−41.9
7	H	*o*-C_2H_5	44.0	10.0	−3.64	10.0	−6.14				
8	H	*p*-C_2H_5	47.7	10.0	−4.78				−8.00		
9	C_2H_5	H	9.6	10.0	−3.65	10.0				115	−16.2
10	H	*o*-$(CH_3)_2$	(43.0)		−3.95	10.0					
11	*N*-Phenylaziridine		27.7	10.0	−3.85	10.0					−47.5

a) Observed shift in Hz from diamagnetic position for ring *ortho* proton at 0.5 M ligand and 0.05 M $Ni(AA)_2$ concentrations in deuterochloroform.
b) Positions somewhat uncertain owing to overlapping of peaks.

TABLE 2. RELATIVE ISOTROPIC SHIFTS IN COMPLEXED ANILINES

	R	R'	Absolute[a] shift	Relative shift							
				Ring proton			Aryl CH_3 or CH_2			NH	N-CH_3 or CH_2
				o	*m*	*p*	*o*	*m*	*p*		
1	H	H	120.0	10.0	0.53	4.83					
2	H	*o*-CH_3	107.0	10.0	0.67	5.32	1.50				
3	H	*m*-CH_3	139.0	10.0	0.55	4.75		2.03			
4	H	*p*-CH_3	113.0	10.0	0.47				−2.39		
5	CH_3	H	38.0	10.0	0.40	4.20					1.32
6	CH_3	*m*-CH_3	57.0	10.0	0.09	4.30		1.76		61.0	0.26
7	H	*o*-C_2H_5	122.0	10.0	0.77	4.83	2.05				
8	H	*p*-C_2H_5	176.0	10.0	0.37				−1.52		
9	C_2H_5	H	21.3	10.0		5.15					5.15(CH_2)
10	H	*o*-(CH_3)	35.0[b]		7.8[b]	35.0		5.8[b]			
11	*N*-Phenylaziridine		125.0	10.0	0.36	3.16					8.32(CH_2)

a) Observed shift in Hz from diamagnetic position for ring *ortho* proton at 0.5 M ligand and 0.05 M $Co(AA)_2$ concentrations in deuterochloroform.
b) Absolute shift for *para* proton at 0.5 M ligand and 0.05 M $Co(AA)_2$.

with $M(AA)_2$ presumably because of steric effects, but the observed isotropic shift ratios for ring protons are almost the same as those observed for non-*N*-substituted anilines.

The N–H and N-CH_3 or N-CH_2 proton resonances exhibit different magnitudes and opposite signs for contact shifts in the $Ni(AA)_2$ system. If the amino group in the coordinated *N*-alkyl anilines takes a coplanar configuration, similar magnitudes but opposite signs for contact shifts of N–H and N-CH_3 or N-CH_2 proton resonances should be observed, as predicted by the theory of McConnell.[4]

A metal-nitrogen bond of the planar configuration would involve a pure *p* atomic orbital on the nitrogen which is orthogonal to the σ-plane and would give rise to similar magnitudes but opposite signs for the contact shifts of N–H and N-CH_3 protons. However, the relatively small value of the observed contact shift for N-CH_3 protons compared with that for N–H rules out this expectation and suggests a non-planar configuration of the amino group for coordinated aniline derivatives.

Now let us enter upon a further quantitative discussion of this problem. The relative value of hyperfine coupling constants for N–H and N-CH_3 protons in which an electron spin is localized on the *p* atomic orbital of the nitrogen is given by McConnell's relation:[4]

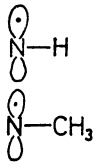

$$a_H = Q\rho_N$$

$$\frac{a_{CH_3}}{a_H} = \frac{Q_{CH_3}}{Q_H} \simeq 1.2$$

The value of a_{CH_3}/a_H can be obtained from the ESR studies.[5] The relative contact shifts for these protons become equal to this value. Table 3 gives the relative contact shifts for *N*-methyl- and *N*-ethylanilines, together with that for benzyl aniline reported by Fitzgerald and Drago.[6] The values are all very small compared with those predicted by McConnell's relation, but they are very close to the value for benzylamine with a non-planar configuration. The rapid attenuation of contact shifts for the N-CH_3 or N-CH_2 group appears to be due to spin delocalization through the σ system.[7,8] The above results and considerations strongly suggest a pyramidal configuration of the nitrogen atom.

Table 3. The ratio of contact shifts for NH and NCH_3 or NCH_2 protons

Ligand	$\Delta\nu_{NCH_3}/\Delta\nu_{NH}$
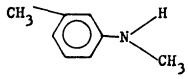	−0.35
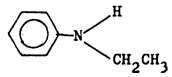	−0.14
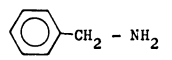	−0.33[a]

a) Taken from Ref. 6.

It should be noted that the value of $\Delta\nu_{CH_2}/\Delta\nu_{NH}$ is much smaller for *N*-ethylaniline than for the *N*-methyl derivative. This singularity is not due to the decrease in electron transfer by hyperconjugation in going from CH_3 to CH_2 groups, but to the more pyramidal nature of the configuration of

Table 4. Molecular orbital calculation of spin densities on aniline derivatives[a]

	Position		Spin densities: Hückel method[b]	Relative values	McLachlan's method		Relative values
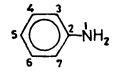	*o*	3, 7	0.0773	10.00	0.0928		10.00
	m	4, 6	0.0020	0.26	−0.0303		−3.26
	p	5	0.0852	11.02	0.1043		11.24
		1 (N)	0.7389	95.59	0.7824		84.31
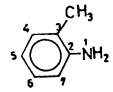	*o*	3	0.0814	9.66	0.0980		11.51
		7	0.0843	10.00	0.0851		10.00
	m	4	0.0003	0.04	−0.0328	−0.0292	−3.43
		6	0.0047	0.56	−0.0256		
	p	5	0.0843	10.00	0.1025		12.10
		1 (N)	0.7265	86.18	0.7689		90.30
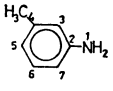	*o*	3	0.0747	0.0711	10.00	0.0891	0.0928	10.00
		7	0.0795			0.0964		
	m	4	0.0022		0.29	−0.0290		−3.12
		6	0.0020		0.28	−0.0308		−3.32
	p	5	0.0874		11.33	0.1079		11.68
		6	0.7367		95.55	0.7800		84.05
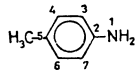	*o*	3, 7	0.0764		10.00	0.0904		10.00
	m	4, 6	0.0046		0.60	−0.0261		−2.89
	p	5	0.0879		11.50	0.1064		11.76
		1	0.7192		94.14	0.7607		84.14

a) Calculated by Hückel approximation with $\alpha_N = \alpha_C + 0.4\beta$, $\beta_{C-N} = 0.6\beta$. A hyperconjugative effect of methyl group is introduced by

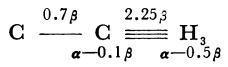

b) Obtained by the square of the AO coefficients in the highest occupied molecular orbital.

5) A. D. McLachlan, *Mol. Phys.*, **1**, 233 (1958).
6) R. J. Fitzgerald and R. S. Drago, *J. Amer. Chem. Soc.*, **89**, 2879 (1967).
7) R. J. Fitzgerald and R. S. Drago, *ibid.*, **90**, 2523 (1968).
8) D. R. Eaton, A. D. Josey and R. E. Benson, *ibid.*, **89**, 4040 (1967).

the *N*-ethyl group, in which the electron spin on the nitrogen atom transfers to the CH_2 proton through a σ delocalization mechanism with a rapid attenuation.

The lone-pair electrons on a nitrogen atom belong to the hybrid (sp^3) orbital, which can overlap with the π atomic orbitals of the phenyl ring; *i.e.*, the lone-pair AO need σ bonding with the metal is conjugated with other π-orbitals of the ligand. Therefore, the spin which is delocalized onto the ligand through the metal-ligand bond may be distributed in the ligand in a typical π-orbital pattern. The delocalized π-orbital occupied by an odd electron can involve either the highest occupied π-orbital (lone-pair orbital) or the lowest-vacant orbital of the ligand. These can be distinguished by comparing the observed contact shifts with the spin densities calculated by a molecular orbital method.

Table 4 shows that a relation can be observed between the experimental data and the spin-density distribution calculated for the highest occupied MO of the ligand. This means that the lowest vacant orbital which is antisymmetric to the molecular axis does not interact with the AO of the metal. The spin correlation is not explicitly included in the standard MO calculations, but small positive spin densities might become negative if spin correlation is introduced. The simplest method of estimating the effects of spin correlation is that of McLachlan,[9] in which the α and β spins are allowed to occupy separate Hückel-type orbitals. The results of this calculation are also shown in Table 4.

Negative spin densities can be predicted at the *meta* position on the basis of the experimental results. A comparison of the experimental relative contact shifts with the theoretical relative spin densities shoes a fairly good agreement. The calculated values for *meta* position are generally somewhat lower than the observed values, particularly for *p*-methyl aniline. However, the correspondence between the spin-density distribution in coordinated *p*-methylaniline and that in the radical anion of its related compound, *N*,*N*-dimethyl-*p*-toluidine (Table 6), is fairly good. A comparison of the spin density distribution in coordinated molecules and in the corresponding radical anions leads to some other interesting conclusions (Table 6). For radicals, the spin density on a *para*-carbon atom is larger than that on a *ortho*-carbon atom. This is also true for the benzyl radical with an isoelectronic structure of coordinated aniline and its radical anion. This trend can be reproduced by a molecular orbital calculation (Table 4). Extended Hückel calculations including non-bonded interaction for planar and non-planar structures of aniline yield unequal spin densities on *ortho* and *para* protons (Table 5). However, the contact shifts for *ortho* and *para* protons are equal; this appears to be characteristic of the paramagnetic metal complex of aniline derivatives. An increase in the positive spin density (downfield contact shifts) on the *ortho* proton may result from additional spin delocalization through direct overlap between the metal *d* orbital and the proton 1*s* orbital in question.

Spin delocalization to the methyl or methylene

TABLE 5. MOLECULAR ORBITAL CALCULATION OF SPIN DENSITIES[a]

	Positions	Spin densities	Relative spin densities	HO orbital energy (eV)	Total electronic energy (eV)
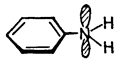	*o*	0.1401	10.00		
	m	0.0282	2.01	−12.21	−648.7878
	p	0.2482	17.72		
$\theta=30°$	*o*	0.1279	10.00		
	m	0.0279	2.18	−12.24	−648.7009
	p	0.2332	18.23		
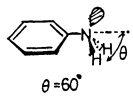 $\theta=60°$	*o*	0.1368	10.00		
	m	0.0306	2.24	−12.25	−649.1771
	p	0.0306	2.24	−12.25	−648.1771
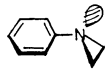	*o*	0.4076	10.00		
	m	0.0060	0.01	−11.46	−812.5641
	p	0.3949	9.69		

a) Calculations were made using extended Hückel method. Geometries for these calculations are referred to structural parameters in Table 9.

9) A. D. McLachlan, *Mol. Phys.*, **3**, 233 (1960).

Table 6. Relative h.f.s. constants and contact shifts for various protons of substituted aniline and related radicals

	Proton	a_H[c]	Relative values	Ref.
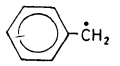	*o*	5.14	10.0	
	m	1.75	3.1	
	p	6.14	12.0	a
	CH_2	16.35	31.6	
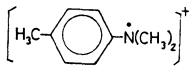	*o*	5.21	10.0	
	m	1.36	2.6	
	p-CH_3	9.97	15.5	b
	N-CH_3	12.22	23.4	
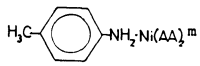	*o*		10.0	
	m		4.44	present work
	p-CH_3		10.0	

a) A. Carrington and I.C.P. Smith, *Mol. Phys.*, **9**, 137 (1965).
b) B. M. Latta and R. W. Taft, *J. Amer. Chem. Soc.*, **89**, 5172 (1967).
c) In gauss.

group adjacent to sp^2-hybridized carbons containing an unpaired electron has been explained by hyperconjugation. A different value of Q should be found for each alkyl group. The Q value for the directly-bonded proton, Q_{CH}, is normally -22.5 G, while that for methyl group ranges from 29 G to 27 G.[10] We evaluated Q_{CH_3} or Q_{CH_2} values for alkyl groups attached to the phenyl ring, using the relation:

$$Q_{CH_3} = Q_{CH}\frac{a_{CH_3}}{a_H} = Q_{CH}\frac{\Delta\nu_{CH_3}}{\Delta\nu_{CH}}$$

where $\Delta\nu_{CH_3}$ and $\Delta\nu_{CH}$ are proton contact shifts for each position (*ortho*, *metha*, and *para*). This relation holds as long as the spin densities on the carbon atoms to which methyl or the proton is attached are equal. This is approximately verified by the MO calculations (Table 4). The Q values thus obtained are listed in Table 7. They decrease in the order: *m*-$>$*o*-methyl$>$*o*-methylene protons. This trend probably reflects an interaction between the coordinated metal and the corresponding methyl or methylene group. This interaction is minimized for the *p*-substituted group, in which the substituent is located far from the metal. The Q_{CH_3} value for aminotroponiminate, in which such an interaction does not operate, shows a normal value of 27.0 G.[10] The Q_{CH_2} value is slightly smaller than the Q_{CH_3} value. This finding is considered to be due to the hindrance of electron transfer through hyperconjugation resulting from the steric interaction between the methyl or ethyl group and coordinated $M(AA)_2$.

Table 7. Q_{CH_3} or Q_{CH_2} value for substituted aniline derivatives

	Ligand molecule	Q_{CH_3} or Q_{CH_2}	
2	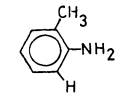	15.3	(14.9)[a]
7	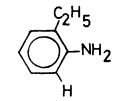	13.8	
3	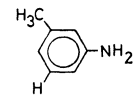	20.6	(27.0)[a]
6	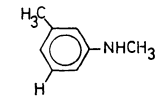	21.8	

a) Taken from D. R. Eaton *et al.*, *J. Amer. Chem. Soc.*, **84**, 4100 (1962) for the system

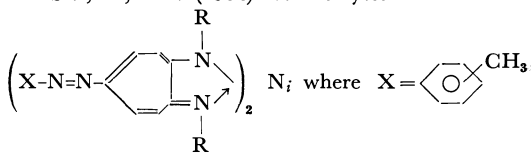

and R=C_2H_5.

The isotropic shift data for $Co(AA)_2$ systems listed in Table 2 show an upfield shift for most of the protons. This upfield bias, compared with the

10) D. R. Eaton, A. D. Josey, R. E. Benson, W. D. Phillips and T. L. Cairsn, *J. Amer. Chem. Soc.*, **83**, 4100 (1962).

TABLE 8. SEPARATION OF ISOTROPIC PARAMAGNETIC SHIFTS IN $Co(AA)_2$ SYSTEM INTO CONTACT AND PSEUDO-CONTACT SHIFTS

$Co(AA)_2$ Compex	l (Å)	Position	Relative value of $\left(\frac{3\cos^2\theta-1}{r^3}\right)$	I.S. (obsd)	P.S. (calcd)	C.S. (calcd)	C.S. (calcd relative)	C.S. (obsd)
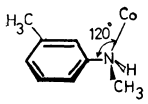	2.2	*o*	1.00	57.0	38.7	18.3	10.0	10.0
		m	0.215	0.5	8.3	−7.8	−4.3	−4.3
		p	0.161	24.5	6.2	18.3	10.0	10.0
		m-CH_3	0.095	10.0	3.7	6.3	3.5	4.1
		N-CH_3	1.80	1.5	69.6	−68.1	−37.3	−41.9
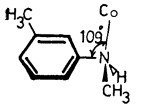	2.2	*o*	1.00	57.0	38.7	18.3	10.0	10.0
		m	0.217	0.5	8.4	−7.9	−4.32	−4.3
		p	0.161	24.5	6.2	18.3	10.0	10.0
		m-CH_3	0.098	10.0	3.8	6.2	3.39	−4.1
		N-CH_3	1.58	61.2	−59.7	−32.6	−32.6	−41.9
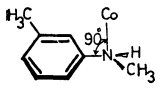	4.3	*o*	1.00	57.0	34.6	22.4	10.0	10.0
		m	0.185	0.5	6.6	−6.1	−2.7	−4.3
		p	0.072	24.5	2.1	22.4	10.0	10.0
		m-CH_3	0.050	10.0	1.7	8.3	3.7	4.1
		N-CH_3	1.61	1.5	58.9	−57.4	−25.6	−41.9
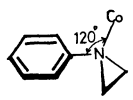	2.0	*o*	1.00	125.0	101.0	24.0	10.0	10.0
		m	0.201	4.5	−15.8	−6.6	−6.6	−4.3
		p	0.155	39.5	15.5	24.0	10.0	10.0
		N-CH_2	1.60	10.4	161.4	−151.0	−63.0	−57.0
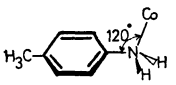	2.8	*o*	1.00	113.0	80.3	32.7	(10.0)	10.0
		m	0.246	5.3	19.8	−14.5	(−4.45)	−4.45
		p-CH_3	0.106	−27.0	8.5	−35.5	−10.9	−10.9
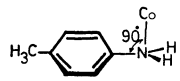		*o*	1.00	113.0	88.2	24.8	(10.0)	10.0
		m	0.185	5.3	16.3	−11.0	(−4.45)	−4.45
		p-CH_3	−0.008	−27.0	−0.8	−26.2	−10.6	−10.9

corresponding $Ni(AA)_2$ data, is due to the pseudo-contact effect, as has been well established for pyridine-type bases complexed with $Co(AA)_2$.[1b]

Here we separate the contact and pseudo-contact shifts in $Co(AA)_2$ systems following the method of Horrocks.[1c] The procedure is as follows. The basic assumption is that the spin density will distribute itself in a manner which is independent of the metal to which it is coordinated; that is, that the ratios of the spin densities at the various carbon atoms (*ortho*, *meta*, *para*) will be the same for the Co(II) and Ni(II) systems, and hence the ratios of the isotropic shifts due to the contact interaction will be the same in these two cases. The pseudo-contact shifts are related to each other by the ratio of calculated geometric factors:

$$\frac{3\cos^2\theta_i - 1}{r_i^3} : \frac{3\cos^2\theta_j - 1}{r_j^3}$$

The bond lengths and bond angles used in estimating the geometric factors listed in Table 8 are given in Table 9. The geometric factor is sensitive to the location of the metal with respect to the amino group, that is, to the metal-nitrogen bond length and to the M–N–C angle. Three angles (90°, 109°, and 129°) and several M–N distances for each angle were adopted. The best geometry was obtained when the agreement of the ratios of the corrected cobalt contact shifts and the observed nickel shifts was obtained. The observed $Co(AA)_2$ isotropic shifts, the necessary pseudo-contact shift correction, and the actual contact shifts for the cobalt complexes of some aniline derivatives are given for three typical geometries of the complex in Table 8. A sizable upfield pseudo-contact shift is evident for the substituted aniline complex of $Co(AA)_2$, implying that $g_{//} < g_{\perp}$. The agreement

TABLE 9. STRUCTURAL PARAMETERS USED IN CALCULATING GEOMETRIC FACTORS AND MOLECULAR ORBITALS

Bond	Distance (Å)	Angle
N-C	1.37	*N*-phenylaziridine
N-CH_3	1.48	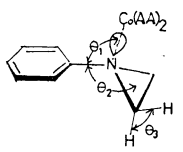
C-C	1.40	
C-H (sp^2)	1.08	
C-CH_3	1.49	
C-H (sp^2)	1.09	
N-CH_2	1.49	
CH_3-CH_2	1.48	$\theta_1=\theta_2=\theta_3=120°$

is satisfactory for the non-planar structure with the M–N–C angle of 120° and the M–N distance of 2.2Å. For the planar structure (I), agreement is obtained only when the M–N distance has the unreasonably large value of 4.3Å. The same situation was found to be true for other aniline derivatives. In these circumstances, the planar structure is ruled out.

To further substantiate the structure of the complexed molecule, we examined *N*-phenylaziridine, for which the M–N–C angle is nearly fixed at 120° because of the hybrid orbital of nitrogen lone pairs. Satisfactory agreement is obtained for the configuration of the M–N–C angle of 120° and the M–N distance of 2.0 Å. The 2.0 Å distance appears to be acceptable for the metal-nitrogen coordination complex.

Thus, studies of contact and pseudo-contact shifts demonstrate conclusively that the geometry surrounding the nitrogen atom of the substituted aniline-$M(AA)_2$ coordination complexes (M=Ni or Co) is pyramidal and that the metal-ligand interaction is essentially σ. In aniline, the nitrogen lone pair is available for σ-bonding with the metal and can overlap with the π atomic orbital of the phenyl ring.

Let us now briefly discuss the non-planarity of the free aniline molecule. It seems premature to draw any firm conclusion about the non-planar structure of free aniline derivatives on the basis of the present study. There have been theoretical and experimental investigations of this problem.[11] From the electronic spectra and theoretical calculations, the configuration of aniline has not yet been established. However, molecular-polarizability (Kerr constant)[12] and microwave studies[3] have provided evidence for a pyramidal structure of the nitrogen atom in aniline. As to the *N*-substituted aniline, the ultraviolet spectra indicate that the $N(CH_3)_2$ group in dimethylaniline is bent out of the ring plane.[12] The angle between the ring-to-N bond and the NH_2 plane is found to be about 45°. This angle would be 54°44′ if the orbitals surrounding the nitrogen atom were oriented tetrahedrally.[11] The angle of nearly 60° found for the aniline-$M(AA)_2$ complex in the present study appears to be slightly larger than that for free aniline. This is probably the result of deformation due to metal-ligand complex formation.

11) J. C. Brand, D. R. Williams and T. J. Cook, *J. Mol. Spectry.*, **20**, 193 (1966).
12) M. J. Aroney, R. J. W. LeFevre, L. Random and G. L. D. Ritchie, *J. Chem. Soc., B*, **1968**, 507.
13) J. Raynaud and A. Lattes, *Compt. Rend.*, **254**, 4054 (1962).

BULLETIN OF THE CHEMICAL SOCIETY OF JAPAN VOL. 43 388—393 (1970)

The Polarographic Behavior of Several α-Keto Acids in Buffered Solutions Containing *o*-Phenylenediamine, and Its Analytical Application

Tamotsu WASA, Morihiko ORITA, Shingo YOSHIDA and Sôichirô MUSHA

Department of Applied Chemistry, College of Engineering, University of Osaka Prefecture, Sakai,

(Received May 20, 1969)

Such α-keto acids as glyoxylic (I), pyruvic (II), α-ketobutyric (III), mesoxalic (IV), oxalacetic (V), and α-ketoglutaric acid (VI) condense with *o*-phenylenediamine (OPD) to form two kinds of products, depending on the pH values of the reaction mixtures. The condensation product formed at pH values lower than 4 gives a well-defined reduction wave ($E_{1/2}$ *vs.* SCE at pH 2.0: −0.490 V for I, −0.587 V for II, −0.592 V for III, −0.181 V for IV, −0.590 V for V, and −0.576 V for VI) at a potential more positive than that of free α-keto acid, while the other product, formed at pH values between 4 and 8, gives an oxidation wave ($E_{1/2}$: −0.1 — −0.2 V *vs.* SCE for all α-keto acids at pH 6.0). From the present polarographic investigations, it was deduced that the condensation product giving the reduction wave is probably 2-hydroxyquinoxaline derivatives and that the product giving the oxidation wave is benzimidazoline derivatives. A linear relation was obtained between the wave height for the reduction of the condensation product and the concentration ($(0.5—20)\times 10^{-4}$ M) for each α-keto acid under appropriate conditions. The reduction wave of the condensation product was used for the determination of II in a commercial product containing II as an impurity.

Since the first work by Shikata and Shoji[1] (1928) on the reduction wave of α-keto acids at a dropping mercury electrode, systematic studies of the polarographic behavior of pyruvic acid and related compounds in buffered solutions have been made by several authors;[2-6] this reduction wave has also been used for the determination of α-keto acids in biological materials.[7] However, the reduction wave is partially reaction-controlled in nature, especially for glyoxylic acid and mesoxialic acid; the limiting current varies intricately with the temperature and with the pH value of the electrolytic solution. For analytical use of this reduction wave, therefore, the experimental conditions must be strictly controlled.

On the other hand, the methods of the chromatographic separation[8,9] and the fluorometric determination[10] of α-keto acids utilizing the 2-hydroxyquinoxalines (HQ)[11] which are formed by the condensation of α-keto acids with *o*-phenylenediamine (OPD) have been developed. The polarographic behavior of several HQ derivatives and a method for the determination of α-keto acids after the paper-chromatographic separation of their HQ's were also reported by Brockelt and Pohloudek-Fabini.[12]

The present authors have previously reported on the polarographic behavior of various carbonyl compounds in buffered solutions containing an excess of OPD, and on the application of the polarograms of the condensation products to the determination of each carbonyl compounds.[13-18]

The present paper will describe the polarographic behavior of several α-keto acids, *i.e.* glyoxylic acid (I), pyruvic acid (II), α-ketobutyric aicd (III),

1) M. Shikata and K. Shoji, *Nippon Nogei Kagaku Kaishi*, **4**, 475 (1928).
2) O. H. Müller and J. P. Baumberger, *J. Amer. Chem. Soc.*, **61**, 590 (1939).
3) R. Bridička, *Collect. Czech. Chem. Commun.*, **12**, 212 (1947).
4) S. Ono, M. Takagi, and T. Wasa, *ibid.*, **26**, 141 (1961).
5) M. Takagi, This Bulletin, **34**, 905 (1961).
6) M. Takagi, *Bull. Univ. Osaka Pref., Ser., B*, **11**, 177 (1961).
7) M. Brezina and P. Zuman, "Polarography in Medicine, Biochemistry, and Pharmacy," Revised English Ed., Interscience, New York (1958), p. 269.
8) D. J. D. Hocknhull and G. D. Floodgate, *Biochem. J.*, **52**, 38 (1952).
9) A. Harjanne, *Suomen Kemistilehti, B*, **28**, 37 (1955).
10) J. E. Spikner and J. C. Towne, *Anal. Chem.*, **34**, 1468 (1962).
11) O. Hinsberg, *Ann.*, **292**, 242 (1896).
12) G. Brockelt and R. Pohloudek-Fabini, *Scintica Pharmaceutica*, **31**, 94 (1963).
13) T. Wasa, M. Takagi, and S. Ono, This Bulletin, **34**, 518 (1961).
14) S. Musha, T. Wasa, and T. Naito, *ibid.*, **39**, 1902 (1966).
15) T. Wasa and S. Musha, *ibid.*, **40**, 1617 (1967).
16) T. Wasa and S. Musha, *ibid.*, **40**, 1624 (1967).
17) T. Wasa and S. Musha, *ibid.*, **41**, 1578 (1968).
18) T. Wasa and S. Musha, *Bull. Univ. Osaka Pref., Ser. A*, **17**, 139 (1968).

mesoxalic acid (IV), oxalacetic acid (V), and α-ketoglutaric acid (VI), in various buffered solutions containing an excess of OPD, and on a method for determining such α-keto acids by using the polarograms of the condensation products.

Experimental

Materials and Reagents. The α-keto acids used were commercial products and were used without further purification: I, sodium glyoxylate monohydrate; IV, calcium mesoxalate trihydrate (Tokyo Kasei Kogyo Co.); II, sodium pyruvate (E. Merck AG.); III, α-ketobutyric acid; VI, α-ketoglutaric acid (Wako Pure Chem. Ind.), and V, cis-oxalacetic acid (Sigma Chem. Co.). The stock solutions (about 10^{-2} M) of α-keto acids, except for IV, were prepared by dissolving the chemicals in redistilled water; IV was dissolved in dilute hydrochloric acid. The HQ derivative corresponding to each of α-keto acids was prepared according to the method of Morrison[19] by condensing α-keto acid with OPD in dilute acetic acid. The HQ derivative of V was not obtained because of the β-decarboxylation[9] which is catalyzed by OPD, and the product obtained was found to be 2-hydroxy-3-methylquinoxaline by thin-layer chromatography. The stock solutions (about 10^{-2} M) of HQ's were prepared by dissolving the products in 50% ethanol or 50% ethanol containing an equimolar amount of sodium hydroxide. OPD was a product for chromatography from E. Merck AG.; the stock solution of about 0.1 M was prepared fresh daily by dissolving OPD in redistilled water or 0.5 N hydrochloric acid. As the buffer solution, the Britton-Robinson buffer (BR) was mainly employed. In the experiments for HQ's without OPD, 0.001% Triton X-100 was used as the maximum suppressor, but in the presence of an excess of OPD in the electrolytic solution no suppressor was added, since the condensation products showed no maximum. All the other chemicals were the same as those in previous works.[14-18]

Apparatus and Procedures. The apparatus and the experimental procedures for the polarographic investigations were almost the same as those reported in previous papers.[14-18] The characteristics of the capillary used were $m=1.96$ mg/sec and $t=3.97$ sec/drop in a buffer solution when the height of the mercury reservoir was 69 cm at 0 V *vs.* SCE. The accuracy of the temperature control was ±0.1°C. The final pH value of the polarographic solution was measured with a glass electrode pH-meter. The pK values of the authentic HQ derivatives were evaluated from the pH-titration curves for 10^{-2} M HQ's containing 50% ethanol and 1 M potassium chloride. The pH-titration was carried out coulometrically at a constant current of about 10 to 20 mA in a titration cell equipped with a platinum cathode, a silver anode, and a glass indicator electrode.[20]

The cyclic voltammetric experiments were carried out using a multipupose instrument employing solid-state operational amplifier circuitry and with a three-electrode configuration, similar to that reported by Goolsby and Sawyer.[21]

19) D. C. Morrison, *J. Amer. Chem. Soc.*, **76**, 4483 (1954).

20) J. J. Lingane, "Electroanalytical Chemistry," 2nd Ed., Interscience, New York (1958), p. 607.

Results and Discussion

When α-keto acid was treated with OPD in buffered solutions of various pH values by the procedure described above, all the α-keto acids examined show a well-defined reduction wave at a potential more positive than that of the original acids at pH values below 4 (Fig. 1a), while there was a well-defined oxidation wave in the pH range between 4 and 8 (Fig. 1c). The relation between

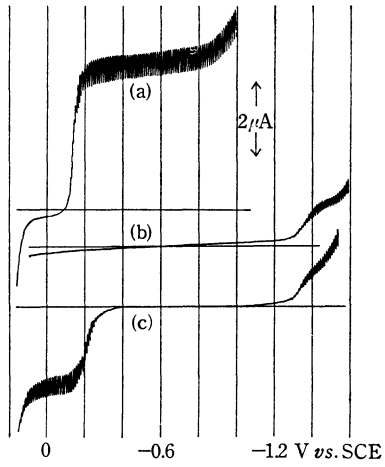

Fig. 1. Polarograms of IV with or without OPD at 25°C.
Mesoxalic acid: 5×10^{-4} M; condensation: 60 min
a) with 5×10^{-2} M OPD in 0.25 N HCl
b) without OPD in BR buffer (pH 6.6)
CO with 4×10^{-2} M OPD in BR buffer (pH 6.4)

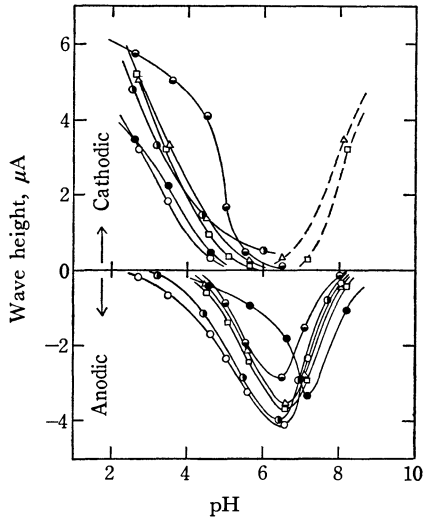

Fig. 2. Effect of pH on the condensation reaction of α-keto acids (about 1×10^{-3} M) with OPD (4×10^{-2} M) at 25°C.
Condensation: 30 min; ● I, □ II, ○ III, ◑ IV, △ V, and ◒ VI.

21) A. D. Goolsby and D. T. Sawyer, *Anal. Chem.*, **39**, 411 (1967).

the heights of the waves and the pH values of reaction media are presented in Fig. 2. The ill-defined reduction wave obtained at pH values above 7 (Fig. 2, dashed line) seems to be due to the reduction of the α-keto acid which had not reacted, because the half-wave potentials are in rough accord with those for free acids. Consequently, it is evident that two kinds of the products were produced by the condensation reactions of α-keto acid with OPD, depending on the pH values of the reaction mixtures.

Reduction Wave of the Condensation Product. Figure 2 shows that the reduction wave rapidly increases in height with a decrease in pH in the range below 4. The effect of the concentration of hydrochloric acid on the condensation reaction of α-keto acid with OPD was examined in the range from 0.05 to 2 N; the results obtained are shown in Fig. 3. The wave height, which is equivalent to the amount of the condensation product, had its maximum value in the range of 0.1 to 1 N hydrochloric acid. The same effect was also observed with sulfuric acid instead of hydrochloric acid.

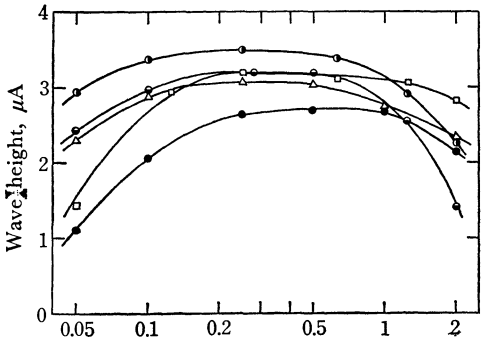

Fig. 3. Effect of the concentration of HCl on the condensation reaction at 25°C.
α-Keto acid: 5×10^{-4} M; OPD: 4×10^{-2} M; Condensation: 30 min
●—I, □—II, ◑—IV, △—V, and ◒—VI

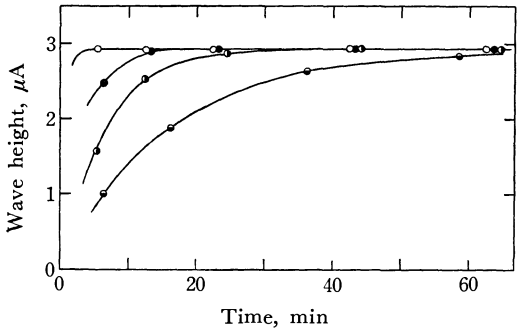

Fig. 4. Effect of the concentration of OPD at 25°C.
α-Ketoglutaric acid: 5×10^{-4} M; OPD: ○—8×10^{-2}, ●—4×10^{-2}, ◑—2×10^{-2}, and ◒—8×10^{-3} M

Figure 4 shows the relation between the wave height of the condensation products and the time elapsed after the addition of VI to the electrolytic solutions containing OPD in various concentrations in 0.25 N hydrochloric acid. With the increase in the concentration of OPD, the growing velocity of the reduction wave increased. A similar effect was also observed for all the other α-keto acids; the time required to reach the maximum value of the limiting current was 20—60 min with the concentrations of OPD higher than 2×10^{-2} M. Moreover, the saturation wave height obtained for each α-keto acid was found apparently to correspond to that of the authentic HQ of the same concentration.

The pH dependence of the wave heights of the condensation products, which were prepared by condensing α-keto acids with OPD in 0.25 N hydrochloric acid and by then neutralizing them with 1 N sodium hydroxide, is given in Fig. 5. The same pH-dependence was obtained for all the α-keto acids other than IV ; the limiting current remains almost constant at pH values lower than 9, while with an increase in pH above 9 a new second reduction wave (curve b), whose half-wave potential of about 100 mV more negative than that of the first wave (curve a), grows at the expense of the latter, which disappears at a pH value of about 11. For the condensation product of IV, a more complicated behavior was observed, as may be seen in Fig. 5 (dashed line): the reduction wave split into two waves at a pH value of about 2.

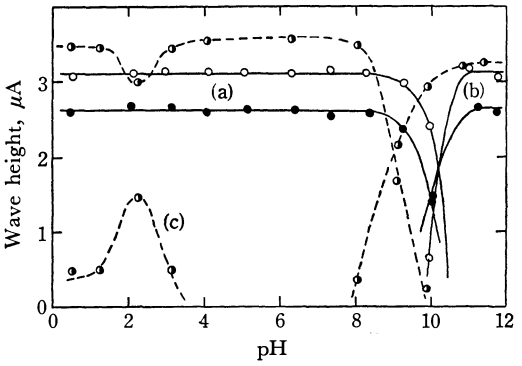

Fig. 5. pH-Dependence of the reduction waves of the condensation products (about 5×10^{-4} M) at 25°C.
—●— I, —○— II (III, V, and VI), --◑-- IV; (a)—1st wave, (b) and (c)—2nd wave

The half-wave potentials of the condensation products are listed in Table 1 as a function of the pH value, together with the pK value. The condensation products for each α-keto acid prepared in acidic media of pH lower than 4 were identical in polarographic behavior with the corresponding authentic HQ's obtained by Morrison's method;[19]

Table 1. Half-wave Potentials and dissociation constants (pK) for the condensation products at 25°C

α-Keto acid		$-E_{1/2}$, V *vs.* SCE						pK*
	pH: (1 N HCl)	2.0	4.0	6.0	8.0	10.0	11.0	
I	R_1	0.313	0.490	0.637	0.782	0.880	0.976	(9.08)
	R_2						1.076	1.097
	Ox				0.12	0.22		
II	R_1	0.439	0.587	0.745	0.876	0.987	1.060	9.8
	R_2						1.160	1.188
	Ox				0.11	0.18		
III	R_1	0.438	0.592	0.739	0.880	1.002	1.050	
	R_2						1.143	1.180
	Ox			0.11	0.12	0.17		
IV	R_1	0.108	0.181	0.363	0.548	0.728		3.2, 9.5
	R_2	0.78	0.92			1.015	1.080	1.146
	Ox			0.24	0.24	0.24		
V	R_1	0.436	0.590	0.739	0.880	0.993	1.065	
	R_2						1.160	1.180
	Ox				0.11	0.18		
VI	R_1	0.428	0.576	0.695	0.827	0.982	1.065	5.4, 10.1
	R_2						1.240	1.276
	Ox				0.14	0.21		

R_1: 1st reduction wave; R_2: 2nd reduction wave; Ox: oxidation wave.
* in 1 M KCl containing 50% ethanol.
( ) A. Albert and J. N. Phillips, *J. Chem. Soc.*, **1956**, 1294.

the present results are also in accordance with the observation by Brockelt and Pohloudek-Fabini,[12] when the pH values of their electrolytic solutions are corrected, taking into account the alcohol error caused by the 50% ethanol addition. As has been reported by Hinsberg,[11] the reaction may be written as:

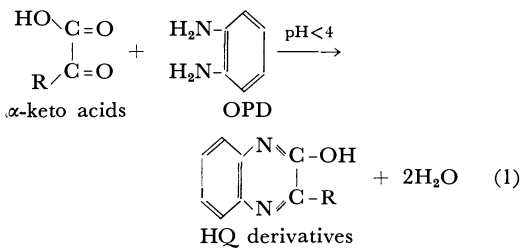

The limiting current for each condensation product at pH values lower than 9 or higher than 11 was the diffusion-controlled current, since the wave height varied in proportion to the square root of the height of the mercury reservoir. By comparing the wave height for the HQ derivatives with that for dimethylquinoxaline[15] at the same concentration, a two-electron reduction was deduced for the reduction wave of HQ.

A cyclic voltammogram of 2-hydroxy-3-methylquinoxaline with a hanging mercury drop electrode is given in Fig. 6 (a); it is typical of the cyclic voltammetric behavior exhibited by the HQ derivatives examined: the electron-transfer step exhibits no reversal peak upon scan reversal about 160 mV past the cathodic peak. Though this result seemingly suggests that the electron transfer is irreversible, a small a. c. peak was observed at the potential crresponding to the d. c. wave for each HQ derivative over all the pH range studied (pH 0—12), the peak height being about one-tenth of that for dimethylquinoxaline at the same concentration. From both of these results, the electrode reaction of HQ derivtives, though a more complete explanation of the mechanism must await further investigation, may be deduced to be a reversible two-electron transfer, followed by a fast chemical reaction.[22]

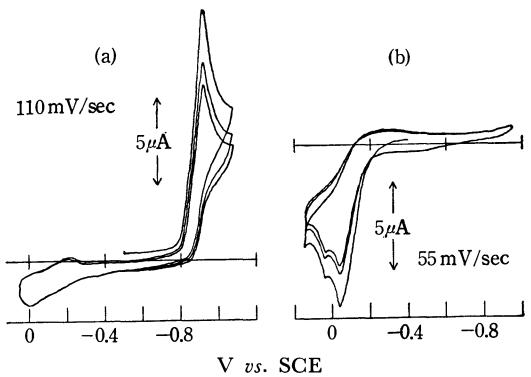

Fig. 6. Cyclic voltammograms of the condensation products of II with OPD at 25°C.
a) cathodic peak of 2-hydroxy-3-methylquinoxaline (5×10^{-4} M) in BR buffer (pH 6.0)
b) anodic peak of II (5×10^{-4} M) in BR buffer (pH 6.0) containing 2×10^{-2} M OPD; condensation: 30 min

22) Joe L. Sadler and Allen J. Bard, *J. Amer. Chem. Soc.*, **90**, 1979 (1968).

From the facts that the pH values, at which the height of the first wave is equal to that of the second wave, were found to be near the pK values (Table 1) for the hydroxyl group of each HQ and that HQ derivatives were proved by the spectrophotometric study[23] to be present in the aqueous solution largely as the amide form, it may be concluded that the first and the second reduction wave of HQ are due to the reduction of the undissociated tautomeric amide form and the dissociated enol form respectively. The electrode reaction may be written as:

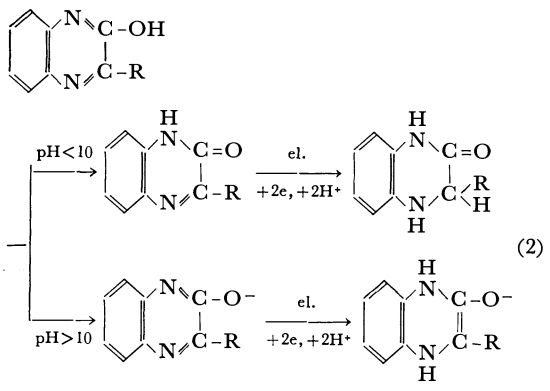

(2)

Oxidation Wave of the Condensation Products. The pH-dependence of the oxidation waves of the condensation products of α-keto acids with OPD (shown in Fig. 2 and Table 1) was, in general, very similar to that observed for monoaldehydes:[16,17,24] the wave heights, which are equivalent to the amount of the condensation product, attain their maximum value in the pH range between 6 and 7.5, and then decrease beyond this pH region. Figure 7 shows the change in the anodic limiting current in buffered solutions (pH: 7.17, 6.10, and 5.30) containing II and OPD with the time elapsed after the addition of OPD. At pH values higher than 6 the condensation reaction was slow (curve b). On the other hand, at pH values lower than 6 the condensation product was unstable (curve c), though the condensation reaction itself was very rapid. At a pH value of about 6 the reaction of every α-keto acid with OPD attained its equilibrium state within 20—60 min after the addition of OPD and the condensation products were comparatively stable (curve a). The oxidation wave was also diffusion-controlled.

A representative cyclic voltammogram of the condensation product is shown in Fig. 6 (b): the electron-transfer step exhibits no cathodic peak upon scan reversal. Moreover, from the facts that no a. c. polarogram was observed with the condensation product and that no reduction wave was obtained with the oxidation product prepared by aeration through the solution containing the condensation product, the electrode reaction may be considered to be irreversible.

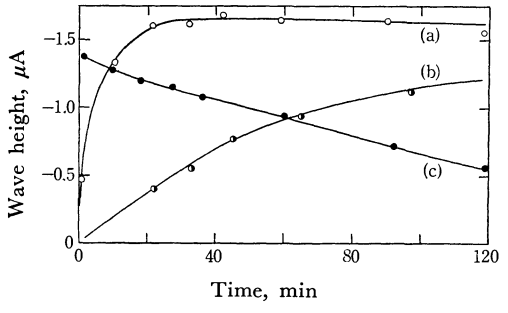

Fig. 7. Change of the oxidation wave for 5×10^{-4} M ,II with time in BR buffer containing 4×10^{-2} M OPD at 25°C.
a) pH 6.10, b) pH 7.17, and c) pH 5.30

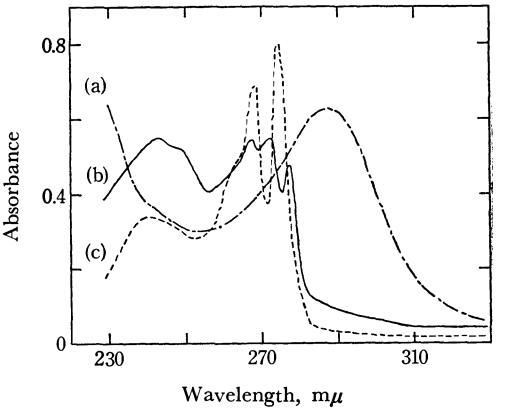

Fig. 8. UV-absorption spectra of the oxidation products corresponding to I (b), II (c), and IV (a) in BR buffer (pH 6.0).
α-Keto acid: 2×10^{-3} M; OPD: about 1×10^{-4} M
Spectrum was recorded for the condensation product after complete oxidation with air.

Figure 8 shows the UV-absorption spectra of the air-oxidation products. The absorption curves obtained for II, III, V, and VI were similar to each other, but they were entirely different from that for IV. The curves for I, II, and III were also identical with those of benzimidazole and the oxidation products from the condensation product of OPD with acetaldehyde and with propionaldehyde respectively. From the results described above, it may be concluded that the condensation products exhibiting oxidation waves are benzimidazolines and that their electro-oxidation products are benzimidazole derivatives, as has previously been reported for aldehydes[16,17] and ketones.[25] Their reactions may be expressed as follows:

23) G. W. H. Cheeseman, *J. Chem. Soc.*, **1958**, 108.
24) M. Fedoroňko, J. Königstein and M. Bullová, *Chem. Zvesti*, **22**, 25 (1968).
25) R. C. Elderfield and J. R. McCarthy, *J. Amer. Chem. Soc.*, **73**, 975 (1951).

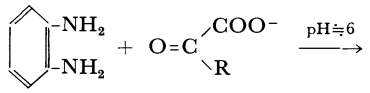

OPD α-keto acids

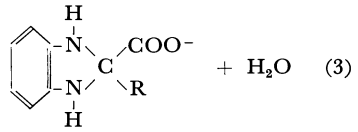

(3)

benzimidazolines

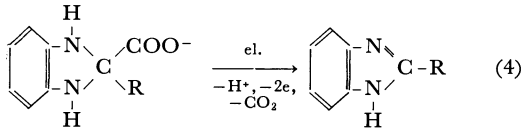

(4)

Analytical Application. From the results described above, the following conditions are recommended for the determintion of α-keto acids by using the reduction wave of the condensation products with OPD: 0.1—1 N for the concentration of hydrochloric acid, (2—4) × 10^{-2} M for the concentration of OPD, 25°C for the temperature, and 20—60 min for the condensation time. To avoid the precipitation of the condensation products, it is desirable to add ethanol (about 10% in volume) to the reaction mixture. Under these conditions, a linear relationship was obtained between the concentration of each α-keto acid in the range of (0.5—20) × 10^{-4} M and the wave height of the corresponding condensation product, as may be seen in Fig. 9.

Alcohols, carbohydrates, monocarbonyl compounds such as aliphatic aldehydes and ketones, and all carboxylic acids except α-keto acids did not interfere with the determination of α-keto acid. Since the condensation products of glyoxals[14,15] behave in a way similar to that of α-keto acids at the dropping mercury electrode, the presence of any glyoxal may interfere with the determination of α-keto acids.

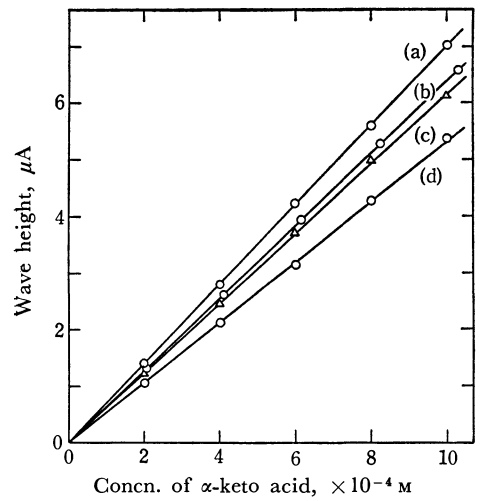

Fig. 9. Relationships between the wave heights (cathodic) of the condensation products and the concentrations of α-keto acids in 0.25 N HCl at 25°C. OPD: 5 × 10^{-2} M; condensation: 30 min a)—IV, b)—II (III and VI), c)—V, and d)—I

As an application, the determination of II in commercial products containing II as an impurity was carried out by means of the standard addition method; some of the analytical results obtained are presented in Table 2, together with those obtained by the direct polarographic method.[7] When no interfering substance is present in the sample, the results obtained by the two methods are in good agreement with each other. Even in the case of the sample containing a substance interfering with the direct polarographic method, the present polarographic OPD method is valid because the half-wave potentials of the condensation products shift to more positive potentials than that of free α-keto acid.

Table 2. The results of the determination of II in commercial products

OPD: 5 × 10^{-2} M, 0.5 N HCl, 25°C, 60 min

Sample	Pyruvic acid content, %	
	Polaro. OPD method	Direct polaro.*
Lactic acid (95%)	0.0112	0.0113
Lactic acid (75%)	0.0084	0.0105
Acidophilus milk (liquid)	0.0119	0.0153
Acidophilus milk (powder)	0.0064	0.504

* According to the procedure of Ref. 7, p. 269.

With regard to the oxidation wave, a linear relationship was also observed between the concentration of each α-keto acid and the wave height under strictly controlled conditions. However, the wave height changes with the concentration of OPD since the equilibrium constant for the condensation reaction seems to be relatively small, much like that for monoaldehydes,[16,17] and it decreases with time since the condensation product is easily oxidizable with the dissolving oxygen. For analytical purposes, therefore, the concentration of OPD in the reaction mixture should be kept in a large excess and should be kept constant, and the dissolving oxygen should be removed by a stream of nitrogen immediately after the preparation of the electrolytic solution.

The authors wish to express their thanks to Dr. Masanosuke Takagi for his helpful discussions and suggestions during this work and to Mr. Iwao Abe for his assistance in the experimental work.

BULLETIN OF THE CHEMICAL SOCIETY OF JAPAN VOL. 43 394—397 (1970)

Isotope Effect of Molten Thallous Nitrate in Countercurrent Electromigration

Isao OKADA and Nobufusa SAITO

Department of Chemistry, Faculty of Science, The University of Tokyo, Hongo, Bunkyo-ku, Tokyo

(Received July 8, 1969)

The isotope effect of the thallous ion in the countercurrent electromigration of molten thallous nitrate has been measured at 219°C. The relative internal mobility difference between $^{203}Tl^+$ and $^{205}Tl^+$, $\Delta V/V_{Tl}$, has been determined to be 0.00035 ± 0.00002. The mass effect $\mu_{Tl}=(\Delta V/V_{Tl})/(\Delta M/M_{Tl})$, has been calculated to be -0.035 ± 0.002, and this value has been compared with those of alkali nitrates previously determined.

Several studies have been made of the mass effects*1 of internal mobilities[1] in countercurrent electromigration with a variety of molten alkali nitrates.[2-7] However, no data on the mass effects have been published for other molten nitrates. This report will be concerned with the mass effect of the internal mobilities of thallous nitrate in a molten state.

Experimental

The experiments were performed in the cell shown in Fig. 1. A mixture of desiccated lithium and potassium nitrates was poured into a quartz beaker and melted by electric heating. On the other hand, a separation tube made of Vycor glass was packed with quartz powder (100—150 mesh size) and placed into a vessel containing molten thallous nitrate. After the molten nitrate had been soaked up to the upper end of the diaphragm of quartz powder in the separation tube, it was transferred into the quartz beaker. Then electromigration was immediately started. A platinum wire and an aluminum tube were used as the anode and the cathode of the electromigration respectively. The temperature of the separation tube was kept at 219 ± 3°C,*2 and a mixture of nitrogen dioxide and oxygen was introduced into the cathode compartment at a constant rate throughout the electromigration. When the electromigration had terminated, the separation tube was taken out from the quartz beaker. After cooling, the surface of the tube was thoroughly cleaned, and the tube was cut into several fractions. The salt in each fraction was leached out with water. In order to determine the thallium content of each fraction, aliquots of the fractions were poured on a column of an anion exchange resin, Dowex-1 (100—200 mesh), of the OH-form. The thallium ion was eluted with distilled water. The thallium in the the effluent was then determined by means of Andrew's titration.

Sodium iodide was added to another aliquot of each fraction. After the resulting precipitate of TlI had been filtered, the potassium in the filtrate was determined gravimetrically as potassium tetraphenylborate. The lithium content of each fraction was determined by spectrophotometry.

The isotopic ratio of thallium in each fraction was measured with an Atlas CH-4 mass spectrometer equipped with a double-filament ion source for surface ionization. The ionizing and vaporizing filaments were made of rhenium ribbons. The distance between these filaments was about 2 mm. Background and memory effects were eliminated by boiling the ionization box in distilled water for 20 min and by then heating *in vacuo* both ionizing and vaporizing filaments at about 2500°C with a current of 5A for 30 min. The sample (about 10 μg as thallium) was painted on the vaporizing filament in the form of thallous nitrate. After the ionization box had been placed in the ion-source compartment of the mass spectrometer, the ionizing filament was slowly heated electrically up to about 1200°C. The ion current of thallium was found to be stable after about 30—50 min. The ion current of ^{205}Tl was controlled to about 3×10^{-12} A at the collector by adjusting the temperature of the ionizing filament.

*1 Mass effect, μ, is defined as the ratio of relative mobility difference, $\Delta V/V$, to relative mass difference, $\Delta M/M$, of two isotopes. It is expressed as $\mu=(\Delta V/V)/(\Delta M/M)$.

*2 The thermogravimetric analysis of thallous nitrate has indicated that no thermal decomposition of the nitrate takes place below 300°C with a heating rate of 2°C/min.

1) A. Klemm, "Molten Salt Chemistry," ed. by M. Blander, Interscience Publishers, New York, London (1963) p. 538.
2) A. Lundén and A. Ekhed, *Z. Naturforsch.*, *A*, **24**, 892 (1969).
3) N. Saito, I. Tomita and I. Okada, unpublished.
4) N. Saito, I. Tomita and I. Okada, *J. Nucl. Sci. Technol. (Tokyo)*, **3**, 140 (1966).
5) A. Lundén and A. Ekhed, *Z. Naturforsch.*, *A*, **23**, 1779 (1968).
6) A. Lundén, C. Reuterswärd and N. G. Sjöberg, *ibid.*, *A*, **10**, 279 (1955).
7) A. Lundén, *ibid.*, *A*, **21**, 1510 (1966).

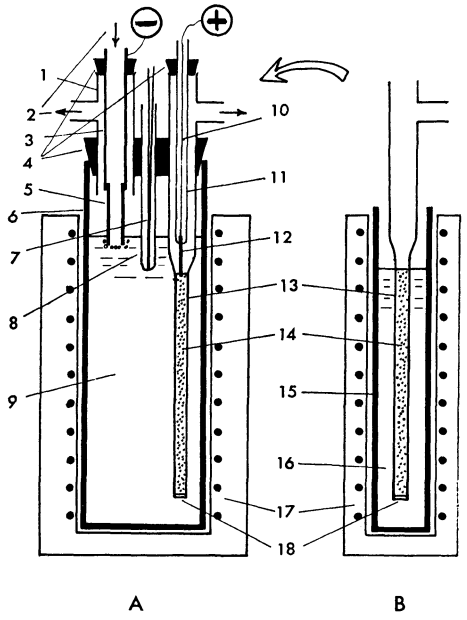

Fig. 1. Electromigration cell.

A: Electromigration cell.
B: Vessel for filling molten $TlNO_3$ into the separation tube.
1: Pyrex glass tube
2: Mixture of NO_2 and O_2
3: Stainless steel tube
4: Silicone stopper
5: Aluminum tube
6: Quartz beaker
7: Thermocouple (Alumel-chromel)
8: Pyrex sheath for thermocouple
9: Mixture of molten $LiNO_3$ and KNO_3
10: Stainless steel lead
11: Pyrex glass tube
12: Platinum wire
13: Separation tube (Vycor glass)
14: Quartz powder of diaphragm
15: Pyrex glass vessel
16: Molten $TlNO_3$
17: Electric oven
18: Quartz frit

Results and Discussion

Four runs of electromigration were carried out. The results of these experiments are summarized in Table 1. For one of these experiments, the detailed experimental conditions and the results obtained are given in Table 2.

For the calculation of the relative internal mobility difference of isotopic ions of thallium, $^{203}Tl^+$ and $^{205}Tl^+$, a formula presented by Klemm[8] can be reformed as follows:

$$\varepsilon = (V_{203}-V_{205})/V_{Tl}$$
$$= (\boldsymbol{F}/Q)\{(x_0+1)/x_0\}\sum_i (x_i-x_0)N_i/(x_i+1) \quad (1)$$

where V_{203}, V_{205}, and V_{Tl} are the internal mobilities of $^{203}Tl^+$, $^{205}Tl^+$, and the thallous ion; where x_i and x_0 are the isotopic ratios of ^{205}Tl to ^{203}Tl in the ith fraction of thallium salt in the separation tube after and before electromigration respectively; where N_i is the equivalent quantity of the thallous ion in the ith fraction; where Q is the transported charge, and where $\boldsymbol{F}$ is the Faraday constant.

The mean square error of the relative internal mobility difference, σ_ε^2, is expressed as:

$$\sigma_\varepsilon^2 = (\partial\varepsilon/\partial x_0)^2\sigma_{x_0}^2 + \sum_i (\partial\varepsilon/\partial x_i)^2\sigma_{x_i}^2 + \sum_i (\partial\varepsilon/\partial N_i)^2\sigma_{N_i}^2$$
$$= (\boldsymbol{F}/Qx_0)^2\sum_i [\{x_i+x_0^2)N_i/(x_i+1)^2\}(\sigma_{x_0}^2/x_0^2)$$
$$+ (x_0+1)^4N_i^2\sigma_{x_i}^2/(x_i+1)^4$$
$$+ (x_0+1)^2(x_i-x_0)^2\sigma_{N_i}^2/(x_i+1)^2] \quad (2)$$

where σ_{x_i} and σ_{x_0} are the standard deviation of the isotopic ratio in the ith fraction of the thallium in the separation tube after and before electromigration respectively, and where σ_{N_i} is the mean deviation of the equivalent quantity of thallous ion in the ith fraction. The values of ε are calculated by Eq. (1) only for the fractions in which ^{205}Tl is enriched. If Eq. (1) is applied to the region of the separation tube where the contents of lithium and potassium nitrates are negligibly small as compared with thallium, the calculated value of ε can be regarded as that of pure thallous nitrate.

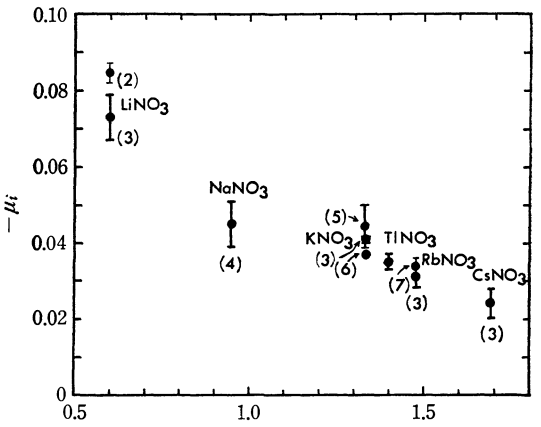

Fig. 2. Relationship between the cationic radius and the internal mass effect of molten nitrates. Figures in parentheses stand for the reference number.

Salt	mp (°C)	Ref.	Temp. (°C)
$LiNO_3$	261	(2)	313—488
		(3)	265—460
$NaNO_3$	308	(4)	340—380
KNO_3	333	(3)	380
		(5)	354—454
		(6)	360
$RbNO_3$	316	(3)	360
		(7)	354
$CsNO_3$	414	(3)	450
$TlNO_3$	206.5	This work	219

8) A. Klemm, *Z. Naturforsch.*, **1**, 252 (1946).

TABLE 1. RESULTS OF THE ELECTROMIGRATION

Experiment No.	1	2	3	4
Electric current (mA)	100—105	60—80	80—100	80—100
Voltage (V)	100	125—130	90	115—120
Duration (hr)	100	74.5	50	50
Transported charge (Coulomb)	37380	16930	15570	15890
Temperature (°C)	219±3	219±3	219±3	219±3
Separation tube				
Length (mm)	99+33	105+29	95+25	143
Int. diam. (mm)	4 5	4 5	4 5	4
Relative internal mobility difference $\{\varepsilon=(\Delta V/V)\}$	0.00031 ±0.00003	0.00031 ±0.00003	0.00037 ±0.00003	0.00037 ±0.00004
Internal mass effect $(-\mu_i)$	0.032 ±0.003	0.032 ±0.003	0.038 ±0.003	0.038 ±0.004

TABLE 2. EXPERIMENTAL CONDITION FOR THE ELECTROMIGRATION

(Exp. No. 3)
Electric current: 80—100 mA,
Voltage: 90 V,
Duration: 50 hr,
Transported charge: 15570 Coulomb,
Temperature: 219±3°C,
Separation tube: 95 mm (int. diam. 4 mm; upper part)
+25 mm (int. diam. 5 mm; lower part).

Fr. No.	Length (mm)	$TlNO_3$ (mM)	$^{205}Tl/^{203}Tl$	$LiNO_3$ (mM)	KNO_3 (mM)	Quartz (mg)
1	—	0.020±0.002	2.470±0.007	0.01	0.03	0
2	12	0.284±0.002	2.540±0.006	0.09	0.02	120
3	16	1.144±0.001	2.451±0.006	0.09	0.05	254
4	18	1.746±0.001	2.392±0.005	0.09	0.09	276
5	10	0.514±0.002	2.378±0.005	0.05	0.03	151
6	14	0.863±0.002	2.371±0.004	0.09	0.04	234
7	17	1.093±0.001	2.374±0.004	0.19	0.39	248
8	18	3.540±0.016	2.363±0.006	0.24	0.11	521
9	15	0.629±0.002	2.346±0.003	—	0.87	397

The isotopic ratio before electromigration: 2.381±0.006

The calculations based on the results of Experiments Nos. 1, 2, 3, and 4 have shown that the mean values of the relative internal mobility difference between ^{203}Tl and ^{205}Tl and of the internal mass effect,[1] μ_{Tl}, for thallous nitrate are 0.00035± 0.00002 and −0.035±0.002 respectively.

In order to compare the mass effect of thallous nitrate with those of the alkali nitrates so far measured, the mass effects of these cations are plotted as a function of the cationic radius[9] in Fig. 2. Figure 2 clearly demonstrates that, the larger the cationic radius, the lower the internal mass effect of molten nitrates.

It is of interest that the linear relationship between the cationic radius and the internal mass effect which is observed for alkali nitrates also holds for thallous nitrate.

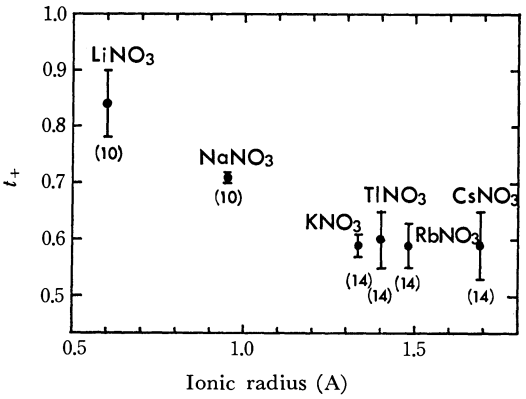

Fig. 3. Relationship between the cationic radius and the transport number of cation in the molten nitrates.
Figures in parentheses stand for the reference number.

9) L. Pauling, "The Nature of the Chemical Bond," 3rd Ed., Cornell Univ. Press, New York (1960) p. 516.

It has been suggested by Duke and Owens[10] that the transport number of cations in pure molten nitrates can be expressed as $t_+=r_-/(r_++r_-)$, where r_+ and $r_-(=2.19$ A,[11] 2.3 A[12]) are the ionic radius of the cation and nitrate ions respectively. Therefore, the transport number of the cation for nitrates is nearly a linear function of the cationic radius, as is shown in Fig. 3: $t_+=1-r_+/(r_++r_-)\fallingdotseq 1-kr_+$ $(r_+\ll r_-)$, where k is a constant.

It can be expected that, as the transport number of the cation increases, the value of the internal mass effect will also increase.[13] In fact, this trend has been observed in these nitrate systems.

10) F. R. Duke and B. Owens, *J. Electrochem. Soc.*, **105**, 548 (1958).

11) O. J. Kleppa and L. S. Hersh, *J. Chem. Phys.*, **34**, 351 (1961).

12) A. F. Wells, "Structural Inorganic Chemistry," 3rd Ed., Oxford Univ. Press, London (1962) p. 171.

13) A. Lundén, *Z. Naturforsch.*, *A*, **14**, 801 (1959).

14) F. R. Duke and G. Victor, *J. Electrochem. Soc.*, **110**, 91 (1963).

BULLETIN OF THE CHEMICAL SOCIETY OF JAPAN VOL. 43 397—400 (1970)

Chromium(III) Complexes with Iminodiacetic Acid or *l*-Aspartic Acid*[1]

Hisayuki MIZUOCHI,*[2] Shuichi SHIRAKATA, Eishin KYUNO and Ryokichi TSUCHIYA

Department of Chemistry, Faculty of Science, Kanazawa University, Kanazawa

(Received July 29, 1969)

The formation constants of chromium(III) complexes with iminodiacetic acid (IDA) and *l*-aspartic acid (Asp) as the terdentate ligands were determined by the pH method in the ionic strength, $\mu=0.1$ and at 25°C: their values were $\log k_1=10.9$ and $\log k_2=10.5$ for IDA and $\log k_1=10.1$ and $\log k_2=9.5$ for Asp, respectively. That the overall formation constants of chromium-(III)-IDA complexes obtained were slightly larger than those of the corresponding -Asp complexes was explained by the stronger chelate effect in the former complexes than in the latter ones. The solid chromium(III) complexes with IDA and Asp were also prepared. Based on chemical analyses and the conductivity measurement or the behavior toward the ion exchangers, the chemical formulas of these complexes are possibly $K[Cr(ida)_2]\cdot 3H_2O$ and $K[Cr(OH)_2asp]$ respectively. X-Ray powder diffraction patterns indicated that the former crystalline complex has tetragonal unit lattice, the axial parameter being $a=14.57$ and $c=12.38$ Å, whereas the latter is amorphous solid.

The formation constants of chromium(III) complexes with glycine and α-alanine as the natural amino acids,[1] anthranilic acid, picolinic acid and 8-hydroxyquinoline,[2] behaving as the (N,O)-type, bidentate ligands, have already been determined. In the series of studies on the formation constants of chromium(III) complexes, the iminodiacetic acid (abbreviated as IDA) and *l*-aspartic acid (abbreviated as Asp) were selected as the (N,O,O)-type, terdentate chelate ligands. We intend first to determine the formation constants of chromium-(III) complexes with IDA and Asp in order to compare their stability with that of glycine and to discuss the difference between them.

A series of the systematic syntheses of the chromium(III) complexes containing diamines and dicarboxylic acids as mixed ligands has been investigated.[3] The complexes with nitrilotriacetic acid and its homologues as the artificial amino acids which can behave as quadridentate ligands were synthesized, and their coordinating structures have been discussed.[4] However, no details of the comparative syntheses of chromium(III) complexes with the amino acids which can behave as the terdentate chelate ligands are known. The second purpose of this study is to prepare chromium(III) complexes with IDA and Asp in the solid phase.

*1 Read at the 19th Annual Meeting and at the 16th Symposium on Coordination Compounds of the Chemical Society of Japan, Tokyo, April and December, respectively, 1966.

*2 Present address: Yamanouchi Rubber Industries Co. Ltd., Hirakata, Osaka.

1) H. Matsukawa, M. Ohta, S. Takata and R. Tsuchiya, This Bulletin, **38**, 1235 (1965).

2) S. Takata, E. Kyuno and R. Tsuchiya, *ibid.*, **41**, 2416 (1968).

3) E. Kyuno, M. Kamada and N. Tanaka, *ibid.*, **40**, 1848 (1967).

4) A. Uehara, E. Kyuno and R. Tsuchiya, *ibid.*, **40**, 2317, 2322 (1967); **41**, 2385, 2393 (1968).

Experimental

Materials. The stock solution of hexaaquochromium(III) perchlorate for the measurement of the formation constants was prepared as described in a previous paper.[1] IDA as a chelating agent used was of highest commercial grade supplied by Dojin Institute of Pharmaceutical Chemistry, and Asp was of special grade by Wako Pure Chemical Industries, Ltd.

Formation Constant Measurements. The formation constants of chromium(III)-IDA and -Asp complexes were determined by the pH method as described.[1] The pH value was measured with a Toa Denpa pH meter, model HM-8. The pH value decreased very slowly as the complex formation proceeds in the mixed solution of hexaaquochromium(III) perchlorate and IDA or Asp, owing to the inertness of chromium(III) complexes. When the decrease of the pH values ceased and the value remained constant for one or one-and-half months, the equilibrium of the complex formation reaction was presumed to be attained. It was also checked by the invariance of the optical density of the reaction solution. In order to see whether some effects upon the pH value due to the unexpected circumstances appear or not, the pH of the solution of the respective chelating agent alone, in the absence of hexaaquochromium(III) perchlorate, was occasionally measured as a blank test for the measurement of the formation constant. It was confirmed that the values remained unchanged during the desired period. Thus, after the pH value of the solution in question became constant, the formation constants were calculated.

Preparation of Complexes. In order to prepare solid chromium(III) complexes with IDA, an aqueous solution of chromium(III) nitrate was mixed with that of IDA in the mole ratio 1 : 3, and then was allowed to boil for a few minutes. After potassium hydroxide was added to the solution to keep the pH value at 3.5—4, it was concentrated to some extent and then ethanol was poured into it. After the solution had been stood for a while, fairly large, red crystals were deposited. If the solution was kept in an ice-box, scale-like, red crystals were produced. Results of chemical and thermal analyses of the crystalline chromium(III)-IDA complex obtained above were as follows: Found: Cr, 12.82; K, 9.73; C, 23.56; N, 6.51; H, 3.75; H_2O, 12.42%. Calcd for $K[Cr(ida)_2]\cdot 3H_2O$: Cr, 12.77; K, 9.60; C, 23.59; N, 6.88; H, 3.93; H_2O, 13.27%.

The content of crystalline water was evaluated from the result of the thermogravimetric analysis by a thermobalance.

Synthesis of crystalline chromium(III) complex with *l*-aspartic acid corresponding to that with IDA which has the composition of 1 : 2 mole ratio was unsuccessful. However, another type of complex was prepared at higher pH. About five grams of *l*-aspartic acid in 500 m*l* of water was warmed on the water bath. After it was dissolved, 5 g of chromium(III) nitrate trihydrate was added and the solution was heated for ten minutes. When 20 g of potassium carbonate were gradually added into the solution with stirring, it turned from reddish-violet to bluish-green. As soon as a scale-like film was formed on the surface of the solution, it was filtered while hot. The yield was very poor, 20 mg at most. The result of analysis was as follows: Found: Cr, 20.56; K, 14.22; C, 21.69; H, 2.13%. Calcd for $K[Cr(OH)_2asp]$: Cr, 20.30; K, 15.26; C, 20.09; H, 2.11%.

Other Measurements. Measurements of the conductivity in an aqueous solution, thermogravimetric analysis and X-ray diffraction in the solid state were carried out with a Yokogawa Universal Bridge, BV-Z-13A, a Shimadzu TM-1A type Thermobalance and a Rigaku-Denki Geiger-flex X-ray Analyzer, respectively.

Results and Discusson

Continuous Variation Method. Prior to determination of the formation constants of the complexes, the continuous variation method was applied to the system of the hexaaquochromium(III) perchlorate and IDA or *l*-aspartic acid. The results obtained by this method at pH 2, and 3—4 are shown in Fig. 1 for IDA complex and in Fig. 2 for *l*-aspartic acid complex, where the increase of the optical density due to the complex formation was plotted against the mole ratio of the ligand to the sum of metal ion and ligand. The optical density of the solution for Cr(III)-IDA system was measured at both the first and second absorption maxima of $[Cr(ida)_2]^-$, 522 mμ and 389 mμ which were reported by Yamasaki and Ito.[5] Those for Cr(III)-Asp system was measured also at the same wavelength since the corresponding absorption maxima of $[Cr(asp)_2]^-$ are close to those of the former complex.

Since the maxima in the curves shown in Fig. 1 are all found to appear in the mole ratio of metal ion

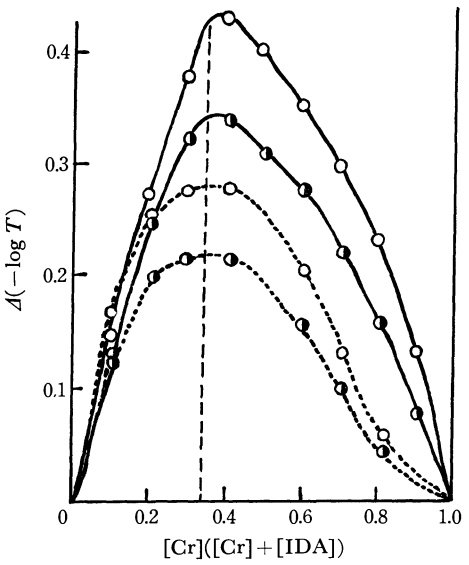

Fig. 1. Continuous variation method for Cr(III)-IDA system.
Full curve: at pH 3—4, Broken curve: at pH 2
○ 522 mμ, ◑ 389 mμ

5) K. Yamasaki and S. Ito, *Proc. Japan Acad.*, **42**, 1077 (1966).

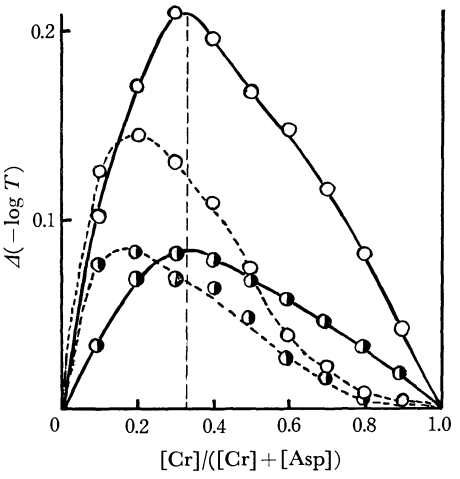

Fig. 2. Continuous variation method for Cr(III)-Asp system.
Full curve: at pH 3—4, Broken curve: at pH 2
○ 522 mμ, ◑ 389 mμ

versus ligand, 1 : 2, the composition of the predominant complex species formed in the solution at pH 2—4 may be $[Cr(ida)_2]^-$. On the other hand, in the case of *l*-aspartic acid complexes as shown in Fig. 2, the maxima in the curves at pH 2 appear in the mole ratio 1 : 3, whereas those at pH 3—4, in the ratio 1 : 2. Hence, the predominant complex species formed may have a composition $[Cr(Hasp)_3]$ at pH 2, and a composition $[Cr(asp)_2]^-$ at pH 3—4.

Conductivity and Behavior toward Ion Exchanger. The results of the molar conductivity of the complex, $K[Cr(ida)_2]\cdot 3H_2O$, in the aqueous solution obtained were 95, 102, 108, 108 and 117 at concentrations of 1/100, 1/250, 1/500, 1/1000 and 1/2000 M, respectively. The complex anion was found to be adsorbed by the anion exchanger, Dowex × 1. It seems that the complex is 1 : 1 valency-type salt and, therefore, the anion is 1 : 2 type complex.

In the solution containing hexaaquochromium(III) perchlorate and *l*-aspartic acid more than three times of chromium(III) salt at pH 2, the complex was found to pass through both cation and anion exchangers, Dowex × 1-Na-form and Dowex-× 50-Cl-form, without being adsorbed, but at pH 4, it was adsorbed only by anion exchanger. Therefore, it is presumed that the anionic complex is 1 : 2 type as given by $[Cr(ida)_2]^-$.

Formation Constants. IDA and Asp seem to dissociate in the following manner in an aqueous solution:

$$^+H_2N\text{-}\langle^{COO^-}_{COOH} \overset{pK_1}{\rightleftharpoons} {}^+H_2N\text{-}\langle^{COO^-}_{COO^-} \overset{pK_2}{\rightleftharpoons} HN\text{-}\langle^{COO^-}_{COO^-}$$

where all the formulas are expressed only by the functional amino and carboxylate groups without describing the detailed skeleton in each molecule, and K_1 and K_2 are the first and second acid dissociation constants, respectively. In order to determine these values, the aqueous solution of these amino acids in the absence of chromium(III) salt was titrated with the standard solution of sodium hydroxide in the ionic strength $\mu=0.1$ and 25°C. In terms of titration these constants were evaluated by[6]

$$K_1 = [H^+](aC_A + [H^+])/\{C_A - (aC_A + [H^+])\}$$

in the lower pH range, and by

$$K_2 = [H^+]\{(a-1)C_A - [H^+]\}/[C_A - \{(a-1)C_A - [OH^-]\}]$$

in the higher pH range, where C_A is the total concentration of amino acid, a, the numbers of moles of base added per mole of amino acid present, $[H^+]$ and $[OH^-]$, the concentrations of hydrogen and hydroxide ions respectively. The values for IDA obtained are $pK_1=2.59$ and $pK_2=9.23$. As those for Asp, $pK_1=3.70$ and $pK_2=9.62$ were used from a reference.[7]

The concentrations of the amino acids non-coordinated to either metal or hydrogen ion, $[A^{2-}]$, and the average number of the ligand coordinated to one mole of metal ion, n were calculated by[6]

$$[A^{2-}] = \{(2-a)C_A - [H^+] + [OH^-]\}/\{2[H^+]^2/K_1K_2 + [H^+]/K_2\}$$

$$\bar{n} = \{C_A - [H^+]/K_1K_2 + [H^+]/K_2 + 1)[A^{2-}]\}/C_M$$

where C_M is the total concentration of metal.

The formation curves, $\bar{n}$ *vs.* $p[A^{2-}]$, are shown in Fig. 3. By applying the successive approximation method to the values of the stepwise formation constants of chromium(III) complexes with the amino acids found in Fig. 3, the correct values were obtained and are summarized in Table 1 together with those of chromium(III) complexes with glycine.[1]

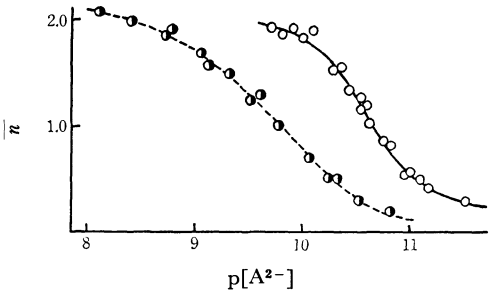

Fig. 3. Formation curve, $\bar{n}$ *vs.* $p[A^{2-}]$ for Cr(III)-IDA (—○—) and Cr(III)-Asp (--◑--) complexes.

6) S. Chaberek, Jr., and A. E. Martell, *J. Amer. Chem. Soc.*, **74**, 5052 (1952).
7) R. F. Lamb and A. E. Martell, *J. Phys. Chem.*, **57**, 690 (1953).

Table 1. Formation constants of chromium(III) complexes with amino acids (μ=0.1, 25°C)

	$\log k_1$	$\log k_2$	$\log k_3$	$\log \beta$*
Cr(III)-IDA	10.9	10.5	—	21.4
Cr(III)-Asp	10.1	9.5	—	19.6
Cr(III)-Gly	8.62	7.65	5	21.3

* β: overall formation constant

As shown in this table, the formation constants of chromium(III) complexes with IDA are slightly larger than those of the corresponding Asp complexes. This fact can be explained by the difference in the coordinating structures, *viz.*, IDA is a terdentate ligand in the complex, forming two five-membered chelate rings with chromium, where Asp seems to form one five-membered and one six-membered chelate rings as terdentate ligand in the complex.

The overall formation constants of Cr-IDA and Cr-Gly (glycine abbreviated as Gly) complexes are apparently equal to each other. This might be explained as follows.

One IDA complex anion, $[Cr(ida)_2]^-$, contains two IDA molecules coordinating totally with two nitrogen and four oxygen atoms, whereas one glycine complex molecule, $[Cr(gly)_3]$ (gly is the abbreviated form of glycinate anion), contains three glycinate anions coordinating entirely with three nitrogen and three oxygen atoms. If the bond energy of nitrogen with chromium is assumed to be larger than that of oxygen atom, the above glycine complex should be more stable than the IDA complex, so far as the coordinating atoms are concerned.

On the contrary, two molecules of IDA anions form four chelate rings in the $[Cr(ida)_2]^-$ complex, but three glycinate anions form three chelate rings in the $[Cr(gly)_3]$ complex, though their chelate rings formed are all five-membered. A large number of chelate rings in IDA complex than in Gly complex will cause larger entropy change in the former complex formation.

Therefore, the result that the overall formation constants of IDA and Gly complexes are comparable with each other can be explained by the fact that the larger chelate effect in IDA complex is balanced by the stronger bonding force in the latter complex formation.

X-Ray Powder Diffraction Analysis. The results of X-ray powder diffraction analysis for the solid IDA complex, $K[Cr(ida)_2]\cdot 3H_2O$, are listed in Table 2, which shows that it is hexagonal with a tetramolecular unit having the axial parameters $a=14.57$ Å and $c=12.38$ Å.

The solid Asp complex, $K[Cr(OH)_2asp]$ was found to be amorphous by X-ray diffraction. When the complex stored over sulfuric acid in a desiccator was exposed to moist air, it gradually began to jump in the same fashion as chromium(III) phthalato[8] and maleato[9] complexes, which was attributed to the absorption of water vapor. The maximum amount of water vapor absorbed by the above chromium(III) aspartato complex was 13.00% for the dried sample. From this value, the solid complex formed by the absorption of water was presumed to have the formula $K[Cr(OH)_2asp]\cdot 2H_2O$, in which the calculated value of the amount of water absorbed is 13.67%.

Table 2. Results of X-ray powder diffraction analyysis

d: lattice distance, *hkl*: Miller's index, *I*: intensity

d	*hkl*	*I*	*a*(Å)	*C*(Å)
9.400	011	100	14.51	12.33
7.880	111	20	14.49	12.32
7.308	020	35	14.61	12.42
4.924	030	21	14.77	12.55
4.716	022	20	14.57	12.38
4.530	031	50	14.59	12.40
4.207	131	30	14.19	12.06
3.630	132	12	14.31	12.16
3.437	123	34	14.36	12.21
3.229	240	22	14.44	12.27
2.838	341	22	14.73	12.52
2.805	124	22	14.61	12.42
2.533	243	20	14.43	12.27
1.796	007	18	14.56	12.34
			mean 14.57	mean 12.38

8) K. Higashi, K. Hori and R. Tsuchiya, This Bulletin, **40**, 2569 (1967).

9) T. Tomita, E. Kyuno and R. Tsuchiya, *ibid.*, **41**, 1130 (1968).

BULLETIN OF THE CHEMICAL SOCIETY OF JAPAN VOL. 43 401—405 (1970)

Separation Factors for Several Lanthanon Pairs Obtained at 60°C in the Ion-Exchange System Involving EDTA

Zenzi HAGIWARA and Masaru NOGUCHI*1

Faculty of Engineering, Tohoku University, Aramaki, Sendai

(Received July 29, 1969)

With a view to the accurate determination of the separation factors of adjacent rare-earth pairs between the aqueous and resin phases, measurements have been carried out at 60°C in the exchange system involving EDTA and Dowex 50W, X-8, 50—100 mesh. Under the same experimental conditions as were used for the isolation of the rare earths by ion exchange, the separation factors at 60°C were found to be 3.43 for Nd-Sm, 1.37 for Eu-Gd, 1.84 for Tb-Y, 1.54 for Y-Dy, 2.83 for Tb-Dy, 1.84 for Dy-Ho, and 2.02 for the Ho-Er and Er-Tm pairs. Further, the observed values were discussed from the viewpoints of both thermodynamics and the real elution of the rare earths by an ion-exchange column.

The isolation of individual rare-earth elements has been intensively performed by the cation-exchange method,[1,2] employing either ethylenediamine-*N*,*N*,*N*′,*N*′-tetraacetic acid (EDTA, H_4Y) or *N*′-(2-hydroxyethyl)ethylenediamine-*N*,*N*,*N*′-triacetic acid(HEDTA) as the eluant. In this case, elutions[3,4] at high temperatures brought about a preferable result for the separation of some lanthanon mixtures as compared to those at lower temperatures. Generally, an increase in the elution temperature gives a larger separation factor (α) and a smaller H.E.T.P. (height equivalent to a theoretical plate)[5-7] due to particle or film diffusion. These two terms are related to the evaluation of column efficiency in the ion-exchange process. The present authors, however, found experimentally that, in the separation of the rare-earth mixture, an increase in the temperature is not always effective for the improvement of α-value for special rare-earth pairs in the presence of a chelating agent. Therefore, a basic study of the temperature dependence of the separation factor is important. In order to make a theoretical treatment of the elution system involving rare earths and EDTA species at a high temperature, it is necessary to get precise information on the separation factors of two adjacent rare earths obtained at the same teaperature as the elution.

Previously, the present authors reported on the separation factors[8] for such adjacent rare-earth pairs as Sm–Nd, Eu–Gd, Tb–Y, Y–Ho, and Er–Tm in the presence of EDTA at 30°C; considerable differences were observed between the calculated values and those determined by experiment. The present study was undertaken in order to find more reliable separation factors for some lanthanon pairs at 60°C, (such factors are necessary for the analysis of a real elution system at the same temperature) and to compare them with the values calculated from the thermodynamic data. Further, with the aid of the experimental results obtained by the ion-exchange elution of the rare earths at 60°C, we determined whether or not the observed α-values at 60°C are correct.

Experimental

Materials Used. The rare earths were supplied in the form of oxides, such as Nd_2O_3, Sm_2O_3, Eu_2O_3, Gd_2O_3, Tb_4O_7, Y_2O_3, Dy_2O_3, Ho_2O_3, Er_2O_3, and Tm_2O_3, by the Shinetsu Chemical Industry Corp.; they all had high purities, greater than 99.99%. Each oxide was dissolved with a slight excess of hydrochloric acid under heating, and the rare-earth ions were adsorbed on a resin of the hydrogen form to prepare the rare-earth form. The other chemicals used were of an analytical grade; a Dowex 50W, X-8, 50—100 mesh was employed as the cation exchanger.

Experimental Procedures. Using the column method, various rare-earth forms of resins containing small amounts of hydrogen and ammonium were prepared. These preparations[8] have previously been described. Thus, the description of the methods is omitted

*1 Present address: Takefu Factory, Shinetsu Chemical Industry Corp.

1) J. E. Powell and F. H. Spedding, *Trans. Met. Soc. AIME (Amer. Inst. Mining. Met., Eng.)*, **215**, 457 (1959).

2) Z. Hagiwara, *Bull. Japan Institute of Metals*, **4**, 311 (1959).

3) J. R. Morton and D. B. James, *J. Inorg. Nucl. Chem.*, **29**, 2997 (1967).

4) Z. Hagiwara, *ibid.*, **31**, 2933 (1969).

5) Z. Hagiwara, *J. Phys. Chem.*, **73**, 3102 (1969).

6) Z. Hagiwara and A. Kamei, *J. Inorg. Nucl. Chem.*, **31**, 3295 (1969).

7) Z. Hagiwara, and H. Ōki, This Bulletin, **42**, 3177 (1969).

8) M. Noguchi, A. Yoshifuji and Z. Hagiwara, *ibid.*, **42**, 2286 (1969).

here. Throughout the experiments, Dowex 50W, X-8, 50—100 mesh was used. The following resins and solutions were prepared for the experiments:

Composition for the Rare-earth Forms of Resins (equivalent fraction).

Sm-resin: $\overline{Sm}=0.8472$; $\overline{NH_4}=0.0547$; $\overline{H}=0.0981$.
Gd-resin: $\overline{Gd}=0.8784$; $\overline{NH_4}=0.0559$; $\overline{H}=0.0657$.
Y - resin: $\overline{Y}=0.9213$; $\overline{NH_4}=0.0312$; $\overline{H}=0.0475$.
Dy-resin: $\overline{Dy}=0.8778$; $\overline{NH_4}=0.0412$; $\overline{H}=0.0809$.
Ho-resin: $\overline{Ho}=0.8665$; $\overline{NH_4}=0.0343$; $\overline{H}=0.0991$.
Er-resin: $\overline{Er}=0.8924$; $\overline{NH_4}=0.0243$; $\overline{H}=0.0833$.
Tm-resin: $\overline{Tm}=0.9096$; $\overline{NH_4}=0.0121$; $\overline{H}=0.0782$.

Composition of the Rare-earth Solutions(mol/l)

Nd-soln.: $Y_f=0.00250$; $Nd_T=0.01374$; $NH_{4T}=0.00997$; pH=2.59.
Eu-soln.: $Y_f=0.00193$; $Eu_T=0.01461$; $NH_{4T}=0.00745$; pH=2.41.
Tb-soln.: $Y_f=0.00169$; $Tb_T=0.01440$; $NH_{4T}=0.00650$; pH=2.21.
Y-soln.: $Y_f=0.00023$; $Y_T=0.01331$; $NH_{4T}=0.00473$; pH=2.19.
Dy-soln.: $Y_f=0.00143$; $Dy_T=0.01487$; $NH_{4T}=0.00575$; pH=2.05.
Ho-soln.: $Y_f=0.00130$; $Ho_T;=0.01449$; $NH_{4T}=0.00503$; pH=2.13.
Er-soln.: $Y_f=0.00082$; $Er_T=0.01488$; $NH_{4T}=0.00353$; pH=2.00.

The barred quantities refer to the composition of the indicated species in the resin, and the subscript quantities, to the concentrations of the indicated species in the aqueous phase. Further, the symbol Y_f represents the excess of anionic species of EDTA present in the uncombined form with the rare earth. Therefore, the total concentration of EDTA is equal to the sum of Ln_T and Y_f, disregarding the presence of Ln^{3+} in the prepared rare-earth solutions. The resin and aqueous phases are expressed in the equivalent fraction and in moles per liter respectively.

Equilibrium Experiment. After mixing a definite amount of the prepared rare-earth resin containing small amounts of hydrogen and ammonium with a proper volume of the rare-earth solution, the resulting mixture was shaken for 96 hr in a constant-temperature bath kept at 60°C. After equilibration, the resin was separated from the aqueous phase, and the rare earths in both phases were determined in order to find the separation factor. The analytical procedures have been described in detail in the foregoing paper.[8]

Resutls and Discussion

The equilibrium compositions of the adjacent rare-earth pairs are listed in Table 1, in which the mole fraction is used as the concentration unit for the two phases. The observed α-values are also given in the same table; they are found from the relation:

$$\alpha_{Ln_2}^{Ln_1}=\left(\frac{m_{\overline{Ln_1}}}{m_{\overline{Ln_2}}}\right)\left(\frac{m_{Ln_2}}{m_{Ln_1}}\right) \quad (1)$$

where $m_{\overline{Ln_1}}+m_{\overline{Ln_2}}=1$ (resin phase) and $m_{Ln_1}+m_{Ln_2}=1$ (aqueous phase). The Ln_1 and Ln_2 symbols represent adjacent rare-earth elements, and m, the mole fraction. The barred quantities refer to the resin phase, and the unbarred, to the aqueous phase. The average values of the separation factors obtained at 60°C are tabulated in Table 2, in which the α-values calculated from the

Table 1. Equilibrium compositions and separation factors for adjacent rare-earth pairs at 60°C

Exp. No.	Sample taken		Mole fraction of adjacent rare earth at equilibrium				$\alpha_{Ln_2}^{Ln_1}$	Ave. $\alpha_{Ln_2}^{Ln_1}$
			Resin phase		Aqueous phase			
	Ln-resin g	Ln-soln. ml	$\overline{Ln_1}$	$\overline{Ln_2}$	Ln_1	Ln_2		
2—4	5.00(Sm)	300(Nd)	0.542(Nd)	0.458(Sm)	0.264(Nd)	0.736(Sm)	3.30	
2—5	5.00(Sm)	450(Nd)	0.677(Nd)	0.323(Sm)	0.373(Nd)	0.628(Sm)	3.53	$\alpha_{Sm}^{Nd}=3.43$
2—6	5.00(Sm)	600(Nd)	0.761(Nd)	0.239(Sm)	0.479(Nd)	0.521(Sm)	3.46	
6—4	5.00(Gd)	300(Eu)	0.482(Eu)	0.518(Gd)	0.398(Eu)	0.602(Gd)	1.41	
6—5	5.00(Gd)	450(Eu)	0.583(Eu)	0.417(Gd)	0.507(Eu)	0.493(Gd)	1.36	$\alpha_{Gd}^{Ed}=1.37$
6—6	5.00(Gd)	600(Eu)	0.661(Eu)	0.339(Gd)	0.595(Eu)	0.405(Gd)	1.33	
4—4	5.00(Y)	300(Tb)	0.506(Tb)	0.494(Y)	0.363(Tb)	0.637(Y)	1.80	
4—5	5.00(Y)	450(Tb)	0.634(Tb)	0.366(Y)	0.485(Tb)	0.515(Y)	1.84	$\alpha_{Y}^{Tb}=1.84$
4—6	5.00(Y)	600(Tb)	0.726(Tb)	0.274(Y)	0.586(Tb)	0.414(Y)	1.87	
6—1	3.00(Dy)	180(Y)	0.462(Y)	0.538(Dy)	0.350(Y)	0.650(Dy)	1.59	
6—2	3.00(Dy)	270(Y)	0.560(Y)	0.440(Dy)	0.459(Y)	0.541(Dy)	1.50	$\alpha_{Dy}^{Y}=1.54$
6—3	6.00(Dy)	360(Y)	0.462(Y)	0.538(Dy)	0.360(Y)	0.640(Dy)	1.53	
5—4	5.00(Ho)	300(Dy)	0.563(Dy)	0.437(Ho)	0.413(Dy)	0.587(Ho)	1.83	
5—5	5.00(Ho)	450(Dy)	0.667(Dy)	0.333(Ho)	0.522(Dy)	0.478(Ho)	1.83	$\alpha_{Ho}^{Dy}=1.84$
5—6	5.00(Ho)	600(Dy)	0.739(Dy)	0.261(Ho)	0.604(Dy)	0.396(Ho)	1.86	
9—1	5.00(Er)	300(Ho)	0.526(Ho)	0.474(Er)	0.360(Ho)	0.640(Er)	1.97	
9—2	5.00(Er)	450(Ho)	0.638(Ho)	0.362(Er)	0.464(Ho)	0.536(Er)	1.04	$\alpha_{Er}^{Ho}=2.02$
9—3	5.00(Er)	600(Ho)	0.712(Ho)	0.288(Er)	0.547(Ho)	0.453(Er)	1.05	
3—4	5.00(Tm)	300(Er)	0.556(Tm)	0.443(Tm)	0.376(Er)	0.624(Tm)	2.08	
3—5	5.00(Tm)	450(Er)	0.667(Tm)	0.333(Tm)	0.516(Er)	0.484(Tm)	1.88	$\alpha_{Tm}^{Er}=2.02$
3—6	5.00(Tm)	600(Er)	0.740(Tm)	0.260(Tm)	0.575(Er)	0.425(Tm)	2.10	

Table 2. Comparison of separation factors for adjacent rare-earth pairs

Rare-earth pair Ln_1-Ln_2	Calcd $\alpha_{Ln_2}^{Ln_1}$ a)		Obsd $\alpha_{Ln_2}^{Ln_1}$		$\alpha_{Ln_2}^{Ln_1}=K_{Ln_2Y}/K_{Ln_1Y}$	
	298°K	333°K	303°K	333°K	298°K	
					$\alpha^{b)}$	$\alpha^{c)}$
La-Ce	1.78	1.77	—	—	3.02	4.68
Ce-Pr	2.09	2.00	—	—	2.63	2.29
Pr-Nd	1.95	1.81	—	—	1.62	2.04
Nd-(Pm)	1.8?	—	—	—	—	—
(Pm)-Sm	1.7?	—	—	—	—	—
Nd-Sm	3.00	3.15	3.77	3.43	3.39	3.09
Sm-Eu	1.32	1.51	—	—	1.62	1.38
Eu-Gd	1.51	1.75	1.30	1.37	1.05	1.02
Gd-Tb	3.08	3.43	—	—	3.63	4.79
Tb-Y	1.13	1.24	1.76	1.84	1.45	1.51
Y-Dy	2.59	2.32	1.61	1.54	1.62	1.55
Tb-Dy	2.92	2.87	2.83*	2.83*	2.35**	2.34**
Dy-Ho	1.82	1.77	1.88	1.84	1.90	3.63
Ho-Er	2.11	1.98	—	2.02	1.86	1.74
Er-Tm	1.97	1.91	2.05	2.02	2.95	3.31
Tm-Yb	2.21	2.06	—	—	1.55	2.09
Yb-Lu	1.48	1.43	—	—	2.09	1.82

* Calcd from the observed α-values of the Tb-Y and Y-Dy pairs.
? Estimated α-values using a value of K_{PmY} found graphically (Fig. 1) and the values of K_{NdY} and K_{SmY}.
** Found from the calcd. α-values of the Tb-Y and Y-Dy pairs.
a) Calcd from calorimetric data.[9]
b) Calcd from data of stability constants.[10]
c) Calcd from data of stability constants.[11]

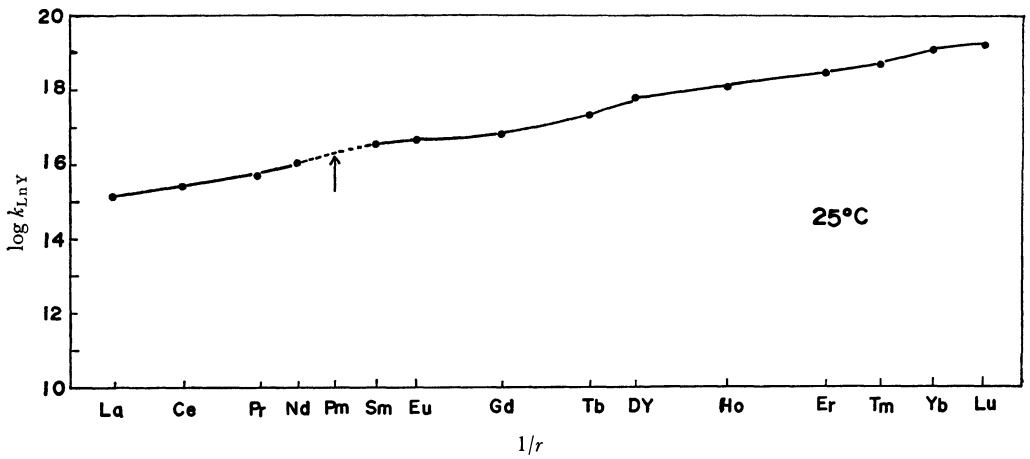

Fig. 1. Plots of stability constants of rare earth-EDTA chelates against the reciprocal value of the ionic radius.
Plots were made using data of Mackey *et al.*[9]

calorimetric data[9] of the formation of the Ln-EDTA chelates and from the ratio of the stability constants[10-11] are also given. The α-values at 30°C are given as well in order to compare the values at different temperatures.

The α-values in the second column in Table 2 were calculated using Eq. (4), which will be given below. The following relationships held, employ-

9) J. L. Mackey, J. E. Powell and F. H. Spedding, *J. Amer. Chem. Soc.*, **84**, 2047 (1962).
10) G. Schwarzenbach, R. Gut and G. Anderegg, *Helv. Chim. Acta*, **37**, 937 (1954).
11) E. J. Wheelwright, F. H. Spedding and G. Schwarzenbach, *J. Amer. Chem. Soc.*, **75**, 4196 (1953).

ing the thermodynamic quantities ($\Delta H°$, $\Delta S°$, and $\Delta F°$):

$$\Delta F^{\circ}_{Ln_1} = -\boldsymbol{R}T \ln K_{Ln_1Y} = \Delta H^{\circ}_{Ln_1} - T\Delta S^{\circ}_{Ln_1} \quad (2)$$

$$\Delta F^{\circ}_{Ln_2} = -\boldsymbol{R}T \ln K_{Ln_2Y} = \Delta H^{\circ}_{Ln_2} - T\Delta S^{\circ}_{Ln_2} \quad (3)$$

The combination of the above equations leads to the following form:

$$\log \alpha^{Ln_1}_{Ln_2} = \log \frac{K_{Ln_2Y}}{K_{Ln_1Y}} = -\frac{(\Delta H^{\circ}_{Ln_2} - \Delta H^{\circ}_{Ln_1}) - T(\Delta S^{\circ}_{Ln_2} - \Delta S^{\circ}_{Ln_1})}{2.303\,\boldsymbol{R}T} \quad (4)$$

The α-values in the fourth column in Table 2 were calculated by means of the following relation[8]:

$$\alpha^{Ln_1}_{Ln_2} = \frac{K_{Ln_2Y}}{K_{Ln_1Y}} \quad (5)$$

As is shown in Table 2, the separation factors for the Nd-Pm and Pm-Sm pairs were calculated using a value of K_{PmY} found by interpolation of the data obtained by Mackey *et al.*[9] (Fig. 1).

In the present study, the temperature dependence of the separation factor is almost identical between the observed and calculated values except for the α-value for the Nd-Sm pair; the experimental results show that the effect of the temperature on α seems to be very small for such rare-earth pairs as Tb-Dy, Dy-Ho, Ho-Er, and Er-Tm. The α-values for the Dy-Ho, Ho-Er, and Er-Tm pairs obtained at 333°K are in good agreement with the calculated values obtained by introducing the thermodynamic data[9] into Eq.(4). On the other hand, the Er-Tm separation factor obtained at temperatures of 298 and 333°K by the use of Eq. (5) seems to be too high. A value of 2.83 for the Tb-Dy separation factor is indirectly found from the experimental data of 1.84 for α^{Tb}_{Y} and 1.54 for α^{Y}_{Dy}; this is consistent with the calculated value of 2.87 at 333°K.

The α^{Y}_{Dy} found at 303°K is too low compared to the value of 2.59 at 298°K obtained by using Eq. (4); the former is rather close to the value obtained from the ratio of the two stability constants of the Ln-EDTA chelates. Further, the observed Tb-Y separation factors at both temperatures show fairly large discrepancies from the calculated values.

As a result of the analysis of the elution behavior of the rare-earth mixture containing Tb, Y, and Dy, the value of α^{Tb}_{Y} and α^{Y}_{Dy} obtained in this study may be concluded to be reasonable. In the temperature range from 25 to 60°C, the elution sequence of these elements with a solution of 0.015 M EDTA buffered with NH_4OH (pH=8.5) is: Dy→Y→Tb. In the elution of a mixture involving Dy, Y, and Tb through a copper-retaining bed with the aid of 0.015 M EDTA (pH=8.5), the rare-earth band arrived at a steady-state condition after travelling for a proper distance on the column. In such a state, the Tb-Y cut at the tail of the adsorption band is obviously sharper than the Dy-Y cut at the front. In other words, the inherent overlap region with Tb and Y is actually less than that with Dy and Y, as is to be expected from a comparison of the H.E.T.P./log α term. This fact supports the observed α-values for these pairs.

Using 0.015 M EDTA (pH=8.5) as the eluant, the following two elution experiments were carried out at 60°C with a flow rate of 10 ml/min (I.D. 22 mm-column). In one of the experiments, the rare-earth-sorption band with an equimolar mixture of Tb and Y (bed dimensions: 2.2×35 cm) was eluted down the retaining bed with Dowex 50 W, X-8, 50—100 mesh (2.2×90 cm). In the other run, the rare-earth band with an equimolar mixture of Dy and Y (bed dimensions: 2.2×70 cm) was eluted down the retaining bed (2.2×180 cm). In both runs, the length of the retaining bed is enough for the steady state to be attained during elution. The rare-earth eluates issuing from the column were analyzed to observe the change in the composition of the overlap region of the rare-earth band.

After a steady state had been established throughout the elution system by the displacement of the rare-earth band, the overlapping area with the two rare-earth components was fixed to a definite composition gradient; the shape of the boundary is independent of further elution distance. In this case, the following relationship[12] finally holds, if the ion exchange is regarded a countercurrent extraction: $\log R_n/R = n \log \alpha = (\log \alpha/\text{H.E.T.P.})L$, where L is the distance between the two points on the resin; n, the number of theoretical plates, and α and R, the separation factor for the adjacent rare earths and their molar ratio respectively. Thus, the plateheight value can be found from the above relationship. Under the previously-described conditions, the H.E.T.P.-values are found to be 1.2 cm for the elution of the Tb-Y mixture and 2.0 cm for the elution of the Dy-Y mixture.

The length of the overlap region with 99.9% pure adjacent Ln_1 and Ln_2 products can be calculated from this relation:

$$L = \frac{6(\text{H.E.T.P.})}{\log \alpha} \quad (6)$$

where the value of 6 as $\log R_n/R$ is found for the above conditions. Therefore, if any pure product is desired, it is necessary for the length of a sorption band of the rare earth in the column to exceed L. Taking H.E.T.P.=1.2 cm and $\alpha^{Tb}_{Y}=1.84$ at 60°C for the Tb-Y pair, L is equal to 27 cm, while a value of 28 cm was experimentally obtained. A good agreement is seen between them. In the case of the Dy-Y pair, taking H.E.T.P.=2.0 cm

12) J. E. Powell and H. R. Burrholder, *J. Chromatogr.*, **29**, 210 (1967).

and $\alpha_Y^{Dy}=1.54$ at 60°C, L is equal to 64 cm; this is near the observed value of 65 cm. In both calculations, the α-value was assumed to be constant throughout the whole mixed zone with rare earths.

One of the present authors deduced the following relationship[4] for film-diffusion control in ion exchange:

$$Z(X_{Ln_2}) = H_f\left\{-\frac{\alpha}{\alpha-1}\ln X_{Ln_2} + \frac{1}{\alpha-1}\ln(1-X_{Ln_2}) - 1\right\} \quad (7)$$

where $Z(X_{Ln_2})$ is the distance of the plane with the concentration of X_{Ln_2} from the gravity center of the rare-earth boundary involving Ln_1 and Ln_2, where α is the separation factor, and where H_f is the plate-height value due to film diffusion. The X_{Ln_2} symbol is expressed in the concentration unit of the equivalent fraction of the Ln_2 species, while both Z and H_f are expressed in centimeters. As Z is a function of X_{Ln_2}, the length of the rare-earth band required to get 99.9% pure products in a steady state can be calculated. The substitution of $\alpha_Y^{Tb}=1.84$ into Eq. (7) gives:

$$Z(X_{Tb}) = H_f\{-5.04\log X_{Tb} + 2.74\log(1-X_{Tb}) - 1\} \quad (8)$$

Therefore, we obtain:

$$Z_1(X_{Tb}) = -9.22\,H_f \text{ at } X_{Tb}=0.999$$

$$Z_2(X_{Tb}) = 14.12\,H_f \text{ at } X_{Tb}=0.001$$

Thus, the length of the overlap region necessary for obtaining 99.9% Tb and Y products can be found by adding the absolute values of Z_1 and Z_2 at $H_f=1.2$ cm:*2

$$L = |Z_1| + |Z_2| = 28 \text{ cm}$$

In the elution of the Y-Dy pair, when $\alpha_{Dy}^{Y}=1.54$ and $H_f=2.0$*2 are introduced into Eq. (7), the length of the band required to get 99.9% Y and Dy products is found to be 65 cm; this value is in excellent agreement with the value obtained in the elution experiments at a steady state. Therefore, it can be concluded that the α-values obtained for the Y-Dy and Tb-Y pairs in the exchange system with EDTA are satisfactory.

On the other hand, an increase in the temperature effects an increase in the Eu-Gd separation factor, as may be seen in Table 2. The α-value at 60°C was 1.37 in the presence of EDTA; this was lower than the value calculated from Eq. (4), while a vlue of 1.5 was obtained for the pair at 92°C by another study.[12] Considering the variation in α with the temperature, the observed value of 1.37 seems to be reasonable.

*2 The H_f-values were found graphically by a curve-fitting method described in a previous paper.[4]

BULLETIN OF THE CHEMICAL SOCIETY OF JAPAN VOL. 43 406—408 (1970)

Cobalt(III) Complexes with Schiff Bases Obtained from Salicylaldehyde Derivatives and Alkanol Amines*[1]

Shoichiro YAMADA,* Yoshio KUGE** and Kuniko YAMANOUCHI*

* *Institute of Chemistry, College of General Education, Osaka University, Toyonaka, Osaka*

** *Public Health Institute, Morimachi, Higashi-ku, Osaka*

(Received July 31, 1969)

Cobalt(III) complexes with Schiff bases (X-SAL.Y-OH) obtained from salicylaldehyde derivatives and alkanol amines ($H_2N.Y$-OH) were synthesized as crystals. Two types of diamagnetic cobalt(III) complexes were obtained, one being green (type A) and the other red (type B). In the complexes of type A with the general formula [Co(H-SAL.R)$_3$], where R=$CH_2CH_2CH_2OH$ and $CH_2CH_2CH_2OCH_3$, the ligands are considered to function as bidentate ligands, the terminal hydroxyl or methoxy groups not being bound with the cobalt(III) ion. In the complexes of type B with the general formula Co(X-SAL.Y-OH)(X-SAL.Y-O), where X=H and 3-CH_3O, and Y=CH_2CH_2, $CH_2CH(CH_3)$ and $C(CH_3)_2CH_2$, the ligands function as terdentate ligands.

In previous papers[1-3] we reported nickel(II) and copper(II) complexes with Schiff bases obtained from salicylaldehyde derivatives and alkanol amines (formula I), and disclosed that the behaviour of the alcoholic hydroxyl group varies depending

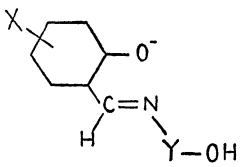

Formula I

upon the kind of the central metal ions on the one hand and upon the nature of the ligands on the other. In this connection, it seems worthwhile to examine the corresponding complexes with other metal ions and to compare the results with the previous ones. The present paper deals with cobalt(III) complexes with the ligands denoted by formula I.

Experimental

Materials. The cobalt(III) complexes, which are shown in Table 1, were prepared according to the following three methods, (1) from cobalt(II) acetate, (2) from bis(salicylaldehydato)- or bis(substituted salicylaldehydato)-cobalt(II) and an alkanol amine, and (3) from cobalt(II) acetate and a Schiff base. These methods are similar to those previously described.[4,5] In methods (1) and (3), sodium carbonate or sodium ethanolate was added to the reaction mixture. Purification was carried out by recrystallizing the crude products from suitable organic solvents like methanol, ethanol or chloroform.

The complexes of the [Co(H-SAL.R)$_3$] type (type A), obtained as dark-green crystals, are insoluble in water but soluble in methanol, ethanol, chloroform, benzene and pyridine.

The complexes of the Co(X-SAL.Y-OH)(X-SAL.-Y-O) type (type B), obtained as red or brownish red crystals, are insoluble in water, slightly soluble in chloroform and benzene, and souble in methanol and ethanol. The solubility in any of these solvents is not high enough to allow any determination of the molecular weights of these complexes.

Analytical data of these complexes are shown in Table 1.

Measurements. Electronic absorption spectra were determined with a Shimadzu MPS-50L spectrophotometer and a Shimadzu QR-50 spectrophotometer. Infrared spectra were determined with a Hitachi-EPI-2 IR-spectrophotometer.

The diamagnetism of the complexes was detected by the Gouy method.

Results and Discussion

Two types of complexes were obtained with the ligands of formula I, one being green (type A) and the other red (type B). Since both these complexes

*1 Presented, in part, at the 20th Annual Meeting of the Chemical Society of Japan, Tokyo, April, 1967.

1) S. Yamada, Y. Kuge and K. Yamanouchi, This Bulletin, **40**, 1854 (1967).

2) S. Yamada, Y. Kuge and K. Yamanouchi, *Inorg. Chim. Acta*, **1**, 139 (1967); S. Yamada, H. Nishikawa, Y. Kuge and K. Yamanouchi, *Sci. Rep. Coll. Gen. Educ. Osaka Univ.*, **16**, 11 (1967).

3) S. Yamada, E. Ohno, Y. Kuge, A. Takeuchi, K. Yamanouchi and K. Iwasaki, *Coordin. Chem. Rev.*, **3**, 247 (1968).

4) S. Yamada, *ibid.*, **1**, 415 (1966).

5) R. H. Holm, G. W. Everett, Jr., and A. Chakravorty, "Progress in Inorganic Chemistry," Vol. VII, ed. by F. A. Cotton, Interscience Publishers, New York, N. Y. (1966), p. 83.

Table 1. Analytical data of [Co(H-SAL.R)$_3$] (type A) and Co(X-SAL.Y-OH)(X-SAL.Y-O) (type B)

X	Y or R	Found, %			Calcd, %			type
		C	H	N	C	H	N	
H	CH_2CH_2	55.48	5.13	6.93	55.96	4.96	7.25	B
	$CH_2CH(CH_3)$	52.87	6.05	5.94	53.34	6.04	6.22	B*
	$CH_2CH_2CH_2OH$	59.78	6.12	6.91	60.70	6.11	7.08	A
	$CH_2CH_2CH_2OCH_3$	62.53	6.70	6.51	62.37	6.62	6.62	A
	$C(CH_3)_2CH_2$	58.75	6.23	5.92	58.54	6.25	6.20	B
3-CH_3O	CH_2CH_2	53.36	5.29	6.22	53.34	6.04	6.22	B*
	$CH_2CH(CH_3)$	50.08	6.51	5.46	50.01	6.29	5.30	B**
	$C(CH_3)_2CH_2$	55.69	6.36	5.44	55.40	6.35	5.38	B***

* With two water molecules of crystallization
** With three water molecules of crystallization
*** With one water molecule of crystallization

are diamagnetic, they are concluded to be cobalt(III) complexes of a low-spin type. It is well known that cobalt(III) (d^6) complexes of a low-spin type usually have an octahedral configuration.

The electronic spectra of these complexes are shown in Fig. 1. The spectra of the complexes of type A are very similar to those of Co(H-SAL.-alkyl)$_3$.[4,6,7] The close similarity in the spectra indicates that these green complexes (type A) may take a configuration similar to that of the Co(H-SAL.-alkyl)$_3$ type, namely a *mer*-configuration.[8]

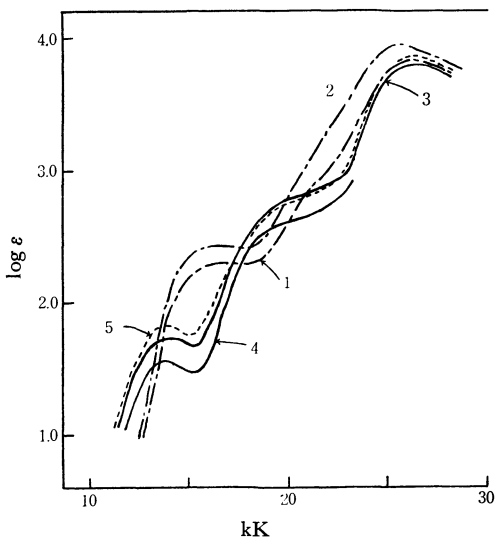

Fig. 1. Electronic absorption spectra of Co(H-SAL.R)$_3$ (type A) and Co(H-SAL.Y-O) (H-SAL.Y-OH) (type B): 1, R=$CH_2CH_2CH_2OH$ (type A), in ethanol; 2, R=*n*-C_3H_7 (type A), in ethanol; 3, Y=$C(CH_3)_2CH_2$ (type B), in methanol; 4, Y=$C(CH_3)_2CH_2$ (type B), in the solid state (by reflectance); 5, Y=$CH_2CH(CH_3)$ (type B), in chloroform.

Their spectra in pyridine are nearly the same as those in non-donor solvents, showing that the configuration of the complexes in non-donor solvents is retained, when dissolved in pyridine. It is thus found that the ligands H-SAL.R function as bidentate ligands in the complexes of type A, the terminal hydroxyl and the methoxy group not being bound with cobalt(III) ion. Inspection of the steric condition shows that the hydroxyl group at the γ-position may not be as favorable as that at the β-position, as in the complexes of the B-type, for coordination with the central metal ion.[1,4,5] It is known that the coordinating ability of the methoxy group is much lower than that of the hydroxyl group.

The red cobalt(III) complexes of type B may be formulated as Co(X-SAL.Y-O)(X-SAL.Y-OH), where Y denotes CH_2CH_2, $CH_2CH(CH_3)$ and $C(CH_3)_2CH_2$ for X=H and 3-CH_3O. The presence of the ligand X-SAL.Y-OH in these complexes is supported by infrared spectra, which have absorption peaks at about 3000 to 3500 cm^{-1} due to the hydroxyl group.*2 The electronic absorption spectra of all the complexes of type B in solution or in the solid state (Fig. 1) are similar to each other, showing that these cobalt(III) complexes have a similar configuration, and that the configuration in the solid state is retained in solution. It should be noted that the main features of these spectra, with absorption maxima at about 14 kK (log ε 1.5—2.0), about 20 kK (log ε 2.5—3.0) and about 26.5 kK (log ε 3.7—4.0), are remarkably similar to those of bis[2-(salicylideneamino)alkanoato]cobaltate(III) complexes, which show absorption maxima at 15.0 kK (log ε 1.95), 19.8 kK (log ε 2.75) and 26.5 kK (log ε 3.7)[9]. It seems, therefore, very likely that the red complexes of type B have a configuration similar to that of the bis[2-(salicylideneamino)alkanoato]-complexes, which were

6) H. Nishikawa and S. Yamada, This Bulletin, **37**, 1154 (1964).
7) S. Yamada, *Coordin. Chem. Rev.*, **2**, 83 (1967).
8) M. Ciampolini, F. Maggio and F. P. Cavasino, *Inorg. Chem.*, **3**, 1188 (1964).
9) R. C. Burrows and J. C. Bailar, Jr., *J. Amer. Chem. Soc.*, **88**, 4150 (1966).

concluded previously to be uninuclear, octahedral cobalt(III) complexes.[9] Thus, in the complexes of type B, the ligands are found to act as terdentate ligands.

For coordination compounds of type $M(ABC)_2$, many isomers are possible, where the notation ABC denotes a terdentate ligand bearing three different ligating atoms. It is to be noted that the *d-d* band maxima at the lowest frequencies of the complexes of type B lie at remarkably low frequencies (about 14.0 kK), as compared with those of the complexes of the $[Co(X\text{-}SAL.alkyl)_3]$ type (about 16.1 kK). It is expected that the complexes of the *trans*-$[Co(N)_2(O)_4]$ type may show remarkable splitting of the *d-d* band, and the splitted component might appear in the region of considerably low frequencies. The arrangement of the ligand atoms shown in Fig. 2(a) or (b) is highly probable for the structure of the complexes of type B, since such a configuration would yield a *d-d* band maximum at the lowest frequency. However, it is not possible at the present stage to draw a definite conclusion about the precise configuration. Another possibility like a binuclear configuration might not be completely excluded. The low solubility of the complexes of type B did not allow any determination of molecular weight.

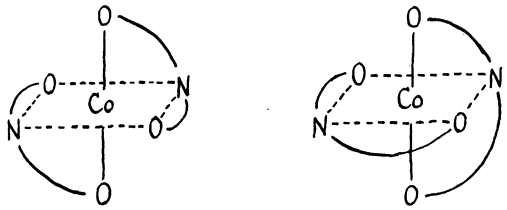

Fig. 2. Proposed configurations for Co(X-SAL.-Y-O)(X-SAL.Y-OH).

It has thus been revealed that all the cobalt(III) complexes obtained are octahedral, six-coordinated. This result, which is different from that for the corresponding nickel(II) and copper(II) complexes,[1,2] is in agreement with the general tendency of cobalt(III) to form much more stable, octahedral complexes as compared with nickel(II) or copper(II).

Financial support of this work by the Ministry of Education is gratefully acknowledged.

*2 It is probable that the hydroxyl group forms a hydrogen bond with an oxygen atom of the neighbouring ligand. More detailed study was not carried out.

BULLETIN OF THE CHEMICAL SOCIETY OF JAPAN VOL. 43 409—414 (1970)

Metal(II) Complexes of Ethylenediaminemonoacetic Acid (EDMA). Polarographic Studies of Cadmium(II) and Lead(II)-EDMA Complexes

Yuki FUJII, Teiko UEDA and Mutsuo KODAMA

Department of Chemistry, Ibaraki University, Mito, Ibaraki

(Received August 2, 1969)

In the present paper, the d.c. polarographic behavior of cadmium(II) and lead(II) ions in ethylenediaminemonoacetate (EDMA) solutions was studied systematically. Since these metal(II) ions in an EDMA solution behave reversibly in a polarographic electrolysis, the compositions and the stability constants of cadmium(II)- and lead(II)-EDMA complexes could be estimated successfully from the shift of the half-wave potential of these metal(II) ions due to the complex formation with EDMA. The cadmium(II) ion was found to form complexes of 1-to-1 and 1-to-2 compositions with EDMA, and the electrode reaction mechanism was established to be:

$$CdX^+ + 2e^- + nH^+ + Hg = Cd(Hg) + H_nX^{n-1}$$
$$\uparrow\downarrow$$
$$CdX_2$$

The successive formation constants of cadmium(II)-EDMA complexes, $(K_1)_{CdX}$ and $(K_2)_{CdX}$, were determined to be 3.01×10^8 and 5.65×10^4 respectively. On the other hand, the lead(II) ion forms only one complex with 1-to-1 composition. In the presence of the chloride ion, the lead(II) ion was found to form a mixed ligand complex involving the chloride ion as well as a normal complex, PbX^+, and the electrode reaction could be formulated as:

$$PbX^+ + 2e^- + nH^+ + Hg = Pb(Hg) + H_nX^{n-1}$$
$$\uparrow\downarrow$$
$$PbXCl^0$$

The equilibrium constants, $(K_1)_{PbX}(=[PbX^+]/([Pb^{2+}]\cdot[[X^-]))$ and $K^{Cl}_{PbX}(=[PbXCl^0]/([PbX^+]\cdot[Cl^-]))$, were determined to be 1.69×10^8 and 1.01×10 respectively. The effect of the zinc(II) ion on the half-wave potential of the cadmium(II) ion in an EDMA solution was also studied. From the positive shift of the half-wave potential due to the presence of the zinc(II) ion, the formation constant of the zinc(II)-EDMA complex with a 1-to-1 composition was estimated to be 1.58×10^8.

Polarographic studies have been made extensively by numerous investigators on the metal complexes of aminopolycarboxylic acids.[1-4] Generally, it has been accepted that cadmium(II) and lead(II) complexes of aminopolycarboxylic acids which have acetic acid groups behave irreversibly in a polarographic electrolysis.[1-3,5] In a previous paper,[6] we ourselves reported that although ethylenediaminetetrapropionic acid (EDTP) has four carboxylate groups and two amino groups, the cadmium(II) ion forms complexes of 1-to-1 and 1-to-2 compositions with EDTP and undergoes a reversible two-electron reduction at the dropping mercury electrode. The formation of the cadmium(II)-EDTP complex with a 1-to-2 composition may indicate that only one propionate group and two amino groups of EDTP anion act as the electron-donating groups in the complex formation reaction with the cadmium(II) ion. Whether or not the reversible nature of the cadmium(II)-EDTP complex can be related to its characteristic structure seems to be very interesting. Therefore, to get much fuller and more accurate information about the above subject, we tried to study the polarographic behavior of the cadmium(II) ion in an ethylenediaminemonoacetic acid (EDMA) which has only one acetate group and compared it with that in the EDTP solution. This attempt was also important in establishing a precise description of the properties of EDMA as a ligand. In this paper, we studied thoroughly the d.c. polarographic

1) N. Tanaka, R. Tamamushi and M. Kodama, *Z. Phys. Chem., N. F.*, **14**, 141 (1959).
2) K. H. Schroder, *Acta Chem. Scand.*, **16**, 1315 (1962).
3) Y. Koike and H. Hamaguchi, *J. Inorg. Nucl. Chem.*, **29**, 473 (1967).
4) Y. Fujii and M. Kodama, This Bulletin, **42**, 3172 (1969).
5) N. Tanaka, M. Kodama, M. Sasaki and M. Sugino, *Bunseki Kagaku*, **6**, 86 (1957).
6) M. Kodama and Y. Tominaga, This Bulletin, **42**, 2267 (1969).

behavior of cadmium(II) and lead(II) ions in the EDMA and determined the solution equilibria between EDMA and these ions. The effect of the zinc(II) ion on the polarographic behavior of the cadmium(II) ion in the EDMA solution was also investigated.

Experimental

Reagents. All the chemicals were of an analytical reagent grade and were used without further purification. The standard solution of cadmium(II) perchlorate was prepared by dissolving pure metallic cadmium in perchloric acid (1+2). Its concentration was determined by EDTA titration, using Eriochrom Black T as the indicator.[7] The methods of the preparation and standardization of the zinc(II) perchlorate solution have been given previously.[8] The standard solution of lead(II) nitrate was prepared by dissolving a known amount of lead nitrate in redistilled water. The preparation and purification of EDMA dihydrochloride were also described in a previous paper.[9]

Apparatus and Experimental Procedures. All the apparatus (polarographs and a glass electrode pH meter) and the experimental procedures employed have been described previously.[4] The rate of the flow of mercury, m, and the drop time, t_d, of the dropping mercury electrode used in the present study were 0.839 mg/sec and 3.92 sec respectively at a mercury height of 60 cm in an air-free 0.10 M acetate buffer solution (μ=0.20) of pH 4.80 at 0.0 V *vs.* SCE.

Results and Discussion

D. C. Polarographic Behavior of the Cadmium(II) Ion in an Ethylenediaminomonoacetate Solution. The polarographic behavior of the cadmium(II) ion in an EDMA solution with an ionic strength of 0.20 was studied in the pH range from 6.00 to 7.00. In this study, no buffer reagent was used, because the sample solutions always contained a large excess of uncomplexed EDMA and had enough buffer capacity to maintain the pH value of the solution constant. Under the above pH conditions, the cadmium(II) ion in the EDMA solution invariably gave a single well-difined polarographic wave (Fig. 1). Although the results are not given here, its wave height was exactly proportional to the square-root of the effective mercury pressure on the dropping mercury electrode and to the bulk concentration of the cadmium(II) ion. The log-plot analysis of the polarogram gave linear relations with reciprocal slopes falling into the range from 33 to 37 mV. The results will not be shown here. From the above experimental facts, it can be concluded that the

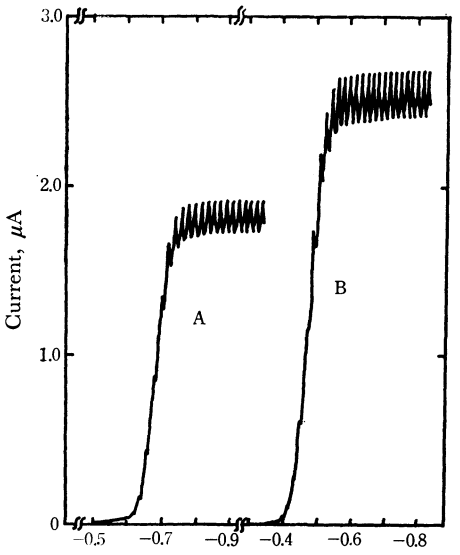

Fig. 1. D.C. polarograms of cadmium(II) and lead(II) ions in the EDMA solution.
A: Concentration of cadmium(II) ion=0.371 mM
Concentration of uncomplexed EDMA=20.0 mM
Concentration of chloride ion=40.0 mM
25°C, μ=0.20, pH=6.95
B: Concentration of lead(II) ion=0.50 mM
Concentration of uncomplexed EDMA =15.0 mM
Concentration of chloride ion=60.0 mM
25°C, μ=0.20, pH=6.45

cadmium(II) ion in the EDMA solution undergoes a two-electron reversible reduction at the mercury electrode. Therefore, the solution equilibria between the cadmium(II) ion and EDMA could be determined successfully by the conventional polarographic method employed previously.[6,10-12] As was mentioned in a previous paper,[4] an EDMA anion X^- can be effected to act as a tridentate ligand. Hence, the cadmium(II) ion will also form complexes with 1-to-1 and 1-to-2 compositions, CdX^+ and CdX_2^0. If both 1-to-1 and 1-to-2 complexes are formed, the electrode reaction of the cadmium(II) ion in the EDMA solution at the DME can be assumed to be:

$$\begin{array}{l} CdX^+ + 2e^- + nH^+ + Hg = Cd(Hg) + H_nX^{n-1} \\ \quad\Updownarrow \\ CdX_2^0 \end{array} \qquad (1)$$

where H_nX^{n-1} indicates protonated EDMA species.

7) W. Biedermann and G. Schwarzenbach, *Chimia*, **2**, 56 (1948).
8) M. Kodama and H. Ebine, This Bulletin, **40**, 1857 (1967).
9) Y. Fujii, E. Kyuno and R. Tsuchiya, *ibid.*, **43**, (1970), in press.
10) M. Kodama, T. Noda and M. Murata, *ibid.*, **41**, 354 (1968).
11) M. Kodama and Y. Tominaga, *ibid.*, **42**, 394 (1969).
12) M. Kodama and Y. Tominaga, *ibid.*, **42**, 724 (1969).

Consequently, as was discussed in connection with the d.c. polarography of the copper(II) ion in an EDMA solution,[4] the shift of the half-wave potential of the cadmium(II) ion due to the complex formation with EDMA can be derived thermodynamically as:

$$\Delta E_{1/2} = (E_{1/2})_{Cd^{2+}} - (E_{1/2})_{CdX} = 0.0296\left[\log\left(\frac{(K_1)_{CdX}}{(\alpha_H)_X}\cdot[X]_f + \frac{(K_1)_{CdX}(K_2)_{CdX}}{(\alpha_H)_X^2}\right)\cdot[X]_f^2 + \log\frac{k_{CdX}}{k_{Cd^{2+}}}\right] \quad (2)$$

where $(E_{1/2})_{CdX}$, $(E_{1/2})_{Cd^{2+}}$, $k_{Cd^{2+}}$, k_{CdX} and $(\alpha_H)_X$ have their usual meanings.[13] $[X]_f$ and (K_i) in Eq. (2) denote the concentration of uncomplexed EDMA and the successive formation constants of cadmium(II)-EDMA complexes.

Equation (2) clearly indicates that when solution's pH is kept constant, the plot of antilog $(\Delta E_{1/2}/0.0296+\log(k_{Cd^{2+}}/k_{CdX}))/[X]_f$ against $[X]_f$ will give a linear relation the slope and the intercept of which will correspond to $(K_1)_{CdX}(K_2)_{CdX}/(\alpha_H)_X^2$ and $(K_1)_{CdX}/(\alpha_H)_X$ respectively. This relation was examined experimentally at pH 6.95. A typical linear relation is shown in Fig. 2. From the intercept and the slope of the linear relation in Fig. 2, the $(K_1)_{CdX}$ and $(K_2)_{CdX}$ values were estimated to be 3.01×10^8 and 5.65×10^4 respectively. The formation of a mixed ligand complex involving the chloride ion could be ruled out, because when the other experimental conditions were kept constant, the half-wave potential was independent of the chloride-ion concentration. If the above conclusion is correct, the dependence of the half-wave potential on the solution pH can be estimated exactly with the aid of Eq. (2) and using the $(K_1)_{CdX}$ and $(K_2)_{CdX}$ values determined. The pH dependence of the half-wave potential was calculated and compared with that observed experimentally (Table 1). The agreement of the caluculated values with those determined experimentally can be regarded as satisfactory. This agreement clearly gives strong support to the electrode reaction mechanism proposed by the present authors.

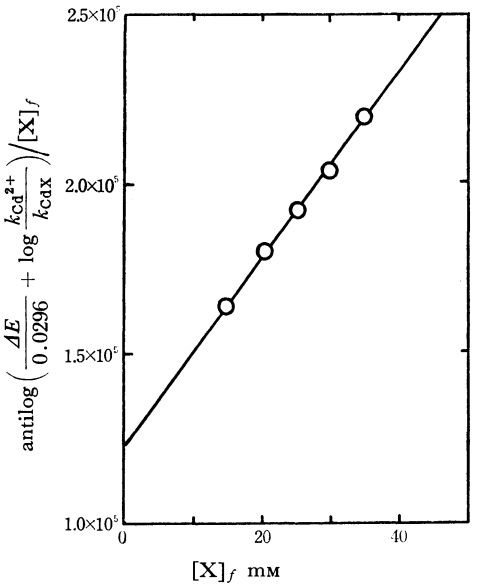

Fig. 2. Determination of successive formation constants of cadium(II)-EDMA complexes. Concentration of cadmium(II) ion=0.371 mM 25°C, μ=0.20, pH=6.95

Table 1. The effect of pH on the half-wave potential

μ=0.20, 25°C
Concentration of cadmium(II) ion=0.371 mM
Concentration of uncomplexed EDMA=20.0 mM

pH	Half-wave potential V *vs.* SCE	$\Delta E_{1/2}$, mV Obsd	$\Delta E_{1/2}$, mV Calcd
6.00	-0.603_0	0	0
6.41	-0.626_5	$23._5$	21.8
6.94	-0.665_0	$62._0$	56.0

The effect of the zinc(II) ion on the half-wave potential of the cadmium(II) ion in the EDMA solution was also studied. The cadmium(II) ion in the EDMA solution containing the zinc(II) ion was also found to behave reversibly in a polarographic sense. The log-plot examination at pH's lower than 7.5 gave linear relations with reciprocal solpes falling in the rang from 30 to 33 mV. The results are not shown here. When the total concentration of the zinc(II) ion added, $[Zn(II)]_t$, is larger than that of EDMA, $[X]_t$, and when all the EDMA species in the solution exist in the form of ZnX^+, the concentration of the uncomplexed cadmium(II) ion can be given by:

$$[Cd^{2+}] = \frac{[Cd(II)]_t}{1+\frac{(K_1)_{CdX}}{(K_1)_{ZnX}}\frac{[ZnX^+]}{[Zn^{2+}]}} \quad (3)$$

where $[Cd(II)]_t$ is the total concentration of the cadmium(II) ion and where $(K_1)_{ZnX}$ is the formation constant of ZnX^+. Therefore, the half-wave potential of the cadmium(II) ion in the solution containing an excess of the zinc(II) ion over EDMA can be expressed as:

$$E_{1/2} = E_{Cd^0} + 0.0296\left[\log\frac{k_{Cd(Hg)}}{k_{Cd^{2+}}} + \log\left(1+\frac{(K_1)_{CdX}}{(K_1)_{ZnX}}\frac{[X]_t}{[Zn(II)]_t-[X]_t}\right) - \log f_{Cd^{2+}}\right] \quad (4)$$

The symbols used in Eq. (4) have their usual meanings.[6] Hence, the difference in the half-wave potential between the cadmium(II) aquo

complex and the cadmium(II) ion in the solution containing EDMA and the zinc(II) ion can be given approximately by:

$$\Delta E_{1/2} = 0.0296\left[\log\left(1+\frac{(K_1)_{CdX}}{(K_1)_{ZnX}}\frac{[X]_t}{[Zn(II)]_t-[X]_t}\right)\right] \quad (5)$$

This relation clearly indicates that the plot of anti log ($\Delta E_{1/2}$/0.0296) *vs.* $[X]_t/([Zn(II)]_t-[X]_t)$ should give the linear relation with an intercept of unity. This relation was examined experimentally on the solution of pH 6.00. A linear relation could be obtained between the antilog ($\Delta E_{1/2}$/0.0296) and $[X]_t/([Zn(II)]-[X]_t)$. A typical linear relation is shown in Fig. 3. This fact clearly indicates that, in the presence of an excess amount of the zinc(II) ion, the EDMA species exists exclusively in the form of ZnX^+. From the slope of the above linear relation, $(K_1)_{ZnX}$ was estimated to be 1.58×10^8. This value seems reasonable, for the stability constants of zinc(II) complexes of polyamines and aminopolycarboxylic acids have been reported to be nearly identical with those of corresponding cadmium(II) complexes.[13]

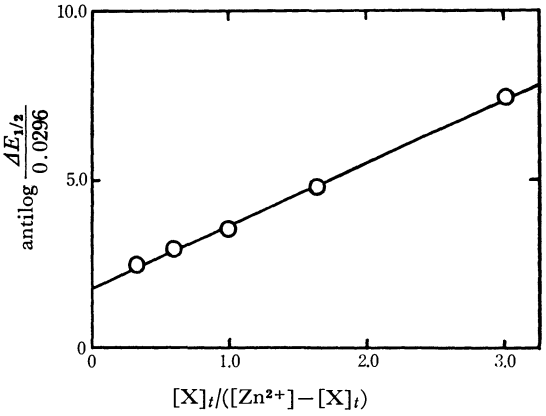

Fig. 3. Determination of formation constant of zinc(II)-EDMA complex.
Concentration of cadmium(II) ion=0.371 mM
Concentration of zinc(II) ion=40.0 mM
Concentration of acetate ion=0.10 M
25°C, μ=20, pH=6.00

D. C. Polarographic Behavior of the Lead(II) Ion in an EDMA Solution. The d.c. polarographic behavior of the lead(II) ion in an EDMA solution was also studied in the pH range from 6.50 to 8.50. The lead(II) ions in the EDMA solution also gave a well-defined single wave (Fig. 1), the height of which was exactly proportional to the square-root of the effective pressure on the DME and to the bulk lead(II) ion concentration. Under the present experimental conditions, the log-plot examination invariably gave linear relations with reciprocal slopes falling into the range from 30 to 33 mV. Therefore, the lead(II) ions in the EDMA solution can also be concluded to undergo a two-electron reversible reduction. The lead(II) ion has been reported to form only the complex of a 1-to-1 composition with nitrilotriacetic acid (NTA).[13] This fact clearly indicates that the coordination number of the lead(II) ion is four under the usual experimental conditions. For this reason, in the presence of the chloride ion, the lead(II) ion can be expected to form a normal complex with a 1-to-1 composition, PbX^+, and a mixed ligand complex involving the chloride ion, $PbXCl^0$, with EDMA. If the lead(II) ion in the EDMA solution containing the chloride ion form a mixed ligand complex as well as a normal complex, the electrode reaction of the lead(II) ion at the mercury electrode can be assumed to be:

$$\begin{array}{l} PbX^+ + 2e^- + nH^+ + Hg = Pb(Hg) + H_nX^{n-1} \quad (6) \\ \quad\Updownarrow \\ PbXCl^0 \end{array}$$

Consequently, the shift of the half-wave potential of the lead(II) ion due to the complex formation with EDMA can be given by:

$$\Delta E_{1/2} = 0.0296\left[\log\frac{(K_1)_{PdX}}{(\alpha_H)_X}(1+K^{Cl}_{PbX}[Cl^-]) + \log[X]_f + \log\frac{k_{PbX}}{k_{Pb^{2+}}}\right] \quad (7)$$

where $k_{Pb^{2+}}$ and k_{PbX} are the diffusion current constants of the lead(II)-aquo and -EDMA complexes respectively, and where $(K_1)_{PbX}$ and K^{Cl}_{PbX} are defined thusly: $(K_1)_{PbX}=[PbX^+]/[Pb^{2+}]\cdot[X^-]$ and $K^{Cl}_{PbX}=[PbXCl^0]/[PbX^+]\cdot[Cl^-]$.

Equation (7) clearly indicates that, if the mixed ligand complex, $PbXCl^0$, is also formed, the plot of the anitilog($\Delta E_{1/2}$/0.0296+log $k_{Pb^{2+}}/k_{PbX}$−log $[X]_f$) against the concentration of the uncomplexed chloride ion, $[Cl^-]$, should give a linear relation when the other experimental conditions are kept constant. This relation was examined experimentally on the solution of pH 6.45. A linear relation was found between the antilog[$\Delta E_{1/2}$/0.0296+log $k_{Pb^{2+}}/k_{PbX}$−log$[X]_f$] and $[Cl^-]$ (Fig. 4). From the slope and the intercept of the above linear relation, the K^{Cl}_{PbX} and $(K_1)_{PbX}$ values were estimated to be 1.08×10 and 1.69×10^8 respectively.

Equation (7) also shows that when the other experimental conditions are kept constant, the following relation should hold between the shift of the half-wave potential and log $(\alpha_H)_X$:

$$\frac{\Delta E_{1/2}}{\Delta\log(\alpha_H)_X} = 29.6\text{ mV} \quad (8)$$

This relation was also examined experimentally. The results are given in Table 2. The shift of the half-wave potential calculated with the aid of Eq. (8) agreed well with that observed. Using the

13) L. G. Sillen and A. E. Martell, "Stability Constants of Metal-Ion Complexes," The Chemical Society, London (1964).

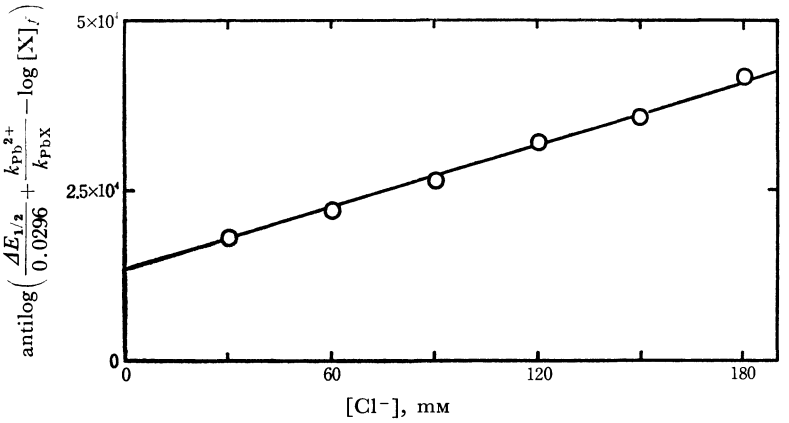

Fig. 4. Determination of formation constants of lead(II)-EDMA complexes.
Concentration of lead(II) ion=0.50 mM
Concentration of uncomplexed EDMA=15.0 mM
25°C, μ=0.20, pH=6.45

TABLE 2. THE EFFECT OF pH ON THE HALF-WAVE POTENTIAL

μ=0.20, 25°C
Concentration of lead(II) ion=0.50 mM
Concentration of uncomplexed EDMA=20.0 mM

pH	Half-wave potential V *vs.* SCE	$\Delta E_{1/2}$, mV	
		Obsd	Calcd
6.75	-0.456_7	0	0
7.29	-0.476_2	$19._5$	19.6
7.85	-0.493_3	$36._6$	39.4
8.36	-0.509_0	$52._3$	55.1

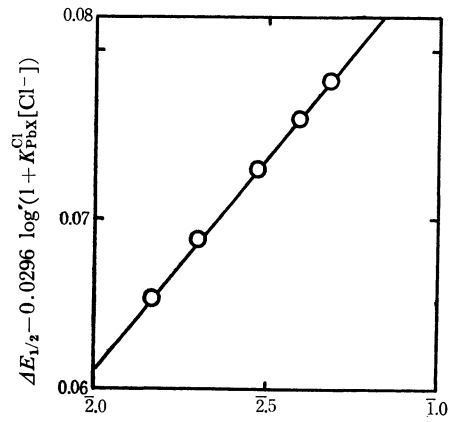

Fig. 5. The plot of $\Delta E_{1/2}-0.0296(1+K^{Cl}_{PbX}\cdot[Cl^-])$ against log $[X]_f$.
Concentration of lead(II) ion=0.50 mM
25°C, μ=0.20, pH=6.45

K^{Cl}_{PbX} value determined, the effect of the concentration of the uncomplexed EDMA on the half-wave potential of the lead(II) ion was also studied. Equation (7) shows that when the solution pH is kept constant, the plot of $\Delta E_{1/2}-0.0296$ log $(1+K^{Cl}_{PbX}\times[Cl^-])$ against log $[X]_f$ should give a linear relation. This was also examined satisfactorily. The results obtained are shown in Fig. 5. From the above results and discussion, it can safely be concluded that, under the present experimental conditions, the lead(II) ion forms PbX^+ and $PbXCl^0$ and the electrode reaction mechanism of the lead(II) ion in an EDMA solution can be given by Eq. (6).

As has been stated above, both cadmium(II) complexes of EDTP and EDMA undergo a reversible two-electron reduction at the dropping mercury electrode. The former complex may contain two six-membered rings involving a metal-oxygen bond, while the latter may contain two five-membered rings involving a metal-oxygen bond. Therefore, the reversible behavior of the cadmium(II)-EDTP complex can hardly be ascribed to the structure of EDTP, in which all acetate groups of ethylenediaminetetraacetate are replaced by propionate groups to give terminal rings of six rather than five members. It should also be mentioned here that cadmium(II)-aminopolycarboxylate complexes which have larger stability constants behave irreversibly, whereas those which have smaller stability constants behave reversibly. Generally, the larger stability constant is considered to correspond to the greater affinity of the ligand for the metal ion. The greater affinity for the metal ion will, then, produce the more pronounced change in the electronic structure of the metal ion. On the basis of the above discussion, the cadmium(II) ion in the EDTP and EDMA complexes may be said to have an electronic structure not significantly different from that of the cadmium(II) aquo complex, which undergoes a typical reversible reduction. This may also account for the reversible behavior of the cadmium(II)-EDTP and -EDMA complexes.

Since the cadmium(II) ion can form complexes

of a 1-to-2 composition with EDTP and EDMA, in both cadmium(II) complexes two ligands are considered to be attached to each cadmium(II) ion with four nitrogens and two oxygens. Considering the well-known fact that the cadmium(II)-amine complex behaves reversibly in a polarographic electrolysis,[14] this may mean that the nature and the number of donor atoms also play an important role in the determination of the polarographic behavior of cadmium(II)-aminopolycarboxylate complexes. In order to describe the precise relation between the polarographic behavior of the cadmium(II)-aminopolycarboxylate complex and its structure, however, further systematic investigations should be conducted.

14) L. Meites, *J. Amer. Chem. Soc.*, **72**, 2293 (1950).

BULLETIN OF THE CHEMICAL SOCIETY OF JAPAN VOL. 43 414—418 (1970)

Preparation of Chromium(III) and Cobalt(III) Complexes with *l*-Leucine-*N*,*N*-diacetic Acid*[1]

Akira UEHARA, Eishin KYUNO and Ryokichi TSUCHIYA

Department of Chemistry, Faculty of Science, Kanazawa University, Kanazawa

(Received August 7, 1969)

l-Leucine-*N*,*N*-diacetic acid (abbreviated as LDA) and the complexes thereof were prepared as follows: $K[Cr(OH)(lda)(H_2O)]\cdot 3H_2O$ (violet) (I), $[Cr(lda)(H_2O)_2]$ (bluish violet) (II), $[Cr(lda)(H_2O)_2]\cdot 2H_2O$ (grayish violet) (III), $(enH_2)_{1/2}[Cr(OH)(lda)(H_2O)_2]$ (green) (IV), $[Cr(lda)(o\text{-phen})]\cdot 2H_2O$ (brownish orange) (V), $K[Cr(lda)(acac)]\cdot H_2O$ (blackish violet) (VI) and $K[Co(OH)(lda)(H_2O)]\cdot H_2O$ (bluish violet) (VII), where lda, en, *o*-phen and acac are the abbreviations of *l*-leucine-*N*,*N*-diacetate ion, ethylenediamine, *o*-phenanthroline and acetylacetonate ion, respectively. Except for Complex IV, LDA behaves as a quadridentate ligand. In Complex IV, it acts as a terdentate one. It was found from electronic absorption spectra that in Complex I, LDA behaves as a quadridentate in a solid state and as a terdentate ligand in an aqueous solution, whereas in cobalt(III) complex VII corresponding to I, LDA behaves as a quadridentate. Stepwise liberation of the coordinated water molecules in Complexes II and III could be detected by means of Derivatograph. Complex VII showed "Dehydration-Dimerization Reaction" upon being heated.

Preparation and properties of chromium(III) complexes with ammoniatriacetic acid (ATA) or with its derivatives have been reported.[1-5] Although these agents have a maximum of four coordinating sites, the coordinating behaviors somewhat differ from each other due to the slight differences in their structures and chemical properties. As an example, the ligands which can form three five-membered chelate rings such as ATA or AIPDA act not only as a quadridentate of $N\text{–}O_3$ type but also as a terdentate ligand of O_3 type.[1,4] ATA, APDA and AEDA can also behave as a terdentate ligand of $N\text{–}O_2$ type.[1,3,5] In spite of the analogous structure of APDA and AEDA, the latter behaves with difficulty as a quadridentate due to the weaker coordinating ability of oxygen atom in the sulfonic than that in carboxylic group.

In a series of studies on chromium(III) and cobalt(III) complexes with ATA and its derivatives, the preparation of *l*-leucine-*N*,*N*-diacetic acid and the complexes thereof were undertaken in order to investigate how LDA behaves toward the two metals.

For the sake of convenience, the rational formula of LDA is given in Table 1 with respect to ATA as the mother chelating agent and the other related agents.[1,3,5]

Experimental

Preparation of *l*-Leucine-*N*,*N*-diacetic Acid, $C_{10}H_{17}O_6N$. Thirteen grams of *l*-leucine was dissolved in 50 m*l* of water containing 6 g of sodium hydroxide

*1 Presented at the 22nd Annual Meeting of the Chemical Society of Japan, Tokyo, April, 1969.

1) A. Uehara, E. Kyuno and R. Tsuchiya, This Bulletin, **40**, 2317 (1967).

2) A. Uehara, E. Kyuno and R. Tsuchiya, *ibid.*, **40**, 2322 (1967).

3) A. Uehara, E. Kyuno and R. Tsuchiya, *ibid.*, **41**, 2385 (1968).

4) A. Uehara, E. Kyuno and R. Tsuchiya, *ibid.*, **41**, 2393 (1968).

5) A. Uehara, E. Kyuno and Tsuchiya, *ibid.*, **42**, 2835, (1969).

Table 1. Chelating agents

Rational formulas	Chelate rings	Chelating agents
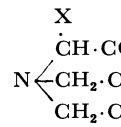	5, 5, 5	X=H : ATA* X=CH_3 : AIPDA* X=$CH_2\cdot CH\cdot(CH_3)_2$: LDA*
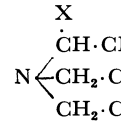	5, 5, 6	X=H, Y=COOH : APDA* X=H, Y=SO_3H : AEDA* X=COOH, Y=COOH : ASDA*

* ATA: Ammoniatriacetic acid, AIPDA: Ammoniaisopropionicdiacetic acid, LDA: *l*-Leucine-*N*,*N*-diacetic acid, APDA: Ammoniapropionicdiacetic acid, AEDA: *β*-Aminoethylsulfonic-*N*,*N*-diacetic acid, ASDA: Aspartic-*N*,*N*-diacetic acid

Table 2. Preparative scheme for Cr-, Co-LDA complexes

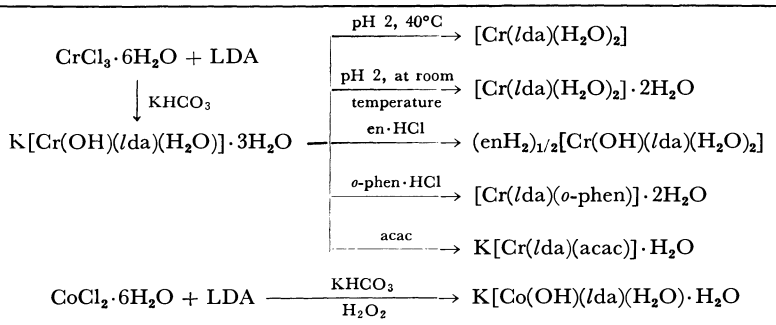

(A). 70 m*l* of water containing 19 g of monochloroacetic acid was gradually neutralized with 17 g of sodium hydrogen carbonate (B). B had to be added gradually to A since rapid addition produces deposit of *l*-leucine. The mixture was heated on a water bath, 30 m*l* of water containing 12 g of KOH being added. Heating was continued for about 1 hr till the condensation reaction was completed. After the solution was cooled, concentrated hydrochloric acid was added little by little to the solution with scrubbing of the wall of the reaction vessel with a glass rod, when white powdered crystals were deposited. Recrystallization was achieved by dissolving the crude products in sodium hydrogen carbonate solution and by adjusting the pH of the solution to 3. Yield about 8 g.

Found: N, 5.66; 48.49; H, 6.86%. Calcd for $C_{10}H_{17}O_6N$: N, 5.63; C, 48.57; H, 6.92%.

Preparation of Complexes. Preparation of the complexes is schematically shown in Table 2.

Potasium Hydroxo-*l*-leucine-*N*,*N*-diacetatoaquochromate(III) Trihydrate, K[Cr(OH)(*l*da)(H_2O)]·$3H_2O$ (I). Twenty five grams of chromium chloride hexahydrate and 24 g of LDA were added to about 300 m*l* of water. The mixture was heated on a water bath until LDA was completely dissolved. To the resulting violet solution, about 10 g of potassium hydrogen carbonate were added, when vigorous bubbling took place. Heating of the solution was continued until the bubbles subsided. When the solution was concentrated, a tar-like residue was deposited out. The supernatant layer was discarded by decantation. The residue was dissolved in about 300 m*l* of water. The pH of the violet solution was then adjusted to 6—7 by adding an appropriate amount of potassium hydrogen carbonate. The resulting solution was concentrated to about 200 m*l* and was stood in a refrigerator. Violet crystals were obtained. Recrystallization was carried out from water. Yield about 5 g. The crystals were used as material to prepare the following complexes, II to VI.

Found: N, 3.31; C, 28.31; 5.43%. Calcd for K[Cr(OH)(*l*da)(H_2O)]·$3H_2O$: N, 3.47; C, 28.58; H, 4.84%.

The use of ammonium carbonate, instead of potassium hydrogen carbonate as described above, produced the corresponding ammonium salt which is also violet.

Found: N, 7.28; C, 31.18; H, 6.48%. Calcd for NH_4[Cr(OH)(*l*da)(H_2O)]·$2H_2O$: N, 7.25; C, 30.90; H, 6.51%.

***l*-Leucine-*N*,*N*-diacetatodiaquochromium(III), [Cr(*l*da)(H_2O)$_2$] (II).** Five grams of Complex I was dissolved in 200 m*l* of hot water and then a few drops of hydrochloric acid were added. As the solution was gradually concentrated at about 40°C, violet crystals were depo-sited out. The crude crystals were recrystallized from a concentrated hot aqueous solution. Yield about 1.5 g.

Found: N, 4.22; C, 36.18; H, 5.43%. Calcd for [Cr(*l*da)(H_2O)$_2$]: N, 4.51; C, 35.56; H, 5.42%.

***l*-Leucine-*N*,*N*-diacetatodiaquochromium(III) Dihydrate, [Cr(*l*da)(H_2O)$_2$]·$2H_2O$ (III).** Preparation was carried out in a manner similar to that used for II, except that the solution was stood at room temperature instead of 40°C. The crystals have a grayish violet

color. Recrystallization was achieved from water. Yield about 2 g.

Found: N, 3.81; C, 32.62; H, 5.38%. Calcd for $[Cr(l\text{da})(H_2O)_2]\cdot 2H_2O$: N, 3.88; V, 32.54; H, 5.19%.

Ethylenediamine Hydroxo-*l*-leucine-*N*,*N*-diacetatodiaquochromate(III) $(enH_2)_{1/2}[Cr(OH)(l\text{da})(H_2O)_2]$ (IV). Five grams of Complex I was dissolved in 200 m*l* of water and then 4 g of ethylenediamine hydrochloride was added. Gradual concentration on a water bath gave a deposit of green crystals. Another crop of crystals were obtained from the resulting cool solution. Recrystallization was carried out from water. Yield about 2 g.

Found: N, 7.37; C, 34.79; H, 6.12%. Calcd for $(enH_2)_{1/2}[Cr(OH)(l\text{da})(H_2O)_2]$: N, 7.22; C, 35.03; H, 5.93%.

***l*-Leucine-*N*,*N*-diacetato-*o*-phenanthrolinechromium(III) Dihydrate, $[Cr(l\text{da})(o\text{-phen})]\cdot 2H_2O$ (V).** Two grams of *o*-phenanthroline was added to 200 m*l* of water containing 5 g of Complex I. After the pH of the solution was adjusted to 4—5, it was heated on a water bath. Heating was continued until brown crystals began to deposit. Although the crystals are slightly soluble in water, recrystallization can be made from hot water. Yield about 3 g.

Found: N, 8.21; C, 51.59; H, 5.08%. Calcd for $[Cr(l\text{da})(o\text{-phen})].2H_2O$: N, 8.43; C, 51.91; H, 4.72%.

Potassium *l*-Leucine-*N*,*N*-diacetatoacetylacetonatochromate(III) Monohydrate, $K[Cr(l\text{da})(\text{acac})]\cdot H_2O$ (VI). Two-hundred milliliters of aqueous solution containing 5 g of Complex I and 1.5 g of acetylacetone was heated on a water bath and then was concentrated to about 50 m*l*. The solution being stood in a refrigerator for a few days, blackish violet crystals were obtained. The crude products were recrystallized from a water-alcohol mixture (1 : 4). Yield about 2 g.

Found: N, 3.09; C, 39.75; H, 5.29%. Calcd for $K[Cr(l\text{da})(\text{acac})].H_2O$: N, 3.03; C, 39.20; 5.19%.

Potassium Hydroxo-*l*-leucine-*N*,*N*-diacetatoaquocobaltate(III) Monohydrate, $K[Co(OH)(l\text{da})(H_2O)]\cdot H_2O$ (VII). One-hundred grams of LDA was added to 300 m*l* of water containing 100 g of cobalt(II) chloride hexahydrate and then the mixture was heated on a water bath. About 50 g of potassium hydrogen carbonate was gradually added. After the pH of the solution was adjusted to 6—7, about 10 m*l* of 28% hydrogen peroxide solution was dropped into the solution in order to oxidize the cobalt(II) ion. Bluish violet crystals were obtained from the solution stood at room temperature. Recrystallization was achieved from water. Yield about 20 g.

Found: N, 3.54; C, 30.41; H, 4.82%. Calcd for $K[Co(OH)(l\text{da})(H_2O)]\cdot H_2O$: N, 3.72; 30.78; H, 4.71%.

Apparatus. Molecular rotatory power was measured with Model MP-IT Polarimeter supplied by Applied Electric Lab., Ltd. The other apparatus used in this paper were the same as described previously.[1-5]

Results and Discussion

IR Spectra. The infrared absorption spectra were measured in their nujol mull state in order to ascertain whether or not the carboxylic group was coordinated. Table 3 shows their IR data. Assignments by Busch and Bailar[6] were also applied in this paper. The bands observed at 1738 and 1580 cm^{-1} in LDA itself were assigned to free carboxylic acid and carboxylate ion, respectively. Only one band was observed in all the complexes in the range ($\sim$1650 cm^{-1}) where the presence of the coordinated carboxylate groups can be detected.

Molar Conductivities. Molar conductivities were measured in an aqueous solution at 25°C for examination of the type of electrolytes for the complexes. The results are given in Table 4, together with their magnetic moments evaluated from magnetic susceptibilities measured at 20—23°C. Numerical data of conductivities for Complexes I, IV, VI and VII are within 110 to 160 mho cm^{-1}, indicating that these complexes are the 1 : 1 type electrolytes. The value for IV (157 mho cm^{-1}) is somewhat larger than that expected. This seems to be due to the partial dissociation of the hydrogen ion from enH_2^{2+}. Small conductivities for II, III and V suggest that they are non-electrolyte complex species.

Magnetic Moments. The effective magnetic moments of these complexes were evaluated from the magnetic susceptibilities measured by the Gouy method. The results are shown in Table 4. The magnetic moments for I to VI are in region of 3.75—

Table 3. IR data (cm^{-1})

Complexes	-COOH	-COO-M	$-COO^-$	Complement
I		1069—1640		
II		1670—1610		
III		1665—1615		
IV		1660—1630		
V		1690—1640		1585, 1529, 860*1
VI		1680—1630		1573, 1528*2
VII		1690—1640		
LDA	1738		1580	

*1 Absorptions arising from *o*-phenanthroline.
*2 Absorptions arising from acetylacetone.

6) D. H. Busch and J. C. Bailar, Jr., *J. Amer. Chem. Soc.*, **75**, 4574 (1953).

Table 4. Molar conductivities (λ) and magnetic moments (μ_{eff})

Complexes	λ* mho cm^{-1}	($^\circ$K)	μ_{eff} B.M.	($^\circ$K)
I	111.2	(298°)	3.76	(293°)
II	11.2	(298°)	3.81	(293°)
III	3.3	(298°)	3.83	(293°)
IV	157.0	(298°)	3.81	(294°)
V	19.6	(298°)	3.93	(294°)
VI	109.0	(298°)	3.86	(296°)
VII	117.8	(298°)	dia	(294°)

* 10^{-3} mol/l aqueous solution was used.

3.95 B.M., being near the spin-only values for tervalent chromium. Complex VII is diamagnetic, indicating that the cobalt is tervalent.

Molecular Rotatory Powers. As LDA is optically active, the measurements of molecular rotatory powers for LDA and each complex were carried out with a Na-D line. The data are summarized in Table 5.

Table 5. Molecular rotatory powers

Complexes	$[M]_D^{25}$	Condition
I	+373	0.3% aqueous solution
II	+298	0.3% aqueous solution
III	+260	0.4% aqueous solution
IV	+362	0.3% aqueous solution
V	+41	0.1% aqueous solution
VI	+299	0.4% aqueous solution
VII	+1132	0.4% aqueous solution
LDA	+22.5	8.7% (0.1 N $KHCO_3$) solution

Electronic Spectra. Electronic spectra of all the complexes were measured in an aqueous solution, and those for solid-state were carried out by a diffusion-reflection method. The spectra are shown in Figs. 1—5, and numerical values of absorption maxima are summarized in Table 6.

Table 6. Absorption maxima

Complexes	ν_1(10^{13}/sec)	(log ε_1)	ν_2(10^{13}/sec)	(log ε_2)
I	51.46	(1.96)	72.64	(2.00)
II	53.57	(2.03)	73.53	(2.01)
III	53.57	(2.04)	73.53	(1.99)
IV	51.46	(1.94)	72.64	(2.01)
V	56.39	(1.95)	76.14	(2.87)
VI	54.45	(1.98)	78.13	(2.28)
VII	53.10	(2.28)	75.38	(2.32)

The spectra for Complex I in an aqueous solution and in a solid state are shown in Fig. 1 together with those for the corresponding ATA complex in a solution. The spectra for Complex I and the corresponding ATA complex both in solution are quite similar, whereas the spectrum for Complex I in a solid state is considerably different from the former two. The facts suggest that, like the ATA complex, LDA actsas a quadridentate (N_1–O_3 type) in a solid state but as a terdentate (O_3 type) in an aqueous solution.

Figure 2 shows the spectra in an aqueous solution for Complexes II, III and [Cr(ata)$(H_2O)_2$] in which ATA acts as a quadridentate ligand. Close resemblance between these spectra suggests that the structures of these complex species are analogous with each other and LDA behaves as a quadridentate.

Figure 3 shows the spectra in solution and solid state for Complex IV and those for the corresponding ATA complex in solution in which ATA behaves as a terdentate ligand (O_3 type). Similarity among these spectra suggests that the structures of Complex IV are identical in solid state and solution, and that LDA behaves toward metal as a terdentate

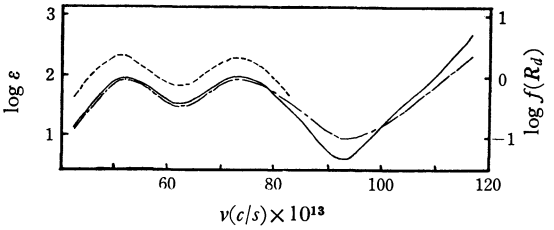

Fig. 1. Electronic Spectra for the solution (——) and the solid (- - -) of Complex I and for the solution of K[Cr(OH)(ata)(H_2O)]·$2H_2O$ (—·—).

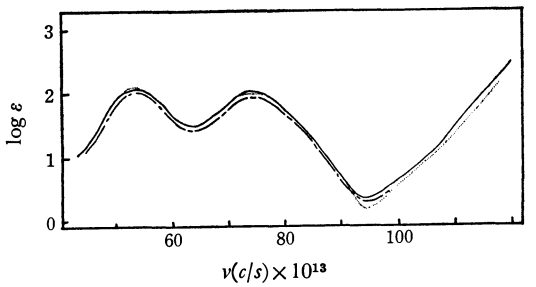

Fig. 2. Electronic spectra for the solutions of Complex II (——), Complex III (……) and [Cr(ata)(H_2O_2)] (—·—).

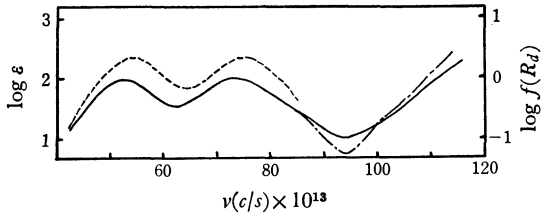

Fig. 3. Electronic spectra for the solution (——) and the solid (- - -) of Complex IV and for the solution of K[Cr(OH)(ata)$(H_2O)_2$]·$3H_2O$.

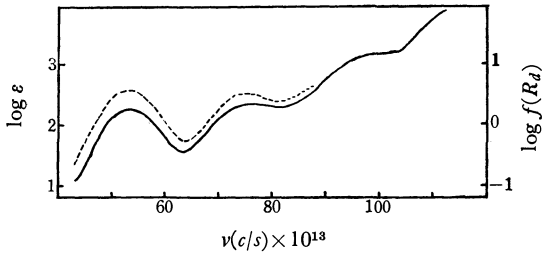

Fig. 4. Electonic spectra for the solution (——) and the solid (·····) of Complex VII.

(O_3 type) as in the case of the ATA complex.

The spectra for Complex VII in a solid state and in an aqueous solution are shown in Fig. 4. We see that both spectra resemble each other, showing the same structures. This is different from Complex I. This might be mainly due to the ease of aquation in the latter complex, *viz.*, the chromium(III) complex may more easily undergo an aquation than the corresponding cobalt(III) complex.

Thermal Decomposition Processes in Complexes II, III and VII. Thermal decomposition of the complexes was measured with a Derivatograph[7,8] in a constant nitrogen stream with heating rate 1°C/min. Five-hundred milligrams of the samples was used in each experiment. The derivatograms for Complexes II, III and VII are given in Fig. 5.

Complex III, first, lost two moles of crystalline water at 100°C and liberated stepwise two moles of coordinated water at 190 to 230°C in the second step.

For Complex II having no crystalline water, a similar liberation of two moles of coordinated water could be detected at 190—235°C as in the second step of III.

Complex VII lost one mole of crystalline water at 100°C and the weight loss, corresponding to one mole of water, was detected at 190—200°C.

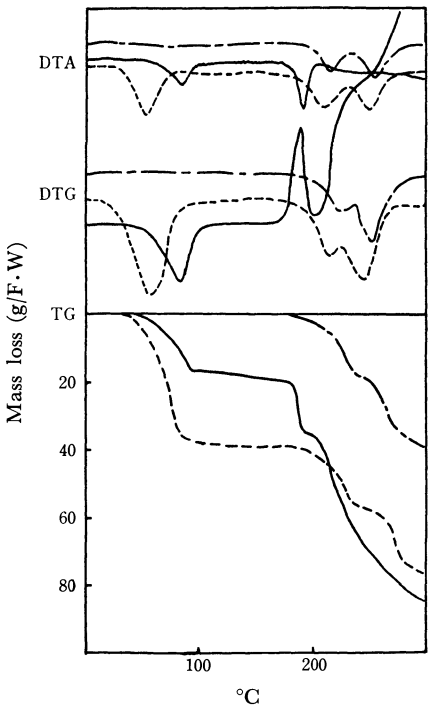

Fig. 5. Derivatograms for Complexes II (—·—), III (- - -) and VII (——).

It is of interest that an exothermic peak appears on DTA curve in the corresponding temperature range. At this step the color of the sample turned from bluish violet to reddish violet. From the results, the dimerization reaction seems to proceed at this step, resulting in the formation of the diol complex as shown by

$$2K[Co(OH)(l\text{da})(H_2O)] \xrightarrow[-2H_2O]{\text{at } 190—200°C} K_2[Co(l\text{da})\langle{}^{H}_{O}\rangle_{O}^{H}(l\text{da})Co].$$

A more detailed discussion and the kinetics for this reaction will be published elsewhere with illustrative examples.

7) R. Tsuchira, Y. Kaji, A. Uehara and E. Kyuno, This Bulletin, **42**, 1881 (1969).

8) R. Tsuchiya, A. Uehara and E. Kyuno, *ibid.*, **42**, 1886 (1969).

BULLETIN OF THE CHEMICAL SOCIETY OF JAPAN VOL. 43 419—423 (1970)

Kinetics of Multidentate Ligand Substitution Reactions. VIII. Substitution Reactions of Diethylenetriaminepentaacetic Acid with Nickel(II) Iminodiacetate and Aspartate Chelates and of Cyclohexane-1,2-diamine-*N*,*N*,*N*′,*N*′-tetraacetic Acid with the Nickel(II) Aspartate Chelate

Mutsuo KODAMA and Teiko UEDA

Department of Chemistry, Ibaraki University, Mito

(Received August 21, 1969)

The substitution reactions of diethylenetriaminepentaacetic acid (DTPA) with nickel(II) chelates of iminodiacetic acid (IDA) and aspartic acid (Asp) and of cyclohexane-1,2-diamine-*N*,*N*,*N*′*N*′-tetraacetic acid (CyDTA) with the nickel(II) chelate of aspartic acid were studied by employing the polarographic method. All the reactions studied were found to proceed through the following two simultaneous reaction paths:

$$\text{i)}\quad \begin{array}{l} NiX^0 + Z^{m-} \rightleftharpoons NiZ^{2-m} + X^{2-} \\ \quad\uparrow\downarrow \text{rapid} \\ NiX_2^{2-} \end{array}$$

$$\text{ii)}\quad \begin{array}{l} NiX^0 + HZ^{1-m} \rightleftharpoons NiZ^{2-m} + HX^- \\ \quad\uparrow\downarrow \text{rapid} \\ NiX_2^{2-} \end{array}$$

where NiX^0 and NiX_2^{2-} denote nickel(II)-IDA or Asp chelates of 1-to-1 and 1-to-2 compositions respectively, and where Z^{m-} indicates a completely-deprotonated DTPA or CyDTA anion. From a comparison of the rate constants of substitution reactions involving the nickel(II)-aspartate chelate with the corresponding rate constants of substitution reactions involving the nickel(II)-iminodiacetate chelate, the six-membered ring of the nickel(II)-aspartate chelate, as compared with its five-membered ring, was concluded to be more labile in the substitution reaction.

In our laboratory, a series of substitution reactions involving nickel(II)- and cobalt(II)-aminopolycarboxylate chelates have been studied kinetically.[1-4] In the substitution reaction involving Eriochrom Black T (BT), from a comparison of the rate constants the reaction intermediate was found to have the structure in which the leaving aminopolycarboxylate anion forms a five-membered ring with the metal ion through one nitrogen group and one oxygen group (Glycinate mechanism).[2]

Diethylenetriaminepentaacetic acid (DTPA) and cyclohexane-2,2′-diamine-*N*,*N*,*N*′,*N*′-tetraacetic acid (CyDTA) were found to displace aspartate and iminodiacetate anions from their nickel(II) chelates at measureable rates. Although both aspartic acid (Asp) and iminodiacetic acid (IDA) have one nitrogen group and two carboxylate groups, the former can form chelates which have one five-membered ring and one six-membered ring with metal ions, while the latter forms chelates which have two five-membered rings. Therefore, by comparing the rate constants for the substitution reactions of the nickel(II)-aspartate chelate with those of the nickel(II)-iminodiacetate chelate, one can determine which of the above two nickel(II) chelates is substitution-inert. In this connection, it would be worthwhile to conduct a kinetic study of the substitution reactions of nickel(II)-aspartate and iminodiacetate chelates with DTPA and CyDTA. This investigation will also provide further important information about the nature of the reaction intermediate in the substitution reaction involving the metal-aminopolycarboxylate chelate. In this paper, the kinetics of the substitution reactions of DTPA with nickel(II)-Asp and IDA chelates and of CyDTA with the nickel(II)-Asp chelate were investigated systematically.

1) M. Kodama, This Bulletin, **40**, 2575 (1967).
2) M. Kodama, C. Sasaki and T. Noda, *ibid.*, **41**, 2033 (1968).
3) M. Kodama, C. Sasaki and K. Miyamoto, *ibid.*, **42**, 163 (1969).
4) M. Kodama, *ibid.*, **42**, 2532 (1969).

Experimental

Reagents. The preparation of the standard nickel(II) nitrate solution was described in a previous paper.[4] The methods of purifying CyDTA and DTPA and preparing their standard solutions have also been given previously.[3] L-Aspartic acid and iminodiacetic acid were recrystallized from their aqueous solutions. The standard solutions were prepared by dissolving known amounts of recrystallized Asp and IDA in redistilled water. All the other chemicals used were of an analytical-reagent grade and were used without further purification.

Apparatus and Experimental Procedures. All the d.c. polarograms and current-time curves were recorded automatically by employing a Yanagimoto pen-recording polarograph PA-102 or a Hitachi recorder QPD-54. The dropping mercury electrode (DME) used in this study was also described previously.[5] All the experimental procedures were the same as these employed previously.[4] All the current-time curves were measured in the pH range from 9.00 to 10.50 in solutions with an ionic strength of 0.20 and containing a large excess of complexed and un-complexed Asp or IDA over DTPA or CyDTA. Therefore, all the substitution reactions could be treated as pseudo first-order reactions. In this study, no buffer reagent was used because all the sample solutions contained un-complexed aspartic acid or iminodiacetic acid, which has enough of a buffer capacity to maintain the solution pH constant over the entire pH range covered.

Results and Discussion

As was found in the substitution reaction of the nickel(II)-NTA chelate with DTPA,[4] in all the substitution reactions studied the plot of $\log(i_0/i_t)$ against time, t, give linear relations which pass through the point of origin, provided that all the other experimental conditions are kept constant (Fig. 1). Here, i_0 and i_t mean the wave-heights of DTPA or CyDTA at time $t=0$ or t respectively.[4] When the other experimental conditions were kept constant, the slope of the above linear relation was not influenced by the addition of a nickel(II)-DTPA or -CyDTA chelate, and it was independent of the initial concentration of DTPA or CyDTA. However, it was exactly proportional to the concentration of the nickel(II)-Asp or -IDA chelate with a 1-to-1 composition, $[NiX]_t/(1+K_2[X]_f/(\alpha_H)_X)$. Here, $[NiX]_t$, $[X]_f$, and $(\alpha_H)_X$ mean the total concentration of the nickel(II)-Asp or -IDA chelate, the concentration of uncomplexed Asp or IDA, and the (α_H) value of Asp or IDA respectively. K_2 is the second successive formation constant of the nickel(II)-Asp or -IDA chelate. Typical results are shown in Tables 1, 2, and 3. As is illustrated in Figs. 2 and 3, the product of the log-plot slope and $2.303\cdot(\alpha_H)_Z\cdot(1+K_2[X]_f/(\alpha_H)_X)/[NiX]_t$ was a linear function of the hydrogen ion concentration,

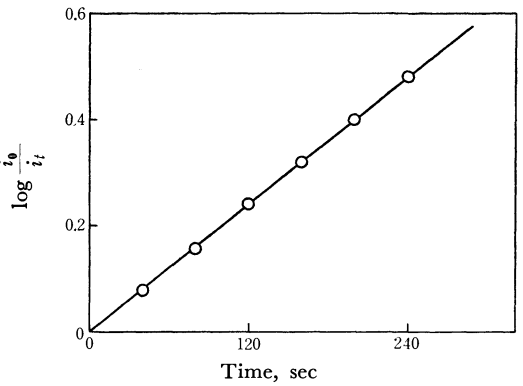

Fig. 1. The plot of $\log(i_0/i_t)$ against time.
Here, i_0 and i_t mean the anodic wave-heights of CyDTA at time $t=0$ and t, respectively.
Ionic strength = 0.20, 1.0°C
Initial concentration of CyDTA = 0.40 mM
Total concentration of Ni(II)-Asp chelate=8.0 mM
Concentration of uncomplexed Asp = 34.0 mM

Table 1. The relation between the log-plot slope and the initial concentration of CyDTA or DTPA
ionic strength=0.20

A) Ni(II)-Asp CyDTA system

Concentration of CyDTA, mM	Slope, sec^{-1}
0.30	2.02×10^{-3}
0.40	2.00×10^{-3}
0.60	2.02×10^{-3}

pH=9.56, 25°C
Concentration of uncomplexed aspartate=34.0 mM
Total concentration of Ni(II)-Asp chelate=8.0 mM

B) Ni(II)-Asp DTPA system

Concentration of DTPA, mM	Slope, sec^{-1}
0.30	2.26×10^{-3}
0.40	2.30×10^{-3}
0.60	2.30×10^{-3}

pH=10.50, 1.0°C
Concentration of uncomplexed aspartate=34.0 mM
Total concentration of Ni(II)-Asp chelate=8.0 mM

C) Ni(II)-IDA DTPA system

Concentration of DTPA, mM	Slope, sec^{-1}
0.366	3.10×10^{-3}
0.610	3.13×10^{-3}
0.854	3.08×10^{-3}

pH=9.30, 25°C
Concentration of uncomplexed iminodiacetate=10.14 mM
Total concentration of Ni(II)-IDA chelate=8.63 mM

5) M. Kodama and A. Kimura, This Bulletin, **40**, 1639 (1967).

Table 2. The relation between the log-plot slope and the concentration of uncomplexed Asp or IDA
ionic strength=0.20

A) Ni(II)-Asp CyDTA system

Concentration of uncomplexed Asp $[X]_f$, mM	Slope sec^{-1}	Slope×$[X]_f$ sec^{-1} mM
24.0	2.83×10^{-3}	6.80×10^{-2}
34.0	2.00×10^{-3}	6.80×10^{-2}
44.0	1.56×10^{-3}	6.80×10^{-2}

pH=9.56, 25°C
Initial concentration of CyDTA=0.40 mM
Total concentration of Ni(II)-Asp = 8.0 mM

B) Ni(II)-Asp DTPA system

Concentration of uncomplexed Asp $[X]_f$, mM	Slope sec^{-1}	Slope×$[X]_f$ sec^{-1} mM
24.0	3.38×10^{-3}	8.10×10^{-2}
34.0	2.30×10^{-3}	7.85×10^{-2}
44.0	1.88×10^{-3}	8.25×10^{-2}

pH=10.50, 1.0°C
Initial concentration of DTPA=0.40 mM
Total concentration of Ni(II)-Asp=8.0 mM

C) Ni(II)-IDA DTPA system

Concentration of uncomplexed Asp $[X]_f$, mM	Slope sec^{-1}	Slope×$[X]_f$ sec^{-1} mM
10.14	3.13×10^{-3}	3.18×10^{-2}
19.34	1.65×10^{-3}	3.19×10^{-2}
28.44	1.10×10^{-3}	3.14×10^{-2}

pH=9.30, 25°C
Initial concentration of DTPA=0.61 mM
Total concentration of Ni(II)-IDA=8.63 mM

and the log-plot slope is given by:

$$\text{log-plot slope} = (k_i + k_{ii}[H^+]) \times \frac{[NiX]_t}{2.303\cdot(\alpha_H)_Z\cdot\left(1+\dfrac{K_2\cdot[X]_f}{(\alpha_H)_X}\right)} \quad (1)$$

where $1+K_2\cdot[X]_f/(\alpha_H)_X$ is practically identical with $K_2\cdot[X]_f/(\alpha_H)_X$ under the present experimental conditions. Therefore, all the substitution reactions studied can be concluded to proceed through the following two simultaneous reaction pathways and, therefore, k_i and k_{ii} in Eq. (1) can be equated with k_1^+ and k_2^+/k_d respectively (here, k_d denotes the k_4 of CyDTA or k_5 of DTPA):

i) $NiX^0 + Z^{m-} \overset{k_1^+}{\rightleftarrows} NiZ^{2-m} + X^{2-}$
$\uparrow\downarrow$ rapid
NiX_2^{2-}

ii) $NiX^0 + HZ^{1-m} \overset{k_2^+}{\rightleftarrows} Ni^{2-m} + HX^-$
$\uparrow\downarrow$ rapid
NiX_2^{2-}

Table 3. The relation between the log-plot slope and the total concentration of nickel(II)-Asp or -IDA chelate
ionic strength=0.20

A) Ni(II)-Asp CyDTA system

Concentration of Ni(II)-Asp mM	Slope sec^{-1}	Concentration ratio	Slope ratio
6.0	1.50×10^{-3}	1.00	1.00
8.0	2.00×10^{-3}	1.33	1.33
10.0	2.52×10^{-3}	1.67	1.68

pH=9.56, 25°C
Concentration of uncomplexed Asp=34.0 mM
Initial concentration of CyDTA=0.40 mM

B) Ni(II)-Asp DTPA system

Concentration of Ni(II)-Asp mM	Slope sec^{-1}	Concentration ratio	Slope ratio
6.0	1.80×10^{-3}	1.00	1.00
8.0	2.30×10^{-3}	1.33	1.28
10.0	3.02×10^{-3}	1.67	1.68

pH=10.50, 1.0°C
Concentration of uncomplexed Asp=34.0 mM
Initial concentration of DTPA=0.40 mM

C) Ni(II)-IDA DTPA system

Concentration of Ni(II)-IDA mM	Slope sec^{-1}	Concentration ratio	Slope ratio
8.63	3.13×10^{-3}	1.00	1.00
13.00	4.52×10^{-3}	1.50	1.45
17.30	6.40×10^{-3}	2.00	2.04

pH=9.30, 25°C
Concentration of uncomplexed IDA=10.14 mM
Initial concentration of DTPA=0.61 mM

where NiX^0 and NiX_2^{2-} denote a nickel(II)-Asp or -IDA chelate with a 1-to-1 or a 1-to-2 composition respectively, and where Z^{m-} means a completely-deprotonated DTPA or CyDTA anion.

From the linear relations shown in Figs. 2 and 3, the k_1^+ and k_2^+ values were determined. These values are listed together with the k_1^+ and k_2^+ values for the substitution reaction of the nickel(II)-IDA chelate with CyDTA,[6] in Table 4. Since the

Table 4. k_1^+ and k_2^+ values
ionic strength=0.20

System	k_1^+ $M^{-1}\cdot sec^{-1}$	k_2^+ $M^{-1}\cdot sec^{-1}$	Temperature °C
Ni(II)-IDA CyDTA[6]	1.7×10^4	3.30×10^2	25
Ni(II)-Asp CyDTA	0	2.50×10^3	25
Ni(II)-IDA DTPA	3.8×10^4	6.13×10^3	25
	$1.3_4\times10^4$	8.26×10^2	1.0
Ni(II)-Asp DTPA	3.0×10^4	6.85×10^3	1.0

6) M. Kodama, This Bulletin, **42**, 3330 (1969).

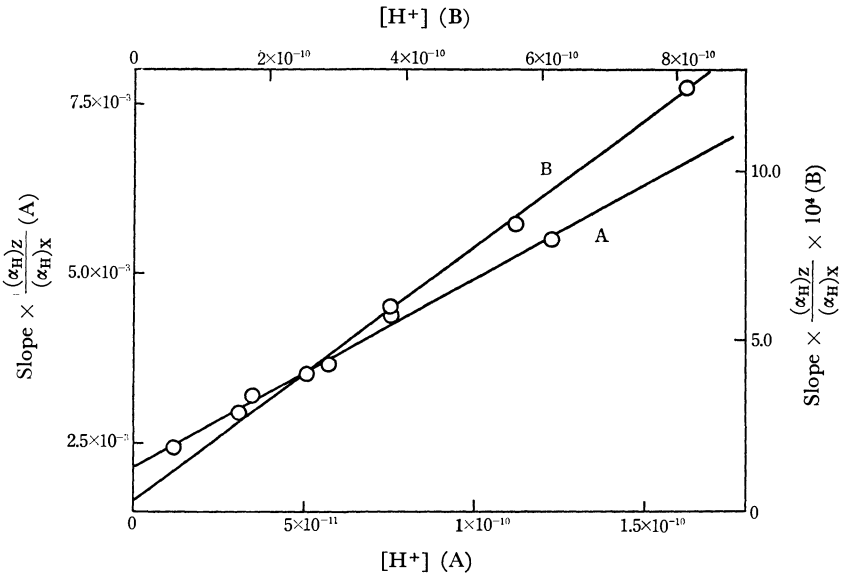

Fig. 2. The plot of log-plot slope$\times(\alpha_H)_Z/(\alpha_H)_X$ against the hydrogen ion concentration.
Ionic strength = 0.20, 1.0°C
Initial concentration of DTPA = 0.40 mM
A) Total concentration of Ni(II)-Asp chelate = 8.0 mM
Concentration of uncomplexed Asp = 34.0 mM
B) Total concentration of Ni(II)-IDA chelate = 10.0 mM
Concentration of uncomplexed IDA = 20.0 mM

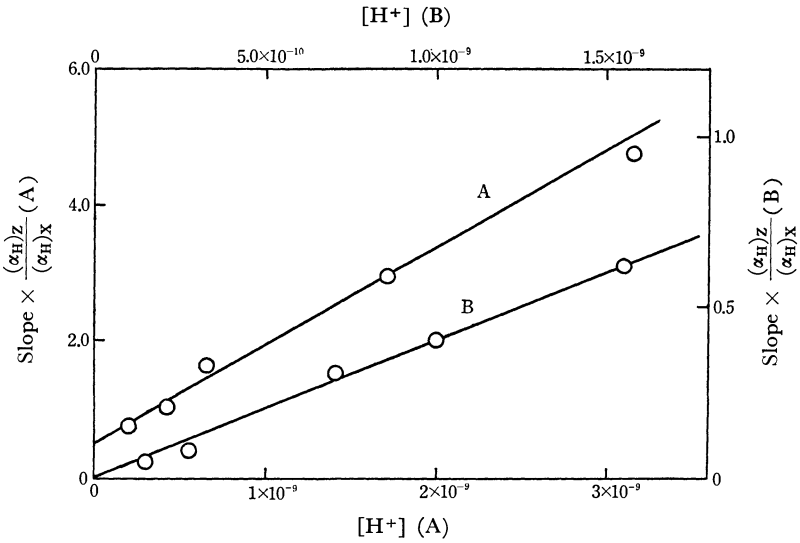

Fig. 3. The plot of log-plot slope$\times(\alpha_H)_Z/(\alpha_H)_X$ against the hydrogen ion concentration.
Ionic strength = 0.20, 25°C
A) Initial concentration of DTPA = 0.40 mM
Total concentration of Ni(II)-IDA chelate = 8.63 mM
Concentration of uncomplexed IDA = 10.14 mM
B) Initial concentration of CyDTA = 0.40 mM
Total concentration of Ni(II)-Asp chelate = 8.0 mM
Concentration of uncomplexed Asp = 34.0 mM

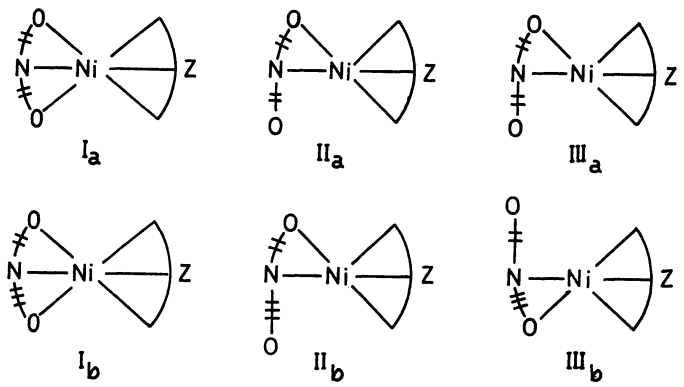

Fig. 4. Reaction intermediates.

substitution reaction of the nickel(II)-Asp chelate with DTPA proceeded too rapidly for us to determine the rate accurately at room temperature, the current-time curves were measured at 1.0°C. The rate constants for the substitution reaction of the nickel(II)-IDA chelate with DTPA determined at 1.0°C are also listed in Table 4.

As is shown in Table 4, the k_2^+ values of the nickel(II)-Asp chelate systems are about seven times as large as those of the nickel(II)-IDA chelate systems. Since the k_1^+ values could be determined less accurately, only the k_2^+ values were used for the comparison of the rate constants. From the above results and discussion, it might be expected that the substitution reaction involving the nickel(II)-Asp chelate proceeds through a mixed ligand reaction intermediate (activated complex) similar to that in the substitution reaction of the nickel(II)-IDA chelate. As was discussed previously,[2] we can estimate the structure of the reaction intermediate by comparing the rate constant calculated on the basis of the proposed reaction intermediate and the observed rate constant. If the Ni(II)-DTPA or -CyDTA segments in the reaction intermediates of both substitution reactions have the same structure, and if the Ni(II)-Asp and Ni(II)-IDA segments in the reaction intermediate have the I_a and I_b structures respectively, the k_2^+ value for the reaction of the nickel(II)-Asp chelate must be equal to that for the reaction of the nickel(II)-IDA chelate, because the rates of dissociation of aspartate and iminodiacetate anions from the reaction intermediate are considered to be identical. If both aspartate and IDA anions in the reaction intermediate form only one five-membered ring with a nickel(II) ion (II_a and II_b), the k_2^+ value for the substitution reaction of the nickel(II)-Asp chelate must be about six times as large as that for the reaction of the nickel(II)-IDA chelate, because the stability constant ratio corrected for the statistical factor between nickel(II)-IDA and -Asp chelates of a 1-to-1 composition[7] is estimated to be 6.0. On the other hand, if the Ni(II)-Asp segment in the reaction intermediate has the six-membered ring and the Ni(II)-IDA segment, a five-membered ring (III_a and III_b), the k_2^+ value for the reaction of the nickel(II)-IDA chelate should be three times as large as that for the reaction of the nickel(II)-Asp chelate. Here, nickel(II) chelates of α-aninate and β-alaninate were used as models. For the reaction intermediates where nickel(II)-IDA and -Asp segment include only one nitrogen bond, the k_2^+ value for the reaction of nickel(II)-Asp must be twelve times as large as that for the reaction of the nickel(II)-IDA chelate.

As is shown in Table 4, the k_2^+ values for the substitution reactions of the nickel(II)-Asp chelate with both DTPA and CyDTA are almost seven times as large as those for the reactions of the nickel(II)-IDA chelate. This fact clearly indicates that all the present substitution reactions also proceed through the glycinate reaction intermediate (II_a and II_b), as in the case of the substitution reaction of BT.[2] With metal ions, the aspartate anion can form the chelate with five- and six-membered rings. Therefore, the finding that the reaction of the nickel(II)-Asp chelate proceeds through the reaction intermediate II_b clearly shows that the five-membered ring, as compared with the six-membered ring, is more inert in the substitution reaction.

The present authors wish to thank the Ministry of Education for its financial support.

7) L. G. Sillen and A. E. Martell, "Stability Constants of Metal-Ion Complexes," The Chemical Society, London (1964).

BULLETIN OF THE CHEMICAL SOCIETY OF JAPAN VOL. 43 424—428 (1970)

Stereochemistry of Trimethylenediaminetetraacetatocobaltate(III)*[1]

Hiroshi OGINO, Masatake TAKAHASHI and Nobuyuki TANAKA

Department of Chemistry, Faculty of Science, Tohoku University Katahira-cho, Sendai

(Received September 5, 1969)

Conformation of trimethylenediaminetetraacetatocobaltate(III) (Cotrdta$^-$) was inferred from the measurement of proton nuclear magnetic resonance spectra. It was found that K[Cotrdta]·$2H_2O$ crystals are mixtures consisting of equimolar amounts of the crystals of K[$(+)_{546}$-Cotrdta]·$2H_2O$ and those of K[$(-)_{546}$Cotrdta]·$2H_2O$; that is, so-called "spontaneous resolution" was found. The absolute configuration of optically active Cotrdta$^-$ was determined by the measurements of optical rotatory dispersion (ORD) and circular dichroism (CD) curves and by the reaction with ethylenediamine to form tris(ethylenediamine)cobalt(III) cation.

The cobalt(III) complexes with ethylenediaminetetraacetate(edta), propylenediaminetetraacetate (pdta) and *trans*-1,2-cyclohexanediaminetetraacetate(cydta) have been extensively investigated. In these complexes, the chelate rings around the central cobalt(III) ions are all five-membered.

Recently, the syntheses of cobalt(III)[1] and chromium(III)[2] complexes with trimethylenediaminetetraacetate(trdta)*[2] have been reported, and it was verified that a quadrivalent trdta anion in each metal complex is hexadentate.[1,2] In trdta complex, a six-membered chelate ring involving two nitrogen atoms is formed, in contrast with complexes with edta, pdta and cydta.

As trdta complex occupies an important position in a series of complexes of edta and its homologues, the stereochemical investigations on Cotrdta$^-$ are dealt with in this paper.*[3]

Experimental

H_4 trdta*[4] and K[Cotrdta]·$2H_2O$ were prepared in the same way as has been reported.[1]

H[Cotrdta]·$3H_2O$. K[Cotrdta]·$2H_2O$ (4.4 g) dissolved in 20 m*l* of water was passed through Dowex 50 W X-8 cation exchange resins in hydrogen form. The equivolume of ethanol was then added to the solution. After the solution had been cooled to 0°C, the reddish violet crystals separated were collected and washed with ethanol and ether. The compound was recrystallized from water by the addition of ethanol.

Ag[Cotrdta]·H_2O. To a solution of 2 g of silver nitrate dissolved in 50 m*l* of water was added 1 g of sodium hydroxide dissolved in 50 m*l* of water. Silver oxide thus obtained was washed several times by decantation. After the total volume of the solution was adjusted to be 50 m*l* with water, 4.5 g of H[Cotrdta]·$3H_2O$ was added to the solution. The solution was stirred at 60°C for 20 min and filtered. To the filtrate, 200 m*l* of ethanol was added. The compound deposited was collected and washed with ethanol and ether and then air-dried. The crystals were recrystallized from water by the addition of ethanol.

Ba[Cotrdta]$_2$·$8H_2O$. To 4.2 g of H[Cotrdta]·$3H_2O$ dissolved in 40 m*l* of water 1.6 g of barium hydroxide was added. The solution was stirred at 65°C for 20 min and filtered. To the filtrate was added 40 m*l* of ethanol. The compound deposited was washed and recrystallized in the same way as Ag[Cotrdta]·H_2O.

Resolution of Cotrdta$^-$. The resolution of Cotrdta$^-$ was carried out by a similar method to that for Copdta$^-$ and Cocydta$^-$.[4,5]

[*d*-Co$(NO_2)_2$en$_2$][$(-)_{546}$Cotrdta]·$3H_2O$.*[5] Resolving agent, *cis*-[*d*-Co$(NO_2)_2$en$_2$]Br (en denotes ethylenediamine) was prepared according to the direction by Dwyer and Garvan.[6] *cis*-[*d*-Co$(NO_2)_2$en$_2$]Br (21.1 g)

---

*[1] Presented at the 18th Symposium on Coordination Chemistry, Kyoto, Oct., 1968.

1) N. Tanaka and H. Ogino, This Bulletin, **37**, 877 (1964).

2) J. A. Weyh and R. E. Hamm, *Inorg. Chem.*, **7**, 2431 (1968).

*[2] trdta denotes

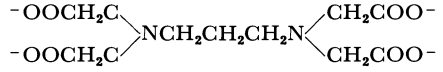

*[3] After the completion of this work, a study on the circular dichroism of cobalt(III) trdta complex was reported by Van Saun and Douglas.[3]

3) C. W. Van Saun and B. E. Douglas, *Inorg. Chem.*, **8**, 1145 (1969).

*[4] H_4 trdta was prepared by heating the solution of the mixture of monochloroacetic acid, potassium hydroxide and trimethylenediamine and following acidification of the condensation mixture.[1] In the previous paper,[1] 16.5 g of potassium hydroxide dissolved in 30 m*l* of water should read 33 g of potassium hydroxide dissolved in 60 m*l* of water.

4) F. P. Dwyer and F. L. Garvan, *J. Amer. Chem. Soc.*, **81**, 2955 (1959).

5) F. P. Dwyer and F. L. Garvan, *ibid.*, **83**, 2610 (1961).

*[5] In this paper, the rotation of *d*- and *l*- refers to the sign of the optical rotation at sodium D line.

6) F. P. Dwyer and F. L. Garvan, "Inorganic Syntheses," Vol. 6, p. 195 (1960).

was suspended in 800 m*l* of water at 60°C. To this suspension, 29.2 g of Ag[Cotrdta]·H_2O dissolved in 200 m*l* of water at 60°C was added and shaken vigorously for 10 min.*6 After filtration of silver bromide, the filtrate was evaporated to 100 m*l* under reduced pressure at a temperature 55°C. The solution was cooled to 0°C, and the brown diastereoisomer [*d*-$Co(NO_2)_2en_2$][(−)$_{546}$Cotrdta]·$3H_2O$ deposited was collected, which was recrystallized from water by the addition of ethanol, washed with ethanol and ether, and then air-dried. An aqueous solution of the diastereoisomer gave $[\alpha]_{546}=-850\pm30°$. The rotation did not change after recrystallization. The filtrate was reserved for the preparation of [*l*-$Co(NO_2)_2en_2$][(+)$_{546}$Cotrdta]·$3H_2O$.

K[(−)$_{546}$Cotrdta]·2H_2O. Fifteen grams of [*d*-$Co(NO_2)_2en_2$][(−)$_{546}$Cotrdta]·$3H_2O$, 15 g of potassium iodide and 40 m*l* of water were ground up in a mortar for 5 min and cooled to 0°C for 1 hr. After removal of the [*d*-$Co(NO_2)_2en_2$]I precipitated, equivolume of ethanol was added to the solution. K[(−)$_{546}$Cotrdta]·$2H_2O$ thus obtained was washed with ethanol and ether, and then air-dried. A solution of K[(−)$_{546}$Cotrdta]·$2H_2O$ gave $[\alpha]_{546}=-1560\pm60°$, and the rotation did not change after recrystallization.

[l-$Co(NO_2)_2en_2$][(+)$_{546}$Cotrdta]·3H_2O. To the filtrate reserved in the resolution of [*d*-$Co(NO_2)_2en_2$][(−)$_{546}$Cotrdta]·$3H_2O$ mentioned above, 20 g of barium iodide was added and shaken vigorously. After the solution had been cooled to 0°C, [*d*-$Co(NO_2)_2en_2$]I precipitated was removed by filtration. Equivolme of ethanol was added to the solution. The solution was cooled to 0°C and allowed crystallization of Ba[Cotrdta]$_2$·$8H_2O$. The compound collected was recrystallized from water by the addition of ethanol.

Three grams of Ba[Cotrdta]$_2$·$8H_2O$ was dissolved in 20 m*l* of water at 60°C. *cis*-[*l*-$Co(NO_2)_2en_2$]Br (2.1g) and 0.94 g of silver sulfate were mixed in 80 m*l* of water at 60°C and the solution was added to the solution of Ba[Cotrdta]$_2$·$8H_2O$. The solution thus obtained was shaken vigorously for 10 min. The silver bromide and bariumsulfate precipitated were removed. Subsequent procedures were the same as those for preparation of [*d*-$Co(NO_2)_2en_2$][(−)$_{546}$Cotrdta]·$3H_2O$. The diastereoisomer [*l*-$Co(NO_2)_2en_2$][(+)$_{546}$Cotrdta]·$3H_2O$ gave $[\alpha]_{546}=870\pm30°$.

K[(+)$_{546}$Cotrdta]·2H_2O. This compound was prepared from [*l*-$Co(NO_2)_2en_2$][(+)$_{546}$Cotrdta]·$3H_2O$ by the same procedure as that for the preparation of K[(−)$_{546}$Cotrdta]·$2H_2O$. The solution of K[(+)$_{546}$Cotrdta]·$2H_2O$ gave $[\alpha]_{546}=1600\pm60°$.

The elementary analyses of the compounds prepared in this work are given in Table 1.

Apparatus The proton nuclear magnetic resonance spectra were recorded with a Varian A-60 NMR spectrometer. Sodium trimethylsilylpropanesulfonate (DSS) was used as internal standard.

Polarimetric measurements at sodium D line were done by a JASCO model DIP-SL automatic polarimeter. ORD and CD curves were recorded with a JASCO model ORD/CD-5 polarimeter.

Goniometric measurements of crystals were carried out by a STOE microscope two-circle-polarizing optical goniometer.

Results and Discussion

Conformation of Cotrdta$^-$. From the measurement of the infrared spectra of K[Cotrdta]·$2H_2O$, it has been reported that a quadrivalent trdta anion in this complex is hexadentate.[1)]

NMR spectrum of Cotrdta$^-$ in deuterium oxide is shown in Fig. 1. From the intensities and the chemical shifts of signals, signals centered at 2.8 ppm can be assigned to the protons attached to the carbon atoms of trimethylenediamine ring, and eight peaks ranged at 3.3 to 4.3 ppm can be assigned to be acetate protons. The latter eight

Table 1. Elementary analyses (%)

Compound		C	H	N	H_2O
H_4trdta	calcd	43.14	5.92	9.15	
	found	43.00	6.09	9.20	
K[Cotrdta]·$2H_2O$	calcd	30.28	4.16	6.42	8.3
	found	30.27	3.93	6.26	8.1
H[Cotrdta]·$3H_2O$	calcd	31.74	5.09	6.73	13.0
	found	31.97	5.31	6.81	13.7
Ag[Cotrdta]·H_2O	calcd	27.13	3.31	5.75	3.7
	found	26.95	3.60	5.64	4.2
Ba[Cotrdta]$_2$·$8H_2O$	calcd	26.33	4.42	5.58	
	found	26.81	4.54	5.58	
	calcd	26.25	5.29	16.33	7.9
[*l*-$Co(NO_2)_2en_2$]-[(+)$_{546}$Cotrdta]·$3H_2O$	found	26.34	5.46	16.22	7.5
[*d*-$Co(NO_2)_2en_2$]-[(−)$_{546}$Cotrdta]·$3H_2O$	found	26.58	5.87	16.21	
	calcd	30.28	4.16	6.42	8.3
K[(+)$_{546}$Cotrdta]·$2H_2O$	found	30.21	4.11	6.53	8.1
K[(−)$_{546}$Cotrdta]·$2H_2O$	found	30.82	4.29	6.40	

*6 Resolution of Cotrdta$^-$ can be done by using Ba[Cotrdta]$_2$·$8H_2O$. The procedure is the same as that given in the preparation of [*l*-$Co(NO_2)_2en_2$]-[(+)$_{546}$Cotrdta]·$3H_2O$.

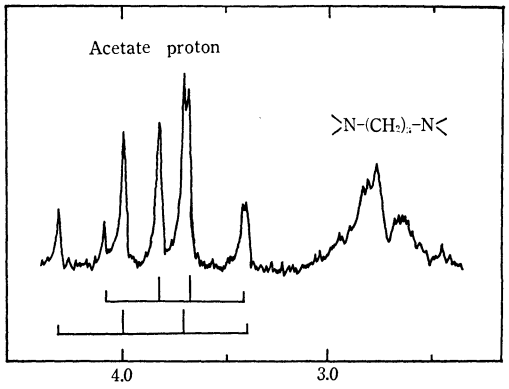

Fig. 1. NMR spectrum of K[Cotrdta]·$2H_2O$ in deuterium oxide.

peaks are attributed to two overlapping AB splitting patterns similar to the eight signals of acetate protons of Coedta$^-$.[7-10] Several parameters of NMR spectra of Cotrdta$^-$ are compared with those of Coedta$^-$ in Table 2.

It is shown in Table 2 that signals of protons attached to the carbon atoms of trimethylenediamine ring are in higher field than those of ethylenediamine ring. This is due to the increasing shielding effect from the applied magnetic field with the increase of methylene group.

The two AB splitting patterns of acetate protons in Cotrdta$^-$ can be attributed to the presence of two acetate rings in N–Co–N plane (in-plane acetates) and of two acetate rings out of N–Co–N plane (out-of-plane acetates), respectively. AB patterns centered at 3.735 ppm were assigned to in-plane acetate and those centered at 3.855 ppm were assigned to out-of-plane acetates, with reference to the data of Coedta$^-$[9,10] and the kinetic study of deuteration reaction of Cotrdta$^-$.*7

The presence of two kinds of AB protons in Cotrdta$^-$ complex means that the magnetic environments of two nitrogen atoms in this complex are equivalent. Unless these magnetic environments are equivalent, it is expected that Cotrdta$^-$ gives four different AB splitting patterns of acetate protons. As an example, it was reported that Copdta$^-$ gives four different AB splitting patterns of acetate protons.[8] In this case, the magnetic environments of two nitrogen atoms are not equivalent by the presence of a methyl group on N–C–C–N chelate ring.

The results of NMR spectra rule out the possibility of the following boat forms as the conformation of trimethylenediamine ring in Cotrdta$^-$:

In the form (A), the magnetic environments of two nitrogen atoms are apparently non-equivalent. In the form (B), as the protons attached to the central carbon atom of trimethylenediamine approach closely one of out-of-plane acetate rings, the equivalence of two nitrogen atoms does not hold. Furthermore, molecular models show that these forms are strained considerably.

It was revealed that the trimethylenediamine chelate ring in tris(trimethylenediamine)cobalt(III) cation is of a chair form.[11] It was, however, found that such a molecular model of Cotrdta$^-$ in which trimethylenediamine chelate ring is of a chair form and trdta anion in the complex is hexadentate could not be constructed.

Figure 2 shows the most probable conformation which explains the experimental results mentioned above, in which cobalt(III) ion, two nitrogen atoms and one central carbon atom of trimethylenediamine (C_6 in Fig. 2) lie in the same plane,

TABLE 2. NMR SPECTRAL PARAMETERS OF Coedta$^-$ AND Cotrdta$^-$

Complex	δ,* ppm	δ_{AB}**, ppm	J_{AB}***, Hz	Number of protons	Assignment	Ref.
Coedta$^-$	3.746	0.333	16.5	4	in-plane acetate	10
	3.916	0.147	18.5	4	out-of-plane acetate	10
	3.61	—	—	4	$>N\,CH_2CH_2\,N<$	9
Cotrdta$^-$	3.735	0.308	16.1	4	in-plane acetate	This work
	3.855	0.529	18.6	4	out-of-plane acetate	This work
	2.8	—	—	6	$>N\,CH_2CH_2CH_2N<$	This work

* Chemical shift of pattern relative to DSS.
** Relative chemical shift of two AB protons.
*** Coupling constant of AB patterns.

7) R. J. Day and C. N. Reilley, *Anal. Chem.*, **36**, 1073 (1964).
8) R. J. Day and C. N. Reilley, *ibid.*, **37**, 1326 (1965).
9) J. I. Legg and D. W. Cooke, *Inorg. Chem.*, **4**, 1576 (1965).
10) J. B. Terrill and C. N. Reilley, *ibid.*, **5**, 1988 (1966).

*7 In acid media, AB protons centered at 3.855 ppm are deuterated faster than those centered at 3.735 ppm. The details will be published elsewhere.

11) Y. Saito, T. Nomura and F. Maruno, This Bulletin, **41**, 530 (1968).

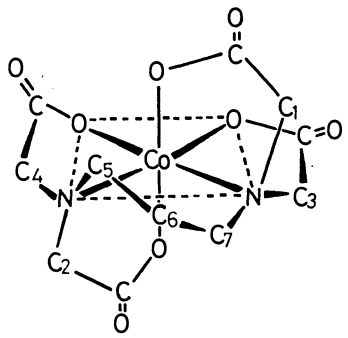

Fig. 2. The most probable conformation of Cotrdta$^-$.
(There is a two-fold axis through Co and C_6.)

and carbon C_5 is above and carbon C_7 below this plane. In this conformation, there is a two-fold axis through a cobalt(III) ion and central carbon atom of trimethylenediamine, C_6. Accordingly, the magnetic environments of two nitrogen atoms in this complex are equivalent. A survey with the use of a molecular model suggested that the in-plane acetate rings in this complex are more strained than the out-of-plane acetate rings.

Spontaneous Resolution of K[Cotrdta]·2-H_2O. When hot solutions saturated with K[Cotrdta]·$2H_2O$ were cooled slowly, fairly large crystals appeared.*8 It was found that each crystal deposited is classified to either forms as shown in Fig. 3. The largest crystal obtained up to date is 1 cm along b axis as shown in Fig. 3. Thus, one can distinguish visually the form to which the crystal deposited belongs. Crystal form A in Fig. 3 is the mirror image of form B. It was found that crystals belonging to A form give *levo* rotation at both 546 mμ and sodium D line and crystals belonging to B form give *dextro* rotation at the same wavelengths. In order to know the accurate value of rotation, single crystals deposited from the solution of racemic K[Cotrdta]·$2H_2O$ were dissolved into 5 m*l* water and the optical rotation of the solutions were measured at sodium D line in 1 cm cell. Fig. 4 shows the results thus obtained. The ordinate in Fig. 4 denotes the value of observed rotation in degree and the abscissa the concentration of K[Cotrdta]·$2H_2O$. The value of rotation of K[$(+)_D$Cotrdta]·$2H_2O$ resolved by using[*l*-$Co(NO_2)_2en_2]^+$ is also plotted in Fig. 4. The plots of crystals belonging to form A lie on a single straight line. The plots of crystals belonging to form B and K[$(+)_D$Cotrdta]·$2H_2O$ resolved with [*l*-$Co(NO_2)_2en_2]^+$ also lie on a straight line. These two straight lines are mirror images of each other within experimental error. This means that each single crystal must contain either *d*- or *l*-isomers. This is a new example of so-called "spontaneous resolution."

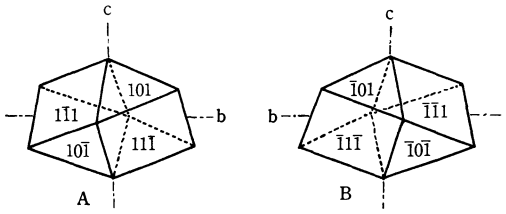

Fig. 3. Two crystal forms of K[Cotrdta]·$2H_2O$.

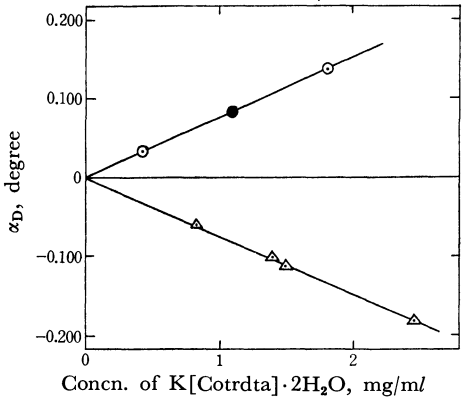

Fig. 4. The relation between optical rotation at sodium D line and the concentration of K[Cotrdta]·$2H_2O$. △ denotes single crystals belonging to form A in Fig. 3 and ○, single crystal belonging to form B in Fig. 3. ● denotes K[$(+)_D$Cotrdta]·$2H_2O$ resolved with [*l*-$Co(NO_2)_2en_2]^+$. Each single crystal is dissolved into 5 m*l* of water.

Table 3. Measured and calculated angle data for K[$(-)_{546}$Cotrdta]·$2H_2O$ crystal obtained by spontaneous resolution

hkl	ρmeasd	φmeasd	ρcalcd	φcalcd
101	51.0°	89.3°	51.1°	90.0°
$\bar{1}$11	55.1	−59.6	54.8	−61.0
$\bar{1}$01	51.4	−90.3	51.1	−90.0
1$\bar{1}$1	55.1	120.7	54.8	119.0
11$\bar{1}$	125.1	61.9	125.2	61.0
$\bar{1}$0$\bar{1}$	128.8	−89.7	128.9	−90.0
$\bar{1}\bar{1}\bar{1}$	126.0	−117.1	125.2	−119.0
10$\bar{1}$	129.0	90.4	128.9	90.0

ρ represents the polar distance and φ, the azimuth of each crystal face.

It was found that crystals shown in Fig. 3 belong to orthorhombic system. The axial ratios are $a : b : c = 0.5534 : 1 : 0.6858$.

Crystal has a cleavage parallel to (010). Accord-

*8 The solubilities of K[Cotrdta]·$2H_2O$ at 10, 15, 20, 25 and 30°C were 18.1, 22.9, 27.3, 31.8 and 37.4 g/100 m*l*, respectively.

Table 4. The reactions of $(+)_{546}$Coedta$^-$ and $(+)_{546}$Cotrdta$^-$ with 50% aqueous ethylenediamine

Reaction	$(+)_D$Co(en)$_3^{3+}$ resulted, %	$(-)_D$Co(en)$_3^{3+}$ resulted, %	Ref.
$(+)_{546}$Cotrdta$^-$ +50% aq. en → Co(en)$_3^{3+}$ + trdta^{4-}	56	44	This work
$(+)_{546}$Coedta$^-$ +50% aq. en → Co(en)$_3^{3+}$ + edta^{4-}	56.6	43.4	14

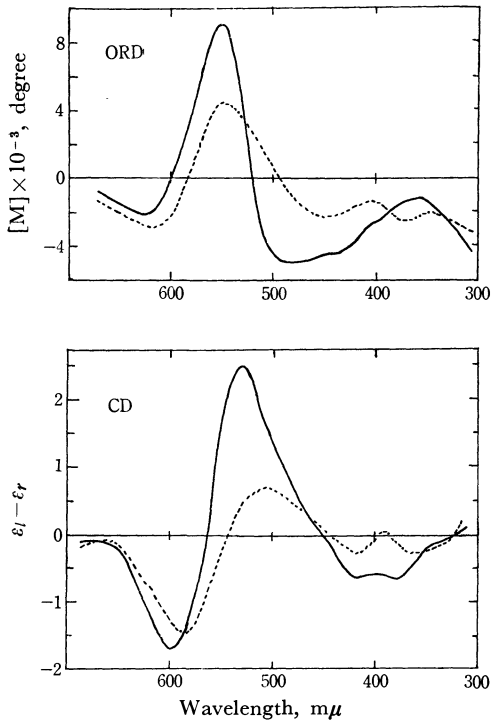

Fig. 5. The ORD and CD curves of $[(+)_{546}$-Cotrdta$]^-$ (——) and $[(+)_{546}$Coedta$]^-$ (----).

ing to this, some modifications of the crystal form shown in Fig. 3 were sometimes found in the crystals of K[Cotrdta]·2H$_2$O.

Absolute Configuration of Optically Active Cotrdta$^-$ Ion. In Fig. 5, the ORD and CD spectra of $[(+)_{546}$ Cotrdta$]^-$ are compared with those of $[(+)_{546}$ Coedta$]^-$. The absolute configuration of $[(+)_{546}$ Coedta$]^-$ has been determined as follows:[12]

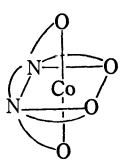

The shape and positions of ORD and CD spectra of $[(+)_{546}$ Cotrdta$]^-$ are quite similar to those of $[(+)_{546}$Coedta$]^-$. Therefore, it can be concluded that the absolute configuration of $[(+)_{546}$ Cotrdta$]^-$ is the same as that of $[(+)_{546}$ Coedta$]^-$. This agrees with the result reported by Van Saun and Douglas.[3]

Busch *et al.*[12-14] reported that [Coedta]$^-$ reacts with ethylenediamine (en) to form tris(ethylenediamine)cobalt(III) cation (Co(en)$_3^{3+}$) with partial retention of optical activity. Weakleim and Hoard[15] reported that in-plane acetate rings in Coedta$^-$ are more strained than out-of-plane acetate rings. From this fact, Busch *et al.* clarified the mechanim of the reaction between Coedta$^-$ and ethylenediamine, in which the first group to be displaced in replacing EDTA by ethylenediamine should be one of the in-plane acetate groups.

In this study the reaction between Cotrdta$^-$ and ethylenediamine was investigated and it was found that Cotrdta$^-$ reacts with ethylenediamine to form Co(en)$_3^{3+}$ similar to Coedta$^-$ system. Table 4 shows a comparison of the reactions of Coedta$^-$[14] and Cotrdta$^-$ with ethylenediamine. The degree of retention of optical activity in reaction between $(+)_{546}$Cotrdta$^-$ and ethylenediamine is essentially the same as that in the reaction between $(+)_{546}$-Coedta$^-$ and ethylenediamine. The results shown in Table 4 support the conclusion that absolute configuration of $(+)_{546}$Cotrdta$^-$ is the same as that of $(+)_{546}$Coedta$^-$ and that the in-plane acetate rings in Cotrdta$^-$ are more strained than the out-of-plane acetate rings.

The authors wish to thank Professors K. Omori and K. Saito, Faculty of Science, and Professor T. Isobe, Research Institute for Chemistry of Non-aqueous Solutions, Tohoku University, for their help and advice in connection with the goniometric and the ORD, CD spectrometric measurements.

12) D. H. Busch and D. W. Cooke, *J. Inorg. Nucl. Chem.*, **23**, 145 (1961).

13) D. H. Busch and K. Swaminathan, *J. Inorg. Nucl. Chem.*, **23**, 150 (1961).

14) D. H. Busch, K. Swaminathan and D. W. Cooke, *Inorg. Chem.*, **1**, 260 (1962).

15) H. A. Weakleim and J. L. Hoard, *J. Amer. Chem. Soc.*, **81**, 549 (1959).

BULLETIN OF THE CHEMICAL SOCEITY OF JAPAN VOL. 43 429—438 (1970)

The Mechanism of Photochromism, Thermochromism and Piezochromism of Dimers of Triarylimidazolyl

Koko MAEDA and Taro HAYASHI*1

Department of Chemistry, Faculty of Science, Ochanomizu University, Bunkyo-ku, Tokyo

(Received October 29, 1968)

A stable free radical, 2,4,5-triphenylimidazolyl, which was produced by oxidation of 2,4,5-triphenylimidazole, dimerizes to yield two dimers, a photochromic dimer and a piezochromic dimer. The photochromic dimer shows thermochromism and photochromism at temperatures between −196°C and about 200°C both in solution and in solid state. The piezochromic dimer shows piezochromism in solid state and thermochromism both in solution and in solid state. Spectroscopic and kinetic studies showed that photochromism, thermochromism and piezochromism are caused by radical dissociation of the dimers of triphenylimidazolyl on irradiation, heating and grinding. Dimers of substituted triphenylimidazolyl also showed these phenomena which are due to the same mechanism as that of the dimers of triphenylimidazolyl.

In the study of the mechanism of chemiluminescence of 2,4,5-triphenylimidazole (lophine)[1] we obtained new compounds by oxidation of lophine.[2] One compound exhibited photochromism[2] and thermochromism both in solution and in solid state[3,4] with irradiation and change of temperature. The other isomeric compound which is convertible to the former by recrystallization exhibited piezochromism[5] on grinding at room temperature, showing a reddish-purple color reversibly. By spectroscopic and kinetic studies it was shown that the photochromic compound is a dimer of triphenylimidazolyl, and the photochromism, thermochromism and piezochromism of the two compounds are due to reversible dissociation of the dimers into triphenylmidazolyl radical which is shown by the following reversible reaction.

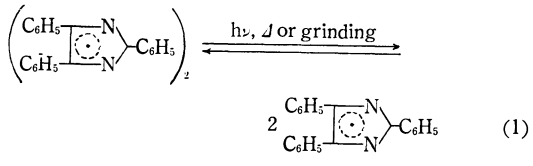

(1)

White and Sonnenberg[6] reported that the photochromic and piezochromic compounds are isomeric dimers which are different in the positions of combination of the 2,4,5-triphenylimidazolyl radical and are in equilibrium with the radical in solution.

We found that[7] besides photochromism at room temperature, showing a reddish-purple color, the photochromic dimer showed photochromism at low temperatures between about −150°C and −196°C, showing a violet color.

In the present paper, the mechanisms of photochromism, thermochromism and piezochromism of the dimers of triarylimidazolyl are reported. The photochromism at low temperatures was reported previously.[8]

Experimental

Materials. The Piezochromic Dimer of Triphenylimidazolyl.[2] To a solution of lophine (1 g) in 2 N ethanolic potassium hydroxide (100 ml) about 500 ml of 2% aqueous solution of potassium ferricyanide was gradually added for 1.5 hr with stirring by a stream of oxygen at 10°C. A reddish-purple color first appeared and then an almost colorless precipitate was formed gradually. The precipitate filtered was washed with water repeatedly and then dried *in vacuo*; 1 g of the piezochromic dimer (piezo-dimer) was obtained; almost colorless fine powder, mp 191—192°C.

Found: C, 84.73; H, 5.28; N, 9.19%. Calcd for $C_{42}H_{30}N_4$ (dimer of triphenylimidazolyl): C, 85.40;

*1 Present address: The Institute of Physical and Chemical Research, Yamato-machi, Kitaadachi-gun, Saitama.

1) T. Hayashi and K. Maeda, This Bulletin, **35**, 2057 (1962); K. Maeda, H. Ojima and T. Hayashi, *ibid.*, **38**, 76 (1965).

2) T. Hayashi and K. Maeda, *ibid.*, **33**, 566 (1960); T. Hayashi, K. Maeda, S. Shida and K. Nakada, *J. Chem. Phys.*, **32**, 1568 (1960).

3) T. Hayashi, K. Maeda and M. Morinaga, This Bulletin, **37**, 1563 (1964).

4) T. Hayashi, K. Maeda and T. Kanaji, *ibid.*, **38**, 857 (1965).

5) T. Hayashi and K. Maeda, *ibid.*, **38**, 685 (1965).

6) D. M. White and J. Sonnenberg, *J. Amer. Chem. Soc.*, **88**, 3825 (1966).

7) T. Hayashi and K. Maeda, This Bulletin, **36**, 1052 (1963); T. Hayashi and K. Maeda, *ibid.*, **40**, 2990 (1967).

8) K. Maeda and T. Hayashi, *ibid.*, **42**, 3509 (1969); T. Shida, K. Maeda and T. Hayashi, *ibid.*, **42**, 3044 (1969).

TABLE 1. PHOTO- AND PIEZO-DIMERS OF TRIARYLIMIDAZOLYL

Imidazolyl radical	Molecular formula of dimer*1 (molecular weight)	Abbreviation of photochromic dimer	Mp °C	Molecular weight of photochromic dimer*2	Abbreviation of piezochromic dimer	Mp °C
2,4,5-Triphenyl-	$C_{42}H_{30}N_4$ (591)	photo-dimer	199—201	600	piezo-dimer	191—192
2,4,5-Tri-*p*-tolyl-	$C_{48}H_{42}N_4$ (633)	photo-dimer $-CH_3$	194—195	600	piezo-dimer $-CH_3$	148—150
2,4,5-Tri-*p*-chlorophenyl-	$C_{42}H_{24}N_4Cl_6$ (695)	photo-dimer -Cl	213—214	680	piezo-dimer -Cl	140—142
2-*p*-Chlorophenyl-4,5-diphenyl-	$C_{42}H_{28}N_4Cl_2$ (526)	photo-dimer -2-Cl	219—220	510	piezo-dimer -2 Cl	205—207

*1 Found: photo-dimer-CH_3: C, 84.78; H, 6.03; N, 8.30%
piezo-dimer-CH_3: C, 84.99; H, 6.17; N, 8.12%
Calcd for $C_{48}H_{42}N_4$: C, 85.43; H, 6.27; N, 8.30%.
Found: photo-dimer-Cl: C, 63.71; H, 3.04; N, 6.86; Cl, 26.95%
piezo-dimer-Cl: C, 62.44; H, 3.34; N, 6.62; Cl, 26.95%
Calcd for $C_{42}H_{24}N_4Cl_6$: C, 63.26; H, 3.03; N, 7.02; Cl, 26.68%.
Found: photo-dimer-2-Cl: C, 76.65; H, 4.18; N, 8.38; Cl, 10.40%
piezo-dimer-2-Cl: C, 76.49; H, 4.70; N, 8.00; Cl, 10.43%
Calcd for $C_{42}H_{28}N_4Cl_2$: C, 76.48; H, 4.28; N, 8.49; Cl, 10.75%.

*2 Determined in a dim light by the cryoscopic method in solutions prepared in the dark.

H, 5.12; N, 9.48%.

Piezo-dimer is soluble in benzene, toluene and other aromatic hydrocarbons, carbon tetrachloride, chloroform, acetone, ethyl acetate and pyridine and slightly soluble in methanol, ethanol, ether and *n*-hexane.

As another method to prepare the piezo-dimer, 200 m*l* of 5% aqueous solution of sodium hydroxide containing 20 g of bromine was added to a solution of lophine (1 g) in 2 N ethanolic solution of potassium hydroxide (100 m*l*) with stirring by a stream of oxygen at 10°C during 1.5 hr. A reddish-purple color first appeared and then an almost colorless precipitate was formed gradually. The precipitate filtered was washed with water repeatedly and dried *in vacuo*; 1 g of piezo-dimer was obtained.

The Photochromic Dimer of Triphenylimidazolyl.[2] By slow recrystallization of piezo-dimer from benzene at 5°C in the dark light yellow crystals of the photochromic dimer (photo-dimer) were obtained.

Found: C, 85.20; H, 5.50; N, 9.41%. Calcd for $C_{42}H_{30}N_4$: C, 85.40; H, 5.12: N, 9.48%.

Photo-dimer is soluble in benzene, acetone, ethyl acetate, pyridine, chloroform and carbon tetrachloride and slightly soluble in ether and *n*-hexane, mp 199—201°C.

Photo-dimer was also prepared by oxidation of lophine according to the method of Khun and Kainer[9] who obtained tetraphenylpyrryl radical by oxidation of tetraphenylpyrrole with lead dioxide. When lophine (0.3 g) was heated in benzene (100 m*l*) with lead dioxide (10 g) for 2 hr at 80°C with stirring by a stream of nitrogen, a reddish-purple solution was obtained. After the solution was cooled to room temperature, lead dioxide was filtered. The reddish-purple filtrate was concentrated under nitrogen atmosphere at room temperature in the dark under reduced pressure. By standing the concentrated solution for 1 day in the dark, a small amount of photo-dimer was obtained.

The Dimers of Substituted Triphenylimidazolyl. Piezo-dimers of substituted triphenylimidazolyl, shown in Table 1, were prepared from the corresponding imidazoles by oxidation with potassium ferricyanide in ethanolic potassium hydroxide. Photo-dimer of these triarylimidazolyls were obtained by recrystallization of the corresponding piezo-dimers.

Spectroscopic Measurements. Measurements of the absorption spectra and kinetic studies were carried out with a Hitachi recording spectrophotometer, EPS 2 type. Temperatures between room temperature and 60°C were controlled within ± 0.5°C by circulating hot water from a thermostat to the cell room of the spectrophotometer. Deaerated solutions were used in all spectroscopic measurements.

Electron Spin Resonance Absorption. Kinetic measurements by the ESR method were carried out by the Japan Electron Optics Laboratory JES 3B type ESR spectrometer (100 kc modulation) with deaerated solutions. Spin concentrations of piezochromic systems were measured by a Japan Electron Optics Laboratory JES P-10 type ESR spectrometer (100 kc modulation) which has a JES 1D-2 type integrator. The hyperfine structure of the ESR spectrum was measured by a Hitachi ESR spectrometer.

Irradiation. Sunlight or the 365 mμ light of a high pressure mercury lamp filtered through a Toshiba glass filter UV-D1B, was used.

Results and Discussion

Formation of Piezo-dimers and Photo-dimers. Lophine which showed an absorption maximum at 303 mμ in ethanol showed a red shift

9) R. H. Kuhn and H. Kainer, *Biochim. Biophys. Acta*, **12**, 325 (1953).

toward 326 mμ in 2N ethanolic potassium hydroxide, whereas *N*-methyl- and *N*-ethyl-lophine phenylimidazole anion in alkaline solution. When lophine was oxidized in a mixture of ethanolic potassium hydroxide and benzene with an aqueous solution of potassium ferricyanide, a reddish-purple substance was produced and transfered to a benzene layer which separated out from an aqueous layer when an excess of the potassium ferricyanide solution was added. The reddish-purple benzene solution showed absorption maxima at 347 and 554 mμ and an ESR signal (*g* 2.003), attributable to the triphenylimidazolyl radical. These facts show that on oxidation of lophine piezo-dimer was produced from triphenylimidazole anion through the triphenylimidazolyl radical.

Because oxidation of monophenylimidazoles did not give the corresponding radicals and diphenylimidazoles gave corresponding radicals only in a small amount, substitution of three phenyl groups in the imidazole ring seems to be favorable for formation of the radicals and their dimers.

Photochromism in Solutions. Light yellow solutions of photo-dimer in various organic solvents quickly turned reddish-purple on irradiation at room temperature and the color gradually reverted to the original color on standing in the dark at room temperature. The change in intensity of photochromic color with time of irradiation, shown in Fig. 1, was measured by the change in absorbance at absorption maximum (347 mμ in benzene, 346 mμ in *n*-hexane). The maximum absorbance at the photo-stationary state depended on the intensity of the irradiation light, concentration of solution, solvent and temperature. The rate of fading in the dark was not accelerated by irradiation with visible light.

Photo-dimer gradually lost photochromic activity in solutions with prolonged irradiation. Duration time of photochromic activity varied with the solvent and also with coexistence of oxygen. For example, in a deaerated benzene solution the duration time was one year or longer, whereas in ethanol and toluene it was very short even in a deaerated solution. The loss of activity is due to hydrogen abstraction from the solvent by triphenylimidazolyl radical which reverts to lophine or oxidation with dissolved oxygen.

A light yellow solution of photo-dimer in *n*-hexane which was prepared in a darkened room at room temperature showed an absorption maximum at 270 mμ (ε 1.6×10^4) which obeyed Beer's law. The reddish-purple solution obtained with

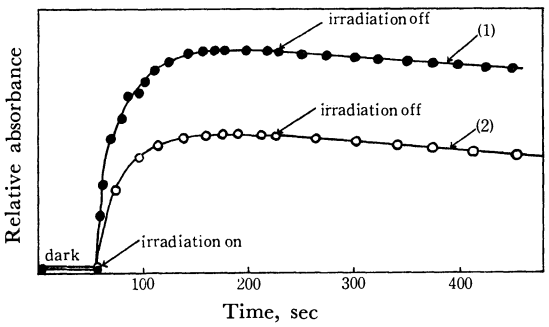

Fig. 1. Photochromic variation of the absorbance of photo-dimer.
(1) 5.28×10^{-5} mol/*l* in benzene; measured at 347 mμ, (2) 5.49×10^{-5} mol/*l* in *n*-hexane; measured at 346 mμ
Irradiation: 365 mμ light, Temp.: 16.0°C

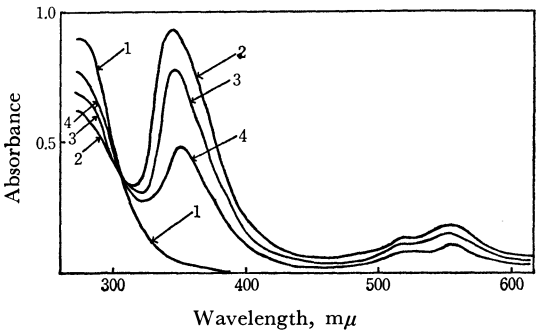

Fig. 2. Photochromic variation of absorption spectrum of photo-dimer in benzene.
(1) before irradiation, (2) immediately after irradiation, (3) 6 min after irradiation, (4) 24 min after irradiation.
Irradiation: 365 mμ light for 3 min, Temp.: 15.0°C. Concentration of photo-dimer: 3.38×10^{-5} mol/*l*.

Table 2. Photochromic changes of the color and the absorption maximum of photo-dimer in ethanol

Dimer	Before irradiation		After irradiation	
photo-dimer	light yellow	(270 mμ)	reddish-purple	(270, 348, 554 mμ)
photo-dimer -CH_3	light yellow	(280 mμ)	bluish-violet	(280, 365, 583 mμ)
photo-dimer -Cl	almost colorless	(274 mμ)	violet	(274, 368, 585 mμ)
photo-dimer -2-Cl	almost colorless	(268 mμ)	violet	(268, 366, 575 mμ)*

* Measured in benzene as the solubility of photo-dimer-2 Cl in ethanol is too low for measurement of the absorption spectrum of the colored form.

irradiation showed new absorption maxima at 346 and 548 mμ with decrease of absorbance at 270 mμ. When the reddish-purple solution was kept in the dark at room temperature, the absorbances of the new bands gradually decreased with recovering of the absorbance at 270 mμ. A similar photochromic variation was also observed in other solvents, for example in benzene, as shown in Fig. 2. Photo-dimers -CH_3, -Cl and -2-Cl also exhibited similar photochromism. The photochromic changes in color and absorption maxima are shown in Table 2.

The absorbances at 347 and 554 mμ of the reddish-purple benzene solution of photo-dimer at different concentrations (7×10^{-6}—5×10^{-5} mol/l) were measured immediately after irradiation. The results are shown in Fig. 3. As can be seen the

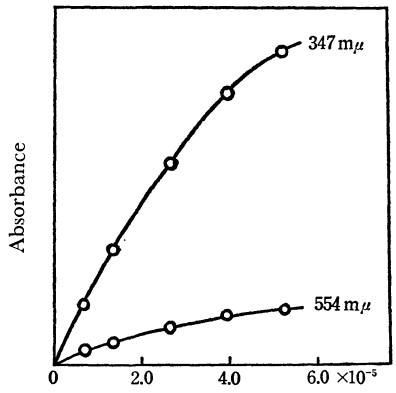

Fig. 3. Variation of the absorbance of the absorption maximum in a photochromic colored benzene solution of photo-dimer, measured immediately after irradiation.
Irradiation: 365 mμ light for 2 min. Temp.: 10.0°C.

absorbances of the photochromic absorption maxima did not obey Beer's law as the absorbances of absorption maxima at 347 and 554 mμ due to thermochromism of photo-dimer were negligibly small under the present conditions.

Photo-dimer and photo-dimers -CH_3, -Cl and -2-Cl also exhibited a similar photochromism in plastics, such as polystyrene and butyral resin.

A light yellow benzene solution of photo-dimer (1.48×10^{-4} mol/l) which was prepared in the dark gave no ESR in the dark at room temperature, whereas the reddish-purple benzene solution produced by irradiation at room temperature showed ESR with g 2.003 (a single peak singal with a line width about 9 gauss). On standing the colored solution in the dark at room temperature, the signal intensity of ESR gradually decreased. The decrease corresponded to the decrease of the absorbance in the visible region. The photochromic colored benzene solutions of photo-dimers -CH_3, -Cl and -2-Cl also showed ESR absorption.

A highly resolved hyperfine structure of an ESR spectrum shown in Fig. 4 was observed in benzene.[10]

Radical formation in the photochromic system was also confirmed by the following chemical evidence. When a light yellow solution of photo-dimer in carbon tetrachloride was brought into contact with oxygen under irradiation with sunlight at room temperature, a reddish-purple color produced on irradiation slowly faded with gradual absorption of oxygen. After about 20 hr the solution turned yellow. A brownish-yellow crystalline residue was obtained by evaporation of the solvent under reduced pressure. It was probably peroxide, because it melted with evolution of gas and liberated iodine from potassium iodide in an acetic acid solution. When nitrogen monoxide was passed into a reddish-purple solution of photo-dimer in oxygen-free benzene under irradiation at room temperature, the solution gradually turned light yellow and almost colorless crystals separated. As the crystals gave a positive Leibermann's test and decomposed at about 105°C with evolution of gas, the colorless crystals are likely to be an addition product of nitrogen monoxide with the radical. When an ethanolic solution of photo-dimer (0.12 g/300 ml) was irradiated for about 5 days with sunlight at room temperature, a reddish-purple color first appeared and then gradually faded. From the solution, lophine (0.11 g) and acetaldehyde which was identified as a dimedone derivative (0.057 g) were obtained. Acetaldehyde seems to arise from ethanol by reaction with the radical under irradiation. When an ethanolic solution of hydroquinone was added to the reddish-purple benzene solution of photo-dimer under irradiation, the color turned almost colorless and lophine was isolated from the solution.

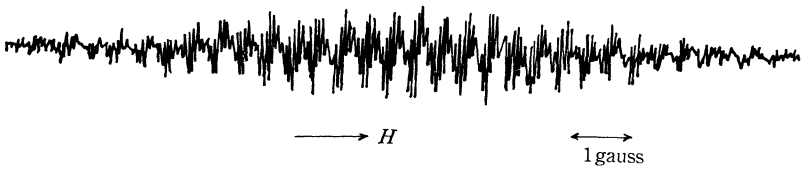

Fig. 4. The ESR spectrum of a photochromic colored benzene solution of photo-dimer.

10) The measurement was carried out by Dr. Koichi Ito of Osaka University.

By using the reaction with hydroquinone the degree of photo-dissociation of photo-dimer in reaction (1) was estimated in benzene at the photostationary state. To a reddish-purple benzene solution (4.7×10^{-5} mol/l, 10 ml) obtained by irradiation with the 365 mμ light for 3 min at room temperature, an ethanolic solution of hydroquinone (9.1×10^{-5} mol/l), was added under a stream of nitrogen. From the volume of hydroquinone solution added to extinguish the color, the degree of the photo-dissociation was estimated to be 0.15 by the following equation.

$$\underset{\text{hydroquinone}}{C_6H_4(OH)_2} + \underset{\text{triphenylimidazolyl radical}}{2C_{21}H_{15}N_2} \longrightarrow$$

$$\underset{\text{benzoquinone}}{C_6H_4O_2} + \underset{\text{lophine}}{2C_{21}H_{16}N_2}$$

The degree of photo-dissociation of photo-dimer was also estimated from molecular weight determination. The molecular weight of photo-dimer determined in a benzene solution under a dim light by the cryoscopic method (0.1127 g in 20.13 g of benzene) was 600 which corresponds to the molecular weight 590 of the dimer $C_{42}H_{30}N_4$, whereas the apparent molecular weight measured immediately after irradiation for 5 min with sunlight at 6°C was 500 (freezing point depression $\Delta t=0.057$°C). From the apparent molecular weight, the degree of photo-dissociation in benzene was estimated to be 0.18. The measurements of the weights of photo-dimers -CH_3, -Cl and -2-Cl in benzene before and after irradiation also showed decrease of the molecular weight on irradiation.

Kinetic Study of Photochromism in Solutions with ESR.[11] In order to confirm the mechanism of photochromism of photo-dimers represented by the reversible reaction (1), the rates of decrease of the radical concentration in the photochromic systems were measured by ESR. The rate of decrease of the radical concentration caused by recombination of the radical to the dimer was expected to obey the second order rate law.

The single peak signal shown by a reddish-purple benzene solution of photo-dimer (1.48×10^{-4} mol/l) gradually decreased with time in the dark. The rate of decrease of the relative signal intensity was successively measured by the height of a signal, h (cm), according to the following procedure. When the recording of the first signal was completed, the sweeping direction of the magnetic field was reversed and the second signal was recorded immediately. Similar procedures were repeated about 20 times for about 15 min at 23.0°C. Since the line width of the signals was 9.3 gauss during the measurement, the height h is assumed to be proportional to the radical concentration. The height h was used in place of the concentration of the radical in the reaction rate expression for the recombination of the radical. The differences between the reciprocals of h at time t and h_0 at $t=0$, $(1/h-1/h_0)$, were plotted against time t. The plots gave a straight line, as shown by (1) in Fig. 5, showing that the rate of decrease of ESR signal intensity obeyed the second order rate law, expressed by $1/h-1/h_0=k't$.[12]

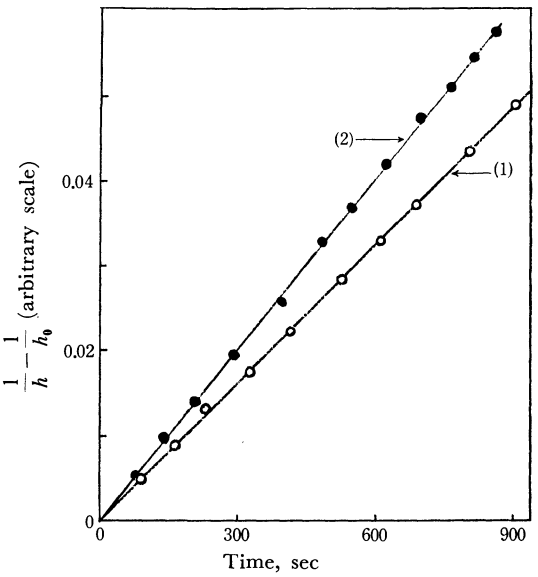

Fig. 5. Plot of $\left(\frac{1}{h}-\frac{1}{h_0}\right)$ against time t in the fading process of photochromism in benzene.
(1) Photo-dimer, (2) Photo-dimer-CH_3
Concentration: Photo-dimer; 1.48×10^{-4} mol/l, Photo-dimer-CH_3; 1.46×10^{-4} mol/l.
Temp.: 23.0°C. Irradiation: 365 mμ light for 3 min.

A similar result was obtained for photo-dimer -CH_3 as shown by the straight line (2) in Fig. 5.

Kinetic Study of Photochromism in Solutions by the Spectroscopic Method.[3] The radical mechanism shown by the reversible reaction (1) is also supported by spectroscopic measurements. The degree of photo-dissociation α of photo-dimer at a photo-stationary state in benzene ($c=3.38\times10^{-5}$ mol/l) at 15.0°C was estimated to be about 0.30 from the change of absorbance at 280 mμ (ε 2.6×10^4) measured before and after irradiation for 3 min (thickness of the solution layer; 1 cm). The degree of photo-dissociation of photo-dimers in the photo-stationary state, shown in Table 3, was estimated in a similar way.

From the absorbances at 347 and 554 mμ and the degree of photo-dissociation α of photo-

11) T. Hayashi, K. Maeda and M. Takeuchi, This Bulletin, **37**, 1717 (1964).

12) M. A. J. Wilks and M. R. Willis, *J. Chem. Soc.*, *B*, **1968**, 1526, reported a result, different from that of the present authors.

Table 3. The degree of photo-dissociation of photo-dimer in the photo-stationary state in benzene at 15.0°C.

Dimer	Concentration (mol/l)$\times 10^5$	Degree of dissociation α
photo-dimer	3.38	0.30
photo-dimer-CH_3	1.60	0.35
photo-dimer-Cl	1.61	0.25
photo-dimer-2-Cl	1.45	0.25

Table 4. Molar absorptivitiy ε of triarylimidazolyl radical at absorption maxima in benzene

Imidazolyl radical	λ_{max}, mμ	($\varepsilon\times 10^{-4}$)
2,4,5-Triphenyl-	347(4.8)	554(0.84)
2,4,5-Tri-*p*-tolyl-	366(6.3)	587(1.6)
2,4,5-Tri-*p*-chlorophenyl-	367(6.5)	588(1.8)
2-*p*-Chlorophenyl-4,5-diphenyl-	366(7.4)	575(1.6)

dimer in benzene, the molar absorptivities of triphenylimidazolyl radical at 347 and 554 mμ were estimated to be about 4.8×10^4 and 8.4×10^3 respectively. The molar absorptivities of other radicals estimated by a similar method are shown in Table 4.

From the measurements of decrease of absorbances at absorption maxima of the triarylimidazolyl radicals the rate of recombination of the radicals

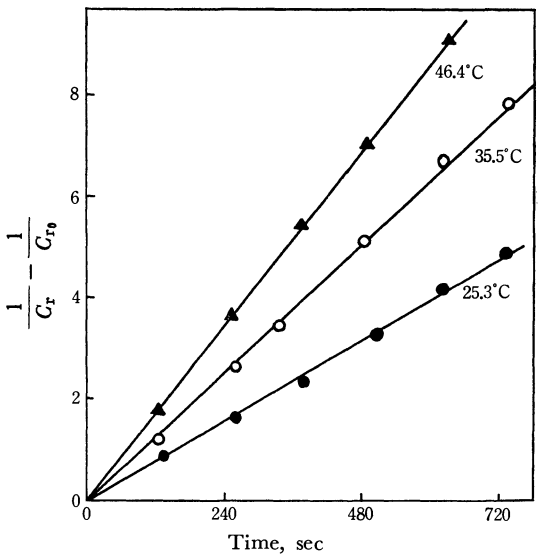

Fig. 6. Plot of $\left(\frac{1}{C_r}-\frac{1}{C_{r_0}}\right)$ against time t in the fading process of photochromism of photo-dimer in benzene.
Concentration of photo-dimer: 1.44×10^{-5} mol/l.
C_r: radical concentration at time t
C_{r_0}: radical concentration at time $t=0$
Irradiation: 365 mμ light for 3 min.

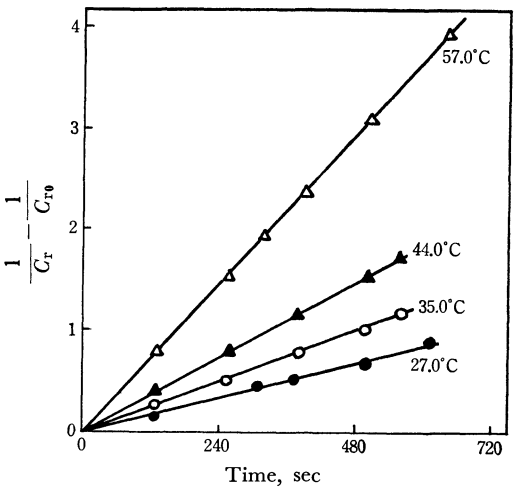

Fig. 7. Plot of $\left(\frac{1}{C_r}-\frac{1}{C_{r_0}}\right)$ against time t in the fading process of photochromism of photo-dimer-CH_3 in benzene.
Concentration of photo-dimer-CH_3: 2.25×10^{-5} mol/l.
Irradiation: 365 mμ light for 3 min.

was obtained. Absorbance at the absorption maximum, A_λ, is the sum of the absorbance A_p due to photochromism and A_t due to thermochromism. A_p was obtained by subtraction of A_t measured before irradiation from A_λ. The concentration of triarylimidazolyl radicals, C_r, at time t were calculated from the relation, $A_p=\varepsilon C_r l$. The values of $(1/C_r-1/C_{r_0})$ increased linearly with time, as shown in Fig. 6 (photo-dimer) and 7 (photo-dimer-CH_3).

Rate constants, activation energies and pre-exponential factors of the Arrhenius equation for the recombination reaction of the triarylimidazolyl radicals in the photochromic systems of photo-dimers are shown in Table 5.

Photochromism of Photo-dimer in Solid State.[4] On irradiation of light yellow fine crystals of photo-dimer at room temperature the color of the crystals turned light reddish-purple. The color hardly faded in the dark at room temperature, whereas the rate of reversion to the original color was accelerated by heating above 40°C. The color rapidly disappeared when the colored solid was subjected to contact the vapor of organic solvents, such as ether, acetone or benzene, at room temperature. This indicates that photo-dimer exhibits photochromism also in solid state. The light reddish-purple crystals also exhibited a strong ESR signal of a single peak (g 2.003) at 20°C at which the signal intensity hardly decreased in the dark. On standing in the dark at 45°C the signal intensity gradually decreased with fading of the photochromic color. The absorption spectrum of the photochromic colored crystals was measured in solid state by both the opal-glass

Table 5. Rate constant, activation energy and pre-exponential factor of the recombination of triarylimidazolyl radical in the photochromic system in benzene

Imidazolyl radical	Temp. °C	k $l\ mol^{-1}\ sec^{-1}$	E_a kcal	A $l\ mol^{-1}\ sec^{-1}$
2,4,5-Triphenyl-	25.3	66	7.4	1.7×10^{7}
	35.5	103		
	46.4	146		
2,4,5-Tri-*p*-tolyl	27.0	14	9.5	1.1×10^{8}
	35.0	22		
	44.0	30		
	57.0	61		
2,4,5-Tri-*p*-chlorophenyl-	29.0	200	6.9	1.9×10^{7}
	35.3	253		
	46.0	354		
2-*p*-Chlorophenyl-4,5-diphenyl-	16.5	62	7.2	1.7×10^{7}
	28.0	108		
	44.0	183		

Table 6. Photochromic change of color and absorption maximum in the visible region measured in solid state

Dimer	Color		λ_{max} (mμ) after irrdiation
	before irradiation	after irradiation	
photo-dimer	light yellow	light reddish-purple	563
photo-dimer-CH_3	light greenish-yellow	light greenishblue	590
photo-dimer-Cl	light greenish-yellow	light blue	591
photo-dimer-2-Cl	almost colorless	light violet	580

* Measured by the opal-glass transmission method.

transmission method and the potassium bromide disk method which gave the same spectrum. The spectrum showed an absorption maximum at 563 mμ as shown in Fig. 8. Although the maximum shifted 9 mμ to wavelengths longer than 554 mμ in the benzene solution, a reddish-purple solution obtained by dissolution of the reddish-purple crystals in benzene in a dim light showed a maximum at 554 mμ immediately after dissolution. These findings indicate that the photochromic color appeared in a solid state is also attributed to triphenylimidazolyl radical produced by dissociation of photo-dimer with irradiation.

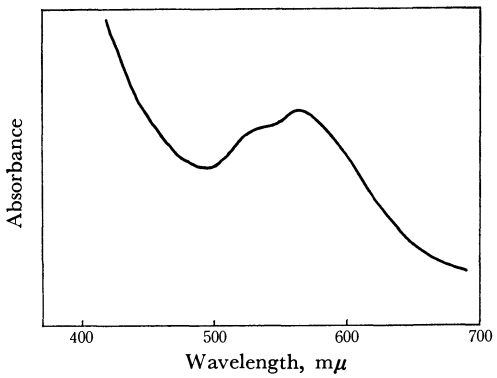

Fig. 8. Absorption spectrum of the photochromic colored solid of photo-dimer, measured by the opal-glass transmission method.

The decay rate of the ESR intensity of the photochromic colored crystals was measured in solid state at 46.0°C and 63.0°C. Differing from the rate in a benzene solution, the decay rate of the signal intensity did not obey the second order rate law.

Photo-dimers -CH_3, -Cl and -2-Cl also exhibited photochromism in solid state. Photochromic changes of the color and absorption maxima measured in solid state by the opal-glass transmission method are shown in Table 6. Benzene solutions prepared by dissolving the photochromic colored crystals in a dim light showed the same absorption maxima as those in the photochromic benzene solutions.

Thermochromism of Photo-dimer in Solutions. When a light yellow benzene solution of photo-dimer was heated in a dim light, a light reddish-purple color and an ESR signal were observed at 40°C and were enhanced with the rise of temperature. On cooling in the dark, the color reverted to the original color with diminution of ESR signal intensity. The fact shows that photo-dimer exhibits thermochromism in solutions above room temperature. Photo-dimer-CH_3, -Cl and -2-Cl also showed thermochromism in solutions. The color and absorption maxima due to thermochromism are the same as those thermochromism of photo-dimers in solutions is

also the same as that of photochromism.

The equilibrium constanst for the thermal dissociation of photo-dimer in benzene were estimated at different temperatures from the variation of the absorbance at 554 mμ with the concentration of the dimer. The measurement was carried out at high concentrations, such as 10^{-3}—10^{-2} mol/l, because coloration due to thermochromism is relatively weak, and at such concentrations the absorption band of λ_{max} 347 mμ overlapped with the tail of the band of the dimer (λ_{max} 273 mμ) but the absorption band of λ_{max} 554 mμ which has a relatively small molar absorptivity did not. The equilibrium constants K shown in Table 7 were calculated by the relation $K=2A^2/\varepsilon(2C\varepsilon-A)$, where ε is the molar absorptivity of λ_{max} at 554 mμ of the radical.

TABLE 7. EQUILIBRIUM CONSTANT OF PHOTO-DIMER OF THE THERMOCHROMIC SYSTEM IN BENZENE

Concn. mol/l	$K\times10^7$		
	49.0°C	53.8°C	60.4°C
1.05×10^{-2}	1.2	2.1	4.9
8.39×10^{-3}	1.3	1.9	5.1
6.29×10^{-3}	1.3	2.0	5.4
5.24×10^{-3}	1.2	1.6	4.8
3.35×10^{-3}	1.2	1.9	4.5
mean $K\times10^7$	1.2	1.9	4.9

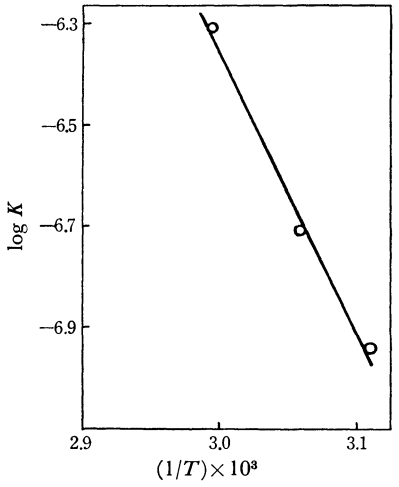

Fig. 9. Plot of logarithm of the equilibrium constant for the thermal dissociation of photo-dimer in benzene against reciprocal of absolute temperature.

From the slope of the straight line shown in Fig. 9, ΔH for the dissociation of photo-dimer in benzene was estimated approximately to be 26 kcal/mol.

Thermochromism of Photo-dimer in Solid State.[4] When light yellow fine crystals of photo-dimer were heated in a dim light, a light reddish-purple color appeared at about 170°C and a deep reddish-purple melt was obtained on melting. On cooling the colored crystals from about 180°C, the light reddish-purple color rapidly reverted to the original light yellow color. A light reddish-purple solution prepared by dissolving a small amount of the reddish-purple crystals in benzene in a dim light showed a weak absorption maximum 554 mμ of triphenylimidazolyl radical immediately after dissolution. When the crystals of photo-dimer which show no ESR signal at room temperature were heated in the dark, a weak signal of a single peak (g 2.003) began to appear at about 50°C and was enhanced with rise of temperature as shown in Fig. 10. On cooling the reddish-purple crystals from about 170°C to room temperature, the signal intensity rapidly decreased to vanish at room temperature.

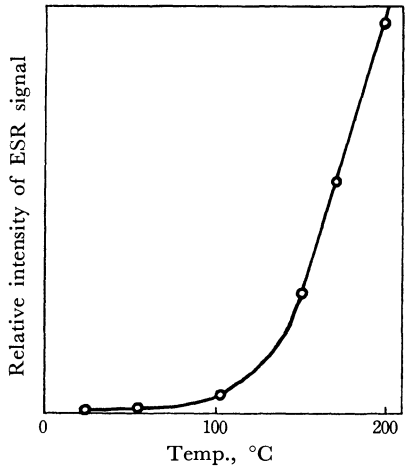

Fig. 10. Variation of the signal intensity of ESR due to thermochromism of photo-dimer in solid state.

This indicates that the mechanism of thermochromism of photo-dimer in solid state is also the same as that of photochromism and thermochromism in solutions. Photo-dimers -CH_3, -Cl and -2-Cl also showed thermochromism in solid state.

Thermochromism of Piezo-dimer in Solid State. When the solid of piezo-dimer was heated, the color turned light reddish-purple at about 180°C. The color rapidly faded on cooling. A deep reddish-purple melt was obtained on melting. When the solid of piezo-dimer which shows a weak ESR signal at room temperature was heated, the signal intensity increased with the rise of temperature. This fact shows that piezo-dimer exhibits thermochromism in solid state above about 180°C. The weak ESR signal observed at room temperature is due to a small amount of triphenylimidazolyl radical produced by the oxidation of lophine and remained without dimerization.

Table 8. Piezochromic change in color and absorption maximum

Dimer	Color		λ_{max} (mμ) after grinding
	before grinding	after grinding	
piezo-dimer	almost colorless	reddish-purple	563
piezo-dimer-CH_3	light violet	greenish-blue	589
piezo-dimer-Cl	light violet	dark blue	591
piezo-dimer-2-Cl	almost colorless	light violet	580

Piezochromism of Piezo-dimer.[5] The solid of piezo-dimer turned deep reddish-purple by grinding in a mortar or pressing at a pressure of about 10—50 kg/cm^2 at room temperature. The colored solid reverted very slowly to the original almost colorless solid on standing for several days in the dark at room temperature. The rate of fading of the color was accelerated by heating to 50°C. These facts show that piezo-dimer exhibits piezochromism. When the solid was ground at 80°C, it showed a reddish-purple color during grinding, but when grinding was stopped, the color quickly disappeared. When the piezochromic colored solid was subjected to contact the vapor of organic solvents, such as ether, ethanol, acetone or benzene at room temperature, the reddish-purple color rapidly disappeared. Since the rate of fading of the piezochromic color at room temperature was very slow and the temperature at which the thermochromic color was first observed was 180°C in solid state, piezochromism is not due to a rise of temperature which may occur by grinding or pressing.

A very intense ESR signal ($g=2.003$) appearing by grinding piezo-dimer decreased very slowly at room temperature, but rapidly at a higher temperature such as 50°C.

The absorption spectrum of the piezochromic colored solid was measured by both the opal-galss transmission method and the potassium bromide disk method which gave a similar spectrum to that of the photochromic colored solid of photo-dimer shown in Fig. 8. The absorption maximum at 563 mμ agreed with that of the photochromic colored solid which showed a red shift of about 9 mμ, as compared with the absorption maximum in the photochromic colored benzene solution.

Piezo-dimers -CH_3, -Cl and -2-Cl also exhibited piezochromism. The changes in color and absorption maxima due to piezochromism are shown in Table 8. These results indicate that the mechanism of piezochromism is due to dissociation of the bond between the imidazolyl radicals into the triarylimidazolyl radicals caused by mechanical work.

The spin concentration of piezo-dimer after grinding for 5 min in an agate mortar was measured with ESR. The spin concentration and the degree of piezochromic dissociation are shown in Table 9. The spin concentration increased with the time of grinding.

Table 9. Spin concentration and degree of piezochromic dissociation of piezo-dimer

Piezo-dimer	Spin concentration (spin/g) (degree of piezochromic dissociation)*1	
	before grinding	after grinding*2
Sample 1	7.2×10^{16} (3.6×10^{-3}%)	3.3×10^{19} (1.6%)
Sample 2	4.3×10^{16} (2.1×10^{-3}%)	5.2×10^{19} (2.6%)

*1 $\frac{1}{2}\times\frac{\text{spin concentration}}{\left(\begin{array}{c}\text{number of molecules in 1 g of}\\ \text{piezo-dimer}\end{array}\right)}\times100$

*2 ground in an agate mortar for 5 min at room temperature.

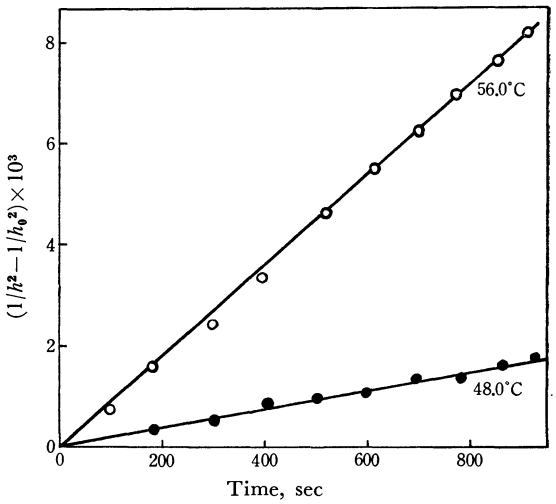

Fig. 11. Plot of $(1/h^2-1/h_0^2)$ against time t in the fading process of piezochromism of piezo-dimer.
h: height of a signal at time t
h_0: height of a signal at time $t=0$

The decay rates of the signal intensity of ESR due to piezochromism of piezo-dimer were measured at 48.0 and 56.0°C. The decrease of the relative signal intensity, h, with time virtually obeyed the relation $1/h^2-1/h_0^2=k't$, as shown in Fig. 11. As the line widths of the signals were almost constant during the measurement, h could be assumed to be approximately proportional to the concentration

of triphenylimidazolyl radical. Differing from the case of photochromism in benzene, the result seems to show that the rate of recombination of the radical in the fading process of piezochromism obeys the third order rate law.

Also in the case of piezo-dimer-CH_3, the decay rates of the signal intensity due to piezochromism, measured at 52.0, 58.0 and 65.0°C were found to obey the third order rate law.

The authors wish to express their cordial thanks to Professor Shoji Shida of Tokyo Institute of Technology, Professor Kazuo Nakada of Niigata University, Dr. Hiroshi Midorikawa of the Institute of Physical and Chemical Research, Professor Saburo Nagakura of The University of Tokyo, Professor Koichi Ito of Osaka University, Mr. Makoto Takeuchi of Japan Electron Optics Laboratory, Professor Taro Tachibana of Ochanomizu University, Professor Heijiro Ojima of Aichi Kyoiku University, Mrs. Midori Mikami and Mrs. Takako Goda for their kind help and to the Ministry of Education for the financial support granted this research.

BULLETIN OF THE CHEMICAL SOCIETY OF JAPAN VOL. 43 438—442 (1970)

Reaction of Alkylidenephosphoranes with Nitrosyl Chloride and Decomposition of α-Hydroxyiminophosphonium Chlorides Formed

Chikahiko EGUCHI, Kin-ya AKIBA and Naoki INAMOTO

Department of Chemistry, Faculty of Science, The University of Tokyo, Hongo, Bunkyo-ku, Tokyo

(Received April 10, 1969)

The reaction of stable alkylidenephosphoranes with nitrosyl chloride in THF gave α-substituted α-hydroxyiminomethyltriphenylphosphonium chloride (A) in high yields. In the case of active alkylidenephosphoranes, "transylidation" took place simultaneously and a mixture of A and α-substituted methyltriphenylphosphonium chloride was obtained along with corresponding amounts of nitrile and triphenylphosphine oxide. By thermal decomposition, all α-hydroxyiminomethyltriphenylphosphonium chlorides (A) afforded nitriles and triphenylphosphine oxide.

Recently we have reported that the reaction of alkylidenephosphoranes with nitric oxide afforded nitriles, aldehydes and phosphine oxide.[1] In connection with this reaction, we attempted the reaction of alkylidenephosphoranes with nitrosyl chloride.[2]

Zbiral and Fenz reported formation of nitriles from acylmethyltriphenylphosphonium salts with ethyl nitrite,[3] but they could not obtain any intermediate.

Trippett, Walker and Hoffmann reported formation of α-substituted α-hydroxyiminomethyltriphenylphosphonium bromides by the reaction of α-bromonitroalkanes ($RCHBrNO_2$) with triphenylphosphine and also formation of nitriles by decomposition of the bromides with alkali.[4] They could isolate the bromides only when the substituents (R) were methyl and ethyl.

We wish to report here formation of α-substituted α-hydroxyiminomethyltriphenylphosphonium chlorides (A) as intermediates and their decomposition to nitriles.

Results and Discussion

When stable α-substituted methylenetriphenylphosphoranes ($Ph_3P{=}CHR$; I: R=COPh and II: R=CO_2Me) were allowed to react with nitrosyl chloride in tetrahydrofuran (THF) solution, α-substituted α-hydroxyiminomethyltriphenylphosphonium chlorides (A-I and A-II) were produced as precipitates in good yields according to reaction (3) (see Table 1).

From the filtrate, benzoyl cyanide and triphenylphosphine oxide were isolated in the case of I, and in the case of II, methyl cyanoformate was determined by g.l.c. In both cases, no α-acylmethyltriphenylphosphonium chlorides (B) were detected in spite of careful examination. This fact suggests that reaction (4) does not take place in these cases.

When α-hydroxyimino-α-benzoylmethyltriphenylphosphonium chloride (A-I) was refluxed in chloroform, benzoyl cyanide (86—98%) and triphenylphosphine oxide (82—93%) were obtained. The

1) K. Akiba, M. Imanari and N. Inamoto, *Chem. Commun.*, **1969**, 166.

2) Preliminary report: K. Akiba, C. Eguchi and N. Inamoto, This Bulletin, **40**, 2983 (1967).

3) E. Zbiral and L. Fenz, *Monatsh. Chem.*, **96**, 1983 (1965).

4) S. Trippett, B. J. Walker and H. Hoffmann, *J. Chem. Soc.*, **1965**, 7140.

Table 1. Formation of α-substituted α-hydroxyiminomethyltriphenylphosphonium chlorides (A)
$Ph_3P{=}CHR + NOCl$ (I: R=COPh and II: R=CO_2Me)

	Temp. (°C)	$[Ph_3\overset{+}{P}C(=NOH)R]Cl^-$ (A) Dec. point (°C)	(%)	$Ph_3P{=}O$* (%)	RCN* (%)
I	0	134—5	70	18	6
	−30—−20		72	16	18
II	−50—−40	128—9	89	5	—
	−50—−40		79	13	19

* Determined from the filtrate of A.

same products were also obtained in 73% yield by the decomposition of A-I in molten state.

However, in a similar decomposition of α-hydroxyimino-α-methoxycarbonylmethyltriphenylphosphonium chloride (A-II), complicated results

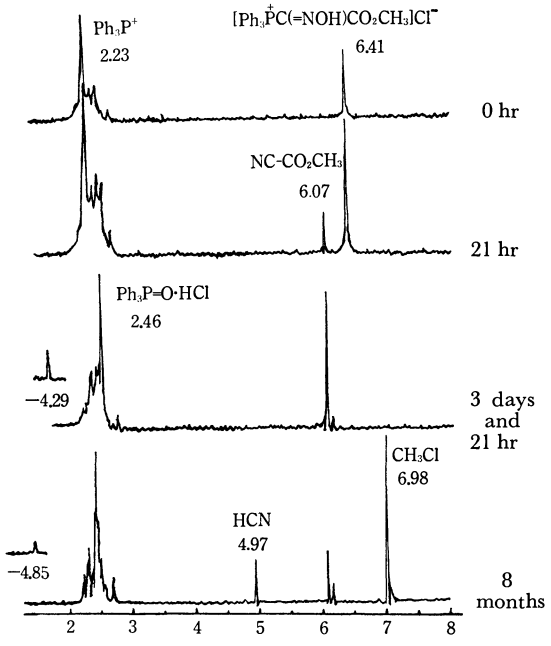

Fig. 1. Decomposition of $[Ph_3\overset{+}{P}C(=NOH)CO_2CH_3]Cl^-$ in $CDCl_3$ at room temperature.

were obtained. When chloroform solution of A-II was allowed to stand at room temperature for 4 days, only methyl cyanoformate and hydrochloride of triphenylphosphine oxide were formed quantitatively (Fig. 1). These yields were determined by NMR (Fig. 1) and also by g.l.c. The signals in Fig. 1 were assigned in comparison with those of authentic samples. On further standing, it was found from Fig. 1 that methyl cyanoformate decomposed into methyl chloride, hydrogen cyanide and carbon dioxide. To realise this fact, stability of methyl cyanoformate was checked under several conditions by NMR.

In chloroform solution, methyl cyanoformate was stable in the presence of triphenylphosphine oxide at room temperature for 4 days but slowly trimerized (in 40% yield after one year) in the presence of hydrogen chloride without decomposition. But when the solution was heated at 40°C for 20 hr in the presence of both triphenylphosphine oxide and hydrogen chloride, the ester was decomposed into methyl chloride, hydrogen cyanide and carbon dioxide. The last result is explicable by reaction (1).

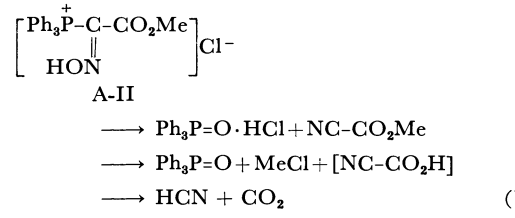

This decomposition of the ester is analogous to the fission of alkyl groups of esters and ethers by triphenylphosphine hydrobromide.[5]

The thermal decomposition of A-II in molten state gave a small amount (9%) of methyl cyanoformate and large amounts of methyl chloride, hydrogen cyanide and carbon dioxide. In this case, a direct decomposition as shown in reaction (2) cannot be ruled out.[6]

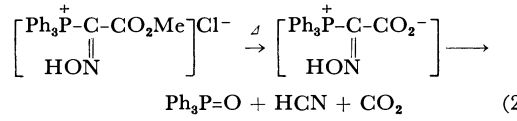

When active α-substituted methylenetriphenylphosphoranes (III: R=Ph and IV: R=*n*-Pr) were allowed to react with nitrosyl chloride in THF, a mixture of α-substituted α-hydroxyiminomethyltriphenylphosphonium chloride (A) and α-substituted methyltriphenylphosphonium chloride (B) precipitated immediately, and the resulting nitrile (RCN-1 in Table 2) and triphenylphosphine oxide were determined from the filtrate. Formation of

5) H. J. Bestmann, L. Mott and J. Lienert, *Ann. Chem.*, **709**, 105 (1967).

6) N. A. Nesmeyanov, Ya. S. Vasyak, V. A. Kalyavin and O. A. Reutov, *Zh. Org. Khim.*, **4**, 385 (1968); *Chem. Abstr.*, **68**, 104379a (1968).

Table 2. Reaction of alkylidenephosphoranes with nitrosyl chloride*
$Ph_3P{=}CHR + NOCl$ (III: R=Ph and IV: R=*n*-Pr)

	Temp. (°C)	$[Ph_3\overset{+}{P}CH_2R]Cl^-$ B (%)	$Ph_3P{=}O$ (%)	RCN-1 (%)	RCN-2 (%)
III	−40—−30	23	21	28	17
	−40—−30	30	29	36	18
IV	−40—−30	32	27	38	15
	−40—−30	23	43	52	

* Yields are based on the initial phosphonium bromide.

these products are ascribable to reaction (4), and this is supported by the fact that B and RCN-1 were obtained in about equal amount.

In order to decompose A in the precipitates (A+B), the precipitates were refluxed in THF or in chloroform. From the filtrate, nitrile (RCN-2 in Table 2) was determined by g.l.c. and B was obtained by usual work up. Unfortunately, isolation of A-III and A-IV from the precipitates was not successful, but their existence is shown by the formation of RCN-2.

These results can be explained by the following scheme.

$$Ph_3P{=}CHR + NOCl \longrightarrow \left[\begin{array}{c} Ph_3\overset{+}{P}\text{-}CHR \\ | \\ O{=}N \end{array}\right]Cl^-$$

I: R=COPh
II: R=CO_2Me
III: R=Ph
IV: R=*n*-Pr

$$\longrightarrow \left[\begin{array}{c} Ph_3\overset{+}{P}\text{-}C\text{-}R \\ \| \\ HON \end{array}\right]Cl^- \quad (3)$$

A

$$\left[\begin{array}{c} Ph_3\overset{+}{P}\text{-}C\text{-}R \\ \| \\ HON \end{array}\right]Cl^- + Ph_3P{=}CHR$$

A

$$\longrightarrow [Ph_3\overset{+}{P}\text{-}CH_2R]Cl^- + RCN + Ph_3P{=}O \quad (4)$$

B

$$\left[\begin{array}{c} Ph_3\overset{+}{P}\text{-}C\text{-}R \\ \| \\ HON \end{array}\right]Cl^- \xrightarrow{\Delta} Ph_3P{=}O + RCN + HCl \quad (5)$$

A

In the cases of stable alkylidenephosphoranes (I and II), reaction (4) was not observed because of their low basicities.[7] On the other hand, in the cases of active alkylidenephosphoranes (III and IV), reaction (4) seems to compete with reaction (3), and a mixture of A and B was obtained as precipitates. The ratio of A-III to B-III was 17 : 23 and that of A-IV to B-IV was 15 : 32, assuming that the amount of RCN-2 correspond to the amount of A.

Although this method is not generally adequate for the synthesis of usual nitriles, it would be useful for preparation of special types of nitriles, because *p*-toluenesulfonyl cyanide[8] was prepared only by this method.

$$RSO_2\text{-}CH{=}PPh_3 + NOCl \xrightarrow{\text{pyridine}} RSO_2\text{-}CN + Ph_3P{=}O$$

Experimental

Materials. Phosphonium salts were prepared from organic halides and triphenylphosphine: phenacyltriphenylphosphonium bromide,[9a,b] mp 268.5—271.0°C; methoxycarbonylmethyltriphenylphosphonium chloride, mp 151—152°C; benzyltriphenylphosphonium bromide,[10] mp 269.0—271.0°C; benzyltriphenylphosphonium chloride,[11] mp 299.5—301.2°C; *n*-butyltriphenylphosphonium bromide,[11,12] mp 232—233°C; and *n*-butyltriphenylphosphonium chloride, mp 217—218.5°C.

Benzoylmethylenetriphenylphosphorane,[9a] mp 180.0—180.5°C, and methoxycarbonylmethylenetriphenylphosphorane,[13] mp 168.0—168.5°C, were prepared by the method described in literature.

Benzylidene- and *n*-butylidenetriphenylphosphoranes were prepared from the corresponding phosphonium bromides and sodium amide prepared *in situ* in liquid ammonia.[14] Evaporation of ammonia, extraction with anhydrous THF and filtration afforded the salt-free solution of the phosphoranes.

Nitrosyl chloride was prepared by Coleman's method[15] and distilled three times before use.

7) K. Issleib and R. Lindner, *Ann. Chem.*, **707**, 120 (1967).

8) A. M. van Leusen, A. J. W. Iedema and J. Strating, *Chem. Commun.*, **1968**, 440.

9) a) F. Ramirez and S. Dershowitz, *J. Org. Chem.*, **22**, 41 (1957). b) I. J. Borowitz and R. Virkhaus, *J. Amer. Chem. Soc.*, **85**, 2183 (1963).

10) M. Grayson and P. T. Keough, *J. Amer. Chem. Soc.*, **82**, 3919 (1950).

11) K. Friedrich and H. G. Henning, *Chem. Ber.*, **92**, 2756 (1959).

12) R. Mechoulam and F. Sondheimer, *J. Amer. Chem. Soc.*, **80**, 4386 (1958).

13) O. Isler, H. Gutmann, M. Montavon, R. Rüegg, G. Ryser and P. Zeller, *Helv. Chim. Acta*, **40**, 1242 (1957).

14) H. J. Bestmann, *Angew. Chem.*, **77**, 609 (1965); H. J. Bestmann, *Chem. Ber.*, **95**, 58 (1962).

15) G. H. Coleman, G. A. Lillis and G. E. Gokeen, "Inorganic Syntheses," Vol. 1, p. 55 (1939).

Methyl cyanoformate as an authentic sample was prepared by dehydration of methyl oxamate with phosphorus pentoxide,[16] bp 99—100°C.

Synthesis of α-Benzoyl- and α-Methoxycarbonyl-α-hydroxyiminomethyltriphenylphosphonium Chlorides. A typical procedure is described below.

a) α-Hydroxyimino-α-benzoylmethyltriphenylphosphonium Chloride (A-I). A solution of 3.40 g (0.052 mol) of nitrosyl chloride in 170 m*l* of anhydrous THF was added dropwise to a solution of 19.0 g (0.050 mol) of benzoylmethylenetriphenylphosphorane in 400 m*l* of anhydrous THF over 50 min at −30—−20°C with stirring. As soon as the solution of nitrosyl chloride was added, white precipitates appeared and the solution showed a light blue color, which disappeared after addition of about half the nitrosyl chloride solution. After the addition, the mixture was stirred for additional 15 min at room temperature. The white precipitates (A-I) were filtered, and washed with anhydrous THF and acetone. Yield 16 g (0.036 mol, 72%), dec. point 134—135°C. IR (in C_4Cl_6): 2500 (ν_{OH}) (shifted to 2600 cm^{-1} in chloroform), 1645 (ν_{CO}), 1275, and 1050 cm^{-1}. $\lambda_{max}^{CHCl_3}$: 266 ($\varepsilon=1.49\times10^4$), 271 ($1.53\times10^4$), and 277.5 mμ ($1.34\times10^4$).

Found: C, 69.94; H, 4.62; N, 3.04%. Calcd for $C_{26}H_{21}NO_2PCl$: C, 70.04; H, 4.75; N, 3.14%.

After removal of THF from the filtrate, the residue was extracted with petroleum ether (bp 40—60°C), and the extract was distilled under reduced pressure to yield 1.25g (0.0095 mol, 18%) of benzoyl cyanide, bp 77—78°C/10 mmHg, mp 31.0—32.1°C, IR (Nujol): 2240 (ν_{CN}) and 1680 cm^{-1} (ν_{CO}).

Insoluble part in petroleum ether was washed three times with ether to afford 2.2g (0.0079 mol, 16%) of triphenylphosphine oxide, mp 153.5—155°C.

b) α-Hydroxyimino-α-methoxycarbonylmethyltriphenylphosphonium Chloride (A-II). This salt was prepared by addition of a solution of 4.00g (0.061 mol) of nitrosyl chloride in 200 m*l* of anhydrous THF to a solution of 20.0g (0.060 mol) of methoxycarbonylmethylenetriphenylphosphorane in 350 m*l* of anhydrous THF at −50 — −40°C. Appearance of the reaction was similar to that of a), except that the color of the solution changed to cherry pink. Yield 19.0g (0.0476 mol, 80%), dec. point 128—129°C. IR (in C_4Cl_6): 2220 (ν_{OH}) (shifted to 2540 cm^{-1} in chloroform), 1730 (ν_{CO}), 1275, and 1070 cm^{-1}. $\lambda_{max}^{CHCl_3}$: 262.5 (shoulder), 270 ($\varepsilon=6.45\times10^3$), and 277.5 mμ ($4.69\times10^3$).

Found: C, 62.97; H, 4.78; N, 3.40%. Calcd for $C_{21}H_{19}NO_3PCl$: C, 63.09; H, 4.79; N, 3.50%.

The filtrate was analyzed by g.l.c. (diisodecyl phthalate, 78°C; dibenzyl ether, 74°C), and found to contain 0.986g (0.0116 mol, 19%) of methyl cyanoformate and a trace of carbon dioxide. Attempt to isolate methyl cyanoformate by distillation was unsuccessful, but 2.24g (0.00805 mol, 13%) of triphenylphosphine oxide was obtained from the residue.

Decomposition of α-Benzoyl- and α-Methoxycarbonyl-α-hydroxyiminomethyltriphenylphosphonium Chlorides (A-I and A-II). *a) For A-I.* 1) In boiling chloroform. A solution of 4.0g (0.09 mol) of A-I in 200 m*l* of chloroform was refluxed for 22 hr. After generation of hydrogen chloride ceased and the chloroform was removed, the residue was treated by the procedure described in "synthesis of A-I" to afford 1.15g (0.0088 mol, 98%) of benzoyl cyanide and 2.2g (0.00785 mol, 87%) of triphenylphosphine oxide.

2) In molten state. Heating of 2.2g (0.0049 mol) of A-I at 140°C (bath temperature) for 45 min gave 0.468 g (0.0036 mol, 73%) of benzoyl cyanide and 0.985 g (0.00353 mol, 72%) of triphenylphosphine oxide.

b) For A-II. 1) In molten state. In an oil bath, 3.16g (0.0079 mol) of A-II was gradually heated and then at 200°C (bath temperature) for further 3 hr under dry nitrogen stream. The liquid collected with a dry ice-ethanol trap was analyzed by g.l.c. and found to contain methyl cyanoformate (9%), methyl chloride and hydrogen cyanide. The residue in the reaction flask was recrystallized from ethyl acetate-petroleum ether to yield 1.8g (0.0065 mol, 82%) of triphenylphosphine oxide.

2) A solution of A-II (*ca.* 2%) was allowed to stand at room temperature for 4 days and the resulting methyl cyanoformate was determined simultaneously both by NMR (91%) and by g.l.c. (95%).

A solution of 1.09g (0.00274 mol) of A-II in 65 m*l* of chloroform was refluxed for 25 hr. The formation of methyl cyanoformate (15%), methyl chloride, and hydrogen cyanide was observed by g.l.c.

Reaction of Benzylidenetriphenylphosphorane with Nitrosyl Chloride. To a solution of 3.30g (0.0505 mol) of nitrosyl chloride in 250 m*l* of anhydrous ether was added dropwise a solution of salt-free benzylidenetriphenylphosphorane (0.050 mol) in 150 m*l* of anhydrous THF under nitrogen at −40 — −30°C with stirring. After the addition, the reaction mixture was stirred for a further 10 min at room temperature. White precipitates (C) thus formed were filtered, washed with anhydrous THF and anhydrous ether, and dried over phosphorus pentoxide *in vacuo*. Yield 12.1g. The filtrate was analyzed by g.l.c. (Apiezon grease M, 197°C) to contain 1.85g (0.018 mol, 36%) of benzonitrile, the isolation of which was unsuccessful. The residue was recrystallized from ether to yield 3.9g (0.014 mol, 29%) of triphenylphosphine oxide.

A suspension of C (3.5g) in 50 m*l* of anhydrous THF was refluxed for 35 hr and 0.269g (0.0026 mol) of benzonitrile was determined by g.l.c. The precipitates insoluble in anhydrous THF were recrystallized twice from chloroform-ethyl acetate to yield 1.7g (0.0048 mol) of benzyltriphenylphosphonium chloride, mp 295.5—297.0°C. A mixed mp with authentic benzyltriphenylphosphonium chloride (mp 299.5—301.2°C) was 299.0 301.0°C and that with benzyltriphenylphosphonium bromide (mp 269.0—271.0°C) was 277.5—281.0°C. From this result, the precipitates C were found to consist of α-hydroxyiminobenzyltriphenylphosphonium chloride (A-III) and benzyltriphenylphosphonium chloride (B-III). The yields were 18 and 30% on the basis of the initial benzyltriphenylphosphonium bromide, respectively.

Reaction of *n*-Butylidenetriphenylphosphorane with Nitrosyl Chloride. The procedure and the reaction scale were the same as those of benzylidenetriphenylphosphorane. The white precipitates (D) thus obtained were very hygroscopic. Yield 10.9g. The filtrate was analyzed by g.l.c. (Polyethylene glycol, 120°C), and found to contain 1.32g (0.019 mol, 38%) of *n*-butyronitrile, the isolation of which was unsuccessful. Chromatography of the residue of distillation on silica gel with benzene gave 3.82g (0.0137 mol, 27%) of tri-

16) A. Weddige, *J. Prakt. Chem.*, **10**, 197 (1874).

phenylphosphine oxide.

A solution of D (2.3g) in 79 m*l* of chloroform was refluxed for 20 hr and the reaction mixture was analyzed by g.l.c., and found to contain 0.109g (0.0016 mol) of *n*-butyronitrile. From the solution chloroform was removed, and the residue was recrystallized three times from chloroform - ethyl acetate to afford 1.20g (0.0034 mol) of *n*-butyltriphenylphosphonium chloride, mp 218.0—219.0°C (Found: Cl, 9.85%). A mixed mp with authentic sample (mp 217.0—218.5°C) was 217.5—218.5°C and that with *n*-butyltriphenylphosphonium bromide (mp 232.0—233.0°C) was 222.5—224.5°C.

From this result, the precipitates (D) were found to consist of α-hydroxyimino-*n*-butyltriphenylphosphonium chloride (A-IV) and *n*-butyltriphenylphosphonium chloride (B-IV). The yields were 15 and 32% on the basis of the initial *n*-butyltriphenylphosphonium bromide, respectively.

BULLETIN OF THE CHEMICAL SOCIETY OF JAPAN VOL. 43 442—446 (1970)

The Stereochemistry of Hydrogenation and Hydrogenolysis. XI.[1] The Stereochemistry of the Reduction of 3-Methyl-4-chromanone*[1]

Kaoru HANAYA

Department of Chemistry, Faculty of Science, Yamagata University, Koshirakawa-cho, Yamagata

(Received April 14, 1969)

3-Methyl-4-chromanone (VIII) was reduced with a metal hydride complex, by the Meerwein-Ponndorf method and by catalytic hydrogenation. When VIII was reduced with a metal hydride complex and the Meerwein-Ponndorf method, *trans*-3-methyl-4-chromanol (IX) was produced as the main product. In the catalytic hydrogenation, VIII gave a *cis*-3-methyl-4-chromanol (X) as the main product over Raney nickel, but over the palladium catalyst the *trnas* isomer was larger than the *cis* isomer. These results indicate that, on Meerwein-Ponndorf and metal hydride reductions, the more stable product was formed as the main product; in the catalytic hydrogenation over the Raney nickel catalyst, VIII seems to be adsorbed mainly on the opposite side of the methyl group of the C-3 position and is hydrogenated to give the *cis* isomer, whereas, over the palladium catalyst, hydrogenation seems to proceed under the effect of "product development control over the catalyst" and the *trans* isomer is produced in a high yield.

In the previous papers of this series, the reductions of 2-phenyl-1-tetralone(I),[2] 2-acetoxy-1-tetralone (II),[3] and 2-methyl-1-tetralone(III)[4] were reported. In the catalytic hydrogenation over the Raney nickel, I and II gave *cis*-2-phenyl-1-tetralol (IV) and *cis*-2-acetoxy-1-tetralol(V) respectively in high yields, whereas III gave a mixture of about equivalent quantities of *cis*-2-methyl-1-tetralol(VI) and *trans*-2-methyl-1-tetralol(VII), but over a palladium catalyst VII was formed in a larger amount than VI, along with hydrocarbons resulting from hydrogenolysis. From these results, it is considered that, on the catalytic hydrogenation, the phenyl or acetoxyl group works as a catalyst hindrance to the adsorption of I or II on a catalyst, while the methyl group does not act as so much a hindrance to the adsorption of III. However, the different behaviour observed in the catalytic hydrogenation of III over Raney nickel and palladium catalysts has not yet been discussed. In the metal hydride reduction of I, II, and III, I and II afforded *cis* isomers as the main products, whereas III gave the *trans* isomer in a larger amount than the *cis* isomer. On the Meerwein-Ponndorf reduction of I and III, if acetone was removed, the *cis* isomer was produced mainly, whereas the *trans* isomer was produced mainly when the reaction mixture was refluxed without removing the acetone. From these results, it can be considered that, in the reduction with metal hydride complex, the phenyl or acetoxyl group sterically hinders the carbonyl carbon atom of I or II from the attack of the hydride ion, but the methyl group of III does not exert any such steric hindrance. On the Meerwein-Ponndorf reduction, if acetone is removed, the reaction may proceed under the effect of steric hindrance. On the other hand, if the reaction mixture is refluxed without removing the acetone, the more stable product is formed as the main product.

In order to obtain further information on the stereochemistry of the reduction of cyclic ketones

1) Part X: K. Hanaya, *Nippon Kagaku Zasshi*, **90**, 314 (1969).

*1 Presented at the 21st Annual Meeting of the Chemical Society of Japan, Osaka, April, 1968.

2) K. Hanaya, *Nippon Kagaku Zasshi*, **87**, 745 (1966).

3) K. Hanaya, This Bulletin, **40**, 1884 (1967).

4) K. Hanaya, *Nippon Kagaku Zasshi*, **87**, 991 (1966).

and on the different behavior of these ketones in catalytic hydrogenation over nickel and palladium catalysts, the reduction of 3-methyl-4-chromanone (VIII) was investigated.

Results and Discussion

The reduction of 3-methyl-4-chromanone (VIII) was carried out by the catalytic, metal hydride complex, and Meerwein-Ponndorf methods. The results of these reductions are shown in Table 1.

The configurations of the product alcohols (IX and X) have been established by the synthesis of *trans*-3-methyl-4-chromanol (X) *via* the hydroboration[5] of 3-methyl-3-chromene (XI), which had itself

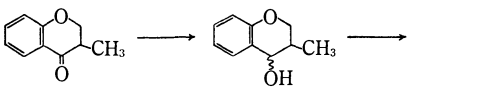

(VIII) (XI) (X)

been prepared by the dehydration of 3-methyl-4-chromanol with *p*-toluenesulfonic acid in benzene, and by the examination of the NMR spectra of IX, X, and their acetates. In the NMR spectra of IX, X, and their acetates, the values of the 3,4-coupling constant ($J_{3,4}$=4.8Hz) of X and its acetate are larger than those ($J_{3,4}$=3.4Hz) of IX and its acetate. In view of the Karplus relationship,[6] these results indicate that, in X and its acetate, the methyl group is *trans* to the hydroxyl or acetoxyl group, while in IX and its acetate it is *cis*.

From the experimental results shown above, the stereochemistry of the reduction of VIII can be considered to be as follows.

VIII is considered to have the conformations shown in Fig. 1, which are similar to those of γ-chromanone proposed by Philbin and Wheeler.[7]

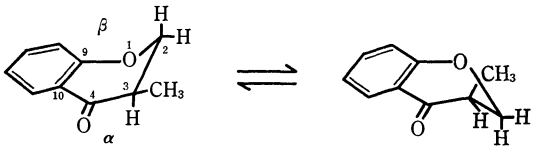

(A) (B)

Fig. 1. Conformations of VIII.*2

The conformation of the methyl group in the 3-position of VIII may be assumed to be quasi-equatorial, as usual. Therefore, the preferable conformation of VIII will be the A-form of Fig. 1.

The reduction of VIII with the metal hydride complex gave the *trans* isomer as the main product. On the Meerwein-Ponndorf reduction VIII, if the acetone was removed, the *cis* isomer was produced mainly, whereas if the reaction mixture was

Table 1. Products of the reduction of 3-methyl-4-chromanone (VIII)

Expt. No.	Reducing agent or catalyst	Conversion %	Products, %		
			IX	X	XII
1	$LiAlH_4$	100	35	65	—
2	$NaBH_4$	100	46	54	—
3	$Al(OC_3H_7)_3$[a]	100	73	27	—
4	$Al(OC_3H_7)_3$[b]	91	37	63	—
5	Raney Ni	96	52	37	11
6	Raney Ni[c]	91	64	36	—
7	5% Pd-C-B (2 hr)	53	35	58	7
8	5% Pd-C-B (4 hr)	84	33	60	7
9	5% Pd-C-B (6 hr)	98	29	61	10
10	5% Pd-C-A	44	27	49	24
11	5% Pd-$CaCO_3$	92	33	49	18
12	5% Pd-$BaSO_4$	94	23	52	25

a) Acetone was removed.
b) The reaction mixture was refluxed without removing acetone for 4 hr.
c) 1/2000 mol of NaOH was added.

5) H. C. Brown and G. Zweifel, *J. Amer. Chem. Soc.*, **81**, 247 (1959); H. C. Brown and G. Zweifel, *ibid.*, **83**, 2544 (1961); E. L. Allred, J. Sonnenberg and S. Winstein, *J. Org. Chem.*, **25**, 26 (1960).

6) M. Karplus, *J. Chem. Phys.*, **30**, 11 (1959).

7) E. M. Philbin and T. S. Wheeler, *Proc. Chem. Soc.*, **1958**, 167.

*2 Philbin and Wheeler have been proposed that five atoms in the heterocyclic, O_1, C_3, C_4, C_9, and C_{10}, are coplanar. However, the present author has considered that C_2, C_3, and the 4-keto group are not coplanar with the adjacent benzene nucleus.[8] A study of the conformations of γ-chromanone derivatives is now in progress.

8) K. Hanaya and K. Furuse, *Nippon Kagaku Zasshi*, **89**, 1002 (1968); K. Hanaya, *ibid.*, **90**, 314 (1969).

refluxed without removing the acetone, the *trans* isomer was produced mainly. These results parallel the findings on III. On reduction with the metal hydride complex, the steric structure near the carbonyl group influences the stereochemical course of the reaction, rather than the whole steric structure of the molecule. When a hydride ion attacks the carbonyl carbon atom, the methyl group of the 3-position of VIII does not seem to exert any steric hindrance; this reaction proceeds under the effect of "product development control." On the Meerwein-Ponndorf reduction of VIII, a consideration of its reaction mechanism[9] suggests that the reaction will proceed under the effect of steric hindrance if the acetone is removed. On the other hand, if the reaction mixture is refluxed without removing the acetone, the reaction mixture will easily reach an equilibrium in which the *trans* isomer predominates.

In the case of the catalytic hydrogenation over the Raney nickel catalyst, VIII afforded the *cis* isomer as the main product, while over the palladium catalyst, VIII gave the *trans* isomer as the main product. In the catalytic hydrogenation of VIII over the palladium-charcoal-B, the *trans* isomer was obtained preferably, even at the initial stage of hydrogenation (Expts. 7, 8, and 9). Therefore, it is considered that the predominant formation of the *trans* isomer was not due to the isomerization of the *cis* isomer.

Generally, the course of the hydrogenation of ketones can be represented as involving three steps, as is shown in Fig. 2: Step 1, the formation of a first adsorbed intermediate; Step 2, the formation of a half-hydrogenated intermediate, and Step 3, the formation and desorption of the product.

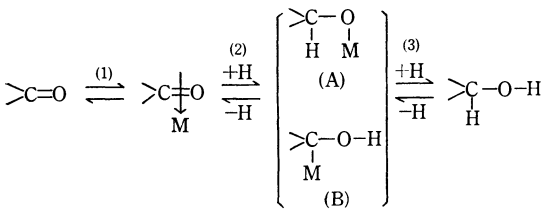

Fig. 2

When the molecule of VIII shown as in Fig. 1-A adsorbs over a catalyst, the adsorption seems to be hindered more at the β-face of the molecule than at the α-face. It is considered that the predominant production of the *cis* isomer in the Raney nickel catalyst hydrogenation of VIII is caused by this catalyst hindrance. The nickel catalyst is considered to have a larger affinity for the oxygen atom than the palladium catalyst.[10] Therefore, on the catalytic hydrogenation of VIII over the Raney nickel catalyst the molecule does not desorb easily, but it will be hydrogenated rapidly when the carbonyl group is strongly adsorbed. That is, on the Raney nickel catalyst, the stereochemistry of hydrogenation may be controlled mainly by the first adsorption step of the molecule and, therefore, by the steric interaction between the molecule and the catalyst surface. On the other hand, since the palladium catalyst does not have a strong affinity for the oxygen atom, the products are not determined by the step of adsorption of the molecule, but, rather, by the step of the transfer of hydrogen from the catalyst surface to the molecule. That is, in the catalytic hydrogenation of VIII over the palladium catalyst, a large contribution of the second or third process will give a stable isomer predominantly. There are two possible states, (A) and (B), to be considered for the half-hydrogenated state, as is shown in Fig. 2. Bent and Keevil[11] reported that the free energy of the addition of sodium to a carbonyl group is at least 5 kcal more negative in the case of the oxygen atom. This fact indicates that sodium is much more firmly attached to oxygen than to carbon. In view of this fact, the oxygen-metal bond may be formed more easily than the carbon-metal bond, and the hydrogenation of ketones may proceed mainly *via* the (A)-type half-hydrogenated state. Besides, in the case of the hydrogenation of VIII, the (B)-type may be expected to be less stable than the (A)-type because of a more severe nonbonded interaction between the quasi-equatorial carbon-metal bond and the hydrogen atom at the peri-position than between the quasi-equatorial oxygen-metal bond and the hydrogen atom in the peri-position. The palladium-catalyzed hydrogenation of VIII will proceed *via* the half-hydrogenated state, as is shown in Fig. 3, and will give the *trans* isomer predominantly.

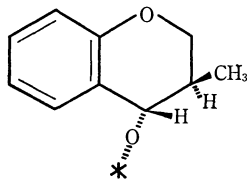

Fig. 3

On the basis of the previous works and the present work, the catalytic hydrogenation of 1-tetralone and 4-chromanone derivatives having the substituent at the α-position of carbonyl group may be summarized as follows. When the substituent is sterically bulky, as in the case of the phenyl or

9) R. B. Woodward, N. L. Wendler and F. J. Brutschy, *J. Amer. Chem. Soc.*, **67**, 1425 (1945); W. E. Doering and R. W. Young, *ibid.*, **72**, 631 (1950); E. D. Williams, K. A. Krieger and A. R. Day, *ibid.*, **75**, 2404 (1953); W. N. Moulton, *J. Org. Chem.*, **26**, 290 (1961).

10) S. Mitsui, Y. Senda and H. Saito, This Bulletin, **39**, 694 (1966).

11) H. E. Bent and N. B. Keevil, *J. Amer. Chem. Soc.*, **58**, 1367 (1936).

acetoxyl group, the molecule is hydrogenated in the adsorbed state on the catalyst surface at the opposite side to the substituent, not dependent on the sort of catalyst. On the other hand, when the substituent is relatively small, as in the case of the methyl group, the catalyst hindrance has the largest influence with nickel catalyst, while the hydrogenation over the palladium catalyst is not influenced by the catalyst hindrance, but will give thermodynamically more stable products predominantly because of the large influence of the reaction process of the transfer of hydrogen from the catalyst surface to the molecule.

Experimental

3-Methyl-4-chromanone (VIII). VIII was prepared by the catalytic hydrogenation of 3-methyl-4-chromone[12] over Raney nickel in ethanol. Bp 125—128°C/11 mmHg; The oxime, mp 154—156°C(lit,[13] mp 156°C). IR(liquid film): 1680(C=O) cm^{-1}. NMR(CCl_4): 1.15 (3H, doublet, J=6.9 Hz, CH_3), 2.75 (1H, multiplet, methine at the 3-position), 4.2(2H, multiplet, methylene at the 2-position), and 7.25 ppm(4H, multiplet, benzene-ring protons).

The Catalytic Hydrogenation of VIII. Two hundredths of a mole of VIII, 40 m*l* of ethanol or 10 m*l* of acetic acid, and the catalyst (0.5 g of Raney nickel, 0.2 g of 5% Pd-C-B, 0.1 g 5% Pd-C-A, 0.2 g of 5% Pd-$CaCO_3$ or 0.2 g of 5% Pd-$BaSO_4$) were shaken under hydrogen at an ordinary temperature and pressure. After the theoretical amount of hydrogen had been absorbed, the catalyst was filtered off and the ethanol or acetic acid was distilled off. The products were analyzed by gas chromatography.

Reduction of VIII with $NaBH_4$. A solution of VIII(5.0 g) in ethanol (100 m*l*) was added over a 30-min period to a well-stirred mixture of sodium borohydride (2.4 g) in ethanol (100 m*l*) at 0°C. After the mixture had then been allowed to stand for 24 hr at room temperature, water (50 m*l*) was added and the ethanol was removed under reduced pressure. The residue was acidified with dilute hydrocholric acid, the solution was extracted with ether, and the ether solution was washed with a sodium bicarbonate solution and then with water, and dried over anhydrous sodium sulfate. After the evaporation of the ether, the residue were analyzed by gas chromatography. The oily residue was dissolved in hot ligroin and then cooled in an ice bath. *trans*-Rich crystals of 3-methyl-4-chromanol were thus obtained. The recrystallization of them from ligroin gave the pure *trans*-chromanol (X) (mp 97—98.5°C) (1.5 g). NMR ($CDCl_3$): 0.97(3H, doublet, J=6.9 Hz, CH_3), 2.01(1H, multiplet, methine at the 3-position), 2.17(1H, singlet, OH), 4.0(2H, multiplet, methylene at the 2-position), 4.3(1H, doublet, J=4.8 Hz, methine at the 4-position), and 7.0 ppm(4H, multiplet, benzene-ring protons).

Found: C, 73.44; H, 7.46%. Calcd for $C_{10}H_{12}O_2$: C, 73.14; H, 7.37%.

12) A. Schonberg and A. Sina, *J. Chem. Soc.*, **1950**, 3344.

13) J. Colonge and A. Guyot, *Bull. Soc. Chim. Fr.*, **1958**, 325.

Reduction of VIII with $LiAlH_4$. To a well-stirred suspension of lithium aluminum hydride (0.3 g) in dry ether (50 m*l*), VIII (0.8 g) dissolved in dry ether (50 m*l*) was added over a 30-min period at 0°C; the mixture was then stirred at room temperature for 12 hr. Water (10 m*l*) and 20% sulfuric acid (5 m*l*) were then added, and the ether layer was separated. The aqueous solution was extracted with ether, and the combined ether extracts were washed with a sodium bicarbonate solution and then with water and dried over anhydrous sodium sulfate, and the ether was removed. The products were analyzed by gas chromatography.

Meerwein-Ponndorf Reduction of VIII. *Method A (The acetone was removed).* The ketone (0.02 mol) was mixed with an aluminum isopropoxide solution (prepared from 2.24 g of aluminum and 80 m*l* of dry isopropyl alcohol) and isopropyl alcohol (20 m*l*), and was then distilled slowly until acetone was no longer detectable in the distillate. The isopropyl alcohol was then removed by vacuum distillation, the residue mixed with water, and diluted hydrochloric acid was added until all the precipitated solid had dissolved. The solution was extracted with ether, and the extract was washed with a 5% sodium carbonate solution and with water, and dried over anhydrous sodium sulfate. After the evaporation of the ether, the residue was analyzed by gas chromatography. The residue oil was then distilled under reduced pressure to give 2.0g of *cis*-chromanol (IX) (bp 140—142°C/12 mmHg). The identity of IX was ascertained by a study of its IR spectrum, by gas chromatography, and by a study of its NMR spectrum. NMR ($CDCl_3$): 1.05(3H, doublet, J=6.9 Hz, CH_3), 2.0(1H, singlet, OH), *ca.* 2.2(1H, multiplet, methine at the 3-position), 4.05(2H, multiplet, methylene at the 2-position), 4.53(1H, doublet, J=3.4 Hz, methine at the 4-position), and 7.0 ppm(4H, multiplet, benzene-ring protons).

Method B (The acetone was not removed but refluxed). A solution of VIII (0.01 mol) and an aluminum isopropoxide solution (prepared from 1.12 g of aluminum and 40 m*l* of dry isopropyl alcohol) and isopropyl alcohol (10 m*l*) were refluxed for 4 hr. The reaction products were then treated as above. The residue was analyzed by gas chromatography.

3-Methyl-3-chromene (XI). 3-Methyl-4-chromanol (2.0 g) was heated with 0.2 g of *p*-toluenesulfonic acid in 200 m*l* of benzene for 10 hr. The water was successively removed by azeotropic distillation; the benzene layer was washed with a sodium bicarbonate solution and water, and the benzene was distilled off under reduced pressure. 1.5 g of XI was thus obtained. This compound was checked by a study of its IR spectrum and by gas chromatography.

The Hydroboration of XI. To a solution of 0.4g of sodium borohydride in 10 m*l* of diglyme containing 1g of XI, there was added 0.85 m*l* of boron trifluoride etherate under cooling with ice. The mixture was stirred for 3 hr at room temperature before the excess hydride was decomposed with water. The organoborane was oxidized at room temperature by the addition of 5 m*l* of a 3N solution of sodium hydroxide, followed by the drop-by-drop addition of 6 m*l* of 30% hydrogen peroxide. The reaction mixture was then extracted with ether, and the extract was washed five times with equal volumes of a saturated salt solution in order to remove the diglyme. The extract was then dried over

anhydrous sodium sulfate, and the solvent was removed. The residue was recrystallized from ligroin to give *trans*-chromanol (X) (mp 97—98°C) (0.8g).

3-Methylchroman (XII). The mixture of 2g of VIII, 0.2g of the 5% Pd-C-A catalyst, and 50 m*l* of ethanol was shaken under hydrogen at an ordinary temperature and pressure. After 2 mol of the hydrogen had been absorbed, the catalyst was filtered off and the residue were distilled under reduced pressure to give 1.2g of XII (bp 94.5—96°C/9 mmHg). This compound was checked by a study of its IR spectrum, by gas chromatography, and by a study of its NMR spectrum. NMR(CCl_4): 1.03 (3H, doublet, J=6.9 Hz, CH_3), 1.9—2.9 (3H, multiplet, methine at the 3-position and methylene at the 4-position), 3.8(2H, multiplet, methylene at the 2-position) and 6.9 ppm (4H, multiplet, benzene-ring protons).

***cis*-3-Methyl-4-acetoxychroman (XIII) and *trans*-3-Methyl-4-acetoxychroman (XIV).** XIII and XIV were prepared by the acetylation of IX and X by means of the acetic anhydride-pyridine method at room temperature overnight. These products were checked by a study of their IR spectra, by gas chromatography, and by a study of their NMR spectra. IR (liquid film): XIII, 1725, 1225 (-O-CO-CH_3) cm^{-1}; XIV, 1735, 1230(-O-CO-CH_3) cm^{-1}. NMR($CDCl_3$): XIII, 0.98(3H, doublet, J=6.9 Hz, CH_3), 2.08(3H, singlet, -O-CO-CH_3), *ca.* 2.4(1H, multiplet, methine at the 3-position), 4.0(2H, multiplet, methylene at the 2-position), 5.98(1H, doublet, J=3.4 Hz, methine at the 4-position), and 7.1(4H, multiplet, benzene-ring protons); XIV, 1.0(3H, doublet, J=6.9 Hz, CH_3), 2.08(3H, singlet, -O-CO-CH_3), *ca.* 2.3(1H, multiplet, methine at the 3-position), 4.14(2H, multiplet, methylene at the 2-position), 5.65(1H, doublet, J=4.8 Hz, methine at the 4-position), and 7.05(4H, multiplet, benzene-ring protons).

Instrumentation. The gas chromatographic analysis of the reduction products were carried out with a Hitachi Model K-53 apparatus, fitted with a 45-m Golay column coated with PEG 4000 and equipped with a flame-ionization detector. The nitrogen carrier-gas inlet pressure was 1.5 kg/cm^2, and the column temperature was 180°C. The NMR spectra were measured on a Hitachi H-60 high-resolution nuclear spectrometer. The sample was dissolved in $CDCl_3$ or CCl_4, containing TMS as the internal reference. The IR spectra were measured with a Hitachi EPI-S infrared spectrometer.

The author wishes to express his deep gratitude to Professor Sekio Mitsui of Tohoku University and to Professor Akira Kasahara of Yamagata University for their kind guidance and encouragement throughout this study.

BULLETIN OF THE CHEMICAL SOCIETY OF JAPAN VOL. 43 446—447 (1970)

Study of the Sapogenins from *Albizzia lebbek* Benth. Seeds

I. P. VARSHNEY and Geeta BADHWAR

Department of Chemistry, G. S. Technological Institute, Indore-3, India

(Received March 25, 1969)

The seeds of *Albizzia lebbek* Benth. from Madhya Pradesh have been found to contain a mixture of saponins which on hydrolysis gives echinocystic acid (I), oleanolic acid (II) as major sapogenins and an unidentified sapogenin (not albigenin) in traces. The albigenic acid (III) earlier reported to be present has been shown to be an alcoholic hydrochloric acid isomerisation product of echinocystic acid.

The seeds and pods of *Albizzia lebbek* Benth. have been found to be a rich source for saponin and sapogenin contents.[1,2] Varshney *et al.*[1,2] have isolated a saponin mixture from the seeds collected from Utter Pradesh (U. P.), which on hydrolysis with 10% sulphuric acid yields three sapogenins, echinocystic acid (I), oleanolic acid (II) and a third sapogenin in trace (in the proportion 75: 20: trace).

Later Barua and Raman[3] studied the whole beans of *Albizzia lebbek* Benth. (containing pods and seeds), collected from Bengal, and reported that the hydrolysis of the crude saponin with hydrochloric acid in ethanol yields four sapogenins, echinocystic acid (I), oleanolic acid (II), albigenic acid (III) and albigenin (IV). It may be noted that the two extra sapogenins (albigenin and albigenic acid) reported by these authors[3] may be either present in pods or in the seeds from Bengal and absent in the seeds from U. P. studied by Varshney *et al.*,[1,2] or may be the artifact of alcoholic hydrochloric acid hydrolysis. To clarify this, the present work has been undertaken.

1) Ch. Sannié, H. Lapin and I. P. Varshney, *Bull. Soc. Chim. Fr.* **1957**, 1440.

2) I. P. Varshney, Thesis, Dr. d'Etat, Etude des Sapogénines d'*Albizzia lebbek* Benth., Soutenue 1956, Université de Paris, France.

3) A. K. Barua and S. P. Raman, *Tetrahedron*, **7**, 19 (1959); *ibid.*, **18**, 155 (1962).

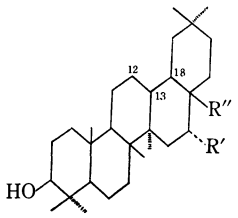

I R'=OH; R''=COOH; Δ^{12-13}
II R'=H; R''=COOH; Δ^{12-13}
III R'=OH; R''=COOH; Δ^{13-18}
IV R'=O; R''=H; Δ^{13-18}

Finely powdered *Albizzia lebbek* Benth. seeds collected from Madhya Pradesh (M. P.) were defatted with petroleum ether and exhausted with ethanol. The ethanolic extract on concentration and subsequent treatment in the usual manner gave a saponin which was purified by dissolving in a small quantity of methanol, and by adding to large amounts of ether/acetone a number of times. This caused precipitation of the saponin as a light brown coloured powder satisfying all the tests for saponins.

Half of the saponin was hydrolyzed with 10% sulphuric acid by heating on a boiling water bath for one hour and then refluxing for another hour (*cf.* Varshney *et al.*[1,2]), and the remainder of the saponin with ethanolic hydrochloric acid (using the same procedure as that of Barua and Raman[3]). The sapogenins obtained by sulphuric acid hydrolysis on thin layer chromatography showed three spots, two present in major quantity and the third one in trace only, *viz.* echinocystic acid (I), oleanolic acid (II) and an unidentified one, as earlier reported by Varshney *et al.*[1,2] The sapogenins obtained by ethanolic hydrochloric acid hydrolysis showed the presence of four prominent spots, corresponding to echinocystic acid (I), oleanolic acid (II), albigenic acid (III), and the fourth may be identical with albigenin (IV), confirmed by alongside chromatography (TLC) with authentic samples. This conclusively showed that albigenic acid (III) and most possibly albigenin (VI) are artifacts formed by the ethanolic hydrochloric acid hydrolysis of the saponin as they are not obtained in the sulphuric acid hydrolysis product of the same saponin. During alcoholic hydrochloric acid hydrolysis the migration of the double bond takes place from 12—13 position to 13—18 position yielding albigenic acid (III) from echninocystic acid (I) (I → III). This type of migration is not rare and was earlier reported by Spring *et al.*[4] All the four sapogenins were separated by repeated column chromatography on silica gel and identified by melting points, (mp obtained (I) 306—308°C (II) 305—306°C, (III) 280—281°C and (IV) 224—226°C; lit. echinocystic acid, 305—312°C, oleanolic acid, 310°C, albigenic acid, 280—281°C and albigenin, 226—228°C).

The possibility of the shifting of the double bond in the case of albigenic acid (III) was ruled out by Barua and Raman[3] by heating echinocystic acid (I) with ethanolic hydrochloric acid. It might be possible that such migration might not have taken place in their case due to some reason such as the variation in the conditions and concentration *etc.* as the experimental details of such experiment are not given.[3] In our repeated attempts, when free echinocystic acid (I) was heated with ethanolic hydrochloric acid (20%) it always yielded a number of products (3 new products and one starting material *i.e.* echinocystic acid) as shown by the thin layer chromatography. Starting with TLC pure echinocystic acid, the major product corresponded with albigenic acid (III) on thin layer chromatography. Therefore albigenic acid (III) is nothing but an alcoholic hydrochloric acid isomerisation product of echinocystic acid (I) and is not present in *Albizzia lebbek* plant, seeds or pods either as free genin or as saponin.

The albigenin (IV) is present in very small quantities in ethanolic hydrochloric acid hydrolysis product only, and this can also be a product of alcoholic hydrochloric acid isomerisation and probably some type of oxidation is taking place in the hydrolysis process itself, which might be giving rise to 16-keto acid by the partial oxidation of the echinocystic acid giving rise to a β-ketonic acid which decarboxylates in the hydrolysis process and the migration of the double bond taking place simaltaneously yielding albigenin (IV). It might also be possible that the third sapogenin (unidentified) present in trace in sulphuric acid hydrolysis product might be isomerising with ethanolic hydrochloric acid hydrolysis process yielding albigenin (IV). Therefore the aqueous sulphuric acid is a better hydrolyzing agent for saponins than alcoholic hydrochloric acid as the latter brings about isomerisation as reported in this paper and by Spring *et al.*[4] and some times corresponding ester is also formed.[5,6]

Thanks are due to the Chemical Research Committee of the Council of Scientific and Industrial Research, New Delhi, for the award of a junior research fellowship to one of the authors (G. B.) and to the authorities of the Shri Govindram Seksaria Technological Institute, Indore for the facilities.

4) G. Brownlie, M. B. E. Fayez, F. S. Spring, R. Stevenson and W. S. Strachan, *J. Chem. Soc.*, **1956**, 1377.

5) C. Djerassi, Festeschraft Arthur Stoll, (Brikhauser, Basal) 1957, 330.

6) I. P. Varshney, *Indian J. Chem.*, **7**, 446 (1969).

BULLETIN OF THE CHEMICAL SOCIETY OF JAPAN VOL. 43 448—452 (1970)

Studies of Hydrogenolysis. LVII.[1] Catalytic Hydrogenation of Benzalacetophenone Oxide

Akiko SOHMA*[1] and Sekio MITSUI

Department of Applied Science, Faculty of Engineering, Tohoku University, Aoba, Sendai

(Received April 5, 1969)

The effects of catalysts and an additive, sodium hydroxide, on the catalytic hydrogenation of benzalacetophenone oxide (I) have been studied for the purpose of elucidating the selectivity of the catalysts on the hydrogenation. The catalytic hydrogenation over palladium or Raney nickel led to the formation of the hydroxyketones as the primary products resulting from the hydrogenolysis of the epoxide ring. 1,3-Diphenylpropane-1,2-diol (III) was obtained by the catalytic hydrogenation over palladium, while 1,3-diphenylpropane-1,3-diol (VI) and III were yielded over Raney nickel. Under the basic conditions III was predominantly produced even over Raney nickel. Over platinum oxide, 2,3-epoxy-1,3-diphenylpropan-1-ol (VIII) was the primary product of the hydrogenation of the carbonyl group of I. In the hydrogenolysis of VIII, 1,2-diol (III) was produced regardless of the species of the catalysts.

It has been shown by Herz[2] that the catalytic hydrogenation of benzalacetophenone oxide (I) gave two diphenylpropanediols, which he considered to be the diastereoisomeric α-glycols, and that the mode of hydrogenation followed I—II—III, regardless of the species of the catalysts and solvents.

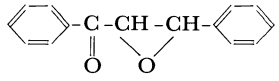

(I)

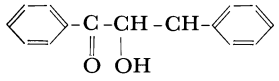

(II)

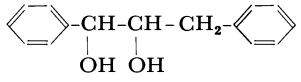

(III)

On the other hand, Mitsui and his co-workers[3] reported that both α-glycol and β-glycol were obtained from the cleavage of the carbon-oxygen bond of the epoxide ring at different positions; α-glycol was obtained from the hydrogenation over palladium-charcoal, and β-glycol, from that over Raney nickel.

In order to study the selectivity of the catalysts and the effect of the additive, sodium hydroxide, on the catalytic hydrogenation of epoxyketones, benzalacetophenone oxide was hydrogenated over Raney nickel, palladium charcoal-B[4] or platinum oxide respectively in ethanol at room temperature and at atmospheric pressure. In addition to these catalytic hydrogenations, metal hydride reduction has also been carried out.

Results and Discussion

A quantitative analysis of the reduction products by gas chromatography was performed as their diastates. A qualitative analysis of the primary reduction product was carried out by means of thin-layer chromatography.

In accordance with the previous report,[3] the catalytic hydrogenation of I over palladium charcoal yielded 2-hydroxy-1,3-diphenylpropan-1-one (II) with the consumption of one mole of hydrogen, and 1,3-diphenylpropane-1,2-diol (III) (65% of *erythro*-III, 25% of *threo*-III), and other substances with the consumption of two moles of hydrogen. Diastereoisomers, *erythro*-, and *threo*-III have been prepared and characterized by Bonner and Raunio.[5] The catalytic hydrogenation of I over palladium charcoal-B to which sodium hydroxide had been added gave 1-hydroxy-1,3-diphenylpropan-2-one (IV) preferentially. The rate of the hydrogenation became slower after the consumption of one mole of hydrogen.

The Raney nickel-catalyzed hydrogenation of I

*1 Present address; Department of Chemistry, University of Hirosaki, Bunkyo-cho, Hirosaki, Aomori.

1) Part LVI; Y. Sugi and S. Mitsui, for publication.

2) W. Herz, *J. Amer. Chem. Soc.*, **74**, 2928 (1952).

3) S. Mitsui, Y. Senda, T. Shimodaira and H. Ichikawa, This Bulletin, **38**, 1898 (1965).

4) Method B: E. C. Horning, "Organic Synthesis," Coll. Vol. III, p. 686, (1955). This was named by Mitsui and Saito as the catalyst containing trace base: S. Mitsui and H. Saito, *Nippon Kagaku Zasshi*, **82**, 890 (1961).

5) W. A. Bonner and E. K. Raunio, *J. Org. Chem.*, **31**, 291 (1966).

yielded 3-hydroxy-1,3-diphenylpropan-1-one (V) and 2-hydroxy-1,3-diphenylpropan-1-one (II) as the initial products; almost equal amounts of 1,3-diphenylpropane-1,3-diol (VI) and 1,3-diphenylpropane-1,2-diols (III) were produced on further hydrogenation. In this case, a considerable amount of the deoxygenation product of the epoxide was obtained.

Semi-hydrogenation over Raney nickel to which sodium hydroxide had been added resulted in the formation of α-hydroxyketones (mainly II), while exhaustive hydrogenation led to α-glycol (80% of *erythro*-III, 10% of *threo*-III) and other substances. The fact that only a small amount of 1,3-diphenylpropan-1-ol (VII) was formed seems to indicate that the sodium hydroxide in the reaction mixture may resist the elimination of the oxygen atom of the epoxide.[6]

Though the hydrogenation over palladium or Raney nickel led to the formation of the hydroxyketones as a result of the cleavage of the epoxide ring, over platinum oxide epoxy alcohol VIII was the primary product resulting from the hydrogenation of the carbonyl group[7] of I. Other primary products formed over platinum oxide were α-hydroxyketone II and β-hydroxyketone V. The exhaustive hydrogenation yielded α-glycol III (rich in *erythro*-III) from VIII and β-glycol VI from V. The deoxygenation product, VII, was obtained over platinum oxide as well as over Raney nickel. On the other hand, hydrogenation over platinum oxide to which sodium hydroxide had been added resulted in the formation of epoxy alcohol VIII as the primary product; then α-glycol III, which was rich in the erythro isomer, was obtained, by adding hydrogen continuously.

The lithium aluminum hydride reduction of benzalacetophenone oxide (I) yielded 77% of 1,2-diols III, 18% of 1,3-diols VI, and a small amount of another product. The metal hydride which was active toward the reduction of carbonyl compounds and epoxide gave epoxy alcohol VIII, α-hydroxyketone II, and β-hydroxyketone VI as the primary products in the course of the reduction. Since sodium borohydride is inactive toward the reduction of the epoxide, epoxy alcohol VIII was the only reduction product. The further hydrogenation of the product, VIII, over palladium charcoal-B yielded 54% of *erythro*-III and 46% of *threo*-III.

From these results, it is obvious that the mode of the hydrogenation of benzalacetophenone oxide is greatly affected by the species of catalysts and the additives (Chart I). Mitsui and Imaizumi have reported that the hydrogenolysis of optically-active α-methyl or α-ethylstyrene oxide gives optically-active products with the retention of the configuration over Raney nickel and with the inversion of the configuration over Raney nickel in the presence of sodium hydroxide, potassium bromide, or cesium chloride as well as over palladium or platinum oxide.[8] Similar trends have been observed in the hydrogenolysis of *trans*-dimethylstilbene oxide.[9]

It is considered that, on the hydrogenolysis over Raney nickel, hydrogen may attack the carbon atom from the same direction as the oxygen atom of epoxide. Consequently, the reaction proceeds with the retention of the configuration. On the other hand, over Raney nickel with a small amount of alkali as well as over palladium or platinum, the hydrogen may attack from behind the carbon-oxygen bond and the reaction proceeds with the inversion of the configuration.

It is known that the catalytic hydrogenolysis of benzylic substituents is relatively easy. The high reactivity of the benzylic substituents on the catalytic hydrogenolysis may be attributed to the ease of formation of the π-benzyl intermediate. This reaction includes the adsorption of the substrate on the catalyst (1 or 1′), the cleavage of the C–X bond (2 or 2′), the formation of the π-benzyl intermediate (3 or 3′), the hydrogenolysis of the π-benzyl intermediate, and the desorption of the product from the catalyst (4 or 4′). The reaction path (A or B) determines the stereospecificity of the product; the hydrogenolysis proceeds with the retention of the configuration in Path B, whereas the configuration is inverted in Path A.[10]

Path A

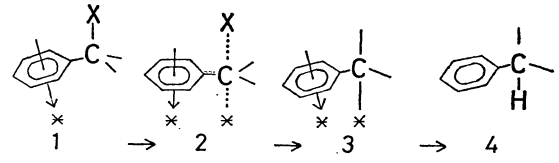

Path B

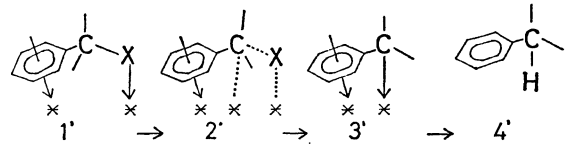

Taking account of the stereochemical results obtained in the catalytic hydrogenolysis of benzylic-

6) D. R. Howton and R. W. Kaiser, *J. Org. Chem.*, **29**, 2421 (1964); O. Gawron, T. P. Fondy and D. J. Parker, *ibid.*, **28**, 700 (1963); G. B. Payne, *ibid.*, **24**, 2408 (1959).

7) P. L. A. Plattner, H. Hausser and A. B. Kulkarm, *Helv. Chim. Acta*, **31**, 1822 (1948); J. Raese, *Ber.*, **75**, 385 (1942).

8) S. Mitsui and S. Imaizumi, *Nippon Kagaku Zasshi*, **86**, 219 (1965).

9) S. Mitsui and Y. Nagahisa, *Chem. Ind.* (London), **1965**, 1975.

10) S. Mitsui, M. Fujimoto, Y. Nagahisa and T. Sukegawa, *ibid.*, **1969**, 241; S. Mitsui, Y. Kudo and M. Kobayashi, *Tetrahedron*, **25**, 1921 (1965); S. Mitsui and Y. Sugi, *Tetrahedron Lett.*, **1969**, 1291.

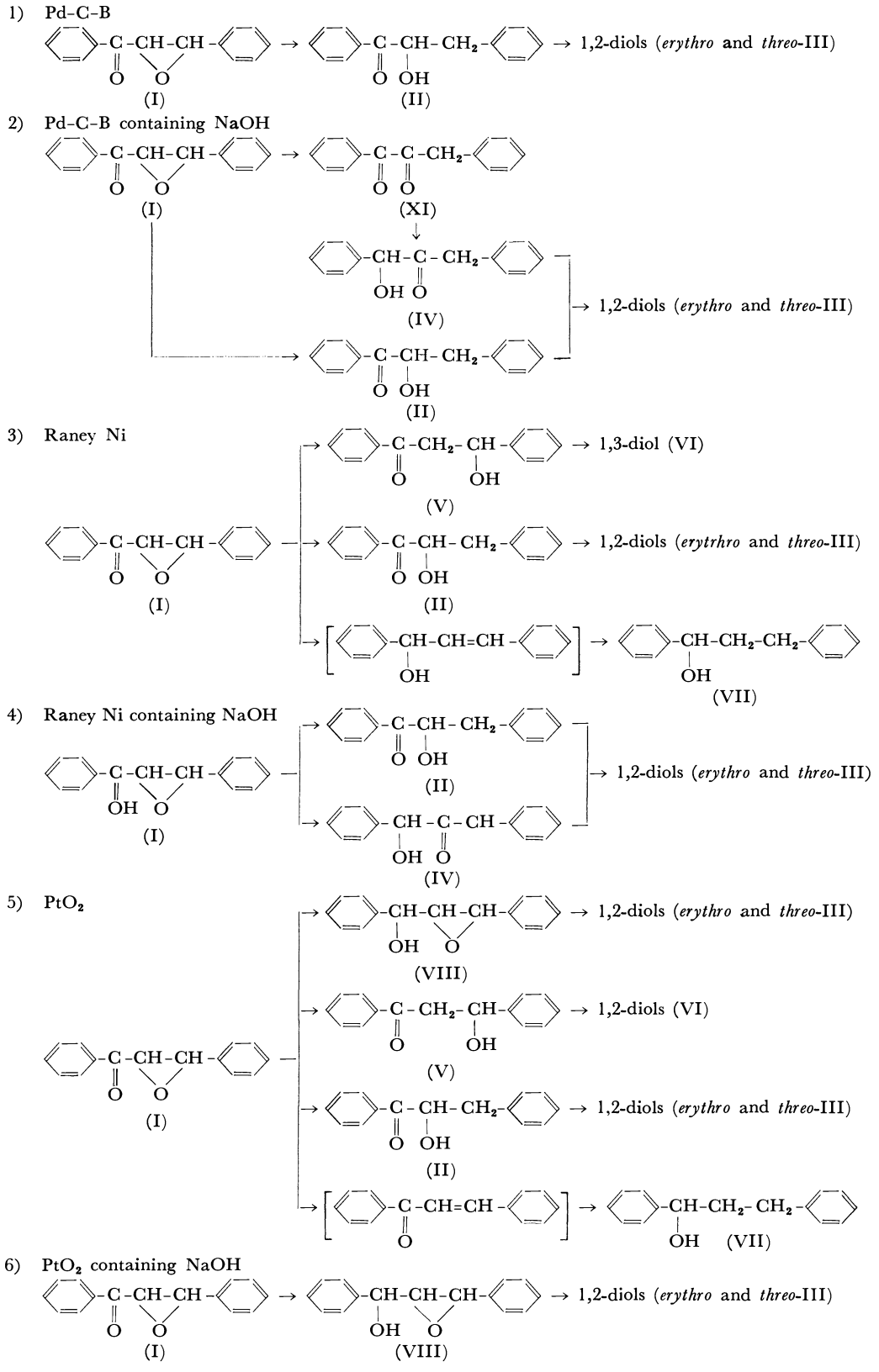

Chart 1. The paths of the catalytic hydrogenation of benzalacetophenone oxide (I).

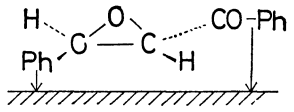

Fig. 1

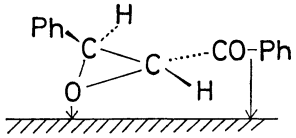

Fig. 2

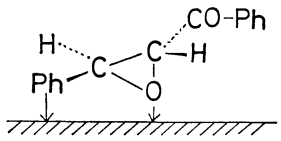

Fig. 3

type compounds, the epoxide ring may be hydrogenolyzed with the inversion of the configuration over a palladium catalyst in such a way as in Fig. 1, in which the cleavage of the benzylic C–O bond occurs selectively. On Raney nickel hydrogenolysis, the rupture of the benzylic C–O bond may occur as is shown in Fig. 2. Moreover, since Raney nickel has a strong affinity for the oxygen atom, the adsorption state shown in Fig. 3 is also plausible. In this case, the hydrogenolysis of the epoxide ring occurs at homobenzylic C–O bond because of its strain, affording β-hydroxyketone V. The addition of an alkaline substance to the Raney nickel catalyst decreases the rate of the reaction of the species, whose epoxide oxygen is adsorbed on the catalyst surface.[8] Consequently, the reaction preferably proceeds taking the adsorption state, as is shown in Fig. 1. Regardless of the species of the catalysts, the cleavage of the oxirane ring of VIII proceeds to give α-glycols selectively, in contrast to the case of the hydrogenolysis of α-ketoepoxide I.

In the case of platinum oxide to which sodium hydroxide had been added, *erythro*-III was favorably obtained from the epoxy alcohol VIII which was produced as a semihydrogenation product; however, reduction with sodium borohydride gave almost equal amounts of *erythro*-VIII and *threo*-VIII.

The catalytic hydrogenation of α-hydroxyketone II lead to the formation of *erythro*-glycol III. This process may be well specurated on the basis of Bonner and Raunio.[5]

The formation of 1-hydroxy-1,3-diphenylpropan-2-one suggests that I was isomerized to phenylbenzylglyoxal (XI) prior to reduction. This isomerization occurred in the presence of palladium charcoal, sodium hydroxide, and hydrogen, while it did not occur if any one of these three components was lacking.

Experimental

The Catalytic Hydrogenation of Benzalacetophenone Oxide (1). The catalyst and I dissolved in

Table 1. Catalytic hydrogenation of benzalacetophenone oxide (I)

Exp. No.	Substrate (mg)	Catalyst (g)	NaOH (mg)	Reduction products (%)					
				IX	X	VII	*erythro*-III	*threo*-III	VI
1	450	Pd-C-B 0.2	—	2	2	5	62	25	4
2	450	Pd-C-B 0.4	40	4	2	3	77	13	1
3	450	Raney Ni 1.0	—	7	trace	39	21	7	26
4	450	Raney Ni 1.0	80	trace	trace	36	27	17	20
5	450	Raney Ni 1.0	400	trace	trace	8	80	10	2
6	400	PtO_2 0.05	—	trace	trace	27	32	10	31
7	450	PtO_2 0.05	5	trace	trace	4	91	4	1

Solvent: 30 m*l* of 99% ethanol

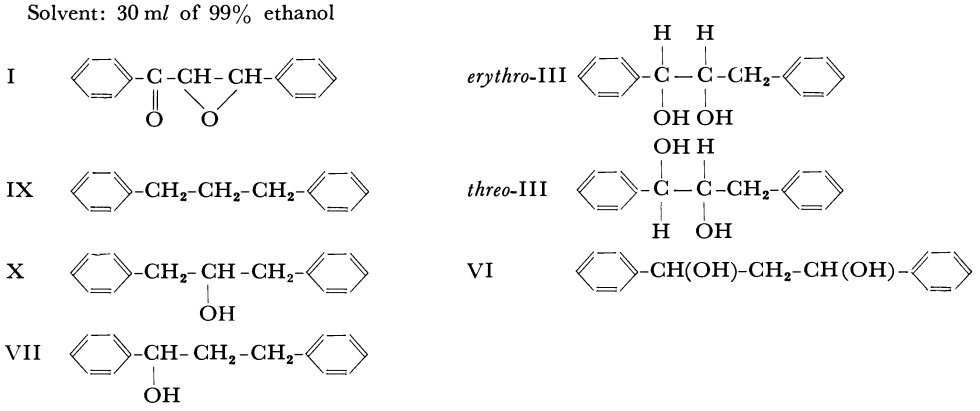

ethanol were stirred with hydrogen at room temperature and at atmospheric pressure. The determination of the initial products in the course of the hydrogenation was done by thin-layer chromatography (T.L.C. on silica gel, chloroform 99 : methanol 1). After the hydrogen uptake had ceased with the absorption of two moles of hydrogen, the catalyst was filtered and ethanol was distilled off. The residue was acetylated with acetic anhydride in pyridine at room temperature. After having been kept standing for 12 hr, the reaction mixture was treated as usual. The products were dissolved in benzene and analyzed by V.P.C. The experimental data are summarized in Table 1.

Benzalacetophenone Oxide (I). I was prepared by the method of Weitz and Scheffer[11] by the epoxidation of benzalacetophenone; mp 90°C; 73% yield.

***threo*-1,3-Diphenylpropane-1,2-diol (*threo*-III).** *threo*-III was prepared by the method of Bonner and Raunio[5] by the *cis* hydroxylation of *trans*-1,3-diphenyl propene;[12] mp 62°C.

***erythro*-1,3-Diphenylpropane-1,2-diol (*erythro*-III).** *erythro*-III was prepared by the catalytic hydrogenation of benzalacetophenone oxide (1) over palladium charcoal-B at an ordinary temperature and at atmospheric pressure. After the hydrogen uptake had ceased with the absorption of two moles of hydrogen, the residue was fractionally recrystallized from the benzene-ligroin mixture to give pure *erythro*-III; mp 82°C; 62% yield.

2-Hydroxy-1,3-diphenylpropan-1-one (II).[13] II was prepared by the catalytic hydrogenation of benzalacetophenone oxide over palladium charcoal-B with the absorption of one mole of hydrogen; mp 66°C (recrystallized from the benzene-ligroin mixture); 50% yield.

1-Hydroxy-1,3-diphenylpropan-2-one (IV).[14] IV was prepared by the catalytic hydrogenation of benzalacetophenone oxide over palladium charcoal-B containing a small amount of sodium hydroxide, with the absorption of one mole of hydrogen; mp 114°C (recrystallized from the benzene ligroin mixture); 70% yield.

1,3-Diphenylpropan-1-ol (VII). VII was prepared by the catalytic hydrogenation of benzalacetophenone over palladium charcoal-B; bp 146—147°C/0.9 mmHg; 90% yield.

2,3-Epoxy-1,3-diphenylpropan-1-ol (VIII). VIII was prepared by reduction with sodium borohydride in methanol at room temperature. The reaction mixture was treated by the usual method. The product was recrystallized from a petroleum ether-benzene mixture. The epoxy alcohol VIII, whose melting point was 65°C, proved to be a mixture of 70% of the *erythro* and 10% of *threo*-isomer. The yield was 30%.

1,3-Diphenylpropan-2-ol (X). X was prepared by the catalytic hydrogenation of 1,3-diphenylpropane-1,2-diol over palladium charcoal-B containing one drop of concentrated hydrochloric acid at an ordinary temperature and at atmospheric pressure.

1,3-Diphenylpropane (IX). IX was prepared by the catalytic hydrogenation of 1,3-diphenylpropene.[12]

The authors are indebted to the Takeda Science Foundation for its financial support.

11) E. Weitz and A. Scheffer, *Ber.*, **54**, 2329 (1921).
12) W. A. Bonner and E. K. Raunio, *J. Org. Chem.*, **31**, 397 (1966).
13) W. Perkin and J. Stenhouse, *J. Chem. Soc.*, **1908**, 59.
14) P. Ruggli and A. H. Lutz, *Helv. Chim. Acta*, **30**, 1070 (1947).

BULLETIN OF THE CHEMICAL SOCIETY OF JAPAN VOL. 43 453—455 (1970)

Reactions of Thioamides with Haloacids*1

Ahmedhusen SHAIKH, Akiko CHINONE and Masaki OHTA

Department of Chemistry, Faculty of Science, Tokyo Institute of Technology, Ookayama, Meguro-ku, Tokyo

(Received May 8, 1969)

The reactions of *S*-carboxymethylisothioamide RC(=NR')SCHRCOOH with acetic anhydride proceeded through various courses depending on the reaction conditions and the structure of thioamides. When *S*-carboxymethylisothiobenzanilide (IIa) was treated with a mixture of acetic anhydride and triethylamine in the cold, an intermediate (A), presumably 2-hydroxy-2,3-diphenylthiazolidin-4-one (V), was isolated which was readily converted to benzoylthioacetanilide (IIIa). Attempts to convert A or IIIa to a mesoionic compound failed. Under the same reaction conditions as for IIa, *S*-carboxymethylisothiobenz-*p*-chloroanilide (IIb) afforded benz-*p*-chloroanilide, while corresponding *p*-anisidide (IIc) gave only tarry product. Attempts to obtain a mesoionic product from pyrrolidine-2-thione or thiocaprolactam and bromoacetic acid were unsuccessful. However, condensation of pyrrolidine-2-thione with α-chlorophenylacetic acid followed by treatment with a mixture of acetic anhydride and triethylamine gave eight-membered rearranged product (XII).

In previous papers,[1,2] we showed that the reaction of thiobenzanilide (Ia) with bromoacetic acid afforded three different products depending on the kinds of condensing agents and the reaction conditions. On refluxing a benzene solution of Ia and bromoacetic acid, benzoylthioglycolic acid anilide (IIIa) was obtained. It was proposed that the reaction proceeded *via* the pseudobase (V). Condensation of Ia with bromoacetic acid in the presence of triethylamine afforded *S*-carboxymethylisothiobenzanilide (IIa) which gave 5-acetyl-2,3-diphenyl-4-thiazone (IVb) by treatment with acetic anhydride, whereas treatment of Ia with a mixture of acetic anhydride and triethylamine gave 2,3-diphenyl-4-thiazone (IVa).

We found that when IIa was treated with a cold mixture of acetic anhydride and triethylamine, a new intermediate (A) of mp 143°C was obtained. When A was treated with ethanol, benzene or chloroform, benzoylthioglycolic acid anilide (IIIa) was obtained. Attempts to convert A or IIIa to IVa by treating with a mixture of acetic anhydride and triethylamine were unsuccessful. Elementary analysis indicated the composition of A to be $C_{15}H_{13}NO_2S$. Two structures having this composition may be taken into consideration, *viz.*, 2-hydroxy-2,3-diphenylthiazolidin-4-one (V) and 4-oxo-2,3-diphenylthiazolinium hydroxide (VI). Although we were unable to determine the structure of A unequivocally by IR or NMR spectra, pseudobase structure V seems to be more preferable to VI.

The mechanism of the formation of IVa from IIa by the action of acetic anhydride in the presence or absence of triethylamine was discussed in a previous paper.[2] The process was assumed to be similar to that proposed for the formation of sydnone from *N*-nitroso-*N*-phenylglycine, in which mixed acid anhydride is formed as an intermediate. From the present observation, it is clear that IVa is not derived from IIIa or A by internal dehydration. For the mechanism of the formation of IIIa, a probable scheme is shown below, which is quite similar to that proposed for the reaction of imidoyl chloride and glycolic acid.[3]

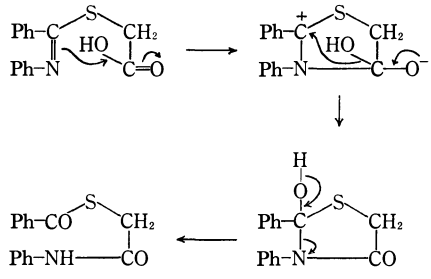

When *S*-carboxymethylisothiobenz-*p*-chloroanilide (IIb) was treated with a mixture of acetic anhydride and triethylamine in the cold, benz-*p*-chloroanilide was obtained instead of the rearranged product. When *S*-carboxymethylisothiobenz-*p*-anisidide (IIc) was treated with acetic anhydride in the presence or absence of triethylamine, only tarry matter was obtained.

*1 Studies on mesoionic compounds. XXXIII. Part XXXII; Ref. 3.

1) M. Ohta, H. Chosho, C. Shin and K. Ichimura, *Nippon Kagaku Zasshi*, **85**, 440 (1964).

2) M. Ohta and C. Shin, This Bulletin, **38**, 704 (1965).

3) A. Chinone, S. Sato, T. Mase and M. Ohta, *ibid.*, **42**, 2310 (1969).

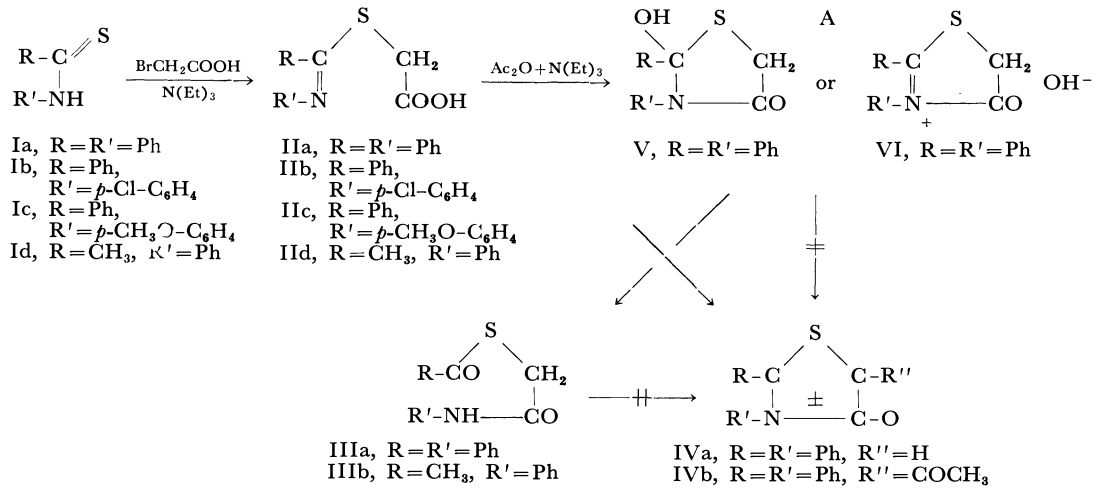

Ia, R=R'=Ph
Ib, R=Ph, R'=*p*-Cl-C_6H_4
Ic, R=Ph, R'=*p*-CH_3O-C_6H_4
Id, R=CH_3, R'=Ph

IIa, R=R'=Ph
IIb, R=Ph, R'=*p*-Cl-C_6H_4
IIc, R=Ph, R'=*p*-CH_3O-C_6H_4
IId, R=CH_3, R'=Ph

V, R=R'=Ph

VI, R=R'=Ph

IIIa, R=R'=Ph
IIIb, R=CH_3, R'=Ph

IVa, R=R'=Ph, R''=H
IVb, R=R'=Ph, R''=$COCH_3$

The mechanism for the formation of benz-*p*-chloroanilide may be explained by assuming that the electron attractive chlorine atom would lower the nucleophilicity of nitrogen atom and enhance the electrophilicity of carbon atom of >C=N- grouping. The latter effect would favor the attack of anion in preference to the attack of nitrogen on carbonyl carbon atom and the cleavage of C–S bond may ensue.

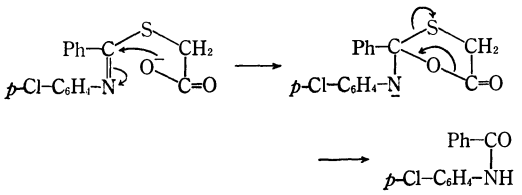

An unexpected result obtained in the case of thiobenz-*p*-anisidide, where the *p*-methoxy group would favor the formation of mesoionic compound by enhancing the nucleophilicity of nitrogen, may be ascribed to the instability of the mesoionic compound which would decompose if formed.

Our findings on the rearrangement of *S*-carboxymethylisothioamide prompted us to extend the reaction to the analogous *S*-(*β*-carboxyethyl)isothiobenzanilide (VII) obtained by condensing thiobenzanilide with *β*-bromopropionic acid in the presence of triethylamine. When VII was treated with a mixture of acetic anhydride and triethylamine in the cold, the intermediate analogous to A was not isolated and by working up the reaction mixture, *β*-benzoylthiopropionanilide (IX) was obtained. In this case, the rearrangement proceeds probably *via* the pseudobase (VIII).

Anticipating some information on the effect of substituents upon the reaction courses and the possibility of preparing 4-thiazone having an aliphatic substituent at 2 or 3 position, reaction of several other *N*-substituted thioamides with bromoacetic acid were attempted. Thioacetanilide (Id), when reacted with bromoacetic acid in the presence of

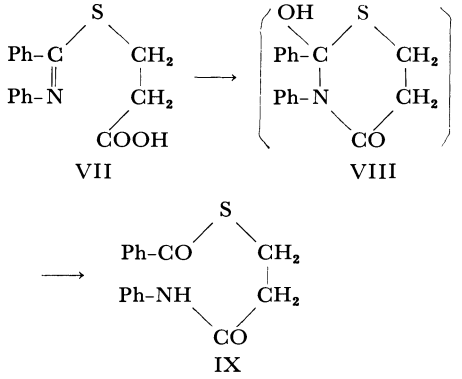

VII VIII IX

triethylamine in benzene at room temperature, gave an oily intermediate (IId). Treatment of this intermediate with a mixture of acetic anhydride and triethylamine gave a rearranged product, acetylthioacetanilide (IIIb). Attempts to obtain mesoionic compound by cyclizing IId with a mixture of acetic anhydride and boron trifluoride or acetic anhydride and triethylamine were unsuccessful.

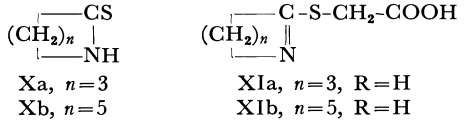

Xa, *n*=3
Xb, *n*=5

XIa, *n*=3, R=H
XIb, *n*=5, R=H

Reaction of pyrrolidine-2-thione (Xa) or thiocaprolactam (Xb) with bromoacetic acid in the presence or absence of triethylamine were also carried out and the intermediate (XIa and XIb or their hydrobromides) were obtained, which could not be cyclized to the mesoionic compounds either amine or with DCC in nitromethane.

The reaction of Xa with *α*-chlorophenylacetic acid in the presence of triethylamine, followed by treatment with a mixture of acetic anhydride and triethylamine, gave the acetylated rearranged product (XII) instead of the mesoionic compound. In a similar reaction, however, Xb did not react

with α-chlorophenylacetic acid to give the rearranged product or the mesoionic compound and tarry substance was obtained.

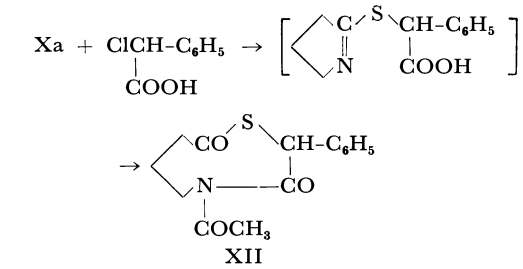

XII

Experimental

Intermediate (A). A solution of 5.0 g of thiobenzanilide, 3.3 g of bromoacetic acid and 5.0 g of triethylamine in 25 m*l* of benzene was heated for 1 hr at 50°C. Triethylamine hydrobromide was filtered off and washed with benzene. The combined filtrates were concentrated in a vacuum to obtain reddish viscous oil, which was dissolved in a cold mixture of 7.5 m*l* of acetic anhydride and 7.5 m*l* of triethylamine. Within a few minutes, crystals separated out. After 10 min the crystals were collected by filtration, washed well with a mixture of petroleum ether and diethyl ether (5 : 1) and dried quickly to give 4 g of pale yellow crystals, mp 143°C.

Found: C, 66.16; H, 5.01; N, 5.44%. Calcd for $C_{15}H_{13}NO_2S$: C, 66.42; H, 4.79; N, 5.16%.

β-Benzoylthiopropionanilide (IX). A solution of 2.1 g of thiobenzanilide, 1.5 g of β-bromopropionic acid and 1.4 g of triethylamine in benzene (25 m*l*) was refluxed for 2 hr. After cooling, triethylamine hydrobromide was filtered off, washed with benzene, and the combined filtrate was concentrated in a vacuum to give reddish viscous oil, which was dissolved in a cold mixture of 3 m*l* of acetic anhydride and 3 m*l* of triethylamine. A small amount of triethylamine hydrobromide separated was filtered off and the filtrate was concentrated in a vacuum to remove acetic anhydride. The resulting reddish oil was allowed to stand for one week over sodium hydroxide in a desiccator. To a partly crystallized mass, a mixture of carbon tetrachloride and petroleum ether (1 : 1) was added, and the crystals were collected and recrystallized from chloroform solution by adding petroleum ether to give colorless crystals, mp 140—141°C. The yield was 1.15 g.

Found: C, 67.53; H, 5.27; N, 5.01%. Calcd for $C_{16}H_{15}NO_2S$: C, 67.36; H, 5.26; N, 4.91%. IR(KBr): 3290 and 1640 cm^{-1} (–CONH–)

Reaction of Thiobenz-*p*-chloroanilide with Bromoacetic Acid. A solution of 3.6 g of thiobenz-*p*-chloroanilide, 2.1 g of bromoacetic acid and 3.0 g of triethylamine in 25 m*l* of benzene was heated at 50°C for 3 hr. The precipitated triethylamine hydrobromide was filtered off and the solvent was removed by evaporation in a vacuum. This left a viscous oil, which was dissolved in 6 m*l* of acetic anhydride and left standing overnight. Acetic anhydride was removed by vacuum distillation. To the residual crystalline mass ether was added and the crystals were collected by filtration and washed with ether to obtain 0.9 g of *p*-chlorobenzanilide identified by its mp (195°C) and by comparison of IR spectrum with that of an authentic sample.

A similar experiment was carried out using a mixture of 5 m*l* of acetic anhydride and 5 m*l* of triethylamine instead of acetic anhydride. Only a minute amount of *p*-chlorobenzanilide was obtained as an identifiable product.

Acetylthioacetanilide (IIIb). To a solution of 3.0 g of Id and 2.8 g of bromoacetic acid in 40 m*l* of benzene, 4.0 g of triethylamine was added and stirred for 3 hr at room temperature. The precipitates were filtered off and the filtrate was concentrated in a vacuum to give reddish oil, which was dissolved in a mixture of 5 m*l* of acetic anhydride and 5 m*l* of triethylamine and left standing overnight. The reaction mixture was then poured into ice water and after several hours the brownish semi solid mass was recrystallized from water to give 1.6 g of colorless needles of mp 94—96°C.

Found: C, 57.70; H, 5.56; N, 7.03%. Calcd for $C_{10}H_{11}NO_2S$: C, 57.41; H, 5.30; N, 6.70%.

IR: 3230, 3185, 3060, 1705, 1650, 1690 cm^{-1}.

2-Carboxymethylthio-1-pyrroline Hydrobromide (XIa-HBr). A solution of 2.5 g of Xa and 3.5 g of bromoacetic acid in 30 m*l* of benzene was heated on a water bath for 1 hr. After cooling the solution, the precipitates were collected and recrystallized from acetonitrile to give 5.8 g of colorless crystals of the hydrobromide of XIa; mp 126—128°C.

Found: C, 30.23; H, 4.26; N, 5.82%. Calcd for $C_6H_{10}NO_2SBr$: C, 30.01; H, 4.16; N, 5.83%. IR: 3450, 3200, 1730, 1605 cm^{-1}.

7-Carboxymethylthio-3, 4, 5, 6-tetrahydro-2*H*-azepine Hydrobromide (XIb-HBr). A solution of 1.2 g of thiocaprolactam and 1.4 g of bromoacetic acid in 30 m*l* of benzene was refluxed for 1 hr and after cooling, the precipitates were collected and recrystallized from acetonitrile to give 2.3 g of colorless crystals of the hydrobromide of XIb; mp 124—125°C.

Found: C, 35.91; H, 5.19; N, 5.47%. Calcd for $C_8H_{14}NO_2SBr$: C, 35.82; H, 5.22; N, 5.22%. IR: 3350, 2940, 1720, 1600 cm^{-1}.

***N*-Acetyl-2-phenyl-hexahydro-1,4-thiazocine-3,8-dione (XII).** A solution of 1.0 g of Xa, 1.7 g of α-chlorophenylacetic acid and 3 m*l* of triethylamine in 30 m*l* of benzene was heated on a water bath for 1 hr. The precipitates were filtered off and the filtrate was concentrated to give brownish oil, to which 5 m*l* of acetic anhydride and 5 m*l* of triethylamine were added and allowed to stand overnight. The precipitates were collected and recrystallized from ethanol to give 1.1 g of colorless crystals; mp 133—134°C.

Found: C, 60.54; H, 5.31; N, 5.04%. Calcd for $C_{14}H_{15}NO_3S$: C, 60.64; H, 5.45; N, 5.05%. IR: 2950, 1765, 1666, 1655 cm^{-1}.

BULLETIN OF THE CHEMICAL SOCIETY OF JAPAN VOL. 43 456—461 (1970)

Studies of Phosphorylation. IV. The Phosphorylation of Nucleosides with Phosphorus Trihalide.[1]

Masaharu YOSHIKAWA, Mitsuru SAKURABA and Koji KUSASHIO

Central Research Laboratories, Ajinomoto Co., Inc., Kawasaki

(Received May 8, 1969)

The treatment of a 2′,3′-*O*-isopropylidene nucleoside with phosphorus trichloride in the presence of trimethyl phosphate and subsequent hydrolysis gave a nucleoside 5′-phosphite in an excellent yield. Triaryl phosphates, trialkylphosphine oxides, and trialkyl phosphites were also found to be potential accelerators of the reaction. Their effects were comparable to that of trimethyl phosphate. The similar treatment of a 5′-*O*-acetyl nucleoside gave mixed nucleoside 2′- and 3′-phosphites in an approximate mole ratio of 4 : 6. The reaction intermediate, nucleoside phosphorodichloridite, was subjected to partial hydrolysis, giving the corresponding monochloridite. The product was readily oxidized to give the 5′-nucleotide. Chlorine was generally suitable as an oxidizing agent, but iodine gave better results for guanosine derivatives than did chlorine or bromine. The treatment of an unprotected nucleoside with phosphorus oxychloride in a trialkyl phosphate, prior to the reaction with phosphorus trichloride, could be used for the synthesis of a nucleoside 2′(or 3′),5′-diphosphate in a good yield.

Two methods have been reported for the preparation of nucleoside 5′-phosphates from 2,′3′-*O*-substituted nucleosides *via* the corresponding 5′-phosphites: phosphorylation with *O*-benzylphosphorous *O*,*O*-diphenylphosphoric anhydride, followed by oxidation with *N*-chlorosuccinimide,[2] and condensation with phosphorous acid by di-*p*-tolylcarbodiimide or dicyclohexylcarbodiimide, followed by oxidation with potassium permanganate.[3,4] The latter method has also been used in the preparation of nucleoside 2′(or 3′)-phosphites and- phosphates from the corresponding 5′-*O*-substituted nucleosides.

Holý *et al.* have reported that the treatment of adenosine with triethyl phosphite in dimethylformamide containing hydrochloric acid, followed by alkaline hydrolysis, gives a mixture of adenosine 2′- and 3′-phosphites in a 60% yield. A similar reaction, but carried out with triphenyl phosphite in place of triethyl phosphite, yielded a mixture of 2′(or 3′)-phosphite and 2′(or 3′),5′-diphosphite.[5]

The phosphorylation of a 5′-*O*-substituted nucleoside to give the corresponding 2′(or 3′)-phosphate has been carried out successfully by the condensation of the nucleoside with 2-cyanoethyl phosphate by dicyclohexylcarbodiimide,[6] but when dibenzyl phosphorochloridate was used, the reaction was not achieved because of the inertness of the chloridate to the secondary hydroxyl groups of nucleoside sugar.[7] The present authors attempted to prepare guanosine 2′(or 3′)-phosphate from 5′-*O*-acetylguanosine and pyrophosphoryl tetrachloride in triethyl phosphate, but the yield was 50% at best. A better method, using P^1,P^1-diphenyl P^2-morpholinopyrophosphorochloridate, has been described by Ikehara and Tazawa.[8]

Recently, Honjo *et al.*[9] have reported that the reaction of 2′,3′-*O*-isopropylideneinosine with phosphorus trichloride in acetone (or methyl ethyl ketone) in an open vessel and subsequent hydrolysis gave inosine 5′-phosphate as the major product, although similar treatment in a closed vessel gave mainly inosine 5′-phosphite. The route *via* nucleoside phosphorodichloridite was considered to be a more plausible mechanism than the phosphorylation with phosphorus oxychloride formed by the air oxidation of phosphorus trichloride.

Secondary alkyl phosphorodichloridites have been prepared by the treatment of secondary alcohols

1) M. Yoshikawa, T. Kato and T. Takenishi, This Bulletin, **42**, 3505 (1969).

2) N. S. Corby, G. W. Kenner and A. R. Todd, *J. Chem. Soc.*, **1952**, 3669.

3) J. A. Schofield and A. R. Todd, *ibid.* **1961**, 2316.

4) A. Holý, J. Smrt and F. Šorm, *Collect. Czech. Chem. Commun.*, **30**, 1635 (1965).

5) A. Holý, *Chem. Ind.* (London), **1965**, 721.

6) P. I. Gilham and G. M. Tenner, *ibid.*, **1959**, 542; G. M. Tenner, *J. Amer. Chem. Soc.*, **83**, 159 (1961); H. J. Thomas, K. Hewson and J. A. Montgomery, *J. Org. Chem.*, **27**, 192 (1962).

7) D. H. Hayes, A. M. Michelson and A. R. Todd, *J. Chem. Soc.*, **1955**, 808.

8) M. Ikehara and I. Tazawa, *J. Org. Chem.*, **31**, 819 (1966).

9) M. Honjo, R. Marumoto, K. Kobayashi and Y. Yoshida, *Tetrahedron Lett.*, **32**, 3851 (1966).

with phosphorus trichloride under mild warming conditions.[10] This method, however, could not be directly adapted to the synthesis of nucleotides because of the highly heat-sensitive nature of nucleoside phosphorodichloridites in an acidic condition.

We have attempted to find some potentially active promotors for the reaction of a nucleoside with phosphorus trichloride at a low temperature. The method involving the reaction of 2′,3′-*O*-isopropylidene and 5′-*O*-acetyl nucleosides with a phosphorus trihalide in the presence of an appropriate organo-phosphorus compound gave nucleoside 5′- and 2′(or 3′)-phosphites respectively. The oxidation of a nucleoside phosphorochloridite with a halogen offered a convenient method for the synthesis of a nucleoside 5′- or 2′(or 3′)-phosphate. The reaction of phosphorus trichloride with a nucleoside 5′-phosphorodichloridate proceeded readily. The subsequent hydrolysis of the product after oxidation gave a nucleoside 2′(or 3′),5′-diphosphate in a good yield. This paper will deal with the synthesis of the nucleoside phosphite and phosphate using phosphorus trihalide.

Results and Discussion

Phosphorylation of 2′,3′-*O*-Isopropylidene Nucleoside. Trialkyl phosphate has shown an excellent effect in the phosphorylation of a wide field of nucleosides with phosphorus oxychloride, as has been reported in a preceding paper.[1] The addition of a trialkyl phosphate to the reaction mixture of 2′,3′-*O*-isopropylideneinosine with phosphorus trichloride caused an even more remarkable promotion and resulted in a high yield of inosine 5′-phosphite after hydrolysis, in contrast with the low yield (14%) in the reaction with phosphorus trichloride alone, as is shown in Table 1. The effect was greater with a lower alkyl phosphate. The addition of a triaryl phosphate, such as triphenyl or diphenyl tolyl phosphate, in place of a trialkyl phosphate was also useful in promoting the reaction.

An increase in the amount of a trialkyl phosphate resulted in an acceleration of the reaction. Hence, the reaction must be discontinued quickly because of the rapid decomposition of the produced 5′-phosphorodichloridite. On the phosphorylation of 2′,3′-*O*-isopropylideneinosine with two mole-equivalents of phosphorus trichloride in trimethyl phosphate, only a quarter of an hour at 0°C was enough to give inosine 5′-phosphite in a 93% yield after hydrolysis; if the reaction period was prolonged, the yield was about 60%.

The oxidation of a nucleoside phosphite was carried out successfully by a halogen and yielded a nucleoside 5′-phosphate in a good yield. After the phosphorylation mixture had been poured into ether, the 2′,3′-*O*-isopropylideneinosine 5′-phosphorodichloridite (II) thus precipitated was centrifuged and dissolved again in fresh trimethyl phosphate.

The direct treatment of the solution with chlorine resulted in a serious decomposition of the nucleoside

Table 1. Phosphorylation of 2′,3′-*O*-isopropylidene nucleosides with phosphorus trihalide*

No.	Isopropylidene nucleoside	Organo-phosphorus compound, mmol	PX_3 mmol	Time hr	Yield of 5′-phosphite mol%
1 (2)**	Inosine	none	PCl_3: 100 (PBr_3: 100)	6 (4)	13 (2)
3 (4)	Inosine	$(CH_3O)_3PO$: 10	PCl_3: 100 (PBr_3: 100)	1 (4)	90 (54)
5 (6)	Inosine	$(C_2H_5O)_3PO$: 10	PCl_3: 100 (PBr_3: 100)	1 (3)	84 (80)
7 (8)	Inosine	$(n\text{-}C_4H_9O)_3PO$: 10	PCl_3: 100 (PBr_3: 100)	2 (6)	74 (72)
9	Inosine	$(C_6H_5O)_3PO$: 10	PCl_3: 100	2	72
10	Inosine	$(C_6H_5O)_2(p\text{-}CH_3C_6H_4O)PO$: 10	PCl_3: 100	3	72
11	Inosine	$(n\text{-}C_8H_{17})_3PO$: 10	PCl_3: 100	6	77
12	Inosine	$(CH_3O)_3P$: 10	PCl_3: 100	1	89
13	Inosine	$(C_2H_5O)_3P$: 10	PCl_3: 100	3	88
14	Inosine	$(i\text{-}C_3H_7O)_3P$: 10	PCl_3: 100	7	68
15	Inosine	$(n\text{-}C_4H_9O)_3P$: 10	PCl_3: 100	7	34
16 (17)	Inosine	$(CH_3O)_3PO$: 100	PCl_3: 10 (PBr_3: 10)	0.25 (2)	93 (80)
18 (19)	Adenosine	$(CH_3O)_3PO$: 10	PCl_3: 100 (PBr_3: 100)	1 (2)	87 (73)
20	Adenosine	$(CH_3O)_3PO$: 100	PCl_3: 15	0.5	78
21 (22)	Guanosine	$(CH_3O)_3PO$: 100	PCl_3: 15 (PBr_3: 15)	2 (2)	87 (83)
23	Uridine	$(CH_3O)_3PO$: 100	PCl_3: 10	3	98
24	Cytidine	$(CH_3O)_3PO$: 10	PCl_3: 100	6	75

* 5 mmol of 2′,3′-*O*-isopropylidene nucleoside was treated at 0°C.

** The results of phosphorylation with phosphorus tribromide comparable to phosphorus trichloride are shown in parentheses.

10) G. M. Kosolapoff, "Organo-phosphorus Compounds," John Wiley & Sons, New York (1950), p. 180.

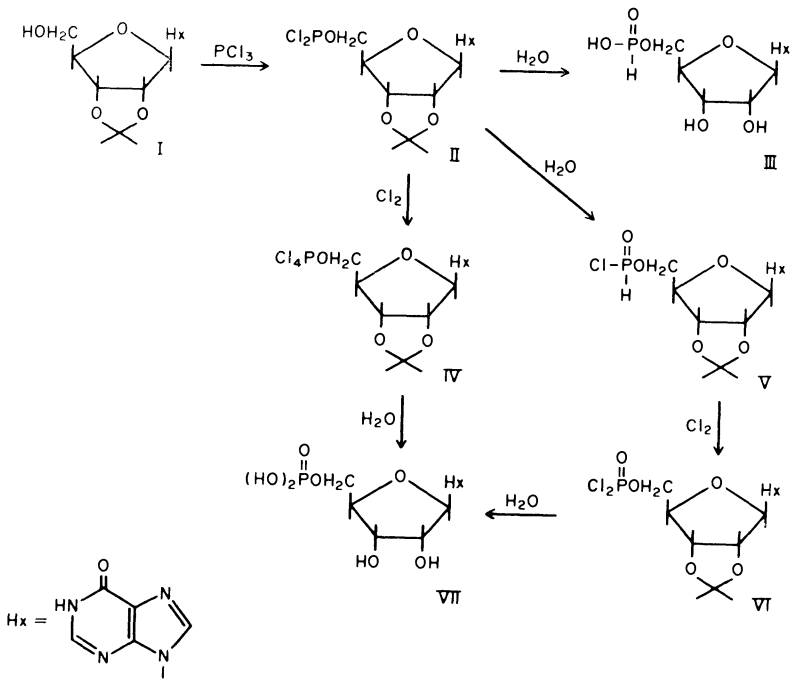

because of the probable instability of the tetrachlorophosphorane (IV) produced during the reaction. However, inosine 5′-phosphate (VII) was obtained in a 73% over-all yield from the starting nucleoside (I) by the careful partial hydrolysis of the phosphorodichloridite (II) by adding about an equimolar amount of water per mole of the intermediate II and by the subsequent oxidation of V with chlorine. Other halogens, such as bromine and iodine, could also be used for oxidation in the same way, but a number of usual oxidizing agents could not be used for this purpose.*1

The use of phosphorus tribromide in place of phosphorus trichloride resulted in a lower yield of a nucleoside 5′-phosphite. Especially, the treatment of 2′,3′-*O*-isopropylideneinosine with phosphorus tribromide alone gave only a trace of inosine 5′-phosphite.

The addition of a trialkylphosphine oxide or trialkyl phosphite to this reaction gave good results in spite of the ineffectiveness of both on phosphorylation with phosphorus oxychloride. However, the latter's effectiveness as an additive decreased sharply according to the increase in the carbon numbers of the alkyl group.

This method is generally applicable to the synthesis of other 5′-nucleotides; the results are shown, along with the results of the investigation of 2′,3′-*O*-isopropylideneinosine, in Table 1.

Phosphorylation of 5′-*O*-Acetyl Nucleoside. The reaction of 5′-*O*-acetyladenosine with a large excess of phosphorus trichloride did not give adenosine 2′(or 3′)-phosphite. The addition of a small amount of triethyl phosphate to the reaction mixture also resulted in only a small percentage of the phosphorylation product, unlike the case of a 2′,3′-*O*-isopropylidene nucleoside. However, adenosine 2′(or 3′)-phosphite was produced in a quantitative yield by the treatment of 5′-*O*-acetyladenosine with two mole-equivalents of phosphorus trichloride in triethyl phosphate and by subsequent hydrolysis. The phosphorylation was completed after a longer period than that needed for 2′,3′-*O*-isopropylideneadenosine. The mole ratio of the adenosine 2′- and 3′-phosphites was 36 : 64, which was very close to the result reported by Holý.[5] Since other 5′-*O*-acetyl ribonucleosides also produced mixtures of the corresponding 2′- and 3′-phosphites in similar mole ratios, as is shown in Table 2, it was clear that the 2′-hydroxyl group was less reactive than the 3′-hydroxyl group.

An oxidation giving a mixture of adenosine 2′- and 3′-phosphates in a 84% yield was carried out by a similar technique to that used for inosine 5′-phosphate. In the course of an investigation of the oxidation of a nucleoside 2′(or 3′)-phosphorodichloridite, it was found that the ease of oxidation depended upon the kind of halogen used and was generally in the order: chlorine > bromine > iodine. However, the oxidation of guanosine 2′(or 3′)-phosphorodichloridite with chlorine gave only a trace of the corresponding phosphate because of the destruction of the heterocyclic nucleus, which was detected by the loss of the ultraviolet absorption. In this case, the highest yield was

*1 The investigation of the oxidation was carried out with the cooperation of Mr. Takashi Yamashita.

Table 2. Phosphorylation of 5'-*O*-acetyl nucleosides with phosphorus trihalide

No.	Acetyl nucleoside mmol	Trialkyl phosphate mmol	PX_3 mmol	Time hr	Yield of 2'(3')-phosphite mol%	Mole ratio 2'	Mole ratio 3'
25	Adenosine: 5	$(C_2H_5O)_3PO$: 5	PCl_3 : 100	6	2	—	—
26	Adenosine: 5	$(C_2H_5O)_3PO$: 20	PCl_3 : 100	6	21	—	—
27	Adenosine: 5	$(C_2H_5O)_3PO$: 125	PCl_3 : 15	1	94	36	64
28	Adenosine: 5	$(CH_3O)_3PO$: 100	PCl_3 : 10	1	97	39	61
29	Adenosine: 5	$(CH_3O)_3PO$: 100	PBr_3 : 10	1	91	35	65
30	Inosine: 5	$(C_2H_5O)_3PO$: 125	PCl_3 : 15	1	97	39	61
31	Inosine: 5	$(CH_3O)_3PO$: 100	PBr_3 : 10	1	88	33	67
32	Guanosine: 5	$(C_2H_5O)_3PO$: 125	PCl_3 : 15	1	95	40	60
33	Guanosine: 5	$(CH_3O)_3PO$: 100	PBr_3 : 10	1	97	47	53

Temperature: 0°C

Table 3. Synthesis of nucleoside 2',5'- and 3',5'-diphosphates*

No.	Nucleoside	Time** hr	Halogen	Yield of diphosphate mol%	Mole ratio 2',5'	Mole ratio 3',5'
34	Adenosine	2	Cl_2	92	43	57
35	Inosine	4	Cl_2	78	48	52
36	Guanosine	9	I_2	64	45	55
37	Cytidine	1	Br_2	78	46	54
38	Uridine	12	I_2	80	46	54

* 0.04 mol of nucleoside was treated successively at 0°C by 0.08 mol of phosphorus oxychloride, 0.08 mol of phosphorus trihalide for 1 hr, 0.48 mol of water and 0.12 mol of halogen for 2 hr in 100 m*l* of trimethyl phosphate.

** This represents the time of the first phosphorylation with phosphorus oxychloride.

achieved by less reactive iodine.

Synthesis of Nucleoside 2'(or 3'),5'-diphosphate. It is known that the 2'- and 3'-hydroxyl groups were inactive compared with the 5'-hydroxyl group. On the other hand, a nucleoside 2'(or 3')-phosphorodichloridite in a reaction mixture was relatively stable even over a prolonged reaction time, despite the sharp decomposition of the 5'-phosphorodichloridite. Thus, the differences in reaction rate between sugar 2'(or 3')- and 5'-hydroxyl groups, and in stability between the corresponding phosphorodichloridites, interfered with the extension of this procedure to the synthesis of a nucleoside 2'(or 3'),5'-diphosphate directly from an unprotected nucleoside.

A combination of phosphorus oxychloride and phosphorus trichloride was utilized for the synthesis. An attempt at the phosphorylation of an unprotected nucleoside in one step with a mixed solution of the combining phosphorylating agents in a trialkyl phosphate resulted in failure. This is considered to be due to the markedly rapid reaction of the unprotected nucleoside with phosphorus trichloride in comparison with that with phosphoryl chloride and to the different properties, described above. However, the treatment of an unprotected nucleoside with phosphorus trichloride, after phosphorylation with phosphorus oxychloride sufficient to give a nucleoside 5'-phosphorodichloridate, and subsequent oxidation gave an excellent yield of the corresponding diphosphate. All of these procedures were carried out in one solution without the isolation of the intermediate.

Experimental

Detection and Analysis of Nucleotides. Paper chromatographies were developed by the ascending technique on Toyo Roshi No. 51 paper with Solvent 1: *n*-propyl alcohol - concentrated ammonium hydroxide - water (20 : 20 : 3), and Solvent 2: isopropyl alcohol - saturated ammonium sulfate - water (2 : 79 : 19). The nucleotides were detected by ultraviolet light and by spraying on a Hanes-Isherwood reagent, as has previously been descrived.[11] The yields were estimated by means of the ultraviolet absorption intensities of the solutions eluted from the spots with 0.1 N hydrochloric acid.

Nucleoside 2'(or 3')-phosphites, 2'(or 3')-phosphates, and 2'(or 3'),5'-diphosphates were chromatographed on thin layers of MN-Cellulose powder 300 (0.25 mm

11) M. Yoshikawa and T. Kato, This Bulletin, **40**, 2849 (1967).

thick) (Macherey, Nagel & Co., Germany) on a glass plate (20×20 cm) using the ascending technique with Solvent 3: isopropyl alcohol - saturated ammonium sulfate - 0.5 M sodium acetate (2 : 79 : 19). For nucleoside diphosphates, the faster-running compounds were assumed to be 2′,5′-diphosphates, judging from the behavior of inosine 2′,5′-diphosphate.

The R_f values are summarized in Table 4.

TABLE 4. R_f VALUES OF NUCLEOTIDES

Nucleotide	R_f Value of chromatogram			
	Paper		Thin-layer	
	Solv. 1	Solv. 2	Solv. 3 2′	3′
Adenosine 2′(3′)-phosphate	0.30	0.29	0.35	0.24
Adenosine 2′(3′)-phosphite	0.55		0.23	0.13
Adenosine 5′-phosphate	0.30	0.32		
Adenosine 5′-phosphite	0.60			
Adenosine 2′(3′),5′-diphosphate	0.15	0.37	0.37	0.32
Inosine 2′(3′)-phosphate	0.34	0.57	0.61	0.52
Inosine 2′(3′)-phosphite	0.54		0.50	0.41
Inosine 5′-phosphate	0.30	0.67		
Inosine 5′-phosphite	0.57			
Inosine 2′(3′),5′-diphosphate	0.16	0.76	0.81	0.76
Guanosine 2′(3′)-phosphate	0.23	0.43	0.50	0.39
Guanosine 2′(3′)-phosphite	0.46		0.36	0.25
Guanosine 5′-phosphate	0.21	0.47		
Guanosine 5′-phosphite	0.50			
Guanosine 2′(3′),5′-diphosphate	0.09	0.55	0.76	0.65
Cytidine 5′-phosphate	0.32	0.73		
Cytidine 5′-phosphite	0.55			
Cytidine 2′(3′),5′-diphosphate	0.23	0.81	0.88	0.81
Uridine 5′-phosphate	0.31	0.69		
Uridine 5′-phosphite	0.61			
Uridine 2′(3′),5′-diphosphate	0.20	0.77	0.87	0.81

Phosphorylation of 2′,3′-*O*-Isopropylideneinosine with Phosphorus Trichloride (as a Typical Example). To a cold mixture of phosphorus trichloride (8.7 m*l*, 100 mmol) and trimethyl phosphate (1.17 m*l*, 10 mmol), 1.54 g (5 mmol) of 2′,3′-*O*-isopropylideneinosine were added; the mixture was stirred for 1 hr at 0°C and then poured into 50 m*l* of ether. The precipitate was separated by a centrifuge and dissolved in about 30 m*l* of ice water, and the aqueous solution was hydrolyzed at 70°C after being adjusted to pH 1.5 with 6 N sodium hydroxide. Paper chromatography showed the presence of inosine 5′-phosphite in a 90% yield, as is shown in No. 3 of Table 1.

The effects of the other additives used in the same manner instead of trimethyl phosphate are summarized in Table 1, along with those of some other 2′,3′-*O*-isopropylidene nucleosides.

The solution was neutralized, absorbed on a Dowex 1×8 ($HCOO^-$) (50—100 mesh) column, and eluted with 0.02 N formic acid. The fraction of inosine 5′-phosphite was neutralized with 6 N ammonium hydroxide and concentrated to about 20 m*l*. Ammonium inosine 5′-phosphite (1.23 g) was separated by the addition of 60 m*l* of ethyl alcohol and purified by reprecipitation from the aqueous solution with ethyl alcohol.

Found: C, 32.96; H, 5.00; N, 19.09; P, 8.77%. Calcd for $C_{10}H_{16}O_7N_5P \cdot H_2O$: C, 32.70; H, 4.94; N, 19.08; P, 8.43%.

The product was converted into inosine 5′-phosphate in a 39% yield by permanganate oxidation according to the method described by Schofield and Todd.[3]

Synthesis of Inosine 5′-Phosphate. To a solution of 0.87 m*l* (10 mmol) of phosphorus trichloride in 11.7 m*l* (100 mmol) of trimethyl phosphate, 1.55 g (5 mmol) of 2′,3′-*O*-isopropylideneinosine were added on cooling; the mixture was then stirred at 0°C for 15 min. The reaction mixture was poured into about 100 m*l* of ether. The precipitate was separated by a centrifuge and dissolved in 10 m*l* of trimethyl phosphate. The solution was partially hydrolyzed with 0.09 m*l* (5 mmol) of water on cooling, and then 1.68 *l* (7.5 mmol) of chlorine was introduced into the sealed vessel of the solution. After having been vigorously stirred for 45 min at 0°C, the solution was treated with 100 m*l* of ether and the precipitate was hydrolyzed at pH 1.5 in a manner similar to that described above. Inosine 5′-phosphate was obtained in an over-all yield of 73%, as estimated by paper chromatographical analysis.

Phosphorylation of 5′-*O*-Acetyladenosine with Phosphorus Trichloride (as a Typical Example). To a solution of phosphorus trichloride (1.3 m*l*, 15 mmol), in 20 m*l* (125 mmol) of triethyl phosphate, 1.55 g (5 mmol) of 5′-*O*-acetyladenosine were added, and the mixture was stirred at 0°C for 1 hr. After the treatment of the reaction mixture with ether, the precipitate was dissolved in concentrated ammonium hydroxide and the solution was allowed to stand overnight at room temperature. This solution was found by chromatographical analysis to contain adenosine 2′- and 3′-phosphites in the mole ratio of 36 : 64 and in a total yield of 94%.

The results of the phosphorylation of several 5′-*O*-acetyl nucleosides with phosphorus trihalide are summarized in Table 2.

The alkaline solution was concentrated to about 10 m*l* and then adjusted to pH 1 with concentrated hydrochloric acid. After the acidic solution had been kept overnight in a refrigerator, the precipitate was filtered and dried. The mixture of adenosine 2′- and 3′-phosphites (1.14 g) thus obtained was reprecipitated from diluted alkali - hydrochloric acid.

Found: C, 35.58; H, 4.33; N, 21.21; P, 9.41%. Calcd for $C_{10}H_{14}O_6N_5P$: C, 36.26; H, 4.26; N, 21.15; P, 9.35%.

Synthesis of Adenosine 2′- and 3′-Phosphates. After working up in the same way with the method described in the previous experiment, the solution of the phosphorylated mixture was hydrolyzed carefully with 0.8 m*l* (45 mmol) of water: 0.5 *l* (22.5 mmol) of chlorine gas was then gradually passed through the solution at 0°C with stirring. After stirring had been continued for 3 hr, the reaction mixture was poured into a cold diluted ammonium hydroxide; analysis by paper chromatography showed adenosine monophosphate to be produced in an over-all yield of 84%. The solution was then concentrated to about 10 m*l* under reduced pressure, acidified to pH 1 with concentrated hydrochloric acid, and kept in a refrigerator. A white powder of adenosine monophosphate (1.08 g) was obtained by filtration; it was identical in paper-chromatographical

behavior in solvents 1 and 2 with authentic adensosine 3′-phosphate. However, on thin-layer chromatography in Solvent 3, it was recognized to be a mixture of adenosine 2′- and 3′-phosphates in a mole ratio of 50 : 50.

Found: C, 33.83; H, 4.22; N, 20.00; P, 8.57%. Calcd for $C_{10}H_{14}O_7N_5P \cdot \frac{1}{2}H_2O$: C, 33.72; H, 4.42; N, 19.66; P, 8.48%.

Synthesis of the Disodium Salt of Guanosine 2′- and 3′-Phosphates. 5′-*O*-Acetylguanosine (1.63 g, 5 mmol) was phosphorylated much as has been described above, hydrolyzed partially, and oxidized for 9 hr at 5—10°C by 5.7 g (22.5 mmol) of iodine in place of chlorine gas. The resulting solution was poured into 100 m*l* of ether, and then the precipitate was dissolved in diluted ammonium hydroxide after centrifuging. Paper chromatography showed the presence of guanosine monophosphate in an 85% yield. The alkaline solution was then evaporated under reduced pressure, and the aqueous solution of the residue was adsorbed on a Dowex 1×2 (Cl^-) (100—200 mesh) column. The column was washed with water and eluted with 0.1 M sodium chloride in 0.003 N hydrochloric acid. The eluate was concentrated and adsorbed again on active carbon. The active carbon was washed with water and eluted with 0.5 N ammonium hydroxide. To the eluate, 6 N sodium hydroxide was added in small portions, with care taken to maintain the pH under 9 until no more ammonia was eliminated by concentration. The solution was then concentrated to about 10 m*l*, and 30 m*l* of ethyl alcohol was gradually added to it. The mixture of the disodium salt of guanosine 2′- and 3′-phosphates (1.19 g) thus obtained was recrystallized from water - ethyl alcohol and identified in a manner similar to that used for adenosine 2′- and 3′-phosphates.

Found: C, 28.74; H, 3.24; N, 16.55; P, 7.34%. Calcd for $C_{10}H_{12}O_8N_5PNa_2 \cdot H_2O$: C, 28.26; H, 3.32; N, 16.47; P, 7.28%.

Synthesis of the Dibarium Salt of Inosine 2′,5′- and 3′,5′-diphosphates (as a Typical Example). After the treatment of inosine (10.7 g, 0.04 mol) with phosphorus oxychloride (7.4 m*l*, 0.08 mol) in 10 m*l* of trimethyl phosphate for 4 hr at 0°C, phosphorus trichloride (7.0 m*l*, 0.08 mol) was added to the solution and the mixture was stirred for 1 hr. Water (8.6 m*l*, 0.48 mol) was then carefully added to the solution, and chlorine gas (2.7 *l*, 0.12 mol) was passed through with stirring. After 2 hr of oxidation at 0°C, the reaction mixture was poured into about 1 *l* of ether; the precipitate was hydrolyzed with 0.5 *l* of ice water and neutralized with 6 N sodium hydroxide. Paper chromatography revealed the presence of inosine diphosphates in a 78% yield.

In a similar manner, nucleoside diphosphates are obtained in high yields. The results are summarized in Table 3. The neutralized solution was passed through a column of a Dowex 1×2 (Cl^-) (50—100 mesh). The column was washed with water and eluted with 0.015 M sodium chloride in 0.003 N hydrochloric acid, and subsequently with 0.2 M sodium chloride in 0.003 N hydrochloric acid. The latter eluate was neutralized with 6 N sodium hydroxide, concentrated to about 100 m*l* under reduced pressure, and filtered to remove the sodium chloride. A saturated solution of 22 g of barium acetate was then added to the filtrate, and the precipitate was collected and dried. The mixture of dibarium inosine 2′,5′- and 3′,5′-diphosphates (15.4 g) thus obtained was dissolved again in 6 N hydrochloric acid, filtered, neutralized with 6 N sodium hydroxide, and reprecipitated by adding a barium acetate solution.

Found: C, 15.87; H, 2.24; N, 7.01; P, 8.24%. Calcd for $C_{10}H_{10}O_{11}N_4P_2Ba_2 \cdot 3H_2O$: C, 15.95; H, 2.14; N, 7.44; P, 8.23%.

Thin-layer chromatography showed the presence of two components with R_f values of 0.81 and 0.76 (mole ratio, 48 : 52). The faster-running component was identical with the inosine 2′,5′-diphosphate which was separated on the column chromatography of a Dowex 1×2 (Cl^-) according to the method reported by Mitsugi *et al.*[12] The slower-moving component was similarly identified as inosine 3′,5′-diphosphate.

The authors are indebted to Dr. Tetsuya Kato for his continuing guidance.

12) K. Mitsugi, E. Nakazawa, S. Okumura, M. Takahashi and H. Yamada, *Agr. Biol. Chem.* (Tokyo), **29**, 1051 (1965).

BULLETIN OF THE CHEMICAL SOCIETY OF JAPAN VOL. 43 462—465 (1970)

Hammett Correlation in Mass Spectra. Substituent Effects for the Migratory Aptitude of the Aryl Group in the Unimolecular Ion Decomposition of Diaryl Sulfones

Toshikazu NAGAI, Tetsuo MAENO and Niichiro TOKURA

Department of Applied Chemistry, Faculty of Engineering, Osaka University, Suita, Osaka

(Received June 16, 1969)

The migratory aptitude of the aryl group in the unimolecular ion decomposition reaction of *p*-substituted diaryl sulfones has been examined. Both electron-donating and -withdrawing substituents showed to be capable of increasing the migratory aptitude. On the other hand, a kinetic treatment allowed a satisfactory Hammett correlation ($\rho=0.3$) on the total abundances of the fragment ions. The energy of the cleaved bond and the production stability were shown to be important factors in the effect of the substituent on the ion decomposition.

In the mass spectra of methyl-substituted diaryl sulfones, the aryl S→O migration has been observed by Meyerson and his co-workers.[1] They have demonstrated that the migratory aptitude apparently increases with an increase in the substitution of the phenyl group by the electron-donating methyl group, and suggested that the electron deficiency is largely localized in a non-bonding oxygen orbital and that, hence, an aryl group better able to function as an electron donor should preferentially migrate (Scheme 1).

In order to obtain further information about substituent effects in the migratory aptitude on diaryl sulfones, we have now dealt with a variety of the *p*-substituted compounds, applying a kinetic method. The results we obtained on the driving

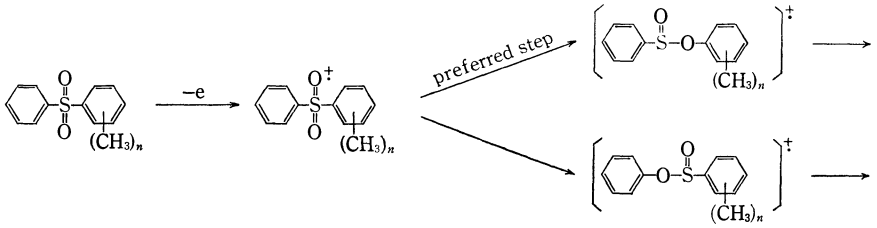

Scheme 1

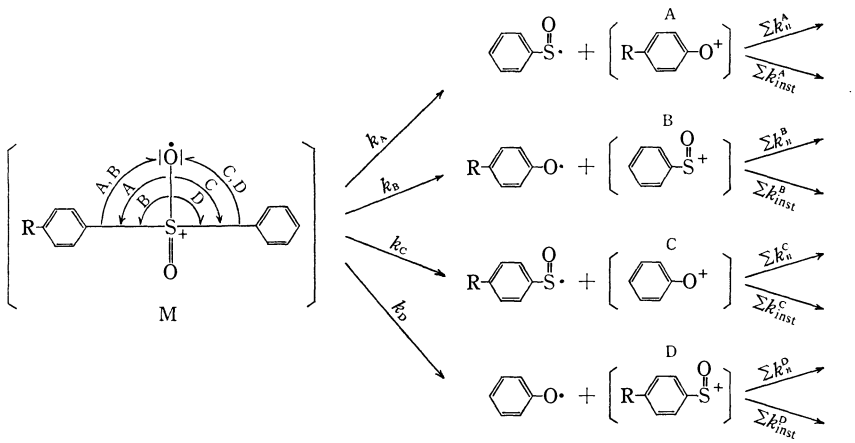

Scheme 2

1) S. Meyerson, H. Drews and E. K. Fields, *Anal. Chem.*, **36**, 1294 (1964).

force of the aryl migration were somewhat different from those obtained by Meyerson and his coworkers.

Results and Discussion

By increasing the electron energy, a variety of fragment ions were formed, along with the A, B, C, and D ions (Scheme 2), as is shown in Fig. 1a. Thus, the voltage of the ionizing electrons used was chosen to be 20 eV in order to keep the products from further decomposition (Fig. 1b).

The ratios of the fragment ions (C+D) due to the migration of the unsubstituted aryl group to those (A+B) of the *p*-substituted aryl group were examined; they are shown in Table 1.

These ratios indicate, interestingly, that both electron-donating and -attracting substituents are capable of increasing their migratory aptitude, indicating a further factor in the migratory aptitude in addition to that proposed by Meyerson *et al.*,[1] that an aryl group better able to function as an electron donor should preferentially migrate.

Thus, we carried out a kinetic study in order to examine the relative rate of bond cleavage. The method by Bursey and McLafferty.[2-4] was modified which was applicable to substituted benzophenone systems involving no phenyl migration.

The concentratioons of ions (A, B, C, and D) in the source of the mass spectrometer were assumed to be dependent on their rates of formation and depletion (whether by further decomposition, $\sum k_n^{A-D}$ or by instrumental removals, $\sum_{inst}^{A-D}$,) according to Scheme 2; the rate of the appearance of A+B+C+D in the source is shown as Eq. 1:

$$\frac{d\{[A]+[B]+[C]+[D]\}}{dt} = (k_A + k_B + k_C + k_D)[M] - \{(\sum k_n^A + \sum k_{inst}^A)[A] + (\sum k_n^B + \sum k_{inst}^B)[B] + (\sum k_n^C + \sum k_{inst}^C)[C] + (\sum k_n^D + \sum k_{inst}^D)[D]\} \quad (1)$$

By the steady-state approximation, Eq. (2) is obtained:

$$(\sum k_n^A + \sum k_{inst}^A)[A] + (\sum k_n^B + \sum k_{inst}^B)[B] + (\sum k_n^C + \sum k_{inst}^C)[C] + (\sum k_n^D + \sum k_{inst}^D)[D] = (k_A + k_B + k_C + k_D)[M] \quad (2)$$

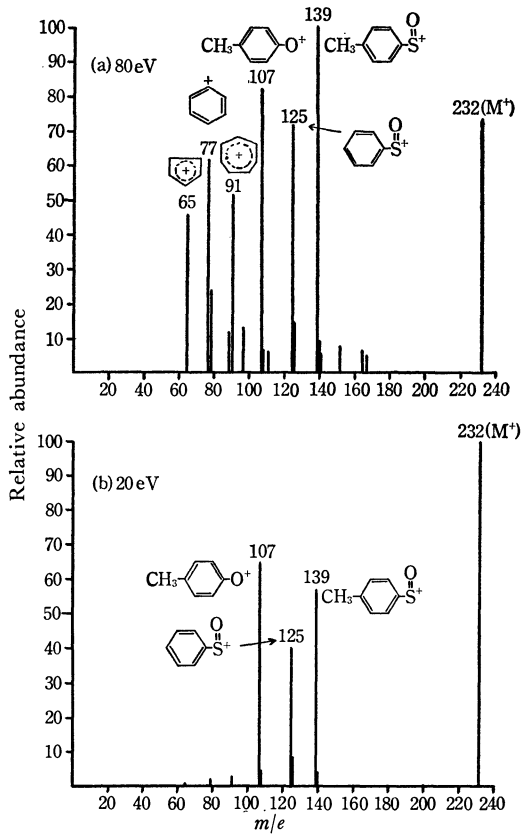

Fig. 1. Relative abundance of the fragment ions of *p*-methyldiphenyl sulfone recorded at 80 eV (a) and 20 eV (b). The peaks below *m/e* 65 are omitted here.

In the present case, if the voltage of the ionizing electrons is so low (20 eV) that no further decomposition products of the A, B, C, and D ions appear in the mass spectrum, then $\sum_n^{A-D}$ vanishes and Eq. (2) is reduced to Eq. (3), since the instrumental parameters do not vary greatly from compound to compound; *i.e.*, $\sum k_{inst}^A = \sum k_{inst}^B = \sum k_{inst}^C = \sum k_{inst}^D \equiv \sum k_{inst}$.

$$\frac{[A]+[B]+[C]+[D]}{[M]} = \frac{k_A + k_B + k_C + k_D}{\sum k_{inst}} \quad (3)$$

Z/Z_0 values defined as in Eq. (4) are given in Table 2, where the suffix zero refers to an unsubstituted compound:

Table 1. The relative abundances of the fragment ions formed by aryl migration

R	NH_2	OCH_3	CH_3	H	Cl	COOH	CN	NO_2
(C+D)/(A+B)	0.132	0.260	0.533	1.000	0.318	0.534	0.375	0.986

2) M. M. Bursey and F. W. McLafferty, *J. Amer. Chem. Soc.*, **88**, 529 (1966).
3) M. M. Bursey and F. W. McLafferty, *ibid.*, **88**, 4484 (1966).
4) M. M. Bursey and F. W. McLafferty, *ibid.*, **89**, 1 (1967).

TABLE 2. RELATIVE INTENSITIES OF THE FRAGMENT IONS IN THE MASS SPECTRA OF *p*-SUBSTITUTED DIPHENYL SULFONE RECORDED AT 20 eV

R	$\frac{[A]}{[M]}$	$\frac{[B]}{[M]}$	$\frac{[C]}{[M]}$	$\frac{[D]}{[M]}$	Z	$\log\frac{Z}{Z_0}$
NH_2	0.700	0.028	0	0.096	0.824	−0.477
OCH_3	1.075	0.021	0	0.285	1.381	−0.253
CH_3	0.660	0.409	0	0.570	1.639	−0.178
H	0	1.235	0	1.235	2.470	0
Cl	0	2.190	0	0.695	2.885	0.068
COOH	0	2.420	0	1.292	3.712	0.177
CN	0	2.068	0.291	0.485	2.844	0.061
NO_2	0	1.655	0.974	0.658	3.287	0.124

$$\frac{Z}{Z_0} \equiv \frac{[A]+[B]+[C]+[D]/[M]}{[A_0]+[B_0]+[C_0]+[D_0]/[M_0]} = \frac{k_A+k_B+k_C+k_D}{k_A^0+k_B^0+k_C^0+k_D^0} \equiv \frac{k}{k^0} \quad (4)$$

The correlation of these data with the Hammett σ^+ constants[5] indicates a small positive ρ value (+0.37), as is shown in Fig. 2.

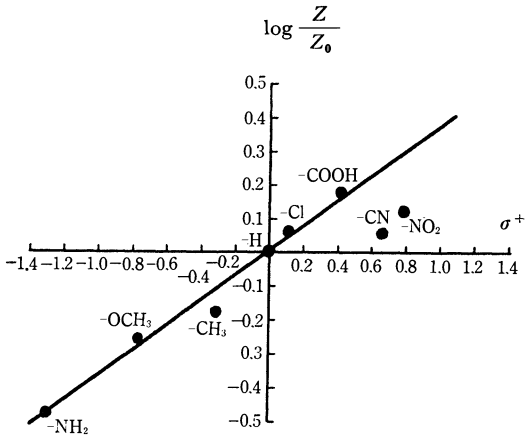

Fig. 2. Relative intensities of the total fragment ions in the mass spectra of *p*-substituted diphenyl sulfones recorded at 20 eV (derived from Eq. (3)) *vs.* σ^+ values.

For this reaction, σ values were less appropriate, indicating the presence of a full positive charge on the substituted molecular ion. Although the total abundances of fragment ions allowed a satisfactory Hammett correlation to be obtained, the effect of a substituent on the abundance of the individual fragment ions was not satisfactorily correlated by the Hammett equation.

In addition to the above-mentioned Z/Z_0 values, we found that Y/Y_0 values as defined in Eq. (5)

$$\frac{Y}{Y_0} \equiv \frac{\ln(1+Z)}{\ln(1+Z_0)} = \frac{k_A+k_B+k_C+k_D}{k_A^0+k_B^0+k_C^0+k_D^0} \equiv \frac{k}{k^0} \quad (5)$$

were applicable to the Hammett correlation, since

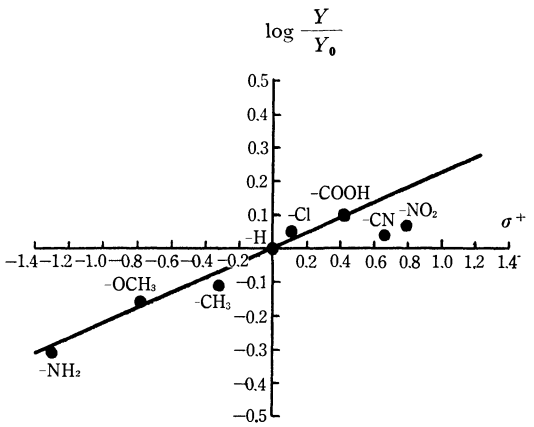

Fig. 3. Relative intensities of the total fragment ions in the mass spectra of *p*-substituted diphenyl sulfones recorded at 20 eV (derived from Eq. (6)) *vs.* σ^+ values.

the proposed values resulted in nearly the same Hammett correlation as in the case of the Z/Z_0 values, as may be seen in Fig. 3.

The coincidence of the two values can be explained by the following considerations.

Applying the general solution of the rate equation of two successive first-order reactions[6] to the present unimolecular competitive reaction shown by Scheme 2 under conditions of negligible $\sum k_n^{A-D}$ rates, Eq. (6) can be obtained by using the equation of $[M]_0 = [M] + \sum_{N=A}^{D}[N]$, where $[M]_0$ is the concentration of [M] at $t=0$:

$$\sum_{N=A}^{D}[N] = \frac{\sum_{N=A}^{D} k_N}{\sum k_{inst} - \sum_{N=A}^{D} k_N}\left([M] + \sum_{N=A}^{D}[N]\right)e^{-\sum_{N=A}^{D} k_N t} - \frac{\sum_{N=A}^{D} k_N}{\sum k_{inst} - \sum_{N=A}^{D} k_N}\left([M] + \sum_{N=A}^{D}[N]\right)e^{-\sum k_{inst} t} \quad (6)$$

5) H. C. Brown and Y. Okamoto, *J. Amer. Chem. Soc.* **80**, 4979 (1958).

6) A. Frost and R. G. Pearson "Kinetics and Mechanism," 2nd Ed., John Wiley & Sons, New York (1961), p. 166.

Assuming $\sum k_{inst} \gg \sum_{N=A}^{D} k_N$, there results:

$$\frac{\sum_{N=A}^{D}[N]}{[M]} = \frac{\sum_{N=A}^{D} k_N([M] + \sum_{N=A}^{D}[N])}{\sum k_{inst}[M]} e^{-\sum_{N=A}^{D} k_N t} \quad (7)$$

$$\ln \frac{[M] + \sum_{N=A}^{D}[N]}{[M]} = \sum_{N=A}^{D} k_N t - \ln \frac{\sum_{N=A}^{D} k_N}{\sum k_{inst}} + \ln \frac{\sum_{N=A}^{D}[N]}{[M]} \quad (8)$$

Equation (9) will be obtained if Eq. (3) is substituted for Eq. (8):

$$\ln \frac{[M] + \sum_{N=A}^{D}[N]}{[M]} = \sum_{N=A}^{D} k_N t \quad (9)$$

This situation yields Eq. (5).

As for the greater deviation from the Hammett correlation in the cases of nitro- and cyano-substituents, as Figs. 2 and 3 show, there is a very large destabilization factor of the substituents, since a large abundance of an ion, M^+–NO or M^+–HCN, was formed.

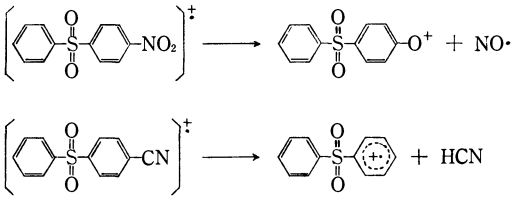

Now, we can explain the findings on the migratory aptitude shown in Table 1.

The ionization potential of sulfur is much lower than that of oxygen, and the ionization of ArSO is much easier than that of ArO; hence, ArO^+ is more sensitive to the substituent effect than $ArSO^+$, as may be seen in Table 2. Namely, the electron-donating group stabilizes ArO^+ more (preferential formation of A) than $ArSO^+$.

Thus, the increase in the migratory aptitude by the electron-donating group is attributable to the product-ion stability, though the over-all rate of bond cleavage is rather slow in the case of the electron-donating substituents, as the Hammett correlation indicates.

On the other hand, it is evident that the electron-withdrawing substituents cause a more rapid cleavage of the bond. In this case, the substituted phenyl carbon-sulfur bond will undergo a readier cleavage than the unsubstituted phenyl carbon-sulfur bond because of the effect of the substituent on the energy of the cleaved bond, for electron-withdrawing substituents destabilize the positive charge.

This may be the reason why the migratory aptitude increases with the substitution of the phenyl ring even by the electron-attracting group, because the effect of the energy of the cleaved bond overcomes the effect of the product-ion stability.

These two effects, the product-ion stability and the energy of cleaved bond, should make an important contribution to the driving force in the ion-decomposition reaction.

Experimental

The compounds used in this study were synthesized by the methods in the literature: diphenyl sulfone,[7] mp 128°C; *p*-aminodiphenyl sulfone,[8] mp 176°C; *p*-methoxydiphenyl sulfone,[9] mp 89—90.5°C; *p*-methyldiphenyl sulfone,[10] mp 124.5°C; *p*-chlorodiphenyl sulfone,[11] mp 91°C; *p*-cyanodiphenyl sulfone,[12] mp 117—118°C; *p*-nitrodiphenyl sulfone,[13] mp 140—141°C, and *p*-phenylsulfonylbenzoic acid,[14] mp 267—268°C. They contained no impurities detectable by mass spectrometry.

The spectra were recorded on a Hitachi RMU-6E single-focusing instrument with both inlet and source temperatures of 250°C.

7) Beilsteins "Handbuch," **EII 6**, 290 (1944).
8) W. R. Waldron and E. E. Reid, *J. Amer. Chem. Soc.*, **45**, 2406 (1923).
9) H. H. Szmant and G. Suld, *ibid.*, **78**, 3400 (1956).
10) Beilsteins "Handbuch," **6**, 418 (1923).
11) *Ibid.*, **EII 6**, 297 (1944).
12) A. T. Fuller, I. M. Tonkin and J. Walker, *J. Chem. Soc.*, **1945**, 637.
13) F. Ullmann and G. Pasdermadjian, *Ber.*, **34**, 1154 (1901).
14) A. Michael and A. Adair, *ibid.*, **11**, 119 (1878).

BULLETIN OF THE CHEMICAL SOCIETY OF JAPAN VOL. 43 466—469 (1970)

Alkoxysilanes. IV. Preparation of Alkoxysiloxy Derivatives of Titanium

Yoshimoto ABE and Ichiro KIJIMA

Department of Industrial Chemistry, Faculty of Engineering, Science University of Tokyo, Kagurazaka, Shinjuku-ku, Tokyo

(Received July 7, 1969)

Alkoxysiloxy derivatives of titanium and polymeric substances with Ti-O-Si bonds were prepared. The reaction of titanium tetra-isopropoxide or bis(acetylacetonato)di-isopropoxytitanium with tri-*t*-butoxysilanol led to the formation of the derivatives of $[(Bu^tO)_3SiO]_nTi(OPr^i)_{4-n}$ ($n=2$ and 3) and those of $[(Bu^tO)_3SiO]_2Ti(AcAc)_2$ respectively. In both of these series, the absorption peak of the Ti-O-Si bond in the IR spectrum shifted toward a lower wave number from the compounds of $n=2$ to those of $n=3$. The reaction of titanium tetra-isopropoxide with di-*t*-butoxysilanediol, as expected, gave a polymeric substance. In the reaction with bis(tri-*t*-butoxysiloxy)-silanediol, however, an unexpected cyclic compound consisting of the Ti-O-Si bond was obtained; its presence was confirmed by a study of the IR and NMR spectra, by elemental analysis, and by molecular-weight determination. In order to obtain a linear polymer, the reaction of the titanium acetylacetonato chelate with the silanediols was carried out to give a reddish-brown, highly viscous liquid or solid. These polymeric substances were soluble in common organic solvents and have an appreciable hydrolytic stability, but only a moderate thermal stability.

In order to obtain thermally-stable polymers, the syntheses of alkylsiloxy derivatives of metals containing the M–O–Si heterosiloxane bond have been studied. However, no alkoxysiloxy derivatives of metals have been investigated. We have already reported on the preparation of alkoxysiloxy derivatives of antimony[1] during the course of an investigation of a series of alkoxysiloxy derivatives of metals. In the present work, the authors have tried to prepare alkoxysiloxy derivatives of titanium.

Alkoxysiloxy derivatives of titanium were afforded by the following reactions:

$$M(OPr^i)_4 + nROH \rightarrow (RO)_nM(OPr^i)_{4-n} + nPr^iOH \quad (I)$$

$$(AcAc)_2M(OPr^i)_2 + 2ROH \rightarrow (AcAc)_2M(OR)_2 + 2Pr^iOH \quad (II)$$

$$M(OPr^i)_4 + (RO)_2Si(OH)_2 \rightarrow \text{polymer} + \text{cyclic compound} \quad (III)$$

$$(AcAc)_2M(OPr^i)_2 + (RO)_2Si(OH)_2 \rightarrow \text{polymer} \quad (IV)$$

where M=Ti, R=$(Bu^tO)_3Si$, and $n=2$ and 3.

In reaction (I), the products of $n=2$ and 3 were obtained, but it was difficult to obtain tetrakis (tri-*t*-butoxysiloxy)titanium ($n=4$) even by the reaction of tris(tri-*t*-butoxysiloxy)isopropoxytitanium with tri-*t*-butoxysilanol in a sealed tube. Molecular-weight determinations showed that these compounds were monomeric.

Breed and Haggerty[2] reported that the reaction of bis(acetylacetonato)di-isopropoxytitanium with triphenylsilanol did not yield the corresponding derivative, but, rather, the disproportionation product, tetrakis(triphenylsiloxy)titanium. In this work we found that the alkoxy groups in the acetylacetonato chelate were easily displaced to form bis (tri-*t*-butoxysiloxy) bis(acetylacetonato)titanium in a good yield (80%) according to reaction (II). The products from reactions (I) and (II) are soluble in all common organic solvents except alcohol, and the acetylacetonato chelate is more stable to hydrolysis than the others. These products were also confirmed, by a study of their IR and NMR spectra, to have the structures shown in Table 1. It has previously been established that the absorption peak due to the titanosiloxane bond Ti–O–Si is in the region from 910 to 930 cm^{-1}.[3] The alkoxysiloxy derivatives of titanium also showed their peaks in the same region. When the absorption in the compound of $n=2$ was compared with that of $n=3$, it was found to shift to a lower wave number by 15 cm^{-1} from the former to the latter. In the NMR spectra of $n=2$, the signal of methyl protons due to isopropyl groups appears as a doublet at 8.82 τ, whereas in $n=3$ it shifts to an appreciably

1) Y. Abe and I. Kijima, This Bulletin, **42**, 1148 (1969).

2) L. W. Breed and W. J. Haggerty, *J. Org. Chem.*, **27**, 257 (1962).

3) K. A. Andrianov, N. P. Gashnikova and E. Z. Asnovich, *Izv. Akad. Nauk. SSSR*, **1960**, 857; V. A. Zeitler and C. A. Brown, *J. Amer. Chem. Soc.*, **79**, 4618 (1957); K. A. Andrianov, Sh. V. Pichzhadze and I. V. Bochkareva, *Vysokomol. Soedin.*, **3**, 1321 (1961).

Table 1. IR and NMR spectra of tri-*t*-butoxysiloxy derivatives of titanium

Compound	IR (cm^{-1}) Ti-O-Si	NMR (τ) *t*-Bu and Me(Pr)	-CH-	=CH-
$(RO)_3TiOPr$	915	8.70(8.73), 8.78	5.10—5.51(q)	
$(RO)_2Ti(OPr)_2$	930	8.71, 8.82(d)	5.11—5.70(sep)	
$(RO)_2Ti(AcAc)_2$	900	9.36(9.45)		5.82
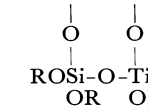	905	8.70(8.73), 8.82	5.28—5.68(q)	

R=$(Bu^tO)_3Si$, Pr=isopropyl, d=doublet, q=quintet, sep=septet
The figures in the parentheses indicate the shoulder.

lower field (8.78 τ, singlet). These facts seem to result from the large difference in proton number between the methyl protons (81H) of the tri-*t*-butoxysiloxy group and those (6H) of the isopropyl group and from the low wave number-shift in the IR spectra of the Ti–O–Si bond. On the other hand, the peak of the tri-*t*-butoxysiloxy derivative of the titanium acetylacetonate chelate due to the Ti–O–Si bond is at a wave number lower by 30 cm^{-1} than that of $n=2$. The NMR spectra of this compound show signals at 5.82 (–CH=) and 9.36, 9.45 τ (shoulder), probably due to the *t*-butyl and methyl groups in the acetylacetonato group. Usually, the tri-*t*-butoxysiloxy group exhibits a signal in the vicinity of 8.70 τ, and the enol type of acetylacetone, at 8.03 and 4.50 τ. Therefore, the high field-shift of the derivative may be attributed to the coordination of acetylacetone to the titanium atom.

Since, in reactions (I) and (II), the exchange reaction between titanium tetraalkoxides and tri-*t*-butoxysilanol had been carried out easily, it was expected that polymers with the Ti–O–Si bond in the molecular main chain might be obtained by reactions (III) and (IV). In the case of R=*t*-Bu, reaction (III) gave only polymeric substances of a pale yellow solid very soluble in organic solvents (it decomposed at about 200°C), although the structure was not confirmed. In the case of R=$(Bu^tO)_3Si$, however, a crystalline substance with a sharp melting point (decomposition) was produced by recrystallization from benzene. The results of the elemental analysis, the molecular-weight determination, and a study of the NMR (Fig. 1) and IR spectra revealed that the structure of the product consisted of an eight-membered ring containing Ti–O–Si bonds, as is shown below:

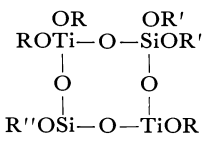

where R=*i*-Pr and R′=$(Bu^tO)_3Si$

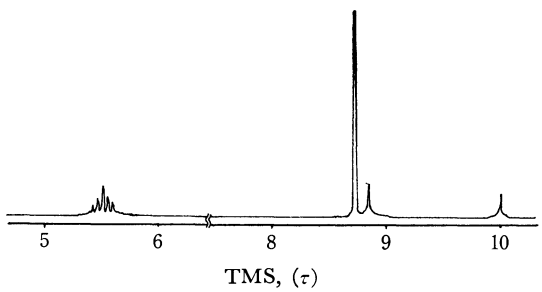

Fig. 1. NMR spectra of cyclic titanosiloxane.

The fact that the reaction of titanium tetraalkoxide with the similar, bifunctional silanediol gave rise to the formation of a polymeric product in one case or a cyclic tetramer in another is thought to be attributed to the difference in the steric hindrance between substituents in the silanediols. Reaction (IV) gave dark reddish, resinous products. These products were treated with active charcoal and activated alumina to give transparent, reddish-orange products which were highly soluble in common organic solvents, able to form a fiber, and resistant to hydrolysis. The results of the elemental analysis were in accordance with the calculated value for a linear structure, 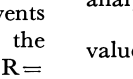 . The molecular-weight determination of the polymeric substances by the vapor-pressure method indicated that the degree of polymerization of the polymer containing the tri-*t*-butoxysiloxy group (about 2) was lower than that with the *t*-butoxy group (27—28). This is probably due to the larger steric effect of the side chain in the former.

As Fig. 2 shows, the decomposition of the polymers takes place at 150 to 200°C and a remarkable weight loss (about 60%) is observed from 200 to 300°C. As compared with the polyalkoxysiloxanes[4]

4) Y. Abe and I. Kijima, This Bulletin, **42**, 1118 (1969).

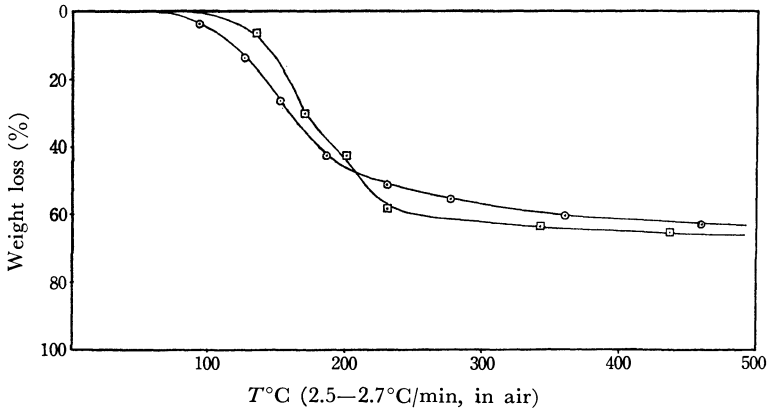

Fig. 2. TGA curve of polybis(acetylacetonato)titanosiloxane.
⊙; $[-Ti(AcAc)_2-O-Si(OBu^t)_2-O-]_n$, ⊡; $[-Ti(AcAc)_2-O-Si[OSi(OBu^t)_3]_2-O-]_n$

and polyalkoxysilanes[5] already reported on, the low thermal stability of the polymers may be attributed to the difference in electronegativity between the heteroatom and silicon in the heterosiloxane bond.

Experimental

All the experiments were carried out under a dry atmosphere or nitrogen purge. The melting points and boiling points were uncorrected.

Materials. Commercially-available titanium tetra-isopropoxide was redistilled before use.[6] The bis(acetylacetonato)di-isopropoxytitanium was obtained by the method described in the literature.[7] The tri-*t*-butoxysilanol and bis(tri-*t*-butoxysiloxy)silanediol were prepared by the method already described.[4] Although di-*t*-butoxysilanediol was obtained by Miner and Bryan,[8] in this work it was prepared by the hydrolysis of di-*t*-butoxydichlorosilane in the presence of aniline: to a solution of 5.0 g (0.281 mol) of water, 26.1 g (0.281 mol) of aniline, and 150 m*l* of ether made homogeneous by adding 50 m*l* of acetone, 34.5 g (0.140 mol) of the dichlorosilane, dissolved in 100 m*l* of dry ether, were stirred in, drop by drop, at from −5 to −10°C. After a 30-min refluxing the aniline hydrochloride was filtered out, and solvent was removed *in vacuo*. The residual white solid was dissolved by adding light petroleum ether. After the precipitate had been removed, the filtrate gave 20.1 g (69%) of needle crystals; mp 101—102°C. Found: C, 47.03; H, 9.79; Si, 13.18%. Calcd for $C_8H_{20}O_4Si$: C, 46.13; H 9.61; Si, 13.46%.

Tris(tri - *t* - butoxysiloxy) - isopropoxytitanium. To a solution of 8.3 g (0.0292 mol) of titanium tetra-*i*-propoxide in 70 m*l* of benzene, 23.1 g (0.0876 mol) of tri-*t*-butoxysilanol were added. The mixture was refluxed for 1 hr, and then the solvent was removed, along with the alcohol formed. On evaporating to dryness *in vacuo*, the residue was recrystallized from *n*-hexane to give 13.4 g (63%) of crystalline plates, mp 157—160°C. Attempts to distil at 250 to 300°C *in vacuo* (1 mmHg) failed because of its decomposition. Found: C, 52.82; H, 10.30; Si, 9.38; Ti, 5.34%. mol wt, 896.

Bis(tri-*t*-butoxysiloxy)di-isopropoxytitanium. A mixture of 29.0 g (0.102 mol) of tri-*t*-butoxysilanol and 100m*l* of benzene was refluxed for 1.5 hr. After the solvent had been removed, along with the alcohol formed, the residue was fractionally distilled to give 41.0 g (60%) of a transparent liquid; bp 161—162°C/1 mmHg, n_D^{20} 1.4304. Found: C, 50.59; H, 10.61; Si, 8.11; Ti, 6.23%; mol wt, 780. Calcd for $C_{30}H_{68}O_{10}Si_2Ti$: C, 51.99; H, 9.88; Si, 8.11; Ti, 6.91%; mol wt, 697.

Bis(tri - *t* - butoxysiloxy)bis(acetylacetonato)titanium. A mixture of 4.7 g (0.0129 mol) of bis(acetylacetonato)di-isopropoxytitanium, 6.8 g (0.0258 mol) of tri-*t*-butoxysilanol, and 60 m*l* of benzene was refluxed for 1 hr. After the subsequent removal of the solvent, the residue was distilled to give 7.7 g (77.5%) of a dark brown liquid, bp 187—188°C/1 mmHg, which solidified at room temperature as soon as distilled; mp 96—98°C. Found: C, 52.41; H, 9.16; Si, 7.39; Ti, 6.12%. Calcd for $C_{34}H_{69}O_{12}Si_2Ti$: C, 52.71; H, 9.07; Si, 7.27; Ti, 6.20%.

Reaction of Titanium Tetra-isopropoxide with Bis(tri-*t*-butoxysiloxy)silanediol. A solution of 4.7 g (0.015 mol) of titanium tetra-isopropoxide and 9.1 g (0.015 mol) of the silanediol in 50 m*l* of benzene was refluxed for 2 hr. The removal of the solvent and subsequent evacuation yielded a white solid (12.7 g), which was recrystallized from benzene to give 5.0 g (44%) of crystalline plates, mp 177—179°C (decomposed). Found: C, 47.67; H, 8.90; Si, 11.22; Ti, 6.65%, mol wt, 1810. Calcd for $C_{60}H_{136}O_{24}Si_6Ti_2$: C, 47.80; H, 9.08; Si, 11.18; Ti, 6.37%; mol wt, 1504.

Preparation of Polybis(acetylacetonato)titanosiloxanes from the Reaction of Bis(acetylacetonato)di-isopropoxytitanium with Silanediols. *From Bis(tri-t-butoxysiloxy)silanediol.* A mixture of 6.3 g (0.0173 mol) of the acetylacetonato chelate, 10.2 g (0.0173 mol) of the diol, and 40 m*l* of toluene was refluxed for 1 hr. After the solvent had been removed, the residue was heated at 110—120°C for 3 hr and then at 150—

5) Presented at the 21st Annual Meeting of the Chemical Society of Japan, Osaka, April, 1968.

6) The authors wish to thank the Matsumoto Pharmaceutical Co. for the supply of titanium tetraalkoxides.

7) A. Yamamoto and S. Kambara, *J. Amer. Chem. Soc.*, **79**, 4344 (1957).

8) C. S. Miner and L. A. Bryan, *Ind. Eng. Chem.*, **39**, 1368 (1947).

160°C for 2 hr more to give 15.7 g of a dark reddish, resinous solid, fusing point, 37—50°C, which was soluble in benzene, *n*-hexane, ether, acetone, and methanol. Attempts to purify this substance by fractional precipitation failed. Therefore, the raw product was subjected to analysis.

Found: C, 47.90; H, 8.81; Si, 9.22; Ti, 10.12%; mol wt, $832 \times n$.

On the other hand, the residue left after the removal of the solvent was heated at 100—120°C under reduced pressure (2—3 mmHg) to give a transparent, highly viscous resinous material. Although the fusing points were raised by heating at elevated temperatures, a remakable discoloration was apt to occur.

From Di-t-butoxysilanediol. After 1 hr's refluxing of a solution of the acetylacetone chelate (7.3 g, 0.0201 mol), the silanediol (4.2 g, 0.0201 mol), and 50 m*l* of toluene, the solvent was removed and the solution heated gave a highly viscous, reddish resinous matter (8.7 g). Due to the difficulty of purification mentioned above, the analytical data were obtained from the crude product.

Found: C, 46.38; H. 7.12; Si, 6.55%; mol wt, 12400. Calcd for $(C_{18}H_{32}O_8SiTi)_n$: C, 47.79; H, 7.13; Si, 6.21%; mol wt, $452 \times n$.

Analysis. The silicon was determined by a method similar to that described by Bradley.[9] The titanium was determined to be titanium dioxide after weighed sample had been decomposed by an aqueous alcohol solution containing ammonia.

We should like to thank Professor Yojiro Tsuzuki for his valuable advice.

9) D. C. Bradley and I. M. Thomas, *J. Chem. Soc.*, **1959**, 3404.

BULLETIN OF THE CHEMICAL SOCIETY OF JAPAN VOL. 43 469—472 (1970)

Anionic Telomerizations of Styrene with Some Aromatic Amines[1)]

Teruzo ASAHARA, Manabu SENŌ and Sadayoshi TANAKA

Institute of Industrial Science, The University of Tokyo, Roppongi, Minato-ku, Tokyo

(Received July 8, 1969)

The anionic telomerizations of styrene with some aromatic amines catalyzed by sodium metal were investigated. *o*-Toluidine, *m*-toluidine, *p*-toluidine, 2,4-xylidine, 2,5-xylidine and 3,4-xylidine were used as the aromatic amines. Each amine reacted with styrene to give an addition product, which was identified as *N*-substituted 2-phenylethylamine. Though both α-hydrogen atoms on α-carbon atoms and hydrogen atoms attached to nitrogen atoms of the aromatic amines are weakly acidic, only the latter hydrogen atoms were detached by alkali species under the present experimental conditions. The formations of the products were discussed from the standpoint of anionic telomerization.

In previous papers, the base-catalyzed reactions of styrene with butylamines[2)] and the telomerizations of this monomer with secondary aliphatic amines[1)] were reported. Wegler and Pieper[3)] investigated the reactions of styrene with various amines in the presence of alkali metal and found that aniline combined with styrene into *N*-phenyl-2-phenylethylamine. Pines and Wunderlich[4)] reported that toluene and ethylbenzene react with styrene in the presence of sodium metal to form monoadducts, 1,3-diphenylpropane and 1,3-diphenylbutane, and diadducts, 1,3,5-triphenylpentane and 1,3,5-triphenylhexane, respectively. Therefore, it is interesting to study which type of compound is produced when aromatic compounds containing both α-hydrogens on α-carbons and an amino group neighboring an aromatic nuclei react with styrene in the presence of alkali matel.

In this paper the reactions of toluidines and xylidines with styrene and the structures of the products will be reported on. The reaction scheme will also be discussed.

Results and Discussion

Reactions of Styrene with Aromatic Amines. *o*-Toluidine, *m*-toluidine, *p*-toluidine, 2,4-xylidine, 2,5-xylidine, and 3,4-xylidine reacted with styrene in the presence of sodium metal to produce *N*-substituted 2-phenylethylamine **1**. The compounds

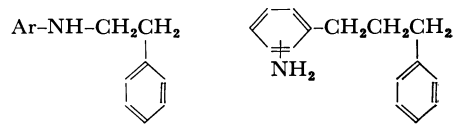

1 **2**

1) Anionic Telomerizations. III. Part II of this series: T. Asahara, M. Senō, S. Tanaka and N. Den, This Bulletin, **42**, 2337 (1969).

2) T. Asahara, M. Senō, S. Tanaka and N. Den, *ibid.*, **42**, 1996 (1969).

3) R. Wegler and G. Pieper, *Chem. Ber.*, **83**, 1 (1950).

4) H. Pines and D. Wunderlich, *J. Amer. Chem. Soc.*, **80**, 6001 (1958).

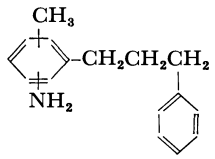

3

of Type **2** and **3** were not produced in the present experiment. The reaction conditions and products are listed in Table 1.

Structure of the Products. The structures of the 1 : 1 addition products obtained in the reactions of styrene with toluidines may be expressed by formula **1** or formula **2**, since both the α-hydro-

Table 1. Reaction products obtained in reactions of styrene with aromatic amines[a)]

Amine	Reaction temp. and time °C	hr	Reaction product		Bp[b)] °C/mmHg	Yield[c)] %
o-Toluidine	150±1	3.0	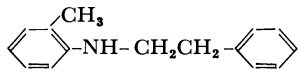	(**1a**)	161—162/4	50.1
m-Toluidine	150±1	3.0	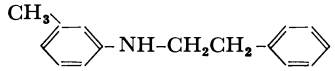	(**1b**)	172—173/4	72.0
p-Toluidine	150±1	3.0	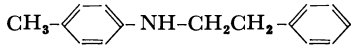	(**1c**)	180—181/4	76.3
2,4-Xylidine	150±1	4.0	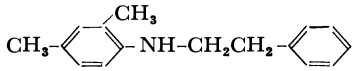	(**1d**)	160—162/2	67.1
2,5-Xylidine	150±1	2.0	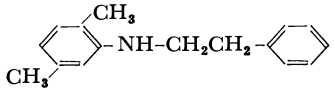	(**1e**)	159—160/2	41.8
3,4-Xylidine	150±1	4.0	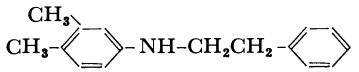	(**1f**)	175—176/2	78.8

a) The molar ratio of styrene to amine was 2 : 1. 0.7 g of sodium was used in each reaction.
b) Boiling points were uncorrected.
c) Yields were calculated on the basis of amine added.

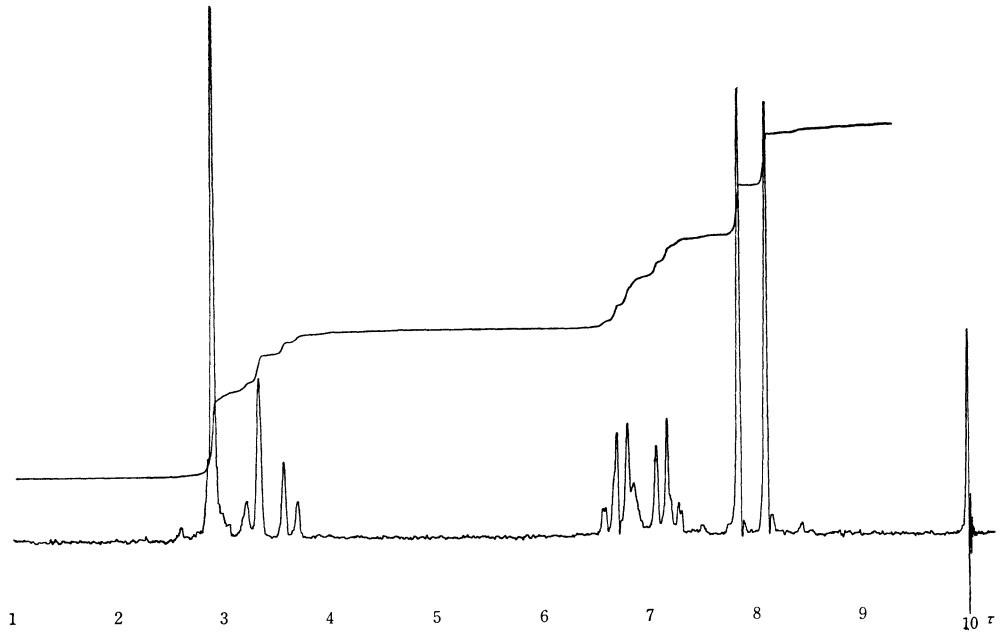

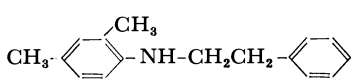

(**1d**)

Fig. 1. The proton NMR spectrum of product **1d**.

gens attached to α-carbon atoms and those connected to the nitrogen of toluidines are weakly acidic. The proton NMR spectrum of each product showed a methyl singlet near 8τ; this is consistent with structure **1**. The reaction products derived from xylidines were analysed in the same way and were identified as **1**. Each product has still six methyl hydrogens and a hydrogen belonging to the –NH– group, whose signal (near 6.8τ) disappeared in the presence of heavy water. The proton NMR spectrum of **1d** is shown in Fig. 1 as an example.

Reaction Scheme. In the first step, sodium metal may add to styrene **4** to give an organometallic compound **5**, which then transmetalates with an aromatic amine.

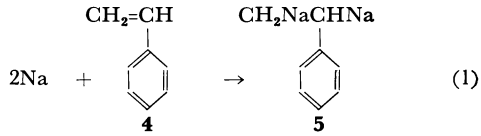

(1)

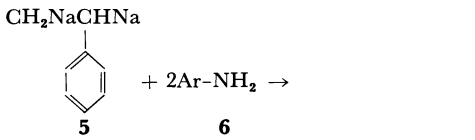

(2)

Compound **7** combines with styrene to produce an organosodium salt **8**, and **8** reacts with the amine **6**. Thus, the product **1** is obtained.

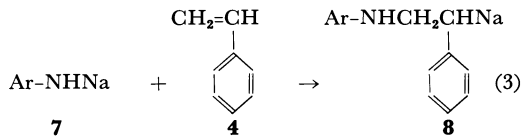

(3)

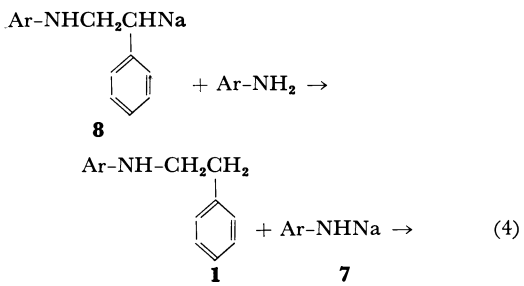

(4)

The organosodium compound **8** may react with styrene, and styrene may compete with the amine **6** for the sodium salt **8**, but the rate of reaction (5) is far slower than that of reaction (4) in the present experiment.

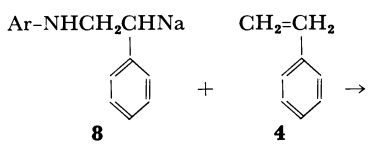

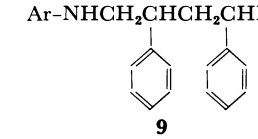

(5)

Carbanions such as **5** and **8** react more readily with hydrogen atoms attached to the nitrogen than with those of the methyl group in the following reactions:

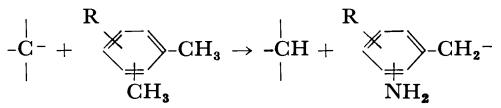

(6)

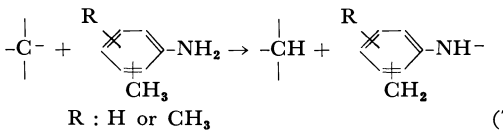

R : H or CH_3 (7)

Following the concept of proton-donors and proton-acceptors, carbanions are bases and hydrogen compounds are acids, and the acid strength of the methyl hydrogens is weaker than that of the hydrogens of amino group. Therefore, reaction (7) exceeds reaction (6) in the reaction rate, and not compound **2** but compound **1** is obtained.

If an aromatic amine and styrene act as a telogen and a taxogen, respectively, the following equation of the telomerization reaction may be presented:

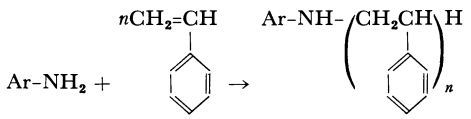

(8)

On combining Eqs. (3) and (4), we obtain Eq. (9):

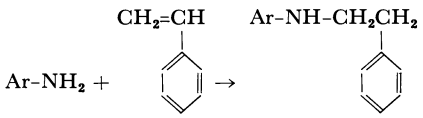

(9)

Thus, reaction (9) may be regarded as a special case among anionic telomerization reactions (8). In other words, when a chain-transfer reaction is much faster than a propagation reaction, anionic telomerization reaction of the type (9) are realized. An organosodium compound, Ar–NNa–CH_2CH_2– , which is a weaker base than Ar–NHNa, may be too stable for another telomerization reaction (10) to take place.

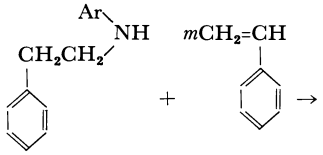

Table 2. Characterization of reaction products

Structural formula Molecular formula		Elementary analysis	Calcd	Found	Molecular weight Calcd	Mass	VPO	Refractive index (25.0°C)
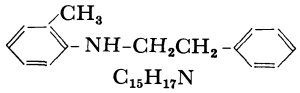 $C_{15}H_{17}N$	(**1a**)	C H N	85.26 8.11 6.63	85.35 8.27 6.74	211.29	211	208	1.5883
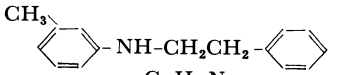 $C_{15}H_{17}N$	(**1b**)	C H N	85.26 8.11 6.63	85.18 8.20 6.76	211.29	211	208	1.5887
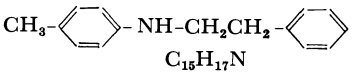 $C_{15}H_{17}N$	(**1c**)	C H N	85.26 8.11 6.63	85.45 8.34 6.93	211.29	211	212	—
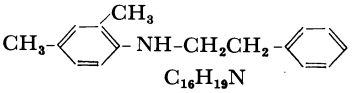 $C_{16}H_{19}N$	(**1d**)	C H N	85.28 8.50 6.22	85.53 8.47 5.96	225.32	225	223	1.5788
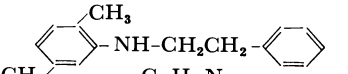 $C_{16}H_{19}N$	(**1e**)	C H N	85.28 8.50 6.22	85.40 8.34 6.28	225.32	225	220	1.5801
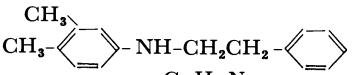 $C_{16}H_{19}N$	(**1f**)	C H N	85.28 8.50 6.22	85.21 8.60 5.93	225.32	225	228	1.5849

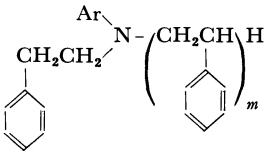

(10)

Experimental

Physical Data. The molecular-weight determination by vapor-pressure osmometry was carried out in benzene at 37°C on a Hewlett Packard Model 302 vapor-pressure osmometer. The proton NMR spectra were recorded on a Hitachi Model R-20A spectrophotometer, using tetramethylsilane as the internal standard in carbon tetrachloride. For mass spectral analysis, a Hitachi RMU-6D mass spectrometer was employed, with the electron beam energy at 80 eV.

Material. The styrene was dried over anhydrous magnesium sulfate and was distilled under reduced pressure. All the aromatic amines except 3,4-xylidine were dried over sodium hydroxide and were distilled *in vacuo*. The 3,4-xylidine was recrystallized from ligroin.

***N*-(2,4-dimethylphenyl)-2-phenylethylamine (1d).** To 37.0 g of 2,4-xylidine and 0.7 g of finely-sliced sodium metal which had been heated to 150±1°C, 62.5 g of styrene was added, drop by drop, over a 0.8-hr; the reaction was then continued for a further 3.2 hr. After 55 m*l* of water and 50 m*l* of benzene had been added to the reaction mixture, the solution was neutralized with hydrochloric acid and washed with water, and the organic layer was separated, dried, and distilled *in vacuo* to give 45.4 g (67.1%) of the product, **1d**, at 160—162°C/2 mmHg. Some parts of the styrene and amines added were recovered unreacted by the distillation, and the residues were very small in quantity.

The other products were synthesized by similar procedures. Table 2 summarizes the results on the characterization of the compounds.

BULLETIN OF THE CHEMICAL SOCIETY OF JAPAN VOL. 43 473—480 (1970)

Anomalous Products Obtained by Nitration of Pentamethylbenzene, Pentaethylbenzene, and Some Mixed Penta-alkylbenzenes[1)]

Hitomi SUZUKI and Kiyomi NAKAMURA

Department of Chemistry, Faculty of Science, Kyoto University, Sakyo-ku, Kyoto

(Received July 9, 1969)

Pentamethylbenzene has been nitrated with fuming nitric acid to give mainly a mixture of nitropentamethylbenzene and 2,3,4,5-tetramethylbenzyl nitrate. Other isomeric nitrates were not formed in any significant amount. 6-Nitro-2,3,4,5-tetramethylbenzyl nitrate, 2,3,4,5-tetramethylbenzyl alcohol, 2,3,4,5-tetramethylbenzaldehyde, 2,2′,3,3′,4,4′,5,5′,6-nonamethyldiphenylmethane, and 2,2′,3,3′,4,4′,5,5′-octamethyl-6-nitroxymethyldiphenylmethane were the minor products. Pentaethylbenzene gave a mixture of nitropentaethylbenzene and α-methyl-2,3,4,5-tetraethylbenzyl nitrate along with some products of oxidation. Preferential side-chain attack occurred at the primary alkyl group *ortho* to the unsubstituted ring position. Thus, 1-methyl-2,3,4,5-tetraethylbenzene was found to give benzyl nitrate and α-methylbenzyl nitrate nearly in equal amounts, while 3-methyl-1,2,4,5-tetraethylbenzene was found to give them in an approximate ratio of 1 : 3. 1,3,4-Trimethyl-2,5-diisopropylbenzene underwent extensive nitrodealkylation, and 3,4-dimethyl-2,5-diisopropylbenzyl nitrate was the only side-chain substituted product identified.

Electrophilic substitution of polysubstituted aromatic systems often gives unusual results which have deviated considerably from the established pathways for lightly substituted compounds. One of such examples is the nitration of penta-alkylbenzenes, where the action of the nitrating agent usually results in the replacement of one of the alkyl groups to form dinitrotetra-alkylbenzenes. Nitration of pentamethylbenzene to dinitroprehnitene was first observed by Gottschalk,[2)] who suggested that hydrocarbon underwent disproportionation to prehnitene and hexamethylbenzene under the influence of acid, and that dinitroprehnitene was formed by nitration of prehnitene. Pentaethylbenzene was also found to behave similarly towards the nitrating agent, giving 3,6-dinitro-1,2,4,5-tetraethylbenzene.[3)] Reinvestigation of the reaction, however, revealed that the products were not so simple as had been described in literature.[4,5)] The present paper deals with anomalous products from nitration of pentamethylbenzene, pentaethylbenzene, and some related mixed penta-alkylbenzenes.

Results and Discussion

When pentamethylbenzene was nitrated at −5—0°C with an excess of fuming nitric acid in chloroform or methylene chloride, the product was a light brown oily solid, the major component of which was readily identified as a benzyl nitrate from very strong infrared bands at 1271 and 1624 cm^{-1} ($-ONO_2$), and a prominent PMR peak at 4.63 τ (CH_2). Weak carbonyl and hydroxylic absorptions were also observed. Careful chromatographic treatment of the crude product on alumina gave unchanged hydrocarbon, polymethyldiphenylmethanes (XV and XXI), nitropentamethylbenzene, and tetramethylbenzyl nitrates from the light petroleum eluates; 6-nitro-2,3,4,5-tetramethylbenzyl nitrate (XII) and 2,3,4,5-tetramethylbenzaldehyde (XIII) from the benzene eluates; and a substantial amount of 2,3,4,5-tetramethylbenzyl alcohol (XI) from the ether eluates. Undoubtedly the alcohol was derived from the benzyl nitrate through the hydrolysis during the elution. Thus, the original mixture was composed mainly of 2,3,4,5-tetramethylbenzyl nitrate (III), the identity of which was further confirmed by comparison with the authentic specimen, prepared from prehnitene (I) through chloromethylation and subsequent treatment of the chloride (II) with silver nitrate in acetonitrile (Fig. 1). Other isomeric tetramethylbenzyl nitrates were also formed, but only in slight amount (less than 5%) as compared to the 2,3,4,5-tetramethylbenzyl isomer. Analysis of these minor products were carried out by gas-liquid chromatography and PMR spectroscopy. Since benzyl nitrates were not thermally so stable, gas-chromatographic analysis was carried out after their conversion into acetates. 2,3,4,6-Tetramethylbenzyl nitrate (IV) greatly exceeded 2,3,5,6-tetramethylbenzyl nitrate (V) in amount.

1) The Reaction of Polysubstituted Aromatics. Part XIV. Part XIII: This Bulletin, **42**, 2618 (1969).
2) M. Gottschalk, *Ber.*, **20**, 3286 (1887).
3) L. I. Smith and C. O. Guss, *J. Amer. Chem. Soc.*, **62**, 2635 (1940).
4) R. Willstätter and H. Kubli, *Ber.*, **42**, 4151 (1909).
5) L. I. Smith and S. A. Harris, *J. Amer. Chem. Soc.*, **57**, 1289 (1935).

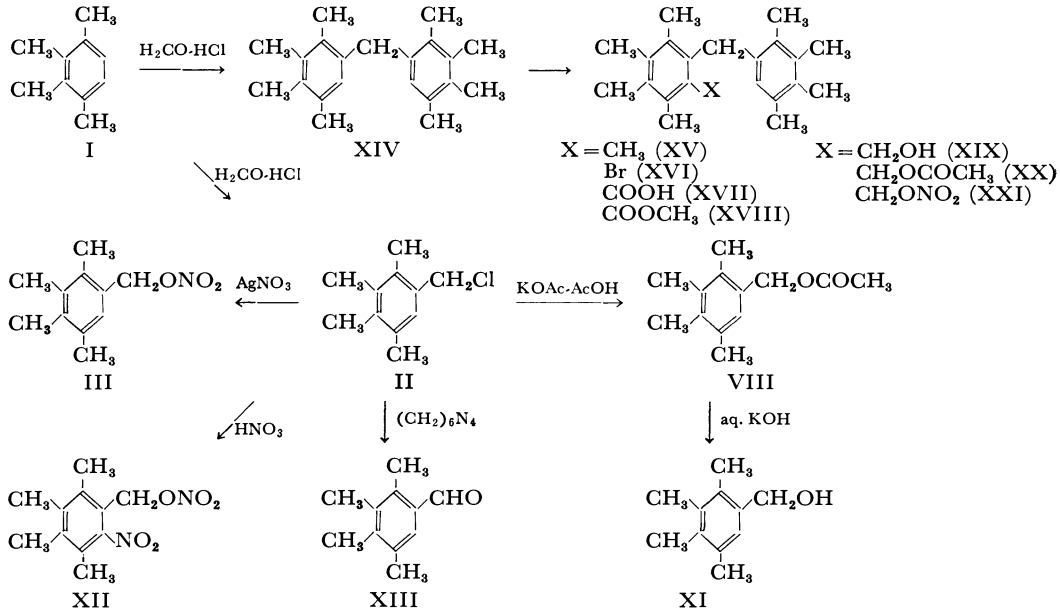

Fig. 1

PMR spectra of the light petroleum eluates showed a pair of weak, ill-resolved peaks of relative areas 1 to 2, at 3.87 and 6.05 τ. As is apparent from the structural correlations,[6] this spectral pattern strongly suggests the presence of polyalkyldiphenylmethanes. Of these the minor component was concentrated in the earlier eluates and readily identified as 2,2′,3,3′,4,4′,5,5′,6-nonamethyldiphenylmethane (XV) by spectral comparison with an authentic specimen. Another diphenylmethane with an extra peak at 4.41 τ could be isolated from a mixture of benzyl nitrates through their conversion into acetates, followed by chromatography on alumina. The later eluates gave a small amount of fine prisms, mp 170—172°C, which had the formula $C_{24}H_{32}O_2$ and showed a sharp infrared peak at 1733 cm^{-1}; PMR peaks at 8.18, 7.71—7.94, 6.09, 5.05, and 4.05 τ with relative areas 3 : 24 : 2 : 2 : 1. The peak at 8.18 τ is due to the acetoxy group, and the peaks at 7.71—7.94 τ due to eight methyl groups of two phenyl groups. The peaks at 5.05 and 6.09 τ arise from the methylene group. The remaining peak at 4.05 τ corresponds to an aromatic proton, the appearance of which at high field indicates its presence *ortho* to the methylene bridge.[6] The above spectral data agree with the structure 2,2′,3,3′,4,4′,5,5′-octamethyl-6-acetoxydiphenylmethane (XX), and therefore the original diphenylmethane is formulated as 2,2′,3,3′,4,4′,5,5′-octamethyl-6-nitroxymethyldiphenylmethane (XXI). These diphenylmethanes were probably derived from the self-condensation of III, or from the condensation of III with pentamethylbenzene. XV may also be derived from XXI through the hydride ion abstraction, as has been demonstrated by the easy conversion of pentamethylbenzyl compounds into hexamethylbenzene.[7] In fact, 2,3,4,5-tetramethylbenzyl chloride (II) heated with trifluoroacetic acid was found to give some XV besides other products.

2,3,4,5-Tetramethylbenzaldehyde (XIII) probably arose from the acid-[8] or base-catalysed[9] conversion of nitrate into aldehyde, and was isolated as a semicarbazone. The semicarbazone showed double melting which may be characteristic for the ones derived from tetramethylbenzaldehydes.[10] In contrast to nitration by mixed acid, the use of fuming nitric acid yielded dinitroprehnitene only in a small amount.

Pentaethylbenzene could be nitrated by fuming nitric acid to give a pale yellow syrup, the main component of which was again a benzyl nitrate since the product showed strong infrared bands at 1275 and 1627 cm^{-1} ($-ONO_2$) and PMR peaks at 8.26 (CH_3, d) and 2.83 τ (CH, q). Absorption due to carbonyl and hydroxylic groups was weak. Repeated chromatography of the crude product on alumina, however, gave 2,3,4,5-tetraethylstyrene (XXVII) accompanied by some unchanged hydrocarbon and nitropentaethylbenzene from the light petroleum eluates; an orange-yellow syrup with a strong carbonyl absorption from the benzene

6) H. Suzuki, This Bulletin, **42**, 2618 (1969).

7) H. Suzuki and K. Nakamura, *ibid.*, **41**, 2197 (1968).

8) S. D. Ross, E. R. Coburn and M. Finkelstein, *J. Org. Chem.*, **33**, 585 (1968).

9) J. W. Baker and A. J. Neale, *J. Chem. Soc.*, **1954**, 3225; J. W. Baker and T. G. Heggs, *ibid.*, **1955**, 616.

10) L. I. Smith and J. Nichols, *J. Org. Chem.*, **6**, 502 (1941).

Table 1. PMR spectral data for tetramethylbenzyl acetates, chlorides, and nitrates

Compound	Mp or bp* (°C)	PMR spectra (in CCl_4, τ)			
		ArH	CH_2	CH_3**	CH_3COO
2,3,4,5-Tetramethylbenzyl series					
Acetate	46—48	3.10	4.97	7.72 (1), 7.78 (2), 7.83 (1)	7.99
Chloride	44—46 (146—148/18 mmHg)	3.21	5.53	7.74 (1), 7.79 (1), 7.85 (1) 7.86 (1)	
Nitrate	45—46	3.07	4.68	7.76 (2), 7.83 (2)	
2,3,4,6-Tetramethylbenzyl series					
Acetate	(166—167/22 mmHg)	3.22	4.89	7.72 (1), 7.79 (2), 7.89 (1)	8.05
Chloride	34—36 (147—149/20 mmHg)	3.25	5.43	7.69 (1), 7.72 (1), 7.80 (1) 7.88 (1)	
Nitrate	42—44	3.19	4.52	7.67 (1), 7.75 (2), 7.85 (1)	
2,3,5,6-Tetramethylbenzyl series					
Acetate	92—93	3.10	4.82	7.77 (4)	8.00
Chloride	67—68 (142—144/20 mmHg)	3.21	5.43	7.76 (2), 7.82 (2)	
Nitrate	115—116	3.04	4.42	7.75 (4)	

* Bp in parentheses.
** Numerals in parentheses refer to the number of methyl groups.

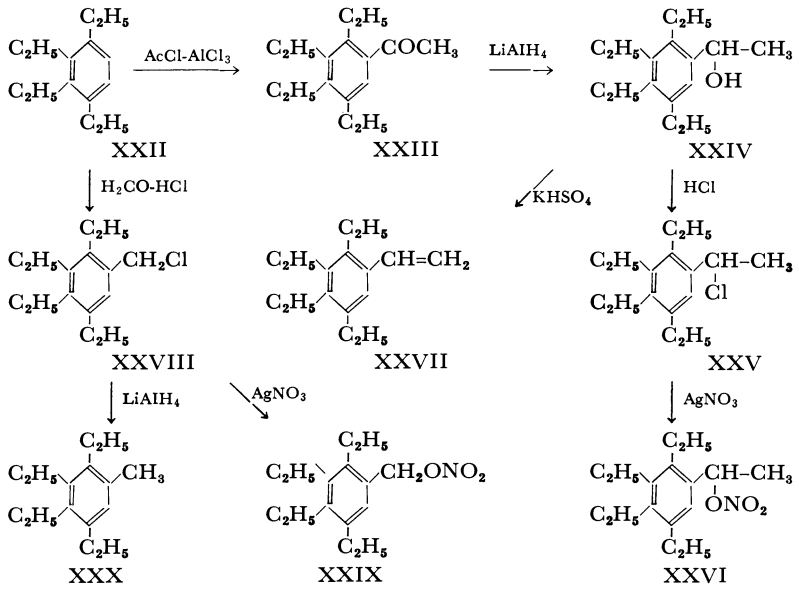

Fig. 2

eluates; and finally a considerable amount of α-methyl-2,3,4,5-tetraethylbenzyl alcohol (XXIV) from the ether eluates. Therefore, the original nitrate was formulated as α-methyl-2,3,4,5-tetraethylbenzyl nitrate (XXVI) which underwent either hydrolysis to alcohol, or β-hydrogen elimination to the unsaturated hydrocarbon during chromatographic treatment. The structure proof of these products was made by a series of syntheses starting from 1,2,3,4-tetraethylbenzene (Fig. 2). The conversion of the α-methylbenzyl chloride (XXV) into the nitrate (XXVI) by treatment with silver nitrate in acetonitrile was not as simple as expected, and gave a mixture of several substances, although nitrate was still the main product.

With pentamethylbenzene and pentaethylbenzene, attack by nitric acid on the side-chain was almost limited to the alkyl groups adjacent to the unsubstituted position. The nuclear-to-lateral migration of the nitro group has been proposed

for such side-chain nitrooxylation of penta-alkylbenzenes.[11]

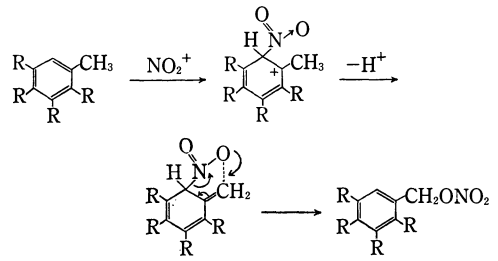

The preferred formation of the 2,3,4,5-tetra-alkylbenzyl nitrate over the 2,3,4,6-tetra-alkyl- and 2,3,5,6-tetra-alkyl isomers may be explained by the greater contribution of the intermediate benzenonium ions XXXV and XXXVII than XXXVI and XXXVIII, and the easier proton removal from the least hindered alkyl groups adjacent to the free ring position.

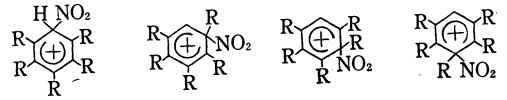

XXXV XXXVI XXXVII XXXVIII

High selectivity in the side-chain substitution is probably concerned with the slow step of the proton transfer from the alkyl groups of the benzenonium intermediate. Kreienbuhl and Zollinger reported that pentamethylbenzene rapidly formed an adduct with nitronium tetrafluoroborate, but showed lower reactivity towards nitration than benzene.[12] Koptyug, Krysin, and Gorfinkel also showed the nitration of 2,3,4,5,6-pentamethyldiphenyl to occur at the unsubstituted ring.[13] These results indicate that the decomposition of benzenonium ion into any side-chain products is a slower step than the nuclear hydrogen replacement, and that both processes can only compete more effectively in such a crowded system as penta-alkylbenzene.

The importance of the steric role in determining the orientation of the side-chain substitution may be understood from the nitration of some mixed penta-alkylbenzenes. The synthesis of these hydrocarbons was carried out by the routes illustrated in Figs. 2 and 3. The PMR spectra of the nitration product from 1-methyl-2,3,4,5-tetraethylbenzene (XXX) showed a methylene singlet at 4.57 τ ($-CH_2ONO_2$) and a methine quartet at 3.79 τ ($-CH(ONO_2)CH_3$), the ratio of signal intensities being 1.8 : 1, while the product from

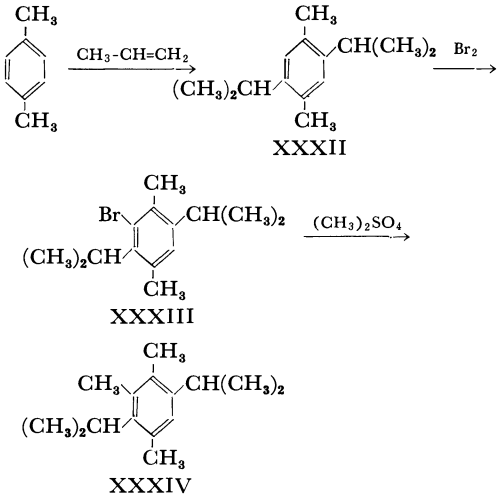

Fig. 3

3-methyl-1,2,4,5-tetraethylbenzene (XXXI) showed these signals at 4.43 and 3.78 τ with relative areas of 1 : 1.9, indicating the preferred proton release from the least hindered side-chain. Appearance of the methine signals nearly at the same position as that (3.82 τ) of XXVI indicates the attack by nitric acid on the ethyl group adjacent to the unoccupied ring position. Otherwise, the signal will appear at lower field owing to the van der Waals interactions between the $-CH(ONO_2)CH_3$ group and the two ortho alkyl groups.[14] A large downfield shift of the ring proton signal relative to the parent hydrocarbons is also consistent with the presence of $-CH(ONO_2)CH_3$ group in its vicinity. In XXX the methyl group is somewhat more reactive than the ethyl group, but the order is reversed in XXXI.

Overcrowding in pentaethylbenzene is readily understood from the marked difference in the ability of hexamethylbenzene and hexaethylbenzene to form complexes with Lewis acids.[15] Thus, the increased attack on the 3-alkyl group of XXXI as compared to XXX may be explained in terms of the increasing contribution of ion XXXVII due to the more favorable steric requirements in XXXI with respect to XXX for the access of the nitronium ion to the 2-position (Fig. 4). Attachment of the nitronium ion at the 2-position of XXXI is also facillitated not only by the favorable orientation of alkyl groups to stabilize ion XXXVII, but also by the relief of the steric strain arising from the vicinal disposition of five alkyl groups.

11) H. Suzuki, K. Nakamura and K. Maruyama, This Bulletin, **41**, 1487 (1968). Also *cf.* H. Suzuki and Y. Tamura, *Chem. Commun.*, **1969**, 244.

12) P. Kreienbuhl and H. Zollinger, *Tetrahedron Lett.*, **1965**, 1739.

13) V. A. Koptyug, A. P. Krysin and M. I. Gorfinkel, *Izvest. SO AN USSR, Ser. Khim.*, **1967** 61.

14) W. A. Gibbons and V. M. S. Gil, *Mol. Phys.*, **9**, 163 (1965).

15) L. J. Andrews and R. M. Keefer, *J. Amer. Chem. Soc.*, **74**, 4500 (1952); M. Tamres, D. R. Virzi and S. Searles, *ibid.*, **75**, 4358 (1953). Also *cf.* L. J. Andrews and R. M. Keefer, *ibid.*, **77**, 2545 (1955).

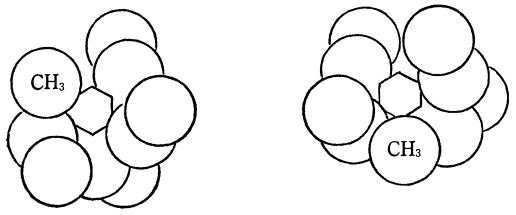

XXX XXXI

Fig. 4

The side-chain nitrooxylation seems to be limited to the methyl and ethyl groups; the isopropyl group remains unchanged or is replaced by a nitro group during the reaction. 2,5-Diisopropyl-1,3,4-trimethylbenzene underwent extensive nitrodealkylation, and the alumina chromatography of the product gave mainly a mixture of nitro compounds. 3,4-Dimethyl-2,5-diisopropylbenzyl alcohol was obtained from the ether eluates as the sole side-chain substituted product identified. The methyl signal due to $-C(ONO_2)(CH_3)_2$ is expected to appear at about 8.0—8.2 τ, between the two clusters of aliphatic and aromatic methyl peaks. Since the PMR spectrum of the reaction product showed only weak absorption in this region, we may conclude that side-chain substitution has not occurred to any significant extent in the isopropyl group. Because of the enhanced stability of the cation, as well as the decreased ease of hyperconjugative proton release from the isopropyl group, nitrodealkylation in this system comes to compete well with the side-chain substitution.

Experimental

Infrared spectra were determined in Nujol on a DS-402G spectrophotometer and only prominent peaks are recorded; PMR spectra were obtained in deuteriochloroform with a Varian A-60A spectrometer against internal tetramethylsilane.

Pentamethylbenzene (mp 50—52°C),[16] pentaethylbenzene (bp 155—156°C/24 mmHg),[17] 1,2,3,4-tetraethylbenzene (bp 134—136°C/23 mmHg),[18] and 1,2,4,5-tetraethylbenzene (bp 129—132°C/23 mmHg)[19] were prepared as described in literature.

2,3,4,5-Tetramethylbenzyl Nitrate (III). A warm solution of silver nitrate (10.2 g) in acetonitrile (30 m*l*) was added all at once to a magnetically stirred solution of 2,3,4,5-tetramethylbenzyl chloride (9.2 g)[20] in acetonitrile (20 m*l*). The mixture was stirred for several hours, and the silver chloride was filtered. After removal of the solvent in a vacuum, the residue was crystallized from light petroleum to yield 9.2 g (88%), mp 45—46°C. IR: 712, 751, 760, 811, 858, 882, 888, 962, 1269 ($-ONO_2$), 1289, 1620, and 1635 cm^{-1} ($-ONO_2$).

Found: C, 63.1; H, 7.4; N, 6.7%. Calcd for $C_{11}H_{15}NO_3$: C, 63.1; H, 7.2; N. 6.7%.

2,3,4,6-Tetramethylbenzyl Nitrate (IV, mp 42—44°C) and **2,3,5,6-Tetramethylbenzyl Nitrate** (V, mp 115—116°C) were prepared in a similar way from 2,3,4,6-tetramethylbenzyl chloride (VI)[21] and 2,3,5,6-tetramethylbenzyl chloride (VII)[22], respectively. The former was less stable than the other two isomers, and underwent slow decomposition on storage under diffused light.

IV: IR; 715, 755, 823, 860, 904, 1115, 1134, 1270 ($-ONO_2$), and 1631 cm^{-1} ($-ONO_2$). Found: C, 63.4; H, 7.3%. Calcd for $C_{11}H_{15}NO_3$: C, 63.1; H, H, 7.2%.

V: IR; 710, 759, 874, 895, 964, 1017, 1273 ($-ONO_2$), 1299, and 1614 cm^{-1} ($-ONO_2$). Found: C, 62.9; H, 7.2%. Calcd for $C_{11}H_{15}NO_3$: C, 62.9; H, 7.2%.

2,3,4,5-Tetramethylbenzyl Acetate (VIII). A mixture of II (3 g), sodium acetate (4.4 g), and acetic acid (7.5 g) was heated under gentle reflux for 6—7 hr. The reaction mixture was diluted with water, extracted with ether, washed with dilute sodium bicarbonate, and dried ($MgSO_4$). The ether was evaporated and the residue was crystallized from light petroleum to give colorless plates, mp 46—48°C. IR; 872, 920, 961, 1026, 1241 ($-O-COCH_3$), and 1732 cm^{-1} ($-COCH_3$).

Found: C, 75.8; H, 9.0%. Calcd for $C_{13}H_{18}O_2$: C, 75.7; H, 8.8%.

The above procedure applied to VI and VII gave **2,3,4,6-tetramethylbenzyl acetate (IX**, bp 166—167°C/22 mmHg) and **2,3,5,6-tetramethylbenzyl acetate (X**, mp 92—93°C), respectively.

IX: IR; 864, 955, 1021, 1233 ($-O-COCH_3$), and 1739 cm^{-1} ($-COCH_3$). Found: C, 75.8; H, 9.2%. Calcd for $C_{13}H_{18}O_2$: C, 75.7; H, 8.8%.

X: IR; 876, 927, 956, 1019, 1077, 1234 ($-O-COCH_3$), and 1733 cm^{-1} ($-COCH_3$). Found: C, 75.4; H, 8.9%. Calcd for $C_{13}H_{18}O_2$: C, 75.7; H, 8.8%.

2,3,4,5-Tetramethylbenzyl Alcohol (XI). The acetate was dissolved in ethanol and hydrolysed with aqueous potassium hydroxide under gentle reflux. The mixture, when poured into water, gave alcohol, which was crystallised from ethanol to give colorless needles, mp 81—82°C. IR; 995, 1025, 1076, 3256, and 3338 cm^{-1}; PMR, 7.88 (CH_3, m), 7.6 (-OH, variable), 5.65 (CH_2), and 3.19 τ (ArH).

Found: C, 79.8; H, 9.9%. Calcd for $C_{11}H_{16}O$: C, 80.4; H, 9.8%.

6-Nitro-2,3,4,5-tetramethylbenzyl Nitrate (XII). A solution of II (3.7 g) in chloroform (10 m*l*) was carefully nitrated at 0—2°C with fuming nitric acid (d= 1.50, 6.5 g). Quenching with water and removal of the solvent gave a syrupy product, which gave nitrate from ethanol as pale yellow leaflets, mp 100—101°C. Yield was poor. IR; 708, 759, 844, 877, 975, 1277 ($-ONO_2$), 1535 ($-NO_2$), and 1636 cm^{-1} ($-ONO_2$); PMR, 7.83 (CH_3), 7.71 (2 CH_3), 7.66 (CH_3), and 4.64 τ (CH_2).

Found: C, 52.0; H, 5.8; N, 10.9%. Calcd for $C_{11}H_{14}N_2O_5$: C, 52.0; H, 5.6; N, 11.0%.

16) "Organic Syntheses," Coll. Vol. II, p. 248 (1948).
17) L. I. Smith and C. O. Guss, *J. Amer. Chem. Soc.*, **62**, 2631 (1940).
18) L. I. Smith and C. O. Guss, *ibid.*, **62**, 2625 (1940);
19) N. Rabjohn, J. W. Fronabarger and W. W. Linstromberg, *J. Org. Chem.*, **20**, 271 (1955).
20) F. Bennington, R. D. Morin and L. C. Clark, *ibid.*, **23**, 2034 (1958).
21) R. C. Fuson and C. A. Sperat, *J. Amer. Chem. Soc.*, **63**, 2643 (1941).
22) R. R. Aitken, G. M. Badger and J. W. Cook, *J. Chem. Soc.*, **1950**, 331.

2,3,4,5-Tetramethylbenzaldehyde (XIII). To a mixture of II (15 g) and ethanol (65 ml) was added with shaking hexamine (12 g) and water (15 ml). The mixture became pale yellow, and the chloride disappeared. After being stood overnight, an additional 50 ml of water was added, and the mixture was heated under reflux for 3 hr, poured into water, and the oily product was extracted with ether. Removal of the solvent, followed by distillation under reduced pressure gave aldehyde boiling at 159—160°C/23 mmHg, which soon solidified to crystalline mass, mp 39—43°C. IR; 755, 792, 836, 887, 1004, 1082, 1208, 1276, 1563, 1596, and 1692 cm^{-1}; PMR, 7.78 (2 CH_3), 7.67 (CH_3), 7.52 (CH_3), and 2.76 τ (ArH).

Found: C, 81.0; H, 9.1%. Calcd for $C_{11}H_{14}O$: C, 81.5; H, 8.6%.

The semicarbazone crystallized from ethanol as white needles. It melted at 209—210°C to a liquid which quickly solidified and remelted at 235—242°C with decomposition. Similar phenomena were reported for semicarbazones from 2,3,4,6-tetramethyl- and 2,3,5,6-tetramethylbenzaldehydes.[10]

Found: C, 65.5; H, 7.9%. Calcd for $C_{12}H_{17}N_3O$: C, 65.7; H, 7.8%.

6-Bromo-2,2',3,3',4,4',5,5'-octamethyldiphenylmethane (XVI). A solution of bromine (13 g) in chloroform (30 ml) was added dropwise to the stirred mixture of 2,2',3,3',4,4',5,5'-octamethyldiphenylmethane (XIV, 21 g)[23] and chloroform (100 ml) using a small amount of iodine as catalyst. Bromination proceeded to completion within a short time. The organic layer was washed with dilute sodium bicarbonate and dried ($CaCl_2$). The solvent was evaporated off to leave white crystals (27.2 g), mp 179—182°C. Chromatography on alumina using ligroin as eluant could raise the mp up to 187—189°C, but some dibromide could not be throughly removed from XVI because of the slight difference in solubility in ordinary solvents.

Found: C, 68.8; H, 7.4%. Calcd for $C_{21}H_{27}Br$: C, 70.2; H, 7.5%.

2,2',3,3',4,4',5,5'-Octamethyldiphenylmethane-6-carboxylic Acid (XVII). The Grignard reagent was prepared from a mixture of XVI (17 g), magnesium turnings (2.7 g), and dry tetrahydrofuran (150 ml) by the dropwise addition of ethyl bromide (10.9 g) over a period of 2 hr. The mixture was heated at 50—55°C for 3 hr, and then poured onto crushed dry ice. Dilute hydrochloric acid was added to dissolve the magnesium salt, and the tetrahydrofuran was evaporated off. The precipitated solid was dissolved in dilute sodium hydroxide and after filtration over Norit was reprecipitated with hydrochloric acid. Recrystallization from ethanol gave prisms (12 g, 78%), mp 231—232°C. IR, 880, 937, 1045, 1089, 1192, 1216, 1281, 1305, 1696 (-CO), and 3430 cm^{-1} (-OH); PMR, 8.02 (2 CH_3), 7.98 (CH_3), 7.93 (3 CH_3), 7.83 (3 CH_3) 7.75 (CH_3), 6.25 (CH_2), and 4.04 τ (ArH).

Found: C, 81.7; H, 8.9%. Calcd for $C_{22}H_{28}O_2$: C, 81.4; H, 8.9%.

Treatment of the acid XVII with ethereal solution of diazomethane gave **2,2',3,3',4,4'5,5'-octamethyl-6-carbomethoxydiphenylmethane (XVIII)**, mp 165—166°C.

Found: C, 81.9; H, 9.0%. Calcd for $C_{23}H_{30}O_2$: C, 81.7; H, 8.9%.

2,2',3,3',4,4',5,5'-Octamethyl-6-hydroxymethyldiphenylmethane (XIX). The direct reduction of the carboxylic acid XVII with lithium aluminum hydride could not be accomplished. Methyl ester XVIII dissolved in dry tetrahydrofuran was reduced with lithium aluminum hydride to give alcohol XIX, which was crystallized from ligroin and melted at 195—196°C. IR, 724, 841, 869, 985, 1032, 1068, and 3300 cm^{-1}; PMR, 7.92 (2 CH_3), 7.86 (CH_3), 7.73 (3 CH_3), 7.66 (2 CH_3), 6.08 (CH_2), 5.58 (CH_2O), and 3.99 τ (ArH).

Found: C, 85.0; H, 9.9%. Calcd for $C_{23}H_{30}O$: C, 85.1; H, 9.7%.

Alcohol XIX was readily acetylated to yield **2,2',3,3',4,4',5,5'-octamethyl-6-acetoxymethyldiphenylmethane (XX)**, mp 175—176°C.

Found: C, 81.7; H, 9.1%. Calcd for $C_{24}H_{32}O_2$: C, 81.8, H, 9.1%.

2,3,4,5-Tetraethylacetophenone (XXIII). To the preformed aluminum chloride (18 g)-acetyl chloride (12 g) complex[24] in carbon tetrachloride (50 ml), a solution of 1,2,3,4-tetraethylbenzene (XXII, 25 g) in the same solvent (50 ml) was added at 0—10°C over a period of 1 hr and the reddish brown mixture was stirred for 4—5 hr, then poured into dilute hydrochloric acid. The organic layer was washed with dilute sodium carbonate followed by water, and dried ($CaCl_2$). The solvent was removed and the residue was distilled to give the ketone (21 g, 68%) as nearly colorless liquid, bp 177—178°C/37 mmHg. IR, 864, 881, 957, 1057, 1160, 1229, 1273, 1352, 1375, 1447, 1548, 1590, and 1684 cm^{-1}; PMR, 8.7—9.0 (4 CH_3, m), 7.55 (-$COCH_3$), 7.0—7.7 (4 CH_3, m), and 2.84 τ (ArH).

Prolonged treatment of the ketone with a sodium acetate-buffered solution of semicarbazide hydrochloride in aqueous methanol separated 2,3,4,5-tetraethylacetophenone semicarbazone as white needles, mp 177—181°C.

Found: C, 70.7; H, 9.7; N, 14.5%. Calcd for $C_{17}H_{27}N_3O$: C, 70.6; H, 9.4; N, 14.5%.

***α*-Methyl-2,3,4,5-tetraethylbenzyl Alcohol (XXIV).** To a suspension of lithium aluminum hydride (2.8 g) in dry ether (100 ml) was added, dropwise and with stirring, XXIII (17 g) in dry ether (80 ml). Following the completion, the mixture was refluxed for 3 hr, and then stood overnight. An excess of the reducing agent was decomposed with ethyl acetate, and dilute sulfuric acid was cautiously added with stirring to the externally cooled solution. The organic layer was separated, washed with dilute sodium carbonate followed by water, and dried ($MgSO_4$). Ether was evaporated and the residue was distilled to yield alcohol XXIV as colorless syrup (12 g, 70%), bp 182—184°C/25 mmHg, which slowly solidified to crystalline mass, mp 43—53°C (lit,[25] 51—52.5°C). IR, 863, 898, 930, 1003, 1057, 1074, 1122, 1270, and 3220—3280 cm^{-1}; PMR, 8.7—9.0 (5 CH_3, m), 7.2—7.6 (4 CH_2, m), 7.0 (OH, s, variable), 4.99 (CH, q), and 2.89 τ (ArH).

Found: C, 82.3; H, 11.4%. Calcd for $C_{16}H_{26}O$: C, 82.0; H, 11.2%.

23) H. Suzuki and K. Nakamura, *Nippon Kagaku Zasshi*, **90**, 105 (1968).

24) M. Lukin and B. B. Corson, *J. Org. Chem.*, **23**, 1007 (1958).

25) H. Hopff and F. Loechner, *Makromol. Chem.*, **84**, 261 (1965).

To a vigorously stirred solution of alcohol in methylene chloride, hydrogen chloride was passed. The reaction mixture was washed with aqueous sodium bicarbonate, dried ($MgSO_4$), and the solvent was removed *in vacuo* to give **α-methyl-2,3,4,5-tetraethylbenzyl chloride (XXV)** as colorless syrup, which on an attempt to distill in a vacuum resulted in decomposition to nondistillable polymeric substances. IR, 885, 981, 1023, 1955, 1075, 1194, 1216, 1265, 1377, and 1450 cm^{-1}; PMR, 8.6—9.0 (4 CH_3, m), 8.19 (CH_3, d, J=6.4 Hz), 7.2—7.7 (4 CH_2, m), 4.18 (CH, q, J=6.4 Hz), and 2.83 τ (ArH).

Chloride XXV in acetonitrile was treated with silver nitrate and a little calcium carbonate. The solution was filtered off from the silver salt, and the solvent was removed under reduced pressure to give a pale yellow syrup, which was identified as impure **α-methyl-2,3,4,5-tetraethylbenzyl nitrate (XXVI)** by infrared and PMR spectroscopy. Nitrate underwent decomposition on heating. IR, 869, 894, 1057, 1279 (-ONO_2), 1378, 1451, and 1635 cm^{-1} (-ONO_2); PMR, 8.6—9.0 (4 CH_3, m), 8.28 (CH_3, d, J=7 Hz), 7.2—7.6 (4 CH_2, m), 3.82 (CH, q, J=7 Hz), and 2.79 τ (ArH).

2,3,4,5-Tetraethylstyrene (XXVII). A mixture of XXIV (12 g), potassium hydrogen sulfate (0.5 g), and *t*-butylcatechol (0.5 g) was slowly distilled under reduced pressure and the fraction boiling at 99—110°C/3 mmHg was collected.[26] The oil was chromatographed on alumina using light petroleum as eluant. Redistillation of the eluate gave pure XXVII as a colorless oil, bp 103—104°C/3 mmHg. Yield, 2.0 g (18%). IR, 888 (isolated ArH), 9.05, 989, and 1624 cm^{-1} (-$CH{=}CH_2$); PMR, 8.7—9.0 (4 CH_3, m), 7.2—7.6 (4 CH_2,m), 4.82, 4.48 and 2.97 (-$CH{=}CH_2$; J_{trans}=17.8 Hz, J_{cis}= 11.0 Hz, J_{gem}=1.8 Hz), and 2.87 τ (ArH).

Found: C, 89.0; H, 11.2%. Calcd for $C_{16}H_{22}$: C, 88.8; H, 11.2%.

2,3,4,5-Tetraethylbenzyl Chloride (XXVIII). A mixture of XXII (17 g), 37%-formalin (30 g), and concentrated hydrochloric acid (300 m*l*) was stirred at 70—80°C, while a stream of hydrogen chloride was introduced with intermittent check of the organic part by gas chromatogaphy. Upon cooling, the chloride precipitated from the reaction mixture as white plates, which were removed, washed, and recrystallized from light petroleum to yield white prisms (14 g, 65%), mp 51—52°C. IR, 713, 887, 1161, 1251, and 1273 cm^{-1}; PMR, 8.6—9.0 (4 CH_3, m), 7.0—7.5 (4 CH_2, m), 4.95 (CH_2), and 3.05 (ArH).

Found: C, 75.6; H, 9.7%. Calcd for $C_{15}H_{23}Cl$: C, 75.4; H, 9.7%.

Treatment of chloride XXVIII with silver nitrate gave **2,3,4,5-tetraethylbenzyl nitrate (XXIX)** as colorless syrup. IR, 756, 855, 916, 938, 963, 1058, 1273 (-ONO_2), and 1635 cm^{-1} (-ONO_2); PMR, 8.7—9.0 (4 CH_3, m), 7.1—7.6 (4 CH_3, m), 4.12 (CH_2), and 3.01 τ (ArH).

Found: C, 67.9; H, 9.0%. Calcd for $C_{15}H_{23}NO_3$: C, 67.9; H, 8.7%.

Lithium aluminum hydride reduction of XXVIII in tetrahydrofuran gave **1-methyl-2,3,4,5-tetraethylbenzene (XXX)**, bp 145—146°C/21 mmHg. PMR; 8.7—9.0 (4 CH_3, m), 7.76 (CH_3, s), 7.2—7.7 (4 CH_2, m), and 3.29 τ (ArH).

Found: C, 88.1; H, 12.1%. Calcd for $C_{15}H_{24}$: C, 88.2; H, 11.8%.

3-Methyl-1,2,4,5-tetraethylbenzene (XXXI) was similarly prepared from 1,2,4,5-tetraethylbenzene, and boiled at 153—155°C/28 mmHg. PMR, 8.7—9.0 (4 CH_3, m), 7.77 (CH_3, s), 7.2—7.6 (CH_2, m), and 3.26 τ (ArH).

3-Bromo - 2, 5 - dimethyl-1, 4-diisopropylbenzene (XXXIII). A solution of 1,4-dimethyl-2,5-diisopropylbenzene (XXXII, 47.5 g)[27] in carbon tetrachloride (150 m*l*) was treated in presence of iodine catalyst with bromine (40 g) in carbon tetrachloride (40 m*l*). The reaction mixture was poured into water, the carbon tetrachloride layer was removed and washed with dilute sodium bisulfite followed by water. After drying ($CaCl_2$), the solvent was removed and the residue was distilled under vacuum to give XXXIII (31 g, 46%), bp 130—131°C/4 mmHg, which soon solidified to prisms, 36—38°C. PMR, 8.89 (2 CH_3, d, J=6.5 Hz) 8.74, (2 CH_3, d, J=6.6 Hz), 7.77 (2 CH_3), 7.07 (CH, sep J=, 6.5 Hz), and 3.60 τ (ArH).

Found: C, 62.7; H, 8.0%. Calcd for $C_{14}H_{21}Br$: C, 62.5; H, 7.9%.

1,3,4-Trimethyl-2,5-diisopropylbenzene (XXXIV). The Grignard reagent was prepared from a mixture of XXXIII (29 g), magnesium turnings (3.3 g), and dry tetrahydrofuran (80 m*l*) using ethyl bromide as the auxiliary halide. The reagent was then treated with vigorous stirring and efficient cooling with a solution of dimethyl sulfate (30 g) in tetrahydrofuran (25 m*l*), and stood overnight. The mixture was poured into dilute hydrochloric acid, and the organic layer was washed, the solvent was removed, and the residue was refluxed with ethanolic sodium ethoxide for 1 hr. Dilution with water, followed by the ordinary working-up yielded hydrocarbon (9.4 g, 42%), bp 127—129°C/11—12 mmHg. PMR, 8.91 (2 CH_3, d, J=8.2 Hz), 8.78 (2 CH_3, d, J=8.3 Hz), 8.01 (CH_3), 7.92 (CH_3), 7.86 (CH_3), 6.6—7.3 (CH, m), and 3.72 τ (ArH).

Found: C, 88.4; H, 12.0%. Calcd for $C_{15}H_{24}$: C, 88.1; H, 11.8%.

Nitration of Pentamethylbenzene. A solution of pentamethylbenzene (14.8 g) in chloroform (50 m*l*) was vigorously stirred and fuming nitric acid (d=1.50, 31.5 g) was added during a period of over 30 min. The mixture was poured into water, and the organic layer was washed with dilute sodium bicarbonate and water. Removal of the solvent in a vacuum gave a partly crystalline, syrupy substance (19.3 g), which showed strong infrared absorption at 1271 (-ONO_2), 1370 (-NO_2), 1460, 1525 (-NO_2), and 1624 cm^{-1} (-ONO_2); PMR peaks at 7.7—7.9, 6.05, 4.63, 4.67, 4.4—4.5, 3.87, 3.26, 3.22, 3.06, an 2.93 τ, indicating the presence of a considerable amount of benzyl nitrates. Weak absorption due to carbonyl and hydroxylic groups was also observed. Thin-layer chromatography of the syrup showed practically no formation of dinitroprehnitene. Chromatography on alumina using light petroleum as eluant gave unchanged pentamethylbenzene (0.8 g), and nitropentamethylbenzene (6.0 g). The latter was obtained as nearly colorless needles from ethanol, mp 158—159°C, and had strong infrared ab-

26) M. S. Newman, J. R. LeBlanc, H. A. Karnes and G. Axerad, *J. Amer. Chem. Soc.*, **86**, 868 (1964).

27) E. C. Kooyman and A. Strang, *Rec. Trav. Chim. Pays-Bas*, **72**, 329 (1953).

sorption at 840 and 1525 cm^{-1} ($-NO_2$); PMR peaks at 7.79 and 7.89 τ. Use of a short alumina column gave tetramethylbenzyl nitrates from light petroleum fractions, but the separation was unsatisfactory. Diphenylmethanes appeared over a wide range of the eluates; XV was concentrated in the early eluates, and XXI came out with tetramethylbenzyl nitrates or nitropentamethylbenzene. A light brown syrupy substance (*ca.* 1 g) from the benzene eluates showed a strong carbonyl absorption and gave a semicarbazone, mp 209—210°C and 235—242°C, which was identified as 2,3,4,5-tetramethylbenzaldehyde semicarbazone by comparison with the authentic specimen. The presence of 6-nitro-2,3,4,5-tetramethylbenzyl nitrate was also confirmed by spectroscopy and thin-layer chromatography. Further elution with ethanol or ether yielded a soft crystalline mass, trituration of which with a little light petroleum gave white needles (*ca.* 7 g, mp 72—78°C) identified as 2,3,4,5-tetramethylbenzyl alcohol.

Nitration of Pentaethylbenzene. A solution of pentaethylbenzene (22 g) in chloroform (50 m*l*) was vigorously stirred and fuming nitric acid (d=1.50, 31.5 g) was introduced at −5—0°C over a period of 30 min. A similar working-up as above gave a light brown, syrupy substance (26 g), which showed prominent infrared peaks at 864, 896, 1059, 1280 ($-ONO_2$), 1381 ($-NO_2$), 1454, 1465, 1526 ($-NO_2$), and 1635 cm^{-1} ($-ONO_2$); PMR peaks at 8.6—9.0 (CH_3, m), 8.26 (CH_3, d, J=7 Hz), 7.2—7.6 (CH_2, m), 3.82 (CH, q, J=7 Hz), 2.35 and 2.64 τ (ArH). Thin-layer chromatography of the syrup showed two main spots, neither of which corresponded to 5,6-dinitro-1,2,3,4-tetraethylbenzene or 3,6-dinitro-1,2,4,5-tetraethylbenzene. The syrup could be separated by repeated chromatography on alumina into several substances; 2,3,4,5-tetraethylstyrene as colorless thick oil (*ca.* 7 g), readily identified by its characteristic twelve peaks due to the vinyl group and confirmed by comparison with the authentic specimen; nitropentaethylbenzene as pale yellow crystals (3.8 g, mp 86—90°C), which showed strong infrared bands at 786, 1059, and 1525 cm^{-1} ($-NO_2$); PMR peaks at 8.95—8.71 (5 CH_3, m) and 7.1—7.7 τ (5 CH_2, m). Found: C, 73.0; H, 9.8; N, 5.6%. Calcd for $C_{16}H_{25}NO_2$: C, 73.0; H, 9.5; N, 5.3%. The minor fractions from the benzene eluates showed strong carbonyl absorptions, but they were not further investigated. A syrup (9.6 g) from the ether eluates gave on cooling a white crystalline mass (5.9 g, mp 43—62°C), which was spectroscopically identical with the authentic α-methyl-2,3,4,5-tetraethylbenzyl alcohol. The original nitrate was undoubtedly converted by repeated chromatography into unsaturated hydrocarbon and alcohol.

Nitration of Mixed Penta-alkylbenzenes. A syrup obtained from nitration of 1-methyl-2,3,4,5-tetraethylbenzene showed prominent infrared peaks at 856, 1060, 1273, 1377, 1451, 1525, and 1634 cm^{-1}; PMR peaks at 8.7—9.0 (CH_3, m), 8.41 (CH_3, d, J=6.7 Hz), 7.72 (CH_3), 7.1—7.5 (CH_2, m), 4.57 (CH_2, s), 3.78 (CH, q, J=6.7 Hz), 3.14 and 2.97 τ (ArH). The methylene signal was readily attributed to 2,3,4,5-tetraethylbenzyl nitrate by comparison with the reference compound. The methine quartet probably arose from 5,α-dimethyl-2,3,4-triethylbenzyl nitrate since its PMR pattern closely resembled that of α-methyl-2,3,4,5-tetraethylbenzyl nitrate.

The nitration product from 3-methyl-1,2,4,5-tetraethylbenzene had strong infrared bands at 854, 1053, 1271, 1376, 1451, and 1632 cm^{-1}; PMR peaks at 8.7—9.0 (CH_3, m), 8.39 (CH_3, d, J=6.8 Hz), 7.77 (CH_3, s), 7.2—7.6 (CH_2, m), 4.43 (CH_2, s), 3.78 (CH, q, J=6.7 Hz), 3.12 and 2.91 τ (ArH).

A light brown syrup from the nitration of 1,3,4-trimethyl-2,5-diisopropylbenzene showed infrared peaks at 857, 1270, 1370, 1461, 1527, 1573, and 1633 cm^{-1}; PMR peaks at 8.6—8.9 (CH_3, m), 7.66 (CH_3, m), 6.2—7.1 (CH, m), 4.47 (CH_2, s), 2.93 and 2.87 τ (ArH). Chromatography on alumina using light petroleum as eluant gave a mixture of nitro compounds as the major product, and from the ether eluates a small amount of white needles was obtained, mp 140—142°C, identified as 3,4-dimethyl-2,5-diisopropylbenzyl alcohol by analysis; infrared spectra, 884, 1008, 1027, 1045, 1108, 1137, 1299, 1548, and 3290 cm^{-1}; PMR spectra, 8.82 (2 CH_3, d, J=6.8 Hz), 8.67 (2 CH_3, d, J=7.5 Hz), 7.83 (CH_3, s), 7.72 (CH_3, s), 6.4—7.2 (CH, m), 5.39 (CH_2, s), and 2.96 τ (ArH).

Found: C, 81.7; H, 11.3%. Calcd for $C_{15}H_{24}O$: C, 81.8; H, 11.0%.

When the crude syrupy product was dissolved in a small amount of carbon tetrachloride and stood in a refrigerator, some white powder (mp 131—133°C) was precipitated. It was poorly soluble in ether and had the composition, C, 45.6, H, 5.3, N, 13.2%.

BULLETIN OF THE CHEMICAL SOCIETY OF JAPAN VOL. 43 481—484 (1970)

Orientation of the Products from the Nitration of Halopentamethylbenzenes[1)]

Hitomi SUZUKI

Department of Chemistry, Faculty of Science, Kyoto University, Sakyo-ku, Kyoto

(Received July 9, 1969)

The action of fuming nitric acid upon chloropentamethylbenzene, bromopentamethylbenzene, and iodopentamethylbenzene has been investigated. 5-Halo-2,3,4,6-tetramethyl- and 6-halo-2,3,4,5-tetramethylbenzyl nitrate were the principal products. 4-Halo-2,3,5,6-tetramethylbenzyl nitrate was never formed in any significant amount. The orientation was consistent with the previously suggested mechanistic scheme. PMR spectral data for nine halotetramethylbenzyl chlorides and nitrates have been presented.

Nitration of polyalkylbenzenes by fuming nitric acid often yields unusual products in which a hydrogen atom in one of the alkyl groups has been replaced by $-ONO_2$ group. The formation of such benzyl nitrates was first observed in 1915 by Huender in the nitration of bromopseudocumene.[2)] Smith and coworkers established that the nitrate formation is a property of the highly alkylated benzenes.[3-7)] But the mode of peculiar substitution has remained undiscussed for long. Our interest in the side-chain substitution of alkyl aromatics under ionic conditions led us to reinvestigate the nitration of penta-alkylbenzenes. The preferred formation of 2,3,4,5-tetra-alkylbenzyl nitrate was explained by a process similar to that postulated for the unconventional chlorination of hexamethylbenzene[8)]; *i.e.*, a process involving the electrophilic attack of the nitronium ion on the ring, followed by the hyperconjugative release of a proton from the neighboring methyl group and the rearrangement of the unstable intermediate (I) to the benzyl nitrite, which will then be transformed into the nitrate.[9)]

In this connection, the nitration of halopentamethylbenzenes seems to be of special interest. According to the suggested mechanism, four intermediate carbonium ion (II—V) are produced by electrophilic attack of nitronium ion on halopentamethylbenzene.

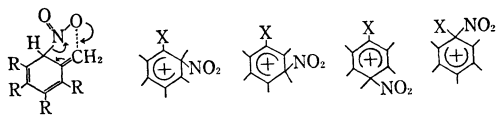

I II III IV V

Except for the case where X is the good leaving group, iodine atom, the fourth ion V, is considered to be less important since the electron-attracting halogen atom is bonded direct to the reaction site. Ion III, in which three methyl groups can contribute to the stabilization of the ion by interaction with the positively polarized centers to which they are adjacent, would be more preferable to II and IV, where there are two such methyl groups. Of the other two ions, II is more favorable than IV not only for statistical reason, but also for more effective stabilization by one methyl group in an ortho position and one in para position than two methyl groups in ortho, as IV. Positive charge distribution in the cyclohexadienyl cation system (VI) has been found to be concentrated in the order para > ortho > meta position.[10)] When the nitronium ion replaces a proton in VI, it follows that an electron-attracting halogen atom should have a more favorable effect on the stability of VII when it is ortho (VII, R_1 = halogen) to the entering

1) The Reaction of Polysubstituted Aromatics. XV. Part XIV: This Bulletin, **43**, 473 (1970).

2) A. Huender, *Rec. Trav. Chim. Pays-Bas*, **34**, 1 (1915). Also *cf.* I. J. Rinkes, *ibid.*, **57**, 1405 (1938); **58**, 538 (1939); **63**, 89 (1944).

3) L. I. Smith and S. A. Harris, *J. Amer. Chem. Soc.*, **57**, 1289 (1953).

4) L. I. Smith and O. Tenenbaum, *ibid.*, **57**, 1293 (1935).

5) L. I. Smith, F. L. Taylor and I. M. Webster, *ibid.*, **59**, 1082 (1937).

6) L. I. Smith and J. W. Horner, *ibid.*, **62**, 1349 (1940).

7) L. I. Smith and C. O. Guss, *ibid.*, **62**, 2635 (1940).

8) E. Baciocchi, A. Ciana, G. Illuminati and C. Pasini, *ibid.*, **87**, 3953 (1965). Also *cf.* P. B. D. de la Mare and H. Suzuki, *J. Chem. Soc., C*, **1967**, 1586.

9) H. Suzuki, K. Nakamura and K. Maruyama, This Bulletin, **41**, 1487 (1968).

10) C. MacLean and E. L. Mackor, *Mol. Phys.*, **4**, 241 (1961); J. P. Colpa, C. MacLean and E. L. Mackor, *Tetrahedron*, **19**, 65 (1963).

reagent (NO_2^+) than when it is para (VII, R_2= halogen). Thus it is understandable that the intermediate cation II will be energetically more preferred than IV.

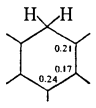

VI*1

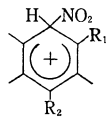

VII

Rearrangement of the ions II and IV according to the suggested sequence will lead to the same nitrate, 5-halo-2,3,4,6-tetramethylbenzyl nitrate (IX). Migration of the nitro group in ion III, however, can occur in two directions, to yield either 4-halo-2,3,5,6-tetramethylbenzyl nitrate (VIII), or 6-halo-2,3,4,5-tetramethylbenzyl nitrate (X). Simple electronic consideration suggests that the hyperconjugative proton release from the methyl group in ortho to the halogen atom would be more preferable than that from the methyl group in a para position, since the former is bonded to the more positively polarized carbon. It follows that the ion III should give rise to X rather than VIII, and if the decomposition of the intermediate benzenonium ion into the side-chain products is quite a slow step, IX and X will be the major products derived from the ordinary nitration of halopentamethylbenzene. The amount of the latter is somewhat greater than that of the former.

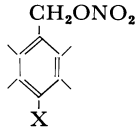

VIII

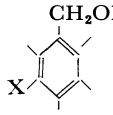

IX

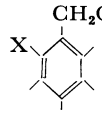

X

Nitration of halopentamethylbenzene has been investigated only by Smith and Horner.[6] They converted the nitration product from bromopentamethylbenzene into a mixture of the amines and separated them by fractional sublimation, and concluded that the action of fuming nitric acid upon bromopentamethylbenzene produced an inseparable mixture of two benzyl nitrates, 5-bromo-2,3,4,6-tetramethylbenzyl nitrate (IX, X= Br) and 6-bromo-2,3,4,5-tetramethylbenzyl nitrate (X, X=Br) in an approximate ratio 3 : 2. No derivative of durene could be obtained from the mixture. Their result seems to be quite consistent with the above discussion, although their conclusion based on the classical method of separation leaves some uncertainty as to the claimed absence of 4-bromo-2,3,5,6-tetramethylbenzyl nitrate (VIII, X=Br) in the reaction mixture. We have carried out nitration of three halopentamethylbenzenes and investigated the product by means of infrared and PMR spectroscopy. Identity of the product has been confirmed by comparison with the authentic specimen, prepared from the corresponding halotetramethylbenzenes by chloromethylation and subsequent treatment of the chlorides with silver nitrate in acetonitrile. PMR spectral data for the chlorides and nitrates derived from each of the three halotetramethylbenzenes are summarized in Table 1.

Chloropentamethylbenzene was nitrated with fuming nitric acid at −5—0°C in methylene chloride to give pale yellow, half-crystalline solid, the PMR spectrum of which showed two prominent peaks due to $-CH_2ONO_2$ at 4.31 and 4.45 τ with average relative areas of 58 : 42. By comparison with the reference compound, a signal at lower field was readily attributed to 6-chloro-2,3,4,5-tetramethylbenzyl nitrate (X, X=Cl). A signal at higher field may be due to either 4-chloro-2,3,5,6-tetramethylbenzyl nitrate (VIII, X=Cl), or 5-chloro-2,3,4,6-tetramethylbenzyl nitrate (IX, X= Cl), since both nitrates absorb at the same position in this region. On the basis of infrared spectra, the absorption at 4.45 τ was assigned to the 5-chloro isomer. Some minor peaks observed at 5.16, 5.36 and 6.60 τ were not investigated further.

A pale yellow oily solid obtained from the nitration of bromopentamethylbenzene showed two methylene peaks at 4.25 and 4.43 τ, to which 6-bromo-2,3,4,5-tetramethyl- and 5-bromo-2,3,4,6-tetramethylbenzyl nitrates respectively, were readily assigned. Of three isomeric nitrates, 4-bromo-2,3,5,6-tetramethylbenzyl nitrate absorb at the highest field, 4.46 τ, and the lack of observable peak at this position excludes the possibility of the formation of this isomer in any significant amount, in line with the previous findings.[6] The ratio of the two nitrates was 56 : 44, which was just opposite to the reported value of 2 : 3, but can be rationalized in terms of the difference in the contribution of the benzenonium intermediates, II and III. Several minor peaks at 5.31, 5.54, an 6.61 τ were not assigned.

Nitration of iodopentamethylbenzene proceeded somewhat differently from that of the other two halopentamethylbenzenes. The reaction was always accompanied by nitrodeiodination. PMR spectra of an oily solid, dark-brown with liberated iodine, showed two sharp methylene signals at 4.19 and 4.37 τ, each attributable to 6-iodo-2,3,4,5-tetramethylbenzyl nitrate (X, X=I) and 5-iodo-2,3,4,6-tetramethylbenzyl nitrate (IX, X=I). The relative intensity of two signals was 53 : 47 on an average. A very weak signal which might arise from 4-iodo-2,3,5,6-tetramethylbenzyl nitrate (VIII, X=I) was also observed at 4.42 τ, but its amount was insignificant as compared with that of the other two isomers. Minor peaks observed below 7 τ were at 4.61, 5.28, 5.50, 6.58, and 6.61 τ.

The orientation of the products is in good agree-

*1 Figures refer to π-electron deficiencies in benzenonium ion calculated from PMR proton shift.

Table 1. PMR spectral data for halotetramethylbenzyl chlorides and nitrates

Compound		Mp °C	PMR spectra (in CCl_4, τ) CH_2	CH_3*
6-Halo-2,3,4,5-tetramethylbenzyl series				
Chloride	6-Chloro,	100—101	5.31	7.63 (2), 7.76 (1), 7.79 (1)
	6-Bromo,	114—116	5.25	7.57 (1), 7.61 (1), 7.73 (1), 7.79 (1)
	6-Iodo,	110—111	5.24	7.50 (1), 7.60 (1), 7.72 (1), 7.82 (1)
Nitrate	6-Chloro,	81— 82	4.30	7.62 (1), 7.67 (1), 7.73 (1), 7.78 (1)
	6-Bromo,	91— 93	4.29	7.56 (1), 7.65 (1), 7.70 (1), 7.79 (1)
	6-Iodo,	98—100	4.18	7.44 (1), 7.61 (1), 7.64 (1), 7.78 (1)
5-Halo-2,3,4,6-tetramethylbenzyl series				
Chloride	5-Chloro,	111—112	5.45	7.51 (1), 7.62 (1), 7.66 (1), 7.75 (1)
	5-Bromo,	113—115	5.43	7.47 (1), 7.56 (1), 7.68 (1), 7.73 (1)
	5-Iodo,	110—112	5.37	7.39 (1), 7.47 (1), 7.71 (2)
Nitrate	5-Chloro,	100—101	4.44	7.52 (1), 7.59 (1), 7.68 (1), 7.74 (1)
	5-Bromo,	105—107	4.43	7.48 (1), 7.53 (1), 7.72 (2)
	5-Iodo,	106—108	4.39	7.38 (1), 7.42 (1), 7.68 (2)
4-Halo-2,3,5,6-tetramethylbenzyl series				
Chloride	4-Chloro,	92— 93	5.49	7.65 (4)
	4-Bromo,	105—107	5.50	7.60 (2), 7.64 (2)
	4-Iodo,	100—101	5.42	7.48 (2), 7.60 (2)
Nitrate	4-Chloro,	112—114	4.47	7.64 (2), 7.68 (2)
	4-Bromo,	113—114	4.46	7.57 (2), 7.65 (2)
	4-Iodo,	116—118	4.44	7.42 (2), 7.57 (2)

* Numerals in parentheses refer to the number of methyl groups.

ment with the suggested mechanism, involving the migration of the nitro group from the nucleus to the neighboring side-chain.[9] The nitro to nitrite rearrangement is quite reasonable in an activated complex, and may be expressed in a fashion similar to those observed in mass spectrometer or photochemistry.[11] It resembles to some extent the base-catalysed oxidation-reduction mechanism and the photochemical oxygen transfer processes widely observed in ortho nitro compounds.[12] In the benzenonium intermediate, proton release from the adjacent alkyl group and the subsequent redistribution of electrons to give nitrite would proceed in a single continuous process, and it does not seem necessary to postulate a discrete intermediate as I in the reaction sequence. The increasing amount of meta substitution as the atomic number of the halogen increases is explained by the steady growth of the contribution of ion II and IV relative to that of III, and is rationalized on the basis of the change in the inductive effect of the substituent.[13] The radical character of the reaction is ruled out by the high selectivity in orientation and the absence of phenylnitromethane or dibenzyl in the reaction product.

Experimental

IR spectra were measured in Nujol with a DS-402G spectrophotometer, and PMR spectra were obtained with a Varian A-60A spectrometer at 60 Mc/sec. with tetramethylsilane as internal standards.

Materials. *Chloropentamethylbenzene* (mp 155—156°C)[14] and *bromopentamethylbenzene* (mp 159—161°C)[15] were prepared as described in literature. *Iodopentamethylbenzene* was prepared by stirring a mixture of pentamethylbenzene (22.2 g), iodine (15.3 g), and periodic acid dihydrate (6.9 g) in 80% acetic acid (60 ml) containing a small amount of sulfuric acid as catalyst, at 70—80°C for about 1 hr until the color of iodine disappeared.[16] The mixture was poured into water, and the solid was removed and recrystallized from ethanol. It weighed 30.4 g (75%) and melted at 140—141°C.[17]

Preparation of Halotetramethylbenzyl Chlorides. A mixture of halotetramethylbenzene, concen-

11) O. L. Chapman, D. C. Heckert, J. W. Reasoner and S. P. Thackaberg, *J. Amer. Chem. Soc.*, **88**, 5550 (1966).

12) J. D. Louden and G. Tennant, *Quart. Rev.*, **18**, 389 (1964).

13) P. B. D. de la Mare and J. H. Ridd, "Aromatic Substitution, Nitration and Halogenation," Butterworth Scientific Publications, London (1959), p. 85.

14) C. Cook, N. Nash and H. Flanagan, *J. Amer. Chem. Soc.*, **77**, 1783 (1955).

15) L. I. Smith and J. Nichols, *J. Org. Chem.*, **6**, 489 (1941).

16) H. Suzuki, K. Nakamura and R. Gotō, This Bulletin, **37**, 1858 (1964).

17) H. Suzuki, T. Sugiyama and R. Gotō, *ibid.*, **39**, 128 (1966).

trated hydrochloric acid, and an excess of 37%-formalin was stirred vigorously and heated on a water-bath, while a stream of hydrogen chloride was passed through. In due course, the benzyl chloride gradually separated as crystalline solid which was removed, washed with water and crystallized from ligroin. The iodotetramethylbenzenes underwent extensive chloromethyldeiodonation at elevated temperature and the product was usually accompanied by an appreciable amount of bis-chloromethyltetramethylbenzenes. Satisfactory results were obtained by stirring the mixture at low temperature for prolonged hours, although under these mild conditions iodoisodurene yielded some bis-chloromethyl compound.

Conversion of Benzyl Chlorides into Nitrates. A warm solution of silver nitrate in acetonitrile was added all at once to a magnetically stirred solution of halotetramethylbenzyl chloride in acetonitrile. The mixture was stirred for several hours, and the silver chloride was filtered. After removal of the solvent the residue was crystallized from light petroleum. Physical properties and spectral data of halotetramethylbenzyl chlorides and nitrates are given in Table 1.

Nitration of Halopentamethylbenzenes. Fuming nitric acid (d=1.50, 31.5 g) was added over a period of thirty minutes to a vigorously stirred solution of halotetramethylbenzene (0.1 mol) in methylene chloride (120 ml). During the reaction the temperature was kept at −5—0°C. The mixture was poured into water and the organic layer was washed with water and dilute sodium bicarbonate. Removal of the solvent left an oily solid which was identified as a mixture of halotetramethylbenzyl nitrates by infrared and PMR spectroscopy.

BULLETIN OF THE CHEMICAL SOCIETY OF JAPAN VOL. 43 484—487 (1970)

A Comparative Study of the Constituents of Volatile Oils of *Zanthoxylum*

Tsutomu SAKAI, Kazuo YOSHIHARA and Yoshio HIROSE

The Institute of Food Chemistry, Dojimanaka, Kita-ku, Osaka

(Received July 18, 1969)

The constituents of the volatile oils of three *Zanthoxylum* species were studied on the basis of the preceding exhaustive analysis of fruit oil from the Japanese pepper. It seems that the fragrance quality among the genera *Zanthoxylum* depends on the content of citronellal in the essential oil. That is, the unripe fruit oil of Japanese pepper with the strongest characteristic aroma contained the largest amount of citronellal. Ripe fruit oil of *Z. simulans* containing a trace amount of citronellal had a poor flavor.

According to Engler,[1] the genus *Zanthoxylum* (15 species) is distributed in the temperate regions of Asia and North America, and the genus *Fagara* (200 species), in the tropics. However, there has been much confusion in the nomenclature because of meager morphological distinction between these genera. A number of *Faraga* species are alternatively named *Zanthoxylum*, and *vice versa*. Since the differences of distribution and chemical constituents have been recognized, these two genera may be differentiated from the chemotaxonomic point of view. In our country, there are two endemic species, *i.e.*, *Z. piperitum* (Linn.) DC and *Z. planispinum* Sieb. et Zucc., and one horticultural species, *i.e.*, *Z. piperitum f. inerme* (Makino) Makino. Generally, the essential oils of *Zanthoxylum* constitute a complex mixture of terpenic compounds and are superior in fragrance. On the other hand, the essential oils of *Fagara* consist of aliphatic ketones and phenolic ethers and are inferior in aroma.

In previous communications, we reported on the compositions of volatile oils obtained from the fruits[2] and the young leaves[3] of *Zanthoxylum piperitum f. inerme*. This paper will present the results of our comparative study of the constituents of volatile oils from the ripe fruits of *Z. planispinium* (Fuyu-sanshoo in Japanese) and from the ripe fruits of *Z. simulans* (Hana-sanshoo, of Red Chinese origin), on the basis of the preceding exhaustive analysis of *Z. piperitum f. inerme* (Asakura-sanshoo).[2]

Experimental

Apparatus. *Gas Chromatography.* Preparative gas chromatography was carried out in a Varian 90-P gas chromatograph, fitted with a 10 ft-by-3/8 inch aluminum column packed with 20% Carbowax 20M or SF-96 on Chromosorb W. The flow rate of the helium carrier gas was 30—60 ml/min. The separated components were trapped in thin-walled glass capillaries. Analytical gas chromatography was performed in a Hitachi K-53 gas chromatograph, wherein two 45 m-by-0.25

1) A. Engler, "Syllabus der Pflanzenfamilien," Band II, Gebrüder Borntraeger, Berlin (1964), p. 263.

2) T. Sakai, K. Yoshihara and Y. Hirose, This Bulletin, **41**, 1945 (1968).

3) S. Kusumoto, A. Ohsuka, M. Kotake and T. Sakai, *ibid.*, **41**, 1950 (1968).

mm stainless steel capillary columns coated with HB-2000 and SF-96 were used.

Infrared Spectroscopy. The infrared spectra were taken as thin films between sodium chloride plates on a Hitachi EPI-G2 spectrometer equipped with a beam condenser.

Nuclear Magnetic Resonance Spectrometry. The NMR spectra were measured on a JEOL Model C-60 spectrometer at 60 MHz in carbon tetrachloride, using tetramethylsilane as the internal reference. The microcell technique was used.

Mass Spectrometry. The mass spectra were obtained on a Hitachi RMU-6 mass spectrometer. The operating conditions were as follows: ionization voltage, 80 eV; ion-accelerating voltage, 2000 V; temperatures of ionization chamber and sample injection block, 250 and 150°C respectively.

Preparation and Separation of the Volatile Oils. The volatile oil of the ripe fruits of Asakura-sanshoo which was used was the same as in a previous study.[2] The volatile oils of the ripe fruits of Hana-sanshoo imported from Szechwan, Red China, and the ripe fruits of Fuyu-sanshoo cultivated at the Botanical Gardens of Osaka City University, Kisaichi, Osaka-fu,[*1] were obtained by steam distillation.

The volatile oil of Hana-sanshoo was fractionated by means of distillation and column chromatography. The volatile oil of Fuyu-sanshoo was divided into two fractions, hydrocarbons and oxygenated compounds, by silicagel column chromatography. Each fraction was further fractionated by preparative gas chromatography utilizing various columns.

Results and Discussion

Figure 1 shows the comparative capillary chromatograms of the ripe fruit oil of Asakura-sanshoo (top of Fig. 1), the ripe fruit oil of Hana-sanshoo (middle), and the ripe fruit oil of Fuyu-sanshoo (bottom). Each chromatogram was obtained by injecting 0.5—1.0 μl of the raw volatile oil into a HB-2000 capillary column. The column temperature was held initially at 80°C for 4 min; then it was programmed at 2°C per minute to 150°C, and run isothermally at 150°C until all the components had emerged. The nitrogen-carrier gas inlet pressure was 1.0 kg/cm^2. Attenuation was kept at 1 except otherwise indicated. The location of each component was determined by a manner reported previously.[2]

The gas chromatogram of the Fuyu-sanshoo oil fairly well resembles that of the unripe fruit oil of the Asakura-sanshoo. Monoterpene hydrocarbon fractions of both oils contain almost the same components. A serious difference was, however, noted in that there were large amounts of citronellal and methyl cinnamate in the Asakura-sanshoo oil, while, on the contrary, there was only a small amount of citronellal and no methyl cinnamate in the Fuyu-sanshoo oil. A considerable amount of nerolidol was found in the Fuyu-sanshoo oil.

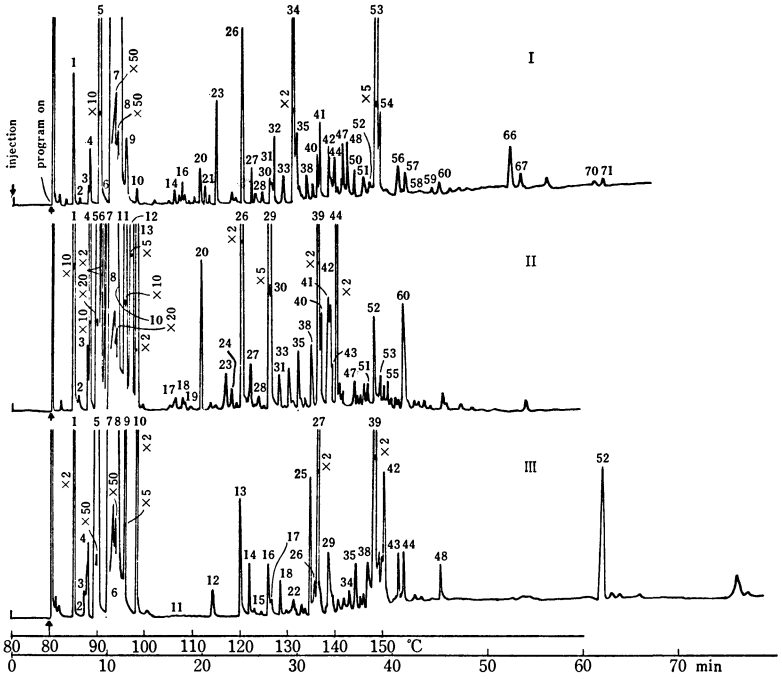

Fig. 1. Gas chromatograms of the genus *Zanthoxylum* I. Asakura-sanshoo oil, II. Hana-sanshoo oil, III. Fuyu-sanshoo oil 45 m×0.25 mm HB-2000 column; temperature isothermal at 80°C for 4 min then programmed at 2°C per minute to 150°C and run isothermal thereafter; sample 0.5—1.0 μl; range 1×1 except as indiated.

*1 The authors thank Botanical Garden of Osaka City University for supplying ripe fruits of Fuyu-sanshoo.

TABLE 1. CONSTITUENTS OF VOLATILE OILS FROM ASAKURA-SANSHOO, HANA-SANSHOO, AND FUYU-SANSHOO

Identified component	Kovats' indices		Peak No. in Fig. 1		
	HB-2000	SF-96	Asakura-sanshoo	Hana-sanshoo	Fuyu-sanshoo
α-Pinene	994	948	1	1	1
Camphene	1025	959	2	2	2
β-Pinene	1060	987	3	3	3
Sabinene	1066	980	4	4	4
Myrcene	1095	987	5	5	5
α-Phellandrene	1105	1007	6	6	6
α-Terpinene	1118	1019		7	
Limonene	1135	1034	7	8	7
1,8-Cineol	1137	1035	7	9	
β-Phellandrene	1145	1034	8	10	8
Ocimene	1156	1089		11	
p-Cymene	1172	1025	9	12	9
γ-Terpinene	1172	1058		12	
Terpinolene	1203	1024	10	13	10
Isobutyl isovalerate	1223	1094	11		
Isobutyl caproate	1274	1142	14		
Alloocimene	1276	1121	14	17	
Perillene	1290	1100		18	
β-Terpinen-3,4-oxide	1307	1048	16		
p-Isopropenyltoluene	1309	1092	17	19	
cis-Linalool oxide	1335	1100		20	
trans-Limonen-1,2-oxide	1341	1146	20		
cis-Limonen-1,2-oxide	1346	1146	21		
Citronellal	1352	1146	23	22	12
Linalool	1376	1101	26	26	13
2-*p*-Menthen-1-ol	1396	—	27	27	14
Isopulegol	1424	1162	28	28	15
Terpinolen-4,8-oxide	1432	1218	28		
trans-2,8-Menthadien-1-ol	—	—	28		
Linalyl acetate	1437	1246	30	29	16
cis-2,8-*p*-Menthadien-1-ol	1438	—	30		
Terpinene-4-ol	1449	1191	31	30	16
Dihydrocarvone	1444	1211	32		
α-Copaene	1455	1389	32	30	17
Cryptone	1501	1200	34	33	22
Methyl chavicol	1498	1200	35	34	
Limonen-4-ol	1501	1071	38	37	24
β-Elemene	1515	1403	39	38	25
α-Terpineol	1516	1204	40	39	26
β-Caryophyllene	1530	1425	41	40	27
Carvone	1531	1246	42		
Piperitone	1548	1260	42	41	29
Citronellyl acetate	1540	1342	43	42	30
Phellandral	1555	1246	44	43	31
Terpinyl acetate	1558	1348	47	44	33
Cuminaldehyde	1562	1271	48	45	34
Perillaldehyde	1586	1280	49		
Humulene	1583	1457	50	47	35
1(7),8-*p*-Menthadien-*trans*-2-ol	—	—	51		
Citronellol	1594	1348	51		
γ-Muurolene	1600	1475	52	51	38
Geranyl acetate	1605	1370	53	52	39
trans-Carveol	1617	1246	54	53	40

TABLE 1. (Continued)

Identified component	Kovats' indices		Peak No. in Fig. 1		
	HB-2000	SF-96	Asakura-sanshoo	Hana-sanshoo	Fuyu-sanshoo
α-Muurolene	1628	1495	55	55	42
cis-Carveol	1633	1255	55		
Geraniol	1653	—	56		
δ-Cadinene	1655	1515	57	60	44
γ-Cadinene	1656	1436	57	60	44
Piperitenone	1676	1216	58		
Calamenene	1693	1513	59	64	48
α-Calacorene	1745	1531	60	66	
Methyl cinnamate	1766	1394	66		
Cuminalcohol	1798	1322	67		
β-Caryophyllene alcohol	1828	1540	70		
Nerolidol	1842	1597	71		52

The gas chromatograms show that the Hana-sanshoo oil is very rich in monoterpene hydrocarbons, we noticed several compounds, such as γ-terpinene, α-terpinene, ocimene, alloocimene, and perillene, which were not found in the oils of the other two species. A large amount of linalool oxide was also found in the Hana-sanshoo oil. It is a remarkable difference that citronellal, methyl cinnamate, and nerolidol were not found in this oil.

Table 1 lists the components, which were confirmed by a comparison of their Kovats' indices and their infrared, nuclear magnetic resonance, and mass spectra with those of authentic samples and the literature data. Kovats' indices were determined under isothermal conditions on 45-m capillary columns (α-pinene through perillene, HB-2000 column at 80°C, 1.0 kg/cm² N_2 : SF-96 column at 100°C, 0.5 kg/cm² N_2; β-terpinen-3,4-oxide through nerolidol, HB-2000, 130°C, 1.0 kg/cm² : SF-96, 130°C, 0.5 kg/cm²).

Obviously, the young leaves and the unripe fruits of Asakura-sanshoo are most fragrant, and their essential oils contained the largest amount of citronellal. A parallelism is observed between the fragrance and the content of citronellal in a downward order from the ripe fruit of the Asakura-sanshoo through the ripe fruit of the Fuyu-sanshoo and Hana-sanshoo oils. The latter had a rather disagreeable odor because of the large amounts of myrcene and ocimene which replaced the citronellal.

As far as was tested, no identified component has been estimated to be essential to the characteristic flavor of the Sanshoo oil. The essential oil of Sanshoo loses its characteristic odor when stored for a week at room temperature in a tightly-sealed tube. The gas chromatogram of this deteriorated oil shows the disappearance of the peak of β-phellandrene and a decrease in the amounts of citronellal, myrcene, and terpinolene. On the other hand, the amounts of isopulegol, *cis*-2,8-*p*-menthadien-1-ol, dihydrocarvone, limonen-4-ol, carvone and piperiton, geranyl acetate, *trans*- and *cis*-carveols, cuminalcohol, β-caryophyllene alcohol, and, especially, cryptone increased.

Therefore, it may be concluded that the fragrance of the genus *Zanthoxylum* consists mainly in the characteristic odor of citronellal and depends on its content.

BULLETIN OF THE CHEMICAL SOCIETY OF JAPAN VOL. 43 488—491 (1970)

The Double Cycloaddition of Disulfene and Its Related Reactions

Koji HIRAI and Niichiro TOKURA

Department of Applied Chemistry, Faculty of Engineering, Osaka University, Suita-shi, Osaka

(Received July 14, 1969)

The reactions of methanedisulfonyl chloride (II) with ketene diethylacetal (III), 1-morpholinocyclohexene (IV), and 1-piperidinopropene (V) in the presence of triethylamine were studied. The products obtained were the double cycloadduct, spiro bithietane tetroxide (VI), and the substitution products (X and XV). These findings suggest that triethylamine dehydrochlorinates methanedisulfonyl chloride to produce disulfene. However, as yet we cannot say whether the formation of disulfene is the one-step dechydrochlorination mechanism ($ClSO_2CH_2SO_2Cl \rightarrow SO_2{=}C{=}OS_2$) or the two-step one ($ClSO_2CH_2SO_2Cl \rightarrow ClSO_2CH{=}SO_2 \rightarrow SO_2{=}\underset{|}{C}{-}\underset{|}{SO_2}$).

In the presence of triethylamine, various alkanesulfonyl chlorides react with compounds containing electron-rich and polarizable double bonds, such as enamines and ketene acetals, to afford four-membered cyclic sulfones (thietane dioxide) or isomeric acyclic compounds, depending on the nature of reactants and the reaction media. These reactions have been formulated as involving the reactive intermediacy of sulfene ($RCH{=}SO_2$).[1-3] However, it has only recently been reported that 1,3-propanedisulfonyl chloride reacts with 1-morpholinocyclohexene or ketene diethylacetal in the presence of triethylamine to yield the corresponding bithietane tetroxide (Fig. 1).[4] These reactions are regarded as proceeding through the intermediacy of disulfene.

In view of these facts, we were prompted to study the possibility of preparing a new disulfene $O_2S{=}C{=}SO_2$ (I) as an analogy to carbon suboxide $OC{=}C{=}CO$. In this paper we now wish to report some of the information obtained from the reactions of methanedisulfonyl chloride (II) with ketene diethylacetal (III), 1-morpholinocyclohexene (IV), and 1-piperidinopropene (V) in the presence of triethylamine. The reaction of II with III and

$$ClSO_2CH_2SO_2Cl + 2\,CH_2{=}C(OEt)_2 \xrightarrow[\text{benzene}\ -5°C\ 10\text{ hr}]{4\text{ or }2\ Et_3N}$$

(II) (III)

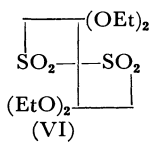

(VI)

triethylamine in benzene at −5°C for 10 hr gave a crystalline substance, which was formulated as spiro bithietane tetroxide (VI), in a 45% yield. The formation of VI is conceived of as proceeding through the intermediacy of disulfene, which then undergoes a double cycloaddition reaction with III.

When VI was dissolved in cold ethanol and set aside at −10——50°C for more than 30 hr, a ring cleavage and proton transfer occurred to give the product, VII, quantitatively. This reaction is

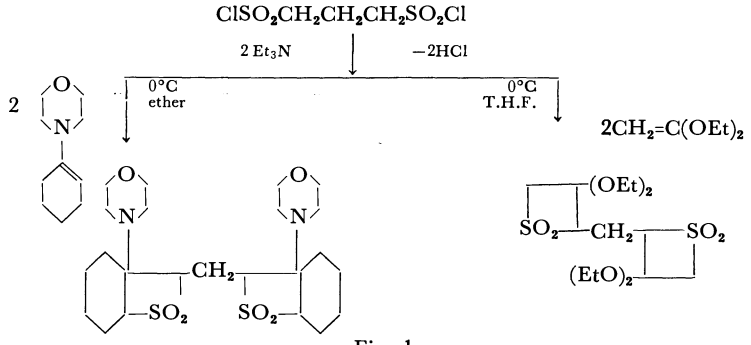

Fig. 1

1) W. E. Truce and J. R. Norell, *J. Amer. Chem. Soc.*, **85**, 3231 (1963).
2) G. Stork and I. J. Borowitz, *ibid.*, **84**, 313 (1962).
3) a) G. Opitz, *Angew. Chem.*, **79**, 161 (1967). b) G. Opitz and H. R. Mohl, *ibid.*, **81**, 36 (1969).
4) T. Nagai, H. Namikoshi and N. Tokura, *Tetrahedron Lett.*, **1968**, 4329.

considered to be due to the strain inherent in VI.

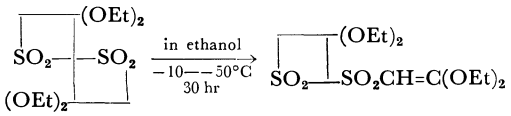

(VI) (VII)

On the other hand, when pure VI was dissolved in ether or ethanol containing a trace of water at 30°C, the diester (IX) was immediately formed quantitatively. Presumably, IX may have arisen from the β-elimination of ethanols from the intermediate diol (VIII), which was produced by the two ring cleavages of VI and the addition of water. The compound VII is found to be stable and does not change to IX under similar or even more vigorous (reflux in ethanol) conditions.

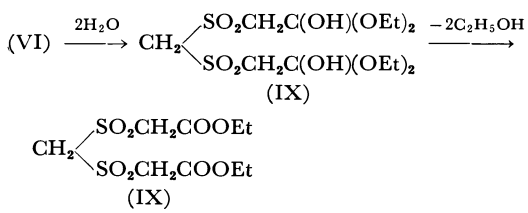

Although the IR and NMR spectra of VI have not yet been obtained because of its instability, the structure VI is adequate judging from elemental analysis and the conversion to VII and IX. The IR spectrum of VII shows strong bands at 1340 and 1130 ($-SO_2-$) and at 1585 cm^{-1}, the latter being attributed to the olefinic double bond; it also shows weak band at 3100 cm^{-1} (CH=). The NMR spectrum is also in harmony with the structure VII. The appearance of the ring methine proton at τ 4.5 as a quartet leads us to attribute the splitting to a 1,3-transannular interaction with the two nonequivalent ring methylene protons (ABX system). A singlet at τ 5.21 was assigned to an olefinic proton, and the abnormal up-field shift of the olefinic proton is considered to be due to the polarization of the double bond by the two electron-donating ethoxyl groups. A double triplet at τ 8.75 accounts for the methyl protons of the ketal moiety. This is regarded as a result of the fact that the two ethoxyl groups of the ketal moiety become unequivalent. Similarly, the methyl protons of the vinyl ether moiety appeared as a double triplet at τ 8.63. The IR spectrum of IX had absorptions at 1740 cm^{-1} (C=O of the ester).

A similar reaction of II with IV in the presence of triethylamine led to the formation of sulfonylenamine (X) in a 34% yield. The acid-catalyzed hydrolysis of X gave the expected corresponding ketosulfone (XI) almost quantitatively. The IR spectrum of X shows an olefin band at 1658 cm^{-1}. A broad triplet at τ 4.55 was assigned to the two olefinic protons, and a multiplet at τ 5.4 was attributed to the two methine protons. This reaction has the possibility of generating different products, for example, the less substituted sulfonylenamine (X) and the more substituted one (XIII) by proton transfer from the 2 and 6 positions of the ring respectively, or a compound like XIV by a double cycloaddition. In this reaction several factors may contribute to the preferred formation of one of the possible isomers. The determining factors may be the particular structure and conformation of the zwitterionic intermediate (XIIa, XIIb) and the nature of the reactants (II, IV, base). For instance, when the intermediate (XIIa, XIIb) bears bulky groups at the electrophilic center, only the less substituted sulfonylenamine (X) is formed.

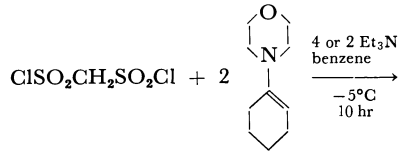

(II) (IV)

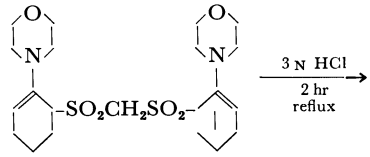

(X)

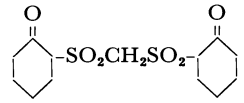

(XI)

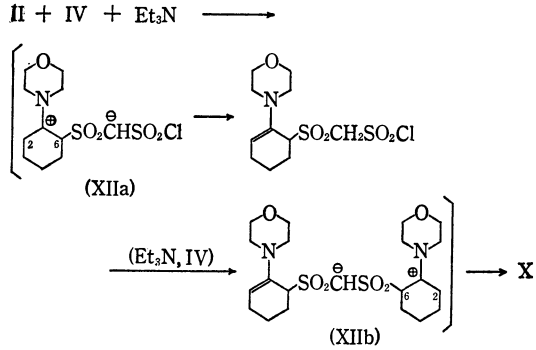

Although the two-step dehydrochlorination mechanism seems to be preferable to the one-step one, more definitive experiments are needed.

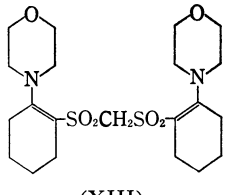

(XIII)

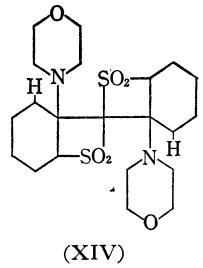

(XIV)

When the reaction time was 1—2 hr, the yields of VI and X were lowered to 2—4% and a white precipitate formed during the reaction immediately decomposed to methanedisulfonic acid, triethylamine hydrochloride, and an intractable dark brown oil on exposure to air. After 10 hr, however, the products obtained did not include this precipitate, but VI (45%) or X (34%) and triethylamine hydrochloride. From these results, it is apparent that these reactions are not complete within 1—2 hr and that this precipitate is the unstable intermediate, from which VI and X result. Methanedisulfonic acid was characterized by its conversion to the dianilide.

In like fashion, the interaction of II, triethylamine, and V under the same conditions led to the formation of XV in a 16% yield. The IR spectrum of XV shows the presence of the olefinic double bond at 1638 cm^{-1}.

The path of this reaction cannot be stated with certainty, but a postulated mechanism is shown below. In this case again, if the steric interference exists, the compound XV would arise from substitution instead of cyclization *via* a zwitterionic intermediate such as XVI (path b), but presumably XV may have arisen from ring cleavages of the intermediacy of spirane (XVII), as is shown in path a, in view of recent articles[5,6] about the reactions of sulfenes and such enamines as V and our own finding regarding ketene diethylacetal, which is not greatly different with regard to its steric circumstances.

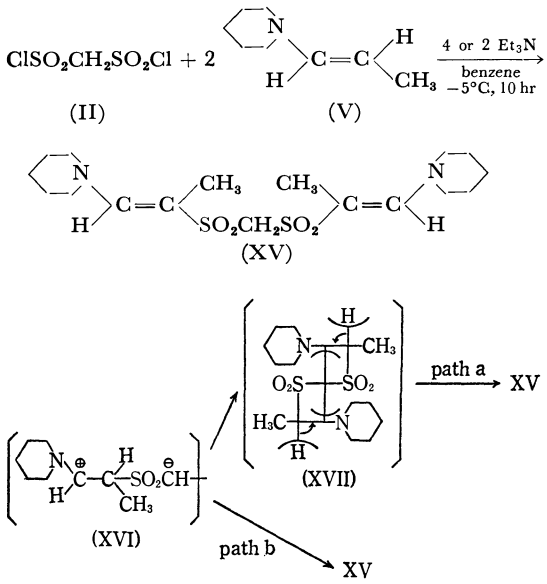

5) G. Opitz and H. Adolph, *Angew. Chem.*, **74**, 77 (1962).

6) G. Opitz and K. Rieth, *Tetrahedron Lett.*, **1965**, 3977.

Experimental

Materials. The methanedisulfonyl chloride,[7] ketene diethylacetal,[8] 1-morpholinocyclohexene,[9] and 1-piperidinopropene[10] were prepared by methods described in the literature.

Reaction of Methanedisulfonyl Chloride with Ketene Diethylacetal. A solution of 5.3 g (0.025 mol) of methanedisulfonyl chloride in 50 m*l* of benzene was stirred, drop by drop, into a solution of 5.8 g (0.05 mol) of ketene diethylacetal and 11.0 g (0.1 mol) of triethylamine in 200 m*l* of benzene at −5°C over a 10-hr period. The amine hydrochloride was then removed by filtration, and the benzene solution was evaporated under reduced pressure to afford 4.15 g (45%) of crude VI, which was then washed with cold petroleum ether - ether and recrystallized from cold ethanol, the temperature being kept below 0°C.

Found: C, 41.70; H, 6.20; S, 17.25%. Calcd for $C_{13}H_{24}O_8S_2$: C, 41.92; H, 6.49; S, 17.21%.

Compound VI (2.0 g) was dissolved in cold ethanol (20 m*l*) and then set aside at −10——50°C for more than 30 hr. The subsequent removal of the ethanol under reduced pressure and recrystallization from ethanol gave 2.0 g of VII. Colorless needles, mp 135.5—136.5°C. IR: 3100 (ν CH=), 1585 (ν C=C), 1340, 1130 cm^{-1} (ν SO_2). NMR ($CDCl_3$): τ 4.5(1H, quartet, SO_2CHSO_2), 5.21 (1H, singlet, $=CHSO_2$), 5.6—6.1 (2H, octet, CH_2SO_2), 5.76 (4H, quartet, $CH_2O-C=$), 6.35 (4H, quartet, CH_2O-C-), 8.63 (6H, double triplet, $CH_3CH_2O-C=$), 8.75 (6H, double triplet, CH_3CH_2O-C-).

Found: C, 41.75; H, 6.55; S, 17.02%. Calcd for $C_{13}H_{24}O_8S_2$: C, 41.92; H, 6.49; S, 17.21%.

The mass spectrum gave a parent peak at 372 *m/e* and other major peaks at 357, 317, 271, 179, 151, 123, 116, 105, 79, 78, 77, 73, 60, 55, 46, 44, and 43 *m/e*.

When VI (2.0 g) was dissolved in ether or ethanol containing a trace of water at 30°C, 1.7 g of IX were immediately formed; the IX was then recrystallized form ethanol. Colorless needles; mp 73.5°C.

IR: 1740 (ν C=O), 1320, 1100 cm^{-1} (ν SO_2). NMR ($CDCl_3$): τ 4.7 (2H, singlet, $SO_2CH_2SO_2$), 5.6 (4H, singlet, SO_2CH_2CO), 5.7 (4H, quartet, OCH_2CH_3), 8.67 (6H, triplet, OCH_2CH_3).

Found: C, 34.14; H, 5.03%. Calcd for $C_9H_{16}O_8S_2$: C, 34.18; H, 5.09%.

The mass spectrum gave a parent peak at 316 *m/e* and other major peaks at 289, 271, 243, 225, 166, 137, 88, 45, 43, and 42 *m/e*.

Reaction of Methanedisulfonyl Chloride with 1-Morpholinocyclohexene. A solution of 5.3 g (0.025 mol) of methanedisulfonyl chloride in 50 m*l* of benzene was stirred, drop by drop, into a solution of 8.4 g (0.05 mol) of 1-morpholinocyclohexene and 11.0 g (0.1 mol) of triethylamine in 200 m*l* of benzene at −5°C over a 10-hr period. The amine hydrochloride was removed by filtration, and the benzene solution was evaporated under reduced pressure to afford 4.0 g

7) H. Goldwhite and M. S. Gibson, *Tetrahedron*, **21**, 2743 (1965).

8) S. M. McElvain, "Organic Syntheses," Coll. Vol. III, p. 506, (1955).

9) S. Hünig, "Organic Syntheses," **41**, 65 (1961).

10) C. Mannich and H. Davidsen, *Ber.*, **69**, 2107 (1936).

(34%) of crude X, which was then washed with ether and recrystallized from methanol. Colorless needles, mp 202°C (dec). IR: 1658 (ν C=C), 1310, 1120 cm^{-1} (νSO_2). NMR($CDCl_3$): τ4.0 (2H, singlet, $SO_2CH_2SO_2$), 4.55 (2H, broad triplet, =CH), 5.4 (2H, multiplet, $CHSO_2$), 6.2 (8H, triplet, O-CH_2), 6.6—7.1 (4H, multiplet, allylic proton), 7.1—8.5 (16H, multiplet, N-CH_2 and other CH_2 groups of the cyclohexene ring).

Found: C, 53.30; H, 7.26; N, 5.74%; mol wt, 474. Calcd for $C_{21}H_{34}N_2O_6S_2$: C, 53.14; H, 7.22; N, 5.90%; mol wt, 474.

Hydrolysis of Sulfonylenamine (X). Compound X was suspended in 200 m*l* of 3 N hydrochloric acid and heated at a gentle reflux for 2 hr, during which time dissolution was completed. The solution was then extracted with benzene, and the bezene layer was washed with water, dried, and concentrated. The solid residue was washed with petroleum ether and recrystallized from ethanol to give 1.35 g (95%) of XI. Colorless plates; mp 158.5°C. IR: 1720 (νC=O), 1320, 1120 cm^{-1} (νSO_2). NMR ($CDCl_3$): τ 4.67 (2H, singlet, $SO_2CH_2SO_2$), 5.5 (2H, multiplet, $CHSO_2$), 7.28—8.4 (16H, multiplet, CH_2 groups of the cyclohexane ring).

Found: C, 46.18; H, 6.21%. Calcd for $C_{13}H_{20}O_6S_2$: C, 46.31; H, 6.00%.

The mass spectrum gave a parent peak at 336 *m/e* and other major peaks at 241, 223, 176, 175, 174, 98, 97, 96, 81, 69, 68, 67, 55, and 41 *m/e*.

Reaction of Methanedisulfonyl Chloride with 1-Piperidinopropene. A solution of 5.3 g (0.025 mol) of methanedisulfonyl cholride in 50 m*l* of benzene was stirred, drop by drop, into a solution of 6.2 g (0.05 mol) of 1-piperidinopropene and 11.0 g (0.1 mol) of triethylamine in 200 m*l* of benzene at −5°C over a 10-hr period. The amine hydrochloride was then removed by filtration, and the benzene solution was evaporated under reduced pressure. The residue was chromatographed on activated alumina. Elution with chloroform gave 1.45 g (16%) of XV, which was then washed with ether and recrystallized from ether. Colorless needles; mp 99—100°C. IR: 1638 (ν C=C), 1300, 1150 cm^{-1} (νSO_2). NMR ($CDCl_3$): τ 3.0 (2H, singlet, =CH), 5.7 (2H, singlet, $SO_2CH_2SO_2$), 6.6 (8H, broad singlet, N-CH_2), 7.9 (6H, singlet, CH_3), 8.35 (12H, broad singlet, other CH_2 groups of the piperidine ring).

Found: C, 52.21; H, 7.76; N, 7.28%. Calcd for $C_{17}H_{30}O_4S_2N_2$: C, 52.27; H, 7.74; N, 7.17%.

The mass spectrum gave a parent peak at 390 *m/e* and other major peaks at 248, 188, 150, 138, 125, 124, 123, 122, 110, 96, 81, 68, 55, and 41 *m/e*.

BULLETIN OF THE CHEMICAL SOCIETY OF JAPAN VOL. 43 491—495 (1970)

A-Substituted 5β-Steroids. III. Synthesis of 2-Oxo-5β-steroids and Their Derivatives

Yasuo SATOH, Akira HORIUCHI and Akira HAGITANI

Department of Chemistry, College of Science, St. Paul's University (Rikkyo Daigaku), Nishi-Ikebukuro, Toshima-ku, Tokyo

(Received July 25, 1969)

The synthesis of 2-oxo-5β-steroids (5β-cholestan-2-one and methyl 2-oxocholanate) and their derivatives have been described. Both oxo-steroids were prepared from 2β-acetoxy-3-oxo-5β-steroids according to the following synthetic pathways: (a) condensation with ethylmercaptan to diethylmercaptol, desulfurization, hydrolysis and oxidation, (b) condensation with ethylmercaptan to diethylmercaptol, hydrolysis to hydroxy-ethylmercaptol, desulfurization and oxidation, and (c) isomerisation to 3α-acetoxy-2-oxo derivative and deacetylation with zinc powder to 2-oxo derivative. In these pathways, it was found that method (b) gave the best yield. On the other hand, desulfurization of the hydroxy-mercaptols with one-half the weight of Raney nickel used for that of method (b) gave 2β-hydroxy-3β-ethylthio derivatives as intermediates. Reductive cleavage of these hydroxy-ethylthio derivatives with Raney nickel produced 2β-hydroxy-5β-steroids in good yields. In the halogenation of these 2-oxo derivatives, the products were 1β-halo-2-oxo-5β-sterodis, not 1α- or 3-halo isomers.

Although most 5α-steroids which possess subtituents on each position in ring A have been thoroughly investigated,[1] only very little information is found in literature concerning the synthesis of 1- and 2-substituted 5β-steroids.[2] On the synthesis of 2-substituted 5β-steroid, Tomoeda and Koga[3] recently repoted that 2α-hydroxy-5β-chloestane was obtained from 4β,5β-epoxycholestan-3-one through

1) L. F. Fieser and M. Fieser, "Steroids," Reinhold Pub. Inc., New York (1959), p. 169; C. Djerassi, "Steroids Reactions," Holden-Day, Inc., San Francisco (1963), pp. 181, 537.

2) Y. Satoh, T. Takahashi, T. Aoki and A. Hagitani, This Bulletin, **42**, 1465 (1969).

3) M. Tomoeda and T. Koga, *Tetrahedron Lett.*, **1965**, 3231.

the epoxy ring opening, condensation with ethanedithiol to an ethylene thioketal, desulfurization, and hydrogenation.

During the course of our studies of A-substituted 5β-steroids, we have found that the substitution reaction of 4β-bromo-3-oxo-5β-steroids (1) with potassium acetate and acetic acid is accompanied with a new rearrangement of a substituent from C_4 to C_2 resulting in the 2β-acetoxy-3-oxo derivative (2) in good yield.[4] In our previous communication, we also reported that the bromination of 2-oxo-5β-steroids affords the 1β-bromo-2-oxo-5β-steroids.[5] In the present paper, we wish to describe in full the details for the synthesis of 1-haloketones from 2β-acetoxy-3-oxo-5β-steroids (2).

Condensation with ethyl mercaptan to diethylmercaptols (3) of the acetoxyketones (2) and hydrogenation of the mercaptols with Raney nickel (W-2) gave acetoxy compounds corresponding in spectroscopic properties to 2β-acetoxy-5β-steroids (4).

In the desulfurization method, considerable amounts of saturated 5β-steroids were formed, and so we attempted another route for the deketonisation; that is, the derivatives (3) were converted to 2β-hydroxy-3-oxo diethylmercaptols (5) by alkaline hydrolysis. In the case of (3b), however, the carbomethoxy group in the side chain was hydrolyzed to carboxylic acid (5c) and then the acid was converted to its methyl ester (5b) with diazomethane. By desulfurization of these 2β-hydroxy-3-oxo-5β-steroid diethylmercaptols with Raney nickel according to the same method for (3), 2β-hydroxy-5β-steroids were formed in good yield. The configuration of these products has been determined by IR spectra and the patterns of NMR spectra. The total yields of 2β-hydroxy-5β-steroids from the 2β-acetoxy-3-oxo-5β-steroids were 80 and 44% (cholestane and 3-bile acid series, respectively).

Acetylation of the 2β-hydroxy-5β-steroids with acetic anhydride and pyridine produced 2β-acetoxy derivatives (4), identical with the specimens described above. In the NMR spectra of 2β-hydroxy- and 2β-acetoxy-5β-cholestanes, it was found that the signals due to C_2-αH were shifted more to the the upper field than those of 2α-isomers.[3] This agreed with the relation of the chemical shifts between *a*- and *e*-H due to the anisotropy of C–C linkage in cyclohexane ring.[6]

When the desulfurization of the hydroxy diethylmercaptols (5) was carried out with one-half the weight of Raney nickel used for that of (3), 2-hydroxy-3-ethylthio derivatives (7) were obtained as intermediates. Small amounts of 2-oxo- and 2β-hydroxy-5β-steroids were also formed. One of the products (7b) could be isolated as needles, but it was so difficult to crystallize the other product (7a) that it was converted to its acetate (8) by treatment with acetic anhydride and pyridine. In the NMR spectra of both crystalline products, (8) has a multiplet at τ 6.60 (Hw=8 Hz, 1H) and a sextet at τ 4.97 (J=4.5, and 10.5 Hz, 1H) and (7b) has multiplets at τ 6.88 (Hw=8 Hz, 1H) and near τ 4.2.*1 From these data, it was found that the intermediates obtained from the desulfurization were 2β-hydroxy-3β-ethylthio-5β-steroids. The reductive cleavages of these hydroxy-ethylthio derivatives with Raney nickel produced 2β-hydroxy-5β-steroids in good yields.

Oxidation of the 2β-hydroxy-5β-steroids with chromic acid and acetic acid gave 2-oxo-5β-steroids (9) showing a double Cotton curve near 310 mμ. One of the products was identical with 5β-cholestan-2-one prepared by Tomoeda and Koga.[3]

In a previous paper, it was reported that the isomerisation of 2β-acetoxy-5β-cholestan-3-one with hydrogen bromide and acetic acid gave 3α-acetoxy-5β-cholestan-2-one (10).[7] In general, α-ketols and their acetates are reduced to the ketone with zinc

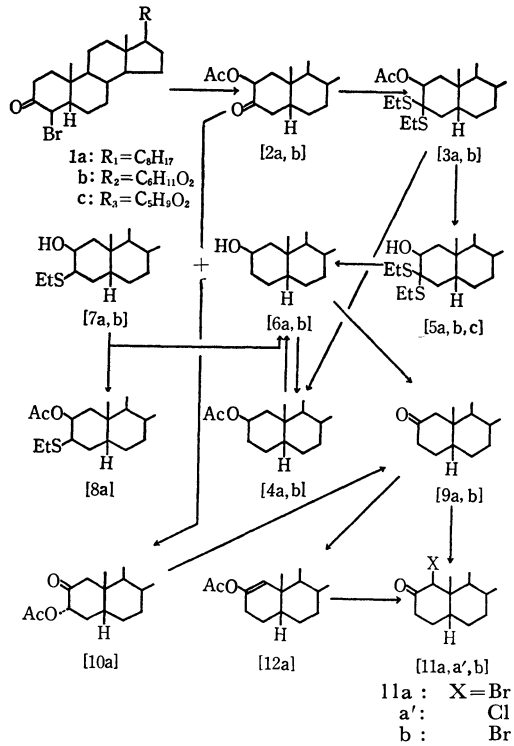

*1 This signal owing to C_2-αH could not be clarified, because it was overlapped by the CH_3-signal of the C_{24}-carbomethoxy group.

4) T. Takahashi, Y. Satoh and A. Hagitani, *Nippon Kagaku Zasshi*, **89**, 974 (1968).

5) Y. Satoh, A. Horiuchi, T. Matsukura and A. Hagitani, This Bulletin, **41**, 3032 (1968).

6) R. U. Lemieux, R. K. Kullnig, H. J. Bernstein and W. G. Schneider, *J. Amer. Chem. Soc.*, **80**, 6098 (1958); N. S. Bhacca and D. H. Williams, "Application of NMR Spectroscopy in Organic Chemistry," Holden-Day, Inc., San Francisco (1964), p. 49.

7) Y. Satoh, T. Kimura, Y. Tajima, T. Takahashi and A. Hagitani, *Nippon Kagaku Zasshi*, **90**, 500 (1969).

and acetic acid.[8] Therefore, the synthesis of 5β-cholestan-2-one from the 3α-acetoxy-2-oxo derivative (10) has been studied according to this method. In a small scale experiment, satisfactory result was obtained, but in a large scale experiment, zinc in great bulk prevented stirring, so that this method was not practical for the synthesis of 5β-cholestan-2-one.

In the bromination of the 2-oxo derivatives, the products were 1β-bromo-2-oxo-5β-steroids, not 1α- or 3-bromo isomers. This was determined by signs of the Cotton effect, Δ[A] (+233 for 5β-cholestan-2-one and +164 for methyl 2-oxocholanate) and $\Delta\lambda_1$-values (+20 and +18 mμ, respectively) in ORD, the shifts of C=O stretching bands (+4 and +2 cm^{-1}, respectively) in IR spectra and the patterns of the NMR spectra.

In connection with the above investigation, we carried out the enol acetylation of 5β-cholestan-2-one according to the directions of Djerassi *et al.* described for the 5α-series.[9] On chromatographical separation of the reaction product, 5β-cholest-1-en-2-ol acetate was obtained. It was found, moreover, that bromination of this enol acetate with bromine in acetic acid gave the same product as described above for that of 5β-cholestan-2-one. From these results, we may conclude that the enolization of the 2-oxo-5β-steroids occurs in the direction of C_1, not C_3, and that the bromination of these ketones forms the 1β-bromo-2-oxo derivatives. The configuration of these bromoketones is consistent with Corey's prediction for the 2-oxo-5β-steroid.[10]

Chlorination of 5β-cholestan-2-one also produced 1β-substituted derivative as in the case of bromination. In the NMR spectra of both 1β-haloketones, it was found that the signal due to C_1-αH in the chloroketone was shifted more to the upper field than that of the bromoketone.

Experimental

Instrumentation. IR and ORD spectra were measured on a Shimadzu model IR-27B infrared spectrometer and a JASCO model ORD/UV-5 spectrometer, respectively. NMR spectra were recorded in deuterochloroform, with TMS as the internal standard with a JEOL model JNM-4H-100 high resolution nuclear spectrometer.

2β-Acetoxy-5β-cholestan-3-one Diethylmercaptol (3a). A current of dry hydrogen chloride was passed into a mixture of (2a) (19.0 g) and ethyl mercaptan (24 m*l*) under cooling with an ice-bath for 10 min. After the reaction mixture had stood for 15.5 hr in a refrigerator, the excess of ethyl mercaptan was removed in a vacuum desiccator on sodium hydroxide. The resulting oil was then extracted with ether. The ether extracts were washed with sodium hydrogencarbonate solution and water, dried, and evaporated under reduced pressure. A slightly brownish oil (21.7 g) was obtained. Attempts to crystallize the diethylmercaptol were unsuccessful, and so it was used in the next step without purification. ν_{max}^{Film} cm^{-1}: 1745 (C=O), 1234 (C–O), 770 (C–S).

Methyl 2β-Acetoxy-3-oxocholanate Diethylmercaptol (3b). The method used here was identical with that described for (3a). No crystalline diethylmercaptol (22.0 g) was obtained from methyl 2β-acetoxy-3-oxocholanate (16.5 g). ν_{max}^{Film} cm^{-1}: 1733 (C=O), 1230, 1165 (C–O), 771 (C–S).

2β-Acetoxy-5β-cholestane (4a). A solution of diethylmercaptol (3a) (9 g) in methanol-acetone (1 : 1, 400 m*l*) was refluxed with Raney nickel (W-2, 90 g) under effecient stirring for 2.5 hr. The hot reaction mixture was filtered and the clear filtrate was evaporated under reduced pressure. The resulting oil (7 g) was chromatographed on silica gel; 5β-cholestane was first eluted by petroleum ether, and the next fraction eluted with benzene - petroleum ether (2 : 1), on crystallization from ethanol gave plates of 2β-acetoxy-5β-cholestane (1.7 g), mp 59—61.5°C, $[\alpha]_D^{24}$ +19.7°C (*c* 1.26, $CHCl_3$), NMR ($CDCl_3$) τ: 5.23 (septet, *J*=5.5 and 11 Hz, 1H), ν_{max}^{KBr} cm^{-1}: 1732 (C=O), 1240 (C–O).

Found: C, 80.55; H, 11.62%. Calcd for $C_{29}H_{50}O_2$: C, 80.87; H, 11.71%.

Methyl 2β-Acetoxycholanate (4b). The desulfurization of the diethylmercaptol (3b) (7.1 g) was carried out using the technique described for the synthesis of (4a). The resulting oil (5.4 g) from the reaction mixture was chromatographed on silica gel; benzene eluted a yellow oil which on crystallization from methanol gave needles of methyl cholanate (3.6 g), mp 85—87°C. The next fraction, eluted by the same solvent, on crystallization from methanol gave plates of methyl 2β-acetoxycholanate (0.3 g), mp 75.5—77°C, $[\alpha]_D^{24}$ +17.9° (*c* 1.12, $CHCl_3$), ν_{max}^{KBr} cm^{-1}: 1739, 1725 (C=O), 1255, 1173 (C–O), NMR ($CDCl_3$) τ: 5.21 (septet, *J*=6.5 and 13 Hz, 1H), 6.36 (s., 3H), 8.01 (s., 3H).

Found: C, 75.33; H, 10.39%. Calcd for $C_{27}H_{44}O_4$; C, 74.96; H, 10.25%.

2β-Hydroxy-5β-cholestan-3-one Diethylmercaptol (5a). A mixture consisting of (4a) (21.7 g), sodium hydroxide (2.4 g), water (2 m*l*), and methanol (800 m*l*) was refluxed for 4.5 hr. After evaporation of the reaction mixture, the residue was dissolved in ether. The ethereal solution was washed with water, dried, and evaporated. Crystallization of the resulting oil from ethanol gave 2β-hydroxy-5β-cholestan-3-one diethylmercaptol as needles (16 g), mp 79—80.5°C, $[\alpha]_D^{24}$ +15.0° (*c* 1.00, $CHCl_3$), ν_{max}^{KBr} cm^{-1}: 3420 (O–H), 770 (C–S), NMR ($CDCl_3$) τ: 6.44 (t., *J*=5 and 10 Hz, 1H), 7.28 (m., 4H).

Found: C, 73.47; H, 11.06; S, 12.49%. Calcd for $C_{31}H_{56}OS_2$: C, 73,16; H, 11.09; S, 12.60%.

Methyl 2β-Hydroxy-3-oxocholanate Diethylmercaptol (5b). A solution of (3b) (6.09 g) in methanol (200 m*l*) was refluxed with potassium hydroxide (2 g) in water (15 m*l*) for 6 hr. After cooling, the reaction mixture was poured into ice-water and acidified with dilute hydrochloric acid. The resulting precipitate

8) R. S. Rosenfeld, *J. Amer. Chem. Soc.*, **79**, 5540 (1957); R. L. Augustine, "Reduction," Marceldekker, Inc., New York (1968), p. 140.

9) C. Djerassi and T. Nakano, *Chem. Ind.*, **1960**, 1385; T. Nakano, M. Hasegawa and C. Djerassi, *Chem. Pharm. Bull.* (Tokyo), **11**, 465 (1962).

10) E. J. Corey, *J. Amer. Chem. Soc.*, **75**, 2301 (1953); **76**, 175 (1954).

was taken up in ether and the ether extracts were washed with water, dilute sodium hydrogencarbonate solution, then water, dried, and concentrated. Crystallization of the residue from methanol gave needles of 2β-hydroxy-3-oxocholanic acid diethylmercaptol (5c) (4.77 g), mp 152—154°C, $[\alpha]_D^{26}$+12.4° (*c* 0.97, $CHCl_3$).

The acid (5c) (4 g) was converted to its methyl ester with diazomethane. After evaporation of the solvent, crystallization of the residue from methanol gave methyl ester (5b) (2.98 g), mp 89—90.5°C, $[\alpha]_D^{24}$+13.5° (*c* 1.13, $CHCl_3$), ν_{max}^{KBr} cm^{-1}: 3450 (O–H), 1735 (C=O), 1166 (C–O), 765 (C–S).

Found: C, 68.32; H, 9.70; S, 12.51%. Calcd for $C_{29}H_{50}O_3S_2$: C, 68.19; H, 9.87; S, 12.55%.

From the mother liquor, a second crop (0.79 g), mp 81.5—85°C, was also obtained.

2β-Hydroxy-5β-cholestane (6a). (i) A solution of 2β-acetoxy-5β-cholestane (4a) (1.4 g) in methanol (5.6 m*l*) and ether (10 m*l*) was refluxed with sodium hydroxide (0.36 g) in water (1.4 m*l*) for 3 hr. After evaporation of the reaction mixture, the residue was dissolved in ether. The ethereal solution was washed with water, dried, and evaporated. Crystallization of the residue from ethanol gave needles of (6a) (0.91 g), mp 100—104°C, $[\alpha]_D^{24.5}$+14.9° (*c* 0.93, $CHCl_3$), ν_{max}^{KBr} cm^{-1}: 3300 (O–H), NMR ($CDCl_3$) τ: 6.28 (septet, *J*=5 and 10 Hz, 1H).

Found: C, 83.10; H, 12.41%. Calcd for $C_{27}H_{48}O$: C, 83.43; H, 12.45%.

(ii) 2β-Hydroxy-5β-cholestan-3-one diethylmercaptol (5a) (12.2 g) was treated with Raney nickel according to the method for the synthesis of (4a) from (3a). Attempts to crystallize the residue were unsuccessful, but this product was identical with 2β-hydroxy-5β-cholestane prepared by the method (i) in t.l.c., g.l.c., and IR spectrum. Acetylation of a part of the product gave 2β-acetoxy-5β-cholestane as plates, which was identical with the specimen prepared from 2β-acetoxy-5β-cholestan-3-one diethylmercaptol with Raney nickel. Thus the oily product was used for the synthesis of 5β-cholestan-2-one (9a) without further purification.

Methyl 2β-Hydroxycholanate (6b). A mixture of (5b) (6.15 g), methanol-acetone, and Raney nickel was treated by the same method as for (6a) (method ii). The resulting oil (4.75 g) was chromatographed on silica gel. A small amount of methyl 2-oxocholanate was first eluted with benzene-ether (20 : 1), and a second fraction, eluted with the same solvent, on crystallization from methanol gave plates of methyl 2β-hydroxycholanate (2.5 g), mp 80—81°C, $[\alpha]_D^{24}$+10.5° (*c* 0.96, $CHCl_3$), ν_{max}^{KBr} cm^{-1}: 3420 (O–H), 1737 (C=O), 1166 (C–O).

Found: C, 76.84; H, 10.76%. Calcd for $C_{25}H_{42}O_3$: C, 76.87; H, 10.84%.

Acetylation of the product (6b) in the usual method produced methyl 2β-acetoxycholanate, which was identical with the product prepared from the mercaptol (3b) by desulfurization.

2β-Acetoxy-3β-ethylthio-5β-cholestane (8a). A solution of (5a) (19.5 g) in methanol-acetone (1 : 1, 300 m*l*) was refluxed with one-half the weight of Raney nickel used for the synthesis of 2β-hydroxy-5β-steroid from diethylmercaptol (5). After 30 min, the reaction mixture was filtered and evaporated. On chromatography of the residue with silica gel, benzene - petroleum ether eluted an oil (5.38 g), which consisted of 2β-hydroxy-3β-ethylthio-5β-cholestane (7a) and 5β-cholestan-2-one (9a). Isolation of (7a) from the mixture was so difficult that the compound was converted to its acetate with acetic anhydride and pyridine. Recrystallization of the acetylation product from ethanol gave needles of 2β-acetoxy-3β-ethylthio-5β-cholestane (8a) (3.6 g), mp 66—68.5C°, $[\alpha]_D^{24}$+2.5°C (*c* 1.22, $CHCl_3$), ν_{max}^{KBr} cm^{-1}: 1744 (C=O), 1238 (C–O), 731 (C–S), NMR ($CDCl_3$) τ: 4.97 (sextet, *J*=4.5 and 10.5 Hz, 1H), 6.60 (m., Hw=8 Hz, 1H), 7.23—7.67 (q., –S– CH_2–), 7.93 (s., 3H).

Found: C, 76.23; H, 11.20; S, 6.45%. Calcd for $C_{31}H_{54}O_2S$: C, 75.86; H, 11.09; S, 6.53%.

Further desulfurization of the mixture consisting of (7a) and (9a) with Raney nickel produced needles of 2β-hydroxy-5β-cholestane.

Benzene eluted a yellow oil which on crystallization from ethanol gave 2α-hydroxy-5β-cholestane (3.7 g).

Methyl 2β-Hydroxy-3β-ethylthiocholanate (7b). A solution of the diethylmercaptol (5b) (1g) in methanol-acetone (1 : 1, 30 m*l*) was treated with Raney nickel according to the procedure described for the synthesis of (7a) except that the reaction was carried out for 1 hr. On chromatography of the residue with silica gel, crystallization of benzene eluates gave needles of methyl 2β-hydroxy-3β-ethylthiocholanate (201 mg), mp 105.5—106.5°C, from methanol. $[\alpha]_D^{24}$ −27.3° (*c* 1.06, $CHCl_3$), ν_{max}^{KBr} cm^{-1}: 3473 (O–H), 1746 (C=O), 1153 (C–O), 766 (C–S).

Found: C, 71.63; H, 10.32; S, 7.09%. Calcd for $C_{27}H_{46}O_3S$: C, 71.95; H, 10.29; S, 7.11%.

Desulfurization of the hydroxy-ethylthio derivative by the method used for (8a) gave methyl 2β-hydroxycholanate.

Further elution with benzene afforded a mixture consisting of a trace of methyl 2-oxo- (9b) and 2β-hydroxycholanate (6b).

5β-Cholestan-2-one (9a). (i) From 2β-Hydroxy-5β-cholestane (6a). A solution of (6a) (8.4 g) in acetic acid (160 m*l*) was treated with chromium trioxide (2.4 g) in 80% acetic acid (14 m*l*) at 10—15°C. After standing for 2 hr, a small amount of methanol was added to the reaction mixture. The solution was slightly warmed on a water bath, cooled, and poured into water, and the resulting precipitate was extracted with ether. The ether extracts were washed with sodium hydrogencarbonate solution and water, dried, and evaporated. Crystallization of the residue from ethanol gave plates of (9a) (5.9 g), mp 86—88°C, ν_{max}^{KBr} cm^{-1}: 1712 (C=O), ORD (*c* 0.49, Di) at 26°C: $[\alpha]_{589}$+16.3°, $[\alpha]_{400}$+24.5°, $[\alpha]_{370}$ 0°, $[\alpha]_{316}$ −321.5° (trough), $[\alpha]_{306}$ −244.9° (sh.), $[\alpha]_{302}$ 0°, $[\alpha]_{275}$+263.3° (peak).

Found: C, 83.29; H, 11.81%. Calcd for $C_{27}H_{46}O$: C, 83.86; H, 11.99%.

(ii) From 3α-Acetoxy-5β-cholestan-2-one (10a). A mixture of (10a) (377 mg), zinc powder (37.7 g), and acetic acid (198 m*l*) was refluxed with stirring for 14 hr. After evaporation of the solvent, the residue was taken up into ether and the ether extracts were washed with sodium hydrogencarbonate solution and water, dried, and concentrated. Crystallization from ethanol gave plates of 5β-cholestan-2-one (50 mg), mp 85—87°C. This product was identical with a sample prepared by method (i) in IR and ORD spectra.

Methyl 2-Oxocholanate (9b). This substance was prepared according to method (i) described above for

the synthesis of (9a). The crystallization of the resulting oil from methanol gave needles of methyl 2-oxocholanate (819 mg), mp 88—89.5°C, from (6b) (1 g). ν_{max}^{KBr} cm^{-1}: 1733, 1708 (C=O), 1162 (C–O), ORD (*c* 0.59, Di) at 26°C: $[\alpha]_{589}$+20.3°, $[\alpha]_{400}$+31.6°, $[\alpha]_{357}$ 0°, $[\alpha]_{317}$ −273° (trough), $[\alpha]_{307}$ −166° (sh.), $[\alpha]_{302}$ 0°, $[\alpha]_{275}$ +509° (peak).

Found: C, 77.27; H, 10.38%. Calcd for $C_{25}H_{40}O_3$: C, 77.58; H, 10.49%.

1β-Bromo-5β-cholestan-2-one (11a). 5β-Cholestan-2-one (4.24 g) was dissolved in acetic acid (100 m*l*) and a few drops of 47% hydrogen bromide were added, followed by addition of bromine (1.75 g) in acetic acid (10 m*l*) with stirring for 25 min at 18°C. The reaction mixture was cooled, and the crystals formed were collected. The crystals were dissolved in ether and the ethereal solution was washed, dried, and evaporated. Crystallization of the residue from methanol-ether gave needles (3.82 g), mp 128—130°C, ν_{max}^{KBr} cm^{-1}: 1714 (C=O), 668 (C-Br), ORD (*c* 0.52, Di) at 26°C: $[\alpha]_{589}$ +9.6°, $[\alpha]_{400}$+421°, $[\alpha]_{336}$+2187° (peak), $[\alpha]_{314}$ 0°, $[\alpha]_{288}$ −2369° (trough), NMR ($CDCl_3$) τ: 5.68 (s., 1H).

Found: C, 69.78; H, 9.80%. Calcd for $C_{27}H_{45}OBr$: C, 69.65; H, 9.74%.

Methyl 1β-Bromo-2-oxocholanate (11b). Bromination of methyl 2-oxocholanate (834 mg) was carried out using the technique for the synthesis of (11a). The reaction mixture was taken up in ether and the ether extracts were washed, dried, and evaporated. On chromatography of the residue with silica gel, elution with benzene gave an oily product (650 mg). Crystallization of this product from methanol afforded needles (81 mg) of (11b), mp 138—140°C, ν_{max}^{KBr} cm^{-1}: 1735, 1710 (C=O), 1171 (C–O), 673 (C–Br), ORD (*c* 0.62, Di) at 25°C: $[\alpha]_{589}$+67.7°, $[\alpha]_{400}$+271°, $[\alpha]_{335}$+1394° (peak), $[\alpha]_{313}$ 0°, $[\alpha]_{289}$−1468° (trough), NMR ($CDCl_3$) τ: 5.66 (s., 1H), 6.35 (s., 3H).

Found: C, 63.33; H, 8.00%. Calcd for $C_{25}H_{39}O_3Br$: C, 64.24; H, 8.41%.

1β-Chloro-5β-cholestan-2-one (11a′). A solution of chlorine (79 mg) in chloroform (3 m*l*) was added to a mixture consisting of 5β-cholestan-2-one (9a) (386 mg), concd. hydrochloric acid (2 drops) and acetic acid (15 m*l*) with stirring at 20°C. After 15 min, the reaction mixture was poured into water, and the chloroform layer was washed, dried, and evaporated. Crystallization of the residue from methanol-acetone gave needles (247 mg), mp 116—118°C, ν_{max}^{KBr} cm^{-1}: 1721 (C=O), ORD (*c* 0.59, Di) at 25°C: $[\alpha]_{589}$+50.8°, $[\alpha]_{400}$+131.4°, $[\alpha]_{327}$+645.8° (peak), $[\alpha]_{321}$+557.6° (trough), $[\alpha]_{316}$+627.1° (peak), $[\alpha]_{298}$ 0°, $[\alpha]_{281}$−314.4° (trough), NMR ($CDCl_3$) τ: 5.83 (s., 1H).

Found: C, 76.49; H, 11.22%. Calcd for $C_{27}H_{45}OCl$: C, 77.01; H, 10.77%.

2-Acetoxy-5β-cholest-1-ene (12a). This substance was prepared according to the directions of Djerassi *et al.* described for 5α-isomer.[9] The reaction product was chromatographed in petroleum ether on silica gel. Elution with benzene gave needles of (12a) from ethanol, mp 103—105°C, $[\alpha]_D^{26}$+52.0°C (*c* 0.997, in $CHCl_3$), ν_{max}^{KBr} cm^{-1}: 1750 (C=O), 1687 (C=C), 1215 (C–O), NMR ($CDCl_3$) τ: 4.66 (s., 1H), 7.93 (s., 3H).

Found: C, 80.52; H, 11.01%. Calcd for $C_{29}H_{48}O_2$: C, 81.25; H, 11.29%.

The authors are indebted to Minophagen Pharmaceutical Co. for gifts of ox bile, to Kawaken Fine Chemicals Co., Ltd., for gifts of Raney nickel (W-2 type), to Japan Electron Optics Laboratory Co., Ltd., for measurement of NMR spectra, to Sankyo Co., Ltd., for elementary analyses, and to Messrs. T. Aoki, T. Matsukura, K. Kaneko, O. Sakamoto, S. Kitoh and H. Toda for collaboration in experimental work. They also thank the Ministry of Education for the financial support granted for this research.

BULLETIN OF THE CHEMICAL SOCIETY OF JAPAN VOL. 43 496—500 (1970)

Addition of Tellurium Tetrachloride to Olefins and Pyrolysis of the Adduct

Masao OGAWA and Ryoji ISHIOKA

Central Research Laboratory, Showa Denko K. K., Tamagawa, Ohta-ku, Tokyo

(Received July 28, 1969)

The tellurium tetrachloride-cyclohexene adduct, 2-chlorocyclohexyltellurium trichloride (I) and bis(2-chlorocyclohexyl)tellurium dichloride (II), both gave, on pyrolysis, chlorocyclohexane as the chlorinated compound. An intermolecular hydrogen transfer is required for the formation of chlorocyclohexane from I. Chloro-*n*-propyltellurium trichloride (III) and bis(chloro-*n*-propyl)-tellurium dichloride (IV) were formed by the addition of tellurium tetrachloride to propylene. The pyrolysis of III afforded allyl chloride, 1,2-dichloropropane, and hydrogen chloride, while tellurium was simultaneously reduced. Besides these products, isopropyl chloride was also obtained from IV. Some properties of the adduct and the effect of the temperature on the thermal decomposition were studied.

In an earlier communication[1] the formation of bis(chloroalkyl)tellurium dichloride by the addition of tellurium tetrachloride (TTC) to olefins and the pyrolysis of the adducts affording organic chlorides were briefly reported. The lower-valent tellurium compounds produced in the pyrolysis are reoxidized by oxygen and hydrogen chloride. Thus, the oxychlorination of olefins for the production of allylic chloride is thought to be possible; the process is now being investigated.[2]

The present paper will deal with the behavior of the TTC-propylene adducts, including the hydrogen transfer observed in the pyrolysis of the TTC-cyclohexene adducts. The results will give a clue to the catalysis of the tellurium compound in the chlorination reaction.

Results and Discussion

Pyrolysis of the TTC-cyclohexene Adducts. In the addition of TTC to cyclohexene,[1] 2-chlorocyclohexyltellurium trichloride (I) was obtained when TTC was allowed to react with less than an equivalent amount of cyclohexene, while bis-(2-chlorocyclohexyl)tellurium dichloride (II) was obtained from the reaction with excess cyclohexene. Both I and II gave, on pyrolysis, chlorocyclohexane, benzene, and cyclohexene, as well as hydrogen chloride and inorganic tellurium compound.

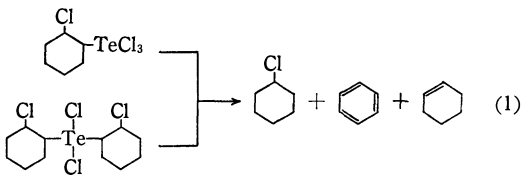

(1)

A certain amount of 3-chlorocyclohexene was expected to be found in the pyrolysate. In fact, it was assumed by gas chromatography. However, its amount was very small; if it was present at all, it was estimated at less than 1% of the products. In contrast to the pyrolysis of the TTC-propylene adducts (Table 3), the yield of allylic chloride was very low, probably because the concurrent dehydrogenation to benzene predominated over the allylic chlorination. The product distribution in the pyrolysis of I is shown in Table 1, along with the corresponding data for II.

TABLE 1. PRODUCTS FROM THE PYROLYSIS OF I AND II

Compound	Organic product (g/g)	Product distribution (%)		
		Chloro-cyclohexane	Ben-zene	Cyclo-hexene
I[a]	0.18	51	28	21
I[b]	0.17	55	28	17
II[a]	0.27	38	13	49

a) Decomposed at 150°C. b) At 200°C.

It seems natural that a tellurium-catalyzed intramolecular hydrogen transfer should be involved in the pyrolysis of II, which has hydrogens available within the molecule, while the intermolecular hydrogen transfer is bound to occur in the pyrolysis of I.

During the thermal decomposition of I and II, an intermediate formation of the tellurium-hydrogen

1) M. Ogawa, This Bulletin, **41**, 3031 (1968).
2) A.G. Höchst, Ger., 1224302 (1967); Japan, 17134 (1966).
3) G. Centini, P. L. Stanghellini, R. Rossetti and O. Gambino, *J. Organometal. Chem.*, **15**, 373 (1968) and the literatures cited therein.

bond, a probable representation of which is shown in Eq. (2), may be implied before the complete cleavage of the tellurium-carbon bond.

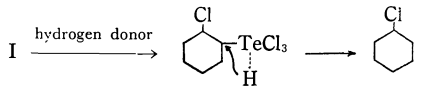

and other products (2)

It is known that the atomic valency of the VIb-group element, particularly that of covalent tellurium,[3] increases to 6 and more upon the participation of vacant *d* orbitals; this character of the element is thought to be related to the hydrogen transfer (perhaps the hydride transfer) observed in the experiment.

Addition of TTC to Propylene. The reaction of propylene with TTC in an organic solvent, after the solvent had been evaporated, afforded the adduct as an faint yellow viscous oil. The IR spectrum showed that the adduct had no double bond in it. The NMR spectrum coincided with the structure of addition compound.

When TTC in acetonitrile was allowed to react, in a sealed tube, with an equivalent amount of propylene, one type of product (named III) was exclusively obtained. On the other hand, another product (named IV) was formed together with III in the reaction with excess propylene. (See Figs. 2 and 3 in the "Experimental" section.) The same results were observed when nitromethane instead of acetonitrile was used as the solvent. Accordingly, compared with the case of cyclohexene, III and IV are thought to be 2-chloropropyltellurium trichloride and bis(2-chloropropyl)tellurium dichloride respectively.

CH_3-CHCl-CH_2-$TeCl_3$ (III)

$(CH_3$-CHCl-$CH_2)_2TeCl_2$ (IV)

Neither the NMR spectrum nor the chemical reaction was conclusive as to the orientation of the addition, but Markownikoff addition was tentatively estimated from the product of the pyrolysis. The Markownikoff additions of aryltellurium trichloride[4] and I[5] to 2,2-disubstituted-penten-4-oic acid, and of selenium tetrachloride[6] to the simple olefins, have been reported, while the random orientation has been manifested in the addition of sulfenyl chloride[7] and sulfur dichloride[8,9] to olefins.

It was suggested in the previous paper[1] that the TTC-butene-1 adduct was a mixture of isomers of bis(chloro-*n*-butyl)tellurium dichloride; this suggestion was based on the analytical method which is now found to involve considerable uncertainties in the determination of tellurium. The estimation must, then, be in error and must be corrected in view of the present results. The TTC-butene-1 adduct can now be thought to be a mixture of bis(2-chlorobutyl)tellurium dichloride and a minor amount of 2-chlorobutyltellurium trichloride.

The effects of the solvent on the addition were investigated, though the number of usable solvents was limited because of the reaction with TTC[10] and the solubility requirements. Gaseous propylene was introduced into a solution of TTC in an organic solvent at room temperature for a sufficiently long period.

Table 2. Solvent effect in addition reaction
TTC 2 g; solvent, 20 m*l*; reaction time, 1 hr

Solvent	Dielectric constant	Time (min)[a]	III (%)[b]	IV
Ethyl acetate[c]	6.03	60	98	2
Acetic acid	6.19	45	83	17
Methylene dichloride[d]	8.9	14	81	19
Acetonitrile	37.5	13	56	44
Nitromethane	39.0	11	32	68

a) The approximate time required for the disappearance of the yellow color of TTC in solution.
b) The ratio of III and IV was calculated approximately from the relative intensity of the NMR signals.
c) The reaction was not completed within an hour.
d) TTC was not fully dissolved in this solvent.

The reaction is generally faster, and IV is more preferentially formed, with increases in the dielectronic constant and in the solvating power of the solvent used. In such a polar solvent, the ionization and the subsequent addition of III to the olefin is accelerated; consequently, the formation of IV, at the expense of III, is favored.

Properties of the TTC-propylene Adduct. The adduct (III or IV) was relatively stable at room temperature, but it began to decompose at approximately 80°C. Sensitive to water, it was hydrolyzed to a white, insoluble mass,[11] losing the chlorine atoms attached to tellurium. With

4) M. De Moura Compos and N. Petragnani, *Chem. Ber.*, **93**, 317 (1960).
5) M. De Moura Compos and N. Petragnani, *Tetrahedron*, **18**, 521 (1962).
6) R. F. Riley, J. Flato and D. Bengels, *J. Org. Chem.*, **27**, 2652 (1962); H. Brintzinger. K. Pfannstiel and H. Vogel, *Z. Anorg. Allgem. Chem.*, **256**, 75 (1948).
7) W. H. Mueller and P. E. Butler, *J. Amer. Chem. Soc.*, **88**, 2866 (1966); *J. Org. Chem.*, **33**, 2111 (1968); *ibid.*, **90**, 2075 (1968).
8) J. R. Nooi and G. J. Huijben, *J. Appl. Chem.* (London), **18**, 84 (1968).
9) F. Lautenschlager, *J. Org. Chem.*, **33**, 2620 (1968).
10) H. Rheinbolt, "Methoden der Organischen Chemie," Vol. IX Georg Thieme Verlag (1956) p. 1156.
11) M. P. Balfe, C. A. Chaplin and H. Phillips, *J. Chem. Soc.*, **1938**, 341.

reducing agents such as sodium sulfite and hydrazine hydrochloride, propylene and elemental tellurium were recovered. When the adduct was dissolved in an acidic solution of potassium perchromate, 1,2-dichloropropane was obtained in a low yield, besides several unidentified compounds.

The tellurium-carbon bond of the adduct was cleaved by the action of bromine. III yielded a mixture of dihalopropanes.

$$\text{III} \xrightarrow{Br_2} CH_2Br\text{-}CHBr\text{-}CH_3 + CH_2Cl\text{-}CHBr\text{-}CH_3 + CH_2Br\text{-}CHCl\text{-}CH_3 + CH_2Cl\text{-}CHCl\text{-}CH_3 \quad (3)$$

Under the same conditions, the chlorine atom in 1,2-dichloropropane or bromochloropropane was not replaced by bromine. This indicates that the chlorine atom in the alkyl remainder of the adduct was activated toward substitution by a neighboring tellurium atom. The activation of the chlorine and the products in Eq. (3) were interpreted in terms of the cyclic tellurium-ion intermediate (V), which had previously been postulated by De Moura Campos and Petragnani[5] in analogy to the episulfonium ion considered in the behavior of the sulfenyl chloride-olefin adduct.[7,12]

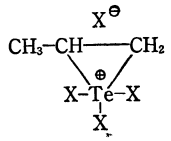

(V) X: Cl or Br

Pyrolysis of the TTC-Propylene Adduct. The pyrolysis of the adducts afforded allyl chloride, isopropyl chloride, 1,2-dichloropropane, and hydrogen chloride as well as inorganic telluride and propylene. It is likely that the adduct was of the Markownikoff type, for if it were of the anti-Markownikoff type *n*-propyl chloride, instead of isopropyl chloride, would be produced by hydrogen transfer at the pyrolysis.

The effect of the temperature on the yield of organic chloride (based on tellurium, mol/atom $\times 100$) was studied by using the adduct obtained from the reaction in an acetonitrile solvent (III 56%, IV 44%).

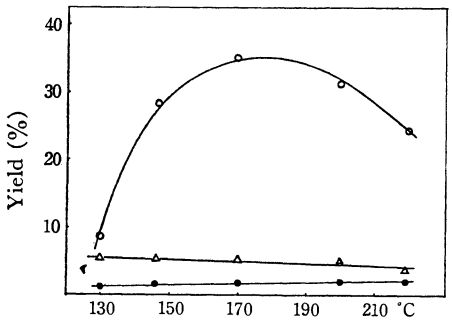

Fig. 1. Effect of temperature on the pyrolysis.
○: Allyl chloride, △: Isopropyl chloride,
●: 1,2-dichloropropane

At a low temperature, the decomposition was incomplete and the residue contained organic tellurides. At a higher temperature, the dissociation (Eq. (8)) predominated over the chlorination. Therefore, the optimum temperature appears in Fig. 1.

The relation between the yield of organic chlorides and the ratio of III and IV in the adduct is shown in Table 3.

Table 3. Pyrolysis of III and IV
170°C, 5 mmHg

III (%)	IV	Isopropyl chloride (%)	Allyl chloride (%)	1,2-dichloropropane (%)
98	2	<1	11	1.2
83	17	1.6	19.9	2.7
81	19	6.0	25.3	2.4
56	44	5.0	34.9	1.7
32	68	9.9	49.0	3.0

Table 3 shows that isopropyl chloride was mainly produced from IV, indicating that intramolecular hydrogen transfer was operating and that intermolecular hydrogen transfer was not important in this case.

$$\begin{array}{l} CH_2\text{-}CHCl\text{-}CH_3 \\ | \\ Cl\text{-}Te\text{-}Cl \\ | \\ CH_2\text{-}CHCl\text{-}CH_3 \end{array} \longrightarrow$$

$$CH_3\text{-}CHCl\text{-}CH_3 + CH_2{=}CH\text{-}CH_2Cl + TeCl_2 \quad (4)$$

The formation of allyl chloride from III and IV is thought to require some type of allylic intermediate, which may be stabilized by the tellurium atom.

$$\text{III, IV} \xrightarrow{-HCl} \text{allylic intermediate} \xrightarrow{-Te} CH_2{=}CH\text{-}CH_2Cl \quad (5)$$

The allylic intermediate illustrates how 3-chloro-1-butene and 1-chloro-2-butene were formed, along with isomeric butenes, from the TTC-butene-1 adduct,[1] and also from the TTC-butene-2[13] adduct.

In this thermal decomposition, the elimination of hydrogen from the carbon bearing both hydrogen and chlorine or the preliminary development of the carbonium ion at the α to tellurium carbon is excluded, because no vinylic chlorides were found in the pyrolysate.

The adduct would give 1,2-dichloropropane by either Eq. (6) or (7), though it is uncertain which process prevails:

12) N. Kharasch, "Organic Sulfur Compounds," Vol. 1, Pergamon Press, New York (1961), p. 382.

13) Unpublished work.

$$\text{III, IV} \longrightarrow \begin{cases} \rightarrow CH_2Cl\text{-}CHCl\text{-}CH_3 + Te & (6) \\ \rightarrow CH_2Cl\text{-}CHCl\text{-}CH_3 + CH_2{=}CH\text{-}CH_3 + TeCl_2 & (7) \end{cases}$$

All these reaction, Eqs. (4)—(7), compete in the rather fast dissociation of the adduct to regenerate TTC and propylene.

$$\text{III, IV} \rightarrow CH_2{=}CH\text{-}CH_3 + TeCl_4 \quad (8)$$

This reaction may be partly responsible for the absence of vinylic chlorides in the pyrolysate.

The results with propylene, described here, can be applied to the study of the behavior of other linear olefins.

Experimental

The IR spectrum was measured using a Nippon Bunko DS-401G-type spectrophotometer. The NMR spectra were recorded on a Japan Electron Optics H-100 spectrometer (100MHz), with benzene as the internal standard. TMS was not used, because it caused precipitation with the organic tellurium compounds described in this report. As has been shown previously,[14] the isotopes of tellurium (^{123}Te and ^{125}Te; nuclear spin, 1/2; natural abundance, *ca.* 25%) hardly affected the NMR spectrum.

The chlorinated organic compounds were analyzed by gas chromatography, using a Carbowax column (at 60°C and 110°C) or a tricresylphosphate column (at 60°C).

2-Chlorocyclohexyl Trichloride (I).[15] Mp 112—113°C (decomp.), Found: C, 20.5; H, 3.8; Cl, 40.0%, mol. wt (cryoscopic), 360.

Addition of TTC to Propylene. Two grams (7.4 mmol) of TTC in 20 m*l* of acetonitrile were mixed with 0.45 m*l* (*ca.* 7.4 mmol) of liquid propylene in a sealed tube. The mixture was then left standing for 2 hr at at room temperature. On removing the solvent *in vacuo*, chloro-*n*-propyltellurium trichloride (III) was obtained as a viscous oil. The characteristics in the NMR spectrum of III (Fig. 2) in deuteriochloroform were similar to those of the sulfenyl chloride-propylene adduct.[7] The terminal methylene and the methine protons form an ABX-type spin system: a double quartet for the methylene protons ($J_{gem} \simeq 12$Hz, $\Delta\nu \simeq 22$Hz) and six symmetrical lines for the methine protons.

The same procedure was repeated using 3.7 mmol of TTC and 77 mmol of propylene. The NMR spectrum of the resulting oil (Fig. 3) suggested that bis(chloro-*n*-propyl)tellurium dichloride (IV) was formed in addition to III. The absorptions that represent the methylene and methine protons also show the features of an ABX-type spin system, though the band for the former protons is distorted and that for the latter is broadened.

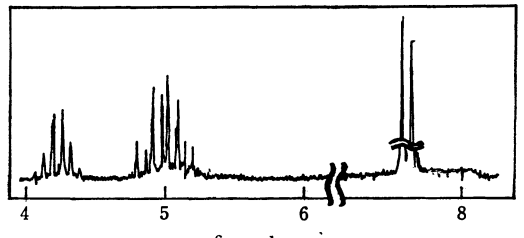

ppm from benzene

Fig. 2. NMR spectrum of III.

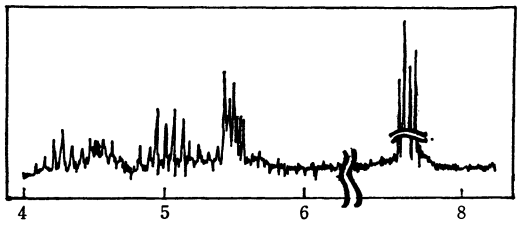

ppm from benzene

Fig. 3. NMR spectrum of III and IV.

Small percentages of impurities, depending on the solvent used in the addition reaction, were also observed in the higher field of the NMR spectra, but they are omitted in the figures cited above.

Attempt to distill or recrystallize the adduct resulted in failure.

The experiments for Table 2 were carried out as follows: two grams of TTC in 20 m*l* of a solvent were transferred to a three-necked flask fitted with a magnetic stirrer, a gas inlet, and an ice-water cooled condenser. After replacing the air with a stream of nitrogen, propylene was bubbled in under vigorous stirring at room temperature for an hour. The solvent was then removed under reduced pressure and a part of the adduct was dissolved in deuteriochloroform in order to measure the NMR spectrum.

The Reaction of the TTC-propylene Adduct with Bromine. One gram of III was dissolved in 10 m*l* of methanol containing 7.0 g of bromine and 1.5 g of potassium bromide. The mixture was warmed at 50°C for 4hr, washed with aqueous potassium hydroxide to remove the excess bromine, and filtered from inorganic tellurium compounds. A mixture of dihalopropanes and unreacted organotellurium compound separated as an oily layer. The dihalopropanes obtained by the distillation of the oil under reduced pressure gave three peaks on gas chromatography; each of them was then separated. By comparing the IR spectra with Sadtler's standard ones, the first and the third fraction, in order of elution, were found to be 1,2-dichloropropane and 1,2-dibromopropane respectively. The second fraction was a mixture of 1-bromo-2-chloropropane and 1-chloro-2-bromopropane, the ratio of which was determined from the NMR spectra. The authentic sample of the bromochloropropanes, in which 1-chloro-2-bromopropane predominates, was prepared from propylene oxide by ring closure with hydrogen chloride, followed by bromination with phosphorus pentabromide. In the NMR spectrum, the doublets for the methyl protons of 1-chloro-2-bromopropane and 1-bromo-2-chloropropane appeared at δ 1.79 (from TMS) and at δ 1.65 respectively. These signals were used to calculate the ratio of the isomers. The composition of the dihalopropanes formed by the reaction of III with bromine was approximately as follows: $CH_3CHCl\text{-}CH_2Cl$ 5%, $CH_3\text{-}CHCl\text{-}CH_2Br$ 6%, $CH_3\text{-}CHBr\text{-}CH_2Cl$ 18%, and $CH_3\text{-}CHBr\text{-}CH_2Br$ 71%. When one gram of III

14) Von Gotthard Klose, *Z. Naturforsch.*, *A*, **16**, 528 (1961).

15) M. De Moura Compos and N. Petragnani, *Tetrahedron Lett.*, **1959**, 11.

was refluxed with 2 g of bromine in methylene dichloride for 10 hr and then worked up as has been described above, the following product distribution was observed: CH_3–CHCl–CH_2Cl 11%, CH_3–CHCl–CH_2Br 20%, CH_3–CHBr–CH_2Cl 38%, and CH_3–CHBr–CH_2Br 31%.

Pyrolysis of the Adducts. Pyrolysis was conducted under a pressure of 1—5 mmHg. About one gram of the adduct in a 25-m*l* flask was immersed into an oil bath maintained at a desired temperature. The decomposition occurred immediately. The products were inorganic tellurium compounds (residue), hydrogen chloride, and organic compounds, the last of which were collected in a dry ice-methanol trap. When necessary, the trap contained a weighed amount of chloroform as an internal standard for gaschromatography. It was ascertained that the simple addition of hydrogen chloride to the olefins did not occur in the cold trap. Each of the organic products from the pyrolysis was separated by distillation or by gas chromatography and was identified by comparing the IR spectrum with that of the authentic sample or with Sadler's standard spectrum.

The authors wish to thank Dr. M. Kitabatake and C. Inoue for their discussions and Mr. N. Tanaka for his measurement of the NMR spectra.

BULLETIN OF THE CHEMICAL SOCIETY OF JAPAN VOL. 43 500—505 (1970)

Polymerization of Vinyl Chloride and Copolymerization of Vinyl Chloride with Styrene by Alkylmagnesium Chlorides

Hiroshi MINATO,* Masayoshi OKU and Nobuyuki HIGOSAKI

Department of Chemistry, International Christian University, Mitaka-shi, Tokyo

(Received July 29, 1969)

t-Butylmagnesium chloride was found to initiate the polymerization of vinyl chloride efficiently at −22—30°C. The best solvent was diethyl ether, but the degree of polymerization was the highest when no solvent was used ($\bar{P}_n = 1940$ at 20°C). The apparent activation energy for the rate of polymerization was 13.2 kcal/mol and the frequency factor was 9.06×10^4. The rate of polymerization, R_p, was equal to const. $\times [VC]^{3.90} \times [t\text{-BuMgCl}]^{1.98}$. Isopropylmagnesium bromide initiated the polymerization with less efficiency, and phenylmagnesium bromide was completely ineffective. Vinyl chloride and styrene were copolymerized in ether by *t*-butylmagnesium chloride at 30°C. The mole % styrene included in the copolymer was considerably different from those obtained by benzoyl peroxide at 48°C or by di-*t*-butylperoxy oxalate at 30°C.

Guyot and Tho investigated the polymerization of vinyl chloride in tetrahydrofuran with *t*-butylmagnesium chlorde, and suggested that the polymerization was anionic.[1-3] Their study was of great interest, since there have been no other papers on the anionic polymerization of vinyl chloride. However, their evidence did not seem convincing, and there was a paper reporting that the polymerization of vinyl chloride with Grignard reagents was of free radical nature.[4] Thus a more detailed study seemed to be desirable. This paper will describe the results of the investigation.

Experimental

Materials. Diethyl ether was shaken with one-tenth volume of a 10% sodium hydrogen sulfite solution for one hour, washed with a saturated sodium chloride solution containing 10% sodium hydroxide, then with a saturated sodium chloride solution containing some sulfuric acid, and twice with a saturated sodium chloride solution, dried over calcium chloride and then over sodium wire, and finally distilled over sodium under a nitrogen atmosphere at 34.5°C.

A *t*-butylmagnesium chloride solution was prepared in a 300 m*l* three-necked, round-bottomed flask from 1.46 g of magnesium turnings, 6.5 m*l* of *t*-butyl chloride and 150 m*l* of absolute ether under a nitrogen atmosphere. The supernatant solution was titrated and then used. The concentration was usually $1.5—2.0 \times 10^{-4}$ mol/*l*. Other Grignard solutions were prepared in a similar manner from halides and magnesium in absolute ether under a nitrogen atmosphere.

Styrene was distilled under reduced pressure before use. Vinyl chloride was passed through a silver nitrate solution and a calcium chloride tube, and then collected

* To whom correspondence should be addressed at Department of Chemistry, Tokyo Metropolitan University, Setagaya-ku, Tokyo.

1) A. Guyot and Pham Quang Tho, *C. R. Acad. Sci. Paris*, **256**, 165 (1963).

2) A. Guyot and Pham Quang Tho, *J. Polymer Sci., C*, **1964**, No. 4, 299.

3) A. Guyot and Pham Quang Tho, "Chemistry of Polymerization Processes," ed. by Society of Chemical Industry, London (1966), pp. 69—81.

4) K. Yoshida and T. Morikawa, *Sci. and Ind.*, **27**, 80 (1953).

in a pressure-tube cooled with a dry ice-methanol bath in a vacuum system.

Polymerization of Vinyl Chloride by *t*-Butylmagnesium Chloride. A pressure tube containing *t*-butylmagnesium chloride dissolved in ether was connected to a vacuum system under a nitrogen atmosphere, and cooled with a dry ice-methanol bath. A measured amount of deaerated vinyl chloride was distilled into the pressure tube, which was then sealed under a nitrogen atmosphere. Tubes were placed in a constant temperature bath and shaken by hand occasionally. After the polymerization was over, the ampoule was opened, and the polymer was washed with 6 N hydrochloric acid, water and methanol, and then dried under reduced pressure.

For the runs containing no ether, the ethereal solution of a Grignard reagent was evaporated to dryness in a vacuum, and then vinyl chloride was added to the residue. The mixture was then polymerized by the same procedure as described above.

Copolymerization of Vinyl Chloride with Styrene or Methyl Methacrylate by *t*-Butylmagnesium Chloride. A measured amount of deaerated vinyl chloride was distilled into the pressure tube containing *t*-butylmagnesium chloride and styrene or methyl methacrylate. The tubes were sealed under a nitrogen atmosphere, and placed in a constant temperature bath at 30.0°C. After appropriate intervals, the tubes were removed from the bath, cooled to −20°C, opened, and the content was poured into methanol. The polymer precipitated was filtered and washed with methanol until the filtrate formed no precipitates with a silver nitrate solution. The copolymer was dried and was burned in platinum wire within a flask, and chloride ions produced were titrated with 0.02 N mercuric nitrate solution.[5]

Copolymerization of Vinyl Chloride with Styrene by *t*-Butylperoxy Oxalate. *t*-Butylperoxy oxalate was prepared according to the method of Bartlett, Benzing and Pincock.[6] Procedures of polymerization and the work-up were the same as described above.

Results and Discussion

At first, the polymerization of vinyl chloride was attempted in tetrahydrofuran, but both the extent of conversion and the degree of polymerization were always smaller than those reported by Guyot and Tho.[3] After various solvents were investigated, diethyl ether was found to be an excellent medium for the polymerization. The degrees of polymerization reported by Guyot and Tho were 66—73, but those of polyvinyl chloride produced in diethyl ether were as large as 1455.[7] It was further found that in the absence of diethyl ether,

Table 1. Polymerization of vinyl chloride with *t*-butylmagnesium chloride

Run	*t*-BuMgCl mol/*l*	$[VC]_0$ mol/*l*	Temp. (°C)	Time (hr)	Conversion (%)	Degree of Polymerization	Remarks
1	0.0286	14.44	−22.0	490	19.3	1530	no ether
2	0.040	12.64	10.0	2	1.4	165	
3	0.040	12.64	10.0	19	7.5	780	
4	0.040	12.64	10.0	42	30	986	
5	0.040	12.64	10.0	120	39	1250	
6	0.040	12.64	10.0	350	48	1455	
7	0.0253	12.64	20.0	46	30.7	780	
8	0.0289	14.44	20.0	46	26.6	1940	no ether
9	0.0253	12.64	30.0	46	50.8	640	
10	0.0289	12.64	30.0	46	18.5	840	no ether
11	0.090	11.23	30.0	22	66	212	
12	0.045	11.23	30.0	22	55	360	
13	0.023	11.23	30.0	22	21	710	
14	0.090	11.23	20.0	22	39	237	
15	0.045	11.23	20.0	22	29	450	
16	0.023	11.23	20.0	22	14	610	
17	0.090	11.23	30.0	22	22	254	
18	0.0735	9.20	30.0	22	22	181	
19	0.0540	6.75	30.0	22	23	159	
20	0.0506	12.64	20.0	22	29	470	
21	0.0450	11.23	20.0	22	30	380	
22	0.0368	9.20	20.0	22	29	280	

5) K. Ono, *Ann. Sankyo Res. Lab.*, **18**, 51 (1966).

6) P. D. Bartlett, E. R. Benzing and R. E. Pincock, *J. Amer. Chem. Soc.*, **82**, 1762 (1960).

7) Recently a detailed investigation on the composition of Grignard compounds has been published, which has established that RMgX (X=Cl, Br, or I) exists as monomeric form in tetrahydrofuran, whereas in diethyl ether RMgCl exists as a dimer in both dilute and concentrated solutions and RMgBr and RMgI are monomeric at low concentrations (0.1 mol/*l*) and polymeric at higher concentrations. (F. W. Walker and E. C. Ashby, *J. Amer. Chem. Soc.*, **91**, 3845 (1969)).

i.e., with a solid Grignard reagent in liquid vinyl chloride, the degree of polymerization was as large as 1940. The results of polymerization are summarized in Table 1.

Run 1 shows that this polymerization proceeds even at −22°C though the rate is small. Runs 2—6 show that the degree of polymerisation increases with the extent of conversion; this behavior is not what is expected for free-radical polymerization. Runs 7—10 indicate that in the absence of ether the degree of polymerization is larger though the rate of polymerization is somewhat

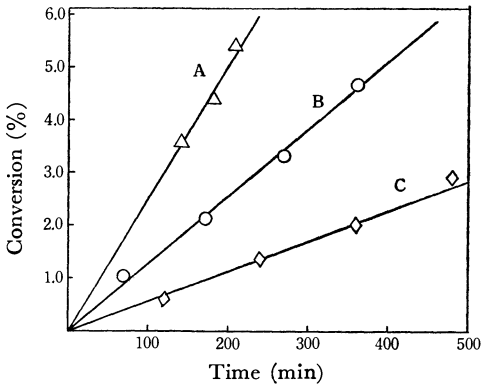

Fig. 1. Rates of polymerization of vinyl chloride at different temperatures.
A, 40.0°C; B, 30.5°C; C, 20.1°C; $[VC]_0=12.64$ mol/l, $[t\text{-BuMgCl}]_0=2.50\times10^{-2}$ mol/l

smaller. Runs 11—16 show that the larger the catalyst concentration the smaller the degree of polymerization. Runs 17—22 indicate that upon dilution of a mixture with ether the extent of conversion is unaltered, but the degree of polymerization decreases.

Figure 1 shows the rates of polymerization at different temperatures with solutions of the same composition. R_p was 1.25, 2.73, and 5.33×10^{-5} mol/l sec at 20.1, 30.5, and 40.0°C, respectively. Plots of log R_p *versus* $1/T$ yielded a straight line, and R_p was expressed as follows.

$$R_p = 9.06\times10^4\, e^{-\frac{13200}{RT}} \qquad (1)$$

The relationship between R_p and the initial concentration of *t*-butylmagnesium chloride is shown in Fig. 2. With $[VC]_0=11.23$ mol/l and at 30.1°C, R_p was 0.333, 3.85 and 9.76×10^{-5} mol/l sec when $[t\text{-BuMgCl}]_0$ was 0.0128, 0.0428 and 0.0711 mol/l, respectively. From the slope of the straight line, R_p was expressed as follows.

$$R_p = \text{const.}\times[t\text{-BuMgCl}]^{1.98} \qquad (2)$$

Figure 3 shows the relationship between the rates of polymerization and the concentration of vinyl chloride. From the slope of the straight line, R_p was expressed as follows.

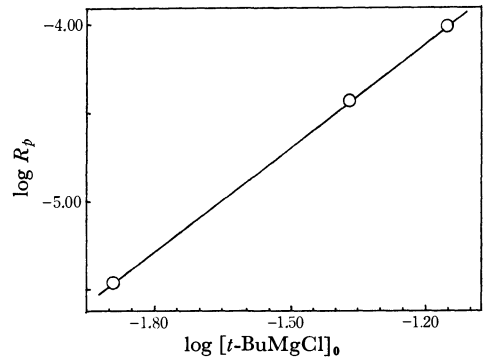

Fig. 2. Rates of polymerization of vinyl chloride with different catalyst concentration at 30.1°C.
($[VC]_0=11.23$ mol/l)

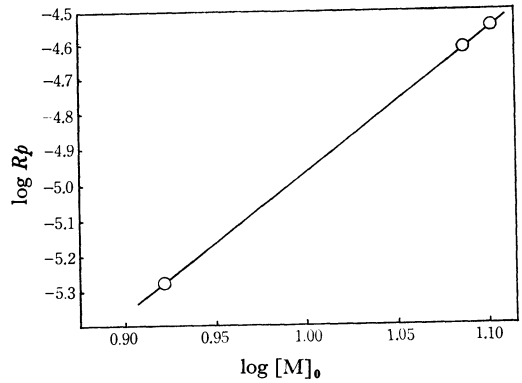

Fig. 3. Rates of polymerization of vinyl chloride with different monomer concentrations at 30.1°C.
($[t\text{-BuMgCl}]_0=2.50\times10^{-2}$ mol/l)

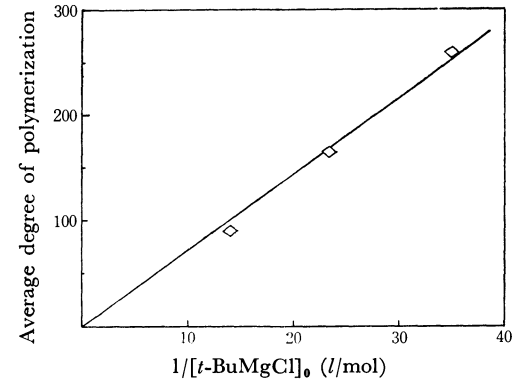

Fig. 4. Relationship between average degree of polymerization and catalyst concentration.
$[VC]_0=11.23$ mol/l, Conversion=3.0%, 30.1°C

$$R_p = \text{const.}\times[VC]^{3.90}[t\text{-BuMgCl}]^{1.98} \qquad (3)$$
(const. = 2.08×10^{-6} at 30°C)

The relationship between the average degree of polymerization and $1/[t\text{-BuMgCl}]_0$ is shown in Fig. 4.

As for other Grignard reagents, isopropylmagnesium bromide was found to initiate the polymerization with less efficiency and phenylmagnesium bromide initiated no polymerization. With $[i\text{-PrMgBr}]_0=0.058$ mol/l and $[VC]_0=12.51$ mol/l at 25.0°C, a polymer with $\bar{P}=625$ was obtained with 13% yield after 16 hr of polymerization. With $[PhMgBr]_0=0.288$ mol/l and $[VC]_0=7.30$ mol/l, no polymer was formed after 20 hr at 20.0°C or after 3 hr at 60°C.

The possible mechanisms of the initiation of the polymerization are (1) monomolecular homolytic decomposition of RMgX, (2) production of free radicals by the reaction between RMgX and vinyl chloride, (3) anionic polymerization, (4) polymerization by an anion-radical, and (5) polymerization by a complex involving magnesium.

The possibility of (1) was definitely excluded from the observation that an ethereal solution of *t*-butylmagnesium chloride underwent no decomposition when it was kept under a nitrogen atmosphere at room temperature for 25 days.

The frequency factor obtained from the Arrhenius plots was 9.06×10^4 which was smaller than the values found for ordinary radical polymerizations (10^6—10^8). Equation (3) is quite different from the equation applicable to ordinary radical polymerizations ($R_p=\text{const.}\times[VC]\times[\text{Initiator}]^{0.5}$).

In an attempt to clarify the mechanism of the initiation of polymerization by *t*-butylmagnesium chloride, copolymerization of vinyl chloride and styrene was investigated. The results are summarized in Table 2, and are compared with the results of a free radical polymerization in acetone by benzoyl peroxide at 48°C in Fig. 5. The mol % styrene included in the copolymer obtained by use of *t*-butylmagnesium chloride is considerably different from that obtained by use of benzoyl peroxide.[8] Since the difference in temperatures and solvents might be the cause for such discrepancy,

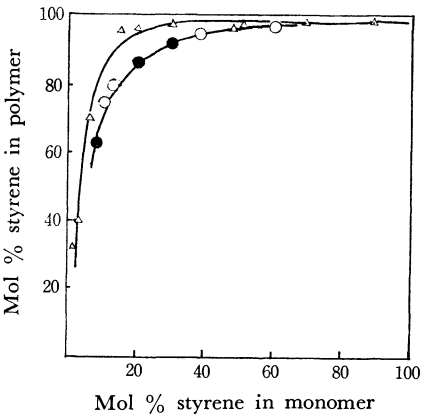

Fig. 5. Copolymerization of vinyl chloride and styrene.
△ with *t*-butylmagnesium chloride in ether at 30°C
○ with benzoyl peroxide in acetone at 48°C
● with di-*t*-butylperoxy oxalate in ether at 30°C

styrene and vinyl chloride were copolymerized in ether at 30°C by use of di-*t*-butylperoxy oxalate. Results are summarized in Table 3 and Fig. 5. These findings indicate that the polymerization initiated by *t*-butylmagnesium chloride is different from ordinary radical polymerization.

Copolymerization of vinyl chloride and methyl methacrylate by *t*-butylmagnesium chloride was attempted, and the results are shown in Table 4. The rates of polymerization were much greater than those of vinyl chloride and styrene, and the polymer obtained was the homopolymer of methyl methacrylate. Apparently the anionic polymerization of only methyl methacrylate took place. It is reasonable that vinyl chloride could not compete with methyl methacrylate, since methoxycarbonylcarbanion is far more stable than chlorocarbanion.

Table 2. Copolymerization of vinyl chloride and styrene by *t*-butylmagnesium chloride at 30.0°C

Mol % styrene in monomers	Catalyst mol/100 mol monomers	Time (hr)	Conversion (%)	Cl (%) in copolymer	Mol % styrene in copolymer
89.1	0.23	3.0	0.253	0.389	98.8
69.1	0.23	2.3	0.715	0.270	99.2
50.5	0.23	2.8	0.282	0.463	98.5
48.4	0.33	333.5	1.92	1.08	96.9
29.9	0.60	70.5	2.35	0.870	97.4
20.0	0.33	70.5	0.318	1.41	96.0
15.0	0.33	355	0.291	1.76	95.0
7.0	0.60	189	1.15	11.58	70.1
3.3	0.60	186	1.10	27.13	39.6
1.0	0.60	186	0.073	31.75	32.1

8) E. C. Chapin, G. E. Han and R. G. Fordyce, *J. Amer. Chem. Soc.*, **70**, 538 (1948).

TABLE 3. COPOLYMERIZATION OF VINYL CHLORIDE AND STYRENE BY DI-*t*-BUTYLPEROXY OXALATE AT 30.0°C

Mol % styrene in monomers	Catalyst mol/100 mol monomers	Time (hr)	Conversion (%)	Cl (%) in copolymer	Mol % styrene in copolymer
29.4	0.30	48	4.62	2.57	92.6
20.1	0.30	50	6.45	4.74	86.9
14.8	0.30	50	2.32	7.46	80.0
7.0	0.30	50	1.06	15.0	62.7
2.95	0.30	50	0.525	22.6	47.5

TABLE 4. COPOLYMERIZATION OF VINYL CHLORIDE AND METHYL METHACRYLATE BY *t*-BUTYLMAGNESIUM CHLORIDE AT 30.0°C

Mol % MMA in monomers	Catalyst mol/100 mol monomers	Time (min)	Conversion (%)	Cl (%) in copolymer	Mol % MMA in copolymer
67.2	0.33	3	9.43	0	100
49.5	0.18	5	4.26	0	100
28.7	0.22	5	8.54	0	100
9.95	0.22	5	6.03	0	100
8.01	0.4	15	4.18	0	100
4.87	0.44	5	4.13	0	100
1.97	0.4	20	1.49	1.82	95.0

From the data on the copolymerization of styrene and vinyl chloride shown in Table 2, the monomer reactivity ratios r_1 and r_2 were calculated by means of Fineman and Ross' plots. The values obtained were r_1(styrene)=56 and r_2(vinyl chloride)=0. The values reported for the copolymerization with benzoyl peroxide were $r_1=35$ and $r_2=0.067$.[8]

Since the rate of conversion in the styrene-vinyl chloride was very low, the rate of polymerization of styrene alone by *t*-butylmagnesium chloride was determined. The initial rate of polymerization of styrene alone was 4.86×10^{-7} mol/*l* sec at 30.0°C when $[t\text{-BuMgCl}]_0$ was 0.57 mol/*l* and $[\text{styrene}]_0$ was 5.46 mol/*l*. The initial rate of polymerization of vinyl chloride alone was 9.76×10^{-5} mol/*l* sec at 30.0°C when $[t\text{-BuMgCl}]_0$ was 0.63 mol/*l* and $[\text{VC}]_0$ was 10.2 mol/*l*.

Gough and Dixon studied the reaction between allyl bromide and *t*-butylmagnesium chloride, and proposed that a radical mechanism is operative. They formulated the reaction as follows.[9]

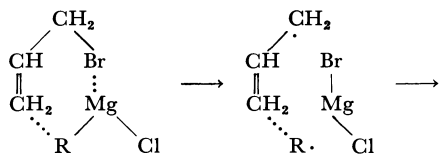

$RCH_2\text{–}CH{=}CH_2$, *etc.*

They found that relative rates of reaction of alkylmagnesium halides with allyl bromide were *t*-BuMgCl 107, *s*-BuMgCl 22.6, *n*-BuMgCl 2.77 and PhMgCl 1.00. This variation in rates is somewhat in parallel with the variation in the efficiency of initiation by *t*-tubyl-, isopropyl-, and phenylmagnesium halides in this investigation. However, as a possible intermediate of the polymerization by *t*-butylmagnesium chloride a free radical is excluded on the basis of the findings that (1) the rate of polymerization was proportional to $[\text{VC}]^4\cdot[\text{Cat}]^2$ instead of $[\text{VC}][\text{Cat}]^{0.5}$, (2) the results of copolymerization by *t*-butylmagnesium chloride were different from those by benzoyl peroxide or *t*-butylperoxy oxalate, and (3) the frequency factor obtained from the Arrhenius plots of rates of polymerization was 9.06×10^4 which was smaller than the values found for ordinary radical polymerizations (10^6—10^8).

Another possible intermediate of this polymerization is an anion, but this possibility can be rejected on the basis of the finding that phenylmagnesium bromide failed to initiate the polymerization of vinyl chloride. It is not reasonable that *t*-butylmagnesium chloride initiates an anionic polymerization whereas phenylmagnesium bromide does not.

Other possible propagating species in this polymerization are an anion-radical or a complex involving magnesium.

Russel, Jansen and Strom have shown that butylmagnesium bromide in a tetrahydrofuran solution forms an anion-radical with a variety of nonbenzenoid aromatic compounds of aromatic ketones such as benzophenone of fluorenone.[10]

9) R. G. Gough and J. A. Dixon, *J. Org. Chem.*, **33**, 2148 (1968).

10) G. A. Russell, E. G. Jansen and E. T. Strom, *J. Amer. Chem. Soc.*, **86**, 1807 (1964).

$$[Bu:]^- + A \rightarrow [Bu\cdot + A^{\overline{\cdot}}] \rightarrow BuA^-$$

Maruyama has found that Grignard reagents react with ketones to form an anion-radical.[11]

$$RMgX + \overset{|}{\underset{|}{C}}{=}O \rightarrow [\overset{|}{\underset{|}{C}}\cdot{-}O^-] \rightarrow R\overset{|}{\underset{|}{C}}OMgX$$

Thus it is probable that an anion-radical is the propagating species in the polymerization by *t*-butylmagnesium chloride. Findings in this investigation excluded three other possible initiation mechanisms, namely (1) radical polymerization by monomolecular decomposition of *t*-butylmagnesium chloride, (2) radical polymerization by a reaction between *t*-butylmagnesium chloride and some other substances, and (3) anionic polymerization. At this stage it is not possible to determine whether the propagating species is an anion-radical or a complex involving magnesium.

Though the mechanism of initiation was not completely clarified, the investigation demonstrated that polymerization of vinyl chloride proceeded efficiently in the presence of *t*-butylmagnesium chloride in diethyl ether or in the absence of solvent at −22°—30°C, and the degree of polymerization of polyvinyl chloride thus obtained was as high as 1940.

Grateful acknowledgement is made to the donors of the Petroleum Research Fund, administered by the American Chemical Society, for support of this research.

11) K. Maruyama, This Bulletin, **37**, 897, 1013 (1964).

BULLETIN OF THE CHEMICAL SOCIETY OF JAPAN VOL. 43 505—509 (1970)

Asymmetric Reactions. IV. An Attempted Asymmetric Reduction by a Solution of $[Co(CN)_5]^{3-}$ and Optically Active α-Amino Acid, and Its Reactive Species[1)]

Yoshiaki OHGO, Seiji TAKEUCHI and Juji YOSHIMURA

Laboratory of Chemistry for Natural Products, Faculty of Science, Tokyo Institute of Technology, Ookayama, Meguro-ku, Tokyo

(Received August 1, 1969)

Reduction of various olefines by a solution of pentacyanocobaltate and glycine or optically active α-amino acid was studied. There is no essential difference between the reactivity of $[Co(CN)_5H]^{3-}$ to olefines and that of the solution of pentacyanocobaltate and α-amino acid. Atropic acid was reduced with the solution containing optically active α-amino acid (L-isoleucine) to give slightly optically active hydratropic acid. It was found that the main reactive species in the solution of $[Co(CN)_5]^{3-}$ and α-amino acid was $[Co(CN)_5H]^{3-}$ (this might be the reason for the asymmetric reduction not taking place effectively), and the reversible change between $[Co(CN)_5]^{3-}$ and $[Co(CN)_5H]^{3-}$ was observed depending on the pH of the solution.

It has been reported by Kwiatek *et al.* that many olefines are hydrogenated catalytically by $[Co(CN)_5]^{3-}$,[2)] and recently by Suzuki and Kwan that an aqueous equimolar solution of $[Co(CN)_5]^{3-}$ and α-amino acids or other acids reduces dienes to monoenes by the following mechanism.[3)]

$$[Co(CN)_5]^{3-} + R\text{-}\underset{\displaystyle NH_2}{\underset{|}{CH}}\text{-}COOH$$

$$\xrightarrow{-CN} \left[(CN)_4Co\begin{array}{l}NH_2\text{-}CH\text{-}R\\ |\\ O\text{-}C{=}O\\ /\\ H\end{array}\right]^{2-} \quad \text{(I)}$$

$$\xrightarrow{\text{electron transfer}} \left[(CN)_4Co\begin{array}{l}NH_2\text{-}CH\text{-}R\\ |\\ O - C{=}O\end{array}\right]^{2-} \quad \text{(II)}$$

$$+ 1/2\,H_2$$

$$2\left[(CN)_4Co\begin{array}{l}NH_2\text{-}CH\text{-}R\\ |\\ O\text{-}C{=}O\\ /\\ H\end{array}\right]^{2-} + CH_2{=}CH\text{-}CH{=}CH_2 \longrightarrow CH_3\text{-}CH{=}CH\text{-}CH_3 + II$$

1) Asymmetric Reaction. III. This Bulletin, **42**, 2957 (1969).

2) J. Kwiatek, I. L. Mador and J. K. Seyler, *J. Amer. Chem. Soc.*, **84**, 304 (1962).

3) T. Suzuki and T. Kwan, *Nippon Kagaku Zasshi*, **88**, 395 (1967); *ibid.*, **88**, 400 (1967).

Table 1. Hydrogenation of monoenes

Substrate	Solvent	Complex	Product and yield
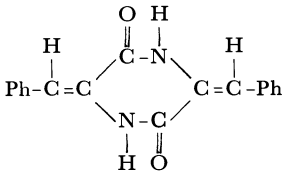	Pyridine and water	$[Co(CN)_5H]^{3-}$ (a)	(c)
		Co-Gly (b)	(d)
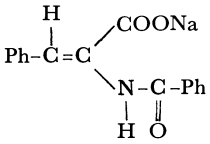	Water	$[Co(CN)_5H]^{3-}$ Co-Gly	(e)
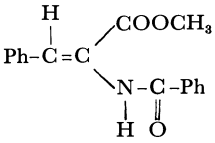	Pyridine and water	$[Co(CN)_5H]^{3-}$ Co-Gly	(e)
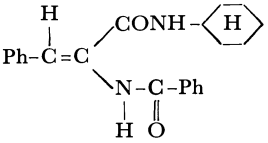	Ethanol and water	$[Co(CN)_5H]^{3-}$ Co-Gly	(e)
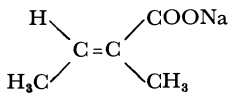	Water	$[Co(CN)_5H]^{3-}$ Co-Gly	(e)
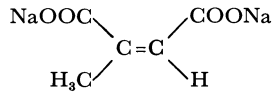	Water	Co-Gly	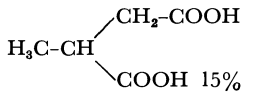
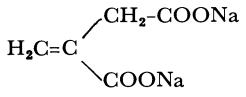 (f)	Water	Co-Gly	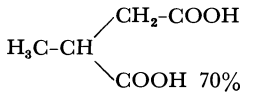
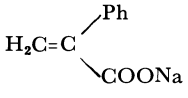 (f)	Water	Co-Gly	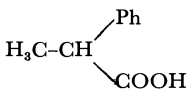 Quantitatively
		Co-L-Isol (b)	(g)

(a) Reaction time of catalytic hydrogenation by $[Co(CN)_5]^{3-}$ was 4 to 5 days at room temperature.

(b) Co-Gly or Co-L-Isol represents the solution of $[Co(CN)_5]^{3-}$ and glycine or L-isoleucine. Reaction time was 1 day at room temperature.

(c) Both double bonds were reduced quantitatively.

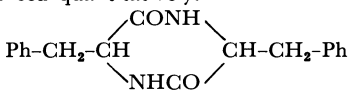

(d) Mixture of fully and partially hydrogenated products was obtained.

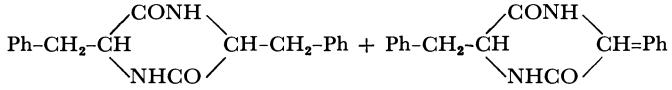

(e) The starting material was recorded quantitatively.

(f) These material were known to be reduced by $[Co(CN)_5H]^{3-}$.[2]

(g) Raw product had $[\alpha]_D$ +0.2° but distillate had slightly negative rotation which was converted to acylthiourea derivative ($[\alpha]_{436}$ −0.2°).

They suggested that dienes are reduced to monoenes *via* coordination to the cobalt (Co^{II}) of the intermediate complex (I).

If monoenes which form asymmetric carbon after reduction can be reduced with the solution of $[Co(CN)_5]^{3-}$ and optically active α-amino acid by the similar mechanism, the coordination of monoenes to the intermediate complex (I) will be affected stereospecifically by the optically active α-amino acid, and an asymmetric reduction will take place.

This paper gives a comparison of the reactivity of a solution of $[Co(CN)_5]^{3-}$ and α-amino acid with that of $[Co(CN)_5H]^{3-}$ to monoenes, and a discussion on whether asymmetric reduction takes place.

Results and Discussion

The results of hydrogenation with a solution of $[Co(CN)_5]^{3-}$ and glycine are summarized in Table 1 in comparison with that of $[Co(CN)_5H]^{3-}$.

As shown in Table 1, the reactivities of $[Co(CN)_5H]^{3-}$ and Co-Gly are similar to each other, and atropic acid is reduced to hydratropic acid quantitatively.

Experiments were carried out to see whether an asymmetric reduction would occur, using atropic acid as substrate and L-isoleucine as an optically active α-amino acid (in an aqueous solution of $[Co(CN)_5^{3-}]$). Atropic acid was reduced by this solution quantitatively to give crude hydratropic acid having slightly positive rotation ($[\alpha]_D+0.2°$), but the optical acivity of hydratropic acid purified by distillation changed to a very small negative value. The acylthiourea derivative of the hydratropic acid was synthesized and the ORD spectrum[4] was measured in order to identify the substance having slightly negative rotation with hydratropic acid. However, because of the very low optical activity ($[\alpha]_{436}-0.2°$) of the purified acylthiourea derivative ($\begin{matrix}Ph\\CH_3\end{matrix}\!\!>\!CH_3\text{-}CH\text{-}CONH\text{-}\overset{\overset{S}{\|}}{C}\text{-}S\text{-}N(C_2H_5)_2$), identification of the optically active material by ORD spectrum failed. Nevertheless, we could not consider it due to contaminant, because the sample was extremely pure. If this optical activity is that of acylthiourea derivative of hydratropic acid, the optical yield is 0.1% (acylthiourea derivative of optically pure hydratropic acid has $[\alpha]_{436}-200°$).

The fact that the reactivities of $[Co(CN)_5H]^{3-}$ and Co-Gly are similar to each other and the optical yield is very small lets us deduce that the intermediate complex such as I to which α-amino acid coordinates directly may not play an essential role in this hydrogenation reaction. On the other hand, it is known that dienes are reduced to monoenes by a solution of $[Co(CN)_5]^{3-}$ and organic or inorganic acids[3] instead of α-amino acids, and the formation of $[Co(CN)_5H]^{3-}$ by aging of an aqueous solution of $[Co(CN)_5]^{3-}$ is promoted by cesium chloride and other salts.[5] Thus, it was deduced that α-amino acid might promote the aging reaction as cesium chloride. As metal hydride signal of $[Co(CN)_5H]^{3-}$ was known to be observed at high magnetic field of the nuclear magnetic resonance spectrum,[6] the NMR spectrum of Co-Gly was measured. The results are shown in Table 2 and Fig. 1.

Fig. 1. NMR spectrum.

Metal hydride signal was observed at high magnetic field and the chemical shift of the hydride formed in Co-Gly was almost the same as that of $[Co(CN)_5H]^{3-}$, and the amount of the hydride did not depend on the amount of α-amino acid (glycine). Thus, this hydride is considered to be $[Co(CN)_5H]^{3-}$ and the main reactive species in the hydrogenation with the aqueous solution of $[Co(CN)_5]^{3-}$ and glycine, *i.e.* α-amino acid. It was also found that the pH of the solution was an important factor in the formation of $[Co(CN)_5H]^{3-}$ from the following experiment. The color of the solution of $[Co(CN)_5]^{3-}$ changes from green to yellow and *vice versa* depnending on the pH:[7]

$$\underset{\text{green}}{[Co(CN)_5]^{3-}} \underset{\text{pH increase on addition of NaOH}}{\overset{\text{pH decrease on addition of glycine}}{\rightleftharpoons}} \text{yellow}$$

The spectrophotometric change of an aqueous solution of $[Co(CN)_5]^{3-}$ and glycine is shown in Fig. 2. Absorption of $[Co(CN)_5]^{3-}$ at 970 mμ[8] decreased gradually on standing for 16 hr at room temperature, and increased on addition of an

4) C. Djerassi, K. Undheim and Anne-Marie Weidler, *Acta Chem. Scand.*, **16**, 1147 (1962).

5) N. K. King and M. E. Winfield, *J. Amer. Chem. Soc.*, **80**, 2060 (1958).

6) W. P. Griffith and G. Wilkinson, *J. Chem. Soc.*, **1959**, 2757.

7) The pH of a solution of $Co(CN)_5^{-3}$ prepared by dissolving $CoCl_2\cdot 6H_2O$ (3.18 g) and KCN (4.5 g) in H_2O (26 m*l*) was about 13. On addition of molar equivalent glycine the pH decreased to 9.5.

8) N. K. King and M. E. Winfield, *J. Amer. Chem. Soc.*, **83**, 3366 (1961).

Table 2. NMR spectra of hydrides

Reaction system	Time (min)	Spacing between chemical shift of hydride and sodium acetate	Co-H/Co
$[Co(CN)_5]^{3-} + H_2O$	20	14.1 ppm	0.18
$[Co(CN)_5]^{3-}$ + 1/2 glycine	24	14.2 ppm	0.50
$[Co(CN)_5]^{3-}$ + glycine	20	14.4 ppm	0.45

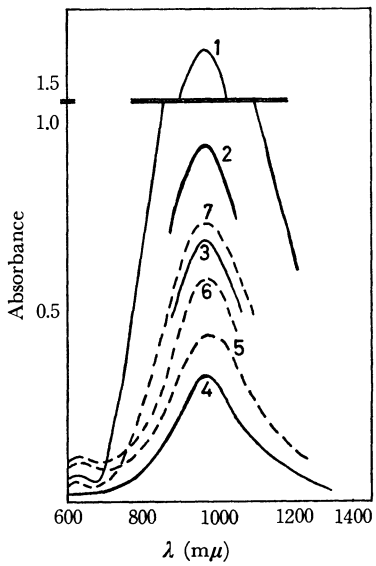

Fig. 2. Spectrophotometric change of a solution $[Co(CN)_5]^{3-}$ and glycine.
1 10 min after preparation of the solution (0.038 M; 0.38 g of $CoCl_2 \cdot 6H_2O$ in 35 ml of water)
2 50 min
3 90 min
4 16 hr aqueous NaOH solution was added
5 10 min after the addition of NaOH solution
6 3 hr
7 19 hr

aqueous sodium hydroxide. From this it is apparent that there is an equillibrium $[Co(CN)_5]^{3-} \rightleftharpoons [Co(CN)_5H]^{3-}$ in the solution of $[Co(CN)_5]^{3-}$ and glycine, and the equillibrium shifts to the right with decrease of pH and to the left by the addition of alkali.[9] Consequently, the following reactions are considered to occur mainly in the hydrogenation with the solution of $[Co(CN)_5]^{3-}$ and α-amino acid.

(A) $2[Co(CN)_5]^{3-} + H_2O \rightleftharpoons [Co(CN)_5H]^{3-} + [Co(CN)_5OH]^{3-}$

(B) $[Co(CN)_5H]^{3-} +$ 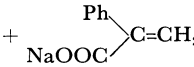 $\xrightarrow{H_2O}$ 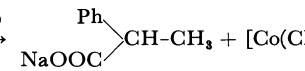 $+ [Co(CN)_5OH]^{3-}$

(C) $[Co(CN)_5OH]^{3-} + R\text{-}CH(NH_2)\text{-}COOH \longrightarrow$ 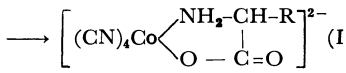 (II) $+ H_2O$

The reactive species $[Co(CN)_5H]^{3-}$ formed in the reaction (A) which is promoted by α-amino acid reduces olefine to saturated compound in the reaction (B). $[Co(CN)_5OH]^{3-}$ formed incidentally with $[Co(CN)_5H]^{3-}$ reacts with α-amino acid to give the complex(II) isolated by Suzuki and Kwan.[3]

Thus, the asymmetric grouping of the optically active amino acid can not effectively control the coordination of olefines to the metal of the reactive species.

Experimental

Reduction of Monoenes by a Solution of $[Co(CN)_5]^{3-}$ and Glycine, or $[Co(CN)_5H]^{3-}$. The solution of $[Co(CN)_5]^{3-}$ and glycine was prepared by Kwan's method.[3] In the case of $[Co(CN)_5H]^{3-}$, 1/2 mole of the substrate was used to 1 mole of cobalt chloride, and 1/3 mole in the case of the solution of $[Co(CN)_5]^{3-}$ and glycine. Water-insoluble substrates were reacted in the mixture of water and organic solvents (see Table 1), and recovered by the addition of a large amount of water. Carboxylic acids were used as sodium salts, and the products were extracted with ether after acidification with hydrochloric acid.

Reduction of Atropic Acid by a Solution of $[Co(CN)_5]^{3-}$ and L-Isoleucine. To a solution of 9.4 g of cobalt chloride (0.04 mol) in 100 ml water, 13.0 g of potassium cyanide (0.20 mol) in 40 ml of water was added. When the solution became homogeneous and dark green, 5.2 g of L-isoleucine (0.04 mol) dissolved in 200 ml of water was added. The color of the solution turned to yellow within 10 min and 2.0 g of sodium atropate (0.013 mol) in 40 ml of water was then added. All the procedure was carried out under nitrogen atmosphere. After 1 day the solution was acidified with

9) An analogous phenomenon was observed in formation of alkylcobaloximes. Near neutral medium only α-substitutedcobaloximes was formed and alkaline solution addition in the β-position took place. In order to explain the differences Schranzer and Windgassen postulated an pH-dependent equilibrium. G. N. Schrauzer and R. J. Windgassen, *J. Amer. Chem. Soc.*, **89**, 1999 (1967).

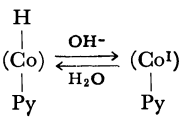

hydrochloric acid and extracted with ether and dried with calcium chloride. The ether solution was evaporated and 1.7 g of residual oil was obtained. This was found to be identical with the authentic hydratropic acid in IR spectrum. The optical activity of the product was slightly positive ($[\alpha]_D+0.2°$, *c* 10, ethanol), and no contamination of L-isoleucine in the product was detected by paper chromatography, using *n*-butanol saturated with water as a developing solvent and ninhydrin or BTB as coloring reagents (R_f: L-isoleucine 0.31, hydratropic acid 0.89, product 0.88). However, the optical activity of the material which was obtained by distillation of the product showed a slightly negative rotation. The main fraction was distilled at 82—83°C/0.05 mmHg and 1.45 g of purified material was obtained. The acylthiourea derivative of the purified hydratropic acid was synthesized[4] and the crude crystals obtained was recrystallized twice from *n*-hexane and about 0.5 g of crystals was obtained, mp 106—7°C. The silica-gel TLC showed one spot (developing solvent; ethyl acetate: pyridine= 1 : 1). Elemental analysis was as follows, Found: C, 63.94; H, 7.54; N, 10.25; S, 12.28%. Calcd for $C_{14}H_{20}N_2OS$: C, 63.61; H, 7.63; N, 10.60; S, 12.13%. The specific rotation was $[\alpha]_{436}$ −0.2° (*c* 12, benzene) and the optical yield was only 0.1%.

Measurement of NMR Spectra. The NMR spectrum was measured with a JNM-4H-100 Spectrometer (Japan Electron Optics Laboratory Co., Ltd.) at 100 Mc/sec. The concentration of the solution of $[Co(CN)_5]^{3-}$ and glycine was 0.5 M (0.18 g) of $CoCl_2 \cdot 6H_2O$ in 25 m*l* of water). As internal standard sodium acetate was used and the quantity of the hydride formed in the solution was estimated from the ratio of the integration of the hydride signal to that of sodium acetate. The average value taken from integration repeated a few times was used.

The authors are grateful to Ajinomoto Co., Inc., for the gift of amino acids, to Dr. Khoko Tanabe for the measurement of ORD spectra and to Mr. Kiyoshi Fukukawa for the measurement of NMR spectra.

BULLETIN OF THE CHEMICAL SOCIETY OF JAPAN VOL. 43 509—514 (1970)

The Thermal Reaction of 3-Acetylguaiazulene with Sulfur

Shinji KUROKAWA

Department of Chemistry, Faculty of Education, Saga University, Honjyô-machi, Saga

(Received August 9, 1969)

When 3-acetylguaiazulene was heated with sulfur at 200°C, three new azulenoids were obtained, in addition to the S-guaiazulene formed by the loss of the acetyl group; the structures were established as 2-acetylguaiazulene, 6-acetyl-, and 7-acetyl-3,5,8-trimethylazuleno[6,5-*b*]thiophenes. From the experimental results it became obvious that a sulfur atom linked one methyl carbon atom of the isopropyl group with the C_6-azulene-ring carbon atom in 3-acetylguaiazulene, resulting in the formation of a thiophene ring, and also that the loss and the migration of the acetyl group took place in 3-acetylguaiazulene as well. The acetyl migration in this compound was ascertained to be a simple thermal reaction and to occur in one direction, from C_3 to C_2.

In the previous works on the thermal reaction of S-guaiazulene or vetivazulene with sulfur, the formations of 3,5,8-trimethylazuleno[6,5-*b*]thiophene[1,2] and 3,5,9-trimethylazuleno[1,2-*b*]thiophene[3] have been reported. The present investigation will be concerned with the thermal reaction between sulfur and 3-acetylguaiazulene (I), which contains both alkyl and acetyl substituents.

Results and Discussion

Structural Elucidation of the Reaction Products. 3-Acetylguaiazulene (I) was heated with sulfur powder at 200°C. When the reaction mixture was subjected to step-by-step elution chromatography, three new compounds were isolated in addition to a small amount of S-guaiazulene (II), as is shown in Table 1. On these compounds, structural elucidation was carried out as follows.

a) 2-Acetylguaiazulene (III). The green crystalline substance, mp 80—81°C, which was isolated as the major product in this reaction had the same molecular formula, $C_{17}H_{20}O$, as the 3-acetylguaiazulene used as the starting material, but it was different in that is easily formed 2,4-dinitrophenylhydrazone, mp 246—247°C. The carbonyl group of this compound was an acetyl group from a methyl singlet (2.72 ppm) which can be assigned to an acetyl group in the NMR spectrum (Fig. 1-B), and from prominent peaks at *m/e* 43 and 197 (m^*= 161.7) in the mass spectrum which may, respec-

1) S. Hayashi, S. Kurokawa, M. Okano and T. Matsuura, *Tetrahedron Lett.*, **1967**, 3443.

2) S. Hayashi, M. Okano, S. Kurokawa and T. Matsuura, *J. Sci. Hiroshima Univ., Ser. A-II*, **31**, 79 (1967).

3) S. Hayashi, S. Kurokawa and T. Matsuura, This Bulletin, **42**, 1404 (1969).

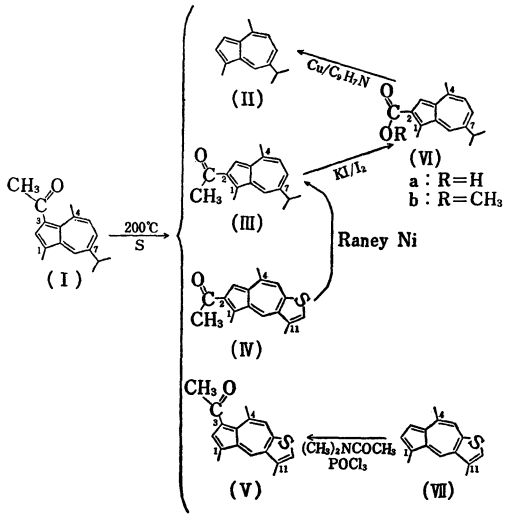

Chart 1*1

tively, be ascribed to CH_3CO^+ and $(M-CH_3CO)^+$ ions.[4]

When the compound was oxidized by hypoiodite and the resulting acid (VIa) of green plates, mp 150—161°C, was subsequently decarboxylated by heating it with copper powder in quinoline, S-guaiazulene (II) was obtained in a good yield. Thus, the compound is thought to be a monoacetyl derivative of S-guaiazulene, which differs from 3-acetylguaiazulene in the position of the acetyl group. This deduction was, furthermore, supported by the fact that the signals of an isopropyl group (1.33 and 3.08 ppm) and a signal of two methyl groups attached to an aromatic ring system (2.83 ppm) were seen in the NMR spectrum of the compound.

The compound exhibited two visible absorption maxima of nearly equal intensities at 637 and 692 mμ. When those hypsochromic shifts from the maximum of S-guaiazulene (607 mμ) are analyzed according to the Plattner rule,[5] three positions of the azulene nucleus, C_2, C_6, and C_8, are possible for the acetyl group.

On the other hand, the aromatic-proton region

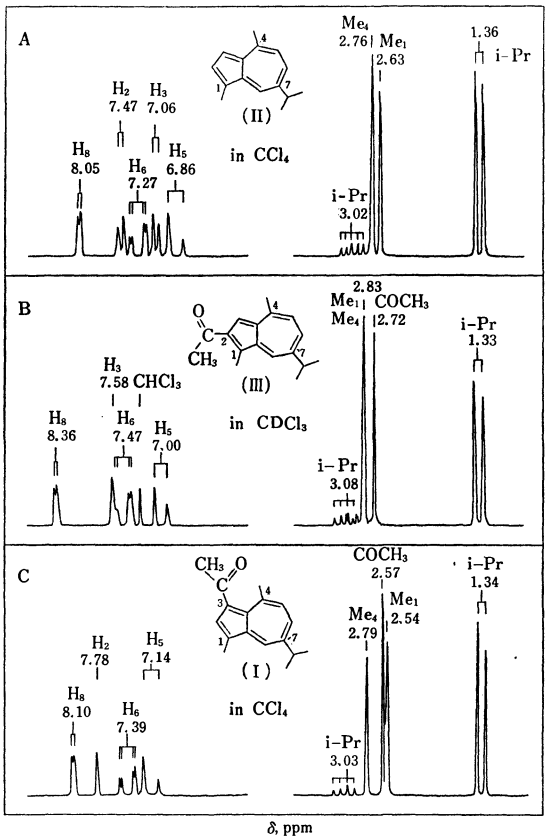

Fig. 1. NMR spectra of S-guaiazulene (A), 2-acetylguaiazulene (B) and 3-acetylguaiazulene (C).

of the NMR spectrum (Fig. 1-B) held four-proton signals. In comparison with the spectra of S-guaiazulene (Fig. 1-A)[6] and 3-acetylguaiazulene (Fig. 1-C), two doublets (2H) at 7.00 and 8.36 ppm can reasonably be assigned to H_5 and H_8, and the remaining signals (2H) from 7.31 to 7.58 ppm, to H_6 and H_3. As for the latter signals, it is thought that a part of a double doublet*2 (J=11.0, 2.0 Hz, 1H) centered at 7.47 ppm, to which H_6 is assigned, overlaps on the foot of the singlet of 7.58 ppm attributed to H_3. By such assignments, the coupling constants, $J_{5,6}$=11.0 Hz and $J_{6,8}$=2.0 Hz, are found to be in good agreement with those of 7-substituted azulene.

From the three positions, C_2, C_6, and C_8, shown to be possible by the visible absorption spectrum, C_6 and C_8 were thus excluded, and the structure of this compound was determined to be 2-acetylguaiazulene (III).

*1 The skeleton numbering of the azulenothiophenes according to the IUPAC nomenclature, used only for the name of the compound, is as follows:

For convenience in comparing these substances with the acetylguaiazulenes in terms of the NMR data, the numbering system in the azulene compounds was generally adopted for the azulenothiophenes in this paper.

4) H. Budjikiewicz, C. Djerassi and D. H. Williams, "Interpretation of Mass Spectra of Organic Compounds," Holden-Day, San Francisco (1964), p. 191.

5) E. Heilbronner, "Non-Benzenoid. Aromatic Compounds," ed. by D. Ginsburg, Interscience Publishers, New York, N. Y. (1959), p. 171.

6) D. Meuche, B. B. Molloy, D. H. Reid and E. Heilbronner, *Helv. Chim. Acta*, **46**, 2483 (1963).

*2 The appearance of the double doublet due to H_6 can be expected from the signals of H_5 and H_8 observed as doublets.

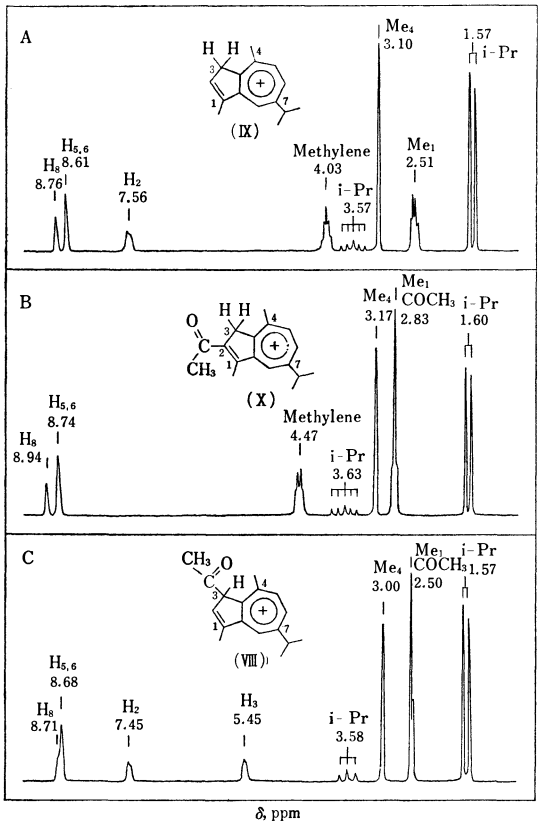

Fig. 2. NMR spectra of conjugate acids of S-guaiazulene (A), 2-acetylguaiazulene (B) and 3-acetylguaiazulene (C) (in CF_3COOH).

In addition, the NMR spectrum (Fig. 2-B) taken in a trifluoroacetic acid solution had no signal to be assigned to an olefinic proton, H_2 (*cf.* Fig. 2-A and 2-C). This fact can be well explained by the structure of the conjugate acid of 2-acetylguaiazulene (III).

b) 6-Acetyl-3,5,8-trimethylazuleno[6,5-b]thiophene (IV). Dark brown needles (mp 162—163°C) with a molecular formula of $C_{17}H_{16}OS$ were isolated from a benzene-eluted fraction in the elution chromatography of the reaction products. This compound gave a green oxime, mp 223—224°C, and exhibited prominent fragment ions of *m/e* 225 (base peak, $m^*=188.8$, $(M-CH_3CO)^+$) and *m/e* 43 (CH_3CO^+) in the mass spectrum. Thus, it is certain that the compound also contains an acetyl group.

When the compound was subjected to reductive desulfurization by heating it with a Raney nickel catalyst, the 2-acetylguaiazulene (III) described in the preceding section was obtained. In the NMR spectrum of this sulfur-containing compound (Fig. 3-B), moreover, there is a singlet (8.34 ppm, 1H) corresponding to the H_8 of 2-acetylguaiazulene, but there are no signals which can be attributed to the isopropyl group or to H_6, which are both present in the spectrum of the original compound. The result of the reductive desulfurization and the NMR evidence lead to the conclusion that the compound is 6-acetyl-3,5,8-trimethylazuleno[6,5-*b*] thiophene (IV), which may be derived from 2-acetylguaiazulene through the formation of a sulfur bond between one methyl carbon atom of the isopropyl group and the C_6 of the azulene nucleus.

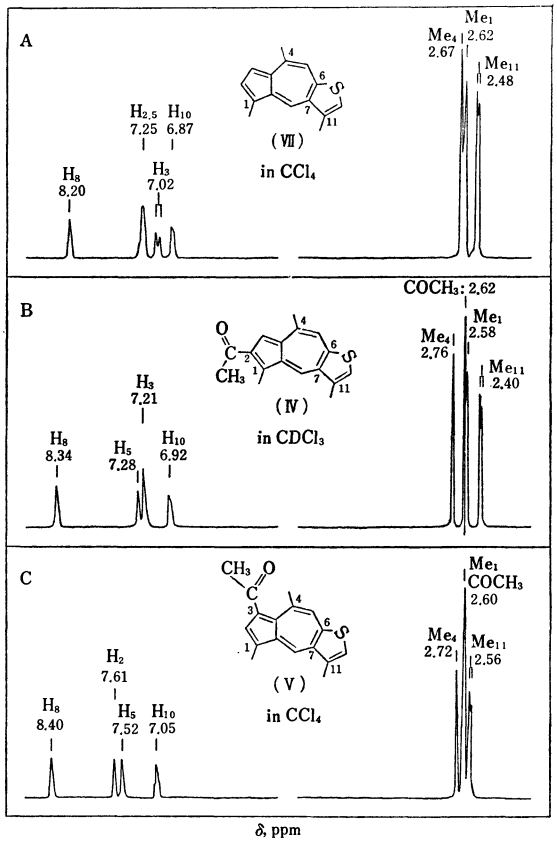

Fig. 3. NMR spectra of 3,5,8-trimethylazuleno-[6,5-*b*]thiophene (A), and its 6-acetyl- (B) and 7-acetyl derivatives (C).

This structure is further supported by the facts that the UV (λ_{max} 324 mμ) and visible absorption spectra (λ_{max} 625 mμ and 668 mμ) show hypsochromic shifts*3 as compared with those of azulenothiophene,[1,2] and that the NMR spectrum (Fig. 4-B) taken in a trifluoroacetic acid solution exhibits the signals assigned to Me_1 (2.95 ppm, 3H) and C_3-methylene (4.49 ppm, quartet, 2H), but has no peak corresponding to H_2 (*cf.* Fig. 4-A).

c) 7-Acetyl-3,5,8-trimethylazuleno[6,5-b]thiophene (V). The third product was brown needles (mp 141—142°C) whose molecular formula,

*3 According to the Plattner rule,[5] this hypsochromic shift of the visible absorption maximum indicates that the acetyl group exists on the C_2 or C_6 of the azulenothiophene nucleus.

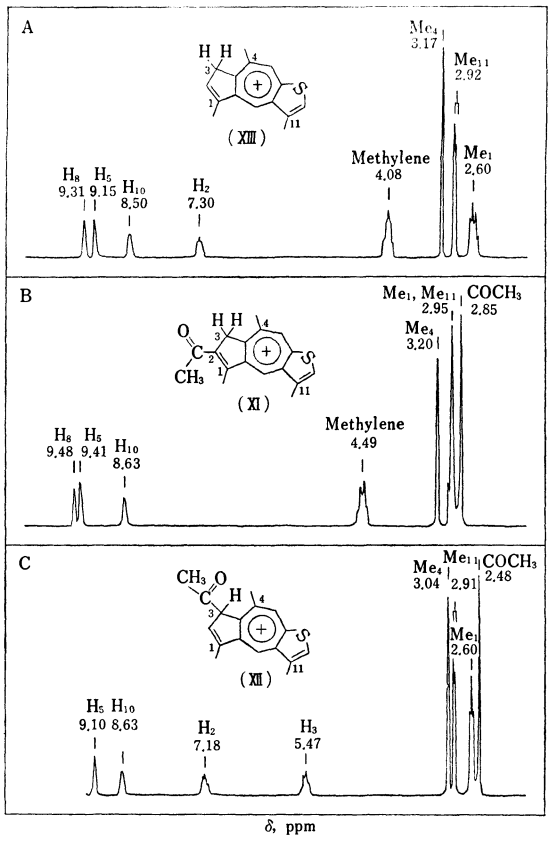

Fig. 4. NMR spectra of conjugate acids of 3,5,8-trimethylazuleno[6,5-*b*]thiophene (A), 6-acetyl-3,5,8-trimethylazuleno[6,5-*b*]thiophene (B) and 7-acetyl-3,5,8-trimethylazuleno[6,5-*b*]thiophene (C)*4 (in CF_3COOH).

$C_{17}H_{16}OS$, was the same as that of the foregoing compound, 6-acetyl-3,5,8-trimethylazuleno[6,5-*b*]-thiophene. This compound also had an acetyl group, as was indicated by the strong carbonyl band at 1650 cm^{-1} and by the fragment ions at *m/e* 253 (base peak, $m^*=238.8$) and at *m/e* 225 ($m^*=200.0$), which were correlated with, respectively, $(M-CH_3)^+$ and $(M-CH_3-CO)^+$. Besides, the NMR spectrum of the compound has a remarkable resemblance to that of 6-acetyl-3,5,8-trimethylazuleno[6,5-*b*]thiophene, as is shown in Fig. 3-C and 3-B. The evidence presented above suggests that the compound has a structure closely related to that of the 6-acetyl derivative.

However, the NMR spectrum (Fig. 4-C) taken in trifluoroacetic acid is extremely different from that of the 6-acetyl derivative (Fig. 4-B); two multiplets similar to those of the 3-acetylguaiazulenium cation (Fig. 2-C) and which can be assigned to H_3 and H_2 appear at 5.47 (1H) and 7.18 ppm (1H) respectively, but a methylene signal seen in the spectra of conjugate acids of azulenothiophene and 6-acetylazulenothiophene (Fig. 4-A and 4-B) is absent. This evidence indicates that this compound is 7-acetyl-3,5,8-trimethylazuleno[6,5-*b*]-thiophene (V).

Furthermore, this structure was proved by its synthesis through the Vilsmeier acetylation[7] of 3,5,8-trimethylazuleno[6,5-*b*]thiophene.

Sequence of the Reaction. As is shown in Table 1, the main product of this reaction was 2-acetylguaiazulene, formed through the migration of the acetyl group in the starting material; the second product was 6-acetyl-3,5,8-trimethylazuleno-[6,5-*b*]thiophene, formed by the reaction of the 2-acetylguaiazulene with sulfur. S-Guaiazulene and 7-acetyl-3,5,8-trimethylazuleno[6,5-*b*]thiophene were obtained as minor products.

In order to clarify the effect of sulfur on the migration and the loss of the acetyl group, 3-acetylguaiazulene was heated at 200°C for 2 hr without sulfur. In this reaction, 2-acetylguaiazulene (16.4%) and S-guaiazulene (1.4%) (*cf.* Experimental section) were obtained in yields similar to those of the thermal reaction of 3-acetylguaiazulene with sulfur. Hence, the migration and the loss of the acetyl group in 3-acetylguaiazulene seem to depend upon the reaction temperature and to be hardly affected at all by sulfur.

On the other hand, when 2-acetylguaiazulene was heated at 200°C in a nitrogen atmosphere or at 300°C in a sealed tube, no appreciable isomerized product was obtained; only the original material was recovered.

Thus, the migration of the acetyl group in the thermal reaction of 3-acetylguaiazulene is not such a reversible reaction as that observed between 1-phenyl and 2-phenylazulenes,[8] but an irreversible reaction proceeding from 3-acetylguaiazulene to 2-acetylguaiazulene. This difference between acetylguaiazulenes and phenylazulenes may result from the fact that the difference in the potential energy between 2-acetyl- and 3-acetylguaiazulenes is much greater than that between phenylazulenes. Further investigation into this point is presently in progress in this laboratory.

Experimental

All the melting points in this paper are uncorrected. The IR spectra were measured using KBr disks. The NMR spectra were obtained at 60 M Hz. The mass spectra were taken at 70 eV. Thin-layer chromatography (TLC) was conducted by the use of silica gel G (Merck), while vapor-phase chromatography (VPC) was carried out by using a stainless steel column (1 m×

*4 The concentration of this sample was so small that the H_8 signal, being covered with the peaks originating from CF_3COOH (spin side band, impurities, *etc.*), could not be identified.

7) K. Hafner and C. Bernhard, *Ann.*, **625**, 108 (1959).

8) Pl. A. Plattner, A. Fürst, M. Gordon and K. Zimmermann, *Helv. Chim. Acta*, **33**, 1910 (1950).

Table 1. The reaction products in the thermal reaction of 3-acetylguaiazulene with sulfur (200°C)

Fr.	Solvent	Compound	Yield mg	Yield %
1	*n*-Hexane	S-Guaiazulene (II)	2.1	1.1
2	Benzene - *n*-hexane (1 : 1)	2-Acetylguaiazulene (III)	52.6	26.4
3	Benzene	6-Acetyl-3,5,8-trimethylazuleno-[6,5-*b*]thiophene (IV)	23.3	11.7
		3-Acetylguaiazulene (I) (unchanged)	117.9	59.3
4	Chloroform	7-Acetyl-3,5,8-trimethylazuleno-[6,5-*b*]thiophene (V)	3.0	1.5

3 mm) packed with 10% NGS on Diasolid L.

3-Acetylguaiazulene (I). This compound was synthesized from S-guaiazulene (II) and acetyl bromide according to the method of Reid *et al.*[9] It was obtained as purple plates (mp 88.2—88.8°C) after being recrystallized from a mixed solvent of petroleum ether and methanol, which showed a single brown spot (R_f, 0.17) in TLC using benzene.

Thermal Reaction of 3-Acetylguaiazulene (I) with Sulfur. 3-Acetylguaiazulene (1.00 g) was heated with half as much powdered sulfur at 200°C on an oil bath for 4 hr under a nitrogen atmosphere. The reaction mixture, which solidified at room temperature, was crushed into small fragments in the reaction vessel; then it was taken out, ground to powder in a mortar, and extracted with benzene. A black oil (320 mg) thus obtained was chromatographed on activated alumina (Merck II—III); after the non-azulenic components had been eluted out with *n*-hexane, the solvents being changed step by step, the four fractions shown in Table 1 were separated depending upon the color.

2-Acetylguaiazulene (III). Green crystals of Fr. 2 (170 mg), which had been collected by repeating the thermal reaction, were developed on a silica-gel column with a mixed solvent of ether and *n*-hexane (1 : 19). The part of a blue-colored main adsorption band was cut off and extracted with the same mixed solvent to yield green crystals (130 mg), which gave green needles (mp 80.0—81.0°C) after being recrystallized twice from methanol. This compound showed a single green spot (R_f, 0.36) in TLC with an ether-*n*-hexane (1 : 19) mixture. IR: 1666 cm^{-1} (C=O). UV: $\lambda_{max}^{cyclohexane}$ mμ (log ε) 250 (4.40), 301.5 (4.63), 345 (3.74), 360 (3.76), 370 sh (3.30). Visible absorption spectrum: $\lambda_{max}^{cyclohexane}$ mμ (ε) 637 (656), 692 (650).

Found: C, 84.83; H, 8.15%. Calcd for $C_{17}H_{20}O$: C, 84.96; H, 8.39%.

The 2,4-dinitrophenylhydrazone of this compound was obtained by using a mixed solvent of ethanol and phosphoric acid[10] as a reddish-brown powder. After being recrystallized twice from benzene, it showed a mp of 246.0—247.0°C. IR: 1526, 1328 cm^{-1} (NO_2).

Hypoiodite Oxidation of 2-Acetylguaiazulene (III). A solution of 2-acetylguaiazulene (III) (170 mg) in dioxane (22 m*l*) was gradually mixed with a 10% aqueous sodium hydroxide solution (23 m*l*). To this mixture, kept at 60°C, an aqueous solution (8.2 m*l*) containing iodine (820 mg) and potassium iodide (1.64 g) was stirred in, drop by drop, over a 10-min period; the stirring was then continued for an additional 20 min at 60°C. At the end of this period, the excess iodine was reduced with a saturated aqueous solution of sodium hydrogen sulfite. The reaction mixture was chilled to 0°C and filtered to remove the precipitate of the iodoform. When the filtrate, from which unchanged 2-acetylguaiazulene was removed by dilution with water (30 m*l*) and subsequent extraction with chloroform, was acidified with 2 N hydrochloric acid, S-guaiazulene-2-carboxylic acid (VIa) (120 mg) was obtained as a green crystalline substance, mp *ca.* 145°C. This crude substance was further purified by sublimation at 220—250°C and 1.5 mmHg to give green prisms, mp 150—161°C. These crystals showed a dispersed blue spot (R_f, 0—0.18) in TLC with benzene; the spot turned yellow when sprayed with a solution of bromocresol green. IR: 1670 (C=O), 1260 (coupled C–O and O–H), 952 cm^{-1} (O–H, out-of-plane deformation). NMR: $\delta_{TMS}^{CDCl_3}$ 2.82 (s, 3H; Me_1), 7.78 (s, 1H; H_3), 2.90 (s, 3H; M_4), 7.03 (d, 1H; H_5), 7.47 (q, 1H; H_6), 1.36/3.08 (d, 6H/m, 1H; *i*-Pr), 8.38 (d, 1H; H_8). $\delta_{TMS}^{CF_3COOH}$ 2.68 (t, 3H; Me_1), 4.23 (q, 1H; H_3), 2.97 (s, 3H; Me_4), 8.66 (s, 2H; $H_{5,6}$), 1.41/3.43 (d, 6H/m, 1H; *i*-Pr), 8.85 (s, 1H; H_8). MS: *m/e* 242 (M^+, $C_{16}H_{18}O_2$), 39.3%; *m/e* 227 $(M-CH_3)^+$ (m*=212.9), 42.3%; *m/e* 197 $(M-COOH)^+$, 11.0%; *m/e* 28 (CO^+), base peak.

Preparation of the Methyl Ester of S-Guaiazulene-2-carboxylic Acid (VIb). Crude S-guaiazulene-2-carboxylic acid (VIa) (70 mg) was dissolved into an ethereal solution of diazomethane prepared from nitrosomethylurea (4 g) in the usual manner; the solution was then allowed to stand at room temperature for 8 hr. After the excess diazomethane had been decomposed by adding a few drops of acetic acid, the solvent was distilled off under reduced pressure to give an oily residue (250 mg). The residue was then eluted through a silica-gel column with a mixed solvent of benzene and ether (1 : 1); the methyl ester of S-guaiazulene-2-carboxylic acid (VIb) (60 mg) was thus isolated as a blue oil. It showed a single blue spot (R_f, 0.47) in TLC using benzene - ether (1 : 1) mixture. IR: 1710 (C=O), 1230 and 1068 cm^{-1} (C–O). UV: $\lambda_{max}^{cyclohexane}$ mμ (log ε) 248.5 (4.29), 290 sh (4.47), 298.2 (4.52), 310 sh (4.33), 340 (3.59), 355.8 (3.69). Visible absorption spectrum: $\lambda_{max}^{cyclohexane}$ mμ (ε) 631 (484), 680 (468). NMR: $\delta_{TMS}^{CCl_4}$ 2.75 (s, 3H; Me_1), 3.88 (s, 3H; COOMe),

9) D. H. Reid, W. H. Stafford and W. L. Stafford, *J. Chem. Soc.*, **1958**, 1118.

10) G. D. Johnson, *J. Amer. Chem. Soc.*, **73**, 5888 (1951).

7.52 (s, 1H; H_3), 2.80 (s, 1H; H_4), 6.86 (d, 1H; H_5), 7.29 (q, 1H; H_6), 1.33/3.02 (d, 6H/m, 1H; i-Pr), 8.22 (d, 1H; H_8). $\delta_{TMS}^{CF_3COOH}$ 2.85 (t, 3H; Me_1), 4.16 (s, 3H; COOMe), 4.41 (q, 1H; H_3), 3.16 (s, 3H; Me_4), 8.75 (s, 2H; $H_{5,6}$), 1.60/3.63 (d, 6H/m, 1H; *i*-Pr), 8.94 (s, 1H; H_8). MS: *m/e* 256 (M^+, $C_{17}H_{20}O_2$), 87.5%; *m/e* 241 $(M-CH_3)^+$(m^*=226.9), base peak; *m/e* 225 $(M-OCH_3)^+$, 17.7%.

Decarboxylation of S-Guaiazulene-2-carboxylic Acid (VIa). A solution of crude S-guaiazulene-2-carboxylic acid (VIa) (30 mg) in quinoline (2 m*l*) was refluxed with copper powder (30 mg) for 1 hr on a sand bath. The reaction mixture was then diluted with *n*-hexane and subsequently filtered. The filtrate, after being washed with 1N hydrochloric acid and then with a 2N aqueous sodium carbonate solution to take quinoline and the unchanged acid away, was concentrated under reduced pressure to give a crude blue oil (30 mg). This oil was subsequently chromatographed on a silica-gel column with *n*-hexane; a blue oil (8.3 mg) was thus isolated in a pure state. The oil thus obtained was identical with an authentic specimen of S-guaiazulene (II) in TLC, VPC, and IR spectrometry.

6-Acetyl-3,5,8-trimethylazuleno[6,5-*b*]thiophene (IV). The purple oil (150 mg) of Fr. 3 (Table 1) was rechromatographed on a silica-gel column with a mixed solvent of ether and benzene (1 : 19), and then with an ether-*n*-hexane (1 : 3) mixed solvent. A green crystalline substance thus isolated was collected by repeating the above process. The substance (40 mg), after recrystallization from a mixed solvent of *n*-hexane and methanol (1 : 1) and again from methanol, gave dark brown needles (10.6 mg), mp 162.0—163.0°C, which exhibited a single blue spot (R_f, 0.37) in TLC with an ether-*n*-hexane (1 : 3) mixture. IR: 1655 cm^{-1} (C=O). UV: $\lambda_{max}^{cyclohexane}$ mμ (log ε) 240.5 (4.10), 290 (4.41), 302 sh (4.60), 324 (4.80), 370 (3.77), 386 (3.82). Visible absorption spectrum: $\lambda_{max}^{cyclohexane}$ mμ (ε) 624.6 (595), 668 (578).

Found: S, 12.38%. Calcd for $C_{17}H_{16}OS$: S, 11.95%.

The oxime of this compound was prepared from a pyridine solution and was obtained as green needles, mp 223.0—224.0°C, after recrystallization from methanol. IR: *ca.* 3400 (O-H), 1638, 1620 and 1592 (C=C and/or C=N), 992 or 910 cm^{-1} (N-O).

Desulfurization of 6-Acetyl-3,5,8-trimethylazuleno[6,5-*b*]thiophene (IV). A solution of 6-acetyl-3,5,8-trimethylazuleno[6,5-*b*]thiophene (IV) (11.3 mg) in methanol (10 m*l*) was stirred with a freshly-activated W-2 Raney nickel catalyst (500 mg) at 50—60°C for 30 min. The reaction mixture was filtered, and the filtrate was concentrated under reduced pressure to give a blue oil (10 mg). The oil was then submitted to elution chromatography using benzene; we separated a green crystalline substance (0.4 mg) which was found to be identical with 2-acetylguaiazulene (III) by TLC and UV spectrometry.

7-Acetyl-3,5,8-trimethylazuleno[6,5-*b*]thiophene (V). Brown crystals of Fr. 4 (15 mg), obtained from several repetitions of the reaction, were recrystallized from ethanol to give brown needles (10 mg; mp 141.0—142.0°C), which showed a single yellow spot (R_f, 0.37) in TLC with benzene. IR: 1650 cm^{-1} (C=O). UV: $\lambda_{max}^{cyclohexane}$ mμ (log ε) 235.5 (4.19), 287 sh (4.28), 300 sh (4.43), 327.4 (4.62). Visible abosorption spectrum: $\lambda_{max}^{cyclohexane}$ mμ (ε) 518 sh (442), 554 (492), 600 sh (370), 660 sh (119).

Acetylation of 3,5,8-Trimethylazuleno[6,5-*b*]thiophene (VII). 3,5,8-Trimethylazuleno[6,5-*b*]thiophene (VII) (80 mg; mp 116.0—116.5°C), prepared by the reaction of S-guaiazulene (II) with sulfur,[1,2] was dissolved in absolute tetrahydrofuran (1 m*l*) together with *N*,*N*-dimethylacetamide (90 mg). To the solution there was then added, drop by drop, another absolute terahydrofuran solution (1 m*l*) of phosphorus oxychloride (150 mg); the mixture was then refluxed on a water bath for 4 hr. The reaction mixture, after being diluted with water (100 m*l*), was made alkaline by adding ammonia water, and a dark brown oil separated was taken up into chloroform. The dark brown oil (140 mg) thus obtained was chromatographed on activated alumina (Merck II—III) with chloroform to afford brown crystals (20 mg). The recrystallization of these crystals from ethanol gave brown needles (12.5 mg; mp 141.5—142.5°C), which were identified as 7-acetyl-3,5,8-trimethylazuleno[6,5-*b*]thiophene by a mixed-melting-point determination and by TLC and IR spectrometry.

Thermal Rearrangement of 3-Acetylguaiazulene (I). In a slow stream of nitrogen, 3-acetylguaiazulene (1.0 g) was heated at 200°C for 2 hr. The reaction mixture was chromatographed on silica gel with benzene to separate it into the following three fractions.

Fr. 1: S-Guaiazulene (II), 10 mg (1.4%). Fr. 2: 2-Acetylguaiazulene (III), 120 mg (16.4%). Fr. 3: 3-Acetylguaiazulene (I), 600 mg (82.2%).

Thermal Reaction of 2-Acetylguaiazulene (III). 2-Acetylguaiazulene (III) (400 mg), which had been isolated from the reaction products of the above thermal isomerization of 3-acetylguaiazulene, was heated at 200°C for 2 hr in the same manner as has been described in the case of 3-acetylguaiazulene. The spots corresponding to 3-acetylguaiazulene and S-guaiazulene (II) were not observed in the TLC of the reaction mixture with benzene, and only the starting material (220 mg) was recovered when the reaction mixture was chromatographed on silica gel with benzene.

Next, 2-acetylguaiazulene (94 mg) was heated in a sealed glass tube at 300°C for 1 hr. In this case also, no spot corresponding to S-guaiazulene or 3-acetylguaiazulene was observed; only the starting material (48 mg) was recovered from the reaction mixture.

The author wishes to thank Professor Tamon Matsuura and Professor Shûichi Hayashi of Hiroshima University for their helpful guidance and advice on this work. Thanks are also due to Professor Shô Itô of Tohoku University for his kind measurement of the NMR and mass spectra and to Dr. Hitoshi Minato of Shionogi Research Laboratory of Shionogi & Co., Ltd., for his kind measurement of the NMR spectra.

BULLETIN OF THE CHEMICAL SOCIETY OF JAPAN VOL. 43 515—520 (1970)

Conformations of Sequential Polypeptides Containing L-Alanyl and Glycyl Residues

Takayoshi Iio and Sho Takahashi

Department of Physics, Faculty of Science, Nagoya University, Chikusa-ku, Nagoya

(Received August 11, 1969)

The conformations of four polypeptides containing ordered sequences of L-alanyl(A) and glycyl (G) residues, $(A)_n$, $(A_3G)_n$, $(A_2G)_n$, and $(AG_2)_n$, are investigated in solution. The optical rotatory dispersion and infrared spectra showed that all the polymers assume both an α-helical conformation and a β-conformation in solution. The stability of the α-helix decreases in the oder: $(A)_n$, $(A_2G)_n$, $(A_3G)_n$, and $(AG_2)_n$; this may be explained in terms of the interaction between methyl groups of L-alanyl residues regularly arranged on the surface of the α-helix.

The study of sequential polypeptides (regular copolymers) is very useful in clarifying the role of the residue sequence in determining the conformations of polypeptides and proteins. For instance, poly-glycyl-L-prolyl-L-alanine was synthesized as an analog of collagen.[1] Recently, three series of sequential polypeptides containing L-valyl and γ-methyl-L-glutamyl residues, S-benzyl-L-cysteinyl and γ-ethyl-L-glutamyl residues, and glycyl and γ-ethyl-L-glutamyl residues have been synthesized and influence of the residues sequence on conformation was reported by Fraser *et al.*[2-4]

Poly-L-alanine takes an α-helical conformation in an organic solvent[5] and in water as a part of a block copolymer with D,L-glutamic acid or D,L-lysine.[6-8] In the solid state, however, poly-L-alanine can take both a β-conformation and an α-helical conformation.[9,10] On the other hand, poly-glycine forms a β-conformation in the solid state.[11] Poly-L-alanylglycine was shown to form a β-conformation similar to that found in *Bombyx mori* silk fibroin in an oriented film.[12]

In this paper we intend to investigate the effect of the residue sequence on the conformation of various sequential polypeptides containing L-alanyl and glycyl residues, because these polymers may reveal simpler types of side chain-side chain interactions and side chain-main chain interactions than do the polymers containing other amino acids.

Experimental

Preparation of Polymers. The several sequential polypeptides, poly-(L-alanyl)$_3$-glycine, poly-(L-alanyl)$_2$-glycine, and poly-L-analyl-glycyl-glycine, were obtained from the corresponding tri- and tetrapeptide-*p*-nitrophenyl esters by treatment with triethylamine. The optical purity of each sequential polypeptide was checked by comparing the specific rotation of the acid hydrolyzate of each polymer with that of L-alanine. The racemization of each polymer was less than 5%. The syntheses of these polymers have previously been reported by one of the present authors (S.T).[13]

The poly-L-alanine was prepared by the polymerization of L-alanyl-N-carboxyanhydride in dioxane, using triethylamine as the initiator. The intrinsic viscosity of each polymer in dichloroacetic acid was 1.80 for poly-L-Ala, 0.15 for poly-(L-Ala$_3$-Gly), 0.26 for poly-(L-Ala$_2$-Gly), and 0.22 for poly-(L-Ala-Gly$_2$). These polymers are abbreviated as $(A)_n$, $(A_3G)_n$, $(A_2G)_n$, and $(AG_2)_n$.

Solution Studies. The polymers can dissolve only in dichloroacetic acid (DCA) or in trifluoroacetic acid (TFA), so the solutions were prepared by dissolving the vacuum-dried polymer in DCA and by then adding

1) S. M. Bloom, S. K. Dasgupta, R. P. Patel and E. R. Blout, *J. Amer. Chem. Soc.*, **88**, 2035 (1966).
2) R. D. B. Fraser, B. S. Harrap, T. P. MacRae, F. H. C. Stewart and E. Suzuki, *J. Mol. Biol.*, **12**, 482, (1965).
3) R. D. B. Fraser, B. S. Harrap, T. P. MacRae, F. H. C. Stewart and E. Suzuki, *ibid.*, **14**, 423, (1965).
4) R. D. B. Fraser, B. S. Harrap, T. P. MacRae, F. H. C. Stewart and E. Suzuki, *Biopolymers*, **5**, 251, (1967).
5) A. R. Downie, A. Elliott, W. E. Hanby and B. R. Malcolm, *Proc. Roy. Soc.* (London), **A 242**, 325, (1957).
6) W. B. Gratzer and P. Doty, *J. Amer. Chem. Soc.*, **85**, 1193, (1963).
7) N. Lotan, A. Berger, E. Katchalski, R. T. Ingwall and H. A. Scheraga, *Biopolymers*, **4**, 239, (1966).
8) R. T. Ingwall, H. A. Scharaga, N. Lotan, A. Berger and E. Katchalski, *ibid.*, **6**, 331, (1968).
9) A. Elliott and B. R. Malcolm, *Proc. Roy. Soc.* (London), **A 249**, 30, (1959).
10) S. D. Dover and A. Elliott, *J. Mol. Biol.*, **30**, 201, (1967).
11) A. Elliott, E. M. Bradbury, A. R. Downie and W. E. Hanby, "Polyamino Acids, Polypeptides, and Proteins," ed. by M. A. Stahmann, The University of Wisconsin Press, Madison (1962), p. 255.
12) R. D. B. Fraser, T. P. MacRae, F. H. C. Stewart and E. Suzuki, *J. Mol. Biol.*, **11**, 706, (1965).
13) S. Takahashi, This Bulletin, **42**, 521, (1969).

DCA and chloroform($CHCl_3$) or TFA and DCA to give a solution of the required solvent ratio. All these solvents except TFA (Nakarai Chemicals, Analytical Grade) were redistilled before use.

The optical rotatory dispersions over the 260—450 mμ wavelength range were measured with a JASCO ORD/UV 5 apparatus made by the Japan Spectroscopic Co., Ltd., using a 0.2 cm, 1 cm, or 5 cm cell set in a water-jacketed cell holder. The temperature in the cell was controlled with flowing water from a Haake constant-temperature bath. The concentrations of solutions were in the range of 0.2—0.7 g/100 cc. Absorption due to the solvents precluded measurements at shorter wavelength below 260 mμ.

To compute $[m']_\lambda$, the reduced mean residue rotation (in degrees·cm^2/dmol) at the λ wavelength from the observed rotation, χ_λ, the following equation was used:

$$[m']_\lambda = \frac{3}{n^2+2} \cdot \frac{\overline{M}}{c} \cdot \frac{\chi_\lambda}{l}$$

Here, n is the refractive index of the solvent calculated by means of Lorentz-Lorenz's equation from the value of the refractive index of each pure solvent; c is the concentration of the polymer in grams per 100 cc; l is the path length in decimeters, and $\overline{M}$ is the mean residue molecular weight of the polymers, that is, 71.08 for $(A)_n$, 67.57 for $(A_3G)_n$, 66.40 for $(A_2G)_n$, and 61.72 for $(AG_2)_n$. We adopted the above values for $\overline{M}$ because it is difficult to estimate the contribution of the glycyl residues to the optical rotations of the sequential polypeptides. The optical rotatory dispersion parameters, a_0 and b_0 were obtained by plotting the original value of the optical rotation in terms of the equation given by Moffitt and Yang:[14]

$$[m']_\lambda = \frac{a_0\lambda_0^2}{\lambda^2-\lambda_0^2} + \frac{b_0\lambda_0^4}{(\lambda^2-\lambda_0^2)^2}$$

Linear relations were obtained between $[m']_\lambda \cdot (\lambda^2-\lambda_0^2)/\lambda_0^2$ and $\lambda_0^2/(\lambda^2-\lambda_0^2)$ using a value of λ_0=212 mμ.

The infrared spectra were measured with a model DS 402 G apparatus made by the Japan Spectroscopic Co., Ltd., using a cell with NaCl windows. The concentrations of the solutions ranged from 2 to 3 g/100 cc. The infrared spectrum of the solution and that of the solvent mixture with the same solvent composition were measured separately, the difference in the spectra was obtained by subtracting the optical density of the latter from that of the former.

Results

Optical Rotatory Dispersion. The dispersion curves of four kinds of polymers in various solvent compositions at 24.5°C are shown in Fig. 1. In the TFA-DCA system, all the polymers exhibit negative rotations; the negative rotation of each polymer decreases as the solvent composition is changed from a high TFA content to 100% DCA, and then to a high $CHCl_3$ content. In 66.7% $CHCl_3$—33.3% DCA, the polymers $(A)_n$ and $(A_2G)_n$ exhibit positive rotations above 355 and 340 mμ respectively.

The parameter, b_0, for the polymers is plotted in Fig. 2 as a function of the solvent composition.

It will be seen that the magnitude of $-b_0$ for each polypeptide is not zero in a DCA solution, and that it decreases as the proportion of TFA increases in the TFA-DCA system; on the other hand, in the DCA-$CHCl_3$ system, the magnitude of $-b_0$ increases as the proportion of $CHCl_3$ increases. Thus, all the polymers assume an α-helical conformation to some extent, although the maximum magnitudes of $-b_0$ and the stabilities of the helices towards DCA and TFA differ markedly from polymer to polymer.

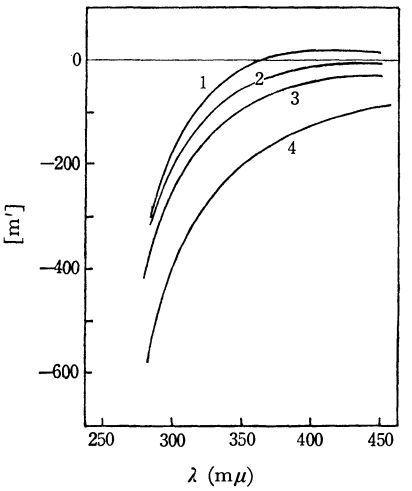

Fig. 1(a). ORD curves of the polymer $(A)_n$ at 24.5°C.
(1): 66.7% $CHCl_3$ - 33.3% DCA, (2); 33.3% TFA - 66.7% DCA, (3); 50% TFA - 50% DCA, (4); 66.7% TFA - 33.3% DCA.

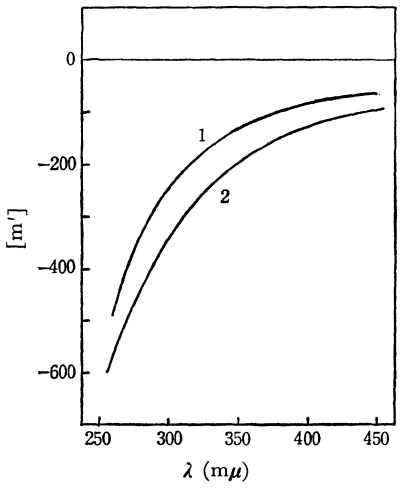

Fig. 1(b). ORD curves of the polymer $(A_3G)_n$ at 24.5°C.
(1); 66.7% $CHCl_3$ - 33.3% DCA, (2); 50% TFA-50% DCA.

14) W. Moffitt and J. T. Yang, *Proc. Nat. Acad. Sci. U.S.*, **42**, 596, (1956).

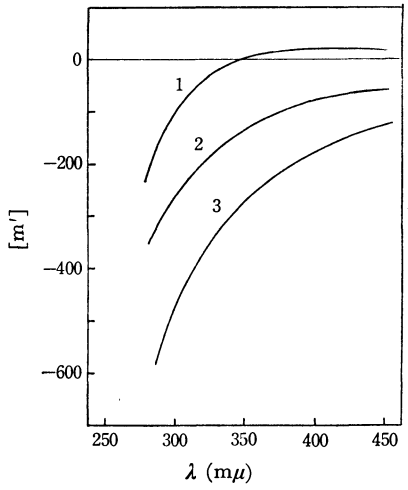

Fig. 1(c). ORD curves of the polymer $(A_2G)_n$ at 24.5°C.
(1); 66.7% $CHCl_3$ - 33.3% DCA, (2); 100% DCA (3); 50% TFA - 50% DCA.

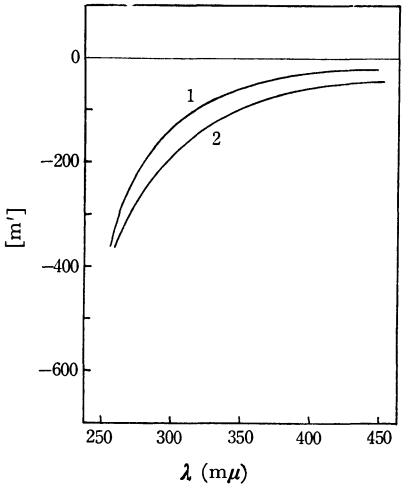

Fig. 1(d). ORD curves of the polymer $(AG_2)_n$.
(1); 66.7% $CHCl_3$ - 33.3% DCA, (2); 100% DCA.

The value of b_0 of the homopolymer $(A)_n$ increases from −200 in 66.7% TFA - 33.3% DCA to −327 in 33.3% TFA - 66.7% DCA; thereafter it increases very slowly to the value of −411 in 66.7% $CHCl_3$ - 33.3% DCA. This behaviour is almost the same as that found by Fasman.[15] Other polymers, having smaller magnitudes of b_0 than $(A)_n$ over the whole range of the solvent composition, exhibit gradual increases in the b_0 values as the solvent composition is changed from a high TFA content to 100% DCA, and then to a high $CHCl_3$ content. However, the magnitude

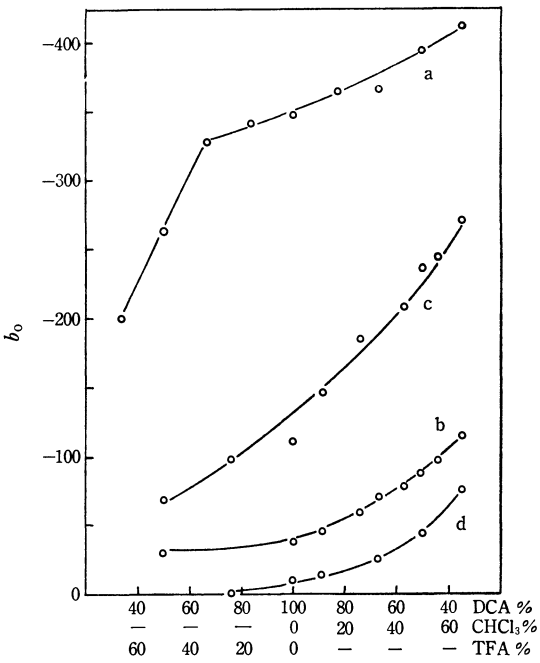

Fig. 2. Variation of the ORD parameter b_0 with solvent composition.
(a); $(A)_n$, (b); $(A_3G)_n$, (c); $(A_2G)_n$, (d); $(AG_2)_n$.

of the value b_0 of each polymer decreases in the order of $(A_2G)_n$, $(A_3G)_n$, and $(AG_2)_n$ over the whole range of the solvent composition.

Each parameter of the polymers in 66.7% $CHCl_3$—33.3% DCA showed only a small change when the temperature of the solution was raised to 57°C, and the values of the parameters returned to the original values when the temperature was

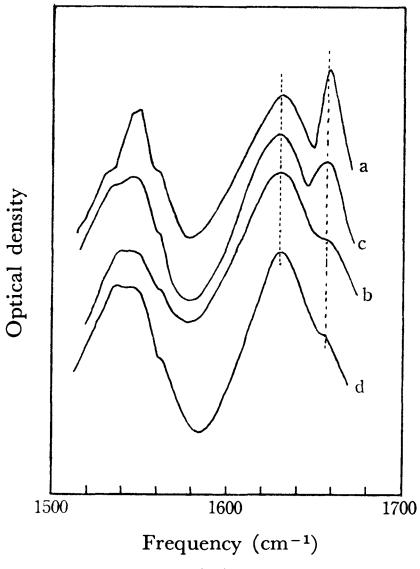

Fig. 3. IR spectra of the polymers.
(a); $(A)_n$, (b); $(A_3G)_n$, (c); $(A_2G)_n$, (d); $(AG_2)_n$.

15) G. D. Fasman, "Polyamino Acids, Polypeptides and Proteins," by M. A. Stahmann, The University of Wisconsin Press, Madison (1962), p. 221.

lowered to 24.5°C. In the same solvent proportion, the $[m']_\lambda$ values of all the polymers were independent of the concentration in the range of 0.1—1.0 g/100 cc.

Infrared Spectra. The infrared spectra over the frequency range from 1500 cm^{-1} to 1700 cm^{-1} are shown in Fig. 3. In the 25% DCA - 75% $CHCl_3$ solution, it was found that all the polymers exhibited an amide I band at about 1630 cm^{-1}, which may be attributed to a β-conformation,[16] and another band at about 1655 cm^{-1} due to an α-helical conformation.[16] This 1655 cm^{-1} component reveals a strong absorption band in the polymers $(A)_n$ and $(A_2G)_n$, but only a weak band in $(A_3G)_n$ and $(AG_2)_n$. The 1655 cm^{-1} component, however, may also contain a contribution from a random-coiled conformation of the polypeptides. Thus, all the polymers assume the β-conformation in addition to the α-helical conformation.

Discussion

Judging from the infrared spectra of the polymers, there is a possibility that all the polymers assume not only the α-helix but also a β-conformation in solution. The behaviour of the β-conformation of these polymers in solution can be investigated on the basis of an analysis of the parameters a_0 and b_0. These parameters can be written in the following forms:[17]

$$a_0 = a_0^R + a_0^H f_H + a_0^\beta f_\beta$$
$$b_0 = b_0^H f_H + b_0^\beta f_\beta$$

Here, a_0^R, a_0^H, and a_0^β are the contributions to a_0 from the random, α-helical, and β-conformations; b_0^H and b_0^β have the usual meanings, and f_H and f_β are the fractions of the α-helical conformation and the β-conformation respectively. For the parameters corresponding to the α-helical conformation, we adopt the values of $a_0^H = 680$ and $b_0^H = -630$.[17]

On the other hand, for the β-conformation various values of the parameters have been reported.[18–23] It, therefore, might be quite difficult to estimate the values of the parameters for the polymers containing L-alanyl and glycyl residues. In this paper we assume tentatively the values of $a_0^\beta = 700$ and $b_0^\beta = 0$. We measured the ORD curve of each polymer in 100% TFA, and we adopted the a_0 value obtained from the curve as the a_0^R of each polymer.

We can now calculate the fraction of the β-conformation from the observed values of a_0 and b_0 according to the above equations. However, it should be emphasized that, because of the ambiguity of the numerical values of the parameters assumed above, the content of the β-conformation thus calculated does not represent the absolute values, but, rather, relative values.

The fraction of the β-conformation, f_β, thus obtained is plotted in Fig. 4 as a function of the solvent composition. In the polymer $(AG_2)_n$, f_β is nearly constant over the whole range of the solvent compositions, while in the polymer $(A_3G)_n$, f_β increases as the proportion of $CHCl_3$ increases. In the polymer $(A_2G)_n$, f_β changes greatly, and in $(A)_n$ f_β has a maximum at 100% DCA and decreases as the proportions of both $CHCl_3$ and TFA increase.

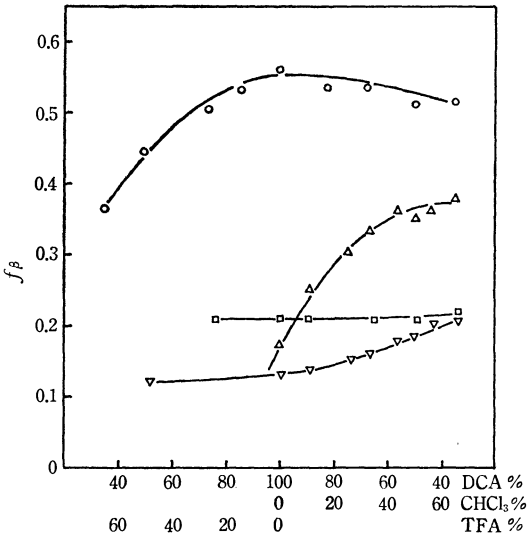

Fig. 4. Variation of the fraction of β-conformation with solvent composition.
-○-; $(A)_n$, -▽-; $(A_3G)_n$, -△-; $(A_2G)_n$, -□-; $(AG_2)_n$.

On the other hand, because of $b_0^\beta = 0$, we can see directly the behaviour of the α-helix of each polymer from the b_0 value in Fig. 2.

The contents of the α-helix conformation and the β-conformation in the highest $CHCl_3$ composition for each of the polymers are shown in Table 1. The ratio of f_H to f_β decreases in the order of $(A)_n$, $(A_2G)_n$, $(A_3G)_n$, and $(AG_2)_n$. This order coincides with the observation of the infrared measurements. In the infrared spectra, the optical density of the 1655 cm^{-1} component

16) T. Miyazawa and E. R. Blout, *J. Amer. Chem. Soc.*, **83**, 712, (1961).
17) P. Urnes and P. Doty, *Advan. Protein Chem.*, **16**, 432, (1961).
18) G. D. Fasman and E. R. Blout, *J. Amer. Chem. Soc.*, **82**, 2262, (1960).
19) A. Wada, M. Tsuboi and E. Konishi, *J. Phys. Chem.*, **65**, 1119, (1961).
20) E. M. Bradbury, A. Elliott and W. E. Hanby, *J. Mol. Biol.*, **5**, 487, (1962).
21) K. Imahori and I. Yahara, *Biopolym., Symp.*, **1**, 421, (1964).
22) S. Ikeda, M. Maeda and T. Isemura, *J. Mol. Biol.*, **10**, 223, (1964).
23) S. Ikeda, *Biopolymers*, **5**, 359, (1967).

Table 1. Comparison of the properties of the polymer

Polymer	% Helix*	% β-Conformation**	Conformation***
$(A)_n$	65	52	α+β
$(A_3G)_n$	18	21	α+β
$(A_2G)_n$	43	38	β+α
$(AG_2)_n$	12	22	β+α

* Percent of α-helix content in 66.7% $CHCl_3$ - 33.3% DCA solution.
** Percent of β-conformation content in the same solution.
*** Obtained from the IR spectra in Fig. 3.

also decreases in the order of $(A)_n$, $(A_2G)_n$, $(A_3G)_n$, and $(AG_2)_n$ compared to that of the 1630 cm^{-1} component (Fig. 3).

As has been mentioned above, the values of the β-contents of the polymers depend largely on the choice of the values of the parameters, so that further quantitative discussions can not be made concerning the behaviour of the β-conformation of the polymers. In the following discussions, we will discuss the behaviour of the α-helix in solution independently of the β-conformation, on the basis of the observation of the paramter b_0.

It is known that the L-alanyl residue stabilizes the α-helical conformation of polypeptide[5-8,24] and that the glycyl residue markedly reduces the α-helical stability.[4,25] In the γ-benzyl-L-glutamateglycine random copolymers[25] and in the sequential polypeptides containing γ-ethyl-L-glutamyl and glycyl residues,[4] the helical stabilities of the polypeptides are reduced as the content of the glycyl residue increases. In this experiment, however, the stability of the α-helix is reduced in the order of $(A)_n$, $(A_2G)_n$, $(A_3G)_n$, and $(AG_2)_n$, as may be seen in Fig. 2. This order does not coincide with the order of the increment of the glycine content. Therefore, the instabilities of the α-helices of these polymers can not be explained merely by the main-chain flexibility at the position of the glycyl residues.[4] It is necessary to consider also the regularity of the residue sequence and the contribution of the side chain of the L-alanyl residue to the α-helical stability.

The distribution of the glycyl (G) and L-alanyl (A) residues on the surface of a 3.6 residue right-handed-turn α-helix is illustrated schematically in Fig. 5 for each of the four polymers. If the residue in the center of each diagram is referred to as the 0 residue, it is convenient to number successive residues +1, +2, *etc.* in the $-CO-C_\alpha-NH-$ direction and −1, −2, *etc.* in the opposite direction. As may be seen in Fig. 5, in the polymer $(A_2G)_n$, if one G is located at the position 0, the 0, ±3, ±6, *etc.* positions are all occupied by G's. In the polymer $(A_3G)_n$, the positions 0, ±4, ±8, *etc.* are all occupied by G's. If the values of b_0 reflect the stabilities of the α-helices, then it should be concluded from the experiments that the introduction of G's decreases the stability of an α-helix, especially in the case of two G's at 0 and 4 as compared with two G's at 0 and 3. The polymer $(AG_2)_n$, where both types of relative arrangements of G's exist, is most unstable.

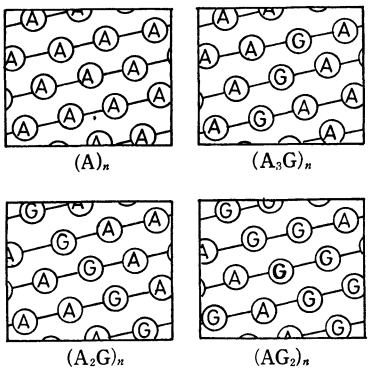

Fig. 5. Radial projection showing the distribution of the residues on an α-helix for each of the polymers.

The α-helix of poly-L-alanine in water is considered to be more stabilized by the hydrophobic bond between the methyl group of the residue A(O) and the $C_\alpha H$ group of the residue A(3).[7,24] This interaction should operate on the poly-L-alanine in the polar organic solvents as the lyophobic bond. This interaction may exist to some extent between A(0) and G(3), but not between G(0) and A(3). Although we do not have accurate knowledge of the magnitudes of these lyophobic interaction energies, we can understand the variation in the α-helical stabilities of the polymers if the energy of this interaction between A(0) and G(3) is assumed to be a half or less than that between A(0) and A(3). We can calculate, based on the above assumption, the total energy of the lyophobic interaction between the residues at 0 and 3 for each repeating unit of the polymers. Of course, the energy between G(0) and G(3) is zero. In the polymer $(A_3G)_n$, where the repeating unit is G(0)-A(1)-A(2)-A(3), the total energy is a sum of the energies of the interactions between G(0) and A(3), between A(1) and G(4). between A(2) and A(5), and between A(3) and A(6); their relative magnitudes are 0, 0.5, 1, and 1 respectively. Therefore, the sum is given by 2.5, and the energy per residue is 0.62. The interaction energy per residue for the other polymers is calculated by the same procedure, resulting in an energy of 1 for $(A)_n$, of 0.67 for $(A_2G)_n$, and of

24) M. Bixon, H. A. Scheraga and S. Lifson, *ibid.*, **1**, 419, (1963).
25) H. Block and J. A. Kay, *ibid.*, **5**, 243, (1967).

0.33 for $(AG_2)_n$. Thus, the average lyophobic interaction energies per residue of the polymer decrease in the order of $(A)_n$, $(A_2G)_n$, $(A_3G)_n$, and $(AG_2)_n$; this order coincides with that of the instabilities of the α-helices observed in the optical rotatory measurements.

The glycyl residue does not have a methyl group, so the polar hydrogen-bond breakers (DCA or TFA) are more easily accessible to the α-helical backbone at the position of the glycyl residue than at that of the L-alanyl residue. It is, therefore plausible that the interaction between A(0) and G(3) is weaker than that between A(0) and A(3).

The authors wish to thank Professor F. Oosawa, Dr. A. Ikegami, and Dr. A. Minakata for their helpful advices and discussions. Professors K. Yamazaki and S. Kubo of the Department of Chemistry, Nagoya University, kindly made available their apparatus for the experiments.

BULLETIN OF THE CHEMICAL SOCIETY OF JAPAN VOL. 43 520—524 (1970)

Aromatic Sulfonylation. II. Attacking Species under Various Conditions.*1

Yoshio KOHARA, Michio KOBAYASHI and Hiroshi MINATO

Department of Chemistry, Faculty of Science, Tokyo Metropolitan University, Fukazawa, Setagaya-ku, Tokyo

(Received August 27, 1969)

p-Toluenesulfonylation of toluene and anisole in the presence of $AlCl_3$, $SbCl_5$ or $TiCl_4$ was investigated in methylene chloride, nitromethane and nitrobenzene. Substitution took place at 8.6—13.4% and 86.6—91.4% *para* positions for toluene in methylene chloride, but 42.0—45.7% *ortho* and 54.2—58.0% *para* isomers were obtained in nitromethane and nitrobenzene. Sulfonylation of toluene with p-$CH_3C_6H_4SO_2^+$ ClO_4^- afforded 44.8—46.3% *ortho* and 53.7—55.2% *para* isomers. Partial rate factors for toluene were $p_f=52.5$ in methylene chloride, $o_f=12.6\pm0.9$, $p_f=31.4\pm2.0$ in nitromethane, and $o_f=16.0\pm1.7$, $p_f=38.3\pm4.2$ with p-$CH_3C_4H_4SO_2^+ClO_4^-$. A plausible mechanism is proposed, in which the attacking species is TsCl-MCl_n complex in methylene chloride, but it is an ion pair, $ArSO_2^+MCl^-_{n+1}$, in nitromethane and nitrobenzene.

In part I of this series we have described the results of kinetic studies on the aluminum chloride-catalyzed *p*-toluenesulfonylation of aromatics in methylene chloride.[1] On the basis of the kinetic data, existence of the kinetic isotope effect and spectroscopic observations, it was concluded that the attacking species of aromatics was TsCl-$AlCl_3$ complex. Jensen and Brown made a kinetic study of Friedel-Crafts sulfonylation of aromatics with aluminum chloride by using nitrobenzene or benzenesulfonyl chloride as solvent, and concluded that either sulfonyl cation or ion pair $ArSO_2^+$ $AlCl_4^-$ was the species which attacked aromatics.[2] Klages and Hoheisel made a study of sulfonyl cations, but did not report the kinetic data of aromatic sulfonylation.[3] In order to clarify the mechanism of sulfonylation, we have investigated the sulfonylation of aromatics with Ts^+ ClO_4^- and with *p*-toluenesulfonyl chloride, using aluminum chloride, antimony pentachloride and titanium chloride as catalysts, and methylene chloride, nitromethane and nitrobenzene as solvents.

Experimental

Materials. The purification of *p*-toluenesulfonyl chloride, toluene, methylene chloride and aluminum chloride was described in a previous paper.[1] Anisole was shaken with sodium carbonate, dried over calcium chloride, and then distilled. Antimony pentachloride and titanium chloride were distilled. Ferric chloride was sublimed. Nitromethane and nitrobenzene were dried over calcium chloride, and then distilled. Silver perchlorate of first grade(Kojima Chemical Co., Ltd.) was used without further prification.

Syntheses of Authentic Samples. *o,p*-Ditolyl sulfone: Reaction between ethyl *p*-toluenesulfinate and *o*-tolylmagnesium bromide, prepared from *o*-bromotoluene and magnesium in ether, gave *o,p*-di-tolyl sulfoxide. Oxidation of sulfoxide, with hydrogen peroxide in acetic acid as solvent, afforded the *o,p*-ditolyl sulfone, mp 55—56°C from methanol(lit, 60°C[4]).

*1 Organic Sulfur Compounds. Part XIX.

1) Aromatic Sulfonylation. I: M. Kobayashi, H. Minato and Y. Kohara, This Bulletin, **43**, 234 (1970).

2) a) F. R. Jensen and H. C. Brown, *J. Amer. Chem. Soc.*, **80**, 4038 (1958). b) F. R. Jensen and H. C. Brown, *ibid.*, **80**, 4042 (1958). c) F. R. Jensen and H. C. Brown, *ibid.*, **80**, 4046 (1958).

3) a) F. Klages and K. Hoheisel, *Chem. Ber.*, **96**, 2057(1963). b) F. Klages and F. E. Malecki, *Ann.*, **691**, 15 (1966).

4) C. Coutot and J. Frenkiel, *Compt. Rend.*, **199**, 557(1934); *Chem. Abstr.*, **29**, 142 (1935).

m,p-Di-tolyl sulfone was prepared in a similar way from *m*-bromotoluene and ethyl *p*-toluenesulfinate, mp 112.5—113.0°C from methanol (lit, 116°C[4]). Di-(*p*-tolyl) sulfone was prepared by aluminum chloride-catalyzed *p*-toluenesulfonylation of toluene in methylene chloride, mp 155°C from methanol(lit, 157—158°C[5]). *p*-Tolyl *o*-methoxyphenyl sulfone: Reaction between sodium *p*-toluenesulfinate and *o*-nitrochlorobenzene in DMSO gave *p*-tolyl *o*-nitrophenyl sulfone. Reduction of the nitro-compound, with hydrochloric acid and stannous chloride, afforded the amino-compound, and hydrolysis of the diazonium chloride in sulfuric acid, prepared from amino-compound, afforded the *p*-tolyl *o*-hydroxyphenyl sulfone. Methylation of hydroxy-compound with dimethyl sulfate gave *p*-tolyl *o*-methoxyphenyl sulfone, mp 118.5—119.0°C from ethanol (lit, 119—120°C[6]). *p*-Tolyl *m*-methoxyphenyl sulfone: A Grignard reagent prepared from 12.5 g of *m*-iodoanisole and 1.3 g of magnesium in 50 m*l* of ether was added drop by drop to 5.0 g of ethyl *p*-toluenesulfinate in 50 m*l* of ether. An excess of dilute hydrochloric acid was then added to the reaction mixture to dissolve the oil. The organic layer was separated, washed with alkali and water, and dried over magnesium sulfate. When the solvent was evaporated, an oily residue was obtained. The oily sulfoxide was purified by elution chromatography over alumina with benzene, and 5.0 g of crystals of *p*-tolyl *m*-methoxyphenyl sulfoxide was obtained (I.R. S-O stretching at 1035 cm^{-1}). To 5.0 g of the sulfoxide in 100 m*l* of acetic acid, 20 g of 30% hydrogen peroxide was added at room temperature, and the reaction mixture was allowed to stand overnight. The solution was warmed to and kept at 50—60°C for about one hour, and the sulfone was extracted with methylene chloride. The solution was evaporated, and the red crystals were purified by elution chromatography over alumina with benzene and ether, and 2.0 g of *p*-tolyl *m*-methoxyphenyl sulfone was obtained, which was recrystallized from methanol, mp 80°C; IR. 1145 cm^{-1}($\nu_s SO_2$), 1285 and 1310 cm^{-1} ($\nu_{as} SO_2$) KBr disc;

Found: C, 63.79; H, 5.55%. Calcd for $C_{14}H_{14}O_3S$: *D*, 64.09; H, 5.39%. *p*-Tolyl *p*-methoxyphenyl sulfone was prepared by aluminum chloride-catalyzed-*p*-toluenesulfonylation of anisole in methylene chloride, mp 103.5—104.0°C from ethanol (lit, 103—104.5°C[7]).

Sulfonylation of Toluene. Two grams of *p*-toluenesulfonyl chloride and 3.0 g of aluminum chloride in 25 m*l* of nitromethane were added to 5.0 g of toluene in 25 m*l* of nitromethane at 10°C. After about 37 hr, a dilute hydrochloric acid was added to the reaction mixture. The residual *p*-toluenesulfonyl chloride was decomposed by steam distillation of organic layer, and then the sulfone which crystallized was extracted with methylene chloride. The isomer ratio of a sulfone obtained was determined by gas-chromatographic analysis on a 2 m column packed with 10% SE-30 on Chromosorb using H_2 as a carrier gas (30 m*l*/min) at 230°C; retention time: *p*-tolyl *o*-tolyl sulfone, 19.9 min, *p*-tolyl *m*-tolyl sulfone, 23.5 min, di-(*p*-tolyl) sulfone, 24.5 min.

Sulfonylation of Anisole. Sulfonylation of anisole was carried out in a manner similar to that used for toluene. Absence of 860 cm^{-1} band showed the absence of *p*-tolyl *m*-methoxyphenyl sulfone in the products. The isomer ratio of a sulfone produced was determined by gas-chromatographic analysis on a 2 m column packed with 10% SE-30 on Chromosorb using H_2 as a carrier gas (30 m*l*/min.) at 250°C; retention time, *p*-tolyl *o*-methoxyphenyl sulfone, 15.8 min, *p*-tolyl *m*-methoxyphenyl sulfone, 16.0 min, *p*-tolyl *p*-methoxyphenyl sulfone, 20.4 min, *p*-tolyl phenyl sulfone, 9.0 min.

Sulfonyation with Sulfonyl Cation. *p*-Toluenesulfonyl perchlorate was prepared from *p*-toluenesulfonyl chloride and silver perchlorate by Klages' method.[3b] The solution of the *p*-toluenesulfonyl perchlorate was added to the solution of an aromatic substrate. The reaction mixture was kept at 10°C overnight, then the sulfone produced was separated by extraction with methylene chloride and analyzed by gas chromatography.

Measurement of Relative Rates by Competitive Sulfonylation. The relative rates were determined by a method similar to that used for measurements of isomer ratios. Gas-chromatographic conditions; 10% SE-30 on Chromosorb, 3 m, H_2 as carrier gas (40 m*l*/min) at 240°C, retention time; *p*-tolyl phenyl sulfone, 15.5 min., *p*-tolyl *o*-tolyl sulfone 19.2 min, *p*-tolyl *m*-tolyl sulfone, 21.0 min, di-(*p*-tolyl) sulfone, 22.5 min.

Results and Discussion

Results concerning the orientation for the *p*-toluenesulfonylation of toluene are summarized in Table 1. The orientation for sulfonylation of toluene with antimony pentachloride and titanium chloride in methylene chloride agreed with the data for aluminum chloride in methylene chloride within the limit of error of gas-chlomatographic analysis. The agreement among the values of orientation for the reactions catalyzed by aluminum chloride, antimony pentachloride or titanium chloride in nitromethane or nitrobenzene is also satisfactory. These values were not in accord with the values obtained in methylene chloride.

Klages and Malecki reported on the formation of sulfonyl cation;[3b] *i.e.* *p*-toluenesulfonyl cation was prepared from *p*-toluenesulfonyl bromide and silver perchlorate in nitromethane. Measurement of electroconductivity indicated that not a free sulfonyl cation but an equilibrium mixture of covalent-bonded(I) and ionized(II) was present in the medium as shown below.

$$\underset{(I)}{Ts\text{-}OClO_3} \rightleftarrows \underset{(II)}{Ts^+ClO_4^-} \xrightarrow{ArH} TsAr + HClO_4 \qquad (1)$$

Sulfonylation of an aromatic substrate with sulfonyl cation (II) took place when the aromatics

5) G. Holt and B. Pagdin, *J. Chem. Soc.*, **1960**, 2508.

6) A. A. Aleykutty and V. Baliah, *J. Indian Chem. Soc.*, **31**, 513(1954); *Chem. Abstr.*, **50**, 219 (1956).

7) H. H. Szmart and G. Suld, *J. Amer. Chem. Soc.*, **78**, 3400 (1956).

TABLE 1. ORIENTATIONS FOR THE *p*-TOLUENESULFONYLATION OF TOLUENE UNDER VARIOUS CONDITIONS AT 10°C

Catalysts \ Solvents		CH_2Cl_2	$PhCH_3$	$PhNO_2$	CH_3NO_2	
$AlCl_3$	*o*	13.4*		42.4	44.6	
	m	0		3.4	—	
	p	86.6		54.2	55.4	
$SbCl_5$	*o*	13.2	31.8	44.1	42.0	
	m	—	—	—	—	
	p	86.8	68.2	55.9	58.0	
$TiCl_4$	*o*	8.6		42.7	45.7	
	m	—		—	—	
	p	91.4		57.3	54.3	
$FeCl_3$	*o*	32.8[a,b]				
	m	—				
	p	67.2				
$Ts^+ClO_4^-$	*o*	35.2[a,b]	37.6[a]	42.7	46.3[a]	44.8
	m	—	—	—	—	—
	p	64.8	62.4	57.3	53.7	55.2

a) at room temperature
b) heterogeneous conditions
* Ref. 1.

was added to this solution.[3b,8]

The orientation for the Lewis acid-catalyzed sulfonylation in nitromethane or nitrobenzene agrees fairly well with the orientation for sulfonylation with tosyl perchlorate solution as seen in Table 1. This fact suggests that the attacking species in the sulfonylation with tosyl perchlorate system was the same as that of the Lewis acid-catalyzed sulfonylation in nitromethane or nitrobenzene, namely sulfonyl cation (II)-like species for both reactions.

Partial rate factors for sulfonylation of toluene are determined by competitive experiments and shown in Tables 2 and 3.

Those values at *para* position were 31.4±2.0 for aluminum chloride-catalyzed sulfonylation in nitromethane and 38.3±4.2 for sulfonylation with sulfonyl cation in nitromethane. The value for the aluminum chloride-catalyzed sulfonylation in methylene chloride was 52.5.[1] Both orientation and partial rate factors clearly indicate that the attacking species in methylene chloride was different from those in nitromethane or nitrobenzene.

TABLE 2. RELATIVE RATES FOR THE ALUMINUM CHLORIDE-CATALYZED *p*-TOLUENESULFONYLATIONS OF TOLUENE AND BENZENE IN NITROMETHANE AT 10°C

Run	$[PhCH_3]_0/[PhH]_0$*	Obs. rel. rate	k_T/k_B
1	0.993	9.00	9.06
2	0.452	4.14	9.15
3	0.263	2.64	10.06

$k_T/k_B = 9.42\pm0.64$
$o_f = 12.6\pm0.9$, $m_f \fallingdotseq 0$, $p_f = 31.4\pm2.0$
* Molar ratio of the initial concentrations.

TABLE 3. RELATIVE RATES FOR THE *p*-TOLUENESULFONYLATION OF TOLUENE AND BENZENE WITH *p*-TOLUENESULFONYL CATION IN IN NITROMETHANE AT 10°C

Run	$[PhCH_3]_0/[PhH]_0$*	Obs. rel. rate	k_T/k_B
1	0.981	10.58	10.78
2	0.472	5.36	11.36
3	0.297	3.86	13.00

$k_T/k_B = 11.72\pm1.28$
$o_f = 16.0\pm1.7$, $m_f \fallingdotseq 0$, $p_f = 38.3\pm4.2$
* Molar ratio of the initial concentrations.

Sulfonylation with a sulfonyl perchlorate in nitromethane and nitrobenzene is less selective than that in methylene chloride and toluene. This finding suggests that the attacking species in the sulfonylation with sulfonyl perchlorate in nitromethane and nitrobenzene were in a relatively free states, whereas the attacking species in methylene chloride or toluene was bulky, less reactive. In order to explain the results of *p*-toluenesulfonylation under various conditions, a plausible mechanism is proposed, which involves several attacking species with various degrees of charge separation. The results of orientation and partial rate factors indicate that; sulfonylations catalyzed by aluminum chloride, antimony pentachloride and titanium chloride in methylene chloride proceed through (2), but sulfonylation in nitromethane and nitrobenzene proceeds through (2), (3) and (4); the

8) H. Burton and H. B. Hopkins, *J. Chem. Soc.*, **1952**, 4457.

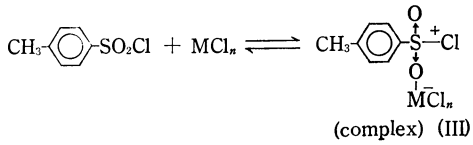

(complex) (III)

$$\xrightarrow{ArH} \text{Sulfone} \quad (2)$$

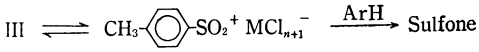

(contact ion pair)
(IV)

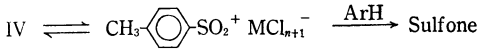

(solvent-separated ion pair)
(V)

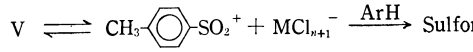

antimony pentachloride-catalyzed sulfonylation in toluene proceeds through (2) and (3); the aluminum chloride-catalyzed benzenesulfonylation of chlorobenzene in benzenesulfonyl chloride as solvent[2b] proceed through (2), (3), (4) and (5). The energy relationship among these attacking species may be represented by a free energy diagram shown in Fig. 1. The formation of various attacking species could be partially attributed to the difference in solvating power of the solvents. Four attacking species expressed in this diagram, namely the complex, contact ion pair, solvent-separated ion pair and free cation should not be considered to be distinctly differentiated from each other as shown in Fig. 1

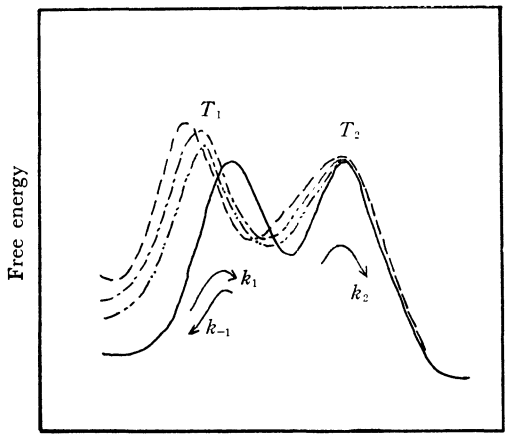

Fig. 1. Free energy diagram for the possible intermediates in the sulfonylation.
——— free cation
——— solvent-separated ion pair
——— contact ion pair
——— complex

and (1)—(5), and the bond strength between sulfonyl group and counter ion varies continuously with the solvents and counter ions. If the aromatic substrate is highly reactive, it can be attacked by sulfonyl chloride-metal chloride complex. Since the reactivity of the complex is low, both its substrate and positional selectivity are high. On the other hand, attacking species similar to free sulfonyl cation is highly reactive and therefore, should have low selectivity. In fact, kinetic evidence supported these suggestions. Kinetic hydrogen isotope effects were observed in sulfonylation with TsCl-$AlCl_3$ complex in methylene chloride,[1] but was not detected in benzenesulfonylation in benzenesulfonyl chloride,[2b] where the sulfonylation was considered to be effected with solvent separated ion pair or free cation. These findings may be explained by the energy diagram in Fig. 1. The difference of energy between reactant and transition states T_1 is small for free cation or ion pair, and considerably large for complex. Transition states T_1 for the complex may be reached in the later stage along the reaction coordinate, where C–H bond length may be stretched much longer than that in T_1 for free sulfonyl cation. On the other hand, the energy difference among transition states T_2 for all attacking species will be very small. Forward rate constant k_2 should be smaller than k_{-1} or at least in comparable order of magnitude with k_{-1} for complex, resulting in kinetic hydrogen isotope effects. For the free cation or solvent-separated ion pair, k_2 should be larger than k_{-1}, and no kinetic isotope effects should be present.

The reaction between arenesulfonyl chloride and such highly reactive aromatics as *m*-dimethoxybenzene in the presence of zinc chloride in aromatic solvent was found to afford a sulfone and attributed to the intermediate formation of the sulfonyl cation.[9] Considering the fact that zinc chloride is a weak Lewis acid and *m*-dimethoxybenzene is a less polar solvent, it seems that a true attacking species was complex or contact ion pair under these reaction conditions.

Orientation for the sulfonylation of anisole is shown in Table 4.

Table 4. Orientation for the sulfonylation of anisole

Catalysts	Solvents	Temp. (°C)	Orientation (%)		
			o-	*m*-	*p*-
$AlCl_3$	CH_2Cl_2	20	38.5	0	61.5
$AlCl_3$	CH_3NO_2	20	40.3	—	59.7
$AlCl_3$	$PhNO_2$	20	42.0	—	58.0
*	CH_3NO_2	10	35.1	—	64.9

* Sulfonylation with $CH_3C_6H_4SO_2^+ClO_4^-$.

9) H. Burton and E. Hoggarth, *ibid.*, **1945**, 14.

The difference in the orientation is less clear than in the cases of other aromatics. It is reasonable that the difference in the reactivity is less clear since anisole is very reactive and reacts with various attacking species of different reactivity more evenly. Partial rate factors for the sulfonylation of anisole catalyzed with aluminum chloride in nitromethane at 10°C were found to be $o_f=50.7$, $m_f \fallingdotseq 0$, $p_f=150$ ($k_{PhOCH_3}/k_{PhH}=41.9$) by competitive experiments. These values are extremely small compared with those of ordinary electrophilic aromatic substitutions ($p_f=1.8\times10^6$ for acetylation[10] and $p_f=1.1\times10^{10}$ for bromination[11]). Plausible explanations for this anomaly is that the reactivity of anisole was depressed by formation of $PhOCH_3$–$AlCl_3$ complex and the concentration of the remaining free anisole was very low for the same reasons.

On the basis of orientation, partial rate factors and other kinetic data, it is concluded that the attacking species varies with the conditions and is a complex, a contact ion pair, a solvent-separated ion pair or a free cation.

10) H. C. Brown and G. Marino, *J. Amer. Chem. Soc.*, **84**, 1658 (1962).

11) L. M. Stock and H. C. Brown, *ibid.*, **82**, 1942 (1960).

BULLETIN OF THE CHEMICAL SOCIETY OF JAPAN VOL. 43 524—530 (1970)

The Non-enzymatic Cleavage of Peptide Bonds. II. The Chemical Cleavage of the Tryptophyl Bond in Several Synthetic Peptides[1,2]

Michiyo MORISHITA and Fumio SAKIYAMA

Institute for Protein Research, Osaka University, Kita-ku, Osaka

(Received September 5, 1969)

Several synthetic peptide derivatives containing tryptophan were examined for the selective cleavage at the tryptophyl residue, according to a new scheme involving ozonization and subsequent treatment with hydrazine. The ozonization reaction of the tryptophyl residue was carried out in the presence and in the absence of resorcinol in formic acid. Then the reaction of the ozonized product with hydrazine was performed at pH 3.6 to bring about the tryptophyl bond cleavage. The yield of the present cleavage reaction ranged from 35 to 68% on the basis of the starting peptide derivative used. The cleavage reaction could be followed spectroscopically in parallel with the exposure of the amino group acylated by the tryptophyl residue. The 2,3,4,5-tetrahydropyridazone derivative derived from the parental tryptophyl residue was identified by a comparison of both its chromatographic behavior and its ultraviolet spectrum with those of the standard sample. Thus it was confirmed that the present cleavage proceeded through the proposed reaction sequence.

In a previous paper, a new approach to effect the selective cleavage of tryptophyl bonds was proposed.[1] The cleavage reaction consists of two reactions; one is the oxidative conversion of the tryptophyl residue into a *N'*-formylkynurenyl residue (the first reaction), and the other is the selective cleavage of the tryptophyl bond by the reaction of the kynurenyl residue with hydrazine. The second step in the cleavage reaction was previously studied by using model compounds.[1] The reaction scheme is thought to be useful not only for the fragmentation of the peptide chain in the structural analysis of the protein molecule, but also for the study of the structure-function relationship of the biologically-active protein by the chemical modification of the particular tryptophyl residue, since the oxidized tryptophan in the protein can be easily characterized by identifying any newly-formed amino terminal amino acid after hydrazine treatment. In the present paper the authors will describe the cleavage reaction of the tryptophyl bond in several synthetic peptide derivatives according to the scheme depicted in Fig. 1.

Results and Discussion

Conversion of the Tryptophyl Residue into a *N'*-Formylkynurenyl Residue by Ozone. Among the oxidation reactions of indoles previously studied, such oxidants as ozone,[3,4] peracids,[5]

1) Part I of this series, M. Morishita, T. Sowa, F. Sakiyama and K. Narita, This Bulletin, **40**, 632 (1967). A part of this report was presented in this Bulletin, **40**, 433 (1967).

2) This investigation was aided in part by a grant from Tanabe Amino Acid Foundation.

3) B. Witkop, *Ann.*, **556**, 103 (1944).

4) A. Previero, E, Scoffone, C. A. Benassi and P. Pajetta, *Gazz. Chim. Ital.*, **93**, 849 (1963).

5) B. Witkop and H. Friedker, *Ann.*, **558**, 91 (1947).

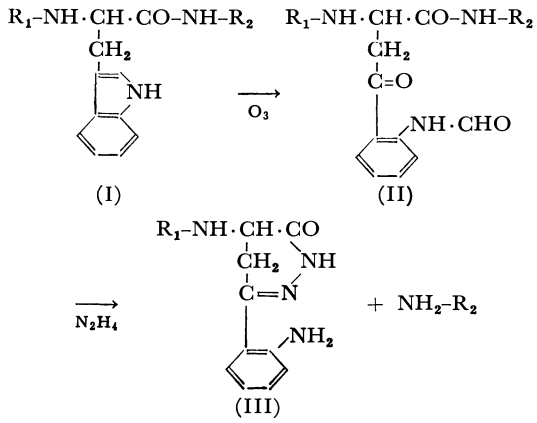

Fig. 1. The reaction sequence for the chemical cleavage of the tryptophyl bond.

and periodate ions[6] have been shown to effect the oxidative scission of the α,β-unsaturated bond of the pyrrole part in the indole nucleus. Molecular oxygen can also act as an oxidizing agent in either physiological[7] or photochemical[8] reactions. For the present purpose, the complete and selective oxidation of the tryptophyl residue in a peptide chain is desirable, and ozone was considered as one of the most favorable oxidants among the above agents. It has previously been reported that, on the controlled ozonization of protein amino acids, tryptophan could be selectively converted into *N'*-formylkynurenine with a side reaction, the oxidation of the sulfur atom of methionine.[9]

The reaction conditions for the quantitative conversion of tryptophan into *N'*-formylkynurenine was first examined since, in the experiment reported by Previero and Bordignon,[9] the amount of ozone to be used for the oxidation of tryptophan was not specified. The oxidation was followed by an increase in the absorption at 322 mμ which was characteristic of the chromophore of *N'*-formylkynurenine. Another determination of the oxidation product was simultaneously achieved by the ninhydrin assay of kynurenine after mild acid hydrolysis and subsequent chromatographic separation on filter paper.

The ozonization of tryptophan was very rapid, and the indole nucleus was oxidized almost completely within one minute either with or without resorcinol. As is shown in Fig. 2, the quantitative formation of kynurenine was observed by the ninhydrin assay when ozonization was carried out in

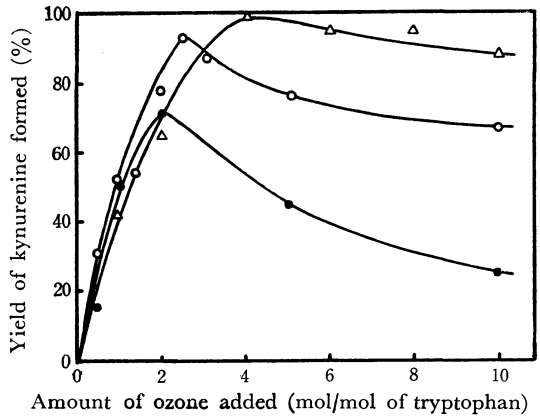

Fig. 2. Ozonization of tryptophan by various amounts of ozone (Formation of kynurenine after acid hydrolysis).
Reaction conditions: concentration of tryptophan was 5 mM in formic acid and ozone was added for a minute. Ozonization in the absence (-●-) or the presence (a molar equivalent (-○-) and twice equivalents (-△-) to the amino acid) of resorcinol was presented.

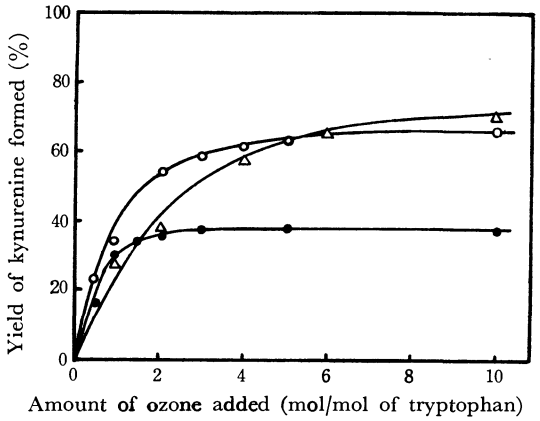

Fig. 3. Ozonization of tryptophan by various amounts of ozone (Formation of *N'*-formylkynurenine).
Reaction conditions and notations are similar with those described in Fig. 2. The amount of *N'*-formylkynurenine was estimated by absorbancy at 322 mμ.

a formic acid containing resorcinol (molar ratio of O_3 : resorcinol : tryptophan = 4 : 2 : 1). However, different features were observed when the same oxidation was monitored by the ultraviolet absorption (322 mμ, Fig. 3). In the presence of resorcinol, the ninhydrin method afforded more kynurenine than did the spectrometric method. It should be noted that no maximal formation of *N'*-formylanthranyl grouping was detected when kynurenine was quantitatively obtained. The same phenomenon was also observed on ozonization without resorcinol. This discrepancy can be explained by the formation of a certain

6) L. J. Dolby and D. L. Booth, *J. Amer. Chem. Soc.*, **88**, 1649 (1965); M. Z. Atassi, *Arch. Biochem. Biophys.*, **120**, 56 (1967).
7) W. E. Knox and A. H. Mehler, *J. Biol. Chem.*, **187**, 149 (1950).
8) Z. Yoshida and M. Kato, *J. Amer. Chem. Soc.*, **76**, 311 (1954).
9) A. Previero and E. Bordignon, *Gazz. Chim. Ital.*, **94**, 630 (1964).

stable intermediate carrying no *N'*-formylanthranyl group; this intermediate was then transformed into kynurenine on acid hydrolysis. Resorcinol was obviously effective in enhancing the ozonization yield of tryptophan and in reducing the over-oxidation of the ozonization products. Phloroglucinol was also effective, but tyrosine was not.

When the carbobenzoxy derivative of tryptophan was ozonized under the best conditions described above, no quantitative formation of kynurenine was observed. In accounting for this phenomenon it was postulated that the bulky aromatic group attached to the tryptophan residue might interfere with the access of ozone to the indole nucleus when the oxidant was added to the reaction media over a short period. Thus, the ozonization of *N*-α-carbobenzoxytryptophylleucine was examined from time to time by both the ninhydrin and spectrometric methods (Fig. 4). The increase in the absorption at 322 mμ reached a plateau after one minute, but the amount of kynurenine estimated by the ninhydrin reaction gradually increased and an almost quantitative formation was observed after half an hour. Such a slow addition of ozone was also recommended by Previero *et al.*[4,9] for the effective conversion of tryptophan to *N'*-formylkynurenine.

Under the same conditions, the ozonization of the tryptophyl residue in several synthetic oligopeptides was undertaken. As is shown in Table 1, on the ozonization of the peptide in the presence of resorcinol the tryptophyl residue could be oxidized to the *N'*-formylkynurenyl residue in a 51—100% yield and, on acid treatment, the formation of kynurenine was estimated to be 80—99%. As long as ozonization is utilized for the first step in the cleavage reaction, it is not relevant to estimate the oxidation of the tryptophyl residue only by absorption at 322 mμ since the *N'*-formylkynurenine would not be a single ozonization product. However, since the second step in the cleavage reaction was performed in weakly acid media, the intermediate ozonization product of the tryptophyl residue can be expected to be readily hydrolyzed to kynurenine during heating in the aqueous media. For the present chemical cleavage of the tryptophyl bond, the carbonyl function at the γ-position is indispensable and the kynurenyl

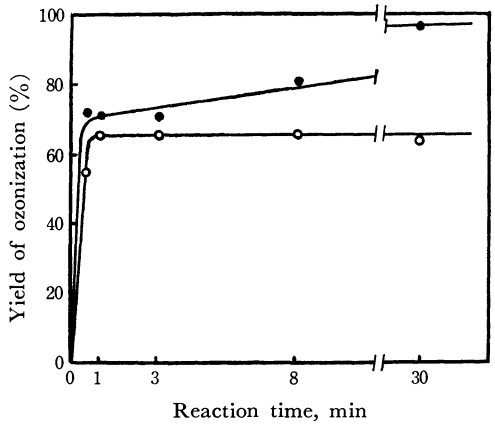

Fig. 4. Ozonization of carbobenzoxytryptophylleucine.
Reaction conditions: concentrations of tryptophan and resorcinol were 5 mM and 10 mM, respectively. Ozone (1—2% in oxygen, total amount was four-fold molar equivalents to tryptophan) was bubbled for half an hour. The extent of ozonization was estimated by both absorbancy at 322 mμ (-○-) and determination of kynurenine after acid hydrolysis (-●-).

TABLE 1. OZONIZATION OF THE TRYPTOPHYL PEPTIDE DERIVATIVE

	Yield of kynurenine formed (%)			
	in the absence of resorcinol		in the presence of resorcinol	
	UV-absorption*	Kynurenine**	UV-absorption*	Kynurenine**
Z-Trp-Gly-OH	51	85	51	88
Z-Trp-Ala-OH	55	83	60	92
Z-Trp-Leu-OH	51	88	55	99
Z-Trp-Phe-OH	54	88	60	96
Z-Trp-Asp-OH	49	77	63	80
Z-Ala-Trp-Leu-OH			60	81
H-Ala-Trp-Leu-OH	46	80	107	96
H-Gly-Trp-Gly-OH	55	75	103	85
H-His-Phe-Arg-Trp-Gly-OH	49		83	87
H-His-Phe-Lys-Trp-Gly-OH			83	82
H-His-Phe-Orn-Trp-Gly-OH			86	86
H-Phe-Arg-Trp-Gly-Ser-Pro-Pro-OH			95	

Z: Carbobenzoxy
* determined as *N'*-formylkynurenine by the absorption at 322 mμ.
** determined by the ninhydrin reaction after acid hydrolysis.

residue is a potent candidate as well as its *N'*-formyl derivative in the second step.[10] Therefore, photooxidation would be another promising reaction for the quantitative, selective conversion of tryptophan into a kynurenine derivative.[11]

Reaction of the Ozonized Product of the Tryptophyl Peptide with Hydrazine (the Second Step). *N*-α-Carbobenzoxytryptophylleucine oxidized by ozone was reacted with hydrazine under the conditions described previously.[1] The formation of the *N'*-formylkynurenyl residue was moderately achieved (66% yield), and about a half of the *N'*-formylkynurenyl bond could be cleaved. The leucine was released in a 31% yield, which was calculated on the basis of the parental tryptophyl peptide. In order to establish more effective conditions for the release of leucine, the reaction of the ozonized tryptophyl peptide with hydrazine was investigated further. The modification of certain parameters usually favorable for the present type of chemical reaction, that is, an increase in the reaction temperature and the reaction period, was not preferable for the selective cleavage reaction of the peptide bond. The effect of the concentration of hydrazine on the release of leucine was first examined. As is shown in Fig. 5, a five-fold molar excess of hydrazine was insufficient for the efficient cleavage reaction of the *N'*-formylkynurenyl bond and the maximal liberation of the amino acid (quantitative from the *N'*-formylkynurenyl residue formed) attained when twenty or more equivalent of the binucleophile were used. Thus, several of the tryptophyl peptides oxidized were submitted to the cleavage reaction: the amino group linked originally with the carboxyl group of the tryptophyl residue could thus obtained in a 35—68% yield (Table 2). The cleavage yield apparently depended on the amount of *N'*-formylkynurenine formed. As the last column in Table 2 shows, the tryptophyl peptide bond was partly hydrolyzed in certain cases when the parental derivative was reacted with hydrazine without ozonization.

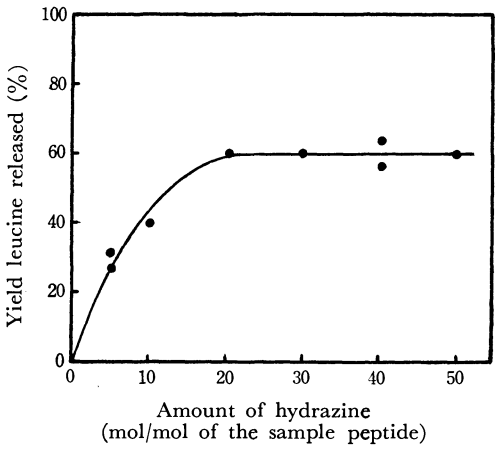

Fig. 5. Effect of concentration of hydrazine on release of leucine from the oxidized product of carbobenzoxytryptophylleucine.

Then the pH-dependence of the cleavage reaction of the *N'*-formylkynurenyl bond was again examined in order to minimize such undesirable non-specific hydrolysis. The release of the amino group was not significantly affected by the concentration of hydrogen ions between pH 3.6 and pH 5.85 (Fig. 6). Furthermore, no remarkable difference in the rate of the cleavage reaction was observed at the more extreme pH's. Therefore, it is expected that the hydrazine treatment at pH 5.85 would give a fruitful result since the non-specific hydrolysis of the peptide bond may occur to a lesser extent at this pH.

Table 2. Yield of the specific cleavage at the tryptophyl bond*

Starting peptide derivative	Released amino acid	Released amino acid by the specific cleavage (%)		Non-specific hydrolysis
		oxidized in the absence of resorcinol	oxidized in the presence of resorcinol	
Z-Trp-Gly-OH	Glycine	22	35	7
Z-Trp-Ala-OH	Alanine	47	57	5
Z-Trp-Leu-OH	Leucine	41	68	0
Z-Trp-Phe-OH	Phenylalanine	31	49	0
Z-Trp-Asp-OH	Aspartic acid	41	52	13
Z-Ala-Trp-Leu-OH	Leucine	—	54	—
H-His-Phe-Arg-Trp-Gly-OH	Glycine	—	45	6
H-His-Phe-Lys-Trp-Gly-OH	Glycine	—	43	7
H-His-Phe-Orn-Trp-Gly-OH	Glycine	—	49	12

* Calculated on the basis of the amount of the starting tryptophyl peptide used.

10) F. Sakiyama, unpublished data.
11) C. A. Benassi, E. Scoffone, G. Galiazzo and G. Jori, *Photochem. Photobiol.*, **6**, 857 (1967).

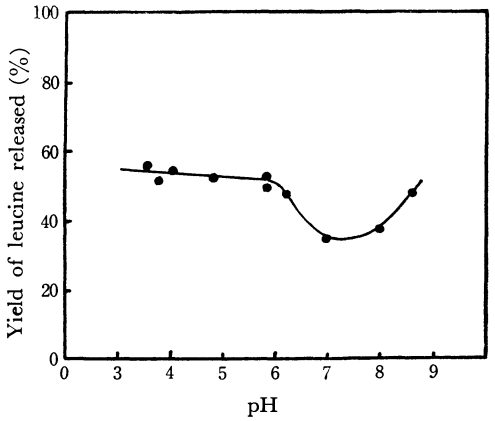

Fig. 6. pH-Profile of release of leucine from the oxidized product of carbobenzoxyalanyltryptophylleucine.

It should be possible to identify the counterpart of the newly-exposed amino group by a conventional technique. The other reaction product which was derived from the tryptophyl residue is probably 4-peptidylamino-6-(*o*-aminophenyl)-2,3,4,5-tetrahydropyridaz-3-one (III). However, little has been known about the chemical properties of the 4-amino-6-(*o*-aminophenyl)-2,3,4,5-tetrahydropyridaz-3-one (IV) derivative. Therefore, two 4-acylamino derivatives of IV, the 4-carbobenzoxy (V) and 4-*N*-carbobenzoxy-L-alanyl (VI) derivatives, were prepared by the reaction of the corresponding α-acylamino-γ-oxo acid ester with hydrazine. Both pyridazones developed an orange color with the Ehrlich reagent, emitted a yellow-orange fluorescence when excited at 260 mμ and showed a characteristic absorption near 350 mμ; this absorption was attributed to a conjugated system composed of the *o*-aminophenyl group and the ketimino function in the tetrahydropyridazone ring.

Then the cleavage reaction of the *N'*-formylkynurenyl bond was spectrophotometrically monitored (Fig. 7). The absorption at 322 mμ due to *N'*-formylkynurenine decreased rapidly in the early stage of the reaction and a new absorption maximum emerged near 350 mμ. This new absorption maximum, however, was gradually shifted to a shorter wavelength after about two hours. In this case the substrate was the carbobenzoxy derivative of tryptophylleucine, and the release of leucine, as expected, was observed in parallel with the increase in the absorption at 350 mμ until the amount of leucine reached a plateau (Fig. 8). However, it has to be noted that the formation of the tetrahydropyridazone derivative was estimated to be less than the concomitant release of leucine throughout the reaction period. For this reason, it was supposed, from the instability of III, that the compound (III), once formed, tended to decompose during the cleavage reaction.

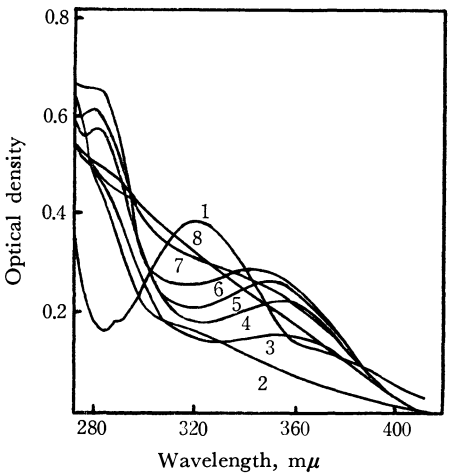

Fig. 7. Change of absorption spectrum during the reaction of the oxidized carbobenzoxytryptophylleucine with hydrazine in a 50% ethanol solution.
1: oxidation product of carbobenzoxytryptophylleucine, 2: after 20 min, 3: after 40 min, 4: after 1 hr, 5: after 1.5 hr, 6: after 2.5 hr, 7: after 3 hr, 8: after 3.5 hr.

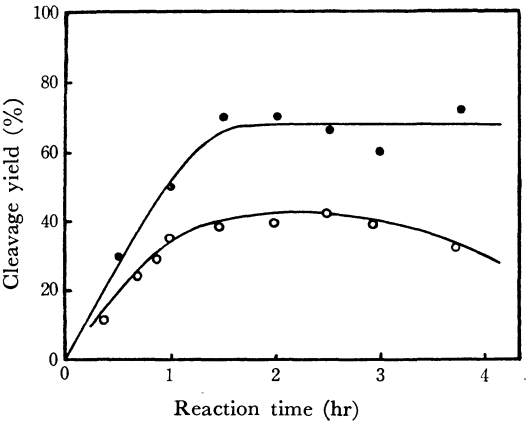

Fig. 8. Relationship between the change of absorbancy at 350 mμ (-○-) and release of leucine (-●-) during the reaction of the oxidized carbobenzoxytryptophylleucine with hydrazine.

By the thin-layer chromatography of the reaction mixture after the reaction of the ozonized carbobenzoxyalanyltryptophylleucine for two hours, two new yellow substances were detected. The major one, slowly moving, was identified as VI, and the other, a minor component, was assumed to be one of decomposition products since this substance showed a spectrum quite different from that of VI. This product was neither alanine nor leucine, and it gave no ninhydrin reaction even after acid hydrolysis.[12] Though no details on the decomposition reaction of VI are available at the present time, it may be concluded that the cleavage reaction of the tryptophyl bond occurred through the series of chemical reactions presented in Fig. 1.

Experimental

Methods and Materials. Paper chromatography on Toyo No. 51 filter paper was carried out using a solvent system, A (*n*-butanol-water-acetic acid, 4 : 1 : 1 by volume) or B (pyridine-*n*-butanol-water-acetic acid, 10 : 15 : 12 : 3 by volume). Thin-layer chromatography (silica gel G, Merck AG) was also performed with either solvent system. The amino acid was determined by Cd-ninhydrin reaction after chromatography on filter paper.[13] The absorption spectra were measured by a Beckmann spectrometer, type DB. Ozone (1—2%) was generated from oxygen by a generator manufactured by the Nippon Ozone Co., Ltd., type 0—3—2, and the ozone concentration was determined by the KI–$Na_2S_2O_3$ method. The formic acid (99—100%) was purchased from Merck AG and was used without purification. Carbobenzoxy-DL-tryptophyl-L-alanine, -L-leucine, -L-phenylalanine, and -L-aspartic acid were prepared by a conventional method. Four tryptophyl peptides related to the adrenocorticotropic hormone were courteously supplied by Dr. H. Yajima of Kyoto University, Kyoto. All the melting points were uncorrected.

Ozonization of Tryptophan with or without Resorcinol. Into 1.0 m*l* of a formic acid solution containing 5 μmol of tryptophan and resorcinol (0, 5 or 10 μmol), the desired amount of ozone was bubbled within one minute at room temperature. Aliquots (0.1 m*l*) of the reaction mixture were then transferred into 3 m*l* of ethanol, and the absorbancies at 322 and 280 mμ were measured. The yield of *N'*-formylkynurenine formed was estimated by the absorbance at 322 mμ on the basis of the molar extinction of *N*-acetyl-*N'*-formylkynurenine ($\varepsilon = 4.25 \times 10^3$ in the mixture of formic acid and ehtanol, 1 : 10 by volume). Another aliquot (0.1 m*l*) was dried up under reduced pressure and incubated in 0.05 m*l* of 1 N hydrochloric acid for one hour at room temperature in order to remove the *N'*-formyl group. Then 10 μ*l* of the above solution was submitted to paper chromatography with either the A solvent or with water in order to determine kynurenine.

Ozonization of Several Synthetic Peptide with Ozone. One milliliter of a formic acid solution containing 5 μmol of the tryptophyl peptide or its derivative was treated by a stream of ozone (20 μmol with, or 10 μmol without, 10 μmol of resorcinol) for half an hour at room temperature. The amount of *N'*-formylkynurenine and kynurenine were estimated much as has been described above except for the procedure of the hydrolysis of kynurenine determination: that is, the hydrolysis of the ozonized peptide derivative was carried out under more drastic conditions (105°C for 20 hr with 6 N hydrochloric acid).

Table 3. Buffers used for the cleavage of the peptide bond of Z-DL-Trp-L-Leu-OH in various concentrations of hydrazine

pH	Final concn. of hydrazine (M)	Final concn. of acetic acid (M)
2.65	0.0	2.0
3.60	0.1	2.0
3.60	0.2	4.0
3.60	0.3	6.0
3.60	0.4	8.0
3.60	0.5	9.0

Effect of the Concentration of Hydrazine and the pH on the Release of Leucine from the Oxidized Product of *N*-α-Carbobenzoxytryptophyl Peptide. Into 10 m*l* of formic acid containing *N*-α-carbobenzoxy-DL-tryptophyl-L-leucine (45.1 mg, 100 μmol), 200 μmol of ozone were bubbled at room temperature within one minute. Aliquots (0.1 m*l*) were taken out and the formic acid was removed under reduced pressure. Into the residue, 0.5 m*l* of the hydrazine-acetate buffer listed in Table 3 was added. The solution or suspension was then heated to boil for two hours. When ten microliters of the reaction mixture were chromatographed on filter paper with the A solvent, the leucine was identified and determined.

For the study of the pH dependence of the hydrazine treatment, the oxidized *N*-α-carbobenzoxy-L-alanyl-L-tryptophyl-L-leucine was similarly treated with a hydrazine-acetate buffer at various pH values (molar ratio of the peptide derivative to hydrazine=1 : 20 in all experiments). (*Cf.* Table 4).

Cleavage Reaction of the Tryptophyl Bond by a Standard Procedure. One milliliter of a formic acid solution containing 5 μmol of the sample peptide derivative was treated with 20 or 10 μmol of ozone for half an hour with or without resorcinol (10 μmol). An aliquot (0.1 m*l*) taken out was evaporated to dryness and treated with a hydrazine(0.1 M)-acetate buffer (pH 3.6) at 105°C for 2 hr in a sealed tube. Then the sample was transferred quantitatively onto filter paper for chromatographic identification, and the amount of amino acid released was determined. A duplicate

Table 4. Buffers used for the cleavage of the tryptophyl bond of Z-L-Ala-L-Trp-L-Leu-OH at various pH's

pH	Final concn. of hydrazine (M)	Final concn. of acetic acid (M)
3.60	0.2	2.0
3.75	0.2	1.0
4.10	0.2	0.5
4.85	0.2	0.28
5.85	0.2	0.175
6.20	0.2	0.17
6.60	0.2	0.165
7.00	0.2	0.16
8.00	0.2	0.11
8.70	0.2	0.00

12) Following reaction was considered as one of possible decompositions of 4-acylaminotetrahydropyridazone.

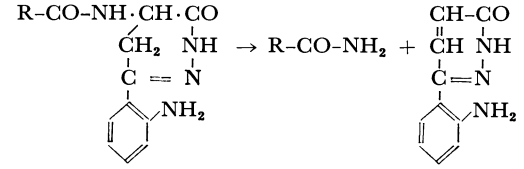

13) R. C. Canfield and C. B. Anfinsen, "The Proteins," Vol. 1, ed. by H. Neurath, Academic Press, New York (1963), p. 318.

experiment was made for the cleavage reaction of each tryptophyl peptide derivative.

The non-specific hydrolysis of *N*-α-carbobenzoxy-tryptophyl amino acids was studied by the same procedure except for the ozonization.

N-α-Acetyl-N'-formyl-DL-kynurenine. *N*-α-Acetyl-DL-tryptophan (2.46 g) dissolved in 100 m*l* of formic acid was oxidized with a stream of ozone at room temperature until the absorption at 280 mμ disappeared almost completely. On the evaporation of the formic acid, the resulting oily product was treated with methanol, and the slightly yellow powder (1.25 g) thus obtained was crystallized from methanol. Mp 194°C. λ_{max} 322 mμ ($\varepsilon=4.25\times10^3$ in ethanol and 4.05×10^3 in ethanol-formic acid (30 : 1 by volume)). ν(Nujol) 3395, 3300, 1729, 1710, 1590 and 1559 cm^{-1}. R_f(A) 0.81 (orange with an Ehrlich reagent).

Found: C, 56.16; H, 5,13; N, 9.74%. Calcd for $C_{13}H_{14}O_5N_2$: C, 56.11; H, 5.07; N, 10.07%.

4-L-(N-carbobenzoxy-L-alanylamino)-6-(o-aminophenyl)-2,3,4,5-tetrahydropyridaz-3-one (VI). By a similar procedure, the *N*-α-carbobenzoxy-L-alanyl-tryptophan methyl ester (400 mg) was oxidized by ozone. After the removal of the formic acid, the oily residue was dissolved in 10 m*l* of ethanol. To the ethanol solution 0.125 m*l* of 80% hydrazine hydrate was added, after which the solution was allowed to stand overnight at room temperature. The slightly yellow crystals thus separated were collected and recrystallized from ethanol (377 mg, 92%). Mp 197.5—198.5°C. R_f(B) 0.87 (orange with an Ehrlich reagent and a yellowish-orange fluorescence under ultraviolet light). λ_{max} 350 mμ ($\varepsilon=8.13\times10^3$), 285 mμ ($\varepsilon=10.5\times10^3$) and 250 mμ ($\varepsilon=16.5\times10^3$) in ethanol. ν(Nujol) 3420, 3270, 1660, 1609, 1558, 1540, 1530 and 1488 cm^{-1}.

Found: C, 61.19; H, 5.46; N, 16.61%. Calcd for $C_{21}H_{23}O_4N_5$: C, 61.60; H, 5.66; N, 17.11%.

4-L-Carbobenzoxyamino-6-(o-aminophenyl)-2,3,4,5-tetrahydropyridaz-3-one (V). By a similar procedure, V was prepared from the *N*-α-carbobenzoxy-L-tryptophan methyl ester. The crude product was recrystallized from methanol. Yield, 37%. Mp 199—200°C. R_f(B) 0.95 and (A) 0.81 (orange with an Ehrlich reagent and a yellowish-orange fluorescence under ultraviolet light). λ_{max} 350 mμ ($\varepsilon=8.10\times10^3$), 285 mμ ($\varepsilon=11.4\times10^3$) and 250 mμ ($\varepsilon=16.0\times10^3$) in ethanol. ν(Nujol) 3450, 3285, 3200, 1609, 1600, 1588, 1544, 1527 and 1488 cm^{-1}.

Found: C, 63.39; H, 5.25; N, 16.10%. Calcd for $C_{18}H_{18}O_3N_4$: C, 63.89; H, 5.36; N, 16.56%.

6-(o-Aminophenyl)-2,3,4,5-tetrahydropyridaz-3-one. This compound was prepared from β-indolepropionic acid in a 15% yield by ozonization and subsequent hydrazine treatment. λ_{max} 350 mμ ($\varepsilon=7.0\times10^3$), 285 mμ ($\varepsilon=10.6\times10^3$) and 250 mμ ($\varepsilon=15.9\times10^3$) in ethanol.

Found: C, 63.26; H, 5.84; N, 21.74%. Calcd for $C_{12}H_{11}ON_3$: C, 63.47; H, 5.84; N, 22.21%.

N-α-Carbobenzoxy-L-alanyl-L-tryptophyl-L-leucine Methyl Ester. *N*-α-Carbobenzoxy-L-alanine was coupled with the L-tryptophyl-L-leucine methyl ester by dicyclohexylcarbodiimide, and the pure, protected tripeptide ester was then obtained by recrystallization from ethyl acetate-petroleum ether. Mp 169.5—170°C. $[\alpha]_D^{26}=-34.5$ (*c* 1.0, glacial acetic acid).

Found: C, 64.74; H, 6.70; N, 10.32%. Calcd for $C_{29}H_{36}O_6N_4$: C, 64.91; H, 6.76; N, 10.44%.

N-α-Carbobenzoxy-L-alanyl-L-tryptophyl-L-leucine. The *N*-α-carbobenzoxy-L-alanyl-L-tryptophyl-L-leucine methyl ester (1.07 g) was suspended in methanol (30 m*l*), and the 2 N sodium hydroxide (2.2 m*l*) was added. The alkaline solution was stirred for an hour under cooling with ice water and then for four hours at room temperature. After the evaporation of the methanol, the aqueous solution was acidified with 1 N hydrochloric acid, and the white precipitates thus separated was collected. Yield, 1.01 g (96.2%). The crude protected tripeptide was dissolved in ethyl acetate (30 m*l*); by the addition of dicyclohexylamine (0.48 m*l*), the dicyclohexylammonium salt (1.30 g, 92.2%) was obtained. Mp 183—185°C.

Found: C, 66.81; H, 8.36; N, 9.95%. Calcd for $C_{40}H_{57}O_6N_5\cdot H_2O$: C, 66.55; H, 8.24; N, 9.70%.

The dicyclohexylammonium salt (1.30 g) suspended in water (50 m*l*) was acidified with 1N hydrochloric acid (2 m*l*), and the white precipitates were extracted into ethyl acetate, which was then dried over anhydrous sodium sulfate and evaporated. Since the protected tripeptide was not crystallized, it was again dissolved in a 5% sodium hydrogencarbonate solution. The pure tripeptide was then separated by acidification with 1N hydrochloric acid. Yield, 0.98 g (96.9%). Mp 156—157°C. $[\alpha]_D^{26}=-29.5$ (*c* 1.0, glacial acetic acid).

Found: C, 64.29; H, 6.52; N, 10.46%. Calcd for $C_{28}H_{34}O_6N_4$: C, 64.35; H, 6.56; N, 10.72%.

The authors wish to express their thanks to Professor Kozo Narita for his discussions throughout this investigation. We also wish to thank Mr. Minoru Kuroda for his technical assistance.

BULLETIN OF THE CHEMICAL SOCIETY OF JAPAN VOL. 43 531—537 (1970)

Studies on Aminosugars. XXIV. The Facile Elimination of the Derivatives of a Pyranosid-4-ulose*1

Tsutomu TSUCHIYA, Kiyohiko SUO and Sumio UMEZAWA

Department of Applied Chemistry, Faculty of Engineering, Keio University, Koganei-shi, Tokyo

(Received September 13, 1969)

Methyl 3-azido-3-deoxy-α and β-D-xylopyranoside are prepared. The oxidation of the 2-*O*-benzoylated derivative of the above-mentioned α-anomer with the Pfitzner-Moffatt reagent leads to the facile elimination of the elements of benzoic acid and the formation of the 4-azido derivative of 5,6-dihydro-α-pyran-5-one. The 3-ethoxycarbonylamido derivative obtained from the above-mentioned 3-azido derivative is oxidized similarly to afford the 4-ethoxycarbonylamido derivative of 5,6-dihydro-α-pyran-5-one. The mechanisms of these elimination reactions are discussed.

In recent years, it has been shown that the oxidation of suitably-protected carbohydrates with dimethyl sulfoxide in the presence of dicyclohexylcarbodiimide and a proton source,[1] phosphorous pentoxide[2] or acid anhydride[3] is a unique and mild method of general application. The reagents oxidize either primary or secondary sugar hydroxyl groups into aldehydes or ketones which are versatile and which are, especially, of potential importance in the synthesis of branched-chain sugars. On the other hand, the oxidation of a secondary hydroxyl group of sugars into a ketone group sometimes results in the elimination of an acyloxyl group and proton in addition to oxidation affording such enones as pyranoid derivatives. Elimination of this kind is useful for introducing a double bond into the pyranoside ring.

In this paper we will present a study of the oxidation of several protected 3-azido-3-deoxy and 3-ethoxycarbonylamido pyranosides with the above-mentioned reagents; this oxidation resulted in the formation of 4-azido and 4-ethoxycarbonylamido derivatives of 5,6-dihydro-2*H*-pyran-5-one.

The first objective of the synthesis was methyl 3-azido-3-deoxy-α-D-xylopyranoside (VIII). 1,2-*O*-Isopropylidene-α-D-xylopyranose (II) was prepared from D-xylose through 1,2 : 3,5-di-*O*-isopropylidene-α-D-xylofuranose (I) by the method of Levene and Raymond[4] and was tritylated to give the 5-*O*-trityl derivative (III). The oxidation of III with the Pfitzner-Moffatt reagent[1] gave a 3-keto derivative (IV) which, on reduction with sodium borohydride, afforded 1,2-*O*-isopropylidene-5-*O*-trityl-D-ribose (V).[5] It should be noted that, when the oxidation of III was effected with dimethyl sulfoxide-acetic anhydride, 1,2-*O*-isopropylidene-3-*O*-methylthiomethyl-5-*O*-trityl-α-D-xylofuranose (IV′) was obtained in addition to IV. A mesyl derivative (VI) prepared from V was treated with sodium azide in dimethyl formamide to afford 3-azido-3-deoxy-1,2-*O*-isopropylidene-5-*O*-trityl-D-xylose (VII). The inversion at C-3 of VI was confirmed by a comparison of the NMR spectra of VI, VII, and the 3-*O*-mesyl derivative (VI′) of III.

The treatment of VII with acidic methanol afforded the desired methyl 3-azido-3-deoxy-D-xylopyranoside in the form of an anomeric mixture. The separation of anomers was effected by column chromatography with Dowex 1×2 (OH form) resin; the α-form (VIII) and β-form (VIII′) were thus obtained in approximately equal amounts. Catalytic hydrogenation over platinum oxide gave the α-form(IX) and β-form (IX′) of methyl 3-amino-3-deoxy-D-xyloside respectively. The melting points and optical rotations of IX and IX′ agreed well with those reported for the corresponding substances prepared by entirely different methods;[6,7] this confirmed the pyranoside structure of the azido compounds. The overall yield of

*1 Presented at the 22nd Annual Meeting of the Chemical Society of Japan, Tokyo, April, 1969. (See Preprints for the Meeting, Vol. 3, p. 1898.)

1) K. E. Pfitzner and J. G. Moffatt, *J. Amer. Chem. Soc.*, **85**, 3027 (1963); for a review, see W. W. Epstein and F. W. Sweat, *Chem. Rev.*, **67**, 247 (1967).

2) K. Onodera, S. Hirano and N. Kashimura, *J. Amer. Chem. Soc.*, **87**, 4651 (1965).

3) J. D. Albright and L. Goldman, *J. Amer. Chem. Soc.*, **87**, 4214 (1965); W. Sowa and G. H. S. Thomas, *Can. J. Chem.*, **44**, 836 (1966).

4) P. A. Levene and A. L. Raymond, *J. Biol. Chem.*, **102**, 317 (1933).

5) The same sequence was developed independently by Sowa in his synthesis of 3-amino-3-deoxy-D-ribose; W. Sowa, *Can. J. Chem.*, **46**, 1586 (1968).

6) R. E. Schaub and M. J. Weiss, *J. Amer. Chem. Soc.*, **80**, 4683 (1958).

7) H. H. Bear and H. O. L. Fischer, *ibid.*, **81**, 5184 (1959).

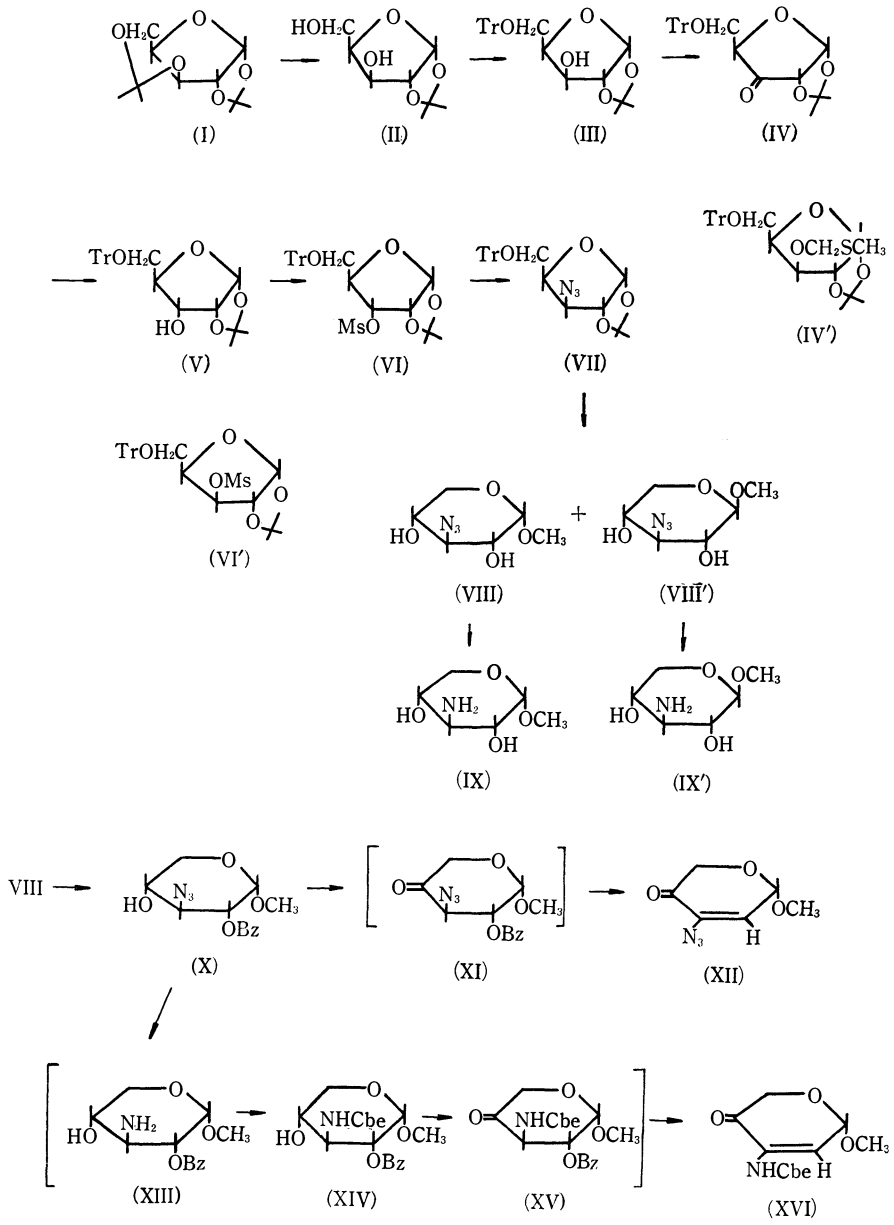

Chart 1. Cbe : $COOC_2H_5$, Bz : COPh, Ms : SO_2CH_3, Tr : CPh_3

the total of IX and IX′ from xylose was about 25%.

The selective benzoylation of the α-anomer (VIII) with benzoyl chloride in pyridine gave 2-*O*-benzoyl derivative (X) in a 70% yield. It is of interest to note that the β-anomer yielded 2 and 4-*O*-benzoylated products in low yields, suggesting that the selectivity is peculiar to the α-anomer.

When the 2-*O*-benzoyl derivative was oxidized with dimethyl sulfoxide-dicyclohexylcarbodiimide-trifluoroacetic acid - pyridine, the product was found to be an azido-ketonic derivative of dihydropyran (XII) which showed a characteristic absorption maximum at 273 mμ (ε 7500). The structural proofs were obtained by infrared and NMR spectroscopy; the patterns, shown in Fig. 1, indicated the structure of XII to be (2S)-4-azido-5,6-dihydro-2-methoxy-α-pyran-5-one. The absence of the expected oxidative product (XI) in the crude product was shown by thin-layer chromatography.

On the other hand, the 2-*O*-benzoyl derivative (X) was hydrogenated over platinum oxide to give an amino derivative (XIII), which was then caused to react with ethyl chloroformate in the presence of sodium bicarbonate to give an ethoxycarbonylamido derivative (XIV). The oxidation

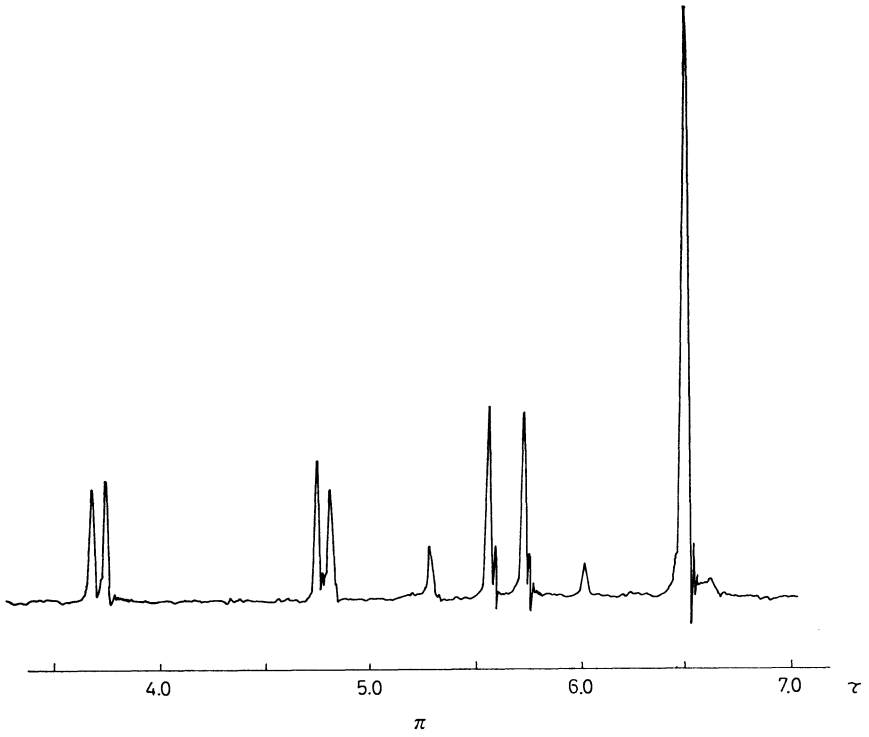

Fig. 1. The NMR spectrum of (2S)-4-azido-5,6-dihydro-2-methoxy-α-pyran-5-one (XII) at 60 MHz in chloroform-*d*.

of XIV with dimethyl sulfoxide-acetic anhydride again afforded a dihydropyran derivative, namely, (2S)-5,6-dihydro-4-ethoxycarbonylamido-2-methoxy-α-pyran-5-one (XVI).

Discussion

Though such an elimination reaction as has been described above appears to be rarely encountered, several definite examples have recently been described. Beynon *et al.*[8] reported that the methyl-3,4,6-tri-*O*-benzoyl-α-D-*arabino*-hexopyranosidulose obtained from methyl 3,4,6-tri-*O*-benzoyl-α-D-glucoside by oxidation with ruthenium tetroxide underwent facile elimination to give an enone, 2-D-*glycero*-benzoyloxymethyl-4-benzoyloxy-6-D-*glycero*-methoxy-5,6-dihydro-α-pyran-5-one. Shibata *et al.*[9] reported that the oxidation of methy 3-acetamido-4,6-di-*O*-acetyl-3-deoxy-α-D-mannopyranoside with the Pfitzner-Moffatt reagent resulted in the formation of 2-D-*glycero*-acetyloxymethyl-4-acetylamido-6-D-*glycero*-methoxy-5,6-dihydro-α-pyran-5-one. Cree *at al.*[10] also found that the oxidation of some partially-acetylated monosaccharides with dimethyl sulfoxide-sulfur trioxide-pyridine-triethyl amine led to the elimination of acetic acid and the formation of 6-aldehydo-4-hexenopyranosides.

Whichever detailed mechanism is involved, these reactions are β-eliminations; the driving force of the elimination is the energy released in forming the double bond, while a potent influence is exerted by the carbonyl and azide group (in the case of XI) in facilitating elimination, as is depicted

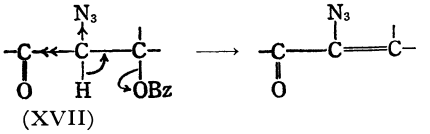

(XVII)

by XVII. The substrates (XI and XV) are favorable for carbanion formation, and, in the elimination, the H and OBz removed are *cis*; those findings support an ElcB mechanism, but not an E2 mechanism, as in the case of the elimination of acetic acid from 2-phenyl-2-acetoxy-1-nitrocyclohexane, in which the H and OAc are *cis*.[11]

A possible alternative mechanism may proceed through such an enol-form as is shown by XI′.

8) P. J. Beynon, P. M. Collins, P. T. Doganges and W. G. Overend, *J. Chem. Soc.*, **1966**, 1131.

9) H. Shibata, I. Takeshita, N. Kurihara and M. Nakajima, *Agr. Biol. Chem.*, **32**, 1006 (1968).

10) G. M. Cree, D. W. Mackie and A. S. Perlin, *Can. J. Chem.*, **47**, 511 (1969).

11) F. G. Bordwell and E. W. Garbisch, Jr., *J. Org. Chem.*, **28**, 1765 (1963); F. G. Bordwell, R. L. Arnold and J. B. Biranowski, *ibid.*, **28**, 2496 (1963).

The electron-withdrawing benzoyloxy group may be oriented pseudoaxially, because a pseudoaxial group at an allylic position is better disposed for a π-orbital overlap than a pseudoequatorial one; thus, carbonium ion formation at the allylic position proceeds more readily upon the departure of a pseudoaxial group than upon the departure of a pseudoequatorial one,[12] and the resulting carbonium ion is stabilized by the allylic delocalization of the positive charge.

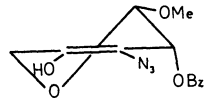

XI′

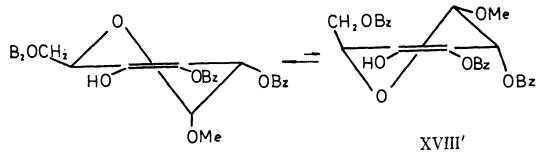

XVIII XVIII′

In connection with the mechanism, we should like to cite the finding by Gabriel,[13] who prepared methyl 2,3,6-tri-*O*-benzoyl-α-D-*xylo*-hexopyranosid-4-ulose by the oxidation of methyl 2,3,6-tri-*O*-benzoyl-α-D-galactopyranoside with dimethyl sulfoxide-acetic anhydride and found it unstable, although he made no study of the decomposition product. This 4-keto-derivative is closely related to our XI and XV; both are derivatives of α-D-xylopyranosid-4-ulose. However, XI and XV differ from the 4-keto-derivative in having no benzoyloxymethyl group (equatorial) at C-5 and in having an azido or ethoxycarbonylamido group at C-3 instead of a benzoyloxy group. When elimination occurs, the 4-keto-derivative may be transformed into a half-chair conformation, XVIII′, which has an axial benzoyloxy group at C-2 (allylic position). As compared with the stability of the conformation XI′, the stability of the conformation XVIII′ differs in having an instability factor caused by a pseudodiaxial interaction between the 5-benzoyloxymethyl group and the anomeric hydrogen atom, the same anomeric effects and $\Delta 2$ effects being involved in both conformations. Consequently, the 4-keto-derivative may have more of a tendency to take a stable conformation such as that of XVIII rather than one such as XI′. This may be the reason why XI and XV are more labile than the 4-keto-derivative.

12) For a general discussion, see E. L. Eliel, N. L. Allinger, S. J. Angyal and G. A. Morrison, "Conformational Analysis," Interscience Publishers, New York (1965), p. 111.

13) O. Gabriel, *Carbohyd. Res.*, **6**, 319 (1968).

Experimental

The NMR spectra were measured with a Varian A-60D spectrometer. Tetramethylsilane (τ 10.00; for the solutions of deuteriochloroform) and sodium 4,4-dimethyl-4-silapentane-1-sulfonate (τ 10.00; for the solutions of deuterium oxide) were used as the internal standards. The abbreviations used were as follows: p: proton, s: singlet, d: doublet, t: triplet, q: quartet, m: multiplet, d.d: doublet of doublets. Thin-layer chromatograms were visualized by spraying them with sulfuric acid at room temperature or by heating them at 110°C.

1,2-*O*-Isopropylidene-5-*O*-trityl-α-D-erythro-pentofuranos-3-ulose (IV). *a)* To a solution of 1,2-*O*-isopropylidene-5-*O*-trityl-α-D-xylofuranose (III) (8.77 g) in anhydrous benzene (60 m*l*) containing dry dimethyl sulfoxide (DMSO) (10 g), pyridine (3.2 m*l*), and trifluoroacetic acid (1.6 m*l*) was added dicyclohexylcarbodiimide (3.5 g×2, at an interval of 0.5 hr); the suspension was then stirred for 2 hr at room temperature. Ether (300 m*l*) and a solution of oxalic acid (2.6 g) in methanol (20 m*l*) were added in turns. After the evolution of gas had ceased, water (150 m*l*) was added, and an insoluble material was filtered off. The ether-layer was washed with a sodium bicarbonate solution and with water successively. After having been dried over sodium sulfate, the ether solution was evaporated to give a syrup which, on trituration with ether or ethanol, gave crystals. The addition of petroleum ether completed the crystallization; 6.97 g (80%), recrystallized from isopropanol; mp 131—132°C, $[\alpha]_D^{25}$ +132° (*c* 1, chloroform). (Sowa[5] reported mp 132°C and $[\alpha]_D$ +132°). Found: C, 75.83; H, 6.42%. Calcd for $C_{27}H_{28}O_5$: C, 75.33; H, 6.09%. R_f 0.60 (benzene-ethyl acetate 30 : 1).

IR (KBr): 1775 (C=O), 1388, 1375 (isopropyl), 703 cm^{-1} (phenyl).

NMR ($CDCl_3$): τ: 8.53 (6-p. s., isopropylidene), 6.67, 6.52 (each 1-p. q., H-5, 5′), 5.60 (1-p. m., H-4), 5.45 (1-p. d.d., H-2), 3.68 (1-p. d., H-1), 2.5—2.85 (15-p. m., phenyl); $J_{1,2}$ 4.5 Hz, $J_{2,4}$ 1 Hz, $J_{5,5'}$ 10.2 Hz, $J_{4,5}$ 2.7 Hz, $J_{4,5'}$ 2.6 Hz.

b) With DMSO-Ac_2O. To an ice-cold solution of III (37.05 g) in DMSO (120 m*l*), acetic anhydride (80 m*l*) was added; the mixture was set aside for 2 hr at that temperature and then for 3 days at room temperature. On thin-layer chromatography (TLC) (silica gel, benzene-ethyl acetate 30 : 1), three spots (R_f 0.67 (IV′), 0.60 (IV), and 0.22 (III)) were detected. Evaporation *in vacuo* gave a syrup, which was then dissolved in chloroform (200 m*l*). The solution was washed with a sodium bicarbonate solution and water successively. After having been dried over sodium sulfate, the solution was evaporated to give a syrup. As the separation of IV and IV′ by column chromatography was unsuccessful, the syrup was reduced with sodium borohydride. To a suspension of the syrup in aqueous ethanol (1 : 3, 750 m*l*), sodium borohydride (3.35 g) was added; the mixture was then agitated for 5 hr. The syrup obtained by evaporation was dissolved in ethyl acetate (900 m*l*) and washed thoroughly with water. Drying over sodium sulfate, followed by evaporation, gave a syrup which was subjected to column chromatography (silica gel, 450 g) with benzene-ethyl acetate (15 : 1). Fractionation gave IV′ between 930

and 1250 m*l* (yield 17.6 g), V between 1330 and 1590 m*l* (12.3 g), III+V between 1590 and 2100 m*l* (11 g), and III between 1200 and 3000 m*l* (4 g). V was recrystallized from benzene-*n*-hexane (1 : 25); 9.39 g; mp 99—100°C. IV′ was recrystallized from ethanol and proved to be 1,2-*O*-isopropylidene-3-*O*-methylthiomethyl-5-*O*-trityl-α-D-xylofuranose (14.6 g); mp 102—103°C, $[\alpha]_D^{15}$ −59.0° (*c* 1, chloroform).

Found: C, 70.94; H, 6.54; S, 6.57%. Calcd for $C_{29}H_{32}SO_5$: C, 70.70; H, 6.55; S, 6.51%.

IR (KBr); 1383, 1375 (isopropyl), 705 cm^{-1} (phenyl).

NMR ($CDCl_3$): τ: 8.68 (3-p. s., isopropylidene), 8.46 (3-p. s., isopropylidene), 8.10 (3-p, s., SCH_3), 6.80 (1-p. q., H-5), 6.48 (1-p. q.. H-5′), 5.75 (1-p. d., H-2 or H-3), 5.3—5.7 (4-p. m., H-3 or H-2, H-4, OCH_2-SCH_3), 4.12 (1-p. d., H-1), 2.35—2.90 (15-p. m., trityl); $J_{1,2}$ 3.9 Hz, $J_{2,3}$ ~0 Hz, $J_{4,5}$ 6.2 Hz, $J_{4,5'}$ 5.8 Hz, $J_{5,5'}$ 9.7 Hz.

1,2-*O*-Isopropylidene-5-*O*-trityl-D-ribofuranose (V). To a suspension of IV (6.97 g) in aqueous ethanol (1 : 3, 80 m*l*), sodium borohydride (0.37 g) was added; the mixture was then shaken gently for a while, a clear solution soon resulted, and then crystals were gradually deposited. After 1 hr's standing, the whole mixture was concentrated to a small volume, and the resultant precipitate was dissolved in ethyl acetate. The solution was washed with water, dried over sodium sulfate, and evaporated to give a solid. To a solution of the solid in benzene (10 m*l*), a 75-m*l* portion of petroleum ether was added all at once; the mixture was then stimulated with a glass rod to give needles (6.1 g); mp 99—100°C, $[\alpha]_D^{18}$ +25.0° (*c* 1, chloroform) (reported[5] mp 117°C, $[\alpha]_D$ +25.8°), R_f 0.53 (silica gel, benzene-ethyl acetate 6 : 1).

Found: C, 75.07; H, 6.45%. Calcd for $C_{27}H_{28}O_5$: C, 74.98; H, 6.52%.

The product was chromatographically homogeneous, and no contamination of the xylo-isomer (III, R_f 0.40) was shown.

IR (KBr): 3460 (OH), 1385, 1377 (isopropyl), 700 cm^{-1} (phenyl).

NMR ($CDCl_3$): τ: 8.64 (3-p. s., isopropylidene), 8.45 (3-p. s., isopropylidene), 7.7 (1-p. d., disappeared on deuteration, OH). 6.63 (2-p. m., H-5, 5′), 6.2—5.95 (2-p. m., H-3, H-4; irradiation at τ 5.49 changed the pattern of this area), 5.49 (1-p. triplet-like pattern, H-2), 4.16 (1-p. d., H-1; collapsed to a singlet on irradiation at τ 5.49), 2.35—2.95 (15-p. m., trityl); $J_{1,2}$ 4.0 Hz.

1,2-*O*-Isopropylidene-3-*O*-mesyl-5-*O*-trityl-D-ribofuranose (VI). To an ice-cold solution of V (6.55 g) in pyridine (60 m*l*), methanesulfonyl chloride (1.77 m*l*) was added drop by drop; the mixture was then allowed to stand for 1 hr under ice-cooling, and then for 24 hr at room temperature. The evaporation of the solution gave a syrup which was then dissolved in chloroform and washed successively with water, a sodium bicarbonate solution, and water. After having been dried over sodium sulfate, the solution was treated with charcoal and coevaporated with toluene to give a thick syrup (7.70 g). The product was chromatographically homogeneous (R_f 0.49 with silica gel, benzene-ethyl acetate 30 : 1) and sufficiently pure for the subsequent reaction. The syrup was crystallized from aqueous 50% ethanol; mp 123—125°C, $[\alpha]_D^{15}$ +64.6° (*c* 0.8, chloroform).

Found: C, 66.11; H, 5.97; S, 6.30%. Calcd for $C_{28}H_{30}O_7S$: C, 65.86; H, 5.92; S, 6.28%.

IR (KBr): ~1365 (broad, isopropylidene), 1180, 835 (mesyl), 703 cm^{-1} (phenyl).

NMR ($CDCl_3$): τ: 8.64 (3-p. s., isopropylidene), 8.45 (3-p. s., isopropylidene), 7.13 (3-p. s., SO_2CH_3), 6.83 (H-5) and 6.47 (H-5′)(eight-line signals, with the inner four being most intense, typical for the AB part of an ABX system), 5.79 (1-p., doublet of triplets in appearance, H-4), 5.17 (1-p. q., H-2), 5.04 (1-p. q., H-3), 4.08 (1-p. d., H-1), 2.9—2.4 (15-p. m., trityl); $J_{1,2}$ 3.5 Hz, $J_{2,3}$ 4.6 Hz, $J_{3,4}$ 8.5 Hz, $J_{4,5}$ 3.5 Hz, $J_{4,5'}$ 2.5 Hz, $J_{5,5'}$ 11.2 Hz. The irradiation at the frequency of H-5 causes H-5′ to become a doublet ($J_{4,5'}$ 2.5 Hz) and H-4 to become a doublet of doublets; the irradiation at the frequency of H-5′ causes H-5 to become a doublet ($J_{4'5}$ 3.5 Hz) and H-4 to become a doublet of doublets; the irradiation at the frequency of H-1 causes H-2 to become a doublet ($J_{2,3}$ 4.6 Hz); the irradiation at the frequency of H-4 causes H-5 and H-5′ to become an AB quartet ($J_{5,5'}$ 11.2 Hz) and H-3 to become a doublet ($J_{2,3}$ 4.6 Hz).

1,2-*O*-Isopropylidene-3-*O*-methyl-5-*O*-trityl-D-xylofuranose (VI′). This compound was prepared from III as has been described in the procedure for the D-ribo isomer (VI); mp 116—117°C, $[\alpha]_D^{15}$ −55.0° (*c* 1, chloroform).

Found: C, 65.69; H, 6.16; S, 5.95%. Calcd for $C_{28}H_{30}O_7S$: C, 65.86; H, 5.92; S, 6.28%.

IR (KBr): 1370 (isopropylidene), 1175, 837 (mesyl), 700 cm^{-1} (phenyl).

NMR ($CDCl_3$): τ: 8.70 (3-p, s., isopropylidene), 8.49 (3-p. s., isopropylidene), 7.28 (3-p. s., SO_2CH_3), 6.72 (H-5) and 6.40 (H-5′)(eight-line signals typical for the AB part of an ABX system), 5.56 (1-p. clear-cut octet, H-4), 5.20 (1-p. d., H-2), 4.90 (1-p. d., H-3). 4.10 (1-p. d., H-1), 2.84—2.4 (15-p. m., trityl); $J_{1,2}$ 3.8 Hz, $J_{2,3}$ 0 Hz, $J_{3,4}$ 3.0 Hz, $J_{4,5}$ 7.6 Hz, $J_{5,5'}$ 9.7 Hz.

3-Azido-3-deoxy-1,2-*O*-isopropylidene-5-*O*-trityl-D-xylofuranose (VII). To a solution of VI (6.38 g) in anhydrous dimethyl formamide (60 m*l*, dried over CaH_2) was added sodium azide (2.1 g). The suspension was heated at 150°C under stirring, and the reaction was pursued by TLC (silica gel, developed with benzene). After 24 hr, the reaction was completed. The organic layer was evaporated *in vacuo*. The resultant brown syrup was dissolved in benzene and passed through a column of silica gel (100 g) with the aid of benzene; after the initial benzene solution had thus been absorbed in the column, the column was set aside for several hours and then treated with benzene as usual. This procedure gave a completely decolorized eluate. The fraction containing the substance with an R_f value of 0.51 was collected and evaporated to give a clear thick syrup: 4.48 g (78%), $[\alpha]_D^{15}$ −42.5° (*c* 0.9, chloroform), IR (KBr): 2108 (N_3), 1385, 1375 (isopropylidene), 703, 697 cm^{-1} (phenyl).

NMR ($CDCl_3$): τ: 8.72 (3-p. s., isopropylidene), 8.50 (3-p. s., isopropylidene), 6.70 (H-5) and 6.46 (H-5′) (eight-line signals typical for the AB part of an ABX system), 6.00 (1-p. d., H-3), 5.67 (1-p. octet, H-4), 5.43 (1-p. d., H-2), 4.20 (1-p. d., H-1), 2.45—2.85 (15-p. m., trityl); $J_{1,2}$ 3.8 Hz, $J_{2,3}$ 0 Hz, $J_{3,4}$ 3.2 Hz, $J_{4,5}$ 7.3 Hz, $J_{4,5'}$ 5.6 Hz, $J_{5,5'}$ 9.7 Hz.

Methyl 3-Azido-3-deoxy-α and β-D-xylopyranoside (VIII, VIII′). A solution of VII (15.26 g) in 1.5% hydrochloric acid in methanol (200 m*l*) was ref-

luxed for 20 hr. Powdered sodium bicarbonate was then gradually stirred in until all gas evolution had ceased. After filtration, the solution was evaporated to give a solid; this solid was boiled with water (30 ml) for a while and then cooled, and the solution was filtered from an insoluble material. The filtrate was evaporated to give a solid, and the procedure was repeated twice more. The resultant solid (6.83 g), which contained a trace amount of tritylcarbinol, was dissolved in a small amount of water and slowly chromatographed on a column of Dowex 1×2 (OH form) resin (220 ml, 20×700 mm) with water. After the removal of the early eluate of 350 ml of water, the fractions were cut into 13-ml portions. An unknown substance (R_f 0.24 with silica gel and benzene - methyl ethyl ketone 3 : 1) appeared between Nos. 6—9 (170 mg after dried), and next the α-anomer (VIII, R_f 0.39) appeared between Nos. 11—37. The β-anomer (VIII′, R_f 0.36) appeared between Nos. 42—80. The second and the third fractions were collected and evaporated to give the α-anomer (2.28 g) and the β-anomer (2.73 g) respectively.

The α-anomer was dissolved in chloroform (30 ml), and filtered, and the filtrate was evaporated to about 5 ml. Gradual cooling at 5°C gave cubic crystals (2.22 g); mp 93—93.5°C, $[\alpha]_D^{20}$ +147° (*c* 0.6, water).

Found: C, 38.29; H, 5.89; N, 22.18%. Calcd for $C_6H_{11}O_4N_3$: C, 38.10; H, 5.86; N, 22.21%.

The β-anomer was crystallized by a similar procedure; cubic crystals (2.48 g), mp 88—89°C, $[\alpha]_D^{20}$ −65.7° (*c* 0.6, water).

Found: C, 38.27; H, 5.89; N, 22.11%.

IR (KBr): α and β-Anomers: 3300—3500 (broad, OH), 2100 (N_3) cm^{-1}. NMR (D_2O) α-Anomer (VIII): τ: 5.31 (1-p. d., H-1), 6.53 (3-p. s., OCH_3); $J_{1,2}$ 2.3 Hz. β-Anomer (VIII′): τ: 5.64 (1-p. d., H-1), 6.45 (3-p. s., OCH_3); $J_{1,2}$ 7.5 Hz.

Methyl 3-Amino-3-deoxy-α- and β-D-xylopyranoside (IX, IX′). Compound VIII (107 mg), dissolved in 50% aqueous ethanol (2 ml), was hydrogenated with hydrogen (50 lb/sq. inch) and preactivated platinum oxide (47 mg) for 2 hr at room temperature. After filtration, the solution was then evaporated to give a solid; this solid was subsequently recrystallized from ethanol to give needles (70 mg); mp 193—195°C (decomp.), $[\alpha]_D^{20}$ +158° (*c* 0.4, water) (lit,[6] mp 195—196°C, $[\alpha]_D$ +155° (*c* 1, pyridine)).

Found: C, 44.54; H, 8.31; N, 8.31%. Calcd for $C_6H_{13}O_4N$: C, 44.16; H, 8.03; N, 8.58%.

β-Anomer (IX′) was obtained by a procedure similar to that used for VIII′; needles, mp 196—199°C (decomp.), $[\alpha]_D^{20}$ −63.2° (*c* 0.5, water) (lit,[7] mp 196—197°C, $[\alpha]_D$ −65° (*c* 1, water)).

The α and β-anomers showed the same R_f values (0.6) on paper chromatography (Toyo Roshi No. 50, sprayed with ninhydrin) with *n*-butanol-pyridine-water-acetic acid (6 : 4 : 3 : 1).

Methyl 3-Azido-2-*O*-benzoyl-3-deoxy-α-D-xylopyranoside (X). Into an ice-cold solution of VIII (6.45 g) in anhydrous pyridine (100 ml), benzoyl chloride (6.78 g) was gradually stirred in; the solution was then set aside for 0.5 hr under ice-cooling, and subsequently for one day at room temperature. TLC (silica gel, benzene-ethyl acetate 6 : 1) showed that the reaction mixture contained three components, with R_f values of 0.82 (dibenzoate), 0.37 (X, main), and 0.09 (VIII). Evaporation *in vacuo* gave a syrup; this syrup was dissolved in chloroform, and the solution was washed successively with a potassium bisulfate solution, water, a sodium bicarbonate solution, and with water again. After drying over sodium sulfate, followed by evaporation, the resultant syrup was chromatographed on silica gel (100 g) with benzene - ethyl acetate (6 : 1). After the removal of the early eluate (120 ml), the fractions were cut into 15-ml portions. Dibenzoate appeared between Nos. 1—5, and X appeared between Nos. 6—20. The latter fractions were collected and evaporated to give a syrup. A solution of the syrup in chloroform was washed with water, dried over sodium sulfate, and concentrated. The addition of petroleum ether gave a syrup. This syrup did not crystallize; 7.02 g (70%), $[\alpha]_D^{16}$ +202.0° (*c* 0.5, chloroform).

Found: C, 53.53; H, 5.49; N, 13.81%. Calcd for $C_{13}H_{15}O_5N_3$: C, 53.24; H, 5.16; N, 14.33%.

IR (KBr): 3450 (OH), 2100 (N_3), 1725 (ester), 710 cm^{-1} (phenyl).

NMR ($CDCl_3$): τ: 6.9 (OH, disappeared on deuteration), 6.62 (3-p. s., OCH_3), 5.88—6.44 (4-p. m., H-3, 4, 5, 5′), 5.10 (1-p. q., H-2), 4.97 (1-p. d., H-1), 1.86—1.97 (2-p.) and 2.3—2.75 (3-p.)(benzoyl); $J_{1,2}$ 3.2 Hz, $J_{2,3}$ 10.0 Hz.

The NMR pattern indicated X to be 2-*O*-benzoate, not 4-*O*-benzozte.

(2S) - 4 - Azido -5,6-dihydro-2-methoxy-α-pyran-5-one (XII). To a solution of X (569 mg) in a mixture of anhydrous benzene (6 ml), dimethyl sulfoxide (6 ml), pyridine (0.32 ml), and trifluoroacetic acid (0.16 ml) was added dicyclohexylcarbodiimide (2.0 g); the suspension was then stirred for 2 hr at room temperature. Ether (50 ml) and a solution of oxalic acid (1.1 g) in methanol (10 ml) were then added in turn. After the evoluation of gas had ceased, water (50 ml) was added; an insoluble material was subsequenty filtered off. The ethereal layer was washed several times with a sodium bicarbonate solution and with water. After having been dried over sodium sulfate, the ethereal solution was evaporated. The resultant syrup was dissolved in a mixture of benzene-ethyl acetate (30 : 1) and chromatographed on a column of silica gel (45 g) with the above-described solvent system. The fractions containing XII were collected and evaporated to give a pale yellow solid; 246 mg (76.3%); mp 58—58.5°C, $[\alpha]_D^{16}$ −23.1° (*c* 0.4, chloroform), λ_{max}^{MeOH} 273 mμ (ε 7500), R_f 0.63 (silica gel, benzene-ethyl acetate 30 : 1).

Found: C, 42.53; H, 4.15; N, 24.40%. Calcd for $C_6H_7O_3N_3$: C, 42.60; H, 4.17; N, 24.85%.

IR (KBr): 2120 (N_3), 1705 (C=O), 1630 (C=C) cm^{-1}.

NMR ($CDCl_3$): τ: 6.49 (3-p. s., OCH_3), 5.80, 5.52 (2-proton AB quartet, H-6, 6′), 4.80 (1-p. d., H-2), 3.71 (1-p. d., H-3); $J_{2,3}$ 3.8 Hz, $J_{6,6'}$ 17.3 Hz.

This substance gradually changes during storage.

(2S) - 4 - Carboethoxyamido-5,6-dihydro-2-methoxy-α-pyran-5-one (XVI). A solution of X (194 mg) in a mixture (2 ml) of equal volumes of 1 N hydrochloric acid and ethanol was hydrogenated with preactivated platinum oxide (30 mg) and hydrogen under pressure (50 lb/sq. inch) for 2 hr. After filtration, the solution was evaporated and an aqueous solution of the residue was treated with charcoal. The aqueous solution was evaporated to give a solid (184 mg), which showed no absorption of the azide group (~2100 cm^{-1}) in the infrared spectrum: it was positive for ninhydrin

coloration.

To an aqueous-acetone (1 : 1) solution (3 ml) of the solid (179 mg) was added ethyl chloroformate (73.2 mg) in the presence of sodium bicarbonate (107 mg); the mixture was then stirred for 1 hr. Evaporation of the solution to about a half volume deposited an oily precipitate; this precipitate was extracted with ether, and the ethereal solution was washed with water, dried over sodium sulfate, and evaporated. The resultant solid (151 mg) was homogeneous on TLC, showing an R_f value of 0.62 with silica gel and ether.

A solution of the solid (104 mg) in DMSO (1.5 ml) and acetic anhydride (0.3 ml) was allowed to stand overnight at room temperature. On TLC (silica gel and chloroform), three sports, with R_f values of 0.05 (starting material), 0.20, and 0.30 (XV), were discerned. After the addition of a saturated sodium bicarbonate solution (15 ml), the reaction mixture was extracted with ether; the ethereal layer was washed thoroughly with water, dried over sodium sulfate, and concentrated. The residue was chromatographed on a silica-gel column with chloroform. The fraction containing XV was evaporated to give a solid; this solid was then recrystallized from ethanol to afford needles (38 mg); mp 64—65°C, $[\alpha]_D^{15}$ +73.8° (*c* 0.4, chloroform), λ_{max}^{MeOH} 271 mμ (ε 8500).

Found: C, 50.50; H, 6.32; N, 6.51%. Calcd for $C_9H_{13}O_5N$: C, 50.23; H, 6.09; N, 6.51%.

IR (KBr): 1745, 1705 (C=O), 1660 (C=O) cm^{-1}.

NMR ($CDCl_3$): τ: 8.72 (3-p. t., CH_2CH_3, J=7.1 Hz), 6.49 (3-p. s., OCH_3), 5.80 (2-p. q., CH_2CH_3), 5.77, 5.47 (2-proton AB quartet, H-6, 6′), 4.71 (1-p. d., H-2), 2.77 (1-p. d., H-3); $J_{2,3}$ 3.8 Hz, $J_{6,6'}$ 17.3 Hz.

The authors wish to thank Mr. Saburo Nakada for his elementary analysis and Mr. Yukio Horiuchi for his technical assistance. This work was supported in part by a grant-in-aid from the Ministry of Education.

BULLETIN OF THE CHEMICAL SOCIETY OF JAPAN VOL. 43 537—542 (1970)

Color Reactions of Polyvinyl Acetate and Its Derivatives with Iodine*[1]

Sadao HAYASHI, Chozo KAWAMURA and Masanari TAKAYAMA

Faculty of Fiber Science and Technology, Shinshu University, Tokiiri, Ueda

(Received July 29, 1969)

It has been found that the addition of a methanol solution containing polyvinyl acetate (PVAc) and iodine to an aqueous solution of potassium iodide results in a red-violet color without precipitating any polymer. The absorption maximum was located at 510 mμ. The absorbance of the PVAc-iodine complex decreased only slightly with an increase in the degree of the polymerization of PVAc. A linear relationship was obtained between the abosrbance and the PVAc concentration. It was found from these results that the color reaction of PVAc with iodine can be used in a colorimetric determination of PVAc, which is insoluble in water. Further, an attempt was made to investigate the complex formation of the vinyl acetate-vinyl propionate copolymer (PVAc-PVPr) and the vinyl acetate-vinyl formacetal copolymer (PVAc-PVFA) with iodine. Although the absorption maximum of the color complex of PVAc-PVPr with iodine appeared at 510 mμ, independent of the copolymer composition, the absorbance decreased with an increase in the number of vinyl propionate units in the copolymer. The absorption maximum of the complex of PVAc-PVFA with iodine was observed to lie at 620 mμ for highly-acetalyzed polyvinyl alcohol and at 520 mμ for polyvinyl alcohol of a low degree of acetalyzation, while a new absorption maximum appeared in the range from 520 to 620 mμ in the intermediate case. The absorbances at the absorption maxima of the complexes of PVAc-PVFA with iodine were approximately the same as those of PVAc. The effect of an elevated temperature on the absorbance was smaller for PVAc-PVFA than for PVAc-PVPr. From these experiments, it became clear that the glass-transition temperature and the color intensity of the polymer-iodine complex have a simple relation.

It is well known that PVAc yields a red-violet-colored complex with iodine; this reaction has previously been applied to the detection of PVAc.[1)] This color development has been carried out in a heterogeneous system which sprays an iodine-potassium iodide solution on the polymer, or immerses the polymer in an iodine-iodide solution. Schweepe[2)] has already reported, regarding the detection of PVAc, that when a few drops of iodine in a potassium iodide solution are added to a sample

*[1] Polyvinyl Acetate and Its Derivatives. VI. Part V: S. Hayashi, M. Takayama and C. Kawamura, *Kogyo Kagaku Zasshi*, **73**, 412 (1970).

1) F. D. Hartley, *J. Polym. Sci.*, **34**, 397 (1959).

2) H. Schweepe, *Paint Technol.*, **27**, 14 (1963).

dissolved in some glacial acetic acid and the solution is diluted with water, the solution develops an intensive red-violet color. We[3] have also found that when both PVAc and iodine are dissolved in a solvent which is easy to mix with water such as methanol or acetone, and the solution is poured into an aqueous solution containing potassium iodide, then, immediately after mixing, the solution exhibits a red-violet color. If the color reaction of PVAc with iodine takes place in a homogeneous system, its reaction might be expected to be applicable to the determination of PVAc and the investigation of the properties of PVAc.

The present work was undertaken in order to examine the optimum conditions of the complex formation of PVAc with iodine in an aqueous phase, and to determine PVAc colorimetrically under the optimum conditions thus obtained. The invessigations of the complex formation of the PVAc copolymers, PVAc-PVPr and PVAc-PVFA, with iodine were also made, and the relationships between the absorbances of the complexes of the copolymers with iodine and the temperature at various temperatures were discussed.

Experimental

Preparations of PVAc and Its Derivatives. It may be expected that the color reaction depends on the degree of polymerization and on the branches in the polymer, as in the cases of amylose and amylopectin.[4] Therefore, two kinds of PVAc samples prepared by different processes were investigated.

PVAc samples made from vinyl acetate: Vinyl acetate was purified by distillation under a reduced pressure in a stream of nitrogen. The polymerization of vinyl acetate was carried out at 60—62°C by using benzoyl peroxide as an initiator. After polymerization for a given time, the contents were poured into a large amount of water in order to precipitate the polymer. The resultant polymer was washed five times with boiling water and then dried in a vacuum.

PVAc samples derived from polyvinyl alcohol (PVA): The various fractionated PVA samples listed in Table 2 were acetylated with acetic anhydride in pyridine. The pyridine solution was then poured into water to obtain the acetylated polymer. The resultant polymer was washed in boiling water until the odor of pyridine completely disappeared; then it was dried in a vacuum. The degree of acetylation of all the samples obtained was over 98 mol %, judging from the saponification values.

The degree of polymerization of PVAc was measured in a Ubbelohde Viscosimeter at 30°C in acetone by using the following equation:[5]

$$[\eta] = 7.94\times10^{-4}P^{0.62}$$

The PVAc samples are summarized in Tables 1 and 2.

PVAc-PVPr was prepared by the acetylation of partially-propionated PVA, which had been propionated in a homogeneous system of water and propionic acid by using hydrochloric acid as a catalyst. These samples are listed in Table 3. PVAc-PVFA was also prepared by the acetylation of partially-formacetalyzed PVA, which had been acetalyzed in a homogeneous system of water and formaldehyde by using sulfuric acid as a catalyst. These samples are presented in Table 4.

Reagents. All the chemicals were of a guaranteed grade and were used without further purification. An iodine stock solution was prepared by dissolving iodine (3.2g) in methanol (250 m*l*). The resultant solution was standardized by sodium thiosulfate and was used by diluting it with methanol to the desired concentration just before its use. A 0.1 N solution of potassium iodide was accurately prepared by dissolving potassium iodide (8.3005 g) in distilled water (500 m*l*); it was used by diluting it with distilled water to the desired concentration before use.

Absorbance Measurements. A Shimadzu spectrometer, Model Spectronic 20, was used for the measurement of the absorption spectra. The color development of PVAc-iodine was done as will be described in the following section. The absorption spectra of the PVAc copolymer-iodine complex were recorded under the optimum conditions established by the use of the PVAc-iodine complex. After 1 m*l* of a methanol solution of the polymer (0.1g/d*l*) had been added to 1 m*l* of a methanol solution of iodine (2.5×10^{-3} mol/*l*), 1 m*l* of the mixture was added to 25 m*l* of an aqueous iodide solution (2×10^{-3} mol/*l*) and the mixture was allowed to stand for an hour at 20°C. The absorbance of the color complex was then measured at the absorption maximum by using the iodine-iodide solution as the reference.

The effect of the temperature on the color development of the polymer-iodine complex was discussed under the above-mentioned conditions. After the color solution had been cooled at 3°C for 24 hr, the solution was permitted to stand for an hour at a definite temperature; then the absorbance was measured at the absorption maximum.

Results and Discussion

The Color Reaction of PVAc with Iodine. A methanol solution containing PVAc and iodine was poured into an aqueous solution of potassium iodide. Immediately after the addition, the solution developed an intensive red-violet color without precipitating any polymer. The spectra of the color complex are indicated in Fig. 1, together with those obtained under different color conditions. The absorption maximum was located at 510 mμ. The absorbance of an iodine-potassium iodide solution at 510 mμ was very small. Even if the contents of PVAc, iodine, and iodide were the same, the order in which iodine was added had a significant effect on the absorbance, as is illustrated in Fig. 1. This is considered to be due to the fact that the penetration of iodine into the polymer was insufficient since molecules of both PVAc and iodine are separately

3) T. Motoyama, S. Hayashi and T. Nakano, *Report of the Poval Committee*, No. 44, 95 (1964).
4) R. M. McCready and W. Z. Hassid, *J. Amer. Chem. Soc.*, **65**, 1154 (1943).
5) A. Nakajima, *Kobunshi Kagaku*, **6**, 451 (1949).

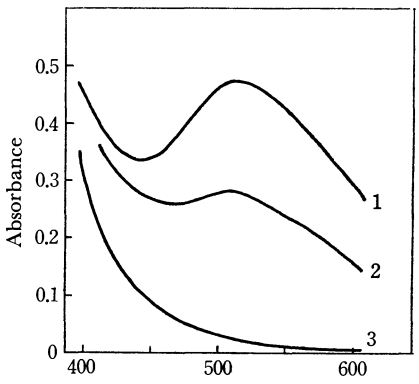

Fig. 1. Absorption spectra of PVAc-iodine complexes. (PVAc : $P=980$).
1: Addition of 1 m*l* of methanol solution containing PVAc 5×10^{-4} g and iodine 2.5×10^{-6} mol to 25 m*l* of aqueous solution of potassium iodide 2×10^{-3} mol/*l*.
2: Addition of 0.5 m*l* of methanol solution containing PVAc 5×10^{-4} g and then 0.5 m*l* of methanol solution containing iodine 2.5×10^{-6} mol to 25 m*l* of aqueous solution of potassium iodide 2×10^{-3} mol/*l*.
3: Blank.

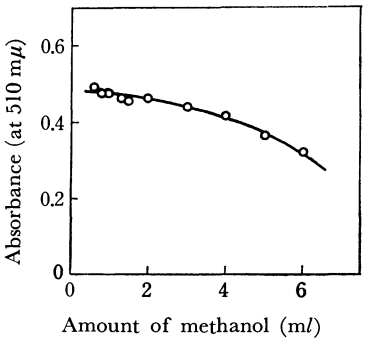

Fig. 2. Effect of amount of methanol on color intensity. (PVAc : $P=980$)
PVAc : 5×10^{-4} g, Iodine : 2.5×10^{-6} mol,
Potassium iodide : 5×10^{-5} mol

dispersed in an aqueous solution. Considering the fact that the PVAc-iodine color reaction did not occur in the absence of potassium iodide, it may be concluded that iodide ions are indispensable to the formation of the complex with PVAc, as in the case of amylose.[6]

The standing time for the color development of the PVAc-iodine complex was investigated at 20°C, while the other components were kept constant. The color of the complex reached its maximum within half an hour after mixing; thereafter the absorbance remained almost constant for three days.

In order to study the effects of the concentrations of iodine and potassium iodide, a series of absorbances was measured under various concentrations of iodine and iodide. It was found from these experiments that the absorbance of the complex at 510 mμ, when the concentration of PVAc was kept at (5×10^{-4} g), reached a higher maximum more than iodine (2.5×10^{-6} mol) and potassium iodide (5×10^{-5} mol).

Figure 2 shows the effect of the amount of methanol on the color development, while the other compoments were kept constant. As is shown by the curve in Fig. 2, the absorbance decreased with an increase in the amount of methanol, but the decrease was only slight in the range of small amounts of methanol.

From the experimental results obtained above, the following procedures were selected as the optimum conditions for the measurement of the PVAc-iodine complex. One volume of a methanol solution of iodine (2.5×10^{-3} mol/*l*) is added to an equal volume of a methanol solution of PVAc, and then 1 m*l* of the mixture is stirred into 25 m*l* of an aqueous solution of iodide (2×10^{-3} mol/*l*). The color solutions are at once transferred into the test tube cells, which are covered with parafilm. The test tube cells are stored for an hour at 20°C, after which the absorbance at 510 mμ is measured with a spectrometer by using an iodine-iodide solution as a reference.

A calibration curve was made under the above-mentioned conditions. A linear relationship was obtained between the absorbance and the PVAc concentration over the range investigated.

The effect of the degree of the polymerization of PVAc on the color development was studied by using the samples shown in Tables 1 and 2. The results are shown in Fig. 3. In both the PVAc obtained from the acetylation of PVA and the PVAc formed by the polymerization of vinyl acetate in methanol, it was found that all the absorption maxima appear at 510 mμ, regardless of the degree of polymerization, while the absorbances of the PVAc-iodine complexes decrease only slightly with an increase in the degree of polymerization.

From the above results, it was found that, if the degree of polymerization of PVAc is known, the color reaction of PVAc with iodine can be used in the colorimetric determination of PVAc, which is itself insoluble in water.

In free-radical polymerization, it is well known that long-chain branches are present in the PVAc molecules.[7] These branches are released during the hydrolysis of PVAc to PVA. Thus, such long-chain branches do not exist in PVA molecules.[8] To ascertain the effect of a branch on the color

6) A. J. Thoma and D. French, *J. Amer. Chem. Soc.*, **82**, 4144 (1960).

7) S. Imoto, J. Ukida and T. Kominami, *Kobunshi Kagaku*, **14**, 101 (1957).

8) R. Inoue and I. Sakurada, *ibid.*, **7**, 221 (1950).

Table 1. Polymerization condition of vinyl acetate and degree of polmerization of PVAc

Vinyl acetate (%)	Methanol (%)	Benzoyl peroxide *vs.* vinyl acetate (%)	Conversion (%)	Degree of polymerization
30	70	1.667	10.7	280
30	70	0.333	10.6	380
40	60	0.020	3.1	920
60	40	0.017	4.5	980
75	25	0.013	6.8	1830
80	20	0.013	5.4	2380

Table 2. Fraction of PVA and degree of polymerization of acetylated PVA

Fraction-ation number	*n*-Propanol (g)	Fractionated PVA (g)	Degree of polymerization of acetylated PVA
1	391	—	—
2	6	3.5592	1660
3	6	1.9106	1640
4	14	4.9394	1390
5	20	2.6024	1110
6	42	2.6262	760
7	60	1.2595	410
8	—	1.5023	210

Used PVA: 500 g of 5% PVA (P=1090) aqueous solution.
Fractionation temperature: at 30°C.

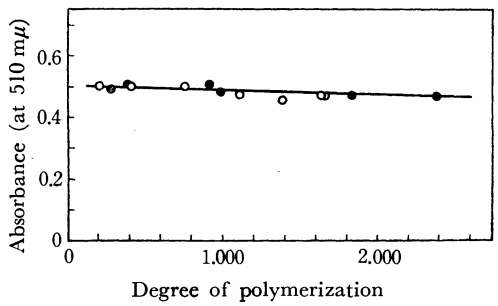

Fig. 3. Degree of polymerization of PVAc and color intensity.
●: PVAc obtained by polymerization of vinyl acetate
○: PVAc derived from acetylation of PVA

reaction, the color reaction was attempted, but the color intensity of the PVAc samples obtained from vinyl acetate was almost identical with that of the PVAc samples derived from PVA, as is indicated in Fig. 3. The long-chain branches in the PVAc molecules may be so small as to be negligible at the low conversion[9] shown in Table 1. However, the effects of nonhydrolyzable long-chain branches formed by the abstration of an α-proton and those of the short-chain branches made by an intramolecular-chain transfer mechanism,[10] as in the case of the free-radical polymerization of ethylene,[11] can not be considered on the basis of the experimental results obtained here. Such discussion must await a detailed investigation of many samples synthesized under various conditions.

The Color Reactions of PVAc Copolymers with Iodine. On the basis of the results obtained above, we then proceeded to examine the absorption spectrum and the temperature dependence of the PVAc copolymer-iodine complex.

Although the color complex of PVAc-PVPr with iodine had its absorption maximum at 510 mμ, as in PVAc, regardless of the copolymer composition, the absorbance decreased with an increase in the number of vinyl propionate units in the copolymer, as is summarized in Table 3.

Table 3. Dependence of degree of propionylation on absorbance of PVAc-PVPr-iodine complex

Degree of propionylation (mol%)	Absorption maximum (mμ)	Absorbance (at 20°C)	T_g (°C)
0	510	0.475	28
5.72	510	0.460	25
11.04	510	0.450	23
16.28	510	0.430	21
22.18	510	0.360	19
27.97	510	0.320	16
30.46	510	0.295	15
32.04	510	0.284	15
33.93	510	0.239	14

Degree of polymerization of PVA used: 1090.

The absorption spectra of the color complex of PVAc-PVFA with iodine are illustrated in Fig. 4. A change in the color from red-violet to green-blue was observed with an increase in the number of vinyl formacetal units in the copolymer. The absorption maximum was observed at 620 mμ for highly-acetalyzed PVA and at 520 mμ for PVA of a low degree of acetalyzation, while a new absorption maximum appeared in the region

9) M. Matsumoto and Y. Ohyanagi, *J. Polym. Sci.*, **46**, 520 (1960).

10) H. N. Fridlandar, H. E. Harris and J. G. Pritchard, *ibid.*, *A-1*, **4**, 649 (1966).

11) M. J. Roedel, *J. Amer. Chem. Soc.*, **75**, 6110 (1953).

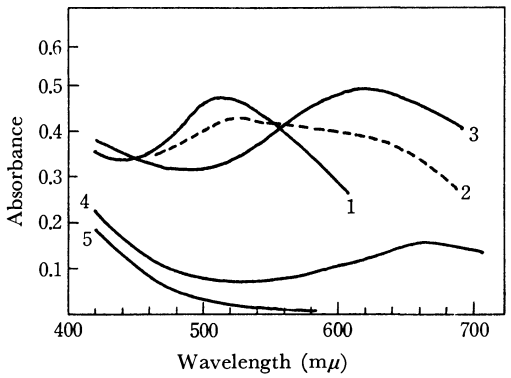

Fig. 4. Absorption spectra of complexes of PVAc, PVc-PVFA and partially formacetalyzed PVA with iodine.
1: PVAc
2: PVAc-PVFA having degree of acetalyzation of 17.11 mol%.
3: PVAc-PVFA having degree of acetalyzation of 31.27 mol%.
4: Partially formacetalyzed PVA having degree of acetalyzation of 31.27 mol%.
5: Blank

Table 4. Dependence of degree of acetalyzation on absorbance of PVAc-PVFA-iodine complex

Degree of acetalyzation (mol%)	Absorption maximum (mμ)	Absorbance (at 20°C)	T_g (°C)
0	510	0.475	28
10.02	520	0.438	32
17.11	520	0.424	35
19.43	600	0.415	36
22.84	620	0.450	38
29.28	620	0.481	42
31.27	620	0.490	43

Degree of polymerization of PVA used: 1090.

between 520 and 620 mμ in the intermediate case. These results are tabulated in Table 4.

Although the PVA used in our experiments did not give the color reaction in a dilute aqueous solution with iodine, partially-formacetalyzed PVA, which had been prepared by the acetalyzation of PVA in a homogeneous system of water and formaldehyde in the presence of sulfuric acid, developed a green-blue color with an increase in the degree of acetalyzation.[12] Since partially-formacetalyzed PVA was insoluble in methanol, the color reaction of the PVA derivatives with iodine was carried out in the aqueous phase, in which methanol as the polymer solvent was replaced by water. The results for formacetalyzed PVA, which had about a 30 mol% degree of acetalyzation, as a representative example are indicated in Fig. 4, together with those of the other PVAc copolymer. The absorption maximum was located at the longer wavelength of 670 mμ, and the absorbance was remarkably lower compared with that of PVAc-PVFA, but with the same degree of acetalyzation. These results clearly suggest that the higher green-blue color development of the copolymer-iodine complex depends not only on the acetal units, but on the vinyl acetate units, and that the red-violet color reaction of PVAc-iodine is based on the long sequence lenght of the vinyl acetate unit in the polymer chain.

Figures 5 and 6 show the results of the temperature dependence of the absorbance at the absorption maximum for the PVAc homopolymer and the PVAc copolymer. In the case of the PVAc homopolymer, it was found that the color intensity is slightly decreased up to about 30°C as the temperature is raised, and that color-fading takes

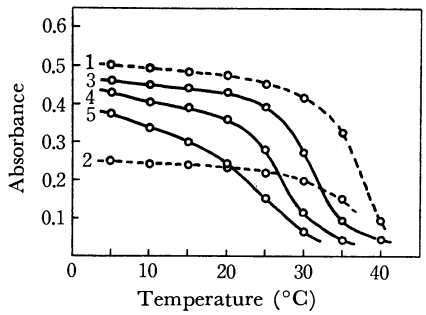

Fig. 5. Effect of temperature on color intensity of complexes of PVAc and PVAc-PVPr with iodine.
PVAc: 1: 5×10^{-4} g, 2: 2.5×10^{-4} g.
PVAc-PVPr, degree of propionylation: 3: 16.28 mol%, 4: 22.18 mol%, 5: 33.93 mol%.

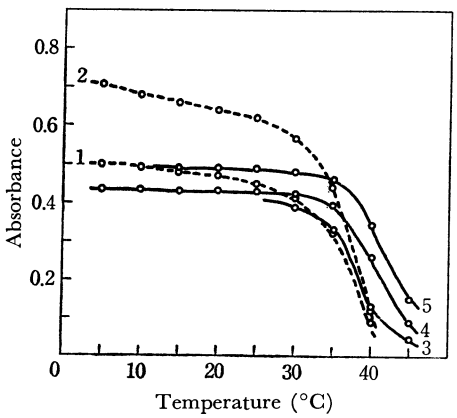

Fig. 6. Effect of temperatue on color intensity of complexes of PVAc and PVAc-PVFA with iodine.
PVAc: 1: 5×10^{-4} g, 2: 7×10^{-4} g.
PVAc-PVFA, degree of formacetalyzation: 3: 10.02 mol%, 4: 23.84 mol%, 5: 31.27 mol%.

12) S. Hayashi, C. Kawamura and M. Takayama, *Preprints for Annual Meeting of Soc. Polymer Sci. Japan*, **19**, 339 (1969).

place in the vicinity of 30°C. This temperature agrees with the glass-transition temperature (T_g) of PVAc. In order to examine this phenomenon more exactly, the effects of the various PVAc concentrations were investigated. These results are given by the broken lines in Figs. 5 and 6, which show that all the color-fadings of PVAc-iodine complexes are in the vicinity of 30°C, independent of the PVAc concentration. For the temperature dependence of the copolymer-iodine complexes, it is of interest to compare these data with the results of PVAc. The difference between the type of curve obtained with the PVAc copolymer and that obtained with the PVAc homopolymer is striking, as Figs. 5 and 6 show. For the copolymer with vinyl propionate, the magnitude of the decrease in the color intensity with the temperature increased with an increase in the number of vinyl propionate units. On the other hand, the absorbances of the complexes of PVAc-PVFA with iodine at the absorption maximum were approximately the same as that of PVAc, and the effect of the elevated temperature on the absorbance appeared to be smaller for PVAc-PVFA than the PVAc, as the vinyl formacetal units as comonomer are introduced into the PVAc chain.

The polymer-iodine complexes generally lose their color intensities at elevated temperatures. The extent of the loss depends on the kind of polymer[12] and on the degree of steric regularity.[13] However, these differences have been difficult to explain satifactorily in the absence of mechanistic studies of polymer-iodine complexes. If it is assumed that the source of the color reaction of polymer with iodine is based on the formation of polyiodine chains in the polymer,[14] the degree of mobility of the polymer molecule at a given temperature at which the color intensity is measured seems to be one of the important causes of the color development. For example, the color-fading temperature of PVAc agreed with the T_g of PVAc. This probably means that the molecular motion of the PVAc polymer over the T_g is so vigorous that the iodine molecules can not be oriented in polyiodine chains in the PVAc polymer. The reason that the effect of the temperature on the color intensity was greater for PVAc-PVPr than for PVAc-PVFA may be also attributed to the T_g of the copolymer. The T_g values of copolymers tabulated in Tables 3 and 4 were calculated by means of the following equation:[15]

$$\frac{1}{T_g} = \frac{W_1}{T_{g1}} + \frac{W_1}{T_{g2}}$$

where T_g, T_{g1}, and T_{g2} are the glass-transition temperatures of the copolymer, the homopolymer 1, and the homopolymer 2, and where W_1 and W_2 are the weight fractions of the homopolymer 1 and the homopolymer 2 respectively.

On comparing these values with the results of the temperature dependence of the absorbance, it is evident that the T_g and the absorbance have a simple relation, that is, the higher the T_g value, the lower the temperature dependence of the absorbance. Therefore, the curves in Figs. 5 and 6 can be explained as follows. As the temperature rises, the color intensity is gradually lowered up to the extent of the T_g of the polymer; then the rate of lowering becames rapid in the vicinity of the T_g. This can be taken as indicating that the polymer in which iodine molecules form the polyiodine chains can not be held in a definite conformation at elevated temperatures.

The authors are grateful to Professor Nobumasa Hojo of Shinshu University for his valuable discussions.

13) M. M. Zwick, *J. Appl. Polym. Sci.*, **9**, 2393 (1965).
14) M. Haisa and H. Itami, *J. Phys. Chem.*, **61**, 817 (1957).
15) W. H. Howard, *J. Appl. Polym. Sci.*, **5**, 303 (1961).

NOTES

BULLETIN OF THE CHEMICAL SOCIETY OF JAPAN VOL. 43 543—545 (1970)

Studies on Reactions of Isoprenoids. VIII.[1] Reactions of Sulfur Dichloride with Certain Cyclic-Acyclic 1,5-Dienes

Tadashi SASAKI, Shoji EGUCHI and Teruhiko ISHII

Institute of Applied Organic Chemistry, Faculty of Engineering, Nagoya University, Chikusa-ku, Nagoya

(Received May 10, 1969)

Although the reactions of sulfur dichloride (SD) with various olefins have been well investigated,[2-7] there seems to have been no study on the reactions of SD with cyclic-acyclic polyolefins. This paper deals with the reactions of SD with 1,5-cyclic-acyclic dienes I-III.[8]

The product from 4-cyano-1-(4-methyl-3-pentenyl)-1,4-cyclohexadiene (I) and SD is a viscous oil, the structure of which was assigned as 3-(1-*p*-cyanophenyl-4-methylene)pentyl sulfide IV on the basis of analytical and spectral data: IV gave a negative Beilstein- and a positive sulfur test[9] and analysis showed a composition of $C_{26}H_{28}N_2S$. IR spectrum (liquid film) exhibited strong bands at 2265 (C≡N), 1605 and 830 (1,4-disubstituted phenyl), and 1650 and 895 (C=CH_2) cm^{-1}. UV spectrum had a λ_{max}^{MeOH} 231 mμ (log ε 4.37) which is very similar to that of *p*-tolunitrile, $\lambda_{max}^{H_2O}$ 234 mμ (log ε 4.2),[10] suggesting the presence of a *p*-alkylcyanobenzene moiety. NMR spectrum had signals at τ 2.38 and 2.68 (*ca.* 8 H, AB-q, J=9.0 Hz, phenyl protons), 4.92 and 5.03 (*ca.* 4H, each broad s, C=CH_2), 6.80—8.25 (6H, broad complex m allylic methylene protons and S–CH), and 8.33 and 8.49 (*ca.* 10H, each s, allylic methyl- and saturated methylene protons). In the mass spectrum at 70 eV, shown in Fig. la, the molecular ion peak could not be observed, as was also the case in the spectrum at 15 eV. However, appearance of ion peaks at *m/e* 269 (0.1%, $C_{17}H_{20}NS^+$) and 268 (0.08%, $C_{17}H_{19}NS^+$) excluded the possibility of a monomeric cyclic sulfide structure in accordance with analytical data. These ions could be formed by the characteristic α-cleavage of a dialkyl sulfide molecule.[11] The dimeric unsaturated sulfide structure was supported by ion peaks at *m/e* 154 (10%, CH_2=$C(CH_3)$–$CH(\dot{C}H_2)$–$\overset{+}{S}$=CH–$C(CH_3)$=CH_2), 153 (8.5%, CH_2=$C(CH_3)$–$C(=CH_2)$–$\overset{+}{S}$=CH–$C(CH_3)$=CH_2), and 141 (10.5%, CH_2=$C(CH_3)$–CH_2–$\overset{+}{S}$=CH–$C(CH_3)$=CH_2). The other main fragmentation resulted from the cleavage of a sulfur-carbon bond to give ion peaks at *m/e* 217 (10%, $C_{13}H_{15}\dot{\overset{+}{N}}S$), 215 (12%, $C_{13}H_{13}\dot{\overset{+}{N}}S$), 213 (24%, $C_{13}H_{11}\dot{\overset{+}{N}}S$), 186 (14%, $C_{13}H_{16}N^+$), 185 (48%, $C_{13}H_{15}N^{+\cdot}$). Sulfur-carbon bond rupture after isomerization of the side-chain double bond and loss of methyl and isopropyl group afforded ion peaks at *m/e* 200 (14%), 168 (22%), 174 (13%), 172 (24%), 142 (10%), and 140 (12%).[12] Appearance of ion peaks at *m/e* 117 (100%) and 116 (43%) in abundance supported structure IV involving a benzene ring but not a cyclic sulfide structure, since these fragmentations are typical for alkyl-

1) Part VII of this series: T. Sasaki, S. Eguchi, and T. Ishii, *J. Org. Chme.*, **45**, 249 (1970), in press.

2) a) J. R. Nooi and G. J. Huijben, *J. Appl. Chem.*, **18**, 84 (1968); b) R. A. Grimm, *J. Amer. Oil Chem. Soc.*, **44**, 567 (1967).

3) H. J. Backer and J. Strating, *Rec. Trav. Chim. Paya Bas*, **54**, 52 (1935).

4) F. Lautenschlaeger, *J. Org. Chem.*, **33**, 2620 (1968).

5) F. Lautenschlaeger, *ibid.*, **33**, 2627(1968) and references cited therein.

6) F. Lautenschlaeger, *ibid.*, **31**, 1679 (1966).

7) E. J. Corey and E. Block, *ibid.*, **31**, 1663 (1966).

8) T. Sasaki, S. Eguchi and T. Ishii, *ibid.*, **34**, 3749 (1969).

9) R. L. Shriner, R. C. Fuson and D. Y. Curtin, "The Systematic Identification of Organic Compounds," 4th Ed., John Wiley & Sons, Inc., New York (1956), pp. 57—62.

10) L. Doub and J. M. Vandenbelt, *J. Amer. Chem. Soc.*, **69**, 2715 (1947).

11) a) H. Budzikiewicz, C. Djerassi and D. H. Williams, "Mass Spectrometry of Organic Compounds," Holden-Day, Inc., San Francisco (1967), pp. 276—296; b) J. H. Beynon, R. A. Saunders and A. E. Williams "The Mass Spectra of Organic Molecules," Elsevier Publishing Co., New York, N. Y. (1968), pp. 252—373

12) For isomerizations before ruptures of terpene molecules in mass spectra, see D. S. Weinberg and C. Djerassi, *J. Org. Chem.*, **31**, 115 (1966).

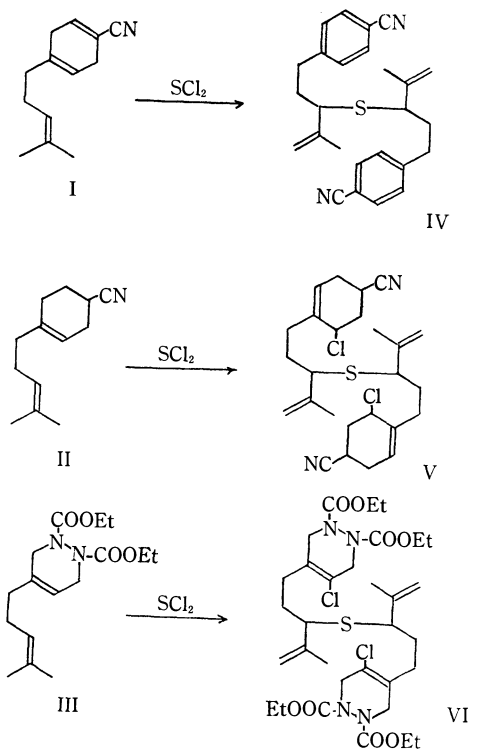

benzene derivatives.[13] All these analytical and spectral data led us to conclude that the product has the unsaturated symmetrical dialkyl sulfide sturcture IV.

The product from 4-cyano-1-(4-methyl-3-pentenyl)cyclohexene II and SD was also an oil, and its structure was assigned as 3-[1-(6'-chloro-4'-cyanocyclohex-1'-enyl)-4-mehylene]pentyl sulfide (V) from analytical and spectral data. V had a composition of $C_{26}H_{34}N_2SCl_2$ from analysis and gave a positive Beilstein- and sulfur test.[9] IR spectrum (liquid film) exhibited strong bands at 2275 (saturated alkyl nitrile), 1645 (C=C), and 892 (C=CH_2) cm^{-1}. NMR spectrum showed signals at τ 4.55 (2 H, broad s, cyclohexenyl vinyl proton),[14] 5.08 (4H, broad s, C=CH_2), 5.45—7.10 (*ca.* 4H, broad complex m, -CHCl- and -CH-S-), 7.30—8.50 (*ca.* 24H, complex m, allylic methyl-, methylene- and methine protons). The mass spectrum at 70 eV is shown in Fig. 1b. The ion peak at *m/e* 255 ($C_{13}H_{17}\overset{+\cdot}{N}SCl$) corresponds to a fragmentation involving a sulfur-carbon bond fission, followed by a hydrogen abstraction.[11] In the other fragmentations, the most characteristic feature is the loss of hydrogen chloride to give ion peaks at *m/e* 219 (18%, $C_{13}H_{16}\overset{+\cdot}{N}S$) and 218 (100%, $C_{13}H_{15}\overset{+}{N}S$). Appearance of ion peaks at *m/e* 154 (2%), 153 (6%), 141 (2%), as well as at 117 (62.5%, $C_7H_7\overset{+\cdot}{N}$) as in the spectrum of IV, supported the unsaturated symmetrical dialkyl sulfide structure V. The spectrum at 15 eV was very simple, having ion peaks originating from a sulfur-carbon bond fission, at *m/e* 219, 218, 204, 186 and 185.

The reaction of 1,2-diethoxycarbonyl-4-(4-methyl-3-pentenyl)-3,6-dihydropyridazine III with SD also gave dimeric sulfide VI. A composition of $C_{32}H_{48}N_4O_8SCl_2$ was indicated by analysis, and by the positive Beilstein and sulfur tests.[9] IR spectrum (liquid film) showed bands at 1710 (C=O), 1650 (C=C) and 898 (C=CH_2) cm^{-1}, and NMR spectrum showed signals at τ 5.08

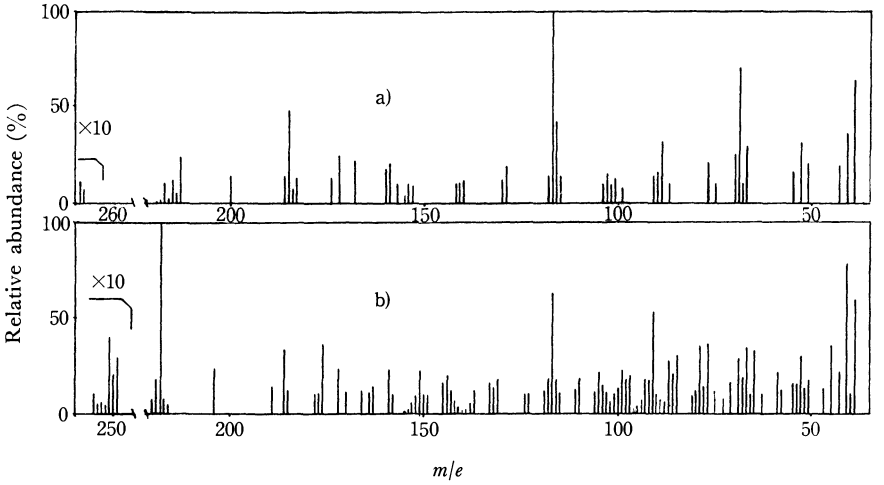

Fig. 1. Mass spectra of IV (a) and V (b) at 70 eV.

13) For example, see Ref. 11b, pp. 122—131.
14) This chemical shift is very similar to that of a cyclohexenyl vinyl proton of II: see Ref. 8.

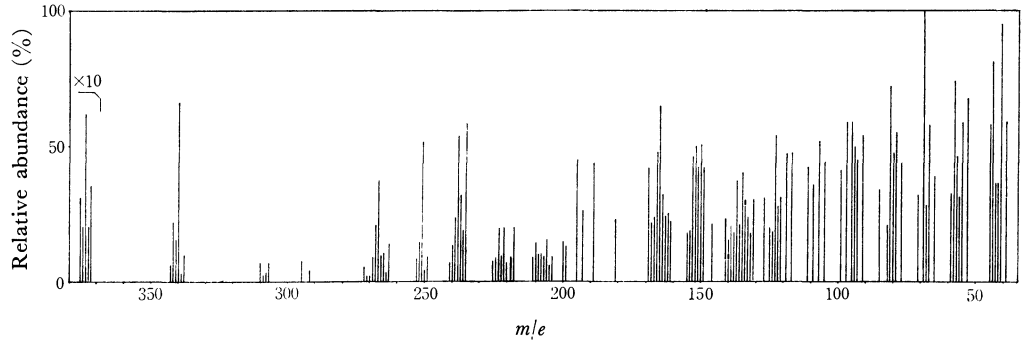

Fig. 2. Mass spectrum of VI at 70 eV.

(4H, broad and unsymmetrical s, C=CH_2), 5.50—7.20 (*ca.* 18H, m, N–CH_2–C=C, –CH–S–, and $COOCH_2C\underline{H}_3$*[1]), 7.45—8.45 (14H, m, allylic methylene-, methyl- and methylene protons of the side-chain), and 8.70 (12H, t, J=6.5 Hz, $COOCH_2C\underline{H}_3$). The mass spectrum (Fig. 2) showed an ion peak at m/e 376 (3.1%, $C_{16}H_{25}N_2\overset{+}{S}Cl$) which originated in a sulfur-carbon bond rupture.[11] The spectrum in the lower *m/e* regions was very complex compared to those of IV and V. Loss of hydrogen chloride from the ion peak at *m/e* 376 affords an abundant ion peak at *m/e* 340 ($C_{16}H_{24}N_2\overset{+}{S}$). Further loss of an ethoxylcarbonyl group from this ion yields an ion peak at *m/e* 267 ($C_{13}H_{19}N_2\overset{+}{S}$), whichcan afford an ion peak at *m/e* 193 ($C_7H_5N_2\overset{+}{S}$) by the loss of another ethoxycarbonyl group. Cleavage of carbon-carbon bond of the side-chain between the positions α and β to a pyridazine ring and the loss of hydrogen chloride afford an ion peak at *m/e* 239 ($C_{11}H_{15}N_2^+$), which can give rise to ion peaks at *m/e* 166, 165, 95, and 93 on the loss of an ethoxycarbonyl group. The base ion peak appeared at *m/e* 69 ($C_5H_9^+$), apparently arising from the side-chain. Ion peaks at *m/e* 154, 153 and 141 *etc.* were observed, supporting the dimeric sulfide structure VI.

All the reactions of SD with I-III occurred between two molecules of the dienes at their side-chain double bond and one molecule of SD to give IV-VI respectively,[15] though these reactions were carried out at high dilutions (2—4 wt% of olefins and 1.5 wt% of SD). The formation of these products can be explained by a facile attack of SD on a side-chain double bond and by chlorinations of cyclohexenyl or cyclohexadienyl moieties with SD.[16]

*[1] The methylene protons of the ethoxycarbonyl group appeared at τ 5.75 in a q, J=6.5 Hz in these overlapped signals.

15) The products seem to be diastereoisomeric mixture since these compounds have two or more asymmetric carbons.

Experimental[17]

Addition Reaction of SD with I. To a mixture of 1.87 g (0.01 mol) of I[8] and 50 m*l* of reagent-grade dichloromethane at *ca.* −50°C under a nitrogen atmosphere in a 200-m*l* three-necked flask fitted with stirrer, addition funnel and nitrogen inlet-outlet, was added with stirring a solution of 0.64 m*l* (0.01 mol) of SD in 50 m*l* of reagent-grade dichloromethane.[7] Addition was carried out for 1 hr and the resulting red solution was allowed to stand at *ca.* 15°C for 5 hr, shaken several times with cold brine and dried over sodium sulfate. After removal of the solvent, the residue was distilled *in vacuo* to give 0.86 g (43%) of IV: bp 117—119°C/0.1 mmHg, $n_D^{22.5}$ 1.5550. Found: C, 77.79; H, 7.50; N, 6.96%. Calcd for $C_{26}H_{28}N_2S$: C, 77.97; H, 7.05; N, 7.00%.

Addition Reaction of SD with II. Similarly 1.89 g (0.01 mol) of II[8] was treated with 0.64 m*l* (0.01 mol) of SD as above, and the product obtained was distilled to give 1.26 g (53%) of V: bp 145—149°C/0.5 mmHg, $n_D^{22.5}$ 1.5544. Found: C, 65.73; H, 7.34; N, 5.63%. Calcd for $C_{26}H_{34}N_2SCl_2$: C, 65.38; H, 7.14; N, 5.87%.

Addition Reaction of SD with III. Similarly 3.10 g (0.01 mol) of III[8] was treated with 0.64 m*l* (0.01 mol) of SD as above. The work-up and distillation afforded 0.97 g (27%) of VI: bp 165—175°C/0.5 mmHg, $n_D^{22.5}$ 1.5227. Found: C, 53.61; H, 7.31; N, 8.33%. Calcd for $C_{32}H_{48}N_4O_8SCl_2$: C, 53.41; H, 6.81; N, 7.79%.

16) a) Ref. 3: b) Chevron Res. Co., Brit. 1084670; *Chem. Abstr.*, **68**, 21528x (1968).

17) Microanalyses were carried out using a Yanagimoto C.H.N. Corder, Model MT-1. IR spectra were recorded on a JASCO Model IR-S IR spectrophotometer and UV spectra, on a JASCO Model ORD/UV-5 spectrophotometer. NMR spectra were obtained with a Hitachi H-60 spectrometer in deuterochloroform and are reported in τ values relative to TMS as an internal standard. Mass spectra were determined with a JEOL Model JMS-OlSG mass spectrometer at 70 and 15 eV of electron energy.

BULLETIN OF THE CHEMICAL SOCIETY OF JAPAN VOL. 43 546—547 (1970)

2,4-Dinitrophenylhydrazones of Benzoin

Yoshie KURIHARA and Rumiko HOSHI*1

Laboratory of Chemistry, Faculty of Education, Yokohama National University, Minami-ku, Yokohama

(Received May 23, 1969)

It is well known that the melting point of the 2,4-dinitrophenylhydrazone (DNP) of benzoin is 234°C.[1] Braude and Jones reported another DNP obtained from benzoin which melted at 174°C.[2] However, they stated nothing about the difference between the two.

Benzoin reacted with 2,4-dinitrophenylhydrazine (DNPH) prepared according to the procedure of Shriner and Fuson[3] at room temperature to give the DNP (I) (mp 236°C). On the other hand, when the reaction was carried out at 80°C for 45 min, the DNP (II) (mp 175°C), which is probably identical with that reported by Braude[2], was isolated as the main product. When the reaction was carried out at a temperature under 80°C, both I and II were formed. The I hydrazone was much more soluble in alcohol than II. The R_f values of I and II on the thin-layer chromatography using benzene-ether (17 : 3) were 0.74 and 0.94 respectively. When the reaction of benzoin and DNPH prepared according to Shriner's method was carried out under refluxing for 2 hr, di-DNP (osazone) of benzoin III, mp 314°C,[4] was obtained. III was also obtained when I or II was treated with Shriner's reagent at the boiling point. Further, I was converted to II when I was warmed at 80°C in ethanolic sulfuric acid.

The structure of II was confirmed as that of the DNP of benzoin ethyl ether on the basis of its elemental and spectral evidence; an absorption band as 1060 cm^{-1} in the infrared spectrum and signals at 8.60 (triplet, 3H, CH_3) and 6.15 τ (quartet, 2H, CH_2) in the NMR spectrum indicate the presence of an ethoxy group in II. Thus, it may reasonably be concluded that the hydroxy group of benzoin may be replaced by the ethoxy group in the reaction with DNPH in a hot alcoholic sulfuric acid solution. As acetoin and propionoin reacted with DNPH to form only sole DNP, even at 80°C, such behavior of benzoin seems somewhat peculiar.

Experimental[5]

Reaction of Benzoin with DNPH. *i) At Room Temperature.* Benzoin (3.5 g, 0.0165 mol) in 10 m*l* of ethanol was stirred into a solution of 18.5 g (0.09 mol) of DNPH in 150 m*l* of ethanol, 140 m*l* of water, and 92.5 m*l* of concentrated sulfuric acid. A nitrogen stream was then bubbled through the mixture. The precipitated product was filtered, washed with alcohol, and recrystallized from ethanol-ethyl acetate (3 : 1).

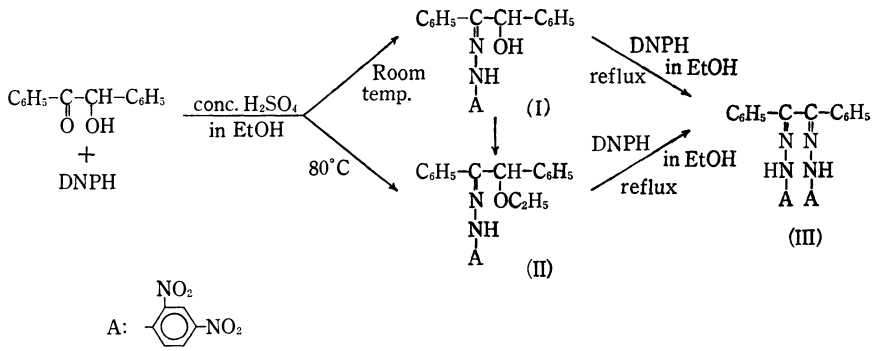

*1 Present address: Dept. of Applied Chem., Faculty of Engineering, Yokohama National University, Yokohama.

1) "Dictionary of Organic Compounds," ed. by J. R. A. Pollock and R. Stevens, 4th Ed., Eyre and Spottiswoode, Britain (1965), p. 344.

2) E. A. Braude and E. R. H. Jones, *J. Chem. Soc.*, **1945**, 501.

3) R. L. Shriner and R. C. Fuson, "The Systematic Identification of Organic Compounds," John Wiley & Sons, New York, N. Y. (1935), p. 148.

4) Mp 317°C in Ref. 1, p. 334.

5) All the melting points were determined on a Mettler electric micromelting-point apparatus and are uncorrected. The infrared spectra (KBr) were recorded on a Hitachi Model EPI-S2 spectrophotometer. The NMR spectra were determined in $(CD_3)_2CO$ on a JEOL NMR spectrometer at 60 MHz, with tetramethylsilane as the internal standard.

Mp 236°C.

Found: C, 61.90; H, 4.35; N, 13.29%. Calcd for $C_{20}H_{16}O_5N_4$: C, 61.22; H, 4.11; N, 14.28%.

ii) At 80°C. After the reaction mixture (the molar ratios were the same as those in the case of i) was heated at 80°C for 45 min, the solution was cooled. The precipitated product was filtered and then washed with ethanol. Recrystallization from ethanol-ethyl acetate (3 : 1) gave red-yellow crystals; mp 175°C.

Found: C, 63.13; H, 5.03; N, 12.72%. Calcd for $C_{22}H_{20}O_5N_4$: C, 62.85; H, 4.79; N, 13.33%.

Conversion of I to II. A few drops of conc. sulfuric acid were added to a solution of I (0.3 g) in 50 m*l* of ethanol. This solution was heated at 80°C for 2 hr. After cooling, the ethanol was evaporated under reduced pressure and the crude product was washed with ethanol. This reaction product indicated two spots on thin-layer chromatography; its R_f values were 0.72 and 0.94, identical with those of I and II.

The authors wish to thank Miss Keiko Inoue for her assistance during this work.

BULLETIN OF THE CHEMICAL SOCIETY OF JAPAN VOL. 43 547—548 (1970)

Polymerization of β-Ethoxypropionaldehyde

Hiroshi SUMITOMO and Junji FUJII

Faculty of Agriculture, Nagoya University, Chikusa-ku, Nagoya

(Received June 18, 1969)

Vogl[1] reported that 3-methoxypropionaldehyde was anionically polymerized with potassium triphenylmethoxide in propylene at −75°C. Takida and Noro[2] attempted the cationic polymerization of methoxybutyraldehyde with use of a magnesium sulfate-sulfuric acid complex at −78°C to give a sticky elastomeric product with a low yield.

The purpose of the present work is to obtain a high molecular weight crystalline polymer from β-alkoxypropionaldehyde.

β-Ethoxypropionaldehyde was prepared by refluxing the mixture of acrolein and ethyl alcohol in the presence of triethylamine and formic acid as catalyst at 65—75°C. Bp 66.0—66.5°C/67 mmHg.

Tetrahydrofuran (THF), methylene chloride, toluene and *n*-hexane used as solvents were purified in the usual way prior to use. Purification of triethylaluminum, diethylaluminum chloride, ethylaluminum dichloride (all of them, from Ethyl Corp.), aluminum trichloride, and titanium tetrachloride was previously described.[3,4] *n*-Butyllithium was prepared by the reaction of *n*-butyl chloride and lithium in a stream of nitrogen.

Polymerization was conducted by the same method as previously described.[3,4] Resulting polymer was isolated by precipitation by pouring the reaction mixture into a large amount of water after adding a mixture of acetic anhydride and pyridine. Waring Blendor was used, when necessary, for crushing and washing the product in water.

In Table 1 are shown the results of polymerization of β-ethoxypropionaldehyde initiated by triethylaluminum at −78°C. It should be noticed that the viscosity numbers, η_{sp}/c, of resulting polymers

Table 1. Polymerization of β-ethoxypropionaldehyde initiated by triethylaluminum at −78°C*

Solv.	Initiator, mol% to monomer	Convn. %	Mp °C	η_{sp}/c**
Methylene chloride	5	62.2	143—152	11.7
Methylene chloride	1	17.4	145—149	—
n-Hexane	5	63.6	137—144	10.5
n-Hexane	1	21.0	155—165	11.1
Toluene	5	78.7	153—160	13.9
Toluene	1	25.6	158—170	12.9

* Monomer, 5 g; solv., 10 g; for 1 day.
** In *o*-cresol; c, 0.2 g/100 m*l*; at 25°C.

Table 2. Polymerization with diethylaluminum chloride*

Solv.	Temp. °C	Time day	Convn. %	η_{sp}/c**
THF	−78	7	0	—
Methylene chloride	−78	7	trace	—
n-Hexane	−78	1	19.4	—
Toluene	−78	1	71.1	12.6
Toluene	−21	5	0	—
Toluene	0	5	0	—

* Monomer, 5 g; initiator, diethylaluminum chloride, 1 mol% to monomer; solv., 10 g;
** In *o*-cresol; c, 0.2 g/100 m*l*; at 25°C.

1) O. Vogl, *J. Polym. Sci. A*, **2**, 4607 (1964).
2) H. Takida and K. Noro, *Kobunshi Kagaku*, **20**, 705 (1963).
3) H. Sumitomo and K. Kobayashi, *J. Polym. Sci. A-1*, **4**, 907 (1966).
4) H. Sumitomo and K. Kobayashi, *ibid.*, **5**, 2247 (1967) and the following papers.

measured at the concentration of 0.2g/100 m*l* in *o*-cresol at 25°C are all extremely high.

The results of polymerization with diethylaluminum chloride are given in Table 2. The rate of polymerization is found to decrease in the order, toluene>*n*-hexane>methylene chloride. No polymer was obtained in THF at −78°C and even in toluene at −21 and 0°C.

Ethylalminum dichloride gave no polymer in all these solvents at −78°C.

Table 3 summarizes the effects of aluminum compounds with different acid strength on the polymerization of β-ethoxypropionaldehyde at −78°C. It was found that diethylaluminum chloride with a moderate acid strength is the most active, whereas aluminum chloride and ethylaluminum dichloride with a high acid strength are inactive in the present system.

Besides these cationic initiators, *n*-butyllithium also induces the polymerization of β-ethoxypropionaldehyde in toluene at −78°C (for example: 1 day; 10.8% convn.; η_{sp}/c, 8.6).

In Fig. 1 are shown the IR spectra of β-ethoxypropionaldehyde and its polymer. The fact that

Table 3. Polymerization with various aluminum compounds*

Initiator	Time day	Convn. %	η_{sp}/c**
$AlCl_3$	7	0	—
$Al(C_2H_5)Cl_2$	7	0	—
$Al(C_2H_5)_2Cl$	1	71.1	12.6
$Al(C_2H_5)_3$	1	25.6	12.9

* Monomer, 5 g; initiator, 1 mol% to monomer; solv., toluene, 10 g; at −78°C.
** In *o*-cresol; c, 0.2 g/100 m*l*; at 25°C.

no carbonyl absorption at 1725 cm^{-1} but four new absorption peaks due to ether linkages appear in the range from 946 to 1100 cm^{-1} in the spectrum of the polymer, suggests that the polymer has the structure of poly(ethoxyethyl)oxymethylene.

$$n CH_3CH_2OCH_2CH_2CHO \longrightarrow \left(\begin{array}{l} -CH-O- \\ | \\ CH_2CH_2OCH_2CH_3 \end{array}\right)_n$$

The result of elementary analysis of the polymer is as follows: Obsd: C, 58.31; H, 9.59%. Calcd for $C_5H_{10}O_2$: C, 58.80; 9.87%.

The monomer is soluble in all common organic solvents. The solubility of the polymer at room temperature is listed in Table 4. It is almost unchanged even at elevated temperature.

A strong birefringence was observed on a polymer film through a polarizing microscope. X-Ray diffraction diagram and data of the polymer are presented in Fig. 2 and Table 5 respectively.

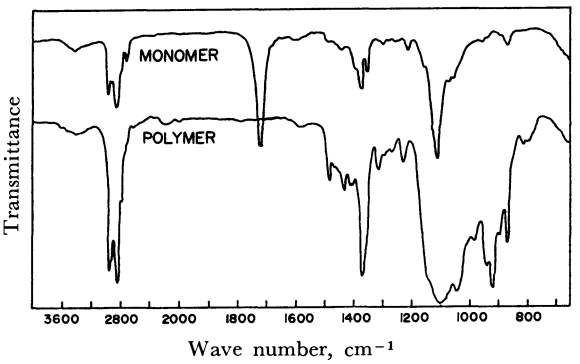

Fig. 1. Infrared absorption spectra of β-ethoxypropionaldehyde and its polymer.

Table 4. Solubility of poly(ethoxyethyl)oxymethylene at room temperature

Soluble in :
phenol, *o*-cresol, and *p*-cresol.

Swelled in :
chloroform, carbon tetrachloride, methylene chloride, ethyl acetate, dimethylformamide, dimethyl sulphoxide, benzene, toluene, xylene, cyclohexane, tetralin, tetrahydrofuran, dioxane, and pyridine.

Insoluble in :
water, methyl alcohol, ethyl alcohol, acetone, methyl ethyl ketone, petroleum ether, *n*-hexane, acetonitrile, ethylene glycol monomethyl ether, and γ-butyrolactone.

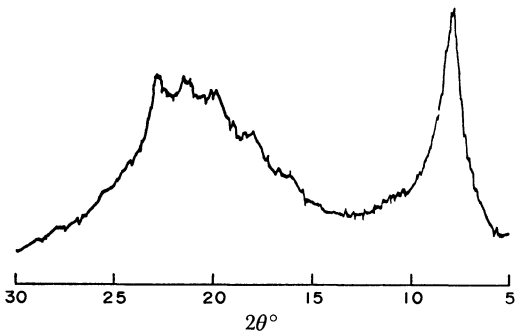

Fig. 2. X-Ray diffraction diagram of poly(ethoxyethyl)oxymethylene (Cu*K*α, Ni filter).

Table 5. X-Ray diffraction data of poly(ethoxyethyl)oxymethylene

Peak	Diffraction angle, 2θ degree	Relative intensity	Spacing *d*, Å
I	8.2	100	10.6
II	20.3	65.4	4.4
III	21.7	70.9	4.1
IV	23.0	71.7	3.9

BULLETIN OF THE CHEMICAL SOCIETY OF JAPAN VOL. 43 549—550 (1970)

Mechanism and Rate of the Intramolecular Energy Transfer in Rare Earth Chelates

Minoru TANAKA, Gentaro YAMAGUCHI, Jiro SHIOKAWA and Chiyoe YAMANAKA

Faculty of Engineering, Osaka University, Yamadakami, Suita, Osaka

(Received July 1, 1969)

The intramolecular energy transfer in rare earth (RE) chelates under excitation by near-ultraviolet light has been the subject of several recent investigations. Three mechanisms by which the excitation energy is transferred from the ligand to the RE ion in RE chelates have been proposed.

As no luminescence is observed from the RE levels higher than T_1,*1 Crosby *et al.* proposed the mechanism I: the energy transfer from S_1 to the *RE* ion *via* T_1 ($S_1 \rightsquigarrow T_1 \rightsquigarrow$ *RE* level$\rightarrow$ emission),[1] while Kleinerman proposed the mechanism II: the direct transfer of energy from S_1 to the *RE* ion ($S_1 \rightsquigarrow$ *RE* level$\rightarrow$emission).[2] Later, Bhaumik *et al.* proposed the mechanism III: the energy is transferred from S_1 to an upper intermediate *RE* level and then is transferred back to T_1 and returns to a lower *RE* level ($S_1 \rightsquigarrow$ *RE* level higher than $T_1 \rightsquigarrow T_1 \rightsquigarrow$ *RE* level lower than $T_1 \rightarrow$emission).[3] Though many other investigators supported the mechanism I on the basis of studies such as that of the intermolecular triplet-triplet energy transfer phenomenon,[4] the possibility of the mechanism II or III has not yet been fully denied. This is mainly due to the fact that the energy-transfer process from the lowest ligand triplet state to the RE ion was too fast to be observed. Bhaumik and El-sayed estimated this time to be $\sim 10^{-10}$ sec.

In this note, we will show some experimental confirmation that the time for this $T_1 \rightsquigarrow$ *RE* level transfer is about $\sim 10^{-8}$ sec and that the intramolecular energy transfer occurs by means of the mechanism I.

Experimental

Synthesis of β-Diketones. Naphthoyltrifluoroacetone (NFA) and benzylidenetrifluoroacetylacetone (BZDTF) were prepared by the condensation of ethyltrifluoroacetate with naphthoyltrifluoroacetone and benzylideneacetone respectively in a manner similar to that described by Reid and Calvin.[5] Some other β-diketones, benzoyltrifluoroacetone (BFA), and thenoyltrifluoroacetone (TTA) were obtained from Tokyo Kasei and were used without further purification.

Synthesis of RE Chelates. The RE chelates used in this study were prepared by the methods described in the literatures.[6-8] Tris and tetrakis chelates of europium, gadolinium, and terbium were prepared.

Luminescence Studies. All the chelates were studied at 300 and 77°K at a concentration of 10^{-3} mol/*l* in the following solvents; (1) EPA: mixed solvent of ether, isopentane, and ethanol (8 : 3 : 5 by volume ratio), (2) ethanol, and (3) acetonitrile. The details of the stroboscopic studies and the numerical calculations undertaken in order to obtain the luminescence rise times are given in Ref. 9.

Results and Discussion

The ligand triplet-state energies were obtained from the phosphorescence spectra of the Gd chelates. These data are presented in Fig. 1, along with several electronic states of Eu^{3+} and Tb^{3+}.

The triplet states of all the Eu chelates except $Eu(BZDTF)_4 \cdot HP$ lie above the $^5D_1$ state of Eu^{3+}. In these cases the time-resolved emission spectra can be accounted for as follows: the population of the $^5D_1$ state occurs in a time of the order of $\sim 10^{-8}$ sec; then the depopulation of the $^5D_1$ sate occurs in about 2 μsec through radiative and nonradiative transitions to the ^7F manifold as well as through simultaneous nonradiative transition to the $^5D_0$ state; On the other hand, the population of $^5D_0$ occurs in about 2 μsec, which is nearly the same as the decay time of $^5D_1$; finally, radiative and nonradiative transitions from $^5D_0$ to the ^7F manifold occur in about 500 μsec. However, in the

*1 Here we used the following abreviations:
S_1: the lowest excited singlet state of the organic ligand.
T_1: the lowest triplet state of the ligand.

1) G. A. Crosby, R. E. Whan and R. M. Alire, *J. Chem. Phys.*, **34**, 743 (1961).
2) M. Kleinerman, *Bull. Amer. Phys. Soc.*, **9**, 265 (1964).
3) M. L. Bhaumik and M. A. El-sayed, *J. Chem. Phys.*, **42**, 787 (1965).
4) Y. Matsuda, S. Makishima and S. Shionoya, This Bulletin, **41**, 1513 (1968).
5) J. C. Reid and M. Calvin, *J. Amer. Chem. Soc.*, **72**, 2948 (1950).
6) R. G. Charles and E. P. Riedel, *J. Inorg. Nucl. Chem.*, **28**, 3005 (1966).
7) R. G. Charles and R. C. Ohlmann, *ibid.*, **27**, 255 (1965).
8) R. G. Charles and E. P. Riedel, *ibid.*, **29**, 715 (1967).
9) G. Yamaguchi, S. Okumura and C. Yamanaka, *Tech. Rep. Osaka Univ.*, **19**, 117 (1968).

Table 1. Rise and decay times of RE-ion luminescence in some RE chelates

Chelate	Solvent	$^5D_1$ rise (μsec) 77°K	300°K	$^5D_1$ decay (μsec) 77°K	300°K	$^5D_0$ rise (μsec) 77°K	300°K	$^5D_0$ decay (μsec) 77°K	300°K	$^5D_4$ rise (μsec) 77°K	300°K	$^5D_4$ decay (μsec) 77°K	300°K
$Eu(BFA)_4 \cdot HP$	EPA	$\sim10^{-2}$		2.45	1.46	2.18	1.28	460	398				
	EtOH		$\sim10^{-2}$	2.45	1.51	2.02	0.98	462	432				
	CH_3CN		$\sim10^{-2}$		1.34		1.23		678				
$Eu(BZDTF)_4 \cdot HP$	EPA	(a)		(a)		$\sim10^{-2}$	(a)	408	(a)				
$Tb(BFA)_4 \cdot HP$	EPA									$\sim10^{-2}$	(b)	485	(b)

a) The luminescence is not sensitized.
b) Data were not obtained because the luminescence is weak.

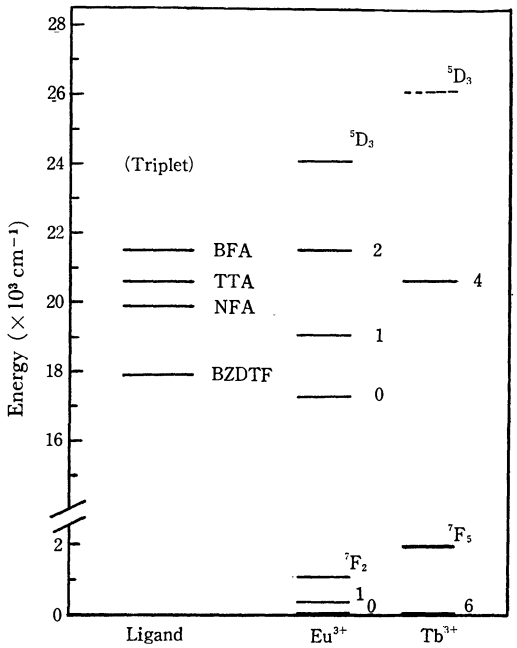

Fig. 1. The triplet states of organic ligands and the f-electronic states Eu^{3+} and Tb^{3+} ion.

case of $Eu(BZDTF)_4 \cdot HP$, where the lowest ligand triplet is situated between $^5D_1$ and $^5D_0$, no emission from the $^5D_1$ level is observed. The population of $^5D_0$ occurs in a time of the order of $\sim10^{-8}$ sec, and this is followed by radiative and nonradiative transitions to the ^7F manifold in about 500 μsec. In the cases of the Tb chelates, $Tb(BFA)_4 \cdot HP$, $Tb(BFA)_3 \cdot 2H_2O$, and $Tb(TTA)_3 \cdot 2H_2O$, the population of $^5D_4$ occurs in a time of the order of $\sim10^{-8}$ sec and decays in about 500 μsec.

The luminescence-rise curve of the $^5D_0 \rightarrow {}^7F_2$ transition (613 mμ) of $Eu(BZDTF)_4HP$ is shown

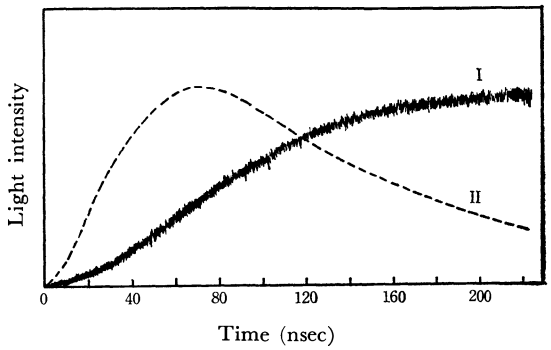

Fig. 2. (I) The typical rise curve of the ion luminescence of Eu, Tb chelates. (II) The rise curve of the excitation flash light.

in Fig. 2. The rise curves of the $^5D_1 \rightarrow {}^7F_1$ transition (538 mμ) in other Eu chelates and of the $^5D_4 \rightarrow {}^7F_5$ transition (545 mμ) in Tb chelates have almost the same behavior as is shown in Fig. 2. These rise times can be estimated to be about 10^{-8} sec. The time-resolved spectroscopic data on several RE chelates are given in Table 1.

From the results stated above, the following conclusions can be reached: First, since the luminescence from RE levels which are higher than T_1 is not observed, as Crosby[1] reported, and since the time for energy transfer is too long to account for the direct transfer from S_1, there is no possibility of the mechanism II. Second, the mechanism III can also be rejected, because the rise times of the RE-ion luminescence in several RE chelates investigated are nearly the same, *i.e.* 10^{-8} sec, in spite of the fact that the energy differences between the intermediate RE level and T_1 are not similar. Therefore, we can conclude that the energy transfer occurs by means of the mechanism I.

BULLETIN OF THE CHEMICAL SOCIETY OF JAPAN VOL. 43 551—552 (1970)

Studies of Aliphatic Hydroxycarboxylic Acids as Antioxidants. III. The Preparation of Two Isomers of Hydroxycitric Acid Lactone (*erythro*- and *threo*-3,4-dicarboxy-3-hydroxy-γ-butyrolactone)

Kazuo HORIKAWA and Shinroku MASUYAMA

The Osaka Municipal Technical Research Institute, Kita-ku, Osaka

(Received July 4, 1969)

In 1883, Lippmann[1] found a hydroxycarboxylic acid in a by-product of beet sugar. He reported that the formula of this compound corresponded to that of hydroxycitric acid, which had already been synthesized by Pawollek.[2] On the other hand, Martius and Maué[3] prepared the hydroxycitric acid lactone by the addition of hypochlorous acid to calcium aconitate. Two isomers were obtained in this reaction; the one with the lower melting point of 152°C was hydroxycitric acid lactone, while the other, with the higher melting point of 182°C was allohydroxycitric acid lactone. The configurations of these two racemic acids have, however, never been described. Therefore, it seemed worthwhile to confirm the configurations of these lactones, since the configuration might be related to the stabilizing effect on the vegetable oil as an antioxidant.

As has been reported previously from our laboratory,[*1,4] erythro lactonic acid (IVa) was synthesized by the oxidation of *trans*-trimethylaconitate with permanganate and by subsequent hydrolysis (Scheme I).

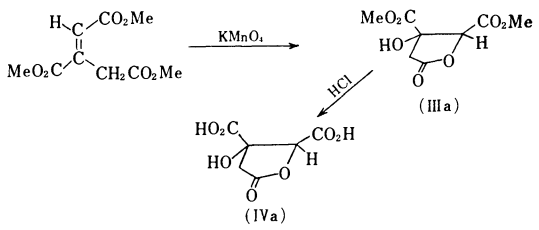

Scheme I

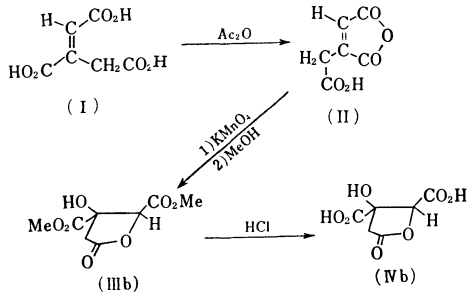

Scheme II

In this paper, another isomer, *threo* lactonic acid (IVb), was similarly prepared from *cis*-aconitic anhydride (II).[5] The oxidation mixture was separated after methylation, and the obtained dimethyl ester (IIIb) was hydrolysed (Scheme II). As for the relative configurations of these two lactonic acids, it was inferred, on the basis of the *cis*-hydroxylation mechanism of permanganate, that IVa was *erythro* and that IVb was *threo*.[*1] These assignments were supported by the reaction of both lactonic acids with acetic anhydride. Thus, when they were treated with this reagent at 60°C for 1.5 hr, the former gave a lactonic anhydride, which exhibited characteristic bands due to the 5-membered anhydride group at 5.31 and 5.75μ, while the latter did not. The NMR spectra of IIIa and IIIb are of interest in connection with the above assignment. The NMR spectra of IIIa and IIIb in chloroform exhibited signals at τ 6.18, 6.22 (each 3 H, $-OCH_3$) and 6.10, 6.23 (each 3 H, $-OCH_3$), 5.04 (1 H, methin proton) and 4.88 (1 H, methin proton), respectively. The methin proton signal of IIIb appeared in a field lower than that of IIIa. The methin proton of IIIb may be more deshielded by the β methoxycarbonyl group, which is situated closer than in IIIa. The IIIb compound has a larger difference in chemical shifts about the *O*-methyl proton (τ 6.10, 6.23) of the two methoxycarbonyl groups than those in IIIa (τ 6.18, 6.22)

1) E. von Lippmann, *Ber.*, **16**, 1078 (1883).
2) A. Pawollek, *Ann.*, **178**, 155 (1875).
3) C. Martius and R. Maué, *Z. Phys. Chem.*, **269**, 33 (1941).
*1 In the preceding paper, the lactonic acid obtained was prefixed with *threo* according to a Fischer projection on the basis of the tartaric acid moiety, but in this paper the lactonic acid obtained was prefixed with *threo* on the basis of the citric acid moiety. Therefore, in order to eliminate this confusion, the authors wish to correct the prefix of the previously-obtained lactonic acid to *erythro*.
4) K. Horikawa and S. Masuyama, *Yukagaku*, **14**, 179 (1965).
5) R. Malachowski, M. Giedroyć and Z. Jerzmanowska, *Ber.*, **61**, 2525 (1928).

Experimental

All the melting points are uncorrected. The infrared spectra were measured in Nujol mull using a Shimadzu IR-27 spectrometer in the 2—15 μ region, while the NMR spectra were determined at 100 Mc with a Japan Electron Optics JNM-4H-100 NMR spectrometer, using TMS as the internal reference. The elemental analyses were done at the Microanalytical Laboratory, Faculty of Science, Osaka City University.

The Preparation of *cis*-Aconitic Anhydride (III). To 240 m*l* of acetic anhydride 240 g of *trans*-aconitic acid (I) were added, after which the reaction mixture was maintained at 60°C for 1.5 hr. The reaction solution was then concentrated *in vacuo* to a syrup, which was crystallized upon the addition of dry benzene. Recrystallization from dry benzene gave pure II. Yield, 125 g; mp 76°C. Found: C, 46.20; H, 2.77%. Calcd for $C_6H_4O_5$: C, 46.17; H, 2.58%.

The Oxidation of *cis*-Aconitic Anhydride (II). A solution of II (30 g) dissolved in 300 m*l* of methanol was neutralized by the addition of sodium bicarbonate and was oxidized with 2% aqueous potassium permanganate for 3 hr at 0—5°C. The reaction solution was then allowed to stand at room temperature overnight. The precipitated inorganic salt was removed by filtration; the filtrate was acidified with hydrochloric acid and then evaporated to a syrup, which was esterified by refluxing for 7 hr with 300 m*l* of methanol and 5 m*l* of concentrated hydrochloric acid. After the methanol had been evaporated *in vacuo*, the syrupy residue was treated as will be described below.

Separation of The Lactonic Ester (IIIb). Five grams of the syrup obtained above were chromatographed on a silica-gel column (140 g). Elution with a large amount of chloroform gave 330 mg of IIIb. Recrystallization from chloroform gave pure IIIb as crystals. Yield, 267 mg; mp 97—98°C.

IR: 2.85, 2.95, 5.55, 5.75 μ. NMR($CHCl_3$): τ 4.88 (1H, singlet, methin), 6.10, 6.23 (2 OCH_3, each 3H, singlet), 7.04 (2H, quartet, methylene). Found: C, 43.99; H, 4.81%. Calcd for $C_8H_{10}O_7$: C, 44.03; H, 4.58%.

Hydrolysis of IIIb. A mixture of 9% hydrochloric acid (10 m*l*) and IIIb (125 mg) was maintained at 80°C for 5 hr. The hydrolysate was then evaporated to dryness under a vacuum. The residue was dissolved in ethyl acetate and crystallized by the addition of small amount of carbon tetrachloride. Mp 180—181°C. IR: 2.92, 5.61, 5.75 μ. Found: C, 37.70; H, 3.11%. Calcd for $C_6H_6O_7$: C, 37.89; H, 3.14%.

The Reaction of IVa and IVb with Acetic Anhydride. A mixture of acetic anhydride (0.5 m*l*) and IVa (81 mg) was maintained at 60°C for 1.5 hr. The reaction solution was then evaporated under a vacuum in order to remove the acetic acid and the acetic anhydride. The residue was treated with dry benzene, after which the benzene was removed *in vacuo*. The infrared spectrum of the product showed the characteristic bands due to the 5-membered anhydride group at 5.31 and 5.75 μ. On the other hand, in the case of IVb the characteristic bands were not observed.

The authors are grateful to Professor T. Kubota and Dr. T. Tokoroyama, Osaka City University, for their valuable discussions and suggestions, and to Professor Y. Izumi, Osaka University, for his NMR spectral measurements.

BULLETIN OF THE CHEMICAL SOCIETY OF JAPAN VOL. 43 553—555 (1970)

A Polarographic Study of Metal Dithio-β-diketonates*1

Akiko FURUHASHI, Shigeyuki KAWAI, Yasumasa HAYAKAWA and Akira OUCHI*2

Department of Chemistry, College of Engineering and Science, Aoyama Gakuin University, Megurisawa, Setagaya-ku, Tokyo

(Received May 10, 1969)

The synthesis and the infrared or visible spectroscopic properties of metal dithio-β-diketonates have been potentially sutided very recently.[1-6] Concerning the abnormal valency states of the central metal ion of the five-membered-ring dithiolate chelates, nickel dithiolate complexes have been extensively studied polarographically,[7-8] and it has been shown that the half-wave potentials of the dithiolates correlate linearly with Taft's substituent constants.[8] However, the polarographic behavior of the six-membered-ring dithio-β-diketonates has not yet been reported on. In our last paper[4] we reported that the dithioacetylacetonate was more stable than the other dithio-β-diketonates, which contain a phenyl or trifluoromethyl group rather than the one or two methyl groups of the former. The correlation between the polarographic and spectroscopic behavior of these chelates will be discussed in this paper.

Experimental

Reagents. All the metal chelates were synthesized by a method reported in previous papers.[3-4] The lithium chloride and the sodium perchlorate were of a guaranteed reagent grade and were used without further purification. The organic solvents were purified by a standard technique.[9]

Apparatuses and Experimental Procedure. A model PA-101 pen-recording d. c. polarograph of the Yanagimoto Mfg. Co., Ltd., and a dropping mercury electrode were employed. The reference electrode was a saturated calomel electrode (SCE); it was connected to the cell by means of a salt bridge (aqueous potassium chloride-agar gel). The liquid junction potential was not measured in this experiment.

Results and Discussion

In a dimethylformamide (DMF) solution, these chelates show three waves. The polarogram of nickel dithioacetylacetonate is shown in Fig. 1. The diffusion-controlled current, i_d, of the sum of the first and the second waves was proportional to the concentration of the chelate in the region of 2×10^{-4}—2×10^{-3}M, and the $i_d/\sqrt{h_{eff}}$ ratio (h_{eff}: the mercury head corrected for the back pressure) of the first wave was almost constant. A plot of $\log i/(i_d-i)$ *versus* the potential, E, of the first wave is shown in Fig. 2. The linear portion of

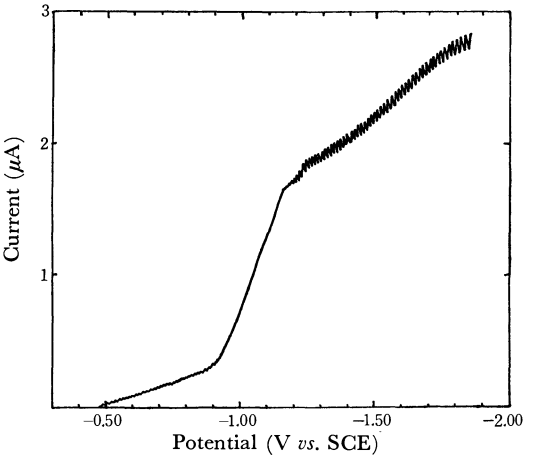

Fig. 1. D.c. polarogram of dithioacetylacetonatonickel(II).
Solvent=dimethylformamide
Concentration of the chelate=2 mM
Concentration of the lithium chloride=1 M

*1 A part of this paper was presented at the 22nd Annual Meeting of the Chemical Society of Japan, Tokyo, 1969.

*2 Department of Chemistry, College of General Education, The University of Tokyo, Komaba, Meguro-ku, Tokyo.

1) R. L. Martin and I. M. Stewart, *Nature*, **210**, 522 (1966).

2) R. Beckett and B. F. Hoskins, *Chem. Commun.*, **1967**, 909.

3) A. Ouchi, M. Hyodo and Y. Takahashi, This Bulletin, **40**, 2819 (1967).

4) A. Ouchi, M. Nakatani and Y. Takahashi, *ibid.*, **41**, 2044 (1968).

5) Y. Takahashi, K. Watanuki and A. Ouchi, *ibid.*, **42**, 274 (1969).

6) A. Furuhashi, K. Watanuki and A. Ouchi, *ibid.*, **42**, 260 (1969).

7) A. Davidson, N. Edelstein, R. H. Holm and A. H. Maki, *J. Amer. Chem. Soc.*, **85**, 3049 (1963).

8) D. C. Olsen, V. P. Mayweg and G. M. Schrauzer, *ibid.*, **88**, 4876 (1966).

9) A. Weissberger (editor), "Technique of Organic Chemistry, Vol. 7, Organic Solvents," 2nd Ed., Interscience Publ., New York (1955), p. 297.

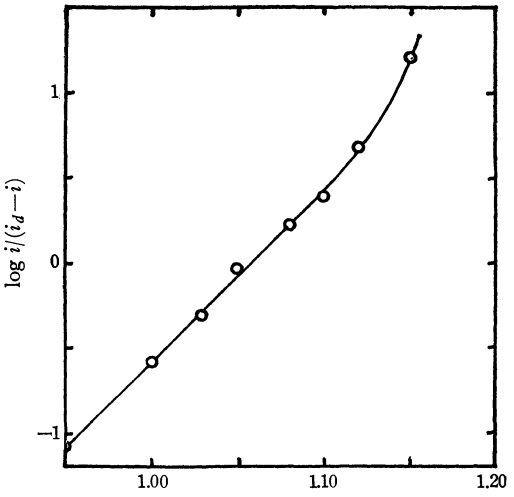

Fig. 2. The d.c. log-plot analysis for bis(dithioacetylacetonato)nickel(II).
Solvent=DMF
Concentration of the chelate=2 mM
Concentration of lithium chloride=1 M

the plot gave a slope of approximately 100 mV. From these results it seems that the wave is somewhat irreversible. The other dithio-β-diketonates give similar polarograms, though they seem to be more irreversible.

The color of the solution of trifluoromethyl derivatives changes from green to red several minutes after dissolution, perhaps because of the fast solvolysis reaction of the chelate. The polarogram of the species was obtained by using the red solution 1 to 5 hr after dissolution. The half-wave potentials of the dithio-β-diketonates and related compounds in various solvents are summarized in Table 1.

The acetonitrile solutions of nickel dithio-β-diketonates show a wave of $E_{1/2}=-1.0$——1.1 V *vs.* SCE. On the other hand, those of nickel(II) chloride show a wave of $E_{1/2}=1.05$ or 1.03 V in a 1 M $NaClO_4$ and a 1 M LiCl aqueous solution respectively, while nickel(II) acetate shows a wave of $E_{1/2}=1.06$ V in 1 M $NaClO_4$. Accordingly, the waves of $E_{1/2}$ = *ca.* -1.0 V *vs.* SCE are probably due to Ni(II)→Ni(0).

In DMF solutions, the first of the three waves seems to be that of the reduction of chelated nickel: Ni(II)→Ni(0). The second wave is lower than the first one and it overlaps with the first one a little. The third wave is unclear because of the superposed wave of the electrolyte; it is probably the reduction wave of the organic part of the ligand.

Since the half-wave potential of the wave of nickel chloride in DMF is close to that of the second wave, the second wave may correspond to the reduction of the nickel chelate, partly solvolysed by the DMF in the solution. In fact, the chelates such as trifluoromethyl derivatives, which are solvolyzed easily by DMF, give larger wave heights. The sum of the heights of the first and the second waves is always approximately the same at any given concentration of the dissolved metal chelate,

Table 1. The half-wave potentials of the chelates and related compounds

Supporting electrolyte	0.5M $NaClO_4$	1M $NaClO_4$				0.2M LiCl			
Solvent	Acetonitrile	Dimethylformamide				Dimethylformamide			
Waves		1st	2nd	3rd	2nd/1st*	1st	2nd	3rd	2nd/1st*
Compound									
$NiCl_2$	1.03		1.20				1.40		
$Ni(sacsac)_2$	1.12	1.09	1.25	1.58	0.29	1.06	1.22	1.66	0.15
$Ni(sbzsac)_2$	1.08	0.96	1.18	1.64	0.75	0.96	1.26	1.77**	0.60
$Ni(sbzsbz)_2$	1.08	0.86	1.12	1.52	0.48	0.80	1.36	1.52**	0.31
$Ni(sfasac)_2$	(0.60) 0.97 (1.27)	0.90	1.04	1.66	3.2	1.01	1.30	1.70	3.5
$Ni(sfasbz)_2$	(0.67) 0.94 (1.50)	0.72	1.09	1.64	1.6	0.78	1.24	1.47**	1.5
$Ni(L_{ss}L_{so})_2$						0.95	1.12	1.71	0.48
$Ni(L_{so})_2$						0.97	1.12	1.70	1.10
$CoCl_2$	1.06		1.34	1.63			>2.00		
$Co(sacsac)_2$	1.06	0.94	1.28		0.20	0.93	1.34		0.36

$Ni(sacsac)_2$: Bis(dithioacetylacetonato)nickel(II)
$Ni(sbzsac)_2$: Bis(dithiobenzoylacetonato)nickel(II)
$Ni(sbzsbz)_2$: Bis(dithiodibenzoylmethanato)nickel(II)
$Ni(sfasac)_2$: Bis(dithiotrifluoroacetylacetonato)nickel(II)
$Ni(sfasbz)_2$: Bis(dithiotrifluorobenzoylacetonato)nickel(II)
$Ni(L_{ss}L_{so})$: Dithioacetylacetonatomonothioacetylacetonatonickel(II)
$Ni(L_{so})_2$: Bis(monothioacetylacetonato)nickel(II)
* The ratio of 2nd and 1st wave heights. (5×10^{-4} M NiL_2; 1 to 3 hr after dissolution)
** Not well-defined owing to the overlapping of the waves.

even if the ligands of the chelates are not the same. This fact also seems to show that both the first and second waves are Ni(II)→Ni(0) reduction waves.

The ratio between the heights of the first and the second waves seems to be related to the ratio between the chelated and solvolyzed species in the solution. However, the evaluation of the stability constants attempted in the present work was not successful because of various unknown factors.

Dithioacetylacetonatomonothioacetylacetonato-nickel(II) and bis(monothioacetylacetonato)nickel-(II) show a small maximum wave between the first and the second wave. The ratio of the second wave height to the first one increases depending on the number of oxygen atoms introduced into the ligands, though the half-wave potentials of both waves do not show any appreciable change.

It is very interesting that the half-wave potential of the first wave of nickel chelates is more positive than that of simple nickel salt in a DMF solution. Perhaps because of the special coordinate bond

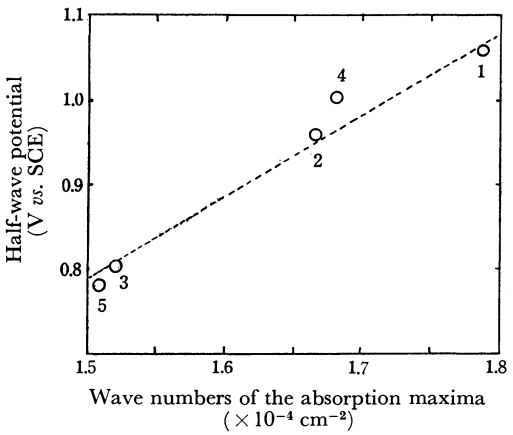

Fig. 3. Relation between the half-wave potential of the first wave and the wave numbers of the absorption maxima.
1. $Ni(sacsac)_2$ 2. $Ni(sbzsac)_2$ 3. $Ni(sbzsbz)_2$
4. $Ni(sfasac)_2$ 5. $Ni(sfasbz)_2$

character between sulfur and the central metal, as well as because of the pseudo-aromaticity of the dithio-β-diketonate chelate ring, electrons are more easily supplied to the central ion than usual complexes; this should cause a positive shift of the wave. On the other hand, the more stable a complex is, the more the wave shifts toward negative potentials. In this case, the former effect is predominant, and the first wave shows a positive shift. The first wave of bis(dithioacetylacetonato)cobalt(II) also shows the same tendency.

The relation between the wave number of the maxima of the electronic spectral band in the 500-to-600 mμ region of the chelates and the half-wave potentials of their first waves is shown in Fig. 3. According to Schrauzer *et al.*,[8] the half-wave potential of the polarograms of five-membered-ring dithiolate chelates shifts toward more positive potentials when Taft's inductive coefficients of ligands are higher. Although this phenomenon is also to be expected for the dithio-β-diketonates, the Taft constants for the six-membered-ring chelates containing a trifluoromethyl group, as calculated by the method of Schrauzer *et al.*,[8] are too high and are not in any linear relation with the $E_{1/2}$ and $\sum\sigma^*$.

In the case of five-membered-ring dithiolate complexes, the waves near −1.0 V and +0.1 V *vs.* Ag/AgCl were assigned to Ni(I)→Ni(0) and Ni(II)→Ni(I) respectively. However, the six-membered-ring dithio-β-diketonato chelates do not give the latter wave; moreover, it is not probable to identify any of the waves as an Ni(I)→Ni(0) one; consequently, it can be said that dianionic or monoanionic species are not stable in the case of six-membered-ring chelates. This is probably because of the weaker aromaticity of the latter chelate ring.

Helpful discussions by Professors Niro Matsuura, Yukichi Yoshino, and Kunihiko Watanuki and by Drs. Kisaburo Umemoto and Toshio Takeuchi are hereby gratefully acknowledged.

BULLETIN OF THE CHEMICAL SOCIETY OF JAPAN VOL. 43 556—558 (1970)

Formation and Absorption Spectra of Mixed Copper(II) Chelates Containing Acetylacetone and 2,2′-Bipyridine or 1,10-Phenanthroline

Yutaka FUKUDA* and Kozo SONE**

* *Department of Chemistry, Faculty of Science, Shizuoka University, Ôya, Shizuoka*

** *Department of Chemistry, Faculty of Science, Ochanomizu University, Ôtsuka, Bunkyo-ku, Tokyo*

(Received July 9, 1969)

The formation and absorption spectra of a number of mixed copper(II) chelates of the general type [CuAB], where A is bip or phen and B is en, gly or ox, were studied by Sone, Utsuno and Ogura.[1] The extension of this study to the systems

(1) $[Cu\ bip_2]^{2+} + [Cu\ aca_2] \rightleftarrows 2[Cu\ bip\ aca]^+$

(2) $[Cu\ phen_2]^{2+} + [Cu\ aca_2] \rightleftarrows 2[Cu\ phen\ aca]^+$

is reported here[2].

Figure 1 shows the visible absorption spectra of the solutions containing $[Cu\ bip_2](NO_3)_2 \cdot H_2O$ and $[Cu\ aca_2]$ in various proportions. The solvent used is 80% (v/v) dioxane, and the total concentration of the two chelates is 10^{-2} M in every case. Existence of two isosbestic points is evident; one at 704 mμ is observed in solutions in which the ratio $[Cu\ bip_2]^{2+}$: $[Cu\ aca_2]$ is 0 : 10 to 5 : 5, and another at 628 mμ is found in solutions where the ratio is 5 : 5 to 10 : 0. In Fig. 1, the curves for the solutions of the ratios 3 : 7, 4 : 6, 6 : 4 and 7 : 3 are not shwon. However, each of them passes the corresponding isosbestic point. The absorption bands of $[Cu\ bip_2]^{2+}$ at 740 and 950 mμ (ε=88 and 78, respectively) disappear almost completely in the solution where the ratio is 5 : 5, and a new band appears, the λ_{max} of which (610 mμ; ε=62) is smaller than those of $[Cu\ bip_2]^{2+}$ and even than that of $[Cu\ aca_2]$ (620 mμ; ε=39). Essentially similar data are obtained with $[Cu\ phen_2](NO_3)_2 \cdot H_2O$ and $[Cu\ aca_2]$ in 72% dioxane, where the

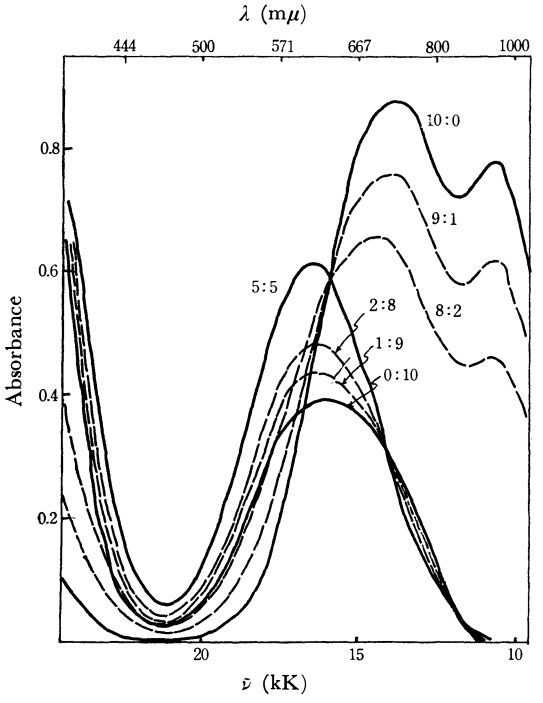

Fig. 1. Absorption spectra of $[Cu\ bip_2]^{2+}$ - $[Cu\ aca_2]$ mixed solutions in 80% dioxane. The molar ratio of the component chelates ($[Cu\ bip_2]^{2+}$: $[Cu\ aca_2]$) is shown for each curve.

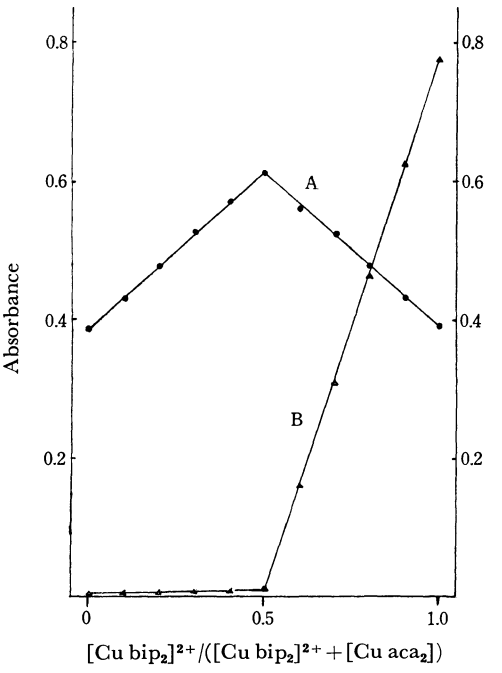

Fig. 2. Application of continuous variation method to the data of Fig. 1. The wavelength used: (A) 600 mμ; (B) 940 mμ.

1) K. Sone, S. Utsuno and T. Ogura, *J. Inorg. Nucl. Chem.*, **31**. 117 (1969).

2) Abbreviations used in this paper are: bip=2,2′-bipyridine; phen=1,10-phenanthroline; en=ethylenediamine; gly=glycinate anion; ox=oxalate anion; aca=acetylacetonate anion.

total concentration of the two chelates is 0.8×10^{-2} M; here the band of $[Cu\ phen_2]^{2+}$ at 720 and 980 mμ ($\varepsilon=46$ and 41, respectively) practically disappears in the 5 : 5 mixture, and a new band appears instead at 615 mμ ($\varepsilon=48$). These facts, and especially the application of continuous variation method to these data (*cf.* Fig. 2), clearly indicate that the mixed chelates $[Cu\ bip\ aca]^+$ and $[Cu\ phen\ aca]^+$ are formed nearly quantitatively in the respective mixed solutions. Estimation from these spectral data indicates that the equilibrium constants (K) of the two systems (1) and (2) are both very large ($K\geqq 10^4$), showing the remarkably high stability of these mixed species. It was also found that dark-green crystalline chelates [Cu bip aca]X and [Cu phen aca]X (X=NO_3 or ClO_4) can be readily obtained by evaporating equimolar mixtures of $[Cu\ aca_2]$ and $[Cu\ bip_2]X_2$ or $[Cu\ phen_2]X_2$ dissolved in aqueous ethanol. The results of elemental analyses are as follows; Found: C, 47.21; H, 3.99; N, 10.96%. Calcd for [Cu bip aca](NO_3): C, 47.29; H, 3.97; N, 11.03%. Found: C, 41.47; H, 4.00; N, 6.50%. Calcd for [Cu bip aca](ClO_4)·H_2O: C, 41.29; H, 3.94; N, 6.42%. Found: C, 47.39; H, 4.23; N, 9.84%. Calcd for [Cu phen aca](NO_3)·1.5 H_2O: C, 47.27; H, 4.21; N, 9.73%. Found: C, 44.37; H, 3.80; N, 6.17%. Calcd for [Cu phen aca](ClO_4)·H_2O: C, 44.35; H, 3.73; N, 6.09%.

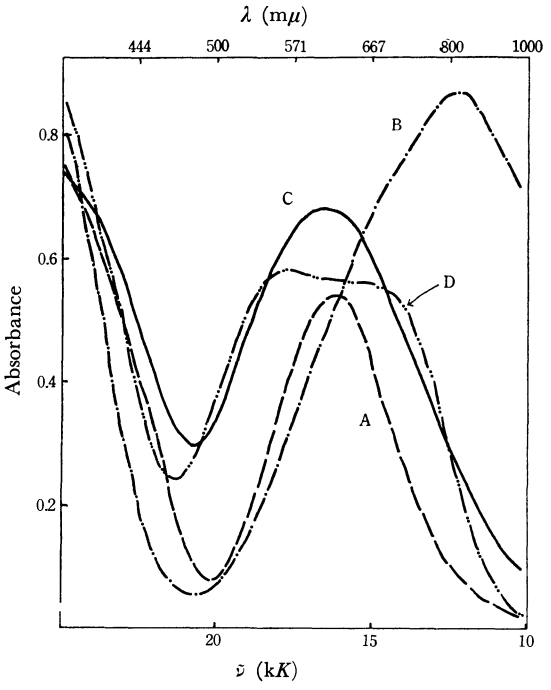

Fig. 3. Spectral data of the chelates in the system $[Cu\ bip_2]^{2+}-[Cu\ aca_2]$. Curve A: absorption spectrum of [Cu bip aca]$^+$ in 80% dioxane; curves B, C and D: reflectance spectra of [Cu bip$_2$](NO_3)$_2$·H_2O, [Cu bip aca](NO_3) and [Cu aca$_2$], respectively.

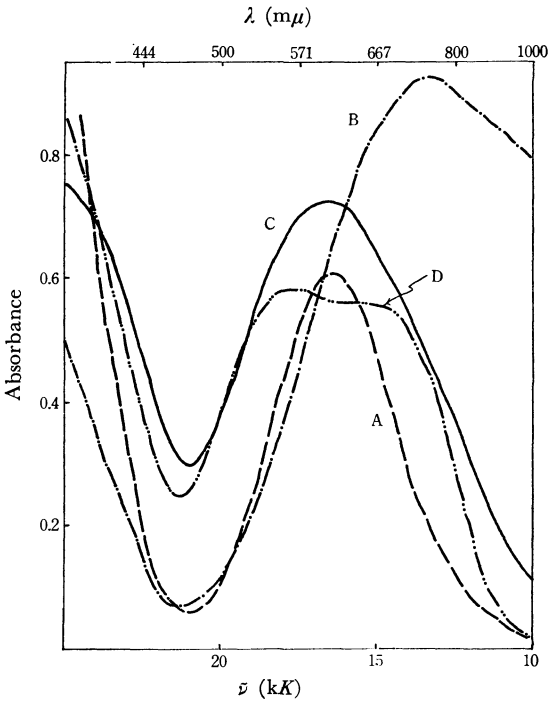

Fig. 4. Spectral data of the chelates in the system $[Cu\ phen_2]^{2+}$-$[Cu\ aca_2]$. Curve A: absorption spectrum of [Cu phen aca]$^+$ in 80% dioxane; curves B, C and D: reflectance spectra of [Cu phen$_2$](NO_3)$_2$·H_2O, [Cu phen aca](NO_3)·1.5H_2O and [Cu aca$_2$], respectively.

Figures 3 and 4 show that the λ_{max} values of the reflectance spectra of these newly obtained chelates agree fairly well with those in the absorption spectra of their 80% dioxane solutions; the latter spectra, on the other hand agree nearly exactly with the spectra of the corresponding 5 : 5 mixtures described above. These facts show that these crystalline chelates are true mixed chelates, and not the mere mixtures of the component chelates.

It is of interest to compare these data with the earlier data of Kida[3] on the formation of [Cu en aca]$^+$ from $[Cu\ en_2]^{2+}$ and $[Cu\ aca_2]$ in water-dioxane. Although his experimental conditions are not exactly the same as ours, it is apparent that the stability of [Cu en aca]$^+$ with respect to its component chelates is very much lower than that of [Cu bip aca]$^+$ and [Cu phen aca]$^+$. The value of K calculated by Kida was only 2.6, and did not differ so much from the statistical value 4. He also found that the absorption band of [Cu en aca]$^+$ was nearly at the middle between those of $[Cu\ en_2]^{2+}$ and $[Cu\ aca_2]$. Thus the behavior of this mixed chelate seems to be quite normal in every respect.

The remarkably greater stability and apparently anomalous spectra of the mixed chelates can now

3) S. Kida, This Bulletin, **29**, 805 (1956).

be ascribed, as in the case of other bip- or phen-containing mixed chelates,[1] to the removal of the steric hindrance existing in $[Cu\ bip_2]^{2+}$ and $[Cu\text{-}phen_2]^{2+}$ by mixed chelate formation. As described in a previous paper,[1] scale model studies show that these chelates are considerably deformed from the square-planar structure normally favored by Cu^{2+}. On the other hand, the same studies show that the mixed chelates $[Cu\ bip\ aca]^+$ and $[Cu\ phen\ aca]^+$ are perfectly square-planar. Therefore, we can expect that they will be very readily formed in solution containing the component chelates, and the value of K will be very much higher than the statistical value. We can also expect that their λ_{max} values will be much smaller than those of $[Cu\ bip_2]^{2+}$ or $[Cu\ phen_2]^{2+}$, and even than that of $[Cu\ aca_2]$ as they are both $[Cu\text{-}N_2O_2]$-type chelates.[1),4] It is apparent that these expectations agree quite well with our observations.

It is of some interest to note that the band of $[Cu\ aca_2]$ in Figs. 3 and 4 is notably split. This can probably be related to its crystal structure in which the chelate molecules are highly planar and each copper atom is practically 4-coordinate.[5]

4) It is noteworthy that the λ_{max} of $[Cu\ aca_2]$, which is a $[Cu\ O_4]$-type chelate, is quite small, and even somewhat smaller than that of $[Cu\ gly_2]$ (635 mμ) which is a $[Cu\ N_2O_2]$-type chelate. However, since the ligand field strength of bip or phen will be more or less comparable with that of en ($[Cu\ en_2]^{2+}$: λ_{max}= 550 mμ), we can anticipate what is stated in the text.

5) E. A. Shugan, *Dokl. Akad. Nauk SSSR*, **1951**, 853; H. Koyama, Y. Saito and H. Kuroya, *J. Inst. Polytech. Osaka City Univ.*, **C4**, 43 (1953); K. Mizutani, K. Sone and T. Sakaki, *Z. Anorg. Allg. Chem.*, **365**, 217 (1969).

BULLETIN OF THE CHEMICAL SOCIETY OF JAPAN VOL. 43 558—560 (1970)

Removability of Oils from Cotton Cloths

Maresuke KASHIWAGI and Tomoko TAMURA

School of Home Economics, Kyoritsu Womens University, Chiyoda-ku, Tokyo

(Received July 22, 1969)

It is well-known that oily substances attached to soiled cloths play an important role in the process of detergency. It seems, however, that the mechanism operating underneath the detergency process has not yet been firmly established.

According to a direct observation of the detergency process, the particulate constituent might give little trouble if the oily constituent could be removed first.[1] However, exactly the opposite may be true, that is, it may be held that it is rather particulate dirt that has become firmly attached to the textile itself, instead of adhering by means of a fatty film.[2] In fact, it seems most likely that the solid and liquid soils are under certain conditions, often removed independently.[3]

Yet it appears that no direct demonstration of the influence of oil on a quantitative basis has ever been made. The present authors, using the gas-chromatographic technique, tried to determine the removability of oily substances from cotton cloths, paying particular attention to the type of oil used. The present report will be concerned with the desorption of three different types of oils with the same carbon chain and with the correlation of the desorption with the detergency.

Experimental

Oils. The three types of oils used were dodecane $C_{12}H_{26}$, dodecyl alcohol $C_{12}H_{25}OH$, and lauric acid $C_{12}H_{24}O_2$, each with a twelve carbon chain. We attempted to use oils with a shorter carbon chain, but we found that alkanes of less than 12 carbons evaporated rather quickly upon gas-chromatographic analysis and upon weight-loss measurement as well. The dodecane and lauric acid were both extremely pure, showing the presence of only one peak on a gaschromatogram. The dodecyl alcohol was purified from commercial lauryl alcohol by repeated distillation under reduced pressure, but it still showed about 7% content of homologous alcohols.

Cloths, Carbon Black, and Carbon Tetrachloride. These were used as assigned by a standard detergency test method.*1

Detergents. The sodium dodecyl sulfate (SDS), which had been purchased from Wako Junyaku Co., Ltd., was purified once by recrystallization from ethanol. The polyoxyethylene condensate of nonyl phenol ($\bar{p}=7.5$ NPE) was used as obtained from the Toho Chemical Co., Ltd. The household detergent mixture

1) T. Fort, Jr., H. R. Billica and C. K. Sloan, *Text. Res. J.*, **36**, 7 (1966).

2) E. Howarth and L. P. S. Piper, *ibid.*, **36**, 856 (1966).

3) K. Durham, "Surface Activity and Degergency," Macmillan Co., London (1961), p. 72.

*1 JIS-C9606 (1968).

was a recently-purchased one. The gaschromatograph used was a Hitachi K-53 type apparatus, equipped with a rising temperature programer. The sensitivity was $10-2\times10^2$. Its column was packed with chromosorb W with phosphoric acid plus polyethyleneglycol.

Procedure. An oil-impregnated cotton cloth was prepared by applying 0.5 cc of an equimolar mixture (2.4×10^{-4} mol of each/cc) of dodecane, dodecyl alcohol, and lauric acid in CCl_4 to a piece of cloth (10×5 cm) by means of a micropipet. After the evaporation of the solvent, the oiled cloths were aged for 3 days before use. The oiled cloth was washed with a scrub-*o*-meter in the usual manner at 30°C for 10 min, and then rinsed for 3 min. Ion-free water was used throughout. Washed cloths from 12 runs were collected and air-dried, and the residual oils were extracted in ether with soxlet for 12 hr. After the removal of the ether, 1 cc of CCl_4 was added to this remaining oil in order to analyze it by gas chromatography. The relative contents of the three oils were calculated by the ordinary triangle method.

By a separate detergency test, we made three types of artificially soiled cotton cloth, in each test using the same amount of a different oil instead of using hardened tallow and paraffin. The cloth was impregnated with carbon black and oil in CCl_4.

The washing time was made 20 min, while keeping the other conditions the same as above.

The detergency may be expressed as; $D=\dfrac{R_w-R_s}{R_o-R_s}$

where R_w: reflectance of the washed cloth
R_s: reflectance of the soiled cloth
R_o: reflectance of the original cloth before soiling.

All the detergency data are averages of four runs made under the same conditions and examined by means of statistical calculations.

Results and Discussion

Table 1 shows the residual oil contents of washed cotton cloths. These are calculated from the gaschromatograms, a sample of which is shown in Fig. 1. As is clearly indicated here, overwhelmingly more dodecyl alcohol remained than the corresponding alkane and acid. In other words, the alcohol was most difficult to remove by any detergent solution including SDS and NPE. Table 2 shows the detergency of water alone, SDS, NPE, and a commercial detergent mixture on cloths artificially soiled with carbon blacks and with one of the three oils. For any of the detergent systems listed in Table 2 except for the commercial detergent, which alone contains alkaline builders, it was found that detergency is strongly dependent on the soiling oil. The influence of oil on the removal of carbon particles from cloths is very clear. In almost all cases, except for the commercial detergent formulation, the detergency for soiled cloths increases in the order of: without oil>alkane>alcohol>acid.

Table 1. Unremovable oils in cotton cloths after washing

Detergent system	Residual oil (ratio against alkane)		
	Alkane	Alcohol	Acid
Water	1	715	10
NPE 0.25%	1	71	44
SDS 0.25%	1	240	34

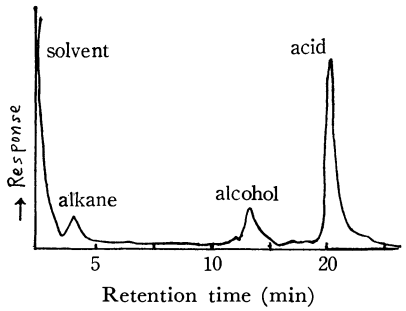

Fig. 1. A GL Chromatogram of residual oil (SDS 0.25%; sensitivity $10-2\times10^2$).

These two results may be summarized by saying that the removability of oil out of cotton cloth by these detergents is definitely: alkane>acid>alcohol in the order of ease, while the removability of carbon soil with regard to the presence of oil is in the order of: without oil>alkane>alcohol>acid. This, in turn, should be interpreted as meaning that the removability of oil is not parallel with that of soiled soil, *i.e.*, carbon black.

The soiled cloth without oil exhibits the highest detergency, and the presence of lauric acid, which should behave like solid, (mp 44°C) interferes with the removal of carbon soil most strongly. The exception of the commercial detergent regarding

Table 2. Detergency on artificially-soiled cloths

Soiling Composition	Detergency %			
	Water	SDS	NPE	Commercial detergent
Carbon black	27.6	51.0	59.2	52.3
Carbon black plus alkane	25.3	54.1	54.2	57.7
Carbon black plus alcohol	19.4	45.8	41.5	48.7
Carbon black plus acid	14.8	30.2	30.0	59.3

(Concentration of detergents: 0.25%)

the order of detergency with respect to acid appears to be very reasonable, because the acid soil may be removed more easily by alkaline builders like sodium tripolyphosphate in detergent formulation. As for the removal of oily dirt, emulsification may be considered to be of importance.[3]

However, it may also be interesting to add that alkane is much more difficult to emulsify than alcohol by these detergent solutions at concentrations of 2.5% or less when emulsification test are carried out by an ordinary method.[4] We have found that alcohol was most easily emulsified, even to a thixotropic gel, while acid, being a solid, never went into emulsion at 30°C.

The author wish to express their appreciation to Mr. H. Uchiki of Hitachi for carrying out the gas-chromatographic analysis and to Mr. H. Akabayashi of the Nissan Co., Ltd., for supplying the samples of alkane and dodecyl alcohol.

4) S. Hayashi and N. Sasaki, *Yukagaku*, **16**, 467 (1967).

BULLETIN OF THE CHEMICAL SOCIETY OF JAPAN VOL. 43 560—561 (1970)

A Simple HMO Treatment of the Acidity of Substituted Tropolones

Kimiaki IMAFUKU and Hisashi MATSUMURA

Department of Chemistry, Faculty of Science, Kumamoto University, Kurokami-machi, Kumamoto

(Received August 4, 1969)

It is known that the dissociation constants of tropolone derivatives which have the phenolic hydroxyl group are linearly correlated with Hammett's substituent constants obtained in benzenoid compounds.[1] In an application of the Hammett equation to tropolone derivatives, we found that the π-electron densities of oxygen atoms and neighboring carbon atoms are correlated with substituent constants.[2]

As a molecular orbital treatment, we examined the energy changes in dissociation of some tropolone derivatives in terms of localization energies. This was on the assumption that the dissociation constants of this type of derivatives are directly proportional to the π-electron energy differences between the unionized and the ionized tropolones.

Calculation Method

The simple Hückel molecular orbital method was used for all calculations as in previously reported.[2]

In the molecular orbital treatment of the energy changes in dissociation equilibrium of tropolones (see below),

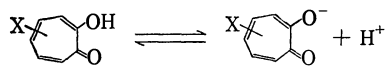

the following localized and delocalized models are assumed. In the dissociation of phenols, the degree of delocalization by the interaction of phenyl group with OH group is smaller than that of phenyl group with O^- group.[3] Similarly, in tropolone derivatives, it is thought that tropolonate anions

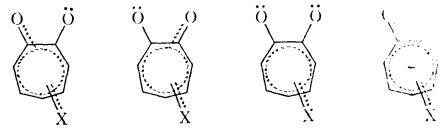

[A] [B] [C] [D]

Fig. 1. The localized models for tropolones and the delocalized model for tropolonate anions.

are more delocalized than tropolones themselves. The localized tropolones can be represented by states [A] or [B] in Fig. 1. However, state [C] was chosen as the model for calculations, since the two oxygen atoms are nearly equivalent in reactivity and the calculation might be simplified. Model [D] was used as the delocalized tropolonate anions. On these assumptions, the energies for the unionized tropolones $(E_\pi)_{AH_I}$ and for the ionized tropolonate anions $(E_\pi)_{A^-_I}$ are calculated, and the energy changes $(\Delta E_\pi)_I$ for dissociation are given by the equation[4]

$$(\Delta E_\pi)_I = (E_\pi)_{A^-_I} - (E_\pi)_{AH_I} = 2\alpha + (\Delta M_I)\beta \quad (1)$$

As the integral parameters for the oxygen atoms and the adjacent carbon atoms, the parameters we obtained previously are used,[2] and Fueno's parameters[3] are applied to all substituents.

1) N. Yui, *Sci. Repts. Tohoku Univ.*, I, **40**, 102 (1956); *Chem. Abstr.*, **51**, 17354^c (1957); *Sci. Repts. Tohoku Univ.*, I, **40**, 114 (1956); *Chem. Abstr.*, **51**, 17354^e (1957).

2) K. Imafuku and H. Matsumura, This Bulletin, **42**, 1772 (1969).

3) T. Fueno, T. Okuyama and J. Furukawa, *ibid.*, **39**, 569 (1966).

Results and Discussion

The ΔM_i terms in the energy changes in dissociation of tropolone derivatives are listed in Table 1, together with their dissociation constants. When the values of ΔM_i are plotted against pK_i (Fig. 2), irrespective of many assumptions, an approximately linear relation holds according to the electron-releasing and the electron-attracting forces of substituents. The relationship between pK_i and ΔM_i is represented by the equation

$$pK_i = 7.77 - 2.87\Delta M_i \quad (2)$$

The calculated pK_i values obtained by this equation are shown with the observed values in Table 1. The correlation coefficient between the observed and the calculated values is 0.98. Thus, the dissociation constants of other tropolone derivatives with substituents in the 4- and 5-positions can be estimated by molecular orbital calculation and equation (2).

Table 1. Energy changes in dissociation and pK values

No.	Substituent	ΔM_i	pK_i	
			calcd	obsd
1	5-OCH_3	0.0610	7.59	7.75
2	5-CH_3	0.1550	7.33	7.32
3	4-CH_3	0.1658	7.29	7.26
4	H	0.2530	7.04	6.92
5	5-Cl	0.5232	6.24	—
6	5-Br	0.5486	6.20	6.32
7	5-NO_2	0.8160	5.43	—

No. of substituents are related to those in Fig. 2.

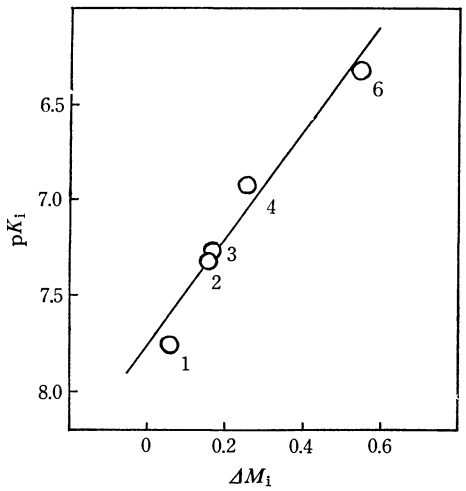

Fig. 2. Correlation of pK_i with ΔM_i.

ΔM_i is correlated with Hammett's substituent constants. This shows that the Hammett relationship is applicable to tropolone derivatives, together with the linearity of the static π-electron densities of oxygen atoms and the neighboring carbon atoms with σ-constants.[2)]

4) A. Streitwieser, Jr., *Tetrahedron Lett.*, **1960**, 23.

BULLETIN OF THE CHEMICAL SOCIETY OF JAPAN VOL. 43 561—563 (1970)

Nuclidic Mass Measurement by Ion Cyclotron Resonance

Shizuo FUJIWARA

Department of Chemistry, Faculty of Science, The University of Tokyo, Hongo, Bunkyo-ku, Tokyo

Katsuyuki AOYAGI and Teruo MIYAMAE

Japan Electron Optics Laboratory, Akishima-shi, Tokyo

(Received August 8, 1969)

Recently Baldeschwieler and his co-workers[1] have applied the double-resonance technique of magnetic resonance to ion cyclotron-resonance spectroscopy (ICRS) and proved it useful for the investigation of the kinetics of organic reactions. Besides the use of ICRS along this line, it is also assumed to be useful for the measurement of the nuclidic masses. This sort of application is important because the atomic masses are, at present, determined by mass spectroscopy[2] as well as by microwave spectroscopy;[3] the effort to build a new and independent method for the determination of nuclidic masses is to be encouraged.[4]

1) L. R. Anders and J. L. Beachamp, R. C. Dunbar and J. D. Baldeschwieler, *J. Chem. Phys.*, **45**, 1062 (1966).

2) H. E. Duckworth "Mass Spectroscopy," Cambridge University Press, Cambridge (1960), p. 97.

3) C. H. Townes and A. L. Schawlow, "Microwave Spectroscopy," McGraw-Hill, New York (1955), p. 42.

4) A. E. Cameron and E. Wichers, Comprehensive Review, Report of the Commission on Atomic Weights, Comptes rendus of IUPAC XXI (1961), p. 20.

The ICRS is based on the motion of charged particles in magnetic and electric fields. The cyclotron frequency, ω_c, is given by Eq. (1), where e is the charge of the particle; H, the magnetic field strength in Gaussian

$$\omega_c = eH/mc \qquad (1)$$

cgs units; m, the particle mass, and, c, the velocity of light. When an alternating electric field, $E_1(t)$, at a certain frequency ω_1, is applied normaly to H with $\omega_1=\omega_c$, an absorption of energy by the ions occurs; this absorption can easily be observed by a bridge-type detector. With a fixed observing frequency, the mass of the ion can be obtained by measuring the intensity of H by the proton magnetic resonance technique.

With this consideration, an experimental set-up has been built according to the descriptions which have been published in the literature.[5)]

The experimental conditions and some results concerning argon 40 will be described below.

Experimental

Since most of the construction of the apparatus is the same as in the literature,[5)] its details will not be given in this paper. A schematic diagram of the apparatus is shown in Fig. 1, where the observing frequency is calibrated as 99.986 kHz; the magnetic field strength is measured by the proton magnetic resonance technique.

Beauchamp *et al.* have shown the dependence of ω_c on the instrumental factors, especially on the trap voltage, V_T, and have shown a relation of:

$$\Delta H_c = (2\times 10^8/\omega_c d^2)V_T \qquad (2)$$

In Eq. (2), ΔH_c is the deviation of the resonant field from the theoretical value of Eq. (1), and d, the distance between the electrodes. Equation (2) has been derived by the consideration that an additional magnetic field, ΔH_c, is produced by V_T in the probe; it implies that the theoretical resonant field will be obtained by extrapolating V_T to 0. However, we assume this condition is not sufficient to produce the state of $\Delta H_c=0$, and it is assumed to be necessary to take the effect of the drift voltage, V_D, into consideration also. Namely, we assume that this condition is realized in the central region of the probe, when V_T is taken as one half of V_D.*1 In other words, Eq. (2) is replaced by Eq. (3):

$$\Delta H_c = (K/d^2\omega_c)(V_T - V_D/2) \qquad (3)$$

where K is an experimental constant.

Measurements have been carried out with respect to Ar 40 under the conditions shown in Table 1.

The values of V_D and V_T have been measured with an experimental error of ± 0.001 V. The resonant field has been measured by the proton resonance technique, it is expressed in terms of the frequency scale shown in Fig. 2. Each point of the observed values in Fig. 2 refers to the average of 5 runs and is assumed to be accurate within 1 Hz.

The observed points present a linear relation with V_T as may be seen in Fig. 2. According to the results of the aforementioned consideration, the real resonant field is determined to be 11.081 MHz in frequency units by the point which refers to the condition of $V_T=-0.1$ V on the extrapolated line of Fig. 2. Hence, the atomic weight of Ar 40, M, is calculated either by

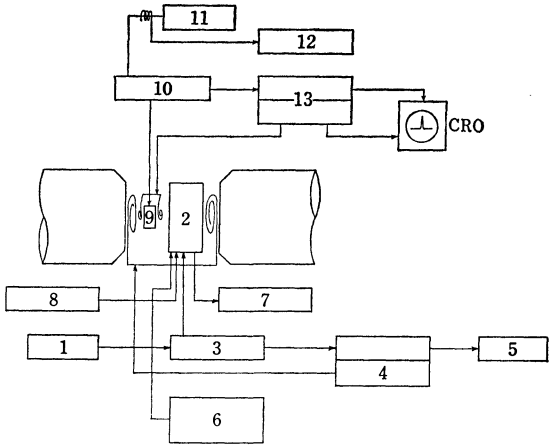

Fig. 1.

ICR part
1. Oscillator
2. Head
3. Detector
4. Amplifier and modulation
5. Recorder
6. Electron regulator (with respect to current and energy)
7. Vacuum control
8. Drift and trapping voltage supplies

NMR part
9. Head
10. Detector
11. Dipmeter
12. Frequency counter
13. Amplifier and modulation source

Table 1.

Observing frequency	$f_c = 99.986$ kHz
Observing electric field	$E_1 = 0.02$ V/cm
Pressure of sample (Argon)	3×10^{-5} Torr
Voltage of electron collector	+20 V
Energy of electrons	70 eV
Trapping voltage (in the resonance region)	$V_T = 0.20$—0.00 V
Drift voltage (in the resonance region)	$V_D = 0.200$ V (plate distance 2.5 cm)
Drift voltage (in the source region)	$V_D = 0.205$ V (plate distance 2.5 cm)
Electron beam	0.025×10^{-6} A

5) J. L. Beauchamp, L. R. Anders and J. D. Baldeschwieler, *J. Amer. Chem. Soc.*, **89**, 4569 (1967).

*1 Dr. Beauchamp has written the present author that he also noticed the same phenomenon. The author's thanks are due to Dr. Beauchamp for sending preprint of his work.

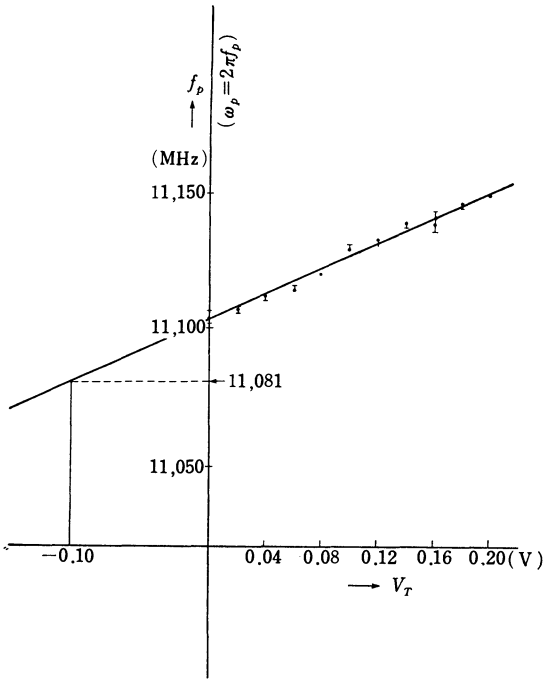

Fig. 2

Eq. (4) or Eq. (5), depending on the choice of the physical constants:

$$M = \frac{e}{c}\frac{N}{\gamma_p}\frac{\omega_p}{\omega_c} \tag{4}$$

$$M = N\frac{m_p}{\mu_p}\frac{\omega_p}{\omega_c} \tag{5}$$

In the sense that the atomic weight thus obtained is still dependent on the mass of the proton, which is determined on the basis of $C=12$ standard, the atomic weight of Ar 40 which has been determined in this experiment still depends on the latter. Calculations after Eqs. (4) and (5) both give a value of 39.970 ± 0.001, which is comparable to that of 39.961324 given in the literature.[6] Agreement between the two values is fairly good, and this agreement gives a sound basis for the assumption involved in Eq. (3) and also for the experimental techniques adopted in this experiment. The latter statement, in turn, implies that the present technique can be utilized for the precise measurement either of the gyromagnetic ratio or the magnetic dipole moment of the proton with the use of the established data on the mass.*2 Further investigation along this line is now in progress.

Table 2.*

N	Avogadro's number	6.002216×10^{23}
e	electric charge unit	4.8029×10^{-10}
c	light velocity	2.9979×10^{10}
γ_p	gyromagnetic ratio of proton	2.6751985×10^{4}
m_p	mass of proton	$1.00727663m_1$ $\left(m_1=\frac{1}{12}C(C=12)\right)$
μ_p	magnetic dipole moment of proton	2.7928 (Bohr magneton)

* After B. N. Taylor, W. H. Parker and D. N. Langenberg, *Rev. Mod. Phys.*, **41**, 375 (1969).

Hearty thanks of the authors are due to Dr. E. Wichers, the chairman of the International Commission of the Atomic Weights for his keeping interest for us throughout this work and to Dr. T. Farrer of the National Burear of Standards, U.S.A., for supplying the information of the values of physical constants.

6) The Atomic Weights as Computed from Nuclidic Masses and Isotope Abundances, P. J. De Bievre, M. G. Gallet and G. H. Debus, 3rd Preliminary Report 1965, Euratom/Geel, Belgium.

*2 The authors' thanks are due to Dr. S. Peiser of the National Bureau of Standards of U.S.A. and to Professor Roth of the University of Paris, who called the notice of the authors to this application.

BULLETIN OF THE CHEMICAL SOCIETY OF JAPAN VOL. 43 564—565 (1970)

Absolute Configurations of 2-Methyl-2-phenylaziridine, 2-Phenylpropylamine, and Their Derivatives

Yoshihiro SUGI and Sekio MITSUI

Department of Applied Science, Faculty of Engineering, Tohoku University, Aoba Aramaki, Sendai

(Received August 11, 1969)

In previous publications,[1,2] we reported the stereoselectivity[1] and the effects of solvent and additive on the stereochemistry[2] of the catalytic hydrogenolysis of optically active 2-methyl-2-phenylaziridine derivatives. We now wish to describe the syntheses and the absolute configurations of 2-methyl-2-phenylaziridine, 2-phenylpropylamine, and their derivatives.

(+)-Ethyl 2-amino-2-phenylpropionate (I) was obtained by the resolution of (±)-I as its tartrate. The subsequent reduction of (+)-I with lithium aluminum hydride gave (+)-2-amino-2-phenylpropanol (II).[1] (+)-II was converted to (+)-2-methyl-2-phenylaziridine (III) *via* its sulfonate.[1] (−)-1-Acetyl-2-methyl-2-phenylaziridine (IV) was obtained by the acetylation of (−)-III. (+)-Ethyl 2-formylamino-2-phenylpropionate (V) was prepared by the formylation of (+)-I. The subsequent reduction of (+)-V with lithium aluminum hydride gave (+)-2-methylamino-2-phenylpropanol (VI). The cyclization of (+)-VI afforded (+)-1,2-dimethyl-2-phenylaziridine (VII). (+)-I has the S configuration.[3] Therefore, (+)-III, (+)-IV, and (+)-VII all have S configurations.

The formylation of (+)-2-phenylpropylamine (VIII) afforded (+)-*N*-2-phenylpropylformamide (IX). (+)-IX was reduced to (+)-*N*-methy-2-phenylpropylamine (X) with lithium aluminum hydride. (−)-*N*-2-Phenylpropylacetoamide (XI) was obtained by the acetylation of (−)-VIII. (+)-VIII has the R configuration.[4,5] Therefore, (+)-IX, (+)-X, and (+)-XI all have R configurations.

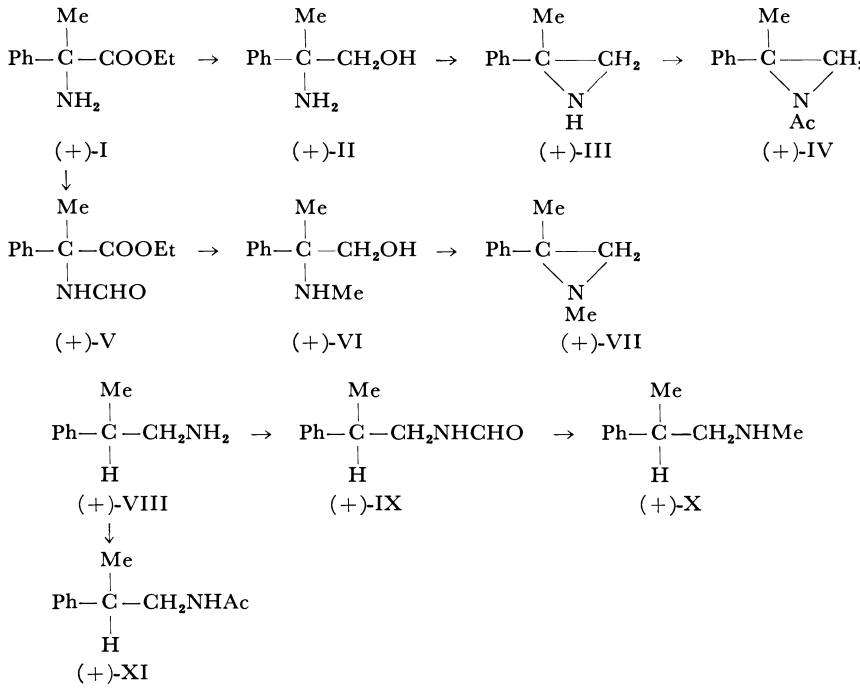

1) S. Mitsui and Y. Sugi, *Tetrahedron Lett.*, **1969**, 1287; Y. Sugi and S. Mitsui, This Bulletin, **42**, 2984 (1969).

2) S. Mitsui and Y. Sugi, *Tetrahedron Lett.*, **1969**, 1291; This Bulletin, **43**, in press.

3) H. Mizuno, S. Terashima, K. Achiwa and S. Yamada, *Chem. Pharm. Bull.* (Tokyo), **25**, 1747 (1967).

4) P. A. Levene, L. A. Mikeska and K. Passoth, *J. Biol. Chem.*, **88**, 27 (1930).

5) E. L. Eliel and J. P. Freeman, *J. Amer. Chem. Soc.*, **74**, 923 (1952).

Experimental

S(+)- and R(−)-Ethyl 2-Amino-2-phenylpropionates (I), S(+)- and R(−)-2-Methyl-2-phenylaziridines (III), and S(+)- and R(−)-2-phenylpropylamines (VIII). These substances were prepared by the procedure previously described.[1] The NMR spectrum of III had signals at 0.40 (broad singlet, >NH); 1.53 (singlet, $-CH_3$); 1.73 (singlet) and 1.78 (singlet), ($-CH_2-$); 7.25 (multiplet, aromatic protons).*1

R(−)-Acetyl-2-methyl-2-phenylaziridine (IV). Acetyl chloride (8.2 g) in ether (25 ml) was added at 0°C to a solution of R(−)-III (13.3 g, α_D^{22} −18.86 (neat), 37.3% optically pure) and triethylamine (15.0 g) in ether (75 ml). The reaction mixture was allowed to proceed to completion by being stirred for 1 hr at this temperature. The triethylamine hydrochloride thus precipitated was filtered off and washed well with ether. After the ether had been removed at room temperature *in vacuo*, the oily residue was distilled to give R(−)-IV; bp 45—47°C/0.01 mmHg, $[\alpha]_D^{24.5}$ −36.2 (*c* 8.98, ethanol), 7.5 g.

Found: C, 75.68; H, 7.67; N, 8.27%. Calcd for $C_{11}H_{13}ON$: C, 75.40; H, 7.48; N, 7.99%.

The NMR spectrum had signals at 1.59 (singlet, $-\overset{|}{C}-CH_3$); 1.94 (triplet, J=0.4 Hz, $-COCH_3$); 3.75 (quartet, J=0.4 Hz, $-CH_2-$); 7.25 (multiplet, aromatic protons).*1

S(+)-Ethyl 2-Formylamino-2-phenylpropionate (V). The procedure described by Tsuboyama[6] was used with slight modifications. To a solution of S(+)-I (39.6 g, $[\alpha]_D^{22}$ +26,6 (*c* 9.70, ethanol), 90.3% optically pure) in 88% formic acid (720 g), acetic anhydride (244 g) was added with stirring at 95°C. The reaction mixture was then allowed to stand at this temperature for 30 min. The excess of the reagents was removed *in vacuo*, and then water (500 ml) was added to the oily residue. The resulting precipitates were filtered and then recrystallized from benzene-*n*-hexane to give S(+)-V; mp 94—95°C, $[\alpha]_D^{23}$ +19.50 (*c* 5.18, ethanol), 25.3 g.

Found: C, 65.20; H, 6.88; N, 6.25%. Calcd for $C_{13}H_{15}O_3N$: C, 65.14; H, 6.83; N, 6.33%.

The filtrate was treated with aqueous ammonia. S(+)-I (17.5 g, $[\alpha]_D^{20.5}$ +26.4 (*c* 9.88, ethanol)) was thus recovered.

For the check of the optical purity, S(+)-V (1.1 g, $[\alpha]_D^{23}$ +19.50 (*c* 5.18, ethanol)) was heated with hydrochloric acid in ethanol for 3 hr. S(+)-I was then isolated in the usual manner; $[\alpha]_D^{20.5}$ +27.8 (*c* 9.25, ethanol), 91.0% optically pure.

S(+)-2-Methylamino-2-phenylpropanol (VI). S(+)-V (24.2 g, $[\alpha]_D^{23}$ +19.50 (*c* 5.18, ethanol), 91.0% optically pure) in tetrahydrofuran (100 ml) was added to lithium aluminum hydride (8.0 g) in tetrahydrofuran (100 ml); the reaction mixture was then heated under reflux for 64 hr. After cooling, water (30 ml) was added with vigorous stirring; the organic layer was then decanted from the precipitates. The resulting precipitates were dissolved with aqueous sodium hydroxide, and the aqueous solution was extracted with ether. The combined extracts were dried over anhydrous sodium sulfate. After the evaporation of the solvents, the oily residue was distilled under a nitrogen stream to give S(+)-VI: bp 94—102°C/0.4 mmHg, $[\alpha]_D^{22.5}$ +21.2 (*c* 4.58, benzene), 16.0 g.

Found: C, 73.00; H, 9.15; N, 8.44%. Calcd for $C_{10}H_{15}ON$: C, 72.69; H, 9.15; N, 8.48%.

S(+)-1,2-Dimethyl-2-phenylaziridine (VII). S(+)-VII was obtained from S(+)-VI by a method similar to that used for the preparation of III.[1] S(+)-VI (16.0 g, $[\alpha]_D^{22.5}$ +21.2 (*c* 4.58, benzene), 91.0% optically pure) afforded S(+)-VII: bp 88—91°C/14 mmHg, $[\alpha]_D^{22}$ +45.0 (*c* 8.95, ethanol), 9.3 g.

Found: N, 9.41%. Calcd for $C_{10}H_{13}N$: N, 9.82%.

R(+)-*N*-2-Phenylpropylformamide (IX). R(+)-IX was prepared by a method similar to that used for the preparation of V. R(+)-VIII (4.0 g, $[\alpha]_D^{19.0}$ +9.84 (*c* 9.71, ethanol), 33.4% optically pure) gave R(+)-IX; bp 130—132°C/0.6 mmHg. $[\alpha]_D^{18.4}$ +8.26 (*c* 10.04, ethanol), 2.2 g.

Found: N, 8.37%. Calcd for $C_{10}H_{13}ON$: N, 8.58%.

R(+)-*N*-Methyl-2-phenylpropylamine (X). R(+)-X was obtained from R(+)-IX by refluxing it with lithium aluminum hydride in ether for 24 hr. R(+)-IX (2.0 g, $[\alpha]_D^{18.4}$ +8.26 (*c* 10.04, ethanol), 33.4% optically pure) afforded R(+)-X; bp 100—103°C/15 mmHg, $[\alpha]_D^{22}$ +8.45 (*c* 9.45, ethanol), 0.3 g (this substance was purified by preparative gas chromatography (10% PEG-10% KOH on fire-brick, 180°C, using helium-carrier gas), for two impurities were present in the crude product).

Found: N, 9.17%. Calcd for $C_{10}H_{15}N$: N, 9.39%.

S(−)-*N*-2-Phenylpropylacetoamide (XI). Acetic anhydride (3.50 g) was added at 0°C to a well-stirred suspension of S(−)-VIII (2.70 g, $[\alpha]_D^{20}$ −8.65 (*c* 9.37, ethanol), 29.3% optically pure) and sodium carbonate (4.2 g) in water (30 ml). The reaction mixture was then stirred for 1 hr at this temperature. The resulting suspension was extracted with ether. The etheral solution was washed with dilute hydrochloric acid, water, and saturated sodium bicarbonate, and was dried over anhydrous sodium sulfate. The evaporation of the ether and the subsequent distillation afforded S(−)-XI: bp 130—132°C/0.6 mmHg, $[\alpha]_D^{19.5}$ −13.83 (*c* 9.55, ethanol), 2.4 g.

Found: N, 7.81%. Calcd for $C_{11}H_{15}ON$: N, 7.90%.

The authors wish to thank Dr. Kaoru Hanaya of Yamagata University for his NMR spectra measurements.

*1 The NMR spectra were determined with a Hitachi model H-6013 spectrometer for the carbon tetrachloride solution, using tetramethylsilane as the internal standard. The chemical shifts are expressed in δ-values.

6) S. Tsuboyama, This Bulletin, **35**, 1004 (1962).

BULLETIN OF THE CHEMICAL SOCIETY OF JAPAN VOL. 43 566—567 (1970)

Asymmetric Hydrogenation of C=O Double Bond with Modified Raney Nickel. XIII.*1 Modification with Peptides

Yoshiharu IZUMI, Susumu TATSUMI,*2 Masami IMAIDA*3 and Kazuo OKUBO

Division of Organic Chemistry, Institute for Protein Research, Osaka University, Kita-ku, Osaka

(Received August 14, 1969)

Previous papers of this series have reported that Raney nickel catalysts (R-Ni) modified with optically-active α-amino acids or α-hydroxy acids asymmetrically catalyze the hydrogenation of methyl acetoacetate to methyl 3-hydroxybutyrate. The relationship between the asymmetric hydrogenation activity of a modified R-Ni catalyst and the structure of its modifying reagent has also been studied in previous papers.[1)]

On the other hand, the silk-palladium asymmetric catalyst prepared as an enzyme model was studied prior to the modified R-Ni catalyst by one of the present authors.[2)] Investigations of R-Ni catalysts modified with peptides have a great importance in elucidating the mechanisms for the substrate specificity of the enzyme action and for the asymmetric hydrogenation of a silk-palladium catalyst. However, no modifications with peptides have been attempted. The influence of the peptide structure used as a modifying reagent on the asymmetric activity of the catalyst was studied, with focussed attention on several leucyl-peptides in the present work. In additionl the asymmetric activity of the catalyst modified with glycyl-L-aspartic acid was tested. The results of the present work are listed in Table 1.

TABLE 1. THE OPTICAL ROTATION OF THE PRODUCTS ON THE MODIFICATIONS WITH DIPEPTIDES

Modifying reagent	Modifying conditions		$[\alpha]_D^{20}$ of methyl 3-hydroxybutyrate
	pH	Temp. °C	
L-Leucine	7.32	0	−1.10*
L-Leucyl-glycine	5.72	0	+1.12
	5.80	40	+1.03
	5.75	70	+0.92
Glycyl-L-leucine	5.70	0	−0.41
	5.55	40	−0.37
	5.50	70	−0.65
L-Leucyl-L-leucine	5.85	0	−0.42
	5.70	40	−0.50
	—	70	−0.46
L-Leucyl-D-leucine	5.80	0	+1.20
	5.80	40	+0.75
	5.80	70	+0.60
L-Aspartic acid	4.65	0	−1.10[3)]
Glycyl-L-aspartic acid	—	0	−1.47
	—	100	−1.09

* Y. Izumi, M. Imaida, H. Fukawa and S. Akabori, This Bulletin, **36**, 155 (1963).

L-Leucyl-glycine (L-Leu-Gly) gives the catalyst a higher asymmetric yield*4 than glycyl-L-leucine (Gly-L-Leu) and the reverse asymmetric direction to Gly-L-Leu or L-leucine as a asymmetric modifying reagent. The asymmetric direction of the catalyst modified with Gly-L-Leu is the same as that with L-leucine, and the asymmetric yield of the former

*1 The previous title of the papers of this series, I-X, was "Asymmetric Hydrogenation with Modified Raney Nickel."

*2 Ajinomoto, Co., Ltd., Takaramachi, Chuo-ku, Tokyo.

*3 Osaka Prefectural Institute of Public Health, Morimachi, Higashinari-ku, Osaka.

1) H. Fukawa, Y. Izumi, S. Komatsu and S. Akabori, This Bulletin, **35**, 1703 (1962); Y. Izumi, M. Imaida, H. Fukawa and S. Akabori, *ibid.*, **36**, 21 (1963); Y. Izumi, M. Imaida, H. Fukawa and S. Akabori, *ibid.*, **36**, 155 (1963); S. Tatsumi, M. Imaida, Y. Fukuda, Y. Izumi and S. Akabori, *ibid.*, **37**, 846 (1964); Y. Izumi, S. Akabori, H. Fukawa, S. Tatsumi, M. Imaida, Y. Fukuda and S. Komatsu, Proc. of the 3rd Int. Cong. on Catalysis, Vol. 2, 1364 (1964); Y. Izumi, S. Tatsumi, M. Imaida, Y. Fukuda and S. Akabori, This Bulletin, **38**, 1206 (1965); Y. Izumi, S. Tatsumi, M. Imaida, Y. Fukuda and S. Akabori, *ibid.*, **39**, 361 (1966); Y. Izumi, S. Tatsumi and M. Imaida, *ibid.*, **39**, 2223 (1966); S. Tatsumi, *ibid.*, **41**, 409 (1968); Y. Izumi, T. Tanabe and S. Yajima, *ibid.*, **41**, 941 (1968); Y. Izumi, K. Matsunaga, S. Tatsumi and M. Imaida, *ibid.*, **41**, 2515 (1968); Y. Izumi, M. Imaida, T. Harada, T. Tanabe, S. Yajima and T. Ninomiya, *ibid.*, **42**, 241 (1969); Y. Izumi, S. Tatsumi and M. Imaida, *ibid.*, **42**, 2373 (1969).

2) S. Akabori, Y. Izumi, Y. Fujii and S. Sakurai, *Nature*, **178**, 323 (1956); S. Akabori, Y. Izumi, Y. Fujii and S. Sakurai, *Nippon Kagaku Zasshi*, **77**, 1374 (1956); **78**, 168 (1957).

*4 The "asymmetric activity" of a catalyst involves two factors. One is the direction of the asymmetric activity, which is expressed as the direction of the specific rotation, (+) or (−), of the hydrogenated product. The other is the degree of asymmetric activity, which is usually presented as the asymmetric yield.

is considerably weaker than that of the latter. It can be expected from the results that the peptide bond existing at the carboxy group of amino acid residue reverses the effect of the asymmetric center of the amino acid itself on the asymmetric direction of the catalyst, and that the peptide bond existing at the amino group of amino acid reduces the effect of the asymmetric center of amino acid on the asymmetric yield of the catalyst.

Since glycine has no asymmetric center, the deviation of the asymmetric activity of the catalyst modified with L-Leu-Gly or Gly-L-Leu from that with L-leucine is considered to occur mainly as a result of the peptide structure.

If the simple additional regulality in the structure of the peptide can be found in the asymmetric activity of the catalyst, it should be possible to calculate the asymmetric activity of the catalyst modified with L-leucyl-L-leucine (L-Leu-L-Leu) or L-leucyl-D-leucine (L-Leu-D-Leu) from those with L-Leu-Gly and Gly-L-Leu. The asymmetric activities of the catalysts modified with L-Leu-L-Leu and L-Leu-D-Leu at 0°C are calculated as follows, respectively;

$$(+1.12) + (-0.41) = +0.71$$

and

$$(+1.12) - (-0.41) = +1.53$$

However, our results, shown in Table 1, are quite far from the above expectations.

Within the limited number of experiments of the present work, the effect of the structure of the peptides as the asymmetric modifying reagent are not simple; there are two possible reasons, either there are two types of adsorption states of peptide on the catalyst surface, as is shown in Fig. 1, or the effect of the structure of the leucine residue is different from that of the glycine residue in the peptide structure as a modifying reagent.

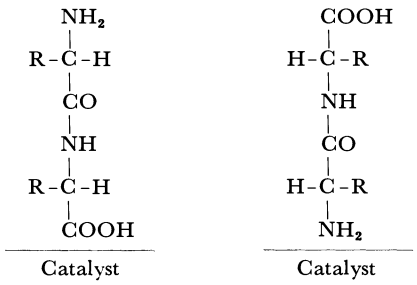

Fig. 1. Adsorption formulas of dipeptide on the catalyst surface.

Although the relationship between the structure of the dipeptide used as a modifying reagent and the asymmetric activity of the catalyst seems to be rather complicated, the following experimental regularity can be presented as the conclusion of the present work. The asymmetric direction of the catalyst modified with dipeptide is ruled by asymmetric center in C-terminal amino acid and has the same sign as the asymmetric direction of the catalyst modified with C-terminal amino acid itself. The glycine residue at the C-terminal reverses the effect of the asymmetric center of N-terminal amino acid itself on the asymmetric direction of the catalyst.

BULLETIN OF THE CHEMICAL SOCIETY OF JAPAN VOL. 43 567—569 (1970)

Initiation of Vinyl Polymerization with Tertiary Amines/Alkylating Agents

Takayuki OTSU and Yasuhiko TAKEMURA

Department of Applied Chemistry, Faculty of Engineering, Osaka City University, Sugimoto-cho, Sumiyoshi-ku, Osaka

(Received August 18, 1969)

It has been reported that the binary system of such tertiary amines as dimethylaniline and such organic halides as benzyl chloride initiates the radical polymerization of methyl methacrylate.[1,2] In this case, a quaternary salt is formed, and then it decomposes at the N^+–C bond into radicals which react with the monomer to initiate the polymerization.[1,3]

On the other hand, several workers[4–6] have found that vinyl pyridine is polymerized in the presence of some alkylating agents, such as methyl iodide and dimethyl sulfate, through a quaternary pyridinium salt. The present paper will describe

1) T. Fueno, H. Okamoto, T. Tsuruta and J. Furukawa, *J. Polym. Sci.*, **36**, 407 (1959).

2) T. Otsu, S. Aoki and K. Itakura, *ibid.*, *Part A-1*, in press.

3) T. Otsu, T. Sato and M. Ko, *ibid.*, in press.

4) V. A. Kabanov, K. V. Aliev and V. A. Kargin, *Vysokomol. Soedin.*, **A**, **10**, 1618 (1968).

5) S. Iwatsuki, T. Kokubo, K. Motomura and Y. Yamashita, *Makromol. Chem.*, **120**, 154 (1968).

6) T. Otsu, M. Ko and T. Sato, *J. Polym. Sci., Part A-1*, in press.

Table 1. Polymerizations of some vinyl monomers with DMA/alkylating agents at 60°C: [DMA]=0.2 mol/l, [DMS]=0.2 mol/l, [MTS]=0.2 mol/l, [Monomer]/[Solvent]=6/4 in volume

Alkylating Agent	Solvent	MMA		St		VAc	
		Time hr	Yield %	Time hr	Yield %	Time hr	Yield %
DMS	C_6H_6	7	0.9	30	2.1	—	—
DMS	C_2H_5OH	7	12.8	30	1.6	20	0.4
MTS	C_6H_6	7	5.0	30	3.7	—	—
MTS	C_2H_5OH	7	11.5	30	6.1	20	3.0

the results of the polymerization of vinyl monomers with the binary system and the quaternary salt of several dialkylanilines, especially dimethylaniline (DMA), and dimethyl sulfate (DMS) or methyl *p*-toluenesulfonate (MTS).

Experimental

The tertiary amines and vinyl monomers were purified in the usual manner from the reagent-grade materials. The commercial DMS and MTS were distilled prior to use.

The quaternary salts of DMA with DMS and MTS were prepared by reacting an equimolar mixture of the two materials in water, followed by recrystallization from water: mp 126 and 167—168°C respectively.

Polymerizations were carried out in a sealed tube in the absence of light with shaking at 60°C.

Results and Discussion

Table 1 shows the results of the polymerizations of methyl methacrylate (MMA), styrene (St), and vinyl acetate (VAc) with the binary initiator system of DMA and DMS or MTS at 60°C.

From Table 1, these binary systems may be seen to have been effective as the initiator of the MMA polymerization in the presence of ethanol, but they showed rather weak activity for the St and VAc ploymerizations. A similar tendency was found in the polymerization with the DMA-benzyl chloride system.[1] From Table 1, these binary systems may be seen to show a lower activity in benzene than in ethanol, for the quaternary salts, which were formed concurrently, were insoluble in benzene and were precipitated in the polymerizing mixture.

Table 2. Polymerization of MMA with quaternary salts of DMA-DMS and of DMS-TMS at 60°C for 22 hr

Quaternary salts	Solvent	Yield %
DMA-DMS	none	1.1
DMA-DMS	C_2H_5OH**	2.3
DMA-MTS	none	1.5
DMA-MTS	C_2H_5OH**	2.1

* The concentration was kept at 2×10^{-2} mol/l.
** MMA (5 ml) and C_2H_5OH (5 ml) were used.

However, the quaternary salts of DMA with DMS and MTS showed very weak activity for the MMA polymerization in ethanol, as is shown in Table 2. This result might indicate that the initiating radical was produced from the unstable intermediate formed through the quaternary reaction.

Table 3 shows the effects of the tertiary amines on the MMA polymerization with these binary initiator systems. From this table, it can be seen

Table 3. Polymerization of MMA with a system of various amines and alkylating agents at 60°C*

Alkylating agent	Amine	Time hr	Yield %
DMS	$C_6H_5N(CH_3)_2$	5.0	15.1
MTS	$C_6H_5N(CH_3)_2$	5.0	13.3
DMS	$C_6H_5N(CH_3)(CH_2C_6H_5)$	5.0	6.9
MTS	$C_6H_5N(CH_3)(CH_2C_6H_5)$	5.0	5.9
DMS	$C_6H_5N(CH_2C_6H_5)_2$	5.0	4.2
MTS	$C_6H_5N(CH_2C_6H_5)_2$	5.0	3.8
DMS	$C_6H_5CH_2N(CH_3)_2$	8.3	2.6
MTS	$C_6H_5CH_2N(CH_3)_2$	8.3	1.1

* Polymerization conditions:
[Amine]=[Alkylating agent]=0.2 mol/l
[MMA]=[C_2H_5OH]=5 ml.

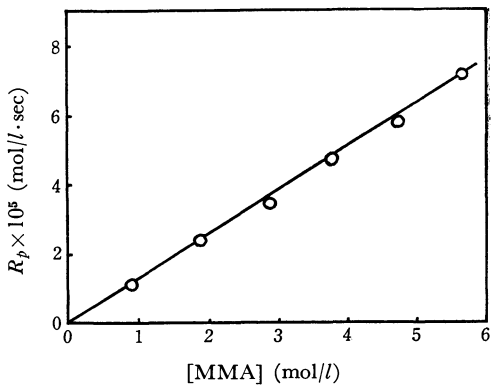

Fig. 1. Relationship between R_p and [MMA] in the polymerization of MMA with DMA/DMS at 60°C: [DMA]=[DMS]=0.2 mol/l, [C_2H_5OH]=6.87 mol/l in benzene.

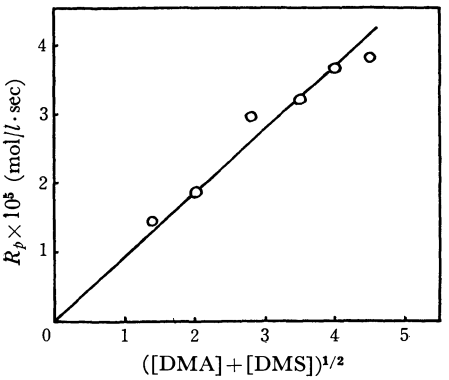

Fig. 2. Relationship between R_p and initiator concentration in the polymerization of MMA with DMA/DMS at 60°C: [MMA]=4.7 mol/l, [C_2H_5OH]=8.58 mol/l in benzene.

that, when the methyl group in DMA was replaced with the benzyl group, the initiator activity of the binary system decreased. The aliphatic tertiary amine, benzyldimethylamine, formed a very weak initiator system with DMS and MTS. This result was the same as that reported in a previous paper.[6]

The polymerization of MMA with an equimolar mixture of DMA and DMS was then investigated kinetically at 60°C. The effects of the monomer and the total initiator concentrations on the rate of polymerization (R_p) are shown in Figs. 1 and 2. From these figures, the following rate equation was obtained:

$$R_p = k([\text{DMA}] + [\text{DMA}])^{1/2}[\text{MMA}]$$

A similar rate equation was observed with the binary system of DMA and MTS at 60°C. It was also found that the copolymers obtained from the copolymerization of an equimolar mixture of MMA and St with DMA-DMS and DMA-TMS contained 49.7 and 47.7 mol% of the St unit respectively; this finding agrees with those reported with azobisisobutyronitrile as the initiator. These findings might suggest that the polymerization proceeded *via* a radical mechanism.

BULLETIN OF THE CHEMICAL SOCIETY OF JAPAN VOL. 43 569—572 (1970)

Kinetics of the Reaction of α-Bromonaphthalene with Carbon Monoxide Catalyzed by Nickel Carbonyl

Mikitake NAKAYAMA and Tsutomu MIZOROKI*1

Government Chemical Industrial Research Institute, Tokyo, Mita, Meguro-ku, Tokyo

(Received August 27, 1969)

In a previous paper,[1] it has been reported that the reaction rate of an aryl halide with carbon monoxide catalyzed by nickel tetracarbonyl to form the corresponding aromatic carboxylic acid is much increased by adding a sufficient amount of potassium acetate; its kinetics showed that the course of the reaction could be represented by the scheme similar to that of an oxo reaction when nickel tetracarbonyl was regenerated rapidly under high temperatures and pressures. On the other hand, nickel carbonyl complexes are more reactive than cobalt carbonyl complexes, and their stoichiometrical reactions with aryl iodides take place under a *ca.* 1 atmosphere of nitrogen and at low temperatures (<100°C), resulting in the formation of aromatic carboxylic compounds.[2] Accordingly, their catalytic carbonylation reactions must take place under milder reaction conditions as long as nickel carbonyls are regenerated smoothly from carbon monoxide. This work was undertaken in order to study the carbonylation reaction of α-bromonaphthalene under milder conditions and to discuss its kinetics.

Experimental

α-Bromonaphthalene obtained from commercial sources was purified by distillation under a vacuum. The other materials used were the same as those in the previous work.[1] The reaction was carried out under a constant temperature and at a constant pressure for a given period by using the same apparatus as that described in the previous paper.[1] The absorption rate of carbon monoxide was also determined. The autoclave used was made of titanium-molybdenum alloy (300 m*l* in vol).

The products were taken out of the autoclave by using sufficient amounts of diethyl ether and water. An aqueous sodium bicarbonate solution was added to the ether phase to separate α-naphthoic acid form α-naphthol and the other organic compunds. α-Naphthoic acid was then precipitated again by adding

*1 Present address: Research Laboratory of Resources Utilization, Tokyo Institute of Technology, Ookayama, Meguro-ku, Tokyo.

1) M. Nakayama and T. Mizoroki, This Bulletin, **42**, 1124 (1969).

2) N. L. Bauld, *Tetrahedron Lett.*, **1963**, 1840.

a sufficient amount of an aqueous hydrochloric acid solution to the sodium α-naphthoate solution. The α-naphthoic acid had been washed well with cold water before its amount was determined by titration with an aqueous potassium hydroxide solution. The amounts of nickel(II) ion and bromide ion were determined according to the EDTA method and the Volhard method respectively.

Results

The absorption rate of carbon monoxide in the reaction of α-bromonaphthalene (0.30—0.55 mol) with carbon monoxide in the presence of water (1.60—4.00 mol), potassium acetate (0.75 mol), and nickel(II) acetate (0.0040 mol) under 100 kg/cm² at 200°C is plotted in Fig. 1. The figure shows that the absorption rate depends neither on the amount of α-bromonaphthalene nor on that of water. The effects of the amounts of nickel(II) acetate and potassium acetate on the absorption rate are shown in Figs. 2 and 3. The rate increases nearly proportionally with the increase in the amount of nickel(II) acetate, which is converted almost quantitatively into nickel tetracarbonyl under these reaction conditions, and also with the increase in potassium acetate. The effect of the

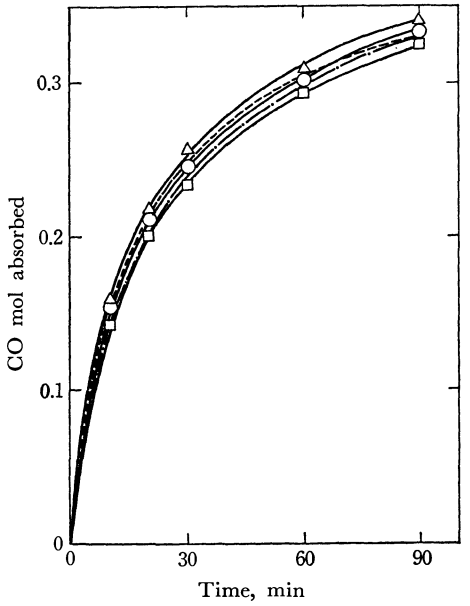

Fig. 1. Effect of the amounts of α-bromonaphthalene and water on absorption rate of carbon monoxide.
Reaction conditions: Temperature 200°C, Pressure 100 kg/cm², $Ni(AcO)_2 \cdot 4H_2O$ 0.004 mol, AcOK 0.75 mol.

	α-$C_{10}H_7Br$	H_2O	Exp. No.
—□—	0.55 mol	2.40 mol	22
—○—	0.40	2.40	7
—△—	0.30	2.40	23
- - -○- - -	0.40	4.00	9
—·-○-·—	0.40	1.60	10

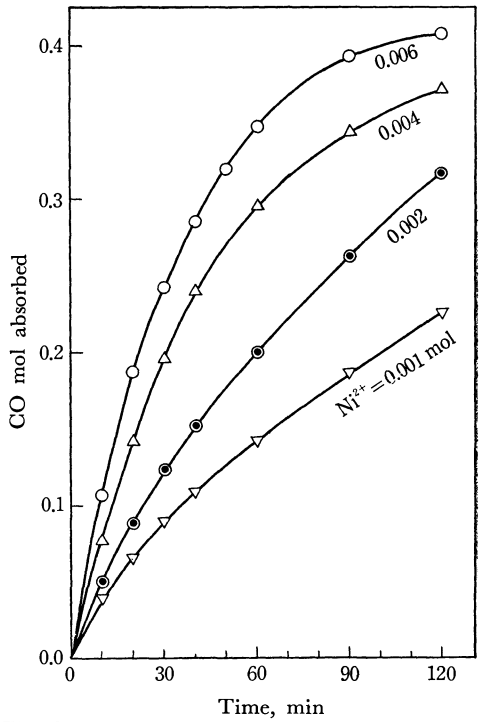

Fig. 2. Effect of the amount of nickel(II) acetate on absorption rate of carbon monoxide.
Reaction conditions: Temperature 200°C, Pressure 100 kg/cm², α-$C_{10}H_7Br$ 0.40 mol, H_2O 2.40 mol, AcOK 0.75 mol

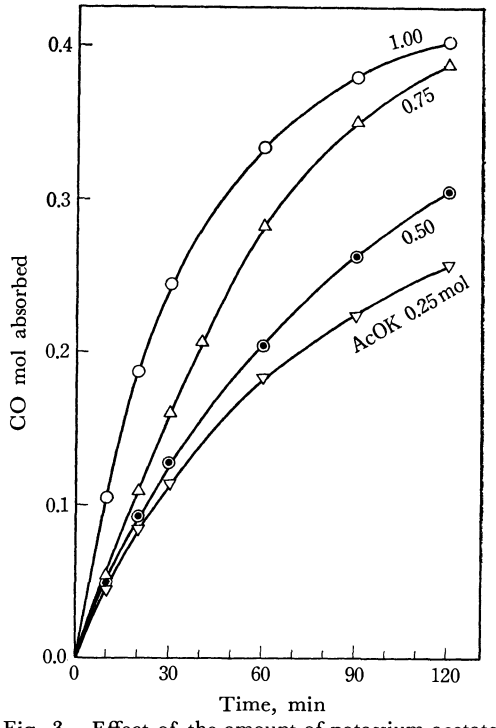

Fig. 3. Effect of the amount of potassium acetate on absorption rate of carbon monoxide.
Reaction conditions: Temperature 200°C, Pressure 100 kg/cm², α-$C_{10}H_7Br$ 0.40 mol, H_2O 2.40 mol, $Ni(AcO)_2 \cdot 4H_2O$ 0.004 mol

Table 1. Experimental results under various conditions
(Standard reaction conditions: α-$C_{10}H_7Br$ 0.40 mol, H_2O 2.40 mol, Ni^{2+} 0.004 mol, AcOK 0.75 mol; temp. 200°C, press. 100 kg/cm², time 90 min)

Exp. No.	Variable		Initial absorp. rate of CO mol/hr	Conversion[a] %	Selectivity %	$Ni(CO)_4$[b] %
22	α-$C_{10}H_7Br$	0.55 mol	0.29	73.3	93.6	16.7
7		0.40	0.31	89.8	98.8	63.2
23		0.30	0.30	84.8	97.9	77.6
9	H_2O	4.00	0.29	82.8	96.0	21.2
7		2.40	0.31	89.8	98.8	63.2
10		1.60	0.29	81.4	97.6	50.7
11	Ni^{2+}	0.006	0.35	103	100	81.7
7		0.004	0.31	89.8	98.8	63.2
12		0.002	0.20	69.5	99.2	56.3
13		0.001	0.14	42.8	97.0	85.6
8	AcOK	1.00	0.33	92.0	98.3	80.8
7		0.75	0.31	89.8	98.8	63.2
5		0.50	0.21	76.0	98.1	45.1
6		0.25	0.18	61.0	98.4	23.5
14	p_{CO}	60 kg/cm²	0.26	65.7	98.8	7.6
15		80	0.31	98.8	99.3	26.3
7		100	0.31	89.8	98.8	63.2
16		120	0.34	95.3	99.2	67.2
17		140	0.31	82.8	98.0	87.1
18		160	0.25	88.9	99.2	82.5
19		200	0.22	56.0	89.5	95.6

a) Obtained from the amount of Br^- formed.
b) Obtained from the amount of Ni(II) ion present in the product.

pressure of carbon monoxide is represented in Table 1, where the other results already shown in Figs. 1, 2, and 3 are also summarized. The absorption rate is almost independent of the pressure of carbon monoxide over the range from 80 to 150 kg/cm². Its decrease under pressures lower than 60 kg/cm² is caused by the fact that these pressures are not high enough to convert nickel(II) acetate into nickel tetracarbonyl quantitatively; the decrease under pressures higher than 200 kg/cm² is probably because these high pressures of carbon monoxide prevent α-bromonaphthalene from coordination to nickel tetracarbonyl, as was discussed in the previous paper.

In summary, the reaction rate of α-bromonaphthalene with carbon monoxide to form α-naphthoic acid increases with an increase in the amounts of nickel tetracarbonyl or potassium acetate, while it depends on neither the amount of α-bromonaphthalene nor on that of water, nor on the partial pressure of carbon monoxide.

Discussion

The course of the reaction with α-bromonaphthalene can be explained by the scheme proposed for the reaction with bromobenzene:[1]

$$\text{Ary-Br} + Ni(CO)_4 \rightleftarrows (\text{Ary-Br})Ni(CO)_3 + CO \quad (1)$$

$$(\text{Ary-Br})Ni(CO)_3 + H_2O \rightarrow \text{Ary-COOH} + (HBr)Ni(CO)_2 \quad (2)$$

$$(HBr)Ni(CO)_2 + \text{AcOK} \rightarrow Ni(CO)_2 + \text{AcOH} + \text{KBr} \quad (3)$$

$$Ni(CO)_2 + 2CO \rightarrow Ni(CO)_4 \quad (4)$$

(Ary-Br=aryl bromide)

Under pressures of carbon monoxide high enough to regenerate nickel tetracarbonyl quickly, Eq. (2) became the rate-determining step of the carbonylation of bromobenzene and its kinetics could be expressed by Eq. (5), where k and K are the rate constant of Eq. (2) and the equilibrium constant of Eq. (1) respectively. Preliminary experiments showed that the carbonylation rate of α-bromonaphthalene could also be expressed by the same equation under pressures higher than 200 kg/cm², while its kinetics under lower pressures of cabon monoxide is very different from Eq. (5) and is, rather, given by Eq. (6):

$$r = \frac{d[C_6H_5COOH]}{dt} = k \cdot K \frac{[Ni(CO)_4][C_6H_5Br][H_2O]}{p_{CO}} \quad (5)$$

$$r = d[\alpha\text{-}C_{10}H_7COOH]/dt \propto [Ni(CO)_4][AcOK] \quad (6)$$

This finding can, however, be understood on the basis of the scheme described above. Lower pressures of carbon monoxide should be favorable for the equilibrium of Eq. (1) to incline much toward the right, and the rate of Eq. (2) must be large enough because α-bromonaphthalene is usually more reactive than bromobenzene, as has been reported in the cases of other organic reactions. The rate of the carbonylation is, accordingly, determined by that of regeneration of nickel tetracarbonyl by Eqs. (3) and (4); we thus find that the rate of the carbonylation is independent of the amounts of α-bromonaphthalene and water. The fact that the rate of carbonylation is also independent of the partial pressure of carbon monoxide, as described in Table 1, suggests that the rate of Eq. (4) is much faster than Eq. (3) and that the true nickel catalyst is nickel tricarbonyl rather than nickel tetracarbonyl.

BULLETIN OF THE CHEMICAL SOCIETY OF JAPAN VOL. 43 572—573 (1970)

ESR Spectra of Irradiated Nitroethane and Polynitroethylene

Kozo TSUJI,*1 Koichiro HAYASHI*2 and Seizo OKAMURA

Department of Polymer Chemistry, Faculty of Engineering, Kyoto University, Sakyo-ku, Kyoto

(Received September 9, 1969)

In a previous paper[1] we have reported that the NO_2·, $CH_2{=}\dot{C}NO_2$, nitroethylene anion radical and some other species showing a very broad ESR spectrum were observed after the γ irradiation of nitroethylene at −196°C. It has also been reported[2] that the ESR spectra of NO_2· and ·CH_3 were observed when nitromethane was irradiated with γ rays at −196°C and that ·CH_2NO_2 was produced after warming the sample to −143°C. Nitrogen dioxide-free radicals seem to be obtained after the radiolysis of every organic compound containing NO_2 groups, while counter radicals are not always detected by ESR spectroscopy.

In this investigation, nitroethane and polynitroethylene were irradiated with electron beams from a Van de Graaff accelerator and the ESR spectra were recorded in order to identify the free radicals produced from these compounds. The change in the ESR spectra with the increase in the temperature was also examined.

Experimental

Polynitroethylene was obtained by radiation-induced polymerization.[3] For nitroethane, we used a commercial sample from the Nakarai Chemical Co., Ltd., without further purification. The experimental techniques have already been described.[1]

Results and Discussion

Nitroethane gave the ESR spectrum shown in Fig. 1a after irradiation at −196°C. This spectrum did not change with the subsequent visible light irradiation. The asymmetric spectrum characteristic of the NO_2· radical can easily be distinguished. Some shoulders of the spectrum may indicate the presence of ethyl radicals.[4] The hyperfine coupling constants and g values of the NO_2· radical are tabulated in Table 1. These values are almost identical with those previously reported.[2,5-9] NO_2· radicals decayed out at about

TABLE 1. HYPERFINE COUPLING CONSTANTS AND g VALUES OF NO_2· RADICALS PRODUCED IN IRRADIATED NITROETHANE AND POLYNITROETHYLENE

Nitroethane	A_x=53.9	g_x=2.006
	A_y=64.6	g_y=2.004
	A_z=43.2	g_z=1.992
	A_{iso}=53.9	g_{av}=2.001
Polynitroethylene	A_x=53.0	g_x=2.006
	A_y=64.6	g_y=2.004
	A_z=44.6	g_z=1.992
	A_{iso}=54.1	g_{av}=2.001

*1 Present address: Central Research Laboratory, Sumitomo Chemical Co., Ltd., Takatsuki, Osaka

*2 Present address: Faculty of Engineering, Hokkaido University, Sapporo

1) K. Tsuji, H. Yoshida, K. Hayashi and S. Okamura, *Kobunshi Kagaku*, **25**, 31 (1968).

2) C. Chachaty, *J. Chim. Phys.*, **62**, 729 (1965).

3) H. Yamaoka, K. Hayashi and S. Okamura, *Trans. Faraday Soc.*, **63**, 376 (1967).

4) R. Fessenden and R. H. Schuler, *J. Chem. Phys.*, **39**, 2147 (1963).

5) P. W. Atkins and M. C. R. Symons, *J. Chem. Soc.*, **1962**, 4794.

6) W. C. Mosley and W. G. Moulton, *J. Chem. Phys.*, **43**, 1207 (1965).

7) J. Tateno and K. Gesi, *ibid.*, **40**, 1317 (1964).

8) H. Zeldes and R. Livingston, *ibid.*, **35**, 563 (1961).

9) R. M. Golding and M. Henchman, *ibid.*, **40**, 1554 (1964).

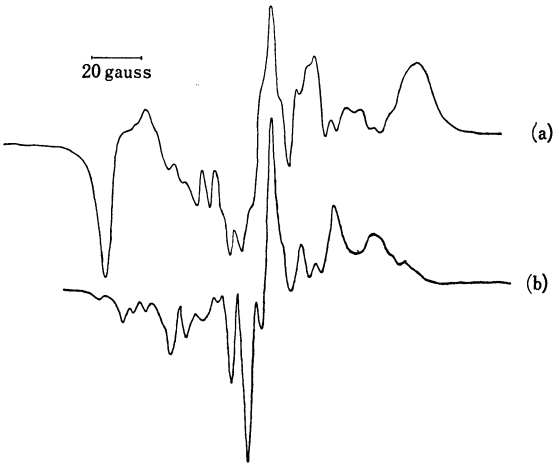

Fig. 1. ESR Spectra of irradiated nitroethane.
a) immediately after irradiation at −196°C 5×10^5 rad $G=100$
b) at −123°C $G=200$

−123°C, and there remained the spectrum shown in Fig. 1b, which may be identified as due to the $CH_3\dot{C}HNO_2$ radical. The coupling constant of the four protons is about 25 gauss, and that of nitrogen is about 7 gauss. These values should be compared with the corresponding values $a_H=20\pm1$ gauss and $a_H=6\pm1$ gauss, for the $\cdot CH_2NO_2$ radical.[2] $CH_3\dot{C}HNO_2$ radicals seem to be produced through hydrogen abstraction by ethyl radicals, since the ESR spectrum due to the $CH_3\dot{C}HNO_2$ radical, which was not observed at −196°C, appeared after the ethyl radicals had decayed out. The same mechanism has been suggested for $\cdot CH_2NO_2$ formation.[2] The spectrum due to $CH_3\dot{C}HNO_2$ radicals decayed out at about −103°C.

From irradiated polynitroethylene, the ESR spectrum shown in Fig. 2a was obtained at −196°C. A spectrum due to the $NO_2\cdot$ radical was clearly observed. The hyperfine coupling constants and g values are shown in Table 1. The $NO_2\cdot$ radical in polynitroethylene was relatively stable at −78°C, but it decayed out after treatment at 0°C for

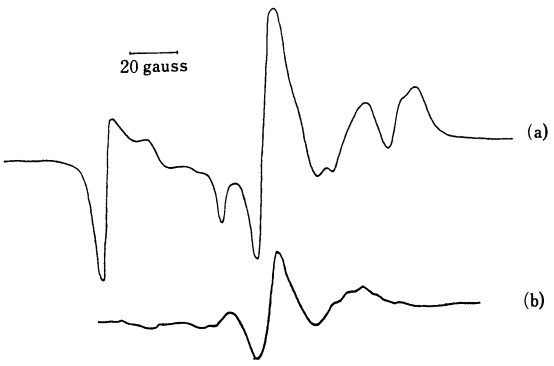

Fig. 2. ESR spectra of irradiated polynitroethylene at −196°C.
a) immediately after irradiation 5×10^5 rad $G=100$
b) after treatment at 0°C for 30 min. $G=630$

30 min. There remained the ESR spectrum shown in Fig. 2(b), which seems to be a slightly asymmetric, five-line spectrum, and this spectrum tentatively attributed to free radicals, $-CH_2-\dot{C}(NO_2)-CH_2-$. For this sample, however, no definite indication of the presence of the $-CH_2-\dot{C}H-CH_2-$ radicals was obtained at −196°C. Therefore, hydrogen abstraction by the $-CH_2-\dot{C}H-CH_2-$ radical at −196°C may possibly cause the formation of $-CH_2-\dot{C}(NO_2)-CH_2-$ radicals. The observation of some shoulders which can be attributed to the later free radicals supports this mechanism.

The authors would like to express their thanks to Professor I. Sakurada for providing us with the opportunity to carry out this investigation at the Osaka Laboratories of the Japanese Association for Radiation Research on Polymers, which is now known as the Osaka Laboratories for Radiation Chemistry, Japan Atomic Energy Research Institute, and to Mr. H. Yamaoka for his kindness in giving us polynitroethylene.

SHORT COMMUNICATIONS

Complete Resolution of the Racemic Trisethylenediaminecobalt(III) Complex into Its Optical Antipodes by Means of Electrophoresis

Hayami YONEDA and Takao MIURA

Department of Chemistry, Wakayama University, Masago-cho, Wakayama

(Received December 4, 1969)

The racemic $[Co\ en_3]^{3+}$ complex can be resolved into its optical antipodes by way of the diastereomers, *d*-$[Co\ en_3]Cl(d\text{-tartrate})\cdot 5H_2O$, separated as crystals, and *l*-$[Co\ en_3]Cl(d\text{-tartrate})$, remaining in solution. This suggests that the tendency of the *d* and *l* forms of the $[Co\ en_3]^{3+}$ complex cation towards ion-pair formation with *d*-tartrate anion is different. In fact, Ogino and Saito[1] showed that the association constant of the *d*-$[Co\ en_3]^{3+}$-*d*-tartrate system differs from that of the *l*-$[Co\ en_3]^{3+}$-*d*-tartrate system by analyzing the increase in the optical density of the charge-transfer band. On the other hand, Yamatera and Fujita[2] measured the rates of amino-hydrogen deuterium exchange for the *d*- and *l*-$[Co\ en_3]^{3+}$ complex in the presence of *d*-tartrate and found that the rate constant was appreciably smaller for *d*-$[Co\ en_3]^{3+}$ than for the *l*-isomer. This also implies that there is some stereoselective interaction in the solution between the isomers of the $[Co\ en_3]^{3+}$ complex cation and the *d*-tartrate anion. Thus, we can expect the complete resolution of the racemic $[Co\ en_3]^{3+}$ complex into its optical antipodes under appropriate conditions by means of electrophoresis.

We would like to report a successful result obtained by paper electrophoresis. Samples tested were *d,l*-$[Co\ en_3]Cl_3\cdot 3H_2O$, *d*-$[Co\ en_3]Cl(d\text{-tratrate})\cdot 5H_2O$ and *l*-$[Co\ en_3]Cl(l\text{-tartrate})\cdot 5H_2O$. Sodium *d*-tartrate was used as a main component of a background electrolyte solution. For electrophoresis a migration apparatus with multicompartment cells was used so that ten samples could be run at one time. Samples were run for 2.5 hr under a potential gradient 250 V/34 cm, keeping the temperature of the migrating box at 25°C. The spot of the sample was easily identified by the orange yellow color of the complex. By spraying a sodium sulfide solution we could visualize the spot more clearly.

When only sodium *d*-tartrate was used in a background electrolyte, the racemic form of the complex appeared always in one spot, irrespective of the concentration of the background solution. This means that resolution by electrophoresis was not successful. However, when aluminum chloride was added to the sodium *d*-tartrate solution, the racemic form was completely separated into two spots, as can be seen in Table 1. This should be taken as a resolution, because the sample of the *d* form showed only one spot just at the same position as the upper spot of the racemic form, and the *l* form showed only one spot corresponding to the lower spot of the racemic form.

TABLE 1. MIGRATION DISTANCE OF THE $[Co\ en_3]^{3+}$ COMPLEX IN VARIOUS BACKGROUND ELECTROLYTE SOLUTIONS

Sample	Background electrolytes		
	0.18M Na_2-*d*-tartrate	0.18M Na_2-*d*-tartrate 0.12M $AlCl_3$	
d,l-$[Co\ en_3]Cl_3$	41 mm	12 mm	59 mm
d-$[Co\ en_3]Cl$-(*d*-tartrate)	41 mm		59 mm
l-$[Co\ en_3]Cl$-(*l*-tartrate)	41 mm	12 mm	

Migration time, 2.5 hr
Potential gradient, 250 V/34 cm

A detailed discussion of the separation mechanism will be reported elswhere. Extension of our new method of resolution to a variety of racemic compounds is in progress.

1) K. Ogino and U. Saito, This Bulletin, **40**, 826 (1967).
2) H. Yamatera and M. Fujita, *ibid.*, **42**, 3043 (1969).

A New Ketol, 1,7-Diphenyl-5-hydroxy-3-heptanone, and *trans*-Stilbene from *Alnus firma* Sieb. et Zucc. (BETULACEAE)

Yoshinori ASAKAWA

Department of Chemistry, Faculty of Science, Hiroshima University, Higashisenda-machi, Hiroshima

(Received October 23, 1969)

I wish to report at this time the occurrence in *A. firma* Sieb. et Zucc. of a new ketol and of *trans*-stilbene, and to outline the biosynthetic pathway of closely-related compounds, such as cinnamic acid, β-phenylethyl cinnamate, pinostrobin (5-hydroxy-7-methoxy-flavanone), and alpinetin (5-methoxy-7-hydroxy-flavanone), which exist together with II and the new ketol (I).

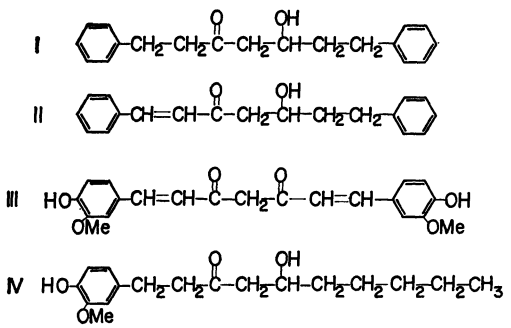

Dihydroyashabushiketol (I). 1,7-Diphenyl-5-hydroxy-3-heptanone. The high-resolution mass-spectral measurement of I isolated from the benzene extract clearly established its molecular formula as $C_{19}H_{22}O_2$. The constituent (I), M^+ 282, mp 36.0—37.0°C, gives positive coloration with 2,4-DNP and with alkali-alkyl xanthate, and is shown by its spectral properties to possess a simple ketone group ($\lambda\lambda_{max}^{EtOH}$: 285 mμ; 1706 cm^{-1}), a monosubstituted benzene ring (3060, 3020, 1600, 1490, 1450, 745 and 698 cm^{-1}), a non-conjugated benzene ring (248 mμ, 254, 261 and 268), active methylene (1409 cm^{-1}), and a hydroxyl group (3440 cm^{-1}). The NMR spectrum (60 MHz) of I in $CDCl_3$ indicates signals at 7.22 ppm (s, 10H, two monosubstituted benzene-ring protons), 4.07 ppm (quintet, 1H, J=7 Hz, $-CH_2-\underline{C}HOH-CH_2-$), 3.10 ppm (s, 1H, O$\underline{H}$), 2.80 ppm (m, 4H, $-\underline{C}H_2-CO-\underline{C}H_2-CHOH-$), 2.55 ppm (t, 4H, J=7 Hz, two $Ar-\underline{C}H_2-CH_2-$), and 1.66 ppm (m, 2H, $-CHOH-\underline{C}H_2-CH_2-$). The mass spectrum shows the parent ion at *m/e* 282, the base peak at *m/e* 91 $(C_7H_7)^+$, and other strong fragment ions at *m/e* 264 (M-18, m*=247.1), *m/e* 177 $(Ar-CH_2-CH_2-CO-CH_2-CH=\overset{+}{O}H)$, *m/e* 159 $(Ar-CH_2-CH_2-CO-CH=CH)^+$, *m/e* 148 $(Ar-CH_2-CH_2-CO-CH_3)^+$, *m/e* 133 $(Ar-CH_2-CH_2-CO)^+$, *m/e* 105 $(Ar-CH_2-CH_2)^+$, *m/e* 104 $(Ar-CH=CH_2)^+$, and *m/e* 43 $(CH_3-CO)^+$. The presence of *m/e* 39, 51, 65, and 77 suggests that I is a benzene derivative. These results have shown the structure of this ketol to be 1,7-diphenyl-5-hydroxy-3-heptanone. Furthermore, this was confirmed by the fact that the TLC R_f value, the mp, and the IR spectrum of I were all completely indentical with those of the hydrogenated product of yashabushiketol (II). In connection with a previous report,[1] I wish to propose the name "dihydroyashabushiketol" for this compound. It is very interesting, from the standpoint of biochemistry, that the ketols (I) and (II) possess the same skeleton as the curcumin (III) isolated from *Curcuma longa* (ZINGIBERACEAE)[2] and are partially similar to the structure of gingeron (IV) isolated from *Zingiber officinalis* Rosc. (ZINGIBERACEAE).[3]

***trans*-Stilbene (V).** The colorless, leaflet crystals (M^+ 180, mp 120.0—121.0°C, R_f=0.75) isolated from the hydrocarbon portion was confirmed to be *trans*-stilbene by a study of the spectral data (UV,[4] IR, NMR, and mass spectra[5]).

It has been reported that oxygen-containing stilbene derivatives are widely distributed and coexist with flavones and flavanones in the family of Pinaceae.[6] According to the shikimate-acetate biosynthesis pathway, dihydroyashabushiketol (I) and yashabushiketol (II) would be formed by the condensation of two molecules of cinnamic acid and a molecule of acetic acid. *trans*-Stilbene, flavanones (pinostrobin and alpinetin), and β-phenylethyl cinnamate would also result from a combination of acetic acid and shikimic acid pathways. It is very interesting, from the biochemical viewpoint, that free *trans*-stilbene and ketol I, ketol II, flavanones (pinostrobin and alpinetin), β-phenylethyl cinnamate, and cinnamic acid have been found to occur together in *A. firma* Sieb. et Zucc.

1) Y. Asakawa, F. Genjida, S. Hayashi and T. Matsuura, *Tetrahedron Lett.*, No. 38 to be published. A New Ketol from *Alnus firma* Sieb. et Zucc. (BETULACEAE).

2) K. R. Srinivasan, *J. Pharm. Pharmacol.*, **5**, 448 (1953); J. Milobedzka, S. V. Kostanecki and V. Lampe, *Ber.*, **43**, 2163 (1910).

3) H. Nomura, *Tohoku Riho*, **7**, 69 (1918).

4) R. N. Beale and E. M. F. Rowe, *J. Chem. Soc.*, **1953**, 2755.

5) R. A. W. Johnstone and A. Millard, *Z. Naturforsch.*, **21a**, 604 (1966).

6) G. Lindstedt and A. Misiorny, *Acta Chem. Scand.*, **5**, 121 (1951).

The Yields of $^{133}Cs(\gamma, xn)$ and $^{133}Cs(\gamma, 2pxn)$ Reactions with 150, 200 and 250 MeV Bremsstrahlung

Toyoaki KATO, Hui-Tuh TSAI and Yoshinaga OKA

Department of Chemistry, Faculty of Science, Tohoku University, Katahira-cho, Sendai

(Received November 11, 1969)

The yields of the reactions (γ, n), $(\gamma, 4n)$, $(\gamma, 6n)$, $(\gamma, 2p)$, $(\gamma, 2pn)$, $(\gamma, 2p5n)$, $(\gamma, 2p7n)$, $(\gamma, 2p8n)$, $(\gamma, 2p10n)$ and $(\gamma, 2p11n)$ in ^{133}Cs have been determined by the residual activity method in order to investigate the reactivity of high-energy bremsstrahlung photons with nuclei in heavy mass region.

Cesium chloride targets were irradiated by bremsstrahlung with maximum energies of 150, 200 and 250 MeV generated by the linear electron accelerator of Tohoku University. The radioactivity measurements were carried out on both the cesium and iodine fractions after radiochemical separation by using a lithium-drifted germanium detector with a sensitive volume of 36 cc coupled to a TMC 1024-channel pulse-height analyzer.

Of the iodine nuclides measured, ^{123}I, ^{121}I and ^{120}I can be formed through decays of the corresponding xenon nuclides generated by $^{133}Cs(\gamma, pxn)$ reactions. In order to reduce such contributions, all irradiations were terminated in 1 hr, and separation was performed very rapidly.

The yield was calculated as the initial disintegration rate of a given radioactive cesium or iodine product. A corresponding saturation rate was computed and expressed relative to that of the $^{133}Cs(\gamma, n)^{132}Cs$ processes. The yield thus obtained are plotted against the difference in mass between the target and product nuclei at each excitation energy in Fig. 1. It can be seen that (1) the yield of cesium nuclides decreases almost exponentially with the number of emitted neutrons, and (2) the more deficient the iodine nuclides in neutron number, the higher their yields, and a yield maximum is found around mass number 123.

The mass number of the center of the stable valley of the nuclear energy surface for iodine ($Z=53$) can be estimated to be 125.[1] Thus the maximum obtained stays at 2 mass unit to the neutron-deficient side. The yield distribution curve shifts 1.5 mass units more towards the neutron-deficient side of the stability line than the photonuclear yield surface in the copper-to-arsenic mass region characterized by Halpern *et al.*[2] The high-energy nuclear reaction mechanism including the initial nucleon cascades and subsequent evaporation steps will be responsible for this behavior. The longer evaporation path will displace the products towards the neutron-deficient side of stability, and thus the fractional yield of heavier iodine nuclides will decrease.

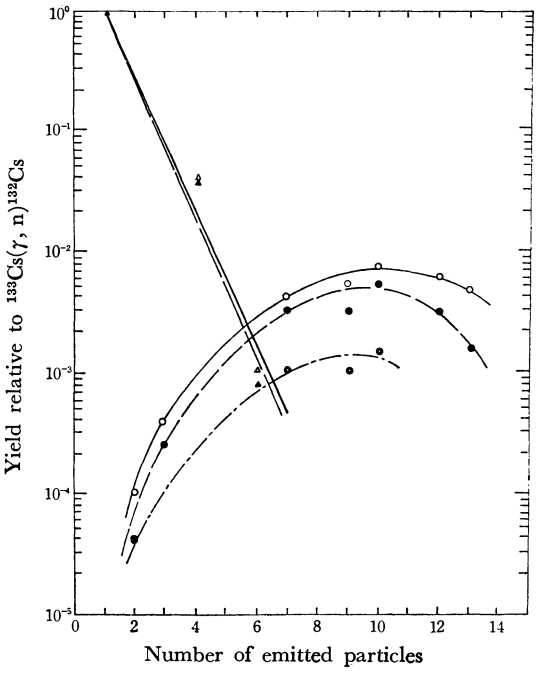

Fig. 1. The relation between yields and the number of emitted particles
△: (γ,xn), 250 MeV ○: $(\gamma,2pxn)$, 250 MeV
▲: (γ,xn), 200 MeV ●: $(\gamma,2pxn)$, 200 MeV
⊙: $(\gamma,2pxn)$, 150 MeV

The exponential decrease in the (γ, xn) reaction yield *versus* the difference in mass between the target and product nuclei has been shown experimentally by photospallation work.[3-5] The yield for the (γ, n) reaction of ^{133}Cs is much greater than that expected from yield surface considerations. This arises from the large contribution of photons in the giant resonance energy region to the production rate of ^{132}Cs.

1) C. D. Coryell, *Ann. Rev. Nucl. Sci.*, **2**, 305 (1953).
2) I. Halpern, R. J. Debs, J. T. Eisinger, A. W. Fairhall and H. G. Richter, *Phys. Rev.*, **97**, 1327 (1955).
3) V. di Napoli, F. Dobici, F. Salvetti and H. G. deCarvalho, *Nuovo Cimento, B*, **43**, 1 (1967).
4) J. M. Wyckoff, *Phys. Rev.*, **159**, 953 (1967).
5) G. G. Jonsson and B. Forkman, *Nucl. Phys., A*, **107**, 52 (1968).

The Crystal Structure of Nitrato-bis(2,2′-bipyridine)copper(II) Nitrate Monohydrate $[Cu(NO_3)(bipy)_2]NO_3 \cdot H_2O$

Hisayoshi NAKAI, Shun'ichiro OOI and Hisao KUROYA

Faculty of Science, Osaka City University, Sugimoto-cho, Sumiyoshi-ku, Osaka

(Received November 27, 1969)

It is well known that the reaction of Cu(II) with bipyridine gives three different products — the 1 : 1-, 1 : 2-, and 1 : 3-complexes — depending on the molar ratio of metal to ligand. Of these three, the structure of the 1 : 2-complex can be guessed to be *trans*-planar, as is shown in Fig. 1.

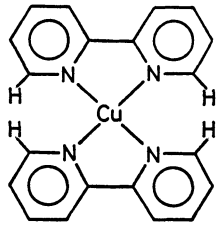

Fig. 1

However, the molecular model indicates that there must be a remarkable steric interference between the hydrogen atoms linked to the 3- and 3′-carbon atoms of the two bipyridine molecules. On the basis of his spectroscopic study, Jørgensen suggested that the complex has the *cis* configuration.[1] In order to elucidate the structure of the complex in detail, a single-crystal X-ray analysis has been carried out on $Cu(bipy)_2(NO_3)_2 \cdot H_2O$.

The blue crystals were prepared by Jaeger's method.[2] The unit cell has these dimensions:

$a=7.53$ $b=10.05$ $c=15.65$ Å
$\alpha=111.8°$ $\beta=91.0°$ $\gamma=90.5°$

The space group is $P\bar{1}$, with $Z=2$. The intensity data of $0kl$—$4kl$, $h0l$, $hk0$ were recorded on Weissenberg photographs ($CuK\alpha$ radiation) and were measured visually, the usual corrections being applied. The structure was solved by Patterson and Fourier techniques and refined by the block-diagonal least-squares method with isopropic temperature factors. The *R*-factor was 0.13 for 3087 independent reflections.

The crystal is essentially ionic and is composed of $[Cu(NO_3)(bipy)_2]^+$, NO_3^-, and H_2O. A schematic drawing of the complex ion is shown in Fig. 2. Four nitrogen atoms of the two bipyridine molecules and one of the oxygen atom of the coordinated nitrate ion form a distorted trigonal bipyramid around the copper atom. Cu, O_1, N_1,

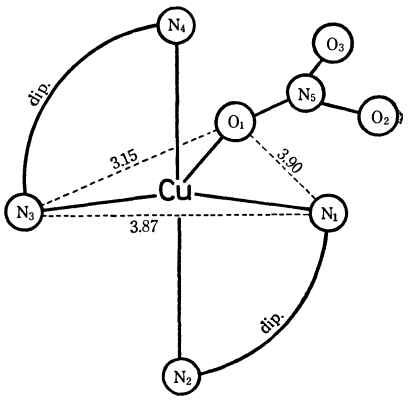

Fig. 2.

and N_3 are equatorially coplanar within the maximum deviation of 0.003 Å, making a dihedral angle of $\sim 10°$ with the O_1—$N_5\langle^{O_3}_{O_2}$ plane; N_5 and O_2 are distant by 0.20 Å, and O_3, by 0.39 Å, from the equatorial plane. The bipyridine molecules are necessarily in the *cis*-planar configuration, and their molecular dimensions are in good agreement with those found in the crystal of bipyridine.[3] The bond lengths and angles are listed in Table 1.

TABLE 1.

Bond length (Å)	Bond angle (degree)
$Cu-N_1=2.04$	$\angle N_4-Cu-N_1=99.3$
	$\angle N_2-Cu-O_1=85.9$
$Cu-N_2=2.01$	$\angle N_4-Cu-N_3=81.8$
	$\angle N_1-Cu-O_1=127.7$
$Cu-N_3=2.07$	$\angle N_4-Cu-O_1=85.4$
	$\angle N_3-Cu-O_1=91.9$
$Cu-N_4=1.99$	$\angle N_2-Cu-N_1=82.4$
	$\angle N_3-Cu-N_1=140.4$
$Cu-O_1=2.30$	$\angle N_2-Cu-N_3=103.3$

In the three-dimensional Fourier synthesis phased on the atomic coordinates of the complex ion, the electron density of the uncoordinated nitrate ion is rather more diffuse than that of the coordinated nitrate ion. The average temperature factor of the four atoms is 15 Å^2 in the former and 4.5 Å^2 in the latter. This fact suggests that the uncoordinated nitrate ion must be loosely bound in the crystal lattice.

1) C. K. Jørgensen, *Acta Chem. Scand.*, **9**, 1362 (1955).

2) F. M. Jaeger and J. A. Dijk, *Z. Anorg. Chem.*, **227**, 273 (1936).

3) L. L. Merritt, Jr., and E. D. Schroeder, *Acta Crystallogr.*, **9**, 801 (1956).

The Phase Transitions of the Anion-radical Salts Containing Mixed Cations; $[(C_6H_5)_3PCH_3]_{1-x}^+[(C_6H_5)_3AsCH_3]_x^+(TCNQ)_2^-$, $(0 \leq x \leq 1)$

Yôichi IIDA

Department of Chemistry, Faculty of Science, Hokkaido University, Sapporo, Hokkaido

(Recieved December 6, 1969)

Much attention has been paid to the solid anion-radical salts of 7,7,8,8-tetracyanoquinodimethane (TCNQ) because of their prominent electrical, magnetic, and optical properties.[1-3] In the course of our study of these salts, we found that the ESR absorption intensity of the salt of methyltriphenylphosphonium, $[(C_6H_5)_3PCH_3]^+(TCNQ)_2^-$, increased abruptly at 40°C when the temperature was raised.[4] The discontinuity was also found in the electrical conductivity at that temperature.[4] This anomaly was ascribed to the phase transition of the crystal, as evidenced by the differential thermal analysis.[5] The methyltriphenylarsonium salt, $[(C_6H_5)_3AsCH_3]^+(TCNQ)_2^-$, exhibits electronic properties almost identical with those of the phosphonium salt; on the other hand, the arsonium salt is known to have no such anomaly. It was suggested that one could prepare the salts containing mixed cations, which may be expressed as $[(C_6H_5)_3PCH_3]_{1-x}^+[(C_6H_5)_3AsCH_3]_x^+(TCNQ)_2^-$, $(0 \leq x \leq 1)$.[6] Therefore, it seemed that it would be interesting to investigate the effect of the composition upon the phase-transition phenomenon. The present investigation was performed by means of a differential scanning calorimeter (DSC).

The six salts with $x=0.00$, 0.20, 0.40, 0.60. 0.80, and 1.00 were prepared according to the method of Melby *et al.*[6] The DSC measurements were made by using powdered α-alumina as a standard substance, with the temperature raised at the rate of 3.0°C/min.

All the salts except for that with $x=1.00$ showed endothermic phase transitions when the temperature was raised. These phase transitions were found to be reversible. The relation of the transition temperature, T_c, to the composition parameter, x, is given in Fig. 1. In DSC measurements, the

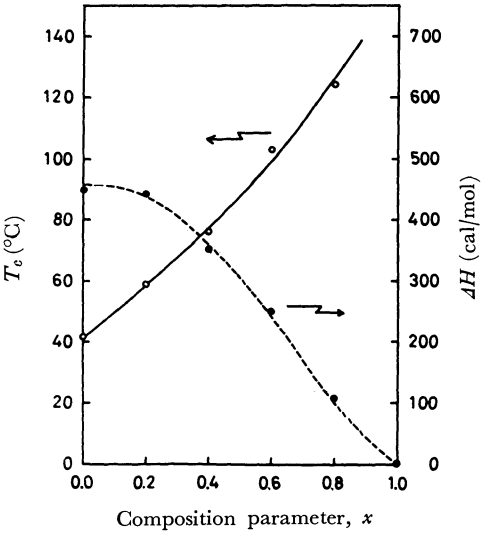

Fig. 1. The relations of the transition temperature, T_c, and of the magnitude of the heat, ΔH, associated with the phase transition, to the composition parameter, x, in $[(C_6H_5)_3PCH_3]_{1-x}^+[(C_6H_5)_3AsCH_3]_x^+(TCNQ)_2^-$, $(0 \leq x \leq 1)$.

peak area of the signal line should be proportional to the magnitude of the heat, ΔH, associated with the phase transition. Therefore, in order to determine the heats associated with the phase transitions of these salts, the area of the signal line of $[(C_6H_5)_3PCH_3]_{1-x}^+[(C_6H_5)_3AsCH_3]_x^+(TCNQ)_2^-$ was compared with that of hexachloroethane or hexamethylbenzene. The phase transition of hexachloroethane is known to take place at 318.1°K with $\Delta H=0.613$ kcal/mol and at 344.4°K with $\Delta H=1.965$ kcal/mol, and that of hexamethylbenzene, at 384.1°K with $\Delta H=0.42$ kcal/mol.[7] The magnitudes of ΔH *versus* x obtained with the above six TCNQ salts are also illustrated in Fig. 1.

It is noteworthy that T_c increases, and the value of ΔH decreases, monotonously with an increase in the value of x, and that the phase transition disappears with $x=1.00$.

1) W. J. Siemons, P. E. Bierstedt and R. G. Kepler, *J. Chem. Phys.*, **39**, 3523 (1963).
2) R. G. Kepler, *ibid.*, **39**, 3528 (1963).
3) Y. Iida, This Bulletin, **42**, 71, 637 (1969).
4) Y. Iida, M. Kinoshita, M. Sano and H. Akamatsu, *ibid.*, **37**, 428 (1964).
5) Y. Iida, M. Kinoshita, A. Kawamori and K. Suzuki, *ibid.*, **37**, 764 (1964).
6) L. R. Melby, R. J. Harder, W. R. Hertler, W. Mahler, R. E. Benson and W. E. Mochel, *J. Amer. Chem. Soc.*, **84**, 3374 (1962).
7) Landort-Börnstein, "Zahlenwerte und Funkutionen aus Physik, Chemie, Astronomie, Geophysik, Technik," II Band, 4 Teil, 6 Auflage, Springer-Verlag, Berlin (1961); Nippon Kagakukai, "Kagaku Binran," Maruzen, Tokyo (1966).

Asymmetric Hydrogenation of C=O Double Bond with Modified Raney Nickel. XIV

Yoshiharu IZUMI and Toshio NINOMIYA

Division of Organic Chemistry, Institute for Protein Research, Osaka University, Kita-ku, Osaka

(Received December 8, 1969)

In the course of the studies of the asymmetric hydrogenation reaction, many kinds of optically-active amino and hydroxy acids have been used as the modifying reagents of Raney nickel catalysts.[1] It has been found that two functional groups, carboxyl and amino or hydroxy groups, are essential in a modifying reagent in order to produce a strong asymmetric activity of the catalyst; that is, the derivative formation of these functional groups of modifying reagents, for example, the acylation of the amino and hydroxy groups or the esterification of carboxyl groups, gives a catalyst which has a lower asymmetric activity than the catalyst modified with the original amino or hydroxy acids.[2] This fact and the physical and physicochemical evidence suggest that the carboxyl and amino or hydroxy groups of the modifiying reagents take part in the binding to the catalyst by chelation, so it seems that these functional groups are indispensable to the adsorption of the modifying reagents on the catalyst surface.

When the metal amino acid chelates are used as the modifiying reagents, all the amino acid molecules on the catalyst surface can adsorb as nickel chelates, so the metal amino acid chelates are expected to have special properties as modifying reagents.

In the present experiment the abilities of the metal chelates of several optically-active amino acids used as modifying reagents were tested. These investigations were carried out with catalysts modified with aqueous or methanolic solutions; the results are summarized in Table 1.

Three points are noticeable in Table 1. The first is the fact that the asymmetric activities of the catalysts modified with the metal chelates of the optically-active amino acids are rather higher than those modified with their original amino acids. The second is the fact that the asymmetric activity depends on the solvent used in the modification of the catalyst; that is, the aqueous solution and the methanolic solution of $[Ni(L\text{-}Ala)_2]\cdot 4H_2O$ give an opposite asymmetric direction to the catalyst. The third is the finding that the modification with the aqueous solution of $[Cu(L\text{-}Ala)_2]$ gives the catalyst with an asymmetric direction opposite to that of the catalyst modified with the aqueous solution of $[Ni(L\text{-}Ala)_2]\cdot 4H_2O$.

The detalis of this investigation will be published after the descriptions of our physical and physicochemical investigations of the adsorption of amino acids on the nickel surface.

TABLE 1. ASYMMETRIC ACTIVITIES OF THE CATALYSTS MODIFIED WITH METAL CHELATES

Modifying solution	$[\alpha]_D^{20}$ of methyl 3-hydroxybutyrate
$[Ni(L\text{-}Val)_2]\cdot 2H_2O$ in MeOH (1% soln.)	−4.21
$[Ni(L\text{-}Ala)_2]\cdot 4H_2O$ in MeOH (1% soln.)	−0.18
$[Ni(L\text{-}Ala)_2]\cdot 4H_2O$ in H_2O (1% soln.)	+0.86
$[Cu(L\text{-}Ala)_2]$ in H_2O (1% soln.)	−0.50
$[Ni(L\text{-}Glu)]\cdot 2H_2O$ in H_2O (1% soln.)	−4.00
L-Val in H_2O (2% soln.)	−2.31*1
L-Ala in H_2O (2% soln.)	+1.08*1
L-Glu in H_2O (2% soln.)	−3.46*2,*3

Substrate: methyl acetoacetate 0.15 mol
Hydrogenation temperature: 60°C
Modifying temperature: 0°C
*1 Y. Izumi, M. Imaida, H. Fukawa and S. Akabori, This Bulletin, **36**, 155 (1963).
*2 Y. Izumi, M. Imaida, H. Fukawa and S. Akoabri, *ibid.*, **36**, 21 (1963).
*3 Obtained at pH 5.0.

1) Part XII of this series: Y. Izumi, S. Tatsujmi and M. Imaida, This Bulletin, **42**, 2373 (1969); Part XIII: Y. Izumi, S. Tatsumi, M. Imaida and K. Okubo, *ibid.*, **43**, 566 (1970).

2) Y. Izumi, M. Imaida, H. Fukawa and S. Akabori, This Bulletin, **36**, 155 (1963).

A Novel Type of Methyl Radical Trapped in Porous Vycor Glass at 77°K

Norio SHIMAMOTO, Yuzaburo FUJITA and Takao KWAN

Faculty of Pharmaceutical Sciences, The University of Tokyo, Hongo, Bunkyo-ku, Tokyo

(Received December 11, 1969)

There has been interest in the study of methyl radicals trapped in various matrices.[1] As has been reported previously, the CH_3 radical photoproduced from methyl iodide in the porous Vycor glass (V. G.) (Corning, # 7930) was very stable even at room temperature.[1a] According to its extraordinary stability over a wide range of temperature, Fujimoto *et al.*[1c] have been able to study the temperature dependence of the hyperfine coupling (hfc) constant of the methyl radical stabilized on the porous V. G. surface.

Recently, in the course of our studies of the photolysis of adsorbed species on the porous V. G. surface at 77°K, we observed a novel type of methyl radical produced by the photolysis of methane; this radical was stable at 77°K and has an abnormally small hfc constant.

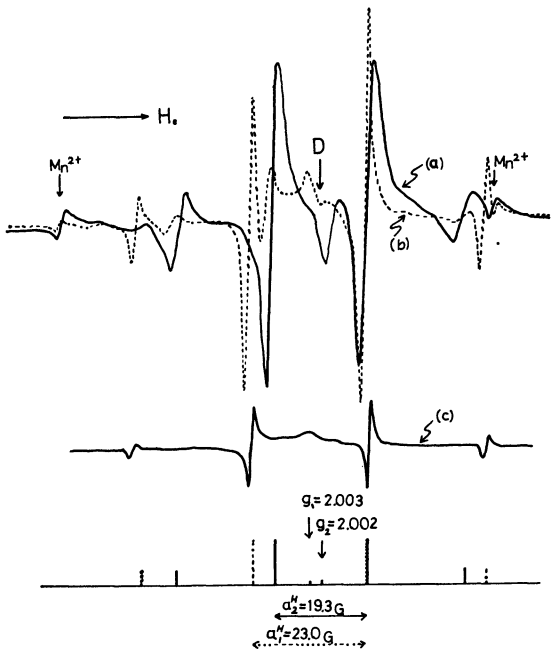

Fig. 1. ESR signals from methane photolysis at 77°K.
(a), Pure methane; (b), In the presence of iodine; (c), After slight warming of (b); Mn^{2+}, hfs of the standard; D, Defect signal

A porous V. G. rod (4 mmϕ, 20 mm in length) was preheated in an oxygen atomosphere at 600°C to remove any adsorbed organic substances. After repeating the pretreatment of the V. G. rod in a quartz sample tube, less than a monolayer amount of purified methane (usually 1/10 of a monolayer) was introduced into the evacuated sample tube at room temperature. Then the sample tube was cooled gradually from room temperature to the temperature of liquid nitrogen in order to secure a homogeneous adsorption of methane on the surface of the porous glass. Irradiation was then carried out at 77°K with the light of a low-pressure mercury lamp (Ushio Electric Co., Ltd., UL 200W). About five minutes' irradiation was enough to observe a methyl-radical signal with a good S/N ratio.

The observed ESR constants of the methyl radical were as follows:

$$|a^H| = 19.3 \pm 0.3 \text{ G}, \quad g = 2.002_3 \pm 0.0003.$$

A linewidth alternation in the proton hf lines was observed, as in the case of the CH_3 obtained from methyl iodide. However, unlike the normal radical from methyl iodide, this methyl radical showed an inverse linewidth alternation; *i. e.*, the higher field lines were broader (Figs. 1a and 1b). The thermal stability was also different, and the abnormal CH_3 decayed rapidly on slight warming, indicating a reactive character. However, this radical was efficiently trapped on the surface and did not decay, at least at 77°K.

When iodine was present during the photolysis of methane, the main signal was a normal one (Fig. 1b). This shows that iodine plays an important role in the stabilization of the normal methyl radical.

The fact that the new type of the methyl radical has a *g*-value close to that of the free electron and an extraordinary small hfc constant compared to that of the planar methyl radical ($a^H = -23$ G, $g = 2.003$) probably indicates a nonplanar (pyramidal) structure, in which an unpaired electron is in an orbital with a larger *s*-character.

The nonplanar structure may be stabilized by the strong interaction between methyl radical and the surface of porous V. G., resulting in the large linewidth. The order of the rotational correlation time of this radical was estimated to be $\tau_c = 10^{-7}$ sec. This value can be compared with that of $\tau_c = 10^{-8}$ sec of the normal methyl radical obtained from methyl iodide.

A detailed analysis is now in progress.

1) a) J. Turkevich and Y. Fujita, *Science*, **152**, 1619 (1966); b) M. Fujimoto, H. D. Gesser, B. Garbutt and A. Cohen, *Science*, **154**, 381 (1966); c) G. B. Garbutt, H. D. Gesser and M. Fujimoto, *J. Chem. Phys.*, **48**, 4605 (1968); d) R. L. Morehouse, J. J. Christiansen and W. Gordy, *ibid.*, **45**, 1751 (1966).

BULLETIN OF THE CHEMICAL SOCIETY OF JAPAN VOL. 43 581—589 (1970)

A Chemical Study on Some Archaeological Samples from Iran and Afghanistan[1)]

Teruko MUROGA

Department of Chemistry, Faculty of Science, Kyoto University, Sakyo-ku, Kyoto

(Received September 28, 1968)

From archaeological interest, chemical analyses were performed on samples which had been collected from Iran and Afghanistan by the Kyoto University Scientific Mission to the Iranian Plateau and Hindukush. As samples were used more than one hundred pieces of glass and glazed material, and two slag-like objects. By analyzing the glass and glazes for major components, it was found that all were made of soda-lime glass except for a fragment of a glaze of tri-colored pottery collected at Kerman, Iran. It is noteworthy that this fragment of tri-colored pottery had a lead content similar to that of Chinese glazes, while Western glasses are rarely found to contain so much lead. Among the minor components detected, detailed consideration was given to the color origins. Although iron and copper were commonly found in blue-colored samples, the origin of the color of the tile from a mosque at Tabriz was confirmed to be cobalt. Investigations of slag-like objects collected from Tepe Sialk have revealed the possibility that these objects are slags from copper smelting. Studies of the silvery effect or of the weathering observed on the surface of glass and glazes of archaeological importance were carried out by semi-quantitative spectrochemical analysis.

Introduction

Until recently, most studies which have been made by historians and archaeologists upon archaeological samples have concentrated on the objects themselves and not on their chemical compositions. It has been and should be recognized, however, that detailed examinations of archaeological materials by physical and chemical methods can bring quite fruitful results in the field of archaeology. Indeed, in discussing age and in estimating the degree of technological accomplishment, furthermore, as part of understanding cultural exchange between the East and the West, archaeology must not neglect the data from the probes of natural science.

In a previous paper,[2)] some results of studies on Chinese and Japanese samples were reported. The author's intention in these works is to contribute to the histories of science and technology through chemical analyses of archaeological samples. The present paper will deal with the results of the chemical analyses of more than one hundred samples of glass, glazes, and slag-like objects, all of which were brought from Iran, Afghanistan, and Pakistan by the Kyoto University Scientific Mission to the Iranian Plateau and Hindukush.

Western Asia is located in a historically-important position through which the interchange of two cultures, the Eastern and the Western, has taken place since most ancient times. Nevertheless, few scientific investigations have been undertaken in that area. Therefore, the project of the Mission was to make a composite study of Western Asia which could serve as one preliminary step to a really thorough plunge into the archaeology of that area. As usual, the collection of these kinds of samples can be neither as systematic nor as complete as one would wish, because the chances of getting samples by excavation can not be foreseen. Moreover, a sample itself is sometimes too valuable for even a part of it to be destroyed; it just has to be kept untouched.

Although the present work was made under these restrictions, care has been taken in choosing samples so that characteristic features of samples from era to era and from area to area may be obtained. The samples chosen here were more than one hundred pieces of glass and glazes and two slag-like objects. For most of the glass and glazes, the major and minor components were qualitatively identified spectrochemically, though for several samples they were determined quantitatively. The main interest in the major components was in finding out whether they were soda-lime glass or lead glass; most Western glass belongs to the former group, while the latter has been manufactured in

1) Presented at The 5th International Congress of Iranian Art and Archaeology (April, 1968, Tehran, Shiraz, Isfahan, Iran).

2) T. Muroga, *Bull. Japanese Studies in The History of Sicence*, **7**, 83 (1968).

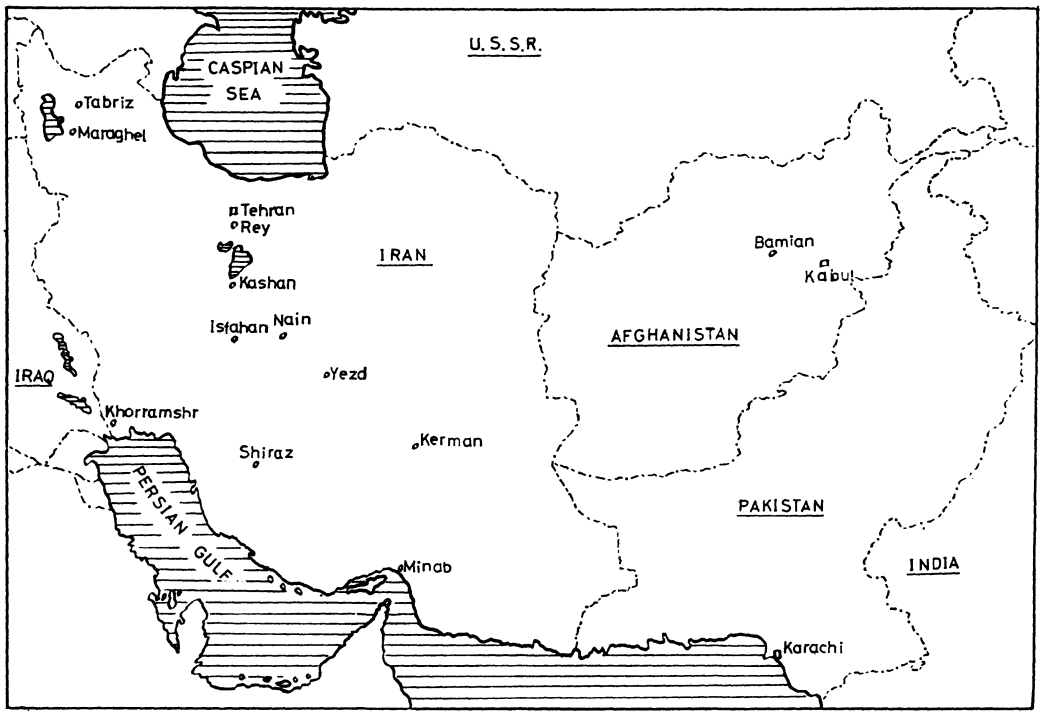

Fig. 1. A map of sampling stations.

China since the ancient period.[3] For the minor components, attention was paid to color origins, which may offer clues to the origin and to the exchange of the techniques of glassmaking. The two slag-like samples, which were picked up at the ruins of a smelting furnace, were subjected to the quantitative determination of their major components. If they were indeed slags of copper smelting, the quality of the techniques of extracting copper from the ore could be estimated from them. The last subject was the silvery effect or weathering which is frequently observed on the surface of glass or glazes of archaeological importance. Semi-quantitative analysis showed a continuous change in composition from the surface to the inner part of the sample.

Experimental

Semi-quantitative spectrochemical analyses were performed on the archaeological samples by using the internal standard (Ge, Pt) method.

The quantitative analytical methods used especially for the glass and glazes were described in the previous report.[4] In brief, the glass and glazes were brought into solution by carbonate fusion and then treated with hydrochloric acid. The analytical methods used subsequently are given in Table 1. In some cases, X-ray micro-probe analysis was performed in order to examine the distribution of elements in a non-destructive way.

TABLE 1. ANALYTICAL METHODS USED

Element	Methods of determination
Si	Gravimetrically as SiO_2
Ca	Chelatometrically
Mg	*ibid.*
Cu	Polarographically
Zn	*ibid.*
Ni	*ibid.*
Pb	*ibid.*
Al	Colorimetrically
Fe	*ibid.*
Co	*ibid.*
Mn	*ibid.*
Ti	*ibid.*
P	*ibid.*
Na	Gravimetrically as $Na(C_2H_3O_2)\cdot Mg(C_2H_3O_2)_2\cdot 3UO_2(C_2H_3O_2)\cdot 6\frac{1}{2}H_2O$
K	Gravimetry as $K_2NaCo(NO_2)_6H_2O$ or $K(ph)_4B$

Results and Discussion

Glasses and Glazes. *Major Components.* All of the samples were soda-lime glass. Representative results are given in Tables 2 and 3. Contrary to

3) M. Yoshida, "Sekai Toji Zenshu" (The Complete Works of Pottery in the World), Vol. 8, Heibonsha, Tokyo (1955), p. 282.

4) T. Muroga and M. Yoshida, *Kagakushi Kenkyu*, **46**, 17 (1958).

TABLE 2. SPECTROCHEMICAL ANALYSES OF GLASSES

No.	Place of collection	Color*	Major						Minor												Trace							
			Si	Na	Al	Ca	Mg	K	Al	Ti	Fe	Mn	Cu	Zn	Pb	Sn	P	Ni	Co	Cr	Ag	Ba	V	B	Sr	Sb	Bi	
1	Tehran	L.B.	○	○		○	○	○	○		○	○	○		○			○	○	○				○				Jug
2	Rey	B.	○	○	○	○	○	○		○	○	○	○							○		○						Bowl
3	Nishapul	G.B.	○	○	○	○	○	○			○	○										○						Bottle
4	Nishapul	L.B.	○	○	○	○	○	○			○	○	○									○						Bottle
5	Nishapul	D.G.	○	○	○	○	○	○			○	○	○							○		○						Bottle
6	Nishapul	L.G.	○	○	○	○	○	○			○	○	○							○								Vessel
7	Nishapul	L.G.	○	○	○	○	○	○			○		○											○				Bottle
8	Nishapul	L.B.	○	○	○	○	○	○			○		○									○						
9	Hirzabad	L.B.	○	○	○	○	○	○		○	○									○		○						
10	Hirzabad	G.	○	○	○	○	○	●			○	○	○							○		○						
11	Hirzabad	B.	○	○	○	○	○	●			○	○	○							○		○						Lump
12	Hirzabad	G.B.	○	○	○	○	○	○			○																	Vessel
13	Hirzabad	Co.	○	○	○	○	○	○			○		○						○	○		○						Lump
14	Atteshekhada	G.Y.	○	○	○	○	○	○			○									○								Vessel
15	Salvistan	L.B.	○	○	○	○	○	○			○									○								Jug
16	Amrash	L.G.	○	○	○	○	○	●		○	○		○										○	○				Bead
17	Amrash	N.B.	○	○	○	○	○	●		○	○		○										○	○				Bead
18	Amrash	Y.	○	○	○	●	●			○	○		○		○								○	○				
19	Amrash	P.	○	○	○	○	○	●		○	○	○								○		○	○		○			Bead
20	Amrash	L.P.	○	○	○	○	○	○		○	○	○								○			○		○			
21	Armash	L.G.	○	○		○	○		○	○	○												○		○			
22	Amrash	Br.	○	○	○	○	○	●		○	○												○	○	○			
23	Amrash	W.	○	○	○	○	○	●		○	○	○											○		○			
24	Tehran	L.G.	○	○		●	●	○	○	○	○	○	○							○			○					
25	Tehran	D.G.	○	○	○	○	○	○		○	○	○	○						○	○		○	○		○			
26	Tehran	G.B.	○	○	○	○	○	○		○	○	○	○						○	○		○	○		○			

No.	Place of collection	Color*	Major						Minor												Trace							
			Si	Na	Al	Ca	Mg	K	Al	Ti	Fe	Mn	Cu	Zn	Pb	Sn	P	Ni	Co	Cr	Ag	Ba	V	B	Sr	Sb	Bi	
27	Tehran	W.	○	○	○	○	○	○			○											○	○		○			
28	Tehran	L.G.	○	○		○	●		○	○	○	○											○	○				
29	Tehran	L.Y.	○	○	○	○	○	●		○	○	○											○					
30	Tehran	D.B.	○	○	○	○	○	●		○	○	○	○						○			○	○		○			
31	Minab	R.	○	○	○	○	●				○		○	○	○					○				○				
32	Minab	Co.	○	○		○	○	○	○		○	○	○	○	○			○	○	○				○				
33	Minab	Co.	○	○		○	○	○	○		○	○	○					○	○	○				○				
34	Minab	D.Br.	○	○	○	○	○	●		○	○	○	○			○				○		○			○			Bracelet
35	Minab	G.B.	○	○	○	○	○	○		○	○	○	○		○	○		○		○	○	○	○	○	○			Bracelet
36	Minab	L.B.	○	○		○	○	○	○		○		○							○				○				Bracelet
37	Minab	L.G.	○	○		○	○	○	○		○	○	○		○	○				○				○				Bracelet
		Y.	○	○		●	○	○	○		○	○	○		○	○				○	○			○				Bracelet
		W.	○	○		●	○	●			○	○	○		○	○				○	○		○	○				Bracelet
38	Minab	M.	○	○		○	○	○	○		○	○	○							○			○	○				Bead
39	Minab	L.G.	○	○		○	○	○	○		○		○							○				○				
40	Minab	G.Y.	○	○	○	○	○	○		○	○	○	○							○		○	○	○	○			
41	Minab	Br.	○	○		○	○	○	○		○		○							○				○				
42	Minab	G.B.	○	○		○	○	○	○		○		○					○		○				○				Jug
43	Minab	L.Br.	○	○	○	○	○	○			○	○	○							○				○				Jug
44	Share-Bonn	D.Br.	○	○		○	○	○	○		○	○	○		○						○							Bracelet
45	Share-Bonn	Bl.	○	○	○	○	○	○			○	○	○											○				Bracelet
46	Share-Bonn	L.B.	○	○	○	○	○	○			○	○	○							○		○		○	○			
47	Share-Bonn	L.G.	○	○	○	○	○	○			○									○			○	○				Jug
48	Share-Bonn	L.Co.	○	○	○	○	○	○			○	○	○					○	○	○				○				
49	Share-Bonn	L.B.	○	○	○	○	○	○			○		○		○	○				○	○			○				Bottle
50	Share-Bonn	G.B.	○	○	○	○	○	○			○	○	○							○				○		○		Jug
51	Share-Bonn	Y.	○	○	○	○	○				○	○	○		○	○		○	○	○	○	○			○		○	Bracelet
		D.G.	○	○		●	○	○	○		○	○	○	○	○	○		○		○	○			○		○	○	Bracelet

○>●

* L.B.: Light-blue, B.: Blue, G.B.: Greenish-blue, D.B.: Dark-blue, L.G.: Light-green, G.: Green, Co.: Cobalt-blue, G.Y.: Greenish-yellow, N.B.: Navy-blue, Y.: Yellow, P.: Purple, L.P.: Light-purple, Br.: Brown, W.: White, L.Y.: Light-yellow, D.G.: Dark-green, R.: Red, D.Br.: Dark-brown, M.: Milky, L.Br.: Light-brown, Bl.: Black, L.C.: Light-cobalt blue, Cr.: Crimson

Table 3. Analyses of glasses

Color / Component	No. 52 Light-blue (%)	No. 53 Light-green (%)	No. 54 Deep-green (%)	No. 55 Green (%)	No. 56 Light-blue (%)	No. 57 Green (%)	No. 58 Green (%)
SiO_2	61.24	61.48	65.60	63.40	78.98	69.81	55.46
TiO_2	2.82	1.72	0.37	0.08	0.02	0.14	0.95
Fe_2O_3	0.15	0.35	1.54	0.32	0.06	0.82	1.90
MnO	0.12	0.03	1.05	5.10	tr	4.25	0.16
Al_2O_3	5.89	8.95	4.15	1.16	1.16	0.38	4.57
MgO	2.37	1.19	3.06	1.13	0.97	2.68	3.16
CaO	3.43	6.26	16.34	3.16	1.83	5.84	7.62
CuO	0.15	tr	0.06	0.27	2.13	0.09	0.25
ZnO	0.32	tr	0.01		0.73	0.71	
Na_2O	17.79	15.12	2.04	14.00	1.57	8.06	16.79
K_2O	4.19	3.63	6.45	4.27	9.92	4.49	9.16
H_2O	1.07	0.87	0.53	0.93	1.53	0.77	
P_2O_5			1.13	0.03	0.02	0.07	0.58
SnO_2				1.07	0.83		
Place collected	Kerman	Kerman	Neyriz	Nain	Malagha	Kerman	Kerman

expectation, specimens containing tin were quite rare in these samples. Only four samples contained tin; the results on these sample, all glass bracelets from Minab and Share-Bonn, were shown in Table 2. It should be emphasized here that the other glass samples from the same area, Minab, were found to be soda-lime glass. This fact is in clear contrast with the case in China, where most of the glass manufactured in ancient periods was lead glass. As Minab was a famous port in old Hormus, a trading center between East and West, much Chinese porcelain was imported there.[5,6] Hormus is said to have prospered between the thirteenth and the fifteenth centuries, and to have declined with the collapse of the Kerman Kingdom; now it is only ruins. It can be thought that the porcelain in Minab was produced under the influence of China. From the results of the chemical analyses of glass samples of many colors and sorts, it can be said that all soda-lime glass; none of these samples was of the lead-glass type. This fact suggests that the glassmaking in Minab was, unlike the porcelain-making, not influenced by Chinese glassmaking. It is very interesting that the glassmaking technique is thus in striking contrast to that of porcelain.

The only sample which contained a large amount of lead was a fragment of tri-colored pottery found at Kare-dokhtal, Kerman. The tri-colored glaze was found to be very similar to that in China, not only in the external appearance but also in the lead content.

The other samples which were found to contain small amounts of lead were beads. Beads which were made in China before the fourth century B.C.[7] have also been found in Iran, but, like the glass from China, the Chinese beads show greater

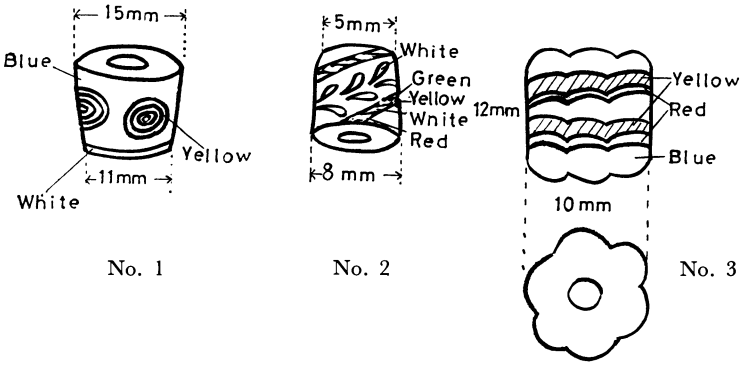

Fig. 2. Schematic diagrams of Beads Nos. 1—3.

5) M. Yoshida and K. Koyama, "Nishi-Ajia no Gijutu" (Western Asia at Work), Kyoto University Scientific Mission to Iranian Plateau and Hindukush, Kyoto (1960).

6) T. Wan, "To-i Shi-ryaku," China, Yuan Dynasty.

7) K. Yamazaki, "Kokogaku Taikei" (The Outline of the Archaeology), Vol. 16, Heibonsha, Tokyo (1962), p. 132.

TABLE 4. SPECTROCHEMICAL ANALYSES OF BEADS

Place of collection	Color*	Major						Minor										Trace							
		Si	Na	Al	Ca	Mg	K	Al	Ti	Fe	Mn	Cu	Zn	Pb	Sn	P	Ni	Co	Cr	Ag	Ba	V	B	Sr	Sb	Bi	As
Tehran B-1	W.	○	○		●	○				○	○	○		○			○	○		○			○		○		
	B.	○	○		○	○	○	○	○	○	○	○		○			○	○	○			○	○				
	Y.	○	○		●	●				○	○	○		○			○	○		○			○		○	○	
B-2	P.	○	○	○	○	○			○	○	○	○		○			○	○	○	○	○	○	○	○		○	
	Y.	○	○			●						○	○	○	○					○					○	○	○
	R.	○	○									○		○						○					○	○	○
	W.	○	○			●				○	○	○		○						○			○			○	○
	B.	○	○									○		○	○					○			○		○	○	○
B-3	B.	○	○	○	○	○	○		○	○	○	○		○	○		○	○	○	○	○		○	○			
	Y.	○	○	○	○	○			○	○		○		○	○		○		○	○	○	○			○		
B-4	W.	○	○	○	○	○	○		○	○	○	○		○	○				○	○	○	○	○	○			
	Y.	○	○	○	○	○	○		○	○	○	○		○	○		○		○	○	○	○	○	○			
	Cr.	○	○		●	○	○	○		○	○	○		○	○		○	○	○	○		○	○				
	B.	○	○	○	○	○			○	○	○	○		○	○				○	○	○		○				
	Y.p.	○	○	○	○	○	○		○	○	○	○		○	○		○		○	○			○	○			
	B.	○	○	○	○	○	○		○	○	○	○		○	○		○		○	○		○	○				

p: projection

TABLE 5. ANALYSIS OF THE BEAD No. 1*

Color / Component	Blue (%)	White (%)	Yellow (%)
SiO_2	77.8	74	64
Al_2O_3	2.2	2.2	2
CaO	23.3	20.1	13.1
TiO_2	0.02	0.03	0.03
PbO			19.6
Fe_2O_3	0.5	0.3	1.26
MnO	0.7	0.3	tr

amounts of lead. The beads of Western Asia are usually larger in size, more colorful, and more complicated in design than those from China, Figure 2 presents an example with the eye pattern and also a bead with cord-design. They were obtained in Tehran and are estimated to have been manufactured in about the fifteenth century A.D. The No. 4 bead has a very complicated structure. The results of the analyses are shown in Tables 4, 5, and 6. The details, shown in Fig. 3, reveal a black cylindrical body upon which white lines have been placed, with a yellow knob at the corners and with larger varicolored knobs imbedded within the square formed by the white line. Lead is detected in all parts of all the beads examined. However, lead might have been put in the glass not for the purpose of making lead glass, as was done in China, but for the purpose of lowering the melting point of glass in order to make it more

TABLE 6. ANALYSIS OF THE BEAD No. 4*

Color / Component	Varicolored knob					Black (%)	White (%)	Yellow (projection) (%)
	Crimson (%)	Blue (%)	Black (%)	White line (%)	White spot (%)			
SiO_2	67	68.5	67	72	70	69.5	70.2	69.5
Al_2O_3	3	3.2	3	1.9	3.2	3	2	1.2
MgO	2	1.5	1.5	1.5	1.5	1.5	3.5	3.5
CaO	13.6	12.6	13.6	17.1	16.4	12.6	19.2	16.5
SnO_2	1.4	1.9	tr	1.7	3.4	0.3	tr	2.8
TiO_2	0.2	0.2	0.2	0.2		0.2	0.03	0.07
PbO	2.1	2.3	tr	2.3	3.7		2.88	0.81
Fe_2O_3	3.4	1.3	0.7	0.7		1.1	0.4	0.5
MnO	0.71	0.7	2.4	1.3	2.1	2.3	0.4	0.5
CuO						0.2		

* Determined by X-ray micro-probe analyzer

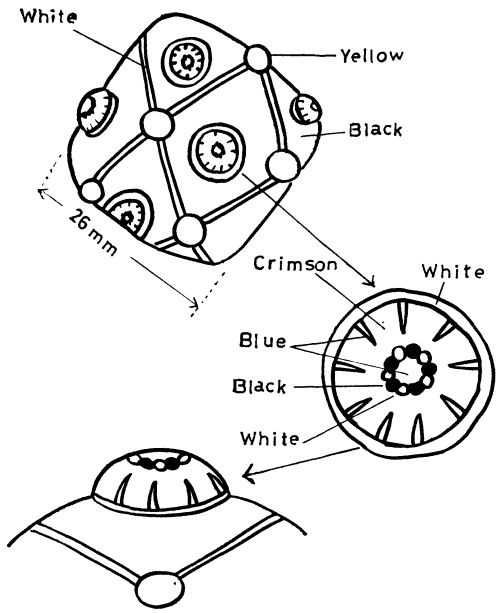

Fig. 3. Schematic diagram of Bead No. 4.

malleable. At any rate, as their specific gravities were less than 3.3 and contained much silicon and sodium, those pieces of glass, on the whole, are of the soda-lime-glass type.

Coloring Materials. As for the color origins of the bead No. 1, the blue color comes from iron, and the yellow, from lead and iron. In the bead No. 2 the purple color is due to the combination of manganese and nickel, and the blue color is due to copper. In No. 3 the blue color may be due to nickel, and the crimson, and the blue, to copper. In the yellow parts of the beads No. 3 and No. 4, more lead was detected than in the other colored parts. A similar fact has been also described by another researcher.[8] Since these beads are unknown provenance, no definitive conclusion can be reached here.

In Iran and Afghanistan there are many mosques decorated with tiles of a blue called "cobalt blue." One fragment of a blue tile was collected from the blue Mosque at Tabriz in Iran, and the other, from Balkh in Northern Afghanistan. The results of chemical analyses, presented in Tables 7 and 8, demonstrate that cobalt was the origin of the color in both cases.

The coloring materials used on the pottery (*ca.* 3000 B.C.) from Tepe Sialk were also investigated. Although a similar pottery in pattern has been found in prehistoric China,[9] the coloring materials have not as yet been closely investigated. A fragment of pottery about 5×5 cm, which appeared to be a part of the base and side of a vessel, was examined. The body was light gray, and upon one surface there

Table 7. Spectrochemical analyses of glazes

No.	Place of collection	Color*	Major					Minor									Trace									
			Si	Na	Al	Ca	Mg	K	Al	Ti	Fe	Mn	Cu	Zn	Pb	Sn	P	Ni	Co	Cr	Ag	Ba	V	B	Sr	Sb	Bi
59	Bara-hissar	L.B.	○	○	○	○	○	○			○	○	○		○	○		○	○	○	○		○	○		○	○
60	Bara-hissar	B.	○	○	○	○	○	○			○	○	○		○	○		○	○	○	○		○	○	○		○
61	Bamiyan	B.	○	○	○	○	○	○		○	○	○	○		○	○		○	○	○	○		○	○			
		W.	○	○	○	○	○	○		○	○	○	○		○			○	○	○	○		○	○	○		
62	Bamiyan	B.	○	○	○	○	○	○			○	○	○		○	○		○		○	○			○		○	○
63	Bamiyan	W.	○	○	○	○	○	○		○	○	○	○		○	○		○		○	○	○	○	○	○	○	○

8) S. Oda, "Dairaman," Vol. I, The University of Tokyo, Tokyo, (1965), p. 45.

9) Kanshuku Saito, (Andersson's Pottery).

TABLE 8. ANALYSIS OF GLAZES

Color / Component	No. 64 Light-green (%)	No. 65 Dark-green (%)	No. 66 Blue (%)	No. 67 Red (%)
SiO_2	67.80	66.52	64.15	61.90
TiO_2	1.08	1.14	0.93	0.92
Fe_2O_3	0.68	0.78	2.42	1.20
MnO	tr	tr	tr	tr
Al_2O_3	12.56	3.87	4.74	2.95
MgO	1.16	0.55	1.24	4.04
CaO	2.75	7.63	3.46	6.59
CuO	0.25	7.43	0.74	0.18
ZnO		0.02		
Na_2O	8.79	8.44	16.38	16.71
K_2O	4.25	2.32	6.34	5.10
H_2O	0.98	0.40		
P_2O_5		0.18	0.53	0.43
SnO_2		1.37		
CoO			0.20	
Place collected	Kerman	Neyriz	Blue-Mosque	Yezde

TABLE 9. ANALYSIS OF THE SEPIA-COLORED MATERIAL OF A SHARD FROM TEPE SIALK

	Fe (%)	Mn (%)	Fe/Mn
Body	3.6	0.2	18.00
Paint	22.7	1.26	18.01
Paint/Body	6.3	6.3	

was a curved painted line. On this line there appeared a node of paint. A part of the body and a part of the node were removed and subjected to chemical analysis. As can be seen in Table 9, approximately 6.3 times as much iron and manganese were found in the sepia-colored part as in the body itself. It is thus obvious that iron was used as the coloring agent. However, it is difficult to state definitely whether manganese was also purposely used as an additive. The ratio of iron to manganese is about the same for both the paint used for the design and the body itself. If the manganese was purposely added to produce this sepia color, it seems to be a highly-advanced technique. The possibility exists, however, that the color was produced by an accidental discovery. Further studies will be necessary to clarify this problem.

Bronze (Slag-like Objects). In 1956 Mitsukuni Yoshida, a member of the Kyoto University Scientific Mission to the Iranian Plateau and Hindukush, discovered rock-like objects in a site at Tepe Sialk, in Iran, which is considered to be the ruins of a refinery (*ca.* 2000 B.C.). From the archaeological point of view, these pieces were obviously pieces of the slag of smelting. Although

TABLE 10. ANALYSIS OF SLAG-LIKE OBJECTS

Sample / Component	Green (%)	Black (%)	Black/Green	Black (Calculated)*
SiO_2	30.83	44.67	1.45	42.19
P_2O_5	0.46	0.21	0.46	
Fe_2O_3	14.30	20.38	1.43	19.57
TiO_2	1.22	1.07	0.88	
CuO	15.52	0.13	0.009	
Al_2O_3	10.52	8.51	0.81	
CaO	9.73	13.75	1.41	13.31
MgO	3.87	3.19	0.82	
MnO	0.06	0.11	1.83	0.83

* See text

they were collected from the same site and layer, however, they were of different colors, one being greenish and the other black. It was believed that this was an important find because it sheds more light upon the actual processes used in the smelting of copper.

Both lumps of slags were about 1.5×1.5 cm in size. Qualitative examinations showed that the chemical compositions of the two were approximately the same. The results of the quantitative determination of the major components are given in Table 10, together with the ratios of the contents of each component in the two samples. As is obvious in the table, the greatest difference between the two samples is in their copper contents. The contents of the other components change to a lesser extent. If, however, one takes the ratios of the contents of the major components, silica, ferric oxide, and calcium oxide, in the two samples, one obtains strikingly constant values, which are shown in the third column of the table.

Another way of comparing the two samples is as follows. The contents of the major components in the green sample are recomputed on the assumption that the black sample is a slag of the green one from which the copper has been almost completely extracted out. In this calculation, the copper content of the green sample was excluded and the contents of the rest of the components were assumed to amount to one hundred percent. The values in the last column of Table 10 were thus obtained; they are in good agreement with the experimental results for the black sample. According to the literature, the ore used in that era (2000 B.C.) was mainly malachite consisting approximately seventy percent of copper,[10] and it was quite precious. Although we could not determine the original ore in the present investigation, the following conclusion may be drawn. It is very probable that there were successive smelting processes; that the green sample is the slag from the first smelting processes of the

10) L. Aitchison, "A History of Metals," Vol. I, MacDonald and Evans Ltd., London (1960), p. 38.

Table 11. Composition of efflorescences

Sample layer	Major						Minor									Trace												
	Si	Na	Al	Ca	Mg	K	Fe	Mn	Mg	Ti	Ca	Cu	Na	K	Al	B	Pb	Sn	Cu	Ag	Na	Cr	Ba	Ni	V	Co	Ti	Fe
Blue-galss bowl																												
Silver	○		○				○	○	○	○	○						○	○	○	○	○	○	○					
Silver-white	○		○	○			○	○	○	○		○					○	○		○	○	○	○	○	○	○		
Purple	○		○	○			○	○	○	○			○				○	○	○			○	○			○		
Body	○	○	○	○	○	○	○	○		○		○				○	○	○		○		○	○	○	○	○		
Greenish-blue glass																												
Surface	○		○				○	○	○		○		○						○			○	○				○	
Body	○	○	○	○	○	○	○	○								○			○	○		○	○		○		○	
Light-green glass																												
Surface	○							○	○		○				○		○		○		○	○	○			○	○	○
Body	○	○	○	○	○	○	○	○				○				○	○			○		○	○	○	○	○	○	
White-glass bead																												
Surface	○			○	○		○	○		○					○	○			○	○		○	○			○		
Body	○	○	○	○	○		○	○		○				○		○			○	○		○	○	○	○			

ore, thus retaining 15.52% copper oxides, and that the black sample is the slag from the second process, in which the residue of the first processes was treated, with only 0.13% copper (II) oxide remaining. Thus, it is obvious that these ancient people had achieved a high level of technique in the process of extracting copper, the major component of bronze.

Weathering. Efflorescence caused by weathering is frequently observed on the surface of glass or glaze samples. A typical example is a fragment of a glass bowl, about 4×4 cm, collected at the ruins of Rey. A schematic picture of the sample is

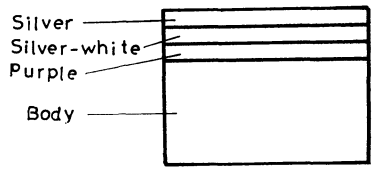

Fig. 4. Schematic diagram of weathering glass.

presented in Fig. 4. The surface of the glass shows the effects of considerable weathering. However, a silvery powder still remained on the surface. Under the weathered surface, there were silvery-white and purple layers beneath which the glass body itself could be seen.

Spectrochemical analysis was performed on each layer of the sample as well as on the sample itself. According to the results, which are shown in Table 11, the contents of such elements as magnesium, sodium, and calcium were found to decrease in proportion to the distance from the inside of the glass to the surface. Potassium was found in substantial amounts only in the glass body; in all the other layers only traces of it were found. The results of other glasses and glazes are also shown in Table 11.

It is very probable, from the chemical point of view, that the ions have partly moved out from the surface to the soil; that is, an ion exchange between the sample and the surrounding materials has taken place, thus forming the outer layers of the sample.

It should be pointed out that the excavation of not only glass objects but also any object should be done carefully, and with the extraction of as much of the surrounding soil as possible, if chemical analyses are desired. It is possible that such ion exchange as occurred with glass objects may occur with other objects. The chemical analyses of surrounding or imbedded soils may yield important clues about this.

The author wishes to express her deep gratitude to Professor Taitiro Fujinaga of the Faculty of Science, Professor Mitsukuni Yoshida of the Research Institute for Humanistic Studies, and Mr. Takenori Sonoda of the Faculty of Engineering of Kyoto University, for their kind guidance and encouragement in the course of this work.

BULLETIN OF THE CHEMICAL SOCIETY OF JAPAN VOL. 43 590—594 (1970)

The Kinetics of the Chromic Acid Oxidation of Phenylphosphonous Acid

Kalyan K. Sen Gupta

Department of Physical Chemistry, Jadavpur University, Calcuta-32, India

(Received December 9, 1968)

The kinetics of the oxidation of phenylphosphonous acid by chromic acid has been investigated. The rate at which gross concentration of chromium(VI) disappears follows a first order law. The rate increased with the increase of hydrogen ion concentration. The activation energy of the reaction was found to be 7.4 kcal. The effect of pyridine on the reaction rate confirmed the findings of Westheimer who showed that pyridine catalyzes the oxidation of isopropyl alcohol. It is suggested that the oxidation appears to proceed through the initial formation of an intermediate compound between the active form of phenylphosphonous acid with chromic acid which finally decomposes slowly by the rate determining step. The inactive form is finally oxidized by chromium(V) by very fast step.

Chromic acid oxidizes several inorganic and organic compounds. Westheimer[1] has reviewed works on this subject. Although chromic acid oxidation of some phosphorus compounds was not studied in detail, the oxidation of phosphorous acid has been studied by Dhar.[2] In the present investigation, the kinetics of the oxidation of phenylphosphonous acid by chromic acid has been reported.

Experimental

Reagents. The materials employed were of the highest purity available. Chromic acid was prepared from 'Anala R' potassium dichromate (E. Merck), and 60% perchloric acid (E. Merck) was used without any further purification. Manganous sulfate used was of 'Anala R' grade. Pyridine (B.D.H.) was purified by redistillation. Sodium perchlorate (Riedel) of analytical grade was also used without any further purification. All other reagents were chemically pure.

Synthesis of Phenylphosphonous Acid.[3] Benzene (205 g) was treated with phosphorous trichloride (109 g) under reflux for 30 hr with stirring in the presence of anhydrous aluminium trichloride (43 g). A stream of nitrogen was passed through the reaction mixture throughout the course of the reaction and 86% H_3PO_4 (15 m*l*) was added with vigorous shaking of the mixture. The precipitate was then removed by filtration using glass wool and excess benzene was removed by distillation. Finally the compound was vacuum-distilled and purified by redistillation to give dichlorophenylphosphine (bp 130°C/18 mmHg).

Found: Cl, 39.8%. Calcd for $C_6H_5Cl_2P$: Cl, 39.6%.

Dichlorophenylphosphine (1 vol) was then added to absolute alcohol (5 vol) with stirring, subsequently diluted with water (2 vol) and boiled for about 10 min. After benzene (2 vol) was added, the excess water and benzene were removed by distillation. The solution was then concentrated and the compound after isolation was purified by recrystallization from benzene. The compound after successive recrystallizations showed 99.6% purity which was checked by cerimetric oxidation[3] method (mp 85—86°C).

Found: C, 50.8; H, 5.1%. Calcd for $C_6H_7O_2P$: C, 50.7; H, 5.0%.

Kinetic Measurements. Rate studies were carried out at constant temperature (±0.1°C). The reactants were brought to thermostat temperature. The reaction was then started by the rapid addition of dichromate solution to phenylphosphonous acid and mixing was achieved by stirring. At definite time intervals, 10 m*l* portions of the reaction mixture were withdrawn and quickly transferred to a flask containing freshly prepared potassium iodide solution (2 g in 20 m*l* water). The liberated iodine was then estimated by standard sodium thiosulphate solution and finally gross concentration of chromium was estimated.

Effect of Light. The hydroxy acids are oxidized by chromic acid in the presence of light.[4] Experiments showed that the reactions in the dark as well as in diffuse daylight proceeded at the same rate and hence the reactions were performed in diffuse daylight.

Results

Rate. The rate at which gross concentration of chromium(VI) disappears follows a first order rate law. It is known[5] that when $[Cr(VI)] \leq 4.0 \times 10^{-3}$M, the concentration of $HCrO_4^-$ ions is the same as the gross concentration of chromium(VI)

1) F. H. Westheimer, *Chem. Rev.*, **45**, 419 (1949).
2) N. R. Dhar, *Ann. Chim.*, **11**, 130 (1919).
3) A. Finch, P. J. Gardner and K. K. Sen Gupta, *J. Chem. Soc., B*, **1966**, 1162.
4) A. K. Bhattacharya and N. R. Dhar, *Z. Anorg. Allg. Chem.*, **169**, 381 (1928).

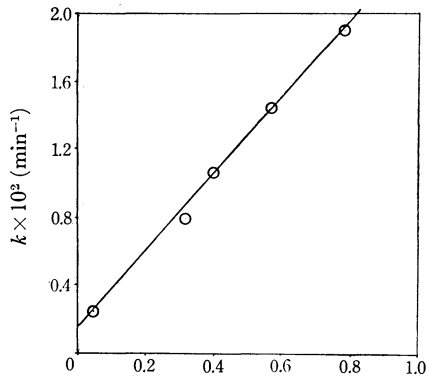

$[PhPO_2H_2]=1.032\times10^{-2}$M
$[Cr(VI)]=1.666\times10^{-3}$M
Temp.=40°C; μ=0.607

Fig. 1. Variation of rate with hydrogen ion concentration.

and the results indicate that $HCrO_4^-$ ions affect the rate of oxidation.

Stoichiometry. The stoichiometry was determined by allowing reaction mixtures containing a large excess of dichromate ion to stand for 48 hr at 30°C. The unreacted oxidant was then estimated by the usual procedure. The reaction may be represented by the following equation:

$$3PhPO_2H_2 + Cr_2O_7^{2-} + 8H^+ \longrightarrow 3PhPO_3H_2 + 2Cr(III) + 4H_2O$$

(Found: 0.31 mol of oxidant per mol of the substrate)

Effect of Hydrogen Ion on the Rate. The experiments were performed at constant ionic strength and temperature. Hydrogen ion concentration was varied by the addition of perchloric acid. The ionic strength was maintained constant with sodium perchlorate. The rate increased with the increase of hydrogen ion concentration. Figure 1 represent the plot of rate constant against [H$^+$].

Effect of Substrate Concentration on the Rate. The rates were investigated at different phenylphosphonous acid concentrations. The experiments were carried out at constant chromium(VI) concentration and temperature. The kinetic evidence indicates that an intermediate ester is formed during oxidation. The plot $1/k$ against 1/ (Substrate) labels the corresponding $1/k$ axis, indicating the formation of an intermediate compound[6] (Fig. 2). Waters and Jones[7] have shown that oxalic acid forms complexes with vanadium (V) and these complexes undergo decomposition. Since vanadium has several chemical similarities to chromium(VI), our assumption regarding the intermediate formation of an ester is quite plausible. In a more recent study, Rao and Ayyar[8] have also shown that the oxidation of oxalic acid by chromic acid proceeded through the initial formation of a metal complex. Similar is the case with glycerol[9] when it is oxidized by chromic acid. The formation of a complex species by interaction of chromium(VI) with several oxyacids has been reported by Lee and Stewart.[10]

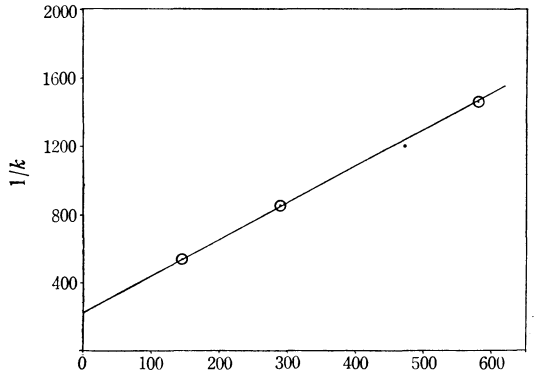

[Cr(VI)]=1.666×10^{-3}M, Temp.=40°C

Fig. 2. Influence of substrate concentration on the rate constant.

$$HCrO_4^- + H^+ + HA \rightleftharpoons HO\text{-}CrO_2\text{-}A + H_2O$$

where,

A = -OAc, $-SO_3H$, $-HCrO_4$, and $-OPO_3H_2$

Influence of Solvent. The reaction was studied in various acetic acid-water binary mixtures. The

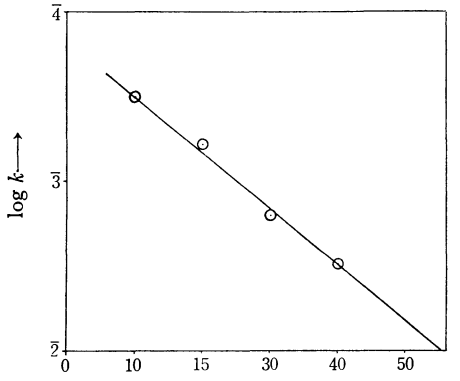

[PhPO$_2$H$_2$]=2.038×10^{-2}M
[Cr(VI)]=3.333×10^{-3}M
Temp=32°C

Fig. 3. Effect of solvent composition on the rate of oxidation.

5) G. V. Bakore and S. Narain, *J. Chem. Soc.*, **1963**, 3421.
6) K. K. Sen Gupta, This Bulletin, **42**, 298 (1969).
7) W. A. Waters and J. R. Jones, *J. Chem. Soc.*, **1961**, 4757.
8) G. G. Rao and R. V. V. Ayyar, *Z. Phys. Chem.*, **236**, 17 (1967).
9) K. K. Rohatgi and P. K. Bhattacharya, *Indian J. Chem.*, **5**, 195 (1967).
10) D. G. Lee and R. Stewart, *J. Amer. Chem. Soc.*, **86**, 305 (1964).

Table 1. Variation of rate with oxidant

$[PhPO_2H_2]=1.032\times10^{-2}$M, Temp.=40°C, $[H^+]=0.325$M

No.	$[Cr(VI)]\times10^{-3}$M	$k\times10^3$ (min^{-1})
1	1.666	5.527
2	3.332	3.070
3	4.998	2.303

dielectric constants of acetic acid-water mixtures are not known. Therefore, if it is assumed that the reciprocal of the dielectric constant of the mixture is proportional to the percentage of acetic acid in the solvent mixture, it has been noticed that the rate increases with the decrease in dielectric constant indicating ion dipole interaction. The increased rate of oxidation of isopropyl alcohol by chromic acid in 86.5% acetic acid has been explained[11,12] on the basis of increased protonation of $HCrO_4^-$ before the reaction in a solvent of low dielectric constant. Figure 3 shows that logarithm of the rate constant increases with the increase in the proportion of acetic acid in the mixture.

Effect of Oxidant. The reaction was also studied at different chromium(VI) concentrations, but the concentrations of phenylphosphonous acid and hydrogen ions were kept constant. Table 1 summarizes the results of the oxidation, which shows that the rate constant decreases with the increase of chromium(VI) concentration. A complication concerning chromic acid oxidation may arise due to the fact that different ionic species of chromium(VI) can exist in solution.[13] The neutral chromate ion, CrO_4^{2-}, has no oxidizing ability and in aqueous solution the dichromate ion, $Cr_2O_7^{2-}$, is formed by the rapid equilibrium

$$2HCrO_4^- \rightleftharpoons (Cr_2O_7)^{2-} + H_2O$$

Thus with the increase of the concentration of chromium(VI), a progressively smaller portion of the total amount of chromium appears in the form of an acid chromate ion, and we observe that the rate constants decrease with increasing chromium(VI) concentration.

Retarding Influence of Added Oxidizable Ions. It has been observed that commonest oxidations involve only a one-electron transfer though instances are not rare where the change involves a two-electron transfer. In the present work, the starting material is chromic acid or the acid chromate ion and the end product is trivalent chromium in a solvated condition. In the present study the rate of oxidation is diminished to one third of that in the absence of manganous ions, when the concentration of manganese(II) is 5.0×10^{-2}M. (Table 2) This is possibly due to the fact that manganous ions catalyze the disproportionation of intermediate valence states of chromium and also indicates that chromium(IV) is probably an intermediate. Since manganese dioxide does not accumulate in the reaction mixture, it may be reasonable to propose the following reaction in the presence of manganous ions.

$$3Cr(IV) + Mn(II) \longrightarrow HCrO_4^- + 2Cr(III) + (Mn(II))$$

and not the reactions

$$Cr(IV) + Mn(II) \longrightarrow Cr(III) + Mn(III)$$

$$2Mn(III) \longrightarrow Mn(II) + MnO_2$$

as suggested by Westheimer[1] for the oxidation of arsenious acid by chromic acid.

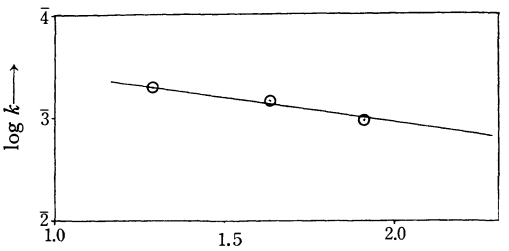

$[PhPO_2H_2]=1.032\times10^{-2}$M
$[Cr(VI)]=1.666\times10^{-3}$M
$[H^+]=0.0548$M, Temp.=40°C

Fig. 4. Variation of ionic strength on the rate of oxidation.

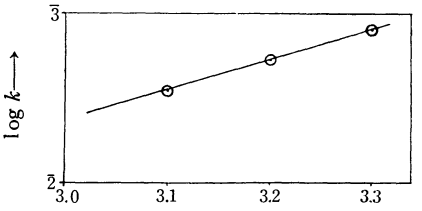

$[PhPO_2H_2]=2.036\times10^{-2}$M
$[Cr(VI)]=1.666\times10^{-3}$M
$[H^+]=0.01862$M
Acetic acid=50%

Fig. 5. Arrhenius plot of log k *vs.* $1/T$.

Effect of Ionic Strength. The rate was studied at different ionic strengths of the reaction mixtures. The ionic strength was varied by the addition of sodium perchlorate. The rate of the reaction was increased with the increase of ionic strength. Figure 4 represents the plot of log k against $\mu^{1/2}$, where μ is the ionic strength.

11) W. A. Waters, "Mechanisms of Oxidation of Organic Compounds," Methuen's Monograph, London (1964), p. 60.

12) M. Cohen and F. H. Westheimer, *J. Amer. Chem. Soc.*, **74**, 4387 (1952).

13) K. B. Wiberg, "Oxidation in Organic Chemistry," Part A, Academic Press, New York (1965), p. 71.

Table 2. Effect of Mn(II) on the rate constant

$[PhPO_2H_2]=1.032\times10^{-2}$M, $[Cr(VI)]=1.666\times10^{-3}$M, $[H^+]=0.0575$M, Temp.=40°C

No.	$[Mn(II)]\times10^2$	$k\times10^3$ (min^{-1})
1	0	0.844
2	3.3	0.4606
3	5.0	0.2763

Table 3. Effect of pyridine on the rate constant

$[PhPO_2H_2]=1.828\times10^{-2}$M, $[Cr(VI)]=1.666\times10^{-3}$M, $[H^+]=0.282$M, $\mu=0.25$, Temp.=40°C.

No.	[Pyridine]	$k\times10^{-3}$ (min^{-1})	$k\times10^{-2}/\{[H^+]-[Py]\}$
1	0	3.137	1.114
2	2×10^{-2}M	3.396	1.295
3	4×10^{-2}M	3.685	1.521
4	6×10^{-2}M	4.012	1.807

Variation of Rate with Temperature. The plot of log k against $1/T$ has been represented in Fig. 5. The experiments were carried out at constant ionic strength and hydrogen ion concentrations. From the slope of log k *vs.* $1/T$ plot, the activation energy has been calculated to be 7.4 kcal/mol. It is interesting that the activation energy calculated in the cases of the oxidation of some hydroxy acids by chromic acid are of the same orders.[5] Such closeness of value suggests that same mechanism may be operative for the rate controlling step of the reaction.

Effect of Pyridine on the Reaction Rate. The rate studies have been carried out in different pyridine concentrations. The results have been recorded in the Table 3. If pyridine catalyzes the oxidation, the value $k/\{[H^+]-[Py]\}$ is expected to increase with the increase in the concentration of pyridine which is in agreement with the experimental finding. It is also known[5] that pyridine effectively removes hydrogen ions and the effective hydrogen ion concentration would correspond to $\{[H^+]-[Py]\}$. The result confirmed the findings of Westheimer who showed that pyridine catalyze the oxidation of isopropyl alcohol.

Discussion

Oxidation of a variety of organic compounds by chromic acid has been investigated. As result of the pioneering work of Westheimer and his co-workers, the details of the mechanism of some reactions have been well elucidated. In connection with the oxidation of isopropyl alcohol by chromic acid, Westheimer[1] considers that the oxidation involves the rapid formation of a chromate ester, followed by the interaction with a base, and water plays the role of base in the slow rate determining step. In our case, we have also evidence for ester formation between phenylphosphonous acid and the acid chromate ion. It is well known that at very low concentration of dichromate solution[5,9] ($\sim4.0\times10^{-3}$M) the hexavalent chromium exists wholly as $HCrO_4^-$. This anion possibly reacts with phenylphosphonous acid to give an ester. But phenylphosphonous acid is said to exist in two forms, normal and active form which are tautomers[14] of the structures:

(I) active (II) normal

Other phosphorous compounds[15] also exhibit the same sort of behaviour. Griffith and McKeown[15] have postulated the interconversion between normal and active forms of phosphorous acid and also dialkyl phosphites to explain their respective results on the oxidation of phosphorous acid and dialkyl phosphites by iodine. The existence of tautomeric equilibrium of phosphorous acid has also been discussed by Finch *et al.*[16] who concluded that both forms of phosphorous acid exist. Carrol and Thomas[17] and recently Gupta and Mishra[18] studied the oxidation of hypophosphorous acid by cerium(IV) ion and showed that the following equilibrium exists in solution.

$$H_3PO_2(\text{normal}) + H^+ \underset{k'_{H^+}}{\overset{k_{H^+}}{\rightleftharpoons}} H_3PO_2(\text{active}) + H^+ \quad (1)$$

followed by the reaction of the active form with the oxidizing agent:

$$H_3PO_2 + OX \xrightarrow{k_{OX}} H_3PO_3 + \text{reaction product} \quad (2)$$

The presence of active form in the case of hypophosphorous acid has also been indicated by Jenkins and Yost[19] who proved that $H-\ddot{P}\begin{smallmatrix}OH\\OH\end{smallmatrix}$ is a better electron donor than the normal form of the structure $\begin{smallmatrix}HO\\H\end{smallmatrix}\!\!>\!P\!<\!\begin{smallmatrix}O\\H\end{smallmatrix}$. Therefore it is quite likely that at high acid concentration, the active form of phenylphosphonous acid is predominating although we cannot totally exclude the presence of normal form in solutions, since the monobasic

14) A. W. Frank, *Chem. Rev.*, **61**, 389 (1961).
15) R. O. Griffith and A. McKeown, *Trans. Faraday Soc.*, **36**, 767 (1940).
16) A. Finch, P. J. Gardner and I. H. Wood, *J. Chem. Soc.*, **1965**, 746.
17) R. L. Carrol and L. B. Thomas, *J. Amer. Chem. Soc.*, **88**, 1376 (1966).
18) S. K. Mishra and Y. K. Gupta, *J. Inorg. Nucl. Chem.*, **29**, 1943 (1967).
19) W. A. Jenkins and D. M. Yost, *ibid.*, **11**, 297 (1959).

character of phenylphosphonous acid can only be explained assuming the normal form of the acid. However, the oxidation of phenylphosphonous acid may proceed in two different ways. Phenylphosphonous acid on initial oxidation may give phenol and phosphorous acid with the consumption of one oxygen atom, followed by the oxidation of the latter to H_3PO_4 with the consumption of another oxygen atom according to the equation

$$PhPO_2H_2 + 2O + H_2O \longrightarrow PhOH + H_3PO_4 \quad (3)$$

Some phosphonous acids also undergo scission[9] of the carbon-phosphorous bond at temperature below the disproportionation temperature. The consumption of one oxygen atom and the absence of phenol in the reaction mixture rule out the possibility of reaction (3). Consequently, phenyl phosphonous acid is oxidized to give phenyl phosphonic acid according to the equation

$$PhPO_2H_2 + O \longrightarrow PhPO_3H_2 \quad (4)$$

It is, therefore, reasonable to suppose that the oxidation of phenylphosphonous acid proceeds in the following manner. The rapid reversible formation of a chromate ester can best be explained by assuming the active form of the acid in the following way:

$$Ph-\ddot{P}\begin{matrix}OH\\OH\end{matrix} + HCrO_4^- + H^+ \overset{\text{fast}}{\rightleftharpoons} Ph-\ddot{P}(OH)-O-\overset{\overset{O}{\|}}{Cr}(=O)-OH + H_2O \quad (5)$$

followed by the decomposition of the ester to give a cation of the type $Ph-\overset{+}{P}(OH)=O$ and chromium(IV) by a slow rate determining step

$$Ph-\ddot{P}(OH)-O-\overset{\overset{O}{\|}}{Cr}(=O)-OH \xrightarrow[\text{slow}]{k} Ph-\overset{+}{P}(OH)=O + Cr(IV) \quad (6)$$

The cation which has been obtained in step (6) reacts with water and by fast step gives phenylphosphonic acid:

$$Ph-\overset{+}{P}(OH)=O + H_2O \overset{\text{fast}}{\longrightarrow} Ph-P(OH)(OH)=O + H^+ \quad (7)$$

Chromium(IV) produced in process (6) is then converted to chromium(V) either by reacting rapidly with chromium(VI) or chromium(IV) itself, undergoes rapid disproportionation in the following manner:

$$Cr(IV) + Cr(VI) \overset{\text{fast}}{\longrightarrow} 2Cr(V) \quad (8)$$

$$2Cr(IV) \overset{\text{fast}}{\longrightarrow} Cr(III) + Cr(V) \quad (9)$$

Similar steps have been considered in many reactions.[8,20] Finally chromium(V) formed oxidizes the inactive form of the phenylphosphonous acid rapidly abstracting two electrons, and is reduced to Cr(III) by fast step as

$$Cr(V) + Ph-\overset{\overset{O}{\|}}{P}(OH)-H + H_2O \overset{\text{fast}}{\longrightarrow} Cr(III) + Ph-\overset{\overset{O}{\|}}{P}\begin{matrix}OH\\OH\end{matrix} + 2H^+ \quad (10)$$

The standard oxidation potential of chromium(V) - chromium(III) couple exceeds 1.75 V whereas the same for chromium(VI)-chromium(III) couple is 1.36 V. This suggests that chromium(V) is a much more active oxidant than chromium(VI) which is possibly responsible for the oxidation of inactive form of phenylphosphonous acid.

Thanks are due to Dr. M. N. Das, Head of the Physical Chemistry Section for laboratory facilities. Part of the investvation was carried out during the tenure of Scientists' Pool.

20) K. K. Sen Gupta and S. D. Bhattacharya, *Z. Phys. Chem.* (Leipzig), **240**, 279 (1969).

BULLETIN OF THE CHEMICAL SOCIETY OF JAPAN VOL. 43 595—597 (1970)

Studies of Ion Exchange Membranes. XXXI. The Hydrogen Peroxide Treatment of the Cation Exchange Membrane of Ferric Ion Form

Yukio MIZUTANI

Tokuyama Soda Co., Ltd., Tokuyama, Yamaguchi

(Received February 3, 1969)

Neosepta CL-2.5T, the cation-exchange membrane prepared by the "Paste Method," of the ferric-ion form was treated with hydrogen peroxide, and the changes in the membrane properties (the thickness, the water content, and the ion-exchange capacity) were measured. The porous membrane, having no ion-exchange capacity, was obtained by the treatment with hydrogen peroxide and the water permeation through the membrane was measured. Assuming the capillary model, the water-permeability data of this membrane suggested that the apparent pore radius of this membrane was 15—17 mμ and that the apparent pore distance was about 40 mμ. This suggests that Neosepta CL-2.5T contains a minute and continuous heterogeneity; *i.e.*, there is a localized distribution of the ion-exchange resin component within the membrane.

The present author has previously proposed the "Paste Method"[1-4] as a practical procedure for the preparation of an ion-exchange membrane. In this procedure, a fine powder of polyvinyl chloride (PVC) and a monomer mixture, mainly consisting of styrene (St) and divinylbenzene (DVB), were mixed to prepare a paste, and then this paste was coated onto Teviron cloth (a reinforcing material). The resultant polymer composite was heated to polymerize the monomers and to convert the PVC powder to a PVC gel. Then, an ion-exchange group was introduced to the base membrane by sulfonation or chloromethylation and amination with trimethylamine. The ion-exchange membrane thus prepared (commercial name, Neosepta) has been used in electrodialytic concentration[5-7] or in the desalination of sea water.[8] One of the characteristic properties of this ion-exchange membrane is its excellent flexibility, which makes it easy to handle the membrane in practical use; this fact also suggests that the structure of the membrane may be different from a rigid gel-structure such as, for example, that of amberlite IR-120.

In a preceding paper,[9] the chemical structure of the ion-exchange membrane prepared by the "Paste Method" was studied by means of extraction with tetrahydrofuran and it was concluded that the fine powdery ion-exchange resin component, extractable through a filter paper with tetrahydrofuran, was present, while the matrix of the ion-exchange resin component was complicatedly entwined with the PVC chain and there was a graft copolymer of the former onto the latter. In this study, the chemical structure of the ion-exchange membrane prepared by the "Paste Method" was investigated by making use of the treatment with hydrogen peroxide.

Experimental

The Sample. Prior to the experiment, Neosepta CL-2.5T was treated alternately with 0.1N aqueous solutions of sodium chloride and hydrochloric acid; thus the membrane properties were made stationary. The ion-exchange capacity, the thickness, and the water content were measured at 21°C by ordinary methods.

The Treatment with Hydrogen Peroxide. After Neosepta CL-2.5T of the hydrogen-ion form had been soaked in an aqueous solution of ferric chloride (0.15 mol/*l*), the surface of the membrane was wiped with a filter paper and the membrane was soaked in an aqueous solution of hydrogen peroxide (5—6%) at room temperature with intermittent stirring.

The Measurement of the Water Permeability. The apparatus is shown in Fig. 1. The pressure difference (Δp) between the both sides of the membrane

1) Y. Mizutani, W. Tesima and S. Akiyama, Japan. 410368.

2) Y. Mizutani, W. Tesima, S. Akiyama, R. Yamane and H. Ihara, Japan. 481838.

3) Y. Mizutani, R. Yamane, H. Ihara and H. Motomura, This Bulletin, **36**, 361 (1963).

4) Y. Mizutani, R. Yamane and H. Motomura, *ibid.*, **38**, 689 (1965).

5) R. Yamane, T. Sata and Y. Mizutani, *Nippon Kaisui Gakkai Shi*, **20**, 313 (1967).

6) R. Yamane, H. Motomura, T. Sata and Y. Mizutani, *ibid.*, **20**, 327 (1967).

7) R. Yamane, M. Ichikawa, Y. Mizutani and Y. Onoue, *Ind. Eng. Chem., Process Des. Develop.*, **8**, 159 (1969).

8) T. Matsuda, S. Ogawa and Y. Onoue, *Desalination*, **3**, 295 (1967).

9) Y. Mizutani, This Bulletin, **42**, 2459 (1969).

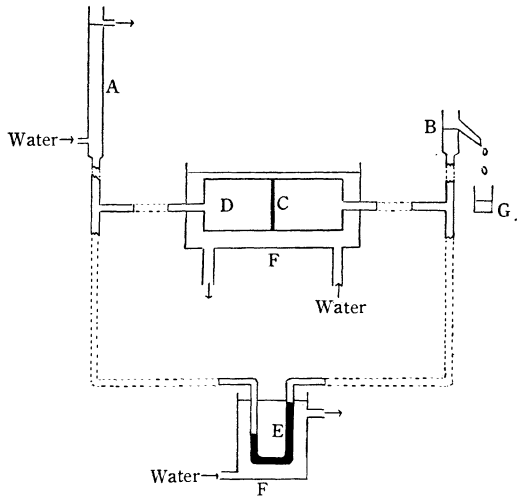

Fig. 1. The apparatus.
A, B: Leveling bulb C: Membrane
D: Cell E: Hg differential manometer
F: Thermostat G: Weighing bottle

was measured by means of the mercury differential manometer (E). While the Δp value was kept constant, the water permeating in a given period was collected in a weighing bottle (G) and weighed. The temperature of the thermostat (F) was 21°C. The effective area of the membrane was 20 cm².

Characterization of the Water Permeability Through the Membrane. The size and the number of pores of a porous diaphragm can be calculated by applying D'Arcy's law and Poiseuille's law, as has been done for a porcelain diaphragm by Sanada.[10] The following equation is well-known as D'Arcy's law, relating to water permeability through a porous membrane:

$$K_p = \frac{Q\eta L}{A\Delta p} \tag{1}$$

where K_p is the specific permeability (cm²); Q, the permeation rate (cm³/sec); A, the effective area of the membrane (cm²); η, the viscosity of water (poise); Δp, the pressure difference (dyne/cm²), and L, the thickness of the membrane (cm).

Assuming that a pore is cylindrical and that it is vertical to the membrane plane and does not intercross with it, Poiseuille's law (Eq. (2)) can be applied to the water permeation through the pore:

$$V = \frac{\pi r^4 \Delta p}{8\eta L} \tag{2}$$

where r is the pore radius (cm) and V, the permeation rate through a pore (cm³/sec). Therefore, the permeation rate through the porous membrane can be expressed as follows:

$$Q = \frac{nA\pi r^4 \Delta p}{8\eta L} \tag{3}$$

where n is the pore number/cm².

On the other hand, the porosity of the membrane (ε) is given by Eq. (4):

$$\varepsilon = \frac{W_e - W_d}{AL\rho_w} = \pi r^2 n \tag{4}$$

where W_e is the wet weight of the membrane (g); W_d, the dry weight of the membrane (g), and ρ_w, the specific gravity of water. By comparing Eqs. (1), (3), and (4), Eqs. (5) and (6) can be derived:

$$r = \sqrt{\frac{8\pi LQ}{\varepsilon A\Delta p}} = \sqrt{\frac{8}{\varepsilon}K_p} \tag{5}$$

$$n = \frac{\varepsilon^2}{8\pi K_p} \tag{6}$$

Assuming the square array of the pores, the apparent pore distance (δ, cm) can be given by Eq. (7).

$$\delta = \frac{1}{\sqrt{n}} \tag{7}$$

Results and Discussion

As a preliminary, it was confirmed that Amberlite IR-120 was completely decomposed by the treatment with hydrogen peroxide, while PVC was essentially stable under the same treatment.

Figure 2 shows the change in the membrane

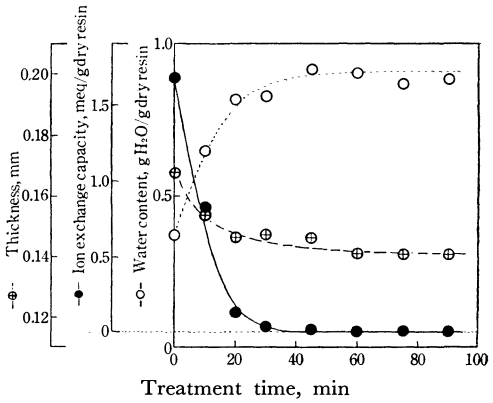

Fig. 2. The membrane properties *vs.* the treatment time with hydrogen peroxide.

properties *vs.* the treatment time with hydrogen peroxide. After 40 min, the thickness and the water content became constant, and the ion-exchange capacity was completely lost. The decrease in the thickness can be attributed to the decrease in the swelling pressure due to lack of the ion-exchange group. Contrary to the decrease in the thickness, the water content increased. This can be explained by the increase in the membrane porosity caused by the decomposition of the ion-exchange resin component within the membrane.

Figure 3 shows the dry weight of the membrane against the treatment time with hydrogen peroxide. After more than 40 min, constant values were observed. Table 1 shows the change in the chlorine content of the membrane *vs.* the treatment time with hydrogen peroxide. The chlorine content gradually decreased with the increase in the treatment time, approaching a constant value after 75—90 min. However, the decreased chlorine contents

10) S. Sanada, *Kogyo Kagaku Zasshi*, **42**, 625 (1939).

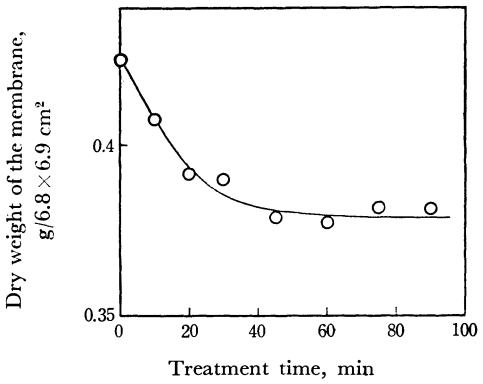

Fig. 3. Dry weight of the membrane *vs.* the treatment time with hydrogen peroxide.

Table 1. The chlorine content of the membrane treated with hydrogen peroxide

Treatment time, min	45	60	75	90
Cl content, %	54.82	54.74	54.08	54.12

are less than that of polyvinyl chloride itself (56.4%). This indicates the treatment with hydrogen peroxide caused not only the decomposition of the ion-exchange resin component but also a slight decomposition of the polyvinyl chloride.

Thus, Neosepta CL-2.5T was transformed to a pale yellowish brown membrane after the complete decomposition of the ion-exchange resin component, and the resultant membrane showed definite properties and an appreciable water permeability, indicating that the membrane was porous. Figure 4

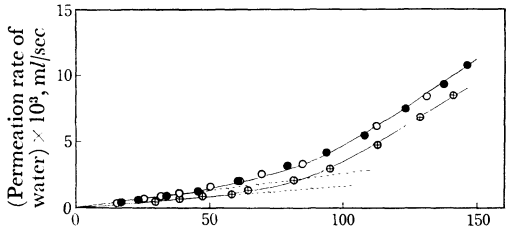

Fig. 4. The permeation rate of water *vs.* the pressure difference between both sides of the membrane.
Treatment time
⊕: 45 min ●: 75 min ○: 90 min

shows the experimental results on the water permeation. When Δp is small, a linear relation was observed between the permeation rate of water and Δp. From the slopes of this straight line, the specific permeation rate was calculated according to Eq. (1). The calculated values are cited in Table 2. As is shown in Table 2, the apparent pore radius is 15—17 mμ, and the apparent pore distance, about 40 mμ.

Table 2. The experimental results

Treatment time, min	45	75	90
$(Q/\Delta p)\times 10^8$, cm⁵/sec·g	1.84	2.65	2.65
$K_p\times 10^{13}$, cm²	1.26	1.81	1.81
ε	0.500	0.509	0.513
$r\times 10^6$, cm	1.5	1.7	1.7
$n\times 10^{-10}$, cm^{-2}	7.9	5.7	5.8
$\delta\times 10^6$, cm	3.6	4.2	4.2

η: 0.981 centipoise at 21°C

These values are in good agreement with the results of the previous paper,[9] in which there was a fine powdery cation-exchange resin component of 50 mμ or less in the cation-exchange membrane prepared by the "Paste Method." Furthermore, the obtained result suggests that the structure of Neosepta CL-2.5T is different from that of both Amberlite IR-120 having a rigid gel-structure and that of a mosaic-type membrane[11,12] having a discontinuous heterogeneity of the ion-exchange resin component.

A membrane structure such as that described above may be comprehended by considering the mechanism of the process of preparing the base membrane. Since St and DVB were polymerized in a gel phase of PVC, the St-DVB matrix should be complicatedly entwined with the PVC chain and the former should be grafted onto the latter. This may be supported by the fact that a graft copolymer is formed when St is polymerized in a PVC film.[13] These facts should be effective in improving the homogeneity of the membrane. However, while a gel phase of PVC is comiscible with both St and DVB, it is immiscible with polystyrene; thus, the resultant polymer should be separated in a fine powdery form. This may be deduced from the fact that a fine powdery polymer is obtained when *n*-heptane, which is comiscible with both monomers but immiscible with polystyrene, is used in place of PVC.[14,15] This should engender the heterogeneity of the membrane and, in fact, is probably the reason why Neosepta CL-2.5T was transformed into the microporous membrane with no ion-exchange capacity upon treatment with hydrogen peroxide.

In conclusion, Neosepta CL-2.5T contains a minute and continuous heterogeneity; *i.e.*, there is a localized distribution of the ion-exchange resin component. Furthermore, the excellent flexibility of Neosepta CL-2.5T may be attributed to the heterogeneity described above. Further details will be investigated in the future.

11) M. R. J. Wyllie and H. W. Patnode, *J. Phys. Chem.*, **54**, 204 (1950).
12) M. R. J. Wyllie and S. L. Kanaan, *ibid.*, **58**, 73 (1954).
13) Y. Mizutani, *Kogyo Kagaku Zasshi*, **65**, 1124 (1962).
14) Y. Mizutani, This Bulletin, **39**, 1088 (1966).
15) Y. Mizutani, *ibid.*, **40**, 1519 (1967).

BULLETIN OF THE CHEMICAL SOCIETY OF JAPAN VOL. 43 598—600 (1970)

Kinetics and Mechanism of the Silver Catalysed Oxidation of Malic Acid by Potassium Peroxydisulphate

G. L. AGRAWAL[*1] and Arun K. BHATTACHARYA[*2]

Department of Chemistry, University of Saugor, India

(Received January 29, 1969)

Preliminary experiments showed that the reaction between malic acid and potassium peroxydisulphate is very slow. The reaction rate becomes a measurable value at 25°C by introducing the Ag^+ ion as a catalyst. The total order of the reaction has been found to be nearly unity. The effect of the concentration of catalyst and malic acid has been studied. The temperature coefficient of the reaction between the temperature range of 30 and 45°C is 1.76 and the mean value of the energy of activation is 10.9 kcal. The frequency factor and entropy of activation are 16.8×10^5 sec^{-1} and −41.1 e.u. respectively. The probable mechanism for the reaction has been suggested.

The reaction between potassium peroxydisulphate and several reducing ions such as oxalate, formate, *etc.*, has been studied by a number of workers and various mechanisms have been suggested to explain the reactions in each case. Ghosh and co-workers[1] following the work of King[2] and Howell[3] studied the catalysed and uncatalysed reaction between oxalic acid and potassium peroxydisulphate. Allen[4] studied the copper catalysed reaction between potassium formate and potassium peroxydisulphate. The kinetics of the reaction between potassium formate and potassium peroxydisulphate also formed a topic of study of Ghosh *et al.*[5] Saxena and Singhal[6] have studied the reduction of peroxydisulphate with tartaric acid.

A study of literature (*loc. cit.*) showed that the reaction between malic acid and potassium peroxydisulphate has not been studied so far. The authors have therefore taken up the study of this in order to arrive at the general mechanism of the reaction.

Preliminary experiments showed that the reaction in the absence of any catalyst is very slow. However, the rate is enhanced by the introduction of Ag^+ ion as a catalyst.

Experimental

All the chemicals used were that of purest quality available. Solutions were prepared in redistilled water. Calculated amounts of malic acid and silver nitrate solutions were taken in a reaction vessel kept in a Townson and Mercer, Croydan Thermostat (adjustable upto ±0.1°C). The flask containing potassium peroxydisulphate was also kept in the thermostat to attain the temperature of the bath. After attaining the required temperature in the bath, the two solutions were mixed in order to initiate the reaction. At suitable intervals of time, 10 m*l* of the reaction mixture were withdrawn and added to 10 m*l* of an ice cold solution of 10% potassium iodide in order to estimate the unreacted potassium peroxydisulphate. The flask was allowed to remain for five minutes in order to liberate the iodine. The liberated iodine was titrated by a standard solution of sodium thiosulphate using starch as an indicator.

Results

Order of Reaction. The total order of the reaction was calculated employing the isolation method. The data of experiments are recorded in Tables 1 and 2. Column 1 gives the time in minutes, colum 2 volume of sodium thiosulphate used to titrate the liberated iodine at various time intervals and column 3 the values of k. "a" is the volume of sodium thiosulphate at the start of the reaction and $a-x$ is the volume of sodium thiosulphate at different time. Since k exhibits satisfactory consistency, the order with respect to potassium peroxydisulphate must be unity.

By making a run at each of two different initial concentrations of any one component, the other concentrations remaining constant, the data will enable the determination of the order of the reac-

*1 Present address: Departmento de quimica, Universidad de oriente, Cumaná, Venezuela.

*2 Present address: 438 Wallce drive, Fairborn, Ohio 45324, U.S.A.

1) S. P. Srivastava and S. Ghosh, *Z. Physik Chem.*, **202**, 191 (1953); **205**, 332 (1956).

2) C. V. King, *J. Amer. Chem. Soc.*, **49**, 2869 (1927); **50**, 2089 (1928).

3) W. J. Howells, *ibid.*, **61**, 463 (1939).

4) T. L. Allen, *ibid.*, **73**, 3589 (1951).

5) S. P. Srivastava and S. Ghosh, *Z. Physik Chem.*, **202**, 198 (1953); **207**, 161, 1957.

6) L. K. Saxena and C. P. Singhal, *J. Ind. Chem. Soc.*, **38**, 346 (1961); *J. Phys. Chem.*, **211**, 161 (1959); *ibid.*, **214**, 179 (1960).

Table 1

(Temperature 25°C)

Reaction mixture	Overall concentration
Malic acid	0.0330M (C_2')
Potassium peroxydisulphate	0.0066M
Silver nitrate	0.00066M

Time (min)	Volume of $Na_2S_2O_3$ (ml)	$k\times10^{-2}=2.303/t\log\frac{a}{a-x}$
1	13.10	—
5	12.00	1.75
10	10.80	1.93
15	9.90	1.87
20	8.90	1.93
25	8.00	1.97
30	7.00	2.10
40	5.95	1.98
	Mean value	1.93

Table 2

(Temperature 25°C)

Reaction mixture	Overall concentration
Malic acid	0.0660M (C_2'')
Potassium peroxydisulphate	0.0066M
Silver nitrate	0.00066M

Time (min)	Volume of $Na_2S_2O_3$ (ml)	$k\times10^{-2}=2.303/t\log\frac{a}{a-x}$
1	13.00	—
5	12.00	1.60
10	11.00	1.67
15	10.20	1.67
20	9.40	1.62
25	8.70	1.61
30	8.00	1.62
35	7.65	1.52
40	7.15	1.50
45	6.50	1.54
50	6.00	1.55
	Mean value	1.59

tion with respect to that component.[7] Using the data given in Tables 1, 2 and 3, the order of reaction with respect to malic acid was determined by means of the equation

$$n=\frac{\log\frac{k_1'}{k_2''}}{\log\frac{C_2'}{C_2''}}$$

where k_1' and k_2'' are the first order rate constants obtained at two different concentrations of malic acid C_2' and C_2''. The value of n is -0.3 which suggests that the rates of reaction are slightly

7) A. A. Frost and R. G. Pearson, "Kinetics and Mechanism," John Wiley, New York (1961), p. 45.

Table 3

$[K_2S_2O_8]=0.0066M$, $[AgNO_3]=0.00066M$

Temperature	[Malic acid]	$k\times10^{-2}$ (min^{-1})	
25°C	0.0330M	1.93	$n=-0.27$
25°C	0.0660M	1.59	
30°C	0.1330M	1.57	
35°C	0.1638M	1.50	$n=-0.32$
35°C	0.3276M	1.21	

dependent on the concentration of reducing ions. Thus the total order of the reaction is 0.7 which may be taken as unity *i. e.* the velocity at any instant is dependent on the peroxydisulphate concentration only.

Effect of Malic Acid. Different sets of experiments were carried out at different concentrations of malic acid in order to study is behaviour on the reaction rates. The results are tabulated in Table 3.

A perusal of the above table shows that the value of the first order rate constant decreases with simultaneous increase in malic acid concentration and temperature. The effect can be seen clearly that even increase in temperature has little effect on the rate indicating the important role of malic acid concentration on the reaction mechanism.

Effect of Silver Nitrate Concentration. In order to decide the role of silver nitrate as catalyst on the kinetics of the reaction, the study was carried out using different concentration of $AgNO_3$. The observations are given below:

Table 4

(Temperature 25°C)

$[K_2S_2O_8]=0.0066M$, [Malic acid]$=0.0660M$

[Silver nitrate]	$k\times10^{-2}$ (unimolecular)
0.00066M	1.57
0.00100M	2.28
0.00133M	3.16

The above data indicates that the rate is dependent on the catalyst concentration. When a graph is plotted between $AgNO_3$ concentration and the rate constant, a linear curve is obtained indicating that the rate is linearly related to $AgNO_3$ concentration *i. e.* $dx/dt\propto[Ag^+]$ (Fig. 1)

Temperature Coefficient. The reaction velocities were measured at four different temperatures. All the four experiments were performed at the identical concentration of the reactants. The values of temperature coefficient calculated are given in Table 5.

Energy and Entropy of Activation. The average value of energy of activation (E) was found to be 10.9 kcal. The value of E is also calculated graphically by plotting $1/T$ *vs.* log k and is found

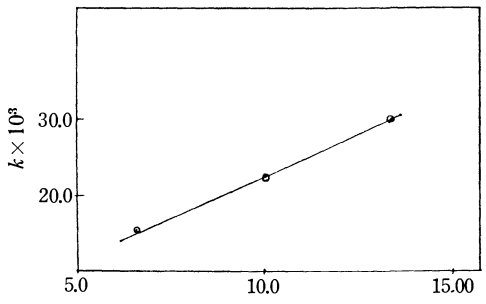

$[AgNO_3]\times10^4$M

Fig. 1. Concentration of $AgNO_3$ *vs.* *K*.

TABLE 5

$[K_2S_2O_8]$=0.0066M, [Malic acid]=0.0660M
$[AgNO_3]$=0.00066M

Temperature	$k\times10^{-2}$ (in units)	Temperature coefficient
30°C	2.28	$k(t+10)/k(t)$
40°C	4.12	1.81 (30—40°C)
35°C	3.64	1.70 (35—45°C)
45°C	6.12	
	Average value 1.76	

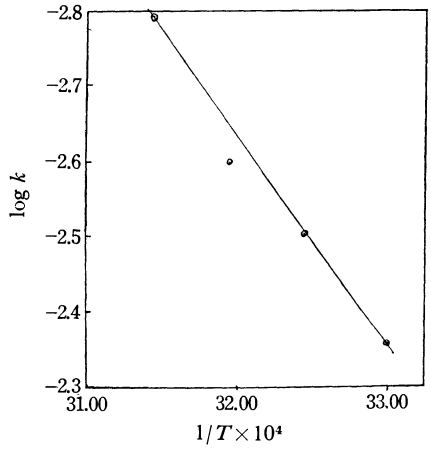

Fig. 2. Plot of log *k* *vs.* $1/T$.

to be 11.4 kcal (Fig. 2). The value of frequency factor with E=10.9 kcal at 40°C is 16.8×10^5 sec^{-1} and entropy of activation at 40°C is −41.1 e. u.

Discussion

The total order of the reaction between potassium peroxydisulphate and malic acid in presence of Ag^+ ion as a catalyst comes out near unity. Then the observed rate equation is

$$-\frac{d(S_2O_8^{2-})}{dt} = k(S_2O_8^{2-})\ (\text{malic acid})^{-0.3}\ (Ag^+)$$

which represents that velocity at any instant is largely proportional to the peroxydisulphate concentration.

Since the rate of reactions catalysed by silver ions are very much independent of the reductant concentrations, it has been suggested[8] that these reactions have a common rate determining step

$$Ag^+ + S_2O_8^{2-} \longrightarrow Ag^{3+} + 2SO_4^{2-} \quad (1)$$

If we take this reaction as a rate determining step, then Ag^{3+} formed reacts with malic acid:

$$\begin{matrix}CH(OH)\cdot COOH\\ |\\ CH_2COOH\end{matrix} + Ag^{3+} + H_2O \longrightarrow \begin{matrix}CH_3CH\begin{matrix}OH\\ \diagdown OH\end{matrix}\end{matrix} + 2CO_2 + Ag^+ + 2H^+ \quad (2)$$

$$\begin{matrix}CH_2CH\begin{matrix}OH\\ \diagdown OH\end{matrix}\end{matrix} \longrightarrow CH_3CHO + H_2O \quad (3)$$

The presence of acetaldehyde in the reaction mixture after completion of the reaction has been confirmed by the spot test method.[9]

It has also been observed that the rate of reaction decreases with an increase in the concentration of malic acid. Decrease in the rate might be due to the complex formation between Ag^{3+} ion and malic acid. If this is the case, part of the trivalent silver will be used to form complex compound and thus the concentration of silver will be reduced in the reaction mixture. Since the rate is linearly related to the catalyst concentration, a decrease in the rate constant is observed with increasing concentration of malic acid

The authors are grateful to the Head of the Chemistry Department for providing the necessary facilities. One of the authors (G.L.A.) thanks the C.S.I.R., New Delhi, for the junior research fellowship.

8) D. A. House, *Chem. Rev.*, **62**, 185 (1962).
9) F. Feigle, "Spot Test in Organic Analysis," Elsevier Publishing Company, New York (1956) p. 208.

BULLETIN OF THE CHEMICAL SOCIETY OF JAPAN VOL. 43 601—608 (1970)

Kinetic Investigations of the Reaction of Brilliant Green with Alkalies. Influence of Ionic Strength

Sarvagya S. KATIYAR

Department of Chemistry, Indian Institute of Technology, Kanpur, India

(Received February 19, 1969)

Kinetic studies of the reaction of brilliant green with alkalies have been made by following the reaction spectrophotometrically at 625 mμ. The reaction has been found to be bimolecular but under experimental condition of excess alkali, it obeyed a first order law. The rate constants was independent of the concentration of brilliant green but it varied linearly with the hydroxyl ion concentration. Effect of neutral salt on the rate of reaction was investigated in aqueous and in 40% acetone-water media. The rate was found to decrease progressively with increasing ionic strength in both media. Analysis of the data by Brønsted-Christiansen-Scatchard equation yielded a value of -1 for $Z_A Z_B$ indicating thereby that the rate-determining step involves oppositely charged species possessing unit charge. The value of inoic interaction parameter, a_i, corresponded to 1.5 and 4.75 Å in aqueous and 40% acetone-water medium respectively. Without attaching too precise a meaning to a_i it is suggested that B.G. ion is presumably solvated to a greater extent in 40% acetone-water than pure water.

Brilliant green (B.G.), chemically known as 4,4'-bisdiethylaminotriphenyl methyl sulfate belongs to a group of dyes known as triphenylmethane

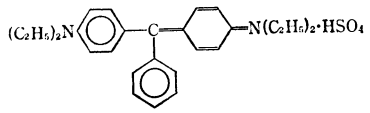

dyes. The physico-chemical[1,2] biological[3,4] and pharmaceutical[5,6] studies of these dyes have attracted the attention of a number of workers. Besides being a compound of biological interest, its major use is in the dye industry where it is used for dyeing and printing all types of fibers, *viz.* cotton, wool, silk, *etc.* Furthermore, it has also been suggested that B.G. can be employed for the colorimetric estimation[7] of Au^{+3}, *etc.*, quantitatively. In biological uses the dye is employed in the biological important pH range 6—7. However, at higher pH the characteristic green color of the dye fades away with time. The kinetic data existing on the instability of B.G. in alkaline solutions are rather scanty[8] while for many other dyes of the series the kinetic data are non-existent. The significance of the stability of these dyes in acidic and alkaline medium, in the course of their biological analytical and dyeing applications, led the author to undertake a systematic kinetic investigation of their reactions. This communication reports the influence of ionic strength, hydroxyl ion concentration and the dye concentration on the reaction responsible for the fading of color of B.G. in alkaline medium, and the data have been employed to detect the species involved in the rate determining step.

Experimental

Materials Used. Brilliant green used was of medicinial quality from British Drug House and was purified by the partition methods[9] described by Lewis, Magel and Lipkin.

Sodium hydroxide employed was a British Drug House 'Anala R' sample.

Potassium nitrate, used for varying the ionic strength of the medium, was a British Drug House 'Anala R' grade reagent which was recrystallized twice from double distilled water.

Acetone employed was a British Drug House 'Anala R' grade reagent and it was further purified[10] before use.

1) T. Azami and T. Hinohara, *Nippon Kagaku Zasshi*, **72**, 515 (1951).
2) R. J. Goldacre and J. N. Phillips, *J. Chem. Soc.*, **1949**, 1724.
3) C. F. Poe and N. F. Witt, *J. Amer. Water Works Ass.*, **22**, 1365 (1930).
4) C. N. Stark and L. R. Curtis, *J. Bacteriol.*, **32**, 385 (1936).
5) F. D. Mann and F. C. Mann, *Amer. J. Digestive Diseases Nutrition*, **6**, 322 (1939).
6) R. H. Aldrich, *Maine Med., J.*, **28**, 5 (1937).
7) N. T. Voskresenkaya, *Zh. Anal. Khim.*, **11**, 585 (1956).
8) N. V. Sidgwick and N. S. Moore, *Proc. Chem. Soc.*, **25**, 123 (1909); *J. Chem. Soc.*, **95**, 889 (1909).
9) G. N. Lewis, T. T. Magel and D. Lipkin, *J. Amer. Chem. Soc.*, **64**, 1774 (1942).
10) A. I. Vogel, "A Text Book of Practical Organic Chemistry," Longmans Green & Co. (1948), p. 170.

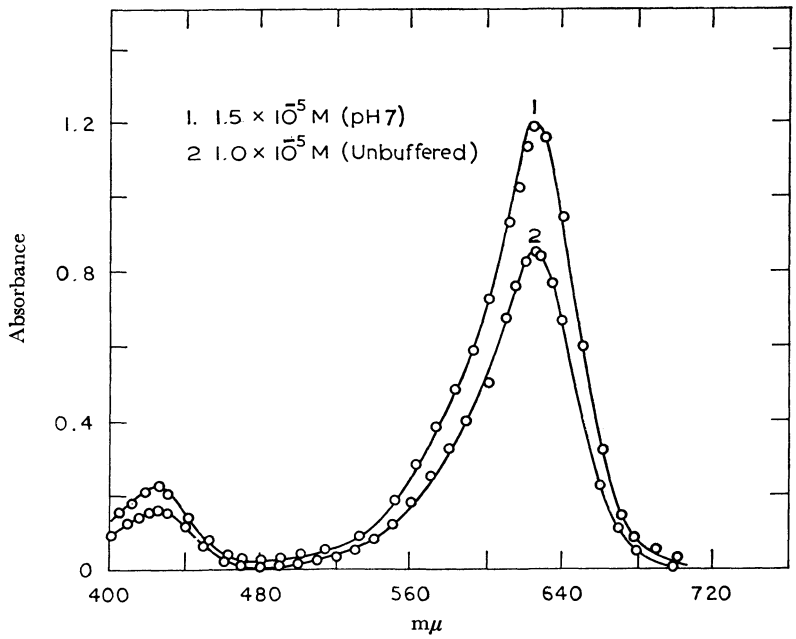

Fig. 1. Absorption spectrum of B.G. in water.

Pre Treatment of Reaction Vessels. B.G. gets adsorbed[11] strongly on the glass surfaces due to which there is a decrease in the effective concentration of the dye. In order to avoid this loss all the vessels used for keeping the solutions of B.G. were coated with a thin layer of purified paraffin wax, which checked the adsorption for sufficiently long durations. The glass cells used for absorbance measurements were rinsed periodically with purified ethanol to remove the adsorbed dye.

Procedure for Following the Reaction. The rate of the chemical change undergone by B.G. in the alkaline medium was studied spectrophotometrically by a Beckman DU spectrophotometer fitted with a dual thermospacer set. The temperature in the cell compartment was regulated by circulating water in the thermospacer set from an external thermostat maintained at 25 ± 0.5°C. The kinetic experiments were carried out in the paraffined flasks kept in the external thermostat and the samples from these flasks were drawn out into 10 mm corex glass cells and their absorbances were noted with time. The absorption measurements were made at λ_{max} of the dye.

Results and Discussion

Absorption Spectrum of Brilliant Green. The absorption spectrum of B.G. in water at two different concentrations in the visible region of the spectrum is given in Fig. 1. It is seen that B.G. exhibits λ_{max} at 625 and 426 mμ. Beer's law held at both these wavelengths as shown by the linear plots of absorbance *vs.* millimicrons in Fig. 2. The value of absorptivity (ε) at 625 mμ corresponded to 8.00×10^4 l mol^{-1}cm^{-1}, which is very high as compared to the absorptivity at 426 mμ. Hence the absorbance measurements during kinetic runs were made at 625 mμ in aqueous solutions. The wavelengths of maximum absorption were unaffected by the buffered or unbuffered nature of the solutions. But in acetone-water mixtures λ_{max} was shifted to 627.5 mμ and therefore the measurements were made at this wavelength in acetone-water mixtures.

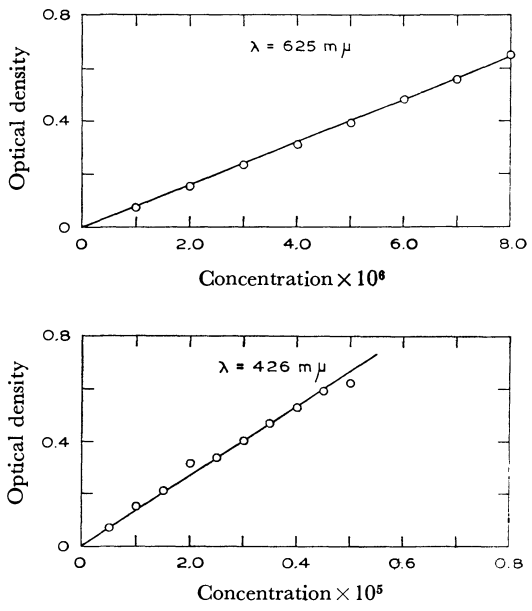

Fig. 2. Applicability of Beer's law.

11) B. P. Gyani, *J. Indian Chem. Soc., Ind. and News Ed.*, 13, No. 1 (1950).

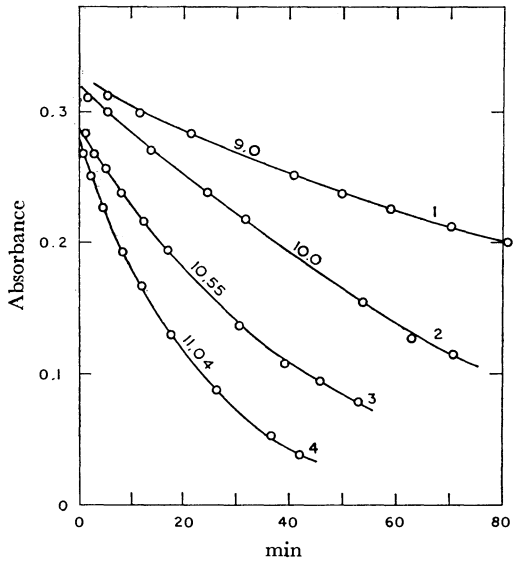

Fig. 3. Typical kinetic runs for the reaction of B.G. in different buffers.

Kinetic studies for the reaction of B.G. and sodium hydroxide could not be carried out at concentrations greater than 5×10^{-5}M of the dye and also at $\lambda=426$ mμ for the following reasons. At concentrations greater than 5×10^{-5}M, turbidity appeared. This was due to the low solubility of the reaction product. At concentrations below 5×10^{-6}M, the absorbance at $\lambda=426$ mμ was so small that spectrophotometric measurements were not feasible.

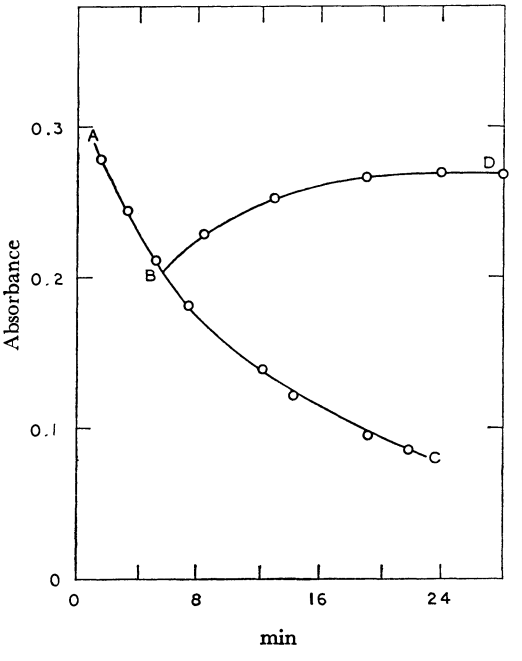

Fig. 4. Reversible nature of the reaction.

Nature of the Reaction. A typical set of kinetic data for the reaction of B.G. in alkaline medium is given in Fig. 3. Here curves 1, 2, 3 and 4 refer to the kinetic runs obtained at pH 9.0, 10.0, 10.35 and 11.04 respectively, the concentration of B.G. being 4×10^{-6}M in all the experiments. In the presence of sufficient hydroxyl ions, the absorbance of the solutions progressively decreased to zero and the solutions became colorless; the color however reappeared gradually with time when the alkali was neutralized by addition of acid. This suggests that the reaction of B.G. with the alkali is reversible in nature, an observation in conformity with that made by Sidgwick and Moore.[8] The reversibility of the reaction was further confirmed by the data presented in Fig. 4. In this figure the portion AB represents the process of fading of color of 4.5×10^{-6}M B.G. solution containing 1.0×10^{-3}M sodium hydroxide. This reaction would have normally proceeded along the curve BC, but as a result of addition of pre-determined quantity of the acid (HCl), which exactly neutralized the alkali present without causing any significant change in volume, the reaction followed the course shown by BD. This portion represents a process in which there is a gradual formation of B.G. This experiment, besides proving the reversibility of the reaction also exposes the complete dependence of the reaction on hydroxyl ion concentration.

In order to make the reaction kinetically simple, sufficient alkali was employed to make the back reaction negligible. Under this condition the equilibrium point of the reaction was shifted to the

Table 1. Order of reaction by equifractional parts method

Concentration of B.G.$=4\times10^{-6}$M
Temperature$=25$°C

pH	Initial absorbance a_1	Initial absorbance a_2	Fraction reacted	Time taken t_1 min	Time taken t_2 min	Order of reaction
10.00	0.325	0.260	0.66	26.75	27.00	1.04
	0.325	0.260	0.50	46.00	46.50	1.05
	0.325	0.260	0.40	58.50	58.50	1.00
10.55	0.280	0.200	0.66	18.00	17.50	0.91
	0.280	0.200	0.50	29.00	28.00	0.90
	0.280	0.200	0.40	37.50	37.00	0.96
	0.280	0.200	0.33	46.00	45.50	0.97
11.04	0.264	0.180	0.66	9.00	9.30	1.09
	0.264	0.180	0.50	16.50	16.00	0.92
	0.264	0.180	0.40	21.00	20.50	0.94
	0.264	0.180	0.33	24.50	24.50	1.00
11.20	0.270	0.180	0.66	2.70	2.90	1.18
	0.270	0.180	0.50	4.35	4.85	1.00
	0.270	0.180	0.40	6.35	6.35	1.00
	0.270	0.180	0.33	8.25	8.20	0.98

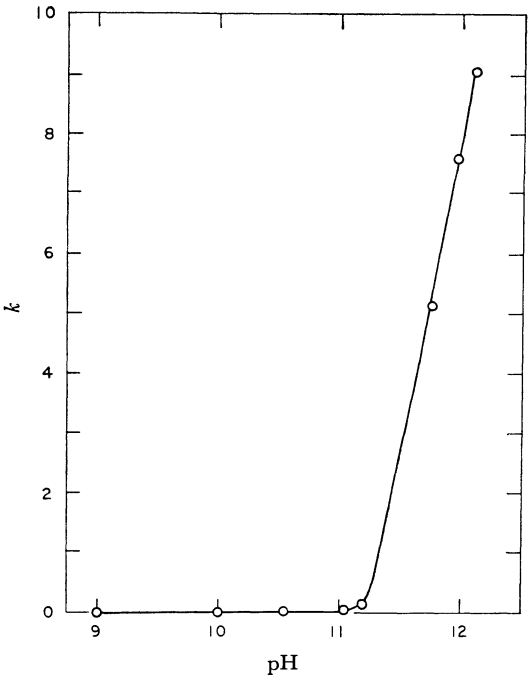

Fig. 5. Variation of velocity constant with pH.

side of the products. Further, less alkali could not be used since spurious rate constants were obtained when the reaction proceeded slowly ($t_{2/1}>1$ hr). The order of the reaction (n) was determined by various methods,[12] *viz.* integration method, graphical method, equifractional parts method, differential method and Guggenheim's method.[13] A typical set of values of n calculated from the data of Fig. 3 by equifractional parts method are given in Table 1. The last column of this table shows that the order of reaction responsible for the decolorization of B.G. corresponds to 1.04 ± 0.14, which indicates that the reaction is first order with respect to B.G. concentration. The values of velocity constant (k) were determined in a number of alkaline buffers in the pH range 9—12. The variation of k with pH is shown in Fig. 5. It is of interest to note from this figure that the value of velocity constant increases slowly up to pH 10.5 but the increase becomes very steep at pH values greater than 10.5. This confirms the marked dependence of the reaction on the OH^- ion concentration.

Dependence of Rate on Hydroxyl Ion Concentration. The dependence of the rate of reaction on the hydroxyl ion concentration was investigated by running the reaction at different concentrations of sodium hydroxide. The data obtained are reported in Fig. 6. In all these experiments the initial concentration of B.G. was 4×10^{-6}M while that of sodium hydroxide was varied in the range $1.0—4.5\times10^{-3}$M. The linear variation of logarithm of absorbance of B.G. with time indicates the applicability of the first order law. The values of the apparent velocity constant (k) obtained from the data of Fig. 6 at different concentrations of hydroxyl ion are given in Fig. 7. It is of interest to note that a linear plot is obtained, which shows that the experimental condition employed in the experiments, *viz.* the excess of OH^- ion concentration, is an important factor responsible for the above observations. This is not an uncommon observation and similar behavior was noticed by Turgeon

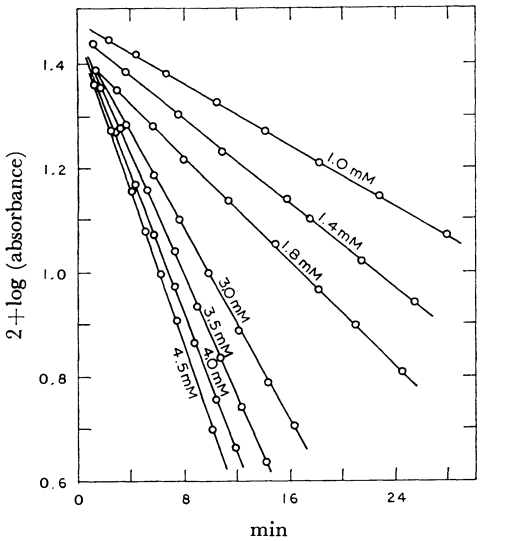

Fig. 6. Kinetic runs at varying sodium hydroxide concentration.

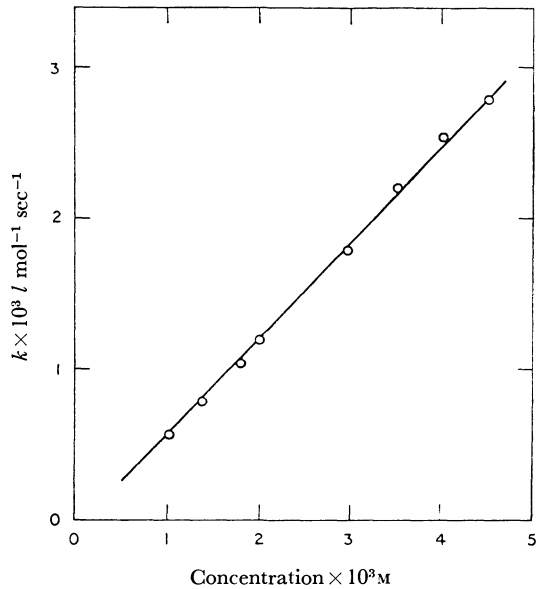

Fig. 7. Dependence of k on sodium hydroxide concentration.

12) See for example, A. A. Frost and R. G. Pearson, "Kinetics and Mechanism," John Wiley & Sons, Inc., New York (1953), p. 40.

13) E. A. Guggenheim, *Phil. Mag.*, **2**, 538 (1926).

and LaMer[14] and Amis and Lamer.[15] The reaction under study is in fact bimolecular but since OH^- present is in much excess, change in its concentration is negligible. The real or true velocity constant was therefore computed by dividing the apparent velocity constant k by the hydroxyl ion concentrations:

$$k' = \frac{2.303(\Delta \log C_{B.G.})\, l}{(\Delta t)(C_{OH^-})\ \text{mol}\cdot\text{sec}} \qquad \text{(i)}$$

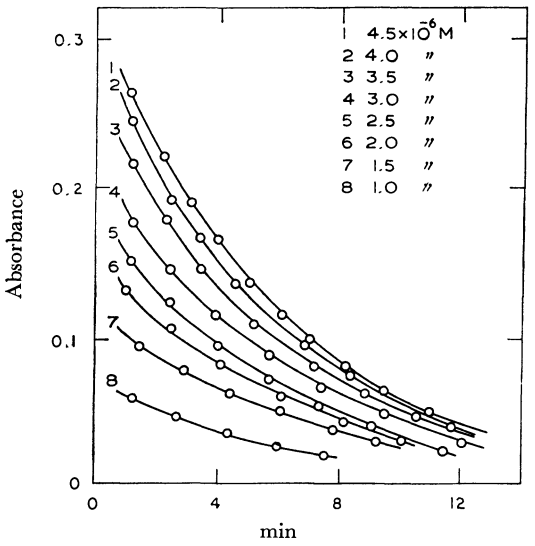

Fig. 8. Dependence of k on B.G. concentration.

Table 2. Effect of concentration of B.G. on k

pH=11.2, Temperature=25°C

Concentration of B.G. $\times 10^{-6}$M	Velocity constant $k \times 10^2$ sec^{-1}
4.5	0.274
4.0	0.274
3.5	0.273
3.0	0.262
2.5	0.260
2.0	0.240
1.5	0.240
1.0	0.211

Dependence of Rate Constant on B.G. Concentration. The effect of concentration of B.G. on the rate constant of the reaction was examined by carrying out the reaction at varying concentrations of B.G. and fixed concentration of hydroxyl ions. The data obtained are given in Fig. 8. It is noted that k is independent of the conecntration of B.G. in the range $(1.0—5.0) \times 10^{-6}$M, as the values of k obtained from Fig. 8 and shown in Table 2 are constant. Similar observations were made earlier for the reaction of murexide[16] and crystal violet[14] with alkali where the value of k' was independent of the initial concentration of murexide and crystal violet. Studies at higher concentrations of B.G. could not be carried out due to low solubility of the reaction product and inapplicability of Beer's Law.

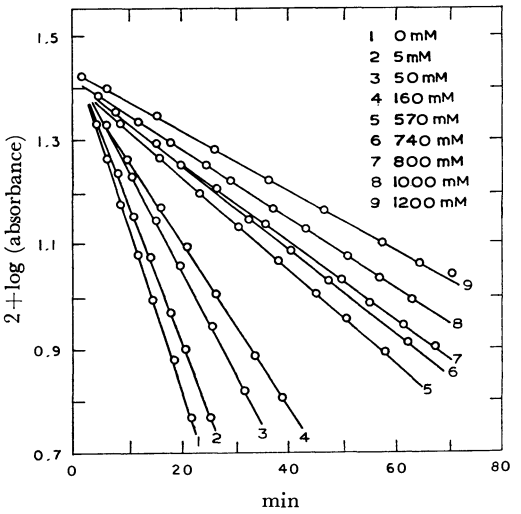

Fig. 9. Kinetic runs at varying ionic strength in aqueous medium.

Table 3. Velocity constants at varying ionic strength in water

Concentration of B.G. $=4 \times 10^{-6}$M

Concentration of NaOH $=2 \times 10^{-3}$M

Temperature=25°C

Ionic strength μ	$\frac{\sqrt{\mu}}{1+\beta a_i\sqrt{\mu}}$ where $a=0.49$	Apparent velocity constant $k \times 10^3$ sec^{-1}	Real velocity constant k' l mol^{-1}sec^{-1}
0.002	0.043	1.180	0.588
0.0036	0.059	1.070	0.537
0.007	0.081	1.020	0.510
0.052	0.205	0.768	0.384
0.162	0.336	0.561	0.281
0.572	0.552	0.341	0.170
0.742	0.605	0.307	0.153
0.802	0.623	0.288	0.144
1.002	0.671	0.258	0.129
1.202	0.713	0.230	0.115

Dependence of the Rate on the Ionic Strength. Figure 9 gives a typical set of kinetic data obtained at varying ionic strength (μ). The

14) J. C. Turgeon and V. K. LaMer, *J. Amer. Chem. Soc.*, **74**, 5988 (1952).

15) E. S. Amis and V. K. LaMer, *ibid.*, **61**, 905 (1939).

16) R. K. Chaturvedi, Doctoral dessertation, Agra Univ., 1960.

concentrations of B.G. and NaOH were kept constant, while the ionic strength was varied in the range 0.002—1.2. In the calculation of μ of the reaction system, the concentration of B.G. (4×10^{-6}M) was not taken into account due to its extreme low value as compared to the added neutral electrolyte. Prior to carrying out investigations on the influence of μ on k', it appeared necessary to examine the effect of the neutral salt, potassium nitrate, on the absorption spectrum of B.G. Experiments indicated that potassium nitrate exerts no influence on the absorption spectrum of B.G. which shows the same characteristic absoprtion maxima at λ=625 and 426 mμ. It may be seen from the data of Fig. 9 that increase in ionic strength of the system decreases the rate of reaction of B.G. The value of k' at different ionic strengths are summarized in Table 3. These data were analyzed by the Brønsted equation, which gives the following relation between k' and μ at 25°C.

$$\log k' = \log k_0' + 1.02 Z_A Z_B \sqrt{\mu} \qquad \text{(ii)}$$

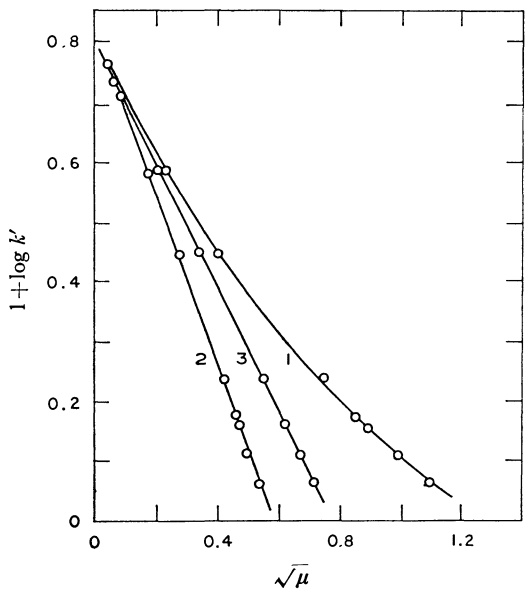

Fig. 10. Variation of velocity constant with ionic strength in water.

where Z_A and Z_B are the charges on the reacting species. According to this equation a plot of log k' *vs.* $\sqrt{\mu}$ should be a straight line with a slope equal to 1.02 $Z_A Z_B$. The variation of log k' *vs.* $\sqrt{\mu}$ is shown in Fig. 10 (curve 1). It may be noted from this plot that at higher values of μ, the points do not lie on a straight line suggesting thereby the non-applicability of Brønsted's equation at higher values of μ. However, if a straight line is drawn by taking into consideration the data below 0.09 μ, the slope of it gives a value of -0.82 for $Z_A Z_B$. The non-applicability of the above equation at higher ionic strengths has been attributed to the inaccurate values of activity coefficients computed from the Debye-Hückel equation, and has been observed by numerous workers. Guntelberg suggested the use of modified form of the Debye-Hückel equation which is as follows:

$$\log k' = \log k_0' + \frac{1.02 Z_A Z_B \sqrt{\mu}}{1+\sqrt{\mu}} \qquad \text{(iii)}$$

Plot 2 of Fig. 10 represents the variation of log k' *vs.* $\sqrt{\mu}/(1+\sqrt{\mu})$. It is instructive to find that the plot is linear over a wide range of μ and the $Z_A Z_B$ as computed from the slope of this plot is -1.36 which is higher than unity. Scatchard[17] made a further modification of the Debye-Hückel equation and this modification when introduced into the Brønsted-Christiansen equation gave the relation

$$\log k' = \log k_0' + \frac{2AZ_A Z_B \sqrt{\mu}}{1+\beta a_i \sqrt{\mu}} \qquad \text{(iv)}$$

A and β are Debye-Hückel constants and a_i is an ionic interaction parameter.[18] The computation of a_i was done by observing the influence of different values of a_i on the constancy of Eq. (iv). The value of a_i which gives a constant value of log k_0' for all the observed values of k' at different μ, over the whole range of ionic strength investigated, was calculated by the method of successive trials. The effect of varying ionic parameter on the constancy of Eq. (iv) is shown in Fig. 11. The calculations were made by taking the values of $2A$ and β as 1.02 and 0.329×10^8 in water at 25°C respectively. According to Eq. (iv) for a correct value of a_i the plot of log k_0' and $\sqrt{\mu}$ will be a straight line parallel to $\sqrt{\mu}$ axis. Interesting enough is to note that curves 1 and 3 of Fig. 11, which give the variation of log k_0' with $\sqrt{\mu}$ at ionic parameter values equal to 0.5 and 4 Å respectively, are not straight lines parallel to x-axis, but are rather diverging lines. This suggests that the correct value for a_i for B.G. in water lies between 0.5 and 4 Å. Plot 2 in Fig. 11 which represents a linear variation of log k_0' *vs.* $\sqrt{\mu}$ was obtained by putting a_i equal to 1.5 Å, suggesting thereby that 1.5 Å is the correct value of interionic attraction parameter for B.G. in water.

Now putting this value of a_i in Eq. (iv) the variation of log k' *vs.* $\sqrt{\mu}/(1+\beta a_i\sqrt{\mu})$ was examined. The plot thus obtained is shown in Fig. 10 (plot 2). From the slope of this plot the value of $Z_A Z_B$ corresponds to -1.01. It is instructive to compare this value with other values of $Z_A Z_B$ computed earlier which corresponded to -0.82 and -1.36. It may, therefore, be concluded that the Brønsted-Christiansen-Scatchard equation gives a value of $Z_A Z_B$ which is nearest to unity. This value suggests that the reaction is taking place between oppositely

17) G. Scatchard, *J. Amer. Chem. Soc.*, **52**, 52 (1930).
18) V. K. LaMer, *J. Franklin Inst.*, **225**, 709 (1938).

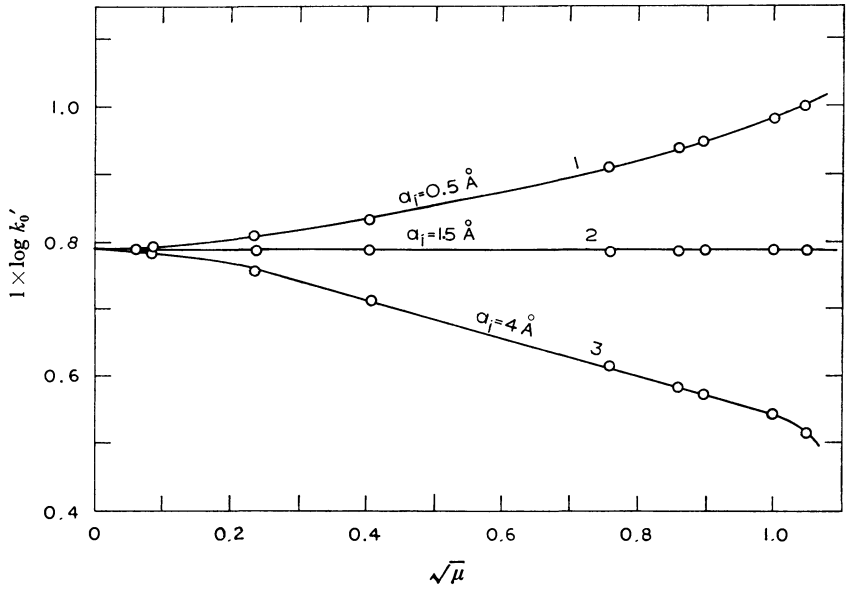

Fig. 11. Effect of varying ionic parameter on the constancy of Eq. (iv) in water.

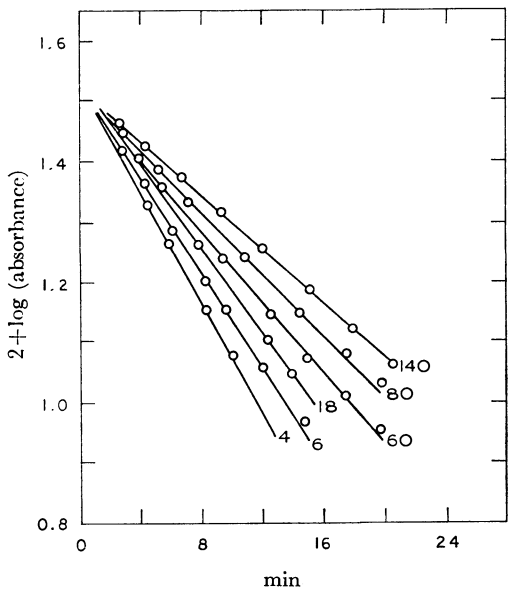

Fig. 12. Kinetic runs at varying ionic strength in 40% acetone-water medium.

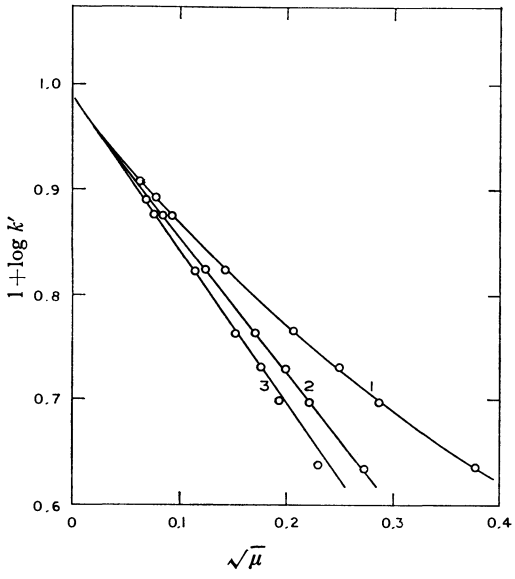

Fig. 13. Variation of k' with ionic strength in 40% acetone-water.

charged species of unit charges.

Salt Effect in 40% Acetone-Water Mixtures. The studies of salt effects were extended to 40% acetone-water mixtures, to determine the value of interionic attraction parameter and hence indirectly the extent of solvation of B.G. in mixed media. To investigate this, kinetic runs were made in 40% acetone-water at varying ionic strength but with fixed concentration of B.G. (4×10^{-6}M) and NaOH (2×10^{-3}M). A typical set of data obtained are given in Fig. 12. The linearity of plots indicates the first order nature of the reaction in this medium. The velocity constant k' was found to decrease with increase in the ionic strength, an observation similar to that obtained in aqueous medium. Analysis of the data for Eqs. (ii) and (iii) yielded the results shown in Fig. 13. Curves 1 and 2 of this figure give the variation of log k' *vs.* $\sqrt{\mu}$ and $\sqrt{\mu}/1+\sqrt{\mu}$ respectively. It is quite evident that plot 1 is a

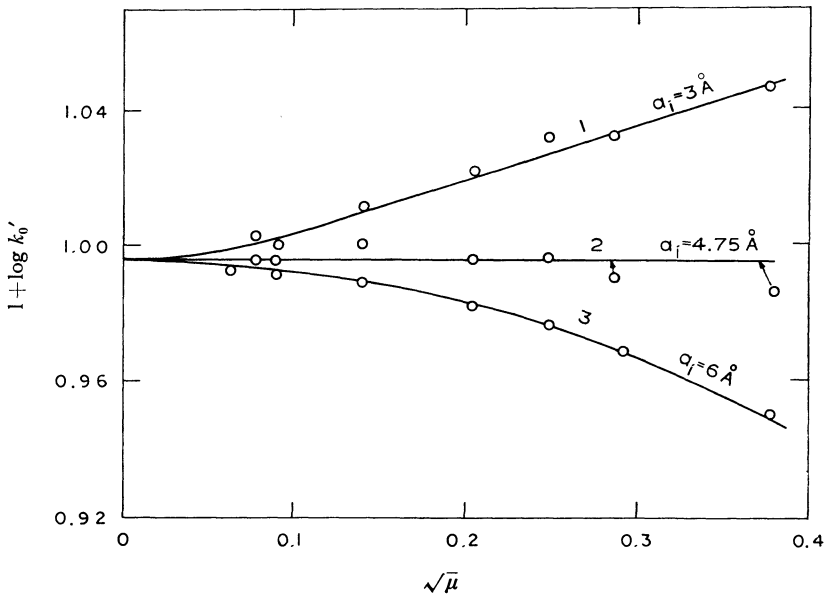

Fig. 14. Effect of varying ionic parameter on the constancy of Eq. (iv) in 40% acetone-water.

curved line and not a straight line, which indicates the non-applicability of Eq. (ii) at higher μ, while plot 2 is linear over a wide range of μ. The slopes of plots 1 and 2 gave a value of Z_AZ_B equal to -0.89 and -1.25 respectively.

For the application of Eq. (iii) the value of a_i of B.G. in acetone-water medium was determined as described earlier. The results obtained are summarized in Fig. 14, which gives the effect of varying ionic parameter on the constancy of Eq. (iv) in 40% acetone-water medium. For the calculations β was taken to be equal to 0.38×10^8 at 25°C. It is of interest to note from Fig. 14 that plots 1 and 3 obtained by putting a_i equal to 3 and 6 Å are non-linear, while plot 2 obtained by putting a_i equal to 4.75 Å is linear. Thus the value of ionic attraction parameter corresponds to 4.75 Å in 40% acetone-water, which is substantially larger than its value in aqueous medium (1.5 Å). Utilizing the value of a_i=4.75 Å in 40% acetone-water, the plot of log k' *vs.* $\sqrt{\mu}/(1+\beta a_i\sqrt{\mu})$ (Fig. 13, plot 3) gave a value of -1.30 for Z_AZ_B, which indicates that the reaction is taking place between oppositely charged species of unit charge. In a ternary system a too precise physical meaning cannot be attached to the parameter a_i. Hence from its larger value in the acetone-water mixture it can be presumed that B.G. ion is solvated to a greater extent in this solvent than in water. In agreement with Sheppard and Geddes[19] it can be suggested that in the B.G. ion the hydrophilic groups at the end of benzene ring are preferentially surrounded by water molecules whereas acetone molecules are probably bound to the hydrophobic parts. These bound acetone molecules will make the B.G. ion appear larger during its reaction in alkaline medium with OH^- ion, as indicated by the larger value of a_i. It appears therefore that it approaches the central carbon atom from a direction perpendicular to the plane of B.G. ion. A similar type of behavior was observed by Turgeon and LaMer[14] in the reaction of crystal violet.

The author is indebted to Professor N. A. Ramaiah of National Sugar Institute, Kanpur for valuable and helpful discussions during the progress of this work.

19) S. E. Sheppard and A. L. Geddes, *J. Amer. Chem. Soc.*, **66**, 1995 (1944).

BULLETIN OF THE CHEMICAL SOCIETY OF JAPAN VOL. 43 609—618 (1970)

Molecular Vibrations and Force Fields of Alkyl Sulfides. I. Dimethyl Sulfide and Its Deuterated Compounds

Yuji SHIRO,*1 Masaru OHSAKU, Michiro HAYASHI and Hiromu MURATA

Department of Chemistry, Faculty of Science, Hiroshima University, Higashisenda-machi, Hiroshima

(Received April 7, 1969)

Dimethyl sulfide and dimethyl sulfide-d_1 were prepared, and their infrared spectra were measured in the gaseous and liquid states. The Raman spectra were measured in the liquid state. The assignments of their spectra were made. On these assigned frequencies, two sets of modified Urey-Bradley force constants and a set of local symmetry force constants were determined by a least-squares technique. The obtained force constants were then transferred to the treatment of the vibrational frequencies of dimethyl sulfide-d_3. The centrifugal distortion constants obtained from the vibrational data were compared with those from the data of the microwave spectra in order to confirm the reasonableness of the obtained force constants.

It would be useful to find a reasonable force field which could reproduce the observed vibrational frequencies and to acertain the assignments of the frequencies of a group of molecules of alkyl sulfides. The present paper, the first of a series of reports on alkyl sulfides, will deal with the molecular vibrations and several force fields of dimethyl sulfide, dimethyl sulfide-d_1, and dimethyl sulfide-d_3.

Although many papers[1-6] on the infrared and Raman spectra of dimethyl sulfide have been reported, the assignments for the methyl group have not consistent with each other. For this reason we have attempted to study the vibrational spectra of dimethyl sulfide in detail. Dimethyl sulfide and dimethyl sulfide-d_1 were prepared, and the observed infrared and Raman bands were newly assigned. Their assigned frequencies were then used to determine the force constants of the modified Urey-Bradley force fields and of the local symmetry force field. When each final set of those force constants was then used in the normal coordinate treatment of dimethyl sulfide-d_3, the calculated frequencies agreed well with the observed frequencies.[4] In order to confirm the reasonableness of the obtained force constants, the centrifugal distortion constants were further calculated from the force constants; their values were found to be consistent with those determined by the microwave study.[7]

Experimental

The dimethyl sulfide was prepared by the reaction of dimethyl sulfate with sodium sulfide.[8] The dimethyl sulfide-d_1 was prepared by the reduction of monochloromethyl methyl sulfide with lithium aluminum deuteride in *n*-buthyl ether, and the monochloro-methyl methyl sulfide was prepared by the reaction of dimethyl sulfide with thionyl chloride.[9]

The infrared spectra of dimethyl sulfide and dimethyl sulfide-d_1 were recorded in the region from 600 to 4000 cm^{-1} in the gaseous and liquid states with Perkin-Elmer Model 112-G and Hitachi Model EPI-S2 Spectrometers. The Raman spectra were measured in the liquid state by the use of a Cary 81 Raman Spectrometer.

Vibrational Assignments

Dimethyl Sulfide. Table 1 shows the observed infrared and Raman data. As the molecule has a C_{2v} symmetry, the fundamental vibrations can be subdivided into these four groups: A_1, A_2, B_1, and B_2. The vibrations belonging to the A_1, B_1, and B_2 species are active in infrared, and all of the A_1, A_2, B_1, and B_2 vibrations are active in Raman. In the gaseous-state absorption spectra, A_1, B_1, and B_2 vibrations have *b*-type, *a*-type, and *c*-type band contours respectively.

*1 Present address: Shinonome Branch School, Faculty of Education, Hiroshima University, Shinonome-3-chome, Hiroshima.

1) I. F. Trotter and H. W. Thompson, *J. Chem. Soc.*, **1946**, 481.
2) H. Siebert, *Z. Anorg. Allgem. Chem.*, **271**, 65 (1952).
3) D. W. Scott and J. P. MacGullough, *J. Amer. Chem. Soc.*, **80**, 3554 (1958).
4) J. P. Perchard, M. T. Forel and M. L. Josien, *J. Chim. Phys.*, **61**, 632 (1964).
5) J. R. Allkins and P. J. Hendra, *Spectrochim. Acta*, **22**, 2075 (1966).
6) W. G. Fateley and F. A. Miller, *ibid.*, **18**, 977 (1962).
7) G. O. Sørensen, *J. Mol. Spectroscopy*, **22**, 325 (1967).
8) W. Strecker, *Ber.*, **41**, 1105 (1908).
9) W. E. Truce, G. H. Birum and E. T. McBee, *J. Amer. Chem. Soc.*, **74**, 3594 (1952).

Table 1. Fundamental frequencies (cm^{-1}) and assignment of the infrared and Raman spectra of dimethyl sulfide

Infrared		Raman	Symmetry species	Assignment
Gaseous	Liquid	Liquid		
2990 sh.	2990 sh.	2991 (3) br.	A_1, B_1, B_2	C–H str.
2915 s.	2920 vs.	2916 (10)	A_1	C–H str.
2850 s.	2850 s.	2860 2852 (2) br. 2837	B_1	C–H str.
1456 s.	1456 s.		A_1	CH_3 deg. def.
1440 vs.	1440 vs.	1440 (10)	B_1	CH_3 deg. def.
1420 sh.	1434 sh.		B_2	CH_3 deg. def.
1329 1317 s.[a] 1303	1317 s.		A_1, B_1	CH_3 sym. def.
1036 1017 s.[b]	1028 s.	1030 vw.	A_1	CH_3 rock.
1005 w.	1005 w.		B_2	CH_3 rock.
972 s.[a]	972 s.	965 vw.	B_1	CH_3 rock.
919 vw.	907 w.			impurity ?
703 w.	723 m.	741 (3)	B_1	C–S str.
694 684 m.[b]	693 m.	691 (7)	A_1	C–S str.
		282 (3)	A_1	CSC def.
	182[c]		B_2	torsion

a) The *a*-type or *c*-type band contours, b) the *b*-type band contour, c) from Ref. 6; s. strong, m. medium, w. weak, v. very, sh. shoulder, br. broad. Values in parentheses of Raman data indicate relative intensities.

The CH_3 rocking vibrations of this molecule may be expected in the region from 900 to 1050 cm^{-1}. In Fig. 1-a, the spectrum of the 900—1050 cm^{-1} region observed in dimethyl sulfide is illustrated. The infrared band at 1028 cm^{-1} is obviously a *b*-type band; therefore, it is assigned to the CH_3 rocking vibration belonging to the A_1 species. The infrared band at 972 cm^{-1} is an *a*-type band; this band is assigned to the CH_3 rocking vibration belonging to the B_1 species. As the B_2 rocking band is expected around the region of 1000 cm^{-1} on the basis of the normal coordinate treatment, as will be discussed later, the weak band at 1005 cm^{-1} can perhaps be assigned to the B_2 vibration. Although the band belonging to the A_2 species of the CH_3 rocking vibration should appear in Raman, the corresponding band is not observed in the Raman spectra. The band at 907 cm^{-1} might be an impurity band, since the absorption intensity is much reduced by the fractional distillation. The infrared band at 1317 cm^{-1} is assigned to the symmetrical deformation vibration. In the gaseous state, as is shown in Fig. 1-b, the band at 1317 cm^{-1} splits into three components, at 1329, 1317, and 1303 cm^{-1}, and is considered to be an *a*-type band belonging to the B_1 species overlapped by a *b*-type band belonging to the A_1 species. Therefore, the bands of the A_1 and B_1 species are considered to have nearly the same frequencies. This was also shown by the results of the normal coordinate treatment. Four CH_3 degenerate deformation vibrations may be expected in the region from 1500 to 1400 cm^{-1}. In this region the infrared bands are made up of three components in the liquid state; these are assigned to the vibrational modes as is shown in Table 1 on the basis of the normal coordinate treatment.

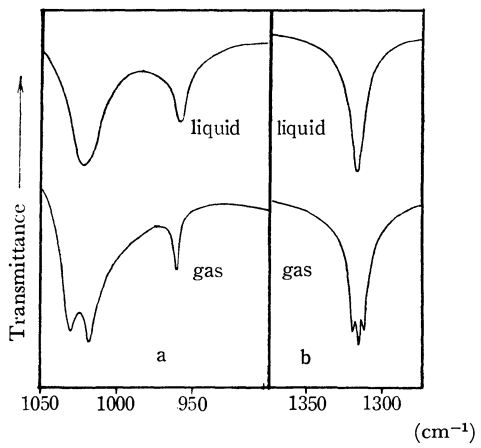

Fig. 1. Infrared spectra of dimethyl sulfide in the gaseous and liquid states in the region of the CH_3 rocking (a) and the CH_3 symmetrical deformation (b) vibrations.

Table 2. Fundamental frequencies (cm^{-1}) and assignment of the infrared and Raman spectra of dimethyl sulfide-d_1

Infrared		Raman	Species	Assignment	
Gaseous	Liquid	Lliquid		Symmetric	Asymmetric
2985 vs.	2985 vs.	2986 (5)	A', A''	C–H str.	C–H str.
2930 vs.	2930 vs.	2919 (10)	A'	C–H str.	C–H str.
		2871 (3)	A'	C–H str.	C–H str.
2202 2189 s. 2179	2185 s.	2189 (10)	A'	C–D str.	C–D str.
1457 1447 sh.	1451 vs. br.	1450 (2)	A'	CH_3 deg. def.	CH_3 deg. def.
1436 s.	1436 vs. br.	1436 (5)	A''	CH_3 deg. def.	CH_3 deg. def.
1424 sh.	1424 sh.	1422 (1)	A'	CH_2 bend.	CH_2 bend.
1340 1327 m. 1315	1327 s.	1329 (3)	A'	CH_3 sym. def.	CH_3 sym. def.
1263 w.	1259 s.	1259 (1)			CH_2 wagg.
1252 s.	1250 sh.	1252 (1)	A'	CH_2 wagg.	
1236 m.	1236 sh.	1236 (1)			CH_2 twist.
1224 1217 w.	1223 vs.	1223 (1)	A''	CH_2 twist.	
1018 1000 vs.	1007 s.		A'	CH_3 rock.	CH_3 rock.
980 sh.	981 s.		A''	CH_3 rock.	CH_3 rock.
961 m.	963 s.		A''	CH_2 rock.	CH_2 rock.
	806 w.	807 (1) br.	A'	SCD def.	
800 m.	789 w.	790 (1) br.			SCD def.
745 w. br.	738 vs.	739 (6)	A'	C–S str.	C–S str.
699 vw.	696 s.	691 (10)			C–S str.
670 659 w.	660 w.	664 (8)	A'	C–S str.	
		274 (2)	A'	CSC def.	CSC def.

Notations are the same to Table 1.

Dimethyl Sulfide-d_1. Table 2 shows the obtained data. The observed infrared spectra of dimethyl sulfide-d_1 are more complicated than those of dimethyl sulfide. For this isotopic species, two rotational isomers, in one of which the deuterium atom is in the plane of the CSC skeleton (sym-dimethyl sulfide-d_1), while in the other it is out of the plane (asym-dimethyl sulfide-d_1), can be expected, as is presented in Fig. 2. Moreover, Pierce and Hayashi[10] have confirmed the existence of the two molecular forms by their analysis of the microwave spectra. The deuterated species has a structure similar to that of monochloro-methyl methyl sulfide, although their atomic masses are different. The CH_2 deformation frequencies of monochloromethyl methyl sulfide have been reported as 1404, 1230, 1149, and 835 cm^{-1}.[11] In the deuterated species, new bands are observed, at 1420, 1260, 1230, and 960 cm^{-1}, which are not observed in the normal species. These frequencies correspond well with those of monochloromethyl methyl sulfide. In view of these aspects of the observed bands, it would be much better to consider the CH_2D group in this isotopic species as two separate groups, one, the CH_2 group and the other, the CD group, much as is the case of monochloromethyl methyl sulfide, rather than to consider the CH_2D group as one group. The experimental result is also confirmed in the $\boldsymbol{L}$ matrix obtained from the normal coordinate treatment. A part of the $\boldsymbol{L}$ matrix of sym-dimethyl sulfide-d_1 is shown in Table 3. Table 3 shows that each normal coordinate has a main contribu-

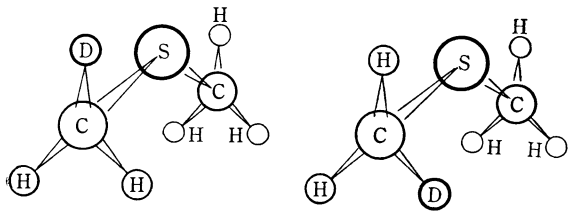

sym-dimethyl sulfide-d_1 asym-dimethyl sulfide-d_1

Fig. 2. Rotational isomers of dimethyl sulfide-d_1.

10) L. Pierce and M. Hayashi, *J. Chem. Phys.*, **35**, 479 (1961).

11) M. Hayashi, *Nippon Kagaku Zasshi*, **80**, 1073 (1959).

TABLE 3. *L*-MATRIX OF sym-DIMETHYL SULFIDE-d_1

	ν_5	ν_6	ν_7	ν_8	ν_9	ν_{10}	ν_{16}	ν_{17}	ν_{18}	ν_{19}
CH_3 deg. def.	1.468	0.048	−0.006	−0.005	0.280	0.017				
CH_3 deg. def.							1.486	0.008	−0.218	−0.049
CH_3 sym. def.	0.146	0.006	1.141	0.005	−0.039	0.016				
CH_3 rock.	−0.390	0.000	0.057	0.016	0.850	0.148				
CH_3 rock.							0.444	−0.017	1.259	0.310
redundancy[a)]	−0.219	−0.001	−0.001	−0.006	−0.006	−0.021				
CH_2 bend.	−0.085	1.509	−0.021	0.005	−0.007	−0.017				
CH_2 wagg.	0.006	−0.014	0.002	1.269	0.042	−0.102				
CH_2 twist.							0.007	1.215	−0.055	−0.156
CH_2 rock.							0.001	0.477	0.231	0.863
SCD def.	0.059	0.003	−0.002	0.232	−0.009	0.553				
redundancy[a)]	−0.012	−0.022	−0.011	−0.010	−0.001	0.006				

a) This coordinate is the sum of six coordinates of bond angles in the CH_3 group or the CH_2 group.

tion from each underlined symmetry coordinate; these coordinates are constructed for the CH_3, CH_2, and CD groups, respectively. The new bands at 1420, 1260, 1230, and 960 cm^{-1} are assigned to the CH_2 bending, wagging, twisting, and rocking vibrations respectively, though these CH_2 group vibrations contain other, slight contributions. This is also the case with asym-dimethyl sulfide-d_1.

Two infrared bands are observed close to each other, at 806 and 789 cm^{-1}, in the liquid state. They could not be assigned to the C–S stretching vibrations or to the CH_3 and the CH_2 deformation vibrations by comparing them with those of dimethyl sulfide. From the results of the normal coordinate treatment, the SCD deformation vibrations can be expected to be observed around 800 cm^{-1} and the splitting due to the rotational isomerism can be expected to be 5—10 cm^{-1}. This spacing of the calculated frequencies explains well the observed frequency (17 cm^{-1}). Therefore, the two bands at 789 and 806 cm^{-1} are assigned to the SCD deformation bands of sym-dimethyl sulfide-d_1 and asym-dimethyl sulfide-d_1 respectively. In the region from 750 to 600 cm^{-1}, four bands can be expected, since each rotational isomer has two C–S stretching modes. In the experiment three bands, at 738, 696, and 660 cm^{-1}, are observed in the liquid state. Two modes among the four might be overlapped. From the normal coordinate treatment, the bands at 738 and 660 cm^{-1} are assigned to the C–S stretching vibrations of sym-dimethyl sulfide-d_1, and the bands at 738 and 696 cm^{-1} are assigned to the C–S stretching vibrations of asym-dimethyl sulfide-d_1.

The complicated infrared absorption bands in the region from 1050 to 950 cm^{-1} are assigned to the overlapped CH_3 and CH_2 rocking vibrations. On the basis of the assignments of the CH_3 rocking vibrations for dimethyl sulfide and the normal coordinate treatment, these bands in the liquid state are assigned as follows: the band at 963 cm^{-1} is assigned to the CH_2 rocking vibration, the band at 981 cm^{-1} is assigned to the CH_3 out-of-plane rocking vibration, and the band at 1007 cm^{-1}, to the CH_3 in-plane rocking vibration. These assignments are summarized in the 5th and 6th columns of Table 2.

The CH_2 wagging and twisting vibrations for the CH_2 group could be observed around 1250 cm^{-1}. The frequency differences between sym-dimethyl sulfide-d_1 and asym-dimethyl sulfide-d_1 can be expected from the calculations to be about 10—20 cm^{-1}. Consequently, the bands at 1250 and 1259 cm^{-1} are assigned to the CH_2 wagging vibrations of sym- and asym-dimethyl sulfides respectively, and the bands at 1223 and 1236 cm^{-1} are assigned to the CH_2 twisting vibrations of sym- and asym- sulfides respectively. The band at 1327 cm^{-1} is so close to the band at 1317 cm^{-1} of normal dimethyl sulfide that it can easily be assigned to the CH_3 symmetrical deformation vibration.

The absorption bands in the region from 1500 to 1400 cm^{-1} are much shifted to frequencies lower than those of normal dimethyl sulfide. The CH_2 bending vibrations of the CH_2D group may be expected to appear at slightly lower frequencies than the CH_3 degenerate deformation vibrations. This is also confirmed by the normal coordinate treatment. Since the band at 1424 cm^{-1} is assigned to the CH_2 bending, the bands at 1451 and 1436 cm^{-1} are assigned to the CH_3 degenerate deformation vibrations.

The sum rule and the product rule are used to check the above assignments, assuming that the potential energy is common to dimethyl sulfide, sym-dimethyl sulfide-d_1, and asym-dimethyl sulfide-d_1. The total sums of the squared frequencies are calculated to be 6.470×10^7 for sym-dimethyl sulfide-d_1 and 6.475×10^7 for asym-dimethyl sulfide-d_1. The difference is 0.1%; the assignments of the

observed frequencies are thus confirmed to be correct. The ratio of the squares of the product of the observed frequencies to the values of the determinants of the G matrices are found to be 0.8650, 0.8594, and 0.8600 for dimethyl sulfide, sym-dimethyl sulfide-d_1, and asym-dimethyl sulfide-d_1 respectively; the differences are 0.5%. Therefore, all of our assignments are acceptable.

Normal Coordinate Treatment

The Urey-Bradley force field has been applied to various molecules by many authors, and several modifications have been found to be necessary for complicated molecules. We assumed two following kinds of potential functions of dimethyl sulfide: 1) a modified Urey-Bradley force field, and 2) a local symmetry force field. It has been also supposed that the potential constants of sym- and asym-dimethyl sulfide-d_1 are the same as those of normal species. The force constants were determined by a least-squares technique. In the treatment, the observed frequencies of dimethyl sulfide-d_1 were used together with those of normal species since the investigation of the CH_2D-group vibrations, which have different vibrational modes from those of normal species, as well as of the CH_3 group vibrations could lead to reliable findings on the force constants of the methyl group. The obtained force constants were then transferred to dimethyl sulfide-d_3. The molecular parameters used in the computation were those reported by Pierce and Hayashi.[10]

1) Modified Urey-Bradley Force Field (MUBFF). At first the normal coordinate treatment was carried out in the simple Urey-Bradley force field. For the CH_3 rocking, CH_3 degenerate deformation, and C–S stretching vibrations, however, we could not reduce the deviation between the calculated and the observed frequencies to less than 5%. In order to get better agreements of their frequencies, the following modifications of the simple Urey-Bradley force field were attempted: the bond interaction constant of C–H bonds (p), the angle interaction constant between ∠HCS and ∠HCH (n), the *trans* and *gauche* coupling constants between ∠HCS and ∠CSC (t and g), and the bond interaction constant of C–S bonds (p'). This is the force field designated as "MUBFF-I" in the present paper.

Table 4. Calculated force constants[a] and their dispersion

	MUBFF-I			MUBFF-II				LSFF		
	Force const.	Dispersion[b] Calcd 1	Calcd 2	Force const.	Dispersion[b] Calcd 1	Calcd 2		Force const.	Dispersion[b] Calcd 1	Calcd 2
K(C–H)	4.286	(0.03)	(0.07)	4.267	(0.04)	(0.04)	f(ts)	4.921	(0.06)	(0.06)
K(C–S)	1.691	(0.03)	(0.18)	1.648	(0.03)	(0.19)	f(ds)	4.903	(0.04)	(0.04)
H(HCS)	0.036	(0.00)	(0.04)	0.050	(0.00)	(0.05)	f(cs)	3.659	(0.10)	(0.15)
H(HCH)	0.366	(0.00)	(0.00)	0.348	(0.00)	(0.00)	f(csc)	0.940	(0.00)	(0.02)
H(CSC)	0.244	(0.02)	(0.20)	0.128	(0.05)	(0.24)	f(sd)	0.582	(0.01)	(0.02)
F(HCS)	0.763	(0.01)	(0.13)	0.815	(0.02)	(0.02)	f(dr)	0.668	(0.01)	(0.02)
F(HCH)	0.2[c]			0.2[c]			f(dd)	0.544	(0.00)	(0.01)
F(CSC)	0.21	—	(0.44)	0.21	—	(0.53)	f(to)	0.054[c]		
κ	0.063	(0.01)	(0.01)	−0.010	(0.01)	(0.01)	f(cs, csc)	0.168	—	(0.44)
Y(C–S)	0.054[c]			0.042	(0.03)	(0.03)	f(cs, sd)	−0.673	(0.16)	(0.17)
t	0.070	(0.04)	(0.09)	—			f(cs, cs)	−0.053	(0.02)	(0.12)
g	−0.075	(0.04)	(0.08)	—			f(dr, dd)	−0.056	(0.02)	(0.02)
p(C–H)	−0.130	(0.02)	(0.03)	−0.140	(0.03)	(0.03)	f(ds, dd)	−0.093	(0.00)	(0.00)
p(C–S)	−0.189	(0.00)	(0.03)	−0.186	(0.03)	(0.03)	f(dr, dr)[d]	0.013	(0.01)	(0.01)
n	0.033	(0.00)	(0.03)	—						
q	—			0.009	(0.02)	(0.02)				
q'	—			0.043	(0.01)	(0.01)				

a) K, stretching (mdyn/Å); H, bending (mdyn/Å); F, repulsion (mdyn/Å); $F'=-0.1F$; κ, intramolecular tension (mdyn·Å); Y, internal rotation (mdyn·Å); t, *trans* coupling (mdyn·Å); g, *gauche* coupling (mdyn·Å); p, bond interaction (mdyn/Å); n, angle interaction (mdyn·Å), and q and q', repulsion between two methyl groups (mdyn/Å); cs, C-S stretching; csc, CSC deformation; ts, CH_3 symmetrical stretching; ds, CH_3 degenerate stretching; dd, CH_3 degrenerate deformation; sd, CH_3 symmetrical deformation; dr, CH_3 rocking; to, torsion.

b) See Ref. 13.

c) Fixed force constants, Calcd 1: F (CSC) or f (cs, csc) is fixed, Calcd 2: F (CSC) or f (cs-csc) is not fixed.

d) Rocking interactions so that diagonal elements with regard to A_1 and B_1 rocking modes are f (dr) $+f$ (dr, dr) and f (dr) $-f$ (dr, dr), respectively.

Table 5. Observed and calculated frequencies of dimethyl sulfide (cm^{-1})

		Observed	Calculated					
			MUBFF-I		MUBFF-II		LSFF	
CH_3SCH_3								
A_1	ν_1	2991	3009	0.6	3015	0.8	3015	0.8
	ν_2	2916	2906	0.3	2910	0.2	2907	0.3
	ν_3	1456	1448	0.5	1455	0.0	1447	0.7
	ν_4	1317	1325	0.6	1337	1.5	1323	0.4
	ν_5	1028	1019	0.9	1004	2.3	999	2.8
	ν_6	691	691	0.0	686	0.7	688	0.5
	ν_7	282	277	1.8	277	1.6	280	0.8
A_2	ν_8		3013		3026		3012	
	ν_9		1446		1433		1438	
	ν_{10}		963		977		989	
	ν_{11}		173		207		173	
B_1	ν_{12}	2991	3008	0.6	3011	0.7	3013	0.8
	ν_{13}	2852	2906	1.9	2905	1.9	2907	1.9
	ν_{14}	1440	1450	0.7	1438	0.1	1444	0.3
	ν_{15}	1317	1323	0.5	1337	1.5	1326	0.7
	ν_{16}	972	971	0.1	976	0.4	969	0.3
	ν_{17}	741	742	0.1	742	0.1	743	0.2
B_2	ν_{18}	2991	3013	0.7	3018	1.1	3012	0.7
	ν_{19}	1434	1446	0.9	1423	0.8	1438	0.3
	ν_{20}	1005	979	2.6	992	1.3	1006	0.1
	ν_{21}	182	182	0.0	180	0.9	182	0.0
CH_2DSCH_3 (Symmetric)								
A'	ν_1	2986	3008	0.8	3013	0.9	3014	0.9
	ν_2	2919	2946	0.9	2974	1.2	2946	0.9
	ν_3	2871	2906	1.2	2907	1.3	2907	1.3
	ν_4	2189	2173	0.7	2169	0.9	2176	0.6
	ν_5	1451	1449	0.1	1449	0.1	1445	0.4
	ν_6	1424	1434	0.7	1420	0.3	1430	0.5
	ν_7	1327	1324	0.2	1337	0.8	1324	0.2
	ν_8	1250	1236	1.1	1227	1.8	1233	1.4
	ν_9	1007	996	1.1	989	1.8	984	2.3
	ν_{10}	806	807	0.1	814	1.0	794	1.5
	ν_{11}	739	741	0.3	741	0.3	742	0.4
	ν_{12}	664	673	1.3	675	1.6	674	1.5
	ν_{13}	274	271	1.0	282	2.8	274	0.0
A''	ν_{14}	2986	3013	0.9	3026	1.4	3012	0.9
	ν_{15}	2986	3013	0.9	3018	1.1	3012	0.9
	ν_{16}	1436	1446	0.7	1429	0.5	1438	0.2
	ν_{17}	1223	1234	0.9	1257	2.8	1233	0.6
	ν_{18}	981	975	0.6	987	0.6	1001	2.1
	ν_{19}	963	957	0.7	946	1.7	980	1.7
	ν_{20}		178		205		178	
	ν_{21}		156		165		156	
CH_2DSCH_3 (Asymmetric)								
	ν_1	2986	3013	0.9	3022	1.2	3014	1.0
	ν_2	2986	3010	0.8	3016	1.0	3013	0.9
	ν_3	2986	3008	0.7	3012	0.9	3012	0.9
	ν_4	2919	2944	0.8	2945	0.9	2947	0.9
	ν_5	2871	2906	1.2	2908	1.3	2907	1.2
	ν_6	2189	2176	0.6	2177	0.5	2173	0.7
	ν_7	1451	1449	0.2	1448	0.2	1445	0.4
	ν_8	1436	1446	0.7	1429	0.5	1438	0.2
	ν_9	1424	1430	0.4	1408	1.1	1421	0.2
	ν_{10}	1327	1324	0.2	1337	0.8	1324	0.2
	ν_{11}	1259	1246	1.0	1271	1.0	1249	0.7
	ν_{12}	1236	1242	0.4	1239	0.2	1238	0.2
	ν_{13}	1007	1010	0.3	994	1.3	998	0.9
	ν_{14}	981	972	1.0	985	0.4	991	1.0
	ν_{15}	963	959	0.4	941	2.3	959	0.4
	ν_{16}	789	793	0.5	805	2.1	799	1.3
	ν_{17}	739	724	2.1	732	1.0	731	1.0
	ν_{18}	691	688	0.5	684	1.0	686	0.7
	ν_{19}	274	270	1.4	282	2.8	274	0.0
	ν_{20}		177		200		179	
	ν_{21}		156		170		156	

The force constants obtained by a least-squares technique and the calculated frequencies are shown in Tables 4 and 5. An effect of anharmonicity was seen with the C–H and C–D stretching frequencies. On the SCD deformation vibration, the effect of anharmonicity was not so clear, since the CH_2 deformation coordinate is coupled with it. For the CH_3 rocking vibrations of dimethyl sulfide, the observed frequencies were 1028 (A_1), 972 (B_1), and 1005 cm^{-1} (B_2), and the calculated frequencies in this force field were 1019 (A_1), 971 (B_1), and 979 cm^{-1} (B_2), although the frequencies in the simple Urey-Bradley force field were 962 (A_1) and 949 cm^{-1} (B_1). The calculated frequencies and difference between the A_1 and B_1 vibrations in MUBFF-I satisfactorily agree with the observed values of the A_1 and B_1 frequencies. The B_2 vibration could not be discussed since the observed frequency was ambiguous. The observed spectra could reasonably be explained by MUBFF-I using the five modification terms.

The set of the force constants of MUBFF-I was then transferred to dimethyl sulfide-d_3. The calculated frequencies are shown in Table 6 together with the reported experimental values.[4] These force constants of MUBFF-I are confirm to reproduce the observed frequencies well except for the CD_3 rocking A' vibration on dimethyl sulfide-d_3. Since the band assigned by Perchard *et al.*[4] to the CD_3 rocking mode is so weak, we can not discuss the disagreement between the calculated and observed frequencies at present. In the calculated results the anharmonicity mentioned above is also seen in the case of the C–H and C–D stretching vibrations.

In MUBFF-I we treated the interactions in methyl groups as modification terms, n, t, and g. However, the nearest atomic distance between two hydrogens

Table 6. Observed and calculated frequencies of dimethyl sulfide-d_3 (cm^{-1})

	Assignment	Observed[a]	Calculated					
			MUBFF-I		MUBFF-II		LSFF	
A'	C–H str.	2970.5	3009	1.3	3012	1.4	3014	1.5
	C–H str.	2917	2908	0.8	2904	0.4	2907	0.3
	C–D str.	2231	2227	0.2	2226	0.2	2230	0.0
	C–D str.	2128	2078	2.3	2074	2.5	2076	2.4
	CH_3 deg. def.	1437.5	1444	0.5	1438	0.0	1445	0.5
	CH_3 sym. def.	1332	1325	0.5	1333	0.1	1324	0.6
	CD_3 deg. def.	1050.5	1054	0.3	1032	1.8	1048	0.2
	CH_3 rock.	1013.5	1006	0.7	988	2.5	990	2.3
	CD_3 sym. def.	961	975	1.5	972	1.1	969	0.8
	CD_3 rock.	740	782	5.7	773	4.5	770	4.1
	C–S str.	705	721	2.3	719	2.0	719	2.0
	C–S str.	656	669	2.0	674	2.7	674	2.7
	CSC def.		261		234		263	
A''	C–H str.	2989	3014	0.8	3018	1.0	3012	0.8
	C–D str.	2240	2292	0.5	2230	0.5	2226	0.6
	CH_3 deg. def.	1428.5	1442	0.9	1420	0.6	1438	0.7
	CD_3 deg. def.	1040.5	1054	1.3	1022	1.7	1046	0.5
	CH_3 rock.	983	974	0.9	981	0.2	998	1.5
	CD_3 rock.	725.5	729	0.5	746	2.8	750	3.4
	torsion		176		155		177	
	torsion		129		115		131	

a) From Ref. 4.

situated at the ends of methyl groups is 2.6 Å, and the second nearest is 3.2 Å (see Fig. 3.). Therefore,

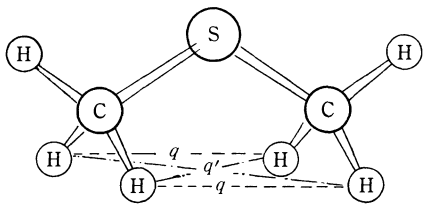

Fig. 3. Repulsion potentials (q and q') between hydrogen atoms.

we could expect the other kind of interaction between methyl groups, namely a direct interaction between two methyl groups. Let us denote the repulsion potentials between the two hydrogen atoms in the case of the nearest and the second nearest atomic distances as q and q' respectively. We then assumed the second modified Urey-Bradley force field (MUBFF-II), in which the modification terms are the bond interaction potential, p, besides the repulsion potentials between two methyl groups, q and q'. The obtained force constants and the calculated frequencies are shown in Tables 4 and 5. This force field reproduces the observed frequencies well. Moreover, the deviation was only about 1%. The determined values of q and q' were 0.009 and 0.043 respectively; these however do not satisfy the relation expected from the van der Waals function ($q \fallingdotseq 2q'$). This suggests that same other weak interactions contribute to the force field of the sulfides.

2) Local Symmetry Force Field (LSFF). In the second place the normal coordinate treatment was carried out using the local symmetry force field reported by Shimanouchi *et al.*[12] All of the diagonal elements and a part of the off-diagonal elements of the $\boldsymbol{F}$ matrix, expressed in terms of local symmetry coordinates, were treated as independent force constants, while the other off-diagonal elements were calculated from the relation of the Urey-Bradley force field. The results thus obtained are shown in Tables 4 and 5. The calculated frequencies agreed well with the observed frequencies. The set of force constants was transferred to the calculation of dimethyl sulfide-d_3. In this force field the calculated frequencies of the CD_3 rocking vibrations agreed fairly well with the observed frequencies. The values of the $\boldsymbol{F}$ matrix elements of LSFF resemble those of MUBFF-I. From these facts it can be said that the off-diagonal elements of the potential energy matrix are, greatly, related to the repulsion force constants.

12) T. Shimanouchi, I. Nakagawa, C. Tanaka, I. Suzuki, H. Takahashi, T. Fujiyama, Y. Abe, T. Ueda, M. Mikami, M. Oka, A. Hirakawa and A. Kurokawa, *Molecular Structure Symposium*, October, 1966, Osaka, Japan.

Discussion

The normal coordinate treatments presented above lead to the conclusion that the interaction terms of the methyl group with the other group are indispensable in the force fields of dimethyl sulfides. If the interaction terms of the methyl group with the other group, t, and g in MUBFF-I, q and q' in MUBFF-II, and f(cs, sd) and f(dr, dr) in LSFF, were not introduced, the observed frequencies could not be reproduced satisfactorily by their force fields. In Table 4 the values in brackets beside the force constants represent the dispersion[13] (Calcd 1) of the force constants around the convergence values. It may be seen that none of the force constants for diagonal and off-diagonal elements relating to the skeletal coordinate are tightly adjusted. At first stage of the calculation by the least-squares technique, some of the force constants for diagonal and off-diagonal elements of the CSC skeletal and C–S stretching vibrational coordinates were reasonablely fixed in several cases. In the final stage, all of the fixed force constants were released from the fixed values. The value of dispersion in this case is shown as Calcd 2 in Table 4. After all, it seems that the force constants relating to the skeleton, especially the off-diagonal elements, can not be exactly determined. Their precise determinations may, however, be accomplished by studies of the isotopic effect of the skeleton or by a completely different approach.

It is well known that the centrifugal distortion constants are closely related to the force constant.[14] We have attempted to compare the centrifugal distortion constants determined on the basis of the force constants with those determined on the basis of the microwave data.[7]

The centrifugal distrotion constants of dimethyl sulfide as determined by microwave measurements have been reported by Rudolph *et al.*,[15] these values were later corrected by Sørensen.[7] He found that none of the six constants could be determined independently when the determinant of the centrifugal distortion matrix (6×6) was almost zero. Therefore, five new linear combinations were selected in such a way that the direct influence of the fixed constant on the observed values was entirely negligible. The determined constants are shown in the 2nd column of Table 7.

The centrifugal distortion constants, $\tau_{\alpha\beta\gamma\delta}$, are defined thus:

$$\tau_{\alpha\beta\delta\gamma} = -\sum_{ij}[J^0_{\alpha\beta}]_i[J^0_{\gamma\delta}]_j[F^{-1}]_{ij}/2\ I^0_{\alpha\alpha}I^0_{\beta\beta}I^0_{\gamma\gamma}I^0_{\delta\delta} \quad (1)$$

Table 7. Centrifugal distortion constants of dimethyl sulfide (kHz)

Centri. Destn. Conts.[c]	Microwave[a]	Normal vibration MUBFF-I	MUBFF-II	LSFF
T_1	−447.8	−450	−710	−480
T_2	−54.84	−53	−3	−56
T_3	−9.626	−9.4	−5.9	−9.5
T_4'	−26.21	−34.1	12.8	−28.3
T_5'	−2.333	−4.1	−2.4	−2.5
T_6	−5[b]	−16.8	1.8	−8.6

a) See Ref. 7.

b) Fixed constant which contributes with less than 1.6×10^{-5} MHz to the centrifugal distortion correction.

c) $T_1 = \tau_{aaaa}$, $T_2 = \tau_{bbbb}$, $T_3 = \tau_{cccc}$,

$$T_4 = \tau_{abab} + \frac{1}{2}\left[\tau_{aabb} - \left(\tau_{cccc} - \left(\frac{C}{A}\right)^4\tau_{aaaa} - \left(\frac{C}{B}\right)^4\tau_{bbbb}\right)\frac{A^2B^2}{2C^4}\right],$$

$$T_5 = \tau_{bcbc} + \frac{1}{2}\left[\tau_{bbcc} - \left(\tau_{cccc} - \left(\frac{C}{A}\right)^4\tau_{aaaa} + \left(\frac{C}{B}\right)^4\tau_{bbbb}\right)\frac{B^2}{2C^2}\right],$$

$$T_6 = \tau_{caca} + \frac{1}{2}\left[\tau_{ccaa} - \left(\tau_{cccc} + \left(\frac{C}{A}\right)^4\tau_{aaaa} - \left(\frac{C}{B}\right)^4\tau_{bbbb}\right)\frac{A^2}{2C^2}\right],$$

$T_4' = T_4 + 0.8426T_6$, $T_5' = T_5 + 0.1574T_6$, $A = 17809.7$, $B = 7621.1$ and $C = 5717.8$ MHz

where $I_{\alpha\alpha}$ denotes the moment of inertia and where $\boldsymbol{F}$ is the potential energy matrix expressed in terms of displacement coordinates, and $[J_{\alpha\beta}{}^0]_i$ is defined by:

$$[J^0_{\alpha\beta}]_i = (\partial I_{\alpha\beta}/\partial q_i) \quad (2)$$

where $I_{\alpha\beta}$ is the inertia tensor and where q_i is the ith displacement coordinate. Using Eq. (2) the centrifugal distortion constants were calculated from the above-mentioned three sets of force constants; the six constants were then recalculated in the same form as the constants obtained by Sørensen. They are shown in the last three columns of Table 7. The calculated centrifugal distortion constants were in good agreement with the observed values in the cases of MUBFF-I and LSFF, while in the case of MUBFF-II the agreement was not sufficient.

Then we examined the change in the centrifugal distortion constants due to the change in the force constants. From Eq. (1) the following equations were deduced:[16]

$$(\partial\tau_{\alpha\beta\gamma\delta}/\partial f_{ij}) = -\sum_{kl}[J^0_{\alpha\beta}]_k[F^{-1}]_{ik}[F^{-1}]_{jl}[J^0_{\gamma\delta}]_l/ I^0_{\alpha\alpha}I^0_{\beta\beta}I^0_{\gamma\gamma}I^0_{\delta\delta} \quad (\text{if } i \neq j)$$

13) T. Ogawa and T. Miyazawa, *Spectrochim. Acta*, **20**, 557 (1964).

14) D. Kivelson and E. B. Wilson, Jr., *J. Chem. Phys.*, **20**, 1575 (1952).

15) M. D. Rudolph, H. Dreizler and W. Maier, *Z. Naturforsh.*, **A 15**, 742 (1960).

16) I. M. Mills, *J. Mol. Spectrosc.*, **5**, 334 (1960).

TABLE 8. CALCULATED VALUES OF DERIVATIVES OF THE CENTRIFUGAL DISTORTION CONSTANTS ($\tau_{\alpha\beta\gamma\delta}$) WITH RESPECT TO THE ELEMENTS (f_{ij}) OF $\boldsymbol{F}$ MATRICES[a] OF DIMETHYL SULFIDE (k·Hz·Å/md)

	CH str.	CH str.	CH_3 deg.	CH_3 sym.	CH_3 rock.	CS str.	CSC def.
τ_{aaaa} (A_1)	−0.1			Symmetric			
	−0.4	−0.7					
	−0.4	−1.5	−0.8				
	−3.6	−11.7	12.9	−51.7			
	2.4	7.9	8.7	70.0	−23.7		
	3.0	9.8	10.8	87.1	−58.9	−36.6	
	−9.4	−30.6	−33.7	−271.0	183.0	228.0	−355.0
τ_{bbbb} (A_1)	0.0			Symmetric			
	0.0	0.0					
	0.1	−0.3	−0.4				
	0.0	0.0	0.0	0.0			
	−0.3	0.7	2.2	−0.1	−3.0		
	0.3	−0.6	−1.7	0.1	4.7	−1.8	
	1.1	−2.6	−7.4	0.5	21.0	−16.1	−35.8
τ_{cccc} (A_1)	0.0			Symmetric			
	0.0	0.0					
	0.0	0.0	0.0				
	−0.2	0.0	−0.1	−0.3			
	−0.2	0.0	−0.1	−0.6	−0.3		
	0.4	−0.2	0.3	1.5	1.5	−1.9	
	0.4	−0.3	0.3	1.6	1.6	−4.0	−2.1
τ_{bbcc} (A_1)	0.0			Symmetric			
	0.0	0.0					
	0.2	0.1	0.0				
	0.0	0.0	0.7	0.0			
	−0.5	0.3	0.7	−2.0	−1.0		
	0.3	−0.6	−1.7	0.1	4.8	−1.8	
	1.8	−1.0	−1.8	0.1	5.1	−16.3	−8.7
τ_{ccaa} (A_1)	0.0			Symmetric			
	0.0	0.0					
	0.0	−0.2	0.0				
	−0.3	−0.9	−1.4	−4.1			
	−0.3	−0.9	0.9	−8.1	2.7		
	1.9	−1.1	1.2	6.8	6.8	−8.3	
	0.7	2.4	−3.6	−21.2	−21.2	−17.6	27.3
τ_{aabb} (A_1)	0.0			Symmetric			
	−0.2	0.2					
	−0.2	0.4	0.6				
	−1.4	3.1	0.0	−0.3			
	0.9	−2.1	−3.1	0.4	8.5		
	2.2	2.2	2.4	19.4	−13.1	−8.2	
	−3.6	8.0	10.7	86.1	−58.3	50.8	113.0
τ_{abab} (B_1)	−0.2			Symmetric			
	0.0	0.0					
	0.2	0.0	0.0				
	−0.8	0.0	0.5	−0.8			
	−0.5	0.0	0.3	−1.1	−0.3		
	2.0	0.1	−1.3	4.4	2.8	−5.8	

TABLE 8. (Continued)

	CH str.	CH_3 deg.	CH_3 rock.	torsion
τ_{caca} (A_2)	0.0		Symmetric	
	0.0	−0.3		
	0.1	1.2	−1.0	
	−1.2	−12.9	23.1	−130.0
τ_{bcbc} (B_2)	0.0		Symmetric	
	0.0	0.0		
	0.0	0.0	0.0	
	−0.3	−0.9	−2.5	−23.9

a) The matrices are expressed with the local symmetry coordinates. The i and j denote the ith and jth coordinates, respectively.

or $$= -\frac{1}{2}\sum[J^0_{\alpha\beta}]_{ik}[F^{-1}]_{ik}[F^{-1}]_{jl}[J^0_{\gamma\delta}]_{lj}/ I^0_{\alpha\alpha}I^0_{\beta\beta}I^0_{\gamma\gamma}I^0_{\delta\delta} \quad (\text{if } i=j)$$

where the i and j denote ith and jth local symmetry coordinates respectively. Therefore, f_{ij} denotes the element of the F matrix represented by the local symmetry coordinates. Normal dimethyl sulfide has a C_{2v} symmetry. Therefore, τ_{aaaa}, τ_{bbbb}, τ_{cccc}, τ_{bbcc}, τ_{ccaa}, and τ_{aabb} are related to the vibrations belonging to the A_1 species; τ_{abab} is related to the B_1 species; τ_{caca}, to the A_2 species, and τ_{bcbc}, to the B_2 species. Table 8 shows the calculated values of $(\delta\tau_{\alpha\beta\gamma\delta}/\delta f_{ij})$ in each symmetry species. The larger values show the more relations between $\tau_{\alpha\beta\gamma\delta}$ and f_{ij}. If $\tau_{\alpha\beta\gamma\delta}$ is completely determined by the microwave analysis, the force constants with a large value of $(\delta\tau_{\alpha\beta\gamma\delta}/\delta f_{ij})$ can be correctly obtained. Such force constants are f(cs), f(cs, csc), f(csc), f(to), and so on. On the other hand, f(ts), f(dd), f(sd), *etc.* can not be correctly determined from the centrifugal distortion constants. In general, the $(\delta\tau_{\alpha\beta\gamma\delta}/\delta f_{ij})$ values related to the vibrational coordinates on hydrogen atoms, *i.e.*, small-mass atoms, are small. Those related to skeletal vibrational coordinates (skeletal stretching, skeletal deformation, and torsional) are large. Therefore, their off-diagonal values are rather larger than the diagonal values. Thus, the force constants related to the hydrogen stretching and deformation vibrations can be determined only with difficulty from the centrifugal distortion constants, whereas those for diagonal and off-diagonal elements related to the skeletal stretching, skeletal deformation, and torsional vibrations can be determined more easily. This fact may be valuable for studies of molecular force fields, since usually it is too hard to determine the force constants related to the skeleton, especially their off-diagonal elements with sufficient accuracy. The determination of the force constants on the basis of the centrifugal distortion constants may be expected to be valuable. In this study, however, we did not calculate the force constants from the centrifugal distortion constants. The comparison of the two sets of centrifugal distortion constants obtained from the vibrational spectra and the microwave spectra reveals that the force field of MUBFF-I and LSFF would be preferable. The application of the force constants we have obtained will be discussed in the near future.

The authors wish to express their gratitude to Professor T. Shimanouchi of the University of Tokyo, for the permission to use the Perkin-Elmer 112-G spectrometer and to Dr. Shinnosuke Saeki of the Tokyo Government Industrial Research Institute for his measurements of the Raman spectra.

BULLETIN OF THE CHEMICAL SOCIETY OF JAPAN VOL. 43 619—622 (1970)

Molecular Vibrations and Force Fields of Dimethyl Selenide and Dimethyl Selenide-d_6

Yuji SHIRO,*1 Masaru OHSAKU, Michiro HAYASHI and Hiromu MURATA

Department of Chemistry, Faculty of Science, Hiroshima University, Higashisenda-machi, Hiroshima

(Received May 6, 1969)

A set of the modified Urey-Bradley force constants and of the local symmetry force constants of dimethyl selenide have been calculated by a least-squares technique, using the vibrational frequencies of the two isotopic species, $(CH_3)_2Se$ and $(CD_3)_2Se$. The calculated frequencies thus obtained are in good agreement with the observed values. Comparison has been made for the force constants among dimethyl ether, dimethyl sulfide, and dimethyl selenide. This has shown the reasonable relation to be expected among the force constant, the bond length, the bond angle, and the atomic number of the central atom. The centrifugal distortion constants, which were calculated from the two sets of force constants, were then compared with those obtained from the microwave spectra; their values are found to be consistent with those obtained from a microwave study in a three-body approximation.

The force fields of dimethyl ether[1-3] and dimethyl sulfide[4] have been extensively investigated. For dimethyl selenide, the vibrational data have been reported by Allkins and Hendra,[5,6] who made a treatment of the simple valence force field for the skeleton. Although Fritz and Keller[7] made a simple computation of the vibrational frequencies of dimethyl ether, dimethyl sulfide, dimethyl selenide, and dimethyl telluride, no study has been made of the Urey-Bradley and the local symmetry force fields. In our paper[4] on the most probable force fields of dimethyl sulfide, we determined two sets of force constants. One of them was a set of modified Urey-Bradley force constants which contained such modification constants as C–H bond interaction, p(C–H); C–S bond interaction, p(C–S); *trans* coupling, t; *gauche* coupling, g, between ∠HCS and ∠CSC, and angle interaction, n, between ∠HCS and ∠HCH. The other set was the local symmetry potential constants. For dimethyl selenide, we have attempted to estimate, by a least-squares technique, a set of the force constants of the modified Urey-Bradley force field (MUBFF) and of the local symmetry force field (LSFF) from the reported vibrational frequencies of the normal[5] and fully-deuterated[6] species. To make sure of the propriety of the two sets of the force constants thus obtained, the centrifugal distortion constants were calculated and compared with those reported by Beecher[8] on the basis of his microwave study.

Calulated Vibrational Frequencies

Assuming that dimethyl selenide and dimethyl selenide-d_6 belong to the same symmetry class as a C_{2v} symmetry, 21 fundamental modes of vibrations can be subdivided by symmetry properties into four species, $7A_1$, $4A_2$, $6B_1$, and $4B_2$. Two types of potential function were treated as in the case of dimethyl sulfide. One is the modified Urey-Bradley force field. This contains the C–H bond interaction term, p(C–H); the C–Se bond interaction term, p(C–Se); the *trans* and *gauche* coupling terms, t, and g, between ∠HCSe and ∠CSeC, and the angle interaction term, n, between ∠HCSe and ∠HCH. The other is the local symmetry force field. Normal coordinate treatments were carried out by a least-squares technique on the basis of the observed frequencies of the normal[5] and fully deuterated[6] species by Allkins and Hendra. Computation has been carried out assuming that the

*1 Present address: Shinonome Branch School, Faculty of Education, Hiroshima University, Shinonome-3-chome, Hiroshima.

1) T. Shimanouchi, I. Nakagawa, C. Tanaka, I. Suzuki, H. Takahashi, T. Fujiyama, Y. Abe, T. Ueda, M. Mikami, M. Oka, A. Hirakawa and A. Kurokawa, Molecular Structure Symposium, October, 1966, Osaka, Japan.

2) R. G. Snyder and G. Zerbi, *Spectrochim. Acta*, **23A**, 391 (1967).

3) P. Labarbe, M. T. Forel and G. Bessis, *ibid.*, **24A**, 2165 (1968).

4) Y. Shiro, M. Ohsaku, M. Hayashi and H. Murata, This Bulletin, **43**, 609 (1970).

5) J. R. Allkins and P. J. Hendra, *Spectrochim. Acta*, **22**, 2075 (1966).

6) J. R. Allkins and P. J. Hendra, *ibid.*, **23A**, 1671 (1967).

7) H. P. Fritz and H. Keller, *Chem. Ber.*, **94**, 1524 (1961).

8) J. F. Beecher, *J. Mol. Spectroscopy*, **21**, 414 (1966).

TABLE 1. OBSERVED AND CALCULATED FREQUENCIES OF DIMETHYL SELENIDE (cm^{-1})

			CH_3SeCH_3					CD_3SeCD_3				
			Obsd[a]	Calcd				Obsd[b]	Calcd			
				MUBFF		LSFF			MUBFF		LSFF	
A_1	ν_1	CH_3,CD_3 deg. str.	2992	3018	0.9	3009	0.6	2256	2239	−0.8	2246	−0.4
	ν_2	CH_3,CD_3 sym. str.	2920	2953	1.1	2942	0.7	2134	2108	−1.2	2118	−0.8
	ν_3	CH_3,CD_3 deg. def.	1423	1426	0.2	1442	1.3	1038	1036	−0.2	1034	−0.4
	ν_4	CH_3,CD_3 sym. def.	1284	1295	0.9	1278	−0.5	983	965	−1.9	971	−1.2
	ν_5[d]	CH_3,CD_3 rock.	954	955	0.1	960	0.6	744	743	−0.1	726	−2.4
	ν_6	C–Se str.	589	581	−1.3	591	0.3	548	555	1.4	547	−0.2
	ν_7	CSeC def.	233[c]	234	0.6	230	−1.3	201[c]	200	−0.5	204	1.3
A_2	ν_8	CH_3,CD_3 deg. str.	2996[f]	3020		3007			2235		2242	
	ν_9	CH_3,CD_3 deg. def.	1424[f]	1425		1428			1033		1026	
	ν_{10}[e]	CH_3,CD_3 rock.	890	886	−0.4	922	3.6	680	660	−2.9	688	1.2
	ν_{11}	torsion		160		160			114		115	
B_1	ν_{12}	CH_3,CD_3 deg. str.	2992	3016	0.8	3008	0.5	2256	2233	−1.0	2243	−0.6
	ν_{13}	CH_3,CD_3 sym. str.	2920	2953	1.1	2942	0.7	2134	2108	−1.2	2118	−0.8
	ν_{14}	CH_3,CD_3 deg. def.	1423	1450	0.5	1431	0.6	1038	1035	−0.3	1029	−0.9
	ν_{15}	CH_3,CD_3 sym. def.	1263	1290	2.1	1278	1.2	968	958	−1.1	971	0.3
	ν_{16}[d]	CH_3,CD_3 rock.	857	888	3.6	862	0.6	658	666	1.2	646	−1.9
	ν_{17}	CSe str.	604	597	−1.2	606	0.3	564	571	1.2	562	−0.4
B_2	ν_{18}	CH_3,CD_3 deg. str.	2992	3020	0.9	3007	0.5	2256	2235	−0.9	2242	−0.6
	ν_{19}	CH_3,CD_3 deg. def.	1423	1425	0.1	1428	0.4	1038	1033	−0.5	1026	−1.1
	ν_{20}[e]	CH_3,CD_3 rock.	908	981	−1.8	927	2.1	696	667	−4.1	695	−0.1
	ν_{21}	torsion		163		164			118		119	
		MUBFF m.d. 1.1% r.m.s.d. 1.4%										
		LSFF m.d. 0.9% r.m.s.d. 1.1%										

a) See Ref. 5. b) See Ref. 6. c) Raman. d) In plane vibration.
e) Out of plane vibration. f) Not used in calculation.

potentials of dimethyl selenide and dimethyl selenide-d_6 are common. The molecular parameters used on the computation were those reported by Beecher.[8] Table 1 shows the observed frequencies and two cases of the calculated frequencies with the deviation between the observed and calculated frequencies.

For normal dimethyl selenide in the modified Urey-Bradley force field, the calculated frequencies of the CH_3 rocking region, $\nu_{16}(B_1)$ and $\nu_{20}(B_2)$, and of CH_3 symmetric deformation, $\nu_{15}(B_1)$, are fairly different from each observed frequency. However, the other vibrations are in good agreement within a deviation of about 1%. In the local symmetry force field the CH_3 rocking vibrations, $\nu_{10}(A_2)$ and $\nu_{20}(B_2)$, also have fairly large deviations.

For dimethyl selenide-d_6 in the modified Urey-Bradley force field, the vibrations of the CD_3 rocking region, $\nu_{10}(A_2)$ and $\nu_{20}(B_2)$, and those in the local symmetry force field, $\nu_5(A_1)$ and $\nu_{16}(B_1)$, of the CD_3 rocking vibrations have also fairly large deviations. That is, CH_3 or the CD_3 rocking vibrations were not reproduced in good agreement either in the modified Urey-Bradley or in the local symmetry force fields. This tendency was also shown in our work on dimethyl sulfides.[4] The calculated mean deviation (m.d.) and the root mean squared deviation (r.m.s.d.) are as follows: MUBFF; m.d. 1.1%, r.m.s.d. 1.4%, LSFF; m.d. 0.9%, r.m.s.d. 1.1%. Thus the modified Urey-Bradley force field and the local symmetry force field are appropriate as the force fields of dimethyl selenide.

Force Constants

Table 2 shows the two final sets of the force constants and their dispersion, together with the sets obtained from dimethyl ether[1] and dimethyl sulfide.[4] Although some modification constants taken into consideration differ from each other, the force constants among the listed molecules will be made compared in order to establish a definite tendency.

The C–X bond length in these compounds with the formula $(CH_3)_2X$ increases and, on the other hand, the CXC angle decreases towards 90°, with an increase in the atomic number of the atom X (X: O, S, and Se). The data provided by the microwave studies are as follows:

Table 2. Calculated force constants with their dispersion

	Modified Urey-Bradley force constants[a]				Local symmetry force constants[b]				
	$(CH_3)_2O$[c]	$(CH_3)_2S$[d]	$(CH_3)_2Se$			$(CH_3)_2O$[c]	$(CH_3)_2S$[d]	$(CH_3)_2Se$	
K(C–H)	4.112	4.286	4.467	0.04	f(ts)	4.613	4.921	4.937	0.13
K(C–X)	3.366	1.691	1.288	0.10	f(ds)	4.851	4.903	4.778	0.09
H(HCX)	0.282	0.036	0.03[e]		f(cx)	5.123	3.659	2.716	0.01
H(HCH)	0.361	0.366	0.355	0.55	f(cxc)	1.169	0.940	0.849	0.02
H(CXC)	0.445	0.244	0.259	0.04	f(sd)	0.670	0.582	0.547	0.04
F(HCX)	0.756	0.763	0.617	0.07	f(dr)	0.942	0.668	0.590	0.03
F(HCH)	0.200	0.2	0.19[e]		f(dd)	0.547	0.544	0.524	0.03
F(CXC)	0.3	0.21	0.2[e]		f(to)	—	0.054	0.047[e]	
κ	0.059	0.063	0.029	0.09	f(cx, cxc)	0.059	0.168	0.12[e]	
Y(CX)	0.074	0.054	0.047[e]		f(cx, sd)	−0.523	−0.673	−0.322	0.04
t	—	0.070	0.09[e]		f(cx, cx)	−0.275	−0.053	−0.008	0.01
g	—	−0.075	−0.211	0.05	f(dr, dd)	−0.043	−0.056	0.006	0.05
p(C–H)	−0.219	−0.130	−0.073	0.03	f(ds, dd)	−0.093	−0.093	0.124	0.14
p(C–X)	−0.302	−0.189	−0.118	0.04	f(dr, dr)	0.067	0.013	0.063	0.01
n	—	0.033	0.003	0.05					

a) K, stretching (mdyn/Å); H, bending (mdyn/Å); F, repulsion (mdyn/Å); $F'=-0.1F$; κ, intramolecular tension (mdyn·Å); Y, internal rotation (mdyn·Å); t., *trans* coupling (mdyn·Å); g, *gaushe* coupling (mdyn·Å); p, bond interaction (mdyn/Å); n, angle interaction (mdyn·Å), and q and q', repulsion between two methyl groups (mdyn/Å).
b) cx, C–X stretching: cxc, CXC deformation; ts, CH_3 symmetrical stretching; ds, CH_3 degenerate stretching; dd, CH_3 degenerate deformation; sd, CH_3 symmetrical deformation; dr, CH_3 rocking; to, torsion.
c) See Ref. 1. d) See Ref. 4. e) Fixed force constants.

∠COC 111°43′, r(C–O) 1.410 Å Ref. 9;
∠CSC 98°52′, r(C–S) 1.802 Å Ref. 10;
∠CSeC 96°11′, r(C–Se) 1.943 Å Ref. 8.

K; Stretching Force Constants. The stretching force constant of K(C–H) does not show any clear tendency. The results due to the simple computation of Fritz and Keller[7] show that the C–X stretching force constants with the general formula of $(CH_3)_2X$ decrease with an increase in the atomic number (X; O, S, Se, and Te). Such a phenomenon is also shown in this work. The force constants of K(C–O) and K(C–S) were found to be 3.366 and 1.691 respectively, and the force constant of K(C–Se) was found to be 1.288, both decreasing with an increase in the atomic number.

H: Bending Force Constants. As the C–X bond length increases and the CXC angle decreases, the bending force constant, H(HCX), decreases, but H(CXC) shows no definite tendency.

F: Repulsion Force Constants. This kind of force constant decreases with an increase in the atomic number of central atom. This shows that the repulsive force in each case decreases with an increase in the C–X bond length.

κ: Internal Tension. These constants also decrease in the order O<S<Se.

Y: Torsional Force Constants. These constants can be calculated from the barrier height (V_3) of each molecule; the barrier heights of the normal species with the formula $(CH_3)_2X$ (X; O, S, and Se) were found to be 2720, 2132, and 1500 cal/mol.[8,10,11] Therefore, the constants also decrease in the order O<S<Se.

Modification Constants. Generally, the modification constants are in the same order, as have been mentioned above. However, most of the modification constants have a fairly large dispersion. This suggests that these potentials bear at the same time the effect of other interactions which are not taken into consideration, and also that these constants are not tightly adjusted. Therefore, the modification constants are fairly arbitrary and a regular comparison could not be made.

In the case of the local symmetry force constants, our results were nearly the same as the modified Urey-Bradley force constants. That is, the constants decrease in the order O<S<Se. However, the physical meanings of the local symmetry force constants are not obvious enough for us to discuss the local symmetry force constants.

Centrifugal Distortion Constants

In order to confirm the reasonableness of the

9) U. Blukis, P. H. Kasai and R. J. Myers, *J. Chem. Phys.*, **38**, 2753 (1963).
10) L. Pierce and M. Hayashi, *ibid.*, **35**, 479 (1961).
11) P. H. Kasai and R. J. Myers, *ibid.*, **30**, 1096 (1959).

obtained force constants, we calculated the centrifugal distortion constants. Table 3 shows the centrifugal distortion constants calculated from the two final sets of the force constants and those from the microwave study by Beecher,[8] who determined the centrifugal distortion constants in the three-body approximation. The two cases of the modified Urey-Bradley force field and the local symmetry force field are in good agreement with those from the microwave study. In comparing Beecher's results and the present results we noticed the following two results; (1) the four observed values of constants, τ_{aaaa}, τ_{bbbb}, τ_{aabb}, and τ_{abab} agreed well with the calculated values, and (2) three constants, τ_{cccc}, τ_{bbcc}, and τ_{ccaa}, which are ignored by Beecher are found in this work to have small values.

Therefore, it is confirmed that the obtained force constants are reasonable in the light of the first finding, while, on the other hand, Beecher's assumption is reasonable as the first approximation in the light of the second finding.

TABLE 3. CENTRIFUGAL DISTORTION CONSTANTS OF DIMETHYL SELENIDE (Mc/sec)

	Microwave[a]	Normal vibration	
		MUBFF	LSFF
τ_{aaaa}	−0.2422	−0.219	−0.223
τ_{bbbb}	−0.0604	−0.046	−0.055
τ_{cccc}	—	−0.005	−0.005
τ_{bbcc}	—	−0.009	−0.011
τ_{ccaa}	—	−0.005	−0.002
τ_{aabb}	0.0721	0.069	0.079
τ_{abab}	−0.0092	−0.014	−0.015

a) See Ref. 8, the values determined on $(CH_3)_2{}^{80}Se$ species.

BULLETIN OF THE CHEMICAL SOCIETY OF JAPAN VOL. 43 622—625 (1970)

n–π^* Electronic Emission Spectrum of *o*-Methoxybenzaldehyde Vapour

M. P. SRIVASTAVA, O. N. SINGH and I. S. SINGH

Department of Spectroscopy, Banaras Hindu University, Varanasi-5, India

(Received March 27, 1969)

The n–π^* vapour emission spectrum of *o*-methoxybenzaldehyde has been excited in transformer discharge in flowing vapours of benzene and the substance. In the spectrum the C=O stretching frequency is the most prominent and its found to form progression of bands. The entire spectrum has been analyzed in terms of several ground state frequencies.

In recent years there has been a growing interest in the study of non-bonding electron transition specially in benzaldehyde derivatives. The n–π^* electronic emission and absorption spectra of benzaldehyde[1–3] and halobenzaldehydes[4–9] have been investigated in detail by many workers. The electronic absorption spectrum due to n–π^* system of *o*-methoxybenzaldehyde in vapour state was recorded by Dwivedi.[10] However, the emission spectrum of *o*-methoxybenzaldehyde was not studied by any earlier worker. The present paper deals with the detailed study of the emission spectrum of the compound in vapour state obtained for the first time in transformer discharge. To make the electronic study more comprehensive the infrared spectrum was also recorded.

Experimental

The emission spectrum has been obtained in transformer discharge through the flowing mixture of benzene and *o*-methoxybenzaldehyde vapour. The discharge tube was of π type 35 cm in length, narrower in the middle (14 mm diam.) and broader at the two ends.

1) S. N. Garg, *J. Sci. Res. Banaras Hindu Univ.*, **4**, 42 (1953—1954).
2) G. W. Robinson, *J. Chem. Phys.*, **22**, 1384 (1954).
3) S. N. Garg and I. S. Singh, *J. Sci. Res. Banaras Hindu Univ.*, **9**, 61 (1957—1958).
4) M. R. Padhey and B. G. Viladkar, *Indian J. Pure Appl. Phys.*, **4**, 92 (1966).
5) D. P. Juyal, *Curr. Sci.*, **6**, 175 (1965).
6) M. P. Srivastava and I. S. Singh, *J. Sci. Res. Banaras Hindu Univ.*, **17** (1), 252 (1966—1967).
7) M. P. Srivastava I. S. Singh, *Curr. Sci.*, **36**, 456 (1967).
8) M. P. Stivatava and I. S. Singh, *ibid.*, **36**, 399 (1967).
9) R. M. P. Jaiswal, *Indian J. Pure Appl. Phys.*, **3**, 405 (1965).
10) C. P. D. Dwivedi, *ibid.*, **3**, 452 (1965).

TABLE 1. EMISSION BANDS OF *o*-METHOXYBENZALDEHYDE

Wave-length Å	Wave number cm^{-1}	Intensity	Separation from (0–0) band in cm^{-1}	Assignment
3750.4	26656	1	496	0+496
3788.8	26386	1	226	0+226
3791.5	26367	1	207	0+207
3800.5	26305	2	145	0+145
2821.5	26160	4	0	0–0
3834.5	26072	1	88	0–88
3840.6	26030	1	130	0–130
3849.8	25968	2	192	0–192
3861.2	25891	2	269	0–270
3879.6	25769	1	391	0–2×192
3892.1	25686	2	474	0–475; 0–270–192
3908.2	25580	2	580	0–580
3929.3	25443	3	717	0–717; 0–580–130
3945.8	25336	3	824	0–824
3971.1	25175	2	985	0–717–270
3974.0	25144	5	1016	0–1016; 0–824–192
3979.3	25123	4	1037	0–1037
3987.2	25073	2	1087	0–824–270
3998.1	25005	1	1155	0–1155
4012.2	24929	2	1231	0–1231
4019.8	24870	2	1290	0–1016–270
4031.7	24796	1	1364	0–1231–130
4039.6	24748	2	1412	0–1155–270
4045.4	24712	4	1448	0–1450
4051.8	24673	4	1487	0–1485
4061.4	24615	5	1545	0–824–717
4070.0	24563	6	1597	0–1597
4074.6	24535	6	1625	0–1155–475
4087.5	24458	9	1702	0–1702
4098.1	24395	5	1765	0–1485–270
4118.6	24273	5	1887	0–1702–192
4132.8	24190	4	1970	0–1702–270
4150.7	24086	2	2074	0–1597–475
4155.4	24058	5	2102	0–1702–2×192; 0–1016–824–270
4167.6	23988	4	2172	0–1702–475
4184.8	23889	2	2271	0–1702–580
4210.7	23742	5	2418	0–1702–717
4228.8	23641	6	2519	0–1702–824
4263.7	23447	5	2713	0–1702–1016
4266.3	23433	5	2727	0–1702–1037
4278.0	23369	4	2791	0–1702–824–270
4304.3	23226	6	2934	0–1702–1231
4313.4	23177	4	2983	0–1702–1016–270
4345.4	23006	4	3145	0–1702–1450
4371.7	22868	5	3292	0–1702–1597
4383.2	22808	5	3352	0–1702–2×824
4392.4	22670	10	3400	0–2×1702
4429.0	22572	7	3588	0–2×1702–192
4445.1	22490	5	3670	0–2×1702–270
4485.6	22287	6	3873	0–2×1702–475
4505.0	22191	4	3969	0–2×1702–580
4534.7	22046	2	4114	0–2×1702–717
4548.4	21980	3	4180	0–2×1702–580–192
4556.4	21914	5	4129	0–2×1702–824
4597.5	21745	4	4415	0–2×1702–1016
4644.7	21524	6	4636	0–2×1702–1231
4692.4	21305	5	4855	0–2×1702–1450
4723.0	21167	6	4993	0–2×1702–1597
4745.8	21065	8	5095	0–3×1702
4791.0	20867	5	5293	0–3×1702–192
4809.8	20785	5	5375	0–3×1702–270
4858.9	20575	3	5585	0–3×1702–2×192
4873.7	20513	3	5647	0–3×1702–2×270
4938.8	20242	4	5918	0–3×1702–824
4988.9	20039	2	6121	0–3×1702–1016
5021.3	19910	1	6250	0–3×1702–1155
5054.2	19780	3	6380	0–3×1702–1016–270
5098.8	19607	2	6553	0–3×1702–1450
5113.1	19552	2	6608	0–2×1702–2×1597
5136.3	19464	4	6696	0–3×1702–1597
5156.7	19387	5	6773	0–4×1702
5209.8	19189	3	6971	0–4×1702–192
5288.9	18902	2	7258	0–4×1702–270
5384.7	18566	2	7594	0–4×1702–824
5446.7	18361	1	7799	0–4×1702–1016; 0–4×1702–824–192

Two separate containers joined to each other in series to hold the substance and benzene, were attached to one end of the discharge tube facing the slit. The benzene container was provided with a fine capillary tube to control the flow of the benzene vapour whereas the substance container was externally heated to a desired temperature to give requisite vapour pressure in the discharge tube. The use of benzene in this experiment is to prevent dissociation of the molecules to a great extent. The stablized discharge condition was obtained at 4500—5000V and the discharge was bright blue in colour.

The spectrum was recorded on a Fuess glass spectrograph and a Q-24 Zeiss medium quartz spectrograph. Ilford HP-3 and ORWO blue rapid plates were used to photograph the spectra. With a slit-width of 40 μ, exposures of 6—10 hr were found sufficient on both the instruments. The wavelength and wave number of the bands, their relative intensities, separation from the 0-0 band and proposed assignments are given in Table 1.

Results

The emission spectrum lies in the region 3750—5447 Å and consists of about 75 bands. The spectrum consists of a long progression of bands. These bands form the head of the groups. The first group is observed with weak intensity but the intensity of the second group abruptly increases and is maximum for the third and then decreases gradually. Between each pair of successive bands in each group there is a recurring pattern of bands. A typical spectrogram of the emission spectrum is shown in Fig. 1.

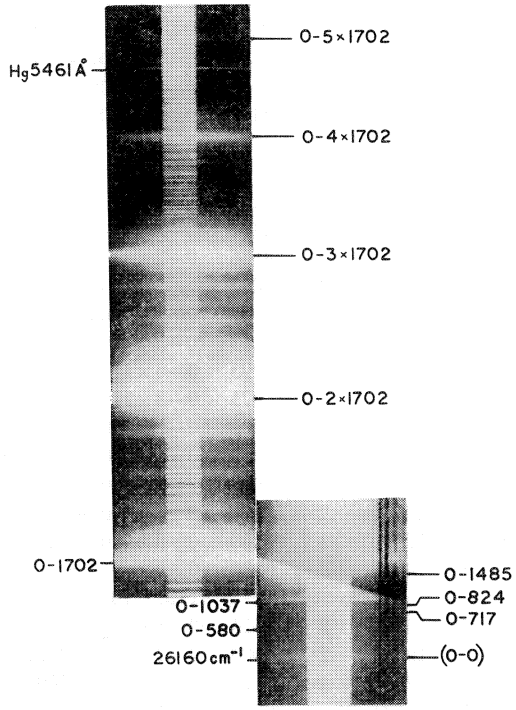

Fig. 1. Emission spectrum of *o*-methoxybenzaldehyde.

Analysis and Discussion

It is well established that the longest wavelength electronic transition of compounds containing carbonyl groups arises from the excitation of a non-bonding (n) electron localized on the oxygen atom to the anti-bonding π^* orbital. The eletronic transition is supposed to be confined to a large extent to the C=O part of the molecule and has been interpreted by McMurry[11] as corresponding to a transition in which a loosely bound electron occupying a non-bonding orbital lying in the molecular plane and across the C=O direction is excited to an anti-bonding π^* orbital with a mode in the plane. Padhye[12] and Sidman[13] have also reviewed the nature and characteristics of such non-bonding electron transition. The electronic transition responsible for the present system is similar to 3714 Å system in benzaldehyde and corresponds to the forbidden transition $^1A_2$–$^1A_1$ of formaldehyde. However, in *o*-methoxy benzaldehyde with lower symmetry C_s (considering the OCH_3 group to behave as a single mass point and CHO group to lie in the plane of the ring), the above forbidden transition becomes allowed and is ascribed to $^1A''$–$^1A'$.

The band 26160 cm^{-1} observed with medium weak intensity in the emission spectrum has been identified as the 0–0 band of the system. In the absorption spectrum of vapour, Dwivedi[10] has assigned the band at 26136 cm^{-1} as the 0–0 band of the system. The choice of the 0–0 band is supported by the smooth vibrational analysis as well as the good agreement of the ground state freqencies observed in the emission spectrum with those recorded in infrared spectrum.

The frequency 1702 cm^{-1} is the most prominent one which dominates the spectrum. Four quanta of it have been observed forming a progression of bands. This frequency with its overtones combines with most of the ground state frequencies giving thereby a recurring pattern of bands. It has been assigned as the C=O stretching frequency in the ground state. Its magnitude in both Raman and infrared spectrum in liquid phase is 1684 cm^{-1}. The difference in the C=O stretching frequency in liquid and vapour phase is probably due to hydrogen bonding resulting from the intermolecular interaction in the liquid phase. The molecules in the liquid phase are very close to each other and due to partial linking of the hydrogen atom of the CHO group of one molecule with the oxygen atom of the CHO group of another molecule, the C–O bond strength is slightly lowered and consequently the magnitude of the C=O stretching frequency is slightly lowered in liquid phase. Such shifts have also been observed in benzaldehyde,[3] fluoro and chlorobenzaldehydes.[5,8]

Another ground state frequency 1037 cm^{-1} is involved in the band at 25123 cm^{-1} occurring with weak intensity. The frequency is correlated with the totally symmetric 1039 cm^{-1} Raman and 1040 cm^{-1} infrared frequency and is assigned to the ring breathing mode corresponding to 992 cm^{-1} (a_{1g}) vibration of benzene.

Other ground state frequencies observed in the emission spectrum are: 130, 192, 270, 475, 580, 717, 824, 1016, 1155, 1231, 1450, 1485 and 1597 cm^{-1}. All these are observed to combine with the 1702 cm^{-1} C=O stretching frequency and its overtones. A correlation of ground state frequencies

11) H. L. McMurry, *J. Chem. Phys.*, **9**, 231 (1941).

12) M. R. Padhye, *J. Univ. Bihar*, **5**, 41 (1958).

13) J. W. Sidman, *Chem. Rev.*, **58**, 689 (1958).

TABLE 2. CORRELATION AND ASSIGNMENT OF GROUND STATE FREQUENCIES OBSERVED IN RAMAN, INFRARED AND EMISSION SPECTRA OF *o*-METHOXYBENZALDEHYDE

Raman (liquid) Kahovec[14]		Infrared (liquid) Present work		Electronic emission (vapour) Present work		Mode of vibration
cm^{-1}	Int.*	cm^{-1}	Int.	cm^{-1}	Int.*	
124	1			136	1	a″ C–CHO twisting
195	1			192	2	a″ C–OCH_3 o.p. bending
270	½b	277	3	269	2	a″ C–C–C o.p. bending
478	2	472	9½	475	2	a′ C–C–C i.p. bending
580	3	575	6½	580	2	a′ C–OCH_3 i.p. bending
719	½	717	5	717	3½	a″ CH_3 wagging
830	1	830	10	824	3½	a′ C–CHO stretching
1018	½	1018	10	1016	3½	a′ C–C–C i.p. bending
1039	4½	1040	10	1037	1	a′ C–C stretching (breathing vibration)
1158	5½	1159	10	1155	1	a′ C–H i.p. bending
1238	9	1242	10	1231	2	a′ C–OCH_3 stretching
1458	1	1460	10	1450	2	a′ C–H asym. bending (in methyl group)
1483	4	1482	10	1485	2	a′ C=C stretching
1597	9	1588	10b	1597	6½	a′ C=C stretching
1684	10	1684	10	1702	10	a′ C=O stretching

* The intensities have been changed to the scale of 10 from the original table.
b=broad; i.p.=in plane; o.p.=out of plane; asym.=asymmetric

observed in Raman, infrared and emission spectra is given in Table 2. Besides these, there are some bands which are observed on the shorter wavelength side of the 0–0 band and involve excited state frequencies and their combination. These are also included in Table 1.

The authors are grateful to Professor N. L. Singh for his interest in the work. One of them (M.P.S.) is thankful to C.S.I.R. (India) for financial assistance.

14) L. Kahovec and K. W. F. Kohlrausch, *Z. Phys. Chem.*, **38**B, 119 (1937).

BULLETIN OF THE CHEMICAL SOCIETY OF JAPAN VOL. 43 625—628 (1970)

Theory of Solvent Effects on Oscillator Strengths for Molecular Electronic Transitions

Takehiro ABE

College of General Education, Tohoku University, Kawauchi, Sendai

(Received April 30, 1969)

A theoretical expression has been presented for an oscillator strength of an electronic transition in a solute molecule immersed in an isotropic dielectric continuum of solvent. It is assumed that a charged particle in the solute is subjected to a force due to a cavity field. The approximate expression derived on the basis of a quantum-mechanical perturbation theory has been successfully tested for nitrobenzene and acetone.

Many theoretical expressions have recently been presented for solvent effects on frequency shifts in electronic absorption spectra. There are, however, few theoretical expressions relating to solvent effects on intensities of electronic transitions in solute molecules. The only explicit expression

relating an oscillator strength of solution to that of vapor was given by Chako[1] who used the classical dispersion theory. Schuyer[2] gave a classical extension relating a molar extinction coefficient of solution to that of vapor. Weigang[3] and Liptay[4] independently presented expressions of an integrated intensity.

In the present work, attempts are made to present a new expression for the oscillator strength of solution on the basis of a quantum-mechanical theory, and to compare the result with previous theories. The approximate expression is applied to the data for nitrobenzene and acetone.

Theoretical

Spectra of solutions are usually measured at very low concentrations. Let us consider a solution containing numerous solvent molecules and one neutral solute molecule, and assume that the solute molecule is contained within a spherical cavity in an isotropic continuous medium of the solvent. According to the Franck-Condon principle the same molecular configurations are assumed for the ground and excited states of the solute. The present theory does not include specific effects like hydrogen bonding and complexing.

Solution spectra are commonly measured by using transparent solvents. Thus we can assume that the electronic absorption region of the solvent is at shorter wavelengths than that of the solute.

We consider an electromagnetic radiation field of frequency ν with an electric field $\vec{E}$. The change of field $\vec{E}$ with time t may be written as

$$\vec{E}(\nu) = -\frac{1}{\sqrt{\varepsilon(\nu)}\,\{c/n(\nu)\}} \times \frac{\partial}{\partial t}\vec{A} \tag{1}$$

where $\vec{A}$ is a vector potential, c is the velocity of light in a vacuum, and $n(\nu)$ and $\varepsilon(\nu)$ are the refractive index and dielectric constant of the solvent at ν, respectively. In Eq. (1) a scalar potential is neglected, since the wavelength of the radiation is much longer than the diameter of the cavity. In electromagnetic theory a radiation density $\rho(\nu)$ is given by:

$$\rho(\nu) = \frac{\varepsilon(\nu)}{4\pi} \times \overline{E^2(\nu)} \tag{2}$$

Applying the Onsager cavity field, the author assumes that a particle of charge e_j in the solute molecule immersed in the solvent in the presence of the electromagnetic field is subjected to the force

$$\vec{F} = e_j \times \frac{3n^2(\nu)}{2n^2(\nu)+1} \times \vec{E}(\nu) \tag{3}$$

Reaction field is neglected herewith, assuming that the effect of the reaction field is much smaller than that of the cavity field. The effect of magnetic intensity of light is also neglected, since the velocity of electrons in the solute is small compared to that of light.

Starting from Eq. (3) and calculating in the same way as Eyring, Walter and Kimball,[5] we can approximately write the Einstein transition probability coefficient $B_{0\to i}$ for an electronic transition from the ground state to the ith-excited state in the solute molecule as

$$B_{0\to i} = \frac{8\pi^3}{3h^2} \times \frac{9n_D^2}{(2n_D^2+1)^2} \times |\vec{\mu}_{0i}^{\,0}|^2 \tag{4}$$

where h is the Planck constant, n_D is the refractive index of the solvent at the frequency of sodium-D line, and $\vec{\mu}_{0i}^{\,0}$ is the transition moment from the ground state to the ith-excited state for the free solute molecule. In Eq. (4) $n(\nu)$ is replaced approximately by n_D.

By the definition of oscillator strength, we find the theoretical expression for the oscillator strength of the transition of the solute molecule in solution from Eq. (4) as

$$f_{0\to i}^{\text{theor}}(\text{soln}) = \frac{mhc\bar{\nu}_{0i}}{\pi e^2} \times B_{0\to i} = \frac{8\pi^2 cm}{3he^2} \times \frac{9n_D^2}{(2n_D^2+1)^2} \times \bar{\nu}_{0i}|\vec{\mu}_{0i}^{\,0}|^2 \tag{5}$$

where e and m are the charge and mass of an electron, respectively, and $\bar{\nu}_{0i}$ is the transition energy of the solute in solution in unit of cm^{-1}. From Eq. (5), we find the relation

$$f_{0\to i}^{\text{theor}}(\text{soln})/f_{0\to i}^{\text{theor}}(\text{vap}) = \frac{9n_D^2}{(2n_D^2+1)^2} \times \frac{\bar{\nu}_{0i}^0}{\bar{\nu}_{0i}^0} \tag{6}$$

where $\bar{\nu}_{0i}^0$ is the transition energy of the free solute.

When the traditional Lorentz field is used instead of the Onsager cavity field, we can derive the following approximate expression by the same method as described above.

$$B_{0\to i} = \frac{8\pi^3}{3h^2} \times \frac{1}{n_D^2} \times \left(\frac{n_D^2+2}{3}\right)^2 \times |\vec{\mu}_{0i}^{\,0}|^2 \tag{7}$$

Thus we have

$$f_{0\to i}^{\text{theor}}(\text{soln}) = \frac{8\pi^2 cm}{3he^2} \times \frac{(n_D^2+2)^2}{9n_D^2} \times \bar{\nu}_{0i}|\vec{\mu}_{0i}^{\,0}|^2 \tag{8}$$

Accordingly, we have the relation

$$f_{0\to i}^{\text{theor}}(\text{soln})/f_{0\to i}^{\text{theor}}(\text{vap}) = \frac{(n_D^2+2)^2}{9n_D^2} \times \frac{\bar{\nu}_{0i}}{\bar{\nu}_{0i}^0} \tag{9}$$

Experimental Expression for Solution Oscillator Strength. The experimental oscillator strength for the solute molecule in solution has been customarily determined by

1) N. Q. Chako, *J. Chem. Phys.*, **2**, 644 (1934).
2) J. Schuyer, *Rec. Trav. Chim. Pays-Bas*, **72**, 933 (1953).
3) O. E. Weigang, Jr., *J. Chem. Phys.*, **41**, 1435 (1964).
4) W. Liptay, *Z. Naturforsch.*, **21A**, 1605 (1966).
5) H. Eyring, J. Walter and G. E. Kimball, "Quantum Chemistry," John Wiley & Sons, Inc., New York (1949), p. 107.

$$\bar{f}^{\exp}_{0\to i}(\text{soln}) = \frac{10^3 \ln 10 \cdot mc^2}{\pi e^2 N}\int \kappa(\tilde{\nu})\mathrm{d}\tilde{\nu} \qquad (10)$$

where N is the Avogadro number, and $k(\tilde{\nu})$ is a molar extinction coefficient. Equation (10) has been derived on the assumption that the velocity of light in the solution is equal to that in a vacuum. When the velocity of light in the solution is considered by replacing c by $c/n(\nu)$, as pointed out by Baba,[6] we can approximately write

$$f^{\exp}_{0\to i}(\text{soln}) = \frac{10^3 \ln 10 \cdot mc^2}{\pi e^2 N} \times \frac{1}{n_D^2}\int \kappa(\tilde{\nu})\mathrm{d}\tilde{\nu} \qquad (11)$$

Thus we can relate $\bar{f}^{\exp}_{0\to i}(\text{soln})$ to $f^{\exp}_{0\to i}(\text{soln})$ as

$$f^{\exp}_{0\to i}(\text{soln}) = (1/n_D^2) \times \bar{f}^{\exp}_{0\to i}(\text{soln}) \qquad (12)$$

Discussion

The Onsager cavity model is adopted in the present theory. Any deviation of the cavity from spherical symmetry would result in a great difference between the observed and theoretical ratios of the oscillator strength of solution to that of vapor. It is, however, probable that a thermal motion makes the cavity nearly spherical.

If the Onsager reaction field is considered in Eq. (3), the expression for the oscillator strength will differ from Eq. (5), but the difference will not be great.

Equations (5) and (8) show that the effective microscopic fields and the dielectric constant of the solvent at ν_{0i} have important roles for the solvent effects on the oscillator strength. It is, of course, better to use the refractive index measured at the frequency of ν_{0i}, although n_D was used herewith for the sake of convenience.

Previous Theories. *(1) Chako's Formula.* Chako's formula[1] based on the classical dispersion theory is usually written as

$$f^{\text{theor}}_{0\to i}(\text{soln})/f^{\text{theor}}_{0\to i}(\text{vap}) = (n_D^2+2)^2/9n_D \qquad (13)$$

(2) Schuyer's Theory. An original formula (Eq. (29) in Ref. 2) derived by Schuyer[2] from the theory of Onsager-Böttcher may be approximately written as

$$\frac{(2n_D^2+1)(n_D^2+1)}{6n_D^3} \times \kappa(\tilde{\nu}_{0i}) = \text{constant} \qquad (14)$$

Combining Eq. (14) with $k^0(\tilde{\nu}_{0i})$=constant for n_D=1, we have

$$\kappa(\tilde{\nu}_{0i}) = \frac{6n_D^3}{(2n_D^2+1)(n_D^2+1)} \times \kappa^0(\tilde{\nu}_{0i}) \qquad (15)$$

Putting Eq. (15) into Eq. (11), we obtain after some calculation

$$f_{0\to i}(\text{soln})/f_{0\to i}(\text{vap}) = 6n_D/(2n_D^2+1)(n_D^2+1) \qquad (16)$$

Assuming the simple relation $f_{0\to i}(\text{soln})/f_{0\to i}(\text{vap}) = k(\tilde{\nu}_{0i})/k^0(\tilde{\nu}_{0i})$ on the basis of Schuyer's theory, Bayliss and Wills-Johnson[7] presented a formula different from Eq. (16).

(3) Weigang's Theory. Applying Moffitt and Moscowitz's formula[8] for dispersion, Weigang[3] presented the expression

$$\int \frac{\kappa(\nu)}{\nu}\mathrm{d}\nu = \frac{8\pi^3 N}{3\times 10^3 \ln 10 \cdot hc} \times \frac{\{n^2(\nu)+2\}^2}{9n(\nu)} \times \frac{|\vec{\mu}_{0i}|^2}{k} \qquad (17)$$

where k is the number of the solute molecules contained in a small cavity, and $\vec{\mu}_{0i}$ is the transition moment for the solute molecule in solution. The Lorentz condition is included in Eq. (17). Using Weigang's expression[3] for $\vec{\mu}_{0i}$, we may write $B_{0\to i}$ as follows

$$\begin{aligned} B_{0\to i} &= \frac{10^3 \ln 10 \cdot (c/n_D)}{hN}\int \frac{\kappa(\nu)}{\nu}\mathrm{d}\nu \\ &= \frac{8\pi^3}{3h^2} \times \frac{(n_D^2+2)^2}{9n_D^2} \times |\vec{\mu}^0_{0i}|^2 \times \left\{1 + A \times \frac{n_D^2-1}{2n_D^2+1} \right. \\ &\quad \left. + B \times \frac{n_D^2-1}{2n_D^2+1} - C\left(\frac{\varepsilon_0-1}{\varepsilon_0+2} - \frac{n_D^2-1}{n_D^2+2}\right)\right\}^2 \end{aligned} \qquad (18)$$

where the coefficients of A, B and C are characteristic of the solute, the cavity radius and the absolute temperature. Equation (18) may be approximated to Eq. (7). Thus we obtain the relation identical to Eq. (9) from Weigang's theory.

(4) Liptay's Theory. Liptay[4] presented the following formula.

$$\begin{aligned} \int \frac{\kappa(\tilde{\nu})}{\tilde{\nu}}\mathrm{d}\tilde{\nu} &= \frac{8\pi^3 N}{2.303\times 10^3 \times 3h(c/n_D)} \times |\vec{\mu}^0_{0i}|^2 \\ &= \frac{8\pi^3 N}{2.303\times 10^3 \times 3h(c/n_D)} \times [|\vec{\mu}^0_{0i}|^2 + \tilde{R}\vec{F}_{RW} \\ &\quad + \tilde{F}_{RW}(\vec{P}+\vec{Q})\vec{F}_{RW} + 2Re\{\tilde{\mu}^0_{0i}\vec{W}_{0i}\}f'] \end{aligned} \qquad (19)$$

Here the notations refer to Liptay's original paper. In Eq. (19), c in the original formula of Liptay is replaced by c/n_D. Carrying out the same calculation as in the case of Weigang's theory, we obtain approximately

$$f_{0\to i}(\text{soln})/f_{0\to i}(\text{vap}) = \tilde{\nu}_{0i}/\tilde{\nu}^0_{0i} \qquad (20)$$

It is obvious from Eq. (19) that Liptay did not consider any effective microscopic field such as the Onsager cavity or Lorentz field.

Application

Equations (6), (9), (13), (16) and (20) were applied to the 240 mμ band of nitrobenzene and to the 280 mμ band of acetone. The results are summarized in Tables 1 and 2.

6) H. Baba, "Zikkenkagaku Koza," Ser. 11, ed. by Chem. Soc., Japan, Maruzen, Tokyo (1965), p. 22.

7) N. S. Bayliss and G. Wills-Johnson, *Spectrochim. Acta*, **24A**, 551 (1968).

8) W. Moffitt and A. Moscowitz, *J. Chem. Phys.*, **30**, 648 (1959).

TABLE 1. THE π–π^* TRANSITION OF NITROBENZENE

Solvent	$\tilde{\nu}_{max}$ cm^{-1}	$\bar{f}^{exp}$	$\frac{f^{exp}(soln)}{f^{exp}(vap)}$	$\frac{f^{theor}(soln)}{f^{theor}(vap)}$				
				Eq. (6) (Abe)	Eq. (9) (Abe, Weigang)	Eq. (13) (Chako)	Eq. (16) (Schuyer)	Eq. (20) (Liptay)
Vapor	41670[9]	0.17[9]	1	1	1	1	1	1
n-Heptane	39740[10]	0.23[10]	0.70_3	0.702	0.848	1.23	0.587	0.954
Cyclohexane	39540[10]	0.26[10]	0.75_2	0.677	0.844	1.27	0.556	0.949
Chloroform	38150[10]	0.25[10]	0.70_4	0.642	0.814	1.29	0.542	0.916

TABLE 2. THE n–π^* TRANSITION OF ACETONE

Solvent	n_D^{20}	$\tilde{\nu}_{max}$[7] cm^{-1}	$\frac{f^{exp}(soln)}{f^{exp}(vap)}$		$\frac{f^{theor}(soln)}{f^{theor}(vap)}$				
			Ref. 7	Ref. 10	Eq.(6)	Eq.(9)	Eq.(13)	Eq.(16)	Eq.(20)
Vapor	1	36100	1	1	1	1	1	1	1
n-Heptane	1.3876	35800	0.636	0.654	0.730	0.882	1.23	0.587	0.992
Isooctane	1.3915	35800	0.584	—	0.728	0.882	1.24	0.584	0.992
Cyclohexane	1.4262	35700	0.502	0.708	0.705	0.879	1.27	0.556	0.989
Benzene	1.5011	35450	0.471	—	0.657	0.876	1.34	0.503	0.982
Carbon tetrachloride	1.4604	35650	0.618	0.896	0.683	0.879	1.30	0.531	0.988
Chloroform	1.4457(19°)	36250	0.626	0.761	0.704	0.893	1.29	0.542	1.004
Dichloromethane	1.4237	36300	0.594	—	0.718	0.894	1.27	0.558	1.006
Diethylether	1.3497 (24.8°)	36050	0.780	—	0.759	0.890	1.20	0.618	0.999

TABLE 3. RATIOS OF CUSTOMARY OSCILLATOR STRENGTHS OF NITROBENZENE

Solvent	n[10] 2800 Å	$\frac{\bar{f}^{exp}(soln)}{\bar{f}^{exp}(vap)}$ (from Refs. 9 and 10)	$\frac{n^2 f^{theor}(soln)}{f^{theor}(vap)}$ (Eq. (6) $\times n^2$)
Vapor	—	1	1
n-Heptane	1.42	1.3_5	1.38
Cyclohexane	1.47	1.5_3	1.41
Chlororoform	1.50	1.4_7	1.38

The ratio of the customary experimental oscillator strength of solution to that of vapor can be directly compared with the theoretical value. Using Eq. (6) and values of refractive indexes for 2800 Å, the values of $\bar{f}^{exp}(soln)/\bar{f}^{exp}(vap)$ were compared with those of $n^2 f^{theor}(soln)/f^{theor}(vap)$, as indicated in Table 3.

The values of $\bar{f}^{exp}$ by Bayliss and Wills-Johnson were computed by assuming the spectra to be symmetric about absorption maxima.[7] As Bayliss and Wills-Johnson[7] mentioned, the determination of oscillator strength is complicated by the fact that the transitions under investigation are overlapped by other transitions. In view of the above discussion, Tables 1—3 seem to show that Eq. (6) best reproduces the experimental results among the five theoretical formulas.

The author is particularly indebted to Professor Yoshito Amako for discussion.

9) S. Nagakura, M. Kojima and Y. Maruyama, *J. Mol. Spectrosc.*, **13**, 174 (1964).
10) N. S. Bayliss and E. G. McRae, *J. Phys. Chem.*, **58**, 1006 (1954).

BULLETIN OF THE CHEMICAL SOCIETY OF JAPAN VOL. 43 629—632 (1970)

Measurement of the Adsorption of Tritium Labelled Sodium Stearate at Air/Water Interface using Thin Windowed Geiger-Müller Counter Tube

Keiichi SEKINE, Tsutomu SEIMIYA and Tsunetaka SASAKI

Department of Chemistry, Faculty of Science, Tokyo Metropolitan University, Setagaya-ku, Tokyo

(Received May 29, 1969)

The adsorption of tritium labelled sodium stearate at various pH values and temperatures was directly measured by using a thin end-windowed Geiger-Müller counter. The disturbances due to the application of high electrical potential and the introduction of counting gas were avoided, which are inevitably encountered in an ordinary windowless 2π counter. Precautions were taken to avoid both surface evaporation effect and contamination of solution due to the absorption of carbon dioxide from the air. The results show that free stearic acid is considered to be the main surface active species in an aqueous sodium stearate.

The radiotracer technique using tritium is particularly suited for the accurate measurement of adsorption because of extreme softness of its beta radiation. But for this same reason the counting of tritium radiation suffers from errors which should not be overlooked. For tritium beta-counting, a windowless gas flow 2π counter is often used because of its high detection efficiency,[1] and the adsorption of tritium labelled detergent at air-water interface has been measured by this method.[2] However, this counter introduces several difficulties in the measurement of the radioactivity from aqueous surface. They arise chiefly from the high electrical potential applied between the solution surface and the anode placed over it for the counting of radioactivity, and from the contamination of the aqueous surface by a counting gas such as propane, though a good counting stability is shown against moisture. These disturbances can be shown by the following.

In the first experiment, the surface tension of water and that of aqueous solution of sodium dodecyl sulfate (SDS) were measured at 20°C by the Wilhelmy method in atmosphere with and without propane gas. No surface tension depression was observed when the water surface was brought to contact with propane gas, whereas for 5×10^{-3} mol/l aqueous SDS solution the surface tension depression of about 2.3 dyne/cm was produced by contact of propane gas with the aqueous surface. This evidently shows the influence of propane gas, presumably producing a change in adsorption of SDS and/or propane due to its contact. Such a change was demonstrated in a separate experiment.

In the second experiment, the effect of applied electric field upon the surface tension of aqueous solution was checked at the same temperature. Using the electrode assemblies which simulate the conditions of the counting chamber of a windowless 2π counter usually employed in such a measurement, the surface tension of aqueous SDS solution was measured with and without an applied electric field of 4000 V in the propane gas atmosphere. In this experiment precaution was taken to avoid the influence of direct electrical interaction, if any, between the anode and the glass plate for the surface tension measurement. The results show a surface tension drop of 3.1 dyne/cm for an aqueous surface of SDS solution (5×10^{-3} mol/l) in propane gas by the application of 4000 V external field, while in the case of water surface only 0.1 dyne/cm drop was observed for the surface tension under the same condition. We can observe the streaming of the solution at the surface caused by applied electrical potential from the motion of talc scattered over the surface. These experiments also show the possibility of undesirable effect of high electrical potential upon the establishment of the true adsorption equilibrium. Therefore measurements free from such disturbances are desired.

In our preceding paper,[4] we stated that soft tritium radioactivity could be measured effectively by using a thin polycarbonate end-windowed Geiger-Müller counter tube without the difficulties which an ordinary windowless flow-counter encounters. It also enables measurements free from the above electrical and surface chemical disturbances. In the present investigation, we employed this method for the measurement of the adsorption of tritium labelled sodium stearate on aqueous surface. Here, precautions were further taken to avoid both

1) G. W. Eulitz, *Rev. Sci. Instrum.*, **34**, 1010 (1963).
2) G. Nilsson, *J. Phys. Chem.*, **61**, 1135 (1957).
4) T. Seimiya, K. Sekine and T. Sasaki, *J. Sci. Insturm.*, **42**, 906 (1965).

the surface evaporation affecting the surface concentration of the solute,[5] and the absorption of carbon dioxide into the solution from atmosphere, which proved to have great effect on the results.[6]

It may be mentioned in this connection that Flengas and Rideal also studied the adsorption of ^{14}C-labelled sodium stearate solutions[7] and obtained results somewhat different from ours as will be described later. Their results, however, involve some uncertainty as to the solubilities of soap,[8] evaporation effect, the constancy of pH and the effect of carbon dioxide[3,6] since no distinct statements concerning them could be found. The present paper described the apparatus and measurement of adsorption of sodium stearate, free of these uncertainties and the errors due to the applied electrical field and contact with gas.

Experimental

Apparatus. The surface concentration was measured by a gas flow GM-counter (FC-16, Japan Radiation and Medical Electronics Inc.), the counter tube being equipped with an end-window of a thin polycarbonate film[4] of 34 mm effective aperture. The tritium-labelled sodium stearate was dissolved in distilled water and the solution was contained in a 120×61 mm rectangular Teflon trough of 5.6 mm depth. The distance between the window of the counting tube and the aqueous surface was kept to 0.5 mm by means of a platinum needle fixed to the window. A movable barrier was placed on the trough and was operated from outside the thermostatted box to sweep the aqueous surface.

Special care was taken to avoid a change of geometry due to the difference in pressure across the thin window, by supporting the film with a perforated thin brass sheet (0.15 mm thick and 50% perforation in area). In order to avoid surface evaporation and absorption of carbon dioxide from the surrounding atmosphere, nitrogen gas which was passed through charcoal and saturated with water, was let to flow gently over the liquid surface. The whole apparatus was put in an air thermostat of 30, 40 and 50°C during the experiment.

Materials. Sodium stearate was prepared by dissolving tritium-labelled stearic acid (specific activity 7 Ci/mol)[9] in absolute alcohol freshly distilled over sodium hydroxide, and a smaller amount of sodium hydroxide than that required for neutralization of the acid was added. The soap solution thus prepared was evaporated to dryness *in vacuo*, and the residue was washed with benzene to remove excess stearic acid using a Soxhlet extractor. The water used in this experiment was obtained by refluxing ordinary distilled water in an acid permanganate solution for 24 hr, then adding excess alkali and distilling. Water thus obtained was further distilled twice from Hysil flasks connected in series.

Procedures. The calibration curve used for calculating the amount of adsorption from the observed counting rate was made by measuring the counting rate of a known amount of radioactive stearic acid monolayer spread on water surface. For this purpose the trough was filled with water of pH controlled to 5.5 by adding distilled hydrochloric acid, and tritium-

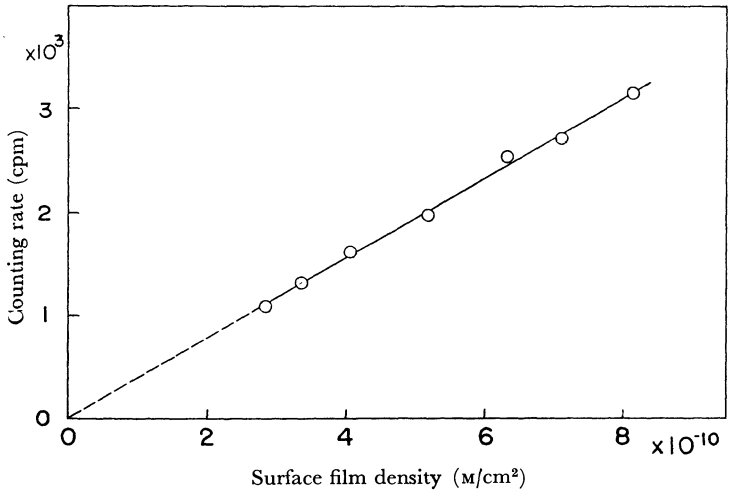

Fig. 1. Surface counting rate against film density for stearic acid monolayer.
Substrate : distilled water, pH 5.5
temperature, 20°C

5) T. Seimiya and T. Sasaki, *J. Colloid Interfac. Sci.*, **21**, 229 (1966).
6) J. Bagg, M. D. Haber and H. P. Gregor, *ibid.*, **22**, 138 (1966).
7) S. N. Flengas and Sir E. Rideal, *Trans. Faraday Soc.*, **55**, 339 (1959).
8) J. W. McBain and W. C. Sierichs, *J. Amer. Oil Chem. Soc.*, **25**, 221 (1948).
3) To be published in the near future.
9) M. Muramatsu, O. Fuji and T. Sasaki, *Radioisotopes* (in Japanese), **10**, 100 (1961).

labelled stearic acid having the same sprecific activity as that of the tritium-labelled sodium stearate was spread on water surface from 2.40×10^{-4} mol/l benzene solution by means of a microsyringe. The plots of the counting rate *versus* surface concentration were obtained from the radioactivity measurements made at various surface concentrations by compressing and expanding the monolayer. The result is shown in Fig. 1.

At low surface concentration, surface heterogeneity and its time dependence were observed for this monolayer by the radioactivity measurement (Fig. 2a). Usually, however, by standing the surface film at 20°C for at least several hours the film became homogeneous and the time dependence practically vanished when detected by means of radioactivity. As the surface concentration increased, the surface film became more homogeneous and time effect also disappeared (Fig. 2b).

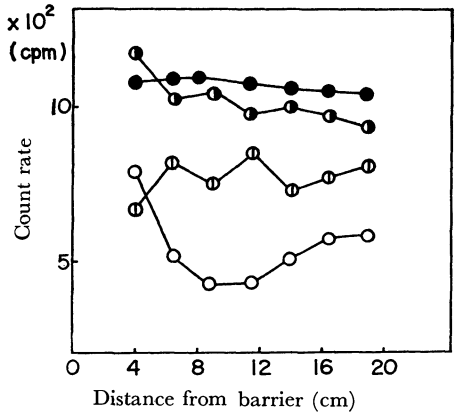

Fig. 2a. Change in homogeneity of monolayer with time.
Substrate : distilled water, pH 5.5
temperature, 20°C
Film density : 55.7 Å²/mol
Age : ○, 0 hr
◑, 1 hr
◑, 2 hr
●, 3 hr

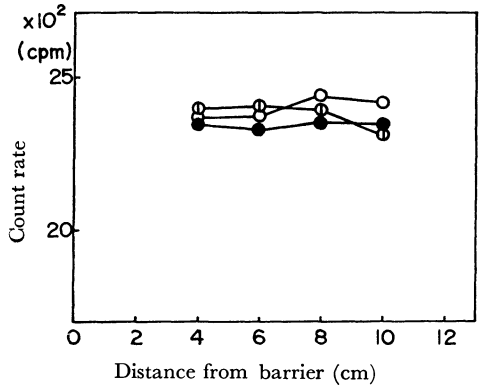

Fig. 2b. Change in homogeneity of monolayer with time.
Substrate : same as Fig. 2a
Film density : 28.0 Å²/mol
Age : ○, 0 min
◑, 30 min
●, 60 min

To measure the adsorption of sodium stearate at solution-air interface the radioactive sodium stearate solution of 2.5×10^{-5} mol/l concentration was put in the same Teflon trough as used in the monolayer measurement, and the counting of surface radioactivity was started immediately after the sweeping of surface by the barrier. The geometry of the whole arrangement including the GM-tube was kept constant.

The counting rate obtained by subtracting the one due to the bulk of the solution[2] from the observed surface counting rate gives the amount of sodium stearate adsorbed at the solution/air interface. In this experiment, the bulk counting rate turns out to be a very small fraction of the total counting rate, being comparable to the back ground counting rate when the monolayer adsorption is established. This fact may be expected from an extremely low concentration of the solution (2.5×10^{-5} mol/l) and the softness of beta-ray. This can also be confirmed by the fact that for some solutions the surface counting rate at the initial stage of measurement is comparable to that of the back ground. Therefore the bulk counting rate can be neglected within the limit of the counting error. The pH of the solution was controlled by hydrochloric acid and sodium hydroxide free from carbon dioxide, and was kept constant throughout the experiment within ±0.1 by keeping the trough in a humidified nitrogen atomsphere. Measurements were made at 30, 40 and 50°C, and the concentration of sodium stearate was kept at 2.5×10^{-5} mol/l throughout the experiment.

Results and Discussion

The equilibrium amount of adsorption Γ was measured and plotted against the pH of the solution at each temperature as shown in Fig. 3. The curves for 30 and 40°C show plateaux in the pH region proper for each system and the Γ values of these plateaux nearly agree with that of monolayer

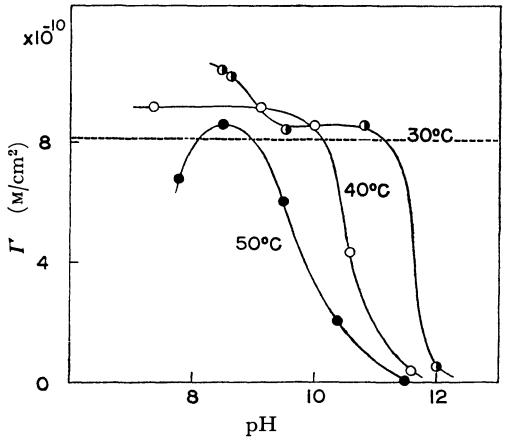

Fig. 3. pH dependence of stearate adsorption at air/solution interface.
Concentration of sodium stearate : 2.5×10^{-5} mol/l

adsorption (dotted line in Fig. 3) calculated by using the value of 20.5 A^2/mol known as the area occupied by a stearic acid molecule on water. In a less alkaline region Γ exceeds the monolayer value at 30°C, while Γ is smaller than the monolayer value at 50°C.

Apart from some irregularities, the agreement of Γ value of the plateaux with that of monomolecular area of stearic acid suggests the possibility that the adsorption layer actually consists of stearic acid instead of stearate ion. We have some evidence to support this view. Lucassen[10] pointed out that the major species of the aqueous solution prepared by dissolving sodium stearate in distilled water is changed to free stearic acid. Harkins[11] also observed a relatively high surface tension for an aqueous sodium laurate solution in an alkaline region, and low surface tension for a neutral solution and gave a similar explanation. Our study on the surface pressure-area curve for sodium stearate by means of the simultaneous measurements of the amount of adsorption and surface tension of the solution suggests that the adsorbed species is stearic acid.[3] Figure 3 shows that at pH higher than 12, the amount of adsorption of the solution is almost reduced to zero. This sudden decrease of adsorption is ascribed to salting out of the soap due to the high concentration of sodium hydroxide added, causing decrease of concentration of stearate ion. To assure the concentration decrease of soap solution at high pH, soap solutions at pH 10.7 and 12.3 were centrifuged, and the concentration of the supernatant solution was determined by radioactivity measurement. The results show a marked decrease of soap concentration in the solution for pH 12.3 while no tendency of decrease is observed for 10.7. Flengas and Rideal[7] reported a higher value of stearate adsorption than ours in this pH region. However, their results do not seem to confirm the presence of carbon dioxide in an atmosphere which influence the amount of adsorption (possibly resulting in an overestimation), since it can be confirmed[6] that the amount of adsorption is quite sensitive to the presence of carbonate ions in solution even in the pH of the solution is kept unchanged.

We note the decrease of adsorption below pH 8 at 50°C. This may be explained by the formation of free stearic acid precipitate[10] as recognized by the turbidity of the solution. However, the increase of adsorption beyond the monolayer at 30°C remains unexplained at present.

An overall trend of decrease of adsorption with temperature is also seen. The adsorption may be affected by temperature in two ways. One, by enhanced degree of bulk hydrolysis at high temperatures, and the other, by the increased solubility of stearic acid at higher temperature. Adsorption is expected to increase in the former case and decrease in the latter case. The result suggests that the latter tendency is dominant as far as the present experimental conditions of temperature and time ranges are concerned.

We are of the opinion that in an aqueous sodium stearate solution the surface active species is exclusively free stearic acid, while stearate ion is less surface active. The adsorption of stearic acid is unexpected although suggestions have been made as to the hydrolysis in bulk of the solution by other investigators. It should be emphasized that the present conclusion is mainly based upon the results of direct adsorption measurements in comparison with the conclusions or predictions obtained more or less theoretically and indirectly.

10) J. Lucassen, *J. Phys. Chem.*, **70**, 1824 (1966).
11) F. A. Long, G. C. Nutting and W. D. Harkins, *J. Amer. Chem. Soc.*, **59**, 2197 (1937).

The authors express their thanks to the Ministry of Education for the Scientific Expenditure given to this work.

BULLETIN OF THE CHEMICAL SOCIETY OF JAPAN VOL. 43 633—636 (1970)

Thinning of Nonionic Detergent Films

Teruko YAMANAKA*1

Department of Chemistry, Faculty of Engineering, Yokohama National University, Minami-ku, Yokohama

(Received June 21, 1969)

The effect of added electrolytes on the thinning of single vertical film formed from nonionic detergent solution has been studied. Addition of the electrolytes did not show an appreciable effect on the thinning of the film in the region of interference fringes. Specific effects of anions upon the "blackening time" (the time necessary for turning the total film area completely into a black film) were observed similarly to those on the cloud point. The order of magnitude of these effects followed the lyotropic series, which may be explained qualitatively by the effects on the dehydration of detergent molecules and on the electrical double layer of the film. The effect of the electrolytes on aqueous ionic detergent film was also examined. It was mainly explained by their influence on the electrical double layer.

Single liquid film is considered to be a very simple colloid system, and is useful in elucidating various colloidal and interfacial phenomena. Interest has been shown by many investigators,[1-4] particularly the kinetic study of single liquid film stabilized by ionic detergent for its influence on the drainage of the film. However, there are few reports on nonionic detergent films.[5,6]

It has been confirmed that the effects of the addition of electrolytes on the foam stability and on the cloud point of aqueous solutions of nonionic detergent are similar.[7] They are both specific for anion and follow the lyotropic series.

The purpose of this work is to study the effect of the addition of electrolytes upon the thinning of single liquid film formed from aqueous nonionic detergent solutions, in connection with the investigation of foaming. In observing the thinning process of liquid film, special attention was paid to the rate of formation of an ultra-thin film, the so called "black film", which always appears in the last stage of the draining process of the liquid film.

Experimental

Materials. Polyoxyethylene nonylphenyl ether (PNP) was obtained from commercially available PNP by molecular distillation. The average chain length of the ethylene oxide adducts obtained by distillation was determined from their hydroxyl values to be 11.4 in ethylene oxide units. The aqueous solutions of this compound exhibited a sharp break in the plots of surface tension against logarithm of concentration, so it is considered to be sufficiently homogeneous. Sodium dodecylsulphate (SDS) was prepared by the reaction of $C_{12}H_{25}OH$ with $ClSO_3H$ and purified by the ordinary procedure. Inorganic electrolytes were of analytical reagent grade and were purified by using a soxhlet extractor with ether as a solvent, except for HCl and NaOH which were used without further purification. Water was distilled first in a hard glass apparatus from potassium permanganate solution to remove organic impurities and then was redistilled in a quartz glass apparatus. All solutions were freshly prepared before use.

Apparatus and Procedure. The method used for these measurements is similar to that discribed by Miles and co-workers[8] and by Lyklema and co-workers.[9] The apparatus consists essentially of a square cell 4×4 cm containing the solution and a rectangular frame supported from above. The rectangular frame is made from a glass rod of about 1 mm in diameter, and is 2.3 cm wide for PNP solutions and 1.4 cm wide for SDS solutions.

After standing the solution in the closed cell for about 17 hr, the frame was vertically withdrawn in about 5 sec

*1 Present address: Laboratory of Chemistry, Faculty of Education, Chiba University, Yayoi-cho, Chiba, Japan.

1) B. V. Derjaguin, "Proc. 2nd. Int. Congr. Surf. Activity," Vol. 1, Butterworths, London (1957), p. 211.

2) K. J. Mysels, K. Shinoda and S. Frankel, "Soap Film; Studies of Their Thinning," Pergamon Press, New York, N. Y. (1959).

3) J. Th. G. Overbeek, *J. Phys. Chem.*, **64**, 1178 (1960).

4) A. Scheludko and D. Exerowa, *Kolloid-Z.*, **168**, 24 (1960).

5) A. Scheludko, *Dokl. Akad. Nauk SSSR*, **123**, 1074 (1958).

6) E. M. Duyvis and J. Th. G. Overbeek, *Konindkl. Ned. Akad. Wetenshap.*, Proc. Ser. B **65** (1), 26 (1962).

7) T. Yamanaka, to be published.

8) G. D. Miles, J. Ross and L. Shedlovsky, *J. Amer. Oil Chem. Soc.*, **27**, 268 (1950).

9) J. Lyklema, P. C. Scholten and K. J. Mysels, *J. Phys. Chem.*, **69**, 116 (1965).

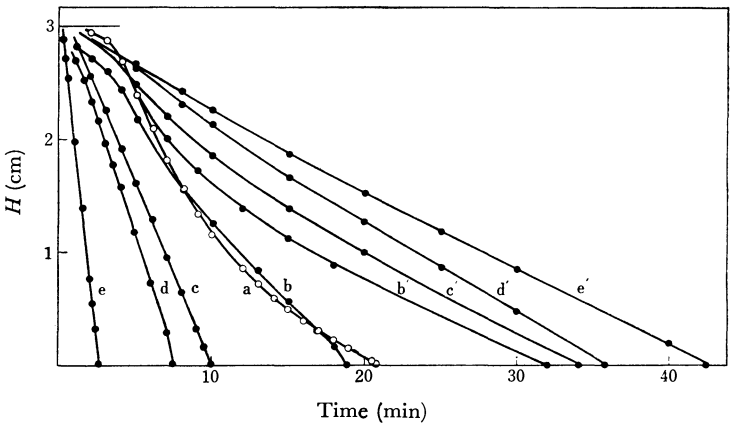

Fig. 1. Effect of increasing concentrations of NaCl and Na_2CO_3 on the rate of formation of black film in liquid films at 30°C.
H: distance between black-silver boundary and solution surface.
Time: time elapsed after formation of liquid film.
Aqueous solutions: 0.1% PNP (a), 0.1% PNP+Na_2CO_3 [0.1N (b) 0.5N (c) 0.8N (d) 1N (e)], 0.1% PNP+NaCl [0.1N (b') 0.5N (c') 1N (d') 2N (e')]

from the solution by manual opperation so that the top of the frame was 3 cm above the solution surface (2.5 cm in the case of SDS solutions). Xenon lamp was used for illuminating the film. By using optical filters, wave length was limited to 400—450 mμ with the maximum at about 417.5 mμ. The positions of interference fringes and boundary between black and silver film were measured and expressed as the distance from the solution surface on the photograph properly enlarged. All the measurements were carried out in a thermostated room of 30±1°C.

Results

The effect of the addition of electrolytes on the thinning process of single liquid film was measured for 0.1% PNP aqueous solutions. For comparison, the observation was made with 1×10^{-2}M SDS solutions in the presence of NaCl and Na_2SO_4.

Freshly formed films quickly drain and the horizontal interference fringes are produced. The film drains further and a silver film appears at the top of the film and spreads downward. Finally a black film develops and its area gradually increases at the expense of silver film. The boundary between black and silver films is very sharp and horizontal except for the place near the frame. Black films so formed are fairly stable, with the exception of those formed from pure SDS solution. Their average life is more than 2 hr.

Aqueous PNP Solutions. Figure 1 shows typical effects of concentration of some electrolytes upon the rate of descent of the black-silver boundary. The positions of the black-silver boundary are plotted against time elapsed after complete formation of the liquid film. The time necessary for turning the whole film area into a black film, which is taken as the standard of the rate of formation of a black film, was also measured in all solutions. For brevity, this is called "blackening time" in this paper.

Curves of the descent of black-silver boundary in liquid films formed from aqueous solutions of PNP with and without added electrolytes can be classified into three types. Type 1 curve shows that the rate of descent of the black-silver boundary is faster in the early period and slower in the later stage, except for the first stage. This type appears in the case of relatively long blackening time. Type 2 curve shows a nearly constant rate of descent. Each instance is shown by (a) and (c) in Fig. 1. In the same electrolytes, curves of the descent tend to change into type 2 from type 1 with increasing concentrations, and the tendency is marked in the case of shorter blackening time. Type 3 curve, which shows a slow rate of descent in the early stage and a fast one in the final stage, only appears in the case of addition of 1N NaOH.

Contrary to these behaviors, the drainage of the film in the region of interference fringes is not affected by the addition of electrolytes.

Figure 2 shows the effect of added electrolytes and their concentrations upon the blackening time. Evidently, blackening time of liquid films formed from PNP solutions is greatly affected by the nature and concentration of the added electrolytes. The effect is classified into two types; namely electrolytes which decrease and those which increase blackening time with increasing concentration. The electrolytes can be arranged in the following series according to the order of magnitude of blackening time. $Na_3PO_4<Na_2CO_3\simeq Na_2SO_4<NaF\simeq NaOH\ll NaCl\simeq KCl\simeq LiCl\simeq NaSCN\simeq HCl$.

Ions such as SCN^- and Cl^- act as an inhibitor whereas PO_4^{3-}, SO_4^{2-}, CO_3^{2-}, F^- and OH^- ions act as a promoter for the black film formation. It is evident that the effect is not so sensitive to the

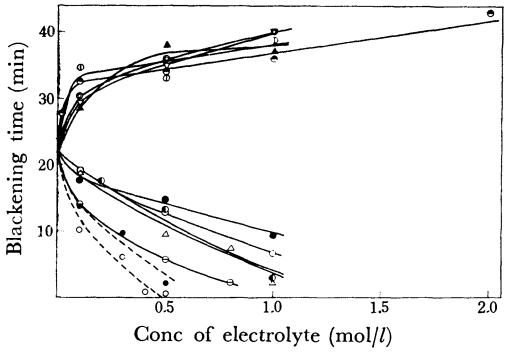

Fig. 2. Effect of added electrolytes on the blackening time of liquid films at 30°C. (average of five films)
Aqueous solutions: 0.1% PNP+electrolyte (◎ NaSCN, ▲ HCl, ▽ LiCl, ⓘ KCl, ◓ NaCl, ● NaOH, ○ NaF, ◐ $1/2Na_2SO_4$, △ $1/2Na_2CO_3$, ⊖ $1/3Na_3PO_4$), 1×10^{-2} mol/l SDS+electrolyte (---●--- $1/2Na_2SO_4$, ---○--- NaCl)

nature of cation, but is specific to the nature of anion, and the series is similar as a whole to the lyotropic series of anions.

With regard to the region of the interference fringes, the change of the film thickness with time at its center is almost independent of the nature and concentration of the electrolytes added as shown in Fig. 3. The film thickness is calculated from the order of interference fringes.

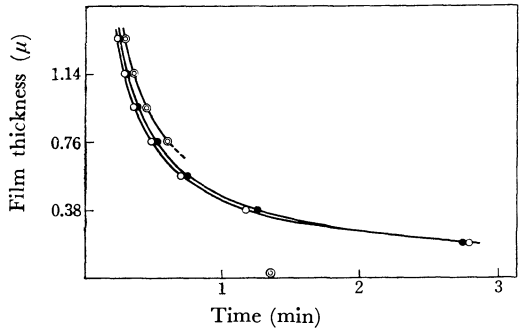

Fig. 3. Time dependence of film thickness at center of films at 30°C.
Aqueous solutions: 0.1% PNP+electrolyte (○ 0, ● 0.5N Na_2CO_3, ◎ 0.8N Na_3PO_4)

Aqueous SDS Solutions. Measurements of the SDS solutions were performed for a smaller film area (width 1.4 cm, height 2.5 cm), because the instability of the liquid film of pure SDS solution prevented the use of a larger frame employed in the measurement of PNP solutions.

The broken lines in Fig. 2 show the effect of added electrolyte upon the blackening time of films formed from 1×10^{-2}M SDS solutions. It is evident that the effect of electrolytes is quite different for the films formed from SDS and PNP solutions. Addition of NaCl prolongs blackening time in the case of PNP solutions, whereas in the case of SDS solutions blackening time is shortened.

Discussion

Thinning of vertical thin film is caused mainly by gravity and the border suction when the film is thick. However, the van der Waals force and electrostatic repulsion become important as the thinning advances by drainage to such an extent that the formation of a black film begins.[10]

Overbeek explained the mechanism of the formation of balck film as follows.[2] The welt at the boundary between black and colored films is a kind of border and sucks the colored film (a thicker film) by border suction to form more black film (a thinner film). An excess liquid accumulates at the welt and later flows down as a two-dimensional droplet. The rate of formation of a black film depends upon the electrostatic repulsion between detergent ions adsorbed on both surfaces of the film, the van der Waals force acting among all the molecules in the film and the viscous resistance in the film.[2] However, a precise interpretation of this kinetic process is not clear.

On the other hand, it has been proved experimentally that the thin film has a sandwich structure, consisting of two surface layers and inner core of solutions.[11] Of the forces acting on the thin film, the force between water molecules gathered around the polar heads of the detergent molecules assumes considerable importance in films of an aqueous nonionic detergent. However, in the case of aqueous ionic detergent film, the electrostatic repulsion between the charged surface layers on both sides of the film becomes important as well.

Thus the influence of electrolyte on black films may be explained as follows.

For nonionic detergent, added electrolytes affect the stability and so the rate of drainage of the film through their influence on the amount of hydration and on the formation of the diffuse double layer.

It is recognized that the solubility of polyoxyethylated detergents is closely related to the hydration of ethylene oxide. The effect of added electrolyte on black film is considered to cause dehydration of the ethylene oxide chains and this results in the decrease of steric repulsion against the thinning of the film. Thus, small or polyvalent and strongly hydrated ions are expected to be more effective in decreasing stability and increasing the rate of drainage than large and weakly hydrated ions. However, to elucidate the increase in stability and the retardation of film drainage produced by some electrolytes the possibility of electrostatic repulsion of surface film should be also taken into account,

10) A. Scheludko, "Colloid Chemistry," Elsevier Pub. Co., Amsterdam, London, N. Y. (1966), p. 173.
11) J. M. Corkill, J. F. Goodman, D. R. Haisman and S. P. Harrold, *Trans. Faraday Soc.*, **57**, 821 (1961).

since the added electrolytes are expected to be adsorbed at the film surface to form a diffuse electrical double layer. This effect would be stronger for weakly hydrated large ions than strongly hydrated small ions.

It may be expected that large ions such as SCN^- and Cl^- increase while small or polyvalent ions such as OH^-, F^-, CO_3^{2-}, SO_4^{2-} and PO_4^{3-} decrease the stability of the film. The results shown in Fig. 2 are in line with this explanation. It should be inferred that such an explanation is in accord with the lyotropic effect of anions. A similar effect of electrolytes on the cloud point of nonionic detergent could be observed.[7]

As regards the effect of electrolyte on the ionic detergent, increase in the rate of black film formation with increasing concentration of electrolyte may be explained by the contraction of the diffuse electrical double layer and the resulting decrease of the repulsion between two surface layers. The minor difference observed in the effect between Na_2SO_4 and NaCl requires further study. It should be noted that the mutually opposite effect of NaCl for ionic and nonionic detergent films can also be understood from the opposite effect of ions on the electrical double layer of the film.

The author expresses her gratitude to Professor K. Kinoshita and to Professor T. Sasaki for their encouragement throughout this study. The study was supported in part by a grant from the Asahi Glass Foundation for the Contribution to Industrial Technology given to Professor Kinoshita.

BULLETIN OF THE CHEMICAL SOCIETY OF JAPAN VOL. 43 636—641 (1970)

Ultrasonic Study of Dilute Aqueous Solutions of Urea, Guanidine Hydrochloride and Dioxane

Kiyoshi ARAKAWA, Nobuo TAKENAKA and Katsutaka SASAKI

Research Institute of Applied Electricity, Hokkaido University, Sapporo

(Received July 21, 1969)

An ultrasonic study on dilute aqueous solutions of urea, guanidine hydrochloride and dioxane was made by means of a pulse method, with the intention of investigating the influence of these solutes upon the structure of water. Ultrasonic absorption coefficient was measured in the range of frequency from 15 to 45 Mc/sec, and ultrasonic velocity was measured at 5 Mc/sec. Temperature was varied from 10 to 40°C. In urea solutions, the magnitude of α/f^2 (α=absorption coefficient, f=frequency) decreases first very slowly with concentration, then rapidly in the range from about 0.5 to 3M and at about 4—6M reaches a nearly constant value. In guanidine hydrochloride solutions a similar change in the relation α/f^2 *vs.* concentration takes place with a smaller amount than in urea solution. This shows that guanidine hydrochloride has greater ability as a structure breaker in liquid water than urea. In the dioxane-water system, absorption increases with the concentration of dioxane. A nearly flat region in the absorption *vs.* concentration curve is found for a small concentration of dioxane.

This feature in the α/f^2 *vs.* concentration curve, which is found in the small concentration region, is ascribed to the "cooperative breaking effect" upon the "open-packed structure" in water.

In preceding papers[1-3] we have reported results of ultrasonic investigation on aqueous solutions of urea, alkyl-substituted urea and dioxane by means of an ultrasonic pulse technique. These materials are known as denaturing agents for proteins. The main purpose of these studies was the investigation of the influence of solutes upon the structure of water. Along this line, we have further made a detailed investigation and have chosen urea, guanidine hydrochloride and dioxane as solutes in the present study.

Experimental

Apparatus and Procedures for Measurements. The ultrasonic velocity and absorption were measured according to the pulse method developed by Pinkerton.[4] The detailed procedures for the measurements were

1) K. Arakawa and N. Takenaka, This Bulletin, **40**, 2739 (1967).
2) K. Sasaki and K. Arakawa, *ibid.*, **42**, 2485 (1969).
3) K. Arakawa and N. Takenaka, *ibid.*, **42**, 5 (1969).
4) J. M. M. Pinkerton, *Proc. Phys. Soc.*, **B62**, 86, 129, 286 (1949).

described in the preceding paper.[5] The sound velocity was measured at a fixed frequency of 5 Mc/sec. The absorption was measured in the frequency range of 15—45 Mc/sec.

Materials. Urea, guanidine hydrochloride and dioxane were obtained from Wako Pure Chemical Industry Co., Ltd. The melting points of the former two materials were 132.5±0.5°C and 175.9±0.5°C, respectively. The urea was the same as that used in the preceding study.[1] The dioxane was used after being treated according to the purification procedure described previously.[3] Its boiling point was 101.1—101.3°C.

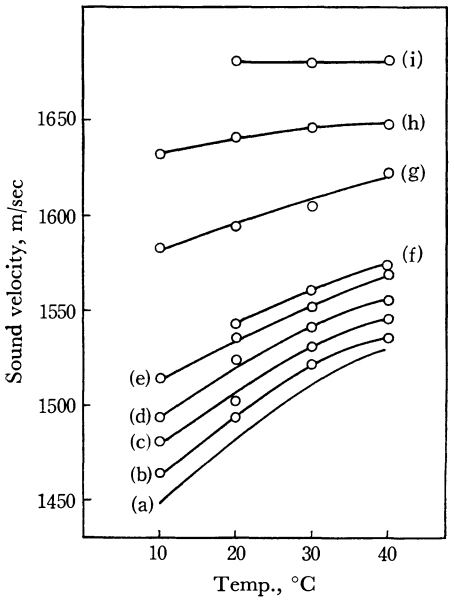

Fig. 1(a). Ultrasonic velocity of aqueous urea solutions.
Concn. (M: mol/l) (a) Pure water, (b) 0.5M, (c) 1M, (d) 1.5M, (e) 2M, (f)[3] 2.3_5M (13.6 wt%), (g)[3] 4.4_5M (25 wt%), (h)[3] 6.4M (35 wt%), (i)[3] 8M (42.9 wt%).

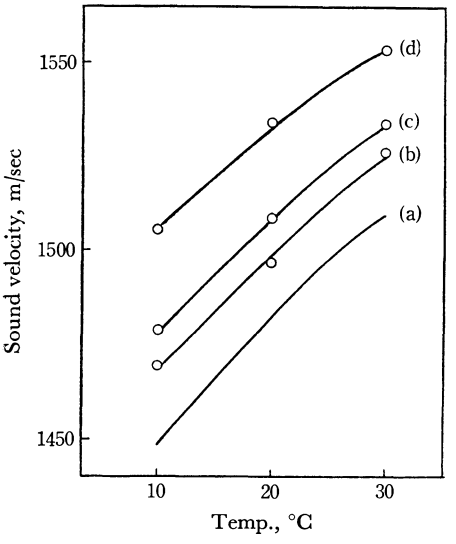

Fig. 1(b). Ultrasonic velocity of aqueous guanidine hydrochloride solutions.
Concn. (M: mol/l) (a) Pure water, (b) 0.3M, (c) 0.5M, (d) 1M

5) K. Arakawa and N. Takenaka, This Bulletin, **40**, 2063 (1967).

Results

Sound Velocity. The ultrasonic velocity at 5 Mc/sec obtained for dilute aqueous solutions of urea and guanidine hydrochloride is plotted against temperature in Figs. 1 (a) and (b). The velocity *vs.* concentration curves obtained for the dilute solutions of dioxane are given in Fig. 2, and those for the entire range composition, including earlier results,[3] are given in Fig. 3.

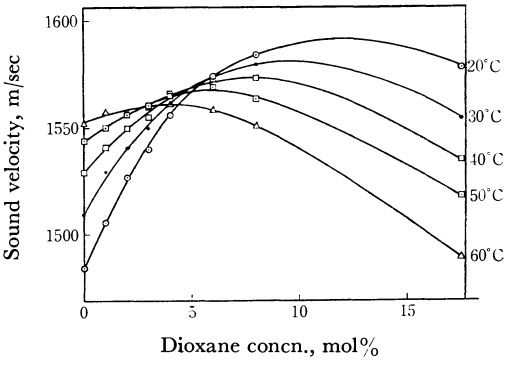

Fig. 2. Ultrasonic velocity of dioxane-water system.

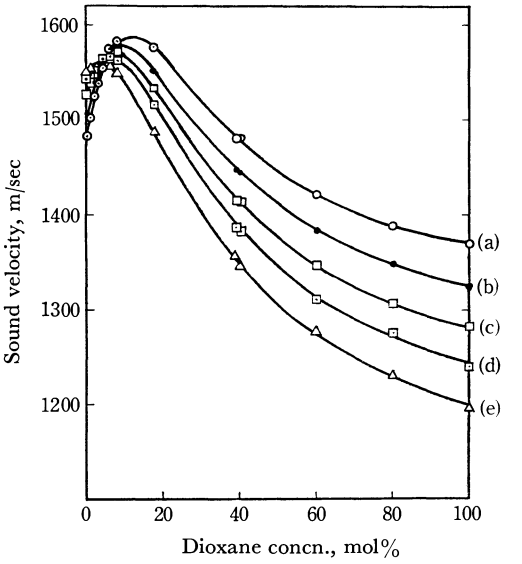

Fig. 3. Concentration dependence of ultrasonic velocity for dioxane-water system.
Temp.: (a) 20°C, (b) 30°C, (c) 40°C, (d) 50°C, (e) 60°C

We see from Fig. 2, that all curves cross at about 4 mol% of dioxane (about 2M of dioxane), but not at one point. The velocity *vs.* temperature curves for urea and guanidine hydrochloride solutions resemble each other. The accuracy of the data of sound velocity was within 2 m/sec.

Ultrasonic Absorption. The absorption coefficient, α, was measured for solutions of urea, guanidine hydrochloride and dioxane. The accuracy of α is within $\pm 2\%$. No relaxation frequency is observed for urea and guanidine hydrochloride solutions, as seen in Fig. 4(a) and (b). For the dioxane-water system, the α/f^2 *vs.* $\log f$ curves given in Fig. 4(c) decrease gradually, but a relaxation frequency can not be determined.[3]

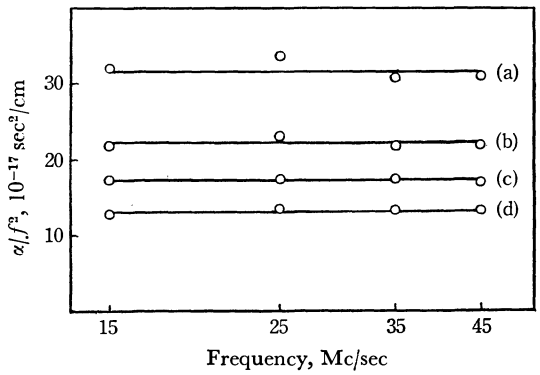

Fig. 4(a). Ultrasonic absorption of aqueous urea solutions. (1.5M urea)
Temp.: (a) 10°C, (b) 20°C, (c) 30°C, (d) 40°C

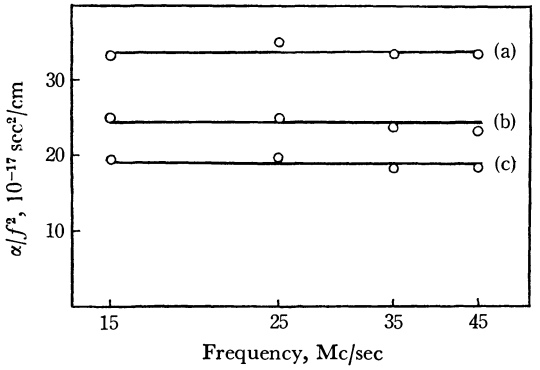

Fig. 4(b). Ultrasonic absorption of aqueous guanidine hydrochloride solutions. (0.5M guanidine hydrochloride)
Temp.: (a) 10°C, (b) 20°C, (c) 30°C

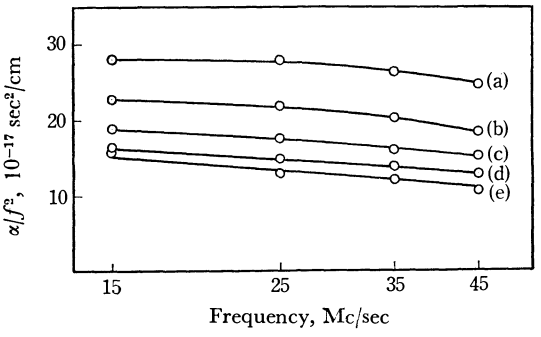

Fig. 4(c). Ultrasonic absorption of dioxane-water system. (4 mol% of dioxane)
Temp.: (a)20°C, (b) 30°C, (c) 40°C, (d) 50°C, (e) 60°C

Concentration Dependence of Ultrasonic Absorption. For urea and guanidine hydrochloride solutions, values of α/f^2 obtained are plotted against concentration by vol% in Figs. 5(a) and (b). In Fig. 6(a) the α/f^2 *vs.* concentration curves for urea solutions are plotted, including the previous data obtained for concentrated solutions,[1] those by Hammes and Schimmel[6] and those by Beauregard and Barrett.[7] In the range of concentration greater than 2M urea (about 9 vol%), the agreement of these data is very good. However, for a smaller concentration a noticeable difference is

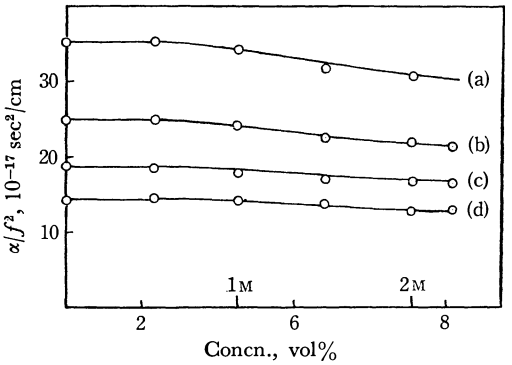

Fig. 5(a). Concentration dependence of ultrasonic absorption for urea solutions.
Temp.: (a) 10°C, (b) 20°C, (c) 30°C, (d) 40°C

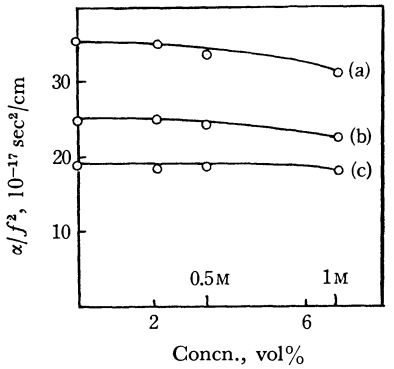

Fig. 5(b). Concentration dependence of ultrasonic absorption for guanidine hydrochloride solution.
Temp. (a) 10°C, (b) 20°C, (c) 30°C

6) G. G. Hammes and P. R. Schimmel, *J. Amer. Chem. Soc.*, **89**, 442 (1967).
7) D. V. Beauregard and R. F. Barrett, *J. Chem. Phys.*, **49**, 5241 (1968).

observed between our present data and those of Hammes and Schimmel.

As seen in Fig. 6(a), the value of α/f^2 decreases first very slowly with concentration. At a concentration greater than 0.5M urea (about 2—3 vol%), it decreases more rapidly, and at about 4—6M becomes nearly constant again.

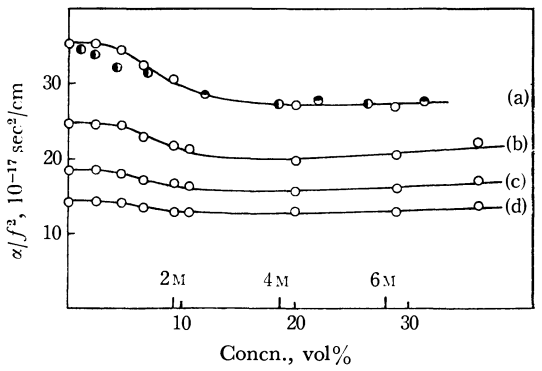

Fig. 6(a). Concentration dependence of ultrasonic absorption for aqueous solution of urea.
Temp.: (a) 10°C, (b) 20°C, (c) 30°C, (d) 40°C
○ Authors, ◐ Hammes and Schimmel,[6]
◓ Beauregard and Barrett[7]

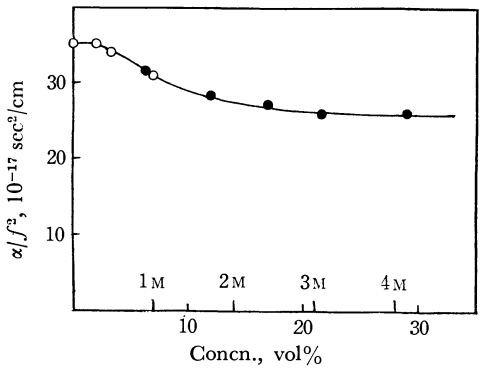

Fig. 6(b). Concentration dependence of ultrasonic absorption for guanidine hydrochloride solution at 10°C.
○ Authors, ● Hammes and Swann[8]

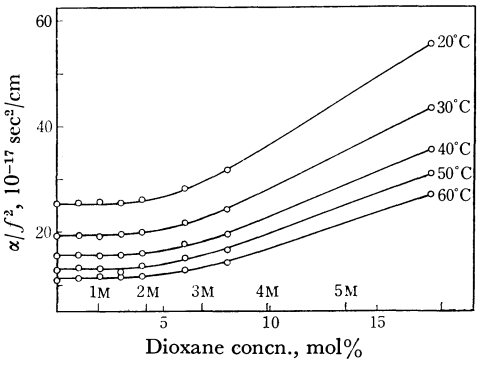

Fig. 7. Concentration dependence of ultrasonic absorption for dioxane-water system at 35 Mc.

In Fig. 6(b) the α/f^2 *vs.* concentration curve of guanidine hydrochloride solution at 10°C is given, including the data reported by Hammes and Swann.[8] In the curve, a tendency similar to that of urea solution is observed, though the decreasing rate of α/f^2 is greater than in urea solution.

For the dioxane-water system concentration dependence of α/f^2 is given in Fig. 7 for a smaller concentration than 17.5 mol% of dioxane. The results for the entire range of composition is given in Fig. 8, including earlier results.[3] As seen in

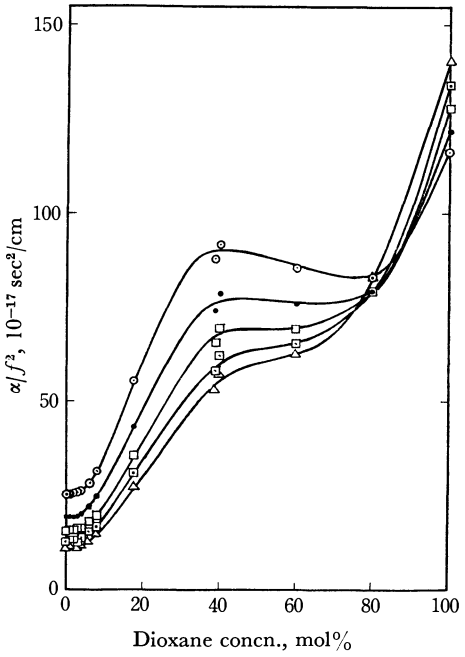

Fig. 8. Concentration dependence of ultrasonic absorption for dioxane-water system at 35 Mc.
Temp.: ⊙ 20°C, ● 30°C, □ 40°C, ⊡ 50°C, △ 60°C

Figs. 7 and 8, the α/f^2 *vs.* concentration curve is nearly flat in the concentration range smaller than about 4 mol% (about 17 vol%; about 2M in molarity). The magnitude of α/f^2 begins to increase rapidly at about 6 mol% of dioxane.

Discussion

The Structure-Breaking Effect of Urea and Guanidine Hydrochloride. Studies have been made on the effect of denaturing agents of urea-guanidium class[9-16] upon the conformation of

8) G. G. Hammes and J. C. Swann, *Biochemistry*, **6**, 1591 (1967).
9) W. Kauzmann, *Advan. Protein Chem.*, **14**, 1 (1959).
10) J. A. Gordon and W. Jencks, *Biochemistry*, **2**, 47 (1963).

protein molecules, and also on the effect of organic solvents such as dioxane,[13,17] ethanol. The effect of denaturing agents seems to be due to two factors: direct interaction between the agent and protein molecules,[10,11] and influence on conformation of protein molecules resulting from the change of the structure of water caused by the agent.[1,6,9,18]

Studies on the effect of denaturing agents upon the structure of water have been made recently by the authors,[1,2,18] Hammes *et al.*[6,8] and Beauregard and Barrett.[7] Concerning the behavior of urea in water, there are ambiguities.[19,20] However, from the results of ultrasonic studies, it has been concluded that urea behaves as a structure breaker for the clusters in water. Recently a statistical mechanical explanation of the behavior of urea as a breaker has been given by Frank and Franks.[21]

The data agree in the range of concentration greater than about 2M,[6,7] as seen in Fig. 6(a). However, for a concentration smaller than 2M, our data are greater than those of Hammes and Schimmel, and the curves by the authors are found to be nearly flat in the range of concentration smaller than about 0.5M. This tendency is seen at temperatures from 10°C to 40°C,*1 as seen in Fig. 6(a). A similar tendency is observed in guanidine hydrochloride solution.

The α/f^2 *vs.* concentration curves for solutions of urea and guanidine hydrochloride are compared in Fig. 9. The magnitude of α/f^2 for guanidine hydrochloride solutions decreases more rapidly than for urea solutions. This supports the idea that guanidine has a greater ability as a structure breaker than urea. It is also seen in Fig. 9 that the constant value of α/f^2 at about 20—30 vol% (4—6M urea) for the urea solution is nearly equal to that for the guanidine solution at about the same volume concentration (3—4M guanidine). This suggests that the "open-packed structure" in water is nearly completely disrupted with addition of 4—6M urea, and nearly the same situation occurs with addition of 3—4M of guanidine hydrochloride.

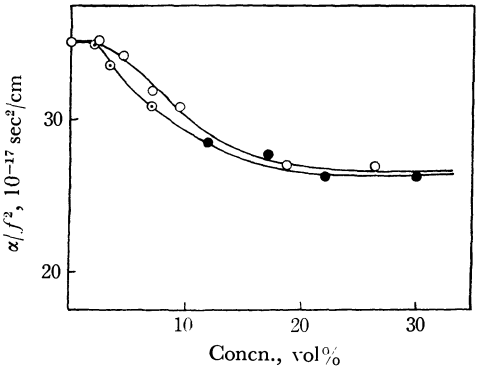

Fig. 9. Comparison between ultrasonic absorption for urea solutions and that for guanidine hydrochloride solution at 10°C.
○ Present data for urea solution, ⊙ Present data for guanidine hydrochloride solution, ● Hammes and Swann's data[8]

Cooperative Breaking[22] of Open-Packed Structure in Water through Addition of Solutes. Frank and Wen[22] have proposed the cooperative formation and breaking of clusters in water. A statistical theory based on the flickering cluster model has been developed by Némethy and Scheraga.[23] We have presented recently a two state theory based on the model proposed by Hall.[24,25]

The source of ultrasonic absorption is attributed to the presence of the "open-packed structure" or "flickering clusters" in water.*2 This "structure" is in equilibrium with a high density region in water as represented by:

open-packed structure $\rightleftarrows$ close-packed structure,
or
flickering clusters $\rightleftarrows$ unbonded monomers. (1)

The lifetime of clusters is believed to be of the order of 10^{-11}—10^{-10} sec,[22,23] and the formation

11) D. R. Robinson and W. Jencks, *J. Amer. Chem. Soc.*, **87**, 2462 (1965).
12) C. Tanford, *ibid.*, **86**, 2050 (1964).
13) C. Tanford, and P. K. De, *J. Biol. Chem.*, **236**, 1711 (1961).
14) C. Tandord, K. Kawahara and S. Lapanje, *ibid.*, **241**, 1921 (1966).
15) P. H. Hippel and K.-Y. Wong, *ibid.*, **240**, 3909 (1965).
16) K. Hamaguchi and A. Kurono, *J. Biochem.* (Tokyo), **54**, 111 (1963).
17) K. Hamaguchi and A. Kurono, *ibid.*, **54**, 497 (1963).
18) M. Watase and K. Arakawa, *Nippon Kagaku Zasshi*, **89**, 383 (1968).
19) M. Abu-Hamdiyyah, *J. Phys. Chem.*, **69**, 2720 (1965).
20) A. Holtzer and M. F. Emerson, *ibid.*, **73**, 26 (1969).
21) H. S. Frank and F. Franks, *J. Chem. Phys.*, **48**, 4746 (1968).

*1 According to Hammes and Schimmel,[6] a shoulder was observed in the curve at 25°C in dilute solutions (Fig. 1), but it disappears at 10°C.

22) H. S. Frank and W. Y. Wen, *Discuss. Faraday Soc.*, **24**, 133 (1957).
23) G. Némethy and H. A. Scheraga, *J. Chem. Phys.*, **36**, 3382 (1962).
24) L. Hall, *Phys. Rev.*, **73**, 775 (1948).
25) K. Arakawa and K. Sasaki, This Bulletin, **42**, 303 (1969).

*2 The situation is different in the case of a uniform state theory,[26] but this theoy can not explain the origin of ultrasonic absorption.

26) M. Falk and T. A. Ford, *Can. J. Chem.*, **44**, 1699 (1966); E. U. Franck and K. Roth, *Discuss. Faraday Soc.*, **43**, 108 (1967).

and breaking of them is supposed to proceed "cooperatively," as proposed first by Frank and Wen. As seen in Fig. 10, the magnitude of α/f^2 for urea solutions is greater than that given by the dotted line in an extremely small concentration. The dotted line represents calculated magnitude of absorption attributed to only water as a solvent under the assumption that no structural change takes place in water.[1,2] The α/f^2 *vs.* concentration curve at 10°C is seen to cross the line at about 1M, and the magnitude of α/f^2 decreases further with concentration. It is concluded, therefore, that the effect of urea as a structure breaker is not appreciable in an extremely dilute solution, and that the effect becomes appreciable with the increase of urea concentration (about 0.5—1M urea). This trend in the concentration dependence of α/f^2 for a small concentration seems to be ascribed to the cooperative nature of cluster formation and breaking.

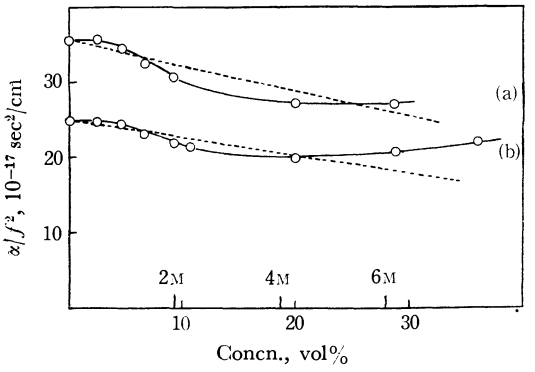

Fig. 10. Concentration dependence of ultrasonic absorption for urea solutions.
Temp. (a) 10°C, (b) 20°C
Dotted line; absorption due to water as solvent.

When a very small amount of urea is added to water, the influence of urea molecules upon the structure of water is isolating, and does not affect the cooperative formation of clusters. Phenomenologically, urea molecules enter the empty space among water molecules with no appreciable influence upon the structure. When the amount of urea becomes greater, the influence becomes appreciable, and urea affects the clusters cooperatively to disrupt them into unbonded monomers. Therefore, for a greater concentration, ultrasonic absorption decreases rapidly with concentration.

The situation is similar in guanidine hydrochloride solutions, the influence being greater than that of urea.

As for the dioxane-water system, the over-all increasing trend of α/f^2 *vs.* concentration curves becomes pronounced because of a large absorption of pure dioxane,[3] but a similar flat region appears for a small concentration. As seen in Figs. 7 and 8, α/f^2 *vs.* concentration curves are nearly flat for a concentration of dioxane less than 4 mol%. This behavior is also attributed to the cooperative nature of cluster formation and breaking. However, the concentration range of nearly flat region is clearly broader than that in urea and guanidine solutions. This is ascribed to the fact that in a dioxane molecule the structure-breaking ability owing to two ether oxygens is diminished in part by the structure-forming ability[27,28] owing to two ($-C_2H_4-$) groups.

Summary and Conclusion

An ultrasonic study on dilute aqueous solutions of urea, guanidine hydrochloride and dioxane has been made by means of a pulse technique in order to investigate the influence of solutes upon the structure of water.

The following conclusions have been obtained.

1) Urea behaves as a structure breaker in water.

2) Guanidine hydrochloride has a greater ability as a breaker than urea.

3) For a small concentration, the structure-breaking effect is not appreciable. This is ascribed to the cooperative nature of cluster formation and breaking in aqueous solutions.

4) In the case of the dioxane-water system, the ability of dioxane as a breaker is diminished in part by the structure-forming effect owing to two ($-C_2H_4-$) groups within a dioxane molecule.

The authors wish to thank Miss Yuko Endo for her cooperation in carrying out this study.

27) G. Némethy and H. A. Scheraga, *J. Chem. Phys.*, **36**, 3401 (1962).

28) D. B. Wetlaufer, S. K. Malik, L. Stoller and R. L. Coffin, *J. Amer. Chem. Soc.*, **86**, 508 (1964).

BULLETIN OF THE CHEMICAL SOCIETY OF JAPAN VOL. 43 642—645 (1970)

Kinetics of Alkaline Hydrolysis of Esters. II.*1 Unsaturated Esters and Oxalic Esters

R. C. SHARMA and M. M. SHARMA

Department of Chemical Technology, University of Bombay, Matunga Road, Bombay-19, India

(Received July 14, 1969)

The kinetics of alkaline hydrolysis of some typical esters, with unsaturation in the alkyl and the acyl portions, was studied. It was found that, in general, unsaturation results in enhancing the rate as compared to that of the corresponding saturated esters, provided that there is no conjugation between the double bond and the carboxyl carbonyl group. Oxalic esters hydrolyze relatively very fast due to the close proximity of the two ester groups. Rate constants for the alkaline hydrolysis of di-*n*-propyl-, di-isopropyl-, di-*n*-butyl-, di-*s*-butyl-, dicyclohexyl- and di-*β*-chloroethyl oxalates were obtained by using the theory of mass transfer accompanied by fast pseudo first-order reaction (diffusion method).

There is limited information in literature concerning the effect of unsaturation, present either on the alkyl or the acyl portion of the ester, on the kinetics of alkaline hydrolysis of esters.[2,3] It was therefore thought desirable to study some typical esters.

In the case of oxalic esters also only limited information is available. The first step of the alkaline hydrolysis of these esters is known to be an extremely fast reaction. Skrabal and coworkers[4-6] have studied the kinetics of this reaction using a phosphate buffer ($HPO_4^{2-}/H_2PO_4^-$) solution. The values of rate constant for the first step of the alkaline hydrolysis of dimethyl and diethyl oxalates obtained by them at 25°C were approximately 20000 and 6300 *l*/g mol sec. Tommila and Stenberg[7] studied the kinetics of alkaline hydrolysis of diethyl oxalate in a flow reactor similar to that used by Hartridge and Roughton.[8] The value of the rate constant was 3900 *l*/g mol sec in water at 30°C. Homan[9] found the value of the rate constant for the alkaline hydrolysis of di-*t*-butyl oxalate in 66.7 per cent (v/v) aqueous dioxane at 25°C to be 21.7 *l*/g mol sec. Sharma and Sharma[1] employed the theory of mass transfer with chemical reaction to obtain the value of the rate constant for the alkaline hydrolysis of di-*n*-butyl oxalate. They reported a value of 1780 *l*/g mol sec in water at 30°C. It was thought desirable to cover a more representative range of oxalic esters.

Experimental

Materials. Vinyl and isopropenyl acetates, methyl-, ethyl- and *n*-butyl acrylates and methyl methacrylate were purified by distillation at reduced pressure. Allyl acetate was synthesized by the reaction of allyl alcohol and acetic anhydride in the presence of one per cent sulphuric acid, and subsequently purified by distillation.

Oxalic diesters of *n*-propyl-, isopropyl-, *n*-butyl-, *s*-butyl, cyclohexyl and *β*-chloroethyl alcohols were synthesized by refluxing anhydrous oxalic acid with appropriate alcohol, taken as two to three times the stoichiometric requirement, in the presence of about three per cent sulphuric acid. The esters were purified by distillation at reduced pressure (10 to 50 mmHg). The physical properties for all the esters are reported in literature. The properties of purified esters agreed with those reported in literature.

Kinetic Measurements. The kinetics of alkaline hydrolysis of esters was studied in the aqueous medium. The rate constants for unsaturated esters were determined by the conventional method. The experimental procedure for this method was reported in a previous paper.[1] In some cases studies were made at lower temperatures (0.2 to 15°C). A constant temperature bath was used, where the temperature could be controlled to within ±0.05°C.

The theory of mass transfer accompanied by fast pseudo first-order reaction was used to study the kinetics of alkaline hydrolysis of oxalic esters. Details of the

*1 The previous paper by the authors[1] may be treated as Part I.

1) R. C. Sharma and M. M. Sharma, *J. Appl. Chem.*, **19**, 162 (1969).
2) E. A. Haloiven, *Acta Chem. Scand.*, **10**, 485 (1956).
3) R. T. Myers, A. R. Collett and C. L. Lazzell, *J. Phys. Chem.*, **56**, 461 (1952).
4) A. Skrabal, *Monatsh.*, **38**, 29 (1917).
5) A. Skrabal and A. Matievie, *ibid.*, **39**, 765 (1918).
6) A. Skrabal and E. Singer, *ibid.*, **41**, 339 (1920).
7) E. Tommila and H. Stenberg, *Suomen Kemistilahiti*, **19B**, 19 (1946).
8) H. Hartridge and F. J. W. Roughton, *Proc. Roy. Soc., Ser. A*, **104**, 376 (1923).
9) J. D. H. Homan, *Rec. Trav. Chim.*, **63**, 181 (1944); *Chem. Abstr.*, **39**, 1587 (1945).

method for the determination of rate constants have already been reported.[1,10-12]

Analysis. Methods of analysis have already been reported[1] except in the case of solid oxalic esters (dicyclohexyl and di-β-chloroethyl). In these cases about 20 ml of 8 N H_2SO_4 solution was added to 25 ml of an aqueous solution containing disodium oxalate. The solution was heated to about 70°C and titrated against standard $KMnO_4$ solution. Under these conditions disodium oxalate is oxidized quantitatively.[13]

Results and Discussion

1) Unsaturated Esters. An unsaturated carbon to carbon linkage near the carbonyl carbon in a carboxylic ester should speed up the rate of alkaline hydrolysis compared to that of the corresponding saturated ester due to the electronegative nature of unsaturation.[14,15] However, if there is conjugation of the unsaturation with the carboxyl (–C(=O)–O–) group then this retards the rate of the alkaline hydrolysis of the ester. Esters considered in this work could be divided in two groups: (i) unsaturation present in the alkyl group, (ii) unsaturation present in the acyl part.

(i) Unsaturation in the Alkyl Group. The presence of unsaturation on the alkyl portion of an ester accelerates the rate of alkaline hydrolysis. The effect decreases when the unsaturation moves away from the reaction centre. The results are given in Table 1.

Table 1. Rate constants for the alkaline hydrolysis of unsaturated esters in aqueous medium

Ester	Temperature °C	k_2 l/g mol sec
Vinyl acetate	0.3	0.392
	5	0.594
	10	0.854
	15	1.17
Isopropenyl acetate	10	0.145
	20	0.285
	30	0.512
Allyl acetate	30	0.23
Ethyl propionate	30	0.119
Methyl acrylate	30	0.198
Ethyl acrylate	30	0.102
n-Butyl acrylate	30	0.074
Methyl methacrylate	30	0.083

Only a limited amount of information is available in literature concerning the kinetics of alkaline hydrolysis of vinyl acetate.

$$CH_3COOCH{=}CH_2 + OH^- \xrightarrow{k_2} CH_3COO^- + H_2C{=}CHOH \quad (1)$$

$$H_2C{=}CHOH \xrightarrow{\text{fast}} CH_3CHO \quad (2)$$

The value of the rate constant for alkaline hydrolysis of vinyl acetate has been reported as 10.3 l/g mol sec by Skrabal and Zahorke.[16] They used a borate buffer solution for kinetic studies. The accuracy of the rate constant will be dependent on a precise knowledge of the hydroxyl ion concentration in the borate buffer solution. The value reported in this work is very different from that given by Skrabal and Zahorke.[16] The kinetics of alkaline hydrolysis of vinyl acetate was studied in the homogeneous phase by the conventional method[17] at lower temperatures (0.2 to 15°C) and data were extrapolated to room temperature. The extrapolated value of 2.6 l/g mol sec at 27°C is in good agreement with that obtained by the "diffusion method" (2.34 l/g mol sec at 27°C).

In the case of isopropenyl acetate, it would be expected that the steric hindrance due to the methyl group at the α-carbon atom of the alkyl portion would considerably decrease the rate of alkaline hydrolysis:

$$CH_3COOC(CH_3){=}CH_2 + OH^- \xrightarrow{k_2} CH_3COO^- + H_2C{=}C(CH_3)OH \quad (3)$$

$$H_2C{=}C(CH_3)OH \xrightarrow{\text{fast}} CH_3COCH_3 \quad (4)$$

The rate constant for this ester is about one sixth of that for vinyl acetate. The ratio of the rate constants for vinyl and isopropenyl acetates may be compared with the ratio for ethyl and isopropyl acetates (0.145 and 0.032 l/g mol sec at 30°C, respectively).

The value of the rate constant for the alkaline hydrolysis of phenyl acetate is about 12 times that of ethyl acetate.[18] The value of the rate constant for phenyl acetate should be obviously higher than that of isopropenyl acetate as there are two more unsaturation linkages present between 2,3- and 4,5-carbon atoms in the phenyl group. Further-

10) M. M. Sharma and A. K. Nanda, *Trans. Instn. Chem. Engrs.*, **46**, T44 (1968).
11) A. K. Nanda and M. M. Sharma, *Chem. Eng. Sci.*, **21**, 707 (1966).
12) A. K. Nanda, M. M. Sharma, *ibid.*, **22**, 769 (1967).
13) A. I. Vogel, "Quantitative Inorganic Analysis," 3rd Ed., Longmans Green & Co., N. Y. (1962), p. 301.
14) H. Olsson, *Z. Phys. Chemie*, **133**, 233 (1928).
15) J. F. J. Dippy, *Chem. Rev.*, **25**, 151 (1939).
16) A. Skrabal and A. Zahorke, *Monatsh.*, **48**, 459 (1927).
17) R. C. Sharma and M. M. Sharma (Paper to be published).
18) A. Skrabal and M. A. Hugetz, *Monatsh.*, **47**, 17 (1926).

more, the rate constant for phenyl acetate should be expected to be less than that of vinyl acetate as the latter is sterically less hindered.

The rate constant for allyl acetate was found to be 0.23 *l*/g mol sec in water at 30°C, which is about one twelfth of that for vinyl acetate. In the case of allyl acetate the double bond is further away from the reaction center. Moreover it is well known that when an electronegative group or atom moves away from the reaction center the rate decreases. For instance, the value of the rate constant for the alkaline hydrolysis of chloromethyl acetate is about twenty times higher than that for β-chloroethyl acetate.[19,20]

(ii) Unsaturation in the Acyl Part. Unsaturation between α-, β-carbon atoms of the acyl portion results in conjugation with the carboxyl carbonyl group (–C(=O)–) of the ester. The effect of conjugation is not very marked in acrylic acid.[21] (The dissociation constants (K_a) of propionic and acrylic acids are 1.33×10^{-5} and 5.56×10^{-5}, respectively). However, the effect is much greater in acrylates, since here the conjugation energy of carbonyl group is approximately 4000 cal lower than that of carbonyl group in the acid.[22]

The values of the rate constant for the alkaline hydrolysis of ethyl propionate, methyl-, ethyl- and *n*-butyl acrylates and methyl methacrylate were obtained in water at 30°C by the conventional method and are given in Table 1.

The value of the rate constant decreases with the increase in the size of the alkyl group of acrylates. The relative decrease was found to be of the same magnitude as that in the case of acetic ester.

The effect of methyl substitution on the acyl portion, near the reaction center, was also investigated. The retardation of the alkaline hydrolysis of methyl methacrylate as compared to that of methyl acrylate was observed. The decrease in the rate constant when a hydrogen atom of the α-carbon atom of the acyl portion is replaced by a methyl group is comparable in the case of methyl acrylate and methyl methacrylate, and ethyl propionate and ethyl isobutyrate.[2] The ratio of the rate constants in these two cases is about 2.5 to 3.

2. Oxalic Esters. In order to obtain the values of the rate constant by the diffusion method, it is necessary to know the values of solubility and diffusivity of the ester in water. Solubilities of oxalic esters in water and aqueous solutions of sodium chloride were determined. The results were correlated by the methods reported in literature[23-25] and are given in Table 2. Diffusivities of esters were estimated by the method of Wilke and Chang[26] and are given in Table 3. The rate constants determined by the diffusion method are also given in Table 3.

In oxalic esters, the two ester groups are in close proximity to each other. The ester group (–COOR′) is a strong electron-attracting group and it is well known that such groups enhance the rate of alkaline hydrolysis. Hence the values of rate constants for alkaline hydrolysis of oxalic esters are relatively very high.

The kinetics of alkaline hydrolysis of dimethyl- and diethyl oxalates could not be studied in this work because of their higher solubilities. However, in the case of di-*n*-propyl oxalate the necessary conditions were satisfied. Extraction of this ester in the stirred cell was carried out only for five minutes to avoid the formation of disodium oxalate in excess of its saturation concentration. However, in the case of di-*n*-butyl oxalate, because of its very low solubility, experiments could be conducted even upto 30 min.

The values of the rate constant for di-*n*-propyl- and di-*n*-butyl oxalates are 2020 and 1780 *l*/g mol·sec, respectively. The ratio of rate constants of diethyl to di-*n*-propyl, and di-*n*-propyl to

TABLE 2. SOLUBILITIES OF OXALIC ESTERS IN WATER AND AQUEOUS SODIUM CHLORIDE SOLUTIONS (1 to 3M)

No.	Ester	Temperature °C	Solubility in water $[E]_w\times10^5$ g mol/cm³	K_s* *l*/g ion
1	Di-*n*-propyl oxalate	30	1.83	0.202
2	Di-isopropyl oxalate	30	4.6	0.164
3	Di-*n*-butyl oxalate[1]	30	0.23	0.264
4	Di-*s*-butyl oxalate	30	0.368	0.223
5	Di-β-chloroethyl oxalate	30	3.71	0.15
		5	1.56	0.15
6	Di-cyclohexyl oxalate	30	0.02	0.18

* $\log_{10}\frac{[E]_w}{[E]} = K_sI$ 1)

[E] = Solubility of the ester in aqueous sodium chloride solution, g mol/cm³

I = Ionic strength, g ion/*l*

19) E. Tommila, S. Hietala and J. Nyrkoo, *Soumen Kemistilehti*, **28B**, 143 (1955).
20) E. K. Euranto and R. A. Euranto, *ibid.*, **35B**, 96 (1962).
21) C. K. Ingold, "Structure and Mechanism in Organic Chemistry," Cornell University Press, Ithaca (1953), p. 328.
22) L. Pauling, "The Nature of the Chemical Bond," Cornell University Press, New York (1945), p. 202.
23) F. A. Long and W. F. McDevit, *Chem. Rev.*, **51**, 119 (1952).
24) D. W. Van Krevelen and P. J. Hoftizer, *Chem. Ind.*, **1948**, 168.
25) P. J. Kothari and M. M. Sharma, *Chem. Engng. Sci.*, **21**, 391 (1966).
26) C. R. Wilke and P. Chang, *A. I. Ch. E. Jl.*, **1**, 264 (1955).

TABLE 3. SPECIFIC RATES OF EXTRACTION, DIFFUSIVITIES AND RATE CONSTANTS FOR ALKALINE HYDROLYSIS OF OXALIC ESTERS IN AQUEOUS SOLUTION

No.	Ester	Concentration of electrolytes g mol/l		Temperature °C	Specific rate of extraction $\frac{\text{g·mol}}{\text{cm}^2\text{·sec}}$	Diffusivity $\times 10^6$ cm^2/sec	Rate constant l/g mol sec
		NaCl	NaOH				
1	Di-*n*-propyl oxalate	1	0.56	30	6.0×10^{-7}	5.65	2020
2	Di-isopropyl oxalate	1	0.6	30	1.27×10^{-6}	5.65	890
3	Di-*n*-butyl oxalate[1]	0	0.3	30	1.18×10^{-7}	6.37	1780
4	Di-*s*-butyl oxalate	1	0.5	30	8.2×10^{-8}	5.11	810
5	Di-β-chloroethyl oxalate	0	0.3	5	6.7×10^{-7}	3.56	2160
6	Dicyclohexyl oxalate	0	0.25	30	8.35×10^{-9}	6.43	1080

di-*n*-butyl oxalates are approximately 2 and 1.2, respectively. For the acetates of the corresponding alcohols the ratio of rate constants for alkaline hydrolysis are about 1.23 and 1.2, respectively. (The values of the rate constant for ethyl, *n*-propyl and *n*-butyl acetates are 0.41, 0.12 and 0.1 l/g mol·sec in water at 30°C, respectively). Oxalic esters, other than dimethyl and diethyl oxalates, seem to follow the normal trend of change in the rate constant due to inductive and steric factors.

The rate constant for di-β-chloroethyl oxalate would be expected to be higher than that of diethyl oxalate due to the electronegative nature of the chlorine atoms present at the β-carbon atoms of the alkyl portions.

It was observed that the solubility of di-β-chloroethyl oxalate (mp 45°C) in water increases with an increase in the temperature. It is so high at 30°C that the necessary conditions for the validity of pseudo first-order reaction mechanism are not satisfied. However, all the conditions were satisfied when the experiments were carried out at 5°C in a bubble column where the temperature was kept constant by circulating water at the desired temperature through the outer jacket. The rate constant was found to be 2160 l/g mol sec at 5°C. If the energy of activation for the alkaline hydrolysis of di-*n*-propyl ester is assumed to be the same as that for other related oxalic esters of about 7 kcal/mol,[7] then the rate constant for di-*n*-propyl oxalate at 5°C works out to be about 700 l/g mol sec. This value is about one-third of that of di-β-chloroethyl oxalate. The rate constant of β-chloroethyl acetate is about 3.5 times higher than that of *n*-propyl acetate.

The steric effect was investigated by studying the kinetics of alkaline hydrolysis of di-isopropyl, di-*s*-butyl and dicyclohexyl oxalates. The value of the rate constant for the alkaline hydrolysis of di-isopropyl oxalate was found to be 890 l/g mol sec and that of di-*s*-butyl oxalate 810 l/g mol sec. These values are very close to each other, probably because of a similar steric effect offered by the isopropyl and *s*-butyl groups. The rate constants for isopropyl and *s*-butyl acetates and the corresponding formates are practically the same. However, the rate constant for dicyclohexyl oxalate is higher than the expected value. The discrepancy might be caused by the error involved in the determination of the solubility of this ester which is relatively very low. A 10 per cent error in the solubility results in about 20 per cent error in the rate constant.[1]

One of the authors (R.C.S.) wishes to thank the University Grants Commission for an award of a scholarship which enabled this work to be carried out.

BULLETIN OF THE CHEMICAL SOCIETY OF JAPAN VOL. 43 646—651 (1970)

Electronic Structures and Electronic Absorption Spectra of Cyclohexadienyl and Related Radicals Produced by γ-Irradiation

Tadamasa SHIDA and Ichiro HANAZAKI

The Institute of Physical and Chemical Research, Yamatomachi, Kitaadachi-gun, Saitama

(Received July 26, 1969)

The electronic absorption spectrum for the cyclohexadienyl radical produced upon γ-irradiation of pure benzene and benzene-alcohol solutions both at 77°K was investigated. In addition to the absorption band at 3.9 eV, a weak band with a prominent vibrational structure was observed at 2.2 eV. An SCF-CI molecular orbital calculation was carried out for the radical taking into account explicitly the hyperconjugation effect of methylene group. The theory predicts the two observed bands with satisfactory accuracy. The calculated spin densities are also in good agreement with the existing ESR data of the radical. Vibrational analysis was carried out for the band system at about 2 eV as well as for the corresponding bands of isotopically mixed radicals, C_6H_6D, C_6D_6H, and C_6D_7. Parallel calculations for hydronaphthyl radicals are also in harmony with the available experimental data of optical and ESR measurements.

Cyclohexadienyl-type radicals are assumed as the reaction intermediates in radical substitution reactions at the benzene ring.[1] They are also known to be important intermediates in the radiolysis of benzene and its derivatives. Both the liquid benzene at room temperature[2] and the solid at 77°K,[3] produce the radical upon γ-irradiation which has been identified by its characteristic absorption band in the near UV and the triplet ESR spectrum. In the irradiated solid benzene the radical is assumed to be formed by the reactions,[3]

$$C_6H_6 \xrightarrow{\gamma} \cdot C_6H_5 + H \quad (1)$$

$$C_6H_6 + H \longrightarrow \cdot C_6H_7 \quad (2)$$

The same radical can also be produced in dilute benzene solutions in alcoholic solvents γ-irradiated at 77°K,[4,5]

$$CH_3OH \xrightarrow{\gamma} CH_3OH^+ + e^- \quad (3)$$

$$C_6H_6 + e^- \longrightarrow C_6H_6^- \quad (4)$$

$$C_6H_6^- + CH_3OH \longrightarrow \cdot C_6H_7 + CH_3O^- \quad (5)$$

Similarly γ-irradiation of naphthalene single crystal or naphthalene in methanol glass at 77°K produces α-hydronaphthyl radical which has been confirmed by ESR and optical absorption measurements.[6,7]

The characteristic feature common to these radicals is the participation of ring methylene group in the π electron system through hyperconjugation. In the present work we have undertaken an open-shell SCF-CI calculation for electronic states of these radicals taking into account explicitly the effect of hyperconjugation. A method previously developed for the benzenium ion and related cations[8] was applied to the neutral radicals.

The results for cyclohexadienyl radical predicts a new electronic absorption band in the visible region in addition to the band in the near UV region.[5] Hence the absorption spectrum of the radical was carefully reexamined for irradiated solid benzene and benzene in alcoholic solvents. We have found the corresponding weak absorption band in the visible region with a marked vibrational structure which can be analyzed directly on the basis of fundamental vibrational frequencies close to those of the benzene molecule.

Experimental

Pure benzene and benzene in alcohols both degassed thoroughly were frozen at 77°K to a polycrystalline and a glassy solid. The samples were kept at the same temperature throughout the measurements of absorption

1) M. Levy and M. Szwarc, *J. Chem. Phys.*, **22**, 1621 (1954); *J. Amer. Chem. Soc.*, **77**, 1949 (1955); M. Szwarc, *J. Phys. Chem.*, **61**, 40 (1957).

2) R. Cooper and J. K. Thomas, *J. Chem. Phys.*, **48**, 5097 (1968).

3) S. Ohnishi, T. Tanei and I. Nitta, *ibid.*, **37**, 2402 (1962).

4) J. A. Leone and W. S. Koski, *J. Amer. Chem. Soc.*, **88**, 224 (1966).

5) T. Shida and W. H. Hamill, *ibid.*, **88**, 3689 (1966).

6) J. A. Leone and W. S. Koski, *ibid.*, **88**, 656 (1966).

7) T. Okubo, N. Itoh and T. Suita, *Molecular Crystals*, to be published.

8) I. Hanazaki and S. Nagakura, This Bulletin, **38**, 1298 (1965).

spectrum before and after irradiation with γ-rays from a 12 kCi (kilocurie) ^{60}Co source. Optical cells of the thicknesses of 2.0 and 1.5 mm were made of Suprasil quartz. A quartz Dewar with flat quartz windows was placed in the sample compartment of a Cary spectrophotometer Model 14RI which was equipped with a high-intensity source attachment 1417200 operated at 110 V. The accessory was indispensable for the optical measurements because pure benzene solidifies at 77°K to an opaque polycrystalline and transmits light only to a small extent. Since the absorption induced by irradiation appears at wavelengths longer than 280 mμ where neither benzene nor methanol absorbs, the difference in the optical density before and after irradiation was taken to be due to the absorption of products formed upon irradiation.

Thiophene-free benzene was purified by distillation with a theoretical plate number of about 40 followed by repeated crystallization. Perdeuterobenzene of a stated atomic purity (>99%) from E. Merck AG was used. Methanol was purified by the standard method.[9] CH_3OD and C_2H_5OD were supplied from CIBA AG. Methanol and methanol-d_1 were added with 4% of water and D_2O respectively which formed clear glass with cracks at 77°K, while the ethanols vitrified without water. The cracks did not interfere with the optical measurement in the thin absorption cells. The aqueous methanols used as a solvent for benzene will be designated simply "methanol" hereafter.

Theoretical

In a previous paper[8] the electronic structures of benzenium ion and some related compounds were studied in the framework of the Pariser-Parr-Pople SCF-CI theory.[10] The hyperconjugation effect of the methylene group was treated explicitly in the following manner. The H_2 unit of CH_2 in the ion is regarded as a pseudo atom which provides a σ- and a π-type valence electrons to the ring system. The ionization potential and electron affinity of the pseudo π atomic orbital (AO) of the H_2 "atom" is calculated non-empirically to be 9.4219 and -0.7007 eV, respectively, by reducing the integrals over the pseudo AO into those over the hydrogen 1s AO's. The two-center Coulomb repulsion and core resonance integrals are also evaluated by the standard method by reducing them into the intergrals over the hydrogen 1s AO's. Satisfactory agreement with the experimental results for the benzenium ion and its derivatives encouraged us to use the same method of calculation for the corresponding neutral radicals. The method developed by Longuet-Higgins and Pople[11] for the open-shell electron system was applied to the radical in combination with the above method of evaluating the molecular integrals.

Results and Discussion

The Cyclohexadienyl Radical. One mol/l of benzene in methanol irradiated at 77°K to the dose of 1.1×10^{19} eV/g produced absorption spectra shown in Fig. 1. In accordance with the previous

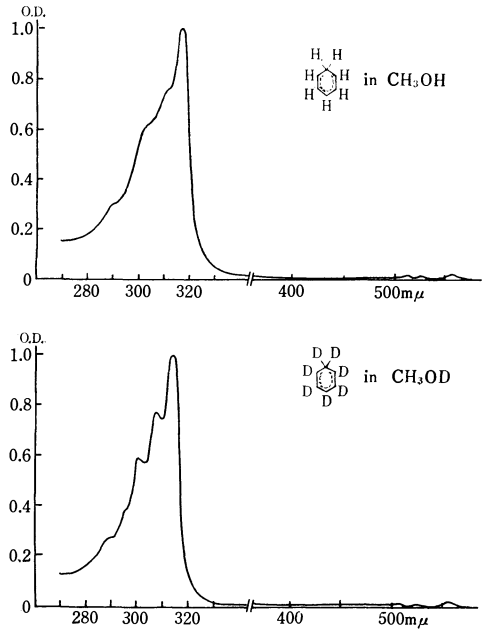

Fig. 1. Absorption spectra of cyclohexadienyl radicals in benzene-methanol solutions γ-irradiated at 77°K.

Upper: C_6H_7 produced from C_6H_6 (1 mol/l) in CH_3OH.
Lower: C_6D_7 produced from C_6D_6 (1 mol/l) in CH_3OD.
Dose$=1.1\times10^{19}$ eV/g for both samples.
A cell 1.5 mm thick was used for both.

conclusion[5] they are associated with cyclohexadienyl radicals, C_6H_7 and C_6D_7 produced by reactions (3)—(5). The band at 3.9 eV was observed for a sample treated similarly, while the band system in the visible region was not detected apparently because of a high level of noise in the previous experiment.[5] By irradiating for a longer period the band system at about 2 eV became intense enough to reveal the structure as shown in Fig. 2 for the two isomeric radicals. The molar extinction coefficient of the most intense peak in the visible band system can be estimated knowing that of the band at 3.9 eV as 1.21×10^4 $l$mol^{-1} cm^{-1}.[12]

9) H. Seki and M. Imamura, *J. Phys. Chem.*, **71**, 870 (1967).
10) R. Pariser and R. G. Parr, *J. Chem. Phys.*, **21**, 466, 767 (1953). J. A. Pople, *Proc. Phys. Soc., A*, **68**, 81 (1955).
11) H. C. Longuet-Higgins and J. A. Pople, *ibid., A*, **68**, 591 (1955).
12) T. Shida, to be published.

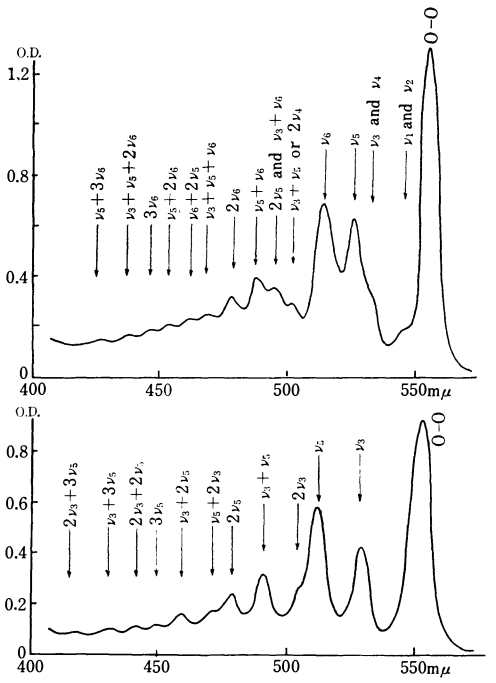

Fig. 2. Weak bands in the visible region of Fig. 1 magnified.

Upper: C_6H_7 in C_6H_6-CH_3OH solution.
Lower: C_6D_7 in C_6D_6-CH_3OD solution.
Dose=2.1×10^{21} eV/g. The cell, 1.5 mm thick.

TABLE 1. ELECTRONIC TRANSITIONS OF CYCLOHEXADIENYL RADICAL, C_6H_7.

Sym-metry[a]	Theroretical Energy (eV)	Theroretical Oscillator strength	Experimental Energy (eV)	Experimental Oscillator strength
A_2	2.030	4.07×10^{-4}	2.22	4.3×10^{-4}
B_1	3.626	3.20×10^{-4}		
A_2	3.950	1.35×10^{-1}	3.92	1.27×10^{-1}
B_1	5.649	4.20×10^{-2}		

a) The molecule has the C_{2v} symmetry.

Table 1 summarizes the theoretical results for the cyclohexadienyl radical together with the experimental results obtained. The prediction that a weak absorption should be observed at 2.03 eV is well substantiated. The first A_2 transition can be correlated to the benzene B_{2u} transition strongly mixed with the charge transfer transitions between the methylene pseudo AO and the π electron system of the aromatic ring. Similarly, the second A_2 transition comes from the benzene E_{1u} transition strongly affected by the charge transfer interactions.

The first B_1 transition predicted at 3.6 eV was not observed. We consider that either the intensity of the band is too small or the band is over-shadowed by the strong absorption at 3.9 eV.*1

The ESR spectrum of the radical has been studied by previous workers[3,4] who attributed the observed splittings of 47.5, 10.4, and 2.5 gauss to the methylene protons, three ring protons at ortho and para positions and two protons at meta position, respectively. The calculated spin densities are given in Fig. 3. The splitting due to the ring protons

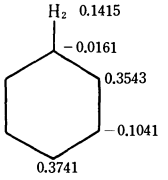

Fig. 3. Calculated spin densities of cyclohexadienyl radical.

are calculated by means of McConnell's relation with the proportionality constant of 30 gauss. The values of 10.6, 11.2, and 3.1 gauss for the ortho, para, and meta protons, respectively, are in fairly good agreement with the observed values. The splitting due to the methylene protons is derived to be 49.9 gauss by the following procedure. The pseudo AO χ is written as

$$\chi = [2(1-S)]^{-1/2}(\chi_1-\chi_2) \quad (6)$$

where χ_1 and χ_2 are the hydrogen $1s$ AO's and S is the overlap integral between them. Assuming the geometrical conformation of methane S is estimated as 0.282 from the table given by Mulliken *et al.*[13] The net atomic spin density ρ^{net} on each $1s$ AO is

$$\rho^{net} = [2(1-S)]^{-1}\rho \quad (7)$$

where ρ stands for the spin density on χ. With this relation and the calculated value of $\rho=0.1415$, we obtain $\rho^{net}=0.09854$. Using the hyperfine splitting of 506.8 gauss for the hydrogen atom the splitting due to the methylene protons is obtained as 49.9 gauss.*2

The general agreement between the theoretical and experimental results on the optical and ESR

*1 We have not succeeded in observing this weak band for radicals of lower symmetry (*e.g.*, the radical derived from ortho xylene),[5] where the intensity of the band might be enhanced a little by the removal of symmetry of the radical.

13) R. S. Mulliken, C. A. Rieke, D. Orloff and H. Orloff, *J. Chem. Phys.*, **17**, 1248 (1949).

*2 The contribution from the "overlap" spin density has been neglected. This gives an error of about 7% for the splitting. The odd electron on the $2p\pi$ AO of methylene carbon may induce an additional spin density on the methylene protons by the mechanism of spin polarization. This effect, however, can also be neglected since the $2p\pi$ spin density on the methylene carbon is minute.

properties of the radical indicates the adequacy of the present theoretical treatment. It must be emphasized that the effect of hyperconjugation is crucial in the electronic behavior of the radical. The striking resemblance of the electronic absorption spectrum of the cyclohexadienyl radical to that of the benzyl[14] may be an indication that the pseudo π electron in the former radical is as important as the $2p\pi$ electron of the methylene group in the latter radical.

The α-Hydronaphthyl Radical. Theoretical results for the electronic transition energies and intensities of α-hydronaphthyl radical are summarized in Table 2. Upon γ-irradiation an H atom

Table 2. Electronic transitions of α-hydronaphthyl radical

Theoretical			Experimental[a]
Energy (eV)	Oscillator strength	Polarization[b] (deg.)	Energy (eV)
2.402	1.20×10^{-3}	−86	2.34
2.986	3.39×10^{-4}	−18	3.14
3.681	1.82×10^{-3}	−14	3.68
3.752	5.38×10^{-2}	−72	
4.029	2.41×10^{-1}	+65	
4.615	1.77×10^{-3}	+18	

a) T. Okubo, N. Itoh and T. Suita; to be published in Molecular Crystals.
b) The direction of transition moment defined as measured from the $x+$ axis toward the $y+$ axis shown in Fig. 4.

may be added to naphthalene at α- and/or β position. The calculation for the total π electron energy predicts a lower value for the α radical by the amount of 4.2 eV. Thus the experimentally observed absorption bands are regarded as predominantly due to the α radical*3

In Table 2 the experimental transition energies obtained for the γ-irradiated naphthalene single crystal are also included.[7] Agreement between the theoretical and observed values is satisfactory. Because of the overlapping of absorption bands due to several species produced in the irradiated crystal, it is difficult to determine the intensity of each band accurately. However, the intensity ratio of the observed three bands seems to be consistent with the calculated oscillator strengths.[7]

The spin densities calculated for the α-hydronaphthyl radical are shown in Fig. 4. By a similar

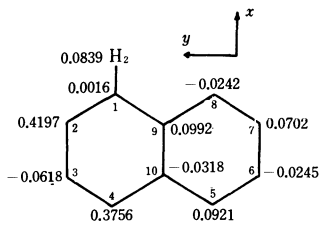

Fig. 4. Calculated spin densities of α-hydronaphthyl radical.

procedure to that for the cyclohexadienyl radical the triplet splitting due to the methylene protons was found to be 29.3 gauss in comparison with the observed 37 gauss.[6] We assign, in conformity with the previous workers,[6] the observed minor triplet of splitting of 12.8 gauss to the ring protons at the 2 and 4 positions whose theoretical splittings are 12.6 and 11.3 gauss, respectively. The calculated spin densities for the β-radical cannot explain the ESR spectrum even qualitatively.

The Vibrational Analysis of the Visible Band System of Cyclohexadienyl Radical. γ-Irradiation of pure solid benzene produced sharp peaks in the region of 400—560 mμ as shown in Fig. 5.

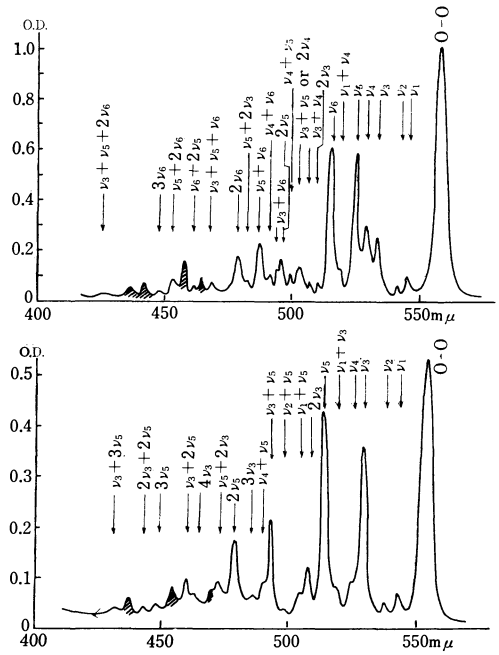

Fig. 5. Absorption spectra of the visible band of cyclohexadienyl radicals produced in pure benzene solids γ-irradiated at 77°K.
Upper: C_6H_7 in C_6H_6
Lower: C_6D_7 in C_6D_6
Dose$=2.1\times10^{21}$ eV/g. The cell, 2.0 mm thick.

Owing to the stability of benzene towards radiation the total dose of the magnitude of 10^{21} to 10^{22} eV/g

14) E. J. Land, "Progress in Reaction Kinetics," Vol. III, ed. by G. Porter, Pergamon Press, London (1965), p. 378

*3 This is consistent with the result of localization energy method which shows a larger methyl affinity for the α-position than the β-position.[15]

15) T. Fueno, T. Tsuruta and J. Furukawa, *Nippon Kagaku Zasshi*, **78**, 1075 (1957).

was required to obtain the optical density of 0.5 to 1.0. In irradiated benzene concomitant reactions could yield species other than the cyclohexadienyl radical,[16] while in the methanol solution reactions (3)—(5) are predominant processes and no other species is expected which absorbs in the visible region.[5] Since Fig. 5 for the irradiated benzene is strikingly corresponding to Fig. 2 for the methanol solution, it can be concluded that in irradiated benzene also cyclohexadienyl radical is the main species responsible for the absorption in the visible region. It is fortunate that only a few minor bands are foreign. The other product of reactions (1) and (2), that is, the phenyl radical, is known to absorb in the region of 432—530 mμ.[17] However, the radical is so reactive that it may not exist as such in the irradiated solid but transform itself to other species transparent in the visible region. Even if the radical survives, it may have eluded our observation because the extinction coefficients of the radical may be extremely small as Porter and Ward implied.[17]

The appearance of the spectrum in Figs. 2 and 5 indicates clearly that the strongest peak is the 0–0 band. This is in accord with the theoretical prediction that the visible band is symmetry-allowed. All other peaks in Figs. 2 and 5 can be readily analyzed in terms of six and five fundamentals for

TABLE 3. VIBRATIONAI ANALYSIS FOR C_6H_7 IN C_6H_6

Wave number (cm^{-1})	Difference (cm^{-1})	Assignment
17904	—	0–0
18350	446	ν_1
18442	538	ν_2
18750	846	ν_3
18890	986	ν_4
19033	1129	ν_5
19331	1427	$\nu_1+\nu_4$
19386	1482	ν_6
19582	1678	$2\nu_3$
19753	1849	$\nu_3+\nu_4$
19886	1982	$\nu_3+\nu_5$ or $2\nu_4$
20018	2114	$\nu_4+\nu_5$
20170	2266	$2\nu_5$
20218	2314	$\nu_3+\nu_6$
20374	2470	$\nu_4+\nu_6$
20522	2618	$\nu_5+\nu_6$
20721	2817	$\nu_5+2\nu_3$
20858	2954	$2\nu_6$
21361	3457	$\nu_3+\nu_5+\nu_6$
21528	3624	foreign
21652	3748	$\nu_6+2\nu_5$
21868	3964	foreign
22003	4099	$\nu_5+2\nu_6$
22346	4442	$3\nu_6$
22636	4732	foreign
22823	4919	$\nu_3+\nu_5+2\nu_6$

The fundamentals above correspond to those of benzene as follows.

ν_1 C–C–C out-of-plane bending;
(e_{2u}) 404(cm^{-1}) Raman(forbidden)
ν_2 C–C–C in-plane bending
(e_{2g}) 605.6 Raman
ν_3 C–H out-of-plane bending;
(e_{1g}) 848.9 Raman
ν_4 C–C stretching;
(a_{1g}) 991.6 Raman
ν_5 C–H in-plane bending;
(e_{1u}) 1037 IR
ν_6 C–C stretching;
(e_{1u}) 1485 IR

TABLE 4. VIBRATIONAL ANALYSIS FOR C_6D_7 IN C_6D_6

Wave number (cm^{-1})	Difference (cm^{-1})	Assignment
18042	—	0–0
18433	391	ν_1
18605	563	ν_2
18891	849	ν_3
18979	937	ν_4
19284	1242	$\nu_1+\nu_3$
19467	1425	ν_5
19736	1694	$2\nu_3$
19855	1813	$\nu_1+\nu_5$
20032	1990	$\nu_2+\nu_5$
20310	2268	$\nu_3+\nu_5$
20396	2354	$\nu_4+\nu_5$
20593	2551	$3\nu_3$
20896	2854	$2\nu_5$
21164	3122	$\nu_5+2\nu_3$
21277	3235	foreign
21646	3604	$4\nu_3$
21739	3697	$\nu_3+2\nu_5$
21978	3936	foreign
22303	4261	$3\nu_5$
22576	4534	$2\nu_3+2\nu_5$
22857	4815	foreign
23164	5122	$\nu_3+3\nu_5$

The fundamentals above correspond to those of benzene as follows.

ν_1 C–C–C out-of plane bending;
(e_{2u}) 337(cm^{-1}) Raman(forbidden)
ν_2 C–C–C in-plane bending;
(e_{2g}) 576.7 Raman
ν_3 C–H in-plane bending;
(e_{1u}) 813 IR
ν_4 C–C stretching;
(a_{1g}) 944.7 Raman
ν_5 C–C stretching;
(e_{1u}) 1333 IR

16) F. S. Dainton and G. A. Salmon, *Proc. Roy. Soc., Ser. A*, **285**, 319 (1965).

17) G. Porter and B. Ward, *ibid.*, **287**, 457 (1965).

the light and the heavy radicals, respectively. Tables 3 and 4 list the assignment for the two radicals. The deduced fundamentals bear close resemblance to those of $^1A_{1g}$ benzene.[18] Because of the wavelength accuracy of the monochromator the reproducibility of the measured wave number is roughly $\pm 10\ cm^{-1}$ for the sharp peaks in solid benzene and $\pm 20\ cm^{-1}$ for the blunt peaks in alcohol solutions.

The 0–0 band of C_6H_7 in CH_3OH is blue-shifted by about 45 cm^{-1} compared with that of the same radical in C_6H_6 (Tables 3 and 5). Similarly C_6D_7 in CH_3OD and C_6D_6 has a difference of about 40 cm^{-1} (Tables 4 and 8). Since the inherent error of the wave number is about 10 cm^{-1}, this amount of difference is quite significant. The wave number difference $\Delta\tilde{\nu}$, however, is more or less similar in the methanol and the benzene matrices. This implies that both C_6H_7 and C_6D_7 are stabilized in their ground electronic state by the dielectric alcohol matrix but that the vibrational levels of the electronically excited radicals are little affected by the environment. Parallel experiments using ethanol instead of methanol show that the stabilization effect is roughly equal for both alcohols (Tables 5 through 8).

Table 5. Vibrational analysis for C_6H_7 in alcohols

Methanol		Ethanol		
Wave number (cm^{-1})	Difference (cm^{-1})	Wave number (cm^{-1})	Difference (cm^{-1})	Assignment
17950	—	17947	—	0–0
19073	1123	19065	1118	ν_5
19425	1475	19420	1473	ν_6
20530	2580	20528	2581	$\nu_5+\nu_6$
20914	2964	20916	2969	$2\nu_6$

Table 6. Vibrational analysis for C_6H_6D in alcohols

Methanol-d_1		Ethanol-d_1		
Wave number (cm^{-1})	Difference (cm^{-1})	Wave number (cm^{-1})	Difference (cm^{-1})	Assignment
17973	—	17968	—	0–0
19087	1124	19080	1112	ν_5
19444	1471	19439	1471	ν_6
20546	2573	20541	2573	$\nu_5+\nu_6$
20928	2955	20922	2954	$2\nu_6$

Table 7. Vibrational analysis for C_6D_6H in alcohols

Methanol		Ethanol		
Wave number (cm^{-1})	Difference (cm^{-1})	Wave number (cm^{-1})	Difference (cm^{-1})	Assignment
18055	—	18054	—	0–0
18918	863	18916	862	ν_3
19475	1420	19477	1423	ν_5
20333	2278	20332	2278	$\nu_3+\nu_5$
20906	2851	20901	2847	$2\nu_5$

Table 8. Vibrational analysis for C_6D_7 in alcohols

Methanol-d_1		Ethanol-d_1		
Wave number (cm^{-1})	Difference (cm^{-1})	Wave number (cm^{-1})	Difference (cm^{-1})	Assignment
18080	—	18071	—	0–0
18941	861	18929	858	ν_3
19512	1432	19493	1422	ν_5
20361	2281	20343	2272	$\nu_3+\nu_5$
20924	2844	20919	2848	$2\nu_5$

The difference in 0–0 band of C_6H_7 in C_6H_6 and C_6D_7 in C_6D_6 amounts to 138 cm^{-1}. Likewise C_6H_7 in CH_3OH and C_6D_7 in CH_3OD has a difference of 130 cm^{-1} (Tables 5 and 8). Similar isotopic shift of about 190 cm^{-1} is observed for another 0–0 band at 3.9 eV as shown in Fig. 1. The shifts between the light and the heavy radicals are attributed to the smaller zero point energies of the heavy radical in the two electronic states concerned.

According to the mechanism of reactions (3)—(5) it is possible to produce two other isotopically different cyclohexadienyl radicals; light benzene in methanol-d_1 and heavy benzene in the normal methanol will yield C_6H_6D and C_6D_6H respectively. Leone and Koski[4] have shown by ESR that both are actually produced, although they did not clarify the reaction mechanism of radical formation.[4,5] We found that both C_6H_6D and C_6D_6H give rise to very similar spectra to those of C_6H_7 and C_6D_7, respectively. Barely significant differences (in the 0–0 band between C_6H_7 and C_6H_6D (Tables 5 and 6), and between C_6D_6H and C_6D_7 (Tables 7 and 8) are again atrributed to the slight difference in the mass of the radicals.

The authors wish to thank Dr. N. Itoh of Nagoya University for informing them of the experimental results on the hydronaphthyl radical prior to publication. They are also indebted to Dr. S. Iwata and Mr. H. Katsumata for writing the computer program and to Dr. M. Imamura for his helpful discussion.

18) G. Herzberg, "Infrared and Raman Spectra of Polyatomic Molecules," D. Van Nostrand Co., Inc., N. Y. (1949).

BULLETIN OF THE CHEMICAL SOCIETY OF JAPAN VOL. 43 652—657 (1970)

Optical and ESR Studies on Triphenylimidazolyl Radicals Produced by Photolysis and Radiolysis at Low Temperature*1

Tadamasa SHIDA,* Koko MAEDA** and Taro HAYASHI

* *The Institute of Physical and Chemical Research Yamato-machi, Kitaadachi-gun, Saitama*

** *Department of Chemistry, Faculty of Science, Ochanomizu University, Bunkyo-ku, Tokyo*

(Received July 29, 1969)

The characteristic temperature-dependent behavior exhibited by the solution of the photochromic dimer of triphenylimidazolyl (photo-dimer) has been reinvestigated by means of optical and ESR spectroscopy. Assuming two conformations for triphenylimidazolyl radical, the spectral change at low temperatures has been elucidated in terms of a conformational isomerization of the radical and dimerization of the radical to a colorless dimer. Photo-dimer in γ-irradiated glassy solutions undergoes a dissociative electron attachment to produce triphenylimidazolyl radical and its anion.

UV-illumination of the photochromic dimer of triphenylimidazolyl in benzene at room temperature produced triphenylimidazolyl radical which was characterized by the absorption spectrum having absorption maxima of 347 and 554 mμ.[1] Upon lowering the temperature of the solution under illumination the intensity of the absorption band diminished gradually, and at sbout -20——150°C the absorption in the visible region disappeared. The phenomenon first studied by Hayashi and Maeda[2] was later interpreted by White and Sonnenberg on the basis of a thermochemical equilibrium between the radical and the colorless piezochromic dimer.[3],*2 It was found that illumination at still lower temperatures gave a color slightly different from that observed at higher temperatures.[4] We attributed the absorption observed at -196°C to the radical cation of photo-dimer produced by photoionization.[4] Later work revealed, however, that the absorption should be associated with triphenylimidazolyl radical produced by the same mechanism as that in solutions at room temperature.[5] Assuming two conformations for the radical, one stable at higher temperatures ($>$*ca.* -20°C), the other at lower temperatures ($<$*ca.* -150°C), we are able to explain the temperature dependence of photochemical reactions of the lophine system.

Experimental

Photo-dimer was dissolved in deaerated solvents in a dimmed room. Methyltetrahydrofuran (MTHF) was mainly used as a solvent, because it forms a clear glass at -196°C. For the optical measurement the solution was transferred in a vacuum to a thin quartz absorption cell. The absorption spectrum of the solution was measured at -196°C in a quartz Dewar with quartz windows using a Cary 14 RI spectrophotometer. Polymer films containing photo-dimer was prepared by dissolving the dimer in polystyrene-benzene gel and solidifying it by evaporation of benzene in nitrogen stream. A 500 W high-pressure mercury lamp in combination with a glass filter passing light of 240 mμ $<\lambda<$ 400 mμ and a 12000 Ci Co 60 γ-ray source were for photolysis and radiolysis. ESR spectra were recorded on a JEOL 3B spectrometer with a 100 kc modulation.

Results and Discussion

Photolysis. When a colorless solution of photo-dimer in MTHF glass at -196°C was exposed to UV light, the glass colored immediately to reddish-

*1 Presented at the Symposium on Photochemistry of the Chemical Society of Japan (T. Shida, K. Maeda and T. Hayashi, Oct., 1968, Sendai).

1) T. Hayashi, K. Maeda and M. Morinaga, This Bulletin, **37**, 1563 (1964).

2) T. Hayashi and K. Maeda, *ibid.*, **36**, 1052 (1963).

3) D. M. White and J. Sonnenberg, *J. Amer. Chem. Soc.*, **88**, 3825 (1966).

*2 The dimer of triphenylimidazolyl, called lophine dimer, has two isomeric forms, one of which is photochromic and is assumed to have structure I. The other is piezochromic presumably having structure II.[3]

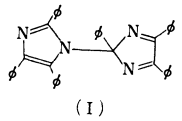

(I)

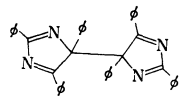

(II)

The two isomers will be designated photo- and piezo-dimers, respectively.

4) T. Hayashi and K. Maeda, This Bulletin, **40**, 2990 (1967).

5) T. Hayashi and K. Maeda, *Nippon Kagaku Zasshi*, **90**, 325 (1969).

purple. The absorption spectrum shown in curve 1 of Fig. 1 was almost the same as that of tri-

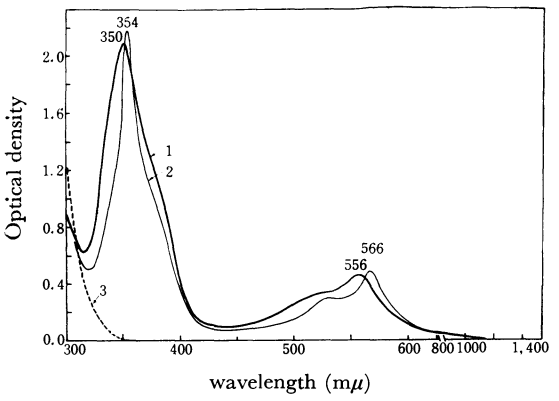

Fig. 1. Absorption spectra of photo-dimer in MTHF UV-illuminated at −196°C. Curve 1: immediately after illumination (R bands). Curve 2: the preceding solution after limited warming (S bands). Curve 3: before illumination. Concentration $=6.7\times10^{-4}$M. Cell thickensss = 0.5 mm.

phenylimidazolyl radical in solutions at room temperature (*e.g.*, the absorption maximum of the visible band at −196° was 556 mμ which corresponded to 552 mμ at room temperature). Apparently photo-dimer dissociates also in the rigid matrix at −196°C. Reaction (1) formulates the process with R· standing for triphenylimidazolyl radical.

$$R_2 \xrightarrow{h\nu} 2R\cdot \qquad (1)$$

In the rigid glass the bulky radicals must be confined in a cage. Strong evidence for the formation

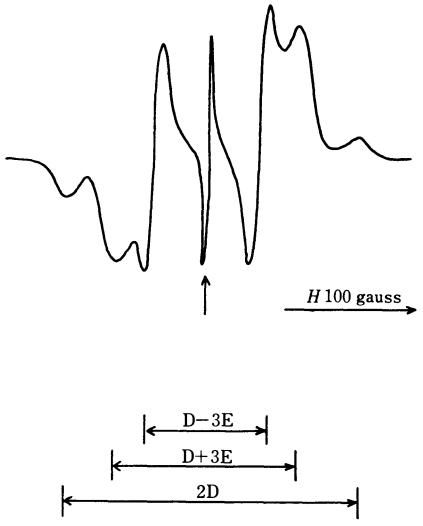

Fig. 2. ESR spectrum of photo-dimer in MTHF UV-illuminated at −196°C.

of radical pair is a broad ESR spectrum shown in Fig. 2. Since the monomeric triphenylimidazolyl radical in solutions at room temperature gives a singlet ESR spectrum of a line width of $\Delta H_{msl}=9.1$ gauss,[6] the spectrum of the width of about 200 gauss must be attributed to the fine structure of the two-spin system. The three pairs of bands connected by leading lines in Fig. 2 were also observed for solutions in several other solvents. The intensity of the central singlet (arrowed) varied with the solvent, illumination time and wavelengths of the exciting light, and was more easily saturated with the microwave power. Following Kommandeur's discussion on the photolyzed tetraphenylhydrazine[7] we identified the outermost pair of a small intensity with the separation of $2D$ and the inner two sets with $D\pm3E$. In view of complexity of the molecules we used a simple relation, $D=3g\beta r^{-3}/2$ to estimate the approximate distance between the two radicals.[8] From the observed $D=112.6$ gauss we obtain $r=6.3$ Å. As in the case of an EPA solution[4] a weak half-field absorption was detected also for the MTHF solution which confirms the triplet state of the two-spin system. The central singlet in Fig. 2, on the other hand, may be due to unknown species produced as byproducts of photolysis.

When the solution photolyzed at −196°C was taken out of the liquid nitrogen, the color of the sample faded with the rise of temperature. Before the rapid fading started, a very subtle color change from reddish-purple to purple took place. The purple solution, quickly dipped again in liquid nitrogen to quench the fading, exhibited the absorption spectrum shown in curve 2 of Fig. 1 which differs from the spectrum in curve 1: (1) the absorption maxima shifted towards red, (2) the bands became narrower with the increase of absorbance at λ_{max}, (3) the band structure manifested slightly. Hereafter we will denote the spectra before and after the heat treatment by R and S bands, respectively. A change from R to S bands was also observed invariably in other glass-forming solvents such as 3-methylpentane, decalin-cyclohexane 3 : 1 mixture, isobutyl chloride. In all cases tested only R and S bands appeared and no intermediate spectrum was observed as long as the temperature was controlled to ensure the color change from reddish-purple to purple. In alcoholic glasses such as EPA and ethanol the absorption maxima of both R and S bands shifted further to red probably because of the general dielectric solvent effect (*e.g.*, the absorption maximum of S bands in EPA was

6) T. Hayashi, K. Maeda and M. Takeuchi, This Bulletin, **37**, 1717 (1964).

7) D. A. Wiersma and J. Kommandeur, *Mol. Phys.*, **13**, 241 (1967).

8) H. van Willigen and S. I. Weissman, *ibid.*, **11**, 175 (1966).

575 mμ compared with 566 mμ of the corresponding band in MTHF).

Since a simple heat treatment transforms the radical R· at −196°C to a species giving rise to the S bands which resemble the R bands in general appearance, we presume that the species responsible for the S bands is a similar radical to R· with the conformation slightly modified, and will designate the species S· radical. The features of S bands enumerated above in relation to the R bands may be associated with the enhancement of planarity in the radical; as the radical becomes more planar, the extent of conjugation would increase to result in a red shift of the absorption band. The variance in the twist angle between the planes of phenyl groups and of imidazole ring would produce a number of potential energy curves for both the ground and the excited electronic states of the radical, and the electronic absorption band would be broadened on account of the Franck-Condon principle.[9] Thus the observed sharpening of the absorption band may be an indication of the enhancement of planarity.

The phenyl groups in the crowded photo-dimer must be twisted considerably from the plane of imidazole ring. The phenyl groups in a monomeric R· radical at room temperature are also considered to be twisted by analogy with orthoterphenyl and hexaphenylbenzene.[10] The rotatory displacement of the phenyl group, however, must have been attained at the sacrifice of conjugation, and at low temperatures a planar conformation might be favored. On the basis of this inference we account for the R· to S· transition in the following way; the radical produced by reaction (1) in a rigid cage is forced to retain the same conformation of twisted phenyl groups as in photo-dimer. However, as soon as the original cage is relaxed by softening the matrix, the radical assumes a more or less planar conformation presumed to be stable at −196°C.

Upon warming the solution the S bands disappeared at about −100——150°C. This can be explained by dimerization of S· radicals to a colorless dimer S_2. When the temperature was further raised to room temperature, the solution regained a reddish-purple color attributable to the regeneration of R· radical.

The R bands also appeared when the MTHF solution containing photo-dimer was illuminated first at room temperature. Upon lowering the temperature, however, the bands diminished and disappeared at temperatures below about −20°C. This phenomenon is essentially the same as reported before for benzene and EPA solutions.[5,11] For the latter systems White *et al.* constructed an energy diagram reproduced in the solid curve of Fig. 3.[3]

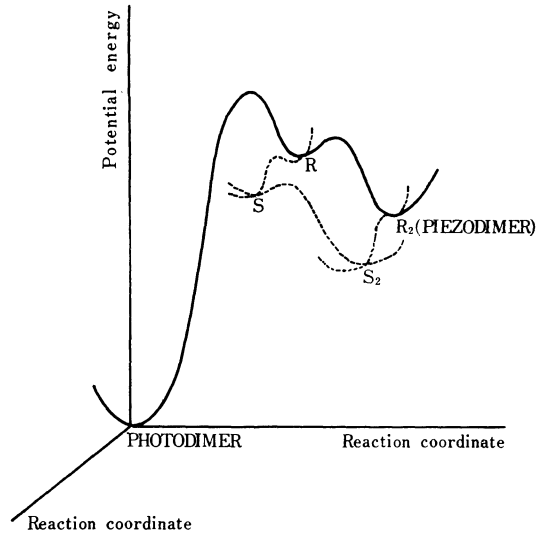

Fig. 3. Possible potential surface of the system of triphenylimidazolyl radicals and dimers.

To incorporate the newly proposed S· and S_2 we modify the diagram as shown in Fig. 3 and account for the processes throughout the whole temperatures; photo-dimer in the matrix at −196°C is "pumped up" by photons to dissociate into R· radicals in a cage. By raising the temperature slightly above −196°C radical R· overcomes a small barrier to become radical S· which successively dimerizes to piezo-dimer R_2 *via* S_2. Dimer S_2 assumed here may be less substantive than S·, because dimerization of S· radicals could lead directly to piezo-dimer, in which case the paths of S· to S_2 and S_2 to R_2 should be replaced by a single path of S· to R_2. Since piezo-dimer is thermochemically unstable in relation to photo-dimer, the former eventually isomerizes to the latter through the thermal dissociation to R· radicals.[3]

The polymer film illuminated at room temperature also exhibited the R bands. In contrast with the MTHF solution the color of the polymer did not fade on cooling, and the bands measured at −196°C showed a spectral change indicative of the transition from R to S. The change is not due to a mere temperature shift of the R bands, because the polymer film illuminated at −196°C produced the same R bands as those obtained by the illumination at room temperature. These results of film samples are also consistent with the diagram of Fig. 3; R· radical produced in the film at room temperature may be prevented from dimerization in the rigid polymer network, and on lowering the temperature the radical may undergo the isomerization to S· radical without the intervention of the formation of piezo-dimer.

9) H. Suzuki, "Electronic Absorption Spectra and Geometry of Organic Molecules," Academic Press, N. Y. (1967).
10) Ref. 9, p. 292.
11) K. Maeda and T. Hayashi, to be published.

Radiolysis. When γ-irradiated at -196°C, pure MTHF glass yields an absorption band in the near IR region ($\lambda_{max} \cong 1.2\ \mu$) which is known as due to the electron trapped by the matrix and is designated $(e^-)_t$.[12] In the presence of photo-dimer (0.67 mM) the $(e^-)_t$ band was suppressed to about 70% and new absorption bands identifiable with the R bands appeared (curve 1 of Fig. 4). The

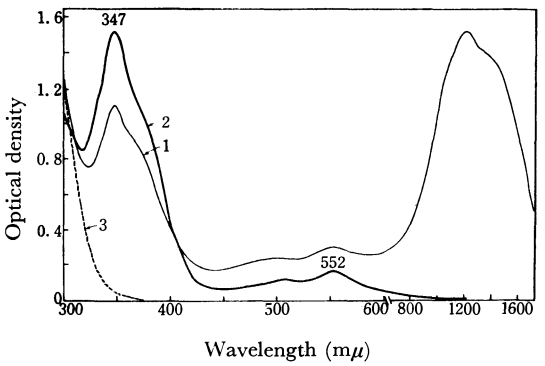

Fig. 4. Absorption spectra of photo-dimer in MTHF γ-irradiated at -196°C. Curve 1: immediately after irradiation. The absorption at λ—600 mμ is due to the trapped electron. Curve 2: the preceding solution after optical bleaching with light of λ—620 mμ. Curve 3: before irradiation.
Concentration $= 6.7 \times 10^{-4}$ M. Cell thickness = 0.5 mm. Dose $= 6.3 \times 10^{19}$ eV/g.

remaining $(e^-)_t$ band was easily photobleached with light of λ—620 mμ. The bleaching enhanced the R bands as shown in curve 2 of Fig. 4. The decrease of the $(e^-)_t$ band with the concomitant enhancement of R bands indicates that the formation of R· radical in the radiolysis is related with electron and not with photon as in the photolysis.

In a study of tetraphenylhydrazine in MTHF we have found that UV-illumination induces the homolysis,

$$(C_6H_5)_2NH(C_6H_5)_2 \xrightarrow{h\nu} 2(C_6H_5)_2N\cdot \qquad (2)$$

while γ-irradiation leads to the heterolytic dissociation,[13]

$$(C_6H_5)_2NN(C_6H_5)_2 + e^- \longrightarrow (C_6H_5)_2N\cdot + (C_6H_5)_2N^- \qquad (3)$$

By analogy with reaction (3) we may assume that the γ-irradiated photo-dimer induces the following reaction.

$$R_2(\text{photo-dimer}) + e^- \longrightarrow R\cdot + R^- \qquad (4)$$

A criterion for this type of reaction is the exothermicity of the reaction; if the electron affinity of the radical exceeds the dissociation energy of the central bond of the dimer, reaction (4) is possible.[14] Although the electron affinity of triphenylimidazolyl radical is not known, reaction (4) may be exothermic owing to the extremely small dissociation energy of photo-dimer($\sim$1 eV[1,5]). If the excess energy is utilized to excite R· or R^- to a luminescent state, reaction (4) should accompany the emission of light which was, in fact, observed; when γ-irradiated solutions corresponding to curve 1 of Fig. 4 was thawed in the dark, a bright yellow light was emitted. However, if, prior to thawing, the $(e^-)_t$ band was photobleached (see curve 2 of Fig. 4), the solution did not luminesce on thawing. Thus electrons released from the trap by thawing seem to produce excited R· or R^-.

Addition of 10 vol% of carbon tetrachloride to the solution of photo-dimer in MTHF prevented the formation of R· radical in the radiolysis, whereas in the photolysis the chloride caused no effect on the production of R· radicals. This can

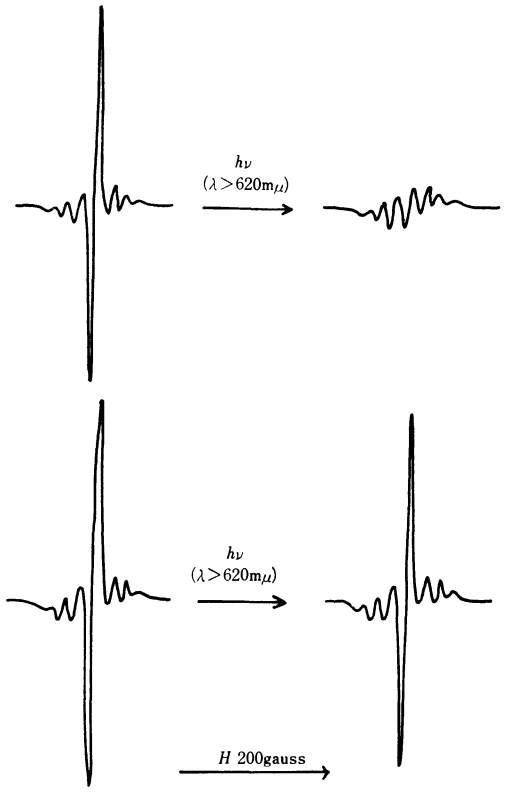

Fig. 5. ESR spectra of pure MTHF and photo-dimer in MTHF both γ-irradiated at -196°C. Upper: pure MTHF. The singlet is due to the trapped electron. Lower: photo-dimer in MTHF. Concentration = 5 mM. Dose $= 6.3 \times 10^{19}$ eV/g for both.

12) F. S. Dainton and G. A. Salmon, *Proc. Roy. Soc., Part A*, **285** 319 (1965).
13) T. Shida and A. Kira, *J. Phys. Chem.*, **73**, 000 (1969).
14) J. B. Gallivan and W. H. Hamill, *Trans. Faraday Soc.*, **61**, 1960 (1965).

be accounted for by the competition for electron between photo-dimer and the chloride which is known to react with electron as follows.[15]

$$CCl_4 + e^- \longrightarrow \cdot CCl_3 + Cl^- \qquad (5)$$

ESR measurements also support reaction (4): Fig. 5 shows the ESR spectra of γ-irradiated pure MTHF and a solution of photo-dimer (5 mM) in MTHF. The singlet in pure MTHF having $\Delta H_{msl}=4.6$ gauss disappears on photobleaching and is attributed to the $(e^-)_t$.[12] The spectrum remaining after the bleaching is due to the MTHF radical.[12] On the other hand, the singlet in the photo-dimer solution, though similar to the $(e^-)_t$ singlet, has a width of $\Delta H_{msl}=8.1$ gauss and did not disappear on the same optical bleaching. It was more resistive against the microwave power saturation than the $(e^-)_t$ singlet. Contrary to the photolysis, the spectrum of the radiolyzed photo-dimer solution showed no sign of radical pairs. These results indicate that the singlet of photo-dimer solution is due to the singlet R· radical produced by reaction (4). The line width of the singlet, $\Delta H_{msl}=$ 8.1 gauss, is comparable with that of the R· radical in solutions at room temperature.[6]

Closer examination of the absorption spectra of photolyzed (curve 1, Fig. 1) and radiolyzed (curve 2, Fig. 4) rigid solutions reveals that the absorption maxima of R bands in the γ-irradiated solution are slightly blue-shifted, compared with the photolyzed solution (347 and 552 mμ for the former and 350 and 556 mμ for the latter). Although the shift is admittedly small, it was reproducible. This shift may reflect the weak interaction between the paired radicals in the photolyzed solution as manifested by the ESR fine structure. The R bands of the radiolyzed solution at -196°C coincide with those of the R· radical in MTHF at room temperature ($\lambda_{max}=552$ mμ). This coincidence may be attributed to the fact that in both media R· radicals are not paired as in the photolyzed rigid solution.

The R bands of the radiolyzed solution also changed to S bands with the heat treatment (Fig. 6). Since the change occurring in the softened matrix was transient, the signal of S bands was liable to disappear by the successive dimerization. However, the disappearance was less rapid in the radiolyzed solution than in the photolyzed and the spectral change is seen more distinctly in Fig. 6 than in Fig. 1 (curve 2). This may be because in the photolyzed solution the radical pairs are ready to recombine geminately whereas in the radiolyzed solution the R· radical from reaction (4) has more chances for the isomerization to S·. Contrary to the R bands which show a slight shift between the radiolyzed and photolyzed rigid solutions, the

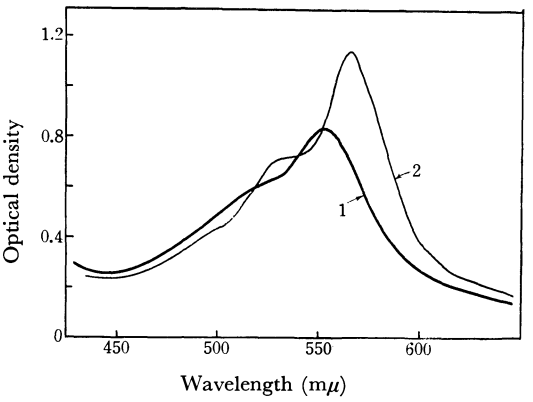

Fig. 6. Absorption spectra of photo-dimer in MTHF γ-irradiated at -196°C. Curve 1: corresponding to curve 2 of Fig. 4. Concentration=5 mM. Cell thickness=1.5 mm. Dose=3.1×10^{19} eV/g. Curve 2: the preceding solution after limited warming.

S bands derived from both photolysis and radiolysis were identical with $\lambda_{max}=566$ mμ. This indicates that the R· radicals in a cage in photolyzed solutions separate from each other upon softening the matrix and the resulting S· radicals are no longer paired to exhibit any spectral shift due to the pairing.

The absorption at 300—400 mμ of the R· radical in the radiolyzed solution (curve 2, Fig. 4) is disproportionately high compared with the spectrum of the photolyzed solution (curve 1, Fig. 1). Since the lophine anion, R^-, produced by reaction (4) is known to have $\lambda_{max}=326$ mμ with $\varepsilon_{326}=2.48\times$

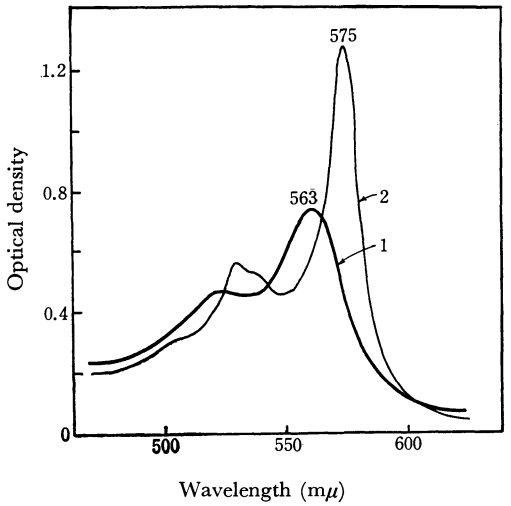

Fig. 7. Absorption spectra of photo-dimer of 2,3,4,5-tetraphenylpyrryl in MTHF UV-illuminated at -196°C. Curve 1: immediately after illumination. Curve 2: the same solution after limited warming. Concentration=1 mM. Cell thickness=1.5 mm.

15) T. Shida and W. H. Hamill, *J. Chem. Phys.*, **44**, 2369 (1966).

10^4,[5] the anion should contribute to the absorption in the near UV region. This contribution can be subtracted by using the known molar extinction coefficients of R bands at 552 mμ (8.4×10^3) and 347 mμ (4.8×10^4).[5] Even after the subtraction, however, the absorption at 300—400 mμ is still high compared with the spectrum of the photolyzed solution. The reason for this discrepancy is not clear at present.

Additional Remark

As in the case of triphenylimidazole, 2,3,4,5-tetraphenylpyrrole produces two isomeric dimers on oxidation, one photochromic and the other piezochromic.[5,16] We have carried out parallel studies on these dimers also and obtained quite analogous results. One example is shown in Fig. 7 where the spectrum in curve 1 was observed immediately after UV-illumination at -196°C, and that in curve 2 was obtained after the limited warming. The two spectra are regarded as corresponding to the R and S bands in the case of lophine dimer.

The authors wish to thank Dr. Masashi Imamura and Dr. Hiroshi Midorikawa of The Institute of Physical and Chemical Research for their helpful discussion.

16) K. Maeda, A. Chinone and T. Hayashi, to be published.

BULLETIN OF THE CHEMICAL SOCIETY OF JAPAN VOL. 43 657—662 (1970)

ESR Spectra of γ-irradiated Linear Aliphatic Polyesters*1

Yasuo NOZAWA

Department of Chemistry, Faculty of Science, Science University of Tokyo, Kagurazaka, Shinjuku-ku, Tokyo

(Received July 28, 1969)

The ESR spectra of γ-irradiated linear aliphatic polyesters (2.2, 2.4, 2.6, 2.7, 2.8 and 6.8 polymer) have been measured at various temperatures ranging from 77°K to room temperature. Two types of spectra are obtained in these polyesters except for 2.2 polymer. The first, the six-line spectrum obtained at low temperatures was relatively short-lived and increased in signal intensity with increasing methylene groups of these polyesters. The well-resolved, second, five-line spectrum is stable even at room temperature in comparison with the former. The possible structures of two radicals were discussed.

Recently a number of ESR studies on the radical produced by γ-irradiation of low molecular weight organic and polymeric substances have been carried out. Correlations between the radical species and chemical structures of various polymers have been extensively found.[1-7] Configurations of the free radical in irradiated polyethlene and polypropylene in particular were discussed with respect to the relation of the radical decay reaction to a molecular motion in the matrices.[8,9]

In the linear aliphatic polyesters, however, no studies on the radical species produced by γ-irradiation or the behaviour of radical decay have been reported except for an anisotropic study on irradiated poly(β-propiolactone).[10] From the data obtained by the observation of ESR spectra of irradiated polyesters, the species and the site of the radical are discussed.

The crystal structures of the polyesters have been

*1 Presented at the 17th Annual Meeting of the Society of Polymer Science, Tokyo, Japan, May, 1968.

1) a) E. J. Lawton, J. S. Balmit and R. S. Powell, *J. Chem. Phys.*, **33**, 396, 405 (1960). b) S. Ohnishi, This Bulltin, **35**, 254 (1962).

2) M. Kashiwagi, *J. Polym. Sci.*, **A-1**, 189 (1963).

3) H. Fisher and K. H. Hellwege, *J. Polym. Sci.*, **56**, 33 (1962).

4) S. Ogawa, *J. Phys. Soc. Jap.*, **16**, 1488 (1960).

5) D. J. Ingram and M. G. Townsend, *Trans. Faraday Soc.*, **54**, 409 (1958).

6) H. N. Rexroad and W. Gordy, *J. Chem. Phys.*, **39**, 399 (1959).

7) F. C. Thryion and M. D. Baijal, *J. Polym. Sci.*, **6**, 505 (1968).

8) S. Nara, S. Shimada, H. Kashiwabara and J. Sohma, *J. Polym. Sci.*, **6**, A-2, 1435 (1968).

9) S. Nara, H. Kashiwabara and J. Sohma, *ibid.*, **5**, A-2, 929 (1967).

10) S. Ohnishi, S. Sugimoto, K. Hayashi and I. Nitta, This Bulletin, **37**, 524 (1964).

extensively studied by many investigators.[11-14] From the results, it is apparent that the crystal structure is similar to that of polyethylene and the molecular chain conformations are planar zigzag except for poly(ethylene adipate) and the glycol parts of the polyesters with ethlene glycols. The chemical structure of the polyesters studied is expressed as $-\left[(CH_2)_n-O-\overset{\overset{O}{\|}}{C}-(CH_2)_m-\overset{\overset{O}{\|}}{C}-O\right]-$, and the polyesters are denoted as *n.m* polymer hereafter. In the present paper the results deduced from ESR spectra of 2.2, 2.4, 2.6, 2.7, 2.8 and 6.8 polymer are mainly discussed.

Experimental

Samples (the 2.2, 2.4, 2.6, 2.7, 2.8 and 6.8 polymer) were prepared by polycondensation between the corresponding diol and dibasic acid using the $ZnCl_2$ as a catalyst. To obtain high molecular weight polymers, the later stage of the reaction was carried out in a vacuum keeping the pressure below 1 mmHg and bubbling argon gas through the reacting mass. The polyesters prepared as above were purified by repeated precipitation from benzene solution with methylalcohol and dried in a high vacuum at room temperature.

The samples used for ESR measurements were prepared in a 5 mmϕ glass tube with dried nitrogen atmosphere, and subjected to irradiation at 77°K. Irradiation dose was about 4 Mrad.

The ESR spectrometer used in the present study was a JES-3BSX type apparatus (Japan Electron Optics Laboratory Co., Ltd.) with 100 kHz field modulation and TE_{011} mode cavity. The ESR measurements were carried out at different temperatures from liquid nitrogen to room temperature using variable attachments for the spectrometer.

The drawn samples of 6.8 polymer were also prepared from the film obtained by means of hot pressing at melting point. Drawing was carried out at room temperature, up to 500% in draw ratio. The ESR spectra were measured on various orientations of the specimen in the applied magnetic field.

Results and Discussion

The ESR spectra of the irradiated 2.4 polymer measured at various temperatures are shown in Fig. 1. At low temperature, a single line spectrum is overlapped on a weak six-line spectrum. By raising the temperature, the signal intensity decreases gradually and the spectrum begins to split at around −140°C. At room temperature, it splits into a five-line spectrum with a hyperfine (hf) constant of about 25 gauss.

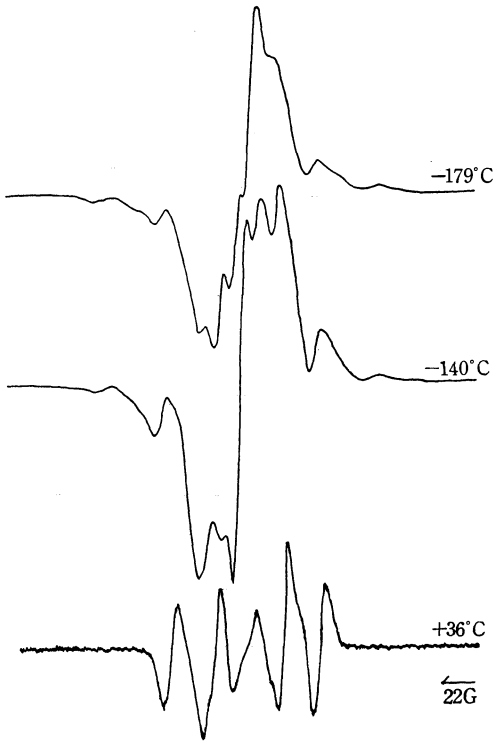

Fig. 1. The ESR spectra of γ-irradiated 2.4 polymer.

As possible species of the radical produced in these polyesters, three kinds of species are expected which are produced by abstraction of hydrogen atom from the acid or the glycol part of the main chain.*2 The three types are those which could be produced by extracting α-hydrogen from the acid

(A) $-\left[(CH_2)_n-O-\overset{\overset{O}{\|}}{C}-\dot{C}H-(CH_2)_{m-1}-\overset{\overset{O}{\|}}{C}-O\right]-$

(B) $-\left[(CH_2)_{n-1}-\dot{C}H-O-\overset{\overset{O}{\|}}{C}-(CH_2)_m-\overset{\overset{O}{\|}}{C}-O\right]-$

(C) $-\left[CH_2-\dot{C}H(CH_2)_{n-2}-O-\overset{\overset{O}{\|}}{C}-(CH_2)_m-\overset{\overset{O}{\|}}{C}-O\right]-$ or

$-\left[(CH_2)_n-O-\overset{\overset{O}{\|}}{C}-CH_2-\dot{C}H(CH_2)_{m-2}-\overset{\overset{O}{\|}}{C}-O\right]-$

11) C. S. Fuller and C. J. Frosh, *J. Phys. Chem.*, **43**, 323 (1939), C. S. Fuller and C. L. Erickson, *J. Amer. Chem. Soc.*, **59**, 344 (1937).

12) A. Turner-Jones and C. W. Bunn, *Acta Crystallogr.*, **15**, 109 (1962).

13) Y. Chatani, A. Ueda and H. Tadokoro, Preprint of the 16th Symposium on Makromolecular Chemistry held by the Polymer Chemistry of Japan (Fukuoka, Oct., 1967) p. 41.

14) K. Tanaka, T. Kanamoto and H. Nagai, Preprint of International Symposium on Makromolecular Chemistry, VII-147, Kyoto (1966).

*2 At the first stage of the analysis we examined the possibility of radical production by chain scission, but the possibility was excluded on the basis of ESR spectra.

part (A), α-hydrogen from glycol part (B) and the other hydrogen from both the acid or glycol parts (C).

Type C is expected to give the same spectrum as that of the alkyl radical which has often been observed in irradiated polyethylene at low temperatures. From the experimental results, the weak six-line spectrum detected at low temperature might be assigned to type C radical, because the hf constant of the signal is about 33 gauss which equals that of polyethylene.

The spectral changes caused by the rise of temperature in the irradiated 2.6, 2.7 and 2.8 polymer are shown in Fig. 2. This behavior is similar to that of 2.4 polymer. At low temperature the weak six-line spectrum with the hf constant of 33 gauss is also observed more strongly than in that of 2.4 polymer. At room temperature the same type of five-line spectrum as detected in 2.4 polymer is also observed in each polymer. The spectrum may be attributed to either type A or type B radical.

The crystal structures of the linear aliphatic polyesters have been extensively studied by Fuller and Frosh,[11] Turner-Johns and Bunn,[12] Chatani *et al.*,[13] and Kanamoto.[14] According to their

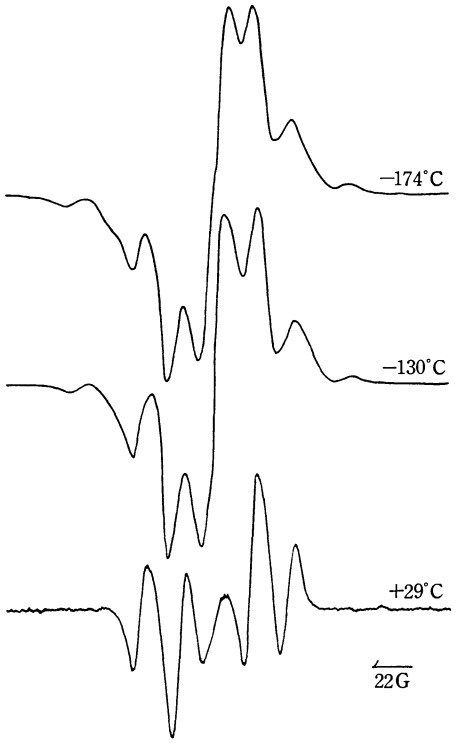

Fig. 2-b. The ESR spectra of γ-irradiated 2.7 polymer.

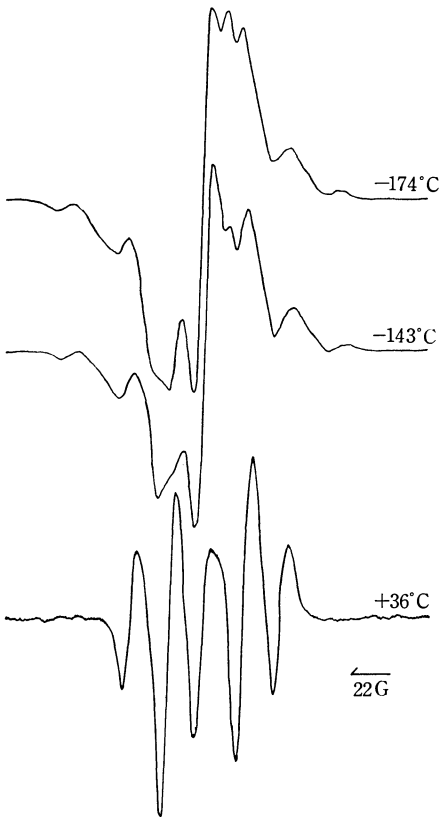

Fig. 2-a. The ESR spectra of γ-irradiated 2.6 polymer.

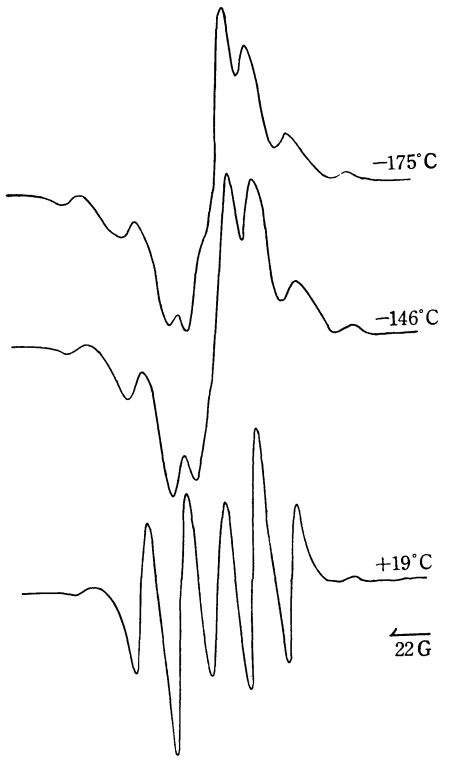

Fig. 2-c. The ESR spectra of γ-irradiated 2.8 (c), polymer.

studies, the crystal structure of these polyesters are very similar to each other and a molecular packing in planes perpendicular to the chain axis is very similar to that of polyethylene. From these results, the chain conformation of the polyesters is found to be nearly planar zigzag except for 2.2 polymer which has helical chain conformations, and for 2.4, 2.6, 2.7 and 2.8 polymers which are slightly distorted around the chain axis in glycol parts. The 6.8 polymer has a substantially planar zigzag chain conformation throughout the chain.

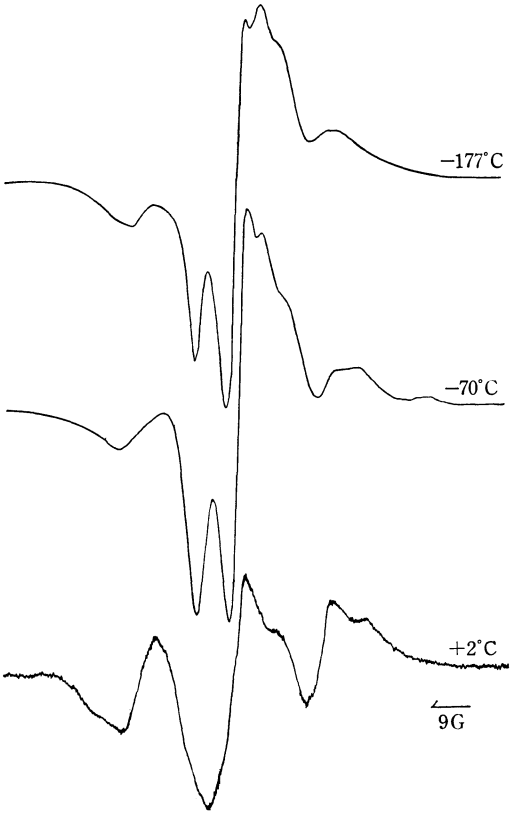

Fig. 3. The ESR spectra of γ-irradiated 2.2 polymer.

In order to obtain further information, the same experiment was performed on 2.2 polymer. As shown in Fig. 3, the spectrum at low temperature is complicated, and is not well resolved even at room temperature. On the other hand, the same type of spectrum has been observed on both irradiated poly(ethylene terephthalate)[15] and powdered succinic acid,[16] and the spectrum has been interpreted as the result of the interaction between an odd electron and three nonequivalent hydrogen atoms (*i.e.*, α and two β-hydrogen atoms). The nonequivalency of these hydrogen atoms in the hf interaction may be caused by distrotions of the methylene groups from the planar zigzag conformation. Considering the chemical structure of 2.2 polymer, the radical produced by irradiations is probably situated on α-carbons of diacid or diol parts. According to the crystal structure of the polymer,[13] methylene groups in both parts are distorted from the planar zigzag chain conformation. From the distortion in the methylene group we can see the coincidence of the ESR spectrum of the 2.2 polymer with that of poly(ethylene terephthalate). In 2.4, 2.6, 2.7 and 2.8 polymer, as mentioned above, it is known that the ethylene glycol part of the polymers have also a slight departure from the planar chain conformation. If type B radical was produced in the polymers, unresolved signals similar to that obtained in 2.2 polymer should be expected. However, only the five-line spectrum is observed in the polyesters. This suggests that the five-line spectrum observed at room temperature could be assigned to the type A radical on the acid parts having planar zigzag chain conformation.

The effect of temperature on the ESR spectra of the 6.8 polymer was studied by raising the tem-

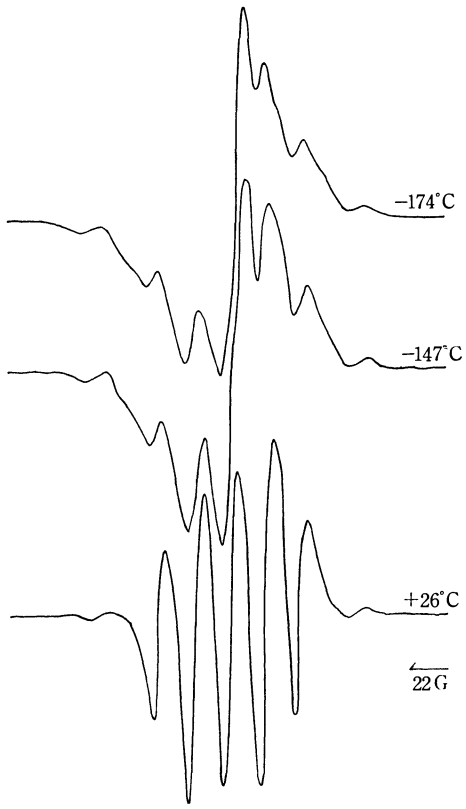

Fig. 4. The ESR spectra of γ-irradiated 6.8 polymer.

15) D. Campbell, K. Araki and D. T. Turner, *J. Polym. Sci.*, **A-4**, 2597 (1966).

16) C. Heller and H. M. McConnell, *J. Chem. Phys.*, **32**, No. 5, 1535 (1960).

perature (Fig. 4). At low temperature the six-line spectrum is larger than that of the 2.4, 2.6, 2.7 and 2.8 polymers, and decreases with rising temperature. At room temperature the five-line spectrum was also observed with a trace of type C, and the spectral pattern and the hf splitting are very similar to those of polymers described above.

The chain conformation of the polymer, as reported by Kanamoto,[14] is planar zigzag in both dibasic acid and the diol parts. If type B radical was produced in the polymer, the spectral pattern and the hf constant of the signal might be different from that of the five-line spectrum. However, the spectrum is in good agreement with that of the polyester with ethylene glycol. This indicates that type A radical is more probable than type B because of the resonance stabilization

As shown in Fig. 5, the integrated intensity ratio of the five-line spectrum is nearly 1 : 2 : 2 : 2 : 1. The intensity distribution is interpreted as the result of the interaction between an odd electron and one α-hydrogen and two equivalent β-hydrogen atoms. To obtain the anisotropic behaviour of α-hydrogen, experiments are carried out in drawn 6.8 polymer. The spectra were measured in orientation axes parallel and perpendicular to the external magnetic field. The radicals trapped in the specimen quickly disappear by the reaction with oxygen, since experiments are carried out in air without sealing the sample tube. The spectra obtained at −80°C are shown in Fig. 6-a, where type C radical remains.

Salovy and Yager[17] have reported the anisotropy in the ESR spectrum of oriented mats of solution-grown polyethylene single crystal.

In the present case, the signal intensity of type C radical will be similar to the alkyl radicals of the polyethylene studied by Salovy and Yager.

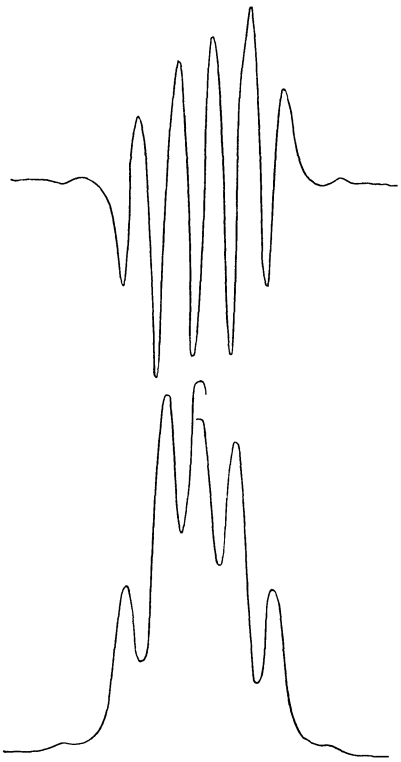

Fig. 5. The ESR spectrum of γ-irradiated 6.8 polymer at 26°C: (top) observed first derivative curve; (bottom) its integrated absorption curve.

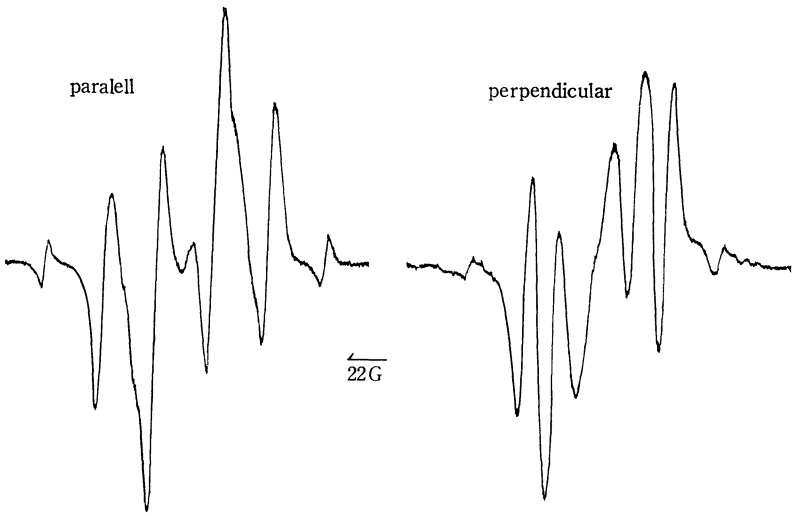

Fig. 6-a. The ESR spectra of γ-irradiated 6.8 polymer measured at −80°C. Magnetic field parallel (left) and perpendicular (right) to chain.

17) R. Salovy and W. A. Yager, *J. Polym. Sci.*, **A-2**, 219 (1964).

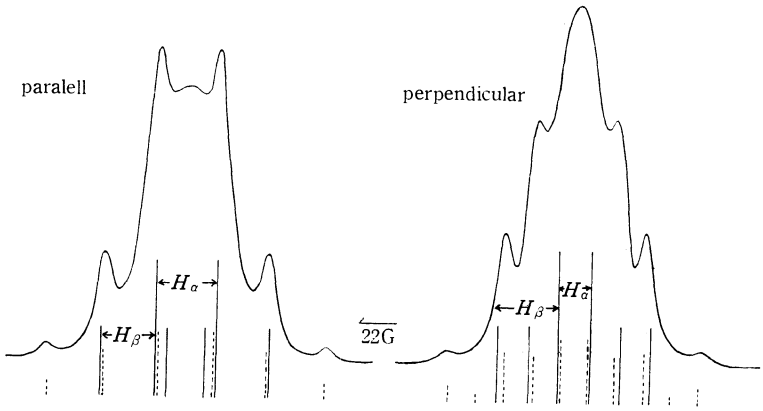

Fig. 6-b. The integrated absorption curves of γ-irradiated 6.8 polymer. Vertical dotted lines show hyperfine pattern obtained by Salovey[17] and solid lines show predicted hyperfine pattern of type A radical.

Thus, by substracting the signal intensity of polyethylene from the integrated absorption curves of our spectrum, the intensity due to type A is obtained in both orientations parallel and perpendicular to the external magnetic field, as shown in Fig. 6-b. The anisotropy of the hf constant of α-hydrogen was estimated as $A^{\alpha}_{//}=34.6$ gauss and $A^{\alpha}_{\perp}=17.3$ gauss. In oriented polymeric substances the molecular chain is aligned to the orientation axis (Y). Thus the hf constant of α-hydrogen to direction (X and Z) normal to the molecular chain is obtained as the average in hf interactions, so that $A^{\alpha}_{//}$ and $A^{\alpha}_{\perp}$ are to be A_y and $(A_x+A_z)/2$, respectively. Consequently, $A_y=34.6$ and $A_x+A_z=34.6$ are evaluated. A values are in close agreement with those of low molecular weight organic compounds.[16,18-20] The fact also permits the five-line spectrum to be attributed to type A radical.

Existence of two kinds of species is concluded. The one is relatively short-lived and gives a six-line spectrum which is attributed to type C. The other gives the five line spectrum which is stable even at room temperature. Based on the chain conformation of the polymer, it is assigned to type A radical in the acid parts.

The author wishes to thank Professor M. Takeda and Dr T. Kanamoto, Department of Chemistry, Science University of Tokyo, for their valuable advice and encouragement.

18) H. M. McConnell, C. Heller, T. Cole and R. W. Fessenden, *J. Amer. Chem. Soc.*, **82**, 766 (1960).
19) D. Pooley and D. H. Whiffen, *Mol. Phys.*, **4**, 81 (1961).
20) I. Miyagawa and K. Itoh, *J. Chem. Phys.*, **36**, 2157 (1962).

BULLETIN OF THE CHEMICAL SOCIETY OF JAPAN VOL. 43 663—669 (1970)

Measurement of the Hydrogen Ion Concentration in the Vicinity of the Anode during Electrodeposition of Water-Soluble Resin*1

Yoshio NAKAMURA, Kimio KOMATA and Hiroshi NOZAKI

Institute of Industrial Science, The University of Tokyo Roppongi, Minato-ku, Tokyo

(Received August 4, 1969)

In order to make clear the mechanism of the electrodeposition of water-soluble resin, the hydrogen ion concentration in the vicinity of the anode during electrodeposition was measured using a quinhydrone reaction on platinum wire. The measured concentration of hydrogen ions in the vicinity of the anode was then compared with that of hydrogen ions which had been calculated according to the diffusion theory. The results show that the most of the hydrogen ions produced at the anode during electodeposition are consumed in the vicinity of the anode. This shows that there is apparently ionic combination of hydrogen ions with organic anions on the anode; this may lead to the deposition of organic anions.

Many reports related to the mechanism of the electrodeposition of water-soluble resin have been published. For example, the results of the analyses of the gas generated at the anode during electrodeposition,[1-3] chemical analyses of the components of the deposited film,[4-6] and electrochemical interpretations of electrode phenomena[2,5,7] have been reported. These reports have supported the idea that the film formation of water-soluble resin is made by coagulation caused by the ionic combination of anionic resin with hydrogen ions according to the following reaction:

$$R(COO^-)_n + nH^+ = R(COOH)n \qquad (1)$$

where $R(COO^-)_n$ represents the organic anion.

Moreover, a current-time relation was observed at a constant voltage deposition, and results which may support the coagulation theory were obtained.[8]

These reports show that the principal electrode reaction at the anode during the electrodeposition of water-soluble resin is the electrolysis of water, which gives hydrogen ions at the anode; these ions then cause the coagulation of organic anions. Therefore, one of the best means to make clear the mechanism of the film formation is the measurement of the concentration of hydrogen ions on the anode surface. However, this measurement is very difficult because the diameter of the glass electrode is not small enough to measure the concentration gradient of hydrogen ions on the anode. Nevertheless, even the results were not rigorous, at first, the concentration gradient of hydrogen ions on the anode was measured using indicating reagents.

In order to obtain detailed results, the concentration of hydrogen ions in the vicinity of the anode was measured using a quinhydrone reaction on the platinum wire; some appreciable results were thus obtained.

Experimental

Sample. Maleic methyleleostearate was used as a water-soluble resin. Methyleleostearate was obtained by the methyl-inter-esterification of china wood oil. A mixture of 150 g of methyleleostearate and 50 g of maleic anhydride was heated for two hours at 180°C and then for additional three hours at 230°C. During the reaction, the mixture was kept in a nitrogen atomosphere. The method of purifying the reaction product was the same as that reported in a previous report.[8] The purified maleic methyleleostearate was dissolved into potassium hydroxide solution, after which this solution was used as a sample. The pH of the solution was adjusted by means only of the potassium hydroxide solution and maleic methyleleostearate. We name this solution simply the MME solution.

The potassium chloride, quinhydrone, and hydroquinone used in this experiment were of a special grade.

Apparatus. The measurement of the pH in the vicinity of the anode was made by means of measuring the potential of the hydroquinone-quinone reaction on platinum wire, as is shown in Fig. 1 (A).

*1 Electrodeposition of Water-Soluble Resin VI.

1) L. R. L. Brass, *J. Paint Technol.*, **38**, 493 (1966).

2) Y. Nakamura, N. Higashiyama and H. Nozaki, *Denki Kagaku*, **36**, 278 (1968); Y. Nakamura, S. Ando and H. Nozaki, *J. Electrochem. Soc. Jap.*, **37**, 13 (1969).

3) S. Yoshizawa, N. Watanabe, I. Tari and I. Totake, 34th Conference of the Electrochemical Soc. of Japan.

4) M. R. Sullivan, *J. Paint Technol.*, **38**, 424 (1966).

5) S. Maeda, N. Hirai, H. Okada and K. Inoue, *Denki Kagaku*, **34**, 705 (1966).

6) T. Nakamura, M. Nagasawa and I. Kagawa, *J. Ind. Chem.* (Japan), **70**, 2 (1967).

7) S. R. Finn, C. C. Mell, *J.O.C.C.A.*, **41**, 219 (1964); A. R. H. Tawn and J. R. Berry, *ibid.*, **28**, 790 (1965), *etc.*

8) Y. Nakamura, H. Oki and H. Nozaki, This Bulletin, **42**, 1534 (1969).

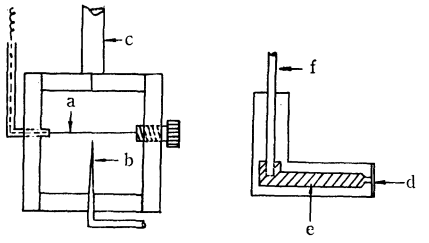

Fig. 1. Platinum wire electrode (A) and electrolysis electrode (B).
a: platinum wire, b: capillary electrolyte bridge, c: arm, d: platinum plate electrode, e: mercury, f: copper rod.

The platinum wire had a diameter of 0.05 mm, all its surface except for a length of 5 mm was insulated by organic resin. The arm of the frame which supported the platinum wire electrode was supported by the arm of the cathetometer. The platinum electrolysis electrode is shown in Fig. 1(B). A polished platinum plate was stuck on the even frame and connected to the copper rod through the mercury pool. The frames of both (A) and (B) were made of acrylic resin. As is shown in Fig. 2, a microscope was arranged above the electrolysis electrode and the wire electrode, so the wire electrode was set at will in the vicinity of the electrolysis electrode.

The circuits of the electrolysis and the measurement of the quinhydrone electrode potential are shown in Fig. 2.

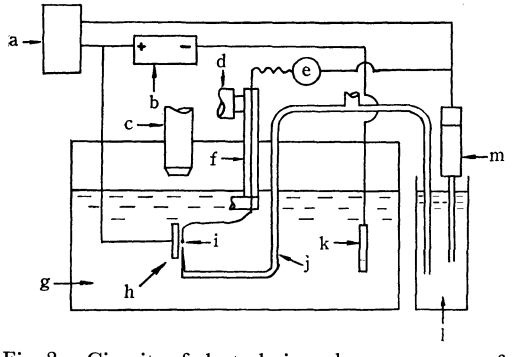

Fig. 2. Circuits of electrolysis and measurement of Q.H. potential.
a: XY recorder, b: current supply, c: microscope, d: arm of cathetometer, e: electrometer, f: arm of wire electrode, g: electrolyte solution, h: platinum plate, i: platinum wire electrode, j: electrolyte bridge, k: cathode, l: saturated KCl solution, m: saturated calomel electrode.

During electrolysis, the electrolysis electrode potential (=anode potential) was recorded by means of a Riken Denshi XY recorder, model F-42. The quinhydrone potential was measured by means of a Keysley electrometer, model 610B. This measurement was made when the electrolysis circuit was open in order to escape the $i \cdot R$ effects, where i and R are the current and the resistance of the electrolyte solution respectively. The quinhydrone potential was measured within 2 sec. However, when the electrolyte solution was a 1N KCl solution saturated with quinhydrone, the quinhydrone potential was measured without cutting the current. We will abbreviate hydroquinone, quinone and quinhydrone H.Q., Q., and Q.H. respectively.

When Q.H. was added to the electrolyte solution, H.Q. was oxidized at the anode as follows:

$$C_6H_4(OH)_2 \rightleftarrows C_6H_4O_2 + 2H^+ + 2e \qquad (2)$$

Then the anode reaction of the electrolyte solution saturated with Q.H. was observed. The pH of the anode part of the cell, which is shown in Fig. 3, was measured.

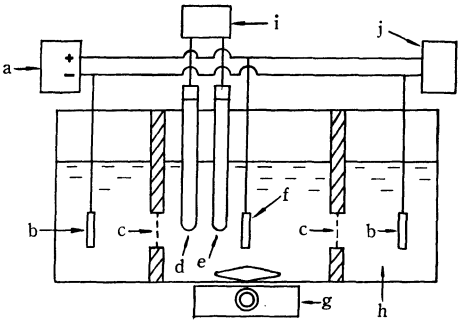

Fig. 3. Apparatus for pH measurement of anode part.
a: current supply, b: cathode, c: milipore filter, d: calomel electrode, e: glass electrode, f: anode, g: stirrer, h: electrolyte solution, i: pH meter, j: XY recorder.

The anode part and the cathode parts of the cell were separated by milipore filters. When a electrolyte solution including a supporting electrolyte is used, most hydrogen ions produced at the anode remain within the anode part because the migration and diffusion of the hydrogen ions into the cathode parts are negligible compared with their production rate. The cells shown in Figs. 2 and 3 were kept 25±0.5°C.

Results

Hydrogen Ion Production at the Anode. The mechanism of the deposition of water-soluble resin is considered to be a coagulation of organic anions occuring by means of ionic combination with hydrogen ions, so the anode reaction of the aqueous electrolyte solution saturated with Q.H. must also be investigated.

Using the cell shown in Fig. 3, the pHs of the anode part during the constant-current electrolysis of a 1N KCl solution and a 1N KCl solution saturated with Q.H.*2 were measured. The results are shown in Fig. 4, which shows that the rate of the production of hydrogen ions is nearly the same whether the electrolyte solution includes Q.H. or

*2 An oversaturated solid substance of Q.H. was filtered out at 25°C.

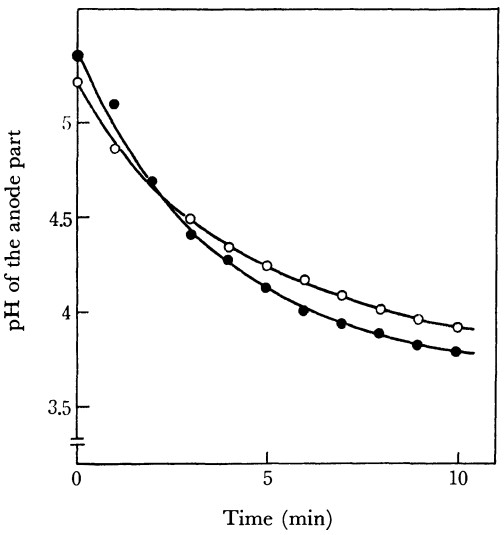

Fig. 4. pH of the anode part against time.
●: 1N KCl solution saturated with Q.H., ○: 1N KCl solution, current density 2.5 mA/cm².

not.

However, the anode potentials during electrolysis were about 0.45 and 1.1 V (*vs.* SCE) in the cases of a 1N KCl solution saturated with Q.H. and a 1N KCl solution respectively. These results can naturally be expected according to Reactions (2), (3), and (4):

$$4OH^- = 2H_2O + O_2 + 4e \quad (3)$$

$$2H_2O = 4H^+ + O_2 + 4e \quad (4)$$

Moreover, the effects on the deposition of the addition of Q.H. to the deposition bath (5% in-weight MME solution) were observed; the results are shown in Table 1, where τ_2 is the transition time as shown in Fig. 9. It is known that after $t=\tau_2$ an organic film is formed on the anode.

Table 1. Effects of the concentration of Q.H. on transition time τ_2 (sec)

Current density (mA/cm²)	Concentration of Q.H. (mol/l)·10²		
	0	0.9	2.0
2.5	86	80	75
5.0	21	20.5	20

The results show that τ_2 decreased as the weight of the addition of Q.H. increased, but the effect was minor.

pH and Q.H. Electrode Potential. The equilibrium potential of Q.H. solution is given by Eq. (5) according to Reaction (2):

$$E = E_0 + (RT/2F)\ln(a_{Q.}/a_{H.Q.}) + (RT/F)\ln a_{H^+} \quad (5)$$

where E, E_0, and a_i are measured potential, the standard potential, and the activity of the i species respectively. As the concentration of Q. equals that of H.Q. in the bulk solution, according to Eq. (6), the second term on the right-hand side of Eq. (5) is zero.

$$C_6H_4(OH)_2 \cdot C_6H_4O_2 = C_6H_4(OH)_2 + C_6H_4O_2 \quad (6)$$

Here we name the second term E_1. However, when the Q.H. electrode potential was measured in the vicinity of the anode where the current flows, the second term (E_1) is not zero but a function of x, t, and I, where x, t, and I are the distance from the anode surface, the time after switch-on, and the current density respectively.

The relations between the pH and the Q.H. equilibrium potential are shown in Fig. 5.

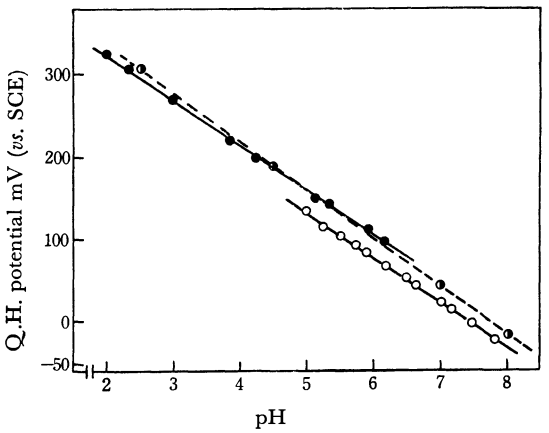

Fig. 5. Q.H. potential against pH.
●: 1N KCl solution, ○: MME solution, ◑: theoretical curve.

The potential was measured at 25°C using a saturated calomel electrode as the reference electrode. The pH was measured by means of a Hitachi-Horiba pH meter, model 5. The pH of the solution was adjusted by means of the addition of hydrogen chloride solution. The same figure also shows theoretical curve given by Eq. (5). The potential-pH curve of a 1N KCl solution differs from that of the 5% (in weight) MME solution.

However, the linear relation between the potential and the pH is satisfied in both solutions, and the values of the slopes of the curves are nearly equal. In the MME solution, a plot of the potential against the same value of pH gradually decreased with time, but the linearity between potential and pH was satisfied at all times and the value of the slope of the line was kept constant. Therefore, by measuring a potential against a value of pH, the relation between potential and pH was obtained as a function of the time.

Electrolysis of KCl Solution and pH Measurements. In order to test the method, the pH in the vicinity of the anode was measured by means of Q.H. potential measurement and was

compared with the results of theoretical calculation. The electrolyte solution was a 1N KCl solution saturated with Q.H.

In Fig. 6, the measured potential at $x=0.1$ mm is shown; the anode potential is also shown in Fig. 6.

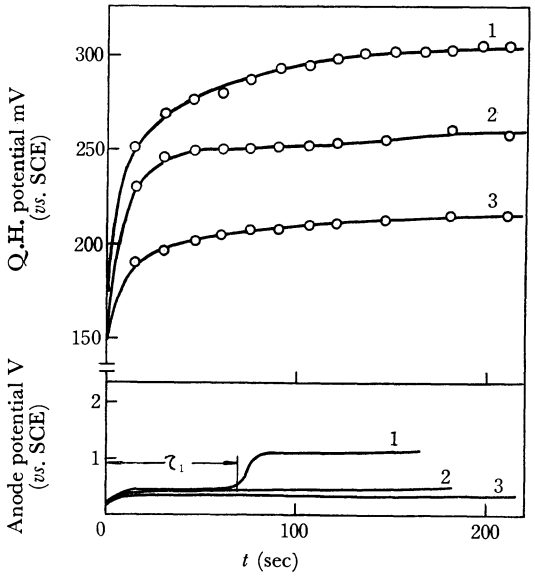

Fig. 6. Q.H. potential at $x=0.1$ mm and anode potential against time in 1N KCl solution saturated with Q.H. current density, 1 : 1.0, 2 : 0.1, 3 : 0.01 mA/cm².

In the range of current density from 0.01 to 0.1 mA/cm², the anode potential during electrolysis was kept about 0.4—0.6 V (*vs.* SCE). However, when the current density was 1 mA/cm², the transition to a more noble potential was observed; we term this transition time τ_1.

The values of the Q.H. potential shown in Fig. 6 were converted to the pH value using the results shown in Fig. 5, and the pH-time curves are shown in Fig. 7. In a solution containing a supporting electrolyte, hydrogen ions produced at the anode will diffuse to the bulk solution from the anode surface. Therefore, it is possible to calculate the hydrogen ion concentration or pH as a function of x, t, and I.[9]

Assuming that the diffusion is one dimension and that the reaction shown in Eq. (2) or (4) occurs at the anode, the values of pH in the vicinity of the anode were calculated; the results are also shown in Fig. 7. The chemical reaction of hydrogen ions and hydroxide ions is negligible when the pH of the electrolyte solution is smaller than 6. Figure 7

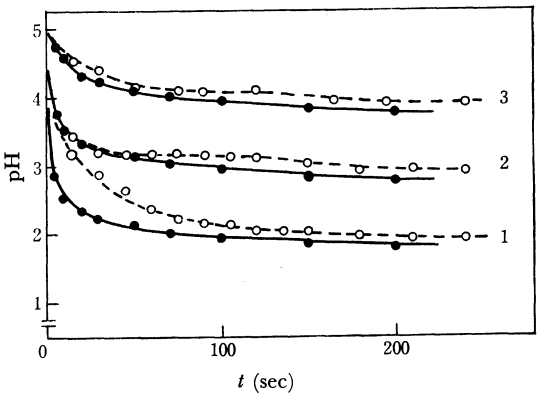

Fig. 7. pH at $x=0.1$ mm against time in 1N KCl solution saturated with Q.H. current density, 1 : 1.0, 2 : 0.1, 3 : 0.01 mA/cm², the dotted lines are experimental curves and the solid lines are theoretical curves.

shows that this method of pH measurement is reproducible, though it is not highly accurate.

Electrodeposition and pH Measurement. Electrodeposition was made at a constant current density. The concentration of MME was 5% (in weight), and the pH of the MME solution was 7.9. The Q.H. potential during deposition was measured, after which the values were converted to the pH values. In Fig. 8, the pH values at $x=0.1$, 0.2, and 0.5 mm are shown against the time after the current has been put on. The dotted line drawn in Fig. 8 shows that film formation begins at that time, that is, $t=\tau_2$.

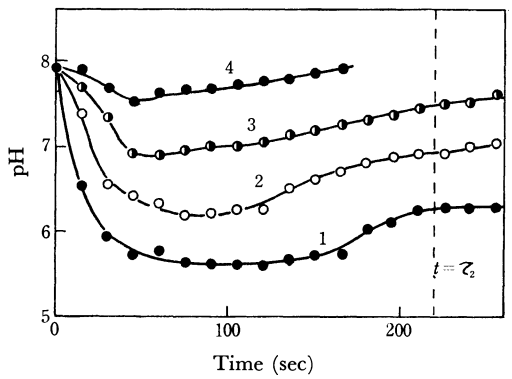

Fig. 8. pH against time.
Current density 2 mA/cm², MME concentration 2.5% (in weight), x, 1 : 0.1, 2 : 0.2, 3 : 0.3, 4 : 0.5 mm.

Deposition was made at several concentration of MME but at a constant current density, 3 mA/cm², and the potential of Q.H. at $x=0.3$ mm was measured. The pHs of the solution were adjusted to 7.9. The results, converted to the pH values are shown in Fig. 9. The anode potentials are also shown in Fig. 9.

9) P. Delahay, "New Instrumental Method in Eelctrochemistry," Interscience Pub. (1954), p. 47; H. S. Carslaw and J. C. Jaeger, "Conduction of Heat in Solids," Clarendon Press (1950), p. 216.

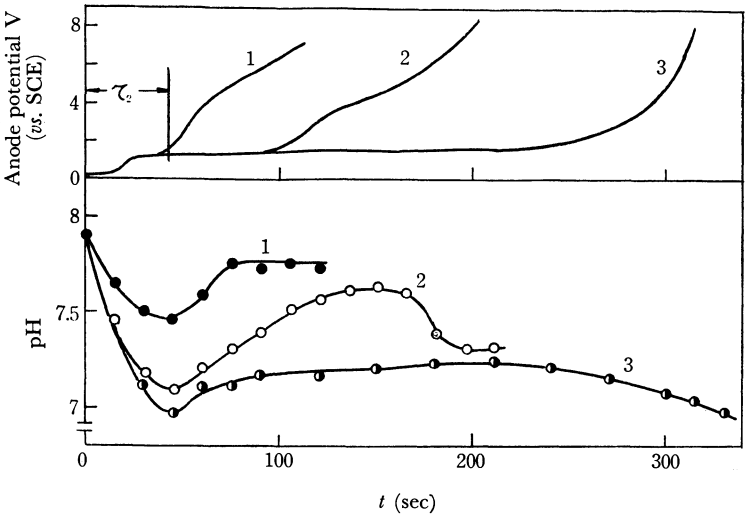

Fig. 9. Anode potential and pH at $x=0.3$ mm against time.
MME concentration, 1 : 5, 2 : 2.5, 3 : 1.25% (in weight), current density 3 mA/cm^2.

τ_2 increases with a decrease in the concentration of MME. On the other hand, the values of pH decrease with an increase in the concentration of MME, and the curves of pH and time have a peak.

The Q.H. potential at several concentrations of MME was measured as a function of x, and t; the values of the potential were then converted to the pH values by using the results shown in Fig. 5. The values of pH at $t=20$ and 75 sec are shown against x in Figs. 10 and 11 respectively. The theoretical values of the pH calculated as before are also plotted in these figures. They show that the concentration of hydrogen ions in the vicinity of the anode is smaller than that of the hydrogen ions which were calculated theoretically.

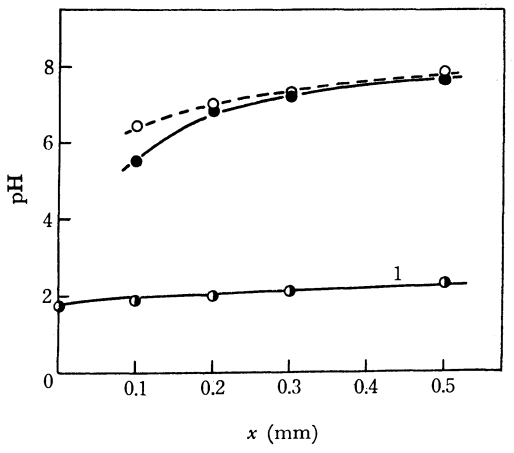

Fig. 10. pH at $t=20$ sec against x.
Current density 3 mA/cm^2, MME concentration, ●: 2.5, ○: 5% (in weight), pH of the bulk solution is 7.9, 1: theoretical curve.

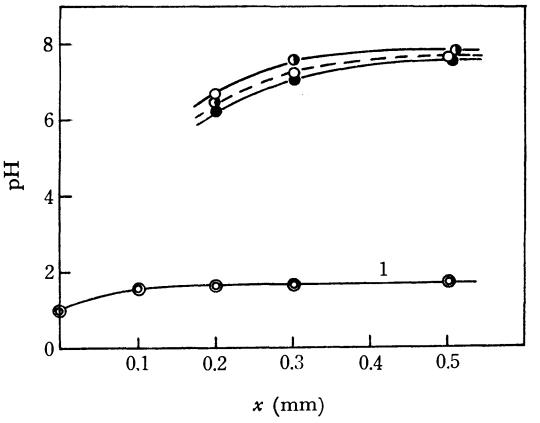

Fig. 11. pH at $t=75$ sec against x.
Current density 3 mA/cm^2, MME concentration, ●: 1.25, ○: 2.5, ◑: 5% (in weight), 1: theoretical curve.

Discussion

When the potential of the reaction shown in Eq. (2) in the vicinity of the anode, where the current flow is measured, the concentration of H.Q. decreases and that of Q. increases in the solution. This causes the E_1 potential. By means of chronopotentiometry, the saturated concentration of Q.H. was measured. $I\cdot\tau_1^{1/2}$ was plotted against the concentration of Q.H. in 1N KCl solution and 5% (in weight) MME solution. Moreover, $I\cdot\tau_1^{1/2}$ was plotted against the concentration of H.Q. in a 1N KCl solution. The results, shown in Fig. 12, show that the concentration of H.Q. is nearly equal to that of Q.H. when Q.H. is dissolved in the solution.

Table 2. Calculated E_1 (mV) at low current density

I (mA/cm²)	x(mm)	(t sec) 5	10	15	20	30	50	70	100	150	200
0.5	0.1	0.5	1.8	2.5	3.6	4.4	6.4	10	13	19	25
	0.2	—	0.3	1.0	1.3	1.6	4.2	6.5	8.7	13	16
	0.3	—	—	—	—	0.8	2.1	3.5	6.2	8.8	12
	0.5	—	—	—	—	—	0.4	0.9	2.0	3.8	6.3
1.0	0.1	1.2	3.3	5.1	7.7	8.2	17	24	(50)		
	0.2	—	0.7	2.1	2.4	3.3	7.8	13	(20)		
	0.3	—	—	0.6	0.7	1.0	4.3	7.4	(12)		
	0.5	—	—	—	—	—	0.9	2.0	(4.0)		

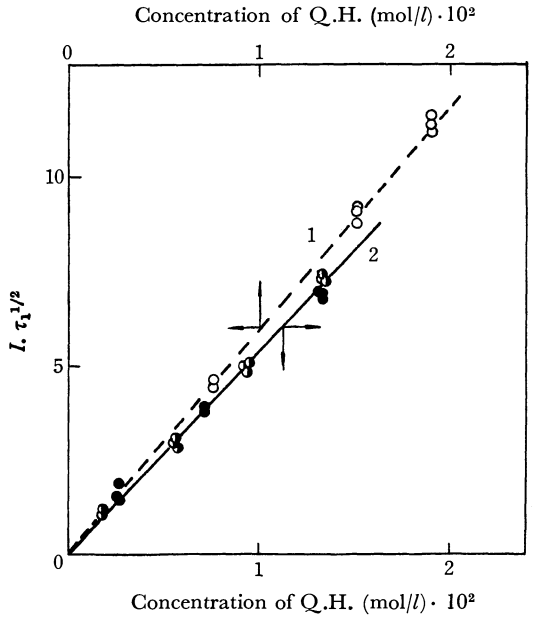

Fig. 12. $I\cdot\tau_1^{1/2}$ against concentration of Q.H. or H.Q.
1: when H.Q. was dissolved into 1N KCl solution,
2: when Q.H. was dissolved into, ●: 5% MME solutionl ◑: 1N KCl solution.

That is, most of the dissolved Q.H. dissociates to H.Q. and Q. From the $I\cdot\tau_1^{1/2}$ values of the saturated solution and the results shown in Fig. 12, the saturated concentrations of Q.H. were found to be about 1.5×10^{-2} and 2.1×10^{-2} mol/l in the 1N KCl solution and in the 5% (in weight) MME solution respectively.

Assuming that the reaction shown in Eq. (2) occurs at a constant current density, I, and that H.Q. and Q. are transported only by diffusion with one dimension, their concentrations can be calculated as functions of x, t, and I. Then, if $C_i(x,t)=a_i(x,t)$, E_1 can be calculated according to Eq. (5), where $C_i(x,t)$ means the concentration at x and t of the i species. In Table 2, the values of E_1 are shown as functions of x, t, and I. The values of E_1 were calculated assuming that $D_{Q.}=D_{H.Q.}$*3 and $(dC_{Q.}(x,t)/dX)_{x=0}+(dC_{H.Q.}(x,t)/dX)_{x=0}=0$.

$I\cdot\tau_1^{1/2}$ in a 1N KCl solution saturated with Q.H. is about 8.5. Therefore, when the current densities are from 0.01 to 0.1 mA/cm², the transition from the oxidation of H.Q. to that of water does not occur within 200 sec, and the value of E_1 is negligibly small compared with the values of the other term in Eq. (5). When the current density is larger than 0.5 mA/cm², E_1 becomes appreciable with the time, as is shown in Table 2, and the transition occurs as is shown in Figs. 6 and 9. In Table 2, the values of E_1 at $I=1.0$ mA/cm² and $t=100$ sec are not obvious because the transition occurs at 75 sec.

However, as is shown in Figs. 8 and 9, the Q.H. potential does not increase so much with the time. After the transition has occurred, the anode reaction will be the reaction shown in Eqs. (3) and (4), so Reaction (2) may be retrained by Reaction (3) and (4).

In the case of high current densities, the approximate concentrations of H.Q. and Q. will be given as follows. When the current density is high, τ_1 becomes very short, so it may be assumed that at $t=0$, the initial concentration of H.Q. at $x=0$ is zero and that the initial concentration of Q. equal to that of H.Q. at $x\neq0$. According to the diffusion theory, the concentrations of H.Q. and Q. were calculated as functions of x and t, and the values of E_1 were calculated. The results are shown in Table 3.

Table 3 shows that, within $t=200$ sec, the value of E_1 is 30 mV at most; this value corresponds the pH value of 0.5, according to Fig. 5. It is considered that the peak of the pH-time curve in Fig. 9 is caused by E_1 and the transition from the oxidation of H.Q. to that of water, for the pH-time curves in Figs. 7—11 were obtained from the value of the

*3 $D_{H.Q.}$ is the diffusion constant of H.Q.; it has value of 7.6×10^{-6} cm²/sec at 25°C.[10]

10) International Critical Table, Vol. 70 (1933); M. Kolthoff and E. F. Lingane, *J. Amer. Chem. Soc.*, **63**, 664 (1941).

TABLE 3. CALCULATED E_1 (mV) AT HIGH CURRENT DENSITY

x (mm)	t (sec)									
	5	10	15	20	30	50	70	100	150	200
0.1	4.0	13	16	18	21	24	28	30	32	34
0.2	1.4	3.6	5.9	7.6	11	14	17	21	23	24
0.3	—	1.0	1.8	4.9	5.2	8.5	12	15	17	18
0.5	—	—	—	—	0.8	2.5	4.5	7.5	10	11

measured Q.H. potential without any correction for E_1. However, the transition time, τ_1, does not correspond to the time at which a peak appears. At present, it is not obvious why a peak appears on the pH-time curve.

As is shown in Figs. 8 and 9, the hydrogen ion concentration in the vicinity of the anode does not increase with the time, but remains lower than the concentration to be expected from only the diffusion process. That is, most hydrogen ions produced at the anode are consumed on the anode surface. This shows that there is an ionic combination of hydrogen ions with MME anions. In Fig. 9, some anode potential-time curves are shown, and the transition time, τ_2, is observed on the curves. As has been noted previously, τ_2 shows that film formation begins. Compared with the pH-time curve, it is found that the rate of the ionic combination of hydrogen ions on the anode does not change at all at $t=\tau_2$.

These results show that the ionic combination of hydrogen ions begins at switch-on.

In this experiment, the pH on the anode surface was not measured. Though the pH-x curves are shown in Figs. 10 and 11, it is not impossible to ascertain the value of pH on the anode surface. In the experiment of the bulk solution without an electric field, the value of pH which the MME solution begins to coagulate was about 5.

BULLETIN OF THE CHEMICAL SOCIETY OF JAPAN VOL. 43 669—672 (1970)

The Dye-sensitized Photolysis of Hexamethyleneammonium Hexamethylenedithiocarbamate by Thiazine Dyes

Toshihiro YAMASE, Hiroshi KOKADO and Eiichi INOUE

Imaging Science and Engineering Laboratory, Tokyo Institute of Technology, Ookayama, Meguro-ku, Tokyo

(Received August 4, 1969)

Hexamethyleneammonium hexamethylenedithiocarbamate (HMTC) was photolyzed by UV light to yield carbon disulfide as the decomposition product. This photolysis could be sensitized by thiazine dyes, such as methylene blue and thionine. New methylene blue was the most effective among the sensitizers of this type examined. Bewteen the reciprocal concentration of HMTC and the reciprocal quantum yield, a linear relation was observed. The presence of oxygen was essential for the sensitization. Systems containing methylene blue appear to be more sensitive to oxygen than those containing thionine or new methylene blue. In the presence of an appropriate reducing agent such as allylthiourea, the quantum yield was decreased. The sensitization mechanism by thiazine dyes was probably different from that by benzophenone previously reported. It seems that the sensitization by thiazine dyes takes place by means of the interaction of the triplet state of the sensitizer with dissolved oxygen.

In previous papers,[1,2] the photochemical reaction of sodium *N,N*-dimethyldithiocarbamate (SMTC) was reported. Carbon disulfide was found in the decomposition products. This photolytic reaction could be sensitized by benzophenone under the light (365 nm wavelength) which was absorbed by benzophenone. The photo-sensitization was observed regardless of whether or not the solution contained dissolved oxygen. It seemed that the sensitization took place by means of energy transfer

1) T. Yamase, H. Kokado and E. Inoue, *Kogyo Kagaku Zasshi*, **71**, 1587 (1968).

2) T. Yamase, H. Kokado and E. Inoue, *ibid.*, **72**, 162 (1969).

from the triplet state of the sensitizer to SMTC molecules.[2)]

We have found that SMTC could be efficiently sensitized by thiazine dyes such as methylene blue if the solution contained dissolved oxygen. However, we encountered difficulty in studying the sensitizing effect of these dyes for the photolysis of SMTC; for their stability is greatly reduced in the alkaline ethanol, while SMTC is stable only under alkaline conditions. This difficulty could be avoided by using HMTC as the photolyzable dithiocarbamate, because this substance is stable in neutral ethanol. This paper will describe the effects of the concentration and the reducing agent on the sensitized-photolysis by thiazine dyes. The effect of oxygen will also be discussed in connection with them.

Experimental

HMTC was prepared by adding carbon disulfide slowly to a petroleum ether solution of hexamethyleneimine cooled to about 5°C. The resultant white precipitate was then filtered off, washed with fresh petroleum ether, and dried in the air. The crystallized HMTC was a pale cream-colored powder. It was recrystallized three times from ethanol to form white needles melting at 147°C. Methylene blue, thionine, and new methylene blue (G. R. grade, Tokyo Kasei Corp.) were purified by three recrystallizations from water. Allylthiourea, triethanolamine, and ethanol were G.R. grade reagents (Tokyo Kasei Corp.). The experimental procedure used in this study was almost the same as that described previously.[1,2)] Oxygen was removed from the solution by a standard freeze-thaw cycle procedure under a vacuum of 10^{-4} mmHg. A 1 kW-tungsten lamp was used as a source of actinic light for the dye-sensitization. Transmitting glass filters which cut off light shorter than 580 and 620 nm were used for thionine or methylene blue, and for new methylene blue, respectively. In most of the experiment a filter absorbing heat (HR 1-69) was also employed. Unfortunately, convenient chemical actinometers for measuring red light are not available. We assumed, therefore, that the quantum yield under the incident red light is the same as that under a 546 nm light. The latter was easily measured using Reinecke's salt as a chemical actinometer. In this case, the concentration of dye has to be increased for it to have enough absorption at 546 nm. The dye concentration was then high enough to absorb 100% of the incident red light. The quantum yields under various dye concentrations were calculated from the dye concentration against decomposed HMTC quantity relationship at a constant illumination time.

Results and Discussion

Photolysis Rate. Typical examples of the degree of photolysis *versus* time relationships under different experimental conditions are shown in Fig. 1. The logarithm of the surviving HMTC concentration changed linearly with the time. Sensitization showed no induction period and proceeded at a considerable speed. Almost no fading of dye was observed, even if the initial HMTC concentration was changed ($2-6\times10^{-4}$M). The slope in Fig. 1 was unchanged within the range of experimental uncertainty, as long as all the other factors were held constant.

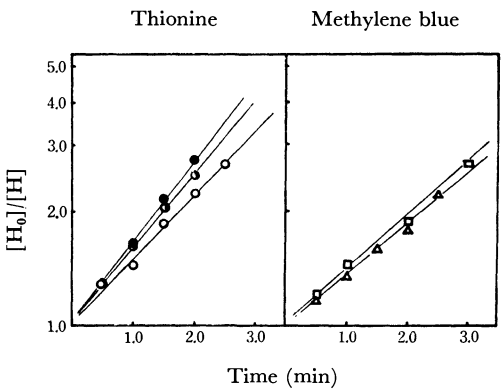

Fig. 1. Photolysis of HMTC as a function of illumination time.
Thionine conc.$=8.0\times10^{-5}$M; methylene blue conc.$=4.0\times10^{-5}$M; initial HMTC conc. ($[H_0]\times10^4=3.69$. (○), 7.51 (●), 2.64 (◑), 3.75 (△), 2.64 (□)

Effect of Dye Concentration. The effects of the concentrations of thiazine dyes are shown in Fig. 2. The reciprocal of the quantum yield changed linearly with the dye concentration.

	Thionine	Methylenene blue	New methylene blue
Intercept	4.3	6.0	3.4
$(\text{Slope})^{-1}$	3.9×10^4	3.4×10^4	1.9×10^4

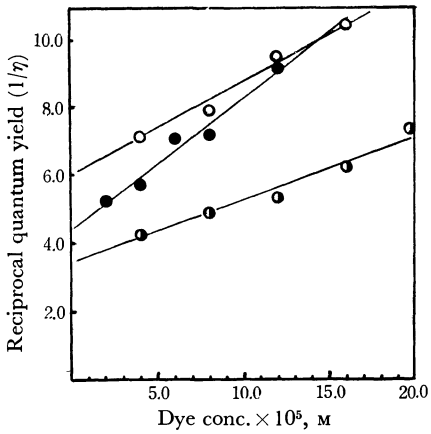

Fig. 2. Dependence of the quantum yield on the dye concentration.
HMTC conc.$=3.7$—3.8×10^{-4}M; methylene blue (○), thionine (●), new methylene blue (◑)

Effect of HMTC Concentration. The results of photolysis at different HMTC concentrations are

	Thionine	Methylene blue	New methylene blue
$(\text{Slope})^{-1}$	5.9×10^{2}	4.5×10^{2}	7.0×10^{2}

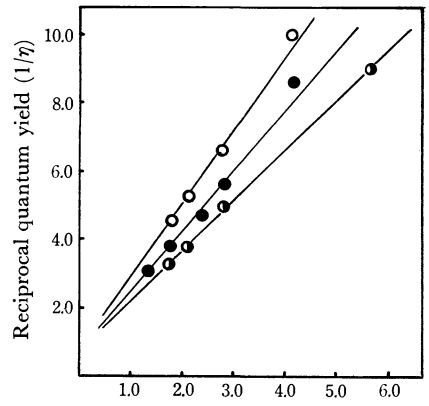

Fig. 3. Dependence of the quantum yield on the HMTC concentration.
Dye conc.$=4.0\times10^{-5}$M; methylene blue (○), thionine (●), new methylene blue (◑)

represented in Fig. 3. Figure 3 shows that a linear relation between the reciprocal of the quantum yield and that of the HMTC concentration holds for all of the dyes investigated. Apparently the efficiency of sensitization increases in the following order: methylene blue<thionine<new methylene blue.

Effect of Reducing Agent, Allylthiourea. The fact that the fluorescence of thionine (or methylene blue) was not quenched by HMTC in ethanol suggests that the excited singlet state of dye does not participate in the sensitization. If the sensitization occurs from the semiquinone radicals which are formed from the excited triplet state of the sensitizer, the efficiency of sensitization will be increased by adding a weak reducing agent, such as triethanolamine or allylthiourea.[3,4] Figure 4 shows the effect of allylthiourea on the sensitization by methylene blue. Allylthiourea did not increase the efficiency of the sensitization. Allylthiourea was regarded rather a quencher for the chemically-active state of the dye. The present investigation suggests that a reducing agent is not necessary for dye-sensitization. It may be inferred that the sensitization does not take place *via* the semiquinone radical, while in the dye-sensitized photopolymerization,[3,4] this type of process is quite common.

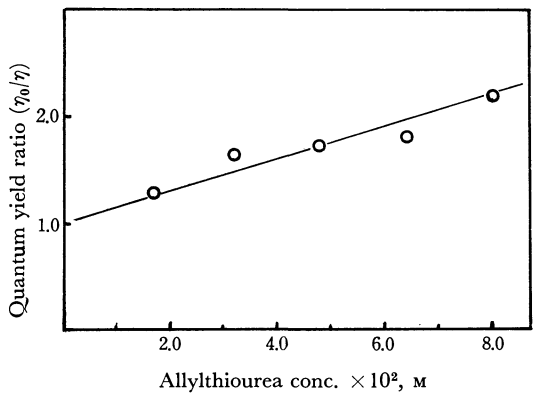

Fig. 4. Effect of allylthiourea on the quantum yield.
initial HMTC conc.$=3.96\times10^{-4}$M; methylene blue conc.$=4.0\times10^{-5}$M; η and η_0 indicate the quantum yields for the system with and without allylthiourea, respectively

Effect of Oxygen. Some representative results of photolysis in a deaerated solution are presented here. Table 1 gives the results for 4.0×10^{-5}M thiazine dye. Table 1 also includes the results obtained in solutions into which oxygen or nitrogen containing a small amount of oxygen had been bubbled in. Remarkable sensitization did not take place in the deaerated systems. This finding indicates the presence of a mechanism different from the photolysis by UV light or sensitized-photolysis by benzophenone, which was almost unaffected by oxygen, as has been reported previously.[1,2] It may be inferred that sensitization by thiazine dyes takes place not by energy transfer from the excited triplet state of the dye to HMTC, as has been proposed in connection with the sensitization of benzophenone,[2] but *via* the interaction of triplet state of dyes with oxygen. Methylene blue appeared to be more sensitive to oxygen than was thionine or new methylene blue. This is identical with what Chaberek has said regarding the effects of thionine and methylene blue on the dye-sensitized photopolymerization.[4]

Sensitization Mechanism. On the basis of the above results, the mechanism of the main reactions may be represented by the following scheme:

	Rate	
$D \xrightarrow{h\nu} D^*$	aI	(1)
$D^* \xrightarrow{k_1} D$	$k_1[D^*]$	(2)
$D^* + D \xrightarrow{k_2} 2D$	$k_2[D^*][D]$	(3)
$D^* + O_2 \xrightarrow{k_3} X$	$k_3[D^*][O_2]$	(4)
$X + \text{HMTC} \xrightarrow{k_4}$ Decomposed HMTC	$k_4[X][H]$	(5)
$X \xrightarrow{k_5} ? \ (D+O_2)$	$k_5[X]$	(6)

where a is the efficiency of the conversion of initially-excited singlets to the triplet states (D*)

3) G. Delzenne, W. Dewinter, S. Toppet and G. Smets, *J. Polym. Sci., Part A*, **2**, 1069 (1964).
4) S. Chaberek and R. J. Allen, *J. Phys. Chem.*, **69**, 647 (1965).

TABLE 1

Sensitizer	$[H]_{ini} \times 10^4$	η[a]	η'[b]	η''[c]	η'''[d]
Thionine	5.33	0.251	0	0.128	—
Methylene blue	5.57	0.227	0	0	0.310
New methylene blue	4.86	0.263	0	0.056	—
Benzophenone	3.78	0.160	0.130	—	—

a) atmospheric condition b) deaerated condition
c) saturated with nitrogen to contain little oxygen d) saturated with oxygen

and where I is the rate of red-light absorption by dye (D) in Einsteins/min. Reaction (2) represents the thermal deactivation of D* to the ground state. Reaction (3) denotes the quenching of D* by the dye of the ground state. Reaction (4) is the interaction between D* and oxygen (O_2) to form an unknown substance, X, which then reacts with HMTC as is shown by Reaction (5). Reaction (6) presents the thermal deactivation of X. According to this scheme, and assuming the steady-state condition, the quantum yield can be expressed by Eq. (7):

$$\eta = a\{k_3[O_2]/(k_1+k_2[D]+k_3[O_2])\}\{k_4[H]/(k_5+k_4[H])\} \quad (7)$$

or by

$$1/\eta = (1/ab)(1+k_5/k_4[H]) \quad (8)$$

$$b = k_3[O_2]/(k_1+k_2[D] + k_3[O_2]) \quad (9)$$

$$1/\eta = (1/ac)\{1+(k_1+k_2[D])/k_3[O_2]\} \quad (10)$$

$$c = k_4[H]/(k_5+k_4[H]) \quad (11)$$

The good fit of the data to Eqs. (8) and (10) is shown in Figs. 3 and 2. To introduce the illumination time into the rate equation, let us consider the following rate equation:

$$-\mathrm{d}t/\mathrm{d}[H] = (1/abI)(1+k_5/k_4[H]) \quad (12)$$

If $k_5/k_4[H]$ is sufficiently large, as is shown in the slope of Fig. 3, Eq. (12) becomes:

$$\log([H]_0/[H]) = (k_4/k_5)abIt \quad (13)$$

where H_0 is the initial concentration of HMTC. Figure 1 shows that a linear relation between log ($[H_0]/[H]$) and t holds experimentally. However, the greater concentration of HMTC will allow the plots to deviate from the relationship of Eq. (13). The presence of oxygen is essential to the sensitization by thiazine dyes, as is shown in Table 1. This finding contrasts with what we had earlier found, that oxygen was not necessary for the sensitization by benzophenone or for the direct photolysis. It is well-known that singlet oxygen can be generated from exogenous photo-sensitizers such as methylene blue in the photooxygenation.[5] The sensitized photolysis of HMTC by thiazine dyes may proceed by means of the singlet oxygen formed by energy transfer from the triplet sensitizer. One conceivable mechanism involves the (a) reaction;

$$^1O_2 + \mathrm{HMTC} \rightarrow {}^3O_2 + {}^3\mathrm{HMTDC} \quad (a)$$

This is tenable only if the triplet energy of HMTC is below or near that of singlet oxygen (the $^1\Delta_g$ state is at 22.5 kcal). Unfortunately, the triplet energy is not known, but such a low energy would be unreasonable. The following reaction, (b) is, thus:

$$^1O_2 + \mathrm{HMTC} \rightarrow \mathrm{Decomposed\ HMTC} \quad (b)$$

This is the only mechanism which is consistent with our present knowledge, though the mechanism is not yet understood in detail. It should be noted that, in the reactions of amines with singlet oxygen, tertiary aliphatic amines are known to yield no reactive products, but rather act as inhibitors of the oxidation of known reactive acceptors of singlet oxygen.[6] Further studies are necessary to examine the above possibility.

5) C. S. Foote and R. W. Denny, *J. Amer. Chem. Soc.*, **90**, 6233 (1968).
6) C. Quannes and T. Wilson, *ibid.*, **90**, 6527 (1968).

BULLETIN OF THE CHEMICAL SOCIETY OF JAPAN VOL. 43 673—676 (1970)

Biradical Spin-Labeled Micelles

Shun-ichi OHNISHI, Theodore J. R. CYR*1 and Hiroko FUKUSHIMA

Department of Biophysics, Faculty of Science, Kyoto University, Sakyo-ku, Kyoto

(Received August 6, 1969)

A biradical spin-label, *N,N'*-di-[4-(1-oxyl-2,2,6,6-tetramethylpiperidyl)] urea, has been used for studying the dynamic structure of a micelle, sodium dodecyl sulfate (SDS). Analysis of the ESR spectra of the label has shown that the biradical was incorporated in the micelle. The tumbling motion of the label in the micelle was not strongly inhibited, suggesting a dynamic character of the micelle structure. The exchange rate of the biradical between the micelle and the water phases was slower than 10^7 sec^{-1}. The partition coefficient expressed as the ratio of the concentration of the biradical in the micelle to that of the biradical in the water phase was approximately 6×10^5 in the SDS concentration lower than 2×10^{-2}M. The biradicals form aggregate in the micelle, when they are present in excess in the solution.

In the present paper we describe the results of a preliminary study of the paramagnetic resonance of a biradical acting as a solubilizate (spin-label) in a micelle system. Micelles may be a simple model of biological membranes, and are chosen in this study to illustrate a possible application of a biradical, such as I, to biological systems.

(I)

The spin-label technique has yielded a great deal of information on the dynamic properties of biological systems such as hemoglobin, enzymes, and nucleic acids.[1] More complex systems, for example membranes, are also examined.[2-4] Labels used for the investigations have been mostly nitroxide *monoradicals*. The rate of tumbling motion of the labels is sensitively reflected in the ESR spectra and indicates some of the dynamic and structural characteristics of the environment of the labels. *Biradicals* can also be used as spin-labels and their ESR spectra can yield more information on the environment, since the spectra depend on the intramolecular spin-spin exchange interaction, in addition to the *g*-factor and hyperfine interaction. The exchange interaction is determined by the molecular configuration which, in turn, may be affected by the environment. Hsia and Piette[5] were the first to use biradical spin-labels in the study of hapten-antibody interactions.

The results of the present investigation complement and extend those of Waggoner *et al.*[6] who used nitroxide monoradical spin-labels to study the same micelle system.

Materials and Methods

The spin-label used for the present study is the nitroxide biradical (I), *N,N'*-di-[4-(1-oxyl-2,2,6,6-tetramethylpiperidyl)] urea. This label was prepared by mixing stoichiometric amounts of 2,2,6,6-tetramethyl-4-aminopiperidine-1-oxyl and phosgene in benzene. After several days the reaction mixture was washed with water and dried. The product was purified first by recrystallization from benzene and then by column chromatography on alumina using benzene, ether, and ethanol, needle crystals of mp 145°C (uncorrected) being obtained. Sodium dodecyl sulfate (SDS) was used as the micelle forming compound in water. Its critical micelle concentration (CMC) and aggregation number in water are reported to be 8.1×10^{-3}M

*1 Grantee of Fellowship of Japan Society for the Promotion of Science for Foreign Researchers, 1967—1968.

1) For example, see C. L. Hamilton and H. M. McConnell, "Structural Chemistry and Molecular Biology," ed. by A. Rich and N. Davidson, W. H. Freeman & Co., San Francisco, Calif. (1968), pp. 115—149.

2) V. K. Koltover, M. G. Goldfield, L. Ya. Hendel and E. G. Rozantzev, *Biochem. Biophys. Res. Commun.*, **32**, 421 (1968).

3) W. L. Hubbel and H. M. McConnell, *Proc. Nat. Acad. Sci. U. S.*, **61**, 12 (1968).

4) A. D. Keith, A. S. Waggoner and O. H. Griffith, *ibid.*, **61**, 819 (1968).

5) J. C. Hsia and L. H. Piette, "Recent Developements of Magnetic Resonance in Biological System," ed. by S. Fujiwara and L. H. Piette, Hirokawa Publishing Co., Inc., Tokyo (1968), pp. 74—82.

6) A. S. Waggoner, O. H. Griffith and C. R. Christensen, *Proc. Nat. Acad. Sci. U. S.*, **57**, 1198 (1967).

and 62, respectively.[7] Commercial SDS from Wako Chemical Co. was purified by recrystallization from hot ethanol.

ESR spectra of the biradical aqueous solutions containing various amounts of SDS were measured at room temperature with a commercial X-band spectrometer (JEOLCO Model JES-P-10S).

Results and Discussion

ESR Spectrum of the Biradical Aqueous Solution. The ESR spectrum of the biradical in water shown in Fig. 1a, can be accounted for in terms of the spin-Hamiltonian,[8]

$$\mathcal{H}_s = g\beta\mathbf{H}\cdot(\mathbf{s}_1+\mathbf{s}_2) + a_N(\mathbf{I}_1\cdot\mathbf{s}_1+\mathbf{I}_2\cdot\mathbf{s}_2) + J\mathbf{s}_1\cdot\mathbf{s}_2$$

where a_N is the isotropic hyperfine coupling constant of the nitroxide N^{14} nucleus and J is the exchange interaction between the two unpaired electrons in a biradical. The spectra in Fig. 1 consist of the "triplet"-"triplet" or T resonances and the "singlet"-"triplet" or S resonances. The J/a_N value can be easily estimated from the relative S resonance positions. The value obtained for the biradical in water was $J/a_N=1.35$ resulting $J=23.1$ G, since $a_N=17.1$ G. The J values of the biradical in organic solvents (for example 18 G in hexane) were always smaller than that in water, suggesting that the biradical assumes a folded configuration in water and more or less extended forms in organic media.[9] This is consistent with the hydrophobic nature of the biradical as judged from solubility data.

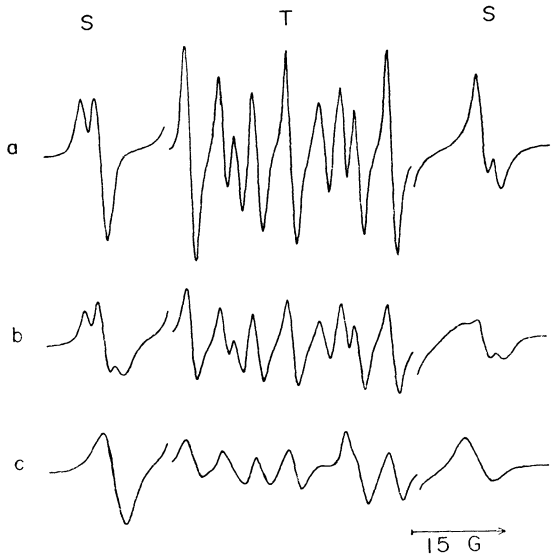

Fig. 1. ESR spectrum of biradical I in a) water, b) aqueous SDS solution of 1.4×10^{-2}M, and c) aqueous SDS solution of 6.9×10^{-2}M. Concentration of the biradical, R_0, is 4.4×10^{-5}M. The "S" resonance spectra are recorded at 6 times higher gain than that of the "T" resonances, since the S resonances are due to the "forbidden" transitions.

Effect of SDS on the Biradical Spectrum. A series of ESR spectra were recorded with aqueous solutions containing a fixed concentration (R_0) of the biradical and various concentrations of SDS. The ESR spectra remained unchanged until the concentration of SDS became larger than the critical value, 7×10^{-3}M, which is very close to the reported CMC of SDS, 8.1×10^{-3}M. At higher concentrations, the spectrum changed in both T and S resonance regions and new peaks became observable at inner field positions (Fig. 1b) in the latter. As the SDS concentration increased, these new peaks grew in intensity at the expense of the initial resonances. The final spectrum is broad (Fig. 1c), slightly asymmetric with respect to the field and corresponds to a slower rate of tumbling motion of the biradical. Moreover, since the new peaks locate at inner field positions, the J value of the biradical is smaller in the presence of micelles ($J/a_N=1.18$, $a_N=16.9$ G, $J=19.9$ G). The biradical has smaller J values in organic solvents. The results suggest that the biradical is incorporated in the micelle, has organic surroundings and experiences a slower rate of tumbling motion.

State of the Biradical in Micelle. The biradical is not strongly immobilized in the micelle, since the spectrum in Fig. 1c is similar to that of the biradical in ethyleneglycol at *ca.* 30°C. A rough estimation of the correlation time for the tumbling motion in the ethyleneglycol medium gives a value of the order of 10^{-9} sec. If the biradical were to tumble with the micelle as a whole, the correlation time would be of the order of 10^{-8} sec and the breadth of the spectral components would be much larger. This reflects the dynamic character of the micelle structure, in agreement with conclusions drawn from a monoradical spin-label study.[6] Exchange of the biradical between micelle and water, however, is not so fast as to average out the two spectra in Fig. 1a and 1c. The exchange rate is, therefore, slower than the difference in J and a_N, *i. e.* 10^7 sec^{-1}.

The S resonance portions of the spectra were recorded on an expanded scale with solutions containing various concentrations of SDS and $R_0=4.4\times10^{-5}$M. It can be seen from Fig. 2 that isosbestic points are present in the superposition

7) For example, see K. Shinoda, T. Nakagawa, B. Tamamushi and T. Isemura, "Colloidal Surfactants," Academic Press, New York and London (1963), Chap. 1.

8) S. H. Glarum and J. H. Marshall, *J. Chem. Phys.*, **47**, 1374 (1967).

9) T. Iwaoka, T. J. R. Cyr, and S. Ohnishi, unpublished results.

of the S resonance spectra. This demonstrates that the biradicals are present in only two environments, *i. e.* in the micelle and in the water phase. The fraction of the biradical in each phase is easily obtained from Fig. 2 and some values are given in Table 1.

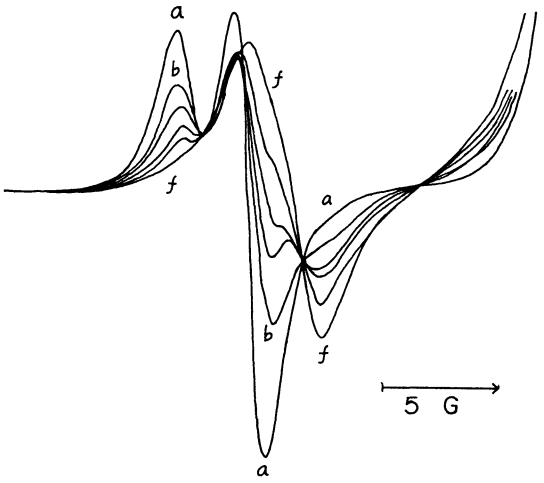

Fig. 2. Superposition of the S resonances of the biradical-SDS solutions. $R_0=4.4\times10^{-5}$M. Concentration of SDS, c_{SDS}, is a) 0, b) 1.0, c) 1.4, d) 1.7, e) 2.1, and f) 14×10^{-2}M.

Table 1

c_{SDS} 10^{-2}M	c_m 10^{-4}M	f_m/f_w a	f_m/f_w b	R_m/c_m a	R_m/c_m b	$P\times10^{-5}$ a	$P\times10^{-5}$ b
1.0	0.6	0.54	0.37	0.27	2.0	5.0	3.5
1.4	1.2	1.2	1.5	0.21	2.3	5.6	7.2
1.7	1.7	1.9	2.6	0.17	1.9	6.0	8.3
2.1	2.3	4.0	3.6	0.16	1.5	11	8.8
2.4	2.8	7.3	5.0		1.3	14	9.8
2.8	3.4	12	6.7	0.12	1.1	19	11
3.1	4.0	14	6.1	0.1	0.96	19	8.5
3.5	4.5	19	5.3	0.095	0.82	23	6.5
6.9	10		19		0.41		10

c_m: Assumed concentration of micelle calculated by $c_m=(c_{SDS}-CMC)/62$, where CMC is 6.7×10^{-3}M.

R_m: Mole of biradical in micelle per liter of aqueous micellar solution.

f_m and f_w: Estimated by comparison of the observed spectra shown in Fig. 2, with calculated spectra assuming various ratios of the fractions.

a and *b*: In these columns are given the data for $R_0=4.4\times10^{-5}$M and $R_0=4.4\times10^{-4}$M, respectively. R_m/c_m and P for $R_0=2.8\times10^{-3}$M solutions are 10 and 7.2×10^5 for $c_m=2.1\times10^{-4}$M, respectively.

P: The partition coefficient defined as $(f_m/f_w)(c_w/c_m)$. The relative error in the evaluation of f_m/f_w is equal to δ/f_mf_w, where δ is the error in f_m and f_w.

Aggregation of the Biradicals in a Micelle. When more concentrated biradical solutions were employed in the above measurements, the isosbestic

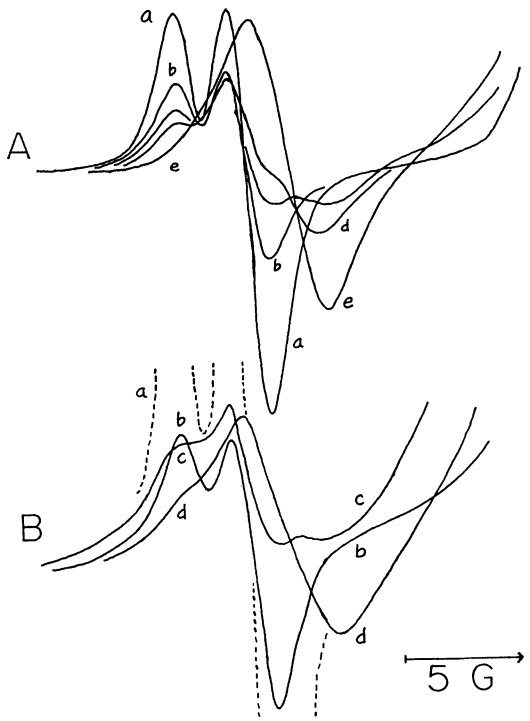

Fig. 3. Superposition of the S resonances of the biradical-SDS solutions.
A: $R_0=4.4\times10^{-4}$M. c_{SDS}; a) 0, b) 1.4, c) 1.7, d) 2.4, e) 3.5×10^{-2}M.
B: $R_0=2.8\times10^{-3}$M. c_{SDS}; a) 0, b) 1.9, c) 5.6, d) 6.9×10^{-2}M. Curve a (dotted) is calculated spectrum.

character was removed. This is evident in Fig. 3 where the S resonance spectra for $R_0=4.4\times10^{-4}$M and $R_0=2.8\times10^{-3}$M are shown. We should note that the solubility limit of the biradical in water is approximately 1×10^{-3}M, and that, in the presence of micelles, the excess biradical beyond this limit is quickly solubilized. Other features seen only at higher biradical concentrations were the decrease in the apparent spectral intensity (*cf.* Fig. 4) and the presence of a background signal increasing monotonously in the field range shown in Fig. 3. The background signal is most pronounced in the spectrum c in Fig. 3B, and from the full spectrum we see that the background is the tail part of a broad single line spectrum. The broadening is interpreted to be due to the interbiradical spin-spin exchange interaction, and can be expected when more than one biradicals dissolve in a micelle particle and the distances among them become small. In Table 1 we listed the number of the biradicals per micelle particle, which was around 2 at low SDS concentrations for $R_0=4.4\times10^{-4}$M. In such cases, the apparent S resonance intensities decrease by an amount equal to the number of biradicals in aggregation. The isosbestic character, observed at lower value of R_0, diappears since there are at

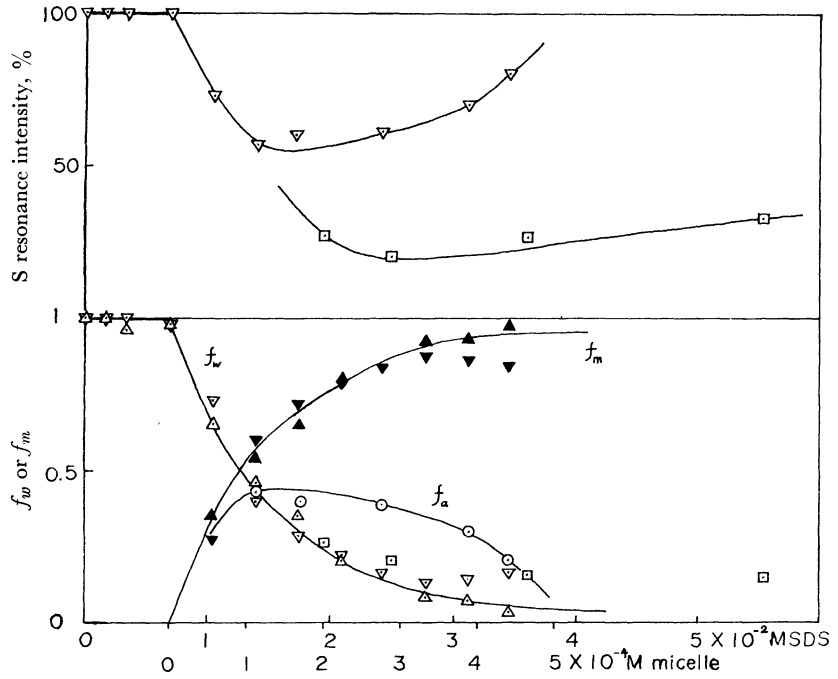

Fig. 4. Upper: The relative S resonance intensity *vs.* SDS concentration. ▽ for $R_0=4.4\times10^{-4}$M and ⊡ for $R_0=2.8\times10^{-3}$M.
Lower: The fraction of biradical in water, f_w, and micelle, f_m, *vs.* SDS concentration. △ and ▲; f_w and f_m for $R_0=4.4\times10^{-5}$M. ▽, ▼, and ⊙; f_w, f_m, and f_a for $R_0=4.4\times10^{-4}$M. ⊡; f_w for $R_0=2.8\times10^{-3}$M. f_a is the fraction of biradical aggregates in micelle.

least three different spectra of various intensities depending on the micelle concentration.

The results suggest that the biradicals in the micellar solutions can be divided into three fractions: those remaining dissolved in water (f_w), those incorporated individually in micelles (f_s), and those forming aggregates in micelles so that the biradicals give exchange-broadened ESR spectra (f_a). The fraction of biradical in a micelle, f_m, is equal to f_a+f_s. The ratio, f_s/f_w, can be estimated from the S resonance spectral shape, and f_a from the decrease in the total S resonance intensity. The values obtained for biradical solutions of various concentrations are given in Table 1 and are plotted in Fig. 4 against the SDS concentration. The micelle concentration, also given on the ordinate, is calculated by assuming that all the SDS molecules form micelles of molecular weight 62×288 above CMC. In the most dilute biradical solution, there is no apparent decrease in the S resonance intensity, suggesting that the biradicals do not aggregate within micelles. At the first measurement above CMC, the calculated micelle concentration, 6×10^{-5}M, is already larger than the biradical concentration, 4.4×10^{-5}M. On the other hand, in the more concentrated biradical solutions, there are fewer micelles than biradicals and the radicals aggregate. The f_a *versus* micelle-concentration curve, after reaching a maximum value, decreases towards zero at higher micelle concentration. If the f_a curve is extrapolated, f_a reaches zero at about 5×10^{-4}M micelles, which is close to the biradical concentration 4.4×10^{-4}M. The radicals, therefore, appear to distribute themselves fairly evenly among the micelles and aggregate only when there are not enough micelles present.

The Partition Coefficient. The f_w and f_m *versus* SDS-concentration curves for the various biradical concentrations fall on the same curve, indicating that the partition of the biradicals in the water and micelle phases is independent of the biradical concentration. The presence of biradical aggregates does not appear to affect the partition. We can define the partition coefficient P as $P=(f_m/f_w)(c_w/c_m)$, where c_w and c_m represent the concentrations of water and micelle in the solution, respectively. The calculated coefficients are fairly constant, 6×10^5 within experimental error, in the smaller SDS concentration region ($<\sim2\times10^{-2}$M) (see Table 1). P seems to tend to increase, however, in the larger SDS concentration region, although the relative error in the evaluation of P becomes greater for larger f_m or f_w values. This might suggest some change in the mode of micelle formation in more concentrated SDS solutions, since, in the calculation of P, we assumed a monotonous linear increase in the micelle concentration.

BULLETIN OF THE CHEMICAL SOCIETY OF JAPAN VOL. 43 677—681 (1970)

The Crystal Structure and the Molecular Behaviour of 2,3-Dibromo-2,3-dimethylbutane at Room Temperature

Yoshiyuki NAMBA, Tsutomu ODA, Nobuto FUKUDA and Osamu TAKADA

Department of Chemistry, Osaka Kyoiku University, Tennoji-ku, Osaka

(Received August 9, 1969)

The crystal structure of 2,3-dibromo-2,3-dimethylbutane at room temperature has a disordered nature. In the crystal, *trans*-form molecules have at least four orientations of equal statistical weight around the axes parallel to the [001] direction. Therefore, in spite of the low symmetry of the molecule, the crystal belongs to the tetragonal system and has the space group of $I\bar{4}/mmm$, while $a=7.38$ Å, $c=8.12$ Å and $Z=2$.

The crystal of 2,3-dibromo-2,3-dimethylbutane has three modifications, phase I (high-temperature modification) appearing above 80°C,[1] phase II (room-temperature modification) existing between −90°C and 80°C, and phase III (low-temperature modification) appearing below −90°C.[2] An X-ray investigation of the room-temperature modification (phase II) has already been carried out by Yardley,[3] who has given useful crystal data and suggested some possible crystal structures. Yamada and Taguchi[4] have pointed out that phase I is cubic, the molecules rotating as a whole in the crystal.

A reexamination of the structure of phase II will be described in this paper.

Experimental

The material was synthesized by mixing hydrogen bromide and pinacol at 0°C (Thiele's method[5]). It was purified by several vacuum sublimations. Single crystals were obtained from an ethanol solution. They were colourless needles which were elongated along the [001] axis and were flexible. The crystals, enclosed in thin-walled terex-glass capillary tube to protect them from sublimation and contamination, were used in the X-ray investigations.

The unit-cell dimensions were determined from Weissenberg photographs superimposed on a powder pattern of pure sodium chloride. The density was measured by the floatation method. Laue photographs were also taken to determine the crystall class.

Crystal data:
2,3-dibromo-2,3-dimethylbutane, $C_6H_{12}Br_2$
mol wt 243.9, mp 182°C.

Tetragonal, $a=7.38$Å, $c=8.12$Å. $U=442.2$Å^3. Density (observed) 1.82 g/cm^3, Density (calculated) 1.83 g/cm^3, $Z=2$. Laue symmetry: $4/mmm$.*1

The absent spectra are:

$$hkl\colon\ h+k+l=2n+1,$$
$$hk0\colon\ h+k=2n+1,$$
$$hhl\colon\ l=2n+1,$$
$$0kl\colon\ k+l=2n+1.$$

Thus, the space group was selected as one of the following: $I422$, $I4mm$, $I\bar{4}m2$, $I\bar{4}2m$, or $I4/mmm$.

The intensity data were obtained from equi-inclination Weissenberg photographs, $hk0$, $hk1$, $hk2$, and $hk3$, taken by means of CuK_α radiation filtered through nickel foil. The multiplefilm technique was used, and the intensities were estimated visually by comparison with a calibrated scale. The intensities were corrected for the Lorentz and polarization factors to obtain the relative values of $|F|^2$.

Structure Determination

Since the body-centered unit cell contains two molecules, the centers of the molecules must be placed at 0,0,0 and 1/2, 1/2,1/2.

Even though the crystals belong to one of the possible space groups mentioned above, the point symmetry of these positions must at least contain a four-fold rotation axis or a four-fold inversion axis. On the other hand, when the configuration of a free molecule is considered, the *trans*-form is taken as the highest symmetric one, for it possesses the symmetry C_{2h}. This symmetry does not, however, satisfy requirement of a high symmetrical nature such as C_4 or S_4 for the molecules in the crystal. This inconsistency in symmetry consideration proves some disordered character in the crystal.

1) A. H. White and W. S. Bishop, *J. Amer. Chem. Soc.*, **62**, 8 (1940).
2) H. Suga, K. Nakatsuka, T. Shinoda and S. Seki, *Nippon Kagaku Zasshi*, **82**, 29 (1961).
3) K. Yardley (Mrs. Lonsdale), *Proc. Roy. Soc., Ser. A*, **118**, 485 (1928).
4) Private communication. See also Ref. 2.
5) Thiele, *Ber.*, **27**, 455 (1894).

*1 It is to be noted that these crystal data are in harmony with those of Yardley.

To obtain preliminary knowledge on the structure, a Patterson map, $P(u,v)$, was synthesized. As is shown in Fig. 1, there is no predominant peak except at the point of origin and at 1/2,1/2, indicating that the Br–Br axis in the molecule is oriented almost parallel to the c-axis. Hence, it is reasonable that the *trans* molecules placed at 0,0,0 and at 1/2,1/2,1/2 with their Br–Br axis parallel to the [001] axis remain some disordered orientation about the [001] axis, thus having, on the average, a symmetry higher than 4 or $\bar{4}$.

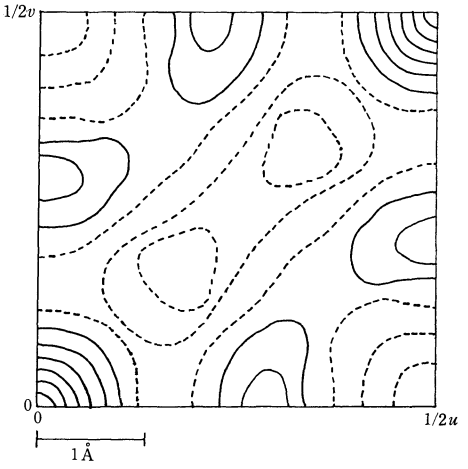

Fig. 1. Patterson map: $P(u,v)$.

Let us now proceed with the structure analysis using the trial-and-error method.

The configuration of molecule used in the trial calculations is an ordinary *trans* one; that is to say, the bond lengths used are 1.54 and 1.91 Å for C–C and C–Br bonds respectively, while normal tetrahedral bonds are taken for the carbon atom. For convenience in calculating, we used the value of $3/2f_c$ for the scattering factor of carbon atoms belonging to methyl groups, moreover, the precise contribution of hydrogen atoms was not calculated, as it is thought to be small.

The adopted arrangements of the molecules in the crystal and the results of the calculated structure factors are as follows:

Case I. Axial Rotation. As the first example in this case, let us consider a model in which the "axial rotation" of the molecule about its Br–Br axis is taking place freely, the Br–Br axis coinciding with the [001] direction. This is called model I. The calculated values of the structure factors are compared with the observed values in Fig. 4a. The general correspondence seems to be satisfactory. However, the aspects in (220), (310), (400), and especially in (hkl) do not give sufficient agreement.

In order to improve this inconsistency in the case of model I, a slightly modified model was considered. That is, in the second model, we assumed that the bromine atoms also rotate about the axis parallel to [001]. This model is shown in Fig. 2b. However, this treatment produces no remarkable improvement, as may be seen in Fig. 4b.

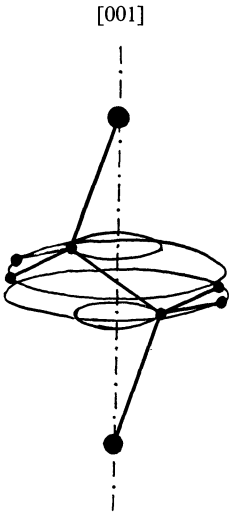

Fig. 2a. Model I.

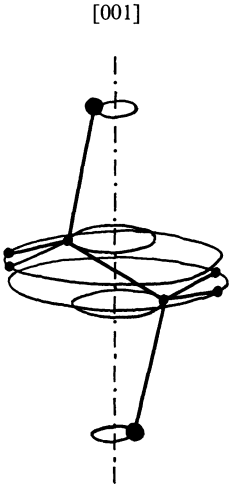

Fig. 2b. Model II.

Case II. Static Statistical Structure. Now, we can also assume static statistical structures in which the *trans* molecules with their Br–Br axis in the direction of the [001] axis occupy laterally four orientations about [001], with an equal statistical weight of 1/4, resulting in a four-fold nature of the [001] axis.

The atomic parameter values selected for this model, III, were as follows:

Br: $x = y = 0.00$, $z = 0.28$;

C: $x = y = 0.06$, $z = 0.05$;

C (methyl group): x=0.26, y=0.016, z=0.018.

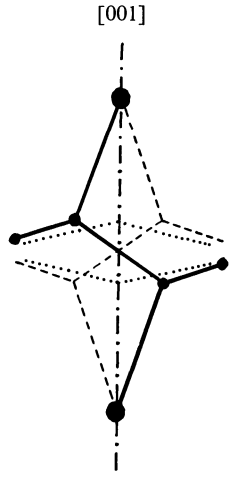

Fig. 3a. Model III.

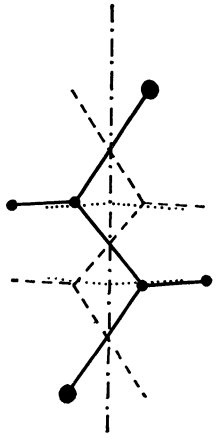

Fig. 3b. Model IV.

The calculated structure factors are shown in Fig. 5a. The correspondence of F_c and F_o is fairly good. This structural model may be said to represent well the structure of the present crystal.

Now, in this case, the central C–C bond of each molecule is on the plane on the (110) type. The methyl groups are, then, lying nearly on the plane of the (100) type. Speaking only on the basis of a consideration of the statistical symmetry, another arrangement of molecules is also possible, one where the central C–C bond is not on the (110)-type plane but on the (100)-type plane. However, in this model the agreement of F_c and F_o is far less than with the model III.

In model III, the Br–Br axis of a molecule has been taken as parallel to the [001] direction. In this arrangement, the intermolecular Br–Br distance along the [001] direction is calculated as 3.73 Å. This value can be seen to be slightly shorter than the normal distance, 3.90 Å, of Van der Waals contact. In view of this, we further assumed the model IV, in which the Br–Br axis of the molecule is slightly inclined to the [001] direction. In this case, four statistical positions must be considered for bromine atoms, also.

The atomic parameter values used were as follows:

Br: $x=y=0.029$, $z=0.278$;

C: $x=y=0.051$, $z=0.068$;

C (methyl group): $x=0.014$, $y=0.257$, $z=0.051$.

The calculated structure factors are shown in Fig. 5b. In this case the coincidence of F_c and F_o is better than in the case of model III.

In the analyses hitherto described, the *trans* configuration has been adopted as that of the free molecule. We have also tried an analysis using the *gauche* form of the molecule. However, such a form does not explain the observed values of the structure factors. Therefore, the *gauche* configuration can be disregarded.

Conclusion

The results obtained above for the present crystal structure can explain the mechanism of the transitions at about 70°C and at −120°C. When the temperatures are raised from room temperature, the thermal motion of the *trans* molecules possessing an orientational or rotational disorder around the Br–Br axes almost parallel to the [001] axis is more and more enhanced, and at 70°C the crystal is transformed to its cubic phase, in which the molecules rotate spherically as a whole, their Br–Br axes being randomly oriented. In this high-temperature modification, it may be possible for the molecules to take the *gauche* configuration.

When the temperatures are lowered from room temperature, the cessation of the axial rotation of the molecules around their Br–Br axes occurs below −120°C, the crystal taking an ordered structure.

Furthermore, it is of interest to compare the present structure with that given for the dichloroethane crystal above its transition temperature at −70°C. It has been reported by Reed and Lipscomb[6] that the molecules in that phase rotate axially about their Cl–Cl axes, the molecules also possessing the *trans* configuration. This structure is quite similar to the present one given for the 2,3-dibromo-2,3-dimethylbutane crystal at room temperature.

However, the 2,3-dibromo-2,3-dimethylbutane crystal shows a high-temperature transition at 70°C, whereas there is no corresponding transition in the case of dichloroethane crystals.

The onset of the spherical rotation of the molecules as a whole in the high-temperature modification

6) T. B. Reed and W. N. Lipscomb, *Acta Crystallogr.*, **6**, 45 (1953).

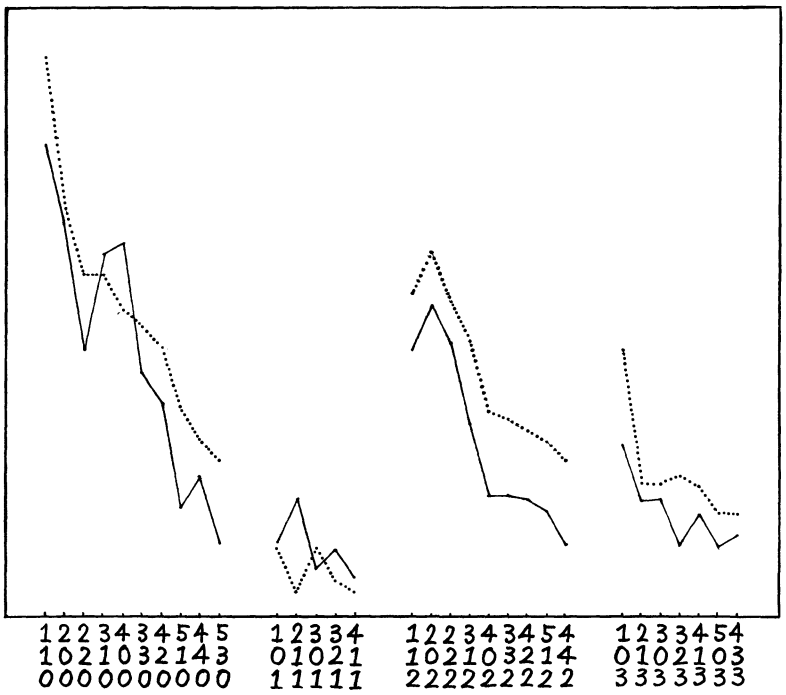

Fig. 4a
F_o —— F_c ……

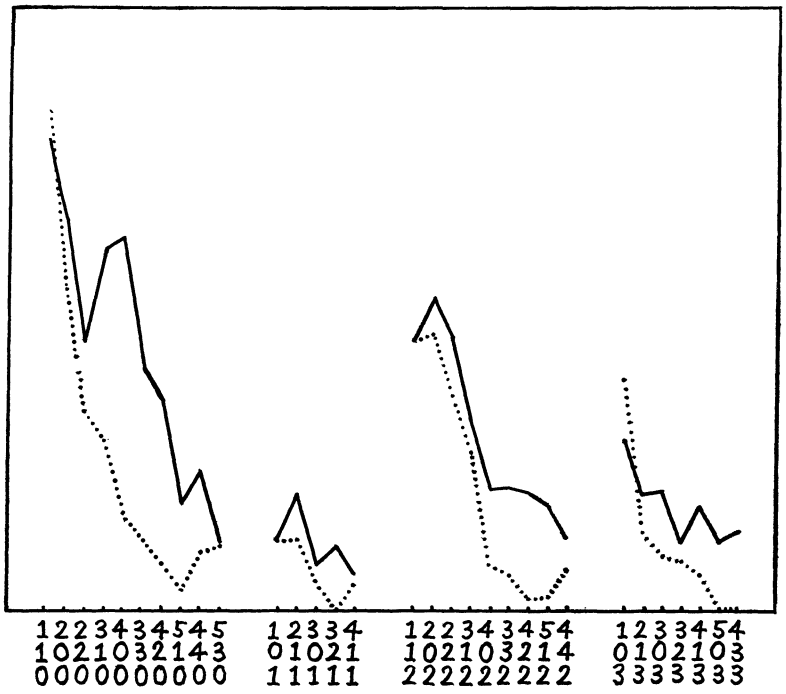

Fig. 4b
F_o —— F_c ……

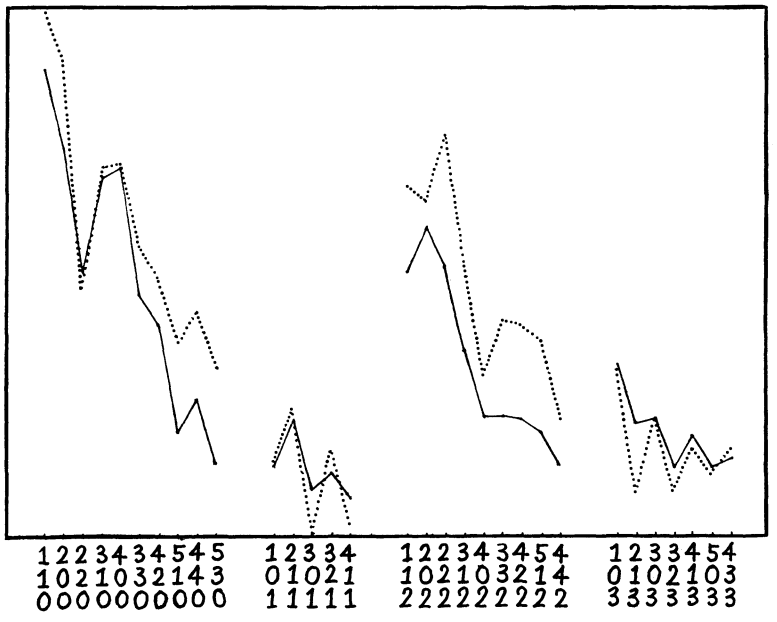

Fig. 5a

F_o —— F_c .....

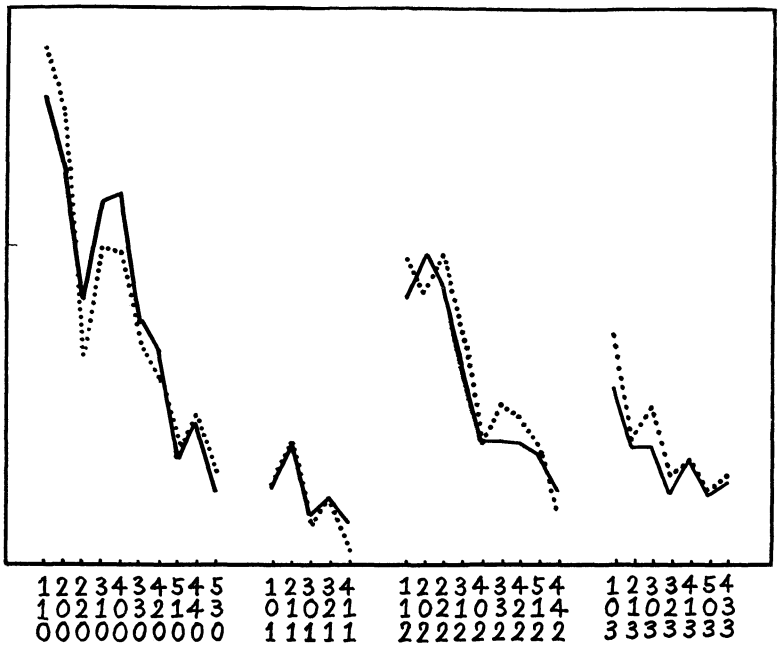

Fig. 5b

F_o —— F_c .....

in the case of 2,3-dibromo-2,3-dimethylbutane may be closely related to the "ellipsoidal" shape of the molecules in contrast to the elongated "rectangular" shape of dichloroethane.

Turning to the low-temperature transition, it is desirable to investigate the crystal structure below -120°C in order to give a precise explanation of the mechanism of the low-temperature transition.

The authors wish to thank Professor S. Seki for his interest in this work and also Professor T. Watanabe for his helpful discussions.

BULLETIN OF THE CHEMICAL SOCIETY OF JAPAN VOL. 43 682—686 (1970)

Studies of the Structure of Polyurethane Elastomers. I. The Number-average MW Determination of the Hard-segment in the Poly(Ether)Urethane Elastomer by Means of Perchloric Acid Depolymerization

Hajime Suzuki and Hiroshi Ono

Katata Research Institute, Toyobo Co., Ltd., Honkatata, Otsu

(Received August 18, 1969)

Urea segment which is called a hard-segment in the poly(ether)urethane elastomer (PEUE) consisting of a polyether segment,urethane segment,and urea segment was isolated by means of perchloric acid depolymerization. The number-average molecular weight (MW) of the urea segment obtained by the above method was determined by elemental analysis and by volumetric analysis. By comparing the analytical results with the results calculated for a random polymerization, the number-average MW of the hard-segment was found to deviate from that expected from the equal reactivity of the two isocyanate groups in 4,4'-diphenyl methane diisocyanate (MDI). Therefore, an apparent reactivity ratio of two isocyanate groups in MDI (A) can be calculated from the number-average MW of the hard-segment isolated by means of perchloric acid depolymerization.

There have been a number of reports concerning the determination of randomness[1] and copolymer compositions[2] by means of the high-resolution NMR, but the determination of the sequence length of the hard-segment in PEUE has not been successful, mainly because of the complication of the spectra of poly (ether) urethane elastomers. Therefore, we have studied the isolation of three segments by means of the difference in the cleavage rate of three segments in a typical PEUE prepared from MDI, polyoxytetramethylene glycol (PTG), and hydrazine (HD). Although the structure of the PEUE can not be written in one formula, it may be expressed by the following three segments:

polyether segment, $(-CH_2CH_2CH_2CH_2O-)_n$

urethane segment,

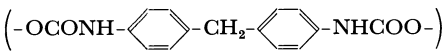

urea segment,

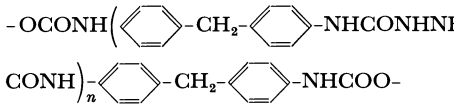

By determining the MW of the urea segment, we were able to show the blockiness in the PEUE, and also the apparent reactivity ratio of two isocyanate groups in MDI. These studies will be very useful for the elucidation of the relationship between the structure and the physical properties of the elastomers.

Experimental

Materials. The PEUE's used in this work were synthesized by the prepolymer method. The prepolymer was prepared by reacting 0.02 mol (20 g) of PTG (MW, *ca.*, 1000) with MDI (0.03—0.07 mol, as in Table 1) in 60 m*l* of *N,N*-dimethyl acetamide at 30°C for 3 hr. The completeness of the prepolymer reaction was ascertained by the *n*-dibutylamine titration method reported by Otey *et al.*,[3] and the PEUE's were prepared from the prepolymer and HD as a chain extender. The molar ratios of the various monomers in the polymers prepared in this way are listed in Table 1.

Poly(ether)urethane (PEU) was synthesized by reacting PTG (MW, *ca.* 1000) with the equivalent mole of MDI as polyether and urethane segment models.

Depolymerization of PEUE. The depolymerization was carried out by placing the PEUE (5 g) in perchloric acid (60%, 60 m*l*) for 24 hr at room temperature, and by then treating it at 70°C for 40 hr in a water bath. An excess of water was added to the mixture to precipitate the perchlorate of the amine end group of the urea segment. The salt was collected by filtration, and then washed with water and dried.

The completeness and the selectivity of depolymerization reaction were ascertained by the following procedure. A mixture of 5 g of model compounds of PEU and 2 g of the urea segment obtained by the above depolymerization was depolymerized by perchloric acid (60%, 60 m*l*) under the same conditions as in the depolymerization of PEUE. After the depolymerization of this mixture,

1) R. Yamadera and M. Murano, *J. Polym. Sci., Part A-1*, **5**, 2259, (1967).

2) T. Harada and N. Ueda, *Kobunshi Kagaku*, **22**, 685 (1965).

3) F. H. Otey, Bornnie L. Zagoren and C. L. Mehltretter, *J. Appl. Polym. Sci.*, **8**, 1985 (1964).

Table 1. Preparation and elementary analysis of the hard-segments of PEUE's

No.	Prepolymer MDI (mol)	Prepolymer PTG (mol)	Chain extender HD (mol)	[Urea]/[Urethane]	Found (%) C	Found (%) H	Found (%) N	Found (%) Cl	Calcd (%) C	Calcd (%) H	Calcd (%) N
1	0.030	0.020	0.010	1/2	53.60	4.33	14.59	7.18	53.85	4.58	14.67
2	0.035	0.020	0.015	1.5/2	54.41	4.17	14.85	6.81	54.36	4.60	14.94
3	0.040	0.020	0.020	2/2	55.23	4.60	15.32	6.33	55.03	4.62	15.29
4	0.050	0.020	0.030	3/2	56.72	4.72	16.21	5.18	56.64	4.69	16.12
5	0.060	0.020	0.040	4/2	57.22	4.65	16.40	4.75	57.23	4.71	16.43
6	0.070	0.020	0.050	5/2	57.87	4.78	16.79	4.22	57.96	4.74	16.81

the weight loss was measured, and the change in the MW of the urea segment was measured by the titration method.

MW Determination of the Hard-segment. The MW of the hard-segment was determined by elemental analysis and by titration. In the elemental analysis the MW was calculated directly from the chlorine content.

In the titration method, about 30 mg of the hard-segment obtained by the above method was immersed in 10 m*l* of a N/100 aqueous solution of NaOH and titrated by a N/100 aqueous solution of HCl, using methyl orange as the indicator. The MW of the hard-segment was calculated by the following equation:

$$\text{MW of hard-segment} = \frac{2\{\text{Weight of hard-segment (mg)} - 100.5 \times (T_B - T_S)(\text{ml}) \times 1/100 \times F\}}{(T_B - T_S)(\text{ml}) \times 1/100 \times F}$$

where F is a factor of an aqueous solution of HCl and where T_S and T_B are the volume of an N/100 aqueous solution of HCl required for the titration of the sample and the blank solution respectively.

Results and Discussion

Depolymerization Reaction. A previous paper[4] has described how THF is formed quantitatively in the reaction of PTG and perchloric acid. After the reaction of PEU and perchloric acid, an aqueous solution of sodium hydroxide was added to the reaction mixture until the pH value reached 9; 4,4′-diaminodiphenylmethane (mp, 93—94°C) was thus obtained. From these findings, the reaction of PEU and perchloric acid may be assumed to proceed as follows:

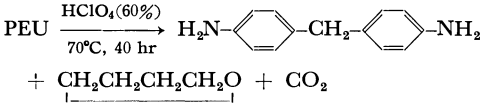

After the depolymerization reaction of PEUE under the conditions described above, precipitates were obtained by adding an excess of water to the reaction mixture. The IR absorption spectrum of the precipitate is shown in Fig. 1. A comparison of the IR absorption spectra of the precipitate (B) and of PEUE (A) shows that the 2900 cm^{-1} region due to the methylene group and the 1700 cm^{-1} region due to the urethane group disappeared in B. The IR absorption spectrum of the precipitate washed with an aqueous solution of sodium hydroxide is shown in C of Fig. 1. The comparison of the IR absorption spectra of C and B in Fig. 1 shows that the absorption at 1100 cm^{-1} can not be seen in C, but this absorption C was again coincident with the IR absorption spectrum of B after this precipitate had been washed with perchloric acid; therefore, the absorption in the 1100 cm^{-1} region in B may be due to the perchlorate of amine. On the other hand, the absorption in the 1100 cm^{-1} region in A is due to the ether segment in PTG. From the above results, the precipitate obtained by the perchloric acid depolymerization can be written by the following formula:

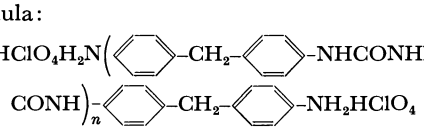

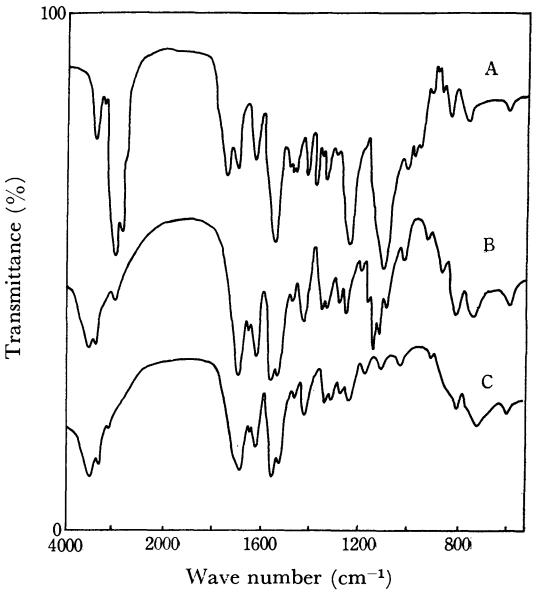

Fig. 1. IR spectra of PEUE and hard-segment. A: PEUE, B: urea segment with the perchlorate of the amine endgroups, C: urea segment with amine endgroups

4) H. Suzuki and H. Ono, *Kogyo Kagaku Zasshi*, **72**, 1593 (1969).

The results of the elementary analysis of the above hard-segments of the PEUE's are given in Table 1. The calculated values shown in Table 1 were obtained from the analytical results of the chlorine.

To ascertain the recovery of the hard-segment from PEUE, the mixture of PEU and the hard-segment obtained by the above experiment was depolymerized by perchloric acid under the same conditions as above. In this experiment, the recovery and the MW of the hard-segment were measured. Table 2 shows these results.

Table 2. Recovery and MW of hard-segment

Recovery (wt%)	MW before re-depolymerization	MW after re-depolymerization
99.7	782	779
99.2	828	808
99.5	931	945
99.7	1213	1215
98.3	1333	1315
99.0	1573	1575

From these results, the reaction of PEUE with perchloric acid can be assumed to proceed as follows:

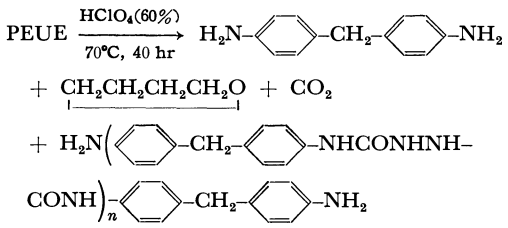

Since 4,4′-diaminodiphenylmethane, which came from the urethane segment, was soluble in perchloric acid, while the hard-segment was insoluble, it could be separated by precipitation.

Table 3. MW of hard-segment

No.	[Urea]/[Urethane] molar ratio	MW of Hard-segment: Titration method	MW of Hard-segment: Elemental analysis method	MW of Hard-segment: Calcd value
1	1/2	782	789	621
2	1.5/2	828	842	691.5
3	2/2	931	921	762
4	3/2	1213	1172	903
5	4/2	1333	1295	1044
6	5/2	1573	1482	1185

Table 3 shows the number-average MW of the hard-segment. The calculated values in Table 3 were obtained in a manner to be shown later.

MW of the Hard-segment. The reactivity between MDI and alcohols has been reported on by many authors.[5,6] Naito and Tanaka[7] have shown the equal reactivity of two isocyanate groups in MDI for the reactions with low-molecular-weight alcohols. Moreover, Ferstandig and Scherrer[8] reported that the reactivity ratio ($A=K_2/K_1$) of two isocyanates in MDI was about 0.33. Although there has been no report concerning the reactivity between the polymer diol and MDI, we assumed an equal reactivity of the isocyanate group in MDI in the prepolymer reaction and in the chain-extender reaction.

The PEUE composition is given by:

$$C = E + H \tag{1}$$

where C, E, and H are the numbers of moles of MDI, PTG, and HD respectively. After the prepolymerization, the concentration ratio of the three structural units could be obtained by a probability calculation, as is shown in Table 4.

Table 4. Concentration ratio of three structural units after prepolymerization

Structural unit	Concentration ratio
$CH_2\left(\bigcirc\text{-NHCOO-}\right)_2$	$P_{E\text{-}I\text{-}E}=E^2/C^2$
$CH_2\left(\bigcirc\text{-NCO}\right)_2$	$P_{H\text{-}I\text{-}H}=(C-E)^2/C^2$
OCN-⬡-CH-⬡-NHCOO-	$P_{H\text{-}I\text{-}H}=1-\{E^2+(C-E)^2\}/C^2$

After the prepolymerization, the prepolymer was polymerized by HD to give the following structure:

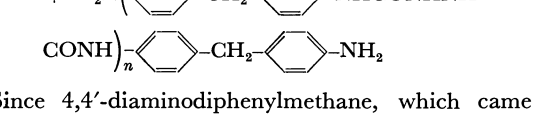

The probability to produce a sequence of $n=1$ is given by:

$$\frac{1/2[1-\{E^2+(C-E)^2\}/C^2]}{(C-E)^2/C^2+1/2[1-\{E^2+(C-E)^2\}/C^2]}=E/C \tag{2}$$

and the probability for $n=2$ is given by:

$$\frac{(C-E)^2/C^2}{(C-E)^2/C^2+1/2[1-\{E^2+(C-E)^2\}/C^2]}\times E/C = \{(C-E)/C\}\times E/C \tag{3}$$

Generally, the probability for $n=m$ is given by:

$$\{(C-E)/C\}^{m-1}\times E/C \tag{4}$$

and the sum of the hard-segment is given by the

5) M. E. Bailey, V. Kriss and R. G. Spaunburgh, *Ind. Eng. Chem.*, **48**, 794 (1956).

6) J. Burkus and C. F. Echert, *J. Amer. Chem. Soc.*, **80**, 5948 (1958).

7) K. Naito and M. Tanaka, Preprints for 19th Annual Meeting of the Chemical Society of Japan, Hiyoshi (1963), p. 76.

8) L. L. Ferstandig and R. A. Scherrer, *J. Amer. Chem. Soc.*, **81**, 4838 (1959).

following equation:

$$\sum_{n=1}^{\infty}\{(C-E)/C\}^{n-1}\times E/C = 1 \qquad (5)$$

The hard-segment obtained by the perchloric acid depolymerization of the PEUE has the following structure:

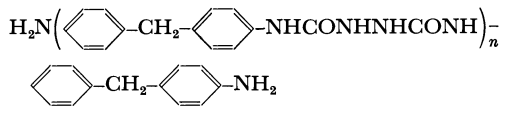

The MW for $n=1$ is 480, and that of the repeating unit is 282, so the number-average MW of the hard-segment is calculated as:

$$\sum_{n=1}^{\infty}\{480+282(n-1)\}\{(C-E)/C\}^{n-1}E/C = 480 + 282(C-E)/E \qquad (6)$$

In the case of the random polymerization, the MW of the hard-segment may be calculated from the monomer content by means of Eq. (6).

The contents of the urea linkage and the urethane linkage in PEUE do not depend on the way of polymerization, as is shown in Table 5.

Table 5. Concentration ratio of each linkage in PEUE

Linkage	Concentration ratio
[NHCONH]	$(C-E)/C=H/C$
[NHCOO]	E/C
[NHCONH]/[NHCOO]	$(C-E)/E=H/E$

A plot of [NHCONH]/[NHCOO] *versus* the absorbance ratio at 1680 cm^{-1} and 1740 cm^{-1} gives a straight line, as is shown in Fig. 2. As may be seen from Fig. 2, the [Urea]/[Urethane] ratio in PEUE is obtained by the IR measurement, and by inserting the above result into Eq. (6), the MW of the hard-segment can be determined. The results are shown in Table 3. These results show that the distribution of the monomer unit deviates from that expected from the equal reactivity of the two isocyanate groups in MDI.

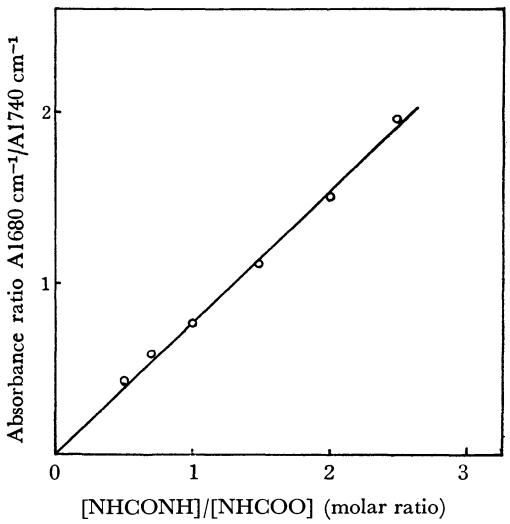

Fig. 2. Absorbance ratio at 1680 cm^{-1} and 1740 cm^{-1} of PEUE.

Apparent Reactivity Ratio of Two Isocyanate Groups in MDI. In the case of the random polymerization, the distribution of monomers in PEUE may be decided by the reactivity ratio of the two isocyanate groups in MDI. The apparent reactivity ratio of the two isocyanate groups is calculated from the MW of the hard-segment in the following way.

In the prepolymerization, the following reaction scheme may hold:

$$\text{OCN–I–NCO} + \text{HO–E–OH} \xrightarrow{k_{11}} \text{HO–E–OCONH–I–NCO} \qquad (7)$$

$$\text{OCN–I–NHCOO–} + \text{HO–E–OH} \xrightarrow{k_{21}} \text{HO–E–OCONH–I–NHCOO–} \qquad (8)$$

$$\text{OCN–I–NCO} + \text{HO–E–OCONH–} \xrightarrow{k_{12}} \text{OCN–I–NHCOO–E–OCONH–} \qquad (9)$$

$$\text{OCN–I–NHCOO} + \text{HO–E–OCONH} \xrightarrow{k_{22}} \text{–OCONH–I–NHCOO–} \qquad (10)$$

where OCN–I–NCO and HO–E–OH denote MDI and PTG respectively and where k denotes a rate constant. Assuming that $k_{11}=k_{12}=k_1$ and that $k_{21}=k_{22}=k_2$, the reactivity ratio of the two isocyanate groups in MDI is given by:

$$A = k_2/k_1$$

Thus, the rate of the reaction may be expressed by the following equations:

$$d[I_1]/dt = -2k_1[I_1][E] \qquad (11)$$

$$d[I_2]/dt = k_1[I_1][E] - k_2[I_2][E] \qquad (12)$$

$$d[E]/dt = -k_1[I_1][E] - k_2[I_2][E] \qquad (13)$$

where $[I_1]$, $[I_2]$, and [E] are the concentrations of isocyanate in MDI, in OCN–I–NHCOO–, and in PTG respectively. From Eqs. (11) and (12),

$$d[I_2]/d[I_1] = (k_2/2k_1)\cdot[I_2]/[I_1] - 1/2 \qquad (14)$$

In the case of $A\neq 2$, the integration of Eq. (14) from time 0 to T, which is the time for the prepolymer reaction, gives the following result:

$$1/(1-A/2)\ln\frac{(1-A/2)[I_2]_T/[I_1]_T+1/2}{(1-A/2)[I_2]_0/[I_1]_0+1/2} = -\ln[I_1]_T/[I_1]_0 \qquad (15)$$

These are also the following relations:

$$[I_1]_0 = 2\times 1 \qquad [I_1]_T = 2\times P_{\text{H–I–H}}$$

$$[I_2]_0 = 0 \qquad [I_2]_T = P_{\text{H–I–E}}$$

By inserting the above relations into Eq. (15), we obtained:

$$2/(2-A)\log\{1-(1-A/2)P_{H\text{-}I\text{-}E}/P_{H\text{-}I\text{-}H}\} = \log(1/P_{H\text{-}I\text{-}H}) \quad (16)$$

Similarly, for $A=2$ we obtained:

$$P_{H\text{-}I\text{-}E}/P_{H\text{-}I\text{-}H} = \ln(1/P_{H\text{-}I\text{-}H}) \quad (17)$$

The values of $P_{H\text{-}I\text{-}E}$, $P_{H\text{-}I\text{-}H}$, and $P_{E\text{-}I\text{-}E}$ are determined by the following known procedure. Inserting the experimental results in Table 3 into Eq. (18), the average sequence length (L_{nH}) of the hard-segment of PEUE is calculated:

$$\overline{L_{nH}} = (\overline{MW}-198)/282 \quad (18)$$

Since the molar fractions of a hard-segment and a soft-segment in PEUE correspond to those of HD and PTG in PEUE respectively, the following equations may be obtained.

$$[\text{Urea}] = [\text{HD}] = P_{H\text{-}I\text{-}H} + \frac{1}{2}P_{H\text{-}I\text{-}E} \quad (19)$$

$$[\text{Urethane}] = [\text{PTG}] = P_{E\text{-}I\text{-}E} + \frac{1}{2}P_{H\text{-}I\text{-}E} \quad (20)$$

The following equation can also be written:

$$P_{H\text{-}I\text{-}H} + P_{E\text{-}I\text{-}E} + P_{E\text{-}I\text{-}H} = 1 \quad (21)$$

Therefore, the number-average sequence length of the hard-segment is given by:

$$\overline{L_{nH}} = \frac{P_{H\text{-}I\text{-}H}+\frac{1}{2}P_{H\text{-}I\text{-}E}}{\frac{1}{2}P_{H\text{-}I\text{-}E}} \quad (22)$$

By inserting the experimental results derived from Table 3 into Eqs. (16) and (17), the reactivity ratio, A, may be calculated. Table 6 shows the reactivity ratio calculated by using an electronic computer.

Table 6. Reactivity ratio of two isocyanate groups in MDI

No.	[Urea]/[Urethane]	$P_{H\text{-}I\text{-}H}$	$P_{H\text{-}I\text{-}E}$	A
1	1/2	0.172	0.322	1.86
2	1.5/2	0.237	0.384	1.68
3	2/2	0.307	0.386	1.79
4	3/2	0.433	0.334	2.40
5	4/2	0.501	0.332	2.25
6	5/2	0.568	0.292	2.69

These calculated apparent reactivity ratios of the two isocyanate groups in MDI (A) are obtained on the assumption of a homogeneous reaction in the prepolymer and chain-extender reactions. It is also necessary to consider the cases of $K_{11} \neq k_{12}$ and $K_{21} \neq k_{22}$. Therefore, thses results deviate from the results obtained by many previous authors.[7,8]

The composition analysis of PEUE's by NMR will become increasingly important since it often provides a direct, simple fingerprint of the various structures.

We should like to express our gratitude to Mr. Hiroo Yanagawa, to Dr. Yasushi Nishimura, and to Dr. Reizo Yamadera for his helpful discussion and examination of this paper. We also wish to express our gratitude to Director Dr. Eiichi Nagai of this Institute for permission to publish this paper.

BULLETIN OF THE CHEMICAL SOCIETY OF JAPAN VOL. 43 687—689 (1970)

Studies of the Structure of Polyurethane Elastomers. II. The Determination of the Blockiness of Poly(Ether)Urethane Elastomes

Hajime SUZUKI and Hiroshi ONO

Katata Research Institute, Toyobo Co., Ltd., Otsu

(Received August 18, 1969)

Two types of poly(ether)urethane elastomers (PEUE), which had the same composition ratio but different degrees of blockiness, were synthesized by the reaction of 4,4′-diphenyl methane diisocyanate (MDI), polyoxytetramethylene glycol (PTG), and hydrazine (HD) or ethylenediamine (EDA) by means of the prepolymer method. The degree of blockiness of the PEUE thus synthesized by the reaction of MDI, PTG, and HD was determined by measuring the molecular weight of a hard segment (urea segment), itself obtained by perchloric acid depolymerization. The values of the blockiness of PEUE which had been synthesized by the prepolymer method without any solvent or in a solvent by means of a prepolymer reaction were about 0.4 and 0.7 respectively. The degree of the blockiness of the PEUE prepared from MDI, PTG, and HD, as measured by the above method, corresponded to the infrared absorbance ratio of the PEUE synthesized by the reaction of MDI, PTG, and EDA at 1740 cm^{-1} and 1720 cm^{-1}. From these results two infrared absorbances, at 1740 cm^{-1} and 1720 cm^{-1}, were assigned to the urethane linkage in a soft segment and at the end of an urea segment respectively.

The determination of the blockiness of PEUE would be very helpful in elucidating the relationship between the structure and the physical properties of the elastomer, but previous attempts to determine the blockiness of PEUE were not successful. Therefore, we have attempted to determine the blockiness by the perchloric acid depolymerization method and by means of infrared spectroscopy.

Although the structure of the PEUE synthesized from MDI, PTG, and HD can not be written in one formula, it may be expressed by the following two segments:

soft segment (poly(ether)urethane segment):

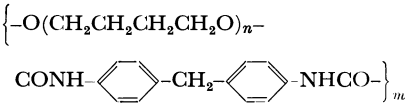

hard segment (urea segment):

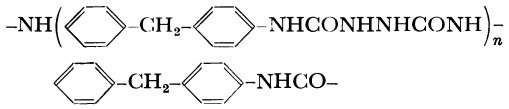

By expressing PEUE by means of the above two segments, the blockiness of PEUE may be determined in the same way as with a vinyl copolymer or a stereoregular polymer.[1,2]

It was thought that the hard segment was composed of a paracrystalline state,[3] and that the soft segment was composed of a liquid-like state; therefore, the infrared absorbance due to an urethane linkage in the soft segment or at the end of the hard segment was assumed to be assignable to two different absorbances.

Experimental

Materials. The PEUE used in this work had been synthesized by the prepolymer method. The prepolymer was prepared by reacting various molar ratios of PTG (MW, *ca.* 1500) and MDI without any solvent at 75°C for 1 hr and the PEUE was prepared from the prepolymer and HD or EDA as a chain extender in *N*,*N*-dimethylacetamide (DMAC) at 7°C. Between the prepolymer reaction and the chain-extender reaction,

TABLE 1. PREPARATION OF PEUE, NUMBER AVERAGE MOLECULAR WEIGHT AND SEQUENCE LENGTH OF HARD SEGMENT SYNTHESIZED FROM MDI, PTG AND HD

No.	Prepolymer MDI (mol)	Prepolymer PTG (mol)	Chain extender MDI (mol)	Chain extender HD or EDA (mol)	$\overline{MW}$	$\overline{L_{nH}}$
1	0.040	0.02	0.000	0.02	1659	5.18
2	0.038	0.02	0.002	0.02	1681	5.26
3	0.034	0.02	0.006	0.02	1960	6.25
4	0.030	0.02	0.010	0.02	2366	7.69
5	0.026	0.02	0.014	0.02	3331	11.1

1) R. L. Miller, L. E. Nielsen, *J. Polym. Sci.*, **46**, 303 (1960).

2) H. J. Harwood and W. M. Ritchey, *ibid.*, **2B**, 601 (1964); **3B**, 419 (1965).

3) R. Bonart, *J. Macromol. Sci-Phys.*, **B2 (1)**, 115 (1968).

MDI was added to make the molar ratio [Urea]/[Urethane]=1.

The various molar ratios of the monomers in the prepolymers prepared in this work are listed in Table 1.

The PEUEs which were synthesized in a solvent by means of the prepolymer reaction were described in a previous paper.[4]

$\overline{MW}$ Determination of the Hard Segment. The hard segment of PEUE prepared from MDI, PTG, and HD was obtained by the perchloric acid depolymerization method described in our previous communication;[4] it was examined by the titration method, and the number-average molecular weight (MW) of the hard segment was calculated by means of the following equation:

$$\overline{MW} = \frac{2\{W(\text{mg}) - 100.5 \times (T_B - T_S)(\text{ml}) \times 1/100 \times F\}}{(T_B - T_S)(\text{ml}) \times 1/100 \times F}$$

where W is the weight of the hard segment, F is a factor of an aqueous solution of HCl, and T_B and T_S are the volumes of an N/100 aqueous solution of HCl required for the titration of the blank and the sample solutions respectively.

Infrared Spectra Measurement. The infrared spectra of PEUE prepared from MDI, PTG, and EDA were obtained with a Hitachi EPI-S2-type infrared spectrophotometer, using thin films cast on glass from the DMAC solution of PEUE. The samples were heat-treated at 100°C for 10 min in order to evaporate the solvent.

Results and Discussion

The structure of the hard segment of PEUE prepared from MDI, PTG, and HD can be written as follows:

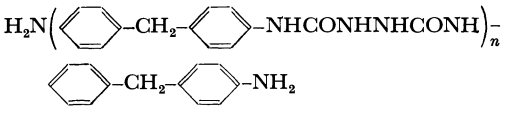

Therefore, the average sequence length of a hard segment can be calculated by the following equation:

$$\overline{L_{n\text{H}}} = (\overline{MW} - 198)/282 \quad (1)$$

Table 1 shows the number-average molecular weight and the sequence length of the hard segment, both values having been measured by the perchloric acid depolymerization method.

If the number-average sequence length of the hard segment is determined to be as is shown in Table 1, one can determine the blockiness of PEUE by the following known procedure.[1,5] If $P_{\text{H-I-H}}$, $P_{\text{H-I-E}}$, and $P_{\text{E-I-E}}$ show the molar fraction of each segment in PEUE, Eq. (2) can be evolved:

$$P_{\text{H-I-H}} + P_{\text{H-I-E}} + P_{\text{E-I-E}} = 1 \quad (2)$$

Since the molar fractions of a hard segment and a soft segment in PEUE correspond to those of HD and PTG respectively in PEUE, the following equations may be obtained:

$$[\text{Urea}] = [\text{HD}] = P_{\text{H-I-H}} + \frac{1}{2}P_{\text{H-I-E}} \quad (3)$$

$$[\text{Urethane}] = [\text{PTG}] = P_{\text{E-I-E}} + \frac{1}{2}P_{\text{H-I-E}} \quad (4)$$

The number-average sequence length of the ($\overline{L_{n\text{H}}}$) hard segment can be determined by inserting the number-average MW of the hard segment into Eq. (5):

$$\overline{L_{n\text{H}}} = (\text{MW} - 198)/282 \quad (5)$$

The values of $P_{\text{H-I-H}}$, $P_{\text{H-I-E}}$, and $P_{\text{E-I-E}}$ are calculated by means of Eqs. (6) and (9). If one could inspect the units along the soft-segment-hard-segment chain in PEUE from one end to the other, the probability of finding a soft segment unit next to a hard segment unit would be:

$$P_{\text{HE}} = \frac{\frac{1}{2}P_{\text{H-I-E}}}{P_{\text{H-I-H}} + \frac{1}{2}P_{\text{H-I-E}}} \quad (6)$$

Similarly, a hard segment unit exists next to a soft segment unit with a probability of:

$$P_{\text{EH}} = \frac{\frac{1}{2}P_{\text{H-I-E}}}{P_{\text{E-I-E}} + \frac{1}{2}P_{\text{H-I-E}}} \quad (7)$$

The degree of blockiness is defined by:

$$B = P_{\text{HE}} + P_{\text{EH}} \quad (8)$$

If $B<1$, these units tend to cluster in blocks of each unit, and finally $B=0$ in a homopolymer mixture, whereas if $B>1$, the sequence length becomes shorter, and $B=2$ in an alternative copolymer.

The number-average sequence length of the $\overline{L_{n\text{H}}}$ hard segment and the $\overline{L_{n\text{E}}}$ soft segment are given by:

$$\overline{L_{n\text{H}}} = 1/P_{\text{HE}} \quad (9)$$

$$\overline{L_{n\text{E}}} = 1/P_{\text{EH}} \quad (10)$$

Table 2 shows the values of the blockiness (B) of the PEUEs listed in Table 1; these values were calculated by means of Eqs. (1)—(10). The value of the blockiness (B) of the PEUEs prepared in DMAC by means of a prepolymer reaction are shown in Table 3. Sample 1 in Table 2 has the same composition ratio as sample 3 in Table 3, but the blockiness of sample 1 in Table 2 is greater than that of sample 3 in Table 3. When there is no solvent in the prepolymer reaction, the reaction between PTG and MDI occurs through the solvation of MDI into PTG: the reaction rate of MDI with PTG may then shows the effects of viscosity and agitation. Therefore, the greater

4) H. Suzuki, H. Ono, This Bulletin, **43**, 682 (1970).
5) R. Yamadera, M. Murano, *J. Polym. Sci., Part A-1*, **5**, 2259 (1967)

Table 2. Molar fraction of the three structural units and degree of the blockiness of PEUE synthesized without solvent at prepolymer

No.	P_{H-I-H}*	P_{E-I-E}*	P_{H-I-E}*	P_{EH}	P_{HE}	B
1	0.403	0.403	0.194	0.193	0.193	0.386
2	0.405	0.405	0.190	0.189	0.189	0.379
3	0.418	0.418	0.164	0.164	0.164	0.328
4	0.434	0.434	0.132	0.133	0.133	0.267
5	0.452	0.452	0.096	0.092	0.092	0.185

* P_{E-I-E}, P_{H-I-H} and P_{H-I-E} represent the molar fractions of the following structures; CH_2–$\left(\bigcirc\!\!\rangle\text{–NHCOO}\right)_2$, $CH_2\left(\bigcirc\!\!\rangle\text{–NHCONH–}\right)_2$ and –OCONH–$\bigcirc\!\!\rangle$–CH_2–$\bigcirc\!\!\rangle$–NHCONH, respectively.

Table 3. Molar fraction of the three structural units and degree of the blockiness of PEUE synthesized in solven at prepolymer

No.	P_{H-I-H}	P_{E-I-E}	P_{H-I-E}	P_{EH}	P_{HE}	B
1	0.172	0.506	0.322	0.241	0.483	0.724
2	0.237	0.379	0.384	0.337	0.448	0.785
3	0.307	0.307	0.386	0.385	0.385	0.770
4	0.433	0 233	0.334	0.418	0.278	0 696
5	0.501	0.167	0.332	0.499	0.249	0.748
6	0.568	0.140	0.292	0.512	0.205	0.717

blockiness of sample 1 in Table 2 in comparison with sample 3 in Table 3 may be due to the heterogeneity of agitation in the prepolymer reaction. On the other hand, the prepolymer reaction in DMAC is a homogeneous reaction; therefore, the difference in the blockiness of sample 3 in Table 3 and the expected blockiness from a random reaction may be small.

The infrared spectra between 1800 cm^{-1} and 1700 cm^{-1} of the PEUE prepared from MDI, PTG, and EDA in Table 1 are shown in Fig. 1.

There have been no reports concerning the two peaks due to urethane linkage, but these peaks are assumed to be assignable to the urethane linkage for two different states, such as the para-crystalline part of a hard segment[3] and a liquid-like state of a soft segment. Figure 2 shows the relationship between the absorbance ratio at 1740 cm^{-1} and 1720 cm^{-1} and the degree of blockiness of PEUE.

From the above results, the absorptions at 1740 cm^{-1} and 1720 cm^{-1} may be assigned to the C=O stretching vibration of urethane linkage in a soft segment without any hydrogen bond and to that of the urethane linkage at the end of the hard segment with a hydrogen bond for the para-crystalline state.

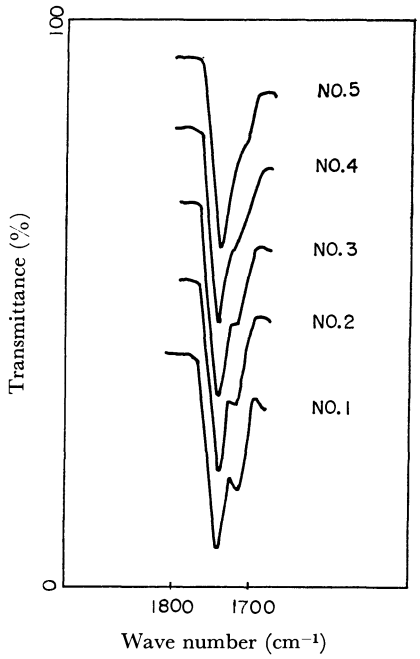

Fig. 1. Infrared spectra of PEUE synthesized from MDI, PTG and EDA in the region 1800—1700 cm^{-1}.

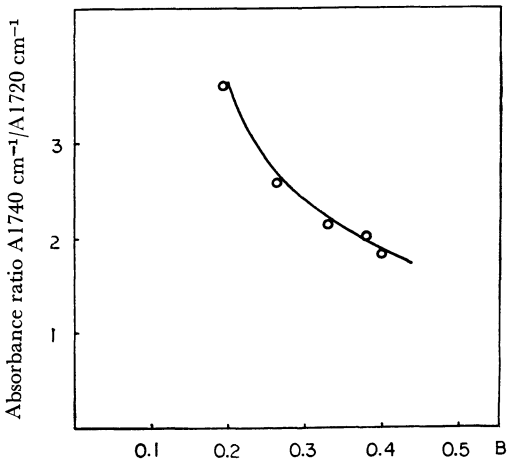

Fig. 2. Relationship between the absorbance ratio at 1740 cm^{-1} and 1720 cm^{-1} and the degree of blockiness.

We should like to express our gratitude to Drs. Yasushi Nishimura and Reizo Yamadera for his helpful discussion and the inspection of this paper. We also wish to express our gratitude to Director Dr. Eiichi Nagai of this institute for permission to publish this paper.

BULLETIN OF THE CHEMICAL SOCIETY OF JAPAN VOL. 43 690—697 (1970)

Far-Infrared Spectra and Lattice Vibrations of Barium Chloride Dihydrate

Kunio FUKUSHIMA and Hiroaki KATAIWA

Department of Chemistry, Faculty of Science, Shizuoka University, Oya-cho, Shizuoka

(Received August 25, 1969)

The far-infrared spectra of barium chloride dihydrate and its deutero analog were measured in the region of 60—4000 cm^{-1}. The assignment of the infrared bands due to crystal water and crystal heavy water was made on the basis of the band frequency shift associated with deuteration. The optically-active lattice vibrations were calculated in order to assign the far-infrared bands and elucidate the nature of the vibrations.

There are many types of crystal water molecules in crystals from the point of view of their coordination to the surrounding ions and the electron-acceptor groups. Chidambaram has classified crystal water molecules on the basis of their coordination to ions and electron-acceptor groups.[1]

In the present study, barium chloride dihydrate (b.c.d.) was adopted as a representative of B-type crystal water molecules in Chidambaram's classification, and a spectroscopic investigation in the IR spectral region and a normal coordinate treatment of the crystal as a whole were made in order to elucidate the nature of the optically-active lattice vibrations and the potential in the crystal. As measurements of the IR spectra in the region of 300—4000 cm^{-1} had already been made by several investigators for b.c.d. and its deutero analog (b.c.d.-d),[2-5] this paper will primarily present the results of the measurement of the far IR spectra in the 60—300 cm^{-1} region of these compounds.

Experimental

The sample for the measurements was obtained by the recrystallization of a special-grade b.c.d. of the Wako Pure Chemical Co., Ltd., from an aqueous solution. The IR spectra of the sample in Nujol mull were measured with a Perkin-Elmer Model 521 spectrophotometer and a Hitachi FIS-3 far-infrared spectrometer. The deuterated sample was made by the recrystallization of b.c.d. from a heavy water solution. The IR spectra of the deuterated sample in Nujol mull were also measured. The results of the measurements are shown in Figs. 1, 2, 3, and 4. The degree of deuteration is manifested in the relative intensities of the O–H stretching bands in the region of 3100—3400 cm^{-1} and of the O–D stretching bands in the region of 2200—2700 cm^{-1} in Fig. 3.

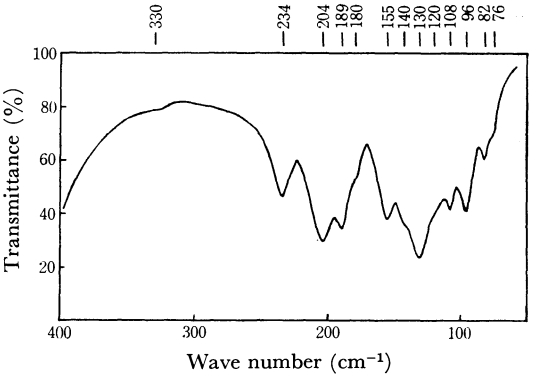

Fig. 1. Far infrared spectra of barium chloride dihydrate in Nujol mull.

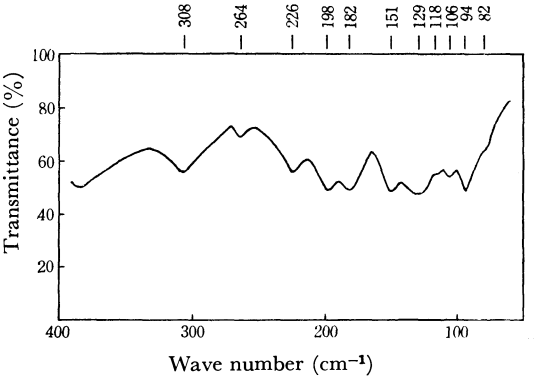

Fig. 2. Far infrared spectra of deuterated barium chloride dihydrate in Nujol mull.

1) R. Chidambaram, A. Sequeira and S. K. Sikka, *J. Chem. Phys.*, **41**, 3616 (1964).

2) T. Noto, H. Sawada, Y. Sato, K. Kotera, M. Goto, N. Fukuba and T. Takahashi, *Tanabe Seiyaku Kenkyu Nempo*, **3**, 48 (1958).

3) O. Salvetti and D. Nobili, *Ann. Chim.* (Rome), **47**, 99 (1952).

4) F. A. Miller and C. H. Wilkins, *Anals. Chem.*, **24**, 1253 (1952).

5) J. Elsken and D. W. Robinson, *Spectrochim. Acta*, **17**, 1249 (1961).

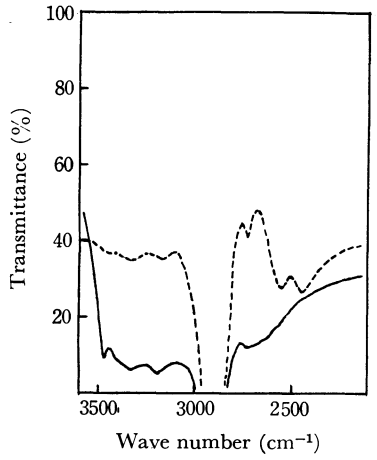

Fig. 3. Infrared spectra of barium chloride dihydrate in Nujol mull (solid line) and deuterated barium chloride dihydrate in Nujol mull (dotted line).

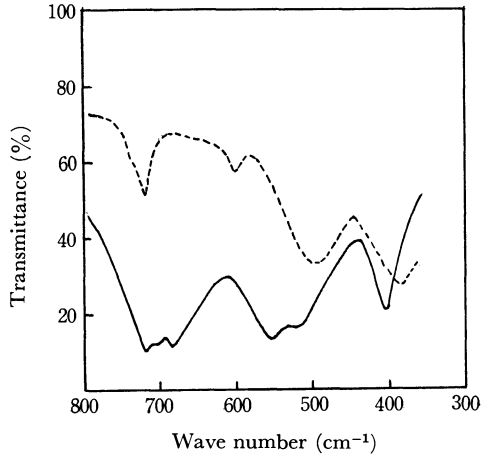

Fig. 4. Infrared spectra of barium chloride dihydrate in Nujol mull (solid line) and deuterated barium chloride dihydrate in Nujol mull (dotted line).

Assignment of IR Absorption Bands

The assignment of the IR absorption bands in the region of 800—4000 cm^{-1} have already been made by several investigators.[2-4] The shift of the IR-band frequencies on deuteration in the present study (3300 cm^{-1}, 3200 cm^{-1}, 1639 cm^{-1}, 1603 cm^{-1} →2545 cm^{-1} 2440 cm^{-1}, 1198 cm^{-1} 1173 cm^{-1}) confirms the assignment[2,3] of the bands at 3300 cm^{-1} and 3200 cm^{-1} to O–H stretching vibrations, and the bands at 1639 cm^{-1} and 1603 cm^{-1} to H_2O bending vibrations. In the region of 300—800 cm^{-1}, Elsken and Robinson found that the bands at 690 cm^{-1}, 560 cm^{-1}, and 520 cm^{-1} shift to lower frequencies on deuteration.[5] This fact was confirmed in the present study, in addition, it was found that the bands at 710 cm^{-1} and 405 cm^{-1} also shift to 500 cm^{-1} and 308 cm^{-1} respectively, as is shown in Figs. 2 and 4. The band at about 720 cm^{-1} in Fig. 4 is due to Nujol, and the weak band at 600 cm^{-1} is considered to be due to an overtone or to a combination band.

In the region of 60—400 cm^{-1}, a comparison of the spectra of b.c.d. with those of b.c.d.-d (Figs. 1 and 2) leads to the following conclusions. The band of b.c.d., which corresponds to the band at 264 cm^{-1} of b.c.d.-d, is considered to be overlapped by the band 405 cm^{-1} of b.c.d., as the frequency ratio (264/405) is close to $1/\sqrt{2}$, which is a rough measure of the frequency ratio of deuteration, while the band at 264 cm^{-1} may be due to a rotational lattice vibration of crystal heavy water. The IR absorption bands in the region of 220—800 cm^{-1}, which are concluded to be due to the rotational lattice vibrations of crystal water and crystal heavy water, are shown in Table 1. Those frequencies in the table correspond to the peak frequencies in neutron-scattering spectra:[6] 710 cm^{-1} (664 ±40 cm^{-1}), 684 cm^{-1} (664±40 cm^{-1}), 555 cm^{-1}

Table 1. Observed fundamental frequencies of infrared absorption bands (4000—400 cm^{-1}) (in cm^{-1})*

$BaCl_2 \cdot 2H_2O$	$BaCl_2 \cdot 2D_2O$
3300 (m)	2545 (m)
3200 (m)	2440 (m)
1639 (s)	1198 (m)
1603 (s)	1173 (m)
710 (s)	500 (m)
684 (s)	488 (sh)
555 (s)	380 (m)
525 (s)	
405 (m)	308 (w)
330 (sh)	264 (w)

* Intensity description:
s, strong; m, medium; w, weak; sh, shoulder

Table 2. Result of the factor group analysis $BaCl_2 \cdot 2H\ O(C_{5h}^2)$ or $BaCl_2 \cdot 2D_2O$ (C_{5h}^2)

	N	T	T'	R'	n
A_g	27	0	15	6	6
A_u	27	1	14	6	6
B_g	27	0	15	6	6
B_u	27	2	13	6	6

N number or the total freedom
T number of the translation
T' number of the translational lattice vibrations
R' number of the rotational lattice vibrations
n number of intramolecular vibrations of H_2O or D_2O

6) H. Boutin, G. J. Safford and H. R. Danner, *J. Chem. Phys.*, **40**, 2670 (1964).

(536 +32cm^{-1}), 525 cm^{-1} (480±24 cm^{-1}), 405 cm^{-1} (384±16 cm^{-1}), 234 cm^{-1} (224±16 cm^{-1}). The figures in parentheses are the peak frequencies in neutron-scattering spectra and their errors.

The number of the observed bands is less than the number derived from a factor group analysis of b.c.d.

This may be interpreted as being due to small frequency differences between A_u and B_u vibrations or to the weak intensities of some bands.

Normal Coordinate Treatment

The crystal structure of b.c.d. was investigated by Jensen,[7] by Padmanabhan *et al.*,[8] and by Padmanabhan *et al.*,[9] the investigators concluded that the space group was $P2_1/n$ for the crystal. In the present study, on the basis of the investigation by Padmanabhan *et al.*,[9] which determined the locations of the hydrogen atoms of crystal water molecules by the neutron diffraction method, the optically-active vibrations were calculated. According to the investigations, b.c.d. is monoclinic and the lattice parameters are $a=6.738$ Å, $b=10.86$ Å, $c=7.136$ Å, and $\beta=90°57'$. The Bravais lattice of the crystal is a simple monoclinic lattice (P), in which four chemical units, $4(BaCl_2\cdot 2H_2O)$, belong to each lattice point.

The optically-active lattice vibrations were calculated according to the method developed by Shimanouchi *et al.*[10]

The optically-active cartesian and internal symmetry coordinate vectors, X_{op} and R_{op}, are expressed by the cartesian and internal symmetry coordinate vectors, $(X_s)^{i,j,k}_{\text{Bravais}}$ and $(R_s)^{i,j,k}_{\text{Bravais}}$ respectively, associated with the Bravais cell (i,j,k).

$$X_{op} = \lim_{n_1,n_2,n_3\to\infty} (n_1n_2n_3)^{1/2} \sum_{i=0}^{n_1}\sum_{j=0}^{n_2}\sum_{k=0}^{n_3} (X_s)^{i,j,k}_{\text{Bravais}}$$

$$R_{op} = \lim_{n_1,n_2,n_3\to\infty} (n_1n_2n_3)^{1/2} \sum_{i=0}^{n_1}\sum_{j=0}^{n_2}\sum_{k=0}^{n_3} (R_s)^{i,j,k}_{\text{Bravais}}$$

The components of the vectors, $(X_s)^{i,j,k}_{\text{Bravais}}$ and $(R_s)^{i,j,k}_{\text{Bravais}}$, are shown in Tables 3 and 4. In the tables, for example, the superscript, I, of X^{I}_i or R^{I}_i represents the chemical unit number, and the underscript, i, of X^{I}_i represents the atom number in one chemical unit. The underscript of R^{I}_i represents simply the coordinate number. In Table 4, $\Delta\alpha_{l(i,j,k)m(i,j,k)n(i,j,k)}$ represents the change in the angle formed by the l atom in the Bravais cell (i,j,k), the m atom in the Bravais cell (i,j,k), and the n atom in the Bravais cell (i,j,k). (In the case of ion, the word "atom" must be replaced by "ion".) The optically-active B matrix, B_{op}, and the optically-active F matrix, F_{op}, are defined as follows:

$$R_{op} = B_{op}X_{op}$$

$$F_{op} = F_{000} + F_{100} + \tilde{F}_{100} + F_{010} + \tilde{F}_{010} + F_{001} + \tilde{F}_{001} + \cdots$$

Here, F_{000} is related to one Bravais cell, and F_{100}, F_{010}, F_{001}, ⋯ are interaction matrices between the Bravais cell and the surrounding Bravais cells.

The lattice vibration frequencies were calculated

Table 3. Cartesian symmetry coordinates (components of the vector, $((X_s)^{i,j,k}_{\text{Bravais}})$*

A_g	$s_{ix} = \Delta(x_i^{\text{I}}+x_i^{\text{II}}-x_i^{\text{III}}-x_i^{\text{IV}})/2$
	$s_{iy} = \Delta(y_i^{\text{I}}+y_i^{\text{II}}-y_i^{\text{III}}-y_i^{\text{IV}})/2$
	$s_{iz} = \Delta(z_i^{\text{I}}-z_i^{\text{II}}-z_i^{\text{III}}+z_i^{\text{IV}})/2$
A_u	$s_{ix} = \Delta(x_i^{\text{I}}-x_i^{\text{II}}+x_i^{\text{III}}-x_i^{\text{IV}})/2$
	$s_{iy} = \Delta(y_i^{\text{I}}-y_i^{\text{II}}+y_i^{\text{III}}-y_i^{\text{IV}})/2$
	$s_{iz} = \Delta(z_i^{\text{I}}+z_i^{\text{II}}+z_i^{\text{III}}+z_i^{\text{IV}})/2$
B_g	$s_{ix} = \Delta(x_i^{\text{I}}-x_i^{\text{II}}-x_i^{\text{III}}+x_i^{\text{IV}})/2$
	$s_{iy} = \Delta(y_i^{\text{I}}-y_i^{\text{II}}-y_i^{\text{III}}+y_i^{\text{IV}})/2$
	$s_{iz} = \Delta(z_i^{\text{I}}+z_i^{\text{II}}-z_i^{\text{III}}-z_i^{\text{IV}})/2$
B_u	$s_{ix} = \Delta(x_i^{\text{I}}+x_i^{\text{II}}+x_i^{\text{III}}+x_i^{\text{IV}})/2$
	$s_{iy} = \Delta(y_i^{\text{I}}+y_i^{\text{II}}+y_i^{\text{III}}+y_i^{\text{IV}})/2$
	$s_{iz} = \Delta(z_i^{\text{I}}-z_i^{\text{II}}+z_i^{\text{III}}-z_i^{\text{IV}})/2$

* $i=1$ though 9; refer to Table 6.

Table 4. Internal symmetry coordinates (compoents of the vector, $(R_s)^{i,j,k}_{\text{Bravais}}$)*

A_g	$\Delta R_{si} = \Delta(R_i^{\text{I}}+R_i^{\text{II}}+R_i^{\text{III}}+R_i^{\text{IV}})/2$
A_u	$\Delta R_{si} = \Delta(R_i^{\text{I}}-R_i^{\text{II}}-R_i^{\text{III}}+R_i^{\text{IV}})/2$
B_g	$\Delta R_{si} = \Delta(R_i^{\text{I}}-R_i^{\text{II}}+R_i^{\text{III}}-R_i^{\text{IV}})/2$
B_u	$\Delta R_i = \Delta(R_i^{\text{I}}+R_i^{\text{II}}-R_i^{\text{III}}-R_i^{\text{IV}})/2$
	$i=1$ through 44

$\Delta R^{\text{I}}_{33} = \Delta\alpha_{6(i,j-1,k)4(i,j-1,k)7(i,j,k)}$
$\Delta R^{\text{I}}_{34} = \Delta\alpha_{8(i,j,k)5(i,j,k)9(i,j,k)}$
$\Delta R^{\text{I}}_{35} = \Delta\alpha_{8(i,j,k)5(i,j,k)1(i,j,k)}$
$\Delta R^{\text{I}}_{36} = \Delta\alpha_{8(i,j,k)5(i,j,k)1(i,j-1,k)}$
$\Delta R^{\text{I}}_{37} = \Delta\alpha_{1(i,j,k)5(i,j,k)1(i,j-1,k)}$
$\Delta R^{\text{I}}_{38} = \Delta\alpha_{1(i,j,k)5(i,j,k)9(i,j,k)}$
$\Delta R^{\text{I}}_{39} = \Delta\alpha_{1(i,j-1,k)5(i,j,k)9(i,j,k)}$
$\Delta R^{\text{I}}_{40} = \Delta\alpha_{6(i,j-1,k)4(i,j-1,k)1(i,j,k)}$
$\Delta R^{\text{I}}_{41} = \Delta\alpha_{6(i,j,k)4(i,j,k)1(i,j,k)}$
$\Delta R^{\text{I}}_{42} = \Delta\alpha_{1(i,j,k)4(i,j-1,k)1(i,j-1,k)}$
$\Delta R^{\text{I}}_{43} = \Delta\alpha_{1(i,j,k)4(i,j-1,k)7(i,j,k)}$
$\Delta R^{\text{I}}_{44} = \Delta\alpha_{1(i,j-1,k)4(i,j-1,k)7(i,j,k)}$
$\Delta R^{\text{II}}_i = \sigma(\Delta R^{\text{I}}_i),\ \Delta R^{\text{III}}_i = i(\Delta R^{\text{I}}_i),\ \Delta R^{\text{IV}}_i = \text{C}_2(\Delta R^{\text{I}}_i)$

* ΔR^{I}_i's for $i=1$ through 32 correspond to R_i's in Table 5. The symbols, $\boldsymbol{\sigma}$, $\mathbf{i}$ and $\mathbf{C}_2$, represent symmetry operations associated with glide plane, inversion and 2-fold screw axis.

7) A. T. Jensen, *Mat. fys. Medd.*, **22**, 22 (1945).

8) V. M. Padmanabhan, V. S. Jakkal and J. Shanker, *Indian J. Pure Appl. Phys.*, **1**, 293 (1963).

9) V. M. Padmanabhan, W. R. Busing and H. A. Levy, *Acta Crystallogr.*, **16**, 13 (1963).

10) T. Shimanouchi, M. Tsuboi and T. Miyazawa, *J. Chem. Phys.*, **35**, 1597 (1963).

by solving the secular equation, $|M^{-1}F_{xs}-\lambda E|=0$. M is diagonal matrix having diagonal elements of masses of atoms or ions, and $F_{xs}=B_{op}F_{op}B_{op}$. The following potential was assumed: $V=V_{H_2O}+V_{inter}$. V_{H_2O} is the Urey-Bradley force field[11] associated with crystal water molecules, and V_{inter} represents the interaction potential between crystal water molecules and ions, between ions, and also between water molecules.

$$\begin{aligned}2V_{inter} = &\sum f_i(Cl^-\cdots H)(\Delta q_i(Cl^-\cdots H))^2\\ &+ f_i(Ba^{2+}\cdots O)(\Delta q_i(Ba^{2+}\cdots O))^2\\ &+ f_i(Ba^{2+}\cdots Cl^-)(\Delta q_i(Ba^{2+}\cdots Cl^-))^2\\ &+ f_i(O\cdots O)(\Delta q_i(O\cdots O))^2\\ &+ \sum f_i(O\cdots Cl^-)(\Delta q_i(O\cdots Cl^-))^2\\ &+ \sum f_i(Cl^-\cdots Cl^-)(\Delta q_i(Cl^-\cdots Cl^-))^2\\ &+ \sum H_i(H\text{–}O\cdots Ba^{2+})r^i_{O\text{-}H}r^i_{Ba^{2+}\cdots O}(\Delta\alpha^i_{HO\cdots Ba^{2+}})^2\\ &+ \sum H_i(Ba^{2+}\cdots O\cdots Ba^{2+})r^i_{Ba^{2+}\cdots O}r^i_{Ba^{2+}\cdots O}\\ &\quad\times(\Delta\alpha^i_{Ba^{2+}\cdots O\cdots Ba^{2+}})^2\\ &+ 2a(\Delta\alpha^k_{H\text{-}O\cdots Ba^{2+}})(\Delta\alpha^l_{H\text{-}O\cdots Ba^{2+}})\\ &+ 2b(\Delta\alpha^m_{Ba^{2+}\cdots O\text{-}H})(\Delta\alpha^n_{Ba^{2+}\cdots O\text{-}H})\end{aligned}$$

In the above equation, the Δq_i's and $\Delta\alpha_i$'s represent changes in the interatomic distances and in the bond angles respectively, and the r's represent equilibrium interatomic distances. The force constants, a and b, are the interaction force constant between two $\Delta\alpha_{H-O\cdots Ba^{2+}}$'s which share a O–H bond and that between two $\Delta\alpha_{Ba^{2+}\cdots O-H}$'s which share a $Ba^{2+}\cdots O$ bond respectively. The atom-atom, atom-ion, or ion-ion interactions with interatomic distances of more than 4.0 Å were neglected. The interactions taken into account are shown for the chemical unit, I, in Table 5.

The first-trial set of force constants are shown in Table 7 as set I. $K(Cl^-\cdots Cl^-)$ and $K(O\cdots O)$ were calculated by the assumed formula: $K=A\exp(-Br)$, in which r represents the interatomic distance. The parameters, A and B, were determined from two values of $Cl^-\cdots Cl^-$ force constants (0.11 mdyn/Å, 0.15 mdyn/Å), corresponding to two values of interatomic distances (3.29 Å, 3.18 Å)[12] and from seven values of O···O force constants (5.14 mdyn/Å, 3.02 mdyn/Å, 3.03 mdyn/Å, 1.74 mdyn/Å, 1.05 mdyn/Å, 0.76 mdyn/Å, and 0.555 mdyn/Å) corresponding to seven values of interatomic distances (2.09 Å, 2.20 Å, 2.21 Å, 2.27 Å, 2.36 Å, 2.47 Å, and 2.48 Å).[13] The formula for $K(Cl^-\text{–}Cl^-)$ was used for the estimation of $K(O\cdots Cl^-)$. $K(H\cdots Cl^-)$ was estimated from the $K(H\cdots Cl^-)$ values in Ref. 14. $H(H\text{–}O\cdots Ba^{2+})$ and $H(Ba^{2+}\cdots O\cdots Ba^{2+})$ were taken from Ref. 13. $K(Ba^{2+}\cdots O)$ and $K(Ba^{2+}\cdots Cl^-)$ were estimated to be twice the $K(Cs^+\cdots O)$ and $K(K^+\cdots Cl^-)$ values in Ref. 14. The results of the calculation showed a good agreement of the calculated frequencies with the frequencies of the far IR bands in the region of 60—250 cm^{-1}. Therefore, only the force constants, K(O–H), H(H–O–H), $H_i(H\text{–}O\cdots Ba^{2+})$'s, $H_i(Ba^{2+}\cdots O\cdots Ba^{2+})$'s, a and b were adjusted by the method of least squares[15] in order to obtain the best fit of the observed frequencies with the calculated frequencies.

Table 5. Atom–atom and atom–ion interactions

	Interacting pair		Distance (Å)
R_1	$1(i,j,k)4(i,j-1,k)$	$Ba^{2+}\cdots O$	2.747
R_2	$1(i,j,k)5(i,j,k)$	$Ba^{2+}\cdots O$	2.865
R_3	$1(i,j,k)2(i-1,j-1,k)$	$Ba^{2+}\cdots Cl^-$	3.178
R_4	$1(i,j,k)3(i-1,j,k)$	$Ba^{2+}\cdots Cl^-$	3.168
R_5	$1(i,j,k)5(i-1,j-1,k)$	$Ba^{2+}\cdots O$	2.874
R_6	$1(i,j,k)5(i-1,j-1,k)$	$Ba^{2+}\cdots O$	2.940
R_7	$1(i,j,k)2(i-1,j-1,k)$	$Ba^{2+}\cdots Cl^-$	3.210
R_8	$1(i,j,k)3(i-1,j-1,k)$	$Ba^{2+}\cdots Cl^-$	3.199
R_9	$4(i,j,k)6(i,j,k)$	O–H	0.967
R_{10}	$4(i,j,k)7(i,j+1,k)$	O–H	1.057
R_{11}	$4(i,j,k)5(i+1,j+1,k)$	O···O	3.236
R_{12}	$5(i,j,k)8(i,j,k)$	O–H	0.965
R_{13}	$5(i,j,k)9(i,j,k)$	O–H	0.953
R_{14}	$6(i,j,k)3(i+1,j+1,k)$	$H\cdots Cl^-$	2.242
R_{15}	$7(i,j,k)3(i,j,k)$	$H\cdots Cl^-$	2.172
R_{16}	$2(i,j,k)8(i+1,j,k)$	$H\cdots Cl^-$	2.222
R_{17}	$9(i,j,k)2(i+1,j+1,k)$	$H\cdots Cl^-$	2.631
R_{18}	$9(i,j,k)3(i+1,j+1,k)$	$H\cdots Cl^-$	2.529
R_{19}	$4(i,j,k)2(i-1,j,k)$	$O\cdots Cl^-$	3.665
R_{20}	$4(i,j,k)2(i,j,k)$	$O\cdots Cl^-$	3.508
R_{21}	$4(i,j,k)2(i-1,j,k)$	$O\cdots Cl^-$	3.936
R_{22}	$4(i,j,k)3(i-1,j,k)$	$O\cdots Cl^-$	3.302
R_{23}	$4(i,j,k)2(i+1,j+2,k)$	$O\cdots Cl^-$	3.372
R_{24}	$5(i,j,k)3(i,j,k)$	$O\cdots Cl^-$	3.365
R_{25}	$5(i,j,k)2(i-1,j-1,k)$	$O\cdots Cl^-$	3.475
R_{26}	$5(i,j,k)3(i,j+1,k)$	$O\cdots Cl^-$	3.439
R_{27}	$2(i,j,k)3(i,j,k)$	$Cl^-\cdots Cl^-$	3.922
R_{28}	$2(i,j,k)2(i+2,j+2,k)$	$Cl^-\cdots Cl^-$	3.986
R_{29}	$2(i,j,k)3(i+1,j+1,k)$	$Cl^-\cdots Cl^-$	3.905
R_{30}	$2(i,j,k)3(i,j+1,k)$	$Cl^-\cdots Cl^-$	3.901
R_{31}	$3(i,j,k)3(i+1,j+1,k)$	$Cl^-\cdots Cl^-$	4.075
R_{32}	$3(i,j,k)2(i+2,j+1,k)$	$Cl^-\cdots Cl^-$	4.072

The computations were carried out making use of the Computation Center, University of Tokyo. The programs, BGLZ and LSMB, were constructed at the Shimanouchi Lab., Department of Chemistry, Faculty of Science, University of Tokyo, while the other programs made by one of the authors, Dr. Fukushima.

11) T. Shimanouchi, *J. Chem. Phys.*, **17**, 245 (1949).
12) J. Hiraishi and T. Shimanouchi, *Spectrochim. Acta*, **22**, 1483 (1966).
13) T. Shimanouchi, *Pure Appl. Chem.*, **7**, 131 (1963).
14) I. Nakagawa and T. Shimanouchi, *Spectrochim. Acta*, **22**, 1707 (1966).
15) D. E. Mann, T. Shimanouchi, J. H. Meal and L. Fano, *J. Chem. Phys.*, **27**, 43 (1957).

The cartesian coordinate values of the atoms and ions in the chemical unit, I, are shown in Table 6. The coordinate axes, X, Y, and Z, are chosen in such a way that the symmetry elements of the factor group, $\mathbf{C}_2$ and σ, coincide with the Z axis and the XY plane respectively. Therefore, the cartesian coordinate values of the atoms and ions in other chemical units, II, III, and IV, can be obtained by the operation of σ, $\mathbf{i}$ and $\mathbf{C}_2$ respectively on the coordinates of the chemical unit, I. Here, σ, $\mathbf{i}$ and $\mathbf{C}_2$ mean (translation, $(\boldsymbol{a}+\boldsymbol{c})/2$)+(reflection with respect to the XY plane), inversion, and (translation, $\boldsymbol{b}/2$)+(rotation of 180°) respectively.

Table 6. Cartesian coordinates of atoms and ions in the chemical unit, I (in Å)

No.	Atom or Ion	X	Y	Z
1	Ba^{2+}	−1.424	−0.742	−0.363
2	Cl^-(1)	4.034	3.884	−1.833
3	Cl^-(2)	2.606	0.369	−1.575
4	O (1)	0.748	4.930	−1.188
5	O (2)	−0.393	1.824	−1.113
6	H (1)	0.592	4.512	−2.046
7	H (2)	1.515	−1.497	−1.352
8	H (3)	−1.097	2.473	−1.229
9	H (4)	−0.081	1.696	−2.005

Table 7. Force constants (in mdyn/Å)

	Set I	Set II	*
$f(Ba^{2+}\cdots O)$	0.250	0.250	
$f(Ba^{2+}\cdots Cl^-)$	0.200	0.200	
$K(OH)$	5.640	5.830	
$f(O\cdots O)$	0.009	0.009	
$f^1(H\cdots Cl^-)$	0.150	0.150	ΔR_{14}, ΔR_{15}, ΔR_{16}
$f^2(H\cdots Cl^-)$	0.100	0.100	ΔR_{17}, ΔR_{18}
$f(O\cdots Cl^-)$	$\ln f=7.070-2.820\,r$		
$f(Cl^-\cdots Cl^-)$	$\ln f=7.070-2.820\,r$		
H^1(H–O–H)	0.640	0.763	ΔR_{33}
H^2(H–O–H)	0.640	0.735	ΔR_{34}
F(H···H)	−0.100	−0.100	
H^1(H–O···Ba^{2+})	0.040	0.0405	ΔR_{35}, ΔR_{36}
H^2(H–O···Ba^{2+})	0.040	0.0400	ΔR_{38}
H^3(H–O···Ba^{2+})	0.040	0.0600	ΔR_{39}
H^4(H–O···Ba^{2+})	0.040	0.0570	ΔR_{40}, ΔR_{41}
H^5(H–O···Ba^{2+})	0.040	0.0375	ΔR_{43}, ΔR_{44}
H($Ba^{2+}\cdots O\cdots Ba^{2+}$)	0.040	0.0400	
a	0.000	0.019**	
b	0.000	−0.019**	

* coordinates representing change of bonds and bond angles for which the force constant was used.
** in mdyn·Å

Discussion

The calculated frequencies and the significant terms of the potential energy distributions for the set II force constants in Table 7 are shown in Tables 8, 9, 10, and 11, along with the observed frequencies. For the vibrations primarily associated with rotational lattice vibrations of crystal water and crystal heavy water, the following coordinates were used for the expression of the potential energy distributions.

$$\Delta R'_{s35} = (\Delta R_{s35}+\Delta R_{s36}+\Delta R_{s38}+\Delta R_{s39})/2$$
$$\Delta R'_{s36} = (\Delta R_{s35}-\Delta R_{s36}+\Delta R_{s38}-\Delta R_{s39})/2$$
$$\Delta R'_{s38} = (\Delta R_{s35}-\Delta R_{s36}-\Delta R_{s38}+\Delta R_{s39})/2$$
$$\Delta R'_{s39} = (\Delta R_{s35}+\Delta R_{s36}-\Delta R_{s38}-\Delta R_{s39})/2$$
$$\Delta R'_{s40} = (\Delta R_{s40}+\Delta R_{s41}+\Delta R_{s43}+\Delta R_{s44})/2$$
$$\Delta R'_{s41} = (\Delta R_{s40}-\Delta R_{s41}+\Delta R_{s43}-\Delta R_{s44})/2$$
$$\Delta R'_{s43} = (\Delta R_{s40}-\Delta R_{s41}-\Delta R_{s43}+\Delta R_{s44})/2$$
$$\Delta R'_{s44} = (\Delta R_{s40}+\Delta R_{s41}-\Delta R_{s43}-\Delta R_{s44})/2$$

$\Delta R'_{s36}$ and $\Delta R'_{s41}$, $\Delta R'_{s38}$ and $\Delta R'_{s43}$, and $\Delta R'_{s39}$ and $\Delta R'_{s44}$ represent H_2O (or D_2O) wagging, H_2O (or D_2O) twisting, and H_2O (or D_2O) rocking motions respectively. As is shown in the potential energy distributions, the IR bands at 710 cm^{-1}, 684 cm^{-1}, 555 cm^{-1}, and 525 cm^{-1} of $BaCl_2\cdot 2H_2O$ are due to the coupled vibrations of H_2O wagging and H_2O twisting vibrations, while the bands at 405 cm^{-1} and 330 cm^{-1} are due to H_2O rocking vibrations. The corresponding bands of the coupled D_2O wagging and D_2O twisting vibrations of $BaCl_2\cdot 2D_2O$ appear at 500 cm^{-1}, 488 cm^{-1}, and 380 cm^{-1}, while the bands due to D_2O rocking vibrations appear at 308 cm^{-1} and 264 cm^{-1}, as shown is in Tables 8 and 9. The frequency, 330 cm^{-1}, of the very weak band of $BaCl_2\cdot 2H_2O$ and the frequency shifts of the Raman lines listed in the Tables 10 and 11[16] were not used for the adjustment of the force constants.

There are two crystal water molecules per chemical unit, $BaCl_2\cdot 2H_2O$; these molecules differ in the type of bonding to the surrounding ions. In order to ascertain the bound state of the crystal water molecules, the force constants for rotation around the principal axes of the moment of inertia, k_A, k_B, and k_C, were calculated as follows. The following symbols were used:

atoms, H, O, H : i, j, k

F : Potential energy matrix having the coordinates which change by the displacement of the i, j, and k atoms as its bases

B : Matrix transforming the displacements of the i, j, and k atoms to the coordinates forming bases of F.

$\Delta\theta_m$ (m=A, B, C) : Angle of rotation around the principal axis, m.

The potential energy change, ΔV_m, due to the displacements of the i, j, and k atoms, ρ_{mn} (m=

16) A. Galy, *Compt. Rend.*, **235**, 1504 (1952).

A,B,C; $n=i,j,k$), is shown as:

$$2\Delta V_m = \sum_n \tilde{\rho}_{mn}\tilde{B}FB\rho_{mn} = k_m(\Delta\theta_m)^2$$

$$\rho_{An} = Y_n\Delta\theta_A e, \quad \rho_{Bn} = X_n\Delta\theta_{BC} \quad (n=i,j,k)$$

$$e = (r_{ji}\times r_{jk})/(|r_{ji}||r_{jk}|\sin\alpha_{ijk})$$

$$\rho_{Ci} = \sqrt{X_i^2+Y_i^2}\,e_1$$

$$e_1 = ((r_{gi}/|r_{gi}|)\cos\alpha_{igj} - (r_{gj}/|r_{gj}|))/\sin\alpha_{igj}$$

$$\rho_{Cj} = \sqrt{X_j^2+Y_j^2}\,e_2$$

$$e_2 = ((r_{gi}/|r_{gj}|)\cos\alpha_{jgk} - (r_{gk}/|r_{gk}|))/\sin\alpha_{jgk}$$

$$\rho_{Ck} = \sqrt{X_k^2+Y_k^2}\,e_3$$

$$e_3 = ((r_{gk}/|r_{gk}|)\cos\alpha_{igk} - (r_{gi}/|r_{gi}|))/\sin\alpha_{igk}$$

Table 8. Calculated frequencies (in cm^{-1}) and significant terms of potential energy distributions (A_u species)

$BaCl_2\cdot 2H_2O$

ν_{obsd}	ν_{calcd}	Significant terms of P.E.D.
3300	3291	$\Delta R_{s9}(0.49)$, $\Delta R_{s10}(0\ 47)$
	3282	$\Delta R_{s12}(0.59)$, $\Delta R_{s13}(0.39)$
3200	3211	$\Delta R_{s13}(0\ 60)$, $\Delta R_{s12}(0.39)$
	3210	$\Delta R_{s10}(0.50)$, $\Delta R_{s9}(0.48)$
1639	1638	$\Delta R_{s33}(0.97)$
1603	1607	$\Delta R_{s34}(0.96)$
710	725	$\Delta R'_{s38}(0.47)$, $\Delta R'_{s36}(0.17)$, $\Delta R_{s17}(0.19)$
684	688	$\Delta R'_{s43}(0.54)$, $\Delta R'_{s41}(0.26)$
555	557	$\Delta R'_{s36}(0.69)$, $\Delta R'_{s38}(0.41)$
525	516	$\Delta R'_{s41}(0.68)$, $\Delta R'_{s43}(0.43)$
405	398	$\Delta R'_{s39}(0.77)$, $\Delta R_{s18}(0.12)$
330	328	$\Delta R'_{s44}(0.94)$
234	235	$\Delta R_{s16}(0.15,)$, $\Delta R_{s37}(0.13)$, $\Delta R_{s6}(0.13)$
	232	$\Delta R_{s1}(0.36)$, $\Delta R_{s14}(0.18)$, $\Delta R_{s22}(0.11)$
···	224	$\Delta R_{s5}(0.33)$
204	212	$\Delta R_{s6}(0.35)$, $\Delta R_{s2}(0.33)$, $\Delta R_{s17}(0.12)$
···	168	$\Delta R_{s15}(0.31)$, $\Delta R_{s8}(0.14)$, $\Delta R_{s14}(0.14)$
155	153	$\Delta R_{s24}(0.20)$, $\Delta R_{s17}(0.15)$, $\Delta R_{s3}(0.14)$
140	137	$\Delta R_{s4}(0.45)$, $\Delta R_{s7}(0.14)$, $\Delta R_{s24}(0.10)$
130	129	$\Delta R_{s3}(0.26)$, $\Delta R_{s8}(0.12)$, $\Delta R_{s26}(0.11)$
120	124	$\Delta R_{s7}(0.55)$
108	106	$\Delta R_{s16}(0.23)$, $\Delta R_{s15}(0.13)$
96	96	$\Delta R_{s8}(0.26)$, $\Delta R_{s26}(0.18)$, $\Delta R_{s3}(0.15)$
82	78	$\Delta R_{s1}(0.24)$, $\Delta R_{s5}(0.17)$
76	70	$\Delta R_{s6}(0.26)$, $\Delta R_{s25}(0.17)$, $\Delta R_{s2}(0.11)$
···	62	$\Delta R_{s22}(0.16)$, $\Delta R_{18}(0.12)$

$BaCl_2\cdot 2D_2O$

ν_{obsd}	ν_{calcd}	Significant terms of P.E.D.
2545	2410	$\Delta R_{s9}(0.49)$, $\Delta R_{s10}(0.48)$
	2401	$\Delta R_{s12}(0.55)$, $\Delta R_{s13}(0.42)$
2440	2329	$\Delta R_{s13}(0.56)$, $\Delta R_{s12}(0.42)$
	2325	$\Delta R_{s9}(0.49)$, $\Delta R_{s10}(0.49)$
1198	1194	$\Delta R_{s33}(0.96)$
1173	1168	$\Delta R_{s34}(0.95)$
500	520	$\Delta R'_{s38}(0\ 39)$, $\Delta R'_{s36}(0.24)$, $\Delta R_{s17}(0.19)$
488	504	$\Delta R'_{s43}(0.40)$, $\Delta R'_{s41}(0.37)$
380	416	$\Delta R'_{s36}(0.61)$, $\Delta R'_{s38}(0.46)$
	385	$\Delta R'_{s43}(0.56)$, $\Delta R'_{s41}(0.51)$
308	310	$\Delta R'_{s39}(0.70)$, $\Delta R_{s18}(0.13)$
264	263	$\Delta R'_{s44}(0.74)$, $\Delta R_{s11}(0.13)$
226	224	$\Delta R_{s16}(0.14)$, $\Delta R_{s37}(0.13)$, $\Delta R_{s6}(0.13)$
···	216	$\Delta R_{s22}(0.15)$, $\Delta R_{s14}(0.10)$, $\Delta R_{s42}(0.10)$
···	210	$\Delta R_{s5}(0.35)$, $\Delta R_{s1}(0.11)$, $\Delta R_{s15}(0.12)$, $\Delta R_{s23}(0.11)$
198	200	$\Delta R_{s6}(0.33)$, $\Delta R_{s2}(0.30)$, $\Delta R_{s17}(0.15)$
151	157	$\Delta R_{s8}(0.22)$, $\Delta R_{s15}(0.20)$, $\Delta R_{s14}(0.11)$
	145	$\Delta R_{s3}(0.22)$, $\Delta R_{s24}(0.15)$, $\Delta R_{s17}(0.14)$
129	136	$\Delta R_{s4}(0.45)$, $\Delta R_{s7}(0.14)$
	126	$\Delta R_{s3}(0.15)$, $\Delta R_{s26}(0.15)$
118	124	$\Delta R_{s7}(0.50)$, $\Delta R_{s3}(0.13)$
106	104	$\Delta R_{s16}(0.23)$, $\Delta R_{s15}(0.11)$
94	90	$\Delta R_{s8}(0.28)$, $\Delta R_{s26}(0.19)$, $\Delta R_{s3}(0.13)$
82	77	$\Delta R_{s1}(0.24)$, $\Delta R_{s5}(0.18)$, $\Delta R_{s22}(0.10)$
···	70	$\Delta R_{s6}(0.26)$, $\Delta R_{s25}(0.17)$, $\Delta R_{s2}(0.10)$
···	59	$\Delta R_{s22}(0.15)$, $\Delta R_{s18}(0.12)$

Table 9. Calculaed frequencies (in cm^{-1}) and significant terms of potential energy distributons (B_u species)

$BaCl_2\cdot 2H_2O$

ν_{obsd}	ν_{calcd}	Significant terms of P.E.D.
3300	3291	$\Delta R_{s9}(0.50)$, $\Delta R_{s10}(0.47)$
	3282	$\Delta R_{s12}(0.58)$, $\Delta R_{s13}(0.39)$
3200	3211	$\Delta R_{s13}(0.60)$, $\Delta R_{s12}(0.39)$
	3210	$\Delta R_{s10}(0.50)$, $\Delta R_{s9}(0.48)$
1639	1638	$\Delta R_{s33}(0.97)$
1603	1607	$\Delta R_{s34}(0.96)$
710	725	$\Delta R'_{s38}(0.47)$, $\Delta R'_{s36}(0.17)$, $\Delta R_{s17}(0.19)$
684	688	$\Delta R'_{s43}(0.54)$, $\Delta R'_{s41}(0.26)$
555	557	$\Delta R'_{s36}(0.69)$, $\Delta R'_{s38}(0.41)$
525	516	$\Delta R'_{s41}(0.69)$, $\Delta R'_{s43}(0.42)$
405	401	$\Delta R'_{s39}(0.75)$, $\Delta R_{s18}(0.13)$
330	334	$\Delta R'_{s44}(0.84)$
···	261	$\Delta R_{s1}(0.27)$, $\Delta R_{s5}(0.23)$
···	256	$\Delta R_{s2}(0.28)$, $\Delta R_{s6}(0.14)$, $\Delta R_{s16}(0.11)$, $\Delta R_{s37}(0.10)$
204	203	$\Delta R_{s15}(0.30)$, $\Delta R_{s22}(0.21)$, $\Delta R_{s8}(0.11)$
189	187	$\Delta R_{s6}(0.25)$, $\Delta R_{s16}(0.19)$, $\Delta R_{s24}(0.19)$
180	173	$\Delta R_{s4}(0.17)$, $\Delta R_{s23}(0.16)$, $\Delta R_{s8}(0.15)$
155	163	$\Delta R_{s7}(0.35)$, $\Delta R_{s3}(0.32)$
140	137	$\Delta R_{s23}(0.21)$, $\Delta R_{s4}(0.16)$, $\Delta R_{s20}(0.10)$,
130	130	$\Delta R_{s17}(0.46)$
108	112	$\Delta R_{s24}(0.22)$
96	90	$\Delta R_{s22}(0.16)$, $\Delta R_{s15}(0.11)$, $\Delta R_{s18}(0.11)$
82	84	$\Delta R_{s18}(0.16)$, $\Delta R_{s8}(0.16)$
···	67	$\Delta R_{s25}(0.27)$, $\Delta R_{s1}(0.12)$
···	48	$\Delta R_{s42}(0.13)$, $\Delta R_{s14}(0.13)$, $\Delta R_{s5}(0.10)$

TABLE 9. (Continued)

$BaCl_2 \cdot 2D_2O$

ν_{obsd}	ν_{calcd}	Significant terms of P.E.D.	ν_{obsd}	ν_{calcd}	Significant terms of P.E.D.
2545	2410	$\Delta R_{s9}(0.49)$, $\Delta R_{s10}(0.48)$	226	229	$\Delta R_{s43}(0.24)$, $\Delta R_{s1}(0.20)$, $\Delta R_{s5}(0.11)$
	2401	$\Delta R_{s12}(0.55)$, $\Delta R_{s13}(0.42)$	198	194	$\Delta R_{s15}(0.23)$, $\Delta R_{s22}(0.17)$, $\Delta R_{s8}(0.15)$
2440	2329	$\Delta R_{s13}(0.56)$, $\Delta R_{s12}(0.42)$	182	174	$\Delta R_{s4}(0.13)$, $\Delta R_{s24}(0.10)$
	2325	$\Delta R_{s10}(0.50)$, $\Delta R_{s9}(0.48)$	...	165	$\Delta R_{s6}(0.18)$, $\Delta R_{s16}(0.14)$
1198	1194	$\Delta R_{s33}(0.96)$	...	161	$\Delta R_{s7}(0.29)$, $\Delta R_{s3}(0.26)$
1173	1168	$\Delta R_{s34}(0.95)$	129	130	$\Delta R_{s23}(0.20)$, $\Delta R_{s4}(0.13)$
500	520	$\Delta R'_{s38}(0.39)$, $\Delta R'_{s36}(0.24)$, $\Delta R_{s17}(0.19)$	118	121	$\Delta R_{s17}(0.44)$
488	502	$\Delta R'_{s43}(0.42)$, $\Delta ER'_{s41}(0.37)$	106	111	$\Delta R_{s24}(0.24)$
380	416	$\Delta R'_{s36}(0.61)$, $\Delta R'_{s38}(0.46)$	94	89	$\Delta R_{s18}(0.16)$, $\Delta R_{s22}(0.14)$, $\Delta R_{s15}(0.12)$
	385	$\Delta R'_{s43}(0.54)$, $\Delta R'_{s41}(0.51)$	82	80	$\Delta R_{s8}(0.14)$, $\Delta R_{s18}(0.10)$
308	316	$\Delta R'_{s39}(0.64)$, $\Delta R_{s18}(0.15)$	...	65	$\Delta R_{s25}(0.27)$, $\Delta R_{s1}(0.13)$
264	281	$\Delta R'_{s44}(0.46)$, $\Delta R_{s5}(0.18)$, $\Delta R_{s14}(0.16)$	...	47	$\Delta R_{s42}(0.13)$, $\Delta R_{s14}(0.12)$, $\Delta R_{s5}(0.10)$
...	242	$\Delta R_{s2}(0.27)$, $\Delta R_{s16}(0.16)$, $\Delta R_{s37}(0.12)$			

TABLE 10. CALCULATED FREQUENCIES (in cm^{-1}) AND SIGNIFICANT TERMS OF POTENTIAL ENERGY DISTRIBUTIONS (A_g species)*

$BaCl_2 \cdot 2H_2O$

ν_{obsd}	ν_{calcd}	Significant terms of P.E.D.
3345	3291	$\Delta R_{s9}(0.49)$, $\Delta R_{s10}(0.47)$
	3282	$\Delta R_{s12}(0.59)$, $\Delta R_{s13}(0.39)$
3285	3211	$\Delta R_{s12}(0.39)$, $\Delta R_{s13}(0.60)$
	3210	$\Delta R_{s9}(0.48)$, $\Delta R_{s10}(0.50)$
...	1638	$\Delta R_{s33}(0.97)$
...	1607	$\Delta R_{s34}(0.96)$
717	725	$\Delta R'_{s38}(0.47)$, $\Delta R'_{s36}(0.17)$, $\Delta R_{s17}(0.19)$
	688	$\Delta R'_{s43}(0.54)$, $\Delta R'_{s41}(0.26)$
560	557	$\Delta R'_{s36}(0.69)$, $\Delta R'_{s38}(0.41)$
...	516	$\Delta R'_{s41}(0.68)$, $\Delta R'_{s43}(0.43)$
405	398	$\Delta R'_{s39}(0.77)$, $\Delta R_{s18}(0.12)$
...	328	$\Delta R'_{s44}(0.94)$
250	235	$\Delta R_{s1}(0.33)$, $\Delta R_{s14}(0.11)$
...	231	$\Delta R_{s5}(0.36)$, $\Delta R_{s15}(0.14)$, $\Delta R_{s23}(0.14)$, $\Delta R_{s22}(0.12)$
...	229	$\Delta R_{s16}(0.17)$, $\Delta R_{s37}(0.15)$, $\Delta R_{s2}(0.12)$
...	221	$\Delta R_{s6}(0.37)$, $\Delta R_{s2}(0.35)$, $\Delta R_{s17}(0.11)$
167	167	$\Delta R_{s4}(0.21)$, $\Delta R_{s24}(0.20)$, $\Delta R_{s8}(0.13)$
...	156	$\Delta R_{s15}(0.26)$, $\Delta R_{s7}(0.14)$, $\Delta R_{s14}(0.12)$
135	136	$\Delta R_{s3}(0.28)$, $\Delta R_{s8}(0.20)$
125	128	$\Delta R_{s7}(0.21)$, $\Delta R_{s4}(0.13)$, $\Delta R_{s25}(0.11)$
	125	$\Delta R_{s15}(0.19)$, $\Delta R_{s8}(0.17)$, $\Delta R_{s7}(0.12)$
...	111	$\Delta R_{s16}(0.21)$, $\Delta R_{s20}(0.15)$, $\Delta R_{s3}(0.13)$
98	94	$\Delta R_{s4}(0.22)$, $\Delta R_{s26}(0.15)$
77	78	$\Delta R_{s18}(0.13)$, $\Delta R_{s24}(0.11)$
...	53	$\Delta R_{s5}(0.15)$, $\Delta R_{s42}(0.12)$
46	48	$\Delta R_{s24}(0.13)$, $\Delta R_{s23}(0.13)$
33	33	$\Delta R_{s29}(0.21)$, $\Delta R_{s32}(0.13)$, $\Delta R_{s23}(0.10)$, $\Delta R_{s28}(0.10)$

$BaCl_2 \cdot 2D_2O$

ν_{obsd}	ν_{calcd}	Significant terms of P.E.D.
...	2410	$\Delta R_{s9}(0.49)$, $\Delta R_{s10}(0.48)$
...	2401	$\Delta R_{s12}(0.55)$, $\Delta R_{s13}(0.42)$
...	2329	$\Delta R_{s13}(0.56)$, $\Delta R_{s12}(0.42)$
...	2325	$\Delta R_{s10}(0.49)$, $\Delta R_{s9}(0.49)$
...	1194	$\Delta R_{s33}(0.96)$
...	1168	$\Delta R_{s34}(0.95)$
...	520	$\Delta R'_{s38}(0.39)$, $\Delta R'_{s36}(0.24)$, $\Delta R_{s17}(0.19)$
...	504	$\Delta R'_{s43}(0.40)$, $\Delta R'_{s41}(0.37)$
...	417	$\Delta R'_{s38}(0.46)$, $\Delta R'_{s36}(0.61)$
...	386	$\Delta R'_{s43}(0.55)$, $\Delta R'_{s41}(0.50)$
...	310	$\Delta R'_{s39}(0.70)$, $\Delta R_{s18}(0.13)$
...	261	$\Delta R'_{s44}(0.77)$, $\Delta R_{s14}(0.12)$
...	222	$\Delta R_{s22}(0.14)$
...	219	$\Delta R_{s2}(0.11)$, $\Delta R_{s5}(0.11)$, $\Delta R_{s16}(0.10)$, $\Delta R_{s37}(0.12)$
...	214	$\Delta R_{s1}(0.30)$, $\Delta R_{s5}(0.25)$
...	209	$\Delta R_{s6}(0.34)$, $\Delta R_{s2}(0.31)$, $\Delta R_{s17}(0.14)$
...	162	$\Delta R_{s4}(0.24)$, $\Delta R_{s8}(0.16)$, $\Delta R_{s24}(0.16)$
...	146	$\Delta R_{s7}(0.23)$, $\Delta R_{s15}(0.16)$
...	133	$\Delta R_{s3}(0.22)$, $\Delta R_{s8}(0.20)$
...	126	$\Delta R_{s4}(0.16)$, $\Delta R_{s3}(0.10)$
...	119	$\Delta R_{s15}(0.24)$, $\Delta R_{s7}(0.21)$
...	108	$\Delta R_{s16}(0.20)$, $\Delta R_{s20}(0.13)$
...	89	$\Delta R_{s4}(0.21)$, $\Delta R_{s26}(0.18)$
...	75	$\Delta R_{s18}(0.12)$, $\Delta R_{s14}(0.11)$, $\Delta R_{s24}(0.11)$
...	53	$\Delta R_{s5}(0.15)$, $\Delta R_{s42}(0.12)$
...	48	$\Delta R_{s21}(0.14)$, $\Delta R_{s23}(0.13)$
...	33	$\Delta R_{s29}(0.21)$, $\Delta R_{s32}(0.13)$, $\Delta R_{s23}(0.10)$, $\Delta R_{s28}(0.10)$

* Observed frequencies were taken from Ref. 16.

TABLE 11. CALCULATED FREQUENCIES (in cm^{-1}) AND SIGNIFICANT TERMS OF POTENTIAL ENERGY DISTRIBUTIONS (B_g species)*

$BaCl_2 \cdot 2H_2O$			$BaCl_2 \cdot 2D_2O$		
ν_{obsd}	ν_{calcd}	Significant terms of P.E.D.	ν_{obsd}	ν_{calcd}	Significant terms of P.E.D.
3345	3291	$\Delta R_{s9}(0.49)$, $\Delta R_{s10}(0.47)$	···	2410	$\Delta R_{s9}(0.49)$, $\Delta R_{s10}(0.48)$
	3282	$\Delta R_{s12}(0.59)$, $\Delta R_{s13}(0.39)$	···	2401	$\Delta R_{s12}(0.55)$, $\Delta R_{s13}(0.42)$
3285	3211	$\Delta R_{s13}(0.60)$, $\Delta R_{s12}(0.39)$	···	2329	$\Delta R_{s13}(0.56)$, $\Delta R_{s12}(0.42)$
	3210	$\Delta R_{s10}(0.50)$, $\Delta R_{s9}(0.48)$	···	2325	$\Delta R_{s9}(0.49)$, $\Delta R_{s10}(0.49)$
···	1638	$\Delta R_{s33}(0.97)$	···	1194	$\Delta R_{s33}(0.95)$
···	1607	$\Delta R_{s34}(0.96)$	···	1168	$\Delta R_{s34}(0.95)$
717	725	$\Delta R'_{s38}(0.47)$, $\Delta R'_{s36}(0.17)$, $\Delta R_{s17}(0.19)$	···	520	$\Delta R'_{s38}(0.39)$, $\Delta R'_{s36}(0.24)$, $\Delta R_{s17}(0.19)$
	688	$\Delta R'_{s43}(0.54)$, $\Delta R'_{s41}(0.26)$	···	504	$\Delta R'_{s43}(0.41)$, $\Delta R'_{s41}(0.37)$
560	557	$\Delta R'_{s36}(0.69)$, $\Delta R'_{s38}(0.41)$	···	416	$\Delta R'_{s38}(0.46)$, $\Delta R'_{s36}(0.61)$
···	516	$\Delta R'_{s41}(0.68)$, $\Delta R'_{s43}(0.43)$	···	386	$\Delta R'_{s43}(0.55)$, $\Delta R'_{s41}(0.51)$
405	398	$\Delta R'_{s39}(0.77)$, $\Delta R_{s18}(0.12)$	···	309	$\Delta R'_{s39}(0.72)$, $\Delta R_{s18}(0.13)$
···	328	$\Delta R'_{s44}(0.94)$	···	260	$\Delta R'_{s44}(0.81)$, $\Delta R_{s14}(0.11)$
250	234	$\Delta R_{s16}(0.17)$, $\Delta R_{s2}(0.17)$, $\Delta R_{s37}(0.15)$	···	222	$\Delta R_{s2}(0.19)$, $\Delta R_{s16}(0.17)$, $\Delta R_{s37}(0.15)$, $\Delta R_{s18}(0.11)$
···	227	$\Delta R_{s5}(0.19)$, $\Delta R_{s42}(0.18)$, $\Delta R_{s22}(0.14)$, $\Delta R_{s6}(0.11)$	···	217	$\Delta R_{s42}(0.17)$, $\Delta R_{s5}(0.16)$, $\Delta R_{s22}(0.14)$, $\Delta R_{s6}(0.11)$
···	224	$\Delta R_{s1}(0.39)$, $\Delta R_{s5}(0.16)$	···	206	$\Delta R_{s1}(0.35)$, $\Delta R_{s5}(0.18)$
205	212	$\Delta R_{s6}(0.34)$, $\Delta R_{s2}(0.26)$, $\Delta R_{s17}(0.11)$	···	200	$\Delta R_{s6}(0.32)$, $\Delta R_{s2}(0.23)$, $\Delta R_{s17}(0.13)$
···	157	$\Delta R_{s14}(0.25)$, $\Delta R_{s8}(0.23)$	···	153	$\Delta R_{s8}(0.41)$, $\Delta R_{s14}(0.18)$, $\Delta R_{s22}(0.13)$
144	149	$\Delta R_{s15}(0.18)$, $\Delta R_{s4}(0.18)$, $\Delta R_{s8}(0.14)$, $\Delta R_{s22}(0.11)$	···	147	$\Delta R_{s4}(0.33)$, $\Delta R_{s3}(0.17)$
	147	$\Delta R_{s15}(0.18)$, $\Delta R_{s4}(0.14)$, $\Delta R_{s3}(0.11)$	···	140	$\Delta R_{s15}(0.21)$, $\Delta R_{s7}(0.18)$
135	130	$\Delta R_{s3}(0.33)$, $\Delta R_{s7}(0.15)$	···	129	$\Delta R_{s3}(0.32)$, $\Delta R_{s4}(0.14)$, $\Delta R_{s7}(0.11)$
125	128	$\Delta R_{s7}(0.36)$, $\Delta R_{s16}(0.10)$, $\Delta R_{s25}(0.10)$	···	125	$\Delta R_{s7}(0.33)$
	123	$\Delta R_{s26}(0.17)$, $\Delta R_{s4}(0.14)$	···	116	$\Delta R_{s16}(0.21)$, $\Delta R_{s23}(0.14)$, $\Delta R_{s15}(0.14)$
98	103	$\Delta R_{s24}(0.18)$, $\Delta R_{s26}(0.14)$, $\Delta R_{s23}(0.13)$, $\Delta R_{s20}(0.10)$	···	99	$\Delta R_{s24}(0.22)$, $\Delta R_{s26}(0.20)$
			···	73	$\Delta R_{s22}(0.15)$, $\Delta R_{s1}(0.14)$, $\Delta R_{s5}(0.11)$, $\Delta R_{s4}(0.11)$
77	75	$\Delta R_{s18}(0.16)$			
···	71	$\Delta R_{s2}(0.22)$, $\Delta R_{s6}(0.15)$, $\Delta R_{s18}(0.11)$	···	70	$\Delta R_{s2}(0.22)$, $\Delta R_{s18}(0.16)$, $\Delta R_{s6}(0.14)$, $\Delta R_{s25}(0.12)$
62	68	$\Delta R_{s25}(0.15)$, $\Delta R_{s22}(0.11)$	···	67	$\Delta R_{s25}(0.11)$, $\Delta R_{s22}(0.10)$
···	55	$\Delta R_{s23}(0.13)$, $\Delta R_{s8}(0.12)$, $\Delta R_{s14}(0.10)$	···	55	$\Delta R_{s23}(0.14)$, $\Delta R_{s8}(0.12)$

* Observed frequencies were taken from Ref. 16.

In the above formulae, g represents the center of gravity of the H_2O molecule, and X_n and Y_n ($n=i, j, k$) represent the cartesian coordinates of the i, j, and k atoms with respect to the cartesian coordinate system, X–Y–Z, having its origin at the center of gravity and the coordinate axes coinciding with the principal axes of the moment of inertia. The vector, from i to j, is expressed by r_{ij}.

Using the above formulae and the force constants in Set II in Table 7, the following values were obtained for k_A, k_B, and k_C:

$k_A = 0.138$ mdyn·Å, $k_B = 0.283$ mdyn·Å,

$k_C = 0.115$ mdyn·Å

for H_2O I $(6(i,j-1,k)4(i,j-1,k)7(i,j,k))$

$k_A = 0.138$ mdyn·Å, $k_B = 0.307$ mdyn·Å,

$k_C = 0.165$ mdyn·Å

for H_2O II $(8(i,j,k)5(i,j,k)9(i,j,k))$

From these values, it can be concluded that both the crystal water molecules, H_2O I and H_2O II, are more strongly bound around the principal axis, B, than around the principal axes, A and C.

The authors express their gratitude to Professor T. Miyazawa of Osaka University for allowing them to use FIS-3 Far Infrared Spectrometer and Perkin-Elmer 521 spectrophotometer and to Dr. T. Kitagawa and Miss M. Tsuchida of Professor Miyazawa's laboratory for their kind assistance during the measurements of IR spectra.

Their thanks are also due to Professor T. Shimanouchi of The University of Tokyo for allowing them to use the programs, BGLZ and LSMA, and to Dr. I. Suzuki of Professor Shimanouchi's laboratory for his kind instruction of use of the programs and also to Professor S. Shibata of our Department for allowing them to use IBM key punch.

BULLETIN OF THE CHEMICAL SOCIETY OF JAPAN VOL. 43 698—704 (1970)

Semi-empirical Unrestricted SCF-MO Treatment for Valence Electron Systems. II. The Angular Dependence of the Methyl Group *hfs* Constants

Hiroshi NAKATSUJI, Hiroshi KATO*1 and Teijiro YONEZAWA

Department of Hydrocarbon Chemistry, Faculty of Engineering, Kyoto University, Sakyo-ku, Kyoto

(Received August 27, 1969)

Since the spin-polarization contribution to the methyl-group *hfs* constant of the ethyl radical has been recognized to be important, the angular dependence of the β-proton *hfs* constants is re-examined for various radicals. Thus, the observed relation, $Q(\theta)=B_0+B_1\cos^2\theta$, is interpreted as being the sum of the following two equations.

$$Q_{SD}(\theta) = (B_1)_{SD}\cos^2\theta$$
$$Q_{SP}(\theta) = (B_0)_{SP} + (B_1)_{SP}\cos^2\theta,$$

where SD and SP denote the spin delocalization and spin polarization contributions respectively. θ is the rotational angle about C–C single bond. A molecular orbital description of the above angular dependences is also given.

The methyl-group proton *hfs* constants of aliphatic and aromatic hydrocarbon radicals have been extensively studied from both experimental[1] and theoretical[2] points of view. The theoretical studies of the methyl proton spin densities have been carried out mainly by two different methods, namely by the valence bond (VB) and molecular orbital (MO) methods,[3] and an interesting view of the spin-appearing mechanisms was presented by Lazdins and Karplus.[2g] They stated that the methyl-group proton spin density in the ethyl radical is due to nearly 60% "exchange polarization" and nearly 40% "electron transfer" contributions. In a previous MO study[4b] it was shown that the methyl-proton spin density is due to 74% "spin delocalization (SD)" and 26% "spin polarization (SP)" contributions.[5]

The angular dependence of the β-proton *hfs* constant on the rotation about the C_α–C_β single bond has been well established experimentally and is explained by the relation[1]:

$$a_\beta^H = Q(\theta)\rho_C^\pi, \tag{1}$$

where ρ_C^π is the spin density in the $2p_{C\alpha}$ atomic orbital of the contiguous π-carbon atom, and where $Q(\theta)$ is expressed as:

$$Q(\theta) = B_0 + B_1\cos^2\theta, \tag{2}$$

where θ is the angle between the axis of the $2p_{C\alpha}$ orbital and the C_β–H bond, both projected on a plane perpendicular to the C_α–C_β bond. Aono and Higuchi[2c] studied the angular dependence of the β-proton *hfs* constant theoretically by considering only the spin delocalization (spin-hyperconjugation) mechanism; they successfully derived the $Q(\theta)=B_1\cos^2\theta$ relation, where B_1 is a constant. However, since the β-proton spin density is in large part due to the SP mechanism, it seems necessary to examine the angular dependence of the SP contribution in order to interpret the observed relation (2).

In the present study, the methyl-proton *hfs* constants of the various doublet radicals (ethyl, *n*-propyl, methyl-substituted allyl radicals, and toluene ion-radicals) are calculated by the unrestricted Hartree-Fock (UHF) method reported

*1 Present address: Department of General Education, Nagoya University, Chikusa-ku, Nagoya.

1) a) C. Heller and H. M. McConnell, *J. Chem. Phys.*, **32**, 1535 (1960). b) A. Horsfield, J. R. Morton and D. H. Whiffen, *Mol. Phys.*, **4**, 425 (1961). c) J. R. Bolton, A. Carrington and A. D. McLachlan, *ibid.*, **5**, 31 (1962). d) J. R. Bolton, A. Carrington, A. Forman and L. E. Orgel, *ibid.*, **5**, 43 (1962). e) A. Horsfield, J. R. Morton and D. H. Whiffen, *ibid.*, **5**, 115 (1962).

2) a) A. D. McLachlan, *ibid.*, **1**, 233 (1958). b) P. G. Lykos, *J. Chem. Phys.*, **32**, 625 (1960). c) S. Aono and J. Higuchi, *Progr. Theor. Phys.* (Kyoto), **28**, 589 (1962). d) E. W. Stone and A. H. Maki, *J. Chem. Phys.*, **37**, 1326 (1962). e) K. Morokuma and K. Fukui, This Bulletin, **36**, 534 (1963). f) J. P. Colpa and E. de Boer, *Mol. Phys.*, **7**, 333 (1964). g) D. Lazdins and M. Karplus, *J. Chem. Phys.*, **44**, 1600 (1966). h) Z. Luz, *ibid.*, **48**, 4186 (1968).

3) T. H. Brown and M. Karplus, *ibid.*, **46**, 870 (1967).

4) a) T. Yonezawa, H. Nakatsuji, T. Kawamura and H. Kato, *Chem. Phys., Letters*, **2**, 454 (1968). b) T. Yonezawa, H. Nakatsuji, T. Kawamura and H. Kato, *J. Chem. Phys.*, **51**, 669 (1969).

5) J. P. Colpa, E. de Boer, D. Lazdins and M. Karplus, *J. Chem. Phys.*, **47**, 3098 (1967).

Table 1. The methyl proton spin density in the ethyl radical

Angle θ	UHF spin density ρ_{uhf}	From Eq. (2)	$(\rho)_{SP}$	From Eq. (3)	$(\rho)_{SD}$	From Eq. (4)	AA ρ_{aa}
0	0.072	(0.072)	0.020	(0.020)	0.053	(0.053)	0.059
15	0.067	0.067	0.018	0.018	0.050	0.049	0.055
30	0.054	0.053	0.014	0.014	0.039	0.039	0.044
45	0.035	0.035	0.009	0.009	0.026	0.026	0.029
60	0.017	0.017	0.003	0.003	0.013	0.013	0.014
75	0.003	0.003	0.000	0.000	0.004	0.004	0.003
90	−0.002	(−0.002)	−0.002	(−0.002)	0.000	0.000	−0.001

in a previous study of this series,[6] and the mechanistic contributions to the *hfs* constants are diveded by means of the method previously proposed by the present authors.[7,4] The conclusions are that the SP contribution to the methyl-proton *hfs* constant has the angular dependence expressed by:

$$Q_{SP}(\theta) = (B_0)_{SP} + (B_1)_{SP}\cos^2\theta \quad (3)$$

and that the observed relation (2) is to be understood as the sum of the angular dependence of the SD contribution.

$$Q_{SD}(\theta) = (B_1)_{SD}\cos^2\theta \quad (4)$$

and that of the SP contribution (Eq. (3)). Thus, the constants, B's, in Eq. (2) are expressed as:

$$B_0 = (B_0)_{SP}$$

and:

$$B_1 = (B_1)_{SP} + (B_1)_{SD}. \quad (5)$$

Moreover, for the isotropic γ-carbon *hfs* constants, one may expect the same dependences as those for the methyl-proton *hfs* constants. This is certainly true for the 2*s* AO spin density of the γ-carbon atom of the *n*-propyl radical.

In the last section, a molecular orbital description of the above angular dependences is given. It is shown that the intrinsic restriction of the UHF method, compared with the configuration interaction method, does not much affect the above conclusions.

Results and Discussion

Angular Dependence. In Table 1 the methyl-proton spin densities in the ethyl radical are given for the various angles, and then they are illustrated in Fig. 1. For the total spin density, ρ_{uhf}, the relation (2) holds fairly satisfactorily, while for the SP and SD contributions Eqs. (3) and (4) excellently represent their angular dependences. The curves obtained from Eqs. (2), (3), and (4) almost overlap with the corresponding curves shown in Fig. 1.

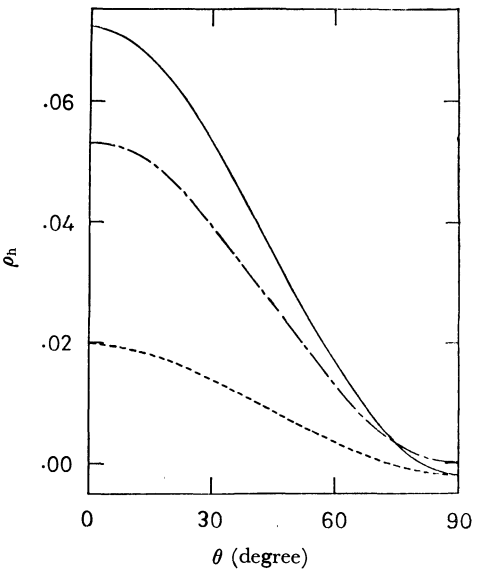

Fig. 1. Angular dependence of the methyl proton spin density in the ethyl radical.
——, ρ_{uhf}; - —, $(\rho_{uhf})_{SD}$; -----, $(\rho_{uhf})_{SP}$

The coefficients, B, calculated from the results shown in Table 1, are given in Table 2.

For the *n*-propyl radical, the situation is very similar to that of the ethyl radical. For the β-proton spin density, the dependences of ρ_{uhf}, $(\rho_{uhf})_{SP}$, and $(\rho_{uhf})_{SD}$ on the rotational angle, θ, is illustrated in Fig. 2. The relation (2) deviates only slightly from the calculated dependence; this deviation is mainly due to the SD contribution. The constants, B, in Eqs. (2), (3), and (4) were obtained by fitting the calculated curves; they are given in Table 2.

For the isotropic γ-carbon *hfs* constants of the *n*-propyl radical, one may expect the same dependences as those for the methyl proton *hfs* constants in the ethyl radical. This is certainly true for the 2*s* AO spin density of the γ-carbon atom. The angular dependences of the 2*s* AO spin density and of the mechanistic contributions are illustrated in Fig. 3. The curves of this figure are very well represented by $\rho_{uhf} = -0.001 + 0.018\cos^2\theta$, $(\rho_{uhf})_{SD} =$

6) T. Yonezawa, H. Nakatsuji, T. Kawamura and H. Kato, This Bulletin, **42**, 2437 (1969).

7) H. Nakatsuji, H. Kato and T. Yonezawa, *J. Chem. Phys.*, **51**, 3175 (1969).

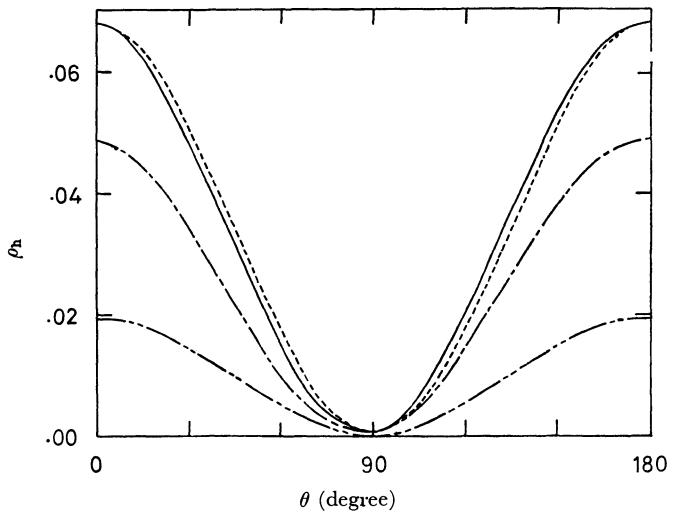

Fig. 2. Angular dependence of the β-proton spin density of the *n*-propyl radical.
——, ρ_{uhf}; - —, $(\rho_{uhf})_{SD}$; - - —, $(\rho_{uhf})_{SP}$; -----, ρ calculated from Eq. (2)

TABLE 2. ANGULAR DEPENDENCE OF THE MECHANISTIC CONTRIBUTIONS[a)]

Radical	B_0[b)]	B_1	$(B_1)_{SP}$	$(B_1)_{SD}$	ρ_C^π
Ethyl	−1.5	55.4	16.0	39.4	1.000
i-Propyl	0.6	50.0	13.7	36.3	1.000
cis-1-Methylallyl	−0.5	49.2	21.4	27.9	0.689
trans-1-Methylallyl	−0.5	50.7	21.7	29.0	0.694
2-Methylallyl	1.6	44.1	44.1	0.0	−0.345
Toluene anion	4.1	39.1	39.1	0.0	−0.135
Toluene cation	−1.0	63.4	23.8	39.6	0.383

a) The values of B are given in gauss unit.
b) $B_0=(B_0)_{SP}$

$0.005\cos^2\theta$, and $(\rho_{uhf})_{SP}=-0.001+0.013\cos^2\theta$.

Among the methyl-substituted allyl radicals, the 2-methylallyl radical is of great interest. Since the singly-occupied π-orbital of this radical has a node on the C_2 atom, the spin density of the methyl group is expected to be due only to the SP mechanism and to be negative in sign. This is certainly true, as Tables 2 and 3 show. Thus, the angular dependence of the methyl proton spin density of the 2-methylallyl radical is well represented *only* by

TABLE 3. THE METHYL PROTON SPIN DENSITY OF THE 2-METHYLALLYL RADICAL

Angle	UHF spin density				AA
θ	ρ_{uhf}	$(\rho)_{SP}$	$(\rho)_{SD}$	From Eq.(2)or(3)	ρ_{aa}
0	−0.020	−0.020	0.000	(−0.020)	−0.006
30	−0.016	−0.016	0.000	−0.016	−0.005
60	−0.006	−0.006	0.000	−0.006	−0.002
90	−0.001	−0.001	0.000	(−0.001)	0.000

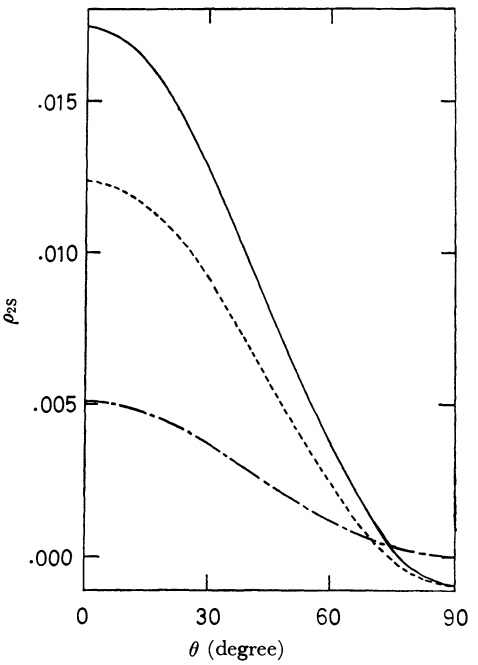

Fig. 3. Angular dependence of the 2*s* AO spin density of the γ-carbon atom of the *n*-propyl ridical.
——, ρ_{uhf}; - —, $(\rho_{uhf})_{SD}$; -----, $(\rho_{uhf})_{SP}$

Eq. (3), as is shown in Table 3.

For the other methyl-substituted allyl radicals (*cis*-1-methylallyl and *trans*-1-methylallyl), the situations are similar to that of the ethyl radical. The SD contributions to the methyl proton spin densities of these radicals are nearly 60%, small compared with those of the ethyl radical (See Table 2). Much

TABLE 4. THE METHYL PROTON SPIN DENSITY OF THE TOLUENE ION-RADICALS

Species	Angle θ	UHF spin density						AA
		ρ_{uhf}	From Eq. (2)	$(\rho)_{SP}$	From Eq. (3)	$(\rho)_{SD}$	From Eq. (4)	ρ_{aa}
Anion	0	−0.008	(−0.008)	−0.008	(−0.008)	0.000	0.000	−0.003
	30	−0.006	−0.006	−0.006	−0.006	0.000	0.000	−0.002
	45	−0.004	−0.005	−0.004	−0.005	0.000	0.000	−0.001
	60	−0.003	−0.003	−0.003	−0.003	0.000	0.000	−0.001
	90	−0.001	(−0.001)	−0.001	(−0.001)	0.000	0.000	0.000
Cation	0	0.033	(0.033)	0.012	(0.012)	0.021	(0.021)	0.025
	30	0.024	0.025	0.009	0.009	0.015	0.016	0.018
	45	0.016	0.016	0.006	0.006	0.010	0.010	0.012
	60	0.007	0.008	0.002	0.003	0.005	0.005	0.006
	90	−0.001	(−0.001)	−0.001	(−0.001)	0.000	0.000	0.000

as with the above examples, the angular dependences of the SP and SD contributions are well represented by Eqs. (3) and (4). The values of B in these equations are given in Table 2.

The methyl-proton spin densities of the toluene-ion radicals are summarized in Table 4. Although the tolune ions have nearly degenerate symmetric and antisymmetric electronic states with respect to the C_2 operation, only their ground electronic states (the symmetric electronic state for the cation and the antisymmetric state for the anion) are calculated for the present purposes. For the antisymmetric state of the anion radical, its singly-occupied π-orbital has a node on the 1-carbon (the carbon to which the methyl group is attached); therefore, the spin density of the methyl proton is due only to the SP mechanism and is negative, similar to that of the 2-methylallyl radical. By referring to Table 4, Eq. (3) is found to apply satisfactorily. For the symmetric state of the cation radical, the SD contribution to the methyl proton spin density is nearly 60%. As is shown in Table 3, Eqs. (2), (3), and (4) hold very satisfactorily. The values of B in these equations are given in Table 2. Note that the B_1 values of the anion and cation differ greatly.

One conclusion from Table 2 is that the methyl proton spin densities are composed of a major (60—75%) SD contribution and of a minor (25—40%) SP contribution, except for the special cases of the 2-methylallyl radical and the antisymmetric state of the toluene anion. Note that the B values of the 2-methylallyl and toluene anion radicals, in which only the SP mechanism is important, deviate greatly from the average B values. Another conclusion of the present study is that the observed relation, (2), can be interpreted as the sum of Eqs. (3) and (4), and that this relation may also hold for the 2*s* AO spin density of the γ-carbon atom (as is shown in the case of the *n*-propyl radical).

***hfs* Constants.** The proton *hfs* constants[8] calculated by assuming the free rotation of the methyl group are compared with the experimental results in Tables 5 and 6. Although the toluene ions have nearly degenerate electronic states, the calculated values given in Table 5 correspond only to the lower electronic states (the symmetric state for the cation and the antisymmetric state for the anion). For a more rigorous discussion of the *hfs* constants, the thermal and vibronic coupling effects must be considered,[1d] as Purins and Karplus did recently.[9] Note, however, that the inclusion of

TABLE 5. CALCULATED PROTON *hfs* CONSTANTS

Radical	Position	*hfs* constant	
		Calcd.[a]	Exptl.
Ethyl	α-H	−25.6	(−) 22.38[b]
	β-H	26.2	(+) 26.87[b]
n-Propyl	α-H	−25.3	(−) 22.08[b]
	β-H	25.6	(+) 33.2[b]
	γ-H	−1.8	(−) 0.38[b]
Toluene anion[c]	*o*-H	−9.0	(−) 5.12[d]
	m-H	−9.6	(−) 5.45[d]
	p-H	−0.1	(−) 0.59[d]
	H(CH_3)	−3.2	(+) 0.79[d]
Toluene cation[e]	*o*-H	−2.7	—
	m-H	−1.1	—
	p-H	−9.1	—
	H(CH_3)	11.8	—

a) The calculated values are obtained by assuming free rotation of the methyl group about the C–C single bond.
b) R. W. Fessenden and R. H. Schuler, *J. Chem. Phys.*, **39**, 2147 (1963).
c) Only the antisymmetric electronic state is calculated.
d) J. R. Bolton, A. Carrington, A. Forman and L. E. Orgel, *Mol. Phys.*, **5**, 43 (1962).
e) Only the symmetric electronic state is calculated.

8) Proton *hfs* constants are calculated by multiplying ρ_{uhf} by 743 gauss.

9) a) D. Purins and M. Karplus, *J. Chem. Phys.*, **50**, 241 (1969). b) D. Purins and M. Karplus, *J. Amer. Chem. Soc.*, **90**, 6275 (1968).

TABLE 6. PROTON *hfs* CONSTANT OF THE ALLYL AND METHYL-SUBSTITUTED ALLYL RADICAIS

Radical	Position	*hfs* constant Calcd.[a]	Exptl.[b]
Allyl			
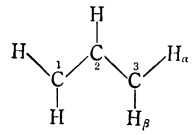	$H_{1,3\alpha}$	−14.19	(−) 14.81
	$H_{1,3\beta}$	−13.97	(−) 13.90
	H_2	3.64	(+) 4.06
cis-1-Methylallyl			
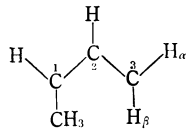	$H(CH_3)$	16.80	(+) 14.01
	$H_{1\alpha}$	−18.87	(−) 14.17
	H_2	4.49	(+) 3.83
	$H_{3\alpha}$	−13.89	(−) 14.94
	$H_{3\beta}$	−13.64	(−) 13.52
trans-1-Methylallyl			
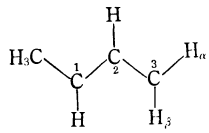	$H(CH_3)$	17.22	(+) 16.43
	$H_{1\beta}$	−18.99	(−) 13.83
	H_2	3.97	(+) 3.85
	$H_{3\alpha}$	−14.12	(−) 14.78
	$H_{3\beta}$	−13.91	(−) 13.83
2-Methylallyl			
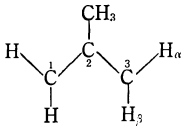	$H(CH_3)$	− 7.89	(−) 3.19
	$H_{1,3\alpha}$	−13.97	(−) 14.68
	$H_{1,3\beta}$	−13.74	(−) 13.82

a) The calculated values are obtained by assuming free rotation of the methyl group about the C–C single bond.

b) J.K. Kochi and P.J. Krusic, *J. Amer. Chem. Soc.*, **90**, 7157 (1968).

these effects, which are expressed by the weighted mean of the *hfs* constants of the symmetric and antisymmetric electronic states, will improve the calculated *hfs* constants of the toluene anion.[10]

Since Fessenden and Schuler[11] observed the different *hfs* constants for the terminal methylene protons of the allyl radical, the observed *hfs* constants have been assigned theoretically by several investigators.[6,12-14] This finding was of particular interest since the well-known McConnell rule cannot interpret the observed difference. Recently, however, Kochi and Krusic[15] settled this assignment by observing the *hfs* constants of the methyl-substituted allyl radicals; they proved that the assignment by the present authors[6,12] was correct. Here, we calculated the proton *hfs* constants of these methyl-substituted allyl radicals. The results are summarized in Table 6. The assignments of the *hfs* constants of the $H_{3\alpha}$ and $H_{3\beta}$ protons of the *cis*- and *trans*-1-methylallyl radicals agree with the experimental results, although the differences in the calculated *hfs* constants of these two protons are rather small compared with the experimental values. In the 2-methylallyl radical, the methyl-proton *hfs* constants are calculated to be due only to the SP mechanism and to be negative in sign. The calculated *hfs* constants of the $H_{1\alpha}$ proton of the *cis*-form and of the $H_{1\beta}$ proton of the *trans*-form are too large (absolute value) compared with the experimental values.

Origin of the Angular Dependence. Here, we shall give a molecular orbital description of the angular dependences expressed by Eqs. (2), (3), and (4). For the present purposes the configuration interaction (CI) treatment may be most suitable. As has been shown previously, the UHF wave-function is expressed by the following CI form to a first-order approximation:[7]

$$\Psi_{\mathrm{uhf}} = \Psi^{\mathrm{rf}} + \sum_i C^{\mathrm{se}}(ii^*)\,\Psi^{\mathrm{se}}(ii^*), \tag{6}$$

where the second term is due to the spin polarization perturbation. Ψ^{rf} is the restricted function composed of the natural orbitals,[16,4b] λ_i and μ, of the UHF wave-function and Ψ^{se} (ii^*) represents the normalized singly-excited configuration expressed by the one-electron jump from λ_i to ν_i:

$$\Psi^{\mathrm{rf}} = |\lambda_1\alpha\ \lambda_1\beta\cdots\lambda_q\alpha\ \lambda_q\beta\mu\alpha|$$

$$\Psi^{\mathrm{se}}(ii^*) = |\lambda_1\alpha\ \lambda_1\beta\cdots\nu_i\lambda_i\ \frac{1}{\sqrt{2}}(\alpha\beta+\beta\alpha)\cdots\lambda_q\alpha\lambda_q\beta\mu\alpha| \tag{7}$$

$2q+1$ is the number of electrons in the radical. The natural orbitals, λ, μ, and ν, correspond, respectively, to the doubly-occupied, singly-occupied, and unoccupied orbitals of the restricted function, Ψ^{rf}, and are orthonormal to each other.[16] Note that λ_i and ν_i correspond to the bonding and antibonding partner MO's of the alternant molecular orbital method.[16,4b]

From Eq. (6), the SP and SD contributions to the UHF spin density are given by[4b]:

$$(\rho_{\mathrm{uhf}})_{\mathrm{SD}} = \langle\Psi^{\mathrm{rf}}|\rho|\Psi^{\mathrm{rf}}\rangle = \mu^2 \tag{8}$$

10) The observed *hfs* constant of the methyl proton of the toluene anion is positive in sign; E. de Boer and J. P. Colpa, *J. Phys. Chem.*, **71**, 21 (1967).

11) R. W. Fessenden and R. H. Schuler, *J. Chem. Phys.*, **39**, 2147 (1963).

12) T. Yonezawa, H. Nakatsuji, T. Kawamura and H. Kato, This Bulletin, **40**, 2211 (1967).

13) A. Hincliffe and H. M. Atherton, *Mol. Phys.*, **13**, 89 (1967).

14) J. A. Pople, D. L. Beveridge and P. A. Dobosh, *J. Amer. Chem. Soc.*, **90**, 4201 (1968).

15) J. K. Kochi and P. J. Krusic, *ibid.*, **90**, 7157 (1968).

16) a) A. T. Amos and G. G. Hall, *Proc. Roy. Soc., Ser. A*, **263**, 483 (1961). b) T. Amos and L.C. Snyder, *J. Chem. Phys.*, **41**, 1773 (1964).

TABLE 7. UHF NATURAL ORBITALS, λ AND μ OF THE ETHYL RADICAL

AO	λ						μ
	$1(\sigma_1)$	$2(\sigma_2)$	$3(\bar{\pi}_1)$	$4(\pi_1)$	$5(\bar{\pi}_2)$	$6(\sigma_3)$	$7(\pi_2)$
			Configuration[a]				
Y(1C)	0.000	0.000	0.310	0.000	−0.341	0.000	0.000
Z(1C)	0.000	0.000	0.000	0.038	0.000	0.001	1.000
Y(2C)	0.000	0.000	0.340	0.000	0.312	0.000	0.000
Z(2C)	−0.001	0.000	0.000	0.458	0.000	0.003	0.013
h(5H)	0.167	−0.118	−0.356	−0.307	−0.410	0.082	0.115
h(6H)	0.167	−0.118	0.356	−0.307	0.410	0.082	0.115
h(7H)	0.161	−0.115	0.000	0.614	0.000	0.089	−0.229
			Configuration[b]				
Y(1C)	0.000	0.000	0.310	0.000	−0.341	0.000	0.000
Z(1C)	0.000	0.000	0.000	0.038	0.000	0.000	1.000
Y(2C)	0.001	0.000	0.340	0.000	0.313	−0.003	0.000
Z(2C)	0.000	0.000	0.000	0.458	0.000	0.000	0.013
h(5H)	0.163	−0.116	−0.206	−0.531	−0.237	0.086	0.198
h(6H)	0.163	−0.116	−0.206	0.531	−0.237	0.086	−0.198
h(7H)	0.169	−0.119	0.411	0.000	0.474	0.079	0.000

a) Configuration I

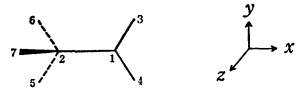

b) Configuration II

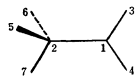

TABLE 8. COEFFICIENTS OF THE SINGLY EXCITED CONFIGURATIONS, $C^{se}(ii^*)$ OF THE ETHYL RADICAL

Geometry[a]	Coefficients, C^{se} (ii^*)					
	11*	22*	33*	44*	55*	66*
Configuration I	0.0013	0.0292	0.0043	0.0049	0.0031	0.0130
Configuration II	0.0015	0.0292	0.0042	0.0048	0.0032	0.0130

a) See footnotes a and b of Table 7.

and:

$$(\rho_{uhf})_{SP} = 2\sum_i C^{se}(ii^*) <\Psi^{rf}|\boldsymbol{\rho}|\Psi^{se}(ii^*)> = 2\sqrt{2}\sum_i C^{se}(ii^*)\,\lambda_i\nu_i, \quad (9)$$

where $\boldsymbol{\rho}$ is the spin-density operator.

Now let us enter upon a description of the angular dependence of the methyl group proton spin density. In Table 7 the natural orbitals, λ and μ, of the ethyl radical, as calculated by the present method, are given for the two rotational configurations, and in Table 8 the coefficients of the singly-excited configurations, $C^{se}(ii^*)$, are summarized.[4] Table 8 shows that the coefficients, $C^{se}(ii^*)$, are almost independent of the rotational angle, θ. Thus, we have only to consider the angular dependence of the AO coefficients of the natural orbitals.

The local-group orbitals constructed from the three hydrogen 1s AO's of the methyl group may be written as:

$$\begin{aligned} \phi_\sigma &= h_1 + h_2 + h_3, \\ \phi_{\bar{\pi}} &= h_1 - h_2, \\ \phi_\pi &= h_1 + h_2 - 2h_3. \end{aligned} \quad (10)$$

ϕ_σ is totally symmetric about the rotation, while $\phi_{\bar{\pi}}$ and ϕ_π are the quasi-π-orbitals and are perpendicular to each other. Thus, the angular dependence of the coefficients of the one particular hydrogen 1s AO, h, in various molecular orbitals (i) may be grouped into the following three types:

$$\begin{aligned} &\sigma\text{-type: } a_i \cdot h, \\ &\bar{\pi}\text{-type: } b_i \sin\theta \cdot h, \\ &\pi\text{-type: } c_i \cos\theta \cdot h, \end{aligned} \quad (11)$$

where a_i, b_i, and c_i are the AO coefficients of the molecular orbital, i, at $\theta=90°$ or at $\theta=0°$. In Table 7 the orbitals are divided into the above three groups. For the π-electron radicals, the angular dependence of the coefficient of the methyl hydrogen is, of course, of the π-type. Hence, the

SD contribution to the methyl-proton spin density is given by:

$$(\rho_{\mathrm{uhf}})_{\mathrm{SD}} = c_{\mu}^{2} \cos^{2}\theta \cdot \qquad (12)$$

From Eqs. (9) and (11) the SP contribution is similarly expressed by:

$$\begin{aligned}(\rho_{\mathrm{uhf}})_{\mathrm{SP}} &= 2\sqrt{2}\{\sum_{i}^{\sigma} C^{\mathrm{se}}(ii^{*})\, a_i a_{i^{*}} \\ &\quad + \sum_{i}^{\pi} C^{\mathrm{se}}(ii^{*})\, b_i b_{i^{*}} \sin^{2}\theta \\ &\quad + \sum_{i}^{\pi} C^{\mathrm{se}}(ii^{*})\, c_i c_{i^{*}} \cos^{2}\theta\} \\ &= (\rho_0)_{\mathrm{SP}} + (\rho_1)_{\mathrm{SP}} \cos^{2}\theta, \qquad (13)\end{aligned}$$

where:

$$(\rho_0)_{\mathrm{SP}} = 2\sqrt{2}\{\sum_{i}^{\sigma} C^{\mathrm{se}}(ii^{*})\, a_i a_{i^{*}} + \sum_{i}^{\pi} C^{\mathrm{se}}(ii^{*})\, b_i b_{i^{*}}\}$$

$$(\rho_1)_{\mathrm{SP}} = 2\sqrt{2}\{\sum_{i}^{\pi} C^{\mathrm{se}}(ii^{*})\, c_i c_{i^{*}} - \sum_{i}^{\pi} C^{\mathrm{se}}(ii^{*})\, b_i b_{i^{*}}\}.$$

$\sum^{\pi}$ denotes the summation over the π-type orbitals. Eqs. (12) and (13), and the sum of them, correspond to Eqs. (4), (3), and (2) respectively.

Note here that the conditions for the local symmetry orbitals expressed by Eq. (10) (the conditions for the definite grouping of MO's by Eq. (11)) are not satisfactorily fulfilled in cases of poor symmetry,[17] and that, in the usual CI treatment, the transitions other than $i \rightarrow i^{*}$ (i and i^{*} have, of course, the same type of local symmetry) must be included.[18] (Compare this with Eq. (6)). In these cases, Eqs. (12) and (13) may include types of angular-dependent terms other than $\cos^{2}\theta$. One example of the poor symmetry is the *n*-propyl radical, where the curves obtained by Eqs. (2), (3), and (4) deviate slightly from the calculated curves. Nevertheless, the relations (2), (3), and (4) are still good approximations to the angular dependences of the β-proton spin density of the *n*-propyl radical (See Fig. 2).

The effects of the inclusion of the $i \rightarrow j^{*}$ ($i \neq j$) transitions are not certainly determined numerically by the present study, but they can be estimated as follows. The $i \rightarrow j^{*}$ transitions may be grouped into two groups; one is composed of the transitions where i and j^{*} have the same local symmetry, and the other is composed of the transitions where i and j^{*} have different local symmetries. By including the former type of transition, the angular dependence expressed by Eq. (13) is not altered. Only the coefficients may be changed. For the latter type of transition, which may produce types of angular-dependent terms other than $\cos^{2}\theta$, their CI coefficients, $C^{\mathrm{se}}(ij^{*})$, can be expected from symmetry considerations to be very small. Thus, the inclusion of the $i \rightarrow j^{*}$ ($i \neq j$) transitions will not much alter the type of angular dependence expressed by Eq. (13).

One of us (H. N.) wishes to thank Dr. T. Kawamura for his helpful discussions. The computation was carried out by a HITAC 5020E computer at the Computation Center of the University of Tokyo.

17) For example, the condition of the local symmetry expressed by Eq. (10) is already broken in the ethyl radical (See Table 7). However, the relations (2), (3) and (4) are very satistactory as shown in the previous section.

18) A. L. H. Chung, *J. Chem. Phys.*, **46**, 3144 (1967).

BULLETIN OF THE CHEMICAL SOCIETY OF JAPAN VOL. 43 704—708 (1970)

Microwave Spectra of *o*-Difluorobenzene in the Excited Vibrational States*1

Aritada HATTA and Kunio KOZIMA

Laboratory of Molecular Spectroscopy, Tokyo Institute of Technology, Ookayama, Meguro-ku, Tokyo

(Received September 6, 1969)

The microwave spectra of *o*-difluorobenzene in various excited vibrational states have been measured in the frequency region from 10- to 30-GHz. The R- and Q-branch transitions of the a-type have been assigned. The rotational constants for the $v_1=1$ state are $A=3254.77$, $B=2226.85$, and $C=1324.67$ MHz, and those for the $v_2=1$ state are $A=3269.76$, $B=2220.48$, and $C=1322.94$ MHz. The inertial defects in the excited states have been used in order to make vibrational assignments. It is very probable that the v_1 and the v_2 mode are the out-of-plane vibration of A_2 and the in-plane vibration of A_1 respectively.

Previous studies[1,2] of the microwave spectrum of *o*-difluorobenzene in the ground vibrational state have shown that the molecule is planar and that the angle made by two C–F bonds is probably

*1 Presented in part at the Symposium on Molecular Structure held by the Chemical Society of Japan, Tokyo, Oct., 1968.

1) A. Hatta, C. Hirose and K. Kozima, This Bulletin, **41**, 1088 (1968).

2) L. Nygaard, E. R. Hansen, R. L. Hansen, J. Rastrup-Andersen and G. O. Sørensen, *Spectrochim. Acta*, **23A**, 2813 (1967).

TABLE 1. TRANSITION FREQUENCIES (in MHz) FOR THE EXCITED VIBRATIONAL STATES OF *o*-DIFLUOROBENZENE

Transition	$v_1=1$ Observed*	$\nu_{obsd}-\nu_{calcd}$	$v_1=2$ Observed*	$\nu_{obsd}-\nu_{calcd}$	$v_1=3$ Observed*	$\nu_{obsd}-\nu_{calcd}$
$2_{11}\rightarrow3_{12}$	11685.0	+0.2	11680.8	+0.3	—	
$3_{13}\rightarrow4_{14}$	11858.6	−0.2	11861.6	+0.2	—	
$3_{12}\rightarrow4_{13}$	14873.4	−0.2	14866.7	+0.2	—	
$3_{21}\rightarrow4_{22}$	16079.3	+0.2	—		—	
$4_{14}\rightarrow5_{15}$	14550.9	+0.2	14554.7	+0.2	14558.7	+0.2
$4_{04}\rightarrow5_{05}$	14591.2	+0.1	14594.0	−0.3	—	
$4_{23}\rightarrow5_{24}$	16911.1	+0.2	—		—	
$4_{13}\rightarrow5_{14}$	17548.3	+0.1	17539.7	0.0	—	
$5_{15}\rightarrow6_{16}$	17212.8	−0.1	—		—	
$5_{05}\rightarrow6_{06}$	17223.8	−0.1	17229.0	+0.1	—	
$5_{14}\rightarrow6_{15}$	20039.2	+0.1	20032.5	+0.1	—	
$5_{23}\rightarrow6_{24}$	23082.0	+0.1	—		—	
$5_{41}\rightarrow6_{42}$	23155.6	0.0	23159.5	0.0	23163.7	0.0
$6_{25}\rightarrow7_{26}$	22479.9	+0.1	—		—	
$6_{15}\rightarrow7_{16}$	22581.6	−0.2	22577.8	−0.3	22574.2	−0.2
$6_{34}\rightarrow7_{35}$	24771.2	0.0	24765.2	0.0	24759.1	0.0
$6_{24}\rightarrow7_{25}$	25719.7	0.0	25702.7	0.0	25685.6	+0.1
$6_{33}\rightarrow7_{34}$	28089.0	−0.2	28077.6	0.0	28065.6	0.0
$7_{35}\rightarrow8_{36}$	27668.0	−0.2	27661.3	+0.4	—	
$6_{15}\rightarrow6_{34}$	11923.7	−0.2	—		—	
$8_{36}\rightarrow8_{35}$	11723.0	+0.3	11710.0	+0.1	—	
8_{26}—8_{45}	14326.8	−0.3	14268.2	−0.4	14209.0	+0.2

Transition	$v_2=1$ Observed*	$\nu_{obsd}-\nu_{calcd}$	$v_1=1+v_2=1$** Observed*	$\nu_{obsd}-\nu_{calcd}$	$v_3=1$ Observed*
$2_{02}\rightarrow3_{03}$	9416.8	+0.3	—		—
$2_{21}\rightarrow3_{22}$	10630.5	+0.2	—		—
$2_{11}\rightarrow3_{12}$	11662.0	−0.1	—		—
$3_{13}\rightarrow4_{14}$	11844.5	+0.1	—		—
$3_{03}\rightarrow4_{04}$	11981.1	+0.4	—		—
$3_{22}\rightarrow4_{23}$	13865.0	−0.3	—		—
$3_{12}\rightarrow4_{13}$	14861.1	+0.4	—		—
$3_{21}\rightarrow4_{22}$	16031.5	+0.1	—		—
$4_{23}\rightarrow5_{24}$	16877.8	+0.2	—		—
$4_{13}\rightarrow5_{14}$	17545.9	+0.1	—		17541.5
$5_{15}\rightarrow6_{16}$	17194.2	+0.1	17201.0	−0.1	—
$5_{05}\rightarrow6_{06}$	17205.7	−0.3	—		—
$5_{14}\rightarrow6_{15}$	20034.5	+0.1	—		—
$5_{23}\rightarrow6_{24}$	23064.8	−0.1	23050.0	−0.2	—
$5_{41}\rightarrow6_{42}$	23055.8	0.0	23058.5	0.0	—
$6_{25}\rightarrow7_{26}$	22459.4	−0.1	—		—
$6_{15}\rightarrow7_{16}$	22570.0	+0.3	—		—
$6_{34}\rightarrow7_{35}$	24736.4	−0.2	24730.5	+0.1	—
$6_{24}\rightarrow7_{25}$	25722.6	−0.3	25705.3	+0.1	—
$6_{33}\rightarrow7_{34}$	28031.4	+0.2	—		28106.6
$8_{26}\rightarrow8_{45}$	14393.9	−0.1	—		($v_3=2$; 28112.2)

* Maximum experimental uncertainty in the frequency measurements is ±0.2 MHz.
** Combination tone of the v_1 and the v_2 mode.

larger than 60°.

The infrared and Raman spectra of *o*-difluorobenzene have been investigated by Green *et al.*,[3] Scott *et al.*,[4] and Nonnenmacher and Mecke.[5] However, the vibrational assignments by these authors in the far-infrared region ($<400\ cm^{-1}$) are different from each other. The present study has been carried out in order to investigate the microwave spectra of *o*-difluorobenzene in the excited vibrational states and to obtain information about their vibrational assignments.

Experimental

The spectra were measured over the frequency range from 10- to 30-GHz with a conventional Stark modulation microwave spectrometer, employing 110-kHz square-wave or sine-wave modulation. The absorption-line frequencies were measured by the same method as has been previously reported by the present authors.[1]

All the measurements were made at room temperature. The sample of *o*-difluorobenzene was prepared from commercial *o*-fluoroaniline by the method of Schiemann and Pillarsky.[6]

Results

The rotational spectra were obtained for six excited vibrational states. The states will be designated hereafter by using the vibrational quantum numbers of v_i.

Assignments of the microwave spectra for the excited states were difficult because of the weakness of the lines and the complexity of the spectra. Because the spectra of the low-J R-branch transitions for the excited states, particularly for the $v_1=1$ state, overlap with the corresponding ground-state lines, an analysis for the low-J transitions was not easy. The lines of the excited states with the relatively high-J values, however, are well separated, and little overlapping occurs. The observations of the qualitative Stark patterns of the spectra were very helpful in the assignments. A least-squares procedure was used to get the best fit between the observed and the calculated frequencies. Agreement is as good as in the case of the ground state. A FACOM 222 digital computer was used in carrying out these calculations. For the $v_3=1$ state, only two transitions are assigned on the basis of their Stark effects and the relative intensities. The rotational constants were obtained for the states of the over-tones ($v_1=1$, 2, and 3, and $v_2=1$) and for that of the combination tone ($v_1=1+v_2=1$). The observed frequencies and the assignments in the excited states are listed in Table 1, together with the differences between the observed frequencies and those calculated by the use of the rigid rotor rotational constants given in Table 2.

As may be seen in Table 1, the centrifugal distortion effect is not important in the transitions studied. The rotational constants and the asymmetry parameters obtained are listed in Table 2. The principal moments of inertia derived from the rotational constants and the resulting inertial defects are listed in Table 3. As is shown in Tabel 3, the inertial defect, $\Delta_{v_1}(=I_c-I_a-I_b)$, becomes progressively more negative as the vibration is excited to higher over-tone states. For the $v_2=1$ state, $\Delta_{v_2=1}$ is also negative, though less in magnitude than $\Delta_{v_1=1}$.

The difference in the inertial defects between the first excited state and the ground state of v_1, $\delta\Delta_1$, is -0.757 amu·Å^2. That of v_2, $\delta\Delta_2$, is -0.197 amu·Å^2.

The measurements of relative intensity were made on the selected transitions of the ground and the first two excited states of v_1 and the first excited state of v_2.

Because of the richness of the spectrum, there were only a few transitions for which reliable measurements could be made. By the use of isolators the relative intensities were obtained by a direct comparison of the line heights on a recorder. The lines are so closely spaced that the variations in the microwave powder were limited to about 10% during these measurements. The results are shown in Table 4.

Discussion

Because the molecule of *o*-difluorobenzene, $^{12}C_6H_4F_2$, has a C_{2v} (or C_2) symmetry, the total wave-function should change in sign under the effect of the rotation operation of 180° about the two-fold axis of symmetry. Since the ratio of the number of the symmetric spin functions to that of the antisymmetric spin functions is 36 : 28, the antisymmetric rotational states (with K_{-1} odd) are more populated than the symmetric rotational states (with K_{-1} even) by this ratio for the ground vibrational state.

In the first vibrationally-excited state the value of the ratio must change to its inverse only for the vibrational mode of B_1 or B_2. As can be seen from Table 4, the relative intensities of the rotational transitions for the same vibrationally-excited state do not depend upon whether K_{-1} is even or odd. Therefore, it can be concluded that the vibration of the v_1 or the v_2 mode belongs to the A_1 or the A_2 type. In this paper the letters representing the frequencies and the relating quantities for different

3) J. H. S. Green, W. Kynaston and H. M. Paisley, *J. Chem. Soc.*, **1963**, 473.

4) D. W. Scott, J. F. Messerly, S. S. Todd, I. A. Hossenlopp, A. Osborn and J. P. McCullough, *J. Chem. Phys.*, **38**, 532 (1963).

5) G. Nonnenmacher and R. Mecke, *Spectrochim. Acta*, **17**, 1049 (1961).

6) G. Schiemann and R. Pillarsky, *Chem. Ber.*, **62**, 3035 (1929).

Table 2. Rotational constants for the excited states of o-difluorobenzene

	Ground state	$v_1=1$	$v_1=2$	$v_1=3$	$v_2=1$	$v_1=1+v_2=1$
A (MHz)	3263.55	3254.77	3246.04	3237.10	3269.76	3260.12
B (MHz)	2227.91	2226.85	2225.82	2224.77	2220.48	2219.21
C (MHz)	1323.87	1324.67	1325.48	1326.33	1322.94	1323.96
κ	−0.06785	−0.06515	−0.06241	−0.05960	−0.07794	−0.07523

Table 3. Moments of inertia* and inertial defects for the excited states of o-difluorobenzene

	Ground state	$v_1=1$	$v_1=2$	$v_1=3$	$v_2=1$	$v_1=1+v_2=1$
I_a (amu·Å^2)	154.854	155.272	155.690	156.120	154.560	155.017
I_b (amu·Å^2)	226.838	226.946	227.051	227.158	227.597	227.727
I_c (amu·Å^2)	381.741	381.510	381.277	381.033	382.009	381.715
Δ_{v_s} (amu·Å^2)	+0.049	−0.708	−1.464	−2.245	−0.148	−1.029

* Conversion factor: 5.05375×10^5, corresponding to $^{12}C=12$ atomic weight scale.

Table 4. Relative intensities* of the excited state transitions

Transition	$v_1=1$ ν cm^{-1}**	$v_1=2$ ν cm^{-1}**	$v_2=1$ ν cm^{-1}**	$v_3=1$ ν cm^{-1}**
$3_{12}\rightarrow4_{13}$	0.36 (206)	0.17 (364)	0.29 (250)	—
$4_{14}\rightarrow5_{15}$	0.33 (224)	0.14 (400)	—	—
$4_{32}\rightarrow5_{33}$	—	—	0.28 (260)	—
$4_{31}\rightarrow5_{32}$	—	—	0.26 (274)	—
$3_{21}\rightarrow4_{22}$	0.36 (206)	—	0.29 (250)	—
$3_{22}\rightarrow4_{23}$	—	—	0.30 (244)	—
$4_{23}\rightarrow5_{24}$	—	—	0.29 (250)	—
$4_{04}\rightarrow5_{05}$	0.37 (200)	0.15 (384)	—	—
$6_{24}\rightarrow7_{25}$	0.38 (194)	0.13 (406)	—	—
$6_{25}\rightarrow7_{26}$	0.34 (216)	—	0.28 (260)	—
$6_{33}\rightarrow7_{34}$	—	—	—	0.18 (298)
Mean value (in cm^{-1})	$\nu_{v_1=0\rightarrow1}$ =208	$\nu_{v_1=0\rightarrow2}$ =389	$\nu_{v_2=0\rightarrow1}$ =255	

* Referred to that the same rotational transition of the ground state.
** The estimated frequencies are shown in the parentheses.

Table 5. Comparison of our vibrational assignments with other authors'

	This study ν_{obsd} cm^{-1}	Green *et al.*[3] ν_{obsd} cm^{-1}	Scott *et al.*[4] ν_{obsd} cm^{-1}	Nonnenmacher and Mecke.[5]* ν_{obsd} cm^{-1}
ω_1	208 A_2	196 (R) A_1 and A_2	197 (R) B_2	197 (R) A_2
ω_2	255 A_1	—	240 (R) A_2	240 (R) B_2
ω_3	~300 B_2	298 (R) B_2	296 (R) A_1	—
ω_4	—	441 (IR) B_1	436 (R) B_1	—
ω_5	—	451 (IR) B_2	451 (IR) B_2	451 (IR) B_2

* Assignments for out-of-plane vibrations.

vibrational modes are designated by the numerical suffixes which number the vibrations from lower to higher. From the data of the intensities, the mean values of the vibrational frequencies of ω_1 and ω_2 were calculated to be 208 cm^{-1} and 255 cm^{-1} respectively. In view of the experimental error for the intensity measurements, these results are in agreement with those obtained by means of the Raman spectra,[4,5] as is shown in Table 5. For the v_3 mode, only two rotational transitions could be observed, as is shown in Table 1. The relative intensity of the $4_{13}\rightarrow5_{14}$ transitions could not be accurately measured because of the overlapping of the other band.

The relative intensity of the $6_{33}\rightarrow 7_{34}$ transitions for the $v_3=0$ and 1 states is shown in Table 4. From this value, the frequency of ω_3 is calculated to be 298 cm^{-1} if the v_3 mode is of the B_1 or the B_2 type. On the other hand, the value is calculated to be 348 cm^{-1} if the v_3 mode is of the A_1 or the A_2 type. As the value of 298 cm^{-1} is in good agreement with that of the Raman spectrum, the former assignment seems to be correct. Therefore, it is reasonable that the v_3 mode is of the B_2 type, according to the assignment given by Green *et al.*[3]

Until now three different assignments for the vibrational type have been reported. However, only for the v_4 and v_5 modes the assignments agree with each other, as is shown in Table 5. Let us, then, proceed to assign the v_1 and v_2 modes by assuming that the assignments for the v_4 and v_5 modes are correct. For this purpose the values of the inertial defect are useful. For a planar molecule a general formula for inertial defect, Δ, has been given by Oka and Morino[7] as follows:

$$\Delta = \Delta_{\text{vib}} + \Delta_{\text{cent}} + \Delta_{\text{elec}}$$

$$\Delta_{\text{vib}} = \sum_r (v_r+1/2)\Delta_r = \sum_r \frac{h}{\pi^2 c}(v_r+1/2) \times \sum_s{}' \frac{{\omega_s}^2}{\omega_r(\omega_r{}^2-\omega_s{}^2)} \{(\zeta_{rs}^{(a)})^2+(\zeta_{rs}^{(b)})^2-(\zeta_{rs}^{(c)})^2\} + \sum_t \frac{h}{\pi^2 c}\cdot\frac{3}{2\omega_t}(v_t+1/2) \quad (1)$$

where ω_r and ω_s are the wave numbers of different modes of vibrations, ζ's are Coriolis coupling constants, and the last term is taken into account only when the modes of r belong to the out-of-plane vibrations. The superscripts refer to the molecular fixed principal axes along which a vibrational angular momentum is produced. From this equation the difference between the total values of the inertial defect for two adjacent vibrational states can be expressed as follows:

$$\Delta v_{r+1} - \Delta v_r = \frac{h}{\pi^2 c}\left[\sum_s{}' \frac{{\omega_s}^2}{\omega_r(\omega_r{}^2-\omega_s{}^2)} \{(\zeta_{rs}^{(a)})^2 + (\zeta_{rs}^{(b)})^2 - (\zeta_{rs}^{(c)})^2\} + \frac{3}{2\omega_t}\right] \quad (2)$$

In Eq. (2) the difference between the values for Δ_{cent} are negligibly small and can be omitted, together with the difference in Δ_{elec}.

From the character table for C_{2v}, it can be seen that the nonvanishing elements of the Coriolis coupling constants for this molecule are $\zeta_{A_1A_2}^{(a)}$, $\zeta_{B_1B_2}^{(a)}$, $\zeta_{A_1B_2}^{(b)}$, $\zeta_{A_2B_1}^{(b)}$, $\zeta_{A_1B_1}^{(c)}$, and $\zeta_{A_2B_2}^{(c)}$, where the subscripts refer to the vibrational modes. The C_2 axis of symmetry is the a-axis, and the axis perpendicular to the molecular plane is the c-axis.

Equation (2) shows that the vibrational modes and their frequencies directly affect the inertial defect through the Coriolis interactions and that the interactions fall off with an increase in the frequency difference because of the $({\omega_r}^2-{\omega_s}^2)$ terms in the denominator. Hence, we can assume that the higher vibrations ($s>5$) are not important in these discussions.

It is very probable that the v_1 and v_2 modes are mainly due to the C–F deformation vibrations. Since it is clear, from symmetry considerations, that the out-of-plane vibrational modes belong to the A_2 and B_2 species and that the in-plane modes belong to the A_1 and B_1 species, the possibility that both the v_1 and v_2 modes belong to A_1 or A_2 can be excluded.

Additional evidence for this can also be obtained from the considerations based on Eq. (2). Therefore, there remain only the following two possibilities:

	ω_1	ω_2	ω_3	ω_4	ω_5
Case (1)	A_2	A_1	B_2	B_1	B_2
Case (2)	A_1	A_2	B_2	B_1	B_2

For Case (1), the following equations can be written on the basis of Eq. (2):

$$\frac{h}{\pi^2 c}\left[\frac{{\omega_2}^2}{\omega_1(\omega_1{}^2-\omega_2{}^2)}(\zeta_{12}^{(a)})^2 - \frac{{\omega^2}_3}{\omega_1(\omega_1{}^2-\omega^2{}_3)}(\zeta_{13}^{(c)})^2 + \frac{3}{2\omega_1}\right] = \delta\Delta_1$$

$$\frac{h}{\pi^2 c}\left[\frac{{\omega_1}^2}{\omega_2(\omega_2{}^2-\omega_1{}^2)}(\zeta_{12}^{(a)})^2 + \frac{{\omega_3}^2}{\omega_2(\omega_2{}^2-\omega_3{}^2)}(\zeta_{23}^{(b)})^2\right] = \delta\Delta_2$$

where the terms containing $(\zeta_{14}^{(b)})^2$ and $(\zeta_{15}^{(c)})^2$ in the former equation and the terms containing $(\zeta_{25}^{(b)})^2$ and $(\zeta_{24}^{(c)})^2$ in the latter equation could be considered to be approximately cancelled out, because the value of ω_4 is not very different from that of ω_5. By using the wave numbers reported by Scott *et al.*,[4] the possible values of the squares of the Coriolis coupling constants could be estimated as follows:

$$(\zeta_{12}^{(a)})^2 = 1.0 - 0.85, \quad (\zeta_{13}^{(c)})^2 = 0.26 - 0.0,$$
$$(\zeta_{23}^{(b)})^2 = 0.83 - 0.72$$

where the conversion factor of $h/\pi_2 C=134.8599$ amu·Å^2·cm^{-1} was used. These values seem to be reasonable. On the other hand, for Case (2) no reasonable values of the squares of the Coriolis coupling constants could be obtained.

Therefore, it can be concluded that the assignments of Case (1) are correct. The assignments obtained are analogous to those obtained for *o*-dichlorobenzene by Nonnenmacher and Mecke[5] and by Scherer.[8]

7) T. Oka and Y. Morino, *J. Mol. Spectrosc.*, **6**, 472 (1961).

8) J. R. Scherer, *Spectrochim. Acta*, **20**, 345 (1964).

BULLETIN OF THE CHEMICAL SOCIETY OF JAPAN VOL. 43 709—712 (1970)

Diffuse Reflection Spectra of Acid Clays Colored with Benzidine and Some Other Diamines

Akihiko HAKUSUI, Yoshio MATSUNAGA*1 and Kenji UMEHARA

Department of Chemistry, Faculty of Science, Hokkaido University, Sapporo

(Received September 9, 1969)

In order to identify the species responsible for the coloration of acid clay upon the addition of benzidine and related aromatic diamines, the diffuse reflection spectra of colored clays in the presence of water, methanol, and benzene were examined in the range from 4 to 29 kK. The coloration appeared to be due to the oxidation of the diamines held between the silicate sheets to the mono- and di-valent cations. The former cations were found to be in various modes of intermolecular interaction, depending on the kind and amount of the liquid. The lightening of the color upon drying was attributed to the disproportionation of the monovalent cations to the divalent cation and the protonated molecule.

It has been known that the addition of benzidine and other aromatic diamines to some clay minerals produces deep colors.[1,2] Examining the absorption spectra of acid clays suspended in benzene and colored by benzidine and its tetramethyl derivative, Hasegawa has concluded that the quinoidal and meriquinoidal forms of the diamines are responsible for the coloration.[3] In recent years much knowledge of the electronic spectra of ion radicals, including those derived from the diamines, has accumulated. It is now clear that the electronic spectra depend considerably on the mode of aggregation, *e.g.*, monomeric, dimeric or polymeric. Even in the solid state the presence of various modes of intermolecular interactions has been pointed out on the basis of the spectra.[4] As the diamine molecules held between the silicate sheets are in the form of a double layer,[5] it is not likely that the cation radicals in colored clays are free from intermolecular interaction. Therefore, no complete identification of the colored species in acid clays as the monovalent cations can be made without considering the mode of aggregation. In addition, a lightening of the colors on drying and a deepening on wetting have been noted by Hauser and Leggett and also by Takahashi.[2,5] To measure the spectral changes in such processes it seemed to us that the method of diffuse reflection has great advantages.

Experimental

Materials. The acid clay supplied by Wako Pure Chemical Industries, Ltd., was refined by repeated elutriations. Colored clays were prepared by mixing a diamine dissolved in a suitable organic solvent and the clay suspended in the same; the mixture was then filtered and washed throughly with the solvent. The samples thus prepared were quickly dried in a vacuum and then moistened with the liquid selected for the spectral measurements. For example, a 0.37-g portion of benzidine dissolved in 20 m*l* of methanol was added to 3.0 g of the clay suspended in 20 m*l* of methanol. The color was blue, but it turned green and finally yellow on drying. The carbon content of the dried sample was found by elemental analysis to be 1.48%, corresponding to a benzidine content of 1.89%. The diamines and the solvents used for sample preparations were as follows: benzidine in methanol, *o*-tolidine in methanol, *N,N,N′,N′*-tetramethylbenzidine in benzene, and 1,6-diaminopyrene in acetone. The cation radical salts of the first three diamines were prepared according to the methods of Hughes and Hush.[6] The solid bromides of the mono- and di-valent 1,6-diaminopyrene cations were made by the oxidation of the diamine dissolved in xylene with bromine, as has been described by Scott *et al.*[7]

Measurements. The difference in reflectance between a colored clay and the dry refined acid clay was recorded by means of a Beckman DK 2A spectroreflectometer. The spectra were plotted using the Kubelka-Munk function, $f(R)=(1-R)^2/2R$, where R is the reflectance. The function is supposed to be equal to the absorption coefficient divided by the scattering coefficient. As both the coefficients are affected by the pres-

*1 To whom inquiries may be addressed.

1) K. Kobayashi and K. Yamamoto, *Kogyo Kagaku Zasshi*, **26**, 289 (1921).

2) E. A. Hauser and M. B. Leggett, *J. Amer. Chem. Soc.*, **62**, 1811 (1940).

3) H. Hasegawa, *J. Phys. Chem.*, **65**, 292 (1961).

4) Y. Iida and Y. Matsunaga, This Bulletin, **41**, 2615 (1968).

5) H. Takahashi, *ibid.*, **28**, 5 (1955).

6) G. K. Hughes and N. S. Hush, *J. Proc. Roy. Soc. N. S. W.*, **81**, 48 (1947).

7) H. Scott, P. L. Kronick, P. Chairge and M. M. Labes, *J. Phys. Chem.*, **69**, 1740 (1965).

ence of a liquid, we must seek a set of conditions such that the change in the absorption coefficient is of major importance in determining the change in the spectra. When colored clays are only slightly moistened, *e.g.*, by a few drops of liquid per gram of the clay, the spectra were found to be approximately comparable with each other. The procedures used for the spectral measurements of the solid ion-radical salts were described in an earlier paper.[4]

Results

Benzidine-acid Clay. The dried sample is yellow, and the spectrum has only one absorption maximum, located at 22.5 kK. As is shown in Fig. 1, a weak, continuous absorption can be seen

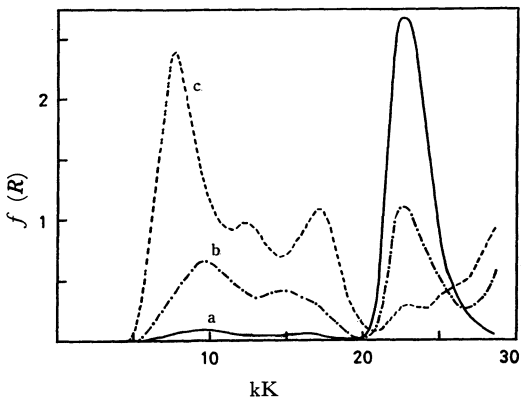

Fig. 1. Diffuse reflection spectra of benzidine-acid clays moistened with water; (a) nearly completely dried, (b) moistened, (c) moistened further.

in the low-energy region if the sample is not quite dry. On slight moistening with water, the absorption in the low-energy region is intensified and that at 22.5 kK is considerably weakened. The presence of maxima at 9.5 and 14.5 kK and a shoulder at 16 kK can be clearly noted. (Hereafter this will be called the pattern B-2). The further addition of water to the sample modifies the spectrum drastically. The absorption at 22.5 kK almost decays out, and absorption maxima at 7.5, 12.0, 17.0, and about 27 kK form the pattern B-1. When the sample is very wet, the pattern remains the same as the pattern B-1, but the intensities may be hundreds of times higher than those shown in Fig. 1.

The spectra of the samples moistened with methanol are shown in Fig. 2. The pattern B-2 can be more clearly observed here than in the clays moistened with water. An absorption maximum now clearly appearing at 26 kK is considered to be a part of this pattern. This figure presents a good example of how the spectral change by the addition of a liquid is reversible. A slightly moistened sample was examined first (curve a). Then the sample

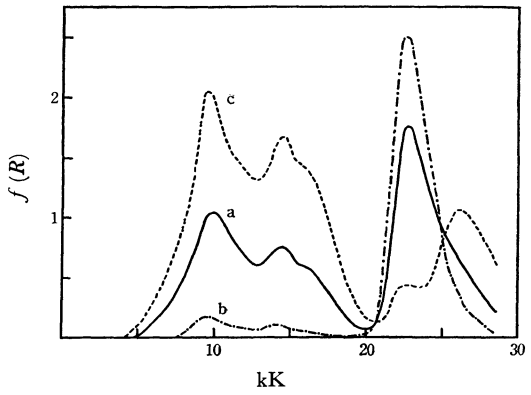

Fig. 2. Diffuse reflection spectra of benzidine-acid clays moistened with methanol; (a) moistened, (b) nearly completely dried, (c) moistened again.

was nearly completely dried (curve b), and finally it was moistened again with methanol (curve c). The pattern B-1 can be observed in this combination, too, provided that the samples are soaking wet.

Moistening the dried samples with benzene results in the appearance of a spectrum entirely different from that described above. The pattern B-3, found in Fig. 3, consists of absorption maxima at 11.5, 15.2, and somewhere around 27 kK.

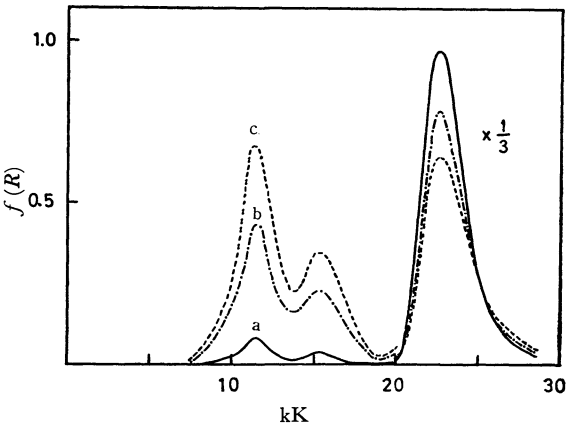

Fig. 3. Diffuse reflection spectra of benzidine-acid clays moistened with benzene; (a) nearly completely dried, (b) moistened, (c) moistened further.

The results given in Figs. 1, 2, and 3 were all obtained using freshly-prepared samples. On storage the absorption at 22.5 kK is slowly intensified and the sample becomes less sensitive to moisture. Long after preparation, the deep color does not develop on either moistening or soaking.

***o*-Tolidine-acid Clay.** In this system the samples moistened with methanol show essentially the same spectra as those moistened with water. Figure 4

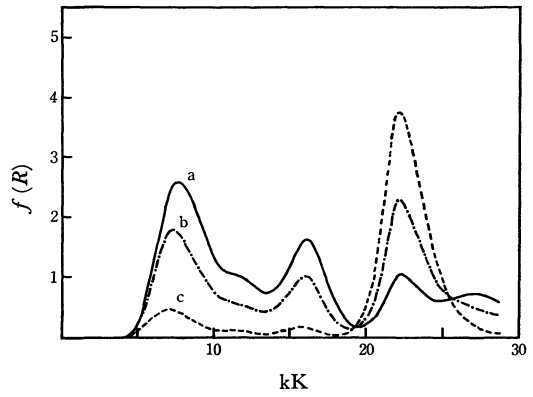

Fig. 4. Diffuse reflection spectra of *o*-tolidine-acid clays moistened with methanol; (a) moistened, (b) moistened less, (c) nearly completely dried.

presents the spectra obtained by the former combination. The pattern T-1 characteristic of the deep-colored clays consists of absorption maxima at 7.5, 16.0, and 27.0 kK and a shoulder at 11.5 kK; it bears a close resemblance to the pattern B-1.

On moistening with benzene absorption maxima are observed at 10.7, 14.5, and 27 kK. The pattern shown in Fig. 5 may be designated as T-3 because

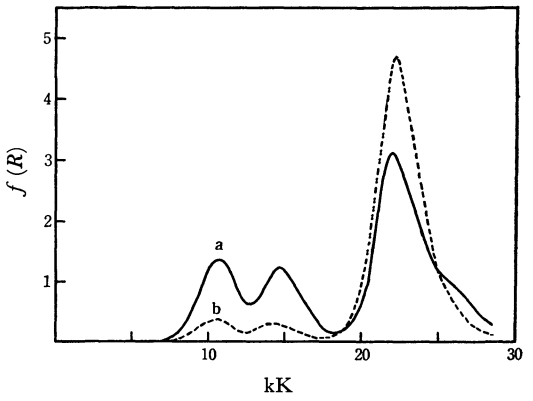

Fig. 5. Diffuse reflection spectra of *o*-tolidine-acid clays moistened with benzene; (a) moistened, (b) nearly completely dried.

of its similarity to the pattern B-3. It should be noted that the spectra given in Figs. 4 and 5 were taken in the process of drying.

Tetramethylbenzidine-acid Clay. The sample prepared in benzene is green. This color lightens only very slowly on drying. The spectrum (curve a) given in Fig. 6 was obtained after three weeks' storage over silica gel. By the addition of methanol, the absorptions at 7—7.5, 14—14.5, and 25 kK are intensified. The spectrum exhibited by the moistest sample in the figure (curve c) is practically the same as that exhibited by the sample freshly prepared in benzene.

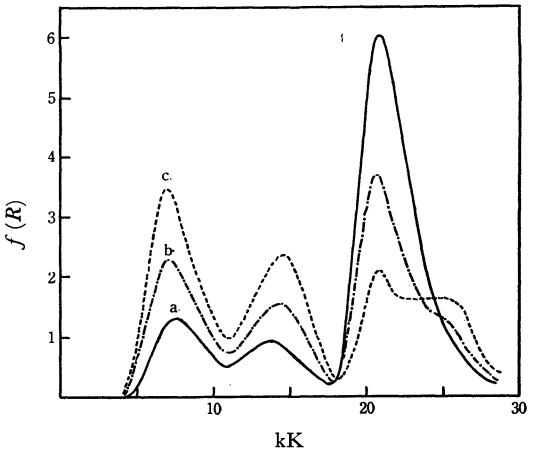

Fig. 6. Diffuse reflection spectra of tetramethylbenzidine-acid clays moistened with methanol; (a) nearly completely dried, (b) moistened, (c) moistened further.

Diaminopyrene-acid Clay. The freshly-prepared sample is dark brown. The color turns to a reddish brown on standing. As is shown in Fig. 7,

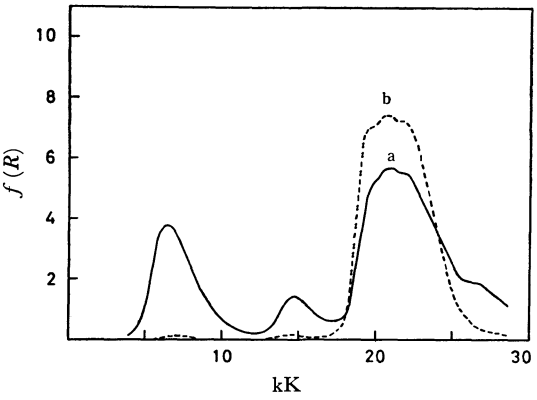

Fig. 7. Diffuse reflection spectra of dry diaminopyrene-acid clays; (a) freshly prepared, (b) stored for three days.

the disappearance of absorptions at 6.5, 14.7 and about 26 kK is the cause of this color change. As grinding and moistening accelerate this change, the effects of the added liquid cannot be ascertained.

Bromides of Mono- and Di-valent Cations. The spectra of the cation radical salts derived from benzidine and its tetramethyl derivative were described in a previous paper.[4] The bromide of the monovalent *o*-tolidine cation gives a spectrum very similar to them. The locations of the absorption maxima are as follows: 6.8, 15.5, and 26.0 kK in the benzidine bromide, 7.5, 16.0, and 27.0 kK and a shoulder at 11.5 kK in the *o*-tolidine bromide, and 8.0, 14.7, and 25.0 kK in the tetramethylbenzidine bromide.

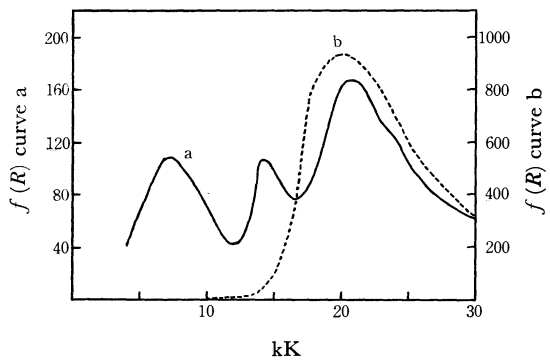

Fig. 8. Diffuse reflection spectra of diaminopyrene bromides; (a) monobromide, (b) dibromide.

The bromides of mono- and di-valent diaminopyrene cations show the spectra given in Fig. 8. It must be added that the intensity of the absorption near 20 kK in the dibromide is about five times stronger than that in the monobromide. In addition to a broad absorption appearing around 21 kK, the monobromide exhibits absorption maxima at 7.0 and 14.0 kK.

Discussion

First of all we must note that none of the spectra of the colored clays studied here exhibits a pattern which can be assigned to the monomeric form of the cation radicals. The patterns B-1 and T-1 and that in the spectra of the clay colored with tetramethylbenzidine resemble those of the solid bromides. Furthermore, the pattern B-3 is close to that of the dimeric cation radicals in solution. The latter is known to consist of absorption maxima at 12.4, 16.4, and 27.8 kK.[8] Perhaps only the cation radicals can show such pronounced variations and coincidence of the spectra. Therefore, the patterns B-1 and T-1 and that in the spectra of the clays colored with tetramethylbenzidine may be assigned to the univalent diamine cations in more-than-by-pairs interactions, while the patterns B-3 and T-3 may be assigned to the cations in pair-by-pair interactions. The presence of the pattern B-2 indicates that there is another mode of more-than-by-pairs interaction in this particular case.

The absorption spectra of the acid clays colored with benzidine and with its tetramethyl derivative reported by Hasegawa[3] are in agreement with those we give in Fig. 3 (pattern B-3) and Fig. 6 respectively. Although the monovalent cations, Hasegawa's meriquinoidal forms, are responsible for the deep colors developed in these two systems, it must be pointed out that the cations are in different modes of intermolecular interaction.

Hasegawa has reported that the quinoidal form, presumably the divalent cation in our nomenclature, of tetramethylbenzidine dissolved in ethanol exhibits an absorption at 21.3 kK. The absorption at 20.8 kK in Fig. 6 may be assigned to this species. We may conclude that the species giving strong absorptions in the range between 20 and 23 kK of Figs. 1—5 are also the divalent diamine cations. This conclusion is in accordance with the observation that these absorptions are slowly intensified on storage until finally these are the only ones to be detected.

1,6-Diaminopyrene has been known to form solid bromides of the mono- and di-valent cations.[7] The spectra in Fig. 8 may well be compared to those of the clays colored with this diamine in Fig. 7. The freshly-prepared sample shows the pattern characteristic of the monobromide, but after three days' storage only the absorption to be assigned to the dibromide can be observed. These findings are consistent with our observations concerning the clays colored with benzidine and its derivatives.

As has been mentioned before, the spectra in each figure from 2—6 are only approximately in the same scale; however, there is no doubt about the presence of isosbestic points. This implies that the mono- and di-valent diamine cations are in equilibrium. Since these two species are in different oxidation states, if follows that the diamine itself is also a participant in the equilibrium. However, the absence of the absorption to be assigned to the diamine, *i. e.*, 30.0 kK for benzidine and 28.7 kK for tetramethylbenzidine in the solid state, suggests that the diamine molecules in acid clay are in the protonated form.

Summing up our conclusions, the following equilibrium may be conceived in acid clay:

$$D^{2+} + DH^{+} \rightleftarrows 2D^{+} + H^{+},$$

where D is a diamine molecule. On being moistened, protonated diamine molecules dissociate into protons and diamine molecules, and the electron transfer from the latter to the divalent cations leads to the formation of deeply-colored aggregates of the monovalent cations. According to the proposed mechanism of the lightening of the color on drying and the deepening on moistening, Hauser and Leggett have observed that mineral and organic acids either inhibit or lighten the color.[2] Moreover, the same equilibrium as that described above has been proposed by Hasegawa to explain the pH dependence of the absorption spectrum of the "meriquinoid compound" of tetramethylbenzidine in a 30% ethanol solution.[3]

8) H. Matsusaka and K. Suzuki, Paper presented at the 19th Annual Meeting of the Chemical Society of Japan, Tokyo, April, 1966.

BULLETIN OF THE CHEMICAL SOCIETY OF JAPAN VOL. 43 713—720 (1970)

Charge-Transfer Complexes of Maleic Anhydride and Dichloromaleic Anhydride with Various Aromatic Compounds

Takayoshi KOBAYASHI,* Suehiro IWATA** and Saburo NAGAKURA*

* *The Institute for Solid State Physics, The University of Tokyo, Roppongi, Minato-ku, Tokyo*

** *The Institute of Physical and Chemical Research, Yamato-machi, Saitama*

(Received September 19, 1969)

Absorption, fluorescence and fluorescence excitation spectra were measured at room temperature and at low temperature for charge-transfer complexes containing maleic anhydride and dichloromaleic anhydride as electron acceptors. Benzene, toluene, mesitylene, durene, hexamethylbenzene, aniline, dimethylaniline, naphthalene and anthracene were used as electron donors. The charge-transfer absorption and fluorescence bands were observed for these complexes, their peak positions being linearly dependent upon the ionization potentials of donors for the same electron acceptor. From the comparison of the charge-transfer absorption or fluorescence peaks of maleic anhydride complexes with the corresponding values of dichloromaleic anhydride complexes, the difference in electron affinity between these two electron acceptors was obtained to be 0.4 eV. The electronic structures of the maleic anhydride complexes with benzene, naphthalene and anthracene were studied theoretically by considering the configuration interaction among the ground, locally-excited and charge-transfer configurations. The stable geometrical configurations in the ground and lower excited states of the complexes were discussed by the aid of the energy levels calculated for various relative orientations between electron donor and acceptor.

Maleic anhydride (abbreviated hereafter to MA) is one of the most important dienophilic substances in the Diels-Alder reaction. The charge-transfer (abbreviated hereafter to CT) complexes between MA and some aromatic hydrocarbons are suggested to take part in some Diels-Alder photoreactions.[1] This seems to be supported by the fact that MA and benzene which can form a CT complex is led to the Diels-Alder reaction.[2] The reaction is sensitized by benzophenone, and is inhibited by benzil.[2,3] The triplet-energy transfer from the sensitizer to the CT complex and therefore the sensitization of the Diels-Alder reaction may be possible, if the lowest triplet state of the former is higher than that of the latter. In this connection, it seems to be important to determine the positions of the lower excited states, especially the lowest triplet state, of CT complexes containing MA as an electron acceptor.

In the present work, we have undertaken to measure the absorption and emission spectra of the complexes between MA and various electron donors such as benzene, toluene, mesitylene, durene, hexamethylbenzene, aniline, dimethylaniline, naphthalene and anthracene. Furthermore, to clarify the character of the MA complexes, the study has been extended to complexes containing dichloromaleic anhydride (DCMA) which is stronger as an electron acceptor than MA.

Furthermore, from the theoretical point of view, we have undertaken to study by the semi-empirical MO method the electronic structures of CT complexes between MA and benzene, naphthalene or anthracene, the calculated energy of CT excited states being discussed in connection with the Diels-Alder photoreaction mechanism.

Experimental

Commercially available MA (Wako, reagent grade) and DCMA (Tokyo Kasei, reagent grade) were purified by sublimation *in vacuo* and by zone refining. Benzene, toluene, mesitylene, aniline and dimethylaniline (abbreviated hereafter to DMA) were purified by distillation. Commercially available durene, hexamethylbenzene (abbreviated hereafter to HMB), naphthalene and anthracene were purified by repeated recrystallizations from ethanol. A mixture 1 : 1 of ethyl ether and isopentane (abbreviated hereafter to EP) was used for the spectrophotometric study at low temperature. The single crystals of complexes between MA or DCMA and aromatic hydrocarbons were prepared by mixing the acceptor and one of the donors in methylene chloride or chloroform and by evaporating slowly the solvent at room temperature.

1) N. J. Turro, "Molecular Photochemistry," W. A. Benjamin, Inc, New York (1965), p. 193.

2) D. Bryce-Smith, A. Gilbert and B. Vickery, *Chem. Ind.* (London), **1960**, 2060; D. Bryce and J-E. Lodge, *J. Chem. Soc.*, **1962**, 2675; D. Bryce-Smith and A. Gilbert, *ibid.*, **1965**, 918.

3) G. S. Hammond and W. M. Hardham, *Proc. Chem. Soc.*, **1963**, 63.

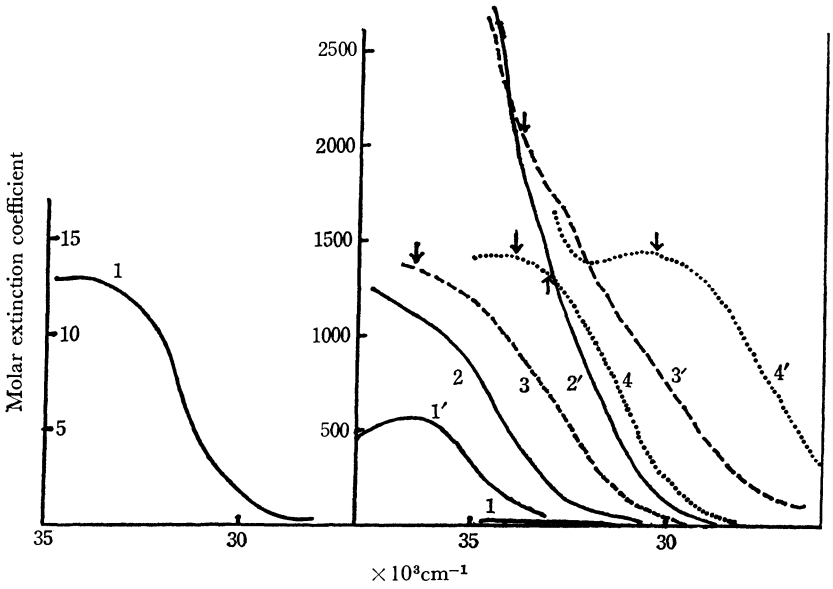

Fig. 1. The absorption spectra of MA and DCMA in various solvents at room temperature.
Curves 1, 2, 3, and 4 are for the MA solutions in chloroform, benzene, toluene and mesitylene, respectively. Curves 1′, 2′, 3′ and 4′ are for the DCMA solutions in chloroform, benzene, toluene and mesitylene, respectively.

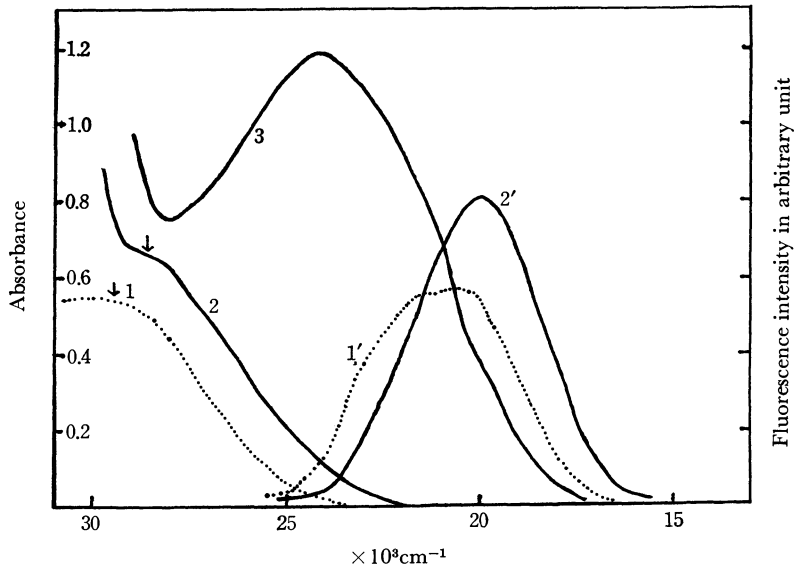

Fig. 2. The absorption and fluoresecnce spectra of some MA complexes at room temperature (in chloroform) and at liquid nitrogen temperature (in rigid EP solution), respectively.
Curve 1, absorption for the MA (0.93×10^{-1} mol/l)–durene (0.33×10^{-2} mol/l) solution.
Curve 2, absorption for the MA (0.93×10^{-1} mol/l)–HMB (0.83×10^{-2} mol/l) solution.
Curve 3, absorption for the MA (0.93×10^{-1} mol/l)–DMA (5.3×10^{-2} mol/l) solution.
Curves 1′ and 2′ are the fluorescence spectra of the MA complexes with durene and HMB, respectively.

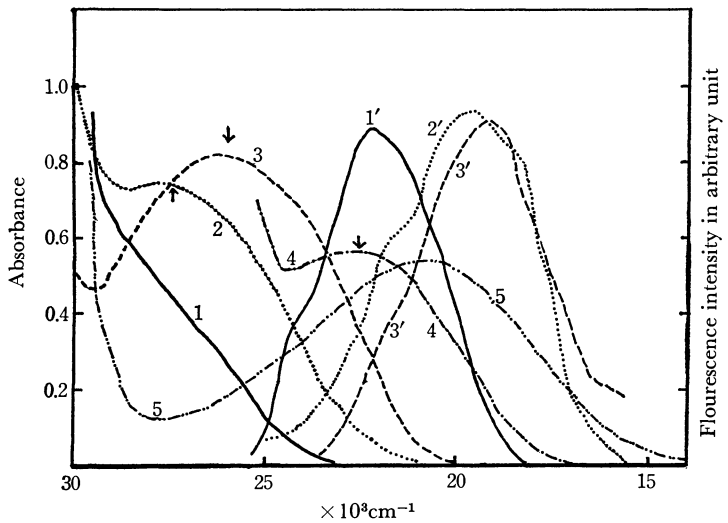

Fig. 3. The absorption and fluorescence spectra of some DCMA complexes at room temperature (in chloroform) and at liquid nitrogen temperature (in rigid EP solution), respectively.
Curve 1, absorption for the DCMA (0.55×10^{-2}mol/l)–durene (0.42×10^{-1} mol/l) solution.
Curve 2, absorption for the DCMA (0.55×10^{-2} mol/l)–HMB (1.1×10^{-1} mol/l) solution.
Curve 3, absorption for the DCMA (0.50×10^{-1} mol/l)–naphthalene (0.45×10^{-1} mol/l) solution.
Curve 4, absorption for the DCMA (0.50×10^{-1} mol/l)–anthracene (0.27×10^{-2} mol/l) solution.
Curve 5, absorption for the DCMA (0.50×10^{-1}mol/l)–DMA (1.5×10^{-1} mol/l) solution.
Curves 1′, 2′, and 3′ are the fluorescence spectra of the complexes with durene, HMB and naphthalene, respectively. The DCMA-durene complex exhibits considerably strong phosphorescence and curve 1′ is the difference between the total emission and the phosphorescence.

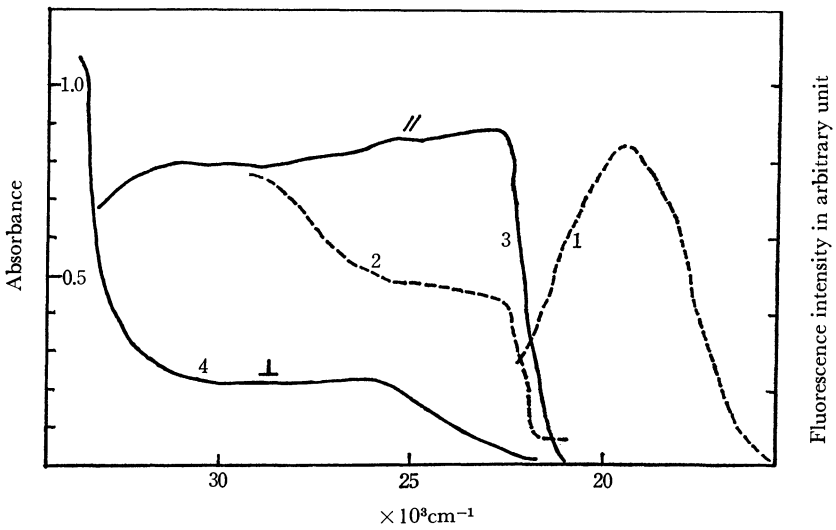

Fig. 4. The fluorescence (curve 1), fluorescence excitation (curve 2) and polarized absorption (curves 3 and 4) spectra of the DCMA-HMB crystal. The polarized absorption was measured in the direction parallel and perpendicular to the crystal growth axis.

TABLE 1. ABSORPTION MAXIMA AND IONIZATION POTENTIALS OF DONORS

Donor	Acceptor	State	Temperature	ν_m	I_D*
MA	Mesitylene	in mesitylene	r.t.	34.0 (10^3 cm^{-1})	8.39 (eV)
MA	Durene	in chloroform	r.t.	31.8	8.03
MA	HMB	in chloroform	r.t.	28.6	7.85
MA	DMA	in chloroform	r.t.	24.0	7.14
DCMA	Mesitylene	in mesitylene	r.t.	30.8	8.39
DCMA	Durene	in chloroform	r.t.	27.8	8.03
DCMA	HMB	in chloroform	r.t.	26.2	7.85
DCMA	Anthracene	in chloroform	r.t.	22.7	7.37
DCMA	DMA	in chloroform	r.t.	20.8	7.14
MA	Aniline	powder	100°K	30.2	7.69
DCMA	HMB	single crystal	77°K	23.2**	7.85

* V. I. Vedeneyev, L.V. Gurvich, V. N. Kondrat'yev, V. A. Madevdev and Ye. L. Frankevich, "Bond Energies, Ionization Potentials and Electron Affinities," Edward Arnold Ltd., London (1966).

** The peak of the polarized absorption parallel to the crystal growth axis.

TABLE 2. FLUORESCENCE MAXIMA AND IONIZATION POTENTIALS OF DONORS

Donor	Acceptor	State*	ν_m	I_D
MA	Mesitylene	in EP	22.4 (10^3 cm^{-1})	8.39 (eV)
MA	Durene	in EP	20.9	8.03
MA	HMB	in EP	20.0	7.85
DCMA	Mesitylene	in EP	22.3	8.39
DCMA	Durene	in EP	19.8	8.03
DCMA	HMB	in EP	19.2	7.85
MA	Aniline	powder	21.3	7.69
DCMA	HMB	single crystal	19.5	7.85

* Fluorescence was measured at 77°K in all cases.

Absorption spectra of solutions and of thin films on quartz plates[4] were measured with a Cary recording spectrophotometer Model 14M. Polarized absorption spectra of small single crystals were measured with a microspectrophotometer constructed in our laboratory.[5]

Emission spectra at liquid nitrogen temperature were measured with a JASCO Model CT-50 grating monochromator with an RCA 1P28 or EMI 9529A photomultiplier tube as a detector, glassy solutions or crystals being irradiated by a high pressure 500 W Hg lamp combined with Toshiba UV D1A and UV D2 filters in order to select 3650 Å light which excites the CT complexes only. The fluorescence spectra and their excitation spectra of powder samples (MA-aniline) were measured with an Aminco-Bowman spectrophotofluorometer (4-8202B) located at Government Chemical Industrial Research Institute.*1

The spectra observed with the MA and DCMA complexes are shown in Figs. 1, 2, 3 and 4, and the peak positions of the absorption and emission spectra are tabulated in Tables 1 and 2.

Theoretical

In the present paper, the interaction between electron donor and acceptor is taken into account by the configuration interaction among the ground, CT and locally-excited (abbreviated hereafter to LE) configurations.[6,7] For this calculation we need the MO's of each component. We adopt the SCF MO's of MA calculated by S. Hosoya and H. Hosoya by the aid of the Pariser-Parr-Pople method.*2 The electron donors taken in the present theoretical study are benzene, naphthalene and anthracene.

For the sake of simplicity, we consider only the highest two occupied MO's (ϕ_1, ϕ_2 and θ_1, θ_2) and the lowest two vacant MO's (ϕ_3, ϕ_4 and θ_3, θ_4) of MA and aromatics. The wave functions

4) T. Sakata and S. Nagakura, This Bulletin, **42**, 1497 (1969).

5) J. Tanaka, *ibid.*, **36**, 833 (1963).

*1 We should like to express our sincere thanks to Dr. Akira Kuboyama, Government Chemical Industrial Research Institute, for his kindness in permitting us to use the instrument.

6) S. Iwata, J. Tanaka and S. Nagakura, *J. Amer. Chem. Soc.*, **88**, 894 (1966).

7) S. Iwata, J. Tanaka and S. Nagakura, *ibid.*, **89**, 2813 (1967).

*2 We are greatly indebted to Dr. Haruo Hosoya and Mrs. Sumie Hosoya for their kindness in permitting us to use their unpublished theoretical result.

of the ground and lowest CT configurations[8] are given by the Slater-type determinant

$$\Phi_G = |\phi_1\bar{\phi}_1\phi_2\bar{\phi}_2\theta_1\bar{\theta}_1\theta_2\bar{\theta}_2|$$

$$\Phi_{CT_1} = 1/\sqrt{2}\{|\phi_1\bar{\phi}_1\phi_2\bar{\phi}_2\theta_1\bar{\theta}_1\theta_2\bar{\phi}_3| - |\phi_1\bar{\phi}_1\phi_2\bar{\phi}_2\theta_1\bar{\theta}_1\bar{\theta}_2\phi_3|\}$$

$$\Phi_{CT_2} = 1/\sqrt{2}\{|\phi_1\bar{\phi}_1\phi_2\bar{\phi}_2\theta_1\bar{\phi}_3\theta_2\bar{\theta}_2| - |\phi_1\bar{\phi}_1\phi_2\bar{\phi}_2\bar{\theta}_1\phi_3\theta_2\bar{\theta}_2|\}$$

$$\Phi_{CT_3} = 1/\sqrt{2}\{|\phi_1\bar{\phi}_1\phi_2\bar{\phi}_2\theta_1\bar{\theta}_1\theta_2\bar{\phi}_4| - |\phi_1\bar{\phi}_1\phi_2\bar{\phi}_2\theta_1\bar{\theta}_1\bar{\theta}_2\phi_4|\}$$

$$\Phi_{CT_4} = 1/\sqrt{2}\{|\phi_1\bar{\phi}_1\phi_2\bar{\phi}_2\theta_1\bar{\phi}_4\theta_2\bar{\theta}_2| - |\phi_1\bar{\phi}_1\phi_2\bar{\phi}_2\bar{\theta}_1\phi_4\theta_2\bar{\theta}_2|\}$$

In addition to the above-mentioned configurations, the following LE configurations corresponding to the lower excited states of the component molecules are taken into consideration.

$\Phi^{MA}_{L_1} = \Phi^{MA}(\phi_2^{-1}\phi_3)$ (5.96 eV)
for local excitation in MA

$\Phi^{B}_{L_1} = 1/\sqrt{2}\{\Phi^{B}(\theta_1^{-1}\theta_4) - \Phi^{B}(\theta_2^{-1}\theta_3)\}$ (4.71 eV)
for $^1B_{2u}$ local excitation in benzene

$\Phi^{N}_{L_1} = 1/\sqrt{2}\{\Phi^{N}(\theta_1^{-1}\theta_3) - \Phi^{N}(\theta_2^{-1}\theta_4)\}$ (4.06 eV)
for $^1B_{3u}^-$ local excitation in naphthalene

$\Phi^{N}_{L_2} = \Phi^{N}(\theta_2^{-1}\theta_3)$ (4.45 eV)
for $^1B_{2u}^+$ local excitation in naphthalene

$\Phi^{A}_{L_1} = \Phi^{A}(\theta_2^{-1}\theta_3)$ (3.31 eV)
for $^1B_{2u}^+$ local excitation in anthracene

$\Phi^{A}_{L_2} = 1/\sqrt{2}\{\Phi^{A}(\theta_1^{-1}\theta_3) + \Phi^{A}(\theta_2^{-1}\theta_4)\}$ (4.93 eV)
for $^1B_{3u}^+$ local excitation in anthracene

The energies of the LE configurations are taken from the transition energies observed with MA, benzene,[9a] naphthalene[9b] and anthracene.[9b] Their values are given in the parentheses after the wave functions of the corresponding LE configurations.

The energies of the CT configurations, the ground configuration energy being taken as the standard, is obtained as follows, for example, for the CT_1 configuration:

$$E_{CT_1} = \varepsilon(\phi_3) - \varepsilon(\theta_2) - \iint \phi_3(1)\phi_3(1)\frac{e^2}{r_{12}}\theta_2(2)\theta_2(2)d\tau_1 d\tau_2$$
$$= I(\theta_2) - A(\phi_3) - C_{23}$$

where $\varepsilon(\phi_3)$ and $\varepsilon(\theta_2)$ are the orbital energies, and $I(\theta_2)$ and $A(\phi_3)$ are the ionization potential of the donor and the electron affinity of the acceptor, respectively. The ionization potentials of benzene, naphthalene and anthracene are 9.245, 8.10 and 7.37 eV, respectively.[10] The electron affinity of MA can be determined to be 0.6 eV from the peak of the first CT band of MA-DMA complex on the assumption that the Coulomb term in Eq. (1) given later is 3.6 eV.[11] The electron affinity for the second lowest vacant orbital can be determined from the value for the lowest vacant orbital by assuming that the difference in the electron affinity is equal to that in the corresponding SCF orbital energies. The off-diagonal matrix elements of the total electron Hamiltonian each of which represents the interaction between two different configurations can be evaluated.[12] For example, those between the CT configuration and the ground or LE configurations can be represented in terms of the core resonance integral β which is approximately represented by the following equation:[13]

$$\beta = -KS_{ij}$$

where K is an experimental parameter and S_{ij} is the overlap integral between the electron donating orbital θ_i and the electron accepting orbital ϕ_j. It is represented by the sum of the overlap integrals between the Slater type atomic orbitals. We set K equal to 10.[6,7]

By solving secular equations constructed by the above-mentioned diagonal and off-diagonal matrix elements, we evaluate the energies of the ground and lower excited states for the MA complexes with benzene, naphthalene and anthracene,[14] taking various geometrical configurations under the following limitations;

1) The molecular planes of electron donor and acceptor are parallel with each other and their distance is 3.4 Å.

2) The C=C bond of MA is parallel to the symmetry axis parallel to a bond of each donor molecule.

Results and Discussion

Complexes in Solution. The absorption spectra of MA and DCMA in chloroform, benzene, toluene and mesitylene are shown in Fig. 1. A very weak absorption of MA (curve 1 in Fig. 1) due to an n–π^* transition[15] appears at 31000 cm^{-1}—34000

8) Since the wave functions include spin functions, strictly speaking, these configurations should be called the "zero-order ground singlet state" and the "zero-order CT singlet state." Here we use "configuration" instead of "zero-order singlet state" because of simplicity.

9) a) H. B. Klevens and J. R. Platt, *J. Chem. Phys.*, **17**, 470 (1949). b) E. Clar, "Aromatische Kohlenwasserstoffe," Springer-Verlag, Berlin (1952).

10) K. Watanabe, *J. Chem. Phys.*, **26**, 542 (1957); J. B. Birks and M. A. Slifkin, *Nature*, **191**, 761 (1961).

11) This is the value calculated for the benzene-tetracyanobenzene system on the point-charge approximation.[7] On this approximation, this value is applicable to various donor-acceptor systems taking structures of parallel molecular planes 3.4 Å distant.

12) J. A. Pople, *Proc. Phys. Soc.*, **68A**, 81 (1955); H. C. Longuet-Higgins and J. N. Murrell, *ibid.*, **68A**, 601 (1955).

13) For example, R. Hoffmann, *J. Chem. Phys.*, **39**, 1397 (1963).

14) Actual calculations were performed by the aid of an electronic computer FACOM 202 of our institute. The authors' thanks are due to the Mr. Yasuho Ishida for his assistance in writing the program.

15) From the low value of the molar extinction coefficient and from the analogy with similar carbonyl compounds, the absorption band near the 360 mμ is clearly attributed to the n–π^* transition.

cm^{-1} in chloroform. In the other solvents, MA exhibits a new band conceivably due to the CT interaction with surrounding molecules. The situation is the same for the DCMA solutions.

Concerning the electron donors other than benzene, toluene and mesitylene, absorption and fluorescence spectra were measured with ternary solutions containing electron donor and acceptor in chloroform, with the results shown in Figs. 2 and 3 for the MA and DCMA complexes, respectively. A new absorption band neither due to electron donor nor acceptor is observed for the MA complexes with HMB and DMA and for the DCMA complexes with DMA, anthracene, HMB and durene. Furthermore, a shoulder appears for the MA complex with durene, and for the DCMA complex with naphthalene. In order to certify that these bands and shoulders are due to the CT transition, we examine the relationship between the peak positions and the ionization potentials of donors.

The peak wave numbers of the CT bands for a series of complexes with a fixed electron acceptor are related to the ionization potentials (I_D) of donors by the following equation:

$$h\nu_{CT} = I_D - C_1 + \frac{C_2}{I_D - C_1} \qquad (1)$$

where C_1 and C_2 are constants to be determined experimentally. C_1 is mainly composed of two factors, the electron affinity of the electron acceptor (A_A) and the Coulomb attraction between the donor and acceptor orbitals (C): that is to say, $C_1 = A_A - C$. Using the observed ionization potentials of the donors and taking the CT band maximum of the MA-DMA or DCMA-DMA complex as the standard, we can calculate the CT band positions for the MA and DCMA complexes. They are indicated by the arrows in Figs. 1, 2 and 3. The calculated peak positions are in good agreement with the observed ones. This supports the CT assignment of the absorption bands under consideration.

Figures 2 and 3 show that the fluorescence spectrum of each complex in EP solution at liquid nitrogen temperature satisfies the mirror image relation with the CT absorption spectrum observed for the chloroform solution at room temperature. This means that the observed fluorescence spectra are of the CT character.

From Eq. (1), we may expect that a linear relation can be approximately satisfied between ν_{CT} and I_D in the case where the latter is changed in a rather narrow range. Plotting these two quantities for both the fluorescence and the absorption spectra observed for a series of complexes containing the fixed electron acceptor, we obtain a straight line relationship, as is shown in Fig. 5. From this figure, it is found that the lines for the absorption maxima observed for the MA and DCMA complexes are parallel with each other and they cross the

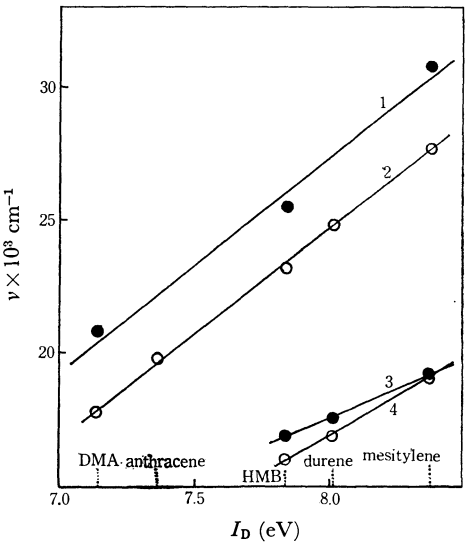

Fig. 5. The plot of the absorption and fluorescence maxima for the MA and DCMA complexes in solution against the ionization potentials (I_D) of donors.
1 and 2; absorption maxima—I_D polts for the MA and DCMA complexes, respectively.
3 and 4; fluorescence maxima—I_D plots for the MA and DCMA complexes, respectively.

ordinate with the energy difference of ~0.4 eV. This is mainly due to the difference in C_1 in Eq. (1) between the DCMA and MA complexes. That is to say, the electron affinity of DCMA may be higher by ~0.4 eV than that of MA.

Complexes in Solid State. The polarized absorption was measured with a single crystal of the DCMA-HMB complex, for the purpose of obtaining an additional support for the CT assignment of the band at ~22000 cm^{-1}. The needlelike crystal of this complex is unstable and decomposed within a few days at 5°C. Therefore the measurement was carried out as quickly as possible after the crystallization. The result is shown in Fig. 4. Furthermore, the fluorescence and fluorescence excitation spectra of this crystal measured at liquid nitrogen temperature are also shown in this figure. An absorption at 22000 cm^{-1} is polarized parallel to the crystal growth axis with the dichroic ratio more than 4. Since crystals of this kind usually grow up in the direction perpendicular to the planes of the stacked component molecules, the above result seems to mean that the transition moment of the band is directed perpendicular to the molecular plane. This supports the interpretation that the absorption band at ~22000 cm^{-1} is the CT one and therefore the corresponding fluorescence at ~20000 cm^{-1} is of the same character.[16]

16) The similar experimental work has been carried out for the single crystal of the DCMA-durene complex. In this case too, the CT absorption polarized parallel to the crystal growth axis is observed.

Theoretical Result. The energies of the ground and lowest CT states were calculated for the MA complexes with benzene, naphthalene and anthracene by the method described in the "Theoretical" part. Concerning the MA complex with benzene, the stable geometrical configuration of the ground state is predicted to be similar to that of the lowest CT state. In both the ground and the lowest CT state, the center of the C=C double bond of MA is located above the point close to the center of benzene. However, the gradient of energy surface is about 10 times steeper in the excited state than in the ground state.

Theoretical results on the MA complexes with naphthalene and anthracene are shown in Figs. 6 and 7, respectively. These figures show energy contour maps for the ground and lowest CT state, which are obtained by plotting the state energies against the positions of the center of the C=C bond of MA.

The MA-naphthalene and MA-anthracene complexes in the ground state have, respectively, two and three energy minima which are located near the center of each benzene ring, while in the excited state they have only one minimum near the center of donor molecule. As an example, the stable geometrical structure of the MA-anthracene complex predicted by the present theoretical consideration is shown in Fig. 8. According to this figure,

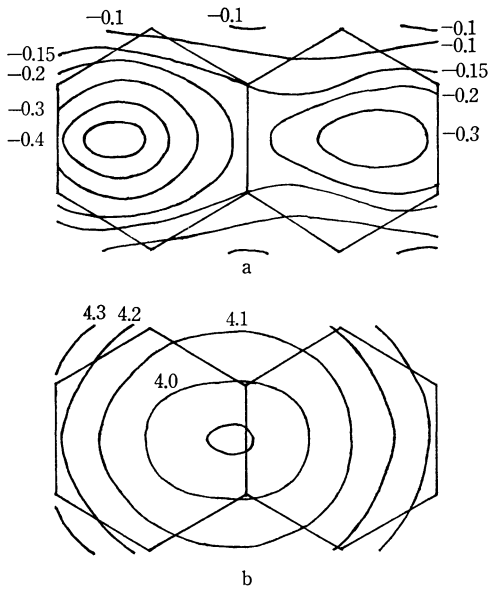

Fig. 6. The dependence of energy (in eV) on the geometrical configuration for the MA-naphthalene complex.
a, ground state
b, lowest CT state

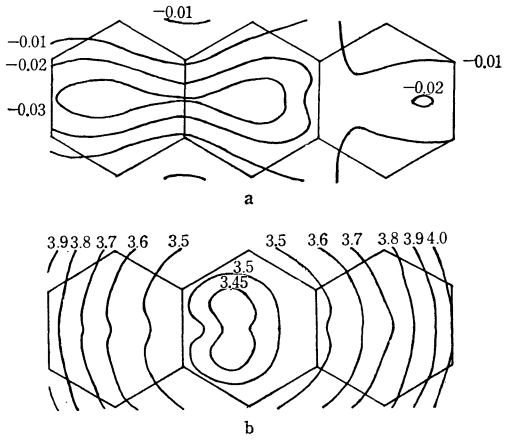

Fig. 7. The dependence of energy (in eV) on the geometrical configuration for the MA-anthracene complex.
a, ground state
b, lowest CT state

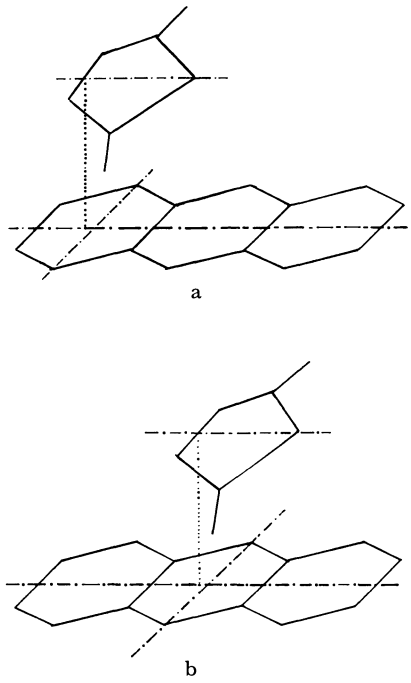

Fig. 8. The stable geometrical configuration of the MA-anthracene complex.
a, ground state
b, lowest CT state

the MA molecule moves to the energy minimum position above the center of the anthracene molecule in the excited state from the position above one of the end benzene rings in the ground state. This seems to be interesting in connection with the fact that in the Diels-Alder reaction the C=C double bond of MA reacts with anthracene on the 9 and 10 positions. The positions of photochemical dienophile addition in this case seems to be reason-

ably explained by assuming that the reaction occurs through the excited CT state of the complex.

Next, we add a brief descrption on the mechanism of thermal Diels-Alder reaction of MA. In view of the electron accepting ability mentioned above, it may be considered that the CT interaction takes part in the reaction. That is to say, in the initial stage of the reaction, we can except the formation of the π (outer)-complex which takes the structure shown in Fig. 8a.[17] In this stage the degree of the electron transfer from anthracene to MA may be small. With the progress of the reaction, the CT degree may increase and the system may approach gradually the structure shown in Fig. 8b. Therefore in the stage of the actual formation of the new C–C bonds between MA and anthracene, the system may probably take the structure similar to that in Fig. 8b.[18] Thus, by the aid of CT state structure shown in Fig. 8b we can explain reasonably the fact that the thermal dienophile addition occurs at the 9 and 10 positions of anthracene.

We are greatly indebted to Dr. Keitaro Yoshihara, the Institute for Solid State Physics, for his helpful advice.

17) The present discussion is made on the assumption that the thermal Diels-Alder reaction proceeds through the π (outer)-complex in the initial stage.

18) The actual process of the bond formation is not clear. There are two possibilities that the two C–C bonds are simultaneously formed, and that each of them is formed separately and the bond formation proceeds in the two steps. In the latter case, we may expect the inner (σ)-complex formation in which electron transfer occurs to a great extent and a new C–C bond is formed between MA and anthracene.

BULLETIN OF THE CHEMICAL SOCIETY OF JAPAN VOL. 43 720—725 (1970)

The Reactivity of the Electron Donor-Accepter Complex—Catalysis by 1,3-Dimethylalloxazine in an Enzymatic Model Reaction

Yasuhiro Iwasawa, Mitsuyuki Soma, Takaharu Onishi and Kenzi Tamaru

Department of Chemistry, The University of Tokyo, Hongo, Bunkyo-ku, Tokyo

(Received September 29, 1969)

The effect of electron donor-accepter(EDA)-complex formation upon the reactivity (or catalytic activity) of 1,3-dimethylalloxazine, a model compound of co-enzyme, FMN, was examined in the redox reaction between methylene blue and ascorbic acid. The 1,3-dimethylalloxazine exhibited a behavior similar to the enzyme, having an optimal pH for the redox reaction. The characteristic behavior of 1,3-dimethylalloxazine was demonstrated in the presence of both 1,3-dimethylalloxazine and pyrene; such behavior was not to be observed upon the addition of either of them. It was accordingly suggested that the EDA complex formation would play an important role in the enzymatic reactions *in vivo*. The influence of various aromatic hydrocarbons upon the enzyme-like catalysis was examined.

It is generally accepted that the electron-transfer process in a living body is frequently associated with the formation of adenosine triphosphate (ATP), thus accumulating energy. As to the mechanism of the electron-transfer process, various hypotheses have been proposed, such as conduction band theories,[1,2] exciton models,[3,4] and charge-transfer models.[5] No crucial evidence, however, has ever been presented to elucidate the reaction mechanism or its reaction intermediate for the redox process catalyzed, for instance, by the flavin enzyme. Especially, the reason why the co-enzymatic action appears, the role of protein in the enzyme, and its reaction site and intermediate still remain important problems to be solved.

The present authors have been working for several years with the problems of the reactivity of electron donor-acceptor (EDA) complexes of

1) D. D. Eley, "Horizons in Biochemistry," Academic Press, New York, (1962), p. 341.

2) M. G. Evans and J. Gergely, *Biochem. Biophys. Acta*, **3**, 188 (1949).

3) M. Kasha, *Rev. Mod. Phys.*, **31**, 162 (1959).

4) M. Calvin, *ibid.*, **31**, 16, 147 (1959).

5) A. Szent-Györgyi, "Introduction to a Submolecular Biology," Academic Press, New York (1960).

aromatic compounds, and they have demonstrated that the reactivity of aromatic compounds, is in general, markedly influenced by the formation of the EDA complexes.[6] Accordingly, in connection with the mechanism of the co-enzyme action, 1,3-dimethylalloxazine*1 has been employed as a model compound of co-enzyme, flavin mononucleotide (FMN),*2 and its reactivity or its catalytic activity and the effects of the EDA complex formation thereon have been examined for the redox process between methylene blue and ascorbic acid from the view point of the EDA-complex formation.

It was found that the 1,3-dimethylalloxazine accelerates the redox reaction and that the formation of the EDA-complexes markedly affects the catalytic activity.

Experimental

The 1,3-dimethylalloxazine (DMA)[7] was synthesized from caffeine and *o*-phenylendiamine, while commercial ascorbic acid and methylene blue were employed. The aromatic hydrocarbons, such as naphthacene, perylene, anthracene, pyrene, *p*-terphenyl and phenanthrene, were purified by sublimation. The reactor consisted of a quartz cell for visible spectra and of three glass tubes, containing solutions of ascorbic acid, methylene blue, and DMA or its EDA-complexes, respectively. The reactants were always handled in the absence of air or oxygen. In the oxidation-reduction reaction, ascorbic acid was used as the hydrogen donor, while methylene blue was used as the hydrogen acceptor. The decrease in the absorption peak of methylene blue at 650 mμ was employed as a measure of the extent of the redox reaction to follow the reaction rate. Three different sorts of experiments were carried out as follows: (1) The DMA was used as a catalyst for the redox reaction between ascorbic acid and methylene blue, and the dependence of the rate upon the pH, the reaction temperature, and the addition of electron-donating and -accepting compounds, such as pyrene and tetracyanoethylene (TCNE), was examined.

As an aqueous solution of ascorbic acid (3.27×10^{-4} mol/*l*, 2 m*l*), a solution of methylene blue (3.27×10^{-4} mol/*l*, 1 m*l*), a tetrahydrofuran (THF) solution of DMA (1.64×10^{-4} mol/*l*, 2 m*l*), and a phosphate buffer (20 m*l*) were mixed in the absence of oxygen and the rate of the reduction of methylene blue was studied at various temperatures and at various pH values, as controlled by the phosphate buffer.

(2) The influence of the EDA-complex formation upon the catalytic activity of DMA was studied. In this case, a 1,2-dichloroethane solution of DMA and pyrene (2 to 1 molar ratio; 3.27×10^{-7} mol and 1.64×10^{-7} mol, respectively, in a 4.5 m*l* solution) was added to a redox system of a 1,2-dichloroethane solution of ascorbic acid (3.27×10^{-4} mol/*l*, 1 m*l*) and methylene blue (3.27×10^{-4} mol/*l*, 1 m*l*).

(3) The reduction of methylene blue by ascorbic acid was affected by the addition of various aromatic hydrocarbons, such as naphthacene, perylene, anthracene, pyrene, *p*-terphenyl, and phenanthrene, as electron-donating compounds for the methylene blue, and the influences of these aromatic additives were examined in the 1,2-dichloroethane solution.

Results and Discussion

(1) Catalysis by 1,3-Dimethylalloxazine (DMA). The reduction reaction of methylene blue by ascorbic acid was accelerated to a facter of 50 by the addition of DMA. The reaction was first-order with respect to methylene blue. The higher the temperature of the reaction, the greater the rate of the reaction, when the pH was constant, as is shown in Fig. 1. When the pH was changed

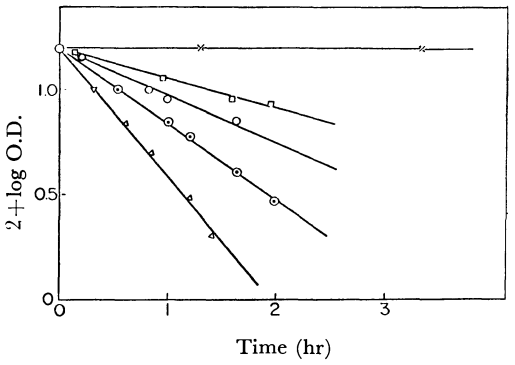

Fig. 1. Dependence of the rate constants *k*, $-d(Mb)/dt=k(Mb)$, upon temperature in the redox reaction between ascorbic acid and methylene blue (Mb) catalyzed by DMA.
O. D. represents the optical density of methylene blue.
—×— at 0°C, pH 10.4, without DMA
—○— at 0°C, pH 10.4
—⊙— at 26°C, pH 10.4
—□— at 0°C, pH 12.0
—△— at 25°C, pH 12.0

at a constant temperature, 13°C, the gradient of the rate against the pH became less steep in the region of pH 10 and approached a saturation value in the region higher than pH 12. At a constant temperature, 0°C, on the other hand, a maximum peak appeared in the reaction rate in the range from pH 9 to pH 10, as is shown in Fig. 2. A minimum activation energy for the reaction was also found in the same region (Table 1). When an electron-donating compound, such as pyrene, or an electron-accepting compound, such as TCNE, for the DMA was added to the system of the redox

6) M. Ichikawa, M. Soma, T. Onishi and K. Tamaru, *Trans. Faraday Soc.*, **63**, 997 (1967), S. Tanaka, M. Ichikawa, S. Naito, M. Soma, T. Onishi and K. Tamaru, This Bulletin, **41**, 1278 (1968).

*1 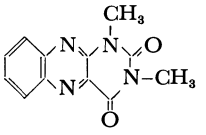

*2 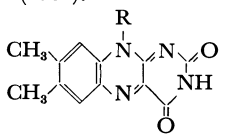

7) H. Biltz, *Ber.*, **45**, 3674 (1912).

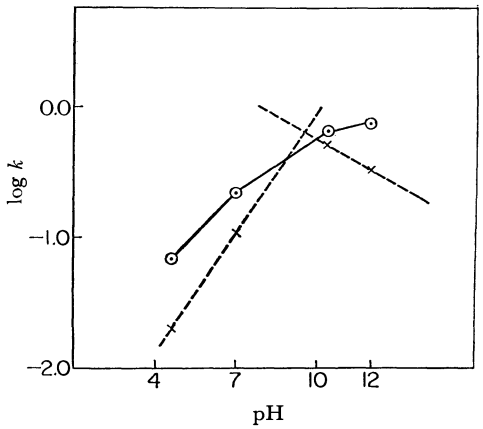

Fig. 2. Dependence of the rate constants k, $-d(Mb)/dt=k(Mb)$, upon pH:
—⊙— at 13°C
—×— at 0°C

TABLE 1. THE REDUCTION OF METHYLENE BLUE BY ASCORBIC ACID CATALYZED BY DMA

pH	Temperatures (°C)	Rate constants (hr^{-1})	Activation energies (kcal/mol)
4.6	0	0.020	14.8
	13	0.069	
7.0	0	0.11	8.0
	13	0.22	
10.4	0*	0.011*	—
	0	0.53	2.8
	26	0.84	
12.0	0	0.35	9.2
	25	1.43	

* Without DMA

reaction of ascorbic acid, methylene blue, and DMA, the rates of the reduction reaction of methylene blue decreased to approximately one-third.

The activity of enzymes is, in general, high in weak alkaline solution and has an optimal temperature range to work in. It is interesting to note that the DMA, a model compound of the co-enzyme, FMN, exhibited a catalysis similar to that of the enzyme and that the optimal pH values were demonstrated in the activity of the redox reaction; this suggests that the behavior of the active site of the enzyme is similar to that of the co-enzyme model.

(2) Effects of the EDA Complex Formation between DMA and Pyrene in the Redox Reaction. The 1,2-dichloroethane solutions of ascorbic acid, methylene blue, and a mixture of DMA-pyrene (2 : 1) were mixed at 0°C in the absence of oxygen. For 10 to 15 min the time-concentration relation for methylene blue exhibited a valley-shaped curve; thereafter, the reaction reached an equilibrium, as Fig. 3 shows. This valley curve can be explained not as an equilibrating reaction

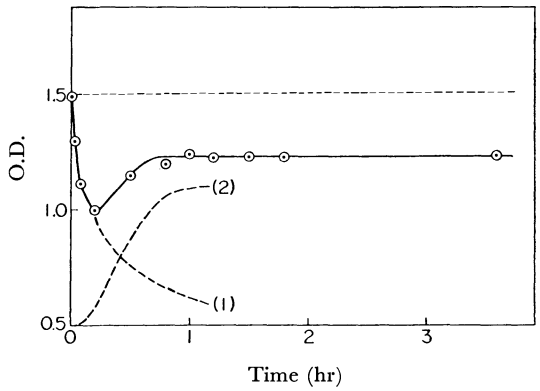

Fig. 3. The reduction of methylene blue by ascorbic acid in the presence of DMA and pyrene at 0°C in 1,2-dichloroethane solution.
------ O.D. of methylene blue at $t=0$.
----(1) forward reaction, Eqs. (b) and (c)+(c').
----(2) back reaction, Eq. (e).

with a single reaction path, but as a successive reaction to consume the methylene blue, followed by its reproduction.

Such characteristic behavior appeared only in the presence of both DMA and pyrene, was not observed upon the addition of either of them or in a phosphate buffer as has been described in Section (1), where the interaction between them is very weak. Consequently, the following experiment was undertaken: first, ascorbic acid and methylene blue were reacted in the presence of only pyrene, and then DMA was introduced into the system during the course of the redox reaction. The results are given in Fig. 4. The results in Fig. 4 exhibit a behavior similar to those shown in Fig. 3.

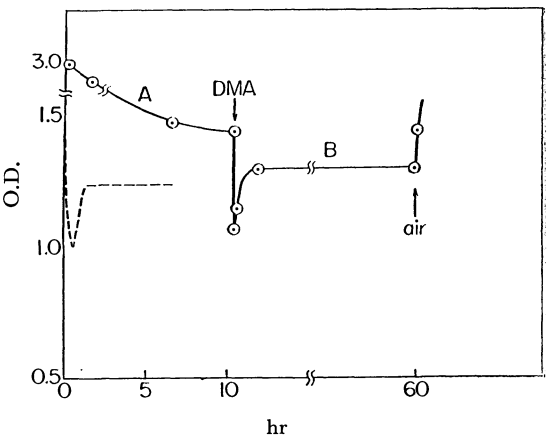

Fig. 4. Effect of the formation of EDA complex in the redox reaction of methylene blue with ascorbic acid at 0°C:
---- in the presence of DMA and pyrene
A: catalyzed by pyrene.
B: DMA addition into A.

When the temperature of the reaction was kept constant at 26°C, the valley in Fig. 3 became more shallow.

The characteristic behavior shown in Fig. 3 was not observed for lower concentrations of both DMA and pyrene in comparison with methylene blue; for instance, when the molar ratios of DMA and pyrene to methylene blue were 1/22.5 and 1/45, respectively or 1/45 and 1/90, respectively, no valley could be detected. When leuco-methylene blue which had been obtained by bubbling hydrogen gas over a platinum catalyst in a dichloroethane solution of methylene blue was introduced into a solution containing both DMA and pyrene, it was oxidized to methylene blue rather rapidly. DMA and pyrene form a solid EDA complex with a molar ratio of 2 : 1 and with a charge-transfer band in the region from 400 to 500 mμ.[8] It was concluded, in accordance to these results, that the appearence of the characteristic curve shown in Fig. 3 is due to the complex formation between DMA and pyrene.

It is also confirmed spectroscopically and theoretically that the enzymes or co-enzymes form EDA complexes.[9-11] When DMA, a model compound of the co-enzyme, FMN, of the flavin enzyme formed an EDA complex with pyrene, there was a controlled reaction; this suggests that the EDA complex formation plays an important role in the enzymatic reaction *in vivo*.

Mechanisms. In the presence of both DMA and pyrene (P), the mechanism of the reduction reaction of methylene blue (Mb) by ascorbic acid (AsH_2) may be as follows:

$$AsH_2 + Mb \underset{k_{-1}}{\overset{k_1}{\rightleftharpoons}} As + MbH_2 \qquad (a)$$

$$AsH_2 + \left(\frac{P}{2}\cdot Mb\right) \underset{k_{-2}}{\overset{k_2}{\rightleftharpoons}} As + \frac{P}{2} + MbH_2 \qquad (b)$$

$$AsH_2 + DMA \underset{k_{-3}}{\overset{k_3}{\rightleftharpoons}} As + DMAH_2 \qquad (c)$$

$$DMAH_2 + Mb \underset{k_{-3'}}{\overset{k_{3'}}{\rightleftharpoons}} DMA + MbH_2 \qquad (c')$$

$$AsH_2 + \left(\frac{P}{2}\cdot DMA\right) \underset{k_{-4}}{\overset{k_4}{\rightleftharpoons}} As + \frac{P}{2} + DMAH_2 \qquad (d)$$

$$MbH_2 + \left(\frac{P}{2}\cdot DMA\right) \underset{k_{-5}}{\overset{k_5}{\rightleftharpoons}} Mb + \frac{P}{2} + DMAH_2 \qquad (e)$$

where (P/2·Mb) and (P/2·DMA) represent the complexes between pyrene and methylene blue, and between pyrene and DMA, respectively. The reaction (a) is first-order with respect to ascorbic acid and also to methylene blue, and it is expressed by the following equation:

$$-\frac{d}{dt}(Mb) = k_1(AsH_2)(Mb)$$

The step (b) is a reaction catalyzed by pyrene, while the steps (c) and (c') show that the redox reaction is catalyzed by DMA. When the steady-state method of Birggs and Haldan is applied to this reaction system, the rate equation of the reaction is given as follows:

$$-\frac{d}{dt}(Mb) = k_3'(DMAH_-)(Mb)$$

$$= k_3'(DMA)_0(Mb)\frac{1}{1 + \dfrac{k_{-3}(As)}{k_3(AsH_2)} + \dfrac{k_3'(Mb)}{k_3(AsH_2)}}$$

where $(DMA)_0$ represents the initial concentration of DMA, and under the conditions when $(DMA)_0 \ll (AsH_2)_0$ and $(Mb)_0$, $16(Mb)_0 = (AsH_2)_0$, and $k_3 \approx k_3'$:

$$\frac{1}{1 + \dfrac{k_{-3}(As)}{k_3(AsH_2)} + \dfrac{k_3'(Mb)}{k_3(AsH_2)}}$$

becomes about unity, following equation is thus obtained:

$$-\frac{d}{dt}(Mb) = k_3'(DMA)_0(Mb) = k_3''(Mb)$$

Under these circumstances, the reaction was first-order with respect to methylene blue, and the rate constant, k_3'', is proportional to the initial concentration of DMA, as is shown in Fig. 5. The dihydro-1,3-dimethylalloxazine ($DMAH_2$) in Eqs.

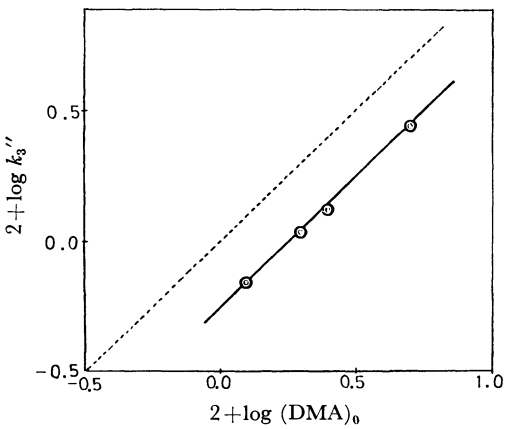

Fig. 5. The dependence of the rate constant k_3'' upon the initial concentration of DMA; $-d(Mb)/dt = k_3'(DMA)_0(Mb) = k_3''(Mb)$, where $(DMA)_0$ and (Mb) represent the concentration of DMA at time zero and methylene blue, respectively. Solid line runs parallel with broken line (slope of 45°).

8) U. Matsunaga, *Nature*, **211**, 182 (1966).
9) A. Pullman and B. Pullman, "Horizons in Biochemistry," Academic Press, New York (1962), p. 553.
10) R. S. Mulliken, *J. Chem. Phys.*, **61**, 20 (1964).
11) L. J. Andrews and R. W. Keefer, "Molecular Complexes in Organic Chemistry," Holden-Day, San Franscisco (1964).

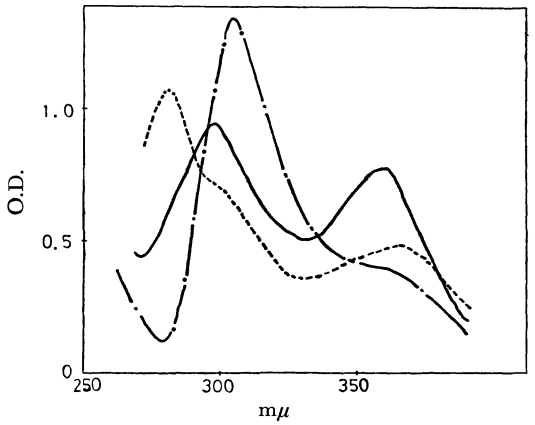

Fig. 6. Spectra of 1,3-dimethylalloxazine (DMA).
—— DMA in THF
---- DMA plus ascorbic acid
---- DMA plus HCl (45°C heating)

Table 2. The reduction of methylene blue by ascorbic acid

Steps		Rate constant
(a)*	k_1	$2.0\times10^2\ l\cdot mol^{-1}\cdot hr^{-1}$
(b)*	k	$0.0058\ hr^{-1}$
(c)(c')*	k_3'	$1.0\times10^4\ l\cdot mol^{-1}\cdot hr^{-1}$
(e)*	k'	$\sim2\ hr^{-1}$

* (a): $-d(Mb)/dt = k_1(AsH_2)(Mb)$
(b): $-d(Mb)/dt = k_2'(Ar)_0{}^{1/2}(Mb) = k(Mb)$
(c)(c'): $-d(Mb)/dt = k_3'(DMA)_0(Mb) = k_3''(Mb)$
(e): $-d(MbH_2)/dt = k'(Mb)$, when $(DMA)_0 \gg (Mb)_0$, where (Mb), (MbH_2), (AsH_2) and $(DMA)_0$ represent the concentrations of methylene blue, leuco-methylene blue, ascorbic acid and the DMA at $t=0$, respectively.

(c) and (c') was detected by UV spectroscopy, as is shown in Fig. 6.[12]

The steps (d) and (e) form another reaction path resulting from the formation of the EDA complex of DMA with pyrene, while the back reaction in Fig. 3 is due to the step (e).

The rate constants of all the steps, (a), (b), (c), (c'), and (e), are given in Table 2.

(3) Influences of Various Aromatic Hydrocarbons in the Redox Reaction. Various aromatic hydrocarbons, such as naphthacene, perylene, anthracene, pyrene, *p*-terphenyl, and phenanthrene, all electron donors for methylene blue but with different ionization potentials, accelerated the reduction reaction of methylene blue by ascorbic acid, though they are generally considered to be inert in the reaction.

When the aromatic hydrocarbons form EDA complexes with methylene blue of a molar ratio of 1 : 2, the reaction equation is given as follows:

$$\tfrac{1}{2}(Ar) + Mb \underset{k_{-1}}{\overset{k_1}{\rightleftharpoons}} (\tfrac{1}{2}Ar\cdot Mb) \qquad (g)$$

$$(\tfrac{1}{2}Ar\cdot Mb) + AsH_2 \xrightarrow{k_2} MbH_2 + \tfrac{1}{2}Ar + As \qquad (h)$$

where (Ar) represents aromatic hydrocarbons:

$$K = \frac{k_1}{k_{-1}} = \frac{(\tfrac{1}{2}Ar\cdot Mb)}{(Ar)^{1/2}(Mb)}$$

Accordingly,

$$\frac{d}{dt}(MbH_2) = k_2(\tfrac{1}{2}Ar\cdot Mb)(AsH_2) = k_2K(AsH_2)(Ar)^{1/2}(Mb).$$

When $(AsH_2)_0 \gg (Mb)_0$:

$$-\frac{d}{dt}(Mb) = k_2K(AsH_2)_0(Ar)_0{}^{1/2}(Mb) = k_2'(Ar)_0{}^{1/2}(Mb) = k(Mb)$$

where $(Ar)_0$ is the initial concentration of the aromatic hydrocarbons.

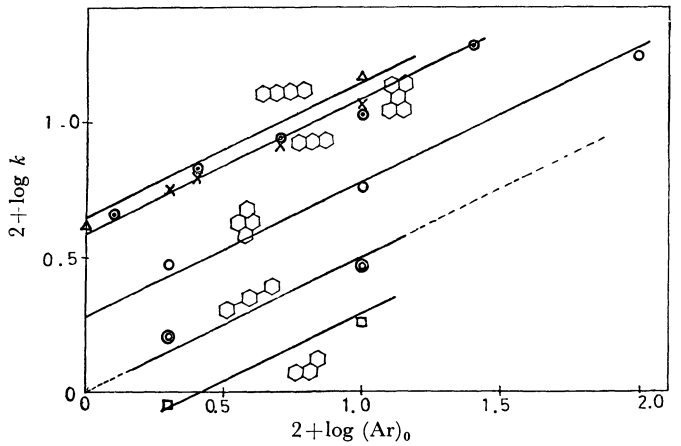

Fig. 7. The linear dependence of rate constants k upon the initial concentrations of aromatic hydrocarbons $(Ar)_0$:
$-d(Mb)/dt = k_2'(Ar)_0{}^{1/2}(Mb) = k(Mb)$.

12) P. Hemmerich, C. Veeger and H. C. S. Wood, *Angew. Chem.*, **77**, 699 (1965).

TABLE 3. THE REDUCTION OF METHYLENE BLUE BY ASCORBIC ACID, CATALYZED BY AROMATIC HYDROCARBONS

Catalysts \ k*	Molar ratios+ 1/4	1/10	1/20	1/40	1/50	1/80	1/100
Naphthacene		0.15					0.043
Perylene		0.12	0.083	0.064	0.058		0.034
Anthracene	0.19	0.11	0.090	0.069		0.038	0.030
Pyrene		0.058			0.030		
p-Terphenyl		0.030			0.017		
Phenanthrene		0.018			0.009		

* $-\mathrm{d(Mb)}/\mathrm{d}t = k_2'(\mathrm{Ar})_0{}^{1/2}(\mathrm{Mb}) = k(\mathrm{Mb})$
where, $(\mathrm{Ar})_0$ represents the initial concentrations of aromatic hydrocarbons.
\+ Molar ratios of aromatic hydrocarbons to methylene blue (1.64×10^{-4} mol/l).

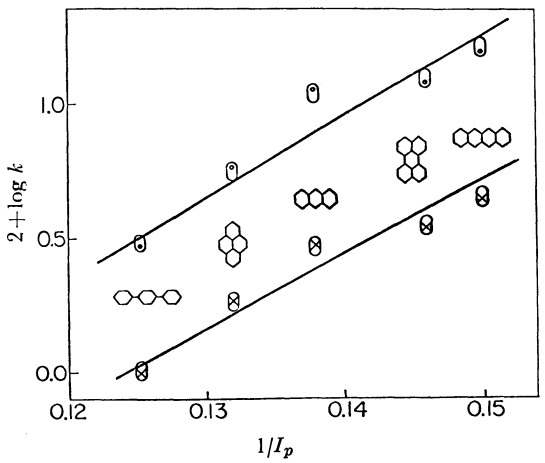

Fig. 8. The relation between the rate constants k, $-\mathrm{d(Mb)}/\mathrm{d}t=k(\mathrm{Mb})$, and ionization potentials (I_p) of aromatic hydrocarbons (Ar):
—⊙— $(\mathrm{Ar})_0$, $1/10\times5.45\times10^{-5}$ mol/l
—⊗— $(\mathrm{Ar})_0$, $1/100\times5.45\times10^{-5}$ mol/l

It can be seen in Fig. 7 that the first-order rate constant, k, is proportional to the square root of the initial concentration of aromatic hydrocarbons.

The rate constants of the redox reaction catalyzed by various aromatic hydrocarbons are given in Table 3.

The stabilization energies for the formation of the EDA complexes of aromatic hydrocarbons with methylene blue have been obtained by the second-order perturbation theory,[13] but if the EDA complex formation makes a contribution to a decrease in the activated state of the redox reaction, some correlation must be found between the stabilization energies and the activation energies. In fact, the plots of the logarithms of the rate constant, a measure of the activation energy, against the reciprocal of the ionization potential, a measure of the stabilization energy, gave a good linear relation, as is shown in Fig. 8.

13) R. S. Mulliken, *J. Amer. Chem. Soc.*, **74**, 811 (1952).

BULLETIN OF THE CHEMICAL SOCIETY OF JAPAN VOL. 43 726—733 (1970)

The Crystal Structure of Copper Yunainate Trihydrate, $Cu(C_5H_8O_3NS)_2 \cdot 3H_2O$

Akio Furusaki and Yujiro Tomiie*1

Faculty of Science, Kwansei Gakuin University, Nishinomiya

(Received September 29, 1969)

The crystal structure of copper yunainate trihydrate, $Cu(C_5H_8O_3NS)_2 \cdot 3H_2O$, has been studied by means of three-dimensional X-ray analysis. The crystal is monoclinic, with two formula units in a unit cell of the dimensions: $a=15.94$, $b=6.33$, $c=8.60$ Å, and $\beta=95.6°$; the space group is $P2_1$. The intensities were measured visually from equi-inclination integrating Weissenberg photographs taken with Cu$K\alpha$ radiation around the b and c axes. The structure was elucidated by Sim's method, and refined by the block-diagonal-matrix least-squares method, assuming anisotropic thermal motions for all the atoms. The final R factor is 9.2%. The copper atom is coordinated by imino nitrogen and carboxyl oxygen atoms of two yunainate groups, and a water oxygen atom. The first four atoms lie almost on a plane and make a square configuration of the *trans* type. The last one is bonded to the copper atom nearly in the direction of the normal of the plane. Thus, the coordination number of copper is five in the present crystal. Of the three sorts of water of crystallization, one is connected with the copper atom, as has already been mentioned, and the remaining two are lattice water, forming a hydrogen-bonded spiral chain around the screw axis. Further, these water molecules connect complex molecules to one another by their hydrogen bonds, forming a three-dimensional hydrogen-bonded structure.

Yunaine (I) is a kind of natural amino acid isolated from a seaweed, *Chondria crassicaulis* Harvey (Japanese name "Yuna"), by Professor Tsunematsu Takemoto.[1] A projection of the crystal structure of the copper salt of this amino acid, *i.e.*, copper yunainate trihydrate, has already been reported.[2] That work not only confirmed the structural formula (I), but also revealed some interesting facts about the molecular and crystal structure. In order to obtain more detailed information about these aspects, a three-dimensional X-ray crystal analysis of the copper salt has now been carried out.

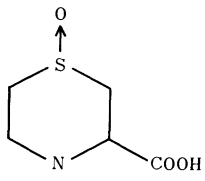

(I)

Experimental

The sample of yunaine was kindly supplied by Professor Tsunematsu Takemoto, Tohoku University. The copper salt was prepared by dissolving copper carbonate in an aqueous solution of yunaine. Single crystals, suitable for the structure determination, were obtained as blue needles from the aqueous solution by slow evaporation in a desiccator.

The crystal data of copper yunainate trihydrate, obtained from oscillation and Weissenberg photographs in the present experiment, are given in Table 1.

Table 1. Crystal data of copper yunainate trihydrate

Monoclinic	$a=15.94\pm0.04$ Å
	$b=6.33\pm0.03$
	$c=8.60\pm0.03$
	$\beta=95.6\pm0.3°$
Space group	$P2_1$
Z	2
$\rho_{calcd.}$	1.70 g/cm³

Equi-inclination integrating Weissenberg photographs were taken with Cu$K\alpha$ radiation from the zeroth to the fourth layer around the b axis and from the zeroth to the sixth layer around the c axis. The intensities were estimated visually by the multiple-film technique and were corrected for the Lorentz and polarization factors. Though the cross-sections of the samples used were about 0.2×0.3 mm² for the b axis and 0.2×0.4 mm² for the c, no correction was made for the absorption effect. The partial resolution of α_1—α_2 doublets was not taken into account, and only the α_1 spot intensities were measured where the doublets were completely resolved.

*1 Deceased 31 May 1967.

1) T. Takemoto, *Yakugaku Kenkyu*, **32**, 645 (1960).
2) A. Furusaki and Y. Tomiie, *Kwansei Gakuin Univ. Ann. Stud.*, **13**, 187 (1964).

The approximate scale and mean temperature factors were estimated by Wilson's method,[3] the latter being 2.83 Å^2. Thus, the absolute values of the structure factors of 1699 independent reflections were obtained out of about 1970 possible reflections.

All the calculations necessary to derive the structure factors in an absolute scale from the intensity data were carried out on a Bendix G-20 at the C. Itoh Electronic Computing Service Co., Ltd., using a program devised in this laboratory.

Structure Determination

A three-dimensional Patterson function, $P(u,v,w)$, was calculated on the computer mentioned above. From the Patterson map, the y parameters of the copper and two sulfur atoms were obtained easily, since the x and z parameters of these atoms had already been determined by two-dimensional analysis.[2] For the elucidation of the positions of the light atoms, the Fourier synthesis using Sim's method[4] was carried out on a HITAC 5020 computer at the University of Tokyo using a program written by the present authors. In case of non-centrosymmetry, the statistical weight for each structure factor, W, is given by the following equation:

$$W = I_1(X)/I_0(X)$$
$$X = 2|F||F_H|/\sum f_L^2$$

where F is the observed structure factor in an absolute scale, F_H is that calculated with heavy atoms alone, $\sum f_L^2$ is the sum of the squares of the scattering factors of the light atoms in a unit cell, and I_0 and I_1 are, respectively, the zero-order and first-order modified Bessel functions of the first kind.

From the Fourier map thus obtained, the peaks corresponding to all twenty-one light atoms could be easily picked out because of the distinct difference in height between these peaks and the ghost peaks. These atomic parameters were refined at first by the diagonal-matrix least-squares method, with individual isotropic temperature factors, on the HITAC 5020 computer. After three cycles of the refinement, the R factor dropped from 0.159 to 0.125. In these calculations, the standard atomic scattering factors listed in "International Tables for X-Ray Crystallography, Vol. III" were used. For the carbon, nitrogen, oxygen, and sulfur atoms, the scattering factors of neutral atoms were used, while for the copper atom, that of the Cu^{2+} ion was used without any correction for the anomalous dispersion. Figure 1 shows a composite diagram of the (010) sections, taken as through the centers of the atoms, of the three-dimensional electron density distribution at this stage. The positional parameters were further refined by the block-diagonal-matrix least-squares method, with anisotropic temperature factors of the form:

$$\exp(-B_{11}h^2-B_{22}k^2-B_{33}l^2-B_{12}hk-B_{23}kl-B_{31}lh)$$

After six cycles of the refinement, including a real dispersion correction of the copper atom for Cu$K\alpha$ radiation, $\Delta f' = -2.1$, the R factor dropped to 0.092, excluding non-observed reflections. The final atomic coordinates and anisotropic temperature factors are given in Table 2.

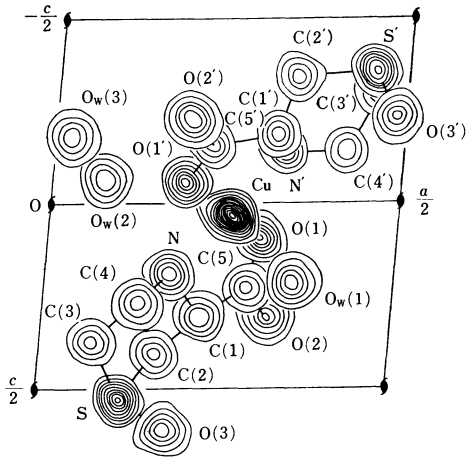

Fig. 1. The electron density distribution of copper yunainate trihydrate. A composite diagram of the (010) sections taken as through the atomic centers. Contours are at intervals of 5 e/Å^3 for a copper atom, 4 e/Å^3 for sulfur atoms and 2 e/Å^3 for the others, beginning at 2 e/Å^3.

Discussion

The molecular framework of the yunainate ions thus obtained is given in Fig. 2. Since the yunaine molecule has been proved to be of the L-type,[1] the yunainate ions should have the absolute configuration shown in Fig. 2, as long as the inversion into the D-type does not occur in the process of the mild reaction of yunaine with copper carbonate.

The two yunainate ions surrounding a copper atom are crystallographically independent. The bond lengths and angles of these two kinds of yunainate ions are given in Fig. 3. The average standard deviations of the atomic coordinates are 0.018 Å for carbon atoms, 0.013 Å for nitrogen and oxygen atoms, 0.005 Å for sulfur atoms, and 0.003 Å for the copper atom. Therefore, the mean standard deviations of various interatomic distances are estimated to be as is shown in Table 3. Some of the corresponding bond lengths and angles of the two kinds of yunainate groups are somewhat different from each other, but these differences do not seem to be significant in view of the accuracy of the present experiment. These bond lengths and

3) A. J. C. Wilson, *Nature*, **150**, 152 (1942).
4) G. A. Sim, *Acta Crystallogr.*, **12**, 813 (1959).

Table 2

(a) The final atomic coordinates

Atom	x/a	y/b	z/c	Atom	x/a	y/b	z/c
Cu	0.2600	0.0002	0.0329	N	0.1774	−0.0703	0.1891
S	0.1202	−0.1322	0.5306	N′	0.3249	0.0552	−0.1505
S′	0.4496	0.3003	−0.3577	C(1)	0.2288	−0.2005	0.3105
O(1)	0.3038	−0.2908	0.0896	C(2)	0.1684	−0.3199	0.4061
O(2)	0.3239	−0.4886	0.3088	C(3)	0.0716	0.0333	0.3745
O(3)	0.1916	−0.0187	0.6126	C(4)	0.1379	0.1138	0.2695
O(1′)	0.1903	0.2365	−0.0531	C(5)	0.2898	−0.3458	0.2281
O(2′)	0.1928	0.4984	−0.2276	C(1′)	0.3157	0.2869	−0.1830
O(3′)	0.4948	0.4208	−0.2266	C(2′)	0.3370	0.3429	−0.3472
$O_w(1)$	0.3578	0.1298	0.2121	C(3′)	0.4551	0.0304	−0.2917
$O_w(2)$	0.0740	−0.3061	−0.0636	C(4′)	0.4178	−0.0166	−0.1359
$O_w(3)$	0.0244	0.0881	−0.1750	C(5′)	0.2267	0.3452	−0.1557

(b) The anisotropic temperature factors in form of exp $(-B_{11}h^2-B_{22}k^2-B_{33}l^2-B_{12}hk-B_{23}kl-B_{31}lh)$

Atom	B_{11}	B_{22}	B_{33}	B_{12}	B_{23}	B_{31}
Cu	0.00213	0.01554	0.00727	0.00131	0.00279	0.00226
S	0.00276	0.02077	0.00823	−0.00128	0.00081	0.00333
S′	0.00236	0.03792	0.01245	−0.00198	0.01085	0.00428
O(1)	0.00373	0.01237	0.00997	0.00032	−0.00415	0.00417
O(2)	0.00453	0.02175	0.01176	0.01129	0.00589	0.00263
O(3)	0.00390	0.02503	0.01050	−0.00043	−0.00773	−0.00003
O(1′)	0.00219	0.01819	0.00904	0.00136	0.00651	0.00410
O(2′)	0.00354	0.03827	0.01965	−0.01097	0.00796	−0.00041
O(3′)	0.00500	0.02104	0.01412	0.00945	0.01582	0.00699
$O_w(1)$	0.00221	0.01611	0.01889	0.00163	−0.00731	−0.00004
$O_w(2)$	0.00406	0.02702	0.01245	−0.00066	−0.00450	0.00407
$O_w(3)$	0.00403	0.02763	0.01687	0.00381	−0.00005	0.00189
N	0.00185	0.01813	0.00651	0.00425	0.00261	0.00146
N′	0.00233	0.01379	0.00831	−0.00042	0.00136	0.00312
C(1)	0.00252	0.00564	0.00778	0.00472	0.00324	0.00287
C(2)	0.00319	0.01393	0.00958	0.00196	0.00537	0.00393
C(3)	0.00328	0.02077	0.00948	0.00505	0.00766	0.00626
C(4)	0.00330	0.01341	0.00923	0.00496	−0.00365	0.00513
C(5)	0.00307	0.02187	0.00884	0.00281	−0.00364	0.00028
C(1′)	0.00185	0.01810	0.00902	−0.00119	0.00175	−0.00127
C(2′)	0.00188	0.03132	0.01066	0.00237	0.01454	0.00143
C(3′)	0.00485	0.02447	0.01788	0.00806	0.00956	0.01138
C(4′)	0.00242	0.03288	0.01492	0.00769	0.01452	0.00720
C(5′)	0.00349	0.02083	0.01011	0.00158	0.00331	0.00357

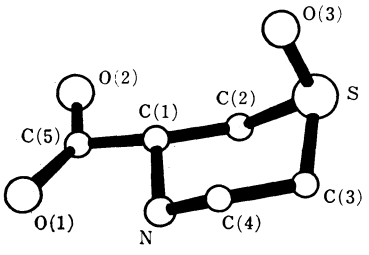

Fig. 2. The framework of a yunainate ion.

angles agree, within the limits of experimental error, with those found in the hydrochloride of cycloalliin, a methyl derivative of yunaine.[5]

In either of the two kinds of yunainate ions, the heterocyclic ring takes a chair form similar to that of cyclohexane. The sulfinyl oxygen atom is attached to the sulfur in the axial configuration, while the carboxyl group, a bulky substituent of the ring, is equatorial. The copper atom occupies the equatorial position of the nitrogen; hence, the hydrogen atom of the imino group should be axial.

The configuration of the atoms bonded to the sulfur is geometrically similar to that in dimethyl

5) K. J. Palmer and Kay Sue Lee, *Acta Crystallogr.* **20**, 790 (1966).

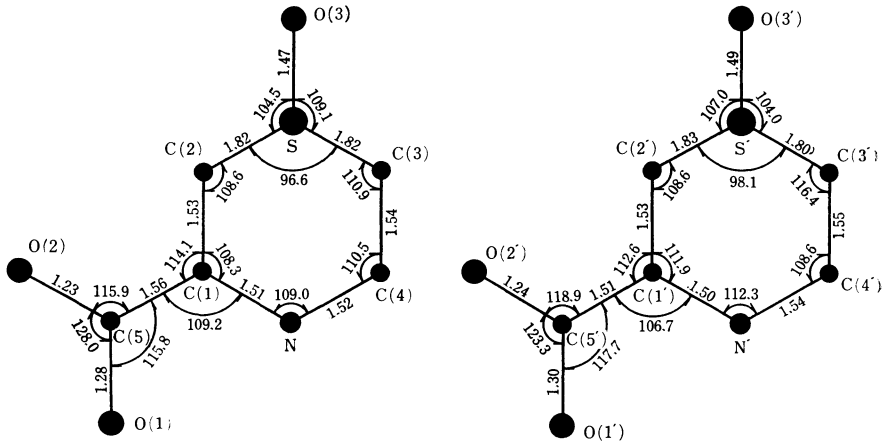

Fig. 3. The bond lengths (Å) and angles (°) of the two yunainate ions.

TABLE 3. THE MEAN STANDARD DEVIATIONS OF VARIOUS INTERATOMIC DISTANCES (in Å)

Cu···Cu	0.005	S···C	0.019
Cu···S	0.006	O···O	0.018
Cu···O	0.013	O···N	0.018
Cu···N	0.013	O···C	0.022
Cu···C	0.018	N···N	0.018
S···S	0.007	N···C	0.022
S···O	0.014	C···C	0.025
S···N	0.014		

sulfoxide.[6] The average length of the four independent sulfur-carbon bonds and that of the two independent sulfur-oxygen bonds found in the present molecules are 1.82 and 1.48 Å respectively, while the corresponding values in dimethyl sulfoxide are 1.82 and 1.47 Å respectively. The mean value of the four C–S–O angles and that of the two C–S–C angles are 106 and 97° respectively, while the corresponding angles in dimethyl sulfoxide are 107 and 100° respectively.

The mean of the two C–N–C angles, 111°, is very close to the tetrahedral angle, 109.5°, while the average value of the four nitrogen-carbon bond distances, 1.52 Å, is nearly in agreement with that in copper D,L-proline dihydrate, 1.525 Å.[7]

The conformation of the carboxyl group around the C(1)–C(5) or C(1′)–C(5′) bond is somewhat different in the two kinds of yunainate ions; that is, the azimuthal angle of the C(1)–N and C(5)–O(1) bonds around the C(1)–C(5) bond is about 19°, while the corresponding angle of the C(1′)–N′ and C(5′)–O(1′) bonds is about 30°.

As is shown in Fig. 4, the copper atom is coordinated by two imino nitrogen atoms, two carboxyl oxygen atoms, and a water oxygen atom.

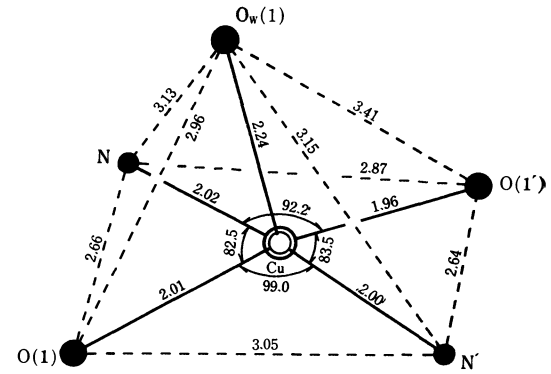

Fig. 4. The tetragonal pyramid of the five coordinating atoms.

The first four atoms lie almost on a plane and make a square configuration of the *trans* type. The last one is bonded to the copper atom nearly in the direction of the normal of the plane.

In the present crystal, there is no atom at a distance smaller than 3.5 Å from the copper atom except for the coordinated five atoms and except for some carbon atoms which are forced to approach the copper in consequence of the formation of the square coordination. On the side of the coordination square opposite to the coordinated water molecule described above, two oxygen atoms are present at distances of 3.57 and 3.67 Å respectively from the copper; one of them is the oxygen atom, $O_W(2)$, of another water molecule, and the other, the sulfinyl oxygen, O(3), of the adjacent complex molecule. However, both of these approaches to the copper seem to be due to the formation of hydrogen bonds with the N and N′ nitrogen atoms respectively rather than to the formation of the coordination bond with the copper. Thus, it is reasonable to conclude that the coordination number of the copper atom is five in the present crystal.

In the present case, the absence of the sixth atom

6) O. Bastiansen and H. Viervoll, *Acta Chem. Scand.*, **2**, 702 (1948).

7) A. M. Mathieson and H. K. Welsh, *Acta Crystallogr.*, **5**, 599 (1952).

to be coordinated to the copper may be closely connected with the fact that, as has already been mentioned, the two oxygen atoms, $O_W(2)$ and O(3), form hydrogen bonds with the N and N′ nitrogen atoms respectively in the axial direction of the six-membered ring and lie just in the neighborhood of the sixth coordination position. If, on the contrary, one of the water oxygen atoms should, for example, occupy the sixth position, neither of the two imino nitrogen could form a normal hydrogen bond because of the steric hindrance of the sixth coordinating atom. It is an interesting fact that, as is actually found, the formation of one of coordination bonds of a copper atom is given up, and instead that of two hydrogen bonds of the nitrogen atoms is achieved.

The five atoms, N, O(1), N′, O(1′), and $O_W(1)$, connected with the copper form a tetragonal pyramid, as is shown in Fig. 4. The lengths of two of the edges, N–O(1) and N′–O(1′), are nearly equal, while those of the other two edges, N–O(1′) and N′–O(1), are somewhat different from each other, the latter being 0.18 Å larger. This distortion of the tetragonal configuration may come from the deformation of the whole complex molecule of copper yunainate, a deformation which is due to the formation of hydrogen bonding at several parts of the complex. It is further found that the orientation of the Cu–$O_W(1)$ bond is inclined to some extent toward the side of the O(1) atom. This inclination may also be due to the strong hydrogen bond formed at a distance of 2.63 Å with the O(1) oxygen atom of the adjoining molecule. The two copper-nitrogen distances, Cu–N and Cu–N′, are 2.02 and 2.00 Å respectively, while the two copper-oxygen distances, Cu–O(1) and Cu–O(1′), are 2.01 and 1.96 Å respectively. These correspond approximately to the ordinary values found in many other copper complexes, such as copper D,L-proline dihydrate (1.99 Å for Cu–N and 2.03 Å for Cu–O).[7] The remaining copper-oxygen bond, Cu–$O_W(1)$, is somewhat weaker than the other two Cu–O bonds, its length being 2.24 Å. This value also nearly corresponds to that in cupric acetate dihydrate, 2.20 Å.

The best plane determined by the least-squares method throughout the four atoms, N, O(1), N′, and O(1′), is described by the equation:

$$0.5577X + 0.5182Y + 0.6484Z = 2.253$$

where X, Y, and Z are rectangular coordinates in the Å unit; $X=x+z\cos\beta$, $Y=y$, and $Z=z\sin\beta$. The deviations of the atoms from this plane are shown in Fig. 5. The copper atom is about 0.23 Å displaced from the plane toward the coordinated water molecule, and the direction of the Cu–$O_W(1)$ bond makes an angle of about 10° with the normal of the plane.

It may be said that the whole complex molecule, composed of a copper atom, a water molecule, and two yunainate groups, has approximately a symmetry of C_2. The centers of all the atoms in the puckered complex molecule lie between two parallel planes, a distance of about 1 Å apart, except in some hydrogen atoms and three oxygen atoms; the latter three oxygen atoms, O(3), O(3′), and $O_W(1)$, stand out to the same side of the plane.

The arrangements of the complex molecules, viewed down along the b and c axes, are shown in Figs. 6 and 7 respectively, together with some intermolecular distances smaller than 4.0 Å. The copper atom, the approximate center of gravity of a complex molecule, is situated very close to the particular position of $x/a=1/4$ and $z/c=0$. Consequently, the arrangement of the copper atoms alone forms nearly a (001) face-centered lattice; the smallest distance among the copper atoms is 6.33 Å along the b axis.

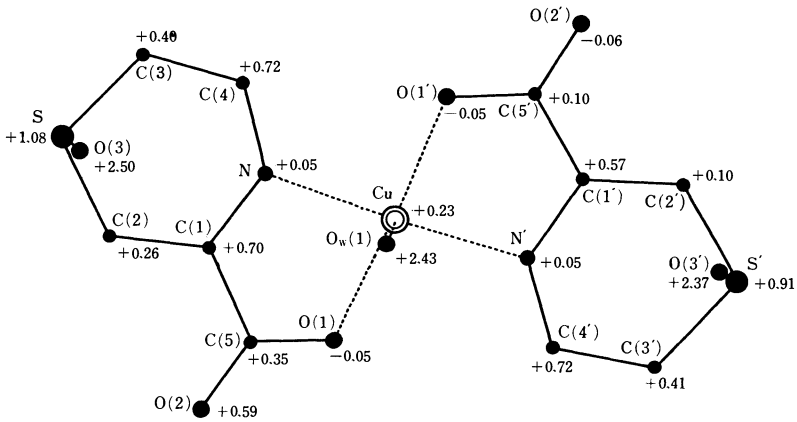

Fig. 5. The deviations (Å) from the square coordination plane, $0.5577X+0.5182Y+0.6484Z-2.253=0$. The complex molecule is viewed down along the normal of this plane.

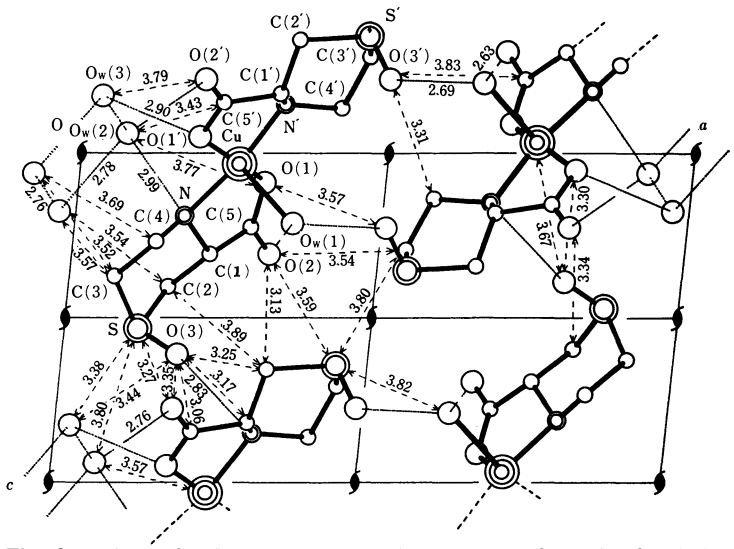

Fig. 6. The molecular arrangement viewed down along the *b* axis in the copper yunainate trihydrate crystal.

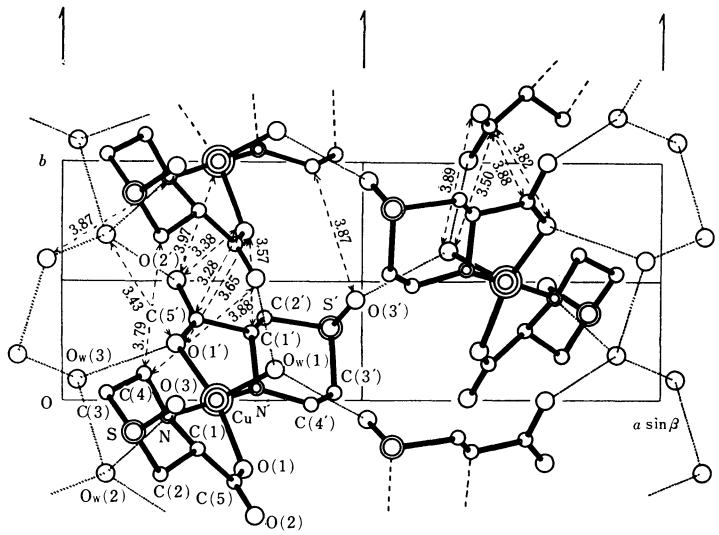

Fig. 7. The molecular arrangement viewed down along the *c* axis in the copper yunainate trihydrate crystal.

The three kinds of water of crystallization contained within the crystal seem to play an important part in connecting the complex molecules with one another. The W(1) water molecule, coordinated to the copper atom, binds not only two complex molecules adjoining along the *b* axis by the Cu-O_W(1) coordination bond and the O_W(1)–H···O(2) hydrogen bond, but also those related by the screw axis with each other, by the O_W(1)–H···O(3′) hydrogen bond. By these bonds and another hydrogen bond, N′–H···O(3), a molecular layer is formed parallel to the (100) plane. Such molecular layers are further connected by several hydrogen bonds formed by water molecules of the two remaining kinds, W(2) and W(3), which form a hydrogen-bonded spiral chain around the two-fold screw axis.

As has been described above, the W(1) water molecule forms two hydrogen bonds, O_W(1)–H··· O(2) and O_W(1)–H···O(3′), their lengths being 2.63 and 2.69 Å respectively. The two hydrogen atoms of the water molecule seem to be considerably off the O···O line, since the O(2)–O_W(1)–O(3′) angle, 130°, is markedly larger than the H–O–H angle of free water molecules in the gas phase, 104.5°.[8] Both of the two hydrogen bonds make

8) R. Mecke and W. Baumann, *Phys. Z.*, **33**, 833 (1932); B. T. Darling and D. M. Dennison, *Phys. Rev.*, **57**, 128 (1940); D. W. Posener and M. W. P. Standberg, *ibid.*, **95**, 374 (1954).

an angle of about 114° with the $O_W(1)$–Cu coordination bond. The total sum of the three angles, O(2)-O_W(1)-O(3′), Cu-O_W(1)-O(2), and Cu-O_W(1)-O(3′), 358°, is very close to the angle (360°) which would be found if the three bonds were coplanar.

The N′–H···O(3) hydrogen bond is the only one formed directly between two complex molecules, its length being 2.83 Å. As is shown in Fig. 8, the direction of this hydrogen bond is fairly much inclined to the side of the carboxyl group (C(1′), O(1′) and O(2′)) from the plane which bisects the C(1′)–N′–C(4′) angle perpendicularly. This may be due to some strong attractive force between the sulfinyl oxygen atom, O(3), and the carboxyl group, since they approach each other quite closely, as will be described later in more detail.

The hydrogen-bonded spiral structure of water molecules alone is one of the remarkable features found in the present crystal. The two kinds of hydrogen bonds, $O_W(2)\cdots O_W(3)$ and $O_W(2)\cdots O_W$-(3′), making the spiral are, respectively, 2.76 and 2.78 Å in length; these lengths are nearly comparable to that found in the hexagonal structure of ice, 2.76 Å, while the angles between the hydrogen bonds, $O_W(2)\cdots O_W(3)\cdots O_W(2')$ and $O_W(3)\cdots O_W$-$(2)\cdots O_W(3')$, are 97 and 108° respectively. The spiral is about 3 Å in diameter if only the nuclei of the water oxygen atoms are taken into account, and it is so right-handed a one that it takes, on the average, a rotation of about 1 radian to move it by 1 Å forward in the direction of the *b* axis.

Besides the hydrogen bonds mentioned above, the W(2) and W(3) water molecules form several hydrogen bonds with the complex molecules around them. The former makes two hydrogen bonds, one with the carboxyl oxygen atom, O(2′), and the other with the nitrogen atom, N; their lengths are 2.76 and 2.99 Å respectively. On the other hand, the latter water molecule forms a hydrogen bond with the carboxyl oxygen atom, O(1′), its length being 2.90 Å. It seems certain that the W(2) and W(3) water molecules direct one of their two hydrogen atoms toward the O(2′) and O(1′) atoms respectively, since neither of these carboxyl oxygen has any hydrogen atom. On the other hand, it is difficult to determine distinctly whether the other hydrogen of W(2) is donated to W(3), and that of W(3), to W(2′), or *vice versa*. Judging only from the angles among the hydrogen bonds shown in Fig. 9, the former case seems to be more reasonable. If, in this case, the hydrogen atoms lie exactly on the O···O lines, the H–O–H angles of the W(2) and W(3) water molecules should be about 115 and 102° respectively.

As is shown in Figs. 6 and 7, in the present crystal some close intermolecular contacts are found aside from the hydrogen-bonded ones already discussed. In particular, the approach between the sulfinyl group (S and O(3)) and the carboxyl

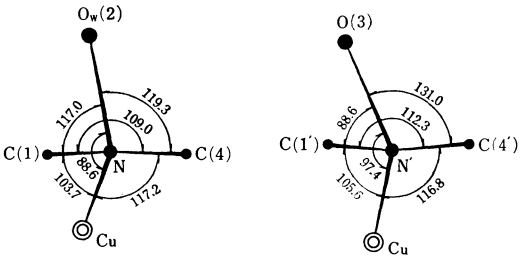

Fig. 8. The bond angles (°) of the imino nitrogen atoms.

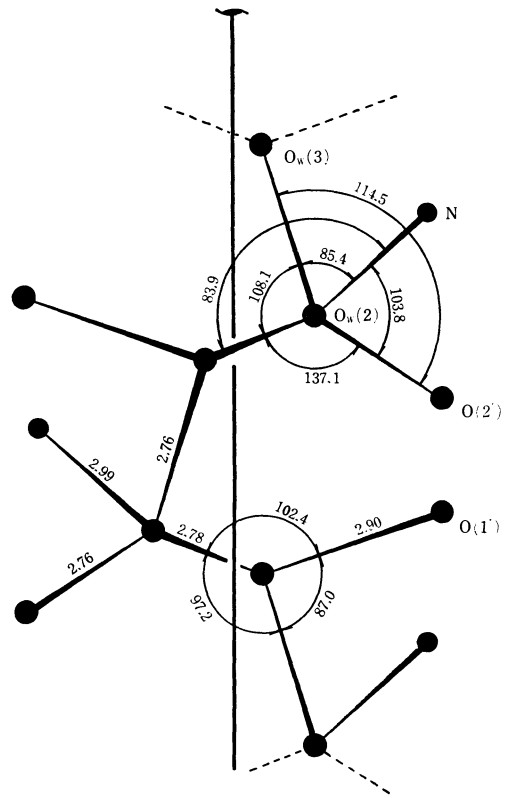

Fig. 9. The hydrogen-bonded spiral chain of the water molecules.

group (O(1′), O(2′), and C(5′)) is of interest in connection with the strong interaction between the two polar groups. The sulfinyl group of a complex molecule is close to the carboxyl groups of the two complex molecules adjoining each other along the *b* axis. The O(3) oxygen atom is in quite close contact with one of the two molecules at four points in all, *i.e.*, O(1′), C(1′), C(2′), and C(5′); the distances of these four atoms from O(3) are, respectively, 3.30, 3.17, 3.25, and 3.06 Å. On the other hand, the sulfinyl group is in contact with the carboxyl oxygen atom, O(2′), of the other complex molecule, the S···O(2′) and O(3)···O(2′) distances being 3.27 and 3.35 Å respectively. The former corresponds nearly to the sum of the van

der Waals radius of sulfur atoms, 1.85 Å, and that of oxygen atoms, 1.40 Å. These close contacts, particularly that of the O(3)···C(5′), seem to suggest that the O(3) sulfinyl oxygen atom and the carboxyl group exert some strong attractive force on each other.

Few atoms are in close contact with the other sulfinyl group (S′ and O(3′)) except for the hydrogen-bonded one which is in close contact with the W(1) water molecule. The sulfinyl groups of this kind are arranged, sufficiently apart from one another, around the two-fold screw axis.

It is interesting to notice that the C(1) carbon atom has no intermolecular contact with a distance smaller than 4.0 Å. This may be partly due to the environment of the other atoms in the same yunainate group, but it does not seem to be attributable to only that cause, since the C(1′) carbon atom, in a similar condition, has contacts with the O(1) and O(3) oxygen atoms of the adjacent molecule. This vacancy around the C(1) atom may be caused by the formation of many hydrogen bonds, which disturb the very close packing of the complex molecules.

Tables of the observed and calculated structure factors are preserved by the Chemical Society of Japan.

The authors are very grateful to Professor Tsunematsu Takemoto, Tohoku University, for providing them with the sample. Thanks are also due to the staff of the C. Itoh Electronic Computing Service Co., Ltd., for allowing the use of their Bendix G-20 computer.

BULLETIN OF THE CHEMICAL SOCIETY OF JAPAN VOL. 43 733—739 (1970)

The Crystal Structure of *cis*-Dinitrotetraamminecobalt (III) Nitrate

Isao OONISHI, Hiroto FUJIMAKI,*1 Fumio MUTO and Yoshimichi KOMIYAMA*2

Department of Applied Chemistry, Faculty of Engineering, Yamanashi University, Kofu

(Received October 3, 1969)

The crystal structure of *cis*-dinitrotetraamminecobalt(III) nitrate, $[Co(NO_2)_2(NH_3)_4]NO_3$, has been determined from three dimensional X-ray diffraction data. The dimensions of the orthorhombic unit cell are: $a=12.19$ Å, $b=7.18$ Å, $c=10.92$ Å, and $Z=4$. The space group is $P2_12_12_1$. The structure has been refined by the three-dimensional Fourier and least-squares methods to $R=0.095$. The complex ion has a slightly distorted octahedral coordination, with six N atoms at 1.96 ± 0.02 Å. The complexes are tightly bound together by N–H···O interactions, thus forming a three-dimensional network.

In our series of investigations into the crystal structures of nitroamminecobalt(III) complexes,[1] the crystal structure of *cis*-dinitrotetraamminecobalt-(III) nitrate, $[Co(NO_2)_2(NH_3)_4]NO_3$, has been determined. In crystals of *trans*-$[Co(NO_2)_2(NH_3)_4]$-$NO_3\cdot H_2O$,[1] $[Co(NO_2)_3(NH_3)_3]$,[2] and $NH_4[Co-(NO_2)_4(NH_3)_2]$[3] in which all the complex ions (or molecules) possess at least a pair of nitro groups coordinated in *trans*-positions, the complex ions form a three-dimensional network connected by N–H···O interactions. Moreover, the arrangement of the cobalt atoms always exhibits a higher symmetry than that of the corresponding space groups.

It seemed that it would be of interest to investigate the crystal structure of a *cis*-form of dinitrotetraamminecobalt(III) salt and compare the results with those for the *trans*-form. In this paper, the crystal structure of *cis*-$[Co(NO_2)_2(NH_3)_4]NO_3$ will be reported on.

Experimental

The crystals were prepared by the method of Jörgensen.[4] Recrystallization from water containing a small amount of acetic acid yielded prismatic crystals. The unit-cell dimensions were determined from the higher-order reflections of Weissenberg photographs (Ni$K\alpha$, $\lambda=1.6591$ Å). The systematic absences were: $h00$ for h odd, $0k0$ for k odd, and $00l$ for l odd. Hence,

*1 Present address: Ashigara Factory, Fuji Photo Co., Ltd., Minamiashigara-cho, Minamiashigara-gun, Kanagawa.

*2 Deceased on Aug. 1, 1968.

1) I. Oonishi, F. Muto and Y. Komiyama, This Bulletin, **42**, 2791 (1969).

2) Y. Tanito, Y. Saito and H. Kuroya, *ibid.*, **25**, 188 (1952).

3) Y. Komiyama, *ibid.*, **30**, 13 (1957).

4) S. M. Jörgensen, *Z. Anorg. Allg. Chem.*, **17**, 477 (1898).

Table 1. Crystal data

cis-$[Co(NO_2)_2(NH_3)_4]NO_3 \cdot H_2O$	
Orthorhombic	$a=12.19\pm0.02$ Å
	$b=7.18\pm0.01$
	$c=10.92\pm0.02$
	$Dx=1.95$ g·cm^{-3}
	$Dm=1.95$ g·cm^{-3}
	$Z=4$

Space group D_2^4-$P2_12_12_1$
Linear absorption coefficient for Ni$K\alpha$, $\mu=44.0$ cm^{-1}

the space group was unequivocally determined. The crystal data are listed in Table 1. Sets of multiple-film equi-inclination Weissenberg photographs were taken about the *c*-axis (0 to 8th layers), the *a*-axis, and *b*-axis (0th layer). Ni$K\alpha$ radiation was used throughout. The intensities were estimated visually with a standard film strip and were converted to $|F_o(hkl)|^2$ and $|F_o(hkl)|$ by applying the usual Lorentz, polarization, and spot-shape corrections. 847 independent reflections were observed. This number is about two-thirds of those within the nickel sphere. The crystal used was a rod with the dimensions of $0.2\times0.15\times1.0$ mm. No correction was made for absorption or extinction.

Structure Analysis

At first, a three-dimensional Patterson synthesis was calculated. From the Patterson maps, the position of the Co atom and the approximate orientation of the complex ion were easily deduced, but those of the nitrate anion could not be fixed. The structure factors were calculated from the parameter values of the atoms of the complex ion. At this stage the discrepancy factor, *R*, was 0.35. Preliminary three-dimensional Fourier syntheses were calculated using all the $F(hkl)$'s except $|F_{obs.}|>2|F_{cal.}|$. From these Fourier maps, the positions of the nitrate ions were determined. The discrepancy factor calculated with the parameter values of all the atoms was 0.26.

The structure thus obtained was refined by three-dimentional difference synthesis to $R=0.143$, and later again by a block-diagonal least-squares method using an HBLS-4 program written by T. Ashida. In this least-squares calculation, anisotropic temperature factors were introduced and six cycles of refinement were carried out. A weighting scheme employed was:

$\sqrt{w}=0.2$ if $F_0 \leqq F_{min.}$ $(=5.5)$
$\sqrt{w}=1.0$ if $F_{min.}<F_0 \leqq F_{max.}$ $(=100.0)$
$\sqrt{w}=F_{max.}/F_0$ if $F_0>F_{max.}$

The final discrepancy factor, $R=\sum||F_0|-|F_c||/\sum|F_0|$, was 0.095 for all the reflections. The atomic scattering factors were taken from the International Tables for X-ray Crystallography.[5] The final atomic parameters and their standard deviations are summarized in Table 2. The observed and calculated structure factors are listed in Table 3.

Description of the Structure and Discussion

A perspective drawing of the complex ion, *cis*-$[Co(NO_2)_2(NH_3)_4]^+$, is given in Fig. 1. The bond lengths and bond angles, with their e.s.d.'s

Table 2. Atomic parameters and their e.s.d.'s* (10^4)

The expression of the temperature factor is $\exp[-(h^2B_{11}+k^2B_{22}+l^2B_{33}+hkB_{12}+hlB_{13}+klB_{23})]$.

Atom	*x/a*	*y/b*	*z/c*	B_{11}	B_{22}	B_{33}	B_{12}	B_{13}	B_{23}
Co	0973 (2)	0361 (3)	4599 (3)	27	91	64	4	5	−19
O(1)	0064 (12)	1262 (20)	2381 (13)	62	137	26	52	−31	−22
O(2)	1501 (9)	−0245 (19)	2143 (11)	32	169	22	−7	42	5
O(3)	2539 (9)	3064 (17)	5024 (12)	36	137	55	−101	43	−70
O(4)	3187 (9)	0785 (22)	4060 (12)	18	306	16	−50	18	−119
O(5)	2435 (12)	3949 (24)	2016 (17)	59	245	141	−100	−58	191
O(6)	3434 (13)	6148 (19)	2856 (13)	92	122	28	55	−14	−6
O(7)	4136 (13)	3997 (21)	1757 (15)	75	169	90	68	−8	−59
N(1)	0844 (9)	0500 (18)	2867 (13)	7	51	45	−18	−10	−61
N(2)	2406 (11)	1557 (20)	4549 (17)	28	132	70	−43	15	39
N(3)	1119 (12)	0229 (22)	6427 (13)	51	133	11	−18	21	−71
N(4)	−0498 (9)	−0864 (19)	4700 (17)	5	113	93	−23	24	−71
N(5)	0259 (11)	2828 (19)	4762 (19)	41	56	102	49	−2	−116
N(6)	1657 (11)	−2150 (19)	4367 (15)	35	68	42	28	35	30
N(7)	3305 (11)	4671 (22)	2223 (14)	30	106	42	−9	0	19

* e.s.d.'s in parentheses

5) "International Tables for X-Ray Crystallography," Vol. III, Kynoch Press, Birmingham (1962), p. 202.

TABLE 3. OBSERVED AND CALCULATED STRUCTURE FACTORS

Columns are k, F_o, F_c. Unobserved marked by *

K FO FC	K FO FC	K FO FC	K FO FC	K FO FC	K FO FC	K FO FC	K FO FC
H,L= 0 0	H,L= 14 0	2 36 15	3 109 115	H,L= 8 3	0 264 269	7 78 107	2 361 368
2 872 943	0 209 226	3 187 178	4 127 147	0 55 57	1 235 242	H,L= 7 5	3 69 74
4 173 155	1 44 38	4 29 32	5 122 144	1 395 402	2 224 242	0 178 154	4 150 133
6 54 0	2 92 71	5 129 127	6 176 181	2 199 205	3 125 121	1 184 180	5 63 47
8 40 44	H,L= 0 1	H,L= 12 1	H,L= 10 2	3 172 165	4 59 42	2 200 161	6 66 62
H,L= 1 0	1 411 377	0 217 232	0 139 140	4 55 61	5 57 58	3 175 162	H,L= 8 6
1 443 404	2 111 115	1 65 54	1 114 137	5 66 43	6 81 90	4 83 93	0 114 113
2 243 277	3 190 191	2 168 161	2 284 289	6 60 56	7 70 69	5 160 166	1 81 93
3 491 449	4 29 9	3 100 113	3 104 118	H,L= 9 3	H,L= 8 4	6 41 14	2 189 188
4 393 415	5 301 313	4 150 145	4 144 166	0 36 32	0 147 150	H,L= 8 5	3 51 14
5 228 227	6 61 57	H,L= 13 1	5 33 23	1 62 50	1 65 64	0 210 199	4 145 160
6 189 183	7 309 319	0 96 105	6 56 38	2 121 125	2 143 134	1 243 254	5 63 60
7 36 13	8 38 39	1 56 57	H,L= 11 2	3 63 71	3 165 191	2 207 194	6 153 165
8 221 238	H,L= 1 1	2 91 87	0 42 22	4 79 76	4 97 98	3 184 191	H,L= 9 6
H,L= 2 0	0 254 222	3 100 109	1 66 65	5 67 74	5 118 125	4 35 15	0 221 202
0 55 75	1 648 633	H,L= 14 1	2 73 51	6 123 122	6 167 167	5 86 82	1 240 66
1 95 87	2 417 404	0 212 230	3 128 147	H,L= 10 3	H,L= 9 4	6 44 27	2 238 236
2 211 236	3 529 462	1 147 152	4 87 90	0 42 39	0 75 77	H,L= 9 5	3 76 58
3 393 370	4 474 447	2 96 102	5 76 93	1 100 89	1 201 218	0 293 258	4 117 122
4 130 97	5 140 112	H,L= 0 2	H,L= 12 2	2 59 45	2 172 160	1 60 37	5 131 123
5 245 243	6 64 64	0 317 259	0 44 16	3 116 131	3 177 170	2 218 198	H,L= 10 6
6 96 74	7 53 43	1 548 574	1 127 140	4 100 88	4 62 54	3 119 131	0 58 33
7 189 198	8 140 152	2 401 275	2 36 35	5 152 159	5 161 174	4 88 64	1 211 216
8 24 3	H,L= 2 1	3 28 24	3 58 47	H,L= 11 3	6 31 28	5 179 179	2 61 38
H,L= 3 0	0 671 754	4 376 362	4 71 78	0 55 47	H,L= 10 4	H,L= 10 5	3 247 216
1 689 727	1 636 641	5 54 45	H,L= 13 2	1 126 123	0 38 20	0 139 137	4 64 70
2 258 237	2 361 398	6 63 61	0 133 123	2 135 135	1 124 127	1 58 48	H,L= 11 6
3 571 562	3 179 148	7 76 75	1 216 230	3 82 76	2 90 80	2 204 188	0 122 108
4 58 46	4 342 362	8 112 105	2 71 85	4 138 142	3 156 150	3 83 83	1 78 60
5 288 281	5 188 184	H,L= 1 2	3 136 151	5 90 89	4 72 72	4 207 199	2 145 131
6 157 163	6 93 93	0 190 222	H,L= 14 2	H,L= 12 3	5 67 60	5 67 67	3 179 178
7 34 5	7 64 49	1 565 530	0 209 212	0 133 128	H,L= 11 4	H,L= 11 5	4 110 96
8 60 63	8 58 60	2 313 224	1 68 87	1 113 121	0 36 29	0 179 159	H,L= 12 6
H,L= 4 0	H,L= 3 1	3 179 182	2 63 68	2 75 69	1 53 45	1 116 103	0 61 70
0 415 380	0 462 395	4 203 170	H,L= 0 3	3 144 146	2 156 161	2 156 146	1 126 118
1 420 354	1 46 44	5 130 133	1 495 541	4 86 96	3 75 67	3 92 85	2 49 54
2 781 827	2 337 323	6 120 133	2 38 70	H,L= 13 3	4 141 143	4 81 84	H,L= 0 7
3 253 250	3 137 111	7 82 87	3 199 183	0 28 17	5 78 83	H,L= 12 5	1 240 194
4 408 399	4 434 439	8 131 161	4 310 315	1 45 12	H,L= 12 4	0 170 173	2 78 94
5 402 466	5 231 215	H,L= 2 2	5 63 62	2 49 60	0 159 148	1 181 170	3 98 97
6 47 34	6 298 303	0 101 66	6 172 180	3 55 51	1 63 54	2 139 123	4 176 141
7 227 221	7 62 74	1 69 53	7 92 88	H,L= 14 3	2 67 74	3 157 125	5 91 70
8 20 21	8 131 139	2 392 368	H,L= 1 3	0 138 125	3 26 27	H,L= 13 5	6 212 203
H,L= 5 0	H,L= 4 1	3 359 338	0 254 232	1 79 78	4 94 109	0 36 28	7 55 62
1 293 220	0 466 466	4 231 207	1 450 451	H,L= 0 4	H,L= 13 4	1 61 52	H,L= 1 7
2 397 398	1 289 258	5 273 275	2 324 278	0 869 960	0 252 263	H,L= 0 6	0 193 300
3 74 57	2 428 381	6 120 133	3 297 300	1 972 595	1 66 73	1 494 529	1 121 83
4 400 418	3 405 409	7 204 196	4 175 172	2 150 164	2 127 111	2 93 73	2 288 316
5 74 67	4 202 177	8 76 102	5 52 33	3 224 222	H,L= 0 5	3 402 317	3 162 131
6 303 332	5 283 281	H,L= 3 2	6 38 51	4 79 67	1 35 33	4 64 57	4 227 226
7 106 126	6 36 33	0 88 34	7 38 54	5 165 147	2 415 380	5 157 126	5 70 51
8 91 107	7 140 142	1 130 170	8 72 85	6 59 30	3 296 318	6 49 34	6 57 41
H,L= 6 0	8 20 16	2 381 351	H,L= 2 3	7 33 17	4 284 296	7 46 43	7 87 104
0 369 382	H,L= 5 1	3 246 246	0 209 252	H,L= 1 4	5 169 149	H,L= 1 6	H,L= 2 7
1 100 63	0 49 16	4 163 154	1 314 259	0 824 806	6 75 79	0 179 234	0 102 77
2 311 319	1 652 669	5 157 163	2 383 363	1 168 113	7 125 162	1 175 187	1 312 361
3 126 117	2 192 209	6 49 27	3 101 83	2 297 299	H,L= 1 5	2 61 55	2 150 113
4 72 75	3 462 450	7 38 24	4 164 151	3 174 164	0 785 826	3 276 293	3 173 177
5 137 133	4 176 165	8 28 34	5 176 175	4 186 178	1 153 112	4 100 70	4 85 93
6 67 62	5 131 136	H,L= 4 2	6 86 80	5 104 100	2 391 383	5 259 255	5 87 61
7 98 107	6 45 47	0 139 78	7 41 26	6 94 81	3 251 240	6 76 62	6 76 62
H,L= 7 0	7 29 23	1 347 301	8 21 15	7 138 140	4 234 217	7 204 196	7 50 30
1 394 435	8 44 59	2 332 332	H,L= 3 3	H,L= 2 4	5 169 152	H,L= 2 6	H,L= 3 7
2 149 134	H,L= 6 1	3 189 169	0 216 213	0 112 106	6 36 12	0 75 42	0 197 211
3 384 398	0 332 337	4 158 147	1 114 111	1 209 210	7 116 153	1 141 145	1 135 133
4 95 90	1 296 266	5 146 138	2 162 162	2 273 260	H,L= 2 5	2 192 173	2 109 113
5 113 119	2 396 372	6 103 113	3 176 173	3 303 272	0 63 140	3 242 218	3 270 293
6 152 172	3 89 87	7 68 61	4 135 122	4 258 262	1 603 567	4 349 340	4 83 89
7 37 11	4 93 85	8 28 33	5 236 244	5 106 96	2 179 180	5 76 80	5 286 252
H,L= 8 0	5 139 160	H,L= 5 2	6 148 157	6 101 91	3 335 360	6 293 244	6 83 42
0 162 151	6 243 239	0 117 97	7 90 96	7 63 39	4 156 166	7 66 39	7 102 108
1 66 46	7 230 221	1 187 174	8 67 70	8 107 113	5 240 218	H,L= 3 6	H,L= 4 7
2 80 75	H,L= 7 1	2 219 223	H,L= 4 3	H,L= 3 4	6 76 61	0 399 446	0 102 94
3 270 246	0 29 5	3 258 277	0 165 111	0 254 258	7 29 16	1 109 114	1 137 149
4 47 12	1 250 247	4 189 194	1 373 390	1 382 379	H,L= 3 5	2 384 424	2 197 190
5 310 328	2 159 151	5 130 139	2 73 76	2 311 305	0 26 8	3 298 293	3 208 184
6 105 102	3 171 155	6 201 209	3 328 327	3 137 123	1 92 85	4 259 225	4 171 152
7 283 282	4 117 128	7 90 118	4 236 266	4 252 259	2 210 185	5 116 121	5 83 80
H,L= 9 0	5 64 65	H,L= 6 2	5 128 118	5 69 69	3 238 240	6 37 11	6 128 113
1 304 313	6 196 202	0 560 531	6 141 141	6 110 122	4 204 191	7 63 61	H,L= 5 7
2 325 311	7 24 18	1 271 281	7 63 63	7 59 40	5 307 301	H,L= 4 6	0 210 193
3 106 98	H,L= 8 1	2 309 324	8 50 76	H,L= 4 4	6 139 112	0 29 43	1 193 160
4 146 149	0 416 430	3 106 114	H,L= 5 3	0 162 127	7 145 176	1 226 234	2 255 252
5 81 71	1 168 168	4 90 101	0 317 313	1 347 374	H,L= 4 5	2 218 205	3 96 101
6 149 132	2 458 486	5 109 114	1 226 241	2 357 355	0 188 182	3 252 245	4 160 157
H,L= 10 0	3 36 17	6 131 156	2 250 272	3 232 242	1 148 134	4 228 212	5 68 33
0 137 125	4 72 80	7 87 92	3 205 198	4 218 209	2 91 73	5 146 138	6 74 76
1 150 132	5 45 39	H,L= 7 2	4 111 115	5 202 191	3 257 250	6 180 163	H,L= 6 7
2 296 290	6 66 58	0 50 25	5 46 23	6 112 117	4 247 263	7 47 40	0 72 52
3 37 7	7 62 66	1 306 313	6 36 24	7 82 91	5 98 87	H,L= 5 6	1 162 157
4 152 150	H,L= 9 1	2 106 131	7 49 46	H,L= 5 4	6 207 188	0 49 40	2 176 159
5 30 19	0 175 147	3 119 132	H,L= 6 3	0 50 32	7 51 50	1 128 111	3 108 98
6 20 15	1 243 256	4 84 89	0 126 124	1 47 52	H,L= 5 5	2 117 112	4 85 89
H,L= 11 0	2 143 153	5 42 50	1 239 244	2 152 120	0 353 368	3 256 239	5 76 60
1 156 163	3 238 236	6 84 82	2 267 274	3 187 159	1 235 193	4 133 118	6 139 138
2 188 191	4 100 117	7 42 47	3 133 142	4 218 209	2 443 485	5 233 216	H,L= 7 7
3 78 67	5 144 154	H,L= 8 2	4 84 60	5 205 222	3 113 112	6 69 91	0 150 157
4 239 259	6 182 193	0 44 26	5 65 57	6 135 139	4 238 243	7 143 169	1 169 181
5 24 22	H,L= 10 1	1 168 136	6 33 21	7 169 153	5 83 106	H,L= 6 6	2 104 103
H,L= 12 0	0 53 2	2 100 110	7 113 109	H,L= 6 4	6 67 68	0 348 352	3 180 209
0 344 354	1 146 140	3 141 144	H,L= 7 3	0 131 127	7 23 12	1 465 506	4 89 72
1 55 32	2 116 107	4 108 117	0 145 131	1 100 87	H,L= 6 5	2 66 52	5 104 94
2 114 125	3 229 234	5 41 29	1 107 112	2 107 94	0 58 36	3 174 146	H,L= 8 7
3 45 16	4 93 109	6 106 132	2 105 125	3 202 201	1 297 296	4 76 71	0 111 114
4 34 48	5 234 238	7 85 85	3 48 26	4 87 93	2 188 178	5 39 4	1 266 275
H,L= 13 0	6 53 75	H,L= 9 2	4 82 98	5 135 141	3 220 198	6 141 145	2 98 90
1 246 234	H,L= 11 1	0 184 174	5 70 70	6 85 83	4 159 143	H,L= 7 6	3 148 133
2 73 75	0 36 2	1 233 248	6 140 150	7 53 50	5 89 78	0 339 370	4 63 42
3 149 143	1 131 139	2 212 210	7 110 119	H,L= 7 4	6 241 245	1 78 76	5 68 62

Table 4. Bond distances and angles and their standard deviations*

Co–N(1)	1.900 (15) Å	N(1)–Co–N(2)	91.3 (7)°
N(2)	1.948 (14)	N(1)–Co–N(4)	90.2 (6)
NH_3(3)	2.006 (14)	N(1)–Co–N(5)	90.4 (7)
NH_3(4)	1.999 (12)	N(1)–Co–N(6)	87.5 (6)
NH_3(5)	1.981 (14)	N(2)–Co–N(3)	88.2 (7)
NH_3(6)	2.003 (14)	N(2)–Co–N(5)	90.1 (6)
N(1)–O(1)	1.218 (19)	N(2)–Co–N(6)	91.1 (6)
O(2)	1.246 (17)	N(3)–Co–N(4)	90.2 (7)
N(2)–O(3)	1.211 (20)	N(3)–Co–N(5)	89.5 (7)
O(4)	1.224 (19)	N(3)–Co–N(6)	92.6 (6)
N(1)–N(2)	2.753 (20)	N(4)–Co–N(5)	89.7 (6)
NH_3(4)	2.764 (21)	N(4)–Co–N(6)	89.1 (5)
NH_3(5)	2.754 (22)	O(1)–N(1)–O(2)	114.7 (14)
NH_3(6)	2.699 (19)	Co–N(1)–O(1)	121.4 (11)
N(2)–NH_3(3)	2.752 (22)	Co–N(1)–O(2)	123.8 (10)
NH_3(5)	2.782 (19)	O(3)–N(2)–O(4)	119.2 (14)
NH_3(6)	2.821 (20)	Co–N(2)–O(3)	120.1 (11)
NH_3(3)–NH_3(4)	2.839 (21)	Co–N(2)–O(4)	120.7 (12)
NH_3(5)	2.809 (22)	O(5)–N(7)–O(6)	124.7 (16)
NH_3(6)	2.900 (21)	O(5)–N(7)–O(7)	118.5 (17)
NH_3(4)–NH_3(5)	2.808 (19)	O(6)–N(7)–O(7)	116.7 (14)
NH_3(6)	2.808 (18)		
N(7)–O(5)	1.202 (21)		
O(6)	1.275 (21)		
O(7)	1.232 (21)		
O(5)–O(6)	2.195 (22)		
O(7)	2.092 (22)		
O(6)–O(7)	2.135 (21)		

* e.s.d.'s $\times 10^3$ are given in parentheses

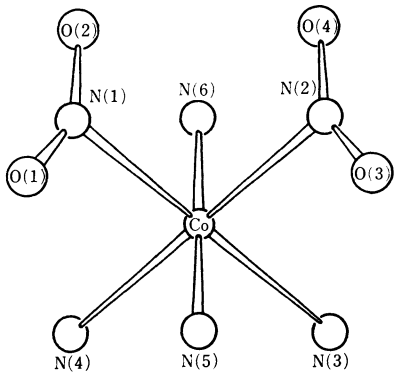

Fig. 1. A perspective drawing of the complex ion, *cis*-$[Co(NO_2)_2(NH_3)_4]^+$

calculated on the basis of the atomic parameters in Table 2, are listed in Table 4. A projection of the contents of one unit cell onto the (010) plane is presented in Fig. 2. The important intermolecular contacts (*i.e.*, those less than 3.5 Å) are listed in Table 5. The interatomic distances and bond angles were calculated by using the RSDA-4 program written by T. Sakurai.

The cobalt atoms are surrounded by nitrogen atoms of two nitro groups and of four ammonia molecules, which form a slightly distorted octahedron. Two nitrogen atoms of nitro groups are coordinated to a cobalt atom in *cis*-positions. The distortion of the coordinated octahedron is more marked than that of the *trans* isomer described in a previous paper.[1] For example, the N(1)–Co–N(6), N(2)–Co–N(3), N(3)–Co–N(6), and N(1)–Co–N(2) angles are 87.5, 88.2, 92.6, and 91.3° respectively. This is partly due to the repulsion of the two nitro groups in *cis*-positions. However, in the *trans* isomer[1] the greatest deviation of N–Co–N angles from 90° are 1.1°; the other deviations are within 1°. Two nitro groups are inclined in the direction opposite to the mean plane consisting of N(1), N(2), N(3), and N(4), with angles of 60 and −64° respectively. Such an inclination in the opposite direction of the nitro groups is also found in $[Co(NO_2)_3(NH_3)_3]$,[2] where the inclination angles are −16, 13, and 18° to the mean plane, consisting of four nitrogen atoms of three nitro groups and one ammonia molecule respectively. In Table 6 the distances between the central cobalt atom and the ligand atoms in various complex ions are compared. The distances are in agreement with those found in the related compounds. Generally

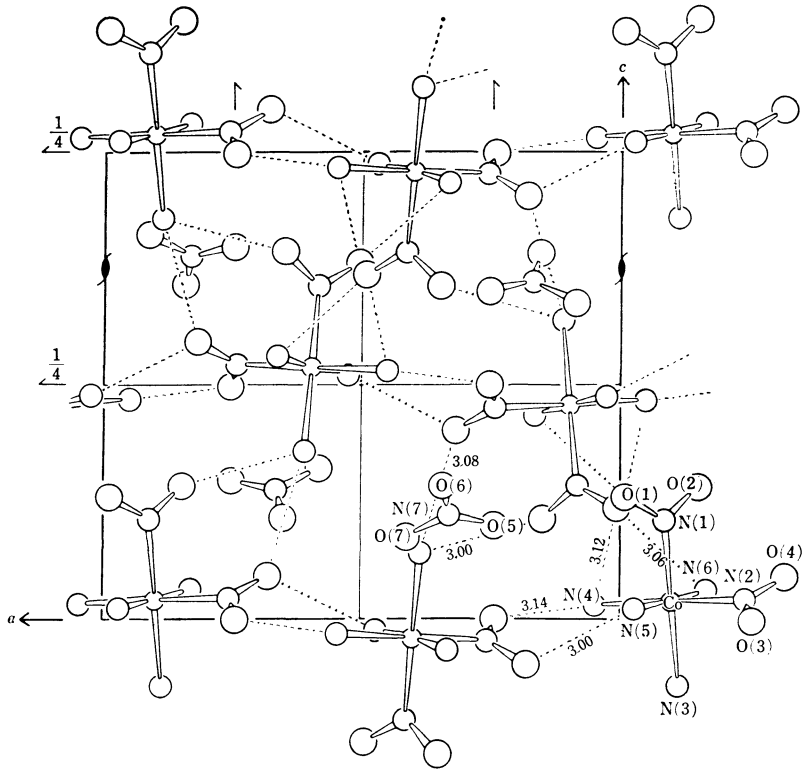

Fig. 2. Projection of the unit cell contents on the (010) plane.

TABLE 5. INTERMOLECULAR CONTACTS NOT EXCEEDING 3.5 Å

N(1)-O(5)(1)	3.280 (21) Å	N(7)-O(3)(1)	3.400 (20) Å
N(2)-O(2)(3)	3.129 (22)	O(3)(3)	3.077 (20)
O(5)(1)	3.256 (26)	O(4)(1)	3.439 (21)
N(3)-O(2)(3)	3.004 (18)	O(1)-O(5)(1)	3.498 (22)
O(4)(3+1′)	3.084 (19)	O(2)(4)	3.194 (19)
O(6)(3)	3.082 (21)	O(2)-O(3)(3)	3.289 (18)
O(7)(2)	3.176 (21)	O(4)(3+1′)	3.411 (18)
O(7)(3+1′)	3.071 (21)	O(3)-O(5)(1)	3.348 (23)
N(4)-O(1)(4+1′)	3.115 (22)	O(5)(3)	3.055 (22)
O(3)(2)	3.140 (17)	O(6)(1)	3.420 (19)
O(5)(4+1′)	3.018 (22)	O(6)(3)	3.360 (20)
O(6)(2+1′)	2.976 (23)	O(7)(3)	3.493 (20)
N(5)-O(2)(4)	3.294 (21)	O(4)-O(5)(1)	3.313 (23)
O(3)(2)	3.385 (18)	1) x, y, z	
O(4)(2)	3.004 (19)	1′) $x, -1+y, z$	
N(6)-O(1)(4+1′)	3.058 (21)	2) $1/2+x, 1/2-y, -z$	
O(5)(3+1′)	3.355 (24)	3) $1/2-x, -y, 1/2+z$	
O(6)(1′)	2.984 (20)	4) $-x, 1/2+y, 1/2-z$	
O(7)(3+1′)	3.083 (22)		

e.s.d.'s $\times 10^3$ in parentheses

the distances of Co–N (NH_3) seem to be longer than those of Co–N (NO_2). An inspection of Table 6 would seem to support in the previous paper[1] that the distances of Co–N (NO_2) increase with an increase in the number of nitro groups. In Table 7 the N–O distances and the O–N–O angles of nitro groups in various complex ions are listed. The N–O distances range from 1.16 to 1.27 Å, and the O–N–O angles, from 114 to 127°.

The nitrate ion has an approximate threefold axis, and the N atom is 0.02 Å apart from the plane composed of three O atoms. The mean value of N–O distances (1.24 Å) agrees with that found in *trans*-$[Co(NO_2)_2(NH_3)_4]NO_3 \cdot H_2O$ (1.25Å).

Table 6. The intratomic distances between cobalt and its ligand atoms

	Co–NH_3	In *trans*-coordination with respect to	Co–NO_2	In *trans*-coordination with respect to
$[Co(NO_2)(NH_3)_5]Br_2$[6]	1.976 (19) Å	NO_2	1.921 (21) Å	NH_3
	1.985 (15)	NH_3		
	1.972 (16)	NH_3		
$[Co(NO_2)_2(NH_3)_5]Cl_2$[7]	1.977 (16)	NO_2	1.912 (14)	NH_3
	1.957 (8)	NH_3		
	1.956 (7)	NH_3		
cis-$[Co(NO_2)_2(NH_3)_4]NO_3$	1.999 (12)	NO_2	1.948 (14)	NH_3
	2.006 (14)	NO_2	1.900 (15)	NH_3
	2.003 (14)	NH_3		
	1.981 (14)	NH_3		
trans-$[Co(NO_2)_2(NH_3)_4]NO_3$ H_2O[1]	1.954 (11)	NH_3	1.933 (11)	NO_2
	1.986 (12)	NH_3	1.937 (11)	NO_2
	1.963 (12)	NH_3		
	1.973 (12)	NH_3		
$[Co(NO_2)_3(NH_3)_3]$[2]	1.97	NO_2	1.97	NO_2
	1.98	NH_3	1.97	NO_2
	1.99	NH_3	1.96	NH_3
$NH_4[CO(NO_2)_4(NH_3)_2]$[3]	2.01	NH_3	1.96	NO_2
	2.01	NH_3	1.96	NO_2
			1.96	NO_2
			1.96	NO_2
$K[Co(NO_2)_4(NH_3)_2]$[8]	2.00	NH_3	1.96	NO_2
	2.00	NH_3	1.96	NO_2
			1.96	NO_2
			1.96	NO_2

e.s.d.'s $\times 10^3$ in parentheses

Table 7. The shape and size of nitro groups in nitroamminecobalt (III) complexes

	N–O		O–N–O
$[Co(NO_2)(NH_3)_5]Br_2$[6]	1.161 (22) Å	1.161 (22) Å	113.9 (19)°
$[Co(NO_2)(NH_3)_5]Cl_2$[7]	1.230 (11)	1.230 (11)	120.8 (14)
cis-$[Co(NO_2)_2(NH_3)_4]NO_3$	1.218 (19)	1.246 (17)	114.7 (14)
	1.211 (20)	1.224 (19)	119.2 (14)
trans-$[Co(NO_2)_2(NH_3)_4]NO_3 \cdot H_2O$[1]	1.215 (16)	1.262 (16)	118.7 (10)
	1.235 (17)	1.260 (17)	119.8 (10)
$[Co(NO_2)_3NH_3)_3]$[2]	1.24	1.25	127
	1.25	1.27	119
	1.25	1.27	121
$NH_4[(Co(NO_2)_4(NH_3)_2]$[3]	1.23	1.23	116
	1.24	1.26	118
	1.20	1.22	119
	1.20	1.23	118
$K[Co(No_2)_4(NH_3)_2]$[8]	1.23	1.24	115
	1.21	1.26	116
	1.20	1.22	118
	1.20	1.23	124

e.s.d.'s $\times 10^3$ in parentheses

The structure is built up of complex cations $[Co(NO_2)_2(NH_3)_4]^+$ and nitrate ions; thus, it is essentially ionic. The closest approach between the complex ion and the nitrate ion occurs between the oxygen atom of the nitrate ion and the nitrogen atom of the coordinated ammonia. The binding

6) F. A. Cotton and W. T. Edwards, *Acta Crystallogr.*, **B24**, 474 (1968).
7) O. Bortin, *Acta Chem. Scand.*, **22**, 2890 (1968).
8) Y. Komiyama, This Bulletin, **29**, 300 (1956).

force between the complex ions is mainly due to the N–H···O interactions between NH_3 and NO_2 groups. By means of these N–H···O interactions the complex ions and the nitrate ions are bound tightly together, forming a three-dimensional network. It is interesting to note here that no special networks consisting of the complex ions are found in this structure such as those found in *trans*-$[Co(NO_2)_2(NH_3)_4]NO_3 \cdot H_2O$,[1] $[Co(NO_2)_3(NH_3)_3]$,[2] and $NH_4[Co(NO_2)_4(NH_3)_2]$,[3] in which all the complex ions (or molecules) possess at least a pair of nitro groups coordinated in *trans*- positions and in which the arrangement of the cobalt atoms themselves have a higher symmetry than that required by the corresponding space group:

	Space group	Pseudo-symmetry
trans-$[Co(NO_2)_2(NH_3)_4]NO_3 \cdot H_2O$	D_2^4-$P2_12_12_1$	D_{2h}^{25}-*Immm*
$[Co(NO_2)_3(NH_3)_3]$	D_2^4-$P2_12_12_1$	D_{2h}^{17}-*Bbmm*
$NH_4[Co(NO_2)_4(NH_3)_2]$	D_2^4-$P2_12_12_1$	D_{2h}^{16}-*Pbnm*

$[Co(NO_2)(NH_3)_5]Br_2$[6] and $[Co(NO_2)(NH_3)_5]Cl_2$[7] also do not possess such a particular type of network nor any such array of cobalt atoms with a higher symmetry.

It may be concluded that the binding force between the complex ions in the crystals of nitroamminecobalt(III) complexes are mainly the N–H···O interactions between NH_3 and NO_2 groups. In particular, if the two nitro groups and the two ammonia groups are both coordinated in *trans*-positions, the two-dimensional network formed by the complex ions possesses a particularly high symmetry and the arrangement of the cobalt atoms exhibits pseudo-symmetry.

The numerical calculations were carried out on the FACOM231 computer of this University and on the HITAC5020 computer of the Computer Center, The Tokyo University. Part of the cost of this investigation has been defrayed by a Scientific Research Grant from the Ministry of Education, to which the authors' thanks are due.

BULLETIN OF THE CHEMICAL SOCIETY OF JAPAN VOL. 43 739—744 (1970)

Substituent Effects on Spectral Properties of Protonated Azo Compounds

G. L. EIAN and Charles A. KINGSBURY

Department of Chemistry, University of Nebraska, Lincoln, Nebraska, U.S.A.

(Received January 29, 1969)

The effect of a remote substituent upon the NMR and visible spectra, and upon hydrogen-deuterium exchange in certain phenylazophenol systems is reported. Electron donating substituents uniformly lower the NMR chemical shift function, $\Delta\delta$, cause bathochromic shifts in the visible spectra, and increase the rate of deuterium exchange. Correlations between the above measurements and also with Hammett constants are reported. In particular the logarithm of $t_{1/2}$ is linear with δ_o, the chemical shift of the position adjacent to the position attacked by deuterium.

Correlations involving the nuclear magnetic resonance (NMR) parameters with the several types of linear free energy parameters have been successful for many classes of organic compounds.[1] In recent years the substituent effects on NMR spectra have been reported for pyridines,[2,3] anilines,[4] amines,[5] aldoximes,[6] phenols,[7,8] alkylbenzenes,[9] styrenes,[10] stilbenes,[11] diphenylethylenes,[12]

1) a) S. Marcus, W. Reynolds and S. Miller, *J. Org. Chem.*, **31**, 1872 (1966). b) C. Heathcote, *Can. J. Chem.*, **40**, 1865 (1962). c) N. Nakagawa and S. Fujigawa, This Bulletin, **34**, 143 (1961).

2) H. Perkampus and U. Krueger, *Chem. Ber.*, **100**, 1165 (1967).

3) Y. Kondo, K. Kondo, T. Takemoto and T. Ikenoue, *Chem. Pharm. Bull.* (Tokyo), **14**, 1332 (1966).

4) I. Rae and L. Dyall, *Aust. J. Chem.*, **19**, 835 (1966).

5) H. Friedrich, *Angew. Chem.*, **77**, 700 (1965).

6) I. Pejković-Tadić, M. Hranisavljević-Jakovljević, S. Nĕsić, C. Pascual and W. Simon, *Helv. Chim. Acta*, **48**, 1157 (1965).

7) a) J. Traynham and G. Knesel, *J. Org. Chem.*, **31**, 3350 (1966). b) R. J. Ouellette, *Can. J. Chem.*, **43**, 707 (1965).

8) V. Bystrov, V. Ershov and V. Lezina, *Op. Spectroscopiya*, **17**, 538 (1964).

9) N. van Meurs, *Rec. Trav. Chim. Pays-Bas*, **86**, 111 (1967).

phenylacetylenes,[13a] esters,[13b] phosphines,[14] acetophenones,[15] pyrazoles[16] and other heterocycles,[17] metalocenes,[18,19] protonated benzophenones,[20] and carbonium ions.[21] In other works, the effect of substituent upon coupling constants in various fluorine systems has been investigated.[22,23]

In particular, the NMR spectra of many types of cations have been investigated, principally by Olah and co-workers.[24] In other work, the chemical shift of the proton donated to the various substituted acetophenones has been correlated with σ^+ parameters.[25]

The deshielded character of certain chemical shifts in carbonium ion systems has been related to the charge delocalization of the ion.[26] In cyclopropenium ions additive ring current effects also have a profound effect on the chemical shifts of the various groups.[27]

One salient feature of the NMR spectrum of *para* substituted benzene derivatives is illustrated in Scheme I.[28]

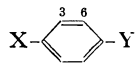

X	Y	δH_A	δH_B	$\Delta\delta$
NO_2	CH_2CN	8.25	7.57	−0.68
NO_2	$NH-CH_3$	8.10	6.55	−1.55
CH_3O	CH_3	6.80	7.05	+0.25
CH_3	CHO	7.02	7.83	+0.81

Scheme I

As noticed by many of the workers cited above, when there is a significant resonance interaction between X and Y, the difference in chemical shift between H_a and H_b (hereafter termed $\Delta\delta$) is large. Little resonance interaction produces a much smaller $\Delta\delta$.

Corio and Dailey[29] have interpreted the chemical shifts of the various ring protons in terms of the same resonance and inductive parameters of a given substituent which enhance or detract from aromatic substitution rates. Jackman[30] however considers the anisotropy of the various groups to be important.

The subject of this work is a series of 4-phenylazophenols (**1**), and their protonated analogues (**1H**). The effect of the remote substituent (ring B)

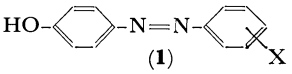

(**1**)

Ring A Ring B

on the chemical shift function ($\Delta\delta$) of ring A is of interest. In this context if should be noticed that any anisotropy effects of X will have little effect on the NMR spectrum of ring A. In other cases the visible spectra in system **1H** will be compared to the NMR data. The influence of X on the hydrogen-deuterium exchange in ring A will also be considered.

Results and Discussion

Table 1 lists the NMR data for the series of azophenols (**1**). The function $\Delta\delta$(ring A) is rather small for electron donating substituents and is largest for $X=NO_2$, but the total change is small, and rather irregular. The effect of substituent of the protons of its own immediate ring are of course much larger. In the two extreme cases, $X=CH_3O$ and $X=NO_2$, $\Delta\delta$(ring B) is large and of opposite sign.

The chemical shift of the *ortho* protons of both rings is relatively constant at δ *ca.* 7.8. This absorption, however, occurs rather far downfield compared to certain stilbenes, in which analogous protons absorb at δ *ca.* 7.0—7.3. Similarily, the chemical shifts of methyls substituted in the 2′

10) J. Dubois, J. Miller and D. Doucet, *J. Chim. Phys.*, **62**, 1783 (1966).
11) H. Güsten and M. Salzweldel, *Tetrahedron*, **23**, 173 (1967).
12) Y. Yukawa, Y. Tsuno and H. Yamada, *Mem. Inst. Sci. Ind. Res. Osaka Univ.*, **23**, 79 (1966).
13) a) Y. Yukawa and H. Yamada, *Nippon Kagaku Zasshi*, **85**, 561 (1964). b) O. Rosaldo Lojo, C. Hancock and A. Danti, *J. Org. Chem.*, **31**, 1899 (1966).
14) S. Grim and W. McFarlane, *Nature*, **208**, 495 (1965).
15) K. Dhami and J. Strothers, *Can. J. Chem.*, **43**, 479 (1965).
16) L. Tensmeyer and C. Ainsworth, *J. Org. Chem.*, **31**, 1878 (1966).
17) G. DiModica, E. Barni and A. Gasco, *J. Heterocycl. Chem.*, **2**, 457 (1965).
18) S. Gubin, *Izv. Akad. Nauk. SSSR, Ser. Khim.*, **1966**, 151.
19) A. Nesmeyanov, E. Fedin, O. Nogina, N. Kochetkova, V. Dubontskii and P. Petrovskii, *Tetrahedron*, Suppl. No. 8, Part II, 389 (1966).
20) G. Eian and C. Kingsbury, *J. Org. Chem.*, **32**, 1864 (1967).
21) R. Taft and J. Rakshys, Jr., *J. Amer. Chem. Soc.*, **87**, 4385 (1965).
22) R. Abraham, D. Macdonald and E. Pepper, *Chem. Commun.*, **1966**, 542.
23) M. Dhingra, G. Gavil and C. Khetrapal, *Proc. Indian Acad. Sci., Sect. A*, **64**, 91 (1966).
24) G. Olah, M. Calin and D. O'Brien, *J. Amer. Chem. Soc.*, **89**, 4736 (1967) plus many earlier papers.
25) T. Birchall and R. Gillespie, *Can. J. Chem.*, **43**, 1045 (1965).
26) H. Richey, Jr., L. Rennick, A. Kushner, J. Richey and J. Philips, *J. Amer. Chem. Soc.*, **87**, 4017 (1965).
27) D. Farnum and C. Wilcox, *ibid.* **89**, 5379 (1967).
28) N. Bhacca, L. Johnson and J. Schoolery, "High-Resolution NMR Spectra Catalog," Varian Associates, 1962, No. 495, 489, 205, and 194.
29) P. Corio and B. Dailey, *J. Amer. Chem. Soc.*, **78**, 3043 (1956).
30) L. M. Jackman, "Applications of Nuclear Magnetic Resonance Spectroscopy to Organic Chemistry," Pergamon Press, London (1959), p. 63.

TABLE 1. PROTON CHEMICAL SHIFTS OF SUBSTITUTED PHENYLAZOPHENOLS[a] (**1**)

Compd.	X	Ring A			Ring B			CH_3
		δ_o[b]	δ_m[c]	$\Delta\delta$	δ_o[b]	δ_m[c]	$\Delta\delta$	
2	4′-OCH_3	7.86	7.04	0.82	7.83	7.02	0.81	
3	4′-CH_3	7.89	7.06	0.83	7.86	7.24	0.62	2.35
4	H	7.92	7.06	0.86		complex		
5	4′-Br	7.89	7.06	0.83	7.92	7.78	0.14	
6	4′-NO_2	7.86	6.99	0.87	7.87	8.24	−0.37	
7	3′-CH_3	7.90	7.05	0.85				2.41
8	2′-CH_3	7.89	7.04	0.85				2.67
9	2′,4′-$(CH_3)_2$	7.84	7.03	0.81				2.63; 2.32
10	2′,5′-$(CH_3)_2$	7.85	7.01	0.84				2.60; 2.32
11	2′,6′-$(CH_3)_2$	7.83	7.02	0.81				2.30

a) Spectra were made of 5 mol% solutions in acetone. Chemical shifts are in ppm downfield from an internal TMS standard.
b) δ_o refers to the protons *ortho* to the azo group.
c) δ_m refers to the protons *meta* to the azo group.

TABLE 2. NMR[a] AND VISIBLE[b] SPECTRAL PARAMETERS OF THE PROTONATED PHENYLAZOPHENOLS (**1H**)

	X	Ring A			Ring B			δ_{CH_3}	λ_{max} (mμ)	ε ($\times 10^{-4}$)
		δ_o[c]	δ_m	$\Delta\delta$	δ_o[c]	δ_m	$\Delta\delta$			
2H	4′-OCH_3	8.14	7.30	0.84	8.21	7.34	0.87		488	4.28
3H	4′-CH_3	8.22	7.32	0.90	7.99	7.52	0.47	2.53	472	4.16
4H	H	8.28	7.35	0.93		complex			461	3.42
5H	4′-Br	8.30	7.37	0.93	7.97	7.86	0.11		477	4.28
6H	4′-NO_2	8.42	7.42	1.00	8.29	8.59	−0.30		473	5.11
7H	3′-CH_3	8.27	7.35	0.92				2.53	466	3.46
8H	2′-CH_3	8.25	7.33	0.92				2.83	472	3.36
9H	2′,4′-$(CH_3)_2$	8.20	*ca.* 7.33	*ca.* 0.87				2.83; 2.56	481	3.60
10H	2′,5′-$(CH_3)_2$	8.26	*ca.* 7.36	*ca.* 0.90				2.81; 2.52	481	3.05
11H	2′,6′-$(CH_3)_2$	8.26	*ca.* 7.38	*ca.* 0.88				2.67	464	2.79

a) Solutions were prepared by dissolving 100 mg of substrate in 1 m*l* of trifluoroacetic acid containing 29.4% sulfuric acid by weight. Chemical shifts are taken relative to tetramethylsilane as 0 ppm.
b) The same solvent mixture was used for the visible spectra (*vide supra*).
c) δ_o refers to the aromatic protons *ortho* to the azo group, in ppm.

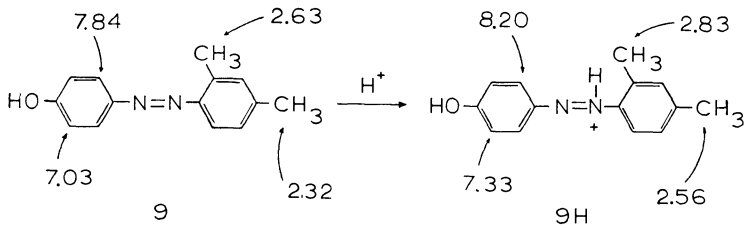

position (ring B) occur considerably downfield of the methyls in the 3′ or 4′ positions. The azo group may be somewhat electron withdrawing compared to the unsaturated carbon analogue in the stilbene system, but more likely the anisotropy of the azo group has a deshielding influence on the neighboring *ortho* protons.

The data for the protonated azophenols are listed in Table 2. Relevant chemical shifts for a typical compound and its conjugate acid are given above. The particular position of protonation is given for illustration purposes only.

Every group in the cation is deshielded compared to its counterpart in the unprotonated structure, as the result of the interplay of resonance, inductive and anisotropy effects. The downfield absorption of the 2′ methyl in **9H** compared to the 4′ methyl is suggestive that the anisotropy of the azo function persists in the cation form. Other types of cations shown the opposite trend, the 4′ methyl

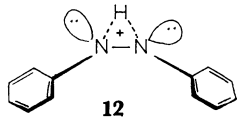

12

Scheme II

being downfield compared to the 2′ methyl.[20]

As Table 2 shows the change in $\Delta\delta$ (ring A) is now larger and quite regular. The increased electron demand of the cationic system renders it more sensitive to the various substituents. Moving from electron donating substituents X to electron withdrawing substituents involves a steady increase in $\Delta\delta$. In fact a plot of $\Delta\delta$ *vs.* σ^+ of the remote substituent is reasonably linear (Fig. 1).

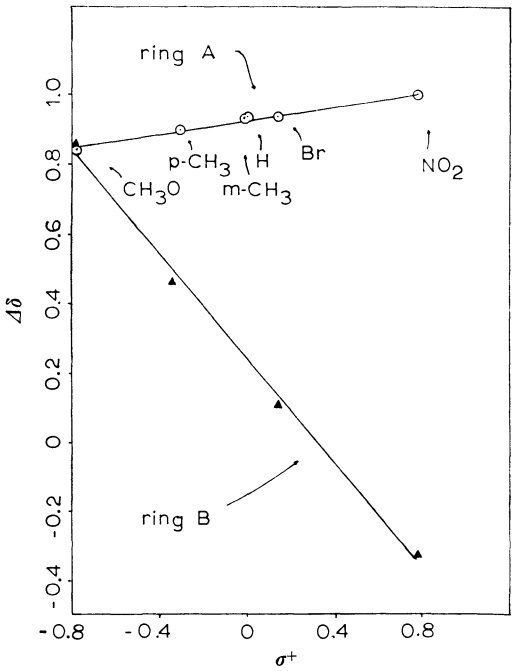

Fig. 1. A plot of the NMR chemical shift function, $\Delta\delta$ *vs.* Okamoto-Brown σ^+ constants.

For ring B, again the effect of the substituent is much greater. The trend of $\Delta\delta$ is now the opposite from that in ring A. Electron withdrawing substitutents produce smaller values of $\Delta\delta$. A plot of $\Delta\delta$ *vs.* σ^+ is again reasonably linear.[31] In ring B the anisotropy of the substituents would be expected to affect the chemical shift of the *meta* protons, thus a linear plot was somewhat unexpected.

The position of protonation of the azo structure remains a question of interest. One likely possibility is that the acid attacks one of the non-bonded pairs on nitrogen. This type of protonation would leave the pi orbitals of the system essentially undisturbed. An equilibrium between structures in which the proton has attacked the α nitrogen and structures resulting from β nitrogen attack seems likely. With electron withdrawing substituents the former structure would seem less probable due to the instability of the resonance froms involving a charge in ring B. In either case the transmission of electronic effects from substituent X through the pi system to affect ring A would be possible.

The symmetrically protonated structure **12** does

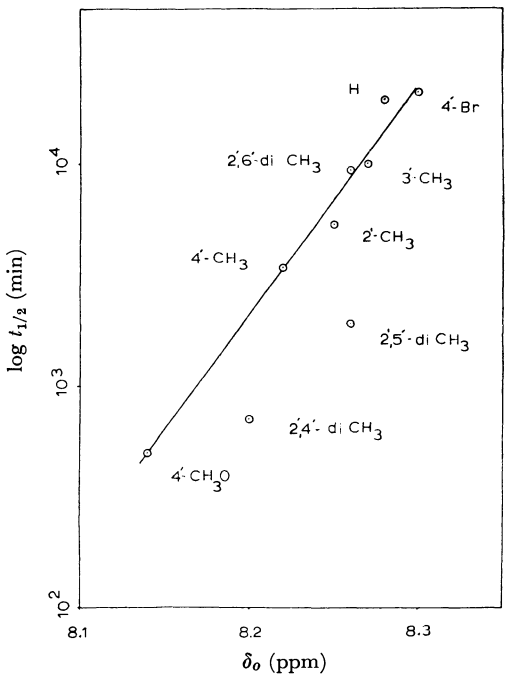

Fig. 2. A plot of log half-life of hydrogen-deuterium exchange in the *meta* position (ring A) *vs.* the chemical shift of the *ortho* proton (ring A) for the various remote substituents indicated.

31) Y. Okamoto and H. C. Brown, *J. Org. Chem.*, **22**, 485 (1957).

not appear to be generally accepted.[32]

For comparison purposes, two model systems have been investigated. The first system, *para* substituted anilinium ions[33] in trifluoroacetic acid, illustrated the effect of a localized charge on a nitrogen attached to one ring. The $\Delta\delta$ values vary with substituent as follows: CH_3O, 0.30; CH_3, *ca.* 0.0; Br, −0.33; $CH_3\overset{O}{\overset{\|}{C}}$, −0.54; NO_2, −0.65. Quite similar values result when small amounts of sulfuric acid are added to the solvent mixture.

The second model system of interest is that of the *para* substituted benzenediazonium chlorides, in which some delocalization of charge from a two nitrogen system into a single ring is possible. The $\Delta\delta$ values vary with substituent as follows: CH_3O, 0.74; Br, 0.32; and NO_2, |0.21|.

Although a strict comparison is not possible due to solvent differences, ring B of system **1H** seems somewhat closer to the anilinium ion model (taking into consideration the anisotropy of the protonated azo function). Thus in the equilibrium between α and β nitrogen protonation, the latter would seem somewhat more important for most substituents.

The visible spectral parameters for the cations **1H** are given in Table 2. The λ_{max} and ε decrease as the electron donating character of X diminishes, in the order **2H**>**3H**>**4H**. However, these parameters increase for **5H** and **6H**. The absorption bands are rather broad and possibly result from the superposition of two or more bands.[34] One band may undergo a bathochromic shift for electron donating substituents X whereas the other band undergoes a bathochromic shift for electron withdrawing substituents. Changes in the site of protonation also would affect λ_{max}, but the direction of change is difficult to predict.

Compound **11H** (2′,6′ dimethyl) exihibits a significantly lower λ_{max} and ε compared to **9H** and **10H**. Although $\Delta\delta$ value is similar, the chemical shifts of the 2′ and 6′ methyl groups occur upfield from the 2′ methyl groups in all other compounds. Ring B in this case (**11H**) appears to be somewhat out-of-plane.

In deuteriotrifluoroacetic acid - deuteriosulfuric acid mixtures, hydrogen-deuterium exchange occurred smoothly in the meta positions of ring A. The half-lives of exchange are recorded in Table 3. It is noteworthy that 4′-electron donating substituents markedly accelerate exchange in the *meta* position (ring A) even though no resonance form can be written in which the 4′ substituent stabilizes the σ complex intermediate. Thus, methyl groups in the 2′ or 4′ of ring B accelerate the exchange in ring A by a factor of 4—5 compared to the case where X=H. A methyl group in the 3′ position is less effective however. The 2′ substituent does not appear to hinder coplanarity of ring B to any great extent, in agreement with the spectral data.

However, the slowness of exchange in ring A of **11H** compared to **9H** is consistent with the out-of-plane character of the former, in which the activating effect of the methyls is reduced. However in ring B, **11H** exchanges much faster than **9H**. Although other explanations are possible, some exchange through a dication intermediate may be in effect. Since ring B of **11H** is not planar with the rest of the pi system, ring B would be less deactivated than the planar system **9H**.

Two aspects of the data in Table 3 are particularly interesting. One aspect concerns compound **7H**. In this case ring B exchanges more rapidly than the much more highly activated ring A. Again exchange directly on the protonated form **7H** may be in effect, rather than exchange *via* the small amount of **7** present in equilibrium with **7H**.

Table 3. Exchange half-lives for substituted phenylazophenols (**1H**) in trifluoroacetic acid-d - 29.4% sulfuric acid-d_2 at 30°C

	X	Ring A	Ring B
2H	4′-CH_3O	500 min	*ca.* 500
3H	4′-CH_3	3400	
4H	H	19000	
5H	4′-Br	21000	
6H	4′-NO_2	very slow[a]	
7H	3′-CH_3	10000	1700[b]
8H	2′-CH_3	5300	
9H	2′,4′-$(CH_3)_2$	700	
10H	2′,5′-$(CH_3)_2$	*ca.* 1900	[c]
11H	2′,6′-$(CH_3)_2$	*ca.* 9200	*ca.* 9200[b]

a) No exchange was observed in 30 days.
b) Three protons exchange.
c) The degeneration of the spectrum over a period of time was probably indicative of sulfonation.

The second aspect worthy of comment is shown in Fig. 2. Although plots of the log exchange half-life ($t_{1/2}$) *vs.* δ_m (ring A) or $\Delta\delta$ are reasonably linear for monosubstituted ring B compounds, the best correlation occurs by plotting log $t_{1/2}$ *vs.* δ_o (ring A). The remote substituent can supply or withdraw electrons from the *ortho* position by resonance. The modified electron density will in turn affect the chemical shift. However, the effect of the electron donation by X to the *ortho* position on hydrogen-deuterium exchange in the adjacent *meta* position is considered to be an inductive effect.

32) H. Jaffé, S. Yeh and R. Gardner, *J. Mol. Spectrosc.*, **2**, 120 (1958).
33) First investigated by G. Fraenkel and J. P. Kim, *J. Amer. Chem. Soc.*, **88**, 4203 (1966).
34) H. Jaffé and M. Orchin, "Theory and Applications of Ultraviolet Absorption Spectroscopy," John Wiley & Sons, Inc., New York, N. Y. (1962), pp. 258, 279.

Experimental

Preparation of 4-Phenylazophenols (1). The phenylazophenols were prepared by the coupling reaction of the appropriately substituted diazonium chloride with phenol. A typical procedure is the preparation of **10**. The diazotization was carried out by dissolving 2,5-dimethylaniline (6.0 g, 0.05 mol) in a solution of 12.5 m*l* of concd. hydrochloric acid in 50 m*l* of water. This solution was cooled in an ice bath and an aqueous solution of sodium nitrite was added until a positive test for nitrous acid was obtained. Sodium hydroxide (4.8 g, 0.12 mol) and phenol (4.6 g, 0.05 mol) in 30 m*l* of water was placed in a three necked flask, equipped with stirrer, *etc.* The diazonium salt was added to the cooled phenoxide solution. The resulting bright orange mixture was filtered and the filtrate acidified with hydrochloric acid. The product was filtered off, thoroughly washed, and recrystallized from benzene, mp 98—100°C, 7.2 g, 65% yield.

Found: C, 74.21; H, 6.25%. Calcd for $C_{14}H_{14}ON_2$: C, 74.31; H, 6.24%.

Compound **11** was prepared similarly, mp 147—148°C.

Found: C, 74.17; H, 6.25%. Calcd for $C_{14}H_{14}ON_2$: C, 74.31; H, 6.24%.

The following were literature preparations: **2**, mp 136—137°C, (lit,[35] 142°C): **3**, mp 150—151°C (lit,[36] mp 151°C); **4**, mp 150—151°C (lit,[37] 152°C); **5**, mp 160—161°C (lit,[38] 162°C); **6**, mp 206—207°C (lit,[39] mp 211°C); **7**, mp 142—143°C (lit,[40] 141°C); **8**, mp 101—102°C (lit,[41] mp 102—103°C); **9**, mp 134—135°C (lit,[35] mp 134°C).

The anilines from which the diazonium salt NMR data were taken were commercial products recrystallized twice, usually from ethanol. In each case the literature melting point was obtained.

Sulfuric acid-d_2 was obtained from Merck, Sharp and Dohme of Canada and was used as received. Trifluoroacetic acid-d was prepared from the anhydride (Mathieson) by the procedure of Taylor and Templeman.[42] On distillation the fraction boiling at 71°C was collected. The isotopic purity was greater than 96%.

The NMR data were taken on a Varian-A-60 instrument. The chemical shift data (taken *vs.* tetramethylsilane or *vs.* tetramethylammonium bromide in acid solutions) are considered good to ±0.03 ppm, and the $\Delta\delta$ values to ~0.01 ppm. The latter are less sensitive to concentration than the chemical shifts. The NMR solvents 29.4% sulfuric acid-d_2 in trifluoroacetic acid-d were made up by weight. Stronger acid solutions showed rather diffuse peaks whereas weaker solutions did not appear to protonate the substrate fully in all cases. For the diazonium salt runs, the solvent was 18% hydrochloric acid in water.

The ultraviolet data were taken on a Cary Model 14 instrument. The λ_{max} data are considered good to ±2—3 mμ due to rather broad peaks in some cases.

The rate solutions were made up and run as described previously.[20]

This work was begun at Iowa State University.

35) P. Jacobson, *Liebig's Ann. Chem.*, **287**, 211 (1895).
36) C. Kimich, *Ber.*, **8**, 1030 (1875).
37) O. Wallach and K. Kiepenhauer, *ibid.*, **14**, 2617 (1881).
38) J. Fox and J. Hewitt, *J. Chem. Soc.*, **93**, 340 (1908).
39) E. Nolting, *Ber.*, **20**, 2997 (1887).
40) R. Paganini, *ibid.*, **24**, 368 (1891).
41) E. Nolting and P. Werner, *ibid.*, **23**, 3257 (1890).
42) M. D. Taylor and M. B. Templeman, *J. Amer. Chem. Soc.*, **78**, 2950 (1956).

BULLETIN OF THE CHEMICAL SOCIETY OF JAPAN VOL. 43 745—749 (1970)

Formation Constants of Chromium(II) Complexes with (O,O)-, (O,N)- and (N,N)-Type Ligands and Comparison with Those of the Other First Transition Metal Complexes*1

Yutaka FUKUDA,*2 Eishin KYUNO and Ryokichi TSUCHIYA

Department of Chemistry, Faculty of Science, Kanazawa University, Kanazawa

(Received March 26, 1969)

The formation constants of the bivalent chromium complexes with various chelating ligands were determined by the pH titration method at the ionic strength $\mu=0.1$ and at 25°C. The values of the formation constants for (O,O)-type complexes were log $k_1=3.85\pm0.05$ and log $k_2=2.96\pm0.05$ for oxalate ion, log $k_1=3.92\pm0.05$ and log $k_2=3.21\pm0.05$ for malonate ion, and log $k_1=9.89\pm0.05$ for sulfosalicylate ion: for (O,N)-type complexes we obtained log $k_1=7.72\pm0.05$ and log $k_2=7.54\pm0.05$ for glycine, log $k_1=9.05\pm0.05$ for 8-hydroxyquinoline, and log $k_1=7.53\pm0.05$ for β-alanine. Based on these values together with the corresponding values of the (N,N)-type complexes, the effect of the coordinating atoms and of the number of members in a chelate ring upon the stabilities was discussed. These values were compared with those for the other transition metal complexes.

There are many unknown formation constants on the complexes of d^4-type metal ions, such as vanadium(I), chromium(II), manganese(III) and iron(IV). This may be mainly attributed to their variable valencies owing to the easy oxidation to d^3-type electronic state as shown by the standard reduction potential such as $E_{298}^0=-0.41$ V[1] for Cr^{2+}–Cr^{3+} system or to the easy reduction to d^5-type state as shown by the standard oxidation potential such as $E_{298}^0=1.51$ V[1] for Mn^{2+}–Mn^{3+} system. The corresponding potentials for V^+–V^{2+} and Fe^{3+}–Fe^{4+} are not known. Thus, because of the instability of the bivalent chromium ion in an aqueous solution, the formation constants have not been determined except for a few complexes, such as sulfosalicylic and salicylic acids,[2] acetylacetone,[3] ethylenediamine[4] and α,α'-bipyridyl.[5]

The present work was undertaken (1) to provide enough data on the formation constants of the chromium(II) complexes to find the effect of the coordinating atoms on the stabilities among the (O,O)-, (O,N)- and (N,N)-type complexes, (2) to know the effect of the number of members forming the chelate upon the stabilities and (3) to clarify the position of the chromium(II) complexes in the series of the stability order.

Experimental

Ligand Materials. The (O,O)-type chelating ligands were oxalic, malonic and sulfosalicylic acids, and the (O,N)-type ligands were glycine, 8-hydroxy-

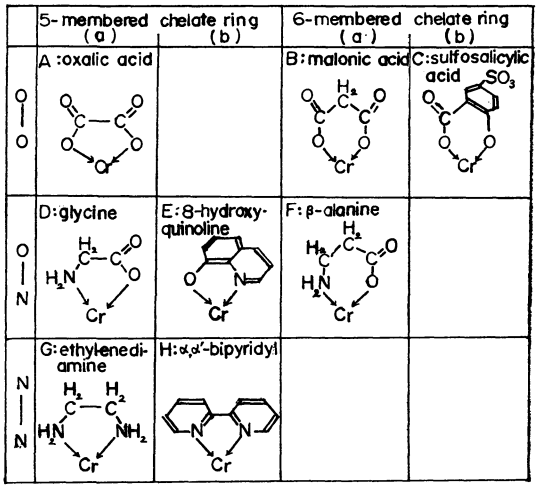

Fig. 1. The coordination structures of the various ligands in the complexes concerned.
(a) column: non-π-character ligands
(b) column: π-character ligands

*1 Presented at the 21st Annual Meeting of the Chemical Society of Japan, Osaka, April, 1968.

*2 Present address: Department of Chemistry, Faculty of Science, Shizuoka University, Shizuoka.

1) W. M. Latimer, "Oxidation Potentials," Prentice-Hall, Inc., Englewood Cliffs, N. J. (1961).

2) R. L. Pecsok and W. P. Schaefer, *J. Amer. Chem. Soc.*, **83**, 62 (1961).

3) W. P. Schaefer and M. E. Mathisen, *Inorg. Chem.*, **4**, 431 (1965).

4) R. L. Pecsok and J. Bjerrum, *Acta Chem. Scand.*, **11**, 1419 (1957).

5) J. M. Crabtree, D. W. Marsh, J. C. Tomkinson, R. J. P. Williams and W. C. Fernelius, *Proc. Chem. Soc.*, **1961**, 336.

quinoline and β-alanine. They were all of special grade reagents from Wako Pure Chemical Industries. For the sake of convenience, the structures of the ligands are given in Fig. 1.

Preparation of Chromium(II) Perchlorate. A solution of chromium(II) perchlorate was prepared by the electrolytic reduction of a solution of hexaaquochromium(III) perchlorate.[6] The cell for electrolysis consists of three compartments:[2] in one compartment the so-called Winkler platinum electrode was inserted as an anode and in another one mercury was used as a cathode. The starting voltage was 2—3 V in the electrolysis. The applied voltage was gradually raised to about 6 V, keeping the electric current at about 0.5 A. Electrolysis was continued under these conditions for 7—8 hr, nitrogen being passed through all the apparatus not only during the electrolysis but also for 2—3 hr before the electrolysis to protect the bivalent chromium ion from oxidation. Nitrogen was purified by passing it through a basic pyrogallol solution and a chromium(II) ion solution.

The color of the electrolytic solution changed from reddish-violet to blue as the reduction proceeded. The absorption spectrum of the resulting solution in a *d–d* transition region was found to coincide with that of aquo chromium(II) complex.[7] Determination of the chromium(II) ion content was carried out iodometrically: a standard solution of potassium iodate, in the presence of potassium iodide and a few drops of starch solution as indicator, was titrated with the chromium(II) perchlorate solution prepared by electrolytic reduction, and the concentration of chromium(II) ion was calculated from the titres. The reactions concerned can be expressed by the following:

$$IO_3^- + 5I^- + 6H^+ \rightarrow 3I_2 + 3H_2O$$
$$3I_2 + 6Cr^{2+} \rightarrow 6I^- + 6Cr^{3+}$$

Total concentration of chromium was spectrophotometrically determined as bichromate. Although the accuracy of the determination of total chromium content is about ten times less than that of the chromium(II) content evaluated from the iodometric titration, it could be confirmed by this procedure that more than 99% of the chromium was reduced.

Formation Constant Measurement. The aqueous solution of each ligand was titrated with alkali hydroxide solution at an ionic strength $\mu=0.1$ and at 25°C, in the presence as well as in the absence of the hexaaquochromium(II) perchlorate. The ligand materials were used in excess in comparison to the chromium(II) perchlorate added. Thus the change of the concentration of the ligands in complex formation can be neglected as compared with the total concentration of the ligands added. The ionic strength of the solution was adjusted to 0.1 by adding an appropriate amount of sodium perchlorate.

Results

When the ligand materials behave as bidentate chelating agents, the acid dissociation constants*3 are given by

$$H_2L = H^+ + HL, \quad K_1 = [H^+][HL]/[H_2L],$$
$$HL = H^+ + L, \quad K_2 = [H^+][L]/[HL],$$

where the square brackets, [ ], express the concentration of relevant species, and the ionic charges are omitted except for hydrogen ion. From the equations, the concentration of the free ligand bound neither with proton nor with metal ions, [L], is calculated by the equation:

$$[L] = K_1K_2[C_L]/\{K_1K_2 + K_1[H^+] + [H^+]^2\}, \quad (1)$$

where $[C_L]$ is the total concentration of the ligand.

The average number of the coordinated ligands per one chromium(II) ion, $\bar{n}$, is expressed by the equation

$$\bar{n} = C_{OH}[OH^-]/2C_MV_M, \quad (2)$$

where C_{OH} and C_M are the initial concentrations of alkali hydroxide and chromium(II) perchlorate solution, respectively, V_M is the titres of the chromium(II) perchlorate solution and $[OH^-]$ is the difference between the titres obtained from pH titration curves in the presence and absence of the metal ion at the same pH value of the solution. $[OH^-]$ corresponds to the amount of the ligand participating in the complex formation.[8]

The values, $\bar{n}$ and the logarithm of the reciprocal concentration of the free ligand, p[L], are calculated by using equations, (1) and (2). The formation curves, $\bar{n}$—p[L], are plotted in Fig. 2.

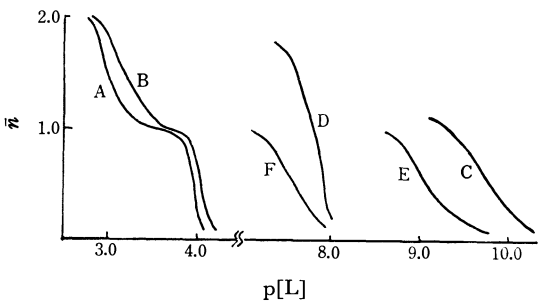

Fig. 2. The formation curves, $\bar{n}$—p[L], for chromium(II)-various ligands systems.
A: oxalic acid, B: malonic acid, C: sulfosalicylic acid, D: glycine, E: 8-hydroxyquinoline, F: β-alanine.

The values of the formation constants of the chromium(II) complexes obtained from Fig. 2 were refined by means of successive approximation. The final values are summarized in Table 1, together with those for salicylic and sulfosalicylic acids,[2] acetylacetone,[3] ethylenediamine,[4] and α,α′-bi-

6) H. Matsukawa, M. Ohta, S. Takata and R. Tsuchiya, This Bulletin, **38**, 1235 (1964).

7) J. P. Fackler, Jr., and D. G. Halah, *Inorg. Chem.*, **4**, 954 (1965).

*3 The values of the acid dissociation constants are cited from literature, and are given in Table 1.

8) M. Calvin and N. C. Melchoir, *J. Amer. Chem. Soc.*, **70**, 3270 (1948).

pyridyl.[5] In Table 1 are also included the acid dissociation constants of the relevant ligands.

Table 1. Formation constants of the chromium(II) complexes with various chelate lidands, and the acid dissociation constants of the ligands

Coordination ligand type	$\log k_1$	$\log k_2$	pK_1	pK_2
(A)	3.85±0.05	2.96±0.05	1.37	3.81[9]
(B)	3.92±0.05	3.21±0.05	2.76	5.29[10]
(C)	9.89±0.05	—	2.62	11.95[11]
	7.14	5.74[2]		
(I)*	5.96	5.74[3]	8.88[3]	
(J)*	8.41	6.95[2]	3.18	13.12[2]
(D)	7.72±0.05	7.54±0.05	2.35	9.68[12]
(E)	9.05±0.05	—	3.97	11.54[13]
(F)	7.53±0.05	—	3.52	10.26[14]
(G)	5.15	4.04[4]	7.44	10.06[4]
(H)	4	6.4[5]	4.44[5]	

* I: acetylacetone, J: salicylic acid

Discussion

Comparison of the Formation Constants. It may be deduced from Fig. 2 that the chromium(II) complexes having two ligand molecules at highest appear in aqueous solution. This may be due to the so-called Jahn-Teller effect in d^4-type complexes, the electronic configuration preferring the high-spin state.

The 1 : 3 complex was found only in α,α′-bipyridyl in an aqueous solution.[5] It was also confirmed by preliminary experiment that the yellow crystalline tervalent chromium complex with α,α′-bipyridyl was obtained by oxidizing the crystalline black chromium(II) complex prepared in nitrogen atmosphere in the air. The fact that chromium(II) forms 1 : 3 complex only with α,α′-bipyridyl may suggest that only the complex with α,α′-bipyridyl is in the low-spin state.

In the case of chromium(III) complexes, the stability is known to increase, in general, in the order of the ligands giving the coordination types, *viz.*, (O,O)<(O,N)<(N,N).[6] This may be due to the fact that the polarizing ability of the chromium(III) ion is relatively stronger owing to its greater ionic charge and smaller ionic radius than that of the chromium(II) ion and that the polarizability of nitrogen as a soft base[15] is larger than that of oxygen.

In chromium(II) complexes, the following results are given in Fig. 2 and Table 1. For the ligands forming five-membered chelate ring with metal, the formation constants of the (O,N)-type complexes such as glycinate and 8-hydroxyquinolinate are larger than those of the (O,O)-type complexes such as oxalate. This is in line with the results obtained with the chromium(III) complexes.[6] The same stability order applies also to the ligands forming six-membered chelate ring: the formation constants of the (O,N)-type complexes such as β-alaninate are larger than those of the (O,O)-type complexes such as malonate or acetylacetonate.

The formation constants of the (N,N)-type complexes such as ethylenediamine and α,α′-bipyridyl are slightly larger than those of the (O,O)-type complexes such as oxalate or malonate. This may be explained as above with respect to the corresponding chromium(III) complexes: the strength as Lewis base is larger in nitrogen than in oxygen atoms, or nitrogen is a more soft base than oxygen.[9]

However, the formation constants of chromium(II) complexes with ethylenediamine and α,α′-bipyridyl are, contrary to expectation, smaller than those of the (O,N)-type complexes such as glycinate and 8-hydroxyquinolinate. This fact was not found with the chromium(III) complexes reported in an earlier paper.[6]

It is known that the complexes having five-membered chelate ring are, in general, more stable than those having six-membered chelate ring. Nevertheless, so far as chromium(II) complexes are concerned, the difference is not appreciable between the formation constants of complexes forming five-membered and those forming six-membered chelate rings as seen in the (O,O)-type complexes such as oxalate and malonate or in the (O,N)-type complexes such as glycinate and β-alaninate.

The salicylate and sulfosalicylate complexes, however, have exceptionally larger formation constants than those of malonate complexes having the same six-membered chelate ring of (O,O)-type. 8-Hydroxyquinolinate complex has a larger value of the formation constants than that of glycinate complex having the same five-membered ring of (O,N)-type. Salicylic and sulfosalicylic acids have benzene ring, and 8-hydroxyquinoline has a pyridine ring besides a benzene ring. The reason why the complexes containing such chelating ligands are extraordinarily stable comes from the possibility of the resonance effect resulting from the presence of a

9) A. McAulley and G. H. Nancollas, *Trans. Faraday Soc.*, **56**, 1165 (1960).
10) M. Yasuda, K. Yamasaki and H. Ohtaki, This Bulletin, **33**, 1067 (1960).
11) D. D. Perrin, *Nature*, **182**, 741 (1958).
12) N. C. Li and R. A. Manning, *J. Amer. Chem. Soc.*, **77**, 5225 (1955).
13) W. D. Johnston and H. Freiser, *ibid.*, **74**, 5239 (1952).
14) H. Irving, R. J. P. Williams, D. J. Ferrett and A. E. Williams, *J. Chem. Soc.*, **1954**, 3494.
15) J. O. Edwards and R. G. Pearson, *J. Amer. Chem. Soc.*, **84**, 16 (1962).

benzene or pyridine ring and/or the change of the electronic configuration in chromium(II) ion from the high-spin to the low-spin state.

In the case of α,α′-bipyridyl complexes, the second stepwise formation constant is larger than the first one as shown by their data.[5] The normal order where the first stepwise formation constant is larger than the second one as seen in most complexes is not applied to the case of α,α′-bipyridyl complexes. Such an abnormal result suggests that the electronic configuration in these complexes may be changed from the high-spin to the low-spin state when the 1 : 1 complex is converted to 1 : 2 complex.

The fact that the acetylacetonate complexes have larger values of formation constants than the malonate ones which have the same six-membered ring as seen in Table 1 may be explained by considering the presence of the quasi-aromaticity in the former.

Comparing the formation constants of chromium(II) complexes with the corresponding acid dissociation constants, we see that, when the latter becomes larger, the former tends to increase. The linear relationships between the logarithmic values of the formation constants and of the respective acid dissociation constants are verified by the approximately constant values of $(\log k_1)/pK_2$ except for oxalate, ethylenediamine and α,α′-bipyridyl complexes. Calculated values are listed in Table 2.

TABLE 2. THE VALUES OF $(\log k_1)/pK_2$

Complex	$(\log k_1)/pK_2$
A	1.01
B	0.74
C	0.83
I	0.66
J	0.64
D	0.80
E	0.78
F	0.73
G	0.51
H	0.90

Position of the Stability of Chromium(II) Complexes in the First Transition Metal Complexes. So far enough data of the formation constants of the bivalent chromium complexes have not been obtained, and the position of the constants in the so-called Irving-Williams series[16] is ambiguous. In order to survey the stability sequence in various complexes of the first bivalent transition metal, ion formation constants of some chelates of these metals ion are plotted against the metal series following their atomic numbers in Fig. 3.

16) H. Irving and R. J. P. Williams, *J. Chem. Soc.*, **1953**, 3192.

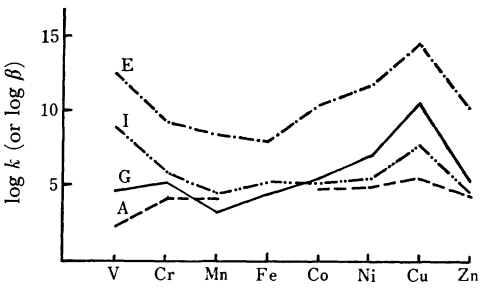

Fig. 3. Comparison of the stabilities of the bivalent metal complexes with various chelate ligands.
E: 8-hydroxyquinoline, I: acetylacetone, G: ethylenediamine, A: oxalic acid.

A approximate order of the stability of the first transition metal complexes including chromium is found to be Zn<Cu>Ni>Co≳Cr>Fe>Mn. The stability of chromium(II) complexes seems to be situated between that of iron(II) and cobalt(II) complexes, so far as the chelating lignads such as 8-hydroxyquinoline and ethylenediamine are concerned.

The order found for cobalt(II), iron(II) and chromium(II) complexes may be explained on the basis of the ligand field theory as follows: if the electronic configuration in these complexes is in the high-spin state as given in Fig. 4, the ligand field stabilization energy can be calculated as $4/5\Delta$, $2/5\Delta$ and $3/5\Delta$ for Co(II), Fe(II) and Cr(II) complexes, respectively, in octahedral environment, where Δ is the splitting energy dependent upon the strength of the ligand field. Since all the values of Δ are not known, the explanation by the ligand field theory is not always applicable to each stability sequence over the first transition metal complexes with various chelating ligands.

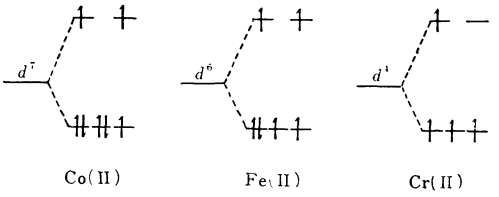

Fig. 4. Ligand field splitting in Co(II), Fe(II) and Cr(II) complexes in high-spin state.

It will be found from Fig. 3 that the stability of the chromium(II) complexes which contain the π-character ligands such as 8-hydroxyquinoline or acetylacetone is lower than that of the corresponding vanadium(II) complexes, whereas, in the case of the complexes containing normal ligands such as oxalic acid or ethylenediamine, their stabilities are in reverse order. The reason might be as follows: since the radius of chromium(II) ion is smaller than that of vanadium(II) ion, the former is a harder acid than the latter, so that the chromium-

(II) complex is more stable than vanadium(II) for a common chelating ligand having no π-character, whereas the strength of the back-coordination is larger in chromium(II) than in vanadium(II) for a π-character ligand, so that the stability order might become reverse.

BULLETIN OF THE CHEMICAL SOCIETY OF JAPAN VOL. 43 749—755 (1970)

On the Ligand Exchange Equilibrium in the Propylene-Mercury(II) Complex

Itsuro KAWAI, Riichiro NAKAJIMA and Tadashi HARA

Department of Chemical Engineering, Faculty of Engineering, Doshisha University, Kamikyo-ku, Kyoto

(Received May 15, 1969)

The equilibrium between the propylene-mercuric complex and either Cl^-, Br^-, I^-, or EDTA, and their dependences on the pH were investigated manometrically. The propylene-mercuric complexes present in the above equilibrium were found to be $(HO^-)_n$-Hg^{2+}-Propylene ($n=0$, 1 and 2) and $(HO^-)_n$-Hg^{2+}(X^-)-Propylene ($n=0$ and 1), and their equilibrium equations were:

$$(HO^-)_n\text{-}Hg^{2+} + \text{Propylene} \overset{K_{p1}}{\rightleftharpoons} (HO^-)\text{-}Hg^{2+}\text{-Propylene}$$

$$X^-\text{-}Hg^{2+}\text{-}(HO^-)_n + \text{Propylene} \overset{K_{p2}}{\rightleftharpoons} (HO^-)_n\text{-}Hg^{2+}(X^-)\text{-Propylene.}$$

By introducing $K_{p1}=K'_{p1}$ and $K_{p2}=K'_{p2}$ when $n=0$, the dependences on the pH were shown by:

$$\log K_{p1} = \log K'_{p1} + 2\cdot\text{pH}, \quad \log K_{p2} = \log K'_{p2} + \text{pH}$$

where $K'_{p1}=2.2\times10^5$, $K'_{p2(Cl)}=4.1\times10^5$, and $K'_{p2(Br)}=2.7\times10^6$ at 25°C and $\mu=0.8$. As was to be expected from the above equilibrium, K'_{p1} was idependent of the presence of Cl^-, Br^-, I^-, and EDTA, while K'_{p1} varied in the presence of Cl^-, Br^-, and I^-. The above relationships were also derived theoretically.

It has been well known that the mercuric ion in an aqueous solution can be made to react with olefin to form a stable complex[1] and that the complex can be decomposed by adding a chloride ion to an olefin and mercuric complex.[2]

Though the mercuric chloride-olefin system has been studied by many people, no satisfactory explanation of the equilibrium has been given. The equilibrium constant for the mercuric chloride-ethylene system was estimated by Allen *et al.*,[2] but they could not explain the effect of sodium chloride and perchloric acid on the equilibrium. The equilibrium between *cis*- or *trans*-butene-2 and mercuric chloride was also investigated by Kreevoy *et al.*,[3] but their study was limited to the range in which $HgCl_3^-$ and $HgCl_4^{2-}$ can be neglected.

The present study was carried out in order to make clear the species present in an aqueous solution and to calculate the equilibrium constants. On the basis of the species and the equilibrium constants thus obtained, the ligand-exchange reactions between the propylene-mercury(II) complex and chloride, bromide, iodide, and ethylenediaminetetraacetate were satisfactorily explained.

It has been reported in a preceding paper[4] that the mercury(II) in an aqueous solution can be determined indirectly by adding such ligand as chloride, bromide, iodide, and ethylenediaminetetraacetate to the propylene-mercury(II) complex and by then measuring the amount of propylene evolved.

The amount of propylene evolved in these ligand-exchange reactions decreased with an increase in the pH in the pH range of >0.15 for chloride, >2.10 for bromide, and >4.00 for iodide, while it decreased with a decrease in the pH in the range of pH<4.90 for ethylenediaminetetraacetate. These phenomena seemed to be very interesting from the standpoint of understanding the mechanism of oxymetallation, they could be explained satisfactorily using the species and the equilibrium con-

1) J. Sand and F. Breest, *Z. Phys. Chem.*, **59**, 424 (1907).

2) E. R. Allen, J. Cartlidge, M. M. Taylor and C. F. H. Tipper, *J. Phys. Chem.*, **63**, 1437 (1959).

3) M. M. Kreevoy, L. L. Schaleger and J. C. Ware, *Trans. Faraday Soc.*, **58**, 2433 (1962).

4) I. Kawai and T. Hara, This Bulletin, **42**, 3466 (1969).

stants, as has been mentioned above.

No discussion including oxymetallation has been given for an equilibrium in the propylene-mercury-(II) system in which the formation constants of mercuric halide are taken into consideration.

In the present paper, all the species, such as $HgX_i^{(2-i)+}(i=1—4)$, $(HO^-)_n$-Hg^{2+}-Propylene ($n=0$, 1 and 2), $(HO^-)_n$-$Hg^{2+}(X^-)$-Propylene ($n=0$ and 1), and $Hg(OH)_i^{(2-i)+}$ ($i=0$, 1 and 2), were taken into consideration in an equilibrium. The above-mentioned phenomena were attributed to the difference in the formation constants of mercuric halide complexes and to the affinity between the α-carbon in propylene and the hydroxyl groups produced by the hydrolysis of the hydrated propylene-mercury(II) complex.

Experimental

The amount of propylene evolved or absorbed was measured by the same apparatus and procedure as in the preceding paper.[4] With the objective of examining the hydrolysis of the aquo mercuric complex, the absorption spectra of 8×10^{-4}M Hg(II) solutions (pH: 0, 1, 2, 3, 5 and 7; ionic strength with sodium perchlorate : 1) were obtained over 210—300 mμ at 25°C by means of a Shimadzu QR-50 spectrophotometer, using 1-cm cells. The acidity was regulated with a 10^{-3}M sodium hydroxide solution after a preliminary run had been made. With the same objective as above, 5×10^{-2}M Hg(II) solutions (0.7N in perchloric acid concentration) in the presence and in the absence of 0.15M chloride or bromide or iodide were titrated with 0.97N NaOH, and the pH during titration was measured by means of a Horiba M-5 pH-meter.

Results

The amounts of propylene absorbed into mercuric solutions at various concentrations are shown in Table 1, along with the apparent formation constant,

TABLE 1. APPARENT FORMATION CONSTANT (K_p) BETWEEN MERCURIC ION AND PROPYLENE

$t=25$°C, P_{tot}=total pressure of propylene=1 atm, $\mu=0.85$, $[HClO_4]=0.7$N, Total volume=7.00 ml

[$\sum$Hg] mol/l	Propylene absorbed sample ml (mol/l)	Formation constants (K_p) l/mol
2.867×10^{-2}	5.70 (3.340×10^{-2})	3.0×10^4
3.584×10^{-2}	6.88 (4.029×10^{-2})	1.5×10^4
4.301×10^{-2}	8.12 (4.756×10^{-2})	2.3×10^4
5.017×10^{-2}	9.30 (5.445×10^{-2})	1.5×10^4
		Av.=2.1×10^4

Blank 0.84 ml (4.92×10^{-3} mol/l)

which was directly estimated from the experimental data. Since the mole ratio of propylene to mercury is 1 : 1, the composition of the propylene-mercury-(II) complex can also be expected to be 1 : 1. The reaction is thus given by Eq. (1):

$$Hg^{2+} + CH_3\text{-}CH{=}CH_2 \overset{K_p}{\rightleftharpoons} \begin{matrix} & CH_3 & \\ & | & \\ HC & & \diagdown Hg^{2+} \\ | & & \\ H_2C & & \end{matrix} \quad (1)$$

The equilibrium constant is, therefore, shown by Eq. (2), and the values of K_p are as shown in Table 1.

$$K_p = \frac{[Hg^{2+}\text{-Propylene}]}{[Hg^{2+}]\cdot[\text{Propylene}]} = \frac{[\text{Total amount of propylene absorbed}] - [\text{Blank}]}{\{[\sum Hg] - [\text{Total amount of propylene absorbed}] + [\text{Blank}]\}\cdot[\text{Blank}]} \quad (2)$$

Where [Blank] indicates the amount of propylene absorbed into the solution containing no mercuric ion, and [Total amount of propylene absorbed] corresponds to the propylene absorbed into the Sample as shown in Table 1. Hereafter, [Propylene] and [Hg^{2+}-Propylene] will be abbreviated as [P] and [Hg^{2+}-P] respectively.

Though the values of K_p were obtained directly from the experimental data, they are not very accurate since the value of [Blank] contains something of an experimental error. Therefoer, the value of K_p was estimated indirectly by means of Eq. (9), using the equilibrium data concerning the Hg(II)-EDTA and propylene-Hg(II)-EDTA systems. For the former system, Eqs. (3), (4), (5) and (6) are given:

$$Hg^{2+} + L^{4-} \overset{K_{EDTA}}{\rightleftharpoons} Hg\text{-}L^{2-} \quad (3)$$

$$K_{EDTA} = \frac{[HgL^{2-}]}{[Hg^{2+}]\cdot[L^{4-}]} \quad (4)$$

$$H_{5-i}L^{1-i} \overset{K_{ai}}{\rightleftharpoons} H_{4-i}L^{-i} + H^+ \quad (5)$$

$$K_{ai} = \frac{[H_{4-i}L^{-i}]\cdot[H^+]}{[H_{5-i}L^{1-i}]} \quad (i=1—4) \quad (6)$$

For the latter system, Eqs. (7), (8) and (9) are given:

$$Hg^{2+}\text{-Propylene} + L^{4-} \overset{K_{p3}}{\rightleftharpoons} Hg\text{-}L^{2-} + \text{Propylene} \quad (7)$$

$$K_{p3} = \frac{[HgL^{2-}]\cdot[P]}{[Hg^{2+}\text{-P}]\cdot[L^{4-}]} \quad (8)$$

$$K_{p1} = \frac{K_{EDTA}}{K_{p3}} \quad (9)$$

where K_{p1} is theoretically equal to K_p, but it is differentiated from K_p since K_{p1} is indirectly calculated. Table 2 shows the experimental data obtained in the preceding paper; these data show the residual amount of the propylene mercuric complex on the addition of chloride, bromide, iodide, and ethylenediaminetetraacetate. The values of K_{p3} were estimated from the data (Table 2) obtained at pH 5 and at varying mole ratios of EDTA to Hg(II); they are shown in Table 3.

Table 2. The residual amount of propylene mercuric complex in an addition of sodium chloride, sodium bromide, sodium iodide and EDTA

t=25°C, P_{tot}=1 atm, μ=0.8, [$HClO_4$]=0.7N for halide, pH=5 for EDTA

Mole ratio [∑L]**/[∑Hg]	Propylene mercuric complex (mol/l) Cl⁻	Br⁻	I⁻	EDTA
1.0	1.1×10^{-2}	9.6×10^{-3}	7.4×10^{-3}	3.1×10^{-3}
1.5	6.9×10^{-3}	5.3×10^{-3}	3.9×10^{-3}	1.7×10^{-3}
2.0	3.5×10^{-3}	2.0×10^{-3}	—*	1.0×10^{-3}
2.5	1.2×10^{-3}	—*	—*	4.4×10^{-4}
3.0	—*	—*	—*	—*

* less than 2.8×10^{-5} mol/l

** stand for [∑Cl], [∑Br], [∑I], and [∑EDTA]

Table 3. Formation constant (K_{p3}) between mercuric EDTA complex and propylene

t=25°C, P_{tot}=1 atm, μ=0.8, pH=5

Mole ratio [∑EDTA]/[∑Hg]	Formation constant K_{p3}
1.25	1.2×10^{7}
1.50	1.2×10^{7}
1.75	1.2×10^{7}
2.00	1.2×10^{7}
2.25	1.2×10^{7}
	Av.=1.2×10^{7}

Formation constant (K_{p3}) were calculated using Schwarzenbach's[5] stability constants; $K_{a1}=1.02\times10^{-2}$, $K_{a2}=2.14\times10^{-3}$, $K_{a3}=6.92\times10^{-7}$, $K_{a4}=5.49\times10^{-11}$, $K_{EDTA}=6.31\times10^{21}$

Table 4. The residual amount of prorylene mercuric complex in an addition of sodium chloride, sodium bromide, sodium iodide and EDTA

t=25°C, P_{tot}=1 atm, μ=0.8, mole ratio: [∑L]/[∑Hg]=3

pH	Propylene mercuric complex (mol/l) Cl⁻	Br⁻	I⁻	EDTA
0.15	—*	—*	—*	—*
1.00	3.2×10^{-3}	—*	—*	—*
2.10	7.6×10^{-3}	—*	—*	2.0×10^{-3}
3.00	1.1×10^{-2}	3.9×10^{-3}	—*	1.6×10^{-3}
4.00	1.3×10^{-2}	7.8×10^{-3}	—*	1.0×10^{-3}
5.00	—*	9.9×10^{-3}	4.7×10^{-3}	—*
6.10	—*	—*	7.9×10^{-3}	—*

* less than 2.8×10^{-5} mol/l

5) G. Schwarzenbach, R. Gut and G. Anderegg, *Helv. Chim. Acta*, **37**, 937 (1954).

The values of K_{p1} were calculated by Eq. (9) using the values of K_{p3} calculated from the data (Table 4) obtained at various pH values and at the mole ratio of EDTA to Hg(II) of 3; they are shown in Table 5 and in Fig. 1. On the basis of

Table 5. Formation constant (K_{p1}) between mercuric ion and propylene

t=25°C, P_{tot}=1 atm, μ=0.8, mole ratio: [∑EDTA]/[∑Hg]=3

pH	Formation constant (K_{p1})
2	2.4×10^{8}
3	9.1×10^{10}
4	1.1×10^{12}
5	5.4×10^{14}

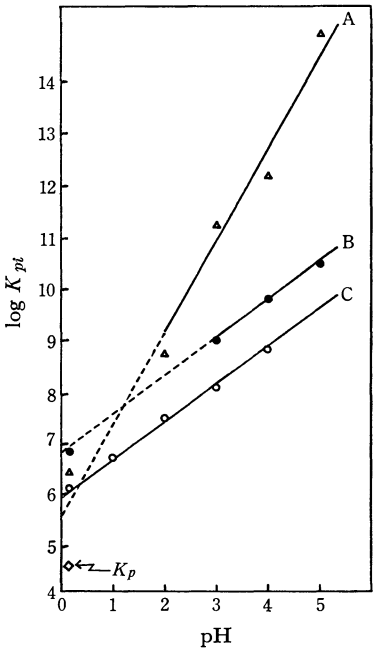

Fig. 1. Relationship among log K_{p1}, log K_{p2} and pH; t=25°C, μ=0.8
i=1: A
i=2: B(Br), C(Cl)

Fig. 1, the relationship between K_{p1} and pH can be expressed by Eq. (10):

$$\log K_{p1} = \log K'_{p1} + 2\mathrm{pH} \qquad (10)$$

where $K'_{p1} = 2.2\times10^{5}$

In the propylene-Hg(II)-halide system, Eqs. (11) and (12), in addition to Eqs. (1) and (2), were taken into consideration:

$$HgX_{i-1}^{(3-i)+} + X^- \overset{K_i}{\rightleftharpoons} HgX_i^{(2-i)+} \qquad (11)$$

$$K_i = \frac{[HgX_i^{(2-i)+}]}{[HgX_{i-1}^{(3-i)+}]\cdot[X^-]} \quad (i=1\text{—}4,\ X\text{: Cl, Br}) \qquad (12)$$

Under the experimental conditions shown in

TABLE 6. FORMATION CONSTANTS (K_{p1} and K_{p2}) IN THE PROPYLENE-MERCURY(II)-HALIDE SYSTEM

t=25°C, P_{tot}=1 atm, μ=0.8, [$HClO_4$]=0.7N

Mole ratio [∑X]/[∑Hg]	K_{p2}		K_{p1}	
	Cl^-	Br^-	Cl^-	Br^-
1.00	7.5×10^5	3.3×10^6	1.4×10^6	1.5×10^6
1.25	6.8×10^5	3.1×10^6	1.3×10^6	1.6×10^6
1.50	6.7×10^5	2.9×10^6	1.3×10^6	1.4×10^6
1.75	6.3×10^5	3.1×10^6	1.3×10^6	1.4×10^6
2.00	6.4×10^5	3.7×10^6		
2.25	6.4×10^5	3.8×10^6		
Av	6.9×10^5	3.3×10^6	1.3×10^6	1.5×10^6

X: Cl, Br

Formation constants (K_{p1} and K_{p2}) were calculated using Sillén's[6] stability constants;

Cl: $K_1=5.49\times10^6$, $K_2=3.02\times10^6$, $K_3=7.08$, $K_4=1.26\times10$

Br: $K_1=1.12\times10^9$, $K_2=1.91\times10^8$, $K_3=2.57\times10^2$, $K_4=1.82\times10$

Table 6, Eqs. (13) and (14) held:

$$[\sum X] = \sum_{i=1}^{4}(i\cdot[HgX_i^{(2-i)+}]) + [X^-] \quad (13)$$

$$[\sum Hg] = \sum_{i=1}^{4}[HgX_i^{(2-i)+}] + [Hg^{2+}] + [Hg^{2+}\text{-P}] \quad (14)$$

By combining Eqs. (11)—(14), Eq. (15) was obtained:

$$\left(\prod_{i=1}^{4}K_i\right)\cdot[X^-]^5 + \left(\prod_{i=1}^{3}K_i\cdot(1-K_4\cdot[\sum X]-4[\sum Hg])\right)\times[X^-]^4 + \left(\prod_{i=1}^{2}K_i\cdot(1-K_3([\sum X]+3[\sum Hg]))\right)\cdot[X^-]^3 + (K_1(1-K_2([\sum X]-2[\sum Hg])))\cdot[X^-]^2 + (1+K_1\cdot([\sum Hg]-[\sum X]))\cdot[X^-] - [\sum X] = 0 \quad (15)$$

The value of [X^-] in Eq. (15) was obtained by the method of halving by a computor, followed by the calculation of the constituent concentration and of K_{p1}. Though the value of K_{p1} was expected to be constant, it varied with the kind and with the concentration of the halide. This seemed to be attributable to the fact that Hg^{2+}-P alone was adopted as the propylene-mercury(II) complex in the above equilibrium. However, those data are not shown since they are not useful in explaining the equilibrium. Paul and Brandt[7] took the monohalogeno propylene mercuric complex alone into consideration in examining an equilibrium of the propylene-Hg(II)-halide system, but the present authors took both the monohalogeno-propylene mercuric complex and the propylene mercuric complex into consideration. Therefore, Eqs. (16) and (17), in addition to Eqs. (1) and (11), were considered:

$$HgX^+ + \text{Propylene} \overset{K_{p2}}{\rightleftharpoons} X\text{-}Hg^+\text{-Propylene} \quad (16)$$

$$K_{p2} = \frac{[X\text{-}Hg^+\text{-P}]}{[HgX^+]\cdot[P]} \quad (17)$$

Eqs. (13) and (14) were rewritten as Eqs. (18) and (19):

$$[\sum X] = \sum_{i=1}^{4}(i\cdot[HgX_i^{(2-i)+}]) + [X^-] + [X\text{-}Hg^+\text{-P}] \quad (18)$$

$$[\sum Hg] = \sum_{i=1}^{4}[HgX_i^{(2-i)+}] + [Hg^{2+}] + [Hg^{2+}\text{-P}] + [X\text{-}Hg^+\text{-P}] \quad (19)$$

By combining Eqs. (12), (17), (18), and (19), the equation corresponding to Eq. (15) was derived; here [Hg^{2+}-P] and [X-Hg^+-P] were included, while K_{p1} and K_{p2} were calculated by the method of trial and error after having assigned arbitrary values to [Hg^{2+}-P] and [X-Hg^+-P]. The results obtained are shown in Table 6, while the mole fraction of the complexes is plotted against the mole ratio of halide to mercury in Fig. 2. Thus, the value of K_{p1} became independent of the kind and of the concentration of the halide. The value of K_{p1} obtained at pH 0.15 from Eq. (10) agreed approximately with those in Table 6; therefore, the values of K_{p2} for chloride and bromide were calculated using the values of K_{p1} at various pH values. The results obtained are shown in Table 7, while the mole fractions of the complexes are shown in Fig. 3. The data concerning K_{p2} and pH in Table 7 are shown as B and C in Fig. 1. From Fig. 1, the relationship between K_{p2} and pH is given by Eq. (20):

$$\log K_{p2} = \log K'_{p2} + \text{pH} \quad (20)$$

where the K'_{p2} values for chloride and bromide are 4.1×10^5 and 2.7×10^6 respectively.

The absorption spectra of mercuric perchlorate solutions are shown in Fig. 4; there are two isosbestic points among the curves (2), (3), (4), and (5).

The titration curves of mercuric perchlorate solutions in the presence and in the absence of chloride, bromide, and iodide are shown in Fig. 5.

Discussion

Since there were two isosbestic points in Fig. 4, the aquo complex seems to be more or less subject to hydrolysis at pH 2—7. The process of hydrolysis can be understood more precisely from the titration curves in Fig. 5. The amount of sodium hydroxide corresponding to $\overline{AB}$ in Fig. 5 is exactly equivalent to the amount of mercury(II) used in the experiment, and the hydrolysis of the aquo complex begins and ends at approximately pH 2. On the other

6) P. Brandt and O. Plum, *Acta Chem. Scand.*, **7**, 97 (1957).

7) L. G. Sillén, *ibid.*, **3**, 539 (1949).

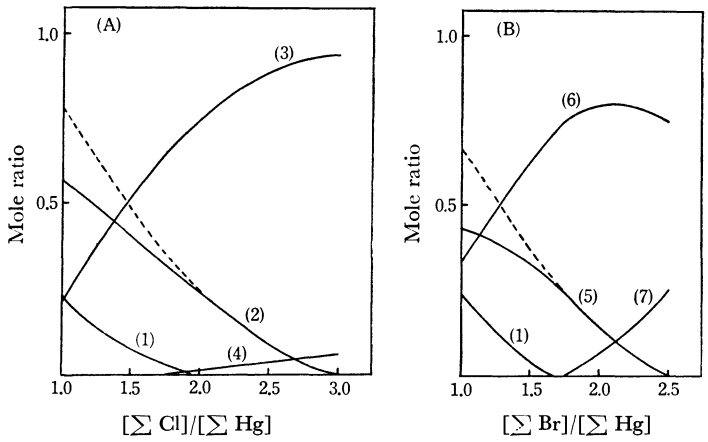

Fig. 2. Composition of the propylene-mercury system containing various amounts of halide; t=25°C, μ=0.8, [$HClO_4$]=0.7N
(A) Propylene-mercury-chloride system
(B) Propylene-mercury-bromide system
(1): [Hg^{2+}-P], (2): [Cl-Hg^{+}-P], (3): [$HgCl_2$], (4): [$HgCl_3^-$], (5): [Br-Hg^{+}-P], (6): [$HgBr_2$], (7): [$HgBr_3^-$]

Table 7. Formation constant (K_{p_2}) in the propylene-mercury(II)-halide system

t=25°C, P_{tot}=1 atm, μ=0.8, mole ratio: [∑X]/[∑Hg]=3

pH	K_{p_2}	
	Cl^-	Br^-
1	3.1×10^6	
2	1.6×10^7	
3	5.9×10^7	5.0×10^8
4	3.0×10^7	4.2×10^9
5		1.3×10^{10}

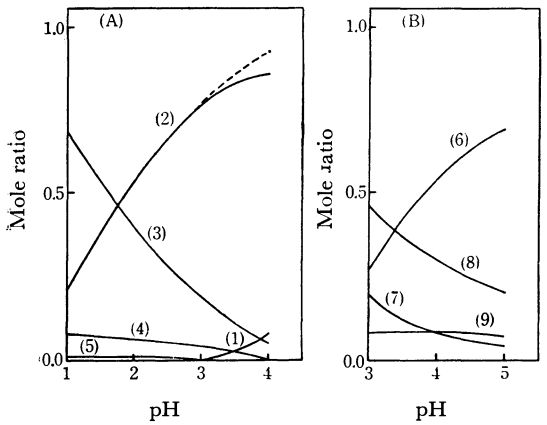

Fig. 3. Compostion of the proyplene-mercury system containing a definite amount of halide; t=25°C, μ=0.8, [∑ X]/[∑ Hg]=3, X^-: Cl^-, Br^-
(A) Propylene-mercury-chloride system
(B) Propylene-mercury-bromide system
(1): [Hg^{2+}-P], (2): [Cl-Hg^{+}-P], (3): [$HgCl_2$], (4): [Hg-Cl_3^-], (5): [$HgCl_4^{2-}$], (6): [Br-Hg^{+}-P], (7): [$HgBr_2$], (8): [$HgBr_3^-$], (9): [$HgBr_4^{2-}$]

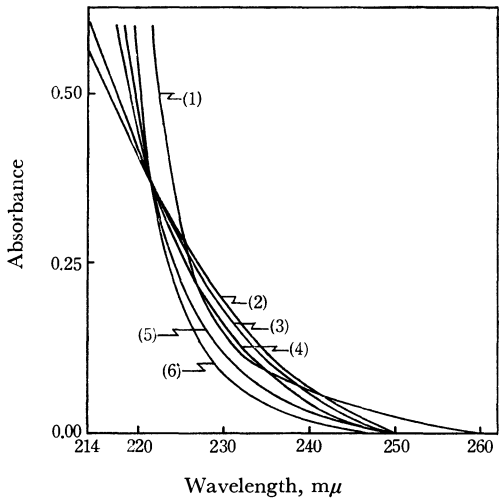

Fig. 4. Absorption spectra of mercuric perchlorate soltuions; t=25°C, μ=1, [∑Hg]=8×10^{-4} mol/l
(1): 1 normal solution, (2): pH=7, (3): pH=5, (4): pH=3, (5): pH=2, (6): pH=1

hand, the hydrolysis of the aquo complex in the presence of halide begins at pH>7, judging from the titration curves (2), (3), and (4). Since a precipitate was produced in the presence of iodide, no further analysis was carried out.

The values of the formation constant (at pH 0.15) shown in Table 1 are smaller than those of K_{p1} in Table 6 and the value of K_{p1} (4.4×10^5) at pH 0.15 as calculated by Eq. (10). This is probably because of the experimental error in the direct method, since the propylene-mercury complex was quite stable and the equilibrium was shifted remarkedly to the right-hand side of Eq. (1).

Eqation (10) is derived as follows. The propyl-

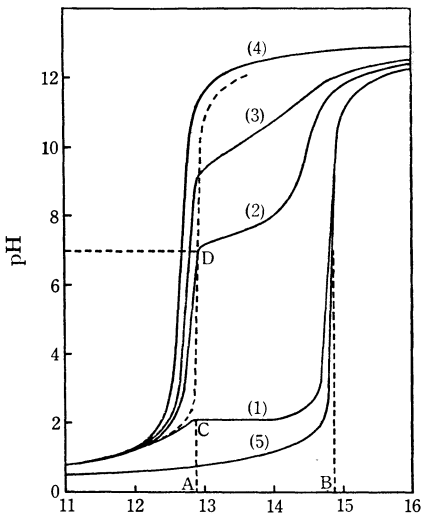

Fig. 5. Titration of mercuric perchlorate solutions; t=25°C, μ=1, [∑Hg]=5×10^{-2} mol/l, [∑X]/[∑Hg]=3, X$^-$: Cl$^-$, Br$^-$, I$^-$
(1): Mercuric perchlorate solution
(2): Solution containing chloride
(3): Solution containing bromide
(4): Solution containing iodide
(5): Perchloric acid solution

enemercury complex seems to undergo hydrolysis at pH 2—5 in accordance with Eq. (21):

$$Hg(OH_2)_2^{2+}\text{-}P \overset{k_1}{\rightleftharpoons} Hg(OH)_2\text{-}P + 2H^+ \quad (21)$$

$$k_1 = \frac{[Hg(OH)_2\text{-}P]\cdot[H^+]}{[Hg(OH_2)_2^{2+}\text{-}P]} \quad (22)$$

$$[Hg(OH)_2\text{-}P] = k_1\cdot[Hg(OH_2)_2^{2+}\text{-}P]\cdot[H^+]^{-2} \quad (23)$$

Since the Hg^{2+}-P in Eq. (8) is actually present as $Hg(OH)_2$-P, the K_{p3} in Eq. (8) is given by K_{p4}:

$$K_{p4} = \frac{[Hg\text{-}L^{2-}]\cdot[P]}{[Hg(OH)_2\text{-}P]\cdot[L^{4-}]} = \frac{[Hg\text{-}L^{2}]\cdot[P]\cdot[H^+]^2}{k_1\cdot[Hg(OH_2)_2^{2+}\text{-}P]\cdot[L^{4-}]} \quad (24)$$

Hence, Eq. (25) is obtained instead of Eq. (9):

$$K_{p1} = \frac{K_{EDTA}}{K_{p4}} = \frac{[Hg(OH_2)_2^{2+}\text{-}P]\cdot k_1}{[Hg^{2+}]\cdot[P]\cdot[H^+]^2} = K_{p1E}\cdot k_1\cdot[H^+]^{-2} \quad (25)$$

where $K_{p1E}=[Hg(OH_2)_2^{2+}\text{-}P]\cdot[Hg^{2+}]^{-1}\cdot[P]^{-1}$
Eqation (25) is then rewritten as Eq. (26);

$$\log K_{p1} = \log K_{p1E} + 2\cdot pH + \log k_1 \quad (26)$$

The K_{p1E} in Eq. (26) indicates the formation constant of the propylene-mercury(II) complex at very low pH values. On the other hand, the K'_{p1} in Eq. (10) indicates the intercept (pH=0) on the ordinate in Fig. 1. Therefore, the values of K_{p1E} and K'_{p1} may be expected to be approximately equal, and $\log k_1$, to be approximately zero. Therefore, Eqs. (10) and (26) become indentical.

Equation (20) is derived as follows. As can be seen form Fig. 5, the aquo complex in the presence of three times as many moles of halide as those of mercury is not subject to hydrolysis up to pH 7. However, the monohalogeno propylene mercuric complex seems to be more or less subject to hydrolysis and to stabilize in accordance with Eq. (27):

$$X\text{-}Hg(OH_2)^+\text{-}P \overset{K_e}{\rightleftharpoons} X\text{-}Hg(OH)\text{-}P + H^+ \quad (27)$$

$$K_e = \frac{[X\text{-}Hg(OH)\text{-}P]\cdot[H^+]}{[X\text{-}Hg(OH_2)^+\text{-}P]} \quad (28)$$

$$[X\text{-}Hg(OH)\text{-}P] = K_e\cdot[X\text{-}Hg(OH_2)^+\text{-}P]/[H^+] \quad (29)$$

Hence, Eq. (17) may be rewritten as Eq. (30):

$$K_{p2} = \frac{[X\text{-}Hg(OH)\text{-}P]}{[X\text{-}Hg^+]\cdot[P]} = \frac{[X\text{-}Hg(OH_2)^+\text{-}P]\cdot K_e}{[X\text{-}Hg^+]\cdot[P]\cdot[H^+]} = K'_{p2}\cdot K_e\cdot[H^+]^{-1} \quad (30)$$

$$\log K_{p2} = \log K'_{p2} + pH = \log K_e \quad (31)$$

Since the K_{p2} values in Eqs. (20) and (31) are identical and since the K'_{p2} values in Eqs. (20) and (31) are approximately equal, $\log K_e$ may be expected to be around zero. Therefore, Eqs. (20) and (31) become identical.

In the practical experiment of the propylene-mercury(II)-halide system, a definite amount of halide is added to the $Hg(OH)_2$-P, and the X-Hg(OH)-P is formed by the replacement of the hydroxyl group with the halide ion. The formation of the X-Hg(OH)-P is considered to proceed with an increase in the stability of the halogeno mercuric complex. This makes K_{p2} in Eq. (30) large and locates the K_{p2}(Br) line over the K_{p2}(Cl) line, as is shown in Fig. 1.

The results obtained are summarized in the following schematic diagram:
EDTA-Mercury(II)-Propylene system, assumed species:

Hg^{2+}-P, $Hg(OH)_2$-P, $Hg(OH^-)_n$ (n=0—2),
Hg-L^{2-}, $H_{5-i}L^{1-i}$ (i=1—4), P, L^{4-}.

$$\begin{array}{ccc} Hg^{2+} & \overset{K'_{p1}}{\underset{\pm P}{\rightleftharpoons}} & Hg^{2+}\text{-}P \\ K_{EDTA}\Big\uparrow\downarrow L^{4-} & & k_1\Big\uparrow\downarrow \pm 2H^+ \\ HgL^{2-} & \overset{K_{p4}}{\underset{\pm P}{\rightleftharpoons}} & Hg(OH)_2\text{-}P \end{array} \quad \left.\begin{array}{l} \\ \overset{K_{p1}}{\underset{\pm P}{\rightleftharpoons}} \ Hg(OH^-)_n \\ (n=0-2) \end{array}\right.$$

$$H_{5-i}L^{1-i} \overset{K_{ai}}{\underset{\pm H^+}{\rightleftharpoons}} H_{4-i}L^{i}$$

Halide-Mercury(II)-Propylene system, assumed species:

$Hg(OH^-)_n$ (n=0—2), Hg^{2+}-P, $Hg(OH)_2$-P, HgX_i^{2-i} (i=1—4), HgX(OH), X-Hg^+-P, X-Hg(OH)-P.

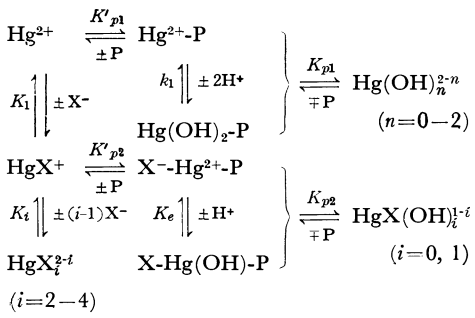

obtained equilibrium constants

$K_p = 2.2 \times 10^4$ (at pH 0.15)

$\log K_{p_1} = \log K'_{p_1} + 2 \cdot \mathrm{pH}$

$K'_{p_1} = 2.2 \times 10^5$

$\log K_{p_2} = \log K'_{p_2} + \mathrm{pH}$

$K'_{p_2} = 4.1 \times 10^5$ (for chloride)

$K'_{p_2} = 2.7 \times 10^6$ (for bromide)

BULLETIN OF THE CHEMICAL SOCIETY OF JAPAN VOL. 43 755—758 (1970)

Hydrodynamic Voltammetry with the Convection Electrode. IV. The Measurements of the Kinetic Parameters of the Electrode Reaction. Part II

Junsuke SUZUKI

Faculty of Education, Shizuoka University, 836, Oya, Shizuoka

(Received June 11, 1969)

The convection electrode system was applied to the determination of the kinetic parameters of the electrode reaction. By analyzing the observed current-voltage curve, the parameters of α and k° were calculated; for the ferric-ferrous system in 0.1M perchloric acid, α and k° were found to be 0.63 and 7.6×10^{-3} cm/sec respectively, while for the hexammine cobaltic-cobaltous system in 1M ammonia-ammonium chloride, they were 0.65 and 4.5×10^{-6} cm/sec respectively.

In the preceding paper[1] the convection electrode system with the rotating disk as a stirrer was applied to the measurement of the rate constant of the electrode reaction. The results were in good agreement with the published data.[2]

In investigating the kinetics of the electrode reaction using the voltammetry, the rate of mass transfer should be faster than that of electron transfer. At the present convection electrode the rate of mass transfer can be increased by increasing the tangential velocity of the rotating disk. That is, any reversible current-voltage curve can apparently be made irreversible due to such an increased mass transfer. Therefore, it is considered that the use of the convection electrode is very suitable for the determination of a moderately fast electron-transfer rate by voltammetry.

In the present investigation, the kinetic parameters for the Fe(III)-Fe(II) system in a 0.1M perchloric acid solution, and for the Co(III)-Co(II) system in an ammonia-ammonium chloride solution, will be measured, and good results will be obtained.

Experimental

Materials. All the chemicals used were of a chemically pure grade.

Electrodes and Apparatus. The electrode system and the apparatus were the same as had been described in a previous paper.[3] In the present investigation, the pretreatment of the platinum electrode was carried out as follows: the platinum electrode was oxidized anodically for 1 min at +1.5 V *vs.* SCE in 0.1M perchloric acid, and then 0 V *vs.* SCE was applied to it for 3 min in nitrogen-bubbled 0.1M perchloric acid.

Measurements. A Yanagimoto Polarograph, Model PA 102, was used for recording the current-voltage curve. A saturated calomel electrode was used as a reference electrode. An electrolytic solution was kept at 25 ± 0.1°C.

Results and Discussion

The Upper Limit of the Tangential Velocity of the Rotating Disk. It would be possible to determine the rate parameters of a moderately rapid electron-transfer process by increasing the

1) J. Suzuki, This Bulletin, **42**, 3487 (1969).

2) Y. Okinaka and I. M. Kolthoff, *J. Amer. Chem. Soc.*, **82**, 324 (1960).

3) J. Suzuki, *Rev. Polarog.* (Kyoto), **15**, 21 (1968).

mass transfer sufficiently, that is, by increasing the tangential velocity of the rotating disk. When the tangential velocity exceeds a certain value, however, the flow passing through the electrode changes from a laminar to a turbulent one. Since the relations derived in the previous paper[1] for the determination of the rate parameters can be applied only to the laminar flow, the tangential velocity of the rotating disk must be limited to the value below which the flow is kept laminar.

On the other hand, one can anticipate, from the value of dimentionless parameter, the Reynolds number (*Re*), whether or not the conditions of the flow passing over the electrode surface will be laminar. However, the critical *Re* value for the present convection electrode, the value at which the flow passing through the electrode changes from a laminar to a turbulent one, is not clear. Nevertheless, assuming that the condition of the flow passing over the convection electrode surface is similar to that of the flow passing through the rotating disk electrode,[4] the critical *Re* value at the convection electrode can be estimated to be of the order of 10^4.

Assuming a diameter of the convection electrode surface (working part plus shield) of 0.50 cm and the kinematic viscosity of an electrolytic solution of 10^{-2} cm^2/sec, the highest velocity for the laminar flow is found to be about 200 cm/sec; this corresponds to a tangential velocity of the rotating disk of about 500 cm/sec.

Upper Limit of the Rate Constant which can be determined. Under the initial condition of $C_R=0$, Eq. (12), which was derived in the preceding paper,[1] is transformed into this form:

$$i = \frac{i_l^c}{1+e^{\zeta}} \cdot \frac{A e^{-\alpha\zeta}(1+e^{\zeta})}{0.61+A e^{-\alpha\zeta}(1+e^{\zeta})} \qquad (1)$$

where:

$$\zeta = \frac{nF}{RT}(E-E_{1/2}^r) \qquad (2)$$

and:

$$A = k^\circ\left(\frac{f_O}{D_O^{2/3}}\right)^{1-\alpha}\left(\frac{f_R}{D_R^{2/3}}\right)^{\alpha}\left(\frac{v}{d}\right)^{-1/2}\nu^{1/6} \qquad (3)$$

Here, i_l^c is the cathodic limiting current; the other symbols have been identified in the preceding paper.[1]

Equation (1) is completely analogous to the general equation of the current-voltage curve, which was derived theoretically by Matsuda, for the reduction or oxidation process in polarography[5] and in voltammetry.[6]

According to the magnitude of k°, the characteristics of the current-voltage curve can be classified into three kinds:[1] (a) reversible, (b) quasi-reversible,[7] and (c) irreversible. The magnitude of k° corresponding to each of these cases can then be estimated, as is shown in Table 1.

Table 1. Characters of the current-voltage curve

Character	Magnitude of k°
Reversible	$>1.5\times10^{-2}(v/d)^{1/2}$
Quasi-reversible	$1.5\times10^{-2}(v/d)^{1/2}>k^\circ>1.3\times10^{-6}(v/d)^{1/2}$
Totally irreversible	$<1.3\times10^{-6}(v/d)^{1/2}$

Assuming $f_O=f_R=1$, $D_O=D_R=10^{-5}$ cm^2/sec, $\alpha=0.5$, and $\nu=10^{-2}$ cm^2/sec.

In order to determine the rate constant by analyzing the current-voltage curve, it is necessary in practice that the curve have a quasi-reversible or an irreversible character. Therefore, the upper limit of the rate constant, k°, which could be determined by the present hydrodynamic voltammetry is considered to be about 1.5×10^{-2} $(v/d)^{1/2}$ (*cf.* Table 1). On the other hand, the highest tangential velocity of the rotating disk, v, for the laminar flow is 500 cm/sec, as has been mentioned above. Consequently, the upper limit of the rate constant so determined can be estimated to be 0.47 cm/sec, when d is 0.50 cm.

Fe(III)-Fe(II) System in Perchloric Acid Media. It is well-known that the redox reaction of a ferric-ferrous system in a perchloric acid solution is a moderately fast one-electron transfer

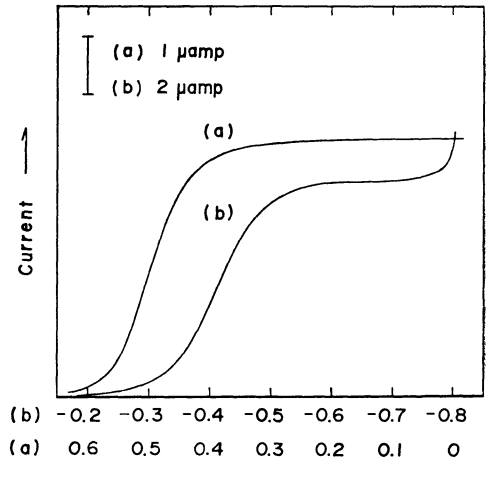

Fig. 1. The typical current-votage curves obtained by using the convection electrode.
(a) 3.72×10^{-4}M Fe^{3+} in 0.1M $HClO_4$
(b) 1×10^{-4}M $Co(NH_3)_6^{3+}$ in 1M NH_3+1M NH_4Cl

4) V. G. Levich, "Physicochemical Hydrodynamics," Prentice-Hall, Inc., Englewood Cliffs, N. J. (1962), p. 71.

5) H. Matsuda and Y. Ayabe, This Bulletin, **28**, 422 (1955).

6) H. Matsuda, *J. Electroanal. Chem.*, **15**, 109 (1967).

7) P. Delahay, *J. Amer. Chem. Soc.*, **75**, 1430 (1953).

process.

The current-voltage curves for the reduction of a ferric ion in absence of a ferrous ion were recorded at the tangential velocities of the rotating disk ranging from 62.8 to 188.4 cm/sec. A typical current-voltage curve thus obtained is shown in Fig. 1.

The rate constant of electron transfer can be evaluated only when the observed current-voltage curve shows a sufficient deviation from a reversible character. Such deviation can be most easily checked by means of the following equation:[8]

$$E_{3/4} - E_{1/4} = \frac{0.059}{n} \text{ V} \qquad (4)$$

where $E_{3/4}$ and $E_{1/4}$ are the potentials at the three-quarter and at the one-quarter limiting currents respectively. That is, if the current is controlled only by mass transfer, the difference between the potentials at $E_{3/4}$ and $E_{1/4}$ on the observed current-voltage curve equals $(0.059/n)$ V. In the present case, this difference was evaluated as 81 mV from Fig. 1 at the tangential velocity of the rotating disk of 188.4 cm/sec.

From the observed current-voltage curve at the tangential velocity of 188.4 cm/sec, a series of values of the rate constants, k_R, at the applied potential, E, were calculated by using Eq. (5), which was itself obtained by rearranging the Eq. (13) derived in the preceding paper.[1] Then the plots of log k_R *vs.* $(E-E^\circ)$ were made for each current-voltage curve.

$$k_R = k^\circ \exp\left[\alpha(E^\circ - E)n\boldsymbol{F}/\boldsymbol{R}T\right] = \frac{1}{\frac{i_l{}^c - i}{i} \cdot \frac{f_O}{m_O} - \frac{f_R}{m_R} \exp\left[(E-E^\circ)n\boldsymbol{F}/\boldsymbol{R}T\right]} \qquad (5)$$

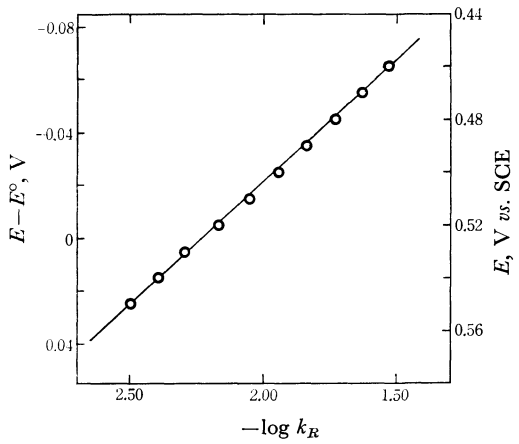

Fig. 2. The plots of log k_R *vs.* E.
Concentration of Fe^{3+}: 3.72×10^{-4}M in 0.1M $HClO_4$
Tangential velocity of rotating disk: 188.4 cm/sec

where m is the mass transfer coefficient.[3,9,10] A typical plot is shown in Fig. 2.

As was predicted by Eq. (5), a linear relation between log k_R and $(E-E^\circ)$ was obtained. Therefore, the slope of this line equals 2.303 $\boldsymbol{RT}/\alpha n$ and the intercept at $E=E^\circ$ equals (2.303 $\boldsymbol{RT}/\alpha n$) log k°. The rate parameters obtained are given in Table 2.

Table 2. Kinetic parameters for Fe(III)-Fe(II) system in 0.1M perchloric acid

k°, cm/sec	α	Ref.
$(7.6\pm1.5)\times10^{-3}$	0.63 ± 0.02	this work
$(1.1\pm0.2)\times10^{-2}$	0.78 ± 0.04	10)
5.3×10^{-3}	—	11)*

* In 1.0M perchloric acid.

The value of k° obtained is considered to be reliable on the basis of a comparison with the results of Jordan and Javick,[10] and of Randles and Somerton.[11]

Co(III)-Co(II) System in Ammonium Buffer Media. It is well-known that ammine complexes of cobalt(III) are inert, and those of cobalt(II), labile. The heterogeneous electroreduction of hexammine cobaltic salts has already been investigated in detail by several workers.[12-15] The results showed that the character of the electrode reaction of cobaltic to cobaltous species is a totally irreversible process, followed by a chemical reaction. This mechanism may be shown as follows:

$$Co(NH_3)_6^{3+} + e \xrightarrow{\text{irrev.}} Co(NH_3)_6^{2+} \qquad (6)$$

$$Co(NH_3)_6^{2+} \overset{\text{fast}}{\rightleftharpoons} \sum_{n=0}^{6} Co(NH_3)_{6-n}^{2+} \qquad (7)$$

The proportions of the complexes with various n values in Reaction (7) depend upon the concentration of free ammonia in the supporting electrolyte solution.

Because the electron transfer step of Reaction (6) is totally irreversible,[14,16,17] the succeeding

8) Z. Galus and R. N. Adams, *J. Phys. Chem.*, **67**, 866 (1963).

9) J. Jordan, *Anal. Chem.*, **27**, 1708 (1955).

10) J. Jordan and R. A. Javick, *Electrochim. Acta*, **6**, 23 (1962).

11) J. E. B. Randles and K. W. Somerton, *Trans. Faraday Soc.*, **48**, 937 (1952).

12) J. B. Willis, J. A. Friend and D. P. Mellor, *J. Amer. Chem. Soc.*, **67**, 1680 (1945).

13) H. A. Laitinen, J. C. Bailar, H. F. Holtzclan and J. V. Quagliano, *ibid.*, **70**, 2999 (1948).

14) H. A. Laitinen and P. Kivalo, *ibid.*, **75**, 2198 (1953).

15) N. Maki, Y. Shimura and R. Tsuchida, This Bulletin, **32**, 23 (1959).

16) A. A. Vlcek, "Proceedings of the Sixth International Conference on Coordination Chemistry," Macmillan, New York (1961), pp. 509—603.

17) L. N. Klatt and W. J. Blaedel, *Anal. Chem.*, **39**, 1065 (1967).

chemical reaction of Reaction (7) has no effect upon the reduction step of hexammine coblat(III) ions. Therefore, the rate constant for the heterogeneous electrode reaction of hexammine cobalt-(III) can be evaluated using the same equation as that used for an ordinary totally irreversible process.[1)]

The kinetics of the electrode reaction of the hexammine cobalt(III) ion in 1 M ammonia-ammonium chloride was investigated by using a convection electrode. A typical current-voltage curve for the reduction of hexammine cobalt(III) is shown in Fig. 1.

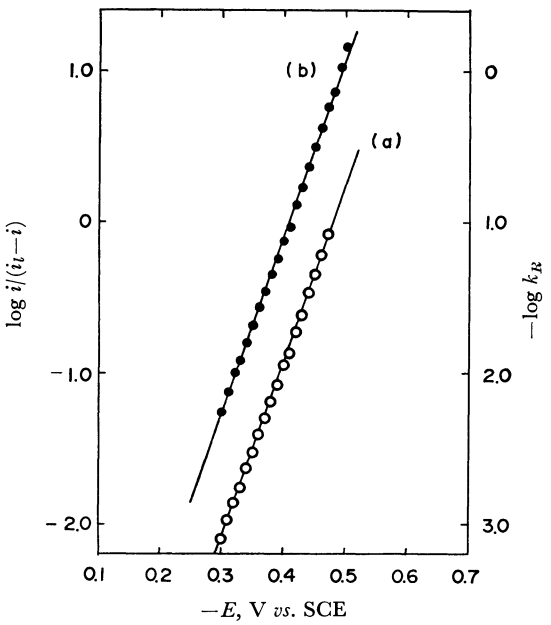

Fig. 3. The polts of $\log k_R$ *vs.* E and of $\log i/(i_l-i)$ *vs.* E.
(a) Plots of $\log k_R$ *vs.* E, (b) Plots of $\log i/(i_l-i)$ *vs.* E. Concentration of $Co(NH_3)_6^{3+}$: 1×10^{-4} M in 1 M NH_3+1 M NH_4Cl. Tangential velocity of the rotating disk: 188.4 cm/sec

The values of the rate constant, k_R, can be calculated from the i/i_l ratio at various potentials on the current-voltage curve. Figure 3 shows the plots of $\log k_R$ *vs.* E and of $\log i/(i_l-i)$ *vs.* E; both plots give straight lines. The kinetic parameters, α and k°, can be estimated from Fig. 3.

The former was calculated from the slope of line (a) or line (b), and the latter, from the intercept at the standard potential, E°, to line (b). The standard potentials of the hexammine cobaltic-cobaltous couple were calculated from Latimer's data[18)] as -0.100 V *vs.* SCE. They are summarized in Table 3.

Table 3. Kinetic parameters for $Co(NH_3)_6Cl_3$ system in 1 M NH_3+1 M NH_4Cl

Tangential velocity v, cm/sec	α	k° $\times10^{-6}$ cm/sec
94.2	0.67±0.01	5.0±0.4
125.6	0.65±0.02	5.5±0.8
157.0	0.64±0.02	3.5±0.5
188.4	0.65±0.02	4.1±0.2
Average	0.65	4.5

The values of the kinetic parameters obtained at the convection electrode are in good agreement with those in a previously-published paper,[17)] in which the parameters of α and k° are 0.61 and 6×10^{-6} cm/sec respectively in 1 F ammonia-ammonium chloride; these values were obtained by using the tubular platinum electrode.

The author wishes to express his thanks to Professors Nobuyuki Tanaka of Tohoku University and Tokuro Ozaki of Shizuoka University for their helpful discussion, and to Misses Mihoko Imura and Junko Takashima for their earnest assistance.

18) W. M. Latimer, "Oxidation Potential" 2nd Ed., Prentice-Hall, New York (1952), p. 214.

BULLETIN OF THE CHEMICAL SOCIETY OF JAPAN VOL. 43 759—763 (1970)

The Reaction between Mercury(II) and Organic Compounds. VIII. Titrimetric Determination of Mercury(II) with *o*-(2-Thiazolylazo)-2,4-dichlorophenol as a Metallochromic Indicator

Fumiaki KAI

Department of Chemistry, Faculty of Science, Kumamoto University, Kurokami-machi, Kumamoto

(Received June 20, 1969)

The reaction between mercury(II) and *o*-(2-thiazolylazo)-2,4-dichlorophenol (TADC) was investigated spectrophotometrically. A mixture containing TADC and a large excess of mercury(II) showed the absorption maxima in the range of pH 2.3—5.0 at 570 mμ. The composition of the chelate was considered to be as Hg(II) : TADC=1 : 2. No homologous color was obtained by the reaction between TADC and the other metal ions in the above pH range. Therefore, TADC was suggested as a suitable metallochromic indicator for the direct titrimetric determination of mercury(II) ions with EDTA at pH 3.8—5 (citric acid plus disodium hydrogenphosphate buffer). Sharp color changes were observed from deep violet to orange or to reddish orange at an equivalence point. The titrimetry could be carried out satisfactorily within a range of error of ±0.5% at mercury(II) concentrations of more than 2×10^{-4}M by the present method.

The stability constants of the complexes formed between the *o*-(2-thiazolylazo)-phenols and mercury(II) and the availability of these reagents as chromogenic or spectrophotometric reagents for the determination of mercury(II) were reported previously.[1-3]

In the present paper, the reactivity of mercury(II) ions with *o*-(2-thiazolylazo)-2,4-dichlorophenol (TADC) was studied spectrophotometrically, and the applicability of TADC as a chromogenic reagent for the determination of mercury(II) ions was examined. In previous papers[1-3] it was reported that titrimetric determinations of mercury(II) ions using *o*-(2-thiazolylazo)-cresol (TAC),[1] *o*-(2-thiazolylazo)-4-methoxyphenol (TAM)[2] and *o*-(2-thiazolylazo)-4-chlorophenol (TACL)[3] as indicators were carried out in a weakly alkaline medium in all cases. As for the titrimetry using TADC as a metalloindicator, the optimum pH range was found to be 3.8—5. (This range was wider than those of Cu-PAN (pH 3—3.5),[4] XO (pH 6),[5] and MTB (pH 6).[6]) Therefore, there was no trouble in precipitating mercury(II) oxide in this acidic medium; thereby a considerably larger amount of mercury(II) ions than those reported in previous papers[1-3] could be determined accurately. Sharp color changes, *i. e.*, from deep violet to orange or to reddish orange, were observed at equivalence points. Except for a few anions and nickel(II), there were no interfering ions. Accordingly, TADC was also considered to be as a suitable metallochromic indicator as TAC, TAM and TACL for the direct titrimetric determination of mercury(II) ions with EDTA in an acidic medium.

Experimental

Preparation of TADC. TADC was prepared according to the method in the literature.[7] Several recrystallizations were repeated from hot ethanol. This crystals were obtained in a yield of 18%; mp 112—116°C (decomp.). Found: C, 40.04; H, 1.90; N, 14.65%. Calcd for $C_9H_5N_3OSCl_2$: C, 39.44; H, 1.84; N, 14.65%. IR: 3420 cm^{-1} (νO–H); 3100 cm^{-1} (νC–H of phenyl); 1248 cm^{-1} (δO–H); 1170 cm^{-1} (νC–O) and 730 cm^{-1} (νC–Cl).

Buffer Solutions. Buffer solutions with definite pHs were prepared by properly mixing 0.1M citric acid and 0.1M disodium hydrogenphosphate solutions.

The methods of purifying dioxane and of preparing a solution of the EDTA titrant and a stock solution of mercury(II) were the same as those described previously.[1-3]

Instruments. The absorption spectra were obtained with a Hitachi recording spectrophotometer (EPS-2) and a Hitachi electric spectrophotometer (EPU-2) with 10-mm silica cells. The infrared spectrum was obtained using an infrared spectrometer (DS-403G, Japan spectro-

1) F. Kai, *Anal. Chim. Acta*, **44**, 129 (1969).
2) F. Kai, *ibid.*, **44**, 242 (1969).
3) F. Kai, This Bulletin, **42**, 2250 (1969).
4) H. Flaschka and H. Abdine, *Chemist-Analyst*, **45**, 58 (1956).
5) H. Körbl, R. Pribil and A. Emf, *Chem. Listy*, **50**, 1440 (1956).
6) H. Körbl, R. Pribil and A. Emf, *ibid.*, **51**, 1061 (1957).
7) A. Kawase, *Bunseki Kagaku*, **11**, 621 (1962).

scopic Co., Ltd.). The pH was measured with a glass electrode pH meter (Hitachi-Horiba, F-5).

Results and Discussion

Acid Dissociation Constant of TADC in a 10% v/v Dioxane-Water Solution. The dissociation scheme of TADC is as follows:

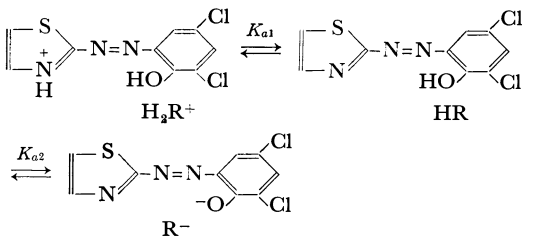

The constants were obtained spectrophotometrically. If the acid dissociation constants are given by:

$$K_{a1} = \frac{[HR][H^+]}{[H_2R^+]} \text{ and } K_{a2} = \frac{[R^-][H^+]}{[HR]} \quad (1)$$

then the second step of the dissociation could be given as:

$$pK_{a2} = pH - \log \frac{A - \varepsilon_{HR}C_R}{\varepsilon_R - C_R - A} \quad (2)$$

where A is the total absorbance; C_R, the analytical concentration of TADC, and ε_x, the molar absorptivity of the species x.

The molar absorptivity was calculated from the horizontal lines of the pH-absorbance plots.

The absorption spectra of TADC scanned over pH 4.8—6.45 are illustrated in Fig. 1. There is an isosbestic point at 463 mμ, and the absorption maximum appears at 505 mμ. At higher pH values than 4.7 it is red or orange.

Though the figure is not given, the absorption curves in the range of pH 3.3—4.7 also showed the absorption maxima near 500 mμ, in accordance with the increasing pH values, but they have no isosbestic point at 463 mμ. The pK_{a2} value, therefore, was calculated from the absorbance at 505 mμ between pH 4.8 and 6.45 having the isosbestic point at 463 mμ, by means of Eq. (2). As a result, the second acid dissociation constant, pK_{a2}, was obtained as 5.3_8 in 10% v/v dioxane-water at μ=0.1 (KNO_3) and at room temperature. This value was, of course, lower than that of the mono-chloro derivative,[3] but was almost the same as that obtained in 20% v/v dioxane-water.[7]

The first step acid dissociation constant, pK_{a1}, was not estimated precisely because it was considered to be at a pH$<$0 value.

Absorbances and Absorption Spectra of the Mercury(II)-TADC Chelate in a Dioxane-Water Solution. A mixture of a large excess of mercury(II) and TADC was a clear violet. The maximum absorbance was obtained when the solution was prepared by mixing mercury(II) of 50-fold against TADC at pH 4.15 (Fig. 2). Figure 3 shows the absorption spectra of this mixture at various pHs, using water as the reference. In the pH range 2.3—5.0, the spectra showed an isosbestic point at 450 mμ and the absorption maxima at 570 mμ. The maxi-

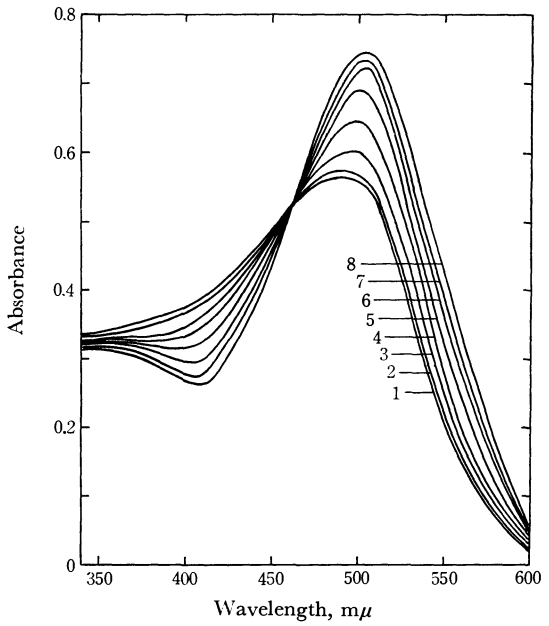

Fig. 1. Absorption spectra of TADC in 10% (v/v) dioxane-water at various pH values.
TADC=8×10^{-5}M; μ=0.1 (KNO_3); room temp.; Ref.=water.
pH: 1=4.80; 2=5.04; 3=5.26; 4=5.50; 5=5.73; 6=6.01; 7=6.26; 8=above 6.45

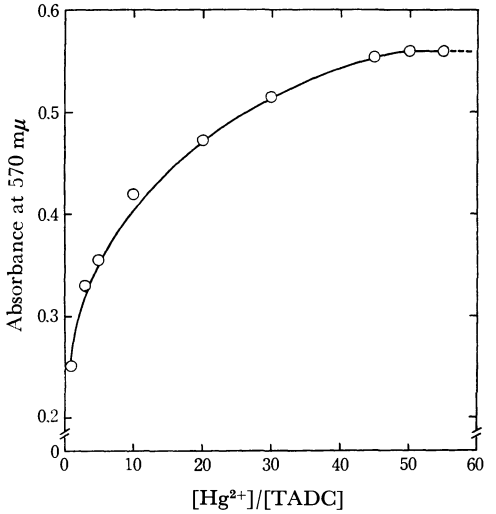

Fig. 2. Absorbances of TADC solutions with increasing mercury(II) concentration in 10% (v/v) dioxane-water at pH 4.15.
[TADC]=1×10^{-4}M; μ=0.1 (KNO_3); room temp.; Ref.=water

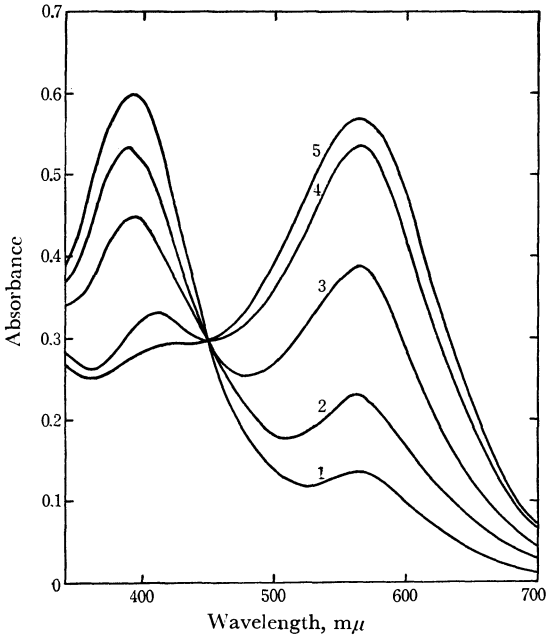

Fig. 3. Absorption spectra of TADC solutions in the presence of excess of mercury(II) at various pH.
10% dioxane; μ=0.1 (KNO_3); room temp.; Ref.=water; TADC=10^{-1}M; Hg(II)=5×10^{-3}M.
pH: 1=2.29; 2=2.78; 3=3.35; 4=4.16; 5=5.03

mum molar absorptivity obtained from Fig. 3 was 11000; this was calculated by assuming the composition of the chelate to be mercury(II) : TADC=1 : 2. No discoloration was observed for 24 hr. Thus, it was suggested that TADC could by used as a suitable metallochromic indicator for the direct titration of mercury(II) ions in an acidic medium.

The absorption spectra of the mixtures containing equimolar solutions could not be scanned because precipitation tended to occur in a 10% v/v dioxane-water solution.

The pH adjustments in all the solutions described above were made with a citric acid and disodium hydrogenphosphate buffer system because the characteristic violet colour of the chelate was shown only when the pH adjustment was made with this buffer, whereas with other buffer systems, *e. g.*, a phosphate system and an acetic acid and sodium acetate system, the colour was not violet, but orange or reddish orange being considered to be a color due to a free reagent at those pHs. The reason of this phenomenon can not be explained.

Compositions of the Chelate. In order to examine the composition of the chelate, continuous variation plots at pH 4.50 and mole-ratio plots at pH 4.00 were made. In the case of continuous variation, the total concentration of mercury(II) plus TADC, and in the case of the mole ratio, the mercury(II) concentration, was kept constant at 10^{-4}M. The results are shown in Fig.4. As is

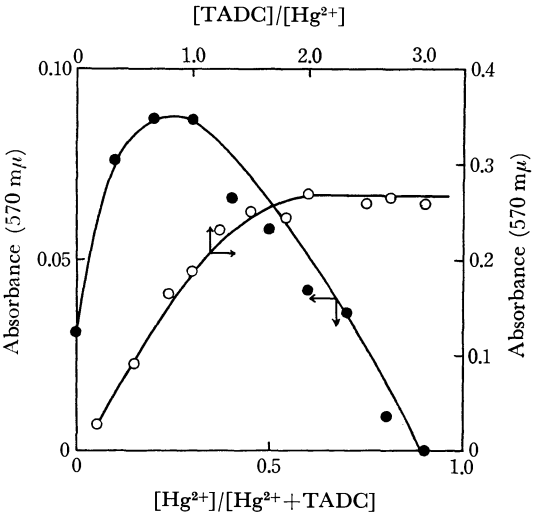

Fig. 4. Composition of the Hg(II)-TADC chelate.
—●— continuous variation. [Hg^{2+}+TADC]=1×10^{-4}M; pH=4.50.
—○— mole ratio. [Hg^{2+}]=1×10^{-4}M; pH=4.00.
10% (v/v) dioxane-water; μ=0.1 (KNO_3); room temp.; Ref.=water

shown in this figure, mercury(II) probably forms only a 1 : 2 chelate with TADC, regardless of the pH value. Moreover, the round refraction points of these plots suggest that the chelate is unstable.

Photometric Titration Curve. Photometric titrations at various pHs were carried out. The concentration of mercury(II) was 10^{-2}M, and several drops of alcoholic TADC solution (*ca.* 10^{-2}M) was added to the sample solution. A deep violet solu-

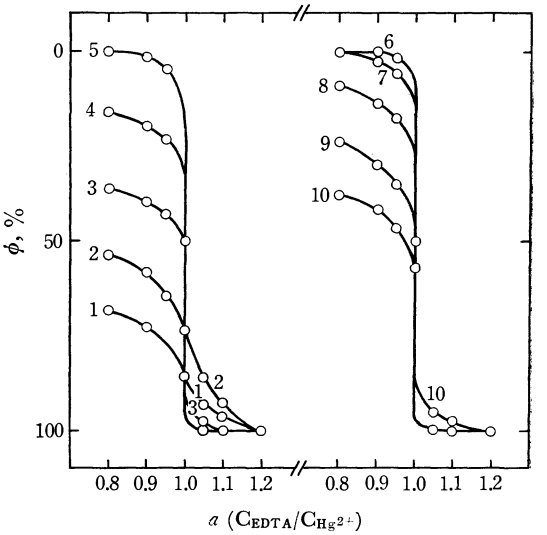

Fig. 5. Photometric titration curves.
$C_{Hg^{2+}}=10^{-2}$M; 10^{-1}M EDTA; Citric acid+Na_2HPO_4 buffer soln.
pH: 1=2.60; 2=2.90; 3=3.20; 4=3.59; 5=3.82; 6=4.49; 7=4.99; 8=5.51; 9=6.00; 10=6.50

tion was thus obtained. The concentration of the aqueous EDTA titrant was 10^{-1}M. The ϕ values were checked by means of the absorbances at 570 mμ. As can be seen in Fig. 5, in the pH range 3.8—5, sharp color changes, *i. e.*, from deep violet to orange or to reddish orange, were observed at the equivalence point. At the other pH values tested, color changes were observed before the equivalence point. In the pH 2.6—3.2 range and at 6.5, a tailing of the color change after the equivalence point was observed. The optimum pH range for the titration, therefore, was pH 3.8—5. This pH range was wider than that of such other indicators as Cu–PAN,[4] XO,[5] and MTB[6] used in acidic media.

Detectable Limit of Mercury(II). The detectable limit of the mercury(II) concentration by the titrimetry using TADC as the indicator was determined by checking the recoveries of mercury(II) ions at pH 4.50. Table 1 shows that there were

Table 1. Recovery of mercury(II) at various concentration at pH 4.50

Taken mg as Hg^{2+}/100 m*l*	Found mg as Hg^{2+}/100 m*l*	Error %
1.35	1.11	−10.4
2.26	2.36	+ 4.6
2.74	2.71	− 1.0
5.61	5.58	− 0.5
88.17	88.43	+ 0.3
104.90	104.79	− 0.1
250.30	251.30	+ 0.4
366.42	367.89	+ 0.4
487.19	485.73	− 0.3

large errors at concentrations of mercury(II) up to 2.74 mg/100 m*l* (corresponding to *ca.* 10^{-4}M as Hg(II)). These large errors can, for the reason mentioned in Fig. 2, be attributed to the weak color intensity of the chelate, which results in an uncertainty of color changes at the equivalence point. On the other hand, small errors within an accuracy range of $\pm 0.5\%$ were given at concentrations of more than 5.61 mg/100 m*l* (corresponding to *ca.* 2×10^{-4}M). Because of the lesser hydrolytic property of mercury(II) owing to an acidic media, the concentration of mercury(II) ions being determined was considerably higher than those*1 reported previously for TAC, TAM, and TACL.

Effect of Diverse Ions. An interference study was carried out. The depressions of the absorbances at 570 mμ were checked after the titration of aqueous sample solutions containing various amounts of diverse ions with an EDTA titrant (10^{-2}M). A 100 m*l* portion of the sample solution (10^{-3}M as Hg(II) ions) was kept at pH 4.5. The results are listed in Table 2. Negative errors were given by anions which form complex ions with mercury(II), whereas positive errors were given by metal ions forming complexes with the EDTA titrant. Cyanide, thiocyanate, ammonium, and halide, except when there is an excess of chloride, gave negative errors. As to metal ions, a large positive error was given by nickel(II) because the Ni(II)–TADC chelate showed an analogous violet color to that of the Hg(II)–TADC chelate at this pH. A 3 mg of cobalt(II), a 5 mg of iron(II) and a 10 mg of cadmium(II) gave small positive

Table 2. Effects of diverse ions (100 m*l* of 10^{-3}M mercury(II)), pH=4.50

Ion	Added amounts as ion, mg	Recovery of mercury(II), %	Error %
Cl^-	5.0	100.0	0.0
	10.0	100.1	+ 0.1
	20.0	100.0	0.0
Br^-	0.5	98.6	− 1.4
	1.0	91.1	− 8.9
I^-	0.5	93.5	− 6.5
	1.0	90.7	− 9.3
CN^-	0.5	96.9	− 5.1
	1.0	89.9	−10.1
SCN^-	0.1	99.1	− 0.9
	0.5	91.5	− 8.5
NH_4^+	5.0	99.8	− 0.2
	10.0	98.9	− 1.1
Ag^+	15.0	100.0	0.0
Cu^+	10.0	100.2	+ 0.2
Ca^{2+}	10.0	100.0	0.0
Sr^{2+}	10.0	99.9	− 0.1
Ba^{2+}	10.0	100.1	+ 0.1
Mn^{2+}	10.0	99.9	− 0.1
Fe^{2+}	5.0	100.3	+ 0.3
	10.0	105.5	+ 5.5
Co^{2+}	3.0	103.4	+ 3.4
	8.0	103.9	+ 3.9
Ni^{2+}	1.0	102.8	+ 2.8
	5.0	109.2	+ 9.2
Cu^{2+}	10.0	99.9	− 0.1
Zn^{2+}	10.0	100.1	+ 0.1
Cd^{2+}	5.0	100.2	+ 0.2
	10.0	101.0	+ 1.0
	15.0	104.4	+ 4.4
Pb^{2+}	10.0	100.0	0.0
Al^{3+}	10.0	100.0	0.0
Cr^{3+}	10.0	99.9	− 0.1
Fe^{3+}	10.0	100.0	0.0

Metal ions were added as nitrate.

*1 In previous papers[1-3] it was reported that the detectable limit was restricted to concentrations below 10^{-2}M, because hydrolysis of mercury(II) is likely to occur at concentrations higher than 10^{-2}M, as a result of the weakly alkaline media.

errors. However, no interference was caused by the presence of silver(I), copper(I), calcium(II), strontium(II), barium(II), manganese(II), lead(II), aluminum(III), chromium(III), and iron(III) ions up to 10 mg. Iron(III) ions seem generally to give a positive error, for the formation constant of FeY ($\log K_{FeY}=25.1$) is larger than that of HgY ($\log K_{HgY}=21.8$). However, there was no error by iron(III) ions in this experiment. It seems reasonable to assume that iron(III) forms, with the citric acid used as the buffer solution, a stable chelate whose formation constant ($\log K_{Fe-citr.}=25.0$[8]) is larger than that of the iron(III)-EDTA chelate.

The titration could be carried out accurately without heating the sample solution.

The above observations demonstrate that TADC can be utilized as a metallochromic indicator of mercury(II) with as high a sensitivity and accuracy as TAC, TAM, and TACL.

The author wishes to thank Professor Daisei Yamamoto of Kumamoto University for his encouragement throughout the work. The author's thanks are also due to the Ministry of Education for its financial support.

8) R. C. Warner and I. Weber, *J. Amer. Chem. Soc.*, **75**, 5086 (1953); R. E. Hamm, C. M. Shull and D. M. Grant, *ibid.*, **76**, 2111 (1954).

BULLETIN OF THE CHEMICAL SOCIETY OF JAPAN VOL. 43 763—769 (1970)

Kinetics of the Ligand Substitution Reaction of the Cobalt(II)-(Ethylene glycol)bis(2-aminoethyl ether)-*N*,*N*,*N*′,*N*′-tetraacetate Complex with 4-(2-Pyridylazo)resorcinol

Shigenobu FUNAHASHI and Motoharu TANAKA

Laboratory of Analytical Chemistry, Faculty of Science, Nagoya University, Chikusa-ku, Nagoya

(Received July 10, 1969)

The kinetics of the ligand substitution reaction of the cobalt(II)-(ethylene glycol)bis(2-aminoethyl ether)-*N*,*N*,*N*′,*N*′-tetraacetate complex (Co(II)-EGTA) with 4-(2-pyridylazo)resorcinol (PAR) have been studied photometrically in the pH range 8—9.4 at an ionic strength of 0.1 and at 25°C. The reaction proceeds simultaneously through two different reaction paths. Thus the rate law can be written as

$$\frac{d[CoR_2^-]}{dt} = k_1[CoY^{2-}][HR^-] + k_2[CoHY^-][HR^-]$$

where Y^{4-} and R^{2-} refer to tetravalent EGTA and divalent PAR respectively. Rate constants, k_1 and k_2 are $3.2 M^{-1}sec^{-1}$ and $2.1\times10^4 M^{-1}sec^{-1}$. Possible mechanism for the substitution is discussed. The stability constants for mercury(II)-EGTA complexes and cobalt(II)-EGTA complexes are determined by the mercury electrode method at $\mu=0.1$ and 25°C in order to analyze the substitution reaction: $K_{HgY}=10^{23.86\pm0.10}$, $K^H_{HgHY}=10^{3.06\pm0.10}$, $K_{CoY}=10^{12.3\pm0.1}$, $K^H_{CoHY}=10^{4.9\pm0.1}$, $K^H_{CoH_2Y}=10^{3.3\pm0.3}$.

In a previous paper,[1] the ligand substitution reaction of the zinc(II)-4-(2-pyridylazo)resorcinol complex (Zn(II)-PAR) with (ethylene glycol)-bis(2-aminoethyl ether)-*N*,*N*,*N*′,*N*′-tetraacetic acid (EGTA) has been reported. The reaction was found to proceed, under the experimental conditions, through one path involving predissociation equilibrium of the Zn(II)-PAR complex. The rate constants were determined and the possible mechanism was discussed.

Since it seemed worth while to extend the study to the substitution reaction involving the other metal ion, the ligand substitution reaction of the cobalt(II)-(ethylene glycol)bis(2-aminoethyl ether)-*N*,*N*,*N*′,*N*′-tetraacetate complex with 4(-2-pyridylazo)resorcinol:

$$\text{Co-EGTA} + \text{PAR} \rightleftharpoons \text{Co-PAR} + \text{EGTA} \quad (1)$$

was undertaken, where EGTA and PAR represent (ethylene glycol)bis(2-aminoethyl ether)-*N*,*N*,*N*′,*N*′-tetraacetic acid and 4-(2-pyridylazo)resorcinol respectively, and are abbreviated as H_4Y (hexadentate) and H_2R (tridentate) respectively. This paper gives the results.

1) M. Tanaka, S. Funahashi and K. Shirai, *Inorg. Chem.*, **7**, 573 (1968).

Experimental

Reagents. *Cobalt(II) Perchlorate.* The reagent grade cobalt(II) chloride was recrystallized twice from distilled water. The recrystallized cobalt(II) chloride was then dissolved in perchloric acid, and hydrochloric acid and excess perchloric acid were expelled by an infrared lamp. The cobalt(II) perchlorate was recrystallized further from distilled water. The concentration of cobalt(II) ion was determined by a standard EDTA solution using xylenol orange as an indicator.

Mercuric Perchlorate. Mercuric perchlorate was prepared from mercuric nitrate by the same method as that for cobalt perchlorate. The solution was standardized against a standard EDTA solution using Erio T as an indicator.

Methods of preparation of all other reagents have been described previously.[1)]

Apparatus. The following instruments were used: a Horiba Model P pH meter; a Sharp Model TEB-10 thermoelectric circulating bath; a Beckman Model DU spectrophotometer with a thermostated cell compartment; a Jasco Model ORD/UV-5 optical rotatory dispersion recorder.

Determination of the Stability Constants of Cobalt(II)-EGTA Complexes. It is necessary to determine the stability constants of cobalt(II)-EGTA complexes in connection with the kinetic study of the substitution reaction. These stability constants were determined at ionic strength $\mu=0.1$ (sodium perchlorate) and 25°C.

Procedure of Measurements of Potential and pH. Potentials were measured by pH meter with the J shape tube mercury electrode using a saturated calomel electrode as a reference electrode. The latter was jacketted with a tube containing 1M potassium nitrate solution in order to avoid contamination of chloride ion. The pH was varied by the dropwise addition of carbonate-free sodium hydroxide or perchloric acid in an atmosphere of nitrogen.

Calculation of Stability Constants of Mercury-(II)-EGTA Complexes. The potential of a mercury electrode at 25°C is given by the following equation:

$$E = E^{\circ}_{Hg} + 0.0296 \log [Hg^{2+}]. \quad (2)$$

The value of the standard potential, E°_{Hg}, of the mercury electrode has been given by Latimer[2)] as 0.612 V *vs.* saturated calomel electrode at 25°C. The conditional stability constant, K'_{HgY}, of the mercury(II)-EGTA complex was determined from potential of the mercury electrode in a solution containing free EGTA and mercury(II)-EGTA complex. The potential is given by the relationship:

$$E = E^{\circ}_{Hg} + 0.0296 \log \frac{[HgY^{2-}]\alpha_{H(Y)}}{[Y']K'_{HgY}}, \quad (3)$$

where $[Y']=[Y^{4-}]\alpha_{H(Y)}$ and $\alpha_{H(Y)}$ is the side reaction coefficient taking into account the protonation of Y^{4-}. $K'_{HgY}=[HgY']/[Hg^{2+}][Y^{4-}]$ and [HgY'] refers to the total concentration of normal and protonated complexes of mercury(II)-EGTA. As the concentration of EGTA added is about twice that of mercury ion added and the stability constant of mercury(II)-EGTA is very high, the following relationships hold with a good approximation:

$$[HgY'] = C_{Hg}, \quad [Y']=C_Y-C_{Hg}, \quad (4)$$

where C_{Hg} and C_Y are the total concentrations of added mercury ion and EGTA respectively. Thus we have

$$E = E^{\circ}_{Hg} + 0.0296 \log \frac{C_{Hg}\alpha_{H(Y)}}{(C_Y-C_{Hg})K'_{HgY}}. \quad (5)$$

Therefore K'_{HgY} can be calculated from potential-pH measurements. Values of log K'_{HgY} at various pH's are tabulated in Table 1.

Table 1. Values of log K'_{HgY} at various pH's for determination of the stability constants of HgY^{2-} and $HgHY^{-}$
$C_{Hg}=2\times10^{-3}$M, $C_Y=4\times10^{-3}$M, 25°C, $\mu=0.1$

pH	log K'_{HgY}	pH	log K'_{HgY}
2.69	24.35	4.28	23.83
2.82	24.33	4.94	23.85
3.09	24.15	6.20	23.92
3.24	25.08	8.32	23.88
3.54	23.98	8.52	23.88
3.94	23.93	9.29	23.80

Since the log K'_{HgY}-pH diagram gives a curve of a limiting slope of unity at lower pH, the presence of protonated complex of mercury(II)-EGTA is anticipated. Thus

$$K'_{HgY} = \frac{[HgY^{2-}]+[HgHY^{-}]}{[Hg^{2+}][Y^{4-}]} = (1+K^{H}_{HgHY}[H^+])K_{HgY}, \quad (6)$$

where

$$K_{HgY} = \frac{[HgY^{2-}]}{[Hg^{2+}][Y^{4-}]} \text{ and } K^{H}_{HgHY} = \frac{[HgHY^{-}]}{[HgY^{2-}][H^+]}.$$

In the pH range 5 to 9 K'_{HgY} is independent of hydrogen ion concentration. This value is obviously equal to K_{HgY} from the definition of K'_{HgY}. The following values are obtained: log $K_{HgY}=23.86\pm0.10$, log $K^{H}_{HgHY}=3.06\pm0.10$. The value of log K_{HgY} compares favorably with the value 23.8 reported by Holloway and Reilley.[3)]

Stability Constants of Cobalt(II)-EGTA Complexes. As the stability constant of HgY^{2-} is higher than that of CoY^{2-} and the total concentration of EGTA and that of cobalt ion added, C_Y and C_{Co}, are about twice that of mercury ion, the following relationships hold:

$$C_{Hg} = [HgY'] \quad (7)$$

$$C_Y - C_{Hg} = [CoY'] + [Y'] \quad (8)$$

$$[Co'] = C_{Hg} + C_{Co} - C_Y + [Y'] = [Co^{2+}]\alpha_{OH(Co)} \quad (9)$$

$$E = E^{\circ}_{Hg} + 0.0296 \log \frac{K'_{CoY}C_{Hg}[Co']}{K'_{HgY}[CoY']\alpha_{OH(Co)}}. \quad (10)$$

where $\alpha_{OH(Co)}$ is the side reaction coefficient taking into account the hydrolysis of cobalt ion. We can calculate

2) W. M. Latimer, "Oxidation Potentials," 2nd Ed., Prentice-Hall, New York (1952), p. 179.

3) J. H. Holloway and C. N. Reilley, *Anal. Chem.*, **32**, 249 (1960).

pY from the following equation:

$$E = E^{\circ}_{Hg} + 0.0296 \log \frac{C_{Hg}}{K'_{HgY}} + 0.0296\,pY. \quad (11)$$

Thus with a knowledge of [Y′], [CoY′] and [Co′] are obtained from Eqs. (8) to (9) respectively, and K'_{CoY} is calculated from Eq. (10). As shown in Fig. 1,

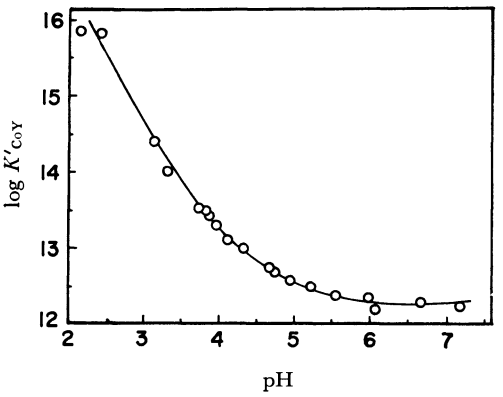

Fig. 1. Determination of the stability constants of CoY^{2-}, $CoHY^{-}$ and CoH_2Y. Solid line is the theoretical curve calculated with values obtained by means of the curve fitting. At μ=0.1, 25°C.

the log K'_{CoY}-pH diagram tends to give a curve of limiting slope of 2 at lower pH. This fact points to the presence of CoY^{2-}, $CoHY^{-}$ and CoH_2Y species. Then

$$K'_{CoY} = \frac{[CoY^{2-}]+[CoHY^{-}]+[CoH_2Y]}{[Co^{2+}][Y^{4-}]}$$

$$= K_{CoY}(1+K^{H}_{CoHY}[H^+]+K^{H}_{Co_2HY}K^{H}_{CoHY}[H^+]^2), \quad (12)$$

where

$$K_{CoY} = \frac{[CoY^{2-}]}{[Co^{2+}][Y^{4-}]}, \quad K^{H}_{CoHY} = \frac{[CoHY^{-}]}{[CoY^{2-}][H^+]}$$

and

$$K^{H}_{Co_2HY} = \frac{[CoH_2Y]}{[CoHY^{-}][H^+]}.$$

By means of a "curve fitting" method the following results were obtained: log K_{CoY}=12.3±0.1, log K^{H}_{CoHY}=4.9±0.1, log $K^{H}_{CoH_2Y}$=3.3±0.3. The value of log K_{CoY} compares favorably with the previous finding 12.3.[3] These constants are used in the analysis of the kinetic data.

Equilibrium. As seen from the values of stability constants of EGTA (log K^{H}_{HY}=9.43, log $K^{H}_{H_2Y}$=8.85, log $K^{H}_{H_3Y}$=2.68, log $K^{H}_{H_4Y}$=2.07[4]), Y^{4-}, HY^{3-}, and H_2Y^{2-} species may be present in the pH range 8 to 9.4 investigated. The 1 : 1 normal cobalt(II)-EGTA complex exists under these experimental conditions. In the pH range 8 to 9.4, the dominant species of PAR is found to be the monoionic species (HR^{-}) from the stability constants of PAR (log $K^{H}_{H_2R}$=2.69, log $K^{H}_{H_2R}$=5.50, log K^{H}_{HR}=12.31[5]). The monoionic species has maximum absorption at 410 nm and the absorbance of PAR is independent of pH in this pH range. The molar absorption coefficient is 8.14×10^2 at 510 nm. The molar ratio of cobalt to PAR in cobalt-PAR complex is 1 : 2.[6,7] Cobalt-PAR complex has maximum absorption at 510 nm and its molar absorption coefficient is 6.40×10^4 at 510 nm.

The equilibrium 1 is much favored to the right under the present experimental conditions, so that the reverse reaction can be neglected in the kinetic study. Therefore the stoichiometry of the present substitution reaction is expressed as

$$CoY^{2-} + 2HR^{-} \rightarrow CoR_2^{-} + Y', \quad (13)$$

where Y′ denotes nonmetallized EGTA.[8]

Procedure of Measurement of the Substitution Reaction Rate. pH of the cobalt-EGTA solution, prepared by mixing cobalt perchlorate solution with EGTA solution in excess, is buffered with borax and boric acid or sodium hydroxide and the ionic strength maintained constant (μ=0.1) with sodium perchlorate. The cobalt-EGTA solution and the PAR solution are brought to the temperature equilibrium in a bath kept at 25±0.2°C. The velocity of the substitution reaction is sufficiently slow to be studied by manual mixing techniques. The reaction is commenced by mixing these two solutions. A portion of the reaction mixture is transferred to a spectrophotometer cell at different intervals, and the absorbance of cobalt-PAR complex is measured at 510 nm, a spectrophotometer being used with a thermostated cell compartment capable of temperature control±0.3°C. All experiments are carried out in a room thermostated at 25±1°C.

Results

Beer's law is obeyed for the cobalt-PAR complex and the reaction(13) goes to completion. Therefore, if the substitution reaction of cobalt-EGTA with PAR in large excess is of the pth order with respect to cobalt-EGTA, the order of the reaction with respect to cobalt-EGTA is given by the slope, p, of the straight line obtained in a plot[1] of log $d(E_t-E_0)/dt$ against log $(E_\infty-E_t)$. The plot gave a straight line of slope 1. Therefore the reaction is of the first order in cobalt-EGTA. Thus for the reactions with a large excess of PAR the rate law is expressed as:

$$\frac{d[CoR_2^{-}]}{dt} = k_{0(R,H)}[CoY^{2-}], \quad (14)$$

4) J. Bjerrum, G. Schwarzenbach and L. G. Sillén, Special Publication No. 6, The Chemical Society, London, 1957, Part I.

5) W. J. Geary, G. Nickless and F. H. Pollard, *Anal. Chim. Acta*, **27**, 71 (1962).

6) A. Corsini, Q. Fernando and H. Freiser, *Inorg. Chem.*, **2**, 224 (1963).

7) A. I. Busev, V. M. Ivanov and Zh. I. Nemtseva, *Zh. Neorg. Khim.*, **13**, 511 (1968).

8) We assume trivalent cobalt to be in the cobalt-PAR complex according to a previous finding (T. Iwamoto and M. Fujimoto, *Anal. Chim. Acta*, **29**, 282 (1963)). However, electron transfer does not seem to make any obstacle in studying the present ligand substitution reaction (see Discussion).

where $k_{0(R,H)}$ denotes the conditional rate constant[1] involving the concentration terms of PAR and hydrogen ion.

The kinetic studies performed with a 20—50-fold excess of the entering group PAR showed that the reaction was of the first order in PAR. The fact is also supported by the good linearity of the second order plots concerning cobalt-EGTA and PAR:

$$\frac{1}{C_{PAR}-2C_{Co}} \ln \frac{C_{Co}(C_{PAR}-2[CoR_2^-])}{C_{PAR}(C_{Co}-[CoR_2^-])} = k_{0(H)}t.$$

Typical second order plots are shown in Fig. 2.

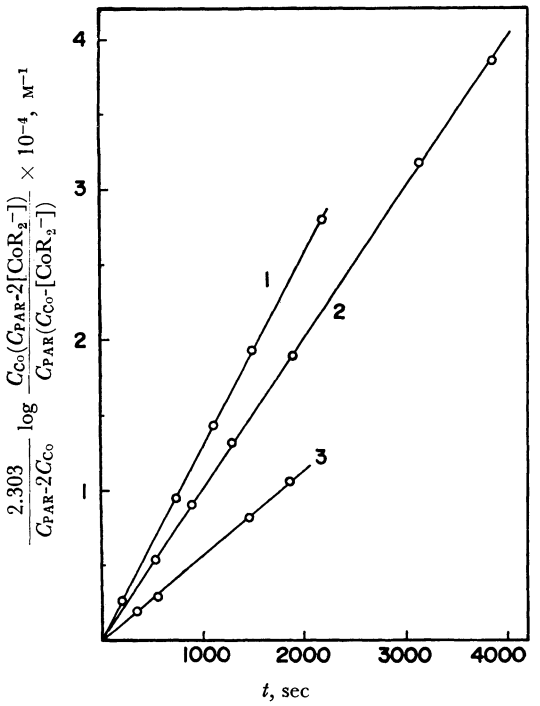

Fig. 2. Typical second order plots. For these runs the experimental conditions were as follows: $C_{Co}=1.09\times10^{-5}$M, $C_{PAR}=7.00\times10^{-5}$M, $C_Y=5.00\times10^{-5}$M, 1: pH=8.33; 2: pH=8.45; 3: pH=8.86, ionic strength=0.1M ($NaClO_4$), reaction temperature=25°C.

Under the experimental condition, predominant species of PAR is HR^- ($K^H_{HR}=10^{12.31}$ and $K^H_{H_2R}=10^{5.50}$).[5] Therefore, the rate law is expressed as

$$\frac{d[CoR_2^-]}{dt} = k_{0(H)}[CoY^{2-}][HR^-], \qquad (15)$$

where $k_{0(H)}$ refers to the conditional second order rate constant. The conditional rate constant $k_{0(H)}$ was determined at various pH's, concentrations of EGTA and concentrations of PAR.

Some results obtained are tabulated in Table 2. The values of $k_{0(H)}$ are plotted against the hydrogen ion concentration in Fig. 3, which indicates a linear relationship between $k_{0(H)}$ and $[H^+]$ within experimental error regardless of the concentration

Table 2. Conditional second order rate constants for the substitution reaction of cobalt-EGTA with PAR

μ=0.1, 25°C, $C_{Co}=9.78\times10^{-6}$M (Runs No. 1—14) or 1.09×10^{-5}M (Runs No. 15—23).

Run No.	C_{PAR} (M)	C_Y (M)	pH	$k_{0(H)}$ ($M^{-1}sec^{-1}$)
1	4.00×10^{-4}	1.00×10^{-3}	8.32	11.7
2	4.00×10^{-4}	1.00×10^{-3}	8.44	9.58
3	4.00×10^{-4}	1.00×10^{-3}	9.13	4.17
4	4.00×10^{-4}	1.00×10^{-3}	9.37	4.00
5	4.00×10^{-4}	2.00×10^{-3}	8.22	13.3
6	4.00×10^{-4}	2.00×10^{-3}	8.28	10.9
7	4.00×10^{-4}	2.00×10^{-3}	8.39	9.38
8	4.00×10^{-4}	2.00×10^{-3}	9.08	4.22
9	4.00×10^{-4}	2.00×10^{-3}	9.29	3.75
10	2.00×10^{-4}	2.00×10^{-3}	8.00	19.0
11	2.00×10^{-4}	2.00×10^{-3}	8.04	19.8
12	2.00×10^{-4}	2.00×10^{-3}	8.09	16.6
13	2.00×10^{-4}	2.00×10^{-3}	8.12	16.8
14	2.00×10^{-4}	2.00×10^{-3}	8.25	12.8
15	7.00×10^{-5}	2.00×10^{-5}	8.63	7.82
16	7.00×10^{-5}	5.00×10^{-5}	8.33	12.9
17	7.00×10^{-5}	5.00×10^{-5}	8.45	10.1
18	7.00×10^{-5}	5.00×10^{-5}	8.86	5.60
19	7.00×10^{-5}	1.00×10^{-4}	8.62	7.85
20	7.00×10^{-5}	1.00×10^{-3}	8.52	8.88
21	7.00×10^{-5}	1.00×10^{-3}	8.18	14.5
22	7.00×10^{-5}	2.00×10^{-3}	8.11	15.9
23	7.00×10^{-5}	2.00×10^{-3}	8.37	9.39

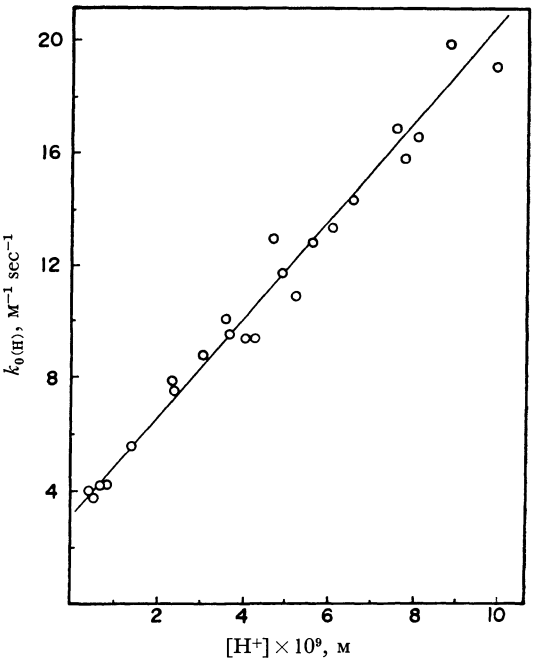

Fig. 3. $k_{0(H)}$ as a function of hydrogen ion concentration C_{Co}=about 10^{-5}M, $C_Y=2\times10^{-5}$ to 2×10^{-3}M, $C_{PAR}=7\times10^{-5}$ to 4×10^{-4}M, μ=0.1, 25°C.

of EGTA. Thus we obtain the following rate expression:

$$\frac{d[CoR_2^-]}{dt} = k_1[CoY^{2-}][HR^-] + k_2'[H^+][CoY^{2-}][HR^-]. \quad (16)$$

From the intercept and slope in Fig. 3 k_1 and k_2' may be obtained: $k_1=3.2\,M^{-1}\,sec^{-1}$ and $k_2'=1.7\times10^9\,M^{-2}\,sec^{-1}$. The second term of Eq. (16) shows the participation of the proton complex $CoHY^-$. Thus substituting the stability constant of $CoHY^-$ determined in the present study, we have

$$\frac{d[CoR_2^-]}{dt} = k_1[CoY^{2-}][HR^-] + \frac{k_2'}{K^H_{CoHY}}[CoHY^-][HR^-]$$
$$= k_1[CoY^{2-}][HR^-] + k_2[CoHY^-][HR^-]. \quad (17)$$

The rate constants k_1 and k_2 at ionic strength $\mu=0.1$ and 25°C are $3.2\,M^{-1}\,sec^{-1}$ and $2.1\times10^4\,M^{-1}\cdot sec^{-1}$, respectively.

Discussion

Mechanism of the Present Ligand Substitution Reaction. PAR forms a 1 : 2 complex with cobalt and the formation of cobalt-PAR is of the first order in the concentration of PAR. The rate of the addition of the second PAR is much faster than the rate of addition of the first PAR.

The first step of complexation is in general rate-determining: the fact that the rate constants increase with increasing degree of association of ligand with metal has been provided by Hammes and Steinfeld[9] in successive substituion of nickel or cobalt with glycine. Honaker and Freiser[10] reported that the addition of the first ligand is rate controlling in the rate of extraction of zinc dithizonate from aqueous solution. Pearson and Ellgen[11] have shown that in the complex formation reactions of nickel(II) ion with dithioxalate or maleonitriledithiolate the formation of monoligand nickel(II) complex is rate-determining. Recently, the labilizing effect of a coordinated ligand in the substitution reaction has been quantitatively accounted for by a study of kinetics of the formation of nickel(II)-PAR complex from some monovalent monoacidopentaaquonickel(II) complexes.[12]

Proton transfer reactions are extremely rapid and the proton will tend to be in the position of the greatest basicity. Usually the reaction rate increases with decreasing pH if the protons are more attracted to the leaving group.[13]

It is suggested therefore that the first order dependence of the cleavage rate on hydrogen ion concentration is due to a rapid acid-base reaction preceding the rate-determining step. From this consideration, in the present case, the second term of Eq. (17) clearly shows the participation of a protonated complex $CoHY^-$ which is in equilibrium preceding the rate-determining step. From the stability constant K^H_{CoHY} of $10^{4.9}$ determined in the present study, the concentration of protonated complex $[CoHY^-]$ is found only 0.1 to 0.01% of that of the total cobalt-EGTA complex in the range of pH 8 to 9. Nevertheless the reaction path through the protonated complex is important in the present substitution reaction, because $CoHY^-$ is much more reactive than CoY^{2-}.

Margerum and Rosen[14] have recently shown a clear evidence for a series of intermediates in equilibrium with one another in the reaction of EDTA with mono- and bis(diethylenetriamine)-nickel(II) complexes. In the present case, there may be a successive dissociation of donor atoms in EGTA, before three sites of coordination at least are available for the incoming PAR. Thus the cleavage of nitrogen atom bonded to the central metal in the mixed ligand intermediates, RCoY and RCoHY, should be rate-determining.[1] The coordination of the second PAR molecule to the resulting 1 : 1 cobalt-PAR complex is fast.[12]

Reactions of CoY^{2-} and $CoHY^-$ with PAR are schematically given in Fig. 4. We assume the partial dissociation of cobalt-EGTA bonds (Steps K_I and K_I') followed by the incorporation of PAR to form the mixed ligand intermediates, RCoY and RCoHY (Steps K_{II} and K_{II}'). According to the proposed mechanism, the rate law (17) can be rewritten as

$$\frac{d[CoR_2^-]}{dt} = k_1[CoY^{2-}][HR^-] + k_2[CoHY^-][HR^-]$$
$$= \frac{k_1}{K_IK_{II}}[RCoY] + \frac{k_2}{K_I'K_{II}'}[RCoHY]$$
$$= k_I[RCoY] + k_{II}[RCoHY],$$

where $k_I=k_1/K_IK_{II}$ and $k_{II}=k_2/K_I'K_{II}'$. The estimation of the ratio k_I/k_{II} may be interesting. We have immediately.

$$\frac{k_I}{k_{II}} = \frac{k_1}{k_2}\frac{K_I'K_{II}'}{K_IK_{II}}$$

As it appears reasonable to assume that $K_I'/K_I=K_{CoY}/K^{HY}_{CoHY}$ and that the value of K_I does not differ appreciably from K_{II}', we put $K_{II}\simeq K_{II}'$. Then with the observed rate and formation con-

9) G. G. Hammes and J. I. Steinfeld, *J. Amer. Chem. Soc.*, **84**, 4639 (1962); *J. Phys. Chem.*, **67**, 528 (1963).
10) C. B. Honaker and H. Freiser, *J. Phys. Chem.*, **66**, 127 (1962).
11) R. G. Pearson and P. Ellgen, *Inorg. Chem.*, **6**, 1379 (1967).
12) S. Funahashi and M. Tanaka, *ibid.*, **8**, 2159 (1969).
13) J. D. Carr, R. A. Libbly and D. W. Margerum, *ibid.*, **6**, 1083 (1967).
14) D. W. Margerum and H. M. Rosen, *ibid*, **7**, 299 (1968).

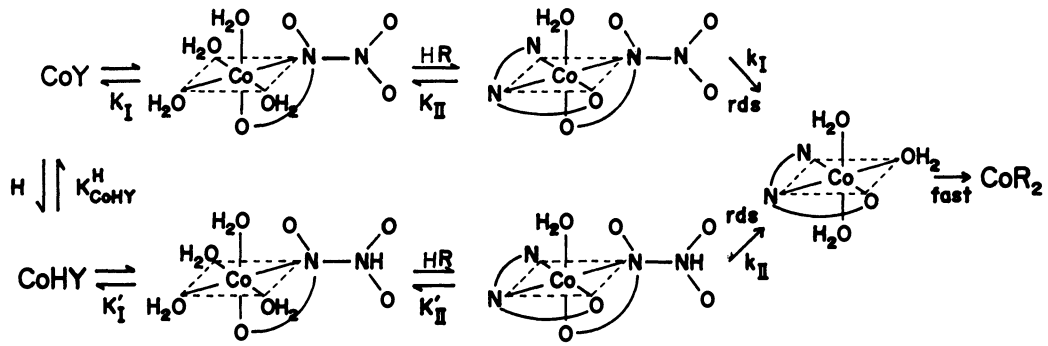

Fig. 4. Proposed mechanism of the substitution reactions of CoY and CoHY with PAR. EGTA and PAR are symbolized respectively as 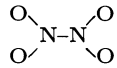 and N–N–O. Charges are omitted for simplicity.

stants, we obtain $k_{II}/k_I=5$, *i.e.*, k_I and k_{II} are of the same order of magnitude. In other words the difference between k_1 and k_2 is mostly determined by the difference between the overall formation constants of the mixed ligand intermediates, $K^R_{RCoY}=K_IK_{II}$ and $K^R_{RCoHY}=K_I'K_{II}'$. The ratio K_{CoY}/K^{HY}_{CoHY} would be a measure of k_2/k_1 in the proposed mechanism.

Oxidation State of Cobalt in the Product CoR_2 and in the Intermediate RCoY. 1-(2-Pyridiylazo)-2-naphthol (PAN) is similar to PAR and forms 1:2 cobalt-PAN complex. On mixing a cobalt(II) solution with an excess of PAN the color of the solution (pH 8) change gradually from red to green in a few minutes. This corresponds to the oxidation of the red cobalt(II)-PAN complex to the green cobalt(III) complex by atmospheric oxygen. On the other hand, mixing a cobalt(II) solution with a PAR solution results immediately in a red solution, which does not change in color. The trivalent state of cobalt in the green PAN complex and in the red PAR complex has been confirmed by magnetic susceptibility measurements.[15]

We studied qualitatively the rate of the acid dissociation reactions of cobalt-PAN and cobalt-PAR complexes. Solutions of red cobalt-PAN, green cobalt-PAN and red cobalt-PAR complexes were made acidic (pH 1 or lower) with 10 M perchloric acid. Then the color of the red cobalt-PAN complex changed immediately to reddish yellow which is the color of protonated PAN, while the color of the green cobalt-PAN and red cobalt-PAR complexes remained unchanged for at least a week. Similar experiments were carried out on nickel complexes. Upon acidification with perchloric acid, the color of the red nickel-PAN and nickel-PAR complexes changed to the color of a free ligand.

As expected from the inertness of trivalent cobalt complexes, the reaction of cobalt(III)-EDTA complex with PAN and that of cobalt(III)-PAN with EDTA do not proceed at all, for at least a week. Thus the cobalt in the labile red cobalt-PAN complex is divalent, while the cobalt in the inert (or thermodynamically very stable) green cobalt-PAN and the inert red cobalt-PAN complexes is trivalent. The result agrees with the previous conclusion drawn from the magnetic susceptibility of these complexes.[15] Trivalent state of cobalt seems to be more stabilized in the cobalt-PAR complex than in the corresponding PAN complex by the effect of the electron flow from the dissociated *para*-hydroxyl group of PAR into benzene ring. The same effect seems to be responsible for the fact that the cobalt(III)-PAR complex absorbs at a shorter wavelength than the cobalt(III)-PAN complex.

The rate of electron transfer in the system of tris-(1,10-phenanthroline)-cobalt(II)——tris(1,10-phenanthroline)-cobalt(III) is faster by about five orders of magnitude than that of cobalt(II)-EDTA ——cobalt(III)-EDTA. This fact has been explained on the basis of the difference in the ligand field strength.[16,17] If the cobalt in the intermediate RCoY were trivalent, the dissociation of EGTA from the intermediate would be impossible. Thus the cobalt in the intermediate RCoY should be divalent. Since the ligand field of PAR is stronger than that of EGTA, it seems reasonable that the oxidation of cobalt(II) occurs immediately after the incorporation of the second PAR molecule.

On the other hand, the substitution of nickel(II)-EGTA complex with PAR[18] is about 10 times slower than the corresponding reaction of cobalt(II) complexes studied in the present work. This is just as expected from the ligand field theory and

15) T. Iwamoto and M. Fujimoto, *Anal. Chim. Acta*, **29**, 282 (1963).

16) B. R. Baker, F. Basolo and H. M. Neumann, *J. Phys. Chem.*, **63**, 371 (1959).

17) F. Basolo and R. G. Pearson, "Mechanisms of Inorganic Reactions," 2nd Ed., John Wiley & Sons, Inc., New York, N. Y. (1967), p. 512.

18) S. Funahashi and M. Tanaka, to be published.

agrees with a great number of experimental results.

It seems plausible that, in the step of the dissociation of EGTA from the intermediate RCoY, cobalt is divalent. The oxidation of cobalt(II) occurs after the dissociation of EGTA followed by the incorporation of the second PAR molecule.

The financial support given by the Ministry of Education (Japan) is gratefully acknowledged.

BULLETIN OF THE CHEMICAL SOCIETY OF JAPAN VOL. 43 769—773 (1970)

Kinetics of the Ligand Substitution Reaction of the Copper(II)-4-(2-Pyridylazo)resorcinol Complex with (Ethylene glycol)-bis(2-aminoethyl ether)-*N*,*N*,*N*′,*N*′-tetraacetic Acid

Shigenobu FUNAHASHI, Shinkichi YAMADA and Motoharu TANAKA

Laboratory of Analytical Chemistry, Faculty of Science, Nagoya University, Chikusa-ku, Nagoya

(Received July 21, 1969)

The kinetics of the ligand substitution reaction of the copper(II)-4-(2-pyridylazo)resorcinol complex (Cu(II)-PAR) with (ethylene glycol)bis(2-aminoethyl ether)-*N*,*N*,*N*′,*N*′-tetraacetic acid (EGTA) has been studied spectrophotometrically at pH 9—10 at μ=0.10 ($NaClO_4$) and at 25.0°C. The reaction proceeds through the 1 : 1 Cu(II)-PAR complex resulting from the predissociation equilibrium of the 1 : 2 Cu(II)-PAR complex:

$$-d[CuR_2^{2-}]/dt = 10^{6.15}[CuR_2^{2-}][H^+][Y']/[HR^-] = 10^{2.9}[CuR][Y']$$

where R^{2-} refers to the divalent anion of PAR (H_2R) and Y′ the free EGTA not combined with any metal. The release of PAR from the mixed ligand intermediate RCuY is the rate-determining step. The substitution reaction for the copper(II)-PAR complex proceeds in the same mechanism with that for the zinc(II)-PAR complex. The difference in reactivity of these complexes is discussed. Cu-PAR bond is weakened in a distorted octahedron of the intermediate RCuY before the release of PAR.

Many works have been devoted to the kinetics and mechanisms of the exchange of polyaminocarboxylic acid anion (*e.g.* EDTA) between metal ions. A general mechanism has been proposed by Margerum and Bydalek[1] for the exchange of a multidentate ligand between metal ions that involves a dinuclear intermediate species, in which the multidentate ligand is partially unwound from the initially complexed metal ion and partially attached to the attacking metal ion. We have studied the substituion of metal chelates with multidentate ligands which are often involved in the complexometric titration and the solvent extraction of metal chelates.

In a previous paper,[2] the ligand substitution reaction of the zinc(II)-4-(2-pyridylazo)resorcinol complex (Zn(II)-PAR) with (ethylene glycol)bis-(2-aminoethyl ether)-*N*,*N*,*N*′,*N*′-tetraacetic acid (EGTA) has been reported. The reaction was found to proceed through one path involving predissociation equilibrium of the zinc(II)-PAR complex, and the possible mechanism was discussed.

It seemed worth while to extend the study to the substitution reaction involving the other metal ion, and the ligand substitution reaction of the copper(II)-4-(2-pyridylazo)resorcinol complex with (ethylene glycol)bis(2-aminoethyl ether)-*N*,*N*,*N*′,*N*′-tetraacetic acid

$$\text{Cu(II)-PAR} + \text{EGTA} \rightleftharpoons \text{Cu(II)-EGTA} + \text{PAR} \quad (1)$$

was undertaken, where EGTA and PAR represent (ethylene glycol)bis(2-aminoethyl ether)-*N*,*N*,*N*′,*N*′-tetraacetic acid and 4-(2-pyridylazo)resorcinol respectively and are abbreviated as H_4Y (hexadentate) and H_2R (tridentate) respectively. This paper gives the results.

Results

It is necessary to determine the stability constants of copper(II)-PAR complexes in connection with

1) T. J. Bydalek and D. W. Margerum, *J. Amer. Chem. Soc.*, **83**, 4326 (1961); *Inorg. Chem.*, **1**, 852 (1962); **2**, 678 (1963); **2**, 683 (1963).

2) M. Tanaka, S. Funahashi and K. Shirai, *Inorg. Chem.*, **7**, 573 (1968).

the equilibria involved in the substitution reaction. Thus the stability constants of the copper(II)-PAR complexes have been determined spectrophotometrically at $\mu=0.10$ ($NaClO_4$) and at 25.0°C:

$$[CuHR^+]/[Cu^{2+}][HR^-] = 10^{9.90\pm0.05},$$
$$[CuHR^+]/[CuR][H^+] = 10^{5.00\pm0.05},$$
$$[CuR]/[Cu^{2+}][R^{2-}] = 10^{17.20\pm0.05},$$
$$[CuR_2^{2-}]/[CuR][R^{2-}] = 10^{9.1\pm0.2}.$$

Details will be reported elsewhere.[3]

Methods of preparation of the reagents and kinetic measurements have been described previously.[2-4]

Under the present experimental conditions the copper(II) forms with PAR quantitatively the 1 : 2 complex CuR_2^{2-}. The absorbance of the copper(II)-PAR complex is constant over a pH range 9 to 10. The molar absorption coefficient is 6.87×10^4 at 515 nm. The dominant species of PAR is the singly charged species (HR^-), and the species of EGTA involves Y^{4-}, HY^{3-} and H_2Y^{2-}. The copper(II)-EGTA complex is the 1 : 1 complex CuY^{2-} ($K_{CuY}=10^{17.8}$).[5] Equilibrium (1) is much favored to the right so that the substitution reaction of the copper(II)-PAR complex with EGTA goes substantially to completion and the reverse reaction can be neglected.

For the reaction with large excesses of PAR and EGTA the rate law can be expressed as

$$-\frac{[CuR_2^{2-}]}{dt} = k_{0(H,R,Y)}[CuR_2^{2-}], \qquad (2)$$

where $k_{0(H,R,Y)}$ is the conditional rate constant[6] involving concentration of PAR, EGTA and hydrogen ion. The rate plots of $\log (E_0-E_\infty)/(E_t-E_\infty)$ *vs.* t were linear at least for over 90% of reaction. The conditional rate constant $k_{0(H,R,Y)}$ was determined from the slope of the straight line. The values of conditional rate constants at various concentrations of PAR, at a concentration of EGTA, and at constant pH are given in Table 1 (Runs No. 1—9). These data indicate clearly a linear relationship between $k_{0(H,R,Y)}$ and the reciprocal concentration of PAR with the zero intercept. In Fig. 1, the values of $k_{0(H,R,Y)}$ determined at various pH's and concentrations of EGTA and PAR are plotted against the hydrogen ion concentration and some data of $k_{0(H,R,Y)}$ are tabulated in Table 1. It is evident from Fig. 1 that $k_{0(H,R,Y)}$ is linearly related to hydrogen ion concentration and that the rate increases with increasing EGTA concentration. The plots give the zero intercept (Figs. 1 and 2). The substitution reaction is of first order with respect to EGTA and hydrogen ion. Thus the rate law is given by

$$-\frac{d[CuR_2^{2-}]}{dt} = k_0\frac{[CuR_2^{2-}][H^+][Y']}{[HR^-]}. \qquad (3)$$

This rate law is consistent with the reaction mechanism:

$$CuR_2^{2-} + H^+ \rightleftharpoons CuR + HR^-, \qquad (4)$$
$$CuR + Y' \rightleftharpoons RCuY \rightleftharpoons CuY^{2-} + HR^-. \qquad (5)$$

EGTA reacts with CuR in equilibrium with CuR_2^{2-}. Substituting the equilibrium constants in Eq. (4),

TABLE 1. FIRST ORDER CONDITIONAL RATE CONSTANTS $k_{0(H,R,Y)}$

At 25.0°C and $\mu=0.10$ ($NaClO_4$), $C_{Cu}=1.00\times10^{-6}$M.

Run No.	10^4C_R (M)	10^3C_Y (M)	pH	$k_{0(H,R,Y)}$ (sec^{-1})
1	1.00	1.00	9.52	3.8
2	1.50	1.00	9.52	2.9
3	2.00	1.00	9.52	2.2
4	3.00	1.00	9.52	1.7
5	1.00	1.00	9.30	6.3
6	1.50	1.00	9.30	4.8
7	2.00	1.00	9.30	3.7
8	1.50	1.00	9.16	6.7
9	2.00	1.00	9.16	5.2
10	1.00	1.00	9.08	11.1
11	1.00	1.00	9.20	8.38
12	1.00	1.00	9.35	4.75
13	1.00	1.00	9.60	2.79
14	1.00	1.00	9.78	1.87
15	1.00	1.00	10.06	0.767
16	1.50	1.00	9.10	8.33
17	1.50	1.00	9.19	6.25
18	1.50	1.00	9.35	4.13
19	1.50	1.00	9.55	2.21
20	1.50	1.00	9.72	1.38
21	2.00	1.00	9.09	6.33
22	2.00	1.00	9.19	4.79
23	2.00	1.00	9.35	2.96
24	2.00	1.00	9.54	1.73
25	3.00	1.00	9.07	5.13
26	3.00	1.00	9.32	2.50
27	3.00	1.00	9.52	1.46
28	1.00	0.500	9.11	5.75
29	1.00	0.500	9.31	3.42
30	1.00	0.500	9.76	0.792
31	1.00	1.50	9.14	13.8
32	1.00	1.50	9.32	8.83
33	1.00	1.50	9.45	6.42
34	1.00	1.50	9.60	3.75
35	1.00	2.00	9.17	16.7
36	1.00	2.00	9.27	13.8
37	1.00	2.00	9.41	9.25

3) S. Funahashi, S. Yamada and M. Tanaka, to be published.

4) S. Funahashi and M. Tanaka, *Inorg. Chem.*, **8**, 2159 (1969).

5) J. H. Holloway and C. N. Reilley, *Anal. Chem.*, **32**, 249 (1960).

6) M. Tanaka, S. Funahashi and K. Shirai, *Anal. Chim. Acta*, **39**, 437 (1967).

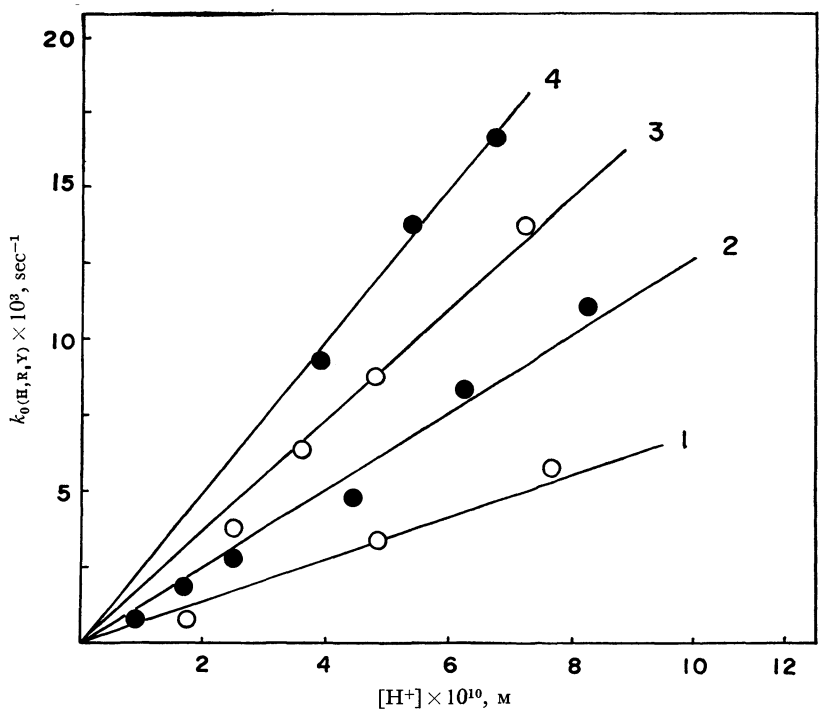

Fig. 1. $k_{0(H,R,Y)}$ as a function of hydrogen ion concentration.
$C_{Cu}=1.00\times10^{-6}$M; $C_R=1.00\times10^{-4}$M; $C_Y=1$, 5.00×10^{-4}M; 2, 1.00×10^{-3}M; 3, 1.50×10^{-3}M; 4, 2.00×10^{-3}M; $\mu=0.10$ ($NaClO_4$); temperature, 25.0°C

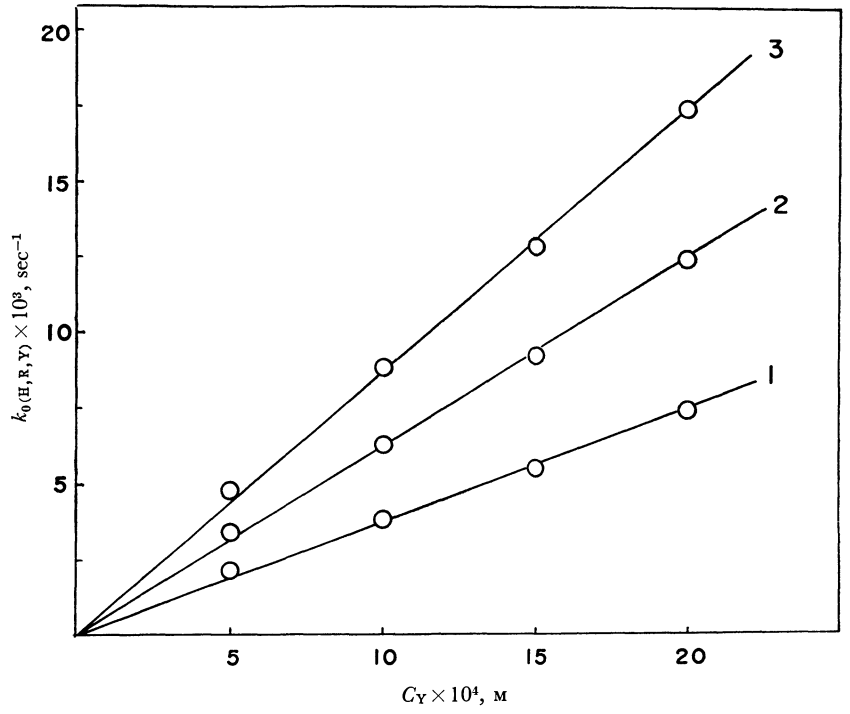

Fig. 2. $k_{0(H,R,Y)}$ as a function of EGTA concentration.
$C_{Cu}=1.00\times10^{-6}$M; $C_R=1.00\times10^{-4}$M; pH=1, 9.52; 2, 9.30; 3, 9.16; $\mu=0.10$($NaClO_4$); temperature, 25.0°C

the rate law can be rewritten as

$$-\frac{d[CuR_2^{2-}]}{dt} = k_0\frac{K^R_{CuR_2}}{K^H_{HR}}[CuR][Y'] = k[CuR][Y'], \quad (6)$$

where

$$K^R_{HR} = [HR^-]/[R^{2-}][H^+] = 10^{12.30}\ ^{6)}.$$

Under the present experimental conditions, Y^{4-}, HY^{3-} and H_2Y^{2-} are present. However, we observe no variation of the rate with varying proportion of these species of EGTA. The rate constants k_0 and k determined in this investigation are $1.4\pm0.4\times10^6$ M^{-1} sec^{-1} and $8.8\pm0.3\times10^2$ M^{-1}·sec^{-1}, respectively.

Discussion

Margerum and Rosen[7] have recently shown a clear evidence for a series of intermediates in equilibrium with one another in the reaction of EDTA with mono- and bis(diethylenetriamine)-nickel(II) complexes. We have reported the kinetics of the ligand substitution reaction of the zinc(II)-4-(2-pyridylazo)-resorcinol complex with (ethylene glycol)bis(2-aminoethyl ether)-*N,N,N',N'*-tetraacetic acid. The substitution reaction of copper(II)-PAR proceeds through the same mechanism with that of zinc(II)-PAR, *i.e.*, the cleavage of PAR bonded to the central metal in the mixed ligand intermediate, RMY, should be rate-determining (M denotes Zn or Cu).[2]

We assume the 1 : 1 M-PAR complex and EGTA are in rapid equilibrium with the mixed ligand complex in which EGTA is bonded to the central metal ion with a segment of EGTA and the rate-determining step is the loss of PAR from the mixed ligand intermediate. Since PAR is not as flexible as aliphatic polyamines, it is not likely that EGTA reacts with PAR complexes *via* a stepwise removal of donor atoms of PAR from the central metal as postulated previously in the substitution of polyamine complexes of nickel with EDTA.[8] As soon as one donor atom of PAR is removed from the central metal ion in the intermediate RMY, the other two will also be detached. This step should be the rate-determining step. Thus the reaction of ZnR and CuR with EGTA is given by

$$MR + Y' \overset{K_{RMY}}{\rightleftharpoons} RMY \overset{k_R^M}{\longrightarrow} MY^{2-} + HR^-, \quad (7)$$

where $K_{RMY}=[RMY]/[MR][Y']$ is the stability constant of the intermediate. If the reaction follows the mechanism given in Eq. (7), the experimentally determined rate constants, k^M, can be equated with the corresponding rate constants for metal-PAR bond rupture, $k_R{}^M$, by

$$k^M = K_{RMY}k_R{}^M. \quad (8)$$

According to the proposed mechanism, the rate law (6) can be rewritten as

$$-\frac{d[MR_2^{2-}]}{dt} = k^M[MR][Y'] = \frac{k^M}{K_{RMY}}[RMY] = k_R{}^M[RMY]. \quad (9)$$

It is interesting to compare the ratio k_R^{Cu}/k_R^{Zn} with the ratio of rate constants of dissociation of PAR from CuR and ZnR. Unfortunately, experimental K_{RMY} values are not available for the system studied. Consequently, it is necessary to rely on estimates. The second stability constants, $K^X_{MX_2}=[MX_2]/[MX][X]$, for copper(II) and zinc(II) with various tridentate ligand similar to PAR and a segment of EGTA are compared. Plots of $\log K^X_{CuX_2}$ *vs.* $\log K^X_{ZnX_2}$ are shown in Fig. 3. The plots lie close to a straight line with a slope of unity and zero intercept: the value of $K^X_{CuX_2}$ does not seem to differ appreciably from $K^X_{ZnX_2}$. Thus it appears reasonable to assume $K_{RCuY}\cong K_{RZnY}$. Then

$$\frac{k_R{}^{Cu}}{k_R{}^{Zn}} = \frac{k^{Cu}/K_{RCuY}}{k^{Zn}/K_{RZnY}} = \frac{k^{Cu}}{k^{Zn}} = 10^{-1.5}, \quad (10)$$

where the value of k^{Zn} is 2.4×10^4M^{-1} sec^{-1} at 25.0°C and $\mu=0.10$.[2]

The release of a water molecule from an aquo metal ion is the rate-determining step in the complex formation.[9-12] Though the rate constants for formation of CuR and ZnR are not yet available, they will very probably be comparable to the rate constants $k^M_{H_2O}$ of the substitution of coordinated water molecules of corresponding aquo metal ion M. Therefore, the rate of dissociation of CuR and ZnR can be estimated from the stability constants and the rate constants of formation of these complexes. We have immediately the ratio of the rate constants of dissociation of PAR from the 1 : 1 M-PAR complexes:

$$\frac{k^{Cu}_{H_2O}/K^R_{CuR}}{k^{Zn}_{H_2O}/K^R_{ZnR}} = 10^{-4.5} \quad (11)$$

where the values of $k^{Cu}_{H_2O}$ and $k^{Zn}_{H_2O}$ are 2×10^8 sec^{-1} at 25°C[13] and 3×10^7 sec^{-1} at 25°C[14], respectively, and the value of K^R_{ZnR} is $10^{11.9}$ at 25°C and

6) W. J. Geary, G. Nickless and F. H. Pollard, *Anal. Chim. Acta*, **27**, 71 (1962).

7) D. W. Margerum and H. M. Rosen, *Inorg. Chem.*, **7**, 299 (1968).

8) D. B. Rorabacher and D. W. Margerum, *Inorg. Chem.*, **3**, 382 (1964).

9) M. Eigen, *Z. Elektrochem.*, **64**, 115 (1960).

10) M. Eigen and N. Tamm, *ibid.*, **66**, 93 (1962).

11) M. Eigen and R. W. Wilkins in "Mechanisms of Inorganic Reactions," Advances in Chemistry Series, No. 49, American Chemical Society, Washington, D. C. (1965).

12) N. Sutin, *Ann. Rev. Phys. Chem.*, **17**, 119 (1966).

13) T. J. Swift and R. E. Connick, *J. Chem. Phys.*, **37**, 307 (1962).

14) M. Eigen, *Pure Appl. Chem.*, **6**, 97 (1963).

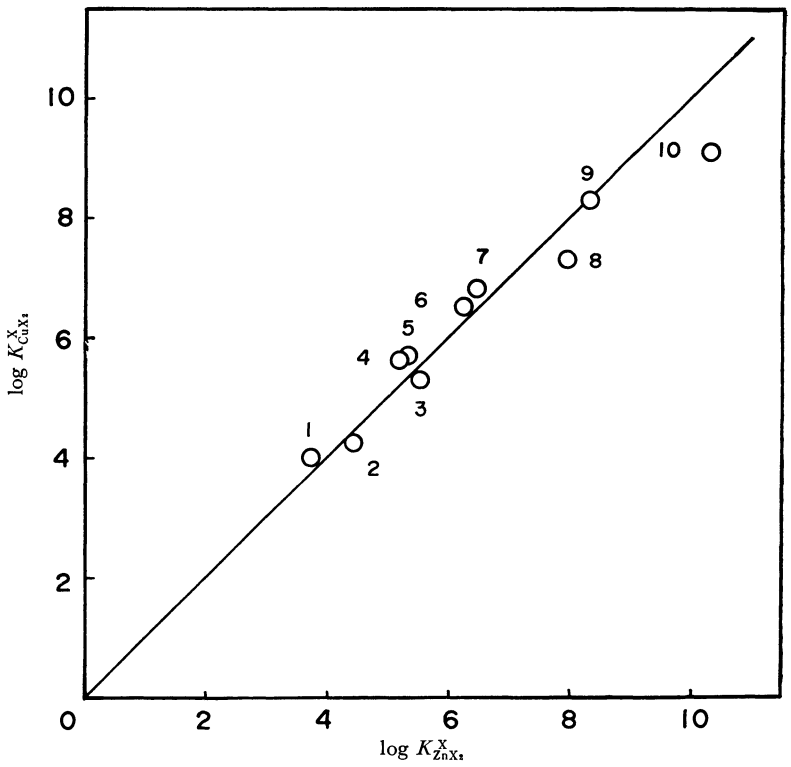

Fig. 3. log $K^{X}_{CuX_2}$ as a function of log $K^{X}_{ZnX_2}$.
1, *N*-2-hydroxyethyliminodiacetic acid; 2, *N*-(2-methoxyethyl)iminodiacetic acid;
3, diethylenetriamine; 4, iminodiacetic acid;
5, *N*-(3-hydroxypropyl)iminodiacetic acid; 6, *N*-(3,3-dimethylbutyl)iminodiacetic acid;
7, *N*-methyliminodiacetic acid;
8, 2-(2-pyridylazo)-4-methoxyphenol (G. Nakagawa and H. Wada, private communication, 1968);
9, 2-(2-pyridylazo)-4-methylphenol (G. Nakagawa and H. Wada, *Nippon Kagaku Zasshi*, **83**, 1190 (1962));
10, 4-(2-pyridylazo)resorcinol (Ref. 2).
Data from L. G. Sillén and A. E. Martell, "Stability Constants of Metal Complexes," Special Publication No. 17, The Chemical Society, London, 1964, except where indicated otherwise.

μ=0.10.[2] The ratio of dissociation rate of PAR from M-PAR (Eq. (11)) is by three orders of magnitude lower than the ratio of the rate constants of dissociation of PAR from the intermediates (Eq. (10)). This difference points to the possible change of the structure of the assumed intermediate RMY during the reaction. Since the *d* electron configuration of copper(II) ion is $(t_{2g})^6(e_g)^3$, we expect to find four short bonds coplanar with the metal atom and two longer ones completing a distorted octahedron (Jahn-Teller distortions). We know that zinc(II) ion with the configuration d^{10} is spherical. In 1 : 1 Cu-PAR complex, PAR is coordinated in the same plane with the central metal and two of the three water molecules in the complex are coordinated weakly with copper. These water molecules are substituted by EGTA in the formation of the intermediate RCuY. The bond Cu-PAR should then be necessarily forced to be longer and weaken in the distorted octahedron of the intermediate before the cleavage of Cu-PAR bond. In other words, the dissociation of PAR in the mixed ligand intermediate RCuY should be strongly driven due to Jahn-Teller distortions.[15]

The financial support given by the Ministry of Education is gratefully acknowledged.

15) The stepwise stability constants of the zinc(II)-PAR complexes are different by less than a factor of 10^2: $K^{R}_{ZnR}=10^{11.9}$ and $K^{R}_{ZnR_2}=10^{10.3}$. [2] The second stability constant of the copper(II)-PAR complex, however, is smaller than the first by a factor of 10^8. The greatly reduced stability of the 1 : 2 copper(II)-PAR complex must be attributed to Jahn-Teller distortions.

BULLETIN OF THE CHEMICAL SOCIETY OF JAPAN VOL. 43 774—778 (1970)

Polarography of Iron(III)- and Europium(III)-Acetylacetonate Complexes in *N,N*-Dimethylformamide

Seizo Misumi, Makoto Aihara and Yasuomi Nonaka

Inorganic Chemistry Laboratory, Faculty of Science, Kyushu University, Fukuoka

(Received July 14, 1969)

The reduction potentials of $Fe(acac)_3$ and $Eu(acac)_3$ in DMF are shifted to more positive potentials by the addition of cations (Li^+ and Mg^{2+}) to the supporting electrolyte of tetraethylammonium perchlorate. Studies of the complexes show that the effect is caused by coordinative relaxation reaction of the $Fe(acac)_3^-$ reduction product in which acetylacetonate ligand becomes transferred to the cation. However, in the case of $Eu(acac)_3^-$, acetylacetonate ligands seemed to be completely stripped off. Cyclic voltammetric data indicate reduction and reoxidation processes of the complexes.

Polarography in non-aqueous solvent is more advantageous for the study of a metal complex than that in aqueous solution, and investigations in non-aqueous solvents have been reported recently. However, the interaction of the supporting electrolyte with either the electrode reactant or product which remains innocuous in aqueous medium, should be taken into consideration in lower dielectric solvents such as in acetonitrile ($\varepsilon=37.5$) and dimethylformamide, DMF ($\varepsilon=36.7$). Schaap[1] developed polarographic theory for ion pairing of metal ion reactant with electrolyte anions. Murray and Hiller[2] studied the interaction of $Fe(acac)_3^-$ reduction product with Li^+ ion in acetonitrile. We are interested in the interaction of the supporting electrolyte with electron transfer products of a neutral complex in non-aqueous solvents and wish to describe cation (Li^+ and Mg^{2+}) effects on the iron(III)- and europium(III)-acetylacetonate complexes, ($Fe(acac)_3$ and $Eu(acac)_3$) in DMF.

Experimental

Solvent and Materials. *N,N*-Dimethylformamide by Wako Junyaku Co. of extra pure reagent grade was used. DMF was shaken with potassium carbonate anhydride and sodium sulfate, left standing for several days and then upper layer of the solution was distilled three times under reduced pressure in a nitrogen atomosphere. Moisture in the distillate was determined by Karl-Fischer titration to be only 0.03%. There were no impurities, which caused a detectable current at negative potentials less than −2.8 V in the polarogram. $Fe(acac)_3$ and $Eu(acac)_3$ were prepared by the ordinary method.[3]

Found: C, 50.90; H, 5.89%. Calcd for $Fe(acac)_3$: C, 51.01; H, 5.99%.

Found: C, 38.07; H, 4.88%. Calcd for $Eu(acac)_3 H_2O$: C, 38.55; H, 4.96%.

Tetraethylammonium perchlorate (abbreviated as TEAP) was prepared through the reaction of tetraethylammonium bromide with perchloric acid, recrystallized in water and dried at 60°C over $Mg(ClO_4)_2$.

Found: C, 41.89; H, 8.71; N, 5.96%. Calcd for $(C_2H_5)_4NClO_4$: C, 41.83; H, 8.77; N, 6.09%.

All other reagents were of extra pure grade.

Apparatus. The electrolysis cell has two diaphragms of sintered glass and consists of three electrodes as shown in Fig. 1. The reference electrode was SCE with a salt bridge devised by Takaoka.[4] DME was used as the working electrode ($m=0.833$ mg/sec, $t=4.50$ sec in 0.1M TEAP-DMF medium at −1.7 V *vs.* SCE).

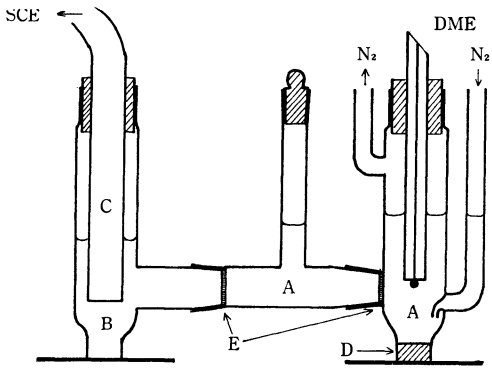

Fig. 1. Electrolysis cell.
A: Sample solution
B: 0.1M TEAP in DMF
C: Agar salt bridge connected with SCE
D: Counter electrode
E: Sintered glass

A Yanagimoto PA 102-type polarograph connected with a liquid resistance compensator P8-PT, was used

1) W. B. Schaap, *J. Amer. Chem. Soc.*, **82**, 1837 (1960).
2) R. W. Murray and L. K. Hiller, Jr., *Anal. Chem.*, **39**, 1221 (1967).
3) J. G. Stites, C. N. McCarthy and L. L. Quill, *J. Amer. Chem. Soc.*, **83**, 4533 (1961); T. Moeller and W. F. Ulrich, *J. Inorg. Nucl. Chem.*, **2**, 164 (1956).
4) K. Takaoka, *Rev. Polarog.* (Kyoto), **14**, 63 (1966).

for recording polarograms. Cyclic voltammograms were recorded by Iwasaki Synchroscope SS-5302 with preamplifier SP-O1H-A.

Triangular potential signals were obtained from a Yokogawa-Hewlett-Packard 3300A Function Generator. A compensator P8-PT was used as a potentiostat. A Pt wire electrode was used for a counter electrode. Current-measuring resistance was 10—30Ω.

Procedure. A sample of 0.1M TEAP-DMF, containing $Fe(acac)_3$ or $Eu(acac)_3$ (10^{-3}M), was taken into a cell. After dried nitrogen gas was passed through it for 20 min, DME and the agar bridge connected with SCE were inserted in the cell. A polarogram was then recorded. The junction potential was measured by using SCE with a slowly flowing-type aqueous saturated KCl salt bridge. All experiments were carried out at 25.0±0.1°C. Cyclic voltammogram was photographed during the growth of a mercury drop and the value of its maximum current was analysed.

Results

$Fe(acac)_3$ in 0.1M TEAP. The polarogram of 1 mM $Fe(acac)_3$ in 0.1M TEAP in DMF developed a well-defined wave (Fig. 2). The half-wave

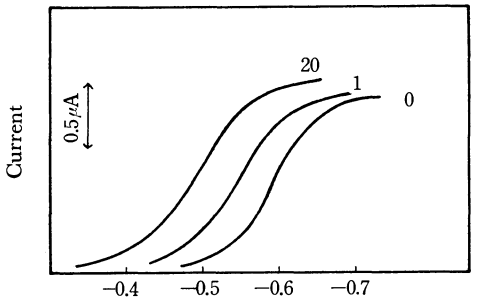

Fig. 2. Polarograms for 1.00 mM $Fe(acac)_3$ in 0.1M TEAP in DMF. Numbers above curves are mM of $LiClO_4$ added.

potential was −0.58 V *vs.* SCE. The electrode reaction was found to be a reversible (reciprocal slope: 52 mV) one-electron reduction and diffusion-controlled.

$Fe(acac)_3$ in TEAP-$LiClO_4$ Electrolyte Mixtures. As shown in Fig. 2 the reduction wave of 1 mM $Fe(acac)_3$ was shifted to less negative potentials by increasing concentrations of $LiClO_4$ in 0.1M TEAP medium. In this case, the electrode reaction was diffusion-controlled. As is seen in Table 1, the half-wave potential is shifted to more negative potential by increasing concentrations of $Fe(acac)_3$ with constant concentration of 30 mM $LiClO_4$.

$Fe(acac)_3$ in TEAP-$Mg(ClO_4)_2$ Electrolyte Mixtures. The same results as those for TEAP-$LiClO_4$ electrolyte mixtures were obtained (Table 2).

Table 1. Polarographic data for $Fe(acac)_3$ in 0.1M TEAP in DMF (Effect of $LiClO_4$)

$[Fe(acac)_3]$ mM	$[LiClO_4]$ mM	$-E_{1/2}$ V *vs.* SCE	i_d μA	Slope E *vs.* $\log((i_d-i)/i^2)$
0.5	30	0.46_7	0.93	a
1.0	0	0.58_5	1.17	0.052
	1	0.54_7	1.26	0.056
	2	0.54_4	1.28	0.056
	5	0.52_4	1.15	0.053
	10	0.51_7	1.25	0.054
	20	0.49_2	1.22	0.057
	30	0.48_2	1.41	0.054
3.0	30	0.51_4	4.64	a

a: plot curved

Table 2. Polarographic data for $Fe(acac)_3$ in 0.1M TEAP in DMF (Effect of $Mg(ClO_4)_2$)

$[Fe(acac)_3]$ mM	$[Mg(ClO_4)_2]$ mM	$-E_{1/2}$ V *vs.* SCE	i_d μA	Slope
0.5	20	0.49_4	0.78	
1.0	0	0.58_5	1.27	0.052
	3	0.54_3	1.31	0.044
	10	0.52_7	1.30	0.044
	20	0.51_2	1.21	0.053
	30	0.50_7	1.29	0.046
2.0	20	0.65_7	3.24	

$Eu(acac)_3$ in 0.1M TEAP. A single wave with the half-wave potential of −1.55 V *vs.* SCE, was obtained for 1 mM $Eu(acac)_3$ in 0.1M TEAP in DMF (Fig. 3). The electrode reaction was diffusion-

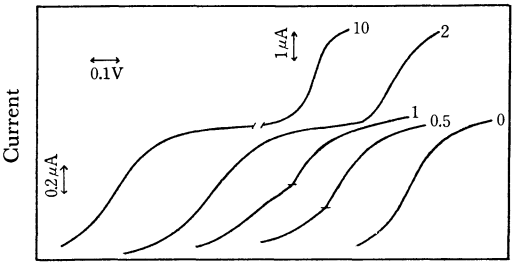

Fig. 3. Polarograms for 1.00 mM $Eu(acac)_3$ in 0.1M TEAP in DMF. Numbers above curves are mM of $LiClO_4$ added.

controlled. Addition of water up to 0.5% has no effect on the half-wave potential and the diffusion current remained. However, addition of water more than 0.5% caused the decrease of the diffusion current.

$Eu(acac)_3$ in 0.1M TEAP-$LiClO_4$ Electrolyte Mixtures. Differing from the case of $Fe(acac)_3$, the original single wave of the complex split into two waves by addition of $LiClO_4$ and a new wave

appeared at less negative potentials than the original. The height of this wave increased with increasing $LiClO_4$ concentrations and the original wave disappeared, whereas the new wave remained and was shifted again to less negative potentials at $[LiClO_4]/[Eu(acac)_3] \geqq 2$ (Fig. 3). The electrode reaction was diffusion-controlled. As shown in Table 3-1, the half-wave potential was shifted to more negative potentials by increasing concentrations of $Eu(acac)_3$ with constant concentration of $LiClO_4$. By addition of $LiClO_4$ at $[LiClO_4]/[Eu(acac)_3] \geqq 2$, a second wave appeared close to the potential of -2.0 V *vs.* SCE. The diffusion current became almost constant at $[LiClO_4]/[Eu(acac)_3] \geqq 10$(Fig. 3 and Table 3-2).

Table 3-1. Polarographic data for $Eu(acac)_3$ in 0.1M TEAP in DMF (Effect of $LiClO_4$)

$[Eu(acac)_3]$ mM	$[LiClO_4]$ mM	$-(E_{1/2})_1$ V *vs.* SCE	i_d μA
0.5	30	1.30_7	0.61
1.0	0.5	——[a], ——[a]	0.25, 1.08
	1	——[a], ——[a]	0.54, 0.78
	2	1.49_5	1.40
	5	1.44_9	1.36
	10	1.41_3	1.26
	20	1.36_8	1.28
	30	1.33_9	1.20
2.0	30	1.35_2	2.80

a) ill defined

Table 3-2. Polarographic data for $Eu(acac)_3$ in 0.1M TEAP in DMF (Effect of $LiClO_4$)

$[Eu(acac)_3]$ mM	$[LiClO_4]$ mM	$-(E_{1/2})_2$ V *vs.* SCE	i_d μA	Slope
1	2	2.08_7	0.85	68
	3	2.08_0	1.70	38
	5	2.06_5	2.27	36
	10	2.05_0	2.61	35
	20	2.04_7	2.65	31
	30	2.03_3	2.70	32

$Eu(acac)_3$ in 0.1M TEAP-$Mg(ClO_4)_2$ Electrolyte Mixtures. Differing from the case of $LiClO_4$, by addition of $Mg(ClO_4)_2$ to 1 mM $Eu(acac)_3$ in 0.1M TEAP medium the wave split into three steps and became considerably complicated.

Positive shifts in the half-wave potentials of the reduction waves of $Fe(acac)_3$ and $Eu(acac)_3$ were observed by addition of the cations (Li^+ and Mg^{2+}). Negative shifts in the half-wave potentials of those waves resulted from the increase of both complex concentrations at a constant concentration of the cation.

Assuming that metal complex ML_p is reduced reversibly with n-electron transfer, the electrode reaction is given by

$$ML_p + ne \rightleftharpoons ML_p^{n-} \quad (1)$$

If metal-ligand bond in ML_p^{n-} reduction product is more labile than that in ML_p complex, then ligand dissociation may occur from ML_p^{n-}. The extent of such dissociation is limited by the nature of the cation C^+. According to Murray and Hiller,[2] this particular interaction is a "theft" of ligand(s) from ML_p^{n-} by C^+ (coordinative relaxation), which produces a positive shift of the reduction potential of the reaction (1). In this case it seems that a sequence of the following coordinative relaxation reaction may occur.

$$\left.\begin{aligned} ML_p^{n-} + C^+ &\rightleftharpoons ML_{p-1}^{(n-1)-} + CL \\ &\vdots \\ ML_{p-q+1}^{(n-q+1)-} + C^+ &\rightleftharpoons ML_{p-q}^{(n-q)-} + CL \end{aligned}\right\} \quad (2)$$

Denoting the overall equilibrium constants of the above relaxations as K_1, K_2, $\cdots$, K_q, and solving for $[ML_p^{n-}]$, we obtain from the Nernst equation

$$E = E^0 + \frac{0.059}{n} \log \frac{[ML_p][1+\sum K_j[C^+]^j/[CL]^j]}{[ML_p^{n-}]_{total}} \quad (3)$$

where $[ML_p^{n-}]_{total}$ is the total concentration of all forms of the product complex.

If $n=q=1$ and essentially complete relaxation to ML_{p-1} is assumed, Eq. (3) is reduced to

$$E = E^0 + 0.059 \log \frac{K_r K_{CL} K_1}{K_0} + 0.059 \log [C^+] + 0.059 \log \frac{i_d - i}{i^2} \quad (4)$$

where K_r, K_0 and K_{CL} are the current-concentration proportionality constants for ML_{p-1}, ML_p and CL, respectively. Eq. (4) shows that the half-wave potential $E_{1/2}$ is shifted positively with increase in $[C^+]$ and is shifted negatively with increase in the concentration of the complex (at $i=i_d/2$, the last term of Eq. (4) is reduced to $0.059 \log (2/i_d)$). Plots of $E_{1/2}$ for $Fe(acac)_3$ and $Eu(acac)_3$ complexes against log $[Li^+]$ are shown in Fig. 4, where the following dissociation constants were used to calculate the concentration of dissociated lithium ions, $[Li^+]$.

$(K_a)_{LiClO_4} = 65.5$ (calculated by using the data of electric conductivity of Prue and Sherrington)[5]

$(K_a)_{TEAP} = 4.0$ (obtained by Peover and Davies)[6]

In the case of $Fe(acac)_3$ complex, $\Delta(E_{1/2})/\Delta\log[Li^+] = 0.062$. This value coincides with the theoretical value 0.059 for $q=1$. Consequently, the overall electrochemical process should be

$$Fe(acac)_3 + e \rightleftharpoons Fe(acac)_3^- \quad (5)$$

$$Fe(acac)_3^- + Li^+ \rightleftharpoons Fe(acac)_2 + Li(acac) \quad (6)$$

5) J. E. Prue and D. J. Sherrington, *Trans. Faraday Soc.*, **57**, 1795 (1967).

6) M. E. Peover, J. D. Davies, *J. Electroanal. Chem.*, **6**, 46, (1963).

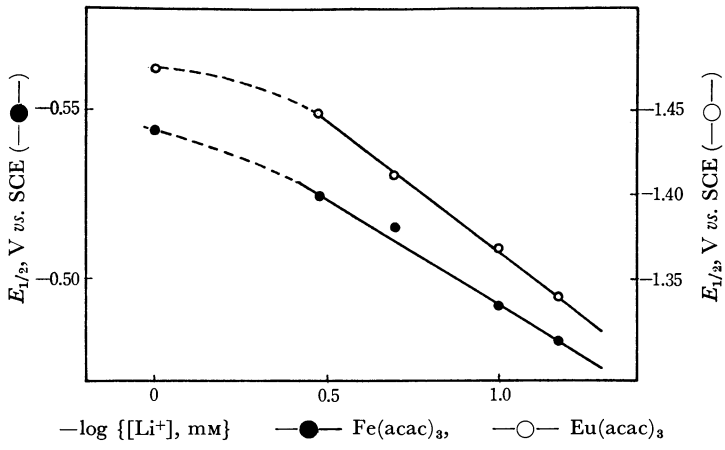

Fig. 4. Plot of $E_{1/2}$ values against log{[Li+]}.

However, in the case of $Eu(acac)_3$ complex we have $\Delta(E_{1/2})/\Delta\log[Li^+]=0.16$. This value is almost equal to the theoretical value of coordinative relaxation reaction of three ligands by Li^+ ions (Eq. (8)). As the half-wave potential of the second wave corresponds to that for the reduction of Eu(II) $\rightarrow$Eu(0) in DMF ($(E_{1/2})_2$: −2.0 V *vs.* SCE), it seems that all ligands of the reduction product of $Eu(acac)_3^-$ are completely stripped off by the addition of $LiClO_4$. The electrode reaction is presumed to be quasi-reversible and one-electron transfer, but the wave denotes apparently the value of the slope of an irreversible wave, caused by the succeeding controlled reaction in coordinative relaxation reaction. Thus, the overall electrochemical reaction would be

$$Eu(acac)_3 + e \rightleftharpoons Eu(acac)_3^- \quad (7)$$

$$Eu(acac)_3^- + 3Li^+ \rightleftharpoons Eu^{2+} + 3Li(acac) \quad (8)$$

$$Eu^{2+} + 2e \rightleftharpoons Eu^0 \quad (9)$$

In a low concentration of $LiClO_4$, a stepwise relaxation reaction of ligand sould occur by the deficiency of Li^+ ions. Though the effect of Mg^{2+} ion on the electrode process of $Fe(acac)_3$ complex is similar to that of Li^+ ion, a quantitative treatment was omitted because of the lack of data for ion association constants.

The cyclic voltammetry for $Fe(acac)_3$ complex was carried out. As shown in Fig. 5, both peaks of reduction and reoxidation were obtained only for $Fe(acac)_3$ complex, the results being ΔE_{peak} equals 60 mV.

An increase in $[LiClO_4]$ shifted the cathodic wave

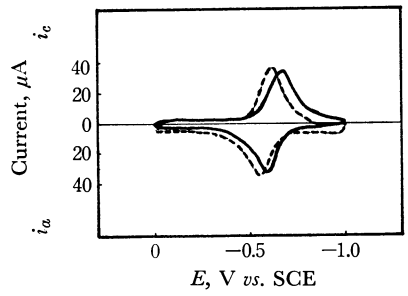

Fig. 5. Cyclic voltammograms for 1.00 mM Fe(acac)3 in 0.1M TEPA in DME.
Scan rate : 1.01 V/sec
——— 0 mM $LiClO_4$, ------- 5 mM $LiClO_4$

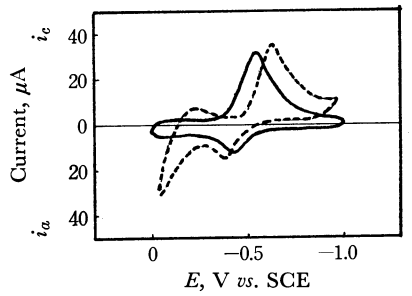

Fig. 6. Cyclic voltammograms for 1.00 mM Fe(acac)3 in 0.1M TEAP in DMF with 20 mM $LiClO_4$.
Scan rate:
——— 1.01 V/sec, ------- 10.1 V/sec

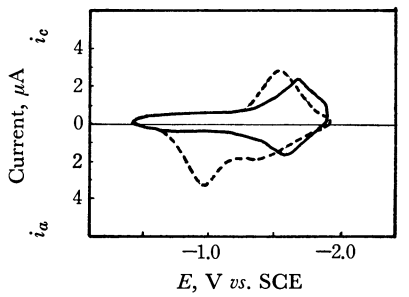

Fig. 7. Cyclic voltammograms for 1.00 mM Eu(acac)3 in 0.1M TEAP in DMF.
Scan rate : 0.151 V/sec
——— 0 mM $LiClO_4$, ------- 20 mM $LiClO_4$

7) G. Gritzner, V. Gutmann and G. Schöber, *Monatsh. Chem.*, **96**, 1056 (1965).

positively and its reoxidation process appeared. These data indicate Eq. (6) to be reversible under this condition. However, as given in Fig. 6, under fast scan of the applied voltage and high lithium concentration, the coordinative relaxation reaction by Li^+ becomes rate-controlled and prevents complete generation of $Fe(acac)_3^-$ species which will give the anodic wave. It was observed that the anodic wave decreased in this case.

In the cyclic voltammetry for $Eu(acac)_3$ complex, as shown in Fig. 7, ΔE_{peak} was found to be approximately 80 mV.

An increase in $[LiClO_4]$ also shifted the cathodic wave positively as the wave in the D.C. polarography. However, the value of ΔE_{peak} became very large and seemed to be an irreversible electrode process controlled by the following coordinative relaxation reaction. This fact supports the results obtained by D.C. polarography of the complex.

The authors wish to thank the Ministry of Education for the financial support given to this work.

BULLETIN OF THE CHEMICAL SOCIETY OF JAPAN VOL. 43 778—782 (1970)

Stability of Tropolone Chelates of the Bi- and Tervalent Metal Ions

Michio HIRAI and Yoshinaga OKA

Department of Chemistry, Faculty of Science, Tohoku University, Katahira-cho, Sendai

(Received July 30, 1969)

The reaction of tropolone with several bi- and tervalent metal ions has been studied spectrophotometrically. Their stability constants (k_1) have been found to be 7.4_0, 3.8_2, 3.0_6, 2.4_5, 7.4_6, 4.6_0, and 6.2_5 for Be(II), Mg(II), Ca(II), Sr(II), Y(III), Cd(II), and La(III) respectively, at 25 ± 0.1°C and at an ionic strength of 0.10. A plot of log k_1 against e^2/r gave a straight line for all the non-polarizable metal ions except Be(II) and Mg(II). The log k_1 values for all the polarizable metal ions are large. The correlation of log k_1 with the second or the third ionization potentials for bi- and tervalent metal ions gave a fairly straight line.

Several metal chelates of troponoid have been studied by many investigators.[1-7] Bryant *et al.* made their studies in 50 per cent dioxane because of the insolubility of metal chelates of troponoid in water.[1-2] The stability constants of copper and zinc chelates with 4-isopropyltropolone have been determined by Dryssen by the solvent extraction technique.[3]

Oka *et al.* have studied the effect of substitution on the stability of iron(III) chelates using 3-, 4- and 5-substituted tropolones.[8-11]

In a previous paper, the present authors have reported the results of their investigations of the tropolone chelates of manganese(II), cobalt(II), nickel(II), copper(II), and zinc(II).[12,13] In this paper their studies of the beryllium(II), magnesium(II), calcium(II), strontium(II), cadmium(II), yttrium(III), and lanthanum(III) chelates with tropolone will be described. In these studies the stability constants have been spectrophotometrically determined.

Experimental

Materials. The tropolone was purified by sublimation at 40°C under reduced pressure, 20 mmHg. All the metal salt solutions were prepared as perchlorate from pure oxides, chlorides or nitrates. The water used was double-distilled. For the adjustment of the ionic strength (0.10), sodium perchlorate was used.

1) B. E. Bryant, W. C. Fernelius and B. E. Douglas, *J. Amer. Chem. Soc.*, **75**, 3784 (1953).
2) B. E. Bryant and W. C. Fernelius, *ibid.*, **76**, 1696, 4864 (1954).
3) D. Dyrssen, *J. Inorg. Nucl. Chem.*, **8**, 291 (1958).
4) J. Rydberg, *Acta Chem. Scand.*, **14**, 157 (1958).
5) B. P. Gupta, Y. Dutt and R. P. Singh, *J. Indian Chem. Soc.*, **43**, 610 (1966); *Indian J. Chem.*, **5**, 214 322 (1967); *J. Inorg. Nucl. Chem.*, **29**, 1806 (1967).
6) A. Beauchamp and R. L. Benoit, *Can. J. Chem.*, **44**, 1607, 1615 (1966).
7) D. L. Campbell and T. Moeller, *J. Inorg. Nucl. Chem.*, **31**, 1077 (1969).
8) Y. Oka, M. Umehara and T. Nozoe, *Nippon Kagaku Zasshi*, **83**, 703, 1197 (1962).
9) Y. Oka and K. Yamamoto, *ibid.*, **85**, 779 (1964).
10) Y. Oka, M. Yanai and C. Suzuki, *ibid.*, **85**, 873 (1964).
11) Y. Oka and M. Yanai, *ibid.*, **86**, 929 (1965).
12) Y. Oka and M. Hirai, *ibid.*, **89**, 589 (1968).
13) Y. Oka, I. Watanabe and M. Hirai, *ibid.*, **89**, 1220 (1968).

Measurements. For the measurement of absorbance, Hitachi Model EPU-2 and EPS-2 spectrophotometers were used. The pH of the solutions was measured with a Hitachi-Horiba Model M-5 pH meter.

Results and Discussion

Acid Dissociation Constant of Tropolone. Tropolone is amphoteric, and its absorption spectrum changes with variations in the pH of the solution. In the pH range from 1.5 to 3.4, the spectrum I in Fig. 1 was obtained; this is the absorption spectrum of tropolone itself. Above pH 9.6, tropolone dissociates completely and gives the spectrum II. In a strong acidic solution, in a 2N $HClO_4$ solution for example, the spectrum III was obtained, indicating the formation of the dihydroxytropylium ion (I).

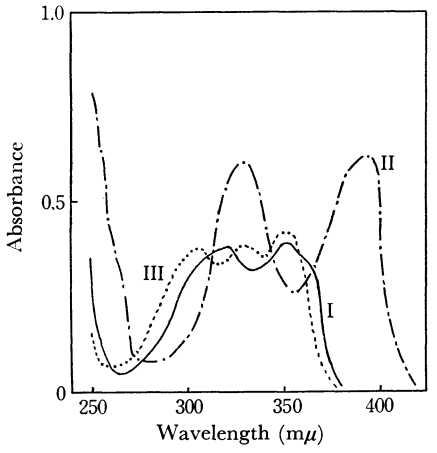

Fig. 1. Absorption spectra of tropolone.
tropolone: 6.06×10^{-5} mol/l
I; pH 1.5—3.4, II; pH >9.6, III; $HClO_4$ 3.2N

The acid dissociation constant, K_a, of tropolone was evaluated spectrophotometrically at an ionic strength of 0.10 and at 25.0±0.1°C.

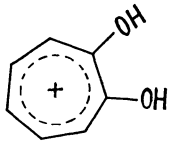

(I) Dihydroxytropylium ion

When tropolone (HL) dissociates as follows:

$$HL = L^- + H^+$$

the following equation is derived, as has been reported previously:[14]

$$\frac{a}{(A-A')} = \frac{1}{(\varepsilon_2-\varepsilon_1)} + \frac{1}{(\varepsilon_2-\varepsilon_1)K_a}\cdot[H^+] \qquad (1)$$

where A is the total absorbance of the solution at various pH values, a is the analytical concentration of tropolone, ε_1 and ε_2 are the molar extinction coefficients of tropolone and the tropolonate ion respectively, and A' is equal to $\varepsilon_1 a$. Equation (1) shows that a plot of $a/(A-A')$ against $[H^+]$ may give a straight line. The acid dissociation constant, K_a, may, then, be calculated from the intercept and the slope of the straight line.

Keeping the analytical concentration of tropolone $1.21_2\times10^{-4}$ mol/l, and varying the pH-values of the solution in the range from 6.40 to 6.91, the total absorbances were measured, the ionic strength being adjusted to 0.10. The plots of $a/(A-A')$ against $[H^+]$ are shown in Fig. 2. Good straight lines were obtained at various wavelengths. The acid dissociation constant calculated is shown in Table 1.

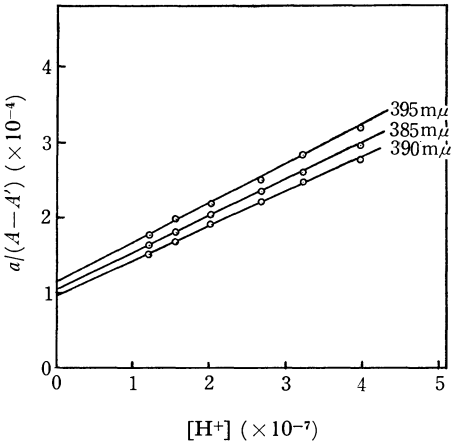

Fig. 2. Correlation of $a/(A-A')$ with $[H^+]$.
Tropolone: $1.21_2\times10^{-4}$ mol/l
25.0±0.1°C, ionic strength; 0.10, pH 6.40±6.91

Table 1. Acid dissociation constant of tropolone (K_a)
25.0±0.1°C, ionic strength: 0.10

Wavelength (mμ)	pK_a
385	6.68
390	6.68
395	6.68
mean	6.68

Stability Constants of Metal Chelates (1 : 1) with Tropolone. Each of the metal perchlorate solutions was added in excess into a tropolone solution, the ionic strength being kept at 0.10 with sodium perchlorate. The pH values of the solutions were varied in the range where the hydrolysis of metal ions does not occur in any appreciable extent. As an example, the absorption spectra of strontium-(II)-tropolone system are shown in Fig. 3. At pH

14) a) Y. Oka and R. Tanaka, *Nippon Kagaku Zasshi*, **81**, 1846 (1960). b) H. A. Benesei and J. H. Hildebrand, *J. Amer. Chem. Soc.*, **71**, 2703 (1949).

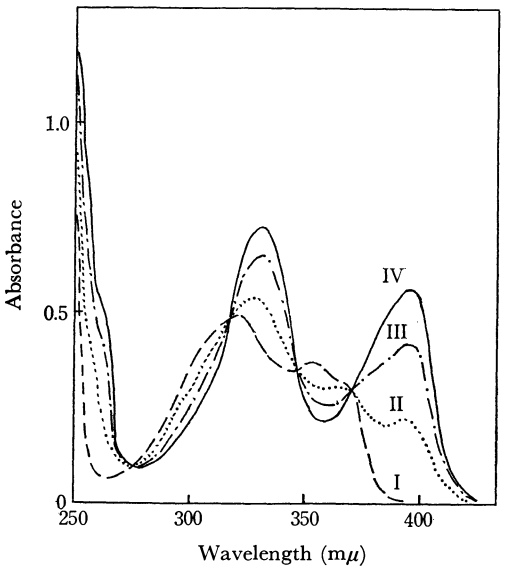

Fig. 3. Change of absorption spectrum of Sr(II)-tropolone system depends on pH in the presence of excess metal ion.
Tropolone: 6.01×10^{-5} mol/l
$Sr(ClO_4)_2$: 1.65×10^{-2} mol/l
I, pH 1.72; II, 5.93; III, pH 6.70; IV, pH 8.41

1.72 a spectrum I identical with that of tropolone was obtained. In this pH region, therefore, it may be considered that tropolone does not react with strontium. Above pH 5.9, the spectra II, III, and IV were obtained.

If, in the presence of an excess of the metal ion, tropolone (HL) reacts following Eq. (2):

$$M^{n+} + HL = ML^{(n-1)+} + H^+ \qquad (2)$$

the equilibrium constant, K_1, can be expressed as follows:

$$K_1 = \frac{[ML^{(n-1)+}][H^+]}{[M^{n+}][HL]} \qquad (3)$$

Then,

$$K_1 = \frac{x[H^+]}{(b-x)(a-x)} \qquad (4)$$

where x is the equilibrium concentration of the metal chelate formed, and a and b are the total concentrations of the tropolone and the metal ion respectively. When the concentration of the metal ion is large enough, we may safely assume that $(b-x)\fallingdotseq b$.

Next, when measurements are made in the wavelength range where the molar extinction coefficient of the metal ion is zero, the total absorbance, A, is expressed as follows:

$$A = \varepsilon_1[HL] + \varepsilon_3[ML^{(n-1)+}] = \varepsilon_1(a-x) + \varepsilon_3 x \qquad (5)$$

where ε_1 and ε_3 are the molar extinction coefficients of the tropolone and the metal chelate respectively.

From Eqs. (4) and (5), Eq. (6) is derived:

$$\frac{a}{(A-A')} = \frac{1}{(\varepsilon_3-\varepsilon_1)} + \frac{1}{(\varepsilon_3-\varepsilon_1)k_1}\cdot\frac{[H^+]}{bK_a} \qquad (6)$$

where k_1 is the stability constant.

In case when a chelate is formed in the pH range above 3.4, the dissociation of tropolone is not negligible. Then, Eq. (7) is derived:

$$\frac{a}{A} = \frac{1}{\varepsilon_3} + \frac{1}{\varepsilon_3 k_1 b}\cdot\frac{(A-A')[H^+]+(A-A'')K_a}{AK_a} \qquad (7)$$

where $A'=\varepsilon_1 a$, $A''=\varepsilon_2 a$, and ε_1 is the molar extinction coefficient of tropolone, and ε_2, that of the tropolonate ion. A plot of $a/(A-A')$ against $[H^+]/bK_a$ or of a/A against $\{(A-A')[H^+]+(A-A'')\cdot K_a\}/AK_a$ will give a straight line.

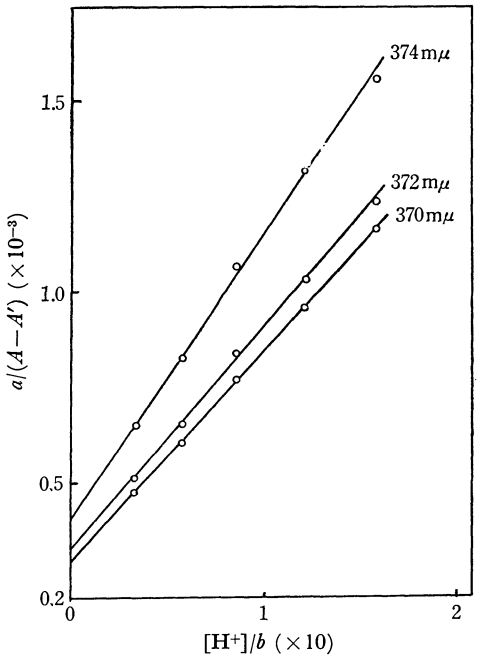

Fig. 4. Correlation of $a/(A-A')$ with $[H^+]/b$ (Be(II)-tropolone system).
Tropolone: $1.20_2\times10^{-4}$mol/l
$Be(ClO_4)_2$: $3.04_8\times10^{-3}$mol/l
25.0±0.1°C, ionic strength 0.10, pH 1.32—1.96

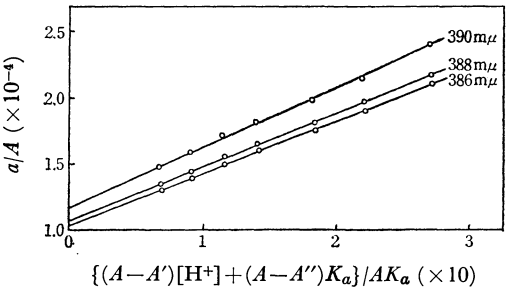

Fig. 5. Correlation of a/A with $\{(A-A')[H^+]+(A-A'')K_a\}/AK_a$ (Ca(II)-tropolone system).
Tropolone: $1.20_2\times10^{-4}$ mol/l
$Ca(ClO_4)_2$: $2.24_1\times10^{-2}$ mol/l
25.0±0.1°C, ionic strength 0.10, pH 5.22—5.82

For the beryllium(II)-, magnesium(II)-, yttrium(III)-, cadmium(II)- and lanthanum(III)-systems, Eq. (6) is used, while for the calcium(II)- and strontium(II)-systems, Eq. (7) is used. In all cases, good straight lines are obtained. Some sample results are shown in Figs. 4 and 5. Therefore, it can be safely concluded that 1 : 1 chelates are formed in such circumstances.

From the slopes and the intercepts of the straight lines, the stability constants are calculated to be as shown in Table 2.

TABLE 2. STABILITY CONSTANTS (k_1) OF METAL CHELATES (1 : 1) WITH TROPOLONE
25.0±0.1°C; ionic strength, 0.10

Metal ion	Wavelength (mμ)	log k_1
Be(II)	370	7.39
	372	7.40
	374	7.40
	average	$7.4_0\pm0.0_1$
Mg(II)	386	3.82
	388	3.82
	390	3.81
	average	$3.8_2\pm0.0_1$
Ca(II)	386	3.05
	388	3.06
	390	3.06
	average	$3.0_6\pm0.0_1$
Mn(II)	average	$4.6_0\pm0.0_1$ [13]
Co(II)	average	$5.5_9\pm0.0_1$ [13]
Ni(II)	average	$5.9_7\pm0.0_1$ [13]
Cu(II)	average	$8.3_5\pm0.0_0$ [12]
Zn(II)	average	$5.8_4\pm0.0_0$ [13]
Sr(II)	386	2.45
	388	2.45
	390	2.46
	average	$2.4_5\pm0.0_1$
Y(III)	376	7.46
	378	7.47
	380	7.47
	382	7.46
	384	7.46
	average	$7.4_6\pm0.0_1$
Cd(II)	380	4.60
	384	4.60
	388	4.61
	390	4.59
	average	$4.6_0\pm0.0_1$
La(III)	380	6.24
	382	6.25
	384	6.25
	386	6.25
	average	$6.2_5\pm0.0_0$

The stability constants increase from strontium to copper in the following order:

Sr(II)<Ca(II)<Mg(II)<Cd(II), Mn(II)<Co(II)<Zn(II)<Ni(II)<La(III)<Be(II)<Y(III)<Cu(II)

For chelates of the primarily "ionic" type, the strength of chelation should increase with an increase in the ionic charge of both metal ion and donor, and with a decrease in the ionic radius of the metal ion. Martell *et al.* have discussed the

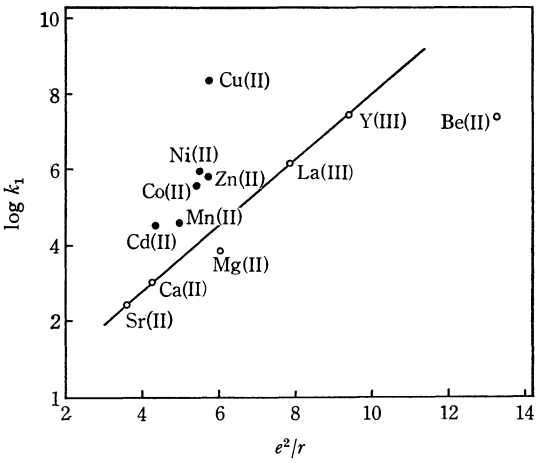

Fig. 6. Correlation of log k_1 with e^2/r for metal complexes (1 : 1) with tropolone.
○: non-polarizable metal ion
●: polarizable metal ion

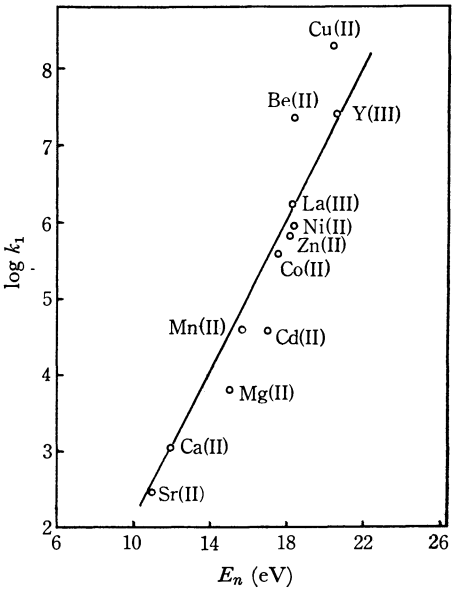

Fig. 7. Correlation of log k_1 with nth ionization potential for metal chelates (1 : 1) with tropolone.
E_n: nth ionization potential
n=2 for bivalent metal ion
n=3 for tervalent metal ion

stability constants with respect to charge(e)/radius(r) and e^2/r for a number of chelates which would be expected to form a primarily ionic bond.[15-17] They have found that e^2/r is superior. Where electrostatic interaction is predominant, $\log k_1$ may have a direct correlation with e^2/r. A similar treatment was attempted in the case of tropolone chelates; the results shown in Fig. 6 were obtained. A good straight line is observed for all the non-polarizable metal ions except beryllium(II) and magnesium(II). Their $\log k_1$ values are smaller than those expected. The ionic radii of these metal ions are small. It seems possible, therefore, that the steric effect hinders the stability. On the other hand, the values of $\log k_1$ for all polarizable metal ions are large. The polarization of the metal ion should be expected to enhance the stability of the chelates. Figure 7 shows the correlation of $\log k_1$ with the second and third ionization potentials for chelates of bi- and tervalent metals.[18] A fairly good correlation is observed.

The authors would like to express their thanks to Dr. Hiroshi Sugiyama, The Chemical Research Institute of Non-Aqueous Solutions, Tohoku University, who kindly provided us with the tropolone.

15) A. E. Martell and M. Calvin, "Chemistry of the Metal-Chelate Compounds," Prentice-Hall, Englewood Cliffs, N. J., (1952) p. 191; J. Lewis and R. G. Wilkins, ed., "Modern Coordination Chemistry," Interscience Publishers, New York, N. Y. (1960) p. 39; F. Basolo and R. G. Pearson, "Mechanisms of Inorganic Reactions," John Wiley & Sons, New York (1958), p. 72.

16) C. W. Davies, *J. Chem. Soc.*, **1951**, 1256.

17) V. N. Kumok and V. V. Serebrennikov, *Zh. Neorg. Khim.*, **10**, 2019 (1965).

18) M. Calvin and N. C. Melchior, *J. Amer. Chem. Soc.*, **70**, 3270 (1948).

BULLETIN OF THE CHEMICAL SOCIETY OF JAPAN VOL. 43 782—786 (1970)

The Cation-exchange Separation of Nitrosylruthenium(III) from Ruthenium(III and IV) and Its Radiochemical Applications

Eiichi MIKI, Tatsujiro ISHIMORI and Hisateru OKUNO

Department of Chemistry, College of Science, Rikkyo University, Toshima-ku, Tokyo

(Received August 12, 1969)

The cation-exchange separation was made on a 0.1 M perchloric acid solution of the evaporated residue of a hydrochloric acid solution which contained nitrosylruthenium(III) of 10 mg—100 μg Ru and ruthenium(III and IV) of 100—10 μg Ru; the nitrosylruthenium species were eluted by the use of 80—90 m*l* of 0.1 M perchloric acid, and the ruthenium species, by the use of 100 m*l* of 3 M hydrochloric acid containing 50 vol% ethyl alcohol for the columns (3—8 m*l*) of the HR type. It was found by means of the separation that a ^{106}Ru-nitrosylruthenium tracer can be quantitatively prepared by passing nitric oxide into a hydrochloric acid solution of ^{106}Ru-ruthenium(III and IV). The separation on dipotassium pentachloronitrosylruthenate(III) irradiated by thermal neutrons indicated that the specific activities caused by ^{103}Ru in the ruthenium fractions are a few hundred times as high as those in the nitrosylruthenium fractions.

In acid aqueous solutions, both ruthenium(III and IV) and nitrosylruthenium(III) species are present as stable species. However, the chemical behavior of nitrosylruthenium(III) is different from that of ruthenium(III) and (IV). The separation of the nitrosylruthenium(III) species from the ruthenium(III or IV) species is necessary in order to study the chemistry of ruthenium. Kepak and Kanka have reported that an efficient separation was achieved by adsorption on iron(II) hydroxide.[1)]

We attempted to separate small amounts of ruthenium(III and IV) and nitrosylruthenium(III) species in hydrochloric acid solutions by the use of the cation-exchange technique.

The separation can be carried out on a perchloric acid solution of the evaporated residue of a hydrochloric acid solution of 10 mg—100 μg nitrosylruthenium(III) and 100—10 μg ruthenium(III and IV). This paper will also report on such applications of the separation to the radiochemistry of ruthenium as preparing the labeled nitrosylruthenium(III) species and the separation of ^{103}Ru with high specific activities from dipotassium penta-

1) *Chem. Abstr.*, **67**, 95533w (1967); F. Kepak and J. Kanka, *Int. J. Appl. Radiat. Isotopes*, **18**, 673 (1967).

chloronitrosylruthenate(III) irradiated by thermal neutrons.

Experimental

Ru(III and IV)*1 in a hydrochloric acid solution was prepared by distilling ruthenium tetroxide into an alcoholic hydrochloric acid solution, evaporating the distillate, and dissolving the evaporated residue with a hydrochloric acid solution, or by dissolving the commercial $RuCl_3 \cdot 3H_2O$ with a hydrochloric acid solution. Ru(III)NO in a hydrochloric acid solution was prepared by bringing nitric oxide into contact with Ru(III and IV) in a hydrochloric acid solution.[2]

The sample solutions for the cation-exchange separation were prepared by evaporating hydrochloric acid solutions of Ru(III and IV) or/and Ru(III)NO, dissolving the evaporated residue in 10 m*l* of a 0.1M perchloric acid solution, and allowing the solution to digest for thirty minutes in a boiling-water bath.

Dipotassium pentachloronitrosylruthenate(III) was prepared by adding an excess of potassium chloride in a hydrochloric acid solution of Ru(III)NO and was recrystallized from a 0.1M hydrochloric acid solution.[3]

The ^{106}Ru was purchased from the Radiochemical Centre, Amersham, England, and was purified by the distillation of the tetroxide. The radiochemical purity of the ^{106}Ru was examined by means of its γ-ray spectrum; no impurity was found with respect to γ-emitters. The tracer solutions of the ^{106}Ru were prepared by the same procedures as the solutions containing the ordinary amount of Ru(III and IV) or Ru(III)NO.

The cation exchanger used was Dowex 50, X-4, with a hydrogen-ion form. The chromatographic procedures were carried out with columns 1 cm in diameter and 3—8 m*l* in volume at the flow rate of 1 m*l*/min.

The ruthenium was determined spectrophotometrically by the phenanthroline method[4] and the thiourea method.[4] The latter could not, however, be applied to the samples containing Ru(III)NO species. The radioactivities of ^{106}Ru or ^{103}Ru in solutions were measured as gross γ-activities with a well-type NaI(Tl) scintillator.

Results and Discussion

Sorption of Ruthenium and Nitrosylruthenium Species in Perchloric Acid Solutions on Cation-exchange Resins. The study of the species of ruthenium(IV) in perchloric acid solutions has indicated that the average charge on the aqueous species is +2, and extensive polymerization was observed in these solutions.[5] In the perchloric acid solution of the ruthenium(III and IV) chloride*2 prepared as has been described above, almost all the ruthenium species were found by iodometric titration to be in the Ru(IV) state and were expected to be cationic from their strong sorption on the cation exchanger. The species in the solution of the nitrosylruthenium(III) chloride*2 will be discussed later.

The distribution coefficients (K_d) of ruthenium and nitrosylruthenium species between the cation exchanger and perchloric acid-hydrochloric acid solutions were determined with ^{106}Ru tracers of the ruthenium and nitrosylruthenium species. A part of the perchloric acid in the solutions was replaced by hydrochloric acid in order to observe the effect of chloride ions on the distribution coefficients. As will later be decribed in more detail, we found a certain abnormal behavior of the radioactive tracer of the ruthenium species on the cation exchanger, and the values of the distribution coefficients obtained were not considered to give a strict measure of the sorption of ruthenium species on the cation exchanger. The values of K_d for the ruthenium species were great over the range of chloride concentration less than 0.04M at the 0.15M hydrogen-ion concentration (log K_d:

Table 1. Separation of the Ru(III and IV) and the Ru(III)NO chlorides

Ru added (mg)		Ru found (mg)	
Ru(III)-NO	Ru-(III and IV)	RuNO-fraction	Ru-fraction
10.9	10.0	10.7 (90)*	6.94 (100)*
10.9	1.00	10.9 (80)	0.642 (270)
10.9	0.400	10.6 (80)	0.362 (100)
10.9	0.200	11.0 (80)	0.176 (30)
0.100	0.104	0.098(90)	0.104 (30)
0.109	0.100	0.109(80)	0.097 (—)
10.9	0.100	10.5 (80)	0.098 (30)
0.130	0.100	0.130(80)	0.094 (30)
2.61	0.100	—	0.098 (30)
10.9	0.050	11.0 (80)	0.053 (20)
10.9	0.025	10.7 (80)	0.026 (20)
10.9	0.010	10.7 (80)	0.011 (20)

* Volume (m*l*) required for the elution.

*1 The Ru(IV) was estimated by iodometric titration to be 20—40%.

2) J. M. Fletcher, I. L. Jenkins, F. M. Lever, F. S. Martin, A. R. Powell and R. Todd, *J. Inorg. Nucl. Chem.*, **1**, 378 (1955).

3) "Gmelins Handbuch der Anorganischen Chemie," Ruthenium (1938), S. 93.

4) E. B. Sandell, "Colorimetric Determination of Traces of Metals," 3rd Ed., Interscience Publishers, New York (1959), p. 784, 781.

5) F. P. Gortsema and Cobble, *J. Amer. Chem. Soc.*, **83**, 4317 (1961).

*2 In this paper, the ruthenium(III and IV) and the nitrosylruthenium(III) chlorides are the evaporated residues of a hydrochloric acid solution of Ru(III and IV) and of Ru(III)NO respectively. The ruthenium chloride has been thought to be $Ru(OH)Cl_3$ (N. V. Sidgwick, "Chemical Elements and Their Compounds," Vol. II, Oxford, (1950), p. 1476). The nitrosylruthenium(III) chloride is considered to be $H_2[RuCl_4OHNO] \cdot 2H_2O$ and $RuCl_3NO \cdot nH_2O$.[3]

Table 2. Behavior of ^{106}Ru-tracer in the separation

Sample	Found in RuNO-fraction			Found in Ru-fraction		
	Activity %	μg	vol (ml)	Activity %	μg	vol (ml)
*Ru[1]	38.2	—	150	61.0	—	200
*Ru, Ru 100 μg[2]	10.8	0	90	89.0	97	100
*Ru, Ru 100 μg[3]	10.2	0	90	89.5	99	100
*Ru, Ru 100 μg, RuNO 100 μg[4]	11.3	91	80	88.4	103	90
**Ru (4 μg)	3.4	—	90	94.6	—	120
**Ru (4 μg), Ru 100 μg[4]	0.3	0	90	98.9	103	30
**Ru (4 μg), Ru 100 μg, RuNO 100 μg[4]	0.9	98	90	98.2	104	20
Ru 100 μg, radioactive RuNO (120 μg)	98.4	130	90	1.6	94	30

*Ru: The ^{106}Ru-tracer stored in 0.2M HCl.
**Ru: The ^{106}Ru-tracer eluted in the ruthenium fraction with a carrier in the separation. This was stored in 3M HCl and used within several days after the preparation.
1) To *Ru solution, an equal volume of 6M HCl was added and then the solution was evaporated.
2) The *Ru was digested as 3M HCl solution and evaporated. Then, the carrier was added and the mixture was evaporated.
3) The *Ru and the carrier were mixed and the mixture was digested as 6M HCl solution after addition of Br_2(aq) and evaporated.
4) The mixture was evaporated.

about 3.0 for $[Ru_{aq}]$=the order of 7×10^{-8}M) and decreased upon the addition of hydrochloric acid to the solution phase ($\log K_d$: 2.9 for $[Cl^-]=0.16$, $[H^+]=0.31$; 1.8 for $[Cl^-]=0.5$, $[H^+]=0.65$, $[Ru_{aq}]=7\times10^{-8}$M). The K_d values for the nitrosylruthenium species were less than 10(ml/g) over the chloride-concentration range of 10^{-3} to 0.1M and the hydrogen-ion concentration range of 0.02 to 0.4M.

Mutual Separation of the Ruthenium(III and IV) and the Nitrosylruthenium(III) Chlorides by Cation-exchange Technique. The separation method was examined using sample solutions of the 0.1M perchloric acid solution of the ruthenium or/and the nitrosylruthenium chlorides and a cation-exchanger column 1 cm in diameter and 8 ml in volume. For ruthenium species less than 100 μg Ru and nitrosylruthenium species less than 10 mg Ru, the separation was satisfactorily done by the following procedure: the sample solution (10 ml) was passed through the column, and then 80—90 ml of 0.1M perchloric acid was passed to elute the nitrosylruthenium species. The ruthenium species absorbed were eluted by 100 ml of 3M hydrochloric acid containing 50 vol% ethyl alcohol. The results of the separation are given in Table 1. The use of a perchloric acid solution in the cation-exchange separation of this type has been reported on the separation of platinum from palladium, rhodium, and iridium.[6]

The recoveries of ruthenium and nitrosylruthenium species were often less than 100%; the average deviation(%) on the recovery was −2.3% for 11 samples of ruthenium species containing 100 μg of Ru and −1.4% for 11 samples of nitrosylruthenium species containing 10.9 mg Ru. When ruthenium species more than 100 μg Ru were present in the sample solutions, the ruthenium species were not eluted quantitatively with an ethanolic hydrochloric acid solution. Incomplete recoveries in the ion-exchange separations have also been described in connection with the separation of platinum metal species.[7] The nitrosylruthenium species eluted were thought to be anionic, neutral, and univalent cationic chloro complexes; the anionic and neutral species were eluted, and then the univalent cationic complex was eluted as a single band. This cationic species was identified as $[RuCl_2(H_2O)_3NO]^{1+}$ by comparing the visible spectrum of its solution with the data provided by Mercer and Campbell.[8] The bivalent and tervalent cationic species of nitrosylruthenium were not present in the perchloric acid solution of the nitrosylruthenium chloride.

It was observed that the behavior of the radioactive ruthenium species was in part different from that of the carrier of ruthenium species in the cation-exchange separation (Table 2). The separations were carried out using columns 1 cm in diameter and 3 ml in volume. The ^{106}Ru-tracer of ruthenium (III and IV) had been stored in 0.2M hydrochloric acid, and its concentration was estimated to be 10^{-7}M. About 40% of the activity was eluted with 0.1M perchloric acid in the nitrosylruthenium fraction. Similar phenomena were observed even when 100 μg ruthenium species was added to the radioactive ruthenium species as a carrier and the mixture was evaporated after the addition of hydrochloric acid. When the radioactive species and the

6) P. Stevenson, A. Frank, R. Berg and W. Nervik, *J. Amer. Chem. Soc.*, **75**, 4876 (1953).

7) O. Samuelson, "Ion-exchange Separations in Analytical Chemistry," John Wiley & Sons, New York (1963), p. 399.

8) E. E. Mercer, W. A. Campbell, Jr., and R. M. Wallace, *Inorg. Chem.*, **3**, 1018 (1964).

carrier eluted in the ruthenium fraction were treated again by the same separation procedure, almost all the activities were found in the ruthenium fraction.

There have been studies[9-12] of a variety of ruthenium(III) and (IV) species in hydrochloric acid solutions, and the equilibria among the species have been considered to be complicated. It can be suggested that part of the radioactive tracers of ruthenium species may form neutral and/or anionic species, or polymers, and that they can not be converted to the species of the carrier even by evaporating them with the carrier in a hydrochloric acid solution.

The data in Table 2 indicate that no appreciable exchange of ruthenium atoms between ruthenium and nitrosylruthenium species occurred under the experimental conditions used.

Preparation of the Radioactive Nitrosylruthenium Tracer. It has been reported that the nitrosylruthenium tracer can be prepared in a good yield by treating the evaporated residue of a hydrochloric acid solution of ^{106}Ru with fuming nitric acid.[13] Nitrosylruthenium(III) in ordinary amounts has been prepared by passing nitric oxide into a dilute hydrochloric acid solution of ruthenium-(III and IV).[2] We determined the yield when the nitrosylruthenium tracer was prepared with fuming nitric acid or with nitric oxide. The method of preparing with fuming nitric acid was as follows; 1 m*l* of a dilute hydrochloric acid solution of ^{106}Ru was evaporated to dryness, and then a few drops of fuming nitric acid were added and the mixture was evaporated on a boiling-water bath. The evaporation with fuming nitric acid was then repeated. The residue was dissolved in 1 m*l* of concentrated hydrochloric acid and evaporated; a 0.1 M hydrochloric acid solution of radioactive nitrosylruthenium(III) was thus prepared. The method of preparing with nitric oxide was as follows; nitric oxide was passed into a dilute hydrochloric acid solution of the ^{106}Ru tracer for about twenty hours; the solution was then evaporated and again evaporated after the addition of hydrochloric acid. A 0.1 M hydrochloric acid solution of radioactive nitrosylruthenium(III) was thus prepared.

The carriers of ruthenium(III and IV) and nitrosylruthenium(III), each containing 100 μg Ru, were added to the radioactive nitrosylruthenium-(III), and a cation-exchange separation was carried out on the mixture in order to determine the yield in the preparation of radioactive nitrosylruthenium-(III). The results are shown in Table 3. It was found that the radioactive nitrosylruthenium tracer was prepared in a much better yield with nitric oxide than with fuming nitric acid. It was also observed that a part of the activity escaped in air in the preparation with fuming nitric acid if the reaction mixture was heated at a considerable temperature by means of a boiling-water bath or an infrared lamp.

Table 3. Examination of the yield in the preparation of radioactive nitrosylruthenium tracer

Method	Activity found in RuNO-fraction %	Activity found in Ru-fraction %
Fuming nitric acid	64.6	32.9
	67.4	32.0
	60.9	36.6
	63.8	35.6
Nitric oxide	98.8	1.0
	98.1	1.6
	98.7	1.1
	97.9	1.8

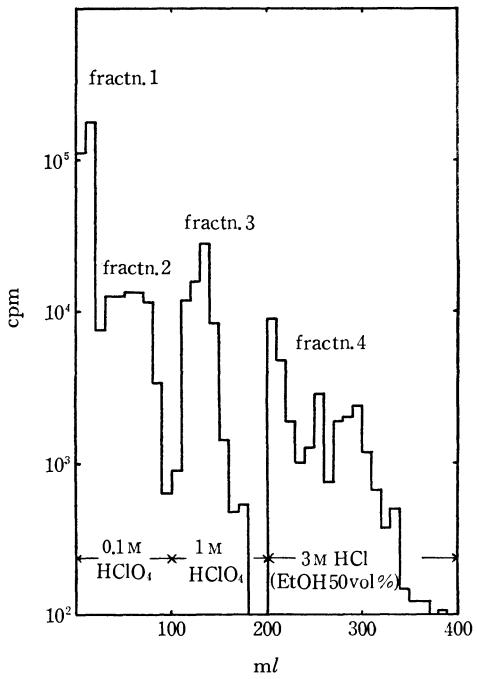

Fig. 1. The cation-exchange separation of the irradiated $K_2[RuCl_5NO]$.
Activities(%), Ru(mg) and specific activities (cpm/mg Ru) found in fractions 1, 2, 3 and 4 were: 58.0, 2.16, 1.06×10^5; 19.4, 0.386, 2.56×10^5; 15.2, 0.001,* 6.02×10^7; and 7.4, 0.001,* 2.89×10^7; respectively. *: less than the detection limit.

9) H. H. Cady and R. E. Connick, *J. Amer. Chem. Soc.*, **79**, 4242 (1957); **80**, 2646 (1958).
10) R. E. Connick, "Advances in the Chemistry of the Coordination Compounds," ed. by S. Kirschner, MacMillan, New York (1961), p. 17.
11) S. K. Shukla, *J. Chromatogr.*, **8**, 96 (1962).
12) A. Ohyoshi, E. Ohyoshi, M. Senoo and M. Shinagawa, *J. Nucl. Sci. Technol.*, **3**, 237 (1966).
13) J. Griess, *J. Electrochem. Soc.*, **100**, 429 (1953); M. H. Lietzke and J. Griess, *ibid.*, **100**, 434 (1953).

The Separation on Dipotassium Pentachloronitrosylruthenate(III) Irradiated by Thermal Neutrons. Dipotassium pentachloronitrosylruthenate(III) was irradiated by thermal neutrons to prepare a ^{103}Ru-tracer with a high specific activity by the use of the hot-atom reactions. The irradiation was carried out on a rotatory specimen rack (about $3.5\times10^{11}n_{th}$ cm^{-2} sec^{-1}) in a nuclear reactor of the TRIGA MARK II type at Rikkyo University.

In a typical example, $K_2[RuCl_5NO]$ (10 mg) was irradiated for 15 hr over 4 days and then cooled at room temperature for several days. The irradiated sample was thereafter dissolved in an ethanolic hydrochloric acid solution and evaporated. The residue was dissolved in a 0.1M perchloric acid solution to prepare the solution for the cation-exchange separation. The separation was carried out with a column 1 cm in diameter and 3 m*l* in volume. The results of the separation are shown in Fig. 1. The γ-activities could be measured excluding the β-activity of ^{35}S produced by ^{35}Cl(n, p)^{35}S. The γ-activities caused by ^{97}Ru and ^{105}Ru, the daughter of ^{105}Ru, were estimated to be very small parts of the total γ-activity. A small contribution by ^{42}K was possible in the activity of fraction 1 in Fig. 1. The γ-activities of fractions 1, 2, 3 and 4 were identified as those of ^{103}Ru by measuring their γ-spectra and their half-lives. The specific activities (cpm/mg Ru) of the ruthenium fractions (fractions 3 and 4) were a few hundred times as large as those of the nitrosylruthenium fractions (fractions 1 and 2). The activity in the ruthenium fraction was 23% of the total activity. The separation included elution with 1M perchloric acid (fraction 3 in Fig. 1); the species eluted was a ruthenium species with a high specific activity.

It was shown that the cation-exchange separation is useful in the preparation from the irradiated nitrosylruthenium complex of a ^{103}Ru-tracer with a high specific activity.

We have prepared ^{15}N-nitrosylruthenium(III) complexes in a semimicro scale.[14,15] The separation method has then been usefully used to examine the formation of nitrosylruthenium(III) by the use of limited amounts of nitric oxide.

14) E. Miki, T. Ishimori, H. Yamatera and H. Okuno, *Nippon Kagaku Zasshi*, **87**, 703 (1966).
15) E. Miki, This Bulletin, **41**, 1835 (1968).

BULLETIN OF THE CHEMICAL SOCIETY OF JAPAN VOL. 43 786—789 (1970)

Cobalt(III) and Chromium(III) Complexes with Ethylenediaminemonoacetic Acid*1

Yuki Fujii,*2 Eishin Kyuno and Ryokichi Tsuchiya

Department of Chemistry, Faculty of Science, Kanazawa University, Kanazawa

(Received August 21, 1969)

Cobalt(III) and chromium(III) complexes with ethylenediaminemonoacetic acid (EDMA), $[Co(edma)_2]Cl \cdot 2H_2O$ and $[Cr(edma)_2]Cl \cdot 3H_2O$, (edma: $H_2NCH_2CH_2NHCH_2COO^-$), were prepared. The former complex was isolated as two geometrical isomers. From the electronic absorption spectra, the two isomers were assigned to *trans* and *cis* forms with respect to the carboxylate oxygen atoms coordinated. Chromium(III) complex was concluded to have the *trans* form by comparing the IR spectrum with those of the above two isomers of cobalt(III) complexes.

Terdentate chelating ligands can take various coordination forms in octahedral environment, depending upon the steric requirements of the ligands and the character of the central metal ion, especially upon the kind of coordination sites the ligands contain. As typical representatives of the terdentate ligands of (N,O,O)-, (N,N,O)- and (N,N,N)-types, iminodiacetic acid, ethylenediaminemonoacetic acid (abbreviated as EDMA)[1] and diethylenetriamine can be chosen.

In the present work EDMA, a simple, artificial and basic amino acid, was selected as the terdentate ligand. There are only a few reports[2,3] on the metal complexes with EDMA. In order to in-

*1 Presented, in part, at the 21st Annual Meeting of the Chemical Society of Japan, Osaka, March, 1968.

*2 Present address: Department of Chemistry, Faculty of Science, Ibaraki University, Mito.

1) T. Goldschmit, *Ger.*, **819**, 402 (1951).
2) M. A. Doran, *Anal. Chem.*, **33**, 1752 (1961).
3) M. Idelson, I. R. Karady, B. H. Mark, D. O. Rickter and V. H. Hooper, *Inorg. Chem.*, **6**, 450 (1967).

vestigate the stereochemistry of the complexes, the following two purposes were presented: (1) preparation of the EDMA complexes of cobalt(III) and chromium(III) ions, and (2) approach to the structures of the complexes by comparing their electronic and IR spectra with those of the related complexes.

Experimental

Preparation of the Complexes. *1) trans-Bis(ethylenediaminemonoacetato)cobalt(III) Chloride Dihydrate, trans*-[Co(edma)$_2$*[3]]Cl·2H$_2$O (I). 25.2 g (0.12 mol) of ethylenediaminemonoacetic acid dihydrochloride monohydrate (Hedma·2HCl·H$_2$O) was dissolved into 50 m*l* of water and the solution was neutralized with 20 g (0.24 mol) of sodium hydrogencarbonate. To this solution was added a solution of 10.4 g (0.044 mol) of cobalt(II) chloride hexahydrate in a very small amount of water and 10 m*l* of hydrogen peroxide (10%), and the mixture was warmed on a water bath to nearly 40°C. After the solution was evaporated to about 60 m*l*, an equal volume of ethanol was added to the resulting solution. The solution was kept in a refrigerator. Reddish purple crystals were separated out and recrystallized from 50% ethanol solution. Yield, 5.2 g (32.5%).

Found; C, 26.04; H, 5.87; N, 15.78%. Calcd for [Co(edma)$_2$]Cl·2H$_2$O: C, 26.34; H, 6.09; N, 15.36%.

2) cis-Bis(ethylenediaminemonoacetato)cobalt(III) Chloride Dihydrate, cis-[Co(edma)$_2$]Cl·2H$_2$O (II). To a solution of hexaamminecobalt(III) chloride (5.4 g, 0.02 mol), 9.4 g (0.045 mol) of Hedma·2HCl·H$_2$O was added and the mixture was warmed to nearly 70°C on a water bath. Potassium hydroxide (6.7 g) in 200 m*l* of water was added slowly to the solution, which was warmed, until the odor of ammonia vanished. After adjusting the pH of the solution to 7 with hydrochloric acid, an equal volume of ethanol was added to the resulting solution. After cooling to 0°C, orange yellow crystals were separated out and recrystallized from the aqueous solution. Yield, about 2.1 g (28.8%).

Found: C, 25.75; H, 6.15; N, 15.19%. Calcd for [Co(edma$_2$)]-Cl·2H$_2$O: C, 26.34; H, 6.09; N, 15.36%.

An orange yellow complex of cobalt(III) of *cis* form was also prepared by using cobalt(II) chloride hexahydrate as the starting material in an aqueous solution at high temperature.

3) trans-Bis(ethylenediaminemonoacetato)chromium(III) Chloride Trihydrate, trans-[Cr(edma)$_2$]Cl·3H$_2$O (III). Two isomers, *cis* and *trans* forms of the cobalt(III) complexes could be prepared by suitably selecting the starting materials as described above, in 1) and 2).[4] However, in the case of chromium(III) complexes, it was impossible to prepare the *cis* form even by starting from hexaamminechromium(III) iodide in a manner similar to that used in the preparation of the corresponding cobalt(III) complex in 2).

Only the *trans* form was obtained for the chromium(III)-EDMA system. To a solution of 5.3 g (0.02 mol) of chromium(III) chloride hexahydrate in a small amount of water, Hedma·2HCl·H$_2$O (9.2 g, 0.044 mol) was added and the mixture was heated on a water bath. After adjusting the pH of the solution to 7, an equal volume of ethanol was added to the resulting solution. When it was cooled to 0°C, red crystals were separated out and recrystallized from 10% ethanol solution. Yield, 5.5 g (72.5%).

Found: C, 25.47; H, 6.46; N, 15.42%. Calcd for [Cr(edma)$_2$]Cl·3H$_2$O: C, 25.57; H, 6.40; N, 14.91%.

Preparation of Ligand. *Ethylenediaminemonoacetic Acid Dihydrochloride Monohydrate,* Hedma·2HCl·H$_2$O. The solution of 94.5 g (1 mol) of monochloroacetic acid in 100 m*l* of water was neutralized with 84 g (1 mol) of sodium hydrogencarbonate, and 60 g (1 mol) of ethylenediamine (98%) was added to the solution. After being added 40 g of sodium hydroxide in 80 m*l* of water, the mixture was acidified with 6N hydrochloric acid and the solvent was then evaporated off. After filtration, ethanol three times in volume was added to the filtrate, when the oilish liquid was produced. This syrupy substance was treated by separating funnel and then concentrated hydrochloric acid was added to the syrup. After being added the mixture of ethanol and ether to the solution, it was kept in a refrigerator for a day. White crystals were separated out and recrystallized from 50% ethanol solution. The method is new and simple for the preparation of the ligand material. Yield, 140 g (70%).

Found: C, 22.94; H, 6.72; N, 12.96%. Calcd for C$_4$H$_{10}$N$_2$O$_2$·2HCl·H$_2$O: C, 22.97; H, 6.76; N, 13.50%.

Results and Discussion

Electronic Absorption Spectra. The visible absorption spectra for all the complexes in aqueous solutions are shown in Figs. 1 and 2, together with those of *cis*-[Co(edda)*[4](en)]Cl·3H$_2$O, *trans*-[Co(edda)(en)]NO$_3$·H$_2$O[5] and [Cr(ox)(en)$_2$]I[6] for

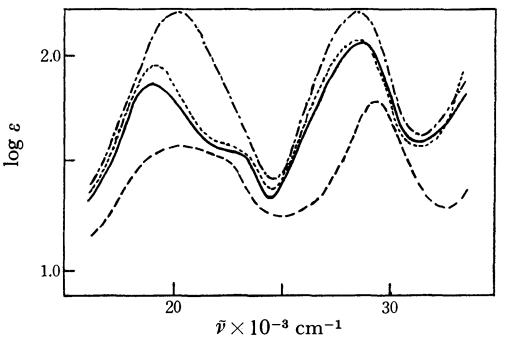

Fig. 1. Electronic absorption spectra: (———) *trans*-[Co(edma)$_2$]Cl·2H$_2$O, (------) *cis*-[Co(edma)$_2$]-Cl·2H$_2$O, (--------) *trans*-[Co(edda)(en)]NO$_3$·H$_2$O and (—·—·—) *cis*-[Co(edda)(en)]Cl·3H$_2$O.

*3 edma is an abbreviated form of H$_2$NCH$_2$CH$_2$-NHCH$_2$COO$^-$.

4) M. Mori, M. Shibata, E. Kyuno and M. Kanaya, This Bulletin, **34**, 1837 (1961).

*4 edda is an abbreviation of $^-$OOCCH$_2$NHCH$_2$-CH$_2$NHCH$_2$COO$^-$.

5) J. I. Legg and D. W. Cooke, *Inorg. Chem.*, **4**, 1576 (1965).

6) H. L. Schlaefer, O. King, L. Mahler and H. P. Opitz, *Z. Phys. Chem.*, **24**, 307 (1960).

Table 1. Absorption maxima ($\times 10^3$ cm^{-1})

Complex	Band Ia $\bar{\nu}$ (log ε)	Band Ib $\bar{\nu}$ (log ε)	Bnad II $\bar{\nu}$ (log ε)
trans-[Co(edma)$_2$]Cl·2H$_2$O	18.87 (1.88)	22.03 (sh)	28.17 (2.05)
cis-[Co(edma)$_2$]Cl·2H$_2$O	20.00 (1.59)	21.51 (1.58)	28.90 (1.77)
trans-[Cr(edma)$_2$]Cl·3H$_2$O	19.80 (1.84)	21.70 (sh)	26.32 (1.88)
trans-[Co(edda)(en)]NO$_3$·H$_2$O[5]	18.90 (1.94)	22.32 (sh)	27.62 (2.05)
cis-[Co(edda)(en)]Cl·3H$_2$O[5]	18.05 (sh)	20.20 (2.23)	27.78 (2.23)
[Cr(ox)(en)$_2$]I[6]	20.33 (1.81)		27.17 (1.83)

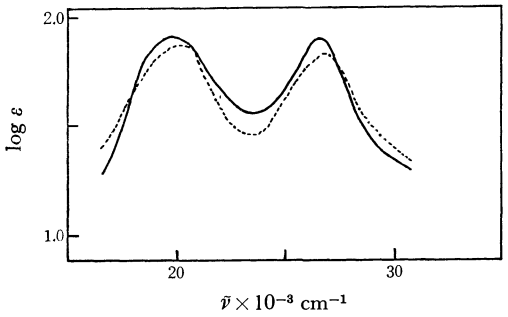

Fig. 2. Electronic absorption spectra: (———) *trans*-[Cr(edma)$_2$]Cl·3H$_2$O and (--------) [Cr(ox)-(en)$_2$]I.

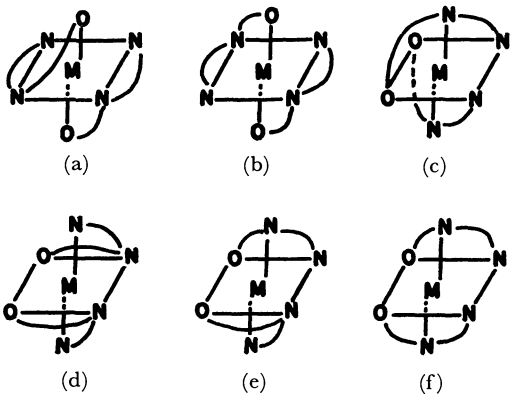

Fig. 3. The possible six geometrical isomers of bis(ethylenediaminemonoacetato)cobalt(III) and chromium(III) ion:
(a) *trans,cis,cis* (with respect to carboxylate oxygen, primary amine nitrogen and secondary amine nitrogen) (b) *trans,trans,trans*, (c) *cis,cis,trans*, (d) *cis,trans,cis*, (e) *cis,cis,cis*, (f) *cis,cis,trans*.

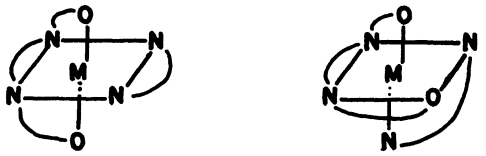

Fig. 4. The possible two geometrical isomers of [Co(edda)(en)]$^+$: (g) *trans* form, (h) *cis* form (with respect to carboxylate oxygen atoms).

comparison. Numerical values concerning their absorption maxima are given in Table 1.

The spectrum of complex I has a band which is remarkably split into two components Ia and Ib, at 18.9 and 22.0 (shoulder). It has another band at 28.2×10^3 cm^{-1}. The shape of the spectrum and the positions of the absorption peaks are in close agreement with those of *trans*-[Co(edda)(en)]-NO$_3$·H$_2$O.

The possible chelate configurations in six geometrical isomers of [M(edma)$_2$]$^+$-type complex and those in two isomers of [Co(edda)(en)]$^+$ complex are given in Figs. 3 and 4, respectively. It is possible to assume from the appearance of the splitting in the first bands of both complex I and *trans*-[Co(edda)(en)]$^+$ in Fig. 1 that the structure of complex I has either configuration (a) or (b) in Fig. 3, which has *trans* configuration with respect to the coordinated carboxylate oxygens.[7,8] However, the choice of (a) or (b) for the structure of complex I is not clear.

The spectrum of complex II has a broad first band, which is slightly split into two components Ia and Ib of nearly equal intensity, at 20.0 and 21.5, and a second band at 28.9×10^3 cm^{-1}.

The spectrum of complex II does not completely agree with that of *cis*-[Co(edda)(en)]$^+$ ion. A slight splitting of the first band makes us believe that complex II has a structure of *cis* configurations. However, the choice of (c), (d), (e) or (f) for the structure of complex II can not be done easily, as they have identical coordination forms except for the difference of the chelating features as seen in Fig. 3.

The spectrum of complex III shows the first band at 19.8 with a small shoulder at 21.7 and the second band at 26.3×10^3 cm^{-1}. On the other hand, the spectrum of [Cr(ox)(en)$_2$]I[5] shows two bands at 20.3 and 27.1×10^3 cm^{-1} with no shoulder near the first band. Since the shoulder at 21.7×10^3 cm^{-1} in complex III is thought to be one of the components of the first band, its configuration is assumed to be *trans* form.

IR Spectra. The infrared absorption spectra

7) J. Hidaka, Y. Shimura and R. Tsuchida, This Bulletin, **35**, 567 (1962).
8) H. Yamatera, *ibid.*, **31**, 95 (1958).

of the three new complexes synthesized were measured in the nujol mull state in the range 4000—700 cm^{-1}. Since the strong band appearing at 1730 cm^{-1}, which is assigned to free carboxylic acid in the ligand itself, is found to be shifted to 1630 cm^{-1} in cobalt(III) complexes and to 1645 cm^{-1} in chromium(III) complex, it is obvious that all the carboxylate groups are coordinated to central metal ions in all the three complexes.[9]

Though all the complexes show very similar spectra, the bands appearing at 1220 cm^{-1} (assigned to C–CN stretching vibration)[4] and at 1040 cm^{-1} (assigned to NH_2 twisting)[4] are split into two bands in the case of complexes I and III but not in II. Appearance of the splitting in IR spectra in complexes I and III also supports the conclusion that both complexes I and III have *trans* configuration with respect to the coordinated carboxylate oxygen atoms, since the splitting is observed in the first band of the electronic spectra.

9) D. H. Bush and J. C. Bailar, Jr., *J. Amer. Chem. Soc.*, **75**, 4574 (1953); *ibid.*, **78**, 716 (1956).

BULLETIN OF THE CHEMICAL SOCIETY OF JAPAN VOL. 43 789—793 (1970)

The Thermal Decomposition of Potassium Trioxalatoferrate(III) Trihydrate

Nobuyuki TANAKA and Katsuya SATO

Department of Chemistry, Faculty of Science, Tohoku University, Katahira-cho, Sendai

(Received August 29, 1969)

The thermal decomposition of $K_3[Fe(C_2O_4)_3]\cdot 3H_2O$ in solid state was studied by the thermogravimetric, the infrared spectroscopic and the manometric methods. It was found that, with elevating temperatures, three moles of water were evolved as the first step to form an anhydrous complex $K_3[Fe(C_2O_4)_3]$, which was then decomposed as the second step by an electron transfer from a ligand to the central iron(III) with the formation of an iron(II) complex. $K_2[Fe(C_2O_4)_2]$, $K_2C_2O_4$ and CO_2 were found as products in the second step. The total pressure of CO_2 gas evolved was measured at suitable time intervals. The shape of a curve of α (the fraction isothermally decomposed) *vs.* t (time) was sigmoidal. The initial part of the decomposition reaction was kinetically of a first-order and the activation energy was obtained to be 43.6 kcal/mol. A main part of it ($0.2<\alpha<0.8$) was of a second-order and obeyed the Prout-Tompkins' law. The activation energy was calculated to be 35.3 kcal/mol.

The thermal decomposition of anhydrous trioxalatoferrate(III) in solid state has been investigated by several researchers. From the polarographic and the infrared studies, Tanaka and Nanjo[1] reported that the thermal decomposition of this complex was initiated by an electron transfer from the coordinated oxalate ion to the central iron(III) forming iron(II) complex. From the thermogravimetric analysis (TGA) and the differential thermal analysis (DTA), Broadbent *et al.*[2] also indicated that a reduction of iron(III) to iron(II) takes place during the decomposition reaction. However, the stoichiometry of this reaction has not been fully determined and no kinetic studies have been reported. Therefore, it is worth while to determine the stoichiometry and to investigate the kinetics of this decomposition reaction. In this paper, the decomposition products which were identified by the thermogravimetric and the infrared spectroscopic methods and the kinetic parameters of this reaction which were obtained by the manometric method are presented. On the basis of the experimental results, possible reaction mechanisms are discussed.

Experimental

Materials. $K_3[Fe(C_2O_4)_3]\cdot 3H_2O$ was prepared with $FeCl_3\cdot 6H_2O$ and $K_2C_2O_4\cdot H_2O$. $K_2[Mn(C_2O_4)_2]$, $K_2[Co(C_2O_4)_2]$ and $K_2C_2O_4$ were prepared from their hydrates. $K_2[Mn(C_2O_4)_2]\cdot 2H_2O$ was prepared with $MnSO_4\cdot 4\sim 6H_2O$, $H_2C_2O_4\cdot 2H_2O$ and $K_2C_2O_4\cdot H_2O$. $K_2[Co(C_2O_4)_2]\cdot 6H_2O$ was prepared with $Co(NO_3)_2\cdot 6H_2O$, $H_2C_2O_4\cdot 2H_2O$ and $K_2C_2O_4\cdot H_2O$.

Apparatus and Procedure. The thermogravimetric curve was recorded with an automatic-recording thermobalance, Shimadzu Thermano Balance Type RT-2, in a nitrogen atmosphere. Two hundred milligrams of sample was used in each measurement. The furnace heating rate was about 4°C per min. The

1) N. Tanaka and M. Nanjo, This Bulletin, **40**, 330 (1967).

2) D. Broadbent, D. Dollimore and J. Dollimore, *J. Chem. Soc.*, *A*, **1967**, 451.

particle size of the sample was smaller than 200 mesh.

A Hitachi EPI-2G double-beam infrared spectrophotometer equipped with a potassium bromide foreprism and gratings was used for the measurement of the infrared absorption spectra. The potassium bromide disk method was employed except the case of the identification of gaseous product.

The reflectance spectra were obtained on a Hitachi photo-electric spectrophotometer EPU-2 equipped with a standard reflectance attachment. Powdered magnesium oxide was used as a standard.

Decomposition pressure-time curves of the isothermal decomposition reaction were obtained by the manometric method. The temperature of the sample was controlled in a range of ± 0.5°C by means of a mercury regulator and an electric furnace. The measurement of isothermal decomposition of anhydrous trioxalato complex was carried out after hydrate sample was previously dehydrated at 120°C for 4 hr in each run. Samples which were smaller than 200 mesh in size weighed 33.5 mg in each run unless otherwise stated. The fraction decomposed in the pyrolysed sample, α, is calculated according to the equation,

$$\alpha = \frac{\text{Total } CO_2 \text{ pressure at time } t}{\text{Total } CO_2 \text{ pressure at the completion of reaction}}$$

The rate constants of the isothermal decomposition were obtained from the kinetic analysis of α-t curves. The kinetic parameters were calculated according to the Arrhenius equation.

Results and Discussion

Stoichiometric Studies. From the TGA curve of the trioxalatoferrate(III) as shown in Fig. 1, it

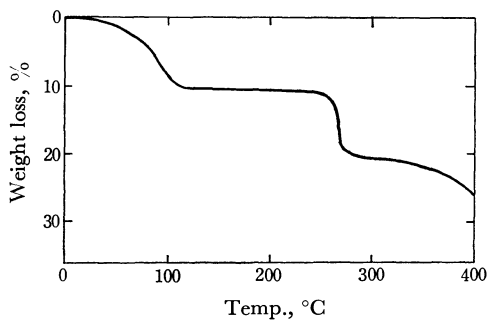

Fig. 1. Thermogravimetric curve of $K_3[Fe(C_2O_4)_3]\cdot 3H_2O$ obtained in nitrogen atmosphere.

can be seen that the first stage in the decomposition reaction begins at 30°C and completes at 120°C. The weight loss in this stage was determined to be 10.6%. This result agrees with the calculated weight loss of 11.00% for the loss of 3 mol of water. This dehydrated complex is thermally stable up to 230°C. The second stage in the decomposition reaction begins at 250°C and completes at 300°C. The weight loss was found to be 9.5% and the color change from green to yellow was observed. This weight loss is compared with the calculated value of 8.96% for the evolution of carbon dioxide, which was identified by the measurement of infrared spectra of the gaseous product.

In order to identify the solid-state decomposition products, infrared spectra were obtained with the samples which were completely decomposed and with some of other anhydrous complexes. They are shown in Fig. 2. The decomposition products

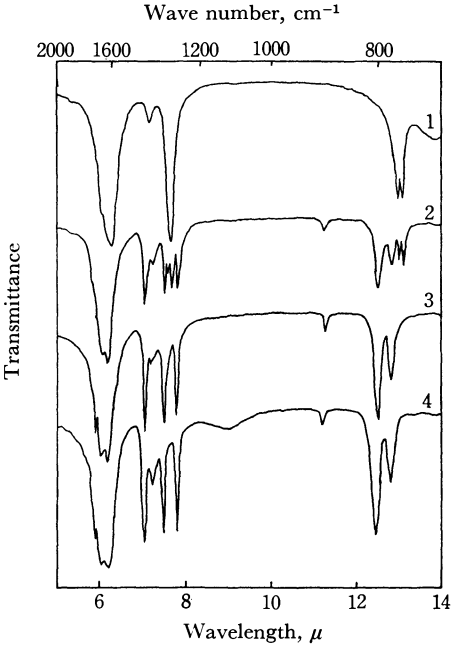

Fig. 2. Infrared absorption spectra of (1) $K_2C_2O_4$, (2) decomposition products, (3) $K_2[Mn(C_2O_4)_2]$ and (4) $K_2[Co(C_2O_4)_2]$. Transmittance scale is displaced arbitrarily.

give absorption bands at 764.5, 771.0 and 1305 cm^{-1} which are also observed with anhydrous potassium oxalate. This means that one component of the solid-state products is anhydrous potassium oxalate. The rests of the absorption bands of the products are similar to those of $K_2[Mn(C_2O_4)_2]$ and $K_2[Co(C_2O_4)_2]$. This indicates that another component of the products will be $K_2[Fe(C_2O_4)_2]$. The absorption band at 1289 cm^{-1} of the product, which was not observed with $K_2[Mn(C_2O_4)_2]$ and $K_2[Co(C_2O_4)_2]$, may be a characteristic one of $K_2[Fe(C_2O_4)_2]$. Unfortunately, however, the infrared absorption spectra of $K_2[Fe(C_2O_4)_2]$ could not be obtained because of the difficulty in the preparation of the complex. From the chemical analysis and the reflectance spectroscopic studies, Wendlandt and Simmons reported that decomposition products of the corresponding complexes of manganese(III)[3] and cobalt(III)[4] were also dioxalato complexes of

3) E. Simmons and W. Wendlandt, *J. Inorg. Nucl. Chem.*, **27**, 2325 (1965).

4) W. Wendlandt and E. Simmons, *ibid.*, **27**, 2317 (1965).

manganese(II) and cobalt(II), respectively. These facts support, though indirectly, the results obtained in this study.

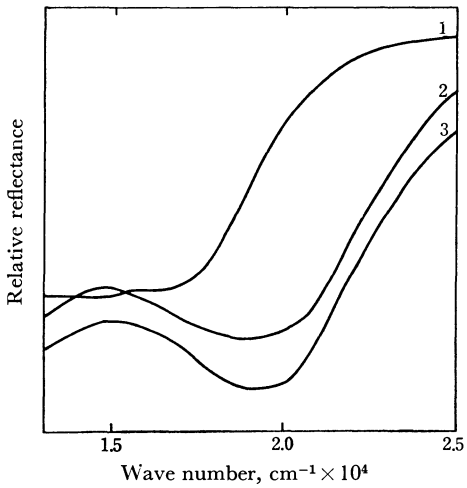

Fig. 3. Reflectance spectra of (1) decomposition products, (2) $K_3[Fe(C_2O_4)_3]$ and (3) $K_3[Fe(C_2O_4)_3]\cdot 3H_2O$. Relative reflectance scale is displaced arbitrarily.

The reflectance spectra of $K_3[Fe(C_2O_4)_3]\cdot 3H_2O$, $K_3[Fe(C_2O_4)_3]$ and its decomposition products are shown in Fig. 3. In the case of $K_3[Fe(C_2O_4)_3]\cdot 3H_2O$ and its anhydride, the absorption bands due to the d–d transition appear at 14925 cm^{-1} and 14706 cm^{-1}, respectively. Above 19000 cm^{-1}, the absorption of both compounds increases with increasing wave numbers. This means that the structure of $[Fe(C_2O_4)_3]^{3-}$ ion in $K_3[Fe(C_2O_4)_3]$ is similar to that in $K_3[Fe(C_2O_4)_3]\cdot 3H_2O$; the structure of $[Fe(C_2O_4)_3]^{3-}$ ion in the latter is octahedral. Of the decomposition products, which must be $K_2C_2O_4$ and $K_2[Fe(C_2O_4)_2]$, $K_2C_2O_4$ is transparent throughout all of the visible region of the spectrum, and therefore the absorption may be due to $K_2[Fe(C_2O_4)_2]$. It can be assumed that the structure of $[Fe(C_2O_4)_2]^{2-}$ ion is either tetrahedral or planar. If it is tetrahedral, only one absorption may appear, whereas if planar, several absorptions may appear because of a lower symmetry of crystal field. Actually, as $K_2[Fe(C_2O_4)_2]$ gives an absorption which increases gradually with increasing wave numbers as shown in Fig. 3 and its color is yellow, its structure may be tetrahedral. From all of these informations obtained in this study, the stoichiometry of the thermal decomposition reaction was estimated to be:

i) $K_3[Fe(C_2O_4)_3]\cdot 3H_2O \rightarrow K_3[Fe(C_2O_4)_3] + 3H_2O$

ii) $K_3[Fe(C_2O_4)_3] \rightarrow K_2[Fe(C_2O_4)_2] + \frac{1}{2}K_2C_2O_4 + CO_2$

In the case of photolysis,[5] the reduction product is a monooxalatoiron(II) complex. This means that the mechanism of the electron transfer to iron(III) is different from each other in the cases of the thermal and the photolytic decomposition.

Kinetic Studies. The kinetics of the decomposition reaction was investigated by the manometric measurements. A plot of α *vs.* t was sigmoidal when the anhydride was decomposed completely. It may be divided from the standpoint of kinetics into two stages; (a) the initial reaction which is fitted to a first-order rate law where α is smaller than 0.05, and (b) the main reaction which is fitted to the Prout-Tompkins' equation[6] where α is between 0.2 and 0.8.

(a) The Initial Reaction. At lower temperatures, the curves of α *vs.* t show the initial stage of the decomposition reaction. (See Fig. 4). The rate constant in this stage, k_1, was expressed by the equation,

$$\frac{d\alpha}{dt} = k_1(1-\alpha) \qquad (1)$$

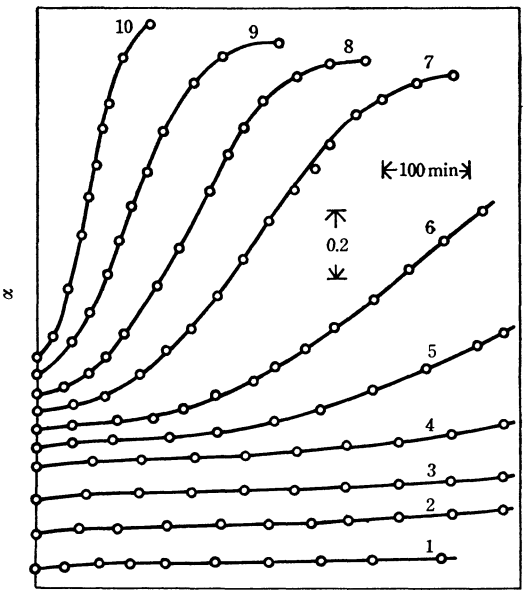

Fig. 4. Fractional decomposition as a function of time at (1) 180.5, (2) 183.2, (3) 184.0, (4) 186.5, (5) 190.5, (6) 195.3, (7) 201.0, (8) 205.0, (9) 210.5, and (10) 216.0°C.

Equation (1) is converted to

$$\ln(1-\alpha) = -k_1 t \qquad (2)$$

and the values of k_1 were determined from the slopes of $\log(1-\alpha)$ *vs.* t (Table 1). The Arrhenius plot for this stage is shown in Fig. 5. The kinetic equation derived from the Arrhenius plot is

5) W. Wendlandt and E. Simmons, *J. Inorg. Nucl. Chem.*, **28**, 2420 (1966).

6) E. Prout and F. Tompkins, *Trans. Faraday Soc.*, **40**, 488 (1944).

TABLE 1. RATE CONSTANTS FOR THE INITIAL REACTION (k_1) AND THE MAIN REACTION (k_2)

Temp. °C	$k_1\times10^6$ sec^{-1}	$k_2\times10^4$ sec^{-1}
180.5	1.03	—
183.2	1.27	—
184.0	1.60	—
186.5	2.00	—
190.5	3.02	1.10
195.3	4.76	1.52
201.0	8.27	2.38
205.0	—	3.40
210.5	—	4.58
216.0	—	8.51

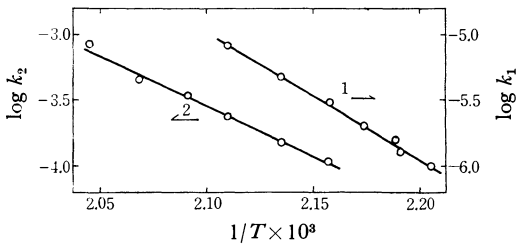

Fig. 5. Arrhenius plots for (1) the initial reaction (k_1) and (2) the main reaction (k_2).

$$\log k_1 = \frac{-43600}{2.3RT} + 14.9 \qquad (3)$$

(b) The Main Reaction. At higher temperatures, the experimental results were fitted to the Prout-Tompkins' equation,

$$\frac{d\alpha}{dt} = k_2(1-\alpha)\alpha \qquad (4)$$

over the range of $\alpha=0.2$ to 0.8. (See also Fig. 4). Equation (4) is converted to

$$\ln\frac{\alpha}{1-\alpha} = k_2 t \qquad (5)$$

The rate constant of the main reaction, k_2, was determined from the slope of $\log \alpha/(1-\alpha)$ *vs.* t (Table 1). The Arrhenius plot for this stage is also shown in Fig. 5. The activation parameters were determined as usual from the Arrhenius equation:

$$\log k_2 = \frac{-35300}{2.3RT} + 12.6 \qquad (6)$$

In the region where the rate obeyed to the Prout-Tompkins' law, the effects on the reaction rate were investigated under several experimental conditions. Changes in sample weight and particle size were found to give little difference in the rate constant as shown in Table 2; sample weight was changed from 10.0 to 33.5 mg and particle size, from 150~200 mesh to smaller than 200 mesh. The effect of pressure of carbon dioxide gas was also investigated. Pressure-time curves A, B and C measured are shown in Fig. 6. When curves B and C are shifted

TABLE 2. EFFECTS OF SAMPLE WEIGHT AND PARTICLE SIZE ON THE RATE CONSTANT k_2 FOR THE REACTION

Temp. °C	Sample weight* mg	Particle size mesh	$k_2\times10^4$ sec^{-1}
210.5	10.0	smaller than 200	4.69
210.5	15.1	smaller than 200	4.51
210.5	20.0	smaller than 200	4.57
210.5	33.5	smaller than 200	4.58
208.0	20.0	smaller than 200	3.92
208.0	20.0	150~200	3.96

* Weight is converted for hydrate.

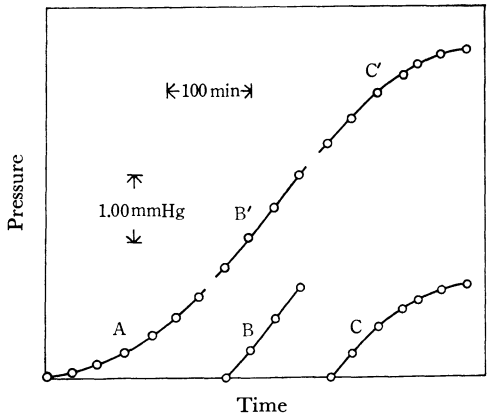

Fig. 6. Decomposition pressure of $K_3[Fe(C_2O_4)_3]$ as a function of time at 201.0°C, when system was evacuated at suitable time intervals (Curves A, B, and C). Curves B′ and C′ are obtained by shifting curves B and C in a proper way.

parallel to pressure axis, curves B′ and C′ are obtained. The shape of curve A-B′-C′ is identical with that obtained under the condition that the decomposition gas was not removed. This means that the rate of the decomposition reaction is not affected by the pressure of carbon dioxide gas. In order to investigate the reaction process, the mixture of $K_3[Fe(C_2O_4)_3]$ and its actual decomposition product and also the mixture of $K_3[Fe(C_2O_4)_3]$ and anhydrous $K_2C_2O_4$ were subjected to the thermal decomposition, because $K_2C_2O_4$ was considered to be one of the decomposition products. The rate constants obtained were compared with those ob-

TABLE 3. EFFECTS OF DECOMPOSITION PRODUCTS AND $K_2C_2O_4$ ON THE RATE CONSTANT k_2 FOR THE REACTION AT 208°C

Material added to $K_3[Fe(C_2O_4)_3]\cdot3H_2O$ and its wieght percentage in parentheses	Total weight mg	$k_2\times10^4$ sec^{-1}
None	20	3.96
Actual decomposition product (16.7%)	25	3.83
$K_2C_2O_4\cdot H_2O$ (20%)	25	4.20

tained with $K_3[Fe(C_2O_4)_3]$ alone, when no significant difference was observed (Table 3). It was found that, as far as the main reaction is concerned, neither products nor potassium oxalate react chemically with $K_3[Fe(C_2O_4)_3]$, and they have no catalytic role in the decomposition reaction. It is said that chemical processes which give α *vs.* t plots of sigmoidal shape usually result from reactions which take place at the reactant-product interface.[7] This indicates that, when the decomposition products are mixed mechanically with the reactant before heating, the effective area of the reactant-product interface is much smaller than that which is actually produced in the course of reaction. The Prout-Tompkins' equation means the existence of the acceleration and the deceleration period. The former corresponds to the increase in the area of the reactant-product interface. In the latter, the reaction interface still continues to grow towards the central unreacted regions of the particle, but the interfacial area begins to overlap, and therefore the rate becomes deceleratory until the decomposition of the reactant is completed. Presumably, this reaction is controlled by the diffusion of the interface. Further evidence is necessary to state the relationship between the reaction mechanism and the Prout-Tompkins' law.

7) A. Galwey, "Chemistry of Solids," Chapman & Hall Ltd. (1967), Chapter 5.

The authors are grateful to Mr. Kenzo Nagase for advice and suggestion which he gave in the course of this study, and to Mr. Mitsuo Sato for the measurement of infrared absorption spectra. They also wish to thank the Ministry of Education for the financial support granted for this research.

BULLETIN OF THE CHEMICAL SOCIETY OF JAPAN VOL. 43 793—796 (1970)

Synergistic Effect in Solvent Extraction—Effect of Oxygen and Nitrogen Containing Organic Bases on the Stability of Zinc(II) and Cobalt(II) β-Diketonate Adducts—

Tsunenobu SHIGEMATSU, Takaharu HONJYO,*1 Masayuki TABUSHI and Masakazu MATSUI

Institute of Chemical Research, Kyoto University, Uji, Kyoto

(Received September 5, 1969)

The effect of the organic Lewis bases acting as a synergist on the extraction of zinc(II) and cobalt(II) with benzoyltrifluoroacetone was studied. *n*-Hexyl alcohol, TBP, TBPO and TOPO were used as oxygen-containing bases, and quinoline, isoquinoline, lepidine, acridine and quinaldine as nitrogen-containing bases. The stability constants between metal chelates and the adduct forming materials in the organic phase were obtained by curve fitting method. The results are summarized as follows: (1) Zinc(II) and cobalt(II) chelates formed adducts including one or two molecules of the bases per metal ion. Adduct formation was carried out successively. (2) The stability of adducts with oxygen-containing organic bases increased in the order, *n*-hexyl alcohol$<$TBP$<$TBPO$\approx$TOPO. This is the same order with that of the basicity of donor oxygen in the compounds. The stability of adducts with nitrogen-containing bases increased in the order, quinaldine$<$acridine$<$quinoline$<$lepidine$<$isoquinoline. In this case, however, the steric effect of the bases preferably contributed to the adduct formation. (3) The overall stability constants of the adducts are affected by the coordination number of the metal ions. Cobalt(II) adducts are more stable than zinc(II) adducts.

In many extraction systems of metal β-diketone chelates, the presence of some neutral organic Lewis bases extremely enhances the extractability. Such phenomena, called "synergistic effect" can be explained by adduct formation between the metal chelates and the Lewis bases. The authors have made a systematic study on synergistic extraction,[1-4]

*1 Present address: Faculty of Science, Kanazawa University, Kanazawa.

1) T. Shigematsu, M. Tabushi, M. Matsui and T. Honjyo, This Bulletin, **39**, 165 (1966).

2) T. Shigematsu, M. Tabushi, M. Matsui and T. Honjyo, *ibid.*, **40**, 2807 (1967).

3) T. Honjyo, *ibid.*, **42**, 995 (1969).

4) T. Shigematsu, M. Tabushi, M. Matsui and K. Utsunomiya, *Bull. Inst. Chem. Res., Kyoto Univ.*, **45**, 290 (1967).

and reported on the influence of terminal groups of β-diketones in zinc-β-diketone-TOPO system.[4] In the present research, the effect of organic Lewis bases on the synergistic extraction of zinc(II) and cobalt(II) with benzoyltrifluoroacetone was studied, and the stability constants of the adducts were determined.

Experimental

The radioisotopes, zinc-65 and cobalt-60 were supplied by the Radiochemical Centre, Amersham, England, as chlorides in hydrochloric acid solution. They were converted to the perchlorates and diluted with 0.01M perchloric acid to make stock solutions. Sodium perchlorate was prepared by dissolving sodium carbonate in perchloric acid and purified by recrystallization from water. Benzoyltrifluoroacetone (BFA) was obtained from the Dojindo Co. Organic bases; TOPO (tri-*n*-octylphosphine oxide), TBPO (tri-*n*-butylphosphine oxide), *n*-hexyl alcohol, quinoline, isoquinoline, lepidine, quinaldine and acridine were obtained commercially. TBP was purified by washing successively with a dilute sodium hydroxide solution, a dilute hydrochloric acid solution and a saturated sodium chloride solution, followed by centrifugation. All the other reagents were GR grade materials and used without further purification.

Experimental procedure was almost the same as previously described.[1-4] Five milliliters of aqueous solution containing zinc(II) or cobalt(II) ions (a few ppm), sodium perchlorate (0.1M) and acetic acid (0.01M) were adjusted to a desired pH, and shaken with 5 m*l* of benzene solution containing 0.05M benzoyltrifluoroacetone and various amount of organic bases, for one to three hours, at 20±1°C. After separating two phases, 2 m*l* of each of the phases was pipetted into test tubes (14 mm in diameter), and radioactivity was measured with a NaI(Tl) well-type scintillation counter. The pH values of the aqueous layers after the extraction were again measured, and the data were used for plotting the distribution curves.

Theoretical

The extraction constants of metal chelates, K, and the stability constants of adducts, β_n, were calculated by the equations

$$K = [MR_2]_o[H^+]^2/[M^{2+}][HR]_o^2, \quad (1)$$

$$\log K = \log D - 2\log [HR]_o - 2pH, \quad (2)$$

$$\beta_n = [MR_2L_n]_o/[MR_2]_o[L]_o^n, \quad (3)$$

$$\log D^*/D = \log(1 + \sum_{n=1}^{n} \beta_n[L]_o^n), \quad (4)$$

where D and D^* were the distribution ratios in the absence or presence of organic bases, M stood for metal, HR for β-diketone and L for organic bases; and [ ] and [ ]$_o$ designated the concentration of the chemical species in the aqueous and organic phase, respectively.

The equilibrium concentration of the bases, $[L]_o$, can be assumed to be equal to the initial concentration, C_L, in the case of oxygen-containing bases, because the amount of metal ions is negligibly small and the bases are scarcely distributed to the aqueous phase. However, nitrogen-containing bases can form the cationic species such as LH^+ in acidic aqueous solution, and accordingly the $[L]_o$ value may not be the same with, but lower than the C_L value. Using the dissociation constant, $K_{LH} = [H^+][L]/[LH^+]$, and the partition coefficient, $P_L = [L]_o/[L]$, the relation between these two concentrations may be given as follows:

$$C_L = [L]_o(1 + P_L^{-1} + P_L^{-1}K_{HL}^{-1}[H^+]) \quad (5)$$

The $\log P_L$ values of quinoline and isoquinoline are about 2 at 20±2°C and the pK_{LH} values are 4.85 (quinoline) and 5.14 (isoquinoline) (Ref. 5). In the pH region studied (pH 4.5—6.0), more than 90 per cent of the base must be present in organic phase, and therefore, the error caused by using C_L for $[L]_o$ can be neglected. The $\log P_L$ and pK_{LH} values of the other three bases are unknown or uncertain. However, as they are almost insoluble in water, and their K_{LH} values may not be so low as to cover their very high P_L, we might assume that the situation is similar to the case of quinoline and isoquinoline.

Results and Discussion

Fugures 1 and 2 show the $\log D$ *vs.* pH plots and the $\log D$ *vs.* $\log [HR]_o$ plots in the extraction of zinc(II) and cobalt(II) with BFA only. All the plots give an almost straight line with a slope of 2, indicating that over all extraction equilibrium can be written as follows:

$$M^{2+} + 2HR(org) \rightleftharpoons MR_2(org) + 2H^+ \quad (6)$$

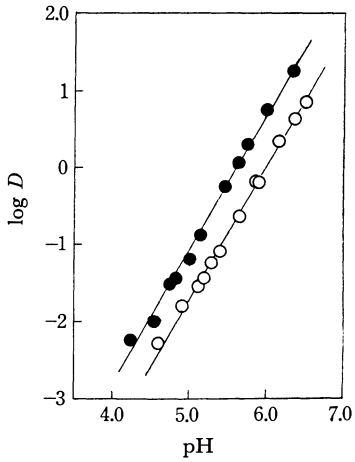

Fig. 1. Variation of the distribution ratio of zinc-(II) (—●—) and cobalt(II) (—○—) as a function of pH.
Organic phase: 0.05M BFA in benzene
Aqueous phase: 0.1M $NaClO_4$

5) H. M. N. H. Irving and N. S. Al-Niaimi, *J. Inorg. Nucl. Chem.*, **27**, 1671 (1965).

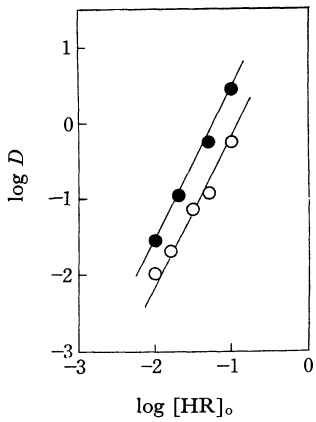

Fig. 2. Variation of the distribution ratio of zinc-(II) (—●—) and cobalt(II) (—○—) as a function of chelate ligand concentration.
Organic phase: BFA in benzene
Aqueous phase: 0.1M $NaClO_4$, pH=5.5

The extraction constants, K, can be calculated by Eq. (2).

The change in the distribution ratio of zinc and cobalt resulting from the addition of organic Lewis bases is shown in Figs. 3 and 4, as the log D^*/D *vs.* log $[L]_o$ plots (actually, log D^*/D *vs.* log C_L plots). When the metal chelates react with organic bases to form adducts in organic phase, the equilibrium may be written as follows:

$$MR_2(org) + nL(org) \rightleftharpoons MR_2L_n(org) \qquad (7)$$

Since the slope of linear log D^*/D *vs.* log $[L]_o$ plots or the slope of an asymptote of curved plots indicates the maximum number of the base molecule, it is considered that cobalt BFA chelate forms MR_2L type adduct with TBPO, TOPO, quinaldine

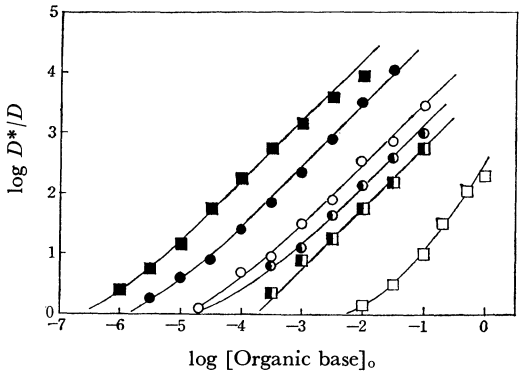

Fig. 3. Variation of the distribution ratio of zinc-(II) as a function of the organic base concentration.
Solvent: benzene BFA: 0.05M
Organic base: —●— Isoquinoline, —◐— Quinaldine, —○— Quinoline, —■— TBPO, —◧— TBP, —□— *n*-Hexyl alcohol

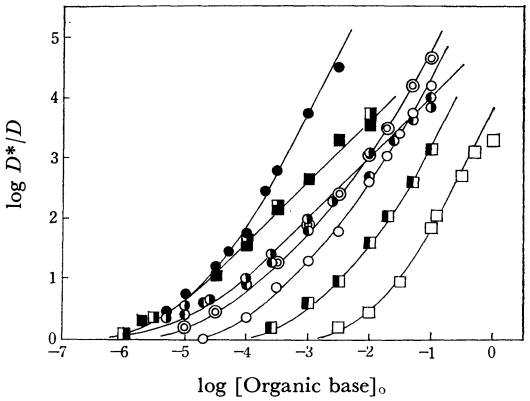

Fig. 4. Variation of the distribution ratio of cobalt-(II) as a function of the organic base concentration.
Solvent: benzene BFA: 0.05M
Organic base: —●— Isoquinoline, —◐— Quinaldine, —◑— Acridine, —◎— Lepidine, —○— Quinoline, —■— TBPO, —◧— TOPO, —◧— TBP, —□— *n*-Hexyl alcohol

and acridine, and both MR_2L and MR_2L_2 type adducts with *n*-hexyl alcohol, TBP, quinoline, isoquinoline and lepidine; while zinc chelate forms MR_2L_2 type adduct only with *n*-hexyl alcohol. The stability constants of the adducts were obtained by analyzing the plots in Figs. 3 and 4 with the curve fitting method.[6] The log β_1, log β_2 and log K values are summarized in Table 1.

Table 1. Extraction constants of zinc(II) and cobalt(II) BFA chelates and stability constants of their adducts with some organic bases

Organic base	Zn(II) log K=−9.9 log β_1	Zn(II) log K=−9.9 log β_2	Co(II) log K=−10.5 log β_1	Co(II) log K=−10.5 log β_2
n-Hexyl alcohol	1.45	2.90	2.20	3.80
TBP	3.75	*	3.45	5.20
TBPO	6.20	*	5.60	*
TOPO	6.24**	*	5.70	*
Quinoline	4.50	*	4.20	6.40
Isoquinoline	5.45	*	5.50	9.80
Lepidine	—	—	4.80	6.80
Quinaldine	4.10	*	4.80	*
Acridine	—	—	5.00	*

* MR_2L_2 type adduct was not observed.
** Taken from Ref. 4.

The stability of zinc and cobalt adducts with oxygen-containing Lewis bases increases in the order, *n*-hexyl alcohol<TBP<TBPO≈TOPO, which is the

6) T. Sekine and D. Dyrssen, *ibid.*, **26**, 1727 (1964).

same with that of the donating power of lone-pair electron of oxygen atom. In other words, the stability directly corresponds to the basicity of the base. A similar tendency has been observed in rare earth metals-BFA,[1] zinc-TTA[6-8] and europium-TTA systems.[9] In the TTA systems, the increasing order of the stability found in carbon tetrachloride was: hexone<TBEP<TBP<TBPO≈TOPO. From the fact that TBPO adducts as well as the TOPO adducts are stable it may be deduced that the length of hydrocarbon chain of alkyl phosphine oxides or alkyl phosphate does not give important effect on the stability of the adducts.

The over all stability of the adducts with nitrogen containing Lewis bases increases in the order, quinaldine<quinoline<isoquinoline for zinc, and quinaldine<acridine<quinoline<lepidine<isoquinoline for cobalt. The order of stability does not only correlate with the basicity, but results preferably from the steric effect by methyl or phenyl groups of the bases. A similar result has been observed in the adduct formation between cobalt acetylacetonate and pyridine derivatives, where the apparent stability of the adducts increases as, α-picoline<2,6-lutidine<2,4-lutidine<β-picoline<γ-picoline.[10]

The effect of the basicity of oxygen-containing Lewis bases and the steric effect of nitrogen-containing bases reflect the maximum number of the base molecule involved in the adduct. *n*-Hexyl alcohol forms MR_2L_2 type adduct with both zinc and cobalt chelates, TBP forms the same type adduct with cobalt chelate, but TBPO and TOPO forms only MR_2L type adduct. Steric hindrance appears similarly in the formation of MR_2L_2 type cobalt adduct with nitrogen-containing bases. Maximum mole ratio of the base to cobalt chelate is 2 for quinoline, isoquinoline and lepidine adducts, but 1 for quinaldine and acridine adducts.

In general, cobalt BFA chelate forms more stable adduct than zinc chelate. This may be due to the fact that cobalt ion has a coordination number of six and takes octahedral configuration, while zinc ion has a coordination number of four and usually forms tetrahedral complexes, although octahedral configuration with a coordination number of six should be expected in some cases.

7) H. M. N. H. Irving and D. N. Edgington, *J. Inorg. Nucl. Chem.*, **27**, 1359 (1965).

8) R. L. Scruggs, T. Kim and N. C. Li, *J. Phys. Chem.*, **67**, 2194 (1963).

9) T. Sekine and D. Dyrssen, *J. Inorg. Nucl. Chem.*, **29**, 1457 (1967).

10) H. Akaiwa and H. Kawamoto, *ibid.*, **29**, 1345 (1967).

BULLETIN OF THE CHEMICAL SOCIETY OF JAPAN VOL. 43 796—800 (1970)

Synergistic Effect in Solvent Extraction—Effect of the Chelating Ligands on the Stability of Lutetium Mixed Chelates with β-Diketones and Their Adducts with TOPO—

Tsunenobu SHIGEMATSU and Takaharu HONJYO*1

Institute for Chemical Research, Kyoto University, Uji, Kyoto

(Received September 5, 1969)

The effect of the chelating ligands on the stability of mixed chelates of lutetium with β-diketones and the stability of their adducts with TOPO in benzene was studied by extracting lutetium with mixtures of two β-diketones, benzoylacetone (BzA) and dibenzoylmethane (DBM), and benzoylacetone and benzoyltrifluoroacetone (BFA), in the absence or in the presence of TOPO. The results are summarized as follows. (1) The extraction constants of Lu-BzA-DBM mixed chelates are almost the same as statistically calculated, while those of Lu-BzA-BFA mixed chelates are somewhat lower than the theoretical values. (2) The stability of the TOPO adducts of the mixed chelates increases in the order, $M(BzA)_2(DBM) \approx M(BzA)(DBM)_2 < M(BzA)_2(BFA) < M(BzA)(BFA)_2$, which is almost the same as that found among the extraction constants of the mixed chelates. The fluoromethyl group stabilizes the adduct more than phenyl group. (3) All the mixed chelates of lutetium β-diketonates bind one molecule of TOPO per metal chelate.

In the solvent extraction of rare earth β-diketonates, the presence of TOPO brings about the considerably enhancement of the extractability, which results from the adduct formation between the metal chelates and TOPO. The authors investigated the

*1 Present address: Faculty of Science, Kanazawa University, Kanazawa

effects of the size of central rare earth metal ions and of the terminal group of β-diketones on the synergistic extraction, and concluded that the stability of the adducts increased as the ionic radius of rare earth metal ions increased[1] or the terminal groups of β-diketones were substituted with aliphatic, aromatic and fluoromethyl groups.[2]

Recently, Sekine and Dyrssen[3,4] described the extraction of copper, zinc, indium and europium with mixtures of TTA and β-isopropyltropolone, and presented the extraction constants of the mixed chelates of these metals and the stability constants of the adducts of europium chelates with undissociated chelating agent, β-isopropyltropolone. However, the stability of the adducts formed between mixed chelates and neutral Lewis bases such as TOPO was reported neither by them nor by other investigators.

As it seems interesting to know how the stability of such adducts depends upon the successive formation of various mixed chelates, and it is also important to obtain more detailed information about the effect of the chelating ligands on the stability of the adducts, the authors attemped to deal with this subject. In the present research, the extraction behaviors of lutetium with mixtures of two β-diketones, benzoylacetone and dibenzoylmethane, and benzoylacetone and benzoyltrifluoroacetone in benzene were studied in the absence or in the presence of TOPO, and the extraction constant of the mixed chelates and the stability constants of their adducts with TOPO were obtained.

Experimental

Materials. The radio-isotope, lutetium-177 was produced by irradiating pure lutetium oxide in a thermal neutron flux of about 5×10^{12}n/cm^2·sec in the Research Reactor of Kyoto University. After the irradiated sample was dissolved in hot hydrochloric acid, lutetium was extracted at pH 5 with 0.05M BFA in benzene and stripped into 0.1M perchloric acid. The resulting solution was evaporated to fume and the residue was dissolved with an appropriate amount of perchloric acid to make a stock solution. Specific activity of the tracer was sufficiently high for this investigation. Sodium perchlorate was prepared by dissolving sodium carbonate in perchloric acid and purified by recrystallization. Benzoylacetone (BzA), dibenzoylmethane (DBM), benzoyltrifluoroacetone (BFA) and tri-*n*-octylphosphine oxide (TOPO) were obtained from the Dojindo Co.

Procedure. Experimental procedure was almost the same as previously described.[1,2] Five milliliters of an aqueous solution containing lutetium (a few ppm), sodium perchlorate (0.1M) and acetic acid (0.01M), and having a desirable pH, were shaken with 5 m*l* of a benzene solution including β-diketones and various amount of TOPO, for one to three hours at 20±1°C. After separating both phases, 2 m*l* of each phase were pipetted into test tubes (14 mm in diameter), and the radioactivities were measured with a NaI(Tl) well-type scintillation counter. The pH value of the aqueous layers after extraction was again measured with a glass electrode pH meter.

Theoretical

When tervalent ions, M^{3+}, are extracted with a mixture of two chelating acids, HA and HB, the ideal extraction equilibrium may be written as

$$M^{3+} + mHA(org) + (3-m)HB(org) \rightleftharpoons MA_mB_{3-m}(org) + 3H^+ \quad (1)$$

The extraction constants of the reaction, $K_{m,3-m}$ and the distribution ratio of the metal, D, can be given by

$$K_{m,3-m} = [MA_mB_{3-m}]_o[H^+]^3[M^{3+}]^{-1}[HA]_o^{-m} \times [HB]_o^{-(3-m)} \quad (m = 0, 1, 2, 3) \quad (2)$$

$$D = \sum_{m=0}^{3}[MA_mB_{3-m}]_o[M^{3+}]^{-1} \quad (3)$$

where [ ] and [ ]$_o$ designate the concentration of chemical species in the aqueous and organic phase, respectively.

From Eqs. (2) and (3), a fundamental equation of the curve fitting method is obtained as follows:

$$\log D[H^+]^3[HB]_o^{-3} - \log K_{0,3} = \log\{1+K_{0,3}^{-1}K_{1,2}([HA]_o/[HB]_o) + K_{0,3}^{-1}K_{2,1}([HA]_o/[HB]_o)^2 + K_{0,3}^{-1}K_{3,0}([HA]_o/[HB]_o)\} \quad (4)$$

Comparing the experimental curves, $Y=\log D\cdot[H^+]^3[HB]_o^{-3}-\log K_{0,3}$, $X=\log([HA]_o/[HB]_o)-\frac{1}{3}\log K_{0,3}K_{3,0}^{-1}$, with the normalized curves, $Y=\log(1+pv+qv^2+v^3)$, $X=\log v$, the following relations can be obtained.

$$K_{1,2} = p(K_{0,3}^2K_{3,0})^{1/3} \quad (5)$$

$$K_{2,1} = q(K_{0,3}K_{3,0}^2)^{1/3} \quad (6)$$

The statistical relation between these equilibrium constants can be given as, $K_{1,2}=3(K_{0,3}^2K_{3,0})^{1/3}$ and $K_{2,1}=3(K_{0,3}K_{3,0}^2)^{1/3}$ (*cf.* Ref. 4).

When metal chelates, MA_mB_{3-m} form the adducts with a neutral Lewis base, L, in the organic phase, the equilibrium may be expressed as

$$MA_mB_{3-m}(org) + nL(org) \rightleftharpoons MA_mB_{3-m}L_n(org) \quad (7)$$

The stability constants of the adducts, β_n, and the distribution ratio, D^*, are given by

$$\beta_n = [MA_mB_{3-m}L_n]_o/[MA_mB_{3-m}]_o[L]_o^n \quad (8)$$

$$D^* = \{[MA_mB_{3-m}]_o + \sum_{n=1}^{n}[MA_mB_{3-m}L_n]_o\}/[M^{3+}] \quad (9)$$

From Eqs. (3) and (9), the following equations can be obtained,

1) T. Shigematsu, M. Tabushi, M. Matsui and T. Honjyo, This Bulletin, **40**, 2807 (1967).
2) T. Honjyo, *ibid.*, **42**, 995 (1969).
3) T. Sekine and D. Dyrssen, *J. Inorg. Nucl. Chem.*, **26**, 2013 (1964).
4) T. Sekine and D. Dyrssen, *ibid.*, **29**, 1489 (1967).

$$D^*/D = 1 + \sum_{n=1}^{n} \beta_n [\mathrm{L}]_o^n \quad (10)$$

or

$$\log D^*/D = \log \left(1 + \sum_{n=1}^{n} \beta_n [\mathrm{L}]_o^n\right) \quad (11)$$

The derivations of the equations are described in previous papers.[1,3,4]

Results and Discussion

Lutetium-β-Diketone System. Figures 1 and 2 show the extraction of lutetium with BzA, DBM and BFA alone in benzene as a function of pH and the chelating agent concentration, respectively. All the plots give almost a straight line with a slope of 3 indicating that the extraction of lutetium is ideally performed.

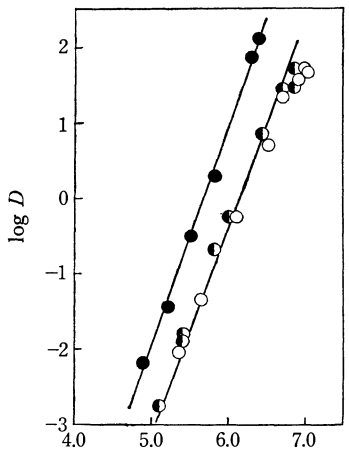

Fig. 1. Variation of the distribution ratio of lutetium as a function of pH.
Organic phase: —●— 10^{-3}M BFA, —◐— 10^{-1}M DBM, —○— 10^{-1}M BzA in benzene
Aqueous phase: 10^{-1}M $NaClO_4$

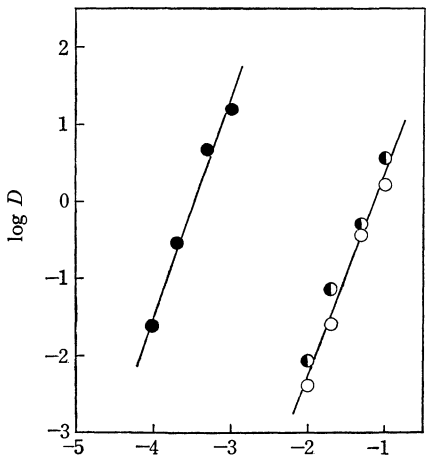

Fig. 2. Variation of the distribution ratio of lutetium as a function of chelate ligand concentration.
Organic phase: —●— BFA, —◐— DBM, —○— BzA in benzene
Aqueous phase: 10^{-1}M $NaClO_4$, pH=6.25

Figure 3 indicates the extraction of lutetium with

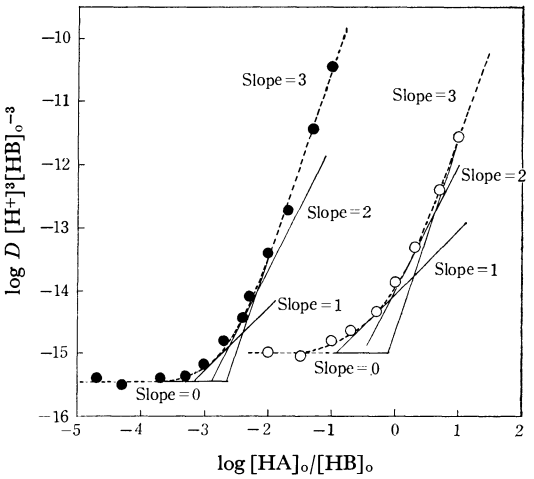

Fig. 3. Extraction of lutetium with mixtures of BFA and BzA (●) or DBM and BzA (○) in benzene at different mixing ratio.
The two dotted curves represent the normalized curves $Y=\log(1+pv+qv^2+v^3)$, $X=\log v$ with $p=1$, $q=1$ (mixtures of BFA and BzA) and $p=3$, $q=3$ (mixtures of DBM and BzA).

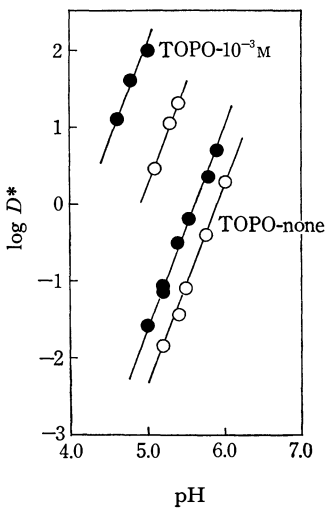

Fig. 4. Variation of the distribution of letetium in the presence or in the absence of TOPO as a function of pH.
Organic phase: —●— mixtures of BFA (5×10^{-4}M) and BzA (10^{-1}M) $\log [HA]_o/[HB]_o = -2.30$, —○— mixtures of DBM ($3.3\times10^{-2}$M) and BzA ($10^{-1}$M) $\log [HA]_o/[HB]_o = -0.48$
Aqueous phase: 10^{-1}M $NaClO_4$

Table 1. Extraction constants of lutetium β-diketonates and stablity constants of their adducts with TOPO

	Chelate	log K (found)	log K (calcd)*	log β_1
BzA-BFA mixed system	$Lu(BzA)_3$	−15.21		5.25
	$Lu(BzA)_2(BFA)$	−12.7	−12.2	6.15
	$Lu(BzA)(BFA)_2$	−10.2	− 9.7	6.65
	$Lu(BFA)_3$	−7.69		7.50
BzA-DBM mixed system	$Lu(BzA)_3$	−15.21		5.25
	$Lu(BzA)_2(DBM)$	−14.7	−14.7	5.60
	$Lu(BzA)(DBM)_2$	−14.7	−14.7	5.70
	$Lu(DBM)_3$	−15.16		6.15

* The values were estimated from Eqs. (5) and (6) by assuming $p=3$ and $q=3$ (theoretical value).

mixtures of BzA and DBM, and BzA and BFA in benzene with different mixing ratios. From the plots, p and q values of the normalized curves were obtained by the curve fitting method, and the extraction constants of mixed chelate, $K_{1,2}$ and $K_{2,1}$ were calculated by Eqs. (5) and (6), using $K_{0,3}$ and $K_{3,0}$ values which were obtained by extraction with each β-diketone. The results are listed in Table 1. The extraction constants experimentally obtained of the BzA-DBM mixed chelates are almost the same with the value statistically calculated, while those of the BzA-BFA mixed chelates are somewhat lower than the calculated values. Similar results have been observed on europium-TTA-IPT and indium-TTA-IPT mixed chelates.[4]

The $\log D[H^+]^3[HB]_o^{-3}$ *vs.* $\log([HA]_o/[HB]_o)$ plots have two asymptotes with the slope of 0 (for $[HA]_o/[HB]_o \to 0$) and 3 (for $[HA]_o/[HB]_o \to \infty$). The slope of the tangent gently changing from 0 to 3, indicates the composition of the metal chelates extracted under the condition. Namely, MA_3, MA_2B, MAB_2 and MB_3 may each exist as a predominant species in the region where the slope of the tangent is 0, 1, 2 and 3, respectively.

Lutetium-β-Diketone-TOPO System. Figures 4 and 5 indicate the log D *vs.* pH plots in the extraction of lutetium ions with the mixtures of two β-diketones in the absence and presence of 10^{-3}M TOPO in benzene: The mixing ratio of two β-diketones lies in the region where the predominant species is MA_2B (Fig. 4) and MAB_2 (Fig. 5). The large enhancement of the extraction observed in the

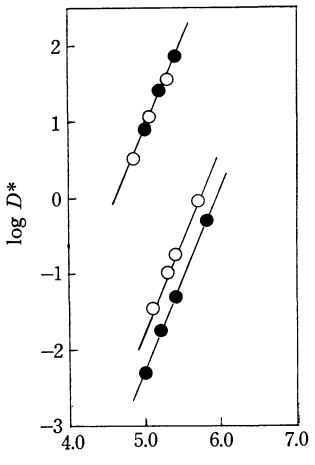

Fig. 5. Variation of the distribution of lutetium in the presence or in the absence of TOPO as a function of pH.
Organic phase: —●— mixtures of BFA (1.25×10^{-4}M) and BzA (10^{-1}M), $\log[HA]_o/[HB]_o=-2.90$ —○— mixtures of DBM (10^{-1}M) and BzA (5×10^{-2}M), $\log[HA]_o/[HB]_o=0.30$

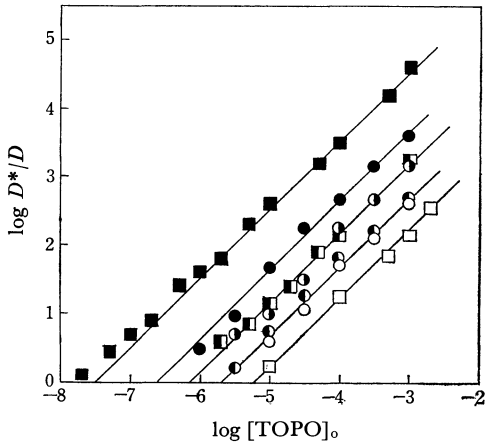

Fig. 6. Variation of the distribution of letetium as a function of TOPO concentration.
Organic phase: —□— BzA (5×10^{-2}M); —○— mixtures of DBM (3.3×10^{-2}M) and BzA (10^{-1}M), $\log[HA]_o/[HB]_o=-0.48$; —◐— mixtures of DBM (10^{-1}M) and BzA (5×10^{-2}M), $\log[HA]_o/[HB]_o=0.30$; —◧— DBM (5×10^{-2}M); —◑— mixtures of BFA (1.25×10^{-4}M) and BzA (10^{-1}M), $\log[HA]_o/[HB]_o=-2.90$; —●— mixtures of BFA (5×10^{-4}M) and BzA (10^{-1}M), $\log[HA]_o/[HB]_o=-2.30$; —■— BFA (5×10^{-2}M).

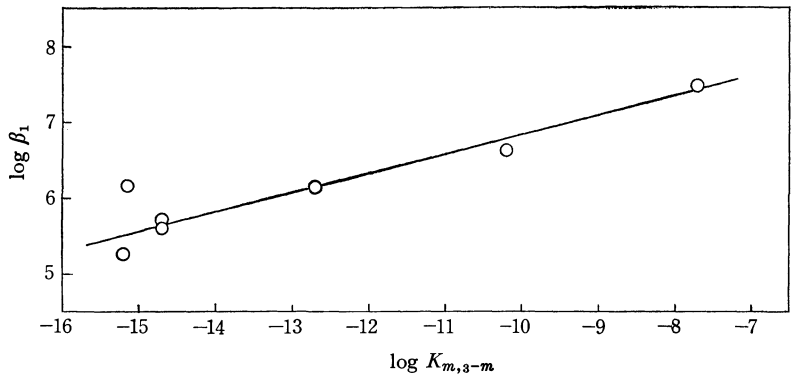

Fig. 7. Stability constant of lutetium β-diketonate adducts with TOPO as a function of the extraction constant of lutetium β-diketonates.

presence of TOPO shows that the mixed chelates, MA_2B and MAB_2 form adducts with TOPO as the simple chelates MA_3 and MB_3.

Figure 6 indicates $\log D^*/D$ *vs.* $\log [TOPO]_0$ plots in the extraction of lutetium with each of three β-diketones or with mixtures of two β-diketones. All the plots give the straight line with a slope of 1, showing that one molecule of TOPO binds to one molecule of the metal chelates. The apparent stability constants of the adducts with TOPO are summarized in Table 1. The stability of the adduct of the mixed chelates increases in the order, $Lu(BzA)_2(DBM) \approx Lu(BzA)(DBM)_2 < Lu(BzA)_2(BFA) < Lu(BzA)(BFA)_2$.

Figure 7 shows the relation between $\log K$ and $\log \beta_1$. Both values linearly correlate with each other and in the BzA-BFA mixed system, increase smoothly without showing any irregularity, as BzA is successively replaced by BFA. The fact leads to the following conclusions: (1) The concept that metal chelates having higher K value form more stable adducts is true of the mixed chelates, as well as of the simple chelates. (2) Asymmetry of the structure of mixed chelates does not give a measurable effect on the adduct formation. (3) Fluoromethyl group, irrespective of simple chelates or mixed chelates, makes the chelates form stable adducts. (3) can be explained by the electron withdrawing effect of fluoromethyl group.[2)]

The authors are grateful to Drs. M. Tabushi and M. Matsui (Institute for Chemical Research, Kyoto University) for their helpful advice and discussions.

BULLETIN OF THE CHEMICAL SOCIETY OF JAPAN VOL. 43 801—804 (1970)

The Thermal Annealing Behavior of Recoil Manganese Atoms Produced in Alkali Metal Permanganates by (n, 2n) and (n, γ) Reactions*1

Takanobu SHIOKAWA and Teikichi SASAKI*2

Department of Chemistry, Faculty of Science, Tohoku University, Sendai

(Received October 3, 1969)

The thermal annealing behavior of recoil manganese atoms produced in alkali metal permanganates by $^{55}Mn(n,2n)^{54}Mn$ and $^{55}Mn(n,\gamma)^{56}Mn$ reactions was studied. In the case of potassium permanganate, the thermal annealing of ^{54}Mn proceeded faster than that of ^{56}Mn. The retention of ^{54}Mn in the annealing curve decreased after an initial increase when it was treated at 180°C, whereas this anomaly was not observed in the case of ^{56}Mn. These differences in the annealing behavior of the two nuclides were ascribed to the effects of background gamma radiation during the neutron irradiation and also to the differences in recoil energies. An effect of the counterpart cations of permanganate was also observed in the thermal annealing behavior, and was interpreted in terms of the ionization potential of alkali metal.

It is well known that the chemical behavior of recoil atoms of the same element produced in a crystal by different nuclear processes is often not exactly the same. However, very little work has been carried out on their thermal annealing behaviors.

Aten and his co-workers[1] studied the thermal annealing of iodine atoms produced in potassium iodate by $^{127}I(n,2n)^{126}I$ and $^{127}I(n,\gamma)^{128}I$ reactions and observed that the thermal annealing of both recoils proceeded at the same rate, while the initial retention of ^{128}I recoils is higher than that of ^{126}I recoils. Jach and Harbottle[2] found that the thermal annealing of ^{82}Br recoils in bromate crystal irradiated with thermal neutrons proceeded faster than that of ^{80m}Br recoils. These isotope effects on thermal annealing behavior have been ascribed to the differences in the initial recoil energies of the various isotopes and also to differences in the electric charge of the recoil atoms. However, more detailed investigations are necessary in order to elucidate the effect of the recoil energy on thermal annealing.

This paper will deal with the thermal annealing behavior of recoil manganese atoms produced in alkali metal permanganates by $^{55}Mn(n,2n)^{54}Mn$, and $^{55}Mn(n,\gamma)^{56}Mn$ reactions from the point of view of the influences of the recoil energy and the effect of the alkali metal cation. The initial kinetic energy of ^{54}Mn recoils produced by the (n,2n) reaction is about 1000 times that of ^{56}Mn recoils produced by the (n,γ) reaction. The differences in the thermal annealing behavior of the two recoil atoms will be discussed in relation to the effects of the recoil damage and of gamma radiation during the neutron irradiation. Further, a remarkable effect of counterpart cations in the permanganate on the thermal annealing of the manganese recoils will be interpreted in terms of the electrostatic character of the alkali metal ion.

Experimental

Sample. The alkali metal permanganates were prepared by the method described in a previous paper.[3] All the samples were sealed in quartz or glass ampoules for neutron irradiation after the ampoules had been evacuated to a pressure below 10^{-4} mmHg.

Neutron Irradiations and Thermal Annealing Procedure. For the $^{55}Mn(n,2n)^{54}Mn$ reaction, about 500 mg of the sample was irradiated with 14 MeV neutrons for 5 hr at room temperature. The neutron flux at the irradiation position was 1×10^{7} n/cm^2/sec, and the gamma dose rate was about 5 R/hr.

On the other hand, for the $^{55}Mn(n,\gamma)^{56}Mn$ reaction, a few mg of the sample were irradiated for 6 min at the reactor temperature (*ca.* 40°C) with thermal neutrons in a pneumatic tube of the KUR at Kyoto University. The thermal neutron flux was 4×10^{12} n/cm^2/sec, and the gamma dose rate was estimated to be 2×10^{7} R/hr.

After irradiation, all the samples were stored at the temperature of dry ice. The thermal annealing ex-

*1 This work was partially supported by the Research Fund for Cooperating Utilization of Kyoto University.

*2 Present address: Japan Atomic Energy Research Institute, Tokai, Ibaraki.

1) A. H. W. Aten, Jr., M. Lindner and L. Lindner, "Chemical Effects of Nuclear Transformations," Vol.II, IAEA (1965), p. 125. G. A. Dupetit and A. H. W. Aten, Jr., *Radiochim. Acta*, **7**, 165 (1967).

2) J. Jach and G. Harbottle, *Trans. Faraday. Soc.*, **54**, 520 (1958).

3) T. Shiokawa, M. Yagi and T. Sasaki, *Radiochim. Acta*, **12**, 54 (1969).

periment was carried out by using an oil bath, its temperature controlled within ± 1°C.

Analytical Procedure for Chemical Species. The irradiated samples were dissolved into redistilled water at room temperature. The chemical species of radioactive manganese were separated into three fractions ($*Mn^{2+}$, $*MnO_2$ and $*MnO_4^-$ ions) by employing a simplified adsorption method based on an earlier worker's.[4] The radioactive permanganate ion was separated from the reduced species by shaking with 200 mg of manganese dioxide, followed by filteration through a glass filter. This procedure was repeated three times, each time using fresh manganese dioxide. Then the manganese dioxide which contained radioactive manganese dioxide and manganous ions was washed with neutral water until the purple color of the permanganate ion disappeared completely. The radioactive manganous ion was then eluted with 20 m*l* of a 10% manganous nitrate solution and 10 m*l* of 3N nitric acid from the manganese dioxide fraction. Finally, the latter was reduced into a solution by hydrochloric acid containing a small amount of hydrogen peroxide.

Radioactivity Measurements. The radioactivity was measured by means of a multi-channel pulse-height analyzer connected with a well-type NaI (Tl) detector (2in × 1¾in). The intensities of 0.84 and 0.85 MeV gamma rays were counted for ^{54}Mn and ^{56}Mn respectively.

Results and Discussion

No radiolytic decomposition of the samples through fast or reactor neutron irradiation was observed, except that the lithium salt was decomposed slightly as a consequences of the $^6Li(n,\alpha)^3H$ reaction in the case of reactor irradiation.

The $*MnO_2$-yield in each of the three fractions described above was independent of the type of nuclear reaction and was 4—8% for all samples except the potassium permanganate annealed at 180°C.

The retentions for the samples irradiated with fast neutrons are listed in Table 1. The tabulated values are the means of at least two determinations. The results of isothermal annealing for the samples irradiated with reactor neutrons are given in Table 2. As may be seen in this table, the yield depends slightly on the heating time when it is longer than 90 min. It is noticeable that the retentions for ^{54}Mn recoils in every permanganate treated at room temperature are higher than those for the ^{56}Mn recoils which were reported in the previous paper.[3]

TABLE 1. CHEMICAL DISTRIBUTIONS OF ^{54}Mn RECOILS IN ALKALI METAL PERMANGANATES TREATED AT ROOM TEMPERATURE

Compound	Yield (%)		
	$^{54}Mn^{2+}$	$^{54}MnO_2$	$^{54}MnO_4^-$
$LiMnO_4$	69.0±2.2	15.7±2.0	15.3±1.7
$NaMnO_4$	70.1±2.1	7.0±1.5	22.9±1.9
$KMnO_4$	61.3±2.5	10.6±2.8	24.5±2.2
$RbMnO_4$	53.7±2.5	13.5±2.0	32.8±2.4
$CsMnO_4$	46.4±0.9	11.2±0.5	43.1±0.6

4) For example, D. J. Apers and G. Harbottle, *Radiochim. Acta*, **1**, 189 (1963).

The isothermal annealing curves of the manganese recoils produced in the potassium permanganate are shown in Figs. 1 and 2. The rapid increase in retention by heating corresponds to the decrease in the $*Mn^{2+}$-yield for both nuclides. In treatment at 180°C, the retention for ^{54}Mn recoils decreased after a rapid initial increase, while the $^{54}MnO_2$-yield increased slowly with the heating time. Nothing similar was observed in the case of ^{56}Mn recoils.

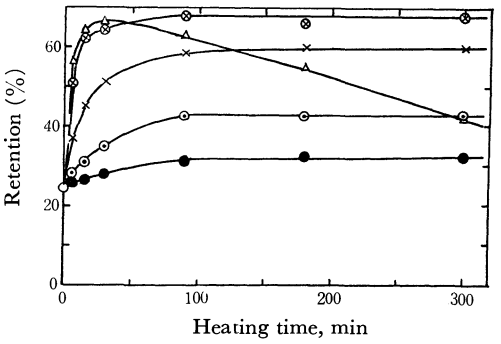

Fig. 1. Isothermal annealing curves for ^{54}Mn recoils in potassium permanganate.
●: 70°C ⊙: 100°C ×: 130°C
⊗: 150°C △: 180°C

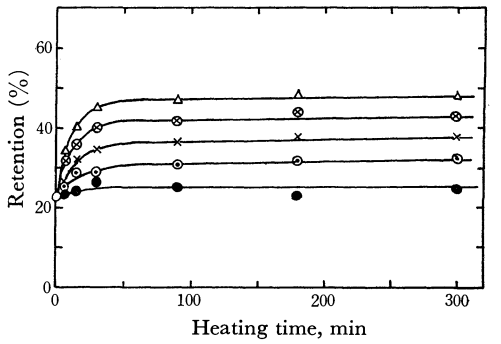

Fig. 2. Isothermal annealing curves for ^{56}Mn recoils in potassium permanganate.
●: 70°C ⊙: 100°C ×:130°C
⊗: 150°C △: 180°C

Figure 3 shows isochronal annealing curves obtained by 5 hr heating, together with the results of the thermal decomposition of the samples which had been irradiated with 14 MeV neutrons for 5 hr before heating. Although, for both nuclides, the difference in retention was not very large in room-temperature treatment, at a higher temperature the thermal annealing of ^{54}Mn recoils proceeded more rapidly. In other words, the thermal annealing

TABLE 2. CHEMICAL DISTRIBUTIONS OF ^{56}Mn RECOILS IN ALKALI METAL PERMANGANATES ANNEALED AT VARIOUS TEMPERATURES FOR 90 AND 180 MIN

Compound	Chemical species*	Yield (%) 100°C 90 min	100°C 180 min	130°C 90 min	130°C 180 min	150°C 90 min	150°C 180 min
$LiMnO_4$	A	78.5±0.8					
	B	9.9±1.3					
	C	11.6±2.1					
$NaMnO_4$	A	67.6±2.3		56.7±1.5	54.5±1.3		
	B	12.8±2.5		14.2±2.0	15.1±2.2		
	C	19.6±1.4		29.1±1.2	30.4±0.9		
$KMnO_4$	A	64.4±1.3	63.2±1.1	57.5±1.3	56.2±1.2	53.0±1.0	49.3±0.9
	B	4.0±2.2	4.8±1.7	5.7±0.8	5.8±1.3	4.0±0.8	7.0±1.2
	C	31.6±1.5	32.0±0.9	36.8±0.9	38.0±0.9	42.2±2.1	43.7±1.7
$RbMnO_4$	A	48.6±1.4			33.9±1.8	30.8±1.8	
	B	6.5±1.1			4.9±0.3	5.4±1.2	
	C	44.9±0.7			61.2±1.5	63.9±2.0	
$CsMnO_4$	A	37.7±1.5		22.1±1.5		22.6±1.9	
	B	6.0±1.8		5.3±0.9		5.1±0.9	
	C	58.3±1.2		72.6±1.8		72.9±2.3	

* A: $^{56}Mn^{2+}$, B: $^{56}MnO_2$, C: $^{56}MnO_4^-$

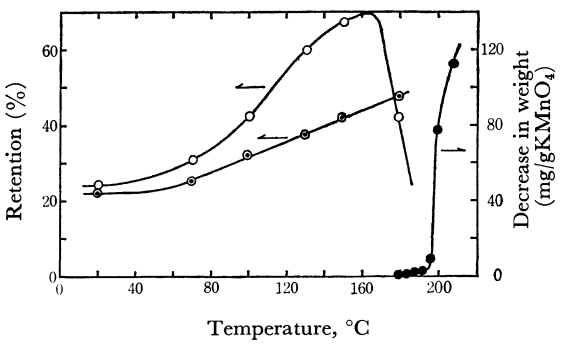

Fig. 3. Isochronal annealing curves (heating time: 5 hr) and the results of thermal decomposition of potassium permanganate irradiated with fast neutrons.
○: ^{54}Mn recoils ⊙: ^{56}Mn recoils
●: results for thermal decomposition

of ^{56}Mn recoils seems to be somewhat prevented at temperatures under 160°C, this tendency becomes more remarkable with the increase in the annealing temperature. On the other hand, the anomalous behavior in the thermal annealing of ^{54}Mn recoils at 180°C was not due to either thermal or radiolytic decomposition, because a macroscopic decomposition of the samples occurred over 190°C.

As is shown in Tables 1 and 2, the retentions of the samples treated at the same temperature increase in the order of the atomic number of the alkali metal in the permanganate. Because the retention values are very low[3,5],*3 in the lower-temperature treatment of the permanganates, the tabulated values may be considered to indicate the fractions annealed at the respective temperatures. These do not depend on any steric character of the crystal,

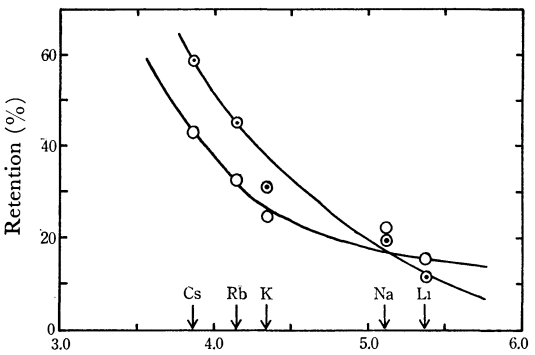

Fig. 4. The relationships between retention and the ionization potential of alkali metal.
○: retention for ^{54}Mn recoils at room temperature
⊙: retention for ^{56}Mn recoils at 100°C (heating time: 90 min)

5) S. R. Veljković and G. Harbottle, *J. Inorg. Nucl. Chem.*, **23**, 159 (1961); **24**, 1517 (1961).

*3 For potassium and rubidium permanganates which were irradiated with thermal neutrons at −196°C and then dissolved in cold acetone of −78°C, the retention values were 5.8±2.1 and 2.0±1.8% respectively.

such as the crystal configuration or the crystal free space of permanganate, but on the electrostatic character of the alkali metal ion. The relationships between the retention and the first ionization potential of alkali metal are shown in Fig. 4. The trends in this figure show that the thermal annealing is promoted by the decrease in the ionization potential of alkali metal or by the increase in the electron density of the inactive permanganate ion. These findings imply that the thermal annealing of manganese recoils proceeds by means of a mechanism similar to the transfer annealing suggested for potassium chromate crystal doped with chromic ions,[6] through interaction between the permanganate ion and the reduced species of those manganese recoils which are positively-charged.

The assumptions listed above may be supported by the experimental results on the thermal annealing of bromine recoils produced in alkali metal bromate crystals,[2,7,8] in which a decrease (ΔR) in annealed fractions was observed with an increase in the first ionization potential of alkali metal. The contradictory results are presumably due to the fact that the reduced species in the permanganate is detected as positive, while that in the bromate is detected as nagative. Thus, it is clear that the electrostatic characteristics of the lattice constituents influence the thermal annealing of the recoils.

These processes are different for each nuclide, as is shown in Fig. 3. In the case of iodine recoils in iodates, Aten and his coworkers[1] have ascribed the isotope effects observed in the thermal annealing to the differences in the de-excitation processes of the compound nucleus and the composite nature of the reduced species of the recoils. However, the following noticeable fact, which may account for the different annealing behavior of the manganese recoils, was found in correlated investigations.

The potassium permanganate which had been irradiated with 14 MeV neutron was exposured to gamma rays of a ^{60}Co source for 1 hr (total gamma dose: 2.0×10^6 R) and then heated for 90 min at 130°C. These gamma rays caused the retention to decrease from 58.7±1.4 to 33.7±2.2%, almost the same as for the samples irradiated with reactor neutrons (36.8±0.9%). These findings for permanganate are peculiar compared with the findings for the other oxianion salts, such as chromate,[9] bromate[10] and phosphate,[11,12] in which the retentions increased upon exposure to gamma radiation. As no macroscopic decomposition of the samples was observed, the present results suggest that the thermal annealing processes in the permanganate crystals are prevented by gamma irradiation. Therefore, the different annealing behavior in the two nuclides at temperatures under 150°C probably resulted from the different total gamma dose, which were 25 and 2.0×10^6 R, respectively, in the fast neutron and in the reactor neutron irradiations.

On the other hand, the anomalous behavior in the thermal annealing of ^{54}Mn recoils observed at 180°C arose from the peculiar properties of the recoil site, because a thermal decomposition of the sample began to occur over 190°C. By approximate calculation, the initial kinetic energy of the recoils is estimated to be 370 keV for the ^{55}Mn(n,2n)^{54}Mn reaction and 330 eV for the ^{55}Mn(n,γ)^{56}Mn reaction. The linear range of ^{54}Mn recoils in the potassium permanganate crystal is calculated to be 6900 Å according to the range-energy relations proposed by Nielsen;[13] hence, a recoil damage of a few ten Å at least may be created. It is well known[14,15] that the temperature of thermal decomposition is lowered when potassium parmanganate contains a small amount of an impurity such as carbon dioxide or manganese dioxide. Therefore, the rapid decrease in retention may be explained as follows: the recoil site of ^{54}Mn acts as an impurity in the crystal, thus promoting catalytically the localized thermal decomposition in the post-thermal treatment, even at a temperature lower than that of thermal decomposition. These conclusions may be supported also by the experimental finding that the $^{54}MnO_2$-yield increased with the lapse of the time of thermal annealing at 180°C. Thus, the recoil energy strongly influences the thermal annealing behavior in the temperature region of thermal decomposition.

The authors wish to thank Dr. K. Yoshihara and Dr. T. Omori for their useful discussions.

6) C. H. Collins, K. E. Collins, Y. F. Ghoos and D. J. Apers, *Radiochim. Acta*, **4**, 211 (1965).
7) T. Shiokawa and T. Sasaki, to be published.
8) G. E. Boyd and Q. V. Larson, *J. Amer. Chem. Soc.*, **90**, 254 (1968).
9) G. Harbottle, *J. Chem. Phys.*, **22**, 1083 (1954).
10) J. Cobble and G. E. Boyd, *J. Amer. Chem. Soc.*, **74**, 1287 (1952).
11) R. F. C. Claridge and A. G. Maddock, *Trans. Faraday Soc.*, **59**, 935 (1963).
12) K. Tanaka, This Bulletin, **37**, 1032 (1964).
13) K. O. Nielsen, "Electromagnetically Enriched Isotopes and Mass Spectrometry," Academic Press, Inc., New York (1956), p. 273.
14) E. Moles and M. Crespi, *Z. Phys. Chem.*, **100**, 337 (1920).
15) W. Komatsu, *Nippon Kagaku Zasshi*, **78**, 1454 (1957).

BULLETIN OF THE CHEMICAL SOCIETY OF JAPAN VOL. 43 805—809 (1970)

Macro Chelate Rings. II.*1 Syntheses and Properties of 2,7-Dimethyl-4,5-bis(salicylideneaminomethyl)xanthone as a Quadridentate Chelating Agent and Its Metal Complexes

Hisashi Okawa and Tamotsu Yoshino

Department of Chemistry, Faculty of Science, Kyushu University, Hakozaki, Fukuoka

(Received October 15, 1969)

2,7-Dimethyl-4,5-bis(salicylideneaminomethyl)xanthone, a new quadridentate chelating agent, was synthesized by a sequence of steps and subsequently characterized. Some divalent metal complexes of the ligand were isolated, and their properties were characterized on the basis of infrared spectra. The non-coplanar structure of the complex derived from the ligand was suggested by the resolution of a cobalt(II) complex into optical isomers.

No detailed study has been reported on the metal chelate with a macro chelate ring, in spite of the great interest in the configuration of the complex. In a preceding paper[1] we studied the syntheses and properties of a quadridentate chelating agent, 2,7-dimethyl-4,5-bis(salicylideneaminomethyl)acridone, and its metal complexes. Neither the complexes nor the ligand, however, was sufficiently stable for our ultimate purpose to utilize it as a catalyst for an assymmetric synthesis. One reason for the unstability of the ligand may be the presence of the acridone nucleus in it; this problem could be overcome by the replacement of the acridone nucleus by another more stable one with a similar structure, such as the xanthone nucleus.

In this work, therefore, the syntheses and the properties of a new quadridentate chelating agent, 2,7-dimethyl-4,5-bis(salicylideneaminomethyl)xanthone (I) (abbreviated as H_2SAX), with the xanthone nucleus in place of the acridone nucleus, were investigated, as were those of its metal complexes.

Results and Discussion

The synthetic scheme of the ligand I is shown in Chart 1. Although there have been some reports upon the synthesis of 2,7-dimethylxanthone V, in which the most reactive sites of xanthone are blocked by methyl groups, all of them are impractical for preparation in large quantities. We newly synthesized 2,7-dimethylxanthone V as follows. Starting from 2-bromo-4,4′-dimethyldiphenyl ether II, which had been obtained from 4,4′-dimethyldiphenyl ether, 2-cyano-4,4′-dimethyldiphenyl ether III was made by means of a modification of the Rosenmund-von

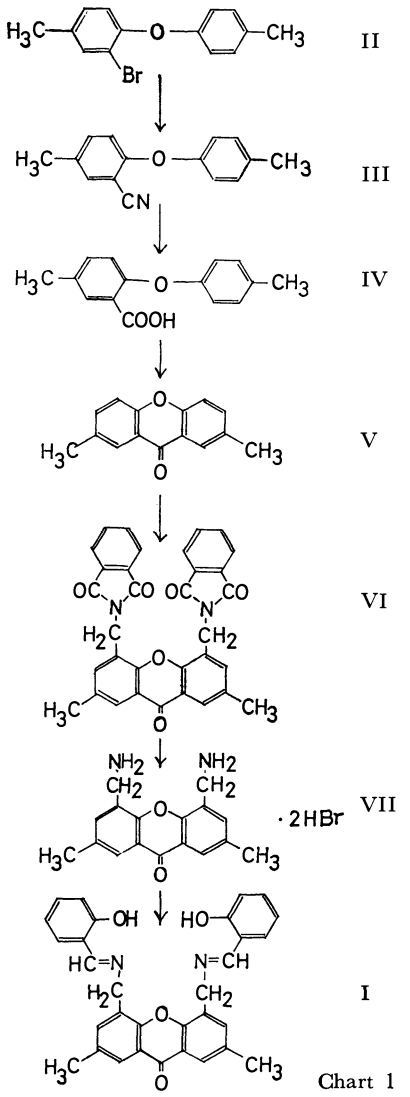

Chart 1

*1 Part I: Ref. 1.

1) H. Okawa and T. Yoshino, This Bulletin, **42**, 1934 (1969).

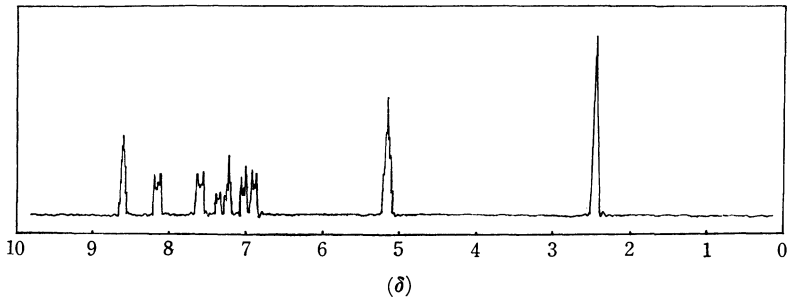

Chart 2. NMR spectrum of H_2SAX.

Braun reaction;[2] the bromide II and cuprous cyanide were treated in *N,N*-dimethylformamide, and then with a ferric chloride solution. The cyanide III thus separated was hydrolyzed with sodium ethoxide to give 4,4′-dimethyldiphenyl ether-2-carboxylic acid (IV), which was then converted to 2,7-dimethylxanthone V by treatment in hot sulfuric acid.

Like 2,7-dimethylacridone,[1] 2,7-dimethylxanthone could also be converted to 2,7-dimethyl-bis-(phthalimidomethyl)xanthone (VI) by treatment with *N*-hydroxymethylphthalimide; the compound VI was hydrolyzed in a mixture of hydrobromic acid and acetic acid to give 2,7-dimethyl-di(aminomethyl)xanthone dihydrobromide (VII). The di-(aminomethyl)derivative VII seemed stable only in its salt form, and the attempt to isolate the free diamine was unsuccessful. Because of the instability of the free diamine of VII, in addition to the insolubility of the compound VI, in most organic solvents, the positions of the substitution were tentatively assigned to 4 and 5 positions from a consideration of the meta-directing action of the carbonyl group in xanthone. The appropriateness of the assignment, however, was supported by the NMR spectrum of the compound I, which could be prepared from the diamine dihydrobromide VII and salicylaldehyde in the presence of an alkali.

The NMR spectrum of the ligand is given in Chart 2. The signal at $\delta=8.18$ can be attributed to protons at the 1 and 8 positions; both are strongly shielded by the carbonyl group in xanthone. On the other hand, the signal at $\delta=7.60$ is to be ascribed to the protons at the 3 and 6 positions, because the coupling constants of the peaks at $\delta=8.18$ and 7.60 are at least 1.7 Hz; this is consistent with the result given by Mathis and Goldstein.[3] The coupling constant, J_{13}, in xanthone itself is 1.78 Hz, while J_{14} is only 0.50 Hz. In this connection, two salicylideneaminomethyl groups must be at the 4 and 5 positions. The protons on the benzene rings are in the range of $\delta=6.95$—7.40. The protons of the methyl and methylene groups are at $\delta=2.45$ and 5.13 respectively, while the protons on the two azomethin groups appear at $\delta=8.61$, strongly shielded both by the phenyl group and by the C=N group.

The structure of the compound I was further confirmed by elementary analysis and by a study of the infrared spectrum, which indicated the existence of the chelated azomethin group at 1636 cm^{-1}. The C=O stretching vibration was observed at 1650 cm^{-1}.

Some stable divalent metal complexes have been derived from the ligand. They are listed in Table 1. Metal acetates were successfully used as a metal source, while metal chlorides and metal sulfates caused the decomposition of the ligand into salicylaldehyde and the diamine salt. The complex XIII was derived from XII by heating it under reduced pressure. Furthermore, we obtained two additional mixed complexes, XIV and XV, starting from XIII. The structures of the complexes thus obtained were confirmed by elementary analyses and by a study of the infrared spectra, which indicated a shift of the C=N stretching vibration from 1636 cm^{-1} in the ligand to near 1600 cm^{-1} and the appearance of a new absorption band in the range of 1535—1540 cm^{-1}; we could not assign the latter phenomenon, but it was useful for detecting a complex formation.

In the comparison of the infrared spectra of the ligand and the complexes, a recognizable blue shift of the C=O stretching vibration was observed in each case, demonstrating some interaction between a central metal atom and the ether oxygen atom. The bonding between them, however, was neglected because the infrared absorption peaks due to the ether bonding in the xanthone nucleus given by Kimoto[4] did not recognizably shift upon the complex formation, as would be expected from the very weak coordinating ability of the oxygen atom in diphenyl ether (Table 1). Thus, the ligand I acts as a quadridentate (Chart 3a) rather than as a quinquedentate chelating agent (Chart 3b). The blue shift (about 5 cm^{-1}) in the complexes XI, XIV and XV, which were characterized by their insolu-

2) L. Friedmann and H. Schechter, *J. Org. Chem.*, **26**, 2522 (1961).

3) C. T. Mathis and J. H. Goldstein, *Spectrochim. Acta*, **20**, 871 (1964).

4) S. Kimoto, *Yakugaku Zasshi*, **75**, 763 (1955).

Table 1. IR absorption peaks of complexes

	Complex	C=O	C=N[a]	New band	Bands due to C–O–C				
I	H_2SAX	1650	1636		—[b]	1240	1213	1173	1150
VIII	CuSAX	1660	(1600)	1538	1315	1247	1215	1170	1153
IX	NiSAX	1659	(1600)	1540	1315	1247	1215	1170	1153
X	ZnSAX	1660	(1600)	1538	1315	1246	1215	1170	1152
XI	$MnSAX \cdot 2H_2O$	1656	(1600)	1537	1316	1249	1215	1175	1153
XII	$CoSAX \cdot H_2O \cdot 2Py$	1660	1597	1534	1318	1265	1217	1175	1153
XIII	$CoSAX \cdot \frac{1}{2}H_2O$	1660	(1600)	1536	1318	1270	1212	1174	1153
XIV	$CoSAX \cdot phen \cdot 2H_2O$	1655	(1600)	1535	1317	1265	1212	1173	1152
XV	$CoSAX \cdot bipy \cdot H_2O$	1655	(1600)	1535	1320	1265	1212	1175	1150

a) The absorption parenthesized could be detected as a shoulder on a strong C=C vibration peak.
b) The peak could not be detected by a strong absorption of phenolic oxygen.

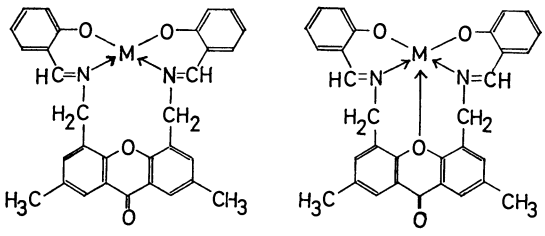

a b

Chart 3

bility in most organic solvents and which were expected to possess an octahedral configuration, was smaller than that (about 10 cm^{-1}) in other, supposedly tetrahedral-configurational complexes (Table 1). The blue shift of the C=O stretching vibration upon a complex formation can be interpreted as the inhibition of the mesomery as a result of interaction between a metal cation and the positively-charged oxygen atom in a canonical form of the xanthone nucleus (Chart 4), while the larger blue shift in

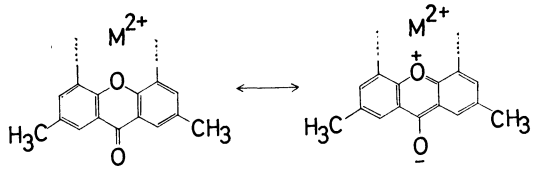

Chart 4

a tetrahedral complex than in an octahedral complex can be explained by the shorter distance between a metal and the ether oxygen in the former than in the latter. That is, the interatomic distance, which was roughly estimated from the model, between a metal and the ether oxygen in an octahedral complex was about 3.5 Å, while that in a tetrahedral complex was about 2.8 Å.

We have already suggested a non-coplanar structure for the complex derived from the ligand similar to I.[1] The visible spectrum of the copper complex, VIII, measured in chloroform had an absorption band centered around 720 mμ; this band was located at a longer wavelength than that at 580 mμ in a typical square planar copper(II) complex, bis-(salicylaldehyde)ethylenediimine-copper(II). This indicated that the copper complex VIII was nearly tetrahedral, but not planar. Another experimental fact regarding a non-coplanar structure was obtained by resolving the complex derived from I into optical isomers. Krebs *et al.*[5] observed that there was no separation unless the compound was soluble in water or an aqueous organic solvent, and that separation was better, in general, in water than in a solvent mixture when starch was used as an adsorbent. However, it seemed possible to resolve a complex using benzene as the eluent when D-glucose was utilized as an adsorbent. The only available complex for the separation was the complex XIII, which easily soluble in benzene and which could be recovered without any change in the complex. The eluate was separated into fifty fractions using a fraction collector. The combined first five fractions showed dextro-rotatory ($[\alpha]_D^{15}$ $+0.32°$), while the combined last ten fractions indicated levo-rotatory ($[\alpha]_D^{15} -0.98°$).

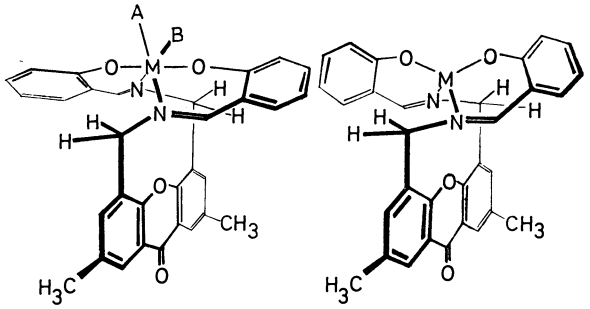

a b

Chart 5. Probable structures for an octahedral complex (a) and a tetrahedral complex (b).

5) H. Krebs, J. Diewald and J. A. Wagner, *Angew. Chem.*, **67**, 705 (1958).

The appropriateness of a non-coplanar structure of a metal and four donor atoms in a complex was, therefore, assured by the partial resolution of the compound XIII into optical isomers. The supposed, most probable structures for an octahedral and a tetrahedral complex are given in Chart 5.

Experimental

Apparatus. The NMR spectrum was recorded on a Varian Associates A-60 model, using tetramethylsilane as the internal standard and $CDCl_3$ as the solvent. A Hitachi infrared spectrometer EPI-S2 was used for the measurement of the infrared absorption spectra in the 4000—650 cm^{-1} region. The visible spectra were measured on a Hitachi EPS-3T spectrophotometer. The specific rotations were measured using a Yanagimoto OR-20 polarimeter.

Syntheses. All melting points and boiling points are uncorrected.

2-Bromo-4,4′-dimethyldiphenyl Ether (II). To a solution of 4,4′-dimethyldiphenyl ether (99 g, 0.5 mol) in acetic acid (300 m*l*) containing iodine (0.1 g), we added bromine (81.6 g, 0.51 mol) at 80°C over a period of two hours. After the reaction mixture had then been heated on a boiling bath for one hour, it was poured into water. The bromide was extracted with benzene and distilled at 155—165°C/7 mmHg. The yield was 113 g.

Found: C, 60.39; H, 4.88%. Calcd for $C_{14}H_{13}OBr$: C, 60.67; H, 4.73%.

2-Cyano-4,4′-dimethyldiphenyl Ether (III). A mixture of the bromide II (110.8 g, 0.40 mol) and cuprous cyanide (45 g, 0.5 mol) in *N,N*-dimethylformamide (200 m*l*) was refluxed on an oil bath for five hours. The reaction mixture was then filtered out and poured into a solution of ferric chloride ($FeCl_3 \cdot 6H_2O$ 180 g, concd. HCl 30 m*l*, water 300 m*l*); after which the mixture was heated on a water bath for half an hour. The nitrile III thus separated was extracted with benzene and purified by distillation at 163—170°C/6 mmHg to give a colorless liquid (57 g), which soon solidified.

Found: N, 5.87%. Calcd for $C_{15}H_{13}NO$: N, 6.27%.

4,4′-Dimethyldiphenyl Ether-2-carboxylic Acid (IV). The nitrile III (57 g) was placed in an alcoholic sodium hydroxide solution (300 m*l*) and heated on an oil bath while being stirred. After forty hours a white mass of sodium salt of 4,4′-dimethyldiphenyl ether-2-carboxylic acid IV separated. It was collected and neutralized with hydrochloric acid; the free acid thus obtained was crystallized from alcohol to give colorless needles with a mp of 112—113°C. The yield was almost theoretical.

Found: C, 74.04; H, 5.84%. Calcd for $C_{15}H_{14}O_3$: C, 74.36; H, 5.82%.

2,7-Dimethylxanthone (V). Crude 4,4′-dimethyldiphenyl ether-2-carboxylic acid IV (50 g) was dissolved in concentrated sulfuric acid (150 m*l*), and then the mixture was heated on a boiling bath for two hours. After it had cooled, the reaction mixture was poured onto ice water to give a white precipitate. This precipitate was collected, washed with a 10% sodium bicarbonate solution and then with water, and crystallized from alcohol as colorless needles with a mp of 144°C. The yield was almost quantitative.

The compound, V, made by this new method was identified by the coincidence of our description with that of Kimoto *et al.*[6]

2,7-Dimethyl-4,5-bis(phthalimidomethyl)xanthone (VI). 2,7-Dimethylxanthone (15 g) and *N*-hydroxymethylphthalimide (25 g) were dissolved in chilled concentrated sulfuric acid (200 m*l*), after which the mixture was left standing at room temperature for a week. Then the reaction mixture was poured onto ice water to give a white precipitate, which was collected and washed with a 10% sodium bicarbonate solution and then with water. A portion was crystallized from acetic acid or dioxane for analysis. It formed colorless prisms with a mp of 262—265°C. The yield was 80—90%.

Found: C, 72.98; H, 4.17; N, 5.09%. Calcd for $C_{33}H_{22}N_2O_6$: C, 73.06; H, 4.09; N, 5.16%.

2,7-Dimethyl-4,5-di(aminomethyl)xanthone Dihydrobromide (VII). The compound VI (10 g) was suspended in a mixture of acetic acid (100 m*l*) and 40% hydrobromic acid (100 m*l*), and then the mixture was heated on an oil bath for eighty hours under stirring. The hot reaction mixture was filtered and cooled to give white needles, which were collected and recrystallized from water as colorless needles. The yield was about 2.5 g.

Found: C, 42.27; H, 5.25; N, 5.96%. Calcd for $C_{17}H_{10}N_2O_2Br_2$: C, 42.52; H, 5.04; N, 5.83%.

2,7-Dimethyl-4,5-bis(salicylideneaminomethyl-xanthone (I). The diamine dihydrobromide VII (2.0 g) and salicylaldehyde (1.5 g) were dissolved in a hot dilute ethanol (50%, 50 m*l*). To it was added a dilute aqueous sodium bicarbonate solution until neutralization; pale yellow needles (1.7 g) were thus obtained. These needles were recrystallized from dioxane as pale yellow needles with a mp of 225—226°C.

Found: C, 75.94; H, 5.58; N, 5.71%. Calcd for $C_{31}H_{26}N_2O_4$: C, 75.90; H, 5.34; N, 5.71%.

CuSAX (VIII). A solution of the ligand I (50 mg) in dioxane (15 m*l*) was added to a solution of copper acetate monohydrate (25 mg) in ethanol (10 m*l*). The mixture was heated on a water bath for one and a half hours. The greenish-brown precipitate which separated was collected and washed with ethanol.

Found: C, 67.48; H, 4.65; N, 5.19; Cu, 11.18%. Calcd for $C_{31}H_{24}N_2O_4Cu$: C, 67.44; H, 4.38; N, 5.09; Cu, 11.51%.

NiSAX (IX). This was obtained from the ligand (50 mg) and nickel acetate tetrahydrate (30 mg) as a green precipitate, which was collected and washed with ethanol.

Found: C, 67.85; H, 4.37; N, 5.30%. Calcd for $C_{31}H_{24}N_2O_4Ni$: C, 68.04; H, 4.05; N, 5.13%.

ZnSAX (X). This was prepared from the ligand (50 mg) and zinc acetate dihydrate (30 mg) as a yellow precipitate.

Found: C, 67.76; H, 4.51; N, 4.71%. Calcd for $C_{31}H_{24}N_2O_4Zn$: C, 67.22; H, 4.37; N, 5.06%.

MnSAX·2H$_2$O (XI). To a solution of I (50 mg) in pyridine (15 m*l*) there was added a solution of manganese acetate tetrahydrate (25 mg) in pyridine (15 m*l*); the mixture was then heated on a water bath for two hours

6) S. Kimoto, S. Sakai and K. Ohkuma, *Yakugaku Zasshi*, **69**, 155 (1949).

to give a whitish-brown precipitate, which was subsequently collected and washed with ethanol.

Found: C, 63.87; H, 4.67; N, 4.80; Mn, 9.89%. Calcd for $C_{31}H_{24}N_2O_4Mn \cdot 2H_2O$: C, 64.25; H, 4.87; N, 4.83; Mn, 9.48%.

CoSAX•H_2O•2Py (XII). A solution of I (100 mg) in pyridine (30 m*l*) was added to a solution of cobalt acetate tetrahydrate (60 mg) in pyridine (30 m*l*), and then the mixture was heated on a water bath for half an hour. After the reaction mixture had been concentrated to 10 m*l* and left standing over night, yellow prisms separated. These prisms were collected, recrystallized from pyridine, and air-dried at room temperature.

Found: C, 68.03; H, 5.11; N, 7.87; Co, 8.31%. Calcd for $C_{31}H_{24}N_2O_4Co \cdot H_2O \cdot 2Py$: C, 68.05; H, 5.01; N, 7.76; Co, 8.14%.

CoSAX•1/2H_2O (XIII). The compound XII was heated at 110°C/30 mmHg for five hours to give a brown powder which could subsequently be crystallized from dry benzene as orange needles.

Found: C, 67.02; H, 4.59; N, 5.20; Co, 10.69%; mol wt, 561(Chf). Calcd for $C_{31}H_{24}N_2O_4Co \cdot \frac{1}{2}H_2O$: C, 66.91; H, 4.59; N, 5.03; Co, 10.59%; mol wt, 556.49.

CoSAX•phen•2H_2O (XIV). The compound XIII (20 mg) and an excess of 1,10-phenanthroline were dissolved in ethanol (20 m*l*), and then the mixture was heated on a water bath for two hours. The orange precipitate which separated was collected and washed with ethanol. It was characterized by its insolubility in most organic solvents.

Found: C, 68.03; H, 4.58; N, 7.15%. Calcd for $C_{43}H_{32}N_4O_4Co \cdot 2H_2O$: C, 67.63; H, 4.75; N, 7.34%.

CoSAX•dipy•H_2O (XV). This was also prepared from the compound XIII (20 mg) and 2,2′-dipyridyl (excess) as a reddish-brown precipitate. It was also insoluble in most organic solvents.

Found: C, 68.33; H, 4.47; N, 4.55%. Calcd for $C_{41}H_{32}N_4O_4Co \cdot H_2O$: C, 68.24; H, 4.47; N, 4.76%.

Resolution of the Complex XIII. The conditions for the separation of the complex XIII were:

Adsorbent: anhydrous D-glucose (guaranteed reagent)
Diameter of column: 1.8 cm
Height of bed: 150 cm
Sample: Complex XIII, 70 mg
Eluent: benzene
Flow rate: about 6 m*l*/min.

The eluate was separated into fifty fractions by the use of a fraction-collector apparatus, Toyo Fraction Collector SF-200A. The first five fractions were combined, and the solvent was evaporated. A solution of the complex (1.25 mg) in chloroform (1.0 m*l*) showed a specific rotation of $[\alpha]_D^{15}$ +0.32°. The last ten fractions were combined, and the benzene was evaporated. A solution of the complex (0.90 mg) in chloroform (1.0 m*l*) showed a levo-rotation of $[\alpha]_D^{15}$ −0.98°.

BULLETIN OF THE CHEMICAL SOCIETY OF JAPAN VOL. 43 809—813 (1970)

Syntheses of Benzodiazepine Derivatives

Shinichi MOTOKI, Chikahiro URAKAWA, Akio KANO, Yukio FUSHIMI, Tōru HIRANO and Katsumi MURATA

Department of Chemistry, Faculty of Science, Science University of Tokyo, Shinjuku-ku, Tokyo

(Received April 30, 1969)

This communication deals with the syntheses of the aza-analogues of benzoheptafulvene. Acetylacetone or benzoylacetone reacted with benzophenone chloride in the presence of sodium ethoxide to form 3-(α-phenylbenzylidene)pentane-2,4-dione (XIVa) or 1-phenyl-2-(α-phenylbenzylidene)butane-1,3-dione (XIVc) respectively. Treatment of *o*-phenylenediamine with XIVa in acetic acid - ethanol resulted in forming 2,4-dimethyl-3-(α-phenylbenzylidene)-3*H*-benzo[*b*]-1,5-diazepine (XVa) which has a 3,6-diaza-4,5-benzoheptafulvene ring skeleton. Similarly, substituted *o*-phenylenediamines reacted with XIVa to give 7-substituted 2,4-dimethyl-3-(α-phenylbenzylidene)-3*H*-benzo[*b*]-1,5-diazepines (XVb)—(XVd). Reaction of XIVa with hydrazine gave only the monohydrazone of XIVa. The ketene dimer reacted with *o*-phenylenediamines to give 4-methyl-2,3-dihydro-2-oxo-1*H*-benzo[*b*]-1,5-diazepines (Xa)—(Xc). However, the condensation of Xa with aldehyde gave an undesirable product.

Although a number of seven membered ring compounds containing nitrogen have been prepared by several workers,[1] aza-analogues of tropone, heptafulvene and fulvene have not been investigated extensively. Only the following are known of the compounds involving such ring systems: 3-hydroxyimino-2,4-dimethyl-3*H*-benzo[*b*]-1,5-diazepine (I),[2] 2,4-diphenyl-3-oxo-3*H*-benzo[*b*]-1,5-diazepine

1) A. Yokoo, *Yuki Gosei Kagaku Kyokai Shi*, **24**, 532 (1966).

2) J. A. Barltrop, C. G. Richard, D. M. Russel and G. Ryback, *J. Chem. Soc.*, **1959**, 1132.

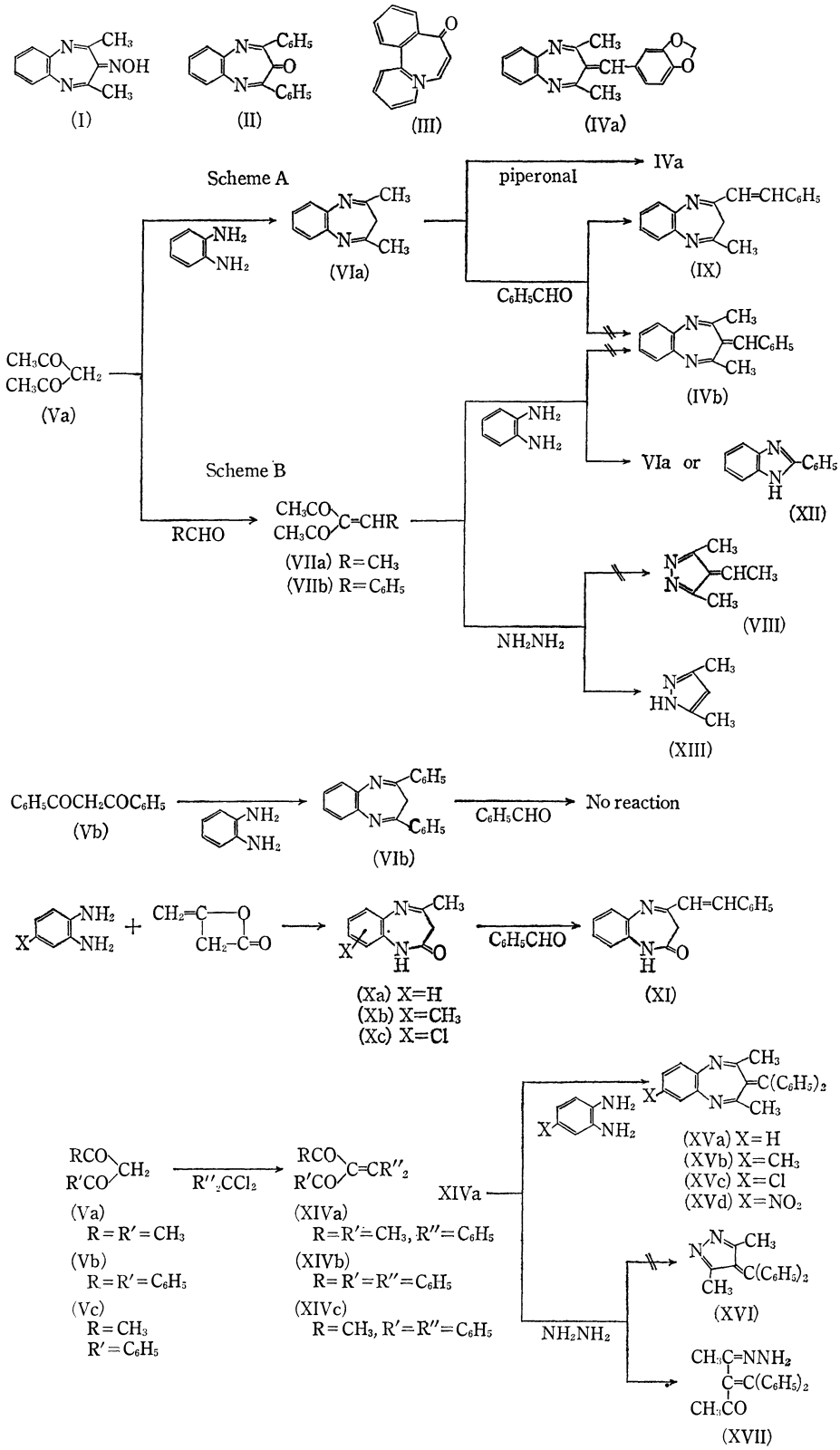
(I)
(II)
(III)
(IVa)
Scheme A
piperonal
IVa
(VIa)
(IX)
C6H5CHO
(IVb)
(Va)
VIa or
(XII)
Scheme B
RCHO
(VIIa) R=CH3
(VIIb) R=C6H5
(VIII)
NH2NH2
(XIII)
(Vb)
(VIb)
C6H5CHO
No reaction
(Xa) X=H
(Xb) X=CH3
(Xc) X=Cl
(XI)
R''2CCl2
(Va)
R=R'=CH3
(Vb)
R=R'=C6H5
(Vc)
R=CH3
R'=C6H5
(XIVa)
R=R'=CH3, R''=C6H5
(XIVb)
R=R'=R''=C6H5
(XIVc)
R=CH3, R'=R''=C6H5
XIVa
(XVa) X=H
(XVb) X=CH3
(XVc) X=Cl
(XVd) X=NO2
(XVI)
NH2NH2
(XVII)

Fig. 1

Table 1. Preparation of unsubstituted and substituted 4-methyl-2,3-dihydro-2-oxo-1*H*-benzo[*b*]-1,5-diazepine

X	g	Ketene dimer* g	Time** hr	Solvent (C_6H_6) m*l*	Products	Yield %	Mp*** °C	Anal. %	Found	Calcd
H	4.3	3.4	3.5	80	Xa	54****	147—148 (lit, 151)		—	—
CH_3	4.9	3.4	4.0	55	Xb	20	174—175	C	69.87	70.18
								H	6.71	6.43
								N	15.05	14.88
Cl	5.7	3.4	5.0	60	Xc	42	174—175	C	57.84	57.55
								H	4.38	4.32
								N	13.42	13.43
								Cl	17.04	17.03

* The ketene dimer was dissolved in 10 m*l* of benzene.
** Temperature was maintained at about 45—55°C during the reaction.
*** The products were recrystallized from benzene.
**** The yield was not recorded in literature.

(II),[3] 8-oxo-8*H*-dibenzo[*a*,*c*]azepine (III)[4] and 2,4-dimethyl-3-piperonylidene-3*H*-benzo[*b*]-1,5-diazepine (IVa).[2] In this paper, the syntheses of various aza-analogues of benzoheptafulvenes (XVa)—(XVd) have been described.

The benzodiazepine such as IVa may be synthesized either by scheme A or scheme B as illustrated in Fig. 1. In scheme A, *o*-phenylenediamine is first condensed with *β*-diketones (V) to benzodiazepines (VI) which are then condensed with aldehydes at their 3 position. In scheme B, *β*-diketones are converted to *α*-alkylidene- or arylidene-*β*-diketones (VII) preceding the ring formation and then condensed with *o*-phenylenediamine. Similarly, a compound such as VIII may be prepared by the reaction of hydrazine and VII in accordance with scheme B. Barltrop *et al.*[2] reported that the condensation of VIa with piperonal gave IVa whereas the reaction with benzaldehyde took place at the methyl group in VIa to give the undesirable compound (IX). In our experiment, the diazepine (VIb) which posseses no methyl group in the side chain was allowed to react with benzaldehyde. However, the reaction did not proceed even under various conditions and the starting materials were recovered.

Accordingly, the condensation of 4-methyl-2,3-dihydro-2-oxo-1*H*-benzo[*b*]-1,5-diazepine (Xa) with aldehydes was examined, since the methylene group of Xa appeared to be more reactive than that of VI. Although several procedures for the preparation of Xa are available,[5-7] the method by the reaction of the ketene dimer with *o*-phenylenediamine[5] was found to be the most convenient. Xa and 7- or 8-substituted 4-methyl-2,3-dihydro-2-oxo-1*H*-benzo[*b*]-1,5-diazepines (Xb and Xc) were prepared by the reaction of the ketene dimer with *o*-phenylenediamine, 3,4-diaminotoluene and 3,4-diaminochlorobenzene. Xa reacted with benzaldehyde in the presence of piperidine to give a condensation product. The NMR spectra of the product in $CDCl_3$ exhibited one methylene singlet but no methyl singlet in contrast with those of Xa. Thus the product was assumed to be 4-styryl-2,3-dihydro-2-oxo-1*H*-benzo[*b*]-1,5-diazepine (XI). Similarly, condensation of Xa with other aromatic aldehydes or furfural occurred at the methyl group of Xa.

As we found that the syntheses of the compound of the type IV were unsuccessful by scheme A, a different synthetic approach was investigated following scheme B. *α*-Alkylidene- or arylidene-*β*-diketones (VII) are readily prepared by the condensation of *β*-diketones with aldehydes. Barltrop *et al.*[2] reported that the reaction of 3-benzylidenepentane-2,4-dione (VIIb) with *o*-phenylenediamine yielded 2-phenylbenz[*d*]imidazole (XII) or diazepine (VIa) depending upon the reaction conditions. We examined the reaction of 3-ethylidenepentane-2,4-dione (VIIa) with *o*-phenylenediamine or hydrazine under various conditions. The attempts were also unsuccessful and the product isolated was diazepine (VIa) or dimethylpyrazole (XIII).

Although the reaction of diamines with VII is complicated and may yield a variety of products depending upon the reaction conditions, Pauly[8] reported that the reaction of ethyl *α*-isopropylideneacetoacetate with phenylhydrazine gave 1-phenyl-3-methyl-4-isopropylidene-5-pyrazolone which contains exo double bond. This fact suggests that the

3) T. Yonezawa, M. Matsumoto and H. Kato, This Bulletin, **41**, 2543 (1968).
4) W. Paterson, G. R. Procter, *J. Chem. Soc.*, **1962**, 3468.
5) W. Ried and P. Stahlhofen, *Chem. Ber.*, **90**, 825 (1957).
6) W. A. Sexton, *J. Chem. Soc.*, **1942**, 303.
7) J. Davoll, *ibid.*, **1960**, 308.
8) H. Pauly, *Ber.*, **30**, 481 (1897).

Table 2. Preparation of unsubstituted and substituted 2,4-dimethyl-3-(α-phenylbenzylidene)-3*H*-benzo[*b*]-1,5-diazepines

X (g)	XIVa g	Time hr	Solvent EtOH ml	Solvent HOAc ml	Products	Yield %	Mp* °C	Anal. %	Found	Calcd
CH_3 2.5	5.3	7	5	2	XVb	40	141—142	C	85.65	85.68
								H	6.52	6.33
								N	8.08	7.99
Cl 2.9	5.3	2	10	2	XVc	50	156	C	77.94	77.73
								H	5.19	5.13
								N	7.53	7.56
								Cl	9.59	9.58
NO_2 3.1	5.3	4	5	3	XVd	7	205—206	C	75.53	75.57
								H	4.98	5.02
								N	10.72	11.02

* The products were recrystallized from methanol.

β-diketone such as XIV would undergo the ring closure with diamines in the desired manner. Compound XIV is extremely inaccessible as compared with VII because the direct condensation of β-diketones with ketones to form XIV is difficult. However, when acetylacetone (Va), dibenzoylmethane (Vb) and benzoylacetone (Vc) was allowed to react with benzophenone chloride in the presence of sodium ethoxide, 3-(α-phenylbenzylidene)pentane-2,4-dione (XIVa) and 1-phenyl-2-(α-phenylbenzylidene)butane-1,3-dione (XIVc) were obtained. In the case of XIVb the reaction product was a waxy solid and could not be identified owing to difficulties in purification.

When XIVa was heated with *o*-phenylenediamine in ethanol-acetic acid, a crystalline product was obtained. The elementary analysis of the product indicated the empirical formula, $C_{23}H_{20}N_2$ and the NMR spectra showed only two signals, one for phenyl protons (2.8 τ, multiplet, 14H) and the other for methyl protons (8.0 τ, singlet, 6H), while the IR spectra showed no NH stretching band. Thus the product was identified as 2,4-dimethyl-3-(α-phenylbenzylidene)-3*H*-benzo[*b*]-1,5-diazepine (XVa) which has a 3,6-diaza-4,5-benzoheptafulvene ring skeleton. Similarly, treatment of XIVa with 3,4-diaminotoluene, 3,4-diaminochlorobenzene and 3,4-diaminonitrobenzene gave the corresponding 7-substituted benzodiazepines (XVb)—(XVd). The reaction of XIVb with *o*-phenylenediamine was also examined but no identified product was obtained. On the other hand, the reaction of XIVa with hydrazine in acetic acid gave high melting white crystals. Its analytical values agreed better with the calculated values for XVII than those for diazafulvene (XVI) and the IR spectra clearly exhibited a broad NH stretching band. Therefore, the product is assumed to be 4-hydrazono-3-(α-phenylbenzylidene)pentan-2-one.

Experimental

4-Methyl-2,3-dihydro-2-oxo-1*H*-benzo[*b*]-1,5-diazepine (Xa). This compound was prepared by the method given in literature.[5]

4,7(or 8)-dimethyl-2,3-dihydro-2-oxo-1*H*-benzo[*b*]-1,5-diazepine (Xb) and 7(or 8)-chloro-4-methyl-2,3-dihydro-2-oxo-1*H*-benzo[*b*]-1,5-diazepine (Xc) were prepared similarly by the reaction of the ketene dimer with 3,4-diaminotoluene and 3,4-diaminochlorobenzene. The results are summarized in Table 1.

4-Styryl-2,3-dihydro-2-oxo-1*H*-benzo[*b*]-1,5-diazepine (XI). A solution of 3.5 g of Xa, 2.0 g of benzaldehyde and three drops of piperidine in 15 ml of benzene was refluxed for 15 hr. After cooling, precipitated product was filtered, recrystallized from ethanol and 1.1 g of XI was obtained; yield 21.2%, yellow needles, mp 218—219°C.

Found: C, 78.10; H, 5.17; N, 10.57%. Calcd for $C_{17}H_{14}ON_2$: C, 77.84; H, 5.38; N, 10.68%.

3-(α-Phenylbenzylidene)pentane-2,4-dione (XIVa). Into a solution of sodium ethoxide, prepared from 15.3 g of sodium and 300 ml of ethanol, 66.7 g of acetylacetone was added. The mixture was then heated under reflux and 79 g of benzophenone chloride was added over a period of 1 hr. After addition of the chloride, the mixture was refluxed a further 2 hr. Carbon dioxide was passed through the cooled reaction mixture for 10 min and the precipitate was filtered and washed with ethanol repeatedly. The filtrate was steam-distilled to remove most of the ethanol and excess of acetylacetone. An oily product separated in the residue was extracted with ether and the extract was dried over anhydrous sodium sulphate. After the ether was removed, the residue was distilled and a fraction boiling at 165—181°C/7 mmHg was collected. The distillate solidified immediately in the receiver and was recrystallized from ligroin to give 34.4 g (39.1%) of XIVa, colorless needles, mp 120—121°C.

Found: C, 81.52; H, 6.23%. Calcd for $C_{18}H_{16}O_2$: C, 81.79; H, 6.10%.

1-Phenyl-2-(α-phenylbenzylidene)butane-1,3-dione (XIVc). As in the preceding procedure, 23.2 g of benzophenone chloride was treated with sodium benzoylacetonate, prepared from 4.6 g of sodium and 32.4 g of benzoylacetone in 100 ml of ethanol. After the reaction was over, carbon dioxide was passed through the reaction mixture and the precipitate was filtered and washed with 10 ml of ethanol. The filtrate was cooled in an ice-salt bath and the crystalline product separated

was collected and recrystallized from ethanol. XIVc was obtained as light yellow needles, mp 126°C, yield 4.7 g (14.7%).

Found: C, 84.78; H, 5.50%. Calcd for $C_{23}H_{18}O_2$: C, 84.64; H, 5.56%.

2,4-Dimethyl-3-(α-phenylbenzylidene)-3*H*-benzo[*b*]-1,5-diazepine (XVa). A solution of 2.6 g of XIVa and 1.1 g of *o*-phenylenediamine in 10 m*l* of ethanol containing 1 m*l* of acetic acid was refluxed for 3 hr. After cooling, the product precipitated was filtered and recrystallized from methanol. XVa was obtained as white needles, mp 156—157°C, yield 2.1 g (62.5%).

Found: C, 85.37; H, 5.67; N, 8.53%. Calcd for $C_{24}H_{20}N_2$: C, 85.68; H, 5.99; N, 8.33%.

Similarly, 7-substituted 2,4-dimethyl-3-(α-phenylbenzylidene)-3*H*-benzo[*b*]-1,5-diazepines (XVb)—(XVd) were prepared by the reaction of XIVa with 3,4-diaminotoluene, 3,4-diaminochlorobenzene and 3,4-diaminonitrobenzene respectively. The results are summarized in Table 2.

4-Hydrazono-3-(α-phenylbenzylidene)pentan-2-one (XVII). A mixture of 2.6 g of XIVa, 0.5 g of hydrazine hydrate and 6 m*l* of acetic acid was refluxed for 1 hr. After cooling, 100 m*l* of water was added and the mixture was allowed to stand for 2—3 hr. Precipitated product was filtered and recrystallized from methanol to give 1.6 g of XVII, mp 217—219°C.

Found: C, 77.71; H, 6.20; N, 9.99%. Calcd for $C_{18}H_{18}ON_2$: C, 77.67: H, 6.52; N, 10.07%.

The authors wish to express their thanks to Professor Yojiro Tsuzuki for his helpful advice and encouragement.

BULLETIN OF THE CHEMICAL SOCIETY OF JAPAN VOL. 43 813—817 (1970)

Effects of Additives on the Alternating Copolymerization of Aziridines with Cyclic Imides

Tsutomu KAGIYA and Teruho ADACHI

Faculty of Engineering, Kyoto University, Sakyo-ku, Kyoto

(Received May 8, 1969)

The effect of the addition of 2-methyl-2-oxazoline, which is an isomer of the growing chain end, was examined. The rate of the copolymerization of ethylenimine with succinimide increased upon the addition of 2-methyl-2-oxazoline. On the basis of this result and of the NMR spectrum of the copolymer, the mechanism of propagation *via* an activated state similar to oxazoline was proposed. The copolymerization was accelerated by the addition of sodium iodide, which is the catalyst of the isomerization of the growing chain end. The property of the copolymer obtained was different from that of the copolymer obtained without sodium iodide. Sodium iodide also affected the copolymerization of *N*-ethylethylenimine with succinimide, while it did not affect that of ethylenimine with *N*-ethylsuccinimide. The reduced viscosity of the copolymer increased with the reaction time. The reaction mechanism of the copolymerization in the presence of the catalyst was discussed on the basis of the facts mentioned above.

The present authors have previously reported[1,2] that the growing chain end in the alternating copolymerization of ethylenimine with cyclic imides

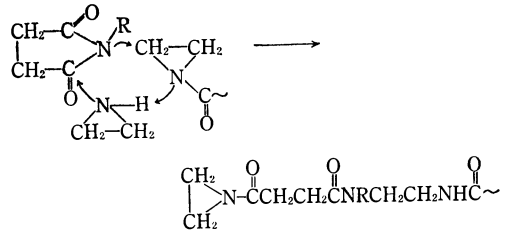

was the *N*-acylethylenimine ring and that the propagation proceeded *via* a six-membered ring by means of the hydrogen migration of the ethylenimine and the ring opening of cyclic imide.

In this mechanism, it is also plausible that the oxygen atom of *N*-acylethylenimine coordinates to the hydrogen atom of ethylenimine. In relation to this coordination, it has been reported[3] that this growing chain end, *N*-acylethylenimine, easily isomerized to the oxazoline ring with a catalyst such as sodium iodide. In this isomerization, it is considered that the oxygen atom of the carbonyl group and the carbon atom of the ring coordinate

1) T. Kagiya, M. Izu, T. Adachi and K. Fukui, *J. Polym. Sci., Part A-1*, **7**, 2659 (1969).

2) T. Kagiya, T. Adachi and K. Fukui, *ibid.*, **7**, 2651 (1969).

3) T. Kagiya, S. Narisawa, T. Maeda and K. Fukui, *Kogyo Kagaku Zasshi*, **69**, 732 (1966).

to the cation and anion of the catalyst respectively.

In order to examine the coordination of the oxygen atom, the effect of the oxazoline or isomerization catalyst on the copolymerization was studied.

Experimental

The methods of preparing and purifying the monomers were described in a previous paper.[1] The 2-methyl-2-oxazoline was prepared by the isomerization of *N*-acetylethylenimine according to the literature.[3] The sodium iodide and *N,N*-dimethylformamide were obtained commercially (G.R. grade) and were used without further purification.

A measured amount of the cyclic imide and a solid additive were placed in a glass ampoule. After the mixture had been dried under reduced pressure, a certain volume of aziridine and a liquid additive were placed in the ampoule with a syringe under a nitrogen atmosphere. The ampoule was then sealed and kept in a constant-temperature bath for a definite period. The reaction products were washed with acetone to remove the residual monomers and then dried *in vacuo*.

The composition of the copolymer was determined by elementary analysis. The infrared spectra were obtained by the potassium-bromide-pellet technique on a Shimadzu infrared spectrophotometer, Model IR-27. The NMR spectra were recorded in D_2O at room temperature with JEOL model JNM-3H-60 at 60 MHz. The reduced viscosity of the copolymer was calculated from the viscosity measurement of a 0.5% solution of formic acid at 35°C.

Results and Discussion

(1) Effect of 2-Methyl-2-oxazoline. In order to examine the oxygen coordination mechanism described above, 2-methyl-2-oxazoline was added to the system of the copolymerization of ethylenimine with succinimide. The results are shown in Table 1.

TABLE 1. EFFECT OF ADDITION OF 2-METHYL-2-OXAZOLINE*

Expt. No.	2-Methyl-2-oxazoline g (mol)	Reaction time min	Yield g	Rate** g/min
1	—	24.0	1.808	0.075
2	0.051 (0.0006)	19.5	2.028	0.104
3	0.128 (0.0015)	11.5	2.037	0.177
4	0.255 (0.0030)	10.0	1.987	0.199
5***	*N*-Acetylethylenimine 0.256 (0.0030)	9.2	2.323	0.252

* Monomer: Ethylenimine 1.291 g (0.03 mol)
Succinimide 2.973 g (0.03 mol)
Reaction temperature: 70°C

** Reaction was stopped at almost the same yield, and a reaction rate was expressed in a value of yield divided by time.

*** Shown as a reference.

The copolymerization was accelerated by the addition of 2-methyl-2-oxazoline, and the copolymer obtained was a white, powdery polymer. The rate was almost the same as that of the copolymerization in the presence of the same amount of *N*-acetylethylenimine (Exp. No. 5). The NMR spectrum of the copolymer shown in Fig. 1-a displayed peaks which could be assigned to the methylene proton of the repeating unit, $-(-C\underset{a}{H_2}C\underset{a}{H_2}-NHCOC\underset{b}{H_2}C\underset{b}{H_2}-CONH-)-$, at $\tau=6.72$ (a), 7.48 (b).[1] It also displayed peaks assignable to the end groups of *N*-acylethylenimine ($\tau=7.56$) and *N*-substituted succinimide ($\tau=7.25$). The peak intensity of the latter was quite small compared with that in the spectrum (Fig. 1-b) of the copolymer obtained without additives. This phenomenon was also observed in the NMR spectrum (Fig. 1-c) of the copolymer obtained by the copolymerization of ethylenimine and succinimide in the presence of *N*-acetylethylenimine. Since the copolymer initiated by 2-methyl-2-oxazoline or *N*-acetylethylenimine has no amide end, it is difficult for the cyclization reaction[2] at the polymer end to form the structure of *N*-substituted succinimide to occur.

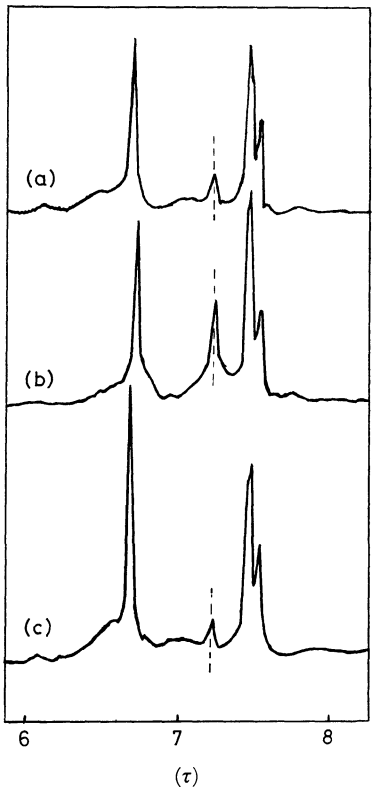

Fig. 1. The NMR spectra of the copolymers of ethylenimine with succinimide obtained in the presence of 2-methyl-2-oxazoline (a), without additive (b) and in the presence of *N*-acetylethylenimine (c).

On the basis of the facts that the acceleration by 2-methyl-2-oxazoline was almost the same as the acceleration by *N*-acetylethylenimine, that the peaks which should be assignable to the oxazoline ring were not observed in the spectrum (a) and that the structure of the copolymer was the same as the structure of the copolymer obtained in the presence of *N*-acetylethylenimine, the following mechanism for initiation by oxazoline is proposed: the oxazoline ring quickly opens *via* the activated state (A) and the *N*-acylethylenimine end is yielded. Moreover, the effect of 2-methyl-2-oxazoline on the copolymerization is similar to that of *N*-acetylethylenimine.

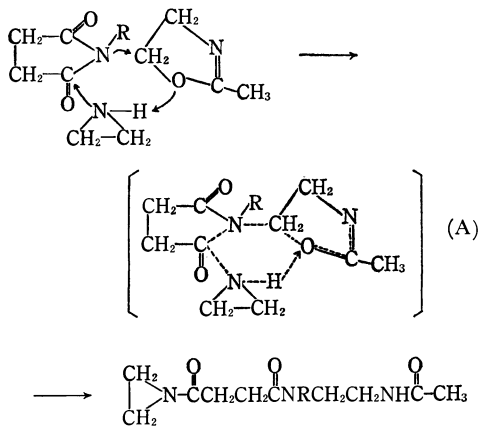

On the basis of the above consideration, the mechanism of the propagation reaction may be considered to be analogous: (i) it is not the nitrogen atom, but the oxygen atom, of the *N*-acylethylenimine end of polymer that coordinates to the hydrogen of ethylenimine, and (ii) the hydrogen-migration-propagation reaction proceeds *via* an activated state (A) similar to that in the oxazoline structure.

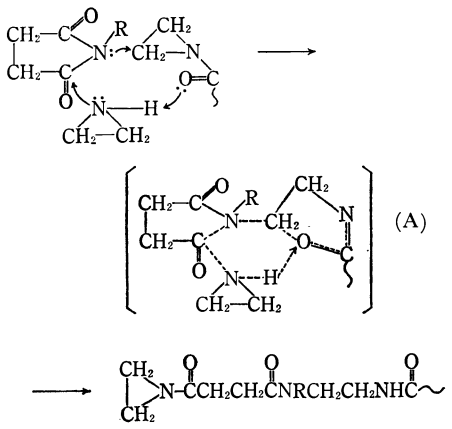

(2) Effect of Isomerization Catalyst. It has been reported that *N*-acylethylenimine is isomerized to oxazoline by a catalyst such as sodium iodide.[3] In case the reaction proceeds *via* the mechanism proposed above and the isomerization is the rate-determining step, it can be expected that the propagation reaction will be accelerated by the addition of sodium iodide. The results shown in Table 2 are in accordance with this expectation.

These findings seem to support the mechanism proposed above, but the copolymer obtained was a yellow or brown, hygroscopic or greasy polymer, and the properties of the copolymer were different from those of a copolymer obtained without sodium iodide. The infrared spectrum of the copolymer displayed the characteristic peaks of amide, but the NMR spectrum (Fig. 2) of the copolymer

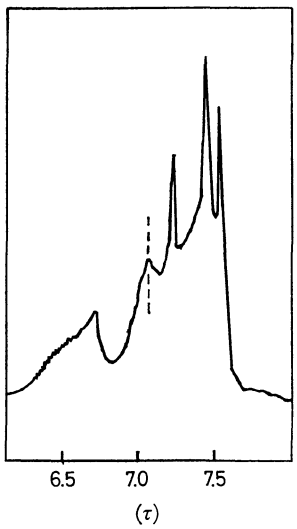

Fig. 2. The NMR spectrum of the copolymer of ethylenimine with succinimide obtained in the presence of sodium iodide.

displayed an extra peak at $\tau=7.07$ which had not been found in the specturm of the copolymer shown in Fig. 1-b.

In order to clarify the role of sodium iodide in the structure of the copolymer obtained, the following experiments were performed (Table 3). Ethylenimine or succinimide was not polymerized by sodium iodide. Moreover, *N*-acetylethylenimine neither copolymerized with succinimide nor homopolymerized in the presence of sodium iodide. Therefore, it can be concluded the structure of the copolymer is neither $-(-CH_2CH_2-N(-COCH_2CH_2CONH-)-)_n$ nor $-(-CH_2CH_2-N(-CO\sim)-)_n$.

In view of the fact that sodium iodide acts as a catalyst of the isomerization of the *N*-acylethylenimine end to oxazoline, the reaction of succinimide with 2-methyl-2-oxazoline was carried out and examined, with particular care. From the

TABLE 2. EFFECT OF SODIUM IODIDE

Expt. No.	Monomers, g (mol)		NaI mol×10⁴	Temp. °C	Time min	Yield g	Composition (mol%)		η_{sp}/c* dl/g
	Ethylenimine	Succinimide					Imine	Imide	
1	1.291 (0.03)	2.973 (0.03)	—	70	24.0	1.808	50.15	49.85	—
2	1.291 (0.03)	2.973 (0.03)	6	70	13.0	2.985	56.25	43.75	0.073
3	0.646 (0.015)	2.973 (0.03)	3	70	20.0	1.410	54.46	45.54	—
4	0.646 (0.015)	1.487 (0.015)	—	30	240	0.000	—	—	—
5	0.646 (0.015)	1.487 (0.015)	3	30	240	0.081	—	—	—
6	1.291 (0.03)	1.487 (0.015)	3	30	240	0.052	—	—	—
7	0.646 (0.015)	2.973 (0.03)	3	30	240	0.058	—	—	—
8	0.646 (0.015)	1.487 (0.015)	15	30	26.0	1.376	—	—	—

* 0.5% solution of formic acid at 35°C.

TABLE 3. REACTIVITIES OF POLYMERIZATION OF VARIOUS MONOMERS BY SODIUM IODIDE*

Expt. No.	Monomer** (mol)		Additive (mol)	Reaction time hr	Yield g
1	Ethylenimine (0.03)		NaI 0.0006	216	0.000
2***	Succinimied (0.01)		NaI 0.0002	44	0.000
3	AEI (0.01)	Succinimide (0.01)	—	119	0.000
4	AEI (0.01)	Succinimide (0.01)	NaI 0.0002	148	0.000
5	AEI (0.01)		NaI 0.0002 Succinimide 0.0002	216	0.000
6	AEI (0.01)		NaI 0.0002	41	0.000
7	Succinimide (0.01)	2-Methyl-2-oxazoline (0.01)	—	69	0.000

* Reaction temperature: 70°C
** AEI = *N*-Acetylethylenimine
*** Solvent: Acetonitrile 5 cc

TABLE 4. EFFECT OF SODIUM IODIDE ON THE COPOLYMERIZATION OF *N*-SUBSTITUTED MONOMERS*

Expt. No.	Momoners (mol)**		NaI mol	Reaction time hr	Yield g
	Imine	Imide			
1	Ethylenimine (0.01)	ESI (0.01)	—	65	0.444
2	Ethylenimine (0.01)	ESI (0.01)	0.0005	70	0.465
3	EEI (0.01)	Succinimide (0.01)	—	170.5	0.000
4	EEI (0.01)	Succinimide (0.01)	0.001	70	0.133

* Reaction temperature: 70°C
** ESI = *N*-Ethylsuccinimide, EEI = *N*-Ethylethylenimine

fact that no polymer was obtained, it may be concluded that sodium iodide does not give the structure of $-(-CH_2CH_2-N(-CO-)CH_2-CH_2CONH-)-_n$ which is that of the copolymer of succinimide with an oxazoline ring.

On the other hand, it is plausible that sodium iodide does not only affect the *N*-acylethylenimine, but also activates either succinimide or ethylenimine to give the copolymer with a different structure. In the light of the mechanism described above, the effect of sodium iodide on the copolymerization of ethylenimine with *N*-substituted succinimide was also examined (Table 4, Nos. 1 and 2). No effect was, however, observed. As has been mentioned in a previous paper.[2] *N*-ethylethylenimine did not copolymerize with succinimide. However, in the presence of sodium iodide, this copolymerization occurred to give a greasy polymer. This result is similar to that in the copolymerization of *N*-ethylethylenimine with succinimide by water.[2]

On the basis of these results, it may be considered that sodium iodide does not affect the ring opening of succinimide, but that it does affect the ring opening of ethylenimine to yield *N*-(β-aminoethyl)-succinimide, which is then able to give a polyamide by polyaddition reaction in analogy with the copolymerization by water.

The copolymerization of ethylenimine with succinimide was carried out quantitatively in an *N,N*-dimethylformamide solution in order to verify the polyaddition mechanism. The polymer yield and the reduced viscosity of the polymer obtained were then plotted against the reaction time (Fig. 3). In the early stage, an acceleration

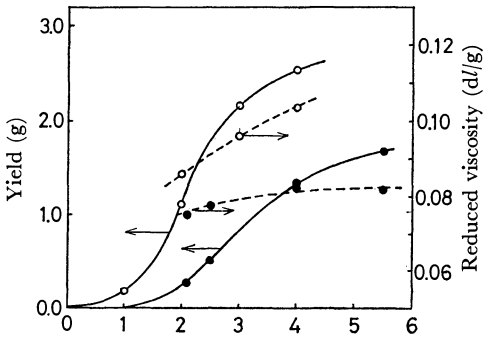

Fig. 3. The plots of polymer yield or reduced viscosity *vs.* reaction time.
Monomers: Succinimide 2.973 g (0.03 mol)
Ethylenimine 1.291 g (0.03 mol)
Additive: ○ NaI 0.0015 mol
● No additive
Solvent: *N,N*-Dimethylformamide 5 cc
Temperature: 70°C

of the rate was observed. The reduced viscosity of the copolymer obtained in the absence of sodium iodide was almost constant regardless of the reaction time, while that obtained in the presence of sodium iodide increased. After the copolymer obtained by sodium iodide was again dissolved in *N,N*-dimethylformamide and kept at 70°C for 47 hr, the reduced viscosity increased from 0.103 to 0.131 (dl/g). These two facts suggest that the reaction between polymers, namely, polyaddition reaction, occurs, at least in part.

On the basis of the facts presented above, the following is proposed as a possible reaction mechanism in the presence of sodium iodide:

(i) The same reaction as that which occurs without a catalyst.

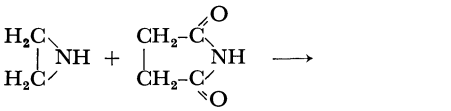

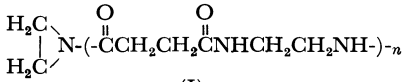

(I)

(ii) Polyaddition of *N*-(*β*-aminoethyl)succinimide. *N*-(*β*-Aminoethyl)succinimide is formed by the ring-opening reaction of ethylenimine with sodium iodide.

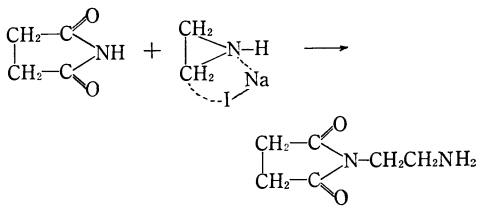

N-(*β*-Aminoethyl)succinimide is considered to give a polyamide by a polyaddition in which the ring of succinimide opens with amine.[2,4,5]

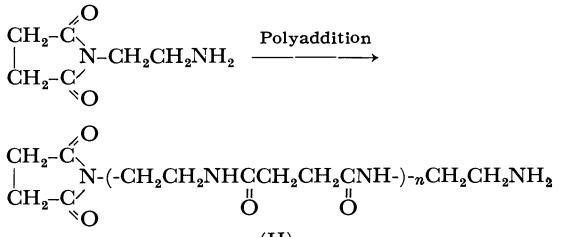

(II)

(iii) Copolymerization of ethylenimine with *N*-(*β*-aminoethyl)succinimide.

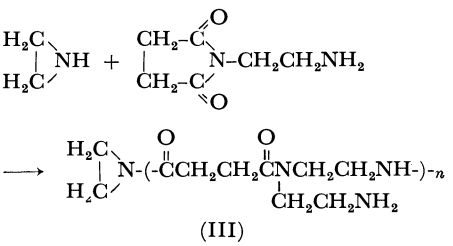

(III)

Since ethylenimine is able to copolymerize with *N*-substituted succinimide, *N*-(*β*-aminoethyl)succinimide may be considered to act as an active *N*-substituted succinimide.

The NMR spectrum of the copolymer obtained by sodium iodide at 30°C displayed the peak assigned to *N*-acylethylenimine. On the other hand, at 30°C, the copolymerization without sodium iodide did not occur (*cf.* Table 2, No. 4). This indicates that the (i) reaction did not occur. Therefore, the *N*-acylethylenimine end was considered to be produced by the reaction (iii). Moreover, the peak of the NMR spectrum at $\tau=7.07$ in Fig. 2 might be assignable to the methylene proton of the *N*-(*β*-aminoethyl) group.

Therefore, it may be concluded that the copolymer obtained by a catalsyt of the isomerization of *N*-acylethylenimine, such as sodium iodide, is a mixture of the copolymers (I), (II), and (III).

Authors gratefully acknowledge the encouragement of Professor Ken-ichi Fukui during this work.

4) T. V. Sheremeteva, V. A. Gusinskaya and V. V. Kudryavtsev, *Izv. Akad. Nauk SSSR, Ser. Khim.*, **1963**, 1821; *Chem. Abstr.*, **60**, 2809 (1964).

5) T. Kagiya, S. Narisawa, K. Manabe, M. Kobata and K. Fukui, *J. Polym. Sci., Part A-1*, **4**, 2081 (1966).

BULLETIN OF THE CHEMICAL SOCIETY OF JAPAN VOL. 43 818—823 (1970)

Studies on the Substrate Specificity of Taka-amylase A. III. Syntheses of Some New Derivatives of Phenyl α-Maltoside

Hitoshi ARITA, Mamoru ISEMURA, Tokuji IKENAKA and Yoshio MATSUSHIMA

Department of Chemistry, Osaka University, College of Science, Toyonaka

(Received June 19, 1969)

In order to obtain information of the interaction between various portions of the substrate molecule and the enzyme protein, mono-*O*-methyl derivatives of phenyl α-maltoside and its analogues were synthesized and the enzymatic action was investigated. The purity and chemical structure of the compounds were confirmed by chromatographic method, phenol determination, and elemen talanalyses. The anomeric configuration of the glycosidic linkage to phenol was presumed to be of an alpha type on the basis of the high positive value of specific rotation. Some regularities in the enzymatic action on these synthetic substrates were observed.

Elucidation of the interaction through definite atoms or atomic groups between the substrate and the enzyme molecule is an important problem in understanding enzymatic action as a whole, as shown by Blake *et al.*[1] in an X-ray crystallographic investigation of hen egg-white lysozyme. A useful chemical approach to this problem will be an investigation of the enzymatic action on the substrates with different but analogous chemical structures. Helferich and Gruenler[2] and Pigman and Richtmyer[3] investigated the action of β-glucosidase of almond emulsion on phenyl β-glucoside and its *O*-methyl derivatives and analogues. The enzyme preparations at that time were far from being pure. Isemura *et al.*[4] studied the Taka-amylase action on partially *O*-methylated amylose, and obtained some information on the substrate specificity of the enzyme.

Taka-amylase A [EC 3.2.1.1. α-1,4-glucan-4-glucanohydrolase, *Aspergillus oryzae*] crystallized by Akabori *et al.*[5] has been known to liberate phenol from a synthetic substrate, phenyl α-maltoside.[6] The present authors synthesized the compounds shown in the following formulae, and investigated the enzymatic action on them. The structure of the compounds and the ratio of the initial rate of phenol liberation by the enzyme are summarized in Table 1.

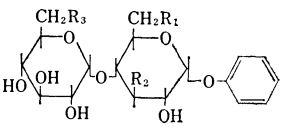

[VI, VII, IX, XI, XIX, XXIV, XXVII, XXXI, XXXIV]

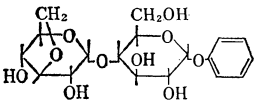

[XXII]

TABLE 1.

Compound	R_1	R_2	R_3	Ratio of the initial rate of phenol liberation by the enzyme
Phenyl α-maltoside	OH	OH	OH	1.00
XI	OCH_3	OH	OH	0.00
XXXIV	OH	OCH_3	OH	0.00
VI	H	OH	OH	0.02
IX	Cl	OH	OH	0.00
VII	I	OH	OH	0.00
XXVII	OH	OH	OCH_3	2.10
XIX	OH	OH	H	0.05
XXXI	OH	OH	Cl	0.24
XXIV	OH	OH	I	0.29
XXII	—	—	—	0.00

The reaction sequences of the syntheses were represented in Schemes 1 and 2. The basic principle of the syntheses was as follows:

1) C. C. F. Blake, L. N. Johnson, G. A. Mair, A. C. T. North, D. C. Phillips and V. R. Sarma, *Proc. Roy. Soc.*, **167B**, 378 (1967).

2) B. Helferich and S. Gruenler, *J. Prakt. Chem.*, [2] **148**, 107 (1937).

3) W. Pigman and N. K. Richtmyer, *J. Amer. Chem. Soc.*, **64**, 374 (1942).

4) M. Isemura, T. Ikenaka and Y. Matsushima, *J. Biochem.*, **64**, 73 (1968).

5) S. Akabori, B. Hagihara and T. Ikenaka, *ibid.*, **41**, 577 (1954).

6) S. Akabori, K. Uehara, Y. Shimazu and K. Nakanishi, Nippon Kwagaku Kwaishi, **64**, 1046 (1943).

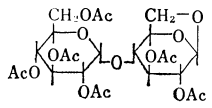

I

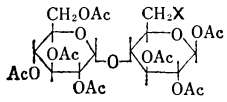

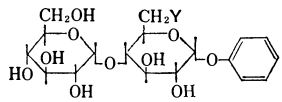

II: X=OH
III: X=OTs
IV: X=I
V: X=H
VIII: X=Cl
X: X=OCH_3

VI: Y=H
VII: Y=I
IX: Y=Cl
XI: Y=OCH_3

(1) I → II(X=OH) → III(X=OTs) → IV(X=I) → V(X=H) → VI(Y=H)
↓
VII(Y=I)

(2) I → II(X=OH) → VIII(X=Cl) → IX(Y=Cl)
↓
X(X=OCH_3) → XI(Y=OCH_3)

Scheme 1

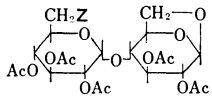

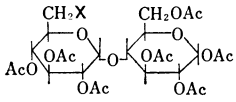

XIII: Z=OTr
XIV: Z=OH
XV: Z=OTs
XVI: Z=I
XVII: Z=H
XXV: Z=OCH_3
XXVIII: Z=Cl

XX: X=OTs
XXIII: X=I
XVIII: X=H
XXVI: X=OCH_3
XXIX: X=Cl

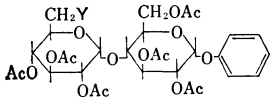

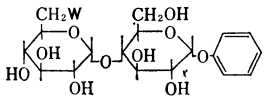

XXI: Y=OTs
XXX: Y=Cl

XIX: W=H
XXIV: W=I
XXVII: W=OCH_3
XXXI W=Cl

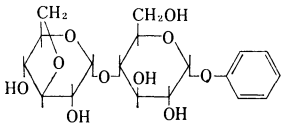

XXII

(1) XIII(Z=OTr) → XIV(Z=OH) → XV(Z=OTs) → XVI(Z=I) → XVII(Z=H) → XVIII(X=H) → XIX(W=H)

(2) XV(Z=OTs)
↓
XX(X=OTs) → XXI(Y=OTs) → XXII
↓
XXIII(X=I) → XXIV(W=I)

(3) XIV(Z=OH) → XXV(Z=OCH_3) →
| XXVI(X=OCH_3) → XXVII(W=OCH_3)
↓
XXVIII(Z=Cl) → XXIX(X=Cl) →
XXX(Y=Cl) → XXXI(W=Cl)

Scheme 2

Maltosan hexaacetate was obtained by the alkali treatment of phenyl β-maltoside followed by acetylation.[7,8] 1,6-Anhydro-ring of maltosan hexaacetate was cleaved by treatment with titanium tetrachloride in chloroform,[9,10] and the hydroxyl on position-6 was set free. The hydroxyl on the position-6′ was set free according to the method of Dutton and Slessor.[11] Introduction of chlorine into the 6- or 6′-position was performed with the use of sulfuryl chloride in pyridine.[12] *O*-Methyl derivatives were prepared through methylation with diazomethane in the presence of boron trifluoride as a catalyst. We found a convenient method for leading 3,6-anhydro-ring into sugar by treating terminal tosyloxy compound with Dowex 1 (OH^-) at room temperature. Using this method, phenyl 3′,6′-anhydro-α-maltoside was prepared from phenyl 6′-*O*-*p*-toluenesulfonyl α-maltoside in good yield. Dick and co-workers[13] havereported that acetylation of β-maltose monohydrate with acetylpyridinium chloride gave acetylated maltose which had free hydroxy at 3-position. This method was used for preparing 3-*O*-substituted phenyl α-maltoside. Phenyl glycosidation was accomplished by the fusion of *O*-acetylated disaccharides with phenol and zinc chloride,[14] followed by deacetylation with sodium methoxide in anhydrous methanol.

In order to eliminate the ambiguity of the structure of the compounds which might arise from the migration of the acetyl groups during the course of syntheses, confirmation was carried out by means of analytical methods: (1) Position of the substitution on the glucose residue. (2) Moiety of the glucose residues which underwent substitution.

Experimental

Maltosan Hexaacetate (I). Maltosan hexaacetate was prepared from phenyl β-maltoside hexaacetate[7] by alkali treatment according to the method of Karrer and Kamienski.[8] Crystallization in methanol gave colorless needles which melted at 182—184°C. Found: C, 50.23; H, 5.58%. Calcd for $C_{24}H_{32}O_{11}$: C, 50.00; H, 5.56%.

1,2,3,2′,3′,4′,6′-Hepta-*O*-acetyl-β-maltose (II). This compound was prepared from I by cleaving 1,6-anhydro ring with titanium tetrachloride following the method

7) B. Helferich and E. Schmitz-Hillebrecht, *Ber.*, **66**, 378 (1933).
8) P. Karrer and L. Kamienski, *Helv. Chim. Acta*, **15**, 739 (1932).
9) L. Asp and B. Lindberg, *Acta Chem. Scand.*, **6**, 941 (1952).
10) G. Zemplen and Z. Csuros, *Ber.*, **62**, 993 (1929).
11) G. C. S. Dutton and K. N. Slessor, *Canad. J. Chem.*, **44**, 1069 (1966).
12) A. G. Cottrell, E. Buncel and J. K. N. Jones, *ibid.*, **44**, 1483 (1966).
13) W. E. Dick, Jr., B. G. Baker and J. E. Hodge, *Carbohyd. Res.*, **6**, 52 (1968).
14) B. Helferich and S. R. Petersen, *Ber.*, **68**, 790 (1935).

of Asp and Lindberg[9] in principle. Crystallization in cold methanol-water (1 : 5) gave colorless needles which melted at 140—142°C. Found: C, 49.59; H, 5.81%. Calcd for $C_{26}H_{36}O_{18}$: C, 49.65; H, 5.66%.

6-*O*-*p*-Toluenesulfonyl-1,2,3,2′,3′,4′,6′-hepta-*O*-acetyl-β-maltose (III). II (4 g) was converted into III by the method of Asp and Lindberg.[9] Recrystallization from methanol gave pure substance (4 g) which melted at 138—141°C. Found: C, 49.06; H, 5.30; S, 3.98%. Calcd for $C_{33}H_{42}O_{20}S$: C, 50.10; H, 5.31; S, 4.03%.

6-Iodo-6-deoxy-1,2,3,2′,3′,4′,6′-hepta-*O*-acetyl-β-maltose (IV). This compound was prepared from III (4.0 g) according to the method of Asp and Lindberg.[9] Crystallization in methanol gave colorless crystals (3.2 g) which melted at 129—131°C. Found: C, 41.69; H, 4.27; I, 16.34%. Calcd for $C_{26}H_{35}O_{17}I$: C, 41.82; H, 4.70; I, 17.00%.

6-Deoxy-1,2,3,2′,3′,4′,6′-hepta-*O*-acetyl-β-maltose (V). IV (3.0 g) was dissolved in a mixture of dioxane (50 m*l*), ethanol (150 m*l*) and pyridine (2 m*l*). Reduction with hydrogen over 10% palladium-charcoal (3.0 g) at 70°C was repeated twice. The solution was extracted with chloroform, and the extract was washed with 5% aqueous sodium thiosulfate and water, and was dried over anhydrous sodium sulfate. After chloroform had been evaporated, the residue was crystallized in methanol (10 m*l*). Colorless crystals thus obtained (2.1 g) melted at 163—164.5°C. $[\alpha]_D^{19}$ +17° (*c*, 1.00, chloroform), Found: C, 50.24; H, 5.81%. Calcd for $C_{26}H_{36}O_{17}$: C, 50.32; H, 5.80%.

Phenyl 6-Deoxy-α-maltoside (VI). Zinc chloride (0.5 g) was dissolved in phenol (3 m*l*), and to this mixture was added V (2.5 g). The mixture was heated for 30 min at 115—120°C under vigorous stirring. Benzene (40 m*l*) was poured into the reaction mixture, which was washed with 1N sodium hydroxide and then with water. The benzene layer was dried over anhydrous sodium sulfate and was evaporated. The residual syrup was dissolved in a solution of 0.1M sodium methoxide in methanol (20 m*l*), and the solution was kept for 20 min at room temperature. The alkoxide was excluded by the addition of Dowex 50×8(H^+ form). The product was purified by passing through a column of Biogel P-2(polyacrylamide gel for chromatographic use, purchased from BIO. RAD Laboratories). The freeze-dried substance gave $[\alpha]_D^{24}$ +176° (*c* 1.00, water). Found: C, 54.05; H, 6.40%. Calcd for $C_{18}H_{26}O_{10}$: C, 53.73; H, 6.47%.

Phenyl 6-Iodo-6-deoxy-α-maltoside (VII). IV (2.0 g) was reacted with phenol (3.5 m*l*) in the presence of zinc chloride (0.35 g) in a manner similar to that described above, followed by deacetylation with sodium methoxide. The product was passed through Biogel P-2 column. The fraction of phenyl 6-iodo-6-deoxy-α-maltoside was lyophilized and crystallized in methanol. The yield of crystals which melted at 174°C (decomp.) was 150 mg. $[\alpha]_D^{24}$ +128° (*c* 0.50, water). Found: C, 40.45; H, 4.81; I, 24.17%. Calcd for $C_{18}H_{25}O_{10}I$; C, 40.92; H, 4.77; I, 24.02%.

6-Chloro-6-deoxy-1,2,3,2′,3′,4′,6′-hepta-*O*-acetyl-β-maltose (VIII). II (2.0 g) was dissolved in anhydrous pyridine (20 m*l*). The solution was cooled in ice-water, and then sulfuryl chloride (2.0 m*l*) was added dropwise under stirring, and the mixture was kept at room temperature for 12 hr. A brown solution thus obtained was extracted with chloroform (2×25 m*l*), and the extract was washed several times with water, dried over calcium chloride and concentrated *in vacuo*. The syrupy residue was dissolved in methanol and decolorized with Norit A. Colorless needles were obtained in a methanol solution, which were recrystallized in the same solvent. The yield of the specimen which melted at 138—139°C was 1.38 g. $[\alpha]_D^{19}$ +50° (*c* 1.00, pyridine). Found: C, 47.51; H, 5.36; Cl, 5.39%. Calcd for $C_{26}H_{35}O_{17}Cl$: C, 47.67; H, 5.38; Cl, 5.41%.

Phenyl 6-Chloro-6-deoxy-α-maltoside (IX). VIII (1.2 g) was reacted with phenol (3 m*l*) and zinc chloride (0.2 g) at 115°C for 30 min. After deacetylation with sodium methoxide, the product was purified by passing through a column of Biogel P-2, and was crystallized in methanol. The yield of the colorless crystals which melted at 184—186°C was 240 mg. $[\alpha]_D^{20}$ +142° (*c*, 0.50, water). Found: C, 49.19; H, 5.82; Cl, 7.86%. Calcd for $C_{18}H_{25}O_{10}Cl$: C, 49.49; H, 5.77; Cl, 8.12%.

6-*O*-Methyl-1,2,3,2′,3′,4′,6′-hepta-*O*-acetyl-β-maltose (X). II (2.5 g) was dissolved in anhydrous dichloromethane (20 m*l*) and methylated with diazomethane in the mixture of ether (100 m*l*) and boron trifluoride (5 m*l* of boron trifluoride etherate-dichloromethane, 1 : 25). The reaction was carried out in a dry ice-acetone bath. After 12 hr, the reaction mixture was filtered off from insoluble substance and extracted with chloroform. The extract was washed with water and dried over calcium chloride. Rapid crystallization occurred in methanol. Recrystallization in the same solvent gave in 80% yield 6-*O*-methyl-1,2,3,2′,3′,4′,6′-hepta-*O*-acetyl-β-maltose which melted at 135—136°C. $[\alpha]_D^{20}$ +60.7° (*c*, 1.36, chloroform). Found: C, 49.56; H, 5.87%. Calcd for $C_{27}H_{38}O_{18}$: C, 49.84; H, 5.88%.

Phenyl 6-*O*-Methyl-α-maltoside (XI). X (1.8 g) was reacted with phenol (4 m*l*) in the presence of zinc chloride (0.3 g) in a similar manner as described above, followed by deacetylation with sodium methoxide. The syrup thus obtained was purified by gel filtration using Biogel P-2. The yield of an amorphous product obtained was 390 mg. $[\alpha]_D^{20}$ +168° (*c*, 0.67, water). Found: C, 52.14; H, 6.56%. Calcd for $C_{19}H_{28}O_{11}$: C, 52.77; H, 6.53%.

Maltosan (XII).[11] Hexa-*O*-acetyl-maltosan (I) was deacetylated with sodium methoxide. Crystals were obtained in methanol which melted at 149—150°C. Found: C, 43.00; H, 6.23%. Calcd for $C_{12}H_{20}O_{10}$: C, 44.44; H, 6.17%.

6′-*O*-Trityl-penta-*O*-acetyl-maltosan (XIII).[11] Maltosan (XII, 11 g) was dissolved in anhydrous pyridine (125 m*l*). To the solution was added freshly recrystallized trityl chloride (15 g). After standing three days at room temperature, the starting material disappeared on a thin layer chromatogram. The mixture was then acetylated with acetic anhydride (20 m*l*) at room temperature for 12 hr. The solution was extracted with chloroform, washed with sodium bicarbonate and then with water, dried over calcium chloride and evaporated *in vacuo*. The acetylated trityl compound contaminated with triphenyl carbinol was used without purification in the next procedure.

2,3,2′,3′,4′-Penta-*O*-acetyl-maltosan (XIV). The product XIII (5 g) was detritylated in 80% aqueous acetic acid (200 m*l*) by the method of Dutton and Slessor.[11] Crystallization in methanol gave XIV (2.4 g) almost free from triphenyl carbinol, which melted at

82—83°C. Found: C, 49.51; H, 5.71%. Calcd for $C_{22}H_{30}O_{15}$: C, 49.44 H, 5.62%.

6′-*O*-*p*-Toluenesulfonyl-penta-*O*-acetyl-maltosan (XV).[11] XIV (5.5 g) was dissolved in anhydrous pyridine (80 ml) and *p*-toluenesulfonyl chloride (7 g) was added to the solution. After 24 hr, needles appeared on addition of water (30 ml). Recrystallization in methanol gave pure 6′-*O*-*p*-toluenesulfonyl-penta-*O*-acetyl-maltosan (6.0 g) which melted at 170—171°C. Found: C, 50.51; H, 5.23; S, 4.44%. Calcd for $C_{29}H_{36}O_7S$: C, 50.58; H, 5.23; S, 4.65%.

6′-Iodo-6′-deoxy-penta-*O*-acetyl-maltosan (XVI).[11] XV (6 g) was dissolved in acetone (120 ml) and sodium iodide (15 g) was added to the solution. The mixture was refluxed for 15 hr and then extracted with chloroform. The extract was evaporated after it had been washed with 5% sodium thiosulfate and then with water. A syrupy residue was crystallized in methanol.

Recrystallization in methanol gave 6′-iodo-6′-deoxy-penta-*O*-acetyl-maltosan (5.5 g) which melted at 193—195°C. Found: C, 40.97; H, 4.57; I, 19.77%. Calcd for $C_{22}H_{29}O_{14}I$: C, 40.99; H, 4.50; I, 19.72%.

6′-Deoxy-penta-*O*-acetyl-maltosan (XVII). XVI (5.5 g) was dissolved in a mixture of ethanol (200 ml), dioxane (100 ml) and pyridine (1 ml), and reduced with hydrogen over 10% palladium-charcoal (6 g) according to the method of Dutton and Slessor.[11] Crystallization in methanol gave XVII (3.2 g) which melted at 140—141°C. $[\alpha]_D^{19}$ +42° (*c*, 1.00, chloroform). Found: C, 50.88; H, 5.88%. Calcd for $C_{22}H_{30}O_{14}$: C, 50.96; H, 5.77%.

6′-Deoxy-hepta-*O*-acetyl-maltose (XVIII). XVII (1.5 g) was dissolved in an acetolysis-mixture (30 ml of sulfuric acid-acetic anhydride-acetic acid, 1 : 70 : 30), and treated according to the method of Dutton and Slessor.[11] Crystallization in ethanol - *n*-hexane (3 : 1) gave XVIII (1.5 g) which was a mixture of α- and β-anomer. Thus the melting point (85—87°C) was different from that (mp 183—185°C) given by Dutton and Slessor.[11] $[\alpha]_D^{19}$ +85° (*c*,1.00, chloroform). Found: C, 49.45; H, 5.83%. Calcd for $C_{26}H_{36}O_{17}$: C, 50.32; H, 5.80%.

Phenyl 6′-Deoxy-α-maltoside (XIX). XVIII (2.0 g) was dissolved in phenol (4 ml), and zinc chloride (0.35 g) was added to the solution. The mixture was treated as described above. After deacetylation with sodium methoxide, the product was passed through a column of Biogel P-2. The fraction of the product was freeze-dried, but it did not crystallize. $[\alpha]_D^{19}$ +170° (*c*, 0.96, water). Found: C, 53.42; H, 6.48%. Calcd for $C_{18}H_{26}O_{10}$: C, 53.73; H, 6.47%.

6′-*O*-*p*-Toluenesulfonyl-hepta-*O*-acetyl-maltose (XX). XV (1.5 g) was dissolved in the above acetolysis mixture. After standing for three hours at room temperature, 10% aqueous barium acetate was added to the mixture, which was extracted with chloroform (3×50 ml), after barium sulfate was removed by centrifugation. A white powder (1.5 g) was obtained by evaporation *in vacuo*. Though the product gave a single spot on a thin-layer chromatogram, it did not crystallize. $[\alpha]_D^{24}$ +100° (*c*, 2.00, dioxane). Found: C, 50.63; H, 5.50; S, 3.96%. Calcd for $C_{33}H_{42}O_{20}S$: C, 50.12; H, 5.35; S, 4.05%.

Phenyl 3′,6′-Anhydro-α-maltoside (XXII). A mixture of XX (2.0 g), phenol (3.5 ml) and zinc chloride (0.35 g) was heated under stirring on an oil bath at 118—120°C for 30 min. Benzene (50 ml) was added to the hot reaction mixture, which was washed with 1N sodium hydroxide, water, and evaporated *in vacuo*. The syrupy product was dissolved in methanol (30 ml), and Dowex 1×4 (OH^- form) was added to the solution under stirring at room temperature. After two hours, the resin was filtered and the filtrate was concentrated *in vacuo*. The product was purified by passing through a column of Biogel P-2. The fraction of the product was crystallized in methanol. The colorless crystals (0.2 g) melted at 194—195°C. $[\alpha]_D^{24}$ +136° (*c*, 0.90, water). Found: C, 53.85; H, 5.99%. Calcd for $C_{18}H_{24}O_{10}$: C, 54.00; H, 6.00%.

6′-Iodo-6′-deoxy-hepta-*O*-acetyl-maltose (XXIII). XX (2.5 g) was dissolved in acetone (30 ml), and sodium iodide (5.0 g) was added to the solution. The solution was refluxed for 10 hr and was extracted with chloroform. The extract was washed with 5% aqueous sodium thiosulfate and then with water. Evaporation of chloroform gave a syrupy product, which did not crystallize. $[\alpha]_D^{20}$ +102° (*c*, 2.00, dioxane). Found: I, 16.41%. Calcd for $C_{26}H_{35}O_{17}I$: I, 17.00%.

Phenyl 6′-Iodo-6′-deoxy-maltoside (XXIV). XXIII (2.0 g) was treated with phenol (4 ml) and zinc chloride (0.3 g) by the method described above. The product was deacetylated with 0.1M sodium methoxide for five minutes under cooling with ice-water bath. Column chromatography using Biogel P-2 gave a single product, which did not crystallize. $[\alpha]_D^{27}$ +130° (*c*, 1.00, water). Found: C, 40.45; H, 4.81; I, 24.17%. Calcd for $C_{18}H_{25}O_{10}I$: C, 40.92; H, 4.77; I, 24.02%.

6′-*O*-Methyl-penta-*O*-acetyl-maltosan (XXV). XIV (3.0 g) was dissolved in dichloromethane (25 ml). After the solution was cooled in a dry ice-acetone bath, diazomethane in ether (140 ml) and boron trifluoride (7 ml of boron trifluoride etherate-dichloromethane, 1 : 25) were added dropwise during two hours. Insoluble substance was filtered off, and the solution was extracted with chloroform. The extract was washed with water and dried over calcium chloride. The chloroform extract was evaporated to a syrup which crystallized in methanol. Recrystallization in the same solvent gave 6′-*O*-methyl-penta-*O*-acetyl-maltosan (2.5 g) which melted at 164°C. $[\alpha]_D^{20}$ +20° (*c*, 1.00, chloroform). Found: C, 50.06; H, 5.95%. Calcd for $C_{23}H_{32}O_{15}$: C, 50.36; H, 5.88%.

6′-*O*-Methyl-hepta-*O*-acetyl-maltose (XXVI). XXV (2.0 g) was dissolved in the acetolysis mixture (40 ml) and the mixture was kept at room temperature for three hours. Five per cent barium acetate solution was added to the reaction mixture, and the resulting barium sulfate was removed by centrifugation. The mixture was extracted with chloroform, and the extract was washed with sodium bicarbonate and repeatedly with water. Evaporation of chloroform gave a syrupy product, which gave a single spot on a thin-layer chromatogram, though it did not crystallize. Found: C, 49.97; H, 5.93%. Calcd for $C_{27}H_{38}O_{18}$: C, 49.98; H, 5.89%.

Phenyl 6′-*O*-methyl-α-maltoside (XXVII). XXVI (1.5 g) was reacted with phenol (3.5 ml) in the presence of zinc chloride (0.4 g) in a similar manner, and the deacetylated product was purified by gel filtration as described above. $[\alpha]_D^{18}$ +183° (*c*, 0.48, water). Found: C, 52.72; H, 6.57%. Calcd for $C_{19}H_{28}O_{11}$: C, 52.77; H, 6.53%.

6′-Chloro-6′-deoxy-penta-*O*-acetyl-maltosan (XXVIII). 2,3,2′,3′,4′-Penta-*O*-acetyl-maltosan (XIV, 3.0 g) was dissolved in freshly distilled pyridine and the solution was cooled in an ice-water bath, and sulfuryl chloride (1 ml) was added dropwise. The reaction was continued for 12 hr at room temperature. Water was poured into the mixture in order to destroy excess sulfuryl chloride, and the mixture was extracted with chloroform. The extract was washed with sodium bicarbonate and water. Evaporation of chloroform *in vacuo* gave a syrup, which crystallized rapidly in methanol. The crystals thus obtained (2.3 g) melted at 129°C. $[\alpha]_D^{18}$ +53.8° (*c*, 1.30, chloroform). Found: C, 47.28; H, 5.60; Cl, 6.07%. Calcd for $C_{22}H_{29}O_{14}Cl$: C, 47.79; H, 5.28; Cl, 6.41%.

6′-Chloro-6′-deoxy-hepta-*O*-acetyl-maltose (XXIX). XXVIII (2.0 g) was dissolved in the acetolysis mixture (40 ml) and the mixture was kept at room temperature for three hours. Aqueous barium acetate was added to the mixture in order to remove sulfuric acid. The chloroform extract was evaporated to a syrup (1.8 g) which did not crystallize.

Phenyl 6′-Chloro-6′-deoxy-hexa-*O*-acetyl-α-maltoside (XXX). XXIX (1.5 g) was converted into a phenyl glycoside in a similar manner, and a syrupy product was obtained which was crystallized in ethanol. Recrystallization from the same solvent gave colorless crystals (0.2 g) which melted at 133—134°C. $[\alpha]_D^{18}$ +186.9° (*c*, 0.57, chloroform). Found: C, 52.55; H, 5.36; Cl, 5.23%. Calcd for $C_{30}H_{37}O_{16}Cl$: C, 52.29; H, 5.41; Cl, 5.14%.

Phenyl 6′-Chloro-6′-deoxy-α-maltoside (XXXI). XXX (0.143 g) was dissolved in chloroform (3 ml) and 0.1M sodium methoxide in methanol (20 ml) was added to this solution. After 20 min, the solution was treated with Dowex 50(H^+ form), followed by filtration and evaporation. A syrup thus obtained was purified by gel filtration through Biogel P-2 column. Found: C, 48.89; H, 5.89; Cl, 7.68%. Calcd for $C_{18}H_{25}O_{10}Cl$: C, 49.49; H, 5.77; Cl, 8.12%.

1,2,6,2′,3′,4′,6′-Hepta-*O*-acetyl-β-maltose (XXXII). Maltose (10 g) was mixed with pyridine (30 ml) and dry benzene (200 ml), and acetylated with acetyl chloride (18 ml) following the method of Dick and coworkers.[13] The syrup (5 g) was chromatographed through a column of silica-gel using an elution solvent (ethyl acetate, benzene, 1 : 1).[15] The syrup obtained (1.4 g) showed a single spot on a thin-layer chromatogram, though it did not crystallize. $[\alpha]_D^{15}$ +77.3° (*c*, 0.97, chloroform). Found: C, 48.82; H, 5.66%. Calcd for $C_{26}H_{36}O_{18}$: C, 49.06; H, 5.70%.

1,2,6,2′,3′,4′,6′-Hepta-*O*-acetyl-3-*O*-methyl-β-maltose (XXXIII). XXXII (2.5 g) was dissolved in dichloromethane (25 ml) and was methylated with diazomethane and boron trifluoride in a dry ice-acetone bath. Methylation was not complete, and the same procedure was repeated three times. The product showed contamination of a small amount of the starting material on a thin-layer chromatogram, and we carried out the next procedure without further purification.

Phenyl 3-*O*-Methyl-α-maltoside (XXXIV). Crude XXXIII (2.0 g) was reacted with phenol and deacetylated in the similar manner as described above. The product was purified by passing through a column of Biogel-P-2. $[\alpha]_D^{17}$ +199° (*c*, 0.80, water). Found: C, 52.25; H, 6.41%. Calcd for $C_{19}H_{28}O_{11}$: C, 52.77; H, 6.53%.

15) M. L. Wolfrom and R. M. de Lederkremer, *J. Org. Chem.*, **30**, 1560 (1965).

Discussion

The purity of the phenyl glycosides obtained was examined by the determination of phenol content using the colorimetric method.[16] It was shown that all samples contained one mole of phenol per mole of sample. The results, together with those of the elemental analyses show a high degree of

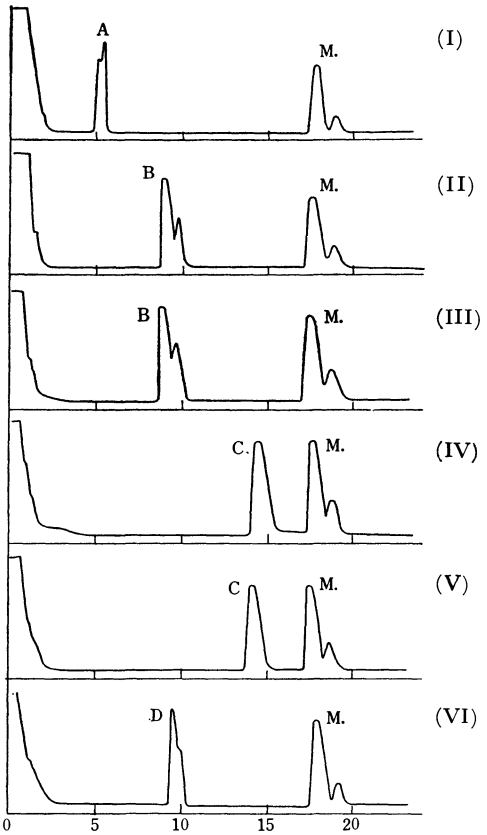

Fig. 1. Gas-liquid chromatograms of methanolyzed and trimethylsilylated compounds.
(I) Phenyl 3′,6′-anhydro-α-maltoside.
(II) Phenyl 6′-deoxy-α-maltoside.
(III) Phenyl 6-deoxy-α-maltoside.
(IV) Phenyl 6′-*O*-methyl-α-maltoside.
(V) Phenyl 6-*O*-methyl-α-maltoside.
(VI) Phenyl 3-*O*-methyl-α-maltoside.
The position of peak (A) is identical with that of authentic methyl 3,6-anhydro-glucoside,[18] (B) with methyl 6-deoxy-glucosides,[19] (C) with methyl 6-*O*-methyl glucoside[20] and (D) with methyl 3-*O*-methyl-glucosides.[21] Peak (M) is of methyl glucosides.[22] The analyses were carried out at 185°C under 1.6 atm pressure of carrier nitrogen.

16) T. Ikenaka, *J. Biochem.*, **54**, 328 (1963).

purity of the specimens.

The position of substitution on the glucose residues, which might be an unexpected one due to possible migration of acetyl groups during the course of synthesis, was confirmed by gas-liquid chromatography. Samples were methanolyzed and trimethylsilylated with hexamethyl disilazane and trimethylsilyl chloride.[17] The peaks in the gas-chromatograms were identified with the authentic derivatives of D-glucose.[18-22] The substitution occurred at the expected positions of glucose residues as shown in Fig. 1. As the iodine derivatives were the precursor of the deoxy compounds in the course of synthesis (Schemes 1 and 2), the position of iodine was also confirmed.

Gas-liquid chromatography was also used for determining which of the two glucose residues in the phenyl maltosides was substituted. As shown in Fig. 2, the precursor disaccharides of the phenyl glycosides were reduced with borohydride, after the *O*-acetyl groups had been removed, and the products were methanolyzed and analyzed by means of gas liquid chromatography. The reducing-end groups of the original disaccharides appeared in the chromatogram as corresponding sugar alcohols.

Compound XXXIII gave 3-*O*-methyl-glucitol and the compounds XXVI, XVIII and XXIX gave glucitol. These results confirm the structure of the phenyl glycosides XXXIV, XXVII, XIX and XXXI. As a counterpart of XIX, compound VI had an identical composition, and showed different behavior toward the enzymatic action (Table 1), the structure of VI was confirmed. Similarly XI was the counterpart of XXVII and IX was of XXXI, and structures of VI and IX were also confirmed. A slight ambiguity remained about the position of chlorine in the chloro-derivatives, because gas-chromatographic analysis of the chloro-deoxy-glucose had been unsuccessful.

Phenyl 3′,6′-anhydro-α-maltoside (XXII) was prepared from tosyloxy derivative (XV) which was a precursor of 6′-deoxy derivative (XVII). Thus the position of 3,6-anhydro ring was confirmed.

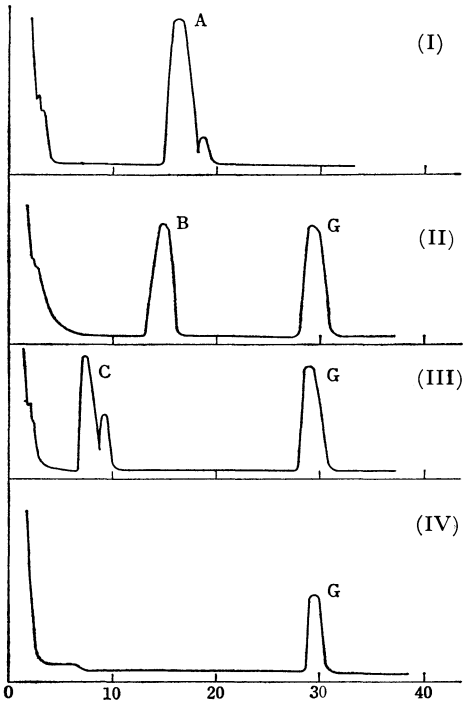

Fig. 2. Reducing-end analyses by gas-liquid chromatography.
(I) 3-*O*-Methyl-maltose derived from XXXIII.
(II) 6′-*O*-Methyl-maltose derived from XXVI.
(III) 6′-Deoxy-maltose derived from XVIII.
(IV) 6′-Chloro-6′-deoxy-maltose derived from XXIX.
The position of peak (A) is identical with that of authentic 3-*O*-methyl-glucitol, (B) with methyl 6-*O*-methyl-glucoside, (C) with methyl 6-deoxy-glucosides and (G) with glucitol. The analyses were performed after borohydride reduction and methanolyzation. All the procedures were carried out at 185°C under a 1.6 atm pressure of carrier nitrogen.

It is of interest that Taka-amylase A showed different hydrolysis rate on each substrate (Table 1). As regards the non reducing-end glucose of substrate, electronegativity at 6-position seems to be very necessary, but the steric factor is not so important for enzymatic action. On the other hand, data for the reducing-end group show that the steric factor has great significance as well as the role of electronegative residues at 6-position. These results are in line with a data presented by Isemura *et al.*[23]

17) C. C. Sweeley, R. Bentley, M. Makita and W. W. Wells, *J. Amer. Chem. Soc.*, **85**, 2497 (1963).
18) W. N. Haworth, L. N. Owen and F. Smith, *J. Chem. Soc.*, **1941**, 97.
19) P. Karrer and A. Boettcher, *Helv. Chim. Acta*, **36**, 570 (1953).
20) L. Hough, J. K. N. Jones and M. S. Magson, *J. Chem. Soc.*, **1952**, 1925.
21) S. Hakomori, *J. Biochem.*, **55**, 205 (1964).
22) B. Helferich, "E. Fischers Anleitung zur Darstellung Organischer Präparate," Braunschweig (1939), p. 93.
23) M. Isemura, T. Ikenaka and Y. Matsushima, *J. Biochem.*, **66**, 77 (1969).

BULLETIN OF THE CHEMICAL SOCIETY OF JAPAN VOL. 43 824—826 (1970)

Synthesis of Furonaphthoquinones

Hiroshi KAKISAWA and Mitsuru TATEISHI

Department of Chemistry, Tokyo Kyoiku University, Otsuka, Bunkyo-ku, Tokyo

(Received June 19, 1969)

The reaction of 2-acetoxy-1,4-naphthoquinone with *N*-(1-propenyl)morpholine in an ordinary atomsphere afforded 3-methylnaphtho[2,3-*b*]furan-4,9-quinone in a modest yield. When this reaction was carried out in an atmosphere of nitrogen, the reaction product was an aminodihydronaphthofuran XII, which was then converted into 3-methylnaphtho[1,2-*b*]-2,3-dihydrofuran-4,5-quinone by succesive treatments with ferric chloride, sodium borohydride, and sufuric acid.

Since the presence of orange-red pigments, the tanshinones, in the roots of *Salvia miltiorrhiza* Bunge was reported by Nakao in 1934,[1] more than ten tanshinones have been isolated from the roots, and their structures have been determined by various groups.[2] These pigments are classified into two groups according to their structural characters: the members of the first group have a furo-*o*-quinone chromophore, while those of the second group have a furo-*p*-quinone chromophore, as is shown by the examples of cryptotanshinone (I)[2a] and isotanshinone-II (II)[2b] respectively.

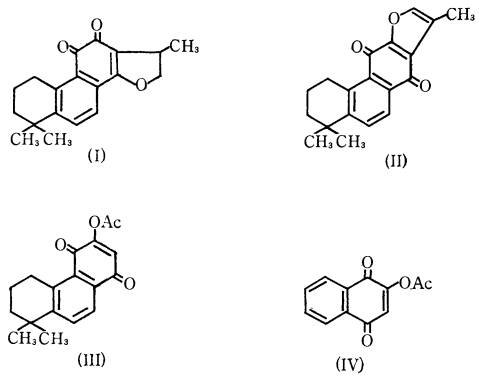

Fig. 1

These tanshinones seem to be synthesized from an intermediate (III) through constructing an appropriate furan group fused to the quinone ring. To develop a synthetic route from the intermediate (III) to the tanshinones, some attempts have been made with a model compound; the present report will deal with a new synthesis of 3-methylnaphtho[1,2-*b*]-furan-4,9-quinone (VIII) and 3-methylnaphtho[1,2-*b*]-2,3-dihydrofuran-4,5-quinone (XV) from 2-acetoxy-1,4-naphthoquinone.

For the synthesis of furonaphthoquinones from the acetoxynaphthoquinone (IV), it is preferable to introduce at the C-3 position of the quinone, an isopropyl group bearing an appropriate oxygen function. The reaction of the quinone with an enamine made from propionaldehyde was expected to give either formylethylnaphthol or an equivalent addition compound. Although a reaction of enamine with unsubstituted quinone (V) has been reported by Brannock *et al.*[3] to give a cyclic addition compound such as VI, no reaction of an acyloxyquinone with an enamine has yet been reported.

When 2-acetoxy-1,4-naphthoquinone (IV) was allowed to react with an equivalent amount of 4-(1-propenyl)morpholine (VII)[4] in methanol, there was obtained, by direct crystallization, a nitrogen-free product, $C_{13}H_8O_3$, in a 44% yield. The structure of this yellow product was identified as 3-methylnaphtho[2,3-*b*]furan-4,9-quinone (VIII) from its spectral properties. The IR spectrum of the product shows a quinonoid carbonyl absorption at 1675 cm^{-1} besides furano absorptions[5] at 3150, 1590, and 1525 cm^{-1}. The presence of the furan group in the reaction product was supported by its NMR spectrum, which exhibits the signal of a methyl group at 2.36 (3H, d. J=2 Hz) and that of an olefinic proton at 7.45 (1H, q. J= 2 Hz), attributable to the coincidence with the CH_3–C(I)=CH–O– group, in addition to aromatic protons at 7.65 and 8.05. The UV spectrum of

1) M. Nakao and T. Fukushima, *J. Pharm. Soc. Jap.*, **54**, 154 (1934).

2) a) K. Takiura, *ibid.*, **61**, 482 (1941). b) F. von Wessely and S. Wang, *Ber.*, **73**, 19 (1940). c) Y. Okumura, H. Kakisawa, M. Kato and Y. Hirata, This Bulletin, **34**, 895 (1961). d) H. Kakisawa, T. Hayashi and T. Yamazaki, *Tetrahedron Lett.*, **1969**, 301.

3) K. C. Brannock, R. D. Burpitt, H. E. Davis and H. S. Pridgen, *J. Org. Chem.*, **29**, 2579 (1964).

4) Propenylmorpholine (VII) was made according to the method explored by C. Mannich and H. Davidsen, *Ber.*, **69**, 2106 (1936).

5) M. Yamaguchi and A. Fujino, "Kagaku no Ryoiki," Supplement No. 3, Nankodo, Tokyo, (1954), p. 101.

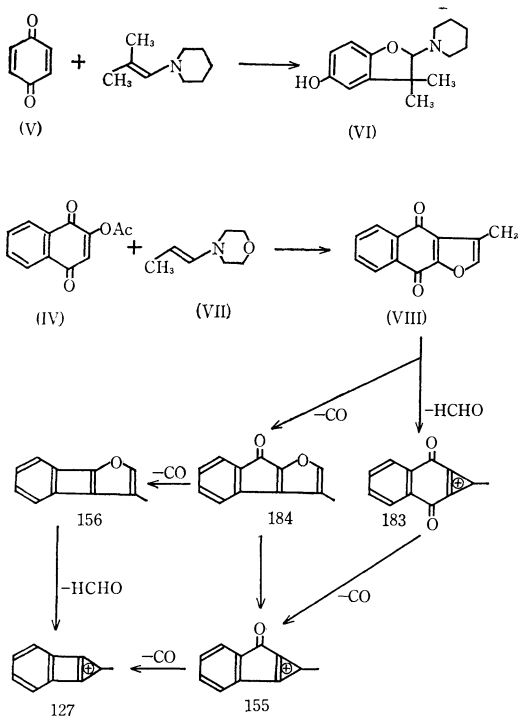

Fig. 2

the product, λ_{max} 246 (21500 sh), 251 (22000), 268 (6100), 305 (4100) and 360 nm (4300), is almost superimposable upon that of isotanshinone-II (II), which has a naphtho[2,3-*b*]furan-4,9-quinone chromophore. The mass spectrum shows main peaks at 212, 184, 183, 156, 155, and 127 mu; these fragmentation patterns are characteristic[6] of the 3-methylnaphtho[2,3-*b*]furan-4,9-quinone derivatives. This reaction, which has made possible the synthesis of the furo-*p*-quinone by a simple reaction from 2-acetoxy-1,4-naphthoquinone, will be useful for the synthesis of isotanshinones.[7]

The above addition reaction of the enamine (VII) to the acetoxynaphthoquinone (IV) was expected first to afford an aminodihydronaphthofuran, either XI or XII, by the nucleophilic addition of the enamine to the quinone and by subsequent cyclization, but the fact that the furonaphthoquinone (VIII) was formed without any oxidative reagent makes it obvious that air oxidation must have taken place during the condensation process. Therefore, the condensation of 4-(1-propenyl)morpholine (VII) to 2-acetoxy-1,4-naphthoquinone (IV) in an atmosphere of nitrogen has been attempted in order to obtain the intermediates, XI and/or XII. The reaction product was formed of white crystals having a molecular composition of $C_{19}H_{21}O_5N$; the UV spectrum (λ_{max} 246 and 305 nm) indicates the presence of a naphthol group, while the IR spectrum (ν_{max} 3350 and 1750 cm^{-1}) shows the presence of hydroxy and enol-acetate groups. Although two structures XI and XII were possible for the reaction product, the possibility of structure XI was disregarded in the following reactions. The oxidation of the adduct XII with ferric chloride gave a substance shown to be XIII. Three carbonyl absorptions, at 1780, 1720, and 1660 cm^{-1}, in the IR spectrum of XIII point to the presence of enol-acetate, unconjugated aldehyde, and quinonoid carbonyl groups respectively, and the NMR spectrum shows the presence of a formylethyl group at 1.35 (3H, d. J=8 Hz), 3.75 (1H, q. J=8 Hz), and 9.6 (1H, s), and of an acetyl group at 2.31 (3H, s). The UV spectrum of the oxidation product, showing absorption maxima at 248, 268, and 335 nm, is almost the same as that of 2-acetoxy-1,4-naphthoquinone.

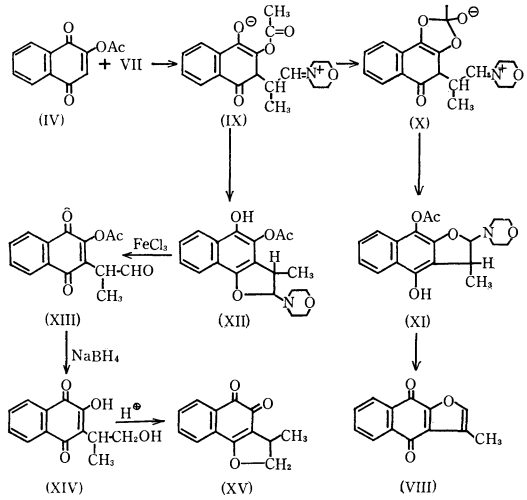

Fig. 3

The sodium borohydride reduction of XIII and the subsequent base hydrolysis of the acetyl group afforded a diol XIV (ν_{max} 3400, 1660 cm^{-1}). The diol XIV was prepared directly from the aminodihydrofuran (XI) by alkaline hydrolysis followed by reduction with sodium borohydride in an ordinary atmosphere. The treatment of the diol (XIV) with cold sulfuric acid in ethanol afforded, selectively, 3-methyldihydronaphtho[1,2-*b*]-2,3-dihydrofuran-4,5-quinone (XV), whose structure was confirmed by spectral data. The IR absorption bands at 1680, 1650, and 1625 cm^{-1} are compatible with the *o*-naphthoquinone. The NMR spectrum has signals at 1.36 (3H, d, J=8 Hz) and 3,40—5.06 (3H, m) assignable to the CH_3–CH–CH_2–O–

6) T. Hayashi, Y. Inouye, M. Ohashi, H. Kakisawa, A. Tatematsu and S. Kinoshita, *Org. Mass Spect.*, **2**, (1970), in press.

7) Recently this reaction has been applied to the synthesis of matsurinone, a natural product having the structure of 3,5-dimethylnaphtho[2,3-*b*]furan-4,9-quinone; H. Kakisawa and Y. Inouye, *Tetrahedron Lett.*, **1969**, 1929.

grouping besides those due to aromatic protons at 7.60 (2H, m) and 8.10 (2H, m). Finally, the structure (XV) is established by the UV spectrum (λ_{max} 262, 333, and 460 nm), whose shape is very similar to that of cryptotanshinone (I). This synthetic method from IV to XV can be applied to the total synthesis of cryptotanshinone.

Experimental

All the melting points are determined in a liquid bath and are uncorrected. The infrared spectra were measured on a Hitachi EPI-S2 spectrophotometer as KBr disks. The UV spectra were determined on a Hitachi EPS-3T spectrometer, and the NMR spectra were recorded on Hitachi R-20 spectrometer, with tetramethylsilane as the internal standard.

3-Methylnaphtho[2,3]furan-4,9-quinone (VIII). 4-(1-Propenyl)morpholine (0.32 g) was added to an ice-cooled mixture of 0.54 g of 2-acetoxyl-1,4-naphthoquinone and 2 m*l* of methanol. The reaction mixture was allowed to stand for 2 hr at room temperature, and then left in a refrigerator overnight in order to separate crystals. The crystals were collected and recrystallized from ethanol to give 0.235 g (44%) of light yellow needles; mp 206°C; λ_{max}^{EtOH} (ε) 246^{sh} (21500), 251 (22000), 268^{sh} (6100), 305 (4100), 360 nm (4300); ν_{max} 3150, 1675, 1590, 1525, 1020 cm^{-1}; NMR ($CDCl_3$) 2.36 (3H, d, J=2 Hz), 7.45 (1H, q, J=2 Hz), 7.65 (2H, m), 8.05 (2H, m); MS 212, 184, 183, 157, 156, 155, 128, 126, 105, 102, 77 mu.

Found: C, 73.69; H, 3.88%. Calcd for $C_{13}H_8O_3$: C, 73.58; H, 3.80%.

2,3-Dihydro-4-acetoxy-5-hydroxy-3-methyl-2-morpholinonaphtho[1,2-*b*]furan (XII). Into a suspension of 2-acetoxy-1,4-naphthoquinone (100 mg) in 0.5 m*l* of methanol was gradually stirred 60 mg of 4-(1-propenyl)morpholine in an atmosphere of nitrogen. The yellow quinone thus dissolved, and white crystals were separated. After standing in a refrigerator for 24 hr, the crystals were filtered and washed with ether several times to give 65 mg (40%) of aminodihydronaphthofuran (XII). Although the product was difficult to purify by recrystallization, the crystals were pure enough for further experiments; mp 150—151°C; λ_{max}^{EtOH} (ε) 246 (48500), 305 (6700) nm; ν_{max}^{KBr} 3350, 1750, 1640, 1590 cm^{-1}.

Found: C, 67.03; H, 6.37; N, 4.26%. Calcd for $C_{19}H_{21}O_5N$: C, 66.46; H, 6.16; N, 4.08%.

2-(3-Acetoxy-1,4-naphthoquinonyl)propionaldehyde (XIII). A solution of 250 mg of ferric chloride hexahydrate and 0.6 m*l* of hydrochloric acid was stirred, drop by drop, into a suspension of 120 mg of aminodihydronaphthofuran (XII) in an atmosphere of nitrogen. After the reaction mixture had then been stirred for 10 min at room temperature, the solution turned orange-red; the mixture was then extracted with ether. The ether extract was washed with water, dried over sodium sulfate, and evaporated *in vacuo* to afford oil; λ_{max}^{EtOH} 248, 268, 335 nm; $\nu_{max}^{CHCl_3}$ 1780, 1720, 1660 cm^{-1}; NMR ($CDCl_3$) 1.35 (3H, d, J=8 Hz), 2.31 (93H, s), 3.75 (1H, q, J=8 Hz), 7.7 (2H, m), 8.1 (2H, m), 9.61 (1H, s).

2-(3-Hydroxy-1,4-naphthoquinonyl)-1-propanol (XIV). To a solution of 95 mg of naphthoquinonylpropionaldehyde (XIII) in 5 m*l* of ethanol, was added 25 mg of sodium borohydride dissolved in 5 m*l* of methanol. After stirring at room temperature for 10 min, 2 m*l* of 2N sodium hydroxide solution was added and the mixture was stirred for a further 10 min. The deep red reaction mixture was neutralized with dilute hydrochloric acid and extracted with ether. The ether extract was washed with water, dried over anhydrous sodium sulfate, and evaporated to give naphthoquinonylpropanol (XIV): $\nu_{max}^{CHCl_3}$ 3400 1660, 1590 cm^{-1}.

This diol XIV was made directly from the adduct XII. To a suspension of the adduct XII (165 mg) in 12 m*l* of ethanol was added 8 m*l* of a 0.1N aqueous potassium hydroxide solution, whereupon the solution turned deep red. After the solution had then been stirred for 1 hr at room temperature, the solution was acidified with dilute hydrochloric acid and extracted with ether. The ether extract was washed with water, dried and evaporated *in vacuo*. The residue was dissolved in 10 m*l* of ethanol and treated with excess sodium borohydride dissolved in aqueous ethanol. After standing for 1 hr at room temperature, the solution was treated with dilute hydrochloric acid and extracted with ether. The treatment of the ether solution as usual afforded oil (50 mg) whose IR spectrum was the same as that of the diol (XIV).

3-Methylnaphtho[1,2-*d*]-2,3-dihydrofuran-4,5-quinone (XV). A solution of 75 mg of diol (XIV) in 1 m*l* of ethanol was treated with a mixture of sulfuric acid and ethanol (1 : 1) at 80°C. After 5 min, the mixture was poured into ice water to give a red solution. The aqueous solution was then extracted with ether. The ether extract was washed with water, dried over magnesium sulfate, and evaporated to give red crystals. Recrystallization from ethanol yielded furonaphthoquinone (XV) (50 mg); mp 150—151°C; λ_{max}^{EtOH} (ε) 253^{sh} (12600), 262 (16800), 271^{sh} (14500), 288^{sh} (4100), 333 (1400), 460 nm (1500); $\nu_{max}^{CHCl_3}$ 1680, 1650, 1625 cm^{-1}; NMR ($CDCl_3$) 1.36 (3H, d, J=8.0 Hz), 3.40—5.06 (3H, m), 7.60 (2H, m), 8.10 (2H, m).

BULLETIN OF THE CHEMICAL SOCIETY OF JAPAN VOL. 43 827—829 (1970)

Spiro Compound Formation. IV.[1] Acid-catalyzed Reactions of 2-Cyclohexylidenecyclohexanone Oxide

Masatomo NOJIMA, Keniti HINOUE and Niichiro TOKURA

Department of Applied Chemistry, Faculty of Engineering, Osaka University, Suita, Osaka

(Received July 16, 1969)

The reactions of 2-cyclohexylidenecyclohexanone oxide in the presence of (i) sulfuric acid, (ii) fluorosulfonic acid, (iii) boron trifluoride etherate, and (iv) antimony pentachloride have been studied. The products consisted of spiro[5.6]dodecane-7,12-dione, 2-(1-cyclohexenyl)-2-hydroxycyclohexanone, and 1,2,3,4,6,7,8,9-octahydrodibenzofuran. The ratio of the products was found to depend on the differences in the catalysts and solvents.

Although the reactions of α,β-epoxyketones under acidic conditions have been performed energetically from synthetic points of view,[2] only a few examinations aiming at a systematic clarification of the effects of catalysts upon the reaction mechanism have been performed.

Reusch, Anderson, and Johnson[3] recently reported that the gas-phase pyrolysis of pulegone oxide (I) at 200°C produced 2,2,5-trimethylcycloheptane-1,3-dione (II); they concluded that this reaction involved the rearrangement of I absorbed at Lewis acid sites on the Pyrex glass surface. Contrary to the above results, however, the reaction of I with *p*-toluenesulfonic acid led to the unsaturated hydroxyketone (III). These results suggest that the mechanism of the reaction of α,β-epoxyketones with Lewis acid is different from the mechanism of the reaction which is performed in the presence of Brønsted acid.

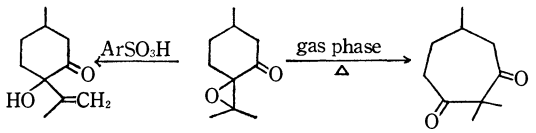

(III) (I) (II)

In order to investigate in more detail the dependence of the reaction pathways upon the difference in catalysts, we examined the reaction of 2-cyclohexylidenecyclohexanone oxide(IV)[4] in the presence of (i) sulfuric acid. (ii) fluorosulfonic acid, (iii) boron trifluoride etherate, and (iv) antimony pentachloride respectively. Liquid sulfur dioxide and cyclohexane were used as the solvents, and the solvent effects upon the reaction were also examined. The reactions were performed under the conditions described in Table 1.

TABLE 1. ACID-CATALYZED REACTIONS[a] OF IV AND VI

Substrate	Catalyst	Solvent	Total yield, %[b,h] V[d]	VI[e]	VII[f]
IV[c]	$SbCl_5$	SO_2	93.2	0	6.8
	BF_3-Et_2O	SO_2	82.8	0	17.2
	FSO_3H	SO_2	27.7	0	72.3
	H_2SO_4	SO_2	41.8	10.6	47.6
	$SbCl_5$	Cyclohexane	30.2	44.3	25.5
	BF_3-Et_2O	Cyclohexane	41.3	35.4	23.3
	FSO_3H	Cyclohexane	6.6	49.2	44.2
	H_2SO_4[g]	Cyclohexane	8.5	0	91.5
VI	H_2SO_4	SO_2	0	13.0	87.0

a) 0.1 g Substrate, 0.1 m*l* catalyst in 10 m*l* of SO_2 at 0°C or in 10 m*l* of cyclohexane at 15°C for 1 hr.
b) Calculated from the glpc peak areas.
c) 2-Cyclohexylidenecyclohexanone oxide.
d) Spiro[5.6]dodecane-7,12-dione.
e) 2-(1-Cyclohexenyl)-2-hydroxycyclohexanone.
f) 1,2,3,4,6,7,8,9-Octahydrodibenzofuran.
g) The reaction was performed for 21 hr.
h) The total yields were almost quantitative.

Gas-liquid partition chromatography showed that the products consisted of spiro[5.6]dodecane-7,12-dione (V), 2-(1-cyclohexenyl)-2-hydroxycyclohexanone (VI), and 1,2,3,4,6,7,8,9-octahydrodibenzofuran (VII). The products were isolated by column chromatography and were characterized by physical measurements and by their chemical transformations.

The compound V was a white crystalline solid of

1) Part III; M. Nojima and N. Tokura, This Bulletin, **42**, 1351 (1969).

2) R. E. Parker and N. S. Issacs, *Chem. Rev.*, **59**, 737 (1959).

3) W. Reusch, D. F. Anderson and C. K. Johnson, *J. Amer. Chem. Soc.*, **90**, 4988 (1968).

4) House and Wasson examined the pyrolytic rearrangement of IV to yield spiro[5.6]dodecane-7,12-dione (V). Although the reaction of IV with BF_3 etherate was also performed in benzene or diethyl ether, they failed to obtain the same compound V; H. O. House and R. L. Wasson, *J. Amer. Chem. Soc.*, **78**, 4394 (1956).

mp 69—70°C. Mass spectroscopy established a molecular formula $C_{12}H_{18}O_2$ (Calcd for $C_{12}H_{18}O_2$: 194, Found: 194). V exhibited a carbonyl absorption at 1682 cm^{-1}, forming a semicarbazone, mp 218—223°C. The treatment of V with aqueous sodium hydroxide gave 6-cyclohexyl-6-oxohexanoic acid (VIII).[4]

VI exhibited carbonyl and hydroxyl absorptions at 1700 and 3460 cm^{-1} respectively. The NMR spectrum displayed signals at 4.35 τ (one-proton multiplet) and 6.25 τ (one-proton singlet). Mass spectroscopy established the molecular formula of $C_{12}H_{18}O_2$ (Calcd for $C_{12}H_{18}O_2$: 194, Found: 194). When the diol obtained by the hydrogenation of VI using Raney Ni as the catalyst was oxidized by chromic acid, it gave VIII. The IR spectrum of VII (ν_{max}, 1600, 1140 cm^{-1}) indicated the presence of a furan ring, and the molecular ion in the mass spectrum was observed at *m/e* 176. Conclusive evidence for the structure assigned to VII was obtained by a comparison of the maleic anhydride adduct of VII with an authentic sample.[5]

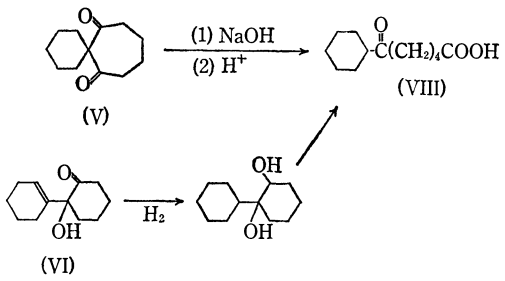

In Table 1 the results obtained from the reactions of IV under various conditions are summarized; it is obvious that the ratio of the products varied drastically with the change in the experimental conditions. From these data, Scheme I may be considered to be the most plausible reaction scheme.

When the Brønsted acid was used as the catalyst, much VI and VII were formed. In addition to this result, we established the selective formation of VII by the reaction of VI with sulfuric acid in liquid sulfur dioxide; this seems to show that VI is the intermediate for the formation of VII. As is shown in Table 1, the spiro compound V was also obtained.

These results seem to show that the reaction of IV with Brønsted acid is very similar to the pinacol rearrangement of 1,1-dihydroxydicyclohexyl[6]; IV is attacked by a proton to form the intermediate B after the ring opening. The B intermediate then probably disappears following one of two pathways; that is, either it rearranges to form V or loses a proton to form VI. The tertiary carbonium ion is

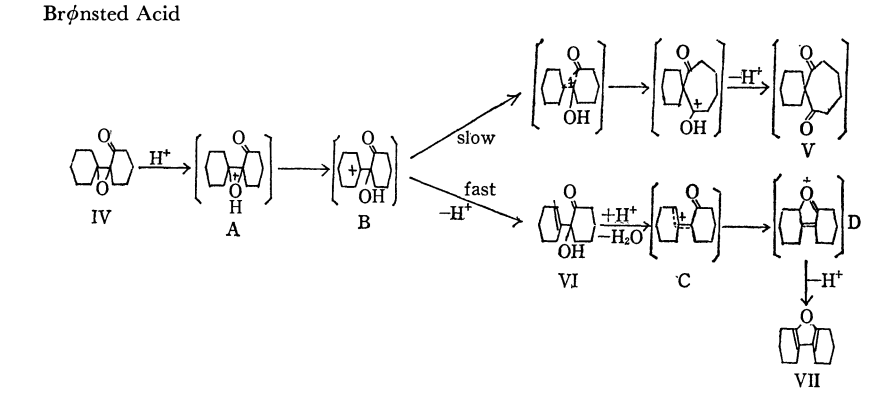

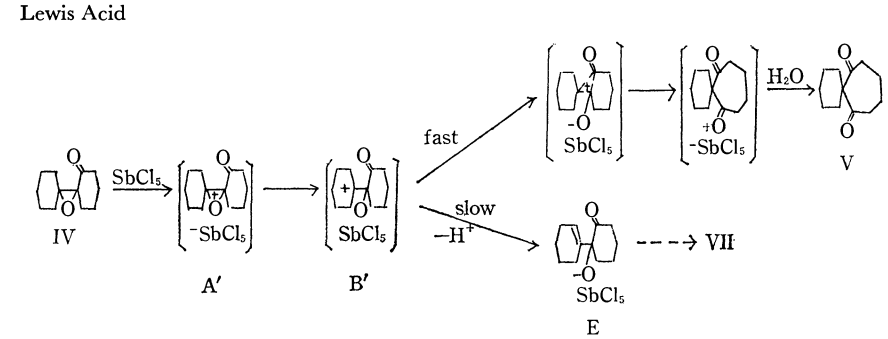

Scheme 1

5) T. A. Spencer, R. W. Britton and D. S. Watt, *J. Amer. Chem. Soc.*, **89**, 5727 (1967).

6) M. Qudrat-I-Kuda and A. K. Ray, *J. Indian Chem. Soc.*, **16**, 525 (1939).

well known to deprotonate very rapidly,[7] and so it may be considered that the rate of deprotonation from B to form VI is very rapid. It is reasonable to consider that the allylic alcohol VI is not stable in the presence of an acid catalyst and that VI is attacked by a proton to form the intermediate C after the dehydration. The cation cite of C may be attacked by the lone-pair electrons of oxygen to form VII with a furan ring after the deprotonation.

For the formation of the spiro compound V, Lewis acid was more effective than Brønsted acid; V was obtained in a 93.2% yield when the reaction was performed with antimony pentachloride in liquid sulfur dioxide. This is probably due to the instability of the intermediates B and E because of the steric hindrance of a large volume of Lewis acid. In order to diminish this steric hindrance, the ring-enlargement reaction to form V seems to be more profitable than the deprotonation to form VI.

We can not propose a good explanation of the solvent effects upon the reaction of IV, but it seems probable that the rearrangement of the intermediate B to form V is accelerated by the stabilization of the transition state due to the solvation of the liquid sulfur dioxide. When cyclohexane is used as the solvent, there is no factor to stabilize the transition state and the deprotonation to form VI seems to be an important part of this reaction.

Experimental

2-Cyclohexylidenecyclohexanone Oxide (IV) was prepared by the method of Reese.[8] From 21.0 g of 2-cyclohexylidenecyclohexanone and 21 m*l* of a 30% hydrogen peroxide solution, we obtained 10.0 g (47.6% yield based on 2-cyclohexylidenecyclohexanone) of 2-cyclohexylidenecyclohexanone oxide; mp 96.5—97°C (lit,[5] mp 96.5—97°C).

1,2,3,4,6,7,8,9-Octahydrodibenzofuran (VII) was prepared by the action of zinc dust with 2-bromocyclohexanone[5]; bp 88—89°C/2 mmHg. The adduct of VII with maleic anhydride was prepared by the following method; maleic anhydride (1 g) and 2 g of VII were dissolved in 5 m*l* of benzene, after which the mixture was allowed to react at room temperature for 24 hr. The solid obtained was recrystallized from cyclohexane; mp 166—167°C (lit,[9] 167—168°C).

The Reaction of 2-Cyclohexylidenecyclohexanone Oxide (IV) in Liquid Sulfur Dioxide. To 200 mg of IV and 10 m*l* of liquid sulfur dioxide, was added 0.1 m*l* of the acid catalyst at −68°C, after which the mixture was allowed to react at 0°C for 1 hr. The reaction mixture was then rapidly cooled, diluted with water, and extracted three times with ether. The combined organic layers were washed with saturated brine and dried over anhydrous sodium sulfate. The volume of the extraction solvent was kept small so that no concentration step was neccesary in vpc analysis.

The products were analyzed by a Hitachi K-53 vpc apparatus, with a flame ionization detector, on a SE 30 column operated at 130—170°C.

The Reaction of 2-Cyclohexylidenecyclohexanone Oxide (IV) in Cyclohexane. To 200 mg of IV and 10 m*l* of cyclohexane was added 0.1 m*l* of the acid catalyst, after which the mixture was allowed to react at 15°C for 1 hr. When sulfuric acid was used as the catalyst, the reaction was performed for 21 hr. The reaction mixture was treated and analyzed as has been described in the preceding experiment.

Reaction Products from 2-Cyclohexylidenecyclohexanone Oxide (IV). 2-Cyclohexylidenecyclohexanone oxide (1.0 g), 0.5 m*l* of sulfuric acid, and 20 m*l* of sulfur dioxide were maintained at 0°C for 1 hr and then extracted with ether and dried over anhydrous sodium sulfate. The residue after the removal of the solvent was chromatographed on 50 g of silica gel. Elution with ten 50-m*l* portions of petroleum ether gave 0.4 g of an oil, which was then fractionated. Vpc on a SE 30 column indicated that this product was 99% pure. The infrared and mass spectra were identical with those of authentic 1,2,3,4,6,7,8,9-octahydrodibenzofuran (VII), and a mixed melting-point determination of the maleic anhydride adduct of the isolated product with the authentic maleic anhydride adduct of VII was undepressed.

Elution with thirteen 50-m*l* portions of benzene gave 0.1 g of a solid, which was then recrystallized from petroleum ether; mp 69—70°C. The physical data were identical with those of spiro[5,6]dodecane-7,12-dione.[4] In order to clarify the structure of this solid (V), the following reaction was performed; a solution of 0.5 g of V and 2.5 m*l* of 6N aqueous sodium hydroxide in 15 m*l* of ethanol was boiled under reflux for 30 min, diluted with water, acidified with hydrochloric acid, and extracted with ether. The extract was dried over anhydrous sodium sulfate and concentrated to leave a white solid. This keto acid was crystallized from petroleum ether as colorless plates; mp 56—58°C, mixed mp 56—58°C.

2-(1-Cyclohexenyl)-2-hydroxycyclohexanone (VI) was also isolated from the reaction mixture by chromatography. Elution with ten 50-m*l* portions of methanol gave 0.4 g of an oil which was then fractionated and thus confirmed to be 99% pure by vpc; bp 104°C/4 mmHg.

VI was hydrogenated using Raney nickel and hydrogen at 40—50°C; a white crystalline solid (IX) was obtained in a quantitative yield; *m/e* 198; ν_{max} 3300 and 3400 cm^{-1}. By the oxidation of IX with chromic acid at 50°C, 6-cyclohexyl-6-oxohexanoic acid (VIII) was obtained; mp 56—58°C (lit,[4] 56.5—58°C).

7) M. Nojima, T. Nagai and N. Tokura, *J. Org. Chem.*, **33**, 1972 (1968).

8) J. Reese, *Ber.*, **75**, 384 (1942).

9) W. Treibs and M. Weissenfels, *Chem. Ber.*, **93**, 1374 (1960).

BULLETIN OF THE CHEMICAL SOCIETY OF JAPAN VOL. 43 830—835 (1970)

The Metal-Catalyzed Autoxidation of Cumene

Yoshio KAMIYA

Department of Fuel Engineering, Faculty of Engineering, The University of Tokyo, Hongo, Bunkyo-ku, Tokyo

(Received July 18, 1969)

The catalysis of metal carboxylates and metal phthalocyanines in the autoxidation of cumene was kinetically studied. The limiting rate of oxidation of cumene was just over half the theoretical rate of $k_p^2(RH)^2/2k_t$ suggesting that the induced decomposition of cumyl hydroperoxide due to cumyloxy radical proceeds rapidly. The effect of metal catalyst in the autoxidation of cumene was concluded to be caused by the decomposition of hydroperoxide and not by the activation of oxygen, since the rate of oxidation increased with the increase in the rate of metal-catalyzed decomposition of hydroperoxide. The synergistic effect on the metal-catalyzed autoxidation of cumene was proved to result from the synergistic effect of metal salts on the decomposition of hydroperoxide. The oxidation products of cumene varied remarkably according to reaction conditions.

The rate of oxidation of hydrocarbons catalyzed by metal salts reaches a constant value as the metal concentration is increased, and the value is in good agreement with the theoretical value of $k_p^2(RH)^2/2k_t$ in the cases of tetralin[1,2] and ethylbenzene.[3] These results strongly suggest that the metal catalysis is caused by the production of radicals from the hydroperoxide decomposition.

$$ROOH + Metal \longrightarrow \text{radicals } (RO\cdot \text{ and } RO_2\cdot) \quad (1)$$

$$R\cdot + O_2 \longrightarrow RO_2\cdot \quad (2)$$

$$RO_2\cdot + RH \xrightarrow{k_p} ROOH + R\cdot \quad (3)$$

$$RO_2\cdot + RO_2\cdot \xrightarrow{k_t} \text{inactive products} + O_2 \quad (4)$$

The autoxidation of cumene has been studied by a number of workers,[4-9] but its metal catalysis has not yet been completely clarified. Blanchard[4] concluded that the role of metal salt in the autoxidation is not to initiate chain by the activiation of oxygen but to produce radicals by the decomposition of hydroperoxide. Kropf[5] suggested that the chain initiation due to copper phthalocyanine-oxygen complex occurs by the hydrogen abstraction from cumene because there is an almost quantitative production of hydroperoxide at temperatures below 105°C when copper phthalocyanine was used as the catalyst. However, Minkov[7] has shown that cumyl hydroperoxide can be decomposed by copper phthalocyanine.

Recently, we found that copper phthalocyanine remarkably initiates the chain of autoxidation of α-methylstyrene[10] by the addition mechanism. The following mechanism can be postulated.

$$CuPc + O_2 \longrightarrow (CuPc)^{\delta+}O_2^{\delta-} \quad (5)$$

$$(CuPc)^{\delta+}O_2^{\delta-} + \rangle C{=}C\langle \longrightarrow (CuPc)^{\delta+}O_2^{\delta-}-\overset{|}{\underset{|}{C}}-\overset{|}{\underset{|}{C}}\cdot \xrightarrow{\text{olefin, } O_2} (-\overset{|}{\underset{|}{C}}-\overset{|}{\underset{|}{C}}-O_2-)_n \quad (6)$$

It was intended to make clear by precise experiments the two kinds of catalytic effect in the autoxidation of cumene owing to metal catalyst, that is, the production of radicals by the decomposition of hydroperoxide and the activation of oxygen molecule.

Experimental

The oxidation technique has been described previously.[1] All experiments were carried out at 60°C except otherwise stated. The catalysts used are cobaltous and manganous acetates and the cobaltous, manganous and cupric decanoates along with cobalt phthalocyanine-(CoPc) and α- and β-copper phthalocyanine(CuPc). Oxygenated copper phthalocyanine was prepared by the oxidation of copper phthalocyanine with 45% nitric acid at −5 to 0°C as reported by Bansho and coworkers.[11] The analysis of oxygenated copper phthalocyanine gave the formula CuPc-O_2-CuPc, which was converted to copper phthalocyanine after reduction.

1) Y. Kamiya, S. Beaton, A. Lafortune and K. U. Ingold, *Can. J. Chem.*, **41**, 2020, 2034 (1963).
2) Y. Kamiya and K. U. Ingold, *ibid.*, **42**, 1027 (1964).
3) Y. Kamiya, *Kogyo Kagaku Zasshi*, **69**, 897 (1966).
4) H. S. Blanchard, *J. Amer. Chem. Soc.*, **82**, 2014 (1960).
5) H. Kropf, *Ann. Chem.*, **637**, 73 (1960).
6) D. G. Hendry, *J. Amer. Chem. Soc.*, **89**, 4433 (1968).
7) A. I. Minkov and N. P. Keier, *Kinetika i Kataliz*, **8**, 160 (1967).
8) T. G. Traylor and C. A. Russell, *J. Amer. Chem. Soc.*, **87**, 3698 (1965).
9) J. A. Howard, K. U. Ingold and M. Symonds, *Can. J. Chem.*, **46**, 1017 (1968).
10) Y. Kamiya, *Tetrahedron Lett.*, **1968**, 4965.
11) T. Sekiguchi, E. Yamazaki and Y. Bansho, *Kogyo Kagaku Zasshi*, **70**, 503 (1967).

The oxidation products of cumene were determined by gas-liquid chromatography.

Results and Discussion

The Limiting Rate of Metal-Catalyzed Autoxidation of Cumene

The effect of three metal decanoates on the rate of oxidation of cumene at 60°C was examined over a range of metal concentrations from 0.001 to 0.1M in Fig. 1.

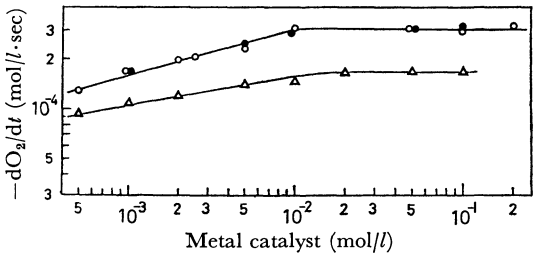

Fig. 1. The steady rate of oxidation of cumene as a function of metal decanoate concentration.
○ cobalt, ● manganese, △ copper.

As in the usual case, the cumene contained about 0.001M of hydroperoxide. In general, oxygen absorption proceeded linearly until several percent of cumene was consumed. The induction period of autoxidation was less than ten minutes and the metal catalysts were slowly deactivated during the oxidation as observed in the case of tetralin.

It can be seen that in the cobalt or manganese concentrations between 0.01 to 0.1M the measured maximum rate (ρ_m) reaches a limit of 3.1×10^{-4}M/sec, which is just over half the theoretical limit 6.0×10^{-4}M/sec. The theoretical value was calculated by the following equation, using the results of azobisisobutyronitrile initiated oxidation of cumene.

$$-dO_2/dt = k_p^2(RH)^2/2k_t \qquad (7)$$

ρ_m reaches a lower limit of 1.7×10^{-4}M/sec in the case of copper salt. This lower value might be due to the solubility as in the case of tetralin.[2]

The rate of oxidation of cumene in acetic acid reaches a limit of 7.8×10^{-5}M/sec in an acetic acid — cumene mixture (1 : 1 by volume) as shown in Fig. 2 at cobalt concentrations above 0.05M. The limiting value after correcting $(RH)^2$ term of equation (7) will be 3.12×10^{-4}M/sec as in the case of neat cumene.

Recently, it was suggested that the rate of oxidation depends on the dielectric function of solvent.[12-14] Therefore, the true rate of oxidation

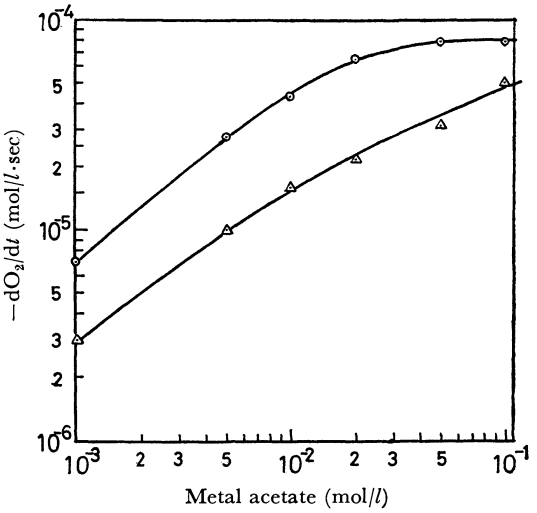

Fig. 2. The steady rate of oxidation of a 1 : 1 by volume cumene acetic acid mixture as a function of the metal acetate concentration.
○ cobalt, △ manganese.

in acetic acid after correcting the dielectric function will be a little lower than 3.12×10^{-4}M/sec and probably around 2.5×10^{-4}M/sec according to the results of tetralin.[14] The disaccordance between the experimental and the theoretical values might be due to the very fast induced decomposition of cumyl hydroperoxide by cumyloxy radical, because the ratio of cumyl alcohol to acetophenone in the oxidation products is higher than 1.7 (see Table 2). Recently, Hiatt and his co-workers,[16] Howard and Ingold[15] have shown that the chain length of the decomposition of tertiary hydroperoxide is as long as ten. If the induced decomposition of hydroperoxide by cumyloxy radical resulting from the metal catalyzed decomposition of hydroperoxide proceeds preferentially to hydrogen abstraction from cumene, the theoretical limiting rate will be $k_p^2(RH)^2/4k_t$, which is just half of the theoretical value and is in good agreement with the experimental values. The possibility of oxidation inhibition due to phenol can be ruled out, since we could not isolate any appreciable amount of acetone or phenol in the oxidation products.

The disaccordance between the theoretical and experimental rates of oxidation of neat tetralin[1] was explained well by the effect of $(RH)^2$ term because the rate of oxidation of tetralin in acetic acid is in excellent agreement with the theoretical limiting rate.

The decomposition of cumyl hydroperoxide by cobalt salt at 2×10^{-4}M was of first order with respect to hydroperoxide, and the half life of 18 min

12) D. G. Hendry and G. A. Russell, *J. Amer. Chem. Soc.*, **86**, 2368 (1964).
13) J. A. Howard and K. U. Ingold, *Can. J. Chem.*, **42**, 1044, 1250 (1964).
14) Y. Kamiya, This Bulletin, **38**, 2516 (1965).
15) J. A. Howard and K. U. Ingold, *Can. J. Chem.*, **46**, 2655 (1968).
16) R. Hiatt, T. Mill, K. C. Irwin and J. K. Castleman, *J. Org. Chem.*, **33**, 1421 (1968).

increased by a factor of one hundred, when acetic acid was used as the solvent instead of chlorobenzene.

These results correspond to the fact that the rate of oxidation in acetic acid reaches a limiting value at higher cobalt concentration than in the case of neat cumene.

In acetic acid, the manganese salt was a weak catalyst compared with cobalt as observed in the case of tetralin[2] and ethylbenzene.[3]

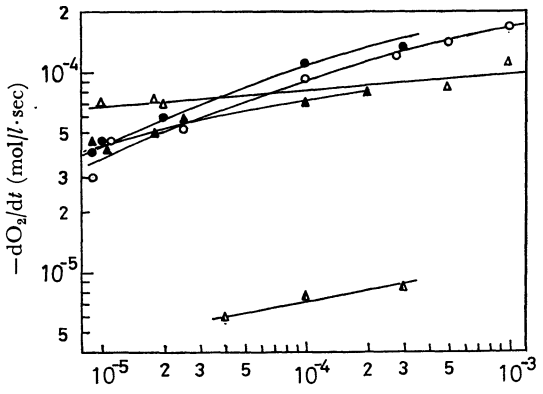

Fig. 3. The steady rate of oxidation of cumene as a function of metal decanoate or metal phthalocyanine concentrations at concentrations from 10^{-5} to 10^{-3} mol/l.
○ cobalt decanoate, △ copper decanoate, ● cobaltphthalocyanine, ◭ α-copper phthalocyanine, ▲ β-copper phthalocyanine

Metal-Catalysis by Phthalocyanines and Decanoates in the Autoxidation of Cumene. The rate of oxidation of cumene at metal concentration below 0.001M is shown in Fig. 3. At metal concentration of 1×10^{-5}M, 0.05M of cumyl hydroperoxide was added before the oxidation in order to reduce the induction period and to obtain a reproducible value of the rate of oxidation, since a metal catalyst was deactivated before reaching the maximum rate.

The chain length in the metal-catalyzed autoxidation of cumene was calculated to be 13 in the case of cobalt decanoate and 8 in the case of copper decanoate at the catalyst concentration of 1×10^{-5}M, using the results in Fig. 3 and the following equation obtained by the azobisisobutyronitrile initiated oxidation of cumene.

$$-dO_2/dt = 9\times10^{-4}(\mathrm{AIBN})^{1/2} \qquad (8)$$

It seems peculiar that the rate of oxidation with copper becomes higher than with cobalt at low metal concentrations. The rate of decomposition of cumyl hydroperoxide with cobalt decanoate was higher than with copper decanoate by a factor of four at metal concentrations from 10^{-3} to 10^{-4}M, suggesting that cobalt gives a two fold higher rate of oxidation than copper.

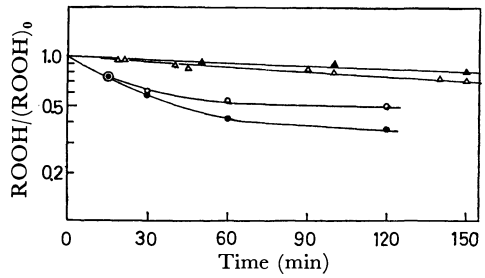

Fig. 4. The decomposition of cumyl hydroperoxide by metal decanoate or metal phthalocyanine at metal concentration of 6.3×10^{-5} mol/l in chlorobenzene.
$[ROOH]_0$ 0.025 mol/l; ○ cobalt de canoate, △ copper decanoate, ● cobalt phthalocyanine, ▲ β-copper phthalocyanine.

However, the plots of hydroperoxide decomposition at catalyst concentration of 6.3×10^{-5}M (Fig. 4) indicate that cobalt catalysts are deactivated quickly at the beginning of hydroperoxide decomposition and copper compounds retain their activity for a longer time.

Cobalt phthalocyanine was deactivated more slowly than cobalt decanoate probably due to its stable structure, and it showed a little higher rate of oxidation than cobalt decanoate.

At the steady state of oxidation (after 30 to 60 min) the reactivity of copper decanoate will be equal to that of cobalt phthalocyanine according to Fig. 4.

The first order rate constant (k) of hydroperoxide decomposition increased by a factor of three in the case of copper decanoate when hydroperoxide concentration was increased from 0.025 to 0.125M, while k remained constant in the case of cobalt decanoate.

Thus, it is not surprising to find that copper compounds give a higher rate of oxidation than the value expected from the rate of hydroperoxide decomposition in Fig. 4, since the concentration of hydroperoxide at the steady state of oxidation will reach a value higher than 0.1M. The higher rate of oxidation by copper decanoate than by cobalt compounds at concentration of 1×10^{-5}M can be attributed to the higher rate of decomposition of hydroperoxide by copper decanoate.

The k value with β-CuPc was higher than with α-CuPc by a factor of sixty at metal concentration 6.3×10^{-5}M. It should be mentioned that α-CuPc, which is a very effective initiator in the autoxidation of α-methylstyrene[10] by the addition mechanism, is exceptionally inactive for the decomposition of hydroperoxide.

For comparison, the autoxidation of tetralin in the presence of various catalysts is shown in Fig. 5. In this case β-CuPc is much more active than α-CuPc. From the hydroperoxide decomposition experiment by copper catalysts at initial hydroperoxide concentration 0.02M and metal concentra-

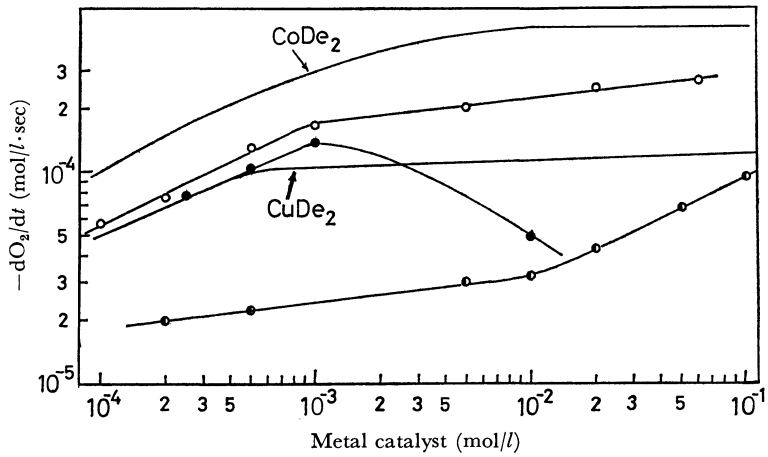

Fig. 5. The steady rate of oxidation of tetralin as a function of metal concentration at 50°C.
○ cobalt phthalocyanine, ◐ α-copper phthalocyanine, ● β-copper phthalocyanine

tion 0.001M in chlorobenzene at 50°C, the half life of tetralyl hydroperoxide decomposition was found to be 80 min in the cases of $CuDe_2$ and β-CuPc and 1500 min in the case of α-CuPc. Thus, the rate of oxidation of tetralin is roughly proportional to the square root of the rate of hydroperoxide decomposition. Although the rate of oxidation with β-CuPc is a little higher than with $CuDe_2$ at concentration of 0.001M, the two rates of oxidation at catalyst concentrations below 5×10^{-4}M coincide well as in the case of half lives of hydroperoxide decomposition.

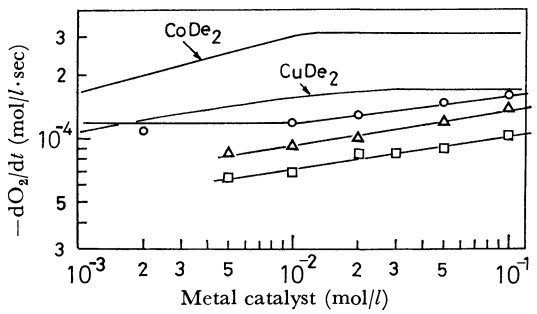

Fig. 6. The steady rate of oxidation of cumene as a function of metal phthalocyanine concentration at concentrations below 0.1 mol/l.
○ cobaltphthalo cyanine, △ α-copper phthalocyanine, □ oxygenat ed copper phthalocyanine

The activation of oxygen by CuPc and the direct oxidation by the oxygenated copper phthalocyanine(CuPcO) were further examined at high concentration of catalyst (Fig. 6). The rate of oxidation of cumene at metal concentrations from 10^{-4} to 10^{-2}M was entirely constant in the cases of CoPc, β-CuPc and CuPcO, but it gradually increased with the increase of metal concentrations above 0.01M. The direct oxidation of cumene by the complex of metal phthalocyanine or by the oxygenated metal phthalocyanine might occur at high concentration of metal complex.

In conclusion, the results of hydroperoxide decomposition account for the relative rate of oxidation with various catalysts. The autoxidation of cumene catalyzed by CuPc should not involve the chain initiation step due to hydrogen abstraction from cumene by $(CuPc)^{\delta+}O_2^{\delta-}$, since the effect of hydroperoxide decomposition is overwhelming. The reactivity of $(CuPc)^{\delta+}O_2^{\delta-}$ is undoubtedly not so large as peroxy radical, although we found that copper phthalocyanine initiates the chain of autoxidation of α-methylstyrene.

According to Kropf,[5] the observed rate of oxidation of cumene by his copper phthalocyanine is about one-hundredth of our value by β-CuPc. The chain initiation due to copper phthalocyanine and oxygen will be about one–ten thousandth of the rate of radical production by the decomposition of hydroperoxide, even if his copper phthalocyanine could not decompose any amount of hydroperoxide. Therefore, production of radicals by the metal-catalyzed decomposition of hydroperoxide occurs predominantly as compared with hydrogen abstraction by copper phthalocyanine and oxygen.

A complex situation arizes from the fact that α-CuPc which is quite inactive for hydroperoxide decomposition can be gradually converted to β-CuPc in an aromatic solvent even at temperatures below 100°C. It was observed that α-CuPc, which was used in the autoxidation of α-methylstyrene at 60°C for 120 min, decomposed cumyl hydroperoxide with the rate as fast as that of $CuDe_2$, that is, the rate of decomposition of hydroperoxide by α-CuPc increases considerably in the course of reaction probably after isomerizing to β-CuPc or another active form of CuPc especially in the presence of peroxy radicals. Minkov[7] has also

TABLE 1. OXIDATION PRODUCTS OF CUMENE

Reaction conditions	Oxidation of neat cumene	Oxidation of cumene acetic acid mixture (1 : 1 by volume)	Decomposition of cumyl hydroperoxide of 0.08M in chlorobenzene
Metal catalyst	Cobalt and manganese decanoates from 0.001 to 0.1M	Cobalt and manganese acetate from 0.01 to 0.1M	Cobalt decanoate from 0.002 to 0.01M
Products distribution of cumene (mol %)			
α-Methylstyrene	3.3	1.7	2.0
Acetophenone	15.8	36.4	36.0
Cumyl alcohol	70.7	61.3	59.3
Dicumyl peroxide	10.2	2.5	2.7
The ratio of cumyl alcohol to acetophenone	4.5	1.7	1.64

pointed out that the activity of CuPc in the decomposition of hydroperoxide shows a maximum as the reaction proceeds.

Oxidation Products of Cumene. The oxidation products were cumyl alcohol, acetophenone, dicumyl peroxide, cumyl hydroperoxide and α-methylstyrene. No acetone or methyl alcohol were detected. Oxidation products other than hydroperoxide are shown in Table 1.

The ratio of alcohol to ketone is about 1.6, when cumyl hydroperoxide is decomposed in chlorobenzene by cobalt decanoate. However, autoxidation in acetic acid gives a value of about 1.7 and the ratio increases to 4.5 in the case of neat cumene. Since α-methylstyrene can be obtained from cumyl alcohol, the true ratio will be higher than the observed value.

The chain termination mechanism of cumyl peroxy radicals can be described as follows,[9]

$$RO_2\cdot + RO_2\cdot \longrightarrow [ROOOOR] \longrightarrow ROOR + O_2$$
$$\searrow\ 2RO\cdot + O_2$$
$$RO\cdot \xrightarrow{O_2} CH_3O_2\cdot + C_6H_5COCH_3$$
$$CH_3O_2\cdot + RO_2\cdot \longrightarrow C_6H_5C(CH_3)_2OH + HCHO + O_2$$

When all alkoxy radicals formed by the decomposition of hydroperoxide due to metal catalysis result in cumyl alcohol, and all methyl peroxy radicals result in cumyl alcohol and formaldehyde after terminating with cumyl peroxy radical, the ratio of alcohol to ketone will be two. Thus, it can be concluded that some alkoxy radicals from the termination reaction in the solvent cage slip out of the cage and abstract hydrogen atom from hydroperoxide or cumene to yield alcohol.

If the solvent cage is composed of a viscous and inactive solvent for hydrogen abstraction, the probability of the alkoxy radical slipping out of the cage and abstracting hydrogen from the substrates will be decreased.

The effect of the amount of solvent was studied using chlorobenzene as a solvent (Table 2). As

TABLE 2. EFFECT OF SOLVENT ON THE RATIO OF ALCOHOL TO KETONE IN THE AUTOXIDATION OF CUMENE CATALYZED BY 0.02M COBALT DECANOATE

Cumene/chlorobenzene (volume/volume)	1/0	1/1	1/3	1/5
Cumyl alcohol/acetophenone (mol/mol)	4.5	2.7	1.94	1.67

the solution is diluted with chlorobenzene, the ratio of alcohol to ketone decreases remarkably. Much lower ratio in acetic acid (Table 1) seems to indicate that the physical properties of solvent affects the strength of the cage.

The formation of alkoxy radical from the bimolecular termination of peroxy radicals gives two different effects on the rate of oxidation. The induced decomposition of hydroperoxide will cause a decrease in the rate of oxidation, since the initiation reaction by the decomposition of hydroperoxide will be retarded. On the other hand, the hydrogen abstraction from cumene will result in the increase in the rate of oxidation. We can not exactly evaluate these influences, since the rate constants of elementary steps are not known and the two reactions will proceed simultaneously.

However, the effect of alkoxy radical from the cage on the rate of oxidation of cumene may not be so large because the rate of oxidation of neat cumene is in excellent agreement with the rate in acetic acid solution after correcting $(RH)^2$ term. Even if the dielectric effect is corrected, the effect on the rate enhancement will probably be about 20% according to the results of tetralin oxidation.[14]

The higher ratio of alcohol to ketone in the case of neat cumene can be attributed to the increase of dicumyl peroxide and to the decrease of acetophenone rather than to the decrease of cumyl alcohol. The bimolecular termination reaction of alkoxy radicals seems to be relatively fast.

Catalysis by Cobalt and Bromide Ions. In Fig. 7 the steady rate of oxidation of cumene is

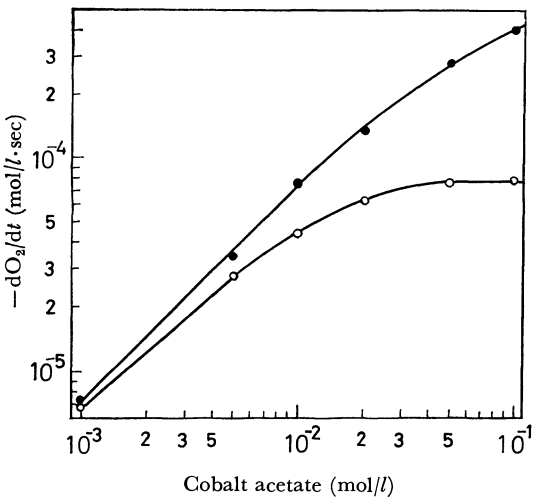

Fig. 7. The steady rate of oxidation of 1 : 1 by volume cumene: acetic acid mixture as a function of cobalt acetate concentration ○ in the presence or ● in the absence of sodium bromide.

plotted against the cobalt concentration in the presence and absence of sodium bromide. Two moles of sodium bromide per one mole of cobalt are used, since at this ratio the rate of oxidation has shown a limiting value as the amount of sodium bromide is varied.

The rate of oxidation of cumene in acetic acid reaches the limiting value 7.8×10^{-5}M/sec at 0.05M of cobalt. The rate of oxidation in the presence of sodium bromide tends to increase as the cobalt is increased. The difference of two rate curves due to the addition of sodium bromide to the solution is very small at cobalt 0.001M and is of first order with respect to cobalt concentration. The effect of bromide ion on the rate of oxidation of cumene is comparable as in tetralin[17] and not so remarkable as in *p*-xylene.[18] However, the steady concentration of cumyl hydroperoxide increased and the rate of decomposition of cumyl hydroperoxide decreased in the presence of bromide ion in contrast to the case of tetralin.[17]

The Synergistic Effect Due to Metal Catalysts. A synergistic effect of metal catalyst was observed, *i.e.*, by replacing 20% of the cobalt acetate of 0.02M by manganese acetate an approximately 1.3 fold increase in the rate of oxidation of cumene was observed (Fig. 8).

However, the synergistic effect could not overcome the experimental limiting rate of oxidation. It is interesting that at total metal concentration of 0.05M no more synergistic effect can be observed as seen in Fig. 8.

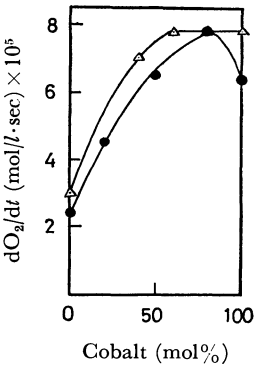

Fig. 8. The synergistic effect by cobalt and manganese acetates on the rate of oxidation of a 1 : 1 by volume cumene : acetic acid mixture at total metal concentration of ● 0.02 mol/l and △ 0.05 mol/l.

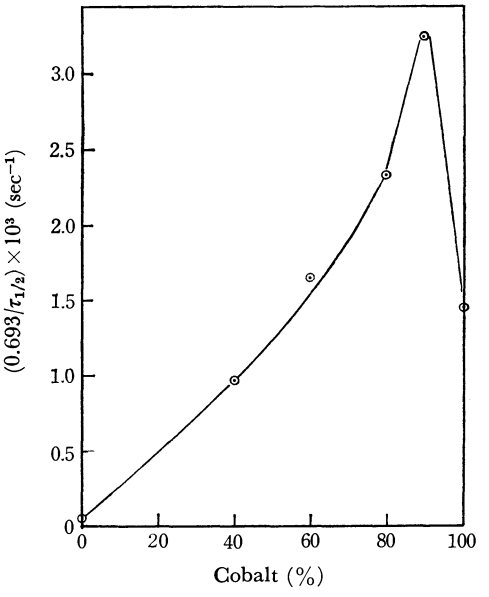

Fig. 9. The synergistic effect of cobalt and manganese acetates on the decomposition of cumyl hydroperoxide in an acetic acid : chlorobenzene mixture (1 : 1 by volume) at total metal concentration of 0.01M. $\tau_{1/2}$ represents the half life of 0.05M hydroperoxide.

A synergistic effect was observed also in the rate of decomposition of cumyl hydroperoxide by metal acetate as shown in Fig. 9, corresponding to the result in which the rate of oxidation is of nearly half order with respect to the first order rate constant of hydroperoxide decomposition. Therefore, the rate enhancing effect by the mixing of metal catalysts can be attributed to the chain initiation step by the metal-catalyzed decomposition of cumyl hydroperoxide.

17) Y. Kamiya, *Tetrahedron*, **22**, 2029 (1966).
18) Y. Kamiya, "Oxidation of Organic Compounds-II," Amer. Chem. Soc., Washington, D. C. (1968), p. 193.

BULLETIN OF THE CHEMICAL SOCIETY OF JAPAN VOL. 43 836—841 (1970)

The Reductive Coupling Reactions of Some Chloromethylbenzene Derivatives with Iron(II) and Copper(I) Complexes*1

Kazuhiko ONUMA, Junzo YAMASHITA and Harukichi HASHIMOTO

Department of Synthetic Chemistry, The University of Tokyo, Bunkyo-ku, Hongo, Tokyo

(Received July 23, 1969)

The reductive coupling reactions of some chloromethylbenzene derivatives with ferrous and cuprous chloride in ethanol or in acetonitrile and the effect of some additives on this reaction have been investigated. Benzotrichloride has been reduced selectively to tolan tetrachloride with ferrous chloride, while with cuprous chloride-ethylenediamine (a stronger reductant than ferrous chloride) mixtures of tolan and tolan dichloride or tolan tetrachloride are obtained depending on the condition. Similarly benzal chloride, diphenylmethyl chloride and diphenyldichloromethane are also reduced to give coupling products. In case of ferrous chloride the addition of ethylenediamine or pyrophosphoric acid raises the yield considerably and in case of cuprous chloride selection of the ratio, organic halide: copper (I): ethylenediamine, makes it possible to control the product distribution. The reaction mechanism and the effect of the additives are discussed.

Progress in the study of the iron- or copper ion catalyzed organic reactions[1-12] has revealed some catalytic features of these ions. As an example, the iron- or copper ion catalyzed addition of organic chloride to olefins[1,2] can be understood through the redox-transfer chain mechanism, metal ion being a chlorine-atom transfer agent.

$$RCl + M^{(n-1)+} \rightarrow R\cdot + M^{n+}Cl \quad (1)$$

$$R\cdot + \text{>C=C<} \rightarrow R\text{–}\overset{|}{C}\text{–}\overset{|}{C}\cdot \quad (2)$$

$$R\text{–}\overset{|}{C}\text{–}\overset{|}{C}\cdot + M^{n+}Cl \rightarrow R\text{–}\overset{|}{C}\text{–}\overset{|}{C}\text{–}Cl + M^{(n-1)+} \quad (3)$$

Reaction (3) is a relatively well studied "ligand transfer oxidation" process.[13-16] On the other hand step (1), which is just the reverse reaction of step (3), may be named tentatively "ligand transfer reduction" and about this much is left to be learned.

From this point of view we investigated previously the reductive coupling reaction of benzyl chloride by copper(I) complexes.[17] In this paper, application of this reductive coupling reaction with ferrous or cuprous chloride to some polyhalomethylbenzene derivatives and the effect of some additives will be studied.

Results and Discussion

Reductive Coupling by Ferrous Chloride. Simple ferrous ion is only a weak reductant compared with iron metal[18-20] and little is known

*1 Oxidation-Reduction Reactions by Transition Metal Complexes. V.

1) M. Asscher and D. Vofsi, a) *Chem. Ind.*, **1962**, 209; b) *J. Chem. Soc.*, **1963**, 1887; c) *ibid.*, **1963**, 3921; d) *ibid.*, **1964**, 4962; e) *ibid.*, **1968**, 947.
2) F. Minisci and R. Galli, *Tetrahedron Lett.*, **1964**, 167; *ibid.*, **1964**, 3197; *ibid.*, **1965**, 1679; *ibid.*, **1966**, 3163.
3) S. Murai, S. Tsutsumi and N. Sonoda, *J. Org. Chem.*, **29**, 2104 (1964); S. Murai and S. Tsutsumi, *ibid.*, **31**, 3000 (1966).
4) D. J. Burton and L. J. Kehoe, *Tetrahedron Lett.*, **1966**, 5163.
5) R. R. Lavine, R. T. Iwamoto and J. Kleinberg, *J. Amer. Chem. Soc.*, **88**, 4304 (1966).
6) J. K. Kochi, *Tetrahedron*, **18**, 483 (1962).
7) G. Sosnovsky and S. O. Lawessen, *Angew. Chem. Intern. Ed.*, **3**, 245 (1964).
8) F. Minisci and R. Galli, *Tetrahedron Lett.*, **1962**, 533; *ibid.*, **1963**, 357.
9) J. K. Kochi, *J. Amer. Chem. Soc.*, **79**, 2942 (1957).
10) C. E. Castro, E. J. Gaugham and D. C. Owsley, *J. Org. Chem.*, **31**, 4071 (1966).
11) R. G. R. Bacon and H. A. O. Hill, *Quart. Rev.*, **19**, 95 (1965).
12) T. Cohen and A. H. Lewin, *J. Amer. Chem. Soc.*, **88**, 4521 (1966).
13) D. C. Nonhebel and W. A. Waters, *Proc. Roy. Soc.*, **242**, 16 (1957).
14) J. K. Kochi, *Tetrahedron*, **18**, 483 (1962); *J. Amer. Chem. Soc.*, **84**, 2785, 3271 (1962); *Science*, **155**, 419 (1967).
15) C. H. Bamford, A. D. Jenkins and R. Johnston, *Trans. Faraday Soc.*, **55**, 421 (1959).
16) K. Wada, J. Yamashita and H. Hashimoto, This Bulletin, **40**, 2410 (1967).
17) K. Wada and H. Hashimoto, *ibid.*, **41**, 3601 (1968).
18) Y. Ogata and T. Tsuruta, *Bull. Inst. Phys. Chem. Res.* (Tokyo), **21**, 616 (1942); Y. Ogata and H. Nakamura, *J. Org. Chem.*, **21**, 1170 (1956).
19) K. Sisido, Y. Udo and H. Nozaki, *J. Amer. Chem. Soc.*, **82**, 434 (1960); H. Nozaki and R. Noyori, *Tetrahedron*, **22**, 2163 (1966).
20) D. W. Hall and E. Hurley, *Can. J. Chem.*, **47**, 1238 (1969).

about the interaction of ferrous ion with organic halides except for the case of ferrous porphyrin.[21] Actually, benzyl chloride does resist ferrous ion. It is well known, however, that the replacement of hydrogen atom attached to methyl carbon by phenyl group or chlorine atom considerably activates the molecule, and several polychloromethylbenzene derivatives were reduced by ferrous chloride. The reactions were carried out mostly in ethanol solvent and in a few cases in acetonitrile, under a nitrogen atmosphere and in the range from 70°C to reflux temperature. The results with benzotrichloride, benzal chloride, diphenyldichloromethane and diphenylmethyl chloride are tabulated in Tables 1—5.

Ethanol is a good solvent for both reactants but the ethanolysis of organic halides is unavoidable and always competes with the reduction reaction. In the case of acetonitrile homogeneity can be reached only at reflux temperature.

Table 1. Reductive coupling of benzotrichloride by ferrous chloride tetrahydrate in ethanol

$C_6H_5CCl_3$: 2.00×10^{-2} mol
Solvent C_2H_5OH: 50—60 m*l*
Reaction temperature: 72.0±3.0°C

Additive	$C_6H_5CCl_3$: $FeCl_2\cdot4H_2O$: additive (mole ratio)	Reaction time hr	$C_6H_5\cdot CCl_2\cdot CCl_2\cdot C_6H_5$[a] %
—	1 : 1	6	49
	1 : 3	6	67
en[b]	1 : 1 : 1	4	54
	1 : 1 : 2	4	74
	1 : 1 : 3	4	87
$H_4P_2O_7$	1 : 1 : 0.5	4	70
	1 : 1 : 1	4	81

a) In every run ethyl benzoate was recognized as a solvolysis product.
b) "en" is ethylenediamine and in this case the reaction system is heterogeneous.

Table 2. Reductive coupling of benzotrichloride by ferrous salts

$C_6H_5CCl_3$: 2.00×10^{-2} mol
Ferrous salt: 2.00×10^{-2} mol
Solvent: 50 m*l*

Ferrous salt	Solvent	Temp. °C	Reaction time hr	$C_6H_5\cdot CCl_2\cdot CCl_2\cdot C_6H_5$ %
$FeCl_2\cdot4H_2O$	CH_3CN	82	6	71[a]
$FeSO_4\cdot6H_2O$[b]	C_2H_5OH	71	2.5	8.1[c]
$FeCl_2\cdot4H_2O$	C_2H_5OH	r.t.	70	9.8[c]

a) 17% of benzoic acid was obtained other than coupling product.
b) Heterogeneous system.
c) Ethyl benzoate and unreacted benzotrichloride were recognized.

21) C. E. Castro, *J. Amer. Chem. Soc.*, **86**, 2310 (1964).

Table 3. Reductive coupling of diphenyldichloromethane by ferrous chloride tetrahydrate in ethanol

$FeCl_2\cdot4H_2O$: 4.00×10^{-2} mol
$(C_6H_5)_2CCl_2$: 2.00×10^{-2} mol
C_2H_5OH: 50—70 m*l*, 71.0±1.0°C, 3 hr

Additive	Fe(II) : additive (mole ratio)	$(C_6H_5)_2C{=}C(C_6H_5)_2$[a] %
—	—	39
en[b]	1 : 2	67
$H_4P_2O_7$	1 : 0.5	36

a) Benzophenone was also obtained as solvolysis product.
b) heterogeneous.

Table 4. Reductive coupling of benzal chloride by ferrous complexes

$C_6H_5CHCl_2$: 2.00×10^{-2} mol
solvent: 50—60 m*l*, 3 hr

Additive	$C_6H_5CHCl_2$: $FeCl_2\cdot4H_2O$: additive (mole ratio)	Solvent	Temp. °C	$C_6H_5\cdot CHCl\text{-}CHCl\cdot C_6H_5$ %
—	1 : 1.5	C_2H_5OH	70	0[a]
$H_4P_2O_7$[b]	1 : 2 : 1	C_2H_5OH	70	0[a]
en[b]	1 : 2 : 2	C_2H_5OH	70	4
en[b]	1 : 1 : 3	C_2H_5OH	78[c]	8
—	1 : 1	CH_3CN	82[c]	trace[d]
en[b]	1 : 1 : 3	CH_3CN	82[c]	3[e]

a) Hydrolyzed benzaldehyde and unreacted benzal chloride were recognized.
b) heterogeneous
c) under reflux
d) all converted to benzaldehyde
e) Organic substance other than coupling product was original benzal chloride.

Table 5. Reductive coupling of diphenylmethyl chloride by ferrous and cuprous chloride

$(C_6H_5)_2CHCl$: 2.00×10^{-2} mol
metal salt: 2.00×10^{-2} mol, CH_3CN; 50 m*l*
under reflux, 3 hr

Metal salt	$(C_6H_5)_2CHCl$: Metal salt : en (mole ratio)	Product (%) $(C_6H_5)_2CH\text{-}CH(C_6H_5)_2$	Product (%) $(C_6H_5)_2CH\text{-}NHCOCH_3$
$FeCl_2\cdot4H_2O$[a]	1 : 1	51	50
$FeCl_2\cdot4H_2O$	1 : 1 : 2	57[b]	
CuCl	1 : 1	0	
CuCl	1 : 1 : 2	100	

a) 1.00×10^{-2} mol of $(C_6H_5)_2CHCl$ was used.
b) 39% of hydrolyzed benzhydrol was obtained.

Reduction Products. From Tables 1 and 2 it can be seen that for benzotrichloride the yield of coupling product increases with increase of ferrous ion concentration, and the additive such as ethylenedi-

amine (en) or pyrophosphoric acid increases the yield considerably. The product is always tolan tetrachloride showing that ferrous ion is a weak reductant and additives have no marked effect on reducing power of ferrous ion.

$$2C_6H_5CCl_3 + 2Fe^{II}Cl_2 \rightarrow C_6H_5CCl_2 \cdot CCl_2C_6H_5 + 2Fe^{III}Cl_3 \quad (4)$$

Low yield in the case of ferrous sulfate seems to be due to the insolubility of the salt.

Table 3 contains the result of diphenyldichloromethane. It is noted that the product is tetraphenylethylene, being all chlorine atom split off. It seems that tetraphenylethylene is formed by step-wise reduction, that is, tetraphenyldichloroethane which is formed intermediately is further reduced because of steric and electronic instability.

$$2(C_6H_5)_2CCl_2 \xrightarrow{2Fe^{II}} (C_6H_5)_2CClCCl(C_6H_5)_2 \xrightarrow{2Fe^{II}} (C_6H_5)_2C{=}C(C_6H_5)_2 \quad (5)$$

However, the possibility of the formation of diphenylcarbene cannot be ruled out since this carbene is known to be fairly stable.[22] It was reported recently that dichlorocarbene was produced from tetrachloromethane and ferrous chloride.[1e]

As seen from Table 4 benzal chloride can not be reduced by ferrous chloride only. However, when ethylenediamine is added as an additive, reduction takes place and stilbene dichloride is obtained though the yield is poor. Some discussions on this effect will be made later.

Diphenylmethyl chloride is also reduced to produce tetraphenylethane (Table 5). It is of interest to note that in case of the use of ferrous chloride *tetrahydrate* in acetonitrile *N*-benzhydrylacetamide is also produced. Evidently this amide results from interaction of diphenylmethyl chloride or its hydrolysis product, benzhydrol with acetonitrile by the aid of ferrous or ferric chloride as a Lewis acid (this is a variation of well known Ritter reaction[23]).

These reactions give only coupling products as the reduction products. No hydrogenated materials are detected in contrast to the case of chromous ion.[24]

Effect of Additives. As pointed out before, when ethanol is used as solvent the solvolysis reaction of organic halides inevitably competes the reduction reaction (Tables 1—4). In addition ferric chloride is known to be a good catalyst for hydrolysis of organic halides. In fact preliminary experiment showed that a) at 70.5°C benzotrichloride is solvolyzed in ethanol and after 4 hr about 20% of the halide is converted to ethyl benzoate b) addition of 1/10 equiv. ferric chloride increases the solvolysis rate twice. If this solvolysis is suppressed by some means, increase of the yield of coupling product will be expected. As mentioned before, additives such as ethylenediamine and pyrophosphoric acid increase the yield of coupling products considerably. It seems reasonable that the primary effect of these additives lies in the suppression of the solvolysis of the organic substrates. Additives which can coordinate to ferric (or ferrous) ion will occupy the catalytic sites and suppress the solvolysis. The reaction of benzal chloride in acetonitrile (Table 4) supports this idea. Here in the presence of ferrous chloride *tetrahydrate* benzal chloride is completely converted to benzaldehyde (hydrolysis product of benzal chloride). But when ethylenediamine is added the starting material is recovered except for 3% of coupling product. This means that ethylenediamine expels water from the metal ion sphere and suppresses hydrolysis.

It may also be necessary to consider some other factors on the effect of ethylenediamine. As seen in Table 4 addition of ethylenediamine gives rise to form stilbene dichloride from benzal chloride which can not be reduced by ferrous ion only. This suggests the coordination of ethylenediamine to ferrous ion enhances the reducing power of the ion just as in the case of cuprous chloride (see below). Instability of Fe(III) complexes of amines is generally explained as Fe(III) state having half-filled d^5 system and, therefore, no CFSE in high spin state. Recently, however, ethylenediamine complex of ferric chloride—$Fe(en)_3Cl_3$—was reported to be synthesized and have spin-paired d^5 system.[25] Thus, it is not improbable to conceive that ethylenediamine has some coordination effect.

Some comments should be made on the possibility of the interaction of the organic halides with ethylenediamine as the reaction of amines with organic halides are fairly well known. Actually products which were thought to be formed from organic halides and ethylenediamine were detected. But they are only trace amount and supplementary experiments on the ethanolysis rate of benzotrichloride showed ethylenediamine has practically no effect on the rate. Moreover electronic spectra of benzotrichloride in ethanol does not change on addition of ethylenediamine in contrast to carbon tetrachloride which forms charge-transfer complexes with some amines.[26,27] These facts indicate that there is no need to consider the specific interaction.

Reductive Coupling by Cuprous Chloride.

22) C. E. Coffey, *J. Amer. Chem. Soc.*, **83**, 1623 (1961).
23) B. Prajsnar, *Chem. Anal.* (Warsaw), **8**, 255 (1963).
24) C. E. Castro and W. C. Kray, *J. Amer. Chem. Soc.*, **88**, 4447 (1966).
25) G. A. Renovitch and W. A. Baker, *ibid.*, **90**, 3585 (1968).
26) D. P. Stevenson and G. M. Coppinger, *ibid.*, **84**, 149 (1962).
27) W. J. Lautenberger, E. N. Jones and J. G. Miller, *ibid.*, **90**, 1110 (1968).

Cuprous chloride as well as ferrous chloride is only a weak reductant. Still it may be surprising that even diphenylmethyl chloride can not be reduced in acetonitrile. In dimethyl sulfoxide solvent, on the other hand, benzal chloride and benzotrichloride were reported to give coupled products by cuprous chloride.[28] Therefore this unusual inertness of cuprous chloride is attributable to a specific interaction with acetonitrile. In fact redox potential of Cu^{I}-Cu^{II} couple shows clearly stability of low valent state.[29,30]

As reported by us previously,[17] however, addition of ethylenediamine enhances the reducing power of cuprous ion strikingly and bibenzyl has been obtained from benzyl chloride. Here some application of this reaction is made and the results are in Tables 5—7. From diphenylmethyl chloride 100% yield is obtained, whereas the yield does not exceed 80% in case of benzal chloride and benzotrichloride. Probably side reactions leading to resinous products have occurred partly by relatively activated Cu(I) - ethylenediamine system.

It is of interest to note that selection of the ratio, organic halide: cuprous chloride: ethylenediamine, can control the product distribution (Tables 6 and 7). This also suggests that the reaction proceeds stepwise, that is, from benzotrichloride tolan tetrachloride is produced first and this tetrachloride is again reduced to dichloride in the presence of excess active reductant.

$$2C_6H_5CCl_3 \xrightarrow{2Cu(I)\text{-}en} C_6H_5CCl_2\text{–}CCl_2C_6H_5$$
$$\xrightarrow{2Cu(I)\text{-}en} C_6H_5CCl{=}CClC_6H_5 \qquad (6)$$

As shown in a previous report,[17] copper complexes which have been taken out after the reaction are $Cu^{II}(en)_nCl_2$ ($n=1$ or 2), and this shows that, in this case too, cuprous complexes of the type $Cu^{I}(en)_nCl$ are the intrinsic reagent. Such reactivity may reflect the effect of ligands on redox potential[31] (see Ref. 17).

An Approach to Reaction Mechanisms. From the mechanism of ligand transfer oxidation by ferric or cupric chloride, the most plausible mechanism of the reduction seems to be the reverse process of the oxidation as follows (in the following equations iron ion is used as metal ion for convenience).[1e,17,32]

$$RCl + Fe^{II}Cl_2 \rightleftharpoons RCl\cdot Fe^{II}Cl_2 \qquad (7)$$
$$RCl\cdot Fe^{II}Cl_2 \rightarrow R\cdot ClFe^{III}Cl_2 \qquad (8)$$

A kinetic study of the reduction of benzotrichloride by ferrous chloride *tetrahydrate* in ethanol has shown that plots of the initial rate of disappearance of Fe(II) *vs.* both initial concentration of organic halide and ferrous ion have first order dependence (Fig. 1), and the rate law is written as follows.

$$R = k[RCl][Fe(II)] \qquad (9)$$

This is compatible with the mechanistic scheme if we take step (8)—electron transfer or in other word chlorine transfer step—as rate determining step.

Another information to support this scheme is available from electronic spectra of cuprous chloride. On addition of benzotrichloride to the system of cuprous chloride - acetonitrile new absorption mixima appear at 310 and 463 mμ (75°C, under nitrogen). The absorption at the same wavelength is also observed in the case of benzal chloride. The fact that these absorption maxima

Table 6. Reductive coupling of benzotrichloride by cuprous chloride-ethylenediamine in acetonitrile

$C_6H_5CCl_3$: 2.00×10^{-2} mol
CH_3CN 50 m*l*, 82°C, 1 hr, heterogeneous

$C_6H_5CCl_3$: CuCl : en (mole ratio)	Product (%)		
	$C_6H_5CCl_2$-$CCl_2C_6H_5$	$C_6H_5\cdot CCl{=}CCl\cdot C_6H_5$[b]	$C_6H_5C{\equiv}CC_6H_5$
1 : 1 : 1	79	—	—
1 : 3 : 3[a]	—	47	8
1 : 3 : 6	—	54	5

a) 5.00×10^{-2} mol of benzotrichloride and 100 m*l* of acetonitrile were used.
b) mixture of *cis*- and *trans*-isomer.

Table 7. Reductive coupling of benzal chloride by cuprous chloride-ethylenediamine in acetonitrile

$C_6H_5CHCl_2$: 2.00×10^{-2} mol
CH_3CN 50 m*l*, 82°C, 1 hr, heterogeneous

$C_6H_5CHCl_2$: CuCl : en (mole ratio)	Product (%)	
	C_6H_5CHCl-$CHClC_6H_5$	*trans*-$C_6H_5CH{=}CHC_6H_5$
1 : 1 : 1	10[a]	—
1 : 2 : 2[b]	—	50
1 : 2 : 4	—	65

a) Unreacted benzal chloride was recognized.
b) 5.00×10^{-2} mol of benzal chloride and 100 m*l* of acetonitrile were used.

28) H. Nozaki, Y. Yamamoto, T. Shirafuji and R. Noyori, Preprint for 21st Annual Meeting, Chem. Soc. Japan, p. 1860 (1968).
29) I. M. Kolthoff and J. F. Coetzee, *J. Amer. Chem. Soc.*, **79**, 1852 (1957).
30) R. C. Larson and R. T. Iwamoto, *ibid.*, **82**, 3526 (1960).
31) J. K. Kochi, D. M. Singleton and L. J. Andrews, *Tetrahedron*, **24**, 3503 (1968); J. K. Kochi and P. E. Mocadlo, *J. Amer. Chem. Soc.*, **88**, 4094 (1966).
32) J. K. Kochi and D. D. Davis, *ibid.*, **86**, 5264 (1964); J. K. Kochi and D. Buchanan, *ibid.*, **87**, 853 (1965).

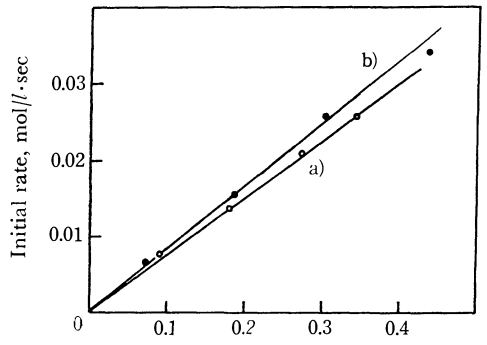

Fig. 1. Rate of reduction of benzotrichloride by ferrous chloride tetrahydrate.
a) $[Fe(II)]_0=0.30\pm0.01$ mol/l, $71\pm1°C$
b) $[C_6H_5CCl_3]_0=0.35\pm0.01$ mol/l, $71\pm1°C$

are the same with both organic halides suggests that the absorption is caused from the interaction between cuprous chloride and acetonitrile with the help of organic halide but it is also possible that the interaction between cuprous chloride and halogen atom of organic chloride is causative of the band. At any rate formation of intermediate complex between organic halide and cuprous chloride is indicative and in case of cuprous ion, unlike ferrous ion, electron transfer in the complex may be sustained.

The latter part of the reaction path is more complicated.[32,33] The formation of cupling products suggests radical feature of the reaction, whereas absence of hydrogen atom abstration products makes it uncertain. It should be noted also that solvent effect on product yield was hardly appreciable in the previous study.[17] From these facts the existence of radical in its free state seems unacceptable. Even if such a radical species is formed intermediately, it may be trapped by ferrous ion immediately (see Ref. 17).

Experimental

Materials. Reagent grade ferrous chloride tetrahydrate, ferrous sulphate hexahydrate and ferric chloride hexahydrate were used without further purification. As the hydration number of ferrous chloride was not accurately 4, Fe(II) equivalent was determined by ceric titration method. Reagent grade anhydrous cuprous chloride was further purified by the usual method.

Reagent grade benzotrichloride and diphenyldichloromethane and first grade benzal chloride, checked by NMR and gas chromatography, were used without further purification. Diphenylmethyl chloride was prepared from benzhydrol by the modification of Grice's method[34] for the preparation of *p*-methoxybenzyl chloride. Ethylenediamine (reagent grade) was distilled and used. Pyrophosphoric acid was used without further purification.

Absolute ethanol was purified by the conventional method and acetonitrile was purified according to O'Donnell's method.[35]

Typical Reaction Procedure. Ferrous or cuprous chloride (2.00×10^{-2} mol for example) was dissolved in 40 m*l* of absolute ethanol or acetonitrile in a four-necked, 50 m*l*, round-bottomed flask equipped with a 30 cm Dimroth condenser, a nitrogen inlet, a thermometer, a dropping funnel and a magnetic stirrer. The solution was then swept with oxygen-free nitrogen and heated to the required temperature. To this a solution of organic halide (2.00×10^{-2} mol) and, if necessary, ethylenediamine or pyrophosphoric acid in 10 m*l* solvent was added through the dropping funnel. The reaction was continued for required time under nitrogen stream.

Product Analyses. *A. Reduction of Benzotrichloride by Ferrous Chloride Tetrahydrate.* When the reaction was carried out in homogeneous system in ethanol solvent, the reaction mixture was cooled and 200 m*l* of water was added. The precipitated organic substance was filtered off and the filtrate was extracted with benzene, dried on sodium sulfate, concentrated to about 5 m*l* volume and the precipitated organic substance was also filtered and combined with the former. The filtrate was analyzed by g.l.c. to check the unreacted benzotrichloride and the solvolysis product, ethyl benzoate. The organic product was dried *in vacuo*, weighed for crude product yield and analyzed by IR, NMR, mp and also elementary analysis after recrystallization. The product was tolan tetrachloride, $C_6H_5\cdot CCl_2CCl_2\cdot C_6H_5$, mp 162.5—163.0°C (Found: C, 52.65; H, 3.13; Cl, 44.59%. Calcd: C, 52.54; H, 3.15; Cl, 44.31%). When the reaction mixture was heterogeneous insoluble iron complexes were filtered, washed four times with 50 m*l* hot benzene and the combined benzene solution was washed with water, dried on sodium sulfate, concentrated to about 5 m*l* volume and analyzed. When acetonitrile was used as solvent the reaction mixture was treated as in section D and the extracted benzene layer was again extracted by aqueous sodium bicarbonate for benzoic acid.

B. Reduction of Diphenyldichloromethane by Ferrous Chloride Tetrahydrate in Ethanol. Reaction mixture was treated as above. The product was 1,1,2,2-tetraphenylethylene, $(C_6H_5)_2C=C(C_6H_5)_2$, mp 223.5—224.0°C (Found: C, 93.80; H, 5.82%. Calcd: C, 93.94; H, 6.06%).

C. Reduction of Benzal Chloride by Ferrous Chloride Tetrahydrate. Reaction mixture was treated as in section A. The product was stilbene dichloride, $C_6H_5\cdot CHCl\text{-}CHCl\cdot C_6H_5$, mp 189.0—191.0°C (lit, for *meso* 191—193°C, racemic 93—94°C) (Found: C, 66.55; H, 4.61%. Calcd: C, 66.95; H, 4.82; Cl, 28.23%).

D. Reduction of Benzotrichloride and Benzal Chloride by Cupurous Chloride in Acetonitrile. As ethylenediamine was used as additive all runs were heterogeneous and the reaction was carried out under reflux temperature.

33) J.K. Kochi and F.F. Rust, *J. Amer. Chem. Soc.*, **83**, 2017 (1961); J.K. Kochi and P.E. Macadlo, *J. Org. Chem.*, **30**, 1134 (1965).

34) R. Grice and L. N. Owen, *J. Chem. Soc.*, **1963**, 1947.

35) J. F. O'Donnell, J. T. Ayres and C. K. Mann, *Anal. Chem.*, **37**, 1161 (1965).

After the reaction was ended the solvent was removed by distillation from the reaction mixture taking an hour, then the remainder was filtered and washed with hot benzene. The benzene filtrate was dried, concentrated and analyzed. The product was, if necessary, pretreated with column chromatography (300 mesh alumina) to remove resinous materials. When the products were mixtures of tolan and tolan dichloride (it was proved by IR, NMR and g.l.c.) the percentage of both substances were calculated from elementary analysis value or by g.l.c. peak area with *p*-nitrotoluene as a marker. The mp of the mixture was 60.5—62.5°C (lit, tolan; 62.5°C; tolandichloride *cis*, 142°C; *trans*, 63°C). *trans*-Stilbene was also produced form benzal chloride, C_6H_5–CH=CH–C_6H_5, mp 124.0—125.5°C (Found: C, 92.90; H, 6.46%. Calcd: C, 93.29; H, 6.71%).

E. Reduction of Diphenylmethyl Chloride by Ferrous Chloride Tetrahydrate of Cuprous Chloride. All runs were treated similarly. When the products were mixtures of tetraphenylethane and *N*-benzhydrylacetamide, they were easily separated from the difference of the solubility to benzene (this amide is hardly soluble to benzene). Hydrolysis product, benzhydrol was also separated because of the easy solubility. 1,1,2,2-Tetraphenylethane, $(C_6H_5)_2 \cdot CH \cdot CH \cdot (C_6H_5)_2$, mp 210.5—211.0°C (Found: C, 93.22; H, 6.53%. Calcd: C, 93.37; H, 6.63%). *N*-Benzhydrylacetamide, $(C_6H_5)_2CH \cdot NH \cdot CO \cdot CH_3$, mp 148.0—149.0°C, (Found: C, 79.62; H, 6.67; N, 6.12%. Calcd: C, 79.97; H, 6.71; N, 6.22; O, 7.10.%)

Other Experimental Procedures. For the rate of the solvolysis of benzotrichloride the modification of Vorhard's method was used and for the kinetics of the reduction of benzotrichloride by ferrous chloride tetrahydrate, the decrease in concentration of Fe(II) ion was followed by titration with cerium(IV) solution, ferroin as indicator.[36]

The visible and ultraviolet spectra were measured using Shimadzu MPS-50L multipurpose spectrophotometer and for g.l.c. a 2-m silicone DC550 column was employed.

36) M. Kolthoff and R. Belcher, "Volumetric Analysis," Vol. III, Interscience Publishers, New York, N.Y. (1957), p. 147.

BULLETIN OF THE CHEMICAL SOCIETY OF JAPAN VOL. 43 841—848 (1970)

Nitroalkenylferrocene. V. New Reactions of α-Halonitroolefins in the Presence of Sodium Alkoxides

Mikio SHIGA, Masaaki TSUNASHIMA, Hiromichi KONO, Izumi MOTOYAMA and Kazuo HATA

Department of Chemistry, Faculty of Science, Tokyo Metropolitan University, Setagaya, Tokyo

(Received August 4, 1969)

The reactions of 1-iodo-2-ferrocenyl-1-nitroethylene (**1**) and β-bromo-β-nitrostyrene (**5**) with various sodium alkoxides were investigated. The reaction in the presence of an excess of alkoxides gave nitroketones, (**2**) and (**6**), and nitroacetals (**3**) and (**7**). The thermal decomposition of the nitroacetals in a nitrogen atmosphere afforded β-alkoxynitroolefins (**8**), which were found to be useful for obtaining asymmetric nitroacetals (**9**) with different alkoxy groups. The reaction mechanism was discussed by postulating the intervention of a nitrocarbene (**12**) and β-alkoxynitroolefin (**8**). The intermediacy of the nitrocarbene was supported by an experiment using vinylferrocene as a carbene scavenger.

Some information has been given[1,2] on the reactivity of the α-carbon of nitroolefins in preceding papers of this series. With a view to get further information, reactions of 1-iodo-2-ferrocenyl-1-nitroethylene (**1**)[2] and the phenyl analogs, β-bromo-β-nitrostyrene (**5**)[3]in the presence of various sodium alkoxides were investigated. The mechanism of the reaction of β-bromo-β-nitrostyrene with sodium methoxide was discussed by the aid of a reaction in the presence of vinylferrocene. The nitroacetals and β-alkoxynitroolefins which were obtained in these reactions have not yet appeared in the literature. Especially, acetals of an asymmetric structure with different alkoxy groups were first prepared in this investigation.

1) M. Shiga, H. Kono, I. Motoyama and K. Hata, This Bulletin, **42**, 798 (1969).

2) H. Kono, M. Shiga, I. Motoyama and K. Hata, *ibid.*, **42**, 3270 (1969).

3) W. E. Parham and J. L. Bleasdale, *J. Amer. Chem. Soc.*, **73**, 4664 (1951).

Results

The Reactions of 1-Iodo-2-ferrocenyl-1-nitroethylene with Sodium Alkoxides. The reaction conditions and the products are summarized in Table 1. The structures of the reaction products

TABLE 1. THE REACTIONS OF 1-IODO-2-FERROCENYL-1-NITROETHYLENE IN THE PRESENCE OF SODIUM ALKOXIDES

Reaction temp., reflux in 20 ml of THF
Reaction time, 2 hr

FcCH=C(NO$_2$)I (1) (g)	(mol)	RONa (g)	(mol)		Products (mp°C)	(g)	(%)
0.38	0.001	CH_3ONa		**2**	97—98	0.16	54
		0.54	0.01	**3a**	oil	0.04	14
0.38	0.001	$C_6H_5CH_2ONa$		**2**	97—98	0.15	55
		1.30	0.01	**3b**	oil	0.037	8
0.38	0.001	*i*-C_3H_7ONa		**2**	97—98	0.14	51
		0.82	0.01				
0.76	0.002	*t*-C_4H_9ONa		**2**	97—98	0.24	45
		0.96	0.01				

were confirmed by their elemental analyses and by a study of their IR and NMR spectra, which are listed in Tables 4 and 5.

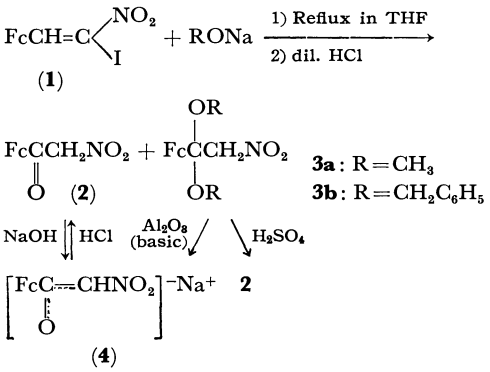

The refluxing of the solution of 1-iodo-2-ferrocenyl-1-nitroethylene (**1**) in tetrahydrofuran with an excess of sodium methoxide gave (nitroacetyl)-ferrocene (**2**) as reddish-orange crystals (mp 97—98°C) and its dimethyl acetal (**3a**) as a dark brown oil, along with a small amount of formylferrocene and an unidentified carbonyl compound.

When an ethereal solution of (nitroacetyl)ferrocene (**2**) was shaken with a dilute solution of sodium hydroxide, the substance easily transferred to the aqueous layer, forming its sodium salt. Because of the strong acidity of **2**, a sodium salt (**4**) was also formed during the chromatographic purification of **2** on basic alumina or on basic Florisil. Especially, the chromatography on basic Florisil using methanol as a solvent gave a pure red solid of the sodium salt, which in turn easily regenerated the original nitroketone by means of dilute hydrochloric acid. The dimethyl acetal (**3a**) was easily converted into nitroketone (**2**) of treating it with sulfuric acid. The chromatography of **3a** on alumina gave sodium salt of the nitroketone (**4**) in a quantitative yield.*1 The results of similar reactions using varying amounts of sodium methoxide are summarized in Table 2, in which the yield of **2** is shown as a total yield of **2** after the coexisting dimethyl acetal has been completely converted into the nitroketone. The maximum yield was attained when ten equivalents of methoxide were used (see also Table 1).

TABLE 2. THE REACTION OF 1-IODO-2-FERROCENYL-1-NITROETHYLENE IN THE PRESENCE OF VARIED AMOUNT OF SODIUM METHOXIDE

Reaction temp., reflux in 20 ml of solvent
Reaction time, 2 hr

FcCH=C(NO$_2$)I (g)	(mol)	CH_3ONa (g)	(mol)	Solvent	Yield* of **2** (g)	(%)
0.38	0.001	0.16	0.003	THF	0.05	20
0.38	0.001	0.27	0.005	THF	0.097	36
0.38	0.001	0.54	0.01	THF	0.19	69
0.38	0.001	0.54	0.01	Benzene	0.16	61
0.38	0.001	1.0	0.02	THF	0.18	67

* The yields were expressed as the nitroketones, the nitroacetals being converted to the former by the treatment with alumina.

The reaction of **1** with sodium benzyl oxide gave nitroketone (**2**) and its dibenzyl acetal (**3b**) in 55% and 8% yields respectively. Though the acetal (**3b**) was obtained as a dark brown oil, it was too unstable to be purified; therefore, its yield was estimated by converting it completely into nitroketone (**2**).

A similar reaction with sodium isopropoxide and *t*-butoxide gave nitroketone (**2**) in 51% and 45% yields respectively, but the corresponding acetals could not be found in the products.

The Reactions of β-Bromo-β-nitrostyrene with Sodium Alkoxides. The reaction conditions and the products are summarized in Table 3. The IR and NMR spectra of the reaction products are listed in Tables 4 and 5.

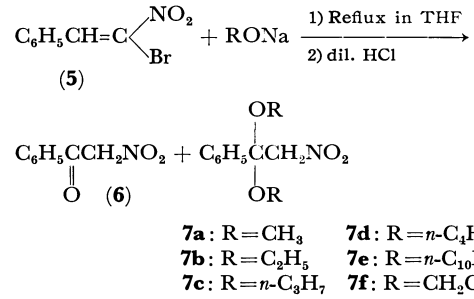

*1 The sodium ion may be supplied from basic alumina for the chromatography.

Table 3. The reactions of β-bromo-β-nitrostyrene in the presence of sodium alkoxides
Reaction temp., reflux in THF, Reaction time, 2 hr.

$C_6H_5CH=C\langle^{NO_2}_{Br}$ (5)		RONa		Product (mp, bp)	Yield	
(g)	(mol)	(g)	(mol)		(g)	(%)
0.57	0.0025	CH_3ONa		**7a** 97.5—98°C/1 mmHg	0.40	76.0
		0.67	0.0125	**6** 108—109°C	trace	
1.14	0.005	CH_3ONa		**7a** 97.5—98°C/1 mmHg	0.82	78.0
		2.7	0.05	**6** 108—109°C	0.10	12.5
1.14	0.005	CH_3ONa		**7a** 97.5—98°C/1 mmHg	0.82	78.0
		5.4	0.1	**6** 108—109°C	0.15	18.0
2.0	8.78×10^{-3}	C_2H_5ONa		**7b** 91.5—92°C/0.6 mmHg	1.49	71.0
		5.9	8.78×10^{-2}	**6** 108—109°C	0.028	2.08
				C_6H_5COOH	0.01	1.4
1.44	6.14×10^{-3}	*n*-C_3H_7ONa		**7c** 104—105°C/0.2 mmHg	1.47	94.4
		5.04	6.14×10^{-2}	**6** 108—109°C	trace	
				C_6H_5COOH	trace	
1.44	6.14×10^{-3}	*n*-C_4H_9ONa		**7d** 120—121°C/0.2 mmHg	1.43	77.4
		6.05	6.14×10^{-2}	**6** 108—109°C	0.06	8.7
				C_6H_5COOH	0.015	1.5
1.13	4.95×10^{-3}	*n*-$C_{10}H_{21}ONa$		**7e** oil	1.82	83.2
		14	4.95×10^{-2}	**6** 108—109°C	trace	
				C_6H_5COOH	trace	
1.14	0.005	$C_6H_5CH_2ONa$		**7f** oil	1.49	82.4
		6.5	0.05	**6** 108—109°C	trace	
				C_6H_5COOH	trace	

Table 4. The IR spectra of nitroacetones, nitroacetals and β-alkoxynitroolefins
(Frequency cm^{-1})

Compound	NO_2 (asym.)	NO_2 (sym.)	C=O	C–O	C=C
2	1553	1317	1673		
3a	1552	1325		1120	
6	1556	1330	1694		
7a	1560	1322		1100	
7b	1562	1326		1100	
7c	1560	1320		1100	
7d	1558	1318		1100	
7e	1550	1342		1100	
7f	1552	1310		1100	
9	1564	1328		1100	
8a	1504	1352			1616
	1488	1322			1600
8c	1518(504)*	1356(671)*			1628
	1498(647)*	1326(647)*			1608
8f	1504(584)*	1356(866)*			1620
	1490(700)*	1320(338)*			1602

* These ε-values were calculated by the usual method on the basis of integrated ratio of *cis* to *trans* isomer obtained from their NMR spectra.

The reaction of β-bromo-β-nitrostyrene (**5**) with an excess of sodium methoxide gave ω-nitroacetophenone (**6**)[4] as white crystals (mp 108—109°C) and its dimethyl acetal (**7a**) as a pale yellow oil (bp 97.5—98°C/1.0 mmHg) in 18% and 78% yields respectively. The increase in the amount of sodium methoxide from five to twenty equivalents to the bromonitroolefin brought about a marked increase in the yield of nitroacetal (**7a**), as is shown in Table 3. The reactions of **5** with sodium ethoxide, *n*-propoxide, and *n*-butoxide gave diethyl, dipropyl, and dibutyl acetal (**7b, c, d**) of ω-nitroacetophenone respectively as the main products, all in good yields. Each reaction also gave small amounts of ω-nitroacetophenone (**6**) and benzoic acid, the latter of which had been found to be formed by the decomposition of the intervening alkoxynitroolefins, as will be described later. The reactions of **5** with sodium decyl oxide and sodium benzyl oxide gave a pale yellow oil consisting of nitroacetals (**7e**) and (**7f**), in 83.2% and 82.4% yields respectively. Besides the oily main product, traces of ω-nitroacetophenone and benzoic acid were obtained as crystalline products in each reaction. Each of the oily products proved to be pure enough, judging from the results of thin-layer chromatography. These nitroacetals are indifferent to aqueous alkali and to dilute acid, and also to heating.

4) A. Lucas, *Ber.*, **32**, 602 (1899).

TABLE 5. THE NMR SPECTRA OF NITROKETONES, NITROACETALS AND β-ALKOXYNITROOLEFINS (τ-Value, in $CDCl_3$)

Compound	Benzene ring protons	$-CH_2NO_2$	$-OCH_2R$	$-CH_2-$	$-CH_3$	$=C<^{H}_{NO_2}$	Cyclopentadienyl ring protons (unsubst.)	(subst.)
2		4.43(s)					5.66(s)	5.22(t)[a] 5.32(t)[b]
6	2.33(m)	4.07(s)						
7a	2.63(m)	5.28(s)	6.77(s)[c]					
7b	2.62(m)	5.23(s)	6.54(m)		8.76(t)			
7c	2.60(m)	5.20(s)	6.54(m)	8.39(m)	8.98(t)			
7d	2.56(m)	5.16(s)	6.52(m)	8.46(m)	9.06(t)			
9	2.59(m)	5.24(s)	6.57(m) 6.74(s)[c]	8.36(q)	9.04(t)			
8a	2.62(d)		6.25(s)[c] 6.28(s)[c]			3.18(s) 3.05(s)		
8c	2.57(d)		6.03(t) 6.11(t)	8.26(m)	8.99(t)	3.15(s) 3.03(s)		
8f	2.60(d)		5.05(s) 4.95(s)			2.94(s) 3.13(s)		

a) 2,5-Protons b) 3,4-Protons c) R=H

Sodium isopropoxide and sodium *t*-butoxide reacted with **5** to give neither nitroacetals nor ω-nitroacetophenone, but it did afford a large amount of benzoic acid.

The Reactions of Nitroketones. The nitroketones (**2** and **6**) were found to act as acids, thus easily forming sodium salts by means of a sodium hydroxide solution or by means of basic alumina during chromatography, as has been described above. When the nitroketones were treated with piperidine and alcohol, they decomposed to give the esters of ferrocenecarboxylic or benzoic acid.

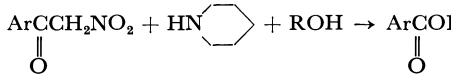

The Reactions of Nitroacetals (7). It was found that the thermal decomposition of nitroacetals (**7**) in air gave alkyl benzoates. On the contrary, the thermal decomposition of nitroacetals (**7**) under an atmosphere of nitrogen afforded quantitatively α-alkoxy-β-nitrostyrene (**8**) and the respective alcohols, the former of which was found to be a mixture of *cis* and *trans* isomers by a

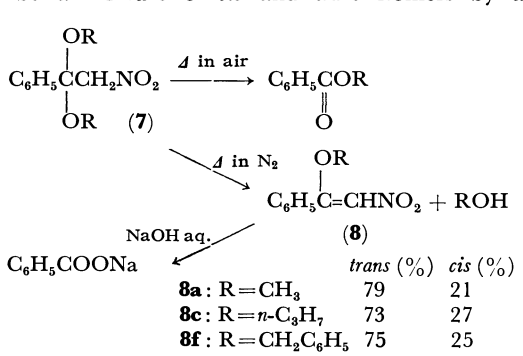

	trans (%)	*cis* (%)
8a: R=CH_3	79	21
8c: R=*n*-C_3H_7	73	27
8f: R=$CH_2C_6H_5$	75	25

study of its IR, UV, and NMR spectra. For example, the IR spectra of α-benzyloxy-β-nitrostyrene (**8f**) (bp 153—154°C/0.005 mmHg) obtained from **7f** showed strong absorption peaks at 1504 cm^{-1} (asym. NO_2) and 1356 cm^{-1} (sym. NO_2) for one isomer, and weak absorption peaks at 1490 cm^{-1} (asym. NO_2) and 1320 cm^{-1} (sym. NO_2) for the other.

The geometric relation between the nitro and phenyl groups in these compounds can be distinguished in the manner described by Watarai *et al.*[5] It is reasonable to consider that the former has a *trans*, and the latter a *cis* configuration with regard to the nitro and phenyl groups, because the absorbance of the asymmetrical NO_2-stretching absorption is weaker than that of the symmetrical one in the case of the former, while the relation is the inverse in the case of the latter.

The UV spectrum of **8f** shows two characteristic absorption maxima, at 268 and 290 mμ, the latter of which can be considered to be due to the *trans* configuration because of the more favorable conjugation of nitro group with the phenyl group. The NMR spectrum of **8f** also indicated the presence of stereoisomers (see Fig. 1); one of these exhibits two singlet peaks, at τ 5.05 and 2.94, due to methylene and olefinic protons respectively, while the other exhibits two corresponding singlet peaks, at τ 4.95 and 3.13 respectively. The signal of the *O*-methylene protons of the *trans* isomer is expected to shift toward a higher magnetic field than that of the *cis* isomers by anisotropy of the nitro group. Since the integrated intensity ratio of the methylene and olefinic protons of the former to those of the

5) S. Watarai, K. Yamamura and T. Kinugasa, This Bulletin, **40**, 1448 (1967).

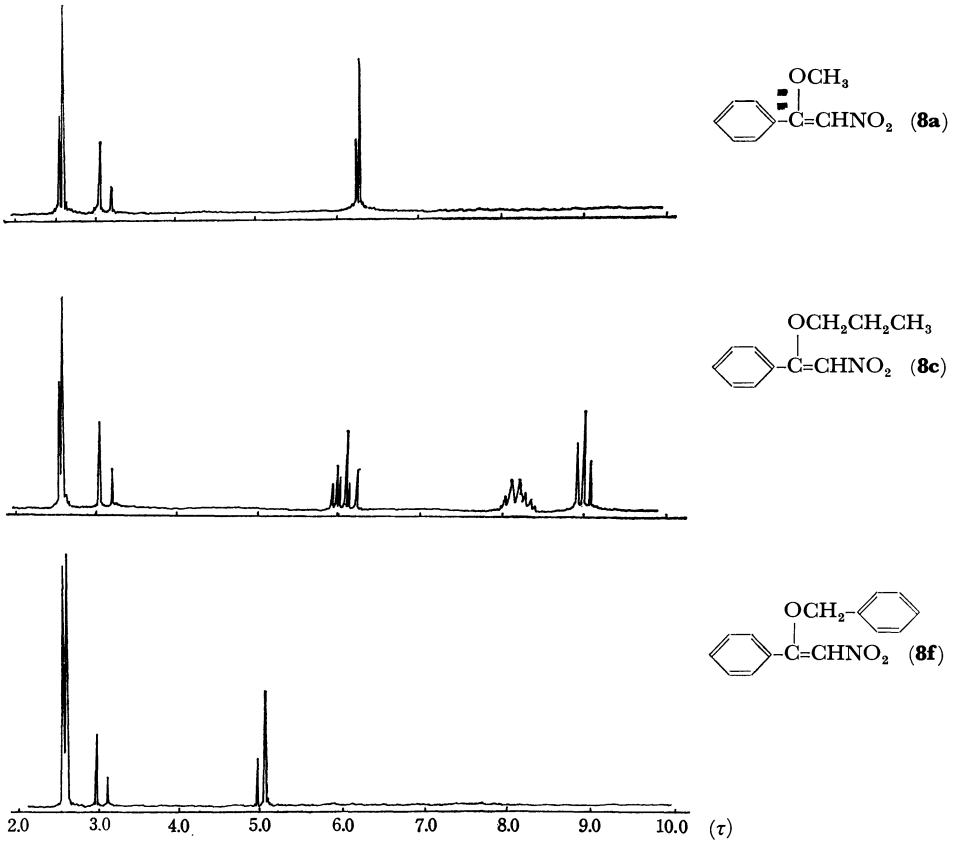

Fig. 1. NMR spectra of α-alkoxy-β-nitrostyrenes.

latter is about 3 : 1, **8f** was considered to be a mixture composed of approximately 75% *trans* and 25% *cis* isomers. The pale yellow viscous oil of **8f** gradually solidified on standing in air. In the IR, UV, and NMR spectra of the solidified product, a decrease in the relative strength of the absorption band to the *cis* isomer was observed. After standing for 5 days, the percentage of the *trans* isomer increased from 75% to 98%, judging from the intensity ratio of the NMR spectra.

ω-Nitroacetophenone dimethyl acetal (**7a**) and dipropyl acetal (**7c**), on being heated under a nitrogen atmosphere, gave a yellow oil of α-methoxy-β-nitrostyrene (**8a**) (bp 110°C/0.35 mmHg) and an α-propoxy analog (**8c**) (bp 115—116°C/0.2 mmHg) in 96% and 95% yields respectively. The ratios of the *trans* to the *cis* isomers in **8a** and **8c** were similarly calculated to be 3.8 : 1 and 2.7 : 1 respectively from their NMR spectra (Fig. 1).

The Reactions of Alkoxynitroolefins. The alkoxynitroolefins (**8**) were easily converted into ω-nitroacetophenone (**6**) or sodium benzoate by treating them with hydrochloric acid or sodium hydroxide solution respectively. The reaction of sodium alkoxide on the alkoxynitroolefins (**8**) leads to the reverse formation of the nitroacetals (**7**). Thus, asymmetric acetals with different alkoxy groups can be prepared by this reaction. For instance, the reaction of sodium propoxide on α-methoxy-β-nitrostyrene (**8a**) afforded ω-nitroacetophenone methyl propyl acetal (**9**) (bp 89—90°C/0.3 mmHg) in an 84% yield. The acetal was obtained as a racemic compound; its resolution into optically active enantiomers has not yet been attempted.

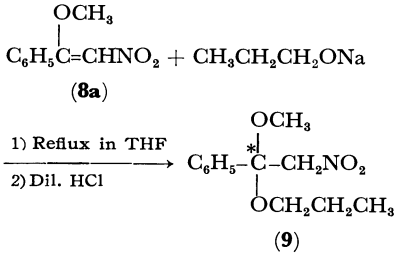

The Reaction of β-Bromo-β-nitrostyrene with Sodium Methoxide in the Presence of Vinylferrocene. Since the reaction of β-bromo-β-nitrostyrene (**5**) with sodium alkoxide to form nitroacetals (**7**) was supposed to proceed through a carbene intermediate, an experiment to capture the

carbene was attempted. When β-bromo-β-nitrostyrene was refluxed with equimolar portions of sodium methoxide and vinylferrocene, 3-ferrocenyl-1-(α-methoxybenzyl)cyclopropene (**10**) was obtained as yellow-brown crystals (mp 88—90°C) in a 6.9% yield, besides small amounts of 1-ferrocenyl-2-nitroethylene,[6] ω-nitroacetophenone dimethyl acetal, and another unidentified nitro compound.

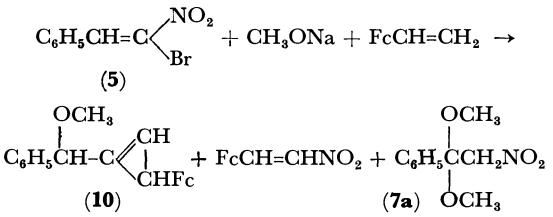

The NMR spectrum of **10** exhibits four singlet peaks, at τ 2.59, 4.79, 5.83, and 6.56, due to phenyl protons, methine in the side chain, ferrocenyl, and methoxy protons respectively, and two doublet peaks, at τ 5.91 and 7.02, corresponding to olefinic and methine protons in the cyclopropene ring. The IR spectrum of **10** shows a strong absorption peak at 1104 cm^{-1} (C–O).

Discussion

As is shown in Scheme 1, sodium alkoxides easily reacted with 1-iodo-2-ferrocenyl-1-nitroethylene (**1**) or β-bromo-β-nitrostyrene (**5**) to give adducts (**11**). The adducts were found to be very stable in organic solvents at room temperature, but they were decomposed into the original halonitroolefins by the action of dilute hydrochloric acid. On the other hand, they were converted into sodium salts of nitroacetals (**13**) or of nitroketones (**14**) when heated above 90°C with an excess of sodium alkoxides. These reactions can be considered to proceed through nitrocarbenes (**12**), which are generated by the α-elimination of sodium halide from the adducts (**11**), followed by an immediate hydride shift to give β-alkoxynitroolefins (**8**). This consideration is based on the fact that alkylcarbenes cause intramolecular insertion into neighboring β- or γ-carbon–hydrogen bonds to give olefins or cyclopropanes respectively.[7]

In order to get evidence of the existence of such a nitrocarbene as a reaction intermediate, the thermal reaction of β-bromo-β-nitrostyrene was attempted in the presence of vinylferrocene. As a result, a small amount of 3-ferrocenyl-1-(α-methoxybenzyl)cyclopropene (**10**) was obtained instead of the expected nitrocyclopropane (**15**), as is shown in Scheme 2. Since Darling and Spanagel have reported that nitrocyclopropane (**19**) was easily

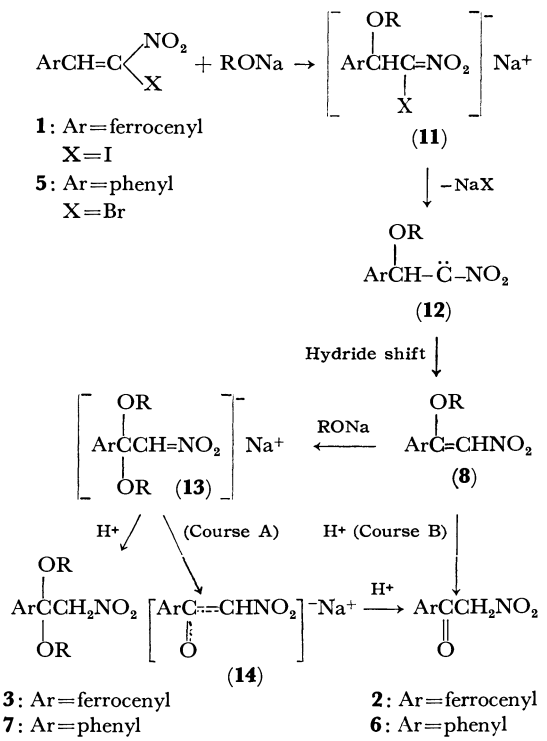

Scheme 1. Reaction mechanism.

converted into cyclopropene (**20**) by the action of sodium methoxide (Scheme 2),[8] the formation of 3-ferrocenyl-1-(α-methoxybenzyl)cyclopropene (**10**) can reasonably be considered to be an indirect evidence of the existence of nitrocyclopropane (**15**) as an intermediate. An alternative cyclopropene derivative (**18**) was not obtained in this reaction. The exclusive formation of **10** may stem from the fact that the intermediate α-ferrocenylcarbanion (**17**) is less stable than the isomeric carbanion (**16**) because of the electron-releasing character of the neighboring ferrocene nucleus.

β-Alkoxynitroolefins (**8**), which were expected to be the hydride-shift products from the nitrocarbene (**12**), could not be isolated in these reactions. The further addition of sodium alkoxide to the β-alkoxynitroolefin (**8**) led to the formation of sodium salts of nitroacetals (**13**), which were then easily converted into nitroacetals (**3** or **7**) by dilute hydrochloric acid. Phenylnitroacetals (**7**) were found to be much more stable than ferrocene analogs (**3**). The difference in stability appears to be due to the larger steric hindrance and the larger electron-releasing character of the ferrocene nucleus.

As for the mechanism affording nitroketones (**2** or **6**) two pathways can be considered, as Scheme 1 shows. Course A involves the thermal decomposition of sodium salts of nitroacetals (**13**) into sodium salts of nitroketones (**14**), while Course B involves

6) M. Shiga, H. Kono, I. Motoyama and K. Hata, This Bulletin, **41**, 1897 (1968).

7) W. Kirmse, "Carbene Chemistry," Academic Press, New York and London (1964), p. 52.

8) S. F. Darling and E. W. Spanagel, *J. Amer. Chem. Soc.*, **53**, 1117 (1931).

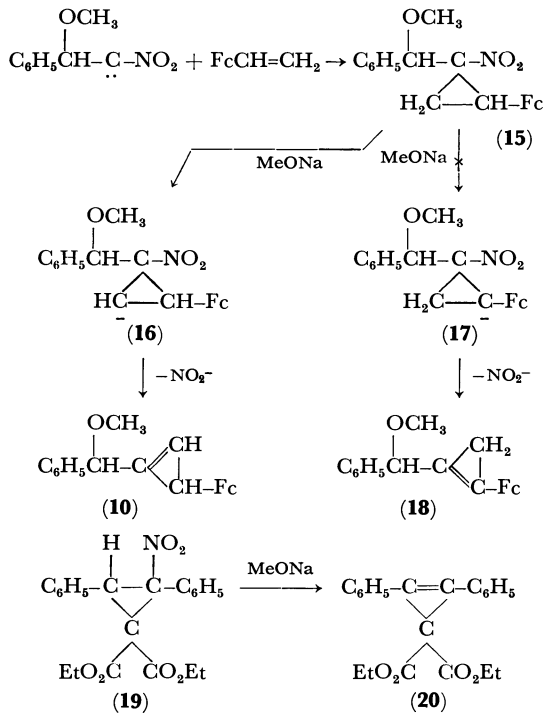

Scheme 2. Reaction of nitrocarbene.

the direct attack of hydrochloric acid on β-alkoxynitroolefins (**8**). Course B can be ruled out on the basis of the observation that the reaction of β-bromo-β-nitrostyrene (**5**) with equimolar sodium methoxide gave neither ω-nitroacetophenone, its dimethyl acetal, nor benzoic acid at all; if the reaction followed course B, ω-nitroacetophenone or benzoic acid should be isolated from the reaction mixture when it was treated with dilute hydrochloric acid. Thus, the nitroketone must be produced *via* sodium salts of nitroacetals (**13**) by means of course A.

The effect of the bulk of the alkyl group in sodium alkoxides was not so evident in the reactions with 1-iodo-2-ferrocenyl-1-nitroethylene, but it was striking in those with the phenyl analog. The reaction of β-bromo-β-nitrostyrene with an excess of sodium isopropoxide or *t*-butoxide gave a large amount of benzoic acid, along with a small amount of ω-nitroacetophenone (**6**), while the ferrocene analog (**1**) gave (nitroacetyl)ferrocene (**2**) as the main product. The difference can be interpreted in terms of the stability of the intermediate sodium salts of nitroacetals (**13**). The intermediate sodium salts (**13**) of ferrocenyl series are so unstable because of their much larger steric crowding that they are predominantly converted into the sodium salts of nitroketones (**14**) rather than decomposed to alkyl benzoates. On the other hand, the corresponding intermdiates (**13**) of the phenyl series are considerably stable and give nitroacetals (**3**) preferably; diisopropyl and di-*t*-butyl acetals of ω-nitroacetophenone or their sodium salts can be easily decomposed to isopropyl or *t*-butyl benzoate, followed by hydrolysis to benzoic acid at the reaction temperature (90—95°C), while primary alkyl acetals such as dimethyl acetal are stable at that temperature and are decomposed to benzoate only at a much higher temperature (180—200°C).

Experimental

(Nitroacetyl)ferrocene (2) and Its Dimethyl Acetal (3a). To 0.001 mol (0.38 g) of 1-iodo-2-ferrocenyl-1-nitroethylene in 20 m*l* of dry THF, 0.01 mol (0.54 g) of sodium methoxide was added. After it had been refluxed for 2 hr on a water bath, the reaction mixture was poured into a mixture of 100 m*l* of a 5% sodium hydroxide solution and 20 m*l* of benzene. The benzene layer was then separated off, and the aqueous layer was washed three times with benzene. After the aqueous solution had been acidified with 5% hydrochloric acid, it was extracted with 30 m*l* of benzene. When the benzene solution was shaken with 100 m*l* of a 5% NaOH solution, the nitroketone moved to the aqueous layer, forming its sodium salt, while the nitroacetal remained in benzene unchanged. The benzene layer was washed three times with 100-m*l* portions of water and dried over anhydrous magnesium sulfate. Then, the benzene was removed by distillation to give 0.04 g (14% yield) of a dark brown oil of **3a**.

Found: C, 51.00; H, 4.83; N, 4.07%. Calcd for $C_{14}H_{17}FeNO_4$: C, 52.66; H, 5.32; N, 4.38%.

The aqueous alkaline layer, on the other hand, was acidified with 5% hydrochloric acid and extracted three times with 20-m*l* portions of benzene, after which the benzene solution was dried over anhydrous magnesium sulfate. After the removal of the solvent, 0.199 g of crude (nitroacetyl)ferrocene (**2**) was obtained. Recrystallization from a mixture of *n*-hexane and methylene dichloride (3 : 1) gave 0.16 g (54% yield) of orange crystals (mp 97—98°C).

Found: C, 53.04; H, 3.77; N, 5.04%. Calcd for $C_{12}H_{11}FeNO_3$: C, 52.74; H, 4.02; N, 5.12%.

(Nitroacetyl)ferrocene Dibenzyl Acetal (3b). Following the procedure described above, (nitroacetyl)-ferrocene dibenzyl acetal was prepared from 1-iodo-2-ferrocenyl-1-nitroethylene and sodium benzyl oxide in an 8% yield. The dark brown oil thus obtained is unstable and is apt to decompose to (nitroacetyl)-ferrocene even on standing in the air.

ω-Nitroacetophenone Dimethyl Acetal (7a). To 0.005 mol (1.14 g) of β-bromo-β-nitrostyrene in 60 m*l* of dry THF, 0.05 mol (2.7 g) of sodium methoxide was added. After having been refluxed for 2 hr on a water bath, the reaction mixture was poured into a mixture of 200 m*l* of 10% hydrochloric acid and 30 m*l* of benzene. The aqueous layer was separated off, and the benzene layer was shaken three times with 100-m*l* portions of water and then with 100 m*l* of a 5% sodium hydroxide solution. Thus, ω-nitroacetophenone was separated as its sodium salt. The benzene layer, which contained the acetal **7a**, was washed three times with 100-m*l* portions of water and then dried over anhydrous magnesium sulfate. The benzene solution, after the removal of the solvent, gave 1.1 g of crude ω-nitroacetophenone dimethyl acetal, which was distilled under reduced

pressure to give 0.82 g (78.0% yield) of **7a** as a pale yellow oil (bp 97.5—98°C/1.0 mmHg).

Found: C, 57.11; H, 6.53; N, 6.76%. Calcd for $C_{10}H_{13}NO_4$: C, 56.87; H, 6.16; N, 6.63%.

The aqueous alkaline layer, which contained the nitroketone, was acidified with 5% hydrochloric acid and then extracted three times with 20-m*l* portions of benzene. The benzene solution thus obtained was dried over anhydrous magnesium sulfate. After the removal of the solvent, the residual pale yellow crystals were dissolved in 3 m*l* of benzene and chromatographed on basic alumina, using methanol as the eluent. The first yellow fraction gave the sodium salt of ω-nitroacetophenone,*2 which was treated with 5% hydrochloric acid and then extracted with 30 m*l* of benzene. The benzene extract gave 0.1 g (12.5% yield) of white crystals of ω-nitroacetophenone (**6**) (mp 108—109°C). ω-Nitroacetophenone was also easily obtained by the chromatography of the acetal (**7**) on basic alumina, using methanol as the eluent.

ω-Nitroacetophenone Diethyl Acetal (7b), Dipropyl Acetal (7c) and Dibutyl Acetal (7d). Following the procedure described above, pale yellow oils of ω-nitroacetophenone diethyl acetal (bp 91.5—92°C/0.6 mmHg), dipropyl acetal (bp 104—105°C/0.2 mmHg) and dibutyl acetal (bp 120—121°C/0.2 mmHg) were obtained by reactions with sodium ethoxide, *n*-propoxide, *n*-butoxide respectively in 71%, 94.4%, and 77.4% yileds.

Found: C, 60.44; H, 6.95; N, 5.84%. Calcd for $C_{12}H_{17}NO_4$ (**7b**): C, 60.25; H, 7.11; N, 5.85%.

Found: C, 63.30; H, 8.10; N, 5.30%. Calcd for $C_{14}H_{21}NO_4$ (**7c**) C, 62.92; H, 7.86; N, 5.24%.

Found: C, 64.74; H, 7.94; N, 4.86%. Calcd for $C_{16}H_{25}NO_4$ (**7d**): C, 65.08; H, 8.47; N, 4.74%.

ω-Nitroacetophenone Didecyl Acetal (7e). A similar procedure using sodium decyl oxide gave the didecyl acetal (**7e**). It was obtained as a yellow oil after 1-decanol had been removed under reduced pressure from the alkali-insoluble fraction of the reaction product. Though an attempt to purify it by vacuum distillation resulted in failure, it was proved to be almost pure nitroacetal (**7e**) by means of thin-layer chromatography and IR spectrum. The yield of **7e** was calculated to be 83.2% after converting it completely into ω-nitroacetophenone by chromatography on alumina.

ω-Nitroacetophenone Dibenzyl Acetal (7f). The dibenzyl acetal was obtained similarly using sodium benzyl oxide; its yield was calculated to be 82.4% in the manner described for **7e**.

α-Methoxy-β-nitrostyrene (8a). ω-Nitroacetophenone dimethyl acetal (**7a**) (1 g) was heated for 2 hr at 180—200°C under an atmosphere of nitrogen. The yellow oil of **8a**, obtained by thermal decomposition, was purified by distillation under reduced pressure (bp 110°C/0.35 mmHg, 0.81 g, 96% yield).

Found: C, 60.41; H, 5.38; N, 7.71%. Calcd for $C_9H_9NO_3$: C, 60.32; H, 5.02; N, 7.82%.

α-Propoxyl-β-nitrostyrene (8c). On heating 1 g of ω-nitroacetophenone dipropyl acetal (**7c**) at 200°C for 2 hr under an atmosphere of nitrogen, a yellow oil of **8c** was obtained. It was purified by distillation under reduced pressure (bp 115—116°C/0.2 mmHg, 0.73 g, 95% yield).

Found: C, 64.51; H, 6.21; N, 6.54%. Calcd for $C_{11}H_{13}NO_3$: C, 63.76; H, 6.28; N, 6.76%.

α-Benzyloxy-β-nitrostyrene (8f). A similar procedure using 1 g of ω-nitroacetophenone dibenzyl acetal (**7f**) (180°C, 1 hr) afforded an orange-yellow oil of **8f** (bp 153—154°C/0.005 mmHg, 0.42 g).

Found: C, 70.97; H, 5.34; N, 5.03%. Calcd for $C_{15}H_{13}NO_3$: C, 70.58; H, 5.09; N, 5.49%.

ω-Nitroacetophenone Methyl Propyl Acetal (9). To 0.005 mol (0.89 g) of α-methoxy-β-nitrostyrene (**8a**) in 50 m*l* of dry THF, 0.02 mol (1.64 g) of sodium *n*-propoxide was added. After having been refluxed for 1 hr on a water bath, the reaction mixture was treated in the manner described for the preparation of **7a**. A pale yellow oil of **9** was then isolated by distillation under reduced pressure (bp 89—90°C/0.3 mmHg, 0.99 g, 84% yield).

Found: C, 60.58; H, 7.31; N, 6.41%. Calcd for $C_{12}H_{17}NO_4$: C, 60.25; H, 7.11; N, 5.85%.

3-Ferrocenyl-1-(α-methoxybenzyl)cyclopropene (10). To 0.005 mol (1.14 g) of β-bromo-β-nitrostyrene in 50 m*l* of dry THF, 0.005 mol (0.27 g) of sodium methoxide and 0.005 mol (1.06 g) of vinylferrocene were added. After having been refluxed for 20 min on a water bath, the reaction mixture was poured into a mixture of 200 m*l* of water and 30 m*l* of benzene. The benzene layer was separated, washed three times with 100-m*l* portions of water, and dried over magnesium sulfate. After the removal of the solvent, the residue was dissolved in 5 m*l* of a mixture of benzene and *n*-hexane (1 : 1) and chromatographed on Florisil, using a mixture of benzene and *n*-hexane (1 : 1) as the eluent. The second blue fraction gave 0.14 g of 1-ferrocenyl-2-nitroethylene. The third fraction gave yellow-brown crystals of 3-ferrocenyl-1-(α-methoxybenzyl)cyclopropene (**10**) (mp 88—90°C, 0.12 g, 6.9% yield).

Found: C, 72.66; H, 5.61%. Calcd for $C_{21}H_{20}FeO$: C, 73.25; H, 5.81%.

The first fraction consisted of recovered vinylferrocene. The fourth fraction gave pale yellow crystals of the sodium salt of ω-nitroacetophenone, which was found to be produced from its dimethyl acetal during the chromatography, because ω-nitroacetophenone was not detected in the original reaction mixture.

Decomposition of Nitroketones in the Presence of Piperidine and Alcohol. A mixture of 1.3 g (0.005 mol) of (nitroacetyl)ferrocene (**2**), 30 m*l* of absolute methanol, and 4 g of piperidine was stirred at 0°C for 20 hr. Then the reaction mixture was poured into a mixture of 10% hydrochloric acid (100 m*l*) and benzene (30 m*l*), followed by stirring for a few more minutes. The benzene layer was washed three times with 50-m*l* portions of water and then dried over magnesium sulfate. After the benzene had been removed by distillation, the residue was dissolved in 3 m*l* of benzene and chromatographed on alumina, using benzene as the solvent. The first fraction of the chromatography gave 0.92 g (76% yield) of methyl ferrocenecarboxylate.

A similar procedure using ethanol instead of methanol afforded ethyl ferrocenecarboxylate (8% yield). Similarly, the reaction of ω-nitroacetophenone with methanol and ethanol in the presence of piperidine gave methyl benzoate and ethyl benzoate respectively in 54 and 9% yields.

*2 ω-Nitroacetophenone was found to be converted into its sodium salt during chromatography on basic alumina.

BULLETIN OF THE CHEMICAL SOCIETY OF JAPAN VOL. 43 849—855 (1970)

The Formation of Pyrazolo[1,5-*a*]pyrimidine Derivatives[1)]

Isaburo Hori, Koji Saito and Hiroshi Midorikawa

The Institute of the Physical and Chemical Research, Yamato-machi, Kitaadachi-gun, Saitama

(Received August 5, 1969)

The combination reactions of 3-alkyl-2-cyano-3-methoxyacrylic esters (I) and their 3-hydrazino derivatives (II) in the presence of pyridine in alcohol at room temperature mostly gave chain intermediates, whose cyclizations led to the formation of only 2,7-dialkyl-5-hydroxypyrazolo-[1,5-*a*]pyrimidine derivatives. On the other hand, the reaction of Ia (3-Me) with the 5-aminopyrazole derivative (IIIa) obtained by the cyclization of IIa (3-Me) gave 7-hydroxy- and 7-aminopyrazolopyrimidine derivatives in alcohol under reflux *via* an intermediate. The reactions of 2-cyano-3-ethoxycrotononitrile with IIa or IIIa both afforded 7-aminopyrazolopyrimidine derivatives directly.

Many pyrazolo[1,5-*a*]pyrimidines, such as the 7-hydroxy and 7-amino derivatives, have, in recent years, been synthesized by the condensation of 1-ethoxyalkylidene-1,3-dicarbonyl compounds with 5-aminopyrazoles.[2-4)] The present investigation will describe mainly the formation of several 5-hydroxypyrazolo[1,5-*a*]pyrimidine derivatives by means of the condensation of 3-alkyl-2-cyano-3-methoxyacrylic esters (I) with their 3-hydrazino derivatives (II),[5)] obtained previously by the action of hydrazine on I.

The reaction of I with the corresponding 3-hydrazino compounds (II) in the presence of pyridine in ethanol at room temperature afforded first the chain intermediates, bis(2-alkoxycarbonyl-1-alkyl-2-cyanovinyl)hydrazines (IV). The symmetrical structure of IV was confirmed by a study of the NMR spectra, shown in Table 1. The intermediates (IV), upon heating in ethanol or even upon treatment in the presence of an acid or base catalyst, readily cyclized to form only 6-cyano-2,7-dialkyl-5-hydroxypyrazolo[1,5-*a*]pyrimidine-3-carboxylic esters (V), with the loss of one molar equivalent of alcohol; they were unchanged upon heating in acetic acid. The saponification of V(a—c) with aqueous sodium hydroxide gave the corresponding 3,6-dicarboxylic acids (VI), which were then decarboxylated by being heated above the melting point to give 2,7-dialkyl-5-hydroxypyrazolo[1,5-*a*]pyrimidines (VIII). The Vd compound on similar alkaline treatment, was converted into 6-carbamoyl-3-carboxylic acid (VII), which gave VIIIc upon further hydrolysis with diluted sulfuric acid.

Table 1. NMR spectra of bis(2-alkoxycarbonyl-1-alkyl-2-cyanovinyl)hydrazines (IV)*

Compound	R	COOR′	NH
IVa	2.31(3)	1.34(3), 4.26(2)	11.09(1)
IVb	2.31(3)	3.82(3)	11.06(1)
IVc	1.29(3), 2.14(2)	3.81(3)	11.12(1)
IVd	0.96(3), 1.20—1.30(4), 2.10(2)	3.82(3)	11.12(1)

* The chemical shifts of protons are expressed as δ value and deuteriochloroform was used as solvent. Relative peak intensities in parentheses.

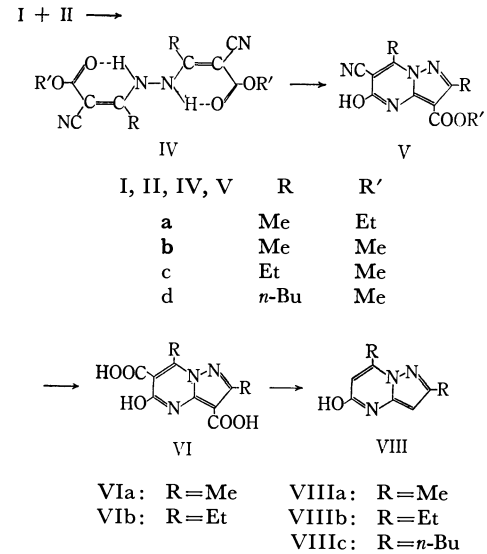

1) Presented in part at the 22nd Annual Meeting of the Chemical Society of Japan, Tokyo, April, 1969.

2) Y. Makisumi, *Chem. Pharm. Bull.* (Tokyo), **10**, 620 (1962).

3) A. Takamizawa and S. Hayashi, *Yakugaku Zasshi*, **83**, 313 (1963); A. Takamizawa, Y. Hamashima, S. Hayashi and R. Kido, *ibid.*, **83**, 745 (1963).

4) S. Hayashi, *ibid.*, **85**, 442 (1965).

5) H. Baba, I. Hori, T. Hayashi and H. Midorikawa, This Bulletin, **42**, 1653 (1969).

The other structures (V′ and V″) considered on the basis of the differential ring closure of IV on dealcoholation can be excluded on the basis of the following chemical evidence.

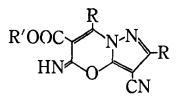

V′

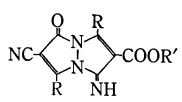

V″

The VIIIa compound was chlorinated, by the action of phosphoryl chloride, to a chloro derivative (IX), which was then catalytically reduced to 2,7-dimethylpyrazolo[1,5-*a*]pyrimidine (X). On the other hand, X could be derived from the condensate (XII) obtained by the reaction of ethyl 2-acetyl-3-ethoxyacrylate (XI) with ethyl 3-methyl-5-aminopyrazole-4-carboxylate (IIIa).

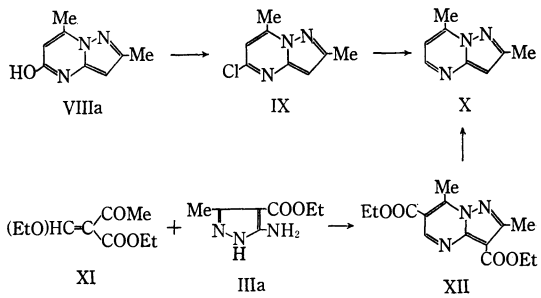

VIIIa IX X

XI IIIa XII

In order to compare this process with the formation of 2,7-dialkyl-5-hydroxypyrazolo[1,5-*a*]pyrimidines described above, the condensation of ethyl 2-cyano-3-methoxycrotonate (Ia) with IIIa, the cyclized compound of IIa, was carried out in ethanol under reflux. The resulting intermediate (XIII) cyclized upon heating in ethanol containing an acid catalyst to give two products, hydroxy- (XIV) and aminopyrazolo[1,5-*a*]pyrimidine derivatives (XV). The hydrolysis and the subsequent decarboxylation of the latter product with diluted sulfuric acid led to the known 7-amino-2,5-dimethylpyrazolo[1,5-*a*]pyrimidine (XVI), prepared by a different procedure.[6] The former gave the 7-hydroxy derivative (XVII) by similar treatment. The compound XVII could also be prepared by acid hydrolysis and by the subsequent decarboxylation of the condensate (XVIII) isolated by means of the reaction of ethyl acetoacetate with IIIa. Isomeric hydroxy derivatives (VIIIa and XVII) were distinguishable from each other by means of IR and NMR spectral comparisons. From these results, it is clear that VIII and its original compound (V) are 2,7-dialkyl-5-hydroxypyrazolo-[1,5-*a*]pyrimidine derivatives.

The reaction of Ic (3-Et) with IIa gave the chain intermediate, 1-(2-cyano-2-ethoxycarbonyl-1-methylvinyl)-2-(2-cyano-1-ethyl-2-methoxycarbonylvinyl)hydrazine (XIX). In its cyclization, two kinds of dealcoholation are possible because XIX has an unsymmetrical structure. In fact, when XIX was heated in ethanol or above the melting point, two condensates, XX and XXI, were obtained as a mixture in approximately a 5 : 3 ratio and were isolated by fractional recrystallization. These two structures, XX and XXI, were confirmed to be methyl 6-cyano-2-ethyl-5-hydroxy-7-methylpyrazolo[1,5-*a*]pyrimidine-3-carboxylate and ethyl 6-cyano-7-ethyl-5-hydroxy-2-methylpyrazolo[1,5-*a*]-pyrimidine-3-carboxylate respectively by means of the molecular formula and by NMR spectral observations.

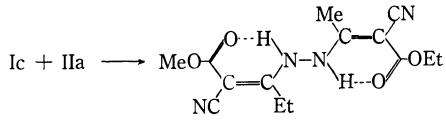

XIX

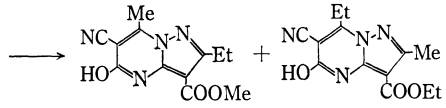

XX XXI

The reaction of Ie (3-Ph) with IIa directly formed two isomeric cyclized products, XXII and

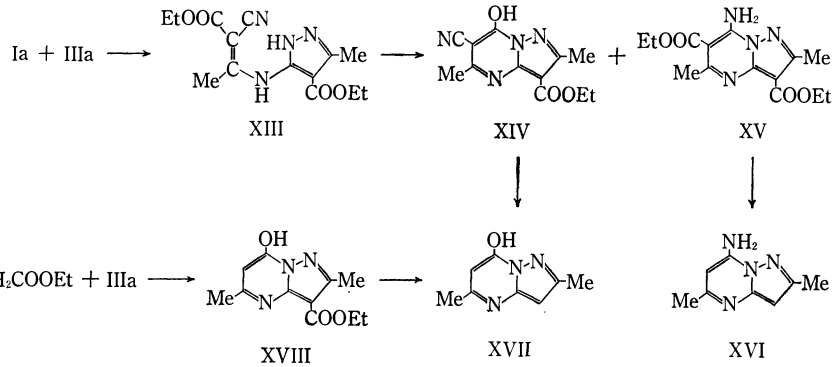

XIII XIV XV

XVIII XVII XVI

6) A. Takamizawa and Y. Hamashima, Japan. 18755 (1965); *Chem. Abstr.*, **64**, 12696g (1966).

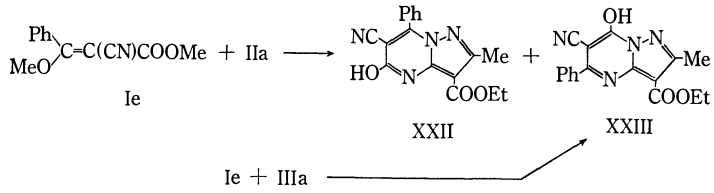

XXIII, but no intermediate could be isolated. The latter product was identical with the condensate prepared from the reaction of Ie with IIIa. Therefore, XXIII is ethyl 6-cyano-7-hydroxy-2-methyl-5-phenylpyrazolo[1,5-*a*]pyrimidine-3-carboxylate, and perhaps XXII is ethyl 6-cyano-5-hydroxy-2-methyl-7-phenylpyrazolo[1,5-*a*]pyrimidine-3-carboxylate.

The reaction of If (3-*i*-Pr) and IIa afforded predominantly IVa and XIII, which were identical with those obtained by the reactions involving the Ia and IIIa related to IIa, as has been described previously, and also a small quantity of methyl 6-cyano-5(or 7)-hydroxy-2,7(or 2,5)-diisopropylpyrazolo[1,5-*a*]pyrimidine-3-carboxylate (XXIV). Though the main products (IVa and XIII) were considered to be formed by the self-condensation of the reactant IIa only, the blank experiment without If did not give any product. These results suggest a certain interaction between the two reactants in this reaction, but the reaction mechanism is not clear.

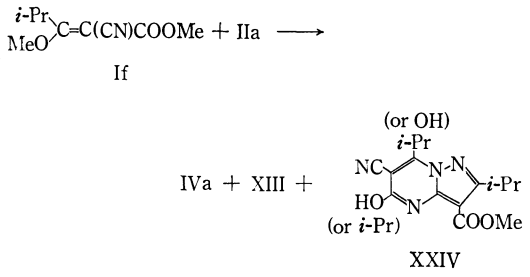

On a similar condensation of 2-cyano-3-ethoxycrotononitrile (XXV) with IIa, the formation of 5-aminopyrazolo[1,5-*a*]pyrimidine derivative can be expected. However, this reaction at room temperature or even below (near 0°C) gave mostly ethyl 2,5-dimethyl-6-cyano-7-aminopyrazolo[1,5-*a*]-pyrimidine-3-carboxylate (XXVI), along with a very small amount of its isomeric substance, mp 301°C (XXVII). The structure of XXVI was proved by the following experiments. The XXVI compound was identical with the product obtained by the reaction of XXV with IIIa in ethanol under reflux, and the treatment of XXVI with diluted sulfuric acid led to the 7-amino-2,5-dimethylpyrazolo[1,5-*a*]pyrimidine (XVI). The minor product (XXVII) seems likely to be the expected 5-amino derivative.

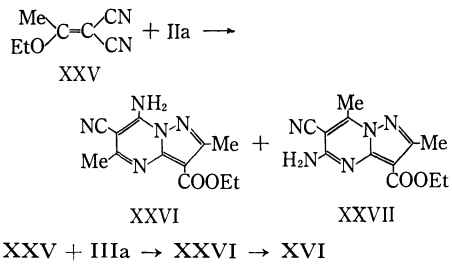

The hydroxyl and amino groups at the 5- and 7-positions of pyrazolo[1,5-*a*]pyrimidine are capable of tautomerism to keto and imino forms respectively. Makisumi[2] has observed, in the IR spectra, that the hydroxyl groups at both positions show the keto form, while the amino group at the 7-position shows the amino form in a neutral medium. The IR data of the pyrazolo[1,5-*a*]pyrimidine derivatives obtained in the present work are presented in Table 2. From these data, it can be said that all the 5-hydroxy compounds exist in the keto form, whereas the 7-hydroxy and 7-amino derivatives exist as tautomeric mixtures in the solid state.

Experimental[7]

Reactions of 3-Alkyl-2-cyano-3-methoxyacrylic Esters (I) with the Corresponding 3-Hydrazino Compounds (II). To a solution of I (3 mmol) and II (3 mmol) dissolved in ethanol at room temperature, a few drops of pyridine were added, and then the mixture was allowed to stand overnight at the same temperature. The precipitate which formed was separated by filtration, washed with ethanol, and recrystallized to give bis(2-alkoxycarbonyl-1-alkyl-2-cyanovinyl) hydrazines (IV) as colorless crystals. The results are given in Table 3.

Cyclization of IV; 6-Cyano-2,7-dialkyl-5-hydroxypyrazolo[1,5-*a*]pyrimidine-3-carboxylic Esters (V). *a*) A mixture of IV in ethanol was refluxed; the IV soon dissolved, and then crystals began to precipitate. After refluxing for 4 hr and cooling, the crystals formed were collected by filtration, washed with methanol,

7) All the melting points are uncorrected. The IR spectra were measured with a Shimadzu 27A spectrophotometer in Nujol mulls. The NMR spectra were obtained with a Nihon-denshi JNM-C-60 high-resolution NMR spectrometer (60 MHz), using tetramethylsilane as the internal reference; the chemical shifts of the protons are presented in terms of δ values; s: singlet, bs: broad singlet, d: doublet, t: triplet, q: quartet, sep: septet, m: multiplet.

Table 2. Characteristic IR data of hydroxy- and aminopyrazolo-[1,5-*a*]pyrimidine derivatives (ν cm^{-1} in Nujol)

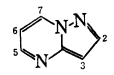

	5-Hydroxy compound				NH	C≡N	C(=O)OR	C=O	
	C_2	C_7	C_3	C_6					
Va	Me	Me	COOEt	CN	3135	2232	1701	1689	1631
Vb	Me	Me	COOMe	CN	3125	2232	1724	1669	1629
Vc	Et	Et	COOMe	CN	3165	2237	1736	1669	1631
Vd	*n*-Bu	*n*-Bu	COOMe	CN	3145	2242	1730	1667	1616
XX	Et	Me	COOMe	CN	3135	2227	1724	1667	1616
XXI	Me	Et	COOEt	CN	3145	2227	1727	1669	1621
XXII	Me	Ph	COOEt	CN	3155	2227	1724	1667	1621
VIIIa	Me	Me	H	H				1701	1587
VIIIb	Et	Et	H	H				1672	1590
VIIIc	*n*-Bu	*n*-Bu	H	H				1669	1587

	7-Hydroxy compound				OH and NH	C≡N	C(=O)OR	C=O	
	C_2	C_5	C_3	C_6					
XIV	Me	Me	COOEt	CN	3145 3058	2227	1695	1678	1618
XVII	Me	Me	H	H	3155 3067			1667	1623
XVIII	Me	Me	COOEt	H	3521 3236		1724	1704	1639
XXIII	Me	Ph	COOEt	CN	3289	2232	1706	1689	1626

	7-Amino compound				NH_2 and NH	C≡N	C(=O)OR		
	C_2	C_5	C_3	C_6					
XV	Me	Me	COOEt	COOEt	3367 3257		1695 1669		1616
XXVI	Me	Me	COOEt	CN	3367 3185 3135	2222	1692		1618
XVI	Me	Me	H	H	3390 3226 3115				1639

Table 3. Reactions of I with the corresponding 3-hydrazino compounds (II)

Product	Mp °C (dec)	Yield %	Recryst. solvent	Formula	Calcd, %			Found, %		
					C	H	N	C	H	N
IVa	183	60	chloroform-ethanol	$C_{14}H_{18}O_4N_4$	54.89	5.92	18.29	54.79	5.72	18.45
IVb	207	54	acetone	$C_{12}H_{14}O_4N_4$	51.79	5.07	20.14	51.77	5.26	20.32
IVc	171—172	56	chloroform-ethanol	$C_{14}H_{18}O_4N_4$	54.89	5.92	18.29	54.65	5.74	18.17
IVd	127—130	37	ethanol	$C_{18}H_{26}O_4N_4$	59.65	7.23	15.46	59.71	7.04	15.55

Table 4. Products obtained by cyclization of IV according to the method *a*)

Product	Mp, °C	Formula	Calcd, %			Found, %		
			C	H	N	C	H	N
Va	227—228	$C_{12}H_{12}O_3N_4$	55.38	4.65	21.53	55.15	4.55	21.66
Vb	261—262	$C_{11}H_{10}O_3N_4$	53.66	4.09	22.76	53.90	4.30	22.54
Vc	229—231	$C_{13}H_{14}O_3N_4$	56.93	5.15	20.43	56.67	4.85	20.44
Vd	195—196	$C_{17}H_{22}O_3N_4$	61.80	6.71	16.96	61.58	6.62	16.80

and recrystallized from chloroform-methanol to afford V as colorless needles. The yields were 80—90%. The products (V) obtained are listed in Table 4.

b) To a mixture of 0.61 g of IVa in 40 m*l* of ethanol, 0.41 g of concentrated hydrochloric acid was added, and then the mixture was refluxed for 2 hr. The resulting crystals were separated by filtration to give 0.38 g of colorless needles, mp 228°C, which did not

show any depression when the needles were mixed with the Va obtained above. The mother layer was concentrated to dryness under reduced pressure, and to the residue 15% hydrochloric acid was added. The solid precipitated was filtered and washed with water to give 0.11 g of a colorless solid, which was found to be a mixture of the starting substance (IVa) and Va by a comparison of their IR spectra. The filtrate did not give any precipitate after the solution had been made alkaline with sodium carbonate.

c) The treatment of 0.61 g of IVa with 3 m*l* of acetic acid at 100°C for 3 hr resulted in the recovery of 0.50 g (90%) of the starting substance.

Hydrolysis of V. *a*) A mixture of 0.26 g of Va in 2.5 m*l* of 20% aqueous sodium hydroxide was heated under reflux for 4.5 hr, thus producing a clear solution. After cooling, the solution was diluted with water and acidified with 15% hydrochloric acid. The precipitate formed was separated by filtration, washed with water, and recrystallized from acetone-water to afford colorless needles of 2,7-dimethyl-5-hydroxypyrazolo[1,5-*a*]pyrimidine-3,6-dicarboxylic acid (VIa), mp 243—244°C (dec); yield, 0.17 g (67%).

Found: C, 47.78; H, 3.45; N, 16.85%. Calcd for $C_{10}H_9O_5N_3$: C, 47.81; H, 3.61; N, 16.73%.

b) From 0.24 g of Vb, 0.18 g of VIa was obtained by the same procedure. Found: N, 16.78%.

c) A suspension of 0.50 g of Vc in 5 m*l* of 20% aqueous sodium hydroxide was refluxed for 5 hr. Water was then added to the reaction mixture, and it was acidified with 15% hydrochloric acid. The precipitate thus formed was collected by centrifugation and recrystallized from acetone to give 0.31 g of colorless needles of 2,7-diethyl-5-hydroxypyrazolo[1,5-*a*]pyrimidine-3,6-dicarboxylic acid (VIb), mp 207°C (dec).

Found: C, 51.32; H, 4.90; N, 15.04%. Calcd for $C_{12}H_{13}O_5N_3$: C, 51.61; H, 4.69; N, 15.05%.

d) Compound Vd (0.25 g) was treated as above (*a*) with 3 m*l* of 20% aqueous sodium hydroxide to form 0.20 g of colorless crystals of 2,7-di-*n*-butyl-6-carbamoyl-5-hydroxypyrazolo[1,5-*a*]pyrimidine-3-carboxylic acid (VII), mp 210°C (dec).

Found: C, 57.21; H, 6.34; N, 16.56%. Calcd for $C_{16}H_{22}O_4N_4$: C, 57.47; H, 6.63; N, 16.76%.

2,7-Dialkyl-5-hydroxypyrazolo[1,5-*a*]pyrimidine (VIII). *a*) Compound VIa (2.25 g) was heated on an oil bath at 250°C until the evolution of carbon dioxide ceased. The crude substance thus formed was treated with charcoal in methanol. After the methanol had been concentrated, the residue afforded 1.25 g of colorless needles of pure VIIIa, mp 244—245°C, by the recrystallization from acetone. NMR in CF_3COOH: 2.72 (s, C_2–Me), 2.85 (s, C_7–Me), 6.63 (overlap, C_3– and C_6–H).

Found: C, 58.72; H, 5.52; N, 25.56%. Calcd for $C_8H_9ON_3$: C, 58.88; H, 5.56; N, 25.75%.

b) At 210—215°C, 0.30 g of VIb was heated. After the evolution of carbon dioxide had ceased, this mixture was treated as above. The residue thus obtained was recrystallized from acetone to yield 0.18 g of light yellow needles of VIIIb, mp 125—125.5°C. NMR in CF_3COOH: 1.47 (t) and 3.02(q) (C_2–Et), 1.51 (t) and 3.14(q) (C_7–Et), 6.63 (overlap, C_3– and C_6–H).

Found: C, 62.62; H, 6.59; N, 21.74%. Calcd for $C_{10}H_{13}ON_3$: C, 62.80; H, 6.85; N, 21.98%.

c) A mixture of 0.20 g of VII and 3 m*l* of 50% sulfuric acid was heated under reflux for 2 hr to make it a clear solution. After cooling, water was added to the mixture, and the resulting crystals were filtered, washed with water, and dried in a desiccator. Colorless needles of VIIIc were thus obtained; mp 82—83°C; yield, 0.14 g. NMR in CF_3COOH: 1.04(t), 1.08(t), 1.35—2.05(m), 3.03(t) and 3.15(t) (C_2– and C_7-*n*-Bu), 6.60 (overlap, C_3– and C_6–H).

Found: C, 67.79; H, 8.77; N, 17.00%. Calcd for $C_{14}H_{21}ON_3$: C, 67.98; H, 8.56; N, 16.99%.

5-Chloro-2,7-dimethylpyrazolo[1,5-*a*]pyrimidine (IX). A solution of VIIIa (0.55 g) in 7 m*l* of phosphorus oxychloride was refluxed for 4 hr. After the excess phosphorus oxychloride had then been removed under reduced pressure, the residual syrup was decomposed with crushed ice. The precipitate thus obtained was collected by filtration, washed with water, and recrystallized from ethanol to form 0.50 g of fine, light yellow needles of IX, mp 100—101°C. NMR in $CHCl_3$: 2.45 (s, C_2–Me), 2.66 (s, C_7–Me), 6.30 (s, C_3–H), 6.50 (s, C_6–H).

Found: C, 52.87; H, 4.51; N, 23.13%. Calcd for $C_8H_8N_3Cl$: C, 52.90; H, 4.43; N, 23.16%.

Reduction of IX; 2,7-Dimethylpyrazolo[1,5-*a*]pyrimidine (X). A suspension of 0.18 g of IX and 0.08 g of sodium acetate in 10 m*l* of ethanol was reduced over 0.08 g of 5% palladised charcoal, and then one equivalent mole of hydrogen was taken up. After the catalyst had been removed by filtration, the solution was concentrated to dryness under reduced pressure, and the residue was dissolved in water and extracted with chloroform. The chloroform extracts were dried over sodium sulfate, and the chloroform was removed to give a colorless oil which solidified after cooling. The recrystallization of this solid from light petroleum-benzene gave 0.12 g of hygroscopic, colorless needles of X, mp 35—36°C. NMR in $CDCl_3$: 2.53 (s, C_2–Me), 2.73 (s, C_7–Me), 6.33 (s, C_3–H), 6.46 (d, J=4.2 Hz, C_6–H), 8.17 (d, J=4.2 Hz, C_5–H).

Found: C, 64.95; H, 6.17; N, 28.13%. Calcd for $C_8H_9N_3$: C, 65.28; H, 6.16; N, 28.55%.

Reaction of Ethyl 2-Acetyl-3-ethoxyacrylate (XI) with IIIa. A mixture of 1.86 g of XI and 1.69 g of IIIa in 15 m*l* of acetic acid was heated on a steam bath for 2.5 hr. After the reaction mixture had been diluted with water, the white precipitate formed was separated by filtration and recrystallized from ethanol-water (3 : 1) to give 2.20 g of colorless needles of diethyl 2,7-dimethylpyrazolo[1,5-*a*]pyrimidine-3,6-dicarboxylate (XII), mp 95—97°C. IR: 1727, 1698, 1610 cm^{-1}.

Found: C, 57.73; H, 5.54; N, 14.59%. Calcd for $C_{14}H_{17}O_4N_3$: C, 57.72; H, 5.88; N, 14.43%.

Hydrolysis of XII. A mixture of 1.00 g of XII and 5 m*l* of 50% sulfuric acid was refluxed for 5 hr. After cooling, the mixture was basified with 20% aqueous sodium hydroxide, and then the violet-brown oil thus formed was extracted with chloroform. The chloroform layer was dried over sodium sulfate and chromatographed on alumina. The benzene eluate was recrystallized from light petroleum-benzene to give 0.58 g of hygroscopic, colorless needles, mp 35—36°C, which did not show any depression when the needles were mixed with X; the IR spectrum of the product was identical with that of X.

Reaction of Ethyl 2-Cyano-3-methoxycrotonate (Ia) with IIIa. A solution of 1.10 g of Ia and 1.10 g

of IIIa in 20 m*l* of ethanol was heated under reflux for 5 hr and then concentrated to about 5 m*l* under reduced pressure. After cooling, the colorless crystals thus obtained were recrystallized twice from ethanol to give 0.80 g of colorless needles of ethyl 2-cyano-3-(4-ethoxycarbonyl-3-methyl-5-pyrazolylamino) crotonate (XIII), mp 175°C. IR: 3215, 3115, 2217, 1704, 1678 cm^{-1}.

Found: C, 54.61; H, 5.77; N, 18.39%. Calcd for $C_{14}H_{18}O_4N_4$: C, 54.89; H, 5.92; N, 18.29%.

Cyclization of XIII; XIV and XV. To a solution of 0.30 g of XIII in 60 m*l* of ethanol, 4 m*l* of concentrated hydrochloric acid was added drop by drop, and then the mixture was refluxed for 3 hr. The solution was concentrated under reduced pressure and diluted with 40 m*l* of water, and then the white precipitate thus formed was separated by filtration. The recrystallization of the precipitate from ethanol gave 0.15 g of colorless needles of ethyl 6-cyano-2,5-dimethyl-7-hydroxypyrazolo-[1,5-*a*]pyrimidine-3-carboxylate (XIV), mp 262—263°C. NMR in CF_3COOH: 2.80 (s, C_2–Me), 2.97 (s, C_5–Me), 1.55(t) and 4.59(q) (COOEt).

Found: C, 55.36; H, 4.36; N, 21.45%. Calcd for $C_{12}H_{12}O_3N_4$: C, 55.38; H, 4.65; N, 21.53%.

The mother layer of the reaction was made basic with aqueous sodium carbonate. The precipitate thus formed was washed with water, dried in a desiccator, and then recrystallized from ethanol-acetic acid to give 0.09 g of colorless needles of diethyl 7-amino-2,5-dimethylpyrazolo[1,5-*a*]pyrimidine-3,6-dicarboxylate (XV), mp 175°C. NMR in CF_3COOH: 2.76 (s, C_2–Me), 3.21 (s, C_5–Me), 1.55(t), 4.60(q) and 4.65(q)(2COOEt), 8.80(bs) and 10.25(bs) (NH_2).

Found: C, 54.94; H, 5.71; N, 18.48%. Calcd for $C_{14}H_{18}O_4N_4$: C, 54.89; H, 5.92; N, 18.29%.

Hydrolysis of XIV; 2,5-Dimethyl-7-hydroxypyrazolo[1,5-*a*]pyrimidine (XVII). A mixture of 0.50 g of XIV and 10 m*l* of 50% sulfuric acid was heated under reflux for 3 hr; then, after cooling, the pH of the reaction mixture was adjusted with ammonium hydroxide to about 5. The precipitate thus formed was separated by filtration, washed with water, and recrystallized from ethanol to give 0.32 g of colorless needles of XVII, mp 250—251°C. NMR in CF_3COOH: 2.65 (s, C_2–Me), 2.74 (s, C_5–Me), 6.34 (s, C_3–H), 6.61 (s, C_6–H).

Found: C, 58.97; H, 5.49; N, 25.52%. Calcd for $C_8H_9ON_3$: C, 58.88; H, 5.56; N, 25.75%.

Reaction of Ethyl Acetoacetate with IIIa. A mixture of 0.60 g of ethyl acetoacetate and 0.80 g of IIIa in 1.5 m*l* of acetic acid was refluxed for 2.5 hr. After the mixture had then been diluted with water, the precipitate thus obtained was collected by filtration, washed with water, and dried in a desiccator. The recrystallization of the precipitate from ethanol and benzene afforded 0.75 g of colorless needles of ethyl 2,5-dimethyl-7-hydroxypyrazolo[1,5-*a*]pyrimidine-3-carboxylate (XVIII), mp 150—151°C. NMR in CF_3COOH: 2.75 (s, C_2–Me), 2.95 (s, C_5–Me), 6.43 (s, C_6–H), 1.55(t) and 4.63(q) (COOEt).

Found: C, 55.91; H, 5.47; N, 17.91%. Calcd for $C_{11}H_{13}O_3N_3$: C, 56.16; H, 5.57; N, 17.86%.

Hydrolysis of XVIII. A mixture of 0.50 g of XVIII and 10 m*l* of 50% sulfuric acid was heated under reflux for 2.5 hr. After cooling, the mixture was treated with ammonium hydroxide to adjust its pH to about 5. The precipitate thus formed was washed with water and then recrystallized from ethanol to give 0.38 g of colorless needles, mp 250—251°C, which did not show any depression when the needles were mixed with the XVII obtained above; the IR and NMR spectra of the product were identical with those of XVII.

Hydrolysis of XV; 7-Amino-2,5-dimethylpyrazolo[1,5-*a*]pyrimidine (XVI). A mixture of 0.50 g of XV and 10 m*l* of 50% sulfuric acid was refluxed for 3.5 hr; then, after cooling, the mixture was diluted with 10 m*l* of water and basified with ammonium hydroxide to give a white precipitate. The recrystallization of the precipitate from ethyl acetate afforded 0.33 g of colorless needles, mp 198—200°C, which did not show any depression on admixture with an authentic sample of 7-amino-2,5-dimethylpyrazolo[1,5-*a*]pyrimidine (XVI).[6] NMR in CF_3COOH: 2.64 (s, C_2–Me), 2.69 (s, C_5–Me), 6.47 (overlap, C_3– and C_6–H), 8.30 (bs, NH_2).

Reaction of Methyl 2-Cyano-3-ethyl-3-methoxyacrylate (Ic) with IIa. Into a solution of 1.32 g of Ic and 1.32 g of IIa dissolved in ethanol at room temperature, a few drops of pyridine were added. After the solution had then been allowed to stand overnight at room temperature, the white precipitate thus formed was collected by filtration and washed with ethanol. The recrystallization of this from chloroform-ethanol (1 : 2) gave 1.36 g of colorless needles of 1-(2-cyano-2-ethoxycarbonyl-1-methylvinyl)-2-(2-cyano-1-ethyl-2-methoxycarbonylvinyl)hydrazine (XIX), mp 165°C (dec). IR: 3165, 2217, 1689, 1672, 1587 cm^{-1}. NMR in $CDCl_3$: 2.33 (s, vinyl Me), 1.28(t) and 2.64(q) (vinyl Et), 3.82 (s, COOMe), 1.34(t) and 4.25(q) (COOEt), 10.95 (s, NH), 11.07 (s, NH).

Found: C, 54.60; H, 5.87; N, 18.39%. Calcd for $C_{14}H_{18}O_4N_4$: C, 54.89; H, 5.92; N, 18.29%.

Cyclization of XIX; XX and XXI. A mixture of 0.55 g of XIX in 40 m*l* of ethanol was heated under reflux; soon the XIX completely dissolved, and then a white precipitate was separated out. The whole mixture was refluxed for 3 hr. After cooling, the precipitate formed was collected by filtration. The treatment of this with fresh boiling ethanol gave 0.16 g of insoluble methyl 6-cyano-2-ethyl-5-hydroxy-7-methylpyrazolo-[1,5-*a*]pyrimidine-3-carboxylate (XX) in hot ethanol as colorless prisms, mp 258—260°C. NMR in CF_3COOH: 1.40(t) and 3.16(q) (C_2–Et), 3.09 (s, C_7–Me), 4.15 (s, COOMe).

Found: C, 55.21; H, 4.68; N, 21.54%. Calcd for $C_{12}H_{12}O_3N_4$: C, 55.38; H, 4.65; N, 21.53%.

The mother layer of the boiling-ethanol treatment was concentrated to give colorless crystals, the recrystallization of which from dioxane afforded 0.21 g of colorless needles of ethyl 6-cyano-7-ethyl-5-hydroxy-2-methylpyrazolo[1,5-*a*]pyrimidine-3-carboxylate (XXI), mp 209—210°C. NMR in CF_3COOH: 2.73 (s, C_2–Me), 1.52(t) and 3.45(q) (C_7–Et), 1.56(t) and 4.62(q) (COOEt).

Found: C, 56.70; H, 5.01; N, 20.17%. Calcd for $C_{13}H_{14}O_3N_4$: C, 56.93; H, 5.15; N, 20.43%.

Reaction of Methyl 2-Cyano-3-methoxycinnamate (Ie) with IIa. Compound Ie (1.08 g) and 0.84 g of IIa were dissolved in 35 m*l* of ethanol by slightly warming the solution, and to this a few drops of pyridine were added; then the mixture was allowed to stand at room temperature for 4 days. The resulting white precipitate was separated by filtration, washed with ethanol, and recrystallized from ethanol to give 0.38 g of

colorless needles of ethyl 6-cyano-5-hydroxy-2-methyl-7-phenylpyrazolo[1,5-*a*]pyrimidine-3-carboxylate (XXII), mp 227—228°C. NMR in CF_3COOH: 2.67 (s, C_2–Me), 7.47 (m, C_7–Ph), 1.53(t) and 4.66(q) (COOEt).

Found: C, 63.27; H, 4.11; N, 17.77%. Calcd for $C_{17}H_{14}O_3N_4$: C, 63.35; H, 4.38; N, 17.38%.

The mother layer of the reaction was concentrated to a small volume under reduced pressure. After the residue had been stored in an ice-box, the precipitate was separated out and washed with ethanol. The recrystallization of this from ethanol gave 0.60 g of the hydrate of ethyl 6-cyano-7-hydroxy-2-methyl-5-phenylpyrazolo[1,5-*a*]pyrimidine-3-carboxylate (XXIII) as colorless plates, mp 144—146°C.

Found: C, 61.16; H, 4.29; N, 16.95%. Calcd for $C_{17}H_{14}O_3N_4 \cdot 1/2H_2O$: C, 61.62; H, 4.56; N, 16.91%.

The water of crystallization could be driven off by heating at 110°C in reduced pressure; XXIII was thus obtained as colorless crystals, mp 190—191°C. NMR in CF_3COOH: 2.90 (s, C_2–Me), 7.80 (m, C_5–Ph), 1.63(t) and 4.67(q)(COOEt).

Found: C, 63.46; H, 4.37; N, 17.58%. Calcd for $C_{17}H_{14}O_3N_4$: C, 63.35; H, 4.38; N, 17.38%.

Reaction of Ie with IIIa. A mixture of 0.54 g of Ie and 0.42 g of IIIa in 5 m*l* of ethanol was heated under reflux for 2 hr. The ethanol was removed under reduced pressure, and the residue was washed with ethanol and recrystallized twice from dioxane-water to give 0.58 g of colorless needles, mp 144—145°C. The heating of the needles at 110°C under reduced pressure afforded colorless crystals, mp 190—191°C, which did not show any depression when the crystals were mixed with the XXIII obtained above; the IR and NMR spectra of the product were identical with those of XXIII.

Reaction of Methyl 2-Cyano-3-isopropyl-3-methoxyacrylate (If) with IIa. To a solution of 2.75 g of If and 2.54 g of IIa in 40 m*l* of ethanol, a few drops of pyridine were added, and then the solution was allowed to stand at room temperature overnight. The precipitate thus formed was collected by filtration, and washed with ethanol; the recrystallization of this from chloroform-ethanol gave 1.25 g of colorless needles, mp 183°C (dec), which were proved to be identical with the IVa obtained from the reaction of Ia and IIa by a mixed-melting-point measurement and by an IR spectral comparison. The second crop was 0.05 g. The mother layer of the reaction was evaporated under reduced pressure, and the residue was dissolved in water and acidified with 15% hydrochloric acid. The precipitate thus formed was collected and recrystallized from ethanol to give 0.32 g of colorless crystals, mp 175°C. This was found to be identical with XIII obtained from the reaction of Ia with IIIa by a mixed-melting-point measurement and by an IR spectral comparison.

The filtrate of the acidic solution contained an oily substance which solidified after having been stored in an ice-box. The solid thus separated was washed with water, dried in a desiccator, and recrystallized from ethanol to give 0.43 g of colorless needles of methyl 6-cyano-5 (or 7)-hydroxy-2,7-(or 2,5)-diisopropylpyrazolo[1,5-*a*]pyrimidine-3-carboxylate (XXIV), mp 164—165°C. IR: 3279, 2212, 1724, 1695, 1610 cm^{-1}. NMR in $CDCl_3$: 1.41(t), 1.43(t) and 3.49(sep) (2 *i*-Pr), 3.45 (s, COOMe).

Found: C, 59.74; H, 5.69; N, 18.85%. Calcd for $C_{15}H_{18}O_3N_4$: C, 59.59; H, 6.00; N, 18.53%.

Blank Experiment without If in the Above Reaction. To a solution of 0.63 g of IIa in 10 m*l* of ethanol, a few drops of pyridine were added; the solution did not give any precipitate after having been allowed to stand at room temperature for 10 days. The evaporation of the solution resulted in the recovery of the starting substance.

Reaction of 2-Cyano-3-ethoxycrotononitrile (XXV) with IIa. *a*) To a solution of XXV (0.68 g) and 0.84 g of IIa dissolved in 25 m*l* of methanol at room temperature, a few drops of pyridine were added, and then the mixture was allowed to stand at the same temperature for 3 days. The precipitate thus formed was collected by filtration and recrystallized from acetone to afford 0.09 g of light brown plates of, probably, ethyl 5-amino-6-cyano-2,7-dimethylpyrazolo[1,5-*a*]pyrimidine-3-carboxylate (XXVII), mp 301°C (dec). IR: 3448, 3247, 3145, 2227, 1698, 1642, 1610 cm^{-1}. NMR in CF_3COOH: 2.73 (s, C_2–Me), 3.18 (s, C_7–Me), 1.55(t) and 4.60(q) (COOEt), 8.25 (bs, NH_2).

Found: C, 55.33; H, 4.89; N, 26.71%. Calcd for $C_{12}H_{13}O_2N_5$: C, 55.59; H, 5.05; N, 27.02%.

The mother layer of the reaction was evaporated under reduced pressure, and the residue thus obtained was recrystallized twice from ethanol-water to give 1.03 g of fine, colorless needles of ethyl 7-amino-6-cyano-2,5-dimethylpyrazolo[1,5-*a*]pyrimidine-3-carboxylate (XXVI), mp 281—282°C. NMR in CF_3COOH: 2.80 (s, C_2–Me), 3.15 (s, C_5–Me), 1.58(t) and 4.66(q) (COOEt), 9.05 (bs, NH_2).

Found: C, 55.70; H, 5.03; N, 26.94%. Calcd for $C_{12}H_{13}O_2N_5$: C, 55.59; H, 5.05; N, 27.02%.

b) When the above reaction was carried out near 0°C, the same results as in *a*) were obtained.

Reaction of XXV with IIIa. A mixture of 0.68 g of XXV and 0.84 g of IIIa in 20 m*l* of ethanol was heated under reflux for 7 hr. After cooling, the precipitate thus obtained was collected by filtration, washed with ethanol, and recrystallized twice from ethanol-water to form 1.17 g of colorless needles, mp 282—283°C, which were proved to be identical with the foregoing XXVI by a mixed-melting-point determination and by IR and NMR spectral comparisons.

Found: C, 55.64; H, 5.01; N, 27.08%.

Hydrolysis of XXVI. Compound XXVI (0.50 g) was dissolved in 10 m*l* of 50% sulfuric acid, and then the mixture was refluxed for 4 hr. After cooling, the reaction mixture was diluted with water and basified with ammonium hydroxide. The precipitate thus formed was collected, washed with water, and dried in a desiccator. The recrystallization of this from ethyl acetate gave 0.35 g of colorless needles, mp 199—201°C, which did not show any depression on admixture with the XVI obtained from the hydrolysis of XV.

BULLETIN OF THE CHEMICAL SOCIETY OF JAPAN VOL. 43 856—860 (1970)

Reactions of Nitrones with Free Radicals. I. Radical 1,3-Addition to Nitrones

Michiko IWAMURA and Naoki INAMOTO

Department of Chemistry, Faculty of Science, The University of Tokyo, Hongo, Bunkyo-ku, Tokyo

(Received August 16, 1969)

Reactions of the aldonitrones with α,α′-azobisisobutyronitrile or dimethyl α,α′-azobisisobutyrate gave trisubstituted hydroxylamines as addition products, whose structures were determined to be radical 1,3-addition products to the nitrones. Reactions of *N*-benzyl-α-phenylnitrone with di-*t*-butyl peroxide and aralkyl hydrocarbons possessing at least one α-hydrogen atom gave similar 1,3-adducts and substituted *N*-benzylaldonitrones. Reaction of α,*N*-diphenylnitrone with phenylazotriphenylmethane gave similarly α,α,*N*-triphenylnitrone. Mechanisms for the formation of these products were discussed.

Inamoto and Simamura found that the reaction of α,α′-azobisisobutyronitrile (AIBN) with nitrobenzene at 100°C gave *N*,*O*-bis(1-cyano-1-methylethyl)phenylhydroxylamine, acetone and hydrogen cyanide in 3% yields.[1,2] In the reaction of AIBN with azoxybenzene or *N*,*N*-dimethylaniline *N*-oxide at 100°C, azobenzene or *N*,*N*-dimethylaniline was isolated in 1—1.5% yield, together with acetone (1—1.5%) and hydrogen cyanide.[3] From the results it was considered that the free radicals generated from AIBN are able to abstract the oxygen atom from some N→O bonds by addition-elimination mechanism.

In connection with the results, the reactions of AIBN or related compounds with aldonitrones were attempted. It was found that two 1-substituted 1-methylethyl radicals add to the nitrones in good yields.[4] This paper describes the addition reactions of free radicals to nitrones in detail.

Results and Discussion

Addition of Free Radicals Generated from Aliphatic Azo Compounds. When AIBN was decomposed in xylene containing an equimolar amount of α,*N*-diphenylnitrone (I) at 90—110°C, an addition product (IV) was obtained in 63% yield. Similar addition products were obtained in the reactions of *N*-benzyl-α-phenylnitrone (II) and glyoxal-bis-*N*-phenylnitrone (III). In the case of the dinitrone (III), an addition product to only one nitrone group was produced even with an excess of AIBN. Dimethyl α,α′-azobisisobutyrate (MAIB) behaved similarly as a radical source under similar conditions. The results are summarized in Table 1.

Table 1. Addition products of 1-substituted 1-methylethyl radicals to nitrones

	Addition product		Elemental analysis (%)			
	%	Mp (°C)		C	H	N
IV	63	142.5—143.5	Found	75.52	6.86	12.65
			Calcd	75.64	6.95	12.65
V	46	114—115	Found	75.94	7.54	12.09
			Calcd	76.05	7.25	12.10
VI	50	55—56	Found	69.47	7.56	3.69
			Calcd	69.15	7.32	3.51
VII	40	51—52	Found	69.56	7.53	3.40
			Calcd	69.71	7.56	3.39
VIII	15	134—134.5	Found	70.24	6.55	15.17
			Calcd	70.18	6.43	14.88

In these reactions, it is required that the nitrones are stable under the reaction conditions. However, most of the nitrones are susceptible to heat and

$$RCH{=}N(\rightarrow O)R' + 2Me_2\dot{C}X \rightarrow RCH(CMe_2X)\text{–}NR'\text{–}OCMe_2X$$

I: R=R′=Ph
II: R=Ph, R′=PhCH$_2$
III: R=PhN(→O)=CH–, R′=Ph

IV: R=R′=Ph, X=CN
V: R=Ph, R′=PhCH$_2$, X=CN
VI: R=R′=Ph, X=CO$_2$Me
VII: R=Ph, R′=PhCH$_2$, X=CO$_2$Me
VIII: R=PhN(→O)=CH–, R′=Ph, X=CN

1) N. Inamoto and O. Simamura, *J. Org. Chem.*, **23**, 408 (1958).
2) N. Inamoto, *Yuki Gosei Kagaku Kyokai Shi*, **16**, 420 (1958).
3) N. Inamoto, *ibid.*, **17**, 170 (1959).
4) Preliminary report: M. Iwamura and N. Inamoto, This Bulletin, **40**, 702 (1967).

undergo isomerization to amides or decomposition.[5] Therefore, the aliphatic aldonitrones were not used.

Structure of Addition Products. Elemental analyses (see Table 1), NMR and IR spectra of the addition products (IV—VIII) support the proposed structures, trisubstituted hydroxylamines. For example, the NMR spectrum of IV in deuteriochloroform showed signals at δ 1.14 (3H), 1.35 (3H), 1.75 (3H), 1.95 (3H), 3.50 (1H, broad), 6.88, 7.05, 7.08 (5H in total), and 7.19 (5H), and the IR spectrum in KBr disk showed absorption peaks at 2220 (CN), 1592, 1277, 1220, 1198, 1160, 1083, 1030, 1015, 970, 950, 925, 915, 902, 890, 764, 740, 713, and 700 cm^{-1} (phenyl and trisubstituted hydroxylamine[6]).

However, some uncertainty remains in the cases of IV, V and VIII for the following reason. It is known that the decomposition of AIBN gives the keteneimine (IX) as an intermediate.[7,8] The nitrones are well known as 1,3-dipolar substrates.[9] If the nitrones react with IX by 1,3-dipolar cycloaddition, it would be expected to yield a five-membered ring compound such as X, which has the same molecular formula as the radical addition product.

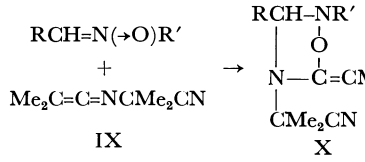

Distinction between the two or more structures was difficult from only the spectral data. Thus dimethyl-*N*-(1-cyano-1-methylethyl)keteneimine (IX) was allowed to react with the nitrone (II) at room temperature for two days. However, only the same compound as the radical addition product (V) was obtained from the reaction mixture, and it was impossible to determine the structure by this method.

The addition product (IV) gave hydrogen cyanide and acetone by heating with hydrochloric acid in ethanol. This fact indicates that one 1-cyano-1-methylethyl group was attached to the oxygen or nitrogen atom. Treatment of the compound (V) with an alkaline hydrogen peroxide gave a nitrile-amide (XI), which was inert to an alkaline hydrogen peroxide even under more vigorous conditions. If the structure (V) is correct, the structure of the nitrile-amide is assumed to be XI, because the 1-cyano-1-methylethyl group bonded to the oxygen atom seems to be sterically more favorable for hydrolysis. These facts support the structures, IV and V, rather than the structure X. However, several attempts to correlate the cyano compound (IV or V) to the methoxycarbonyl compound (VI or VII) were unsuccessful.

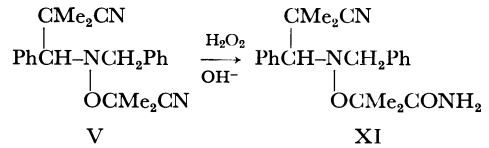

Compound (VI) was reduced with lithium aluminum hydride to a diol (XII). The same treatment of compound (VII) was assumed to afford diol (XIII), but pure substance was not obtained.

1-Methoxycarbonyl-1-methylethyl radicals generated from MAIB can not give a keteneimine type of intermediate. Similar addition products were also obtained by the reactions of MAIB with nitrones. As an example, the NMR spectrum of VI in carbon tetrachloride exhibited signals at δ 0.85 (3H), 1.24 (3H), 1.42 (3H), 1.52 (3H), 2.99 (3H), 3.75 (3H), 4.55 (1H, broad), 6.97 (5H), and 7.10 (5H). Therefore, it is reasonable that the addition products (IV—VIII) are trisubstituted hydroxylamines produced by the 1,3-addition of two radicals to the carbon and oxygen atoms in the nitrone system.

Addition of Other Carbon Radicals. The reaction of *N*-benzyl-α-phenylnitrone (II) with di-*t*-butyl peroxide (DTBP) in *t*-butylbenzene at 135°C for 12 hr gave only the decomposition products and no starting nitrone was recovered. In the aralkyl hydrocarbons possessing at least one α-hydrogen, however, reaction products with radicals were isolated. In these cases, nitrone II was mainly used, because it is considerably stable during heating for a long time. Toluene, ethylbenzene, isopropylbenzene, tetralin and diphenylmethane were used as aralkyl hydrocarbons. These facts show that the nitrones have an ability as a radical scavenger.

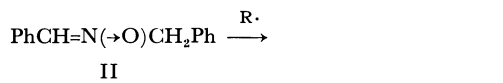

XIVa: R=$PhCH_2$ XVa: R=$PhCH_2$
XIVb: R=PhCHMe XVb: R=PhCHMe
XIVc: R=$PhCMe_2$
XIVd: R=$C_{10}H_{11}$ XVd: R=$C_{10}H_{11}$
($C_{10}H_{11}$: α-tetralyl) XVe: R=Ph_2CH

As the reaction products, an addition product (XIV) and a new aldonitrone (XV) were isolated from the reaction mixture in the cases of most

5) J. Hamer and A. Macaluso, *Chem. Rev.*, **64**, 473 (1964).
6) B. A. Gingras and W. A. Waters, *J. Chem. Soc.*, **1954**, 1920.
7) M. Talât-Erben and S. Bywater, *J. Amer. Chem. Soc.*, **77**, 3710, 3712 (1955).
8) G. S. Hammond, C. S. Wu, D. O. Trapp, J. Warkentin and R. T. Keys, *ibid.*, **82**, 5394 (1960).
9) R. Huisgen, *Angew. Chem.*, **75**, 604, 741 (1963).

aralkyl hydrocarbons described above. However, the new aldonitrone was not isolated in the case of isopropylbenzene, and the addition product derived from diphenylmethane was not detected. The results and elemental analyses of XIV and XV are summarized in Tables 2 and 3.

Table 2. Reaction products of aralkyl radicals to nitrone (II) at 135°C

Radical	Reaction condition*	Addition product (XIV) Yield (%)	Addition product (XIV) Mp (°C)	Nitrone (XV) Yield (%)	Nitrone (XV) Mp (°C)
$PhCH_2\cdot$	a)**	2.6	79—86.5	6.2	152.5—153.5
PhCHMe·	a)	29	oil	17	181—184
	b)	60		5	
$PhCMe_2\cdot$	a)	35	oil	—	
	b)	47		—	
	a)	59	oil	15	148.5—150
	b)	79		8	
$Ph_2CH\cdot$	b)	—		trace	187—189

* a) II (0.01 mol), DTBP (0.03 mol), and RH (25 ml)
b) II (0.01 mol), DTBP (0.02 mol), and RH (0.2 mol)
** At the refluxing temperature

Table 3. Elemental analyses of XIV and XV

		Calcd (%) C	Calcd (%) H	Calcd (%) N	Found (%) C	Found (%) H	Found (%) N
Addition product (XIV)							
XIVa	$C_{28}H_{27}NO$	85.46	6.92	3.56	85.53	7.00	3.53
XIVb	$C_{30}H_{31}NO$	85.47	7.41	3.80	85.43	7.12	3.53
XIVc	$C_{32}H_{35}NO$	85.48	7.85	3.12	85.42	7.98	2.97
XIVd	$C_{34}H_{35}NO$	86.21	7.45	2.96	86.24	7.63	3.02
Nitrone (XV)							
XVa	$C_{21}H_{19}NO$	83.69	6.35	4.65	83.48	6.28	4.63
XVb	$C_{22}H_{21}NO$	83.77	6.71	4.44	83.90	6.54	4.18
XVd	$C_{24}H_{23}NO$	84.42	6.79	4.10	84.45	6.69	3.89
XVe	$C_{27}H_{23}NO$	85.91	6.14	3.71	85.76	5.99	3.60

The addition products (XIV) are determined to be 1,3-radical addition products, trisubstituted hydroxylamines, from the spectral data. All the 1,3-adducts except for that derived from toluene are colorless oils.

The structures of the new aldonitrones (XV) were confirmed by NMR spectra. For instance, the NMR spectrum of XVa shows an AMX spin system (at 60 MHz in $CDCl_3$) in the region of δ 3—5.3 (H_M 3.18, H_A 4.02, H_X 5.05; $J_{AX}=9$, $J_{MX}=5$, $J_{AM}=15$ Hz), and the result ruled out an isomeric structure (XVI).

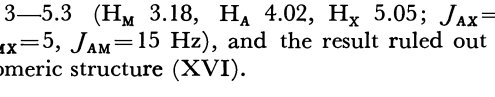

XVI XVa

The nitrones (XVa, XVb, and XVd) have the coupling constant J_{AX} of about 10 Hz, indicating that H_A and H_X are located in a *trans* position to each other.

A similar reaction was attempted with α,N-diphenylnitrone (I), using isopropylbenzene or tetralin as an aralkyl hydrocarbon. In both cases, crude 1,3-adducts were obtained as viscous oil by means of column chromatography, but attempts to isolate pure adducts were unsuccessful.

As seen from Table 2, the yields of the 1,3-adduct are affected by the amount of DTBP; that is, the yields are better in condition b), where a smaller amount of DTBP was used, than in condition a). The results indicate that the addition reaction to the nitrone competes with decomposition of the nitrones by DTBP.

Reaction of α,N-diphenylnitrone (I) with phenylazotriphenylmethane in refluxing benzene gave α,α,N-triphenylnitrone.

Formation Mechanism. It was confirmed that the rate of evolution of nitrogen gas from AIBN was almost the same either in the presence or in the absence of the nitrones. This finding shows that the nitrones react with free radicals generated from AIBN.

As the addition products are trisubstituted hydroxylamines, it is reasonable to consider that two radicals could add to the nitrones in a 1,3-fashion. It has been found that nitroxides were formed instead of expected trisubstituted hydroxylamines in the cases of the *N-t*-butylnitrones.[10] In the reaction of a cyclic nitrone, 5,5-dimethyl-Δ^1-pyrroline *N*-oxide, with AIBN, it was confirmed by ESR technique that nitroxide was the intermediate of the 1,3-adduct.[10] These facts indicate that, in the reaction of the nitrones with free radicals, radicals first add to the carbon atom and then to the oxygen atom of the nitrone system.

The fact that the reaction of α,N-diphenylnitrone (I) with phenyl radical generated from phenylazotriphenylmethane gave α,α,N-triphenylnitrone supports that a radical first adds to the carbon atom to produce nitroxide radical, from which reactive phenyl radical abstracts a hydrogen atom to afford a new ketonitrone, as shown below.

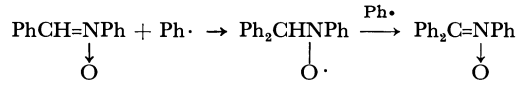

It was recently reported that the reaction of 4,5,5-trimethyl-Δ^1-pyrroline *N*-oxide (XVII) with substituted benzenediazonium salts gave the 2-aryl derivatives (XVIII) in the presence of sodium acetate, sodium sulfite and cupric sulfate.[11]

10) Preliminary report: M. Iwamura and N. Inamoto, This Bulletin, **40**, 703 (1967); *ibid.*, **43**, 860 (1970). (Part II).

11) R. F. C. Brown, L. Subrahmanyan, and C. P. Whittle, *Aust. J. Chem.*, **20**, 339 (1967).

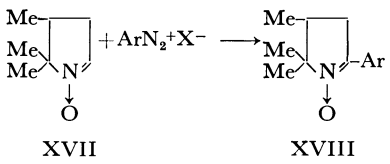

XVII XVIII

This result also supports the mechanism mentioned above.

The ketonitrone such as α,*N*-dimethyl-α-phenylnitrone, did not afford a 1,3-adduct with AIBN. This result is analogous to the fact that Grignard reagents add to the aldonitrones in a 1,3-fashion but the reactions with ketonitrones produce Schiff bases.[5]

As for the mechanism of the formation of the new aldonitrones in the reactions of nitrone II with DTBP and aralkyl hydrocarbons, the following two processes might be conceivable.

Process A

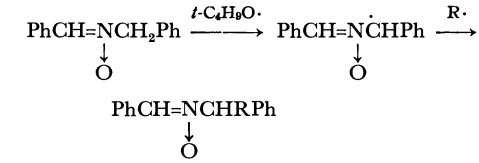

Process B

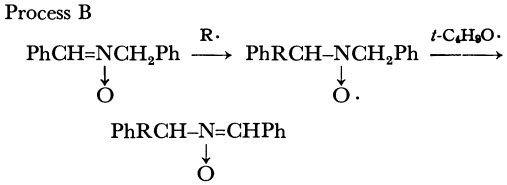

If the nitroxide was assumed to be a common intermediate in formation of both nitrone and 1,3-adduct as shown in Process B, the nitroxide might afford an isomeric ketonitrone instead of the isolated aldonitrone, because abstraction of a tertiary hydrogen atom is usually easier than that of a secondary one. Therefore, it is considered that Process A might be more reasonable than Process B.

Experimental

Materials. Commercial α,α′-azobisisobutyronitrile (AIBN) was recrystallized from ethanol, mp 103—105°C. Dimethyl α,α′-azobisisobutyrate (MAIB) was prepared from AIBN,[12] mp 29—31°C. Commercial di-*t*-butyl peroxide (DTBP) was dried over anhydrous calcium chloride and distilled at 21—22°C/17 mmHg. Benzene, toluene, xylene, ethylbenzene, cumene, tetralin, and diphenylmethane were used after usual purification. Phenylazotriphenylmethane was prepared by Gomberg's method,[13] mp 111—112°C (dec). Nitrones were prepared by the methods described in literature: α,*N*-diphenylnitrone (I),[14] mp 112—114°C; *N*-benzyl-α-phenylnitrone (II),[15] mp 81—83°C; glyoxal-bis-*N*-phenylnitrone (III),[16] mp 181—182°C; α,*N*-dimethyl-α-phenylnitrone,[17] mp 113—114°C.

Addition Reactions of Nitrones with AIBN. A typical procedure is described for α,*N*-diphenylnitrone (I). Nitrone I (18.7 g, 0.1 mol) in 80 m*l* of xylene was heated on a steam bath and AIBN (15.6 g, 0.1 mol) was added little by little to the solution. The mixture was heated for 7 hr, and distilled with steam. Acetone was isolated as its 2,4-dinitrophenylhydrazone (0.22 g, 0.924 mmol, 0.46%) from the distillate. From the residue, a crude addition product (IV), which was recrystallized from methanol, was obtained in a 63% yield (19.8 g). The same product (IV) could be isolated by the following procedure. From the reaction mixture, xylene and other volatile compounds were distilled off under reduced pressure, and then petroleum ether was added to the residue. The precipitate thus obtained was recrystallized from methanol. The results are summarized in Table 1.

Addition Reactions of Nitrones with MAIB. A typical procedure is described for the reaction of *N*-benzyl-α-phenylnitrone (II). Nitrone (II) (7.0 g, 0.033 mol) and MAIB (7.0 g, 0.030 mol) in 35 m*l* of xylene were heated at 120—125°C with stirring. After the evolution of nitrogen gas had ceased, xylene and other volatile components were distilled off *in vacuo*. The residual oil was chromatographed on silica gel with petroleum ether (60—80°C). From the fractions eluted with petroleum ether, 8 g of colorless oil was obtained. The IR spectrum of this oil was different from that of the dimethyl tetramethylsuccinate derived from MAIB. After standing for ten days, it solidified, and then was recrystallized from petroleum ether. The results are summarized in Table 1.

Decomposition of Adduct (IV) with Hydrochloric Acid. IV (1.2 g) dissolved in 30 m*l* of 10% aqueous hydrochloric acid by adding ethanol was refluxed for 10 hr, during which hydrogen cyanide was detected. From the ethanol distilled from the reaction mixture, acetone was detected as its 2,4-dinitrophenylhydrazone (70 mg).

Formation of Nitrile-amide (XI) from Adduct V. V (7.0 g, 0.021 mol) was dissolved in 48 m*l* of 10% hydrogen peroxide containing 2 m*l* of 6N sodium hydroxide by adding 200 m*l* of ethanol. The solution was heated at 50°C for 2 days, and then poured into 500 m*l* of water. Crude nitrile-amide (6.5 g, 89%) was collected by filtration and recrystallized from 95% ethanol, mp 182.5—183°C. IR (in Nujol): 3500(NH), 3180(NH), 2230(C≡N), and 1690 cm^{-1} (C=O).

Found: C, 72.56; H, 7.47; N, 11.62%. Calcd for $C_{22}H_{27}N_3O_2$: C, 72.30; H, 7.45; N, 11.50%.

Formation of Diol (XII) from Adduct VI. An anhydrous ether solution of VI (2 g, 0.005 mol) and lithium aluminum hydride (0.4 g, 0.01 mol) was refluxed for 4 hr. The excess lithium aluminum hydride was decomposed by ethyl acetate and the solution was poured into alkaline water. The solution was extracted

12) J. Thiele and K. Hauser, *Ann. Chem.*, **290**, 1 (1896).
13) M. Gomberg, *Ber.*, **30**, 2043 (1897).
14) G. E. Utzinger, *Ann. Chem.*, **556**, 50 (1944).
15) H. E. De La Mare and G. M. Coppinger, *J. Org. Chem.*, **28**, 1068 (1963).
16) G. E. Utzinger and F. A. Regenass, *Helv. Chim. Acta*, **37**, 1892 (1954).
17) O. Exner, *Collect. Czech. Chem. Commun.*, **16**, 258 (1951); *Chem. Abstr.*, **47**, 5884 (1953).

with ether and dried over anhydrous magnesium sulfate. By chromatography on silica gel and then recrystallization from benzene and petroleum ether, 1 g of diol (XII) was obtained, mp 89—90°C. NMR (in $CDCl_3$): δ 0.84 (3H), 1.10 (3H), 1.15 (3H), 1.20 (3H), 2.98, 3.23, 3.42, 3.70, 3.88 ($2CH_2$+2OH, 6H in total), 4.08 (1H), 7.00 (5H), and 7.12 (5H).

Found: C, 73.14; H, 8.58; N, 4.07%. Calcd for $C_{21}H_{29}NO_3$: C, 73.43; H, 8.51; N, 4.08%.

Reaction of Nitrone II with Aralkyl Hydrocarbons and DTBP. A typical procedure is described for the reaction of II with ethylbenzene and DTBP. A mixture of II (32.11 g, 0.01 mol), ethylbenzene (21.2 g, 0.2 mol) and DTBP (2.90 g, 0.02 mol) was heated at 135°C for 12 hr under nitrogen with frequent shaking. Ethylbenzene and other volatile products were then distilled off under reduced pressure. The residue was chromatographed on silica gel. With petroleum ether-benzene, 2,3-diphenylbutane was eluted and then 2.56 g of addition product (XIVb) was eluted. With benzene-ethyl ether, nitrone (XVb) (0.18 g) was eluted. After XVb had been eluted, a small amount of II was eluted. The crude addition product (XIVb) was diluted with ethyl ether dried over anhydrous sodium sulfate. Ether was then evaporated and XIVb was dried *in vacuo* under nitrogen. The crude nitrone (XVb) was recrystallized from benzene and petroleum ether. The results are summarized in Tables 2 and 3.

Reaction of Nitrone I with Phenylazotriphenylmethane. Phenylazotriphenylmethane (7.4 g, 0.021 mol) was allowed to react with a solution of the nitrone I (4.2 g, 0.021 mol) in 80 m*l* of benzene for 2 hr at 70—80°C with stirring under argon atmosphere. After addition of petroleum ether, precipitates thus obtained (mainly α,α,N-triphenylnitrone) were recrystallized from benzene as white needles, mp 216—219°C (dec.) (lit, 216—217°C (dec.)[18] or 220°C[19]). Yield 2.2 g (38%) (Found: C, 83.64; H, 5.72; N, 5.09%). This reaction was carried out qualitatively, and no further treatment was done.

18) H. Staudinger and K. Miescher, *Helv. Chim. Acta*, **2**, 568 (1919).

19) A. Dornow, H. Gehrt and F. Ische, *Ann. Chem.*, **585**, 226 (1954).

BULLETIN OF THE CHEMICAL SOCIETY OF JAPAN VOL. 43 860—863 (1970)

Reactions of Nitrones with Free Radicals. II. Formation of Nitroxides

Michiko Iwamura and Naoki Inamoto

Department of Chemistry, Faculty of Science, The University of Tokyo, Hongo, Bunkyo-ku, Tokyo

(Received August 16, 1969)

Reactions of *N*-*t*-butylaldonitrones with free radicals gave stable nitroxides, one of which was isolated in pure state. The stability of the nitroxides was explained by the steric effect around the nitrogen and α-carbon atoms. In the reaction of 5,5-dimethyl-Δ^1-pyrroline *N*-oxide with AIBN, nitroxide was detected by ESR technique, and 1,3-adduct and ketonitrone were isolated from the reaction mixture. From the results, it was confirmed that nitroxide is the intermediate of the 1,3-adduct formation and that a radical first adds to the carbon atom and then adds to the oxygen atom of the nitrones.

In the reactions of the aldonitrones with several carbon radicals, we have found new radical 1,3-addition to the carbon and oxygen atoms of the nitrone system.[1] We found that *N*-*t*-butylaldonitrones and the related compounds reacted with carbon radicals to give extremely stable nitroxides. This paper describes the formation of nitroxides by the addition reactions to the nitrones.[2]

Results and Discussion

Formation of Nitroxides from *N*-*t*-Butylaldonitrones.

The reaction of α,α′-azobisisobutyronitrile (AIBN) with *N*-*t*-butyl-α-phenylnitrone (I) in xylene at 110°C gave *N*-*t*-butyl-*N*-[α-(1-cyano-1-methylethyl)benzyl]nitroxide (III) in a 3.2% yield. Analysis of the ESR spectrum and elemental analysis support the structure (see Table 1 and Experimental). The nitroxide (III) is quite stable to a diffused light, at temperatures below 100°C and also during chromatography on alumina. No change was observed after over one year in air. However, one drop of hydrochloric acid or aqueous sodium hydroxide quenches ESR signals. Addition of one drop of benzyl mercaptan to a benzene solution of III gave almost no change in ESR spectrum, but, when the mixture was warmed for a little while, ESR signals were almost quenched.

The reaction of nitrone I with dimethyl α,α′-

1) a) M. Iwamura and N. Inamoto, This Bulletin, **40**, 702 (1967); b) *ibid.*, **43**, 856 (1970).

2) Preliminary report: M. Iwamura and N. Inamoto, *ibid.*, **40**, 703 (1967).

azobisisobutyrate (MAIB), and the reactions of glyoxal-bis-*N*-*t*-butylnitrone (II) with AIBN or MAIB under similar reaction conditions also gave stable nitroxides (IV—VI), which were detected by ESR spectra but not isolated in pure state. The reaction of nitrone I with tetraphenylsuccinodinitrile at 160°C in *t*-butylbenzene similarly produced the nitroxide VIII. The data are summarized in Table 1.

Table 1. ESR spectra of nitroxide radicals

Reactant	Nitroxide	a_N*1	a_H*1	Solvent
I+AIBN	III*2	14.6	3.07	THF
I+MAIB	IV	13.4	3.7	Xylene
II+AIBN	V	14.5	0.8	Xylene +*o*-$Cl_2C_6H_4$
II+MAIB	VI	15.7	*3	Xylene +*o*-$Cl_2C_6H_4$
I+$PhCHMe_2$ +DTBP	VII	15.1	3.6	$PhCHMe_2$
I+$(Ph_2CCN)_2$	VIII	14.0	8.7	*t*-C_4H_9Ph

*1 In gauss. *2 g=2.0044.
*3 Not determined because of broadening of signals.

The reaction of nitrone I with di-*t*-butyl peroxide (DTBP) and cumene also gave stable nitroxide (VII) which was detected by means of ESR spectroscopy (Table 1). In the cases of toluene, ethylbenzene and tetralin in the place of cumene, however, ESR spectra showed only triplet, whose splitting constants (a_N) are 14.7, 14.4 and 14.4 gauss, respectively. The structures of the nitroxides remain uncertain. A characteristic common to these cases is that the radicals generated from aralkyl hydrocarbons are RR'ĊH; always having at least one α-hydrogen atom. As the nitroxides (IX) are considered to be the intermediate, abstraction of the β-hydrogen atom from the nitroxides (IX) would be easier than that from the starting hydrocarbon $RR'CH_2$, and thus the following reactions would give the nitroxide (X) possessing no α-hydrogen atom.

$$RCH{=}N(\rightarrow O)\text{-}t\text{-}C_4H_9 + R'\cdot \rightarrow R'RCH\text{-}N(t\text{-}C_4H_9)O\cdot$$

I: R=Ph
II: R=*t*-C_4H_9-N(→O)=CH-
III: R=Ph, R'=Me_2CCN
IV: R=Ph, R'=Me_2CCO_2Me
V: R=*t*-$C_4H_9N(\rightarrow O)$=CH-, R'=Me_2CCN
VI: R=*t*-$C_4H_9N(\rightarrow O)$=CH-, R'=Me_2CCO_2Me
VII: R=Ph, R'=$PhCMe_2$
VIII: R=Ph, R'=Ph_2CCN

$$RR'\overset{\beta}{C}H\text{-}\overset{\alpha}{C}HPh\text{-}N(t\text{-}C_4H_9)\text{-}O\cdot \xrightarrow{t\text{-}C_4H_9O\cdot}$$

IX

$$RR'\dot{C}\text{-}CHPh\text{-}N(t\text{-}C_4H_9)\text{-}O\cdot \xrightarrow{t\text{-}C_4H_9O\cdot}$$

$$RR'C{=}CPh\text{-}N(t\text{-}C_4H_9)\text{-}O\cdot$$

X

Therefore, it is probable that the detected nitroxides may be the nitroxides X.

Janzen and Blackburn[3] recently reported detection and identification of short-lived free radicals by ESR trapping technique with *N*-*t*-butyl-α-phenylnitrone (I), using our preliminary results.[2] Vincent and Grubbs also reported the formation of the corresponding nitroxide by the reaction of *N*-benzhydryl-α,α-diphenylnitrone with AIBN.[4]

It is known that the reactions of the nitroso compounds with free radicals give trisubstituted hydroxylamines,[5] and that the nitroxides are the intermediate in the above addition reactions.[6]

$$R\text{-}N{=}O + R'\cdot \rightarrow RR'N\text{-}O\cdot \xrightarrow{R'\cdot} RR'N\text{-}OR'$$

Thus, it is considered that the reactions of the nitrones with free radicals are analogous to those of the nitroso compounds.

After a xylene solution of *N*-benzyl-α-phenylnitrone or glyoxal-bis-*N*-phenylnitrone was heated with AIBN at 130°C for 5 min, ESR spectra were measured immediately, but there was no paramagnetic species, indicating the very short lifetime of the corresponding nitroxides.

Reaction of Δ^1-Pyrroline *N*-Oxides with AIBN. The reaction of 5,5-dimethyl-Δ^1-pyrroline *N*-oxide (XI) with AIBN in xylene at 105—110°C gave a 1,3-adduct (XIII) and a new ketonitrone (XIV). Their yields are listed in Table 2.

Table 2. Reaction of XI with AIBN

XI (g)	AIBN (g)	Xylene (ml)	Products (%) XIII	XIV
5.65	10	10	47.5	23
2.82	5	10	44.2	6.5

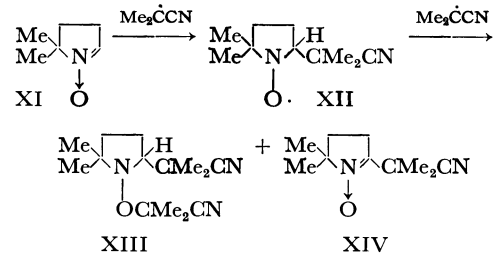

The reactions of 2,4,4-trimethyl- (XV) and 3,3,5,5-tetramethyl-Δ^1-pyrroline *N*-oxides (XVI) with AIBN gave no radical addition product.

3) E. G. Janzen and B. J. Blackburn, *J. Amer. Chem. Soc.*, **90**, 5909 (1968).
4) J. S. Vincent and E. J. Grubbs, *ibid.*, **91**, 2022 (1969).
5) B. A. Gingras and W. A. Waters, *J. Chem. Soc.*, **1954**, 1920.
6) A. Mackor, Th. A. J. W. Wajer and Th. J. de Boer, *Tetrahedron Lett.*, **1966**, 2115.

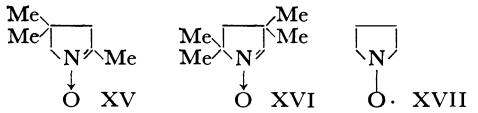

XV XVI XVII

It was shown by ESR technique that there were two kinds of nitroxides in the reaction mixture of the nitrone (XI) with AIBN. The ESR spectrum of one of the nitroxides showed doublet of triplets ($a_N=14.6$, $a_H=20.4$ gauss), from which the structure was confirmed to be XII by comparison with the hyperfine coupling constants ($a_N=14.9$, $a_H=19.6$ gauss) of pyrrolidine-*N*-oxyl (XVII).[7] Although the nitroxide (XII) was stable at least for two days, it was not isolated by column chromatography on silica gel. The other nitroxide, which is more stable, showed nitrogen splitting constant of 14.6 gauss and no further splitting was observed. The structure remains uncertain.

The results in Table 2 indicate that the radical addition to the nitrone is more favorable than the disproportionation of XII in a lower concentration, and that radical addition is almost independent of concentration. It is plausible that the nitroxide is the intermediate in the radical 1,3-additions and that a radical adds first to the carbon atom of the nitrone group and then to the oxygen atom.

Since ketonitrones did not react with free radicals,[1b] we see that nitrone XV did not give addition product. In the case of nitrone (XVI), it is assumed that the geminal dimethyl groups at the C-3 atom sterically hinder the addition of a radical to the C-2 atom, although the nitroxide derived from XVI would be considered to be very stable if it was once formed.

Stability of Nitroxides. Unhindered aliphatic nitroxides such as dimethylnitroxide[7] or diethylnitroxide[8] are known to decompose through disproportionation. The nitroxides containing aromatic rings such as *N*-*t*-butyl-*N*-phenylnitroxide[9] and diphenylnitroxide[10] decompose to disproportionation products by oxygen-atom transfer.

The stability of bis(trifluoromethyl)nitroxide[11] is attributed to impossibility of disproportionation. The stability of nitroxides such as di-*t*-butylnitroxide[12] and 2,2,5,5-tetramethyl-4-oxopiperidine-*N*-oxyl[13] is attributed to steric effect by bulky groups attached to the nitrogen atom.

It is known that nitroxides having at least one α-hydrogen atom may disproportionate to a nitrone and a hydroxylamine.[7] Recently, it was reported that norpseudopelletierine-*N*-oxyl[14] was stable in spite of the presence of α-hydrogen atom. The reason is attributed to prohibition from the disproportionation by Bredt's rule. Therefore, it is noteworthy that the nitroxides (III—VIII) we obtained are quite stable in spite of the presence of α-hydrogen atom. Thus these nitroxides are a new type of stable nitroxides, and regarded as the first examples of nitroxides prohibited from disproportionation because of a spatial congestion around the α-hydrogen atom.

Although nitroxide XII is similar to the nitroxides (III—VIII) it is less stable. This indicates that the steric effect around the α-carbon atom in XII might be not so large as III—VIII, because the nitroxide group of XII is fixed in the ring.

In conclusion, the aldonitrones react with free radicals to give trisubstituted hydroxylamines as addition product or stable nitroxides, and the difference seems to be explicable in terms of the steric effect around the nitrogen and α-carbon atoms of the nitrone group.

Experimental

Materials. The nitrones were prepared by the methods in literature. *N*-*t*-Butyl-α-phenylnitrone (I),[15] mp 75—76°C; glyoxal-bis-*N*-*t*-butylnitrone,[15] mp 193—194°C; 5,5-dimethyl-Δ^1-pyrroline *N*-oxide,[16] bp 75°C/1.5 mmHg; 2,4,4-trimethyl-Δ^1-pyrroline *N*-oxide,[16] bp 92—95°C/3 mmHg; 3,3,5,5-tetramethyl-Δ^1-pyrroline *N*-oxide,[16] mp 31—32°C. Tetraphenylsuccinodinitrile was prepared by Kharasch's method,[17] mp 217—218°C (dec.).

***N*-*t*-Butyl-*N*-α-(1-cyano-1-methylethyl)benzylnitroxide (III).** Nitrone (I) (4.5 g, 0.025 mol) and AIBN (5 g, 0.03 mol) in xylene (30 ml) were heated at 115—120°C until the evolution of nitrogen ceased. Xylene was evaporated *in vacuo* and the reaction mixture was heated at 100—110°C under a pressure of 2 mmHg in order to sublimate most of tetramethylsuccinodinitrile derived from AIBN. The residue was chromatographed on silica gel. Nitroxide (III) was eluted with petroleum ether (bp 30—60°C), and recrystallized from methanol as red needles, mp 121—122°C. λ_{max}^{EtOH}: 437 mμ ($\varepsilon=22$).*1 Yield 0.2 g (3.2%).

Found: C, 73.25; H, 8.70; N, 11.47%. Calcd for $C_{15}H_{21}N_2O$: C, 73.43; H, 8.63; N, 11.42%.

The analysis of the ESR spectrum in tetrahydrofuran

7) G. Chapelet-Letourneux, H. Lemaire and A. Rassat, *Bull. Soc. Chim. Fr.*, **1965**, 3283.

8) G. M. Coppinger and J. D. Swallen, *J. Amer. Chem. Soc.*, **83**, 4900 (1961).

9) A. R. Forrester and R. H. Thompson, *Nature*, **203**, 74 (1964).

10) K. Tokumaru, H. Sakuragi and O. Simamura, *Tetrahedron Lett.*, **1964**, 3945.

11) W. D. Blackley and R. R. Reinhard, *J. Amer. Chem. Soc.*, **87**, 802 (1965).

12) A. K. Hoffmann and A. T. Henderson, *ibid.*, **83**, 4671 (1961).

13) E. G. Rozantsev and M. B. Neiman, *Tetrahedron*, **20**, 131 (1964).

14) R.-M. Dupeyre and A. Rassat, *J. Amer. Chem. Soc.*, **88**, 3180 (1966).

15) W. D. Emmons, *ibid.*, **79**, 5749 (1957).

16) R. Bonnett, R. F. C. Brown, V. M. Clark, I. O. Sutherland and A. Todd, *J. Chem. Soc.*, **1959**, 2094.

17) M. S. Kharasch and G. Sosnovsky, *Tetrahedron*, **3**, 97 (1958).

*1 The value reported previously ($\varepsilon=48$)[2] is erroneous.

(THF) is listed in Table 1.

Solutions of Nitroxides. The solutions of nitroxides were prepared by the reaction of *N*-*t*-butylaldonitrones with an equimolar AIBN or MAIB in a suitable solvent at 110—120°C until the evolution of nitrogen ceased. In the cases of the reactions with DTBP and aralkyl hydrocarbons, the solutions of nitroxides were prepared by the reaction of nitrone I (*ca.* 0.2 g) with an aralkyl hydrocarbon (5 m*l*) and DTBP (1 m*l*) at 130—140°C for 1.5 hr. In the reaction of nitrone (I) with tetraphenylsuccinodinitrile, the equimolar mixture was heated in *t*-butylbenzene at 160°C for 2 hr. After the reaction had completed, the reaction mixture was transferred to an ESR sampling tube and then ESR spectra were taken after evacuation. To avoid any broadening due to dipole-dipole interaction, the reaction mixture was sometimes diluted with the dry solvent.

ESR Measurement. ESR spectra were taken on an X-band TES-3B spectrometer. Calibration was carried out with the NMR signal of water.

Reaction of 5,5-Dimethyl-Δ^1-pyrroline *N*-Oxide (XI) with AIBN. A typical procedure is as follows. *N*-Oxide (5.65 g, 0.05 mol) and AIBN (10 g, 0.06 mol) were dissolved in 10 m*l* of xylene and the solution was heated at 105—110°C with stirring until the evolution of nitrogen ceased. Xylene was evaporated *in vacuo* and the reaction mixture was chromatographed on silica gel. With petroleum ether, 7 g of the 1,3-adduct (XIII) (47.5%) was eluted. Tetramethylsuccinodinitrile (3.8 g) was eluted with benzene. A small amount of the starting *N*-oxide was eluted with ether, and the nitrone (XIV) (2.7 g, 23%) was eluted with acetone. The crude 1,3-adduct (XIII) was recrystallized from benzene, mp 88—88.5°C. NMR (in CCl_4): δ 1.23 (3H), 1.32 (3H), 1.35 (3H), 1.45 (3H), 1.69 (3H), 1.74 (3H), 1.2—1.8 (4H, broad), and 3.34 (1H, multiplet).

Found: C, 67.45; H, 9.33; N, 16.92%. Calcd for $C_{14}H_{23}N_3O$: C, 67.43; H, 9.30; N, 16.85%.

The crude nitrone (XIV) was recrystallized from benzene and methanol, mp 93.5—94.5°C. NMR (in CCl_4): δ 1.35 (6H), 1.70 (6H), 2.02 (2H, triplet, J=7.5 Hz), and 2.78 (2H, triplet, J=7.5 Hz).

Found: C, 66.83; H, 8.95; N, 15.43%. Calcd for $C_{10}H_{16}N_2O$: C, 66.63; H, 8.95; N, 15.55%.

BULLETIN OF THE CHEMICAL SOCIETY OF JAPAN VOL. 43 863—867 (1970)

Aromatic Substitution of Olefin. X. Formation of Biphenyl Derivatives by Means of Olefin-Palladium Chloride Complexes and Silver Nitrate*1

Yuzo FUJIWARA, Ichiro MORITANI, Katsuhiko IKEGAMI, Ryohei TANAKA and Shiichiro TERANISHI

Department of Chemistry, Faculty of Engineering Science, Osaka University, Machikaneyama, Toyonaka, Osaka

(Received August 20, 1969)

The system, olefin-palladium chloride complex-silver nitrate has been shown to cause the oxidative coupling reaction of the aromatic compounds to afford biphenyl derivatives. The mechanism was also discussed in connection with the aromatic substitution of olefins by palladium salts.

We have reported a novel method of arylation by substitution of aromatic compounds for hydrogen on the double bond of the olefin.[1)]

In the course of this work, it has been found that the system, olefin-palladium(II) chloride complex-silver(I) nitrate does cause the oxidative coupling reaction of aromatic compounds to give biaryl derivatives easily.

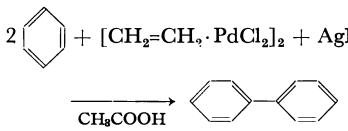

On the formation of biaryl derivatives by palla-

*1 Presented at the Symposium on Homogeneous Catalytic Reactions Involving Palladium, American Chemical Society, Minneapolis, U. S. A., April 1969.

1) a) I. Moritani and Y. Fujiwara, *Tetrahedron Lett.*, **1967**, 1119; b) Y. Fujiwara, I. Moritani and M. Matsuda, *Tetrahedron*, **24**, 4819 (1968); c) Y. Fujiwara, I. Moritani, M. Matsuda and S. Teranishi, *Tetrahedron Lett.*, **1968**, 633; d) Y. Fujiwara, I. Moritani, M. Matsuda and S. Teranishi, *ibid.*, **1968**, 3868; e) Y. Fujiwara, I. Moritani, R. Asano and S. Teranishi, *ibid.*, **1968**, 6015; f) Y. Fujiwara, I. Moritani, S. Danno, R. Asano and S. Teranishi, *J. Amer. Chem. Soc.*, **91**, 7166 (1969); g) S. Danno, I. Moritani and Y. Fujiwara, *Tetrahedron*, **25**, 4809 (1969); h) Y. Fujiwara, I. Moritani, R. Asano, H. Tanaka and S. Teranishi, *ibid.*, **25**, 4815 (1969); i) S. Danno, Y. Fujiwara and I. Moritani, *ibid.*, **25**, 4819 (1969).

dium salts, van Helden and Verberg[2] have reported that benzene gives biphenyl in the presences of palladium(II) chloride and sodium acetate in an 82% yield, and Davidson and Trigg[3] have described a similar biphenyl formation by palladium(II) acetate and that when perchloric acid is used with palladium(II) acetate, the yield of biphenyl increases up to 55%.

We have investigated the biaryl derivative formation reaction involving palladium chloride complexes and silver nitrate. Interesting aspects of the present reaction are that the olefin palladium(II) chloride complex and silver(I) nitrate are employed together and that the yield of biphenyl is almost quantitative (99%) with respect to palladium(II) when the ethylene-palladium(II) chloride complex is used with silver(I) nitrate.

The present paper reports a study of the coupling reaction of benzene derivatives by means of the olefin-palladium(II) chloride complex and silver(I) nitrate.

Results and Discussion

In the course of the study on the aromatic substitution of olefin, we have performed the reaction of the ethylene-palladium(II) chloride complex with benzene in the presence of silver(I) nitrate in a hope of preparing styrene directly.[4] Unexpectedly, no styrene was formed, but biphenyl was obtained in almost quantitative yield[5] with a very small amount of chlorobenzene. The result is reproducible on triplicate reactions. This higher yield of biphenyl comparing to van Helden (82%) and Davidson's results (55%) prompted us to investigate the oxidative coupling of benzene derivatives in the system, olefin-palladium(II) chloride complex-silver(I) nitrate in detail.

The oxidative coupling of benzene derivatives takes place in the homogeneous solution of olefin-palladium(II) chloride complexes, silver(I) nitrate (equal mol equivalent to Pd(II) in the olefin-palladium complex)[6] and the benzene derivatives (large excess) in acetic acid. The solution is stirred in the presence of air for 20 hr to give several per cent to 99% yield of biphenyl derivatives.

Effect of Olefin-$PdCl_2$ Complex. As the ethylene complex-silver nitrate system affords biphenyl from benzene quantitatively, the effect of the similar olefin complexes such as styrene or cyclohexene has been investigated under the same condition. Table 1 shows the yields of biphenyl.

TABLE 1. BIPHENYL FORMATION BY OLEFIN-PALLADIUM CHLORIDE COMPLEX-SILVER NITRATE SYSTEM

Olefin-complex	Biphenyl yield, %[a]
$[CH_2{=}CH_2 \cdot PdCl_2]_2$	99[b]
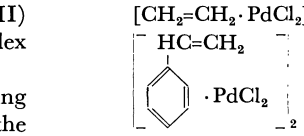	68[c]
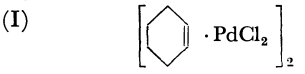	3[d]
$PdCl_2$	40

a) Yields are based on palladium(II) of the complex.
b) A trace amount of chlorobenzene was also obtained.
c) A 22% yield of 1-phenylethyl acetate and a 7% yield of tetraphenylethylene were also formed.
d) A 9% yield of isomeric terphenlys was also obtained.

It can be seen that the yield of biphenyl decreases in the following sequence:

ethylene > styrene > cyclohexene

That this sequence is consistent with the stability of the olefin-complex[7] suggests that the reactivity depends upon the ease with which the olefin ligand on Pd(II) exchanges with benzene. Table 1 also shows that biphenyl can be formed in the presence of $PdCl_2$ and $AgNO_3$, but the yield is low indicating

TABLE 2. EFFECT OF METAL SALTS[a]

$PdCl_2$	Metal slat	Biphenyl yield, %[b]
○	$AgNO_3$	40
○	×	×
×	$AgNO_3$	×
○	AgOAc	45
○	Ag_2O	24
○	HgOAc	23
○	$Cu(OAc)_2$	22

a) Reactions were carried out at 80°C with stirring for 20 hr, charging 25 mmol of $PdCl_2$, an equal mole amount of $AgNO_3$, 280 m*l* of benzene, and 40 m*l* of acetic acid.
b) Yields are based on palladium (II) chloride.

2) R. van Helden and G. Verberg, *Rec. Trav. Chim. Pays-Bas*, **84**, 1263 (1965).
3) J. M. Davidson and C. Trigg, *Chem. Ind.* (London), **1966**, 457.
4) It has been known that styrene can be prepared directly from ethylene and benzene by palladium acetate.[1f]
5) Interestingly, in the absence of siliver nitrate, no biaryl derivatives are formed except the arylated products in the aromatic substitution of olefins by means of palladium salts.[1]
6) When 1/2 mol equivalent of $AgNO_3$ to Pd(II) was used, a greenish black complex was obtained after the reaction. As it has a function to cause the coupling of benzene, it can be considered to be one of the reaction intermediates. Owing to the insolubility, purification is not practical, but approximate composition is $Ag_2Pd_2(OAc)_2Cl_4$.
7) M. S. Kharasch, R. C. Seiler and F. R. Mayo, *J. Amer. Chem. Soc.*, **60**, 882 (1938).

that the ethylene-$PdCl_2$ complex is the most effective for the oxidative coupling of benzene.

Effect of Metal Salts. Further, the effect of metal salts was studied. The results are shown in Table 2.

It can be seen that $PdCl_2$ alone or $AgNO_3$ alone can not effect the coupling of benzene, indicating that coexistence of $PdCl_2$ and $AgNO_3$ is necessary for the present reaction.[8] Of metal salts, mercuric or copper salts, rather than $AgNO_3$ can also act as cocatalysts but silver salts are the most effective. From these results, it becomes clear that the system, ethylene-$PdCl_2$ complex-$AgNO_3$ is the most useful one for the oxidative coupling of benzene.

Now, we have investigated the coupling reactions of benzene derivatives using the present system.

Reaction of Benzene Derivatives. The coupling reactions of toluene, chlorobenzene, nitrobenzene, and *p*-xylene are carried out using the ethylene-$PdCl_2$-$AgNO_3$ system at 80°C. Table 3 summarizes the results.

Table 3. Coupling reaction of benzene derivatives

Benzene derivative	Product, %[a]
Toluene	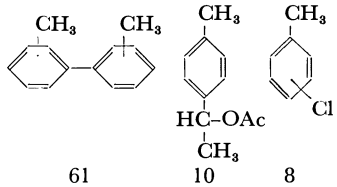 61 10 8
Nitrobenzene	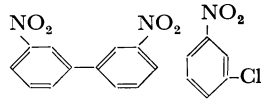 60 21
Chlorobenzene	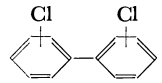 70
p-Xylene	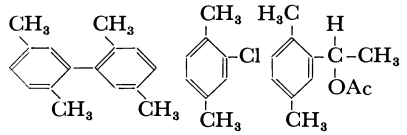 38 25 13

a) Yields are based on palladium (II) of the complex.

In the cases of toluene and chlorobenzene, five isomeric dimethylbiphenyls[9] and dichlorobiphenyls are formed in 61% and 70% yields respectively. Contrary to this, nitrobenzene gives only *m,m'*-dinitrobiphenyl as the coupling product. *p*-Xylene also undergoes a coupling reaction in lower yield (38%) due to the steric hindrance of methyl groups. From the data in Table 3, it seems that the reactivity of benzene derivatives such as toluene or nitrobenzene will not be influenced by the substituent. In order to clarify this point, the relative reactivities were examined by competitive reactions. The typical examples are shown in Table 4.

Table 4. Competitive reactions of some benzenes[a]

Benzene derivative	Product ratio (mole)
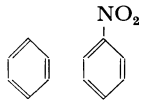	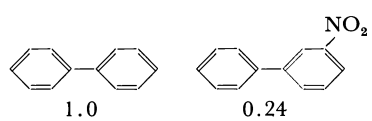 1.0 0.24
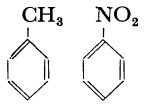	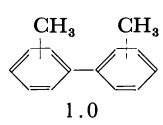 1.0

a) Reactions were performed at 80°C with stirring for 20 hr, charging an equal amount (1.5 mol) of two benzene derivatives, the ethylene-$PdCl_2$ complex (25 mmol as a monomer), $AgNO_3$ (25 mmol), and acetic acid (40 m*l*).

It can be seen that the yield of mononitrobiphenyl decreases sharply and none of the dinitro derivative was detected in the reaction mixture. This result shows that the substituent on a benzene ring excerts an effect, that is, a methyl group (electron donating) increases the reactivity, and a nitro group (electron attracting) decreases it.[2] This is marked contrast to the fact that the substituent on a benzene ring does not influence on the reactivity in the aromatic substitution of olefins by palladium salts.[1h]

Finally, the mechanism of the present coupling reaction appears to be closely related to the aromatic substitution of olefins proposed in a previous paper.[1i] The reaction may proceed through a sigma bonded benzene-palladium complex.[10] This benzene-palladium sigma bond formation step is fast in the aromatic substitution of olefins and hence the substituent did not influence the reactivity.[1h] However, in the present case, this must be included in the rate determining step, and therefore, the reactivity becomes a function of the substituent.

The present reaction provides a convenient method for the synthesis of biphenyl derivatives.

Experimental

All melting points and boiling points are uncorrected.

8) That $PdCl_2$ without $AgNO_3$ or NaOAc can not cause both the oxidative coupling and the aromatic substitution of olefins shows the role of $AgNO_3$ or NaOAc to be that Ag^+ or Na^+ abstracts the Cl^- ligand from the Pd(II) and then, it becomes possible for benzene to coordinate with Pd(II).[1f]

9) M. O. Unger and R. A. Fouty, *J. Org. Chem.*, **34**, 18 (1969).

10) J. M. Davidson and C. Trigg, *J. Chem. Soc., A*, **1968**, 1324.

Infrared spectra were recorded by a Hitachi EPI-S2 IR spectrometer and UV spectra were recorded on a Hitachi EPS-2U spectrophotometer. The NMR spectra were obtained by a Japan Electron Optics JNM-4H-100 spectrometer using tetramethylsilane as an internal standard. Chemical shifts are given in τ units together with splitting patterns and relative integrated area. Analyses of products were carried out by a column chromatograph or a Yanagimoto GCG-3 gas chromatograph using an Apiezon L column. Identities with the products formed were proved by mixture melting point, IR and NMR comparison with authentic samples. Olefin-$PdCl_2$ complexes used were prepared according to the method described by Kharasch *et al.*[7] Benzene, toluene, *p*-xylene were refluxed with sodium metal and distilled. Chlorobenzene and nitrobenzene were dried over Na_2SO_4 and distilled. Acetic acid was dried over P_2O_5 and distilled.

Coupling of Benzene with Ethylene-$PdCl_2$ Complex and $AgNO_3$. In a 500-m*l*, three necked flask provided with a condenser and a stirrer, was placed a solution of 4.13 g (25 mmol as a monomer) of the ethylene-complex, 4.25 g (25 mmol) of $AgNO_3$, 280 m*l* of benzene, and 40 m*l* of acetic acid. The solution was stirred for 20 hr at 80°C. During the reaction, ethylene gas, hydrogen chloride gas, and nitrogen dioxide gas evolved. The resulting mixture was filtered to remove palladium metal and AgCl, and the filtrate was poured into water and then the organic layer was separated. The organic layer was treated with aqueous sodium bicarbonate solution, washed with water to free it from acetic acid and then dried over Na_2SO_4. After evaporation of the benzene, the residue was chromatographed on a column of alumina. Elution with petroleum ether and recrystallization yielded 3.81 g, mp 69—70°C (lit,[11] 70°C) (99%, based on Pd(II) in the complex) of a colorless crystalline material which was assigned as biphenyl by comparison of the IR spectra and mixture melting point. IR (Nujol): 2995, 1575, 1480, 900, 728, and 695 cm^{-1}. Found: C, 93.38; H, 6.62%. Calcd for $C_{12}H_{10}$: C, 93.50; H, 6.52%.

From the benzene evaporated, a trace amount of chlorobenzene was also detected by glpc.

Coupling of Benzene with Styrene-$PdCl_2$ Complex and $AgNO_3$. The same procedure was followed as above, charging 25 mmol (as a monomer) of the syrene-complex, 25 mmol of $AgNO_3$, 280 m*l* of benzene, and 40 m*l* of acetic acid. After work-up as described above there were obtained biphenyl (68%), tetraphenylethylene (7%),[1f] mp 219.5—221°C (lit,[12] 223—224°C) and 1-phenylethyl acetate (22%).[1b]

Coupling of Toluene with Ethylene-$PdCl_2$ Complex and $AgNO_3$. The same procedure was followed as above. After evaporation of toluene, the residue was distilled under reduced pressure (10 mmHg), to give 0.45 g (10%) of the colorless liquid, bp 120—121°C (10 mmHg) which was assigned as *p*-(1-acetoxylethyl)toluene. IR (neat): 3015, 1750, 1240, 1085, 890, 820, and 745 cm^{-1}. NMR (CCl_4): 2.9 (multiplet, 4), 4.3 (quadruplet, 1), 7.8 (singlet, 3), 8.1 (singlet, 3), 8.6 (doublet, 3). Found: C, 74.28; H, 7.91%. Calcd for $C_{11}H_{14}O_2$: C, 74.15; H, 7.86%.

The distillation residue was chromatographed on a column of alumina. Elution with *n*-hexane yielded a colorless substance which crystallized partly. Recrystallization from ether gave 0.86 g (19%) of *p,p'*-dimethylbiphenyl, mp 123—124°C (lit,[13] 121°C). IR (Nujol): 3020, 1500, 1210, 810 cm^{-1}. Found: C, 92.51; H, 7.63%. Calcd for $C_{14}H_{14}$: C, 92.26; H, 7.74%.

The oil part (1.91 g, 42%) was subjected to gas chromatograph (Apiezon L, 2m, 190°C) to detect four components. The four components were separated into A and B by preparative glpc.

The component A: IR (neat): 3040, 1600, 1480, 1100, 820, 755, 726, 708 cm^{-1}. Found: C, 92.32; H, 7.68%. Calcd for $C_{14}H_{14}$: C, 92.26; H, 7.74%.

The component B: IR (neat): 3040, 1610, 1480, 1092, 880, 820, 775, 700 cm^{-1}. Found: C, 92.40; H, 7.78%. Calcd for $C_{14}H_{14}$: C, 92.26: H, 7.74%. From these results, the oil part (A and B) can be considered to be a mixture of four isomeric dimethylbiphenyls. Further elution with benzene afforded 0.25 g (8%) of isomeric chlorotoluenes, mp 153—158°C. IR (Nujol): 3020, 1600, 1475, 1080, 885, 810, 750, 715 cm^{-1}. Found: C, 66.30; H, 5.51; Cl, 28.20%. Calcd for C_7H_7Cl: C, 66.41; H, 5.53; Cl, 28.06%.

Coupling of Chlorobenzene with Ethylene-$PdCl_2$ Complex and $AgNO_3$. The same procedure was followed as above. After evaporation of the chlorobenzene, the residue was chromatographed on a column of alumina. Elution with petroleum ether gave 0.78 g (14%) of a crystalline material which was assigned as *p,p'*-dichlorobiphenyl by comparison with an authentic sample. Mp 147—148°C (EtOH) (lit,[14] 148—149°C), IR (Nujol): 3050, 1590, 1090, 1000, 810, 700 cm^{-1}. Found: C, 64.65; H, 3.70; Cl, 32.12%. Calcd for $C_{12}H_8Cl_2$: C, 64.57; H, 3.60; Cl, 31.84%. Further elution with petroleum ether resulted 3.12 g (56%) of a liquid substance which was gas chromatographed to detect four components. The four components were separated into C and D by preparative glpc.

The component C: IR (neat): 3000, 1575, 1030, 825, 785, 750, 700 cm^{-1}. Found: C, 64.77; H, 3.48; Cl, 32.02%. Calcd for $C_{12}H_8Cl_2$: C, 64.57; H, 3.60; Cl, 31.84%.

The component D: IR (neat): 3000, 1580, 1555, 1450, 1085, 1055, 750, 700 cm^{-1}. Found: C, 65.00; H, 3.64; Cl, 32.16%. Calcd for $C_{12}H_8Cl_2$: C, 64.57; H, 3.60; Cl, 31.84%. From these results, the liquid substance (C and D) can be considered to be a mixture of four isomeric dichlorobiphenyls.

Coupling of Nitrobenzene with Ethylene-$PdCl_2$ Complex and $AgNO_3$. The products were *m,m'*-dinitrobiphenyl (60%) and *m*-chloronitrobenzene (21%): *m,m'*-Dinitrobiphenyl: mp 201—202°C (*n*-hexane-benzene) (lit,[14] 198.5—199°C). IR (Nujol): 2950, 1515, 1340, 1260, 1100, 855, 800, 726, 700 cm^{-1}. Found: C, 59.08; H, 3.28; N, 11.49%. Calcd for $C_{12}H_8N_2O_4$: C, 59.02; H, 3.28; N, 11.48%.

Coupling of *p*-Xylene with Ethylene-$PdCl_2$ Complex and $AgNO_3$. The products were 2,5,2',5'-tetramethylbiphenyl (38%), 2-chloro-*p*-xylene (25%) and

11) M. Gomberg and W. E. Bachman, *J. Amer. Chem. Soc.*, **46**, 2343 (1924).

12) N. Rabjohn, Ed., "Organic Syntheses," Coll. Vol. IV, p. 914 (1941).

13) Th. Zincke, *Ber.*, **4**, 397 (1871).

14) B. Williamson and W. H. Rodebush, *J. Amer. Chem. Soc.*, **63**, 3018 (1941).

2-(1-acetoxyethyl)-1,4-dimethylbenzene (13%).

2,5,2′,5′-Tetramethylbiphenyl: mp 50.5—52°C (*n*-hexane) (lit,[15] 52°C). UV λ_{max}^{EtOH} 270 (log ε 3.20), 277 (3.18). Found: C, 91.28; H, 8.52%. Calcd for $C_{16}H_{16}$: C, 91.37; H, 8.63%.

15) G. H. Beaven and E. A. Johnson, *Spectrochim. Acta*, **14**, 67 (1957).

BULLETIN OF THE CHEMICAL SOCIETY OF JAPAN VOL. 43 867—872 (1970)

β-Ferrocenyl-α,β-unsaturated Ketones. II.[1] The Reduction of β-Ferrocenyl-α,β-unsaturated Ketones and Their Relative Reactivities

Hiromichi KONO, Masayoshi ISHIGE, Koji SAKAI, Mikio SHIGA, Izumi MOTOYAMA and Kazuo HATA

Department of Chemistry, Faculty of Science, Tokyo Metropolitan University, Setagaya, Tokyo

(Received August 21, 1969)

The catalytic reduction of several β-ferrocenyl-α,β-unsaturated ketones was investigated using Urushibara nickel A (U-Ni-A) or precipitated nickel (ppt-Ni) as the catalyst, and their relative reactivities toward the catalytic reduction were discussed in comparison with those of the phenyl analogs. Some anomalies observed in the NMR spectra of the reduction products was also discussed.

The preceding paper[1] in this series has reported on synthetic and spectroscopic studies of β-ferrocenyl-α,β-unsaturated ketones. This paper will deal with a study of the reduction of these unsaturated ketones and related compounds. Although a considerable number of works on the hydrogenation of α,β-unsaturated ketones have previously reported in some detail,[2-5] the reduction of the unsaturated ketones conjugated with the ferrocene group has scarcely been studied at all. Recently, the reduction of various organic compounds with water as a hydrogen donor in the presence of precipitated metal as a catalyst has been extensively investigated in our laboratory.[6,7] When 1,3-diferrocenyl-2-buten-1-one (**1**) was refluxed in a mixture of water and dioxane in the presence of precipitated nickel (ppt-Ni in abbreviation), 1,3-diferrocenyl-1-butanone was obtained almost quantitatively, while the reduction of dypnone (**2**) under the same conditions yielded 1,3-diphenylbutane exclusively. This interesting

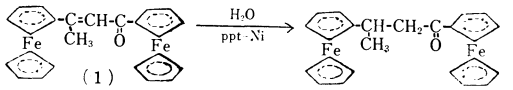

(1)

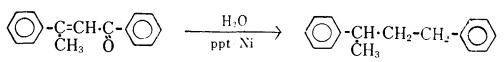

(2)

observation prompted us to more detailed investigations of the catalytic reduction of β-ferrocenyl-α,β-unsaturated ketones and related compounds in the hope of getting some information about the particular effect of the ferrocenyl group on the conjugated system.

Catalytic Hydrogenation of β-Ferrocenyl-α,β-unsaturated Ketones. β-Ferrocenyl-α,β-unsaturated ketones were hydrogenated with Urushibara nickel A (abbreviated as U-Ni-A)[8] under an atmospheric pressure of hydrogen at room temperature, using dioxane as the solvent. When the reaction was stopped after the absorption of equimolar hydrogen, the corresponding saturated ketones were obtained in most cases. The reaction conditions and the results are listed in Table 1. The products were purified by chromatography on alumina, and they were identified by means of elemental analyses and by a study of their IR and NMR spectra. The NMR data are summarized in Table 2.

1) Part I: H. Kono, M. Shiga, I. Motoyama and K. Hata, This Bulletin, **42**, 3273 (1969).

2) M. Delepine and C. Hanegraaff, *Bull. Soc. Chim. Fr.*, [5] **4**, 2087 (1937).

3) R. Cornubert and J. Phelisse, *C. R. Acad. Sci., Paris*, **227**, 1131 (1948).

4) H. Adkins, *Ind. Eng. Chem.*, **32**, 1191 (1940).

5) K. Hoshiai *et al.*, *Kogyo Kagaku Zasshi*, **59**, 236 (1956); **60**, 40, 253, 1150, 1527 (1957).

6) K. Sakai and K. Watanabe, This Bulletin, **40**, 1548 (1967).

7) K. Sakai, M. Ishige, H. Kono, I. Motoyama and K. Hata, *ibid.*, **41**, 1902 (1968).

8) Y. Urushibara, S. Nishimura and H. Uehara, *ibid.*, **28**, 446 (1955).

Table 1. Hydrogenation of β-ferrocenyl-α,β-unsaturated ketones in the presence of U-Ni-A under ordinary atmospheric pressure of hydrogen
Solvent, dioxane; Shaking, 200 strokes/min

Compound	(g)	Cat. (g)	React. temp. (°C)	React. time (min)	Sol. (ml)	Product	Yield (%)
Fc-CH=CH-CO-CH_3 (**3**)	1.00	1.0	17.2	209	20	Fc-CH_2-CH_2-CO-CH_3 (**3a**)	80
	1.00	1.0	18.8	140	20		79
	0.50	0.5	22.4	80	10		85
	0.80	0.8	24.1	30	16		80
Fc-CH=CH-CO-C_2H_5 (**4**)	1.34	1.0	26.1	93	20	Fc-CH_2-CH_2-CO-C_2H_5 (**4a**)	77
Fc-CH=CH-CO-CH_2-$CH(CH_3)_2$ (**5**)	1.48	1.0	23.2	60	20	Fc-CH_2-CH_2-CO-CH_2-$CH(CH_3)_2$ (**5a**)	80
Fc-CH=CH-CO-CH=CH-Fc (**6**)	1.13	0.5	24.0	410	10	Fc-CH=CH-CO-CH_2CH_2-Fc (**6a**)	18.1
						Fc-CH_2CH_2-CO-CH_2CH_2-Fc (**6b**)	35.1
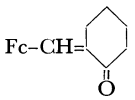 (**7**)	0.74	0.5	23.0	415	10	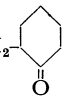 (**7a**)	41
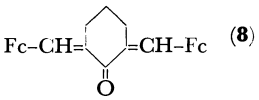 (**8**)	0.37	0.3	25.4	199	5	no reaction	
Fc-C(-CH_3)=CH-CO-Fc (**1**)	1.50	0.5	20.0	280	10	Fc-CH(-CH_3)-CH_2-CO-Fc (**1a**)	30

Table 2. NMR spectra of the hydrogenation products of β-ferrocenyl-α,β-unsaturated ketones

Compound	τ Value (Intensity, signal pattern[a])						
	Unsubst. c.p. ring	Subst. c.p. ring	1	2	3	4	5
$FcCH_2^1CH_2^2COCH_3^3$ (**3a**)	5.91 (5H, s)	5.97 (4H, s)		7.39 (4H, s)	7.89 (3H, s)		
$FcCH_2^1CH_2^2COCH_2^3CH_3^4$ (**4a**)	5.89 (5H, s)	5.95 (4H, s)		7.38 (4H, s)	7.57 (2H, q)[b]	8.94 (3H, t)[b]	
$FcCH_2^1CH_2^2COCH_2^3CH^4(CH_3)_2^5$ (**5a**)	5.90 (5H, s)	5.97 (4H, s)		7.42 (4H, s)		7.98 (1H, m)	9.10 (6H, s)
$FcCH_2^1CH_2^2COCH_2CH_2Fc$ (**6b**)	5.89 (5H, s)	5.94 (4H, m)		7.39 (8H, s)			
$FcCH_2^1CH_2^2COCH^3{=}CHFc^4$ (**6a**)	5.85 (10H, s)	5.52 (4H, s) 5.88 (4H, m)		7.25 (4H, s)	2.49 (1H, d)[c]	3.65 (1H, d)[c]	
$FcCH_2^1CH^2-CO-(CH_2^3)_4$ (**7a**)	5.90 (5H , s)	5.97 (4H, s)		7.07 (1H, m)	7.50—8.80 (10H, c)		
$FcCH_2^1CH_2^2CO$- 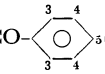 (**9**)[d]		5.89 (9H, m)	7.25 (2H, m)	6.82 (2H, m)	2.05 (2H, m)	2.59 (3H, m)	
$FcCH_2^1CH_2^2CO$- 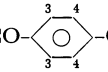 -CH_3^5 (**10**)[d]		5.92 (9H, s)	7.26 (2H, m)	6.78 (2H, m)	2.14 (2H, d)[e]	2.79 (2H, d)[e]	7.64 (3H, s)

a) s: singlet, d: doublet, t: triplet, q:quartet, m: multiplet, c: complex.
b) J=7 Hz. c) J=16 Hz.
d) A preparation of this product will be reported in the following paper.
e) J=8 Hz.

The hydrogenation of 4-ferrocenyl-3-buten-2-one (**3**), 1-ferrocenyl-1-penten-3-one (**4**), and 1-ferrocenyl-5-methyl-1-hexen-3-one (**5**) gave the corresponding saturated ketones in good yields. The C=C stretching absorption bands at 1615 and 1591 cm^{-1} and the C=O stretching absorption bands at 1665 and 1684 cm^{-1}, due, respectively, to *s-trans* and *s-cis* isomerism observed in the spectrum of the unsaturated ketone (**3**), completely disappear in that of the hydrogenation product (**3a**), in which only the C=O absorption band at 1703 cm^{-1} appears.[1)]

The hydrogenation of 1,5-diferrocenyl-1,4-pentadien-3-one (**6**) proceeded at only a slow rate and gave a dark orange reaction mixture, the chromatographic separation of which on alumina gave 1-ferrocenyl-1-penten-3-one (**6a**) from the first fraction in an 18.1% yield and 1-ferrocenyl-3-pentanone (**6b**) from the second one in a 35.1% yield. There is some obscurity in the structural elucidation of **6** in terms of its IR spectrum, since the ethylenic absorption band at 1614 cm^{-1} was observed to be unusually stronger (ε'*1=1740/2) than the carbonyl absorption bands at 1649 (ε'=416) and 1665 cm^{-1}. However, the spectroscopic data of the reduction products, **6a** and **6b**, provided decisive evidence as to the cross-conjugated structure for the original ketone (**6**); that is, distinct carbonyl absorption bands were observed at 1660 and 1690 cm^{-1} for **6a**, and at 1710 cm^{-1} for **6b**.

The reduction of 2-(ferrocenylmethylene)cyclohexanone (**7**) afforded 2-(ferrocenylmethyl)cyclohexanone (**7a**), mp 75—77°C, in a 41% yield, whereas 2,6-di(ferrocenylmethylene)cyclohexanone (**8**) could not be hydrogenated under the conditions employed here, probably because of steric hindrance to the adsorption of the unsaturated system on the surface of the calalyst.

1,3-Diferrocenyl-2-buten-1-one (**1**) was slowly hydrogenated to the corresponding saturated ketone, 1,3-diferrocenyl-1-butanone (**1a**), in a 30% yield under the conditions shown in Table 1.

An interesting result was obtained with regard to the NMR signal of four methylene protons between the ferrocenyl and carbonyl groups in the reduction products, **3a**, **4a**, **5a**, **6a**, and **6b**. That is, these protons gave only one signal as a singlet peak in the τ 7.25—7.42 region, whereas the phenyl analogs, for example, 4-phenyl-2-butanone and 1,5-diphenyl-3-pentanone, gave the corresponding methylene signals as multiplet peaks[9)] at τ 7.47 and 7.26, and at τ 7.63 and 7.26, respectively. The present observations suggest that the two methylenes between the ferrocenyl and carbonyl groups are equivalent in magnetic field. A similar observation, that [3]ferrocenophane gave only a singlet peak for its six methylene protons, has been presented by Rosenblum *et al.*, who interpreted their observation by assuming a rapid inversion of the bridged methylene groups.[10)] Different alkyl groups on the carbonyl group do not cause any splitting of the signal, although the position of the signal is somewhat shifted. However, the corresponding aryl ketones, such as **9** and **10**, showed a multi-splitting of the methylene signal in their NMR spectra (see Table 2). The reason for the apparent magnetic equivalence of the four methylene protons in the ferrocenylethyl ketones (**3a**—**6b**) is not yet clear, but the following consideration may be pertinent. The chemical shift of the methyl protons of methylferrocene is found at τ 8.04,[11)] while that of toluene is found at τ 7.66.[12)] Thus, the deshielding effect exerted by a ferrocenyl group can be expected to be somewhat smaller than that by a phenyl group, and this might bring about an accidental coincidence of the chemical shifts of both methylene protons on α- and β-carbons to the carbonyl group. Moreover, the consideration may be extended to the possibility that some kind of participation of the iron atom of the ferrocene nucleus contributes to averaging the chemical shifts of these methylenes.

Ppt-Ni Catalyzed Reduction of β-Ferrocenyl-α,β-unsaturated Ketones. The effectiveness of ppt-Ni, which is prepared from an aqueous nickel chloride solution and zinc dust,[8)] as a catalyst for the reduction of various unsaturated compounds has been demonstrated in previous papers.[6,7)] Several β-ferrocenyl-α,β-unsaturated ketones were reduced by refluxing them with water in the presence of ppt-Ni. In this reaction water served as a hydrogen donor, and dioxane was used in order to keep the reaction mixture homogeneous. The results of these experiments are summarized in Table 3.

The reaction generally gave a reduction product, in an excellent yield, consisting of a mixture of a ketone and an alcohol. For example, 4-ferrocenyl-2-butanone (**3a**) and 4-ferrocenyl-2-butanol (**3b**) were obtained from 4-ferrocenyl-3-buten-2-one (**1**) in 10% and 90% yields respectively. The formation of alcohol as the main product suggests that the ppt-Ni-catalyzed reduction may be more drastic than the U-Ni-A-catalyzed one. The survival of the carbonyl group in the reduction of 1-ferrocenyl-5-methyl-1-hexen-3-one (**5**) may be attributed to the steric hindrance around it.

Relative Reactivity of β-Ferrocenyl-α,β-unsaturated Ketones and Related Compounds in

*1 $\varepsilon' = \frac{1}{cl} \log \frac{T_0}{T}$; c=concentration of **6**.

9) F. A. Bovey, "NMR Data Tables for Organic Compounds," Vol. I, John Wiley & Sons, N. Y. (1969), pp. 277, 440.

10) M. Rosenblum, A. K. Banerjee, N. Danieli, R. W. Fish and V. Schlatter, *J. Amer. Chem. Soc.*, **85**, 316 (1963).

11) Data in our laboratory.

12) Ref. 9, p. 169.

TABLE 3. REDUCTION OF β-FERROCENYL-α,β-UNSATURATED KETONES WITH WATER IN THE PRESENCE OF ppt-Ni
Refluxing with 10 ml water and 5 ml dioxane; Reaction time 18 hr

Compound	(g)	ppt-Ni (g)*	Product	(%)
Fc-CH=CH-CO-CH_3 (**3**)	0.30	4.0	Fc-CH_2-CH_2-CO-CH_3 (**3a**)	10
			Fc-CH_2-CH_2-CH(OH)-CH_3 (**3b**)	90
Fc-CH=CH-CO-CH_2-$CH(CH_3)_2$ (**5**)	0.13	3.0	Fc-CH_2-CH_2-CO-CH_2-$CH(CH_3)_2$ (**5a**)	95
Fc-CH= 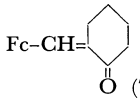 (**7**)	0.32	4.0	Fc-CH_2- (**7a**)	25
			Fc-CH_2- (**7b**)	60
Fc-CH=CH-CO-CH=CH-Fc (**6**)	0.12	3.0	mixture {Fc-CH_2-CH_2-CO-CH_2-CH_2-Fc (**6b**) / Fc-CH_2-CH_2-CO-CH=CH-Fc (**6a**)}	>80

* Every 10 g of ppt-Ni contains 1 g of nickel.

Catalytic Hydrogenation. It is known that the hydrogenation of an α,β-unsaturated carbonyl compound proceeds competitively through several reaction pathways, which involve either the 1,2- or the 1,4-addition of hydrogen.[13,14] The kinetic investigation of the hydrogenation of β-ferrocenyl-α,β-unsaturated ketones with U-Ni-A is expected to be useful for the elucidation of the reaction pathway, since U-Ni-A has been found to be particularly effective for the hydrogenation of ethylenic compounds over carbonyl compounds. The reaction rate was followed by measuring the hydrogen uptake. During the initial stage of the reaction, a linear relation holds between log $(H_\infty - H)$ and the reaction time (t) as a first-order reaction, where H_∞ is the total hydrogen uptake at the end point of the reaction and where H is the hydrogen uptake at each point of time. The slope of the straight line represents the initial rate constant (k) of the reaction. Thus, the initial rate constant in the first order (k) was calculated for each compound; these constants are listed in Table 4. The rate constants, obtained from the hydrogenation of several α,β-unsaturated ketones other than ferrocene derivatives under the same conditions as those employed in the ferrocene series, are listed in Table 5.

TABLE 4. RELATIVE REACTIVITY IN HYDROGENATION OF β-FERROCENYL-α,β-UNSATURATED KETONES IN THE PRESENCE OF U-Ni-A
Conc. 2.5×10^{-1} mol/l; U-Ni-A, 1.0 g; solvent, dioxane; shaking, 200 strokes/min

Compound	React. temp. (°C)	Rate const. k $(min^{-1}) \times 10^{-2}$
Fc-CH=CH-CO-CH_3 (**3**)	17.2	5.76
	18.8	6.06
	22.4	6.72
	24.1	11.0
Fc-CH=CHCO-C_2H_5 (**4**)	26.1	6.45
Fc-CH=CH-CO-CH_2-$CH(CH_3)_2$ (**5**)	23.2	5.66
Fc-CH=CH-CO-CH=CH-Fc (**6**)	24.0	0.44
Fc-C(CH$_3$)=CH-CO-Fc (**1**)	20.0	0.68
Fc-CH= 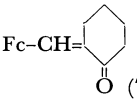 (**7**)	23.0	2.02
Fc-CH= 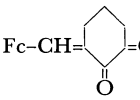 =CHFc (**8**)	25.4	0.00

TABLE 5. RELATIVE REACTIVITY IN HYDROGENATION OF α,β-UNSATURATED KETONES AND RELATED COMPOUND IN THE PRESENCE OF U-Ni-A
2.5×10^{-1} mol/l; 200 strokes/min; solvent, dioxane; U-Ni-A, 1.0 g

Compound	React. temp. (°C)	Rate const. k $(min^{-1}) \times 10^{-2}$
$(CH_3)_2$C=CH-CO-CH_3 (**11**)	19.7	3.84
Ph-CH=CH-CO-CH_3 (**12**)	20.8	28.5
Ph-C(CH$_3$)=CH-CO-Ph (**13**)	21.7	1.57
Ph-CO-CH=CH-CO-Ph (**14**)	21.9	8.40

Although the bulkiness of the ferrocenyl group had been expected to retard the reaction, the reaction rates of the hydrogenation of β-ferrocenyl-α,β-unsaturated ketones were found to be relatively high. This fact implies that the ferrocenyl group

13) K. Hotta and T. Kubomatsu, The 21st Annual Meeting of the Chemical Society of Japan, Osaka, April, 1968, Proceeding Vol. I, p. 154.

14) F. J. McQuillin, W. O. Ord, and P. L. Simpson, *J. Chem. Soc.*, **1963**, 5996.

in the molecule approaches the surface of the catalyst with its less hindered side in the adsorbed transition state, as is shown sketchily in Fig. 1 (a).

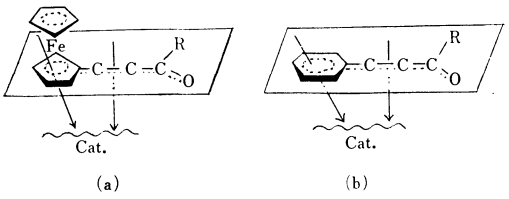

Fig. 1

Thus, the fact that 4-ferrocenyl-3-buten-2-one (**3**) was reduced easier than mesityl oxide (**11**) can be explained in terms of the cooperation of the ferrocenyl group. The larger rate constant of benzylideneacetone (**12**) can also be interpreted in the same manner. As is shown in Fig. 1 (b), the planar structure of the benzylideneacetone molecule may permit the facile adsorption of the conjugated system on the surface of the catalyst from either side of the molecule. On the other hand, the adsortpion of 4-ferrocenyl-3-buten-2-one (**3**) is permitted from only one side of the conjugated system, the other side being sterically hindered by a cyclopentadienyliron moiety. Hence, the reaction rate of the ferrocenyl compound (**3**) can naturally be expected to be considerably smaller than that of the phenyl analog.

Compounds with ferrocenyl groups at both ends of the molecule, such as **6** and **1**, were found to have far smaller reaction rates, as would be expected from the above-mentioned consideration. In the ferrocenylmethylene derivatives of cyclohexanone (**7** and **8**), the conjugated system is largely distorted from coplanarity. The steric environment retards the approach of the ethylenic bond to the surface of the catalyst, and results in a decrease in the rate constant. Especially, 2,6-di(ferrocenylmethylene)-cyclohexanone (**12**) could not be reduced under the conditions employed.

The steric effect of the alkyl groups on the carbonyl group was apparently not observed in this U-Ni-A catalyzed reaction, though it may be expected to affect the conformation of the ketone.[1] This fact implies that the coordination of the substrate molecule to the catalyst might occur preferentially on the part of the ferrocenyl and ethylenic groups.

The reaction pathways for the hydrogenation of β-ferrocenyl-α,β-unsaturated ketones can be considered to be as is shown in Scheme 1.[14]

From the results mentioned above, it can be concluded that the path A, involving α,β-addition, is more favored than the others, while there may be some reaction by the path B at a higher reaction temperature, forming alcohol as a by-product. The path C, which may give an unsaturated alcohol, does not play any important role in this hydrogenation, for the reaction rate is not significantly affected by the nature of the alkyl substituent on the carbonyl group. On the other hand, the striking drops in the reaction rates of 1,3-diferrocenyl-2-buten-1-one (**1**) and the phenyl analog (**13**) clearly support the mechanism *via* the path A.

There is no evidence that any kind of electronic effect of the ferrocenyl group was operative in the reduction of these unsaturated ketones, though remarkable steric effects of the ferrocenyl group were observed.[7]

The electronic effects of the ferrocenyl group have been discussed by several authors,[15-17] especially the effect on the unusual stability of α-ferrocenylcarbonium ions. If such an anchimeric assistance by the *d*-orbital of the iron atom cooperates in the delocalization of the π-electron system of the α,β-unsaturated ketone, it would favor the coplanarity of the conjugated system including the ferrocenyl group, thus promoting the reaction *via* the path A.

Experimental

Materials. The β-ferrocenyl-α,β-unsaturated ketones

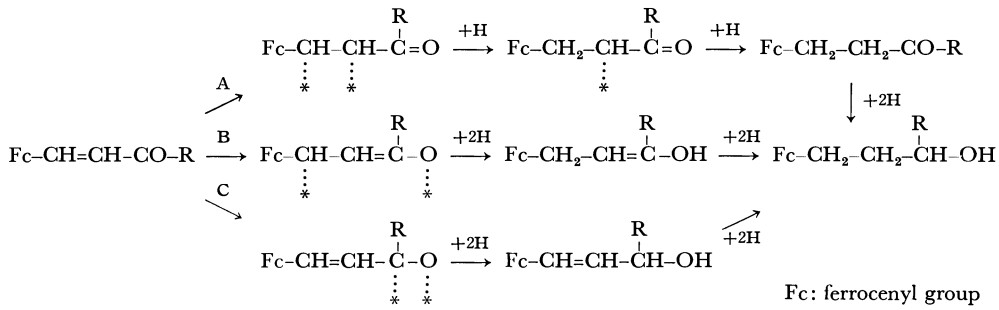

Scheme 1. A schematic diagram of the hydrogenation pathways of β-ferrocenyl-α,β-unsaturated ketones.

15) E. A. Hill and J. H. Richard, *J. Amer. Chem. Soc.*, **83**, 3840 (1961).
16) G. R. Buell, W. E. McEwen and J. Kleinberg, *ibid.*, **84**, 40 (1962).
17) T. G. Traylor and J. C. Ware, *ibid.*, **89**, 2304 (1967).

used in this study were synthesized according to the procedures reported in a preceding paper.[1]

Catalyst. Ppt-Ni. Ppt-Ni was prepared by a procedure reported previously.[6]

U-Ni-A. U-Ni-A was prepared from the ppt-Ni by digesting it with a 13% aqueous acetic acid solution, but the usual digestion procedure reported previously[8] was somewhat modified as follows: 10 g of ppt-Ni was placed in a 200-m*l* Erlenmeyer flask, and then about 20 m*l* of 13% aqueous acetic acid solution was added all at once. With occasional shaking, the temperature of the solution was kept at about 30°C for several minutes; then 100 m*l* of the acetic acid was added in 20-m*l* portions over a period of about 20 min. After the evolution of gas had become gentle, the supernatant liquid was decanted away and the solid was washed several times with 50-m*l* portions of distilled water, methanol, and finally dioxane by decantation. Thus, 1 g of U-Ni-A was obtained.

General Procedure for Hydrogenation Using U-Ni-A. Freshly-prepared U-Ni-A (1 g) was placed, together with 10 m*l* of dioxane, in a hydrogenation vessel which was connected with a gas-buret containing hydrogen and stirred vigorously for about half an hour after the air in the vessel had been replaced with hydrogen. When the absorption of hydrogen by the catalyst ceased, a solution containing 5×10^{-3} mol of the respective unsaturated ketone in 10 m*l* of dioxane was introduced into the vessel. Then, the shaking was continued until the absorption of hydrogen in the buret became almost unrecognizable.*2 At this time, the reaction was stopped and the reaction mixture was filtered. The solid on the filter was washed several times with methanol. The filtrate and the washings were then combined and dried over anhydrous magnesium sulfate. After the solvent had been removed under reduced pressure, a crude reaction product was purified by chromatography on alumina, using *n*-hexane except otherwise stated.

4-Ferrocenyl-2-butanone (3a). A yellow solid which had been obtained by chromatography was recrystallized from *n*-hexane to give yellow needles, mp 42—43°C,*3 in about an 80% yield. IR (KBr disk): 3100, 2940, 1708, 1470, 1410, 1360, 1162, 1104, 1040, 1020, 999, and 816 cm^{-1}.

Found: C, 66.48; H, 5.54%. Calcd for $C_{14}H_{16}OFe$: C, 65.66; H, 6.25%.

1-Ferrocenyl-3-pentanone (4a). Yellow crystals; mp 51—52°C. IR (KBr disk): 3120, 2950, 1712, 1412, 1360, 1104, 1039, 1020, 998, and 817 cm^{-1}.

Found: C, 66.72; H, 6.50%. Calcd for $C_{15}H_{18}OFe$: C, 66.70; H, 6.67%.

1-Ferrocenyl-5-methyl-3-hexanone (5a). Yellow oil. IR (liq. film): 3110, 2950, 1710, 1467, 1408, 1367, 1288, 1224, 1102, 1070, 1039, 1020, 998, and 813 cm^{-1}.

Found: C, 68.27; H, 6.96%. Calcd for $C_{17}H_{22}OFe$: C, 68.49; H, 7.40%.

2-(Ferrocenylmethyl)cyclohexanone (7a). Yellow crystals; mp 75—77°C; 41% yield. IR (KBr disk): 3100, 2940, 2860, 1707, 1475, 1446, 1410, 1355, 1309, 1269, 1243, 1219, 1123, 1100, 1032, 1014, 994, 812, 749, and 670 cm^{-1}.

Found: C, 68.94; H, 6.39%. Calcd for $C_{17}H_{20}OFe$: C, 68.95; H, 6.78%.

1,5-Diferrocenyl-1-penten-3-one (6a) and 1,5-Diferrocenyl-3-pentanone (6b). A reddish-orange, oily product, which had been obtained by the reduction of 1,5-diferrocenyl-1,4-pentadien-3-one (**6**), was chromatographed on alumina using a mixture of benzene and *n*-hexane (1 : 1) as the solvent. 1,5-Diferrocenyl-3-pentanone (**6b**) was obtained from the first fraction as greenish-yellow needles, mp 110—111°C, in a 35% yield, while 1,5-diferrocenyl-1-penten-3-one (**6a**) was obtained from the second fraction as reddish-orange plates, mp 113—114°C, in an 18.1% yield. IR (KBr disk): (**6a**) $\nu_{C=O}$ 1660, 1690 cm^{-1}; $\nu_{C=C}$ 1604, 1621 cm^{-1}. (**6b**) $\nu_{C=O}$ 1710 cm^{-1}.

General Procedure for Hydrogenation Using Ppt-Ni. A solution of a given amount of unsaturated ketone (Table 3) in a mixture of dioxane (5 m*l*) and water (10 m*l*) was refluxed vigorously in the presence of 3.0—4.0 g of ppt-Ni for 18 hr. Then, the reaction mixture was filtered while hot, and the ppt-Ni on filter was washed several times with ether. The filtrate was extracted with ether. All the ethereal solutions were combined and dried over anhydrous magnesium sulfate. After the removal of the solvent, a yellowish-orange residue was chromatographed on alumina using a mixture of *n*-hexane and benzene (1 : 1) as the solvent to fractionate the products shown in Table 3.

4-Feffocenyl-2-butanol (3b). The crude mixture, obtained by the ppt-Ni-catalyzed reduction of 4-ferrocenyl-3-buten-2-one (**3**), was carefully chromatographed on deactivated alumina (100—200 mesh, exposed to air for 1.5 hr) in order to prevent such a reoxidation of the alcohol (**3b**) in the crude mixture to the ketone (**3a**) during alumina chromatography as was observed by Decombe *et al.*[18] 4-Ferrocenyl-2-butanone (**3a**) was obtained in a 10% yield as the first fraction, using a mixture of *n*-hexane and benzene (1 : 1) as the solvent. After the ketone (**3a**) had been completely removed, elution with ether gave 4-ferrocenyl-2-butanol (**3b**) as red oil (90% yield). The structure of **3b** was established by means of its IR and NMR spectra. IR (liquid film): 3400 (OH), 3100, 2940, 1455, 1415, 1376, 1125, 1105, 1040, 1020, 998, 950, 925, and 812 cm^{-1}. NMR (in $CDCl_3$): Fc–$\overset{1}{CH_2}$–$\overset{2}{CH_2}$–$\overset{3}{CH}$($\overset{4}{OH}$)–$\overset{5}{CH_3}$; τ 5.89 (5H, unsub. ring H, singlet), 5.93 (4H, sub. ring H, singlet), 6.15 (1H, H^3, multiplet), 7.56 (2H, H^1, multiplet), 8.39 (3H, H^2 and H^4, complex) and 8.83 (3H, H^5, doublet, J=7 Hz).

2-(Ferrocenylmethyl)cyclohexanol (7b). A dark brownish-red product, which had been obtained by the ppt-Ni-catalyzed reduction of 2-(ferrocenylmethylene)-cyclohexanone (**7**), was chromatographed on deactivated alumina using a mixture of *n*-hexane and benzene (1 : 1) as the solvent. 2-(Ferrocenylmethyl)cyclohexanone (**7a**) was obtained in a 25% yield from the first fraction. After the ketone (**7a**) had been completely removed, elution with ether afforded 2-(ferrocenylmethyl)cyclohexanol (**7b**) as a red oil in a 60% yield; this was identified by means of its IR spectra. IR (liquid film): 3430 (OH), 3100, 2940, 2870, 1450, 1104, 1038, 1018, 998, 972, 924, and 810 cm^{-1}.

*2 When the hydrogenation was continued further, a very slow absorption of hydrogen was again observed due to the hydrogenation of the carbonyl group.

*3 The melting point was observed to be somewhat lower than that previously reported (mp 45—46°C[18]).

18) J. Decombe, J. P. Ravoux and A. Dormont, *C. R. Acad. Sci., Paris, Ser. C*, **258**, 2348 (1964).

BULLETIN OF THE CHEMICAL SOCIETY OF JAPAN VOL. 43 873—876 (1970)

The Structure of Salts of β-Dione Dioximes

Yoshio IWAKURA, Keikichi UNO and Kazuo HAGA*1

The Department of Synthetic Chemistry, Faculty of Engineering, The University of Tokyo, Bunkyo-ku, Tokyo

(Received August 21, 1969)

Cyclohexane-1,3-dione dioxime hydrochloride was prepared and investigated with reference to its structure. Analysis and a study of its NMR and IR spectra suggested that the salt is the enamine form of the oxime. Further, the salts of 5-methylcyclohexane-1,3-dione dioxime, 5,5-dimethylcyclohexane-1,3-dione dioxime and acetylacetone dioxime were prepared and found to have the same structure.

For the structure of ketoxime salt, the structure of cyclohexanone oxime hydrochloride was investigated by Saito.[1] The proton was known to be attached to the nitrogen of the hydroxyimino group as in Eq. (1). Further, an excess of strong acid was found to make another kind of salt containing two molecules of acid. Here, protons bond with the nitrogen and the oxygen of oxime as in Eq. (2). The salt with two molecules of acid, however, is so unstable that it easily releases one molecule of hydrogen chloride at room temperature.

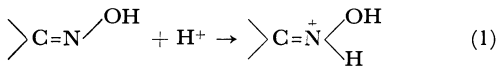

(1)

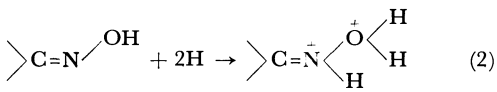

(2)

In our series of studies to synthesize cyclic diamides, the Beckmann rearrangement of the dioximes of alicyclic diones has been carried out. During the study of the rearrangement, the characteristic structures of the salts of β-dione dioximes were found. β-Dione dioxime gave only one kind of stable salt, with one molecule of hydrogen chloride, in spite of the presence of two hydroxyimino groups. In the present study, the structure of the salt of β-dione dioxime will be discussed on the basis of a study of the NMR and IR spectra.

Results and Discussion

The β-dione dioximes were derived from β-diones according to the usual method. The β-diones used as starting materials were cyclohexane-1,3-dione, 5-methylcyclohexane-1,3-dione, 5,5-dimethylcyclohexane-1,3-dione and acetylacetone. The salts of these β-dione dioximes were obtained as crystals on adding various acids in acetic acid solutions. The results are summarized in Table 1, along with the data of elementary analyses.

Cyclohexane-1,3-dione dioxime was expected to act as a diacid base. An elementary analysis of the salt, however, showed that the salt contains only one molecule of hydrogen chloride. Even if an excess of hydrogen chloride was added, dihydrochloride was not obtained.

Since the results obtained seemed to be anomalous, a further attempt to prepare various salts of β-dione dioximes was made to confirm that β-dione dioximes act as monoacid bases. In every case here, the salts of β-dione dioximes contained an equivalent of acid. The addition of a half mole of sulfuric acid to 1 mol of cyclohexane-1,3-dione dioximes gave a quantitative yield of the salt; this salt, on the addition of another half mole of sulfuric acid, dissolved in acetic acid again, we could not isolate the product. For the sake of comparison, we studied how to obtain γ-dione dioxime monohydrochloride by the same method, but in the case of cyclohexane-1,4-dione dioxime, monohydrochloride was not obtained, rather, hygroscopic crystals of dihydrochloride were precipitated by the addition of an excess of hydrochloric acid. In view of the above facts, the salts of β-dione dioximes seemed to have structures different from those of the salts of the other oximes such as cyclohexanone oxime.

The Structure of 5,5-Dimethylcyclohexane-1,3-dione Dioxime. As a structure of cyclohexane-1,3-dione dioxime, the presence of three kinds of isomers were proposed, as is shown below:

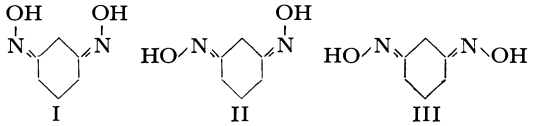

I II III

Here, in the NMR spectrum of the dioxime, methylene protons at the 2 position gave three peaks

*1 Present address: Department of Industrial Chemistry, Faculty of Engineering, Utsunomiya University, Ishii-machi, Utsunomiya

1) H. Saito, *Nippon Kagaku Zasshi*, **85**, 728 (1964).

TABLE 1. SALTS OF β-DIONE DIOXIMES AND ELEMENTARY ANALYSES

Dioxime	Acid HX	Method	Yield (%)	Mp (°C)	Elementary analyses	C (%)	H (%)	N (%)
Cyclohexane-1,3-dione dioxime	HCl	A	100	190 (d)	C.	40.34	6.21	15.68
					F.	40.20	5.92	15.17
	$\frac{1}{2}H_2SO_4$	A	100	180 (d)	C.	37.70	5.80	14.62
					F.	37.80	5.87	13.80
	$CH_3C_6H_4SO_3H$	A	66	180—180.5	C.	49.68	5.54	8.91
					F.	49.27	5.77	9.08
	$C_6H_2(NO_2)_3OH$	B	60	166—167	C.	38.92	3.53	18.87
					F.	38.55	3.54	19.54
5-Methylcyclohexane-1,3-dione dioxime	HCl	B	80	179 (d)	C.	44.00	6.83	14.69
					F.	43.64	6.80	14.54
5,5-Dimethylcyclohexane-1,3-dione dioxime	HCl	B	81	177—178	C.	46.50	7.24	13.57
					F.	47.02	7.40	13.92
Acetylacetone dioxime	$\frac{1}{2}H_2SO_4$	B	50	104—105	C.	33.33	6.21	15.27
					F.	33.52	6.19	15.64

d: decomposition C.: Calcd for dioxime·HX F.: Found Method A and B: *cf.* experimental

corresponding to the protons of the structures I, II, and III, while the methylene protons at the 4, 5, and 6 positions gave very complicated signals.[2] In the present study the NMR spectrum of 5,5-dimethylcyclohexane-1,3-dione dioxime was found to give a rather simple chart, as is shown in Fig. 1, because the carbon at the 5 position has no hydrogen.

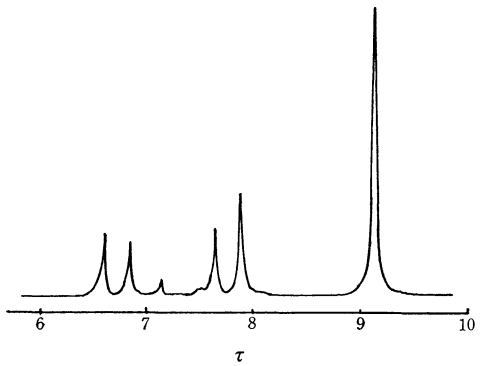

Fig. 1. NMR spectrum of 5,5-dimethylcyclohexane-1,3-dione dioxime. (DMSO-d_6 60MHz)

The methylene protons at the 2 position are observed around τ 6.5—7.2 as three signals. The central signal of these three can be assigned to the structure II analogous to results previously reported.[2] The assignment of the other two signals, one of which corresponds to the syn-syn or anti-anti form, has not been made. The ratio of the intensities of the three signals of the methylene protons at the 2 position in 5,5-dimethylcyclohexane-1,3-dione dioxime is 6 : 3 : 1.

The signals of the methylene protons at the 4 and 6 position are observed as two peaks around τ 7.5—8.0. These seemed to correspond to syn and anti protons with respect to the hydroxyimino group. The protons at the 4- and 6-methylene of Form I are all anti protons, and those of Form III are all syn; moreover in Form II either the protons of 4-methylene or those of 6-methylene are syn, and the other are anti protons. Finally, without regard to the differences between Forms I, II, and III, the methylene protons at the 4 and 6 positions are divided into just two classes. From the ratio of the intensities of the signals of 2-methylene, the ratio of syn and anti protons at 4- and 6-methylenes, was calculated to 1 : 3. This calculated value coincides with the experimental result. The separation between the two peaks indicates the difference in the shielding constants of the syn and anti protons. The value obtained is 0.24 ppm, which is expected to be consistent with the separations between both side peaks and the central one of 2-methylene; however, the actual values related to 2-methylene are 0.24 and 0.29 ppm. A further, detailed discussion of this point is required.

NMR Spectra of Salts of β-Dione Dioximes. The NMR spectra of the β-dione dioxime monohydrochlorides are shown in Fig. 2.

If the structure of the salt of β-dioxime is IV, as is expressed in Eq. (3), in which the proton is attached to one of the two nitrogens, the signal of the methylene protons between the two oxime groups would shift toward a lower field by about 0.3 ppm because of the influence of protonated oxime, as has been indicated by Saito, and the signal would be observed as a doublet due to the anisotropic effect of the syn and anti forms of the oxime group which was not protonated. The spectrum actually obtained, however, gave a quite

2) H. Saito and K. Nukada, *Tetrahedron Lett.*, **1965**, 2117.
3) H. Saito, *J. Mol. Spectrosc.*, **18**, 355 (1965).

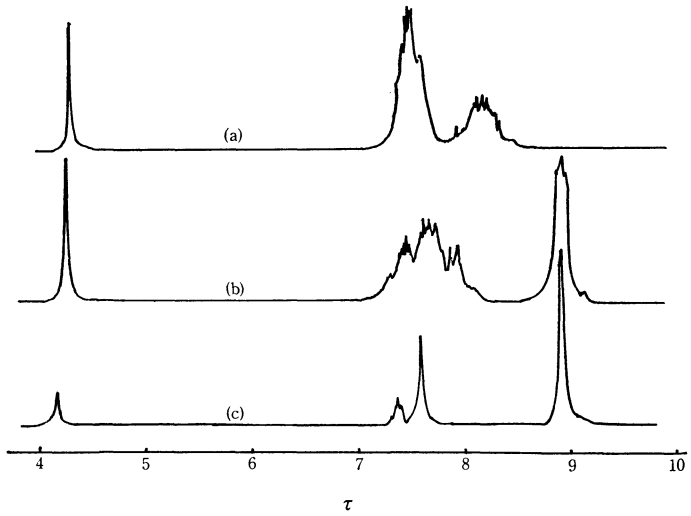

Fig. 2. NMR spectra of cyclohexane-1,3-dione dioxime hydrochloride (a), 5-methylcyclohexane-1,3-dione dioxime hydrochloride (b), 5,5-dimethylcyclohexane-1,3-dione dioxime hydrochloride (c), (DMSO-d_6 60MHz).

different figure from that assumed from the above consideration.

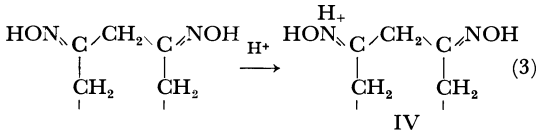

(3)

IV

The methylene signals which have been observed in 5,5-dimethylcyclohexane-1,3-dione dioxime around τ 6.5—7.2, disappear completely, and a new signal is found at about τ 4. Further, the same phenomenon is observed in each of our experiments. The number of the proton which gave the signal at τ 4 is estimated by comparison with those of the other methylene or methyl protons to be one. Therefore, it is reasonable to consider that the structure of β-dione dioxime changes from the imine form to the enamine form V by means of salt formation, as is shown in Eq. (4):

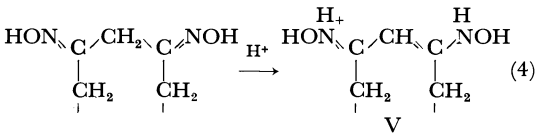

(4)

V

It is well known that β-diketone exists mainly as an enol form, while β-dione dioxime does not take an enamine form. This is interpreted as being due to the difference in electron-withdrawing tendencies between carbonyl and oxime groups. If β-dione dioxime is protonated, the electron-withdrawing character of the oxime will increase very much and the hydrogens of methylene between the two oxime groups will become acidic. Consequently, the salt of β-dione dioxime will have a structure of an enamine, as is shown in Eq. (5):

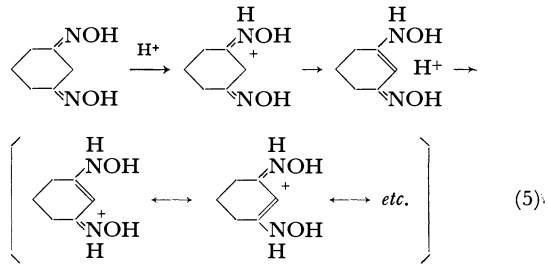

(5)

This resonance stabilization can explain how the β-dione dioxime acts as a monoacid base. The structure described above is also supported by the fact that the protons of the 4 and 6 positions of 5,5-dimethylcyclohexane-1,3-dione dioxime hydrochloride show a single signal.

IR Spectra of the Salts. The absorption band of the carbon nitrogen double bond of cyclohexanone oxime (1669 cm^{-1}) was reported to shift to the higher-wave-number region of 1696 cm^{-1} upon salt formation.[1] However, 5,5-dimethylcyclohexane-1,3-dione dioxime gave just the opposite result.

The IR spectra of 5,5-dimethylcyclohexane-1,3-dione dioxime and its hydrochloride are illustrated in Fig. 3. The absorption at 1655 cm^{-1} shifts to the lower-wave-number region of 1578 cm^{-1} upon salt formation. Further, a new absorption, which seems to be attributable to a C=C double bond, appears at 1610 cm^{-1}. Some bands of the IR absorptions of various β-dione dioximes and other oximes, and of these hydrochlorides, are shown in Table 2.

If the structure of the salt of β-dione dioxime were IV, in which the proton is added to one nitrogen of the two hydroxyimino groups, two peaks related to C=N and C=N$^+$ streching would

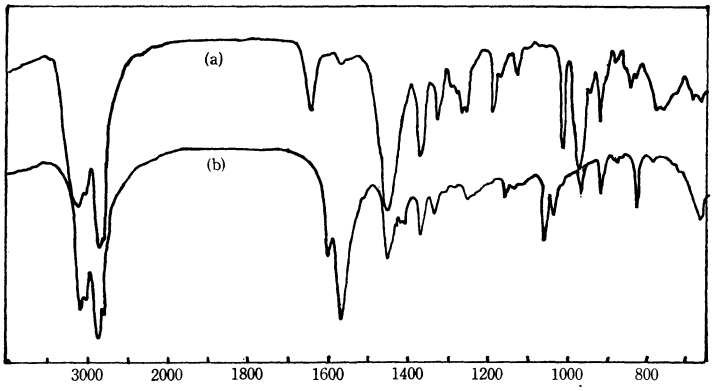

Fig. 3. IR spectra of 5,5-dimethylcyclohexane-1,3-dione dioxime (a) and its hydrochloride (b).

TABLE 2. INFRARED ABSORPTION FREQUENCIES OF THE DIOXIMES AND THEIR SALTS (cm^{-1})

	Dioximes		The oxime hydrochlorides		
	OH	C=N	OH	N^+H	$C=N^+$
Cyclohexane-1,3-dione dioxime	3200, 3100	1665	3200, 3100	3000—2500	1595
5-Methylcyclohexane-1,3-dione dioxime	3200, 3080	1655	3140, 3080	3000—2500	1582
5,5-Dimethylcyclohexane-1,3-dione dioxime	3200, 3080	1655	3150, 3070	3000—2500	1578
Acetylacetone dioxime	3200, 3100	1670	3200, 3100	2650	1610
Cyclohexane-1,4-dione dioxime	3200, 3100	1665	3300	2600	1710
Cyclohexanone oxime	3190, 3110	1650	3350	2600	1695

appear. In the case of the structure V, the resonance of $C=N^+$ and C=N can explain why the peak shifts to a low-frequency region and the intensity is very strong. Therefore, the experimental results of the IR absorption spectra seem to support the structure V, too.

The wave number of the carbon-nitrogen stretching of the salt of β-dione dioxime varies with the number of methyl groups at the 5 position. The chemical shift of the methine proton of the salt varies also, as is shown in Table 3. These differences seem to have some correlation with the change of the conformation of the ring, though this question has not yet been elucidated.

TABLE 3. THE CHEMICAL SHIFTS OF THE METHINE PROTON AND IR ABSORPTION FREQUENCIES OF CN^+ STRETCHING OF THE DIOXIME HYDROCHLORIDES

	τ (ppm)	$C=N^+$ (cm^{-1})
Cyclohexane-1,3-dione dioxime hydrochloride	4.28	1595
5-Mthylcyclohexane dioxime hydrochloride	4.26	1582
5,5-Dimethylcyclohexane-1,3-dione dioxime hydrochloride	4.15	1578

Experimental

The cyclohexane-1,3-dione,[4] 5-methylcyclohexane-1,3-dione,[5] and 5,5-dimethylcyclohexane-1,3-dione[6] were synthesized by the methods given in the literature. The acetylacetone was obtained from a commercial source. The dioximes of these diones were prepared by the usual method.

Cyclohexane-1,3-dione Dioxime Hydrochloride. Cyclohexan-1,3-dione dioxime was dissolved in acetic acid. An equivalent weight of concentrated hydrochloric acid was added to the solution, and then the hydrochloride was precipitated. The hydrochloride was reprecipitated from methanol by the addition of ether (Method A).

5-Methylcyclohexane-1,3-dione Dioxime Hydrochloride. 5-Methylcyclohexane-1,3-dione dioxime was dissolved in acetic acid. After the addition of an equivalent weight of hydrochloric acid, a small amount of ether was added, and then hydrochloride was precipitated (Method B).

Other salts of the dioximes were prepared by the method A or B, as is shown in Table 1.

4) R. B. Thompson, "Organic Syntheses," Coll. Vol. III, p. 279 (1955).
5) A. W. Crossley, *J. Chem. Soc.*, **107**, 602 (1915).
6) R. L. Shriner and H. R. Todd, "Organic Syntheses," Coll. Vol. II, p. 200 (1948).

BULLETIN OF THE CHEMICAL SOCIETY OF JAPAN VOL. 43 877—879 (1970)

Synthetic Reactions by Complex Catalysts. XVI. The Dimerization of Acrylonitrile and Acrylate by Means of the Metal-Isocyanide Complex

Takeo SAEGUSA, Yoshihiko ITO, Hideo KINOSHITA and Shimpei TOMITA

Department of Synthetic Chemistry, Kyoto University, Sakyo-ku, Kyoto

(Received August 29, 1969)

Acrylonitrile and acrylate were dimerized to 2-methyleneglutaronitrile and 2-methyleneglutarate respectively by the binary catalyst system of a copper compound and an isocyanide in the presence of a protic solvent such as *t*-butanol. Transition metal acetylacetonates, such as Fe(II and III), Co(II and III), and Ni(II), in combination with isocyanide were also effective for this dimerization. A mechanistic discussion has been presented.

This paper will describe the dimerization of acrylonitrile and acrylate by a new type of catalyst, a metal-isocyanide complex. The catalytic dimerization of acrylonitrile and methyl acrylate has been extensively investigated. Trialkylphosphines and transition metal compounds are known to be excellent catalysts. By the phosphine catalyst, acrylonitrile[1a] and methyl acrylate[1b] can be dimerized to produce α-methylene-glutaronitrile (Ia) and glutarate (Ib) respectively.

$$CH_2{=}CHX \xrightarrow{P(n\text{-}C_4H_9)_3} CH_2{=}\underset{\displaystyle CH_2CH_2X}{\overset{\displaystyle |}{C}}{-}X \qquad (1)$$

a: X=CN [I]
b: X=CO_2CH_3

On the other hand, rhodium- and ruthenium-trichloride catalyzes the dimerization of methyl acrylate[2a] and acrylonitrile[2b] to produce dimethyl 2-hexendioate (IIa) and 1,4-dicyanobutene-1 (IIb) respectively.

$$CH_2{=}CHX \xrightarrow{RhCl_3 \text{ or } RuCl_3} XCH{=}CHCH_2CH_2X \qquad (2)$$

a: X=CO_2CH_3 [II]
b: X=CN

The binary system of cuprous oxide and alkyl isocyanide is a new type of catalyst for the dimerization of polar olefins. Previously, we reported[3a] the dimerization of β-alkyl-α,β-unsaturated carbonyl and such nitrile compounds as methyl crotonate and crotononitrile by means of a cuprous oxide-alkyl isocyanide system:

$$RCH{=}CHX \xrightarrow{Cu_2O\text{-}RNC} RCH{=}\underset{\displaystyle RCHCH_2X}{\overset{\displaystyle |}{C}}{-}X \qquad (3)$$

a: X=CO_2CH_3 [III]
b: X=CN

When acrylonitrile was treated with the system of cuprous oxide and cyclohexyl isocyanide, acrylonitrile was polymerized in an almost quantitative yield, even at room temperature. The IR spectrum of the acrylonitrile polymer thus obtained resembled that of the polymer produced by the anionic catalyst. This finding prompted us to explore the dimerization of acrylonitrile. The treatment of acrylonitrile with the cuprous oxide-cyclohexyl isocyanide system in the presence of a mixture of *t*-butanol and acetonitrile produced Ia, along with a low-molecular-weight polymer.

$$CH_2{=}CH{-}CN \xrightarrow{Cu_2O\text{-}C_6H_{11}NC} \left(CH_2CH\right)_n \quad [III]$$

$$CH_2{=}CH{-}CN \xrightarrow[\text{in } t\text{-}C_4H_9OH\text{-}CH_3CN]{Cu_2O\text{-}C_6H_{11}NC} CH_2{=}\underset{\displaystyle CH_2CH_2CN}{\overset{\displaystyle |}{C}}{-}CN \quad [Ia]$$

$$+ \left(CH_2CH\right)_m \quad [IV]$$

$n > m$

The polymeric product was soluble in acetone, and its average molecular weight was about 1500. The yield of the dimer was low (6%). The structure of the dimer was confirmed by a comparison of its IR and NMR spectra with those of the authentic sample prepared by means of a trialkylphosphine catalyst. The combination of copper acetylaceto-

1) a) M. M. Baizer and J. D. Anderson, *J. Org. Chem.*, **30**, 1357 (1965). b) American Cyanamide Co., U.S. 3074999 (1963).

2) a) T. Alderson, E. L. Jenner and R. V. Lindsey, Jr., *J. Amer. Chem. Soc.*, **87**, 5638 (1965). b) A. Misono, Y. Uchida, M. Hidai, H. Shinohara and Y. Watanabe, This Bulletin, **40**, 931 (1967).

3) a) T. Saegusa, Y. Ito, S. Kobayashi and S. Tomita, *Chem. Commun.*, **1968**, 273. b) T. Saegusa, Y. Ito, S. Tomita and H. Kinoshita, *J. Org. Chem.*, in press.

nate and alkyl isocyanide in the presence of a mixture of *t*-butanol and acetonitrile gave much better results; *i. e.*, this system produced Ia exclusively. The presence of a protic solvent mixture was essential for dimerization. In the absence of a protic solvent mixture, the copper acetylacetonate-isocyanide system induced only the acrylonitrile polymerization. Cuprous and cupric chlorides with isocyanide were quite inactive in the dimerization and polymerization of acrylonitrile.

Besides copper acetylacetonate, the acetylacetonates of iron(II and III), cobalt(II and III), and nickel(II) in combination with isocyanide and a protic solvent were also active in the acrylonitrile dimerization. The results of the dimerization of acrylonitrile are summarized in Table 1.

Table 1. Dimerization of acrylonitrile and methyl acrylate catalyzed by metal compounds—isocyanide*

Olefin	Metal compound	Yield of Dimer (%)	
		t-C_4H_9NC	$C_6H_{11}NC$
CH_2=CHCN	$Cu(acac)_2$	31	34
	$Co(acac)_2$	26	32
	$Co(acac)_3$	40	50
	$Fe(acac)_2$	52	14**
	$Fe(acac)_3$	49	11**
	$Ni(acac)_2$	3	—**
CH_2=$CHCO_2CH_3$	Cu_2O	11	11
	$Cu(acac)_2$	2	1
	$Co(acac)_2$	2	—

* Olefin (20 mM), isocyanide (20 mM), metal compound (0.4 mM), *t*-butanol (2 m*l*), acetonitrile (5 m*l*) at 110°C, 20 hr.

** Cyclohexyl isocyanide was polymerized in these reactions.

When acetylacetonates of iron(II and III), and nickel(II) were used as the catalyst components, cyclohexyl isocyanide was polymerized; hence, the catalyst activity was decreased. Generally, *t*-butyl isocyanide was not polymerized, and so it could be usefully employed.

Acrylate is much less reactive than acrylonitrile in a reaction by a metal-isocyanide system. In the absence of a protic solvent, methyl acrylate is scarcely polymerized at all by the cuprous oxide-cyclohexyl isocyanide system and remains unchanged under room-temperature conditions. The treatment of methyl acrylate in *t*-butanol and acetonitrile by a copper-isocyanide system at a higher temperature produced the dimer Ib in a lower yield. The dimer was identified by a comparison of its IR and NMR spectra with those of dimethyl α-methyleneglutarate.

Mechanism

The catalytic behavior of the cuprous oxide-alkyl isocyanide system has been characterized on the basis of several important observations in the dimerization of β-alkyl-α,β-unsaturated nitrile and carbonyl compounds:[3b] (i) β,γ-unsaturated nitrile compounds are rapidly isomerized to the corresponding α,β-unsaturated species by the catalyst system; (ii) the *cis-trans* isomerization of β-alkyl-α,β-unsaturated nitrile and carbonyl compounds is caused by the catalyst system, and (iii) the exchange between the hydrogen at the α-position and that of the γ-position in β-alkyl-α,β-unsaturated nitrile and carbonyl compounds is caused by the catalyst system. A reaction mechanism involving an allyl carbanion copper isocyanide complex (V) was proposed to explain these findings:

$$\underset{\ominus}{\text{RCHCH=CHX}} \longleftrightarrow \text{RCH=}\underset{\ominus}{\text{CH}}\text{CHX}$$

[V] (X=CN, CO_2CH_3)

By analogy with the allyl carbanion copper isocyanide complex obtained from β-alkyl-α,β-unsaturated species, a vinyl carbanion complex (VI) may be assumed to be the key intermediate in the dimerization of acrylonitrile and acrylate. In the complex (VI), the vinyl carbanion probably exists as a ligand of the copper-isocyanide complex. The formation of VI is supported by the deuterium/hydrogen exchange at the α-position of acrylonitrile upon treatment with the copper acetylacetonate-cyclohexyl isocyanide system in the presence of *t*-butanol-d.

$$\text{CH}_2\text{=CH-CN} \xrightleftharpoons{\text{Cu compd.-RNC}} [\text{CH}_2\text{=}\underset{\ominus}{\text{C}}\text{CN}]$$

[VI]

The nucleophilic addition of VI to the second molecule of acrylonitrile in a Michael-type addition produces the dimeric anion (VII). The protonation of VII by a protic solvent gives rise to the formation of a dimer. On the other hand, in the absence of a potent proton donor the successive addition of carbanion to the acrylonitrile monomer takes place to produce a polymer.

$$\text{CH}_2\text{=CHX} \xrightleftharpoons{\text{catalyst}} [\text{CH}_2\text{=}\underset{\ominus}{\text{C}}\text{X}] \xrightarrow{\text{CH}_2\text{=CHX}}$$

[VI]

$$\left[\begin{array}{l}\text{CH}_2\text{=CX}\\ \quad\ \ |\\ \quad\text{CH}_2\underset{\ominus}{\text{C}}\text{HX}\end{array}\right] \xrightarrow{\text{H}^+} \begin{array}{l}\text{CH}_2\text{=CX}\\ \quad\ \ |\\ \quad\text{CH}_2\text{CH}_2\text{X}\end{array}$$

[VII] $\xrightarrow{\text{CH}_2\text{=CHX}}$ polymer $\left(\text{-CH}_2\text{CH(X)-}\right)_n$

The copper acetylacetonate-isocyanide system also catalyzes the Michael-type addition.[4] The addition of VI to the second monomer corresponds to the

4) T. Saegusa, Y. Ito, S. Tomita and H. Kinoshita, unpublished results.

addition of the anion to an α,β-unsaturated nitrile in the usual Michael addition. Furthermore, the Michael addition catalyzed by the copper-isocyanide system is characterized by the coordination of α,β-unsaturated compounds to the catalyst.[4] In the dimerization, the coordination of acrylonitrile may facilitate the addition of VI.

Experimental

Reagents. The acrylonitrile and the methyl acrylate were commercial reagents and were purified by distillation. The cuprous oxide and the acetylacetonates of copper, iron(II and III), cobalt(II and III), and nickel(II) were commercial reagents; all were used without purification. The cyclohexyl and the *t*-butyl isocyanide were prepared according to Ugi's procedure.[5]

Oligomerization and Dimerization of Acrylonitrile. A mixture of 2.18 g (20 mmol) of cyclohexyl isocyanide, 40 mg (0.28 mmol) of cuprous oxide, and 1.06 g (20 mmol) of acrylonitrile in 2 m*l* of *t*-butanol and 5 m*l* of acetonitrile was heated at 65°C for 20 hr. The reaction mixture was then poured into about 100 m*l* of methanol, after which the insoluble oligomer of acrylonitrile was removed by filtration. The oligomer was dissolved in acetone, and the acetone solution was filtrated and poured into methanol. The purified oligomer (0.334 g (32%)) was soluble in acetone and *N,N*-dimethylformamide. The methanol solutions were concentrated and subjected to gas-liquid-phase chromatography (glpc) analysis. The yield of the dimer was 6%. The dimer was isolated by preparative glpc and was identified by a comparison of its glpc retention time and NMR and IR spectra with those of an authentic sample which had been prepared by means of a tri-*n*-butyl phosphine catalyst.

NMR of the dimer (in CCl_4): τ 4.00 ppm and 4.11 $\left(2s, \underline{H}\!>\!C\!=\!C\!<\underline{H}\right)$, 7.39 (s, $-C\underline{H}_2C\underline{H}_2-$).

Principal IR bands (neat): 2325 (w) and 1624 (w) cm^{-1}.

Dimerization of Acrylonitrile. A mixture of 2.18 g (20 mmol) of cyclohexyl isocyanide, metal acetylacetonate (0.4 mmol), and 1.06 g (20 mmol) of acrylonitrile in 2 m*l* of *t*-butanol and 5 m*l* of acetonitrile was heated at 110°C for 20 hr. The reaction mixture was then distilled at 62—64°C/0.1 mmHg. The distillate was subjected to glpc analysis.

Dimerization of Methyl Acrylate. A mixture of 2.18 g (20 mmol) of cyclohexyl isocyanide (or 1.66 g (20 mmol) of *t*-butyl isocyanide), cuprous oxide (57 mg (0.4 mmol)), and 1.72 g (20 mmol) of methyl acrylate in 2 m*l* of *t*-butanol and 5 m*l* of acetonitrile was heated at 110°C for 20 hr. The reaction mixture was then distilled at 82—84°C/3 mmHg. The distillate was subjected to glpc analysis. The product was identified by a comparison of its glpc retention time and NMR and IR spectra with those of an authentic sample which had been prepared by the tri-*n*-butyl phosphine-catalyzed reaction of methyl acrylate. The yield of the dimer was 11%.

NMR of dimer (in CCl_4): τ 3.89 ppm and 4.42 $\left(2d, J_{H-H}=2.0\ Hz, \underline{H}\!>\!C\!=\!C\!<\underline{H}\right)$, 6.26 and 6.37 (2s, $-COO-C\underline{H}_3$), 7.50 (s, $-C\underline{H}_2C\underline{H}_2-$).

Principal IR bands (neat): 1725 (s) and 1629 (w) cm^{-1}.

5) I. Ugi and R. Meyr, *Chem. Ber.*, **93**, 239 (1960).

BULLETIN OF THE CHEMICAL SOCIETY OF JAPAN VOL. 43 879—883 (1970)

Intermediate Stages of the Nitration of Hexamethylbenzene to Dinitroprehnitene[1)]

Hitomi SUZUKI

Department of Chemistry, Faculty of Science, Kyoto University, Sakyo-ku, Kyoto

(Received August 29, 1969)

A syrupy substance formed in quantity during the nitration of hexamethylbenzene to dinitroprehnitene has been found to be a complex mixture of varying amounts, depending markedly on the conditions, of 2,3,4,5,6-pentamethylbenzyl nitrate, 5,6-bis(nitrooxymethyl)-1,2,3,4-tetramethylbenzene, nitropentamethylbenzene, 6-nitro-2,3,4,5-tetramethylbenzyl nitrate, 2,3,4,5,6-pentamethylphenylnitromethane, bis(2,3,4,5,6-pentamethylbenzyl) ether, pentamethylbenzaldehyde, and several other unidentified carbonyl compounds, nitrite esters, and aliphatic nitro compounds. On the basis of the products isolated, a possible path by which hexamethylbenzene can be converted into dinitroprehnitene has been suggested.

Electrophilic attack on hexaalkylbenzenes usually leads to the replacement of alkyl groups by the attacking reagent.[2)] However, some instances are known in which the result is the side-chain sub-

1) The Reaction of Polysubstituted Aromatics. XVI, Part XV: This Bulletin, **43**, 481 (1970).

2) K. Galle, *Ber.*, **16**, 1744 (1883); P. Jannasch and A. Bartels, *ibid.*, **31**, 1716 (1898); L. I. Smith and C. O. Guss, *J. Amer. Chem. Soc.*, **62**, 2635 (1940); H. Hopff and A. K. Wick, *Helv. Chim. Acta*, **43**, 1473 (1960); *ibid.*, **44**, 19 (1961).

stitution, and the replacement of alkyl group by nitro group during the nitration of polyalkylbenzenes has been suggested to proceed through the intermediacy of the nitrate.[3] Recently, Illuminati and co-workers explained the side-chain chlorination of hexamethylbenzene in acetic acid by stating that the attacking reagent undergoes the rearrangement from nucleus to side chain to yield a benzylic compound.[4] An extension of this idea to the nitration and sulfonation of polyalkylated benzenes has been presented.[5,6] In this connection, hexamethylbenzene seems to be a convenient substrate for investigating the mode of alkyl replacement since there is no nuclear hydrogen atom to be replaced and all the methyl groups are equivalent. The reduced complexity of the products is expected—a very considerable advantage over the other polyalkylated systems.

Hitherto little has been reported on the direct nitration of hexamethylbenzene. Willstätter and Kubli treated hydrocarbon with benzoyl nitrate in carbon tetrachloride and obtained bis(2,3,4,5,6-pentamethylbenzyl) ether and a bis(nitromethyl)-tetramethylbenzene in an unspecified yield.[7] No mention was made on the details of the reaction. Smith and Harris carried out nitration with fuming nitric acid in the presence of sulfuric acid and obtained as much as 22% yield of dinitroprehnitene (5,6-dinitro-1,2,3,4-tetramethylbenzene).[8] However, a significant proportion of the starting material remained unaccounted for. The present study was undertaken in order to separate and identify the various intermediate products formed when hexamethylbenzene is nitrated to dinitroprehnitene.

When hexamethylbenzene was nitrated in methylene chloride with excess of fuming nitric acid (d=1.5), at temperatures between −5 and 0°C, there resulted a white crystalline product, which showed strong infrared bands at 1272 and 1612 cm^{-1} ($-ONO_2$); PMR peaks at 4.41 τ ($-CH_2ONO_2$) in accord with the expected formation of 2,3,4,5,6-pentamethylbenzyl nitrate (I) as the initial product. If the dark brown mixture was allowed to stand at room temperature, a further reaction soon took place under active liberation of brown fume to give a slightly pasty, pale yellow solid, the infrared spectrum of which showed strong absorptions at 1277 and 1626 cm^{-1} ($-ONO_2$); PMR peak at 4.36 τ ($-CH_2ONO_2$). Neglecting the minor peaks due to by-products and comparing it with an authentic specimen, the major product was readily identified as 5,6-bis(nitrooxymethyl)-1,2,3,4-tetramethylbenzene (II). A close inspection of the infrared spectra ruled out the possibility of the concurrent formation in significant amounts of other isomers, 4,6-bis-(nitrooxymethyl)-1,2,3,5-tetramethylbenzene (III) or 3,6-bis(nitrooxymethyl)-1,2,4,5-tetramethylbenzene (IV).

Chromatography of the nitration products on alumina gave an appreciable amount of bis(2,3,4,5,6-pentamethylbenzyl) ether (V) as an early light petroleum eluate. In the presence of a strong acid, the benzyl nitrate or nitrite will form the conjugate acid,[9] VI or VII, which can act as an alkylating agent when there is appropriate nucleophile in the system.

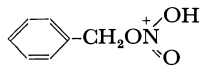

(VI)

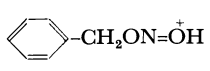

(VII)

Thus, V seems to be derived from the nucleophilic displacement of the ester oxygen on the benzylic carbon.[10] A similar case has been reported by Paraille during the decomposition of p-nitrobenzyl perchlorate in nitromethane to give bis(p-nitrobenzyl) ether.[11] Pentamethylbenzaldehyde (VIII) and other carbonyl compounds were obtained from the late light petroleum eluates, or from the benzene eluates. Nitrate I was hydrolyzed during the elution and appeared as 2,3,4,5,6-pentamethylbenzyl alcohol (IX), but dinitrate II was adsorbed so firmly on alumina that chromatographic treatment did not give satisfactory results at all. Even the prolonged elution with ether gave only small amounts of 5,6-bis(hydroxymethyl)-1,2,3,4-tetramethylbenzene (X) besides some non-crystallizable syrupy substances.

When the reaction mixture was allowed to stand overnight in an ice-bath, a light brown oily solid was obtained. Its PMR spectrum contained six peaks in the nitrooxymethylene proton region. Besides two strong peaks due to I (4.41 τ) and II (4.37 τ), the third peak at 4.31 τ became prominent. Its infrared spectrum showed an increased broad absorption due to $-NO_2$ group at 1545—1565 cm^{-1}, suggesting the presence of some aliphatic nitro

3) L. I. Smith and J. W. Horner, *J. Amer. Chem. Soc.*, **62**, 1349 (1940).

4) E. Baciocchi, A. Ciana, G. Illuminati and C. Pasini, *ibid.*, **87**, 3953 (1965).

5) H. Suzuki, K. Nakamura and K. Maruyama, This Bulletin, **41**, 1487 (1968).

6) H. Suzuki and Y. Tamura, *Chem. Commun.*, **1969**, 244.

7) R. Willstätter and H. Kubli, *Ber.*, **42**, 4151 (1909).

8) L. I. Smith and S. A. Harris, *J. Amer. Chem. Soc.*, **57**, 1289 (1935).

9) R. Boschan, R. T. Merrow and R. W. van Dolah, *Chem. Rev.*, **55**, 485 (1955).

10) Treatment of fully substituted benzyl nitrates with a catalytic amount of sulfuric acid usually gives some bis-benzyl ether. However, if nuclear hydrogen atom is available, preference for the ring substitution is observed. Thus, nitration of pentamethylbenzene yields as by-products 2,2′,3,3′,4,4′,5,5′,6-nonamethyldiphenylmethane and 2,2′,3,3′,4,4′,5,5′-octamethyl-6-nitrooxymethyldiphenylmethane rather than bis(2,3,4,5-tetramethylbenzyl) ether (H. Suzuki and K. Nakamura, This Bulletin, **43**, 473 (1970).

11) P. F. G. Paraille, *J. Chem. Soc.*, **1957**, 3162.

compounds. If the concentration of the nitrous acid formed was lowered either by passing a gentle stream of dry nitrogen into the mixture, or by using a large excess of nitric acid, the peak could be weakened.

Evidence of nitroalkane formation was obtained by the isolation of a crystalline product. Nitration of hexamethylbenzene in methylene chloride saturated with nitrogen trioxide gave a yellow pasty solid. Chromatography of this product on alumina gave unchanged hydrocarbon and the ether V from the light petroleum eluates; some carbonyl compounds from the benzene eluates; and the alcohol IX from the early ether eluates. Further prolonged elution with ether gave a dark yellow syrup, which gradually separated prisms (mp 80—84°C) and was identified as 2,3,4,5,6-pentamethylphenylnitromethane (XI) by comparison with the authentic specimen. Since the homolytic reaction was less probable under these conditions, aliphatic nitro compounds seem to have been formed by the union of the benzylic portion of the conjugate acid, VI or VII, with the nitrogen atom of the nitrite ion. The process is analogous to that of the Victor Meyer reaction in which phenylnitromethane and benzyl nitrite are formed from benzyl halide and silver nitrite.[12] When the above reaction mixture was kept overnight in an ice-salt bath, to which no further amount of ice was added, there resulted a non-crystallizable, sticky, pale yellow syrup. The mixture was found to contain, in addition to the anticipated products, appreciable amounts of nitrite esters, carbonyl compounds and aliphatic nitro compounds. Chromatographic separation did not give any satisfactory results.

Treatment of hexamethylbenzene with fuming nitric acid alone always gave nitrates as the principal product. Dinitroprehnitene (XII) was not formed in any significant amount. Since XII was obtained by Smith and Harris as much as in 22% yield by carrying out the reaction in presence of a large excess of sulfuric acid,[8] the effect of sulfuric acid on the product composition has been examined. Addition of a small amount of sulfuric acid to the reaction mixture was found to facilitate the side-chain substitution greatly, and the hydrocarbon was readily converted into the mono or dinitrate, depending on the amount of nitric acid used. With the increase of sulfuric acid, the yield of V fell rapidly, while those of nitropentamethylbenzene (XIII), 6-nitro-2,3,4,5-tetramethylbenzyl nitrate (XIV) and XII rose progressively. Carbonyl compounds (aldehyde and carboxylic acid) also increased, but aliphatic nitro compounds diminished. The results are consistent with the proposal by Smith and Horner that the group $-CH_2ONO_2$ can be replaced by a nitro group in the presence of sulfuric acid.[3]

While the results reported here do not provide a basis for describing in a precise way the mode of the alkyl replacement, they seem to provide valuable insights. Noteworthy is the marked increase in the formation of carbonyl compounds, especially aldehyde such as VIII when some sulfuric acid is added to the nitrating system. Considering the ease of electrophilic displacement of the formyl group at suitably activated or blocked positions,[13] a mechanism involving the preliminary transformation of the benzyl nitrate into the aldehyde, followed by the nitrodeformylation now seems worthy of consideration. One of the possible courses which can lead hexamethylbenzene to dinitroprehnitene is shown below:

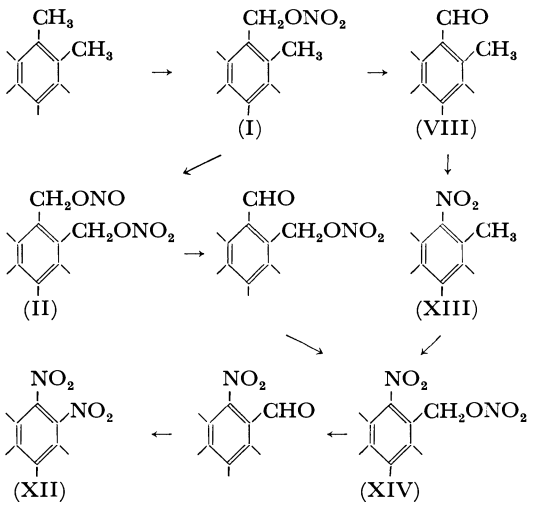

In fact, a catalytic quantity of sulfuric acid can lead the benzyl nitrate to the benzaldehyde as well as benzoic acid,[14] and the replacement of formyl group by nitro group is a quite common occurrence.[15] The behavior of various polysubstituted benzyl nitrates towards sulfuric and nitric acids are now being investigated. We hope to clarify the role of the aldehyde in these anomalous nitrations in a later paper.

Experimental

Infrared spectra were run as Nujol mulls on a DS-402G

12) N. Kornblum, R. A. Smiley, R. K. Blackland and D. C. Iffland, *J. Amer. Chem. Soc.*, **77**, 6269 (1955); N, Kornblum, J. W. Jones and D. E. Hardies, *ibid.*, **88**, 1704 (1966).

13) W. M. Suhubert and R. Kintner, "The Chemistry of the Carbonyl Group," ed. by S. Patai, Interscience Publishers, London (1966), p. 695; J. Strating, L. Thijs and B. Zwanenburg, *Rev. Trav. Chim.*, **85**, 291 (1966).

14) S. D. Ross, E. R. Coburn and M. Finkelstein, *J. Org. Chem.*, **33**, 585 (1968).

15) D. V. Nightingale, *Chem. Rev.*, **40**, 117 (1947); P. B. D. de la Mare and J. H. Ridd, "Aromatic Substitution, Nitration and Halogenation," Butterworths, London (1959).

spectrophotometer. Only prominent peaks were recorded. PMR measurements were carried out on a Varian A-60A spectrometer with deuteriochloroform as solvent and tetramethylsilane as internal standard. All melting points were determined in hot stage and not corrected.

Hexamethylbenzene was prepared by methylation of commercial xylene mixture and crystallized from ethanol.[16] Pentamethylbenzaldehyde (VIII) was prepared from 2,3,4,5,6-pentamethylbenzyl chloride[17] by oxidation with 2-nitropropane.[18] Bis(2,3,4,5,6-pentamethylbenzyl) ether (V) was prepared from 2,3,4,5,6-pentamethylbenzyl alcohol[19] according to Rhoad and Flory.[20]

2,3,4,5,6-Pentamethylbenzyl Nitrate (I). A solution of silver nitrate (12 g) in acetonitrile (30 m*l*) was added all at once to a solution of 2,3,4,5,6-pentamethylbenzyl chloride (12 g) in acetonitrile (20 m*l*). The mixture was stirred for 5 hr at room temperature. Silver chloride was removed by filtration and the solvent was pumped off. The product was crystallized from light petroleum to yield 12.2 g (90%) of white leaflets, mp 95—97°C. IR: 760, 855, 875, 900, 962, 1272 ($-ONO_2$), 1301, 1612, and 1625 cm^{-1} ($-ONO_2$); PMR (in CCl_4), 7.80 (3*[1] CH_3), 7.72 ($2CH_3$), and 4.42 τ (CH_2).

Found: C, 64.4; H, 7.9; N, 6.0%. Calcd for $C_{12}H_{17}NO_3$: C, 64.6; H, 7.7; N, 6.3%.

5,6-Bis(nitrooxymethyl)-1,2,3,4-tetramethylbenzene (II). A warm solution of silver nitrate (2.0 g) in acetonitrile (10 m*l*) was added all at once with stirring, to a hot solution of 5,6-bis(chloromethyl)-1,2,3,4-tetramethylbenzene (1.5 g, mp 133—137°C; lit,[21] 138—139°C) in acetonitrile (30 m*l*). The mixture was stirred for several hours, and silver chloride was separated by filtration. Evaporation of the solvent *in vacuo*, followed by crystallization of the residue from ligroin gave white needles (0.7 g), mp 127—129°C. IR: 697, 732, 755, 859, 876, 954, 964, 1277 ($-ONO_2$), and 1626 cm^{-1} ($-ONO_2$); PMR, 7.74 ($2CH_3$), 7.68 (2*[1]CH_3), and 4.36 τ (CH_2).

Found: C, 50.9; H, 5.8%. Calcd for $C_{12}H_{16}N_2O_6$: C, 50.7; H, 5.6%.

A product of low purity first separated as an oil from the solution and gradually turned into a powder-like solid. Repeated recrystallization gave no improved result.

The above procedure applied to 4,6-bis(chloromethyl)-1,2,3,5-tetramethylbenzene (mp 115—117°C)[20] and 3,6-bis(chloromethyl)-1,2,4,5-tetramethylbenzene (mp 194—196°C)[20] gave *4,6-bis(nitrooxymethyl)-1,2,3,5-tetramethylbenzene (III,* mp 126—128°C) and *3,6-bis(nitrooxymethyl)-1,2,4,5-tetramethylbenzene (IV,* mp 203—205°C), respectively. IR: (III), 694, 757, 818, 873, 950, 1275 ($-ONO_2$), and 1622 cm^{-1} ($-ONO_2$); (IV), 727, 759, 871, 895, 964, 1014, 1274 ($-ONO_2$), 1297, 1614, and 1625 cm^{-1} ($-ONO_2$). PMR: (III), 7.78 (CH_3), 7.68 ($2CH_3$), 7.60 (CH_3), and 4.44 (CH_2); (IV), 7.70 ($4CH_3$) and 4.43 τ (CH_2).

2,3,4,5,6-Pentamethylphenylnitromethane (XI). A solution of 2,3,4,5,6-pentamethylbenzyl chloride (4 g) in acetonitrile (10 m*l*) was poured into a stirred mixture consisting of silver nitrite (5 g), a small amount of calcium carbonate, and acetonitrile (30 m*l*). After 5 hr, the reaction mixture was worked up as usual, and the residue obtained after removal of the solvent was taken up in ethanol and boiled for some minutes to destroy the accompanying nitrite ester. The solution was evaporated to dryness *in vacuo* and the residue was extracted with three portions each of 20 m*l* cold light petroleum to separate from the less soluble alcohol IX. Spontaneous evaporation of the combined extracts gave XI as large plates, and recrystallization from light petroleum gave prisms (0.6 g),[22] mp 86—88°C. IR: 711, 764, 834, 1065, 1271, 1304, 1369 ($-NO_2$), and 1547 cm^{-1} ($-NO_2$); PMR, 7.78 ($3CH_3$), 7.73 ($2CH_2$), and 4.46 τ (CH_2).

Found: C, 69.8; H, 8.3%. Calcd for $C_{12}H_{17}NO_2$: C, 69.6; H, 8.2%.

5,6-Bis(hydroxymethyl)-1,2,3,4-tetramethylbenzene (X). 5,6-Bis(chloromethyl)-1,2,3,4-tetramethylbenzene was converted into the diacetate,[20] which without further purification was saponified by refluxing in 10% ethanolic potassium hydroxide for several hours. The product was recrystallized from benzene-ligroin mixture to give white needles, mp 174—175°C.

Found: C, 74.1; H, 9.2%. Calcd for $C_{12}H_{18}O_2$: C, 74.2; H, 9.3%.

Nitration of Hexamethylbenzene. Typical examples are shown below. Products were identified by spectral comparison and mixed melting as far as the authentic specimens were available.

i) Fuming nitric acid (16.8 g, d=1.5) was added over a period of thirty minutes to a vigorously stirred solution of hexamethylbenzene (8.1 g) in methylene chloride (50 m*l*), keeping the temperature between −5 and 0°C by the use of an ice-salt bath. The organic layer was separated and washed with dilute sodium bicarbonate and then with water. Removal of the solvent left a white crystalline solid, chromatography of which (5 g) on alumina gave the unchanged hydrocarbon (1.2 g) and V (0.5 g) from the light petroleum eluates; carbonyl compounds (0.3 g) from the benzene eluates; and finally IX (0.8 g) from the ether eluates.

ii) Nitration of the hydrocarbon (8.1 g) with the 1 : 1 mixture of fuming nitric acid (23.4 g) and sulfuric acid (23.4 g) under a similar condition gave an orange-yellow pasty solid. The product (5 g) dissolved in a minimum amount of methylene chloride was placed on the top of the alumina column. Elution with light petroleum gave XIII (0.1 g), XIV (0.3 g),[5] and XII (0.5 g); and with benzene some carbonyl compounds. Dinitrate II which constituted the bulk of the nitration product could not be eluted successfully even with ether.

iii) When the hydrocarbon (8.1 g) was treated with fuming nitric acid (15.8 g) in the presence of an excess of sulfuric acid (48 g), a light brown oily solid was obtained. Because of the difficulties encountered in the

16) L. I. Smith, "Organic Syntheses," Coll. Vol. 2, p. 248 (1943).

17) F. Bennington, R. D. Morin and L. C. Clark, *J. Org. Chem.*, **23**, 2034 (1958).

18) M. G. Beets, W. Meerburg and H. van Essen, *Rec. Trav. Chim. Pays-Bas*, **78**, 570 (1959).

19) M. S. Newman and N. C. Deno, *J. Amer. Chem. Soc.*, **73**, 3644 (1951).

20) M. J. Rhoad and P. J. Flory, *ibid.*, **72**, 2216 (1950).

21) M. S. Newman, J. R. LeBlanc, H. A. Karnes and G. Axelrad, *ibid.*, **86**, 868 (1964).

*1 Numerals refer to the number of methyl groups.

22) Resourse to chemical separation gave even poorer yield of the product.

chromatographic separation, a part of the product (14.2 g) was fractionally extracted with light petroleum using a Soxhlet's extractor. Each extract was monitored by infrared spectroscopy and those of a similar composition were combined. Chromatography of the earlier extracts on alumina gave, besides some unchanged hydrocarbon, V (0.4 g); VIII (0.4 g); XII (1.9 g); an unidentified carbonyl compound (0.5 g; Found: C, 70.9; H, 7.3%. $C_{12}H_{15}NO_2$ requires C, 70.2; H, 7.3%) which melted partly at 150—153°C, soon solidified in another crystalline form, and remelted at 223—227°C with partial sublimation and decomposition; IX (0.6 g); and an unidentified hydroxy compound (0.6 g; mp 153—154°C; Found: C, 74.6; H, 9.1%; strong IR bands at 993, 1524, and 3310 cm^{-1}) as well as a little X. Later extracts were mainly a complicated mixture of several carbonyl compounds (1.5 g). A light brown half-resinous substance (5.2 g) which had broad, deep absorptions due to –OH, >C=O, and $-NO_2$, was left in the thimble.

iv) A solution of hexamethylbenzene (8.1 g) in methylene chloride (50 m*l*) was saturated with nitrogen trioxide at −10—−5°C. Fuming nitric acid (15.8 g) was introduced with vigorous stirring over a period of 30 min and the mixture was worked up as usual. A pasty yellow product (5 g) was chromatographed on alumina to give the recovered hydrocarbon (2.5 g), V (0.2 g), aldehydes (0.3 g), and IX (0.7 g). A further prolonged elution with ether gave a yellow syrup, which was dissolved in a small amount of light petroleum and set aside. A solid product (0.2 g, mp 74—84°C) separated out and recrystallized from the same solvent to give prisms, mp 80—84°C, identical with the authentic specimen of XI.

BULLETIN OF THE CHEMICAL SOCIETY OF JAPAN VOL. 43 883—890 (1970)

Photochemical Studies of the Esters of Aroylphosphonic Acids

Ken-ichi TERAUCHI and Hiroshi SAKURAI

The Institute of Scientific and Industrial Research, Osaka University, Suita, Osaka

(Received September 2, 1969)

The photochemical behavior of several dialkyl benzoylphosphonates and *para*-substituted benzoylphosphonates in various solvents has been studied using product isolation, ultraviolet-spectral change, the electron spin resonance (ESR) technique, and quantum yield measurements. Upon irradiation to a degassed solution of these benzoylphosphonates through a Pyrex filter, the photo-pinacolization reaction was observed, except in the case of diethyl benzoylphosphonate; it was effectively quenched by 1,3-pentadiene or oxygen. On the other hand, the ESR spectra of photo-irradiated aroylphosphonates at 77°K have a large anisotropic doublet of 53—128 gauss separation; this separation is thought to be due to the interaction between an unpaired electron and the phosphorus nucleus. The structure of these radicals is also discussed. From these observations, it can be considered that the photochemical reaction proceeds *via* the ketyl radical formed by the hydrogen abstraction of the lowest excited triplet state of these aroylphosphonates. Irradiation to the diethyl benzoylphosphonate solutions in various solvents gave, not the pinacolized product, but 2,4,6-triphenyl-2,4,6-tris[diethylphosphoryl]-1,3,5-trioxane almost quantitatively. The quantum yields (Φ) of the disappearance of several *para*-substituted derivatives are highly sensitive to the electron-inductive abilities of the substituents; that is, Φ drops from 2.10 in the *p*-methoxybenzoylphosphonate derivative to 1.79 in the *p*-chloro derivative at room temperature. Such a substituent effect can be considered to result in the difference in the conformation between the carbonyl and phosphoryl groups. On the basis of these studies, the mechanism of the photochemical reaction of aroylphosphonates is described and discussed.

In a previous paper,[1] we demonstrated that dialkyl aroylphosphonates had a moderately strong n-π^* transition of the carbonyl group occurring around 320—390 mμ because of the interaction with the phosphorus *d*-orbitals. Therefore, as an extension of the previous work, we wish now to report on the photochemical behavior and on the reaction mechanism of these aroylphosphonates.

The photochemistry of organo-phosphorus derivatives has received only a little attention. In general, photochemical studies of organo-phosphorus compounds have been undertaken out of an interest in synthesis; that is, Griffin and his co-worker[2] have demonstrated the synthesis of a variety of nuclear

1) K. Terauchi and H. Sakurai, This Bulletin, **42**, 821 (1969).

2) R. Obrycki and C. E. Griffin, *J. Org. Chem.*, **33**, 632 (1968).

substituted phenylphosphonates and other aryl-(1-naphthyl-, 2-thienyl-, 2-furyl-) phosphonates by the photolysis of the corresponding aryl iodides in an excess of trialkyl phosphite. Also, Petrellis and his co-worker[3] have reported that the irradiation of a solution of 1,3,2-dioxaphospholans in 2-methyl-2-butene or 2,3-dimethyl-2-butene provided the corresponding phenylcyanocyclopropanes. However, the study of the reactivity is important to the same extent for the photochemistry of organophosphorus compounds. From this point of view, we have studied the effect of substituents on the reactivity and the low-lying excited-state structure of these aroylphosphonates.

Results and Discussion

1) Irradiation to Dialkyl Benzoylphosphonates. Before describing the experimental results, it will be useful to clarify the primary photochemical process of dialkyl benzoylphosphonates.

The ultraviolet absorption spectra of a solution of dialkyl benzoylphosphonates are very similar to those of diethyl benzoylphosphonate.[1] The spectra of all the degassed cyclohexane solutions of dialkyl benzoylphosphonates were drastically altered by irradiation through a filter cutting off below 3200 Å; such a filter causes the light to be almost completely absorbed by only the n–π^* transition bands of benzoylphosphonates.

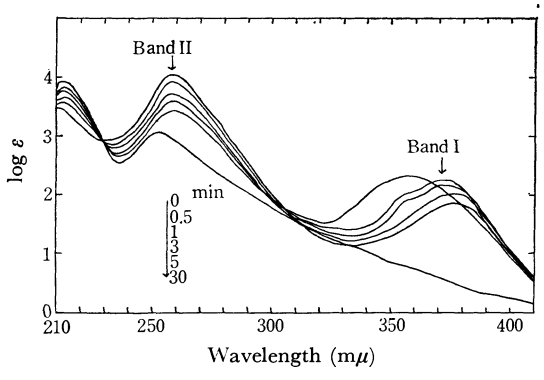

Fig. 1a. The progressive spectral change of diethyl benzoylphosphonate on irradiation in cyclohexane. Numbers refer to irradiation time.

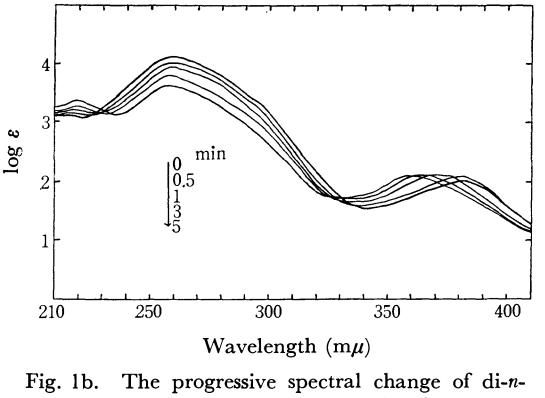

Fig. 1b. The progressive spectral change of di-*n*-butyl benzoylphosphonate on irradiation in cyclohexane. Numbers refer to irradiation time.

a) Photochemical Reactions of Diethyl Benzoylphosphonate. Figure 1a shows the progressive spectral change in a cyclohexane solution of diethyl benzoylphosphonate at an irradiation above 3200 Å. The absorption band II (258 mμ) decreased, and a new band appeared with maxima of 213 and 245 mμ, as the irradiation time increased. On the other hand, the I absorption band (379 mμ) increased with the hypsochromic shift and disappeared after 30 min, as is shown in Fig. 1a. One isosbestic point was observed, at 228 mμ. It may reasonably be considered that the increase in the n–π^* absorption is due to the formation of the ketyl radical or the kethyl radical ion, which might serve as reaction intermediates. Such an intensification of the n–π^* absorption has also been observed in a solution of the other aroylphosphonates used in the present work. The photoproduct, which had its absorption maxima at 213 and 245 mμ in a cyclohexane solution, as can be seen from Fig. 1a, was confirmed to 2,4,6-triphenyl-2,4,6-tris-[diethylphosphoryl]-1,3,5-trioxane (III) by a study of its infrared spectra, by elemental analysis, and by molecular-weight measurements.

b) Photochemical Reactions of Diisopropyl- and Di-n-butyl benzoylphosphonates. Figure 1b shows the progressive spectral change in a solution of di-*n*-butyl benzoylphosphonate. The absorption band II (259 mμ) decreased and a new band with the maximum of 220 mμ gradually appeared, but no clear isosbestic point was observed. As is shown in Fig. 1b, the absorption band I (380 mμ) increased for only the first 10 min in a pattern similar to that of diethyl benzoylphosphonate. A similar progressive spectral change was also observed in the case of diisopropyl benzoylphosphonate.

On the other hand, the photochemical reaction of diisopropyl- and di-*n*-butyl benzoylphosphonates solutions afforded the corresponding pinacols, IIb and IIc respectively, which were identified by means

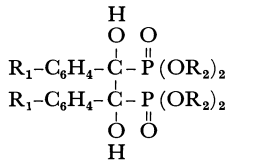

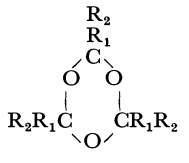

IIb: R_1=H, R_2=iso-C_3H_7
c: R_1=H, R_2=*n*-C_4H_9
d: R_1=*p*-Cl, R_2=C_2H_5
e: R_1=*p*-*t*-Bu, R_2=C_2H_5
f: R_1=*p*-CH_3O, R_2=C_2H_5

III: R_1=C_6H_5
R_2=P(O)$(OC_2H_5)_2$

3) P. Petrellis and G. W. Griffin, *Chem. Commun.*, **1968**, 1099.

of elemental analysis, a study of their infrared and UV spectra, and molecular-weight measurements, as is shown in Tables 6 and 7.

2) Irradiation to *para*-Substituted Benzoylphosphonates. The photochemical reactions of three *para*-substituted benzoylphosphonates, *p*-chloro, *p*-*t*-butyl, and *p*-methoxy derivatives, were investigated in the same manner. The spectra of all the degassed cyclohexane solutions of *p*-substituted benzoylphosphonates were also markedly changed by irradiation.

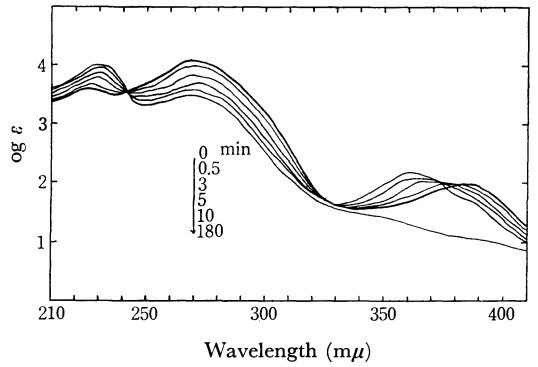

Fig. 2a. The progressive spectral change of diethyl *p*-chlorobenzoylphosphonate in cyclohexane.
Numbers refer to irradiation time.

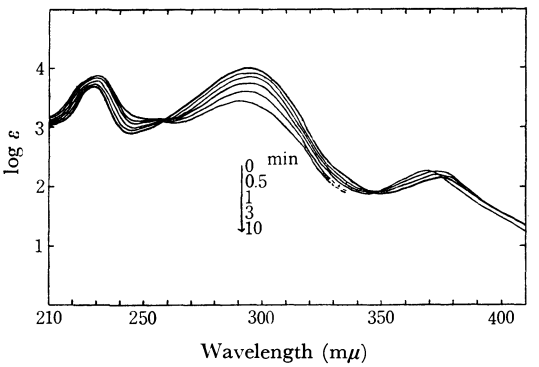

Fig. 2b. The progressive spectral change of diethyl *p*-methoxybenzoylphosphonate on irradiation in cyclohexane.
Numbers refer to irradiation time.

Photochemical Reactions of p-Chloro-, p-t-Butyl- and p-Methoxybenzoylphosphonates. The progressive spectral change in the absorption spectrum of *p*-chlorobenzoylphosphonate at an irradiation above 3200 Å is shown in Fig. 2a, where an isosbestic point is observed at 241 mμ. As the irradiation time increases, both the absorption bands, II (270 mμ) and I (385 mμ), decrease, and new bands, with maxima at 228 mμ and 360 mμ, appear. The new absorption band at 360 mμ, however, began to decrease at the irradiation time of 95 min and completely disappeared within 180 min.

The isolated photoproduct from the irradiated solution was identified as the corresponding pinacol, IId. As is to be expected from the findings on the spectral change, this pinacol has only one high, intense band, at 228 mμ, with no shoulders in the 320—450 mμ region. Similar results have been observed from the experiments with *p*-*t*-butylbenzoylphosphonate.

On the other hand, in *p*-methoxybenzoylphosphonate the photoproduct had very poor solubility in cyclohexane at room temperature, and hence no data on the spectral change over 3 min could be obtained. Figure 2b shows the progressive spectral change in a solution of *p*-methoxybenzoylphosphonate. In this case, the II absorption band (295 mμ) decreased, new bands with maxima at 227 and 366 mμ appeared, and an isosbestic point was observed at 258 mμ.

3) Solvent Effects on the Photochemical Reactions. In order to examine the solvent effect on the photochemical reaction, irradiation through a Pyrex filter was carried out in degassed solutions of aroylphosphonates in various solvents at room temperature. The solvents used in this study were methanol, acetonitrile, carbon tetrachloride, benzene, *N*,*N*-dimethylformamide, dioxane, and *n*-pentane.

The results thus obtained are summarized in Table 8 in the Experimental section. As is obvious from Table 8, the photoproduct from the photolysis of the diethyl benzoylphosphonate solution was the trioxane derivative III in any solvent. On the other hand, the photolysis of di-*n*-butyl benzoylphosphonate under similar conditions in benzene, acetonitrile, and carbon tetrachloride afforded the pinacol IIc in every case much as in cyclohexane.

In the case of the methanol solution, we found, by the observation of the NMR and UV spectra, that the following reaction could proceed in the dark slowly at room temperature.

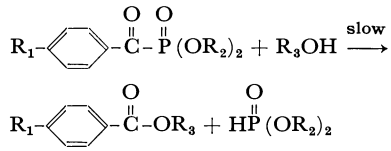

R_1=H, *p*-Cl, *p*-*t*-Bu, *p*-CH_3O
R_2=C_2H_5, iso-C_3H_7, *n*-C_4H_9
R_3=CH_3, C_2H_5, iso-C_3H_7

Further, it has been confirmed that any aroylphosphonate used in this study similarly reacts with alcohols, methanol, ethanol, and isopropyl alcohol. This reaction (for example, R_1=H, R_2=C_2H_5, R_3=CH_3) was observed to proceed to a 73% conversion in 17 hr in the dark at room temperature.

In addition, we could not find any evidence in these photochemical reactions for the corresponding products to undergo a Norrish type-I cleavage, that is, the predissociation of the C–P bond in the phosphonates by irradiation.

These results, obtained in various solvents, afford useful information on photochemical reaction mechanism. The finding of photopinacol formation in the aprotic solvents that the photochemical-excited state of di-*n*-butyl benzoylphosphonate must be able to abstract a hydrogen atom from the other phosphonate molecules to from ketyl radicals. Such a process are similarly suggested by the experiments on the quantum yield of aroylphosphonate disappearance in various solvents, as will be discussed in the next section. If this reaction is operative, the overall quantum yield of aroylphosphonate disappearance may then be greater than unity.

4) Quantum Yields of the Disappearance of Aroylphosphonates. *a) p-Substituted Aroylphosphonates.* The quantum yields of the disappearance of *p*-chloro-, *p-t*-butyl-, and *p*-methoxybenzoylphosphonates in a cyclohexane solution were determined in spectrophotometry. We found that the quantum yield of disappearance depended significantly upon the concentration of the solution in all cases; that is, the higher the concentration, the higher was the quantum yield obtained. A plot of the Φ^{-1} *vs.* the resiprocal of the phosphonate concentration is shown in Fig. 3.

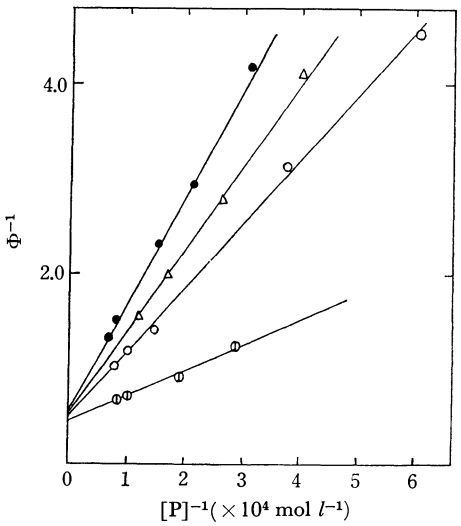

Fig. 3. Plot of Φ^{-1} against the reciprocal of diethyl *p*-substituted aroylphosphonate concentration.
● Cl; ○ $(CH_3)_3C$; △ H; ⓘ CH_3O

As can be seen from Fig. 3, the relation does result in a good linear relationship. These results are of particular interest. Although it is considered that many processes are probably operative in a photochemical reaction, a quantitative treatment of the dependence of quantum yield on the aroylphosphonate concentration will require knowledge concerning the extremely complex inhomogeneous distribution of radicals throughout the volume of the cell.

Furthermore, it was observed that the limited quantum yields of disappearance were significantly altered by the introduction of substituents into the aromatic ring of the phosphonate.

TABLE 1. SUBSTITUENT EFFECTS ON THE QUANTUM YIELD OF DISAPPEARANCE OF AROYLPHOSPHONATE

Substituent	Φ	σ
p-CH_3O	2.100	−0.268
p-$(CH_3)_3C$	2.000	−0.197
p-H	1.850	0
p-Cl	1.792	+0.227

The results obtained are shown in Table 1. Such a substituent effect on the quantum yield has previously been reported in *para*-substituted benzoylphosphonates by Pitts and his co-workers;[4] they demonstrated that the quantum yields of the disappearance of *para*-substituted benzophenones decreased with an increase in the electron-donating ability of the substituent.

However, as is shown in Table 1, we found that, on the contrary, the quantum yields of the disappearance of *para*-substituted aroylphosphonate dropped from 2.10 in *p*-methoxybenzoylphosphonate to 1.79 in *p*-chloro derivatives. This is also evident from Fig. 4, a plot of Φ *vs.* the Hammett σ constants, in which the trend toward a lower quantum yield with an increase in the σ value is pronounced.

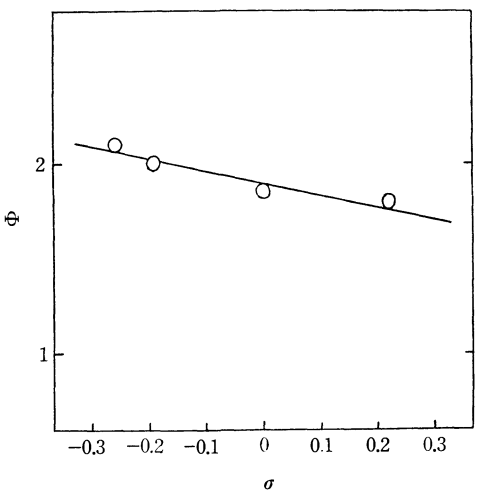

Fig. 4. Plot of Φ against Hammett σ values.

Assuming that a reduction of electronic density occurs on the carbonyl oxygen atom during an n–π^* transition, the Φ *vs.* σ relation indicates that

4) J. N. Pitts, Jr., H. W. Johnson, Jr., and T. Kuwana, *J. Phys. Chem.*, **66**, 2456 (1962); L. H. Piette, J. H. Sharp, T. Kuwana and J. N. Pitts, Jr., *J. Chem. Phys.*, **36**, 3094 (1962); E. J. Baum, J. K. S. Wan and J. N. Pitts, Jr., *J. Amer. Chem. Soc.*, **88**, 2652 (1966).

electronwithdrawing substituents reduce the reactivity of the excited carbonyl group. These facts may be explained in terms of the steric effect concerning the preferred conformation in the aroylphosphonates. The NMR data suggest free rotation around the C–P bond.[5] Dipole-moment measurements have been reported the values of 2.93D for Ia, 3.20D for If, and 2.64D for Id.[6] These values of Id and If are lower and higher respectively than those of the corresponding aldehydes (reported[7] as 3.70D and 2.03D respectively), suggesting that the powerful electron-inductive abilities of the methoxy and chloro functions cause a change in the electron density on the carbonyl carbon atom. That is, the more the electron density on the carbonyl carbon increases, the more the life-time of the conformation in which the carbonyl and phosphoryl groups are opposite may increase. Therefore, it is reasonable to consider that the conformation between the carbonyl and phosphoryl groups can alter the intermolecular hydrogen atom-abstracting ability of the excited carbonyl group.

Although it is recognized that the quantum yield data indicate the excited state reactivities, while, on the other hand, the σ constants and the dipole moment involve ground states only, such a linear relationship between the Φ and σ values appears worthy of comment. Unfortunately, no kinetic data involving σ constants for *para*-substituted benzoylphosphonate in a reaction in which a hydrogen atom or ion is transferred have yet been reported.

However, such a substituent effect is significant and may apply to rate constants.

b) Quenching Effect of 1,3-Pentadiene and O_2. In order to examine this photoreduction mechanism, the effect of the addition of such a quencher as 1,3-pentadiene and oxygen, both of which are well-known as triplet quenchers, was investigated. The quenching efficiency of these additives was found to be significantly sensitive. The quantum yields of the di-*n*-butyl benzoylphosphonate disappearance against the 1,3-pentadiene (piperylene) concentrations are summarized in Table 2. The concentration of benzoylphosphonate was essentially constant throughout these measurements. As is obvious from Table 2, the quantum yield of disappearance in cyclohexane decreased markedly with an increase in the quencher concentration. A plot of Φ^{-1} *vs.* the quencher coccentrations is given in Fig. 5.

Table 2. Quenching effect of 1,3-pentadiene on photoreduction of 3.11×10^{-4}M cyclohexane solutions of di-*n*-butyl benzoylphosphonate

[1,3-Pentadiene] $\times 10^5$	Φ
0	1.309
0.126	1.250
0.530	1.144
1.060	0.925
2.120	0.776

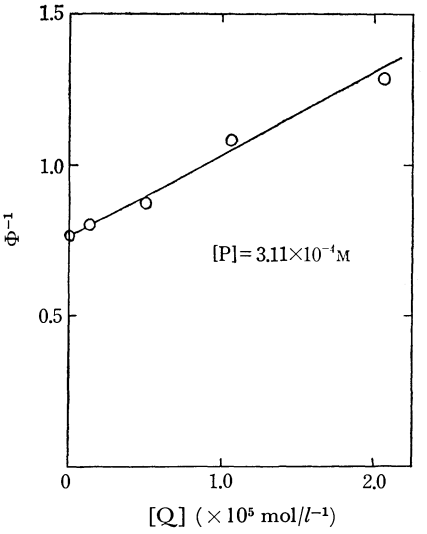

Fig. 5. Plot of Φ^{-1} against 1,3-pentadiene concentration.

A linear relationship of Φ^{-1} against the concentration of piperylene was obtained. Therefore, it is clear that the photochemical reaction proceeds *via* the excited triplet state of aroylphosphonate.

Moreover, the quenching effect of oxygen was examined. In a 1.14×10^{-4}M solution of di-*n*-butyl benzoylphosphonate, the value of the quantum yield of disappearance was 0.870 in a degassed solution, while in a nondegassed solution was 0.377; this observation may be considered to provide evidence for the quenching action of the presence of dissolved oxygen.

c) Solvent Effects on the Quantum Yield of Disappearance. The quantum yields of di-*n*-butyl benzoylphosphonate disappearance were determined in various solvents. The results obtained are summarized in Table 3. As can be seen from Table 3, the quantum yields of disappearance in aprotic solvents indicate smaller values than those in hydrogen-donating solvents. These facts suggest that the excited phosphonate molecule can be abstracting, to a smaller extent, a hydrogen atom from the solvent to form a ketyl radical. However, it should be noted that the quantum yield of disappearance indicates only a little variation depending on whether the solvent is hydrogen-deficient or -donating. As compared with the hydrogen-donating

5) K. D. Berlin and H. A. Taylor, *J. Amer. Chem. Soc.*, **86**, 3862 (1964).

6) See Ref. 5. These values were measured in methyl esters.

7) L. G. Wesson, "Tables of Electric Dipole Moment," The Technology Press, Cambridge, Mass. (1948).

TABLE 3. THE QUANTUM YIELDS OF DISAPPEARANCE OF PHOSPHONATE IN VARIOUS SOLVENTS AT ROOM TEMPERATURE

Solvent	λ_{max} (mμ)	ε	Φ	conc. (mol·l^{-1})
Cyclohexane	259	12880	0.745	1.0×10^{-4}
Ether	259	8850	0.782	1.1×10^{-4}
n-Pentane	259	10380	0.752	1.0×10^{-4}
Acetonititle	261	7920	0.660	1.0×10^{-4}
Carbon tetrachloride	259	8990	0.621	1.0×10^{-4}

solvents, it would be reasonable to conclude that such a high quantum yield of disappearance in aprotic solvents implies the formation of ketyl radicals. As has been mentioned earlier, we know that the solvent effect in photochemical reaction is almost negligible. Consequently, it can be deduced that the excited triplet state of the phosphonate abstracts a hydrogen atom from other phosphonate molecules in the ground state in a photochemical reaction.

5) Electron Spin Resonance Spectra of Irradiated Aroylphosphonates. A low-temperature (77°K) ESR technique was used to investigate whether the triplet state of phosphonate could be detected. When a degassed solution of aroylphosphonate Ia-f was irradiated at 77°K with a filter transparent above 3200 Å, the ESR signal (at *ca.* 1500 gauss) attributable to the triplet state of benzoylphosphonate caused by the transitions between the highest and lowest sublevels and corresponding to $\Delta Ms=2$ was not detected. However, a strong phosphorescence was noted during irradiation in a rigid medium, and an ESR signal (at *ca.* 3000 gauss) attributable to a free radical species of benzoylphosphonate was observed at 77°K. These ESR spectra have a large anisotropic doublet of 53—128 gauss separation and a *g* value almost close to the free spin value.

In a previous paper,[8] we proposed, on the basis of the calculation of these signals, that the greater part of an unpaired electron was localized in the carbonyl carbon atom and was partially delocalized over the P–O group, perhaps through the vacant d orbitals on phosphorus.

In connection with the experimental results on the photochemical reactions in solution, it seems most reasonable to conclude that the structure of the observed radicals is previously postulated for the ketyl radical, which is produced by the hydrogen abstraction of an electron-deficient oxygen atom in the n–π^* triplet state of the carbonyl group in aroylphosphonate Ia-f.

6) Estimated Mechanism of Photopinacolization Reaction. On the basis of these studies, the possible photochemical reaction scheme of aroylphosphonates at an irradiation above 3200 Å can be written as is shown in Eqs. (1)—(8), where P, PH, Q, and RH are the phosphonate molecule, the ketyl radical, the quencher, and the solvent respectively.

$$\mathrm{P} \xrightarrow{h\nu} \mathrm{P}^* \quad (1)$$

$$\mathrm{P}^* + \mathrm{RH} \rightarrow \mathrm{PH} + \mathrm{R}\cdot \quad (2)$$

$$\mathrm{P}^* \rightarrow \mathrm{P} \quad (3)$$

$$\mathrm{P}^* + \mathrm{P} \rightarrow \mathrm{PH} + \mathrm{P}'\cdot \quad (4)$$

$$\mathrm{P}^* + \mathrm{Q} \rightarrow \mathrm{P} + \mathrm{Q}^* \quad (5)$$

$$\mathrm{P}'\cdot + \mathrm{RH} \rightarrow \mathrm{P} + \mathrm{R}\cdot \quad (6)$$

$$\mathrm{R}\cdot + \mathrm{P} \rightarrow \mathrm{PH} + \mathrm{R}' \quad (7)$$

$$2\mathrm{PH} \rightarrow \mathrm{P\text{–}P} \quad (8)$$

It is unlikely that the reaction (7) will occur in the solvents used in this study. The fact that the observed quantum yields of aroylphosphonate disappearance tend toward near 2 can be explained if the reaction (4) is operative. At high concentrations of phosphonate, reaction (4) is thought to become relatively more important.

Finally, we are now investigating the reason why the difference in the alkyl function in the phosphoryl group or the introduction of *para*-substituents drastically changes the product in a photochemical reaction in solution.

Experimental

Preparation of Dialkyl Aroylphosphonates Ia-f. The acid chloride was stirred, drop by drop, into the trialkyl phosphite at 10—20°C in a nitrogen atmosphere. The temperature was raised slowly to room temperature during about a 1-hr period.

The reaction mixture was then distilled under reduced pressure to give dialkyl aroylphosphonate as a yellow oil. The data are listed in Table 4.

TABLE 4. PREPARATION OF AROYLPHOSPHONATES

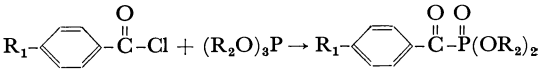

Compound	R_1	R_2	bp °C	bp mm	Yield %	Phosphite: Acid chloride
Ia	H	C_2H_5	142	1.0	70	4 : 3
Ib	H	iso-C_3H_7	127	0.8	55	4 : 3
Ic	H	*n*-C_4H_9	175	4.0	32	4 : 3
Id	*p*-Cl	C_2H_5	159	2.0	57	4 : 3
Ie	*p*-$(CH_3)_3C$	C_2H_5	163	0.8	29	4 : 3
If	*p*-CH_3O	C_2H_5	158	0.5	79	4 : 3

Repeated distillation under reduced pressure was used to purify all the compounds needed. The purity was confirmed by the presence of only one spot after development by the thin-layer chromatographic method. Carbon tetrachlorde, benzene, acetonitrile, *n*-hexane, *n*-pentane, dioxane, *N*,*N*-dimethylformamide (DMF),

8) K. Terauchi and H. Sakurai, This Bulletin, **42**, 2714 (1969).

methanol, and ethanol were purified by ordinary methods.

Steady-light Experiment. The light source employed was a Toshiba high-pressure mercury lamp (Model HLS-4002Å type), while for cutting off below 3200 Å a UV-35 Toshiba filter was used. Aliquots (4 m*l*) of solutions in various concentrations were pipetted into the Pyrex tube equipped with a quartz spectroscopic cell (path-length 10 mm) at the side-arm, and then tubes degassed in four cycles of the freeze-melt technique.

The absorption spectra were taken with a Hitachi EPU-2 spectrophotometer.

Measuremtnt of the Quantum Yield. The chemical change occurring in the photolyte was determined from the change in the optical density at the wavelength of the absorption maximum. The quantum yields of the disappearance of the photolyte were calculated from the form of the absorption spectrum before and after irradiation. The extinction coefficients of aroylphosphonates in cyclohexane which were used for the calculation of the quantum yields are given in Table 5.

Table 5. Extinction coefficients of aroylphosphonates in cyclohexane

Compound	λ_{max} (mμ)	ε, $l\ mol^{-1}\cdot cm^{-1}$
Ia	258	11220
	379	83
Ib	258	11880
	379	82
Ic	259	12880
	380	103
Id	268	12600
	385	93
Ie	271	11500
	375	145
If	294	10250
	373	152

The amount of irradiation absorbed by the solution was determined by the use of a potassium ferrioxalate actinometer[9] with filtered irradiation from a Toshiba high-pressure mercury lamp (HLS-4002A). After irradiation, aliquots of the ferrioxalate solution were treated with phenanthroline and analyzed for the ferrous ion. The mean value for the irradiation absorbed was 3.22×10^{16} quanta/sec without the photolyte solution and 3.189×10^{16} quanta/sec with the photolyte solution. The difference between these two quantities, 3.507×10^{14} quanta/sec, is the quantity of irradiation absorbed by the aroylphosphonate solution.

General Procedure of the Photolysis of Aroylphosphonates in Cyclohexane. A mixture of 1.0 g of aroylphosphonate and 30 m*l* of cyclohexane in a Pyrex tube was degassed by the freezement technique and then irradiated with a 400-Watt high-pressure mercury are at room temperature. The irradiation was carried out until the yellow color of the solution was entirely bleached out. After irradiation evaporating the solvent at reduced pressure, either a white solid or a colorless, oily photoproduct was obtained. These products were dried under a high vacuum for several hours. The analytical and spectral data of these photoproducts are summarized in Tables 6 and 7.

Table 6. Analytical data for the photoproducts from aroylphosphonates Ib—f

Compound	Irrad. hr	Formula	Molecular weight* Found	Molecular weight* Calcd.	Anal. Found (Calcd) C (%)	H (%)	P (%)
Ib	5	$C_{26}H_{40}O_8P_2$	551	542	57.22 (57.50)	7.37	11.42 (11.44)
Ic	5	$C_{30}H_{48}O_8P_2$	596	598	59.98 (60.20)	8.25	9.96 (10.37)
Id	4	$C_{22}H_{30}O_8P_2Cl_2$	553	555	47.29 (47.56)	5.88	11.50 (11.79)
Ie	5	$C_{30}H_{48}O_8P_2$	589	598	59.88 (60.20)	8.27	10.30 (10.37)
If	4	$C_{24}H_{36}O_{10}P_2$	544	546	52.52 (52.74)	6.60	11.47 (11.35)

* Measured by the vapor phase osmometry in benzene at 45°C.

Table 7. The spectral data for the photoproducts from aroylphosphonates Ib—f

Compound	IR (cm^{-1})	UV (λ_{max} mμ, log ε)
Ib	3300 (ν OH), 1595 (phenyl), 1380 (δ_s CH_3), 225 (ν P=O), 1130, 1020 (P-O-C)	240 (3.11) alone
Ic	3200 (ν OH), 1595 (phenyl), 1225 (ν P=O), 1130, 1025 (P-O-C)	237 (3.01) alone
Id	3300 (ν OH), 1588 (phenyl), 1220 (ν P=O), 1160, 1010 (P-O-C)	224*(4.11), 268*(3.79)
Ie	3300 (ν OH), 1595 (phenyl), 1225 (ν P=O), 1160, 1015 (P-O-C)	228 (4.19), 266 (3.40)
If	3350 (ν OH), 1590 (phenyl), 1230 (ν P=O), 1160, 1020 (P-O-C)	288*(3.52)alone

* Measured in acetonitrile solution.

On the basis of these data, the photoproducing agent was identified as the pinacol II. The treatment of the photopinacol II with dilute or concentrated hydrochloric acid in an attempt to produce the phosphonic acid derivative was unsuccessful, giving only tar. After alkaline hydrolysis with a 17% potassium hydroxide solution, treatment with 2,4-dinitrophenylhydrazine in ethanol gave the hydrazone derivatives. This hydrazone was washed by 20% aqueous methanol and dried under reduced pressure over calcium chloride. The benzaldehyde 2,4-dinitrophenylhydradrazone

9) C. G. Hatchard and C. A. Parker, *Proc. Roy. Soc.*, **A235**, 518 (1956).

Table 8. Analytical data for the photoproducts from Ia and Ic in various solvents

Compound irradiated	Solvent	Irrad. hr	Molecular weight* Found	Anal. Found C (%)	H (%)	P (%)
Ia	Cyclohexane	5	721	54.28	6.41	12.72[a]
	n-Pentane	5	724	54.38	6.29	12.60
	Acetonitrile	6	725	54.10	6.19	12.58
	Dioxane	5	722	54.29	6.37	12.55
	CCl_4	10	724	54.22	6.43	12.59
	Benzene	5	725	54.28	6.28	12.66
	DMF	8	718	54.24	6.55	12.49
Ic	Acetonitrile	5	597	59.55	8.32	10.11[b]
	Benzene	5	591	59.80	8.22	10.26
	CCl_4	10	592	59.92	8.27	10.17

a) Calcd for $C_{33}H_{45}O_{12}P_3$: Mol wt; 726, C, 54.54; H, 6.20; P, 12.81%.

b) Calcd for $C_{30}H_{48}O_8P_2$: Mol wt; 598, C, 60.20; H, 8.02; P, 10.37%.

* Measured by the vapor phase osmometry in benzene at 45°C.

melted at 241—242°C (lit, mp 237°C). These observation suggest that the pinacol undergoes carbon-carbon bond cleavage to form the α-hydroxy phosphonic ester, which is then further hydrolyzed by the excess base to yield the aldehyde.

Photolysis of Ia and Ic in Various Solvents. The photolyses were carried out by a similar method. The analytical data of the photoproducts are summarized in Table 8.

The IR spectrum of the photoproduct from no solution of Ia showed any carbonyl absorption. IR(KBr disk); 1600, 1440 (phenyl), 1220 (P=O), 1160, and 1020 (P–O–C) cm^{-1}. The UV spectrum had only one high intense band ($\lambda_{max}^{CH_3CN}$ 245 mμ, log ε 3.27), with no shoulders in the 280—450 mμ region. Attempts to lead from this compound to the phosphonic acid by acid or alkaline hydrolysis under any conditions were unsuccessful.

No useful information on the structure could be obtained from the NMR spectrum. Although the structure of the trimer contains several configurations, the structure, III, we have proposed seems to accord best with the observed data.

On the other hand, the product from Ic was identified as the IIc pinacol by means of the same spectral data, as is shown in Table 7, and by means of the analytical data (Table 8).

BULLETIN OF THE CHEMICAL SOCIETY OF JAPAN VOL. 43 890—897 (1970)

Stereospecific Polymerization of Allyl Vinyl Ether by $BF_3 \cdot OEt_2$

Heimei YUKI, Koichi HATADA, Koji OHTA and Takashi SASAKI

Department of Chemistry, Faculty of Engineering Science, Osaka University, Toyonaka, Osaka

(Received September 8, 1969)

The polymerization of allyl vinyl ether was carried out by means of $BF_3 \cdot OEt_2$. The reaction proceeded through the vinyl double bond, and a polymer with allyl ether side chains was obtained. The effects of the polymerization conditions on the stereoregularity of the polymer were studied by means of NMR spectroscopy using a spin decoupling technique. A highly isotactic polymer was obtained at −78°C in toluene. The isotacticity of the polymer decreased slightly with a rise in the reaction temperature and with an increase in the initial monomer concentration. When the reaction was carried out in a mixture of toluene and nitroethane, a marked decrease in the isotacticity and the solution viscosity of the polymer was observed with an increase in the amount of nitroethane. The solution viscosity of the polymer decreased with an increase in the polymerization temperature and the catalyst concentration, and increased with an increase in the initial monomer concentration. The reaction between the polymer and HBr in acetic acid yielded a ternary copolymer consisting of vinyl alcohol, vinyl acetate, and vinyl bromide units.

Many papers have been published on the stereospecific polymerization of vinyl ethers.[1-6] However, only a few investigations have been done on the

1) C. E. Schildknecht, S. T. Gross, H. R. Davidson, J. M. Lambert and A. O. Zoss, *Ind. Eng. Chem.*, **40**, 2104 (1948).

2) H. Yuki, K. Hatada, K. Ohta, I. Kinoshita, K. Ono, S. Murahashi and Y. Ito, *J. Polym. Sci.*, Part *A-1*, **7**, 1517 (1969).

3) S. Murahashi, S. Nozakura and M. Sumi, *Polym. Lett.*, **3**, 245 (1965).

4) S. Murahashi, S. Nozakura, M. Sumi and K. Matsumura, *ibid.*, **4**, 59 (1966).

5) G. J. Blake and A. M. Carlson, *J. Polym. Sci.*, Part *A-1*, **4**, 1813 (1966).

6) S. Okamura, T. Kodama and T. Higashimura, *Makromol. Chem.*, **53**, 180 (1962).

polymerization of allyl vinyl ether (AVE) by cationic catalysts,[7,8] and there have been no information concerning the stereospecific polymerization of this monomer.

The present authors studied the polymerization of AVE by $BF_3 \cdot OEt_2$ and found that the polymerization proceeded through the vinyl double bond and that a polymer containing one allyl double bond per monomer unit was obtained. The tacticity of the polymer were analyzed by means of NMR spectroscopy using a spin decoupling technique, and the effects of the polymerization conditions on the stereoregularity of the polymer were investigated. The reaction of poly(allyl vinyl ether) (PAVE) with hydrogen bromide was also studied.

Experimental

Reagents. AVE was prepared from isobutyl vinyl ether and allyl alcohol by transetherification using mercuric acetate as the catalyst.[9] The crude product was purified by refluxing it over calcium hydride and then over lithium aluminum hydride under nitrogen pressure, after which it was distilled *in vacuo*. Bp, 67.0°C. The purified AVE was sealed in an ampule under dry nitrogen and stored at −20°C.

The isobutyl vinyl ether was purified by shaking it several times with 5% aqueous sodium hydroxide, dried with anhydrous potassium carbonate, and then refluxed over calcium hydride. It was finally distilled from calcium hydride using an efficient column. Bp, 82.8—83.0°C.

The allyl alcohol was dried with molecular sieves 4A and distilled under nitrogen pressure. Bp, 96.0—97.0°C.

The toluene was purified and dried by a usual method and was distilled from calcium hydride. Then the distillate was mixed with a small amount of *n*-butyllithium in a toluene solution and distilled on a vacuum line before use.

The *n*-hexane and *n*-heptane were purified by usual methods and stored over calcium hydride. Each was mixed with a small amount of *n*-butyllithium in the same solvent and distilled on a vacuum line just before use.

The nitroethane was purified by distillation, dried with molecular sieves 4A, and distilled under a high vacuum just before use.

The methylene chloride was shaken with concentrated sulfuric acid, washed with aqueous sodium hydroxide and water, dried over calcium chloride, and distilled. The distillate was dried with a mixture of calcium hydride and molecular sieves 4A and then distilled again under a vacuum just before use.

The tetralin, dioxane, and acetic acid were purified and dried by usual methods.

The hydrogen bromide was prepared by dropping dry bromine into tetraline at 60°C under nitrogen pressure.

The nitrogen was dried by being passed through molecular sieves 4A cooled at −78°C.

The boron trifluoride etherate ($BF_3 \cdot OEt_2$) was purified by distillation under reduced nitrogen pressure and was used as a toluene solution.

Polymerization. A vessel equipped with a three-way stop-cock was flushed with dry nitrogen. The monomer and a solvent were introduced with hypodermic syringes. To this solution, cooled at a given temperature, the catalyst solution was then added, drop by drop, using a syringe. The polymerization was stopped by adding a small amount of ammoniac methanol which had been cooled at the same temperature as the reaction mixture. The mixture was then poured into a large amount of methanol containing a small amount of phenyl-β-naphthylamine. The precipitated polymer was collected by filtration, washed thoroughly with the same methanol, and dried *in vacuo* at room temperature for 2 days. The polymer was stored under nitrogen atmosphere at −20°C to avoid the formation of cross-linked insoluble polymer. When the polymer was low-molecular and was soluble in methanol, the solution was concentrated to dryness under a high vacuum; the residual polymer was then redissolved in benzene in order to free it from inorganic materials and dried by the freeze-drying method.

Reaction of PAVE with HBr. Dry hydrogen bromide was bubbled through a solution of PAVE in toluene at room temperature under nitrogen pressure. After the reaction has been completed, dry nitrogen was passed through the reaction mixture in order to remove the excess hydrogen bromide, and then the mixture was poured into a large amount of methanol in order to precipitate the product. After the mixture had stood overnight, the resultant polymer was collected, washed with methanol, and dried *in vacuo*.

When the reaction was carried out in acetic acid, the polymer was not completely soluble in the medium at the begining, but it was gradually dissolved in the course of the reaction. In the reaction the formation of poly(vinyl acetate) was expected. However, the reaction product did not contain a methanol-soluble part.

Measurements of NMR Spectra. NMR spectra were obtained with a JEOL JNM-4H-100 spectrometer at 100 MHz by using a 5 w/v% solution containing a small amount of tetramethylsilane as an internal standard. The spectra of the polymer and AVE were measured in carbon tetrachloride at 60°C and in chloroform at 22.5°C respectively.

Measurements of IR Spectra. The IR spectra of the polymer were taken on a JASCO IR-S spectrometer, casting the polymer film on a rock salt plate from a benzene solution.

Viscosity Measurements. The solution viscosity of the polymer was measured on its benzene solution (0.1 g/dl) at 30.0±0.03°C using an Ostwald viscometer.

Results

NMR Spectra and Structure of PAVE. Figure 1 shows the NMR spectrum of PAVE obtained at −78°C in toluene, together with the spectrum of AVE. The spectrum of PAVE consists of five peaks which correspond to the β-methylene, α-methine, allyl methylene protons, and terminal methylene and methine protons in an allyl double

7) R. Paul, G. Roy, M. Fluchaire and G. Collardeau, *Bull. Soc. Chim. Fr.*, **1950**, 121.

8) J. Lal, *J. Polym. Sci.*, **31**, 179 (1958).

9) W. H. Watanabe and L. E. Conlon, *J. Amer. Chem. Soc.*, **79**, 2828 (1957).

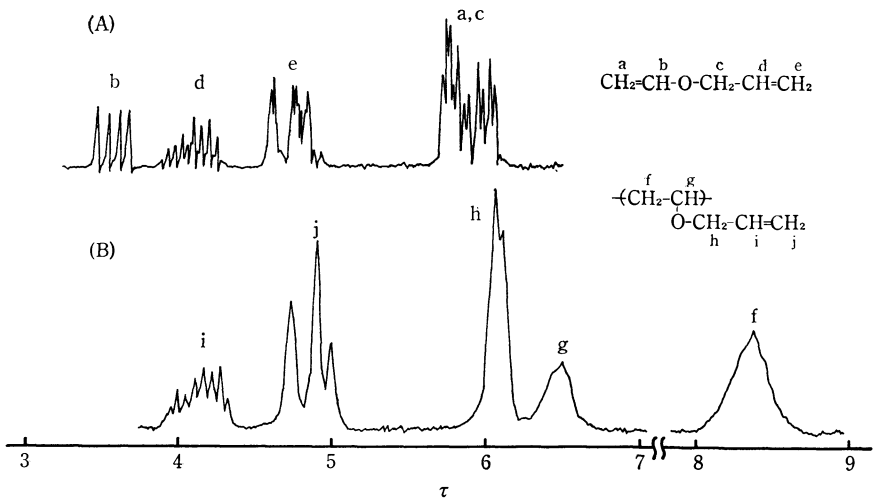

Fig. 1. NMR spectra of allyl vinyl ether (A) and poly (allyl vinyl ether) polymerized by $BF_3 \cdot OEt_2$ at −78°C in toluene (B).

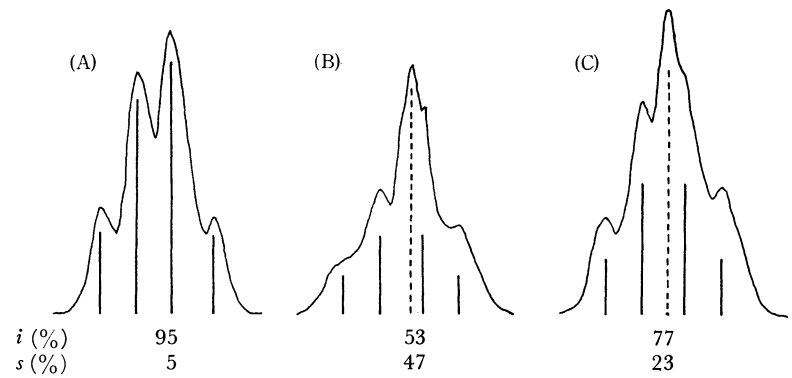

Fig. 2. β-Proton resonance spectra decoupled from α-proton of poly (allyl vinyl ether)s prepared at −78°C by $BF_3 \cdot OEt_2$ in toluene (A), by $BF_3 \cdot OEt_2$ in nitroethane (B) and by $EtAlCl_2$ in toluene (C).
——— isotactic dyad, ------ syndiotactic dyad

bond with a decrease in the magnetic field. The intensity ratio of these five peaks is 2.1 : 1.0 : 2.0 : 1.9 : 1.1. There is no resonance at about 3.6 and 5.6—6.0 τ, where the resonances due to the protons of vinyl group in the polymer may appear, if they exist, as is observed in the spectrum of AVE. These results suggest that AVE polymerizes exclusively through the vinyl double bond and that the polymer contains one pendant allyl group per monomer unit.

The polymers obtained under various conditions showed the same spectra as that of PAVE obtained at −78°C in toluene, suggesting that the mode of polymerization did not depend on the reaction conditions.

Determination of Tacticity of PAVE. In the undecoupled spectrum of PAVE (Fig. 1B) it was impossible to discriminate the respective multiplets arising from the nuclei in different stereochemical sequences because the spin-spin coupling complicated the spectrum greatly. However, the resonance of the β-protons appeared to be sensitive to the stereochemical configuration in the spin decoupled spectrum, as is shown in Fig. 2.

The β-proton resonance of PAVE obtained at −78°C in toluene showed a typical AB quartet (Fig. 2A) when decoupled from the α-proton, suggesting that the polymer is highly isotactic.

On the other hand, the decoupled resonance of PAVE obtained in nitroethane exhibited five components, as is shown in Fig. 2B. Generally in cationic polymerization vinyl ether gives a less isotactic polymer as the reaction medium is more polar.[10-12] Therefore, the above resonance may

10) T. Higashimura, T. Watanabe, K. Suzuoki and S. Okamura, *J. Polym. Sci.*, **C**, **No. 4**, 361 (1963).
11) T. Higashimura, K. Suzuoki and S. Okamura, *Makromol. Chem.*, **86**, 259 (1965).
12) M. Sumi, S. Nozakura and S. Murahashi, *Kobunshi Kagaku*, **24**, 424 (1967).

be considered to be the overlap of an AB quartet due to the isotactic methylene and a singlet due to the syndiotactic methylene, which are equivalent. Although the spectral resolution was not sufficient, the fraction of the tactic dyad can be estimated from the relative areas of the AB quartet and singlet within an error of $\pm 5\%$.

The resonance of the α-proton seems not to be so sensitive to the stereochemical configuration of the polymer chain that the fraction of the tactic triad can not be determined by NMR spectroscopy.

Effect of Polymerization Temperature. The polymerizations were carried out in toluene at various temperatures ranging from -78 to 0°C. The results are shown in Fig. 3. The polymerization

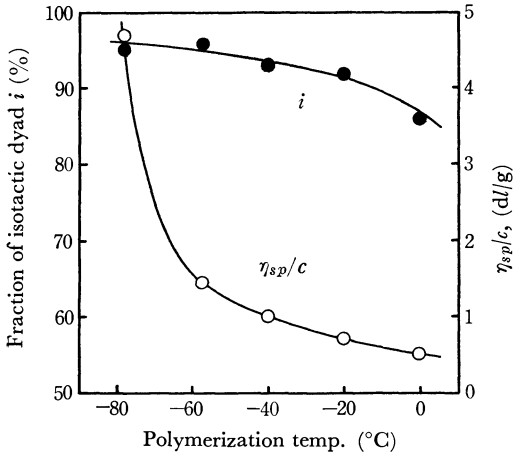

Fig. 3. Effect of temperature on the polymerization of allyl vinyl ether by $BF_3 \cdot OEt_2$ in toluene for 1 hr.
Monomer 20 mmol, $BF_3 \cdot OEt_2$ 0.1 mmol, total volume of the system 22 m*l*

was always almost completed within one hour even at -78°C. The isotacticity of the polymer decreased slightly with a rise in the polymerization temperature. On the other hand, a marked decrease was observed in the molecular weight of the polymer at higher polymerization temperatures. The polymer obtained at 0°C was a viscous oil and was soluble in methanol.

Effect of Catalyst Concentration. Figure 4 shows the results of the polymerizations carried out with various catalyst concentrations at -78°C in toluene. The polymerization was always almost completed in one hour at any catalyst concentration above 4.6×10^{-3} mol/*l*. The solution viscosity of the polymer remarkably decreased with an increase in the catalyst concentration.

Effect of Monomer Concentration. The polymerization was carried out at various monomer concentrations in toluene at -78°C. The results are given in Fig. 5. The isotacticity of the polymer was enhanced with a decrease in the initial monomer concentration. The solution viscosity of the polymer

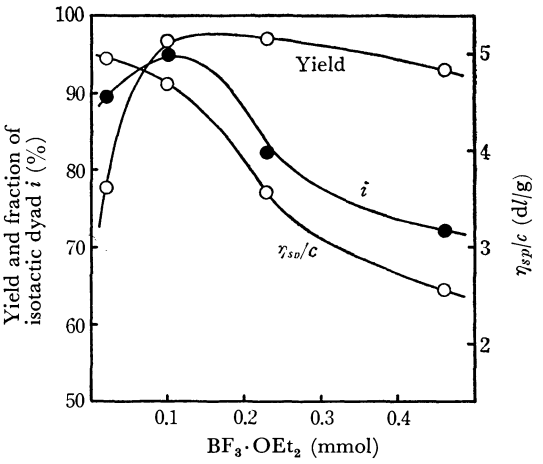

Fig. 4. Effect of catalyst amount on the polymerization of allyl vinyl ether by $BF_3 \cdot OEt_2$ in toluene at -78°C for 1 hr.
Monomer 20 mmol, total volume of the system 22 m*l*

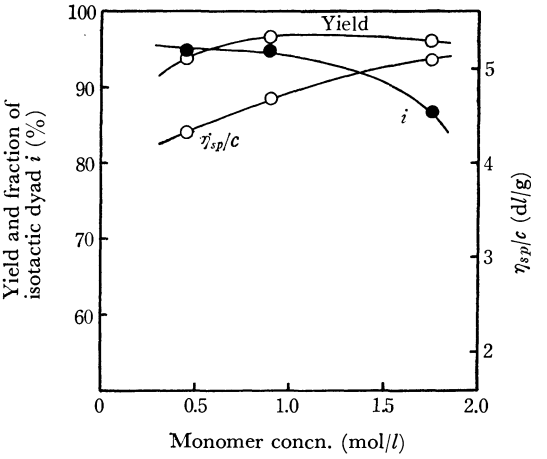

Fig. 5. Effect of monomer concentration on the polymerization of allyl vinyl ether by $BF_3 \cdot OEt_2$ in toluene at -78°C for 1 hr.
$BF_3 \cdot OEt_2$ 0.1 mmol, total volume of the system 22 m*l*

increased with an increase in the initial monomer concentration.

Polymerization in Various Solvents. The results of polymerizations in various solvents at -78°C are listed in Table 1. The isotacticity of the polymer was lowered in a polar solvent. In the polymerization in *n*-hexane or *n*-heptane, the polymer produced was precipitated during the course of the reaction, and the yield and the isotacticity of the polymer were both lowered.

The polymerization was carried out in toluene-nitroethane mixtures at -78°C. The results are shown in Fig. 6. A gradual decrease in the isotacticity and a rapid decrease in the solution viscosity of the polymer were observed with an

TABLE 1. POLYMERIZATION OF ALLYL VINYL ETHER IN VARIOUS SOLVENTS AT −78°C FOR 1 hr
Monomer 20 mmol, $BF_3 \cdot OEt_2$ 0.1 mmol, total volume of the system 22 m*l*

Solvent	Polymer			
	Yield (%)	Tacticity (%)		η_{sp}/C^a (d*l*/g)
		i	*s*	
Toluene	96.6	95	5	4.70
$EtNO_2$	94.1	53	47	0.55
CH_2Cl_2	82.6	87	13	1.81
n-Hexane	37.4	69	31	2.05
n-Heptane	47.8	63	37	3.45

a) Determined at 30.0°C with a benzene solution at 0.1 g/d*l*

increase in the fraction of nitroethane in the medium.

Reaction of PAVE and HBr. The reactions of PAVE with HBr were carried out in toluene, dioxane, and acetic acid. The results are given in Table 2. The reaction products in toluene and dioxane were not soluble in usual organic solvents and contained a considerable amount of bromine.

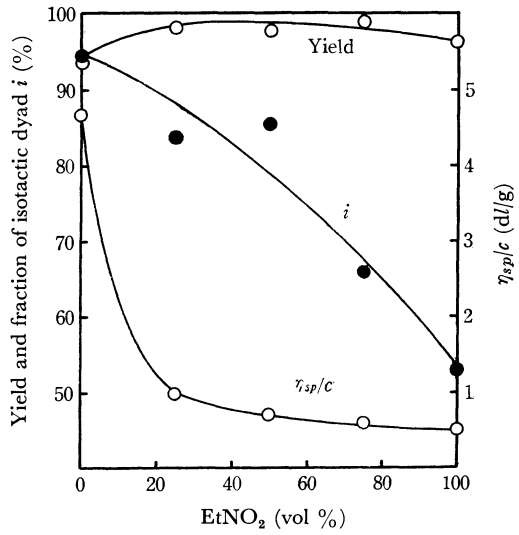

Fig. 6. Polymerization of allyl vinyl ether by $BF_3 \cdot OEt_2$ at −78°C for 1 hr in toluene-nitroethane mixed solvent.
Monomer 20 mmol, $BF_3 \cdot OEt_2$ 0.1 mmol, total volume of the system 22 m*l*

TABLE 2. REACTION OF PAVE WITH HBr IN VARIOUS SOLVENTS

No.	Solvent	(m*l*)	PAVE		Reaction time (hr)	Reaction product				
			(g)	η_{sp}/C (d*l*/g)		Yield (g)	Elementary analysis (%)			
							C	H	O	Br
A-82	Toluene	60	0.957	2.7	1	0.788	48.77	7.54	20.74	22.95
B02	Toluene	150	1.448	2.6	5	1.103	48.08	7.68	24.49	19.75
B03	Dioxane	200	1.460	2.6	5	0.959	55.63	8.03	23.72	12.62
B04	Acetic acid	80	0.783	1.2	3	0.684	38.83	5.09	16.99	39.09
K-15	Acetic acid	110	1.010	—	2.5	1.163	37.85	4.81	15.85	41.49

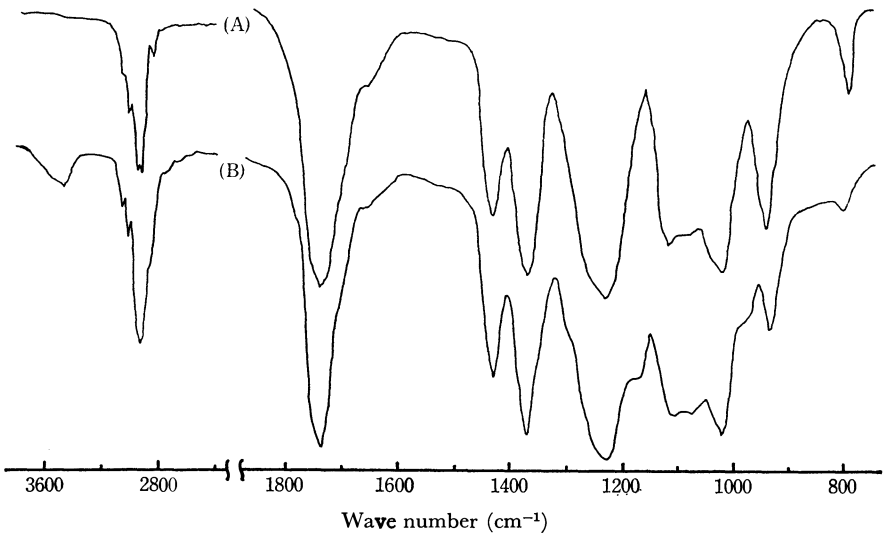

Fig. 7. Infrared spectra of PVAc polymerized by AIBN (A) and reaction product of PAVE with HBr in glacial acetic acid (B).

Table 3. Possible structural units for the reaction product of PAVE and HBr

	Structure	Mol. formula	C (%)	H (%)	O (%)	Br (%)
I	$-\left(-CH_2-CH(OCH_2-CH=CH_2)-\right)_n-$	C_5H_8O	71.39	9.59	19.02	0
II	$-\left(-CH_2-CH(OH)-\right)_n-$	C_2H_4O	54.52	9.17	36.31	0
III	$-\left(-CH_2-CH(OCH_2-CH(Br)-CH_3)-\right)_n-$	C_5H_9OBr	36.40	5.50	9.70	48.43
IV	$-\left(-CH_2-CH(O-COCH_3)-\right)_n-$	$C_4H_6O_2$	55.80	7.03	37.17	0
V	$-\left(-CH_2-CH(OCOCH_2Br)-\right)_n-$	$C_4H_5O_2Br$	29.12	3.05	19.39	48.43
VI	$-\left(-CH_2-CBr(OCOCH_3)-\right)_n-$	$C_4H_5O_2Br$	29.12	3.06	19.39	48.43
VII	$-\left(-CH_2-CH(Br)-\right)_n-$	C_2H_3Br	22.45	2.83	0	74.73

When the reaction was performed in acetic acid, the product was not soluble in methanol, but it was soluble in toluene, benzene, acetone, and chloroform. It also contained about 40% of bromine. As is shown in Fig. 7 the infrared spectrum of this product was almost identical with that of poly(vinyl acetate) except for an absorption at 3490 cm^{-1} due to an OH group. These results suggest that the product was composed of vinyl acetate and vinyl alcohol units, plus a unit containing bromine. The possible structures for the constituent units are summarized in Table 3. Among the bromine-containing units, the vinyl bromide unit is most relevant because the other three units have a bromine content close to that of the product, which may be assumed to contain considerable amounts of vinyl acetate and vinyl alcohol units.

The NMR spectrum of the reaction product of PAVE and HBr is shown in Fig. 8 and compared with that of poly(vinyl acetate). In the spectrum there are a sharp singlet resonance of the acetoxy methyl proton, a broad multiplet probably due to the β-methylene proton overlapping with the methyl resonance, and three peaks, at 6.40, 5.93, and 4.93 τ, in the region of the methine proton resonance. The literature[13] indicates that the τ values corresponding to the methine protons in the structures of –CH(OH)–, –CHBr–, and –CH(OCOCH$_3$)– are 6.4, 5.9, and 5.0 τ respectively. Therefore, the three peaks at 6.40, 5.93, and 4.93 τ may be tentatively assigned to the methine protons in the structural units of vinyl alcohol, vinyl bromide, and vinyl acetate respectively.

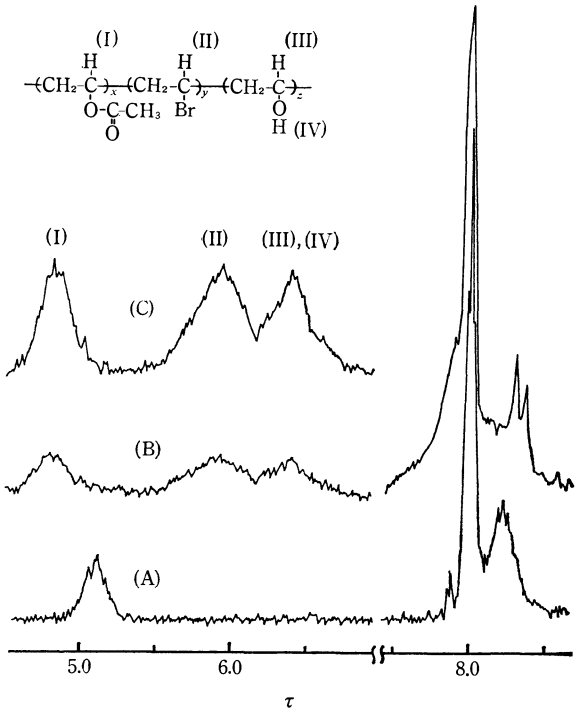

Fig. 8. NMR spectra of (A) PVAc prepared by AIBN, (B) reaction product of PAVE with HBr in AcOH and (C) the slow sweep of B.

On the basis of this assignment, the fraction of the three structural units in the reaction product can be estimated from the intensity ratio of these three methine resonances, assuming that the resonance of the hydroxy proton in the vinyl alcohol

13) R. M. Silberstein and G. C. Bassler, "Spectrometric Identification of Organic Compounds," 2nd Ed., John Wiley & Sons Inc., N. Y. (1963). p. 137.

TABLE 4. COMPOSITION OF THE REACTION PRODUCT OF PAVE AND HBr

No.	$-\left(-CH_2-CH(OCOCH_3)-\right)_x-\left(-CH_2-CH(Br)-\right)_y-\left(-CH_2-CH(OH)-\right)_z$			Elementary Analysis* (%)		
	x	y	z	C	H	Br
K-15	1	1.38	0.67	36.99	4.92	41.88
				(37.40)	(4.99)	(40.88)
B04	1	1.34	0.60	36.99	4.90	41.85
				(38.19)	(5.10)	(39.11)

* Values in parentheses are calculated for the ratio x, y, and z determined.

unit overlaps with its methine resonance at 6.40 τ. The results are shown in Table 4. The elementary compositions calculated for the determined ratio of the three structural units is in good agreement with that observed by the analysis. This shows the validities of the assignment of the NMR spectrum and the structure of the reaction product presumed to be a ternary copolymer of vinyl acetate, vinyl alcohol, and vinyl bromide.

Discussion

Two double bonds in AVE are expected to participate in the polymerization reaction, either independently or together as in the cyclopolymerization of α,ω-diolefin.[14] However, all the PAVEs obtained by $BF_3 \cdot OEt_2$ under various conditions gave NMR spectra in which the resonances characteristic of the vinyl protons disappeared and the peaks due to the protons of the allyl double bond remained unchanged (Fig. 1). This shows that, by means of the $BF_3 \cdot OEt_2$ catalyst, this monomer polymerized exclusively through the vinyl double bond, leaving the allyl double bond unaffected during the polymerization. The polymer could subsequently be cross-linked through the allyl side chains over a long period at room temperature.

The solution viscosity of the PAVE obtained in toluene at -78°C increased with the increase in the monomer concentration (Fig. 5). This suggests that there is no or only a little chain-transfer reaction to the monomer in the polymerization. The marked decrease in the viscosity of the polymer with a rise in the polymerization temperature (Fig. 3) indicates that the contribution of the chain-transfer or termination reaction becomes greater at elevated temperatures. The decrease in the viscosity with an increase in the catalyst concentration (Fig. 4) will indicate the existence of a chain-transfer reaction to the catalyst. However, this is not conclusive, because a temporary elevation of the temperature in the reaction mixture was observed at a higher concentration of catalyst; this may cause the depression of the molecular weight of the polymer.

A number of NMR studies of poly(alkyl vinyl ether) have been reported, and the tacticity of polymer has been determined with[15] and without[2,16,17] the spin decoupling technique. In this work we have determined the fraction of the tactic dyad in PAVE by analysis of the decoupled spectrum, in which the resonance of β-protons decoupled from the α-proton was sensitive to the stereochemical configuration.

Generally the cationic polymerization at a low temperature gave an isotactic polymer in a non-polar solvent and a syndiotactic one in a polar solvent. This was explained by the ion-pair mechanism in a non-polar system and by the free-ion propagation in a polar system.[11,3] *t*-Butyl vinyl ether[11] and trimethylsilyl vinyl ether[18] gave isotactic polymers in toluene and rather syndiotactic polymers in nitroethane or methylene chloride. On the other hand, in the polymerization of benzyl vinyl ether[2] a fairly isotactic polymer was obtained even in a polar solvent and the isotacticity of the polymer decreased only slightly at elevated temperatures. The specific participation of the benzyl group was suggested in this stereoregulated polymerization.

Allyl vinyl ether gave a highly isotactic polymer at -78°C in toluene, and the decrease in the isotacticity was very small at higher temperature (Fig. 3), although it was observed remarkably in a polar medium (Table 1 and Fig. 6). This behavior of AVE may be attributable to the similarity between the allyl group and the benzyl group in benzyl vinyl ether.

It has been previously reported that an isotactic poly (benzyl vinyl ether) gave an isotactic poly(vinyl alcohol) by debenzylation reaction with HBr in toluene.[19] The reaction of PAVE with HBr in

14) N. D. Field, *J. Org. Chem.*, **25**, 1006 (1960).

15) K. C. Ramey, N. D. Field and A. E. Borchert, *J. Polym. Sci.*, **A3**, 2885 (1965).

16) S. Brownstein and D. M. Wiles, *ibid.*, **A2**, 1901 (1964).

17) K. C. Ramey, N. D. Field and I. Hasegawa, *ibid.*, **B2**, 865 (1964).

18) S. Murahashi, S. Nozakura, M. Sumi, H. Yuki and K. Hatada, *Kobunshi Kagaku*, **23**, 605 (1966).

19) S. Murahashi, H. Yuki, T. Sano, U. Yonemura. H. Tadokoro and Y. Chatani, *J. Polym. Sci.*, **62**, No. 174, S 77 (1962).

toluene or dioxane gave an insoluble product containing a considerable amount of bromine. It was probably cross-linked through the allyl side chains by a cationic mechanism. In the reaction in acetic acid, the product was revealed to be a ternary copolymer of vinyl alcohol, vinyl acetate, and vinyl bromide by IR and NMR spectroscopies. The vinyl acetate unit must have been produced by a further reaction of the vinyl alcohol unit and acetic acid. It is not certain at present whether the vinyl bromide unit was formed by the reaction of the vinyl alcohol unit and HBr or by the cleavage of the ether linkage by HBr on the opposite side.

The authors wish to express their sincere thanks to Mr. Y. Terawaki for the NMR experiments and to Mr. K. Nagata and Mrs. F. Yano for clerical assistance in preparing the manuscript.

BULLETIN OF THE CHEMICAL SOCIETY OF JAPAN VOL. 43 897—901 (1970)

The Total Synthesis of Dehexyl-deisovaleryloxy-antimycin A_1*1

Mitsuhiro KINOSHITA and Sumio UMEZAWA

Department of Applied Chemistry, Faculty of Engineering, Keio University, Koganei-shi, Tokyo

(Received September 8, 1969)

A biologically active prototype of antimycin A series has been synthesized. The dilactone moiety was synthesized from a masked L-threonine and γ-hydroxyvalerate and condensed with an *O*-masked derivative of 3-nitrosalicylic acid *N*-hydroxysuccinimide ester. Hydrogenation followed by formylation afforded the anti-fungal substance. This synthesis established a possible general synthetic pathway to the members of antimycin A.

In 1949 F. M. Strong and his co-workers[1] isolated antimycin A and by later works[2] it was revealed that the crystalline antibiotic was a complex of at least four closely related active components. Antimycin A is a potent antibiotic against fungi and, especially, owes its interest to the fact that it is remarkably effective in inhibiting the hydrogen transport systems of aerobic organisms.[3]

The structures of antimycin A_1 (**1b**) and A_3 (**1c**) were elucidated by several research groups[4] on chemical and spectral evidences, and variations in the higher alkyl side chains account for structural differences between the members of the antimycin complex.

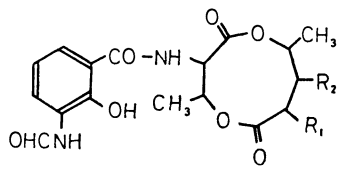

	1a	**1b**	**1c**
R_1:	H	n-C_6H_{13}	n-C_4H_9
R_2:	H	i-C_4H_9COO	i-C_4H_9COO

The most striking characteristic of the structure of antimycin A is its dilacton ring linked *via* an amide linkage to 3-formamidosalicylic acid. We were interested in the total synthesis of antimycin A, and attempted, in the first place, to synthesize a prototype in which the structure of dilactone moiety was made somewhat simpler than that in the natural antimycin A. This paper presents the total synthesis of dehexyl-deisovaleryloxy-antimycin A_1 (**1a**) which differs from natural antimycin A

*1 Part XXXIX of "Studies on Antibiotics and Related Substances" by Sumio Umezawa. This paper was read before the 22nd Annual Meeting of the Chemical Society of Japan, Tokyo, April, 1969. (See Preprints for the Meeting, Vol. 3, p. 1874). A part of this work has been briefly communicated: M. Kinoshita and S. Umezawa, This Bulletin, **42**, 854 (1969).

1) B. R. Dunshee, C. Lebens, G. W. Keitt and F. M. Strong, *J. Amer. Chem. Soc.*, **71**, 2436 (1949).

2) H. G. Schneider, G. M. Tenner and F. M. Strong, *Arch. Biochem. Biophys.*, **37**, 147 (1951); J. L. Lockwood, C. Lebens and G. W. Keitt, *Phytopathology*, **49**, 438 (1954).

3) For a general review, see J. S. Rieske, "Antimycin A" in "*Antibiotics*," Vol. I., Mechanism of Action, ed. by D. Gottlieb and P. D. Shaw, Springer-Verlag (1967), p. 542.

4) F. M. Strong, J. P. Dickie, M. F. Loomans. E. E. van Tamelen and R. S. Deway, *J. Amer. Chem. Soc.*, **82**, 1513 (1960); E. E. van Tamelen, J. P. Dickie, M. F. Loomans, R. S. Deway and F. M. Strong, *ibid.*, **83**, 1639 (1961); A. J. Birch, D. W. Cameron, Y. Harada and R. W. Rickard, *J. Chem. Soc.*, **1961**, 889; H. Yonehara and S. Takeuchi, *J. Antibiot.* (Tokyo), *Ser. A*, **11**, 122, 254 (1958); K. Uzu, H. Kato, K. Kumabe and Y. Harada, *ibid.*, *Ser. A*, **14**, 209 (1961).

in that the acyloxy and higher alkyl side chains in its dilactone ring are replaced by hydrogen atoms.

As for the amino acid moiety in the dilactone ring, L-threonine was incorporated as it was in the natural antimycin A, because the characteristic antibiotic activity of antimycin A seems to be strictly dependent upon the maintenance of the stereochemical feature of the amino acid moiety.

t-Butyl levulinate was prepared from levulinic acid and isobutene by a modification of the method of Gal and Sletzimyer[5] in a good yield.

Catalytic reduction of *t*-butyl levulinate over Raney Ni W-5 afforded *t*-butyl γ-hydroxyvalerate in a 91.8% yield.

t-Butyl γ-hydroxyvalerate was allowed to react with *N*-benzyloxycarbonyl-*O*-*t*-butyl-L-threonine[6] in the presence of *N*,*N*′-dicyclohexylcarbodiimide and pyridine in ether according to the condition in which Hassall *et al.*[7] had obtained the excellent result on the preparation of benzyl β-(*N*-benzyloxycarbonyl-*O*-*t*-butyl-DL-seryloxy)propionate. In our case, however, the reaction was accompanied by byproduction of a considerable amount of acyl dicyclohexyl urea. Separation of the condensation product from the by-product was effected on a silica gel column chromatography with a *n*-hexane-diisopropyl ether-ether (2 : 2 : 1) system to afford *t*-butyl γ-(*N*-benzyloxycarbonyl-*O*-*t*-butyl-L-threonyloxy) valerate (**2**) in a 45% yield as a syrup.

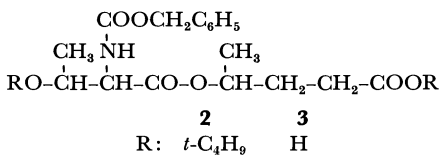

	2	**3**
R:	*t*-C_4H_9	H

Treatment of **2** with trifluoroacetic acid, followed by purification through a silica gel column with *n*-hexane-ethyl acetate-acetic acid (20 : 10 : 1) system gave γ-(*N*-benzyloxycarbonyl-L-threonyloxy)-valeric acid (**3**) in a 90% yield. The free linear ester acid **3** was cyclized by high dilution technique in a benzene solution by adding 2 mol of trifluoroacetic anhydride at 75°C during 19 hr.[8]

Treatment of the reaction product with ether gave crystal **A** in a 2.6% yield. The mother-liquor was concentrated and chromatographed on a silica gel column with a benzene-diisopropyl ether-ether (6 : 2 : 1) system to give two fractions. The first fraction gave crystal **B** in a 16.7% yield. On the basis of elemental analysis, infrared spectrum and molecular weight determination by mass spectrum, the crystal **B** was found to be the desired intramolecular cyclization product, namely, 3-(benzyloxycarboxamido)-4,9-dimethyl-1,5-dioxa-2,6-cyclononadione (**4**).

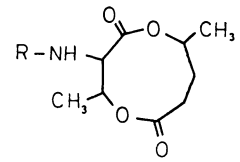

4 **5**

R:	$C_6H_5CH_2OCO$	NO_2 $OCH_2C_6H_5$ -CO

The second fraction of the chromatography gave a crystalline solid, which, on treatment with ether, was further devided into crystal **C** and syrup **D**. Each of the crystal **A** and **C** and syrup **D** proved to be a diastereomer of dimeric intermolecular cyclization products by the results of elemental analyses, IR-spectra, molecular weight determinations and optical rotatory powers.

When the cyclization reaction was carried out by directly using a freshly prepared crude ester-acid **3** without purification through a silica gel column, the yields of cyclization products markedly increased (about twice).

On NMR spectrum of the compound **4**, the proton signals of the two methyl groups were observed as four doublets having coupling constant $J=7.5$ Hz at τ values in deuteriochloroform 8.53, 8.60, 8.69 and 8.76 (Fig. 1). This indicates that the compound **4** is a mixture of two diastereomers. The presence of the two diastereomers is natural because racemic *t*-butyl γ-hydroxyvalerate was used as one of the starting materials, and the diastereomeric rela-

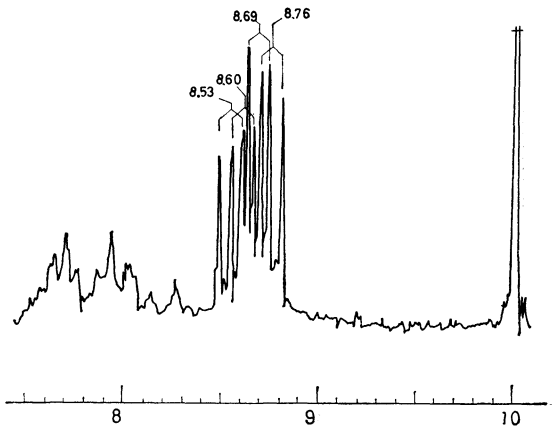

Fig. 1. Partial NMR spectrum of the compound **4** in $CDCl_3$ at 60 MHz.

5) Levulinic anhydride was used instead of levulinic acid in a patent by G. Gal and M. Sletzimyer, Fr. 1384248 (1965); *Chem. Abstr.*, **62**, 16197b (1965).

6) E. Schröder, *Ann.*, **670**, 127 (1963).

7) C. H. Hassall, T. G. Martin, J. A. Schofield and J. O. Thomas, *J. Chem. Soc., C*, **1967**, 997.

8) O. Th. Schmidt and W. Staab, *Chem. Ber.*, **81**, 388 (1954).

tionship is concerned with the two possible configurations at C-9 of the dilactone molecule.[9]

The formation of three kinds of cyclic dimers may reasonably explained by the theoretical combinations of *N*-benzyloxycarbonyl-L-threonine (Z-L-Thr), D- and L-γ-hydroxyvaleric acid (D-HV, L-HV) as shown in the schematic diagram.

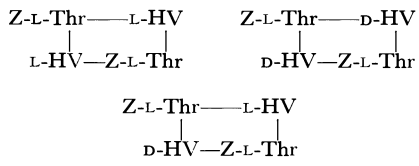

The benzyloxycarbonyl group of **4** was removed by catalytic hydrogenolysis over palladium black in methanol to give the free amino dilactone, which was directly *N*-acylated with an active ester, *O*-benzyl-3-nitrosalicylic acid *N*-hydroxysuccinimide ester in tetrahydrofuran. A silica gel column chromatography of the reaction product with *n*-hexane-ethyl acetate (5 : 3) system gave 3-(*O*-benzyl-3-nitrosalicyloylamido)-4,9-dimethyl-1,5-dioxa-2,6-cyclononadione (**5**) as crystals in a 72.4% yield.

The compound **5** was then hydrogenolysed over palladium black in methanol to yield *N*-(3-aminosalicyloyl)amino dilactone which was immediately *N*-formylated with 98% formic acid and dicyclohexylcarbodiimide. Column chromatography of the crude product followed by recrystallization afforded dehexyl-deisovaleryloxy-antimycin A_1 (**1a**) which was considered to be a diastereomeric mixture in a 54% yield based on the compound **5**.

The UV spectrum of **1a** showed the characteristic absorption maxima at 226 and 320 mμ which correspond to the *N*-formyl-3-aminosalicyloyl chromophore as a constituent portion of antimycin A.

The IR spectrum of **1a** also was similar to that of antimycin A in respect of the characteristic absorptions assignable to ester carbonyl, formamido and aromatic amido groups.

Bioassay: The synthetic dehexyl-deisovaleryloxy-antimycin A_1 showed strong inhibition against certain fungi. Minimal inhibitory concentrations (mcg/ml) of the synthetic specimen against tested fungi were as follows: *Corticium rosii* 50, *Gloeosporium lacticola* 100, *Glomerella cingulate* 100, *Leptosphaeria sulvinii* 50 by dilution method with Sabouraud medium, 27°C 5 days; *Piricularia oryzae* 0.1, *Trichophyton asteroides*-429 12.5 by agar dilution method with 1% glucose nutrient agar, 27°C 42 hr.

9) A possibility of racemization at C-4 which may occur during the ring closure reaction with trifluoroacetic anhydride might be excluded on the basis of the fact that Taub *et al.* had elucidated in their synthetic studies on zearalenone;[9] D. Taub, N. N. Girotra, R. D. Hoffsommer, C. H. Kuo, H. L. Slates, S. Weber and N. L. Wendler, *Tetrahedron*, **24**, 2443 (1968).

Experimental

Melting points were determined on a micro hot stage and were uncorrected. Thin-layer chromatography (TLC) was conducted by the use of silica gel (Daiichi Pure Chemical Co., Inc.). Silica gel column chromatography was carried out by using the silica gel (Kanto Chemical Co., Inc. and Junsei Chemical Co., Inc.) which was activated at 110°C for 1 hr. Infrared spectra were recorded on a Hitachi IPI-2 spectrometer. Ultraviolet spectra were taken in a Hitachi Perkin-Elmer UV-VIS spectrometer 139. NMR spectra was recorded on a Varian A-60D spectrometer (TMS as an internal standard). In general, all concentrations were carried out in a rotary evaporator at reduced pressure below 40°C.

***t*-Butyl Levulinate.** Liquid isobutene (100 ml, *ca.* 1.2 mol) was added to a solution of levulinic acid (20 g, 0.172 mol) in a mixture of dichloromethane (100 ml) and conc. sulfuric acid (1 ml) which was cooled at −30°C in a 500-ml round-bottomed flask. The stoppered flask was allowed to stand at room temperature for 70 hr. The reaction mixture was neutralized with triethylamine (2.52 ml) and evaporated. The residue was taken with ethyl acetate (100 ml) and the solution was washed with water (20 ml × 3) and saturated sodium chloride solution (20 ml) and dried over sodium sulfate. After evaporation of the solvent, the residue was distilled at reduced pressure. The fraction boiling at 49.5—51.0°C/0.8 mmHg was collected: yield 25.8 g (87%); n_D^{20} 1.4232; $\nu_{max}^{CHCl_3}$ 1735 cm^{-1} (C=O and ester). [lit,[5] bp 72—74°C/2 mmHg].

Found: C, 62.94; H, 9.50%. Calcd for $C_9H_{16}O_3$: C, 62.76; H, 9.36%.

***t*-Butyl γ-Hydroxyvalerate.** *t*-Butyl levulinate (14 g) was hydrogenated with Raney Ni W-5 (1.5 ml) in an initial hydrogen pressure of 75 kg/cm^2 at 66—68°C for 2 hr. After removal of the catalyst, the filtrate was distilled at reduced pressure to afford a colorless liquid: yield 13.27 g (91.8%); bp 70—73°C/1 mmHg; n_D^{20} 1.4291; $\nu_{max}^{liq.}$ 3420 (OH) and 1735 cm^{-1} (ester).

Found: C, 62.26; H, 10.58%. Calcd for $C_9H_{18}O_3$: C, 62.04; H, 10.41%.

***t*-Butyl γ-(*N*-Benzyloxycarbonyl-*O*-*t*-butyl-L-threonyloxy)valerate (2).** A solution of *N*-benzyloxycarbonyl-*O*-*t*-butyl-L-threonine[6] (8.00 g, 25.9 mmol) in dry ether (15 ml) was added dropwise during 40 min to a stirred solution of *t*-butyl γ-hydroxyvalerate (4.50 g, 25.9 mmol), *N,N'*-dicyclohexylcarbodiimide (DCCI) (5.89 g, 28.6 mmol) and dry pyridine (2.2 ml, 25.9 mmol) in dry ether (20 ml) cooled to 0°C. Stirring at 0°C was continued for a further 1 hr. After standing at 0°C for 23 hr, the precipitate of *N,N'*-dicyclohexylurea (3.54 g, 55.2%) was filtered off and the filtrate was treated with acetic acid (2 ml) under stirring at 0°C for 2 hr. An additional urea was removed by filtration and the filtrate was diluted with ether. The solution was then washed with 5% sodium hydrogen carbonate solution, 5% citric acid solution and saturated sodium chloride solution, dried over sodium sulfate, and concentrated to dryness. The oily residue (13.4 g) was chromatographed on a silica gel column (2.2 kg, 8 × 54 cm). Elution with a *n*-hexane-diisopropyl ether-ether (2 : 2 :1) system gave a straw-colored syrup (5.42 g, 45%) as a first fraction which behaved as a homogeneous compound

having R_f-value of 0.66 on TLC using the same solvent system as in the column chromatography: $[\alpha]_D^{19}$ −4.1°C (c, 2.0, ethanol); $\nu_{max}^{liq.}$ 3480, 3380 (NH), 1740 (ester and amide I) and 1510 cm^{-1} (amide II).

Found: C, 64.78; H, 8.60; N, 3.22%. Calcd for $C_{25}H_{39}O_7N$: C, 64.49; H, 8.44; N, 3.01%.

The second fraction of the column chromatography gave a syrup (3.05 g) having R_f-value of 0.56 on TLC. A part of the syrup was purified through a silica gel column with the same solvent system to afford *N*-(*N*-benzyloxycarbonyl-*O*-*t*-butyl-L-threonyl)-*N*,*N*'-dicyclohexylurea as a colorless glass.

Found: C, 67.61; H, 8.44; N, 7.80%. Calcd for $C_{29}H_{45}O_5N_3$: C, 67.54; H, 8.80; N, 8.15%.

γ-(*N*-Benzyloxycarbonyl-L-threonyloxy)valeric Acid (3). A mixture of **2** (692 mg) and trifluoroacetic acid (12 m*l*) was kept at room temperature with occasional swirling for 20 min, after which the reaction mixture was evaporated below 20°C. The residual syrup was then dissolved in ether and again evaporated. This procedure was repeated thrice to remove trifluoroacetic acid. The final residue was chromatographed on silica gel (25 g) with a *n*-hexane-ethyl acetate-acetic acid (20 : 10 : 1) system. The eluents containing **3** were evaporated to afford the pure sample of **3** (475 mg, 90%) as a pale-yellow syrup: $[\alpha]_D^{21}$ −16.4°C (c 2.0, ethanol); $\nu_{max}^{liq.}$ 3340 (NH and OH), 2700—2500 (carboxyl OH), 1720 (ester, carboxyl and amide I) and 1525 cm^{-1} (amide II).

Found: C, 57.91; H, 6.85; N, 4.08%. Calcd for $C_{17}H_{23}O_7N$: C, 57.78; H, 6.56; N, 3.96%.

Cyclization of 3. a) A mixture of **3** (991 mg, 2.81 mmol) purified by column chromatography, dry benzene (70 m*l*) and trifluoroacetic anhydride (0.39 m*l*, 2.81 mmol) was heated at 75°C for 10 hr, after which additional trifluoroacetic anhydride (0.39 m*l*) was added and again heated at the same temperature for 9 hr. The reaction mixture was evaporated and the resulting syrup was dissolved in absolute ether. On ice-cooling of the solution, there was obtained a crystalline product **A**, which was collected by filtration: mp 206—208°C; yield 24.5 mg (2.6%). Recrystallization of the product **A** from ethyl acetate-petroleum ether (bp 40—60°C) gave colorless needles: mp 208—210°C; $[\alpha]_D^{11}$ −45° (c 2.0, chloroform); m/e 670; ν_{max}^{KBr} 3340 (NH), 1732 (ester), 1715 (amide I) and 1530 cm^{-1} (amide II).

Found: C, 61.44; H, 6.16; N, 4.41%. Calcd for $(C_{17}H_{21}O_6N)_2$: C, 60.88, H, 6.31; N, 4.18%.

The mother liquor of the crystal **A** was concentrated and chromatographed on silica gel (200 g) with a benzene-diisopropyl ether-ether (6 : 2 : 1) system to afford two fractions having R_f-values, 0.55 and 0.43 on TLC with the same solvent stysem. The first fraction (R_f 0.55) gave a crystalline product **B** (158 mg, 16.7%); mp 99—103°C. Recrystallization of **B** from ethyl acetate-petroleum ether gave a pure sample of 3-benzyloxycarboxamido-4,9-dimethyl-1,5-dioxa-2,6-cyclononadione (**4**): mp 105—107°C; $[\alpha]_D^{21}$ +14° (c 2.0, ethanol); $[\alpha]_D^{21}$ +31° (c 1.0, chloroform), m/e 335; ν_{max}^{KBr} 3320 (NH), 1745 (ester), 1693 (amide I) and 1539 cm^{-1} (amide II); τ^{CDCl_3} 8.53, 8.60, 8.69 and 8.76 (d, C_4- and C_9-CH_3, J=7.5 Hz).

Found: C, 61.21; H, 6.70; N, 4.37%. Calcd for $C_{17}H_{21}O_6N$: C, 60.88; H, 6.31; N, 4.18%.

The second fraction (R_f 0.43) afforded a crystalline product melting at 151—154°C (26.6 mg, 2.8%). The product (71 mg) was washed with ether (4 m*l*) and the resulting crystal (46 mg) was recrystallized from ethyl acetate-petroleum ether to afford crystals **C**: mp 167—169°C; $[\alpha]_D^{13}$ +1.3° (c 2.0, chloroform); ν_{max}^{KBr} 3340 (NH), 1732 (ester), 1710 (amide I) and 1525 cm^{-1} (amide II); m/e 670.

Found: C, 61.00; H, 6.57; N, 4.23%. Calcd for $(C_{17}H_{21}O_6N)_2$: C, 60.88; H, 6.31; N, 4.18%.

The ether washing was concentrated and worked up with petroleum ether to give additional crystals **C** (5 mg). The filtrate was evaporated to afford a syrup **D** (14 mg): $[\alpha]_D^{18}$ +15° (c 1.0, chloroform); $\nu_{max}^{CCl_4}$ 3450 (NH), 1746—1732 (ester and amide I) and 1505 cm^{-1} amide II); m/e 670.

Found: N, 4.35%. Calcd for $(C_{17}H_{21}O_6N)_2$: N, 4.18%.

b) Treatment of **2** (162 mg) with trifluoroacetic acid (2.6 m*l*) for 10 min, followed by rapid evaporation below 10°C afforded crude **3**, which was immediately subjected to cyclization by the same procedures as described above. The concentrated reaction mixture afforded the product **A** (3.6 mg, 3.08%, mp 205—208°C), product **B** (**4**) (38 mg, 32.5%, mp 98—101°C, and product **C**+**D** (6.3 mg, 5.38%, mp 151—154°C).

***O*-Benzyl-3-nitrosalicylic Acid *N*-Hydroxysuccinimide Ester.** To a solution of *O*-benzyl-3-nitrosalicylic acid[10] (1.38 g, 5.05 mmol) and *N*-hydroxysuccinimide (0.58 g, 5.05 mmol) in dry tetrahydrofuran (16 m*l*) was added a solution of DCCI (1.04 g, 5.05 mmol) in tetrahydrofuran and the mixture was kept at room temperature overnight. The precipitated *N*,*N*'-dicyclohexylurea (1.08 g, 95.6%) was filtered off and the filtrate was evaporated to dryness. The residue (1.92 g) was recrystallized from ethanol (80 m*l*) to afford pure title compound as pale-yellow needles: yield 1.62 g (87%); mp 140—141°C; ν_{max}^{KBr} 1810, 1780, 1741, 1600, 1540, 1360, 770 and 700 cm^{-1}.

Found: C, 58.56; H, 3.79; N, 7.27%. Calcd for $C_{18}H_{14}O_7N_2$: C, 58.38; H, 3.81; N, 7.57%.

3-(*O*-Benzyl-3-nitrosalicyloylamido)-4,9-dimethyl-1,5-dioxa-2,6-cyclononadione (5). A solution of **4** (crystal **B**) (138 mg, 0.413 mmol) in methanol (6 m*l*) was stirred with palladium black (*ca.* 15 mg) for 50 min under bubbling with hydrogen. The filtered reduction mixture was evaporated to yield the free amino dilactone (85 mg) which showed a single ninhydrin positive spot on TLC with a benzene-diisopropyl ether-ether (6 : 2 : 1) system. The free amino dilactone (83 mg, 0.413 mmol) was dissolved in dry tetrahydrofuran (2 m*l*) and *O*-benzyl-3-nitrosalicylic acid *N*-hydroxysuccinimide ester (153 mg, 0.413 mmol) was added. The mixture was kept for 20 hr at room temperature, after which it was allowed to stand for 27 hr at 36°C in an incubator. The resulting solution was concentrated to afford a yellow crystalline mass which was purified through silica gel (45 g) column. Elution with *n*-hexane-ethyl acetate (5 : 3) system gave the title compound (**5**) as pale-yellow crystals: yield 135 mg (72.4%), mp 186—189°C. Recrystallization from tetrahydrofuran-petroleum ether (bp 60—70°C): mp 188—189.5°C; $[\alpha]_D^{23}$ +20° (c 2.0, tetrahydrofuran); ν_{max}^{KBr} 3300 (NH), 1743 (ester), 1645 (amide I) and 1532 cm^{-1} (amide II and NO_2).

Found: C, 60.57; H, 5.48; N, 6.11%. Calcd for

10) F. S. Okumura, M. Masumura and T. Horie, *J. Amer. Chem. Soc.*, **81**, 5215 (1959).

$C_{23}H_{24}O_8N_2$: C, 60.52; H, 5.30; N, 6.14%.

Dehexyl-deisovaleryloxy-antimycin A_1 (1a). A solution of **5** (62.6 mg, 0.137 mmol) in methanol (10 m*l*) was stirred with palladium black (*ca.* 45 mg) under bubbling with hydrogen gas for 40 min. The filtered yellow-green reduction mixture was concentrated to give a yellow oil (48.4 mg, 100%). The product (46.1 mg, 0.137 mmol) was dissolved in tetrahydrofuran (2 m*l*) and to the solution was added DCCI (28.2 mg, 0.137 mmol) and 98% formic acid (6.8 mg) under ice-cooling. After standing for 15 hr in a refrigerator, the reaction mixture was filtered to remove *N,N'*-dicyclohexylurea (23.2 mg, 72.4%). The filtrate was evaporated and the residue was chromatographed on silica gel (10 g) with a *n*-hexane-ethyl acetate (4 : 3) system to afford **1a** (31.7 mg) as crystals. The crystals were again chromatographed on silica gel (7 g) with the same solvent system to give a practically pure of **1a** (26.1 mg, 54%). Recrystallization from ethyl acetate-*n*-hexane: mp 154—156°C; *m/e* 364; $[\alpha]_D^{19}$ +70° (*c* 1.0, chloroform); λ_{max}^{MeOH} 226 (log ε 4.62), 320 mμ (log ε 3.93); $\nu_{max}^{CHCl_3}$ 3435 (NH), 1747 (ester), 1706 (NHCHO), 1647 (ArCONH), 1614 (Ar–H) and 1531 cm^{-1} (ArCONH).

Found: C, 56.29; H, 5.76; N, 7.77%. Calcd for $C_{17}H_{20}O_7N_2$: C, 56.04; H, 5.53; N, 7.69%.

We wish to thank Professor H. Umezawa for his helpful advice, Mr. S. Nakada for the microanalyses and Mr. F. Kishimoto for his technical assistance. We also wish to thank Professor S. Zen of Kitasato University for the measurement of mass spectra, Dr. M. Hamada of Institute of Microbial Chemistry and Mr. S. Fukatsu of Meiji-Seika Co. for their microbiological tests.

BULLETIN OF THE CHEMICAL SOCIETY OF JAPAN VOL. 43 901—904 (1970)

Syntheses of 2,3-Dihydro-4(1*H*)-pyridones

Noboru SUGIYAMA, Makoto YAMAMOTO and Choji KASHIMA

Department of Chemistry, Tokyo Kyoiku University, Otsuka, Bunkyo-ku, Tokyo

(Received September 10, 1969)

The condensation of β-diketones with benzaldazine yields 1-benzylidenimino-2,3-dihydro-4-pyridones, which may be catalytically hydrogenolyzed to the corresponding 2,3-dihydro-4(1*H*)-pyridones. Some reactions of 2,3-dihydro-4(1*H*)-pyridones are discussed.

Previously we described that β-diketones may be condensed with benzylidenaniline in the presence of three molar equivalents of potassium amide in liquid ammonia to produce 1-phenyl-2,3-dihydro-4-pyridones.[1] We also reported that these 1-phenyl-2,3-dihydro-4-pyridones were prepared by the cyclization of the correspoding aminodiketones.

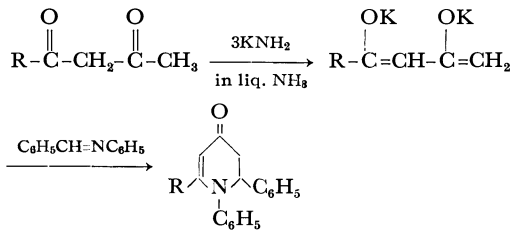

Fig. 1

However, the 1-unsubstituted dihydropyridones, namely 2,3-dihydro-4(1*H*)-pyridones are more important than 1-phenyl ones in view of the organic reactions and biochemical studies. Now we wish to report that β-diketones when condensed with benzaldazine give 1-benzylidenimino-2,3-dihydro-4-pyridones, which on hydrogenolysis lead to 2,3-dihydro-4(1*H*)-pyridones. The present paper also described some of the reactions of these compounds.

Results and Discussion

Acetylacetone (II) was condensed with benzaldazine (I) in the presence of three molar equivalents of sodium amide in liquid ammonia to give 1-benzylidenimino-6-methyl-2-phenyl-2,3-dihydro-4-pyridone (V). The yield was 6.2%. When potassium amide was used instead of sodium amide, the yield of V increased to 11.0%.

The structure of V was determined from the spectral data and the elemental analyses (see Experimental). The nuclear magnetic resonance spectrum supported the structure of V, *i.e.*, the two singlets at τ 7.52 and 4.82 were assigned to the methyl and the olefinic protons. The ABX type signals in the region τ 6.49—7.70 were assigned to the C-3 methylene protons coupled with C-2 methine proton at τ 4.50 as a quartet. The signal at τ 2.40—3.05 displayed 10 aromatic protons and

1) N. Sugiyama, M. Yamamoto and C. Kashima, This Bulletin, **42**, 1357 (1969).

TABLE 1. SPECTRAL DATA OF 2,3-DIHYDRO-4(1*H*)-PYRIDONES

Compound	IX	X	XI	XII
IR (cm^{-1}): ν_{NH}	3250 (m)[a]	3275 (m)	3250 (m)	3250 (s)[b]
$\nu_{C=O}$	1610 (s)	1615 (s)	1605 (s)	1610 (s)
$\nu_{C=C}$	1585 (s)	1555 (m)	1570 (m)	1575 (m)
UV: λ_{max}^{EtOH} mμ (ε)	315 (14500)	245 (14000) 339 (12200)	318 (14400)	318 (14100)
$\lambda_{max}^{EtOH\text{-}HCl}$ mμ (ε)	310 (10300)	277 (13300) 333 (10200)	312 (9950)	312 (10100)
NMR (in $CDCl_3$): (τ)				
NH	4.10 bs[c]	4.50 bs	4.41 bs	4.70 bs
Olefinic	5.07 s[d]	4.54 s	5.08 s	5.05 s
C-2 methine	5.34 q	5.12 q[e]	5.52 q	5.67 d[f]
J_{AX} (Hz)	12.0	12.0	12.0	
J_{BX} (Hz)	7.5	7.4	7.5	
C-3 methylene	7.2—7.9 m[g]	6.9—7.6 m	6.9—7.8 m	7.0—7.3 m

a) (m) medium b) (s) strong c) bs, broad singlet d) s, singlet e) q, quartet
f) d, doublet g) m, multiplet

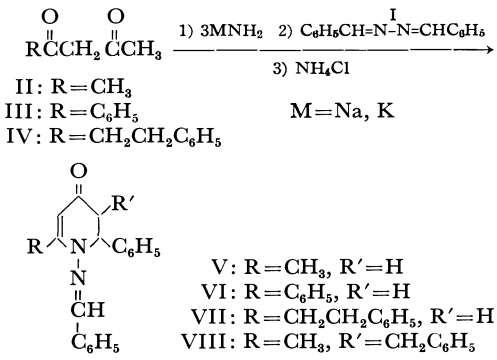

Fig. 2

a proton of –N=CH– group as a multiplet.

By the same procedure, 1-benzylidenimino-2,6-diphenyl-2,3-dihydro-4-pyridone (VI) was obtained in 9.2% yield from I and benzoylacetone (III). Using I and 6-phenyl-2,4-hexanedione (IV), 1-benzylidenimino-6-phenethyl-2-phenyl-2,3-dihydro-4-pyridone (VII) and its isomer 3-benzyl-1-benzylidenimino-6-methyl-2-phenyl-2,3-dihydro-4-pyridone (VIII) were obtained in the yields of 52% and 21%, respectively. In the reaction of I and IV, the condensation took place not only at C-1 but also C-5 position of IV. The ratio of VII to VIII was about 5 : 2, similar to that of the reaction of IV with benzylidenaniline.

Schiff bases are reduced to secondary amines by hydrogen in the presence of nickel or platinum catalyst,[2] and hydrazocompounds are reduced to amines.[3] On the other hand, neither the carbonyl group nor the double bond of 2,3-dihydro-4-pyridone ring is hydrogenolyzed by platinum oxide catalyst in methanol or ethanol solution.[4] However, 2,3-dihydro-4-pyridone is reduced in the presence of platinum oxide to a corresponding 4-piperidinol or 4-piperidone in acetic acid solution.[5] When 1-benzylidenimino-2,3-dihydro-4-pyridone is catalytically hydrogenolyzed in the presence of platinum oxide in alcohol solution, 1-benzylamino- or 2,3-dihydro-4(1*H*)-pyridone may be expected. Hydrogenolysis of VII in ethanol catalyzed by platinum oxide gave only 2,3-dihydro-4(1*H*)-pyridone, 6-phenethyl-2-phenyl-2,3-dihydro-4(1*H*)-pyridone (XI), but no 1-benzylaminodihydropyridone. The structure of XI was confirmed by the spectral data and the results of elemental analyses (see Table 1).

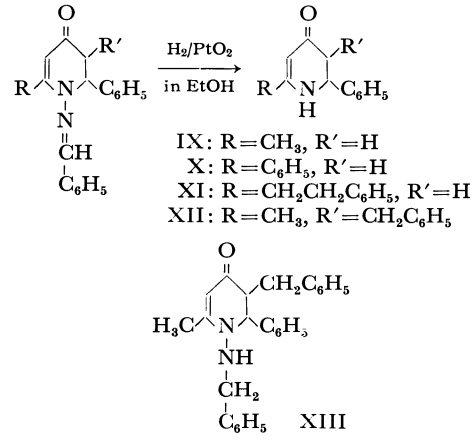

Fig. 3

By the same procedure, 6-methyl-2-phenyl-2,3-dihydro-4(1*H*)-pyridone (IX), 2,6-diphenyl-2,3-dihydro-4(1*H*)-pyridone (X) and 3-benzyl-6-methyl-2-phenyl-2,3-dihydro-4(1*H*)-pyridone (XII) were

2) a) C. F. Winans, *J. Amer. Chem. Soc.*, **61**, 3566 (1939). b) A. Skita and F. Keil, *Chem. Ber.*, **61**, 1682 (1928). c) A. Skita, F. Keil and H. Havemann, *ibid.*, **66**, 1400 (1933). d) A. Skita and F. Keil, *ibid.*, **61**, 1452 (1928).

3) G. Schultz, *Ber.*, **17**, 472 (1884).

4) Unpublished data by N. Sugiyama, M. Yamamoto and C. Kashima.

5) N. Sugiyama, M. Yamamoto and C. Kashima, This Bulletin, **42**, 2690 (1969).

obtained from V, VI and VIII, respectively. The spectral data are summarized in Table 1.

When equimolar hydrogen is absorbed, 1-benzylamino-2,3-dihydro-4-pyridone may be expected to be formed as an intermediate. However, after absorbing about 3/2 molar hydrogen, VIII gave 20% of 1-benzylamino-3-benzyl-6-methyl-2-phenyl-2,3-dihydro-4-pyridone (XIII) together with 45% of XII.

The structure of XIII was proved by the spectral data. The infrared spectrum showed bands at 3300, 1630 and 1550 cm^{-1} for NH, conjugated carbonyl and C=C double bonds. The nuclear magnetic resonance spectrum showed at τ 6.33—6.66 (broad triplet, 1H) and τ 6.13 (doublet, 2H) for amino proton and methylene protons of 1-benzylamino group. By treatment with D_2O, the former disappeared and the latter changed to a singlet. The other signals are similar with those of VIII. From these results it is apparent that 1-benzylidenimino-2,3-dihydro-4-pyridone was first hydrogenolyzed to 1-benzylamino-2,3-dihydro-4-pyridone and this benzylamino compound underwent hydrogenolysis to yield the corresponding 2,3-dihydro-4(1*H*)-pyridone.

In a previous paper, we reported that 1-phenyl-2,6-disubstituted dihydropyridones were dehydrogenated in the presence of a hydrogen acceptor.[5] XI was also dehydrogenated by treating with chloranil in tetrahydrofuran to yield the corresponding pyridone, 6-phenethyl-2-phenyl-4(1*H*)-pyridone (XIV). XIV was identical with the authentic sample[6] on thin-layer chromatography. However, conversion from XIV into XI with tetrachlorohydroquinone was not successful. This proved that XI was easily oxidized with chloranil to XIV and the reaction was not of the equilibrium type.

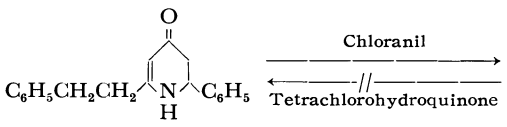

(XI)

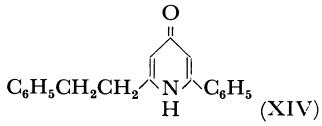

(XIV)

Fig. 4

It is well known that I is decomposed to hydrazine and benzaldehyde by treating with dilute acid. Taylor *et al.* reported[7] that the isopropylidenimino group of 3-isopropylidenimino-4(3*H*)-pteridinone undergoes a reductive elimination in dilute acid solution to give 3-amino-4(3*H*)-pteridinone. If VII is treated with dilute acid, the corresponding *N*-amino dihydropyridone is expected to produce.

Compound VII was treated with dilute hydrochloric acid, but *N*-aminodihydropyridone was not obtained, and instead of *N*-aminodihydropyridone, a red viscous substance, which could not be purified, was obtained.

The present method is generally applicable for the synthesis of 2,3-dihydro-4(1*H*)-pyridones.

Experimental

Syntheses of 1-Benzylidenimino-dihydropyridone. General Procedure: In a 500 m*l* three necked flask, about 300 m*l* of anhydrous liquid ammonia was introduced. A small amount of potassium was then added and completely dissolved. A catalytic amount of ferric chloride was then added to the stirred blue solution, followed by 4.7 g (0.12 g atom) of potassium in small portions. The solution turned dark gray within 90 min. To this solution was added 0.04 mol of β-diketone in 30 m*l* of anhydrous ether. After stirring for 45—60 min, 0.02 mol of I[8] in 50 m*l* of anhydrous ether was added. After stirring for another 3.5—4 hr at −33°C, 100 m*l* of ether was added from a dropping funnel, followed by the rapid evaporation of ammonia on a water both. To the ethereal solution, excess ammonium chloride (10 g) in 100 m*l* water was added. The ethereal layer was then separated and the aqueous layer was extracted with 100 m*l* of ether. The ethereal layer was washed with water and dried over anhydrous sodium sulfate. The remaining aqueous layer was acidified with dilute hydrochloric acid, and again extracted with 200 m*l* of chloroform. The chloroform extract was dried over calcium chloride. After concentration under reduced pressure, both residue gave condensation products.

The crude product was chromatographed on a silica gel (Merck 7734, 0.05—0.2 mm) column with a benzene-ethyl acetate mixture. The fraction showing a green color on a ferric chloride test was collected and concentrated *in vacuo* to give crude 1-benzylidenimino-2,3-dihydro-4-pyridone. The latter was then crystallized from ethyl acetate to yield pure dihydropyridone. By this procedure, V, VI, VII and VIII were obtained.

1-Benzylidenimino-6-methyl-2-phenyl-2,3-dihydro-4-pyridone (V). From I and II, V was synthesized. Fractionating solvent: Benzene-ethyl acetate 2 : 1 (*v*/*v*) mixture. Pale yellow prisms, mp 176—177°C.

Found: C, 78.40; H, 6.42; N, 9.59%. Calcd for $C_{19}H_{18}N_2O$: C, 78.59; H, 6.25; N, 9.65%. IR (KBr): ν_{max} 1635 (νC=O), 1580 (νC=N) and 1560 cm^{-1} (νC=C). UV(mμ(ε)): λ_{max}^{EtOH} 229(9900), 234(9500), 282(3600) and 364(44000).

In this reaction, 72% of II and 49% of I were recovered. In spite of elongation of the reaction time (for 6.5 hr), the yield of V was 10.2% and 65% of II, 35% of I also recovered.

1-Benzylidenimino-2,6-diphenyl-2,3-dihydro-4-pyridone (VI). VI was prepared from I and III in

6) C. Kashima, M. Yamamoto, S. Kobayashi and N. Sugiyama, *ibid.*, **42**, 2389 (1969).

7) E. C. Taylor, O. Vogl and P. K. Loeffler, *J. Amer. Chem. Soc.*, **81**, 2479 (1959).

8) H. T. Bucherer and M. Schmidt, *J. Prakt. Chem.*, **79**, 369 (1909).

9.2% yield. Fractionating solvent: Benzene-ethyl acetate 4 : 1 (*v/v*). Yellow plates, mp 178—179°C.

Found: C, 81.88; H, 5.83; N, 8.06%. Calcd for $C_{24}H_{20}N_2O$: C, 81.79; H, 5.72; N, 7.95%. IR (KBr): ν_{max} 1645 (νC=O), 1570 (νC=N) and 1550 cm^{-1} (νC=C). UV(mμ(ε)): λ_{max}^{EtOH} 238(15400), 281(9430) and 368 (31700). NMR (in $DCCl_3$): τ6.36—6.76 (ABX type, quartet, 1H, C-3 methylene proton, J_{AB}=16.5 Hz, J_{AX}=7.5 Hz), 6.96—7.34 (ABX type, quartet, 1H, C-3 methylene proton, J_{BX}=1.5 Hz), 4.68 (singlet, 1H, C-5 olefinic proton), 4.40(quartet, 1H, C-2 methine proton) and 2.35—2.84 (multiplet, 16H, a proton of -N=CH- group and aromatic protons).

In this reaction, 57% of II was also recovered. But III was merely 18.5% recovered.

1-Benzylidenimino-6-phenethyl-2-phenyl-2,3-dihydro-4-pyridone (VII). VII was prepared from I and IV[9] in 52% yield. Fractionating solvent: Benzene-ethyl acetate 2 : 1 (*v/v*). Yellow plates, mp 118—121°C.

Found: C, 81.71; H, 6.34; N, 7.35%. Calcd for $C_{26}H_{24}N_2O$: C, 82.07; H, 6.36; N, 7.36%. IR (KBr): ν_{max} 1635 (νC=O), 1575 (νC=N) and 1550 cm^{-1} (νC=C). UV(mμ(ε)): λ_{max}^{EtOH} 231(12000), 236(11100), 283(3850) and 365(39000). NMR (in $CDCl_3$): τ 6.88 (singlet, 4H, phenethyl ethylene protons), 4.51—4.91(ABX type, quartet, 1H, C-3 methylene proton, J_{AB}=16.2 Hz, J_{AX}=7.4 Hz), 7.11—7.43(ABX type, quartet, 1H, C-3 methylene proton, J_{BX}=1.5 Hz), 4.81(singlet, 1H, C-5 olefinic proton), 4.50 (quartet, 1H) and 2.40—2.96 (multiplet, 16H).

3-Benzyl-1-benzylidenimino-6-methyl-2-phenyl-2,3-dihydro-4-pyridone (VIII). VIII was obtained from the same reaction mixture as VII. On column chromatography with benzene-ethyl acetate 2 : 1 (*v/v*) VIII eluted ahead of VII. On silica gel (Wako gel B-500) thin layer chromatography with benzene-ethyl acetate 2 : 1 (*v/v*), VIII showed the R_f 0.37, while that of VII was 0.29. VIII was concentrated and recrystallized from benzene-*n*-hexane giving 21% yield. Yellow neeldes, mp 129—131°C.

Found: C, 81.32; H, 6.51; N, 7.27%. Calcd for $C_{26}H_{24}N_2O$: C, 82.07; H, 6.36; N, 7.36%. IR(KBr): ν_{max} 1640 (νC=O), 1580 (νC=N) and 1560 cm^{-1} (νC=C). UV(mμ(ε)): λ_{max}^{EtOH} 228(11800), 234(11100), 284(3280) and 363(28200). NMR (in $CDCl_3$): τ 6.68—7.32 (multiplet, 3H), 7.48 (singlet, 3H), 4.96 (singlet, 1H), 4.81 (singlet, 1H) and 2.40—3.30 (multiplet, 16H).

Reduction of 1-Benzylidenimino-2,3-dihydro-4-pyridones by Catalytic Hydrogenolysis: Using 100 mg of platinum oxide, 200—300 mg of 1-benzylidenimino-2,3-dihydro-4-pyridone in 30 m*l* ethanol was hydrogenolyzed at room temperature and atmospheric pressure. After absorbing about two molar equivalents of hydrogen the catalyst was filtered off. The ethanol solution was concentrated *in vacuo*, and the residue was chromatographed on a silica gel (Merck 7729, 0.08 mm) column with benzene-ethyl acetate 2 : 1 (*v/v*). Fractions showing a dark brown color with ferric chloride were collected, concentrated and recrystallized to give 2,3-dihydro-4-pyridone. IX, X and XI were prepared by this method. The spectral data are listed in Table 1.

6-Methyl-2-phenyl-2,3-dihydro-4(1*H*)-pyridone (IX). IX was prepared by using 210 mg of V. Yield 62 mg (46%), colorless needles, mp 160—161°C.

Found: C, 76.92; H, 7.10; N, 7.73%. Calcd for $C_{12}H_{13}NO$: C, 76.97; H, 7.00; N, 7.48%.

2,6-Diphenyl-2,3-dihydro-4(1*H*)-pyridone (X). X was prepared from 200 mg of VI. Yield 92 mg (65.0%), yellow cubics, mp 149—151°C.

Found: C, 81.50; H, 6.13; N, 5.69%. Calcd for $C_{17}H_{15}NO$: C, 81.90; H, 6.06; N, 5.62%.

6-Phenethyl-2-phenyl-2,3-dihydro-4(1*H*)-pyridone (XI). XI was obtained from 300 mg of VII in 92% (201 mg) yield, mp 124—126°C, colorless needles.

Found: C, 82.08; H, 6.95; N, 5.22%. Calcd for $C_{19}H_{19}NO$: C, 82.28; H, 6.91; N, 5.05%.

3-Benzyl-6-methyl-2-phenyl-2,3-dihydro-4(1*H*)-pyridone (XII). VIII (250 mg) was hydrogenolyzed by the procedure described above. Twenty m*l* of hydrogen (calculated 31 m*l*) was absorbed and the product was chromatographed on a silica gel (Merck 7729) column with a benzene-ethyl acetate 2 : 1 (*v/v*) mixture. Fractions with R_f values 0.23 were collected and concentrated to give 65 mg (45%) of XII, colorless prisms, mp 159—160°C.

Found: C, 82.20; H, 6.89; N, 5.05%. Calcd for $C_{19}H_{19}NO$: C, 82.28; H, 6.91; N, 5.05%.

3-Benzyl-1-benzylamino-6-methyl-2-phenyl-2,3-dihydro-4-pyridone (XIII). From the same column, XIII was obtained. R_f value: 0.42. Yield, 51 mg (20%) as a yellow oil. UV(mμ): λ_{max}^{EtOH} 328. NMR(in $CDCl_3$): τ 7.80 (singlet, 3H, methyl protons), 7.20—6.70 (multiplet, 3H, C-3 methine proton and benzyl methylene protons), 6.66—6.33 (broad triplet, 1H, amino proton), 6.13 (doublet, 2H, methylene protons of benzylamino group), 5.41 (quartet, 1H, C-2 methine proton), 5.03 (singlet, 1H, C-5 olefinic proton) and 3.11—2.60 (multiplet, 15H, aromatic protons).

Dehydrogenation of XI. In 30 m*l* tetrahydrofuran were dissolved 80 mg of XI and 75 mg of chloranil. After refluxing for 5.5 hr, the mixture was cooled and the formation of XIV was confirmed on thin layer by the comparison with the authentic sample.[6]

Hydrolysis of VII. Compound VII (0.8 g) was dissolved in 40 m*l* of 50% aqueous ethanol and then 5 m*l* of concentrated hydrochloric acid was added. The mixture was refluxed for one hour on a water bath, and was made alkaline with sodium hydroxide. Extraction with chloroform and analysis of extract by means of silica gel (Wako gel B-500) thin layer chromatography (benzene-ethyl acetate, 2 : 1 *v/v*) showed two spots with R_f value 0.00 and 0.30. The latter was identified as VII. The former was a red viscous substance which could not be purified.

9) R. B. Meyer and C. R. Hauser, *J. Org. Chem.*, **25**. 158 (1960).

BULLETIN OF THE CHEMICAL SOCIETY OF JAPAN VOL. 43 905—908 (1970)

Mechanism of Decomposition of Carboxylic Sulfurous Anhydrides*1

Michio KOBAYASHI, Hiroshi MINATO and Yoshikuni OGI

Department of Chemistry, Tokyo Metropolitan University, Setagaya, Tokyo

(Received September 11, 1969)

Ethyl benzoyloxysulfinate, prepared from ^{18}O-labeled benzoic acid and ethyl chlorosulfite, was decomposed and the products were analyzed. The ^{18}O analyses showed that; 1) prior to decomposition the ^{18}O of the mixed anhydride was scrambled due to the formation and the internal return of an ion-pair, $C_6H_5C^{+}{}^{-}OSOEt$ (O O); 2) ethyl benzoate, benzoic anhydride and diethyl sulfite were produced *via* an ionic chain mechanism involving successive attack of ethoxide anion and benzoate anion on the carbonyl carbon and sulfinyl sulfur of the mixed anhydride.

In the thermal decomposition of mixed anhydride (I), formed from a carboxylic acid and an alkyl hydrogen sulfite, products are sulfur dioxide, a carboxylic ester, a carboxylic anhydride, and dialkyl sulfite, as shown in Eqs. (1) and (2).[1] In a previous paper[2] we described the isolation and the infrared spectra of I with various R and R′, and discussed the mechanism of the formation of a carboxylic ester by use of ^{18}O-labled methyl and phenyl benzoyloxysulfinates.

In order to clarify the mechanism of the formation of all the decomposition products, the ^{18}O contents of all the products from the decomposition

$$R\text{-}CO_2Na \text{ (or } RCO_2^{-}{}^{+}NEt_3) + Cl\text{-}S\text{-}OR' \rightarrow$$

(H, O)

$$R\text{-}C(=O)\text{-}O\text{-}S(O)\text{-}OR' + NaCl \quad (1)$$

(I)

$$(I) \rightarrow R\text{-}C(=O)\text{-}O\text{-}R' + SO_2 \quad (2)$$

$$(I) \rightarrow R\text{-}C(=O)\text{-}O\text{-}C(=O)\text{-}R + R'O\text{-}S(O)\text{-}OR' + SO_2 \quad (3)$$

of ^{18}O-labeled ethyl benzoyloxysulfinate (Ia, R= -Ph, R′=$-C_2H_5$) have been analyzed in detail, and the results are presented in this paper.

Results and Discussion

When ^{18}O-labeled sodium benzoate and ethyl chlorosulfite were mixed and the sirupy mixture formed was heated at 110—120°C, it decomposed with vigorous evolution of sulfur dioxide. The sulfur dioxide was collected in a dry ice-acetone trap, and was converted to benzyl phenyl sulfone for the ^{18}O analysis according to the equation.

$$SO_2 \xrightarrow{PhMgBr} (PhSO_2)_2Mg \xrightarrow{Na_2CO_3} Ph\text{-}SO_2Na$$

$$\xrightarrow{PhCH_2Br} Ph\text{-}S(=O)(=O)\text{-}CH_2Br \quad (4)$$

After the decomposition was complete, the products were separated by repeated fractional distillation. In order to distinguish the carbonyl oxygen and the ether oxygen in the benzoic anhydride, the anhydride was converted to benzoic acid and benzanilide by reaction with aniline in dichloromethane as shown in the equation.[5]

$$Ph\text{-}C(=O)\text{-}O\text{-}C(=O)\text{-}Ph + Ph\text{-}NH_2 \rightarrow$$

$$Ph\text{-}CO_2H + Ph\text{-}C(=O)\text{-}NH\text{-}Ph \quad (5)$$

(O)

Table 1. Specificity of ^{18}O-labeling

Sample	% ^{18}O-excess	% ^{18}O-calcd	
Starting $PhCO_2Na$	1.30	(1.30)	1
$PhCOOC_2H_5$*	0.67	0.65	1/2
$(EtO)_2SO$*	0.31	0.22	1/6
$PhSO_2CH_2Ph$ (←SO_2*)	0.60	0.65	1/2
PhCOCPh* (O O)	1.00	1.08	5/6
$PhCO_2H$**	1.00	1.07	13/16
PhCONHPh**	1.00	1.14	7/8

* Direct reaction products.
** Derived from benzoic anhydride.

*1 Organic Sulfur Compound. XX.

1) M. Kobayashi and A. Yamamoto, This Bulletin, **39**, 961 (1966).

2) M. Kobayashi and R. Kiritani, *ibid.*, **39**, 1782 (1966).

3) D. B. Denney and M. A. Greenbaum, *J. Amer. Chem. Soc.*, **79**, 3701 (1957).

The results of ^{18}O analyses of all the reaction products are shown in Table 1.

The ^{18}O-atom % of ethyl benzoate was one half of that of the starting sodium benzoate. This finding indicates that, as shown previously, the ester was formed not by the reaction between ethyl chlorosulfite and benzoic anhydride, but formed directly by the decomposition of the mixed anhydride Ia. It should be noted that diethyl sulfite contained an appreciable amount of ^{18}O, and the ^{18}O content observed for benzoic anhydride was smaller than the value calculated on the basis of the reaction

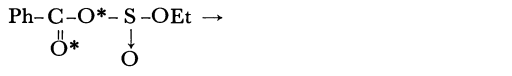

$$\text{Ph-C(=O*)-O-S-OEt} \rightarrow \tfrac{1}{2}\text{Ph-C(=O*)-O-C(=O*)-Ph} + \tfrac{1}{2}(EtO)_2SO + SO_2 \quad (6)$$

The unexpected data can be explained by the assumption that Ia dissociates reversibly to form an ion pair of benzoyl cation and ethoxysulfinate anion according to Eq. (7). When the scrambling of ^{18}O due to internal return of the ion pair is taken into consideration, the ^{18}O contents and distribution in other products are also explained.

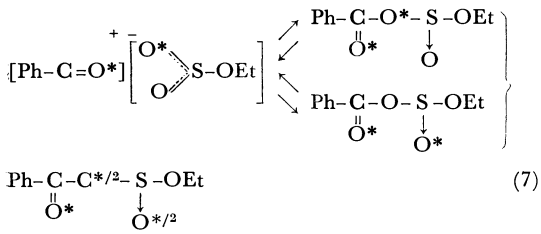

$$[\text{Ph-C(=O*)}]^{+}\left[\text{O*, O, S-OEt}\right]^{-} \rightleftharpoons \text{Ph-C(=O*)-O-S-OEt} \rightleftharpoons \text{Ph-C(=O*)-O-S-OEt (O*)} \quad (7)$$

Reaction between Ia and Bases. Piperidine and *p*-chloroaniline were used as examples of a strong base and a weak base respectively. The only product isolated from the reaction between piperidine and Ia was the S-attack product, II,[4] whereas the only product isolated from the reaction between *p*-chloroaniline and Ia was the C-attack product, III, as shown in the following equation.

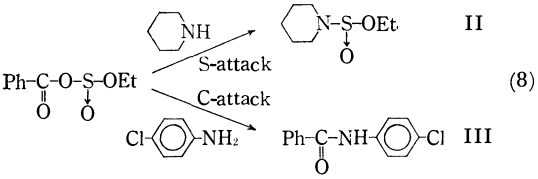

$$\text{Ph-C(=O)-O-S(=O)-OEt} \xrightarrow{\text{NH, S-attack}} \text{N-S-OEt (=O)} \quad \text{II}$$

$$\text{Ph-C(=O)-O-S(=O)-OEt} \xrightarrow{\text{Cl-C}_6\text{H}_4\text{-NH}_2,\ \text{C-attack}} \text{Ph-C(=O)-NH-C}_6\text{H}_4\text{-Cl} \quad \text{III} \quad (8)$$

Since each of two derivatives contains a carbonyl oxygen and a sulfinyl oxygen, respectively, it is possible to determine the ^{18}O-distribution in Ia by the analyses of these two derivatives. The ^{18}O atom % found for II and III are shown in Table 2.

The ^{18}O content of the S-attack product, II, increased with time between the formation of Ia and the addition of piperidine, whereas that of the C-attack product, III, remained constant and was equal to that of the original benzoic acid. These findings indicate that it takes a little while for the oxygens to be scrambled completely through formation and internal return of ion-pairs at room temperature.

TABLE 2. SPECIFICITY OF ^{18}O-LABELING

Sample	% ^{18}O-excess
Starting PhCOOH	1.32
II (12 hr after formation of Ia)*	0.19
II (36 hr after formation of Ia)*	0.22
III	1.32

* at room temperature

Both the reaction between Ia and aniline and that between Ia and hydrazine yielded unidentifiable brown tar, which was probably produced from the decomposition of the S-attack products, Ph-NH-S-OEt and H_2NNH-S-OEt. Neither *p*-nitroaniline nor 2,5-dichloroaniline reacted with Ia when they were mixed with Ia and the mixture was allowed to stand at room temperature for several hours.

Isolation of Ia. Ia was unstable to water and was hydrolyzed rapidly. However, it was thermally stable, and it was possible to obtain white crystals of Ia by distillation in a high vacuum.

Reaction Mechanisms. The observed ^{18}O contents of all the reaction products are best explained by the reaction steps involving formation and internal return of the ion-pair and the successive attack of both benzoate anion and ethoxide anion to Ia by an ionic chain mechanism.

The most plausible route for formation of ethyl benzoate is direct attack of ethoxide anion to the carbonyl carbon of Ia, Eq. (9), or to that of the ion pair, Eq. (7). However, an S_Ni-type mechanism, as shown in Eq. (10) cannot be ruled out by the results of the ^{18}O analyses alone. The fractions shown in the parentheses under the ^{18}O-containing compounds indicate the ratio of the excess ^{18}O content calculated for the compound versus the excess ^{18}O content of the starting benzoic acid.

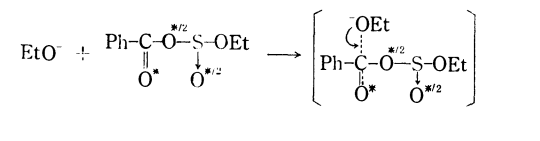

$$EtO^- + \text{Ph-C(=O)-O-S(=O)-OEt} \longrightarrow \left[\text{Ph-C(=O)(OEt)-O-S(=O)-OEt}\right]^- \longrightarrow \text{Ph-C(=O)-OEt} + SO_2 + {}^-OEt \quad (9)$$

(1/2) (1/2)

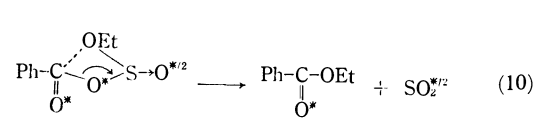

$$\text{Ph-C(=O)(OEt)-O-S(=O)} \longrightarrow \text{Ph-C(=O)-OEt} + SO_2 \quad (10)$$

4) G. Zinner, *Chem. Ber.*, **91**, 969 (1958).

The attack of the ethoxide anion on the sulfinyl sulfur atom of Ia will yield ethyl sulfite and benzoate anion, and the attack of the benzoate anion thus formed on the carbonyl carbon of Ia will yield benzoic anhydride, according to Eqs. (11) and (12). The analyses of the ^{18}O content of the products should determine whether or not Eq. (11) or (12) represent the reaction taking place in this medium. The benzoic anhydride was converted to benzanilide and benzoic acid according to Eq. (13). The result of the ^{18}O analyses of benzoic anhydride, benzoic acid, ethyl sulfite and sulfur dioxide (see Table 1) shows that Eqs. (11) and (12) actually represent the reaction taking place in this medium.

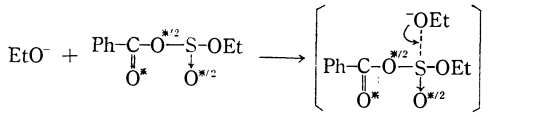

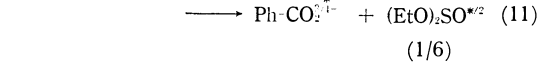

(1/6)

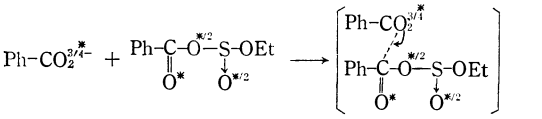

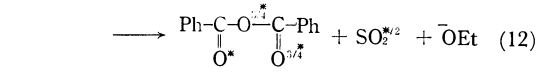

(5/6)

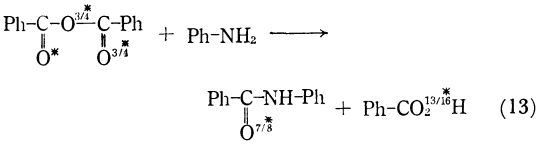

Experimental

^{18}O-Labeled Benzoic Acid. According to a previous method[2] a mixture of 25 g of benzotrichloride and of $H_2{}^{18}O$ (1.30 excess-^{18}O atm %) was refluxed and shaken for 20 hr in a bath at 110°C. After the hydrogen shaken for 20 hr in a bath at 110°C. After the hydrogen chloride formed and excess water were removed under reduced pressure, and the crystals of the benzoic acid remaining were converted to sodium benzoate by addition of the equimolar amount of a sodium hydroxide solution. The sodium salt was recrystallized from distilled water, ground to fine powder, and then dried in a vacuum at 100°C for 2 hr. Yield 14.2 g.

Ethyl Chlorosulfite. To 100 g of thionyl chloride 35.8 g of methanol was slowly added while the temperature was kept low with ice-cooling. The mixture was allowed to stand at room temperature for three days. Distillation under reduced pressure gave 61.5 g of ethyl chlorosulfite (bp 34.5°C/23 mmHg). Yield 61.5%.

Thermal Decomposition of Ethyl Benzoyloxysulfinate (Ia). When 17.85 g of ethyl chlorosulfite was added to 10 g of well-dried sodium benzoate-^{18}O, a slightly exothermic reaction occurred. The milky reaction mixture was then heated at 110—130°C for 2 hr. The sulfur dioxide which evolved vigorously during this period was dried with calcium chloride and introduced into an ethereal solution of phenylmagnesium bromide.[5] The yield of sodium benzenesulfinate was 6.63 g. After the salt was recrystallized from absolute methanol and dried, it was converted to phenyl benzyl sulfone by heating it with benzyl bromide in a sealed tube at 110°C for 5 hr.

The residual reaction mixture was refluxed at 190°C for 2 hr to complete the decomposition. The cooled reaction mixture was treated with 40 m*l* of methylene chloride, and the sodium chloride precipitated was filtered off. After the solvent was removed in a vacuum, repeated fractional distillation of the residue under reduced pressure yielded 2.1 g of diethyl sulfite (bp 68°C/30 mmHg), 0.7 g of ethyl benzoate (bp 105—108°C/30 mmHg), and 2.1 g of benzoic anhydride (bp 190—200°C/30 mmHg).

The benzoic anhydride obtained above was converted to benzanilide and benzoic acid by allowing a mixture of 1.0 g of benzoic anhydride and 0.5 g of aniline to stand at room temperature for a few minutes. White crystals of benzanilide which precipitated were filtered off and recrystallized from ethanol; yield, 500 mg. The filtrate was shaken well with a sodium carbonate solution, and the aqueous layer yielded, upon acidification with a diluted hydrochloric acid, crystals of benzoic acid, which were recrystallized from *n*-hexane; yield, 300 mg.

Reaction between Ia and Piperidine. To 500 m*l* of a carbon tetrachloride solution containing 2 g of benzoic acid and 2.1 g of ethyl chlorosulfite was added 2 g of triethylamine drop by drop with ice-cooling. When 1.7 g of piperidine was added to this mixture, the solution turned pale yellow. After it was allowed to stand overnight at room temperature, 50 m*l* of water was added to remove triethylamine hydrochloride. The organic layer separated was dried over magnesium sulfate. After the solution was removed in a vacuum, the residual yellow-brown liquid was distilled under reduced pressure and 0.5 g of an oil boling at 90°C/5 mmHg was obtained, which was found to be II by comparison of its infrared spectrum with that of the authentic sample prepared from ethyl chlorosulfate and piperidine.

Reaction between Ia and *p*-Chloaniline. To 30 m*l* of benzene solution containing 2 g of benzoic acid and 2.1 g of ethyl chlorosulfite was added 2 g of triethylamine with ice-cooling. The triethylamine hydrochloride precipitated was filtered off, and 30 m*l* of a carbon tetrachloride solution containing 2 g of *p*-chloroaniline was added to the filtrate. After the mixture was allowed to stand at room temperature for one hour, white crystals of *p*-chlorobenzanilide precipitated; yield, 130 mg.

Isolation of Ia. When 5 g of well-dried sodium benzoate and 10 g of ethyl chlorosulfite were mixed, an exothermic reaction takes place and the mixture became sirupy. Distillation in a high vaccum yielded a crystalline distillate at 94 °C/4×10^{-3} mmHg, which was found to be Ia on the basis of its infrared spectrum and the finding that upon addition of an ethereal solution of

5) C. F. H. Allen and S. Converse, "Organic Syntheses," Coll. Vol. I, 226 (1956).

p-chloroaniline it yielded crystalline *p*-chlorobenzanilide.

^{18}O-Analyses. The ^{18}O analyses were carried out according to the method of Rittenberg and Ponticorvo.[6] Each sample was pyrolyzed in the presence of mercuric chloride and mercuric cyanide at 400°C for 4 hr, and the ^{18}O atom % of the carbon dioxide produced was determined by use of a Hitachi RMU-6D type mass spectrometer.

6) D. Rittenberg and L. Ponticorvo, *Int. J. Appl. Rad. Isotopes.*, **1**, 208 (1956).

BULLETIN OF THE CHEMICAL SOCIETY OF JAPAN VOL. 43 908—914 (1970)

Studies of Diazosulfides. I.*1 A Kinetic Study of the Reaction of Diaryldiazosulfides with β-Naphthol in Alkaline Ethanol

Takashi YAMADA,*2 Nobuo TANAKA, Takao MORISAWA,*3
Masao NISHIKURI and Aritsune KAJI

Department of Chemistry, Faculty of Science, Kyoto University, Sakyo-ku, Kyoto

(Received September 16, 1969)

It was found that diaryldiazosulfides (I) reacted at an appreciable rate with β-naphthol in alkaline ethanol to produce azo-dyes. This is contrary to Hantzsch's observation. The initial-rate constants of the reaction were determined at various temperatures. The electron-donating substituents accelerated the rate when they were in the *N*-aryl part of I (substituent X) but retarded when in the *S*-aryl part of I (substituent Y). A set of ρ-values which have opposite signs, $\rho_X = -2.96$ and $\rho_Y = 3.93$, suggested that the rate-determining step in this reaction is the heterolytic rupture of the N–S bond of I. This was supported by the negative values of the entropy of activation and by such a solvent effect as that the rate was significantly increased when the polarity of the solvent increased. As the change in the concentration of β-naphthol affected the rate, the possibility of the participation of the transition state or of the intermediate including β-naphthol was also discussed.

It has been known that the thermolysis of diaryldiazosulfides is available as a preparative route for the generation of aromatic thiyl radicals.[1] Recently, Zwet and Kooyman[2] also reported on kinetic studies of the homolysis of diazosulfides. However, few reports have been presented on the ionic reaction of diazosulfides. Hantzsch and Freese[3] reported that diazosulfides dissociate to diazonium chloride and thiophenol in concentrated hydrochloric acid and that they do not give the coupling product with β-naphthol in alkaline ethanol.

We found that diaryldiazosulfides (I) reacted at an appreciable rate with β-naphthol in alkaline ethanol, thus producing azo-dyes (II).

In this paper, we wish to report our findings in a kinetic study of the reaction of diaryldiazosulfides with β-naphthol in alkaline ethanol.

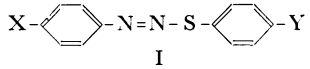

I

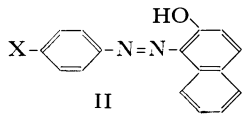

II

Results and Discussion

Diaryldiazosulfides. The diaryldiazosulfides (I)

*1 Presented at the 21st Annual Meeting of the Chemical Society of Japan, Osaka, April 1968.

*2 Present address: Laboratory of Chemistry, Faculty of Science, Kōnan University, Okamoto, Higashinada-ku, Kobe.

*3 Present address: Yokkaichi Division, Mitsubishi Petrochemical Co., Ltd., Toho-cho, Yokkaichi-shi, Mie.

1) a) E. C. Kooyman, "Organosulfur Chemistry," ed. by M. J. Janssen, Interscience Publishers, New York (1967), p. 9. b) W. B. Reynolds and E. W. Cotten, *Ind. Eng. Chem.*, **42**, 1905 (1950). c) S. Yamashita, J. Furukawa and T. Yamawaki, *Nippon Gomu Kyokaishi*, **31**, 534 (1958).

2) a) H. van Zwet and E. C. Kooyman, *Chem. Commun.* (London), **1965**, 313. b) H. van Zwet and E. C. Kooyman, *Rec. Trav. Chim. Pays-Bas*, **86**, 993 (1967). c) H. van Zwet and E. C. Kooyman, *ibid.*, **86**, 1143 (1967).

3) A. Hantzsch and H. Freese, *Ber.*, **28**, 3237 (1895).

Table 1. Rate constants for the reaction of diazosulfides with β-naphthol in alkaline ethanol at various temperatures*

	Substituent		$k \times 10^5$ (sec^{-1})			
	X	Y	15.0°C	25.0°C	35.0°C	45.0°C
Ia	OCH_3	Cl	—	223	370	589
Ib	CH_3	Cl	65.3	122	207	353
Ic	H	Cl	23.0	53.8	122	248
Id	Cl	Cl	1.08	3.45	9.50	24.0
Ie	$COCH_3$	Cl	0.295	0.825	2.47	6.15
If	CN	Cl	—	0.0257	0.106	0.320
Ig	NO_2	Cl	—	—	0.0245	0.0717
Ih	Cl	OCH_3	—	0.0363	0.105	0.158
Ii	Cl	CH_3	0.0282	0.0945	0.278	0.752
Ij	Cl	H	0.107	0.320	1.03	2.62
Ik	Cl	$CONH_2$	4.37	13.9	36.2	87.2
Il	Cl	$COCH_3$	17.3	51.7	131	310
Im	Cl	CN	61.7	166	400	828

* [Diazosulfide] $= 1.0 \times 10^{-4}$M, [β-Naphthol] $= 1.0 \times 10^{-3}$M, [KOH] $= 1.1 \times 10^{-3}$M

used in the present work all have their absorption maxima at 330—350 mμ (Table 6). According to the UV spectral discussion by Zwet and Kooyman,[2b] all the diaryldiazosulfides (I) prepared in the present work may be assigned as the *trans* form. This assignment of their configuration is supported by such a phenomenon as the polymorphism; that is, the crystals of I prepared at a low temperature change in forms when left standing at room temperature (see Experimental Section). This change is probably to be ascribed to the isomerization from the *cis* form to the *trans*.

Reaction of Diaryldiazosulfides (I) with β-Naphthol in Alkaline Ethanol. Contrary to Hantzsch's observation,[3] diazosulfides (I) reacted at an appreciable rate with β-naphthol in alkaline ethanol, thus producing azo-dyes (II). The products were identified by thin-layer chromatography (TLC).

The first-order rate plots of the reaction tended to curve more or less with the increase in the time (Fig. 1). This may be ascribed to the concurrent decomposition of I to diarylsulfides or disulfides,[2c] the rates of which, in alkaline ethanol, are comparable to the rate of the reaction of I with β-naphthol,[4] although the decomposition is overwhelmed by the coupling with β-naphthol and, accordingly, prevented fairly well in the presence of excess β-naphthol. Therefore, the initial-rate constants summarized in Table 1 will be utilized in the following discussion.

The electron-donating substituents accelerated the rate when they were in the *N*-aryl part of I, but retarded it when in the *S*-aryl part of I. A Hammett correlation of the rate constants at 35°C for diazosulfides (I) with substituents (Y) in the *S*-aryl part gives an excellent straight line, with

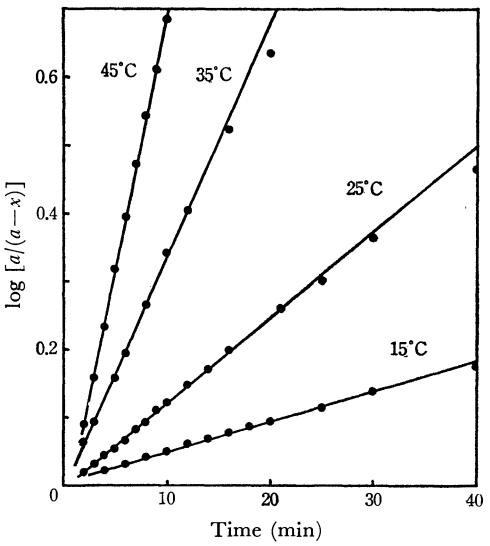

Fig. 1. First-order plots for the reaction of diazosulfide (Il) with β-naphthol in alkaline ethanol at various temperatures.

a slope ρ_Y of 3.93 ($r = 0.9997$) (Fig. 3), whereas a Hammett correlation for diazosulfides with substituents (X) in the *N*-aryl part shows a little poorer linearity, with a slope ρ_X of -3.92 ($r = 0.979$). However, this latter linearity can be improved by eliminating the points for *p*-CN and *p*-NO_2 ($\rho_X = -2.96$, $r = 0.985$) (Fig. 2). The deviation of these points below the line in Fig. 2 may be ascribed to an additional conjugation such as III and IV, which decreases the positive charge upon the diazonium part. Similar behavior was observed in the substituent effect on the rearrangement of *N*-methyldiaryltriazenes.[5]

4) T. Yamada and N. Tanaka, unpublished work.

5) T. Yamada, This Bulletin, **42**, 3565 (1969).

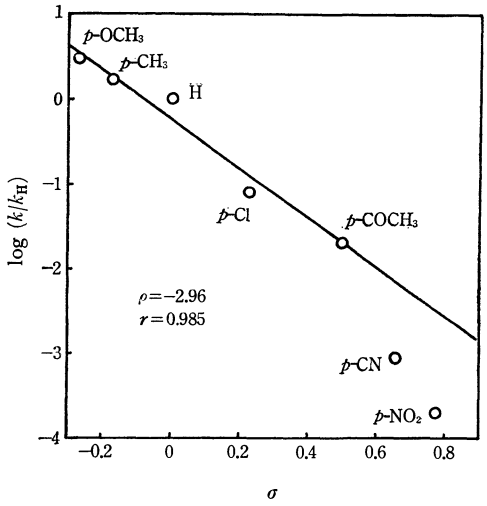

Fig. 2. Hammett plot for the reaction of diazosulfides (Ia—g), *p*-X-C_6H_4-N=N-S-C_6H_4-Cl-*p*, with *β*-naphthol in alkaline ethanol at 35.0°C.

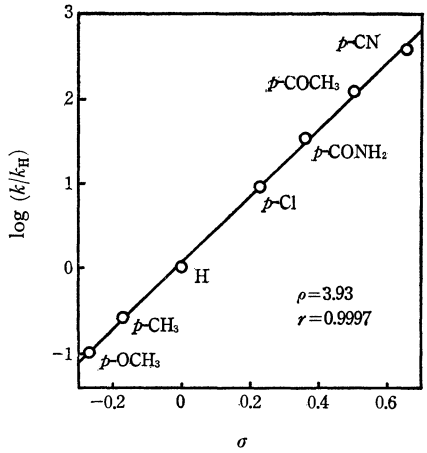

Fig. 3. Hammett plot for the reaction of diazosulfides (Ih—m, Id), *p*-Cl-C_6H_4-N=N-S-C_6H_4-Y-*p*, with *β*-naphthol in alkaline ethanol at 35.0°C.

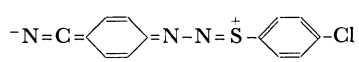

III

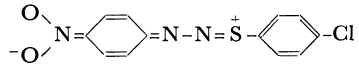

IV

A set of ρ-values which have opposite signs suggests that the heterolytic rupture of the N–S bond of diazosulfides (I) is the rate-determining step in this reaction, because a negative ρ_X-value and a positive ρ_Y-value suggest the stabilization of the diazonium cation by the substituents (X) in the *N*-aryl part and that of the thiophenoxide anion by the substituents (Y) in the *S*-aryl part. Similar substituent effects have been previously reported; for example, the following triazene rearrangement showed $\rho = -3.63$ (at 30.0°C).[5] The rate-determining step in the rearrangement was, therefore, concluded to be the dissociation of protonated triazene.

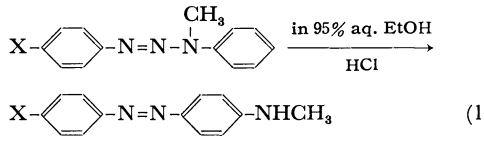

(1)

On the other hand, for the dissociation of *m*- and *p*-substituted thiophenols in 95% aqueous ethanol, $\rho = 2.847$ (at 20—22°C) has been reported.[6] In this case, the use of σ^- rather than σ reduced the scatter in Hammett correlation. According to Tsuno,[7] the dissociation constants of *m*- and *p*-substituted thiophenols gave a good correlation with a value, 0.52, of the parameter, *r*, in the Yukawa-Tsuno equation. However, in the present reaction of I with substituents (Y) in the *S*-aryl part, a Hammett correlation using σ shows an excellent linearity ($r = 0.9997$). Therefore, the contribution of the additional resonance stabilization by electron-withdrawing substituents seems to be less important in stabilizing the transition state in this reaction than in the case of the dissociation of thiophenols. This may be because the transition state of the reaction of I with *β*-naphthol may have a smaller charge separation than that of the dissociation of thiophenols.

TABLE 2. ACTIVATION PARAMETERS FOR THE REACTION OF DIAZOSULFIDES WITH *β*-NAPHTHOL IN ALKALINE ETHANOL

Diazosulfide	Substituent X	Substituent Y	E_a kcal/mol	$\Delta S^{\neq}$(35°C) e.u.
Ia	OCH_3	Cl	9.1	−34.0
Ib	CH_3	Cl	10.3	−31.5
Ic	H	Cl	14.5	−18.0
Id	Cl	Cl	18.8	− 9.7
Ie	$COCH_3$	Cl	18.5	−13.7
Ii	Cl	CH_3	20.1	−12.3
Ij	Cl	H	20.0	−10.4
Ik	Cl	$CONH_2$	18.1	− 9.3
Il	Cl	$COCH_3$	17.5	− 8.9
Im	Cl	CN	15.7	−12.4

The thermodynamic parameters (Table 2) also suggest that the ionization of diazosulfides is rate-determining, because the values of E_a and $\Delta S^{\neq}$ fall within the range of the values found for a case in which the dissociation of neutral molecules to

6) H. H. Jaffe, *Chem. Rev.*, **53**, 191 (1953).
7) Y. Tsuno, "Summary of the Symposium on the Hammett Relationship," the Chemical Society of Japan (1967), p. 4.

ions is rate-determining.[8] A plot of E_a against $\Delta S^{\neq}$ is found to show a linearity ($\beta \fallingdotseq 470°K$) (Fig. 4). The large negative values of $\Delta S^{\neq}$ for Ia and Ib may due to the substantial contribution of the entropy term to the reaction.

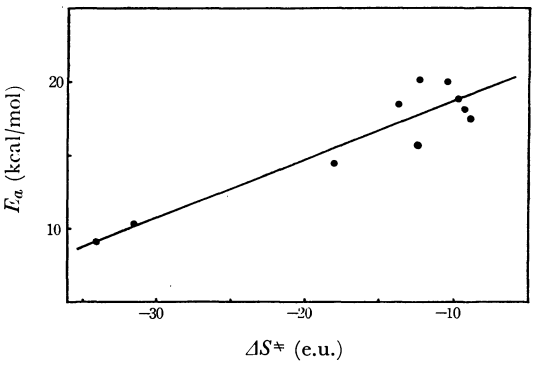

Fig. 4. Plot of E_a *vs.* $\Delta S^{\neq}$ for the reaction of diazosulfides with β-naphthol in alkaline ethanol.

According to Ingold's criterion,[9] this consideration can be supported by the findings concerning the solvent effect upon the rate constants; the rate significantly increased when the polarity of the solvent, ethanol, was increased by the addition of water (Table 3).

Table 3. Effect of water concentration on the rate constants in the reaction of diazosulfide (Id) with β-naphthol in aqueous alkaline ethanol at 35.0°C*

H_2O (vol%)	$k \times 10^4$ (sec^{-1})
0	0.950
10	5.98
20	12.7
30	17.2
50*2	26.3

* [Diazosulfide] $= 1.0 \times 10^{-4}$M, [β-Naphthol] $= 1.0 \times 10^{-3}$M, [KOH] $= 1.1 \times 10^{-3}$M

*2 [Diazosulfide] $= 5.0 \times 10^{-5}$M, [β-Naphthol] $= 5.0 \times 10^{-4}$M, [KOH] $= 5.5 \times 10^{-4}$M

Table 4 shows that the increment in the concentration of KOH resulted in only a slight increase in the rate, while the addition of KCl also increased the rate in aqueous ethanol. These results can reasonably be interpreted in terms of the salt effect.

From the available evidence, the most probable mechanism can be assumed to be as follows: dia-

Table 4. Effect of alkali concentration on the rate constants in the reaction of diazosulfides with β-naphthol at 35.0°C

	[Diazosulfide] $\times 10^4$M	[β-Naphthol] $\times 10^4$M	[KOH] $\times 10^4$M	Solvent	$k \times 10^5$ sec^{-1}
Id	1.0	10	11	EtOH	9.50
Id	1.0	10	22	EtOH	10.0
Ic	1.0	10	11	EtOH	122
Ic	1.0	10	22	EtOH	136
Id	0.5	5.0	5.5	EtOH (50%) $-H_2O$ (50%)	263
Id	0.5	5.0	0*	EtOH (50%) $-H_2O$ (50%)*	243
Id	1.0	10	11*2	EtOH (50%) $-H_2O$ (50%)	333

* Buffer solution (pH=9.4) was added.
*2 KCl was added (1.0×10^{-3}M).

zosulfide dissociates to the diazonium cation and the thiophenoxide anion, and, then the former cation couples with the β-naphthoxide anion to produce azo-dye. The rate-determining step is the dissociation of diazosulfide; *i. e.*, $k_1 \ll k_2$, k_{-1}.

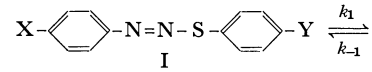

I

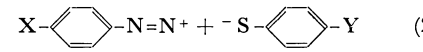

(2)

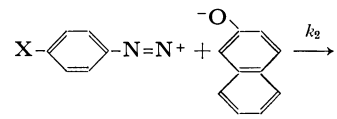

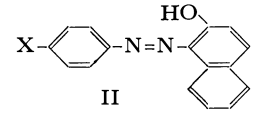

II (3)

However, it is possible that the intermediate is an ion pair (V) rather than a free diazonium cation; that is, the ion pair intermediate (V) may be formed in the rate-determining step (Eq. (4)) and attacked by β-naphthol to produce II (Eq. (5)) ($k_1 \ll k_2$, k_{-1}).

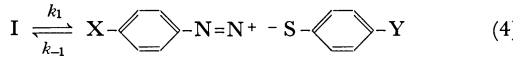

(4)

V, ion pair

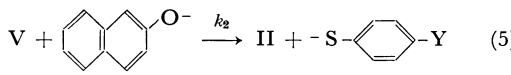

(5)

As is shown in Table 5, the change in the concentration of β-naphthol has an effect on the rate. The rate enhancement with the increase in β-naphthol is fairly large, but not so large that the order of reaction is one with respect to β-naphthol. Therefore, we may suggest the possibility of a

8) A. A. Frost and R. G. Pearson, "Kinetics and Mechanism," John Wiley & Sons, Inc., N. Y. (1961), p. 135.

9) C. K. Ingold, "Structure and Mechanism in Organic Chemistry," Cornell University Press, Ithaca, N. Y. (1953), p. 345.

TABLE 5. EFFECT OF THE MOLAR RATIO OF β-NAPHTHOL TO DIAZOSULFIDE ON THE RATE CONSTANTS IN THE REACTION OF DIAZOSULFIDE (Id) WITH β-NAPHTHOL AT 35.0°C*

[β-Naphthol]/[Diazosulfide]	$k \times 10^5$ (sec^{-1})		
	A	B	C
5	7.4	80.8	162
10	9.5	127	243
15	—	—	288
20	11.3	190	320

* [Diazosulfide] = 1.0×10^{-4}M
A: solvent, EtOH; [KOH]/[β-Naphthol] = 1.1
B: solvent, 80% aq. EtOH, [KOH]/[β-Naphthol] = 1.1
C: solvent, EtOH (50%) + Buffer solution (pH 9.4) (50%)

"borderline" case[10] between S_N1 and S_N2; *i.e.*, in Eqs. (4) and (5), the rate of step 1 is comparable that of step 2. On the other hand, the possibility of an alternative mechanism through a loose "complex" (VI) containing β-naphthoxide cannot be disregarded (Eq. (6)).

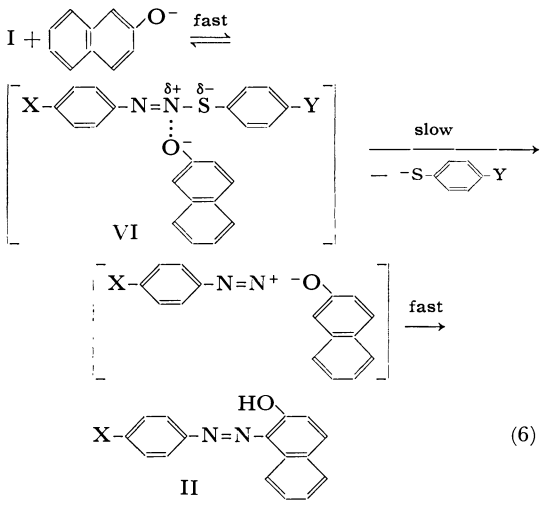

(6)

However, the determination of the reaction order was difficult because the decomposition of I became predominant and made the rate plot complex in the presence of a low concentration of β-naphthol; thus, the role of β-naphthol in the rate enhancement is ambiguous.

On the basis of the above results, we consider the mechanism through the ion pair (Eqs. (4) and (5)) to be most likely in the reaction of I with β-naphthol. The rate enhancement with the increase in β-naphthol may be ascribed to the salt effect.

Zwet and Kooyman[2b] reported that the *cis* isomers react with β-naphthol in alkaline ethanol to form red azo-dye, whereas the *trans* isomers do not. Thus, they concluded that the ionization of diazosulfide could occur with only the *cis* isomers.

According to our present data on the substituent effect and the difference in the thiol acidities,[11] there is a considerable possibility that the following is true: the *trans*-diazosulfides studied by Zwet and Kooyman may also dissociate only very slowly, and this very slow dissociation seems to have led them to the mistaken conclusion that the *trans* isomer cannot undergo ionization. The same possibility may hold in the case of Hantzsch's report;[3] the diaryldiazosulfides used by Hantzsch and Freese may dissociate very slowly, judging from our results, and thus it seems that they failed to observe the reaction of diazosulfides with β-naphthol.

However, it becomes necessary to question whether or not the *trans* isomers dissociate through the *cis* forms. We intend to pursue this question through the isolation of *trans* and *cis* isomers of diazosulfides and by studying them kinetically in a subsequent paper.

Experimental

Preparation of Materials. *Most of the diaryldiazosulfides (I)* were synthesized by the following general method:[12]

A solution of 0.02 mol of *p*-substituted aniline in 20 m*l* of 7% hydrochloric acid was diazotized with 0.023 mol of sodium nitrite in 5 m*l* of water. The diazonium solution was then slowly added to an ice-cold, stirred solution of 0.02 mol of *p*-substituted thiophenol in 20 m*l* of a 10% aqueous sodium hydroxide solution. The yellow crystals which immediately formed were filtered, thoroughly washed with cold water, and dried *in vacuo* over calcium chloride. The crude products were dissolved in acetone at room temperature and recrystallized by cooling them in an acetone-dry ice refrigerant.

In the preparation of I, the following phenomena were observed. When the *S*-coupling was carried at 5—10°C, pale yellow crystals were first formed, but they soon rose to the surface of the liquid and became brownish. The brown solids were recrystallized from acetone to give pure yellow diazosulfide. On the other hand, when the *S*-coupling was carried below 0°C, the pale yellow crystals were obtained in a fairly stable form. However, they turned brownish upon filtration or desiccation at room temperature. Especially, when a large amount (0.1 mol) of Id was prepared, the yellow crystals turned exothermically into a brown mass, but a pure Id was obtained by several recrystallizations of the crude material. After recrystallization, no such change in I could be observed besides a gradual thermal decomposition.

10) R. A. Sneen and J. W. Larsen, *J. Amer. Chem. Soc.*, **91**, 362 (1969).

11) B. Dmuchovsky, F. B. Zienty and W. A. Vredenburgh, *J. Org. Chem.*, **31**, 865 (1966); the pK_a values at 27°C in 3 : 1 (*v/v*)-acetone-water are 11.1 for triphenylmethanethiol, 9.3 for 4-methylbenzenethiol, 8.6 for benzenethiol and 7.8 for 4-chlorobenzenethiol.

12) *Cf.* Refs. 1c, 2b and 3.

TABLE 6. THE ANALYTICAL DATA AND ULTRAVIOLET SPECTRAL DATA OF DIARYLDIAZOSULFIDES:

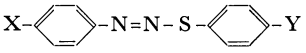

	Substituent		Mp °C	λ_{max} mμ	log ε	Analysis (calcd)		
	X	Y				C%	H%	N%
Ia	OCH_3	Cl	55.5—56.0	345	4.19	55.87 (56.01)	4.08 (3.98)	10.08 (10.05)
Ib	CH_3	Cl	66.0—66.5	336	4.13	59.24 (59.42)	4.19 (4.22)	10.75 (10.66)
Ic	H	Cl	34.0	332	4.06	57.70 (57.95)	3.63 (3.65)	11.36 (11.26)
Id	Cl	Cl	97.0—97.5	337	4.13	50.65 (50.90)	3.04 (2.85)	
Ie	$COCH_3$	Cl	80.5—81.0	342	4.17	58.13 (57.83)	3.79 (3.81)	9.64 (9.63)
If	CN	Cl	112.5—113.5	340	4.14	57.31 (57.04)	2.87 (2.95)	15.50 (15.35)
Ig	NO_2	Cl	111.5—112.0	350	4.16	48.92 (49.06)	2.57 (2.75)	14.43 (14.31)
Ih	Cl	OCH_3	59.0—59.5	333	4.11	56.27 (56.01)	4.00 (3.98)	10.00 (10.05)
Ii	Cl	CH_3	78.5—79.0	336	4.12	59.55 (59.42)	4.31 (4.22)	10.60 (10.66)
Ij	Cl	H	59.0—59.5	337	4.12	57.91 (57.95)	3.63 (3.65)	11.34 (11.26)
Ik	Cl	$CONH_2$	150	345	4.17	53.51 (53.53)	3.48 (3.46)	14.31 (14.41)
Il	Cl	$COCH_3$	104.5—105.5	349	4.22	57.68 (57.83)	3.84 (3.81)	9.82 (9.63)
Im	Cl	CN	109.0—109.5	346	4.22	56.84 (57.04)	2.88 (2.95)	

Diazosulfides (Im and Ik) were prepared as follow: *p*-aminobenzonitrile (5.9 g) was treated by the usual procedure[13] to convert an amino group to a mercapto group, but in order to avoid the hydrolysis of a cyano group, the hydrolysis of the intermediate, *p*-cyanophenyl ethyl xanthate, was carried out by standing overnight at room temperature. Nevertheless, a mixture of *p*-cyanothiophenol and *p*-carbamoylthiophenol was obtained. From this mixture, a mixture (9 g) of diazosulfides, Im and Ik, was obtained by the procedure described above. The mixture was added to benzene (90 m*l*), stirred well at room temperature, and filtered from the insoluble material. To filtrate, after the benzene was distilled off *in vacuo*, was purified by elution chromatography over the activated alumina, using benzene as the eluent. The compound that was first eluted, the predominant component, was identified as diazosulfide (Im) on the basis o the elementary analysis and a study of the infrared spectrum (ν_{CN}=2270 cm^{-1}). The yield of Im was 6 g. On the other hand, the insoluble material (1.2 g) was recrystallized from acetone and gave diazosulfide (Ik) ($\nu_{C=O}$=1693 cm^{-1}, ν_{NH_2}= 3480, 3590 cm^{-1}). The analytical data and the ultraviolet spectral data of I are summarized in Table 6.

α-(p-Substituted phenylazo)-β-naphthols (II) were prepared by the reaction of the corresponding aryldiazonium chlorides and β-naphthol in an aqueous alkaline solution by the usual procedure, and were purified by several recrystallizations from ethanol (Table 7). The λ_{max} and ε values for II, summarized in Table 7, were measured, under conditions similar to those holding in the reaction of diazosulfides with β-naphthol, as follows: an ethanol solution (1 m*l*) of II (10^{-3}M), 1 m*l* of a 1.1×10^{-2}M KOH ethanol solution, and 0.9 m*l* of $1.0\times$

TABLE 7. PHYSICAL CONSTANTS AND ULTRAVIOLET SPECTRAL DATA* OF α-ARYLAZO-β-NAPHTHOLS (II)

Substituent X	Mp °C	λ_{max} mμ	ε
OCH_3	136—137	458	15000
CH_3	132.5—134	476	13400
H	133—134	476	14300
Cl	165—166	476	15900
Cl	165—166	486*2	19000*2
$COCH_3$	186—187	485	22800
CN	239—240	480	20400
NO_2	251—252	494	20600

* Solvent: EtOH
*2 Solvent: EtOH (50%)-water (50%)

13) D. S. Tarbell and D. K. Fukushima, "Organic Syntheses," Coll. Vol. III, p. 809 (1955).

10^{-2}M β-naphthol ethanol soultion were placed in a 10-m*l* measuring flask, and then, by the subsequent addition of ethanol, the solution was made up to volume. This solution was used as the sample for the visible spectra measurements.

Kinetic Measurements. The rate constants were determined spectrophotometrically. A Hitachi Perkin-Elmer 139 UV-VIS spectrophotometer equipped with a thermostated cell compartment was used.

One m*l* of a β-naphthol ethanol solution (10^{-2}M), 1 m*l* of a KOH ethanol solution (1.1×10^{-2}M), and about 6.5 m*l* of ethanol were placed in a 10-m*l* measuring flask immersed in a thermostated water bath. The reaction was initiated by the addition of 1 m*l* of an ethanol solution of diazosulfide (10^{-3}M), freshly prepared at the same temperature, to the flask. The entire solution was then quickly made up to volume with ethanol, and the solution was transferred into a 10-mm stoppered quartz cuvette set in a thermostated cell compartment.

The optical densities were measured at appropriate intervals at the maximum-absorption wavelength of the azo-dye produced.

In the present work, it was assumed that the amount of azo-dye produced (x) was equal to that of diazosulfide consumed; thus, the rate constants were evaluated from the slope of the plot of log ($a/(a-x)$) against t, where a is the initial concentration of diazosulfide. A typical example is shown in Fig. 1. In most of the reactions, the rate decreased with time, and so the initial rates were measured (Table 1).

On the reaction in a mixture of ethanol and a buffer solution, Clark-Lubs's buffer solution (pH 9.4) was used, and the initial concentrations of I and β-naphthol were half as much as those in the general procedure described above because of the low solubility of the azo-dye produced in this solvent.

The authors wish to thank Professor Ryozo Goto for his encouragement of this work. They are also indebted to Dr. Jun-ichi Hayami for his valuable discussions.

BULLETIN OF THE CHEMICAL SOCIETY OF JAPAN VOL. 43 914—917 (1970)

Studies of Peptide Antibiotics. XV. The Synthesis of *cyclo*-(L-Valyl-L-ornithyl-L-leucyl-D-phenylalanyl-L-prolyl-glycyl-glycyl)

Okitoshi ABE,[1] Kenji KUROMIZU, Michio KONDO[2] and Nobuo IZUMIYA[3]

Laboratory of Biochemistry, Faculty of Science, Kyushu University, Hakozaki, Fukuoka

(Received September 17, 1969)

A cyclic heptapeptide, *cyclo*-(L-Val-L-Orn-L-Leu-D-Phe-L-Pro-Gly-Gly-), was synthesized in order to investigate a contribution for an antibacterial activity of a ring size of a cyclic peptide. A linear heptapeptide *p*-nitrophenyl ester, in which an δ-amino function of ornithine residue was protected with benzyloxycarbonyl group, was transformed to the cyclic benzyloxycarbonyl-substituted heptapeptide which was hydrogenated to afford the desired cyclic heptapeptide as hydrochloride. The cyclic peptide thus obtained showed no activity against any of microorganisms tested.

In studies of the relationship between chemical structure and biological activity of antibacterial cyclic peptides, the cyclic penta- and hexapeptide, cyclosemigramicidin S[4] and *cyclo*-(L-Val-L-Orn-L-Leu-D-Phe-L-Pro-Gly-)[5], which contain the partial amino acid sequence found in gramicidin S and tyrocidines, were prepared, and their biological activities examined. However, in spite of its apparent resemblance to those natural antibiotics, the cyclic penta- and hexapeptide were found to be inactive. Furthermore, a cyclic hexapeptide designated as gramicidin J_2 was synthesized, and the peptide showed no activity.[6] Although the reason for the inactivity is not yet clear, other structural features such as appropriate ring sizes may be necessary in this type of molecule for the exhibition of the activity. Therefore, it became of interest to determine whether or not a larger cyclic peptide with an appropriate amino acid sequence would exhibit the antibacterial properties.

This paper is concerned with the synthesis and an antibacterial assay of a cyclic heptapeptide,

1) Present address: Institute for Muscle Disease, New York, N. Y., U.S.A.

2) Present address: Department of Chemistry, Saga University, Honjo, Saga.

3) To whom the reprint request should be addressed.

4) M. Waki and N. Izumiya, *J. Amer. Chem. Soc.*, **89**, 1278 (1967); This Bulletin, **40**, 1687 (1967).

5) T. Kato, M. Kondo, M. Ohno and N. Izumiya, This Bulletin, **38**, 1202 (1965).

6) T. Kato and N. Izumiya, *J. Biochem.*, **59**, 629 (1966); This Bulletin, **39**, 2242 (1966).

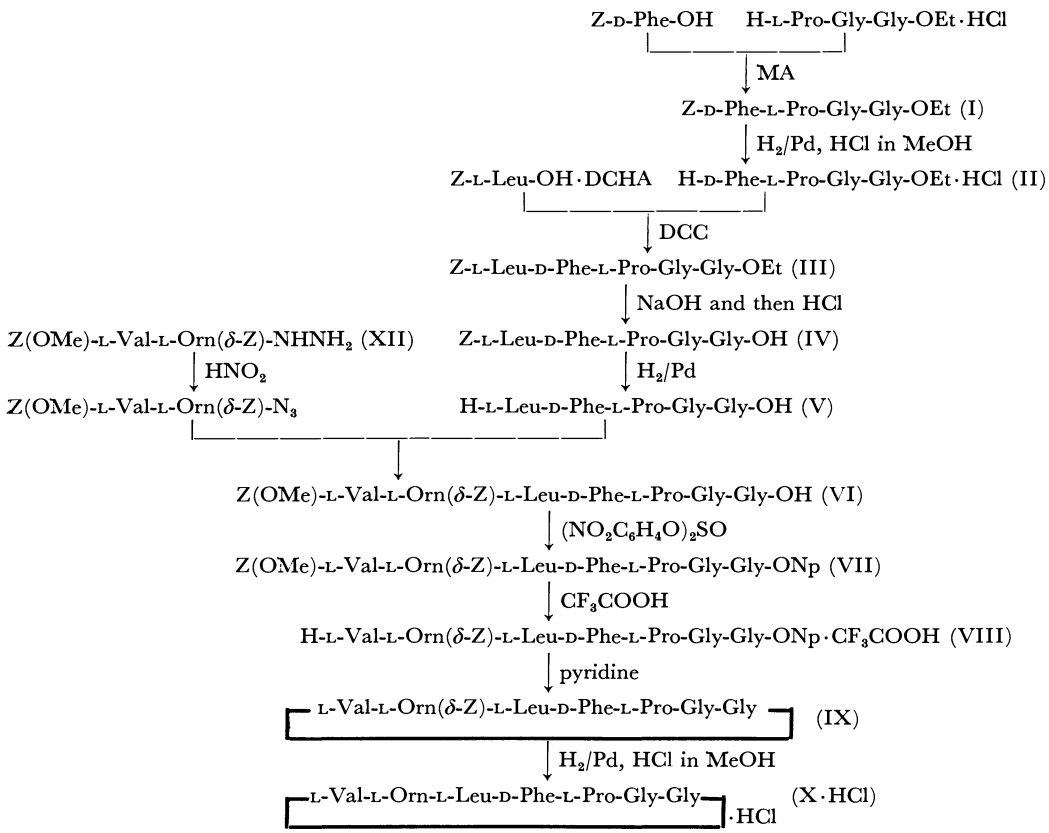

Fig. 1. Cyclization of linear heptapeptide active ester

cyclo-(L-Val-L-Orn-L-Leu-D-Phe-L-Pro-Gly-Gly-), which contains the partial sequence -L-Val-L-Orn-L-Leu-D-Phe-L-Pro- found in the natural antibiotics mentioned above.

Figure 1 indicates the route for the synthesis of the cyclic heptapeptide (X·HCl). *p*-Methoxybenzyloxycarbonyl-heptapeptide acid (VI) was prepared by the coupling reaction of the acyl-dipeptide azide derived from XII with the neutral pentapeptide (V), and then VI was converted to the benzyloxycarbonyl-substituted heptapeptide *p*-nitrophenyl ester trifluoroacetate (VIII). The cyclization reaction of the trifluoroacetate in pyridine gave the benzyloxycarbonyl-substituted cyclic peptide (IX) which was purified by passing it through columns of Dowex 50 and Dowex 1. The molecular-weight determination demonstrated that the molecular size of IX corresponds to that of cyclic heptapeptide. The final product, X·HCl, was obtained upon the hydrogenolysis of IX in the presence of one equivalent of hydrogen chloride as crystals with five moles of water; its homogeneity was demonstrated by several chromatographic techniques.

The antibacterial activity of the cyclic peptide (X) toward several microorganisms was examined. The compound X showed no activity against any of the microorganisms even at 100 μg per m*l* of the assay medium. Hence, it appears that even the presence of seven amino acid residues in a cyclic peptide does not satisfy the requirements for antibacterial activity.

Experiments on the preparations and the properties of several cyclic peptides with larger ring sizes, such as a cyclic octapeptide, are in progress in this laboratory in order to extend this study further.

Experimental

All the melting points are uncorrected. Prior to analysis, the compounds were dried over phosphorus pentoxide to a constant weight at 80°C and 2 mmHg, except for the cyclic peptide (X·HCl·5H_2O).

Z-D-Phe-Pro-Gly-Gly-OEt (I).[7] To a solution of benzyloxycarbonyl-D-phenylalanine (2.57 g, 8.5 mmol), H-Pro-Gly-Gly-OEt·HCl[8] (2.54 g, 8.6 mmol) and triethylamine (1.2 m*l*) in tetrahydrofuran (40 m*l*) was

7) The following abbreviations are used according to *Biochemistry*, **5**, 2485 (1966); Z-, benzyloxycarbonyl; Z(OMe)-, *p*-methoxybenzyloxycarbonyl; -ONp, *p*-nitrophenyl ester; -OEt, ethyl ester; DCC, dicyclohexylcarbodiimide; DMF, dimethylformamide. Amino acid symbols except D-Phe denote the L configuration.

8) H. N. Rydon and P. W. G. Smith, *J. Chem. Soc.*, **1956**, 3642.

added DCC (1.77 g, 8.6 mmol) at 0°C. After the stirring had been continued for 2 hr at 0°C, the mixture was left to stand for overnight at room temperature. The mixture was then evaporated *in vacuo*, and ethyl acetate was added to the residue. After the dicyclohexylurea was filtered off, the filtrate was washed successively with 4% sodium bicarbonate solution and 2% hydrochloric acid and dried over sodium sulfate. The filtrate was evaporated *in vacuo*. The residual foam weighed 4.07 g (88%); R_f 0.95.[9]

H-D-Phe-Tro-Gly-Gly-OEt·HCl (II). A solution of I (4.07 g) in 0.4N methanolic hydrogen chloride (20.8 ml) was subjected to hydrogenolysis in the presence of palladium black. The filtrate from the catalyst was evaporated to dryness *in vacuo*; yield of oil, 3.37 g (102%); R_f 0.80[9] and 0.95.[10]

Z-Leu-D-Phe-Pro-Gly-Gly-OEt (III). To a solution of benzyloxycarbonyl-L-leucine dicyclohexylamine salt[11] (3.35 g, 7.5 mmol) and II (4.03 g) in chloroform (50 ml) was added DCC (1.45 g, 7.5 mmol) at 0°C. The reaction mixture was treated as has been described for the preparation of I. The residual foam weighed 4.61 g (94%); R_f 0.94.[9]

Z-Leu-D-Phe-Pro-Gly-Gly-OH (IV). To a solution of III (4.37 g, 6.7 mmol) in methanol (50 ml), N sodium hydroxide (13.4 ml) was added. After the solution had been allowed to stand two days at room temperature, N hydrochloric acid (27 ml) was added and the solution was evaporated *in vacuo*. The oily product was extracted with ethyl acetate and the solution was dried over sodium sulfate. The filtrate was evaporated, and the residue was crystallized by the addition of ether. It was recrystallized from ethanol-ether; yield, 2.97 g (71%); mp 178—180°C; $[\alpha]_D^{20}$ −4.4° (*c* 1, MeOH).

Found: C, 61.49; H, 6.69; N, 10.98%. Calcd for $C_{32}H_{41}O_8N_5$: C, 61.62; H, 6.63; N, 11.23%.

H-Leu-D-Phe-Pro-Gly-Gly-OH (V). A solution of IV (2.50 g, 4.01 mmol) in a mixture of acetic acid-methanol-water (6 : 4 : 1, 40 ml) was subjected to hydrogenolysis in the presence of palladium black. The filtrate was evaporated to dryness *in vacuo*, and the residual crystals were collected with the aid of ether. It was recrystallized from ethanol-ether; yield, 1.76 g (90%); mp 158—159°C (dec.); $[\alpha]_D^{20}$ −20.0° (*c*, 1, MeOH); R_f 0.64.[9]

Found: C, 57.07; H, 7.42; N, 13.47%. Calcd for $C_{24}H_{35}O_4N_5 \cdot H_2O$: C, 56.78; H, 7.36; N, 13.80%.

Z(OMe)-Val-Orn(δ-Z)-Leu-D-Phe-Pro-Gly-Gly-OH (VI). The azide[5] derived from Z(OMe)-Val-Orn(δ-Z)-$NHNH_2$ (XII) (1.63 g, 3 mmol) was added to a solution of V (1.47 g, 3 mmol) and triethylamine (0.42 ml) in DMF (50 ml). The mixture was stirred for 3 days at 0°C and evaporated *in vacuo*. The resideu was triturated with 10% citric acid, and the precipitate was collected by filtration and washed with water. It was recrystallized from methanol-ether-petroleum ether; yield, 2.71 g (90%); mp 119—120°C $[\alpha]_D^{20}$ −8.0° (*c* 1, DMF); R_f 0.75.[9]

Found: C, 59.26; H, 6.82; N, 10.85%. Calcd for $C_{51}H_{68}O_{13}N_8 \cdot 2H_2O$: C, 59.05; H, 7.01; N, 10.80%.

***cyclo*-(Val-Orn(δ-Z)-Leu-D-Phe-Pro-Gly-Gly-) (IX).** To a solution of VI (0.50 g, 0.5 mmol) in pyridine (25 ml), di-*p*-nitrophenyl sulfite[12] (1.62 g, 5 mmol) was added, and the reaction mixture was then allowed to stand for 24 hr at room temperature. After evaporation of the solvent, the product was triturated with petroleum ether and washed repeatedly with a mixture of ether and petroleum ether (1 : 1) by decantation (yield of VII, 578 mg). The *p*-nitropheynl ester content was estimated to be 90% by measuring the optical density at 412 mμ.[13]

To VII (576 mg) thus obtained were added anisole (1 ml) and trifluoroacetic acid (6 ml) at 0°C. After 20 min, the solution was evaporated, and the solid was collected with the aid of a mixture of ether and petroleum ether. The heptapeptide *p*-nitrophenyl ester trifluoroacetate (VIII) thus obtained was dissolved in DMF (10 ml) with acetic acid (0.5 ml). The solution was added dropwise into pyridine (300 ml) at 55—60°C during 5 hr and the stirring was continued for additional 2 hr. After removal of the solvent, the residue was dissolved in a mixture of methanol-water (5 : 1, 150 ml). The solution was treated with columns (1.8×15 cm) of Dowex 1 (OH^- form) and Dowex 50 (H^+ form). The columns were washed with the same solvent (400 ml), and the combined effluent was evaporated to dryness. The residual product was collected by filtration with the aid of water and dried (249 mg). It was recrystallized from dioxane-methanol-ether; yield of air-dried product, 202 mg (50% form VI); mp 149—151°C (decomp.); $[\alpha]_D^{20}$ −4.0° (*c* 1, MeOH); R_f 0.94.[9]

Found: C, 60.69; H, 7.17; N, 13.25%; mol wt, 850.[14] Calcd for $C_{42}H_{58}N_8O_9 \cdot \frac{1}{2}H_2O$: C, 60.91; H, 7.20; N, 13.53%: mol wt, 828.

The air-dried product lost 1.00% of its weight after

Table 1. Inhibitory activity of the compounds on microorganisms

Minimum inhibitory concentration, μg/ml

Compound	Synthetic medium[a]		Bouillon agar medium[b]	
	E. coli	*B. subtilis*	*R. coli*	*B. substilis*
The cyclic heptapeptide (X)	>100	>100	>100	>100
Gramicidin S	>100	10	>100	2—5

a) Stephenson-Whetham's medium (modified); K_2HPO_4 0.1%, NaCl 0.1%, $MgSO_4 \cdot 7H_2O$ 0.05%, Na-glutamate 0.4%, casamino acid 0.2%, yeast-extract 0.05% and agar 2.0%, pH 7.0.
b) Usual boulillon agar medium, pH 7.0.

9) The R_f values refer to the thin-layer chromatography with Merck silica gel G and to the *n*-butanol-acetic acid-pyridine-water (4 : 1 : 1 : 2, *v/v*) system. Compounds possessing a free amino group were detected by spraying them with ninhydrin, and those with blocked amino groups, by spraying them with 47% hydrobromic acid, and then with ninhydrin.

10) The R_f of the paper chromatography with Toyo Roshi No. 52 refers to the *n*-butanol-acetic acid-pyridine-water (4 : 1 : 1 : 2, *v/v*) system.

11) E. Klieger, E. Schröder and H. Gibian, *Ann.*, **640**, 157 (1966).

12) B. Iselin and R. Schwyzer, *Helv. Chim. Acta*, **43**, 1760 (1960).

13) R. Schwyzer and P. Sieber, *ibid.*, **40**, 624 (1957).

14) The molecular weight was determined on a Hitachi Osmometer, type 115, using DMF as the solvent.

being dried for 2 hr at 110°C, 2 mmHg. Calcd for $\frac{1}{2}H_2O$: 1.09%.

***cyclo*-(Val-Orn-Leu-D-Phe-Pro-Gly-Gly-)·HCl(X·HCl).** A solution of VII (82 mg; 0.1 mmol) dissolved in 0.126N methanolic hydrogen chloride (0.88 m*l*) was subjected to hydrogenolysis in the presence of palladium black. The solution, after being filtered from the catalyst, was evaporated to dryness *in vacuo*. The crystals were collected with the aid of ether; yield of the air-dried product, 60.8 mg (84%); mp 150—153°C (decomp.); R_f 0.78[9] and 0.94;[10] $R_{\text{gramicidin S}}$ of paper electrophoresis,[15] 0.76; $[\alpha]_D^{20}$ −18.0° (*c* 1, MeOH); amino acid ratios in acid hydrolysate, $Val_{0.9}Orn_{1.1}$-$Leu_{1.0}Phe_{0.9}Pro_{1.0}Gly_{2.2}$.

Found: C, 50.21; H, 7.44; N, 13.52%. Calcd for $C_{34}H_{52}N_8C_7Cl\cdot 5H_2O$: C, 50.38; H, 7.73; N, 13.83%.

Microbiological Assays.[16] The microorganism employed are listed in Table 1. The minimum amount of the compound necessary for the complete inhibition of growth was determined by a dilution method using a bouillon agar medium and a synthetic medium. As is shown in Table 1, the cyclic heptapeptide was found to be devoid of activity in reaction against any of the microorganisms utilized.

15) Detail of the experiment has been described in the previous publication; H. Aoyagi, T. Kato, M. Waki, O. Abe, R. Okawa, S. Makisumi and N. Izumiya, This Bulletin, **42**, 782 (1969).

16) We are indebted to Dr. M. Shibata of Takeda Chemical Industries, Ltd. for the assay.

BULLETIN OF THE CHEMICAL SOCIETY OF JAPAN VOL. 43 917—920 (1970)

Hydrogenation and Hydrogenolysis. XII.[1] The Hydrogenation of Isomeric Dimethoxybenzenes with Platinum Metal Catalysts*1

Yuzuru TAKAGI and Sadayoshi ISHII

The Institute of Physical and Chemical Research, Yamato-machi, Saitama

and Shigeo NISHIMURA

Department of Industrial Chemistry, Tokyo University of Agriculture and Technology, Koganei-shi, Tokyo

(Received September 26, 1969)

The catalytic hydrogenation and hydrogenolysis of isomeric dimethoxybenzenes over six platinum metals have been investigated at elevated temperature and pressure. The hydrogenolysis of methoxyl group occurred more extensively over Group $VIII_3$ metals than over Group $VIII_2$ metals. The *meta* isomer hydrogenolyzed to greater extent and gave smaller *cis*/*trans* ratio of dimethoxycyclohexane, than the *ortho* and *para* isomers. The greater tendency of the *meta* isomer toward hydrogenolysis supports the previously proposed explanation according to which the electron-releasing group at *meta* position would promote hydrogenolysis.

Only few studies have been described in the literature on the catalytic hydrogenation of dimethoxybenzenes and most of them are not comparative or not quantitative.[2-6] Smith and Thompson[5] studied the hydrogenation of various methoxybenzenes with Adams platinum and rhodium-on-alumina catalysts in acetic acid at 20—50°C under the initial hydrogen pressure of 40—60 psi. Their results indicated that the hydrogenolysis of methoxyl group was less extensive over the supported rhodium catalyst than over the platinum catalyst and that it increased with respect to the three isomers of dimethoxybenzene in the order *ortho*>*meta*>*para* over the platinum catalyst, while with the rhodium catalyst the *meta* isomer underwent slightly more hydrogenolysis than the *ortho* and *para* isomers.

In this study the catalytic hydrogenation and hydrogenolysis of isomeric dimethoxybenzenes over six platinum metals have been investigated at elevated temperature and pressure, mainly with the object to know the behaviors of the three isomers toward hydrogenolysis.

Experimental

Materials. Tokyo Kasei G. R. dimethoxybenzenes were purified by distillation. *o*-Dimethoxybenzene:

1) Part XI: S. Nishimura and H. Yoshino, This Bulletin, **42**, 499 (1969).

*1 Presented partly at the Research Meeting of the Catalysis Society of Japan, Sendai, October, 1968.

2) R. Amatatsu, *Nippon Kagaku Kwaisi*, **52**, 585 (1931).

3) E. M. van Duzee and H. Adkins, *J. Amer. Chem. Soc.*, **57**, 147 (1935).

4) R. H. Martin and R. Robinson, *J. Chem. Soc.*, **1943**, 491.

5) H. A. Smith and R. G. Thompson, "Advances in Catalysis," Vol. 9, Academic Press Inc., New York, N. Y. (1957), p. 727.

6) Y. Takagi, T. Naito and S. Nishimura, This Bulletin, **38**, 2119 (1965).

bp 105°C/26 mmHg, n_D^{25} 1.5316; *m*-dimethoxybenzene: bp 106.5°C/26 mmHg, n_D^{20} 1.5248; *p*-dimethoxybenzene: bp 110°C/26 mmHg, mp 55°C.

Catalysts. Unsupported ruthenium, rhodium, iridium and platinum catalysts were prepared by reducing the corresponding hydroxides in water at 80°C (at 30°C for platinum hydroxide) for 20 min under 80 kg/cm² of hydrogen. Unsupported osmium catalyst was prepared by reducing osmium tetroxide in isopropyl alcohol at 60°C for 20 min under 80 kg/cm² of hydrogen. The metals thus prepared were washed with distilled water until the filtrate became neutral and then dried in vacuum at room temperature. The palladium-on-carbon catalyst (5% Pd) was obtained from the Nippon Engelhard Co.

Hydrogenation. Dimethoxybenzene (0.1 mol) was hydrogenated in a 100-ml bomb of up-and-down stirring type driven electromagnetically, using 20 mg of unsupported catalyst at 80°C or 200 mg of the supported catalyst at 120°C under the hydrogen pressure of 80—100 kg/cm².

Analysis of Products. Hydrogenation products were analyzed by gas chromatography using 10% PEG 20M on 60—80 mesh Chromosorb W (column dimension: 3 mm × 2.25 m; column temperature: 128°C; carrier gas: helium at 70 ml/min). Relative retention times of dimethoxybenzenes and their hydrogenation products are summarized in Table 1. Table 2 summarizes the mol percent composition of reaction mixtures.

TABLE 1. RELATIVE RETENTION TIMES OF DIMETHOXYBENZENES AND THEIR HYDROGENATION PRODUCTS

Compound	Relative retention time
Cyclohexane	1.0
Methanol	1.2
Methoxycyclohexane	1.9
Cyclohexanone dimethyl acetal	3.4
trans-1,2-Dimethoxycyclohexane	3.8
cis-1,2-Dimethoxycyclohexane	4.8
o-Dimethoxybenzene	24.0
trans-1,3-Dimethoxycyclohexane	4.9
cis-1,3-Dimethoxycyclohexane	6.8
m-Dimethoxybenzene	27.3
trans-1,4-Dimethoxycyclohexane	5.3
cis-1,4-Dimethoxycyclohexane	6.3
p-Dimethoxybenzene	25.2

Results

Table 3 shows the amount of hydrogenolysis which occurred during hydrogenation of dimethoxybenzenes over platinum metal catalysts. The figures in the table are based on the amount of the cleaved methoxyl group. It is seen that in most cases the hydrogenolysis is more extensive over Group $VIII_3$ metals (osmium, iridium and platinum) than over Group $VIII_2$ metals (ruthenium, rhodium and palladium). It can also be seen that the *meta* isomer hydrogenolyzes more extensively than the *ortho* and *para* isomers with only one exception in osmium, where the *para* isomer underwent slightly more hydrogenolysis than the *meta* isomer. The greater tendency of the *meta* isomer toward hydrogenolysis is more prominent over Group $VIII_2$ metals than over Group $VIII_3$ metals.

Figures 1 and 2 compare the rates of hydrogenation of isomeric dimethoxybenzenes with ruthenium and rhodium catalysts, respectively. The decreasing

TABLE 2. MOL PERCENT COMPOSITION OF REACTION MIXTURE IN HYDROGENATION OF DIMETHOXYBENZENES OVER PLATINUM METAL CATALYSTS

Dimethoxybenzene	Catalyst	Reac. time (min)	Composition of reaction mixture, mol %				
			Dimethoxybenzene	Dimethoxycyclohexane	Methoxycyclohexane	Cyclohexane	Unidentified product
Ortho	Ru	39	0.0	98.5	1.5	0.06	—
Meta	Ru	74	0.0	81.8	16.9	0.2	1.2
Para	Ru	50	0.8	96.9	2.3	0.04	—
Ortho	Rh	55	0.0	98.9	1.0	0.1	—
Meta	Rh	120	2.4	87.0	7.6	0.7	2.2
Para	Rh	46	0.4	97.7	1.9	0.05	—
Ortho	Pd/C	120	80.1	19.2	0.6	0.03	—
Meta	Pd/C	120	75.4	20.0	4.0	trace	0.6
Para	Pd/C	120	64.3	34.0	1.6	0.08	—
Ortho	Os	60	28.9	67.5	3.3	0.3	—
Meta	Os	60	39.4	51.2	8.6	0.2	0.6
Para	Os	60	53.5	38.3	7.2	1.0	—
Ortho	Ir	90	15.3	79.0	4.6	1.1	—
Meta	Ir	160	12.4	61.9	23.4	1.5	0.9
Para	Ir	40	24.9	62.0	10.4	2.8	—
Ortho	Pt	60	86.9	12.6	0.5	0.01	—
Meta	Pt	60	89.0	9.9	0.9	0.07	0.06
Para	Pt	60	84.5	14.2	1.2	0.03	—

Table 3. Amount of hydrogenolysis in hydrogenation of dimethoxybenzenes over platinum metal catalysts

Catalyst	Hydrogenolysis, mol%[a]		
	Ortho	*Meta*	*Para*
Ru	1.6	17.5	2.4
Rh	1.2	9.4	2.0
Pd/C	3.3	17.0	4.9
Os	5.5	15.0	19.8
Ir	8.0	30.4	21.3
Pt	4.0	9.5	8.1

a) Mol% hydrogenolysis is given by:

$$\frac{\left[\text{mol(methoxycyclohexane}\right.}{\left.\text{+cyclohexane}\times 2)\times 100\right]}$$
$$\overline{\left[\text{mol(dimethoxycyclohexane}\right.}$$
$$\left.\text{+methoxycyclohexane+cyclohexane)}\right]$$

rate during the hydrogenation of the *meta* isomer is noteworthy with both catalysts. This decrease in the rate is probably caused by the methanol produced by hydrogenolysis which occurs extensively in the case of the *meta* isomer. The addition of methanol to reaction mixture was found to retard the hydrogenation of *o*- and *m*-dimethoxybenzene with ruthenium catalyst as indicated in Fig. 1.[7]

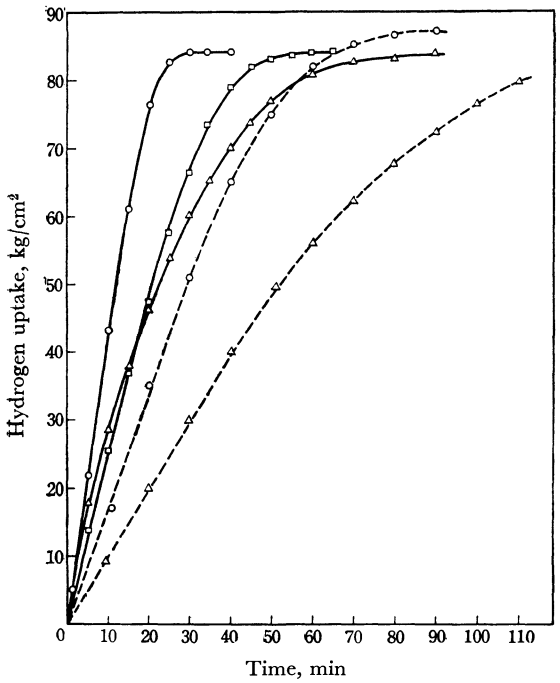

Fig. 1. Hydrogenation of dimethoxybenzenes with ruthenium catalyst: the effect of the addition of methanol.
—○—: *o*-Dimethoxybenzene; ---○---: *o*-Dimethoxybenzene and 0.8 m*l* methanol; —△—: *m*-Dimethoxybenzene; ---△---: *m*-Dimethoxybenzene and 0.5 m*l* methanol; —□—: *p*-Dimethoxybenzene

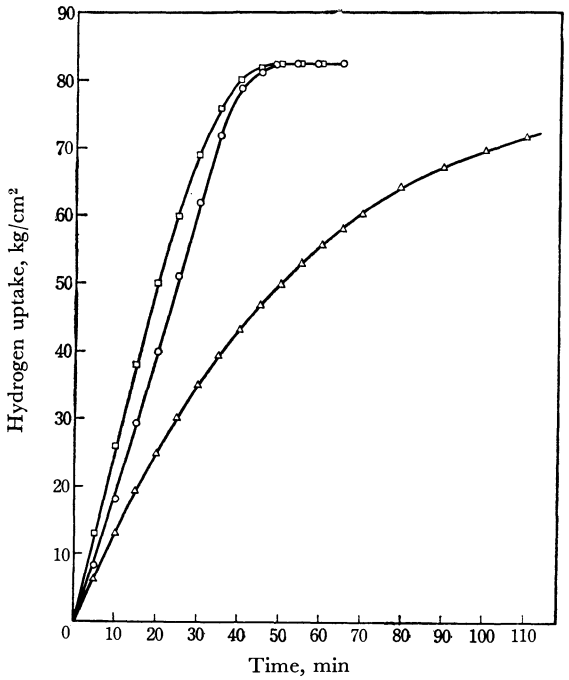

Fig. 2. Hydrogenation of dimethoxybenzenes with rhodium catalyst.
—○—: *o*-Dimethoxybenzene; —△—: *m*-Dimethoxybenzene; —□—: *p*-Dimethoxybenzene

Table 4. Percent *cis* isomer in dimethoxycyclohexane from hydrogenation of dimethoxybenzene with platinum metal catalysts

Catalyst	*cis*-Dimethoxycyclohexane, %		
	1,2-	1,3-	1,4-
Ru	82	73	80
Rh	87	67	81
Pd/C	86	56	64
Os	90	73	80
Ir	92	77	82
Pt	91	73	81

Table 4 summarizes the percent *cis* isomer in the dimethoxycyclohexane formed in hydrogenation of the corresponding dimethoxybenzene. It is of

7) This retardation caused by methanol is probably due to the formation of dimethyl acetals which may result from the addition of methanol to vinyl type ethers formed during hydrogenation. A small amount of cyclohexanone dimethyl acetal has been detected in the product from *m*-dimethoxybenzene. Formation of a considerable amount of 4-methylcyclohexanone diethyl acetal has been observed in hydrogenation of ethyl *p*-tolyl ether over a rhodium catalyst in ethanol, with a decreasing rate in the course of the hydrogenation [S. Nishimura, M. Uramoto and T. Watanabe, *Shokubai*, **11**, 149 (1969)].

interest that formation of *cis* isomer is greater in the *ortho* and *para* isomers than in the *meta* isomer.

Discussion

The results shown in Table 3 clearly indicate that *m*-dimethoxybenzene hydrogenolyzes more readily than the *ortho* and *para* isomers. This conclusion is also true when the rates of formation of hydrogenolysis products (*cf.* Ref. 1) are compared. Although osmium caused slightly less hydrogenolysis in the *meta* isomer than in the *para* isomer, the same conclusion can also be obtained in this case if we compare the rate of formation of hydrogenolysis products which is greater for the *meta* isomer than for the *para* isomer. The greater tendency of the *meta* isomer toward hydrogenolysis has also been observed in the hydrogenation of methoxy- and ethoxyanilines with ruthenium catalyst and for this an explanation based on the ionic cleavage of the carbon-oxygen bond has been proposed.[1] According to this explanation the electron-releasing group at the *meta* position may stabilize the transition states of carbonium ion character when the allyl type ethers formed on the catalyst undergo hydrogenolysis, as shown below in one example of dihydro intermediates.

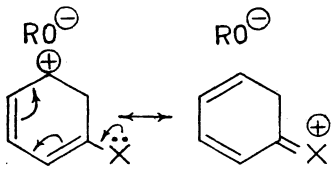

The same effect may also be expected in the allyl type tetrahydro intermediates. In *m*-dimethoxybenzene both methoxyl groups can take part in such stabilization of the transition states leading to hydrogenolysis products and therefore the tendency of the *meta* isomer toward hydrogenolysis is expected to be more pronounced in dimethoxybenzenes than in methoxyanilines. The results in Table 3 which are in accord with this expectation may provide a strong support to the explanation proposed previously. It is to be noted that the more extensive hydrogenolysis in the *meta* isomer was not observed or less pronounced in the hydrogenation of dimethoxybenzenes in acetic acid.[8]

Another important factor which may have an effect on the relative amount of hydrogenolysis between *ortho*, *meta* and *para* isomers is the probability of the formation of allyl type ethers from parent aromatic compounds.[9] It will be difficult, however, to discuss on this point from the data now available and further detailed studies are needed for this purpose.

The stereochemistry of hydrogenation of dimethoxybenzenes is noteworthy in that the *meta* isomer gave smaller yields of the *cis* isomer than the *ortho* and *para* isomers, when compared with the hydrogenation of isomeric xylenes where formation of *cis* isomer decreases in the order *ortho*>*meta*>*para*.[10] It might be possible that the extensive hydrogenolysis in *m*-dimethoxybenzene would decrease the *cis* content of the resulting dimethoxycyclohexane, if the hydrogenolysis of the methoxyl group would occur by the S_N2 type mechanism.[11] But this fails to account for the results with osmium catalyst in which the *meta* isomer underwent less hydrogenolysis than the *para* isomer, whereas the *cis* content of dimethoxycyclohexane was smaller in the *meta* isomer.

8) The *meta* isomer hydrogenolyzes to less extent than the *ortho* and *para* isomers in the rhodium-catalyzed hydrogenation of methoxy- and ethoxyanilines in isopropyl alcohol added by one equivalent of acetic acid (S. Nishimura and Y. Takagi, Abstracts of the Research Meeting of the Catalysis Society of Japan, p. 31, Sendai, October, 1968). In *t*-butyl alcohol differences in the amount of hydrogenolysis are small between three isomers of methoxy- or ethoxyaniline [S. Nishimura, H. Uchino and H. Yoshino, This Bulletin **41**, 2194 (1968)].

9) Hydrogenolysis in vinyl type ethers may also be possible over some platinum metals. But the contribution of this type hydrogenolysis seems not important, especially in hydrogenation with Group $VIII_2$ metals, and was not considered here (Unpublished observations; *cf.* also Ref. 10, p. 444).

10) See, for instance, P. N. Rylander, "Catalytic Hydrogenation over Platinum Metals," Academic Press Inc., New York, N. Y. (1967), p. 324.

11) *Cf.* a) S. Nishimura and K. Mori, This Bulletin, **36**, 318 (1963). b) R. K. Callow and G. A. Thompson, *J. Chem. Soc.*, **1964**, 3106. c) S. Mitsui and Y. Nagahisa, *Chem. Ind.* (London), **1965**, 1975 and references cited therein.

BULLETIN OF THE CHEMICAL SOCIETY OF JAPAN VOL. 43 921—925 (1970)

Syntheses of Optically Active α-Amino Acids from Esters of α-Keto Acids by Hydrogenolytic Asymmetric Transamination, A Solvent Effect[1]

Kaoru HARADA and Takao YOSHIDA

Institute of Molecular Evolution and Department of Chemistry, University of Miami, Coral Gables, Florida 33134, U. S. A.

(Received September 29, 1969)

Optically active α-amino acids were synthesized from esters of α-keto acid azomethines by catalytic hydrogenation. Solvent effect of the reaction was studied and the possible steric courses are discussed.

Several studies on the asymmetric syntheses of α-amino acids from their corresponding α-keto acids have been reported.[2-10] Hiskey and Northrop[4] demonstrated the synthesis of optically active amino acids by catalytic hydrogenation and subsequent hydrogenolysis of the Schiff bases of α-keto acids with optically active α-methylbenzylamine (hydrogenolytic asymmetric transamination). The steric course of the hydrogenolytic asymmetric transamination reactions has been studied in this laboratory.[8,9] It was proposed that the possible conformation of the substrate in the catalytic hydrogenation could be a five-membered cyclic complex with the catalyst, as shown in structure I.[8] The

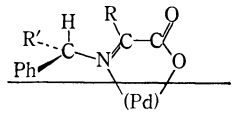

I

proposed intermediate I was supported by the study of a solvent effect of the asymmetric synthesis.[9]

In this investigation, the Schiff bases of α-keto acid esters with optically active amines were subjected to hydrogenation in order to examine the existence of structure I type chelated intermediates in these reactions. α-Keto acids used were ethyl pyruvate and ethyl α-ketobutyrate. Optically active amines used were (S)(−) and (R)(+)-α-methylbenzylamine, (R)(+)-α-ethylbenzylamine, and (R)(+)-1-(1-naphthyl)ethylamine. Solvents used in these reactions were benzene, ethyl acetate, isopropyl alcohol, ethanol, and methanol. Results are summarized in Table 1.

In each six sets of reactions, a solvent effect of the asymmetric synthesis was examined by the use of methanol, ethanol, propanol-2, ethyl acetate, and benzene (dielectric constant ranging from 32.6 to 2.3; Table 1). It was found that when a polar solvent was used, the optical purity of the resulting amino acid was lower and when less polar solvent was used the optical purity increased steadily. These solvent effects in the reactions suggest that the conformations of the substrate molecule changed depending on the solvent used. These results are similar to those obtained in the study of solvent effect in the hydrogenolytic asymmetric transamination between α-keto acids and optically active amine.[9] Therefore, similar conformation of the substrate in the hydrogenolytic asymmetric transamination between optically active amine and α-keto acid ester could be assumed as shown in structure II. Because electrostatic attraction between substrate and catalyst in a less polar solvent is stronger than in a polar solvent and also the solvation of the substrate in the less polar solvent is weak, so that the substrate could react easily with the catalyst to form the intermediate complex II. On the other hand, when polar solvent was used, electrostatic attraction between substrate and catalyst was weaker and the stronger solvation of the

1) Sterically Controlled Synthesis of Optically Active Organic Compounds VIII. For part VII. K. Matsumoto and K. Harada, *J. Org. Chem.*, **33**, 4526 (1968). Contribution No. 124 of the Institute of Molecular Evolution, University of Miami.

2) F. Knoop and C. Martius, *Z. Phys. Chem.*, **258**, 238 (1939).

3) J. B. Herbst and E. A. Swart, *J. Org. Chem.*, **11**, 366 (1946).

4) R. G. Hiskey and R. C. Northrop, *J. Amer. Chem. Soc.*, **83**, 4798 (1961).

5) A. Kanai and S. Mitsui, *Nippon Kagaku Zasshi*, **89**, 183 (1966).

6) K. Matsumoto and K. Harada, *J. Org. Chem.*, **31**, 1956 (1966).

7) K. Harada, *Nature*, **212**, 1571 (1966); *J. Org. Chem.*, **32**, 1790 (1967).

8) K. Harada and K. Matsumoto, *J. Org. Chem.*, **32**, 1794 (1967).

9) K. Harada and K. Matsumoto, *ibid.*, **33**, 4466 (1968).

10) K. Matsumoto and K. Harada, *ibid.*, **33**, 4526 (1968).

TABLE 1. AMINO ACIDS OBTAINED BY HYDROGENOLYTIC ASYMMETRIC TRANSAMINATION BETWEEN ESTERS OF α-KETO ACID AND OPTICALLY ACTIVE AMINES

Amino acid		Keto acid ester[a)]	Amine[b)]	Solvent	Catalyst	Yield (%)	Config'n	Free amino acid		DNP-Amino acid	
								$[\alpha]_D^{25}$ 5N HCl	Optical purity (%)[d)]	$[\alpha]_D^{25}$ 1N NaOH	Optical purity (%)[e)]
Ala	1	Et-Py	(R) (+)-Me	MeOH	$Pd(OH)_2/C$	74	R	−3.1	21	−43.9	31
	2	Et-Py	(R) (+)-Me	EtOH	$Pd(OH)_2/C$	77	R	−4.7	32	−56.0	39
	3	Et-Py	(R) (+)-Me	i-PrOH	$Pd(OH)_2/C$	73	R	−4.7	32	−67.3	47
	4	Et-Py	(R) (+)-Me	AcOEt	$Pd(OH)_2/C$	78	R	−6.5	44	−88.7	62
	5	Et-Py	(R) (+)-Me	Benzene	$Pd(OH)_2/C$	70	R	−7.5	52	−80.8	56
	6	Et-Py	(S) (−)-Me	MeOH	$Pd(OH)_2/C$	75	S	+4.5	31	+46.4	32
	7	Er-Py	(S) (−)-Me	EtOH	$Pd(OH)_2/C$	74	S	+5.9	40	+59.4	41
	8	Et-Py	(S) (−)-Me	i-PrOH	$Pd(OH)_2/C$	79	S	c	c	+64.5	45
	9	Et-Py	(R) (−)-Me	AcOEt	$Pd(OH)_2/C$	73	S	+5.6	39	+91.8	64
	10	Et-Py	(S) (−)-Me	Benzene	$Pd(OH)_2/C$	75	S	+6.7	46	+82.5	57
	11	Et-Py	(R) (+)-Et	MeOH	$Pd(OH)_2/C$	83	R	−1.5	10	−21.0	15
	12	Et-Py	(R) (+)-Et	EtOH	$Pd(OH)_2/C$	82	R	−2.0	14	−33.5	23
	13	Et-Py	(R) (+)-Et	i-PrOH	$Pd(OH)_2/C$	80	R	−3.3	23	−46.3	32
	14	Et-Py	(R) (+)-Et	AcOEt	$Pd(OH)_2/C$	77	R	−7.0	48	−80.8	56
	15	Et-Py	(R) (+)-Et	Benzene	$Pd(OH)_2/C$	73	R	−5.9	41	−72.6	50
	16	Et-Py	(R) (+)-Naph	MeOH	$Pd(OH)_2/C$	83	R	−7.0	49	−82.8	58
	17	Et-Py	(R) (+)-Naph	EtOH	$Pd(OH)_2/C$	82	R	−8.2	56	−93.2	65
	18	Et-Py	(R) (+)-Naph	i-PrOH	$Pd(OH)_2/C$	c	R	−7.3	50	−95.3	66
	19	Et-Py	(R) (+)-Naph	AcOEt	$Pd(OH)_2/C$	68	R	−7.9	54	−118.0	82
	20	Et-Py	(R) (+)-Naph	Benzene	$Pd(OH)_2/C$	70	R	−8.7	60	−100.7	70
	21	Et-Py	(S) (−)-Me	MeOH	Pd/C and $Pd(OH)_2/C$	64	S	+5.1	35	+69.1	48
	22	Et-Py	(S) (−)-Me	EtOH	Pd/C and $Pd(OH)_2/C$	62	S	+4.7	32	+73.2	51
	23	Et-Py	(S) (−)-Me	i-PrOH	Pd/C and $Pd(OH)_2/C$	65	S	+5.5	38	+78.6	55
	24	Et-Py	(S) (−)-Me	AcOEt	Pd/C and $Pd(OH)_2/C$	62	S	+6.4	44	+87.4	61
	25	Et-Py	(S) (−)-Me	Benzene	Pd/C and $Pd(OH)_2/C$	57	S	+5.8	40	+94.2	65
α-NH_2-Bu	26	Et-Bu	(S) (−)-Me	MeOH	Pd/C and $Pd(OH)_2/C$	51	S	+5.5	27	+27.9	28
	27	Et-Bu	(S) (−)-Me	EtOH	Pd/C and $Pd(OH)_2/C$	45	S	+5.5	27	+30.6	31
	28	Et-Bu	(S) (−)-Me	i-PrOH	Pd/C and $Pd(OH)_2/C$	43	S	+5.7	28	+33.5	34
	29	Et-Bu	(S) (−)-Me	AcOEt	Pd/C and $Pd(OH)_2/C$	42	S	+5.7	28	+37.6	38
	30	Et-Bu	(S) (−)-Me	Benzene	Pd/C and $Pd(OH)_2/C$	39	S	+8.3	40	+45.3	46

a) Et-Py: ethyl pyruvate; Et-Bu: ethyl α-ketobutyrate.

b) (S) (−)-Me, (S) (−)-α-methylbenzylamine; R(+)-Me, (R) (+)-α-methylbenzylamine; (S) (−)-Et, (S) (−)-α-ethylbenzylamine; R(+)-Et, (R) (+)-α-ethylbenzylamine; R(+)-Naph, (R) (+)-1-(1-naphthyl)ethylamine.

c) The samples are lost.

d) Defined as $[\alpha]_D$ obsd/$[\alpha]_D$ lit × 100. (S)-Alanine, $[\alpha]_D^{25}$ +14.6° (5N HCl); (S)-α-Amino-*n*-butyric acid, $[\alpha]_D^{25}$ +20.6° (5N HCl). J. P. Greenstein and Winitz, "Chemistry of the Amino Acids," Vol. 3, John Wiley & Sons, Inc., New York, N. Y. (1961) (alanine, p. 1819; α-amino-*n*-butyric acid, p. 2401).

e) Defined as $[\alpha]_D$ obsd/$[\alpha]_D$ lit × 100. DNP-(S)-ala, $[\alpha]_D$ +143.9° (1N NaOH); DNP-(S)-α-NH_2-But, $[\alpha]_D$ +98.8° (1N NaOH). K. R. Rao and H. A. Sober, *J. Amer. Chem. Soc.*, **76**, 1328 (1954).

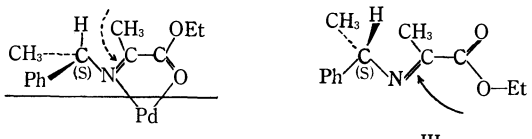

II

III

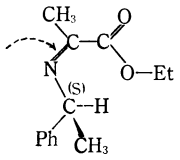

IV

substrate interfered with the attraction between substrate and catalyst to form the intermediate complex II. Therefore, it could be assumed that the conformation of substrate in polar solvent could be more in the form of structures III and IV. Structure IV is rather sterically hindered so that the structure III could be increased in proportion by the use of polar solvent. Structures II and III would be adsorbed at the less bulky side of the molecule and the hydrogenation takes place. When (S)-amine was used, (S)- and (R)-amino acid would be expected from structures II and III respectively. Therefore the use of polar solvent increases the proportion of structure III, and this would result in the formation of amino acid of lower optical purity. From the results obtained, structure II could be the major conformation throughout the reactions.

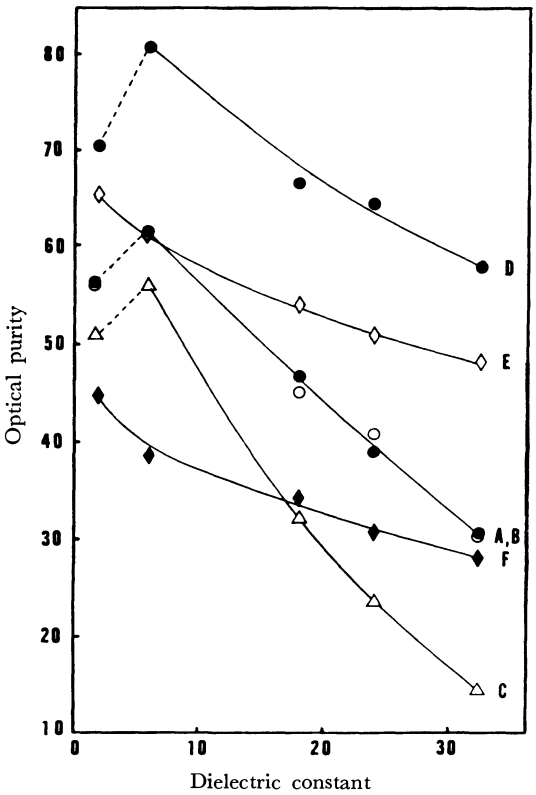

Fig. 1. Relationship between optical activities of synthesized amino acids and dielectric constants of the solvents used.
A. ala, reactions 1—5 (see Table 1)
B. ala, reactions 6—10
C. ala, reactions 11—15
D. ala, reactions 16—20
E. ala, reactions 21—25
F. α-NH_2-Bu, reactions 26—30

Figure 1 shows the relationship between the dielectric constants of the solvents used and the optical activities of synthesized amino acids. The effect of the catalyst, palladium hydroxide on charcoal or palladium on charcoal, was observed. By the use of palladium hydroxide on charcoal,[4] optical activity of amino acids dropped when benzene was used as a solvent (Fig. 1). Optical activities of amino acids increased rapidly when less polar solvents were used. On the other hand, by the use of palladium on charcoal optical activities of amino acids obtained increased slowly in the less polar solvents. A decrease in optical activity of amino acid by the use of benzene was not observed. High optical activity of amino acid (82%) was observed when R(+)-1-(1-naphthyl)-ethylamine was used. The reason for this is understandable from the steric effect in the intermediate complex II.

In the previous studies, hydrogenation of oximes and Schiff bases of α-keto acid *l*-menthyl esters has been studied. It was discussed that the conformation of the substrate might be transoidal, as shown in structure IV.[6,8] From the results obtained in the present investigation, it could also be possible

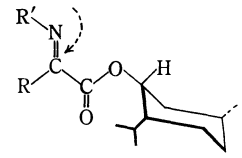

IV

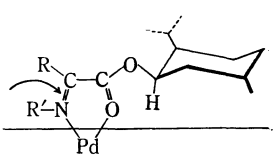

V

to explain the steric course by a cisoidal conformation which forms chelate intermediate with the catalyst as shown in structure V. The menthyl group would be situated as in structure V because of the steric hindrance between menthyl residue and catalyst. Then, the structure V could be adsorbed on the catalyst at the less bulky side of the molecule, and hydrogenation would take place. From structure V, R-amino acid would be expected, which agrees with the experimental results.[6]

In order to examine the newly postulated intermediate (V) in the hydrogenation of α-keto acid *l*-menthyl ester oxime, a similar study of solvent effect was carried out. The substrates used were *l*-menthyl pyruvate oxime, *l*-menthyl α-ketobutyrate oxime, and the Schiff base of *l*-menthyl pyruvate

TABLE 2. AMINO ACIDS OBTAINED FROM α-KETO ACID MENTHYL ESTERS[a)]

Amino acid		Keto acid esters[b)]	Solvent	Yield[c)] (%)	Config'n	Free amino acid		DNP-Amino acid	
						$[\alpha]_D^{25}$ (5N HCl)	Optical purity (%)[d)]	$[\alpha]_D^{25}$ (1N NaOH)	Optical purity (%)[e)]
Ala	31	Py-M-OX	MeOH	87	R	−2.6	18	−28.2	20
	32	Py-M-OX	EtOH	82	R	−2.5	17	−31.3	22
	33	Py-M-OX	i-PrOH	73	R	−2.4	17	−23.6	16
	34	Py-M-OX	AcOEt	74	R	−2.5	17	−28.1	20
	35	Py-M-OX	Benzene	75	R	−3.4	23	−32.2	22
α-NH_2-Bu	36	Bu-M-OX	MeOH	85	R	−3.3	16	−16.4	17
	37	Bu-M-OX	EtOH	71	R	−3.6	18	−22.4	23
	38	Bu-M-OX	i-PrOH	81	R	−2.7	13	−15.4	16
	39	Bu-M-OX	AcOEt	54	R	−3.4	17	−17.2	17
	40	Bu-M-OX	Benzene	60	R	−4.2	20	−22.2	23
Ala	41	Py-M-(R)-Me	MeOH	46	R	−8.1	55	−82.0	57
	42	Py-M-(R)-Me	EtOH	51	R	−8.1	56	−84.5	59
	43	Py-M-(R)-Me	i-PrOH	50	R	−7.5	52	−65.5	46
	44	Py-M-(R)-Me	AcOEt	48	R	−7.9	54	−66.7	46
	45	Py-M-(R)-Me	Benzene	47	R	−8.6	59	−88.8	62

a) All hydrogenation reactions were carried out by the use of 5% palladium on charcoal.
b) Py-M-OX: *l*-menthyl pyruvate oxime; Bu-M-OX: *l*-menthyl α-ketobutyrate oxime; Py-M-(R)-Me: Schiff base of *l*-menthyl pyruvate with R(+)-α-methylbenzylamine.
c) Reactions 31—40: the yields are calculated from oximes of α-keto acid menthyl esters. Reactions 41—45: the yields are calculated from *l*-menthyl pyruvate.
d) Defined as $[\alpha]_D$ obsd/$[\alpha]_D$ lit × 100. (S)-Alanine, $[\alpha]_D^{25}$ +14.6° (5N HCl); (S)-α-amino-*n*-butyric acid, $[\alpha]_D^{25}$ +20.6° (5N HCl). J. P. Greenstein and Winitz, "Chemistry of the Amino Acid," Vol. 3, John Wiley & Sons, Inc., New York, N. Y. (1961) (alanine, p. 1819; α-amino-*n*-butyric acid, p. 2401).
e) Defined as $[\alpha]_D$ obsd/$[\alpha]_D$ lit × 100. DNP-(S)-ala, $[\alpha]_D$ +143.9° (1N NaOH); DNP-(S)-α-NH_2-Bu, $[\alpha]_D$ +98.8° (1N NaOH). K. R. Rao and H. A. Sober, *J. Amer. Chem. Soc.*, **76**, 1328 (1954).

with (R)(+)-α-methylbenzylamine. Results are summarized in Table 2.

However, in these reactions, the solvent effect observed was rather small compared with that of the previous study[9] or with the results summarized in Table 1. Also observed was the discontinuation of optical purities of amino acids in these series of reactions (Fig. 2). The optical purities increased by the use of ethanol compared to that use of methanol. However, optical purities dropped by the use of isopropyl alcohol and increased steadily by the use of less polar solvent. The factors which affect the optical purity of amino acids in these reactions seem to be complex and it is difficult to explain these results at the present time. However, from the results obtained from the hydrogenolytic transamination summarized in Tables 1 and 2 the existence of intermediate complex structure V seems likely.

On the other hand, catalytic reduction of α-keto acid esters with optically active alcohols has been discussed and the reduction was found to follow the Prelog rule.[11] The results obtained in the present study suggest that the formation of α-hydroxy acid from α-keto acid ester with optically active alcohol by catalytic hydrogenation could also be explained by the chelated intermediate hypothesis.[8,9] The study on the synthesis of optically active α-hydroxy acid from α-keto acid amide with optically active amine also supports the chelation hypothesis.[12]

Optically active free amino acids were obtained by the use of a Dowex 50 column. However, these amino acids still contain some impurities. To avoid fractionation of optically active isomers during the purification process, all amino acids were treated with 2,4-dinitrofluorobenzene.[13] The resulting DNP-amino acids were purified by the use of celite column[14] treated with pH 7.0 citrate buffer without fractionation of partially optically active amino acids. Therefore, the values of optical purities of DNP-amino acids are more reliable and consistent (Table 1).

11) V. Prelog, *Bull. Soc. Chim. Fr.*, **1956**, 987.

12) K. Harada and K. Matsumoto, Presented at the 1st American Peptide Symposium at Yale University (1968).

13) F. Sanger, *Biochem. J.*, **39**, 507 (1945); K. Rao and H. A. Sober, *J. Amer. Chem. Soc.*, **76**, 1328 (1954).

14) J. C. Perrone, *Nature*, **167**, 513 (1951); A. Court, *Biochem. J.*, **58**, 70 (1954).

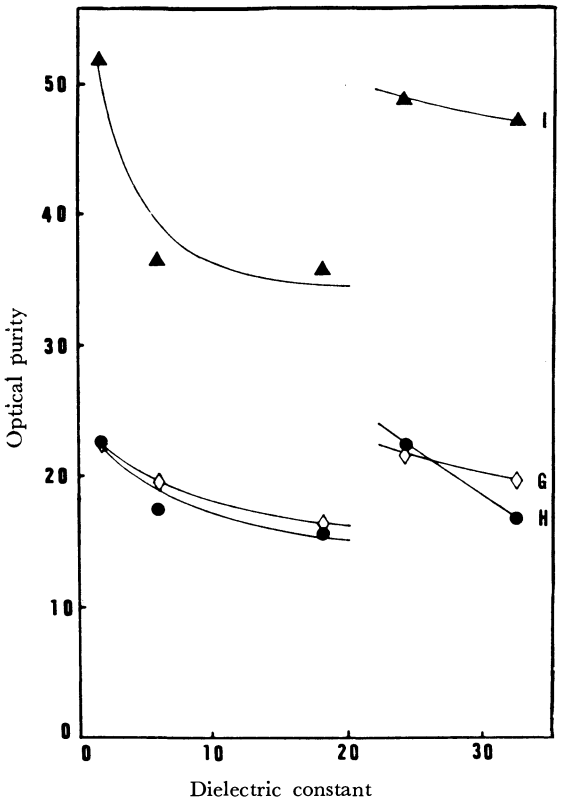

Fig. 2. Relationship between optical activity of synthesized amino acids and dielectric constants of the solvents used.
G. ala, reactions 31—35 (see Table 2)
H. α-NH_2-Bu, reactions 36—40
I. ala, reactions 41—45

Experimental[15]

Alanine from Ethyl Pyruvate and S (−)-α-Methylbenzylamine. Ethyl pyruvate (1.16 g, 0.01 mol) and S(−)-α-methylbenzylamine (1.21 g, 0.01 mol) were dissolved in 20 m*l* of benzene at room temperature. After about ten minutes the solution became cloudy by separation of water. Anhydrous sodium sulfate was added and the mixture was stirred for one hour at room temperature. Sodium sulfate was removed by filtration and the sodium sulfate was washed with benzene. The combined benzene solution was evaporated to dryness under reduced pressure on a water bath (45°C). A light yellow oil was obtained. This was dissolved in 30 m*l* of methanol and the solution was subjected to hydrogenation and hydrogenolysis by the use of 1.0 g of palladium hydroxide on charcoal[4] for 12 hr. The first mole of hydrogen was absorbed in a few minutes. However, the second mole of hydrogen for hydrogenolysis required a much longer time. After the reaction was over, the catalyst was removed by filtration. The catalyst was washed with hot methanol several times. The combined methanol solution was evaporated under reduced pressure at 40°C. The residue was hydrolyzed under reflux with 60 m*l* of 3N hydrochloric acid for 4 hr. The hydrolyzate was extracted once with ether and the hydrochloric acid solution was evaporated to dryness under reduced pressure. Water was added to the residue and it was evaporated again to minimize the remaining free hydrochloric acid. The residual amino acid hydrochloride was dissolved in 10 m*l* of water and the solution was applied to a Dowex 50×2 column (hydrogen form, 100—200 mesh, 25×1.8 cm). The acidic component was washed with water, then alanine was eluted with 1N aqueous ammonia. Fractions containing alanine were combined and were evaporated to dryness. Free alanine, 0.67 g, was obtained. This is pure on paper chromatograph. $[\alpha]_D^{25}=+4.5°$ (*c* 4.0, 5N HCl), optical purity 31%. After one recrystallization with water and ethanol, elemental analysis was carried out.

Found: C, 40.65; H, 8.01; N, 15.58%. Calcd for $C_3H_7ON_2$: C, 40.44; H, 7.92; N, 15.72%.

A part of the unrecrystallized alanine (100 mg) was converted to DNP-alanine in a conventional manner.[13] DNP-Alanine obtained was purified by the use of celite column treated with pH 7 citrate buffer (0.2M).[14] These procedures are similar to those described in earlier reports.[6,8]

DNP-Alanine, mp 172—174°C dec., $[\alpha]_D^{25}=+46.4°$ (*c* 1.1, 1N NaOH), optical purity 32%.

Found: C, 42.42; H, 3.66; N, 16.64%. Calcd for $C_9H_9N_3O_6$: C, 42.36; H, 3.55; N, 16.47%.

Other experiments were carried out in the same way as described above. Results are summarized in Table 1.

Amino Acids from α-Keto Acid *l*-Menthyl Ester. The experimental procedures for the synthesis of optically active amino acids from α-keto acid *l*-menthyl esters were similar to those already described in the earlier papers[6,8] except for the use of different solvents. Alanine and α-aminobutyric acid obtained by saponification of menthyl esters were converted to their DNP-derivatives. These DNP-amino acids were similarly purified by the use of celite column.[14] Results are summarized in Table 2.

This work was supported by grant number NGR 10-007-052 from the National Aeronautics and Space Administration.

15) All hydrogenations and hydrogenolyses were carried out by the use of the Parr 3910 shaker type hydrogenation apparatus. All optical rotations were measured by the use of Durrum-JASCO ORD/UV-5 automatic spectropolarimeter. Some of the optical rotations of free amino acids were measured by the use of the Rudolph model 80 polarimeter with a PEC-101 photometer.

BULLETIN OF THE CHEMICAL SOCIETY OF JAPAN VOL. 43 926—930 (1970)

Effect of Pressure on Graphitization of Carbon. VII. Effect of Pre-Heat-Treatment on Graphitization of Carbon under High Pressure

Kan-ichi KAMIYA, Michio INAGAKI, Hajime SAITO and Tokiti NODA

Faculty of Engineering, Nagoya University, Chikusa-ku, Nagoya

(Received September 24, 1969)

The soft carbon samples PV-15, -17 and -20, and the hard carbon samples PH-15 and -20, which were prepared by pre-heat-treatment of a polyvinylchloride coke PV-7 at 1500, 1700 and 2000°C and a phenolformaldehyde resine char PH-7, at 1500 and 2000°C, respectively, under reduced pressure, were re-heat-treated under quasi-hydrostatic pressure of 5 kbar. The structural changes in these carbons by the re-heat-treatment under pressure were studied by X-ray diffraction analysis. On the soft carbons, the rate of development of graphitic component was found to become small with the increase in temperature of pre-heat-treatment. On these samples, especially on PV-20, the normal homogeneous graphitization of turbostratic component was observed above about 1700°C besides the heterogeneous graphitization. However, the hard carbon samples PH-15 and PH-20 showed the same abrupt heterogeneous graphitization at around 1500°C as the original PH-7. These results suggest that the structure of carbon sample is related to the heterogeneous graphitization under high pressure. One can deduce a conclusion from the results of this series of experiments that the heterogeneous graphitization is more dominant in a carbon sample having a lower degree of graphitization, for example, a larger c_0-spacing and a smaller crystallite size.

Both soft and hard carbons have been found to be graphitized very rapidly around 1400—1500°C under high pressure.[1-5] Under high pressure, the graphitization proceeds heterogeneously, that is a part of original carbon transforms directly to graphite having three dimensional ordering, while the other part of the specimen remains almost unchanged. The direct transformation of turbostratic structure to graphitic structure occurs in whole domain without going through intermediate state of graphitization. This heterogeneous graphitization under high pressure is reflected in the composite (00*l*) diffraction profile of the sample. The observed composite profile consists of two kinds of component profiles which correspond to turbostratic and graphitic components.

Under normal or reduced pressure, however, the graphitization proceeds homogeneously as being demonstrated by the continuous shift of almost symmetrical (00*l*) diffraction line toward higher angle side.

In the preliminary experiment,[1] the carbons pre-heat-treated above 1500°C under reduced pressure was found not to show any abrupt graphitization around 1400—1500°C under the pressure of 10 kbar. The purpose of the present work is to investigate more precisely the effect of pre-heat-treatment on graphitization of carbon under high pressure.

Experimental

Preparation of Samples. The original samples used were a polyvinylchloride coke (PV-7), which was carbonized to 680°C[1] and a phenolformaldehyde resine char (PH-7), which was carbonized to 700°C. Pre-heat-treated soft carbons PV-15, -17 and -20 were prepared by the heat-treatment of PV-7 at 1500, 1700 and 2000°C, respectively, for 60 min under the reduced pressure of 10^{-2} Torr. The c_0-spacings of these samples were 6.885, 6.858 and 6.845 Å, respectively. Pre-heat-treated hard carbons PH-15 and PH-20 were prepared at 1500 and 2000°C, respectively, from PH-7, through the same procedure as the soft carbons. The c_0-spacing of the samples PH-15 and -20 was 6.959 and 6.927 Å, respectively. Only the c_0-spacing of PV-20 was smaller than 6.85 Å and those of the other samples were larger. Therefore, PV-20 was on the second stage[6] of graphitization process and the other samples were on its first stage.

The furnace and the procedure used for the pre-heat-

1) T. Noda and H. Kato, *Carbon*, **3**, 289 (1965).
2) T. Noda, K. Kamiya and M. Inagaki, This Bulletin, **41**, 485 (1968).
3) M. Inagaki, K. Kamiya and T. Noda, *Kogyo Kagaku Zasshi*, **71**, 652 (1968).
4) M. Inagaki, K. Kamiya and T. Noda, *ibid.*, **71**, 812 (1968).
5) K. Kamiya, M. Inagaki, M. Mizutani and T. Noda, This Bulletin, **41**, 2169 (1968).
6) M. Inagaki, *Tanso*, No. **53**, 61 (1968); M. Inagaki Y. Murase and T. Noda, *ibid.*, No. **54**, 80 (1968).

treatments were the same as those reported in detail elsewhere.[7] Time necessary for heating and cooling to and from pre-heat-treatment temperature was both less than a few minutes.

Heat-Treatment under High Pressure and X-Ray Diffraction Analysis. A piston-cylinder type high pressure apparatus,[2,3] made from tool steel, was used for heat-treatments of the samples under 5 kbar. The pressure cell arrangement used was exactly the same as reported previously.[2] The heat-treatment temperature (HTT) was determined by using the relation between specimen temperature and consumed electric input power, which was established beforehand for each sample from the measurement of temperature by using a thermocouple inserted into the specimen under 5 kbar. The heat-treatments under 5 kbar were performed at various temperatures ranging from 1200 to 1900°C.

The central part of the heat-treated specimen was sampled for X-ray diffraction analysis. In this part, the temperature gradient along axial direction has been hardly observed.[4]

Profiles of (004) and (002) diffraction lines of the heat-treated samples were measured by using Ni-filtered Cu $K\alpha$ radiation and a recording goniometer. The composite profile observed was graphically separated by trial and error method into two component profiles which corresponded to the graphitic component G and turbostratic one A. The details of the separation procedure were reported previously.[2,5,8] The c_0-spacing and crystallite size Lc were measured for each separated component profile by referring to the inner standard of silicon, and the content of the graphitic component G_S* or G_H* was obtained from the ratio of the area under the profile of the graphitic component to the total area of the composite profile. The area ratio was corrected for crystallite orientation in the X-ray specimen.[3]

Results

Soft Carbon Samples. Change of (004) diffraction profile of the sample PV-15 with HTT under 5 kbar is shown in Fig. 1a). Above 1500°C, a profile corresponding to the graphitic component G_S appeared on the high angle side of the profile of the turbostratic component A_S. The intensity of diffraction of the component G_S gradually increased

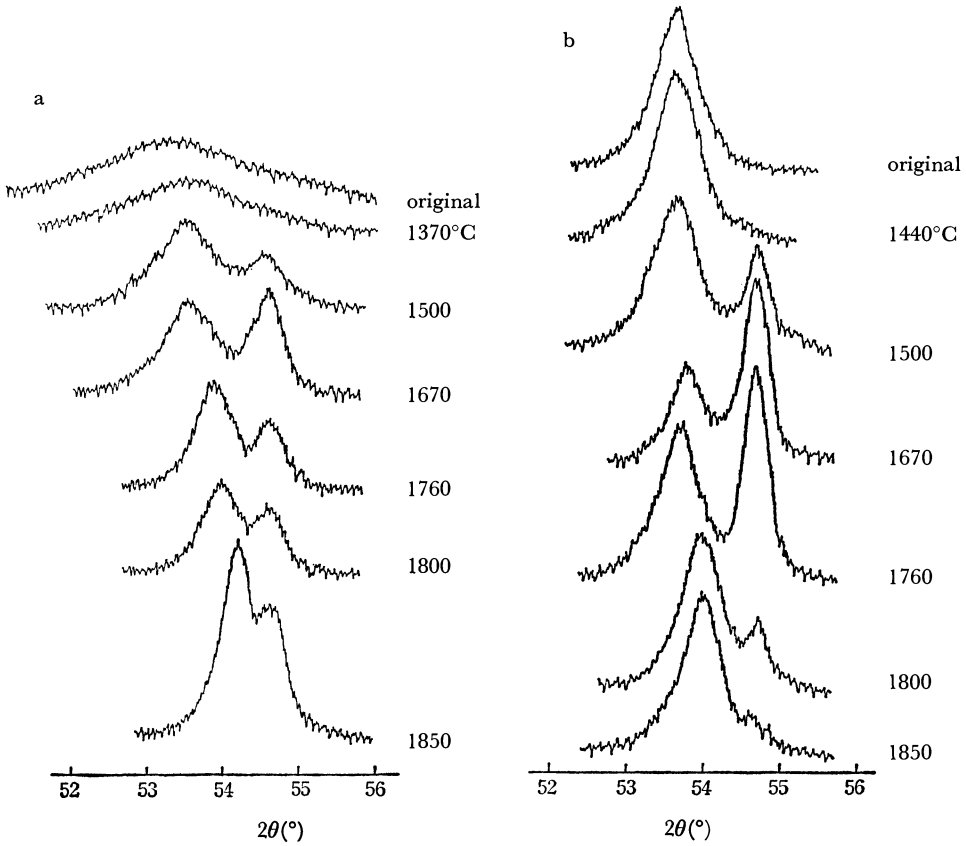

Fig. 1. Changes of Profile of (004) diffraction line with HTT under 5 kbar for 60 min.
a) PV-15 b) PV-20

7) M. Inagaki, Y. Murase and T. Noda, *Yogyo Kyokai Shi*, **76**, 184 (1968).

8) K. Kamiya, M. Inagaki and H. Saito, This Bulletin, **42**, 1425 (1969).

*1 Suffixes S and H show whether the original sample is soft carbon (PV-7) or hard one (PH-7).[5]

up to 1670°C. This change in profile had the same trend as that observed previously for the original sample PV-7,[2] except that the temperature of appearance of the component G_S in PV-15 was somewhat higher than that in PV-7. Above 1670°C, the intensity of diffraction of the component G_S did not increase or rather decreased gradually and the profile of the component A_S began to shift to higher angle side together with sharpening. For the sample PV-17, change of (004) diffraction profile with HTT was similar to that observed for the sample PV-15. The same but more marked trend of change in diffraction profile with HTT can be seen in the case of PV-20, which is shown in Fig. 1b). The component A_S had a little higher diffraction angle, that is, a smaller c_0-spacing than those of the sample PV-7, -15 and -17. The profile of the component G_S appeared at 1500°C and developed gradually with the increase in HTT. Above 1800°C, it became markedly small, and the profile for the component A_S began to shift to higher angle side.

The content of the component G_s for the samples PV-15, -17 and -20 is plotted against HTT in Fig. 2. The variation of content of the component

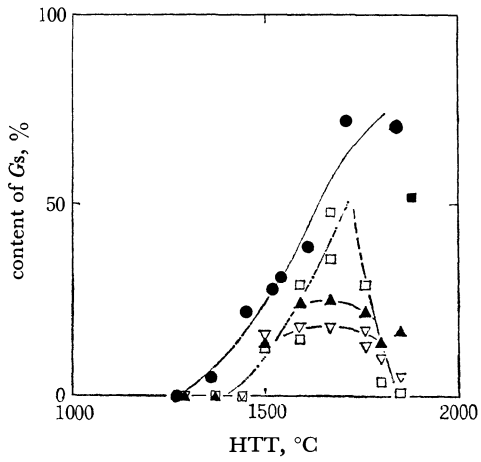

Fig. 2. Variations of content of G_S with HTT under 5 kbar for 60 min for pre-heat-treated soft carbons.
●; PV-7, ▲; PV-15, ▽; PV-17, □; PV-20, ■; PV-20 heat-treated at 1740°C and then at 1880°C under 5 kbar.

G_S for the original sample PV-7 is shown in the same figure. An anomalous change of content of G_S for the sample PV-20 is seen in this figure. In the case of PV-20, the content of the component G_S increased gradually up to 1700—1800°C and became small above this temperature. The similar but small decrease in the content of the component G_S was also observed in the cases of PV-15 and -17 above about 1700°C. The point marked by solid square in Fig. 2 represents the content of G_S for the sample PV-20 which was heat-treated at 1740°C for 60 min and then, without cooling, heat-treated further at 1880°C for 60 min under 5 kbar. It shows a large content of G_S which corresponds to the value for the temperature of the first heat-treatment, that is, 1740°C.

The variations of content of the component G_s with residence time at 1590 and 1800°C under 5 kbar are shown in Figs. 3a) and 3b). In the

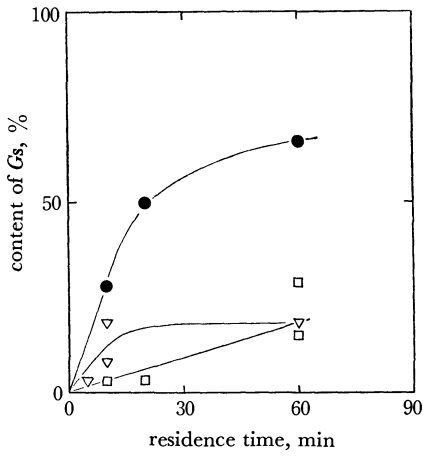

Fig. 3a

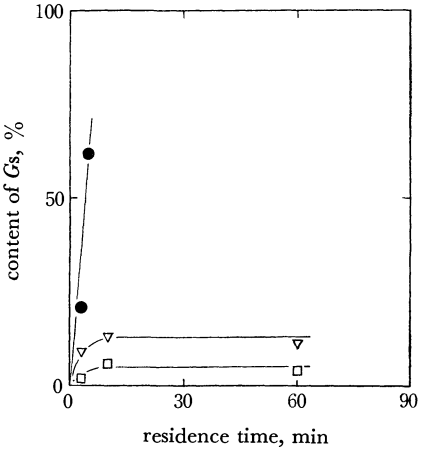

Fig. 3b

Fig. 3. Variations of content of G_S with residence time of HTT under 5 kbar for pre-heat-treated soft carbons.
●; PV-7, ▽; PV-17, □; PV-20
a) at 1590°C under 5 kbar, b) at 1800°C under 5 kbar

case of PV-7, the content of G_S increased very rapidly with residence time. In the cases of PV-17 and -20, the rate of development of the component G_S was depressed and seemed to approach a small limiting value.

The variations of the c_0-spacing of the component A_S and G_S with HTT are shown in Fig. 4. The

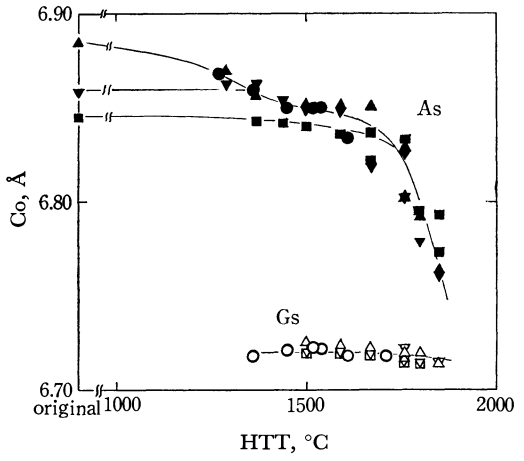

Fig. 4. Variations of c_0-spacing of the component A_S and G_S with HTT under 5 kbar for 60 min for pre-heat-treated soft carbons.

	PV-7	PV-15	PV-17	PV-20
A_S	●	▲	▼	■
G_S	○	△	▽	□

samples PV-15 and -17 showed gradual decrease in the c_0-spacing of the component A_S down to about 6.85 Å. After the c_0-spacing of the component A_S reached about 6.85 Å, it remained almost constant and the component G_S, whose c_0-spacing was about 6.72 Å, began to appear. Above around 1700°C, however, the c_0-spacing of the component A_S decreased rapidly. The sample PV-20, whose c_0-spacing was smaller than 6.85 Å, showed no change in the c_0-spacing of the component A_S until about 1700°C, while the component G_S was detected even at 1500°C. Above about 1750°C, the c_0-spacing of the component A_S for PV-20 decreased rapidly along the same line as PV-15 and -17.

The mutual relation in the change of crystallite size L_c of the component A_S with HTT among the four soft carbon samples PV-7, -15, -17 and -20 was the same as that in the c_0-spacing and is shown in Fig. 5.

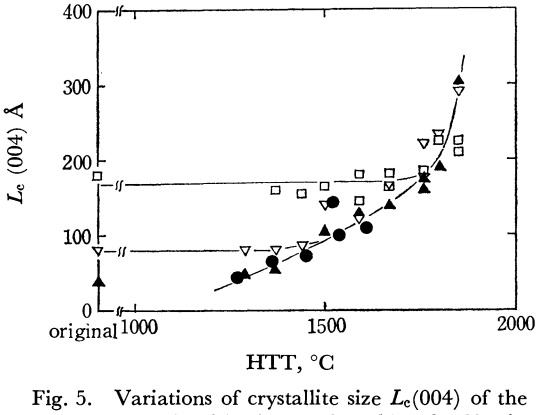

Fig. 5. Variations of crystallite size L_c(004) of the component A_S with HTT under 5 kbar for 60 min for pre-heat-treated soft carbons.
●; PV-7, ▲; PV-15, △; PV-17, □; PV-20

Hard Carbon Samples. Changes of (002) diffraction profile with HTT for the samples PH-15 and PH-20 were almost the same as that for the original sample PH-7, which was previously reported.[5] The variations of content of the graphitic component G_H with HTT for the samples PH-7, -15 and -20 are shown in Fig. 6. No appreciable difference in the change of content of the component G_H among three samples can be made, because there was a relatively large error in the determination of HTT in the case of the hard carbon.[9] The c_0-spacing of the turbostratic component A_H had a constant value of about 6.88 Å and the graphitic component G_H of about 6.72 Å.

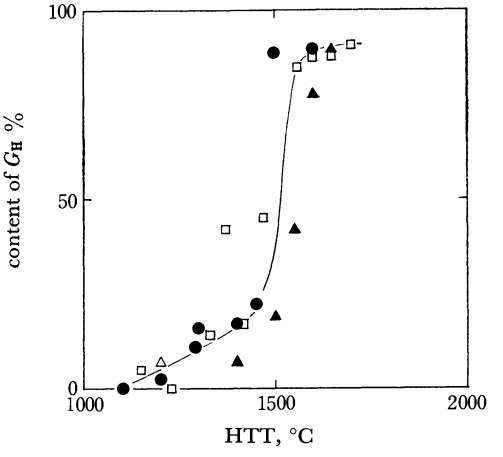

Fig. 6. Variations of content of G_H with HTT under 5 kbar for pre-heat-treated hard carbons
●; PH-7, ▲; PH-15, □; PH-20

Discussion

The starting of the heterogeneous graphitization under pressure, that is, the first appearance of the graphitic component G_S, of the pre-heat-treated soft carbons was retarded about 100°C from that of the original un-treated carbon sample PV-7. In the case of the sample PV-7, the content of the component G_S increased with increase in HTT, but in the cases of the pre-heat-treated carbons, a maximum value at about 1700°C was observed in the plot of the content of G_S against HTT. The apparent decrease of the content of G_S dose not mean the actual disappearance of the graphitic component once formed, but it comes from the fact that the formation of G_S largely depressed at higher HTT in the cases of the pre-heat-treated carbons, as it can be seen from Fig. 3. This conclu-

9) K. Kamiya, S. Yugo, M. Inagaki, H. Saito and T. Tsuzuku, This Bulletin, **41**, 2782 (1968).

sion is also confirmed by an experimental result represented by a solid square mark in Fig. 2. The sample PV-20 was first heat-treated at 1740°C for 60 min and then further at 1880°C for 60 min. The content of G_S of the sample after these heat-treatments was about 50%. This value corresponds to the one which can be obtained by the first heat-treatment at 1740°C. This suggests that the high content of G_S formed by the heat-treatment at 1740°C remained unchanged by the subsequent heat-treatment at 1880°C.

For the sample PV-15 and -17, the heterogeneous graphitization process was dominant in the range around 1400°C to 1700°C, in which the c_0-spacing of the structural components A_S and G_S remained unchanged at 6.85 and 6.72 Å, respectively. However, above 1700°C the homogeneous graphitization process became dominant and the profile of the turbostratic component A_S shifted to higher angle side. For the sample PV-20, the heterogeneous graphitization process began from about 1500°C and was dominant up to about 1800°C. It seemed that the direct transformation of the turbostratic component A_S to the graphitic component G_S, without having the intermediate structure, was slowed down when the c_0-spacing of the component A_S decreased below 6.85 Å. For the sample PV-7, only the heterogeneous graphitization has been observed by the heat-treatment under pressure, because it proceeded so rapidly that almost all of the component A_S transformed to the component G_S at temperatures below about 1700°C. For the pre-heat-treated carbons, one could observe the homogeneous graphitization of the component A_S, because the rate of the direct transformation of A_S to G_S was slowed down by the pre-heat-treatment.

In the previous work,[1] it was reported that the pre-heat-treated soft carbons showed no heterogeneous graphitization under 10 kbar. The residence time in that work was 3 min, but this residence time seems not to be enough for the graphitic component to develope, as it can be deduced from Fig. 3. Therefore, heterogeneous graphitization under pressure was probably not detected. It has been also mentioned that the graphitization of carbon under high pressure might be related to the dehydrogenation of carbon. This assumption was deduced from the fact that, under high pressure, carbon containing hydrogen, such as PV-7, was graphitized more rapidly than pre-heat-treated carbons which had been deprived of hydrogen. In the present work, however, the pre-heat-treated hard carbons PH-15 and PH-20 were shown to be graphitized as rapidly as original un-treated hard carbon sample PH-7. The sample PH-20 seemed to be almost completely dehydrogenated. This suggests that the dehydrogenation of the sample is not important factor for the rapid graphitization under high pressure.

The c_0-spacing of the samples, PH-7, PH-15, PH-20, PV-7, PV-15, PV-17 and PV-20, used in the present work was 7.01, 6.96, 6.93, 6.91, 6.885, 6.858 and 6.845 Å, respectively and the crystallite size $L_C(002)$ was 17, 17, 21, 28, 72, 150 and 260 Å, respectively. Among these seven samples PH-7, PH-15, PH-20 and PV-7 showed only heterogeneous graphitization under high pressure. However, for other samples, which had smaller c_0-spacings and larger crystallite sizes than the above four samples, the homogeneous graphitization was observed to occur side by side with the heterogeneous one even under high pressure. From this fact one can conclude that the heterogeneous graphitization is more dominant in a carbon sample which has a lower degree of graphitization.

The course of developement of the component G_S and A_S of the sample PV-20 was a little different from the other pre-heat-treated samples as shown in Figs. 1b) and 2. It seems to be related to the fact that the sample PV-20 was already on the second stage of normal graphitization process, while the others were on its first stage. However, the reason why the maximum value of the content of G_S was so large for PV-20 can not be understood.

The authors wish to thank Mr. M. Mizutani for his assistance. The carbon materials used were supplied by Tokai Electrode Mfg. Co.

NOTES

BULLETIN OF THE CHEMICAL SOCIETY OF JAPAN VOL. 43 931—932 (1970)

Thin-layer Chromatography of Inorganic Salts. III. Study of the Hydration of Anions by Means of Chromatography of Crystal Violet Cation

Tetsuo BABA,*1 Koji SAKUSHIMA*2 and Hayami YONEDA*3

Department of Chemistry, Wakayama University, Masago-cho, Wakayama

(Received March 29, 1969)

Our object was to obtain information concerning the behavior and the dissolved state of ions in solution by means of chromatography. We suggested that a complex cation is eluted mainly through ion-pair formation with anions contained in a developer.[1] The ion-pair formation reduces the apparent positive charge of a complex cation, which results in the decrease of the electrostatic attraction of an adsorbent and the increase of the R_f value of the complex.

It is well known that a number of anions can be extracted from an aqueous solution into an organic solvent through ion-pair formation between anions and dyestuff cations.[2] The extractability of anions seems to depend largely on the kind of anion and to reflect the behavior of anions towards ion-pair formation. Thus different R_f values of the dyestuff are expected when it is developed with solutions of various salts.

The object of this work is to clarify the effect of hydration of anions on ion-pair formation by means of chromatography of the dyestuff.

Experimental

As an adsorbent, Merck's silica gel H, prepared for thin-layer chromatography was used without further purification. This was spread on glass plates of 20 cm length with 0.25 mm thickness.

The dyestuff used was crystal violet. This was dissolved in ethanol to make 1/1000M solution, and 0.25 μl of the solution was applied at a starting point, 5 cm above the lower edge of the plate.

The following thirteen anions were chosen to form an ion-pair with the crystal violet cation: Cl^-, Br^-, I^-, NO_2^-, NO_3^-, ClO_3^-, ClO_4^-, $CH_3CO_2^-$, $CH_2ClCO_2^-$, $CHCl_2CO_2^-$, CO_3^{2-}, SO_3^{2-} and SO_4^{2-}. The sodium salts of these anions were dissolved in 50% ethanol-water solution to make 0.2M solutions, and they were used as a developer (In the case of sulfate and sulfite, 30% ethanol-water solution was used). Development was carried out at room temperature (17—18°C), until the solvent front rose to about 12—13 cm from the starting point. No special procedure was necessary for visualization of the spot, as it was sufficiently colored.

Results and Discussion

In Table 1 are listed the R_f values of crystal violet developed with alcoholic aqueous solutions of various salts, and typical examples of the chromatograms are shown in Fig. 1. As is seen in these data, the R_f value of the dyestuff cation depends

TABLE 1. R_f VALUES OF CRYSTAL VIOLET DEVELOPED WITH ALCOHOLIC AQUEOUS SOLUTIONS OF SALTS

a) Developed with 50% alcoholic aqueous solutions containing monovalent anions in 0.2M

Anions	R_f values	Anions	R_f values
$CH_3CO_2^-$	0.48	ClO_3^-	0.53
$CH_2ClCO_2^-$	0.59	ClO_4^-	0.57
$CHCl_2CO_2^-$	0.63	Cl^-	0.48
NO_2^-	0.44	Br^-	0.52
NO_3^-	0.51	I^-	0.53

b) Developed with 30% alcoholic aqueous solutions containing divalent anions or monovalent anions in 0.1M

Anions	R_f values	anions	R_f values
CO_3^{2-}	0.05	Cl^-	0.14
SO_4^{2-}	0.05	Br^-	0.21
SO_3^{2-}	0.55	I^-	0.22

*1 On leave from the Minoshima High School, Arita-shi, Wakayama.

*2 On leave from the Kainan High Scool, Kainan-shi, Wakayama.

*3 Correspondence to be addressed to this author.

1) T. Baba, H. Yoneda and M. Muto, This Bulletin, **41**, 1965 (1968).

2) As examples, the crystal violet-benzene system was used for extraction of ClO_4^- and IO_4^- (C. E. Hedrick and B. A. Berger, *Anal. Chem.*, **38**, 791 (1966)), and for $[Ag(CN)_2]^-$ (J. J. Markham, *Anal. Chem.*, **39**, 241 (1967)). The methylene blue-dichloroethane system was used for extraction of BF_4^- (J. Mrozinski, *Chem. Anal.* (Warsaw), **12**, 93 (1967)).

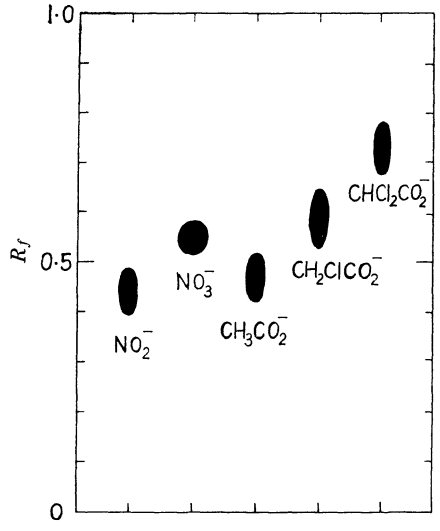

Fig. 1. Chromatogram of crystal violet developed with 50% aqueous alcoholic solutions containing monovalent anions in 0.2M concentration.

on the kind of anion in a developer. Comparison of the R_f values in the pairs (ClO_4^->ClO_3^- and NO_3^->NO_2^-) and the set ($CHCl_2CO_2^-$>$CH_2ClCO_2^-$>$CH_3CO_2^-$) leads us to the following conclusion. The crystal violet cation is dissolved from the adsorbing silica gel surface more easily with a stronger acid anion than with a weaker acid anion. The surface of silica gel is charged negatively in contact with water and adsorbs cations strongly.[4] Thus, the increase of the R_f value of the dyestuff in the salt solution seems to result from the decrease of the apparent positive ionic charge of the dyestuff cation due to the ion-pair formation between the anions and the dyestuff cations. The results suggest that a stronger acid anion can form an ion-pair with a dyestuff cation more easily than a weaker acid anion. As is seen from the structural formula

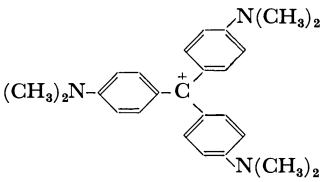

the crystal violet cation seems to be very poorly hydrated in solution. Presumably a weaker acid anion is more hydrated than a stronger one. Thus we might conclude as follows. The poorly hydrated dyestuff cation can form an ion-pair more easily with the less hydrated anion than with the more hydrated one. In fact, the R_f values of crystal violet increase in the order Cl^-<Br^-<I^-. This is just the order of the decrease of hydration. The R_f value in the divalent sulfate and carbonate anions is much lower than that in the monovalent anion. The large R_f value was obtained in the case of the sulfite anion. This can be explained as a result of the reduction of the dyestuff. Thus, the R_f value of the dyestuff is considered to give the relative measure of the degree of hydration of various anions.

One of the authors, T. Baba, wishes to express his thanks to the Ministry of Education for financial support.

BULLETIN OF THE CHEMICAL SOCIETY OF JAPAN VOL. 43 932—934 (1970)

Coordination Chemistry of Lanthanide Elements. II.[1] Cationic Lanthanide Complexes of Trimorpholino Phosphine Oxide

J. T. DONOGHUE

Department of Chemistry, University of Arkansas, Fayetteville, Arkansas, U.S.A.

(Received July 12, 1969)

In earlier studies,[2,3] it was found that the phosphoryl donor, hexamethyl phosphoramide (HMPA), formed six coordinate complexes with lanthanide ions. The occurrence of coordination number six for lanthanide ions, although not unique for this ligand, is unusual enough to warrant further study of the factors which give rise to it. The ligand, trimorpholino phosphine oxide exhibits behavior similar to that of HMPA[3] in forming complexes with transition metals. It was found that this ligand also gives complexes of the type $LnCl_3 \cdot 3L$.[4] It was of interest to investigate cationic lanthanide complexes of this phosphoryl donor.

1) Part I: This Bulletin, **43**, 271 (1970).

2) J. T. Donoghue and D. A. Peters, *J. Inorg. Nucl. Chem.*, **31**, 467 (1969).

3) J. T. Donoghue, E. Fernandez, J. A. McMillan and D. A. Peters, *Inorg. Chem.*, in press.

4) J. T. Donoghue and E. Fernandez, This Bulletin, **43**, 271 (1970).

TABLE 1. ANALYTICAL DATA[a)]

Compound	% Carbon		% Hydrogen		% Nitrogen	
	Calcd	Found	Calcd	Found	Calcd	Found
L[b)]	46.2	46.0	8.0	8.3	13.8	13.5
$La(ClO_4)_3 \cdot 6L$	38.1	38.0	6.4	6.3	11.1	11.2
$Ce(ClO_4)_3 \cdot 6L$	38.1	37.8	6.4	6.8	11.1	11.2
$Pr(ClO_4)_3 \cdot 6L$	38.1	37.9	6.4	6.7	11.1	11.0
$Nd(ClO_4)_3 \cdot 6L$	38.0	37.9	6.4	6.4	11.1	11.0
$Pm(ClO_4)_3 \cdot 6L$	38.0	37.9	6.4	6.4	11.1	11.1
$Sm(ClO_4)_3 \cdot 6L$	37.9	38.1	6.4	6.4	11.1	11.1
$Eu(ClO_4)_3 \cdot 6L$	37.9	38.0	6.4	6.8	11.1	11.3
$Gd(ClO_4)_3 \cdot 6L$	37.8	37.6	6.3	6.7	11.0	11.0
$Tb(ClO_4)_3 \cdot 6L$	37.8	37.7	6.3	6.8	11.0	11.2
$Dy(ClO_4)_3 \cdot 6L$	37.7	37.6	6.3	6.5	11.0	11.2
$Ho(ClO_4)_3 \cdot 6L$	37.7	37.9	6.3	6.5	11.0	11.4
$Er(ClO_4)_3 \cdot 6L$	37.7	37.9	6.3	6.1	11.0	11.2
$Tm(ClO_4)_3 \cdot 6L$	37.6	37.9	6.3	6.1	11.0	11.1
$Yb(ClO_4)_3 \cdot 6L$	37.6	37.6	6.3	6.3	11.0	11.0
$Lu(ClO_4)_3 \cdot 6L$	37.5	37.5	6.3	6.3	10.9	11.0
$Y(ClO_4)_3 \cdot 6L$	38.9	38.5	6.5	6.3	11.4	11.1
$Sc(ClO_4)_3 \cdot 6L$	39.0	38.6	6.9	6.5	11.5	11.1

a) Nitrogen analyses by A. Bernhardt and W. Germany; C, H-analyses obtained on Coleman Analyzer.

b) L designates trimorpholino phosphine oxide $\left(O\begin{smallmatrix}CH_2CH_2\\ \\CH_2CH_2\end{smallmatrix}N\right)_3PO$.

Experimental

Synthesis of Complexes. The complexes were synthesized by metathesis according to the equation

$$LnCl_3 + 3AgClO_4 + 6L \longrightarrow Ln(ClO_4)_3 \cdot 6L + 3AgCl.$$

0.001 mol of lanthanide halide was dissolved in 15 m*l* of hot alcohol. To this was added a solution of 0.003 mol of $AgClO_4$ in 15 m*l* of hot alcohol. The precipitated silver chloride was filtered after cooling. The filtrate, under nitrogen, was treated with 0.006 mol of ligand in 15 m*l* of hot alcohol. After the resulting solutions had cooled to room temperature, they were treated with 75 m*l* of absolute ether to precipitate the complexes. The solid complexes were filtered and dried under nitrogen and were stored *in vacuo* over H_2SO_4. Analytical results are presented in Table 1.

Infrared Spectra. Infrared spectra of Nujol mulls of the complexes and free ligand were obtained using a Perkin-Elmer, model 337, recording infrared spectrophotometer. In all complexes studied, the phosphoryl frequency of the ligand was displaced to lower energies on complexation. The results are shown in Table 2.

Conductance Measurements. Conductances of 0.001M solutions in nitromethane were obtained using an Industrial Instruments Conductivity Bridge which was frequently calibrated with 0.01N KCl. Results are presented in Table 3.

Reagents. The lanthanide halides were obtained from Trona Chemicals and were of 99.9+% purity.

Trimorpholino phosphine oxide was obtained from Aldrich Chemical Co. and was used without further purification.

All other chemicals employed in this study were of reagent-grade quality.

TABLE 2. PHOSPHORYL ABSORPTION FREQUENCY, $\nu_{P=O}$ IN cm^{-1}

Complex	$\nu_{P=O}$	Complex	$\nu_{P=O}$
L	1204	Tb	1191
La	1191	Dy	1192
Ce	1191	Ho	1191
Pr	1192	Er	1192
Nd	1191	Tm	1192
Pm	1193	Yb	1191
Sm	1192	Lu	1189
Eu	1190	Y	1191
Gd	1190	Sc	1192

TABLE 3. MOLAR CONDUCTIVITIES OF 10^{-3}M NITROMETHANE SOLUTIONS

Complex	Λ_{molar}	Complex	Λ_{molar}
La	258	Tb	257
Ce	265	Dy	255
Pr	267	Y	270
Nd	263	Ho	253
Pm	260	Er	252
Sc	261	Tm	253
Sm	261	Yb	251
Eu	258	Lu	251
Gd	256		

Results

Analytical. Analytical data for the ligand and its lanthanide complexes are given in Table 1.

Infrared. Absorption frequencies for the P=O group in the complexes are given in Table 2.

Conductivity. Molar conductivities obtained for 10^{-3}M solutions of the complexes in CH_3NO_2 are given in Table 3.

Discussion

The ligand trimorpholino phosphine oxide is similar to hexamethyl phosphoramide in many ways in that the infrared phosphoryl frequencies are nearly identical at 1204 cm^{-1} and 1208 cm^{-1} respectively. The coordination behavior of the two ligands toward transition metals is very similar in that both form pseudo tetrahedral complexes with nickel(II) and cobalt(II).[5,6] However, in terms of steric requirements, trimorpholino phosphine oxide, $\left(O\langle\begin{smallmatrix}CH_2CH_2\\CH_2CH_2\end{smallmatrix}\rangle N\right)_3PO$, is expected to show a stronger resemblance to triphenyl phosphine oxide $(C_6H_5)_3PO$ than to HMPA, $[(CH_3)_2N]_3PO$.

The conductivity results indicate that the perchlorate anion is not coordinated in nitromethane. Unfortunately, strong ligand absorption in the infrared in the region expected for perchlorate absorption made it impossible to determine if perchlorate is weakly coordinated in the solid state. It must be assumed that the perchlorate anion is uncoordinated in the solid state as well as in nitromethane solution.

The behavior of trimorpholino phosphine oxide toward lanthanides was observed to be quite similar to that of HMPA and other oxygen donor ligands, such as diphenyl sulfoxide.[7,8]

On the basis of the data reported above, it is concluded that the apparent coordination number of the lanthanide elements in these complexes is uniformly six.

Obviously, the steric requirements of triphenyl phosphine oxide and trimorpholino phosphine oxide should be similar, but the coordination numbers exhibited for trimorpholino phosphine oxide in complexes of the type $[LnL_6]^{+3}$ are apparently six. Since the cationic lanthanide complexes of triphenyl phosphine oxide are unknown, a direct comparison between triphenyl phosphine oxide and trimorpholino phosphine oxide is not possible but is desirable. Future work will involve investigation of the cationic lanthanide complexes of triphenyl phosphine oxide.

I would like to acknowledge the aid of the Donors of the Petroleum Research Fund of the American Chemical Society through Grant No. 1108-G3.

5) J. T. Donoghue and R. S. Drago, *Inorg. Chem.*, **2**, 578 (1963).

6) J. T. Donoghue and E. Fernandez, *ibid.*, in press.

7) S. K. Ramalingam and S. Soundararajan, *J. Inorg. Nucl. Chem.*, **20**, 1963 (1967).

8) V. Krishnamurthy and S. Soundararajan, *Can. J. Chem.*, **45**, 189 (1967).

BULLETIN OF THE CHEMICAL SOCIETY OF JAPAN VOL. 43 934—935 (1970)

The Photolysis of Sodium *N,N*-Dimethyldithiocarbamate and Hexamethyleneammonium Hexamethylenedithiocarbamate

Toshihiro YAMASE, Hiroshi KOKADO and Eiichi INOUE

Imaging Science and Engineering Laboratory, Tokyo Institute of Technology, Meguro-ku, Tokyo

(Received July 29, 1969)

We have previously reported that sodium *N,N*-dimethyldithiocarbamate (SMTC) is photolyzed by light of the wavelength of 2537 Å. The absorption was attributed to the excitation of a sulphur-conjugated system. We also found carbon disulfide in the photo-decomposition products.[1] It was then considered desirable to make a more quantitative assessment of carbon disulfide for the purpose of elucidating the kinetics of the photolytic process.

Unless otherwise stated, the experiments were carried out with SMTC or hexamethyleneammonium hexamethylenedithiocarbamate (HMTC) solutions of $3—6\times10^{-5}$M. A deaerated solution was photolyzed in the same manner as before.[1] The produced carbon disulfide was transformed into potassium methylxanthate, which shows an optical absorption at 300 nm in methanol. The amount of the methylxanthate produced, and consequently the yield of carbon disulfide, increased as the

1) T. Yamase, H. Kokado and E. Inoue, *Kogyo Kagaku Zasshi*, **72**, 162 (1969).

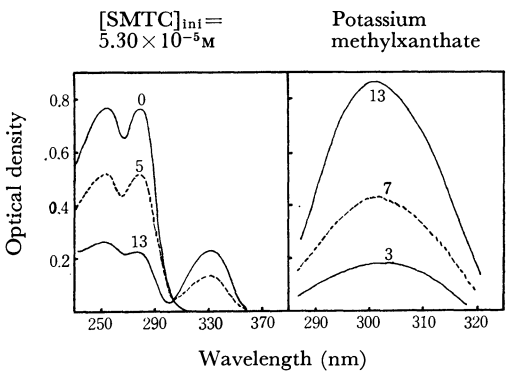

Fig. 1. Absorption spectra of SMTC solution and formed potassium methylxanthate.
Numbers indicate the illumination time (min) of SMTC solution

dithiocarbamate was photolyzed (Fig. 1). The experimental results can be represented as in the following equation, as was anticipated in the previous paper[1]:

$$-dC/dt=kC=dC'/dt=k(C'_\infty-C')$$

where C is the concentration of dithiocarbamate in mol/l and where C' and C'_∞ are the concentrations of carbon disulfide in mol/l at the illumination times of $t=t$ and $t=\infty$ respectively. Representing the concentration by the optical density of each absorption, some log plots derived from the rate formula are shown in Fig. 2. Juging from Fig. 1, the quantity of produced carbon disulfide

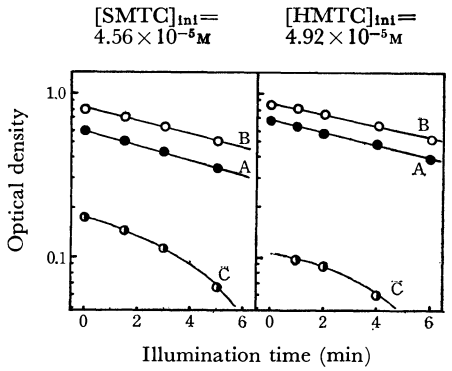

Fig. 2. Optical density as a function of illumination time:
A indicates optical density (O.D) of SMTC and HMTC at 280 nm and 282 nm, respectively.
B and C indicate $O.D_\infty$—O.D at 300 nm and 330 nm, respectively.

can be regarded as the same as the decrease in dithiocarbamate. When the initial concentrations of SMTC were 5.92×10^{-5}M and 4.56×10^{-5}M, the amounts of carbon disulfide produced by prolonged photolysis were 5.70×10^{-5}M and 4.49×10^{-5}M respectively. There remains scarcely any doubt that carbon disulfide is produced by a unimolecular reaction and that the photolysis proceeds by first-order kinetics.

After the photolysis of SMTC, the optical density at 330 nm was decreased and a new absorption appeared at 264 nm. It may be inferred that a stable species was produced *via* an unstable species with the absorption maximum at 330 nm. The change in the absorption of the solution after photolysis is shown in Fig. 3. Such a spectrum was

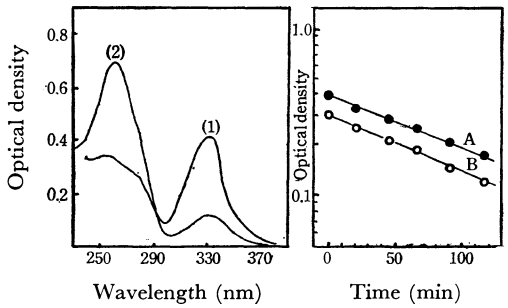

Fig. 3. Dark reaction after photolysis.
(1) and (2) indicate spectra of SMTC after 0 and 170 min, respectively;
A indicates optical density (O.D) at 330 nm.
B indicates $O.D_\infty$—O.D at 264 nm.
$[SMTC]_{ini}=1.06\times10^{-4}$M

not identified with that of dimethylamine, acetaldehyde, formaldehyde, or *N*-methylformaldehyde in an aqueous solution of pH 10, although all those substances had been anticipated as photoproducts. The quantum yield was unknown with regard to HMTC; however, we can easily infer that the quantum yield of HMTC is not far from the 0.11 which is observed in SMTC. This is evident from the fact that those two dithiocarbamates had almost the same slopes of photolytic rates and almost the same absorption coefficients[2]. The substance which has the absorption at 330 nm may be ascribed to an amine or imine derivative which reacts by the first-order process to show an absorption at 264 nm.

2) T. Yamase, H. Kokado and E. Inoue, *ibid.*, **71**, 1587 (1968).

BULLETIN OF THE CHEMICAL SOCIETY OF JAPAN VOL. 43 936—937 (1970)

Dynamic Differential Effect of Alkali Ions on the Desorption of Calcium Ion from Lipid Film

Hideo KIMIZUKA, Shōzō NISHIDA and Taketoshi HIDESHIMA

Department of Chemistry, Faculty of Science, Kyushu University, Hakozaki, Fukuoka

(Received August 8, 1969)

The study of the interaction between the surface film and the solute of an underlying solution is essential in order to elucidate the reactions occurring at the interface of the cellular membrane. Recently, some evidence has been accumulated to show that Ca^{2+} is involved in regulating the ion movement across the cell membrane.[1] It is of importance, therefore, to examine the interactions between Ca^{2+} and other ions within lipid film. Since the phenomenon of ion movement is kinetic in nature, it may be more intimately related to the rate of adsorption or desorption than to any static property such as the equilibrium adsorption. It was shown in the preceding papers that the rate of desorption of Ca^{2+} brought about by K^+ was greater than that brought about by Na^+, whereas the equilibrium adsorptions were almost the same.[2] This differential effect was tentatively explained by assuming that the rate-determining step in the exchange reactions is the removal of the water molecule from the hydrated K^+ and Na^+. A further test of this hypothesis would require similar experiments by the use of other alkali ions such as Li^+, more hydrated than Na^+, and such as Cs^+ and Rb^+, less hydrated than K^+. This paper will describe the result of experiments carried out with these ions.

The samples as well as the apparatus used have been described elsewhere;[2] the temperatures were 25±1°C. The films of stearic acid or phospholipid were spread over the 5 m*l* of a solution containing radioactive calcium, and the calcium bound to the lipid film was measured with the G–M counter. When the equilibrium had been attained, 1 m*l* of a solution of alkali chloride was injected into the underlying solution by means of a syringe and the time-dependence of the desorption of Ca^{2+} was measured.[2] The results are shown in Figs. 1 and 2 together with the preceding results.[2] It may be seen in these figures that Li^+ acts like Na^+, whereas Rb^+ and Cs^+ behave like K^+, *i. e.*, the former indicates the induction period prior to the Ca^{2+} desorption, while the latter cause the desorption immediately. In contrast to the desorption behavior, the equilibrium adsorptions were nearly the same. These phenomena were found to be reproducible regardless of the concentrations of the alkali chloride solutions.

The results of the present paper, together with those of preceding papers,[2] suggest that the alkali ions may be classified into two groups, the 1st consisting of Li^+ and Na^+, and the 2nd, of K^+, Rb^+, and Cs^+, according to their dynamic behaviors at the interface. In addition, it may be pointed out that this classification may be attributed to the kinetic property of the alkali ion itself, since the phenomena are independent of the kind of anionic site.

According to Samoilov,[3] alkali ions are divided

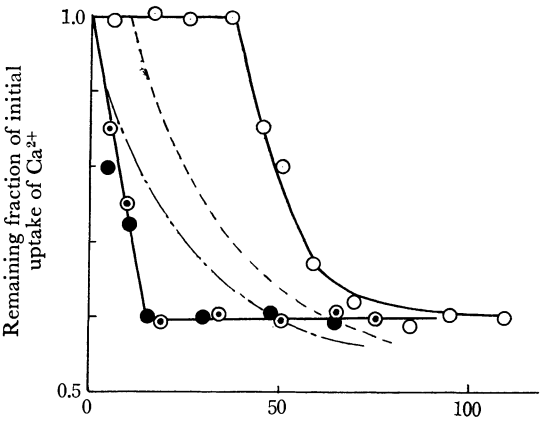

Fig. 1. Desorption of Bound Ca^{2+} from stearate film with time.
Open, dotted and filled circles indicate the effect of Li^+, Rb^+ and Cs^+, respectively. Concentration of Ca^{2+} was 4.72×10^{-5}M and those of the alkali ions, 0.1M (pH, 7.1—7.2).
Dotted and broken lines indicate the effect of Na^+ and K^+, respectively.[2] Concentration of Ca^{2+} was 1.62×10^{-5}M and those of Na^+ and K^+, 0.4M (pH, 8.0—8.2).

1) F. Brink, *Pharmacol. Rev.*, **6**, 243 (1954); J. A. Tobias, *J. Cell. Comp. Physiol.*, **52**, 89 (1958); H. Kimizuka and K. Koketsu, *J. Gen. Physiol.*, **47**, 379 (1963); L. G. Abood, *Int. Rev. Neurobiol.*, **9**, 223 (1966).

2) H. Kimizuka, T. Nakahara, H. Uejō and A. Yamauchi, *Biochim. Biophys. Acta.*, **137**, 549 (1967); A. Yamauchi, A. Matsubara, H. Kimizuka and L. G. Abood, *ibid.*, **150**, 181 (1968).

3) O. Ya. Samoilov, *Discuss. Faraday Soc.*, **24**, 141 (1957).

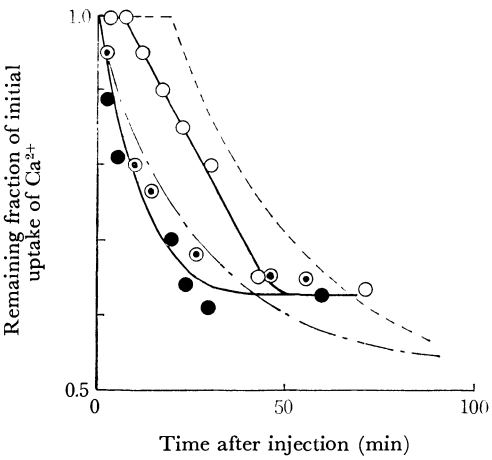

Fig. 2. Desorption of bound Ca^{2+} from lipid film with time.
Open, dotted and filled circles indicate the effect of Li^+, Rb^+ and Cs^+, respectively. Concentration of Ca^{2+} was 2.15×10^{-4}M and those of alkali ions, 1M (pH, 7.1—7.2).
Dotted and broken lines indicate the effect of Na^+ and K^+, respectively.[2] Concentration of Ca^{2+} was 5×10^{-4}M and those of alkali ions, 1.12M (pH, 7.1—7.2).

into two groups on the basis of the kinetic features of hydrated water, *i. e.*, the ions of positive hydration, Li^+ and Na^+, and those of negative hydration, K^+, Rb^+, and Cs^+. The hydrated water molecules of the former and of the latter are, respectively, less and more labile than molecules of pure water. This proposal corresponds to the concept of the structural temperature[4] or the order-disorder structure[5] of hydrated water.

Thus, this concept of the state of hydration may offer a plausible explanation for the present results providing that the rate-determining step of the ion-exchange reaction occurring at the surface film is the dehydration process of the alkali ion.

The similar differentiation has already been established in some biophysicochemical properties, such as the movements of alkali ions across the cell membrane[6] and the activation phenomena of some enzymes by those ions.[7] Since these phenomena are also kinetic in nature, it is conceivable that these biophysicochemical properties are closely related to the kinetic behavior of alkali ions at boundaries.

This research has been supported by a grant-in-aid for special-project research in biophysics from the Ministry of Education, Japan.

4) J. D. Bernal and R. H. Fowler, *J. Chem. Phys.*, **1**, *Ser. A*, 515 (1933).
5) W. M. Cox and J. H. Wolfenden, *Proc. Roy. Soc.*, *Ser. A*, **145**, 475 (1934).
6) W. K. Chandler and H. Meves, *J. Physiol.*, **180**, 788 (1965); I. Tasaki, I. Singer and T. Takenaka, *J. Gen. Physiol.*, **48**, 1095 (1965).
7) M. Dixon and E. C. Webb, "Enzymes," Longmans, Green & Co., London (1964).

BULLETIN OF THE CHEMICAL SOCIETY OF JAPAN VOL. 43 937—939 (1970)

Synthesis of 4-(2-Thienyl)pyrimidine Derivatives. Studies on Heterocyclic Chemistry. VI[1]

Tarozaemon NISHIWAKI

Department of Chemistry, Yamaguchi University, Yamaguchi City

(Received August 11, 1969)

4-(2-Thienyl)pyrimidines are little studied.[2,3] In connection with other programmes some of their derivatives (IX, X, XI, XII) were prepared from the corresponding β-diketones having a thiophene ring and guanidine or urea.

The Wolff-Kishner reduction of 2-isovalerylthiophene (I) gave 2-isoamylthiophene (II) in better yield of 77% than the reported Clemmensen procedure of 32% yield.[4] Reduction of I with lithium aluminum hydride afforded an alcohol III, which was obtained in a pure state only by its acetylation to IV and subsequent hydrolysis to III, because repeated fractional distillations of the crude reaction product could not give an analytically pure sample.

1) Part V. T. Nishiwaki, T. Kitamura, and A. Nakano, *Tetrahedron*, **26**, 453 (1970).

2) S. Gronowitz and J. Röe, *Acta. Chem. Scand.*, **19**, 1741 (1965).

3) H. Bredereck, R. Gompper, and H. Herlinger, *Chem. Ber.*, **91**, 2832 (1958).

4) W. Steinkopf and I. Schubart, *Ann.*, **424**, 1 (1920).

Table 1. NMR spectra of 4-(2-thienyl)pyrimidines IX, X, XI, XII[a,b]

Compound	Chemical Shifts (τ Values, J (Hz))			
	Pyrimidine	Thiophene		
	C_5–H	C_3–H	C_4–H	C_5–H
IX	3.06	2.22 (dd, J_{34}=4.5) (J_{35}=1.5)	2.87 (dd, J_{45}=5.3) (J_{34}=4.5)	2.36 (dd, J_{45}=5.3) (J_{35}=1.5)
X	3.00	2.30 (d, J_{34}=4.2)	2.71 (d, J_{34}=4.2)	
XI	3.14[c]	2.40 (d, J_{34}=4.2)	3.14[c]	
XII	3.18	1.97 (dd, J_{34}=4.2) (J_{35}=1.5)	2.65 (dd, J_{34}=4.2) (J_{45}=5.4)	2.08 (dd, J_{45}=5.4) (J_{35}=1.5)

a) The spectra were determined in dimethyl sulfoxide or its d_6-analogue at room temperature or at 60°C (for XII).
b) dd, double doublet.
c) Broad peak due to overlapping.

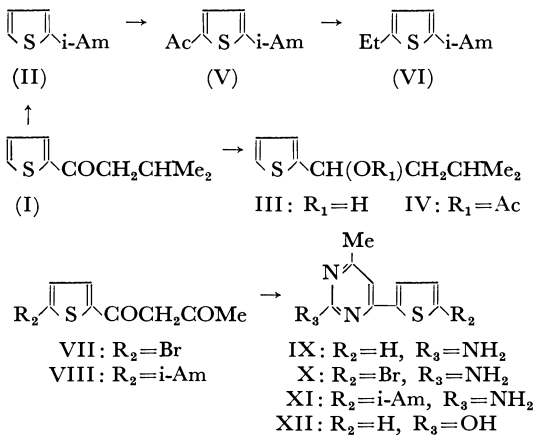

Friedel-Crafts reaction of II with acetic acid in the presence of polyphosphoric acid produced 2-isoamyl-5-acetylthiophene (V), from which a β-diketone VIII was derived. The structure of V was verified by NMR spectrum,[5] which showed in carbon tetrachloride two β-protons of thiophene ring at τ 3.22 (dd, J=4.0 Hz and J=1.0 Hz,*1 C_3–H) and τ 2.52 (d, J=4.0 Hz, C_4–H). An additional support is provided by reduction of V to 2-isoamyl-5-ethylthiophene (VI), the NMR spectrum of which exhibited in carbon tetrachloride only one signal at τ 3.60 corresponding to two β-protons. A β-diketone VII was similarly derived from 2-bromo-5-acetylthiophene.

2-Hydroxy-4-(2-thienyl)-6-methylpyrimidine(XII) was prepared by the cyclization of an intermediate uramido compound which has two possible structures, XIII and XIV.

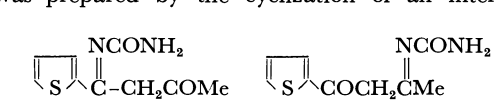

The structures of the pyrimidines (IX—XII) were characterized by NMR spectra in the aromatic region as shown in Table 1.

Experimental

Melting points were determined on a Yanagimoto hot stage and uncorrected. NMR spectra were taken at 60 MHz with a JNM-3H-60 spectrometer with TMS as an internal standard.

2-Isoamylthiophene (II). 2-Isovalerylthiophene[4] (I) (29.9 g, 0.18 mol), hydrazine hydrate (80%) (34 m*l*, 0.70 mol), and ethylene glycol (400 m*l*) were stirred at 120—130°C for 2 hr. After cooling the mixture to 50°C, a solution of potassium hydroxide (30.0 g) in ethylene glycol (100 m*l*) was added at once to this mixture. The mixture was heated at 130—140°C for 1 hr with stirring, left overnight and distilled at atmospheric pressure up to 220°C. The distillate was extracted with ether and the extracts were washed with water, 2N hydrochloric acid, and water successively, dried (Na_2SO_4), and distilled to give II, 21.2 g (77%), bp 56—57°C/2 mmHg, n_D^{20} 1.4951, (lit,[4] bp 72—77°C/11 mmHg). (Found: C, 70.0; H, 9.0; S, 21.0%).

Reduction of 2-Isovalerylthiophene (I) with Lithium Alminum Hydride. A solution of the ketone (I) (13.4 g, 0.08 mol) in anhydrous ether (40 m*l*) was slowly added to a suspension of lithium aluminum hydride (6.0 g, 0.16 mol) in anhydrous ether (200 m*l*). The mixture was refluxed for 3 hr and worked-up in the usual manner to afford an oil, the gas chromatogram of which showed the presence of at least five components. This oil was heated with a mixture of acetic anhydride (11.5 g) and anhydrous sodium acetate (1.5 g) at 100°C for 2 hr and poured into water. Ether extraction and distillation afforded an acetate (IV), 10.1 g (60%), bp 69—70°C/0.4 mmHg, $\nu_{C=O}^{Neat}$ 1745 cm^{-1}.

Found: C, 62.5; H, 7.8; S, 15.8%. Calcd for $C_{11}H_{16}O_2S$: C, 62.2; H, 7.6; S, 15.1%.

This acetate (9.8 g, 0.05 mol) was refluxed with potassium hydroxide (3.1 g) in ethanol (30 m*l*) for 2 hr. The mixture was poured into water and extracted with ether. Distillation of the dried (Na_2SO_4) extracts gave an alcohol (III), 5.4 g (68%), bp 71—72°C/0.8

*1 Coupling with the side chain.

5) R. White, "Physical Method in Heterocyclic Chemistry," Vol. 2 ed. by A. R. Katritzky, Academic Press, New York, (1964), p. 103.

mmHg, n_D^{20} 1.5168, ν_{OH}^{Neat} 3280 cm^{-1}.

Found: C, 63.5; H, 8.5; S, 18.6%. Calcd for $C_9H_{14}OS$: C, 63.5; H, 8.3; S, 18.8%.

2-Isoamyl-5-acetylthiophene (V). A mixture of polyphosphoric acid (200 g), acetic acid (33.3 g) and 2-isoamylthiophene (II) (30.0 g, 0.19 mol) was stirred at 80—85°C for 1 hr and the mixture was poured into water and extracted with ether. The etheral extracts were dried (Na_2SO_4) and distilled at 89—92°C/0.2 mmHg to give a compound (V), 31.5 g (83%), n_D^{20} 1.5277, $\nu_{C=O}^{Neat}$ 1660 cm^{-1}.

Found: C, 67.2; H, 8.5; S, 16.4%. Calcd for $C_{11}H_{16}OS$: C, 67.3; H, 8.2; S, 16.3%.

The 2,4-dinitrophenylhydrazone, mp 170—171°C (from benzene-ligroin), (Found: C, 53.9; H, 5.3; S, 8.4%. Calcd for $C_{17}H_{20}N_4O_4S$: C, 54.2; H, 5.4; S, 8.5 %). The semicarbazone, mp 215—216°C (from methanol), (Found: C, 56.9; H, 7.85; N, 16.14%. Calcd for $C_{12}H_{19}N_3OS$: C, 56.9; H, 7.6; N, 16.6%).

2-Isoamyl-5-ethylthiophene (VI). A mixture of the ketone (V) (10.0 g, 0.05 mol), diethylene glycol (150 m*l*), and hydrazine hydrate (80%) (10 m*l*, 0.26 mol) was heated at 120°C for 2 hr. After cooling to 50°C, a solution of potassium hydroxide (10.0 g) in diethylene glycol (50 m*l*) was added to this mixture at once and heated at 140°C for 1 hr. The mixture was distilled up to 230°C and the distillate was treated as before to give VI, 8.0 g (86%), bp 58—60°C/0.6 mmHg, n_D^{20} 1.4930.

Found: C, 72.1; H, 10.0%. Calcd for $C_{11}H_{18}S$: C, 72.5; H, 9.95%.

2-Isoamyl-5-thenoylacetone (VIII). A solution of V (9.8 g) in ethyl acetate (15.0 g) was added to a suspension of powdered sodium (1.3 g) in anhydrous ether (70 m*l*). The mixture was refluxed for 2 hr with stirring. The sodium salt was filtered off, dissolved in water and extracted with ether. The aqueous solution was acidified and extracted with ether. The dried (Na_2SO_4) extracts afforded the β-diketone by distillation at 102—106°C/0.2 mmHg, 2.6 g (22%), n_D^{20} 1.5676.

Found: C, 65.9; H, 7.7%. Calcd for $C_{13}H_{18}O_2S$: C, 65.5; H, 7.6%.

2-Bromo-5-thenoylacetone (VII). This was prepared similarly from 2-bromo-5-acetylthiophene in 38% yield after recrystallization from methanol, mp 132—133°C.

Found: C, 38.8; H, 2.85%. Calcd for $C_8H_7BrO_2S$: C, 38.9; H, 2.85%.

2-Amino-4-(5-isoamyl-2-thienyl)-6-methylpyrimidine (XI). The β-diketone (VIII) (1.7 g) and guanidine carbonate (0.8 g) were melted at 140—150°C for 1 hr. After cooling, the mixture was washed with water and insoluble product (1.6 g, 84%) was recrystallized twice from *n*-heptane as pale yellow needles, mp 126°C.

Found: C, 64.2; H, 7.3%. Calcd for $C_{14}H_{19}N_3S$: C, 64.3; H, 7.3%.

2-Amino-4-(2-thienyl)-6-methylpyrimidine (IX). This compound was obtained from 2-thenoylacetone and guanidine carbonate in 79% yield and recrystallized from ethanol, mp 173—174°C.

Found: C, 56.4; H, 5.0%. Calcd for $C_9H_9N_3S$: C, 56.5; H, 4.75%.

2-Amino-4-(5-bromo-2-thienyl)-6-methylpyrimidine (X). This compound was prepared from VII and guanidine carbonate in 90% yield and recrystallized from acetone, mp 200—201°C.

Found: C, 40.2; H, 3.0%. Calcd for $C_9H_8BrN_3S$: C, 40.0; H, 3.0%.

2-Hydroxy-4-(2-thienyl)-6-methylpyrimidine (XII). A mixture of 2-thenoylacetone (8.4 g), urea (3.00 g), anhydrous ethanol (50 m*l*), and hydrochloric acid (0.5 m*l*) was left for 40 hr at room temperature with occasional shaking. Homogeneous solution resulted after a few hours and then pale yellow soild began to precipitate. Two recrystallizations from ethanol gave an uramido compound, 5.39 g (51%), as pale yellow plates, mp 192—194°C (decomp.).

Found: C, 51.5; H, 5.0; N, 13.2; S, 15.1%. Calcd for $C_9H_{10}N_2O_2S$: C, 51.4; H, 4.8; N, 13.3; S, 15.25%.

This compound (1.18 g) was heated with potassium hydroxide (0.5 g) in water (10 m*l*) until a clear solution had resulted. After cooling, the solution was acidified and precipitates (0.90 g, 84%) were recrystallized from water as colourless needles, mp 280—282°C (decomp).

Found: C, 56.3; H, 4.0; N, 14.2; S, 16.7%. Calcd for $C_9H_8N_2OS$: C, 56.2; H, 4.2; N, 14.6; S, 16.7%.

BULLETIN OF THE CHEMICAL SOCIETY OF JAPAN VOL. 43 939—941 (1970)

Successive and Simultaneous Solubilizations of Two Different Water-insoluble Dyes by Detergents

Fumikatsu TOKIWA

Research Laboratories, Kao Soap Company, Wakayama

(Received August 15, 1969)

Although the solubilization of water-insoluble materials by detergents is a familiar phenomenon,[1] this subject is not neccessarily well understood. During the course of other work,[2,3] the present author observed an interesting aspect of behavior,

1) M. E. L. McBain and E. Hutchinson "Solubilization and Related Phenomena," Academic Press, New York (1955).

2) F. Tokiwa, *J. Phys. Chem.*, **72**, 1214 (1968).

3) F. Tokiwa, *J. Colloid Interfac. Sci.*, **28**, 145 (1968).

as will be described below, with respect to the solubilization of two different water-insoluble dyes.

This note will describe two types of solubilization for two different dyes. The first type is a successive solubilization in which two dyes are solubilized step-by-step in a detergent solution after the saturation of either of the two. The second type is a simultaneous solubilization in which two dyes are solubilized at the same time. From among the many water-insoluble dyes, two sets of dye combinations, Yellow OB and Sudan Blue GN, and Yellow OB and Aniline Blue, have been chosen by taking into account the possibility of an easy, separate determination by their optical densities. As solubilizing agents, anionic, cationic, and nonionic detergents were used to ascertain the effect of their electrical character on the solubilization.

Experimental

Materials. The sodium dodecyl sulfate ($NaC_{12}S$) and dodecyl nonaoxyethylene ether ($C_{12}(EO)_9$) were samples similar to those used in previous works.[2,3] Dodecyltrimethylammonium chloride ($C_{12}NCl$) was a laboratory-prepared sample purified by repeated recrystallization from acetone. The yellow OB (YW), 1-*o*-tolyl-azo-2-naphthylamine, was described in a previous paper.[2] The Sudan Blue GN (SB), 1-*m*-toluidine-4-methylaminoanthraquinone, and Aniline Blue (AB), *N*-phenylated rosaniline, which were both of a reagent grade, were obtained from Chroma-Gesellschaft, Germany. They were purified by recrystallization from a methanol-water solvent and an acetone-water solvent respectively. Mixed solubilizates were prepared by dissolving two different dyes in an acetone-benzene solvent and by then evaporating the solvent at 50°C.

Solubilization and Absorption Spectra. Solubilization runs were carried out in a water bath at 25°C for 50 hr, a method described elsewhere[2] being employed. The determination of the amount of solubilized dye was made by optical-density measurements at the wavelength of the absorption maximum. The absorption spectra of the dyes were measured by using a Shimadzu Model MPS-50 spectrophotometer at about 25°C.

Results and Discussion

Before discussing the successive and simultaneous solubilizations, the common solubilization of single dyes will be described briefly. Table 1 gives the saturation values of YW, SA, and AB in the aqueous solutions of $NaC_{12}S$, $C_{12}NCl$, and $C_{12}(EO)_9$. These values were obtained from the slope of the linear portion of the solubilization curve, in which the amount of the solubilized dye is plotted against the concentration of the detergent, as has been described in a previous paper.[2] The saturation value of YW in a $C_{12}NCl$ or $C_{12}(EO)_9$ solution is quite high as compared with the other values. It has been shown from spectral study[2] that, in the $NaC_{12}S$ solution, the solubilization of YW occurs mainly in the hydrocarbon interior of the micelle, while in the $C_{12}(EO)_9$ solution it occurs in both the hydrocarbon core and the polyoxyethylene shell of the micelle. This explains the large value for YW in the $C_{12}(EO)_9$ solution. With YW in the $C_{12}NCl$ solution, the probable locus of solubilization is the surface of the micelle (otherwise, we can not explain such a large value).

Table 1. Saturation values of oil-soluble dyes in detergent solutions

Detergents	Saturation Values (g of dye/g of detergent $\times 10^3$)		
	YW	SB	AB
$NaCl_{12}S$	10.7	4.45	18.0
$C_{12}NCl$	67.8	5.00	10.7
$C_{12}(EO)_9$	52.9	4.34	5.90

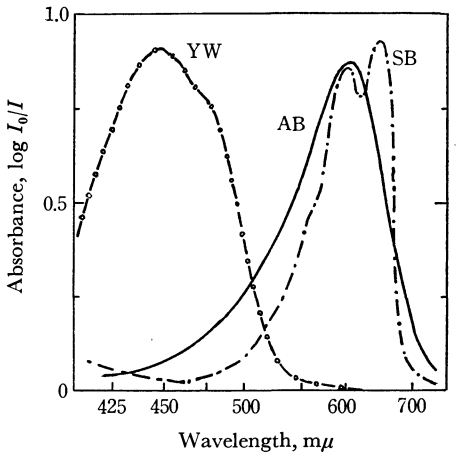

Fig. 1. The absorption spectra of YW, SB and AB in ethanol: concentration, approximately 1.7×10^{-3}%.

Successive Solubilization. The absorption spectrum of each of these three dyes in ethanol is shown in Fig. 1. The spectra indicate that each dye can be separately determined from its optical density in the presence of the other if YW-SB and YW-AB are chosen as the solubilizates.

Table 2 gives the saturation values of YW and SB in detergent solutions when they were solubilized step-by-step through the processes of YW→SB and SB→YW. In the YW→SB process, for example, YW is solubilized before SB; SB is solubilized after the saturation of YW. This table also gives the saturation values of YW and AB obtained through the YW→AB and AB→YW processes. When we compare the values shown in Table 2 with those in Table 1, we can see that the saturation value of each dye in any detergent solution is not very much influenced by the order of solubilization. For example, the YW once solubilized remains

Table 2. Saturation values of oil-soluble dyes by successive solubilization

Combination of Dyes	Order of Solubilization	Saturation Values (g of dye/g of detergent × 10^3)								
		In $NaC_{12}S$ Soln.			In $C_{12}NCl$ Soln.			In $C_{12}(EO)_9$ Soln.		
		YW	SB	AB	YW	SB	AB	YW	SB	AB
YW & SB	YW→SB	10.6	4.21	—	67.3	4.89	—	52.1	4.38	—
	SB→YW	10.6	4.38	—	68.4	4.76	—	52.9	4.54	—
YW & AB	YW→AB	10.9	—	17.4	69.2	—	10.7	53.6	—	5.75
	AB→YW	10.4	—	18.6	69.9	—	11.3	55.0	—	5.70

in the micelle after the solubilization of SB or AB; further, the saturation value of YW in the detergent solution containing solubilized SB or AB is roughly equal to the value in the same detergent solution containing no other dye. The following explanation seems plausible in according for this.

Let us assume that each dye, at least each of those examined here, has a specific locus of solubilization in the micelle where the dye is to be solubilized. With $NaC_{12}S$ and $C_{12}NCl$, the probable locus is the hydrocarbon interior and/or its charged surface, while with $C_{12}(EO)_9$ it is the hydrocarbon core and the polyoxyethylene shell of the micelle. If this is the case, the dye first solubilized in its own locus remains in the micelle without being influenced by the second dye, which will also be solubilized in the other locus irrespective of the presence of the first dye, as long as the solubilization is carried out step-by-step.

It is known that the addition of small amounts of long-chain alcohols or hydrocarbons to a detergent solution enhances the solubilization capacity of the detergent for oil-soluble dyes.[1,4] This has been ascribed to an increase in the space available to dye molecules by the penetration of the additive into the micelle. However, this type of solubilization is essentially different from the successive solubilization described here.

Simultaneous Solubilization. The solubilization of the mixture of two dyes, *e. g.*, YW and SB, or YW and AB, in detergent solutions was achieved by changing the mixing ratio from 0.2 to 4.0 by weight. However, reproducible saturation values could not be obtained for all of the three dyes, and the values are generally smaller, although in some cases they are larger, than those given in Table 1. As examples, typical results for the simultaneous solubilization of the mixture of YW and SB in the solutions of $NaC_{12}S$ and $C_{12}(EO)_9$ are shown in Fig. 2. In these two cases, the saturation

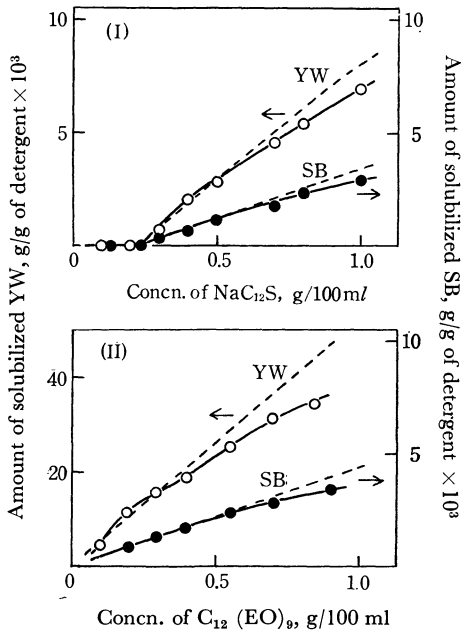

Fig. 2. The simultaneous solubilization of YW (○) and SB (●) mixed in a ratio of 1 : 1 in the solutions of $NaC_{12}S$ (I) and $C_{12}(EO)_9$ (II). The broken line indicates the solubilization curve for single YW or SB.

value of YW or SB at a fixed detergent concentration is neither constant nor reproducible, and the points given in Fig. 2 are only examples of scattered, observed values. The interpretation of these results is difficult at this stage. Probably, interactions between the two dyes, and between the micelles and the dyes in the process of solubilization, are related to the above phenomenon in a complicated way.

The author expresses his thanks to Dr. Hisahiro Kita for encouragement and permission to publish this paper.

4) See, *e.g.*, H. B. Klevens, *Chem. Rev.*, **47**, 1 (1950).

BULLETIN OF THE CHEMICAL SOCIETY OF JAPAN VOL. 43 942—943 (1970)

Kinetic Studies of the Graphitization Process. III. Stages of Graphitization Process

Michio INAGAKI,* Yoshio MURASE,* Hajime SAITO* and Tokiti NODA**

* *Faculty of Engineering, Nagoya University, Chikusa-ku, Nagoya*

** *Mie University, Tsu, Mie-ken*

(Received August 29, 1969)

The dependence of the graphitization degree of carbon on residence time has been studied by many authors.[1-13] However, the rate equations of graphitization have not been clarified. In the present work, the dependence of c_0-spacing on residence time was measured on a coke in a limited range of heat treatment temperature, and the results were discussed in relation to the stages of graphitization process.

The sample used was a polyvinylchloride coke (PV-7) calcined to 680°C and pulverized to particle size 0.4—1.2 mm. The sample was heat-treated at temperatures 1950, 2000, 2100, 2200, 2300 and 2400°C for various residence times under a reduced pressure of about 0.01 Torr. The details on the procedure of heat treatment were reported.[11] When a graphite heater was used for the heat treatment above 2000°C under reduced pressure, the wall of the heater became thin due mostly to evaporation, and partly probably to the oxidation of graphite. This reduced the stability of heat treatment temperature (HTT). Therefore, the long time run of heat treatment was carried out by the repetition of short time runs (mostly 60 min), by replacing the used heater with a new one each time. It was confirmed previously[11] that the repeated heat treatment has the same effect on the c_0-spacing of the carbon sample as the continuous one if the total residence time is equal in each case.

For each heat-treated sample, mean value of c_0-spacing was measured from (004) diffraction line by referring to the inner standard of silicon. Diffraction profile of the line was obtained by using Ni-filtered CuKα radiation and a recording goniometer with a Geiger counter.

The changes of c_0-spacing with total residence time at different HTT are shown in Fig. 1, by means of the plot of c_0-spacing against logarithm of residence time, log t. The rate of change of the c_0-spacing with residence time is found to increase at about 6.84 Å and decrease again at about 6.76 Å for every HTT. Thus, the dependence of

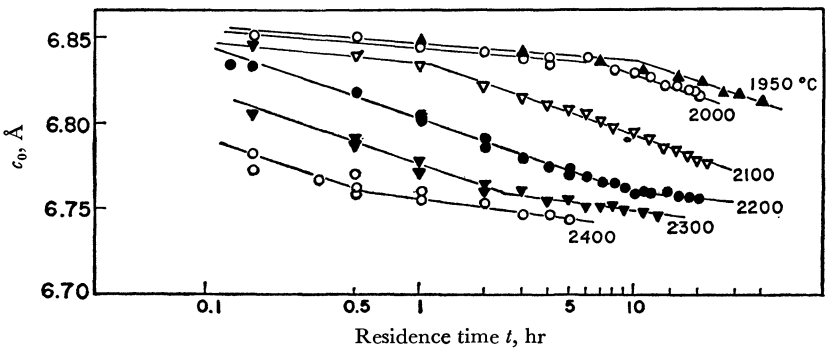

Fig. 1. The relation between c_0-spacing and logarithm of residence time.

1) A. Tarpinian and G. Tedmon, Tech, Rept. WAL TR 851.5/1 Watertown Arsenal Laboratories (1962).
2) F. V. Fair and F. M. Collins, "Proceedings of the Fifth Conference on Carbon," Vol. I Pergamon Press (1963), p. 503.
3) S. Mizushima, "*ibid.*," Vol. II (1963) p. 439.
4) D. B. Fischbach, *Nature*, **200**, 1281 (1963); *Appl. Phys. Lett.*, **3**, 168 (1963); *Tech. Rept.*, No 32—532, Jet Propulsion Laboratory (1966).
5) M. Mazza, *J. Chim. Phys.*, **61**, 721 (1964).
6) M. Mazza, H. Gasparoux and J. Amiell, *ibid.*, **61**, 729 (1964).
7) A. Forchioni, F. Boisard and P. Delhaes, *ibid.*, **61**, 1289 (1964).
8) T. Noda, M. Inagaki and T. Sekiya, *Carbon*, **3**, 175 (1965).
9) A. Pacault and H. Gasparoux, *C. R. Acad. Sci., Paris, Ser. C* **264**, 1160 (1967).
10) A. Pacault, A. Marchand, H. Gasparoux and S. Flandrois, *ibid.*, **260**, 4999 (1965).
11) M. Inagaki, Y. Murase and T. Noda, *Yogyo Kyokai Shi*, **76**, 184 (1968).
12) V. I. Kasatochikin and A. T. Kaberov, *Dokl. Akad. Nauk. SSSR*, **117**, 837 (1957).
13) E. Wege, *Ber. Deut. Keram. Ges.*, **43**, 224 (1966).

c_0 on log t can be divided into three stages, *i. e.*, $c_0>6.84$, $6.84>c_0>6.76$, and $6.76\,\text{Å}>c_0$. In the stage $6.84>c_0>6.76$ Å, the c_0-spacing seems to decrease linearly with logarithm of residence time, and the lines for every HTT are parallel to each other.

The superimposing method[4] can be applied to the present result, and the amount of shifting is determined more accurately. The effective activation energy obtained was 200 kcal/mol which was close to those obtained in previous works.[8,9,11] The dependence of c_0 on residence time t in the stage $6.84>c_0>6.76$ Å is expressed by the equation

$$c_0 - c_0^0 = \beta \log (t/t_0),$$

where c_0^0 is a constant independent of HTT, β the slope of the line shown in Fig. 1 and t_0 is the value of t for $c_0=c_0^0$. t_0 corresponds to the amount of shift in the superimposing method.

In the figures of c_0 *vs.* log t, the linear relation between c_0 and log t can be found only in a small range of c_0.[4,8,9,11] A pyrolytic carbon reported by Fischbach[4] showed a linear dependence of c_0 on log t in the range 6.82—6.73 Å.

The same data were analysed by the method proposed by Murty *et al.*[14] The relations obtained between $\log\{(6.910-c_0)/t\}$ and $\log(6.910-c_0)$ are shown in Fig. 2, where the value of 6.910 Å is the

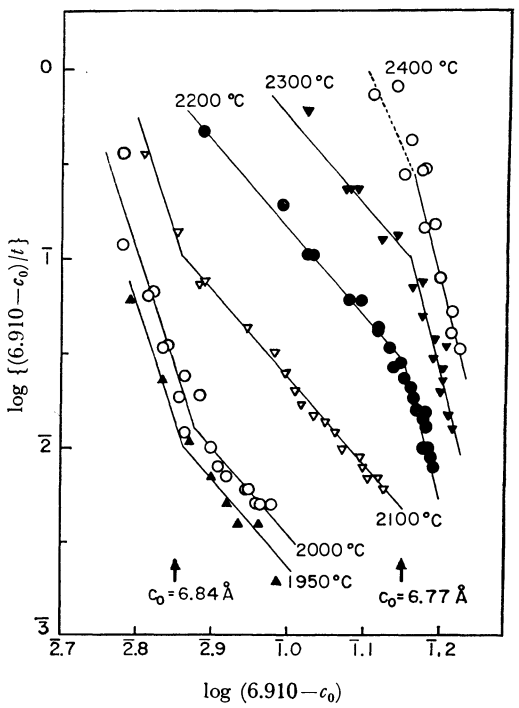

Fig. 2. The relation between $\log\{(6.910-c_0)/t\}$ and $\log(6.910-c_0)$.

14) H. N. Murty, D. L. Biederman and E. A. Heintz, *J. Phys. Chem.*, **72**, 746 (1968).

c_0-value of the original sample PV-7. In this case, the relation between $\log\{(6.910-c_0)/t\}$ and $\log(6.910-c_0)$ seems also to be linear. However, it appears to break at the c_0-values 6.84 and 6.77 Å. The lines are nearly parallel to each other in the range $6.84>c_0>6.77$ Å. The dependence of c_0 on t can be expressed by

$$(6.910-c_0) = A\cdot t^n.$$

The value of n was obtained as 0.18 from the slope of these lines, and the activation energy of 200 kcal/mol was obtained from the linear dependence of intercept of the lines on HTT.

For the stages, *i. e.*, $c_0>6.84$ and $6.76\,\text{Å}>c_0$, no details on the residence time dependence of c_0-spacing could be discussed, because of insufficient data.

From the results, the graphitization process of soft carbon can be concluded to consist of three successive stages, $c_0>6.84$, $6.84>c_0>6.76$, and $6.76\,\text{Å}>c_0$. In the second stage, the change of c_0 from 6.84 to 6.76 Å is fairly large, though the corresponding range of HTT is narrow as 1950—2400°C.

The dividing of the graphitization process at c_0-spacing of about 6.85 Å is consistent with the results of other authors. Kuroda[15] has shown, by means of electron microscopy, that above 1850°C (below the c_0-spacing 6.85 Å in the petroleum coke) c-axes of crystallites align parallel to the normal of the grain. Mazza,[5] Mazza *et al.*,[6] and Forchioni *et al.*[7] have studied the development of the properties, including X-ray parameters, and shown that the graphitization process is divided into two stages, below HTT of 1900°C and above 1900°C (corresponding to the c_0-spacing 6.84 Å in the pitch coke). Inagaki *et al.*[16,17] have reached almost the same conclusion as that of Mazza *et al.*[6] on a petroleum coke and a polyvinylchloride coke from X-ray parameters. The main structural change in the first stage is the development of two-dimensional graphite-like layers. In relation to this stage, Inagaki[18] has proposed the idea of dewrinkling of carbon layers.

The dividing of the graphitization process around 6.76 Å has been reported only by Maire and Mering.[19] They have shown by Fourier analysis of (00l) diffraction lines that below the g-value of about 0.6 (above 6.77 Å in c_0-spacing), the crystallite size L_C increases and above 0.6 the strain decreases with graphitization.

15) H. Kuroda, This Bulletin, **32**, 728 (1959).
16) M. Inagaki, *Tanso*, **1968**, (No. 53) 61.
17) M. Inagaki, Y. Murase and T. Noda, *ibid.*, **1968** (No. 54) 80.
18) M. Inagaki, This Bulletin, **42**, 2371 (1969).
19) J. Maire and J. Mering, "Proceedings of the Fourth Conference on Carbon," Pergamon Press (1959), p. 345.

BULLETIN OF THE CHEMICAL SOCIETY OF JAPAN VOL. 43 944—945 (1970)

Photolysis of *meta*-Disubstituted Benzenes in Low Temperature Matrices

Akio EGAWA, Katsumi KIMURA[1] and Hiroshi TSUBOMURA

Department of Chemistry, Faculty of Engineering Science, Osaka University, Toyonaka, Osaka

(Received September 4, 1969)

Photolysis of *para*-disubstituted benzenes in low temperature matrices has been studied extensively in our laboratory.[2] It has been concluded that photo-ionization occurs predominantly for the compounds having amino-substituents, and the β-fission in the side-chain occurs predominatly for the compounds having hydroxyl or methoxyl groups. In the present note, studies on the photolysis of *m*-aminophenol, *m*-phenylenediamine, *m*-anisidine and *m*-methoxyphenol are reported.

Organic solvents used as transparent matrices are ethanol, EPA (ether-isopentane-ethanol, 5 : 5 : 2 by volume), EP (ether-isopentane, 1 : 1), EM (ether-methylcyclohexane, 1 : 1), and MP (methylcyclohexane-isopentane, 1 : 3). Approximately 8 m*l* of a 1×10^{-4}M solution was put into a quartz cell of 1 cm path length, degassed by the freeze-pump-thaw technique, and the cell was sealed. The transparent samples in liquid nitrogen contained in a quartz Dewar were illuminated for 20—60 sec using a 250 W high-pressure mercury lamp and appropriate filter combinations.

Assignment of the Species Formed by the Photolysis Electronic absorption spectra of free radicals formed by ultraviolet irradiation of *m*-aminophenol are shown in Fig. 1a (region B). It is concluded that the products are cation radicals by reasons similar to those discussed in Ref. 1, that is to say: (1) When biphenyl, as an electron acceptor, was added to the EPA solution of *m*-aminophenol irradiated at 77°K, the absorption spectrum of biphenyl anion appeared together with the cation spectrum. (2) The absorption spectrum was obtained by irradiation in polar solvents, but not in non-polar solvents. (3) By irradiation in the infrared region or by heating the photo-product, luminescence attributable to the recombination of cation radicals and ejected electrons was observed.

By the similar reasons to those for the case of *m*-aminophenol, it has been concluded that the products of photolysis of *m*-phenylenediamine and *m*-anisidine at 77°K are assigned to their cation radicals. For the case of *m*-phenylenediamine irradiated at 77°K a spectrum (from 420 to 490 mμ) appeared at first which is undoubtedly attributable to the cation radical. On prolonged irradiation, the spectrum in this region gradually weakened and after irradiation for 15 min, a new spectrum began to appear in the region from 330 to 350 mμ. At least a large part of this new spectrum remained after warming to room temperature, and hence seems to be due to a permanent dissociation product.

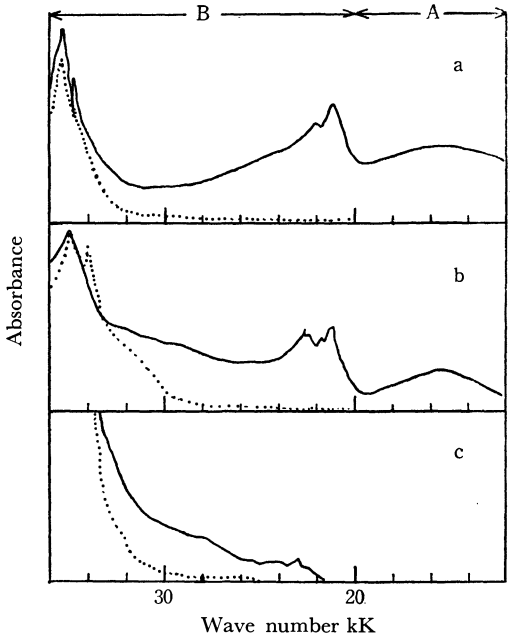

Fig. 1. Electronic absorption spectra of free radicals (region B) and solvated electrons (region A).
The dotted line shows the spectrum before UV irradiation. a, *m*-aminophenol. b, *m*-aminophenol in an alkaline EPA solution. c, *m*-methnoxyphenol.

The irradiation of *m*-aminophenolate anion in alkaline EPA solution caused a spectrum shown in Region B of Fig. 1b. The product has been assigned to the radical $H_2NC_6H_4O\cdot$ by the similar reasons as those described in a previous paper.[2] For *m*-methoxyphenol, it has been concluded by the following reasons that the irradiation yielded the neutral radical, $H_3COC_6H_4O\cdot$, whose spectrum is shown in Fig. 1c.: (1) The radical was produced even in a non-polar solvent, MP. (2) The broad absorption spectrum of the solvated electron did not appear in the near infrared region. (3) Even if biphenyl was added to the MP solution of *m*-

1) Present address: Research Institute of Applied Electricity, Hokkaido University, Sapporo.

2) K. Kimura, K. Yoshinaga and H. Tsubomura, *J. Phys. Chem.*, **71**, 4485 (1967).

methoxyphenol, the absorption bands of biphenyl anion did not appear. (4) The shape of the absorption spectrum is similar to that of *m*-benzosemiquinone radical, $HOC_6H_4O\cdot$, obtained by Land and Porter using flash photolysis.[3]

Solvated Electron Spectra. When *m*-aminophenol in various organic matrices is irradiated at 77°K in the ultraviolet region using a Toshiba UV-D25 glass filter which transmits light from 275 to 370 mμ and from 700 to 750 mμ, the matrix colored yellow owing to the formation of cation radicals. On the other hand, when a Toshiba UV-D25 filter was combined with an aqueous nickel sulfate (transmitting light from 275 to 370 mμ), the matrix colored bluish yellow. The absorption spectrum is shown in Fig. 1a, and the broad absorption band in the near infrared region (region A) can be attributable to the solvated electrons by the following reasons: (1) The sample showed a very feeble afterglow at 77°K to dark-adapted eye. It also showed emission stimulated by the infrared light or by warming. The luminescence spectra was found to correspond to the fluorescence and phosphorescence of *m*-aminophenol. (2) The intensity of the broad absorption band in the near infrared region decreased by the infrared irradiation of the sample. (3) The absorption maximum in the near infrared region shifts to the shorter wavelength as the solvent becomes more polar (Fig. 2). The similar shift was observed by Dorfman and his co-workers for the spectra of solvated electrons obtained by pulse-radiolysis.[4] For *m*-phenylenediamine and *m*-anisidine, similar absorption spectra of solvated electrons are also observed.

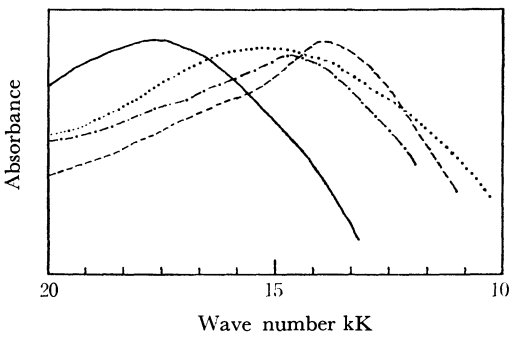

Fig. 2. Electronic absorption spectra of solvated electrons formed by UV irradiation of *m*-aminophenol in various solvents.
——— ethanol, ····· EPA, ------ EP, —·—· EM

Albrecht states that the great majority of electrons photoejected from TMPD have a very limited range in rigid 3-methyl pentane, each electron finding a matrix trap within the coulomb field of its partner TMPD cation radical.[5] In our results, it may also be concluded that the solvated electrons are under the influence of the cation radicals since a small but definite shift of the absorption maxima is observed for different cation radicals (Fig. 3).

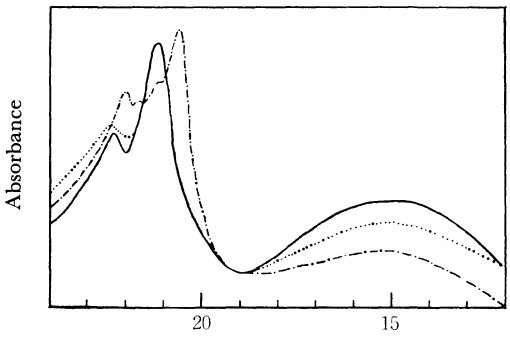

Fig. 3. Electronic absorption spectra of solvated electrons formed by UV irradiation of *m*-aminophenol (———), *m*-anisidine (·····), and *m*-phenylenediamine (—·—·).

It has been reported by McClain and Albrecht that TMPD cation radicals cannot be bleached perfectly by infrared irradiation in 3-MP at 77°K, and some more energetic photons (385 mμ) did bleach some of the $TMPD^+$ remaining after the infrared effect was exhausted.[5] They concluded that the incompleteness of the IR bleaching was due to very deep trapping of some of the electrons. However, in our work the broad absorption band of solvated electrons (300—800 mμ) disappeared completely by irradiation with red light (wavelengths longer than 600 mμ). The intensity of the absorption spectrum of the cation radicals decreased only slightly. This decrease was still more slight in the solvents containing ethanol. From these facts, the following conclusion may be drawn: The traps of the solvated electrons are not very deep, but rather shallow. A small part of the electrons stimulated by irradiation recombine with cation radicals and the remaining part of them react with impurities or with the solvent itself, especially with ethanol.

3) E. J. Land and G. Porter, *Trans. Faraday Soc.*, **59**, 2016 (1963).

4) M. C. Sauer, Jr., S. Arai and L. M. Dorfman, *J. Chem. Phys.*, **42**, 708 (1964). I. A. Taub, M. C. Sauer, Jr., and L. M. Dorfman, *Discuss. Faraday Soc.*, **No. 36**, 206 (1963). I. A. Taub, D. A. Harter, M. C. Sauer, Jr., and L. M. Dorfman, *J. Chem. Phys.*, **41**, 979 (1964).

5) W. M. McClain and A. C. Albrecht, *J. Chem. Soc.*, **44**, 1594 (1966).

BULLETIN OF THE CHEMICAL SOCIETY OF JAPAN VOL. 43 946—947 (1970)

The Non-sensitized Photoreaction of Azoxybenzene

Masaaki IWATA and Sakae EMOTO

The Institute of Physical and Chemical Research, Yamato-machi, Kita-Adachi-gun, Saitama

(Received September 5, 1969)

Since Knipscheer[1] reported the photochemical rearrangement of azoxybenzene to 2-hydroxyazobenzene, its rearrangement has been postulated to be intramolecular[2] and, by means of tracer methods, this postulation has been confirmed.[3-5] Through a recent study of the photoreduction of azoxybenzene, Tanikaga concluded that the irradiation of azoxybenzene without benzophenone as a sensitizer never affords azobenzene in an ethanol solution and, thus, that azobenzene is formed from an excited triplet state of azoxybenzene,[6] while the rearrangement product of azoxybenzene and its isomerization product are formed through an excited singlet state of *trans*-azoxybenzene.[7] This paper will describe some different results from Tanikaga's photoreduction product of azoxybenzene and the overlooked irradiation product.

trans-Azoxybenzene was irradiated with a high-pressure mercury lamp in a chloroform (fairly concentrated) solution at room temperature for 113 hr. After the removal of the solvent under mild conditions, the irradiated mixture was chromatographed on silica gel by elution with benzene. In the column, the mixture showed at least eight colored adsorption bands. These components were designated as A, B, C, D, E, F, G, and H in their order of separation. After the removal of the solvent under reduced pressure, petroleum ether was added to each fraction, if possible, in order to crystallize it. Of these eight components, A, B, and G were obtained in a crystalline form. Then high-resolution mass spectroscopic measurements were made of all of these components. The mass spectra of both the products A and F showed a parent peak at 182 *m/e*, a base peak at 77 *m/e*, and similar fragmentational patterns between these peaks in each fragment. Exact mass measurements showed that both A and F had the molecular formula of $C_{12}H_{10}N_2$. On the basis of these results, and also their IR spectra and melting points, the products A and F were deduced to be *trans*- and *cis*-azobenzene respectively, as a similar phenomenon appeared when the mixture of *trans*- and *cis*-azoxybenzene was chromatographed; the former was eluted faster than the latter by benzene. Product B, the main product, was shown to be 2-hydroxyazobenzene from its mass spectral fragmentational pattern, its exact mass measurement (molecular formula, $C_{12}H_{10}N_2O$), its IR spectrum, and its melting point. Product G was postulated to be 4-hydroxyazobenzene on the basis of its melting point and its fragmentational pattern in the mass spectrum, which was extremely analogous to that of the product B. From these two spectra, the relatively intensive fragment, 121*m/e*, could be used to distinguish hydroxyazobenzene from azoxy-[8] and azobenzene. Fraction C was the starting material. For the other products, D, E, and H, the structural analyses attempted using by the method of mass spectroscopic analysis and exact mass measurements were unsuccessful because of impurities present in each case.

In our experimental results, it is interesting that we detected the reductive formation of azobenzene from azoxybenzene and the production of 4-hydroxyazobenzene which results from the unusual photochemical rearrangement of azoxybenzene. First, the formation of azobenzene without a sensitizer leads us to suggest that this may be due to the solvent effect or to the yield of azobenzene being detectable only in a large-scale experiment. Recent studies have progressively clarified the solvent effects on the photochemical pathway;[9] however, more information is required before we can decide that the difference in results between Tanikaga's and ours are due only to the solvent effect. Now, it seems better to consider that the formation of azobenzene had been overlooked because of its low yield. This may also be true for the formation of 4-hydroxyazobenzene. This compound is a well-known Wallach rearrangement

1) H. M. Knipscheer, *Rec. Trav. Chim.*, **22**, 14 (1903).
2) G. M. Badger and R. G. Buttery, *J. Chem. Soc.*, **1954**, 2243.
3) M. M. Shemyakin, V. J. Maimind and B. K. Vachichunaite, *Chem. & Ind.*, **1958**, 755.
4) M. M. Shemyakin, T. E. Agadzhanyan, V. J. Maimind, R. V. Kudryavtsev, and D. N. Kursanov, *Dokl. Akad. Nauk. SSSR.*, **135**, 346 (1960).
5) S. Oae, T. Fukumoto and M. Yamagami, This Bulletin, **34**, 1873 (1961), and *ibid.*, **36**, 601 (1963).
6) R. Tanikaga, *ibid.*, **41**, 1664 (1968).
7) R. Tanikaga, *ibid.*, **41**, 2151 (1968).
8) J. H. Bowie, R. G. Cooks and G. E. Lewis, *Aust. J. Chem.*, **20**, 1601 (1967).
9) About this see the most recent review; T. Matsuura, *Kagaku no Ryoiki*, **23**, (7) 653 (1969).

product of azoxybenzene[10] upon heating with concentrated sulfuric acid. The photochemical mechanism of its formation suggests that it might be accompanied by an intermolecular reaction or a solvated oxygen atom, one which comes from the reduction of azoxybenzene, with its photoreaction to the extent that azobenzene is produced.

Experimental

As the light source, a UVL-100p (Rikoh Kagaku Co., Ltd.) high-pressure mercury lamp was used; mass spectra and exact mass measurements were performed and measured by means of a JMS-OlSG (Japan Electron Optics Lab.) double-beam focused high-resolution mass spectrometer with an ionizing voltage of 75 eV. The mp's are uncorrected.

Irradiation of Azoxybenzene. The azoxybenzene (Tokyo Kasei, once chromatographed on silica gel before use) (2 g) was dissolved in 25 m*l* of chloroform, sealed in an Erlenmeyer flask, and then irradiated with the lamp for 113 hr at room temperature. After the removal of the solvent under reduced pressure, the mixture was chromatographed on silical gel (Kieselgel, 7734, Merck); upon elution with about 3 *l* of benzene, the eight components described above were separated in aliphabetical order. The yields (in weight) were 6 mg for A, 79.8 mg for B, 1.8 g for C, 3.0 mg for D, 2.08 mg for E, 2.18 mg for F, and 2.68 mg for G (H was not weighed, but it appeared to be almost the same amount as E.).

Product A showed IR absorption bands at 690, 770, 920, 1018, 1065, 1150, 1220, 1300, 1456, 1480, 1580, 1700—2000, and 3030 cm^{-1} (KBr) and fragments in the mass spectrum (relative abundance) at 182 (96.2), 154 (2.9), 105(20.8), and 77(100)*m/e*, and it melted at 67.0—67.5°C (rhombic). These data and exact mass measurements supported the idea that this was azobenzene.

Product B showed IR absorption bands at 670, 750, 760, 805, 910, 930, 990, 1010, 1020, 1060, 1100, 1140, 1180, 1210, 1240, 1280, 1305, 1310, 1360, 1410, 1455, 1485, 1530, 1550, 1595, 1700—2000, and 3030 cm^{-1} (KBr) and fragments in mass spectrum (relative abundance) at 198(100), 121(13.3), 105(4.7), 93(21.7), and 77(37.4)*m/e*, and it melted at 83.5—84.0°C (needles). These data and exact mass measurement supported the idea that this was 2-hydroxyazobenzene.

Product F showed almost the same IR spectrum as A, and its mass spectral fragmentational pattern was quite coincident with that of A. Thus, it was deduced to be a isomer of A, that is, *cis*-azobenzene. Product G melted at 131.8—132.1°C (orange prisms), and its mass spectrum had almost the same characteristic fragments for hydroxyazobenzene as B. Therefore, this may be deduced to be a isomer of B, that is, 4-hydroxyazobenzene. Component C was the starting material; for the other products, D, E, and H, the structural analyses were unsuccessful for the reason presented above.

10) O. Wallach and L. Belli, *Ber.*, **13**, 525 (1880).

BULLETIN OF THE CHEMICAL SOCIETY OF JAPAN VOL. 43 947—950 (1970)

The Reaction of *o*-Lithio-*N*,*N*-dimethylbenzylamine with Metal Carbonyls

Ilsong RHEE, Yoshikazu HIROTA, Membo RYANG and Shigeru TSUTSUMI

Department of Chemical Technology, Faculty of Engineering, Osaka University
Yamadakami, Suita, Osaka

(Received September 6, 1969)

We have previously reported that lithium aroyl or acylmetal carbonylates, $Li[RCOM(CO)_n]$ (M= Ni, Fe), are formed as intermediates in the reaction of organolithium compounds with mononuclear metal carbonyls at low temperature (−50—−70°C). Fischer and Maasböl[1] have also described the formation of lithium benzoylmetal pentacarbonylate by the reaction of phenyllithium with metal hexacarbonyl (metal=Cr, Mo and W); they also revealed that these carbonylates are stable mononuclear-transition metal carbene complexes.

Although an attempt to isolate the pure complexes of the corresponding nickel or iron carbonylate was unsuccessful, their synthetic applications were investigated since lithium aroyl or acylmetal carbonylates showed useful reactivities in organic reactions. However, the nickel complexes showed different reaction behavior from the iron or the Group VI transition metal complexes. For example, lithium aroylnickel carbonylate gave acyloins by hydrolysis,[2] 1,4-diketones by reaction with acetylenes,[3] and α-diketones by thermal decomposition[4] (Eq. 1), while lithium aroyl or acylmetal carbonylates (metal=Fe,[5a] Cr, Mo and W[5b]) gave alde-

1) E. O. Fischer and A. Maasböl, *Angew. Chem.*, **76**, 645 (1964); *Chem. Ber.*, **100**, 2445 (1967).

2) M. Ryang, K-M. Song, Y. Sawa and S. Tsutsumi, *J. Organometal. Chem.*, **5**, 305 (1966).

3) Y. Sawa, I. Hashimoto, M. Ryang and S. Tsutsumi, *J. Org. Chem.*, **33**, 2159 (1968).

4) K-M. Song, Y. Sawa, M. Ryang and S. Tsutsumi, This Bulletin, **38**, 330 (1965).

5) a) M. Ryang, I. Rhee and S. Tsutsumi, *ibid.*, **37**, 341 (1964). b) E. O. Fischer and A. Massböl, German Pat. 1214233 (1966).

hydes in good yields by hydrolysis, but did not give 1,4-diketones from the reaction with acetylenes.[3]

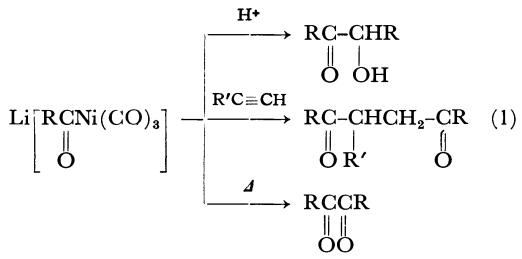

Furthermore, lithium aroylnickel carbonylates gave acyloins by a reaction with benzyl bromide and en-diol-diesters by a reaction with benzoyl chloride (Eq. 2), whereas lithium aroyliron carbonylates yielded ketones[6] (Eq. 3).

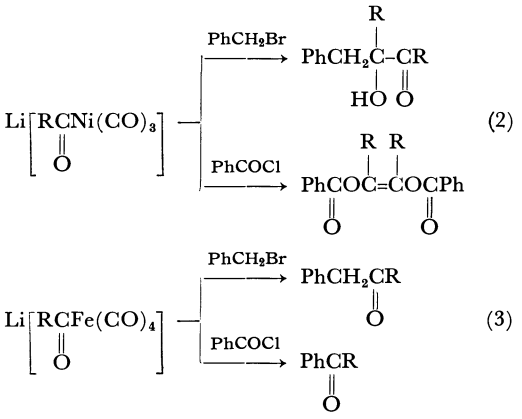

The above results suggest that lithium aroylnickel and -iron carbonylates behave toward various reagents as if the former is a dinuclear, and the latter, a mononuclear complex, for two aroyl or acyl groups are introduced into the products in the case of the nickel complex and one aroyl or acyl group in the case of the iron complex, although the relationship between the structure of the intermediate and the products has not yet been established. Furthermore, it has been reported that the mononuclear iron carbonylate anion exists, but no mononuclear nickel carbonylate anion exists.[7] These results provide one suggestion regarding the structure of the present nickel complexes.

Hereupon, it was considered to be probable that when a nitrogen-containing substituent which has a coordinating ability with the transition metal is present at the *ortho* position of phenyllithium, the nickel carbonylate would also behave as a mononuclear intermediate complex similar to iron carbonylate. In this paper, we wish to report on our study of the reactions of lithium-*o*-*N*,*N*-dimethylaminomethyl phenylmetal (iron or nickel) carbonylates with such organic halides as benzyl bromide or benzoyl chloride and the decomposition of the carbonylates with an iodine-methanol solution.

Results and Discussion

In general, alkyl or aryllithium is very reactive toward nickel carbonyl and the reaction proceeds exothermically even at −70°C, but the reaction of *o*-lithio-*N*,*N*-dimethylbenzylamine[8] with nickel carbonyl took place at −20°C. After stirring had been continued for 10 hr, organic halide was added and the mixture was stirred at 12°C for 2 hr. The resulting reaction mixture was treated and the products were isolated by ordinary methods; the results are summarized in Table 1.

Table 1. The reactions of *o*-lithio-*N*,*N*-dimethylbenzylamine with organic halide and iodine–methanol

	Li[RCOFe(CO)$_n$]		Li[RCONi(CO)$_m$]*	
$PhCH_2Br$	I	II	I	II
	26.7%**	trace	5.0%	11.1%
PhCOCl	III		III	
	12.6%		27.2%	
I_2/CH_3OH	IV		IV	
	18.1%		5.2%	

* R=*o*-*N*,*N*-dimethylaminomethylphenyl.

** All the yields in this paper are based on the *N*,*N*-dimethylbenzylamine used. Unreacted *N*,*N*-dimethylbenzylamine was recovered, while the high-boiling residue formed in these reactions was not examined.

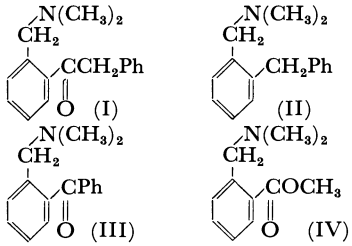

As may be seen in Table 1, the same products are formed in the cases of both nickel and iron, although the yields of the products are low, while such results have not yet been observed from the reaction of nickel carbonyl with aryllithium which does not contain an amino group at the *ortho* position. Consequently, it may be considered that the structure of the nickel complex becomes similar to that of the iron complex by an intramolecular

6) Y. Sawa, M. Ryang and S. Tsutsumi, unpublished work.

7) H. Wakamatsu, "Organometallic Chemistry," Kagaku Dojin, Japan (1966), p. 107.

8) A. C. Cope, *J. Organometal. Chem.*, **8**, 531 (1967).

coordination of the nitrogen to the nickel atom; that is, a mononuclear nickel carbonylate complex will be formed.

Cope[8] has reported that the stable carbon-cobalt σ-bonding complex was isolated from the reaction of cobalt dichloride with *o*-lithio-*N*,*N*-dimethylbenzylamine. However, cobalt dichloride reacts with phenyllithium or phenylmagnesium bromide to give an unstable diphenylcobalt, which then decomposes to form biphenyl above $-20°C$.[9]

In an attempt to isolate the intermediate nickel complex which would be stabilized by the coordination of nitrogen, a white solid was obtained after the solvent had been removed under nitrogen, but the structure has not yet been determined. Although the structures of the intermediates are not clear, the present reaction may be considered to proceed according to the following paths;

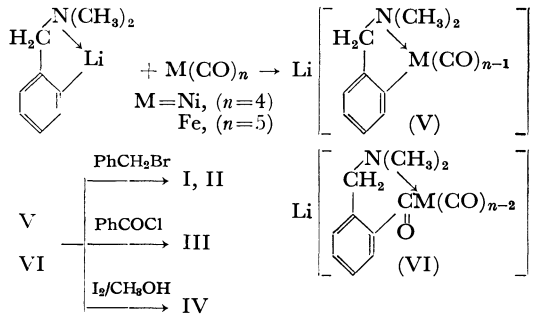

Namely, in the reaction with benzyl bromide (V) and (VI) react to give ketone (I) and coupling product (II), and in the reaction with benzoyl chloride to give ketone (III) (α-diketone was not detected), although it is not evident whether the carbonyl group in ketone came from benzoyl chloride or from (VI). In the reaction with an iodine-methanol solution, (VI) reacts first with iodine; methanolysis then gives the ester (IV).

Fischer and Kiener[10] have recently reported that a dinuclear iron complex was isolated from the reaction of lithium aroyliron carbonylate with trityl chloride. However, the complex isolated does not necessarily reflect the precise structure of the proceeding anionic complex, since the possibility can not be completely neglected that the oxidation of the anionic mononuclear complex with trityl chloride results in the dimerization of the neutral complex thus produced.

The structures of the synthetically useful anionic complexes of iron and nickel are still open to question, and the relationship between the structure of a complex and its reactivity is one of the most interesting problems in organic synthesis using metal carbonyls.

Experimental

The *N*,*N*-dimethylbenzylamine, benzyl bromide, and benzoyl chloride used were obtained by the purification of commercial reagents by fractional distillation. A hexane solution of *n*-butyllithium was used without purification. The diethyl ether was dried over sodium wire, and all the reactions were carried out under a dry argon atomosphere.

a) The Reaction of Benzyl Bromide with Lithium *o*-*N*,*N*-dimethylaminomethylphenylmetal Carbonylate. *N*,*N*-dimethylbenzylamine (0.04 mol) was added to *n*-butyllithium (0.048 mol) in *n*-hexane (60 m*l*), and then the mixture was refluxed for 16 hr. The reaction mixture thus changed from a colorless solution to a suspension of a white solid of *o*-lithio-*N*,*N*-dimethylbenzylamine. The ether solution (60 m*l*) of iron pentacarbonyl (0.04 mol) was added to the mixture at $-50°C$, and the reaction mixture was stirred for 10 hr at $-20°C$; the color of the mixture thus changed from orange-red to red-brown. After the addition of the ether solution (15 m*l*) of benzyl bromide (0.04 mol), the reaction was carried out at an elevated temperature (12°C) for 2 hr, after which the reaction mixture was separated into a benzene-soluble and a benzene-insoluble part. The benzene solution was distilled under reduced pressure to give the following fractions: (1) bp~120°C (1.0 mmHg), 1.3 g; (2) bp 140°C (1.0 mmHg), a trace, and (3) bp 150°C (1.0 mmHg), 2.7 g. Fraction (1) was found by vpc analysis to be a mixture of the following materials: bibenzyl (0.4 g, 11.0%) and dibenzyl ketone (0.8 g, 19.2%) [Column, S. E. 30, 2.25 m; column temperature, 230°C; flow rate of carrier gas (helium), 7 m*l*/min; flame ionization detecter; retention time, 4.8 and 9.7 min]. Fraction (2) was identified as *o*-benzyl-*N*,*N*-dimethylbenzylamine on the basis of the following data: Found: C, 85.28; H, 8.50%. Calcd for $C_{16}H_{19}N$: C, 85.04; H, 8.77%. NMR (τ): 7.90 (6H, singlet), 6.80 (2H, singlet), 5.91 (2H, singlet) and 2.95 (9H, multiplet). Mass (m^+/e): 225. IR: ν_{NCH} 2800 cm^{-1}. Fraction (3) was confirmed to be *o*-*N*,*N*-dimethylaminomethylphenyl benzyl ketone (26.7%); Found: C, 80.33; H, 7.73%. Calcd for $C_{17}H_{19}ON$: C, 80.57; H, 7.56%. NMR (τ): 7.83 (6H, singlet), 6.41 (2H, singlet), 5.86 (2H, singlet) and 2.73 (9H, multiplet). Mass (m^+/e): 253. IR ν_{CO} 1700, ν_{NCH} 2800 cm^{-1}.

In the case of nickel carbonyl, the reaction and treatment were carried out by a method similar to that described in the case of iron pentacarbonyl. The benzene solution was distilled under reduced pressure to give the following materials: *o*-*N*,*N*-dimethylaminomethylphenyl benzyl ketone (0.5 g, 5.0%), *o*-benzyl-*N*,*N*-dimethylbenzylamine (1.0 g, 11.1%), bibenzyl (1.1 g, 30.2%) and dibenzyl ketone (0.2 g, 4.8%).

b) The Reaction of Benzoyl Chloride with Lithium *o*-*N*,*N*-dimethylaminomethylphenylmetal Carbonylate. The reaction and treatment were similar to those described in (a). In the case of iron pentacarbonyl, the following fraction was given by distillation under reduced pressure: bp 113°C (1.0 mmHg), 1.2 g (12.6%). This material was confirmed to be *o*-*N*,*N*-dimethylaminomethyl benzophenone: Found: C, 80.13;

9) M. Ryang, K. Yoshida, H. Yokoo and S. Tsutsumi, This Bulletin, **38**, 636 (1965).

10) E. O. Fischer and V. Kiener, *Chem. Commun.*, **1968**, 1378.

H, 7.25%. Calcd for $C_{16}H_{17}ON$: C, 80.30; H, 7.16%. NMR (τ): 8.08 (6H, singlet), 6.61 (2H, singlet), and 2.67 (9H, multiplet). Mass (m^+/e): 239. IR :ν_{CO} 1670, ν_{NCH} 2800 cm^{-1}.

In the case of nickel carbonyl, *o-N,N*-dimethylaminomethyl benzophenone was given in a yield of 27.2%. The reaction of benzoyl chloride with *N,N*-dimethylbenzylamine under these conditions as well as those described above did not give that ketone.

c) The Reaction of Iodine-methanol Solution with Lithium *o-N,N*-dimethylaminomethylphenylmetal Carbonylate. An iodine-methanol solution (11 g/50 m*l*) was added to lithium *o-N,N*-dimethylaminomethylphenyliron carbonylate, which had been prepared in the manner described in (a) at −20°C. Stirring was continued for 4 hr at room temperature, followed by refluxing for 3 hr. The benzene-soluble part obtained by the ordinary method was distilled under reduced pressure to give the following fraction: bp 105°C (13 mmHg), 1.4 g. The fraction was identified as methyl *o-N,N*-dimethylaminomethylbenzoate (18.1%): Found: C, 68.21; H, 7.80; N, 7.20%. Calcd for $C_{11}H_{15}NO_2$: C, 68.37; H, 7.82; N, 7.25%. NMR (τ): 7.81 (6H, singlet), 6.32 (2H, singlet), 6.17 (3H, singlet) and 2.56 (4H, multiplet). Mass (m^+/e): 193. IR: ν_{CO} 1740, ν_{COC} 1280, 1130 and ν_{NCH} 2800 cm^{-1}.

In the case of nickel carbonyl, methyl *o-N,N*-dimethylaminomethylbenzoate was obtained in a yield of 5.2%.

BULLETIN OF THE CHEMICAL SOCIETY OF JAPAN VOL. 43 950—952 (1970)

Amylose-Iodine Complex. V. An Estimation of Number of Anhydroglucose Units of Helical Segments in Amylose-Iodine Complex*1

Takehiko WATANABE, Kozo OGAWA*2 and Sôzaburo ONO

Laboratory of Biophysical Chemistry, College of Agriculture, University of Osaka Prefecture, Sakai

(Received September 9, 1969)

The amylose molecules in neutral or acidic aqueous solution would take a conformation of deformed helix;[1-5] the individual helical segments are connected by random segments. The dissolved amylose-iodine complex has a similar structure as stated above, *i. e.* a single amylose molecule contains more than one independent polyiodine chains. According to Szejtli *et al.*[5] the number of anhydroglucose units composing the helical segment was about 120 which was obtained from the study of the correlation between the degree of polymerization of amylose molecule and the iodine-binding capacity or the wavelength of the maximum absorption peak of amylose-iodine complex.

In the present paper, the number of anhydroglucose units per helical segment was estimated from spectrophotometric measurement of the change in the absorbance at 288, 352 and 630—660 mμ with addition of amylose to iodide-iodine solution.

Experimental

The amylose subfraction used is the one described in the previous report[4], having viscosity-average molecular weight ($\bar{M}_v$) 1×10^6 calculated from limiting viscosity number, $[\eta]$ (ml/g) in dimethyl sulfoxide at 25°C, using the following equation proposed by Everett and Foster[6], $[\eta]=3.06\times10^{-2}\ \bar{M}_v^{0.64}$.

The spectrophotometric measurements were carried out by using Hitachi Recording Spectrophotometer Model EPS-3 with silica cells 1.00 cm thick.

Results and Discussion

The iodide-iodine solution possesses two absorption peaks (at wavelength, 288 and 352 mμ), which have been attributed by Awtrey and Connick[7] to the I_3^- ion. On the addition of amylose to the solution, blue colored complex is formed and the complex solution possesses three absorption peaks at 288, 352 and 630—660 mμ. Absorbance of iodide-iodine solution with and without amylose

*1 Presented at the 18th Symposium of the Colloid Chemistry, Matsue, Oct. 4, 1965.

*2 Present address: Radiation Center of Osaka Prefecture, Shinke-cho, Sakai.

1) J. Holló and J. Szejtli, *Period. Polytech., Chem. Eng.* (Budapest) **1**, 223 (1957); *Stärke*, **10**, 49 (1958).

2) T. Kuge and S. Ono, This Bulletin, **34**, 1264 (1961).

3) V. S. R. Rao and J. F. Foster, *Biopolymers*, **1**, 527 (1963).

4) S. Ono, T. Watanabe, K. Ogawa and N. Okazaki, This Bulletin **38**, 643 (1965).

5) J. Szejtli, S. Augustat and M. Richter, *Stärke*, **18**, 38 (1966); *Biopolymers*, **5**, 5 and 17 (1967); **6**, 27 (1968).

6) W. W. Everett and J. F. Foster, *J. Amer. Chem., Soc.*, **81**, 3464 (1959).

7) A. D. Awtrey and R. E. Connick, *ibid.*, **73**, 1842 (1951).

changes with the concentration of iodide as shown in Figs. 1 and 2. In the solution of iodide-iodine-amylose, the following equilibria will hold

$$\mathrm{Am(h)} + n\mathrm{I_2} + m\mathrm{I^-} \rightleftharpoons \mathrm{Am(h)(I_2)}_n(\mathrm{I^-})_m \quad (1)$$

$$\mathrm{I_2} + \mathrm{I^-} \rightleftharpoons \mathrm{I_3^-} \quad (2)$$

where Am(h) is the helical segment of amylose molecule and $\mathrm{Am(h)(I_2)}_n(\mathrm{I^-})_m$ is the iodine complex. The dissociation constant of $\mathrm{I_3^-}$ in Eq. (2), K, was given by Davies and Gwynne[8] as follows.

$$K = 1.22 \times 10^{-3} \quad (\text{at } 20^\circ\mathrm{C}) \quad (3)$$

The concentration of $\mathrm{I_3^-}$ ion in iodide-iodine solution can be calculated from the molar extinction coefficients given by Awtrey and Connick;[7] 40000 at 288 mμ and 26400 at 352 mμ.

As shown in Figs. 1 and 2, absorbance at 352 mμ of iodide-iodine solution increases with the addition of amylose in the range of low iodide concentration, therefore the complex is assumed to have appreciable contribution to this absorption peak as well as the $\mathrm{I_3^-}$ ion in solution. On the other hand, absorbance at 288 mμ of the iodide-iodine solution is always suppressed by the addition of amylose. However, the amount of iodine in the complex calculated by the following equation, was not in agreement with that predicted from the experimental results shown in Figs. 1 and 2.

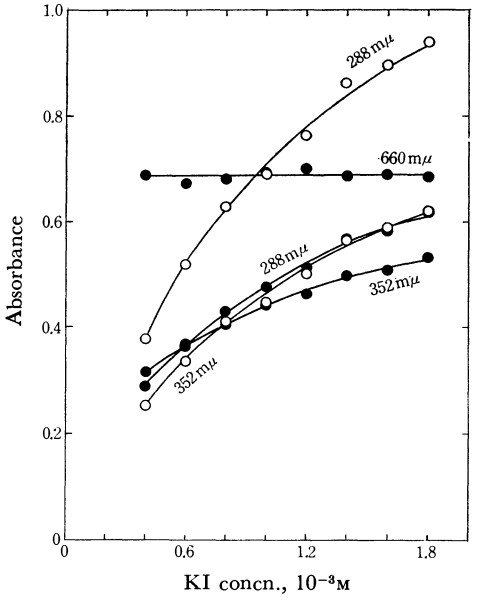

Fig. 1. Relation between the absorbance (at 288, 352 and 660 mμ) and KI concentration of iodide-iodine solution with (—●—) and without (—○—) amylose: concn. of $\mathrm{I_2}$, 4×10^{-5}M; concn. of amylose, 0.02 g/l; at 20°C.

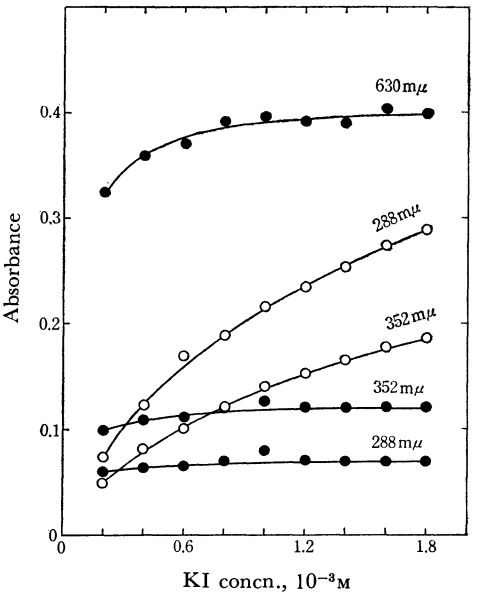

Fig. 2. Relation between the absorbance (at 288, 352 and 630 mμ) and KI concentration of iodide-iodine solution with (—●—) and without (—○—) amylose: concn. of $\mathrm{I_2}$, 1.2×10^{-5}M; concn. of amylose, 0.02 g/l; at 20°C.

(amount of iodine in the complex)
= (amount of iodine dissolved)
$$-\left[\begin{pmatrix}\text{amount of iodine present as } \mathrm{I_3^-} \text{ ion calculated}\\ \text{from the relation, } \{\text{absorbance at 288 m}\mu/40000\}\end{pmatrix} + \begin{pmatrix}\text{amount of iodine in equilibrium with}\\ \text{the } \mathrm{I_3^-} \text{ ion calculated by Eq. (3)}\end{pmatrix}\right] \quad (4)$$

Therefore, polyiodine chain in the complex may have some contribution to the peak at 288 mμ. Thereupon, the molar extinction coefficient of the iodine complex was evaluated by trial-and-error solution and the most probable values per mol iodine obtained were as follows; 0.7×10^4 at 288 mμ, 1.2×10^4 at 352 mμ and 4×10^4 at 630—660 mμ. The latest value at 630—660 mμ is in good agreement with the proposed one by Rundle *et al.*[9] The above values of extinction coefficient were obtained on the basis of the following assumption; both ends of the polyiodine chain are in the form of $\mathrm{I_3^-}$ and these $\mathrm{I_3^-}$ as well as the free $\mathrm{I_3^-}$ ion in solution, take part in the equilibrium, existing in solution according to Eq. (2), with free iodine. The most probable values of n and m were obtained as 11 and 2, respectively. Therefore, the polyiodine chain in the complex is assumed to be composed of linearly linked 11 iodine molecules and the both ends of the chain are in the form $\mathrm{I_3^-}$ such as shown as follows; $^-\mathrm{I_3(I_2)_9I_3^-}$. When one helical turn

8) M. Davies and E. Gwynne, *ibid.*, **74**, 2748 (1952).

9) R. E. Rundle, J. F. Foster and R. R. Baldwin, *ibid.*, **66**, 2116 (1944).

consists of 6 anhydroglucose units, the helical segment will be expected to be composed of $6\times 11=66$ anhydroglucose units provided the condition for the complex formation *i. e.* one iodine molecule per one turn of the helix is maintained. This amount 66 is in good agreement with the maximum number of anhydroglucose units composing a stable single helix obtained from the correlation between the wavelength of the maximum absorption peak of iodine-complex and the degree of polymerization of maltodextrin.[10] The amount of iodine combined in the complex in the presence of excess amount of iodine in solution (Fig. 1), was about 83% of the saturation (2.06×10^{-5} mol iodine per 0.02 g amylose), therefore a random segment between two helical segments in the helical segments may be assumed to be composed of about 14 anhydroglucose units.

10) K. Sakon, T. Watanabe and S. Ono, This Bulletin, **43**, in press.

BULLETIN OF THE CHEMICAL SOCIETY OF JAPAN VOL. 43 952—953 (1970)

The Effect of Urea on the Viscosity of Polymer Aqueous Solutions

Kunio TAMAKI, Yōko ŌHARA and Katsuhide KOMORI

Department of Chemistry, Yokohama City University, Kanazawa-ku, Yokohama

(Received September 10, 1969)

The effect of urea on the behavior of such hydrocolloids as proteins, synthetic polymers, and micelles of amphiphilic compounds in the water phase has been studied by several investigators. We will here report our experimental results on the change in the viscosity of the aqueous solutions of polyvinylpyrrolidone and sodium polystyrenesulfonate upon the addition of urea.

Experimental

Two kinds of polyvinylpyrrolidone (PVP), K-30 and K-90, with molecular weights of 4×10^4 and 9×10^5 respectively, were purchased from the Tokyo Kasei Kogyo Co. Sodium polystyrenesulfonate (NaPSS) was prepared by the neutralization of polystyrenesulfonic acid with a sodium hydroxide solution. Polystyrenesulfonic acid was prepared by the sulfonation of polystyrene (molecular weight 2.0×10^5) with concentrated sulfuric acid in the presence of silver sulfate, and it was purified by successive dialysis.[1] The degree of sulfonation was found to be 0.73. The urea was a reagent-grade product of the Koso Chemical Co. The 1,3-dimethylurea was an E. P.-grade product of the Tokyo Kasei Kogyo Co.; it was recrystallized from a chloroform-ether mixture.

The viscosity measurements were carried out with Ostwald viscometers with an outflow time for water of about 90 sec and with a total volume of 5 m*l* in a water bath at 25 ± 0.02°C.

Results and Discussion

It was found that the change in the reduced viscosities of PVP upon the addition of urea and 1,3-dimethylurea was very small, as is indicated in Figs. 1 and 2. Jirgenson[2] has reported that the reduced viscosities of PVP were reduced by the addition of urea and guanidine hydrochloride, whereas Klotz and Russell[3] have shown that urea had very little effect on the reduced viscosities of

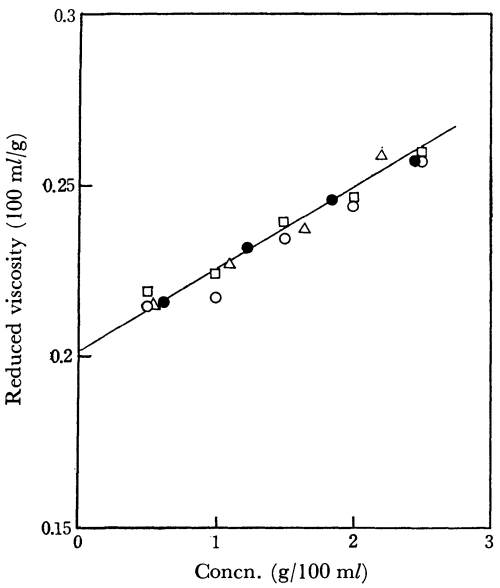

Fig. 1. Reduced viscosity of PVP, K-30, as a function of concentration in g per 100 m*l*; ● in water, ○ in 2M urea, □ in 4M urea, △ in 6M urea.

1) M. Kato, T. Nakagawa and H. Akamatu, This Bulletin, **33**, 322 (1960).

2) B. Jirgenson, *Makromol. Chem.*, **6**, 30 (1951).

3) I. M. Klotz and J. W. Russell, *J. Phys. Chem.*, **65**, 1274 (1961).

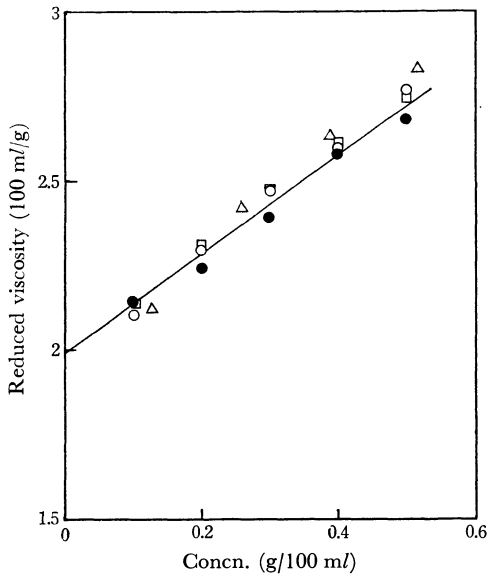

Fig. 2. Reduced viscosity of PVP, K-90, as a function of concentration in g per 100 ml; ● in water, ○ in 2M urea, □ in 2M 1,3-dimethylurea, △ in 4M urea.

PVP. Our results are in agreement with those of Klotz and Russell.[3]

Several different results regarding the change in the viscosity of other water-soluble polymers upon the addition of urea have been reported. Urea did not affect the reduced viscosities of polyacrylamide;[4] this behavior is similar to that of PVP discussed in this paper. Urea addition increased the reduced viscosities of polyvinylalcohol,[5-7] polyethylene glycol,[8] and un-ionized polyacrylic acid in hydrochloric acid.[4] Urea addition decreased the reduced viscosities of un-ionized polymethacrylic acid in hydrochloric acid.[4]

Urea, a well-known protein denaturant, is believed to behave as a structure breaker of water,[9-11] although a contrary opinion has also been reported.[12] Klotz[13] proposed the idea that the modification of water structure by the addition of urea can change the conformation and behavior of macromolecules, markedly different even in their primary structure, in a similar way. However, the experimental results reported in this paper as well as in the literature suggest the existence of some kinds of specificity[14] in the interaction of polymers with urea.

The reduced viscosities of NaPSS were greatly diminished by the addition of urea, as is shown in Fig. 3. NaPSS belongs to a strongly-ionized polyelectrolyte. The depression of ionization seems to be improbable, because the dielectric constant of aqueous urea solutions is slightly higher than that of pure water. Iso[15] obtained results showing a decrease in the reduced viscosities of sodium polyacrylate in the presence of urea. The decrease in the viscosity of strongly-ionized polyelectrolytes by the addition of urea seems to be a common feature, although the mechanism is still unknown.

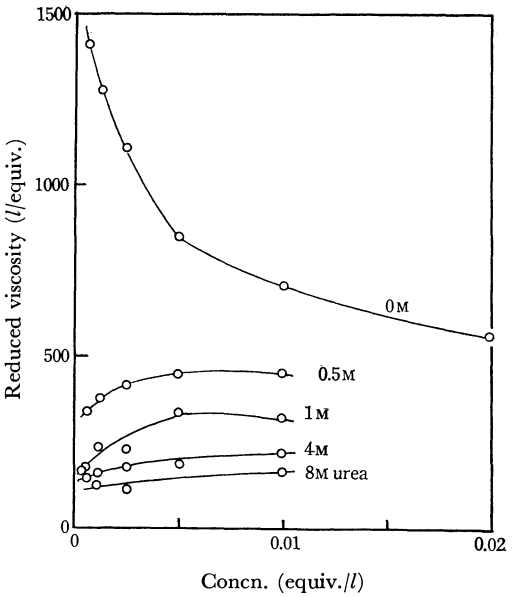

Fig. 3. Reduced viscosity of NaPSS as a function of concentration in equiv. per liter.

4) J. Eliassaf and A. Silberberg, *J. Polym. Sci.*, **41**, **33** (1959).
5) H. Maeda, T. Kawai and S. Sekii, *ibid.*, **35**, 288 (1959).
6) N. Noguchi and J. T. Yang, *J. Phys. Chem.*, **68**, 1609 (1964).
7) T. Suzawa and T. Shimada, *Kogyo Kagaku Zasshi*, **72**, 903 (1967).
8) G. G. Hammes and P. R. Schimmel, *J. Amer. Chem. Soc.*, **89**, 442 (1967).
9) K. Arakawa and N. Takenaka, This Bulletin, **40**, 2739 (1967).
10) G. E. Walrafen, *J. Chem. Phys.*, **44**, 3726 (1966).
11) J. A. Rupley, *J. Phys. Chem.*, **68**, 2002 (1964).
12) M. Abu-Hamdiyyah, *ibid.*, **69**, 2720 (1965).
13) I. M. Klotz, *Fed. Proc.*, **24**, S24 (1965).
14) D. R. Robinson and W. P. Jencks, *J. Amer. Chem. Soc.*, **87**, 2462 (1965).
15) K. Iso, *Nippon Kagaku Zasshi*, **84**, 201 (1963).

BULLETIN OF THE CHEMICAL SOCIETY OF JAPAN VOL. 43 954—955 (1970)

Study on Oxazolopyrimidines. II. Conversion of 7-Aminooxazolo-[5,4-*d*]pyrimidines into Hypoxanthine Derivatives

Yozo Ohtsuka

Sagami Chemical Research Center, Onuma, Sagamihara, Kanagawa

(Received September 16, 1969)

Several 7-aminooxazolo[5,4-*d*]pyrimidines have been synthesized from oxazole derivatives.[1] During the examination of the chemical behavior of these compounds, a new transformation of 7-aminooxazolopyrimidines into hypoxanthine derivatives was found.

Hitchings *et al.*[2] have converted some oxazolopyrimidines into purine derivatives by heating with alcoholic ammonia at 160°C for a long period. These conditions are similar to those of the well-known conversion of oxazoles into imidazoles.[3,4] In these cases, severe conditions are required for the substitution of oxygen atom by imino group. On the other hand, Ishidate and Yuki[5] found that 7-mercaptooxazolopyrimidine derivative was converted into 7-hydroxythiazolopyrimidine derivative under such mild conditions as by boiling with dilute acid for 20 min or by heating the crystals at 270—300°C.

The conversion of 7-aminooxazolopyrimidines into hypoxanthines proceeds under mild conditions. Thus, the treatment of the oxazolopyrimidines with aqueous 4N sodium hydroxide solution at room temperature followed by warming at 60—80°C, was found to be the most appropriate for the transformation.

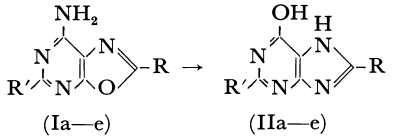

(Ia—e) (IIa—e)

a: R=R′=H
b: R=H, R′=CH_3
c: R=CH_3, R′=H
d: R=R′=CH_3
e: R=H, R′=OC_2H_5

By this treatment, 2- and/or 5-substituted 7-aminooxazolopyrimidines can be converted into the corresponding hypoxanthines. The yields of the hypoxanthines were 60 to 80% but more careful workup seemed to improve them. The structures of the products, IIa—d, were confirmed by comparison with authentic samples. The structure of IIe was confirmed by acid hydrolysis to afford xanthine.

All the hypoxanthines examined here are easily soluble in aqueous alkaline solution, while oxazolopyrimidines have sparing solubilities in the solvent. Therefore, it was thought that completion of the initial step of the reaction could be estimated from the time required for complete dissolution of the starting materials.

Table 1. The time of complete dissolution of several 7-aminooxazolopyrimidine
(45°C aq 4N NaOH solution)

Compound	Time (hr)
Ia	0.2
Ib	2.5
Ic	2.7
Id	7.5
Ie	5.0

The results in Table 1 show that when R and R′ are substituted by CH_3 or OEt, a longer time is needed for dissolution of the starting materials. This would mean the initial attack by alkali is retarded by these substituents.

The reaction proceeds through oxazole ring rupture by attack of OH^- followed by imidazole ring formation. This reaction provides a new route to hypoxanthine derivatives under mild conditions. The scope and applications of the reaction are under investigation.

Experimental

The IR, NMR and mass spectra were recorded with Perkin-Elmer 337, Varian HA-100 and Hitachi RMU-6E spectrometer respectively. The synthesis of the starting material has been described in the previous paper.[1]

Conversion of 7-Aminooxazolopyrimidines into Hypoxanthine Derivatives. General method: 7-Aminooxazolo[5,4-*d*]pyrimidine (1 g) and aqueous 4N sodium hydroxide solution (10 ml) were stirred at room temperature for 30 min. Then the mixture was warmed at 60—80°C for 30 min, and after cooling, the reaction

1) Y. Ohtsuka, This Bulletin, **43**, 187 (1970).
2) E. A. Falco, G. B. Elion, E. Burgi and G. H. Hitchings, *J. Amer. Chem. Soc.*, **74**, 4897 (1952).
3) K. Hoffmann, "Imidazole and Its Derivatives," Part I, Interscience Pub., New York (1953), pp, 43—44.
4) G. Theilig, *Chem. Ber.*, **86**, 96 (1953).
5) M. Ishidate and H. Yuki, *Chem. Pharm. Bull.* (Tokyo), **8**, 137 (1960).

mixture was acidified with conc. HCl. The resultant precipitates were filtered, and the products, about 60—80% yields, were recrystallized from water. These were identified by the comparisons of their IR, NMR and mass spectra with authentic samples (IIa: commercial product, IIb and IId,[6] and IIc[7]; prepared by known procedures). 2-Ethoxyhypoxanthine (IIe); colorless needles, mp >330°C. Found: C, 46.69; H, 4.49; N, 31.14%. Calcd for $C_7H_8N_4O_2$: C, 46.66; H, 4.48; N, 31.10%. NMR in DMSO-d_6 (δ-values): 7.90 (C_8-proton), 1.33, 4.35 (OEt).

7-Aminooxazolopyrimidine, Ia, was most easily converted into hypoxanthine, IIa; heating of Ia at the melting point, solids which were confirmed to be hypoxanthine deposited while other oxazolopyrimidines gave only degraded products. Moreover, on refluxing with acetic anhydride for 2 hr, Ia afforded IIa (60%). With more dilute alkali or at higher initial temperature, 7-aminooxazolopyrimidines were decomposed to acid soluble materials, which by the IR spectra are probably aminohydroxypyrimidine derivatives although they have not been confirmed.

Acid Hydrolysis of 2-Ethoxyhypoxanthine. 2-Ethoxyhypoxanthine (1 g) and 4N hydrochloric acid (20 m*l*) were heated under reflux for 4 hr. After neutralization of the reaction mixture with alkali, 0.7 g of product was obtained. The IR and NMR spectra of the product were identical with those of authentic xanthine.

Determination of the Time of Complete Dissolution. 7-Aminooxazolopyrimidines (2 mg) were suspended in aqueous 4N NaOH solution (1 m*l*) and the mixtures were stirred in the temperature-controlled bath. The time of complete dissolution was measured two or three times in each samples, and the mean deviation of those data were about ±20%.

6) F. Craveri and G. Zoni, *Boll. Chim. Farm.*, **97**, 393 (1958).

7) F. Bergmann and M. Tamari, *J. Chem. Soc.*, **1961**, 4468.

BULLETIN OF THE CHEMICAL SOCIETY OF JAPAN VOL. 43 955—957 (1970)

The Conductances of Alizarine Saphirol SE in Water-dioxane Mixtures at Various Temperatures

Masaru MITSUISHI, Mieko HASHIZUME, Akira KATAYAMA*1 and Nobuhiko KUROKI*1

Faculty of Textile Science and Technology, Shinshu University, Ueda, Nagano

(Received September 16, 1969)

It was reported, in our previous paper,[1] that Alizarine Saphirol SE forms the ion-associates in water-dioxane mixtures with low dielectric constants.

In the present paper, the thermodynamic properties of the ion-association reactions of Alizarine Saphirol SE in 70 and 82% dioxane are examined.

Experimental

Materials. The Alizarine Saphirol SE (sodium salt of 1,5-dihydroxy-4,8-diaminoanthraquinone-2-sulfonic acid) was a laboratory stock used in a previous work.[1]

The dioxane was purified by the same method as that described in the previous work.[1]

Conductance Measurements. These measurements were carried out at 15, 25, and 35°C by the same procedures as those described in the previous work.[1]

Results and Discussion

The conductances of Alizarine Saphirol in water-dioxane mixtures at 15, 25, and 35°C are shown in Fig. 1.

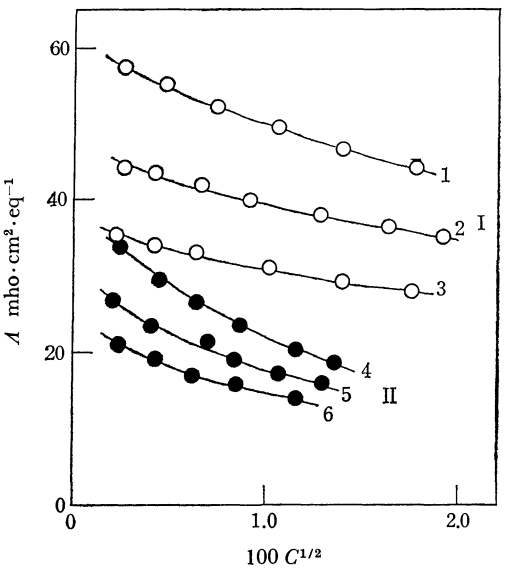

Fig. 1. Equivalent conductances of Alizarine Saphirol SE in 70 and 82 %dioxane. I, 70% dioxane (1 : 35, 2 : 25, 3 : 15°C), II 82% dioxane (4 : 35, 5 : 25, 6 : 15°C).

*1 College of Engineering, University of Osaka prefecture, Sakai, Osaka.

1) M. Mitsuishi, Y. Funatsu and N. Kuroki, This Bulletin, **42** 2384 (1969).

From the results of the conductance measurements indicated in Fig. 1, the equivalent conductances at an infinite dilution, Λ_0, and the ion-association constants, K_A, were calculated by means of Shedlovsky's treatment[2] based on the Onsager limiting equation in a manner similar to that described in the previous work;[1] the results are shown in Table 1.

Table 1. Calculated parameters

Dioxane	t °C	D	100 η poise	Λ_0	$\Lambda_0\eta$	K_A
70.0%	15	18.72	2.483	35.6	0.884	1.31×10^3
	25	17.69	1.918	45.3	0.869	1.39×10^3
	35	16.72	1.522	58.2	0.886	1.63×10^3
82.0%	15	10.01	2.106	23.0	0.484	8.67×10^3
	25	9.53	1.671	27.5	0.460	9.86×10^3
	35	9.06	1.356	36.5	0.495	1.30×10^4

D: Dielectric constant of the solvent.
η: Viscosity coefficient of the solvent.[3]

From Table 1, the K_A values of the dye in water-dioxane mixtures are found to increase with the rise in the temperature of the solvents. The Walden products, $\Lambda_0\eta$, are essentially constant in the solvents of a constant composition, even if the temperatures are different.

The relation among K_A, the dielectric constant, D, and the temperature, T, of the solvent is given by this equation:[4]

$$K_A = e^b, \tag{1}$$

where,

$$b = e^2/aDkT. \tag{2}$$

In Eq. (2), e is the electron charge, a is the center-to-center distance of the ions in an associate and k is the Boltzmann constant.

In accordance with Eq. (1), the plot of log K_A against DT must be linear. The plots of log K_A *vs.* the DT of Alizarine Saphirol in 70 and 82% dioxane are shown in Fig. 2; the plots are found to be linear. These evidences suggest that the ion associates of Alizarine Saphirol in 70 and 82% dioxane are due entirely to the electrostatic interactions between the dye ion and the counter ion.

The a values of Alizarine Saphirol in 70 and 82% dioxane can be obtained from the slopes of the plot of log K_A *vs.* DT; they are indicated in Table 2. As can be seen from Table 2, the a value in 70% dioxane is larger than that in 82% dioxane.

In the ion-association reaction of Alizarine Saphirol in water-dioxane mixtures, the enthalpy change (ΔH) and the entropy change ($\Delta S°$) can be obtained from Eqs. (3) and (5) respectively:

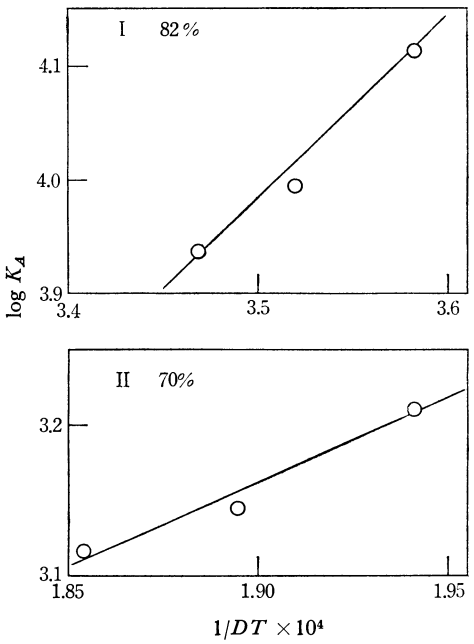

Fig. 2. The relation between log K_A and $1/DT$ in 82% (I) and 70% dioxane (II).

Table 2. Thermodynamic parameters of the ion association reaction of Alizarine Saphirol SE in water–dioxane mixtures at 25°C

Dioxane	$K_{A_{298}}$	ΔH (kcal/mol)	$\Delta G°$ (kcal/mol)	$\Delta S°$ (cal/deg·mol)	a (Å)
70.0%	1.39×10^3	1.93	−4.3	21.1	6.72
82.0%	9.86×10^3	3.57	−5.5	30.5	4.74

$$\mathrm{d}\ln K_A/\mathrm{d}(1/T) = -\frac{\Delta H}{R}, \tag{3}$$

$$\Delta G° = -RT\ln K_A, \tag{4}$$

$$\Delta G° = \Delta H - T\Delta S°, \tag{5}$$

where R is the gas constant.

From the best straight line given by the method of least squares for the log K_A *vs.* $1/T$ plot over the whole temperature range, the ΔH values are obtained, the $\Delta S°$ values are obtained from Eq. (5), and are as indicated in Table 2.

As is shown in Table 2, since the ΔH values are positive, the reaction is endothermic; these ΔH values are comparable to those of the ion-association reactions of several inorganic salts in water.[5,6]

The $\Delta S°$ values of the reactions are positive.

2) T. Shedlovsky, *J. Franklin Inst.*, **225**, 739 (1938).
3) H. S. Harned and B. B. Owen, "The Physical Chemistry of Electrolytic Solutions," Reinhold, New York (1963), p. 713.
4) J. T. Denison and J. B. Ramsay, *J. Amer. Chem. Soc.*, **77**, 2615 (1955).
5) R. P. Bell and J. H. B. George, *Trans. Faraday Soc.*, **49**, 619 (1953).
6) G. H. Noncolls, *Discuss. Faraday Soc.*, **24**, 108 (1957).

These results are considered to reflect the evidence that the degree of freedom of the system increases, since the solvent molecules are removed from the solvation sphere of the ions when the dye ion forms an ion associte with the counter ion.

The authors wish to thank Professors Haruo Gotoh and Masatoki Yokoi for their helpful discussions.

BULLETIN OF THE CHEMICAL SOCIETY OF JAPAN VOL. 43 957—958 (1970)

The Electrochemical Fluorination of *s*-Triazines

Takashi ABE, Shunji NAGASE and Kazuo KODAIRA

Government Industrial Research Institute, Nagoya Kita-ku, Nagoya

(Received September 26, 1969)

A great many papers have described the fluorination of nitrogen compounds with a carbon - nitrogen multiple bond.[1] However, the information given in the literature about the electrochemical fluorination of nitrogen compounds has not extended to nitriles and imines other than acetonitrile[2] and guanidine.[3] The present investigation was undertaken mainly in order to study the general behavior of the carbon - nitrogen multiple bond upon electrochemical fluorination.*1 Trifluoroacetonitrile and perfluoroalkyl iminosulfur difluorides were subjected to electrochemical fluorination. Furthermore, such *s*-triazines as cyanuric fluoride, thiocyanuric acid and 1,3,5-triamino-*s*-triazine were also fluorinated.

It was found that, upon electrochemical fluorination, these samples were cleaved extensively, giving fluorocarbons, nitrogen trifluoride, and perfluoroamines. The evolution of nitrogen gas was also observed. In addition, sulfur hexafluoride was obtained from the compounds containing sulfur.

When trifluoroacetonitrile (bp 65°C) was subjected to fluorination electrochemically (reaction conditions: sample feed rate, 14 ml/min, He, 20 ml/min; anodic current density, 2.0 A/dm^2; cell voltage, 5.7—6.7 V; cell temp, 13°C; NaF added, 5 g), the product consisted of tetrafluoromethane (28 mol%), trifluoromethane (2%), hexafluoroethane (28%), and nitrogen trifluoride (42%). When the sample feed rate was increased (27.1 ml/min), pentafluoroethyldifluoroamine was obtained in a very low yield (<1%), along with other fluorinated compounds. The product composition (mol%) was as follows: tetrafluoromethane (21%), trifluoromethane (1%), hexafluoroethane (33%), nitrogen trifluoride (44%) and pentafluoroethyldifluoroamine (1%). Similarly, trifluoromethyl iminosulfur difluoride (bp −7——5°C), pentafluoroethyl iminosulfur difluoride (bp 22—24°C), and *N*-fluoroformyl iminosulfur difluoride (bp 54°C) underwent breakdown upon electrochemical fluorination, giving the compounds depicted below:

Sample	Products*2
$CF_3N{=}SF_2$	→ CF_4, NF_3, SF_6, CF_3NF_2, $(CF_3)_2NF$ and CHF_3
$C_2F_5N{=}SF_2$	→ C_2F_6, SF_6, NF_3, CF_4, $C_2F_5NF_2$, C_2F_5H and CHF_3
$FC(=O)N{=}SF_2$	→ COF_2, NF_3, SF_6, CF_4 and CF_3OF

The reaction conditions and the results with the electrochemical fluorination of *s*-triazines as well as methyl thiocyanate and methyl isothiocyanate are shown in Table 1. In this fluorination, only cleaved products were yielded; tetrafluoromethane and nitrogen trifluoride were the main products from these starting materials. The results are in contrast to those obtained by the fluorination of these compounds with elementary fluorine. It has been reported by Ruff that the fluorination of trifluoroacetonitrile[4] and perfluoroalkyl iminosulfur difluoride[5] with fluorine gave fully-fluorinated,

1) G. E. Coates, J. Harris and T. Sutcliffe, *J. Chem. Soc.*, **1951**, 2762; J. A. Cuculo and L. A. Bigelow, *J. Amer. Chem. Soc.*, **74**, 710 (1952); P. Robson, V. C. R. McLoughlin, J. B. Hynes and L. A. Bigelow, *ibid.*, **83**, 5010 (1961); H. J. Emeléus and G. L. Hurst, *J. Chem. Soc.*, **1962**, 3276; B. C. Bishop, J. B. Hynes and L. A. Bigelow, *J. Amer. Chem. Soc.*, **84**, 3409 (1962); R. D. Dresdner, J. Merritt and J. P. Royal, *Inorg. Chem.*, **4**, 1228 (1965).

2) J. H. Simons, U. S. 2519983 (1950).

3) A. Engelbrecht and E. Nachbaur, *Monatsh. Chem.*, **90**, 371 (1955).

*1 The electrochemical fluorination of hydrogen cyanide and cyanogen will be described elsewhere.

*2 The products are shown in the order of the amounts formed.

4) J. K. Ruff, *J. Org. Chem.*, **32**, 1675 (1967).

5) M. Lustig and J. K. Ruff, *Inorg. Chem.*, **4**, 1444 (1965).

Table 1. Reaction conditions and the results with the fluorination of *s*-triazines

Run No.	Sample	Sample fed (mol)	Electricity passed*a (A. hr)	Fluorocarbons obtained (g)	Molar ratio*b	Product composition (mol %)							
						CF_4	CHF_3	NF_3	CF_3NF_2	$(CF_3)_2NF$	$CF_2(NF_2)_2$	SF_6	CF_3SF_5
1	$(CNF)_3$	0.148	79	56.3	4.64	48		47	5	+			
2	$(CNSH)_3$	0.150	122	41.4	2.39	24		30	7	6		33	
3	$(CNNH_2)_3$	0.150	176	52.4	3.26	26		64	5	4	1		
4	CH_3SCN	0.150	90	26.8	1.81	34	11	39	1			3	12
5	CH_3NCS	0.150	113	32.7	2.67	42	30	25	+			3	+

*a Electrolysis was continued until the cell voltage was raised up to 7.6 V.
*b (total mol of products/mol of sample)

saturated compounds as the main products, without any fission of the carbon - nitrogen bond or the nitrogen - sulfur bond. However, upon electrochemical fluorination, no formation of any fluorinated compounds, such as R_fNFSF_5 (R_f = trifluoromethyl, pentafluoroethyl and fluoroformyl) and *N,N*-difluoroaminosulfur pentafluoride, was detected from the corresponding starting material, even when an increased amount of sample was fed into anhydrous hydrogen fluoride; a higher feed rate of the sample makes the reaction milder.[6] Further perfluoroalkylazo compounds (*e. g.*, $CF_3N{=}NCF_3$ and $C_2F_5N{=}NC_2F_5$) which have been reported to be found in the products of the direct fluorination of these compounds with an unsaturated carbon - nitrogen bond[7] were not detected in the present fluorination reaction.

Experimental

Materials. Trifluoroacetonitrile,[8] trifluoromethyl iminosulfur difluoride, pentafluoroethyl iminosulfur difluoride,[9] *N*-fluoroformyl iminosulfur difluoride,[10] cyanuric fluoride[11] and thiocyanuric acid[12] were prepared and purified by the method in the literature. The 1,3,5-triamino-*s*-triazine, methyl thiocyanate, and methyl isothiocyanate were obtained commercially.

The purity of the anhydrous hydrogen fluoride was better than 99%.

Apparatus and Procedures. Two types of electrolytic cells were employed in these experiments. For the fluorination of trifluoroacetonitrile, trifluoromethyl iminosulfur difluoride, pentafluoroethyl iminosulfur difluoride, and *N*-fluoroformyl iminosulfur difluoride, an iron cell (300 m*l* capacity) was employed. A monel cell (1 *l* capacity) was employed for the others. The anodic surface areas were 7.7 dm^2 and 9.2 dm^2 respectively. The bottoms of these cells were equipped with a bubbler. In both cases, the anodic current density was 2.0 A/dm^2.

As for the gaseous samples, the procedures are essentially the same as those described in the preceding paper,[13] but the reflux condenser was kept at −20°C and the gaseous product was analysed by studying the G.C. (column; FC 43*3 66% on Celite 545 SK, KelF #3*3 30% on Chromosorb PAW) and IR spectra, taking the sample directly from the sampling valve fixed next to the hydrogen fluoride absorber.

For the other samples the electrolysis were carried out by batch. The procedures thereafter were the same as have been described previously.[6] The tetrafluoromethane and nitrogen trifluoride were analysed by G.C. (conditions: column, silica gel 60—80 mesh, 1.5 m length × 3 mm id; carrier gas, He; temp., 0°C).

6) S. Nagase, T. Abe and H. Baba, This Bulletin, **40**, 684 (1967).
7) J. B. Hynes and L. A. Bigelow, *J. Amer. Chem. Soc.*, **84**, 2751 (1962); J. A. Attaway, R. H. Groth and L. A. Bigelow, *ibid.*, **81**, 3599 (1959).
8) H. Gilman and R. G. Jones, *ibid.*, **65**, 1458 (1943).
9) W. C. Smith, C. W. Tullock, R. D. Smith and V. A. Engelhardt, *ibid.*, **82**, 551 (1960).
10) U. Biermann and O. Glemser, *Chem. Ber.*, **100**, 3795 (1967).
11) A. F. Maxwell, J. S. fry and L. A. Bigelow, *J. Amer. Chem. Soc.*, **80**, 548 (1958).
12) A. W. Hofmann, *Ber.*, **18**, 2201 (1885).
13) S. Nagase, T. Abe and H. Baba, This Bulletin, **42**, 2062 (1969).
*3 Minnesota Mining and Manufacturing Co., Ltd.

BULLETIN OF THE CHEMICAL SOCIETY OF JAPAN VOL. 43 959—960 (1970)

Photolysis of Tetraphenylcyclobutadienenickel Bromide

Takahiro HOSOKAWA and Ichiro MORITANI

Department of Chemistry, Faculty of Engineering Science, Osaka University, Machikaneyama, Toyonaka, Osaka

(Received September 27, 1969)

Thermal behavior of some cyclobutadiene-metal complexes has been well studied.[1] Much less is known, however, about the photochemical reaction of the complexes except for the results of the photolysis of cyclobutadieneiron tricarbonyl by Masamune *et al.*[2] An interesting point in such a reaction is the photochemical behavior of the unstable cyclobutadiene-ligands which are liberated by photodecomposition. Therefore, we have investigated the photolysis of tetraphenylcyclobutadienenickel bromide (I).

The complex I was prepared from 1,1-dimethyl-2,3,4,5-tetraphenylstannole by Freedman's method.[3] The irradiation of I was carried out in a chloroform solution under a nitrogen atmosphere at 10—16°C for 12 hr by using a 500 W high pressure mercury lamp.[4] After irradiation, the insoluble material which resulted from the reaction was filtered off and characterized as nickel bromide. Thus it can be considered that in the reaction the complex I is decomposed by light, thus liberating tetraphenylcyclobutadiene. After the solvent had been evaporated *in vacuo*, the reaction products were separated by alumina-column chromatography. Elution with petroleum ether and recrystallization gave colorless needles (A). The other products were a large quantity of a tarry matrial and an uncharacterized complex. The compound A was found to be 1-chloro-2,3,4-triphenylnaphthalene by an elemental analysis, a molecular-weight determination, and a study of its spectroscopic data. The structure of A was further confirmed by converting it to 1,2,3-triphenylnaphthalene[5] by treatment with metal lithium and then methanol.

The photochemical reaction of diphenylacetylene in *n*-hexane has previously been reported to give 1,2,3-triphenylnaphthalene and 1,2,3-triphenylazulene *via* a tetraphenylcyclobutadiene intermediate.[6] In contrast to this reaction, interestingly, only a chlorinated naphthalene was obtained in our reaction, not azulene. Accordingly, a chlorine atom must be abstracted from the solvent in one stage of the reaction. Therefore, we propose the following reaction scheme including the diradical intermediate (II). The diradical II abstracts the chlorine atom more easily to afford the monoradical III than II rearranges itself intramolecularly since no azulene is formed in this reaction.[7]

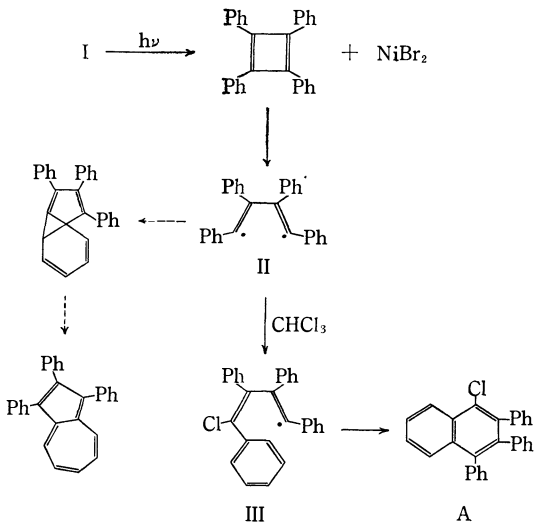

Thus, it can be said that this may depend upon the ease with which the chlorine atom is abstracted from the solvent. In fact, when (4-bromo-1,2,3,4-tetraphenyl-*cis*,*cis*-1,3-butadienyl)dimethyltin bromide was irradiated in benzene, only 1,2,3-tri-

1) As leading references for the reaction of cyclobutadienemetal complexes; see a) P. M. Maitlis, "Advances in Organometallic Chemistry," Vol. 4, Academic Press, New York, N. Y. (1966), p. 95. b) M. P. Cava and M. J. Mitchell," Cyclobutadiene and Related Compounds," Academic Press, New York, N. Y. (1967), p. 88.

2) W. J. R. Tyerman, M. Kato, P. Kebarle, S. Masamune, O. P. Strausz and H. E. Gunning, *Chem. Commun.*, **1967**, 497.

3) H. H. Freedman, *J. Amer. Chem. Soc.*, **83**, 2194, 2195 (1961).

4) At intervals of about 3 hr, the wall of the internal, water-cooled high-pressure mercury arc lamp (Eikosha Co. Ltd., Oyodo-ku Osaka model PIH-500S), which had been coated with a tarry material during the reaction, was washed with hydrochloric acid.

5) L. I. Smith and H. H. Hoehn, *J. Amer. Chem. Soc.*, **63**, 1184 (1941).

6) G. Buchi, C. W. Perry and E. W. Robb, *J. Org. Chem.*, **27**, 5106 (1962).

7) Very recently such an intermolecular naphthalene formation has been reported for the dimerization of phenylpropiolic acid by H. W. Whitlock, Jr., E-M. Wu and B. J. Whitlock in *J. Org. Chem.*, **34**, 1857 (1969).

phenylazulene was formed,[8] whereas in chloroform only the naphthalene A was obtained.[9]

Experimental

Irradiation of Tetraphenylcyclobutadienenickel Bromide (I). A solution of 2.43 g (4.23 mmol) of I[3] in 1 liter of chloroform, agitated by the bubbling of nitrogen gas, was irradiated with a 500 W high pressure mercury lamp, and then the reaction vessel was cooled with ice water. The reaction was followed by studying the ultraviolet spectrum. After the solution had been irradiated for 12 hr, the characteristic ultraviolet peak near 300 mμ, present in I, disappeared. The nickel bromide (*ca.* 718 mg, 3.29 mmol) which appeared during the irradiation was filtered off, and the chloroform was evaporated *in vacuo*. Into the residue, there was added petroleum ether, and then the undissolved amorphous material was filtered off. The filtrate was chromatographed on a column of alumina (48 g). Elution with petroleum ether (55 m*l*) gave pale yellow crystals (133 mg), which were then further chromatographed and recrystallized from petroleum ether. We thus obtained 76 mg (0.19 mmol) of 1-chloro-2,3,4-triphenylnaphthalene (A) as colorless crystals, mp 187—188°C. IR (Nujol): 1070, 1028, 883, 763, 700, and 645 cm^{-1}. UV: λ_{max}^{EtOH} 238 (log ε=4.79), 270[sh] (4.20), and 297 mμ (4.04). NMR (CCl_4): multiplet at τ 1.65—1.70 (1H), multiplets centered at τ 2.55 (3H), 2.97 (11H), and 3.27 (4H). Its UV and NMR spectra were very similar to those of 2,3,4-triphenyl-1-naphthol.[11]

Found: C, 85.38; H, 4.87; Cl, 9.01%. Calcd for $C_{28}H_{19}Cl$: C, 86.03; H, 4.89; Cl, 9.07%.

Reduction of A with Lithium, 1,2,3-Triphenylnaphthalene. A solution of 58 mg of A in 10 m*l* of dry ether was refluxed with stirring in the presence of 10 mg of clean lithium shavings. A purple-brown lithium compound was formed after 8 hr, after which the reflux was continued for an additional 3 hr. The excess lithium was decomposed with methanol, and then the mixture was poured into water. The organic layer was extracted with ether, dried over anhydrous sodium sulfate, and concentrated. The residue was chromatographed on a column of alumina (3.9 g). Elution with petroleum ether (40 m*l*) gave 45 mg of 1,2,3-triphenylnaphthalene (mp 153—156°C (from ethanol-benzene)). The IR spectrum of this compound was superimposable upon that of an authentic material prepared from diphenylacetylene and lithium,[5] and a mixed melting point was undepressed.

8) H. H. Freedman, *J. Org. Chem.*, **27**, 2298 (1962). This reaction has been reported to proceed *via* a tetraphenylcyclobutadiene-like intermediate.

9) Unfortunately, the complex I could not be irradiated in benzene since I is quite insoluble in this solvent.

10) Petroleum ether refers to a fraction with a bp of 40—60°C, the melting points are uncorrected.

11) N. Obata and I. Moritani, This Bulletin, **39**, 1975 (1966).

BULLETIN OF THE CHEMICAL SOCIETY OF JAPAN VOL. 43 960—963 (1970)

Syntheses of Optically Active Amino Acids by Reduction of Schiff Bases with Sodium Borohydride[1)]

Kaoru HARADA and Jun-ichi OH-HASHI

Institute of Molecular Evolution and Department of Chemistry, University of Miami, Coral Gables, Florida 33134, U.S.A.

(Received September 29, 1969)

Several nonenzymatic asymmetric syntheses of α-amino acids from their corresponding α-keto acids have been reported.[2-12)] An asymmetric synthesis of α-amino acids by catalytic hydrogenation and subsequent hydrogenolysis of the Schiff bases of

1) Sterically controlled synthesis of optically active organic compounds IX. Part VIII. K. Harada and T. Yoshida, This Bulletin, **43**, 111 (1970). Contribution No. 133 of the Institute of Molecular Evolution, University of Miami.

2) F. Knoop and C. Martius, *Z. Phys. Chem.*, **258**, 238 (1939).

3) J. B. Herbst and E. A. Swart, *J. Org. Chem.*, **11**, 366 (1946).

4) R. G. Hiskey and R. C. Northrop, *J. Amer. Chem. Soc.*, **83**, 4798 (1961).

5) K. Matsumoto and K. Harada, *J. Org. Chem.*, **31**, 1956 (1966).

6) K. Harada, *Nature*, **212**, 1571 (1966); *J. Org. Chem.*, **32**, 1790 (1967).

7) A. Kanai and S. Mitsui, *Nippon Kagaku Zasshi* **89**, 183 (1966).

8) R. G. Hiskey and R. C. Northrop, *J. Amer. Chem. Soc.*, **89**, 1753 (1965).

9) K. Harada and K. Matsumoto, *J. Org. Chem.*, **32**, 1794 (1967).

10) K. Harada and K. Matsumoto, *ibid.*, **33**, 467 (1968).

11) K. Matsumoto and K. Harada, *ibid.*, **33**, 4526 (1968).

12) K. Harada and T. Yoshida, This Bulletin, **43**, 111 (1970).

Table 1. Amino acids prepared from α-keto acid esters

	Keto acid[a]	Amine[b]	Solvent	$NaBH_4$ (mole)	Amino acid	Yield[d] (%)	Confign.	DNP-Amino acid $[\alpha]_D^{25}$ 1N NaOH[f]	DNP-Amino acid Optical purity[g]
1	Et-Py	(−)-Me	Diglyme	0.01	ala	13	S	+36.2 (0.51)	25
2	Et-Py	(+)-Me	Diglyme	0.01	ala	15	R	−34.9 (0.49)	24
3	Et-Py	(−)-Me	THF	0.01	ala	18	S	+41.5 (0.46)	29
4	Et-Py	(+)-Me	THF	0.01	ala	18	R	−40.8 (0.56)	28
5	Bz-Py	(−)-Me	Diglyme	0.01	ala	16	S	+42.1 (0.49)	29
6	Bz-Py	(+)-Me	Diglyme	0.01	ala	17	R	−40.3 (0.45)	28
7	Bz-Py	(−)-Et	Diglyme	0.01	ala	10	S	+23.6 (0.51)	16
8	Bz-Py	(+)-Et	Diglyme	0.01	ala	11	R	−24.5 (0.46)	17
9	Bz-Py	(−)-Me	THF[c]	0.01	ala	12	S	+52.7 (0.49)	37
10	Bz-Py	(+)-Me	THF[c]	0.01	ala	11	R	−49.5 (0.43)	34
11	Bz-Py	(−)-Et	THF[c]	0.01	ala	9	S	+32.3 (0.52)	22
12	Bz-Py	(+)-Et	THF[c]	0.01	ala	8	R	−30.9 (0.54)	22
13	Bz-Py	(−)-Me	EtOH	0.01	ala	5	S	+34.6 (0.44)	24
14	Bz-Py	(+)-Me	EtOH	0.01	ala	5	R	−32.3 (0.45)	23
15	Bz-Py	(−)-Me	THF[c]	0.01	ala	12(8)[e]	S	+50.1 (0.49)	35(33)[h]
16	Bz-Py	(+)-Me	THF[c]	0.01	ala	12(9)[e]	R	−51.2 (0.50)	36(37)[h]
17	Bz-Py	(−)-Me	THF[c]	0.005	ala	12(9)[e]	S	+48.2 (0.51)	34(34)[h]
18	Bz-Py	(+)-Me	THF[c]	0.005	ala	12(9)[e]	R	−51.8 (0.61)	36(35)[h]
19	Bz-Py	(−)-Me	THF[c]	0.0025	ala	11(8)[e]	S	+48.4 (0.51)	34(35)[h]
20	Bz-Py	(+)-Me	THF[c]	0.0025	ala	12(7)[e]	R	−49.6 (0.49)	34(36)[h]
21	Et-Bu	(−)-Me	THF[c]	0.01	NH_2-but	23	S	+15.3 (0.42)	16
22	Et-Bu	(+)-Me	THF[c]	0.01	NH_2-but	27	R	−15.2 (0.52)	15
23	Et-Bu	(−)-Et	THF[c]	0.01	NH_2-but	22	S	+ 9.1 (0.39)	9.2
24	Et-Bu	(+)-Et	THF[c]	0.01	NH_2-but	26	R	− 8.4 (0.58)	8.5
25	Bz-Bu	(−)-Me	THF[c]	0.01	NH_2-but	23	S	+19.3 (0.56)	20
26	Bz-Bu	(+)-Me	THF[c]	0.01	NH_2-but	20	R	−19.4 (0.55)	21
27	Bz-Bu	(−)-Et	THF[c]	0.01	NH_2-but	23	S	+15.9 (0.49)	16.1
28	Bz-Bu	(+)-Et	THF[c]	0.01	NH_2-but	21	R	−16.0 (0.40)	16.2

a) Et-Py, ethyl pyruvate; Bz-Py, benzyl pyruvate; Et-Bu, ethyl α-ketobutyrate; Bz-Bu, benzyl α-ketobutyrate.
b) (−)-Me, (S)-(−)-α-methylbenzylamine ($[\alpha]_D^{25}$ −42.3°, benzene); (+)-Me, (R)-(+)-α-methylbenzylamine ($[\alpha]_D^{25}$ +41.5°, benzene); (−)-Et, (S)-(−)-α-ethylbenzylamine ($[\alpha]_D^{25}$ 21.0°, benzene); (+)-Et, (R)-(+)-α-ethylbenzylamine ($[\alpha]_D^{25}$ +21.7°, benzene).
c) THF, tetrahydrofuran.
d) Yields are calculated from α-keto acids.
e) Yields represent alanine (reactions 15—20) prepared at room temperature and at 0°C (with parentheses).
f) Optical rotations were measured in 1N sodium hydroxide.
g) Defined as ($[\alpha]_D$ observed/$[\alpha]_D$ lit) × 100. DNP-(S)-ala, $[\alpha]_D$ +143.9° (1N NaOH); DNP-(S)-α-NH_2-but, $[\alpha]_D$ +98.8° (1N NaOH): K. R. Rao and H. A. Sober, *J. Amer. Chem. Soc.*, **76**, 1228 (1954).
h) Optical purities represent alanine (reactions 15—20) prepared at room temperature and at 0°C (with parentheses).

α-keto acids with optically active amines were studied[4] and the steric course of the asymmetric synthesis was studied and a chelated intermediate structure of the substrate with the catalyst was suggested.[9,10]

Several methods of hydrogenation of the azomethine group have been reported. These are: catalytic hydrogenation,[13] reduction using metals,[14] lithium aluminum hydride,[15] sodium borohydride,[16] dimethylamine-borane,[17] formic acid,[18]

13) W. S. Emerson, *Org. Reactions*, **5**, 174, John Wiley & Sons, Inc., New York (1948).

14) A. R. Surrey and H. F. Hammer, *J. Amer. Chem. Soc.*, **66**, 2127 (1944).

15) J. H. Billman and K. M. Tai, *J. Org. Chem.*, **23**, 535 (1958).

16) G. N. Walker, M. A. Moor and B. N. Weaver, *ibid.*, **26**, 2740 (1961).

17) J. H. Billman and J. W. McDowell, *ibid.*, **26**, 1437 (1961).

18) R. Baltzly and O. Kauder, *ibid.*, **16**, 173 (1951).

Table 2. Amino acids prepared from sodium salts of α-keto acids

Keto acid[a]	Amine[b]	Solvent	$NaBH_4$ (mole)	Amino acid	Yield[c] (%)	Confign.	DNP-Amino acid: $[\alpha]_D$, 1N NaOH[d]	DNP-Amino acid: Optical purity[e] (%)
Na-Py	(−)-Me	MeOH–H_2O (1:3)	0.01	ala	6	S	+39.2 (0.59)	27
Na-Py	(+)-Me	MeOH–H_2O (1:3)	0.01	ala	7	R	−37.0 (0.44)	26
Na-Py	(−)-Et	MeOH–H_2O (1:3)	0.01	ala	6	S	+36.2 (0.52)	25
Na-Py	(+)-Et	MeOH–H_2O (1:3)	0.01	ala	8	R	−40.0 (0.59)	25
Na-Bu	(−)-Me	MeOH–H_2O (1:3)	0.01	NH_2-but	19	S	+ 9.0 (0.48)	9
Na-Bu	(+)-Me	MeOH–H_2O (1:3)	0.01	NH_2-but	18	R	−10.8 (0.51)	11
Na-Bu	(−)-Et	MeOH–H_2O (1:3)	0.01	NH_2-but	17	S	+ 8.2 (0.52)	8
Na-Bu	(+)-Et	MeOH–H_2O (1:3)	0.01	NH_2-but	18	R	− 9.1 (0.50)	9

a) Na-Py, sodium pyruvate; Na-Bu, sodium α-ketobutyrate.
b) (−)-Me, (S)-(−)-α-methylbenzylamine ($[\alpha]_D^{25}$ −42.3°, benzene); (+)-Me, (R)-(+)-methylbenzylamine ($[\alpha]_D^{25}$ +41.5°, benzene); (−)-Et, (S)-(−)-α-ethylbenzylamine ($[\alpha]_D^{25}$ −21.0°, benzene); (+)-Et, (R)-(+)-α-ethylbenzylamine ($[\alpha]_D^{25}$ +21.7°, benzene).
c) Yields are calculated from α-keto acids.
d) Optical rotations were measured in 1N sodium hydroxide.
e) Defined as ($[\alpha]_D$ observed/$[\alpha]_D$ lit) × 100. DNP-(S)-ala, $[\alpha]_D$ +143.9° (1N NaOH); DNP-(S)-α-NH_2-but, $[\alpha]_D$ +98.8° (1N NaOH): K. R. Rao and H. A. Sober, *J. Amer. Chem. Soc.*, **76**, 1328 (1954).

and electrolytic reduction.[19] In the present study, the Schiff bases of α-keto acids with optically active α-alkylbenzylamines were reduced with sodium borohydride. The reduced compounds were further hydrogenolyzed and hydrolyzed to afford α-amino acids. The α-keto acid esters used were: ethyl pyruvate, ethyl α-ketobutyrate, and benzyl pyruvate. The optically active α-alkylbenzylamines used were: S(−)-α- and R(+)-α-methylbenzylamine, S(−)-α- and R(+)-α-ethylbenzylamine. Solvents used were: diglyme, tetrahydrofuran, and ethanol. The Schiff base was dissolved in a solvent and was reduced with sodium borohydride at room temperature (or at 0°C). After the reaction was over, the boron complex was decomposed with hydrochloric acid. The resulting *N*-alkyl amino acid ester was hydrolyzed and then hydrogenolyzed by the use of palladium hydroxide on charcoal. A part of the reduction product was applied to an amino acid analyzer to estimate the yield of amino acid. The other part was desalted and then applied to a Dowex 50×2 column (H form). Free amino acids were obtained by elution with aqueous ammonia. The resulting amino acids still contained some impurities, so that the measurements of optical rotation at this stage were meaningless. The crude amino acids were converted to their corresponding DNP-amino acids by the use of 2,4-dinitrofluorobenzene in a conventional manner.[20] The resulting DNP-amino acids were purified without fractionation of optical isomers by the use of Celite column chromatography,[21] as reported in the previous papers.[5,6] Results are summarized in Tables 1 and 2.

The yields of the asymmetric synthesis were rather low (5—27%). The optical purity of synthesized amino acids was in a range of 9—36%. When (S)-α-alkylbenzylamines were used, (S)-amino acids were synthesized. Yields of amino acids prepared at lower temperature (0°C) were smaller than that prepared at room temperature. However, optical purities of amino acids prepared at 0°C and at room temperature (25°C) were found to be the same (Table 1, 15—20). Yields of amino acids were almost constant dependent on the amount of sodium borohydride used (Table 1, 15—20). When α-methylbenzylamine was used, higher optical activity of amino acid was obtained than by the use of α-ethylbenzylamine. The optical purities of alanine were generally higher than that of α-amino butyric acid. These results are similar to those obtained by the hydrogenolytic asymmetric transamination of α-keto acids,[9,10] or α-keto acid esters,[12] with optically active α-alkylbenzylamine.

Experimental

Amino Acids from Benzyl Esters of α-Keto Acids. Benzyl pyruvate (1.78 g, 0.01 mol) and S(−)-α-methylbenzylamine (1.21 g, 0.01 mol) were dissolved in 50 ml of benzene and the solution was gently refluxed for 30 min using a Dean and Stark distillation tube. After dehydration was over, benzene was evaporated under reduced pressure. The residual syrup was dissolved in 30 ml of tetrahydrofuran. To this, sodium

19) H. D. C. Rapson and A. E. Bird, *J. Appl. Chem.* (London), **13**, 233 (1963).
20) F. Sanger, *Biochem. J.*, **39**, 507 (1945).
21) J. C. Perrone, *Nature*, **167**, 513 (1951).

borohydride (0.380 g, 0.01 mol) was added under stirring at room temperature. No heat generation was observed. After 2 hr of stirring, 10 m*l* of 2N hydrochloric acid was added to decompose unreacted sodium borohydride and boron complex. The solvent was removed under reduced pressure. The residual material was dissolved in a mixture of 10 m*l* of water and 5 m*l* of methanol. Sodium hydrogencarbonate was added to the solution to adjust the pH to about 8.0. Palladium hydroxide on charcoal (0.50 g) was added to the solution and hydrogenolysis was carried out for 30 hr. After hydrogenolysis was over, the catalyst was filtered and washed with water. A part of the combined solution was used for amino acid analysis to determine the yield of amino acid.

To the main reaction mixture, 10 m*l* of 2N hydrochloric acid was added and the solution was evaporated to dryness under reduced pressure. To the residual material, absolute ethanol (20 m*l*) was added to extract amino acid hydrochloride. Undissolved sodium chloride was removed by filtration. The alcoholic solution was evaporated to dryness *in vacuo* and the residue was dissolved in 10 m*l* of water. The amino acid solution was applied to a Dowex 50×2 column (H form, 2× 15 cm). The column was washed with water until the effluent became neutral. Then amino acid was eluted with 5% pyridine (*v*/*v*). Fractions containing alanine were combined and evaporated, 0.16 g (18%).

The crude alanine was treated with 2,4-dinitrofluorobenzene in a conventional manner.[20] The resulting DNP-alanine was purified by the use of a Celite column treated with pH 7.0 buffer as described in the earlier reports.[5,6] Results are listed in Table 1.

DNP-(S)-Alanine (reaction 3): $[\alpha]_D^{25}$ +41.5° (*c* 0.46, 1N NaOH).

Found: C, 42.48; H, 3.63; N, 16.38%. Calcd for $C_9H_9N_3O_6$: C, 42.36; H, 3.55; N, 16.47%.

DNP-(R)-Alanine (reaction 4): $[\alpha]_D^{25}$ −40.8° (*c* 0.56, 1N NaOH).

Found: C, 42.53; H, 3.67; N, 16.30%. Calcd for $C_9H_9N_3O_6$: C, 42.36; H, 3.55; N, 16.47%.

Amino Acids from Ethyl Esters of α-Keto Acids. When ethyl esters of α-keto acids were used, the reaction mixture was hydrolyzed with 50 m*l* of 2N hydrochloric acid for 3 hr after reduction and evaporation of the solvent.

DNP-(S)-α-Aminobutyric acid (reaction 21): $[\alpha]_D^{25}$ +15.3° (*c* 0.42, 1N NaOH).

Found: C, 44.68; H, 4.18; N, 15.58%. Calcd for $C_{10}H_{11}N_3O_6$: C, 44.62; H, 4.12; N, 15.61%.

DNP-(R)-α-NH_2-Butyric acid (reaction 22): $[\alpha]_D^{25}$ −15.2° (*c* 0.52, 1N NaOH).

Found: C, 44.73; H, 4.13; N, 15.57%. Calcd for $C_{10}H_{11}N_3O_6$: C, 44.62; H, 4.12; N, 15.61%.

Amino Acids from Sodium Salts of α-Keto Acids. The experimental procedures using α-keto acid sodium salt are similar to those described above. The results are summarized in Table 2.

Amino Acid Analysis of the Products. Synthesized amino acids were analyzed by the use of a Phoenix 5000 K automatic amino acid analyzer. Alanine and α-aminobutyric acid appeared in the ranges of elution volume 148—159 m*l* and 157—159 m*l*. In each of the reactions using benzyl and ethyl esters of α-keto acid and also the α-keto acid sodium salt, few unknown peaks signifying trace amounts were observed in both long (for acidic and neutral amino acid) and short column (for basic amino acid) analyses. The elution volume of alaninol is in a range of 88—90 m*l* in the short column. Because trace amounts of a peak which might correspond to alaninol were found in the reduction products, the low yield of amino acid in this reduction could not be due to the formation of alaninol.

This work was supported by Grant No. NSG 10-007-052 of the National Aeronautics and Space Administration.

BULLETIN OF THE CHEMICAL SOCIETY OF JAPAN VOL. 43 963—965 (1970)

Reaction of Acetonitrile with Carboxylic Esters

Akira UCHIDA, Akio DOYAMA and Sumio MATSUDA

Faculty of Engineering, Osaka University, Yamadakami, Suita

(Received June 21, 1969)

Acetonitrile is metalated by means of alkali amide,[1,2] sodium,[2] alkyllithium,[3] lithium diethylamide[4] or sodium with naphthalene,[5] using ether, petroleum ether, benzene or ethylene glycol dimethyl ether as the solvent.

In a previous paper, a large excess of acetonitrile was treated with sodium, and then the reaction of the resultant cyanomethylsodium with aromatic carbonyl compounds was attempted.[7]

It is well known that cyanomethyl carbanion

1) H. Lettré, G. Meiners and H. Wickmann, *Naturwissenschaften*, **33**, 158 (1946).
2) R. Holtzwart, *J. Prakt. Chem.* [2], **39**, 230 (1885).
3) E. M. Kaiser, *J. Org. Chem.*, **33**, 3402 (1968).
4) K. Ziegler and H. Ohlinger, *Ann.*, **495**, 84 (1932).
5) Du Pont de Memours & Co., U. S. 2307643 (1940).
6) E. Mohr, *J. Prakt. Chem.* [2], **56**, 125 (1897).
7) A. Uchida, S. Saito and S. Matsuda, This Bulletin, **42**, 2989 (1969).

adds to acetonitrile to form diacetonitrile (β-aminocrotononitrile or β-iminobutyronitrile),[2,4,5] and that diacetonitrile condenses with carbonyl compounds.[6] However, when the reaction of cyanomethylsodium with aromatic carbonyl compounds was attempted in acetonitrile, the derivatives of hydroxypropionitrile or the derivatives of cinnamonitrile were obtained.[7] These results suggest that the cyanomethyl carbanion in acetonitrile did not add to the solvent molecule, but instead reacted predominantly with aromatic carbonyl compounds.

The present study will deal with the reaction of cyanomethyl carbanion (or cyanomethylsodium) with carboxylic esters in acetonitrile.

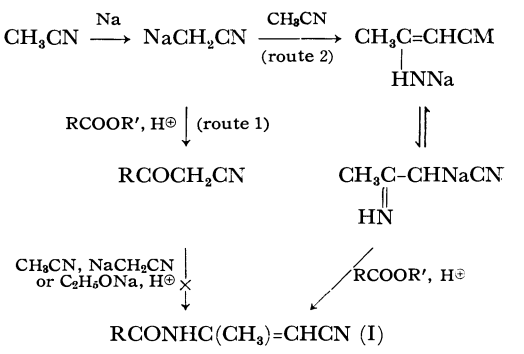

Results and Discussion

Lettré *et al.* attempted the condensation reaction of acetonitrile with various esters using sodium amide in ether and obtained the derivatives of acylacetonitrile.[1] According to the results described in a previous paper,[7] the formation of acylacetonitrile can be expected in the reaction of cyanomethylsodium with esters in acetonitrile.

When a solution of ethyl acetate and cyanomethylsodium in acetonitrile was heated under reflux for an hour, a crystalline solid was formed in a fairly good yield. This solid was identified as β-acetamidocrotononitrile from the spectroscopic data and from the results of elementary analysis, although the mp was not identical with that reported in the literature.[8] Similarly, β-benzamidocrotononitrile was obtained by the reaction of methyl benzoate.

The reaction of diethyl carbonate with acetonitrile in ether or alcohol, using sodium amide[9,10] or sodium ethoxide[11] as the catalysts, has been reported to give ethyl cyanoacetate. The reaction of diethyl carbonate with cyanomethylsodium in acetonitrile, however, resulted in the production of β-ethoxycarbonylaminocrotononitrile. These results are completely different from those to be expected on the basis of the previous paper.[7]

There might be at least two possible routes for the formation of β-acylaminocrotononitrile (I) by the reaction of an ester with cyanomethylsodium in acetonitrile.

If acylacetonitrile is formed by the reaction of cyanomethylsodium with esters, and if the resultant acylacetonitrile is added to a solvent molecule, any rearrangement will give I (route 1). On the other hand, if the reactivities of esters towards cyanomethylsodium are less than that of acetonitrile, cyanomethylsodium will add to acetonitrile preferentially to form diacetonitrile and the reaction of diacetonitrile with the esters will give I (route 2).

When a mixture of acetonitrile, acylacetonitrile (α-cyanoacetophenone or ethyl cyanoacetate,) and sodium ethoxide or cyanomethylsodium was heated under reflux for an hour, almost all of the acylacetonitrile was recovered. This means that the most plausible process is not the route 1 but the route 2. The discrepancies which exist between the aromatic carbonyl compounds and the esters may be supposed to be due to the differences in the reactivities of these two kinds of reactants towards cyanomethyl carbanion.

In the case of the reaction of the α,β-unsaturated ester with cyanomethylsodium in acetonitrile, the Michael-type addition was expected to occur. However, no Michael-type addition product was obtained; only the derivative of dihydropyridone (II) was obtained.

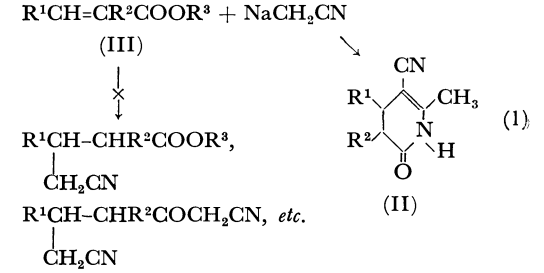

		R^1	R^2	R^3
II, III	a	H	H	CH_3
	b	H	CH_3	C_2H_5
	c	C_6H_5	H	CH_3
	d	CH_3	H	C_2H_5
	e	CH_3	$COOC_2H_5$	C_2H_5

Although the mechanism of the reaction (1) is not clearly known, the following process seems plausible.

8) Du Pont de Memours & Co., U. S. 2333493 (1941).

9) R. Levine and C. R. Hauser, *J. Amer. Chem. Soc.*, **68**, 761 (1946).

10) Mallinchrodt Chem. Works, U.S. 2342385 (1941).

11) V. H. Wallingford, D. M. Jones and A. H. Homeyer, *J. Amer. Chem. Soc.*, **64**, 577 (1942).

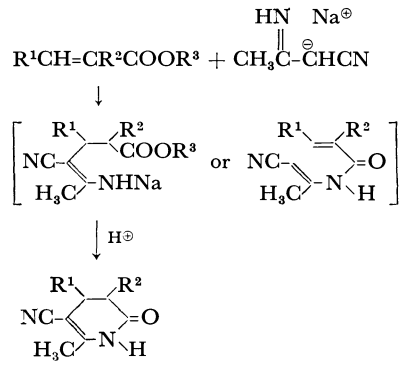

Experimental

The same instruments as those described in the previous paper[7] were used for the spectroscopic measurements.

The esters (unless otherwise noted, 0.5 mol per 1.0-g atom of sodium) was added to a solution which had previously been prepared by the dissolution of sodium in acetonitrile (375 m*l* per 1.0-g atom of sodium)and was cooled in an ice-water bath. Then the mixture was heated under reflux for an hour and neutralized with dilute sulfuric acid. The organic phase was separated and dried over anhydrous magnesium sulfate, and the solvent was removed by distillation. From the residues, the following products were isolated.

β-Acetamidocrotononitrile, from ethyl acetate, in a 64% yield; mp 107—110°C (ethanol-water) (lit,[8] mp 53°C); IR (KBr Disk) 2220 cm^{-1} (CN), 1720 cm^{-1} (CO), 1640 cm^{-1} (C=C); NMR ($CDCl_3$) τ 7.89, 7.85 (3H×2, s, $C\underline{H}_3$), 3.60 (1H, s, C=C$\underline{H}$), 1.79 (1H, broad, CON$\underline{H}$).

Found: C, 57.82; H, 6.75; N, 22.72%; M^+, 124. Calcd for C_6H_8ON: C, 58.05; H, 6.50; N, 22.75%; mol wt, 124.14.

β-Benzamidocrotononitrile, from 0.46 mol of methyl benzoate per 1.0-g atom of sodium, in an 88% yield; mp 81—83°C (benzene); IR (KBr Disk) 2220 cm^{-1} (CN), 1685 cm^{-1} (C=C); NMR ($CDCl_3$) τ 7.75 (3H, s, $C\underline{H}_3$), 3.47 (1H, s, C=C$\underline{H}$CN), 2.5 (6H, m, aryl $\underline{H}$+N$\underline{H}$).

Found: C, 70.67; H, 5.46; N, 15.09%; M^+, 186. Calcd for $C_{11}H_{10}ON_2$: C, 70.95; H, 5.41; N, 15.05%; mol wt, 186.21.

β-Ethoxycarbonylaminocrotononitrile, from diethyl carbonate, in a 69% yield; mp 87—90°C(acetone); IR (KBr Disk) 2200 cm^{-1} (CN), 1750 cm^{-1} (CO), 1640 cm^{-1} (C=C); NMR ($CDCl_3$) τ 8.71 (3H, t, J=7 Hz, $C\underline{H}_3CH_2$), 7.82 (3H, s, $C\underline{H}_3$), 5.81 (2H, q, J=7 Hz, $CH_3C\underline{H}_2$), 4.04 (1H, s, C$\underline{H}$CN), 2.65 (1H, broad, CON$\underline{H}$).

Found: C, 54.67; H, 6.86; N, 18.17%; M^+, 154. Calcd for $C_7H_{10}O_2N_2$: C, 54.53; H, 6.54; N, 18.17%; mol wt, 154.17.

3,4-Dihydro-5-cyano-6-methyl-2-pyridone (IIa), from methyl acrylate, in a 69% yield; mp 213—214°C (THF); IR (KBr Disk) 3200, 3150 cm^{-1} (NH), 2200 cm^{-1} (CN), 1690 cm^{-1} (CO), 1650 cm^{-1} (C=C); NMR ($CDCl_3$) τ 7.88 (3H, s, $C\underline{H}_3$), 7.57 (4H, s, $C\underline{H}_2C\underline{H}_2$), 1.50 (1H, broad, CON$\underline{H}$).

Found: C, 61.58; H, 6.05; N, 20.43%; M^+, 136. Calcd for $C_7H_8ON_2$: C, 61.75; H, 5.92; N, 20.85%; mol wt, 136.15.

3,4-Dihydro-3,6-dimethyl-5-cyano-2-pyridone (IIb), from ethyl methacrylate, in a 75% yield; mp 148—150°C (ethanol); IR (KBr Disk) 3200, 3100 cm^{-1} (NH), 2200 cm^{-1} (CN), 1690 cm^{-1} (CO), 1650 cm^{-1} (C=C); NMR ($CDCl_3$) τ 8.77 (3H, d, J=6.0 Hz, $C\underline{H}_3$-CH), 7.86 (3H, s, $C\underline{H}_3$), 7.1—7.7 (3H, m, $C\underline{H}_2C\underline{H}$), 1.10 (1H, broad, CON$\underline{H}$).

Found: C, 64.00; H, 7.02; N, 18.77%; M^+, 150. Calcd for $C_8H_{10}ON_2$: C, 63.98; H, 6.71; N, 18.65%; mol wt, 150.18.

3,4-Dihydro-4-phenyl-5-cyano-6-methyl-2-pyridone (IIc), from 0.4 mole of methyl cinnamate per 1.0-g atom of sodium, in a 72% yield; mp 188—190°C (methanol); IR (KBr Disk) 3200, 3100 cm^{-1} (NH), 2200 cm^{-1} (CN), 1685 cm^{-1} (CO), 1634 cm^{-1} (C=C); NMR ($CDCl_3$) τ 7.86 (3H, s, $C\underline{H}_3$), 7.16 (2H, m, $C\underline{H}_2$), 6.12 (1H, m, $C_6H_5C\underline{H}$), 2.73 (5H, m, aryl $\underline{H}$), 1.12 (1H, broad, CON$\underline{H}$).

Found: C, 73.65; H, 5.45; N, 13.23%; M^+, 212. Calcd for $C_{13}H_{12}ON_2$: C, 73.56; H, 5.70; N, 13.20%; mol wt, 212.24.

3,4-Dihydro-4,6-dimethyl-5-cyano-2-pyridone (IId), from ethyl crotonate, in a 57% yield; mp 130—132°C (acetonitrile); IR (KBr Disk) 3200, 3100 cm^{-1} (NH), 2200 cm^{-1} (CN), 1670 cm^{-1} (CO), 1620 cm^{-1} (C=C); NMR ($CDCl_3$) τ 8.78 (3H, d, J=6.3 Hz, $C\underline{H}_3$-CH), 7.87 (3H, s, $C\underline{H}_3$C=C), 7.85—7.04 (3H, m, C$\underline{H}$-$C\underline{H}_2$), 1.02 (1H, broad, CON$\underline{H}$).

Found: C, 64.04; H, 7.08; N, 19.07%; M^+, 150. Calcd for $C_8H_{10}ON_2$: C, 63.98; H, 6.71; N, 18.69%; mol wt, 150.18.

3,4-Dihydro-3-ethoxycarbonyl-4,6-dimethyl-5-cyano-2-pyridone (IIe), from 0.4 mole of diethyl ethylidenemalonate per 1.0-g atom of sodium, in 60% yield; mp 91—93°C (ethanol-water); IR (neat) 3250 cm^{-1} (NH), 2200 cm^{-1} (CN), 1700 cm^{-1} (CO), 1640 cm^{-1} (C=C); NMR ($CDCl_3$) τ 8.73 (3H, d, J=7.0 Hz, $C\underline{H}_3CH$), 8.70 (3H, t, J=7.0 Hz, $C\underline{H}_3CH_2$), 7.83 (3H, s, $C\underline{H}_3$ C=C), 6.6—7.2 (2H, m, $CH_3C\underline{H}C\underline{H}COOC_2H_5$), 5.73 (2H, q, J=7.0 Hz, $CH_3C\underline{H}_2$), 1.20 (1H, broad, CON$\underline{H}$).

Found: C, 59.17; H, 6.40; N, 12.60%; M^+, 222. Cacld for $C_{11}H_{14}O_3N_2$: C, 59.45; H, 6.35; N, 12.60%; mol wt, 222.24.

SHORT COMMUNICATIONS

Thermal Dimerization of Tropilidene*1

Keigo TAKATSUKI,*2 Ichiro MURATA*2 and Yoshio KITAHARA

Department of Chemistry, Faculty of Science, Tohoku University, Katahira-cho, Sendai

(Received December 12, 1969)

We have found an example of a [6+4] combination between two hydrocarbon molecules[1] in the Diels-Alder reaction for the first time. Although the photochemical dimerization of tropilidene (I) to give a dimer (II)[2] is known, comparable studies with thermal reactions have not hitherto been reported. In the course of our research on the Diels-Alder reactions of tropilidene, we have found that the thermal reaction of I gave a dimer (III).

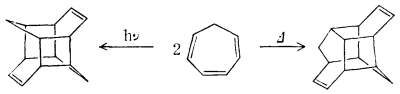

(II) (I) (III)

Fig. 1

When I was heated in an ampoule at 170°C for 100 hr, vacuum distillation (40—43°C/1 mmHg) of the product followed by silicagel chromatography (pentane) gave colorless prisms (from methanol), mp 157—162°C, $C_{14}H_{16}$, in 26% yield, IR, 3020, 2910, 1641, 1436, 889, 731 cm^{-1}; UV, end absorption; MS, *m/e* 184 (M^+), the base peak was found at *m/e* 92 corresponding to the tropilidene ion $C_7H_8^+$ and the second intense peak at *m/e* 91 (79%) corresponding to the tropylium ion $C_7H_7^+$. The NMR specrtum[3] showed the asymmetric complex olefinic protons multiplet at 6.4—5.2 (4H) and the three groups of multiplets centered at 2.8 (4H, allylic methine), 2.3 (4H, methine) and 1.9 (4H, methylene) respectively. These data strongly suggest the structure of pentacyclo[7,5,0,$0^{2,7}$,$0^{5,13}$, $0^{6,12}$]tetradeca-3,10-diene (III) for this dimer. III was identical in all respects with the authentic sample[4] which was obtained by the Wolf-Kishner reduction of the cycloaddition product of tropone and I.[5]

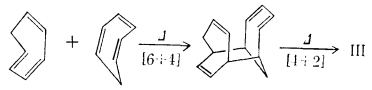

Fig. 2

The formation of III, which may be considered as a concerted [6+4]-cycloaddition[6] followed by an intramolecular Diels-Alder addition, is an additional evidence for the *trans*-[6+4]-cycloaddition.[5,7]

*1 This paper was presented at the 21st Annual Meeting of the Chemical Society of Japan, Osaka, April, 1968.

*2 Present address: Department of Chemistry, Faculty of Science, Osaka University, Toyonaka-shi, Osaka.

1) Thermal [6+4] co-cycloaddition of two azepine molecules has recently been discovered. I. C. Paul, S. M. Johnson, J. H. Barrett and L. A. Paquette, *Chem. Commun.*, **1969**, 6.

2) G. O. Schenck, J. Kuhls and C. H. Krauch, *Ann. Chem.*, **639**, 20 (1966).

3) Determined on a Varian A-60 instrument in deuteriochloroform and reported as δ units relative to TMS ($\delta=0$).

4) Y. Fujise, Ph. D. Thesis (1967) of Tohoku University (under supervision of Professor Shô Itô). We thank Professor Shô Itô for comparison of this compound.

5) Shô Itô, Y. Fujise and M. C. Woods, *Tetrahedron Lett.*, **1967**, 1059.

6) R. Hoffmann and R. B. Woodward, *J. Amer. Chem. Soc.*, **87**, 2046, 4388 (1965).

7) R. C. Cookson, B. V. Drake, J. Hudec and A. Morrison, *Chem. Commun.*, **1966**, 15; Shô Itô, Y. Fujise, T. Okuda and Y. Inoue, This Bulletin, **39**, 1351 (1966).

Fluorescence Spectrum of Pyrene Vapor: Emission from the Second Excited Singlet State*[1]

Akira NAKAJIMA and Hiroaki BABA

Division of Chemistry, Research Institute of Applied Electricity, Hokkaido University, Sapporo

(Received November 22, 1969)

It is generally believed that in isolated polyatomic organic molecules, with the exception of azulene, internal conversion occurs at such a high efficiency that fluorescence cannot be observed from excited singlet states other than the first.[1-5] We have recently measured the fluorescence spectrum of pyrene vapor and detected an emission which can be assigned to fluorescence from the second excited singlet.

Fluorescence and excitation spectra were measured with a Hitachi fluorescence spectrophotometer of type MPF-2A, to which an electric furnace was attached. All the spectra were corrected for instrumental factors. Pyrene was highly purified by chemical treatment, chromatography, vacuum sublimation and zone melting.

Figure 1 shows fluorescence spectra of pyrene vapor. In the near ultraviolet region, pyrene has four electronic absorption bands denoted by I, II, III and IV. In Fig. 1, the wavelengths of the exciting light, 323, 268 and 236 mμ correspond

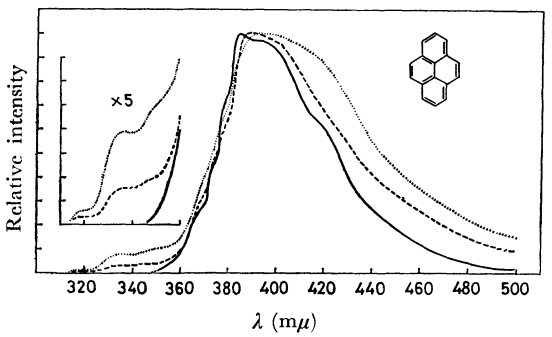

Fig. 1. Fluorescence spectra of pyrene vapor at 200°C and ~3 mmHg obtained by excitation at different wavelengths: solid line, 323 mμ; dashed line, 268 mμ; dotted line, 236 mμ.

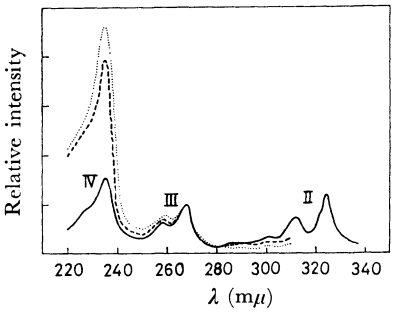

Fig. 2. Excitation spectra of pyrene vapor at 205°C and ~3 mmHg obtained by monitoring at different wavelengths: solid line, 370 mμ; dashed line, 340 mμ; dotted line, 330 mμ.

to the 0–0 transitions for II, III and IV, respectively. It is seen that excitation into the third or fourth excited singlet gives rise to an additional emission between 320 and 360 mμ, *i. e.*, in the region adjacent to the absorption band II. The fluorescence excitation spectrum obtained by monitoring the emission in the above region was different from that obtained by monitoring at a wavelength longer than 360 mμ (Fig. 2). The excitation spectrum monitored at 370 mμ is normal and is in agreement with the absorption spectrum. On the contrary, the excitation spectrum monitored at 340 or 330 mμ differs markedly from the absorption spectrum in intensity distribution, although both spectra have essentially the same vibrational structure. Thus, the quantum yield of the emission between 320 and 360 mμ increases rapidly with excitation into successively higher singlet states. These experimental results can be explained by attributing the emission in the 320—360 mμ region to the fluorescence which originates from the second excited singlet of the pyrene molecule.

*[1] Presented at the 22nd Annual Meeting of the Chemical Society of Japan, Tokyo, April, 1969; Preprints for the Meeting, Vol. I (1969), p. 102.

1) B. Stevens and E. Hutton, *Mol. Phys.*, **3**, 71 (1960).
2) R. Williams and G. J. Goldsmith, *J. Chem. Phys.*, **39**, 2008 (1963).
3) R. J. Watts and S. J. Strickler, *ibid.*, **44**, 2423 (1966).
4) J. E. Haebig, *J. Phys. Chem.*, **71**, 4203 (1967).
5) M. Bixon and J. Jortner, *J. Chem. Phys.*, **48**, 715 (1968).

Thiocarbonyl Compounds as Potential Scavengers of Carbon Radicals

Gen-ichi TSUCHIHASHI, Makiko YAMAUCHI and Atsuyoshi OHNO

Sagami Chemical Research Center, Ohnuma, Sagamihara-shi, Kanagawa

(Received December 15, 1969)

Stable free radicals, such as di-*t*-butylnitroxide,[1] garvinoxyl,[2] or DPPH,[3] are known to act as scavengers for carbon radicals. We would like to report that thiocarbonyl compounds function as powerful, *molecular-type* scavengers toward carbon radicals.

When azobisisobutyronitrile (AIBN) was decomposed in refluxing toluene containing an equimolar amount of thiobenzophenone (I), the yield of tetramethylsuccinonitrile (TMSN), a dimerization product of 1-cyano-1-methylethyl radicals, decreased from 89% (without I) to 21%. 1-Cyano-1-methylethyl radicals were efficiently captured by I, and as a result the adduct IIa was produced in 78% yield. IIa[4]: mp 168°C; IR 2200 and 2240 cm^{-1} (CN); NMR[5] 1.17 (s,6H), 1.34 (s,6H), and 7.3—7.8(m,10H); mass M^+ 334.

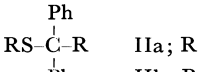

IIa; R=1-cyano-1-methylethyl

IIb; R=1-phenylethyl

Similarly, the addition of I for the decomposition of azobis(1-phenylethane) in toluene resulted in a marked decrease of the formation of 2,3-diphenylbutane:[6] 90% (without I) and 12% (with I). 1-Phenylethyl radicals were trapped by I and the addition product was obtained in 80% yield. This addition product proved to be a 1 : 1 mixture of two diastereomers of IIb, as shown by NMR: 0.86 (d,3H), 1.25(d,3H), 3.10(q,1H), 4.12(q, 1H), and ~7.1(m, 20H) for one isomer and 1.15(d,3H), 1.23(d,3H), 3.06(q,1H), 4.14(q,1H), and ~7.1 (m, 20H) for the other. The mass spectrum was also consistent with this structure, but the most convincing evidence is that oxidation of IIb with hydrogen peroxide in acetic acid produces soley methyl triphenylmethyl ketone in 98% yield. This presumably arises from oxidation of IIb to the sulfone, elimination of the sulfinic acid to form the olefin, and epoxidation, followed by rearrangement of the epoxide:

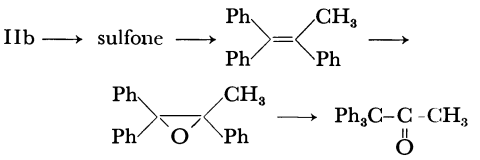

Thioacetophenone (III) also appears to be an efficient radical-capturing agent. Thus, when AIBN was decomposed in toluene with two molar equivalents of III, TMSN was formed in only 23% yield and the adduct (IVa) was produced instead of the dimer in a yield of 71%.

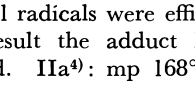

IVa; R=1-cyano-1-methylethyl

IVb; R=1-phenylethyl

IVa: mp 176°C; IR 2230 cm^{-1} (CN); NMR 0.97 (s,6H), 1.62(s,6H), 2.27(s,6H), and ~7.1(m,10H). Desulfurization of IVa with Ra-Ni(W-2) in ethanol gave *trans*-2,3-diphenyl-2-butene (79%). By a similar reaction of azobis(1-phenylethane) with III, adduct (IVb) was formed in 69% yield and the formation of 2,3-diphenylbutane was reduced to 27%. IVb: mp 204—205°C; NMR 1.30(d,6H), 1.45(s,6H), 3.26 (q,2H), and 6.9—7.2(m, 20H). Desulfurization of IVb with Ra-Ni(W-2) gave *trans*-2,3-diphenyl-2-butene(57%), *meso*-2,3-diphenylbutane (18%), and ethylbenzene(42%).

Hence these thioketones appear as potential radical scavengers. The capturing power is particularly strong toward a neutral carbon radical. 1-Phenylethyl radicals were trapped by I (five-fold excess)[7] and III (five-fold excess)[7] quite effectively, cutting down the yields of dimer to 6.0 and 8.2%, respectively, whereas the addition of thiophenol, in place of thioketones, to the system allowed formation of the dimer in a higher yield of 28%.[8] Apparently, these thioketones are much better scavengers than thiophenol. The use of these thioketones is further advantageous, because they possess visible absorption maxima at around 600 mμ. The extent of scavenged radical can be followed easily by measuring the disappearance of this visible absorption.

Studies on the relationship between the radical capturing power and the structure of thiocarbonyl compounds are in progress.

1) A. K. Hoffmann, A. M. Feldman, E. Gelblum and W. G. Hodgson, *J. Amer. Chem. Soc.*, **86**, 639 (1964).

2) P. D. Bartlett and T. Funahashi, *ibid.*, **84**, 2596 (1962).

3) C. E. H. Bawn and S. F. Mellish, *Trans. Faraday Soc.*, **47**, 1216 (1951); G. S. Hammond, J. N. Sen and C. E. Boozer, *J. Amer. Chem. Soc.*, **77**, 3244 (1955).

4) Satisfactory elemental analyses were obtained for all new compounds reported here.

5) The NMR spectra were measured by a Varian HA-100 spectrometer. Chemical shifts are shown as δ (in ppm) from TMS in $CDCl_3$.

6) A 1 : 1 mixture of *dl* and *meso* isomers.

7) The concentrations of the thioketones and the azo compound are 1.3×10^{-2}M and 2.5×10^{-3}M, respectively.

8) F. D. Greene and M. A. Berwick, Abstracts, 156th ACS National Meeting, Atlantic City, N. J., Sep., 1968, ORGN-112.

The Structures of Nigakilactones E and F

Tatsushi MURAE, Tôru IKEDA, Takahiko TSUYUKI, Tadaaki NISHIHAMA and Takeyoshi TAKAHASHI

Department of Chemistry, Faculty of Science, The University of Tokyo, Hongo, Bunkyo-ku, Tokyo

(Received December 16, 1969)

The isolation and determination of the structure of bitter principles (nigakilactones A, B, C and D (quassin)) of *Picrasma ailanthoides* Planchon have already been reported.[1] Two additional bitter principles have now been isolated from the same plant. These new bitter principles, nigakilactones E ($C_{24}H_{34}O_8$) and F($C_{22}H_{32}O_7$), contain one hydroxyl group more than nigakilactones C and B, respectively.

Nigakilactone F (I, R_1=OH, R_2=H, R_3=OH), mp 265—265.5°C, M^+ 408, $[\alpha]_D$ +46° (*c* 0.20, in EtOH), λ_{max}^{MeOH} 272 nm (ε 4500), IR (Nujol): 3530, 3470 sh, 3450, 1732, 1684, 1675, 1642, 1634 cm^{-1}, was obtained by the alkaline hydrolysis of nigakilactone E (I, R_1=OAc, R_2=H, R_3=OH), mp 280°C, M^+ 450, $[\alpha]_D$ +36° (*c* 0.22, in EtOH), λ_{max}^{MeOH} 264 nm (ε 4600), IR (Nujol): 3460, 1740, 1725 sh, 1717, 1642, 1255 cm^{-1}, which was not acetylated with acetic anhydride and pyridine.

The NMR spectra (Table 1) of nigakilactones E and F are best interpreted on the basis of the skeletal structures of two known nigakilactones C (I, R_1=OAc, R_2=H, R_3=H) and B (I, R_1=OH, R_2=H, R_3=H), respectively. The spectra of nigakilactones C and B show the presence of two secondary and two tertiary methyls. However, those of nigakilactones E and F indicate the presence of one secondary and three tertiary methyls.

TABLE 1. NMR SPECTRAL DATA (δ in ppm, in $CDCl_3$)

Nigakilactones	E	F	B	C
s-C<u>H</u>$_3$	1.08 d *J*=7	1.11 d *J*=7	1.00 d *J*=6.5	1.01 d *J*=6
			1.13 d *J*=6.5	1.06 d *J*=7
t-C<u>H</u>$_3$	1.25 s	1.22 s	1.21 s	1.27 s
	1.27 s	1.46 s	1.45 s	1.27 s
	1.53 s	1.46 s		
-O-CO-C<u>H</u>$_3$	1.98 s			1.95 s
<u>H</u>-C-OCH$_3$	3.38 d *J*=9	3.03 d *J*=9		
-O-C<u>H</u>$_3$	3.55 s	3.58 s	3.60 s	3.42 s
	3.57 s	3.73 s	3.65 s	3.54 s
<u>H</u>-C-OH		4.00 q *J*=11; 9		
C | C-C<u>H</u>-O-	4.21m	4.13m	4.15m	4.14m
<u>H</u>-C-OAc	5.54 q *J*=11; 9			5.22 q *J*=11; 9
C=C<u>H</u>	5.17 d *J*=2.5	5.43 d *J*=2	5.45 d *J*=2.5	5.10 d *J*=2.5

On oxidation with $Na_2Cr_2O_7$ in acetic acid, nigakilactone F yielded a ketone (I, R_1, R_2=O, R_3=OH), mp 256.5—257°C, $C_{22}H_{30}O_7$, M^+ 406, λ_{max}^{MeOH} 264 nm (ε 5700), IR (Nujol): 3550, 3480, 1730, 1696, 1630 cm^{-1}, which was then converted to quassin (II)[2] by dehydration with acetic anhydride and sodium acetate.

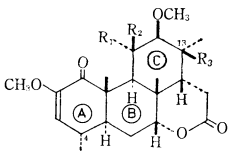

I

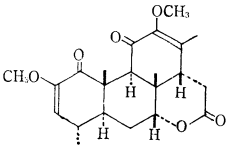

II

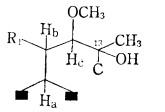

III-a: R_1=OAc
III-b: R_1=OH
(■ indicates carbon with no proton)

These observations, along with the spectral data (Table 1), show that a hydroxyl group is located on C-13 (not on C-4) and lead to partial structures of III-a and -b for the ring C of nigakilactones E and F, respectively. The coupling costants of H_a–H_b (J=11 Hz) and H_b–H_c (J=9 Hz) indicate that two adjacent protons are in axial-axial relationships. One secondary methyl of nigakilactone E (and F) should be located on C-4. The facile dehydration of the ketone (I, R_1, R_2=O, R_3=OH) to yield II suggests that the hydroxyl group at C-13 is in axial conformation.

Thus, the structures of nigakilactones E and F are shown to be I (R_1=OAc, R_2=H, R_3=OH) and I(R_1=OH, R_2=H, R_3=OH), respectively.

1) T. Murae, T. Tsuyuki, T. Nishihama, S. Masuda and T. Takahashi, *Tetrahedron Lett.*, **1969**, 3013.

2) Z. Valenta, A. H. Gray, D. E. Orr, S. Papadopoulos and C. Podešva, *Tetrahedron*, **18**, 1433 (1962).

Vapor-phase Sample Supply of Metals as β-Diketonates in Atomic Absorption Spectroscopy[1]

Hisao KAWAMURA,* Giichiro TANAKA,* Norio KURITA** and Yoshihiko OHYAGI**

*Division of Environmental Contamination, National Institute of Radiological Sciences, Anagawa, Chiba
**Department of Chemistry, Faculty of Science, Chiba University, Yayoi-cho, Chiba

(Received December 27, 1969)

In atomic absorption and other flame spectroscopy, the nebulization technique has been widely employed to supply the analytical flame with liquid samples. Instead of the conventional nebulization, though, methods have recently been reported in which metal fumes or vapors are introduced to flames or absorption cells.[2] In the present work a volatilizer-premix burner system has been developed and a vapor-phase sample supply has been extended by the use of some β-diketonates of metals.[3]

The volatilizer-premix burner was constructed with a volatilizer unit and a pre-heated mixing chamber-type premix burner unit, which were connected to each other in a gas-tight manner. The volatilizer unit consisted of a volatilization chamber (a Pyrex tube, 1 cm I.D. × 13 cm L.) and an electric heater. This chamber was used with or without a small column packed in its rear end which worked as a "spoiler." The temperature inside the volatilization chamber was adjusted to any level between 100 and 250°C. The premix burner unit consisted of a metal mixing chamber with an electric heater and a 5 cm-slot burner head. The mixing chamber was heated to any temperature in the 150—250°C range. Dried nitrogen (up to 170 ml/min) was supplied to the volatilization chamber. Air (4.8 l/min) and acetylene (1.2 l/min) were supplied to the mixing chamber. A Perkin-Elmer Model 303 atomic absorption spectrophotometer was used to record the absorptions at the most sensitive line of each metal. Samples were prepared by dissolving the laboratory-prepared trifluoroacetylacetonates of copper, chromium and iron[4] in chloroform and commercially obtained acetylacetonates of copper and chromium in a chloroform-methanol mixture. Samples of 0.2—10 μl (containing about 0.1—5 μg metal) were injected by a microsyringe into the volatilization chamber through a silicone rubber septum.

Higher temperatures of the volatilization and mixing chamber, and larger nitrogen flow rates, generally gave higher peak absorptions. The analytical curves obtained with a 1 cm glass-microbead column spoiler are shown in Fig. 1. The absolute sensitivity was found to be considerably higher than that estimated with the conventional nebulization (about eight-fold in the case of chromium). With a 4 cm gas-liquid partition column spoiler (30% SE-30 on Shimalite W), the metal β-diketonates were completely separated from the solvent and from each other. Background absorption caused by chloroform was eliminated. These results indicate that the vaporphase sample supply in atomic absorption spectroscopy makes possible a rapid, highly sensitive, and interference-free determination of metals as volatile β-diketonates and possibly also as organometallic compounds. We have also noted the possibility of identifying any particular ligand of metal chelates.

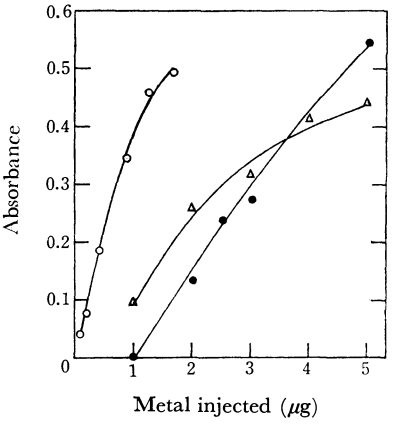

Fig. 1. Analytical curves for chromium acetylacetonate (○), copper trifluoroacetylacetonate (●), and iron trifluoroacetylacetonate (△).

	○	●	△
Volatilization chamber temp. (°C)	202	180	220
Mixing chamber temp. (°C)	200	238	199
Nitrogen flow rate (ml/min)	168	164	164

Precision in C.V.(%): 3.4(○), 13(●), 4.4(△)

1) Presented partly at the 22nd Annual Meeting of the Chemical Society of Japan, Tokyo, April, 1969 and at the 18th Annual Meeting of the Japan Society for Analytical Chemistry, Sapporo, October, 1969.

2) Y. Ohyagi, *Bunseki Kagaku*, Annual Review 1969, 27 R (1969).

3) R. S. Juvet, Jr., and R. P. Durbin, *Anal. Chem.*, **38**, 565 (1966).

4) E. W. Berg and J. T. Truemper, *J. Phys. Chem.*, **64**, 487 (1960).

The Crystal and Molecular Structure of 2,2′-Bipyridinium Tetrabromocobaltate(II)

Shigetaka KODA, Shun'ichiro OOI and Hisao KUROYA

Department of Chemistry, Faculty of Science, Osaka City University, Sumiyoshi-ku, Osaka

(Received December 29, 1969)

2,2′-Bipyridine (=bip) reacts with $CoBr_2$ in a HBr solution to yield a moderately stable crystalline compound. Elemental analysis indicates the composition $[bipH_2][CoBr_4]$; this formula was confirmed by the X-ray analysis. We wish here to report the structural features of the $[CoBr_4]^{2-}$ ion and the conformation of the bipyridinium ion in the crystal.

Crystal data: monoclinic, space group $P2_1/c$: $a=8.420\pm0.005$, $b=14.00\pm0.01$, $c=12.878\pm0.006$ Å, $\beta=98.6\pm0.1°$; $Z=4$, $Dc=2.34$ g·cm^{-3}, $\mu=187.0$ cm^{-1} (for Ni$K\alpha$). Multiple-film equi-inclination Weissenberg photographs were taken with Ni$K\alpha$ radiation about the a and c axes, while the intensities of 1551 independent reflections were obtained by visual estimation.

The structure was solved by Patterson and Fourier methods, and the positional and isotropic thermal parameters were refined by the least-squares procedure. The conventional R-factor is 15.7% at this stage; further refinements are now in progress.

The crystal consists of bipyridinium cations and $[CoBr_4]^{2-}$ anions. In the anions, each cobalt atom is surrounded tetrahedrally by four bromine atoms. The mean value of the four Co–Br bond distances is 2.42 Å; this is presumably the first example found for the Co(II)–Br length. It is known that the configuration of the 2,2′-bipyridine molecule in the crystalline state is planar, the two nitrogen atoms being in the *trans* positions with respect to the C–C bond connecting the two pyridine rings.[1] However, this is not the case for our bipyridinium ion. As is shown in the figure, the pyridine rings are inclined toward one another, thus departing from the *trans*-coplanar configuration; the dihedral angle between the ring planes is 37.4°. The bipyridinium cation is isoelectronic with biphenyl, in which the angle of twisting is 45°.[2] The small discrepancy in those values may be attributable to the formation of rather strong hydrogen bonds between the two N^+–H groups in the cation and bromine atoms (N^+–H···Br^-=3.24 and 3.32 Å respectively). The bond distances and angles in the rings are normal within the range of standard deviation (~0.06 Å).

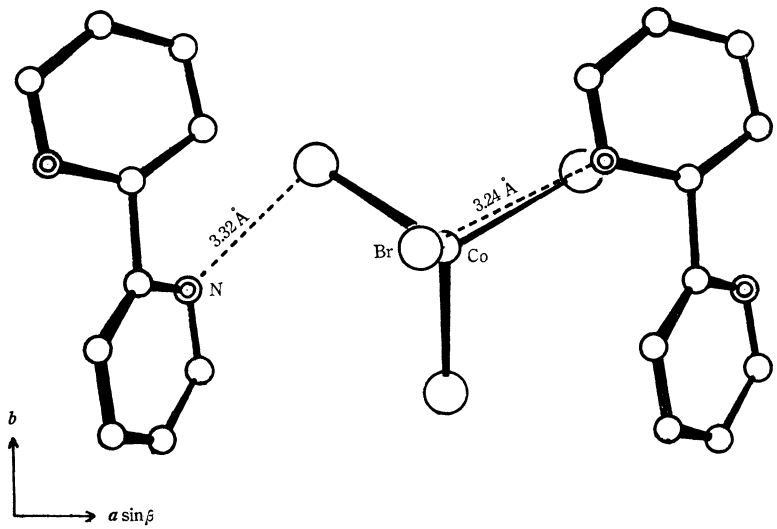

Fig. 1. The crystal structure viewed along the c axis.

1) L. L. Merritt, Jr., and E. D. Schroeder, *Acta Crystallogr.*, **9**, 801 (1956).

2) P. W. Allen and L. E. Sutton, *ibid.*, **3**, 46 (1950).

An Unusual Photochemical Reaction of Friedelin

Makoto TAKAI, Reiko AOYAGI, Shūzō YAMADA, Takahiko TSUYUKI and Takeyoshi TAKAHASHI

Department of Chemistry, Faculty of Science, The University of Tokyo, Hongo, Bunkyo-ku, Tokyo

(Received January 6, 1970)

The photochemical reaction of friedelin has already been reported.[1-3] We now wish to describe a photochemical cleavage of friedelin to form an unusual product whose formation is not known.

Photochemical Cleavage of Friedelin in *n*-Hexane. The suspension of friedelin (I, 1.00 g) in *n*-hexane (500 g) was heated under reflux with bubbling of argon for 1 hr. The solution was then irradiated with a high pressure mercury lamp (100 W) under an argon atmosphere for 8 hr at room temperature. After the solvent was distilled off under reduced pressure, the products were separated to hydrocarbon, aldehyde, ketene, ketone and carboxylic acid with silica gel chromatography.

From TLC examination (SiO_2; PhH : Et_2O, 10 : 1), the carboxylic acid was shown to be a mixture of two components. One of the components, with a lower R_f value, was identical with 3,4-secofriedelan-3-oic acid (II, R=H),[1,2] and the other was an unknown carboxylic acid.

After the ketene fraction was dissolved in benzene and heated with water for 2 hr, the same mixture was obtained as an acid fraction. The carboxylic acids were then esterified with diazomethane and separated to methyl 3,4-secofriedelan-3-oate (II, R=Me, 135 mg) and the other methyl ester (105 mg, about 10 per cent based on I). On mass spectra, the molecular ion peak of the latter appeared at *m/e* 444, which was 14 mass units (due to CH_2) lower than that of II(R=Me). Moreover, the peaks of $(M-56)^+$ were seen in the spectra of the two methyl esters. A loss of 56 mass units could be interpreted by the fragmentation 'a' (Fig. 1).

From these facts, the latter ester was inferred to be 5α-ethyl-10β-carbomethoxymethyl-des-A-friedelane (III, R=Me). This material was identical (mp, GLC, IR, mass and NMR spectra) with the authentic sample, obtained by the following method (Barbier-Wieland degradation) from ethyl 3,4-secofriedelan-3-oate (II, R=Et).

Synthesis of 5α-Ethyl-10β-carbomethoxymethyl-des-A-friedelane (III, R=Me). Irradiation of friedelin in ethanol gave ethyl 3,4-secofriedelan-3-oate (II, R=Et),[2] which afforded 3,3-diphenyl-3,4-secofriedelan-3-ol (IV) [mp 189—190°C, ν_{O-H} 3560 cm^{-1}, $C_{42}H_{62}O$] on Grignard reaction with phenylmagnesium bromide in tetrahydrofuran. IV gave 3,3-diphenyl-3,4-secofriedel-2-ene (V) [mp 202—203°C, $C_{42}H_{60}$] by dehydration with iodine and benzene. On oxidation of V with acetic acid and chromium trioxide, 5α-ethyl-10β-carboxymethyl-des-A-friedelane (III, R=H) [mp 249—250°C, $\nu_{C=O}$ 1695 cm^{-1}, $C_{29}H_{52}O_2$] was obtained. III(R=H) was esterified with diazomethane to give 5α-ethyl-10β-carbomethoxymethyl-des-A-friedelane (III, R=Me) [mp 173—174°C, $\nu_{C=O}$ 1735 cm^{-1}, mw 444 (mass). Found: C, 81.27; H, 11.81%. Calcd for $C_{30}H_{52}O_2$: C, 81.02; H, 11.79%].

Thus the unknown carboxylic acid was confirmed to be 5α-ethyl-10β-carboxymethyl-des-A-friedelane (III, R=H). This type of photochemical process giving rise to III(R=H) has never been reported. Studies to clarify this process are under way.

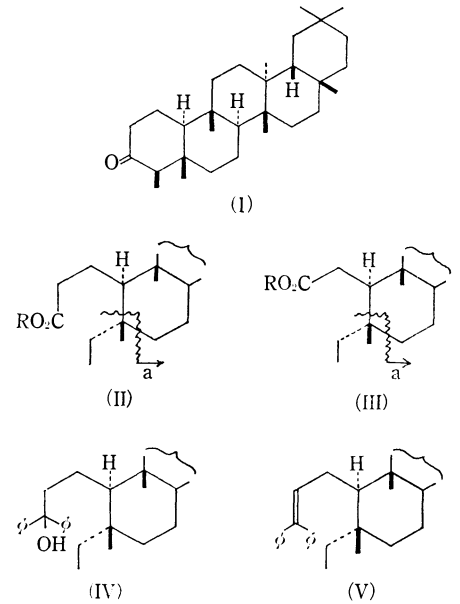

Fig. 1

1) F. Kohen and R. Stevenson, *Chem. Ind.*, **1966**, 1844; F. Kohen, A. S. Samson, S. J. and R. Stevenson, *J. Org. Chem.*, **34**, 1355 (1969).

2) T. Tsuyuki, S. Yamada and T. Takahashi, This Bulletin, **41**, 511 (1968).

3) T. Tsuyuki, R. Aoyagi, S. Yamada and T. Takahashi, *Tetrahedron Lett.*, **1968**, 5263.

COS as an Electron Scavenger in Liquid-phase Radiolysis

Shun-ichi HIROKAMI, Seishi SHISHIDO and Shin SATO

Department of Applied Physics, Tokyo Institute of Technology, Ookayama, Meguro-ku, Tokyo

(Received January 16, 1970)

Although many compounds such as alkyl halides are known to dissociate after capturing an electron,[1] there are a few compounds which produce stable products after the dissociation.[2] Nitrous oxide is one such exceptional compound and has been extensively used in radiation chemistry.[3] The discovery of more such compounds is eagerly desired.

In the study of the γ-radiolysis of benzene, we have recently used COS as one of the solutes and have found that this compound produces CO as much as N_2 when nitrous oxide is used as a solute. Figure 1 shows the results obtained when the competition of COS and N_2O was examined. Obviously, the CO production from a COS-benzene solution decreased as the concentration of N_2O increased; the decrease in CO was about a half of the difference between the amounts of N_2 produced in the absence and in the presence of COS.*1 Since the G-value of N_2 from a N_2O-benzene solution is known to be approximately twice that of the electrons captured by N_2O,[4] the above observation can easily be explained by assuming the following reaction:

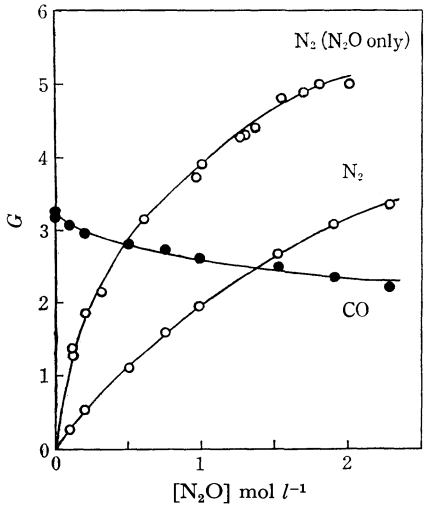

Fig. 1. The competition of COS and N_2O in the radiolysis of a benzene solution. The COS concentration is about 0.4 mol l^{-1}. (Direct decomposition of solutes is not corrected.)

$$e^- + COS \longrightarrow CO + S^-$$

or:

$$e^- + COS \longrightarrow COS^-$$

$$COS^- + C_6H_6^+ \longrightarrow CO + \text{residue}$$

At higher concentrations of N_2O, however, the amount of CO produced did not approach zero, but seemed to level off at a certain value. This is probably due to the reaction of COS with excited benzene molecules. If so, quantitative measurements will help the estimation of the ratio of ionization to excitation in the radiolysis of benzene.

We are now experimenting with COS as an electron scavenger in the radiolysis of saturated hydrocarbons. The results suggest that this compound is a little reactive to the radicals produced. This may cause some complications when analyzing the data. The details will be reported shortly.

1) J. M. Warman, K.-D. Asmus and R. H. Schuler, Advances in Chemistry Series, **82**, 25 (1968).

2) M. Matsui and M. Imamura, This Bulletin, **42**, 3362 (1969).

3) S. Sato, R. Yugeta, K. Shinsaka and T. Terao, *ibid.*, **39**, 156 (1966).

*1 Strictly speaking, this statement cannot be applied to the solutions with low N_2O concentrations.

4) R. R. Hentz and W. V. Sherman, *J. Phys. Chem.*, **73**, 2676 (1969).

Mechanism of the H_2–D_2 Exchange Reaction over ZnO—Dynamic Behaviour of Chemisorbed Hydrogen as a Reaction Intermediate during the Course of the Reaction

Shuichi NAITO, Hazime SHIMIZU, Etsuko HAGIWARA, Takaharu ONISHI and Kenzi TAMARU

Department of Chemistry, The University of Tokyo, Hongo, Bunkyo-ku, Tokyo

(Received November 24, 1969)

The mechanism of the H_2–D_2 exchange reaction over ZnO at lower temperatures (from −70°C to room temperature) was studied by measuring the adsorption during the course of the reaction by the volumetric method as well as by the infrared spectroscopic technique.[1)]

The zinc oxide employed was Kadox 15 and Kadox 25 of the New Jersey Zinc Company; it was evacuated for more than five hours at 400°C prior to the reaction. The infrared spectra of the adsorbed hydrogen and deuterium on ZnO were observed at 3490 (ZnOH), 2584 (ZnOD), 1712 (ZnH), and 1233 (ZnD) cm^{-1}, as has been reported by Eischens, Pliskin and Low.[2)]

Below room temperature, the rate of hydrogen chemisorption over ZnO was rapid, while the rate of desorption was slow. No isotope effect was detected, within the limits of experimental error, in the rate of hydrogen and deuterium chemisorption or in the adsorption equilibrium over ZnO, as has been reported previously.[3)]

When H_2 (9.4 cmHg) was pre-adsorbed over ZnO and D_2 (9.6 cmHg) was then added to the system, the pre-adsorbed H(a) was displaced by D(a) as the exchange proceeded. The rate of HD formation obeyed the first-order rate equation as to H(a), a uniform reactivity of H(a) being demonstrated. Similar experiments were carried out by the infrared technique. The rate of the total decrease in the ZnH and ZnOH-band intensities was equal to that of the increase in the ZnD and ZnOD-band intensities, and it was revealed that the rate of HD formation is proportional to the amount of exchangeable hydrogen chemisorbed which is observed by the infrared technique, and to the D_2 pressure in the ambient gas. At 0°C, the rate of HD formation in the volumetric experiment and the rate of the total decrease in the ZnH and ZnOH-band intensities in the infrared spectroscopic technique were in reasonable agreement. These results lead to the conclusion that the chemisorbed hydrogen observed by the infrared technique exhibits a behaviour similar to that measured volumetrically and that it is the real intermediate of the exchange reaction.

When a mixture of H_2 and D_2 (1 : 1) (total 22.2 cmHg) was introduced, the amounts of ZnH, ZnOH, ZnD, and ZnOD were equal at the beginning of the adsorption, but as the exchange reaction proceeded the amounts of ZnH and ZnOD increased at different rates, whereas those of ZnD and ZnOH decreased correspondingly; this demonstrated the rearrangement of the chemisorbed species through the exchange reaction. No such rearrangement was detected in the absence of the ambient gas, which shows no appreciable mobility to be involved between the hydrogen on zinc and that on oxygen. When one mixture of H_2 and D_2 (2 : 1) (total 24.2 cmHg) was introduced over ZnO, the rate of HD formation was about one and half times as great as that when another H_2 and D_2 (1 : 2) (total 24.3 cmHg) mixture was introduced. Consequently, though no isotope effect is involved in the chemisorption, as has been described above, a considerable kinetic isotope effect is observed in the rate of the exchange reaction.

As the behaviour of the four chemisorbed species, ZnH, ZnD, ZnOH, and ZnOD, may be separately examined by the infrared technique over a wide range of ambient pressures and chemisorbed amounts, and with various isotope contents, the exchange reaction through one of those species and ambient molecules, or through their recombinations, may be studied. It was, consequently, concluded that the rate of the HD formation from the recombination of the chemisorbed species (the Langmuir mechanism), which corresponds to the desorption rate, is at least one or two orders of magnitude slower than the exchange reaction between the molecular hydrogen in the ambient gas and the chemisorbed species (the Eley-Rideal mechanism).

If the repetition of the dissociative chemisorption and desorption of hydrogen results in the H_2–D_2 exchange reaction, as neither process has any kinetic isotope effect, the exchange reaction rate would exhibit no kinetic isotope effect. The marked isotope effect demonstrated in the exchange reaction proves this not to be the case.

---

1) K. Tamaru, *Adv. Catalysis* (Academic Press Inc.), **15**, 65 (1964); *Nippon Kagaku Zasshi*, **87**, 1007 (1966).

2) R. P. Eischens, W. P. Pliskin and M. J. D. Low, *J. Catalysis*, **1**, 180 (1962).

3) J. Pace and H. S. Taylor, *J. Chem. Phys.*, **2**, 578 (1934).

BULLETIN OF THE CHEMICAL SOCIETY OF JAPAN VOL. 43 975—984 (1970)

Statistical Thermodynamics of Binary Liquid Mixtures

Kiyoshi ARAKAWA and Osamu KIYOHARA

Research Institute of Applied Electricity, Hokkaido University, Sapporo

(Received May 29, 1969)

By means of the cell method and using the Sutherland type potential function for pair interactions between molecules, a statistical theory was formulated for binary liquid mixtures consisting of rigid spherical molecules differing in size. A formula was derived for cohesive energy as a function of the volume of liquid, and studied in combination with the radial distribution function. The applicability of the square-well type potential function within a cell was also examined. Formulas for excess thermodynamic functions were derived and their applicability investigated. For 22 binary systems consisting of nearly spherical molecules, excess thermodynamic functions were calculated and compared with data in literature. The results show that the theory is applicable to the mixtures.

The present paper deals with the statistical theory of non-electrolyte solutions. The principal problem in the statistical thermodynamics of liquid mixtures is to calculate the thermodynamic properties of mixtures from the forces between molecules. Many attempts have been made since the designation of "regular solutions" by Hildebrand[1] and Scott.[1,2] The following theories are remarkable: "strictly regular solution theory" based on the lattice model developed by Guggenheim[3] and Rushbrooke,[4] the "conformal solution" theory by Longuet-Higgins,[5] theories by the cell method developed mainly by Prigogine and co-workers,[6-9] by Salsburg and Kirkwood,[10] and by Scott,[11] theories based on the explicit combination of the cell method and the "corresponding state theorem" developed by Prigogine and coworkers[12] and by Scott,[11] and the significant structure theory by Eyring and coworkers.[13]

Recently, Flory and Abe have presented a simple corresponding state theory of liquid mixtures of nonpolar molecules,[14] which is applicable to mixtures of molecules differing in size, based on Prigogine's treatment of *r*-mer molecules.[15]

Theories based on the radial distribution function, which have been developed by Kirkwood, Born, Green, and others,[16] are more rigorous than the theories described above, but they are mathematically laborious, and inconvenient for practical use.

The present statistical theories of solutions are unsatisfactory as a whole, as the agreement between calculated and observed values is only qualitative, and the underlying assumptions need further examination.

The authors present a statistical theory of binary liquid mixtures by the cell method in combination with the radial distribution function, where the interaction potential between molecules is assumed to be of Sutherland type.

Part I. Theory

Formulation of the Partition Function. *Mean*

1) J. H. Hildebrand and R. L. Scott, "The Solubility of Non-electrolyte," 3rd Ed., Reinhold, New York (1953) p. 46.

2) R. L. Scott, *Discuss. Faraday Soc.*, **15**, 44 (1953).

3) E. A. Guggenheim, *Proc. Roy. Soc., Ser. A* **148**, 304 (1935); *ibid.*, **A183**, 203, 213 (1944). R. H. Fowler and E. A. Guggenheim, "Statistical Thermodynamics," Cambridge Univ. Press Inc. (1939) p. 351.

4) G. S. Rushbrooke, *Proc. Roy Soc., Ser. A* **166**, 296 (1938).

5) H. C. Longuet-Higgins, *ibid., Ser. A* **205**, 247 (1951).

6) I. Prigogine and V. Mathot, *J. Chem. Phys.*, **20**, 49 (1952).

7) V. Mathot and A. Desmyter, *ibid.*, **21**, 782 (1953).

8) I. Prigogine and A. Bellemans, *ibid.*, **21**, 561 (1953).

9) I. Prigogine and A. Bellemans, *Discuss. Faraday Soc.*, **15**, 80 (1953).

10) Z. W. Salsburg and J.G. Kirkwood, *J. Chem. Phys.*, **21**, 2169 (1953).

11) R. L. Scott, *ibid.*, **25**, 193 (1956).

12) I. Prigogine, A. Bellemans and A. Englert-Chowles, *ibid.*, **24**, 518 (1956).

13) H. Eyring, A.T. Ree and N. Hirai, *Proc. Nat. Acad. Sci. U.S.*, **44**, 683 (1958); S. Ma and H. Eyring, *J. Chem. Phys.*, **42**, 1920 (1965).

14) P. J. Flory, *J. Amer. Chem. Soc.*, **87**, 1833 (1965); A. Abe and P.J. Flory, *ibid.*, **87**, 1838 (1965).

15) I. Prigogine, A. Bellemans and C. Naar-Colin, *J. Chem. Phys.*, **26**, 751 (1957).

16) J. G. Kirkwood and E.M. Boggs, *ibid.*, **10**, 394 (1942). J.G. Kirkwood and F.P. Buff, *ibid.*, **19**, 774 (1951). M. Born and H. S. Green, *Proc. Roy. Soc.*, **A188**, 10 (1946). G. J. Throop and R. J. Bearman, *J. Chem. Phys.*, **44**, 1423 (1966). H. S. Chung and W.F. Espensheid, *ibid.*, **47**, 219 (1967).

Field for a Molecule within a Cell. In the following treatment we assume that molecules are rigid spheres, and the potential of interaction between two molecules is a function of the intermolecular separation. As the potential function for two molecules a distance a apart, a Sutherland type function, $\varepsilon(a)$, is used,[17] where a is the average distance between the centers of nearest neighbors.

$$\varepsilon(a) = \begin{cases} -\varepsilon^*\left(\frac{r^*}{a}\right)^6 & \text{for } a>r^* \\ \infty & \text{for } a<r^* \end{cases} \quad (1)$$

where ε^* is an energy constant. For a pure liquid, a molecule with a diameter r* is assumed to be wandering in a spherical cell of radius a. The average potential function of mutual interaction, $\bar{\varepsilon}(r)$, in the cell is evaluated according to the same averaging procedure as made by Lennard-Jones and Devonshire,[18] where r is the distance from the center of the cell.*1.

$$\bar{\varepsilon}(r) = \frac{1}{2}\int_0^\pi \varepsilon((r^2+a^2-2ar\cos\theta)^{1/2})\sin\theta \mathrm{d}\theta = \begin{cases} -\varepsilon^*(r^*/a)^6 & \text{for } r=0 \\ -\varepsilon^*\dfrac{r^{*6}(a^2+r^2)}{(a^2-r^2)^4} & \text{for } r<a-r^* \\ \infty & \text{for } r>a-r^* \end{cases} \quad (2)$$

The shape of the function is of nearly square-well type.

We have calculated the magnitude of $\bar{\varepsilon}(a-r^*)/\bar{\varepsilon}(0)$ (the ratio between the depth of the potential at the center and that at its periphery) in order to investigate the extent of deviations of the potential function $\bar{\varepsilon}(r)$ from the perfect square-well type. The results are given in Table 1 for various magnitudes of (a/r^*). In ordinary liquids, the ratio $(a/r^*)^3$ is believed to be not larger than 1.3.

Thus the function $\bar{\varepsilon}(r)$ could be approximated by a perfect square-well type whose depth is given in Eq. (2)

Table 1. Potential field within a cell

a/r^*	$(a/r^*)^3$	$\bar{\varepsilon}(a-r^*)/\bar{\varepsilon}(0)$
1.05	1.16	1.01
1.1	1.33	1.04
1.2	1.73	1.15

In order to obtain the average potential, $\omega(r)$, for a wandering molecule within a cell for $r<a-r^*$, the influence of the outer neighbors is taken into account, and the following integration has been made, where $g(l)$ is the radial distribution function[16,19] at distance l in the liquid consisting of N molecules and occupying a volume V.

$$\omega(r) = \int_{r^*}^\infty \bar{\varepsilon}(r)\cdot 4\pi l^2 \frac{Ng(l)}{V}\mathrm{d}l = -\int_{r^*}^\infty \varepsilon^*\frac{r^{*6}(l^2+r^2)}{(l^2-r^2)^4}\cdot\frac{4\pi l^2}{V}Ng(l)\mathrm{d}l = -\gamma\varepsilon^*\left(\frac{N\cdot\frac{4}{3}\pi r^{*3}}{V}\right)\times\left[1+3\left(\frac{\gamma'}{\gamma}\right)\left(\frac{r}{r^*}\right)^2+\mathrm{O}\left(\left(\frac{r}{r^*}\right)^4\right)\right] \quad (3)$$

where

$$\gamma = \int_{r^*}^\infty \frac{g(l)}{l^4}\mathrm{d}l \Big/ \int_{r^*}^\infty \frac{\mathrm{d}l}{l^4}, \qquad \gamma' = \int_{r^*}^\infty \frac{g(l)}{l^6}\mathrm{d}l \Big/ \int_{r^*}^\infty \frac{\mathrm{d}l}{l^6} \quad (4)$$

As described above, $r/r^* \lesssim 0.1$ for ordinary liquids, and γ and γ' are of the same order (Table 2). Therefore, $\omega(r)$ can be approximated by the first term in Eq. (3), similar to the case of the mutual potential energy $\bar{\varepsilon}(r)$. Throughout the present calculations the potential energy function $\omega(r)$ of square-well type, as given in the following, is used for a wandering molecule within a cell.

$$\omega(r) = \begin{cases} -\gamma\varepsilon^*\left(\frac{\frac{4}{3}\pi r^{*3}N}{V}\right) & \text{for } r<a-r^* \\ \infty & \text{for } r>a-r^* \end{cases} \quad (5)$$

The wandering molecule behaves like a gas molecule within a cell. The depth of the potential well, $\omega(0)$, is related to the heat of vaporization ΔH_V for the liquid as shown by

$$-\frac{N}{2}\omega(0) = \frac{2}{3}\pi N^2\gamma\varepsilon^* r^{*3}\frac{1}{V} = \Delta H_V - \boldsymbol{R}T, \quad (6)$$

where $\boldsymbol{R}$ is gas constant and T temperature.

Partition Function for a Binary Liquid Mixture. Thermodynamic properties of a solution consisting of N_A molecules of species A and N_B molecules of species B, are derived from the following partition function Z formulated by the cell method assuming the square-well type potential within each cell in the solution.

$$Z = \frac{N!}{N_A!N_B!}f_A^{N_A}f_B^{N_B}\times\exp\left[-\frac{1}{2\boldsymbol{k}T}(N_A\omega_A(0)+N_B\omega_B(0))\right]$$

$$f_A = \frac{4\pi}{3}(a_A-r_A^*)^3 j_A, \quad f_B = \frac{4\pi}{3}(a_B-r_B^*)^3 j_B \quad (7)$$

where $j_A(T)$ and $j_B(T)$ are internal partition functions for each molecule of species A and B, and

17) J. O. Hirshfelder, C. F. Curtiss and R. B. Bird, "Molecular Theory of Gasses and Liquids," Wiley, New York (1954), p. 32.

18) J. E. Lennard-Jones and A. F. Devonshire, *Proc. Roy. Soc.*, **A163**, 53 (1937), **A165**, 1 (1938).

*1 Readers should refer to "Theory of Liquids," A. Harashima (Iwanami), pp. 41—42, Fig. 8—1 (1954).

19) J. G. Kirkwood, E. K. Maun and B. J. Alder, *J. Chem. Phys.*, **18**, 1040 (1950).

$\omega_A(0)$ and $\omega_B(0)$ are the depth of the potential well for the molecules of species A and B in each cell, respectively. a_A and a_B are the radius of the spherical cell for each species in the solution. They are related to the volume per molecule v by the formula

$$\frac{V}{N} = v(a_A, a_B) = x_A\beta a_A^3 + x_B\beta a_B^3, \tag{8}$$

where x_A and x_B are the mole fraction for each species. The applicability of the common packing parameter β is assumed. r_A^* and r_B^* are the collision diameter of the molecule within each cell. They are assumed to be related to the diameters of each species in the pure state r_{AA}^* and r_{BB}^* by the formula

$$r_A^* = x_A r_{AA}^* + x_B r_{AB}^*, \quad r_B^* = x_A r_{AB}^* + x_B r_{BB}^*, \tag{9}$$

where

$$r_{AB}^* = \frac{1}{2}(r_{AA}^* + r_{BB}^*).$$

The energy $\omega_A(0)$ and $\omega_B(0)$ for the molecules within cell, and $\omega_A^\circ(0)$ and $\omega_A^\circ(0)$ for the molecules within cells in each pure liquid, are given by

$$\begin{aligned}
\omega_A(0) &= -\gamma\varepsilon_A^*\left(\frac{\frac{4}{3}\pi r_A^{*3}}{v}\right),\\
\omega_B(0) &= -\gamma\varepsilon_B^*\left(\frac{\frac{4}{3}\pi r_B^{*3}}{v}\right),\\
\omega_A^\circ(0) &= -\gamma\varepsilon_{AA}^*\left(\frac{\frac{4}{3}\pi r_{AA}^{*3}}{v_A^\circ}\right),\\
\omega_B^\circ(0) &= -\gamma\varepsilon_{BB}^*\left(\frac{\frac{4}{3}\pi r_{BB}^{*3}}{v_B^\circ}\right)
\end{aligned} \tag{10}$$

according to Eq. (5),
where v_A° and v_B° are the volume per molecule in each pure state. The energy parameters ε_A^* and ε_B^* are given by

$$\varepsilon_A^* = x_A\varepsilon_{AA}^* + x_B\varepsilon_{AB}^*, \quad \varepsilon_B^* = x_A\varepsilon_{AB}^* + x_B\varepsilon_{BB}^*, \tag{11}$$

where ε_{AB}^* is the energy parameter of the Sutherland type pair interaction between species A and B (Eq. (1)) in the solution.

Determination of Parameters a_A and a_B, and the Equation of State. The two parameters a_A and a_B, which are the radius of the spherical cell for each species in the solution, are determined by the minimization of the Helmholtz energy A under the condition of a given volume (Eq. (8)) as well as that of vanishing external pressure by procedures similar to those adopted by Prigogine and Bellemans.[9]

$$A = A(a_A, a_B, T) = A(a_A, v, T) = -kT\ln Z \tag{12}$$

$$\left(\frac{\partial A}{\partial a_A}\right)_{v,T} = \left(\frac{\partial A}{\partial a_A}\right)_{a_B,T} + \left(\frac{\partial A}{\partial a_B}\right)_{a_A,T}\left(\frac{\partial a_B}{\partial a_A}\right)_v = 0 \tag{13}$$

$$-p = \left(\frac{\partial A}{\partial v}\right)_{T,a_A} = \left(\frac{\partial A}{\partial a_B}\right)_{a_A,T}\left(\frac{\partial a_B}{\partial v}\right)_{a_A} = 0 \tag{14}$$

Combinining Eqs. (13) and (14), we obtain

$$\left(\frac{\partial A}{\partial a_A}\right)_{a_B,T} = \left(\frac{\partial A}{\partial a_B}\right)_{a_A,T} = 0. \tag{15}$$

From Eqs. (7) and (12), the Helmholtz energy A is expressed as follows.

$$\begin{aligned}
A = {} & \frac{N}{2}(x_A\omega_A(0) + x_B\omega_B(0))\\
& + NkT(x_A\ln x_A + x_B\ln x_B)\\
& - NkT(x_A\ln f_A + x_B\ln f_B)
\end{aligned} \tag{16}$$

Introducing Eq. (16) into Eq. (15), and assuming $(\partial\gamma/\partial v)=0$,[*2] we obtain

$$\begin{aligned}
a_A^2(a_A - r_A^*) &= a_B^2(a_B - r_B^*)\\
&= \frac{3v^2kT}{2\pi\gamma\beta(x_A\varepsilon_A^* r_A^{*3} + x_B\varepsilon_B^* r_B^{*3})}.
\end{aligned} \tag{17}$$

In principle, we can determine the magnitude of a_A and a_B from Eq. (17). However, it is difficult to obtain analytical solutions of a_A and a_B because Eq. (17) is 3rd power with respect to a_A and a_B. Thus putting

$$\frac{a_A - r_A^*}{r_A^*} = \rho_A, \quad \frac{a_B - r_B^*}{r_B^*} = \rho_B \tag{18}$$

and using the conditions $\rho_A < 1$, $\rho_B < 1$ for ordinary liquids, we obtain the following relation, where Eq. (8) is used and higher order terms than the first with respect to ρ_A and ρ_B are ignored.

$$\frac{v - \beta(x_A r_A^{*3} + x_B r_B^{*3})}{v^2} = \frac{9kT}{2\pi(x_A\gamma\varepsilon_A^* r_A^{*3} + x_B\gamma\varepsilon_B r_B^{*3})} \tag{19}$$

$$\begin{aligned}
\rho_A &= \frac{3v^2kT}{2\pi\beta r_A^{*3}(x_A r_A^{*3}\gamma\varepsilon_A^* + x_B r_B^{*3}\gamma\varepsilon_B^*)}\\
\rho_B &= \frac{3v^2kT}{2\pi\beta r_B^{*3}(x_A r_A^{*3}\gamma\varepsilon_A^* + x_B r_B^{*3}\gamma\varepsilon_B^*)}.
\end{aligned} \tag{20}$$

Excess Thermodynamic Functions of the Binary Liquid Mixture. Various excess thermodynamic functions can be obtained from the equations described above. The excess Helmholtz energy $A_E = A - x_A A_A^\circ - x_B A_B^\circ - T\Delta S_{\text{mix}}^{\text{id.}}$ is given in Eq. (21) from Eq. (16).

$$\begin{aligned}
A_E = {} & \frac{N}{2}\{x_A(\omega_A(0) - \omega_A^\circ(0)) + x_B(\omega_B(0) - \omega_B^\circ(0))\}\\
& - NkT\left(x_A\ln\frac{f_A}{f_A^\circ} + x_B\ln\frac{f_B}{f_B^\circ}\right)
\end{aligned} \tag{21}$$

where $\omega_A(0)$, $\omega_B(0)$, $\omega_A^\circ(0)$, $\omega_B^\circ(0)$, f_A, and f_B are given in Eqs. (7) and (10). The superscript $^\circ$ represents the values for pure liquids. The excess

[*2] As will be discussed later, γ is slightly dependent on volume. However, in the present treatment γ is replaced by its average value.

energy $E_E=E-x_AE_A^\circ-x_BE_B^\circ$ is obtained from Eq. (21) and the thermodynamical relations, assuming $(\partial\gamma/\partial T)_V=0$ and the invariance of internal partition function by the transfer from pure liquid to solution.

$$E_E=\frac{N}{2}\{x_A(\omega_A(0)-\omega_A^\circ(0))+x_B(\omega_B(0)-\omega_B^\circ(0))\} \tag{22}$$

Introducing Eq. (10) into Eq. (22), we obtain

$$E_E=-\frac{2\pi N}{3}\left\{\frac{1}{v}(x_Ar_A^{*3}\gamma\varepsilon_A^*+x_Br_B^{*3}\gamma\varepsilon_B^*)-\left(\frac{x_Ar_{AA}^{*3}\gamma\varepsilon_{AA}^*}{v_A^\circ}+\frac{x_Br_{AA}^{*3}\gamma\varepsilon_{BB}^*}{v_B^\circ}\right)\right\} \tag{22'}$$

The excess entropy $S_E=S-x_AS_A^\circ-x_BS_B^\circ-\Delta S_{\text{mix}}^{\text{id.}}$ is obtained as follows.

$$S_E=-3Nk\left(x_A\ln\frac{a_A^\circ-r_{AA}^*}{a_A-r_A^*}+x_B\ln\frac{a_B^\circ-r_{BB}^*}{a_B-r_B^*}\right)=-3Nk\left(x_A\ln\frac{\rho_A^\circ r_{AA}^*}{\rho_Ar_A^*}+x_B\ln\frac{\rho_B^\circ r_{BB}^*}{\rho_Br_B^*}\right) \tag{23}$$

The excess volume $V_E=V-x_AV_A^\circ-x_BV_B^\circ$ is obtained from Eq. (19)

$$V_E=N\left[\beta\{x_A(r_A^{*3}-r_{AA}^{*3})+x_B(r_B^{*3}-r_{BB}^{*3})\}+\frac{9kT}{2\pi}\left\{\frac{(x_Av_A^\circ+x_Bv_B^\circ)^2}{x_A\gamma\varepsilon_A^*r_A^{*3}+x_B\gamma\varepsilon_B^*r_B^{*3}}-\frac{x_Av_A^{\circ2}}{\gamma\varepsilon_{AA}^*r_{AA}^{*3}}-\frac{x_Bv_B^{\circ2}}{\gamma\varepsilon_{BB}^*r_{BB}^{*3}}\right\}\right]\Big/\left[1-\frac{9kT}{\pi}\left(\frac{x_Av_A^\circ+x_Bv_B^\circ}{x_A\gamma\varepsilon_A^*r_A^{*3}+x_B\gamma\varepsilon_B^*r_B^{*3}}\right)\right]. \tag{24}$$

From Eq. (19) we obtain the following equation, when $x_A=1$ and $x_B=0$.

$$\gamma\varepsilon_{AA}^*=\frac{9kT}{2\pi}\cdot\frac{v_A^\circ}{r_{AA}^{*3}}\cdot\frac{v_A^\circ}{v_A^\circ-\beta r_{AA}^{*3}} \tag{25}$$

Introducing Eqs. (10) and (25) into Eq. (22), the approximate relation between E_E and V_E is derived.

$$\frac{E_E}{3NkT}=\left\{\left(\frac{x_Av_A^\circ}{v_A^\circ-\beta r_{AA}^{*3}}+\frac{x_Bv_B^\circ}{v_B^\circ-\beta r_{BB}^{*3}}\right)-\left(\frac{\bar v_0}{\bar v_0-\bar v^*}\right)\right\}+\left\{\frac{\bar v^*}{(\bar v_0-\bar v^*)^2}\right\}v_E \tag{26}$$

where $\bar v_0=x_Av_A^\circ+x_Bv_B^\circ$ and $\bar v^*=x_A(\beta r_{AA}^{*3})+x_B(\beta r_{BB}^{*3})$, and the conditions $v_E\ll\bar v_0$ and $v_E\ll\bar v_0-\bar v^*$ are satisfied.

Discussion on the Potential $\omega(r)$ and the Physical Meaning of the Parameter γ. *Volume Dependency of the Potential within a Cell.* For the volume dependency of the potential energy the inverse first power relation has been proposed by Hildebrand *et al.*,[20] and adopted by Flory and Abe[14] in their solution theory. Assuming that the energy is proportional to V^{-n}, Hildebrand and co-workers showed the power n for various organic liquids to be not far from unity. Their result was confirmed experimentally by Beninga and Scott.[21]

We have derived the average potential as a function of the volume of liquid on the basis of the Sutherland type interaction, and have obtained an explicit representation of the potential with molecular parameters using the radial distribution function $g(l)$.

In the derivation of the equation of state, Eq. (17), from Eq. (15), we have assumed that γ is independent of volume. The potential function $\omega(r)$ (Eq. (5)) within a cell is found to be proportional to $(1/V)$ in accordance with the earlier results.[20,21] The value of γ is maintained to be 2.0 within the range of fluctuation of 0.1 for ordinary liquids (Table 3 and Appendix). The underlying assumption is regarded to be reasonable as an approximation. However, as seen in Table 2 γ decreases gradually with volume. This means that $n>1$. Recently, it has been found experimentally that n is 1.4 for alkanes which are non-spherical in molecular shape.[22]

Temperature Dependence of the Parameter γ. Using the values of $g(l)$ calculated by Kirkwood *et al.*[19] for liquids consisting of rigid spherical molecules, we have determined the magnitude of γ (Table 2) for various magnitudes of a parameter λ which is related to density.[19]

Table 2. Values of parameter γ

	Rigid sphere with no attractive forces*[19]				
λ	5	10	20	27.4	33
V/V^*	5.15	3.20	2.10	1.73	1.53
γ	1.19	1.36	1.59	1.72	1.82
γ'	1.29	1.50	1.81	1.99	2.13

	Lennard-Jones fluid, (Kirkwood *et al.*[23])		
	$\lambda=27.4$	$V/V^*=1.73$	
kT/ε	0.833	1.111	1.667
γ	1.63	1.69	1.78

	Lennard-Jones fluid (Verlet[24])		
		$V/V^*=1.885$	
kT/ε	0.827		1.304
γ	1.49		1.49
		$V/V^*=1.663$	
kT/ε	0.719	0.880	1.273
γ	1.60	1.60	1.57

* $V^*=N\beta r^{*3}$

As seen from Eq. (4), γ is dependent on temperature through the temperature dependence of $g(l)$. In the derivation of Eq. (22) the temperature dependence of γ is ignored. Taking the temperature dependence into account, the excess energy E_E is obtained as

20) Ref. 17, p. 280; Ref. 1, Chapter V.

21) H. Beninga and R. L. Scott, *J. Chem. Phys.*, **23**, 1911 (1955).

22) V. Fried and G. B. Schneider, *J. Phys. Chem.*, **72**, 4688 (1968).

$$E_E = \frac{\partial(A_E/T)}{\partial(1/T)_V} = E_E^\circ\left(1-\left(\frac{\partial \log \gamma}{\partial \log T}\right)_V\right), \quad (27)$$

where E_E° is the excess energy given in Eq. (22), and the same temperature dependence of γ is assumed for all species.

According to the Kirkwood-Born-Green theory[16,19] the temperature dependence of the radial distribution function g for a fluid of rigid spheres with no attraction comes from that of a parameter λ, which is related to only density, and thus, only from the temperature dependence of (V^*/V). Thus, for a fluid consisting of rigid spherical molecules with no attractive pair interactions, we have

$$(\partial g/\partial T)_V = 0$$

and

$$(\partial \ln \gamma/\partial \ln T)_V = 0. \quad (28)$$

Thus Eq. (27) reduces to Eqs. (22) and (22′).

In all the theories based on a cell model, the number of nearest neighbors was always assumed to be constant. This is equivalent to the assumption that γ is independent of temperature.

When attractive forces act between molecules, it is difficult to calculate $(\partial \log \gamma/\partial \log T)_V$ analytically. The values of γ are calculated numerically for fluids in which the interaction potential between molecules is of Lennard-Jones type, using the values of g given by Kirkwood *et al.*[23] and Verlet.[24] The results are given in Table 2. It is seen that the temperature dependence of γ, is very small. Thus, the application of condition (28) is justified.

Recently Fried and Schneider[22] have reported from experimental grounds that the parameter a (the cohesive energy is given by $-a/V^n$ in their paper) is slightly temperature-dependent at ordinary temperatures, and that the variation of a is less than 3% over a wide range of temperature. The parameter a is supposed to be proportional to our parameter γ. Thus, their results seem to support our result with respect to the temperature dependence of γ.

Estimation of Parameters λ and γ. The values of parameter λ are determined for liquids consisting of rigid spherical molecules with no attractive interactions, by means of the formula[16]

$$\lambda = 3((2\Delta H_V)/(NkT) - \log (V_g/V_l)) \quad (29)$$

where V_l and V_g are the volume of liquid and gas respectively.[16] It is difficult to determine λ for fluids in general. Thus, we use Eq. (29) as an approximate formula for the determination of λ. Values of λ for various liquids are given in Table 3, together with values of γ determined by extrapolation along the γ *vs.* λ curve given in Fig. 1. It is shown in the appendix[25,26] that the estimation of γ is reasonable.

Table 3. Values of parameters λ and γ for various liquids

	T (°K)	V^l (cm³)	ΔH_v (cal/mol)	λ	γ
A	87	28	1560	35.9	1.84
N_2	77	35	1330	36.2	1.86
CH_4	112	38	1960	36.1	1.86
CCl_4	298	97	7830	62.3	2.1
C_6H_6	298	89	8090	64.6	2.1
	353	96	7350	45.4	1.9_5
c-C_6H_{12}	298	109	7900	63.3	2.1
	354	116	7190	43.5	1.9_5

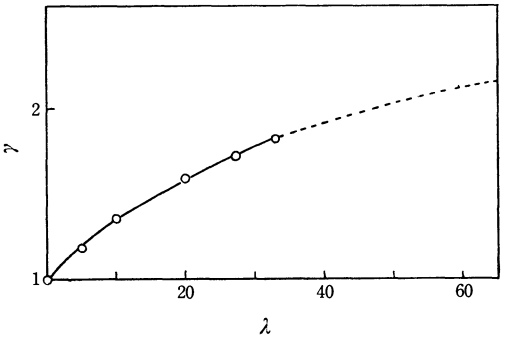

Fig. 1. The values of parameter γ for the liquid composed of rigid spherical molecules with no attractive forces.

Part II. Numerical Computations.

We present here with an analysis of excess functions V_E, E_E, and S_E for binary liquid mixtures. The binary systems consist of pairs of molecules which are approximately spherical and not greatly different in size. Random mixing is assumed. The excess thermodynamic functions for 22 binary liquid mixtures are calculated.

Procedure of Calculation. *Excess Thermodynamic Function.* Combining Eq. (22) with Eqs. (19) and (25), we have

$$E_E = 3RT\left\{\left(\frac{x_A v_A^\circ}{v_A^\circ-\beta r_{AA}^{*3}}+\frac{x_B v_B^\circ}{v_B^\circ-\beta r_{BB}^{*3}}\right) - \frac{v}{v-\beta(x_A r_A^{*3}+x_B r_B^{*3})}\right\}. \quad (30)$$

For the excess volme V_E, we obtain from Eq. (30)

$$\frac{V_E}{N} = \beta(x_A r_A^{*3}+x_B r_B^{*3})\left(\frac{K-E_E}{K-E_E-3RT}\right)-\bar{v}_0 \quad (31)$$

23) J. G. Kirkwood, V. A. Lewinson and B. J. Alder, *J. Chem. Phys.*, **20**, 929 (1952).

24) L. Verlet, *Phys. Rev.*, **165**, 201 (1968).

25) A. Harashima, "Theory of Liquids," Iwanami (1954), p. 42.

26) A. Eisenstein and N. S. Gingrich, *Phys. Rev.*, **62**, 261 (1942).

where

$$K = 3RT\left\{\left(\frac{x_A v_A^\circ}{v_A^\circ - \beta r_{AA}^{*3}}\right) + \left(\frac{x_B v_B^\circ}{v_B^\circ - \beta r_{BB}^{*3}}\right)\right\}.$$

From Eqs. (19), (20) and (23), we obtain the following equation for TS_E.

$$TS_E = 3RT\left[x_A \ln\left\{\left(\frac{v_A^\circ - \beta r_{AA}^{*3}}{v - \beta(x_A r_A^{*3} + x_B r_B^{*3})}\right)\left(\frac{r_A^*}{r_{AA}^*}\right)^2\right\} + x_B \ln\left\{\left(\frac{v_B^\circ - \beta r_{BB}^{*3}}{v - \beta(x_A r_A^{*3} + x_B r_B^{*3})}\right)\left(\frac{r_B^*}{r_{BB}^*}\right)^2\right\}\right] \quad (32)$$

Determination of Parameters for Pure Components. From Eq. (17) we obtain the following equation for $\gamma\varepsilon_{AA}^*$ of pure component A, when $x_A=1$ and $x_B=0$.

$$N\gamma\varepsilon_{AA}^* = \frac{3NkT}{2\pi}\left(\frac{v_A^\circ}{r_{AA}^{*3}}\right)\left(\frac{v_A^{\circ 1/3}}{v_A^{\circ 1/3} - (\beta r_{AA}^{*3})^{1/3}}\right) \quad (33)$$

$\gamma\varepsilon_{AA}^*$ is related to the heat of vaporization ΔH_V in Eq. (6). Eq. (25) is regarded as an approximate representation of Eq. (33).

Differentiating Eq. (33) with respect to temperature assuming that $(d\gamma/dT)_V=0$, we obtain

$$v_A^* = \beta r_{AA}^{*3} = v_A^\circ\left(\frac{1+\alpha_A T}{1+\frac{4}{3}\alpha_A T}\right)^3, \quad (34)$$

where α_A is the thermal expansion coefficient for pure component A. Eq. (34) is found to be similar to that given by Abe and Flory.[14] This may be due to the similarity in the volume dependence of energy.

By means of Eq. (34), $\beta r_{AA}{}^{*3}$ is obtained from thermal expansion coefficient. $N\gamma\varepsilon_{AA}^*$ is determined using Eq. (33). When ΔH_V is known, we can obtain $N\gamma\varepsilon_{AA}^*$ directly by means of Eq. (6). The results are given in Table 4 for 15 liquids. The values given in column 7 are calculated by means of Eq. (33) and those in column 8 by means of Eq. (6). The values in column 7 and those in column 8 are in good agreement with each other. This shows applicability of the present theory. For the calculation of excess thermodynamic functions the values in column 7 are used.

Calculation of Excess Thermodynamic Functions for Equimolar Binary Mixtures. Substituting the observed values of excess energy*3 given in Table 5

Table 4. Molecular parameters of pure liquids

Substance	T (°C)	V (cc/mol)	$\alpha\times10^3$ (deg^{-1})	βr^{*3} (cc/mol)	ΔH^v (kcal/mol)	$N\gamma\varepsilon^{*1)}$ (kcal/mol)	$N\gamma\varepsilon^{*2)}$ (kcal/mol)
CCl_4	0	94.21	1.191	74.42	8.09	3.07	3.23
	20	96.49	1.219	74.97	7.85	3.14	3.16
	25	97.08	1.229	75.10	7.79	3.15	3.14
	40	98.91	1.265	75.43	7.64	3.19	3.11
	70	102.88	1.363	76.00	7.29	3.25	3.02
$SiCl_4$	20	114.64	1.415	86.67		2.92	
	25	115.47	1.442	86.71	7.19	2.92	2.97
$TiCl_4$	20	109.80	1.026	87.88		3.43	
$SnCl_4$	20	116.92	1.171	91.50		3.20	
$C(Me)_4$	0	118.03	1.811	86.24	5.61	2.53	2.34
Ar	84°K	28.20	4.370	22.11	1.56(87°K)	0.92	0.60
O_2	77°K	26.50	3.960	21.16		0.90	
	84°K	27.28	4.270	21.18		0.90	
N_2	77°K	34.62	5.670	25.92	1.33	0.75	0.53
	84°K	36.10	6.320	26.00		0.76	
C_6H_6	20	88.86	1.214	69.11		3.14	
	25	89.40	1.223	69.21	8.09	3.16	3.27
	40	91.07	1.256	69.54		3.20	
	70	94.69	1.346	70.13		3.27	
$C_6H_5CH_3$	25	106.83	1.055	84.21	9.08	3.33	3.64
c-C_5H_{10}	25	94.73	1.390	71.63	6.84	2.97	2.79
c-C_6H_{12}	25	108.75	1.217	84.27	7.84	3.17	3.16
	40	110.79	1.264	84.51	7.69	3.19	3.13
	70	115.25	1.365	85.12	7.31	3.24	3.03
c-C_7H_{14}	25	121.62	1.000	97.47	9.19	3.50	3.62
C_6H_5F	40	96.04	1.197	73.97		3.28	
$C_2H_4Cl_2$	20	78.99	1.132	62.55		3.33	

1) The values calculated by means of Eq. (33)
2) The values calculated by means of Eq. (6)

*3 They are excess enthalpy, not excess energy. However, the difference is very small, and can be ignored.

TABLE 5. EXCESS THERMODYNAMIC QUANTITIES OF EQUIMOLAR MIXTURES

System A-B	T (°C)	H_E (cal/mol)	V_E (cc/mol)		TS_E (cal/mol)		$\theta \times 10^3$	$\theta_{disp} \times 10^3$	$V_{E,size}$ (cc/mol)	$V_{E,int}$	$E_{E,calc}$ (cal/mol)
		Obsd	Obsd	Calcd	Obsd	Calcd					
CCl_4-C(Me)$_4$	0	75[a]	−0.50[a]	−0.76	−1[a]	3	−9.2	−3.3	−0.21	−0.55	−98
CCl_4-$SiCl_4$	25	36[b,c]	0.02[d]	−0.19	16[e]	9	−1.9	−0.5	−0.20	0.01	4
CCl_4-$TiCl_4$	20	42[c]	0.08[f]	−0.01		9	−8.1	−0.9	−0.22	0.21	24
CCl_4-$SnCl_4$	20	69[c]	0.46[f]	0.03		22	−5.0	0	−0.37	0.4	121
$SiCl_4$-$TiCl_4$	20	38[c]	−0.36[f]	−0.24	(15)[g]	−4	−11.7	−2.8	0	−0.24	−88
$SiCl_4$-$SnCl_4$	20	64[c]	0.13[f]	0.18		15	−14.3	−0.8	−0.03	0.21	28
$TiCl_4$-$SnCl_4$	20	45[c]	0.08[f]	0.05		9	−7.2	−0.5	−0.02	0.07	22
Ar-O_2	84°K	14[h]	0.14[h]	0.05	5[h]	4	−2.2	−0.1	0	0.05	41
Ar-N_2	84°K	12[h]	−0.18[h]	−0.33	4[h]	−3	1.5	−3.5	−0.08	−0.25	−33
O_2-N_2	77°K	11[i]	−0.21[j]	−0.27	1[i]	−1	−1.7	−2.8	−0.11	−0.16	−46
CCl_4-*c*-C_6H_{12}	25	35[k]	0.16[l]	0.05	18[k]	11	−4.3	0	−0.12	0.17	42
	40	34[k]	0.16[l]	0.06	18[k]	12	−4.0	0	−0.12	0.18	39
	70	30[k]	0.17[l]	0.06	16[k]	12	−2.9	0	−0.14	0.2	34
CCl_4-C_6H_6	25	26[m]	0.01[n]	0.05	6[m]	8	−5.5	0	−0.06	0.11	3
	40	31[m]	0.04[n]	0.07	12[m]	10	−6.1	0	−0.06	0.13	11
	70	(41)[m]	0.11[n]	0.14	(23)[m]	15	−7.2	0	−0.06	0.15	25
CCl_4-$C_6H_5CH_3$	25	10[o]	−0.04[o]	−0.04		2	−2.8	−0.3	−0.12	0.06	−11
C_6H_6-*c*-C_5H_{10}	25	150[p]	0.30[p]	0.50		45	−30.7	−0.3	−0.01	0.51	80
C_6H_6-*c*-C_6H_{12}	25	195[q]	0.65[r]	0.50	117[q]	61	−32.1	0	−0.34	0.84	178
	40	180[q]	0.66[r]	0.49	109[q]	60	−28.0	0	−0.35	0.84	166
	70	155[q]	0.67[r]	0.49	95[q]	59	−21.9	0	−0.39	0.87	142
C_6H_6-*c*-C_7H_{14}	25	181[p]	0.67[p]	0.02		52	−25.0	−1.2	−1.06	1.08	202
$C_6H_5CH_3$-*c*-C_5H_{10}	25	87[p]	0.08[p]	0.15		20	−18.9	−1.2	−0.24	0.39	21
$C_6H_5CH_3$-*c*-C_6H_{12}	25	149[p]	0.57[p]	0.53		41	−25.1	−0.2	0	0.53	154
$C_6H_5CH_3$-*c*-C_7H_{14}	25	141[p]	0.53[p]	0.37		37	−22.8	−0.3	−0.21	0.58	156
C_6H_6-$C_6H_5CH_3$	25	14[o]	0.07[o]	0.14		5	0.5	−0.3	−0.33	0.19	21
C_6H_{12}-C_6H_5F	40	212[s]	0.71[s]	0.71	98[s]	67	−36.7	0.1	−0.17	0.88	180
C_6H_6-$C_2H_4Cl_2$	20	17[t]	0.25[t]	−0.07	9[u]	4	5.2	−0.3	−0.07	0	88

a) A. Englert-Chwoles, *J. Chem. Phys.*, **23**, 1168 (1955).
b) R. D. Vold, *J. Amer. Chem. Soc.*,**59**, 1515 (1937).
c) A. Kolbe and H. Sackmann, *Z. Phys. Chem.*, **31**, 281 (1962).
d) A. Hildebrand and J. M. Carter, *J. Amer. Chem. Soc.*, **54**, 3592 (1932).
e) S. E. Wood, *ibid.*, **59**, 1510 (1937).
f) H. Sackmann and H. Arnold, *Z. Electrochem.*, **63**, 565 (1959).
g) R. B. Crookston and L. N. Canjar, *J. Chem. Eng. Data*, **8**, 544 (1963).
h) R. A. H. Pool, G. Saville, T. M. Herrington, B. D. C. Shields and L. A. K. Staveley, *Trans. Faraday Soc.*, **58**, 1692 (1962).
i) C. M. Knobler, R. J. J. Van Heijningen and J. J. M. Beenakker, *Physica*, **27**, 296 (1961).
j) H. F. P. Knaap, M. Knoester and J. J. M. Beenakker, *ibid.*, **27**, 309 (1961).
k) D. S,. Adock and M. C. McGlashan, *Proc. Roy. Soc.*, (London), **A226**, 266 (1954).
l) S. E. Wood and J. A. Gray, *J. Amer. Chem. Soc.*, **74**, 3729 (1952).
m) J. R. Goates, R. J. Sullivan and J. B. Ott, *J. Phys. Chem.*, **63**, 589 (1959).
n) S. E. Wood and J. P. Brusie, *J. Amer. Chem. Soc.*, **65**, 1891 (1943).
o) R. P. Rastogi, J. Nath and J. Misra, *J. Phys. Chem.* , **71**, 1277 (1967).
p) A. E. P. Watson, I. A. McLure, J. E. Bennett and G. C. Benson, *ibid.*, **69**, 2753 (1965).
q) A. Abe and P. J. Flory, *J. Amer. Chem. Soc.*, **87**, 1838 (1965).
r) S. E. Wood and A. E. Austin, *ibid.*, **67**, 480 (1945).
s) A. V. Anantaraman, S. N. Bhattacharyya and S. R. Palit, *Trans. Fraday Soc.*, **59**, 1101 (1963).
t) L. H. Ruiter, *Rec. Trav. Chim. Pays-Bas*, **74**, 1131 (1955).
u) L. Sieg, J. L. Crützen and W. Jost, *Z. Phys. Chem.*, **198**, 18 (1951).

into Eq. (31), the excess volume V_E for 22 equimolar binary mixtures is calculated. From the values of V_E calculated and those of βr_{AA}*[3] given in Table 4, the values of TS_E are calculated using Eqs. (32) and (9). The values obtained are given in Table 5, and compared with the observed values.

The agreement between calculated and observed values for V_E and TS_E in satisfactory, as seen in Table 5. The standard deviation of the calculated values from the observed values with respect to V_E, is calculated to be 0.12_5 cc/mol*[4] for the binary mixtures given in Table 5.

It is seen that the calculated entropy is less than the value observed. This is especially remarkable for the systems which include aromatic species as a constituent.

From the observed values of E_E and V_E, substituting the values of $\gamma\varepsilon_{AA}$* and $\gamma\varepsilon_{BB}$* given in Table 4 into Eq. (22′), we can determine the magnitude of the parameter θ defined as follows.

$$\theta = (\varepsilon^*_{AB} - (\varepsilon^*_{AA} + \varepsilon^*_{BB})/2)/\varepsilon^*_{AA} \tag{35}$$

The values of θ thus obtained are given in column 8 of Table 5, together with those of θ_{disp}, in column 9 which are calculated by assuming the Bertholet relation

$$\varepsilon^*_{AB} = (\varepsilon^*_{AA}\varepsilon^*_{BB})^{1/2}. \tag{36}$$

It is observed that for nearly all systems given in Table 5, the sign of θ is negative and $\theta < \theta_{\text{disp}}$. This means that the mutual interactions between different species are less attractive than those within each species in the systems, and that the interactions between molecules can not be ascribed only to dispersion forces.

From Eq. (24) we can divide the excess volume V_E into two terms,[27] $V_{E,\text{size}}$ and $V_{E,\text{int}}$, where $V_{E,\text{size}}$ corresponds to the first term in the numerator in Eq. (24) and $V_{E,\text{int}}$ to the second term:

$$V_E = V_{E,\text{size}} + V_{E,\text{int}}. \tag{37}$$

The values of $V_{E,\text{size}}$ and $V_{E,\text{int}}$ are calculated using the values of θ in Table 5, and are also given in Table 5. The formula for $V_{E,\text{size}}$ is transformed as follows.

$$\begin{aligned} V_{E,\text{size}} &= \beta N\{x_A(r_A{}^{*3} - r^{*3}_{AA}) + x_B(r_B{}^{*3} - r^{*3}_{BB})\}/ \\ &\quad \left[1 - \frac{9kT}{\pi}\left(\frac{x_A v_A{}^\circ + x_B v_B{}^\circ}{x_A\gamma\varepsilon_A{}^* r_A{}^{*3} + x_B\gamma\varepsilon_B{}^* r_B{}^{*3}}\right)\right] \\ &= -\frac{\beta N}{4} x_A x_B (r^*_{AA} - r^*_{BB})^2 \left[\left(4 + \frac{3x_A - x_B}{2}\right) r^*_{AA} \right. \\ &\quad \left. + \left(4 + \frac{3x_B - x_A}{2}\right) r^*_{BB}\right] \Big/ \\ &\quad \left[1 - \frac{9kT}{\pi}\left(\frac{x_A v_A{}^\circ + x_B v_B{}^\circ}{x_A\gamma\varepsilon_A{}^* r_A{}^{*3} + x_B\gamma\varepsilon_B{}^* r_B{}^{*3}}\right)\right] \end{aligned} \tag{38}$$

As is evident in Eq. (38), we have

$$\begin{aligned} V_{E,\text{size}} &< 0 \quad \text{for} \quad r^*_{AA} \neq r^*_{BB} \\ &= 0 \quad \text{for} \quad r^*_{AA} = r^*_{BB} \end{aligned} \tag{39}$$

where the denominator in Eq. (38) has turned out to be always positive for the systems. The values of $V_{E,\text{size}}$ and $V_{E,\text{int}}$ calculated are given in columns 10 and 11 of Table 5.

The numerator in Eq. (38) is regarded to represent the excess volume for the mixture of rigid spherical particles with no mutual attraction. Thus, the fact that the values of $V_{E,\text{size}}$ can not be positive means that the excess volume for the mixture of rigid spherical particles with no attractive forces is always negative or zero. This is supported by the experimental results reported by Westman and Huggil.[28]

The values of $V_{E,\text{int}}$ are observed to be positive or negative. This term is regarded as the excess volume which occurs from an interaction*[5] between molecules.

In order to investigate the relation between E_E and V_E, the second term in Eq. (26) which is taken for the part of E_E apparently attributable to V_E, is calculated using the observed values of V_E, and given in column 12 of Table 5.

Comparison with Other Theories. The calculated values of various excess thermodynamic functions for three equimolar mixtures, benzene-carbon tetrachloride, carbon tetrachloride-cyclohexane and cyclohexane-benzene are given in Table 6(a), and those for equimolar mixtures of aromatic-alicyclic systems in Table 6(b) for comparison with calculated values from other theories. In Table 6(a) the values calculated by means of various theories which were reported previously,[5,9,10,11,14,16] are given together with our results. The Bertholet relation has been assumed in the calculation given in rows (a) to (d), but not in rows (e) to (g) where the calculation was made using the observed values of H_E.

There is not such a large difference in the calculated quantities, A_E, E_E and TS_E by various theories. The difference in the values of V_E is found to the most remarkable. Thus, it seems that the excess volume gives the most sensitive test to the applicability of the theory. With respect to excess volume, the results of Salsburg and Kirkwood,[10] and those of Chung and Espensheid[16] are too large. The results of Scott,[11] Abe and Flory[14] and the authors are of the same order of magnitude compared with the observed values.

In Table 6(b) the values of V_E and θ, calculated

*[4] The value for the system C_6H_6-c-C_7H_{14} is excluded, where an extraordinary large deviation is observed.

27) R. K. Nigam and P. P. Singh, *Trans. Faraday Soc.*, **65**, 950 (1968); R. P. Rastogi, J. Nath and J. Mishra, *J. Phys. Chem.*, **71**, 1278 (1967).

28) A. E. R. Westman and H. R. Huggil, *J. Amer. Cer. Soc.*, **13**, 767 (1930); E. Manegold, R. Hofmann and K. Solf, *Kolloid Z.*, **56**, 142 (1931).

[5] The designation of $V_{E,\text{size}}$ and $V_{E,\text{int}}$ is conventional, as an interaction parameter ε_{AB} is included in the common denominator of the two parts of V_E.

Table 6. (a) Comparison with the results previous theories (25°C)

System	Ref.	A_E	H_E (cal/mol)	TS_E	V_E/V (%)
C_6H_6–CCl_4	Obsd	20	27±1	7	0.01
	(a)	25	37	12	0.10—0.2
	(b)	26	30	4	0.25
	(c)	10	16	6	0.09
	(d)	(19)	30	11	0.09
	(e)	20	(27)	7	0.08
	(f)	25	42.7	17.7	0.70
	(g)	18	(26)	8	0.05
CCl_4–c-C_6H_{12}	Obsd	17	35	18	0.16
	(a)	12	18	6	0.05—0.15
	(b)	44	52	8	0.46
	(c)	23	38	15	0.28
	(d)	(17)	27	10	0.09
	(e)	26	(35)	9	0.12
	(f)	15.4	27.4	12	0.54
	(g)	24	(35)	11	0.05
C_6H_6–c-C_6H_{12}	Obsd	78	195	117	0.63
	(a)	65	100	35	0.20—0.35
	(b)	146	171	25	1.32
	(c)	63	105	42	0.68
	(d)	(74)	116	42	0.36
	(e)	142	(195)	53	0.63
	(f)	79.2	133.7	54.5	2.45
	(g)	134	(195)	61	0.50

a) I. Prigogine, A. Bellemans, *Disscuss. Faraday Soc.*, **15**, 80 (1953).
b) Z. W. Salsburg and J. G. Kirkwood, *J. Chem. Phys.*, **21**, 2169 (1953).
c) R. L. Scott, *ibid.*, **25**, 193 (1956).
d) H. C. Longuet-Higgins, *Proc. Roy. Soc., Ser. A* **205**, 247 (1951).
e) A. Abe and P. J. Flory, *J. Amer. Chem. Soc.*, **87**, 1838 (1965).
f) H. S. Chung and W. F. Espensheid, *J. Chem. Phys.*, **44**, 1433 (1966).
g) Present work.

Table 6(b). Comparison with the result of other theory (Aromatic-Alicyclic Systems at 25°C)

Systems	$H_{E,\text{obs}}$ (cal/mol)	$V_{E,\text{obs}}$ (cal/mol)	$V_{E,\text{calc}}$ (cm^3/mol)		$\theta\times10^3$	
			(a)	(b)	(a)	(b)
C_6H_6–c-C_5H_{10}	151	0.30	0.41	0.50	−25.3	−30.7
C_6H_6–c-C_6H_{12}	195	0.65	0.98	0.50	−12.4	−32.1
C_6H_6–c-C_7H_{14}	181	0.67	2.10	0.02	31.8	−25.0
C_6H_6–c-C_8H_{16}	181	0.58	3.82	−0.42	87.9	−22.8
$C_6H_5CH_3$–c-C_5H_{10}	87	0.08	0.70	0.15	1.2	−18.9
$C_6H_5CH_3$–c-C_6H_{12}	149	0.57	0.36	0.53	−22.9	−25.1
$C_6H_5CH_3$–c-C_7H_{14}	141	0.53	0.59	0.37	−12.8	−22.8
$C_6H_5CH_3$–c-C_8H_{16}	148	0.51	1.41	0.15	11.7	−21.7

(a) I. Prigogine, "The Molecular Theory of Solution," North Holland Pub. Co., Amsterdam (1957), Chaps. 10, 11.
(b) Present work

for equimolar mixtures of aromatic-alicyclic systems by Benson and co-workers[29] using Prigogine's theory[9,30] are compared with our results. we see

29) L. A. McLure, J. E. Benett, A. E. P. Watson and G. C. Benson, *J. Phys. Chem.*, **69**, 2759 (1965).

30) I. Prigogine "The Molecular Theory of Solutions," North Holland Pub. Co., Amsterdam (1957), Chapts. 10, 11.

that the agreement between calculated and observed values is better in the present theory than in Prigogine's theory. The present theory gives slightly smaller values than the observed, while Prigogine's theory gives larger values.

Discussion on the Results of Numerical Computations. In Table 5 the values of θ which are calculated for the observed values of E_E and V_E are compared with those obtained from the Bertholet relation. The former are larger than the latter in absolute magnitude.

In Table 5 appreciable differences are observed between the systems containing an aromatic constituent and other systems. For aromatic-alicyclic systems the values of $|\theta|$ are 0.02—0.03, and are seen to be larger by one order than those of other systems. Benson and coworkers have reported[29] that the values of $|\theta|$ calculated using Scatchard-Hildebrand theory[31] and Barker's quasi-lattice theory[32] are about 0.03 for aromatic-alicyclic systems. Their results agree with our results. The values of θ calculated by Prigogine's theory, shown in column 6, Table 6(b) (cited from Benson *et al.*[29]) vary greatly. This is unreasonable when the similar properties of these systems are taken into account.

For the aromatic-alicyclic systems the observed values of H_E are positive and large compared with those of other systems in Table 5, which correspond to fairly large values of $|\theta|$. We see that the excess entropy calculated is larger for the aromatic-alicyclic systems than for the other systems, and that the observed values of excess entropy for the systems are larger than for the calculated values. A certain ordered arrangement seems to be present in liquid benzene and disturbed by the addition of non-aromatic constituents.[14]

For aromatic-carbon tetrachloride systems the values of $|\theta|$ and those of TS_E are very small. It seems that the systems are to some extent ideal from a thermodynamical point of view, compared with the non-ideal behavior of aromatic-alicyclic systems.

For the benzene-ethylene dichloride system,[33] the situation is different, compared with other systems containing one aromatic constituent. In spite of some positive values of V_E observed, the value of TS_E is small, and the value of θ is positive. The calculated values given in column 12, Table 5, are seen to be fairly larger than the observed value of H_E in column 3. For the aromatic-alicyclic systems in Table 5, the values in column 3 are nearly equal to those in column 12. From the results it seems that an ordered arrangement between benzene and ethylene dichloride molecules occurs in the mixture, and that it reduces the magnitude of TS_E and H_E in spite of the observed positive value of V_E. This explains the fact that the value of V_E calculated from the observed value of H_E is fairly smaller than the observed value of V_E.

The authors wish to thank Miss Yuko Endo of the laboratory for her co-operation in carrying out this study.

Appendix

Estimation of the Number of Nearest Neighbors for Pure Liquid. From Eq. (5) we can estimate the effective number of nearest neighbors, $Z_{\text{eff.}}$ for pure liquid, as follows.

$$\omega(0) = \gamma\varepsilon^* - \left(\frac{N\cdot\frac{4}{3}\pi r^{*3}}{V}\right) = -\gamma\left(\frac{4\sqrt{2}\,\pi}{3}\right)\left(\frac{r^*}{a}\right)^3\varepsilon^* \tag{40}$$

where

$$V = Na^3/\sqrt{2}.$$

On the other hand we can put

$$\omega(0) = -Z_{\text{eff.}}\varepsilon^*\left(\frac{r^*}{a}\right)^6 \tag{41}$$

where $Z_{\text{eff.}}$ is the effective number of nearest neighbors, which includes the influence of outer neighbors.

Equating Eq. (40) and Eq. (41), we have

$$Z_{\text{eff.}} = \gamma\left(\frac{4\sqrt{2}\,\pi}{3}\right)\left(\frac{a}{r^*}\right)^3 = \gamma\left(\frac{4\sqrt{2}\,\pi}{3}\right)\left(\frac{V}{V^*}\right) \tag{42}$$

where V^* is a "hard core volume"[14] and is taken to be equal to $N\beta r^{*3}$.

The influence of outer neighbors is estimated to increase the potential energy within a cell by about 20%, compared with the potential occuring from the first nearest neighbors only.[18,25] Thus, we can estimate the number of the first nearest neighbors approximately equal to $Z = Z_{\text{eff.}}/1.2$.

From the values of γ given in Table 3, estimating the values of (V/V^*) to be 1.3 for ordinary conditions of liquids, we can determine the values of Z to be 11.8 for liquid argon and to be 12.8 for C_6H_6, c-C_6H_{12}, and CCl_4. The values are supposed to be of reasonable magnitudes, though slightly larger than the observed.[26] This seems to support the adequacy of the present theory.

31) J. H. Hildebrand and R. L. Scott, "Regular Solutions" Prentice-Hall Inc., Engewood Cliffs, N. J. (1962), Chapt. 7.

32) J. A. Barker, *J. Chem. Phys.*, **20**, 1526 (1952).

33) A. Neckel and H. Volk, *Z. Elektrochem.*, **62**, 1104 (1958); L. A. K. Staveley, W. I. Tupman, and K. R. Hart, *Trans. Faraday Soc.*, **51**, 323 (1955).

BULLETIN OF THE CHEMICAL SOCIETY OF JAPAN VOL. 43 985—991 (1970)

Phosphorescence of Quinoxaline-Durene Mixed Crystal — Analysis of Fine Structures and Decay Characteristics

Yasuko NAKANO*1 and Tohru AZUMI*2

The Institute for Solid State Physics, The University of Tokyo, Roppongi, Minato-ku, Tokyo

(Received July 26, 1969)

The phosphorescence spectrum of quinoxaline doped in durene crystal is observed at 4.2°K. The spectrum is composed of a number of sharp bands, many of which being interpreted as arising from the coupling with the ground state molecular vibrations of quinoxaline. Associated with the 0,0 and vibronic bands three weak bands were observed which are separated from the vibronic band by 19, 30 and 52 cm^{-1}. The nature of these three bands is not well understood, but it is certain that they are not due to the lattice vibrations of the durene host. The decay of the phosphorescence is investigated at fifteen different temperatures between 4.21 and 1.59°K. Above 2.41°K the decay is single exponential with a lifetime of 0.246 sec. Below 2.19°K, however, the decay is expressed as a sum of two exponential decays whose lifetimes are 0.757 and 0.093 sec. The shorter one is approximately one third of the lifetime at 4.21°K. The change of the decay characteristics at a temperature between 2.19 and 2.41°K is interpreted to be associated with the spin alignment. In terms of these data, together with the polarization ratio observed by Chaudhuri and El-Sayed, radiative and radiationless rate constants are estimated for each of the three magnetic subcomponents of the triplet state. The experimental results and their interpretation are partly in disagreement with the work by de Groot, Hesselmann and van der Waals, and the source of the discrepancy is analyzed.

Quinoxaline exhibits relatively intense phosphorescence of π,π^* nature. As is revealed from the polarization measurements carried out for rigid glass solution by El-Sayed and Brewer,[1] the phosphorescence is polarized normal to the molecular plane. This out-of-plane polarization of the phosphorescence is in line with the π,π^* nature of the phosphorescence.[2] Namely, if the contribution from the two-electron operators for spin-orbit coupling is neglected, the π,π^* triplet state of a planar aza-aromatic molecule mixes only with π,σ^* or σ,π^* singlet states, from which the transition to the ground state is polarized normal to the molecular plane.

The situation is more complicated when quinoxaline is doped in durene host. As Chaudhuri and El-Sayed[3] showed, a significant part of the phosphorescence is polarized in-plane along the long axis of the molecule. This abnormal in-plane polarization was interpreted by Chaudhuri and El-Sayed to be due to the host-guest interaction. The exact nature of the host-guest interaction is, however, not well understood.

Vibrational analysis of the phosphorescence might give us more information on the host-guest interaction. The phosphorescence spectrum at 77°K or above is, however, broad and detailed fine structure analysis is not feasible. In the present paper, effort was made to accomplish the detailed fine structure analysis for the phosphorescence spectrum observed at 4.2°K.

The path of excitation and deexcitation of the triplet state were analyzed with emphasis on the three individual magnetic subcomponents of the triplet state. For this purpose analysis of the phosphorescence decays at very low temperatures was carried out in some detail.

At temperatures not very low, the decay constant of the phosphorescence is a population weighted average of the three individual rate constants for the three magnetic subcomponents. Specifically, the rate constant k for the triplet state as a whole is expressed as

$$k = \sum_i^3 n_i k_i \qquad (1)$$

where n_i and k_i are the fraction of the population and the decay constant for the ith subcomponents, respectively. This averaging results from the fact that, in ordinary condition, spin-lattice relaxation

*1 Present Address: Government Chemical Industrial Research Institute, Tokyo.

*2 The Present Address: Department of Chemistry, Faculty of Science, Tohoku University, Sendai.

1) M. A. El-Sayed and R. G. Brewer, *J. Chem. Phys.*, **39**, 1623 (1963).

2) S. P. McGlynn, T. Azumi and M. Kinoshita, "Molecular Spectroscopy of the Triplet States," Prentice Hall, New Jersey (1969).

3) N. K. Chaudhuri and M. A. El-Sayed, *J. Chem. Phys.*, **44**, 3728 (1966).

time is much shorter than the phosphorescence lifetime and that the population of any one sublevel is strayed over all the three levels. However, at very low temperatures, the spin-lattice relaxation time is expected to become longer than the phosphorescence lifetime. If this condition is realized, the phosphorescence emission would now start from each sublevel independently. The decays observed under this condition directly reflect the rate constants for the individual subcomponents. One may also obtain information regarding the population of the sublevels too.

The notations for states, rate constants and axes to be used in the following discussion are schematically shown in Fig. 1. Three magnetic subcomponents are denoted by T_x, T_y and T_z, which transform like rotations around x, y and z axis, respectively. The energy separations among three sublevels are obtained from the results of the ESR studies of Vincent and Maki.[4] The ordering of energies is consistent with the assumption of positive D and negative E. The radiative and radiationless decay constants for T_x are denoted by k_{px} and k_{qx}, respectively, and the sum of these two simply by k_x. Similar notations are adopted for decay constants for T_y and T_z. In C_{2v} point group, if the lowest triplet state is assumed to be of π,π^* $^3B_2$, the emission from T_x, T_y and T_z should be z-polarized, forbidden and x-polarized, respectively.

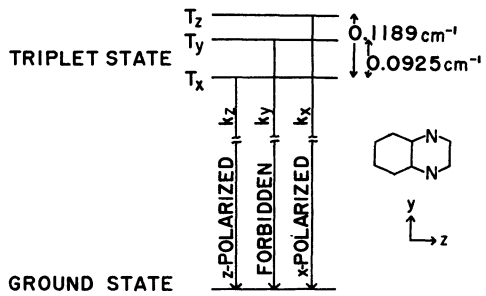

Fig. 1. Notation for states, rate constants and axes concerned with quinoxaline phosphorescence.

Experimental

Quinoxaline was purified by sublimation in a vacuum. Durene was purified by recrystallization from ethanol and by zone refining. Emission was observed for mixed crystals of 10^{-3} mol/mol in a polycrystalline form.

Emission spectra were obtained by a Spex 1700-II grating monochromator (reciprocal dispersion of 11 Å/mm) either photographically with a Kodak 103a-F plate or photoelectrically with an EMI 6256S photomultiplier tube. The locations of phosphorescence bands are determined from the photographic plates by reference to the iron arc spectrum.

The decays of the phosphorescence were measured at 462 nm using a JASCO CT-50 grating monochromator with an EMI 9529 A photomultiplier tube connected to an oscilloscope. In measurements of both spectra and decays, the exciting radiation was obtained from a 500 W high pressure mercury lamp. A Becquerel type phosphoroscope was used to separate the phosphorescence from the exciting light.

Temperature below 4.2°K was obtained by reducing the pressure above boiling helium, and the temperature was estimated from the known temperature-pressure curve.[5]

Infrared spectra of quinoxaline crystal were measured[6] at room temperature by a JASCO 402G spectrometer for the range from 4000 to 650 cm^{-1}, a Hitachi EPI-L spectrometer for the range from 700 to 250 cm^{-1}, and a Hitachi FIS-I spectrometer for the range from 300 to 50 cm^{-1}. Raman spectra of quinoxaline crystal were measured at 77°K in these laboratories by a three prism spectrograph by Yoko Kaizu, a low pressure mercury lamp being used as an exciting source.

Fine Structure Analysis

The phosphorescence spectrum of quinoxaline in durene host observed at 4.2°K is shown in Fig. 2a. The highest energy band at 21639 cm^{-1} is quite sharp and intense, and, in view of the vibrational analyses discussed below, is considered as the 0,0 band. Following this band, three relatively broad and weak bands were observed which are 19, 30 and 52 cm^{-1} apart from the 0,0 band (see Fig. 2b). As seen in Fig. 2, these four bands appear repeatedly in the whole spectral region. The fine structure analysis of the spectrum is attempted in Table 1, in which the wavenumber differences from the 21639 cm^{-1} band are compared with the molecular vibrations observed in infrared and Raman spectra. As shown in Table 1, the wavenumber separations among groups of the above mentioned four bands are in good agreement with the intramolecular vibrations of quinoxaline. Thus, as far as progressions of intramolecular vibrations are concerned, no immediate influence of the host-guest interaction is revealed.

The nature of the three weak bands always accompanied by the intense and sharp bands, however, remains unsolved. The energy separations of 19, 30 and 52 cm^{-1} are, of course, too small to be ascribed to intramolecular vibrations. One might then suppose that these fine structures are due to lattice vibration of the durene host. In fact, Hochstrasser and Small[7] interpreted some

4) J. S. Vincent and A. H. Maki, *ibid.*, **39**, 3088 (1963).

5) G. K. White, "Experimental Techniques in Low Temperature Physics," Oxford Univ. Press, London (1959).

6) We acknowledge Professor Takehiko Shimanouchi, Department of Chemistry, The University of Tokyo for the use of these spectrometers. We also thank Dr. Masako Suzuki for the experimental assistance.

7) R. M. Hochstrasser and G. J. Small, *J. Chem. Phys.*, **45**, 2270 (1966).

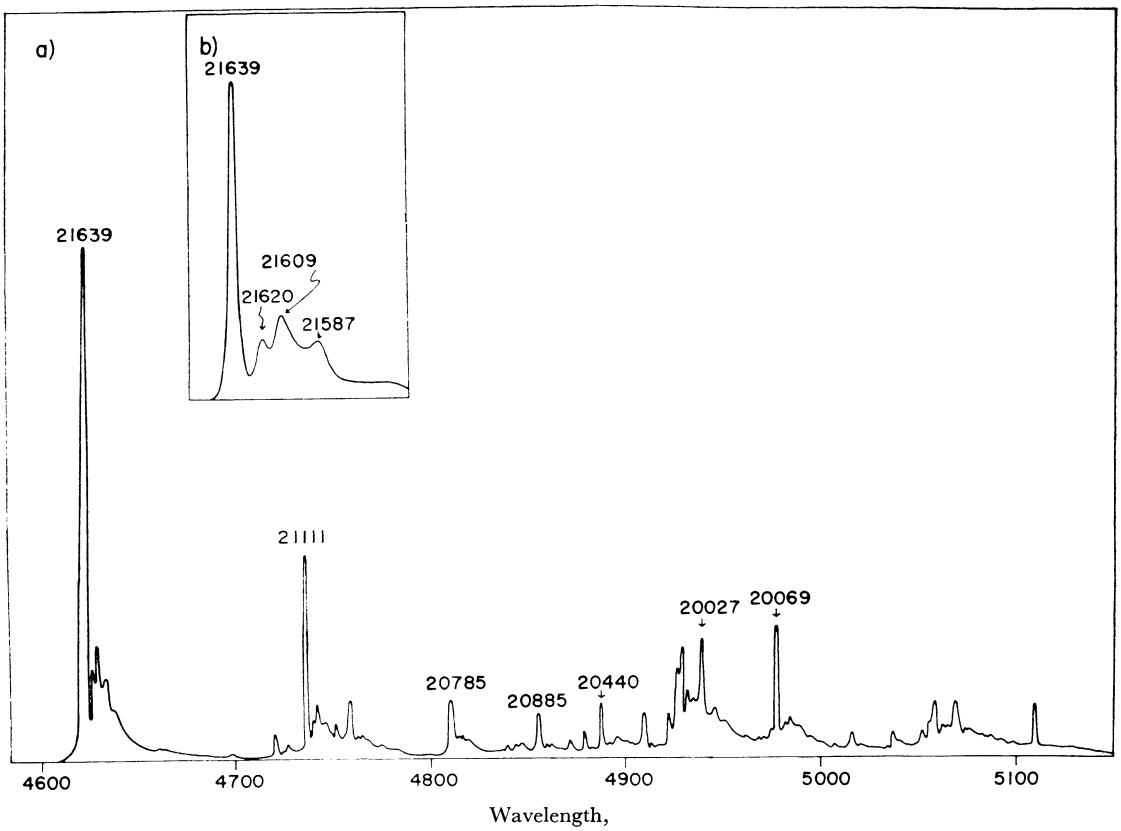

Fig. 2. a) Phosphorescence spectrum of quinoxaline-durene mixed crystal at 4.2°K. The numbers shown in the figure represent the frequencies of the main peaks in wavenumber unit.
b) Enlarged spectrum in the neighborhood of 0,0 band.

of the fine structures observed in phenanthrene fluorescence in biphenyl host to be due to the lattice vibrations of the biphenyl. Similar interpretations have also been given by Shigeoka, Koyanagi and Kanda[8] for fine structures observed in the phosphorescence of pyrazine in various hosts. In order to see if such supposition is also applied in this case, we compare the above mentioned energy intervals with the observed lattice vibrations. Raman spectra of durene crystal observed by Ito, Suzuki and Yokoyama[9] are at 50, 84 and 116 cm^{-1}; in each of these bands two rotational lattice vibrations are considered to be overlapped. As is evident, the intervals of 19 and 30 cm^{-1} are too small even compared with the rotational lattice vibrations. The translational lattice vibrations have not been observed. These frequencies may be a little smaller than the rotational lattice vibrations, but never as low as 19 cm^{-1}. If a lattice vibration of such low frequency existed, because of too large amplitude, it would manifest some unexpected specific heat properties, but such is not the case. All of these considerations lead us to conclude that the fine structures with small frequency intervals observed in the phosphorescence spectrum are not due to the lattice vibrations of the durene host.

A question still remains as to what the fine structures are due to, but cannot be answered at the moment. However, from our efforts in the defect phosphorescence observed in the crystalline states of azaaromatics[10] we regard it not meaningless to surmise that, in this case too, the phosphorescence originates from various perturbed quinoxaline molecules. It might be the guest-host interaction which causes this perturbation. Researches focussing on this point are under way and will be discussed in later publications.

Whatever the origins of the three weak bands associated with the 0,0 and other vibronic bands, the fine structure analysis presented in Table 1 clearly demonstrates that the phosphorescence

8) T. Shigeoka, M. Koyanagi and K. Kanda, Conference on Molecular Spectroscopy, Oct. 7, 1967, Sapporo.

9) M. Ito, M. Suzuki and T. Yokoyama, "Excitons, Magnons and Phonons in Molecular Crystals," ed. by A. B. Zahlan, Cambridge Univ. Press (1968).

10) T. Azumi and Y. Nakano, *J. Chem. Phys.*, **51**, 2515 (1969).

TABLE 1. VIBRATIONAL ANALYSIS OF THE PHOSPHORESCENCE SPECTRUM OF QUINOXALINE-DURENE MIXED CRYSTAL
(All figures are wavenumbers *in vacuo*.)

Phospho-rescence	Inte-nsity	Difference from the 21639 cm^{-1} band	Assignment	IR and Raman frequen-cies	Phospho-rescence	Inte-nsity	Difference from the 21639cm^{-1} band	Assignment	IRamd Raman frequen-cies
21639	vs	0	0		20350	m	1289	1289	1289(R)
21620	m	19	19		20296	m	1343	1343	
21609	m	30	30		20280	m	1359	1359	1361(R)
21587	m	52	52		20268	s	1371	1371	1378(R)
21179	m	462	462	467(IR)	20246	m	1393	528+858	
21149	w	490	490	487(IR)	20227	s	1412	1412	1412(IR,R)
21111	s	528	528	525(IR)	20069	s	1570	1570	1570(R)
21092	w	547	528+19		20051	w	1588	1570+18	
21080	m	559	528+31		20038	w	1601	1570+31	
21061	w	578	528+50		20018	w	1621	1570+51	
21037	w	603	603	603(IR,R)	19911	vw	1729	528+1199	
21006	m	633	633	637(R)	19821	vw	1818	1818	1825(IR)
20988	w	651	633+18		19767	w	1872	528+1343	
20975	w	664	633+30		19752	w	1887	528+1359	
20781	m	858	858	862(IR)	19738	w	1901	528+1371	
20764	w	875	858+17		19698	w	1941	528+1412	
20751	w	888	858+30		19541	w	2098	528+1570	
20729	w	910	858+52		19419	w	2220	858+1359	
20585	m	1054	528+528		19412	w	2227	858+1371	
20567	w	1072	528+528+18		19368	w	2271	858+1412	
20555	w	1084	528+528+30		19215	w	2424	858+1570	
20532	w	1107	528+528+53		18910	w	2729	1359+1359	
20511	vw	1128	1128	1125(IR)	18883	vw	2750	528+528+1359	
20479	w	1160	633+528		18866	w	2773	1359+1412	
20440	m	1199	1199	1202(IR,R)	18860	vw	2779	1371+1412	
20421	w	1218	1199+18		18712	vw	2912	1359+1570	
20409	w	1230	1199+31		18658	vw	2981	1412+1570	

comes from the quinoxaline molecules and not from any impurities. This conclusion is important in interpreting the decay results discussed in the following section, especially in analyzing the discrepancies of experimental results from the work by other workers; any possible complication due to impurity emissions is eliminated.

Spin Alignment as Revealed from Decay Characteristics

The decay of the phosphorescence was measured at fifteen different temperatures between 4.21 and 1.59°K. At any temperature above 2.41°K (and below 4.21°K) decay is found to be identical; it is single exponential decay with lifetime of 0.246 sec. These lifetime data indicate that the phosphorescence is of π,π^* nature, and validate the sublevel specifications shown in Fig. 1. The shortening of lifetime, by a factor of about 10, as compared with the lifetime of π,π^* phosphorescence of aromatic hydrocarbons, say, naphthalene, is due to the presence of n,π^* singlet states, which enhance the spin-orbit coupling.[11]

Below 2.19°K, however, a drastic change in decay characteristics is observed. First, the significant part of intensity is decayed with a rate approximately three times as fast as the decay rate at 4.21°K. In addition to this decay, there exists some component of longer lifetime. At all the temperatures observed below 2.19°K, the decay is expressed as a sum of two exponential decays with lifetimes of 0.757 and 0.093 sec, the component of shorter lifetime emitting more intensely. The manner in which decay is separated into two exponential decays is shown in Fig. 3b.

Such decay behavior at lower temperatures is due to spin alignment as has already been discussed by de Groot, Hesselmann and van der Waals[12] and by Hall, Armstrong, Moomaw and El-Sayed.[13] At very low temperatures, the spin-lattice relaxation time becomes much longer than the phosphorescence lifetime, and consequently "straying" among the spin states is frozen. For quinox-

11) H. Baba and T. Takemura, This Bulletin, **40**, 2215 (1967).

12) M. S. de Groot, I. A. M. Hesselmann and J. H. van der Waals, *Mol. Phys.*, **12**, 259 (1968).

13) L. Hall, A. Armstrong, W. Moomaw and M. A. El-Sayed, *J. Chem. Phys.*, **48**, 1395 (1968).

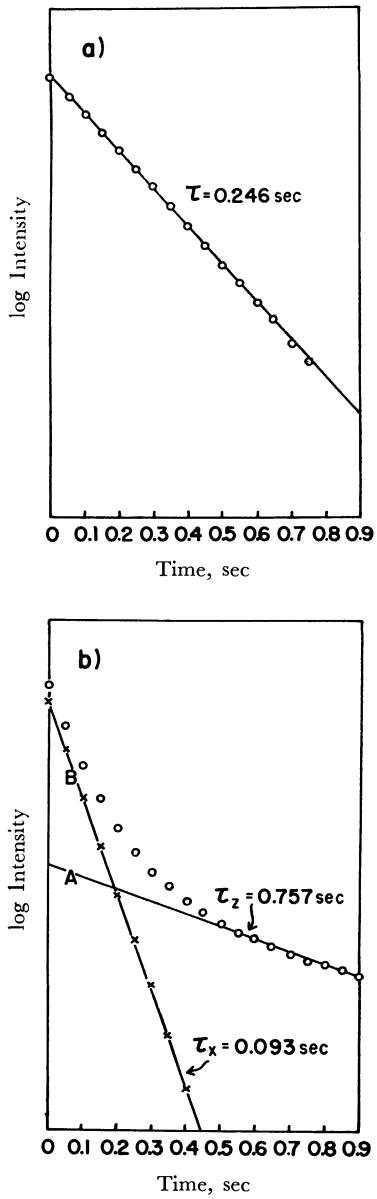

Fig. 3. Decay of phosphorescence in semilogarithmic plot. The points are experimental.
a) Observation at 77, 4.21, 4.00, 3.80, 3.45, 2.74, 2.58 and 2.41°K. The decay is single exponential, and the lifetime is 0.246 sec.
b) Observation at 2.19, 2.02, 1.97, 1.94, 1.84, 1.81, 1.74 and 1.59°K. The decay is expressed as a sum of two exponential decays whose lifetimes are 0.093 and 0.757 sec. Line A is as extrapolation from the long-time decay region. The × marks on the lower curve are differences between the experimental points and the corresponding points on Line A. Line B is drawn through these latter difference intensities.

aline-durene mixed crystal, de Groot *et al.* found that the inversion in magnitude between the spin-lattice relaxation time and the phosphorescence lifetime takes place at a temperature between 4.21 and 1.56°K. Our data indicate that this takes place somewhere between 2.19 and 2.41°K. The fact that the complete inversion of the order of the lifetimes at some temperatures in the narrow range of 0.2° may indicate that the spin-lattice relaxation time is very strongly dependent on temperature.

We shall next see if the above data could be used to estimate the decay constants for each of the magnetic subcomponents. First we note that the decay characteristics are identical at any temperatures between 1.59 and 2.19°K and also between 2.41 and 4.21°K. The identity of the decays indicates that decay constants are unchanged in the two temperature ranges. Thus we could assume that they keep constant all through 1.59 to 4.21°K.

The lifetime observed at temperatures above 2.41°K should be expressed by Eq. (1), thus

$$(k_x+k_y+k_z)/3 = 1/0.246 \tag{2}$$

Since the emission from T_y is forbidden, the two phosphorescence components observed at lower temperatures should be associated with the emission from T_x and T_z. The correspondence between the two components and the two emitting states is not determined uniquely. However, in view of the observation by Chaudhuri and El-Sayed[3] that the significant part of intensity comes from T_x, we shall assign the component of shorter lifetime as the emission from T_x.
Thus

$$k_x = 1/0.093 \tag{3}$$

$$k_z = 1/0.757 \tag{4}$$

From Eqs. 2—4, we obtain

$$\begin{aligned} k_x &= k_{px} + k_{qx} = 10.72\ \text{sec}^{-1} \\ k_y &= k_{qy} = 0.15\ \text{sec}^{-1} \\ k_z &= k_{pz} + k_{qz} = 1.32\ \text{sec}^{-1} \end{aligned} \tag{5}$$

Note that even though the emission from T_y is forbidden, the radiationless decay from this state takes place with a rate of $k_y=0.15\ \text{sec}^{-1}$.

We shall next separate the above rate constants into the radiative and radiationless parts. The polarization ratio observed by Chaudhuri and El-Sayed[3] indicates that

$$k_{px}/k_{pz} = 9 \tag{6}$$

We assume that the rates of radiationless decays are indentical for the three subcomponents. This assumption is only based upon the observation that the rates of radiationless transitions are mostly governed by energy difference.[14] No further justification exists and we admit that the assumption might not represent reality. However, we shall examine what information we could get.

14) R. E. Kellogg and N. C. Wyeth, *J. Chem. Phys.*, **45**, 3156 (1966); W. Siebrand, *ibid.*, **47**, 2411 (1962).

We obtain

$$k_{qx} = k_{qz} = 0.15 \text{ sec}^{-1} \tag{7}$$

which coincides with the k_{qy} value obtained independently. The coincidence is consistent with the above assumption that all of the three radiationless decay rates are the same. The radiative rate constants are then obtained as

$$\begin{aligned} k_{px} &= 10.75 \text{ sec}^{-1} \\ k_{pz} &= 1.17 \text{ sec}^{-1} \end{aligned} \tag{8}$$

From the above estimation, we view the path of excitation and deactivation in the following way: The T_y component is non-emissive, but radiationless deactivation from this state is not nonexisting. Both of the other two states, T_x and T_z, are emissive. Observation of emission from the two states in lower temperatures reveals that at least two subcomponents are populated by intersystem crossing from singlet excited states. Contrary to our view, however, de Groot *et al.*[15] concluded, for the same system, that only the T_z component is populated by intersystem crossing and phosphorescence comes exclusively from the same states. This discrepancy is puzzling, and we try to analyze the source of the discrepancy in the following.

Comparison with, and Comment on, the Work by de Groot, Hesselmann and van der Waals. The most significant source of discrepancy between the two groups of authors is apparently the difference in experimental results. Specifically, we found, at the temperatures where spins are aligned, decays consisted of *two* different exponential decays, whereas de Groot *et al.*[12,15] reported that the decay is always *single* exponential. A question immediately arises why the two sets of experiments, both concerned with apparently the same quinoxaline-durene mixed crystals, give different results. In the experiment of de Groot *et al.*, excitation is effected for a period of 1 msec by a xenon flash lamp, whereas in our case excitation is continued for about 10 sec until further irradiation does not increase the phosphorescence signals. Apparently, excitation is more efficient in our case. We believe that this difference in excitation efficiency is the primary cause of the differences in the observed decay behaviors.

In general, the rise time of the phosphorescence is shorter than or equal to the decay time; lower efficiency in the excitation leads to longer rise time.[16] Now, suppose we have two emitting states characterized by two different decay constants. When excitation is carried out for a sufficiently long time, the population of the two states are increased to their maximum (saturated) values, and consequently the decays from the two states may be separated without much difficulty. On the other hand, if excitation is interrupted after a very short time, as in the case of flash excitation, the state of the longer lifetime is not populated as much as in that of the shorter lifetime. Consequently the emission from the state of longer lifetime may be hidden under the emission from the state of shorter lifetime. It is probably due to this latter effect that de Groot *et al.* did not find the phosphorescence component of longer lifetime. From this viewpoint we emphasize that the phosphorescence decay measurement for a system of more than one emitting states must be carried out with high efficiency of excitation.

In view of what is discussed above, let us for a moment disregard the results of the decay measurements by de Groot *et al.* and see what information concerning the decay rates is available from other data. The most meaningful experiment in this regard is the optical detection of magnetic resonance (hereafter abbreviated as ODMR) carried out by Schmidt, Hesselmann, de Groot and van der Walls[15] for perdeuterated quinoxaline and also by Forman and Kwiram[17] for perhydrated quinoxaline. In this experiment one sees how application of microwave corresponding to magnetic resonance varies the phosphorescence intensity. Both of the above two groups of authors obtained identical results. Analysis of their experimental results leads to the following three inequalities:

$$\begin{aligned} 2k_{pz} &> k_{px} + k_{py} \\ k_{py} + k_{pz} &> 2k_{px} \\ k_{px} + k_{pz} &> 2k_{py} \end{aligned} \tag{9}$$

where no assumptions or preliminary knowledge regarding the values of the rate constants are introduced. If now, in view of our experimental results, k_{py} is set equal to zero, then inequality (9) is reduced to

$$k_{pz} > 2k_{px} \tag{10}$$

This indicates that k_{pz} is larger than twice of k_{px}; it does not indicate that k_{px} is zero. It is therefore not correct to conclude that emission comes exclusively from the T_z component. If, and only if, it becomes certain that only one of the three states is emissive, then conclusion that only k_{pz} is non-zero is justified. From this viewpoint, we suggest that when one tries to see the path of deexcitation from experiments on ODMR, other data such as polarization measurements or decay measurements followed by high efficiency of excitation should be consulted.

One more comment should be added with regard to inequality (10). The inequality, which was derived from the analysis of experimental results

15) M. S. de Groot, I. A. M. Hesselmann, J. Schmidt and J. H. van der Waals, *Mol. Phys.*, **15**, 17 (1968).

16) M. Nakamizo and T. Matsueda, *J. Mol. Spectrosc.*, **27**, 450 (1968).

17) A. Forman and A. L. Kwiram, *J. Chem. Phys.*, **49**, 4714 (1968).

on ODMR, clearly contradicts the polarization results, Eq. 6, reported by Chaudhuri and El-Sayed. At this moment we have no way of judging which of the results are correct; however, if the polarization data be erroneous, the rate constant estimate given in this paper would be meaningless.

The unambiguous determination of the x and z axes of quinoxaline molecule is not an easy task since in durene host x axis of a molecule is nearly parallel to the z axis of another molecule in the same cell.[18] Nonetheless attempts to decide which of the conflicting results are correct are under way and will be treated in the future.

We wish to express our appreciation to Professor Saburo Nagakura, Professor Mitsuo Ito and Mr. Yasuo Udagawa for fruitful discussions.

18) J. M. Robertson, *Proc. Roy. Soc.*, **141A**, 594 (1933); *ibid.*, **142A**, 659 (1933).

BULLETIN OF THE CHEMICAL SOCIETY OF JAPAN VOL. 43 991—995 (1970)

Conformers and Intramolecular Hydrogen Bond of *trans*-2-Halocyclohexanols

Etsuko FUJIMOTO, Yoshiko TAKEOKA*1 and Kunio KOZIMA

Laboratory of Molecular Spectroscopy, Tokyo Institute of Technology, Ookayama, Meguro-ku, Tokyo

(Received August 19, 1969)

By infrared studies it has been ascertained that *trans*-2-halocyclohexanols possess two conformers, namely, the ee-isomer and the aa-isomer, both in the liquid and in a solution, while only the ee-isomer exists in the solid. In a dilute solution the ee-isomer is more stable and exists exclusively in the form with an intramolecular hydrogen bond. The values of the energy difference between the two isomers are 1.3, 1.9, and 2.2 kcal/mol for the chloro-, the bromo-, and the iodo-derivative respectively. The magnitude of the frequency shifts of the O–H stretching bands increases in the order: Cl<Br<I. These facts show that the intramolecular hydrogen bond stabilizes the ee-isomer and that the strength of the hydrogen bond increases in the order: Cl<Br<I. The electrostatic energy increases in the order: Cl>Br>I, while the delocalization energy due to the charge-transfer increases in the opposite order. Therefore, it can be concluded that the energy due to the charge-transfer contributes dominantly to the energy of the intramolecular hydrogen bond formed in the ee-isomer of *trans*-2-halocyclohexanols.

It is very probable that *trans*-2-halocyclohexanols possess two conformers which are interconvertible by the inversion of the ring, and that both the halogen X and the O–H group attach to the e-positions of a ring in one conformer and to the a-positions of a ring in the other, as in the case of *trans*-1,2-dihalocyclohexanes.[1] The conformers hereafter will be referred to as the ee-isomer and the aa-isomer respectively.

Since, of the two isomers, only the ee-isomer is expected to have an intramolecular hydrogen bond between the X atom and the H atom of the O–H group, as in the case of ethylene chlorohydrin,[2] it seemed that it would be interesting to study the energy differences between the isomers.

Experimental

Materials. *trans*-2-Chlorocyclohexanol was prepared[3] by adding hypochlorous acid to cyclohexene obtained according to the method of Osterberg and Kendall.[4] The product was then purified by fractional distillation; bp 71.2—72.5°C/10 mmHg.

trans-2-Bromocyclohexanol was prepared according to the method of Winstein[5] by adding 1,2-epoxycyclohexane to 48% hydrobromic acid, the reaction temperature being maintained below 5°C over a period of about an hour. The product was purified by fractional distillation; bp 61.5—61.8°C/2 mmHg.

trans-2-Iodocyclohexanol was prepared by a method[6]

*1 Present address: Ohtsuma Women's University, Chiyoda-ku, Tokyo.

1) K. Kozima, K. Sakashita and S. Maeda, *J. Amer. Chem. Soc.*, **76**, 1965 (1954).

2) S. Mizushima, T. Shimanouchi, T. Miyazawa, K. Abe and M. Yasumi, *J. Chem. Phys.*, **19**, 1477 (1951).

3) G. H. Coleman and H. F. Johnstone, "Organic Syntheses," Coll. Vol. I, p. 158 (1948).

4) A. E. Osterberg and E. C. Kendall, *J. Amer. Chem. Soc.*, **42**, 2620 (1920).

5) S. Winstein, *ibid.*, **64**, 2794 (1942).

6) S. Winstein, E. Grunwald, R. E. Buckles and C. Hanson, *ibid.*, **70**, 816 (1948).

similar to that used for *trans*-2-bromocyclohexanol. The product was recrystallized from petroleum ether; mp 40.0—41.7°C.

Carbon disulfide of an extra pure grade was used as a solvent after distillation.

Infrared Spectra. The spectra were measured with a Perkin-Elmer 112 spectrometer equipped with a potassium bromide, a sodium chloride, or a lithium fluoride prism. To study the solid-state spectra, the chloro-derivative was cooled by ice,*2 and the bromo-derivative by a mixture of dry ice and ethyl alcohol. The temperature of the samples was determined by means of a copper-constantan thermocouple. The thickness of the cell used for the infrared studies of dilute solutions was 6 mm.

The wavenumber readings for the liquid- and the solid-state spectra are listed in Table 1.

Measurements of the Integrated Intensities. As the contours of the bands used in the intensity measurements were usually represented by Lorentz's curve, the true integrated absorption intensity per mole, a, corrected for finite slit widths was calculated by means of the equation:

$$a = K(1/CL)\log_e(T_0/T)_{max}\Delta\nu^a_{1/2}$$

where the letters have their usual meanings.[7] The values of K were obtained from the table of Ramsay.[7]

In order to determine the energy difference between the isomers, the relative intensities of bands due to the two isomers as a function of temperature were measured in a dilute carbon disulfide solution. The O–H stretching band due to the intramolecular hydrogen bond overlaps with the free O–H stretching band for the three derivatives. However, these bands could be separated only for the iodo-derivative by assuming that the band shapes are given by Lorentz's equation. The measurements for such compounds having an O–H group should be made in a very dilute solution, for which no band assigned to the intermolecular hydrogen bond can be detected in the 3 μ region spectra, because even a small amount of the intermolecular hydrogen bond markedly affects the observed energy difference.

By using the data of the change in the relative intensity with the temperature, the energy difference between the isomers could be estimated by the following equation, as has been described in a previous paper:[8]

$$\log_e \frac{(C_1a_1/C_2a_2)_{T'}}{(C_1a_1/C_2a_2)_{T''}} = -\frac{\Delta E}{R}\left(\frac{1}{T'} - \frac{1}{T''}\right)$$

where ΔE denotes $E_1 - E_2$, $(C_1a_1/C_2a_2)_{T'}$, and $(C_1a_1/C_2a_2)_{T''}$ denote the relative intensities at the T' and T'' °K temperatures, and where the suffixes 1 and 2 refer to the value of each isomer. The results obtained are shown in Tables 3.

Results and Discussion

Since several bands of the liquid-state spectra of these compounds disappear on passing from the liquid to the solid, as is shown in Table 1, it is sure that the two isomers, the ee-isomer and the aa-isomer, exist in the liquid and that the equilibrium between them breaks down in the course of crystallization until only one isomer persists in the solid, as in the cases of *trans*-1,2-dichloro- and *trans*-1,2-dibromocyclohexane.[1]

The infrared spectra of *trans*-2-halocyclohexanols in a dilute carbon disulfide solution were measured in the 3 μ region. As can be seen in Table 2, there are two absorption bands in this region. Concerning the iodo-derivative, in the spectra of which the frequency difference between these bands is relatively large, it was ascertained that the relative intensity of these bands changes with the dilution and that it becomes constant when the concentration is less than 0.03 mol/l. This shows that there are intramolecular hydrogen-bonded molecules in this solution. The lower frequency band can be assigned to the O–H stretching vibration of the hydrogen-bonded molecules, and the other to that of the non-bonded molecules. This behavior of the iodo-derivative is similar to that in the cases of the chloro-derivative and the bromo-derivative. It can be safely assumed that the lower frequency band is due to the ee-isomer, while the higher one may be due to the aa-isomer, because, in view of its molecular geometry, only the ee-isomer is able to form an intramolecular hydrogen bond.

In both the liquid- and the solid-state spectra for these three compounds, we could observe a very broad and weak band extending from 800 to beyond 550 cm^{-1}. Since this band disappears in the spectra of the dilute solution, it may be safely assigned to the out-of-plane deformation vibration of the intermolecular hydrogen-bonded O–H group.[9]

In order to determine the energy difference between the two isomers of the iodo-derivative, we selected a pair of bands, namely the 1030-cm^{-1} band which persists in the solid and the 1001-cm^{-1} band which disappears on passing from the liquid to the solid, and measured the temperature dependence of the relative intensity; the results are shown in Table 3—3a. From these data, the energy difference is calculated to be 2.2 kcal/mol, the isomer which exists in the solid being more stable.

To determine the stable isomer, the change in the relative intensity of the two O–H stretching bands, one of which is due to the intramolecular hydrogen bond, and the other of which is due to the free O–H bond, was measured with the change in the temperature in the dilute solution. The results obtained are shown in Table 3—3b. From these data the energy difference between the two isomers is calculated to be 2.4 kcal/mol, the intramolecular hydrogen-bonded isomer being more

*2 In order to avoid supercooling, this refrigerant is used; it is adequate for this substance.

7) D. A. Ramsay, *J. Amer. Chem. Soc.*, **74**, 72 (1952).

8) K. Kozima and Y. Yamanouchi, *ibid.*, **81**, 4159 (1959).

9) A. V. Stuart and G. B. B. M. Sutherland, *J. Chem. Phys.*, **20**, 1977 (1952).

TABLE 1. INFRARED SPECTRA OF *trans*-2-HALOCYCLOHEXANOL (cm^{-1})

Chloro-derivative		Bromo-derivative		Iodo-derivative	
Liquid	Solid	Liquid	Solid	Liquid	Solid
477 (m)	475 (s)	465 (wb)	467 (wb)	462 (wb)	465 (m)
			550 (w)		
559 (m)	560 (m)	556 (m)	560 (m)	554 (m)	561 (s)
705 (w)		650 (w)		632 (w)	
735 (vs)	732 (vs)	688 (s)	688 (vs)	657 (s)	656 (s)
798 (s)	797 (s)	792 (m)	791 (m)	791 (m)	790 (m)
812 (w)		809 (w)		807 (w)	
843 (m)	845 (m)	841 (m)	841 (m)	839 (m)	838 (m)
			846 (m)		
867 (s)	866 (s)	863 (s)	863 (m)	859 (s)	859 (s)
896 (m)	898 (m)	896 (m)	897 (m)	892 (m)	893 (m)
907 (w)		904 (w)		900 (w)	
946 (m)	945 (sh)	943 (m)	948 (w)	932 (m)	941 (sh)
959 (s)	956 (s)	956 (s)	959 (s)	951 (s)	951 (s)
976 (m)		971 (m)		967 (m)	
1009 (m)		1007 (m)		1002 (m)	
1037 (m)	1037 (sh)	1034 (m)	1032 (m)	1034 (m)	1033 (w)
1045 (sh)	1050 (w)	1045 (sh)	1048 (vw)		1046 (w)
1072 (vs)	1077 (vs)	1074 (vs)	1075 (vs)	1072 (vs)	1075 (vs)
1109 (vw)	1116 (w)	1100 (vw)	1104 (w)		
1126 (m)	1130 (w)	1119 (m)	1122 (m)	1113 (m)	1123 (m)
1152 (vw)		1147 (vw)		1162 (s)	1158 (s)
1205 (sh)	1192 (s)	1185 (s)	1189 (s)	1190 (w)	1195 (w)
1215 (s)					
1229 (m)	1221 (s)	1229 (m)	1228 (m)	1225 (w)	1230 (w)
	1241 (vw)				
1259 (m)	1260 (m)	1251 (m)	1254 (m)	1248 (w)	1246 (m)
1268 (sh)	1281 (w)	1270 (w)	1278 (m)	1267 (w)	1279 (w)
1291 (w)	1309 (w)	1300 (w)	1309 (w)		1302 (w)
1329 (m)	1330 (s)	1322 (m)	1333 (m)	1324 (w)	1328 (w)
			1347 (m)		
1364 (s)	1350 (s)	1363 (s)	1364 (s)	1353 (s)	1350 (s)
1418 (wb)	1419 (wb)	1417 (wb)	1395 (w)	1415 (wb)	1419 (w)
1449 (vs)	1450 (vs)	1449 (vs)	1446 (vs)	1445 (vs)	1447 (vs)
2665 (vw)	2665 (vw)	2671 (vw)	2668 (vw)	2667 (vw)	2677 (vw)
2871 (s)	2871 (s)	2862 (s)	2866 (s)	2862 (s)	2862 (s)
2940 (vs)	2940 (vs)	2939 (vs)	2937 (vs)	2930 (vs)	2932 (vs)
3368 (vs)	3336 (vs)	3370 (vs)	3287 (vs)	3365 (vs)	3193 (vs)

w=weak, m=medium, s=strong, v=very, b=broad and sh=shoulder

TABLE 2. FREQUENCY OF THE O-H STRETCHING BAND IN THE CS_2 SOLUTION (cm^{-1})

Compound	Free band	Hydrogen-bonded band	Frequency shift
$C_6H_{10}Cl(OH)$	3607	3582	25
$C_6H_{10}Br(OH)$	3605	3571	34
$C_6H_{10}I(OH)$	3599	3558	41

stable. When taking into account the experimental error usually introduced in the intensity measurements, the two values of the energy difference are considered to agree with each other. This fact indicates that the isomer which exists in the solid is the ee-isomer and that it exists exclusively in the form having the intramolecular hydrogen bond in the dilute solution.

For the bands assigned to the C-halogen stretching vibration of various halogen derivatives of cyclohexane, one of the present authors has previously pointed out the empirical rule[10] that the frequencies of the bands which are due to the halogen atoms attached to the e-positions of the ring are higher than those of the bands due to the same halogen atoms attached to the a-positions. For the iodo-derivative, the 632- and the 657-cm^{-1} band can be

10) K. Kozima, *Bull. Tokyo Inst. Tech.*, **1952**, 49.

TABLE 3. TEMPERATURE DEPENDENCE OF THE RELATIVE INTENSITIES AND ENERGY DIFFERENCE BETWEEN ISOMERS IN THE CS_2 SOLUTION

(1) *trans*-2-Chlorocyclohexanol
Concentration: 0.016 mol/*l*
Prism: NaCl
Spectral slit width: 3.3 cm^{-1} at 1007 cm^{-1}
3.5 cm^{-1} at 1034 cm^{-1}

Temp. (C)	Wave-number	Isomer	$\log_e (T_0/T)_{max}$	$\Delta\nu^a_{1/2}$ (cm^{-1})	K	C_1a_1/C_2a_2
29	1007	1=aa	0.0945	9.6	1.51	0.059
	1034	2=ee	1.04	14.5	1.55	
−23	1007	1=aa	0.0690	9.8	1.51	0.038
	1034	2=ee	1.30	13.4	1.56	

$E_{aa}-E_{ee}=1.3$ kcal/mol

(2) *trans*-2-Bromocyclohexanol
Concentration: 0.015 mol/*l*
Prism: NaCl
Spectral slit width: 3.3 cm^{-1} at 1005 cm^{-1}
3.5 cm^{-1} at 1033 cm^{-1}

31	1005	1=aa	0.0881	11.0	1.51	0.061
	1033	2=ee	1.42	10.2	1.56	
−23	1005	1=aa	0.0518	11.0	1.51	0.031
	1033	2=ee	1.66	10.8	1.57	

$E_{aa}-E_{ee}=1.9$ kcal/mol

(3a) *trans*-2-Iodocyclohexanol
Concentration: 0.013 mol/*l* Prism: NaCl
Spectral slit width: 3.3 cm^{-1} at 1001 cm^{-1}
3.5 cm^{-1} at 1030 cm^{-1}

31	1001	1=aa	0.109	9.5	1.51	0.067
	1030	2=ee	1.25	12.0	1.56	
−24	1001	1=aa	0.0655	8.2	1.49	0.030
	1030	2=ee	1.64	10.5	1.57	

$E_{aa}-E_{ee}=2.2$ kcal/mol

(3b) *trans*-2-Iodocyclohexanol
Concentration: 0.017 mol/*l*
Prism: LiF
Spectral slit width: 3.6 cm^{-1} at 3558 cm^{-1}
3.7 cm^{-1} at 3599 cm^{-1}

28	3599	1=f	0.203	25.6	1.56	0.17
	3558	2=h	1.26	23.7	1.57	
−16	3599	1=f	0.119	25.7	1.56	0.087
	3558	2=h	1.48	23.6	1.57	

$E_f-E_h=2.4$ kcal/mol

safely assigned to the C-I stretching vibrations. Therefore, according to this rule, the same conclusion as that described above for the stable isomer can be drawn, since only the higher frequency band persists in the solid.

The liquid-state spectrum of the chloro- or the bromo-derivative was divided into two groups according to whether or not the band persists in the solid. For the chloro- or the bromo-derivative, an adequate band for the intensity measurements was selected from each group and the change in the relative intensity with the temperature was measured. The results are shown in Tables 3—1 and 3—2. From these data, the energy differences are calculated to be 1.3 and 1.9 kcal/mol for the chloro- and the bromo-derivative respectively, the isomer which exists in the solid being more stable. By comparing the two groups of the bands of the three compounds, it can be seen that the spectra show striking similarities. Therefore, it is very probable that the stable isomer is the ee-isomer for the chloro- or the bromo-derivative, as is the case for the iodo-derivative. Furthermore, additional evidence is obtained by the following considerations. The 735 and 705-cm^{-1} band of the chloro-derivative, and the 688 and the 650-cm^{-1} band of the bromo-derivative, can be safely assigned to the C–Cl and the C–Br stretching vibrations respectively. According to the rule described above, the same conclusion can be drawn from the fact that the higher frequency bands persist in the solid for the two derivatives.

The energy differences between the two isomers of *trans*-2-halocyclohexanols, $\Delta E=E_{aa}-E_{ee}$, increase in the order: Cl<Br<I. For *trans*-1,2-dihalocyclohexanes it has been reported[1] that the energy difference between the two isomers is 50 cal/mol or 500 cal/mol in the dilute carbon tetrachloride solution for the dichloro- or the dibromo-derivative respectively, the aa-isomer being the more stable. Comparisons of the energy differences show that the ee-isomer of the dibromo-derivative is less stable than that of the dichloro-derivative. This is contrary to the case of *trans*-2-halocyclohexanols. These facts suggest that the intramolecular hydrogen bond formed in the ee-isomer of *trans*-2-halocyclohexanols stabilizes the ee-isomer and that the strength of the hydrogen bond increases in the order: Cl<Br<I. This suggestion is supported by the following experimental evidence.

The magnitude of the frequency shifts of the O–H stretching band, which may be considered to be a measure of the strength of the hydrogen bond, increases in the order: Cl<Br<I. Since the sequence of the hydrogen-bonding power of halogens is opposite to the sequence of electronegativity, the energy due to the electrostatic interaction between the halogen and the hydrogen of the O–H group, which may increase with an increase in the electronegativity of halogens, does not seem to be dominant in this system.

It is well known[11] that, for a proper understanding of the hydrogen bond, we must use the charge-transfer theory. For this it may be assumed that the delocalization effect can be represented as due

11) C. A. Coulson, "Valence," 2nd Ed., Oxford Univ. Press (1961), p. 352.

to the existence of terms corresponding to two structures, namely:

(i) —O—H X—; no bond structure

(ii) —O$^-$ H—X$^+$—; dative structure.

According to Mulliken's theory,[12] the delocalization energy, ε, for these charge-transfer systems of a common electron acceptor can be represented approximately as follows:[13]

$$\varepsilon \propto \frac{S^2_{HX}}{I_D - k}$$

where S_{HX} is the overlap integral over the lone-pair AO of halogen, φ_X, and hydrogen 1*s*-AO, φ_H, *viz.*, $S_{HX}=\int\varphi_H\varphi_X d\tau$, I_D is the ionization potential of the electron donor, and k is taken to be a constant for the three compounds. Therefore, the delocalization energy increases as S_{HX} increases or I_D decreases.

In order to estimate the values of the overlap integrals, we calculated the H---X distance (r_{HX}) and the angle between the C–X bond and the hydrogen bond ($\pi/2-\alpha$), assuming that the most stable hydrogen bond is formed in the position where r_{HX} is at a minimum. The result are shown in Table 4. When we assume the structure of the hydrogen-bonded system shown in Fig. 1, an orbital of the lone-pair of the halogen can be represented as follows:

$$\varphi_X = \sqrt{\frac{1}{3}}\{\sqrt{1-s^2}\,\psi_s + (\sqrt{2}\cos\alpha - s\sin\alpha)\psi(p_x) - (\sqrt{2}\sin\alpha + s\cos\alpha)\psi(p_y)\}.$$

Here s^2 denotes the *s* character of the *s*–*p* hybridization of the halogen-bonding orbital, while ψ_s, $\psi(p_x)$, and $\psi(p_y)$ denote, respectively, the *ns*-, np_x-, and np_y-AO's of the electrons of the halogen atom, where *n* is the principal quantum number. When Slater's AO's are tentatively assumed and the *s* character is assumed to be 18%,[14] the overlap integrals are calculated to be 0.143 and 0.188 for the chloro- and the iodo-derivative respectively.

Although the r_{HX} value of the iodo-derivative is larger than that of the chloro-derivative, the value of the overlap integral of the iodo-derivative is not less than that of the chloro-derivative. By considering this result and the fact[15] that the first ionization potentials of alkyl halides decrease in the order: Cl>Br>I, it can be concluded that the delocalization energies due to the charge-transfer increase in the following order: the chloro- <the bromo- <the iodo-derivative. This conclusion is in accord with the experimental results.

Therefore, it can be concluded that the delocalization energy due to the charge-transfer contributes dominantly to the energy of the intramolecular hydrogen bond formed in the ee-isomer of *trans*-2-halocyclohexanols.

Table 4. Intramolecular hydrogen-bonded system formed in the ee-isomer

Compound	r_{HX} (Å)	α	S_{HX}
$C_6H_{10}Cl(OH)$	2.42	23°44′	0.143
$C_6H_{10}Br(OH)$	2.49	26°52′	
$C_6H_{10}I(OH)$	2.59	30°35′	0.188

Assumed values: -C=1.54, Å, C–O=1.43, Å, O–H=0.94, Å, C–Cl=1.78, Å, C–Br=1.94 Å, C–I=2.14 Å, ∠COH=106° and other bond angles are tetrahedral.

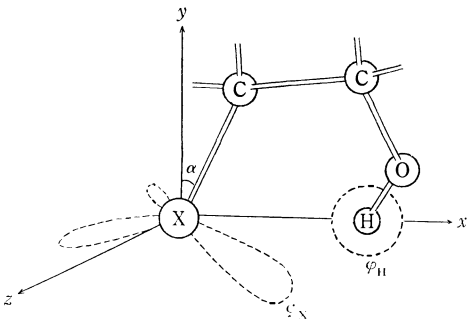

Fig. 1. The assumed structure of the hydrogen-bonded system of the ee-isomer.

12) R. S. Mulliken, *J. Amer. Chem. Soc.*, **74**, 811 (1952).

13) S. P. McGlynn, *Chem. Rev.*, **58**, 1113 (1958).

14) C. H. Townes and B. P. Dailey, *J. Chem. Phys.*, **17**, 782 (1949).

15) *E. g.*, K. Higasi, I. Omura and T. Tsuchiya, "Tables of Ionization Potentials of Molecules and Radicals," Monograph Series of the Research Institute of Applied Electricity, Hokkaido University (1957).

BULLETIN OF THE CHEMICAL SOCIETY OF JAPAN VOL. 43 996—1000 (1970)

The Catalytic Oxidation of Carbon Monoxide on Titanium Dioxide; Anatase and Rutile

Yoshito ONISHI and Takuya HAMAMURA

Department of Chemistry, Faculty of Industrial Arts, Kyoto Technical University, Matsugasaki, Sakyo-ku, Kyoto

(Received September 16, 1969)

For the purpose of investigating the correlation between the crystal structure of titanium dioxide and its catalytic activity, the catalytic oxidation rate of carbon monoxide and the desorption rate of oxygen from the sample surface have been measured on anatase, rutile, and an anatase-rutile mixture. The oxidation of carbon monoxide was investigated by a static method at temperatures of 250—550°C and under gas pressures of 10^{-2}—150 mmHg. The desorption of oxygen was carried out at 600—750°C. The reaction rate was proportional to P_{CO} and did not depend on either P_{O_2} or P_{CO_2}. The activation energy was 16.0 kcal/mol for anatase and 6.7 kcal/mol for rutile. The catalytic activity per unit of the surface area of rutile was 3—6 times as much as that of anatase. The reaction rate almost coincided with the rate of the reduction of titanium dioxide by carbon monoxide. The electric resistance of the sample was little affected by the P_{O_2}. The following reaction mechanism is proposed to explain the results. The rate-determining step is the reaction between the surface oxygen of the sample and the carbon monoxide physisorbed or that which has just collided with the surface coming from the gas phase; the oxygen vacancy thus formed on the surface is quickly filled with oxygen of the gas phase. The difference in the activation energy of the catalytic action between the two structures is based upon the difference in the activation energy of the oxygen desorption from the surface structure; the activation energies are 57.8 kcal/mol for anatase and 38.4 kcal/mol for rutile.

It is generally accepted that there is an intimate relationship between the catalytic activity of a solid catalyst and its crystal structure. Many investigations[1-4] as to these points have been carried out on the metals, but few on metallic oxide catalysts; thus, we have chosen titanium dioxide, TiO_2, as the subject of the present investigation. Titanium dioxide has three polymorphic forms, that is, anatase, rutile, and brookite; among these, rutile can be transformed from anatase by heating it to high temperatures, and so it is easy to obtain samples with the same chemical constitutions but different polymorphic forms. Therefore, titanium dioxide is suitable as a sample to investigate the relationship between the catalytic activity and the crystal structure.

The aim of this series of investigations is to ascertain the difference between anatase and rutile in their catalytic activity in response to the oxidation reaction. This paper will be concerned with the oxidation of carbon monoxide on the surface of titanium dioxide.

There have been several reports[5] on the pure or doped titanium dioxide catalyst used for the CO-oxidation, but there seems to have been no systematic investigation of the catalyst relating to the polymorphic forms. Moreover, most of the investigations of the catalytic reactions reported so far were carried out using an apparatus with greased stop cocks; these might contaminate the catalyst and so might cause some errors in the results. For this reason, the present experiments were performed with strict care taken to prevent the sample from contamination with grease vapor.

Experimental

The samples used in the present experiment are listed in Table 1. The sample A_1 was a reagent of a guaranteed grade obtained from the East Merck Company. Anatase transforms into rutile[6] and decreases in specific surface area when it is heated to high temperatures, so the samples of anatase, rutile, or an anatase-rutile mixture with the desired surface areas were obtained by selecting a suitable temperature and period

1) J. A. Becker, *Advan. Catal.*, **7**, 135 (1955).
2) A. T. Gwathmey and R. E. Cunningham, *ibid.*, **10**, 57 (1958).
3) G. Ehrlich, *ibid.*, **14**, 255 (1963).
4) F. S. Stone, *ibid.*, **13**, 1 (1962).
5) I. L. Mikhailova, I. S. Sazonova and N. P. Keier, *Kinet Katal.*, **6**, 704 (1965). *Chem. Abstr.*, **63**, 17197a (1965).
6) A. W. Czanderna, C. N. R. Rao and J. M. Honig, *Trans. Faraday Soc.*, **54**, 1069 (1958).

Table 1. Samples

No.	Temperature and time of heating		Polymorphic forms	Weight %	Specific surface areas (m^2/g)
A_1	—	—	Anatase	100	10.3
A_2	900°C	1 hr	Anatase	100	7.7
A_3	1000	1 hr	Anatase	100	4.3
R_1	1150	1 hr	Rutile	100	1.3
R_2	1150	3 hr	Rutile	100	1.0
AR_1	1050	1 hr	Anatase Rutile	87.3 12.7	3.8
AR_2	Mixture of A_1 and R_2		Anatase Rutile	87.4 12.6	4.7

of heat treatment. The heat treatments were carried out as follows. The sample A_1 (about 60 g) in a fused quartz tube 3 cm in diameter was put in an electric furnace which had been preheated to a desired temperature, and kept there for the desired period. It was then taken out of the furnace, quenched in air, and pulverized by using an agate mortar. The temperature, time of heating, weight percentages of anatase and rutile, and specific surface areas of the samples are listed in Table 1. The weight percentages of anatase and rutile were estimated by the ordinary method of X-ray analysis, while the specific surface areas were determined by the B.E.T. method,[7,8] using nitrogen as the adsorbate. The crystal structures of A_2 and A_3 are the same as that of A_1, but the specific surface areas of A_2 and A_3 are less than that of A_1. The crystal structures of R_1 and R_2 are rutile, but the specific surface areas differ from each other. The AR_1 is A_1 partly transformed into rutile.

Carbon monoxide prepared by the decomposition of sodium formate by sulfuric acid, and oxygen prepared from a commercial bomb, were purified by fractional distillation using liquid nitrogen.

The apparatus shown schematically in Fig. 1. was used for the experiment under pressures of 10—150 mmHg. It was made of glass and had a circulating pump of the piston type. The stop cocks, A, B, and C, were metallic cocks, with Viton used as the sealing material to keep grease vapor out. The trap T_1 was cooled by liquid nitrogen in order to collect the reaction product, (CO_2), while the trap T_2 was cooled to keep grease and mercury vapor out of the sample. This apparatus could be evacuated to a pressure lower than 10^{-6} mmHg by means of a mercury-diffusion pump. A sample tube of fused quartz, in which a pair of electrodes of gold were mounted, was connected with the glass system by means of a graded seal.

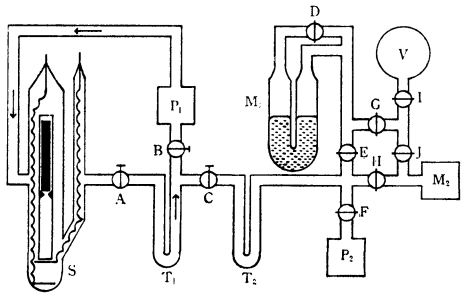

Fig. 1. The apparatus.
A—C: Metal cocks D—J: Grease cocks
M_1: Mercury manometer M_2: McLeod gauge
P_1: Circulating pump P_2: Mercury diffusion pump
S: Sample tube T_1, T_2: Traps V: Gas reservoir

The electric resistance of the catalyst was measured as follows. The catalyst (about 10 g) was put between two electrodes, about 1 cm apart, and was loaded with an iron rod (about 80 g) enclosed in a glass tube; then a constant D.C. voltage was applied, and the current was measured with an electric micro-micro ammeter produced by Takeda-Riken, type TR-16. The voltage was applied only when the current was to be measured.

By preliminary experiments, the followings were confirmed: the electric resistance of the sample was proportional to its length, the contact resistance between the electrodes and the catalyst was negligible, and both the catalytic reaction on the gold electrodes and the gas-phase reaction were negligible.

The apparatus used for the experiments under a gas pressure of about 10^{-2} mmHg consisted of a reaction tube, a Pirani gauge, and a liquid nitrogen trap. Under such low pressures, the diffusion velocity of gas was fast enough, so the circulating pump was not used.

When a mixture of carbon monoxide and oxygen was introduced into the reaction system, a catalytic oxidation reaction occurred to form carbon dioxide, which then condensed in the trap; the rate of reaction could be determined by measuring the rate of decrease of the total pressure. When the reaction rate was too small, however, the following method was employed to get the reaction rate: at the end of the run, the residual carbon monoxide and oxygen were pumped out, the carbon dioxide condensed in the trap was vaporized to a definite volume, and the pressure was measured. The rate of the reaction was obtained from the amount of carbon dioxide thus determined.

In the experiment with a powder catalyst, the rate of reaction is, in general, apt to be affected by the rate of the diffusion of gas into the catalyst, so the rate of the reaction should vary with the amount of the catalyst and this effect should become more remarkable as the reaction rate becomes faster. In order to examine this effect, the rate of reaction per unit amount of the catalyst was estimated from the results of runs using different amounts of the catalyst; it was thus found that, in the present experiment, the effect of the amount of the catalyst is negligible. However, the same amount of the catalyst was used in each of the series of experiments.

Gebhardt and Herrington[9] reported that, in order to clean the rutile surface, it was necessary to heat it at 600°C in oxygen for 30 min. In the present experiments, too, this fact was confirmed on both rutile and anatase. The pretreatment carried out in the present

7) S. Brunauer, P. H. Emmett and E. Teller, *J. Amer. Chem. Soc.*, **60**, 309 (1938).

8) K. Kodera and Y. Onishi, This Bulletin, **33**, 338 (1960).

9) J. Gebhardt and K. Herrington, *J. Phys. Chem.*, **62**, 120 (1958).

experiment was to heat the sample at 600°C for 3 hr in circulating oxygen at a pressure of 70 mmHg until the electric resistance became constant. In the experiment under the lower pressure, the gas could not be forced to circulate in the apparatus, so the pretreatment of the sample was carried out by renewing the oxygen several times.

For obtaining reproducible results with a sample of a low catalytic activity, such as titanium dioxide, it seems necessary to use an apparatus without greased stop cocks and to clean the sample with oxygen prior to the experiment.

Results and Discussion

The Relation of Catalytic Activities to Specific Surface Areas and Polymorphic Forms. The catalytic activity of each sample was measured by using reacting gas with a composition of $CO/O_2=2/1$. At temperatures of 250—550°C and under gas pressures of 10^{-2}—150 mmHg, the reaction rates were found to be proportional to the total pressure of the reacting gas; they can be expressed by the following equation:

$$d(CO_2)/dt = 2/3\, k \cdot P \qquad (1)$$

where k is a constant. The Arrhenius plots of each sample are shown in Fig. 2. It can be seen from the figure that the k value of the sample A_1 is almost equal to that of the smaple A_3 and that the k value of R_1 is almost equal to that of R_2. Therefore, the catalytic activity per unit of the surface area is the same for all samples with the same crystal form, even when they have different surface areas per unit of weight. The sample AR_1 consists of particles with both anatase and rutile forms in each particle. The ratio of the area of anatase-type faces to that of rutile-type faces in the sample may be estimated on the assumption that the catalytic activity of an anatase-type face in AR_1 is equal to that in A_1 and that the catalytic activity of a rutile-type face in AR_1 is equal to that in R_2. From the data at 550°C, the ratio was estimated to be: anatase/rutile=86.8/13.2. At temperatures other than 550°C, the k values of AR_1 can be calculated by using the surface-area ratio presented above, assuming that the k values of the two crystalline faces on AR_1 are equal to those of A_1 and R_2 respectively. These calculated values are plotted as the curve AR_1 in Fig. 2; this curve is convex downward. On the other hand, the measured values of k are plotted in Fig. 2 by the mark ○; this mrak shows that the calculated values agree well with the measured values at every temperature.

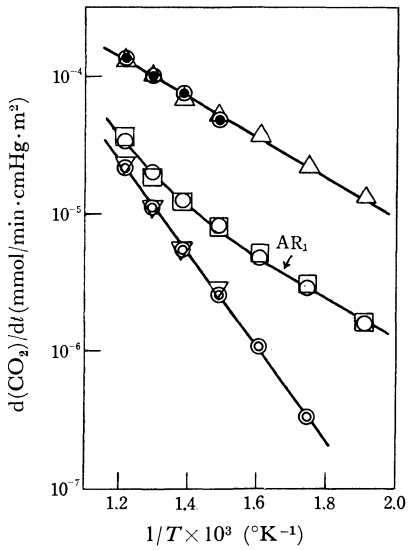

Fig. 2. Effect of temperature on the reaction rate constant.
◎: A_1 ▽: A_3 ⊙: R_1: △: R_2 ○: AR_1
□: AR_2

From these results, it was found that the k value was characteristic for the crystal form and was not affected by the value of the specific surface area nor by the coexistence of two crystalline faces.

The Relation between the Reaction Rate and the Partial Pressure of Carbon Monoxide. The effect of the partial pressures of oxygen and carbon monoxide upon the reaction rate was studied at temperatures of 350—550°C and under gas pressures of 10^{-2}—100 mmHg by changing the CO/O_2 ratio at each pressure. It follows that the reaction rate is proportional to P_{CO} and that it does not depend on the P_{O_2} for all samples and does not change even if a small amount of CO_2 is intentionally introduced into the reaction system. From these results, together with Eq. (1), the following equation can be obtained:

$$d(CO_2)/dt = k \cdot P_{CO} \qquad (2)$$

The activation energies of the reaction using anatase and rutile, as calculated from Fig. 2, are 16.0 kcal/mol and 6.7 kcal/mol respectively.

The Reaction of Carbon Monoxide with the Surface Oxygen of Titanium Dioxide. The catalyst pretreated in oxygen at 600°C was cooled down to the reaction temperature and evacuated.*1 When carbon monoxide, at a pressure of about 10^{-2} mmHg, was introduced into the reaction system, it reacted slowly with the surface oxygen of the catalyst and the carbon dioxide thus formed was caught in the trap. In this experiment, the amount of carbon monoxide which disappeared from the gas phase agreed well with that of the carbon dioxide caught in the trap, showing that the consumed carbon monoxide is entirely converted to carbon dioxide and that the amount of carbon monoxide adsorbed on the surface of the catalyst is negligible compared with that of the carbon monoxide oxidized to carbon dioxide. It was found that the rate of the formation of carbon dioxide

*1 At this time, the electric resistance of the catalyst did not change upon the evacuation.

is proportional to P_{CO}:

$$d(CO_2)/dt = k' \cdot P_{CO} \quad (3)$$

The k' values determined for all the samples are shown in Fig. 3. On the other hand, when reacting

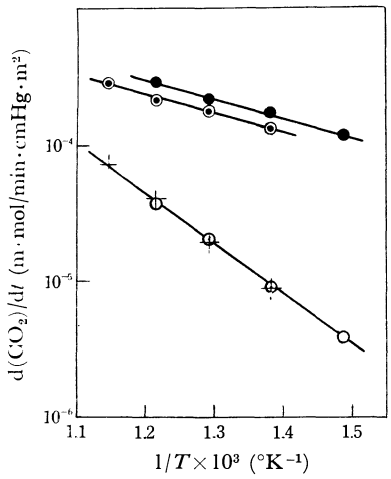

Fig. 3. Effect of temperature on the reaction rate constant.
Anatase, +: k' ○: k Rutile, ⊙: k' ●: k

gas with the composition of $CO/O_2=2/1$ is introduced into the reaction system at a pressure of 10^{-2} mmHg, catalytic oxidation occurs. The k values of this reaction, as calculated by Eq. (1), are shown in Fig. 3. It is clear that the rate constant of the catalytic oxidation of carbon monoxide, k, almost agrees with that of the reaction of carbon monoxide with the surface oxygen of titanium dioxide, k'.

On the catalytic oxidation of carbon monoxide on cupric oxide and nickel oxide,[10-15] it has been reported that the rate of the formation of carbon dioxide is proportional to P_{CO} and independent of P_{O_2}, and that the reaction consists of two processes: 1) carbon monoxide which collides with the surface of the catalyst or is physisorbed on the surface reacts with the surface oxygen of the catalyst, and the carbon dioxide thus formed is desorbed immediately, leaving an oxygen vacancy on the surface, and 2) the oxygen vacancy thus formed is filled with oxygen from the gas phase. Therefore, the reaction mechanism can be expressed as follows:

$$CO(g) + O(s) \rightarrow CO_2\uparrow + (s) \quad (4)$$

$$(s) + 1/2\ O_2 \rightarrow O(s) \quad (5)$$

where O(s) refers to the surface oxygen of the catalyst and (s), to the oxygen vacancy on the surface. The rate of step (5) is much faster than that of step (4); therefore, the overall reaction rate is proportional only to P_{CO}.

In the present investigation, it is believed that the catalytic oxidation of carbon monoxide on titanium dioxide proceeds through the steps (4) and (5), as is the case with cupric oxide or nickel oxide, because the rate of the formation of carbon dioxide is proportional to P_{CO} and the uptake rate of oxygen on the catalyst is much faster than that of carbon monoxide, as will be discussed below.

The Pressure of Oxygen and the Amount of Surface Oxygen. The electric resistance of the catalyst which had been pretreated in oxygen at 600°C was measured under the oxygen pressures from 10^{-2} to 100 mmHg, with the temperature kept constant. The results, given in Fig. 4, can be represented by:

$$R = R_0 \cdot P_{O_2}^n$$

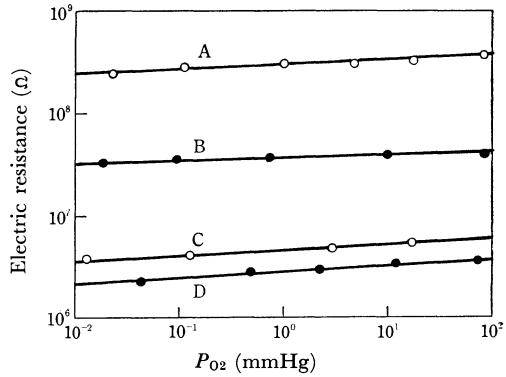

Fig. 4. Effect of oxygen pressure on electric resistance of the catalyst under the constant temperature.
A: 350°C (n=0.04) B: 450°C (n=0.02) C: 550°C (n=0.09) D: 600°C (n=0.10)

where R_0 is a constant at each temperature and n is 0.02—0.10. It is clear from this result that the electric resistance at a fixed temperature is practically independent of the oxygen pressure; this shows that the surface of the catalyst is saturated with oxygen, even at a pressure as low as 10^{-2}mmHg, so the amount of surface oxygen is almost constant, independent of the oxygen pressure. This fact seems to show that the uptake rate of oxygen is extremely fast.

The Desorption of the Surface Oxygen. The catalyst pretreated in oxygen at 600°C was evacuated at this temperature until the gas desorption became almost imperceptible. When the catalyst thus pretreated was heated to a temperature above 600°C, the oxygen desorption was detected and the desorption rate of oxygen could be deter-

10) G. Parravano, *J. Amer. Chem. Soc.*, **75**, 1448 (1953).
11) G. Parravano and M. Boudart, *Advan. Catal.*, **7**, 47 (1955).
12) E. R. S. Winter, *J. Chem. Soc.*, **1955**, 2726.
13) I. Matsuura, Y. Kubokawa and O. Toyama, *Nippon Kagaku Zasshi*, **81**, 1003 (1960).
14) A. Kanome and T. Chitani, *ibid.*, **63**, 36 (1942).
15) S. Nakata, *ibid.*, **63**, 41 (1942).

mined by measuring the pressure of the oxygen, which was collected in a fixed volume by a compressing pump. In this experiment, reproducible results could be obtained as long as the catalyst was pretreated in oxygen for each run and the desorption rate was not too large. The experimental results on anatase and rutile are shown in Fig. 5. The activation energies for anatase and rutile are 57.8 kcal/mol and 38.4 kcal/mol respectively. The difference in activation energy between anatase and rutile is about 20 kcal/mol.

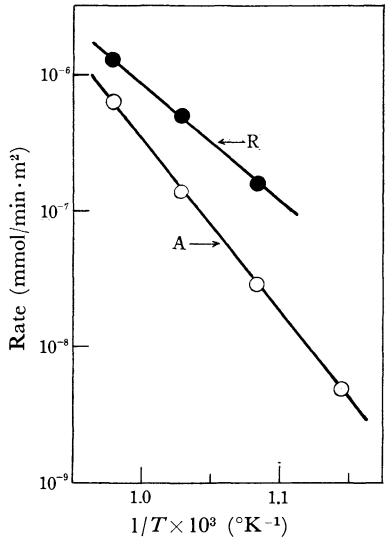

Fig. 5. Effect of temperature on the oxygen desorption rate.

As it is believed[1,16] that the surface oxygen of catalyst exists in the form of O^{2-} at these high temperatures, the desorption of the surface oxygen can be expressed by $2\ O^{2-} \rightarrow O_2(g) + 4e$; the difference of 20 kcal/mol mentioned above would result from this process. Therefore, the difference becomes about 10 kcal/mol for the process $O^{2-} \rightarrow 1/2\ O_2(g) + 2e$. This value is comparable to the 10 kcal/mol difference between the activation energy of anatase and that of rutile which was found in the catalytic oxidation of carbon monoxide and also in the reaction of carbon monoxide with the surface oxygen of the catalyst.

The authors wish to express their deep thanks to Professor Kumasaburo Kodera of Kyoto University for his kind advice and discussions.

16) E. R. S. Winter, *Advan. Catal.*, **10**, 196 (1958).

BULLETIN OF THE CHEMICAL SOCIETY OF JAPAN VOL. 43 1000—1005 (1970)

Amylase Action in Maltodextrin-Sodium Dodecylsulfate Solution

Ken-ichi SAKON,*1 Takehiko WATANABE and Sôzaburo ONO

Laboratory of Biophysical Chemistry, College of Agriculture, University of Osaka Prefecture, Sakai, Osaka

(Received September 19, 1969)

Enzyme catalyzed hydrolysis of maltodextrin was studied with enzyme-maltodextrin and enzyme-maltodextrin-sodium dodecylsulfate systems. Sodium dodecylsulfate (SDS) is a complex forming agent for maltodextrin. When endo-enzyme such as Taka-amylase A was used as the enzyme, ratio of the initial velocity of the hydrolysis of the system containing SDS to that without SDS decreases with the increase of degree of polymerization (D.P.) of the maltodextrin and becomes zero with the maltodextrin of D. P. above about 60. When the liquefying α-amylase of Bacillus subtilis was used as an endo-enzyme, a similar result was also obtained. When exo-enzyme such as Glucoamylase of Rh. Delemar was used, the ratio decreases gradually with the increase of D.P. of maltodextrin, and remains in a relatively high level even in the case of maltodextrin of D.P. above 60. In the case of Taka-amylase A, the enzyme action is suppressed by the presence of the stiff helical segments of SDS complex and the initial velocity of the system with SDS decreases compared with the one without SDS. In the case of Glucoamylase, the presence of the stiff helical segment does not distinctively induce such a depression of the enzyme action as that in the case of Taka-amylase A. The depression is partly dependent on the inhibitory interaction of SDS with the enzyme.

According to recent studies on the conformation of amylose (or maltodextrin*2) molecules in

*1 Permanent address: Research Laboratory, Nakayama Taiyodo Co., Ltd., Mizusaki-cho, Naniwa-ku, Osaka.

*2 Maltodextrin is a degraded amylose, *i. e.* a relatively low molecular weight linear polysaccharide linked by α-1,4 glucosidic linkages.

water,[1-4] amylose behaves like a random coil, while a relatively large percentage of molecule has a helical structure, the individual helical segments being connected by random segments. The amylose-iodine complex in solution is assumed to have a similar structure as stated above in which the polyiodine chain is formed in the axis of the helical segment. The amylose-sodium dodecylsulfate complex[3,5,6] is assumed to have a similar structure as the iodine complex. The character of the helical segment of amylose in the absence of the complexing agent is different from that of the complex. In the absence of the complexing agent, the thermal fluctuation in the conformation of the molecular chain occurs between the helical and random segments. Thus the helical segment has a relatively flexible character and the conformation is designated as deformed helix.[1,2,7] The helical segment in the complex is assumed to be relatively stiff owing to the holding of the iodine or sodium dodecylsulfate molecules inside the helical segment.

Studies have been carried out to elucidate the difference in the characteristics of the enzyme actions of two types of amylases (*i.e.* endo type and exo type) in enzyme-maltodextrin-sodium dodecylsulfate system.

Experimental

Enzyme. Endo-type: Taka-amylase A (TAA) (molecular weight, 53000) was prepared from "Taka-diastase Sankyô" according to the method of Akabori *et al.*[8] and kept as 4.25% aqueous solution containing 0.02M calcium acetate.

Liquefying α-amylase of Bacillus subtilis (BLA) (molecular weight, 45000) was supplied by Ueda Chemical Industry.

Exo-type: Glucoamylase of Rh. Delemar (GA) (molecular weight, 47000) was supplied by Professor J. Fukumoto of Osaka City University and Dr. Y. Tsujisaka of Osaka Municipal Technical Research Institute.

Concentration of these enzymes was determined by absorbance at 280 mμ, assuming $E^{1\%}_{1cm}$=22.0, 25.0 and 14.0 for TAA, BLA and GA, respectively.

Substrate. Maltodextrins: fractionated maltodextrins were prepared according to Hiromi *et al.*[9] A commercial product of potato amylose from Pierce Chemical Co., Illinois was partially hydrolyzed by using TAA at pH=4.5 and at 35°C for 45 min. The partially degraded amylose was precipitated by the addition of ethanol and washed with distilled water and dried. Using this preparation, the fractionation was carried out according to Everett and Foster[10] by employing dimethyl sulfoxide as solvent and ethanol as precipitant. Five subfractions were obtained and designated as maltodextrin I, II, III, IV and V. Maltodextrin VI was prepared according to the method of Hizukuri *et al.*[11] as a crystalline product from a highly concentrated aqueous solution (about 70%) of an acid hydrolyzed dextrin mixture. Determination of the carbonyl groups as the reducing end of each maltodextrin was made by a modified Somogyi-Nelson method.[12] The values of number-average molecular weight and degree of polymerization (D.P.) are listed in Table 1. These maltodextrins were the same as those used for the polarographic studies of starches by Takagi *et al.*[13]

Table 1. Number-average molecular weight ($\bar{M}_n$) and degree of polymerization (D.P.) of substrates

Substrate	$\bar{M}_n$	D.P.
Maltodextrin I	19000	116.6
II	12000	71.5
III	8200	50.5
IV	6200	38.4
V	4600	28.4
VI	2040	12.6
Maltoheptaose	1150	7.0
Maltose	342	2.0

Maltoheptaose was prepared from β-Shardinger's dextrin according to the method of French *et al.*[14]

Maltose was a commercial product and was used after recrystallization four times.

Helical Complex Forming Agent. Sodium dodecylsulfate (SDS), used as the complex forming agent with the substrate molecules, was a commerical product of Ishizu Pure Chemicals and was extracted by ethyl ether using Soxhlet extractor for 15 hr in order to remove unreacted higher alcohol.

Procedure. For the preparation of the reaction mixture suitable to the present experiment, the following three factors were considered.

(1) There should be a linear relationship between the increase of the number of reducing ends produced

1) J. Holló and J. Szejtli, *Period. Polytech.*, **1**, 223 (1957); **2**, 25 (1958); *Stärke*, **10**, 49 (1958).
2) T. Kuge and S. Ono, This Bulletin, **34**, 1264 (1961).
3) V. S. R. Rao and J. F. Foster, *Biopolymers*, **1**, 527 (1963).
4) J. Szejtli, S. Augustat and M. Richter, *Biopolymers*, **5**, 5, 17 (1967); **6**, 27 (1968).
5) T. Takagi and T. Isemura, This Bulletin, **33**, 437 (1960).
6) E. M. Osman, S. J. Leith and M. Fles, *Cereal Chem.*, **38**, 449 (1961).
7) S. Ono, T Watanabe, K. Ogawa and N. Okazaki, This Bulletin, **38**, 643 (1965).
8) S. Akabori, B. Hagihara and T. Ikenaka, *J. Biochem.*, **41**, 577 (1954).
9) K. Hiromi, K. Ogawa, N. Nakanishi and S. Ono, *J. Biochem.*, **60**, 439 (1966).
10) W. W. Everett and J. F. Foster, *J. Amer. Chem. Soc.*, **81**, 3459 (1959).
11) S. Hizukuri, Z. Nikuni, Y. Hattori and S. Wada, *Nippon Nogeikagaku Kaishi*, **33**, 615 (1959).
12) K. Hiromi, Y. Takasaki and S. Ono, This Bulletin, **36**, 563 (1963).
13) M. Takagi, T. Nishio, M. Mizutani, N. Kamatani, Y. Imaoka and S. Ono, *Stärke*, **21**, 2 (1969).
14) D. French, M. L. Levine and J. H. Razur, *J. Amer. Chem. Soc.*, **71**, 356 (1949).

and the reaction time.

(2) The amount of SDS in reaction mixture must be high enough for the formation of a sufficient quantity of helical complex in order to detect the influence of the presence of the complex on the reaction velocity.

(3) The concentration of SDS must be lower than the one where inactivation of enzyme owing to the interaction between SDS and enzyme, and/or the formation of aggregates or precipitates of the SDS-maltodextrin complex occurs.

The procedure adopted for following the reaction of the TAA-substrate-SDS system was as follows. Twenty m*l* of 0.05% substrate solution with or without 0.015% SDS was taken into a reaction vessel immersed in a constant-temperature water bath controlled at 25°C. After about 30 min the reaction was commenced by introducing 10 μl of 2.5×10^{-2}% TAA solution to the substrate solution, and at 2 min intervals the reaction mixture was pipetted into 3 m*l* of Somogyi's reagent, and the reaction was stopped. The number of reducing ends produced was determined by means of Somogyi-Nelson method and was expressed by the value of absorbance observed at the wavelength of 530 mμ. A similar procedure as stated above was adopted for the other enzyme reaction systems. The final recipes for the reaction mixtures were as follows: TAA; 2.0×10^{-9}M, substrate; 0.05%, SDS; 0.5×10^{-3}M, and pH=5.3 for TAA system; BLA; 2.8×10^{-9}M, substrate; 0.1%, SDS; 1.0×10^{-3}M, and pH=5.85 for BLA system; GA; 1.0×10^{-8}M, substrate; 0.05%, SDS; 0.5×10^{-3}M, and pH=4.5 for GA system.

The amount of SDS in the above reaction mixture satisfies the condition of one SDS molecule per one helical turn, provided that all anhydroglucose units of maltodextrin (or amylose) take part in helix formation and 6 anhydroglucose units form one helical turn. Under this condition the complex, SDS-maltodextrin I, II or III showed a slight tendency to form an aggregate in solution, and the reaction was made under continuous stirring to prevent the formation of a large visible aggregate.

Results and Discussion

Typical examples of the change in absorbance with reaction time are shown in Figs. 1, 2 and 3. Each plot was found to show a good linear relationship within the interval of 18 min. The initial velocity was obtained from the slope of the plot shown in these figures. The ratio of the initial velocity of the system containing SDS to that without SDS was expressed in % and designated as "reactivity factor" or *R*. The value of *R* may be primarily determined by the ratio of the number of hydrolyzable α-1,4 glucosidic linkage present in the reaction mixture at the initial stage of reaction

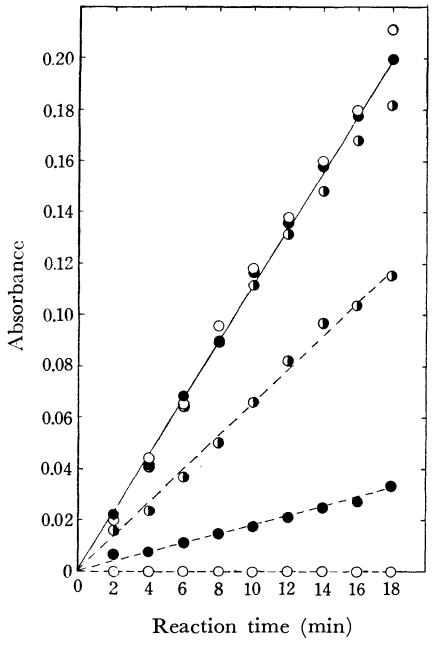

Fig. 1. The plot of absorbance *vs.* reaction time obtained with the system of TAA: 2×10^{-9}M, Substrate: 0.05%, with or without 0.5×10^{-3}M SDS, pH: 5.3, and at 25°C.
—○—: TAA-Maltodextrin I, ···○···: TAA-Maltodextrin I-SDS, —●—: TAA-Maltodextrin IV,···●···: TAA-Maltodextrin IV-SDS, —◑—: TAA-Maltodextrin VI, ···◑···: TAA-Maltodextrin VI-SDS

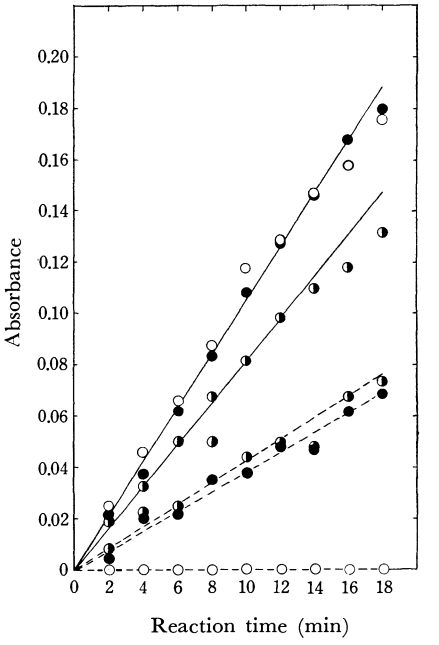

Fig. 2. The plot of absorbance *vs.* reaction time obtained with the system of BLA: 2.8×10^{-9}M, Substrate: 0.10%, with or without 1.0×10^{-3}M SDS, pH: 5.85, and at 25°C.
—○—: BLA-Maltodextrin I, ···○···: BLA-Maltodextrin I-SDS, —●—: BLA-Maltodextrin IV, ···●···: BLA-Maltodextrin IV-SDS, —◑—: BLA-Maltodextrin VI, ···◑···: BLA-Maltodextrin VI-SDS

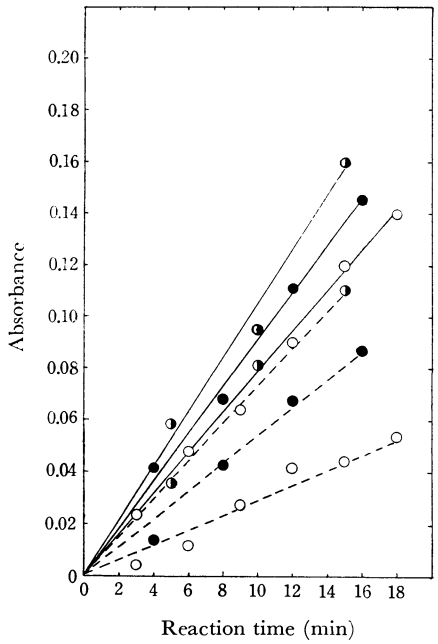

Fig. 3. The plot of absorbance *vs.* reaction time obtained with the system of GA: 1.0×10^{-8}M, Substrate: 0.05%, with or without 0.5×10^{-3}M SDS, pH: 4.5, and at 25°C.
—○—: GA-Maltodextrin I, ···○···: GA-Maltodextrin I-SDS, —●—: GA-Maltodextrin IV, ···●···: GA-Maltodextrin IV-SDS, —◑—: GA-Maltodextrin VI, ···◑···: GA-Maltodextrin VI-SDS

in the system containing SDS to that without SDS.

Figures 4,5 and 6 and Table 2 show the change of R with D.P. of substrate. In TAA (endo-enzyme) system where TAA can hydrolyze α-1,4 glucosidic linkage at random along the linear chain of substrate, the initial velocity of TAA-low D.P. substrate (maltoheptaose)-SDS system was as high as that without SDS, and the value of R

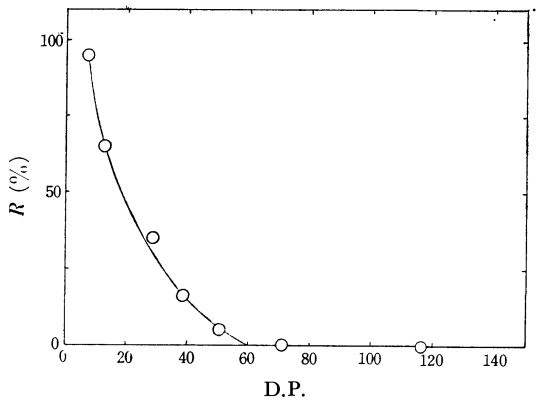

Fig. 4. The plot of R *vs.* D.P. with TAA-Maltodextrin-SDS system (TAA: 2.0×10^{-9}M, SDS: 0.5×10^{-3}M, Substrate: 0.05%, pH: 5.3, at 25°C).

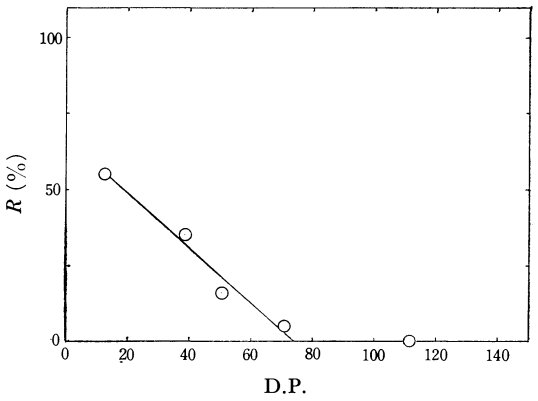

Fig. 5. The plot of R *vs.* D.P. with BLA-Maltodextrin-SDS system (BLA: 2.8×10^{-9}M, SDS: 1.0×10^{-3}M, Substrate: 0.10%, pH: 5.85, at 25°C).

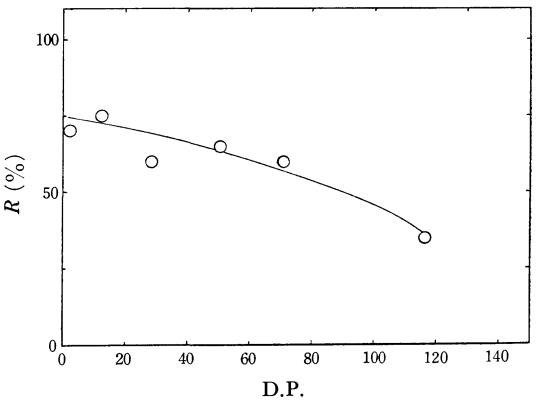

Fig. 6. The plot of R *vs.* D.P. with GA-Maltodextrin-SDS system (GA: 1.0×10^{-8}M, SDS: 0.5×10^{-3}M, Substrate: 0.05%, pH: 4.5, at 25°C).

Table 2. The relation between R and D.P. of substrate with three kinds of systems using TAA, BLA and GA as enzyme, respectively

D.P.	R (%)		
of substrate	TAA	BLA	GA
116.6	0	0	35
71.5	0	5	60
50.5	5	17	65
38.4	20	35	60
28.4	30	—	—
12.6	70	55	75
7.0	95	—	70

was as high as 95%. The value of R decreases rapidly with the increase of D.P. of the substrate and tends to 0% at the D.P. value of about 60 (molecular weight, 1×10^4). In the presence of SDS, the substrate having higher D.P. value than

60, was not hydrolyzed by TAA within the reaction time of 18 min.

As shown in Fig. 5, in BLA (endo-enzyme) system, a similar result was obtained between R and D.P. of substrate as in the case of TAA system.

In GA system (Fig. 6) where GA is an exo-enzyme which catalyzes the hydrolysis of maltodextrin producing glucose from its non-reducing end, the value of R for the substrate of low D.P. value was lower than that in the case of TAA system. However, the rate of decrease of R with the increase of D.P. was slight compared with that in the case of TAA, and a fairly high value of R of 60—65% was obtained with the substrate of D.P. 60—70 to which TAA and BLA could not react in the presence of SDS.

The difference in the characteristics of the enzyme action between the endo-enzyme and exo-enzyme as described above is expected to be brought about primarily by the difference in the contribution of the helical segments of the SDS complex on the reaction. The following experiments on the iodine complex of maltodextrin were carried out to elucidate the conformation of maltodextrin and the SDS complex in solution.

The absorption spectra of the maltodextrin-iodine complex were recorded by a Hitachi Recording Spectrophotometer Model EPS-3 at 25°C. Figure 7 shows the relation between λ_{max} (wave-

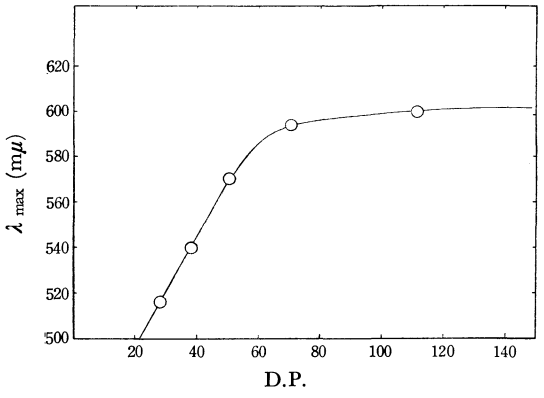

Fig. 7. The relation between the λ_{max} and D.P. of maltodextrin; maltodextrin: 3.7×10^{-3}%, KI: 8.0×10^{-3}M, I_2: 8.0×10^{-5}M, pH: 5.3, at 25°C. (This composition corresponds to the one containing minimum amount of iodine, where the value of λ_{max} takes the longest wavelength, irrespective of the values of D.P. of maltodextrins.)

length of the maximum of absorption spectra observed in the range of wavelength of 400—600 mμ) and D.P. at pH=5.3. As shown in Fig. 7, with increasing D.P. the value of λ_{max} shows a remarkable shift toward longer wavelength up to the D.P. value of about 60, and the plot of λ_{max} *versus* D.P. revealed a break point at about D.P.=60. Above D.P.=70 the value of λ_{max} changes only slightly with the increase of D.P. and the same result was also obtained at pH 4.5. In a previous publication[15] one of the present authors (S.O.) showed that the λ_{max} of the iodine complex shifts toward longer wavelength with the increase of the length of the polyiodine chain. Thus the shift of λ_{max} with the increase of D.P. up to about 60, corresponds to the increase of the length of the single polyiodine chain in the complex. We (T.W. and S.O.) also showed that the helical segments of amylose molecule (molecular weight: 1×10^6) were composed of 66 anhydroglucose units.[16] Therefore the value of about 60 corresponds to the maximum number of anhydroglucose units which take part in the formation of the helical segment.

From the results obtained with the iodine complex, the conformation of the maltodextrin of D.P. above 60—70 in the absence of complexing agent in acidic solution may be a deformed helix. The individual helical segments are connected by random segments which are composed of a certain number of the anhydroglucose units. There are the freely rotating endgroups of a certain number of anhydroglucose units which do not take part in the helix formation. The maltodextrin of D.P. below about 60 consists of a single helix with the freely rotating endgroups.

As shown in Fig. 4, in the case of TAA-substrate-SDS system, the substrates of D.P. from 7 to 60 were hydrolyzed by the enzyme. The initial velocity obtained with the system of low D.P. substrate as maltoheptaose in the presence of SDS was essentially the same as the one without SDS. It may be assumed that the SDS molecules do not inhibit the TAA action under the present experimental conditions. The decrease in the value of R with the increase of D.P. of substrate shows that the SDS complex is difficult to be hydrolyzed by TAA compared with maltodextrin uncoupled with SDS. When the length of the freely rotating endgroups is assumed to be constant independent of the D.P. of the substrate, the ratio of the number of anhydroglucose units in endgroups to that of the helical segment decreases with the increase of D.P. of substrate. Therefore the number of hydrolyzable α-1,4 glucosidic linkage decreases with the increase of D.P. and the value of R decreases with the increase of D.P. In the case of substrate of D.P. above 60 where the helical segments are stabilized by the complex formation, both random segments and endgroups which can be hydrolyzed by TAA in the absence of SDS, would not be hydrolyzed by TAA due to the steric hindrance of the stiff helical segments.

As shown in Fig. 6, in the case of GA-substrate-

15) S. Ono, S. Tsuchihashi and T. Kuge, *ibid.*, **75**, 3601 (1953).

16) T. Watanabe, K. Ogawa and S. Ono, This Bulletin, **43**, 950 (1970).

SDS system, the enzyme action can be assumed to be inhibited by free SDS in solution to some extent, since the value of R was only 70% with the system using maltose as the substrate which can not form the helical complex with SDS. The inhibition of the enzyme action of GA by SDS can be suggested by the result of the measurement of difference spectra.

Absorption spectra obtained with GA solution and GA-SDS solution are shown in Fig. 8. A

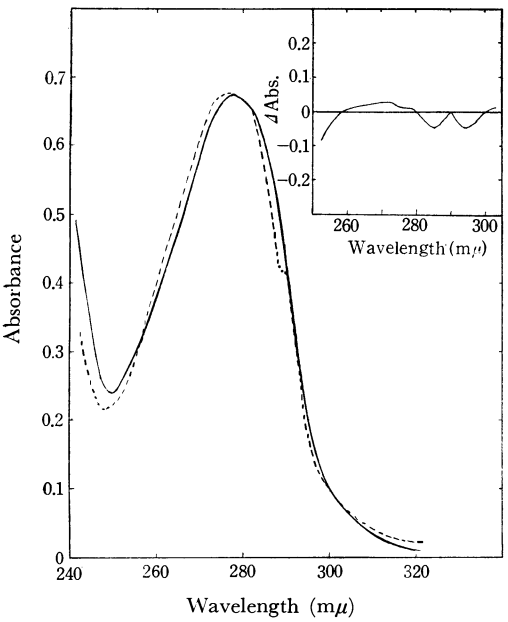

Fig. 8. Absorption spectra of 0.453% GA solution (solid line) and 0.453% GA and 0.2% SDS solution (broken line) at 25°C and difference spectrum (inset).

distinct difference in shape was observed between the two curves. The difference spectrum was recorded by a Hitachi Recording Spectrophotometer Model EPS-3, using four cells; two of them were put on one side of the light path in series, one containing enzyme solution and the other SDS solution, respectively, and on the other side were put the other two cells containing a mixture of enzyme and SDS in one cell, and the buffer solution only in the other, respectively. The spectrum is shown in the inset of Fig. 8. From these results, some interaction is expected to occur between GA and SDS. This interaction suggests the inhibition of the enzyme action of GA. The difference in absorption spectra as in the case of GA was not observed between TAA and TAA-SDS solutions.

In spite of the inhibition of GA action by SDS, the enzyme GA still hydrolyzed the SDS complex of the substrate of D.P. above 60, *i.e.* the values of R are 60% for D.P. 70 and 35% for D.P. 117 (Table 2). These results are markedly different from those obtained with TAA and BLA. When the number of anhydroglucose units of the freely rotating endgroups of maltodextrin chain is assumed to be constant independent of chain length, the ratio of the number of anhydroglucose units in the helical segment to that in whole molecule would become larger with the increase in D.P. in the case of the substrate of D.P. below 60. Thus the amount of SDS combined with the substrate would be smaller and that of SDS free in solution larger in the lower D.P. substrate system compared with the case of the higher D.P. system. In the system containing substrate of D.P. above 60, the concentration of free SDS is assumed to be constant according to the results obtained with the iodine complex as shown in Fig. 7. Thus the enzymatic activity would be more inhibited by free SDS with the system containing lower D.P. substrate, and the value of R is expected to increase with the increase of D.P. of the substrate up to about 60 and become constant with the further increase of D.P. Contrary to expectation, the value of R actually observed decreases gradually with the increase of D.P. of the substrate, though it is fairly high with the complex of high D.P. substrate which was not hydrolyzed by TAA and BLA. The fact that a relatively high value of R was obtained with the system of higher D.P. substrate may support the assumption that the endgroups of the complex are freely rotating and can be hydrolyzed by GA, irrespective of the value of D.P. of the substrate. The decrease in the value of R with the increase of D.P. of the substrate may be explained by the following reasons.

(1) The length of the endgroups of the substrate molecule becomes shorter with the increase of D.P. and consequently the affinity of the substrate for GA becomes smaller.

(2) Even though the length of the endgroups is constant, the stiff helical structure of the complex interferes with the enzymatic action.

(3) Effective concentration of the substrate decreases, which has endgroups with favorable number of anhydroglucose units to be hydrolyzable with GA.

The authors are grateful to Professor Juichiro Fukumoto of Osaka City University and Dr. Yoshio Tsujisaka of Osaka Municipal Technical Research Institute and to Ueda Chemical Industry for the gift of amylase and to Sankyô Co., Ltd. for the supply of "Taka-diastase Sankyô." We are also greatly indebted to Dr. Keitaro Hiromi of Kyoto University and Dr. Masanosuke Takagi for their interest and helpful discussions and to Mr. Yasunori Nitta for his technical assistance.

BULLETIN OF THE CHEMICAL SOCIETY OF JAPAN VOL. 43 1006—1010 (1970)

The Three-dimensional Structure of Macromolecules. I. The Conformation of Ethylene Polymers by the Monte Carlo Method

Keizo SUZUKI and Yoshiro NAKATA

Department of Chemistry, Tokyo Kyoiku University, Otsuka, Tokyo

(Received October 3, 1969)

The Monte Carlo method is employed on a high-speed digital computer in order to generate non-intersecting random chains simulating polymer molecules. For this purpose the GT-model of polyethylene is used. Suitable potential functions are used to calculate the energy and the probability of each chain conformation thus generated. The nonbonded-interaction energy is calculated by the Lennard-Jones "6—12" potential function. The average dimensions are then calculated by using this energy. It is suggested that the hydrogen atoms contribute largely to the statistical properties of the ethylene polymers.

The Monte Carlo procedure is used to simulate non-self-intersecting random walks on a high-speed digital computer. Most of the works up to this time have considered the restricted walks confined to a multidimensional lattice,[1] but the stability of the real molecule (intramolecular energy) is not considered.

Using a more realistic model, we estimate the intramolecular conformational energy of each conformation. The average dimensions are calculated by using this energy.

The lower members of the normal hydrocarbon series have been fully discussed in terms of "Conformation Analysis,"[2] "Molecular Geometry,"[3] *etc.* We use the results of these discussions, and then consider the higher members of the normal hydrocarbon series by means of the Monte Carlo Method.

Model

In this paper we discuss the GT-model of polyethylene. The fully-extended conformation of polyethylene is shown in Fig. 1. The hydrogen atoms are bonded to the ith carbon atom as H_i and H_i'. The backbone of the molecule is considered to begin with the atom H_0, continue on through n carbon atoms, and end with the atom H_{n+1}. All the bond lengths and bond angles are kept constant. The bond lengths are taken to be 1.08 Å for the C–H bonds and 1.54 Å for the C–C bonds, while all the bond angles are taken to be tetrahedral. We assume that each bond in a polyethylene molecule can exist in three rotational isomeric states, *trans*(180°), *gauche*(60°), and *gauche'*(300°). This model is equal to the diamond lattice model if we consider only the skeletal carbon atoms. The *trans* form is chosen with the probability of $p_T=1/2$, and the *gauche* forms, with the probabilities, $p_G=p_G'=1/4$.*1

Calculation

Steric hindrances are examined on the basis of

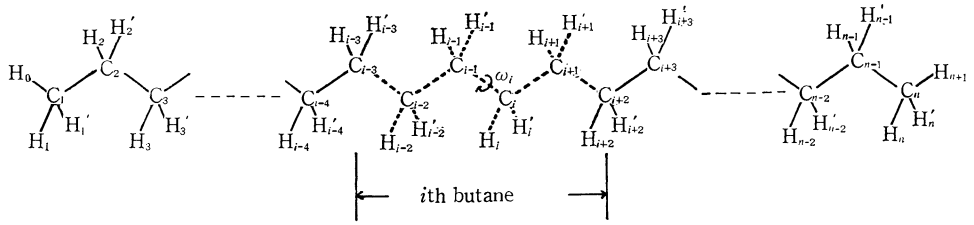

Fig. 1. The polyethylene molecule in the fully extended state.

1) F. T. Wall, S. Windwer and P. J. Gans, *Methods Computation Phys.*, **1**, 217 (1963).

2) R. A. Scott and H. A. Scheraga, *J. Chem. Phys.*, **44**, 3054 (1966).

3) E. J. Jacob, H. B. Thompson and L. S. Bartell, *ibid.*, **47**, 3736 (1967).

*1 This operation is a method to get long chains rapidly, but the generated chain has an unequal *a priori* probability. This inequality is corrected when we calculate the average quantities (see Eq. (4)). However the inequality corresponds roughly to the energy difference between the *trans* and *gauche* forms so that the generated chains have comparable weights.

the van der Waals radii. When the nonbonded interaction energy (see next section) becomes positive, the whole molecule is discarded. Long, non-self-intersecting random walks are difficult to achieve even when the walks are confined to a lattice.[4] When the walks are off the lattice, this problem is much greater. In order to overcome this extreme attrition, use is made of the enrichment technique previously developed by one of the present authors.[5] The scheme of the program is as follows:

1) MAKE AN M-BOND CHAIN AT RANDOM. ($M=12$, FOR EXAMPLE).
2) IF THE NONBONDED INTERACTION ENERGY IS POSITIVE, GO TO 1.
3) $N=M$.
4) IF ANOTHER N-BOND CHAIN IS NOT STORED, STORE THE NEW CHAIN AND GO TO 1.
5) CONNECT THE STORED CHAIN TO THE NEW CHAIN AND MAKE A $2N$-BOND CHAIN.
6) IF THE NONBONDED INTERACTION ENERGY IS POSITIVE, OUTPUT AND CLEAR BOTH THE N-BOND CHAINS AND THEN GO TO 1.
7) $N=2N$, AND GO TO 4.

Energy Equations

The intramolecular conformational energy of each conformation is calculated by using the semi-empirical potential functions. The energy equation is:

$$E = U_{rot} + U_{nb} \tag{1}$$

where:

$$U_{rot} = \sum_i U_{rot}(\omega_i) \tag{2}$$

Table 1. The sets of potential function's constants

Atom pair	a (kcal·Å^{12}/mol)	b(kcal·Å^6/mol)	r_{min} (Å)
H·····H	4.5×10^3	47	2.4
C·····C	286×10^3	370	3.4
C·····H	38×10^3	128	2.9

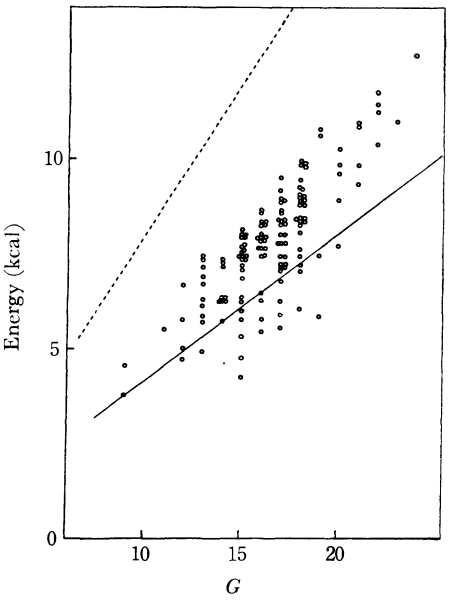

Fig. 2. Plot of total energy against number of *gauche* forms at $N=48$.
The dotted line indicates the energy which is calculated by Eq. (2). The molecules with equal value of $g\cdot\exp(-E/kT)$ at 300°K are equidistant from the solid line.

Table 2. Values of $\langle R^2\rangle$ (Å^2)

N	3	6	12	24	48	96	192
m[a]			256	148	163	39	13
$T=\infty$	10.7	35.0	107.8	308.2	863.8	2230.7	6624.8
$T=1000$°K	11.3	36.7	106.8	300.9	791.0	1811.9	4826.3
$T=360$°K	12.5	40.4	108.5	276.5	576.3	1343.3	3644.3
$T=340$°K	12.6	40.8	109.0	276.1	555.9	1313.7	3677.3
$T=320$°K	12.7	41.2	109.7	276.2	532.9	1281.6	3737.6
$T=300$°K	12.8	41.7	110.6	277.1	506.9	1247.4	3833.5
$T=280$°K	12.9	42.3	111.9	279.4	477.6	1212.2	3966.8
trans[b]	15.0	56.9	227.7	910.7	3642.7	14571.0	58284.0
F. R. [c]	10.8	24.9	53.4	110.3	224.1	451.8	907.1

a) Total number of sample chains.
b) All rotational angles take *trans* forms.
c) Theoretical values for free rotation.
$R^2/r^2=2N+3/2(-1+1/3^N)$, $r=1.54$Å

4) F. T. Wall and J. J. Erpenbeck, *J. Chem. Phys.*, **30**, 634 (1959).
5) K. Suzuki, This Bulletin, **41**, 538 (1968).

TABLE 3. VALUES OF $\langle S^2 \rangle$ (Å^2)

N	3	6	12	24	48	96	192
m[a]			256	148	163	39	13
$T=\infty$	1.91	4.84	13.44	38.71	108.14	285.89	813.83
$T=1000$°K	1.94	4.99	13.61	38.99	102.25	225.15	684.53
$T=360$°K	2.01	5.29	14.47	38.51	80.52	176.21	551.73
$T=340$°K	2.02	5.32	14.12	38.59	78.86	174.04	544.55
$T=320$°K	2.03	5.35	14.19	38.72	77.12	171.63	535.03
$T=300$°K	2.03	5.39	14.28	38.92	75.31	168.90	522.33
$T=280$°K	2.04	5.44	14.39	39.21	73.45	165.82	506.37
trans[b]	2.17	6.52	22.33	82.41	316.41	1239.70	4907.80
F. R.[c]	1.91	4.10	8.70	18.09	37.01	74.93	150.81

a) Total number of sample chains.
b) All rotational angle take *trans* forms.
c) Theoretical values for free rotation.
$S^2/r^2=N/3-5/12+[7/6+3(-3+1/3^N)/8(N+1)]/(N+1)$, $r=1.54$Å

and with ω_i designating the rotation angle about the $C_{i-1}-C_i$ bond.

$$U_{nb}=\sum_{i<j}(a_{ij}/r_{ij}^{12}-b_{ij}/r_{ij}^{6}) \quad (3)$$

We assume that the polyethylene molecule (C_nH_{2n+2}) is formed by overlapping $n-3$ butanes in regard to the internal rotation energy. The energy difference between the one *trans* and the two *gauche* forms is taken as 0.8 kcal/mol from the experimental values of butane. The first term in Eq. (1) is a sum over this energy difference. The second term in Eq. (1) is a sum over the nonbonded interactions between atoms separated by six or more bonds (long-range interaction). In treating the nonbonded interaction, we have used the Lennard-Jones "6—12" potential functions.

The sets of constants[6] in Eq. (3) are summarized in Table 1.

Results and Discussion

The influence of the nonbonded interaction energy on the total intramolecular energy is shown in Fig. 2. The unstabilization by *gauche* forms is fully compensated by the nonbonded interaction energy.

$\langle R_N^2 \rangle$ and $\langle S_N^2 \rangle$. The mean-square end-to-end distance, $\langle R_N^2 \rangle$, and the mean-square radius of gyration, $\langle S_N^2 \rangle$, are calculated by an equation of the form:

$$\langle J_N^2 \rangle = \sum_i J_i^2 g_i \exp(-E_i/kT)/\sum_i g_i \exp(-E_i/kT) \quad (4)$$

where N is the number of C–C bonds and is equal to $n-1$, where J represents R or S, and where g is the weight which corrects the uneven selection.*2

These values are calculated only with carbon atom coordinates. The variation in the molecular dimension with the temperature is calculated by changing the temperature in the Boltzmann factor, $\exp(-E_i/kT)$.

These results fit an equation of the form:

$$\langle J_N^2 \rangle = kN^{\alpha} \quad (5)$$

where k and α are constants.

The results are summarized in Tables 2 and 3. Figure 3 shows plots of $\log\langle S_N^2 \rangle$ *vs.* $\log N$ at

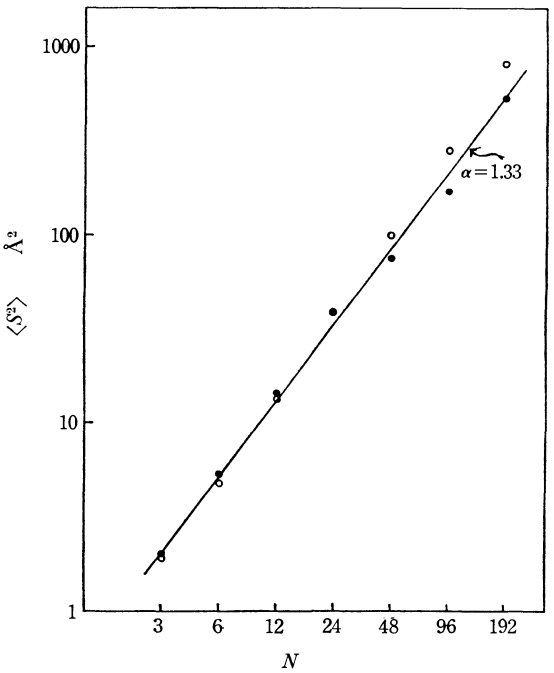

Fig. 3. Values of $\langle S^2 \rangle$ *vs.* N on a log-log plot.
○ $T=\infty$
● $T=300$°K

6) R. A. Scott and H. A. Scheraga, *J. Chem. Phys.*, **45**, 2091 (1966).

*2 The values of g_i are calculated by means of the number of *gauche* forms G; $g_i=(p_T/p_G)^G$. We adopted the uneven selection in order to have a narrow distribution of $g\cdot\exp(-E/kT)$.

Table 4. Values of $(\log\langle R_{2N}^2\rangle - \log\langle R_N^2\rangle)/\log 2$

N	3	6	12	24	48	96	192
$T=\infty$	1.705	1.622	1.516	1.487	1.369	1.570	
$T=1000$°K	1.693	1.543	1.495	1.394	1.196	1.413	
$T=360$°K	1.697	1.426	1.349	1.060	1.221	1.440	
$T=340$°K	1.699	1.419	1.340	1.010	1.241	1.485	
$T=320$°K	1.702	1.413	1.332	0.948	1.266	1.544	
$T=300$°K	1.706	1.407	1.325	0.871	1.299	1.620	
$T=280$°K	1.711	1.403	1.321	0.773	1.344	1.710	
trans[a]	1.928	2.000	2.000	2.000	2.000	2.000	
F. R.[b]	1.100	1.086	1.057	1.033	1.018	1.009	

a) All rotational angles take *trans* forms. b) Theoretical values for free rotation.

Table 5. Values of $\langle S^2\rangle/\langle R^2\rangle$

N	3	6	12	24	48	96	192
$T=\infty$	0.178	0.138	0.125	0.126	0.125	0.128	0.123
$T=1000$°K	0.171	0.136	0.127	0.130	0.129	0.124	0.142
$T=360$°K	0.162	0.131	0.133	0.139	0.140	0.131	0.151
$T=340$°K	0.161	0.131	0.129	0.140	0.142	0.132	0.148
$T=320$°K	0.160	0.130	0.129	0.140	0.145	0.134	0.143
$T=300$°K	0.159	0.129	0.129	0.140	0.149	0.135	0.136
$T=280$°K	0.158	0.129	0.129	0.140	0.154	0.137	0.128
trans[a]	0.145	0.115	0.098	0.090	0.087	0.085	0.084
F. R.[b]	0.177	0.164	0.163	0.164	0.165	0.166	0.166

a) All rotational angles take *trans* forms. b) Theoretical values for free rotation.

$T=\infty$ and at $T=300$°K.

α, the exponent in Eq. (5), is calculated by the equation:

$$\alpha = (\log\langle J_{2N}^2\rangle - \log\langle J_N^2\rangle)/\log 2. \quad (6)$$

These values are summarized in Table 4.

$\langle S_N^2\rangle/\langle R_N^2\rangle$. Table 5 lists the $\langle S_N^2\rangle/\langle R_N^2\rangle$ ratios for the different values of N obtained in this study. These values are small compared with the values determined in a previous investigation.[7] The major reason for this may be the influence of hydrogen atoms.

The variation in R^2 with S^2 is shown in Fig. 4.

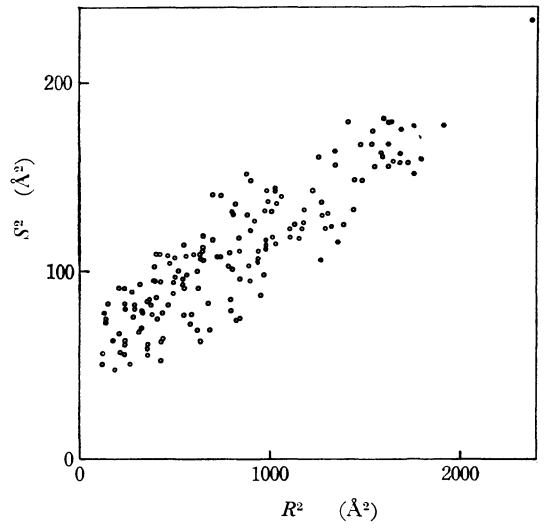

Fig. 4. Plot of S^2 against R^2 at $N=48$.

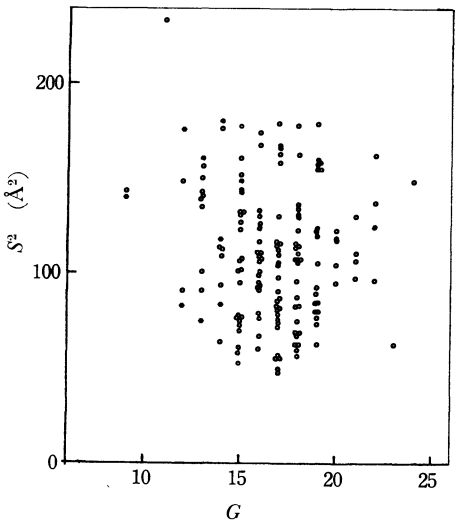

Fig. 5. Plot of S^2 against number of *gauche* forms at $N=48$.

7) S. Windwer, *J. Chem. Phys.*, **43**, 115 (1965).

It is noticeable in Fig. 3 that the temperature coefficient of the dimensions is reversed between $N=24$ and $N=48$. This means that the average dimensions of the long ethylene polymer are affected more strongly by the "long range" interaction than by the "short range" interaction. In this case the van der Waasl attraction is stronger than the *trans-gauche* energy difference. Figure 5 shows that the number of *gauche* forms has little effect on the dimensions.

Our model is a simple one compared with real molecules, but the use of much more realistic models would not alter the general features of the result; the long-range interaction, including interactions by the solvent, will overcome the short-range interaction at the early stage of the chain length.

BULLETIN OF THE CHEMICAL SOCIETY OF JAPAN VOL. 43 1010—1016 (1970)

Electronic Structures of Unsaturated Molecules Containing Hetero-atoms, — Configuration Interaction Treatment Including Doubly Excited Configurations

Fumihiko HIROTA and Saburo NAGAKURA

The Institute for Solid State Physics, The University of Tokyo, Roppongi, Minato-ku, Tokyo

(Received October 14, 1969)

The π-electron structures of several unsaturated molecules containing hetero-atoms were studied by SCFMO-CI scheme employing the Pariser-Parr-Pople method, special attention being paid to the effect of doubly excited configurations upon calculated transition energies, transition moments and π-electron distributions in the ground and lower excited states. The transition energies and oscillator strengths calculated for pyridine, phenol, aniline, pyrrole and furan were compared with their experimental values. Consequently, the inclusion of doubly excited configurations was found to improve the coincidence between the theoretical and observed values and to remove some difficulties in the application of the Pariser-Parr-Pople method to molecules containing hetero-atoms. One-center integrals W_P and γ_{PP} for hetero-atoms were taken as parameters in the calculations of phenol and aniline. Their fittest values were determined reasonably to be $W_N=-24.71$, $W_O=-30.08$, $\gamma_{NN}=13.75$, and $\gamma_{OO}=16.78$ eV.

The Pariser-Parr-Pople (P-P-P) method[1,2] has been successfully applied to many unsaturated organic molecules. The adequateness of several approximations adopted in this method has been discussed from several points of view. For example, the adequateness and limitations of the zero differential overlap approximation have been studied by use of the Löwdin orbitals.[3,4] Furthermore, the *I-A* approximation for the one-center Coulomb repulsion integrals has been discussed on the basis of the correlation effect,[5] the σ-π interaction,[6] and the expansion of excited orbitals.[7]

One of the fundamental problems of the P-P-P method is the treatment of the σ-π interaction, especially of the change in the σ-core caused by π-electron excitation. The development of the CNDO method[8] and other theoretical calculations including both σ and π electrons has brought about some progress in the direction of overcoming this difficulty.

Another important problem is concerned with the application of the P-P-P method to molecules containing hetero-atoms. The results calculated for them are generally sensitive to parameters. Several methods have been presented for the purpose of improving the prediction and interpretation of charge distributions in the ground states of the molecules. They include the VESCF method by Brown and Heffernan[9] and the method of in-

1) R. Pariser and R. G. Parr, *J. Chem. Phys.*, **21**, 466 (1953), 767 (1953).
2) J. A. Pople, *Trans. Faraday Soc.*, **49**, 1357 (1953).
3) R. McWeeny, *Proc. Roy. Soc.* (London), **A227**, 288 (1955).
4) I. Fischer-Hjalmars, *J. Chem. Phys.*, **42**, 1962 (1965); "Advances in Quantum Chemistry," Vol. II, ed. by P. O. Löwdin, Academic Press Inc., New York (1965), p. 25.
5) T. Arai and P. Lykos, *J. Chem. Phys.*, **38**, 1447 (1963).
6) M. O. Orloff and O. Sinanoglu, *ibid.*, **43**, 49 (1965).
7) S. Huzinaga, *ibid.*, **36**, 453 (1962).
8) J. A. Pople, D. P. Santry and G. A. Segal, *ibid*, **43**, S129 (1965).
9) R. D. Brown and M. L. Heffernan, *Trans. Faraday Soc.*, **54**, 757 (1958).

cluding penetration integrals.[10] Furthermore, continuing efforts have made to find improved methods which give reliable results to excitation energies of molecules containing hetero-atoms, and consequently some progress has been achieved in the direction of determining appropriate core resonance integrals[11,12] and of considering the influence of electron cloud polarization upon the two center Coulomb integrals.[13] In the present study we undertake to make some contribution to this problem from the standpoint of attaching some importance to the configuration interaction (CI).

In the P-P-P type calculation, the CI procedure is usually made only among singly excited configurations (SECI treatment). The results in benzene[14-20] and other several hydrocarbons,[18-21] however, point out the importance of some doubly excited configurations. The CI procedure may be expected to have an important meaning in theoretical studies of the π-electron structures of molecules containing hetero-atoms. For example, if the core potential of a hetero-atom is too deep, the single configuration picture gives too large electron density on that atom, but the CI procedure relieves obviously this tendency. In addition, in molecules containing hetero-atoms, the charge distribution is not uniform, and is reorganized by a π-electron excitation. This reorganization in the molecules gives relatively larger effect on charge distributions in excited states and on π-electron levels than on those in hydrocarbons. This effect can be taken into account by the CI procedure. In the present paper, we study the effect of CI including the doubly excited configurations upon the calculated results of π-electron levels, transition moments and electron distributions in some molecules, paying a special attention to the parameters associated with hetero-atoms.

Method of Calculation

In the present study, pyridine, aniline, phenol, pyrrole and furan were taken as the typical molecules containing hetero-atoms and their π-electron structures were calculated by the P-P-P method combined with CI including doubly excited configurations (DECI treatment).

In the evaluation of SCF orbitals of pyridine, the Pariser-Parr parameters[1,2] were employed; that is to say, one-center Coulomb integral γ_{pp} was taken to be the difference between the ionization potential I_p and the electron affinity A_p for an appropriate valence state, and the two-center Coulomb integral γ_{pq} was calculated by the uniformly charged sphere model with the effective nuclear charge Z_p determined by Salter's rule. Concerning W_p representing the diagonal matrix element of the χ_p atomic orbital with respect to the one-electron Hamiltonian consisting of the kinetic energy and the core attraction due to atom p, its absolute value was taken to be equal to the ionization potential of an appropriate valence state.

Several discussions have been made concerning the problem which $|W_p|$ value should be adopted for the nitrogen atoms of aniline and pyrrole, the first or second ionization potential. We have the same problem for the oxygen atoms of phenol and furan, too. Some authors insisted upon the superiority of using the first ionization potentials as the $|W_p|$ values of these atoms.[22,23] Our opinion is that the most suitable $|W_p|$ value for each of these atoms exists between the first and second ionization potentials. Therefore, we carried out several calculations for each of the aniline and phenol molecules, regarding the W_p and γ_{pp} values of the heteroatoms of these molecules as parameters. The best values determined for aniline and phenol were used for the calculation of pyrrrole and furan, respectively. The W_p and γ_{pp} values for the carbon atom and the γ_{pq} values necessary for the calculation of these four molecules were evaluated by the same procedures as described in the case of pyridine.

The core resonance integral (β_{CC}) for the carbon-carbon bond of the benzene and pyridine rings was taken to be equal to -2.61 eV. This value is the optimum one for interpreting the observed benzene spectrum.[24] The core resonance integrals necessary for the calculation of pyrrole and furan were evaluated by two formulas presented by

10) J. D. Dahl and A. E. Hansen, *Theor. Chim. Acta*, **1**, 199 (1963).
11) See, for example, K. Ohno, "Advances in Quantum Chemistry," Vol. III, ed. by P. O. Löwdin, Academic Press Inc., New York (1967) p. 240.
12) K. Nishimoto and L. S. Forster, *Theor. Chim. Acta*, **4**, 155 (1966).
13) K. Nishimoto, *ibid.*, **5**, 74 (1966); **7**, 207 (1967).
14) F. A. Gray, I. G. Ross and J. Yates, *Aust. J. Chem.*, **12**, 347 (1959).
15) T. Anno and A. Sado, *J. Chem. Phys.*, **39**, 2293 (1963).
16) W. E. Donath, *ibid.*, **40**, 77 (1964).
17) H. Itoh and Y. I'Haya, *Theor. Chim. Acta*, **2**, 247 (1964).
18) N. L. Allinger, J. C. Tai and J. W. Stuart, *ibid.*, **8**, 101 (1967).
19) J. Koutecky, J. Cizek, J. Dubsky and K. Hlavaty, *ibid.*, **2**, 462 (1964).
20) J. Koutecky, K. Hlavaty and P. Hochmann, *ibid.*, **3**, 341 (1965).
21) N. L. Alliger and T. W. Stuart, *J. Chem. Phys.*, **47**, 4611 (1967).
22) S. Kwiatokowski, *Theor. Phys.* (Poland), **13**, 817 (1965).
23) S. Kwiatokowski, *Acta Phys. Poland*, **27**, 477 (1966); **30**, 529 (1966).
24) H. Kashiwagi, presented at the Symposium on Molecular Structure and Spectroscopy, Sapporo, on October, 1967.

Mulliken[25] and by Ohno.[26] For the other molecules, the core resonance integral (β_{cx}) for the bond including the hetero-atom was regarded as a parameter.

In the CI calculation, we took all the singly and doubly excited configurations for pyridine, pyrrole and furan, but for phenol and aniline disregarded several doubly excited configurations which include the excitation from the lowest occupied orbital.*1 These configurations are higher than the ground configuration by more than 16 eV and seem to have only little influence on lower excited states.

There are five types of doubly excited configurations,[27] and the total numbers of configurations taken in the actual calculation are 55 for pyridine, 58 for aniline and phenol, and 37 for pyrrole and furan.

In actual calculations we need the data on the geometrical configurations of the molecules under consideration. Pyridine and the benzene rings of aniline and phenol were assumed to have the same geometrical configurations as benzene, that is, all the bond lengths were taken to be 1.397 Å.*2 The C–N and C–O bond lengths in aniline and phenol were assumed to be 1.38 Å and 1.36 Å, respectively, from those of similar compounds given in Sutton's table.[28] The structure of pyrrole was also taken from the same table. The calculation of furan was caried out on the basis of its geometrical structure determined by Bak *et al.*[29]

The computation was carried out by a HITAC 5020E located at the Computer Center, the University of Tokyo.

Results and Discussion

Effect of Parameters. The DECI treatment reduces somewhat the effect of the W_p value upon the calculated energy levels of lower excited states compared with the SECI treatment, (at least) when the change of W_p is limited to ± 4 eV. This is clear form Fig. 1 which exhibits, taking aniline as an example, the W_p dependency of lower excited levels calculated by the P–P–P method without CI and with the SECI and DECI procedures. The same tendency was found for the other molecules under consideration. It is noteworthy that the effect of W_p upon the calculated results is reduced by the DECI treatment.

The effect of one-center Coulomb integrals, γ_{pp}'s upon the calculated energy levels is scarcely reduced by the DECI treatment. Some energy levels are more sensitive to γ_{pp} in the DECI treatment than in the SECI one. This may conceivably be attributed to the fact that γ_{pp} contributes directly to the matrix element of the DECI calculation.

Concerning aniline and phenol, calculations were carried out by the use of several sets of the parameters, W_p and γ_{pp}, with the step of about 2 and 1 eV, respectively, and we looked for the most suitable set which gives the best agreement with the observed transition energies. Consequently, we obtained the values given in Table 1. The selected W_p values, as expected, are the intermediates between the first and the second ionization potentials. Kwiatokowski[22,23] calculated the tran-

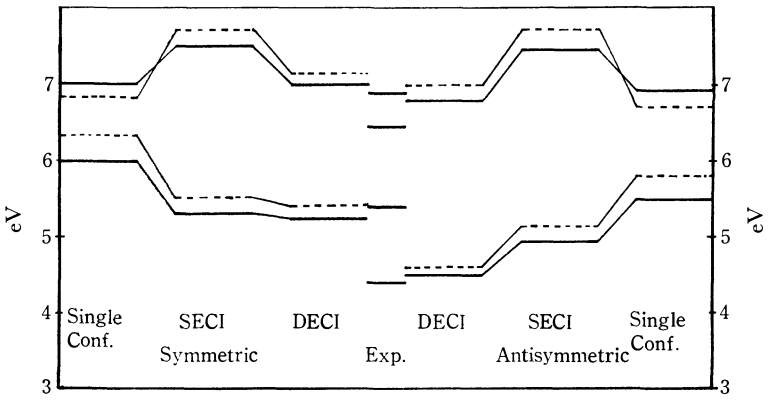

Fig. 1. Dependence of the calculated energy levels of aniline upon the W_N value.
———$W_N=-26.71$, ·····$W_N=-24.71$

25) R. S. Mulliken, *J. Chem. Phys.*, **46**, 521 (1949).
26) K. Ohno, *Theor. Chim. Acta*, **2**, 215 (1964).
*1 This neglect reduces the time necessary for the CI calculation to about a half.
27) J. N. Murrell and K. L. McEwen, *J. Chem. Phys.*, **25**, 1143 (1956).
*2 According to Sutton's Table, the C–C bond lengths of pyridine are 1.3945 and 1.3944 Å and therefore the assumption on its geometry seems to be reasonable concerning the estimation of β_{CC}.
28) "Tables of Interatomic Distances and Configuration in Molecules and Ions," ed. by L. E. Sutton, the Chemical Society, London (1958) and its Supplement.
29) B. Bak, L. Hansen and J. Rastvup-Andersen, *Discuss. Faraday Soc.*, **19**, 30 (1955).

Table 1. Selected parameters for the P-P-P calculation including doubly excited configurations

Atom	From I_p and I_p-A_p		Optimized values	
	$\lvert W_p\rvert$	γ_{pp}	$\lvert W_p\rvert$	γ_{pp}
C	11.22	10.60[b]	—	—
N pyridine type	14.12	12.34[c]	—	—
pyrole type	28.71[a]	16.75[a,c]	24.71	13.75
O ketone type	17.70	15.23[c]	—	—
furan type	34.08[a]	18.78[a,c]	30.08	16.78

a) W_p for these two cases is the second ionization potential, and γ_{pp} is the difference between the first and second ionization potentials.
b) G. Pilcher and H. A. Skinner, *J. Inorg. Nucl. Chem.*, **24**, 937 (1962).
c) J. Hinze and H. H. Jaffé, *J. Amer. Chem. Soc.*, **84**, 540 (1962).

sition energies of aniline by the P-P-P method with the SECI treatment and using Nishimoto-Mataga's formula[30] for γ_{pp}, and obtained the results coincident with the observed transition energies by adopting the $|W_N|$ value (22.49 eV) lower than the second ionization potential of nitrogen, and γ_{pp} for the neutral atom.*3 His parameter values are similar to ours, although the γ_{pp} value in the present calculation is a little greater than that of Kwiatokowski. Since in the SCF calculation the $(W_p + 1/2P_{pp}\gamma_{pp})$ is (P_{pp} is the π-electron density on atom p) mainly effective for the evaluated energies, there may be several sets of W_p and γ_{pp} to give a good agreement between the theoretical and experimental transition energies.

The absolute value of the core resonance integral β_{C-X} for aniline and phenol is somewhat larger in the DECI treatment than in the SECI one. The same tendency was found for β_{C-C}.[15] For pyrrole and furan, the better results were obtained with the aid of the core resonance integrals derived by Ohno's formula than by Mulliken's formula, although the difference is rather small and too much

Table 2. Experimental and theoretical excitation energies (ΔE, eV) and oscillator strengths (f) of pyridine

Experimental[a]		Mataga-Nishimoto[b]		Present work			
				SECI		DECI	
ΔE	f	ΔE[c]	f	ΔE[c]	f	ΔE[c]	f
4.96	0.03	5.01(A)	0.024	5.01(A)	0.038	4.93(A)	0.030
6.36	0.20	6.25(B)	0.026	5.65(B)	0.02	6.26(B)	0.01
7.04	1.36	7.23(A)	1.04	7.30(A)	1.15	7.26(A)	1.09
		7.16(B)	1.24	7.49(B)	1.12	7.39(B)	1.01

a) B. Pickett and B. Pullman, "Quantum Biochemistry," Interscience Publishers, New York (1963).
b) N. Mataga and K. Nishimoto, *Z. Phys. Chem.* (Frankfurt), **13**, 140 (1959).
c) Symmetry of each level is shown in parentheses.

Table 3. Exprimental and theoretical excitation energies (ΔE, eV) and oscillator strengths (f) of aniline

Experimental[a]		Fischer-Hjalmars[b]		Present work			
				SECI		DECI	
ΔE	f	ΔE[c]	f	ΔE[c]	f	ΔE[c]	f
4.40	0.028	4.70(A)	0.015	4.68(A)	0.031	4.38(A)	0.020
5.39	0.144	5.58(B)	0.19	5.30(B)	0.220	5.27(B)	0.130
6.40	0.510	6.50(A)	0.55	6.82(A)	0.63	6.70(A)	0.430
6.88	0.570	6.67(B)	0.68	7.08(B)	0.73	6.91(B)	0.506
7.87	(0.68)	7.50(A)	0.61	8.29(A)	0.99	8.03(A)	0.510
		7.40(B)	0.41	8.37(B)		8.11(B)	

a) K. Kimura and S. Nagakura, *Mol. Phys.*, **9**, 117 (1965).
b) I.Fischer-Hjalmars, *Ark. Fysik*, **21**, 123 (1962).
c) Symmetry of each level is shown in parentheses.

30) K. Nishimoto and N. Mataga, *Z. Physik. Chem.* (Frankfurt), **12**, 335 (1957).

*3 Exactly speaking, this corresponds to the γ_{pp} value for the anion.[6]

TABLE 4. EXPERIMENTAL AND THEORETICAL EXCITATION ENERGIES (ΔE, eV) AND OSCILLATOR STRENGTHS (f) OF PHENOL

Experimental[a]		Bloor, Peradedejordi[b]		Present work SECI		Present work DECI	
ΔE	f	ΔE[c]	f	ΔE[c]	f	ΔE[c]	f
4.59	0.020	4.80(A)	0.10	4.52(A)	0.037	4.66(A)	0.021
5.82	0.132	5.96(B)	0.60	5.16(B)	0.156	5.69(B)	0.159
6.70	0.636	6.82(A)	1.20	6.61(B)	0.950	6.92(A)	0.754
6.93	0.467	6.84(B)	1.09	6.74(A)	1.59	7.06(B)	0.840

a) K. Kimura and S. Nagakura, *Mol. Phys.*, **9**, 117 (1965).
b) J. E. Bloor and F. Peradejordi, *Theor. Chim. Acta*, **1**, 83 (1962).
c) Symmetry of each level is shown in parentheses.

TABLE 5 EXPERIMENTAL AND THEORETICAL EXCITATION ENERGIES (ΔE, eV) AND STATE SYMMETRIES OF PYRROLE

Experimental[a]	Chiorboli *et al.*[b]		Present work SECI		Present work DECI	
ΔE	ΔE	symm.	ΔE	symm.	ΔE	symm.
5.87	5.89	B_1	5.92	B_1	5.80	A_1
6.77	6.80	A_1	6.46	A_1	6.51	B_1
7.22	7.18	A_1	7.43	A_1	7.35	B_1
—	7.45	B_1	7.94	B_1	7.83	A_1

a) See Ref. 32
b) Ref. 32

TABLE 6. EXPERIMENTAL AND THEORETICAL EXCITATION ENERGIES (ΔE, eV) AND OSCILLATOR STRENGTHS (f) OF FURAN

Experimental[a]		Suppenfield, Kreevoy[a]		Present work SECI		Present work DECI	
ΔE	f	ΔE[b]	f	ΔE[b]	f	ΔE[b]	f
6.05	0.12	5.92(A)	0.11	6.10(A)	0.20	5.89(B)	0.14
6.47	0.078	6.49(B)	0.07	6.53(B)	0.04	6.45(A)	0.10
7.55	—	7.—(A)	—	7.54(A)		7.36(A)	

a) D. S. Suppenfield and M. Dreevoy, *Tetrahedron*, **19**, Suppl. 2, 286 (1963). In this calculation, the following parameters were used and the penetration integrals were included: $\gamma_{oo}=14.79$ eV, $W_o=-34.16$ eV.
b) Symmetry of each level is shown in parentheses.

importance should not be attached to it.

Energy Levels. The energy levels calculated by the DECI method are shown in Tables 2—6, together with the experimental values and the results obtained by the SECI method. In these tables, the results obtained by other authors are also given for the purpose of compariosn, only one example being taken from many calculations for each molecule. The comparison of the energy levels calculated by the DECI method with those by the SCF scheme and by the SECI method are schematically shown in Figs. 2—5[*4] for pyridine, aniline, phenol and pyrrole. From these figures, it is clear that the energy levels changes to a considerable extent by the DECI treatment compared with the results by the SECI calculation. The DECI calculation stabilizes the ground states of these molecules by 0.5—1 eV and improves greatly the agreement between the theoretical and experimental excitation energies.

The most remarkable effect of the DECI treatment is found for the separation between the lowest and the second lowest excited states. In the case

[*4] For the convenience of comparison, in these figures the energy levels calculated by the DECI treatment are corrected in such a way as the ground state is equal to that calculated by the SECI treatment.

of the SECI method, the calculated separation is too small compared with the observed value for pyridine, aniline and phenol. The DECI treatment improves this point to a great extent and gives the reasonable values. This is also the case for benzene.[15] In this connection, it is worth noticing

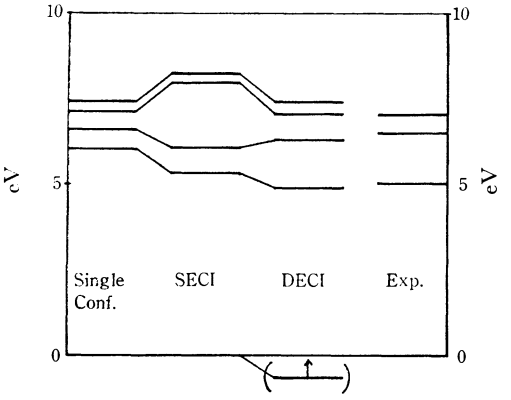

Fig. 2. Calculated Energy Levels of Pyridine.

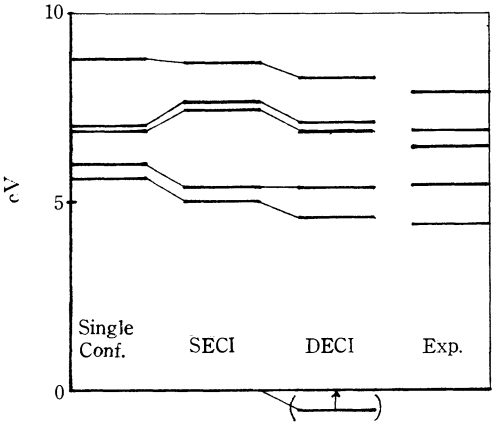

Fig. 3. Calculated and observed energy levels of aniline.

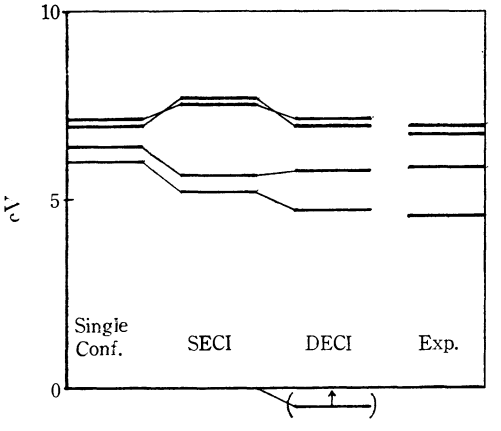

Fig. 4. Calculated and observed energy levels of phenol.

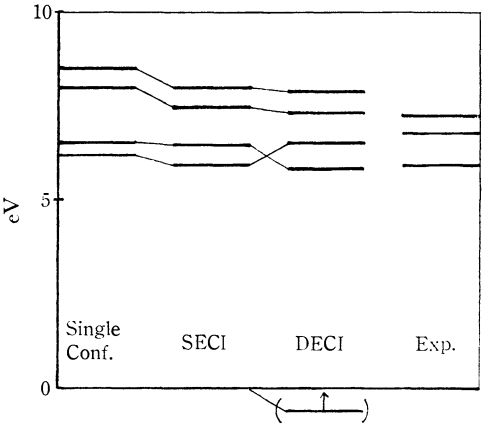

Fig. 5. Calculated and observed energy levels of pyrrole.

that the great separtion between these two states can be obtained[29] by the SECI treatment, when we use Nishimoto-Mataga's formula[31] for γ_{pq} instead of the uniformly charged sphere model. The former gives the smaller γ_{pq} value by 1—2 eV than the latter in the important region of interatomic distance. This seems to mean that the inclusion of the doubly excited configurations has effectively the effect similar to that of the decrease in γ_{pq}. This may be a correlation effect by screening.*5

In phenol, the third and fourth excited levels are inverted in the DECI calculation compared with the result by the SECI treatment. Since the composite-molecule method[32] and also the modified P-P-P method[12] support the results of the DECI treatment, this inversion is thought to be rather important.

In our calculation, the higher excited levels evaluated for aniline and phenol have a tendency to be a little higher than the observed ones. In order to lower these levels, it may be necessary to take doubly excited configurations higher than those taken in the present calculation.

In pyrrole and furan the inversion occurs between the lowest and second lowest levels more vividly than in phenol. We explain the details taking pyrrole as an example. In this case, the first excited state which is of the B_1 character in the SECI calculation turns out to be of the A_1 character in the DECI treatment. Dahl and Hansen[10] obtained by the SECI treatment the same result concerning the order of the excited levels as the present DECI calculation, adopting Nishimoto-Mataga's formula for γ_{pq} and including the penetra-

31) See, for example, K. Nishimoto and L. S. Forster, *Theor. Chim. Acta*, **3**, 407 (1965).

*5 There is a possibility that this is due to the other effects, such as the effective σ-core change and the expansion of π-orbitals.

32) K. Kimura, H. Tsubomura and S. Nagakura, This Bulletin, **37**, 1336 (1964).

tion integrals. Here, again, the DECI treatment shows the effect effectively similar to that of reducing γ_{pq}. In this case, however, the relative change between the two levels (1.5 eV) caused by the inclusion of the doubly excited configurations is too large to be attributed to the correlation effect. Furthermore, Chiorboli *et al.*[33] showed that, in spite of the adoptation of Nishimoto-Mataga's formula, the SECI calculation gives the order of the excited levels different from that of Dahl and Hansen when the penetration integrals are different from theirs. From these facts it is revealed that the effect of the doubly excited configurations upon the calculated energy levels is more complicated for pyrrole than for phenol and aniline.

Transition Moment. As is well known, the transition moment or oscillator strength calculated by the P-P-P method including SECI is usually too large (2—3 times) compared with the experimental value. This is corrected to a great extent by the DECI treatment. This improvement is mainly attributed to the fact that in the DECI treatment excited wavefunctions include many doubly excited configurations, the transition moments from the ground configuration to which are zero. This tendency is vivid in the transitions to higher excited levels of aniline and phenol, and the moments calculated for them are sometimes smaller than the observed values.

π-Electron Densities and Dipole Moments of Aniline. By the aid of the wavefunctions calculated by the present study, π-electron densities were evaluated for the ground state of aniline as shown in Fig. 6. This figure shows that the

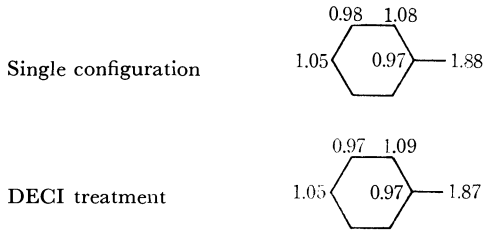

Fig. 6. Electron densities in the ground state of aniline.

nonbonding electrons of the nitrogen atom migrate by 0.12—0.13 *e* toward the benzene ring and consequently the carbon atoms at the *o*- and *p*-positions turn out to have excess π-electrons by 0.08—0.09 *e* and 0.05 *e*, respectively. From these π-electron densities we calculated the dipole moment due to the π-electrons to be 1.82—1.89 D. The values are close to the π-electron moment estimated by analyzing the observed dipole moment of aniline, 1.41—1.52 D.[34,35]

The calculated π-electron densities in the first excited state of aniline are shown in Fig. 7. The

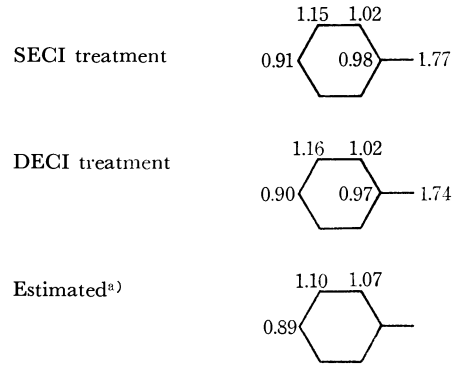

Fig. 7. Electron densities in the first excited state of aniline.

corresponding quantities were estimated[36] from the analysis of the peak positions of the absorption band observed for various aminopyridines. The estimated values are also shown in Fig. 7 for the purpose of comparison, although the estimation includes much ambiguity and therefore too much importance should not be attached to them. The theoretical π-electron densities in the first excited state are qualitatively coincident with the estimated ones in the sense that excess amounts of π-electrons are located on the carbon atoms of *o*- and *m*-positions. In this connection, it may be noticed that the difference ($\Delta\mu_\pi$) in the π-electron moment between the ground and the first excited state was estimated to be~5 D from the analysis of the solvent effect on the absorption and fluorescence spectra observed for aniline.[36] The corresponding quantity was calculated by the SECI and DECI treatment to be 1.45 D and 2.44 D, respectively. The calculated $\Delta\mu_\pi$ values are smaller than the estimated value, although the latter includes much ambiguity. From this it is revealed that the present calculation underestimates a little the π-electron migration from the nitrogen atom toward the benzene ring and therefore that a little smaller $|W_p|$ value than that in the present calculation may give better results for the π-electron distribution. Anyhow, it may be concluded from the both theoretical and experimental points of view that the π-electron migration from the nitrogen atom toward the benzene ring much increases in the first excited state compared with in the ground state.

The authors wish to thank Dr. Haruo Hosoya, Ochanomizu Women Univeristy, Dr. Suehiro Iwata, the Institute of the Chemical and Physical Research, and Dr. Hiroshi Kashiwagi, Hokkaido University for their helpful discussions.

33) P. Chiorboli, A. Rastelli and F. Momicchioli, *Theor. Chim. Acta*, **5**, 1 (1966).
34) L. G. Groves and S. Sugden, *J. Chem. Soc.*, **1937**, 1992.
35) S. Nagakura and H. Baba, *J. Amer. Chem. Soc.*, **74**, 5693 (1952).
36) J. N. Murrell, *Tetrahedron*, **19**, *Suppl.*, 2, 277 (1963).

BULLETIN OF THE CHEMICAL SOCIETY OF JAPAN VOL. 43 1017—1022 (1970)

Excitation Transfer in the Radiolysis of Solid Hydrocarbons as Studied by ESR Spectroscopy and Product Analysis

Terunobu WAKAYAMA, Toyoaki KIMURA, Tetsuo MIYAZAKI, Kenji FUEKI and Zen-ichiro KURI

Department of Synthetic Chemistry, Faculty of Engineering, Nagoya University, Chikusa-ku, Nagoya

(Received October 17, 1969)

The effect of carbon tetrachloride on the radiolysis of isobutane and methylcyclohexane at 77°K is studied by ESR spectroscopy and by product analysis. The yields of solvent radicals from the γ-irradiation of isobutane and methylcyclohexane are not changed by the presence of conventional electron scavengers. This indicates that solvent radicals are not formed by the neutralization of solvent cations with electrons. On the contrary, the yields of solvent radicals decrease remarkably upon the addition of CCl_4. Though the yield of propylene from the γ-irradiation of isobutane is not affected by the addition of electron scavengers, it decreases significantly upon the addition of CCl_4. Though the decrease in the hydrogen yield in the radiolysis of methylcyclohexane at 77°K upon the addition of electron scavengers is only about 1G-unit, it amounts to more than 3.5G-units upon the addition of CCl_4. These characteristic effects of CCl_4 can possibly be explained in terms of excitation transfer from the excited solvent molecule to CCl_4. A kinetic treatment suggests that its mechanism may be an exciton transfer.

Product analysis and the observation of reaction intermediates have been two major methods for the study of the reaction mechanism of radiolysis. Since these two methods reveal different aspects of mechanisms, however, it is desirable to make a study of the radiolysis mechanism using both methods. Along this line we have previously studied the reaction of nitrous oxide with electrons in organic glass[1] and the radiolysis of phenylacetate in the solid states[2] at −196°C.

We reported in a previous communication[3] that the yield of the isobutyl radical produced in γ-irradiated isobutane at −196°C decreases upon the addition of carbon tetrachloride, while it is not affected by the addition of other electron scavengers, such as nitrous oxide, sulfur hexafluoride, and ethyl iodide. Here we will study in more detail, by ESR spectroscopy and by product analysis, the characteristic effect of carbon tetrachloride in the radiolysis of isobutane and methylcyclohexane at −196°C.

Experimental

The isobutane and the methylcyclohexane were more than 99.9% pure. The gas-chromatographic analysis did not show any detectable impurity. They were used after degassing and distillation on a vacuum line. The carbon tetrachloride (99.9%) was used after vacuum distillation. The additives, such as phenyl iodide, ethyl iodide, nitrous oxide, sulfur hexafluoride, *n*-butyl chloride, carbon dioxide, and ethylene, were all of a high purity and were used after vacuum distillation.

The samples were irradiated with γ-rays from Co-60 at a dose rate of 4.2×10^5 rad/hr. The photobleaching of the γ-irradiated samples was carried out at 77°K with the light from a tungsten lamp.

The ESR measurements were made on a JES-3BX ESR spectrometer. The gaseous products not condensable at the temperature of liquid nitrogen were analyzed by a gas burette connected to a Toepler pump and a cupric oxide furnace kept at 240°C. The hydrocarbon products were analyzed by a Hitachi K53 gas chromatograph equipped with a flame-ionization detector (activated alumina column, 2 m, 100°C).

The *G*-value is expressed here by the number of product molecules per 100 eV absorbed in isobutane or methylcyclohexane. The *G*-values of the radicals were determined by ESR measurements by assuming $G(\text{radical})=1.6$ for the radicals produced in the γ-irradiated 3-methylpentane at −196°C.[4]

Results and Discussion

Radiolysis of Isobutane. *A) The Effect of Carbon Tetrachloride on Solvent Radical Formation.* Isobutane forms a polycrystal at −196°C, and when irradiated with γ-rays it produces the isobutyl

1) T. Wakayama, T. Kimura, T. Miyazaki, K. Fueki and Z. Kuri, This Bulletin, **42**, 266 (1969).

2) Y. Noro, M. Ochiai, T. Miyazaki, A. Torikai, K. Fueki and Z. Kuri, *J. Phys. Chem.*, **74**, 63 (1970).

3) T. Wakayama, T. Miyazaki, K. Fueki and Z. Kuri, This Bulletin, **42**, 1164 (1969).

4) M. Shirom and J. E. Willard, *J. Phys. Chem.*, **72**, 1702 (1968).

Fig. 1. (A) Fig. 1. (B)

Fig. 1. A) ESR spectrum of isobutyl radical in the radiolysis of isobutane at 77°K.
B) ESR spectrum of γ-irradiated isobutane containing 4.8 mol% ethylene at 77°K. ○-represents main signals of ethyl radical.
Dose: 1.7×10^5 rad.

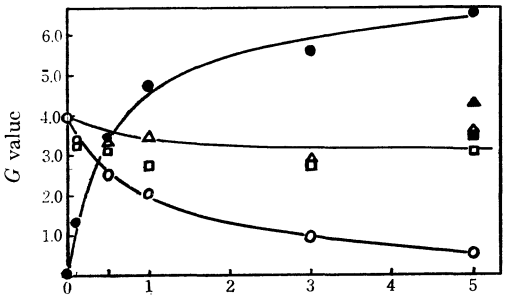

Fig. 2. Effect of additives on the formation of radical in the radiolysis of isobutane at 77°K studied by ESR.
Dose: 1.7×10^5 rad.
Yields of isobutyl radical are shown by the following plots:
○ CCl_4
△ C_6H_5I
□ C_2H_5I
▲ N_2O
■ SF_6
} Additives
Yields of CCl_3 radical in the radiolysis of i-C_4H_{10}-CCl_4 system are also shown by plots (●).

radical whose ESR spectrum is shown in Fig. 1(A). The yield of the isobutyl radical is not affected by the addition of electron scavengers, such as phenyl iodide, C_2H_5I, N_2O, and SF_6 (Fig. 2). When isobutane containing ethyl iodide was γ-irradiated at −196°C, an ethyl radical was observed by ESR measurement. The ethyl radical is produced by dissociative electron attachment to ethyl iodide (reactions (1) and (2)).

$$C_4H_{10} \rightsquigarrow C_4H_{10}^+ + e^- \quad (1)$$

$$e^- + C_2H_5I \longrightarrow C_2H_5 + I^- \quad (2)$$

Nitrous oxide suppresses the formation of the toluene anion in the γ-irradiated isobutane-toluene system, as will be described in the next section, and it also acts as an effective electron scavenger.

Therefore, it can be said that the isobutyl radical is not produced by the neutralization reaction in the radiolysis of solid isobutane. The effect of CCl_4 on the formation of isobutyl radical is shown in Fig. 2. Here the remarkable points are the rapid decrease in the yield of the solvent radical and the increase in the yield of the CCl_3 radical with the increase in the concentration of CCl_4. The yield of the CCl_3 radical amounts to 6.5G-units at $[CCl_4]=5$ mol/100 mol of i-C_4H_{10}. The large yield of the CCl_3 radical cannot be explained only by the dissociative electron attachment:

$$e^- + CCl_4 \rightarrow CCl_3 + Cl^- \quad (3)$$

but suggests the participation of some other reactions. Since the ionization potential of isobutane (10.8 eV) is lower than that of carbon tetrachloride (11.5 eV), isobutane ion in the ground state cannot transfer its charge to CCl_4. The quantity of mobile excited butane ions is considered to be rather small because of the fact that the toluene cation was not formed in the γ-irradiated isobutane matrix containing toluene (*cf.* next section). Therefore, the effect of CCl_4 on the formation of the isobutyl radical may not be due to charge transfer from the excited isobutane ion to carbon tetrachloride.

Let us tentatively ascribe this effect to excitation transfer from the excited isobutane molecule to carbon tetrachloride and the suppression of the decomposition of the excited isobutane (reactions (4)—(6)):

$$C_4H_{10} \rightsquigarrow C_4H_{10}^* \quad (4)$$

$$C_4H_{10}^* \longrightarrow C_4H_9 + H \quad (5)$$

$$C_4H_{10}^* + CCl_4 \longrightarrow C_4H_{10} + CCl_4^* \quad (6)$$

A portion of CCl_4^* may decompose further to produce CCl_3 and Cl radicals:

$$CCl_4^* \rightarrow CCl_3 + Cl \quad (7)$$

The presence of H atoms produced in reaction (5) is demonstrated by the fact that the ethyl radical is observed by ESR measurements in the γ-irradiated isobutane-ethylene system (Fig. 1(B)):

$$H + C_2H_4 \rightarrow C_2H_5 \quad (8)$$

B) The Effect of Toluene on Solvent Radical Formation. The effect of toluene on the formation of the isobutyl radical is shown in Figs. 3 and 4. Here the remarkable points are the rapid decrease in the yield of the solvent radical and the appearance of a new ESR spectrum with the increase in the concentration of toluene. The new spectrum disappears easily upon illumination with light from a tungsten lamp, and it decreases upon the addition of nitrous oxide to the i-C_4H_{10}-$C_6H_5CH_3$ system (Fig. 4a, b and c). These results suggest that the species responsible for this spectrum may be assigned to the toluene anion. The spectrum consists of five lines with a splitting constant of 4.2 G.

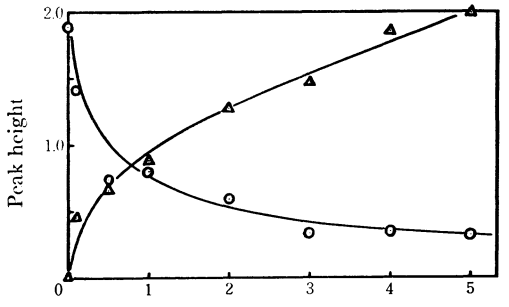

Fig. 3. Effect of toluene on the formation of radical in the radiolysis of isobutane at 77°K studied by ESR.
Dose: 1.7×10^5 rad.
○, isobutyl radical; △, toluene anion

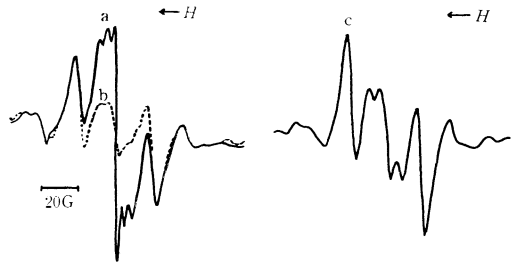

Fig. 4. a) ESR spectrum of γ-irradiated isobutane containing 4.8 mol% toulene at 77°K.
b) The same sample as (a) after 5 min illumination with visible light.
c) ESR spectrum of γ-irradiated isobutane - toluene (4.8 mol%) - nitrous oxide (0.9 mol%) system at 77°K.
Dose: 1.7×10^5 rad.

The ESR spectrum of the toluene anion produced chemically consists mainly of five lines with a splitting constant of 4.0 G,[5] these lines arising from hyperfine interactions with ortho- and meta-protons. The formation of the toluene anion and the related reactions may be written as follows:

$$i\text{-}C_4H_{10} \rightsquigarrow C_4H_{10}^+ + e^- \quad (9)$$

$$e^- + C_6H_5CH_3 \rightarrow C_6H_5CH_3^- \quad (10)$$

$$C_6H_5CH_3^- \xrightarrow[\text{(visible light)}]{h\nu} C_6H_5CH_3 + e^- \quad (11)$$

$$e^- + N_2O \rightarrow N_2 + O^- \quad (12)$$

The absence of the toluene cation suggests that the amount of the mobile excited ion may be negligibly small in the γ-irradiated solid isobutane. Since the yield of isobutyl radical is not altered by the photodetachment of an electron from a toluene anion (reaction (11)), the isobutyl radical is not formed by the neutralization of an electron with an isobutane cation.

5) S. P. Solodovnikov, *Zh. Strukt. Khim.*, **2**, 282 (1961).

Since the addition of toluene suppresses the formation of the isobutyl radical, as does carbon tetrachloride, toluene may also act as an acceptor of excitation energy:

$$C_4H_{10}^* + C_6H_5CH_3 \rightarrow C_4H_{10} + C_6H_5CH_3^* \quad (13)$$

C) The Effect of Carbon Tetrachloride on the Final Products. The fragment products in the radiolysis of isobutane at −196°C are mainly hydrogen, methane, propane, propylene, and isobutene. The hydrogen and propylene decrease in amount upon the addition of CCl_4 (Figs. 5 and 6). The

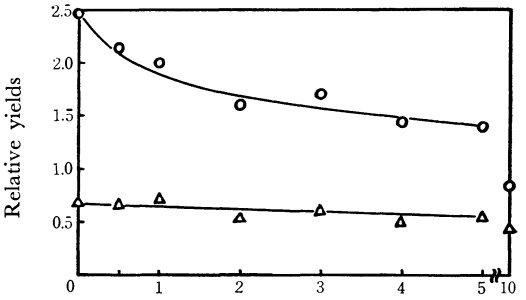

Fig. 5. Effect of CCl_4 on the formation of hydrogen and methane in the radiolysis of isobutane at 77°K.
Dose: 3.4×10^6 rad.
○, H_2; △, CH_4

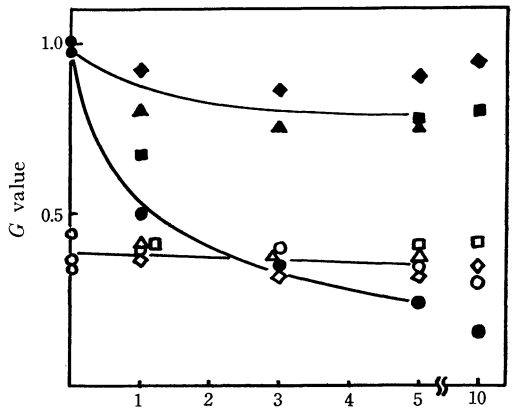

Fig. 6. Effect of additives on the formation of propylene and propane in the radiolysis of isobutane at 77°K.
Dose: 3.4×10^6 rad.

Yields of C_3H_6	Yields of C_3H_8
● CCl_4	○ CCl_4
▲ C_2H_5I	△ C_2H_5I
■ SF_6	□ SF_6
◆ N_2O	◇ N_2O

fact that the yield of propylene is not affected by the addition of electron scavengers, such as N_2O, SF_6, and C_2H_5I, indicates the absence of the follow-

ing neutralization reactions:

$$C_4H_{10}^+ + e^- \rightarrow C_3H_6 + CH_4 \quad (14)$$

$$C_3H_7^+ + e^- \rightarrow C_3H_6 + H \quad (15)$$

The yield of propane in the radiolysis of isobutane at −196°C are 0.3—0.4 G-unit in the presence of SF_6, while the yields amount to 1.4 in the radiolysis in the liquid phase.[6] This is because the fragmentation of the electronically-excited isobutane ion (reaction (16)) may be suppressed in the solid state by the dissipation of the electronic excitation energy to the solvent matrix; thus, the reaction of the $C_3H_7^+$ ion, reaction (15), for example, may play a minor role in the radiolysis of solid isobutane:

$$C_4H_{10}^{+*} \rightarrow C_3H_7^+ + CH_3 \quad (16)$$

The possibility that propylene may be produced directly from the fragmentation of the excited isobutane ion may be unimportant for two reasons. (i) The amounts of the CH_4^+ and $C_3H_5^+$ ions are rather small in the mass spectrum of isobutane, which may be correlated to C_3H_6 (reactions (17)—(20)):

$$C_4H_{10} \rightsquigarrow C_4H_{10}^{+*} + e^- \quad (17)$$

$$C_4H_{10}^{+*} \longrightarrow C_3H_6 + CH_4^+ \quad (18)$$

$$\searrow\ C_3H_5^+ + CH_3 + H_2 \quad (19)$$

$$C_3H_5^+ + C_4H_{10} \longrightarrow C_3H_6 + C_4H_9^+ \quad (20)$$

(ii) Even if $C_4H_{10}^{+*}$ is formed, its fragmentation may be suppressed in the condensed phase by collisional deactivation (reaction (21)).[7]

$$C_4H_{10}^{+*} + C_4H_{10} \rightarrow C_4H_{10}^+ + C_4H_{10} \quad (21)$$

It is suggested, therefore, that propylene is formed mainly by the fragmentation of the excited isobutane molecule:

$$C_4H_{10} \rightsquigarrow C_4H_{10}^* \quad (4)$$

$$C_4H_{10}^* \longrightarrow C_3H_6 + CH_4 \quad (22)$$

$$\searrow\ C_3H_6 + CH_3 + H \quad (23)$$

Lias and Ausloos[8] have reported that propylene is one of the main products in the fragmentation of excited or superexcited isobutane molecules in the photolysis of isobutane in the gas phase.

The addition of carbon tetrachloride suppresses the formation of propylene in the radiolysis of solid isobutane. When ethylene (3 mol/100 mol of i-C_4H_{10}) is added to the i-C_4H_{10}-CCl_4 system in order to protect propylene from the occurrence of reaction (24) while the irradiated sample is being warmed to room temperature, CCl_4 suppresses the formation of propylene to the same extent as in the absence of ethylene. This confirms that the effect of CCl_4 is not due to the secondary reaction of propylene with CCl_3 radicals.

$$C_3H_6 + CCl_3 \rightarrow C_3H_6CCl_3 \quad (24)$$

Therefore, the excitation transfer from the excited isobutane molecule to carbon tetrachloride (reaction (6)) may compete with Reactions (22) and/or (23). Since the yield of methane is not affected by the addition of carbon tetrachloride, Reaction (22) may be unimportant in the formation of propylene. The failure to detect the methyl radical, which would be produced by Reaction (23), may be due to its rapid combination with other radicals, for example butyl radicals, in a spur.

Radiolysis of Methylcyclohexane. As is shown in Fig. 7, the yield of solvent radicals decreases

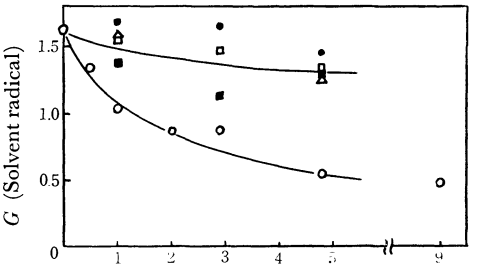

Fig. 7. Effect of additives on the formation of solvent radical in the radiolysis of methylcyclohexane at 77°K studied by ESR.
Dose: 2.1×10^5 rad.
○, CCl_4; □, n-C_4H_9Cl; △, CO_2; ●, N_2O; ■, SF_6

upon the addition of CCl_4. The reaction scheme for the radiolysis of methylcyclohexane may be depicted as follows:

$$C_7H_{14} \rightsquigarrow C_7H_{14}^+, C_7H_{14}^{+*}, C_7H_{14}^*, e^- \quad (25)$$

$$\left.\begin{matrix} C_7H_{14}^+ \\ C_7H_{14}^{+*} \end{matrix}\right\} + e^- \longrightarrow C_7H_{14}^* \quad (26)$$

$$C_7H_{14}^* \longrightarrow C_7H_{13} + H \quad (27)$$

$$\searrow\ C_7H_{12} + H_2 \quad (28)$$

$$2H \longrightarrow H_2 \quad (29)$$

The electron scavengers, such as CO_2, N_2O, SF_6, and n-C_4H_9Cl, but not CCl_4, do not suppress the yield of the solvent radical (Fig. 7). In these cases it was found, by ESR or product analysis, that CO_2^-, N_2,[9] and n-C_4H_9 radicals are formed by electron attachement to CO_2, N_2O, and n-C_4H_9Cl respectively. Moreover, when the trapped electron is bleached by infrared light, the solvent radical does not increase. Therefore, it can be said that the solvent radical is not produced by the neutralization reaction, (26).

6) a) K. Tanno, S. Shida and T. Miyazaki, *J. Phys. Chem.*, **72**, 3496 (1968). b) T. Miyazaki, K. Tanno and S. Shida, This Bulletin, **42**, 362 (1969).

7) T. Miyazaki, *J. Phys. Chem.*, **71**, 4283 (1967).

8) S. G. Lias and P. Ausloos, *J. Chem. Phys.*, **48**, 392 (1968).

9) T. Kimura, T. Miyazaki, K. Fueki and Z. Kuri, This Bulletin, **41**, 2861 (1968).

The characteristic effects of CCl_4 in the radiolysis of methylcyclohexane at 77°K were also observed on the production of hydrogen (Fig. 8). The

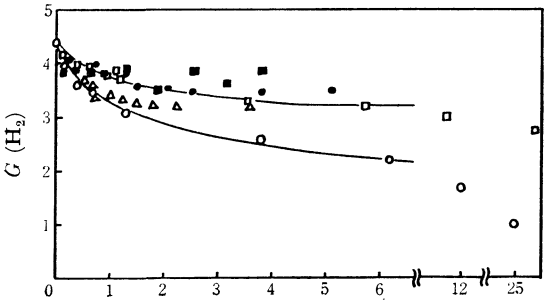

Fig. 8. Effect of additives on the formation of hydrogen in the radiolysis of methylcyclohexane at 77°K.
Dose: 3.6×10^5 rad.
○, CCl_4; □, n-C_4H_9Cl; △, C_6H_5I; ■, SF_6; ●, N_2O

decrease in the amount of hydrogen upon the addition of CCl_4 exceeds 3.5 G-units at the highest concentration, while the decreases upon the addition of n-C_4H_9Cl, SF_6, N_2O,[9] and C_6H_5I[9] are 1.3, 0.7, 0.8, and 1.3 G-units respectively.

Since the ionization potential of methylcyclohexane (9.9 eV) is lower than that of carbon tetrachloride (11.5 eV), the methylcyclohexane ion in the ground state cannot transfer its charge to CCl_4. Though the excited methylcyclohexane ion might transfer its charge to CCl_4, let us tentatively ascribe the effect of CCl_4 to the excitation transfer (reaction (30)):

$$C_7H_{14}^* + CCl_4 \longrightarrow C_7H_{14} + CCl_4^* \qquad (30)$$

Mechanism of Excitation Transfer. From the above results it can be assumed that the isobutyl radical is formed mainly by the decomposition of excited molecules in the radiolysis of solid isobutane and that CCl_4 acts as an acceptor of the excitation energy. Recently it was found, in a study of ultraviolet-induced luminescence of benzene, that CCl_4 is an efficient excitation quencher.[10] The mechanism of excitation transfer will now be discussed on the basis of the effect of CCl_4 on the formation of the isobutyl radical. A possible kinetic scheme is the following:

$$C_4H_{10} \overset{I}{\rightsquigarrow} C_4H_{10}^* \qquad (4)$$

$$C_4H_{10}^* \overset{k_d}{\longrightarrow} C_4H_9 + H \qquad (5)$$

$$C_4H_{10}^* + CCl_4 \overset{k_q}{\longrightarrow} C_4H_{10} + CCl_4^* \qquad (6)$$

where I is the rate of reaction (4) and where k is the rate constant. The rate of excitation transfer (reaction (6)) cannot be expressed *a priori* as that of the bimolecular reaction. Therefore, the following expression may be adopted:[11]

$$R_q = k_q\,[C_4H_{10}^*][CCl_4]^{n/3} \qquad (I)$$

where R_q is the rate of reaction (6). Since the rate of excitation transfer is usually some integral power function of the distance between two interacting molecules, it is natural to assume $R_q \propto [CCl_4]^{n/3}$, where n is an integer. $[CCl_4]^{1/3}$ is proportional to the reciprocal of the average distance between the molecules of carbon tetrachloride and excited butane.

The rate of excitation transfer for various theoretical models may be expressed as follows:[12]

a) Exciton transfer:

$$R_q \propto \frac{1}{r^3}$$

b) Vibrational-relaxation resonance transfer:

$$R_q \propto \frac{1}{r^6}$$

c) Polak's treatment:[11]

$$R_q \propto \frac{1}{r^2}$$

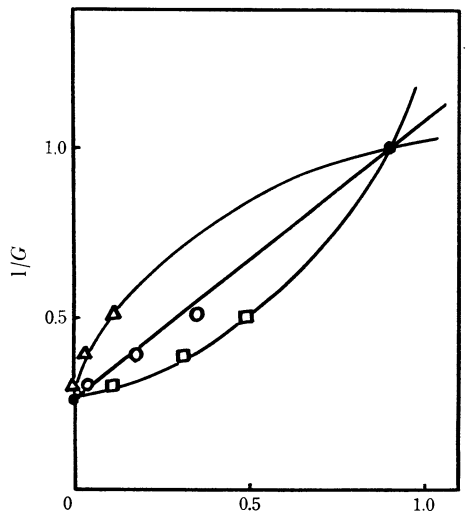

Fig. 9. Relations between $1/G(C_4H_9)$ and $[CCl_4]$. When $[CCl_4]=0.45$M, $[CCl_4]^{n/3}$is normalized to be 1.
—△—, $n=6$; —□—, $n=3$; —○—, $n=2$

10) P. K. Ludwig and C. D. Amata, *J. Phys. Chem.*, **72**, 3725 (1968).

11) a) U. A. Kolanovsky and L. S. Polak, *Dokl. Acad. Nauk SSSR*, **135**, 361 (1960). b) "Radiolysis of Hydrocarbons," ed. by A. V. Topchiev, Elsevier Publishing Company, Amsterdam-London-New York (1964), p. 138.

12) a) M. Kasha, *Radiat. Res.*, **20**, 55 (1963). b)Th. Förster, "Comparative Effects of Radiation," ed. by M. Burton, J. S. Kirby-Smith and J. L. Magee, John Wiley and Sons, New York (1960), p. 300.

where r is the distance between interacting molecules.

The steady-state treatment leads to:

$$\frac{1}{G(C_4H_9)} = \frac{1}{I} + \frac{k_d}{Ik_q}[CCl_4]^{n/3} \qquad (II)$$

where n is taken to be 2, 3, or 6, depending upon the models. Kinetic plots of our data for these cases are shown in Fig. 9. The experimental points fall reasonably well on a straight line for $n=3$; thus,

$$R_q \propto [CCl_4] \propto \frac{1}{r^3}$$

The kinetic treatment suggests that the mechanism of excitation transfer in our system is exciton transfer.

The slope-to-intercept ratio gives $k_q/k_d = 7.3\,\text{M}^{-1}$. The C–H bond rupture of the excited butane molecule may occur in the period of one vibration (10^{-12}—10^{-13} sec). It seems reasonable to assume $k_d = 10^{12}$—$10^{13}\,\text{sec}^{-1}$. Therefore, we obtain:

$$k_q = 7 \times 10^{12}\text{—}10^{13}\ \text{M}^{-1}\text{sec}^{-1}$$

This suggests that the rate of excitation transfer is extremely high as compared with the rate of diffusion-controlled reactions in the liquid phase ($\sim 10^{10}\ \text{M}^{-1}\text{sec}^{-1}$). k_q is of approximately the same order of magnitude as the theoretical value[12] (10^{12}—$10^{13}\,\text{M}^{-1}\,\text{sec}^{-1}$) of the transfer rate of the localized exciton.

BULLETIN OF THE CHEMICAL SOCIETY OF JAPAN VOL. 43 1022—1027 (1970)

Solvent Effects on the *g* Factors of Semiquinones

Teijiro YONEZAWA, Takashi KAWAMURA, Masaru USHIO and Yukimichi NAKAO

Department of Hydrocarbon Chemistry, Faculty of Engineering, Kyoto University, Yoshida, Sakyo-ku, Kyoto

(Received October 17, 1969)

The dependence of the *g* factors of *p*-benzosemiquinone and its tetrahalogenated derivatives on the solvent composition has been studied in the dimethyl sulfoxide-water system. When the water content of the solvent increases, the *g* factor of *p*-benzosemiquinone decreases, that of tetrachloro-*p*-benzosemiquinone scarcely changes, and the *g* factors of tetrabromo- and tetraiodo-*p*-benzosemiquinones increase. These phenomena are interpreted qualitatively by assuming that the water molecule solvates to the carbonyl oxygen atom of semiquinones and by using Stone's equation for the *g* factor of the polyatomic radical. The dependence of the *g* factor of *p*-benzosemiquinone on the solvent composition is quantitatively studied by means of the theory of solvent effects proposed by Gendell, Freed and Fraenkel and by using the 2-site model of Stone and Maki and also the 4-site model. The former model assumes that one carbonyl oxygen atom has one site occupied by a solvent molecule, thus resulting in a dominant *g* shift. In the later model, two solvent molecules interact with one carbonyl oxygen atom. Both models predict the same relation between the *g* shift and the solvent composition; this experiment cannot confirm which model is more adequate, although the deduced values of the equilibrium constants indicate that the 4-site model is preferable.

In two previous papers[1,2] we have studied the effects of solvents on the *g* factors of diphenyl nitric oxide and di-*t*-butyl nitric oxide; these investigations gave useful information about solvent-solute interactions, especially regarding the hydrogen-bond.

Although the solvent effects on the hyperfine coupling constants of the proton, carbon-13, and oxygen-17 of semiquinones have been extensively investigated,[3-7] the solvent effects on their *g* factors have attracted little attention[8]; therefore, a further extensive investigation of the solvent

1) T. Kawamura, S. Matsunami, T. Yonezawa and K. Fukui, This Bulletin, **38**, 1935 (1965).

2) T. Kawamura, S. Matsunami and T. Yonezawa, *ibid.*, **40**, 1111 (1967).

3) E. W. Stone and A. H. Maki, *J. Chem. Phys.*, **36**, 1944 (1962).

4) J. Gendell, J. H. Freed and G. K. Fraenkel, *ibid.*, **37**, 2832 (1962).

5) E. W. Stone and A. H. Maki, *J. Amer. Chem. Soc.*, **87**, 454 (1965).

6) M. R. Das and G. K. Fraenkel, *J. Chem. Phys.*, **42**, 1350 (1965).

7) W. M. Gulick, Jr., and D. H. Geske, *J. Amer. Chem. Soc.*, **88**, 4119 (1966).

8) R. J. Zandstra, *J. Chem. Phys.*, **41**, 3655 (1966).

effect on the g factors of semiquinones seems to be required.

p-Benzosemiquinone and its tetrahalogenated derivatives are generated electrochemically in the mixed solvent system of water and dimethyl sulfoxide (DMSO). The g factors of these radicals are measured in solvents of various compositions. These data are quantitatively explained in terms of the Gendell, Freed, and Fraenkel (GFF) theory;[4] this procedure accounts for these solvent effects on the assumption that the solvent forms localized complexes with oxygen atoms in carbonyl groups. Moreover, the shifts in the g factors of these semiquinones can be quantitatively explained by means of Stone's theory[9] regarding g factor of the polyatomic radical.

Experimental

p-Benzoquinone and chloranil were obtained commercially and were purified by recrystallization. The bromanil and iodanil were synthesized by the method of Torrey and Hunter[10] and were subsequently purified by recrystallization.

Semiquinones were generated by diffusion-controlled electroreduction within the microwave cavity of a 10^{-3} mol/l solution of quinone in DMSO, water, and various mixtures of both solvents under a vacuum. The reduction potential was controlled as the yellow color of the semiquinone arose near the mercury cathode. The supporting electrolyte was 0.05M tetraethylammonium perchlorate or sodium perchlorate in solutions with mole fractions of water less than or greater than 0.5 respectively.[5]

The water content of the mixed solvent was determined by means of the Karl-Fisher method.[11]

The electron spin resonance (ESR) spectra were observed by means of a JEOL JES-3BSX instrument with a 100 kHz field modulation and operating at a nominal frequency of 9.4 GHz.

For the measurement of the g factor, a glass capillary was attached to the sample tube. The capillary was filled with a reference compound, an alkaline aqueous solution of the potassium peroxylamine disulfonate or the tetracene cation radical in concentrated sulfuric acid, the g factors of which were assumed to be 2.005590 or 2.002604[12] respectively.

Results and Discussion

Table 1 lists the experimental values of the g factor of *p*-benzosemiquinone (I) for various mole fractions of water, designated by N_W, in mixture with DMSO. The values of the g factors decrease

Table 1. g Factor of *p*-benzosemiquinone in mixtures of water and dimethyl sulfoxide

N_w [a]	g [b]
0.000	2.005182±0.000003
0.014	2.005169±0.000003
0.043	2.005147±0.000002
0.083	2.005125±0.000004
0.196	2.005065±0.000002
0.268	2.005030±0.000004
0.489	2.004928±0.000007
0.650	2.004845±0.000003
0.777	2.004778±0.000004
0.892	2.004722±0.000004
0.950	2.004693±0.000006
0.980	2.004670±0.000002
1.000	2.004659±0.000003

a) Mole fraction of water.
d) Determined by using an alkaline aqueous solution of potassium peroxylamine disulfonate as a reference, g factor of which is assumed to be 2.005590.

Table 2. g Factor of tetrachloro-*p*-benzosemiquinone in mixtures of water and dimethyl sulfoxide

N_w [a]	g [b]
0.00	2.005859±0.000005
0.10	2.005852±0.000007
0.20	2.005847±0.000005
0.40	2.005868±0.000008
0.60	2.005875±0.000008

a) Mole fraction of water. Maximum error: ±0.02.
d) Determined by using tetracene cation radical in conc. sulfuric acid as a reference, g factor of which is assumed to be 2.002604.

Table 3. g Factor of tetrabromo-*p*-benzosemiquinone in mixtures of water and dimehyl sulfoxide

N_w [a]	g [b]
0.00	2.008433±0.000016
0.10	2.008482±0.000007
0.20	2.008486±0.000016
0.40	2.008596±0.000007
0.60	2.008700±0.000007

a) Mole fraction of water. Maximum error: ±0.02.
d) Determined by using an alkaline aqueous solution of potassium peroxylamine disulfonate as a reference, g factor of which is assumed to be 2.005590.

9) A. J. Stone, *Proc. Roy. Soc. Ser. A* **271**, 424 (1963); *Mol. Phys.*, **6**, 509 (1963).
10) H. A. Torrey and W. H. Hunter, *J. Amer. Chem. Soc.*, **34**, 702 (1912).
11) C. D. McKinney, Jr., and R. T. Hall, *Ind. Eng. Chem.*, **15**, 460 (1943).
12) B. G. Segal, M. Kaplan and G. K. Fraenkel, *J. Chem. Phys.*, **43**, 4191 (1965).

TABLE 4. g FACTOR OF TETRAIODO-p-BENZOSEMIQUINONE IN MIXTURES OF WATER AND DIMETHYL SUIFOXIDE

N_W[a)]	g[b)]
0.000	2.011399±0.000003
0.049	2.011439±0.000003
0.090	2.011469±0.000003
0.211	2.011559±0.000010
0.282	2.011631±0.000007
0.394	2.011791±0.000010
0.503	2.011971±0.000003

a) Mole fraction of water.
b) Determined by using an alkaline aqueous solution of potassium peroxylamine disulfonate as a reference, g factor of which is assumed to be 2.005590.

with the increase in N_W.

The experimental values of the g factors of tetrachloro-p-benzosemiquinone (II), tetrabromo-p-benzosemiquinone (III), and tetraiodo-p-benzosemiquinone (IV) are summarized in Tables 2, 3, and 4 respectively. Since tetrahalogenated derivatives of p-benzoquinone do not dissolve in water, the g factors of semiquinones derived from these quinones can not be obtained for high values of N_W.

Shifts of the g Factors of p-Benzosemiquinone and Its Tetrahalogenated Derivatives. Figure 1 shows plots of the g factors of p-benzosemiquinone and its tetrahalogenated derivatives against N_W. As N_W increases, the g factor of I decreases, and that of II scarcely changes, while that of III increases and the g factor of IV increases even more steeply than that of III.

According to Stone's equation for the g factor of a polyatomic radical,[9] the g factors of these semiquinones can be approximately given as:[13]

$$g \simeq 2.00232 + 2\Delta g_O + 4\Delta g_X \qquad (1)[14]$$

$$\Delta g_O = \frac{a\zeta_O C_{O\sigma}^2 \rho_O^{\pi}}{\Delta E_O} \qquad (2)$$

$$\Delta g_X = \frac{b\zeta_X C_{X\sigma}^2 \rho_X^{\pi}}{\Delta E_X} \qquad (3)$$

where a and b are positive constants; ζ_O and ζ_X are the L–S coupling constants about oxygen and halogen nuclei; $C_{O\sigma}^2$ or $C_{X\sigma}^2$ implies the square of the coefficient of the p_σ atomic orbitals of oxygen or halogen in lone-pair orbitals on it, and ρ_O^{π} and ρ_X^{π} denote the odd-electron density on the oxygen and on the halogen atoms respectively. ΔE_O or ΔE_X is the energy for a transition of a lone pair electron localized on oxygen or halogen atoms to the odd electron π orbital, respectively.

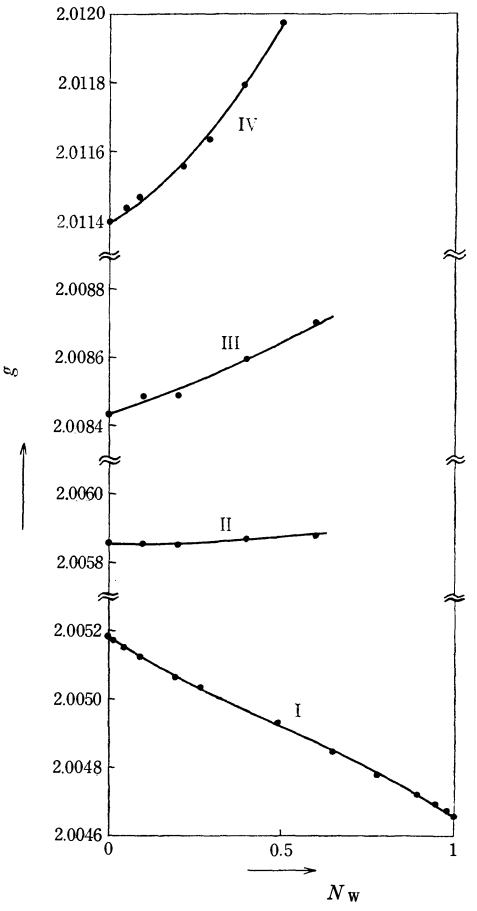

Fig. 1. Observed g factors of p-benzosemiquinone (I), tetrachloro-p-benzosemiquinone (II), tetrabromo-p-benzosemiquinone (III), and tetraiodo-p-benzosemiquinone (IV) *vs.* mole fraction of water in solution of DMSO-water.
The curve for I expresses calculated behavior (See text).

Δg_X and Δg_O then, indicate the contributions of lone parirs on oxygen and halogen respectively to the g factor. The L–S coupling constants of oxygen and halogen are greater than that of carbon (ζ_C=28 cm^{-1}, ζ_O=152 cm^{-1} ζ_{Cl}=587 cm^{-1}, ζ_{Br}=2460 cm^{-1}, ζ_I=5060 cm^{-1}),[15] and the σ-π* and π-σ* transition energies are greater than ΔE_O and ΔE_X; hence, the other terms contribute only a little to the g factors of semiquinones and are neglected in this discussion. Changes in the electronic structure and a resulting shift in the g factor, accompanied by a change in the solvent from DMSO to water, are denoted by δ. For example, when g is the g factor in DMSO, $g+\delta g$ is that in water.

13) See also H. M. McConnell and R. E. Robertson, *J. Phys. Chem.*, **61**, 1018 (1957).
14) In the case of p-benzosemiquinone, the last term in Eq. (1) should be ignored.
15) D. S. McClure, *J. Chem. Phys.*, **17**, 905 (1949).

We assume that semiquinones in water form a hydrogen bond between their lone pairs on the oxygen atom and the solvent molecule, but not between their halogen atoms and the water molecule. Hydrogen-bond formation to the oxygen atom in a carbonyl group affects the odd-electron distribution through increasing the effective electronegativity of oxygen, while it decreases the odd-electron density on oxygen and increases that on halogen.

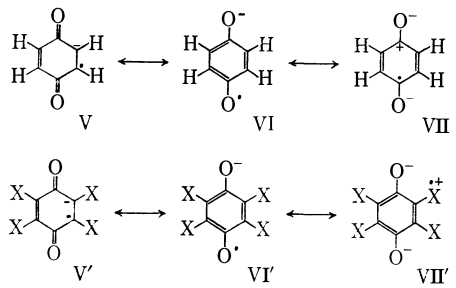

(X: halogen) (4)

When the effective electronegativity of oxygen increases, the weight of the structure VII or VII′ can be expected to increase in resonance (4). Therefore, as to the changes in ρ_0^{π} and ρ_X^{π},

$$\delta\rho_0^{\pi} < 0 \tag{5}$$

$$\delta\rho_X^{\pi} > 0 \tag{6}$$

are expected. Broze, Luz, and Silver[16] have reported that the absolute values of the oxygen-17 hyperfine coupling constants of p-benzosemiquinone and tetrachloro-p-benzosemiquinone in aprotic solvents are larger than those in protic solvents. These results also confirm the inequality (5).

A hydrogen-bond formation changes ΔE_0 and $\Delta C_{0\sigma}^2$ thus:

$$\delta\Delta E_0 > 0 \tag{7}$$

$$\delta C_{0\sigma}^2 < 0, \tag{8}$$

these phenomena are known as the blue-shift of the n–π^* transition and the delocalization of lone-pair electrons onto hydrogen respectively.[17] By comparing Eqs. (2) and (3) and the inequalities, (5)—(8), we obtain:

$$\delta\Delta g_0 < 0 \tag{9}$$

$$\delta\Delta g_X > 0. \tag{10}$$

Since the L–S coupling constants of halogens decrease in the following order:

$$\zeta_{Cl} < \zeta_{Br} < \zeta_I, \tag{11}$$

we may expect:

$$0 < \delta\Delta g_{Cl} < \delta\Delta g_{Br} < \delta\Delta g_I.$$

The discussion above can explain the interesting feature shown in Fig. 1, since:

$$\delta g_I = 2\delta g_0 < 0$$

$$\delta g_{II} = 2\delta g_0 + 4\delta\Delta g_{Cl} \simeq 0$$

$$\delta g_{III} = 2\delta\Delta g_0 + 4\delta\Delta g_{Br} > 0$$

$$\delta g_{IV} = 2\delta\Delta g_0 + 4\delta\Delta g_I > \delta g_{III}.$$

Analysis of the Dependence of the g Factor of p-Benzosemiquinone on N_W. Gendell, Freed, and Fraenkel[4] assume that the electronic structure of a radical is affected by radical-solvent complexing, and that each type of complex is characterize by a unique value of the coupling constant, a. The formation and decomposition of complexes is so rapid in our case, however, that only a single averaged coupling constant, $\bar{a}$, is observed, *i. e.*:

$$\bar{a} = \sum_i p_i a_i \quad (\text{with } \sum_i p_i = 1) \tag{12}$$

where a_i is the coupling constant characteristic of the ith solvent-radical complex, with represents a fraction, p_i, of the total concentration of the radical. The p_i can be evaluated in terms of a series of solvent-radical association equilibria. Although the GFF theory has been proposed in accounting for solvent effects on the coupling constant, this theory is also applicable at discussion of solvent effects on the g factor, for

$$\bar{g} = \sum_i g_i p_i, \tag{13}$$

where $\bar{g}$ is an observed g factor, g_i denotes the g factor of the ith complex, and p_i has the same meaning as in Eq. (12).

Stone and Maki[5] studied the ^{13}C coupling constant of p-benzosemiquinone-1-^{13}C in a DMSO-water mixed solvent and explained their data quantitatively by assuming three types of solvated species, DRD, WRD, and WRW, where R is the radical anion, D is a DMSO molecule, and W is a water molecule. Their model for solvated complexes assumes that two solvent molecules solvate to one semiquinone molecule; it is referred to as the 2-site model in this work. We used this model in discussing solvent effects on the g factor of p-benzosemiquinone. We also analyzed the present data with the 4-site model. This model assumes that 4 solvent molecules solvate to one semiquinone molecule.

2-Sitie Model. The equilibria proposed by Stone and Maki[5] are:

$$\text{DRD} + \text{W} \overset{K_1}{\rightleftarrows} \text{DRW (and WRD)} + \text{D}$$

$$\text{DRW} \overset{K_3}{\rightleftarrows} \text{WRD}$$

$$\text{W} + \text{DRW (and WRD)} \overset{K_2}{\rightleftarrows} \text{WRW} + \text{D}. \tag{14}$$

They assumed, in the complex formation, that one carbonyl group of the radical has one site occupied by a solvent molecule and that the electronic state of the radical is perturbed. In Eq. (14), DRW

16) M. Broze, Z. Luz and B. L. Silver, *J. Chem. Phys.*, **46**, 4891 (1967).

17) G. C. Pimentel and A. L. McClellan, "The Hydrogen Bond," Freeman Co., San Francisco (1960).

or WRD refers to a complex in which the water molecule is complexed with one carbonyl or with the other carbonyl respectively, and it is assumed that $K_3=1$. When the equilibria in (14) are assumed to explain the solvent effects on the g factor of p-benzosemiquinone, the g factor is given by:

$$\bar{g}=\frac{g_1+K_1g_2S+K_1K_2g_3S^2}{1+K_1S+K_1K_2S^2} \tag{15}$$

where $S=[W]/[D]$ is the ratio of the mole fraction of water and DMSO. The notations, g_1, g_2, and g_3, are the g factors of DRD, of the average of DRW and WRD, and of WRW respectively.

If these radical-solvent complexes are assumed, g_2 becomes

$$g_2=(g_1+g_3)/2$$

and Eq. (15) simplifies to:

$$\bar{g}=\frac{g_1(2+K_1S)+g_3(K_1S+2K_1K_2S^2)}{2(1+K_1S+K_1K_2S)} \tag{16}$$

Since we have taken three types of equilibria (14) into consideration, g_1 and g_3 may be interpreted as the experimental g factors in nonaqueous DMSO and in pure water respectively.

According to Stone and Maki's treatment, an equation equivalent to Eq. (16) is given with the $Q\equiv S^{-1}$ parameter as the variable:

$$\bar{g}=\frac{g_3(2+K_2^{-1}Q)+g_1[2(K_1K_2)^{-1}Q^2+K_2^{-1}Q]}{2[1+K_2^{-1}Q+(K_1K_2)^{-1}Q^2]} \tag{17}$$

Taking the experimental values of 2.005182 and 2.004659 for g_1 and g_3 respectively, we obtain $K_1=2.6$ from the initial slope of Eq. (16):

$$\left(\frac{d\bar{g}}{dS}\right)_{S=0}=K_1(g_3-g_1)/2$$

and $K_2=0.41$ from the initial slope of Eq. (17):

$$\left(\frac{d\bar{g}}{dQ}\right)_{Q=0}=K_2^{-1}(g_1-g_3)/2.$$

By adopting the equilibrium constants thus obtained, we have plotted the g factors calculated by means of Eqs. (16) and (17) in Fig. 1, with N_W as the abscissa. The experimental plots agree with Eqs. (16) and (17) over the entire range of solvent composition.

The obtained values of the equlibrium constants of $K_1=2.6>1$ and $K_2=0.41<1$ show that the first solvation of the water molecule to one carbonyl group of the semiquinone tends to occur and that the second solvation of the water molecule to the other carbonyl group of the radical is, rather, prevented. The distance between the two carbonyl oxygen atoms is 5.4 Å.[18] The interaction of the hydrogen bond is a rather localized one. Therefore, the results of $K_1>1$ and $K_2<1$ obtained with Stone and Maki's 2-site model of solvent-radical complexing seems somewhat unreasonable.

4-Site Model. Senti and Harker[19] and Pasternak[20] showed that, in a crystal of acetoamide or succinamide, two N–H hydrogen atoms interact with one carbonyl oxygen atom to form a planar hydrogen-bond structure. On the basis of the infrared spectroscopic study of a hydrogen-bond formation between p-benzoquinone and phenol in a carbon tetrachloride solution, Fritzsche[21] reported that each carbonyl group of p-benzoquinone has two sites occupied by a phenol molecule forming a hydrogen-bond between its OH hydrogen and the lone-pair electrons of the quinone.

On the basis of these experimental observations, we attempted to analyze solvent effects on the g factor of p-benzosemiquinone with a model (4-site model) in which each carbonyl group has two sites which the solvent molecule occupies, thus shifting the g factor of the radical dominantly. The postulated equilibria are:

$$\begin{aligned}
&\text{DDRDD} + \text{W} \overset{K_1'}{\rightleftharpoons} \text{WDRDD (DWRDD, DDRWD, and DDRDW)} + \text{D}\\
&\text{DWRDD (WDRDD, DDRWD, and DDRDW)} + \text{W} \overset{K_2'}{\rightleftharpoons} \text{WWRDD (and DDRWW)} + \text{D}\\
&\text{DWRDD (WDRDD, DDRWD, and DDRDW)} + \text{W} \overset{K_1'}{\rightleftharpoons} \text{DWRDW (DWRWD, WDRDW, and WDRWD)} + \text{D}\\
&\text{WWRDD (and DDRWW)} + \text{W} \overset{K_1'}{\rightleftharpoons} \text{WWRWD (WWRDW, DWRWW, and WDRWW)} + \text{D}\\
&\text{DWRDW (WDRDW, DWRWD, and WDRWD)} + \text{W} \overset{K_2'}{\rightleftharpoons} \text{WWRDW (WWRWD, DWRWW, and WDRWW)} + \text{D}\\
&\text{WWRWD (WWRDW, DWRWW, and WDRWW)} + \text{W} \overset{K_2'}{\rightleftharpoons} \text{WWRWW} + \text{D},
\end{aligned} \tag{17}$$

where WWRWD refers to the complex in which two water molecules solvate to one carbonyl group and in which the other carbonyl group interacts with one water molecule and one DMSO molecule. It is assumed that solvent molecules complexed with one carbonyl group do not affect the equilibrium constants concerned in the solvation of the other carbonyl, and that the number of solvated water molecules determines the g factor of the com-

18) S. M. Swingle, *J. Amer. Chem. Soc.*, **76**, 1409 (1954).

19) F. Senti and D. Harker, *ibid.*, **62**, 2008 (1940).

20) R. A. Pasternak, *Acta Cryst.*, **6**, 808 (1953).

21) H. Fritzsche, *Z. Phys. Chem. Neue Folge*, **43**, 154 (1964).

plex and is proportional to the shift of the g factor; for example,

$$g_{WWRDD} = g_{WDRWD} = g_{DDRDD} + \frac{1}{2}(g_{WWRWW} - g_{DDRDD}).$$

g_{WWRWW} and g_{DDRDD} may be interpreted as the experimental g factors in pure water, g_W, and in nonaqueous DMSO, g_D, respectively.

On the assumptions stated above, the (17) equilibria and Eq. (13) give, as the g factor in the mixed solvent:

$$\bar{g} = g_D + \frac{K_1'K_2'S^2 + K_1'S}{K_1'K_2'S^2 + 2K_1'S + 1}(g_W - g_D). \qquad (18)$$

Eq. (18) coincides with the equation of the 2-site model, Eq. (15), when $K_1' = K_1/2$ and $K_2' = 2K_2$; that is, $K_1' = 1.3$ and $K_2' = 0.82$.

In the 4-site model, the obtained values of K_1' and K_2' are reasonable. $K_2' < 1$ shows that the second solvation of the water molecule, forming a hydrogen bond between an oxygen atom of a carbonyl group and a hydrogen atom of water, is hindered by the water molecule which has solvated to the same oxygen atom.

Stone and Maki's[5] data on the solvent effects on ^{13}C coupling constants can be interpreted by means of the 4-site model as well as by means of their 2-site model. They reported that the solvation to the nonlabeled carbonyl group scarcely changes the odd-electron distribution near the labeled carbonyl of *p*-benzosemiquinone-1-^{13}C (see Eq. (5) of Ref. 5). Therefore, their a_1 value, the ^{13}C coupling constant in DMSO, may be regarded as the constants of the DDRSS complexes; their a_3 value, the ^{13}C coupling constant in water, as those of the WWRSS complexes, and their a_2 value, as those of the DWRSS and WDRSS complexes, where S denote D or W. In the complex representation above, the two prefixed letters refer to the solvent molecules solvated to the labeled carbonyl. With the approximations above, the equation derived from the 4-site model coincides with the 2-site model equation of solvent effects on the ^{13}C coupling constant.

Both Stone and Maki's 2-site model and the present 4-site model can interpret solvent effects on the g factor as well as on the ^{13}C coupling constant of *p*-benzosemiquinone. Although the 4-site model may be preferred on the basis of the physical meaning of the obtained values of K_2 and K_2', which are smaller than 1, neither the present experimental data on solvent effects on the g factor nor Stone and Maki's study of the ^{13}C coupling constant can experimentally confirm which model is more adequate.

The further study of such things as solvent effects on the ESR parameters of 2,6-di-*t*-butyl-*p*-benzosemiquinone and 2,5-di-*t*-butyl-*p*-benzosemiquinone seems to be desirable in order to ascertain how many water molecules, one or two, can solvate to one carbonyl oxygen atom forming hydrogen-bond in solution.

BULLETIN OF THE CHEMICAL SOCIETY OF JAPAN VOL. 43 1027—1032 (1970)

A One-dimensional Model of a Conduction Calorimeter*1

Masaru HATTORI

Department of Machine Engineering, Tokyo Institute of Technology, Ookayama, Meguro-ku, Tokyo

and Satohiro TANAKA and Kazuo AMAYA

Government Chemical Industrial Research Institute, Tokyo, Shibuya-ku, Tokyo

(Received October 17, 1969)

An idealized one-dimensional model of a conduction calorimeter, composed of a container in which thermal change occurs, a thermal bath, and a solid thermal conductor connecting the container with the thermal bath, is presented. The boundary-value problem of heat conduction in the model calorimeter is solved by the Laplace transformation method. A proportionality relation between the quantity of heat evolved in the calorimeter container and the area enclosed by the recorded temperature curve and the time axis is established.

The quantity of heat given off in a reaction or process can be determined by various types of calorimeters.[1-3] One of these types consists of

*1 Any communications concerning this work should be sent to Mr. Tanaka.

1) "Experimental Thermochemistry," Vol. 1, ed. by F. D. Rossini, Interscience Publishers, New York, N. Y. (1956).

conduction or heat-flow calorimeters which have already found successful application in measurements of the quantity of heat and in studies of thermokinetics.[4-14]

A calorimeter consists essentially of a container in which the thermal phenomena under investigation are carried out and studied. In general, this container is placed in a cavity the walls of which are kept at a constant temperature (a "constant temperature environment" calorimeter) or, alternatively, at a temperature which can be varied at will (an "adiabatic" calorimeter). Calvet and Prat refer to the walls of the calorimeter container as the "internal boundary," and to the walls of the surrounding cavity as the "external boundary.[7]"

In the conduction calorimeter, all or nearly all of the heat evolved or absorbed in the calorimeter container is conducted to or from the surrounding "external boundary," which is kept at a constant temperature. The measurement of the quantity of heat or the study of thermokinetics depends entirely on the calculation of the heat exchange. This, in turn, depends on a knowledge of the temperatures of the calorimeter container and the surrounding external boundary at all times during the measurement and on a knowledge of the rate of heat transfer as a function of these temperatures.

In the case of processes which cause only slow variations in the temperature of the container, the simplified theory of Tian is very useful.[4,5,7] In the theory of Tian, the rate of the heat transfer, ϕ, between the calorimeter container and the surrounding external boundary is assumed to be given by Newton's cooling law; thus:

$$\phi = p(\theta_i - \theta_e) = p\theta, \tag{1}$$

where θ_i=container temperature, θ_e=external boundary temperature, $\theta=\theta_i-\theta_e$, and p=leakage modulus of the system. Let W be the calorific power developed in the container at time t. During the dt time, the quantity of heat given off is $W\mathrm{d}t$. This heat, $W\mathrm{d}t$, is in part lost from the container as a flow of heat, represented by $\phi\mathrm{d}t=p(\theta_i-\theta_e)\mathrm{d}t$; the remaining part of the $W\mathrm{d}t$ causes an increase, $\mathrm{d}\theta$, in the container temperature (assuming that the temperature, θ_e, is basically constant). If the thermal capacity of the container is μ, the container heating consumes power by $\mu\mathrm{d}\theta$. Hence, it follows that:

$$\begin{aligned} W\mathrm{d}t &= p(\theta_i-\theta_e)\mathrm{d}t + \mu\mathrm{d}\theta \\ &= p\theta\mathrm{d}t + \mu\mathrm{d}\theta \end{aligned} \tag{2}$$

or that:

$$W = p\theta + \mu\frac{\mathrm{d}\theta}{\mathrm{d}t}\ , \tag{3}$$

(the later is called "Tian's equation").

The finite quantity of heat, $Q=\int W(t)\mathrm{d}t$, produced in the time interval, $[0,\infty)$, is obtained from Eq. (2) by integration:

$$Q = \int_0^\infty W\mathrm{d}t = p\int_0^\infty \theta\mathrm{d}t + \mu(\theta_\infty-\theta_0), \tag{4}$$

where $\theta=\theta_0$ at $t=0$ and $\theta=\theta_\infty$ at $t=\infty$. In an experiment, it is possible to make $\theta_0=\theta_\infty$. Therefore, a very simple relation

$$Q = p\int_0^\infty \theta dt = pA \tag{5}$$

can be obtained. The integral, $\int_0^\infty \theta\mathrm{d}t$, is equal to the area, A, under the recorded curve and the time-axis over the interval $[0,\infty)$. The expression (5) relates the heat of the reaction of the sample to the area of the recorded curve through the use of the proportionality constant, p, which is independent of the heat capacity of the sample. This expression is perhaps one of the most simple, useful and, fundamental theorems in calorimetry by means of the conduction method.

The above expressions by Tian are, however, only approximate relationships. One of the inherent limitations of Tian's theory is the assumption that the rate of heat transfer between the container and the external boundary is given by Newton's cooling law (1). Newton's law of cooling has been proposed for the transfer of heat from the surface of a solid to a fluid flowing past; in fact, the expression is a rather approximate one, and the coefficient, p, in (1) depends not only on the fluid but on the temperature differences $(\theta_i-\theta_e)$.[15,16] This limitation is considered to be very important

2) "Experimental Thermochemistry," Vol. 2, ed. by H. A. Skinner, Interscience Publishers, New York, N. Y. (1962).
3) R. C. Wilhoit, *J. Chem. Educ.*, **44**, A571 (1967).
4) E. Calvet, "Experimental Thermochemistry," Vol. 1, Chap. 12, ed. by F. D. Rossini, Interscience Publishers, New York, N. Y. (1956).
5) E. Calvet, *ibid.*, Vol. 2, Chap. 17, ed. by H. A. Skinner, Interscience Publishers, New York, N. Y. (1962).
6) H. Prat, *ibid.*, Chap. 18.
7) E. Calvet and H. Prat, "Recent Progress in Microcalorimetry," ed. and translated by H. A. Skinner, Pergamon Press, London (1963).
8) K. Amaya and S. Hagiwara, Preprints for the 1st Japanese Calorimetry Conference, 2 (1965), Osaka.
9) K. Amaya, S. Hagiwara and S. Takagi, Preprint for the 2nd Japanese Calorimetry Conference, 1—8 (1966), Tokyo.
10) K. Amaya and S. Hagiwara, *ibid.*, 1—9 (1966).
11) K. Amaya, S. Hagiwara and M. Uetake, Preprint of the 3rd Japanese Calorimetry Conference, B210 (1967), Osaka.
12) K. Amaya, S. Hagiwara and J. Suzuki, Preprint of the 4th Japanese Calorimetry Conference, 14Ba5 (1968), Tokyo.
13) K. Amaya, *Kogyo Kagaku Zasshi*, **69**, 1571 (1966).
14) K. Amaya, *Bunseki Kiki*, **5**, No. 5, Sangyo Kaihatsu Co. (1967), p. 6.
15) W. H. McAdams, "Heat Transmission," McGraw-Hill, New York (1942), p. 3.
16) U. Grigull, "Die Grundgesetze der Warmeubertragung," Springer-Verlag, Berlin (1961), §8.5.1.

when the heat flow from or to the container is conducted by a solid thermal conductor and when the thermal process is rapid one. In actuality, nearly all of the heat flux is conducted away by the thermocouple wires (Tian-Calvet calorimeter)[4,7] or by the thermoelement (Amaya-Hagiwara calorimeter).[8-12]

Calvet has developed a theory of a more general form applicable to the study of a rapid process.[5,7] He has proposed the expression:

$$\theta = a_1\int_0^t W(u)e^{-\omega_1(t-u)}du + a_2\int_0^t W(u)e^{-\omega_2(t-u)}du + \cdots \tag{6}$$

for the temperature of the calorimeter container, θ, where $W(t)$ is the calorific power produced in the container as a function of the time t and where the heating time extends from $u=0$ to $u=t$. The coefficients, a_1, a_2, $\cdots$ and ω_1, ω_2, $\cdots$, are constants of the calorimeter for a given arrangement. However, the model on which his theory is based and the mechanism of the heat transfer are both obscure; therefore, the parameters, a_1, a_2, $\cdots$ and ω_1, ω_2, $\cdots$, must be determined from a calibration experiment and cannot be evaluated *a priori* before the construction of the calorimeter.

It is, then, necessary to develop a definite model of the calorimeter considering a distinct mechanism of heat transfer.

An Idealized One-dimensional Model of a Conduction Calorimeter

In the actual case of a conduction calorimeter, a heat flux from or to the container is conducted in part by conduction and in part by convection and radiation through the space formed by the internal and external boundaries of the calorimeter. To obtain a precise theory, it is necessary to consider all these processes. However, it is so difficult to take into account all the mechanism of the heat transfer and the complex shape of the boundaries of a calorimeter that the calculation must start from a simplified model. As a first step, an idealized one-dimensional model, in which heat transfer by only conduction is considered, can be adopted; it may be a fairly good approximation for a calorimeter in which a considerable amount of the heat flux is conducted by such solid thermal conductors, as thermocouple wires (Tian-Calvet's calorimeter) or a thermoelement (Amaya-Hagiwara's calorimeter).

Figure 1 illustrates a one-dimensional model

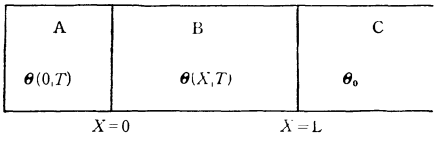

Fig. 1. A one-dimensional model of conduction calorimeter.

of a conduction calorimeter with a container, A, a solid thermal conductor, B, and a thermal bath, C, kept at a constant temperature. The following assumptions are adopted:

1) Calorific power, $W(T)$, is developed in the container at time T, and the temperature of the container is uniform. Let C_0 be the thermal capacity of the container.

2) The solid thermal conductor is a bar with its lateral surface insulated against the flow of heat; the area of its cross section is S, and its ends are $X=0$ and $X=L$. Let $\Theta(X,T)$ denote the temperature at any point in the thermal conductor, and K, the thermal diffusivity of the material.

3) The container is in perfect thermal contact with the $X=0$ side face of the thermal conductor. Heat transfer from or to the container takes place only through the $X=0$ side face of the conductor according to the basic postulate for the conduction of heat in solids, so the quantity of heat per unit of time transferred across the $X=0$ face is given by:

$$-\Lambda S\left(\frac{\delta\Theta}{\delta X}\right)_{X=0},$$

where Λ is the thermal conductivity of the conductor.

4) The thermal bath kept at a constant temperature, Θ_0, is in perfect thermal contact with the $X=L$ side face of the thermal conductor, so that:

$$\Theta_{X=L} = \Theta_0.$$

5) The initial temperature of the calorimeter, $\theta_{T=0}$, is Θ_0 throughout the container, the conductor, and the thermal bath.

6) The C_0, K, and Λ quantities are always constant while the thermal change in the container is taking place. The boundary-value problem for this calorimeter is then:

$$\frac{\partial\Theta}{\partial T} = K\frac{\partial^2\Theta}{\partial X^2} \qquad (0<X<L,\ T>0), \tag{7}$$

$$W(T) = C_0\left(\frac{\partial\Theta}{\partial T}\right)_{X=0} - \Lambda S\left(\frac{\partial\Theta}{\partial X}\right)_{X=0} \tag{8}$$

$$\Theta_{X=L}=\Theta_0, \tag{9}$$

$$\Theta = \Theta_0 \qquad (T\leqq 0). \tag{10}$$

It is convenient to introduce the following dimensionless reduced variables and quantities for the universal forms of the solution of the problem:

$$\left.\begin{aligned} x &= \frac{X}{L} \\ t &= \frac{K}{L^2}T \\ \theta(x,t) &= \frac{\Theta(X,T)-\Theta_0}{\Theta_0} \\ w(t) &= \frac{L^2}{KC_0\Theta_0}W(T) \\ h &= \frac{L\Lambda S}{KC_0}. \end{aligned}\right\} \tag{11}$$

The boundary-value preblem can, then, be written;

$$\frac{\partial\theta}{\partial t} = \frac{\partial^2\theta}{\partial x^2} \qquad (0<x<1,\ t>0) \tag{12}$$

$$w(t) = \left(\frac{\partial\theta}{\partial t}\right)_{X=0} - h\left(\frac{\partial\theta}{\partial x}\right)_{X=0} \tag{13}$$

$$\theta = 0,\ x = 1 \tag{14}$$

$$\theta = 0,\ t = 0. \tag{15}$$

Solution of the Boundary-value Problem by the Laplace Transformation Method[17,18]

Let $\bar{\theta}(x,s)$ be the Laplace transform of $\theta(x,t)$;

$$\bar{\theta}(x,s) = \int_0^\infty e^{-st}\theta(x,t)dt, \quad \mathrm{Re}\{s\}>0.$$

If the Laplace transformation is applied to (12), the transformed equation is:

$$\int_0^\infty e^{-st}\frac{\partial\theta}{\partial t}\,dt = \int_0^\infty e^{-st}\frac{\partial^2\theta}{\partial x^2}\,dt. \tag{16}$$

This becomes, in view of the initial condition (15), and by a formal integration by parts:[19]

$$s\bar{\theta}(x,s) = \frac{d^2}{dx^2}\bar{\theta}(x,s). \tag{17}$$

The boundary conditions, (13) and (14), treated in the same way, give:

$$\bar{w}(s) = s\bar{\theta}(0,s) - h\frac{d}{dx}\bar{\theta}(0,s), \tag{18}$$

$$\bar{\theta}(1,s) = 0, \tag{19}$$

where $\bar{w}(s)$ is the Laplace transform of $w(t)$.

A convenient form of the general solution of Equation (17) is:

$$\bar{\theta}(x,s) = Ae^{\sqrt{s}x} + Be^{-\sqrt{s}x}, \tag{20}$$

where A and B may be functions of s. When this equation is substituted into Eqs. (18) and (19), these equations become:

$$\bar{w}(s) = A(s-\sqrt{s}) + B(s+\sqrt{s}), \tag{21}$$

$$Ae^{\sqrt{s}} + Be^{-\sqrt{s}} = 0. \tag{22}$$

From (21) and (22), the values of A and B are found to be:

$$A = \bar{w}(s)\frac{e^{\sqrt{s}}}{(s-h\sqrt{s})e^{-\sqrt{s}} - (s+h\sqrt{s})e^{\sqrt{s}}}, \tag{23}$$

$$B = -\bar{w}(s)\frac{e^{\sqrt{s}}}{(s-h\sqrt{s})e^{-\sqrt{s}} - (s+h\sqrt{s})e^{\sqrt{s}}}. \tag{24}$$

When these values are substituted into (20), Eq. (20) can be written as:

$$\bar{\theta}(x,s) = \bar{w}(s)\frac{\sinh\sqrt{s}(1-x)}{\sqrt{s}(\sqrt{s}\sinh\sqrt{s}+h\cosh\sqrt{s})} = \bar{w}(s)\bar{f}(s), \tag{25}$$

where:

$$\bar{f}(s) = \frac{\sinh\sqrt{s}(1-x)}{\sqrt{s}(\sqrt{s}\sinh\sqrt{s}+h\cosh\sqrt{s})}. \tag{26}$$

Now the inverse transform of the $\bar{\theta}(x,s)=\bar{w}(s)\bar{f}(s)$ gives $\theta(x,t)$ as the convolution[20] of the $w(t)$ and $f(t)$ functions:

$$\theta(x,t) = \int_0^t w(\tau)f(t-\tau)d\tau. \tag{27}$$

The $f(t)$ function is the inverse transform of $\bar{f}(s)$ and is given by the use of the Inverse Theorem for the Laplace transformation.[21]
This states that:

$$f(t) = \frac{1}{2\pi i}\lim_{\beta\to 0}\int_{\gamma-i\beta}^{\gamma+i\beta} e^{zt}\bar{f}(z)dz = \sum_{n=1}^{\infty}\rho_n(t), \tag{28}$$

where:

$\rho_n(t)$ = the residue of $e^{zt}\bar{f}(z)$ at $z=s_n$

and where:

$z = s_n$ = the singular point of $\bar{f}(z)$.

The singular points $\bar{f}(z)$are:

$$z = 0 \tag{29}$$

and the roots of the equation are:

$$\sqrt{s}\sinh\sqrt{s} + h\cosh\sqrt{s} = 0. \tag{30}$$

The roots of Eq. (30) are given by[22]:

$$s = -\alpha_n^2, \tag{31}$$

where α_n are the positive roots of the equation:

$$\alpha\sin\alpha - h\cos\alpha = 0. \tag{32}$$

The residue for the singular point, $z=0$, is given by:

$$\lim_{s\to 0} s\bar{f}(x,s)e^{st} = 0, \tag{33}$$

while the residues, ρ_n, for the singular points, $z=-\alpha_n$ are given by:[21]

$$\begin{aligned}\rho_n(t) &= \lim_{s\to-\alpha_n^2}(s+\alpha_n^2)\bar{f}(x,s)e^{st}\\ &= \left[\frac{\sinh\sqrt{s}(1-x)}{\frac{d}{ds}\sqrt{s}(\sqrt{s}\sinh\sqrt{s}+h\cosh\sqrt{s})}e^{st}\right]_{s=-\alpha_n^2}\\ &= \frac{2\sin\alpha_n(1-x)}{(1+h+\frac{\alpha_n^2}{h})\sin\alpha_n}e^{-\alpha^2 nt}.\end{aligned} \tag{34}$$

Thus, from (27), (28), (33) and (34), the expression for $\theta(x,t)$ can be obtained as:

17) H. S. Carlslaw and J. C. Jager, "Conduction of Heat in Solids," 2nd Ed., Oxford (1959), Chap. XII.
18) R. V. Churchill, "Operational Mathematics," 2nd Ed., McGraw-Hill, New York, N. Y. (1958).
19) R. V. Churchill, *ibid.*, p. 112.
20) R. V. Churchill, *ibid.*, p. 37.
21) R. V. Churchill, *ibid.*, Chap. 6.
22) H. S. Carlslaw and J. C. Jager, *ibid.*, p. 119.

$$\theta(x,t)=\sum_{n=1}^{\infty}\frac{2\sin\alpha_n(1-x)}{(1+h+\frac{\alpha_n^2}{h})\sin\alpha_n}\int_0^t w(\tau)e^{-\alpha_n^2(t-\tau)}\,d\tau, \tag{35}$$

where α_n are the positive roots of the equation:

$$\alpha\sin\alpha - h\cos\alpha = 0.$$

The final result (35) thus obtained is in a form similar to that of Calvet's general expression (6). The coefficients, a_n and ω_n, in Calvet's expression correspond to those in (35) as follows:

$$a_n \sim \frac{2\sin\alpha_n(1-x)}{(1+h+\frac{\alpha_n^2}{h})\sin\alpha_n}$$

$$\omega_n \sim \alpha_n^2.$$

The coefficients in (35) are physically clear and can be evaluated a priori from the materials and the dimensions of the calorimeter, while a_n and ω_n in Calvet's expression are experimental and physically obscure.

Let us now deduce a property of the series on the right hand of (35), which can be useful in proving the proportionality relation (5). When the quantity $w(t)$ is constant and equals w_0, the series (35) becomes:

$$\theta(x,t)=\sum_{n=1}^{\infty}\frac{2\sin\alpha_n(1-x)}{(1+h+\frac{\alpha_n^2}{h})\sin\alpha_n}\int_0^t w_0e^{-\alpha_n^2(t-\tau)}d\tau$$

$$=\sum_{n=1}^{\infty}\frac{2w_0\sin\alpha_n(1-x)}{\alpha_n^2(1+h+\frac{\alpha_n^2}{h})\sin\alpha_n}(1-e^{-\alpha_n^2t}).$$

The steady temperature, $\theta(x,\infty)$, is obtained as:

$$\theta(x,\infty)=\lim_{t\to\infty}\theta(x,t)$$

$$=\sum_{n=1}^{\infty}\frac{2w_0\sin\alpha_n(1-x)}{\alpha_n^2(1+h+\frac{\alpha_n^2}{h})\sin\alpha_n}. \tag{36}$$

On the other hand, the steady temperature, $\theta(x,\infty)$, can be easily obtained from the steady-state solution of the boundary-value problem, (12), (13), (14), and (15), as:

$$\theta(x,\infty)=w_0\frac{(1-x)}{h}. \tag{37}$$

From (36) and (37), the relation:

$$\sum_{n=1}^{\infty}\frac{2\sin\alpha_n(1-x)}{\alpha_n^2(1+h+\frac{\alpha_n^2}{h})\sin\alpha_n}=\frac{1-x}{h} \tag{38}$$

is obtained.

Proof of Proportionality Relation between the Quantity of Heat and the Integral, $\int_0^\infty\theta dt$

When the rate of heat transfer between the calorimeter container and the thermal bath is given by Newton's cooling law (1), it has easily been shown that the proportionality relation (5) between the quantity of heat, Q, and the "area", $\int_0^\infty\theta dt$, holds. On the other hand, when the container is connected with the thermal bath by a solid thermal conductor, as has been discussed above, and when the rate of heat transfer given by Fourier's Eq. (12), we cannot expect a clear answer to the question of whether the proportionality relation (5) holds or not. However, it will be proved below that the relation is also valid in this case.

The area enclosed by the recorded curve and the time axis is:

$$\int_0^\infty\theta dt=\sum_{n=1}^{\infty}\frac{2\sin\alpha_n(1-x)}{(1+h+\frac{\alpha_n^2}{h})\sin\alpha_n}\int_0^\infty\int_0^t w(\tau)e^{-\alpha_n^2(t-\tau)}d\tau dt. \tag{39}$$

By a formal integration by parts, the integral part on the right hand of (39) becomes:

$$\int_0^\infty\int_0^t w(\tau)e^{-\alpha_n^2(t-\tau)}d\tau dt$$

$$=\frac{1}{\alpha_n^2}\left\{-\lim_{t\to\infty}e^{-\alpha_n^2t}\int_0^t w(\tau)e^{-\alpha_n^2\tau}d\tau+\int_0^\infty w(t)dt\right\}. \tag{40}$$

Now, it can be shown that the first term on the right-hand side of Eq. (40) becomes zero if the total quantity of heat, either evolved or absorbed in the container, has a limited value:

$$Q=\int_0^\infty w(t)dt. \tag{41}$$

A necessary and sufficient condition[23] for the convergence of $\int_0^\infty w(\tau)d\tau$ is that, corresponding to any one positive number, ε, another positive number T should exist so that:

$$\left|\int_T^t w(\tau)d\tau\right|<\varepsilon \tag{42}$$

wherever $t>T$. Therefore,

$$\left|e^{-\alpha_n^2t}\int_0^t w(\tau)e^{\alpha_n^2\tau}d\tau\right|$$

$$=\left|e^{-\alpha_n^2t}\left\{\int_0^T w(\tau)e^{\alpha_n^2\tau}d\tau+\int_T^t w(\tau)e^{\alpha_n^2\tau}d\tau\right\}\right|$$

$$\leqq\left|e^{-\alpha_n^2t}\int_0^T w(\tau)e^{\alpha_n^2\tau}d\tau\right|+\left|e^{-\alpha_n^2t}\int_T^t w(\tau)e^{\alpha_n^2\tau}d\tau\right| \tag{43}$$

The function $e^{\alpha^2n\tau}$ is a positive increasing function and has an upper boundary., e^{α^2nt}, in the $[T,t]$ range:

$$e^{-\alpha_n^2t}\left|\int_T^t w(\tau)e^{\alpha_n^2\tau}d\tau\right|\leqq e^{-\alpha_n^2t}\left|\int_T^t w(\tau)e^{\alpha_n^2t}d\tau\right|$$

$$=e^{-\alpha_n^2t}\left|e^{\alpha_n^2t}\int_T^t w(\tau)d\tau\right|$$

$$=\left|\int_T^t w(\tau)d\tau\right|<\varepsilon.$$

23) E. T. Whittaker and G. N. Watson, "A Course of Modern Analysis," 4th Ed., Cambridge University Press (1965), p. 70.

Therefore, (43) becomes:

$$\left|e^{-\alpha_n^2 t}\int_0^t w(\tau)e^{\alpha_n^2\tau}d\tau\right| < e^{-\alpha_n^2 t}\left|\int_0^T w(\tau)e^{\alpha_n^2\tau}d\tau\right| + \varepsilon. \quad (44)$$

As $t\to\infty$, (44) becomes:

$$\lim_{t\to\infty}\left|e^{-\alpha_n^2 t}\int_0^t w(\tau)e^{\alpha_n^2\tau}d\tau\right| < \varepsilon,$$

or, by the definition of the limit,

$$\lim_{t\to\infty} e^{-\alpha_n^2 t}\int_0^t w(\tau)e^{\alpha_n^2\tau}d\tau = 0. \quad (45)$$

From (38), (39), (40), and (45), it can be shown that:

$$\int_0^\infty \theta(x,t)dt = \sum_{n=1}\frac{2\sin\alpha_n(1-x)}{\alpha_n^2(1+h+\frac{\alpha_n^2}{h})\sin\alpha_n}\int_0^\infty w(t)dt$$

$$= \frac{(1-x)}{h}\int_0^\infty w(t)dt$$

$$= \frac{(1-x)}{h}Q. \quad (46)$$

This is what we desired to prove. It can thus be concluded that the simple method of evaluating the total quantity of heat generated in a thermal process by the simple proportionality relation (5) can well be used when using a conduction calorimeter in which the heat transfer between the container and the surrounding external boundary is effected by conduction.

The authors wish to thank Mrs. K. Sasaki and Mr. I. Takeda of this Institute for their interest and discussions.

BULLETIN OF THE CHEMICAL SOCIETY OF JAPAN VOL. 43 1032—1035 (1970)

Verification of the Conduction Method in Calorimetry

Satohiro TANAKA and Kazuo AMAYA

Government Chemical Industrial Reaserch Institute, Tokyo, Shibuya-ku, Tokyo

(Received November 18, 1969)

An ideal three-dimensional model of a conduction calorimeter is presented. In the model, the heat transfer takes place only by conduction. The proportionality relation between the quantity of heat and the area enclosed by the recorded temperature curve and the time axis is proved under several sets of ideal conditions under which the proportionality relation is valid are examined, and thermal compensation is recommended for more precise measurements of heat and for convenience in obtaining thermogenesis curves.

Calorimetric studies are now made of various systems under a wide range of conditions. The wide range of systems and conditions studied in calorimetry requires a large variety of specific calorimeters and techniques. One of these calorimeters is the conduction or heat-flow calorimeter, which has been used for a long time by many investigators. The technique which the calorimeter requires may be called the "conduction method"; it has also been widely not only for static but also for dynamic calorimeters. Some popular calorimeters of this type are the Tian-Calvet calorimeter,[1] the Benzinger-Kitzinger microcalorimeter,[2] the Amaya-Hagiwara calorimeter,[3] and Ozawa's quantitative differential thermal analyzer.[4] Of these calorimeters, Ozawa's is of the dynamic type.

In the conduction method, all or nearly all of the heat evolved or absorbed in the calorimeter container is conducted to or from the jacket through the space formed by the walls of the container and the jacket. The space between the walls of the container and the jacket is sometimes called the cavity[1] or the thermal barrier.[4] The measurement of the heat depends on the calculation of the heat exchange between the container and the jacket. This depends on a knowledge of the temperatures of the jacket and the container at all times during the measurement and on a knowledge of the rate of heat transfer as a function of these temperatures. The rate of the transfer of heat from the jacket to

1) E. Calvet and H. Prat, "Recent Progress in Microcalorimetry," ed. and translated by H. A. Skinner, Pergamon Press, London (1963).

2) T. H. Benzinger and C. Kitzinger, "Microcalorimetry, New Methods and Objectives," in C. M. Herzfeld (ed.), "Temperature; Its Measurement and Control in Science and Industry," Vol. 3, Part 3, Reinhold, New York (1963).

3) K. Amaya and S. Hagiwara, Preprint for the 1st Japanese Calorimetry Conference, Vol. 2 (1965), Osaka.

4) T. Ozawa, This Bulletin, **38**, 1881 (1965).

the container, ϕ, is nearly always represented by Newton's cooling law:

$$\phi = p_c(\theta_c - \theta_j) = p\theta, \tag{1}$$

where θ_c = the temperature at a point on the outside surface of the container, θ_j = the temperature at a point on the inside surface of the jacket, $\theta = \theta_c - \theta_j$, and p = the leakage modulus of the system. If once Newton's law (1) is adopted as the expression for the rate of the heat transfer, it is easy to show that the total quantity of heat evolved or absorbed in the container, Q, is proportional to the area under the curve of the temperature difference, θ, and the time axis;[1-3]

$$Q = p\int_0^\infty \theta \mathrm{d}t, \tag{2}$$

where t = time and p = the leakage modulus of the calorimeter, independent of the heat capacity of the calorimeter container.

In the dynamic experiment of DTA, the proportionality relation (2) also holds approximately; in this case, θ denotes the temperature difference between the sample and the thermally inert reference substance rather than the difference between the container and the jacket.[5]

Although Newton's law (1) is widely used as an expression for the rate of heat transfer in a calorimeter, it is only an approximate one, since the value of the coefficient, p, depends on the temperature difference, θ, the nature of the fluids, and other factors.[6,7] In particular, when the heat flow between the container and the jacket is conducted mainly by conduction in solids, as in the case of the Amaya-Hagiwara calorimeter and Ozawa's quantitative differential thermal analyzer, we must use Fourier's law for the conduction of heat rather than Newton's law.

Hattori *et al.*[8] have presented a one-dimensional model of a conduction calorimeter, solved the boundary-value problem of the heat conduction in the model, and verified that the proportionality relation (2) is also valid in the case of heat flow conducted by conduction in solids. Ozawa[4] also solved the boundary-value problem of a cyrindrical model of the differential thermal analyzer and also concluded that the proportionality relation holds in good approximation if some devices are used to decrease the temperature gradient in the sample cell. The present work to be descrived in this paper was undertaken to see if the proportionality relation hold in a three-dimensional model of a conduction calorimeter and to investigate the foundation of the conduction method in calorimetry.

An Idealized Three-dimensional Model of a Conduction Calorimeter

Figure 1 illustrates an idealized three-dimensional

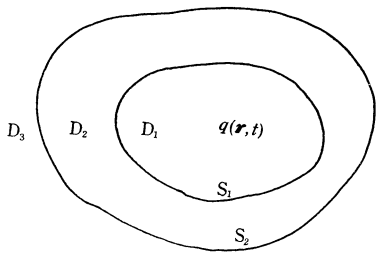

Fig. 1. Three-dimensional model of conduction calorimeter.

model of a conduction calorimeter composed of three solid domains, D_1, D_2, and D_3. The D_1 domain, in which heat is evolved or absorbed, is surrounded by the D_2 domain. The D_2 domain is surrounded by the D_3 domain, the temperature of which is kept constant. The three domains, D_1, D_2, and D_3 correspond, respectively, to the calorimeter container, the space of the solid thermal conductor between the surfaces of the container and the jacket, and the jacket.

The boundary value problem may then, in this case, be written as follows:

1. the D_1 domain:

$$c_1\rho_1\frac{\partial\theta_1}{\partial t} = \lambda_1\Delta\theta_1 + q \tag{3}$$

2. the D_2 domain:

$$c_2\rho_2\frac{\partial\theta_2}{\partial t} = \lambda_2\Delta\theta_2 \tag{4}$$

3. the D_3 domain:

$$\theta_3 = 0 \tag{5}$$

4. the S_1 boundary surface:

$$\theta_1 = \theta_2 \tag{6}$$

$$\lambda_1\frac{\partial\theta_1}{\partial n_1} = \lambda_2\frac{\partial\theta_2}{\partial n_1} \tag{7}$$

5. the S_2 boundary surface:

$$\theta_2 = \theta_3 = 0 \tag{8}$$

6. the initial conditions:

$$\theta_1 = \theta_2 = \theta_3 = 0 \qquad t \leqq 0,\ t = \infty \tag{9}$$

$$q(\boldsymbol{r}, t) = 0 \qquad t \leqq 0,\ t > t_0 \tag{10}$$

$$q(\boldsymbol{r}, t) \neq 0 \qquad 0 < t < t_0, \tag{11}$$

where:

5) W. W. Wendlandt, "Thermal Methods of Analysis," Interscience Publishers, New York (1964), p. 136.

6) U. Grigull, "Die Grundgesetze der Wärmeübertragung," Springer-Verlag, Berlin (1961), §8.5.1.

7) H. A. Skinner, "Experimental Thermochemistry," Vol. 2, Interscience Publishers, New York, (1962), p. 159.

8) M. Hattori, S. Tanaka and K. Amaya, This Bulletin, **43**, 1027 (1970).

θ = temperature measured from the temperature of D_3,
t = time,
r = coordinate vector,
q = the heat evolved or absorbed per unit of time and unit of volume in D_1.
c = the specific heat capacity,
ρ = the density,
λ = the thermal conductivity,
$\partial/\partial n_1$ = differentiation in the direction of the out-ward normal to the surface,
Δ = the Laplacian,

The subscripts, 1, 2, and 3, denote the quantity in the D_1, D_2, and D_3 domains respectively.

Treatments of the Boundary-value Problem and the Proportionality Relation

Let the volume integral extended throughout D_1 apply to (3). Equation (3) then becomes:

$$c_1\rho_1\int_{D_1}\frac{\partial\theta_1}{\partial t}\mathrm{d}v=\lambda_1\int_{D_1}\Delta\theta_1\mathrm{d}v_1+\int_{D_1}q(\boldsymbol{r},t)\mathrm{d}v,$$

where it is assumed that the values of c, ρ, and λ are constant throughout the process of the thermal change. By Green's theorem,

$$\int_{D_1}\Delta\theta_1\mathrm{d}v=\int_{S_1}\frac{\partial\theta_1}{\partial n_1}\mathrm{d}s.$$

The quantity

$$w(t)=\int_{D_1}q(\boldsymbol{r},t)\mathrm{d}v$$

denotes the quantity of heat evolved or absorbed per unit of time in the D_1 domain. Therefore,

$$c_1\rho_1\int_{D_1}\frac{\partial\theta_1}{\partial t}\mathrm{d}v=\lambda_1\int_{S_1}\frac{\partial\theta_1}{\partial n_1}\mathrm{d}s+w(t). \tag{12}$$

The integration of (12) with respect to t from zero to infinity gives:

$$c_1\rho_1\int_0^\infty\int_{D_1}\frac{\partial\theta_1}{\partial t}\mathrm{d}v\mathrm{d}t=\lambda_1\int_0^\infty\int_{S_1}\frac{\partial\theta_1}{\partial n_1}\mathrm{d}s\mathrm{d}t+\int_0^\infty w(t)\mathrm{d}t.$$

When the order of integration can be interchanged, the left-hand side of the above equation becomes:

$$\begin{aligned}c_1\rho_1\int_0^\infty\int_{D_1}\frac{\partial\theta_1}{\partial t}\mathrm{d}v\mathrm{d}t&=c_1\rho_1\int_{D_1}\mathrm{d}v\int_0^\infty\frac{\partial\theta_1}{\partial t}\mathrm{d}t\\&=c_1\rho_1\int_{D_1}\{\theta_{1,t=\infty}-\theta_{1,t=0}\}\mathrm{d}v\\&=0,\end{aligned}$$

considering the initial condition (9). The quantity

$$Q=\int_0^\infty w(t)\mathrm{d}t=\int_0^\infty\int_{D_1}q(\boldsymbol{r},t)\mathrm{d}v\mathrm{d}t$$

is the total quantity of heat evolved or absorbed in D_1. Therefore, the integration of (12) becomes:

$$0=\lambda_1\int_0^\infty\int_{S_1}\frac{\partial\theta_1}{\partial n_1}\mathrm{d}s\mathrm{d}t+Q. \tag{13}$$

By applying the same calculation to (4) in D_2 we obtain:

$$\begin{aligned}0&=\lambda_2\int_0^\infty\int_{S_1+S_2}\frac{\partial\theta_2}{\partial n}\mathrm{d}S\mathrm{d}t\\&=-\lambda_2\int_0^\infty\int_{S_1}\frac{\partial\theta_2}{\partial n_1}\mathrm{d}S\mathrm{d}t+\lambda_2\int_0^\infty\int_{S_2}\frac{\partial\theta_2}{\partial n_2}\mathrm{d}S\mathrm{d}t.\end{aligned} \tag{14}$$

From (7), (13) and (14),

$$\begin{aligned}Q&=-\lambda_1\int_0^\infty\int_{S_1}\frac{\partial\theta_1}{\partial n_1}\mathrm{d}S\mathrm{d}t\\&=-\lambda_2\int_0^\infty\int_{S_1}\frac{\partial\theta_2}{\partial n_1}\mathrm{d}S\mathrm{d}t\\&=-\lambda_2\int_0^\infty\int_{S_2}\frac{\partial\theta_2}{\partial n_2}\mathrm{d}S\mathrm{d}t.\end{aligned} \tag{15}$$

The main purpose of calorimetry is to obtain the Q quantity; Equation (13) shows that the measurement of the $\partial\theta/\partial n$ quantity over the boundary surface enables us to obtain the Q quantity. However, it is not easy to measure the $\partial\theta/\partial n$ quantity.

On the other hand, from Green's formula the temperature at a point, P, inside D_2, $\theta_2(\mathrm{P})$, is given by:

$$4\pi\theta_2(\mathrm{P})=-\int_{D_2}\frac{\Delta\theta_2}{r}\mathrm{d}v+\int_{S_1+S_2}\left\{\frac{1}{r}\frac{\partial\theta_2}{\partial n}-\theta_2\frac{\partial}{\partial n}\left(\frac{1}{r}\right)\right\}\mathrm{d}S, \tag{16}$$

where r is the distance from P to points on the boundary surfaces, S_1 and S_2. The integration of $\theta_2(\mathrm{P})$ with respect to t from zero to infinity then gives:

$$\begin{aligned}4\pi\int_0^\infty\theta_2(\mathrm{P})\mathrm{d}t=&-\int_0^\infty\int_{D_2}\frac{1}{r}\Delta\theta_2\mathrm{d}v\mathrm{d}t\\&+\int_0^\infty\int_{S_1+S_2}\left\{\frac{1}{r}\frac{\partial\theta_2}{\partial n}-\theta_2\frac{\partial}{\partial n}\left(\frac{1}{r}\right)\right\}\mathrm{d}S\mathrm{d}t.\end{aligned} \tag{17}$$

The first term on the right-hand side of Eq. (17) becomes zero, because, from (4) and (9);

$$\begin{aligned}\int_0^\infty\int_{D_2}\frac{1}{r}\Delta\theta_2\mathrm{d}v\mathrm{d}t&=\int_{D_2}\frac{\mathrm{d}v}{r}\int_0^\infty\Delta\theta_2\mathrm{d}t\\&=\int_{D_2}\frac{\mathrm{d}v}{r}\int_0^\infty\frac{c_2\rho_2}{\lambda_2}\frac{\partial\theta_2}{\partial t}\mathrm{d}t\\&=\frac{c_2\rho_2}{\lambda_2}\int_{D_2}\frac{\mathrm{d}v}{r}\{\theta_{2,t=\infty}-\theta_{2,t=0}\}\\&=0.\end{aligned}$$

Therefore, (17) becomes:

$$\begin{aligned}4\pi\int_0^\infty\theta_2(\mathrm{P})\mathrm{d}t&=\int_0^\infty\int_{S_1+S_2}\left\{\frac{1}{r}\frac{\partial\theta_2}{\partial n}-\theta_2\frac{\partial}{\partial n}\left(\frac{1}{r}\right)\right\}\mathrm{d}S\mathrm{d}t\\&=\int_0^\infty\int_{S_1}\left\{\frac{1}{r}\frac{\partial\theta_2}{\partial n}-\theta_2\frac{\partial}{\partial n}\left(\frac{1}{r}\right)\right\}\mathrm{d}S\mathrm{d}t\\&\quad+\int_0^\infty\int_{S_2}\left\{\frac{1}{r}\frac{\partial\theta_2}{\partial n}-\theta_2\frac{\partial}{\partial n}\left(\frac{1}{r}\right)\right\}\mathrm{d}S\mathrm{d}t\\&=\int_0^\infty\int_{S_1}\left\{-\frac{1}{r}\frac{\partial\theta_2}{\partial n_1}+\theta_2\frac{\partial}{\partial n_1}\left(\frac{1}{r}\right)\right\}\mathrm{d}S\mathrm{d}t\\&\quad+\int_0^\infty\int_{S_2}\frac{1}{r}\frac{\partial\theta_2}{\partial n_2}\mathrm{d}S\mathrm{d}t,\end{aligned} \tag{18}$$

considering $\theta_2=0$ on the S_2 surface, as (8) shows.

Now, if we assume that:

(1) $\partial\theta_2/\partial n_1$ and θ_2 are equal everywhere over the S_1 boundary surface and are functions of the time, t, only, and that
(2) $\partial\theta_2/\partial n_2$ is equal everywhere over the S_2 boundary surface and is a function of t, (19)

Equation (15) becomes:

$$\begin{aligned} Q &= -\lambda_1 S_1 \int_0^\infty \frac{\partial\theta_1}{\partial n_1}\mathrm{d}t \\ &= -\lambda_2 S_1 \int_0^\infty \frac{\partial\theta_2}{\partial n_1}\mathrm{d}t \\ &= -\lambda_2 S_2 \int_0^\infty \frac{\partial\theta_2}{\partial n_2}\mathrm{d}t, \end{aligned} \tag{20}$$

where S_1 and S_2 are the areas of the S_1 and S_2 surfaces respectively. Also (18) becomes, considering (20):

$$\begin{aligned} 4\pi\int_0^\infty \theta_2(\mathrm{P})\mathrm{d}t &= -\int_{S_1}\frac{\mathrm{d}S}{r}\int_0^\infty \frac{\partial\theta_2}{\partial n_1}\mathrm{d}t - \int_{S_1}\frac{\partial}{\partial n}\left(\frac{1}{r}\right)\mathrm{d}S\int_0^\infty \theta_2\mathrm{d}t \\ &\quad + \int_{S_2}\frac{\mathrm{d}S}{r}\int_0^\infty \frac{\partial\theta_2}{\partial n_1}\mathrm{d}t \\ &= \frac{Q}{\lambda_2 S_1}\int_{S_1}\frac{\mathrm{d}S}{r} - \int_{S_1}\frac{\partial}{\partial n}\left(\frac{1}{r}\right)\mathrm{d}S\int_0^\infty \theta_2\mathrm{d}t \\ &\quad - \frac{Q}{\lambda_2 S_2}\int_{S_1}\frac{\mathrm{d}S}{r} \\ &= \frac{Q}{\lambda_2}\left\{\frac{1}{S_1}\int_{S_1}\frac{\mathrm{d}S}{r} - \frac{1}{S_2}\int_{S_2}\frac{\mathrm{d}S}{r}\right\} \\ &\quad - \int_{S_1}\frac{\partial}{\partial n}\left(\frac{1}{r}\right)\mathrm{d}S\int_0^\infty \theta_2\mathrm{d}t, \end{aligned} \tag{21}$$

where the integrals, $\int_S \frac{\mathrm{d}s}{r}$ and $\int_S \frac{\partial}{\partial n}\left(\frac{1}{r}\right)\mathrm{d}S$, are not functions of t but are determined by the geometric shapes of the boundary surfaces. The boundary surfaces, which fulfill the assumptions (19), are symmetrical surfaces, for example, the surface of a sphere, a circular cylinder, or a plane.

If the P point is taken on the S_1 surface, $\theta_2(\mathrm{P})=\theta_2$, and if the S_1 and S_2 surfaces do not coincide, the rearrangement of (21) gives:

$$\begin{aligned} Q &= \frac{\lambda_2\left\{4\pi + \int_{S_1}\frac{\partial}{\partial n}\left(\frac{1}{r}\right)\mathrm{d}S\right\}}{\frac{1}{S_1}\int_{S_1}\frac{\mathrm{d}S}{r} - \frac{1}{S_2}\int_{S_2}\frac{\mathrm{d}S}{r}}\int_0^\infty \theta_2\mathrm{d}t \\ &= p\int_0^\infty \theta_2\mathrm{d}t, \end{aligned} \tag{22}$$

where the coefficient:

$$p = \frac{\lambda_2\left\{4\pi + \int_{S_1}\frac{\partial}{\partial n}\left(\frac{1}{r}\right)\mathrm{d}S\right\}}{\frac{1}{S_1}\int_{S_1}\frac{\mathrm{d}S}{r} - \frac{1}{S_2}\int_{S_2}\frac{\mathrm{d}S}{r}} \tag{22'}$$

is a constant determined only by the shape of the boundary surface of the calorimeter.

Conditions for the Reliability of the Proportionality Relation

Let us summarize the main conditions under which the proportionality relation (22) is valid and the conduction method in calorimetry is possible:

(1) The heat transfer in the calorimeter takes place by conduction.

(2) The boundary surfaces of the calorimeter should be symmetrical.

(3) The c, ρ, and λ values of the materials of which the calorimeter is constructed are constant throughout the process of the thermal change in the container.

In the case of an actual conduction calorimeter, none of these conditions are fulfilled. The heat is conducted not only by conduction but by convection and radiation. The surface of the calorimeter container and the inner surface of the jacket are not perfectly symmetrical. Moreover, the values of c, ρ, and λ sometimes change considerably during the process of a thermal change, *e. g.*, phase-change or chemical reactions.

Therefore, the proportionality relation fundamental in conduction calorimetry is only an approximate one in any actual experiment; this is thought to be one of the main causes of the accuracy being less than with an isothermal or adiabatic jacket calorimeter.

For precise heat measurement, it is necessary to compensate the heat of the process being studied.[9] Although it is difficult to achieve a precise thermal compensation, recent progress in servo mechanism and electronic devices favors a precise compensation. When the calorimeter is compensated, it then behaves essentially as an isothermal calorimeter. Since the heat compensated is equal to the rate of heat production or absorption, $w(t)$, it is not necessary to use Calvet's complex method[10] of transforming the recorded curve $\theta=\theta(t)$ into a thermogenesis curve $w=w(t)$.

The authors wish to thank to Miss K. Sasaki and Mr. I. Takeda of this Institute for their interest and discussions.

9) E. Calvet and H. Prat, "Recent Progress in Microcalorimetry," ed. and translated by H. A. Skinner, Pergamon Press, London (1963), p. 10.

10) E. Calvet, "Experimental Thermochemistry," Vol. 2, Interscience Publishers, New York, N. Y. (1962), p. 388.

BULLETIN OF THE CHEMICAL SOCIETY OF JAPAN VOL. 43 1036—1040 (1970)

The Density and Molar Volume of a Binary Liquid, B_2O_3-H_2O

Hiroshi KODAMA,*1 Toshio YOKOKAWA and Kichizo NIWA

Department of Chemistry, Faculty of Science, Hokkaido University, Sapporo

(Received October 22, 1969)

The density of the binary B_2O_3-H_2O liquid system with concentrations of from 4.9 to 83.0 mol% B_2O_3 has been measured, and the mean volume expansivity has been calculated. The molar volume and the expansivity of this system has then been compared with those of other binary borates. The experimental results suggest a change in the boron-to-oxygen coordination number between the $3B_2O_3 \cdot H_2O$ and $B_2O_3 \cdot H_2O$ compositions. The thermal expansivity of this system shows a different trend from those of alkali borate melts.

On the structure of B_2O_3 in glass and liquid states many investigations[1] have been made. While the presently-available data are insufficient for any structural conclusions to be drawn particularly for the molten state, it can be said that the oxide is formed from a random network structure constructed of planar BO_3 triangular units in the two states except for the high-temperature range, *e.g.*, the temperature range far above the liquidus. The network link is gradually disrupted by the addition of alkali oxides, alkaline earth oxides[1] and other basic oxides.[2,3] These are, therefore, called "network modifiers." The thermodynamic and kinetic properties of the binary oxidic melts change continuously with their composition. In addition to this trend, binary metal borate melts show a so-called boron anomaly, which has been interpreted in terms of the structural change from BO_3 triangular to BO_4 tetrahedral units in the network.[4-6] This change in coordination number also takes place on binary alkali germanates.[7]

As to the binary B_2O_3-H_2O system, so far the experimental investigations have been restricted to a dilute aqueous solution of boric acid, on the one hand, and to a boron trioxide melt with trace of water, on the other hand. On the basis of the experimental evidence on the latter, such as the B–OH absorption band and the dependence of the solubility of water on its partial pressure, it seems that the dissolution can be expressed by the following equation:[8]

$$\rangle B\text{–}O\text{–}B\langle + H_2O = 2\,\rangle B\text{–}O\text{–}H \qquad (1)$$

Thus, the water molecule modifies the network as do alkali metal oxides. The solubility decreases with the alkali content in the melt. In other works, water behaves as a base weaker than the alkali oxides. On the other hand, boric acid dissociates at three steps in a dilute aqueous solution, the dissociation being, respectively, promoted and inhibited by the presence of a basic and a strong acid substance.

The purpose of the present study is to make a structural examination of this binary system over the whole composition range by studying the molar-volume trend especially. The electrical conductivity of this system is now being studied.

Experimental

Materials and Reagent. Specimens with the desired compositions were prepared by mixing proper amounts of two reagents from among boric acid, metaboric acid, and boron trioxide of a guaranteed reagent grade, and distilled water. It was useful to start from combinations of H_3BO_3 and B_2O_3, and of HBO_2 and B_2O_3 corresponding to the desired composition except in the range of water content higher than 75 mol% (boric acid). The mixture was heated in a sealed Pyrex glass tube in order to make a uniform solution. The melts' compositions were determined from the quantities of chemicals employed over the H_2O and H_3BO_3 range. Otherwise, the quenched samples were analyzed by volumetric titration with NaOH in the presence of manitol.

Apparatus and Procedure. In order to cover the melt of the whole composition, the temperature had to be raised to a point where the vapor pressure was

*1 Present address: National Institute for Research in Inorganic Materials, Honkomagome 2-29, Bunkyo-ku, Tokyo.

1) See for review, J. D. MacKenzie, "Modern Aspects of the Vitreous State," Vol. 1, Butterworths, London (1960).

2) H. Kodama, Y. Kimura, T. Yokokawa and K. Niwa, This Bulletin, **42**, 681 (1969).

3) T. Maekawa, T. Yokokawa and K. Niwa, *ibid.*, **42**, 677 (1969).

4) L. Shartsis, W. Capps and S. Spinner, *J. Amer. Ceram. Soc.*, **36**, 319 (1953).

5) L. Shartsis and H. F. Shermer, *ibid.*, **37**, 544 (1954).

6) J. Krogh-Moe, *Phys. Chem. Glass*, **3**, 1 (1962).

7) E. F. Riebling, *J. Chem. Phys.*, **39**, 3022 (1963).

8) H. Franz, *J. Amer. Ceram. Soc.*, **49**, 473 (1966).

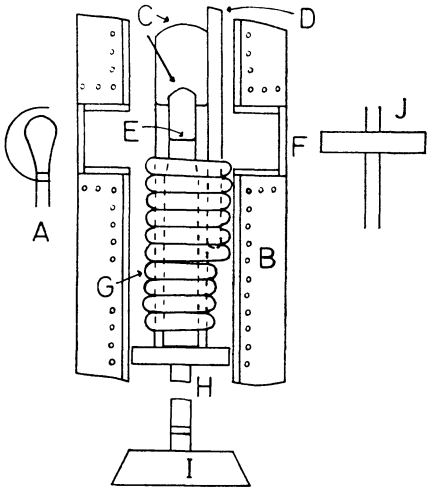

Fig. 1. Apparatus for measurement of density.
A: light source, B: electrical furnace, C: glass tube, D: thermocouple sheath, E: liquid level, F: glass window, G: cupper wire, H: alumina tube, I: lift, J: cathetometer

as high as seven atm.[9] A diagramatic sketch of the apparatus for measuring the density is given in Fig. 1. The Pyrex glass tube shown in Fig. 2 was employed as a densimeter. Figure 1 shows how it was wound with a copper wire and set at the center of an electric resistance furnace, through the windows of which the liquid level could be observed. The densimeter tube was moved up and down at the rate of 2.11 mm/min by means of a lifting device equipped with a synchronus motor. The time needed to drive the motor to reach a given liquid level gave the height. The relation between the height of the liquid column and its volume was calibrated with distilled water at room temperature.

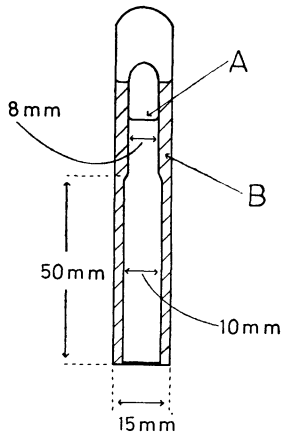

Fig. 2. Specimen cell.
A: liquid level of sample after melting.
B: octhyl alcohol or air

As is shown in Fig. 2, the densimeter was sealed in a second Pyrex tube in order to moderate the stress due to differences in pressure. Sometimes a third enclosure was employed. The measurements were carried out in the temperature range from the liquidus points to 50—150°C above them. The temperature was controlled within ±1°C. The accuracy of the measured density was found to be 99.5% by the use of distilled water at 153°C.

Results

The data on the density isotherms for the B_2O_3-H_2O system are presented in Fig. 3. They were obtained by the intra- or by the extrapolation of the density temperature relations. The densities

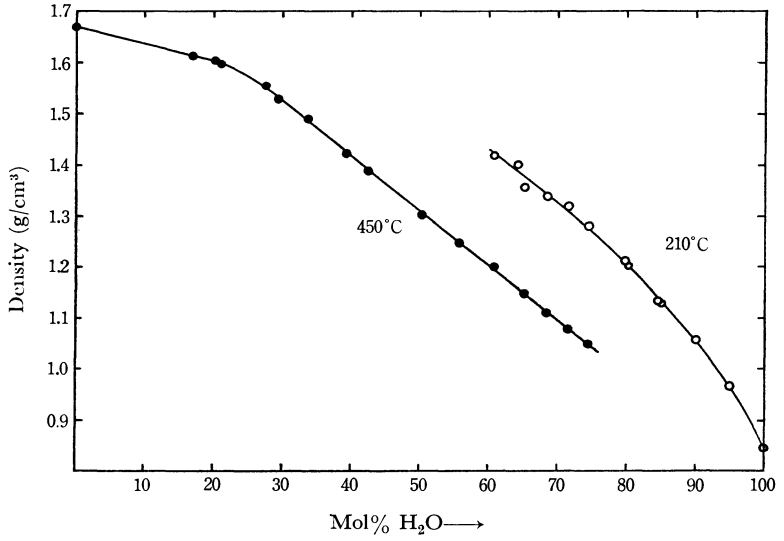

Fig. 3. Density as a function of composition at 210°C and 450°C.

9) F. C. Kracek, G. W. Morey and H. E. Merwin, *Amer. J. Sci.*, **35A**, 143 (1938).

TABLE 1. DENSITY OF B_2O_3-H_2O

450°C		210°C	
Mol% H_2O	Density (g/cm³)	Mol% H_2O	Density (g/cm³)
17.0	1.612	60.9	1.420
20.4	1.604	64.4	1.402
21.0	1.600	65.3	1.358
27.5	1.556	68.4	1.340
29.4	1.531	71.6	1.320
33.7	1.489	74.6	1.288
39.3	1.423	79.9	1.214
42.5	1.388	80.3	1.205
50.4	1.304	85.0	1.146
55.8	1.246	85.2	1.131
60.9	1.202	90.2	1.058
65.3	1.149	95.1	0.967
68.4	1.111		
71.6	1.079		
74.6	1.051		

at two temperatures are summarized in Table 1. For the density of liquid B_2O_3, numerous values have been reported.[10-13] Among them, the value of Napolitano *et al.* is quoted in Fig. 1. The density of water was quoted from "The Chemical Handbook."[14] The measurement could not be done with a B_2O_3 content of over 83.0 mol%, because of the considerable difficulty of obtaining a uniform solution due to the high viscosity. Although a small contamination from the glass tube was observed with melts of a high B_2O_3 content, the amounts of the impurity were less than 1.5 wt%, and so the effect on the density was neglected. The mean volume expansivities of the melts for the temperature range covered are shown in Fig. 4. The value for the liquid B_2O_3 was estimated for the 450—600°C temperature range from the data of Napolitano *et al.*

Discussion

Molar and Partial Molar Volume. The molar volume isotherms presented in Fig. 5 were calculated from Eq. (2).

$$MW = X_{B_2O_3} MW_{B_2O_3} + X_{H_2O} MW_{H_2O} \quad (2)$$

where X is the mole fraction of each component and where MW is the molecular weight. The molar volume is defined by:

$$V_M = MW/\rho \quad (3)$$

where ρ is the density (g/cm³). The addition of H_2O to molten B_2O_3 decreased the molar volume of this mixture below the 41.7 cm³/mol value for B_2O_3. Attention should be paid to the abrupt change in the rate of decrease in the vicinity of the $3B_2O_3 \cdot H_2O$ composition. This suggests some structural change near this composition. There are, generally

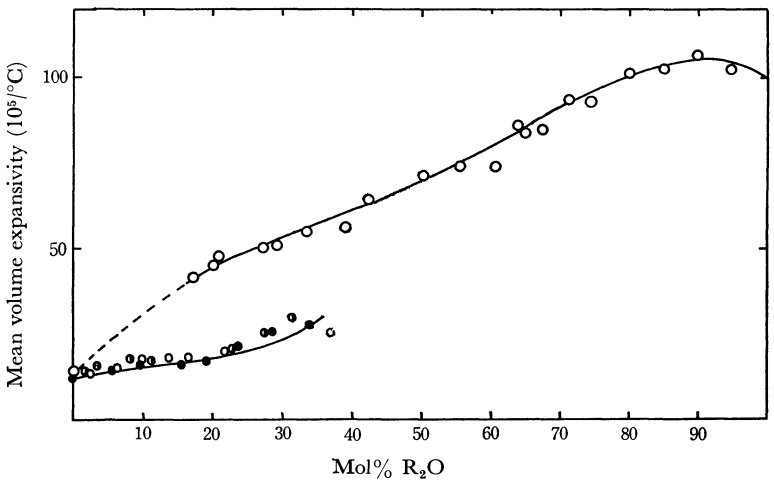

Fig. 4. Mean volume expansivity of $B_2O_3.H_2O$ and alkali borates. Values of the latter were quoted from Ref. 16.
○ $R_2O=H_2O$
◑ K_2O
● Na_2O
○ Li_2O
} at 700—1000°C

10) L. Shartsis, W. Capps and S. Spinner, *ibid.*, **36**, 35 (1953).
11) J. D. MacKenzie, *J. Phys. Chem.*, **63**, 1875 (1959).
12) Pei-Ching Li, A. C. Ghose and G. Jen Su, *J. Amer. Ceram. Soc.*, **45**, 89 (1962).
13) A. Napolitano, P. B. Macedo and E. G. Hawking, *ibid.*, **48**, 613 (1965).
14) Japan Chemical Association, "Chemical Handbood," Fundamental Volume II, Maruzen, Tokyo (1966).

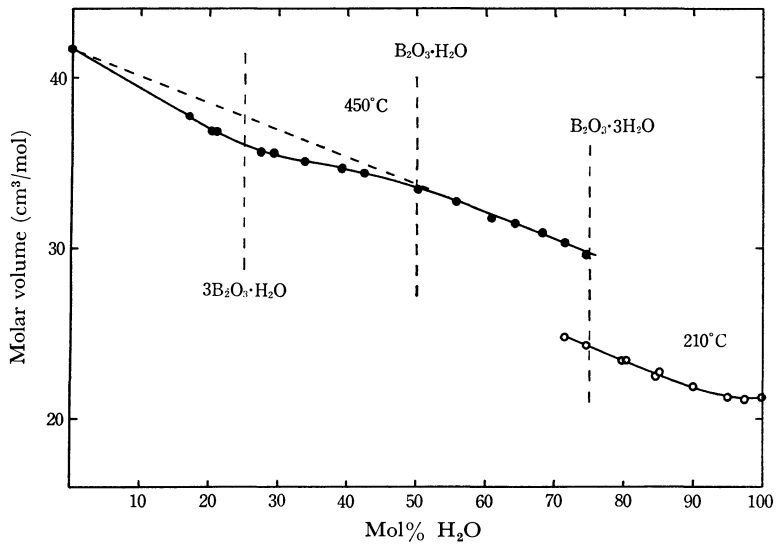

Fig. 5. Molar volume isotherms for B_2O_3-H_2O.

speaking, two types of molar volume decrease arising from the addition of another oxide to molten B_2O_3. One type is seen in the systems of borosilicate,[15] borogermanate[15] and aluminoborate,[16] in which the added oxide can be called a "network former." In these systems, the molar volume changes almost linearly with the addition of the second oxide. That is, the partial molar volume of B_2O_3 in the solution is nearly the same as that of B_2O_3. The coordination number probably remains unchanged. The other type is observed in the alkali,[10] alkaline earth borate,[5] and silver borate[17] systems, in which the decrease in the molar volume results in a convex curve downward. That is, the partial molar volume of B_2O_3 decreases rapidly below the volume of the pure B_2O_3. The latter type can be interpreted by the change in coordination from BO_3 to BO_4. In our system, the linear decrease in the molar volume over the B_2O_3·H_2O range belongs to the former type in spite of the fact that H_2O has been regarded as a network modifier. Therefore, there is no change in coordination number over that range. Milberg and Meller[18] studied the structure of vitreous B_2O_3·H_2O, glass with a composition of B_2O_3, B_2O_3·0.42 H_2O-B_2O_3·0.5H_2O and B_2O_3·0.63H_2O by means of the X-ray scattering method. They indicated that the fundamental triangle coordination characteristic of vitreous B_2O_3 was maintained in the water-containing glasses, although the possibility that a small fraction of the boron atoms was coordinated by four oxygen atoms could not be completely excluded. Their results coincide well with the present result. With the increase in the water content to near the composition of 3B_2O_3·H_2O, the partial molar volume of B_2O_3, which is read out from the intercept of the tangential line with the B_2O_3 axis, decreases abruptly to about 38 cm³/mol, then it returns gradually to the starting value. The decrease might be explained by the change in the coordination number, as in the case of binary metal borate. Silver[19] investigated the system over the B_2O_3 to B_2O_3·3H_2O range by the NMR method and confirmed that all the substances contained a planar BO_3 triangular unit. He also concluded that the BO_4 tetrahedral unit existed only in B_2O_3·0.6H_2O and B_2O_3·0.5H_2O glass samples and in monoclinic acid, not in B_2O_3 and B_2O_3·0.4H_2O. Thus, there is a good correspondence between his results in glass and the present results in liquid. The partial molar volume of the B_2O_3·3H_2O composition returns exactly to that of pure B_2O_3.

The change in the coordination number may be expressed by the following process:

$$\rangle B\text{–}O\text{–}B\langle + Na_2O = 2\,\rangle B\text{–}O^- + 2Na^+ \qquad (4)$$

$$\rangle B\text{–}O^- + -B\langle = \rangle B\text{–}O\text{–}\underset{|}{\overset{|}{B}}\text{–} \qquad (5)$$

Krogh-Moe[20] observed an example in solid Cs_2O·3B_2O_3. That is,

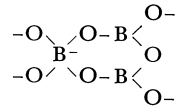

Likewise, a similar equation can be written for the

15) E. F. Riebling, *J. Amer. Ceram. Soc.*, **47**, 478 (1964).
16) E. F. Riebling, *ibid.*, **49**, 19 (1966).
17) Y. Ono, T. Yokokawa and K. Niwa unpublished
18) M. E. Milberg and F. Meller, *J. Chem. Phys.*, **31**, 126 (1959); F. Meller and M. E. Milberg, *J. Amer. Ceram. Soc.*, **43**, 353 (1960).
19) A. H. Silver, *J. Chem. Phys.*, **32**, 959 (1960).
20) J. Krogh-Moe, *Acta Crystallogr.*, **13**, 889 (1960).

B_2O_3-H_2O system;

$$\rangle B\text{–}O\text{–}B\langle + H_2O = 2\,\rangle B\text{–}O\text{–}H \quad (6)$$

$$\rangle B\text{–}O\text{–}H = \rangle B\text{–}O^- + H^+ \quad (7)$$

$$\rangle B\text{–}O^- + -B\langle = \rangle B\text{–}O\text{–}\overset{|}{\underset{|}{B}}\text{–} \quad (5)$$

or equivalently to the last two equations:

$$B\text{–}O\text{–}H + -B\langle = \rangle B\text{–}O\text{–}\overset{|}{\underset{|}{B}}\text{–} + H^+ \quad (8)$$

The above experimental results suggest that, while the (4) and (5) reactions proceed at the same time on the addition of Na_2O to B_2O_3, the (7) and (5) reactions preceed appreciably only after the H_2O content becomes higher than $3B_2O_3 \cdot H_2O$.

Thermal Expansivity. The volume expansivity (the mean values over the measured temperature) is shown in Fig. 4. The corresponding data on the binary alkali borates show a different trend. Any alkali oxide keeps a low expansivity at first as a result of BO_4 formation, and then it rises, probably because of the ionic nature of the melt. Water steadily increases the expansivity. The comparatively moderate increase in the range between $3B_2O_3 \cdot H_2O$ and $B_2O_3 \cdot H_2O$ confirms the notion that BO_4-unit formation occurs in this range.

BULLETIN OF THE CHEMICAL SOCIETY OF JAPAN VOL. 43 1040—1048 (1970)

The Crystal and Molecular Structure of Bis(2-hydroxyethyliminosalicylaldehydato)copper(II)

Kinya IIJIMA,*1 Isao OONISHI, Fumio MUTO, Akitsugu NAKAHARA* and Yoshimichi KOMIYAMA*2

Department of Applied Chemistry, Faculty of Engineering, Yamanashi University, Kofu

* *Institute of Chemistry, College of General Education, Osaka University, Toyonaka, Osaka*

(Received October 30, 1969)

The crystal structure of bis(2-hydroxyethyliminosalicylaldehydato)copper(II) has been determined by means of an X-ray diffraction study of a single-crystal specimen. Four formula units are contained in the monoclinic unit cell, the $P2_1/c$ space group, with lattice parameters of: $a=18.41$ A, $b=4.82$ Å, $c=19.86$ Å, and $\beta=99.1°$ ($Dm=1.50$ g·cm^{-3}; $Dx=1.50$ g·cm^{-3}). The structure has been refined, by means of three-dimensional difference syntheses and the least-squares method, to $R=0.095$. It has been confirmed that copper(II) links to the 2-hydroxyethyliminopyruvate anion through the phenolic oxygen and the nitrogen of the Schiff base linkage, while the alcoholic oxygen in the ethanol-amine moiety is free from coordination. The two Schiff-base ligands are coordinated around copper(II) in the *trans*-configuration. All the bond distances and angles in the complex are within the range of normal values. The N-Cu-O angles (91.3 and 91.8°) in the chelate rings are close to a right angle, showing that there is less strain in the chelate structure than in the case of a similar chelate of the pyruvate Schiff base (84.6°).

Although the ethanolamine molecule is provided with two functional groups for chelate formation, it can not always be coordinated as a bidentate ligand around a metal ion. The Schiff base derived from salicylaldehyde and ethanolamine is, for instance, coordinated around copper(II) to produce not only a one-to-one-type, but also a one-to-two-type, copper(II) Schiff-base complex, (I), in which the two hydroxyl groups of the ethanol-amine moieties are free from coordination.[1] In addition, the Schiff base derived from pyruvic acid and ethanolamine reacts with copper(II) to form, exclusively, a one-to-two-type copper(II) Schiff base complex, (II); consequently, the corresponding one-to-one-type complex is hardly ever obtained regardless of the molar ratio of copper(II) to the Schiff base employed in the preparation.[2] These findings can be explained by taking into account the rather weak binding ability of alcoholic oxygen, on the one hand, and, on the other hand, the geometrically unfavorable structure[3] of the fused

*1 Present address: Department of Chemistry, Faculty of Science, Shizuoka University, Shizuoka.

*2 Died Aug. 1, 1968.

1) A. Nakahara, H. Yamamoto and H. Matsumoto, *Sci. Rep., College of General Education, Osaka Univ.*, **12**, 11 (1963).

2) K. Iijima, I. Oonishi, F. Muto, A. Nakahara and Y. Komiyama, This Bulletin, **42**, 1509 (1969).

3) A. Nakahara, H. Yamamoto and H. Matsumoto, *ibid.*, **37**, 1137 (1964).

chelate ring in the imaginary one-to-one-type complex of copper(II) 2-hydroxyethyliminopyruvate. In order to estimate the validity of the latter assumption, a comparison of the molecular structure of the copper(II) chelates, I and II, seemed valuable. From this point of view, X-ray studies of the two complexes have recently been performed; the crystal structure of II has already been descrived.[2] This paper will describe the molecular and crystal structure of bis(2-hydroxyethyliminosalicylaldehydato)-copper(II).

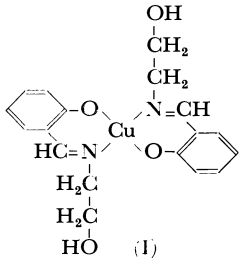

(I)

Bis(2-hydroxyethylimino-salicylaldehydato) copper-(II)

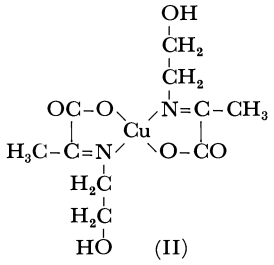

(II)

Bis(2-hydroxyethyl-iminopyruvato)copper(II)[2]

Experimental

Bis(2-hydroxyethyliminosalicylaldehydato)copper(II) was prepared and purified according to the procedure described in a previous paper.[1] The final pure product appears as thin yellow-brown needles elongated along the *b*-axis. The unit-cell dimensions were determined from the higher-order reflections of Weissenberg photographs (Cu$K\alpha$, λ=1.5418 Å). The systematic absences were *h0l* for *l* odd and 0*k*0 for *k* odd. Hence, the space group was unequivocally determined. The crystal data are listed in Table 1. Sets of multiple-film equi-inclination Weissenberg photographs were taken about the *b*-axis (0 to 4th layers), the *a*-axis and the *c*-axis (0th layer). Cu$K\alpha$ radiation was used throughout. The crystal used was a rod with dimensions of 0.07×0.16×0.46 mm. The intensities were estimated visually with a standard film strip and were converted to $|F_o(hkl)|^2$ and $|F_o(hkl)|$ by applying the usual Lorentz, polarization, and spot-shape corrections. No correction was made for absorption and extinction. The range of relative intensities was from 1 to 30000. 2243 independent reflections fell within this range, whereas 1092 others were too weak to be observed.

Table 1. Crystal data

[Cu(HOCH$_2$CH$_2$N=CHC$_6$H$_4$O)$_2$]
Monoclinic
a = 18.41 ± 0.02 Å
b = 4.82 ± 0.01
c = 19.86 ± 0.02
β = 99.1 ± 0.5°
Dx = 1.50 g·cm^{-3}
Dm = 1.50 g·cm^{-3}
Z = 4
Sapce group C_2^{5h}—$P2_1/c$
Linear absorption coefficient for Cu$K\alpha$, μ = 22.9 cm^{-1}

Structure Analysis

At first, two-dimensional Patterson syntheses projected along the *b*-axis and the *c*-axis were calculated. From these Patterson projections it was apparent that the copper atoms occupy two sets of two-fold positions. They could easily be placed at (000 and $\frac{1}{2}\frac{1}{2}\frac{1}{2}$) and at ($\frac{1}{2}\frac{1}{2}0$ and $\frac{1}{2}0\frac{1}{2}$). Attempts were made to deduce the x and y parameters of the lighter atoms from a three-dimensional Patterson function and from Fourier syntheses of the electron density, $\rho(x,z)$, the signs of which were calculated from the parameter values of the copper atoms. It was possible to locate all the atoms except those belonging to ethanol groups. Two-dimensional difference syntheses revealed ethanol groups, and all the x and y parameters of the lighter atoms were refined by a series of two-dimensional Fourier and difference syntheses to R_{h0l}=0.17. Consideration of the projected bond lengths made the estimation of approximate y coordinates possible. With these coordinates, a subsequent series of three-dimensional Fourier syntheses and difference syntheses reduced the R value to 0.15.

The structure thus obtained was refined by a block-diagonal, least-squares method with a HBLS-4 program written by T. Ashida. In this least-squares calculation, anisotropic temperature factors were introduced and four cycles of refinement were carried out. The following weighting scheme was employed:

$w = 0.2$ if $F_o \leqq F_{\min.}$ (=4.0)
$w = 1.0$ if $F_{\min.} < F_o \leqq F_{\max.}$ (=100.0)
$w = F_{\max.}/F_o$ if $F_o > F_{\max.}$

The final discrepancy factor, $R=\sum||F_o|-|F_c||/\sum|F_o|$, was 0.095 for all the observed reflections. The atomic scattering factors were taken from the International Tables for X-ray Crystallography.[4] The final atomic parameters and their estimated standard deviations are summarized in Table 2. The agreement between the observed and calculated structure amplitudes is reasonable (Table 3).

Description of the Structure and Discussion

The structure projected upon a plane normal to the *b*-axis is shown in Fig. 1. The intramolecular distances and angles are listed with their estimated standard deviations in Tables 4 and 5, and are shown in Figs. 2 and 3. The intramolecular distances and angles were calculated by using program DAPH written by T. Ashida.

4) International Tables for X-Ray Crystallography, Vol. III, Kynoch Press, Birmingham (1962), p. 202.

Table 2. Atomic parameters and their e.s.d.'s* ($\times 10^4$)

The expression of the temperature factor is: $\exp[-(h^2B_{11}+k^2B_{22}+l^2B_{33}+hkB_{12}+hlB_{13}+klB_{23})]$

Atom	x/a	y/b	z/c	B_{11}	B_{22}	B_{33}	B_{12}	B_{13}	B_{23}
Molecule I									
Cu(1)	0000	0000	0000	25	353	22	2	9	5
O(1)	722(4)	−0590(15)	763(3)	36	382	20	41	4	−15
O(2)	−2024(3)	2236(15)	795(3)	26	405	27	3	18	24
N(1)	−0479(4)	2986(16)	485(4)	19	298	19	−10	9	14
C(1)	872(5)	820(21)	1345(5)	28	315	18	−17	6	0
C(2)	1523(6)	63(28)	1800(5)	32	568	23	27	−1	24
C(3)	1687(6)	1423(27)	2420(5)	36	574	23	−19	−3	27
C(4)	1245(6)	3541(28)	2615(5)	43	569	23	−77	2	−27
C(5)	613(6)	4307(25)	2172(5)	38	454	24	−43	10	−28
C(6)	417(5)	2884(21)	1522(5)	27	307	19	−22	6	19
C(7)	−0235(5)	3892(21)	1096(5)	25	324	20	−9	13	−3
C(8)	−1157(5)	4402(20)	139(5)	22	242	26	12	11	18
C(9)	−1845(5)	2588(22)	119(5)	24	308	24	−5	8	23
Molecule II									
Cu(2)	5000	5000	0000	25	423	27	−2	9	−4
O(3)	5036(4)	1504(17)	4138(4)	27	549	34	66	15	32
O(4)	2689(3)	2256(15)	4064(3)	26	362	25	−15	5	3
N(2)	4106(4)	2652(18)	54(4)	25	315	23	13	3	34
C(10)	5562(5)	1453(25)	3751(5)	28	447	23	−30	8	2
C(11)	5481(7)	3191(29)	3166(6)	44	596	28	−11	17	2
C(12)	6033(7)	3217(29)	2750(6)	45	627	27	−110	14	−30
C(13)	6662(6)	1435(30)	2896(6)	39	751	25	−87	17	−72
C(14)	3270(5)	4711(27)	1546(5)	29	619	24	22	16	61
C(15)	3817(5)	4691(24)	1104(5)	27	426	23	29	12	29
C(16)	3714(5)	2811(22)	546(5)	24	376	23	1	3	57
C(17)	3873(5)	4424(21)	4524(5)	27	276	29	−4	6	20
C(18)	3399(5)	3072(24)	3907(5)	26	454	25	−9	8	1

* e.s.d.'s in parentheses

The new complex, bis(2-hydroxyethyliminosalicylaldehydato)copper(II) is in a *trans*-configuration. The 2-hydroxyethyliminosalicylaldehyde groups are coordinated to copper(II) as a bidentate chelate, through the terminal phenolic oxygen and the nitrogen of the Schiff-base linkage, while the alcohol groups are free from coordination. This is quite reasonable since the donating tendency of the alcohol oxygen has been estimated to be comparatively weak, as in bis(2-hydroxyethyliminopyruvato)-copper(II) tetrahydrate.[2]

The coordination configurations about the copper atoms in the molecules I and II are both square-planar. Square-planar configurations are also found in bis(salicylaldiminato)copper(II),[5] bis(*N*-*n*-butylsalicylaldiminato)copper(II),[6] and bis(*N*-phenylsalicylaldiminato)copper(II),[7] in which all the Cu(II) atoms occupy the positions of a center of symmetry.

The Cu–O distances of 1.872 and 1.869 Å are shorter than the value of 1.92 Å found in bis(2-hydroxymethyliminopyruvato)copper(II) tetrahydrate.[2] The Cu–N distances of 2.011 and 2.015 Å agree with the value of 2.00 Å in bis(2-hydroxymethyliminopyruvato)copper(II) tetrahydrate.[2] The N–Cu–O angles of 91.7 and 91.3° in the chelate rings are close to a right angle, showing that there is less strain in the chelate structure than the case of the similar chelate of the pyruvate Schiff-base (84.6°),[2] because the chelate rings in this Cu(II) complexes are six-membered, while it is five-membered in the latter.[2] The C–C and C–O bond distances in the ethanol moieties agree well with those in bis(2-hydroxymethyliminopyruvato)copper-(II) tetrahydrate,[2] but the N–C bond distances appear to be longer than that observed in the latter. It is interesting to note here that the distances of C(8)–O(1′) and C(17)–O(3′) (both 2.77 Å) are shorter than the corresponding value (3.10 Å) in bis(2-hydroxymethyliminopyruvato)copper(II) tetrahydrate. These differences in the interatomic distances seem to be caused by the difference in the chelate structure described above.

5) E. N. Baker, D. Hall and T. N. Waters, *J. Chem. Soc.*, **1966**, 680.

6) D. Hall, R. H. Sumner and T. N. Waters, *ibid.*, **1969**, 420.

7) L. Wei, R. M. Stogsdill and E. C. Lingafelter, *Acta Crystallogr.*, **17**, 1058 (1964).

TABLE 3. OBSERVED AND CALCULATED STRUCTURE FACTORS

L FO FC	L FO FC	L FO FC	L FO FC	L FO FC	L FO FC	L FO FC	L FO FC	L FO FC	L FO FC
H,K=-22 0	20 49 60	8 81 -49	H,K= 12 0	10 46 -57	10 58 76	6 152 164	2 190-148	4 67 -64	4 67 -64
2 67 74	22 55 67	10 177-167	0 221 224	11 107 110	11 259 265	7 387 421	3 572 601	5 169 202	5 169 202
4 59 62	24 36 70	12 178 166	2 289 300	12 69 -81	12 31 39	8 46 -32	4 141-121	6 139 139	6 139 139
6 95 104	H,K= -9 0	14 120 109	4 224 218	13 70 76	13 184 184	9 248 268	5 272 298	7 128 138	7 128 138
8 59 59	2 180-173	16 35 -39	6 195 189	15 52 60	14 62 -60	11 207 229	6 115 -92	8 121 121	8 121 121
10 27 30	4 92 -89	H,K= 2 0	8 135 116	17 48 57	15 108 104	12 98 94	7 282 283	9 222 245	9 222 245
12 52 68	6 273 254	0 845 846	10 204 189	19 57 67	16 73 -85	13 234 235	8 191-180	10 105 95	10 105 95
H,K=-21 0	8 160 170	2 598 628	12 214 208	H,K=-16 1	17 78 88	14 135 134	9 306 331	11 140 134	11 140 134
4 26 -33	10 76 -70	4 326 377	14 180 198	1 39 -41	19 102 107	15 263 248	10 98 85	12 50 -51	12 50 -51
6 13 26	12 22 -16	6 556 589	16 89 86	2 51 56	21 78 90	16 70 76	11 288 301	13 72 86	13 72 86
8 34 -46	16 72 67	8 306 346	18 37 40	3 24 26	23 43 61	17 173 176	13 178 183	14 39 -59	14 39 -59
10 26 -28	22 21 -37	10 370 369	H,K= 13 0	4 41 -39	H,K= -8 1	18 19 28	15 143 141	15 94 101	15 94 101
H,K=-20 0	H,K= -8 0	12 178 178	0 106-102	7 27 -30	1 32 -2	19 80 86	17 27 34	17 91 92	17 91 92
2 44 59	2 314 308	14 239 245	2 77 -79	9 51 -60	2 140 116	20 32 36	19 60 68	19 63 64	19 63 64
4 94 95	4 228 248	16 169 174	6 29 -16	12 23 -33	3 129-117	21 41 54	21 74 82	21 32 40	21 32 40
6 138 135	6 171 196	18 160 158	8 58 -58	H,K=-15 1	4 138 123	23 66 84	23 46 63	H,K= 10 1	H,K= 10 1
8 52 58	8 292 321	20 131 130	10 48 -45	1 273 269	5 150 142	H,K= -2 1	H,K= 4 1	0 53 59	0 53 59
10 62 66	10 317 308	22 109 109	14 32 -46	2 84 91	6 85 65	1 223 201	0 306-237	1 67 65	1 67 65
12 64 66	12 229 227	24 45 56	16 20 24	3 220 221	8 79 -82	2 709-712	1 50 26	2 65 -55	2 65 -55
14 47 53	14 161 150	H,K= 3 0	H,K= 14 0	4 27 28	9 55 -67	3 431 396	2 82 100	3 31 -29	3 31 -29
16 29 32	16 132 125	0 120 102	0 143 136	5 67 62	10 52 54	4 88 60	3 296-244	4 66 -55	4 66 -55
H,K=-19 0	18 149 192	2 558-538	2 55 66	6 61 69	11 92-113	5 13 21	4 425 383	5 16 -13	5 16 -13
2 23 26	20 121 132	4 241-212	4 26 28	7 80 89	12 74 89	6 28 39	5 11 26	11 157-156	11 157-156
4 33 44	22 73 88	6 86 103	6 91 83	9 127 142	13 28 26	7 74 75	6 43 -45	12 119-116	12 119-116
6 16 24	H,K= -7 0	8 240 187	8 91 79	10 63 65	14 155 165	9 31 -41	7 186 181	14 19 -31	14 19 -31
8 82 -84	2 155-131	12 175-168	10 152 137	11 143 143	15 19 -24	10 216-188	8 27 -26	15 45 49	15 45 49
10 57 -54	4 116-109	16 156-155	12 93 92	13 84 79	17 19 -32	11 29 30	9 45 42	16 31 -36	16 31 -36
H,K=-18 0	6 351 316	18 89 77	14 89 100	15 67 64	18 58 -65	12 57 -63	10 120-121	17 23 26	17 23 26
2 73 75	8 258 257	20 74 77	16 79 86	17 67 72	19 39 44	13 56 54	11 25 36	18 18 -32	18 18 -32
4 138 149	10 19 -4	H,K= 4 0	H,K= 15 0	19 39 49	21 23 30	16 26 28	12 40 29	H,K= 11 1	H,K= 11 1
6 140 128	14 38 -43	0 14 65	0 59 65	21 30 43	23 13 18	18 36 40	13 22 30	0 74 80	0 74 80
8 50 55	16 135 98	2 443 481	4 38 -24	H,K=-14 1	H,K= -7 1	20 63 -67	15 47 45	1 299 320	1 299 320
10 67 80	H,K= -6 0	4 20 56	6 114-105	1 95 100	1 266 277	21 30 31	16 58 63	2 59 63	2 59 63
12 44 46	2 110 155	6 120 177	8 57 -63	2 74 74	2 134-123	22 22 -36	17 39 -49	3 260 248	3 260 248
14 48 52	4 222 246	8 194 185	10 45 52	3 52 -59	3 294 294	H,K= -1 1	19 22 32	4 29 -33	4 29 -33
16 55 52	6 347 355	10 421 428	12 26 26	4 83 90	4 27 19	1 540 510	H,K= 5 1	5 248 253	5 248 253
18 64 63	8 188 192	12 401 424	16 31 -40	5 26 -30	5 574 573	2 539-511	0 193 170	6 74 -74	6 74 -74
H,K=-17 0	10 375 385	14 119 101	H,K= 16 0	6 64 -66	6 94 80	3 205 234	1 372 361	7 197 188	7 197 188
2 17 17	12 227 216	16 100 -80	0 188 180	8 66 -57	7 206 212	4 86 -69	2 246-230	8 75 75	8 75 75
4 264 263	14 227 218	18 100 86	2 180 182	10 67 -67	8 82 86	5 178 207	3 261 251	9 117 111	9 117 111
6 90 81	16 146 141	20 69 59	4 189 200	14 63 63	9 222 243	6 73 -80	4 285-271	10 19 35	10 19 35
8 34 37	18 105 105	22 93 80	6 64 51	15 22 28	10 81 -91	7 345 378	5 487 453	11 54 56	11 54 56
10 21 -28	20 149 153	H,K= 5 0	8 44 42	H,K=-13 1	11 243 224	8 178 171	6 173-146	12 48 55	12 48 55
H,K=-16 0	22 38 50	0 106 93	10 52 47	1 335 332	12 62 -51	9 272 267	7 304 288	13 140 140	13 140 140
2 225 192	24 22 31	2 152 142	12 53 69	3 222 201	13 219 226	10 96-100	8 57 65	15 52 60	15 52 60
4 128 117	H,K= -5 0	4 299 247	14 67 85	4 25 -37	16 58 -61	11 293 291	9 243 252	17 50 58	17 50 58
6 149 131	2 216 184	6 137 129	H,K= 17 0	5 242 228	17 104 113	13 339 325	11 251 234	19 32 38	19 32 38
8 170 167	4 103 103	8 21 24	0 80 -83	6 62 71	19 110 114	14 75 -76	12 105 -97	H,K= 12 1	H,K= 12 1
10 167 149	6 49 -44	10 56 -59	4 40 46	7 93 92	20 31 -38	15 217 208	13 221 223	1 50 31	1 50 31
12 120 110	8 122 80	14 39 -48	6 31 34	8 105 103	21 72 91	17 186 183	14 177-159	2 118 129	2 118 129
14 76 78	10 99 65	18 30 25	8 38 41	9 165 157	22 15 -30	18 34 36	15 112 117	4 140 144	4 140 144
16 94 88	16 174 157	22 20 23	12 19 22	11 197 207	23 47 63	19 47 48	16 53 54	5 29 -31	5 29 -31
18 81 79	18 185 168	H,K= 6 0	14 31 45	13 127 141	H,K= -6 1	20 45 58	17 89 97	6 97 97	6 97 97
20 44 55	H,K= -4 0	0 446 406	H,K= 18 0	15 102 104	1 131-109	21 41 41	19 108 110	7 25 37	7 25 37
H,K=-15 0	2 587 593	2 296 308	0 181 187	16 57 58	2 102 -75	23 60 75	21 48 50	10 34 -27	10 34 -27
2 34 -34	4* 8 40	4 388 389	2 111 108	17 74 84	3 38 11	H,K= 0 1	23 45 62	11 33 -32	11 33 -32
4 83 79	6 320 316	6 311 314	4 64 66	19 63 76	4 104 -83	1 92-124	H,K= 6 1	16 15 23	16 15 23
6 76 72	8 174 217	8 311 338	6 38 29	21 42 55	5 141 124	2 86 50	0 96 71	17 36 45	17 36 45
8 48 51	10 312 308	10 177 165	8 100 104	H,K=-12 1	6 205 221	3 34 24	1 82 -76	18 31 -32	18 31 -32
10 75 65	12 126 142	12 270 283	10 67 77	1 73 66	7 51 -47	4 160-150	2 69 40	H,K= 13 1	H,K= 13 1
12 24 29	14 277 282	16 86 86	12 40 47	2 112 101	9 81 77	5 48 38	3 89 76	0 43 -39	0 43 -39
14 61 63	16 275 256	18 124 108	H,K= 19 0	4 84 92	10 15 -15	6 91 -88	4 15 23	1 252 258	1 252 258
18 38 37	18 24 23	20 73 70	0 30 -22	5 28 -26	11 25 -22	7 115-116	5 130 104	2 57 -51	2 57 -51
20 16 -26	20 126 117	H,K= 7 0	H,K= 20 0	6 73 -70	12 44 -47	8 344-315	6 191-189	3 197 204	3 197 204
H,K=-14 0	22 33 40	0 258 226	0 69 81	7 17 11	13 57 -67	9 190-158	7 141 127	5 181 175	5 181 175
2 303 332	24 29 47	2 247-197	2 88 102	8 95-101	14 28 -36	10 31 -35	9 44 33	6 35 35	6 35 35
4 239 221	H,K= -3 0	4 384 349	4 53 54	9 65 79	15 29 -23	12 74 72	10 43 53	7 190 188	7 190 188
6 59 62	2 676 651	6 141 148	6 39 38	10 91 -86	16 43 51	13 47 39	11 71 67	8 55 62	8 55 62
8 80 80	4 340-300	8 114 112	8 20 25	11 38 44	17 65 70	15 43 29	12 50 51	9 57 63	9 57 63
10 213 188	6 143-119	10 99 97	H,K= 22 0	15 33 32	20 18 27	16 27 -31	13 19 -27	11 98 99	11 98 99
12 216 204	8 270-260	12 95 75	0 58 65	18 54 -62	H,K= -5 1	17 48 50	14 27 -31	13 93 105	13 93 105
14 133 120	10 166-115	14 143-139	2 54 68	20 22 30	1 472 491	19 70 -87	17 44 40	15 79 90	15 79 90
16 89 80	12 239-237	16 43 32	4 47 65	21 24 28	2 338-300	20 22 -40	18 31 -34	17 36 41	17 36 41
18 87 83	14 103 82	20 45 43	H,K=-22 1	H,K=-11 1	3 722 687	21 29 40	H,K= 7 1	H,K= 14 1	H,K= 14 1
22 53 75	18 178 167	H,K= 8 0	7 17 30	1 310 288	4 242-217	22 27 -44	0 335 286	7 31 42	7 31 42
H,K=-13 0	20 72 79	0 242 249	8 29 -40	2 29 26	5 553 572	23 17 26	1 325 300	8 67 81	8 67 81
2 109-116	22 44 -59	2 494 512	9 26 33	3 167 158	6 138 136	H,K= 1 1	2 337 322	10 53 55	10 53 55
6 76 75	H,K= -2 0	4 412 410	H,K=-21 1	5 181 182	7 210 225	0 95 -92	3 176 221	11 41 42	11 41 42
8 52 -52	2 453 452	6 144 159	1 63 74	6 46 34	8 207 201	1 641 609	4 56 41	12 17 29	12 17 29
10 90 -84	4 303 304	8 249 246	2 27 -35	7 238 217	9 187 210	2 390-420	5 311 324	H,K= 15 1	H,K= 15 1
12 158-143	6 246 286	10 229 217	3 58 69	9 235 219	10 204 206	3 276 316	7 202 229	0 47 -48	0 47 -48
14 27 31	8 327 338	12 140 145	5 48 60	10 102 -95	11 219 224	4 145 109	9 231 231	1 129 128	1 129 128
16 103 95	10 121 114	14 104 99	7 85 101	11 256 251	13 232 235	5 122 165	10 51 59	2 119 131	2 119 131
20 48 -61	12 113 131	18 67 61	9 67 77	12 26 -30	15 145 131	6 105 90	11 207 193	4 27 -37	4 27 -37
H,K=-12 0	14 221 193	20 70 68	11 56 59	13 191 180	16 122-124	7 288 309	12 41 -50	5 107 104	5 107 104
2 48 48	16 212 195	22 28 38	13 46 59	15 189 186	17 67 76	8 36 -55	13 105 110	6 33 -36	6 33 -36
4 176 166	18 139 130	H,K= 9 0	H,K=-20 1	17 44 47	18 19 -30	9 309 305	14 27 -21	7 114 112	7 114 112
6 236 242	20 29 24	0 250-224	10 36 39	19 90 104	19 100 102	11 316 320	15 160 167	8 32 -39	8 32 -39
8 407 408	22 39 51	2 35 -66	H,K=-19 1	21 77 94	21 93 109	12 20 -25	17 110 116	9 96 94	9 96 94
10 286 276	24 37 46	4 75 -20	1 42 48	23 37 54	23 50 62	13 217 211	19 86 89	11 95 96	11 95 96
12 154 149	H,K= -1 0	6 98 106	2 43 -46	H,K=-10 1	H,K= -4 1	14 60 73	21 47 58	13 72 76	13 72 76
14 72 68	2 12 34	8 30 34	3 65 74	1 86 -78	1 277-232	15 206 199	22 17 27	15 61 72	15 61 72
16 63 61	4 390-399	10 100 114	5 95 99	2 45 -46	3 492 459	17 73 62	H,K= 8 1	16 34 -47	16 34 -47
18 52 53	6 42 32	12 40 -40	6 82 -79	4 65 56	4 158-126	20 44 -46	0 167-154	H,K= 16 1	H,K= 16 1
20 28 26	8 153 99	16 31 27	7 91 94	5 37 39	5 155 157	21 93 98	1 192-179	2 27 -38	2 27 -38
22 30 44	10 112-104	H,K= 10 0	8 17 -22	6 174 176	7 26 36	23 32 39	2 55 58	H,K= 17 1	H,K= 17 1
H,K=-11 0	12 77 -70	0 270 278	9 86 91	8 97 91	8 25 36	H,K= 2 1	4 53 43	1 110 115	1 110 115
2 79 -98	22 20 -22	2 485 522	11 85 92	12 25 -30	9 23 37	0 193 153	5 138 138	3 50 49	3 50 49
4 82 -86	H,K= 0 0	4 375 395	13 77 82	13 26 28	10 24 -21	1 387-346	6 30 38	4 38 -46	4 38 -46
6 156-145	2 676 722	6 183 193	15 65 70	16 46 -42	11 35 39	2 666 628	7 31 45	5 99 60	5 99 60
8 53 43	4 347 347	8 176 171	17 54 74	17 38 -43	12 114 111	3 384-343	8 28 -34	7 87 88	7 87 88
10 59 65	6 72 102	10 240 239	H,K=-18 1	18 48 -64	13 29 -21	4 32 -8	9 32 -48	8 95 97	8 95 97
14 53 -66	8 439 440	12 165 173	2 52 65	19 48 -54	14 47 44	5 98 92	10 40 -48	9 57 63	9 57 63
18 57 -70	10 381 414	14 146 148	3 48 52	21 15 27	15 18 24	6 71 66	11 89 -88	11 49 61	11 49 61
20 25 -19	12 339 359	16 39 45	4 35 38	23 27 41	16 19 12	7 39 -23	12 117-128	13 41 -36	13 41 -36
22 22 34	14 259 245	18 101 96	6 40 -48	H,K= -9 1	17 53 53	8 111-106	13 41 -36	H,K= 18 1	H,K= 18 1
H,K=-10 0	16 167 166	20 31 36	8 37 -46	1 223 248	19 47 46	9 123-109	14 39 41	1 39 -36	1 39 -36
2 336 341	18 164 162	H,K= 11 0	H,K=-17 1	2 36 38	20 41 -52	12 36 41	15 25 32	3 45 55	3 45 55
4 284 267	20 118 112	0 39 -38	1 119 123	3 224 241	21 30 -35	13 41 35	19 22 24	5 15 -25	5 15 -25
6 200 202	22 87 91	2 136 138	3 111 117	4 172-150	H,K= -3 1	15 70 67	20 32 -38	H,K= 19 1	H,K= 19 1
8 444 435	24 45 57	4 89 -72	4 31 35	5 124 155	1 435 399	16 63 74	H,K= 9 1	1 99 109	1 99 109
10 256 264	H,K= 1 0	6 35 39	5 43 49	6 49 -60	2 18 -8	17 41 -39	0 93 -89	2 21 -33	2 21 -33
12 310 297	2 144-161	12 34 -32	7 101 102	7 243 267	3 862 806	18 107 115	1 252 265	5 48 50	5 48 50
14 274 267	4 621 590	16 66 72	8 27 -40	8 54 52	4 136 132	H,K= 3 1	2 24 6	7 68 72	7 68 72
16 184 170	6 100 -66	20 17 -22	9 122 120	9 243 264	5 230 266	1 422 393	3 276 291	9 60 67	9 60 67

TABLE 3. (Continued)

L	FO	FC
H,K= 20 1		
3	38	-35
4	34	-43
H,K= 21 1		
0	35	48
1	69	78
3	69	84
5	53	60
H,K=-20 2		
1	21	-30
2	48	59
4	71	78
6	75	79
7	32	39
8	45	47
10	34	40
12	25	26
H,K=-19 2		
10	35	36
H,K=-18 2		
2	102	97
4	130	122
6	124	117
7	40	43
8	114	104
9	27	31
10	90	90
12	70	69
14	74	76
16	60	60
H,K=-17 2		
4	30	-26
6	38	-43
14	41	48
16	17	19
H,K=-16 2		
2	175	183
3	45	-49
4	141	135
6	58	60
7	55	54
8	112	108
10	96	98
11	34	-35
12	93	95
13	40	-43
14	127	134
16	83	83
18	65	67
H,K=-15 2		
3	63	-62
6	28	30
9	17	24
10	87	-85
12	21	-24
18	23	26
H,K=-14 2		
2	85	76
3	92	-89
4	107	105
5	24	-27
6	134	133
8	152	156
10	142	140
12	119	122
14	111	112
16	99	107
18	83	83
20	43	51
H,K=-13 2		
1	57	46
2	72	66
4	112	-95
5	17	13
6	85	-86
7	51	-45
8	55	49
9	69	-67
10	44	38
12	44	39
20	20	28
21	21	-31
H,K=-12 2		
1	54	-49
2	173	161
3	37	-35
4	184	180
5	50	-51
6	142	140
8	34	32
9	65	59
10	53	51
12	147	146
14	101	104
16	105	101
18	46	41
20	38	44
21	21	-31
H,K=-11 2		
1	26	-21
2	21	-40
3	56	61
6	27	-32
9	87	-101
10	40	-36
11	30	29
13	38	41
14	31	28
16	34	30
H,K=-10 2		
1	57	36
2	161	179
3	93	-91
4	135	136
5	30	-27
6	238	244
7	57	-69
8	257	248
9	151	133
10	88	76
11	88	69
14	35	24
16	43	51
18	64	71
19	36	38
20	69	86
22	30	47
H,K= -9 2		
1	36	42
5	40	-37
6	35	44
7	157	-122
8	37	37
9	22	26
12	107	107
13	143	132
14	31	30
16	71	-78
17	35	39
20	32	46
22	15	24
H,K= -8 2		
2	285	323
3	15	-9
4	261	281
6	327	380
7	100	-86
8	240	250
9	26	27
10	212	206
11	35	51
12	236	222
13	43	-35
14	71	77
15	65	-65
16	110	110
17	43	41
18	100	101
20	55	64
22	36	50
H,K= -7 2		
1	33	35
2	28	38
3	37	-40
4	86	78
5	91	-86
6	169	172
7	88	-75
9	71	74
17	40	42
18	27	29
20	26	37
21	17	-20
H,K= -6 2		
1	133	-116
2	252	284
3	121	98
4	343	372
5	212	-201
6	373	394
7	29	-21
8	191	192
9	17	19
10	214	223
11	65	69
12	263	269
13	102	-98
14	127	123
15	71	-73
16	153	142
18	151	153
20	93	111
21	20	30
22	44	57
H,K= -5 2		
1	46	32
2	132	-116
3	187	149
4	83	86
5	157	-144
6	43	47
7	72	76
8	83	-95
9	52	-62
12	131	-129
13	101	-93
14	133	-127
H,K= -4 2		
1	44	-43
2	328	363
3	69	-98
4	491	506
5	102	-103
6	315	336
7	41	45
8	265	286
9	64	-64
10	322	353
11	226	225
12	39	36
13	116	-102
14	148	148
15	35	-26
16	111	122
18	123	114
20	85	72
22	48	48
H,K= -3 2		
1	212	232
2	63	-49
3	249	258
4	63	-48
5	60	-56
6	79	-70
7	32	-26
8	17	12
10	38	45
11	103	-81
12	40	28
13	48	-49
14	109	96
15	17	-30
16	17	27
17	37	-35
18	20	-21
19	17	14
H,K= 4 2		
0	113	141
1	94	-85
2	126	157
3	89	-100
4	372	415
5	180	-161
6	229	268
7	46	55
8	314	312
9	17	12
10	183	164
12	180	155
14	184	186
15	17	-28
16	142	149
18	127	128
20	74	72
22	45	48
H,K= 5 2		
0	203	-189
1	60	66
2	77	-73
3	69	72
4	284	-295
5	75	77
6	205	-193
7	102	-102
8	63	50
9	74	-78
13	35	29
14	58	-65
15	25	-25
17	47	-45
18	40	36
20	25	26
H,K= 6 2		
0	255	269
1	53	-49
2	220	222
3	41	44
4	196	199
5	150	-159
6	307	323
7	13	-23
8	266	243
9	127	117
10	209	181
12	142	131
13	43	33
14	107	98
16	60	60
18	68	57
19	20	-21
20	60	60
H,K= 7 2		
1	26	-25
2	41	22
4	58	-60
5	29	38
6	139	-126
7	52	46
8	141	-125
9	65	-76
10	55	-47
13	58	55
15	30	33
19	19	-26
H,K= 8 2		
0	311	319
1	41	28
2	337	364
3	86	-91
4	259	272
5	23	23
6	252	244
8	258	242
9	131	138
10	191	190
12	76	74
14	87	91
15	29	-29
16	122	132
18	74	67
20	63	66
H,K= 9 2		
0	60	55
1	56	-54
2	144	138
3	43	-43
4	107	96
6	54	57
8	41	51
9	37	-38
10	50	-47
11	40	-32
13	59	-73
14	41	42
H,K= 10 2		
0	221	239
1	102	-88
2	237	258
3	62	-54
4	191	159
5	23	31
6	134	131
7	46	45
8	132	127
10	93	89
12	103	96
14	96	88
16	102	100
18	72	74
H,K= 11 2		
1	81	-77
2	85	76
3	34	-30
4	31	23
6	52	54
7	30	27
8	53	53
9	60	-68
10	21	-25
14	27	29
H,K= 12 2		
0	247	233
1	96	-110
2	150	145
3	26	37
4	58	61
6	158	148
8	69	69
9	76	-80
12	77	75
14	58	63
16	32	39
H,K= 13 2		
0	155	163
1	32	-26
2	49	58
3	55	56
5	45	44
7	25	28
8	47	-47
9	74	-78
10	17	23
12	15	26
H,K= 14 2		
0	158	152
1	35	-32
2	167	164
4	198	202
5	33	36
6	161	160
8	71	69
9	24	-27
10	78	74
12	70	67
13	52	60
H,K= 15 2		
1	33	47
2	40	-31
3	35	45
5	35	41
6	29	23
7	32	-35
8	31	-30
11	17	-19
H,K= 16 2		
0	130	130
2	48	51
4	80	81
5	24	33
6	119	115
8	119	118
10	107	110
12	41	53
H,K= 17 2		
1	36	40
2	120	124
4	99	98
6	83	88
8	57	58
10	40	49
H,K= 19 2		
2	27	-33
4	21	33
6	39	53
8	20	30
H,K= 20 2		
0	33	36
2	48	50
3	21	-34
4	68	76
6	34	51
H,K=-20 3		
5	14	16
6	21	-25
7	24	36
8	14	-18
H,K=-19 3		
1	45	45
3	48	54
5	74	88
7	52	60
9	32	38
11	45	52
H,K=-18 3		
2	19	-25
3	197	218
4	72	72
5	105	102
6	124	120
7	179	182
8	161	161
9	121	123
10	121	123
11	206	194
12	43	47
13	68	63
15	114	109
17	60	65
19	60	72
21	20	22
H,K=-16 3		
2	47	44
4	44	37
6	23	23
8	23	7
H,K=-15 3		
1	93	89
2	27	-27
3	144	142
5	143	137
7	121	118
9	78	70
10	25	-26
11	80	80
13	53	60
15	52	50
17	35	32
H,K=-14 3		
7	17	27
9	30	25
12	25	24
H,K=-13 3		
1	90	82
3	142	142
5	137	133
6	21	26
7	142	141
9	75	64
10	56	-63
11	120	117
13	95	77
15	87	80
17	63	64
19	16	22
H,K=-12 3		
2	44	-40
3	16	9
6	30	35
7	21	-32
8	30	-32
9	75	79
11	63	74
12	85	97
13	41	42
14	30	25
16	27	37
H,K=-11 3		
1	115	108
2	16	-18
3	135	120
4	20	-31
5	161	155
6	30	-40
7	168	162
9	172	166
11	35	29
13	131	116
15	130	111
17	88	88
19	21	30
H,K=-10 3		
1	15	24
4	16	-12
6	28	-41
7	16	-26
8	137	-144
9	55	50
10	68	-65
11	97	83
12	50	54
13	24	27
18	22	-22
H,K= -9 3		
1	105	98
3	103	104
5	157	167
7	206	184
8	111	-121
9	249	246
11	65	62
13	93	89
15	116	111
17	76	73
19	44	53
21	17	26
H,K= -8 3		
1	39	-38
2	58	-59
3	84	-70
5	105	-106
6	24	11
7	59	51
9	113	102
10	16	-21
11	30	22
12	86	-91
13	43	40
14	79	-72
15	99	86
16	29	-34
17	118	123
18	95	105
20	13	-23
21	35	46
H,K= 0 3		
5	114	120
7	174	182
9	166	161
10	121	123
11	206	194
12	43	58
13	68	63
15	114	109
17	60	65
19	60	72
21	20	22
H,K= -7 3		
1	47	44
2	74	72
3	17	-5
5	20	7
6	26	-31
7	22	-2
9	24	-34
10	60	63
11	24	-25
15	50	48
20	15	-18
H,K= -6 3		
1	93	-46
2	40	38
3	123	149
5	202	227
6	209	206
9	172	157
10	29	-30
11	169	151
13	120	106
15	81	71
17	86	67
19	59	64
H,K= -5 3		
1	162	169
2	96	45
3	236	249
4	118	117
5	193	227
6	62	61
7	242	241
8	25	26
9	204	197
11	96	74
12	84	-75
13	98	90
15	140	140
16	52	52
17	114	119
18	23	23
19	75	81
21	44	61
H,K= -4 3		
1	94	91
2	53	-61
3	99	-98
4	17	-11
9	127	124
11	125	114
12	24	32
13	108	108
15	78	71
17	53	46
19	57	54
21	44	52
H,K= -3 3		
1	196	246
2	123	-160
3	249	307
4	67	-81
5	211	242
6	20	28
7	114	127
8	61	67
9	165	169
10	56	-44
11	91	85
12	152	-130
13	181	165
14	86	-88
15	146	144
16	27	-36
17	120	123
19	58	73
21	54	75
H,K= -2 3		
1	125	172
2	28	38
3	43	-44
4	73	93
5	118	-110
6	14	-14
7	22	35
8	45	55
9	32	-27
10	22	-23
11	43	-48
12	29	-31
13	71	72
14	17	33
15	44	53
16	20	19
H,K= -1 3		
1	187	268
2	43	-44
3	144	186
4	39	40
5	214	236
6	24	11
7	218	233
8	34	-29
9	144	-133
10	163	160
11	96	74
12	45	-33
13	100	88
14	30	36
15	99	86
16	31	36
H,K= 0 3		
1	127	118
3	43	47
4	121	131
5	45	-47
6	117	120
8	76	67
9	59	-58
10	83	-86
12	55	-61
15	53	45
H,K= 1 3		
1	206	248
2	46	38
3	202	227
4	209	206
9	172	157
10	29	-30
11	169	151
13	120	106
15	81	71
17	86	67
19	59	64
21	36	51
H,K= 2 3		
1	48	55
2	37	42
3	20	24
5	53	-62
6	23	-15
7	18	-14
8	33	-34
10	44	-53
11	24	24
13	38	-40
14	20	24
H,K= 3 3		
1	191	232
2	56	47
3	223	248
4	17	15
5	258	279
6	114	127
7	172	168
8	103	96
9	127	124
11	125	114
12	24	32
13	108	108
15	78	71
17	53	46
19	57	54
21	44	52
H,K= 4 3		
0	79	90
1	54	53
2	38	45
3	50	42
4	103	-94
5	71	-79
6	110	-112
7	37	27
8	40	-26
9	102	-99
10	71	61
11	56	60
12	56	60
15	42	-44
H,K= 5 3		
0	68	63
1	219	240
2	82	82
3	224	228
5	281	298
7	274	287
8	101	102
9	90	74
10	48	45
11	140	133
12	52	54
13	99	86
15	59	51
17	66	64
19	71	71
H,K= 6 3		
0	83	-80
1	12	20
2	61	-54
3	23	-21
4	84	-64
5	87	88
6	21	23
7	46	-44
8	101	102
9	79	68
10	44	-53
11	27	24
12	38	-40
13	69	75
14	37	-42
15	58	56
16	48	47
H,K= 8 3		
0	61	57
1	62	60
2	55	-48
3	54	49
4	115	-115
5	84	67
7	109	-99
8	61	63
9	35	-33
10	24	29
11	75	69
12	37	44
H,K= 9 3		
0	59	68
1	73	57
2	27	-21
3	181	186
4	112	-103
5	175	173
6	31	-31
7	137	133
8	57	-63
9	150	158
11	72	74
13	63	66
15	75	77
17	56	59
H,K= 10 3		
0	75	65
1	61	-58
3	41	43
4	41	54
6	90	82
7	35	38
8	17	25
H,K= 11 3		
0	35	-33
1	156	145
2	76	-72
3	161	153
4	24	25
5	60	85
6	75	77
7	97	96
8	28	36
9	115	104
11	103	107
13	66	66
15	33	35
H,K= 12 3		
0	30	37
2	37	-44
4	41	-43
6	28	-23
8	30	-30
11	36	38
13	38	44
H,K= 13 3		
1	138	130
3	123	118
4	45	50
5	129	110
7	72	69
9	94	86
11	45	46
13	48	52
H,K= 14 3		
0	47	-46
1	32	-34
2	58	-56
3	224	228
10	34	-39
11	25	35
13	24	34
H,K= 15 3		
1	101	102
6	34	40
7	42	40
8	15	15
9	92	94
10	25	30
11	88	83
12	54	52
13	84	83
14	50	57
15	28	43
H,K= 16 3		
0	28	-27
1	39	-39
2	56	57
3	110	112
5	28	43
H,K= 20 3		
4	106	-200
H,K= 17 3		
1	50	48
3	75	73
5	30	28
7	40	-44
9	53	60
11	44	44
H,K= 18 3		
0	25	34
2	18	24
4	18	19
6	24	31
H,K=-16 4		
1	21	27
2	53	55
3	55	60
4	59	58
5	28	-40
6	69	69
7	28	-40
8	54	69
9	47	53

TABLE 3. (Continued)

L	FO	FC	L	FO	FC	L	FO	FC	L	FO	FC	L	FO	FC	L	FO	FC	L	FO	FC	L	FO	FC
H,K=-15	4		6	54	-61	16	62	75	12	27	29	12	78	76	7	13	-11	7	124	-129	0	124	108	13	7	-3
4	18	28	7	27	-36	18	45	61	14	34	50	14	85	79	8	64	-72	8	117	108	2	83	82	H,K=	12	4
10	22	33	8	27	-34	H,K=	-7	4	15	56	-76	16	54	62	9	34	-31	9	44	-43	3	68	54	0	86	60
11	28	-40	10	81	74	1	95	-86	16	27	40	18	39	51	14	21	41	10	65	67	4	125	107	1	27	-21
12	40	52	12	20	20	3	37	-30	H,K=	-4	4	H,K=	-1	4	H,K=	2	4	12	91	100	6	134	105	2	127	109
H,K=-14	4		13	19	23	5	42	-48	1	24	-27	1	18	35	0	59	73	14	65	61	7	38	35	4	113	95
2	94	82	16	22	-29	9	27	32	2	122	130	3	18	-10	1	13	-9	16	38	36	8	90	82	5	20	30
4	115	109	H,K=	-10	4	11	50	58	4	159	166	5	32	42	2	111	127	H,K=	5	4	10	45	63	6	108	95
6	81	67	2	161	147	12	22	28	6	106	87	6	21	13	3	29	39	0	77	78	14	40	49	8	95	82
7	20	-25	3	74	69	19	34	-39	7	34	24	7	18	-12	4	186	245	2	90	91	H,K=	9	4	10	48	67
8	24	23	4	135	125	17	16	-17	8	126	125	9	79	-68	5	43	46	3	75	70	0	48	-46	11	36	-52
9	33	-44	5	45	33	18	17	-25	10	94	84	11	22	27	6	105	105	4	61	50	2	49	-45	12	49	76
10	56	47	6	103	86	H,K=	-6	4	12	95	89	13	27	36	7	112	-118	6	33	20	3	22	-17	H,K=	13	4
11	42	-50	7	45	39	1	10	-11	14	107	112	15	25	34	8	152	130	7	72	-69	7	38	42	2	29	-30
12	70	73	8	125	114	2	139	146	16	48	54	16	19	-30	9	53	-63	8	27	16	9	50	52	H,K=	14	4
13	24	-26	10	121	117	3	42	-46	18	31	36	H,K=	0	4	10	80	69	9	22	-20	H,K=	10	4	0	72	56
14	42	40	12	99	90	4	135	125	H,K=	-3	4	0	216	221	12	78	65	11	15	-23	0	129	107	2	51	27
H,K=-13	4		14	115	113	5	46	-46	2	27	33	2	236	253	14	86	90	H,K=	0	4	2	123	103	4	36	40
0	30	-34	16	68	72	6	145	123	3	29	-31	3	36	56	16	65	73	0	111	107	3	35	31	6	32	32
9	24	33	H,K=	-9	4	8	113	94	4	31	29	4	124	159	18	36	53	2	91	76	4	124	118	8	47	60
11	35	-37	2	37	31	10	100	85	5	38	48	5	49	50	H,K=	3	4	4	124	112	6	122	106	H,K=	15	4
13	20	-25	7	38	37	11	38	-43	7	81	79	6	177	192	0	26	31	6	179	194	8	124	101	0	27	32
H,K=-12	4		9	31	21	12	81	82	10	38	-61	7	43	-44	2	47	-41	8	115	95	10	68	73	2	22	29
1	38	41	12	30	31	14	52	57	12	20	29	8	91	87	3	51	-45	9	47	54	11	29	-45	4	17	-22
2	86	67	H,K=	-8	4	16	45	54	14	19	29	9	52	-52	4	34	-35	10	47	38	12	34	50	H,K=	16	4
4	116	101	2	117	128	18	28	33	H,K=	-2	4	10	122	122	5	96	-86	12	45	49	14	22	28	1	57	54
6	134	126	4	104	84	H,K=	-5	4	1	22	-26	12	133	131	6	23	-22	13	24	-31	H,K=	11	4	2	65	68
7	92	93	5	26	-28	1	24	-23	2	81	116	14	87	91	7	87	-74	14	81	81	1	55	-53	4	45	56
10	88	92	6	95	80	3	49	-57	3	40	-48	15	29	37	8	47	45	16	56	62	3	13	-4	6	25	43
12	81	67	8	118	99	4	45	27	4	149	167	16	47	53	11	22	32	H,K=	7	4	4	13	8	H,K=	17	4
14	40	36	9	38	44	5	38	-41	5	23	-20	18	49	64	H,K=	4	4	1	79	54	5	13	11	2	19	17
16	31	42	10	95	94	6	24	20	6	163	172	H,K=	1	4	0	114	114	3	78	56	7	13	13			
H,K=-11	4		11	31	44	7	24	31	7	59	62	1	33	-35	1	70	64	4	43	29	8	12	12			
1	90	69	12	58	54	8	25	20	8	108	93	2	25	29	2	91	73	6	73	64	9	12	1			
2	47	44	13	36	39	9	37	43	9	20	27	3	49	-61	3	34	22	9	59	51	10	11	-6			
3	38	23	14	43	40	10	31	42	10	43	49	4	28	25	4	149	138	10	53	57	11	10	9			
4	22	11	15	30	-39	11	22	29	11	49	51	5	23	20	6	113	116	H,K=	8	4	12	9	12			

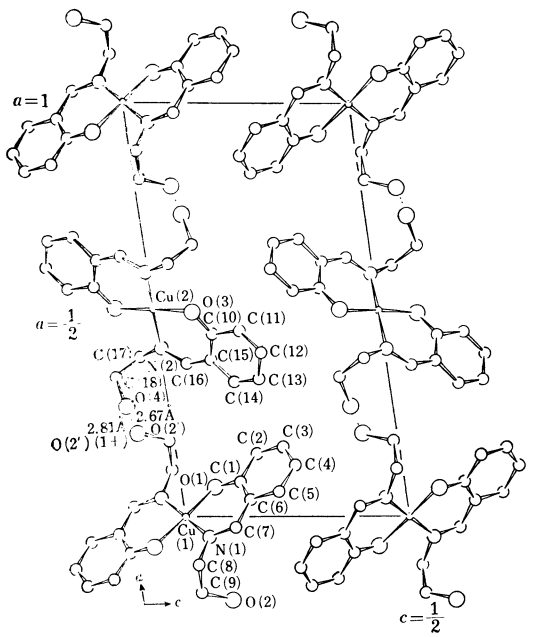

Fig. 1. Projection of the unit cell contents on the (010) plane.

In Table 5 the distances in various related complexes are compared with the values obtained in the present work. These latter values generally agree well with those found in the related compounds. The molecules may be described in terms of a set of various planar groups. Tables 6 (molecule I) and 7 (molecule II) list the equations for various least-square planes, the angles between them, and the deviations of the atoms therefrom. The benzene rings in salicylaldimine groups are almost planar (the maximum deviations of the atoms from the mean planes are 0.007 Å in the molecule I and 0.014 Å in the molecule II), but the nitrogen atoms are slightly, but significantly, out of the plane (0.104 and 0.092 Å). The two salicylaldimine groups in the molecules I and II are, of course, parallel, as is required by the centrosymmetry, but they are far from coplanar. The perpendicular distances between the two parallel salicylaldimine planes in the molecules I and II are 0.29 and 0.50 Å, while these range from 0.13 to 0.89 Å in other, similar complexes with planar configurations about Cu(II) atoms.[5-7] Each salicylaldimine group makes an angle of 5.5° (in the molecule I) and 9.9° (in the molecule II) with the coordination plane. Thus, the planarity of the molecule I is slightly better than that of the molecule II. This difference seems to be caused by the

TABLE 4. BOND DISTANCES AND THEIR ESTIMATED STANDARD DEVIATIONS*

Molecule I		Molecule II	
Cu(1)-O(1)	1.872(7) Å	Cu(2)-O(3)	1.869(8) Å
N(1)	2.011(8)	N(2)	2.015(9)
C(1)-O(1)	1.331(12)	C(10)-O(3)	1.329(14)
C(2)	1.429(17)	C(11)	1.421(18)
C(6)	1.381(14)	C(15)	1.417(17)
C(3)-C(2)	1.386(19)	C(12)-C(11)	1.408(20)
C(4)	1.397(19)	C(13)	1.434(20)
C(5)-C(4)	1.393(18)	C(14)-C(13)	1.375(20)
C(6)	1.457(16)	C(15)	1.435(18)
C(7)-C(6)	1.439(14)	C(16)-C(15)	1.422(16)
N(1)	1.302(13)	N(2)	1.306(14)
C(8)-N(1)	1.492(12)	C(17)-N(2)	1.465(13)
C(9)	1.534(14)	C(18)	1.534(16)
C(9)-O(2)	1.443(13)	C(18)-O(4)	1.445(14)

* e.s.d.'s in parentheses

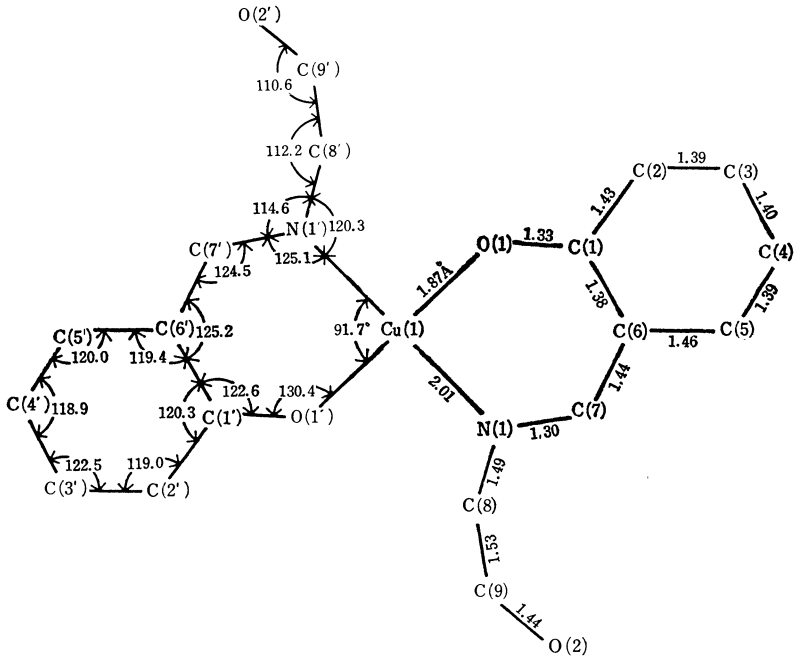

Fig. 2. The environment of the copper atom in the molecule I, showing bond distances and angles.

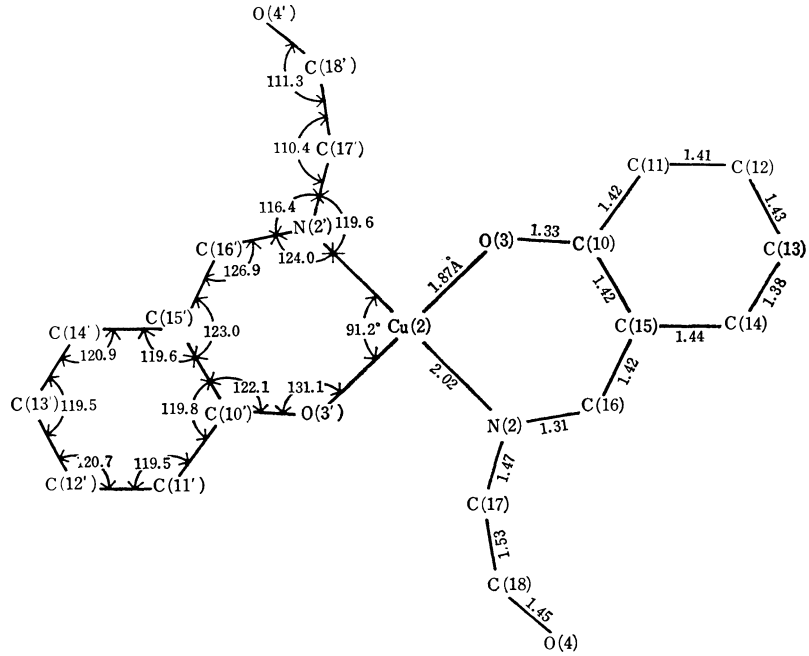

Fig. 3. The environment of the copper atom in the molecule II, showing bond distances and angles.

TABLE 5. BOND ANGLES AND THEIR ESTIMATED STANDARD DEVIATIONS*

Molecule I		Molecule II	
N(1)-Cu(1)-O(1)	91.7(3)°	N(2)-Cu(2)-O(3)	91.2(4)°
Cu(1)-O(1)-C(1)	130.4(7)	Cu(2)-O(3)-C(10)	131.1(8)
O(1)-C(1)-C(6)	122.6(9)	O(3)-C(10)-C(15)	122.1(11)
O(1)-C(1)-C(2)	117.2(9)	O(3)-C(10)-C(11)	118.1(11)
C(2)-C(1)-C(6)	120.3(10)	C(11)-C(10)-C(15)	119.8(11)
C(1)-C(2)-C(3)	119.0(12)	C(10)-C(11)-C(12)	119.5(12)
C(2)-C(3)-C(4)	122.5(12)	C(11)-C(12)-C(13)	120.7(13)
C(3)-C(4)-C(5)	118.9(12)	C(12)-C(13)-C(14)	119.5(13)
C(4)-C(5)-C(6)	120.0(11)	C(13)-C(14)-C(15)	120.9(12)
C(5)-C(6)-C(1)	119.4(10)	C(14)-C(15)-C(10)	119.6(11)
C(5)-C(6)-C(7)	115.3(9)	C(14)-C(15)-C(16)	117.5(11)
C(7)-C(6)-C(1)	125.2(9)	C(16)-C(15)-C(10)	123.0(11)
C(6)-C(7)-N(1)	124.5(9)	C(15)-C(16)-N(2)	126.9(10)
C(7)-N(1)-Cu(1)	125.1(7)	C(16)-N(2)-Cu(2)	124.0(7)
C(7)-N(1)-C(8)	114.6(8)	C(16)-N(2)-N(17)	116.4(9)
C(8)-N(1)-Cu(1)	120.3(6)	C(17)-N(2)-Cu(2)	119.6(6)
N(1)-C(8)-C(9)	112.2(8)	N(2)-C(17)-C(18)	110.4(9)
C(8)-C(9)-O(2)	110.6(8)	C(17)-C(18)-O(4)	111.3(9)

* e.s.d.'s in parentheses

TABLE 6. BOND DISTANCES IN SALICYL COMPLEXES WITH COPPER(II)

	Cu-O	Cu-N	O-C1	C1-C2	C2-C3	C3-C4	C4-C5	C5-C6	C1-C6	C6-C7	C7-N	N-C8
(1)	1.90	1.99	1.32	1.40	1.39	1.40	1.37	1.39	1.42	1.44	1.31	1.52
(2)	1.92	1.94	1.36	1.39	1.38	1.36	1.36	1.44	1.40	1.45	1.25	—
(3)	1.91	1.96	1.33	1.40	1.38	1.40	1.36	1.40	1.44	1.44	1.26	—
(4)	1.91	1.90	1.31	1.42	1.39	1.41	1.38	1.42	1.38	1.44	1.28	—
(5)	1.90	2.02	1.30	1.41	1.39	1.41	1.38	1.43	1.40	1.46	1.31	1.48
(6)	1.87	2.01	1.33	1.43	1.39	1.40	1.39	1.46	1.38	1.44	1.30	1.49
(7)	1.87	2.02	1.33	1.42	1.41	1.43	1.38	1.44	1.42	1.42	1.31	1.47
(8)	1.88	1.99	1.31	1.42	1.40	1.37	1.37	1.42	1.40	1.44	1.30	1.44
(9)	1.90	1.96	1.29	1.41	1.40	1.39	1.39	1.42	1.42	1.43	1.27	1.48
(10)	1.89	1.95	1.28	1.42	1.40	1.44	1.39	1.38	1.44	1.46	1.28	1.53
(11)	1.89	2.01	1.30	1.43	1.40	1.38	1.40	1.41	1.42	1.46	1.25	1.51
(12)	1.89	1.99	1.33	1.42	1.40	1.39	1.37	1.44	1.42	1.41	1.26	1.49
(13)	1.87	1.98	1.31	1.44	1.43	1.41	1.40	1.44	1.41	1.42	1.33	1.51
(14)	1.93	1.97	1.36	1.44	1.45	1.41	1.42	1.42	—	1.43	1.30	1.56
(15)	1.89	2.01	1.31	1.41	1.40	1.40	1.41	1.42	—	1.45	1.30	1.51

(1) Bis-(*N*-methylsalicylaldiminato)-Cu(II)[8] (2) Bis-(salicylaldoximato)-Cu(II)[9]
(3) Bis-(5-chlorosalicylaldoximato)-Cu(II)[10] (4) Bis-(salicylaldiminato)-Cu(II)[5]
(5) Bis-(*N*-*n*-butylsalicylaldiminato)-Cu(II)[6] (6) Molecule I in present work
(7) Molecule II in present work (8) Bis-(*N*-phenylsalicylaldiminato)-Cu(II)[7]
(9) Bis-(*N*-ethylsalicylaldiminato)-Cu(II)[11] salicyl group I
(10) Bis-(*N*-ethylsalicylaldiminato)-Cu(II)[11] salicyl group II
(11) Bis-(*N*-*t*-buthylsalicylaldiminato)-Cu(II)[12]
(12) Bis-(*N*-isopropylsalicylaldiminato)-Cu(II)[13] salicyl group I
(13) Bis-(*N*-isopropylsalicylaldiminato)-Cu(II)[13] salicyl group II
(14) Bis-(*N*-α-phenylethylsalicylaldiminato)-Cu(II)[14] salicyl group I
(15) Bis-(*N*-α-phenylethylsalicylaldiminato)-Cu(II)[14] salicyl group II

(1), (2), and (3) octahedral (4), (5), (6), (7), and (8) planar
(9), (10), (11), (12), (13), (14), and (15) tetrahedral

8) E. C. Lingafelter, G. L. Simmons, B. Morosin, C. Scheringer and C. Freiburg, *Acta. Crystallogr.*, **14**, 1222 (1961).
9) M. A. Jarski and E. C. Lingafelter, *ibid.*, **17**, 1109 (1964).
10) P. L. Orioli, E. C. Lingafelter and B. W. Brown, *ibid.*, **17**, 1113 (1964).
11) C. Panattoni, G. Bombieri and R. Graziani, *ibid.*, **23**, 537 (1967).
12) T. P. Cheeseman, D. Hall and T. N. Waters, *J. Chem. Soc.*, **1966**, 685.
13) P. L. Orioli and L. Sacconi, *J. Amer. Chem. Soc.*, **88**, 277 (1966).
14) Z. A. Starikova, *Acta Crystallogr.*, **A154**, 21 (1966).

Table 7. Least-squares planes in the molecule I

Coefficients of least-squares plane equations
$AX + BY + CZ + D = 0$

	A	B	C	D
		($\times 10^4$)		
Coordination plane (α)	6440	6861	−3384	0
Chelate ring plane (β)	6253	6618	−4136	11647
Cu-chelate ring plane (β')	6278	6736	−3900	4933
Benzene plane (γ)	5986	6776	−4275	15378
Salicylaldimine plane (δ)	6134	6645	−4269	14444
Cu-salicylaldimine plane (δ')	6128	6723	−4153	9335

X(Å) $= ax + cz\cos\beta$ $\quad Y = by$ $\quad Z = cz\sin\beta$

Angles between the least-squares planes

	β	β'	γ	δ	δ'
			(degree)		
α	4.6	3.2	5.7	5.5	4.8
β		1.5	2.0	1.0	1.0
β'			2.7	2.4	1.7
γ				1.1	1.1
δ					0.8

Distances from least-squares planes

	α	β	β'	γ	δ	δ'
			($\times 10^3$)			
Cu(1)	0	(117)	49	(154)	(144)	93
O(1)	0	−9	−42	(−27)	−15	−52
N(1)	0	29	−1	(104)	61	33
C(1)	(−141)	27	30	3	7	−11
C(2)	(−268)	(77)	(99)	6	31	19
C(3)	(−375)	(74)	(133)	−6	13	21
C(4)	(−384)	(45)	(123)	−1	−8	13
C(5)	(−271)	(8)	(67)	7	−21	−6
C(6)	(−131)	−16	4	−6	−28	−34
C(7)	(− 59)	−17	−14	(40)	−4	−15
C(8)	(36)	(49)	(8)	(174)	(105)	(75)

( ) not included in the least-squares calculations

Table 8. Least-squares planes in the molecule II

Coefficients of least-squares plane equations
$AX + BY + CZ + D = 0$

	A	B	C	D
		(10^4)		
Coordination plane (α)	−5284	7371	−4216	30853
Chelate ring plane (β)	−4308	7280	−5333	24104
Cu-chelate ring plane (β')	−4746	7235	−5013	26896
Benzene plane (γ)	−4084	7219	−5586	23075
Salicylaldimine plane (δ)	−4142	7241	−5515	23175
Cu-salicylaldimine plane (δ')	−4460	7151	−5383	25172

X(Å) $= ax + cz\cos\beta$ $\quad Y = by$ $\quad Z = cz\sin\beta$

Angles between the least-squares planes

	β	β'	γ	δ	δ'
			(degree)		
α	8.5	5.6	10.5	9.9	8.3
β		3.1	2.0	1.4	1.2
β'			5.0	4.5	2.7
γ				0.5	2.5
δ					2.0

Distances from least-squares planes

	α	β	β'	γ	δ	δ'
			($\times 10^3$)			
Cu(2)	0	(199)	64	(288)	(250)	136
O(3)	0	−29	−98	(5)	−17	−105
N(2)	0	36	−18	(92)	62	11
C(10)	(237)	18	20	8	−2	−46
C(11)	(389)	(30)	(67)	−14	−15	−49
C(12)	(661)	(99)	(213)	9	20	33
C(13)	(735)	(105)	(262)	2	17	69
C(14)	(557)	(62)	(185)	−7	−3	41
C(15)	(311)	24	69	2	17	69
C(16)	(112)	−46	31	(−35)	−52	−63
C(17)	(−162)	(−26)	(97)	(56)	(18)	(−29)

( ) not included in the least-squares calculations

difference in the packing of the molecules. The C(8) (in the molecule I) and C(17) (in the molecule II) of ethanolamine groups are displaced from the planes of the chelate ring, the deviations being 0.049 and 0.026 Å. The angles between the C–C single bonds in ethanolamine groups and the planes are 62 and 67° respectively.

The closest approach, less than 3.5 Å, between adjacent molecules occurs between the free alcoholic oxygens of the adjacent molecules. The distances of O(2′)–O(4) and O(2′)–O(4) $(x,-1+y,z)$ are 2.67 and 2.81 Å, as is shown in Fig. 1. These short distances suggest the presence of hydrogen bonds between them. By these hydrogen bonds, the complexes are held together to form layers parallel to the (001) plane. Between adjacent layers there exists no hydrogen bond.

The numerical calculations were carried out on the FACOM231 computer at this University and the HITAC5020E computer at the Computer Center, Tokyo University.

Part of the costs of this investigation has been defrayed by a Scientific Research Grant of the Ministry of Education, to which the authors' thanks are due.

BULLETIN OF THE CHEMICAL SOCIETY OF JAPAN VOL. 43 1049—1053 (1970)

The Zero-point Average Structure of Acetone

Takao IIJIMA

Department of Chemistry, Faculty of Science, Hokkaido University, Sapporo

(Received November 4, 1969)

The zero-point average structure of acetone has been determined from the moments of inertia obtained by means of microwave spectroscopy by Nelson and Pierce, as incorporated with the average distances from gas-electron diffraction by Kato *et al.* In addition to the normal species $(CH_3)_2CO$, three isotopically-substituted species, $(^{13}CH_3)_2CO$, $(CH_3)_2C^{18}O$, and $(CD_3)_2CO$, have been used in the analysis. The following values of the r_Z-parameters have been determined: C=O, 1.2122±0.0025 Å; C–C, 1.5190±0.0008 Å; C–H, 1.0614±0.0010 Å; ∠HCH, 108°30′± 6′; and ∠CCC, 116°9′±10′ (∠CCC for $(CD_3)_2CO$, 115°51′±10′). The slightly smaller value of ∠CCC found for the deuterated species has been reasonably attributed to the anharmonicity associated with the symmetric rocking motion of the two methyl tops. The equilibrium values for C–H(D) and ∠CCC have also been estimated to be 1.078 Å and 115°0′ respectively.

The molecular structure of acetone was studied by Nelson and Pierce[1] by means of microwave spectroscopy. They obtained the moments of inertia of $(CH_3)_2CO$ and three isotopically-substituted molecules $(^{13}CH_3)_2CO$, $(CH_3)_2{}^{18}O$ and $(CD_3)_2CO$, and determined the so-called r_s-structure of this molecule. For the deuterated species $(CD_3)_2CO$, they used the spectra which had previously been observed by Swalen and Costain.[2] The moments of inertia calculated by the use of their r_s-parameters differed from the observed moments by as much as 0.4 amu.Å^2. This is not surprising, however, because correction is necessary for the vibrational effect on the observed effective moments of inertia in order to find a set of parameters which will account for all the moments of inertia of isotopically-substituted species.

In the present study, the observed effective moments of inertia for the ground vibrational state have been reduced to the zero-point moments of inertia by applying vibrational correction, and the zero-point average structure has been determined. In the process of the structure determination, the previous electron-diffraction results by the present author and his collaborators[3] have also been used. As a result, an isotope effect has been found in the zero-point average values of the CCC angles.

Determination of r_z-Parameters

The procedure of applying the vibrational correction to the observed effective moments of inertia, $I_\alpha^{(0)}$, in order to obtain the zero-point moments of inertia, $I_\alpha^{(z)}$, is the same as that reported in the previous paper on the zero-point average structure of acetaldehyde.[4] Accordingly, only the results are shown in the present paper (Table 1). The

Table 1. Moments of inertia of acetone (in amu.Å^2 units)

		$I_\alpha^{(0)}$ a)	$I_\alpha^{(z)}$
$(CH_3)_2CO$	a	49.7296	49.5970
	b	59.3698	59.3108
	c	102.9559	102.9230
$(^{13}CH_3)_2CO$	a	50.6695	50.5198
	b	62.6916	62.6339
	c	107.2219	107.1782
$(CH_3)_2C^{18}O$	a	53.0613	52.9124
	b	59.3701	59.3046
	c	106.2938	106.2482
$(CD_3)_2CO$	a	59.6897	59.4442
	b	78.7481	78.6188
	c	126.0280	125.9675

a) Determined by Nelson and Pierce.[1]

quadratic force field by Cossee and Schachtschneider[5] (the set VF3) was used in the calculation of the vibrational correction. The vibrational averages of the linear displacements along the equilibrium bond direction were also calculated for the C–H and C–D bonds in order to estimate the possible isotope effect on the r_z(C–H), or r_z(C–D) value of each isotopically-substituted species. As

1) R. Nelson and L. Pierce, *J. Mol. Spectry.*, **18**, 344 (1965).

2) J. D. Swalen and C. C. Costain, *J. Chem. Phys.*, **31**, 1562 (1959).

3) C. Kato, S. Konaka, T. Iijima and M. Kimura, This Bulletin, **42**, 2148 (1969).

4) T. Iijima and M. Kimura, *ibid.*, **42**, 2159 (1969).

5) P. Cossee and J. H. Schachtschneider, *J. Chem. Phys.*, **44**, 97 (1966).

may be seen from Table 2, the r_z value of the C–D bond can be expected to be longer than r_z(C–H) by 0.007 Å.

Table 2. Calculated values of $\langle \Delta z \rangle_0$ of C–H(D)[a] (in Å units)

	$\langle \Delta z \rangle_0$
$(CH_3)_2CO$	−0.017
$(^{13}CH_3)_2CO$	−0.016
$(CH_3)_2C^{18}O$	−0.017
$(CD_3)_2CO$	−0.010

a) Morse anharmonicity constant a_3 was assumed to be 1.98 Å^{-1}.

The angle between the axes of the two methyl tops is denoted by 2θ; it was determined by Nelson and Pierce[1] as 119° 54′±30′*1 by an analysis of the multiplet separation of the spectrum caused by the coupling between the internal rotation and the overall rotation of the molecule. Since the value of 2θ was determined independently of the other structure parameters, the Nelson and Pierce value, namely, 119°54′, has been assumed in the present study.

The r_g distances of C–C and C=O, as determined by gas-electron diffraction, were converted to the r_z values shown in Table 3 in order to afford additional information for the structure determination. The details of the process of conversion have been reported in a previous paper.[4]

Table 3. Conversion from r_g to r_z (in Å units)

	r_g	l_T^2	l_0^2	K_0
C–C	1.517	0.00262	0.00254	0.0023
C=O	1.211	0.00154	0.00153	0.0032

	δr_{cent}[a]	a_3[b]	r_z
C–C	0.0002	2.1	1.514
C=O	0.0002	2.4	1.208

a) assumed.
b) Morse anharmonic constant.

We assumed that the molecule including the methyl hydrogens had a C_{2v} symmetry and that the outer two hydrogens were on the plane formed by the molecular frame. However, the results of the present study are independent of the assumed conformation of the methyl hydrogens. In other words, no definite information has been obtained on the conformation of the methyl hydrogens by either the present analysis or the previous studies.[1-3]

For the value of $I_a^{(z)}+I_b^{(z)}-I_c^{(z)}$, the out-of-plane coordinate (c-coordinate) of the hydrogen atom was determined for each isotopically-substituted species. As is shown in Table 4, the coincidence between the c-coordinates of the H-atoms is quite satisfactory, while the larger value for the D-atom is well accounted for by assuming that r_z(C–D) is longer than r_z(C–H) by 0.006 Å. This amount of difference between r_z(C–D) and r_z(C–H) is in good agreement with the expected value, 0.007 Å, estimated by the use of $\langle \Delta z \rangle_0$, shown in Table 2. A similar situation has already been reported in the cases of ethane[6] and acetaldehyde.[4]

Table 4. Out-of-plane coordinates of H and D atoms[a] (in Å units)

$(CH_3)_2CO$	0.8616
$(^{13}CH_3)_2CO$	0.8609
$(CH_3)_2C^{18}O$	0.8604
$(CD_3)_2CO$	0.8664

a) Calculated from $I_a^{(z)}+I_b^{(z)}-I_c^{(z)}$.

By keeping 2θ fixed at 119°54′, we tried to adjust the five structure parameters, r_z(C–O), r_z(C–C), r_z(C–H), α_z(CCC), and α_z(HCH), so as to make the calculated moments of inertia fit all the observed moments well, with the additional condition that r_z(C–D) was longer than r_z(C–H) by 0.006 Å. The α_z(DCD) was assumed to be equivalent to α_z(HCH). However, it was revealed that no satisfactory set of parameters could be obtained as long as the moments of inertia of the deuterated species were included. This implies that, in addition to r_z(C–D), at least one r_z-parameter of the deuterated species should take different values from those of other species provided the procedure of data handling is appropriate. Accordingly, the structure parameters were determined without the moments of inertia of the deuterated molecule.

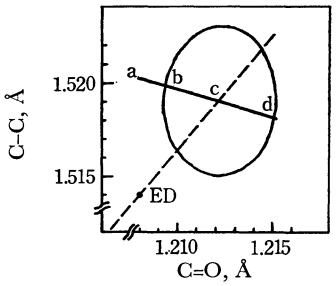

Fig. 1. The parameters r_z(C=O) *vs.* r_z(C–C) of acetone. The solid line gives sets of parameters which account almost equally well for the observed moments of inertia. The diffraction values are denoted by ED, which may vary along the broken line if an uncertainty of the scale factor is allowed for. The circle shows the errors of the ED-values without those originating in the scale factor.

*1 The values of 2θ for $(^{13}CH_3)_2CO$ and $(CD_3)_2CO$ were also determined by them to be 119° 42′ and 119° 54′ respectively.

6) K. Kuchitsu, *J. Chem. Phys.*, **49**, 4456 (1968).

Table 5. Deviations of the calculated moments of inertia from the observed[a] (in amu.Å²)

		Set a	Set b	Set c	Set d
$(CH_3)_2CO$	I_a	+0.016	+0.016	+0.015	+0.015
	I_b	−0.001	+0.003	+0.009	+0.014
$(^{13}CH_3)_2CO$	I_a	−0.013	−0.013	−0.013	−0.014
	I_b	−0.009	−0.007	−0.003	0.000
$(CH_3)_2C^{18}O$	I_a	−0.022	−0.025	−0.013	−0.016
	I_b	+0.011	+0.015	+0.003	+0.008
$(CD_3)_2CO$	I_a	—	—	+0.154 (−0.012)[b]	—
	I_b	—	—	−0.220 (−0.002)[b]	—

a) Values of (obs'd)—(calc'd) are tabulated.
b) With CCC angle reduced by 18′.

As is shown in Fig. 1 and Table 5, a rather wide range of variation in parameters accounts equally well for the observed values of $I_a^{(z)}$ if the mutual correlation between the parameters is properly taken into account. The situation graphically shown in Fig. 1, where a point on the solid line indicates a definite set of parameters which gives a good fit between the calculated $I_a^{(z)}$ and observed $I_a^{(z)}$ values. Although the values of the parameters other than r_z(C–O) and r_z(C=C) are not explicitly shown in Fig. 1, a definite value for each parameter corresponds to each point on the solid line.

The strong correlation between parameters was alleviated by the use of electron-diffraction results as additional information, as has been successfully done in the cases of acetaldehyde[4] and also several other molecules.[7] The point ED in Fig. 1 shows the diffraction values. By allowing for an uncertainty in the scale factor of the ED data, the set ED may vary along the broken line. Therefore, the cross point of the broken line and the solid line, namely, the set c, was obtained as the most reliable set of structure parameters.*2 The region of the solid line cut out by the error circle of the ED data determines the error of the parameters of the set c. The error circle does not, however, include the error associated with the uncertainty of the scale factor. The values of the parameters of the set c are listed in Table 6.

Table 6. The r_z-parameters of acetone (in Å units)

C–C	1.5190±0.0008
C=O	1.2122±0.0025
C–H	1.0614±0.0010[a]
∠HCH	108°30′±6′
∠CCC	116°9′±10′[b]
2θ	119°54′±30′ (assumed)

a) 1.0674 for C–D of $(CD_3)_2CO$
b) 115°51′ for CCC of $(CD_3)_2CO$

For the deuterated species which has been left out, the set c still leaves a rather large deviation of the calculated $I_a^{(z)}$ value from the observed value, as is shown in Table 5. This deviation, however, can be eliminated only if α_z(CCC) is reduced by 18′ for the deuterated species.*3 Accordingly, the present author takes the view that the zero-point average value of the CCC angle of $(CD_3)_2CO$ is less than that of $(CH_3)_2CO$ by 18′. This can most easily be understood as an effect of the bending anharmonicity, which makes it harder for the CCC angle to narrow than to widen. The anharmonicity will be discussed further below.

The above conclusion on the isotope effect found in the CCC angle is not vulnerable to the ambiguity of the value of 2θ. Even if the value of 2θ for $(CD_3)_2CO$ were 1° less than that of $(CH_3)_2CO$, the CCC angle of the deuterated species would be required to be only 1.4′ smaller from I_a value and 1.5′ larger from I_b value; that is, substantially no change would be required in the sense of a least-squares fitting. It should be noted, however, that the question of whether the 2θ value obtained by the spectroscopic analysis can be interpreted as $2\theta_z$, *i. e.*, the angle between the two top-axes in the zero-point average structure, is still unsettled. The equivalence of 2θ and $2\theta_z$ within the reported area of uncertainty has been assumed in the present study.

From the difference between 2θ and α_z(CCC), it is seen that the methyl tops are tilted outwards by nearly 2°.

Discussion

The Effect of Bending Anharmonicity on α_z(CCC). If it is assumed that a cubic term of the kth symmetry coordinate is present in the intramolecular potential function in such a form as:

$$V' = F_k^{(3)} S_k^3, \qquad (1)$$

the zero-point average of the lth symmetry coordinate can be given by a rather simple relation (see

7) References 6 through 10 cited in the reference 4: S. Konaka and M. Kimura, "Determination of the molecular structures of AsF_3 and $AsCl_3$ by gas electron diffraction." This Bulletin, to be published.

*2 It may be seen in Fig. 1 that an error of 0.3% was included in the scale factor of the ED value. This is slightly larger than the limit of error reported in current ED studies. Since there is evidence which strongly suggests that the stabilizing circuit of the accelerating voltage of the electron beam was in a threatening condition at the time acetone was studied, a reinvestigation of this molecule by electron diffraction is now under way.

*3 A similar situation was observed by Swalen and Costain[2] in their determination of r_0-parameters. The difference between the CCC angles of the normal and the deuterated species was 32′ in their case.

Appendix for the derivation) as:

$$\langle S_l \rangle_0 = -3F_k^{(3)}(F^{-1})_{lk}\langle S_k^2 \rangle_0, \quad (2)$$

where F^{-1} is the inverse of the symmetrized F matrix. The symmetry coordinates, S_l and S_k, must belong to the totally symmetric species.

In the case of acetone, the average of the vibrational displacement of the CCC angle is expressed as*4:

$$\langle \Delta\alpha(\mathrm{CCC}) \rangle_0 = \frac{2}{\sqrt{6}}\langle S_8 \rangle_0 = -\sqrt{6}F_k^{(3)}(F^{-1})_{8k}\langle S_k^2 \rangle_0. \quad (3)$$

It can be seen from Eq. (3) that the difference in α_z between the normal and the deuterated species must be caused by the difference in $\langle S_k^2 \rangle_0$, if any. By rewriting Eq. (3) simply as:

$$\langle \Delta\alpha \rangle_0 = a\langle S_k^2 \rangle_0, \quad (4)$$

a relation which enables one to estimate $\langle \Delta\alpha \rangle_0$ values from the difference in α_z, that is, the difference in $\langle \Delta\alpha \rangle_0$, between the normal and the deuterated species, can be obtained as:

$$\langle \Delta\alpha \rangle_0^{\mathrm{H}} = [\langle \Delta\alpha \rangle_0^{\mathrm{H}} - \langle \Delta\alpha \rangle_0^{\mathrm{D}}] \cdot \frac{\langle S_k^2 \rangle_0^{\mathrm{H}}}{\langle S_k^2 \rangle_0^{\mathrm{H}} - \langle S_k^2 \rangle_0^{\mathrm{D}}}. \quad (5)$$

The mean square values, $\langle S_k^2 \rangle^{\mathrm{H}}$ and $\langle S_k^2 \rangle^{\mathrm{D}}$, are quantities which are easily calculated, and the $\langle \Delta\alpha \rangle_0^{\mathrm{H}} - \langle \Delta\alpha \rangle_0^{\mathrm{D}}$ has been estimated to be 18′. The superscripts H and D denote the normal and the deuterated species respectively. The values of $\langle \Delta\alpha \rangle_0^{\mathrm{H}}$ have been calculated by Eq. (5) for each of the k-numbers, from 5 through 9, corresponding to the bending symmetry coordinates of the totally symmetric species of this molecule. The results are tabulated in Table 7.

TABLE 7. ESTIMATED VALUES OF $\langle \Delta\alpha \rangle_0^{\mathrm{H}}$

k	Mode of vibration	$\langle \Delta\alpha \rangle_0^{\mathrm{H}}$
5	HCH bending (nearly redundant)	1°7′
6		1°16′
7		1°16′
8	CCC bending	9°
9	CH_3 rocking	1°9′

If it is accepted as a reasonable judgment that a value of 9° is too large for $\langle \Delta\alpha \rangle_0^{\mathrm{H}}$, the coordinate of CCC bending ($k=8$) is excluded as a possible source of the anharmonicity. Among the rest, the coordinates with the k numbers of 5, 6, and 7 all represent an intra methyl-top bending motion.

*4 The correspondence between the vibrational mode and the sequence number of the symmetry coordinate is arbitrary. In the present treatment, the number 8 has happened to be assigned to the symmetry coordinate of the CCC bending.

In the present results, as well as in the case of acetaldehyde, the zero-point average values of the HCH angle and the DCD angle of the methyl top have been found to be equivalent. Therefore, it is implausible that an appreciable amount of anharmonicity is associated with the intra-methyl bending motion. Accordingly, the coordinate of the rocking motion of the tops ($k=9$) must be the source of the anharmonicity which brings about the difference between $\langle \Delta\alpha \rangle_0^{\mathrm{H}}$ and $\langle \Delta\alpha \rangle_0^{\mathrm{D}}$. A strong anharmonicity of the rocking motion is the most plausible in view of the fact that the methyl tops are tilted outwards, most probably by mutual repulsive interaction.

From the $\langle \Delta\alpha \rangle_0^{\mathrm{H}}$ value thus estimated, the equilibrium value, α_e(CCC), has been evaluated to be 115°0′ by the relation:

$$\alpha_z = \alpha_e + \langle \Delta\alpha \rangle_0. \quad (6)$$

The numerical value of the cubic constant, $F_9^{(3)}$, could be calculated if $(F^{-1})_{89}$ were known. In the present case, however, $(F^{-1})_{89}$ is simply zero because the quadratic force field used is a rather simplified one. Accordingly, $F_9^{(3)}$ is left undetermined, although it would be very interesting to evaluate it by the use of a more sophisticated set of quadratic force constants.[8]

Equilibrium C-H(D) Bond Length. From the r_z-values thus determined and from the $\langle \Delta z \rangle_0$ values in Table 2, the equilibrium bond length, r_e, can be estimated by the relation:

$$r_z = r_e + \langle \Delta z \rangle_0. \quad (7)$$

From both r_z(C–H) and r_z(C–D), the r_e-value of 1.077—1.078 Å was obtained. This is close to the value, 1.078 Å, obtained for the methyl C–H of acetaldehyde.[4] It should be noted that the rather smaller value of the r_z(C–H) of acetone is simply due to the environment effect, that is, the larger torsional amplitude of the methyl top around the axis.

The author wishes to thank Professor M. Kimura for his helpful advice and Mr. C. Kato for his help in the early stages of this study. The numerical calculations were performed on a HITAC 5020E of the Computing Center of the University of Tokyo and on a FACOM 270-20 in the laboratory of Professor Kimio Ohno, Hokkaido University, to whom the author's thanks are also due.

Appendix

Derivation of Eq (2). By applying the theorem that the expectation value of the force with respect to any coordinate should be zero for a system in a stationary state,[9] the following simultaneous linear equations for

8) G. Dellepiane and J. Overend, *Spectrochim. Acta*, **22**, 593 (1966).

9) L. S. Bartell, *J. Chem. Phys.*, **38**, 1827 (1963).

$<S_l>$'s are obtained:

$$\left\langle \frac{\partial V}{\partial S_j} \right\rangle = \sum_l F_{jl}\langle S_l\rangle + 3F_k^{(3)}\langle S_k^2\rangle\delta_{kj} = 0 \qquad (A1)$$

$$(j = 1, 2, \cdots)$$

where the potential function, V, is given as:

$$V = \frac{1}{2}\sum_{j,l} F_{jl}S_lS_j + F_k^{(3)}S_k^3 \qquad (A2)$$

in terms of the symmetry coordinates. By solving Eq. (A1) for $<S_l>$, this relation:

$$\langle S_l\rangle = -3F_k^{(3)}(F^{-1})_{lk}\langle S_k^2\rangle \qquad (A3)$$

can easily be derived. In the event that the cubic potential is given by such a sum of terms as $\sum_k F_k^{(3)} S_k^3$, $<S_l>$ is obtained simply by taking a sum of the right-hand side of Eq. (A3) over k.

BULLETIN OF THE CHEMICAL SOCIETY OF JAPAN VOL. 43 1053—1056 (1970)

Solvent Effect on the Electronic Spectra of Bis(8-quinolinolato)-nickel(II) at 80°C*1,2

Yoshiki MORIGUCHI*3 and Keihei UENO

Department of Organic Synthesis, Faculty of Engineering, Kyushu University, Hakozaki, Fukuoka

(Received June 11, 1969)

The visible absorption spectra were observed on bis(8-quinolinolato)nickel(II) in molten 8-quinolinol as well as in other solvent systems such as molten naphthalene, molten β-methoxynaphthalene or toluene containing various amounts of 8-quinolinol at 80°C. Little interaction was found between the solute and naphthalene or toluene. However, a weak interaction was observed between the solute and β-methoxynaphthalene or 8-quinolinol. The extent of interaction between the solute and 8-quinolinol in toluene was evaluated spectrophotometrically.

Concerning the zone-melting process of the systems containing metal chelates of 8-quinolinol,[1] we are interested in the behavior of 8-quinolinolato metal chelates in molten 8-quinolinol or other solid solvents such as naphthalene or β-methoxynaphthalene. Bis(2,4-pentanedionato)nickel(II) exists as a hexa-coordinate trimeric form in a solid state, but exists as a solvated octahedral monomeric form in donating solvents and as a polymeric or a tetrahedral monomeric form in non-donating solvents.[2] In this connection, it is of interest to study the interaction between the solute, bis(8-quinolinolato)nickel(II), and the solvents such as molten 8-quinolinol or other solvents.

The visible absorption spectra were observed on bis(8-quinolinolato)nickel(II) in molten 8-quinolinol as well as in other solvent systems such as molten naphthalene, molten β-methoxynaphthalene or toluene containing various amounts of 8-quinolinol at 80°C. The analysis of the spectra showed that there was definitely a weak interaction between the dissolved chelate and β-methoxynaphthalene or 8-quinolinol. As the observed absorption bands are due to d–π transition, and as the d–d band was too weak to be observed no significent discussion could be made on the coordinating structure of dissolved 8-quinolinolato metal chelate.

Experimental

Materials. 8-Quinolinol was purified by steam distillation and was dried over phosphorus pentoxide. Bis(8-quinolinolato)nickel(II) was obtained according to the standard procedure as dihydrate,[3] which was then dehydrated by heating at 100°C for 6 hr in a vacuum over phosphorus pentoxide. The dehydrated sample was found to have a composition of $Ni(ox)_2 \cdot 1/2H_2O$. It was a brownish yellow powder relatively soluble in hot toluene or in pyridine at room temperature. Although we tried to obtain a completely dehydrated sample,[4] further dehydration under severer conditions

*1 Contribution No. 172 from the Department of Organic Synthesis, Faculty of Engineering, Kyushu University.

*2 Presented at the 18th Symposium on Coordination Chemistry sponsored by the Chemical Society of Japan, October, 1968, Kyoto University.

*3 Present Address: Department of Chemistry, Fukuoka University of Education, Munakata-machi, Munakata-gun, Fukuoka.

1) H. Kaneko, H. Kanagawa, H. Kobayashi and K. Ueno, *Talanta*, **14**, 1411 (1967).

2) F. A. Cotton and J. P. Fackler, Jr., *J. Amer. Chem. Soc.*, **83**, 2818 (1961).

3) H. Goto, *Sci. Rep. Tohoku Univ. Ist Series*, **26**, 391 (1937).

4) M. Borrel and R. Paris, *Anal. Chim. Acta*, **4**, 272 (1950).

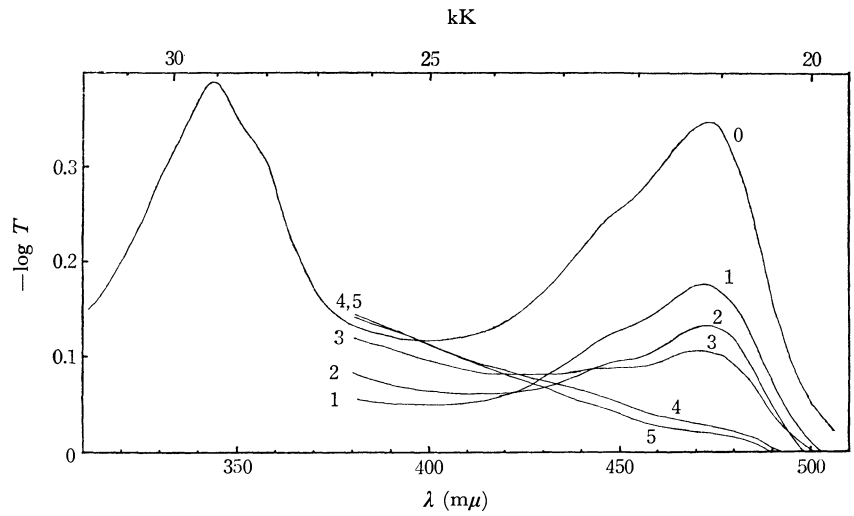

Fig. 1. Absorption spectra of bis(8-quinolinolato)nickel(II) in toluene containing various amounts of 8-quinolinol at 80°C. Concentration of nickel chelate 2.76×10^{-5}M. Concentration of 8-quinolinol increases from curve 0 to 5; zero, 1.95×10^{-4}M, 1.01×10^{-3}M, 1.95×10^{-3}M, 1.08×10^{-2}M and 1.95×10^{-2}M respectively.

resulted in the decomposition of the chelate.

Other solvents were purified and dried according to standard procedures.

Apparatus. Absorption spectra in a visible region were measured with a Hitachi Model 124 recording spectrophotometer, and the optical densities at controlled temperature were measured with a Hitachi-Perkin Elmer Model 139 spectrophotometer equipped with a constant temperature cell compartment which was heated by circulating silicone oil. The temperature fluctuation in the compartment was kept within ±1°C. The spectra were measured against the composite solvent which has exactly the same composition as the solution. However, no reliable specrta could be observed in a region shorter than 390 mμ where a strong absorption of 8-quinolinol was observed, since both solvent and solution contained relatively high concentration of 8-quinolinol.

The molecular weight of 8-quinolinol in toluene was determined by a Mechrolab Model 301A vapour pressure osmometer.

Result and Discussion

The absorption spectrum of bis(8-quinolinolato)-nickel(II) in toluene at 80°C is shown in Fig. 1. The spectrum is characterized by a peak at 473 mμ with an intensity of log $\varepsilon\approx4$, and is interpreted as a d–π transition band of the chelate.[5] Almost similar spectrum was observed for the nickel chelate in molten naphthalene at 83°C. Thus, this spectrum may represent the chelate species which is dissolved in non-donating solvents. On the other hand, when 8-quinolinol is added to the toluene solution of nickel chelate, the peak at 473 mμ diminishes with increasing concentration of 8-quinolinol as illustrated in Fig. 1. Further increase of 8-quinolinol concentration does not change the spectrum appreciably. The spectrum is almost the same as that of nickel chelate in molten 8-quinolinol at 82°C.

When the spectra of nickel chelate are observed in weak donating solvents such as β-methoxynaphthalene, dioxane, cyclohexanol or toluene-methanol, a similar diminution of the 473 mμ peak is noticed, but to a lesser extent than in the case of 8-quinolinol as illustrated in Fig. 2. When the spectra are observed in strong donating solvents, such as pyridine or benzylamine, the spectra changed completely and a new band appeared at 410 mμ. Thus, the absorption band of nickel chelate at 473 mμ was found to be rather sensitive against the donating solvents. The curve 5 in Fig. 1 may be assumed to represent the chelate species which is fully solvated with 8-quinolinol.

In order to estimate the extent of interaction between the nickel chelate and 8-quinolinol, an equilibrium constant of the reaction

$$\mathrm{Ni(ox)_2\cdot\tfrac{1}{2}H_2O} + n\,\mathrm{Hox} \overset{K}{\rightleftharpoons} \mathrm{Ni(ox)_2\cdot(Hox)_n\cdot\tfrac{1}{2}H_2O} \qquad (1)$$

was determined by means of a modified Benesi-Hildebrand method[6] using the spectrophotometric data of Fig. 1.

5) a) K. Sone, *J. Amer. Chem. Soc.*, **75**, 5208 (1953); b) A. S. Bailey, R. J. P. Williams and J. D. Wright, *J. Chem. Soc.*, **1965**, 2579; c) J. Szoke, *Acta Chim. Acad. Sci. Hung.*, **35**, 179 (1963); d) R. Yamaguchi, H. Takahashi and T. Asano, *The Annual Report of the Hoshi College of Pharmacy*, **11**, 9 (1962), *Chem. Abstr.*, **59**, 1195 g (1963).

6) a) H. A. Benesi and J. H. Hildebrand, *J. Amer. Chem. Soc.*, **71**, 2703 (1949); b) Y. Oka, "Jikken Kagaku Koza" Supl. Vol. 7, ed. The Chem. Soc. of Japan, Maruzen, Tokyo (1966), p. 202.

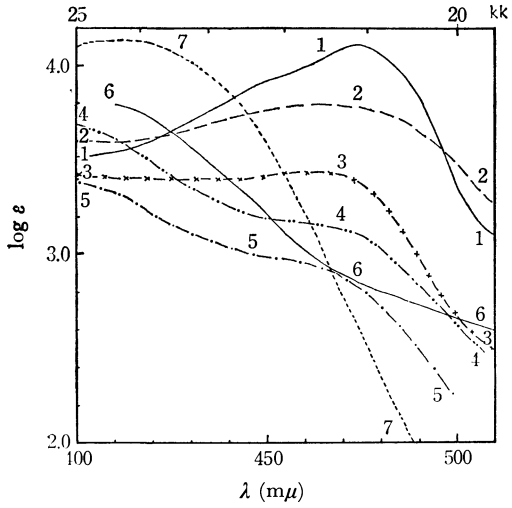

Fig. 2. Absorption spectra of bis(8-quinolinolato)-nickel(II) in various solvents.
Curve 1, in toluene at 80°C; Curve 2, in β-methoxynaphthalene at 77°C; Curve 3, in dioxane at 80°C; Curve 4, in toluene containing 0.5M methanol at 80°C; Curve 5, in cyclohexanol at 60°C; Curve 6, 8-quinolinol at 82°C, Curve 7, in pyridine at room temperature. The values of ε are approximate for the solution of β-methoxy-naphthalene (curve 2) and of 8-quinolinol (curve 6), because no volume corrections were made for those solutions. However, these values are still meaningful for the sake of comparison with other solvent systems.

As we did not succeed in obtaining the completely dehydrated nickel chelate, we could not confirm whether the 8-quinolinol adduct still holds water ($Ni(ox)_2\cdot(Hox)_n 1/2H_2O$) or the chelate releases water when the adduct is formed ($Ni(ox)_2\cdot(Hox)_n$). Thus, the equilibrium constant under discussion is merely an apparent one. However, it may still be useful to estimate the extent of interaction between the nickel chelate and 8-quinolinol.

The equilibrium constant, K, for Eq. (1) is defined by

$$K = \frac{x}{(a-x)(b-nx)^n}, \qquad (2)$$

where a and b are the initial molar concentrations of nickel chelate and 8-quinolinol, respectively, and x is the molar concentration of nickel chelate-8-quinolinol adduct in the equilibrium solution. Eq. (2) may be simplified to

$$K = \frac{x}{(a-x)b^n}, \qquad (3)$$

under the conditions, $b \gg a$ and $b \gg x$.

On the other hand, the optical density of the above system at the given wave length, A_s, can be expressed by

$$A_s = (a-x)\varepsilon_1 + (b-nx)\varepsilon_2 + x\varepsilon_3, \qquad (4)$$

where ε_1, ε_2, and ε_3 are the molar absorption coefficients of nickel chelate, 8-quinolinol and the adduct, respectively.

Thus, we have

$$\frac{a}{(A_s-A_{s_1}-A_{s_2})} = \frac{1}{(\varepsilon_3-\varepsilon_1-n\varepsilon_2)} + \frac{1}{(\varepsilon_3-\varepsilon_1-n\varepsilon_2)K}\cdot\frac{1}{b^n} \qquad (5)$$

by eliminating x from Eqs. (3) and (4), where, $A_{s_1}=a\varepsilon_1$ and $A_{s_2}=b\varepsilon_2$.

Equation (5) can be written as follows, because the molar absorption coefficient of 8-quinolinol, ε_2, at 476 mμ in toluene solution is assumed to be zero.

$$\frac{a}{(A_s-A_{s_1})} = \frac{1}{(\varepsilon_3-\varepsilon_1)} + \frac{1}{(\varepsilon_3-\varepsilon_1)K}\cdot\frac{1}{b^n} \qquad (6)$$

As illustrated in Fig. 3, the plot of $a/(A_s-A_{s_1})$ *vs.* $1/b^n$ becomes a straight line when n is assumed to be 0.5. From the slope of the line, the apparent equilibrium constant is obtained as 5.0 which is comparable to that of hydrogen bond formation in systems such as phenol-dioxane-iso-octane.[7]

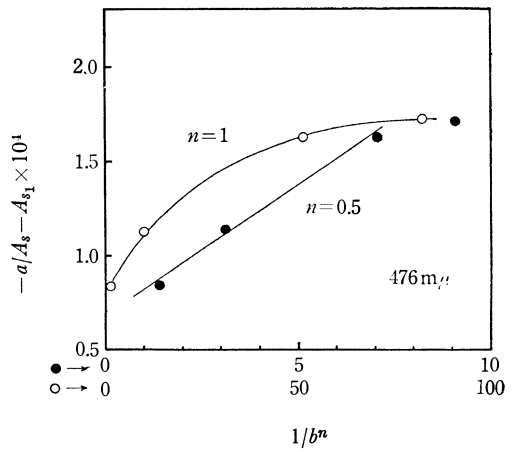

Fig. 3. Determination of equilibrium constant by the modified Benesi-Hildebrand plots.

The combining ratio of 0.5 suggests that one half mole of dimeric 8-quinolinol in toluene interacts with one mole nickel chelate. However, this was denied by the fact that 8-quinolinol exists as monomeric species in toluene as proved by the molecular weight determination.

Formation of 8-quinolinol adducts with 8-quinolinolato metal chelate was reported for several metals, and the equilibrium constant for the reaction

$$Zn(ox)_2 + Hox \rightleftharpoons Zn(ox)_2\cdot(Hox) \qquad (7)$$

in water-chloroform system, was studied by means

7) S. Nagakura and H. Baba, *J. Amer. Chem. Soc.*, **74**, 5693 (1952).

of the solvent extraction technique, and was found to be larger than $10^{2.6}$ at 25°C.[8] The value we obtained is much lower.

Thus, it may be concluded that the extent of interaction of bis(8-quinolinolato)nickel(II) and 8-quinolinol in toluene at 80°C is an order of hydrogen bond formation if the entropy effect is small enough to be neglected.

The authors wish to thank the Ministry of Education, Japanese Government, for financial support of this work. They are also grateful to Miss A. Itoh for the molecular weight determination.

8) Fa-Chu Chou, Q. Fernando and H. Freiser, *Anal. Chem.*, **37**, 361 (1965).

BULLETIN OF THE CHEMICAL SOCIETY OF JAPAN VOL. 43 1056—1061 (1970)

Optimum Geometric Position for Radioactivation by Fast Neutron with a Neutron Generator

Toshiaki KISHIKAWA and Chiro SHINOMIYA

Department of Industrial Chemistry, Faculty of Engineering, Kumamoto University, Kurokami-cho, Kumamoto

(Received June 19, 1969)

With a 14 MeV neutrol generator the optimum irradiation position of disk or square samples of appropriate numbers are given as a function of the configuration of the sample relative to the source. Calculated values are compared with experimental data.

In working with a 14 MeV neutron generator, the need arose to irradiate simultaneously several samples at the same flux. When only one sample is irradiated, the position nearest the deuteron beam spot provides the highest neutron flux.[1,2] When several samples are irradiated, the optimum irradiation position should be chosen at which the neutron flux gives the maximum value, and the radioactivation reaction gives the highest induced activity.

In a previous paper[1] geometry of irradiation was derived and calculated as a function of a generator-sample configuration. The calculated values were compared with the measured values of relative neutron flux. The geometry of irradiation is essentially the same as the geometry of radioactivity measurement. Extensive calculation of solid angles has been carried out.[3-9]

In this paper we report the optimum irradiation position of plane samples as a function of generator-sample configuration. Calculated values are compared with experimental data.

Theoretical

The following assumptions are made:

1. The shape of the neutron source is a point or a disk, emitting neutrons which are distributed uniformly throughout the source.
2. Mono-energetic neutrons (14 MeV) are emitted isotropically.
3. Thermalization and absorption by target holder, water cooling cap and air are neglected.

Geometry of Irradiation and Its Calculation. Neutron flux is different in various irradiation configuration. The flux to be measured is proportional to the numbers of neutron passing through the sample. The fraction of the flux ϕ in n/cm^2-sec to the neutron output N in n/sec is equal to the relative solid angle $\Omega/4\pi$ subtended by the sample. This is defined as the geometry G of irradiation corresponding to the geometry of instruments to measure radioactivity.

$$G = \phi/N = \Omega/4\pi \tag{1}$$

The solid angle Ω_P at a point source P subtended by the sample is given by

$$\Omega_P = \int_A \cos\gamma \frac{dA}{r^2} \tag{2}$$

1) C. Shinomiya and T. Kishikawa, *Tech. Repts. Kumamoto Univ.*, **16**, 68 (1968).
2) P. E. Wilkniss and G. J. Wynne, *Int. J. Appl. Radiat. Isotopes*, **18**, 77 (1967).
3) A. K. Kovarik and N. I. Adams, Jr., *Phys. Rev.*, **40**, 718 (1932).
4) B. P. Buritt, *Nucleonics*, **5**, 28 (1949).
5) M. Calvin, C. Heidelberger, J. C. Reid, B. M. Tolbert and P. Y. Yankwich, "Isotopic Carbon," John Wiley & Sons, New York (1949) p. 304.
6) A. H. Jaffey, *Rev. Sci. Instr.*, **25**, 349 (1954).
7) A. V. H. Masket, R. L. Macklin and H. W. Schmitt, ORNL-2170 (1956).
8) A. V. H. Masket, *Rev. Sci. Instr.*, **28**, 191 (1957).
9) F. Paxton, *ibid.*, **30**, 254 (1959).

Table 1. Typical classification of geometry calculation

Sample form	Source	Distance from Axis[a)]	Calculation		Ref.
			Equation	Solution	
Disk	Point	On axis	5	Given	5
Disk	Point	Off axis	6	Numerically integrated	
Square	Point	On axis	8	Solved	
Square	Point	Off axis	10	Solved	
Disk	Spread	On axis	11	Numerically integrated	
Disk	Spread	Off axis			1
Square	Spread	On axis			1
Square	Spread	Off axis			1

a) The expression "axis" means the direction which passes through a point or the center of a spread source, and which is normal to sample plane (see Fig. 1).

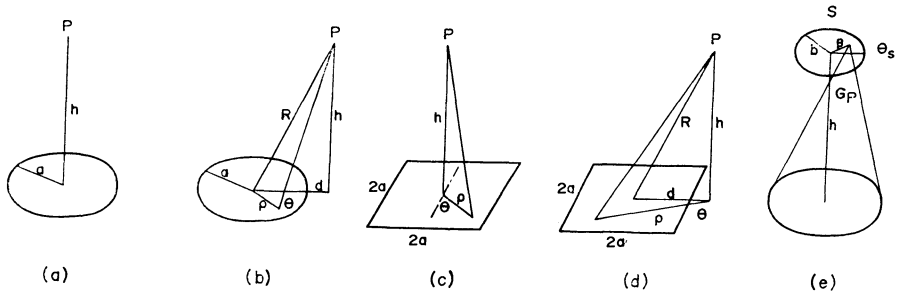

Fig. 1. Typical assemblies of source (point P or spread S) and a sample.

where

A = surface bounded by the sample.
r = distance from the source to a point Q on the sample.
γ = angle between the normal to the surface element dA at Q and the line PQ.

Substituting Eq. (2) into Eq. (1), we obtain

$$G_P = \frac{1}{4\pi}\int_A \cos\gamma \frac{dA}{r^2} \tag{3}$$

If the area of the source is too large to be approximated by a point, the average value of the geometry G_S of a spread source may be calculated by the equation[6)]

$$G_S = \frac{1}{N_S}\int_S G_P N_P dS \tag{4}$$

where

S = surface bounbed by neutron generation.
N_P = relative neutron output at a point P.
N_S = total neutron output.
G_P = geometry at a point P (Eq. 3).

It is possible only in a few cases to carry out the integration analytically where the symmetry of the configuration simplifies the calculation.

Geometry equations were derived for disk and square as functions of the generator-sample configuration in orthogonal coordinates. Typical classification of the geometry calculation is given in Table 1. The schematic configuration and summary of symbol definitions are given in Fig. 1.

The results of the derivation are as follows. Results which cannot be evaluated in closed form are expressed in integral forms.

A. Geometry of a point source coaxial with a disk (Fig. 1a) is derived by means of solid geometry elsewhere[5)]

$$G_P = \tfrac{1}{2}\left\{1 - \frac{h}{(a^2+h^2)^{1/2}}\right\} \tag{5}$$

B. Geometry in which the normal to the center of the disk does not pass the point source (Fig. 1b), is found to be

$$G_P = \frac{1}{4\pi}\int_0^a\int_0^{2\pi} \frac{\rho h d\rho d\theta}{(d^2+\rho^2+h^2-2d\rho\cos\theta)^{3/2}}$$

or

$$G_P = \frac{h}{2\pi}\int_0^{\pi} d\theta \left\{\frac{ad\cos\theta + R^2}{(d^2\cos^2\theta - R^2)(R^2+a^2-2ad\cos\theta)^{1/2}} - \frac{R}{d^2\cos^2\theta - R^2}\right\} \tag{6}$$

where

$$R^2 = d^2 + h^2$$

If the sample is on the axis of the source, *i.e.* d is 0 in Eq. (6), then Eq. (6) can be reduced to Eq. (5).

C. Geometry of a point source coaxial with the

square (Fig. 1c) is given by

$$G_P = \frac{2}{\pi}\int_0^{a\sec\theta}\int_0^{\pi/4}\frac{\rho h\,d\rho\,d\theta}{(\rho^2+h^2)^{3/2}} \tag{7}$$

Equation (7) is then reduced to

$$G_P = \frac{1}{2} - \frac{2}{\pi}\sin^{-1}\frac{h}{(2a^2+2h^2)^{1/2}} \tag{8}$$

D. Geometry in which the normal to the center of the square dose not pass the point source (Fig. 1d) is found to be

$$G_P = \frac{1}{2\pi}\left[\int_{(d-a)\sec\theta}^{(d+a)\sec\theta}\int_0^{\tan^{-1}a/(d+a)}\frac{\rho h\,d\rho\,d\theta}{(\rho^2+h^2)^{3/2}} + \int_{(d-a)\sec\theta}^{a\operatorname{cosec}\theta}\int_{\tan^{-1}a/(d-a)}^{\tan^{-1}a/(d+a)}\frac{\rho h\,d\rho\,d\theta}{(\rho^2+h^2)^{3/2}}\right] \tag{9}$$

Equation (9) is then reduced to

$$G_P = \frac{1}{2\pi}\left[\sin^{-1}\frac{ah}{\{(d-a)^2+h^2\}^{1/2}\{(d-a)^2+a^2\}^{1/2}} - \sin^{-1}\frac{ah}{\{(d+a)^2+h^2\}^{1/2}\{(d+a)^2+a^2\}^{1/2}} + \sin^{-1}\frac{(d-a)h}{(a^2+h^2)^{1/2}\{(d-a)^2+a^2\}^{1/2}} - \sin^{-1}\frac{(d+a)h}{(a^2+h^2)^{1/2}\{(d+a)^2+a^2\}^{1/2}}\right] \tag{10}$$

E. Geometry of a spread source coaxial with a disk (Fig. 1e) is given from Eqs. (4) and (6) by replacing d with β in Eq. (6). We have

$$G_S = \frac{2}{b^2}\int_0^b \beta G_P(\beta)\,d\beta$$

or

$$G_S = \frac{h}{\pi b^2}\int_0^b\int_0^\pi \beta\,d\beta\,d\theta_S \times\left[\frac{\beta^2+h^2-2a\beta\cos\theta_S}{\{\beta^2\cos^2\theta_S-(\beta^2+h^2)\}\{a^2+\beta^2+h^2-2a\beta\cos\theta_S\}^{1/2}} - \frac{(\beta^2+h^2)^{1/2}}{\beta^2\cos^2\theta_S-(\beta^2+h^2)}\right] \tag{11}$$

Numerical data of the derivations A—E and a summary of the geometry (F) in which the normal to the center of the disk does not pass the center of the source, (G) in which the normal to the center of the square passes the center of the source, and

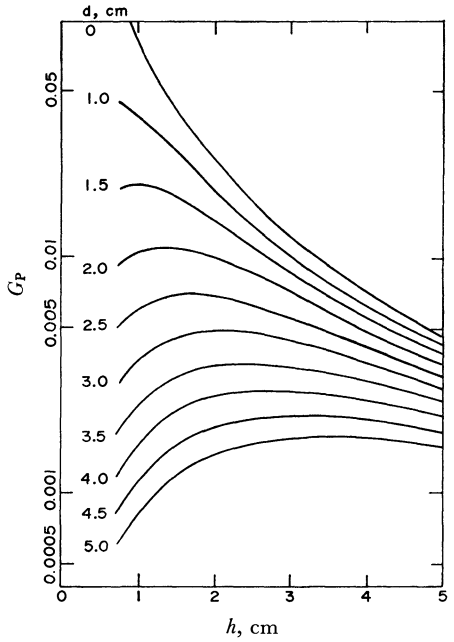

Fig. 2. Geometry value G_P of a point source of a disk (radius 0.665 cm). The G_P curve is given for each distance from axis d.

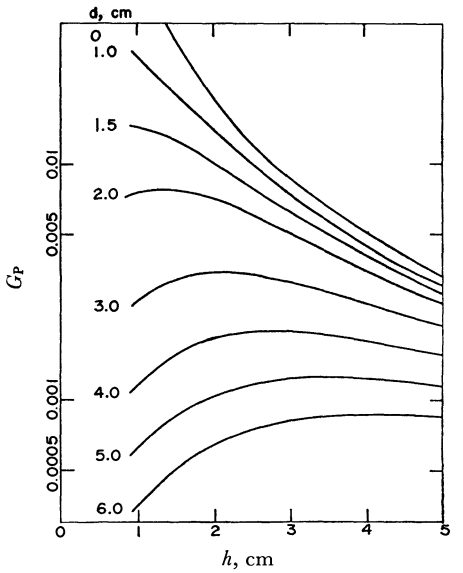

Fig. 3. Geometry value G_P of a point source of a square (side 1 cm). The G_P curve is given for each distance from axis d.

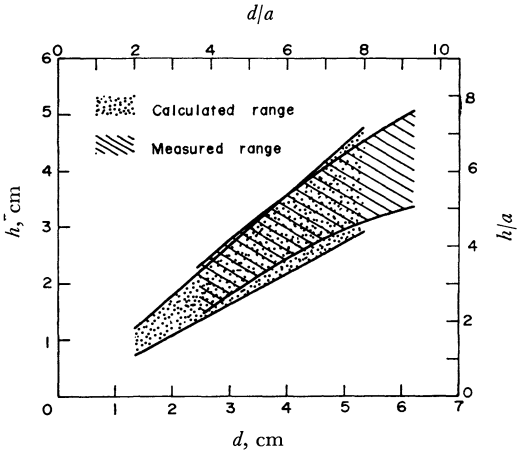

Fig. 4. The optimum geometric position of 97% confidence range of a disk sample with a radius of a=0.665 cm or with an unit radius.

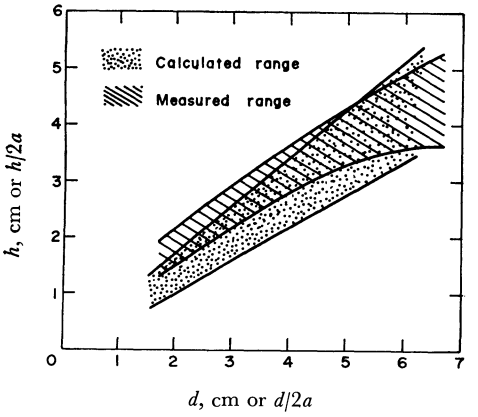

Fig. 5. The optimum geometric position of 97% confidence range of a square sample with a side of $2a=1$ cm or with an unit side.

(H) in which the normal to the center of the square dose not pass the center of the source, have been reported.[1)]

For disk (radius $a=0.665$ cm) and square (side $2a=1$ cm) the geometry values of the series A—D are numerically integrated and shown in Figs. 2 and 3.

The optimum geometry with respect to h can be given analytically by solving the equation $(\partial G/\partial h)_{a,b,d}=0$. This was obtained graphically in Figs. 2 and 3. The optimum geometric position of 97% confidence range in (d, h) with a radius of $a=0.665$ cm or with a side of $2a=1$ cm, so obtained, are shown in Figs. 4 and 5.

Experimental

Neutron Generator. Monochromatic 14 MeV neutrons were produced by $^{3}H(d, n)^{4}He$ reaction with a vertical-type neutron generator made by Hitachi Ltd. A thin tritiated titanium target (*ca.* 5 Ci; copper based) was bombarded with a deuteron beam of *ca.* 200 μA and *ca.* 100 kV. The neutron output was kept constant by controlling the accelerating voltage of the generator. The output was recorded by a BF_3 counter with a counting-rate meter.

Determination of Deuteron Beam Position. It was important to keep the position of deuteron beam spot, or the center of the neutron emission constant. The determination was made by irradiating a small copper foil. The foils ($5\times5\times0.5$ mm) were placed square or crosswise on the cooling cap in the plane parallel to the tritiated target. From the distribution of the induced activity of the foils, the center of the neutron emission was determined by plotting the activity *versus* position. Typical examples are shown in Figs. 6a and 6b.

In the case of the squares method, a contour map (see Fig. 6a) was obtained. The limited numbers of the foil made it difficult to draw a contour of an appropriate level of activity. In the case of the cross method, the plot of activity against position axes gave bloken lines. The ordinates of the folds showed the center (see Fig. 6b). The method was found to be useful.

Determination of Irradiation Geometry. Variation of neutron flux at the irradiation position with respect to the generator-sample configuration was determined by measuring the induced activity of the sample. Copper foil was chosen as a sample. It was a disk (radius 0.665 cm) or a square (side 1 cm).

In order to determine flux at a particular position,

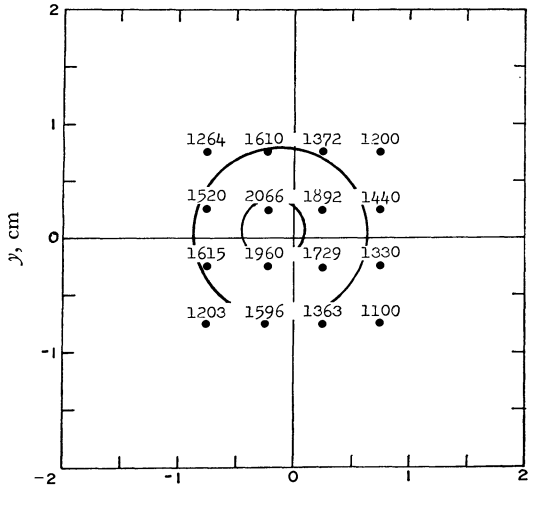

(a) Squares method; center $(-0.2_0, 0.0_6)$

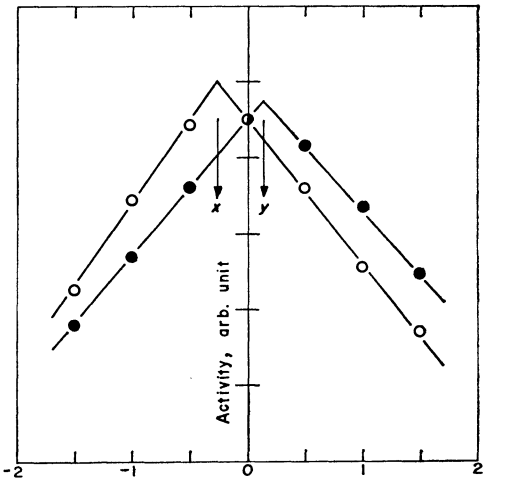

(b) Cross method; center $(-0.2_5, 0.1_3)$

Fig. 6. Determination of the center of the deuteron beam spot, or the center of neutron emission by activating copper foils. In the figure (a) activity values in cpm are superimposed. Contours are 1500 and 2000 cpm level.

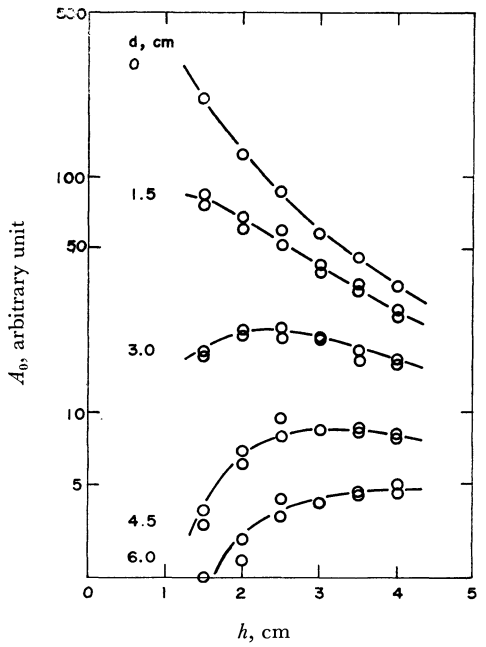

Fig. 7. Induced activity values of disk samples. The radius is 0.665 cm.

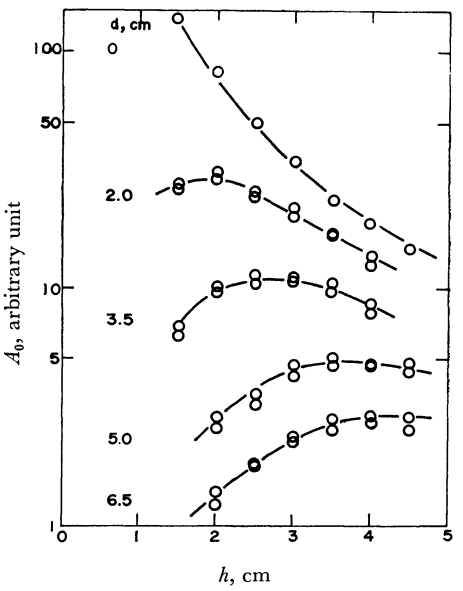

Fig. 8. Induced activity values of square samples. The side is 1 cm.

TABLE 2. RATIO OF INDUCED ACTIVITY TO GEOMETRY OF SPREAD SOURCE COAXIAL WITH A DISK SAMPLE

Axial distance h, cm	Induced activity A_0, cpm	A_0/G_S values $\times 10^{-5}$ at b in cm					
		0[a)]	0.1	0.2	0.3	0.4	0.5
1.5	22200	5.12	5.19	5.22	5.29	5.38	5.49
2.0	13600	5.33	5.33	5.36	5.40	5.46	5.53
2.5	8820	5.25	5.26	5.27	5.30	5.34	5.39
3.0	6310	5.33	5.33	5.34	5.36	5.39	5.43
3.5	4550	5.12	5.18	5.19	5.20	5.23	5.25
	average	5.230	5.258	5.276	5.310	5.310	5.418
	S. D., %	1.807	1.235	1.249	1.294	1.707	1.926

a) Point source, A_0/G_P values.

the foils were placed normal to the direction of deuteron beam and irradiated for several minutes. In order to give uniform neutron emission to the foils, they were rotated with the sample mounting. The induced activity of each foil was then measured in turn to follow its decay with an end-window G-M counter. The decay curve showed the presence of ^{62}Cu (half-life 9.8 min). Possible influence of ^{66}Cu (half-life 5.1 min) produced from ^{65}Cu(n, γ)^{66}Cu reaction and the other nuclides (^{64}Cu and ^{65}Ni) produced from the fast neutron activation could be neglected. Counting rates of the individual samples were corrected for slight weight differences. All the samples were not irradiated at the same time. A comparator technique was used to correlate separate irradiation at different output levels.

The relation between induced activity A_0 at the end of irradiation and flux ϕ can be given by

$$A_0 = N_0\phi\sigma(1-e^{-\lambda t}) \qquad (12)$$

When a foil with known N_0 is irradiated for a certain time t, the term $N_0\sigma(1-e^{-\lambda t})$ in Eq. (12) remains constant. Thus the induced activity is proportional to the neutron flux at the irradiation position or the irradiation geometry. The results are shown in Figs. 7 and 8.

Size of Deuteron Beam Spot. If samples along the direction of the deuteron beam are irradiated (radius of the focus b in cm), the ratio of induced activity to geometry $A_0(h)/G_S(h)$ may remain constant independent of the irradiation distance h. The calculated ratio with the values of $G_S(h)$ given previously[1] at appropreate values of b are listed in Table 2. In the case that b is 0.0, the ratio is equal to $A_0(h)/G_P(h)$. If the value of b is equal to the radius of the neutron emitting spot at which the percent standard deviation of the values of $A_0(h)/G_S(h)$ is minimized, the radius of *ca.* 0.1 cm can be obtained.

The actual size of the focus of the deuteron beam can be seen directly by replacing the tritiated target with a quartz plate. Induced fluorescence showed an

ellipse-like figure, whose diameters are found to be *ca.* 3 mm and *ca.* 5 mm. Its color showed non-uniform intensity. With quartz plate the calculated value was smaller than the observed value. It is probably because (1) the neurton emission is assumed to be distributed unformly throughout the beam spot, and (2) the shape of the spot is assumed to be a disk.

Optimum Irradiation Geometry. The observed values of induced activity at various distances d against distance h shown in Figs. 7 and 8 indicate the presence of maximum values of A_0 and that at d is zero. The experimentally obtained optimum position of 97% confidence range expressed in the coordinates (d, h) which can be found in Figs. 7 and 8 are shown in Figs. 4 and 5. The ranges obtained are in fairly good agreement with the theoretically derived ranges which are shown in the same figures.

As the value of geometry is only a function of the source-sample configuration, the ratio $a : d : h$ is constant. (If the radius of a disk is greater than or equal to 0.665 cm, the value of $G_S(h)$ becomes nearly equal to the value of $G_P(h)$ for $h=1.5$ cm.[1]) This indicates that it is sufficient, under the appropriate empirical conditions, to assume the beam focus to be a point.) This leads to the homologous relation. If the value of a is set up, an optimum position (d, h) is found in scale of d/a and h/a respectively in Fig. 4 or 5. If definite numbers n of disk or square sample (appropreate size a) are irradiated simultaneously under the same neutron flux, the optimum distance d from the axis can be found by means of the relation

$$d = a\mathrm{cosec}\pi/n \quad \text{for disk} \tag{13}$$

or

$$d = \mathrm{a}(1+\cot\pi/n) \quad \text{for square} \tag{14}$$

Hence the optimum configuration can be obtained in Fig. 4 or 5.

As the capsule used for the irradiation of powder or liquid is cylindrical, and the optimum range of irradiation geometry is fairly wide, the present data can be utilized for the choice of the generator-cylindrical sample configuration.

The authors wish to express their gratitude to Dr. Shoichi Sato, Dept. of Mathematics, for his advice and encouragement, and to Professor Kimikazu Matsuyama, Dept. of Electrical Engineering, Chief of the Computing Center, for providing facilities of FACOM-231 computer and for his help with programming. Thanks are also due to Mr. Masaya Tanizaki for the operation of the neutron generator.

BULLETIN OF THE CHEMICAL SOCIETY OF JAPAN VOL. 43 1061—1065 (1970)

Cobalt(III) Complexes with Nitrilotriacetic Acid, Nitrilopropionicdiacetic Acid and Nitriloisopropionicdiacetic Acid*1

Mitsuo TACHIBANA, Akira UEHARA, Eishin KYUNO and Ryokichi TSUCHIYA

Department of Chemistry, Faculty of Science, Kanazawa University, Kanazawa

(Received August 13, 1969)

The following cobalt(III) complexes containing nitrilotriacetic acid (NTA), nitrolopropionicdiacetic acid (NPDA) and nitriloisopropionicdiacetic acid (NIPDA) were prepared: $(NH_4)_3[Co(nta)_2]\cdot 2H_2O$ (pink) (I), $NH_4[Co(Hnta)_2]\cdot 2H_2O$ (pale pink) (II), $K_3[Co(npda)_2]\cdot 2H_2O$ (pink) (III), $K[Co(Hnpda)_2]\cdot 3H_2O$ (pale pink) (IV), [Co(npda)(*o*-phen)]·H_2O (reddish violet) (V), [Co(npda)(bipy)] (reddish violet) (VI), $K[Co(OH)(nipda)(H_2O)]\cdot H_2O$ (bluish violet) (VII) and [Co(nipda)(*o*-phen)] (reddish violet) (VIII); where nta, npda, nipda, *o*-phen and bipy are the abbreviations of nitrilotriacetate-, nitrilopropionicdiacetate-, nitriloisopropionicdiacetate-ion, *o*-phenanthroline and 2,2′-bipyridyl, respectively. On the basis of electronic spectra, it was found that complexes I to IV have the *trans* form, while complexes V, VI and VIII have the *mer* form structure with respect to the nitrogen atoms in the coordinating ligands. Complex VII showed a dehydration-dimerization reaction on heating by "Derivatograph". Comparison of chemical and physical properties of the complexes with those of the corresponding chromium(III) complexes was made.

All the chelating agents discussed in this paper, NTA, NPDA and NIPDA,*2 can behave as $(N\text{–}O_3)$, $(N\text{–}O_2)$ or (O_3) type ligands toward metals. Some behaviors of NTA in cobalt(III)[1] and chromium(III) complexes[2] have been reported. Several

*1 Presented at the 22nd Annual Meeting of the Chemical Society of Japan, Tokyo, April, 1969.

*2 The abbreviations used in this paper, NTA, NPDA and NIPDA, correspond to ATA in Ref. 2, APDA in Ref. 11 and AIPDA in Ref. 12 respectively.

1) M. Mori, M. Shibata, E. Kyuno and Y. Okubo, This Bulletin, **31**, 940 (1958).

2) A. Uehara, E. Kyuno and R. Tsuchiya, *ibid.*, **40**, 2317 (1967).

Table 1. Preparative schemes of complexes

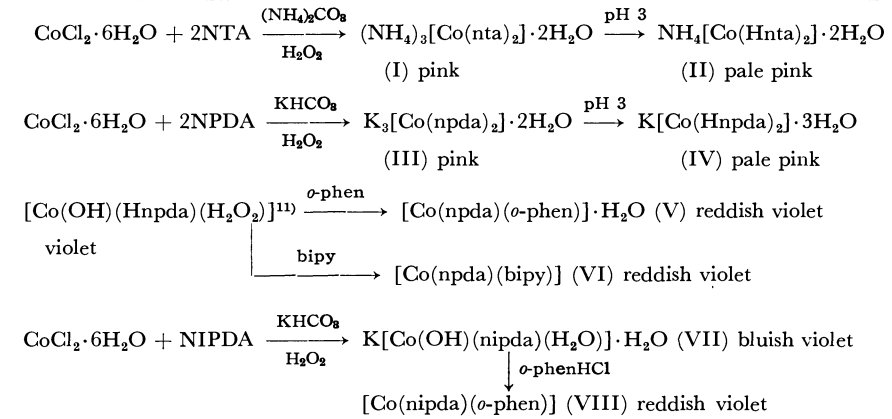

mixed complexes of cobalt(III) with NTA and with natural amino acids have been prepared and discussed in relation to the structural isomers.[3] The bis type complexes of cobalt(III)[4-7] and chromium(III)[8,9] with aminodicarboxylic acids have been reported by many workers, and speculations for their geometrical isomers have also been made. The chromium(III) complexes with aminotricarboxylic acids such as NTA or NPDA have been reported by the authors,[10-12] who pointed out that the coordinating behaviors of these agents toward chromium appreciably vary with each other due to the difference of their structures and properties. However, no report has been given about the corresponding cobalt(III) complexes.

In this study we have undertaken to (1) prepare various kinds of the cobalt(III) complexes with these ligands, (2) ascertain the coordinating behaviors of these ligands toward cobalt(III), (3) predict their structures, especially those of bis type complexes, and (4) compare the structures of the cobalt(III) complexes with those of the corresponding chromium(III) complexes.

Experimental

Preparation of Ligands. NTA,[2] NPDA,[11] and NIPDA[12] were prepared by the methods given in literature.

Preparation of Complexes. The preparative methods of the complexes are schematically shown in Table 1.

Ammonium Bis-(nitrilotriacetato)cobaltate(III) Dihydrate, $(NH_4)_3[Co(nta)_2]\cdot 2H_2O$ (pink) (I). 100 m*l* of water containing 38 g of NTA was gradually neutralized with 17 g of ammonium carbonate. To this solution, 100 m*l* of aqueous solution containing 24 g of cobalt(II) chloride hexahydrate was added. After the pH of the mixed solution was adjusted to 6—7 by means of ammonium carbonate, 10 m*l* of 28% hydrogen peroxide solution was added in order to oxidize the cobalt(II) solution. On being heated on a water bath, the solution turned to pink from violet. The pink crude crystals were obtained from the resulting solution evaporated almost to dryness. The crude products were recrystallized from 5% ammonium carbonate solution. Yield about 8 g.

Found: N, 13.53; C, 27.30; H, 5.21%. Calcd for $(NH_4)_3[Co(nta)_2]\cdot 2H_2O$: N, 13.32; C, 27.41; H, 5.34%.

Ammnoium Bis-(hydrogennitrilotriacetato)cobaltate(III) Dihydrate, $NH_4[Co(Hnta)_2]\cdot 2H_2O$ (pale pink) (II). Five grams of complex I was dissolved in about 50 m*l* of water. When the pH of the solution was adjusted to 3 by adding a few drops of hydrochloric acid, pale pink crystals came out easily. Recrystallization was achieved from an aqueous solution. Yield about 3 g.

Found: N, 8.58; C, 27.78; H, 4.62%. Calcd for $NH_4[Co(Hnta)_2]\cdot 2H_2O$: N, 8.55; C, 27.31; H, 4.48%.

Potassium Bis-(nitrilopropionicdiacetato)cobaltate(III) Dihydrate, $K_3[Co(npda)_2]\cdot 2H_2O$ (pink) (III). These crystals were prepared by a procedure analogous to that in complex I except for the use of 40 g of NPDA and 9 g of potassium hydrogen carbonate instead of 38 g of NTA and 17 g of ammonium carbonate. Yield 6 g.

Found: N, 4.73; C, 27.89; H, 3.13%. Calcd for $K_3[Co(npda)_2]\cdot 2H_2O$: N, 4.54; C, 27.25; H, 3.24%.

Potassium Bis-(hydrogennitrilopropionicdiacetato)cobaltate-(III) Trihydrate, $K[Co(Hnpda)_2]\cdot 3H_2O$ (pale pink)

3) N. Koine, N. Sakota, J. Hidaka and Y. Shimura, This Bulletin, **42**, 1583 (1969).
4) M. Mori, M. Shibata, E. Kyuno and F. Maruyama, *ibid.*, **35**, 75 (1962).
5) J. I. Legg and D. W. Cooke, *Inorg. Chem.*, **5**, 594 (1966).
6) D. W. Cooke, *ibid.*, **5**, 1141 (1966).
7) J. Hidaka, Y. Shimura and R. Tsuchida, This Bulletin, **35**, 567 (1962).
8) K. Yamasaki and S. Ito, *Proc. Japan Acad.*, **42**, 1077 (1966).
9) J. A. Weyh and R. E. Hamm, *Inorg. Chem.*, **7**, 2431 (1968).
10) A. Uehara, E. Kyuno and R. Tsuchiya, This Bulletin, **40**, 2322 (1967).
11) A. Uehara, E. Kyuno and R. Tsuchiya, *ibid.*, **41**, 2385 (1968).
12) A. Uehara, E. Kyuno and R. Tsuchiya, *ibid.*, **41**, 2393 (1968).

(IV). These crystals were also prepared by a procedure similar to that in complex II except that complex III was used instead of complex I as the starting material.

Found: N, 5.11; C, 29.96; H, 4.60%. Calcd for $K[Co(Hnpda)_2]\cdot 3H_2O$: N, 5.00; C, 30.11; H, 4.30%.

Nitrilopropionicdiacetato-o-phenanthrolinecobalt(III) Monohydrate, $[Co(npda)(o\text{-phen})]\cdot H_2O$ (reddish violet) (V). Two grams of hydroxonitrilopropionicdiacetatodiaquocobalt(III)[13] was dissolved in 100 m*l* of water and 1 g of *o*-phenanthroline was then added. On heating the color of the solution gradually turned to reddish violet from violet. From the resulting solution which was kept in a refrigerator, reddish violet crystals were obtained. Recrystallization was achieved from water. Yield 1 g.

Found: N, 9.37; C, 49.58; H, 4.02%. Calcd for $[Co(npda)(o\text{-phen})]\cdot H_2O$: N, 9.15; C, 49.69; H, 3.95%.

Nitrilopropionicdiacetato-2,2′-bipyridylcobalt(III), [Co(npda)(bipy)] (reddish violet) (VI). The preparative method is similar to that described in the case of complex V except that 1 g of 2,2′-bipyridyl was used in place of *o*-phenanthroline. Yield 1 g.

Found: N, 10.01; C, 47.16; H, 3.82%. Calcd for [Co(npda)(bipy)]: N, 10.07; C, 47.93; H, 3.86%.

Potassium hydroxonitriloisopropionicdiacetatoaquocobaltate-(III) Monohydrate, $K[Co(OH)(nipda)(H_2O)]\cdot H_2O$ (bluish violet) (VII). 200 m*l* of water containing 20 g of NIPDA was neutralized with 24 g of potassium hydrogen carbonate. To the solution, 24 g of $CoCl_2\cdot 6H_2O$ was added. After the pH of the solution was adjusted to 6—7 by the addition of potassium hydrogen carbonate, 10 m*l* of 28% hydrogen peroxide solution was added in order to oxidize cobalt(II) solution. From the resulting solution kept at room temperature for a few days, bluish violet crystals were obtained. They were recrystallized from water. Yield 8 g.

Found: N, 3.74; C, 24.02; H, 3.92%. Calcd for $K[Co(OH)(nipda)(H_2O)]\cdot H_2O$: N, 3.98; C, 23.80; H, 3.71%.

Nitriloisopropionicdiacetato-o-phenanthrolinecobalt(III) Monohydrate, $[Co(nipda)(o\text{-phen})]\cdot H_2O$ (reddish violet) (VIII). After two grams of complex VII was dissolved in 100 m*l* of hot water, 1 g of *o*-phenanthroline neutralized with hydrochloric acid was added. The color of the solution turned from violet to reddish violet. From the cooled solution, reddish violet crystals separated. Recrystallization was carried out from water. Yield 0.4 g.

Found: N, 8.58; C, 47.48; H, 4.28%. Calcd for $[Co(nipda)(o\text{-phen})]\cdot H_2O$: N, 8.80; C, 47.82; H, 4.22%.

Apparatus. The same apparatus as described previously was used.[11]

Results and Discussion

Magnetic Properties and Molar Conductivities. Magnetic susceptibilities were measured by the Gouy method in order to ascertain whether the cobalt in the complexes is tervalent or not. The results are listed in Table 2 together with the values of molar conductivities. All the complexes showed diamagnetic properties, indicating that the tervalent cobalt of low-spin type participates in coordination in these complexes.

Table 2. Magnetic properties and molar conductivities

Complexes	Magnetic Properties*	Molar Conductivities** (mho cm^{-1})
I	diamagnetic	325
II	diamagnetic	366
III	diamagnetic	333
IV	diamagnetic	372
V	diamagnetic	<10
VI	diamagnetic	<10
VII	diamagnetic	102
VIII	diamagnetic	<10

* measured at 293°K
** 10^{-3} mol/*l* of aqueous solution was used.

Molar conductivities were measured to investigate to what valency-type the complexes belong in an aqueous solution. As can be seen from Table 2, the values for complexes I and III are 325 and 333 mho cm^{-1}, showing that they are 1 : 3 valency-type electrolytes. The larger values for complexes II (366 mho cm^{-1}) and IV (372 mho cm^{-1}) than those for I and III may be due to the partial dissociation of the hydrogen ion of free carboxylic acid. The very small conductivities of V, VI and VIII suggest that they are non-electrolytes. The value 102 mho cm^{-1} for complex VII is fairly reasonable for the 1 : 1 type electrolyte.

IR Spectra. The infrared absorption spectra of the complexes were measured at a nujol mull state to inspect how the carboxylic groups in the ligands behave toward metals. The numerical data of the absorption bands arising from the free carboxylic (–COOH), the coordinated carboxylic (–COO–M) and the ionic carboxylic groups ($-COO^-$) are given in Table 3 together with the values assigned to the other ligands coordinated. Assignments of the bands were also followed

Table 3. IR data (cm^{-1})

Complexes	–COOH	COO–M	COO^-	Complements
I		1620 (vs)	1595 (sh)	
II	1753 (s)	1610 (vs)		
III		1628 (vs)	1598 (sh)	
IV	1715 (s)	1626 (vs)		
V		1655 (vs)		850, 1590*
VI		1665 (vs)		780, 1590**
VII		1650 (vs)		
VIII		1658 (vs)		865, 1595*

* The absorptions arising from *o*-phenanthrolorine
** Those from 2,2′-bipyridyl

13) R. Tsuchiya, A. Uehara and E. Kyuno, This Bulletin, **42**, 1886 (1969).

by Busch and Bailar.[14] In the spectra of all the complexes, the bands assigned to the coordinated carboxylic group are confirmed. The bands arising from the free carboxylic acid appeared in both the spectra of complexes II and IV. The spectra of complexes I and III show the bands due to the ionic carboxylic groups.

Coordinating Structures of the Complexes. From the results, the coordinating structures of the complexes are discussed.

It has been mentioned from MO treatments that in the cobalt(III) complexes of N_2–O_4 type, the *trans* form with respect to nitrogen atoms shows the splitting in the first absorption band at the longer wave length region,[15] and it has been established in the complexes such as K[Co(ox)(gly)$_2$][16] and K[Co(ida)$_2$].[7]

The numerical data of the absorption maxima of the complexes due to *d–d* transitions are summarized in Table 4.

TABLE 4. ABSORPTION MAXIMA

Complexes	$\nu_1(10^{13}/\text{sec})$ (log ε_1)	$\nu_2(10^{13}/\text{sec})$ (log ε_2)
I	57.58 (1.83)	81.97 (2.27)
II	57.58 (1.81)	81.74 (2.25)
III	58.71 (1.90)	82.87 (2.10)
IV	58.71 (1.91)	82.64 (2.15)
V	56.29 (2.34)	77.92 (2.34)
VI	55.76 (2.36)	77.92 (2.34)
VII	53.00 (2.23)	75.95 (2.31)
VIII	56.07 (2.35)	78.13 (2.36)

The spectral data are obtained in an aqueous solution unless otherwise stated. Figure 1 shows the spectra of complex I, *cis*-K[Co(ida)$_2$] and *trans*-K[Co(ida)$_2$]. The splitted first band of complex I suggests that it takes the *trans* structure with respect to the nitrogen atoms. As regard to these *trans* structures, two possible coordinating structures can be assumed, *i. e.*, facial configuration (Fig. 2 (A)) with respect to O–N–O and meridional one. However, the former seems to be more reasonable than the latter because the observations of NMR[5,6] and electronic spectra[9] and the consideration on the favorable bond angles[7] in the *trans* IDA or MDA complexes suggests that the *trans* facial is prefered to *trans* meridional configuration.

The shapes of the absorption bands of the complexes II, III and IV are essentially analogous to that of complex I. It is reasonable from these facts to consider that complexes II, III and IV

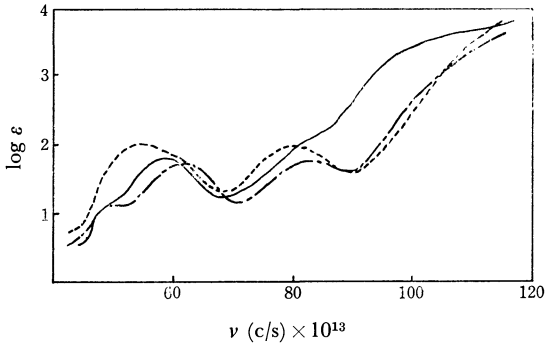

Fig. 1. Absorption spectra for complex I (——), *trans*-K[Co(ida)$_2$](— · —) and *cis*-K[Co(ida)$_2$] (·····).

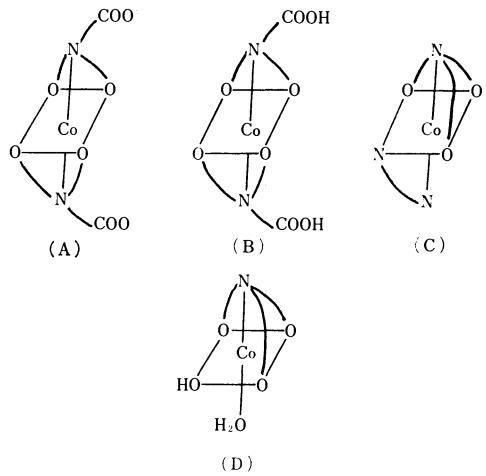

Fig. 2. Possible structures.

may also have the *trans* structure. The IR data show the existence of free carboxylic acid in complexes II and IV, and they seem to have (B) structure as given in Fig. 2.

As for complexes V, VI and VIII, only the *mer* structure with respect to the nitrogen atoms as shown in Fig. 2 (C) can be considered.

Two possible coordinating structures are considered for the structure of complex VII. In the one, the OH group is situated in the *cis* position in relation to the nitrogen atoms of NIPDA, and in the other, in the *trans* position. It has been suggested that K[Co(OH)(nta)(H$_2$O)] has such two isomers; the isomer corresponding to the former was named α type (*cis*) and that corresponding to the latter named β type (*trans*).[1] Comparison of IR spectrum for Complex VII with that for the α or β type of NTA complex indicates that the spectrum of complex VII resembles the former type, and it would be better to assign the *cis* structure to complex VII as shown in Fig. 2 (D).

Comparison of the Properties of Cobalt(III)- with Those of Chromium(III)-Com-

14) D. H. Busch and J. C. Bailar, Jr., *J. Amer. Chem. Soc.*, **75**, 4574 (1953).
15) H. Yamatera, This Bulletin, **31**, 95 (1958).
16) N. Matsuoka, J. Hidaka and Y. Shimura, This Bulletin, **40**, 1868 (1967).

plexes. It will be of interest to compare the difference in properties between the cobalt(III)- and the corresponding chromium(III) complexes.

It has been stated on the basis of electronic spectra that the chromium(III) complex corresponding to I is successively aquated as follows:

$$[Cr(nta)_2]^{3-} \rightarrow [Cr(OH)(nta)(H_2O)]^- \rightarrow [Cr(OH)(nta)(H_2O)_2]^-.$$ [2]

Complex I does not undergo such an aquation. It has been found that the chromium(III) complex corresponding to complex VII turns from $[Cr(OH)(nipda)(H_2O)]^-$ to $[Cr(OH)(nipda)(H_2O)_2]^-$ in an aqueous solution.[12] Complex VII does not show such a change. These facts suggest that the chromium(III) complexes more easily undergo an aquation than the corresponding cobalt(III) complexes in these cases, probably due to the stronger affinity of the metal ion aganist oxygen than aganist nitrogen in the chromium(III) complexes, and *vice versa* in cobalt(III) complexes.

The Coordination Behaviros of the Ligands Toward Chromium(III) or Cobalt(III) Ions. On the basis of the above consideration, the coordinating behaviors of NTA, NPDA and NIPDA toward the metals are summarized in Table 5. The symbol ○ means the possibility of coordination to metals and × the reverse. As seen in Table 5, all the ligands can act as N_1–O_3 type to both cobalt(III) and chromium(III). NIPDA can not behave as N_1–O_2 type for both metals. This may be due to some steric hindrance of CH_3 group and/or the lesser acidities of NIPDA than the other two. NPDA can not behave as O_3 type. This is because the ligand of the 5,5 and 6 membered rings (NPDA) makes the more stable complex than that of 5,5 and 5 membered rings (NTA and NIPDA).[11,17] However, NTA and NIPDA can not act O_3 type to cobalt(III). This may mean that the cobalt has greater affinity to nitrogen than to oxygen.

Table 5. Chelating behaviors of ligands

Ligands	Type	Number of coordinated doner atoms	Chromium(III)	Cobalt (III)
NTA	N_1–O_3	4	○	○
	N_1–O_2	3	○	○
	O_3	3	○	×
NIPDA	N_1–O_3	4	○	○
	N_1–O_2	3	×	×
	O_3	3	○	×
NPDA	N_1–O_3	4	○	○
	N_1–O_2	3	○	○
	O_3	3	×	×

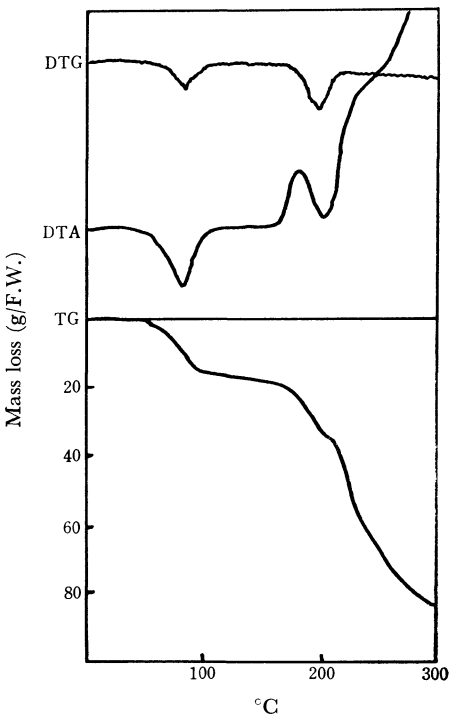

Fig. 3. Derivatogram for complex VII.

Observations of Thermal Decomposition Processes on Complex VII. The thermal decomposition processes of the complex VII were investigated by means of Derivatograph. The measurement was carried out in a constant nitrogen stream at a heating rate of 1°C/min. 500 mg of the samples was used. The derivatogram is shown in Fig. 3. Complex VII lost one mole of crystalline water at 100°C, and the mass loss corresponding to one mole of water is detected at *ca.* 180—200°C. It is of interest to note that the exothermic reaction is detected on DTA curve even in the dehydration process. At this step the color of the sample changed from bluish violet to reddish violet as in the case of the corresponding LDA complex (LDA: *l*-leucine-*N*,*N*-diacetic acid).[18] From this result, it is considered that dimerization may occur at this step, and result in the formation of diol complex such as $K_2[(nipda)Co\langle^{OH}_{OH}\rangle Co(nipda)]$.

The authors wish to thank the Ministry of Education for the financial support granted for this research.

17) S. Chaberek, Jr., and A. E. Martell, *J. Amer. Chem. Soc.*, **75**, 2888 (1953).

18) A. Uehara, E. Kyuno and R. Tsuchiya, This Bulletin, **43**, 414 (1970).

BULLETIN OF THE CHEMICAL SOCIETY OF JAPAN VOL. 43 1066—1078 (1970)

Spectral and Magnetic Studies on Bi- and Tri-Nuclear Complexes Derived from Copper(II) Complexes with Tetradentate Schiff Base and One of the Chlorides, Nitrates and Perchlorates of Copper(II), Nickel(II), Cobalt(II) and Zinc(II)*1

Michinobu KATO,* Yoneichiro MUTO,** Hans B. JONASSEN,*** Kyoko IMAI,* and Tadashi TOKII**

* *Aichi Prefectural University, Mizuho-ku, Nagoya*
** *Department of Chemistry, Saga University, Saga*
*** *Department of Chemistry, Tulane University, New Orleans, La., U.S.A.*

(Received September 16, 1969)

We have prepared a variety of binuclear and trinuclear complexes of the composition Cu(TDSB)·MX_2 and 2Cu(TDSB)·$M(ClO_4)_2$, where Cu(TDSB)=*N,N'*-ethylenebis(salicylideneiminato)copper(II) or *N,N'*-1,2-propylenebis(salicylideneiminato)copper(II), and M=Co, Ni, Cu and Zn. A few higher polynuclear species were also prepared. The previously reported empirical rule found in binuclear copper(II) complexes, where the two copper ions are in the same environment, that the "higher energies of *d–d* bands - lower magnetic moments," was proved to hold in the binuclear copper complexes of the present study, even though the two copper ions are in different environments. For a series of complexes with M = Cu or other metals, and with X = NO_3 or ClO_4, it was observed that "*d–d* bands of Cu(TDSB) apperas at the shortest wavelengths when M = Cu." For perchlorate complexes, the energy of the *d–d* band is in the order, Co<Ni<Cu>Zn, the same as the Irving and Williams' order of complex stability. It can then be generalized that in a hetero-polynuclear complex molecule, the strengthening of the coordinate bonds around one metal ion strengthens the coordinate bonds around the other metal ion or ions.

Previously we reported the correlation between the magnetism and spectra in binuclear copper(II) halide complexes with pyridine *N*-oxides or salicylideneimines.[1-4] As an extension of these investigations we have been studying a variety of polynuclear complexes derived from copper(II) chelates with tetradentate salicylaldimine-Schiff's base and one of the following metal salts: Cu(II), Ni(II), Co(II) and Zn(II) as the chloride, nitrate, and perchlorate. About the time of the completion of this study, Gruber reported magnetic and spectral studies of similar polynuclear complexes.[5-8]

We are therefore reporting in this paper only the data of the complexes which were not included in their papers except those which are necessary for our discussion. Many of Gruber's and our complexes are adducts with different solvent molecules. Often, too, the numerical values of the data differ in details from each other. The spectral data necessary for the discussion of the stereochemistry are shown in the attached figures.

The present study was initiated to investigate the change in magnetic interaction or spectral properties of binuclear copper(II) complexes when the two copper ions were present in different environments. The rule, "higher energies of *d–d* band - lower magnetic moments," previously observed for the homo-binuclear copper(II) complexes, was to be tested for hetero-binuclear copper(II)

*1 A part of this study was presented a) by M. Kato, Y. Muto, H. N. Ramaswamy, H. B. Jonassen, K. Imai and the late K. Ito at the 19th Annual Meeting of the Chemical Society of Japan, Tokyo, April, 1966, Preprints, Vol. II, p. 135; b) by M. Kato, Y. Muto, H. N. Ramaswamy, H. B. Jonassen and K. Imai at the 16th Conference on Coordination Chemistry of the Chemical Society of Japan, Tokyo (November, 1966), Proceedings, p. 68.

1) M. Kato, Y. Muto and H. B. Jonassen, This Bulletin, **40**, 1738 (1967).

2) Y. Muto, M. Kato, H. B. Jonassen, H. N. Ramaswamy and K. Imai, Proceedings of 10th International Conference on Coordination Chemistry, Nikko, September, 1967, p. 337.

3) Y. Muto, M. Kato, H. B. Jonassen and L. C. Cusachs, This Bulletin, **42**, 417 (1969).

4) M. Kato, Y. Muto, H. B. Jonassen, K. Imai, K. Katsuki and S. Ikegami, *ibid.*, **42**, 2555 (1969).

5) S. J. Gruber, C. M. Harris and E. Sinn, *Inorg. Nucl. Chem. Lett.*, **3**, 495 (1967).

6) S. J. Gruber, C. M. Harris and E. Sinn, *Inorg. Chem.*, **7**, 268 (1968).

7) S. J. Gruber, C. M. Harris and E. Sinn, *J. Inorg. Nucl. Chem.*, **30**, 1805 (1968).

8) S. J. Gruber, C. M. Harris and E. Sinn, *J. Chem. Phys.*, **49**, 2183 (1968).

Table 1. List of the complexes by Gruber and co-workers and the present authors†1,†2,†3

Main part of complexes	Solvent molecules attached to the main part of complexes	
	Gruber's	Present study
Cu(En-Sal)		non-adduct (dark green)
$Cu(En\text{-}Sal)\cdot CuCl_2$	non-adduct	$0.5CH_3OH$ (dark purple)
	H_2O	$0.5C_2H_5OH$ (light purple)
$Cu(En\text{-}Sal)\cdot Cu(NO_3)_2$	X	non-adduct (purple)
	X	$1.5CH_3OH$ (purple)
	X	$1.5CH_3OH\cdot H_2O$ (brownish purple)
	X	4py (smoked olive)
$Cu(En\text{-}Sal)\cdot Ni(NO_3)_2$	X	$2C_2H_5OH$ (purple)
$Cu(En\text{-}Sal)\cdot Co(NO_3)_2$	X	$1.5C_2H_5OH\cdot 0.5H_2O$ (purple)
$4Cu(En\text{-}Sal)\cdot 3Zn(NO_3)_2$	X	non-adduct (brick-red)
$Cu(En\text{-}Sal)\cdot CoCl_2$	non-adduct	$0.5C_2H_5OH$ (greyish violet)
$Cu(En\text{-}Sal)\cdot ZnCl_2$	non-adduct	non-adduct (yellowish pink)
$2Cu(En\text{-}Sal)\cdot Cu(ClO_4)_2$	$3H_2O$	$CH_3OH\cdot 2H_2O$ (dark violet)
$2Cu(En\text{-}Sal)\cdot Ni(ClO_4)_2$	$3H_2O$	$2H_2O$ (salmon-pink)
$2Cu(En\text{-}Sal)\cdot Co(ClO_4)_2$	$2.5H_2O$	$2H_2O$ (pink)
$2Cu(En\text{-}Sal)\cdot Zn(ClO_4)_2$	$1.5H_2O$	$2.5H_2O$ (salmon-pink)
Cu(Pn-Sal)		non-adduct (greyish violet)
$Cu(Pn\text{-}Sal)\cdot CuCl_2$	non-adduct	non-adduct (dark violet)
$Cu(Pn\text{-}Sal)\cdot Cu(NO_3)_2$	X	non-adduct (purple)
$Cu(Pn\text{-}Sal)\cdot Ni(NO_3)_2$	X	$2C_2H_5OH$ (purple)
$Cu(Pn\text{-}Sal)\cdot Co(NO_3)_2$	X	$1.75C_2H_5OH\cdot 0.5H_2O$ (purple)
$Cu(Pn\text{-}Sal)\cdot Zn(NO_3)_2$	X	non-adduct (salmon-pink)
$2Cu(Pn\text{-}Sal)\cdot Zn(NO_3)_2$	X	$1.5CH_3OH\cdot 2H_2O$ (greyish purple)
$Cu(Pn\text{-}Sal)\cdot CoCl_2$	X	$0.5H_2O$ (greyish violet)
$Cu(Pn\text{-}Sal)\cdot ZnCl_2$	non-adduct	non-adduct (salmon-pink)
$2Cu(Pn\text{-}Sal)\cdot Cu(ClO_4)_2$	$2H_2O$	$2H_2O$ (dark violet)
$2Cu(Pn\text{-}Sal)\cdot Cu(ClO_4)_2$	X	en (greyish green)
Cu(En-AcAc)		non-adduct (dark violet)
$2Cu(En\text{-}AcAc)\cdot Cu(NO_3)_2$	X	H_2O (greyish brown)

†1 The symbol(X) in column of Gruber's indicates the complexes which are reported in the present study but not described by Gruber and co-workers.

†2 Cu(En-Sal), Cu(Pn-Sal) and Cu(En-AcAc) are used as abbreviations for *N,N'*-ethylenebis (salicylideneiminato)copper(II), *N,N'*-1,2-propylenebis (salicylideneiminato) copper (II) and *N,N'*-ethylenebis (acetylacetoneaminato) copper (II) respectively. en=ethylenediamine, py=pyridine

†3 Color of the complexes was given in parentheses in the third column.

complexes.*2 The mutual stereochemical interaction between local metal complexes which may occur when more than two metal atoms were present in a molecule, was another interesting point under examination.

The complexes of this study is given in Table 1; some of Gruber's complexes are also included to indicate the difference in the solvation.

Experimental

I. Preparation of Complexes. *A. Materials.* Salicylaldehyde, ethylenediamine, 1,2-propylenediamine (Tokyo Kasei Kogyo's Guaranteed Reagent), metal nitrates, chlorides (Wako Pure Chemical Industries' JIS Special Grade), anhydrous cupric chloride (Fisher Certified Reagent) and perchlorates (K & K Laboratories) were obtained commercially.

B. General Method of Preparation. In a typical preparation, an ethanolic solution of a metal salt was added through a quantitative filter paper to one of the recrystallized parent copper(II) complexes, Cu(En-Sal), Cu(Pn-Sal) or Cu(En-AcAc) in a flask equipped with a condenser. For binuclear complexes, the mole ratio of a chloride or a nitrate to parent complex was 1.1 : 1, *i. e.*, ten per cent excess of the metal salt over the stoichiometric quantity. For the preparation of trinuclear complexes, the mole ratio of the perchlorate or nitrate to the parent complex was 1.1 : 2. The ethanolic mixture in the flask was stirred on a hot plate for two hours to complete the reaction. The product was

*2 In this paper, the words, hetero- and homo-, are used to indicate the ligand field environments in a polynuclear complex molecule which are essentially different and the same respectively.

filtered off on a glass filter, washed several times with ethanol and once with ether, and dried at 40—50°C.

C. Preparation of Specific Complexes. a) Cu(En-Sal). $Cu(NO_3)_2$. A crude product was prepared by stirring a mixture of Cu(En-Sal) and $Cu(NO_3)_2 \cdot 3H_2O$ in a 1 : 1 mole ratio in ethanol at room or at an elevated temperature. The product was filtered off, washed with a mixture of ether and ethanol, and dried at 50°C. The pure compound can be prepared by refluxing a recrystallized Cu(En-Sal)·$Cu(NO_3)_2 \cdot 1.5CH_3OH$ in ethanol.

b) Cu(En-Sal)·$Cu(NO_3)_2 \cdot 1.5CH_3OH$. Crude Cu(En-Sal)·$Cu(NO_3)_2$(5 g) was dissolved by heating in 150 m*l* of methanol containing one gram of $Cu(NO_3)_2 \cdot 3H_2O$. The hot solution was filtered through a quantitative filter paper into a flask. To the filtrate were slowly added 30 m*l* of ether and then 120 m*l* of petroleum ether. The precipitated complex was filtered off, washed with ether containing a small amount of methanol and then with a large amount of ether, and dried at 40—45°C. Yield 2.4 g.

c) Cu(En-Sal)·$Cu(NO_3)_2 \cdot 1.5CH_3OH \cdot H_2O$. Crude Cu(En-Sal)·$Cu(NO_3)_2$(5 g), dissolved in 190 m*l* methanol on a hot plate and the hot solution was passed once through a quantitative filter paper. To the filtrate, 15 m*l* of ether and then 130 m*l* of petroleum ether were slowly added. The product was collected on a glass filter, methanol and ether were added with stirring, and then sucked off. After washing with ether it was dried at 40—45°C, yield 2.9 g.

d) Cu(En-Sal)·$Cu(NO_3)_2 \cdot 4Py$. Three grams of Cu(En-Sal)·$Cu(NO_3)_2$, dissolved in 190 m*l* of pyridine on a hot plate were filtered through a quantitative filter paper into a flask. Petroleum ether was added until precipitation just occurred. The mixture was allowed to stand for one to two weeks at room temperature with occasional shaking. The product was washed with ether several times, and dried at 50°C,

TABLE 2. ANALYTICAL DATA OF COMPLEXES

Complexes	C %		H %		N %		Metal %	
	Found	Calcd	Found	Calcd	Found	Calcd	Found	Calcd
Cu(En-Sal)							19.20	19.26
Cu(En-Sal)·$CuCl_2 \cdot 0.5CH_3OH$	41.50	41.26	3.46	3.36	5.98	5.83	26.40	26.46
Cu(En-Sal)·$CuCl_2 \cdot 0.5C_2H_5OH$	42.40	41.90	3.47	3.52	6.09	5.75	26.13	26.08
Cu(En-Sal)·$Cu(NO_3)_2$	37.42	37.14	2.89	2.73	10.59	10.83	24.34	24.56
Cu(En-Sal)·$Cu(NO_3)_2 \cdot 1.5CH_3OH$	36.82	37.17	3.01	3.57	11.25	9.91	22.32	22.47
Cu(En-Sal)·$Cu(NO_3)_2 \cdot 1.5CH_3OH \cdot H_2O$	36.02	36.03	3.70	3.80	10.48	9.60	21.84	21.78
Cu(En-Sal)·$Cu(NO_3)_2 \cdot 4py$	52.05	51.86	4.18	4.11	12.99	13.44	15.31	15.24
Cu(En-Sal)·$Ni(NO_3)_2 \cdot 2C_2H_5OH$	39.89	39.73	4.25	4.33	9.19	9.27	20.60	20.21
Cu(En-Sal)·$Co(NO_3)_2 \cdot 1.5C_2H_5OH \cdot 0.5H_2O$	38.79	38.62	3.78	4.09	9.57	9.48	20.38	20.73
$4Cu(En\text{-}Sal) \cdot 3Zn(NO_3)_2$	40.25	40.73	2.87	2.99	10.38	10.39	23.87	23.86
Cu(En-Sal)·$CoCl_2 \cdot 0.5C_2H_5OH$	42.48	42.30	3.24	3.55	5.97	5.80	25.71	25.37
Cu(En-Sal)·$ZnCl_2$	41.06	41.23	3.01	3.03	5.98	6.01	27.51	27.66
2Cu(En-Sal)·$Cu(ClO_4)_2 \cdot CH_3OH \cdot 2H_2O$	40.71	40.03	3.94	3.66	5.63	5.66	19.40	19.26
2Cu(En-Sal)·$Ni(ClO_4)_2 \cdot 2H_2O$	40.70	40.31	3.55	3.38	5.51	5.88	19.43	19.49
2Cu(En-Sal)·$Co(ClO_4)_2 \cdot 2H_2O$	40.55	40.31	3.52	3.38	5.60	5.88	19.43	19.51
2Cu(En-Sal)·$Zn(ClO_4)_2 \cdot 2.5H_2O$	40.12	39.66	3.41	3.43	5.84	5.78	20.03	19.86
Cu(Pn-Sal)							18.49	18.48
Cu(Pn-Sal)·$CuCl_2$	42.68	42.69	3.78	3.37	5.97	5.86	26.60	26.57
Cu(Pn-Sal)·$Cu(NO_3)_2$	38.54	38.42	3.26	3.03	10.44	10.54	23.74	23.91
Cu(Pn-Sal)·$Ni(NO_3)_2 \cdot 2C_2H_5OH$	40.64	40.77	4.62	4.56	8.95	9.06	19.67	19.76
Cu(Pn-Sal)·$Co(NO_3)_2$ $1.75C_2H_5OH \cdot 0.5H_2O$	39.84	39.94	4.23	4.50	9.35	9.09	19.73	19.87
Cu(Pn-Sal)·$Zn(NO_3)_2$	38.11	38.29	3.00	3.02	10.45	10.51	24.04	24.18
2Cu(Pn-Sal)·$Zn(NO_3)_2 \cdot 1.5CH_3OH \cdot 2H_2O$	44.41	44.36	4.31	4.40	8.78	8.74	20.12	20.02
Cu(Pn-Sal)·$CoCl_2 \cdot 0.5H_2O$	42.56	42.30	3.52	3.55	5.80	5.80	25.39	25.37
Cu(Pn-Sal)·$ZnCl_2$	42.25	42.53	3.40	3.36	5.66	5.83	26.89	26.85
2Cu(Pn-Sal)·$Cu(ClO_4)_2 \cdot 2H_2O$	41.89	41.41	3.92	3.68	5.55	5.68	19.39	19.33
2Cu(Pn-Sal)·$Cu(ClO_4)_2 \cdot en$	42.90	42.80	4.14	3.99	8.23	8.32	19.01	18.87
Cu(En-AcAc)							22.11	22.23
2Cu(En-AcAc)·$Cu(NO_3)_2 \cdot H_2O$	37.13	37.09	5.09	4.93	10.76	10.81	24.52	24.53

yield 1.9 g.

e) $2Cu(Pn\text{-}Sal)\cdot Cu(ClO_4)_2\cdot en$. To a mixture of recrystallized $Cu(en)_2(ClO_4)_2$(2.8 g) and Cu(Pn-Sal) (5.2 g) in a flask, was added a solution of $Cu(ClO_4)_2\cdot 6H_2O$ (3 g) in methanol (130 m*l*). The methanolic mixture was stirred on a hot plate under reflux for three hours. The reaction product was carefully poured into another flask in order to separate it from the small amount of unreacted $Cu(en)_2(ClO_4)_2$. To this, was added 0.2 g of pure $Cu(Pn\text{-}Sal)\cdot Cu(ClO_4)_2\cdot 2H_2O$ and, with stirring, refluxed for five hours more. The dark green fine crystals were washed on a glass filter several times with methanol and once with ether and dried at 80°C, yield 6 g.

f) $2Cu(Pn\text{-}Sal)\cdot Zn(NO_3)_2\cdot 1.5CH_3OH\cdot 2H_2O$. Cu-(Pn-Sal) (2.5 g) and $Zn(NO_3)_2\cdot 6H_2O$ (2.5 g), dissolved in methanol (25 m*l*) by heating gently, was filtered into a flask and allowed to stand until precipitation started. Ether was added to the supernatant to complete the precipitation. The crude material (3.2 g), after dissolving by warming in methanol (20 m*l*), and filtering through a quantitative filter paper into a flask, was placed in a vacuum desiccator. The filtrate was concentrated to one third of its original volume by warming gently under gentle suction. Ether was added to it and the precipitated violet powder was washed on a glass filter with a mixture of ether and methanol several times and once with ether, and dried at 40°C. Yield 2.5 g.

g) $Cu(Pn\text{-}Sal)\cdot Zn(NO_3)_2$. The crude material was prepared by treating a mixture of Cu(Pn-Sal) (3 g) and $Zn(NO_3)_2\cdot 6H_2O$ (3 g) in 30 m*l* of ethanol according to the method of (f). Yield 3.8 g. This was dissolved in methanol (30 m*l*) and filtered through a quantitative filter paper into a flask. By alternatively adding small portions of ether and petroleum ether in volume ratio of 2 : 1 at a time precipitation occurred. The precipitate was filtered, washed with a mixture of ether and methanol twice and once with ether, dried at 95°C, yield 2.7 g.

h) $2Cu(En\text{-}AcAc)\cdot Cu(NO_3)_2\cdot H_2O$. A mixture of Cu(En-AcAc) and $Cu(NO_3)_2\cdot 3H_2O$ in mole ratio of 2 : 1 was dissolved in methanol. The brown solution was concentrated to a certain volume in an evaporator and ether was added to it. The crude product (2.7 g) was dissolved in hot methanol (13 m*l*), filtered through a quantitative filter paper into a flask, and concentrated in an evaporator until precipitation began to occur. After slowly adding 20 m*l* of ether to it, the product was washed with a mixture of ether and methanol several times and once with ether, and dried at 40°C, yield 2 g.

The analytical data for all the complexes are listed in Table 2.

II. Magnetic Susceptibility Determinations. These data were obtained by the Gouy method at room temperature. The molar susceptibility, χ_M, was corrected using Pascal's constants, for the diamagnetism

Table 3. Magnetic data of complexes

Complexes	Susceptibility $\chi_g\cdot 10^6$ (cgs, emu)	Temperature (°K)	μ_{eff} (B.M.)	$\mu_{eff}^{25°C}$ (B.M.)
Cu(En-Sal)	3.77	292	1.81	
$Cu(En\text{-}Sal)\cdot CuCl_2\cdot 0.5CH_3OH$	3.67	290	1.52	1.54
$Cu(En\text{-}Sal)\cdot CuCl_2\cdot 0.5C_2H_5OH$	3.74	289	1.55	1.56
$Cu(En\text{-}Sal)\cdot Cu(NO_3)_2$	2.06	304	1.25	1.23
$Cu(En\text{-}Sal)\cdot Cu(NO_3)_2\cdot 1.5CH_3OH$	2.69	301	1.46	1.45
$Cu(En\text{-}Sal)\cdot Cu(NO_3)_2\cdot 1.5CH_3OH\cdot H_2O$	4.06	300	1.76	
$Cu(En\text{-}Sal)\cdot Cu(NO_3)_2\cdot 4py$	2.99	301	1.87	
$Cu(En\text{-}Sal)\cdot Ni(NO_3)_2\cdot 2C_2H_5OH$	8.28	304	3.59	
$Cu(En\text{-}Sal)\cdot Co(NO_3)_2\cdot 1.5C_2H_5OH\cdot 0.5H_2O$	16.26	285	4.75	
$4Cu(En\text{-}Sal)\cdot 3Zn(NO_3)_2$	2.67	284	1.82	
$Cu(En\text{-}Sal)\cdot CoCl_2\cdot 0.5C_2H_5OH$	22.11	284	4.98	
$Cu(En\text{-}Sal)\cdot ZnCl_2$	2.60	284	1.81	
$2Cu(En\text{-}Sal)\cdot Cu(ClO_4)_2\cdot CH_3OH\cdot 2H_2O$	2.17	303	1.45	
$2Cu(En\text{-}Sal)\cdot Ni(ClO_4)_2\cdot 2H_2O$	6.15	299	3.88	
$2Cu(En\text{-}Sal)\cdot Co(ClO_4)_2\cdot 2H_2O$	12.72	298	5.48	
$2Cu(En\text{-}Sal)\cdot Zn(ClO_4)_2\cdot 2.5H_2O$	2.50	297	1.84	
Cu(Pn-Sal)	3.81	284	1.84	
$Cu(Pn\text{-}Sal)\cdot CuCl_2$	3.66	300.5	1.55	1.54
$Cu(Pn\text{-}Sal)\cdot Cu(NO_3)_2$	2.40	304	1.35	1.34
$Cu(Pn\text{-}Sal)\cdot Ni(NO_3)_2\cdot 2C_2H_5OH$	7.87	293	3.48	
$Cu(Pn\text{-}Sal)\cdot Co(NO_3)_2\cdot 1.75C_2H_5OH\cdot 0.5H_2O$	15.79	293	4.85	
$Cu(Pn\text{-}Sal)\cdot Zn(NO_3)_2$	2.08	295	1.77	
$2Cu(Pn\text{-}Sal)\cdot Zn(NO_3)_2\cdot 1.5CH_3OH\cdot 2H_2O$	2.48_5	295	1.83	
$Cu(Pn\text{-}Sal)\cdot CoCl_2\cdot 0.5H_2O$	21.39	293	4.98	
$Cu(Pn\text{-}Sal)\cdot ZnCl_2$	2.36	294	1.79	
$2Cu(Pn\text{-}Sal)\cdot Cu(ClO_4)_2\cdot 2H_2O$	1.83	303	1.35	
$2Cu(Pn\text{-}Sal)\cdot Cu(ClO_4)_2\cdot en$	2.21	302	1.48	
$2Cu(En\text{-}AcAc)\cdot Cu(NO_3)_2\cdot H_2O$	4.80_6	286	1.76	

TABLE 4. DATA OF DIFFUSE REFLECTANCE SPECTRA OF COMPLEXES*)

Complexes	Band maxima, λ_{max}, mμ
Cu(En-Sal)	395vs,sh 588s,br* 1705vw
Cu(En-Sal)·$CuCl_2$·0.5CH_3OH	375vs,sh 536s,br* 985s,br* 1950vw
Cu(En-Sal)·$CuCl_2$·0.5C_2H_5OH	375vs,sh 536s,br* 990s,br* 1950vw
Cu(En-Sal)·$Cu(NO_3)_2$	516s,br* (860 1020)* m,br,dp 1680vw
Cu(En-Sal)·$Cu(NO_3)_2$·1.5CH_3OH	514s* (855 1015)*m,br,dp 1660vw 1970vw
Cu(En-Sal)·$Cu(NO_3)_2$·1.5CH_3OH·H_2O	375vs,sh (515s 750m 960m,br)* 1700vw
Cu(En-Sal)·$Cu(NO_3)_2$·4py	390vs,sh 585s,br* 1005m,br* 1680vw
Cu(En-Sal)·$Ni(NO_3)_2$·2C_2H_5OH	355vs,sh 539s* 735m,sh† 1210m,br† 1700vw 1980vw
Cu(En-Sal)·$Co(NO_3)_2$·1.5C_2H_5OH·0.5H_2O	385vs,sh (536* 580sh)s, dp 1255m,br† 1690vw 1975vw
4Cu(En-Sal)·3$Zn(NO_3)_2$	385vs,sh 528s,br* 1695vw
Cu(En-Sal)·$CoCl_2$·0.5C_2H_5OH	565vs† (640sh 662)† vs,dp (1370m,sh 1520s)† br,dp 1975s,br
Cu(En-Sal)·$ZnCl_2$	(516* 570sh)s,dp 700vw,sh 1695vw
2Cu(En-Sal)·$Cu(ClO_4)_2$·CH_3OH·2H_2O	505vs,br* (980 1110)*s,br,dp 1950vw
2Cu(En-Sal)·$Ni(ClO_4)_2$·2H_2O	350vs,sh 524s* (705sh 785)†w,dp 1310w,br† 1690w 18985vw
2Cu(En-Sal)·$Co(ClO_4)_2$·2H_2O	360vs,sh 527s* 680vw,br,sh 1100w,sh 1415w,br† 1690vw 1985vw
2Cu(En-Sal)·$Zn(ClO_4)_2$·2.5H_2O	355vs,sh 526s* 1690vw 1990vw
Cu(Pn-Sal)	385vs,br,sh 566s* 1695vw
Cu(Pn-Sal)·$CuCl_2$	355vs,sh 515s,br* 945s,br* 1680vw
Cu(Pn-Sal)·$Cu(NO_3)_2$	360vs,sh 506s,br* (910 1030)* m,br,dp
Cu(Pn-Sal)·$Ni(NO_3)_2$·2C_2H_5OH	540* (675 750)† m,sh,dp 1205m,br† 1715vw 1985vw
Cu(Pn-Sal)·$Co(NO_3)_2$·1.75C_2H_5OH·0.5H_2O	532s* 1215m,br† 1710vw 1985vw
Cu(Pn-Sal)·$Zn(NO_3)_2$	520s* 580s,sh 1700vw 1980vw
2Cu(Pn-Sal)·$Zn(NO_3)_2$·1.5CH_3OH·2H_2O	355vs,sh 533s* 1705w 1685w
Cu(Pn-Sal)·$CoCl_2$·0.5H_2O	565vs† (640sh 660)†vs,dp (1380m,sh 1525s)†dp 2000m,br
Cu(Pn-Sal)·$ZnCl_2$	355vs,sh (520* 560sh)s,dp 1700vw
2Cu(Pn-Sal)·$Cu(ClO_4)_2$·2H_2O	365s 505s,br* (1005 1150)*m,br 1945vw
2Cu(Pn-Sal)·$Cu(ClO_4)_2$·en	(370vs 420s,sh)dp 583s,br* 730m,sh 1700vw
Cu(En-AcAc)	365vs,sh (545* 620sh)s,dp 1735w 1950vw
2Cu(En-AcAc)·$Cu(NO_3)_2$·H_2O	415s,sh (552s,br 915m,br)* 1740vw

*) vs=very strong s=strong w=weak vw=very weak sh=shoulder br=broad dp=double peak, two bands in succession

*, † =the main *d–d* bands of copper(*) and of metal other than copper (†) which were employed in the discussion of the structure of complexes.

of all the atoms in the complexes.[9,10] For the complexes containing only copper atom as paramagnetic ions, the magnetic moments were calculated per copper atom from the expression $\mu_{eff}=2.83\sqrt{\chi_M/n\cdot T}$ B.M., where n is the number of copper atoms in a molecule. For the complexes in which paramagnetic ions other than copper are present, the magnetic moments were calculated using $\mu_{eff}=2.83\sqrt{\chi_M\cdot T}$ B.M. The temperature-independent paramagnetism associated with the paramagnetic ions was not included in the calculation of μ_{eff} throughout this work. For binuclear copper(II) complexes with subnormal magnetic moments, the moments observed at room temperature were corrected for minor room temperature variations to those at 25°C, $\mu_{ref}^{25°C}$, by using Bleaney and Bowers' equation assuming $g=2.2$.[11,12] These results are given in Table 3.

III. Diffuse Reflectance Spectral Measurements. The 340—2000 mμ region was investigated on a Hitachi EPS-3T recording spectrophotometer with the use of a reflectance attachment, and optical grade lithium fluoride was used as the standard of light reflectance. Instead of diluting the compounds with the reference material, appropriate absorbancy ranges were selected by controlling the sensitivity knobs on the spectrophotometer. The band maxima of these complexes are recorded in Table 4.

IV. Infrared Spectral Measurements. Infrared spectra were taken in 4000—1200 cm^{-1} region on Low-Polymerized Trifluoroethylene mulls and in 1300—400 cm^{-1} region on Nujol mulls on a Hitachi EPI-G2 model of infrared spectrophotometer. A part of the data are given in Table 5.

9) G. Foëx, C. J. Gorter and L. J. Smits, "Constantes Sélectionneés, Diamagnétisme et Paramagnétisme, Relaxation Paramagnétique," Masson & Cie, Paris (1957), p. 222.

10) P. W. Selwood, "Magnetochemistry," Interscience Publishers, New York (1956), pp. 78, 91.

11) B. Bleaney and K. D. Bowers, *Proc. Roy. Soc.* (London), *Ser.* **214**, 451 (1952).

12) M. Kato, Y. Muto, H. B. Jonassen, K. Imai and A. Harano, This Bulletin, **41**, 1864 (1968).

Table 5. Data of infrared spectra of complexes**

Complexes	Vibrational frequencies, ν, cm^{-1}				
	ν_{C-O}	ν_{NO_3}			
Cu(En-Sal)	1528vs				
Cu(En-Sal)·$CuCl_2$·0.5CH_3OH	1548s,sh 1536s				
Cu(En-Sal)·$CuCl_2$·0.5C_2H_5OH	1549s,sh 1538s				
Cu(En-Sal)·$Cu(NO_3)_2$	1549m	1499s	1295m,br?	1019w 1003m	804w,br
Cu(En-Sal)·$Cu(NO_3)_2$·1.5CH_3OH	1554m	1498vs	1296vs,br	1020m 1004s	806m
Cu(En-Sal)·$Cu(NO_3)_2$·1.5CH_3OH·H_2O	1544m	1493m	1288vs,br	1020m 1003w	822vw,br 806w
Cu(En-Sal)·$Cu(NO_3)_2$·4py	1530s	1496vw 1486w	1296vs,br	1025m 1015s	821m,spw 805v
Cu(En-Sal)·$Ni(NO_3)_2$·2C_2H_5OH	1552m	1512s,br	1291vs,br	1022m	822w,sp 805w,sp
Cu(En-Sal)·$Co(NO_3)_2$·1.5C_2H_5OH·0.5H_2O	1549m	1509vs,br	1295vs,br	1021m,sp	
4Cu(En-Sal)·3$Zn(NO_3)_2$	1550m 1539m	1490vs	1284vs,br	1020s	810m,sp
Cu(En-Sal)·$CoCl_2$·0.5C_2H_5OH	1550s				
Cu(En-Sal)·$ZnCl_2$	1552s				
2Cu(En-Sal)·$Cu(ClO_4)_2$·CH_3OH·2H_2O	1549s,br				
2Cu(En-Sal)·$Ni(ClO_4)_2$·2H_2O	1548s				
2Cu(En-Sal)·$Co(ClO_4)_2$·2H_2O	1541s				
2Cu(En-Sal)·$Zn(ClO_4)_2$·2.5H_2O	1550m				
Cu(Pn-Sal)	1530m				
Cu(Pn-Sal)·$CuCl_2$	1547m,sh 1531m				
Cu(Pn-Sal)·$Cu(NO_3)_2$	1551m	1501s	1285vs,br?	1016w 1002m?	804w,br
Cu(Pn-Sal)·$Ni(NO_3)_2$·2C_2H_5OH	1552s	1513s, 1503s dp	1289vs,br?	1019s,sp	820w 807m
Cu(Pn-Sal)·$Co(NO_3)_2$·1.75C_2H_5OH·0.5H_2O	1551m	1510vs,br	1303vs,br?	1019s,sp	820w 809m
Cu(Pn-Sal)·$Zn(NO_3)_2$	1550s	1510s, sh?	1294vs,br	1017s,br	810m,sp
2Cu(Pn-Sal)·$Zn(NO_3)_2$·1.5CH_3OH·2H_2O	1544s		1298s,sh?	1017s	826w
Cu(Pn-Sal)·$CoCl_2$·0.5H_2O	1552m				
Cu(Pn-Sal)·$ZnCl_2$	1551m				
2Cu(Pn-Sal)·$Cu(ClO_4)_2$·2H_2O	1550s				
2Cu(Pn-Sal)·$Cu(ClO_4)_2$·en	1541s				
Cu(En-AcAc)	1113w†				
2Cu(En-AcAc)·$Cu(NO_3)_2$·H_2O	1112w†		1292vs,br	1010s?	815w? 808w? 792m?

** sp=sharp For other symbols, see the footnote of Table 4. The band(†) was assigned to the C–O stretching vibration in chelation by K. Ueno and A. E. Martell (*J. Phys. Chem.*, **59**, 998 (1955)).

Results and Discussion

I. General Discussion of Complex Structures. One of the interesting points of studies of polynuclear complexes would be in the observation of the reaction conditions whose minor difference yields different type of complexes (*cf. e. g.*, C-(f) and -(g), the formation of a binuclear and trinuclear complex by reaction of Cu(Ph-Sal) and $Zn(NO_3)_2$). Sometimes, even minor change in the structure of a parent complex or difference in anion part of salts with the same metal gives rise to occurrence of metal exchange reactions; *e. g.*, the copper atom in Cu(Pn-Sal) was exchanged with nickel in ethanol when nickel chloride was employed but no such reaction occurred when nickel nitrate or perchlorate was used under the same reaction condition.

Although the structure of these complexes is unknown at present, Gruber and his co-workers fully discussed probable structures from the con-

sideration of steric hindrance.[7] They proposed the following type of binuclear structure for complexes with the chemical formula, Cu(TDSB)·$CuCl_2$.*3

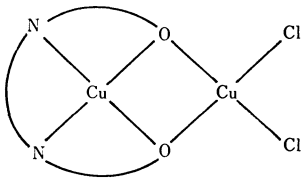

(i)

The most powerful supporting evidence for the binuclear structure is the conformation of the magnetic properties of these complexes to the Bleaney and Bowers' equation.[5-7,11]

The complexes with the chemical formula, Cu(TDSB)·$Cu(NO_3)_2$ (*cf.* Table 1) have not been reported by Gruber and co-workers. We assume for these nitrato complexes a binuclear structure of the same type as the chloro complexes based upon the following observations:

1. The observed subnormal magnetic moments are even lower than those of the corresponding chloro complexes.

2. The appearance of C–O stretching vibration near 1550 cm^{-1}, which is a powerful indication of the presence of bridging phenolic oxygens.[7,13,14] The properties of Cu(TDSB)·$M(NO_3)_2$(M=Ni, Co and Zn) will be discussed assuming that their structures are the same as those of Cu(TDSB)·$Cu(NO_3)_2$.

To complexes with formula, 2Cu(TDSB)·$M(ClO_4)_2$(M=Cu, Ni, Co, Zn and other metals), Gruber and co-workers proposed three probable trinuclear structures shown below (ii-A, B and C).

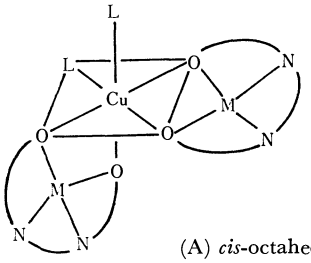

(A) *cis*-octahedral type

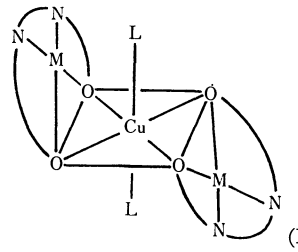

(B) chair type

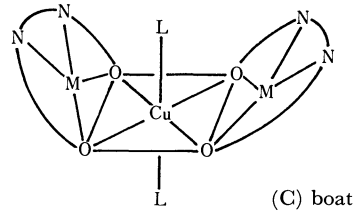

(C) boat type

(ii)

L = solvent molecule attached to the central copper atom

They preferred the *cis*-octahedral type (ii-A). Their recent study of temperature variations of magnetic susceptibilities supported the trinuclear structure for this series of complexes; no appreciable magnetic interaction exists between terminal magnetic ions.[8] However, such magnetochemical studies do not distinguish among a number of probable trinuclear structures.

II. Binuclear Complexes. *A. Infrared Spectra.* a) Band of Bridging Phenolic Oxygen. A shift of the phenolic C–O stretching band of Schiff's base complexes from 1530 cm^{-1} to near 1550 cm^{-1}, can be taken as diagnostic of the formation of polynuclear complexes with bridging phenolic oxygen. Such shift of C–O stretching band toward higher wave numbers was also observed for these complexes.

b) Band of Nitrato Group. The following bands due to coordinately bound nitrato groups[15-22] were observed for Cu(TDSB)·$M(NO_3)_2$,

*3 In this paper, Cu(TDSB) is used for the abbreviation for a copper(II) complex with a tetradentate Schiff's base, and it is schematically expressed as

13) G. E. Batley and D. P. Graddon, *Aust. J. Chem.*, **20**, 877 (1967).
14) G. E. Batley and D. P. Graddon, *ibid.*, **20**, 885 (1967).
15) K. Nakamoto, "Infrared Spectra of Inorganic and Coordination Compounds," John Wiley & Sons, Inc., New York (1963), pp. 92, 161.
16) B. M. Gatehouse, S. E. Livingstone and R. S. Nyholm, *J. Chem. Soc.*, **1957**, 4222.
17) B. M. Gatehouse, S. E. Livingstone and R. S. Nyholm, *J. Inorg. Nucl. Chem.*, **8**, 75 (1958).
18) C. C. Addison and B. M. Gatehouse, *J. Chem. Soc.*, **1960**, 613.
19) F. A. Cotton, D. M. L. Goodgame and R. H. Soderberg, *Inorg. Chem.*, **2**, 1162 (1963).
20) R. L. Carlin and M. J. Baker, *J. Chem. Soc.*, **1964**, 5008.
21) N. F. Curtis and Y. M. Curtis, *Inorg. Chem.*, **4**, 804 (1965).
22) D. E. Billing, A. E. Underhill, D. M. Adams and D. M. Morris, *J. Chem. Soc. (A)*, **1966**, 902.

ν_4 1490—1510 cm^{-1}

ν_1 1290—1310 cm^{-1}

ν_2 1000—1020 cm^{-1}

ν_6 805— 825 cm^{-1}

The band designation follows Gatehouse and others.[16-18] In most cases, two peaks appeared in the respective absorption regions. This may be due to one of the following:

1. Further splitting of the respective bands may be caused because of a lower symmetry of the nitrato group in complexes possibly due to solid state effects.

2. Two differently bound nitrato groups may be present in the complex. According to Curtis and Curtis,[21] the band (ν_4) of a bi-dentate nitrato region appears at a higher frequency than that of a mono-dentate nitrato group. The other bands (ν_1, ν_2 and ν_6) of a bi-dentate nitrato group appear at lower frequencies compared to those of a mono-dentate nitrato group.

At present infrared spectral study in the NaCl region alone can not distinguish between these possibilities.

The (ν_2) band was taken by Nyholm *et al.* as a criterion of the degree of covalency of metal-nitrate bond.[16,17] A low frequency of this band indicates a high degree of covalency of the bond and *vice versa*. The observed frequency range of the band (ν_2) of the complexes in the present study, near 1000 cm^{-1}, indicates a fairly strong covalent character of the metal-nitrate bond in these complexes.

B. Magnetic Moments and d-d Bands. a) General Consideration for Chloro and Nitrato Complexes. These copper(II) complexes showed, in general, two *d-d* bands which appeared at two distinctly different wavelength regions (*cf.* Fig. 1 and Table 4). These two *d-d* bands are assigned to the two copper ions which are placed in different environments. From the spectrochemical series the *d-d* bands of higher energies of the chloro and nitrato complexes are assigned to Cu_1 and those of lower energies to Cu_2.[23]

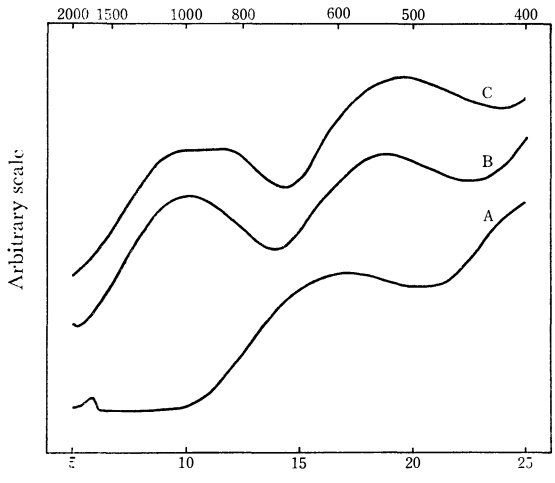

Fig. 1. Reflectance spectra of Cu(En-Sal) (curve A), Cu(En-sal)·$CuCl_2$·0.$5C_2H_5OH$ (curve B) and Cu(En-Sal)·$Cu(NO_3)_2$ (curve C).

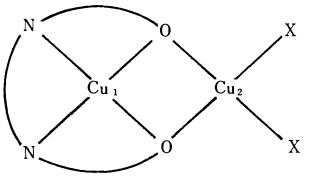

(X=Cl and NO_3) (iii)

Gruber's χ-T study have indicated that the chloro complexes should have a dimeric structure. At present, no χ-T data are available for the nitrato complexes. The complexes with the chemical formula, Cu(TDSB)·$Cu(NO_3)_2$, could be higher polymers such as [Cu(TDSB)·$Cu(NO_3)_2$]$_n$(n=2,3, ···). When n=2, one probable structure is as such given in (iv), where outer nitrate groups may be bound weakly to the metal atoms in the complex ion. Even though such a structure is not inconsistent with the infrared spectral data (*cf.* II-A-b), we

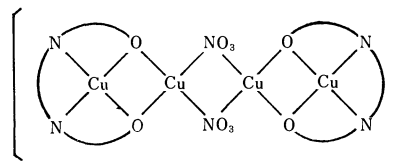

(iv)

shall assume a dimeric structure resembling to those of the chloro complexes.

Gruber and co-workers pointed out that when Cu(TDSB) complexes with metal halides or metal perchlorates, the main ligand field transitions shift to higher energies. This was confirmed in the present study and shown to hold also for complexes with metal nitrates. The main *d-d* band of Cu(En-Sal) appears at a much longer wavelength (590 mμ). This fact is consistent with its dimeric structure in which each copper atom is five coordinated with a pyramidal arrangement.[24] The band of Cu(Pn-Sal) appears at 566 mμ.

On complexing, the main *d-d* band of these Cu(TDSB) shifts towards 540—505 mμ, which is at shorter wavelengths than that of bis(ethylenediamine)copper(II) ions in various ligand field

23) C. K. Jørgensen, "Absorption Spectra and Chemical Bonding in Complexes," Pergamon Press, New York, N. Y. (1962), p. 107.

24) D. Hall and T. N. Waters, *J. Chem. Soc.*, **1960**, 2644.

environments,[25,26] and quite close to that of the copper(II) complexes of planar type.[27-29]

The *d–d* transitions of Cu_1 and Cu_2 occur at 515—536 and 945—983 mμ for the chloro complexes and at 506—516 and 855—910 mμ for nitrato complexes respectively. The *d–d* band energy of Cu_2 is greater for nitrato complexes than for chloro complexes in line with their relative positions in the spectrochemical series.[22,23,30]

The magnetic moments of nitrato complexes ranging from 1.25 to 1.45 B. M., are apparently smaller than those of chloro complexes. The empirical rule "higher energies of *d–d* bands - lower magnetic moments" established for dimeric copper(II) halide complexes with pyridine *N*-oxides[3] or salicylideneimines[2,4] where the two copper ions are in essentially the same environment, is apparently also valid for the complex systems of the present study even though each copper ion is placed in a different environment in a dimeric molecule. Gruber and co-workers[7] showed that, for the system,

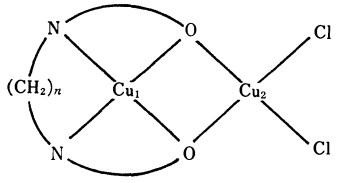

(n=2, 3,···) (v)

as n increases, the deviation of the stereochemistry of Cu_1 from planarity increases thus bringing about a shift of the *d–d* bands of both Cu_1 and Cu_2 to lower energies indicating "mutual influence of complex moieties in a molecule" in the direction $Cu_1 \rightarrow Cu_2$. However, the present study indicates that the influence in the reverse direction $Cu_1 \leftarrow Cu_2$ also occurs. A shift of *d–d* band of copper(II) complexes to lower energy is correlated with the deviation of stereochemistry of the copper ion from planar to tetrahedral symmetry.[30-33] These are in line with the fact that the more planar the copper(II)-stereochemistry in a binuclear complex, the greater the orbital overlap effective for superexchange interaction between copper ions.[3,4]

b) $Cu(TDSB)\cdot M(NO_3)_2$ (M=Ni, Co and Zn). A binuclear structure of the same type as that for copper(II) nitrate complexes shall be assumed for these nitrato complexes since all showed bridging phenolic oxygen band.[7,13,14] The stereochemistry of M greatly influences the properties of these compounds. Reflectance spectra give reasons for many of these properties.

1) M=Ni(II): Spectral data rule out square-planar, tetrahedral[34-40] and the five coordinated configurations.[34-36,41-44] The spectra best fit those

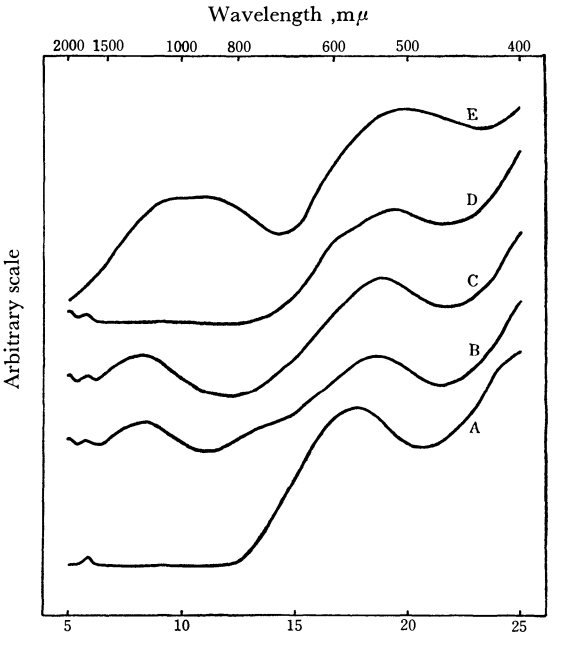

Fig. 2. Reflectance spectra of Cu(Pn-Sal) (curve A), $Cu(Pn\text{-}Sal)\cdot Ni(NO_3)_2\cdot 2C_2H_5OH$ (curve B), $Cu(Pn\text{-}Sal)\cdot Co(NO_3)_2\cdot 1.75C_2H_5OH\cdot 0.5H_2O$ (curve C), $Cu(Pn\text{-}Sal)\cdot Zn(NO_3)_2$ (curve D) and $Cu(Pn\text{-}Sal)\cdot Cu(NO_3)_2$ (curve E).

25) K. Sone and S. Utsuno, This Bulletin, **39**, 1813 (1966).
26) I. M. Procter, B. J. Hathaway and P. Nicholls, *J. Chem. Soc.* (*A*), **1968**, 1678.
27) M. Kato, Y. Komuro and K. Sone, *Nippon Kagaku Zasshi*, **78**, 896 (1957).
28) S. Yamada and S. Miki, This Bulletin, **36**, 680 (1963).
29) S. Miki and S. Yamada, *ibid.*, **37**, 1044 (1964).
30) C. M. Harris, H. R. H. Patil and E. Sinn, *Inorg. Chem.*, **6**, 1102 (1967).
31) L. Sacconi and M. Ciampolini, *J. Chem. Soc.*, **1964**, 276.
32) T. P. Cheeseman, D. Hall and T. N. Waters, *J. Chem. Soc., A*, **1966**, 694.
33) W. J. Eilbeck, F. Holmes, C. E. Taylor and A. E. Underhill, *J. Chem. Soc., A*, **1968**, 128.
34) L. Sacconi, *Coordin. Chem. Rev.*, **1**, 192 (1966).
35) S. Yamada, *Kagaku no Ryoiki*, **22**, 681 (1968).
36) S. Yamada, *Coordin. Chem. Rev.*, **1**, 415 (1966).
37) L. Sacconi, *ibid.*, **1**, 126 (1966).
38) D. M. L. Goodgame, M. Goodgame and F. A. Cotton, *J. Amer. Chem. Soc.*, **83**, 4161 (1961).
39) L. Sacconi, P. Paoletti and M. Ciampolini, *ibid.*, **85**, 411 (1963).
40) C. D. Burbridge and D. M. L. Goodgame, *J. Chem. Soc., A*, **1968**, 237.
41) M. Ciampolini, N. Nardi and G. P. Speroni, *Coordin. Chem. Rev.*, **1**, 222 (1966).
42) L. Sacconi, "Plenary Lectures presented at the 10th International Conference on Coordination Chemistry in September, 1967," Butterworths, London, p. 95.
43) L. Sacconi, P. Nannelli, N. Nardi and U. Campigli, *Inorg. Chem.*, **4**, 943 (1965).
44) M. Ciampolini and G. P. Speroni, *ibid.*, **5**, 45 (1966).

of Ni(II) complexes with octahedral configurations (*cf.* Fig. 2).[35,45-47] The bands at *ca.* 1200 mμ were assigned to $^3A_{2g}\rightarrow{}^3T_{2g}$ transition and those at 740—750 mμ to $^3A_{2g}\rightarrow{}^3T_{1g}$(F). The characteristic feature of the latter band, which occurs often in double peaks ($^3A_{2g}\rightarrow{}^3T_{1g}$(F) and $^3A_{2g}\rightarrow{}^1E_g$), has become partly hidden by the absorption end of the stronger band of the Cu(TDSB) moiety. The band due to transition, $^3A_{2g}\rightarrow{}^3T_{1g}$ (P), expected at *ca.* 400 mμ, could not be observed, being hidden by the stronger absorption due to *d–d* transition of Cu(TDSB) as well as the strong absorption of charge transfer region.

2) M=Co(II): For Co(II) complexes with nitrato groups, the most probable stereochemical environment of Co(II) is octahedral based on a similar consideration to that for Ni(II).[20,34-36,42,46-60] The bands at *ca.* 1200 mμ were assigned to $^4T_{1g}$(F)$\rightarrow{}^4T_{2g}$(F). The absorption due to transition, $^4T_{1g}$(F)$\rightarrow{}^4T_{1g}$(P) which is expected at *ca.* 500 mμ, was not observed, being hidden by the stronger copper(II) band at 520 mμ.

3) M=Zn(II): Surprisingly the *d–d* band of Cu(TDSB) of this compound appeared at a shorter wavelength (520 mμ) than those for Co(II) and Ni(II) complexes (540—532 mμ). The same trend was observed for Cu(TDSB)·$ZnCl_2$ (*cf.* Table 4 and Fig. 4). The "mutual influence of complex moieties" is out of line here compared to that observed in Cu(TDSB)·CuX_2 (X=Cl and NO_3). It is rather difficult to give a clear-cut explanation for this inconsistency. However, a conceivable mechanism for this conflict may be found in the tetrahedral coordination of the Zn(II) ion and subsequent steric influences. This may decrease the ligand field exerted from neighboring molecules or ions on the fifth or sixth coordination positions of the copper(II) ion in Cu(TDSB).[3,4] Such steric effect might then exceed the effect of the "mutual influence of complex moieties" in a dimeric complex molecule.

c) Other Nitrato Complexes. 1) Cu(En-Sal)·$Cu(NO_3)_2\cdot 1.5CH_3OH\cdot H_2O$: The band ν_{C-O} of this compound appeared at 1544 cm^{-1}. This frequency is somewhat low compared to the band due to bridging phenolic oxygen present in the most binuclear complexes (*ca.* 1550 cm^{-1}).[7,13,14] The *d–d* band appearance of this compound makes it difficult to distinguish between Cu_1 and Cu_2 bands.

The spectral feature of this compound differes from that of most binuclear chloro and nitrato copper(II) complexes but resembles that of the pseudo-tetrahedral binuclear complexes, $[Cu(\overset{1}{O}\cdot C_6H_4\cdot\overset{2}{C}H{=}N{-}R)Cl]_2$ (R=alkyl or aryl groups) (*cf.* Fig. 3).[4,30-33,37,53] The magnetic moment of this compound, 1.75 B.M., is consistent with these facts.

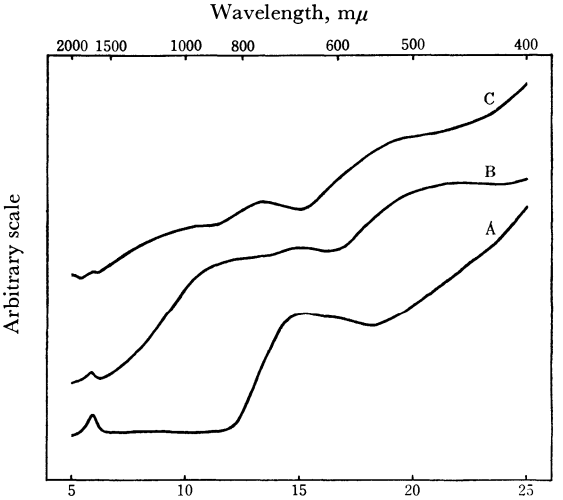

Fig. 3. Reflectance spectra of Cu(Sal·N-CH_3)$_2$ (curve A), [Cu(Sal·N-CH_3)Cl_2] (curve B) and Cu(En-Sal)·$Cu(NO_3)_2\cdot 1.5CH_3OH\cdot H_2O$ (curve C). Sal·N-$CH_3{=}\overset{1}{O}\cdot C_6H_4\cdot\overset{2}{C}H{=}N{-}CH_3$

2) Cu(En-Sal)·$Cu(NO_3)_2$·4Py: The ν_{C-O} frequency of this compound (1530 cm^{-1}) indicates the absence of bridging phenolic oxygen. The magnetic moment, 1.87 B.M., is consistent with this observation. This compound showed two main *d–d* bands at 585 and 1005 mμ due to two copper(II) ions in different ligand fields.

d) Cu(TDSB)·MCl_2(M=Co and Zn). 1) M=

45) R. S. Drago, "Physical Methods in Inorganic Chemistry," Reinhold Publishing Corporation, New York (1967), pp. 167, 410.
46) D. W. Meek, R. S. Drago and T. S. Piper, *Inorg. Chem.*, **1**, 285 (1962).
47) J. H. Nelson, L. C. Nathan and R. O. Ragsdale, *ibid.*, **7**, 1840 (1968).
48) Ref. 45, p. 411.
49) F. A. Cotton and M. Goodgame, *J. Amer. Chem. Soc.*, **83**, 1777 (1961).
50) A. Sacco and F. A. Cotton, *ibid.*, **84**, 2043 (1962).
51) L. Sacconi, M. Ciampolini, F. Maggio and F. P. Cavasino, *ibid.*, **84**, 3246 (1962).
52) J. A. Bertrand and D. L. Plymale, *Inorg. Chem.*, **3**, 775 (1964).
53) R. Longhi and R. S. Drago, *ibid.*, **4**, 11 (1965).
54) D. E. Billing and A. E. Underhill, *J. Chem. Soc., A*, **1968**, 5.
55) D. E. Billing and A. E. Underhill, *ibid.*, **1968**, 29.
56) L. Sacconi, M. Ciampolini and G. P. Speroni, *Inorg. Chem.*, **4**, 1116 (1965).
57) L. Sacconi, M. Ciampolini and G. P. Speroni, *J. Amer. Chem. Soc.*, **87**, 3102 (1965).
58) M. Ciampolini and N. Nardi, *Inorg. Chem.*, **5**, 41 (1966).
59) L. Sacconi and I. Bertini, *J. Amer. Chem. Soc.*, **88**, 5180 (1966).
60) S. Yamada and E. Yoshida, This Bulletin, **40**, 1298 (1967).

Co(II): These greyish violet complexes showed three main absorption bands in the 340—2000 mμ region near 565, 660 and 1520 mμ respectively. No peak was observed in the 520 mμ region where most of these complexes showed a broad band due to the *d–d* transition of Cu(TDSB). Instead, a sharp band appeared in the region at *ca.* 565 mμ. This band can not be assigned to the *d–d* band of Cu(TDSB) because of its shape and absorption position (*cf.* Fig. 4). It seems reasonable that in

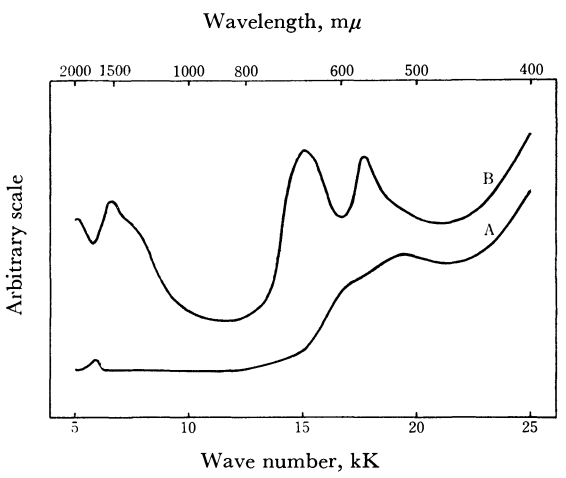

Fig. 4. Reflectance spectra of $Cu(En\text{-}Sal)\cdot ZnCl_2$ (curve A) and $Cu(En\text{-}Sal)\cdot CoCl_2\cdot 0.5C_2H_5OH$ (curve B).

these complexes the band of Cu(TDSB) is hidden under the stronger absorption of Co(II).[50,52] The observed spectra are different from those of octahedral and planar cobalt(II) complexes[35,36,46,47] and are similar to that of tetrahedral Co(II);[34,35,48-55] they have also a resemblance to those of trigonal bipyramidal Co(II).[36,41,42,44,56-60] X-ray analysis of metal complexes often shows them as an intermediate of fundamentally different geometries.[42] An environment of Co(II) for such an intermediate of tetrahedral and trigonal bipyramidal configurations in the presence of ligand A is shown below.

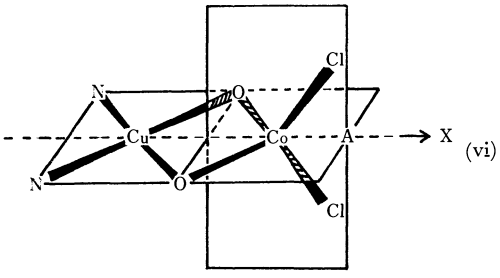

(vi)

Here, A=a solvated molecule or a neighboring molecule or ion which exerts a ligand field on the Co(II) ion in the x direction.

2) M=Zn(II): discussed previously (*cf.* (b)-3).

III. $2Cu(TDSB)\cdot M(ClO_4)_2$. *A. Formation.*[*4] The ease of formation of trinuclear complexes from metal perchlorate and Cu(TDSB) in alcoholic solution is partly due to the very weak coordinating ability of perchlorate ion. In complex formation from Cu(TDSB) and $M(ClO_4)_2$, the ligands to coordinate to M^{2+} are firstly the complex ligand (Cu(TDSB)) and secondly solvent molecules. In a metal with coordination number of six, two molecules of Cu(TDSB) acting as a bidentate ligand, will occupy four positions, and the remaining two coordinating sites will be occupied by solvent molecules. Steric consideration does not allow three molecules of Cu(TDSB) to attach to one metal without a large amount of strain, *i. e.*, the formation of a tetranuclear complex of the following type does not seem possible for the first transition elements.[7] Such steric condition encountered here

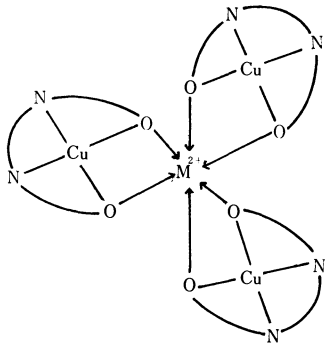

(vii)

is similar to that observed for complex formation of nickel (II) with 2,9-dimethylphenanthroline, where even a large excess of the ligand gave only a bis-complex for steric reason.[61]

Recent X–T studies by Gruber and co-workers supports the trinuclear formation for these perchlorate complexes.[8] For metal chloride or nitrate, the anions have a much greater coordinating ability than the perchlorate ion, and the central metal coordinates with either of the complex ligand and chloride or nitrate ion. Under such conditions, it becomes difficult for one central metal ion to combine with more than a molecule of the complex ligand, leading to the formation of a binuclear complex rather than a trinuclear one. However, in some cases metal nitrates can form trinuclear

[*4] Metal analysis does not distinguish between the chemical compositions of a binuclear and a trinuclear complex. For instance, per cent of copper is 19.36% for $Cu(En\text{-}Sal)\cdot Cu(ClO_4)_2\cdot 2CH_3OH$(dimer) and 19.26% for $2Cu(En\text{-}Sal)\cdot Cu(ClO_4)_2\cdot CH_3OH\cdot 2H_2O$(trimer) respectively, practically the same values within the accuracy of our metal analysis, ±0.5%. At the meeting[*1-b] this was pointed out and a trimeric formula was presented for the dimeric one in the proceedings based on Cu and C.H.N. analysis.

61) K. Sone and M. Kato, *Naturwissenschaften*, **45**, 10 (1958).

complexes as in 2Cu(Pn-Sal)·$Zn(NO_3)_2$ or 2Cu(En-AcAc)·$Cu(NO_3)_2$, where nitrate ion has a stronger coordinating ability than chloride ion in line with the spectrochemical series. This suggests that coordinating ability of the anions is not the only factor determining the formation of these polynuclear complexes. Packing or steric effect, or other factors must be considered to be cooperating in this phenomenon.

B. Spectral Features. The spectra of complexes with Cu(En-Sal) are given in Fig. 5. Of all the

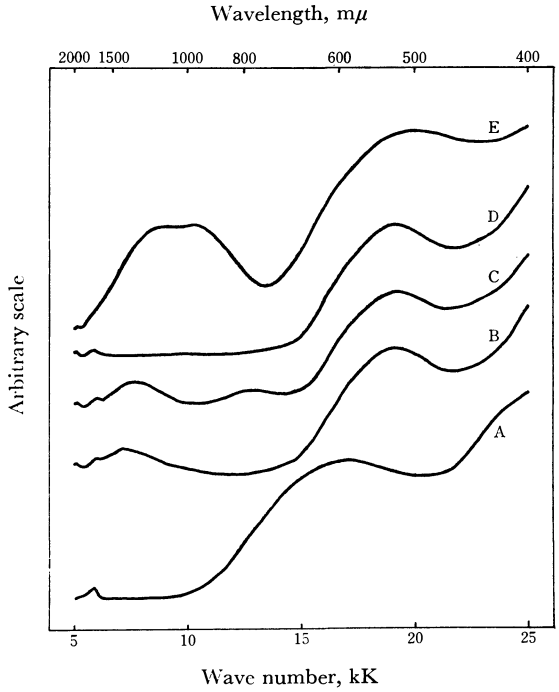

Fig. 5. Reflectance spectra of Cu(En-Sal) (curve A), 2Cu(En-Sal)·$Co(ClO_4)_2$·$2H_2O$ (curve B), 2Cu(En-Sal)·$Ni(ClO_4)_2$·$2H_2O$ (curve C), 2Cu(En-Sal)·$Zn(ClO_4)_2$·$2.5H_2O$ (curve D) and 2Cu(En-Sal)·$Cu(ClO_4)_2$·CH_3OH·$2H_2O$ (curve E).

chloride, nitrate and perchlorate complexes, the *d–d* transitions of Cu(TDSB) always occur at shortest wavelengths when they combine with copper(II) salts. The spectral features of Co(II) and Ni(II) complexes indicate octahedral complexes though the absorptions at wavelengths shorter than 600 mμ are hidden by the stronger absorption of the complex ligand (Cu(TDSB)).

The bands of the central metal ions in perchlorate complexes appear at a lower energy than those of the nitrate complexes. This makes it possible to observe the familiar doublet band of nickel(II) complexes (near 700 mμ) separate from the absorption due to the complex ligand. It is noteworthy that for the perchlorate complexes the *d–d* transitions due to Cu(En-Sal) are in the order from lower to higher energy, Co<Ni<Cu>Zn or Co<Zn<Ni<Cu, the same as the Irving and Williams' sequence for complex stability.[62]

The antiferromagnetic exchange interaction of trinuclear perchlorate complexes, 2Cu(TDSB)·$M(ClO_4)_2$ increases in the order, M=Co<Ni<Cu,[8] is the same as observed for the energy of copper(II) band of Cu(TDSB) in trinuclear complexes of the same type.

C. Some Specific Complexes. a) 2Cu(Pn-Sal)·$Cu(ClO_4)_2$·en. This compound has a chemical formula in which the two water molecules in 2Cu(Pn-Sal)·$Cu(ClO_4)_2$·$2H_2O$ are replaced with one ethylenediamine molecule. Such an apparently minor change in the chemical formula, however, gives rise to a great deal of change in its properties. The ethylenediamine compound is greyish green, and the dihydrate compound is violet. The former has only one *d–d* band due to copper(II) at 583 mμ but the dihydrate, as most polynuclear copper(II) complexes of the present study, has two copper(II) bands at greatly different wavelengths, *i.e.*, at *ca.* 520 and 900—1000 mμ respectively (*cf.* Fig. 6).

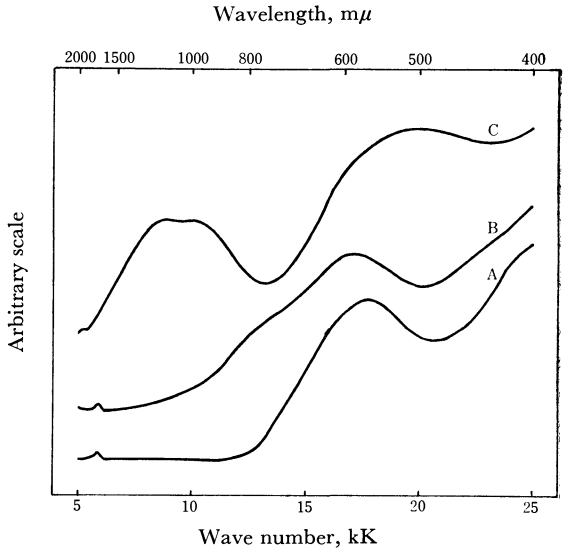

Fig. 6. Reflectance spectra of Cu(Pn-Sal) (curve A), 2Cu(Pn-Sal)·$Cu(ClO_4)_2$·en (curve B) and 2Cu(Pn-Sal)·$Cu(ClO_4)_2$·$2H_2O$ (curve C).

This suggests that in the ethylenediamine complex the copper ions are in practically the same environment whereas in the dihydrate the environment is greatly different for each copper(II) ion. The mechanism by which the two copper(II) ion bands merge into one absorption, and the coordination behavior of ethylenediamine in this complex are under study.[63]

62) F. J. C. Rossotti, "Modern Coordination Chemistry," ed. by L. Lewis and R. G. Wilkins, Interscience Publishers, New York, N. Y. (1960), p. 1.
63) Ref. 15, p. 186.

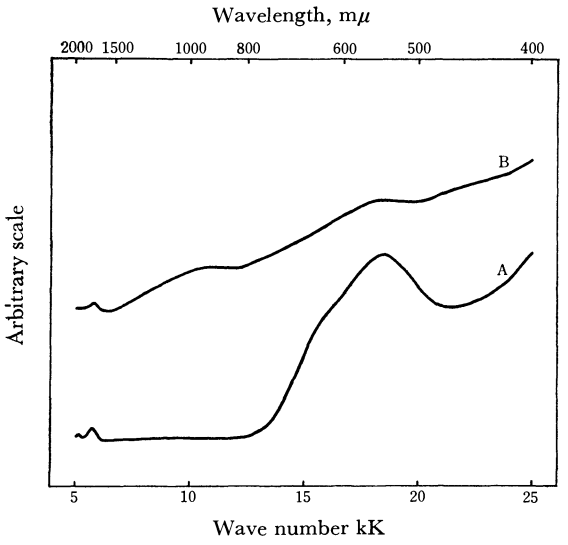

Fig. 7. Reflectance spectra of Cu(En-AcAc) (curve A) and $2Cu(En\text{-}AcAc)\cdot Cu(NO_3)_2\cdot H_2O$ (curve B).

b) $2Cu(En\text{-}AcAc)\cdot Cu(NO_3)_2\cdot H_2O$. The spectral features of this compound indicate a pseudo-tetrahedral copper(II) complex (*cf.* Fig. 7).[30-33,37] The structures of Cu(En-Sal)[24] and Cu(En-AcAc)[64] determined by X-ray analysis indicate that the steric hindrance due to these complex ligands in the formation of the polynuclear complexes is greater in Cu(En-AcAc) than in Cu(En-Sal). The magnetic moment, 1.76 B.M. suggests the existence of an antiferromagnetic interaction in this compound.[3,4]

One area of the further development of the present study will involve the systematic research for the conditions under which even minor changes in the structure of the parent compound lead to the formation of different type of polynuclear complexes, bi-nuclear or tri-nuclear ones, in the cooperation of the specific property of the respective anion of the metal salt employed in the preparation.

64) D. Hall, A. D. Rae and T. N. Waters, *J. Chem. Soc.*, **1963**, 5897.

BULLETIN OF THE CHEMICAL SOCIETY OF JAPAN VOL. 43 1078—1083 (1970)

ESR Studies of Some Copper(II) β-Diketone Chelate Complexes in Heterocyclic Basic Solvents

Hiroshi Yokoi, Mitsuru Sai and Taro Isobe

Chemical Research Institute of Non-aqueous Solutions, Tohoku University, Katahira-cho, Sendai

(Received September 9, 1969)

Three representative copper(II) β-diketone chelate complexes, bis-(ethylacetoacetato)copper-(II), bis-(salicylaldehydato)copper(II), and bis-(acetylacetonato)copper(II), have been investigated by the ESR method in order to estimate their structures in various solvents. The super-hyperfine structures due to the equal coupling of the unpaired electron with two nitrogen atoms were clearly observed for the first two complexes dissolved in pyridine or γ-picoline. The structures of these two complexes in pyridine or γ-picoline could be estimated to be as follows; a new square-planar coordination occurs through two nitrogen atoms of these basic solvent molecules and two oxygen atoms of the four originally-coordinating ligand oxygen atoms, and the other oxygen atoms are coordinated as apical ligand atoms with less strength. On the other hand, the ESR spectra of the latter complex dissolved in pyridine or γ-picoline show a significantly strong ligand field only in the axis normal to the molecular plane; this indicates that the coordination of the basic solvent molecules along the axis normal to the molecular plane occurs.

It has been reported by several authors that the reaction of copper(II) β-diketone chelate complexes with some heterocyclic bases generally produces 1 : 1- or 1 : 2-adducts.[1-3] The absorption spectral features of bis-(ethylacetoacetato)copper(II), one of the copper(II) β-diketone chelate complexes, in pyridine and piperidine are quite different from those in other ordinary solvents.[4] The ESR is a powerful and unique technique for the structural

1) D. P. Graddon, *Nature*, **183**, 1610 (1959); D. P. Graddon and E. C. Watton, *ibid.*, **187**, 1021 (1960).

2) D. P. Graddon and E. C. Watton, *J. Inorg. Nucl. Chem.*, **21**, 49 (1961).

3) Y. Muto, This Bulletin, **31**, 56 (1958).

4) D. P. Graddon, *J. Inorg. Nucl. Chem.*, **14**, 161 (1960).

investigation of the copper(II) complexes in the following specific points: it gives much information about the strength and symmetry of the ligand field of the complexes,[5-8] and it is a method of determining decisively whether or not coordination occurs through nitrogen atoms.[9] The purpose of this paper is to estimate the structures of some copper(II) β-diketone chelate complexes in various solvents by the ESR method.

Experimental

Materials. The copper(II) β-diketone chelate complexes employed in this study are bis-(acetylacetonato)-copper(II), bis-(ethylacetoacetato)copper(II), and bis-(salicylaldehydato)copper(II); they are abbreviated as $Cu(acac)_2$, $Cu(acest)_2$, and $Cu(sal)_2$ respectively. Commercially-available $Cu(acac)_2$ was recrystallized from chloroform. The $Cu(acest)_2$ was prepared and purified according to the method in the literature.[2] The $Cu(sal)_2$ was obtained in the usual way reported in the literature by mixing an aqueous solution of cupric acetate with an ethanolic solution of salicylaldehyde, the green product being then filtered off, washed, and dried.[3,10] The adduct of $[Cu(acest)_2(\gamma\text{-picoline})_2]$ was prepared according to the method of Graddon and Watton.[2]

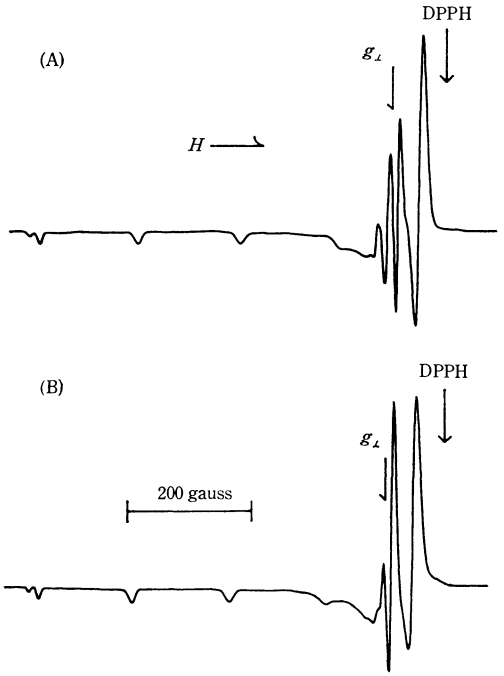

Fig. 1. The X-band ESR spectra of $Cu(acac)_2$ at 77°K.
(A) in 50% chloroform - 50% ethanol
(B) in 20% pyridine - 40% chloroform - 40% ethanol

Measurements. The ESR spectra were measured in solutions at the temperature of liquid nitrogen with a Hitachi X-band ESR spectrometer, Model MES-4001, equipped with a 100 kHz field modulation unit. Furthermore, the second derivative ESR spectra were obtained using 100 kHz-40 Hz field modulations in order to resolve the nitrogen super-hyperfine structure clearly. The field was calibrated with an NMR probe and then with a benzene solution of vanadyl acetylacetonate or with Mn(II) ions in MgO powder. Some of the ESR spectra observed are shown in Figs. 1—7, while the analyzed results are listed in Table 1. All the solvents used were mixed solvents. Almost no change in the ESR results was observed when we varied to some extent the mixing ratios of the solvents listed in Table 1.

Results and Discussion

$Cu(acac)_2$. It has been suggested, on the basis of the optical absorption and ESR spectra, that the physical and chemical properties of the β-diketone copper(II) chelate complexes in solution vary to an appreciable extent according to the kind of solvent used.[4, 11-14] The ESR data of Table 1 also clearly support the above description.

(A) in Fig. 1 shows the ESR spectrum of $Cu(acac)_2$ in 50% chloroform - 50% ethanol (volume %). This spectrum is sharp in its line width and is typical of an axial symmetry in the ligand field. (B) in Fig. 1, where the solvent is 20% pyridine - 40% chloroform - 40% ethanol, is also sharp in its absorption line width and shows the ligand field of an axial symmetry. The ESR spectrum of the complex in 10% pyridine - 90% toluene was quite similar to the (B) in Fig. 1. The absorption line shapes of these spectra indicate that there are not two or more molecular species in solution.

The ESR results of $Cu(acac)_2$ in Table 1 indicate that the addition of pyridine causes the g values to increase and the $|A_{//}|$ value to decrease. This

5) A. Abragam and M. H. L. Pryce, *Proc. Roy. Soc. Ser. A* **205**, 135 (1951); K. W. H. Stevens, *ibid., Ser. A* **219**, 542 (1953).
6) A. H. Maki and B. R. McGarvey, *J. Chem. Phys.*, **29**, 31, 35 (1958); D. Kivelson and R. Neiman, *ibid.*, **35**, 149 (1961).
7) B. G. Malmstöm and T. Vänngard, *J. Mol. Biol.*, **2**, 118 (1960); A. H. Maki, N. Edelstein, A. Davison and R. H. Holm, *J. Amer. Chem. Soc.*, **86**, 4580 (1964); M. Scharnoff, *J. Chem. Phys.*, **42**, 3383 (1965); R. C. Slade, A. A. G. Tomlinson, B. J. Hathaways and D. E. Billing, *J. Chem. Soc.*, **1968**, 61.
8) H. Yokoi and T. Isobe, This Bulletin, **42**, 2232 (1969).
9) A. K. Wiersma and J. J. Windle, *J. Phys. Chem.*, **68**, 2316 (1964).
10) P. Pfeiffer, E. Breith, E. Lubbe and T. Tsumaki, *Ann.*, **503**, 84 (1933).
11) R. L. Belford, M. Calvin and G. Belford, *J. Chem. Phys.*, **26**, 1165 (1957).
12) T. N. Waters and D. Hall, *J. Chem. Soc.*, **1959**, 1200.
13) H. Yokoi and T. Isobe, This Bulletin, **39**, 2054 (1966).
14) S. Antosik, N. M. D. Brown, A. A. McConnell and A. L. Porte, *J. Chem. Soc., A*, **1969**, 545.

Table 1. Magnetic parameters

Copper(II) complex	Solvent[a)]	$g_{//}$	$g_{\perp}$	$\times 10^4 cm^{-1}$			
				$A_{//}$[b)]	$A_{//}$ (^{65}Cu)	$A_{//}$ (^{65}Cu)	$A_N{}_{//}$
$Cu(acac)_2$	A[c)]	2.256	2.056	197			
	B	2.288	2.057		169	181	
	C*	2.304	2.060		160	173	
	E	2.297	2.062		163	175	
$Cu(acest)_2$	A	2.281	2.062		171	183	
	B	2.315	2.068		155	167	
	C	2.320	2.064	158			
	D	2.322	2.068	165			
	E	2.319	2.070	159			
	F	2.313	2.067		159	171	9.8
	G	2.318	2.070		162	174	9.7
$Cu(sal)_2$	B	2.299	2.069		153	165	
	E	2.317	2.068	162			
	F	2.312	2.070	156			
	G	2.311	2.064	168			

a) A: toluene, B: 50% chloroform-50% ethanol, C: 20% pyridine-80% toluene, C*: 10% pyridine-90% toluene, D: 20% γ-picoline-80% toluene, E: 20% pyridine-40% chloroform-40% ethanol, F: 20% pyridine-80% chloroform, G: 20% γ-picoline-80% chloroform (volume %).

b) This value was determined from the hyperfine splitting between the $I_z = \pm 1/2$ components.

c) The data were cited from a literature.[13] The almost same results were reported by Antosik *et al.*[14]

tendency of the g and $A_{//}$ values means that the ligand field of the complex on the axis normal to the molecular plane is strengthened on the addition of pyridine; the pyridine molecules coordinate to the complex as apical ligands.[8, 13, 14]

$Cu(acest)_2$ and $Cu(sal)_2$. The ESR spectra of $Cu(acest)_2$ and $Cu(sal)_2$ in 50% chloroform-50% ethanol are sharper in absorption line width than are those in other solvents, as may be seen in Figs. 2—5. An exception is the ESR spectrum of $Cu(acest)_2$ in toluene, which is shown in (B) in Fig. 2. This spectrum is different in its absorption line shape from the other spectra; it consists of a very sharp absorption-line spectrum and a broad one superposed upon each other. The former spectrum could be analyzed in the usual way; the results are listed in Table 1. The latter spectrum may be due to the triplet dimer of the complex. The observation of the broad signal at $g \fallingdotseq 2.0$ for the triplet dimers of some copper(II) complexes has been reported.[15] Many planar copper(II) complexes are known to have a dimer structure in the crystal,[16,17] and the dimer formation of those complexes seems to be possible in such a non-coordinating solvent as toluene. A similar spectrum

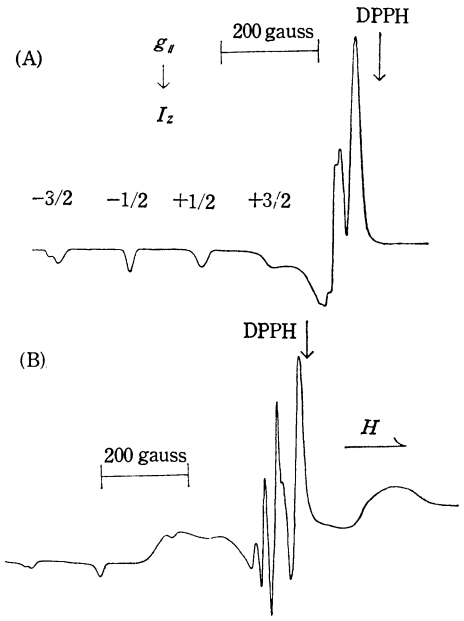

Fig. 2. The X-band ESR spectra of $Cu(acest)_2$ at 77°K.
(A) in 50% chloroform-50% ethanol
(B) in toluene

was observed for $Cu(acac)_2$ in toluene. A detailed investigation of these problems is now in progress.

The addition of pyridine causes the absorption line width to broaden. The (A) of Fig. 3 is very broad in line width, in contrast with the (A) of

15) J. R. Pilbrow, A. D. Toy and T. D. Smith, *J. Chem. Soc., A* **1969**, 1029.

16) H. Koyama, Y. Saito and H. Kuroya, *J. Inst. Polytech. Osaka City Univ.*, **C4**, 43 (1953).

17) T. N. Waters and D. Hall, *J. Chem. Soc.*, **1959**, 1203; D. Hall and T. N. Waters, *ibid.*, **1960**, 2644.

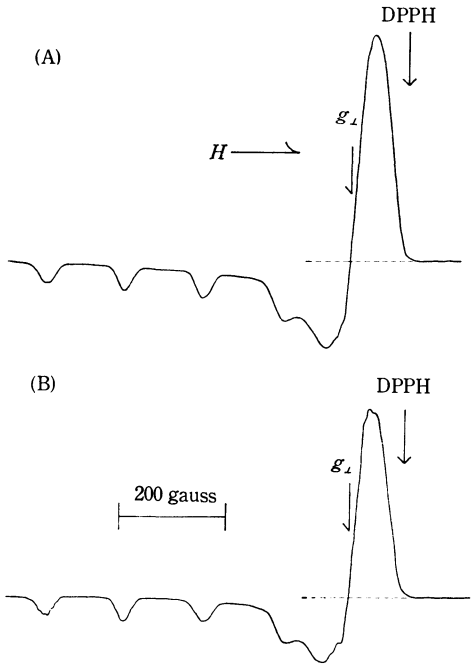

Fig. 3. The X-band ESR spectra of $Cu(acest)_2$ at 77°K.
(A) in 20% pyridine - 40% chloroform - 40% ethanol
(B) in 20% pyridine - 80% chloroform

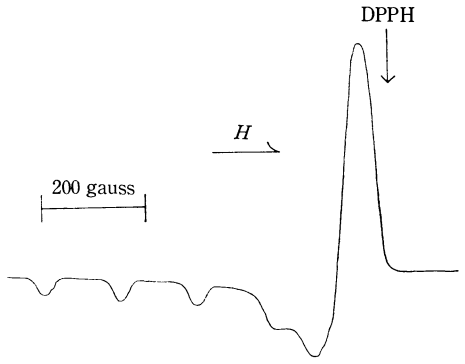

Fig. 4. The X-band ESR spectrum of $Cu(acest)_2$ in 20% γ-picoline - 80% toluene at 77°K. This spectrum was quite the same as the one of [$Cu(acest)_2(\gamma\text{-picoline})_2$] in toluene at 77°K.

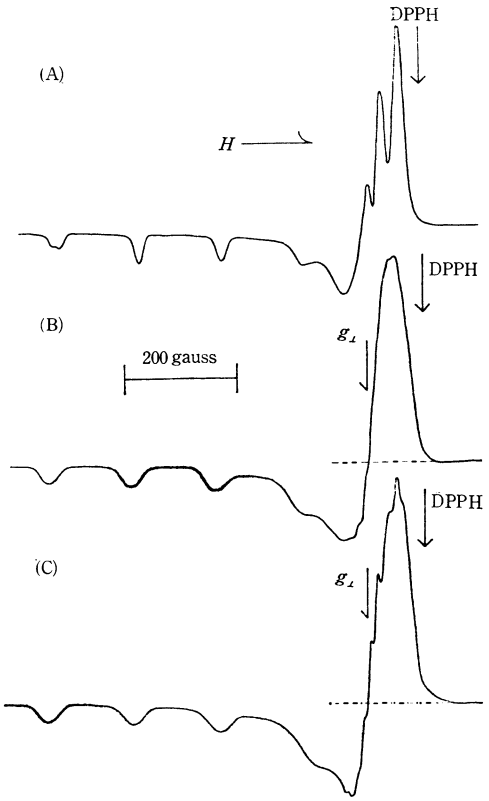

Fig. 5. The X-band ESR spectra of $Cu(sal)_2$ at 77°K.
(A) in 50% chloroform - 50% ethanol
(B) in 20% pyridine - 40% chloroform - 40% ethanol
(C) in 20% γ-picoline - 80% chloroform

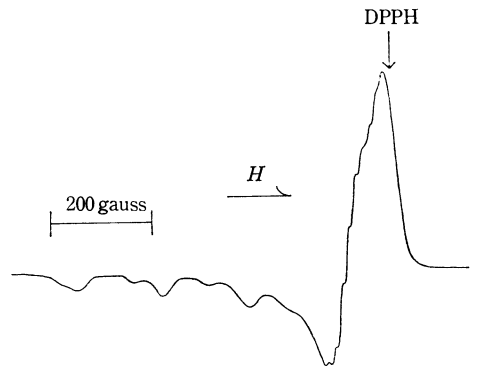

Fig. 6. The X-band ESR spectrum of $Cu(acest)_2$ in 20% piperidine - 40% chloroform - 40% ethanol at 77°K.

Fig. 2. On the other hand, piperidine, which is more basic than pyridine and γ-picoline, has a different effect on the complexes; for example, the ESR spectrum of $Cu(acest)_2$ in 20% piperidine - 40% chloroform - 40% ethanol, as is shown in Fig. 6, is due to two molecular species.

(B) in Fig. 3 shows the ESR spectrum of $Cu(acest)_2$ in 20% pyridine - 80% chloroform; this spectrum has almost the same absorption-line shape as the (A) in Fig. 3. However, the former spectrum shows more clearly than the latter one that the super-hyperfine structures appear at the most intense absorption line in the high-field part and in the hyperfine components of $I_z = -3/2$ and $-1/2$ in the low-field part. These super-hyperfine structures are considered most likely to be due to

nitrogen nuclei.

The second derivative ESR spectra were measured in order to observe the super-hyperfine structures more clearly; some of them are shown in Fig. 7.

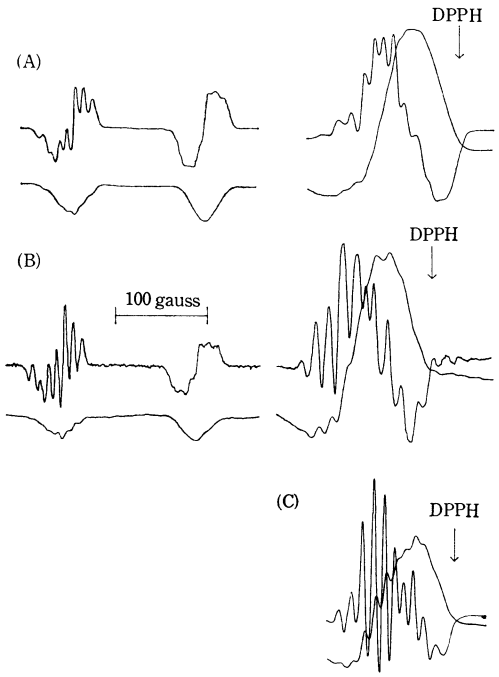

Fig. 7. The second derivative X-band ESR spectra at 77°K.
(A) $Cu(acest)_2$ in 20% pyridine-80% chloroform
(B) $Cu(acest)_2$ in 20% γ-picoline-80% chloroform
(C) $Cu(sal)_2$ in 20% γ-picoline-80% chloroform

The hyperfine and super-hyperfine structures at the most intense absorption line in the high-field part are too complex to be analyzed completely. On the other hand, the super-hyperfine structure in the hyperfine absorption lines of $I_z=-3/2$ and $-1/2$ in the low-field part were analyzed on the assumption of an equal coupling of the unpaired electron with two nitrogen atoms. The results are shown in Fig. 8, which shows a fairly good correspondence in the position and intensity of the super-hyperfine absorption line between the second derivative spectrum and its reconstruction.

The ESR spectrum of (B) in Fig. 3 shows that the ligand field of $Cu(acest)_2$ in 20% pyridine (or γ-picoline) - 80% chloroform is of an axial symmetry; the complex dissolved in the solvent has a square-planar structure. As has been described in the foregoing paragraph, the ESR spectra of $Cu(acac)_2$ in the solvents containing pyridine or γ-picoline also showed the ligand field of an axial symmetry; furthermore, it was concluded that, in the solvents, pyridine or γ-picoline molecules coordinate to the complex as apical ligands. However, no super-hyperfine structure could be observed in these spectra of $Cu(acac)_2$.

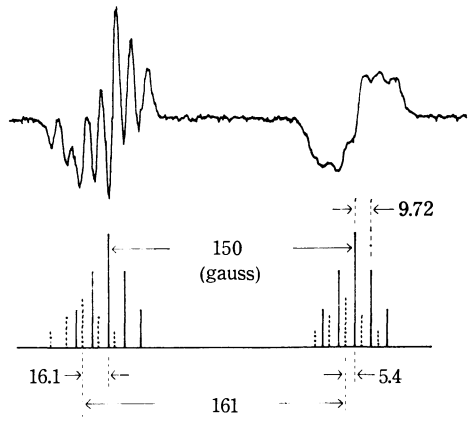

Fig. 8. The second derivative ESR spectrum (the hyperfine absorption lines of $I_z=-3/2$ and $-1/2$) of $Cu(acest)_2$ in 20% γ-picoline - 80% chloroform at 77°K and its reconstruction (solid line : ^{63}Cu dotted line : ^{65}Cu; the hyperfine intensity ratio of ^{63}Cu to ^{65}Cu of 7 : 3 was assumed).

The super-hyperfine interaction between the unpaired electron spin and the nuclear spin of the surrounding ligand atoms is mainly due to the dipole interaction and Fermi contact interaction with the spin density produced in the ligands by the covalent mixing of ligand wavefunctions into the antibonding orbitals.[18-21] The super-hyperfine interaction energies listed as $A_N//$ in Table 1, which were determined from the super-hyperfine structure observed in the hyperfine absorption lines of $I_z=-3/2$ and $-1/2$ in the low-field part, are comparable in magnitude to those previously reported for the square-planar copper(II) complexes containing nitrogen atoms as coordinating ligand atoms.[6,9,22] When the unpaired electron orbit is on the molecular plane, the super-hyperfine interaction between the electron spin and the nuclear spin of the apical

18) W. Marshall, "Paramagnetic Resonance," Vol. 1, ed. by W. Low, Academic Press, New York (1963), p. 347; W. Marshall and R. Stuart, *Phys. Rev.*, **123**, 2048 (1961).

19) T. P. P. Hall, W. Hayes, R. W. H. Stevenson and J. Wilkens, *J. Chem. Phys.*, **38**, 1977 (1963); **39**, 35 (1963).

20) M. Tinkham, *Proc. Roy. Soc. Ser. A* **236**, 535, 549 (1956).

21) B. R. McGarvey, "Transition Metal Chemistry," Vol. 3, ed. by R. L. Carlin, Marcel Dekker, New York (1967), p. 89; G. F. Kokoszka and G. Gordon, "Technique of Inorganic Chemistry," Vol. 7, ed. by H. B. Jonassen and A. Weissberger, Interscience Publishers, New York (1967), p. 151.

22) A. G. Gersmann and J. D. Swalen, *J. Chem. Phys.*, **36**, 3221 (1962); S. E. Harrison and J. M. Assour, "Paramagnetic Resonance," Vol. 2, ed. by W. Low, Academic Press, New York (1963), p. 855; W. Schneider and A. V. Zelewsky, *Helv. Chim. Acta*, **48**, 1529 (1965).

ligand atoms which are 2 Å or more from the metal atom, such interaction proceeding by means of direct dipole interaction or other possible mechanisms, can be estimated to be of an order of magnitude lower than the observed energies.[18-21] Therefore, it can be concluded that, in the system under discussion, two nitrogen atoms are equally introduced into the unpaired electron orbital of the complex and that a new square-planar coordination occurs through the two nitrogen atoms and the two oxygen atoms of the four originally-coordinating oxygen atoms. Needless to say, the two nitrogen atoms are those of the pyridine or γ-picoline used as the solvent.

The question next arises: what are the apical ligands in these systems. Figure 4 shows the ESR spectrum of $Cu(acest)_2$ in 20% γ-picoline - 80% toluene; this spectrum was in complete agreement with the ESR spectrum of $[Cu(acest)_2(\gamma\text{-picoline})_2]$ in toluene. This experimental fact establishes that the apical ligands are not γ-picoline molecules in either of the solutions. Furthermore, all the ESR spectra of $Cu(acest)_2$ in 20% pyridine - 80% chloroform, 20% pyridine - 40% chloroform - 40% ethanol, and 10% pyridine - 90% toluene are almost the same in line shape. This indicates that the apical ligands of the complex are same in all these solutions. From all the above discussion, it can be concluded that the apical ligand atoms are the two oxygen atoms of the four originally-coordinating oxygen atoms of $Cu(acest)_2$, whereas, as has been described above, the other oxygen atoms form a square-planar coordination. Therefore, the structure of $Cu(acest)_2$ in pyridine or γ-picoline can be visualized as is shown in Fig. 9. Such is also the case with $Cu(sal)_2$, since $Cu(acest)_2$ and $Cu(sal)_2$ are quite similar in their ESR spectral behavior.

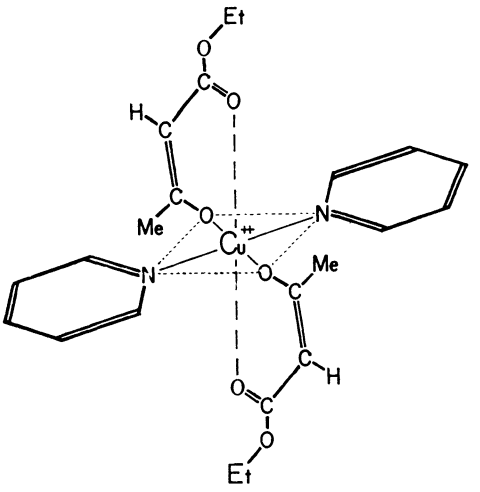

Fig. 9. The estimated structure of $Cu(acest)_2$ in pyridine.

BULLETIN OF THE CHEMICAL SOCIETY OF JAPAN VOL. 43 1083—1087 (1970)

Determination of Niobium by Photon-Activation Analysis Based on Internal-Reference Method*1

Yoshinaga OKA, Tong-Chuin PUNG and Tatsuya SAITO

Department of Chemistry, Faculty of Science, Tohoku University, Katahira-cho, Sendai

(Received September 27, 1969)

The internal-reference method proposed previously has been applied to the photon-activation analysis of niobium using molybdenum as the reference element. For the determination of niobium, ^{92m}Nb produced by the (γ,n) reaction was utilized and ^{95m}Nb or ^{96}Nb activities coming from molybdenum by the (γ,p) processes were used as reference. A series of molybdenum and niobium mixtures with known compositions were irradiated by bremsstrahlung photons with a maximum energy of 17 MeV for an hour. After niobium activities were separated chemically, their γ-ray spectra were measured with a lithium-drifted germanium detector. A good proportionality was obtained between the activity ratio, R_{A_0}, and the weight ratio, R_W. Niobium down to 50 μg can be determined with a relative error within $\pm 3\%$ under the present experimental conditions.

Thermal neutron activation analysis for niobium has been studied by several workers.[1-3] Kim and

*1 Study on the Activation Analysis using Internal-Reference Method. XII., Part XI: Y. Oka, T. Kato and Y. Konami, *Bunseki Kagaku*, **18**, 971 (1969).

1) C. K. Kim, "Production and Use of Short-lived Radioisotopes from Reactors," I.A.E.A., 1963, Vol. II, 73.

Meinke,[2] and Verbeek[3] measured the 16.6 KeV X-ray of 6.3 min-^{94m}Nb produced by (n,γ) reaction. Rapid separation is necessary in their methods, and low energy of the X-ray makes the measurement difficult. Athavale *et al.*[4] have taken advantage of the reaction ^{93}Nb(n,α)^{90}Y induced by fast neutrons in a pile. Tomita and Saisho[5] used the ^{93}Nb(p,n)^{93m}Mo reaction for the same purpose.

In the present paper we describe a method of photon-activation analysis using molybdenum as the internal-reference element.

Experimental

Materials and Irradiation. Niobium, in the form of metallic powder of analytical-reagent grade was supplied from Johnson Mathey Co. Molybdenum was metallic powder of 99.9% purity from Wako Pure Chemical Industries, Ltd.

A linear electron accelerator of the Tohoku University and that of the Japan Atomic Energy Research Institute were the bremsstrahlung sources.

0.1—1.5 g of each element or mixtures of known compositions were sealed either in small quartz or pyrex tubes with an internal diameter of 6 mm. They were placed in a target holder immediately behind the converter*2 and irradiated. Typical irradiation was performed for an hour.

Measurement of Radioactivity. For measurements of γ-ray spectra a lithium-drifted germanium detector with a sensitive volume of 36 cm^3 coupled to a TMC 1024-channel pulse-height analyzer was used. Nuclide identification was made by energies and decay curve analysis of the specified γ-ray photopeaks.[6]

Separation of Niobium. Niobium activities were separated from irradiated samples with anion exchange

TABLE 1. NUCLEAR REACTION AND MASS THRESHOLD

Target nuclide (abundance)	Reaction type	Product nuclide	Threshold energy (MeV)	Coulomb barrier (MeV)	Half-life	γ-Ray energy (MeV)		
^{93}Nb(100%)	(γ, n)	^{92m}Nb	8.95[7]		10.16d	0.90	0.934	1.83
	(γ, 2n)	^{91m}Nb	17.18[7]		62d	1.21		
	(γ, 3n)	^{90}Nb	28.78		14.6 hr	0.142	0.511	1.14
						1.30	2.18	2.32
^{92}Mo(15.16%)	(γ, p)	^{91m}Nb	7.45[7]	6.72	62d	1.21		
	(γ, pn)	^{90}Nb	19.65	6.73	14.6 hr	0.142	0.511	1.14
						1.30	2.18	2.32
	(γ, d)	^{90}Nb	17.28[7]	6.71	14.6 hr	0.142	0.511	1.14
						1.30	2.18	2.32
^{94}Mo(9.12%)	(γ, pn)	^{92m}Nb	17.45	6.70	10.16d	0.90	0.934	1.83
	(γ, d)	^{92m}Nb	15.09[7]	6.66	10.16d	0.90	0.934	1.83
^{96}Mo(16.50%)	(γ, p)	^{95m}Nb	9.53[7]	6.64	90 hr	0.235		
	(γ, p)	^{95}Nb	9.30[7]	6.64	35d	0.765		
^{97}Mo(9.45%)	(γ, p)	^{96}Nb	9.18[7]	6.62	23.35 hr	0.459	0.569	0.778
						0.811	0.851	1.092
						1.200	1.499	
	(γ, pn)	^{95m}Nb	16.44	6.64	90 hr	0.235		
	(γ, d)	^{95m}Nb	14.13	6.61	90 hr	0.235		
	(γ, pn)	^{95}Nb	16.20	6.64	35d	0.765		
	(γ, d)	^{85}Nb	13.89[7]	6.61	35d	0.765		
^{98}Mo(23.75%)	(γ, p)	^{97}Nb	9.79[7]	6.59	72 min	0.655		
	(γ, pn)	^{96}Nb	17.60	6.62	23.35 hr	0.459	0.569	0.778
						0.811	0.851	1.092
						1.200	1.499	
	(γ, d)	^{96}Nb	15.60[7]	6.59	23.35 hr	0.459	0.569	0.778
						0.811	0.851	1.092
						1.200	1.499	
^{100}Mo(9.62%)	(γ, pn)	^{98}Nb	17.97	6.58	51 min	0.720	0.787	1.16
						1.44	1.52	1.68
						1.88	1.93	
	(γ, d)	^{98}Nb	15.81[7]	6.55	51 min	0.720	0.787	1.16
						1.44	1.52	1.68
						1.88	1.93	

2) C. K. Kim and W. W. Meinke, *Anal. Chem.*, **35**, 2135 (1963).

3) A. A. Verbeek, *Anal. Chim. Acta*, **33**, 131 (1965).

4) V. T. Athavale, H. B. Desai, S. Gangadharan, M. S. Pendharkar and M. Sankardas, *Analyst*, **91**, 638 (1966).

5) I. Tomita and H. Saisho, *Nature*, **195**, 1189 (1962).

*2 3 mm thick platinum plate (Tohoku University linac) or 2 mm thick platinum plate (JAERI linac).

6) "Table of Isotopes" was used for specification: C. M. Lederer, J. M. Hollander and I. Perlman, "Table of Isotopes," 6th Ed., John Wiley & Sons, Inc., New York (1967).

7) C. Maples, G. W. Goth and J. Cerny, 'Nuclear Reaction *Q*-Values,' "Nuclear Data," K. Way Ed., Sec. A, Vol. 2, Academic Press, Inc., New York (1966), p. 429.

resin using hydrofluoric acid-hydrochloric acid mixture as the eluting agent.[8] The irradiated sample was dissolved in 3 m*l* of 40 (w/v) % hydrofluoric acid containing a few drops of nitric acid in a teflon beaker, and the content was evaporated to dryness under an infrared lamp. After dissolving the residue with 5 m*l* of 1N hydrofluoric acid, 9.711 mg of niobium in 1N hydrofluoric acid solution was added as carrier. The resulting solution was poured into a Dowex 1×8 column.*3 Yttrium activities were eluted with 1N hydrofluoric acid, and zirconium activities were eluted with 80 m*l* of 0.01N hydrofluoric acid-9N hydrochloric acid mixture. Niobium was then eluted with 80 m*l* of 0.2N hydrofluoric acid-9N hydrochloric acid mixture. To this niobium fraction, 5 m*l* of saturated boric acid solution was added. The solution was heated nearly to boiling for about 1 min and niobium was precipitated by the addition of aqueous ammonium hydroxide solution. The precipitate was filtered and washed with dilute ammonium hydroxide solution and then ignited to obtain niobium oxide. The chemical yield of niobium was 90—95%.

Results and Discussion

Photonuclear Reaction. The photonuclear reactions on niobium and molybdenum were studied with Bremsstrahlung of several different maximum energies. The nuclear characteristics of radionuclides of present importance, mass threshold energies of possible reactions and the Coulomb barrier heights are summarized in Table 1.

When niobium samples were irradiated with Bremsstrahlung, with maximum energies 17, 30, 45 and 60 MeV, the γ-ray spectra of the resultant activities were obtained as shown in Fig. 1. As shown in spectrum I in Fig. 1, an intense photopeak at 0.934 MeV was observed. Minor peaks at 0.90 and 1.83 MeV were also measured. From the γ-ray energies and decay curve analysis, the production of ^{92m}Nb could be confirmed. This might be acceptable from the threshold consideration listed in Table 1. With 30 MeV bremsstrahlung, the production of ^{91m}Nb by (γ,2n) reaction could also be expected. However, as seen in spectrum II in Fig. 1, the activity strength of the 1.21 MeV γ-ray photopeak was very weak. This would be due to the fact that the irradiation period was too short to produce enough 62 d-^{91m}Nb activity and that the branching decay ratio of the 1.21 MeV γ-ray is only 3%. From mass threshold energy, the ^{93}Nb (γ,3n) ^{90}Nb reaction may not be expected at 30 MeV, but it was apparent with 45 and 60 MeV bremsstrahlung.

It should be noted that knowledge of a mass threshold energy of a given photonuclear reaction gives only the possibility of its production: The relative probability of forming each product by the (γ,*x*n) reactions depends on the shape of the excitation functions which determines the yield value over the energy range of given Bremsstrahlung.

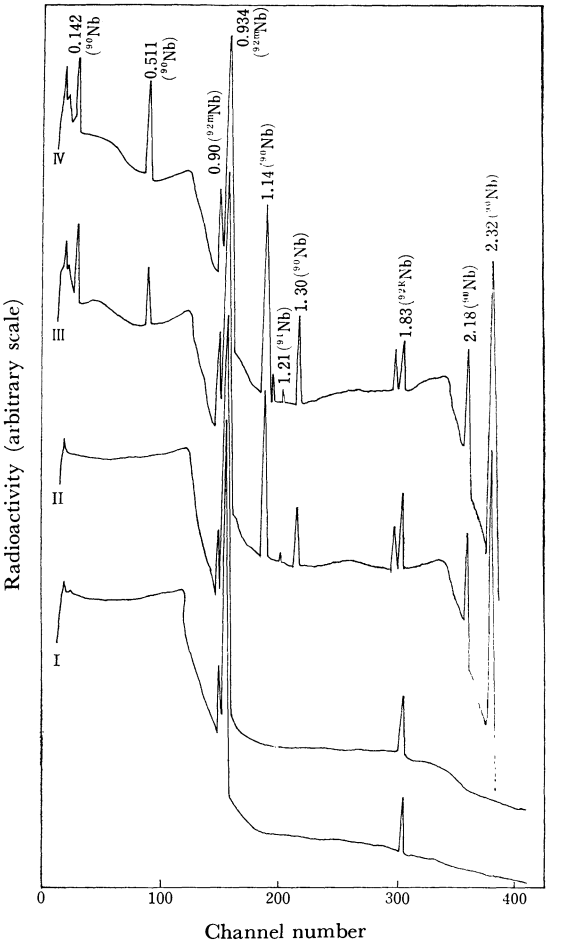

Fig. 1. γ-Ray spectra of niobium targets irradiated by Bremsstrahlung with various maximum energies.
I: 17 MeV bremsstrahlung for 60 min, 10.4 d after irradiation
II: 30 MeV bremsstrahlung for 100 min, 2.0 hr after irradiation
III: 45 MeV bremsstrahlung for 60 min, 1.8 d after irradiation
IV: 60 MeV bremsstrahlung for 105 min, 1.9 d after irradiation

Studies have been done on the niobium activities produced by the (γ,p*x*n) reactions in molybdenum samples irradiated with bremsstrahlung of maximum energies varying from 17 MeV to 65 MeV. Their γ-ray spectra are given in Fig. 2. In spectrum I in Fig. 2, the productions of ^{95m}Nb and ^{96}Nb can be seen. The former can be formed by the ^{96}Mo (γ,p), ^{97}Mo (γ,pn) or ^{97}Mo (γ,d) reactions, and the latter by the ^{97}Mo (γ,p), ^{98}Mo (γ,pn) or ^{98}Mo (γ,d) reactions. From mass threshold and Coulomb barrier consideration as given in Table 1,

8) E. J. Dixon and J. B. Headridge, *Analyst*, **89**, 185 (1964).

*3 1 cmϕ×40 cm, 100—200 mesh.

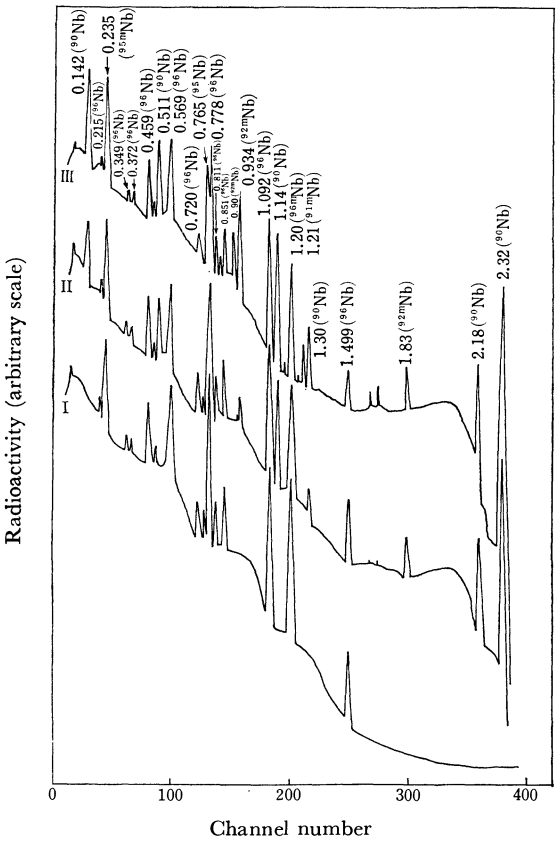

Fig. 2. γ-Ray spectra of niobium fractions separated from irradiated molybdenum targets.
I: Irradiated with 17 MeV bremsstrahlung for 60 min, spectrum obtained 1.33 d after irradiation
II: Irradiation with 30 MeV bremsstrahlung for 30 min, spectrum obtained 3.03 d after irradiation
III: Irradiated with 65 MeV bremsstrahlung for 25 min, spectrum obtained 3.96 d after irradiation

the possible reactions to produce ^{95m}Nb and ^{96}Nb can be concluded to be (γ,p) reactions on ^{96}Mo and ^{97}Mo respectively at 17 MeV. From a similar consideration, ^{95}Nb may be formed only by the (γ,p) reaction on ^{96}Mo at 17 MeV. Its production rate would not be appreciable in a short irradiation period. With bremsstrahlung maximum energies above 30 MeV, the formation of ^{90}Nb, ^{92m}Nb and small amount of ^{95}Nb can be found as shown in Fig. 2.

As has been stated on the yields of the (γ,n), (γ,p), (γ,2n), (γ,pn) and (γ,α) reactions with 20 MeV Bremsstrahlung, the (γ,n) reaction gives the highest yield for most of nuclei in the medium-to-heavy mass region.[9-11] Accordingly, ^{92m}Nb, the (γ,n) reaction product, should be preferably used for the determination of niobium with respect to sensitivity. The formation of ^{92m}Nb, therefore, should be necessarily avoided in an irradiated molybdenum sample. As seen in Table 1, the possible reactions leading to the production of ^{92m}Nb from molybdenum are the (γ,pn) or the (γ,d) reaction on ^{94}Mo. The sum of their mass threshold energies and Coulomb barrier heights are 24.15 and 21.75 MeV, respectively, which are both well beyond an excitation energy of 20 MeV. Hence interference of this sort could be avoided in the irradiation with 20 MeV bremsstrahlung, provided that the tunnel effect was not taken into account. Figure 3 shows the experimental results.

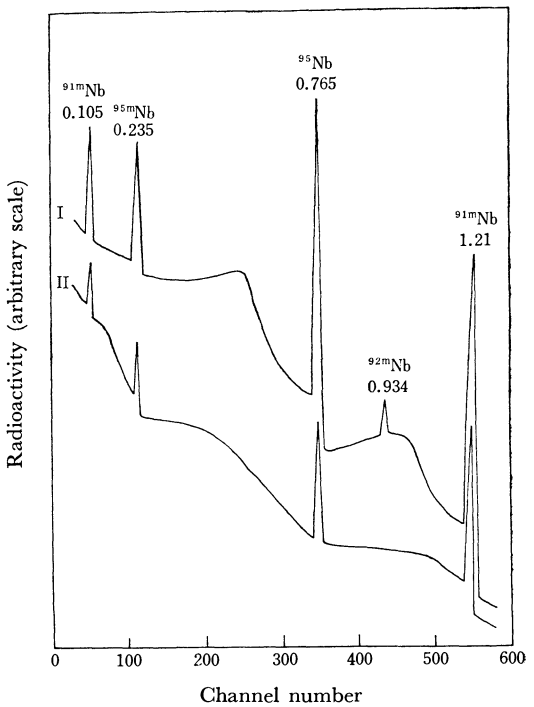

Fig. 3. γ-Ray spectra of niobium fractions separated from irradiated molybdenum targets.
I: Irradiated with 20 MeV bremsstrahlung for 1 hr, spectrum obtained 1.83 d after irradiation
II: Irradiated with 17 MeV bremsstrahlung for 1 hr, spectrum obtained 10.4 d after irradiation

The 0.934 MeV γ-ray of ^{92m}Nb can still be found as shown in spectrum I but its formation was completely suppressed at 17 MeV. Consequently, the irradiation was performed by 17 MeV bremsstrahlung in the determination of niobium using

9) Y. Oka, T. Kato, K. Nomura and T. Saito, This Bulletin, **40**, 575 (1967).

10) Y. Oka, T. Kato, K. Nomura, T. Saito and H.-T. Tsai, *ibid.*, **41**, 380 (1968).

11) Y. Oka, T. Kato, K. Nomura, T. Saito and H.-T. Tsai, *ibid.*, **41**, 2660 (1968).

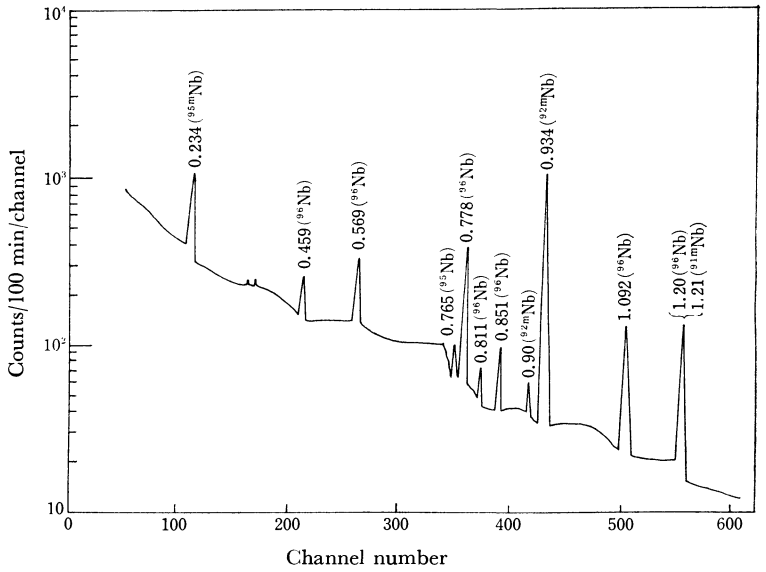

Fig. 4. γ-Ray spectrum of niobium fraction separated from irradiated niobium-molybdenum mixture (Nb/Mo=2.36×10^{-3}). Spectrum obtained
2.1 d after irradiation.

TABLE 2. R_W *vs.* R_{A_0} FOR NIOBIUM-MOLYBDENUM MIXTURES

R_W (Nb/Mo)	R_{A_0}		R_W/R_{A_0}	
	^{92m}Nb (0.932 MeV) / ^{95m}Nb (0.235 MeV)	^{92m}Nb (0.934 MeV) / ^{96}Nb (1.092 MeV)	^{92m}Nb / ^{95m}Nb	^{92m}Nb / ^{96}Nb
4.356×10^{-3}	9.74×10^{-1}	2.55	4.47×10^{-3}	1.71×10^{-3}
3.190×10^{-3}	6.78×10^{-1}	1.99	4.71×10^{-3}	1.60×10^{-3}
1.117×10^{-3}	2.41×10^{-1}	6.63×10^{-1}	4.63×10^{-3}	1.68×10^{-3}
5.694×10^{-4}	1.21×10^{-1}	3.51×10^{-1}	4.71×10^{-3}	1.62×10^{-3}
1.470×10^{-4}	3.33×10^{-2}	8.78×10^{-2}	4.41×10^{-3}	1.67×10^{-3}
		Mean:	4.59×10^{-3}	1.66×10^{-3}
		Std. dev.:	$\pm0.12\times10^{-3}$	$\pm0.04\times10^{-3}$

molybdenum as the internal-reference element.

The Determination of Niobium. The synthetic niobium-molybdenum mixtures were irradiated with 17 MeV Bremsstrahlung for an hour at a photon flux of 4.3×10^5 roentgens/min. After irradiation, niobium activities were separated chemically as described above. In Fig. 4, a typical γ-ray spectrum of niobium fraction is shown. Photopeak area under the 0.934 MeV photopeak of ^{92m}Nb was measured against that of either the 0.235 MeV photopeak area from ^{95}Nb or the 1.092 MeV photopeak area from ^{96}Nb.

The results are shown in Table 2. In each case, a good proportionality was obtained between R_W and R_{A_0}, where R_W is the weight ratio of niobium to molybdenum and R_{A_0} is the ratio of photopeak activities corrected at the end of one hour irradiation. The determination of niobium content in a sample can be achieved by using this relationship.

When a 10 cpm of photopeak activity is selected as the limit of determination, niobium content down to about 50 μg in a 1.5 g sample of molybdenum will be determined with a relative error within $\pm3\%$. Further applicability of this method will be found in the determination of niobium content in various samples by adding a proper amount of molybdenum as internal-reference element. An increase in sensitivity would be expected by using the higher bremsstrahlung dose and with a longer period of irradiation.

BULLETIN OF THE CHEMICAL SOCIETY OF JAPAN VOL. 43 1088—1093 (1970)

Syntheses and Properties of Metal Chelates of Ethanediylidenetetrathiotetraacetic Acid (ETTA) and Some Other Thioglycolic Acid Derivatives

Akira Ouchi, Yayoi Ohashi, Toshio Takeuchi and Yukichi Yoshino

Department of Chemistry, College of General Education, The University of Tokyo, Komaba, Meguro-ku, Tokyo

(Received October 17, 1969)

Some new metal chelate compounds of ethanediylidenetetrathiotetraacetic acid (H_4ETTA), $Co_2L\cdot 5H_2O$, $Cu_2L\cdot 4H_2O$, $Zn_2L\cdot 3H_2O$, $Ni_2L\cdot 6H_2O$, and $FeHL\cdot 3.5H_2O$, where H_4L is H_4ETTA, were obtained. The infrared spectra and other properties of these compounds were compared with those of the metal complexes of other thioglycolic acid derivatives, some of which are also new compounds. Judging from the wave numbers of the stretching bands, the carboxyl group of these complexes can be said to be rather ionic. Though the bond is not very strong, thioglycolic acid derivatives seem to bond with the central metal ion with both the sulfur atom and the carboxyl group.

Many kinds of chelate compounds of various metals with ethylenediaminetetraacetic acid (H_4EDTA) and its analogous ligand have already been synthesized and their properties investigated.[1] Recently many ligands which bond with the central metal ion by one or more sulfur atoms, or by one sulfur atom and some others, such as nitrogen or oxygen atoms, have been investigated very actively.[2,3] Therefore, it seemed that it would be interesting to study multidentate sulfur containing ligands and their metal complexes. The ethanediylidenetetrathiotetraacetic acid (H_4ETTA) is one of the ligands in this line of the research; moreover, as the structure of ETTA resembles that of EDTA, it led us to study the synthetic method and the properties of the metal chelates of this ligand. Only a few reports have been published about ETTA metal chelates. Longo and others have, though, prepared H_4ETTA and its chelate compounds of silver(I), iron(III), and mercury(II).[4] Saini and others have reported that the mole ratio of copper to ETTA in the chelate is 1 : 1 in the solution.[5]

Therefore, we have newly synthesized solid ETTA chelates of other metals; nickel(II), cobalt(II), copper(II), zinc(II) and cadmium(II). The iron(III) complex was also synthesized. The mole ratio of ETTA to iron was 1 : 1, unlike Longo's product, which had the mole ratio of 1 : 2.

In order to study the structure of the ETTA complexes and of the several thioglycolic acid derivatives shown below, their metal complexes were synthesized and investigated; they were benzylidenebisthioglycolic acid $C_6H_5CH(SCH_2CO_2H)_2$ (H_2BzS_2), ethylidenebisthioglycolic acid $CH_3CH(SCH_2CO_2H)_2$ (H_2EtS_2), methylenebisthioglycolic acid $CH_2(SCH_2CO_2H)_2$ (H_2MeS_2), benzylthioglycolic acid $C_6H_5CH_2SCH_2CO_2H$ (H_1BzS_1), and ethylthioglycolic acid $C_2H_5SCH_2CO_2H$ (H_1EtS_1). Their structure are shown in Fig. 1. The metal chelates of some of these compounds were studied by the solution-chemistry method. Ethylthioglycolic acid,

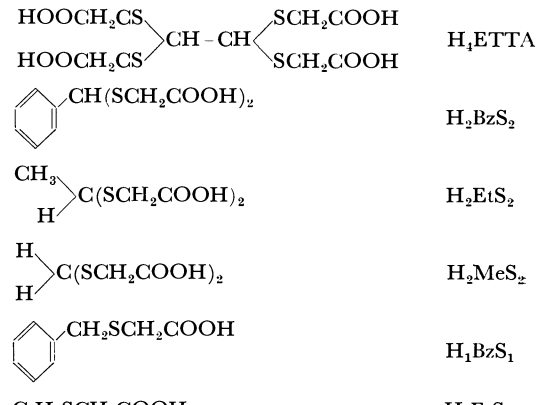

Fig. 1. The chemical formulae of the thioglycolic acid derivatives.

1) F. P. Dwyer and D. P. Meller, "Chelating Agents and Metal Chelates," Academic Press, New York (1964), p. 283.

2) S. E. Livingstone, *Quart. Rev.* (London), **19**, 386 (1965).

3) C. K. Jørgensen, "Inorganic Complexes," Academic Press, New York (1963), p. 131.

4) F. R. Longo, A. Ventresca, Jr., J. E. Drach, J. McBride and R. F. Sauers, *Chemist-Analyst*, **54**, 101 (1965).

5) G. Saini, G. Ostocoli, E. Compi and N. Cibrario, *Gazz. Chim. Ital.*, **91**, 904 (1961).

for example, has been studied by several authors;[6,7] according to their results, the ligand bonds to the central metal ion not only by its carboxyl group, but also by its sulfur atom. Although Yamasaki and Suzuki[8] have reported that the sulfur atom of phenylthioacetic acid seems not to be bonded with the metal ion in their metal complexes, the same authors wrote that ethylenedithiodiacetic acid seems to coordinate to a metal ion by means of sulfur atoms. The behavior of the former may be partly due to some steric interference with the chelate formation.

The chemical properties and the infrared spectra of the metal chelates of H_4ETTA and these thioglycolic acid derivatives resemble each other; accordingly, the structure of all of these chelates seem to be similar. The results obtained below seem to show that these ligands bond to the central metal ion as a multidentate, using both the sulfur atom and the carboxyl group, though the sulfur-metal bond is not very strong.

Experimental

Instruments. The infrared spectra were obtained by the Nujol or hexachloro-1,3-butadiene mull procedure, using a DS 301-type infrared spectrophotometer of the Japan Spectroscopic Co., Ltd. The electronic spectra were obtained with a Hitachi EPS-2-type automatic recording spectrophotometer. The reflectance spectra were obtained by using a reflectance attachment and a magnesium oxide standard. The magnetic moments were measured with a Gouy balance at room temperature (25°C).

Materials. The H_4ETTA was synthesized by Longo's method[4] by means of a condensation reaction between glyoxal and thioglycolic acid. The bisthioglycolic acid derivatives, H_2BzS_2, H_2EtS_2, and H_2MeS_2, were synthesized by Bongartz's method[9] and by Mattisson's method.[10] The monothioglycolic acid derivatives, $HBzS_1$ and $HEtS_1$, were synthesized by Larsson's method.[11]

The Syntheses of the Metal Chelates of ETTA. *(i) Cobalt(II), Copper(II), Nickel(II), Zinc(II) and Cadmium(II) Complexes.* The metal hydroxide of these metals was made from their nitrate and sodium hydroxide. It was suspended in water, about one fourth (mol/mol) of H_4ETTA was added, and the mixture was stirred for about 10 to 30 min at room temperature. The residue was then filtered off, and to the filtrate an equivolume of ethanol was added. The precipitate thus obtained was filtered off and washed by ethanol and acetone, in that order, before being dried in a vacuum desiccator at room temperature.

(ii) Iron(III) Complex. 1.3 g (1/300 mol) of H_4ETTA and 0.53 g (4/300 mol) of sodium hydroxide were dissolved in water. In a separate vessel, an aqueous solution of 2.7 g (1/100 mol) of iron(III) chloride hexahydrate was prepared; the pH of this solution was kept lower than 1 by perchloric acid. The two solutions were then mixed and stirred. The pH of the supernatant fluid was kept at 0.8 by adding perchloric acid. A precipitate thus appeared. It was filtered off, washed by acetone and ether, and dried in a vacuum desiccator at room temperature.

The Syntheses of Metal Complexes of Other Thioglycolic Acid Derivatives. The method of synthesizing the ETTA chelates can be used with slight modifications. Some examples are shown as follows.

(i) Copper(II) Complex of H_1BzS_1. Copper(II) hydroxide was obtained from 1 g of copper(II) chloride dihydrate. After suspending it in water, 2 g of H_1BzS_1 were added; the mixture was stirred well and boiled, and the insoluble residue was filtered off while hot. When the filtrate was cooled in an ice bath, pale blue $Cu(BzS_1)_2 \cdot 2H_2O$ deposited. The $Cu(BzS_1)_2 \cdot 2H_2O$, when boiled with an equivolume mixture of absolute ethanol and benzene, produced a green precipitate, $Cu(BzS_1)_2$. This was washed repeatedly with benzene and dried in a vacuum desiccator at room temperature.

(ii) Nickel(II) Complex of H_2EtS_2. Newly-made wet nickel(II) hydroxide obtained from 0.5 g of nickel(II) chloride hexahydrate and alkali was mixed with 0.7 g of H_2EtS_2(liquid). Ethanol was added to the mixture, after which the mixture was stirred, warmed, and filtered. The solid product thus obtained was washed well with ethanol and ethyl ether successively and then dried in a vacuum desiccator at room temperature.

Results and Discussion

The elemental analyses and the chemical formulae of the complexes thus obtained are shown in Table 1. Judging from these analytical results, many of these complexes can be said to contain water molecules and some of them seem to be coordinated complexes though the coordination number of the metals of these complexes cannot be determined from only these data.

The magnetic moments of these complexes, as measured by Gouy's balance at 25°C, are shown in Table 2. The cobalt complexes show magnetic moments of 4.5—4.9 B.M. per mole of metal. As these complexes are pink in color and have the oxidation number of +2, these cobalt(II) complexes can be said to be in a d^7 high spin configuration. Because of the orbital contribution, the observed magnetic moments are always higher than the spin-only values; they are 4.7—5.2 B.M. for octahedral- and 4.4—4.8 B.M. for tetrahedral-configuration complexes.[12] Consequently, the cobalt(II) complexes of ETTA and thioglycolic acid derivatives probably have an octahedral configuration.

6) R. J. Irving and W. C. Fernelius, *J. Phys. Chem.*, **60**, 1427 (1956).
7) A. Sandell, *Acta, Chem. Scand.*, **15**, 190 (1961).
8) K. Suzuki and K. Yamasaki, *J. Inorg. Nucl. Chem.*, **24**, 1093 (1962).
9) J. Bongartz, *Ber.*, **21**, 478 (1888).
10) B. Holmberg and K. Mattisson, *Ann. Chem.*, **353**, 123 (1907).
11) E. Larsson, *Ber.*, **63**, 1347 (1930).
12) A. Earnshaw, "Introduction to Magnetochemistry," Academic Press, New York (1968), p. 34.

Table 1. The analyses of complexes (Figures are given in %)

		Metal	C	H	S
H_4ETTA	Calcd		30.80	3.59	
	Found		30.85	3.69	
$Co_2(ETTA)\cdot 5H_2O$	Calcd	19.85	20.25	3.38	21.45
	Found	20.10	20.21	3.70	21.38
$Cu_2(ETTA)\cdot 4H_2O$	Calcd	21.70	20.51	3.10	21.90
	Found	20.50	21.84	3.33	22.46
$Zn_2(ETTA)\cdot 3H_2O$	Calcd	22.90	21.02	2.81	22.43
	Found	23.00	21.14	3.05	22.47
$Ni_2(ETTA)\cdot 6H_2O$	Calcd	19.20	19.45	3.61	20.90
	Found	19.10	19.26	4.03	20.71
$Cd_2(ETTA)\cdot 4H_2O$	Calcd	32.98	17.60	2.64	18.73
	Found	33.16	17.51	2.77	18.62
$Fe(HETTA)\cdot 3.5H_2O$	Calcd	11.05	23.73	3.57	25.37
	Found	11.17	23.31	3.19	25.26
$Ni(BzS_2)\cdot 2H_2O$	Calcd	16.08	36.19	3.87	17.57
	Found	16.82	34.84	3.67	18.10
$Co(BzS_2)$	Calcd	17.90	40.13	3.06	19.48
	Found	18.05	36.53	3.08	19.60
$Cu(EtS_2)\cdot H_2O$	Calcd	21.93	24.88	3.45	22.07
	Found	22.25	24.72	3.47	22.93
$Ni(EtS_2)\cdot H_2O$	Calcd	20.72	25.26	3.51	22.46
	Found	21.01	25.39	3.18	22.92
$Co(EtS_2)$	Calcd	22.09	26.98	3.00	23.98
	Found	21.93	26.91	3.18	24.13
$Cu(MeS_2)\cdot H_2O$	Calcd	23.00	21.77	2.90	23.22
	Found	22.62	21.74	3.00	22.97
$Ni(MeS_2)\cdot H_2O$	Calcd	21.72	22.15	2.95	23.61
	Found	20.65	22.45	2.84	22.80
$Co(MeS_2)$	Calcd	23.14	22.59	2.69	24.96
	Found	22.90	23.27	2.69	24.64
$Cu(BzS_1)_2\cdot 2H_2O$	Calcd	13.77	46.78	4.76	13.85
	Found	13.67	46.97	4.86	13.70
$Cu(BzS_1)_2$	Calcd	14.91	50.78	4.23	15.04
	Found	14.98	50.07	4.46	14.43
$Co(BzS_1)_2\cdot 2H_2O$	Calcd	12.91	47.30	4.82	14.00
	Found	13.38	47.05	4.71	14.36
$Ni(BzS_1)\cdot H_2O$	Calcd	13.42	49.20	4.56	14.58
	Found	13.51	49.90	4.49	14.11
$Cu(EtS_1)_2\cdot 2H_2O$	Calcd	18.84	28.43	5.33	18.97
	Found	18.80	28.69	5.33	18.40
$Co(EtS_1)_2\cdot 2H_2O$	Calcd	17.71	28.85	5.41	19.23
	Found	17.68	28.84	5.32	18.50
$Ni(EtS_1)_2\cdot 2H_2O$	Calcd	17.71	28.85	5.41	19.23
	Found	17.40	28.95	5.34	18.78

In the case of nickel complexes, the observed magnetic moment values are in the range of 3.0—3.7 B.M. The nickel(II) complexes in an octahedral configuration show magnetic moments of 2.9—3.4 B.M., whereas the tetrahedral-configuration complexes show 3.5—4.2 B.M.[12] Therefore, these complexes are possibly in an octahedral configuration too, not in the planar or tetrahedral configurations. Although this method cannot be used with the complexes of other metals, they are probably in a hexacoordinated octahedral form, too, for the properties of all of these complexes resemble each other. Therefore, in order to make a hexacoordinate configuration not only the carboxyl group, but also the sulfur atoms and water should be coordinated to the central metal ion.

In the case of copper(II) complexes, the magnetic moments are about 1.7—1.9; therefore, the metal-metal bond of copper(II) acetate-type compounds does not exist. In the case of the copper(II)

Table 2. Magnetic moments (B.M.) of the metal complexes at 25°C
(The numbers of the crystalline water are shown in parentheses)

Metal	Cu	Co	Ni	Zn	Cd	Fe
Ligand						
H_4ETTA	1.71(4)	4.94(5)	3.04(6)	dia(3)	dia(4)	4.01(3.5)
H_2BzS_2		4.55(0)	3.13(2)			
H_2EtS_2	1.87(1)	4.85(0)	3.54(1)			
H_2MeS_2	1.95(1)	4.85(0)	3.71(1)			
H_1BzS_1	1.72(0)	4.68(2)	3.30(1)			
	1.82(2)					
H_1EtS_1	1.73(2)	4.79(2)	3.13(2)			

Table 3. The maximum wave numders and the absorption coefficients of the visible spectra of some metal complexes

Figures are given kK for wave numbers and log ε for intensities (in parentheses)
abs: the absorption spectra of aqueous solutions.
ref: the reflection spectra of solid samples.

$Ni_2(ETTA)\cdot 6H_2O$	abs.	9.10(1.39)	14.7(1.09)		25.4(1.42)	37.7(3.72)sh
	ref.		14.9		25.0sh	
$Co_2(ETTA)\cdot 5H_2O$	abs.	8.1 (1.01)	8.9(1.02)		21.0(1.70)	26.9(1.78)sh
	ref.		16.7sh		20.0	
$Cu_2(ETTA)\cdot 4H_2O$	ref.		14.6			
$Fe(HETTA)\cdot 3.5H_2O$	ref.	12.8sh	18.5sh		24.4sh	
$Ni(EtS_1)_2\cdot 2H_2O$	abs.	8.8(0.79)	14.3(0.65)		25.3(1.02)	
	ref.		15.6		26.3	
$Co(EtS_1)_2\cdot 2H_2O$	abs.	7.5(0.60)	18.9(0.87)			
	ref.		17.1		20.2	22.9
$Cu(EtS_1)_2\cdot 2H_2O$	ref.	13.5sh	13.9sh	15.6	22.2sh	26.3

complex of benzylthioacetic acid, both $Cu(BzS_1)_2\cdot 2H_2O$ and $Cu(BzS_1)_2$ were obtained. The extraordinarily low magnetic moment of the iron(III) ETTA complex seems to be due to the low spin-high spin equilibrium reported by Ewald and others.[13]

The visible spectral data, absorption as well as reflection spectra data, of colored complexes are shown in Table 3. Some of these complexes are not soluble in water or other organic solvents, and so it is difficult to study their absorption spectra. The spectra of soluble samples show relatively low absorption peaks in the visible region; the log ε is about 1, except for those in the ultra-violet region, which seem to be the absorptions of the ligands themselves. Consequently, from the visible spectral data, too, the complex species in the solution seem to be in a hexacoordinate octahedral configuration, although some solvolysis may change the configuration in the solution from that in the solid state. The solid complex salts are not deeply colored, either, and the tetrahedral configuration is less probable even in the solid state. The d–d bands of the cobalt(II) and nickel(II) complexes are observed at about 7.5—8.0 kK and about 9 kK respectively. Therefore, the coordination bond strength of the chelates is not very strong; possibly it is comparable to those of water or of usual amino acids in the spectrochemical series.

The infrared absorption bands of the carboxyl group are most useful for a study of the coordination structure of these complexes. The wave numbers of the antisymmetric and symmetric stretching bands of the carboxyl group of the metal complexes as well as of the free acids, H_4ETTA, and other thioglycolic acid derivatives are shown in Table 4. The antisymmetric stretching bands of the free acids appear at about 1700 cm^{-1}; they shift to about 1570 to 1600 cm^{-1} in the cases of metal chelates. In some cases, the band splits into two peaks. For example, the bands appear at 1715 cm^{-1} as well as at 1610 cm^{-1} in the case of the Fe(III) HETTA complex. Therefore, some carboxyl groups of the ligand bond to the central metal ion, while others are in a free –COOH form. As the wave numbers of the peaks of metal chelates make such a big shift to the lower-wave number side, the carboxyl group of the ligand must have an ionic character in these compounds. Therefore the group seems to bond with the central metal ion, but the bond seems not to be a purely

13) A. H. Ewald, R. L. Martin, I. G. Ross and A. H. White, *Proc. Roy. Soc., Ser. A*, **280**, 235 (1964).

Table 4. The wave numbers of the stretching band of the carboxyl group and their separation in the metal complexes of various thioglycolic acid derivatives (cm^{-1})
(The numbers of the crystalline water of metal complexes are the same as Table 2.)

	H^+	Cu^{2+}	Ni^{2+}	Co^{2+}	Zn^{2+}	Fe^{3+}
$\tilde{\nu}(COO)_{asym}$						
ETTA	1703	1583	1583	1580	1590	1608
BzS_2	1693		1580	1580		
EtS_2	1697	1596	1578	1577		
MeS_2	1698	1590	1580	1579		
BzS_1	1692	1585	1598	1588		
EtS_1	1700	1632	1608	1605		
$\tilde{\nu}(-COO)_{sym}$						
ETTA	1397	1382	1375	1390	1383	1420
BzS_2	1390		1417	1400		
EtS_2	1408	1378	1387	1400		
MeS_2	1390	1384	1392	1384		
BzS_1	1449	1449	1452	1469		
EtS_1	1420	1441	1432	1443		
$\tilde{\nu}(-COO)_{asym}-(-COO)_{sym}$						
ETTA	306	201	208	190	207	188
BzS_2	303		163	180		
EtS_2	289	218	191	177		
MeS_2	308	206	188	195		
BzS_1	243	132	146	119		
EtS_1	280	191	176	162		

covalent one.[14,15] The symmetric stretching band of the carboxyl group of the free acids appeared at about 1400 cm^{-1}; the shift of the band of metal complexes should be another index of the bond type. According to Nakamoto,[16] the direction of the shift of the band depends on the symmetry of the carboxyl group in the metal complexes. If the carboxyl group in the complexes is not symmetric, antisymmetric and symmetric stretching bands shift to the higher- and lower-wave number sides respectively. On the other hand, if the coordination occurs symmetrically, both stretching bands shift in the same direction. Thus, the difference in the wave numbers of the antisymmetric and symmetric stretching bands of the carboxyl group of these compounds is useful for judging the structure of the chelate compounds.[17,18] Therefore, the observed values are also shown in Table 4. The values of carboxylic acid complexes increase in the following order of the central metals:

$$Ni(II) < Zn(II) < Cu(II) < Co(II).$$

The covalent character of the M–O bond also seems to increase in this order.[16]

In this case, however, the direction of the shift of the symmetric stretching band is not clear, and the values of the complexes of different metals are almost random; therefore, no meaningful conclusion could be drawn from the results. Two reasons for this are that the bonds between the metal-ligand bonds of all of these compounds are weak and that the bond strengths by different central metal ions are not very different. Moreover, if the sulfur atom bonds with the metal ion and forms a chelate ring, the order of the coordination bond strength of the simple carboxyl acid complexes should be modified. Whether or not sulfur is bonded to the central metal ion is not clear from the infrared spectral data in the 4000—600 cm^{-1} region, because the sulfur atoms in thio-ether-type compounds do not give strong bands in this region and so it is difficult to distinguish them from other bands. The weak band near 2550 cm^{-1} of the H_4ETTA seems to be due to dimerization by the hydrogen bond. It was not recognized in the spectra of its metal complexes.

Conclusions

From these data it may be concluded that the stabilities of the first-transition metal complexes of H_4ETTA and other thioglycolic acid derivatives are

14) D. T. Sawyer and J. M. McKinnie, *J. Amer. Chem. Soc.*, **82**, 4191 (1960).
15) K. Nakamoto, "Infrared Spectra of Inorganic and Coordination Compounds," John Wiley & Sons, New York (1963), pp. 201—210.
16) K. Nakamoto and P. J. McCarthy, "Spectroscopy and Structure of Metal Chelate Compounds," John Wiley & Sons, New York (1968), p. 269.

not high. Even ETTA acts at most as a tetradentate for each metal ion, and the chelate is not very stable. This is probably due to the weak coordination ability of the sulfur atoms of the thio-ether-type compounds. Moreover, the steric configuration of ETTA also shows that it finds difficult to act as a octadentate ligand for one metal atom with each four sulfur atoms and carboxyl groups. All of these metal complexes, however, are probably hexa-coordinated octahedral complexes, and the ligand bonds with the central metal ion by means of sulfur atoms and an ionized carboxyl group. Sometimes water molecules are also coordinated. In some cases, the polymerized form where a carboxyl group is coordinated with two metal ions is also possible.

The authors wish to express their appreciation to Professor Kunihiko Watanuki and to their colleagues of our laboratory for their helpful discussions.

BULLETIN OF THE CHEMICAL SOCIETY OF JAPAN VOL. 43 1093—1097 (1970)

Mössbauer Studies of the Thermal Decomposition of Iron(II) Pyridine and Picoline Complexes

Takeshi TOMINAGA, Masuo TAKEDA, Takeshi MORIMOTO and Nobufusa SAITO

Department of Chemistry, Faculty of Science, The University of Tokyo, Hongo, Bunkyo-ku, Tokyo

(Received October, 20, 1969)

The thermal decomposition of tetrakispyridineiron(II) chloride, tetrakis(γ-picoline)iron(II) chloride, and tetrakispyridineiron(II) isothiocyanate has been studied in nitrogen. These complexes presumably decompose in the following sequences:

$Fe(py)_4Cl_2 \rightarrow Fe(py)_2Cl_2 \rightarrow Fe(py)Cl_2 \rightarrow Fe(py)_{2/3}Cl_2 \rightarrow FeCl_2$,
$Fe(\gamma\text{-pic})_4Cl_2 \rightarrow Fe(\gamma\text{-pic})Cl_2 \rightarrow FeCl_2$ and $Fe(py)_4(NCS)_2 \rightarrow Fe(py)_2(NCS)_2 \rightarrow Fe(NCS)_2$.

The Mössbauer spectra of these complexes and of their decomposition products have been studied in terms of the structural change about the iron atom during the thermal decomposition process.

The Mössbauer spectroscopy has become a useful technique to investigate the oxidation state and the electronic configuration of iron in iron compounds. Since the Mössbauer study of the radiolysis and photolysis of ferric oxalate[1] indicated that this new technique was useful for directly investigating the chemical changes induced in solids, we applied this method to the study of the thermal decomposition of tetrakispyridineiron(II) chloride.[2]

After our preliminary work had been submitted for publication, we learned of an earlier Mössbauer work on some complex oxalates of iron(III).[3] In those iron oxalates, the oxidation state of iron was found to fluctuate between +2 and +4 during the course of the thermal decomposition.

According to our work on the thermal decomposition behavior of the iron(II) pyridine complexes,[2] the oxidation state of iron remains unchanged during the process in nitrogen. The thermal decomposition of these complexes proceeds through the step-by-step formation of octahedral polymers. Therefore, the purpose of our present work is to study the change in the Mössbauer parameters at different phases of the thermal decomposition in terms of the structural change about the iron atom, or the growth of the polymer structure during the decomposition process.

In the present paper, we will give a more complete report on the system which was studied in our earlier work,[2] as well as new data on some other complexes which have been studied recently.

Experimental

Samples. Tetrakispyridineiron(II) chloride, tetrakis(γ-picoline)iron(II) chloride, and tetrakispyridineiron(II) isothiocyanate were prepared and used for the thermal decomposition studies.

(i) $Fe(py)_4Cl_2$. Tetrakispyridineiron(II) chloride was prepared as has been described in the literature.[4,5]

1) N. Saito, H. Sano, T. Tominaga and F. Ambe, This Bulletin, **38**, 681 (1965).

2) T. Tominaga, T. Morimoto, M. Takeda and N. Saito, *Inorg. Nucl. Chem. Lett.*, **2**, 193 (1966).

3) P. K. Gallagher and C. R. Kurkjian, *Inorg. Chem.*, **5**, 214 (1966).

4) R. Weinland, K. Effinger and V. Beck, *Arch. Pharm.*, **265**, 352 (1927).

5) H. S. Booth, "Inorganic Syntheses," Vol. 1, McGraw-Hill Book Co. Inc., New York (1939), p. 184.

Intense yellow crystals were obtained and dried in a vacuum desiccator containing pyridine vapor. Found: Fe, 12.6; Cl, 15.0%. Calcd for $Fe(py)_4Cl_2$: Fe, 12.6; Cl, 14.2%.

(ii) $Fe(\gamma\text{-pic})_4Cl_2$. This was prepared by a procedure similar to (i). To 20 m*l* of γ-picoline we added 5 m*l* of a saturated $FeCl_2$ solution. Yellow crystals of the complex were obtained. Found: Fe, 11.3: Cl, 16.5%. Calcd for $Fe(\gamma\text{-pic})_4Cl_2$: Fe, 11.2; Cl, 16.0%.

(iii) $Fe(py)_4(NCS)_2$. This compound was prepared by the method described in the literature.[6] The yellowish white crystals obtained were dried in a vacuum desiccator. Found: Fe, 11.5; C, 54.1; H, 4.28; N, 17.2%. Calcd for $Fe(py)_4(NCS)_2$: Fe, 11.5; C, 54.1; H, 4.14; N, 17.2%.

Thermal Decomposition. The thermal decomposition studies were carried out on a Shimadzu Thermal Balance at a rate of heating of 2°C/min. All the thermal decompositions were carried out in a nitrogen atmosphere.*1

The powder X-ray patterns of tetrakispyridineiron(II) chloride, isothiocyanate, and their thermal decomposition products were made using a Rigaku Denki Geigerflex and Fe$K\alpha$ radiation.

The infrared spectra of these compounds were measured by using Hitachi EPI-G2 and EPI-L Spectrophotometers and a Hitachi FIS-1 Far-infrared Spectrophotometer.

Mössbauer Measurements. The Mössbauer absorption spectra of the starting materials and of the thermal decomposition products were obtained at room temperature and at lower temperatures*2 (163°K or 100°K) by using a mechanical constant-velocity drive spectrometer with a source of ^{57}Co diffused into copper or platinum foil. The spectrometer was calibrated with sodium nitroprusside dihydrate powder.

Results and Discussion

Thermal Decomposition of the Iron(II) Pyridine and γ-Picoline Complexes. Although several studies have been made of the thermal decomposition of various metal complexes of pyridine and its derivatives,[7-11] the thermal decomposition of the iron pyridine complexes had never been reported before our preliminary work on $Fe(py)_4Cl_2$[2] was published.

As may be seen in Fig. 1, the thermal decomposition of $Fe(py)_4Cl_2$ in air produced no distinct intermediate phase other than $Fe(py)_2Cl_2$, presumably because of the oxidation taking place at about 100°C or higher temperatures. This was verified by the Mössbauer spectrum of the decomposition product obtained at 150°C (above the temperature for the formation of $Fe(py)_2Cl_2$), which indicated the presence of Fe(III) (δ ~0.5 mm/sec; ΔE_Q

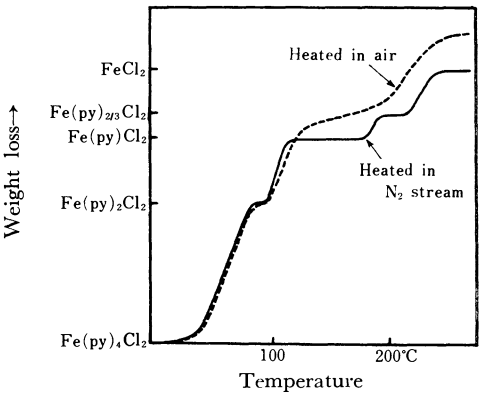

Fig. 1. Thermal decomposition of $Fe(py)_4Cl_2$.

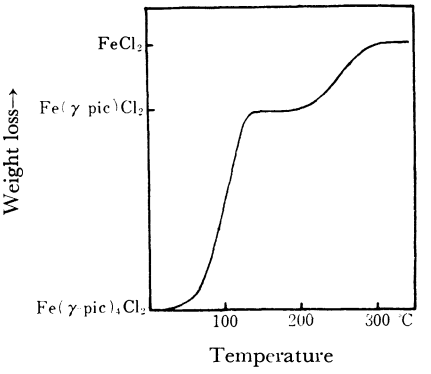

Fig. 2. Thermal decomposition of $Fe(\gamma\text{-pic})_4Cl_2$.

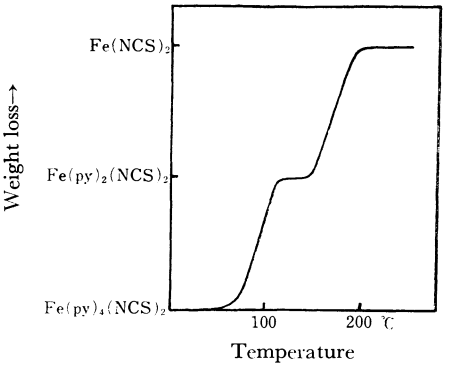

Fig. 3. Thermal decomposition of $Fe(py)_4(NCS)_2$.

6) Gmelins Handbuch der Anorganischen Chemie, Eisen, System-Nummer 59, Teil B.

*1 For purposes of comparison, the thermal decompositions of $Fe(py)_4Cl_2$ were also conducted in air.

*2 For the lower temperature measurements, samples were cooled by conduction through a thick copper plate dipping into liquid nitrogen in a styrofoam-insulated dewar.

7) L. R. Ocone, J. R. Soulen and B. P. Block, *J. Inorg. Nucl. Chem.*, **15**, 76 (1960).

8) D. H. Brown, R. H. Nuttall and D. W. A. Sharp, *ibid.*, **25**, 1067 (1963).

9) J. R. Allan, D. H. Brown, R. H. Nuttall and D. W. A. Sharp, *ibid.*, **26**, 1895 (1964); *ibid.*, **27**, 1529, 1865 (1965).

10) I. G. Murgulescu, E. Segal and D. Fatu, *ibid.*, **27**, 2677 (1965).

11) W. W. Wendlandt and S. I. Ali, *Z. Anorg. Allg. Chem.*, **337**, 6 (1965).

~0.5 mm/sec). Accordingly, all the thermal decompositions of the iron(II) complexes were carried out in a nitrogen atmosphere.

Figures 1 to 3 show the weight-loss curves of $Fe(py)_4Cl_2$, $Fe(\gamma\text{-pic})_4Cl_2$, and $Fe(py)_4(NCS)_2$, respectively. Four distinct phases can be observed during the thermal decomposition of $Fe(py)_4Cl_2$ in a nitrogen atmosphere (Fig. 1). These four phases correspond to the products which can be obtained by the successive loss of two, one, one-third and two-thirds molecules of pyridine from the starting material, $Fe(py)_4Cl_2$. The results of analyses for the iron and chlorine contents were in good agreement with the values calculated for the assumed products. The X-ray powder patterns and Mössbauer spectra confirmed that all of these phases are separate and distinct entities. Therefore, it may be concluded that the thermal decomposition of $Fe(py)_4Cl_2$ proceeds in a nitrogen atmosphere as follows:

$$Fe(py)_4Cl_2 \rightarrow Fe(py)_2Cl_2 \rightarrow Fe(py)Cl_2 \rightarrow Fe(py)_{2/3}Cl_2 \rightarrow FeCl_2.$$

Similarly, the thermal decompositions of $Fe(\gamma\text{-pic})_4Cl_2$ and $Fe(py)_4(NCS)_2$ were found to proceed according to the sequences:

$$Fe(\gamma\text{-pic})_4Cl_2 \rightarrow Fe(\gamma\text{-pic})Cl_2 \rightarrow FeCl_2,$$

and

$$Fe(py)_4(NCS)_2 \rightarrow Fe(py)_2(NCS)_2 \rightarrow Fe(NCS)_2.$$

In addition, it may be worthwhile mentioning that, according to our preliminary work,[12] $Fe(py)_4Br_2$ and $Fe(\gamma\text{-pic})_4Br_2$ decompose through the following steps:

$$Fe(py)_4Br \rightarrow Fe(py)Br_2 \rightarrow FeBr_2,$$

and

$$Fe(\gamma\text{-pic})_4Br_2 \rightarrow Fe(\gamma\text{-pic})Br_2 \rightarrow FeBr_2.$$

Structures of the Decomposition Products. No X-ray study of the structure of $Fe(py)_4Cl_2$ has been reported to date. However, the electronic spectra[13] suggest that $Fe(py)_4Cl_2$ has a trans-octahedral configuration about the iron atoms. We confirmed this conclusion, since the powder X-ray patterns of $Fe(py)_4Cl_2$ are quite similar to those of $Co(py)_4Cl_2$ and $Ni(py)_4Cl_2$, whose structures are known.[14,15] The X-ray powder photography[16] indicated that $Fe(py)_2Cl_2$ has a structure analogous to that of $\alpha\text{-}Co(py)_2Cl_2$, an octahedral polymer with bridging chloride ions.[17] This conclusion was also confirmed by our powder X-ray data. The electronic spectra[13] suggest that $Fe(py)Cl_2$ also has an octahedral polymeric structure. Our powder X-ray data indicate that $Fe(py)_{2/3}Cl_2$ is isomorphous with $Co(py)_{2/3}Cl_2$, which may, according to the electronic spectra,[18] be supposed to have an octahedral polymer structure. Therefore, the thermal decomposition of $Fe(py)_4Cl_2$ proceeds with the formation of the polymer structure: the successive removal of pyridine molecules from the complex gives single, double, and triplechain polymers, and finally the chains are converted to the infinite plane structure of $FeCl_2$.[19] The structural changes which might take place during the thermal decomposition of $Fe(py)_4Cl_2$ are shown in Fig. 4. The structure of

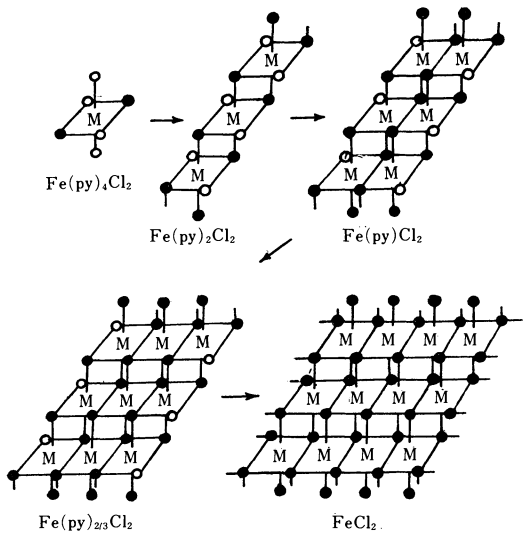

Fig. 4. Structures of $Fe(py)_xCl_2$.
M: Fe; O: py; ●: Cl.

$Fe(py)_4(NCS)_2$ was determined by the X-ray investigation.[20] It has a trans-octahedral arrangement about the iron atoms (nitrogen atoms are bonded to iron). Since the powder X-ray patterns of $Fe(py)_2(NCS)_2$ were found to be quite similar to those of $Co(py)_2(NCS)_2$, whose structure is known,[21] we assume that $Fe(py)_2(NCS)_2$ has an octahedral polymeric structure with bridging NCS ions (sulfur atoms occupy trans positions to iron). The comparison of the IR spectra of $Fe(py)_4(NCS)_2$ and

12) N. Saito, T. Tominaga, T. Morimoto and M. Takeda, Proc. 10th Intern. Conf. Coordination Chem. Nikko, Japan, p. 174 (1967).
13) D. M. L. Goodgame, M. Goodgame, M. A. Hitchman and M. J. Weeks, *Inorg. Chem.*, **5**, 635 (1966).
14) M. A. Porai-Koshits and A. S. Antsishkina, *Dokl. Akad. Nauk SSSR*, 333 (1953).
15) M. A. Porai-Koshits, L. M. Dickareva and E. K. Jukhnov, *Acta Crystallogr.*, **10**, 784 (1958).
16) N. S. Gill, R. S. Nyholm, G. A. Barclay, J. C. Christie and P. J. Pauling, *J. Inorg. Nucl. Chem.*, **18**, 88 (1961).
17) J. D. Dunitz, *Acta Crystallogr.*, **10**, 307 (1958).
18) J. R. Allan, D. H. Brown, R. H. Nuttall and D. W. A. Sharp, *J. Inorg. Nucl. Chem.*, **26**, 1895 (1964).
19) W. G. Wyckoff, "Crystal Structures," Vol. 1, John Wiley & Sons, Inc. New York (1963), p. 272.
20) I. Sϕtofte and S. E. Rasmussen, *Acta Chem. Scand.*, **21**, 2028 (1967).
21) M.A. Porai-Koshits, *Kristallografiya*, **4**, 239 (1959).

$Fe(py)_2(NCS)_2$ also suggests the presence of bridging thiocyanate groups.

The Mössbauer Spectra of the Decomposition Products. The Mössbauer spectra (room temperature) of $Fe(py)_4Cl_2$, $Fe(\gamma\text{-pic})_4Cl_2$, $Fe(py)_4(NCS)_2$ and their decomposition products are represented in Figs. 5 to 7. All the Mössbauer spectra are composed of two absorption peaks. The isomer shifts and quadrupole splittings of these compounds obtained at various temperatures are summarized in Table I.

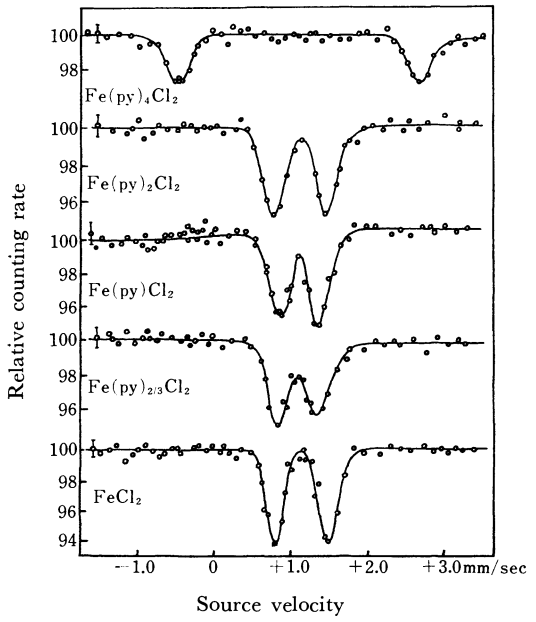

Fig. 5. Mössbauer spectra of $Fe(py)_xCl_2$.

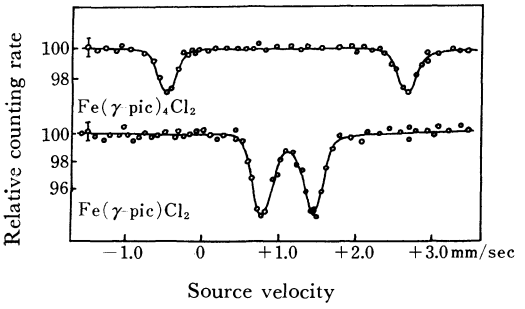

Fig. 6. Mössbauer spectra of $Fe(\gamma\text{-pic})_xCl_2$.

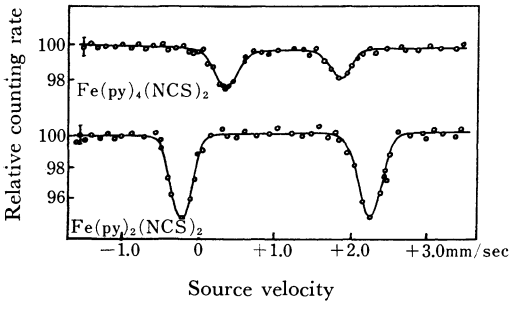

Fig. 7. Mössbauer spectra of $Fe(py)_x(NCS)_2$.

Table I. Mössbauer spectra of iron(II) pyridine and γ-picoline complexes and their decomposition products

Compound	Isomer shift* δ(mm/sec)		Quadrupole splitting ΔE_Q(mm/sec)	
	290°K	163°K	290°K	163°K
	(±0.03)		(±0.04)	
$Fe(py)_4Cl_2$	1.10	1.18**	2.94	3.44**
$Fe(py)_2Cl_2$	1.13	1.26**	0.56	1.26**
$Fe(py)Cl_2$	1.15	1.24	0.38	0.69
$Fe(py)_{2/3}Cl_2$	1.15	1.27	0.51	0.84
$FeCl_2$	1.16	1.29	0.75	0.88
$Fe(\gamma\text{-pic})_4Cl_2$	1.12	1.21**	2.94	3.43**
$Fe(\gamma\text{-pic})Cl_2$	1.14	1.18	0.64	0.90
$Fe(py)_4(NCS)_2$	1.11	1.24**	1.53	1.99**
$Fe(py)_2(NCS)_2$	1.07	1.20**	2.54	3.00**

* Vs. stainless steel (310SS) ** Obtained at 100°K

From the Mössbauer data on $Fe(py)_4Cl_2$ and its thermal decomposition products, we may draw the following conclusions:

(1) The isomer shifts (δ) of the different phases show only small variations during the thermal decomposition process in a nitrogen atmosphere. All the δ values fall within the range of δ values for a typical high-spin Fe(II) state. Thus, it is obvious that the oxidation state of iron in the starting material, $Fe(py)_4Cl_2$, remains unchanged throughout the decomposition process.

(2) The quadrupole splitting (ΔE_Q) is appreciably changed as the thermal decomposition proceeds; at room temperature, the quadrupole splitting of $Fe(py)_4Cl_2$ is 2.94 mm/sec, whereas the quadrupole splittings of the decomposition products are significantly decreased and fall within a range between 0.38 and 0.75 mm/sec. The changes in the quadrupole splitting may reflect the structural changes about the iron atoms.*3

(3) The intensities of absorption peaks are generally larger for the polymeric compounds than for the monomer, $Fe(py)_4Cl_2$. This may be due to the "polymer effect" suggested for organotin

*3 Since the quadrupole splitting of these high spin iron(II) compounds is closely related to the ligand-field splitting of d_ε orbitals, the temperature dependence of the quadrupole splittings of various iron pyridine complexes is now being studied in our laboratory. The results will be published elsewhere.

compounds[22-25] and α-$Co(py)_2Cl_2$[26]; the polymer structures may restrict the motion of the iron atoms and give higher recoilless fractions.

(4) In order to examine the mechanism of the primary step of decomposition, *i. e.*, $Fe(py)_4Cl_2 \rightarrow Fe(py)_2Cl_2$, the Mössbauer spectra were taken of the products obtained at intermediate stages before the $Fe(py)_2Cl_2$ phase was completely attained (Fig. 8). As may be seen in Fig. 8, only the absorption peaks of $Fe(py)_4Cl_2$ and $Fe(py)_2Cl_2$ are observed in the intermediate stages. The intensities of the $Fe(py)_4Cl_2$ peaks are decreased, whereas the intensities of the $Fe(py)_2Cl_2$ peaks are increased, as the decomposition proceeds. Therefore, it seems unlikely that any stable entity such as $Fe(py)_3Cl_2$ could exist as an intermediate phase for the $Fe(py)_4Cl_2 \rightarrow Fe(py)_2Cl_2$ transition. This suggests the possibility of the application of the Mössbauer spectroscopy to the study of the kinetics and the mechanism of solid-phase reactions.

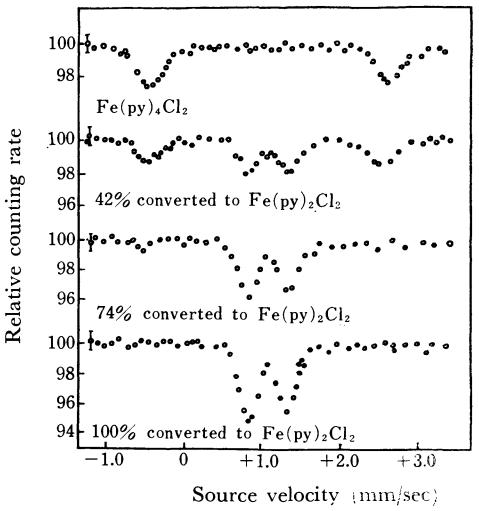

Fig. 8. Mössbauer spectra of the $Fe(py)_4Cl_2 \rightarrow Fe(py)_2Cl_2$ transition.

22) H. A. Stöckler and H. Sano, *Phys. Lett.*, **25A**, 550 (1967).

23) H. A. Stöckler, H. Sano and R. H. Herber, *J. Chem. Phys.*, **47**, 1567 (1967).

24) H. A. Stöckler and H. Sano, *Phys. Rev.*, **165**, 406 (1968).

25) H. A. Stöckler and H. Sano, Proc. 2nd Materials Research Symposium on Molecular Dynamics and Structure of Solids (National Bureau of Standards, U. S. Department of Commerce, Washington, D. C., 1967).

26) H. Sano, M. Aratani and H. A. Stöckler, *Phys. Lett.*, **26A**, 559 (1968).

BULLETIN OF THE CHEMICAL SOCIETY OF JAPAN VOL. 43 1097—1100 (1970)

The Hydrolysis of the Uranyl Ion in Heavy Water*1

Masunobu MAEDA and Hidetaka KAKIHANA

Research Laboratory of Nuclear Reactor, Tokyo Institute of Technology, Ookayama, Meguro-ku, Tokyo

(Received October, 24, 1969)

The hydrolysis equilibria of the UO_2^{2+} ion in heavy water containing 3M $NaClO_4$ as an ionic medium were studied at 25°C by potentiometric titrations, employing a technique of constant-current coulometry. The deuterium-ion concentration was measured by means of a glass electrode. The most probable hydrolysis scheme chosen in the range of the total uranyl concentration from 1 to 10 mM was: $(UO_2)_2(OD)_2^{2+}-(UO_2)_3(OD)_4^{2+}-(UO_2)_3(OD)_5^{+}$; the respective stability constants were $-\log \beta_{2,2}=6.80\pm0.02$, $-\log \beta_{4,3}=14.00\pm0.07$, and $-\log \beta_{5,3}=18.63\pm0.02$. The above results reveal that the composition of the hydrolysis species in heavy water are generally the same as those in light water, while the values of the stability constants are smaller in heavy water than in light water.

In a previous paper[1] we described the hydrolytic reaction of the beryllium ion in heavy water and concluded that the compositions of the hydrolysis species are the same in heavy water as in light water and that the values for the stability constants in heavy water are smaller than those in light water.

In this work, the hydrolytic reaction of the uranyl ion was studied, and the results obtained were compared with those in light water.

*1 Ionic Equilibria in Heavy Water, Part IV.

1) H. Kakihana and M. Maeda, This Bulletin, **43**, 109 (1970).

Symbols

The symbols used are the same as those described in Part II of this series.[1]

Expermental

Reagents and Apparatus. *The reagents used* were, unless otherwise stated, prepared and analyzed as has been described in Refs. 1 and 2.

Uranyl perchlorate in heavy water was prepared by the repeated evaporation of uranyl perchlorate in light water (which had been prepared and analyzed as has been described in Ref. 3), under an infrared lamp, while adding heavy water.

NaOD solution was prepared by the electrolysis of sodium perchlorate in heavy water, using a procedure similar to that described in Ref. 4.

All the apparatuses employed were the same as those used in Refs. 1 and 2.

Experimental Procedures. The hydrolysis of the UO_2^{2+} ion was investigated by measuring the deuterium-ion concentration using a glass electrode. $NaClO_4$ was added to all the test solutions so that they contained 3M ClO_4^-; the total UO_2(II) concentration was maintained within the 1—10 mM range.

The deuterium-ion concentration and the generation of the deuterium ions in a test solution were measured by the use of the same cell assembly as that employed in Part II[1] of this series.

The emf of the cell at 25°C can be denoted by Eq. (1),[5] since the concentration of the deuterium ions was maintained at less than 0.01M in the present work:

$$E = E_0 + 59.15 \log d \qquad (1)$$

The potentiometric titrations were carried out as follows. First, a partially-hydrolyzed solution of the uranyl ion was made by adding the solutions T_1 and T_2 to a test solution, S. The compositions of the solutions T_1, T_2, and S were as follows;

$$T_1 = A\text{M NaOD} + 3\text{M NaClO}_4$$

$$T_2 = 2B\text{M UO}_2(\text{ClO}_4)_2 + X\text{M DClO}_4 + (3-4B-X)\text{M NaClO}_4$$

$$S = B\text{M UO}_2(\text{ClO}_4)_2 + D\text{M DClO}_4 + (3-2B-D)\text{M NaClO}_4.$$

The partially-hydrolyzed solution made thereby was kept standing overnight, while nitrogen gas was passed through the solution; the next morning no precipitate was detected in the test solution.

The partially-hydrolyzed solution was gradually acidified by generating the deuterium ions coulometrically.

During the measurements, the test solution was stirred by a stream of nitrogen gas which had been purified by leading it through heavy water and 3M $NaClO_4$ in heavy water.

All the measurements were carried out in a paraffin-oil thermostat kept at 25.00±0.01°C in a room kept by a thermostat at 25±1°C.

Results and Discussion

The values of Z and $\log d$ in each series of B, which were calculated from the potentiometric measurements by the use of Eq. (1), are represented graphically in Fig. 1.

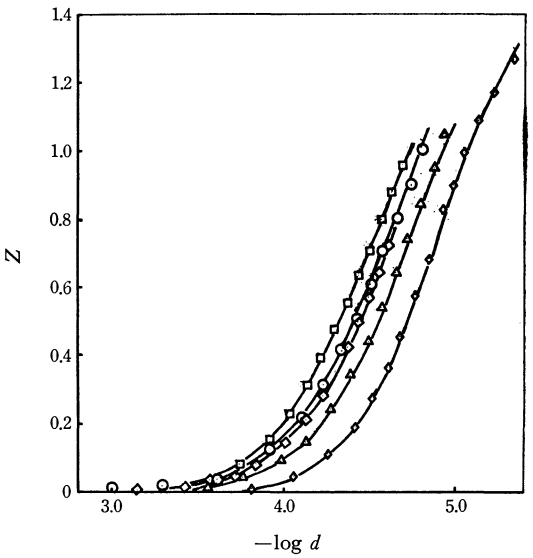

Fig. 1. Average number, Z, of OD bound per UO_2, as a function of $\log d$. Drawn curves were calculated with the stability constants given in Table 2.

B			
□	9.0506 mM	◇	5.231
○	6.177	△	2.971
		◆	1.227

The experimental data were analyzed by a graphical method and by computer calculations.

First, the hydrolysis data were submitted to graphical analysis in order to obtain some preliminary information on the composition of the hydrolysis species formed; then, on the basis of the information thus obtained, computer analysis was made in order to evaluate the most probable hydrolysis scheme and the stability constants of the species formed.

1) The Evaluation of the Composition of the Hydrolysis Products by Graphical Analysis. In order to ascertain the mean composition of the polynuclear species formed, *i. e.*, $\bar{p}$ and $\bar{q}$, the general integration method presented by Sillén[6] was employed. The results of the calculations are

2) H. Kakihana and M. Maeda, This Bulletin, **42**, 1458 (1969).

3) S. Hietanen, B. R. L. Row and L. G. Sillén, *Acta Chem. Scand.*, **17**, 2735 (1963).

4) H. Ohtaki, *Inorg. Chem.*, **6**, 808 (1967).

5) H. Kakihana, M. Maeda and T. Amaya, This Bulletin, **43**, No. 5 (1970), in press.

6) L. G. Sillén, *Acta Chem. Scand.*, **15**, 1981 (1961).

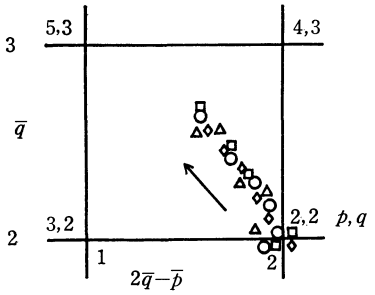

Fig. 2. Average composition of the hydrolysis species in the form of $\bar{q}$ *vs.* $(2\bar{q}-\bar{p})$.
Direction of an arrow corresponds to the increase in Z. Symbols are the same as those in Fig. 1.

shown in Fig. 2 as $\bar{q}$ *vs.* $(2\bar{q}-\bar{p})$.[7] From this figure, it may be seen that the (2,2) species exists at low Z values, while the (5,3) species may be present at high Z values, judging from the directions of the plots.

2) The Evaluation of the Composition and the Stability Constants of the Hydrolysis Products by Computer Analysis. The generalized, least-squares method was, with the help of an electronic computer (HITAC 5020), used to determine the most probable hydrolysis scheme containing the lowest number of species which would suffice to account for the experimental data and for the stability constants of the species formed. The least-squares calculations on the electronic computer were carried out using same procedure as that described in Ref. 1.

Several combinations of the hydrolysis species were attempted by starting with the species which had been suggested by the graphical analysis of the present work and by the investigations previously made by several researchers[8] in light water with the ClO_4^- anion. The results of the computations for several combinations of these species are shown in Table 1.

Table 1. The error square sums and the values of the stability constants for the schemes chosen

$\beta_{1,1}$ $\times 10^7$	$\beta_{2,2}$ $\times 10^7$	$\beta_{4,3}$ $\times 10^{14}$	$\beta_{5,3}$ $\times 10^{19}$	$\beta_{6,4}$ $\times 10^{22}$	U $\times 10^2$
—	1.89	—	3.14	—	1.72
17.8	1.71	—	3.16	—	1.70
—	1.58	1.02	2.32	—	1.27
8.26	1.33	1.56	1.95	—	1.73
—	1.58	0.969	2.29	1.46	1.30

7) H. S. Dunsmore, S. Hietanen and L. G. Sillén, *ibid.*, **17**, 2644 (1963).
8) "Stability Constants," ed. by L. G. Sillén and A. E. Martell, The Chemical Society, London (1964).

The (2,2) - (4,3) - (5,3) species scheme had the least error-square sum and the least systematic errors of the schemes chosen; also, it showed a satisfactory agreement with the experimental data. It is shown in Fig. 1 as solid lines superimposed on the experimental data. The (2,2) - (4,3) - (5,3) - (6,4) species scheme, which had the second least error-square sum, gave rise to slight larger systematic errors than the (2,2) - (4,3) - (5,3) species scheme at higher Z values.

In the present work, no further attempt was made to search for new species other than those listed in Table 1.

From the results described above, it was concluded that the present experimental data in heavy water could be explained by assuming the (2,2) - (4,3) - (5,3) species scheme within the limits of experimental error.

The final values for the stability constants for the system of heavy water are listed in Table 2, together with those for the system of light water described by Dunsmore, Hietanen, and Sillén.[7]

3) Distribution of the Species. The distribution of the hydrolysis species in heavy water and in light water, calculated at the total uranyl concentration of 10 mM, and assuming the values of the stability constants in Table 2, is represented

Table 2. The values for the stability constants of the hydrolysis species of the beryllium ion in heavy water and in light water containing 3M $NaClO_4$ as an ionic medium

	Present work* (in heavy water)	Ref. 7** (in light water)
$-\log \beta_{2,2}$	6.80±0.02	6.04±0.02
$-\log \beta_{4,3}$	14.00±0.07	13.21(>12.97)
$-\log \beta_{5,3}$	18.63±0.02	16.53±0.03
$-\log \beta_{1,1}$	—	6.10(>5.86)

* The uncertainties of the constants were estimated by multiplying by three the standard deviations.
** Range with up to 0.1M UO_2^{2+}

graphically in Fig. 3. There is a general shift toward less hydrolysis in heavy water at a given pH. The dominance of the (2,2) and (5,3) species in the accessible pH region is apparent in both heavy water and light water.

In the present work, it has been found that the compositions of the species formed in heavy water, *i.e.*, $(UO_2)_2(OD)_2^{2+}$, $(UO_2)_3(OD)_4^{2+}$, and $(UO_2)_3(OD)_5^+$, are generally the same as those in light water, although the (1,1) species or of the (6,4) species, which had previously been found, was not found in the present heavy water - system. It has also been found that the values of the stability

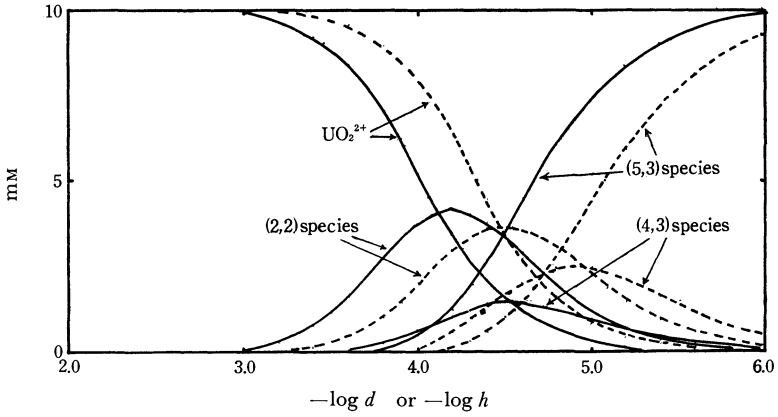

Fig. 3. The calculated distribution of the hydrolysis species in heavy water and in light water at the total uranyl concentration of 10 mM.
Dashed curves denote the distribution of the species in heavy water and full curves the distribution in light water.

constants of the hydrolysis products in heavy water are smaller than those in light water; this tendency is in agreement with that of the beryllium ion.[1)]

The authors wish to express their gratitude to Dr. Hitoshi Ohtaki, Nagoya University, for his valuable advice and discussions.

BULLETIN OF THE CHEMICAL SOCIETY OF JAPAN VOL. 43 1100—1109 (1970)

Circular Dichroism of Chromium(III) Complexes. II.[1] Correlation between Behavior in the Spin-forbidden Absorption Band Region and Absolute Configurations

Sumio KAIZAKI, Jinsai HIDAKA and Yoichi SHIMURA

Department of Chemistry, Faculty of Science, Osaka University, Toyonaka, Osaka

(Received October 31, 1969)

The absorption and circular dichroism (CD) spectra of twelve optically active chromium(III) complexes containing three bidentate ligands have been measured in the near-infrared to ultraviolet region. CD spectra in the spin-forbidden *d–d* absorption band region have been considered mainly in relation to the CD bands in the first spin-allowed *d–d* absorption band region. It has been concluded that the absolute configurations of chromium(III) complexes can be determined on the basis of the signs of the CD bands in the spin-forbidden band region. The splitting components of the CD bands in the spin-forbidden band region have been discussed considering the crystal field treatment by Macfarlane.

There have been a number of studies concerning the relationship between the absolute configurations of dissymmetric d^3 and d^6 metal complexes and their CD spectra in the region of *d–d* absorption bands.[2-5] In these cases, the absolute configurations have been assigned from a comparison of the signs of the CD bands in the spin-allowed *d–d* absorption band region with those of the electronically corresponding CD bands of a reference complex, *e. g.* $(+)_{546}$-$[Co(en)_3]^{3+}$, whose absolute configuration had been conclusively determined by an

1) Part I of this series: S. Kaizaki, J. Hidaka and Y. Shimura, This Bulletin, **42**, 988 (1969).

2) A. J. McCaffery and S. F. Mason, *Trans. Faraday Soc.*, **59**, 1 (1963).

3) A. J. McCaffery, S. F. Mason and R. E. Ballard, *J. Chem. Soc.*, **1965**, 2883.

4) A. J. McCaffery and S. F. Mason, *Mol. Phys.*, **6**, 359 (1963).

5) S. F. Mason, Plenary Lecture presented at XII ICCC, Sydney (1969).

X-ray method.[6] However, it was difficult to decide which band corresponded electronically to the key band of the reference complex. As a means to solve the problem the ion-pairing effect on the CD bands by selenite or phosphate ion in solutions has been proposed by Mason *et al.*

Kling and Woldbye[7] obtained the rotatory dispersion of $(+)_{546}$-$[Cr(en)_3](ClO_4)_3$ and $(+)_{546}$-$[Cr(tn)_3]Cl_3$ in their spin-forbidden band region and found many inversive dispersions superimposed with each other. McCaffery and Mason[2] reported the CD spectra of tris(L-tartrato)chromium(III) ion in the spin-forbidden band region. In the corresponding region, Mason[8] found the splitting of the CD bands due to the ^2E_g transition of $(-)_{546}$-$[Cr_2(OH)_2(dip)_4]^{4+}$ and $(-)_{546}$-$[Cr_2(OH)_2(phen)_4]^{4+}$, and suggested the spin-spin coupling in these binuclear complexes. In a previous paper,[1] we reported the CD spectra of three oxalato- and two L-tartratochromium(III) complexes in the spin-forbidden band region and proposed a tentative assignment of the sharp but weak CD bands observed.

In this paper, the CD and electronic absorption spectra of twelve optically active tris-chelate chromium(III) complexes, which belong to the types, $[Cr(N)_6]$, *cis*-$[Cr(O)_2(N)_4]$ and *cis*-$[Cr(O)_4(N)_2]$, will be reported and the assignment of the CD bands in the spin-forbidden band region will be confirmed on the basis of the ion-pairing effect on the CD bands of the tris-diamine chromium(III) complex ions. The correlation of the CD bands in the spin-forbidden band region with those in the spin-allowed absorption band region as well as with the exciton CD bands of tris- or bis-α-diimine metal complexes will be discussed in connection with the absolute configurations. Macfarlane's analysis[9] using the crystal field model will be applied to the splitting components of the CD spectra in the spin-forbidden band region. The values for the electron repulsion parameter B and the trigonal parameter v and v' will be estimated and considered.

Experimental

Preparation and Optical Resolution. 1) $(+)_{546}$-$[Cr(ox)(en)_2]Cl$. This complex was prepared by Werner's method[10] and resolved by the method of Vaughn and Walkwitz.[11]

2) $(+)_{546}$-$[Cr(ox)(dip)_2]Cl$ and $(+)_{546}$-$[Cr(ox)(phen)_2]ClO_4 \cdot 2.5H_2O$. These 2,2′-dipyridyl(=dip) and 1,10-phenanthroline(=phen) complexes were prepared and resolved by the method of Broomhead *et al.*[12] The CD spectra of $(+)_{546}$-oxalatobis(dip)chromium(III) complex were measured after converting the diastereomer, $(+)_{546}$-$[Cr(ox)(dip)_2] \cdot (+)_{546}$-$[Cr(ox)_2(phen)]$, into the chloride with anion exchange resin of chloride type.

3) $(+)_{546}$-$[Cr(en)_3](ClO_4)_3$. Trisethylenediaminechromium(III) perchlorate was prepared by the method of Linhard and Weigel[13] and resolved by the method of Werner.[14]

4) $(+)_{546}$-$[Cr(tn)_3](ClO_4)_3$. The preparation and optical resolution of this complex was performed by the method of Schläfer and Kling.[15]

5) $(-)_{546}$-$[Cr(BH)_3]Cl_3$.*1 The trisbiguanide complex was obtained by the reaction with potassium chromium(III) alum and biguanide sulfate in an alkaline solution.[16] The optical resolution of this complex was carried out by Michelsen's method.[17]

6) $(+)_{546}$-$[Cr(phen)_3](ClO_4)_3$. The synthesis of optically active tris(1,10-phenanthroline)chromium(III) complex was performed by the second order asymmetric process of Lee *et al.*[18]

7) $(+)_{546}$-$K[Cr(ox)_2(dip)] \cdot 3H_2O$, $(+)_{546}$-$K[Cr(ox)_2(phen)] \cdot 4H_2O$, $(+)_{546}$-$K[Cr(ox)_2(en)] \cdot 2H_2O$, $Ba[Cr_2(L\text{-}tart_2H)(dip)_2]_2 \cdot 9H_2O$ and $NH_4[Cr_2(L\text{-}tart_2H)(phen)_2] \cdot 6.5H_2O$. The preparation and optical resolution of these bisoxalato complexes and the syntheses of the L-tartrato complexes have been described in Part I of this series.[1]

8) Sodium $(+)_{589}$-Nitrocamphoronate. The resolving agent with which $[Cr(en)_3]^{3+}$ and $[Cr(tn)_3]^{3+}$ were resolved was prepared from $(+)_{589}$-camphor.[19] Preparation of $(+)_{589}$-bromocamphor as a starting material was carried out by treating $(+)_{589}$-camphor with bromine. The $(+)_{589}$-bromonitrocamphor was obtained by refluxing with nitric acid for about 50 hr. The resulting $(+)_{589}$-bromonitrocamphor was treated with sodium alcoholate and the crude product obtained was recrystallized from alcohol. The pure sodium $(+)_{589}$-nitrocamphoronate was obtained as pale yellow crystals.

Measurements. Absorption spectra were measured by a Beckman DU spectrophotometer. CD spectra were recorded with a Roussel-Jouan dichrograph. The CD spectra of $(+)_{546}$-$[Cr(en)_3](ClO_4)_3$ in the second spin-allowed *d–d* absorption band region were recorded with a Jasco Model ORD/UV-5 spectrophotometer. The concentrations of complexes for the CD measurements in the spin-forbidden absorption band region were 10^{-1}—10^{-2} F, and the cell lengths employed were 5 and 7 cm.

---

*1 The abbreviation, BH, represents a biguanide.

6) Y. Saito, K. Nakatsu, M. Shiro and H. Kuroya, This Bulletin, **30**, 158 (1957).

7) O. Kling and F. Woldbye, *Acta Chem. Scand.*, **15**, 704 (1961).

8) S.F. Mason and J.W. Wood, *Chem. Commun.*, **1968**, 1512; S. F. Mason, *Inorg. Chim. Acta, Rev.*, **2**, 89 (1968).

9) R. M. Macfarlane, *J. Chem. Phys.*, **39**, 3118 (1963).

10) A. Werner, *Ann.*, **406**, 286 (1914).

11) J. W. Vaughn and D. J. Walkwitz, *Inorg. Chem.*, **5**, 1082 (1966).

12) J. A. Broomhead, M. Dwyer and N. A. P. Kane-Maguire, *Inorg. Chem.*, **7**, 1388 (1968).

13) M. Linhard and M. Weigel, *Z. Anorg. Allg. Chem.*, **271**, 115 (1952).

14) A. Werner, *Ber.*, **45**, 865 (1912).

15) H. L. Schläfer and O. Kling, *Z. Anorg. Allg. Chem.*, **302**, 1 (1959).

16) R. G. Rochow, *Inorg. Synth.*, **6**, 68 (1960).

17) K. Michelsen, *Acta Chem. Scand.*, **19**, 1175 (1965).

18) Ching S. Lee, E. M. Gorton, H. M. Neuman and H. R. Hunt, Jr., *Inorg. Chem.*, **5**, 1397 (1966).

19) V. Steele and T. M. Lowry, *J. Chem. Soc.*, **107**, 1038 (1915).

The CD measurements for the ion-pairing effect were made throughout the spin-forbidden and first spin-allowed absorption band region in solutions with the constant molar concentrations of both the complex perchlorates and sodium selenite, using cells with 7, 5, 2 and 1 cm path-length. The solvent employed was water for the complexes except $(+)_{546}$-$[Cr(ox)(phen)_2]$-ClO_4. The absorption and CD spectra of this 1,10-phenanthroline complex were measured in 70% $HClO_4$, because of very small solubility in water to measure the CD spectrum in the spin-forbidden band region. In the first spin-allowed *d–d* absorption band region, the CD spectra in water show only one positive CD band, whereas the CD spectra in 70% $HClO_4$ show two CD bands, (−) and (+), listing from the longer wavelength side. In 70% $HClO_4$, however, the absorption spectra and the exciton CD bands in the ultraviolet region corresponding to the ligand transition (300—250 mμ) are similar to those in water. This fact indicates that the geometrical sturcture and absolute configuration are retained in 70% $HClO_4$ as they were in water.

Results and Discussion

General Features of the Spin-forbidden Bands. The absorption and CD spectra of the present complexes are shown in Figs. 1—8. Their characteristics are summarized in Table 1. In the spin-forbidden *d–d* absorption band region, the CD spectra of the complexes show a group of sharp and narrow peaks with weak intensity as may be seen in Figs. 1, 2 and 5—8. The intensities of the CD bands in this region are found to be one fraction of a few hundred times as weak as those in the first spin-allowed *d–d* absorption band region as shown in Table 1. The half-widths of these CD bands are found to be about 200 to 400 cm^{-1} with the exception of the case of $(-)_{546}$-$[Cr(BH)_3]Cl_3$, whose half-width is about 800 cm^{-1}. The experimental

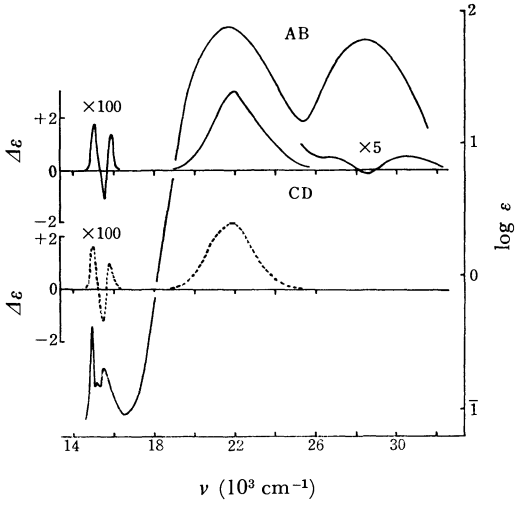

Fig. 1. Absorption (AB) and CD curves of $(+)_{546}$-$[Cr(en)_3](ClO_4)_3$ (———) in water and (·····) in 0.4F Na_2SeO_3 aqueous solution.

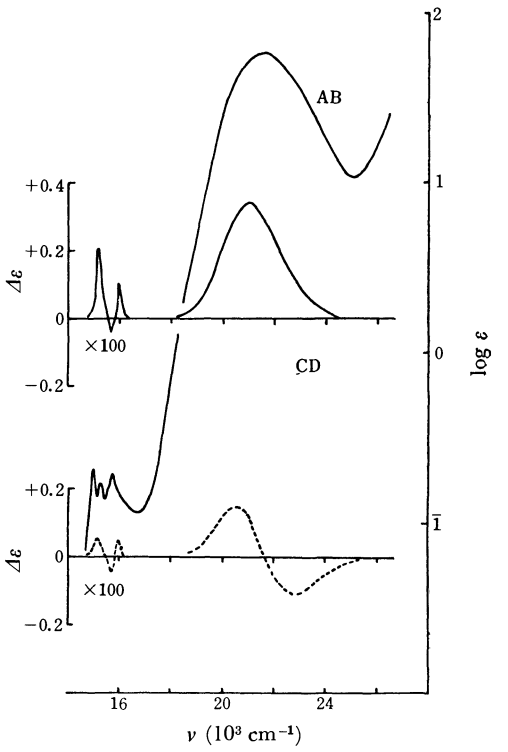

Fig. 2. Absorption (AB) and CD curves of $(+)_{546}$-$[Cr(tn)_3](ClO_4)_3$ (———) in water and (--------) in 0.6F Na_2SeO_3 aqueous solution.

rotational strengths of the spin-forbidden transitions are found to be about 0.1% of that of the first spin-allowed transitions. This value is about one tenth of the value estimated for cobalt(III) complexes by Ballhausen.[20] The anisotropy factor, *g*, for the CD bands in the spin-forbidden band region is nearly equal to that of the CD bands in the first spin-allowed *d–d* absorption band region. This fact suggests that the rotational strength of the spin-forbidden transition originates from that of the first spin-allowed transition which is magnetically dipole allowed in O_h symmetry, rather than from that of the second spin-allowed transition which is magnetically dipole forbidden in O_h symmetry.

The CD bands of trisoxalato- and trismalonato-chromium(III) complexes were also observed in the spin-forbidden band region. However, the CD spectra of both complexes in this region are very complicated, because of the superposition upon the minor but broad CD band related to the longest wavelength component of the first spin-allowed absorption band.

According to the crystal field theory,[21] the

20) C. J. Ballhausen, *Mol. Phys.*, **5**, 461 (1963).

21) Y. Tanabe, *Progr. Theor. Phys. Suppl.*, **14**, 17 (1960); H. Kamimura, S. Sugano and Y. Tanabe, "Ligand Field Theory and Its Applications," Syokabo Book Co., Tokyo (1969).

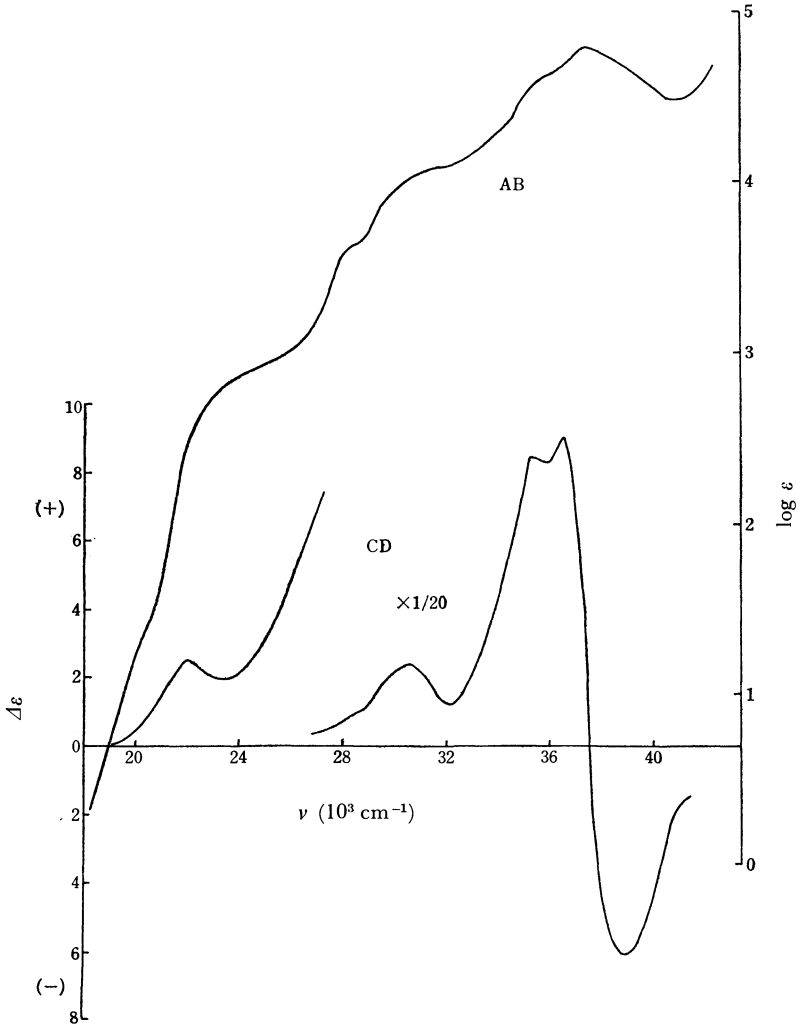

Fig. 3. Absorption (AB) and CD curves of $(+)_{546}$-$[Cr(phen)_3](ClO_4)_3$ in water.

narrow and sharp absorption bands of chromium(III) complexes appearing at 800—600 mμ are considered to be due to the spin-forbidden transitions within the t_{2g} shell and to be assigned to the $^4A_{2g}$–^2E_g and $^4A_{2g}$–$^2T_{1g}$ transitions in O_h symmetry. Furthermore, the ^2E_g state seems to occur at the longer wavelength side and to be of stronger intensity than the $^2T_{1g}$ state.[21] On the other hand, Schläfer *et al.*[22-24] have extensively studied the phosphorescence spectra of a number of chromium(III) complexes. It has been revealed that the relatively intense spin-forbidden absorption band lying at the longest wavelength side are the zero-zero band of the ^2E_g transition and the remaining bands are due to the vibrational transitions associated with the electronic transition to the ^2E_g state rather than the electronic transitions to the $^2T_{1g}$ state. Now, in D_3 symmetry, to which most of the present complexes belong, the T_{1g} state breaks down into the E_b and A_2 states and the E_g state remains as the E_a one. Accordingly, from the fact that most of the complexes studied here exhibit a close correspondence between the positions of the lowest frequency CD band and those of the absorption and phosphorescence bands in the spin-forbidden band region,[22-24] the lowest frequency CD band may be assigned to the ^2E_a transition. Assuming that the remaining CD bands are due to the electronic transitions to the $^2T_{1g}$ state in O_h symmetry, these CD bands may be tentatively assigned to the $^2A_2$ and ^2E_b states in D_3 symmetry.[1] However,

22) G. B. Porter and H. L. Schläfer, *Z. Phys. Chem.*, **38**, 227 (1963); G. B. Porter and H. L. Schläfer, *ibid.*, **40**, 280 (1964).

23) J.L. Laver and P.W. Smith, *Chem. Commun.*, **1968**, 769.

24) K. DeArmond and L. S. Forster, *Spectrochim. Acta*, **19**, 1403 (1963).

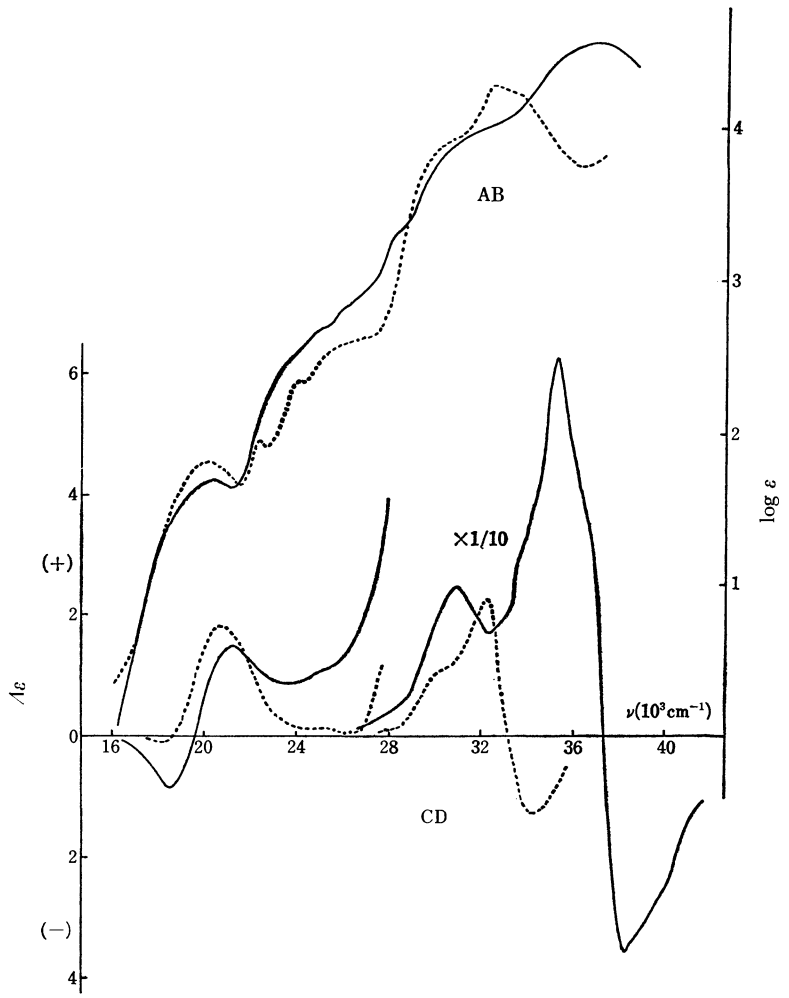

Fig. 4. Absorption (AB) and CD curves of $(+)_{546}$-[Cr(ox)(phen)$_2$]ClO_4 (———) in 70% $HClO_4$ and $(+)_{546}$-[Cr(ox)(dip)$_2$]Cl (·····) in water.

it is difficult to determine whether these CD bands are due to the vibrational transitions associated with the electronic transitions to the $^2E_g(O_h)$ state or to the electronic transitions to the $^2T_{1g}(O_h)$ state from the following reasons. Firstly, the ^2E_g and $^2T_{1g}$ states with $(t_{2g})^3$ configuration are theoretically expected to be split neither to the first order by means of the spin-orbit coupling nor in terms of lowering of symmetry.[21] Secondly, these CD bands in the spin-forbidden band region show rather simpler patterns than the corresponding absorption bands.

$(+)_{546}$-[Cr(en)$_3$]$(ClO_4)_3$ and $(+)_{546}$-[Cr(tn)$_3$]-$(ClO_4)_3$. The absorption spectra of trisethylenediamine- and tristrimethylenediaminechromium-(III) complexes coincide with those reported.[15] The CD spectra of $(+)_{546}$-trisethylenediamine complex in the first spin-allowed *d–d* absorption band region coincide with those reported by Mathieu.[25] In the second spin-allowed *d–d* absorption band region, however, the CD spectra of the complex obtained here are quite different from those reported by Mathieu.[25] According to the present measurement, three weak CD peaks, (+), (−) and (+) listing from the longer wavelength side, are evidently observed in the corresponding region as may be seen in Fig. 1. This result is inconsistent with the theory[26] that the d^3 or d^6 complex with D_3 symmetry should give only one CD component in the second absorption band region.

Mason *et al.*[27-29] have intensively studied the

25) J.-P. Mathieu, *J. Chim. Phys.*, **33**, 78 (1936).
26) W. Moffitt, *J. Chem. Phys.*, **25**, 1189 (1956).
27) S. F. Mason and B. J. Norman, *J. Chem. Soc.*, *A*, **1966**, 307.
28) P. G. Beddoe and S. F. Mason, *Inorg. Nucl. Chem. Lett.*, **4**, 433 (1968).
29) J. R. Gollogly and C. J. Hawkins, *Chem. Commun.*, **1968**, 689.

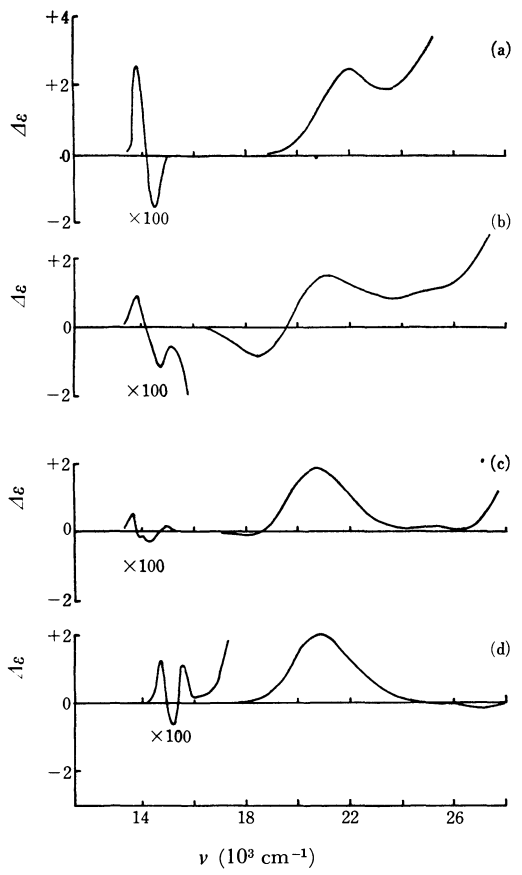

Fig. 5. CD curves of tris(phen) and *cis*-$[Cr(O)_2(N)_4]$ type complexes in the *d–d* absorption band region.
(a) $(+)_{546}$-$[Cr(phen)_3](ClO_4)_3$ in water
(b) $(+)_{546}$-$[Cr(ox)(phen)_2]ClO_4$ in 70% $HClO_4$
(c) $(+)_{546}$-$[Cr(ox)(dip)_2]Cl$ in water
(d) $(+)_{546}$-$[Cr(ox)(en)_2]Cl$ in water

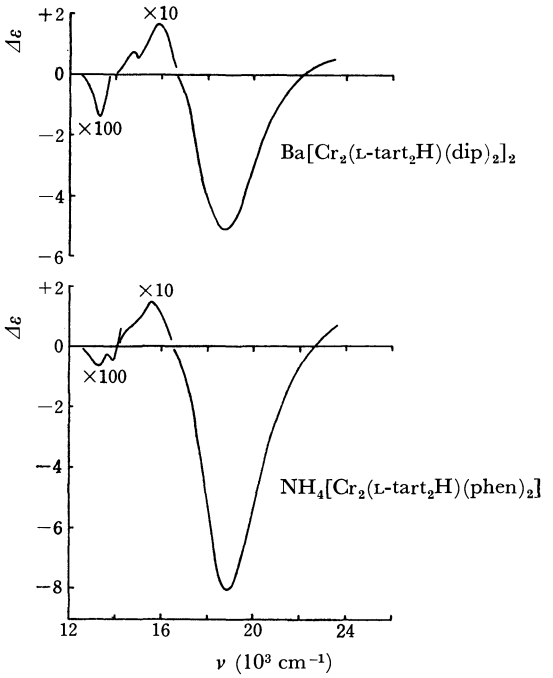

Fig. 6. CD curves of the two L-tartrato complexes in the *d–d* absorption band region. (The intensities are given per one complex, *i.e.*, per two chromium(III) ion.)

ion-pairing effect on the CD spectra of trisdiamine metal complexes. It has been reported that the diminution or increase of the intensity of the CD bands by the ion-pairing effect are observed in the first spin-allowed absorption band region, and it has been proposed that the diminished CD band is assigned in the case of chromium(III) complexes to the ^4E component and the increased CD band to the $^4A_1$ in D_3 symmetry. In the first spin-allowed *d–d* absorption band region, the intensity of the positive CD band of $(+)_{546}$-trisethylenediaminechromium(III) complex is diminished with the addition of sodium selenite to the solution as may be seen in Fig. 1 and Table 1.[27] Since the diminished positive CD band is due to the ^4E component, the $(+)_{546}$-isomer of trisethylenediamine complex seems likely to have a $\Delta(C_2)$ absolute configuration. The same CD behavior due to the ion-pairing effect is also more markedly observed for the $(+)_{546}$-tristrimethylenediamine complex as seen in Fig. 2.

In this complex, the intensity of a positive CD band at 477 mμ is diminished and a new CD band appears at 435 mμ with the addition of sodium selenite to the solution.[28] Thus, the diminished positive band is assigned to the ^4E component and the newly appearing negative band to the $^4A_1$ component.[28] From this fact, the $(+)_{546}$-tristrimethylenediaminechromium(III) complex was determined to have a $\Delta(C_2)$ absolute configuration. The CD spectra in the region corresponding to the spin-forbidden transitions for the $(+)_{546}$-trisethylenediamine- and tristrimethylenediaminechromium(III) complexes with a $\Delta(C_2)$ configuration show three sharp and narrow peaks, (+), (−) and (+). For the $(+)_{546}$-trisethylenediamine complex, the CD intensity of the positive component at the longest wavelength side is diminished by the ion-pairing effect as shown in Table 1. The CD behavior in the corresponding region for the tristrimethylenediamine complex is similar to that for the ethylenediamine complex. That is, the CD intensity of the positive band due to the ^2E_a transition of the trimethylenediamine complex is markedly reduced with the addition of sodium selenite as shown in Fig. 2 and Table 1. From this parallel reduction in the CD intensity by the ion-pairing effect between the ^4E and ^2E_a transitions and from the above-mentioned anisotropy factor, it is suggested that the excited doublet and quartet states with the same orbital symmetry are mixed with

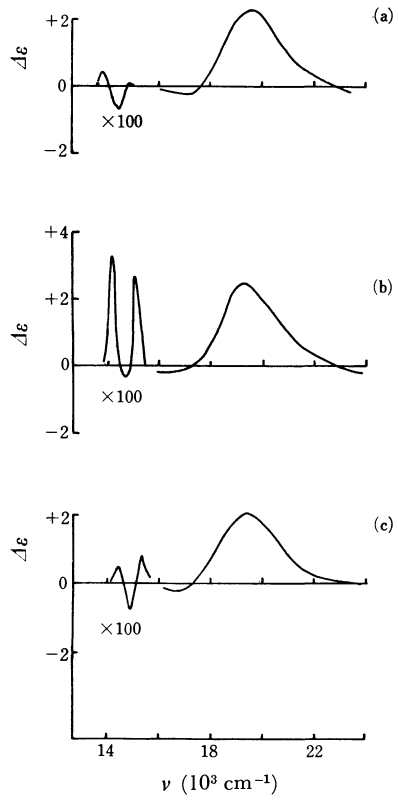

Fig. 7. CD curves of *cis*-$[Cr(O)_4(N)_2]$ type complexes in the *d–d* absorption band region.
(a) $(+)_{546}$-K$[Cr(ox)_2(dip)]$
(b) $(+)_{546}$-K$[Cr(ox)_2(phen)]$
(c) $(+)_{546}$-K$[Cr(ox)_2(en)]$

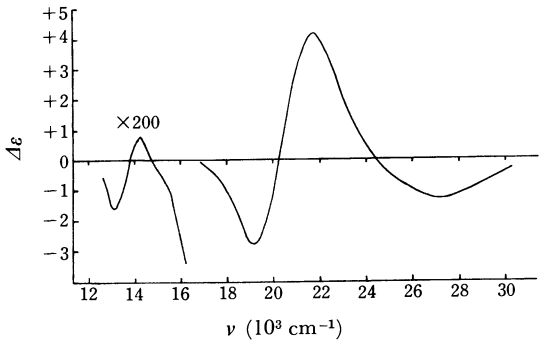

Fig. 8. CD curve of $(-)_{546}$-$[Cr(BH)_3]Cl_3$ in water.

each other by means of the spin-orbit coupling, which allows the ^2E_a transition to acquire a rotational strength by borrowing both the magnetic and electric transition dipole moments from the upper ^4E transition and to have the same sign of rotational strength as that of the ^4E transition. The central negative and the highest frequency positive CD bands in the spin-forbidden band region may be tentatively assigned to the $^2A_2$ and ^2E_b transition with octahedral $^2T_{1g}$ parentage, respectively, though for the $^4A_2$–$^2A_2$ transition the corresponding spin-allowed transition ($^4A_2$–$^4A_2$) is both electrically and magnetically dipole forbidden. From this consideration, it can be proposed that chromium(III) complexes with the positive ^4E CD band of the first spin-allowed *d–d* transition exhibit the positive ^2E_a CD band and have a $\Delta(C_2)$ configuration. This proposal is consistent with the result from the determination of absolute configurations on the basis of the exciton CD bands and of stereospecificity as will be mentioned below.

1,10-Phenanthroline and 2,2′-Dipyridyl Complexes. Mason *et al.*[30-32] and Bosnich[33] have developed the nonempirical method for determining the absolute configurations of tris- or bis-α-diimine metal complexes on the basis of CD spectra in the ultraviolet region, where long-axis-polarized π–π* ligand transition occurs. According to their consideration, the simple electrostatic treatment of the exciton theory neglecting the central metal ion predicts that tris- or bis-α-diimine metal complexes should take a $\Delta(C_2)$ configuration, if these complexes show a positive and a negative CD band at the longer and shorter wavelength side, respectively, in the exciton band region. This prediction has been recently confirmed by X-ray determination[34] of the absolute configuration of $(-)_{589}$-$[Fe(phen)_3]^{2+}$ and has been shown to be consistent with the result of the empirical method on the basis of the CD bands in the first spin-allowed *d–d* absorption band region.[8,31] In the region from 300 mμ to 250 mμ, the CD spectra of tris- or bis-1,10-phenanthroline- and bis-2,2′-dipyridylchromium(III) complexes studied show two large typical exciton bands, which have signs opposite each other and are of nearly equal intensity. As may be seen in Figs. 3 and 4, $(+)_{546}$-$[Cr(phen)_3](ClO_4)_3$, $(+)_{546}$-$[Cr(ox)(phen)_2]ClO_4$ and $(+)_{546}$-$[Cr(ox)(dip)_2]Cl$ give two exciton CD bands, namely, (+) and (−) bands, and a positive major CD band in the first spin-allowed *d–d* absorption band region.[8,35] Consequently, on the basis of the CD bands, the absolute configuration of these phen and dip complexes

30) A. J. McCaffery and S. F. Mason, *Proc. Chem. Soc.*, **1963**, 211; A. J. McCaffery and S. F. Mason, *ibid.*, **1964**, 259; E. Larsen, S. F. Mason and G. H. Searle, *Acta Chem. Scand.*, **20**, 191 (1966); J. Mason and S. F. Mason, *Tetrahedron*, **23**, 1919 (1967).
31) S. F. Mason and B. J. Norman, *Inorg. Nucl. Chem. Lett.*, **3**, 285 (1967).
32) A. J. McCaffery, S. F. Mason and B. J. Norman, *J. Chem. Soc., A*, **1969**, 1428; S. F. Mason and B. J. Norman, *ibid.*, **1969**, 1442.
33) B. Bosnich, *Inorg. Chem.*, **7**, 178 (1968); B. Bosnich, *ibid.*, **7**, 2379 (1968).
34) D. M. Templeton, A. Zalkin and T. Ueki, *Acta Crystallogr.*, **21**, A 154 (1966).
35) J. Ferguson, C. J. Hawkins, N. A. P. Kane-Maguire and H. Lip, *Inorg. Chem.*, **8**, 771 (1969).

TABLE 1. CD DATA OF THE CHROMIUM(III) COMPLEXES IN THE d–d ABSORPTION BAND REGION
(The wave numbers are given in 10^3 cm^{-1}, and the intensities, $(\varepsilon_1-\varepsilon_d)$, in parentheses.)

Complex	Solvent	CD peaks in the region of spin-forbidden band	CD peaks in the region of spin-allowed band
$(+)_{546}$-$[Cr(en)_3](ClO_4)_3$	water	15.0 $(+8.85\times10^{-3})$ 15.5 (-5.70×10^{-3}) 15.8 $(+6.75\times10^{-3})$	21.9 (+1.49) 26.5 (+0.55) 28.5 (−0.08) 30.4 (+0.58)
	0.4F Na_2SeO_3 solution	15.0 $(+7.80\times10^{-3})$ 15.5 (-6.00×10^{-3}) 15.8 $(+4.50\times10^{-3})$	21.9 (+1.28)
$(+)_{546}$-$[Cr(tn)_3](ClO_4)_3$	water	15.1 $(+2.08\times10^{-3})$ 15.6 (-0.45×10^{-3}) 15.9 $(+1.04\times10^{-3})$	20.9 (+0.34)
	0.6F Na_2SeO_3 solution	15.1 $(+0.50\times10^{-3})$ 15.7 (-0.36×10^{-3}) 16.0 $(+0.54\times10^{-3})$	20.5 (+0.14) 22.9 (−0.11)
$(+)_{546}$-$[Cr(phen)_3](ClO_4)_3$	water	13.8 $(+12.4\times10^{-3})$ 14.5 (-7.50×10^{-3})	21.9 (+2.48)
$(+)_{546}$-$[Cr(ox)(phen)_2]ClO_4$	70% $HClO_4$	13.8 $(+4.50\times10^{-3})$ 14.8 (-6.00×10^{-3})	18.4(−0.83) 21.2(+1.50)
$(+)_{546}$-$[Cr(ox)(dip)_2]Cl$	water	13.6 $(+5.48\times10^{-3})$ 14.0 (-1.63×10^{-3}) 14.3 (-2.96×10^{-3}) 14.9 $(+1.92\times10^{-3})$	17.8(−0.06) 20.6 (+1.40)
$(+)_{546}$-$[Cr(ox)(en)_2]Cl$	water	14.7 $(+12.9\times10^{-3})$ 15.2 (-6.40×10^{-3}) 15.5 $(+11.4\times10^{-3})$	20.8 (+1.97) 26.9 (−0.14)
$Ba_{0.5}$ $[Cr_2(L\text{-}tart_2H)(dip)_2]$	water	13.3 (-14.2×10^{-3})	15.7 (+0.14) 18.3 (−5.10)
$NH_4[Cr_2(L\text{-}tart_2H)(phen)_2]$	dmf-water mixture	13.3 (-6.40×10^{-3}) 13.9 (-4.60×10^{-3})	15.5 (+0.15) 18.3 (−8.11)
$(+)_{546}$-$K[Cr(ox)_2(dip)]$	water	13.8 $(>+4.50\times10^{-3})$ 14.3 $(<-5.40\times10^{-3})$ 14.5 $(<-6.60\times10^{-3})$ 14.8 $(>+1.70\times10^{-3})$	17.0 (<-0.12) 19.5 $(>+2.22)$
$(+)_{546}$-$K[Cr(ox)_2(phen)]$	water	13.9 $(>+32.0\times10^{-3})$ 14.4 $(<-3.00\times10^{-3})$ 14.7 $(>+27.0\times10^{-3})$	16.4 (<-0.13) 19.0 $(>+2.46)$
$(+)_{546}$-$K[Cr(ox)_2(en)]$	water	14.5 $(>+7.50\times10^{-3})$ 14.9 $(<-10.3\times10^{-3})$ 15.3 $(>+11.3\times10^{-3})$	16.8 (<-0.05) 19.4 $(>+2.00)$
$(-)_{546}$-$[Cr(BH)_3]Cl_3$	water	13.1 (-7.77×10^{-3}) 14.3 $(+3.89\times10^{-3})$	19.2 (−2.78) 21.7 (+4.16)

will be determined to be a $\Delta(C_2)$ configuration.*2 The CD spectra in the spin-forbidden band region show two peaks, (+) and (−), for $(+)_{546}$-[Cr(phen)$_3$]$^{3+}$ and $(+)_{546}$-[Cr(ox)(phen)$_2$]$^+$ and four peaks, (+), (−), (−) and (+), for $(+)_{546}$-[Cr(ox)(dip)$_2$]$^+$, listing from the longer wavelength side as may be seen in Fig. 5. That is, the sign of the lowest frequency CD band due to the ^2E_a transition for the phen and dip complexes having the $\Delta(C_2)$ absolute configuration is always positive. In the case of $(+)_{546}$-[Cr(ox)(en)$_2$]Cl, which has a *cis*-[Cr(O)$_2$(N)$_4$] type structure similar to that of bis(phen)- and bis(dip)oxalato complexes, the CD band in the region of the spin-forbidden band is also related to that in the first spin-allowed absorption band region. Namely, the CD spectra of $(+)_{546}$-[Cr(ox)(en)$_2$]Cl show a positive band in the first absorption band region and three sharp peaks, (+), (−) and (+), in the spin-forbidden band region, as seen in Fig. 5. Thus, it can be determined that $(+)_{546}$-[Cr(ox)(en)$_2$]Cl giving the positive ^4E and ^2E_a CD components take a $\Delta(C_2)$ configuration.

L-*Tartrato and Oxalato Complexes.* We have revealed that the L-tartratochromium(III) (1:1)-complexes, Ba[Cr$_2$(L-tart$_2$H)(dip)$_2$]$_2\cdot 9H_2O$ and NH_4[Cr(L-tart$_2$H)(phen)$_2$]$\cdot 6.5H_2O$, are formed completely stereospecifically to have a bis(L-tartrato)-bridged binuclear structure with a $\Lambda(C_2)$–$\Lambda(C_2)$ configuration. The L-tartrato complexes gave apparently positive weak CD bands in the spin-forbidden band region superimposing on the positive CD component related to the first spin-allowed absorption band.[1] Upon detailed remeasurements, however, another sharp but weak negative CD bands are observed at longer wavelengths in the spin-forbidden band region as shown in Fig. 6. It is evident that the L-tartrato complexes with the $\Lambda(C_2)$ absolute configuration give the negative CD peaks at the longest wavelength side in the spin-forbidden band region and the negative major CD band in the first spin-allowed *d–d* absorption band region. The L-tartrato complex containing 1,10-phenanthroline exhibits splitting of the negative CD band of the spin-forbidden transition (Fig. 6). This fact suggests the existence of the spin-spin coupling between the two chromium(III) ions also in this binuclear complex as reported by Mason[8] in the case of $(-)_{546}$-[Cr$_2$(OH)$_2$(dip)$_4$]$^{4+}$ and $(-)_{546}$-[Cr$_2$(OH)$_2$(phen)$_4$]$^{4+}$. For the oxalato complexes, $(+)_{546}$-K[Cr(ox)$_2$(dip)], $(+)_{546}$-K[Cr(ox)$_2$(phen)] and $(+)_{546}$-K[Cr(ox)$_2$(en)], which have the geometrical structure identical to that of the L-tartrato complex, *cis*-[Cr(O)$_4$(N)$_2$] type, the major CD band in the first spin-allowed absorption band region and the lowest frequency CD band in the spin-forbidden band region have a positive sign, as seen in Fig. 7. Thus, the oxalato complexes take a $\Delta(C_2)$ absolute configuration.

Trisbiguanide Complex. The biguanide complex, $(-)_{546}$-[Cr(BH)$_3$]Cl$_3$, shows two intense CD bands in the first spin-allowed absorption band region, (+) one at 460 mμ and (−) one at 520 mμ.[17] In the region of the spin-forbidden band, this complex gives two weak and broad CD bands, (−) and (+), as seen in Fig. 8. The absolute configuration of this complex may be assumed to be a $\Delta(C_2)$ one on the basis of the sign of the major CD band in the first spin-allowed band region.[17] On the contrary, a $\Lambda(C_2)$ configuration may be assumed from the theory that the ^2E_a CD component is at the longest wavelength side. However, this contradiction may be solved as follows. Since a biguanide forms a six membered chelate ring, the energy ordering of the trigonal splitting for this complex is assumed to be similar to that of tristrimethylenediamine complex with six membered chelate rings. Thus, the positive major CD component at the shorter wavelength side may be assigned to the $^4A_1$ and the negative minor CD component at the longer wavelength side to the ^4E component. Therefore, the ^4E CD component has a negative sign similar to the ^2E_a CD component. It is thus concluded that the $(-)_{546}$-trisbiguanidechromium(III) complex has a $\Lambda(C_2)$ absolute configuration.

It is concluded that the absolute configurations of tris-chelate chromium(III) complexes can be determined on the basis of the sign of the lowest frequency CD component corresponding to the ^2E_a transition derived from the octahedral ^2E_g parentage. Namely, if the ^2E_a CD component show a positive sign, the absolute configuration of the complexes can be determined to be a $\Delta(C_2)$.

Analysis of the CD Bands. On analysis of the spectra of d^3 ions in a trigonal field in terms of the weak field perturbation, Macfarlane[9] has estimated the contribution of the ligand field parameter Δ, the trigonal parameters v and v', and the electronic repulsion parameters B and C, to the transition energies of the doublet states as shown in Table 2.

*2 When the metal-ligand and ligand-ligand bonding are taken into consideration, the relative energies of the exciton splitting are affected by the central metal ion and also by the kind of conjugated ligand. According to Ferguson *et al.*,[35] the sign of the exciton splitting has been experimentally determined on the basis of analysis of the ligand absorption bands and it has been found that the sign for $(+)_{546}$-[Cr(ox)(dip)$_2$]$^+$ is opposite that of $(+)_{546}$-[Cr(ox)(phen)$_2$]$^+$.

In consequence, it has been concluded that the two $(+)_{546}$-isomers have been assigned to have opposite configurations to each other. It is doubtful, however, that the difference in the π-bonding between 2,2′-dipyridyl and 1,10-phenanthroline gives rise to such drastic modification of the relative energies of the exciton splitting, because the contributions of the metal-ligand or ligand-ligand bonding to the exciton splitting are expected to be small and almost the same for the dip and phen chromium(III) complexes.[8,32] Therefore, the simple dipole-dipole interaction theory may be adopted here as a good approximation.

Table 2. Representation of the transition energies of the doublet states

$$\nu(^2E_a) = 0.0317\Delta - 0.241v - 0.178v' + 6.54B + 3.06C$$
$$\nu(^2A_2) = 0.0250\Delta - 0.217v' + 7.63B + 3.00C$$
$$\nu(^2E_b) = 0.0176\Delta - 0.052v - 0.109v' + 7.81B + 3.01C$$

A similar treatment neglecting the spin-orbit coupling was applied for the trisdiamine complexes on the basis of the above-mentioned assignment for three CD peaks observed in the spin-forbidden band region, on the assumption that the ligand field splitting Δ equals the energy of the first absorption band maximum and that the Racah parameter C is equal to 4B. The values of the parameters B, v and v' obtained are given in Table 3. The values obtained for the parameter B are so reasonable that they are closer to those from Schäffer's treatment[36] including the non-diagonal elements rather than values from strong field approximation with only diagonal elements.[23] The sign of the trigonal parameter v of $[Cr(tn)_3]^{3+}$ obtained is in agreement with the result from the CD measurement. However, the sign for $[Cr(en)_3]^{3+}$ is opposite that from the polarized crystal spectra.[37]

Table 3. Values for the parameters (cm^{-1})

Complexes	B	v	v'
$[Cr(en)_3]^{3+}$	772	+104	+912
$[Cr(tn)_3]^{3+}$	776	+303	+862

36) C. K. Jørgensen, *Progr. Inorg. Chem.*, **4**, 101 (1962); C. K. Jørgensen, *Advan. Chem. Phys.*, **5**, 72 (1963).

37) S. Yamada and R. Tsuchida, This Bulletin, **33**, 98 (1960).

BULLETIN OF THE CHEMICAL SOCIETY OF JAPAN VOL. 43 1109—1119 (1970)

Imidazole Catalyses in Aqueous Systems. III. Formation of the Catalyst-Substrate Complex in the Hydrolysis of a Phenyl Ester Catalyzed by a Naphthylimidazole Derivative*1

Toyoki KUNITAKE, Seiji SHINKAI and Chuji ASO

Department of Organic Synthesis, Faculty of Engineering, Kyushu University, Fukuoka

(Received June 7, 1969)

Catalytic hydrolysis of *p*-acetoxybenzoic acid by 1-[4(5)-imidazolyl]-4-aminomethylnaphthalene was carried out at 30°C in aqueous systems using a pH-stat. The catalytic rate leveled off at high substrate concentrations and increased remarkably at high pH. The data indicated that both the neutral catalytic species (AmIm) and the monoprotonated catalytic species (Am^+Im) acted as enzyme-like catalysts, the catalytic rate conforming to the Michaelis-Menten kinetics, although their catalytic efficiencies were quite different: K_m (dissociation constant of the catalyst-substrate complex)$=0.011$ M and k_3 (pseudo-intramolecular rate constant of the product-formation)$=0.19$ min^{-1} for AmIm, and $K_m=0.041$ M and $k_3=0.036$ min^{-1} for Am^+Im. The binding function was attributed to hydrophobic interaction, on the ground that K_m was smaller for AmIm than for Am^+Im and that an increase in the ionic strength of the medium caused rate enhancement. The hydrolysate showed an inhibitory action. The wide variation of the catalytic efficiency between AmIm and Am^+Im may be related to the structural difference of the Michaelis complexes. 1-Aminomethylnaphthalene similarly catalyzed the hydrolysis and showed a substrate binding phenomenon, though the saturation phenomenon was much less pronounced as compared with the imidazole catalyst.

In the previous publications of this series, it was shown that imidazole-containing copolymers (I and II) catalyzed the hydrolysis of 3-nitro-4-acetoxybenzoic acid according to the Michaelis-Menten kinetics as in enzymatic reactions.[1)]

*1 Contribution No. 169 from this department. Presented at the 22nd Annual Meeting of the Chemical Society of Japan, March, 1969, Tokyo, Japan. A preliminary account of this work was given in C. Aso, T. Kunitake and S. Shinkai, *Chem. Commun.*, **1968**, 1483.

1) a) C. Aso, T. Kunitake and F. Shimada, *J. Polymer Sci., Part B*, **4**, 467 (1968). b) T. Kunitake, F. Shimada and C. Aso, *J. Amer. Chem. Soc.*, **91**, 2716 (1969).

$$\text{catalyst} + \text{substrate} \overset{K_m}{\rightleftarrows} \text{catalyst}\cdot\text{substrate} \xrightarrow{k_s} \text{catalyst} + \text{product} \quad (1)$$

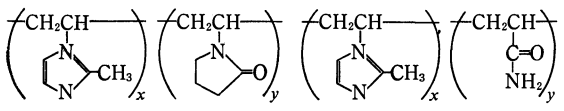

I II

The influence of the copolymer composition of I on the catalytic behavior was accounted for by assuming that the catalytic site was made of a loop of a polymer segment surrounding a substrate molecule. The binding function of the catalytic site was attributable to hydrophobic forces. It was shown that the catalytic action was inhibited competitively by several organic compounds, supporting its enzyme-like catalytic behavior.[2] In the case of catalysis by II, it was not necessary to consider loop formation. The binding function was similarly attributed to the hydrophobic interaction.[1b]

Molecular associations of organic compounds due to hydrophobic forces are frequently encountered in aqueous systems. Dye associations and the micelle formation of detergents are typical examples.

Apart from polymeric systems, there have been several investigations in which formation of catalyst-substrate complexes preceded the chemical transformation of substrates. For instance, Cramer and coworkers found that cyclodextrins catalyzed decarboxylation of substituted cyanoacetates and acetoacetates[3] and fission of pyrophosphates[4] in enzyme-like manners (Eq. (1)). Bender *et al.*[5,6] studied in detail phenyl ester cleavages catalyzed by cycloamyloses. The formation of a 1 : 1 complex between catalyst and substrate molecules with detergent-like structures of opposite charge has been proposed by Wagner *et al.*[7]

Thus, it was expected that small molecules which consist of hydrophobic and catalytic groups might show an enzyme-like catalytic behavior. The first compound we selected for this purpose was 1-[4(5)-imidazolyl]-4-aminomethylnaphthalene (III). The naphthalene ring is considered to show sufficiently strong hydrophobic interaction, since naphthalenesulfonic acid was shown by NMR spectroscopy to associate with acetone or methanol in an aqueous system,[8] and the imidazole group is known to be present in the active site of many hydrolytic enzymes.[9a]

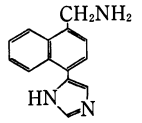

III

In the following we describe an investigation of the enzyme-like catalysis by III for hydrolysis of 4-acetoxybenzoic acid into 4-hydroxybenzoic acid and acetic acid.

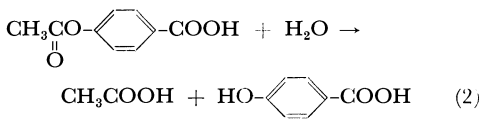

(2)

Experimental

Preparation of 1-Acetyl-4-bromonaphthalene (IV).[10,11] α-Bromonaphthalene was prepared in 70% yield from naphthalene and bromine in CCl_4,[12] and subsequently acetylated with acetyl chloride and $AlCl_3$ in CS_2 at room temperature. Yield 71%, mp 47.0—47.5°C (lit,[10] 47.0—47.5°C).

Preparation of 1-Acetyl-4-cyanonaphthalene (V). The reaction was carried out following the preparative method of 1-cyanonaphthalene.[13] Into a 300-m*l* three-necked flask equipped with a mechanical stirrer, a reflux condenser and a thermometer were added 83 g (0.33 mol) of IV, 35 g (0.38 mol) of cuprous cyanide and 65 m*l* of dimethylformamide (DMF). The reaction mixture was stirred for 6 hr with gentle refluxing at 150—160°C. A warm solution of 133 g (0.50 mol) of ferric chloride in 33 m*l* of concentrated hydrochloric acid and 200 m*l* of water was added to the reaction mixture. Some solid residues left in the flask were dissolved in warm DMF. The solutions were combined and maintained for 20 min at 60—70°C. Black precipitates were filtered and the solution was extracted with 750 m*l* (in three portions) of toluene. After distilling toluene,

2) T. Kunitake, F. Shimada and C. Aso, *Makromol. Chem.*, **126**, 276 (1969).

3) F. Cramer and W. Kampe, *J. Amer. Chem. Soc.*, **87**, 1115 (1965).

4) N. Heinrich and F. Cramer, *ibid.*, **87**, 1121 (1965).

5) M. L. Bender, R. L. VanEtten, G. A. Clowes and J. F. Sebastian, *ibid.*, **88**, 2318 (1966); R. L. VanEtten, J. F. Sebastian, G. A. Clowes and M. L. Bender, *ibid.*, **89**, 3242 (1967).

6) M. L. Bender, R. L. VanEtten and G. A. Clowes, *ibid.*, **88**, 2319 (1966); R. L. VanEtten, G. A. Clowes, J. F. Sebastian and M. L. Bender, *ibid.*, **89**, 3253 (1967).

7) T. E. Wagner, C.-J. Hsu and C. S. Pratt, *ibid.*, **89**, 6366 (1967); R. G. Shorenstein, C. S. Pratt, C.-J. Hsu and T. E. Wagner, *ibid.*, **90**, 6199 (1968).

8) E. S. Hand and T. Cohen, *ibid.*, **87**, 133 (1965).

9) T. C. Bruice and S. J. Benkovic, "Bioorganic Mechanisms," W. A. Benjamin, Inc., New York, N.Y. (1966). a) Chapter 2; b) p. 46.

10) T. L. Jacobs, S. Winstein, J. W. Ralls and J. H. Robson, *J. Org. Chem.*, **11**, 27 (1946).

11) S. Berkovic, *Israel J. Chem.*, **1**, 1 (1963).

12) H. T. Clark and M. R. Brefhen, "Organic Synthesis," Coll. Vol. I, p. 121 (1941).

13) L. Friedman and H. Shechter, *J. Org. Chem.*, **26**, 2522 (1961).

red-brown needles were obtained on cooling. Recrystallization from methanol gave 7 g (11% yield) of yellow needles: mp 130—132°C. The black precipitate was extracted with toluene in a Soxhlet extractor. Solvent removal from the extract gave red-brown needles, which were recrystallized from methanol to yield yellow needles. The combined yield amounted to 90%. Elemental analysis. Found: C, 80.30; H, 4.56; N, 7.09%. Calcd for $C_{13}H_9NO$: C, 79.98; H, 4.65; N, 7.17%. The infrared spectrum showed peaks at 2220 ($\nu_{C\equiv N}$), 1695 ($\nu_{C=O}$, conjugated), 833 (δ_{CH}, aromatic, out of plane) and 758 cm^{-1} (δ_{CH}, aromatic, out of plane).

Oxidation of V with SeO_2. The reaction was carried out by modifying the preparative method of naphthylglyoxal.[14] In a 100-m*l* three-necked flask equipped with a mechanical stirrer, a reflux condenser and a thermometer, 11.1 g (0.1 mol) of SeO_2 was dissolved in 50 m*l* of dioxane containing 2 m*l* of water at 50—55°C. 19.5 g (0.1 mol) of V was then quickly added and the reaction mixture was refluxed with stirring for 6.5 hr, and stirred at room temperature for additional 12 hr. The precipitated selenium metal and filtered and the solvent removed *in vacuo*. The residue was dissolved while still warm in 30 m*l* of acetone and the precipitate formed (Se metal) was filtered. Acetone was evaporated and the resulting brown residue (1-(4-cyanonaphthyl)-glyoxal, VI) dissolved in 200 m*l* of methanol was used for the next step without further purification. When a shorter oxidation period was employed (refluxing for 4 hr and stirring for 2 hr), the yield of the copper complex in the next step did not decrease.

Preparation of 1-[4(5)-Imidazolyl]-4-cyanonaphthalene (VII). The general procedure for preparation of imidazoles from glyoxals[15] was followed. To a 300-m*l* three-necked flask equipped with a mechanical stirrer, a reflux condenser and a thermometer was added 140 m*l* of 28% aqueous ammonia and 8 m*l* of 37% formalin. The mixture was warmed to 40°C on a water bath, and 20 g of cupric acetate and 100 m*l* of a methanol solution of VI were added with stirring. Stirring was further continued for 40 min at 55—58°C, and the copper salt of the imidazole compound was obtained as precipitates. The crude copper complex was purified by refluxing for 1 hr each in the following solvents: a. 1 : 1 aqueous methanol; b. ethyl acetate, twice; c. acetone, twice; d. chloroform, twice. The yield of the purified copper complex was 15 g (30% based on V).

The imidazole was freed from copper by treating with H_2S. The copper complex (50 g) was suspended in 2 *l* of 1 : 1 aqueous methanol and H_2S gas was introduced for 4 hr with gentle refluxing. The hot mixture was filtered, and, on cooling, 40 g of crude VII was obtained as red-brown precipitates. The crude VII was dissolved in dilute hydrochloric acid, and the hydrochloride of VII (VII-HCl) was recovered by concentration and purified by recrystallization from water with charcoal treatment. The overall yield of VII-HCl from V was approximately 10%. Colorless needles, mp 219—220°C. Found: C, 57.68; H, 4.88; N, 13.75%. Calcd for $C_{14}H_{10}N_3Cl\cdot 2H_2O$: C, 57.63; H, 4.83; N, 14.41%.

Its infrared spectrum showed a broad peak characteristic of the imidazole group at 2800—3200 cm^{-1}, a sharp peak at 2220 cm^{-1} ($\nu_{C\equiv N}$), and peaks at 762 and 833 cm^{-1} (δ_{CH} aromatic, out of plane).

The free imidazole derivative, VII, was obtained by treating VII-HCl with concentrated aq. $NaHCO_3$: Colorless crystals, mp 216—218°C. Its infrared spectrum was consistent with what was expected for VII.

Reduction of VII with $LiAlH_4$. In a 300-m*l* three-necked flask equipped with a mechanical stirrer, a dropping funnel and a reflux condenser connected to a soda lime tube were placed 100 m*l* of carefully-purified tetrahydrofuran (THF) and 1.2 g of $LiAlH_4$. Finely powdered VII (0.6 g) was suspended in 50 m*l* of THF and slowly added over 30 min from the dropping funnel. The color of the mixture turned green. The reaction mixture was refluxed during the addition and for the subsequent 90 min. Excess $LiAlH_4$ was decomposed with 50 m*l* of water, and 70 m*l* of 10% aqueous NaOH was added. The pale yellow organic layer was separated and acidified with 10 m*l* of 4N hydrochloric acid, and THF was removed *in vacuo*. When separation of the two layers was difficult, addition of concentrated aqueous NaOH or of an aqueous solution of Rochelle salt was effective for the phase separation. Slow addition of concentrated aqueous alkali to the organic residue gave rise to white precipitates, which again went into solution on standing. When the dissolution became sluggish, an aqueous solution of excess Na_2CO_3 was added to yield 0.4 g of white precipitates (III). mp 172—175°C. Yield 70%. Reprecipitation was carried out by neutralization of an acidic aqueous solution as metioned above, and the precipitate was dried *in vacuo*.

Found: C, 75.03; H, 5.85; N, 17.75%. Calcd for $C_{14}H_{13}N_3$: C, 75.31; H, 5.87; N, 18.82%.

Its infrared spectrum showed the presence of a broad peak between 2900—3400 cm^{-1} (imidazole). The peak at 2220 cm^{-1} was absent, indicating disappearance of the cyano group. Peaks at 827 and 756 cm^{-1} showed that the naphthalene ring remained intact. Titration of III (10.9 mg) was carried out as described below (30°C, 1M KCl) and the alkali consumption to neutralize the protonated imidazole group was 95±3% of the calculated amount.

Preparation of 1-Aminomethylnaphthalene (VIII). Naphthalene was reacted with paraformaldehyde and concentrated hydrochloric acid to give 1-chloromethylnaphthalene[16] in 83% yield: bp 168—172°C/25 mmHg (lit,[16] 148—153°C/14 mmHg). 1-Chloromethylnaphthalene was converted to 1-aminomethylnaphthalene by treating with hexamethylenetetramine in chloroform.[17] Bp 192—198°C/25 mmHg (lit,[17] bp 200—205°C/30 mmHg). Yield 61%. 1-Aminomethylnaphthalene hydrochloride (VIII-HCl) was obtained by introducing dry HCl gas into an ether solution of VIII. Colorless plates, mp 261—263°C (lit,[17] 260—262°C).

Preparation of *p*-Acetoxybenzoic Acid. Commercial *p*-hydroxybenzoic acid, 27.6 g (0.2 mol), was dis-

14) R. C. Fuson, W. S. Emerson and H. W. Gray, *J. Amer. Chem. Soc.*, **61**, 480 (1939).

15) P. Ruggli and E. Henzi, *Helv. Chim. Acta*, **12**, 362 (1929) [*Chem. Abstr.*, **24**, 116 (1930)].

16) O. Grummit and A. Buck, "Organic Synthesis," Coll. Vol. III, p. 195 (1955).

17) F. F. Blicke and C. E. Maxwell, *J. Amer. Chem. Soc.*, **61**, 1781 (1939).

solved in 80 ml (0.8 mol) of acetic anhydride and the solution was refluxed for 3 to 4 hr. The reaction mixture was poured into ice water, and the white precipitates formed were recrystallized twice from water and dried. Additional recrystallization from benzene gave colorless flakes in 85—92% yield. Mp 192—194°C (lit,[18] 186°C).

Titration and Hydrolysis Procedures. Titration and hydrolysis were carried out at 30.0±0.05°C using a pH-stat connected with a recorder (TOA Electronics Ltd., Models HS-1B and EPR-2T, respectively). Details of the procedures have been described previously.[1b]

Miscellaneous. Imidazole and KCl, guaranteed reagents, were dried and used without further purification. Infrared spectra were obtained with a Jasco DS 301 spectrometer.

Results

Synthesis of 1-[4(5)-Imidazolyl]-4-aminomethylnaphthalene (III). III was synthesized by the following sequences.

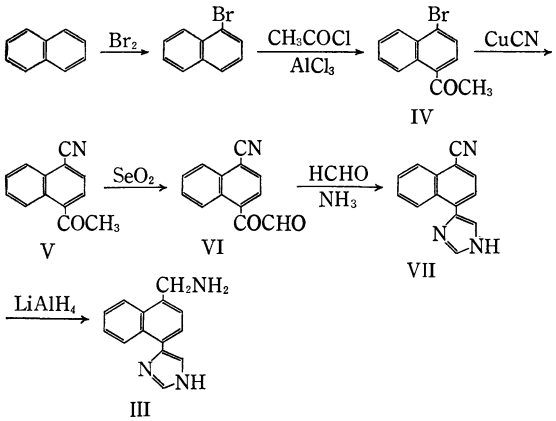

IV was obtained in good yields by acetylating 1-bromonaphthalene with acetyl chloride and $AlCl_3$ in CS_2 at 15—17°C. The conversion from IV to V proceeded smoothly with CuCN in DMF. Oxidation of V was carried out with SeO_2. Since the resulting glyoxal, VI, was unstable in air, a methanol solution of VI was used for the next step without purification. Formation of the imidazole ring was done with HCHO and NH_3 from VI. In order to obtain pure VII, extensive solvent extraction of the VII-copper complex was necessary. Otherwise, VII was accompanied by tarry materials which were difficult to remove. Reduction of the cyano group of VII was readily carried out using $LiAlH_4$. III was rather unstable in air and underwent ready discoloration, while III-HCl was sufficiently stable.

Titration. The titration behavior of the catalysts and the substrate were investigated at 30.0±0.05°C in 1M aqueous KCl. The free naphthylimidazole catalyst (III) was dissolved in 1M aqueous KCl at 30°C and the solution was adjusted to pH 3 by adding a small amount of hydrochloric acid. Titration was carried out by adding aqueous alkali in small portions. When pH of the solution reached approximately 9.8, the catalyst started to precipitate. This compound can exist in the form of the following species:

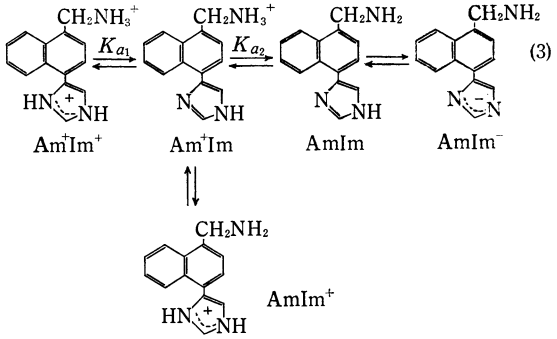

The titration curve of this compound shown in Fig. 1 indicates the presence of two dissociation steps. Since species $AmIm^-$ need not be considered in this pH range and the amount of $AmIm^+$ appears negligible, the two dissociation steps observed were concluded to correspond to processes Am^+Im^+ to Am^+Im and Am^+Im to AmIm. pK_a values determined from the titration curve by the method of Noyes[19] are given in Table 1.

The hydrolysis product, *p*-hydroxybenzoic acid, similarly gives the following two dissociation steps.

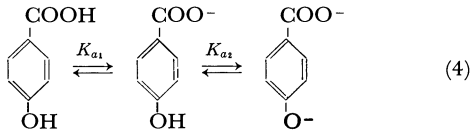

The pK_a values of III obtained from the titration curve of Fig. 1 are shown in Table 1. The titration of imidazole and 1-aminomethylnaphthalene was carried out in the same way and the pK_a (half neutralization point) is given in Table 1. The titration curve of the latter compound (Fig. 1), however, did not show a sharp transition, and the estimation of pK_a was less precise.

The pH dependence of the fractions of each species of III present in the system was calcluted as shown in Fig. 2 from the pK_a values obtained.

Spontaneous Hydrolysis. The substrate underwent spontaneous hydrolysis at higher pH. The results of the spontaneous hydrolysis at pH 8.0 are given in Fig. 3. Its rate was proportional to the substrate concentration, *viz.*,

18) E. R. Marshall, J. A. Kuck and R. C. Elderfield, *J. Org. Chem.*, **7**, 450 (1942).

19) A. Albert and E. P. Serjeant "Ionization Constants of Acids and Bases. A Laboratory Manual," Methuen, 1962, Translated by S. Matsuura, Maruzen Co., Tokyo (1964), p. 45.

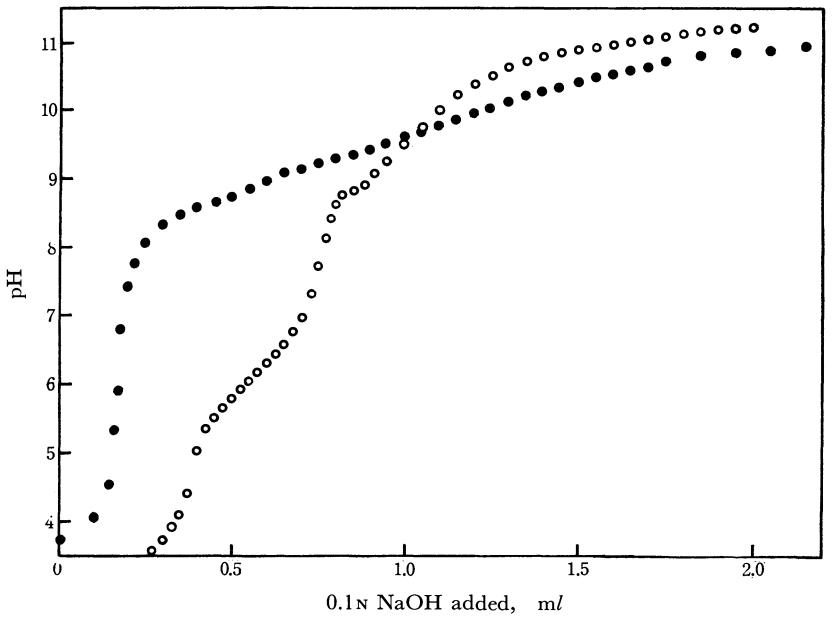

Fig. 1. Titration curves of catalysts.
30°C; μ=1.0M KCl
○: 1-[4(5)-imidazolyl]-4-aminomethylnaphthalene
●: 1-aminomethylnaphthalene

TABLE 1. pK_a VALUES[a)]

Compound	pK_{a1}	pK_{a2}
III	5.92±0.05	8.95±0.08
VIII	9.95±0.09	
Imidazole	7.13±0.03	
p-Hydroxybenzoic acid	4.44±0.04	9.17±0.04

a) 30°C, 1M aqueous KCl

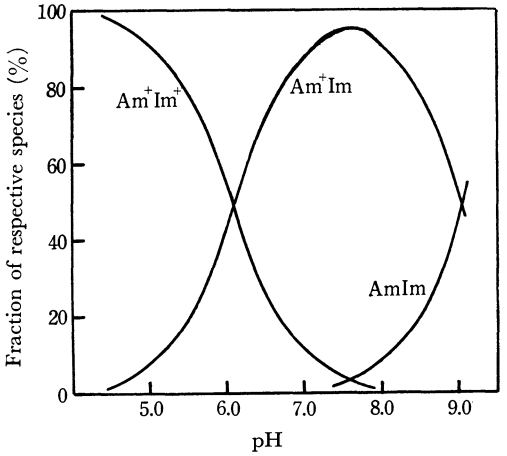

Fig. 2. pH dependence of the fractions of the species of compound III.
30°C; μ=1.0M KCl

$$v_{spont} = k_{spont} \cdot [S] \quad (5)$$

k_{spont} determined by the least square method was

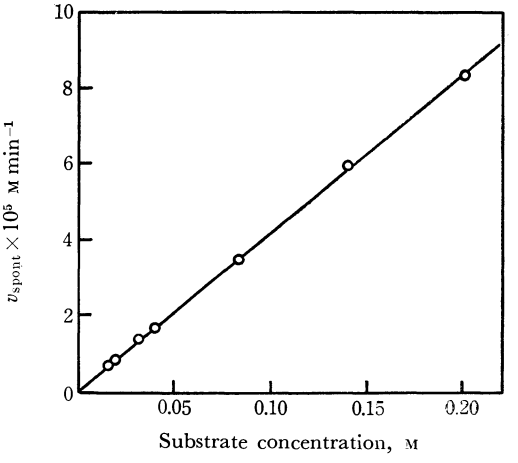

Fig. 3. Spontaneous hydrolysis.
30°C; pH 8.0; 1.0M KCl

$(4.23\pm0.02) \times 10^{-4}$ min^{-1}. The spontaneous hydrolysis was not detectable at pH 7.0.

Catalytic Hydrolysis. The overall rate of hydrolysis is the sum of the rates of the catalytic hydrolysis and of the spontaneous hydrolysis, *viz.*,

$$v_{total} = v_{cat} + v_{spont} \quad (6)$$

The amount of the substrate which was spontaneously hydrolyzed prior to the addition of the catalyst solution was determined by estimating the amount of substrate and alkali used for neutralization. The extent of the spontaneous hydrolysis was 0.8% for 0.04M substrate and about 4% for 0.20M substrate

at pH 8.0. This decrease in the substrate concentration was taken into account. The inhibitory effect of the hydrolysate was rather small and neglected in the determination of the initial rate of the catalytic hydrolysis (see below).

These corrections were not necessary at pH 7.0, because spontaneous hydrolysis was not detected. The amount of alkali necessary to compensate the acid formed by hydrolysis depends upon the pH of the system and on pK_a of the substrate. For instance, 1.063 mol of alkali is required for hydrolysis of 1.000 mol of the substrate at pH 8.0.

The relationships between v_{cat} and [S] at pH 7.0 and 8.0 are shown in Fig. 4. In both cases, v_{cat} showed substrate saturation phenomena. As already shown for polymer catalysts in previous publication,s[1,2] these kinetic patterns are typical of the enzyme-catalyzed reaction, indicating formation of the Michaelis complex between catalyst and substrate (Eq. (1)). The correspondin catalytic rate is given by

$$v_{cat} = \frac{k_3 \cdot [C][S]}{K_m + [S]} \tag{7}$$

As mentioned in the previous publication,[1b] k_3 values for the imidazole catalysts studied so far are rather small, and the Michaelis constant K_m may be considered to represent the true dissociation constant in the following discussion. The kinetic constants in this equation are determined from the following equation by plotting $1/v_{cat}$ *vs.* 1/[S] (the Lineweaver-Burk plots[20]).

$$\frac{1}{v_{cat}} = \frac{K_m}{V_{max}} \cdot \frac{1}{[S]} + \frac{1}{V_{max}} \tag{8}$$

where

$$V_{max} = k_3[C].$$

Since III is present in various forms, depending on pH of the system (Eq. (3)), the large difference between v_{cat} values at pH 7.0 and 8.0 suggests that catalytic efficiencies among various species of III vary to an appreciable extent. In the pH range studied, the catalytic species can be limited to Am^+Im and AmIm. If these two species show the enzyme-like catalysis indepnedently, the overall rate consists of the two terms as follows:

$$v_{cat} = \frac{k_3[C][S]}{K_m + [S]} + \frac{k_3'[C'][S]}{K_m' + [S]} \tag{9}$$

where the first term of the right side refers to AmIm and the second term to Am^+Im.

At $[S] \gg K_m, K_m'$, the maximum rate is given by

$$V_{max} = k_3[C] + k_3'[C'] \tag{10}$$

The Lineweaver-Burk plots of the data of Fig. 4 are given in Figs. 5 and 6. The reciprocal rela-

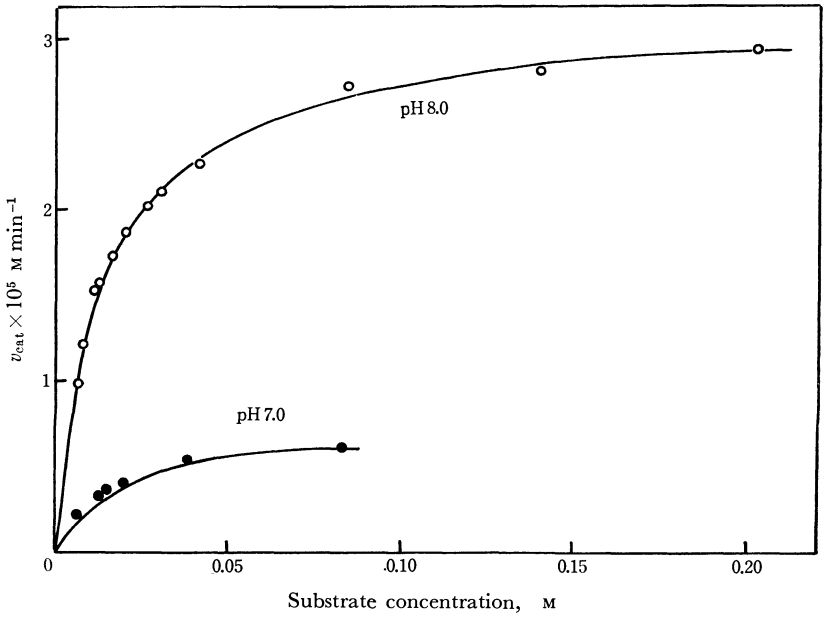

Fig. 4. Catalytic hydrolysis.
30°C; 1.0M KCl; Catalyst III 1.39×10^{-3}M; ○ at pH 8.0; ● at pH 7.0. The solid lines were obtained using K_m and k_3 values for the two catalytic species (Table 2).

20) H. Lineweaver and D. Burk, *J. Amer. Chem. Soc.*, **56**, 658 (1934).

tionships were seemingly linear,*2 and the values of V_{max} at the respective pH were determined from the intercepts. Since the fractions of each catalytic species are known from Fig. 2, k_3 and k_3' were determined to be 1.9×10^{-1} and 3.6×10^{-3} min^{-1}, respectively, by solving Eq. (10) for two values of pH.

The determination of the Michaelis constants was done by a computational trial and error as follows: K_m and K_m' were varied by an interval of 0.001M in Eq. (9) and the corresponding v_{cat} was calculated for respective substrate concentrations (v_{calcd}) from the known k_3, k_3', [C] and [C'] values. v_{calcd} was then compared with the observed rate of the catalytic hydrolysis (v_{obsd}). A set of K_m and K_m' was obtained which minimized the relative error.

$$E_{rel} = \{[\sum_{i=1}^{N}((v_{obsd})_i/(v_{calcd})_i-1)^2]/N\}^{1/2} \quad (11)$$

where N is the number of experimental runs.

When these procedures were carried out for the hydrolysis data at pH 8.0, E_{rel} was minimal (2.7%) for K_m=0.011M and K_m'=0.041M. In Table 2 are given the kinetic constants for the two catalytic species, together with the apparent kinetic constants at the two values of pH as obtained from the overall Lineweaver-Burk plots (Figs. 5 and 6). The kinetic constants obtained for catalysis of 1-aminomethylnaphthalene (see below) were also included in the table. Using these kinetic constants and the fractions of the catalytic species present, the substrate saturation curves were calculated as shown by the solid curve in Fig. 4. The agreement between v_{obsd} and v_{calcd} was satisfactory at pH 8.0 while v_{calcd} was somewhat lower than v_{obsd} at pH 7.0.

Table 2. Kinetic constants

Catalytic species	K_m (mM)	k_3 (min^{-1})	k_3/K_m (M^{-1}min^{-1})
Overall (pH 8.0)	13	0.023	1.3
Overall (pH 7.0)	16	0.053	0.32
AmIm	11	0.19	18
Am$^+$Im	41	0.0036	0.088
VIII	280	1.8	6.5

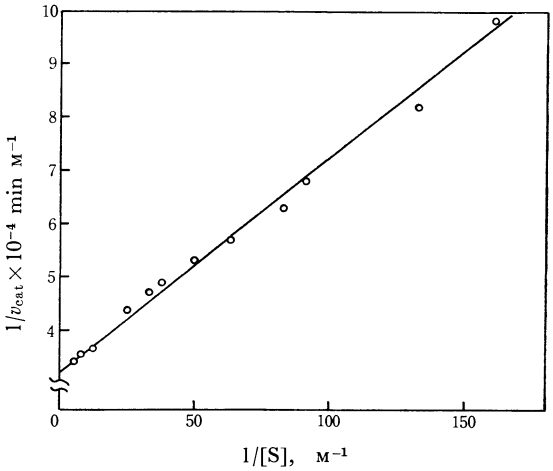

Fig. 5. Lineweaver-Burk plots of the rate data at pH 8.0.
The solid line was obtained by the least squares method.

Effect of pH and Inoic Strength on v_{cat}. The rates of catalytic hydrolysis were measured for [S]=0.010M at several values of pH (Fig. 7). The

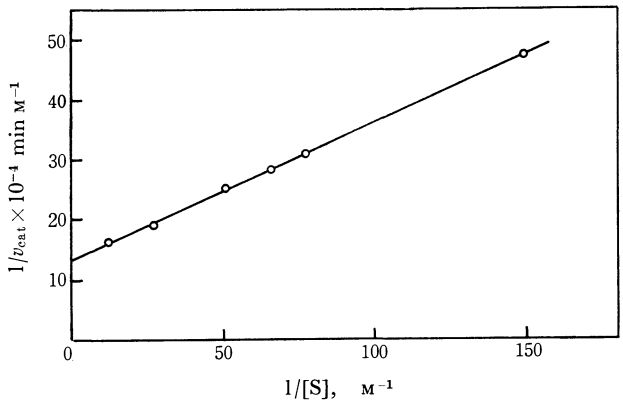

Fig. 6. Lineweaver-Burk plots of the rate data at pH 7.0.
The solid line was obtained by the least squares method.

*2 The Lineweaver-Burk plots of the overall catalytic rate are not necessarily linear, when more than one catalytic species with different K_m values are present.[1b] In the present case, K_m values for AmIm and Am$^+$Im are fairly close and the Lineweaver-Burk plotting of the overall catalytic rate did not deviate much from linearity. Thus, the linear extrapolation of the reciprocal plots to obtain k_3 values at 1/[S]=0 (Eq. (10)) may be justified.

rate was much greater at higher pH, supporting the higher catalytic efficiency of AmIm as compared with Am+Im. When v_{cat} was calculated from the kinetic constants of Table 2 for $[C]=1.39\times10^{-3}$M, the calculated rate was greater at higher pH and somewhat lower at lower pH than the observed rate. They were comparable at pH 7 to 8.

The influence of ionic strength on v_{cat} is shown in Table 3. v_{cat} decreased with decrease in the ionic stregth.

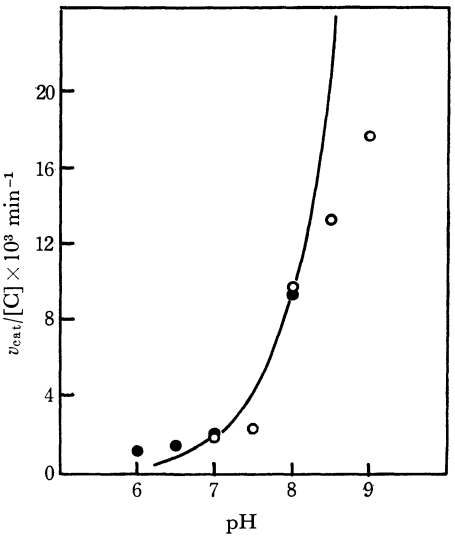

Fig. 7. pH dependence of the catalytic rate.
30°C; 1.0M KCl; substrate 0.010M
○: catalyst, III 1.98×10^{-3}M
●: catalyst, III 1.39×10^{-3}M
The solid curve was obtained by using the kinetic constants of Table 2.

TABLE 3. EFFECT OF IONIC STRENGTH ON v_{cat}[a)]

Ionic strength	$v_{cat}\times10^{6}$(M min^{-1})
0.012	8.1
0.112	10.3
1.01	14.7

a) Reaction condition: pH 8.0; 30°C; substrate 0.010M; catalyst 1.39×10^{-3}M.
b) The sum of KCl added and NaCl formed by neutralization by the time at which the initial rate was measured.

Product Inhibition. Figure 8 shows the rate-depressing effect of *p*-hydroxybenzoic acid (product of hydrolysis). v_{cat} decreased with increase in the amount of the product added, and the rate decrease was appreciable when the amount of the product was greater than 4 mM. Addition of 8 mM of the product lowered v_{cat} to about 30% of the original value. Further analysis of the inhibition was not attemped considering the kinetic complexity of this system.

It was mentioned above that the substrate underwent spontaneous hydrolysis during its dissolution process in the reaction mixture at pH 8.0. However, considering the limited extent of spontaneous hydrolysis and the small rate-depressing effect at low concentrations of *p*-hydroxybenzoic acid (Fig. 8), it was concluded that the correction of v_{cat} due to the inhibitory action of the product was not necessary.

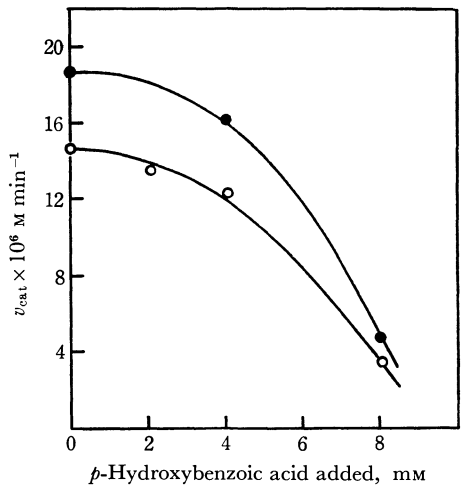

Fig. 8. Effect of *p*-hydroxybenzoic acid on v_{cat}
30°C; pH 8.0; μ=1.0M KCl; catalyst, III 1.39×10^{-3}M; ○, substrate 0.020M; ●, substrate 0.010M.

Recovery of the Catalyst. The imidazole catalyst III was precipitated from the reaction mixture by adding a few drops of 1.7N aqueous NaOH (pH>10). The precipitate was separated by centrifugation and subjected to infrared analysis. Hydrolysis was carried out under standard conditions with $[C]=1.39\times10^{-3}$M and [S]=0.010M. On an average, one mole of the catalyst had hydrolyzed 0.47 mol of the substrate when the catalyst was recovered. No amide absorption was found for the recovered catalyst, indicating that the amino group of the catalyst was not acetylated.

Catalytic Hydrolysis by 1-Aminomethylnaphthalene. The relationship between v_{cat} and [S] is shown in Fig. 9 for the catalytic hydrolysis by 1-aminomethylnaphthalene. A tendency of substrate saturation was observed, although it was much less pronounced than that observed for catalysis of III. The corresponding Lineweaver-Burk plots (Fig. 10) were linear and yielded the following data: $K_m=0.28$M and $V_{max}=5.7\times10^{-5}$M min^{-1}. Since the fraction of the non-protonated catalyst was calculated to be 2.2% at pH 8.0 from its pK_a value, k_3 for the neutral species was 1.8 min^{-1}.

In order to see the catalytic role of the amino group, hydrolysis was carried out at a higher catalyst concentration: $[C]_{total}=0.010$M, [S]=0.044M, μ= 1.0M KCl, 30°C, pH 8.0. The reaction was stopped

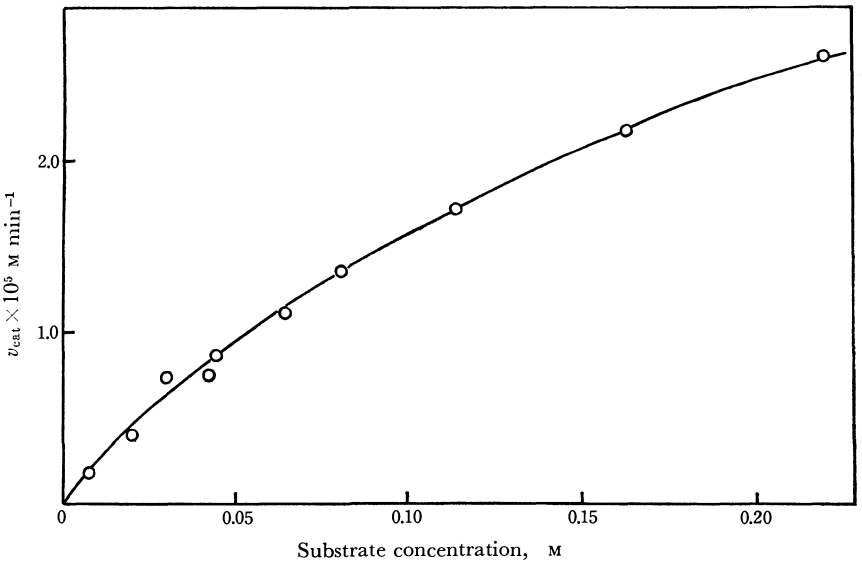

Fig. 9. Catalytic hydrolysis by 1-aminomethylnaphthalene. 30°C; pH 8.0; μ=1.0M KCl; catalyst, 1.39×10^{-3}M.
The solid line was obtained from the kinetic constants given in Table 2.

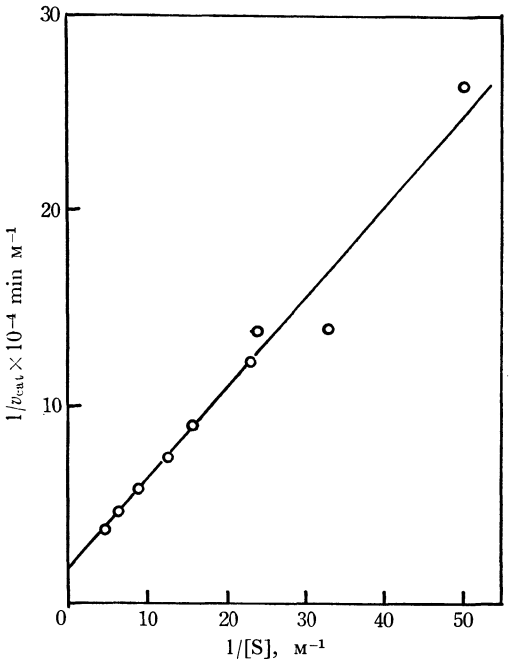

Fig. 10. Lineweaver-Burk plots of the data of Fig. 9.
The solid line was obtained by the least squares method.

when the amount of phenyl ester hydrolyzed reached 4.5×10^{-3}M (0.005M alkali consumption). The catalyst was recovered by ether extraction, drying and evaporation of ether. An IR spectrum of the recovered material (brown oil) did not show amide absorption.

Catalytic Hydrolysis by Imidazole. When imidazole was used as a catalyst, the catalytic rate of hydrolysis was first order with respect to the substrate concentration, as shown in Fig. 11. The fraction of the neutral imidazole was 88.1% at pH 8.0. The second-order rate constant obtained from the slope was 0.325M^{-1} min^{-1}.

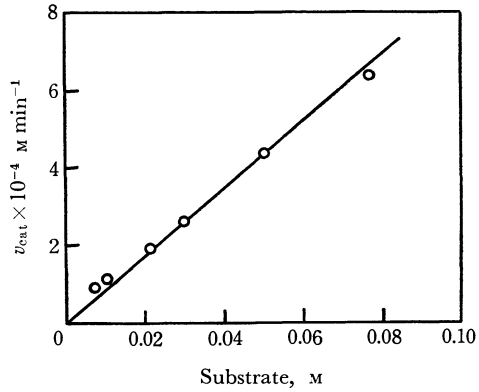

Fig. 11. Catalytic hydrolysis by imidazole.
30°C; pH 8.0; μ=1.0M KCl; imidazole, 0.0278M.
The solid line was obtained by the least squares method.

Discussion

Validity of the Enzyme-like Catalytic Mechanism. Catalytic hydrolysis with the naphthylimidazole derivative, III, showed substrate saturation phenomena, one of the important characteristics of enzyme-catalyzed reactions, as shown in Fig. 4.

The substrate saturation phenomenon, however, cannot exclude the possible coexistence of the common bimolecular catalysis by the uncomplexed imidazole catalyst (Eq. (12)) with the enzyme-like process (Eq. (1)).

$$\text{catalyst} + \text{substrate} \xrightarrow{k'} \text{catalyst} + \text{product} \qquad (12)$$

When these two catalytic processes coexist,[1b] the overall catalytic rate is given by

$$v_{cat} = k_3[CS] + k'[C]_{uncomplexed} \cdot [S] \qquad (13)$$

$$= (k_3 + k'K_m) \cdot \frac{[C]_{total} \cdot [S]}{K_m + [S]} \qquad (14)$$

This means that substrate saturation phenomena will be observed even in the presence of the second-order process (Eq. (12)), as long as the complexation occurs, and the relative importance of the two processes is determined from a comparison of k_3/K_m and k'. The catalytic hydrolysis of the substrate by imidazole was first-order with respect to substrate, the second-order rate constant being 0.325 $M^{-1}min^{-1}$. Since the nucleophilic reactivity of imidazole derivatives towards *p*-nitrophenyl acetate increased exponentially with the increases in pK_a,[21] the hypothetical second-order reactivity (k') of the imidazole group in III ($pK_a = 5.92$) would be much smaller than that of imidazole ($pK_a = 7.13$, $k' = 0.325$ $M^{-1}min^{-1}$). Therefore, the overall second-order reactivity of III expressed by the k_3/K_m term (0.32 at pH 7 and 18 at pH 8) may be assumed to be much greater than the hypothetical second-order reactivity of the imidazole group in III. Thus, the enzyme-like process (Eq. (1)) is concluded to be the major pathway of the catalytic hydrolysis under the present experimental conditions.

Substrate Binding. In the hydrolysis of a phenyl ester catalyzed by imidazole-containing copolymers,[1] the binding function of the catalyst was ascribed to hydrophobic forces. The results in the present system point to the same conclusion.

There are several investigations which showed rate enhancement[22-24] and substrate saturation[25,26] due to the electrostatic interaction of catalysts and substrates. Recently, Bruice *et al.*[27] considered the possible cooperative action of electrostatic and hydrophobic forces between catalysts and substrates of the detergent-like structure. Similarly, at the biginning of the present study, we assumed that an analogous cooperative action for III, as shown by IX, would be observed. However, the Michaelis constant K_m for species AmIm was smaller than that of Am$^+$Im (11 mM *vs.* 41 mM), indicating that

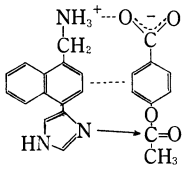

IX

protonation of the aminomethyl group resulted not in an electrostatic attraction toward the anionic substrate but in a decrease of the binding capacity of the catalyst. Thus, the hydrophobic interaction must be responsible for formation of the Michaelis complex for both of the catalytic species (AmIm and Am$^+$Im) at least under the hydrolysis conditions used. This conclusion was further supported by the fact that v_{cat} decreased when the ionic strength of the reaction system decreased (Table 3). If the electrostatic interaction were responsible for the substrate binding, a decrease in the ionic strength would have caused rate enhancement.

Pseudo-Intramolecular Process. The chemical nature of the product-forming step in the present catalytic system remains to be elucidated.

Since III was recovered after hydrolysis at pH 8.0 without undergoing acetylation of its amino group, it is clear that the naphthylimidazole derivative acted as a true catalyst. The imidazole group in III may act as either a nucleophilic or general-base catalyst,[9b] and these two processes are indistinguishable from the kinetic data alone. The amino group, protonated and unprotonated, can also reinforce the catalytic action of the imidazole group as a general-acid and general-base catalyst, respectively. Involvement of the protonated amino group in catalysis, however, appears less likely, considering the much smaller k_3 for Am$^+$Im as compared with that for AmIm (0.0036 min^{-1} *vs.* 0.19 min^{-1}).

This large difference in k_3 is interesting, and is conceivably related to the structural variation of the Michaelis complex. The greater pseudo-intramolecular catalytic efficiency of AmIm may be explicable on the basis of either or both of the following hypotheses: a) The spacial arrangement of the imidazole and ester groups in the Michaelis

21) T. C. Bruice and G. L. Schmir, *J. Amer. Chem. Soc.* **80**, 148 (1958).

22) R. L. Letsinger and T. J. Savereide, *ibid.*, **84**, 114, 3122 (1962).

23) C. G. Overberger, T. St. Pierre, N. Vorchheimer, J. Lee and S. Yaroslavsky, *ibid.*, **87**, 296 (1965).

24) C. G. Overberger, R. Sitaramaiah, T. St. Pierre and S. Yaroslavsky, *ibid.*, **87**, 3270 (1965).

25) R. L. Letsinger and I. S. Klaus, *ibid.*, **87**, 3380 (1965).

26) C. G. Overberger, T. St. Pierre, N. Vorchheimer, J. Lee and S. Yaroslavsky, *Macromolecules*, **1**, 331 (1968).

27) T. C. Bruice, J. Katzhendler and L. R. Fedor, *J. Phys. Chem.*, **71**, 1961 (1967); *J. Amer. Chem. Soc.*, **90**, 1333 (1968).

complex is less favorable for catalysis when the amino group is protonated than when it is not; b) the imidazole and amino groups in AmIm catalyze the ester cleavage cooperatively, while the protonated amino group in Am^+Im cannot be involved in catalysis.

In the above discussion, the catalyst molecules were assumed to be molecularly dispersed. Considering the poor solubility of III it is possible that the catalyst molecules, AmIm in particular, were extensively associated. If the associated catalytic species show different catalytic activities from those of the molecularly dispersed species, the simple allotment of the overall catalytic activity to the two species AmIm and Am^+Im becomes questionable. In fact, as shown in Fig. 7, there was considerable discrepancy between the pH dependence of the observed and calculated catalytic rates. Since AmIm would associate more readily than Am^+Im in the case where the catalyst molecules are not molecularly dispersed, the pH dependence of v_{cat} would be correspondingly complex. Then association of the catalyst molecules could be the cause for the discrepancy. However, the fact that v_{cat} did not vary with the catalyst concentration at pH 7 and 8 (Fig. 7) speaks against this hypothesis, since association of the catalyst molecules, if any, must be concentration dependent, leading to the dependence of $v_{cat}/[C]$ on the catalyst concentration. Another possible cause for the discrepancy might be either or both of underestimation of the catalytic activity of AmIm and of overestimation of the catalytic activity of Am^+Im. At present, experimental data are not sufficient to warrant further discussion on these problems. However, the remarkable variation of the catalytic efficiency with pH (hence the nature of the catalytic species) suggests that catalytic efficiency is much more widely variable when the enzyme-like kinetics are observed than when the common second order kinetics are observed.

Catalysis of 1-Aminomethylnaphthalene. K_m for 1-aminomethylnaphthalene, VIII, was quite large (280 mM), showing the small binding capacity of this catalyst as compared with those of the imidazole derivatives. Since the substrate saturation phenomenon was not very clear in this system, it is not certain if the catalytic action consisted only of the enzyme-like process (Eq. (1)), in spite of the linear Lineweaver-Burk plots obtained. Assuming that the enzyme-like pathway is predominant, the large difference in K_m between III and VIII suggests that the imidazole group made an important contribution to the binding function. It is interesting that the primary amino group in VIII acted as a catalyst without undergoing acetylation. This was also the same with AmIm. The lack of acetylation indicates that VIII was a general-base catalyst, in marked contrast with the commonly observed nucleophilic reaction of the primary amino group with phenyl acetates. This result may be an indication of the particular geometry of the Michaelis complex, in which the nucleophilic attack of the amino group toward the ester group is not favored. The large k_3 value (1.8 min^{-1}) is probably related to the high basicity of the amino group ($pK_a = 9.95$) as well as to the particular geometry of the complex. Although high K_m and k_3 values observed for VIII catalysis is in sharp contrast to those for the imidazole catalysts, it is not warranted to discuss the difference more fully, since substrate saturation with VIII was not sufficient and its catalytic behavior can be more complex than it appears.

BULLETIN OF THE CHEMICAL SOCIETY OF JAPAN VOL. 43 1120—1126 (1970)

On the Photochemical Hydrogen Shifts in Arylcycloheptatrienes*1

Takahiro TEZUKA, Masaru KIMURA, Aiya SATO and Toshio MUKAI

Department of Chemistry, Faculty of Science, Tohoku University, Katahira-cho, Sendai

(Received June 6, 1969)

Photochemically-induced hydrogen shifts in 7-(*p*-chlorophenyl), 7-phenyl, 7-(*p*-methoxyphenyl) and 7-*p*-tolylcycloheptatrienes (Ia—d) were studied. The possibility of hydrogen 1,7 and 1,3 shifts in these compounds was examined on both experimental and theoretical grounds. It was concluded that the hydrogen 1,7 shift is the only suprafacial hydrogen shift possible in the excited cycloheptatriene system. In this study all the isomers of *p*-chlorophenylcycloheptatriene were separated by applying the Diels-Alder reaction to the photo-reaction mixture; the method of preparing each of those isomers will also be described.

The specific hydrogen shifts in substituted cycloheptatrienes have been one of the most interesting topics in photochemistry.[1-5] In 1965 Woodward and Hoffmann[6] successfully interpreted the specific mode of the hydrogen shift in the conjugated allyl system on the basis of molecular orbital symmetry considerations; they implied that the suprafacial hydrogen 1,3 and 1,7 shifts are permitted photochemically in the cycloheptatriene. ter Borg and Kloosterziel,[3] in 1965, reported the unexpected formation of 2-phenylcycloheptatriene (IIIb) from 7-phenylcycloheptatriene (Ib) upon irradiation with a high-pressure mercury lamp. They explained this transformation as a consequence of successive hydrogen 1,7 shifts *via* 1-phenylcycloheptatriene (IIb). However, Murray and Kaplan[5] have recently suggested this to be a possible case of a symmetry-allowed suprafacial hydrogen 1,3 shift.

We now wish to report on our studies of photohydrogen shifts in 7-arylcycloheptatrienes (Ia—Id); these studies have led us to the conclusion that the 1,3 shift is not a favorable mode of the hydrogen shift, while the hydrogen 1,7 shift is the only probable mode in the 7-substituted cycloheptatrienes when a Xenon or mercury lamp is used as the light source.

Results

Upon the irradiation of an ethereal solution of 7-(*p*-substituted-phenyl)cycloheptatriene (Ia—Id) in a quartz vessel with 150 W Xenon lamp, Ia and Ib afforded the isomers IIIa and IIIb, while Ic and Id yielded IIc and IId respectively. The formation of IIc from Ic, and that of IId from Id, can be interpreted in terms of the photo-hydrogen 1,7 shift. Such a type of photoisomerization reaction has been found to occur commonly in 7-methoxy, 7-ethoxy,[4] and 7-deuterio-cycloheptatrienes.[2] However, interpretation of the formation of IIIa from Ia, and that of IIIb from Ib, seems to be more complicated.

Two possible mechanisms can be assumed for the formation of IIIa from Ia and/or IIIb from Ib: (1) the hydrogen migrates from C_7 to C_2 in one step by the suprafacial hydrogen 1,3 shift; or (2) the hydrogen migrates from C_7 to C_1, and then from C_1 to C_2 by pepeating the suprafacial hydrogen 1,7 shift. ter Borg and Kloosterziel[3] have proposed the second mechanism, while Murray and Kaplan[5] suggested the first mechanism for the formation of IIIb from Ib.

In order to elucidate this point we investigated the photochemical isomerization of 7-(*p*-chlorophenyl)cycloheptatriene (Ia) and of 7-phenylcycloheptatriene (Ib) in detail. As 7-(*p*-chlorophenyl)-cycloheptatriene was easier to work with, we studied the photoisomerization reaction of this compound first.

The isomer IIIa formed from Ia on the photolysis was separated as a pure form by applying the Diels-Alder reaction. When a benzene solution of the reaction mixture of the photolysis of Ia was heated with maleic anhydride, only Ia afforded the Diels-Alder adduct (V). An unreacted oil was purified by vacuum distillation to give IIIa. The structure

*1 Organic Photochemistry. XIII. This is also Photochemical Hydrogen Shift in the Cycloheptatriene System. Part I.

1) W. von E. Doering and P. P. Gasper, *J. Amer. Chem. Soc.*, **85**, 3042 (1963).
2) W. R. Roth, *Angew. Chem.*, **25**, 921 (1963).
3) A. P. ter Borg and H. Kloosterziel, *Rec. Trav. Chim., Pays-Bas*, **84**, 241 (1965).
4) G. W. Borden, O. L. Chapman, R. Swindell and T. Tezuka, *J. Amer. Chem. Soc.*, **89**, 2979 (1967).
5) R. W. Murray and M. Kaplan, *ibid.*, **88**, 3527 (1966).
6) R. B. Woodward and R. Hoffmann, *ibid.*, **87**, 2511 (1965).

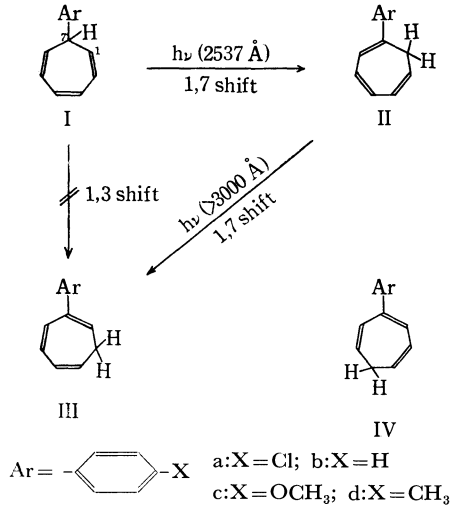

of IIIa was established on the basis of the following physical properties: mass spectrum, *m/e* 202 (M); ultraviolet spectrum, λ_{max}^{MeOH} (log ε), 247 (3.61) with tailing up to 310 mμ; infrared spectrum (oil), 3030, 2841, 1495, 1006, 820, 747, 707 cm^{-1}; NMR spectrum (in $CDCl_3$), 7.65 ($2\times H_7$; triplet, $J_{1,7}=7.0$ Hz), 4.40 (H_1; triplet), 4.47 (H_6; broad quartet), 3.75 (H_5; multiplet), 3.20 (H_3 and H_4; multiplet), 2.7 τ (aromatic protons) (Fig. 2). The isomer IIIa could be differentiated from the other isomers, IIa and IVa, by a comparison of their physical properties. IIa; ultraviolet spectrum, λ_{max}^{MeOH} (log ε), 303 (3.88), 242 (4.24) mμ; infrared spectrum (oil), 3040, 2849, 1490, 1009, 826, 736, 719 cm^{-1}; NMR spectrum (in $CDCl_3$), 7.35 ($2\times H_7$; doublet, $J_{6,7}=$ 7.1 Hz), 4.60 (H_6) around 3.60 τ (H_2, H_3, H_4 and H_5; complex multiplet) (Fig. 3). IVa; ultraviolet spectrum, λ_{max}^{MeOH} (log ε), 285 (3.96), 241 (4.17) mμ; infrared spectrum (oil), 3030, 2833, 1493, 1092, 1014, 824, 744 cm^{-1}; NMR spectrum (in benzene), 7.85 ($2\times H_7$; triplet, $J_{1,7}=7.0$ Hz), 4.75 (H_1; doublet of triplet, $J_{1,2}=9.1$ Hz), 4.65 (H_6; doublet of triplet, $J_{5,6}=9.1$ Hz), 3.75 (H_2; doublet, $J_{1,2}=9.1$ Hz), 3.85 (H_5; quartet), 3.29 τ (H_1; doublet, $J_{4,5}=4.6$ Hz) (Fig. 4).*2

The isomer IVa was obtained by heating Ia at 150°C, as has been described in literatures,[7] while IIa was obtained by the irradiation of Ia for a short period of time with a 6 W low pressure mercury lamp (*vide infra*), followed by the application of the Diels-Alder reaction as described in the case of the isolation of IIIa.

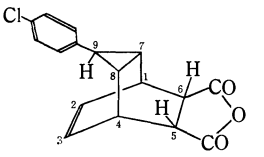

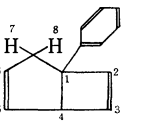

If the first mechanism (1) is correct, there are no intermediate products to be trapped. On the other hand, if the second mechanism (2) is correct, the isomer IIa must be trapped as an intermediate when appropriate photolysis conditions are used. In addition, the isomer IIIa must be formed from IIa at a rate faster than that of the formation of IIa from Ia, or of IIIa from Ia. With these facts in mind the photolysis of Ia and IIa was monitored under several sets of conditions.

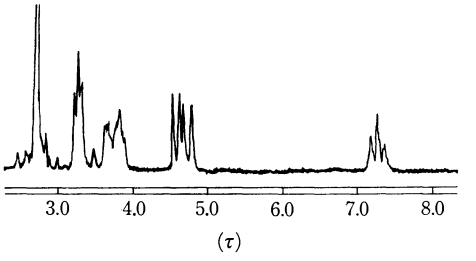

Fig. 1. NMR spectrum of 7-(*p*-chlorophenyl)cycloheptatriene (Ia) in $CDCl_3$.

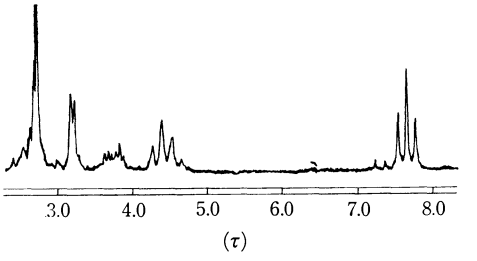

Fig. 2. NMR spectrum of 2-(*p*-chlorophenyl)cycloheptatriene (IIIa) in $CDCl_3$.

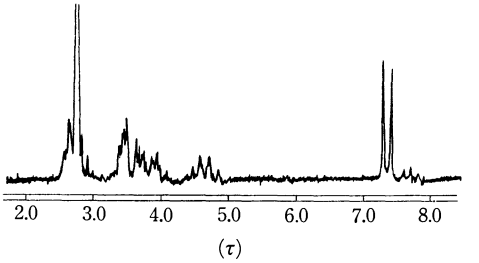

Fig. 3. NMR sepctrum of 1-(*p*-chlorophenyl)cycloheptatriene (IIa) in $CDCl_3$.

*2 A triplet due to the H_7 and $H_{7'}$ appeared at 7.69 τ in $CDCl_3$.

7) a) G. Buchi and E. M. Burgess, *J. Amer. Chem. Soc.*, **84**, 3104 (1962); b) A. P. ter Borg, H. Kloosterziel and N. van Meurs, *Proc. Chem. Soc.*, **1962**, 359; c) A. P. ter Borg, H. Kloosterziel and N. van Meurs, *Rec. Trav. Chem., Pays-Bas*, **82**, 717, 741, 1189 (1963); d) E. Weth and A. S. Dreiding, *Proc. Chem. Soc.*, **1964**, 59; e) A. P. ter Borg and H. Kloosterziel, *Rec. Trav. Chim., Pays-Bas*, **84**, 245 (1965); f) T. Nozoe and K. Takahashi, This Bulletin, **38**, 665 (1965).

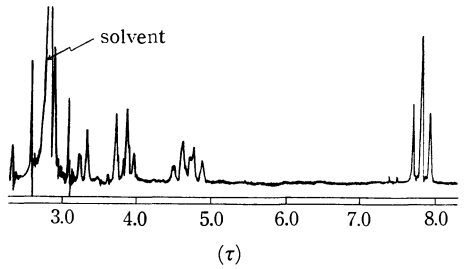

Fig. 4. NMR spectrum of 3-(*p*-chlorophenyl)cycloheptatriene (IVa) in benzene.

In order to trap the intermediate IIa, the Xenon lamp was replaced by a 6 W low-presure mercury lamp with very weak emission bands around 3000 Å, where the intermediate (IIa) has an absorption maximum. Under this condition the formation of IIIa was suppressed, and the only product identified by NMR spectroscopy during the first period of irradiation was the isomer IIa. For further confirmation of the isomer, the product (IIa) was separated from the reaction mixture by applying the Diels-Alder reaction and its structure was established by means of spectral data (*vide supra*). On prolonged irradiation, however, the gradual formation of IIIa was observed at consumption of IIa. The relative ratio of the formations of Ia, IIa, and IIIa under this irradiation condition, which was estimated from the methine or methylene signal in the NMR spectra, was plotted *vs.* the irradiation time (Fig. 5). The plot indicates that the isomer IIIa was apparently produced after the formation of IIa; *i. e.*, IIa must be the precursor of the isomer IIIa. This was supported by the fact that when Ia was irradiated with filtered 2537 Å light, IIa was produced selectively and the formation of IIIa was suppressed. In addition, the irradiation of IIa with a Xenon lamp gave the isomer IIIa at a rate approximately

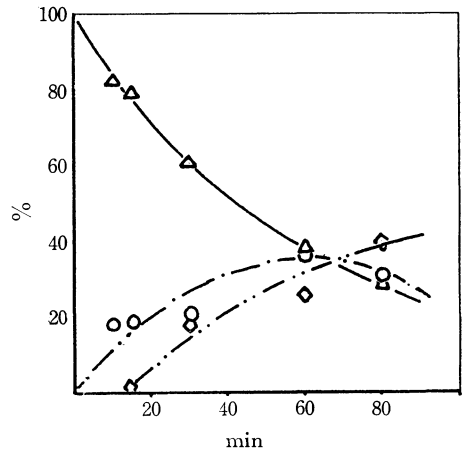

Fig. 5. Relative yields of Ia (△), IIa (○) and IIIa (◇) *vs.* time.

ten times as fast as that of the formation of IIIa from Ia.

These evidences support the second mechanism (2), and the formation of IIIa from Ia can be interpreted in terms of successive hydrogen 1,7 shift. By absorbing light around 2500 Å, Ia isomerizes to IIa, and this is, in turn, rapidly converted into IIIa upon the further absorption of light above 3000 Å by the hydrogen 1,7 shift. Therefore, the fact that the isomer IIa was not identified by NMR spectroscopy in the case of the irradiation of Ia with a Xenon lamp can be explained as a consequence of the rapid transformation of IIa to IIIa.

A similar trend of photoisomerization was observed in the case of 7-phenylcycloheptatriene (Ib). The only isomer identified by NMR spectoscopy was IIIb when Ib was irradiated with a Xenon lamp. On the other hand, the irradiation of Ib with a 6 W low-pressure mercury lamp afforded IIb after a short period of irradiation. On prolonged irradiation, however, the isomer IIIb and the bicyclic compound,[3] for which the structure (VI) is tentatively assigned from the NMR analysis were formed.

Plots of the relative ratio of Ib, IIb, and IIIb *vs.* the irradiation time indicated that the isomer IIIb was formed from IIb, which was itself produced from Ib by the hydrogen 1,7 shift. The bicyclic compound (VI) may arise from the isomer IIa.[4] This may be supported by the fact that the VI was formed after the formation of IIa, which was identified by means of gas chromatographic analysis.

The irradiation of IIb with a Xenon lamp gave IIIb very rapidly. The formation of IIIb from Ib *via* IIb is sensitive to the light source used. Thus, when filtered 2537 Å light was used the formation of IIIb from IIb was suppressed; even after the irradiation of Ib for more than ten hours, the isomer IIIb was not detected; the only isomer detected by NMR spectrum was IIb.

Therefore, it may be concluded that the 1,7 shift is the only mode of hydrogen shift occurring on the photolysis of Ia—Id. This is in accord with the conclusion reached by ter Borg and Kloosterziel[3] regarding the photolysis of Ib, but it is inconsistent with Murry and Kaplan's suggestion[5] that IIIb may be formed from Ib by the hydrogen 1,3 shift.

It may be noted that in both cases, the isomers III and IV were relatively stable to Xenon light and did not afford the other isomers during several hours irradiation.[3,14] This may be due to the electronic effect of the aryl group on the excited triene system, but the details of this effect are not clear at present.

Discussion

Woodward and Hoffmann's selection rule has predicted that the symmetry-allowed suprafacial hydrogen 1,3 and 1,7 shifts would occur photochemi-

cally while the 1,5 shift would occur thermally, in the cycloheptatriene.[6] The process of the thermal 1,5 hydrogen shift has been established in many cycloheptatriene derivatives.[5,7,8] However, there are some problems as to the photochemical hydrogen shifts in the cycloheptatriene series. One of the problems is that only the hydrogen 1,7 shift has been identified experimentally, though the possibility of the occurrence of the hydrogen 1,3 shift has been suggested theoretically[6,12] for the photochemical isomerization of the cycloheptatrienes.

Perhaps the photochemically induced suprafacial hydrogen 1,3 shift has not occurred in the cycloheptatriene for either of following two reasons: (1) geometrical, (2) the molecular orbital symmetry relationship. Geometrically, however, the suprafacial hydrogen 1,3 shift is possible, since the distance between C_7 and C_2, through which the hydrogen 1,3 shift could occur, is approximately 2.8 Å.[9] This distance is comparable with that between C_7 and C_3, through which the hydrogen 1,5 shift occurs. In fact, a base-catalyzed hydrogen 1,3 migration has been observed in 7-cyanocycloheptatriene.[10] Therefore, it is necessary to reexamine whether or not the photo-hydrogen 1,3 shift is really a symmetry-allowed mode in the excited cycloheptatriene.

Woodward and Hoffmann's selection rule[6] for the sigmatropic rearrangement of the order $[1,j]$ is based on the molecular orbital symmetry relation of the terminal carbon atoms C_1 and C_j, in the conjugated allyl radical system containing j π-electrons. It has been stated[6] that a reverse symmetry relation exists between the highest occupied and the first excited molecular orbital at C_j. This relation always holds when C_j is located in the terminal position in the j π-electron system, but it does not hold when C_j is in a half-way position of the π-electron system containing more than j electrons. This may be seen, for example, in the heptatrienyl radical system, which is a model system taken by Woodward and Hoffmann for explaining the specific hydrogen shifts in the cycloheptatriene. The reverse relation between the highest occupied (VII) and the first excited molecular orbitals (VIII) of the heptatrienyl radical exists at the terminal position, C_7, while this relation does not exist at the C_3 position. This implies that the suprafacial hydrogen 1,3 shift is not a symmetry-allowed mode, while the 1,7 shift is the only symmetry-allowed mode of the suprafacial hydrogen shift when the excited heptatrienyl radical system (VIII) is produced by excitation in the cycloheptatriene. Jones also pointed out this point in the photochemical methyl migration of 7,7′,3-trimethylcycloheptatriene.[11]

The suprafacial hydrogen 1,3 shift, however, may schematically become a symmetry-allowed mode if an excited propenyl radical (IX) or an excited pentadienyl radical (X) is produced in the cycloheptatriene molecule. Here, such an excited radical exists as an independent part in the molecule. Practically, however, the introduction of such a limited excited radical system in the cycloheptatriene molecule may be difficult, since the excitation of the

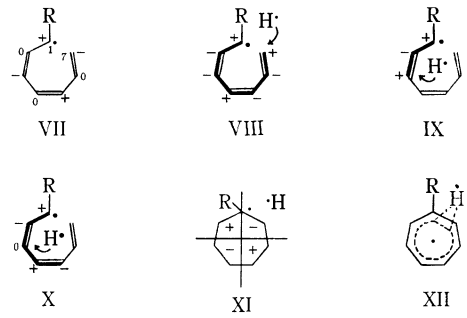

VII VIII IX

X XI XII

triene chromophore occurs preferentially in the cycloheptatriene molecule when 2537 Å light is absorbed and, as a concequence the excited heptatrienyl radical system (VIII) is produced in the molecule.

In general, the selection rule for the photochemical hydrogen shift must be used in terms of the excited radical system, but not in terms of the length of the conjugation in the ground state molecule. Such hydrogen shifts in terms of several excited radical systems can be deduced on the basis of the symmetry relation of the Hückel molecular orbital of the acyclic model.[6] Several such are presented in Table 1. Here, the length of the conjugation of double bonds in a ground state molecule is not a decisive factor, but the nature of a specific excited radical system introduced in this

Table 1

Excited radical system	Type of permissive suprafacial hydrogen shift
Propenyl	1,3
Pentadienyl	1,3
Heptatrienyl	1,7
Nonatetraenyl	1,5 1,7

8) The occurrence of the thermal hydrogen 1,5 shift in Ia, Ic, and Id at 120—150°C, giving IVa, IVc, and IVd respectively, was confirmed by the present work.

9) This is the distance of the ground-state molecule as estimated by the Dreiding model. In the excited state the distance may be somewhat different from what it is in the ground state. However, in a rigid system such as cycloheptatriene the geometrical difference between the two states may be small.

10) a) K. Yamamoto, Master's Thesis, Tohoku University, 1966. b) K. Takahashi, H. Yamamoto and T. Nozoe, This Bulletin, **43**, 200 (1970).

11) L. B. Jones and V. K. Jones, *J. Amer. Chem. Soc.*, **89**, 1880 (1967).

molecule by excitation is important in determining the mode of the photochemical hydrogen shift. Whether or not such a specific excited radical system can be produced in the conjugated allyl depends on the irradiation conditions (the wave length of light used) and the geometrical conditions (the inhibition of the full conjugation of the double bonds in the molecule).

Recently, Anastassiou[12] has proposed a cyclic model (XI) for predicting the specific mode of the hydrogen shifts in the cycloheptatriene. According to Anastassiou's selection rule, all of the hydrogen 1,3 and 1,5 and 1,7 shifts can occur photochemically in the cycloheptatriene. However, this selection rule is not consistent with the observation that the photochemical hydrogen 1,3 and 1,5 shifts have not been found in the cycloheptatriene series.

It is instructive to reconsider the model system of the transition state of the hydrogen shift in the cyclic conjugated allyl system. Anastassiou has mentioned that the acyclic model employed in the derivation of Woodward and Hoffmann's selection rule is incapable of allowing for the necessary cyclic π-interaction introduced by the developing p-orbital at the migration origin of the cyclic system. In this we agree with Anastassiou's comments. However, it seems that Anastassiou's cyclic model does not consider the interaction between a migrating hydrogen and a remnant conjugated system. On the basis of a theoretical consideration including the above discussion, we would like to propose, for the hydrogen shift in the cyclic allyl system, new model system in which the interaction of the migrating hydrogen and the cyclic π-interaction is taken into consideration. For example, according to this treatment the transition state of the hydrogen 1,7 shift in the cycloheptatrienes is represented as XII, where a three-member part including a hydrogen atom, interacts with a dienyl radical system. With this model several modes of the hydrogen shift in the cyclic allyl system can be interpreted. A detailed interpretation and application will not be made in this report, but will appear elsewhere.

It is interesting to consider the substituent effect upon the relative rate of the formation of the bicyclic compound from 1-substituted cycloheptatriene. It has been reported that 1-methoxy- and 1-ethoxycycloheptatrienes isomerize very rapidly to 1-methoxy- and 1-ethoxy-bicyclo[3.2.0]hepta-3,6-dienes upon irradiation by light above 3000 Å.[4] In these cases, the formation of 2-methoxy- and 2-ethoxycycloheptatriene by the hydrogen 1,7 shift has not been observed.[4] On the contrary, the photolysis of 1-phenyl-, 1-(p-chlorophenyl)-, and 1-deuterio-cycloheptatrienes[3] afforded preferentially 2-phenyl-, 2-(p-chlorophenyl)-, and 2-deuterio-cycloheptatrienes respectively, instead of the bicyclic compounds. It may be noted that the substituent at the C_1 position of the cycloheptatrienes potentially affects the rate of the bond formation between C_1 and C_4 as well as the rate of the hydrogen shift. These substituent effects may be electronic in nature; electron-donating substituents facilitate the bond formation at C_1 and C_4, while electron-attracting substituents tend to retard it. However, a detailed interpretation of the mechanism of the substituent effect on the excited state must await further study.[14]

Experimental

Preparation of 7-(p-Chlorophenyl)cycloheptatriene (Ia). To a solution of p-chlorophenylmagnesium bromide which had been prepared from p-bromochlorobenzene (16.89 g) and magnesium (2.14 g) in absolute ether (50 m*l*), there was added a solution of 7-ethoxycycloheptatriene (10.0 g) in absolute ether (50 m*l*) at 0°C; the mixture was then stirred continuously for several hours. The reaction mixture was then treated with 2N hydrochloric acid and extracted with ether. The resultant oil was distilled to give a colorless oil, bp, 107°C/0.2 mmHg (9 g), which crystallized on standing at 0°C; after recrystallization from petroleum ether it gave colorless needles, mp 41—42°C. Ultraviolet spectrum, $\lambda_{max}^{cyclohexane}$ (log ε), 265 mμ (3.52); infrared spectrum (KBr), 3012, 2857, 1492, 1026, 826, 754, 709 cm^{-1}; mass spectrum (*m/e*), 202 (M); the NMR spectrum is shown in Fig. 1.

Found: C, 77.18; H, 5.48%. Calcd for $C_{13}H_{11}Cl$: C, 77.10; H, 5.48%.

The Formation of 1-(p-Chlorophenyl)cycloheptatriene (IIa) from Ia by Irradiation with a Low-pressure Mercury Lamp. a) A solution of 7-(p-chlorophenyl)cycloheptatriene (Ia) (1.5 g) in absolute ether (180 m*l*) was irradiated with an internal 6 W low-pressure mercury lamp for 15 min under a nitrogen stream; 15% of Ia was thus converted to IIa, which was estimated by means of the doublet signal due to methylene protons of IIa at 7.35 τ in NMR spectroscopy. The oily reaction mixture was heated with maleic anhydride (500 mg) in absolute benzene (10 m*l*) for 1 hr. The evaporation of the solvent afforded an Diels-Alder adduct of Ia as white crystals; mp, 186.5°C (V) (300 mg). Infrared spectrum (KBr), 3039, 2985, 1869, 1824, 1785, 1226, 1089, 918, 792, 755 cm^{-1}; NMR spectrum (in $CDCl_3$), 2.95 (aromatic protons; quartet), 3.96 (H_2 and H_3; sextet), 6.38 (H_1 and H_4; multiplet), 6.76 (H_5 and H_6; triplet, $J_{1,5}=J_{4,5}=2.5$ Hz), 8.36 (H_9; triplet, $J_{8,9}=J_{7,9}=3.2$ Hz), 8.60 τ (H_7 and H_8; $J_{1,7}=J_{4,8}=5.0$ Hz).

12) A. G. Anastassiou, *Chem. Commun.*, **1968**, 15.

13) a) Concerning the substituent effects, Professor ter Borg has found that the substituents which facilitate the valence-isomerization reaction end to retard the hydrogen-migration reaction in 1-substituted cycloheptatrienes. The authors wish here to thank Professor ter Borg for his communication on this point prior to publication. b) A. P. ter Borg, E. Razenberg and H. Kloosterziel, *Chem. Commun.*, **23**, 1210 (1967).

14) For example, the photochemical 1,7 migration of the phenyl group in competition with the hydrogen 1,7 shift in 7-phenylcycloheptatriene has recently been reported. *Cf.* K-W Shen, W. E McEwen and A. P. Wolf, *Tetrahedron Lett.*, **1969**, 827.

Found: C, 68.11; H, 4.42%. Calcd for $C_{17}H_{13}O_3Cl$: C, 67.89; H, 4.36%.

The filtrate was purified by alumina chromatograpy, followed by vacuum distillation, to give a colorless oil (IIa); bp, 120—125°C/0.5 mmHg (80 mg).

Found: C, 77.24; H, 5.43%. Calcd for $C_{13}H_{11}Cl$; C, 77.10; H, 5.48%.

b) The photolysis of Ia under the same conditions was monitored, and the amounts of isomers formed was estimated by NMR spectroscopy. The relative ratio of the isomers *vs.* the time was estimated by the integration of the triplet at 7.31 (for Ia), the doublet at 7.33 (for IIa), and the triplet at 7.69 τ (for IIIa), in the NMR spectrum. The results are shown in Fig. 5.

The Formation of 2-(*p*-Chlorophenyl)cycloheptatriene (IIIa) from Ia by Irradiation with a Xenon Lamp. a) A solution of 7-(*p*-chlorophenyl)cycloheptatriene (Ia) (954 mg) in absolute ether (180 m*l*) in a quartz vessel was irradiated with a Xenon lamp (Toshiba XD-150) for 16 hr under a nitrogen stream. The reaction was followed by the appearance of the triplet signal due to IIIa at 7.69 τ in the NMR spectroscopy. The reaction mixture was treated with maleic anhydride (300 mg) as has been described in the case of IIa. The filtrate was purified by alumina chromatography, and subsequent vacuum distillation afforded a colorless oil, bp, 130—135°C/0.2 mmHg (246 mg), which on standing at −60°C afforded colorless needles; mp, 41—42°C (IIIa).

Found: C, 77.44; H, 5.45%. Calcd for $C_{13}H_{11}Cl$; C, 77.10; H, 5.48%.

b) A solution of Ia (20 mg) in absolute ether (5 m*l*), saturated with nitrogen, was irradiated in a sealed quartz vessel with a Xenon lamp for a few hours. The reaction mixture was analyzed by means of NMR spectroscopy, which indicated that the only isomer produced during the irradiation was IIIa. Within 90 min the Ia was converted to IIIa in 50% yield.

Irradiation of 1-(*p*-Chlorophenyl)cycloheptatriene (IIa) with a Xenon Lamp. A solution of 1-(*p*-chlorophenyl)cycloheptatriene (IIa) (20 mg) in absolute ether (5 m*l*) saturated with nitrogen was irradiated in a sealed quartz vessel with a Xenon lamp. The reaction was followed by NMR spectroscopy. The amounts of the isomers IIIa and IIa was estimated from the integrated signals at 7.69 (triplet for IIIa) and 7.35 τ (doublet for IIa) in the NMR spectrum. Within 90 min the IIa was converted into IIIa in 43% yield.

Irradiation of Ia with a 2537 Å Light. A solution of Ia (20 mg) in absolute ether (5 m*l*) saturated with nitrogen was irradiated in a sealed quartz vessel with a 2537 Å light. The reaction was followed by NMR spectroscopy. Within 6 hr the Ia was converted into IIa in 17% yield. No formation of IIIa was detected even after 14 hr of irradiation.

Irradiation of IIa with a High-pressure Mercury Lamp through a Pyrex Filter. A solution of IIa (20 mg) in absolute ether (5 m*l*) saturated with nitrogen was irradiated in a sealed quartz vessel with high pressure mercury lamp through Pyrex filter. The reaction was followed by NMR spectroscopy. Within 25 min the IIa was canverted to IIIa in a 70% yield.

Preparation of 3-(*p*-Chlorophenyl)cycloheptatriene (IVa). 7-(*p*-Chlorophenyl)cycloheptatriene (Ia) (757 mg) was heated at 150—155°C for 90 min. The crude oil was distilled to give a colorless oil, bp 120—125°C/0.5 mmHg (650 mg), which was identified by NMR spectroscopy as a mixture composed of 98% of IVa and 2% of IIa.

Found: C, 77.49; H, 6.05%. Calcd for $C_{13}H_{11}Cl$: C, 77.10; H, 5.48%.

Irradiation of 3-(*p*-Chlorophenyl)cycloheptatriene (IVa) with a Xenon Lamp. A solution of 3-(*p*-chlorophenyl)cycloheptatriene (IVa) (20 mg) in absolute ether (5 m*l*) saturated with nitrogen, was irradiated in a sealed quartz vessel with a Xenon lamp for several hours. The reaction was followed by NMR spectroscopy. No change around the methylene proton region in the NMR spectrum was observed even after 6 hr of irradiation.

Irradiation of 2-(*p*-Chlorophenyl)cycloheptatriene (IIIa) with a Xenon Lamp. A solution of 2-(*p*-chlorophenyl)cycloheptatriene (IIIa) (20 mg) in absolute ether (5 m*l*) saturated with nitrogen, was irradiated in a sealed quartz vessel with a Xenon lamp for 12 hr. No change around the methylene proton region in the NMR spectrum was observed during the time of irradiation.

Preparation of 7-Phenylcycloheptatriene (Ib). To a solution of phenylmagnesium bromide which had been prepared from bromobenzene (41.6 g) and magnesium (6.44 g) in absolute ether (129 m*l*), there was added a solution of 7-ethoxycycloheptatriene (30 g) in absolute ether (100 m*l*) at 0°C; the mixture was then continuously stirred for several hours. The reaction mixture was then treated with a 2N ammonium chloride solution and extracted with ether. The crude oil was distilled to give a pale yellow oil, bp 99—103°C/0.9 mmHg (23 g). This oil crystallized on standing at 0°C; recrystallization from petroleum ether gave colorless needles, mp, 32°C (Ib). The structure of Ib was identified by means of the following physical properties.[15,16] Ultraviolet spectrum, λ_{max}^{MeOH} 262 mμ (logε 3.53); infrared spectrum (KBr), 2994, 1592, 1493, 746, 704 cm^{-1}; mass spectrum (*m/e*), 202 (M).

Irradiation of 7-Phenylcycloheptatriene (Ib) with a Low-pressure Mercury Lamp. a) A solution of 7-phenylcycloheptatriene (Ib) (1.5 g) in absolute ether (180 m*l*) was irradiated with a 6 W low pressure mercury lamp under a nitrogen stream for 30 hr. The reaction products were then separated by means of gas chromatography (Silicon Grease), 1-phenylcycloheptatriene (IIb) (300 mg) and bicyclic product (VI) (35 mg) were thus obtained. The structure of these products was suggested on the basis of the NMR spectrum.

IIb: Infrared spectrum (oil), 3031, 2941, 1600, 1477, 1449, 759, 711, 698 cm^{-1}; NMR spectrum (in $CDCl_3$), 7.34 (H_7 and H_7; doublet, $J_{6,7}=J_{1,7}=7.1$ Hz) 4.72 (H_6; multiplet, $J_{5,6}=9.2$ Hz), 3.60 τ (H_2 and H_5, multiplet).

Bicyclic compound(VI): NMR spectrum*[3] (in $CDCl_3$), 6.87 (H_4), 6.18 (H_7; doublet with small coupling), 6.42 (H_8; doublet with small coupling), 4.35 (H_5; doublet with small coupling, $J_{5,6}=5$ Hz), 4.02 (H_6; doublet

15) a) W. von E. Doering and L. H. Knox, *J. Amer. Chem. Soc.*, **76**, 3203 (1954); b) A. P. ter Borg and H. Kloosterziel, *Rec. Trav. Chem., Pays-Bas*, **82**, 741 (1963).

16) H. Horino, Master's Thesis, Tohoku University (1962).

*[3] An assignment is only tentative.

with small coupling), 3.79 (H_3; quartet, $J_{3,4}=1.4$ Hz), 3.61 (H_2; doublet, $J_{2,3}=3.0$ Hz), around 3.0 τ (aromatic).

b) A solution of 7-phenylcycloheptatriene (Ib) (20 mg) in absolute ether (5 m*l*) saturated with nitrogen was irradiated in a sealed quartz vessel with a low-pressure mercury lamp. The relative ratio of the isomers, (IIb) and (IIIb), was estimated by the integration of the doublet signals at 7.34 and 7.70 τ (in $CDCl_3$) respectively.

Irr. time (min)	% of IIIb	% of IIb	% of Ib
15	0	25	75
35	33	33	33
60	15	53	30

Irradiation of 7-Phenylcycloheptatriene (Ib) with a Xenon Lamp. A solution of 7-phenylcycloheptatriene (Ib) (20 mg) in absolute ether (5 m*l*) saturated with nitrogen was irradiated in a sealed quartz vessel with a Xenon lamp. The reaction was followed by NMR spectroscopy. The only product identified by means of the NMR spectrum was IIIb, which showed a triplet at 7.70 τ (in $CDCl_3$) during several hours irradiation.

Irradiation of 1-Phenylcycloheptatriene (IIb). A solution of 1-phenylcycloheptatriene (IIb) (20 mg) in absolute ether (5 m*l*) saturated with nitrogen was irradiated in a sealed quartz vessel with a Xenon lamp. The reaction was followed by means of NMR spectrum at intervals. The results are as follows.

Irr. time (min)	% of IIb	% of IIIb
5	90	10
10	82	18
30	60	40
60	42	53
90	47	47

Preparation of 7-(*p*-Methoxyphenyl)cycloheptatriene (Ic). To a Grignard solution of *p*-methoxyphenylmagnesium bromide which had been prepared from *p*-bromoanisole (8.25 g) and magnesium (1.07 g) in absolute ether (50 m*l*) was added 7-ethoxycycloheptatriene (5 g) in absolute ether (30 m*l*) at 0°C; the mixture was continuously stirred for 5 hr. The reaction mixture was treated as has been described in the case of Ib. The oily product was distilled to give a yellow oil, bp, 114—115°C/0.3 mmHg (5.6 g), which crystallized on standing at −60°C to give, after recrystallization from petroleum ether, colorless needles, mp, 28°C.

Found: C, 84.58; H, 7.35%. Calcd for $C_{13}H_{14}O$; C, 84.81; H, 7.12%.

Mass spectrum (*m/e*), 198 (M); ultraviolet spectrum, $\lambda_{max}^{cyclohexane}$ (log ε), 270 mμ (3.70); infrared spectrum (oil) 3002, 2994, 1605, 1508, 1250, 1176, 1034, 830, 747, 707 cm^{-1}; NMR spectrum (in $CDCl_3$), 7.34 (H_7 and H_7; triplet, $J_{1,7}=J_{6,7}=6.0$ Hz), 6.30 (OCH_3; singlet), 4.65 (H_1 and H_6; quartet, $J_{5,6}=J_{1,2}=9.1$ Hz), 3.82 (H_2 and H_5; multiplet), 3.32 (H_3 and H_4; multiplet), 2.96 τ (aromatic; quartet).

Irradiation of 7-(*p*-Methoxyphenyl)cycloheptatriene (Ic) with a Xenon Lamp. A solution of 7-(*p*-methoxyphenyl)cycloheptatriene (Ic) (20 mg) in absolute ether (5 m*l*), saturated with nitrogen, was irradiated in a sealed quartz vessel with a Xenon lamp for several hours. The reaction was followed by NMR spectroscopy. The only product identified by means of the NMR spectrum was IIc, which showed a doublet peak at 7.37 τ (in $CDCl_3$).

Preparation of 7-*p*-Tolylcycloheptatriene (Id). To a Grignard solution which had been prepared from *p*-bromotoluene (7.64 g) and magnesium (1.0 g) in absolute ether (20 m*l*) was added 7-ethoxycycloheptatriene (5 g) in absolute ether (20 m*l*) at 0°C; the mixture was then stirred continuously for several hours. The reaction mixture was treated as had been described in the case of Ib. The resultant oil was distilled to give a yellow oil, bp 85—89°C/0.5 mmHg (4 g), which crystallized on standing at −60°C to give, after recrystallization from petroleum ether, yellow needles, mp, 31°C.

Found: C, 91.98; H, 7.68%. Calcd for $C_{14}H_{14}$; C, 92.26; H, 7.74%.

Mass spectrum (*m/e*), 182 (M); ultraviolet spectrum, $\lambda_{max}^{cyclohexane}$ 265 mμ (logε 3.569); infrared spectrum, (KBr) 3040, 1603, 1520, 1391, 814, 746, 704 cm^{-1}; NMR spectrum (in $CDCl_3$) 7.70 (CH_3; singlet), 7.33 (H_7 and H_7; triplet, $J_{1,7}=J_{6,7}=5.5$ Hz), 4.66 (H_1 and H_6; quartet, $J_{5,6}=J_{1,2}=6.0$ Hz), 3.82 (H_2 and H_5; multiplet), 3.34 (H_3 and H_4; multiplet) and 2.89 τ (aromatic; multiplet).

Irradiation of 7-*p*-Tolylcycloheptatriene (Id) with a Xenon Lamp. A solution of 7-*p*-tolylcycloheptatriene (Id) in absolute ether (5 m*l*), saturated with nitrogen, was irradiated in a sealed quartz vessel with a Xenon lamp for several hours. The only product identified by NMR spectroscopy was IId, which showed a doublet peak at 7.40 τ (in $CDCl_3$).

BULLETIN OF THE CHEMICAL SOCIETY OF JAPAN VOL. 43 1127—1131 (1970)

Telomerization of Vinyl Chloride with Carbon Tetrachloride Using Amine-Cupric Chloride. Effects of Amines and Solvents[1]

Teruzō Asahara, Manabu Senō and Cheng-Ching Wu*1

Institute of Industrial Science, The University of Tokyo, Roppongi, Minato-ku, Tokyo

(Received July, 3 1969)

Telomerization of vinyl chloride with carbon tetrachloride was investigated in reaction systems containing amines and cupric chloride. The yield of telomers $CCl_3(CH_2CHCl)_nCl$ and the content of the telomer with $n=1$ were high when aliphatic amines with relatively long chains were used. An increase in basicity of amines raised the yield of telomers. When bifunctional amines such as diamines and alkanolamines were used, the yield of telomers was low and the content of higher telomers was high. The effect of added solvents on the yield of telomers was not so remarkable and an increase in the dielectric constant of solvents decreased the yields. The results were examined on the basis of Asscher-Vofsi mechanism, but could not be explained satisfactorily. A partly modified scheme was proposed for the radical addition in the cage complex stabilized with amine.

In a previous paper,[1] we reported that the telomerization of vinyl chloride and carbon tetrachloride was initiated by *n*-butylamine in the presence of metals (cupper and iron) and metallic salts (Cu(I) or Cu(II) chloride and Fe(II) or Fe(III) chloride). While the reactions initiated by ordinary radical initiators such as benzoyl peroxide and azobisisobutyronitrile afford telomers with higher average molecular weights, the main products obtained in the *n*-butylamine - metallic salt systems were telomers lower average molecular weights. The content of $CCl_3CH_2CHCl_2$, the 1 : 1 adduct of vinyl chloride with carbon tetrachloride, is as high as 80%.

Since Collins noticed that amines change into amine hydrochlorides in carbon tetrachloride under day-light, the reaction of amines with carbon tetrachloride under mild conditions has been investigated by many authors.[2] Amines form charge-transfer complexes with carbon tetrachloride. However, the formation constants are rather small. The complexes decompose with the formation of trichloromethyl radicals under the influence of light or metallic salts.[3-5]

Miller[5] proposed the following mechanism for the photo-decomposition:

$$RNH_2 \cdot CCl_4 \xrightarrow{h\nu} RNH_2^+Cl^- + \cdot CCl_3$$

On the other hand, Asscher and Vofsi[6] proposed the following redox mechanism with participation of metallic ions, *e. g.* cupper ions:

$$RNH_2 \cdot CCl_4 + Cu^+ \rightarrow [Cu^{(+)} \cdot Cl]RNH_2 + \cdot CCl_3$$

When a vinyl compound is present in such a system, trichloromethyl radicals enter into polymerization. However, this mechanism has not been confirmed to be plausible through our investigation on the telomerization of vinyl compounds with carbon tetrachloride in amine-metallic salt systems.[1] In the present paper, the results on the effect of amines on the reaction will be presented.

Experimental

Amines and cupric chloride of commercial special grade were used without purification. Carbon tetrachloride was purified by distillation and vinyl chloride was washed with a 5% sodium hydroxide solution and dried by passing through a calcium chloride tube.

Telomerization was carried out in a stainless steel autoclave with a magnetic stirrer. Definite amounts of carbon tetrachloride, amine and $Cu(II)Cl_2$ were placed in the autoclave chilled with dry ice-acetone, and vinyl chloride which had been liquified was added.

1) Studies on Telomerization. Part V. Part IV of this series, T. Asahara, M. Senō and C. C. Wu, *Kogyo Kagaku Zasshi*, **72**, 1526 (1969).

*1 Present address: Department of Chemical Engineering, Univ. of Taiwan, Taipei, Taiwan.

2) a) R.F. Collins, *Chem. Ind.* (London), **1957**, 704. b) N.H. Cromwell, P.W. Foster and M.M. Wheeler, *ibid.*, **1959**, 228. c) G. J. Beichl, J. E. Colwell and J. G. Miller, *ibid.*, **1960**, 203. d) R. Foster, *ibid.*, **1960**, 1354. e) H. Williams, *ibid.*, **1960**, 900. f) T. G. Bonner and R. A. Hancock, *ibid.*, **1965**, 267.

3) D. P. Stevenson and G. M. Coppinger, *J. Amer. Chem. Soc.*, **84**, 149 (1962).

4) K. M. C. Davis and M. F. Farmer, *J. Chem. Soc., B*, **1967**, 28.

5) W. J. Lautenberger, E. N. Jones and J. G. Miller, *J. Amer. Chem. Soc.*, **90**, 1100 (1968).

6) M. Asscher and D. Vofsi, *J. Chem. Soc.*, **1961**, 2261.

Table 1. Effects of the basicity of amines on the yield and composition of telomers*

Run No.	Amine	pK_B	Yield g/mol CCl_4	Composition of telomers (wt%)		
				$n=1$	$n=2$	$n\geq 3$
119	*n*-Butylamine	3.39	40.1	85	10	5
180	Isobutylamine	3.59	56.4	74	5	21
181	*s*-Butylamine	—	46.8	79	7	14
201	*t*-Butylamine	3.55	43.7	79	5	16
189	*n*-Hexylamine	3.30	53.6	79	7	14
182	Cyclohexylamine	3.31	44.4	75	7	18
198	Benzylamine	4.63	53.3	69	8	23
190	Dodecylamine	3.10	50.2	77	13	10
186	Diethylamine	3.01	29.1	70	10	20
187	Di-*n*-propylamine	3.10	46.3	76	14	10
177	Di-*n*-butylamine	2.79	55.6	84	3	13
183	Dicyclohexylamine	—	46.9	73	26	1
188	Triethylamine	3.07	19.2	62	7	31
178	Tri-*n*-butylamine	4.09	44.4	74	20	6
193	Pyrrolidine	2.73	16.9	69	3	28
192	Piperidine	2.80	28.4	75	6	19
185	Pyridine	8.85	26.3	69	30	1
184	Aniline	9.42	7.1	30	26	44**
197	Pyrrole	—	7.0	9	3	88
191	Ethylenediamine	4.09	12.6	8	4	88**
202	Hexamethylenediamine	—	34.8	20	5	75
139	Monoethanolamine	4.56	9.1	17	6	77**
140	Diethanolamine	5.05	13.1	3	2	95**
141	Triethanolamine	6.18	11.1	8	3	89**
200	Diethylaminoethanol	—	12.1	60	2	38
199	2-Pyrrolidinone	—	4.1	72	2	26**

* Added amount of amine, 0.01 mol/mol CCl_4; Added amount of $CuCl_2$, 0.0025 mol/mol CCl_4; Reaction time, 2.5 hr; Reaction temperature, 130°C; Molar ratio CCl_4/vinyl chloride, 4.

** Determined by gas chromatography.

The autoclave was then sealed and the air inside was replaced several times by nitrogen gas. The autoclave was heated up to the desired temperature and kept for 2.5 hr.

The reaction conditions were as follows. The molar ratio of carbon tetrachloride to vinyl chloride was 4, cupric chloride 0.0025 mol/mol CCl_4, amine 0.01 mol/mol CCl_4, temperature 130°C and reaction time 2.5 hr.

After the autoclave was cooled to room temperature, the reaction mixture was filtered, washed with water to remove soluble amine hydrochloride and the solvent and carbon tetrachloride were recovered by distillation. The mixture of telomers was fractionated into $n=1$, $n=2$ and $n=3$ fractions by distillation. Each fraction was examined by gas chromatography, infrared and NMR spectroscopy to confirm its structure.

Results

Effect of Amines. Telomerization was carried out in the presence of various amines. The result is shown in Table 1. When the amine with lower value of pK_B is used, the yield of telomers becomes higher. The following order which gives higher yields of telomers should be noted; diethylamine<di-*n*-propylamine<di-*n*-butylamine and *n*-butylamine <tri-*n*-butylamine<di-*n*-butylamine. When amines with two functional groups such as diamines and alkanolamines are used, the yield of telomers becomes lower. The result is inconsistent with that obtained on the telomerization of ethylene with carbon tetrachloride, where the presence of alkanolamines raises the yield of telomers.[7] When the yield of total telomers is high, the composition ratio of the telomer with $n=1$ is also high in most cases. However, some heterocyclic amines such as pyridine, piperidine and pyrrolidine give lower yield of telomers, but higher ratio of telomer with $n=1$.

The effect of added amount of di-*n*-butylamine on the yield of telomers is shown in Fig. 1. We see that the yield of telomers increases rapidly at first, then slowly with the increase of added amounts

7) T. Asahara and J. Hirano, *Kogyo Kagaku Zasshi*, **69**, 1512 (1966).

Table 2. Effects of reaction time on the yield and composition of telomers

Run No.	Amine*	$CuCl_2$**	Temp., °C	Time, hr	Yield g/mol CCl_4	Composition (wt%) $n=1$	$n=2$
238	0.01	0.0025	130	1.0	46.8	83	4
239	0.01	0.0025	130	1.5	54.4	83	4
240	0.01	0.0025	130	2.0	55.1	83	4
177	0.01	0.0025	130	2.5	55.6	84	3

* Di-*n*-butylamine, mol/mol CCl_4; Molar ratio CCl_4/vinyl chloride, 4.
** mol/mol CCl_4

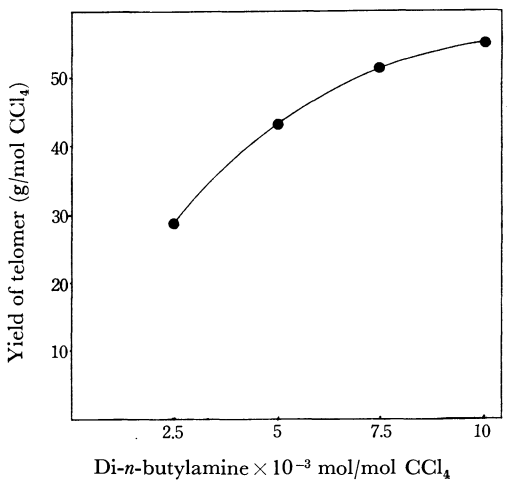

Fig. 1. Effect of added amount of amine on the yield of telomer
Reaction time, 2.5 hr; Reaction temp., 130°C; Molar ratio of CCl_4/VC=4, Added amount of $CuCl_2$: 0.0025 mol/mol CCl_4

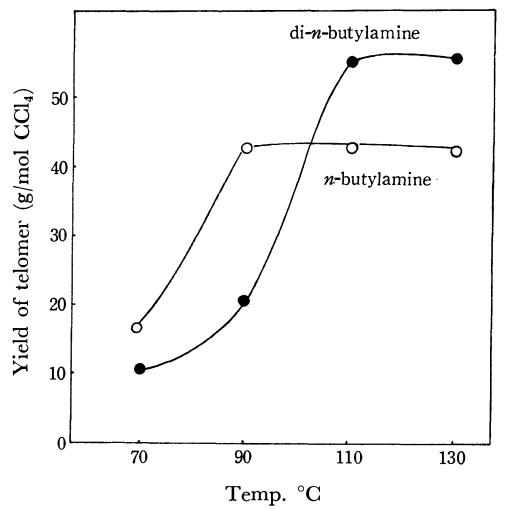

Fig. 2. Effect of temperature on the yield of telomers.
Reaction time, 2.5 hr: Molar ratio of CCl_4/VC=4, Added amount of amine, 0.01 mol/mol CCl_4; Added amount of $CuCl_2$, 0.0025 mol/mol CCl_4

of di-*n*-butylamine.

Effect of Reaction Temperature and Time. The effects of reaction temperature on the yield of telomers when di-*n*-butylamine and *n*-butylamine are used are shown in Fig. 2. The yield of telomers increases abruptly in a relatively low temperature range and shows a maximum at 90 and 120°C in the cases of *n*-butylamine and di-*n*-butylamine, respectively. The composition ratio of the 1 : 1 telomer exhibits a similar behavior.

The effect of reaction time in the system of di-*n*-butylamine and cupric chloride is shown in Table 2. The yield of telomers increases abruptly within 1 hr of the initial stage of reaction. The composition of telomers does not change remarkable during the course of the reaction.

Effect of Solvents. The basicity and ability of complex formation of amines are affected by the solvent. Thus it is probable that telomerization is affected in various stages by addition of solvents. The effect of solvent on the yield and composition of telomers was examined by using mixtures of carbon tetrachloride and various solvents. The

Table 3. Effects of solvents on the yield and composition of telomers*

Run No.	Solvent	Dielectric const.	Yield g/mol CCl_4	Composition (wt%) $n=1$	$n=2$
225	*n*-Heptane	1.92	24.5	67	9
224	Cyclohexane	2.02	50.3	72	6
228	1,4-Dioxane	2.04	42.8	67	17
119	Carbon tetrachloride	2.22	40.1	85	10
223	Benzene	2.27	39.5	75	17
216	*t*-Butyl alcohol	12.5	52.0	83	2
214	1-Butanol	17.1	66.8	73	4
212	2-Propanol	18.3	56.0	73	4
213	Methanol	32.6	43.7	85	10
218	*s*-Butanol	—	39.8	56	3

* Amount of solvent added, 100 ml/100 ml CCl_4; Amount of *n*-butylamine added, 0.01 mol/mol CCl_4; Amount of $CuCl_2$ added, 0.0025 mol/mol CCl_4; Molar ratio CCl_4/vinyl chloride, 4; Reaction time, 2.5 hr; Reaction temperature, 130°C.

results are shown in Table 3. As shown in this table, the effect of solvent is not remarkable, except for the cases where solvents take part in reactions.

Discussion

The amine-metallic salt initiating systems afford a high yield of lower telomers. This might be due to an effective chlorine-transfer mechanism. Asscher and Vofsi supposed some complexes consisting of cuprous ions and chlorine radicals or cupric ions and chloride ions with coordinated amines for a reaction intermediate to take an essential role in this chlorine-transfer mechanism. Assuming the existence of such complexes the following reaction scheme would follow.

$$M^{(+)} + nRNH_2 \rightarrow M^{(+)}(RNH_2)_n$$

$$M^{(+)}(RNH_2)_n + CCl_4 \rightarrow [M^{(+)}\cdot Cl](RNH_2)_n + \cdot CCl_3$$

$$\cdot CCl_3 + CH_2CHCl \rightarrow CCl_3CH_2CHCl\cdot$$

$$CCl_3CH_2CHCl\cdot + [M^{(+)}\cdot Cl](RNH_2)_n \rightarrow CCl_3CH_2CHCl_2 + M^{(+)}(RNH_2)_n$$

The result of kinetic treatments based on this scheme is inconsistent with experimental result. As an example, the increasing stability of the complex $[M^{(+)}\cdot Cl](RNH_2)_n$ gives rise to the increase in the rate of formation of trichloromethyl radicals, and the decrease in the rate of abstraction of chlorine radical from the complex. This conflicts with the result where the increasing yield of total telomers is accompanied by the increasing content of the telomer with $n=1$.

Thus the above reaction scheme should be modified. It seems most probable that the reaction step to form the telomer with $n=1$ takes place in cages stabilized by amines. The reaction scheme is written as follows:

$$M^{(+)} + nRNH_2 \overset{K_1}{\rightleftharpoons} M^{(+)}(RNH_2)_n$$

$$M^{(+)}(RNH_2)_n + CCl_4 \overset{K_2}{\rightleftharpoons} [M^{(+)}Cl\cdot\cdot CCl_3](RNH_2)_n$$

$$[M^{(+)}Cl\cdot\cdot CCl_3](RNH_2)_n + CH_2CHCl \overset{k_1}{\longrightarrow} CCl_3CH_2CHCl_2 + M^{(+)}(RNH_2)_n$$

$$[M^{(+)}Cl\cdot\cdot CCl_3](RNH_2)_n \overset{k_2}{\longrightarrow} (M^{(2+)}Cl^-)(RNH_2)_n + \cdot CCl_3$$

$$\cdot CCl_3 + CH_2CHCl \overset{k_3}{\longrightarrow} CCl_3CH_2CHCl\cdot$$

$$CCl_3CH_2CHCl\cdot + CH_2CHCl \overset{k_4}{\longrightarrow} CCl_3(CH_2CHCl)_2\cdot$$

$$CCl_3CH_2CHCl\cdot + CCl_4 \overset{k_5}{\longrightarrow} CCl_3CH_2CHCl_2 + \cdot CCl_3$$

The following reactions are induced by trichloromethyl radicals:

$$\cdot CCl_3 + \cdot CCl_3 \overset{k_6}{\longrightarrow} C_2Cl_6$$

$$\cdot CCl_3 + RNH_2 \overset{k_7}{\longrightarrow} \dot{R}NH + CHCl_3$$

$$\dot{R}NH + CCl_4 \overset{k_8}{\longrightarrow} RNClH + \cdot CCl_3$$

$$RNClH + RNH_2 \overset{k_9}{\longrightarrow} R'CHNH + RNH_3Cl$$

By kinetic treatment of this reaction scheme, the following formulas are derived on the assumption that reaction intermediate $\cdot CCl_3$, $CCl_3CH_2CHCl\cdot$ and $\dot{R}NH$ are in stationary states.

If the condition $k_3k_4[V]^2/(k_4[V]+k_5[C]) < 4k_2k_6 \times [com]$ is satisfied, the rate of formation of the telomer with $n=1$ is given by

$$\frac{d[CCl_3CH_2CHCl_2]}{dt} = k_1[V][com] + \frac{k_2^{1/2}k_3k_5[C][V]}{k_6^{1/2}(k_4[V]+k_5[C])}[com]^{1/2} \quad (1)$$

and the rate of formation of the telomers with $n \geq 2$, by

$$\frac{d[CCl_3(CH_2CHCl)_nCl]}{dt} = \frac{k_2^{1/2}k_3k_4[V]^2}{k_6^{1/2}(k_4[V]+k_5[C])}\cdot[com]^{1/2} \quad (2)$$

On the other hand, if the reverse condition

$$k_3k_4[V]^2/(k_4[V] + k_5[C]) > 4k_2k_6[com]$$

is satisfied, the corresponding equations are obtained as follows:

The rate of formation of the telomer with $n=1$,

$$\frac{d[CCl_3CH_2CHCl_2]}{dt} = [com]\left(k_1[V]+\frac{k_2k_5[C]}{k_4[V]}\right) \quad (3)$$

and the rate of formation of the telomers with $n \geq 2$,

$$\frac{d[CCl_3(CH_2CHCl)_nCl]}{dt} = k_2[com] \quad (4)$$

In these equations, the following abbreviations are used,

V: CH_2=CHCl, C: CCl_4

and com: $[M^{(+)}Cl\cdot\cdot CCl_3](RNH_2)_n$

and the concentration of this complex is

$$[com] = K_1K_2[M^{(+)}][CCl_4][RNH_2]^n \quad (5)$$

The cage complex as a reaction intermediate would be formed through the interaction of chlorine radical with metal ion and the stabilization by coordinated amines. The attack of vinyl chloride on this cage complex affords tetrachloropropyl radical, and the resulting radical instantly abstracts chlorine radical from the complex. The presence of such cage complexes greatly decreases activation energy for the insertion of vinyl chloride into the Cl–CCl_3 bond.

This scheme gives a plausible explanation for the effect of amines as shown in Table 1. The increasing basicity of amines enhances the stabilization of cage complexes and decreases the activation energy for the insertion reaction. On the other hand, bifunctional amines possess strong chelating ability to Cu(II) ions and, therefore, make the decomposition of cage complexes feasible. Bulkiness of amines do not show any steric hindrance, for the site of reaction is not on the metallic ions and mechanically stabilize the cage complex. This is the reason why the amine with two or three long alkyl chains is effective.

The slight effect of solvents is understandable if the reaction proceeds primarily in cages. However, the increase in dielectric constants might decrease the stability of cages.

Of the alternative conditions mentioned above, the latter would be satisfied in most cases, because k_2 and [com] are relatively small. In this case, from Eqs. (1) and (2), the product ratio of the telomers with $n=1$ and $n\geq 2$ is given by

$$\frac{[CCl_3CH_2CHCl_2]}{[CCl_3(CH_2CHCl)_nCl]} = \frac{k_1}{k_2}[V] + \frac{k_5[C]}{k_4[V]} \simeq \frac{k_1}{k_2}[V] \quad (6)$$

Table 1 shows that the ratio $k_1[V]/k_2$ is 3—5.

The high reaction rate observed in this system supports the mechanism. In telomerization of vinyl chloride and chloroform, the main product of the 1 : 1 adducts is $CCl_3CH_2CH_2Cl$ when benzoyl peroxide or azobisisobutyronitrile is used as an initiator, but the main product is $CHCl_2CH_2CHCl_2$ when the amine-$CuCl_2$ is used.[8] This observation supports the mechanism proposed in this paper. However, further examination would be necessary in order to establish this mechanism. The EPR measurement on copper ion-amine-carbon tetrachloride systems and a detailed analysis on the distribution of products in the reaction of vinyl chloride with chloroform are now in progress. The results will be presented in the near future.

8) T. Asahara, C. C. Wu, *Kogyo Kagaku Zasshi*, **70,** 1197 (1967).

BULLETIN OF THE CHEMICAL SOCIETY OF JAPAN VOL. 43 1131—1135 (1970)

Aromatic Arylation with Aryl Radicals. I. A Novel Method for Generating Aryl Free Radical

Michio KOBAYASHI, Hiroshi MINATO, Nobumasa KOBORI and Eiichi YAMADA

Department of Chemistry, Tokyo Metropolitan University, Fukazawa, Setagaya, Tokyo

(Received July 15, 1969)

Benzenediazonium tetrafluoroborate in DMSO decomposed instantaneously with evolution of nitrogen upon addition of a DMSO solution of sodium nitrite. Orientations and partial rate factors for phenylation of substituted benzenes indicated that not phenyl cation but phenyl radical was produced as an intermediate. Hammett's plots of partial rate factors of meta and para positions yielded good straight lines with $\rho_m = 0.46$ and $\rho_p = 1.67$. Plausible mechanisms were discussed. From *m*-dinitrobenzene 2,6- and 2,4-dinitrobiphenyl were produced in 47 and 23% yields, respectively, and the synthetic value of this method was pointed out.

Aryldiazonium salts decompose with evolution of nitrogen in aprotic polar solvents, and phenyl cation is considered to be the intermediate on the basis of the kinetic studies[1] and the partial rate factors for arylation of substituted benzenes.[2]

$$ArN_2^+ \rightarrow Ar^+ + N_2$$

However, it has been reported that aryldiazonium salts undergo homolytic decomposition in methanol[3] or pyridine.[4]

$$ArN_2^+ + CH_3O^- \rightarrow Ar\text{–}N{=}N\text{–}OCH_3 \rightarrow Ar\cdot + N_2 + \cdot OCH_3$$

or

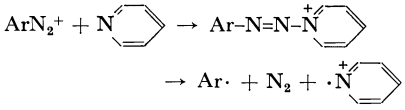

1) E. S. Lewis, *J. Amer. Chem. Soc.*, **80**, 1371 (1958); K. Ishida, N. Kobori, M. Kobayashi and H. Minato, This Bulletin, **43**, 285 (1970).

2) a) R. A. Abramovitch and F. F. Gadallah, *J. Chem. Soc., B*, **1968**, 497. b) M. Kobayashi, H. Minato, E. Yamada and N. Kobori, This Bulletin, **43**, 215 (1970).

3) D. F. DeTar and M. N. Turetzky, *J. Amer. Chem. Soc.*, **77**, 1745 (1955); **78**, 3925 (1956).

4) R. A. Abramovitch and J. G. Saha, *Tetrahedron*, **21**, 3297 (1965).

During a systematic investigation on the decomposition of aryldiazonium salts in aprotic polar solvents in our laboratories, it has been found that aryldiazonium salts decompose instantaneously with evolution of nitrogen upon addition of sodium nitrite in dimethyl sulfoxide (DMSO) at room temperature. In this paper, the results of this investigation will be described, and the evidence for the homolytic nature of the decomposition will be presented. Synthetic utility of this reaction will be also pointed out.

Experimental

Materials. Preparation of benzenediazonium tetrafluoroborate and substituted biphenyls, and purification of DMSO and substituted benzenes were described in our previous paper.[2b] *m*-Dinitrobenzene, *p*-nitrotoluene, *p*-chloronitrobenzene, 1,3,5-trinitrobenzene and sodium nitrite were the first grade chemicals of Wako Pure Chemical Industries, and were used without further purification.

Phenylation of Monosubstituted Benzenes. Under nitrogen atmosphere a solution of 2.00 g of benzenediazonium tetrafluoroborate in 20 g of DMSO was added drop by drop at 10°C into a vigorously stirred solution of sodium nitrite (3 mol/mol of PhN_2BF_4) and a substituted benzene (50 mol/mol of PhN_2BF_4) in 60 g of DMSO. Evolution of nitrogen was instantaneous upon addition of each drop of the diazonium salt solution, and the addition was completed in about ten minutes. Ether was added to the solution, and the mixture was washed with water in order to remove DMSO and excess sodium nitrite. After it was dried over magnesium sulfate, ether and about 70% of the remaining substituted benzene was evaporated, and biphenyl isomers in the residue was analyzed by a Hitachi Gas-Chromatograph K-53. Biphenyl isomers were identified by comparison of the retention times with those of the authentic samples on a 1 m to 6 m-column (depending upon the ease of separation) packed with Chromosorb W (10% Apiezon L). Quantitative determinations were made by use of calibration curves.

Not benzene but chlorobenzene was used as the standard for the competitive phenylation, since non-substituted biphenyl easily sublimes and the evaporation of a remaining substituted benzene will bring forth a great error. The reactivity of each position of substituted benzenes was calculated relative to the reactivity of the ortho position of chlorobenzene. A competitive phenylation between benzene and chlorobenzene was carried out without evaporation in order to determine the partial rate factor of the ortho position of chlorobenzene. The partial rate factors of various substituted benzenes were calculated by the following equation.

$$k_X/k = (k_X/k_{o\text{-}Cl}) \times (k_{o\text{-}Cl}/k)$$

Phenylation of Poly-substituted Benzenes. The experimental procedure was the same as that described for mono-substituted benzenes except where otherwise stated.

***p*-Nitrotoluene.** A solution of *p*-nitrotoluene (10.0 g) and sodium nitrite (2.5 g) in DMSO (30 g) was added to a stirred solution of benzenediazonium tetrafluoroborate (3.717 g) in DMSO (30 g). Biphenyl isomers were separated by a gas chromatograph, and the fractions isolated were identified by infrared spectroscopy, NMR spectroscopy (in $CDCl_3$) and elemental analyses, and quantitative determinations were made by gas chromatography. 3-Methyl-6-nitrobiphenyl. H^2: 2.64 τ (singlet); H^4: 2.71 τ (doublet, J_{45}=9.0 Hz); H^5: 2.20 τ (doublet, J_{54}=9.0 Hz). Found: C, 73.75; H, 5.72%. Calcd for $C_{13}H_{11}O_2N$: C, 73.22; H, 5.20%. 2-Methyl-5-nitrobiphenyl. H^3: 2.76 τ (multiplet); H^4 and H^6: 1.90 τ (multiplet). Found: C, 73.46; H, 5.50%. Calcd for $C_{13}H_{11}O_2N$: C, 73.22; H, 5.20%.

***p*-Nitrochlorobenzene.** A solution of *p*-nitrochlorobenzene (16.0 g) and sodium nitrite (4.0 g) in DMSO (30 g) was added to a stirred solution of benzenediazonium tetrafluoroborate (3.445 g) in DMSO (20 g). Biphenyl isomers were separated by a gas chromatograph, and the fractions isolated were identified by infrared spectroscopy, NMR spectroscopy (in $CDCl_3$) and elemental analyses, and determined quantitatively by gas chromatography. 3-Chloro-6-nitrobiphenyl. H^2: 2.24 τ (singlet); H^4: 2.55 τ (doublet, J_{45}=9.0 Hz); H^5: 2.16 τ (doublet, J_{54}=9.0 Hz). Found: C, 61.29; H, 3.46%. Calcd for $C_{12}H_8O_2NCl$: C, 61.69; H, 3.45%. 2-Chloro-5-nitrobiphenyl. H^3: 2.37 τ (doublet, J_{34}=9.0 Hz); H^4: 1.86 τ (doublet, J_{43}=9.0 Hz); H^6: 1.77 τ (singlet). Found: C, 61.9; H, 3.14%. Calcd for $C_{12}H_8O_2NCl$: C, 61.69; H, 3.45%.

***m*-Dinitrobenzene.** A solution of *m*-dinitrobenzene (10.0 g) and sodium nitrite (5.0 g) in DMSO (22 g) was added to a stirred solution of benzenediazonium tetrafluoroborate (4.237 g) in DMSO (10 g). Chloroform instead of ether was used for extraction. Substituted biphenyl isomers were separated on an alumina column with hexane-benzene as the eluant, and recrystallized from ethyl acetate. 2,4-Dinitrobiphenyl, 2.1 g (47%), mp 108°C (lit,[5] 110°C). 2,6-Dinitrobiphenyl, 1.1 g (23%), mp 186—187°C (lit,[6] 188—189°C).

1,3,5-Trinitrobenzene. A solution of 1,3,5-trinitrobenzene (4.0 g) and sodium nitrite (5.0 g) in DMSO (30 g) was added to a stirred solution of benzenediazonium tetrafluoroborate (4.50 g) in DMSO (10 g). Chloroform was used for extraction. 2,4,6-Trinitrobiphenyl was isolated by elution chromatography on a silica gel column with hexane-benzene as the eluant; 2.55 g (55%), mp 129°C (lit, 130°C).[5]

Results and Discussion

Benzenediazonium tetrafluoroborate in DMSO decomposed instantaneously with evolution of nitrogen upon addition of a DMSO solution of sodium nitrite. Since in the absence of sodium nitrite the diazonium salts slowly undergoes a first-order decomposition *via* phenyl cation,[2b] the mechanism of this rapid decomposition must be different from that involving phenyl cation. The difference of the mechanism is also suggested from the absence of 1,3-benzoxathian in the products, which was always produced when phenyl

5) H. C. Gull and E. E. Turner, *J. Chem. Soc.*, **1929**, 491.

6) J. Forrest, *ibid.*, **1960**, 566.

Table 1. Orientation and partial rate factors for the phenylation of PhX with PhN_2BF_4 in DMSO in the presence of $NaNO_2$ at room temperature

PhX	Yield[a] (%)	Orientation (%)			Partial rate factors		
		o-	*m*-	*p*-	k_o/k	k_m/k	k_p/k
$PhOCH_3$	—	72.4	14.2	13.4	5.66	1.11	2.09
PhC_2H_5	—	49.8	32.9	17.3	2.49	1.64	1.73
PhCl	22.6	58.8	25.4	15.8	3.89	1.68	2.09
PhCl	18.5	57.1	25.4	17.5	3.24	1.44	1.98
PhCl[b]	15.6	56.8	24.7	18.5	3.51	1.53	2.29
$PhCO_2CH_3$	—	32.4	20.2	47.4	1.90	1.19	5.57
PhCN	—	46.5	13.7	39.8	5.71	1.68	9.80
$PhNO_2$	76.3	67.8	5.4	26.9	26.6	2.12	21.1

a) Mole percent per mole diazonium salt.
b) Reaction was carried out in water under heterogeneous conditions.

cation was generated in DMSO.[2b]

Table 1 shows the orientations and partial rate factors for phenylation of substituted benzenes with benzenediazonium tetrafluoroborate and sodium nitrite in DMSO. All the substituents behaved as *o,p*-directors, and partial rate factors were always larger than 1. These data are similar to those of phenylation with phenyl radical produced from benzoyl peroxide[7a] or *N*-nitrosoacetanilide[7b] and quite different from those of phenylation with phenyl cation.[2,8] These findings indicate that the benzenediazonium salt reacts with sodium nitrite and produces phenyl radical. Plausible mechanisms are the following two.

$$PhN_2^+ + {}^-O\text{-}N{=}O \rightarrow Ph\text{-}N{=}N\text{-}O\text{-}N{=}O \quad (I)$$

Scheme 1

$$Ph\text{-}N{=}N\text{-}O\text{-}N{=}O \rightarrow Ph\cdot + N_2 + NO_2$$

Scheme 2

$$2Ph\text{-}N{=}N\text{-}O\text{-}N{=}O \rightarrow Ph\text{-}N{=}N\text{-}O\text{-}N{=}N\text{-}Ph + N_2O_3 \quad (II)$$

$$Ph\text{-}N{=}N\text{-}O\text{-}N{=}N\text{-}Ph \rightarrow Ph\cdot + N_2 + Ph\text{-}N{=}N\text{-}O\cdot$$

Since NO_2 and $PhN{=}NO\cdot$ are rather stable radicals, it is possible that compound I or II decomposes quickly as they are formed.

It is generally recognized that excess sodium nitrite should not be present when aryldiazonium salts are prepared, but no satisfactory explanation for the harmful action of nitrites has been proposed yet. The results of this investigation show that the excess nitrite not only decompose the aryldiazonium salts but also produce very reactive phenyl radical, which attacks various compounds present in the medium, producing a mixture of complicated products.

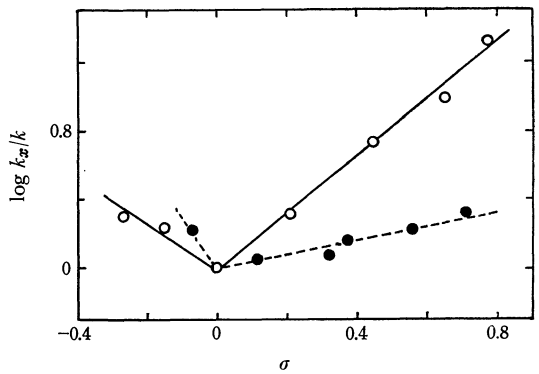

Fig. 1. The Hammett' plots for the phenylation with $PhN_2BF_4NaNO_2$ in DMSO.
---●---: $\log k_m/k$, $\rho_m=0.46$
—○—: $\log k_p/k$, $\rho_p=1.67$

Figure 1 is the Hammett's plots of partial rate factors of meta and para positions. Satisfactory linear relationships of V-shape are observed for meta and para data with $\rho_m=0.46$ and $\rho_p=1.67$. ρ Values were calculated from the right half of the V-shape which contained larger number of experimental data than the left half. Figure 2 shows

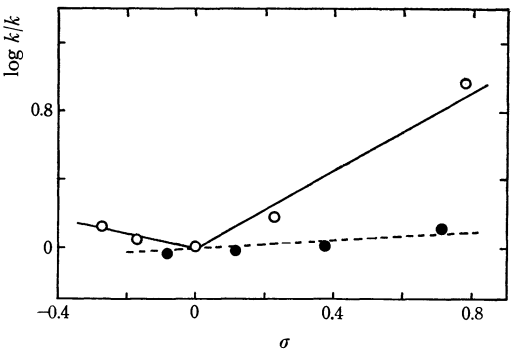

Fig. 2. The Hammett' plots for the phenylation with $PhN(NO)COCH_3$ at 20°C.
---●---: $\log k_m/k$, $\rho_m=0.07$
—○—: $\log k_p/k$, $\rho_p=1.27$

7) a) G. H. Willlams "Homolytic Aromatic Substitution," Pergamon Press, Oxford (1960), p. 73. b) R. Ito, T. Migita, N. Morikawa and O. Simamura, *Tetrahedron*, **21**, 955 (1965).
8) M. Kobayashi, H. Minato and N. Kobori, This Bulletin, **43**, 219 (1970).

the Hammett's plots of partial rate factors obtained by Ito, Migita, Morikawa and Simamura[7b] for phenylation with *N*-nitrosoacetanilide (without consideration of the conjugative effect τ_p). It is a satisfactory linear relationship of V-shape with $\rho_m=0.07$ and $\rho_p=1.27$. Both ρ_m and ρ_p of this investigation were greater than those of *N*-nitrosoacetanilide. The difference might be ascribed to solvent effect, *i.e.*, the use of the polar solvent, DMSO, in this investigation. However, it has been found in our laboratories that the ρ value for the partial rate factors for phenylation with phenyl radical generated from phenylazotriphenylmethane in PhX-DMSO is not greater than that in PhX alone,[9] and this finding shows that the greater ρ value in this investigation is not due to solvent effect. Since sodium nitrite is insoluble in less polar organic solvents, it is not possible to investigate the reaction between benzenediazonium tetrafluoroborate and sodium nitrite in other solvents.

The greater ρ values may be ascribed to the difference in the species abstracting hydrogen from the intermediate phenylcyclohexadienyl radicals. The hydrogen abstractor in Scheme 1 is NO_2, and that in Scheme 2 is PhN=N-O· or N_2O_3. As for the hydrogen abstractor for *N*-nitrosoacetanilide, Ruchardt and his coworkers reported that PhN=NO· is the species which abstracts hydrogen,[10] whereas Chalfont and Perkins reported that Ph(Ac)N-(Ph)N-O· abstracts hydrogen.[11] If the hydrogen abstractor in the case of *N*-nitrosoacetanilide is Ph(Ac)N-(Ph)N-I·, the difference in the ρ values may be ascribed to the difference in the hydrogen-abstracting species. If the hydrogen abstractor in the case of *N*-nitrosoacetanilide is is PhN=N-O·, the difference in the ρ values can be ascribed to the difference in the hydrogen-abstracting species only when the hydrogen abstractor in the PhN_2BF_4-$NaNO_2$ system is NO_2 or N_2O_3, and not PhN=N-O·. At present it is not possible to determine what the true hydrogen abstractor in this system is. In our laboratories phenylation with phenylazotriphenylmethane in the presence of N_2O_4 is being investigated and the capacity of N_2O_4 as a hydrogen abstractor is being examined.[9]

It is interesting to note that the values of $\rho_p-\rho_m$ are approximately the same in both cases (1.27−0.07=1.20 for *N*-nitrosoacetanilide and 1.67−0.46=1.21 for PhN_2BF_4-$NaNO_2$). This fact seems to indicate that the contributions of the direct conjugative effect of *p*-substituents are similar in both cases.

Table 1 shows that the yield of phenylation of nitrobenzene is 76.3%, which is much better than those of chlorobenzene. Williams and his coworkers observed that in the decomposition of benzoyl peroxide in benzene the yield of biphenyl increased from 50% to 90% when aromatic compounds with nitro group were added to the media, and they called the phenomenon "nitro group effect.[12]" However, in Fig. 1 the nitro group

TABLE 2. PHENYLATION OF NITRO COMPOUNDS WITH PhN_2BF_4 AND $NaNO_2$ IN DMSO

Compound	Product	Yield (%)
p-Nitrotoluene	3-Methyl-6-nitrobiphenyl	38
	2-Methyl-5-nitrobiphenyl	4
p-Nitrochlorobenzene	3-Chloro-6-nitrobiphenyl	44
	2-Chloro-5-nitrobiphenyl	6
m-Dinitrobenzene	2,6-Dinitrobiphenyl	47
	2,4-Dinitrobiphenyl	23
1,3,5-Trinitrobenzene	2,4,6-Trinitrobiphenyl	55

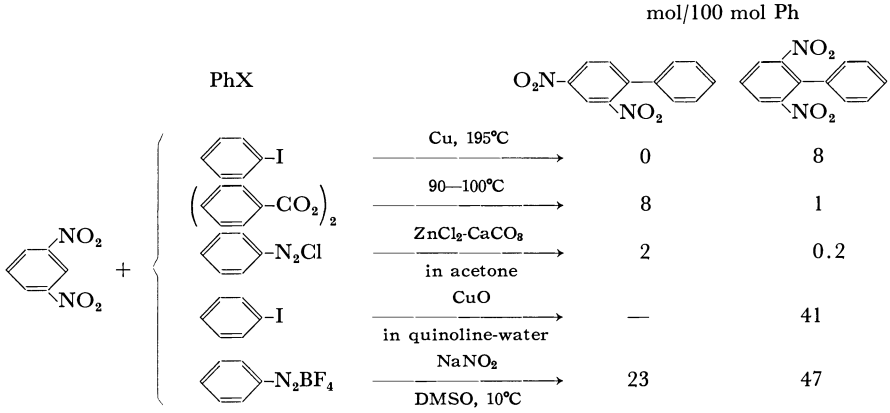

9) to be published

10) C. Rüchardt and E. Merz, *Tetrahedron Lett.*, **1964**, 2431; C. Rüchardt and B. Freudenberg, *ibid.*, **1964**, 3623; C. Rüchardt, *Angew. Chem.*, **77**, 974 (1965).

11) G. R. Chalfont and M. J. Perkins, *J. Amer. Chem. Soc.*, **89**, 3054 (1967).

12) D. H. Hey, K. S. Y. Liang, M. J. Perkins and G. H. Williams, *J. Chem. Soc., C*, **1967**, 1153; G. B. Gill and G. H. Williams, *ibid., B*, **1966**, 880.

does not appear to be peculiar on the straight line representing a satisfactory Hammett relationship, and it seems that the high yield of nitrobiphenyl can be explained in terms of the conjugative effect alone.

This phenylation reaction appears to be a good method for the syntheses of substituted biphenyls. This method is more advantageous than Gomberg reaction in that even solid substrates can be phenylated in homogeneous media under very mild and non-alkaline conditions. The phenylations of several solid aromatic compounds were investigated, and the results are summarized in Table 2. Yields are fairly large and better than those of Ullmann reaction. It is interesting to note that the substitution with phenyl group takes place at the position ortho to sterically large nitro group in good yields. As an example, phenylations of *m*-dinitrobenzene by several methods[13] are compared above, and the comparison reveals the synthetic utility of the phenylation with PhN_2BF_4-$NaNO_2$ in DMSO.

13) P. E. Fanta, *Chem. Rev.*, **64**, 613 (1964); C. Björklund and M. Nilsson, *Tetrahedron Lett.*, **1966**, 675.

BULLETIN OF THE CHEMICAL SOCIETY OF JAPAN VOL. 43 1135—1138 (1970)

Formation of 4-Hydroxycarbostyrils in the Reaction of Carbon Suboxide with Aromatic Amines

Akira Omori, Noboru Sonoda and Shigeru Tsutsumi

Department of Chemical Technology, Faculty of Engineering, Osaka University, Yamadakami, Suita

(Received July 18, 1969)

The reactions of carbon suboxide with aromatic amines were found to give various 4-hydroxycarbostyril derivatives. The reaction between aniline and carbon suboxide usually gives malonanilide. However, it was found that the reaction of aniline with carbon suboxide in ether in the presence of aluminum chloride produced phenylcarbamoylacetic acid in a good yield and that cyclization to 4-hydroxycarbostyril occurred when the solvent was replaced by benzene before the decomposition of the reaction mixture with water. The solvent effect on the formation of 4-hydroxycarbostyrils and the possible reaction mechanism were discussed.

The reaction between carbon suboxide and several enolizable ketones have been reported to give pyrone and pyronopyrone derivatives.[1-3] In our recent publications,[3,4] we have reported the reaction of carbon suboxide with acetylacetone in the presence of sulfuric acid, thus producing 3-acetyl-6-hydroxy-2-methyl-4-pyrone. The reaction includes the cyclization of the *O*-acetylated ketenic intermediate to the pyrone, as is indicated below:

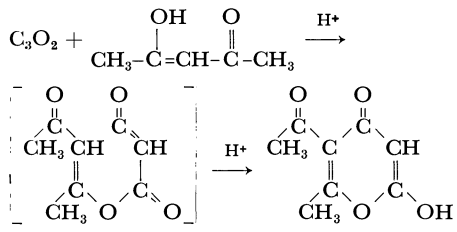

It has been reported that the reaction of carbon suboxide with aniline[5] gave malonanilide (I) quantitatively. In this case, the reaction may proceed *via* the *N*-acylated ketenic intermediate (IIa), which may be expected to produce 4-hydroxycarbostyril (II) if the intramolecular cyclization occurs.

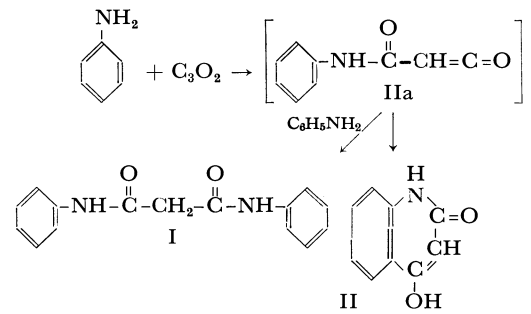

In the present paper, we wish to report on the formation of various 4-hydroxycarbostyril derivatives in the reaction of carbon suboxide with aromatic amines.

1) E. Ziegler and H. Bieman, *Monatsh. Chem.*, **93**, 34 (1962).

2) F. Haadetzky and E. Ziegler, *ibid.*, **97**, 398 (1966).

3) A. Omori, N. Sonoda, S. Okano and S. Tsutsumi, *Tetrahedron Lett.*, **1968**, 3647.

4) A. Omori, N. Sonoda and S. Tsutsumi, *J. Org. Chem.*, **34**, 2480 (1969).

5) L. H. Reyerson and K. Kobe, *Chem. Rev.*, **7**, 479 (1930).

Results and Discussion

Reaction with Aniline. The reaction of carbon suboxide with aniline in ether gave I quantitatively. The presence of a catalytic amount of sulfuric acid did not affect the reaction, and no II was obtained. A further attempt with aluminum chloride in carbon disulfide failed to give either II or phenylcarbamoylacetic acid (III), only I was isolated. However, the reaction of carbon suboxide with aniline in the presence of aluminum chloride in ether at room temperature gave III in a 78% yield when the reaction mixture was decomposed with water. On the other hand, II was obtained in a 17.3% yield when, before the decomposition of the reaction mixture with water, benzene was used in the place of ether and the benzene solution was refluxed at 80°C. The structures of II and III were confirmed by comparison with authentic samples in terms of their mass, infrared, and ultraviolet spectra. The results obtained in the reaction of carbon suboxide with aniline are summarized in Table 1.

Table 1. Reaction of carbon suboxide with aniline under various conditions

Reactant $C_6H_5NH_2$/ C_3O_2	Solvent	Catalyst	Reaction temp.	Product (yield)
1/1	CS_2	$AlCl_3$	r. t.	I (95%)
1/2	CS_2	$AlCl_3$	r. t.	I (100%)
1/2	Et_2O	none	r. t.	I (100%)
1/2	Et_2O	H_2SO_4	r. t.	I (100%)
1/2	Et_2O	$AlCl_3$	r. t.	III (78%)
1/3	$Et_2O \rightarrow C_6H_6$	$AlCl_3$	80°C	II(17.3%)

* Mole ratio

A possible reaction path for the formation of II is illustrated below. The first step in the reaction is considered to be the *N*-acylation to give an *N*-acylated intermediate (IIa), which, on cyclization, gives II and which, on reaction with one molecule of aniline and with water, gives I and III respectively.

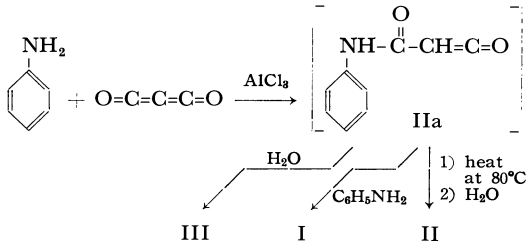

As is shown in Table 1, the solvent effect on the reaction with aniline is remarkable. In the first two cases in Table 1, I was formed quantitatively in carbon disulfide with aluminum chloride. However, in ether III was produced in a 78% yield under similar conditions. The reason for this solvent effect is that aluminum chloride may be catalytically inactive for the formation of I due to the formation of a complex ($\overset{\delta+}{Et_2O} \rightarrow \overset{\delta-}{AlCl_3}$); since no such complex is formed when carbon disulfide is used, it is thought that the activity of aluminum chloride remains such as to give I.

Reaction with Anisidines. The reaction of carbon suboxide with *o*,- *p*-, and *m*-anisidines (IV, V, and VI respectively) gave 4-hydroxy-methoxycarbostyrils in 29—67% yields under conditions similar to those used in the case of aniline. In the reaction with IV, 4-hydroxy-8-methoxycarbostyril (VII) was obtained in a 28.5% yield. With V, 4-hydroxy-6-methoxycarbostyril (VIII) was obtained in a 58.7% yield. The structures of VII and VIII were confirmed by comparison with authentic samples in terms of their infrared, ultraviolet, and mass spectral data. In the reaction of carbon suboxide with VI, a carbostyril derivative (mp 330°C) (IX) was obtained. In this case, 4-hydroxy-5-methoxy- and/or 4-hydroxy-7-methoxycarbostyril would normally be expected.

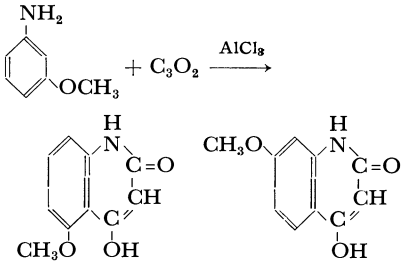

The structure of IX was examined by a comparison of its infrared and ultraviolet spectra with

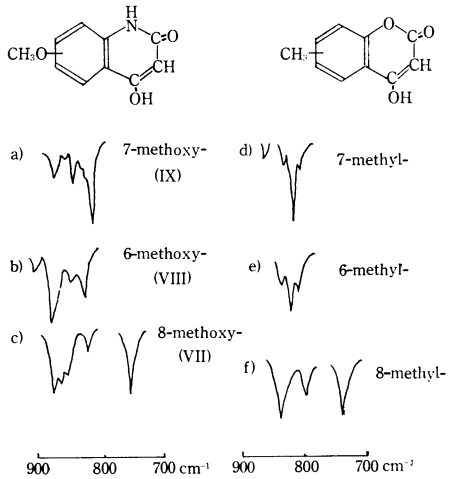

Fig. 1. The IR spectra between 900 cm^{-1} and 700 cm^{-1} of carbostyrils and coumarins.

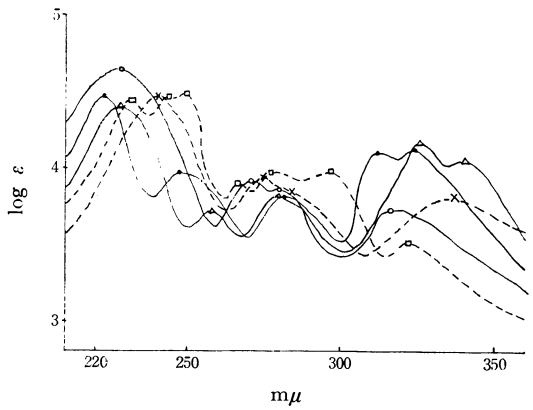

Fig. 2. The UV spectra of carbostyril derivatives.

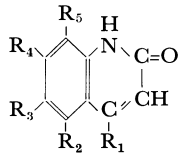

1) $R_1,R_2,R_3,R_5=H$, $R_4=CH_3$ (—△—△)
2) $R_1=OH$, $R_2,R_3,R_4=H$, $R_5=OCH_3$ (—□—□)
3) $R_1=OH$, $R_2,R_4,R_5=H$, $R_3=OCH_3$ (—×—×)
4) $R_1=OH$, $R_2,R_3,R_4,R_5=H$ (—○—○)
5) IX (—●—●)

those of other 4-hydroxycarbostyril and 4-hydroxycoumarin derivatives (Fig. 1 and Fig. 2).

The 1,2,3-trisubstituted benzene rings of 4-hydroxy-methylcoumarin and 4-hydroxy-methoxycarbostyril show characteristic absorption bands due to hydrogen on the benzene ring between 800 cm^{-1} and 700 cm^{-1}. However, IX shows no absorption bands in this region, and the spectrum between 900 cm^{-1} and 800 cm^{-1} can be interpreted rather as that for the 1,2,4-trisubstituted benzene derivative. The spectral data of some 1,2,4-trisubstituted benzene derivatives related to 4-hydroxycarbostyril are also shown in Fig. 1. This speculation is also supported by the ultraviolet spectral data shown in Fig. 2. On the basis of these facts, the structure of IX was assigned to 4-hydroxy-7-methoxycarbostyril. The results obtained in the reactions of anisidines are shown in Table 2.

Table 2. Reaction of carbon suboxide with anisidines

Reactant	Solvent	Catalyst	Reaction temp.	Product (yield)
IV	$Et_2O \rightarrow C_6H_6$	$AlCl_3$	80°C	VII(28.5%)
V	$Et_2O \rightarrow C_6H_6$	$AlCl_3$	80°C	VIII(58.7%)
VI	$Et_2O \rightarrow C_6H_6$	$AlCl_3$	80°C	IX (66.8%)

The reaction path for the formation of 4-hydroxy-methoxycarbostyrils may also include the cyclization of the *N*-acylated intermediate (X).

The better yields of carbostyril derivatives from anisidines than from aniline may be ascribed to

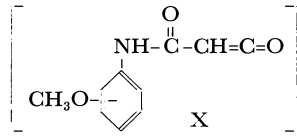

the electron-donating effect of the methoxyl group on the benzene ring in X. In the case of VI, the steric interaction between the methoxyl group and the ketenic group in the intermediate may affect the course of cyclization so as to favor the production of the 7-methoxycarbostyril rather than the 5-methoxy derivative.

Experimental

Preparation of Carbon Suboxide. Carbon suboxide was prepared by the pyrolysis[6] of diacetyltartaric anhydride at about 700°C and trapped at −78°C (a dry ice-methanol bath), and it was purified by distillation from trap to trap. The identification was established by the preparation of malonanilide by means of a reaction with aniline.

Reaction of Carbon Suboxide with Aniline in Carbon Disulfide. Into a suspension of aluminum chloride (15.2 g, 0.14 mol) in carbon disulfide (15 m*l*), we stirred a solution of carbon suboxide (8.8 g, 0.14 mol) in carbon disulfide (20 m*l*) at −70°C under nitrogen. Then a solution of aniline (11.8 g, 0.14 mol) in carbon disulfide (50 m*l*) was stirred, drop by drop, into this reaction mixture over a period of one hour. The reaction mixture was then maintained at −70°C for 6 hr, at 0°C for 9 hr and at room temperature for 9 hr. The reaction mixture was then poured into ice-water. The solid (19.5 g, 95%) which was deposited was recrystallized from ethanol to give I, mp 225°C.

Reaction of Carbon Suboxide with Aniline in Ether. The same procedure as described above was applied using aluminum chloride (6.9 g, 0.05 mol), carbon suboxide (3.4 g, 0.05 mol), and aniline (1.7 g, 0.017 mol), and ether (170 m*l*) instead of carbon disulfide. The reaction mixture was poured into ice water. The ether layer was dried over anhydrous magnesium sulfate, and the solid residue was recrystallized from chloroform to give III (2.2 g, 78%); mp 128°C; ν_{max}^{KBr} 1730 (C=O), 1670 (–NH–C(=O)–) cm^{-1}; an acidic test by $NaHCO_3$ was positive.

Found: C, 60.25; H, 4.90; N, 7.86%. Calcd for $C_9H_9NO_3$: C, 60.33; H, 5.06; N, 7.82%.

4-Hydroxycarbostyril (II). The same procedure as described above was applied using aluminum chloride (6.5 g, 0.04 mol), carbon suboxide (3.3 g, 0.049 mol), aniline (1.5 g, 0.016 mol), and ether (250 m*l*). After mixing the reactants, benzene (150 m*l*) was added, drop by drop, to the mixture, and at the same time the ether was evaporated by warming. After the ether had been removed completely, the benzene solution was refluxed at 80°C for 4 hr and then poured into ice water. A yellow solid, extracted with methanol from the solid deposited, was recrystallized from ethanol to give II; 0.46 g (17.3%); mp 333—335°C (decomp.); ν_{max}^{KBr} 2900 (–OH, –NH), 1680 (C=O), 1600 (C=C)

6) E. Ott, *Ber.*, **47**, 2388 (1914).

cm^{-1}; λ_{max}^{EtOH} 228 (log ε, 4.64), 270 (3.91), 315 (3.74) mμ; enolic –OH (by $FeCl_3$ test); $C_9H_7NO_2$ (M^+, 161).

4-Hydroxy-8-methoxycarbostyril (VII). By the treatment of carbon suboxide (2.2 g, 0.032 mol) with *o*-anisidine (1.3 g, 0.011 mol) in the presence of aluminum chloride (4.3 g, 0.032 mol) as has been described in the formation of II, VII was obtained; 0.58 g (28.5%); mp 243—243.5°C; ν_{max}^{KBr} 3200, 2950 (–NH, –OH), 1640 (C=O), 1600(C=C) cm^{-1}; λ_{max}^{EtOH} 231 (logε, 4.44), 243 (4.47), 249 (4.49), 266(3.91), 276(3.98), 286(3.98), 321(3.53) mμ; $C_{10}H_9NO_3$ (M^+, 191).

Found: C, 62.43; H, 4.95; N, 6.75%. Calcd for $C_{10}H_9NO_3$: C, 62.82; H, 4.75; N, 7.33%.

4-Hydroxy-6-methoxycarbostyril(VIII). By the treatment of carbon suboxide (2.8 g, 0.04 mol) with *p*-anisidine (1.7 g, 0.014 mol) in the presence of aluminum chloride (5.4 g, 0.04 mol) as has been described above, VIII was obtained; 1.52 g (58.7%); mp 305°C (decomp.); ν_{max}^{KBr} 3400, 2950(–NH, –OH), 1660(C=O), 1610(C=C) cm^{-1}; λ_{max}^{EtOH} 240 (logε, 4.45), 274(3.93), 283(3.86), 336(3.81) mμ; $C_{10}H_9NO_3$ (M^+, 191).

Found: C, 63.09; H, 4.70; N, 7.56%. Calcd for $C_{10}H_9NO_3$: C, 62.82; H, 4.75; N, 7.33%.

4-Hydroxy-7-methoxycarbostyril (IX). By the treatment of carbon suboxide (2.8 g, 0.04 mol) with *m*-anisidine (1.7 g, 0.014 mol) in the presence of aluminum chloride (5.4 g, 0.04 mol) as has been described above, IX was isolated; 1.73 g (66.8%); mp 330°C (decomp.); ν_{max}^{KBr} 3100, 2900(–NH, –OH), 1690, 1640 (C=O), 1615(C=C) cm^{-1}; λ_{max}^{EtOH} 222 (logε, 4.47), 247 (3.98), 281(3.84), 311(4.10), 323(4.12) mμ; $C_{10}H_9NO_3$ (M^+, 191).

Found: C, 63.21; H, 4.69; N, 7.92%. Calcd for $C_{10}H_9NO_3$: C, 62.82; H, 4.75; N, 7.33%.

BULLETIN OF THE CHEMICAL SOCIETY OF JAPAN VOL. 43 1138—1141 (1970)

The Optical Rotatory Dispersion and Circular Dichroism of Aromatic Amino Acids*1,2

Naokazu SAKOTA, Kozo OKITA and Yasuhiko MATSUI

Department of Industrial Chemistry, Faculty of Engineering, Ehime University, Bunkyo-cho, Matsuyama

(Received August 8, 1969)

The CD and ORD of D-phenylglycine and L-phenylalanine were measured at various pH's. The superficial small pH dependence of the CD maximum around 220 mμ and the anomalous large $[\theta]$ value at the CD maximum in both aromatic amino acids suggest an interaction between the ^1L_a transition of the benzene ring and the $n\rightarrow\pi^*$ transition of the carboxyl group. The ORD and CD of L-α-amino-β-benzalpropionic acid, L-α-amino-β-benzylpropionic acid, and L-2-amino-4-phenyl-butanol-1 were also measured, and the screening effect of the methylene groups which exist between a benzene ring and an asymmetric carbon atom was discussed.

Studies of the optical rotatory dispersion (ORD) and circular dichroism (CD) of optically active aromatic compounds have revealed that in some compounds, ^1L_a and ^1L_b transitions of the benzene ring in Platt's notation[1] are optically active.[2,3] It has also been reported that the ^1L_b transition of the benzene ring is optically active in such aromatic amino acids as tyrosine,[3] tryptophan,[3] and phenylalanine.[4] However the absorption maximum corresponding to the ^1L_a transition is situated so close to that of the $n\rightarrow\pi^*$ transition of the carboxyl group that it is not obvious whether the ^1L_a transition of aromatic amino acid is optically active or not.

Sakota (one of the present authors) has previously shown[5] that the CD curve of an aromatic amino acid is closely related to that of its acryloyl derivative, although a new CD maximum around 230 mμ appears in the acryloyl derivatives of aliphatic amino acids. These facts suggest that a Cotton effect in 220 mμ regions of aromatic amino acids corresponds to the phenyl chromophore rather than to the carboxyl chromophore. Furthermore, in comparing the ORD curves of phenylalaninol and tyrosinol with those of the corresponding amino acids, Rosenberg[6] has suggested that the ^1L_a transition of the benzene ring is optically active.

In the present experiment, the present authors have measured the ORD and CD curves of D-

*1 Studies of Optical Rotatory Dispersion, Part V. Part IV: N. Sakota, T. Tanigaki, K. Okita and N. Koine, *Nippon Kagaku Zasshi*, **90**, 593 (1969).

*2 Presented at the 22nd Annual Meeting of the Chemical Society of Japan, Tokyo, 1969.

1) J. R. Platt, *J. Chem. Phys.*, **16**, 832 (1948).

2) L. Verbit and Y. Inoue, *J. Amer. Chem. Soc.*, **89**, 5717 (1967).

3) E. Iizuka and J. T. Yang, *Biochem.*, **3**, 1519 (1964).

4) A. Moscowitz, A. Rosenberg and A. E. Hansen, *J. Amer. Chem. Soc.*, **87**, 1813 (1965).

5) N. Sakota, *Nippon Kagaku Zasshi*, **89**, 425 (1968).

6) A. Rosenberg, *J. Biol. Chem.*, **241**, 5119 (1966).

phenylglycine and L-phenylalanine at various pH's, and also, the ORD and CD curves of three more optically active aromatic amino acids synthesized. The results gave direct support to the above-mentioned suggestions, indicating the screening effect of the methylene groups which exist between an asymmetric carbon atom and a benzene ring in aromatic amino acids.

TABLE 1

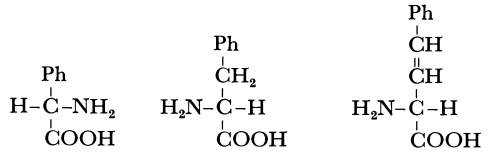

D-Phenylglycine (I) | L-Phenylalanine (II) | L-α-Amino-β-benzalpropionic acid (III)

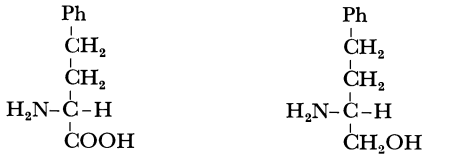

L-α-Amino-β-benzylpropionic acid (IV) | L-2-Amino-4-phenylbutanol-1 (V)

Experimental

Materials. Chromatographically- and optically-pure D-phenylglycine (I) and L-phenylalanine (II) were purchased from the Yoneyama Chemical Industry Co., Ltd.

Preparations. *L-α-Amino-β-benzalpropionic Acid (III).* DL-α-Amino-β-benzalpropionic acid (11 g, 0.0615 mol), prepared from cinnamaldehyde and sodium cyanide by the method of Ref. 7, was dissolved in 32 m*l* of 2N NaOH (0.062 mol). To this solution 6.4 g (0.062 mol) of acetic anhydride and 32 m*l* (0.062 mol) of 2N NaOH were added at 0°C over a period of about 1 hr. Then, the mixture was stirred for one more hour, after which the pH of the solution was adjusted with 6N HCl to 2.0 and the acetyl-DL-α-amino-β-benzalpropionic acid thus precipitated was filtered out in order to dry it. The yield was 11 g (81%), mp 133—134°C. Acetyl-DL-α-amino-β-benzalpropoinic acid (11 g, 0.05 mol) was dissolved in 25 m*l* of 2N LiOH and adjusted to pH 7.5, the clear upper solution of a suspension of 2.5 g of Biodiastase (purchased from the Amano Pharmaceutical Co., Ltd.) in 10 m*l* of water was then added. After the mixture had stood at 37°C for 5 hr, the crystalline precipitate (III) was filtered off and recrystallized from methanol-water. Yield 3 g (75%), $[\alpha]_D^{20}$ −20° (*c* 1, 0.1N HCl).

Found: C, 67.50; H, 6.10%. Calcd for $C_{10}H_{11}O_2N$: C, 67.77; H, 6.45%.

L-α-Amino-β-benzylpropionic Acid (IV). L-α-Amino-β-benzalpropionic acid (2.5 g, 0.014 mol) was dissolved in 10% acetic acid, 200 mg of 10% palladium charcoal (purchased from the Kawaken Fine Chemical Co., Ltd.) was added, and the mixture was hydrogenated at room temperature for 5 hr. Then, the catalyst was filtered off and the filtrate was concentrated *in vacuo*. IV was precipitated by the addition of methanol and filtered off. Yield 2.3 g (95%), $[\alpha]_D^{20}$ −18° (*c* 1, 0.1N HCl). Ref.[8] $[\alpha]_D^{20}$ −17.7° (*c* 1, 0.1N HCl).

L-2-Amino-4-phenylbutanol-1 (V). L-α-Amino-α-benzylpropionic acid (2 g, 0.012 mol) was added to a solution of 1.2 g (0.032 mol) of $LiAlH_4$ in 30 m*l* of ether over a 20-min period. Stirring was continued for 30 more min, and then water was added to decompose the unreacted $LiAlH_4$. The precipitate was filtered off and washed with ether. The ether solution was dried over anhydrous magnesium sulfate and concentrated *in vacuo*. The crystalline material was filtered off and recrystallized from ethyl acetate. Yield 0.4 g (24.4%), mp 95—96°C, $[\alpha]_D^{20}$ −12° (*c* 1, MeOH).

Found: C, 72.60; H, 9.21%. Calcd for $C_{10}H_{15}ON$: C, 72.65; H, 9.28%.

Measurements. The optical rotatory dispersion and circular dichroism were measured at room temperature with a Jasco-model ORD/UV-5 optical rotatory dispersion recorder with a CD attachment. The cells used were 1 mm long except for III (0.1 mm). Samples of I and II were dissolved in distilled water (about 0.1—0.5 mg/m*l*), and the pH was adjusted with aqueous sodium hydroxide or hydrochloric acid.

Results and Discussion

The CD curves of D-phenylglycine (I) and L-phenylalanine (II) are shown in Fig. 1 and Fig. 2 respectively. The pH-dependent CD measure-

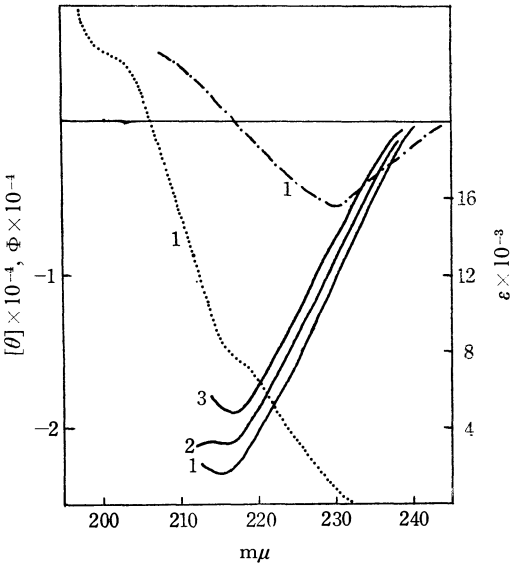

Fig. 1. CD (———), ORD (— • —) and UV (·····) spectra of D-phenylglycine (I).
(1: pH 2.45, 2: pH 6.40, 3: pH 9.75)

7) S. Pinner and A. Spilker, *Ber.*, **22**, 689 (1989).

8) P. E. Gagnon and B. Nolin, *Can. J. Res.*, **B27**, 742 (1949).

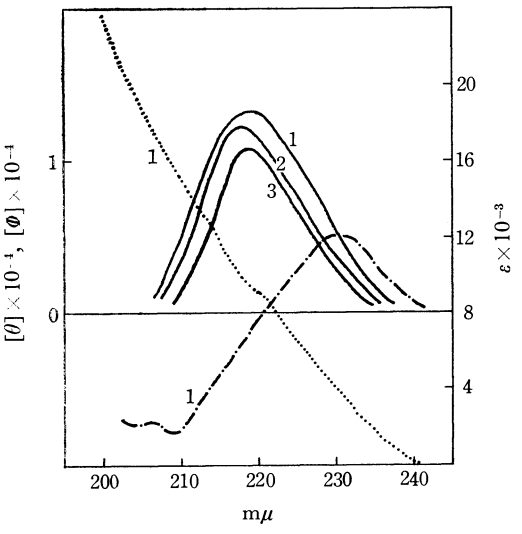

Fig. 2. CD (———), ORD (—·—) and UV (·····) spectra of L-phenylalanine (II).
(1: pH 2.45, 2: pH 6.40, 3: pH 9.81)

ments had little influence on the wavelength of the CD maximum in the 220 mμ region, though in the case of aliphatic amino acids dramatic changes have been reported.[9] These facts suggest that the CD maximum in the 220 mμ region for I and II is attributable to the aromatic chromophore rather than to the carboxyl chromophore. However, the 220 mμ CD maximum should be partly ascribed to the carboxyl $n\rightarrow\pi^*$ transition, because the superficial small pH dependence of the 220 mμ CD maximum observed in these two aromatic amino acids is presumably associated with the anomalous large contribution of the ^1L_a transition of the aromatic chromophore.

In fact, the molecular ellipticities [θ] at the 220 mμ CD maximum of I and II are about 20000—23000 and 11000—13000 respectively, though the aliphatic amino acids show the value of 3000—5000,[9] and the aromatic compounds without a carboxyl group, about 3000.[6] Therefore, it may be deduced that the 220 mμ CD maximum in aromatic amino acids should not be ascribed to the mere sum of the contributions of an aromatic chromophore and a carboxyl chromophore, but, rather, to the results of the interaction of the two chromophores.

Lucas[10] measured the UV spectra of the compounds with the general formulae of $C_6H_5(CH_2)_n$-$CH{:}CH_2$ and $C_6H_5(CH_2)_nCH(COOH)CH_2COOH$; he suggested the presence of the interaction of the two chromophores in the case of $n=1$. As in the case of I, there exists an aromatic chromophore interacted with a carboxyl group through an asymmetric carbon atom, it can be proved that I should show a [θ] value larger than the sum of the contributions of the two chromophores.

On the other hand, II contains a methylene group and an asymmetric carbon atom between carboxyl and phenyl chromophores, so it is difficult to explain the relatively large [θ] value at 220 mμ by Lucas's theory. Recently, Cavanaugh[11] mentioned that in light of the NMR measurements, the conformer, (A) or (B), in which the phenyl group

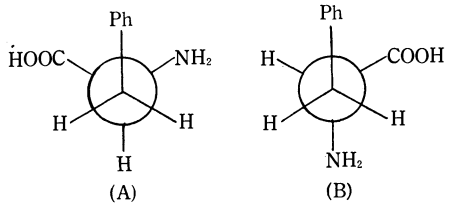

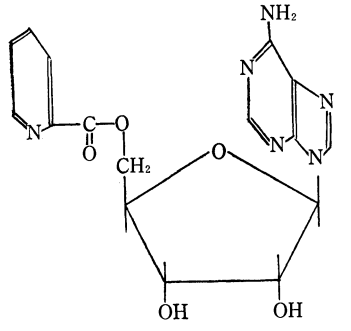

(C)

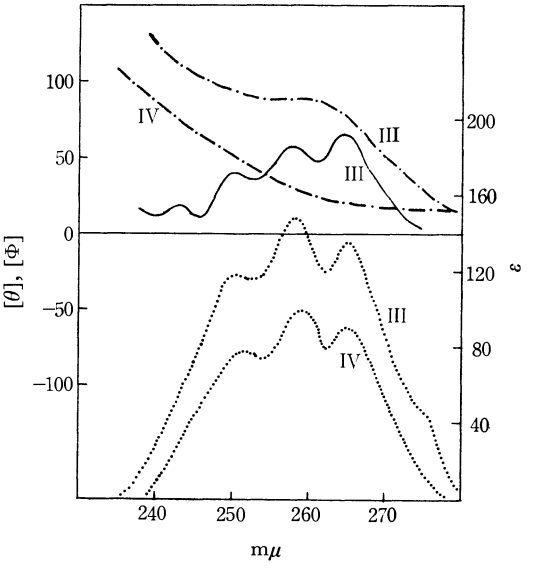

Fig. 3. CD (———), ORD (—·—) and UV (·····) spectra of L-α-amino-β-benzalpropionic acid (III) and L-α-amino-β-benzylpropionic acid (IV) (in 0.1N HCl).

9) M. Legland, *Bull. Soc. Chim. Fr.*, **1965**, 679.
10) R. Lucas, *ibid.*, **1932**, 51, 289, 965.
11) J. R. Cavanaugh, *J. Amer. Chem. Soc.*, **90**, 4533 (1968).

is gauche to the carboxyl group is considerably predominant in the phenylalanine anion and in the dipolar ion. Urry[12] has also concluded that the large molecular ellipticity for adenosine-5′-mononicotinate (C) is caused by the reciprocal relation between the adenine and the nicotinic acid residue. In phenylalanine, it may be suggested that the benzene-ring plane can run nearly parallel to the carboxyl group, therefore, the $[\theta]$ value at 220 mμ becomes larger by means of interaction between the aromatic ^1L_a transition and the carboxyl $n\rightarrow\pi^*$ transition.

Figure 3 shows the ORD, CD, and UV spectra in the 260 mμ region for L-α-amino-β-benzalpropionic acid (III) and L-α-amino-β-benzylpropionic acid (IV) in 0.1N HCl. III reveals a multiple-humped positive CD maximum corresponding to the 250—265 mμ absorption maximum, and a weak Cotton effect in the ORD curve, these characteristics show that the ^1L_b transition of III is optically active. Although IV also shows the multiple-humped absorption band of the ^1L_b transition in 250—265 mμ, neither the CD maximum nor the anomalous dispersion curve are observed. The results imply that the ^1L_b transition is not optically active in the case of IV. From these facts, it is evident that the ^1L_b transition of the compounds with the $C_6H_5(CH_2)_nCH(NH_2)COOH$ formula is optically active in $n=0$ or $n=1$, but inactive in $n=2$.

The ORD, CD and UV spectra for III and IV in the 220 mμ region are shown in Fig. 4. The ORD and CD curves of III shows the CD maximum and an anomalous dispersion, these characteristic may be explained in a manner similar to that used for I. Although IV has a CD maximum at 207 mμ, it is not obvious that this CD maximum is to be attributed to either the ^1L_a transition of the aromatic chromophore or to the $n\rightarrow\pi^*$ transition of the carboxyl chromophore. The CD, ORD and UV spectra of L-2-amino-4-phenylbutanol-1 (V), which was synthesized from IV by the reduction of the carboxyl group, were measured in 0.1N HCl (Fig. 5).

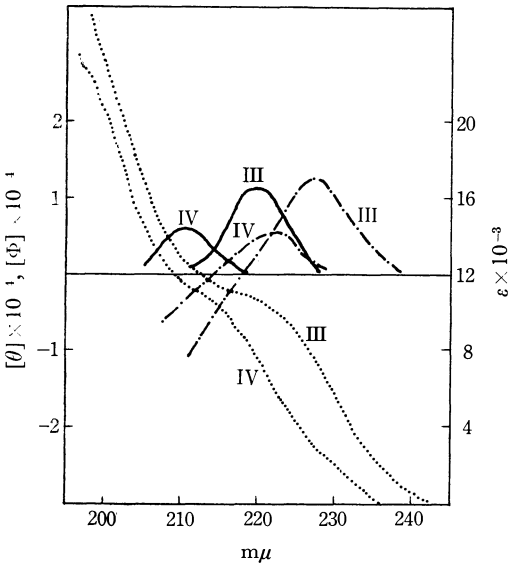

Fig. 4. CD (———), ORD (—·—) and UV (·····) spectra of L-α-amino-β-benzalpropionic acid (III) and L-α-amino-β-benzylpropionic acid (IV).

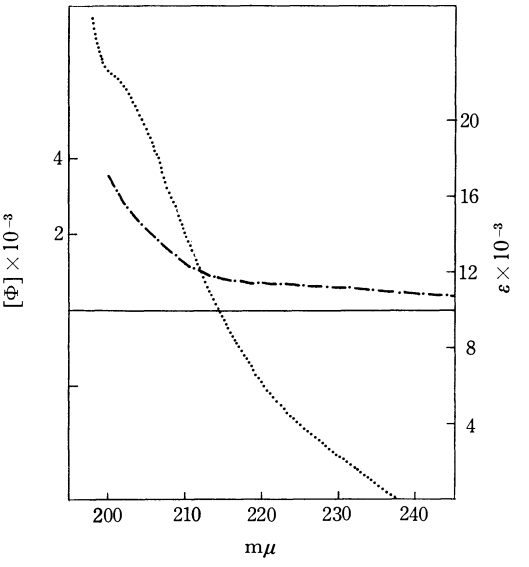

Fig. 5. ORD (—·—) and UV (·····) spectra of L-2-amino-4-phenylbutanol-1 (V) (in 0.1N HCl).

V had a large shoulder of ^1L_a transition in the 200—205 mμ region of the UV absorption spectrum, but no anomalous dispersion was observed. Therefore, it is evident that the ^1L_a transition of V is not optically active; this implies that the 207 mμ CD maximum of IV is to be attributed not to the ^1L_a transition of the benzene ring but to the carboxyl $n\rightarrow\pi^*$ transition.

12) D. W. Miles and D. W. Urry, *J. Phys. Chem.*, **71**, 4448 (1967).

BULLETIN OF THE CHEMICAL SOCIETY OF JAPAN VOL. 43 1142—1147 (1970)

Syntheses and NMR Spectra of the Substituted Methylferrocenes

Masaru SATO, Michinao KOGA, Izumi MOTOYAMA and Kazuo HATA

Department of Chemistry, Faculty of Science, Tokyo Metropolitan University, Setagaya-ku, Tokyo

(Received September 8, 1969)

Several 1′- and 2-substituted 1-methylferrocenes were prepared, and their NMR spectra were measured. From the consideration of the chemical shifts, the transmission coefficient of the electronic effect through the ferrocene nucleus was calculated to be 0.28. 1′-Substituted 1-acetylferrocenes were also prepared, and their NMR spectra were discussed in connection with those of methylferrocenes.

Since the discovery of the fact that the unsubstituted ring of acetylferrocene was acetylated about 10^4 times slower than those of ferrocene itself,[1] the transmissivity of the electronic effect of substituents through the ferrocene system has been widely studied. For example, linear relationships have been observed between the Hammett σ constants and various reaction constants, such as the dissociation constants of various heteroannularly-substituted ferrocenecarboxylic acids,[2,3] the quarter-wave potentials in the chronopotentiometric oxidation of mono- and disubstituted ferrocenes,[4] the shifts of the carbonyl stretching frequencies in the IR spectra of substituted ferrocenecarboxylic acids and esters,[5] the rates of the esterification of heteroannularly-substituted ferrocenecarboxylic acids with diphenyldiazomethane,[6] the rates of the desilylation of 1′-alkyl-1-(trialkylsilyl)ferrocenes,[7] the rates of the protodemercuration of bis(1′-substituted ferrocenyl)mercury,[8] and the rates of the solvolysis of 1′-substituted ferrocenylmethylcarbinyl acetates.[9] However, the electronic effect of homoannular substituents has been little studied. Only a few investigations concerning the chemical shifts of the ring protons in monosubstituted ferrocenes[10] and *p*-substituted phenylferrocenes,[11] and the rates of the acetylation of alkylferrocenes[7] are available.

The chemical shifts of the benzene protons or the side-chain protons in the substituted benzene derivatives have been reported to correlate with Hammett σ constants. For example, the chemical shifts of the methyl groups in *p*-substituted toluenes have linear correlations with the σ^+ constants.[12] In the present study, the NMR spectra of 1′- and 2-substituted methylferrocenes and of 1′-substituted acetylferrocenes were measured in order to get some information about the transmission of the electronic effect through the ferrocene system. An improved method for preparing these compounds will be presented, together with a discussion of the NMR spectra.

Results and Discussion

Syntheses of 1′-Substituted Methylferrocenes. Since methylferrocene is more reactive toward electrophilic reagents than is ferrocene itself, it always affords a mixture of three isomers on acetylation, dimethylaminomethylation, and chloromercuration.[13] Because of the difficulty of separating the isomers each other, some indirect routes which lead selectively to 1′-isomers were devised in the following manner. When formyl-

1) M. Rosenblum, J. O. Santer and W. G. Howells, *J. Amer. Chem. Soc.*, **85**, 1450 (1963).
2) A. N. Nesmeyanov and O. A. Reutov, *Dokl. Akad. Nauk SSSR*, **115**, 518 (1957).
3) W. F. Little and R. Eisenthal, *J. Org. Chem.*, **26**, 3609 (1961).
4) W. F. Little, C. N. Reilley, J. D. Johnson and A. P. Sanders, *J. Amer. Chem. Soc.*, **86**, 1382 (1964).
5) L. A. Kazitsyna, B. V. Lokshin and A. N. Nesmeyanov, *Dokl. Akad. Nauk SSSR*, **127**, 333 (1959).
6) W. F. Little and R. Eisenthal, *J. Amer. Chem. Soc.*, **83**, 4936 (1961).
7) R. A. Benkeser, Y. Nagai and J. Hooz, *ibid.*, **86**, 3742 (1964).
8) A. N. Nesmeyanov, E. G. Perevalova, S. P. Gubin and A. G. Kozlovskii, *Dokl. Akad. Nauk SSSR*, **178**, 616 (1968).
9) D. W. Hall, E. A. Hill and J. H. Richards, *J. Amer. Chem. Soc.*, **90**, 4972 (1968).
10) G. G. Dvoryantseva, S. L. Partnova, K. I. Grandgerg, S. P. Gubin and Yu. N. Sheinker, *Dokl. Akad. Nauk SSSR*, **160**, 1075 (1965).
11) M. Rosenblum, "Chemistry of the Iron Group Metallocenes," Part 1, John Wiley and Sons, Inc., New York, N. Y. (1965), p. 215.
12) Y. Yukawa, M. Sakai, K. Kabazawa and Y. Tsuno, *Mem. Inst. Sci. Ind. Research Osaka Univ.*, **17**, 185 (1960).
13) G. R. Knox, I. G. Morrison, P. L. Pauson, M. A. Sandhu and W. E. Watts, *J. Chem. Soc., C*, **1967**, 1853.

ferrocene was acetylated with three molar amounts of acetyl chloride and aluminum chloride in dichloromethane under cooling, only 1′-acetyl-1-formylferrocene was obtained in a 41% yield. Under somewhat severer conditions, two additional products were isolated. The minor product of the two, which was eluted ahead of 1′-acetyl-1-formylferrocene on chromatographic separation on alumina, seemed to be 3-acetyl-1-formylferrocene, judging from its IR and NMR spectra. The other (1.2% yield), which was eluted after 1′-acetyl-1-formylferrocene, was identified to be 1-(1′-formylferrocenyl)-3-(1″-acetylferrocenyl)-2-propen-1-one (**1**) on the basis of its IR and NMR spectra and

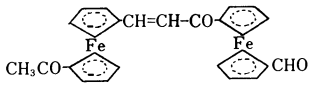

(**1**)

its elemental analysis. In view of the large coupling constant (15.7 Hz) of the vinyl protons of **1**, it can be concluded that **1** has a *trans* configuration with respect to the olefinic double bond. On the reduction of 1′-acetyl-1-formylferrocene by lithium aluminum hydride-aluminum chloride compelx,[14] 1′-ethyl-1-methylferrocene was obtained in a good yield.

We have reported in a previous paper[15] that when 1,1′-diiodoferrocene was treated with copper(I) cyanide in boiling pyridine, 1′-iodo-1-cyanoferrocene was exclusively obtained. This compound proved to be useful as a starting material for the preparation of 1′-substituted methylferrocenes. On the hydrolysis of 1′-iodo-1-cyanoferrocene in a boiling 40% aqueous potassium hydroxide solution for 15 hr, 1′-iodo-1-ferrocenecarboxylic acid was obtained in a 74% yield, whereas the reaction for 4 hr gave 1′-iodo-1-ferrocenecarboxamide as the main product (77% yield). This can be explained by assuming that the reaction may be suppressed by the electron-attracting effect of the iodo group, since 1′-ethyl-1-cyanoferrocene can be hydrolyzed within a shorter period to give, quantitatively, 1′-ethyl-1-ferrocenecarboxylic acid.[16] 1′-Iodo-1-ferrocenecarboxylic acid gave its methyl ester when treated with diazomethane in an ice bath. The reduction of the ester with lithium aluminum hydride and aluminum chloride afforded 1′-iodo-1-methylferrocene in a poor yield. Since no dehalogenated product was detected, this low yield seems to be due to the decomposition of the starting material by the action of the reducing agent. 1′-Iodo-1-methylferrocene was converted into 1′-cyano- and 1′-chloro-1-methylferrocene when treated with copper(I) cyanide and chloride respectively.[15]

Syntheses of 2-Substituted 1-Methylferrocenes. It has recently been reported that 2-haloferrocenylmethanol[17] could be obtained from 2-lithio-1-(dimethylaminomethyl)ferrocene.[18,19] This procedure has now been applied to the synthesis of 2-halo-1-methylferrocenes; 2-bromo- and 2-chloro-1-ferrocenylmethanol thus obtained were reduced with lithium aluminum hydride-aluminum chloride complex to give the corresponding 2-halo-1-methylferrocene in a moderate yield. When 2-chloro-1-methylferrocene was heated with copper(I) cyanide in γ-picoline at 145°C, 2-cyano-1-methylferrocene was obtained in a 22% yield. On the other hand, 2-ethyl-1-methylferrocene was obtained in a good yield on the Clemmensen reduction of 2-acetyl-1-methylferrocene.[20]

NMR Spectra. The NMR spectra of 2- and 1′-substituted methylferrocenes thus obtained were measured as about a 20% solution in carbon tetrachloride, while those of 1′-substituted acetylferrocenes were measured in deuteriochloroform.

Table 1. The chemical shifts of acetyl protons in 1′-substituted 1-acetylferrocenes in deuteriochloroform

	Substituent (X)	Chemical shift(δ) (Hz)	Δδ (Hz)
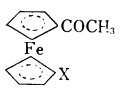	C_2H_5	142.1	−1.1
	H	143.2	0.0
	Cl	144.1	0.9
	CN	145.7	2.5
	$COCH_3$	140.8	−2.4
	$COOCH_3$	141.8	−1.4

Table 2. The chemical shifts of methyl protons in 1′-substituted 1-methylferrocenes in carbon tetrachloride

	Substituent (X)	Chemical shift (δ) (Hz)	Δδ (Hz)
	C_2H_5	116.2	−1.0
	H	117.2	0.0
	Cl	118.1	0.9
	CN	120.5	3.3

14) K. Schlögl, A. Mohar and M. Peterlik, *Monatsh. Chem.*, **92**, 921 (1961).

15) M. Sato, T. Ito, I. Motoyama, K. Watanabe and K. Hata, This Bulletin, **42**, 1976 (1969).

16) A. N. Nesmeyanov, V. A. Sazonova and V. N. Drozd, *Dokl. Akad. Nauk SSSR.*, **137**, 102 (1961).

17) G. Marr, R. E. Moore and B. W. Rockett, *J. Chem. Soc., C*, **1968**, 24.

18) D. W. Slocum, B. W. Rockett and C. R. Hauser, *J. Amer. Chem. Soc.*, **87**, 1241 (1965).

19) R. L. Gay, T. F. Crimmins and C. R. Hauser, *Chem. Ind.* (London), **1966**, 1635.

20) E. A. Hill and J. H. Richards, *J. Amer. Chem. Soc.*, **83**, 4216 (1961).

Table 3. The chemical shifts of methyl protons in 2-substituted 1-methylferrocenes in carbon tetrachloride

	Substituent (X)	Chemical shift (δ) (Hz)	$\Delta\delta$ (Hz)
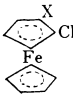	C_2H_5	114.8	−2.4
	H	117.2	0.0
	Cl	121.9	4.7
	CN	129.5	12.3
	$COCH_3$	134.3	17.1

The chemical shifts of these methyl and acetyl protons are summarized in Tables 1, 2, and 3.

In order to examine the substituent effects, the relative chemical shifts ($\Delta\delta$) of the protons in each series were plotted *versus* the Hammett σ_p constants. These results are shown in Fig. 1 for 1′-substituted acetylferrocenes and in Fig. 2 for 1′- and 2-substituted methylferrocenes. It is clear from Fig. 1 that an excellent linear correlation is present between the Hammett σ_p constants and the chemical shifts of the acetyl protons of 1′-substituted 1-acetylferrocenes and acetylferrocene itself, except for those of 1′-acetyl- and 1′-methoxycarbonyl-1-acetylferrocene. An irregularity observed in the compounds containing an extra carbonyl substituent is considered to be due to the large magnetic anisotropy of the carbonyl group.[21] Therefore, the substituent effects will be discussed on the basis of the shifts observed with substituents other than the carbonyl-containing substituent. The same limitation was applied in the consideration of the chemical-shift differences between 1′- and 2-substituted methylferrocenes, and good correlations were observed between the chemical shifts of the methyl protons and the

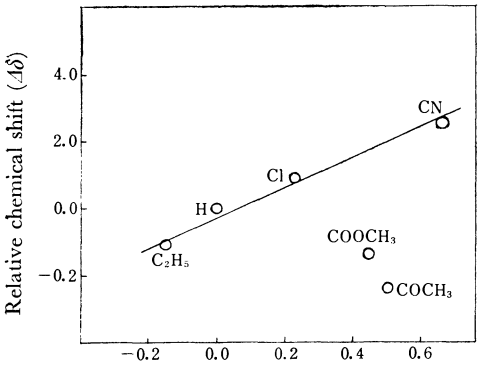

Fig. 1. Plot of the relative chemical shifts of 1′-substituted 1-acetylferrocenes against Hammett σ_p constant.

21) M. I. Levenberg and J. H. Richards, *J. Amer. Chem. Soc.*, **86**, 2634 (1964).

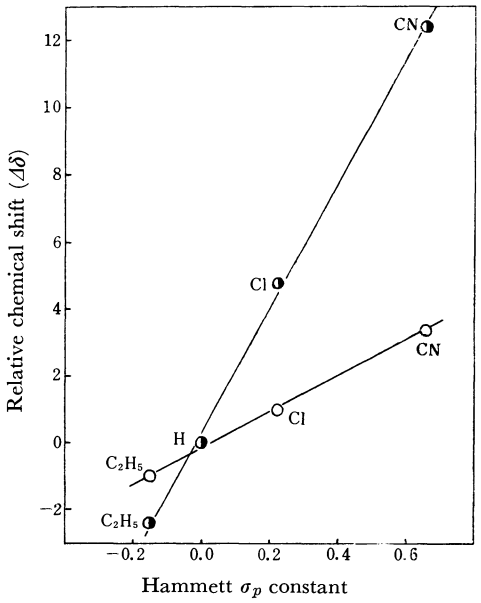

Fig. 2. Plot of the relative chemical shifts of substituted methylferrocenes against Hammett σ_p constant: ◑, 2-derivatives; ○, 1′-derivatives.

Hammett σ_p constants in either series. The following equations are those of the regression lines, shown in Figs. 1 and 2, which were calculated by the method of least squares:

$$\Delta\delta = 4.4\,\sigma_p + 0.1$$

for 1′-substituted 1-acetylferrocenes,

$$\Delta\delta = 5.2\,\sigma_p - 0.2$$

for 1′-substituted 1-methylferrocenes, and

$$\Delta\delta = 18.3\,\sigma_p + 0.3$$

for 2-substituted 1-methylferrocenes.

It is quite interesting that an excellent linear relationship, one with a correlation coefficient more than the 0.99 for the methylferrocene series, was found between the chemical shifts in the acetylferrocenes or methylferrocenes and the Hammett σ_p constants, while good correlations were not found with the other σ constants, such as σ_m, σ^+, and σ^*. In accordance with these observations, there have been reported many findings that various chemical behaviors of ferrocene derivatives correlated with Hammtt σ_p constants.[2-9]

As may be seen in Fig. 2, the chemical shifts of methyl protons in 2-substituted 1-methylferrocenes were found to correlate with Hammett σ_p constants, while no linear correlation was found with the σ^+ constants. A similar tendency had already been reported for those of the cyclopentadienyl ring protons in *p*-substituted phenylferrocenes, but without any detailed discussion.[11] On the other hand, it has been found that the chemical shifts of methyl protons in *p*-substituted toluenes and acetyl protons in *p*-substituted acetophenones correlated linearly

with the σ^+ constants.[12] The difference between the observations of ferrocene derivatives and of benzene derivatives suggests that the transmission of an electronic effect in 2-substituted methylferrocene might be through some way different from such a resonance effect of the substituent as was seen in benzene derivatives. The transmission of an electronic effect in ferrocene derivatives is probably through the total electron density of the ferrocene nucleus, without the loss of its stability due to the aromaticity.

It is clear from Fig. 2 that the regression lines for 1′- and 2-substituted methylferrocenes have different slopes. These differences can undoubtedly be attributed to the differences in the transmissivity of the electronic effect of the substituent. Hence, the ratio of these slopes, 0.28, may be considered to be the transmission coefficient of the electrnoic effect through the ferrocene nucleus. A similar value (0.22) was reported by Butter and Beachell,[22] who calculated it on the basis of the data reported by Nagai *et al.*[23] On the other hand, a transmission coefficient through a benzene ring was reported to be 0.37;[24] this was calculated on the basis of the dissociation constants of substituted 4-biphenylcarboxylic acids. In view of the intervention of an iron atom in the transmission of the electronic effect through the ferrocene ring, a smaller value is to be expected for the transmission coefficient through the ferrocene nucleus than for that through the benzene ring. Therefore, the value (0.28) obtained in this investigation seems reasonable.

Experimental

1′-Iodo-1-ferrocenecarboxylic Acid. 1′-Iodo-1-cyanoferrocene (1.12 g), which had been prepared from 1,1′-diiodoferrocene by a procedure reported previously,[15] was refluxed for 15 hr with 7.5 m*l* of a 40% aqueous potassium hydroxide solution and 16 m*l* of ethanol. The dark reaction mixture was then filtered out. The filtrate was acidified with dilute hydrochloric acid and extracted with ether, and then the ethereal solution was dried over anhydrous magnesium sulfate. The evaporation of the solvent gave red-orange crystals of 1′-iodo-1-ferrocenecarboxylic acid in a 73.7% yield; the acid was then recrystallized from benzene, mp 138.5°C (decomp.).

Found: C, 37.43; H, 2.42%. Calcd for $C_{11}H_9IFe$: C, 37.08; H, 2.52%.

The dark orange solid remaining after the filtration of the reaction mixture was dissolved in chloroform. After the insoluble matters had been filtered off, the filtrate was washed with water and dried over anhydrous magnesium sulfate. By evaporating the solvent, orange crystals of 1′-iodo-1-ferrocenecarboxamide were obtained (0.21 g, 18.7% yield); these were recrystallized from *n*-hexane, mp 136—137.5°C.

Found: C, 37.76; H, 3.17; N, 4.11%. Calcd for $C_{11}H_{10}ONIFe$: C, 37.18; H, 2.82; N, 3.94%.

When the same reaction was stopped after 4 hrs' heating, the main product was the amide (77.1% yield), while the minor product was the acid (14.6%). No recovery of unchanged nitrile was observed in either reaction.

Methyl 1′-Iodo-1-ferrocenecarboxylate. A solution of 1′-iodo-1-ferrocenecarboxylic acid (1.27 g) in 20 m*l* of ether was added, drop by drop, with vigorous stirring into an ethereal solution of diazomethane prepared from 1.0 g of nitrosomethylurea. After the addition of the acid had been completed, stirring was continued further an additional hour. After the solvent had been removed under reduced pressure, the residue was dissolved again in ether. The solution was washed successively with an aqueous sodium hydroxide solution and with water, and then dried. After the removal of the solvent, the residue was chromatographed on alumina to give methyl 1′-iodo-1-ferrocenecarboxylate in a 75.8% yield; the ester was recrystallized from *n*-hexnae, mp 71—72.5°C.

Found: C, 39.19; H, 3.03%. Calcd for $C_{12}H_{11}O_2$-IFe: C, 38.92; H, 3.00%.

From the sodium hydroxide solution, 0.30 g (23.6%) of the starting material was recovered.

1′-Iodo-1-methylferrocene. Methyl 1′-iodo-1-ferrocenecarboxylate (1.2 g, 3.2 mmol) was added, little by little, to a suspension of 0.25 g (6.5 mmol) of lithium aluminum hydride in 20 m*l* of dry ether, and then a solution of 0.47 g (3.5 mmol) of aluminum chloride in 15 m*l* of dry ether was added, drop by drop, to the reaction mixture under a nitrogen atmosphere and in an ice-water bath. After stirred for 15 min, the mixture was poured into cold water and the aqueous layer was extracted with ether. The combined ethereal solution was washed with dilute hydrochloric acid and dried over anhydrous magnesium sulfate. After the removal of the solvent, the residue was chromatographed on alumina to give an orange liquid which was then distilled under reduced pressure, bp 102—104°C/0.2 mmHg. The yield of 1′-iodo-1-methylferrocene was 0.49 g (18.8%).

Found: C, 40.62; H, 3.65%. Calcd for $C_{11}H_{11}IFe$: C, 40.49; H, 3.37%.

1′-Chloro-1-methylferrocene. 1′-Iodo-1-methylferrocene (0.2 g, 0.6 mmol) and copper(I) chloride (0.12 g, 1.2 mmol) were refluxed in 2 m*l* of pyridine for 2 hr. After the reaction had been completed, a small amount of pyridine was added; then the reaction mixture was cooled. The cooled mixture was diluted with ether and filtered. The residue was then washed with ether. The combined ethereal solution was washed several times with dilute hydrochloric acid, and finally with water; it was then dried over anhydrous magnesium sulfate. After the removal of the solvent, the residue was purified by chromatography on alumina with *n*-hexane to give 0.07 g (51% yield) of 1′-chloro-1-methylferrocene, which was recrystallized from methanol, mp 47.5—48.5°C.

Found: C, 56.54; H, 5.11%. Calcd for $C_{11}H_{11}ClFe$: C, 56.38; H, 4.69%.

1′-Cyano-1-methylferrocene. After a mixture of 0.129 g (0.4 mmol) of 1′-iodo-1-methylferrocene, 0.180 g

22) S. A. Butter and H. C. Beachell, *Inorg. Chem.*, **5**, 1820 (1966).

23) Y. Nagai, J. Hooz and R. A. Benkeser, This Bulletin, **37**, 53 (1964).

24) E. Berliner and E. A. Blommers, *J. Amer. Chem. Soc.*, **73**, 2479 (1951).

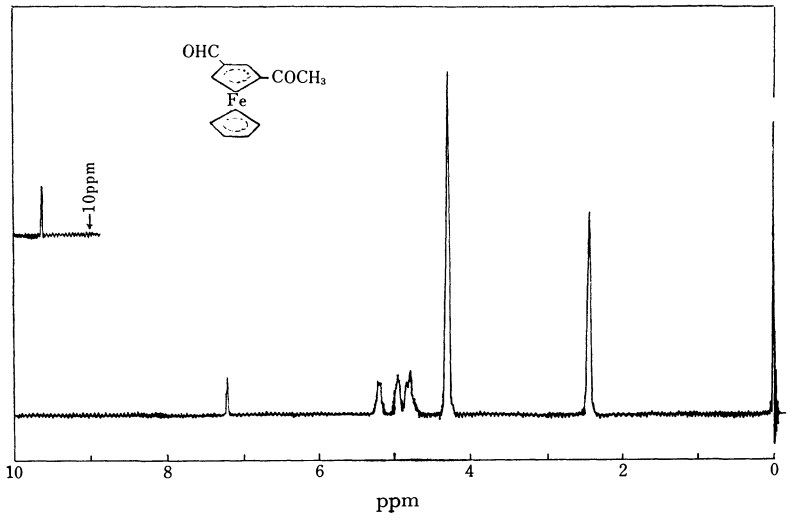

Fig. 3. NMR spectrum of 3-acetyl-1-formylferrocene (in $CDCl_3$).

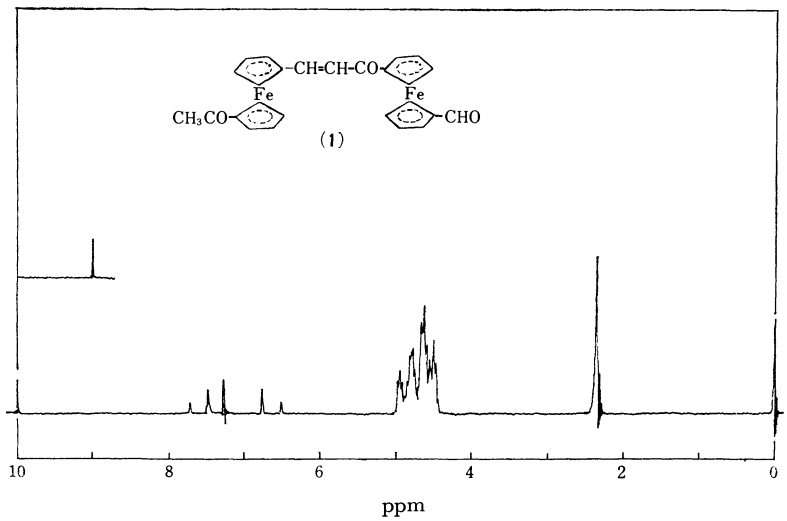

Fig. 4. NMR spectrum of compound **1** (in $CDCl_3$).

(2 mmol) of copper(I) cyanide, and 1 m*l* of pyridine had been heated at 120°C for 2.5 hr in a sealed tube, the mixture was treated in the manner described above to give 0.041 g (52% yield) of 1′-cyano-1-methylferrocene, mp 72.5—73.5°C (lit,[25] mp 72—73°C).

1′-Acetyl-1-formylferrocene. A solution of the complex, which had been prepared in advance from 2.2 m*l* (0.03 mol) of acetyl chloride and 4.0 g (0.03 mol) of anhydrous aluminum chloride in 20 m*l* of dichloromethane, was added to a solution of 2.2 g (0.01 mol) of formylferrocene in 50 m*l* of dichloromethane over a period of 15 min in an ice bath and with stirring under a nitrogen atmosphere. In order to keep the reaction out of the light, the flask was covered with aluminum foil during the reaction. After being stirred for 4 hr in the ice bath, the reaction mixture was hydrolyzed by ice and water containing tin(II) chloride as a reducing agent. The aqueous layer was extracted with dichloromethane, and then the combined dichloromethane solution was washed with water and dried over anhydrous magnesium sulfate. After the removal of the solvent under reduced pressure, the residue was chromatographed on alumina which had previously been deactivated by exposure to the air for 0.5 hr. The chromatography gave 0.62 g (28.2% recovery) of formylferrocene from the first fraction, eluted by ether-*n*-hexane (1 : 1), and then 1.08 g (41.1% yield) of 1′-acetyl-1-formylferrocene from the second fraction, eluted by ether. The product was recrystallized from *n*-hexane-ether, mp 94—95°C (lit,[26] mp 90—93°C).

When the same reaction was carried out initially in

25) G. G. Dvoryantseva, Yu. N. Sheinker, L. P. Yur'eva and A. N. Nesmeyanov, *Dokl. Akad. Nauk SSSR*, **156**, 873 (1964).

26) K. Schlögl, M. Peterlik and H. Seiler, *Monatsh. Chem.*, **93**, 1309 (1962).

an ice bath for 1 hr, and subsequently at room temperature for 3 hr, the chromatographic separation of the product gave different results. After the recovery of the starting material (40.4%), the second fraction with *n*-hexane–ether (1 : 1) gave a trace of orange crystals. This compound was identified to be 3-acetyl-1-formyl ferrocene, mp 106—107.5°C, by a study of its IR and NMR spectra. The NMR spectrum is shown in Fig. 3.

Found: C, 60.70; H, 4.69%. Calcd for $C_{13}H_{12}O_2Fe$: C, 60.94; H, 4.69%.

From the third fraction, which was eluted with ether, 1′-acetyl-1-formylferrocene was obtained in a 33% yield. Further elution with ether gave a fourth fraction consisting of reddish-violet crystals (1.2% yield), which were then recrystallized from benzene–dichloromethane, mp 163°C (decomp.). This compound was identified to be 1-(1′-formylferrocenyl)-3-(1″-acetylferrocenyl)-2-propen-1-one (**1**) by means of its IR and NMR spectra. The NMR spectrum is shown in Fig. 4.

Found: C, 63.26; H, 4.43%. Calcd for $C_{26}H_{22}O_3Fe$: C, 63.16; H, 4.45%.

1′-Ethyl-1-methylferrocene. A solution of 1′-acetyl-1-formylferrocene (190 mg, 0.75 mmol) in 10 m*l* of dry ether was added, drop by drop, to a solution of lithium aluminum hydride (280 mg, 7.4 mmol) and aluminum chloride (1.0 g, 7.5 mmol) in 10 m*l* of dry ether in an ice bath and under an atmosphere of nitrogen. After being stirred for 0.5 hr, the mixture was poured into cold water. Then the ethereal layer was separated, and the aqueous layer was extracted with ether. The combined ethereal solution was then washed with dilute hydrochloric acid and dried over anhydrous magnesium sulfate. After the removal of the solvent, the residue was chromatographed on alumina to give an orange liquid; the liquid was then distilled under reduced pressure, bp 75—77°C/0.21 mmHg. The yield of 1′-ethyl-1-methylferrocene was quantitative.

Found: C, 68.87; H, 6.92%. Calcd for $C_{13}H_{16}Fe$: C, 68.44; H, 7.08%.

2-Chloro-1-methylferrocene. 2-Chloro-1-ferrocenylmethanol (1.45 g, 6 mmol), prepared by Marr's method,[17] was treated for half an hour with a solution of a complex composed of 0.46 g (12 mmol) of lithium aluminum hydride and 0.80 g (6 mmol) of aluminum chloride in 40 m*l* of dry ether under a nitrogen atmosphere. The chromatographic purification of the crude product thus obtained gave 0.94 g (69% yield) of 2-chloro-1-methylferrocene, which was recrystallized from methanol, mp 55.2—56.0°C.

Found: C, 56.68; H, 4.80%. Calcd for $C_{11}H_{11}ClFe$: C, 56.38; H, 4.69%.

2-Bromo-1-methylferrocene. Similarly, 1.01 g (3.4 mmol) of 2-bromo-1-ferrocenylmethanol[17] was converted into 0.57 g (59.7% yield) of 2-bromo-1-methylferrocene, which was then recrystallized from methanol, mp 64—65°C.

Found: C, 47.31; H, 3.94%. Calcd for $C_{11}H_{11}BrFe$: C, 47.45; H, 4.19%.

2-Cyano-1-methylferrocene. 2-Chloro-1-methylferrocene (0.47 g, 2 mmol) was refluxed with 1.8 g (0.02 mol) of copper(I) cyanide for 4 hr in the presence of 1 m*l* of γ-picoline. After the reaction mixture had been treated as has been described for the preparation of 1′-cyano-1-methylferrocene, 0.10 g (22.2% yield) of 2-cyano-1-methylferrocene was obtained and subsequently recrystallized from *n*-hexane, mp 49—50.0°C (lit,[25] mp 51—52°C).

2-Ethyl-1-methylferrocene. A solution of 0.145 g (0.6 mmol) of 2-acetyl-1-methylferrocene in 2 m*l* of acetic acid and 2 m*l* of concentrated hydrochloric acid was added, drop by drop, to amalgamated zinc dust, after which the mixture was refluxed for 5 min. After cooling, the reaction mixture was filtered and the residual zinc dust was thoroughly washed with ether. The filtrate, diluted with water, was also extracted with ether. The combined ethereal solution was washed with a dilute aqueous sodium hydroxide solution and then with water, and subsequently dried over anhydrous magnesium sulfate. After the removal of the solvent, the residue was chromatographed on alumina to give 2-ethyl-1-methylferrocene in an 87% yield as a yellow liquid, bp 68—69°C/0.16 mmHg (lit,[27] bp 70—80°C/0.02 mmHg).

NMR Spectra. The NMR spectra were measured on a Varian Associates A-60 NMR spectrometer.

27) K. Schlögl, M. Fried and H. Falk, *ibid.*, **95**, 576 (1964).

BULLETIN OF THE CHEMICAL SOCIETY OF JAPAN VOL. 43 1148—1153 (1970)

Reaction of Olefin-Palladium(II) Chloride Complexes with *n*-Butylamine

Hidefumi HIRAI, Hiroaki SAWAI and Shoji MAKISHIMA

Department of Industrial Chemistry, Faculty of Engineering, The University of Tokyo, Bunkyo-ku, Tokyo

(Received September 12, 1969)

Olefin-palladium(II) chloride complexes reacted with *n*-butylamine to form Schiff's bases. *N*-Ethylidene-*n*-butylamine was obtained by the reaction of the ethylene complex with *n*-butylamine, accompanied by reduction of palladium(II) to the metal. A tris(*n*-butylamine)palladium chloride complex was formed simultaneously by ligand substitution reaction. The yield of *N*-ethylidene-*n*-butylamine was 15—19 mol% (calcd on palladium) in 2.5 hr at 25°C, and decreased at temperatures higher than 60°C with increasing reduction of palladium(II), owing to conversion of *N*-ethylidene-*n*-butylamine into either *N*-crotylidene-*n*-butylamine or a tarry polymeric substance by aldol type condensation reaction. The *n*-butylamine-palladium(II) chloride complex did not react with ethylene at 25°C, but reacted with ethylene at 150°C to form a large amount of tarry polymer and a small amounts of *N*-ethylidene-*n*-butylamine and *N*-crotylidene-*n*-butylamine. The propylene complex and the cyclohexene complex reacted with *n*-butylamine to yield both 2- and 1-*N*-propylidene-*n*-butylamine, and *N*-cyclohexylidene-*n*-butylamine respectively. The yield of Schiff's bases from olefin complex decreased in the order, ethylene$>$propylene$\gg$cyclohexene.

The reaction of olefin-palladium(II) chloride complexes with nucleophilic reagents have been studied by many workers[1,2] in recent years. Aldehydes,[3] ketones,[3] vinyl ethers[4,5] and vinyl acetates[4,5] were sythesized by the reaction of the olefin complex, or by the reaction of olefin in the presence of palladium(II) salt as catalyst, with nucleophilic reagents such as water, alcohols and acetic acid. These reagents containing nucleophilic oxygen atoms attack on a positively charged carbon atom of the olefin to give the product containing a C–O bond. Olefin-palladium(II) complexes were also reported to react with benzene,[6] cyanide,[7] ethylmalonate[8] and carbon monoxide[9] to yield styrene derivatives, unsaturated nitriles, malonate derivatives and carbonyl compounds, respectively. In these cases the nucleophiles attack with their negatively charged carbon atoms to form C–C bond.

Reaction of olefin-palladium(II) complexes with nucleophiles containing nitrogen, however, has been very scantily reported. Stern and Spector reported briefly the formation of *n*-butylisopropylamine by the reaction of propylene and palladium chloride with *n*-butylamine in the presence of disodium hydrogen phosphate with subsquent hydrogenation.[5] There has been, however, very little information on the reaction of olefin complexes with the compounds containing nitrogen on account of the complicatedness of the reaction. The nucleophilic reagents containing nitrogen such as amines and amides make stable complexes with metal satls. This is a great difference from the case of the reagents containing oxygen such as water or alcohols. Further, both the nucleophiles and the reaction products would form the stable complexes with palladium chloride, which prevent the occurrence of the expected reaction making the analysis of the products complicated. On the other hand, these complex formations can be expected, in view of coordination chemistry, to be useful for elucidation of the mechanism of the reaction where palladium(II) complexes play an important role. Paiaro, Renzi and Polumbo reported the reaction of diene-palladium(II) chloride complex with primary amines, in which a new amine-palladium(II) complex containing a Pd–C bond was formed quantitavely at room temperature.[10] Independently,

1) C. W. Bird, "Transition Metal Intermediates in Organic Synthesis," Logos Press, London (1966), pp. 88—112.

2) A. Guilo, "Advances in Organometallic Chemistry," Vol. 5, ed. by F. G. A. Stone and R. West, Academic Press, New York (1967), p. 321.

3) J. Smidt, W. Hafner, R. Jira, J. Seldmeier, R. Sieber, R. Ruttinger and H. Kojer, *Angew. Chem.*, **71**, 176 (1959).

4) I. I. Moiseev, M. N. Vergaftik and Y. K. Syrkin, *Dokl. Akad. Nauk SSSR*, **133**, 377 (1960).

5) E. W. Stern and M. L. Spector, *Proc. Chem. Soc.*, **1961**, 370.

6) I. Moritani and Y. Fujiwara, *Tetrahedron Lett.*, **1967**, 1119.

7) Y. Odaira, T. Oishi, T. Yukawa and S. Tsutsumi, *J. Amer. Chem. Soc.*, **88**, 4105 (1966).

8) J. Tsuji and H. Takahashi, *ibid.*, **87**, 3275 (1965).

9) J. Tsuji, M. Morikawa and J. Kiji, *ibid.*, **86**, 4581 (1964).

10) G. Paiaro, A. D. Renzi and R. Palumbo, *Chem. Commun.*, **1967**, 1150; R. Palumbo, A. D. Renzi, A. Panunzi and G. Paiaro, *J. Amer. Chem. Soc.*, **91**, 3874 (1969).

we have found the formation of Schiff's bases on the reaction of olefin-palladium(II) chloride complexes with *n*-butylamine.[11] In the present paper, the formation of the Schiff's bases will be described under various temperature, pressure and amount of *n*-butylamine. The reaction mechanism will be discussed on the basis of the results.

Results and Discussion

Reaction of Ethylene-Palladium(II) Chloride Complex with *n*-Butylamine. Ethylene-palladium(II) chloride complex reacted with *n*-butylamine at 25°C for 2.5 hr under 5 atm of ethylene pressure. *N*-Ethylidene-*n*-butylamine (**1**) was obtained in 16 mol% yield based on palladium(II) chloride, accompanying the formation of palladium metal. The reddish brown solution of reaction mixture turned white-yellow forming tris(*n*-butylamine)palladium(II) chloride complex (**2**), the structure of which was confirmed by elemental analysis. These facts indicate two types of reaction, a Schiff's base formation and a ligand substitution.

$$\tfrac{1}{2}\,[PdCl_2(C_2H_4)]_2 + n\text{-}C_4H_9NH_2 \rightarrow \underset{\mathbf{1}}{CH_3CH{=}NC_4H_9} + Pd + 2HCl \quad (1)$$

$$\tfrac{1}{2}\,[PdCl_2(C_2H_4)]_2 + 3\ n\text{-}C_4H_9NH_2 \rightarrow [PdCl(n\text{-}C_4H_9NH_2)_3]Cl + C_2H_4 \quad (2)$$

Hydrochloric acid formed by reaction(1) was mostly caught by an excess of *n*-butylamine as *n*-butylamine hydrochloride.

The effect of the reaction temperature on the yield of the reaction products is shown in Table 1. Compound **1** was obtained at 25°C in a yield nearly equal to that of palladium metal. The formation of the palladium metal increased at temperatures higher than 60°C, and palladium(II) was reduced almost completely to metal at 150°C. The yield of **1**, however, decreased with increasing temperature and only a trace amount was obtained at 150°C, while *N*-crotylidene-*n*-butylamine (**3**) and a tarry reddish substance were obtained in fairly good yields. The infrared spectrum of the tarry substance was essentially the same as that of the tarry substance which was prepared by heating **1**. The molar amount of **2** decreased with the elevation of temperature and was in good agreement with the moles of palladium(II) which was not reduced.

Formation of amine complex by ligand substitution seems to be favored, and a *n*-butylamine-palladium(II) chloride complex was too stable to react with ethylene at room temperature. Thus, the extent of the Schiff's base formation (1) at 25°C was not very high. Formation of **3** and tarry substance at elevated temperature can be explained by the reaction.

Table 1. Effect of temperature on the reaction of ethylene-palladium(II) chloride complex with *n*-butylamine

Temp. °C	Yield mol%				Tarry substance[b] mg
	CH_3-CH=NBu	CH_3CH=CHCH=NBu	Pd (metal)	[PdCl(*n*-BuNH$_2$)$_3$]Cl	
25	16	0	14	86	0
65	16	4	19	81	trace
85	13	5	35		
100	15	15	59	44	190
150	1	42	99	0	510

a) Molar conversion based on palladium chloride.
b) Crude substance.
Conditions: Initial pressure of ethylene, 5 atm; Reaction time, 2.5 hr; Palladium chloride, 0.005 mol; *n*-Butylamine, 0.02 mol.

$$\underset{\mathbf{1}}{CH_3CH{=}NC_4H_9} \xrightarrow{\Delta} \underset{\mathbf{3}}{CH_3CH{=}CHCH{=}NC_4H_9} \xrightarrow{\Delta} CH_3CH(=CH\text{-}CH)_n{=}NC_4H_9$$

Elevation of temperature promoted not only the formation of **1** by reaction (1), but also the conversion of **1** either into **3** or into tarry substance through aldol type condensation reaction. Aliphatic Schiff's bases containing α-methylene group have been reported to undergo aldol type condensation easily at elevated temperature.[12] The formation of palladium metal indicates the extent of the Schiff's base formation reaction (1). Thus, the difference between the yield of palladium metal and that of **1** means the extent of the aldol type condensation. The condensation reaction was not observed at 25°C in 2.5 hr. However, it increased with elevating temperature becoming predominant at 150°C.

Table 2 shows the effect of molar ratio of *n*-butylamine to palladium(II) chloride on the yield of **1** and on the species of *n*-butylamine-palladium(II) chloride complex. The yield of **1** determined by g.l.p.c. increased with the molar ratio and saturated at a ratio of four. In the range of ratios smaller than four, the yield of **1** increased by addition of pyridine to the mixture of reaction products, bacause a part of **1** which had formed a complex with palladium(II) could be made free by pyridine.

The composition of *n*-butylamine-palladium(II) complex changed with the amount of *n*-butylamine as shown in Table 2. Bis(*n*-butylamine)palladium(II) chloride (**4**) was produced at the molar ratio of two, while the complex **2** was obtained at that of more than four. The formation of **2** and **4**

11) H. Hirai, H. Sawai and S. Makishima, Presented at the 20th Annual Meeting of the Chemical Society of Japan, Tokyo, April, 1967.

12) R. W. Rayer, *Chem. Rev.*, **13**, 489 (1963).

TABLE 2. EFFECT OF AMOUNT OF *n*-BUTYLAMINE

[*n*-BuNH$_2$]/[PdCl$_2$][a]	Yield of CH$_3$-CH=NBu, mol%[b]		*n*-Buthylamine complex
	free[c]	free+complexed[d]	
1	3	6	(*n*-C$_4$H$_9$NH$_3$)$_2$$^+$(PdCl$_4$)
2	5	7	PdCl$_2$(*n*-C$_4$H$_9$NH$_2$)$_2$
4	16	16	[PdCl(*n*-C$_4$H$_9$NH$_2$)$_3$]Cl
10	15	15	[PdCl(*n*-C$_4$H$_9$NH$_2$)$_3$]Cl
40	16	16	[PdCl(*n*-C$_4$H$_9$NH$_2$)$_3$]Cl

a) Molar ratio.
b) Based on palladium chloride.
c) Yield of CH$_3$CH=NBu analyzed by gaschromatography on reaction mixture.
d) Yield of CH$_3$CH=NBu analyzed by gaschromatography on reaction mixture after addition of pyridine.
Conditions: Initial pressure of ethylene, 5 atm; Reaction time, 2.5 hr; Reaction temperature, 25°C; Palladium chloride, 0.005 mol.

respectively is nearly equal to the remaining amount of palladium(II). At the molar ratio of one, *n*-butylammonium tetrachloropalladate(II) (**5**) was obtained in a yield approximately equal to that of **1**. Palladium(II) chloride reacted with both *n*-butylamine and hydrochloric acid to form **5**.

The ethylene-palladium(II) chloride complex was prepared either by the reaction of palladium(II) chloride with ethylene under 50 atm in 6 hr, or by the reaction of bis(benzonitrile)palladium(II) chloride complex with ethylene under 10 atm in 1 hr. These two methods were approximately equal in yields of **1** on reaction with *n*-butylamine at 25°C under 5 atm of ethylene pressure. Table 3 shows

TABLE 3. EFFECT OF PESSURE OF ETHYLENE ON THE YIELD OF *N*-ETHYLIDENE-*n*-BUTYLAMINE

Pressure atm[a]	Time[a] hr	Reaction pressure[b] atm	Yield mol%
50	6	1	15
50	6	5	16
50	6	10	18
50	6	25	19
50	6	50	19
10	1	1	4
10	2	25	10
10	1	5	16[c]

a) Pressure of ethylene and reaction time for preparation of the ethylene complex from palladium chloride with ethylene.
b) Pressure of ethylene for the reaction of ethylene complex with *n*-butylamine.
c) Bis(benzonitrile) palladium chloride complex was used instead of palladium chloride.
Conditions: Temperature, 25°C; Reaction time, 2.5 hr; Palladium chloride, 0.005 mol; *n*-Butylamine, 0.02 mol.

that the ethylene complex was prepared completely from palladium(II) chloride in 6 hr under 50 atm, but incompletely in 1 hr under 10 atm. The yield of **1** increased with increasing pressure of ethylene on reaction with *n*-butylamine up to 50 atm as shown in Table 3. The promotion of the yield of **1** can be explained by assuming that the pressure of ethylene not only promoted the coordination of ethylene but also suppressed the ligand substitution reaction resulting in a small acceleration of Schiff's base formation.

Reaction of Tris(*n*-butylamine)palladium-(II) Chloride Complex with Ethylene. *n*-Butylamine-palladium(II) chloride complex **2** was very stable and did not react with ethylene at room temperature. This complex, however, was found to react easily with ethylene at a higher temperature; for example, 95% of palladium (II) in the complex was reduced to the metal at 150°C, yielding **1**, **3** and tarry polymeric substance, as shown in Table 4. These products were consistent with those obtained by the reaction of the ethylene-palladium(II) chloride complex with *n*-butylamine.

TABLE 4. REACTION OF TRIS (*n*- BUTYLAMINE)-PALLADIUM CHLORIDE COMPLEX WITH ETHYLENE

Temp. °C	Yield, mol%[a]			Tarry substance[b]
	CH$_3$CH=NBu	CH$_3$CH=CH=CH=NBu	Pd (metal)	mg
25	0	0	0	0
150	1	11	95	500

a) Based on palladium chloride.
b) Crude substance.
Conditions: Tris(*n*-butylamine)palladium chloride, 0.005 mol; Pressure of ethylene, 50 atm; Reaction time, 2.5 hr.

Reaction of Other Olefin-Palladium(II) Chloride Complexes with *n*-Butylamine. The reaction of propylene-palladium(II) chloride complex with *n*-butylamine gave 2- and 1-*N*-propylidene-*n*-butylamine as shown in Table 5. The yield of 2- and 1-*N*-propylidene-*n*-butylamine were in the ratio of the yield of 6 : 1 approximately, which is in fair agreement with the ratio of the yield of acetone to that of propionaldehyde obtained by reaction of palladium(II) chloride with propylene and water.[3]

$$\tfrac{1}{2}\,[PdCl_2(C_3H_6)]_2 + n\text{-}C_4H_9NH_2$$

$$\swarrow \qquad \searrow$$

$CH_3CH_2CH{=}NC_4H_9$ (1-*N*-proylidene-*n*-butylamine) $\qquad$ $(CH_3)_2C{=}NC_4H_9$ (2-*N*-propylidene-*n*-butylamine)

Cyclohexene-palladium(II) chloride complex yielded a small amount of *N*-cyclohexylidene-*n*-butylamine. Schiff's base formation proceeded to remarkably smaller extent in the case of higher

olefins than in that of ethylene. This tendency is greater than that of aldehydes or ketones obtained by the reaction of palladium(II) chloride with higher olefins and water.[3]

Table 5. Reaction of olefin - palladium(II) chloride complexes with *n*-butylamine at 25°C

Olefin	Reaction time hr	$[n\text{-BuNH}_2]/[PdCl_2]$	Product	Yield mol%
C_2H_4[a]	2.5	4	$CH_3CH{=}NBu$	16
C_3H_6[a]	5	5	$CH_3CH_2CH{=}NBu$	1.3
			$(CH_3)_2C{=}NBu$	7.6
C_6H_{10}	5	5		trace[b]

[a] Pressure, 5 atm.
[b] Less than 1 mol%.

Effect of Small Amount of Water on the Reaction. Schiff's bases are usually obtained from aldehydes and primary amines. Acetaldehyde can be formed from ethylene-palladium(II) chloride complex with water,[3] which remains in a very small amount in the reaction system in spite of careful treatment to prevent contamination with water. Consequently, **1** could be formed by reaction of the acetaldehyde with *n*-butylamine as follows.

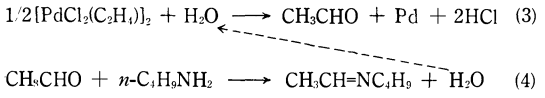

$$1/2[PdCl_2(C_2H_4)]_2 + H_2O \longrightarrow CH_3CHO + Pd + 2HCl \quad (3)$$

$$CH_3CHO + n\text{-}C_4H_9NH_2 \longrightarrow CH_3CH{=}NC_4H_9 + H_2O \quad (4)$$

For examination of this possibility, the formation of acetaldehyde was determined by g.l.p.c. before addition of *n*-butylamine. The result shows that the amount of acetaldehyde is less than 0.8 mol% based on palladium(II) chloride. If **1** were formed by reactions (3) and (4), water should be used twenty times repeatedly to obtain **1** in 16 mol% yield at 25°C, and the yield of **1** could be expected to increase on addition of a small amount of water with *n*-butylamine. The yield, however, decreased from 16 mol% to 9 mol% by the use of *n*-butylamine which contained water in equimolar amount to palladium(II) chloride, instead of dried *n*-butylamine. The fact that the added water played a role of inhibitor indicates that the most of **1** was not formed by reactions (3) and (4), but formed by the direct reaction of *n*-butylamine with ethylene complex. This is consistent with the fact that the ethylene-palladium(II) chloride complex yields *N*-vinylpyrrolidone on reaction with pyrrolidone, which attacks coordinated ethylene with its >NH group to form C–N bond.[13,14] Pyrrolidone cannot react with acetaldehyde under such mild conditions as used in this study.

Reaction Mechanism. The reaction mechanism of direct attack of *n*-butylamine on ethylene-palladium(II) chloride complex will be discussed. The ethylene-palladium(II) chloride complex with equimolar *n*-butylamine was a homogeneous solution under ethylene pressure, and evolved a gas of ethylene with precipitation of complex **5** on standing for several minutes under ordinary pressure of air. Addition of methanol to the homogeneous solution produced palladium metal and methyl vinyl ether. The results indicate the presence of some ethylene-palladium(II) complex in the homogeneous solution. On the other hand, an amine has a stronger coordinating affinity to palladium(II) than ethylene. It is reasonable to suppose that both *n*-butylamine and ethylene coordinate palladium (II) under ethylene pressure to form a complex such as $PdCl_2$(olefin)(amine), which is so unstable as to evolve ethylene under ordinary pressure of air. A platinum complex such as $PtCl_2$(olefin)-(amine) is well known,[15] while a corresponding palladium(II) has never been isolated. The fact that the *n*-butylamine-palladium(II) complex can react with ethylene to give **1** at 150°C indicates the coordination of ethylene to *n*-butylamine-palladium-(II) complex. The complex coordinating both ethylene and *n*-butylamine can be considered to be a reaction intermediate of Schiff's base formation. That the formation of this intermediate is essential for the reaction has been supported also by the results of the allylamine-palladium(II) chloride complexes in dry tetrahydrofuran.[16] The 1 : 1 allylamine-palladium(II) complex which can coordinate olefinic double bond besides amino group could react at 50°C to form palladium metal and Schiff's base, while the 3 : 1 allylamine-palladium-(II) chloride complex, which coordinates only amino group, could not.

The following reaction scheme can be proposed

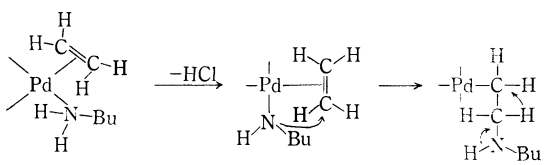

$\xrightarrow{-HCl}$ $CH_3CH{=}NBu + Pd$

1

13) J. E. Mckeon and P. S. Stracher, U. S. 3318906; *Chem. Abstr.*, **68**, 39466k (1968).

14) H. Hirai, H. Sawai and S. Makishima, Presented at the 21st Annual Meeting of the Chemical Society of Japan, Osaka, April, 1968.

15) G. E. Coates and F. Glockling, "Organometallic Chemistry," ed. by H. Zeiss, Reinhold Publishing Co., New York, (1960), p. 456.

16) H. Sawai and H. Hirai, Presented at the 19th Annual Meeting of Coordination Chemistry, Sendai, Sept., 1969.

involving an ethylene-*n*-butylamine-palladium(II) complex as the intermediate. The proton of coordinated *n*-butylamine would be withdrawn by palladium(II) to form amido-palladium(II) complex. Then the coordinated ethylene would enter the Pd–N bond to form Schiff's base **1**. The withdrawal of proton of coordinated amine has been proposed by Tsuji and Iwamoto for the carbonylation reaction of amine catalyzed by palladium(II) chloride.[17]

The following reaction scheme can be also considered.

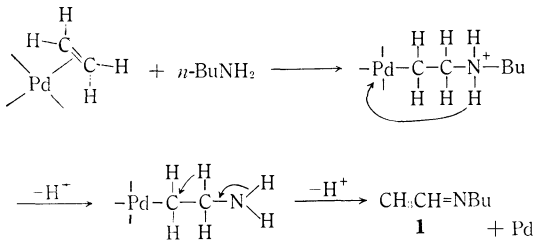

In this case uncoordinated *n*-butylamine attacks coordinated ethylene to form an intermediate complex which is an alkyl palladium derivative containing a quaternary ammonium group. Palladium(II) withdraws two protons from the ammonium group to form Schiff's base. The metal alkyl derivative containing a quaternary ammonium group was isolated in the case of platinum complex prepared from dichloro(olefin)(*t*-phosphine)platinum complex with amine.[18]

The facts that amines have strong coordinating affinity to palladium(II) chloride, and that *n*-butylamine-palladium(II) chloride complex reacts with ethylene at 150°C, suggest that the former scheme is preferable. In either scheme, the elevation of reaction temperature is expected to make the *n*-butylamine complex so labile that the coordination of ethylene becomes possible, and to promote both the withdrawal of proton of *n*-butylamine and the formation of Schiff's base **1** with the subsequent aldol type condensation. These tendencies are supported by the fact that total yield of Schiff's base including the products of condensation increased extensively at higher temperatures and that *n*-butylamine-palladium(II) chloride complex which could not react with ethylene at room temperature reacted at 150°C in a high yield.

Experimental

Materials. Bis(benzonitrile)palladium chloride complex was prepared as described by Kharasch.[19] Ethylene and propylene were from Nihon Petrochemical Co. and used without further purification. Cyclohexene and *n*-butylamine were obtained commercially, dried over calcium hydride and distilled. Tetrahydrofuran used as solvent was dried over calcium hydride and distilled over sodium immediately before use.

Reaction of Ethylene-Palladium(II) Chloride Complex with *n*-Butylamine. Palladium chloride (0.9 g, 0.005 mol) and tetrahydrofuran (20 m*l*) were put into in a magnetically stirred 100 m*l* autoclave in a slow stream of nitrogen. A glass reaction tube containing the reaction mixture was used in the autoclave. The stirrer was gilded with gold to prevent palladium(II) chloride from reacting with steel. Ethylene-palladium(II) chloride complex was prepared under 50 atm of ethylene pressure for 6 hr. The autoclave was then opened and *n*-butylamine (2 m*l*, 0.02 mol) was added. The reaction was carried out at a given pressure of ethylene (1—50 atm) and temperature (25—150°C) by stirring for 2.5 hr. The formation of the ethylene-palladium(II) chloride complex depended on pressure of ethylene and reaction time. To confirm the complete formation of the ethylene complex, bis(benzonitrile)palladium chloride complex was used instead of palladium chloride. In this case the ethylene complex was prepared completely.[19]

The reaction products were analyzed by gaschromatography; 3 m Carbowax 1500 on Diasolid A column at 65°C and a nitrogen flow rate of 60 m*l*/min; 2 m Apiezon Grease L on Diasolid A column at 50°C and a nitrogen flow rate of 50 m*l*/min. Identification of product **1** was carried out by comparison of gas chromatogram and infrared spectrum with that of the authentic sample prepared according to Campbell.[20] Yield data were obtained by gas chromatography using cyclohexane as an internal standard. White crystalline insoluble in tetrahydrofuran was obtained remarkably at elevated temperature. Recrystallization from methanol gave purified *n*-butylamine hydrochloride (mp 195—197°C). Infrared spectrum and melting point of this crystals were identical with those of the authentic sample prepared from *n*-butylamine and hydrochloric acid. The soluble reaction mixture was evaporated to dryness and recrystallization from methanol gave cream yellow crystals, which was **2**, $[PdCl(n\text{-}C_4H_9NH_2)_3]Cl$; mp 149.5—150.5°C.

Found: C, 36.30; H, 8.56; N, 10.16%. Calcd for $PdCl_2C_{12}H_{33}N_3$: C, 36.38; H, 8.38; N, 10.60%.

Analysis of Reaction Products at Elevated Temperature. Product **3** was analyzed by gaschromatography under the same conditions as in **1**. Tarry substance was obtained as follows. The reaction mixture was evaporated and **2** was removed by crystallization from methanol. The black red filtrate was evaporated to dryness under reduced pressure at 60°C for 8 hr and weighed without further purification. Identification of **3** and the tarry substance was made by comparison of gaschromatogram and infrared spectra with those of authentic sample prepared from **1** by heating.[12] The infrared spectrum of the tarry substance showed a broad absorption at 1600—1650 cm^{-1} referred to $\nu_{C=C}$ and $\nu_{C=N}$, but no clear absorption at 3200—3300 cm^{-1} referred to ν_{N-H}.

17) J. Tsuji and N. Iwamoto, *Chem. Commun.*, **1966**, 828.

18) A. Panunzi, A. D. Renzi, R. Palumbo and G. Paiaro, *J. Amer. Chem. Soc.*, **91**, 3879 (1969).

19) M. S. Kharasch, R. C. Seyler and F. R. Mayo, *ibid.*, **60**, 882 (1938).

20) K. N. Campbell, A. H. Sommers and B. K. Campbell, *ibid.*, **66**, 82 (1944).

Analysis of Reaction Products with a Small Amount of *n*-Butylamine. Analysis of **1** was carried out by gas chromatography before and after the addition of pyridine. *n*-Butylamine-palladium(II) chloride complexes which were obtained at molar ratios of *n*-butylamine to palladium chloride of 1 and 2 were different from **2**. When the molar ratio of *n*-butylamine to palladium chloride was 1, *i. e.* $[n\text{-}C_4H_9NH_2]/[PdCl_2]=1$, the reaction mixture was reddish orange and homogeneous immediately after the reaction. In a few minutes copper-red crystals precipitated evolving gas of ethylene. Recrystallization from methanol gave **5**: $(PdCl_4)(n\text{-}C_4H_9NH_3)^+_2$; mp (decomp.) 240—260°C.

Found: C, 24.14; H, 6.07; N, 9.06%. Calcd for $PdCl_4C_8H_{24}N_2$: C, 24.14; H, 6.05; N, 9.05%.

The infrared spectrum was similar to that of *n*-butylamine hydrochloride. Isolation of other complexes was unsuccessful.

At the molar ratio of 2, *i. e.* $[n\text{-}C_4H_9NH_2]/[PdCl_2]=2$, the reaction mixture was yellow and homogeneous. Orange yellow crystals was obtained by the same method as **2**. Recrystallization from methanol gave **4**; $PdCl_2(n\text{-}C_4H_9NH_2)_2$: mp 146—147°C.

Found: C, 29.74; H, 6.66; N, 8.60%. Calcd for $PdCl_2C_8H_{22}N_2$: C, 29.72; H, 6.81; N, 8.67%.

Complex **3** was obtained at the ratio of more than **4**.

Reaction of Tris(*n*-butylamine)palladium(II) Chloride Complex 2 with Ethylene. Both 1.834 g of **2** and 20 m*l* of dry tetrahydrofuran were placed in the autoclave. Ethylene was compressed to 50 atm and stirred for 2.5 hr at 25°C or 150°C. Analysis of the products was carried out by the same method as described in the reaction of ethylene complex.

Reaction of Propylene-Palladium(II) Chloride Complex with *n*-Butylamine. Bis(benzonitrile)palladium chloride complex (1.9 g) and dry tetrahydrofuran (20 m*l*) were put into the autoclave. Propylene was compressed to 10 atm and stirred for 30 min to prepare the propylene complex. The autoclave was opened and *n*-butylamine (2 m*l*) was added. The reaction was carried out under 5 atm of propylene pressure by stirring for 5 hr at 25°C. Analysis of the reaction products was carried out by gas chromatography; 2 m Apiezon Grease L on Diasolid A column at 74°C and a nitrogen flow rate of 50 m*l*/min. Identification of the products was carried out by comparison of gaschromatogram with an authentic sample prepared according to Campbell.[20] Yield data were obtained by gaschromatography using toluene as an internal standard.

Reaction of Cyclohexene-Palladium(II) Chloride Complex with *n*-Butylamine. In a 30-m*l* conical beaker, 0.394 g of bis(benzonitrile)palladium chloride complex, 10 m*l* of dry tetrahydrofuran and 1 m*l* of cyclohexene were stirred by magnetic stirrer for 10 min to prepare the cyclohexene complex. To this reaction mixture 0.4 m*l* of *n*-butylamine was added gradually with stirring. Reaction was carried out at 25°C by stirring for 5 hr. The reaction product was analyzed by gaschromatography; 2 m Apiezon Grease L on Diasolid A column at 144°C and a nitrogen flow rate of 50 m*l*/min. Identification of the product was carried out by comparison of gas chromatogram with an autnentic sample prepared from cyclohexanone and *n*-butylamine.

BULLETIN OF THE CHEMICAL SOCIETY OF JAPAN VOL. 43 1153—1157 (1970)

Oxidation by Transition Metal Complexes. I. Oxidation of Styrene and Triphenylphosphine Catalyzed by O_2-Ir Complex

Kiyotomi TAKAO, Yuzo FUJIWARA, Toshinobu IMANAKA and Shiichiro TERANISHI

Department of Chemical Engineering, Faculty of Engineering Science, Osaka University, Machikaneyama, Toyonaka, Osaka

(Received September 16, 1969)

In order to investigate the oxidation reaction which is catalyzed by transition metal complexes in a homogeneous system under mild conditions, the oxidation reactions of styrene and triphenylphosphine catalyzed by various iridium complexes have been studied. The Vaska complex ($IrX(CO)(PPh_3)_2$) and the biphosphine chelate complex have been found to be effective as oxidation catalyst. It was found that the $SnCl_3$ ligand which has a strong *trans* effect promotes the oxidation of styrene. For the sake of comparison with the iridium compounds, oxidation with palladium salts was also studied.

Extensive studies on heterogeneous oxidation reactions by means of various metal oxides or inorganic metal salts have been carried out.[1] Much less is known about oxidation reactions involving organo-transition metal compounds as a catalyst in homogeneous systems.

Recently, some transition metal complexes having

1) See, for example, K. B. Wiberg, Ed., "Oxidation in Organic Chemistry," Academic Press, New York (1965).

an oxygen molecule as a ligand were prepared.[2-6] These complexes could thus be expected to be effective as oxidation catalyst.

However, only a few workers have studied the homogeneous catalyzed oxidation reaction in the presence of these metal-oxygen complexes.[4-7] Collman has reported briefly that cyclohexene can be oxidized to cyclohexanone and cyclohexene oxide in the presence of the Vaska compelx.[7]

In order to investigate the oxidation reaction which is catalyzed by the transition metal-O_2 complexes in a homogeneous system under mild conditions, we have studied the oxidation reactions of styrene and triphenylphosphine catalyzed by various iridium complexes prepared by Vaska *et al.*[3,8] and others.[9-11]

It has been found that some organoiridium complexes can cause the oxidation reaction of styrene in the presence of oxygen to give styrene oxide, benzaldehyde or acetophenone catalytically. In addition, triphenylphosphine has been found to be easily oxidize to give triphenylphosphine oxide catalytically.

We report in this paper a study on oxidation reactions of styrene and triphenylphosphine by means of iridium complexes under an oxygen atmosphere.

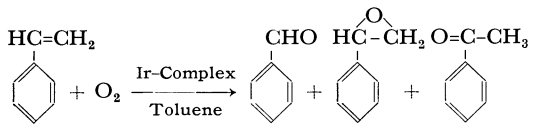

Results and Discussion

The oxidation reactions catalyzed by the iridium complexes were carried out under conditions where homogeneous solutions of reactant styrene (or triphenylphosphine) and iridium complexes in a solvent such as benzene or toluene are heated with a constant bubbling of oxygen for 8 hr.

Oxidation of Triphenylphosphine. Triphenylphosphine has been oxidized easily by the Vaska complexes ($IrX(CO)(PPh_3)_2$; X=Cl, Br, I) to afford triphenylphosphine oxide catalytically, and the catalyst is recovered without decomposition after the reaction. The results are summarized in Table 1.

Table 1. Oxidation of triphenylphosphine with Vaska complex

Catalyst	Reaction temp. °C	Time, hr	Solvent	Triphenylphosphine oxide Yield[a] %
$IrClCO(PPh_3)_2$	110	9	Toluene	426
$IrBrCO(PPh_3)_2$	110	9	Toluene	854
$IrICO(PPh_3)_2$	110	9	Toluene	737

a) Yields are based on catalyst used.

Although it is well known that nickel, palladium, or platinum complexes are effective catalysts for the oxidation of phosphine,[4,5] the present result is the first example of the oxidation by iridium complex catalysts.

Of Vaska complexes, the yield of triphenylphosphine oxide increases in the order: X=Cl<I<Br as shown in Table 1. The fact that the Vaska complexes coordinate with the oxygen molecule easily under oxygen atmosphere, suggests that the present oxidation reaction proceeds *via* an Ir-O_2 complex.

According to La Placa and Ibers[12], and McGinnety *et al.*,[13] the O–O bond lengths of the Ir-O_2 complexes prepared by Vaska *et al.* are 1.30 Å and 1.51 Å for the chloride complex and the analogous iodide complex respectively. That increasing bond length of O–O increases the yield of the oxide formed seems to show that the oxygen molecule is highly activated by coordinating with iridium(I) metal. Heating of Ir-O_2 complex resulted in the formation of triphenylphosphine oxide in the absence of oxygen.

From these results, it appears that the Vaska complex-catalyzed oxidation may proceed through the coordination of both oxygen and triphenylphosphine to iridium(I) metal as is shown in the following scheme:

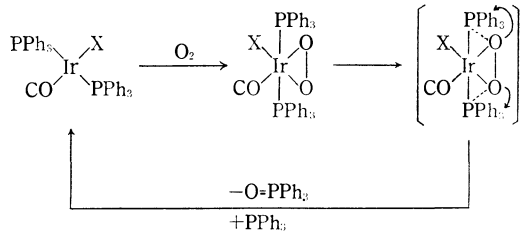

2) L. Vaska, *Science*, **140**, 809 (1963).
3) L. Vaska and D. L. Caton, *J. Amer. Chem. Soc.*, **88**, 5324 (1966).
4) G. Wilke, H. Schott and P. Heimbach, *Angew. Chem.*, **79**, 62 (1967).
5) S. Takahashi, K. Sonogashira and N. Hagihara, *Nippon Kagaku Zasshi*, **87**, 610 (1966).
6) S. Otsuka, A. Nakamura and Y. Tatsuno, *Chem. Commun.*, **1967**, 836.
7) J. P. Collman, M. Kubota and J. Hosking, *J. Amer. Chem. Soc.*, **89**, 4809 (1967).
8) L. Vaska and J. W. Diluzio, *ibid.*, **83**, 2784 (1961).
9) P. B. Chock and J. Halpern, *ibid.*, **88**, 3511 (1966).
10) R. C. Taylor, J. F. Young and G. Wilkinson, *Inorg. Chem.*, **5**, 20 (1966).
11) R. S. Nyholm and K. Vrieze, *J. Chem. Soc.*, **1965**, 5337.
12) S. J. LaPlaca and J. A. Ibers, *J. Amer. Chem. Soc.*, **87**, 2581 (1965).
13) J. A. McGinnety, R. J. Doedens and J. A. Ibers, *Inorg. Chem.*, **6**, 2243 (1967).

Table 2. Oxidation of styrene with iridium compounds

Catalyst	Reaction		Solvent	Product and yield,[a] %		
	Temp. °C	Time, hr		Benzaldehyde	Styrene oxide	Acetophenone
None	110	8	Toluene	0	0	0
$IrClCO(PPh_3)_2$	110	8	Toluene	0	0	84
$IrClCO(PPh_3)_2$	100	8	Toluene	0	0	65
$IrClCO(PPh_3)_2$	80	8	Toluene	0	0	37
$IrClCO(PPh_3)_2$	6.5	8	Toluene	0	0	0
$IrClCO(PPh_3)_2$	100	8	Toluene[b] +Ethanol	0	0	64
$IrClCO(PPh_3)_2$	100	8	Dioxane	0	0	55
$IrClCO(PPh_3)_2$	100	8	Acetic acid	1280	0	152
$IrBrCO(PPh_3)_2$	110	8	Toluene	0	0	4
$IrICO(PPh_3)_2$	110	8	Toluene	0	0	0
$Ir(P\text{-}P)_2Cl$[d]	110	8	*n*-Propanol	469	315	85
$Ir\text{-}SnCl_3$	110	8	Toluene	1212	477	trace
$Ir\text{-}HgCl_2$	110	8	Toluene	253	110	trace
$IrCl_3$[c]	110	8	Toluene	566	418	10
$IrCl_3$	110	8	Acetic acid	1385	51	89

a) Yields are based on the catalyst utilized.
b) A mixture of 250 m*l* of toluene and 50 m*l* of ethanol was used.
c) Phenylethyleneglycol was also obtained in 102% yield.
d) $[Ir(PPh_2CH_2CH_2PPh_2)_2]Cl$

Oxidation of Styrene. Since the Vaska complexes have been found to be active catalysts for the oxidation of triphenylphosphine, we have undertaken a further study on the oxidation of olefins which are not easily oxidized especially under mild conditions.

It has been found that styrene can be smoothly oxidized by the use of iridium complexes under an oxygen atmosphere. The results are given in Table 2.

As apparent from Table 2, the Vaska complexes (X=Cl, and Br) can cause the oxidation of styrene to give acetophenone in considerable yields. In the absence of the complexes, no oxidation product was formed indicating that these complexes function as a catalyst for the oxidation of styrene.

Solvent Effect. The oxidation of styrene catalyzed by the iridium complexes appears to suffer no solvent effect. That is, styrene gave acetophenone in almost similar yields as in the cases of toluene, a non-polar solvent, ethanol, a protic solvent, or dioxane, a polar solvent. However, in the case of acetic acid, a different result was obtained, namely benzaldehyde was formed as a major product in 1280% yield and acetophenone in 152% yield.[14] This peculiar effect of acetic acid will be discussed in the following publication.

Ligand Effect. *1. Halide Ligand.* The effects of varying the halide ligands of the Vaska complex upon the styrene oxidation are shown in Table 2. The yield of acetophenone increases in the order: X=I<Br<Cl which is different from that observed in the oxidation of triphenylphosphine. This may be explained in the following way: Styrene is a weaker ligand than triphenylphosphine, and the steric hindrance of the halide ligand of the Vaska complex increases in the order, Cl<Br<I. Thus styrene is greatly hindered from coordinating with iridium metal because its forming an iridium-styrene-oxygen complex.

2. $SnCl_3$ and HgCl Ligand. The ligand effects are more clearly obtained when $SnCl_3$[15] or HgCl ligand is introduced to the iridium metal (Table 2).

With the iridium-tin chloride complex,[10] styrene gave 1212% yield of benzaldehyde, 477% yield of styrene oxide and a trace of acetophenone. The higher reactivity of the complex might arise from the strong *trans* effect of the $SnCl_3$ ligand which promotes the formation of an iridium-styrene-oxygen complex intermediate.

It is of interest that the oxidative cleavage of the C=C double bond of styrene takes place easily by the iridium complex catalyst under mild conditions indicating that oxygen is highly activated by coordinating with the iridium metal.[12,13] A similar result was obtained in the case of the HgCl ligand[11] though less reactive than the former.

An interesting aspect of the oxidation is that no benzoic acid is formed even under such an oxidative condition, though benzaldehyde is formed in a high

14) Yields of the oxidation products which appear hereafter in this paper are all based on the amount of the complexes ultilized.

15) $SnCl_3$ ligand is known to have a large *trans* effect and to be a strong π-accepter and a weak donor.[16]

16) R. V. Lindsey, Jr., G. W. Parshall and V. G. Stolberg, *J. Amer. Chem. Soc.*, **87**, 658 (1965).

Table 3. Oxidation of styrene with palladium salts

Catalyst	Reaction		Solvent	Product and yield[a] %		
	Temp.°C	Time, hr		Benzaldehyde	Styrene oxide	Acetophenone
$PdCl_2$[b]	110	8	Toluene	1098	184	17
$PdCl_2$	110	8	Acetic acid	969	19	60
$Pd(OAc)_2$	110	8	Toluene	103	68	7
$Pd_2(C_8H_8)Cl_4$[c]	110	8	Toluene	23	9	2

a) Yields are based on the catalyst used.
b) *trans*-Stilbene (64%) and unidentified compound (0.24 g, mp 77—79°C) were also obtained.
c) 1,3-Diphenylbutene (104%) and *trans*, *trans*-1,4-diphenylbutadiene (44%) were also formed.

yield. This was confirmed by the fact that when benzaldehyde was treated with $IrCl_3$ under the oxygen atmosphere, no benzoic acid was detected.

3 *Bisdiphenylphosphinoethane Ligand.* In the oxidation reaction catalyzed by the four coordinated biphosphine chelate complex,[3] bis,bis(1,2-diphenylphosphine)ethane *iridium(III)* monochloride, $[Ir(PPh_2CH_2CH_2PPh_2)_2]Cl$, styrene was also oxidized easily to give a similar result as above. In this case, an oxygen molecule will be also activated through coordination to iridium metal.[17]

Oxidation with $IrCl_3$. Oxidation of styrene catalyzed by iridium trichloride resulted in the formations of benzaldehyde, styrene oxide and acetophenone in high yields suggesting that the Vaska type complex is formed as an intermediate species[9] which causes the oxidation.

Oxidation with Palladium Salts. For the sake of comparison, the oxidation reactions of styrene using palladium(II) salts were performed. The data in Table 3 show that palladium(II) salts such as palladium(II) chloride can cause the oxidation of styrene to afford benzaldehyde, styrene oxide and acetophenone in excellent yields.

It is well known that acetophenone is obtained by the nucleophilic attack of the hydroxyl anion on the olefinic carbon atom of styrene in the presence of palladium(II) chloride and water.[19] The present oxidation reaction was carried out in the absence of water. Thus acetophenone formed can not be derived from the nucleophilic attack of the hydroxy anion on styrene suggesting that in the present system, an oxygen-palladium complex[4,5] is also formed which behaves as an oxidation catalyst.

In conclusion, it has been revealed that the Vaska complexes and some iridium complexes have a catalytic function for the oxidation of triphenylphosphine and styrene under an oxygen atmosphere.

17) The O_2-complex of this biphosphine chelate was synthesized by Vaska, and it has been reported that the O-O bond length in this complex is 0.45 Å larger than in free oxygen molecule.[18]

18) J. A. Connor and E. A. V. Ebsworth, *Adv. Inog. Chem. Radiochem.*, **6**, 280 (1964).

19) J. Smidt, W. Hafuer, R. Jira, R. Seiber, J. Sedlmeier and A. Sabel, *Angew. Chem.*, **71**, 176 (1959); **24**, 73 (1961), See also, A. Aguilo in "Advances in Organometallic Chemistry," Vol. 5, F. G. A. Stone and R. West, ed., Academic Press Inc., New York, N. Y. (1967), p. 321.

Experimental

Materials and Analysis. All temperatures were uncorrected. The IR-spectra were recorded on a Hitachi EPI-S2 spectrometer and NMR spectra were measured on a Japan Electron Optics JNM-4H-100 spectrometer. Chemical shifts are given in τ units together with splitting patterns and relative integrated area. The VPC analysis was made by a Yanagimoto GCG-3 gaschromatograph using an Apiezon L column. Iridium trichloride and palladium chloride were of commercial grade. $Pd(OAc)_2$ was prepared according to the method of Stephenson *et al.*[20] The styrene-$PdCl_2$ complex was prepared according to the method of Kharasch *et al.*[21]

Toluene was refluxed with sodium metal and distilled. Acetic acid was dried over phosphorus pentoxide and distilled. Styrene was dried over anhydrous magnesium sulfate and distilled.

Preparation of Complexes. (1) *trans*-Chloro(carbonyl)bis(triphenylphosphine)iridium. *The Vaska Complex.* *trans*-$IrCl(CO)(PPh_3)_2$ was prepared by a modification of the method of Vaska.[8] Iridium trichloride was dissolved in a mixture of triethyleneglycol and a ten fold excess triphenylphosphine. After heating the mixture at 280°C for 24 hr, the solvent was evaporated to dryness. The residue was recrystallized twice from benzene, affording a yellow crystalline complex (80%). IR: ν(Nujol) 1950 cm^{-1} (C=O) (lit,[8] 1950 cm^{-1}). NMR ($CDCl_3$): 2.00—2.90 (m).

Found: C, 57.23; H, 4.16%. Calcd for $C_{37}H_{30}OClP_2Ir$: C, 56.91; H, 3.88%.

(2) *trans*-Bromo(carbonyl)bis(triphenylphosphine)iridium. *trans*-$IrBr(CO)(PPh_3)_2$ was prepared by the method of Chock *et al.*[9] IR: ν(Nujol) 1955 cm^{-1} (C=O) (lit,[9] 1955 cm^{-1}). NMR ($CDCl_3$): 2.00—3.00 (m).

Found: C, 54.11; H, 3.95; Br, 9.34%. Calcd for $C_{37}H_{30}OBrP_2Ir$: C, 53.89; H, 3.67; Br, 9.69%.

(3) *trans*-Iodo(carbonyl)bis(triphenylphosphine)iridium. *trans*-$IrI(CO)(PPh_3)_2$ was prepared by the

20) J. A. Stephenson, S. M. Morehouse, A. R. Powell, J. P. Heffer and G. Wilkinson, *J. Chem. Soc.*, **1965**, 3632.

21) M. S. Kharasch, R. C. Seiler and F. R. Mayo, *J. Amer. Chem. Soc.*, **60**, 882 (1938).

method of Chock *et al.*[9] IR: ν (Nujol) 1973 cm^{-1} (C=O) (lit, 1975 cm^{-1}). NMR ($CDCl_3$): 2.05—2.80 (m).

Found: C, 50.66; H, 3.55%. Calcd for $C_{37}O_{30}OIP_2Ir$: C, 50.98; H, 3.47%.

(4) Bis,bis(1,2-diphenylphosphino)ethane Iridium Monochloride. $[Ir(Ph_2PCH_2CH_2PPh_2)]Cl$ was prepared according to the method of Vaska and Coton.[3] Mp 225—227°C (lit,[3] 225°).

Found: C, 60.62; H, 4.86; Cl, 3.80%. Calcd for $C_{52}H_{48}ClP_2Ir$: C, 60.94; H, 4.72; Cl, 3.46%.

(5) *trans*-Dichloro(carbonyl)bis(triphenylphosphine)chloromercuryl Iridium. *trans*-$IrCl_2(CO)(PPh_3)_2HgCl$ was prepared by the method of Nyholm and Vrieze.[11] IR: ν (Nujol) 2020 cm^{-1} (C=O) (lit,[11] 2030 cm^{-1}).

Found: C, 42.58; H, 3.42%. Calcd for $C_{37}H_3OCl_3P_2HgIr$: C, 42.25; H, 2.88%.

(6) Dichloro(carbonyl)triphenylphosphine Trichlorostanato Iridium. $IrCl_2(CO)(PPh_3)(SnCl_3)$ was prepared by the method of Taylor *et al.*[10] IR: ν (Nujol) 2070 cm^{-1} (C=O) (lit,[10] 2077, 2072 cm^{-1}). Mp 268—272°C (lit,[10] 270—275°C).

Found: C, 28.91; H, 2.16; Cl, 23.53%. Calcd for $C_{19}H_{15}OCl_5PSnIr$: C, 29.31; H, 1.95; Cl, 22.77%.

General Procedure for Oxidation by the Iridium Complexes Catalysts. The iridium complex and styrene (or triphenylphosphine) were dissolved in a solvent (usually, toluene). Oxygen was bubbled through the solution at reflux for 8 hr (in case of triphenylphosphine, 9 hr). After the evaporation of the solvent, the products were isolated by column or gaschromatography. Specific examples of reaction are given in detail below.

Reaction of Vaska Complex with Triphenylphosphine. In a 500-m*l*, three necked, round-bottomed flask, provided with condenser with a calcium chloride tube at the top and an oxygen inlet tube reaching nearly to the bottom, was placed a solution containing 300 m*l* of toluene, 2.00 g (7.6 mmol) of PPh_3 and 0.50 g (0.64 mmol) of $IrCl(CO)(PPh_3)_2$. The solution was refluxed with continued bubbling of oxygen for 9 hr and then the solvent was evaporated to dryness. The residue was subjected to a column chromatography of alumina (100 g). Elution with 500 m*l* of methanol resulted in 0.76 g (426%) of colorless crystals (I), which was assigned as triphenylphosphine oxide by comparison of IR spectrum and mixture melting point with those of an authentic sample. IR: ν (Nujol) 1420, 1185, 1115, 745, 692 and 535 cm^{-1}. After the reaction the Vaska complex catalyst used was recovered quantitatively.

Reaction of Vaska Complex with Styrene. In a flask similar to that mentioned above was placed a mixture containing 0.50 g (0.64 mmol) of $IrCl(CO)(PPh_3)_2$, 10.0 g (97 mmol) of styrene and 300 m*l* of toluene. The solution was refluxed with continued bubbling of oxygen for 8 hr. After evaporation of solvent under reduced pressure, the residual material was chromatographed on alumina (80 g). Elution with 500 m*l* of methanol and recrystallization gave 0.28 g (79%) of triphenylphosphine oxide (I). Although further elution with methanol resulted in no product, 0.2 g of an iridium complex remained at the upper part of the column, which was not further examined. From the solvent evaporated, we obtained styrene and 0.065 g (84%) of liquid substance (IIa) which was assigned as acetophenone by comparison of the IR spectrum and retention time with those of an authentic sample. IR: ν (neat) 1675, 1262, 759, 688, and 587 cm^{-1}.

Reaction of Biphosphine Chelate Complex with Styrene. In a 100 m*l* flask similar to that described above, was placed a mixture containing 0.66 g (0.64 mmol) of $[Ir(PPh_2CH_2CH_2PPh_2)_2]Cl$, 10.0 g (97 mmol) of styrene and 60 m*l* of *n*-propanol. The solution was refluxed with continued bubbling of oxygen for 8 hr. Resulting reaction mixture was treated as usual, and the liquid phase was analysed and separated by VPC to give IIa (0.065 g), IIb (0.32 g) and IIc (0.24 g). IIb was assigned as benzaldehyde by comparison of NMR spectrum, IR spectrum and retention time with those of an authentic sample. IR: ν (neat) 1675, 1573, 1200, 825, 744, 685 and 647 cm^{-1}. NMR (CCl_4): 0.15 (s,1) and 2.10—2.70 (m,5). IIc was assigned as styrene oxide by comparison of retention time with that of an authentic sample.

The solid substance was recrystallized from petroleum ether-benzene to give 0.46 g of white crystalline complex containing iridium metal. Its structure is not yet established.

BULLETIN OF THE CHEMICAL SOCIETY OF JAPAN VOL. 43 1158—1160 (1970)

Scrambling of Oxygen in the Diester Produced from Labeled Diacyl Peroxide-Olefin Reaction

Michio KOBAYASHI, Hiroshi MINATO and Yoshikuni OGI

Department of Chemistry, Tokyo Metropolitan University, Setagaya-ku, Tokyo

(Received September 17, 1969)

dl-Dihydroanisoin bis-*m*-bromobenzoate produced from the reaction between *p,p'*-dimethoxy-*trans*-stilbene and *m,m'*-dibromobenzoyl peroxide labeled with oxygen-18 at the carbonyl oxygen was found to possess completely equilibrated oxygens, and this finding indicated that a four-centerd mechanism was unlikely.

Formation of cyclohexyl acetate from the decomposition of diacetyl peroxide in cyclohexene was explained by the direct attack of cyclohexene on peroxidic oxygen,[1] but such mechanism was ruled out by a later publication describing the formation of cyclohexyl acetate and 1,2-diacetoxycyclohexane having completely scrambled oxygen-18 from the acetyl peroxide labeled specifically at the carbonyl oxygen.[2]

We have recently reported that phenyl benzoate formed from the photochemical decomposition in benzene of the benzoyl peroxide labeled with oxygen-18 at the carbonyl oxygen possesses completely scrambled oxygen and that direct reaction between benzoyl peroxide and benzene must be denounced.[3] Greene, Adam and Cantrill studied the decomposition of *m,m'*-dibromobenzoyl peroxide in benzene containing, *p,p'*-dimethoxy-*trans*-stilbene, isolated *meso*-dihydroanisoin bis-bromobenzoate (28%) and the *dl*-diester (57%), and proposed that the major course of the reaction proceeded by direct reaction between peroxide and olefin according to the four-centered mechanism shown below.[4]

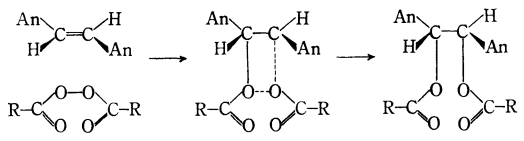

dl-diester

(An=*p*-CH_3O-C_6H_4, R=*m*-Br-C_6H_4)

We have investigated this reaction by use of oxygen-18, and have obtained evidence against such four-centered mechanism.

1) J. C. Martin and E. H. Drew, *J. Amer. Chem. Soc.*, **83**, 1232 (1961).

2) J. C. Martin, J. W. Taylor and E. H. Drew, *ibid.*, **89**, 129 (1967).

3) M. Kobayashi, H. Minato and Y. Ogi, This Bulletin, **42**, 2737 (1969).

4) F. D. Greene, W. Adam and I. E. Cantrill, *J. Amer. Chem. Soc.*, **83**, 3461 (1961).

Experimental

m-Bromobenzaldehyde-^{18}O. *m*-Bromobenzylideneaniline (bp 135°C/0.5 mmHg) was prepared by the reaction with *m*-bromobenzaldehyde and aniline. When a mixture of $H_2{}^{18}O$ (5 g) (^{18}O atom % 1.52) and 9.8 g of concentrated sulfuric acid was added to 26.5 g of *m*-bromobenzylideneaniline, a slightly exothermic reaction took place and white crystals of anilinium sulfate precipitated. After the precipitates were filtered off, 50 m*l* of benzene was added. The organic layer was separated and dried over magnesium sulfate. After the solvent was removed in vacuum, the residual yellow-brown liquid was distilled under reduced pressure and 15.2 g of *m*-bromobenzaldehyde-^{18}O (bp 80.5°C/5 mmHg) was obtained.

m,m'-Dibromobenzoyl Peroxide Carbonyl-^{18}O. Chlorine gas was bubbled through a mixture of 50 m*l* of carbon tetrachloride and 15.2 g of *m*-bromobenzaldehyde-^{18}O at room temperature for 85 min. After the solvent was removed in vacuum, the residual liquid was distilled to give 13 g of *m*-bromobenzoyl chloride-^{18}O; yield, 73.0%.

According to the procedure described by Doering, Okamoto and Krauch[5] 13 g of *m*-bromobenzoyl chloride-^{18}O was let to react with sodium peroxide, and 8.7 g of *m,m'*-dibromobenzoyl peroxide was obtained; mp 117.8°C, yield, 79.5%.

Reaction between m,m'-Dibromobenzoyl Peroxide Carbonyl-^{18}O and p,p'-Dimethoxy-*trans*-stilbene. A benzene solution (35 m*l*) containing *m,m'*-dibromobenzoyl peroxide-^{18}O (1.33 g) and *p,p'*-dimethoxy-*trans*-stilbene (0.88 g) was frozen and degassed for three times in vacuum (10^{-2}—10^{-3} mmHg), and then was heated in a sealed ampoule at 78°C for 24 hr. According to the procedure described by Greene *et al.*,[4] the reaction mixture was treated with alkali for removal of *m*-bromobenzoic acid, and the *meso*-diester was obtained as crystals from ether. The main component of the residue was the *dl*-diester which was then purified by elution chromatography on silica gel. The carbonyl oxygen of the *dl*-diester was separated from the ether

5) W. E. Doering, K. Okamoto and H. Krauch, *ibid.*, **82**, 3579 (1960).

oxygen by reaction with hydrazine in ethanol.[6] The content of oxygen-^{18}O was determined by mass-spectrometric analysis of the carbon dioxide obtained by pyrolysis of a sample.

Results and Discussion

The oxygen-18 analysis were performed for the starting peroxide, two products of the peroxide-olefin reaction (*m*-bromobenzoic acid and the *dl*-diester) and *m*-bromobenzhydrazide derived from the *dl*-diester. The results are summarized in Table 1.

Table 1. Specificity of ^{18}O labeling

Sample	Atom % ^{18}O-excess	% ^{18}O-calcd
Starting peroxide	0.516	(0.516)
m-Br-C_6H_4COOH	0.518	0.516
dl-Diester	0.459	0.516**
m-Br-$C_6H_4CON_2H_3$*	0.525	1.032**

* Derived from the *dl*-diester by reaction with N_2H_4.
** Calculated according to Greene's mechanism.

The fact that oxygen-18 content of the benzhydrazide is approximately the same as that of the *dl*-diester indicates that carbonyl oxygen and ether oxygen of the *dl*-diester are almost completely equilibrated. If the peroxide decomposes *via* the four-centered mechanism corresponding to the direct reaction, the oxygen-18 of the peroxide must be completely retained at the carbonyl oxygen of the *dl*-diester, and the ^{18}O content of the benzhydrazide must be twice that of the *dl*-diester.

The possibility of the scrambling of the ^{18}O of the starting peroxide due to the recombination of benzoyloxy radicals in cage must be considered since such scrambling occurs in the cage of acetyl peroxide,[7] but we have recently demonstrated that such scrambling does not take place in the case of benzoyl peroxide labeled with oxygen-18 at the carbonyl oxygen.[8]

Thus the mechanism of the molecule-induced homolysis does not appear to be so straightforward as usually written.[9] The following radical-induced mechanism is rejected, at least as the major reaction, of the basis of the isotopic results in Table 1 and the finding of Greene *et al.* that in the presence of galvinoxyl the rate of the peroxide-olefin reaction was reduced by only 25%.

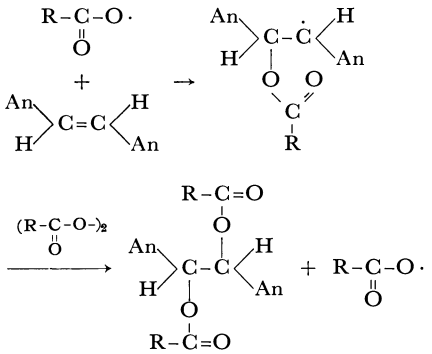

A mechanism which is consistent with various data obtained so far seems to be the following one, in which the diester is produced by combination of two radicals in a cage.

Certainly more detailed study is necessary in order to clalify the mechanism of this reaction completely. However, the above mechanism is consistent with the finding of Greene *et al.* that an

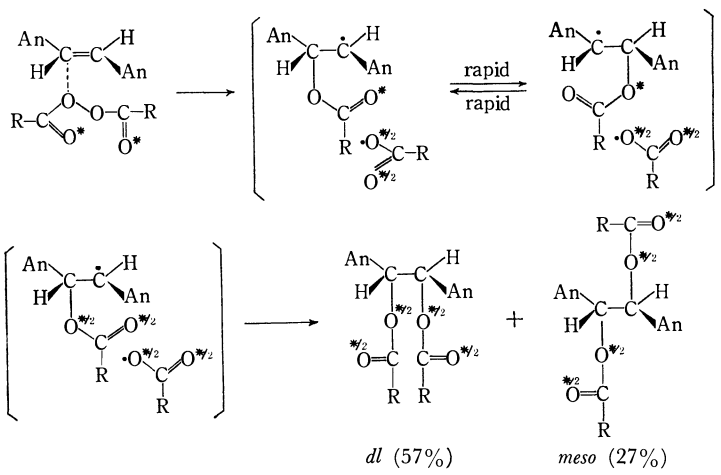

6) D. Z. Denney, T. M. Valga and D. B. Denney, *ibid.*, **86**, 46 (1964).
7) J. W. Taylor and J. C. Martin, *ibid.*, **88**, 3650 (1966).
8) M. Kobayashi, H. Minato and Y. Ogi, This Bulletin, **41**, 2822 (1968).
9) For instance, W. A. Pryor, "Free Radicals," McGraw-Hill, New York, N. Y. (1966), p. 119.

almost identical products mixture (29% *meso*-diester and 57% *dl*-diester) was obtained from the reaction between *p,p'*-dimethoxy-*cis*-stilbene and *m,m'*-dibromobenzoyl peroxide. The above mechanism is also similar to the mechanism proposed for the reaction between acetyl peroxide and cyclohexene.

Grateful acknowledgement is made to the donors of the Petroleum Research Fund, administered by the American Chemical Society, for support of this research.

BULLETIN OF THE CHEMICAL SOCIETY OF JAPAN VOL. 43 1160—1163 (1970)

The Preparation and Reaction of Disubstituted Aminophosphonium Bromide. Reaction of Triphenylphosphine Dibromide with Secondary Amines

Kiyoshi FUKUI and Rokuro SUDO

Laboratory of Organic Chemistry, Tokyo Institute of Technology, Ookayama, Meguro-ku, Tokyo

(Received September 19, 1969)

Disubstituted aminotriphenylphosphonium bromides were obtained in excellent yields from the reaction of triphenylphosphine dibromide and the secondary amines using simple procedures. This method has an advantage in the preparation of cyclic aminophosphonium salts, such as those of morpholine or piperidine. The treatment of the disubstituted aminophosphonium salt with bases resulted in dehydrohalogenation, followed by a Hofmann-like decomposition, and gave imine and triphenylphosphine.

Triphenylphosphine dihalide (**1**) has been used as a halogenation reagent, like phosphorus pentachloride, or as a dehydrating reagent.[1] There have also been several reports on the use of this reagent for the activation of compounds like the malonic ester[2] or primary amines[2b,3] in the form of phosphonium salt or ylide.

In this paper, the preparation of the salt by the reaction of triphenylphosphine dibromide with secondary amines will be reported; the activation of the carbon adjacent to the amino group was also attempted by converting the salt to ylide through the elimination of hydrogen bromide (Eq. (1)).

$$\underset{(\mathbf{1})}{Ph_3PBr_2} + \underset{(\mathbf{2})}{HN\begin{matrix}R^1\\ \diagdown\\ CH_2R^2\end{matrix}} \longrightarrow \underset{Br^-}{Ph_3P^+}\text{–}\underset{(\mathbf{3})}{N\begin{matrix}R^1\\ \diagdown\\ CH_2R^2\end{matrix}}$$

$$\cdots\cdots\rightarrow Ph_3P^+\text{–}N\begin{matrix}R^1\\ \diagdown\\ \underline{C}HR^2\end{matrix} \quad (\mathbf{4}) \qquad \text{Eq. (1)}$$

Disubstituted aminophosphonium salt was obtained by Staudinger[4] through the addition of alkyl halide to phosphoimine, and the scope and the limitations of the dialkylaminophosphonium salt were studied by Zimmer.[3] The disubstituted aminophosphonium salt is obtained by the method used in the preparation of monosubstituted aminophosphonium salt, *i.e.*, directly by the reaction of triphenylphosphine dibromide and secondary amine in the presence of triethylamine.

The reaction of triphenylphosphine dibromide with *N*-ethylaniline (**2a**) in acetonitrile in the presence of an equimolar amount of triethylamine gave *N*-ethylanilinotriphenylphosphonium bromide (**3a**) in an 82% yield. On the other hand, the addition of ethyl bromide or ethyl iodide to tetraphenylphosphoimine gave the corresponding salts in 29% and 73% yields respectively, even after refluxing in benzene for 24 hr. When diethylamine (**2b**), *N*-methylbenzylamine (**2c**), piperidine (**2d**), or morpholine (**2e**) was used as the secondary amine, the corresponding salts were obtained almost quantitatively by this method. In the case of *N*-benzylaniline (**2f**), which would exert a rather large steric hindrance in the salt, there was only a 19% yield of salt after 5 hr refluxing.

In sum, except for the case of bulky amines, the preparations of disubstituted aminophosphonium

1) R. F. Hudson, "Structure and Mechanism in Organo-Phosphorus Chemistry," Academic Press, London and N. Y. (1965), p. 214.

2) a) L. Horner and H. Oediger, *Chem. Ber.*, **91**, 437 (1958). b) L. Horner and H. Oediger, *ibid.*, **95**, 2526 (1962).

3) H. Zimmer and G. Singth, *J. Org. Chem.*, **28**, 483 (1963).

4) H. Staudinger and E. Hauser, *Helv. Chim. Acta*, **4**, 861 (1921).

TABLE 1. PREPARATION OF TRIPHENYLPHOSPHINE DIBROMIDE

All the reactions were carried out in acetonitrile.

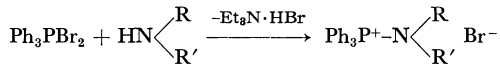

No.	R	R′	Temp.	Time (hr)	Yield	Mp °C	Elemental anal. (%) (Found/Calcd) C	H	N
a.	C_2H_5	Ph	25°	8	82%	242—242.5	67.38	5.67	2.94
							67.53	5.41	3.16
b.	C_2H_5	C_2H_5	25°	8	68%	136.5—137	62.14*	6.30	3.16
							63.77	6.04	3.38
c.	CH_3	CH_2Ph	25°	24	81%	222	67.60	5.16	3.19
							67.53	5.14	3.03
d.	HN⟨ ⟩		25°	8	68%	226.5—229	64.96	6.13	3.33
							64.79	5.86	3.28
e.	HN⟨O⟩		25°	24	42%	245—247	61.43	5.09	2.98
							61.69	5.38	3.27
f.	Ph	CH_2Ph	82°	5	19%	221	71.49	5.34	2.54
							70.99	5.16	2.67

* This compound seems to be contaminated with triethylamine salt, and the purification from the triethylamine salt was extremely difficult because of the solubility of both the salts in water.

salts by the reaction of triphenylphosphine dibromide (**1**) with secondary amines (**2**) quantitatively proceed readily and under mild conditions. The cyclic aminophosphonium salts can be also obtained by this procedure. The results are summarized in Table 1.

In an attempt to obtain β-phosphonium ylide (**4**), *N*-methyl-*N*-benzylaminotriphenylphosphonium bromide (**3c**) was treated with sodium methoxide in methanol. However, the products were triphenylphosphine oxide and dimethylamine; this was similar to the case of the hydrolysis of disubstituted aminophosphonium salt with sodium hydroxide.[3] *N*-Methylbenzylamine was also obtained; it is probably a hydrolysis product.

When *N*-methyl-*N*-benzylaminotriphenylphosphonium bromide (**3c**) was treated with an equimolar amount of butyllithium in THF, triphenylphosphine (**6**; 40%), benzylidenemethylamine (**7**; 25%), an unidentified amine, and two hydrolysis products, triphenylphosphine oxide (**5**; 14%) and

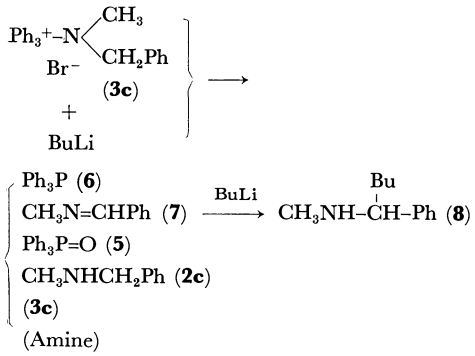

Fig. 1

N-methyl-*N*-benzylamine (**2c**; 41%), were obtained. Thirteen per cent of the unreacted phosphonium salt was recovered.

The unidentified amine is probably the reaction product from benzylidene-methylamine (**7**) and butyllithium, because the treatment of *N*-methyl-*N*-benzylaminotriphenylphosphonium bromide (**3c**) with two mole equivalents of butyllithium gave *N*-methyl-*N*-(1-phenylpentyl)amine (**8**).

These results indicate that the following processes take place in the reaction:

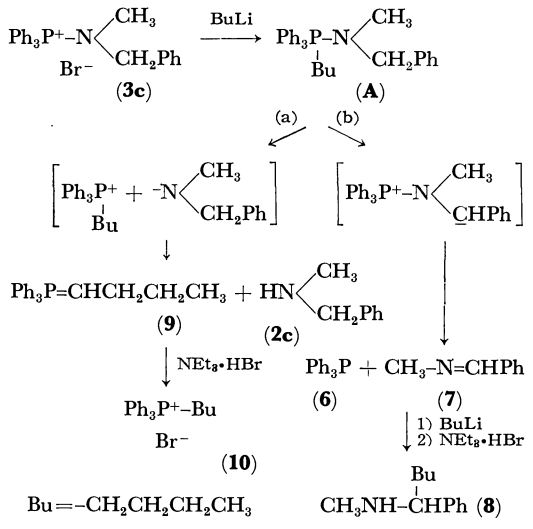

Fig. 2

In the first step, an intermediate, **A**, is formed from the reaction of *N*-methyl-*N*-benzylaminotriphenylphosphonium bromide (**3c**) and butyllithium.

Two different reaction paths from **A** may be considered:

a) The decomposition of **A** produces the amine (**2c**) and butylidenetriphenylphosphorane (**9**), which then, yield phosphonium salt (**10**) after treatment with triethylamine hydrobromide. In this case, the most stable anion, the *N*-methylbenzylamide anion, would leave from the five ligands around the phosphorus atom in **A**.[5]

b) The β-deprotonation of **A** by the butyl anion, followed by a Hofmann-like decomposition gives benzylidenemethylamine (**7**). A similar decomposition of phosphonium salt has been reported by Trippett and[6] Bestmann.[7] The last compound (**7**) was converted to amine (**8**) by the excess butyllithium. If a trace of water is present in the reaction mixture, a portion of the butyllithium will be changed to lithium hydroxide, which will then hydrolyze the phosphonium salt (**3c**) to triphenylphosphine oxide (**5**) and *N*-methylbenzylamine (**2c**).

$$\mathbf{3c} \xrightarrow{\text{LiOH}} \underset{(\mathbf{5})}{Ph_3PO} + HN\begin{matrix}CH_3\\ CH_2Ph\ (\mathbf{2c})\end{matrix}$$

The expected ylide from the elimination of the hydrogen halide of disubstituted aminophosphonium salt was found to be very unstable; as a result, the activation of the carbon adjacent to the amino group as an anion was unsuccessful. However, the results indicate the possibility of the use of this reaction in the preparation of imines and in the reduction of triphenylphosphine dihalide to triphenylphosphine.

In fact, the treatment of *N*-methyl-*N*-benzylaminotriphenylphosphonium bromide with sodium hydride in acetonitrile at room temperature gave triphenylphosphine (**6**; 42%) and benzylidenemethylamine (**7**; 25%). Sodium hydride was used in place of butyllithium to avoid the side reaction of the reagent with the imines.

Experimental

Preparation of Disubstituted Aminophosphonium Salts. *a) From Triphenylphosphine Dibromide (**1**) and Secondary Amines.* Into a solution of triphenylphosphine (2.62 g, 10 mmol) in acetonitrile (50 m*l*), a solution of bromine (1.60 g, 10 mmol) in the same solvent (15 m*l*) was stirred, drop by drop, at room temperature. A solution of *N*-ethylaniline (**2a**) (1.21 g, 10 mmol) in acetonitrile (15 m*l*) and a solution of triethylamine (1.01 g, 10 mmol) in 15 m*l* of the same solvent were then added to the mixture from a dropping funnel. After stirring at room temperature for 8 hr the solvent was removed under reduced pressure at 40—50°C. The concentrated residue was triturated with benzene, and the precipitates were collected by filtration. The precipitates were dissolved in 50 m*l* of water, and the insoluble solids were filtered off. *N*-Ethylanilinotriphenylphosphonium bromide (**3a**) was obtained in an 82% (3.8 g) yield. The crude product was recrystallized from chloroform-ethyl acetate and gave white crystals, mp 242—242.5°C.

The reactions of **1** with all the other secondary amines were carried out by a similar procedure under the reaction conditions shown in Table 1. The solvent for the recrystallization of the crude products was chloroform-ethyl acetate, except for the case of *N*-benzylanilinotriphenylphosphonium salt (**3f**), where water was used as the solvent. The results of elementary analysis and the melting points are listed in Table 1.

b) From the Addition Reaction of Alkyl Halide to Tetraphenylphosphoimine. A solution of tetraphenylphosphoimine[2] (3.53 g) and ethyl bromide (15 m*l*) in benzene (30 m*l*) was refluxed for 24 hr, and then the precipitated crystals were collected at room temperature. **3a** was obtained in a 29% (1.3 g) yield. The crude product was recrystallized from a chloroform-ethyl acetate mixture. The melting point was 242—242.5°C, and there was no depression shown in a mixed-melting point determination with the product from a). Unreacted tetraphenylphosphoimine (2.2 g; 62%) was recovered from the concentrated benzene solution by the addition of isopropyl alcohol.

In a similar fashion, the reaction of ethyl iodide or benzyl chloride with tetraphenylphosphoimine was carried out. The resulting salts were recrystallized from water. The melting points and the results of elementary analysis are as follows: *N*-Ethylanilinotriphenylphosphonium iodide, mp 221—221.5°C. *N*-Benzylanilinotriphenylphosphonium chloride, mp 205—206°C. Found: C, 77.07; H, 5.88; N, 2.92%. Calcd for $C_{31}H_{27}ClNP$: C, 77.60; H, 5.84; N, 2.92%.

Reaction of *N*-Methyl-*N*-benzylaminophosphonium Bromide (3c) with Sodium Methoxide. To a methanol (50 m*l*) solution of sodium (0.5 g), **3c** (9.46 g) in methanol (50 m*l*) was added under cooling. After standing at room temperature for one day, the mixture was refluxed for 3 hr and then concentrated under reduced pressure. Benzene and water were added to the residue. The benzene layer was washed with water and dried over anhydrous sodium sulfate. The solvent was removed to give an oily product, which was then dissolved in *n*-hexane. The insoluble solids were filtered off. Triphenylphosphine oxide was thus obtained in a 97% (5.4 g) yield. The *n*-hexane solution was concentrated and subsequently distilled. A distillate with a bp 80—83°C/26 mmHg was analyzed by gas-liquid chromatography, using an Apiezon Grease M column (10%, 3 mm×2 m); column temperature, 100°C, carrier gas, He. It gave two peaks, whose relative retention times were equal to those of authentic dimethylamine and *N*-methylbenzylamine (**2c**).

Reaction of 3c with Equimolar Butyllithium. To a suspension of **3c** (6.95 g) in THF (50 m*l*) cooled by ice, a *n*-hexane solution of butyllithium (10.5 m*l*) was added, drop by drop, under a nitrogen atmosphere. The mixture was then stirred at room temperature for one day. The precipitated crystals were collected. **3c** (0.9 g, 13%) was recovered. The filtrate was concentrated to give an oily residue. The residue was dissolved in methanol,

5) A. W. Johnson, "Ylid Chemistry," Academic Press, N. Y. and London (1966), pp 59—61.

6) S. Trippett, *Proc. Chem. Soc.*, **1963**, 19.

7) H. J. Bestmann and R. Zimmerman, *Chem. Ber.*, **101**, 2185 (1968).

and the insoluble products were filtered off. By repeating these procedures twice, triphenylphosphine was obtained in a 40% (1.65 g) yield. The filtrate was concentrated and distilled. Benzylidenemethylamine (**7**) was thus obtained in a 40% (0.6 g) yield. The IR spectrum of **7** was equal to that of an authentic sample. The residue of the distillation was dissolved in *n*-hexane. Insoluble solids were thus collected. Triphenylphosphine oxide (**5**) was obtained in a 14% (0.6 g) yield.

Reaction of 3c with 2 Molar Equivalents of Butyllithium. To a suspension of **3c** (23.1 g) in THF (100 m*l*) cooled by a dry ice-acetone mixture, a *n*-hexane solution of butyllithium (68 m*l*) was added, drop by drop, under a nitrogen atmosphere. After keeping the mixture under 0°C for 8 hr, triethylammonium bromide (9 g) and then 50 m*l* of ethanol was added. The crystals were filtered off after 2 hr and washed with water. Butyltriphenylphosphonium bromide (**10**) (8 g, 40%) was thus obtained. The product was recrystallized from water; mp 238°C. Found: C, 65.82; H, 5.99%. Calcd for $C_{22}H_{24}BrP$: C, 66.1; H, 6.01%.

The filtrate was then concentrated and distilled. *N*-Methylbenzylamine (**2c**) (bp 87°C/20 mmHg, 2.5 g, 41%) was thus obtained. Benzene and water was added to the residue of distillation. The precipitated crystals were **10** (2.15 g, 10%). The separated benzene solution was washed with water and dried over anhydrous sodium sulfate. The benzene solution was concentrated and distilled. The distillate with a bp 107—142°C/17 mmHg was identified as *N*-methyl-*N*-(1-phenylpentyl)amine (**8**) (0.55 g, 7%) by IR, bp, and elemental analysis. Found: C, 81.31; H, 10.55; N, 7.91%. Calcd for $C_{12}H_{19}N$: C, 81.3; H, 10.72; N, 7.91%.

Reaction of 3c with Sodium Hydride. To a mixture of **3c** (9.24 g) and sodium hydride (1.0 g), acetonitrile (50 m*l*) was added. A violent gas evolution was observed. The mixture was stirred at room temperature for 8 hr, and then triethylammonium bromide (3.64 g) was added and the mixture was stirred for 2 more hours. After the precipitate had been removed the filtrate was concentrated. To the residue, 2 *N*-hydrochloric acid (10 m*l*), water (20 m*l*), and benzene (30 m*l*) were added, and the two layers were separated. The aqueous solution was neutralized with a sodium bicarbonate solution and was made alkaline by sodium hydroxide. The precipitates were extracted with benzene, washed with water, and dried over anhydrous sodium sulfate. HCl gas was passed through the solution, and the precipitated crystals were collected. The crystals (0.75 g, 24%) showed an IR spectrum identical with that of *N*-methylbenzylammonium chloride prepared from **2c** and hydrogen chloride. The benzene filtrate was washed with water, dried over anhydrous sodium sulfate, and concentrated under reduced pressure. *n*-Hexane (30 m*l*) was added to the residue, and the precipitated crystals were collected. **5** (2.2 g, 40%) was thus obtained. The *n*-hexane solution was concentrated under reduced pressure, the residue was triturated with isopropyl alcohol, and the precipitated crystals were collected by filtration. By repeating these procedures twice, 2.2 g (42%) of triphenylphosphine (**6**) were obtained.

BULLETIN OF THE CHEMICAL SOCIETY OF JAPAN VOL. 43 1163—1172 (1970)

Synthesis of Corticotropin Peptides. XI. Synthesis and Biological Properties of [1-β-Alanine]-ACTH(1-18)-Octadecapeptide Amide

Ken INOUYE, Akira TANAKA and Hideo OTSUKA

Divisions of Biochemistry and Pharmacology, Shionogi Research Laboratory, Shionogi & Co., Ltd., Fukushima-ku, Osaka

(Received September 24, 1969)

The synthesis is described of an octadecapeptide amide, β-alanyl-tyrosyl-seryl-methionyl-glutamylhistidyl-phenylalanyl-arginyl-tryptophyl-glycyl-lysyl-prolyl-valyl-glycyl-lysyl-lysyl-arginyl-arginine amide, corresponding to the first eighteen amino acid residues of corticotropin except for the amino end which has been substituted by a β-alanine for the serine in native hormone. The adrenalstimulating activities of the octadecapeptide amide are compared with those of the corresponding l-serine or l-glycine octadecapeptide amide to show that the l-β-alanine peptide is remarkably more active than the latter when assayed by *in vitro*, subcutaneous and intamuscular approaches, and that the activities of the former are maintained for a longer period of time than those of the latter. The l-β-alanine peptide as a lipotropic agent is also shown to be more active than the synthetic analogs and a native corticotropin on rat adipose tissue. The differences among these octadecapeptide analogs in the biological properties are discussed in terms of their susceptibility toward the action of aminopeptidase.

Syntheses of a large number of highly active corticotropin (ACTH) peptides have been reported from various laboratories. Among these studies it is of special interest that the amino end can be

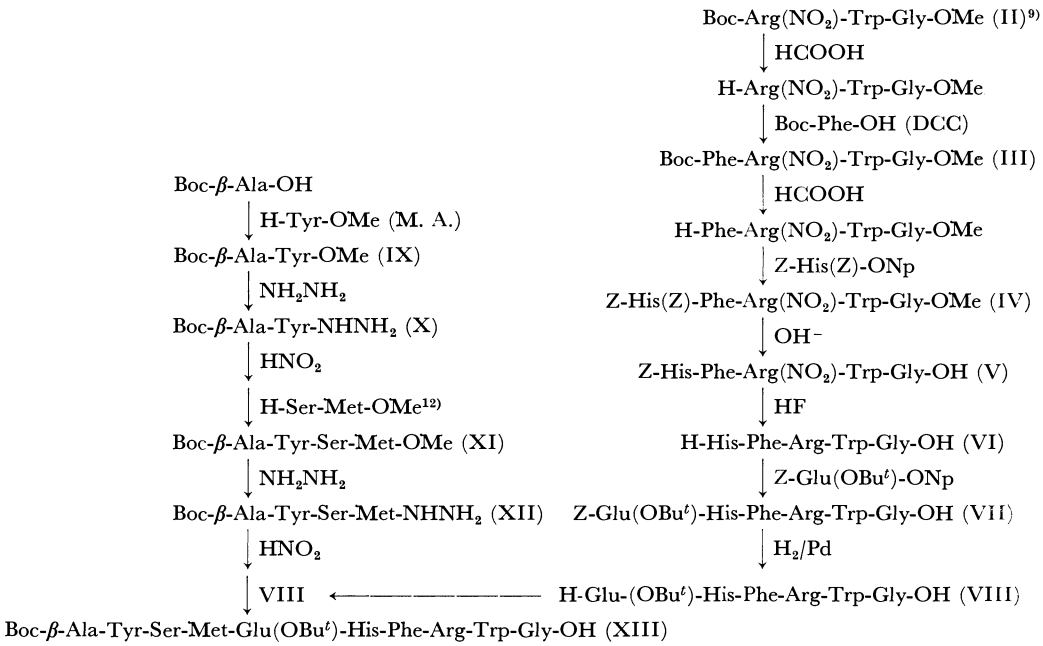

Fig. 1. Procedure for the synthesis of decapeptide intermediate.
Z, benzyloxycarbonyl; Boc, *t*-butyloxycarbonyl; Me, methyl; Bu^t, *t*-butyl; ONp, *p*-nitrophenoxy; M.A., mixed acid anhydride method; DCC, *N,N'*-dicyclohexycarbodiimide method.

replaced by D-serine[1,2] or D-alanine[2] for the native L-serine in corticotropin peptides resulting in a marked increase in the biological activities. Since hormones generally require the cellular organization to exert their biological properties, there must be a number of factors affecting the observed level of activities. It seems, however, most likely that the apparent increase in activities observed with the 1-D-serine and 1-D-alanine analogs of corticotropin peptides is a consequence of the decreased susceptibility of peptides toward the action of aminopeptidase owing to the presence of D-amino acid at the amino end. This is also suggested by the fact that the replacement by glycine of the amino-terminal serine in porcine corticotropin,[3] ACTH-(1-18)-NH_2[4] and ACTH(1-23)-NH_2[5] has made no remarkable change in the adrenal-stimulating activity. If this is correct, such an amino acid, which forms amide bonds resisting the aminopeptidase action, should as well improve the biological properties of a corticotropin peptide as do the D-amino acids, when it is substituted for the amino terminal residue of peptide. In order to confirm this of view, the synthesis of an octadecapeptide amide, β-alanyl-tyrosyl-seryl-methionyl-glutamyl-histidyl-phenylalanyl-arginyl-tryptophyl-glycyl-lysyl-prolyl-valyl-glycyl-lysyl-lysyl-arginyl-arginine amide (I), [β-Ala^1]-ACTH(1-18)-NH_2,[6] corresponding to the first eighteen amino acid residues of corticotropin with the exception of amino end was undertaken. β-Alanine is one choice, because it is known to form acid amides which are not hydrolyzed by hog kidney leucine aminopeptidase.[7] Biological properties of I were then compared with those of the corresponding 1-L-serine and 1-glycine

R-Tyr-Ser-Met-Glu-His-Phe-Arg-Trp-Gly-Lys-Pro-Val-
1 2 3 4 5 6 7 8 9 10 11 12 13
Gly-Lys-Lys-Arg-Arg-NH_2
14 15 16 17 18

ACTH(1-18)-NH_2 (Ia): R=NH_2-CH(CH_2OH)-CO-

[Gly^1]-ACTH(1-18)-NH_2 (Ib): R=NH_2-CH_2-CO-

[β-Ala^1]-ACTH(1-18)-NH_2(I): R=NH_2-CH_2-CH_2-CO-

1) R. A. Boissonnas, St. Guttmann and J. Pless, *Experientia*, **22**, 526 (1966).

2) H. Kappeler, B. Riniker, W. Rittel, P. Desaulles, R. Maier, B. Schär and M. Staehelin, "Peptides" Proceedings of the 8th European Peptide Symposium, ed. by H. C. Beyerman, North-Holland Publishing Co., Amsterdam (1967), p. 214.

3) H. E. Lebovitz and F. L. Engel, *Endocrinol.*, **73**, 573 (1963).

4) H. Otsuka, M. Shin, Y. Kinomura and K. Inouye, This Bulletin, **43**, 196 (1970).

5) R. Geiger, K. Sturm, G. Vogel and W. Siedel, *Z. Naturforsch.*, **19b**, 858 (1964).

6) All amino acid residues are of the L-configuration, unless otherwise indicated. The abbreviated designation of amino acids, peptides and their derivatives accords with the proposal of the IUPAC-IUB Commission on Biochemical Nomenclature.

7) D. H. Spackman, E. L. Smith and D. M. Brown, *J. Biol. Chem.*, **212**, 255 (1955).

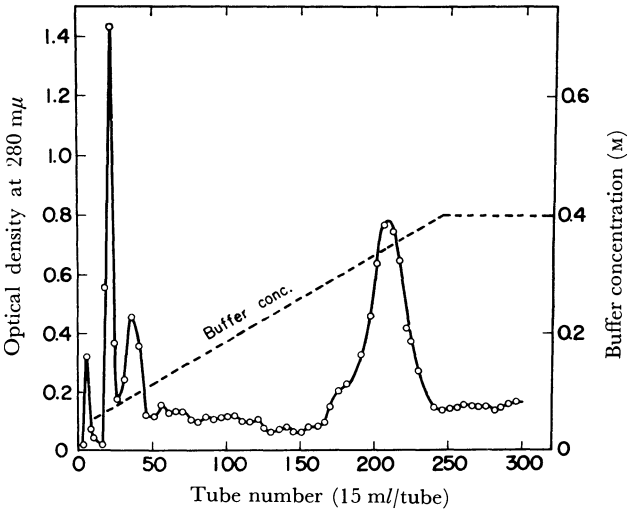

Fig. 2. Chromatography of synthetic octadecapeptide amide. Material: crude [β-Ala[1]]-ACTH(1-18)-NH_2 (I), 0.513 g. Column: carboxymethyl cellulose (Serva, 0.6 meq/g), 2.7×12 cm. Buffer: ammonium acetate (pH 6.84). Flow rate: 6 ml/min.

analogs, ACTH(1-18)-NH_2 (Ia) and [Gly[1]]-ACTH-(1-18)-NH_2 (Ib), whose syntheses were reported previously.[4,8]

A synthetic procedure of the decapeptide intermediate corresponding to the positions 1—10 of I is shown in Fig. 1. The procedure involves a new synthesis of H-Glu(OBu[t])-His-Phe-Arg-Trp-Gly-OH (VIII),[9] in which *t*-butyloxycarbonyl (Boc) groups were removed from Boc-Arg(NO_2)-Trp-Gly-OMe (II) and Boc-Phe-Arg(NO_2)-Trp-Gly-OMe (III) by treatment with formic acid[10] instead of trifluoroacetic acid formerly used,[9] and the conversion of Z-His-Phe-Arg(NO_2)-Trp-Gly-OH (V) into a pentapeptide VI was carried out in anhydrous hydrogen fluoride.[11] In these deprotection steps it was found that no detectable decomposition of the tryptophan residue occurred. The coupling of Z-Glu(OBu[t])-ONp with VI led to the formation of a protected hexapeptide (VII), which was readily converted into VIII by catalytic hydrogenolysis. Boc-β-Ala-Tyr-Ser-Met-$NHNH_2$ (XII) was synthesized by the same procedure as that described for Boc-Gly-Tyr-Ser-Met-$NHNH_2$,[12] except that a mixed acid anhydride method was used to prepare Boc-β-Ala-Tyr-OMe (IX). The azide derived from XII was then coupled with VIII to give a decapeptide Boc-β-Ala-Tyr-Ser-Met-Glu-(OBu[t])-His-Phe-Arg-Trp-Gly-OH (XIII).

In the final coupling step leading to the formation of a protected octadecapeptide amide, Boc-β-Ala-Tyr-Ser-Met-Glu(OBu[t])-His-Phe-Arg-Trp-Gly-Lys(Boc)-Pro-Val-Gly-Lys(Boc)-Lys(Boc)-Arg-Arg-NH_2 (XV), compound XIII was esterified with *N*-hydroxysuccinimide by the carbodiimide method[13] and the resulting active ester, which was isolated, was allowed to react with a partially protected octapeptide amide (acetate), H-Lys(Boc)-Pro-Val-Gly-Lys(Boc)-Lys(Boc)-Arg-Arg-NH_2 (XIV),[14] in the presence of triethylamine. The product, without further purification, was treated with 90% trifluoroacetic acid to remove all the protecting groups. The deprotection has been found to be achieved by the anhydrous hydrogen fluoride treatment;[15] formic acid may also be useful for the same purpose. The crude octadecapeptide amide (I, trifluoroacetate) was converted by treatemnt with Amberlite CG-400 (acetate) into the acetate form, which was, after having been incubated with mercaptoethanol, submitted to chromatography on a carboxymethyl cellulose (CMC) column using an ammonium acetate buffer (pH 6.8) with a linear concentration gradient. The results of chromatography are shown in Fig. 2. An over-all yield of peptide I for the final coupling step was 54%.

8) H. Otsuka, K. Inouye, F. Shinozaki and M. Kanayama, *J. Biochem.* (Tokyo), **58**, 512 (1965).

9) K. Inouye, This Bulletin, **38**, 1148 (1965).

10) B. Halpern and D. E. Nitecki, *Tetrahedron Lett.*, **31**, 3031 (1967).

11) S. Sakakibara and Y. Shimonishi, This Bulletin, **38**, 1412 (1965); S. Sakakibara, Y. Shimonishi, M. Okada and Y. Kishida, "Peptides" Proceedings of the 8th European Peptide Symposium, ed. by H. C. Beyerman, North-Holland Publishing Co., Amsterdam (1967), p. 44.

12) H. Otsuka, K. Inouye, F. Shinozaki and M. Kanayama, This Bulletin, **39**, 1171 (1966).

13) G. W. Anderson, J. E. Zimmerman and F. M. Callahan, *J. Amer. Chem. Soc.*, **86**, 1839 (1964); *ibid.*, **85**, 3039 (1963).

14) H. Otsuka, K. Inouye, M. Kanayama and F. Shinozaki, This Bulletin, **39**, 882 (1966).

15) H. Otsuka and M. Shin, unpublished.

TABLE 1. ADRENAL-STIMULATING ACTIVITIES OF ACTH AND RELATED SYNTHETIC OCTADECAPEPTIDE AMIDES*

Method	Administration route	Peptide			
		Ia	Ib	I	α_s-ACTH
Adrenal ascorbic acid depletion[19]	subscutaneous	45.4	25.6 (3)	135 (2)	120
In vitro steroidogenesis[20]	*in vitro*	13.7 (3)	20.8 (3)	237 (3)	120
In vivo steroidogenesis[21]	intravenous	92.0 (9)	167 (11)	125—285 (4)	100—180
In vivo steroidogenesis in:					
dexamethasone-Nembutal-mouse[22]	intravenous	139	70—168 (2)	259 (2)	—
hypophysecotomized rat peripheral blood	intramuscular	—	35.4 (4)	124	—

* The activities are expressed in USP units/mg, relative to the Third USP Corticotropin Reference Standard. The figures in parentheses are the number of independent assays. Ia: ACTH(1-18)-NH_2, Ib:[Gly^1]ACTH(1-18)-NH_2, I:[β-Ala^1]-ACTH(1-18)-NH_2, and α_s-ACTH: native sheep ACTH

A rechromatography on CMC afforded in an 86% recovery the pure material of I, which was found to be homogeneous to ninhydrin, Pauly, Ehrlich, Sakaguchi and methionine (PtI_6'') reagents in paper chromatography and paper electrophoresis. Quantitative amino acid analysis[16] showed that an acid hydrolysate of the product contained individual amino acids in the ratios expected by theory with the exception of tryptophan. The tryptophan-tyrosine ratio of intact I was determined spectrophotometrically to be unity.[17]

The susceptibility of β-Ala^1-octadecapeptide amide (I) toward the action of hog kidney leucine aminopeptidase (LAP) is compared in Fig. 3 with those of the corresponding Ser^1-analog (Ia) and Gly^1-analog (Ib). A commercial LAP preparation was found to hydrolyze [β-Ala^1]-ACTH(1-10)-OH and I, but not β-Ala-Tyr-Ser-Met-$NHNH_2$. Since there was no β-alanine detected in the enzymic digests on an amino acid analyzer,[16] the observed hydrolysis may be due to the presence of an endopeptidase in the LAP preparation. This apparent susceptibility of β-alanyl peptides to LAP was completely lost when the enzyme preparation had been treated with diisopropyl fluorophosphate (DFP). By the DFP-treated LAP, Ser^1-peptide (Ia) was hydrolyzed faster than Gly^1-peptide (Ib) and no hydrolysis was observed with β-Ala^1-peptide (I) within the error of measurements (Fig. 3). The results confirm and extend the finding of Spackman *et al.*[7] that hog kidney LAP does not split β-alanyl amide bonds.

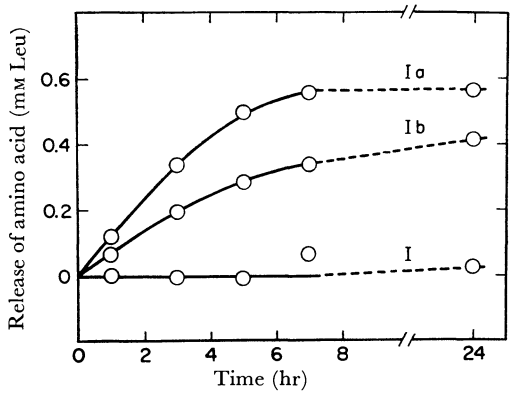

Fig. 3. Action of DFP-treated leucine aminopeptidase on synthetic octadecapeptide amides. Enzyme: DFP-treated hog kidney leucine aminopeptidase, 1.95 units/ml (see Experimental section for the definition of unit). Substrates: I, [β-Ala^1]-ACTH(1-18)-NH_2; Ia, ACTH(1-18)-NH_2; Ib, [Gly^1]-ACTH(1-18)-NH_2; concentration, 0.04 mM. Reactions were carried out in 0.02M Tris buffer (pH 8.3) at 37°C.

The adrenal-stimulating activities of β-Ala^1-octadecapeptide amide (I) were compared with those of the synthetic analogs (Ia and Ib) and sheep corticotropin (α_s-ACTH)[18] by five different assay procedures: 1) adrenal ascorbic acid depletion,[19] 2) *in vitro* steroidogenesis,[20] 3) *in vivo* steroidogenesis,[21] 4) *in vivo* steroidogenesis in the dexamethasone-pentobarbital-blocked mouse[22] and 5) steroidogenesis in the hypophysectomized rat by the intramuscular administration. The results are summarized in

16) D. H. Spackman, W. H. Stein and S. Moore, *Anal. Chem.*, **30**, 1190 (1958).

17) G. H. Beaven and E. R. Holiday, *Advan. Protein Chem.*, **7**, 319 (1952); T. W. Goodwin and R. A. Morton, *Biochem. J.*, **40**, 628 (1946).

18) We thank Professor Choh Hao Li, Hormone Research Laboratory, University of California, San Francisco, California, for his generous supply of the pure preparation of native hormone.

19) The United States Pharmacopeia, XVII, 147 (1965).

20) M. Saffran and A. V. Schally, *Endocrinol.*, **56**, 523 (1955).

21) H. S. Lipscomb and D. H. Nelson, *ibid.*, **71**, 13 (1962).

22) A. Tanaka and M. Nakamura, "Integrative Mechanism of Neuroendocrine System," Hokkaido University Medical Library Series, Vol. 1, 49 (1968).

Table 1, in which some of the data for peptides Ia and Ib are revised by the present assays from those reported previously.[4] As shown in Table 1, peptide I is highly active in any respect to the adrenal-stimulating properties. The *in vivo* steroidogenic activity of I is in the same order of magnitude as those of Ia, Ib and α_s-ACTH, when administered by intravenous injection. However, peptide I exhibited a strikingly higher activity than those of Ia and Ib, when assayed by *in vitro* steroidogenesis and adrenal ascorbic acid depletion methods. It is noteworthy that the potency ratios of subcutaneous or *in vitro vs.* intravenous administration are 1—0.5 for peptide I, whereas the ratios for peptides Ia and Ib are 1/7—1/8. Peptide I is, in this respect, much closer than Ia and Ib to the native hormone (α_s-ACTH) which gives the ratio of unity. Figure 4 shows that the β-Ala^1-peptide (I) can remain active for a longer period of time than Gly^1-peptide (Ib), when administered by intramuscular injection; the steroidogenic activity is expressed in terms of the 11-hydroxycorticosteroid (11-OHCS) level in plasma.

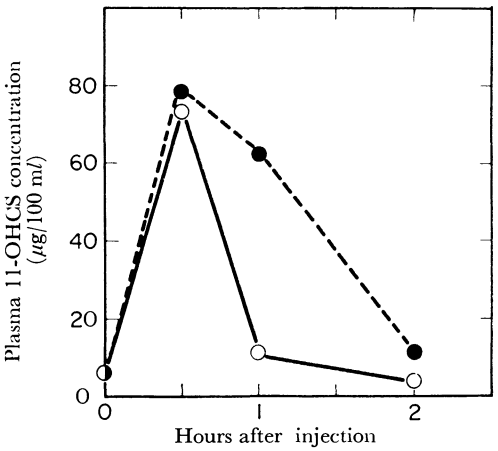

Fig. 4. Time course of synthetic octadecapeptide amides in steroidogenesis.
○—○, [Gly^1]-ACTH(1-18)-NH$_2$ (Ib); ●---●, [β-Ala^1]-ACTH(1-18)-NH$_2$ (I). Peptide (5 μg/rat) was administered into the thigh muscle of hypophysectomized rat and 11-OHCS concentration in blood was measured. See Experimental section for details.

TABLE 2. *In vitro* LIPOTROPIC ACTIVITY OF ACTH AND RELATED SYNTHETIC OCTADECAPTIDE AMIDES[23]

	Minimal effective dose (10^{-6} mg/50 mg tissue)			
	Ia	Ib	I	α_s-ACTH
Rat adipose tissue	3.0	6.3	0.62	6.0
Rabbit adipose tissue	0.004	0.35	0.065	7.1
Rat/rabbit ratio, approx.	750	20	10	1

Ia: ACTH(1-18)-NH$_2$, Ib: [Gly^1]-ACTH(1-18)-NH$_2$, I: [β-Ala^1]-ACTH(1-18)-NH$_2$, and α_s-ACTH: native sheep ACTH.

Peptide I also exhibits a high lipotropic activity, which is compared in Table 2 with the activities of synthetic peptides Ia and Ib, and a native hormone (α_s-ACTH).[23] β-Ala^1-peptide (I) was roughly ten times more active than Ia, Ib and α_s-ACTH, when assayed in the rat. A lesser amount of I can exert the activity in the rabbit as compared to that in the rat. This is the case with the other peptides as well. However, it is to be noted that the ratio of the minimal effective dose in rat fat *vs.* that in rabbit fat is smaller for I than those for Ia and Ib. Figures 5A and B show the inactivation patterns of I and Ib as lipotropic agents in the fresh plasma and in the buffer containing rat muscle fragments, respectively. There was no significant difference between I and Ib in the case of plasma,

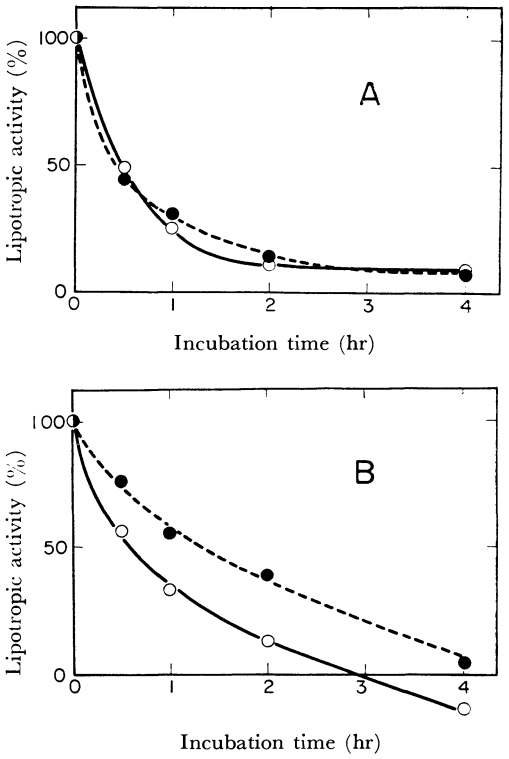

Fig. 5. Inactivation of the lipotropic activity of synthetic octadecapeptide amides.
A: by plasma. B: by tissue. ○—○, [Gly^1]-ACTH(1-18)-NH$_2$ (Ib) 1 μg/fat pad; ●---●, [β-Ala^1]-ACTH(1-18)-NH$_2$ (I) 0.1 μg/fat pad. Incubations were carried out at 37°C in the plasma of anesthetized rat in A and in the buffer containing rat muscle fragments in B. See Experimental section for details.

23) A. Tanaka, B. T. Pickering and C. H. Li, *Arch. Biochem. Biophys.*, **99**, 294 (1962).

whereas the inactivation of I was markedly delayed compared with that of Ib in the case of tissue.

The results described above clearly demonstrate that the introduction of β-alanine into the amino terminal position of ACTH(1-18)-octadecapeptide amide causes not only remarkable enhancement but also prolonged duration of the adrenocorticotropic and the lipotropic activities of the peptide. Whether a similar effect as that produced by β-alanine is expected by other amino fatty acids, such as aminobutyric acids and aminovaleric acids, remains to be examined. In any case, one can not exclude the possibility that the distance between the terminal amino group and the center of active site of the hormone peptide may become another important factor which affects the activities. Since no direct comparison has been made between the β-Ala^1-peptide and its corresponding D-Ala^1-analog in the present studies, it is not clear whether the former differes from the latter in the activity levels, solely owing to the fact that the terminal amino group of the former is located one methylene unit away from the regular position.

The present results also indicate that the remarkable changes in activities, which are produced when the amino terminal residue of octadecapeptide amide (Ia or Ib) is replaced by a β-alanine, are quite smilar in characteristics to those which were reported to occur when the relpacement was made by a D-amino acid for the amino end of the corticotropin peptides.[1,2,24] On the other hand, it is known that the adrenocorticotropic activity of corticotropin peptides is little affected by the replacement by glycine[3-5] and even by the deletion[5] of the amino terminal residue. The present results as well as the other observations support the view that the increased biological activities and their prolonged duration, which were found with the analogs bearing a D-amino acid[1,2] or a β-alanine at the amino end, are the consequence of the diminished susceptibility of peptides toward the action of intracellular aminopeptidase. By analogy, the findings that the peptide amides[8,25] and the peptide terminating with a prolinol[26] are more active than the corresponding acids and the proline amide analog, respectively, would be partly explained by the fact that an amide group at the carboxyl end protects the peptide from the action of carboxypeptidase, and by assuming that a prolinol residue assures the resistance of peptide toward the prolidase action.

As has been pointed out above, the potency ratio of subcutaneous *vs.* intravenous administration in the assay for adrenocorticotropic activity changes from 1/8—1/7 up to 0.5—1, when the amino end of octadecapeptide amide (Ia or Ib) is replaced by a β-alanine, approaching the ratio of α_s-ACTH (Table 1). This probably means that the difference in *s.c./i.v.* ratio between the synthetic peptide (Ia or Ib) and the native hormone mostly depends on the inactivation rate of peptide in the tissue, where an aminopeptidase must act predominantly on the peptide. In blood the inactivation seems to involve another type of enzyme, by which both the synthetic and the native peptides are attacked fairly equally. An enzyme inactivating thenative hormone in blod has been suggested to be an endopeptidase.[27] However, the above view remains to be elucidated by comparing the inactivation patterns of the synthetic peptides (I, and Ia or Ib) and the native hormone. Such work is in progress in this laboratory.

Experimental

All melting points were uncorrected.

***t*-Butyloxycarbonyl-β-alanine.** β-Alanine (8.91 g, 0.1 mol) was dissolved in N sodium hydroxide (100 m*l*), and sodium bicarbonate (21 g) and dioxane (70 m*l*) were added. To this was slowly added a solution of *t*-butyl azidoformate (11.2 g, 0.12 mol) in dioxane (30 m*l*) and the mixture was stirred at 50°C for 42 hr. After removal of dioxane by evaporation *in vacuo*, the residue was acidified at 0°C with ice-cold 4N hydrochloric acid to pH 2 and the desired product was extracted with cold ethyl acetate. The extracts were combined, dried over sodium sulfate and evaporated *in vacuo* to give a sirupy residue which crystallized from ethyl acetate-petroleum ether; yield 12.7 g (67%), mp 77—78°C. Recrystallization from the same solvent did not alter the melting point.

Found: C, 50.99; H, 8.06; N, 7.47%. Calcd for $C_8H_{15}NO_4$: C, 50.78; H, 7.99; N, 7.40%.

***t*-Butyloxycarbonyl-β-alanyl-tyrosine Methyl Ester (IX).** To a solution of *t*-butyloxycarbonyl-β-alanine (1.89 g, 0.01 mol) and tri-*n*-butylamine (2.04 g, 0.01 mol) in anhydrous tetrahydrofuran was added dropwise ethyl chloroformate (1.19 g, 0.01 mol) at an ice-salt bath temperature and the mixture was stirred for 10 min, and a suspension of tyrosine methyl ester (1.95 g, 0.01 mol) in tetrahydrofuran was then introduced. The reaction mixture was stirred at the above temperature for 30 min and at room temperature for 3 hr. After removal of the solvent by evaporation *in vacuo* the residue was dissolved in ethyl acetate. The solution was washed with ice-cold N hydrochloric acid, 5% sodium bicarbonate and water, dried over sodium

24) W. Rittel, Advan. Extl. Med. Biol., Vol. 2, "Pharmacology of Hormonal Polypeptides and Proteins" ed. by N. Back *et al.*, Plenum Press, New York (1968), p. 35.

25) J. Ramachandran, D. Chung and C. H. Li, *J. Amer. Chem. Soc.*, **87**, 2696 (1965).

26) W. Oelofsen and C. H. Li, *ibid.*, **88**, 4252 (1966).

27) a) G. Pincus, T. F. Hopkins and O. Hecter, *Arch. Biochem.*, **37**, 408 (1952); b) E. B. Astwood, M. S. Raben and R. W. Payne, *Recent Progress in Hormone Research*, **7**, 1 (1952); c) H. H. Tomizawa and R. H. Williams, *J. Biol. Chem.*, **217**, 685 (1955); d) W. F. White and A. M. Gross, *J. Amer. Chem. Soc.*, **79**, 1141 (1957).

sulfate and evaporated *in vacuo* to afford a sirupy residue, which crystallized upon addition of ether; yield 2.99 g (82%), mp 139—141°C. Recrystallization from methanol-ether afforded the product with mp 141—142°C, $[\alpha]_D^{23}$ +8.2±0.5° (*c* 1.020, methanol).

Found: C, 59.03; H, 7.12; N, 7.63%. Calcd for $C_{18}H_{26}N_2O_6$: C, 59.00; H, 7.15; N, 7.65%.

***t*-Butyloxycarbonyl-β-alanyl-tyrosine Hydrazide (X).** To a solution of IX (2.56 g) in ethanol (25 m*l*) was added hydrazine hydrate (1.7 m*l*) and the mixture was kept at room temperature for 5 hr. Crystals which separated were, after having been kept in a refrigerator overnight, filtered off, washed with cold ethanol and ether and dried; yield 2.54 g (99%), mp 210—212°C. These crystals were recrystallized from water in an 85% recovery, mp 214—215°C, $[\alpha]_D^{23}$ +3.6±0.6° (*c* 0.978, 50% acetic acid).

Found: C, 55.74; H, 7.11; N, 15.30%. Calcd for $C_{17}H_{16}N_4O_5$: C, 55.72; H, 7.15; N, 15.29%.

***t*-Butyloxycarbonyl-β-alanyl-tyrosyl-seryl-methionine Methyl Ester (XI).** Compound X (1.10 g, 3 mmol) was dissolved in ice-cold N hydrochloric acid (7.5 m*l*) and to this was added 2M sodium nitrite (1.6 m*l*) at an ice-salt bath temperature. The azide which separated was extracted with ice-cold ether. The ethereal extracts were combined, washed with ice-cold M sodium bicarbonate, dried over sodium sulfate and evaporated *in vacuo*. The residue was dissolved in ice-cold acetonitrile together with seryl-methionine methyl ester (0.76 g, 3 mmol)[14] and the mixture was kept at 4°C for 2 days. The solvent was removed by evaporation *in vacuo* and the residue was dissolved in a mixture of ethyl acetate and water. The organic phase was washed successively with ice-cold N hydrochloric acid, 5% sodium bicarbonate and water, dried and evaporated *in vacuo* to yield a gelationous residue, which was twice reprecipitated from ethyl acetate; yield 1.04 g (60%), mp 121—123°C, $[\alpha]_D^{23}$ −13.0±0.6° (*c* 0.997, methanol).

Found: C, 52.94; H, 6.85; N, 9.65; S, 5.48%. Calcd for $C_{26}H_{40}N_4O_9S$: C, 52.41; H, 6.90; N, 9.58; S, 5.48%.

***t*-Butyloxycarbonyl-β-alanyl-tyrosyl-seryl-methionine Hydrazide (XII).** To a solution of XI (0.97 g) in dimethylformamide (6 m*l*) was added hydrazine hydrate (0.5 m*l*) and the mixture was kept at 4°C for 2 days. Addition of ethyl acetate yielded gelatinous precipitates, which were washed with cold ethyl acetate and dried *in vacuo* (1.01 g). The product cyrstallized upon heating with water; yield 0.85 g (88%), mp 187—188°C, $[\alpha]_D^{23}$ −20.1±0.5° (*c* 1.346, 50% methanol).

Found: C, 49.72; H, 7.04; N, 14.50; S, 5.15%. Calcd for $C_{25}H_{40}N_6O_8S\cdot H_2O$: C, 49.82; H, 7.02; N, 13.94; S, 5.32%.

Nitroarginyl-tryptophyl-glycine Methyl Ester Formate. *t*-Butyloxycarbonyl-nitroarginyl-tryptophyl-glycine methyl ester (II, 5.77 g)[28] was dissolved in formic acid (98—100%, 50 m*l*) and the solution was allowed to stand for 3.5 hr. The formic acid was removed by evaporation at 40—45°C and the residue was dissolved in water. The solution was washed with ether and lyophilized; yield 4.76 g (91%), mp 107—111°C, $[\alpha]_D^{23}$ +13.0±0.5° (*c* 2.062, methanol).

Found: C, 47.25; H, 6.03; N, 20.90%. Calcd for $C_{20}H_{28}N_8O_6\cdot HCOOH\cdot \frac{1}{2}H_2O$: C, 47.45; H, 5.88; N, 21.08%.

***t*-Butyloxycarbonyl-phenylalanyl-nitroarginyl-tryptophyl-glycine Methyl Ester (III).** This compound was synthesized in exactly the same manner as described previously, except for using the tripeptide ester formate obtained above instead of the trifluoroacetate.[9] Mp 176—177°C, $[\alpha]_D^{23}$ −20.4±0.2° (*c* 2.040, methanol); lit,[9] mp 172—173°C, $[\alpha]_D^{25}$ −20.1±1° (*c* 2.054, methanol).

Found: C, 56.34; H, 6.22; N, 17.58%. Calcd for $C_{31}H_{45}N_9O_9$: C, 56.42; H, 6.27; N, 17.42%.

Phenylalanyl-nitroarginyl-tryptophyl-glycine Methyl Ester Formate. Compound III (1.81 g) was dissolved in formic acid (98—100%, 18 m*l*) and the solution was kept at room temperature for 3.5 hr. After removal of the formic acid the residue was crystallized from *n*-butanol. The crystalline product was filtered off, washed with ether and dried *in vacuo*; yield 1.71 g (92%), mp 124—125.5°C, $[\alpha]_D^{23}$ −9.0±0.5° (*c* 0.977, methanol).

Found: C, 53.00; H, 6.10; N, 17.79%. Calcd for $C_{29}H_{37}N_9O_7\cdot HCOOH\cdot \frac{1}{2}C_4H_9OH$: C, 54.38; H, 6.28; N, 17.84%.

***N*$^{\alpha}$, *N*$^{\mathrm{Im}}$-Dibenzyloxycarbonyl-histidyl-phenylalanylnitroarginyl-tryptophyl-glycine Methyl Ester (IV).** This compound was synthesized in exactly the same manner as described previously, except for using the tetrapeptide ester formate obtained above instead of the corresponding trifluoroacetate,[9] in a 75% yield; $[\alpha]_D^{27}$ −22.3±0.3° (*c* 2.084, dimethylformamide). Lit,[9] $[\alpha]_D^{25.5}$ −21.5±0.5° (*c* 2.429, dimethylformamide).

Found: C, 58.63; H, 5.70; N, 15.89%. Calcd for $C_{51}H_{56}N_{12}O_{12}\cdot H_2O$: C, 58.50; H, 5.58; N, 16.05%.

Histidyl-phenylalanyl-arginyl-tryptophyl-glycine Monoacetate (VI). Benzyloxycarbonyl-histidyl-phenylalanyl-nitroarginyl-tryptophyl-glycine (V, 0.72 g)[9] and anisole (0.72 m*l*) were dissolved in anhydrous hydrogen fluoride (7—8 m*l*) at a dry-ice-acetone bath temperature and the mixture was stirred at 0°C for 30 min. After removal of hydrogen fluoride by evaporation the residue was dried over sodium hydroxide pellets overnight *in vacuo*. The residue was dissolved in water (20 m*l*) and the solution was washed thoroughly with ethyl acetate and then passed through a small column of Amberlite CG-400 (acetate form). The column was washed with portions of water. The aqueous effluents were combined and lyophilized; yield 0.64 g (98.5%), $\lambda_{max}^{0.1N\ HCl}$=279 mμ ($E_{1cm}^{1\%}$ 66.2), 288 mμ ($E_{1cm}^{1\%}$ 53.5) and $\lambda_{max}^{0.1N\ NaOH}$=280 mμ ($E_{1cm}^{1\%}$ 65.0), 288 mμ ($E_{1cm}^{1\%}$ 54.5). Paper chromatography (*n*-butanol : acetic acid : pyridine : water=30 : 6 : 20 : 24 by volume, BAPW, as solvent) showed the presence of one major component (R_f=0.47—0.53) and two traces, all of which were reactive to ninhydrin, Pauly and Ehrlich reagents; only the major one was reactive to Sakaguchi reagent. The product was used in the subsequent coupling reaction without further purification.

Benzyloxycarbonyl-γ-*t*-butyl-glutamyl-histidyl-phenylalanyl-arginyl-tryptophyl-glycine Monoacetate (VII). A solution of compound VI (0.83 g, 1 mmol) and triethylamine (0.28 m*l*, 2 mmol) in 90% dimethyl-

28) In a previous communication compound II was reported as amorphous solid with mp 112—114°C.[9] Later it was obtained in a crystalline state from methanol, mp 189—190°C, $[\alpha]_D^{23}$ −13.6±0.5° (*c* 1.026, dimethylformamide). Found: C, 51.94; H, 6.23; N, 19.26%. Calcd for $C_{25}H_{36}N_8O_8$: C, 52.07; H, 6.29; N, 19.53%.

formamide (10 ml) was stirred at 0°C and to this was added benzyloxycarbonyl-γ-*t*-butyl-glutamic acid *p*-nitrophenyl ester (0.46 g, 1 mmol),[29] and the mixture was stirred at 4°C overnight. An additional quantity (0.46 g) of the active ester was introduced and the mixture was kept at 4°C until the peptide VI became indetectable in thin-layer chromatography (BAPW as solvent). The reaction mixture was then added dropwise into ice-cold ethyl acetate (100 ml) to afford gelatinous precipitates, which were filtered off, washed with ethyl acetate and dried *in vacuo*. The product was reprecipitated from acid-water to give the desired hexapeptide (VII); yield 0.84 g (70%), $[\alpha]_D^{23}$ −26.6±0.5° (*c* 1.377, 50% acetic acid). Lit,[30] $[\alpha]_D$ not given.

Found: C, 52.86; H, 6.74; N, 13.98%. Calcd for $C_{51}H_{64}N_{12}O_{11}\cdot CH_3COOH\cdot 7H_2O$: C, 52.73; H, 6.85; N, 13.92%.

γ-*t*-Butyl-glutamyl-histidyl-phenylalanyl-arginyl-tryptophyl-glycine Monoacetate (VIII). Compound VII (0.265 g) in 50% acetic acid (10 ml) was hydrogenolyzed in the presence of palladium black for 2.5 hr. After the catalyst had been removed by filtration the filtrate was evaporated *in vacuo* at a bath temperature of 45—50°C. The residue was lyophilized from acetic acid and dried over sodium hydroxide pellets *in vacuo*; yield 0.22 g. The product behaved as a single component in paper chromatography (*n*-butanol: acetic acid : water=4 : 1 : 2 by volume, BAW, as solvent).

Found: C, 49.46; H, 6.77; N, 15.49%. Calcd for $C_{43}H_{58}N_{12}O_9\cdot CH_3COOH\cdot 8H_2O$: C, 49.53; H, 7.21; N, 15.40%.

***t*-Butyloxycarbonyl-β-alanyl-tyrosyl-seryl-methionyl-γ-*t*-butyl-glutamyl-histidyl-phenylalanyl-arginyl-tryptophyl glycine (XIII).** To a solution of XII (0.45 g, 0.75 mmol) in 90% dimethylformamide (4.5 ml), which had been chilled in an ice-salt bath, were added ice-cold N hydrochloric acid (2.0 ml) and ice-cold M sodium nitrite (0.83 ml) and the mixture was stirred for 4 min. Ice-cold saturated sodium chloride (20 ml) and ice-cold ethyl acetate were then introduced. The aqueous layer which separated was extracted twice with ethyl acetate. The organic solutions were combined, washed with cold 5% sodium bicarbonate, dried over sodium sulfate and added to a solution of VIII (0.50 g, 0.5 mmol) and triethylamine (0.21 ml, 1.5 mmol) in dimethylformamide (15 ml) and the mixture was evaporated at a bath temperature of 10—15°C *in vacuo* to remove ethyl acetate. The resulting clear solution was kept at 4°C overnight. An additional quantity of the azide (prepared from 0.23 g of XII as has been described above) was introduced and the reaction mixture was kept at 4°C for one more day. It was then added dropwise into ice-cold ethyl acetate (200 ml) to afford amorphous precipitates, which were filtered off, washed with ethyl acetate and dried *in vacuo*; yield 0.69 g (94%). Reprecipitation from dimethylformamide-methanol (2 : 5) gave the pure decapeptide derivative (XIII) in a 66 per cent recovery; $[\alpha]_D^{23}$ −19.4± 0.7° (*c* 0.882, dimethylformamide). The product behaved as a single component (R_f=0.54—0.57) in thin-layer chromatography (dimethylformamide : ethyl acetate : acetic acid=15 : 10 : 2 by volume as solvent).

Found: C, 51.62; H, 6.66; N, 14.06; S, 2.64%. Calcd for $C_{68}H_{94}N_{16}O_{17}S\cdot 8H_2O$: C, 51.57; H, 7.00; N, 14.15; S, 2.02%.

β-Alanyl-tyrosyl-seryl-methionyl-glutamyl-histidyl-phenylalanyl-arginyl-tryptophyl-glycyl-lysyl-prolyl-valyl-glycyl-lysyl-lysyl-arginyl-arginine Amide, [β-Ala[1]]-ACTH(1-18)-NH_2 (I). To a solution of compound XIII (0.37 g, 0.25 mmol) in dimethylformamide (10 ml) was added ice-cold N hydrochloric acid (0.25 ml) at 0°C and the solution was immediately added to ice-cold ethyl acetate-ether (1 : 1, 200 ml). The resulting precipitates were filtered off, washed with ether and dried *in vacuo*; 0.36 g. These precipitates were dissolved in dimethylformamide (5 ml) and to this were added *N*-hydroxysuccinimide (0.115 g, 1 mmol) and *N*,*N*′-dicyclohexylcarbodiimide (0.21 g, 1 mmol) successively and the mixture was stood at 4°C overnight. After removal of the urea which separated, the filtrate was introduced into ice-cold ethyl acetate-ether (1 : 1, 200 ml). The precipitates were filtered off, washed with ether and dried *in vacuo* to give the decapeptide active ester; 0.39 g.

The triacetate of N^{ε}-t-butyloxycarbonyl-lysyl-prolyl-valyl-glycyl-N^{ε}-*t*-butyloxycarbonyl-lysyl-N^{ε}-*t*-butyloxycarbonyl-lysyl-arginyl-arginine amide (0.23 g, 0.155 mmol)[14] was dissolved in dimethylformamide (3 ml) and triethylamine (0.24 ml) was added. To this was then added a solution of the decapeptide active ester obtained above (0.39 g, 0.24 mmol) in dimethylformamide and the reaction mixture (total volume *ca.* 5 ml) was allowed to stand at 4°C for 60 hr. The crude protected octadecapeptide was obtained as amorphous solid when the reaction mixture was introduced into cold ethyl acetate (100 ml); yield 0.55 g.

The protected peptide obtained above (0.55 g) was dissolved, for deprotection, in 90% trifluoroacetic acid (6 ml) and the solution was kept at room temperature for 60 min, after which the solvent was removed by evaporation *in vacuo*. The residue was dissolved in water and the solution was passed through a column (2.2×7 cm) of Amberlite CG-400 (acetate form); the column was washed with portions of water. The aqueous solutions were combined and concentrated to 10—15 ml *in vacuo*. To the concentrate was added M mercaptoethanol (1 ml) and the mixture was incubated at 37°C overnight and lyophilized. The crude deblocked peptide (0.51 g) thus obtained was subejcted, for purification, to chromatography on a column (2.7×12 cm) of carboxymethyl cellulose (CMC, Serva, 0.6 meq/g) using an ammonium acetate buffer (pH 6.8, 4000 ml) with a linear concentration gradient of 0.05—0.4M.[31] The results of chromatography are shown in Fig. 2. The fractions (15 ml/tube) corresponding to a main peak (tubes 166—245) were combined and the bulk of the solvent was removed *in vacuo*. The residue was lyophilized repeatedly to constant weight to give the partially purified I; 0.22 g (54%). The product (0.2 g) was chromatographed, for further purification, on a column (2.2×18 cm) of CMC (Serva, 0.6 meq/g) using an

29) K. Hofmann, R. Schmiechen, R. D. Wells, Y. Wolman and N. Yanaihara, *J. Amer. Chem. Soc.*, **87**, 611 (1965).

30) R. Geiger, K. Sturm and W. Siedel, *Chem. Ber.*, **96**, 1080 (1963).

31) A buffer with a particular concentration, for example 0.05M, was prepared by adding the reagent grade aqueous ammonia (28%, w/w) to 0.05N acetic acid until the desired pH was obtained.

ammonium acetate buffer (pH 6.8, 2000 m*l*) with a linear cocentration gradient of 0.05—0.8M. The fractions (7.5 m*l*/tube) corresponding to a main peak (tubes 125—160) were combined, concentrated and lyophilized to obtain the pure peptide I; 0.17 g, $[\alpha]_D^{27}$ $-54.0\pm1.8°$ (*c* 0.515, 0.1N acetic acid). $\lambda_{max}^{0.1N\ HCl}$=280 m$\mu$ ($E_{1cm}^{1\%}$ 23.0), $\lambda_{shoulder}^{0.1N\ HCl}$=288.5 m$\mu$ ($E_{1cm}^{1\%}$ 17.5) and $\lambda_{max}^{0.1N\ NaOH}$= 281.5 m$\mu$ ($E_{1cm}^{1\%}$ 24.9), 288 mμ ($E_{1cm}^{1\%}$ 24.3). The peptide behaved as a single component to ninhydrin, Pauly, Ehrlich, Sakaguchi and methionine (PtI_6'') reagents in paper chromatography (BAPW as solvent) and in paper electrophoresis (600 V/36 cm, in 2N acetic acid). Amino acid ratios in acid hydrolysate:[16] Ser 0.75, Glu 0.90, Pro 0.91, Gly 1.89, Val 1.00, Met 0.96, Tyr 1.01, Phe 0.97, β-Ala 1.00, Lys 2.83, His 0.92, Arg 2.82, Trp 0.55, NH_3 1.42. The Trp/Tyr ratio in intact I was determined spectrophotometrically to be 1.16.[17]

Enzymic Studies. A commercial preparation of hog kidney leucine aminopeptidase (LAP) was obtained from Worthington Biochemical Corporation, Freehold, New Jersey, U. S. A.; LAP-C 7HB.[32]

The enzyme preparation (a suspension in 75% saturated ammonium sulfate) was dialyzed against 0.005M trishydroxymethyl aminomethane (Tris) buffer (pH 8.0, 0.005M $MgCl_2$) at 4°C before use. A DEP-treated LAP was obtained in the following way: the LAP suspension (5 mg enzyme) was diluted five fold with 0.005M Tris buffer and to this was added 0.08 m*l* of M diisopropyl fluorophosphate (DFP) in isopropyl alcohol, and the mixture was incubated at 37°C for 45 min and then dialyzed against 0.005M Tris buffer at 4°C. The LAP activity of the enzyme solutions was determined at pH 8.3 and 25°C according to Tuppy *et al.*[33] with some modifications, using L-leucine *p*-nitroanilide (LNA) as substrate. One LAP unit was temporarily defined as the amount of enzyme that produced, in the present assay procedure,[34] an increase in absorbance at 400 mμ of 0.001 per minute above the blank, using 1-cm cells in a Hitachi photoelectric spectrophotometer.

The syntheses of ACTH(1-18)-NH_2 (Ia) and [Gly^1]-ACTH(1-18)-NH_2, (Ib), used as substrates, were described previously.[4,8] [β-Ala^1]-ACTH(1-4)-$NHNH_2$ and [β-Ala^1]-ACTH(1-10)-OH as substrates were prepared from compounds XIV and XIII, respectively, by the treatment with formic acid.[10]

For the measurements of the cleavage of synthetic substrate by LAP, a mixture comprising one part of 0.1 mM substrate (in water), one part of 0.05M Tris buffer (pH 8.3) and a half part of enzyme (4.88 units/m*l*, LNA as substrate) was incubated at 37°C. From the incubation mixture 0.5-m*l* samples were withdrawn and immediately mixed with 0.5 m*l* of ninhydrin reagent[35] and the mixture was then heated in a boiling water bath for 15 min and chilled; after appropriate dilution with 50% ethanol, the absorbance at 570 mμ was determined in a Hitachi spectrophotometer. For each run, control incubation mixtures without substrate or without enzyme were analyzed. In the ninhydrin reaction a standard solution of L-leucine was also checked every time as a reference. The results of the enzymic cleavage of peptides, I, Ia, and Ib, by DFP-treated LAP are shown in Fig. 3, where the release of amino acids is expressed in terms of the leucine concentration.

Characterization of Biological Properties. *1) Adrenal-stimulating Activity.* Assays for adrenal-stimulating activities were carried out according to five different procedures. The adrenal ascorbic acid depleting activity in the hypophysectomized rat was assayed by the method of United States Pharmacopeia, XVII.[19] The *in vitro* steroidogenic activity was assayed by the Saffran and Schally method.[20] The *in vivo* steroidogenic activity by the intravenous administration to hypophysectomized rat was assayed by the method of Lipscomb and Nelson[21] with a minor modification.[36] The *in vivo* steroidogenic activity was also assayed in the dexamethasone-pentobarbital-primed mouse.[22] In addition, the steroidogenic activity by the intramuscular administration to hypophysectomized rat was determined, where a preparation (0.05 m*l*/rat) was injected into the thigh muscle and a blood sample was collected from the abdominal aorta 30 min after the injection. Throughout the experiments, the Third USP Corticotropin Reference Standard was used as a standard and the production of 11-hydroxycorticosteroids (11-OHCS) was determined by the fluorophotometric method of Peterson.[37] For each assay method several determinations were performed and the data obtained independently were submitted to statistical treatment by the Sheps and Moore procedure.[38] The results of these assays are summarized in Table 1.

2) Time Course of Steroidogenesis. The change in steroidogenic activity of the peptides I and Ib, administered by intramuscular injection, was followed: 5-μg/rat samples (1 mg peptide/m*l*) were injected into the thigh muscle of the hypophysectomized rats and blood samples were collected from the abdominal aorta in appropriate time intervals starting 30 min after the injection. The plasma 11-OHCS level was determined fluorophotometrically.[37] The results are shown in Fig. 4.

3) Lipotropic Activity. Assays were carried out according to the method described by Tanaka *et al.*[23] with the rat epididymal and the rabbit perirenal adipose tissues. The increase of nonesterified fatty acid concentration in both medium and tissue is the parameter. The results are summarized in Table 2, in which the activity is expressed in terms of the minimal effective dose per 50 mg itssue.

32) The manufacturer denotes that the preparation has an activity of 150 units/mg (L-leucine amide as substrate) and is free from the activities toward benzoyl-L-tyrosine ethyl ester and benzoyl-L-arginine ethyl ester or tosyl-L-arginine methyl ester.

33) H. Tuppy, U. Wiesbauer and E. Wintersberger, *Z. Physiol. Chem.*, **329**, 278 (1962).

34) A 10-m*l* assay medium is composed of 0.625 mM substrate solution (4 m*l*), 0.1M phosphate buffer (pH 8.3, 4 m*l*) and an enzyme test solution (2 m*l*), which has been prepared from a stock solution by appropriate dilution with 0.005M Tris buffer (pH 8.0, 0.005M $MgCl_2$). With a single run in this assay medium four consecutive determinations are usually possible in appropriate time intervals.

35) S. Moore and W. H. Stein, *J. Biol. Chem.*, **211**, 907 (1954).

36) A. Tanaka and C. H. Li, *Endocrinol. Japonica*, **13**, 180 (1966).

37) R. E. Peterson, *J. Biol. Chem.*, **225**, 25 (1957).

38) M. C. Sheps and E. A. Moore, *J. Pharmacol. Extl. Therap.*, **128**, 99 (1960).

4) Inactivation of Lipotropic Activity by Plasma and by Tissue. A peptide sample was dissolved in the fresh plasma of anesthetized rat and in the Krebs-Ringer bicarbonate buffer containing bovine serum albumin, thigh muscle fragments of rat and glucose. These mixtures were then incubated at 37°C and the aliquots taken from the incubation mixtures were assayed for the lipotropic activity by the above method at 0.5, 1, 2 and 4 hr of incubation time. The results are shown in Fig. 5A and 5B.

Grateful acknowledgement is made to Miss Keiko Namba, Mr. Kunio Watanabe (synthesis), Miss Kazuko Kondo (enzymic work), Mr. Kunihiro Odaguchi, Mr. Takayoshi Furukawa and Mr. Kuniyoshi Nakayama (biological assays) for able technical assistance. The authors also thank Dr. Mitsuo Ebata and staff for amino acid analysis, Dr. Kaoru Kuriyama and staff for optical rotation measurements, and Dr. Satoshi Mizukami and staff for elemental microanalysis.

BULLETIN OF THE CHEMICAL SOCIETY OF JAPAN VOL. 43 1172—1177 (1970)

A Novel Reduction in the Presence of Precipitated Metals. II. The Behavior of Precipitated Metals and Water in Catalytic Reduction

Koji SAKAI, Masayoshi ISHIGE,*1 Ken-ichi WATANABE and Kazuo HATA

Department of Chemistry, Faculty of Science, Tokyo Metropolitan University, Setagaya-ku, Tokyo

(Received September 26, 1969)

The ppt-metal-catalyzed reduction, which is performed by refluxing the substrates with water in the presence of ppt-metals, was investigated in detail. The participation of water as a hydrogen donor was demonstrated by the fact that benzaldehyde was reduced to the corresponding deuterated alcohols when heated with D_2O in the presence of ppt-Ni. The scope of the reduction was established by the reaction of cyclohexanone with ppt-metals and water. The most preferable H_2O/cyclohexanone molar ratio was found to be about 15 : 1. The reaction was accelerated when a 0.25N aqueous solution of sodium chloride was used instead of water. It was found that the order of the abilities of various ppt-metals to decompose water is different from that of the abilities to catalyze the reduction of cyclohexanone. The values of the activation energies for the reduction catalyzed by ppt-Ni and ppt-Ni,Co were found to be 4.0 kcal/mol and 7.5 kcal/mol respectively. From these facts, it was concluded that the ppt-metal-catalyzed reduction consists of two steps: the reaction of water with zinc or zinc compounds to supply a hydrogen source necessary for the hydrogenation, followed by ordinary catalytic hydrogenation.

In previous papers,[1,2] the utilization of precipitated metals (abbreviated as ppt-metals) as catalysts for the reduction of various compounds, with water as the hydrogen donor, has been described. The reduction was easily attained by refluxing with water in the presence of ppt-metal, the co-existence of any acids or bases being unnecessary. It has already been proposed[2] that this catalytic reaction might involve a reaction step similar to that in the ordinary catalytic hydrogenation. The present paper will deal with an extensive study of this reaction, a study covering the behavior of water and the function of catalyst metals.

Results

Deuteration of Benzaldehyde with D_2O. In order to provide direct evidence for the participation of water as a hydrogen donor, the reduction of benzaldehyde with D_2O in the presence of ppt-Ni was investigated.

The experiment was carried out in a sealed tube by heating benzaldehyde with 99.75% D_2O in the presence of ppt-Ni; deuterated benzyl alcohol was thus obtained in a good yield. However, the attempt to determine the deuterium distribution in the product by the spectroscopic method failed because of the rapid exchange between the D and H in the hydroxyl group by means of the moisture in the air. Therefore, the product, which was assumed to be a mixture of C_6H_5-CHD-OD and

*1 Present address: Chemical Laboratory, Ochanomizu University, Ootsuka, Bunkyo-ku, Tokyo.

1) K. Sakai and K. Watanabe, This Bulletin, **40**, 1548 (1967).

2) K. Sakai, M. Ishige, H. Kono, I. Motoyama, K. Watanabe and K. Hata, *ibid.*, **41**, 1902 (1968); M. Ishige, K. Sakai, K. Watanabe and K. Hata, *Shokubai (Catalyst)* (Tokyo), **11**, 50 (1969).

C_6H_5–CD_2–OD, was completely changed to C_6H_5–CHD–OH and C_6H_5–CD_2–OH by vigorous shaking with a large amount of water. The NMR spectrum of the sample thus obtained showed only three sharp singlets, at τ 2.85, 5.60, and 6.35; these singlets are assignable to phenyl, methylene, and hydroxyl protons, and the intensities correspond to 5, 0.4, and 1 protons respectively. From the proton intensities in NMR, the ratio between C_6H_5–CHD–OH and C_6H_5–CD_2–OH was estimated to be approximately 40 : 60. The IR spectram of the deuterated alcohols showed an intense band at 2200 cm^{-1} assignable to the stretching vibration of the CD group. The disappearance of the OD band at 2510 cm^{-1} showed the complete exchange of the D in the hydroxyl group for H. The absorption bands in the 650—900 cm^{-1} region, observed in a *n*-hexane solution (0.014 mol/*l*), distinctly showed the presence of a monosubstituted benzene ring, thus demonstrating that no deuterium exchange of ring protons had occurred during the reduction.

These experimental results prove that water acts as a hydrogen donor as well as a solvent in this reduction. This participation of D_2O as a hydrogen donor in the reduction led to the suggestion that this reduction with D_2O would be useful for the synthesis of various deuterated organic compounds as a simpler method than the well-known reduction with $LiAlD_4$ or $NaBD_4$.

The Reduction of Cyclohexanone Using a Varying Amount of Water. Though the presence of water is indispensable for the reduction, the use of an excess of water may be unfavorable because of the low concentration of the reactants. We tried to ascertain the adequate quantity of water suitable for the reduction by using cyclohexanone as a substrate. The reduction reaction of cyclohexanone to cyclohexanol in the presence of ppt-Ni was apparently first-order in the disappearance of the ketone. Typical examples of the apparent first-order rate constants of cyclohexanone in the reactions with various quantities of water are summarized in Table 1. In order to keep the reaction mixture homogeneous, a given quantity of dioxane was added to the aqueous solution. As is shown in Table 1, when a comparatively small quantity of water is used the rate constant increases with the increase in the quantity of water used. However, the reaction rate gradually decreased when the quantity of water exceeded a certain limit, as had been expected from the decreased concentration of cyclohexanone. The most favorable result was obtained when the H_2O/cyclohexanone mole ratio was about 15 : 1 (Exp. 3).

Table 1. The effect of water on the rate of the reduction of cyclohexanone under refluxing

cyclohexanone 9.8 g (0.1 mol), ppt-Ni 20 g

Exp. No.	Water ml	Water mol	Dioxane ml	Concentration of cyclohexanone %	Rate constant $k(\times 10^2)$ (hr^{-1})
1	16.2	0.9	13	24.8	6.49
2	21.6	1.2	13	21.8	11.30
3	27.0	1.5	15	18.8	13.30
4	32.4	1.8	16	16.7	11.10
5	37.8	2.1	20	14.4	9.00
6	43.2	2.4	20	13.3	9.34

The Promoting Effect of Sodium Chloride[2,3] on the Reduction of Cyclohexanone. The ppt-Ni is generally prepared by the rapid addition of a hot aqueous solution of nickel chloride to slushy zinc dust. When nickel nitrate was used in place of nickel chloride, a ppt-Ni with a lower catalytic activity was obtained. On the other hand, when a nickel chloride solution containing a suitable amount of sodium chloride was used, the activity of the ppt-Ni increased. These findings suggest that the catalytic properties are greatly affected by a small amount of contaminant in the catalyst. In order to get further information on the effect of the chloride ion, the rates of the reduction of cyclohexanone with ppt-Ni in the presence of an aqueous sodium chloride solutions of various concentrations were compared with each other. The results are given in Table 2. As is shown in the table,

Table 2. The effect of NaCl on the reduction of cyclohexanone

Cyclohexanone 9.8 g; Dioxane 13 m*l*; Aqueous NaCl solution 18 m*l*; ppt-Ni 20 g

Exp. No.	Concentration of NaCl N	Rate constant $k(\times 10^2)$ (hr^{-1})
7	0.000	5.21
8	0.080	5.40
9	0.165	4.31
10	0.250	8.58
11	0.500	6.74

the reaction was accelerated by the addition of sodium chloride, the most favorable concentration found to be 0.25N. On the other hand, no promoting effect on the reaction was observed when a potassium chloride was used instead of sodium chloride.

X-Ray diffraction studies revealed the composition of the ppt-Ni. As is shown in Fig. 1, the X-ray diffraction diagram[1,4] of ppt-Ni showed several sharp bands assignable to Zn, Zn(OH)Cl, and ZnO. Besides these constituents, ppt-Ni

3) T. Nakabayashi, *J. Amer. Chem. Soc.*, **82**, 3900 (1960).

4) Y. Urushibara, M. Kobayashi, S. Nishimura and H. Uehara, *Shokubai* (*Catalyst*) (Tokyo) **12**, 163 (1956).

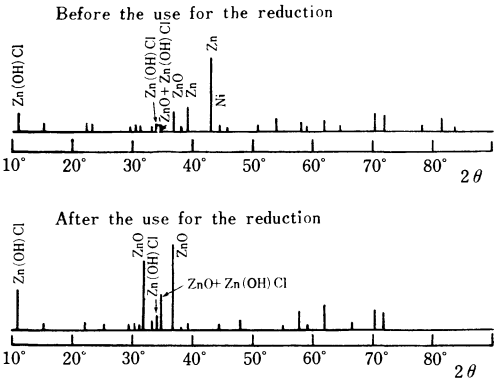

Fig. 1. X-ray diffraction diagrams of ppt-Ni.

also contains Ni, $ZnCl_2$, and $Zn(OH)_2$, though they are not revealed in the X-ray diffraction diagram. On the other hand, a ppt-Ni recovered after being used for the reduction by refluxing with water showed a different diffraction diagram, one in which the bands of Zn disappeared almost completely, while those of ZnO and Zn(OH)Cl were enhanced. This implies that the Zn and $ZnCl_2$ in the ppt-Ni were converted into ZnO, $Zn(OH)_2$, and Zn(OH)Cl in the course of the reaction. It is noteworthy that, when the reaction was carried out in a sodium chloride solution, a remarkable increase in Zn(OH)Cl was observed in the recovered ppt-Ni. From these experimental results, it is concluded that the reaction of water with zinc or zinc chloride is responsible for the supply of hydrogen necessary for the hydrogenation.

The Relationship between the Volume of Generated Hydrogen and That of the Reacted Hydrogen in the Reduction of Cyclohexanone. The reduction with water in the presence of ppt-Ni may be supposed to be composed of two steps: the generation of hydrogen from water and the reduction of organic compounds with the hydrogen.

It has been shown that the generation of hydrogen from water is attributable to the reaction of zinc in the catalyst with water, and also to the difference in ionization potential between zinc and other metals, such as nickel, in the ppt-metal, because the reaction of water with zinc dust alone is extraordinarily slow. Therefore, the amount of hydrogen generated during the reaction depends greatly upon the kind of ppt-metal used. It has previously been reported that the ppt-metal is not useful for ordinary catalytic hydrogenation.[2] However, it has been found*2 that cyclohexene can be hydrogenated under an ordinary pressure of hydrogen in the presence of ppt-Ni, though the reaction velocity is slow. In this hydrogenation, the activity of the catalyst was found to be dependent on the procedure of its preparation and on the amount of nickel in it. Therefore, it may be presumed that the behavior of ppt-metals in the reduction step is analogous to that of the ordinary hydrogenation catalysts. In this step, metals other than zinc in the ppt-metals, such as nickel or cobalt, may play an important part, while zinc may serve for the step of decomposing water.

In the present study, the activities of several ppt-metals were compared for each of the two steps. The hydrogen gas generated when water was refluxed with the ppt-metal alone was introduced into a gas burette and then estimated volumetrically. The volume of hydrogen gas generated when the reaction was carried out in the presence of cyclohexanone under the same conditions was measured in a similar way. Then the volume of hydrogen reacted with cyclohexanone was calculated and compared with the amount of cyclohexanol, determined by gas chromatography. The results are listed in Table 3.

As may be seen in the table, the abilities of the ppt-metals to decompose water were found to increase in the order: ppt-Ni<ppt-Cu<ppt-Ni, Co<ppt-Ni,Cu. This order may be expected if the ability of the ppt-metal to produce hydrogen originates mainly in the difference in ionization potential between the metal in question and zinc.

On the other hand, the ability of each ppt-metal to catalyze the reduction of cyclohexanone was considered to be represented by the ratio of the amount of hydrogen reacted with cyclohexanone

TABLE 3. THE RELATIONSHIP BETWEEN VOLUME OF GENERATED HYDROGEN AND OF THE REACTED HYDROGEN

ppt-metal 0.8 g; H_2O 1.4 m*l*; dioxane 1 m*l*; cyclohexanone 0.5 g; reaction time 2.5 hr

Catalyst	Volume of generated H_2		Hydrogen reacted V_1-V_2	Ratio of reacted hydrogen	Yield of cyclohexanol
	in the absence of cyclohexanone V_1 (m*l*)	in the presence of cyclohexanone V_2 (m*l*)	V_3 (m*l*)	V_3/V_1 (%)	(%)
ppt-Ni	90.6	56.5	34.1	38	24
ppt-Cu	120.6	106.4	14.2	12	15
ppt-Ni,Co	138.3	96.4	41.9	30	25
ppt-Ni,Cu	160.5	142.8	17.7	11	9

*2 A private communication from Y. Urushibara and H. Tomoda.

to the total amount of hydrogen generated by the decomposition of water. The catalytic activity may also be represented by the yield of cyclohexanol. As may be seen in Table 3, the ratio of the amount of reacted hydrogen was approximately parallel to the yield of cyclohexanol. Thus, the catalytic abilities of the ppt-metals were found to increase in the order: ppt-Ni,Cu<ppt-Cu<ppt-Ni <ppt-Ni,Co. This order coincides with that of the catalytic activities of the corresponding Urushibara catalysts which are prepared from these ppt-metals. The fact suggests that the reduction step of the ppt-metal-catalyzed reaction may be similar to that of oridnary catalytic hydrogenation.

The Relative Activities of ppt-Metals in the Reduction of Cyclohexanone.[2] The rate constant was determined for the reduction of cyclohexanone by water in the presence of several ppt-metals. The results are summarized in Table 4 and Fig. 2.

TABLE 4. THE RATE CONSTANTS OF THE REDUCTION OF CYCLOHEXANONE AT 111.5±2°C CATALYZED BY VARIOUS PPT-METALS

Cyclohexanone 0.26 m*l*; H_2O 0.68 m*l*; dioxane 0.50 m*l*; ppt-metal 0.4 g; in a sealed tube

Catalyst	Rate constant $k(\times 10^2)(hr^{-1})$
ppt-Ni,Co	24.5
ppt-Ni,Fe	17.1
ppt-Ni	14.8
ppt-Co	7.17
ppt-Cu	3.76
ppt-Ni,Cu	1.75
ppt-Fe	0.924

The relative activities are found to be in the order: ppt-Fe<ppt-Ni,Cu<ppt-Cu<ppt-Co<ppt-Ni<ppt-Ni,Fe<ppt-Ni,Co. This order is approximately analogous to what has been proposed on the basis of a comparison of the yields of the reduction products.[2]

The Effect of Temperature on the Reduction of Cyclohexanone. The rate constant of the reduction of cyclohexanone was observed at various reaction temperatures; the results are shown in Table 5. Figure 3 shows the Arrhenius plots of the rate constants shown in Table 5. The values of the activation energies and the activation entropies were calculated (from Fig. 3) to be 4.0 kcal/mol and −72 e.u./mol, and 7.5 kcal/mol and −59 e.u./mol, respectively, for the reductions catalyzed by ppt-Ni and by ppt-Ni,Co.

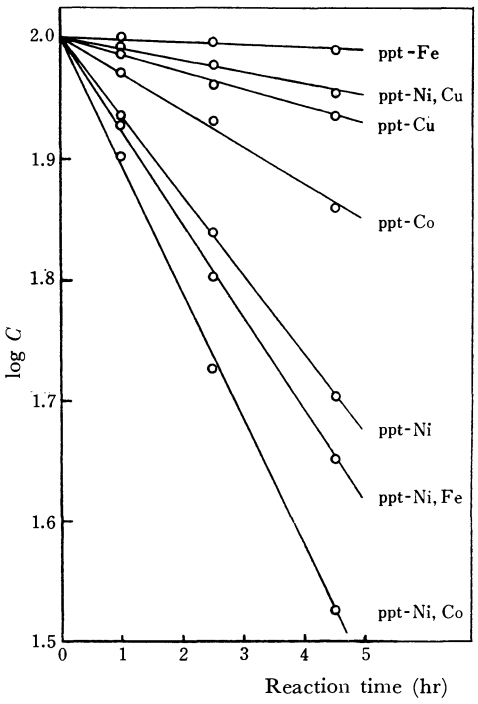

Fig. 2. The first order rate plots for the reduction of cyclohexanone.

$$C=\frac{[\text{cyclohexanone}]}{[\text{cyclohexanone}]+[\text{cyclohexanol}]}\times 100,$$

where [ ] denotes the molar concentration.

Discussion

A mixture of dioxane and water has proved to be an excellent solvent for studies of the ppt-metal-catalyzed reaction because dioxane is almost entirely indifferent to the reaction. Besides the indifference of dioxane to the reaction, the dioxane-water mixed

TABLE 5. THE RATE CONSTANTS OF THE REDUCTION OF CYCLOHEXANONE UNDER VARIOUS REACTION TEMPERATURE (71—100°C)

Reaction temp.		$k(\times 10^2)(hr^{-1})$		log k	
°C	$1/T$ ($\times 10^3$)	ppt-Ni	ppt-Ni,Co	ppt-Ni	ppt-Ni,Co
71.0	2.91	4.40	5.39	−1.35655	−1.28641
80.0	2.83	5.26	7.38	−1.29901	−1.13194
90.0	2.75	5.61	8.78	−1.25104	−1.05651
100.0	2.68	6.90	12.20	−1.16115	−0.91304

Cyclohexanone 0.26 m*l*; H_2O 0.68 m*l*; dioxane 0.50 m*l*; ppt-metal 0.40 g

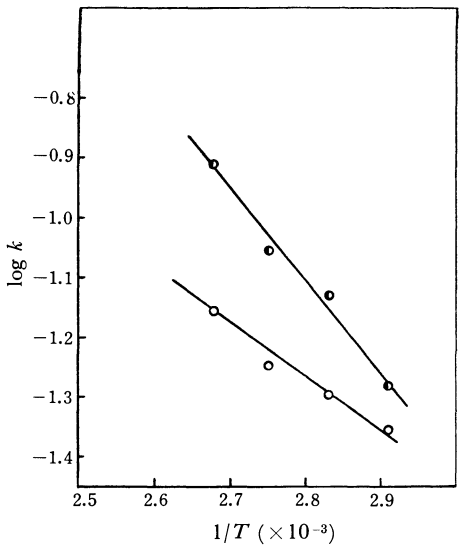

Fig. 3. The Arrhenius plots for the reduction reaction of cyclohexanone.
—◐— ppt-Ni,CO —○— ppt-Ni

solvent*3 has the following merits: (1) it can dissolve almost all organic compounds, (2) it can easily be separated from the reaction mixture in most cases, and (3) the closeness of the boiling points of the two components of the solvent makes it easy to keep the reaction temperature constant, even during refluxing over a long period.

It has been demonstrated, by an X-ray diffraction study, that ZnO and Zn(OH)Cl are produced during the reduction reaction by refluxing with water.*4 The increase in ZnO suggests that the difference in ionization potentials between a catalyst metal, such as nickel, and zinc may lead to the decomposition of water through a coordination of the water to the zinc. The increase in Zn(OH)Cl may be explained in terms of the participation of $ZnCl_2$, which is necessarily present in ppt-metal. The catalytic behavior of such metal halides as Lewis acids is well known.[5] In a ppt-metal-catalyzed reduction, a donor-acceptor complex may be formed by the combination of water, as a Lewis base, with zinc chloride in the ppt-metal, thus, leading to a protonic acid,[6] for example:

$$H_2O + ZnCl_2 \rightarrow \begin{matrix} H \\ H \end{matrix}\!\!>\!O \rightarrow ZnCl_2 \rightarrow H^+[Zn(OH)Cl_2]^-$$

The formation of Zn(OH)Cl during the reaction may be through this protonic acid.

The activation energy of the catalytic hydrogenation of cyclohexanone with U-Ni-B at room temperature under an ordinary pressure was reported by Nishimura to be 5.3 kcal/mol.[7] The value resembles that of the ppt-Ni-catalyzed reduction of cyclohexanone by water. This fact suggests that the function of ppt-Ni as a catalyst is similar to that of the ordinary hydrogenation catalysts.

Whereas the Clemmensen-type reduction of a ketone often affords dimerization of rearrangement products, the ppt-Ni-catalyzed reduction never produces such by-products. However, when the reduction of ketones in the presence of ppt-Ni was carried out in an acidic or an alkaline solution,*5 a different result, one which rather resembles that of the Clemmensen reduction, was observed.

In ppt-metals used as catalysts, active sites for hydrogenation are presumably arranged on the surface of such metals as nickel and cobalt, not on the surface of zinc. This presumption is supported by the facts that, on the one hand, the rate of reduction is dependent on the kind of ppt-metal, and that, on the other hand, the rate stays constant in spite of the consumption of zinc during the reaction.

The fact that the activation energy for ppt-Ni differs from that for ppt-Ni,Co suggests the intervention of a transition state in which cyclohexanone forms a certain complex with the catalyst metal. Thus, the mechanism of the reduction may be considered to be as follows. The coordination of water to zinc or zinc chloride leads to a protonic acid, through which hydrogen is then transferred to active sites for the hydrogenation on the surface of nickel or cobalt. The following step is the reaction of cyclohexanone and hydrogen, each of which is adsorbed on the active sites of the catalyst metal, in just the same way as in ordinary catalytic hydrogenation.

Experimental

Materials. *Benzaldehyde.* Commercial benzaldehyde was purified by fractional distillation under reduced pressure.

Deuterium Oxide. Commercial 99.75% D_2O (Showa Denko K. K.) was used.

Cyclohexanone. Commercial cyclohexanone was purified as follows. About 100 m*l* of commercial cyclohexanone was stirred with a solution of potassium dichromate (4 g) and concentrated sulfuric acid (5 m*l*) in 50 m*l* of water at room temperature. When the color of the

*3 The high suitability of dioxane-water mixtures as solvents for physico-chemical studies has been verified by several authors; *cf.*, *e. g.*, G. Åkerlöf and O. A. Short, *J. Amer. Chem. Soc.*, **58**, 1241 (1936); F. Hovorka, R. A. Schaeffer and D. Dreisbach, *ibid.*, **58**, 2264 (1936).

*4 It has been reported that the Raney alloy reacted with, and was developed by, water, thus forming bayerite; S. Nishimura, This Bulletin, **32**, 61 (1959).

5) Edited by A. Ozaki, K. Tanabe, K. Tamaru and S. Nishimura, "Shokubai Kogaku Koza (Catalytic Engineering)," Vol. 10, Chijinshokan & Co., Tokyo (1967), p. 107.

6) H. Meerwein, *Ann. Chem.*, **455**, 227 (1927); *Angew. Chem. Int. Ed. Engl.*, **5**, 335 (1966).

7) S. Nishimura, *Nippon Kagaku Zasshi*, **79**, 56 (1958).

*5 Y. Urushibara and H. Tomoda, unpublished work.

solution turned dark green (after about 30 min), the cyclohexanone layer was separated, washed with water several times, dried over anhydrous magnesium sulfate, and distilled. A fraction boiling at 153—154°C was collected. The purity of the sample was verified by gas-chromatographic analysis to be over 99%.

The Reduction of Benzaldehyde with D_2O. A mixture of 1 m*l* of benzaldehyde, 4 m*l* of D_2O, and 3 g of ppt-Ni was heated at 100°C in a sealed tube for 12 hr. After the reaction was over, the reaction mixture was filtered quickly. The filtrate was extracted with ether, and the solid on the filter was washed with ether. All the ethereal solution was combined, and the ether was carefully evaporated away. The residue was shaken vigorously with an excess of water to exchange the D in the hydroxyl group for H, and the deuterated benzyl alcohol was extracted with ether.

Kinetic Measurements. *(1) The Reduction of Cyclohexanone with H_2O* (Table 1). In a 100-m*l*, three-necked, round flask equipped with a reflux condenser, a given amount of water and dioxane (shown in Table 1) was placed together with 9.8 g of cyclohexanone (0.1 mol). The solution was heated to 92.5°C, and then 20 g of ppt-Ni (containing 2 g of nickel) was rapidly added. While the mixture was kept at a constant temperature, 0.2—0.3 m*l* portions of the suspending solution were pipetted out at appropriate intervals. Each sample was kept standing for a while until a small amount of the suspending particles had settled, and was then analyzed by gas chromatography.

(2) The Activity of ppt-Metals (Table 4). For each run of the experiment, several sealed ampoules were prepared, each of them containing 0.26 m*l* of cyclohexanone, 0.50 m*l* of dioxane, 0.68 m*l* of water, and 0.4 g of ppt-metal. The tubes were immersed side by side in an oil bath which had been previously kept at 111.5 ± 2°C. At definite intervals tubes were taken out, one after another, and cooled to 0°C with ice. The composition of the reaction mixture was analyzed immediately by gas chromatography. The decrease in the concentration of cyclohexanone was plotted on a graph for each ppt-metal (Fig. 3).

(3) Measurement of the Hydrogen Gas Liberated (Table 3). In a round, 20-m*l* flask connected to a gas-burette through a reflux condenser, 1 m*l* of dioxane and 1.4 m*l* of water were placed. The mixture was heated to boiling, and then 0.8 g of a ppt-metal was rapidly added. After heating for 2.5 hr, the volume of hydrogen generated was measured by a gas-burette. Another run was carried out by the same procedure and under the same conditions except that it was in the presence of 0.50 g of cyclohexanone. Besides the measurement of the volume of the hydrogen generated, cyclohexanol produced in the solution was analyzed by gas chromatography.

The authors wish to express their hearty thanks to Professor Dr. Michio Kobayashi for his helpful advice and discussions.

BULLETIN OF THE CHEMICAL SOCIETY OF JAPAN VOL. 43 1177—1181 (1970)

The Photosensitized Reaction of Deoxyguanosine in the Presence of Methylene Blue*1

Hitoshi FUJITA and Hideo YAMAZAKI*2

Chemistry Division, National Institute of Radiological Sciences, Anagawa, Chiba

(Received September 27, 1969)

The kinetics of the photosensitized decomposition of deoxyguanosine with methylene blue was studied by means of spectrophotometric measurements. The reaction rate increased with an increase in the concentration of the reactant or of oxygen up to a saturation level for each case at a given concentration of the dye. In a buffer solution of a lower phosphate concentration, a larger rate was observed. On the basis of these dependencies of the rate, the reaction scheme was discussed, and the ratios of some rate constants were estimated based on Schenck's mechanism. A preliminary NMR measurement of the protons of deoxyguanylic acid in D_2O suggested that the base-part of the nucleotide was specifically attacked by this photosensitized reaction.

Photodynamic action, namely, a dye-sensitized reaction of biological systems, is known in a wide variety of organisms.[1,2] For example, the muta-

*1 Presented at the 18th Annual Meeting of the Chemical Society of Japan (1965).

*2 Present address: Department of Chemistry, Tokyo Institute of Technology, Meguro-ku, Tokyo.

1) J. D. Spikes and C. A. Ghiron, "Physical Processes in Radiation Biology," ed. by L. Augenstein, R. Mason and B. Rosenberg, Academic Press, New York (1964), p. 309.

2) J. D. Spikes and B. W. Glad, *Photochem. Photobiol.*, **3**, 471 (1964).

tions of bacteria and viruses are induced,[3,4] and the transforming DNA of *Diplococcus pneumoniae* is inactivated by the photodynamic action with methylene blue, acridine orange, *etc.*[5,6] Thus, deoxyribonucleic acid (DNA) seems to be a main target for this action in living organisms. In order to interpret the photosensitivity of organisms, knowledge about the relationship between the chemical alterations of DNA and the resultant biological phenomena is required. Studies of the dye-sensitized reaction of the components of nucleic acids would give basic information. Simon and van Vunakis[7-9] found that guanine derivatives in the components of DNA or RNA were preferentially destroyed by the sensitization of methylene blue. Each derivative consumes one mole of oxygen for each mole of substrate (reactant), accompanied by the loss of ultraviolet absorbance,[7] and the destructive reaction of deoxyguanosine is of the first-order.[8] They also studied the effects of dye concentration, light intensity, temperature, and pH on this reaction.[8]

In this article, we will discuss the reaction kinetics of the methylene blue-sensitized destruction of deoxyguanosine, with an emphasis on the effects of the concentrations of the substrate, oxygen, and the phosphate buffer on the reaction rate.

Experimental

Materials. Methylene blue was obtained from E. Merck Ag., while deoxyguanosine, deoxyadenosine, deoxycytidine, thymidine, deoxyguanylic acid, and 2-deoxy-D-ribose were from Sigma Chemical Co. All the reagents were used without purification. The molar extinction coefficient of methylene blue was measured to be 74000 at 665 mμ.

Irradiation. Methylene blue and the substrate were dissolved in a phosphate buffer. This mixed solution in silica cuvettes (1 cm in path length) was irradiated with visible light. Four photoflood lamps (500 W—100 V) were used at 75 V. Circulating-water filters (5 cm thick) were interposed between the lamps and the cuvettes to absorb thermic rays. The alignment for irradiation is shown in Fig. 1. The light intensity was adjusted so as to be the same at each cuvette. The reaction temperature was not controlled, since the rate constant of the destruction of deoxyguanosine did not vary between 6 and 58°C.[8]

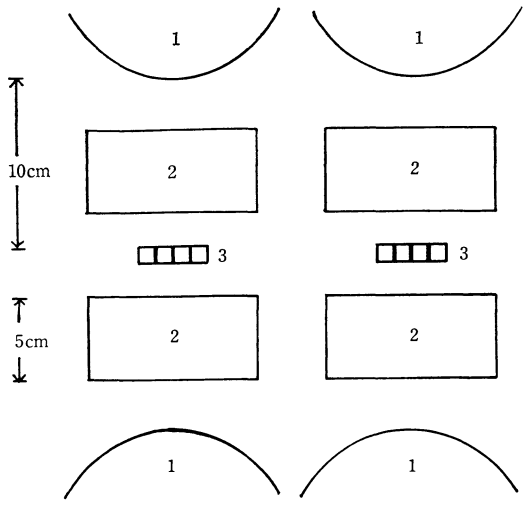

Fig. 1. Alignment of lamps (1), water-filters (2) and cuvettes (3).

Control of the Oxygen Concentration. Some cuvettes were designed to have provisions for bubbling mixtures of air and nitrogen gas in various ratios through sample solutions prior to and during irradiation. The concentration of oxygen in a solution was estimated from the solubility of gas at the experimental temperature. Nitrogen gas was passed through an alkaline-pyrogallol solution to eliminate the contaminating oxygen, and then through water, before being led into the reaction mixture.

Analysis. After irradiation, twenty mg of cation exchange resin (Dowex-50, Na-form) were added to the reaction mixture (3 m*l*) in order to remove methylene blue. The resin was added before the irradiation for the reference sample. The concentration of the substrate in the supernatant solution was measured with a Cary-14-spectrophotometer.

NMR Measurements. Deoxyguanylic acid and methylene blue were dissolved in D_2O to be 5% ($=1.7\times10^{-1}$M) and 3.3×10^{-4}M respectively. One milliliter of this mixed solution was poured into a cylindrical Pyrex reaction vessel (2.6 cm in diameter, 1.7 cm deep) with an inlet and an outlet tube. The thickness of the solution in this vessel was only 1.9 mm. After the inlet and the outlet had been sealed, the solution was irradiated using a photoflood lamp (500 W—100 V) working at 80 V at a distance of 8 cm over the vessel. The circulating water filter was also used in this case. The NMR spectra of the solution before and after the irradiation were measured with a Varian NMR spectrometer, HR-100. The relative signal intensity was determined by measuring the area of each signal on recording paper.

Results

Specificity of the Reaction. Our first interest was in ascertaining whether all the nucleosides constituting DNA submit to the sensitizing reaction of methylene blue. The specific destruction of deoxyguanosine in an aerated aqueous solution was confirmed by measuring the ultraviolet absorp-

3) R. W. Kaplan, *Nature*, **163**, 573 (1949).
4) H. Bohme and A. Wacker, *Biochem. Biophys. Res. Commun.*, **12**, 137 (1963).
5) J. S. Bellin and G. Oster, *Biochim. Biophys. Acta*, **42**, 533 (1960).
6) H. Fujita, E. Saito, K. Suzuki and A. Wada, *J. Rad. Res.*, **11**, (1970), in press.
7) M. I. Simon and H. van Vunakis, *J. Mol. Biol.*, **4**, 488 (1962).
8) M. I. Simon and H. van Vunakis, *Arch. Biochem. Biophys.*, **105**, 197 (1964).
9) M. I. Simon, L. Grossman and H. van Vunakis, *J. Mol. Biol.*, **12**, 50 (1965).

tion; this is in agreement with the finding of Simon and van Vunakis.[8] In connection with the specificity, the red shift of the visible absorption peak of the dye upon the addition of various nucleosides was measured (Fig. 2). The interaction of methylene blue with deoxyadenosine or deoxyguanosine is stronger than that with deoxycytidine or thymidine.

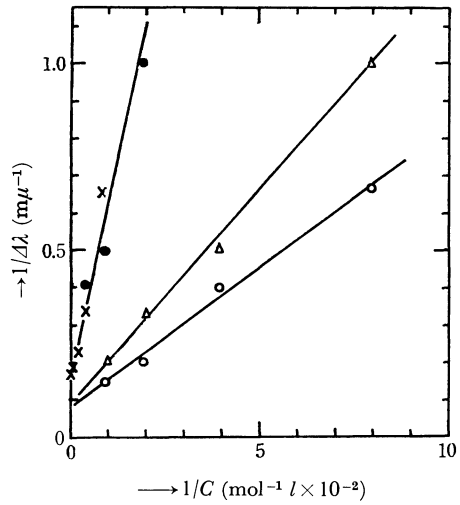

Fig. 2. Reciprocal plottings of extents of red shift ($\Delta\lambda$) and concentrations of nucleosides.
methylene blue, 5×10^{-6}M; phosphate, 1/15M. (pH 6.8); ×, thymidine; ●, deoxycytidine; △, deoxyguanosine; ○, deoxyadenosine.

The remaining concentration of the substrate decreased exponentially with an increase in the irradiation time up to 20 min, at least under the present conditions. Each reaction rate was estimated from the initial slope of the curve in the semi-logarithmic plotting. Deoxyguanylic acid was also decomposed by the irradiation of visible light in the presence of methylene blue when air was dissolved in the solution. Its reaction rate was found to be lower than that of deoxyguanosine (Fig. 3).

It was confirmed that the reaction rate of deoxyguanosine was independent on the pH between 5.4 and 6.6; this is consistent with the data of Simon and van Vunakis.[8] Thus, all the experiments below were performed with solutions in this pH range.

Effects of the Concentrations of Phosphate, the Substrate, and Oxygen. The reaction of deoxyguanosine was examined in 1×10^{-3} and 1×10^{-2}M phosphate buffers. The reaction rate increased with an increase in the concentration of the substrate up to a saturation level at a constant concentration of methylene blue (1×10^{-5}M), as may be seen in Fig. 3. In the solution with a lower phosphate concentration, a larger rate was observed. The phosphate anion may be connected with some irreversible reaction(s) of methylene blue in an aerated solution as well as in a deaerated solution.[10] The present finding may be interpreted as a result of competition between deoxyguanosine and phosphate.

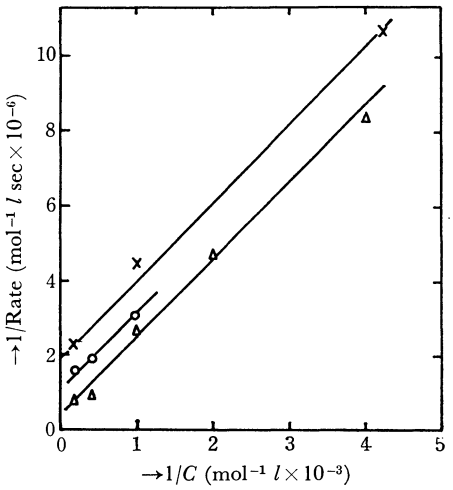

Fig. 3. Dependency of the reaction-rate on the concentration of substrate.
methylene blue, 1×10^{-5}M; air saturated; △ and ○, deoxyguanosine in 1×10^{-3} and 1×10^{-2}M phosphate buffer respectively; ×, deoxyguanylic acid in 1×10^{-2}M phosphate buffer.

It was also observed that the reaction proceeded with a larger rate with an increase in the concentration of oxygen up to a saturation level (Fig. 4). The reaction did not take place in a deaerated solution.

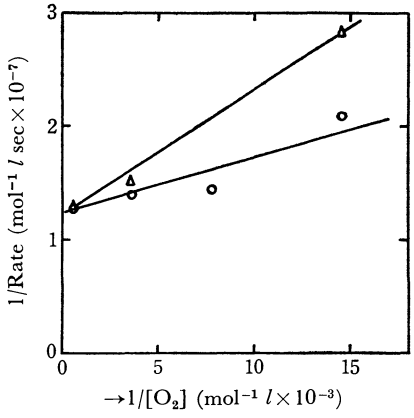

Fig. 4. Oxygen-effect on the reaction-rate.
methylene blue, 1×10^{-5}M; deoxyguanosine, 1×10^{-4}M; phosphate, 1×10^{-3}M (○) and 1×10^{-2}M (△).

Independency on Added 2-Deoxy-D-ribose. Varying amounts of 2-deoxy-D-ribose, which is

10) Y. Usui, H. Obata and M. Koizumi, This Bulletin, **34**, 1049 (1961), Y. Usui and M. Koizumi, *ibid.*, **34**, 1651 (1961).

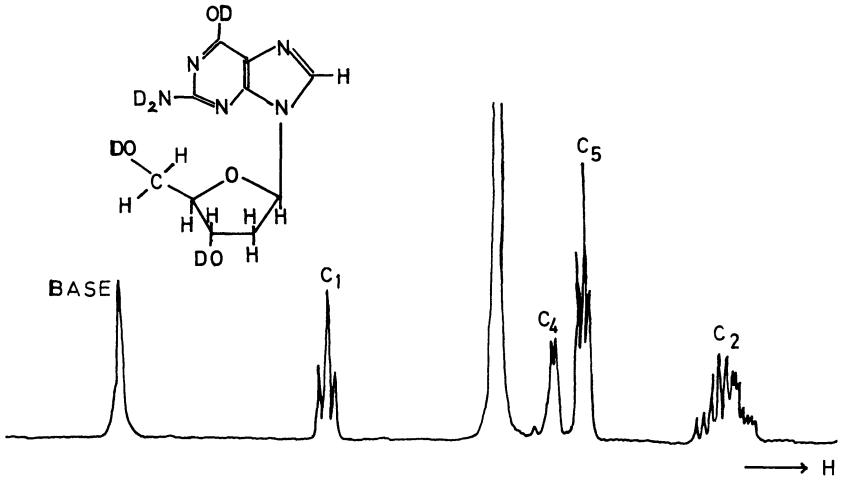

Fig. 5. NMR-Spectrum of deoxyguanylic acid in D_2O.

a component of deoxyguanosine, were added to a reaction mixture of deoxyguanosine (5×10^{-5}M) and methylene blue (1×10^{-5}M) in a phosphate buffer (1×10^{-3}M). Even if the additive was increased as high as 1×10^{-3}M, it however did not affect the photosensitized reaction.

NMR Measurements. As a preliminary experiment, the reaction of deoxyguanylic acid in D_2O was followed by NMR measurements. It did not have an adequate quantitative accuracy, but the decrease in the proton signal from the guanine base caused by the reaction was remarkable compared with that of the C_1-proton of the deoxyribose ring (See Fig. 5). The ratio between the signal intensity of the base and that of C_1 is plotted against the irradiation time in Fig. 6. Since methylene blue itself is also decomposed by such a long irradiation, this curve does not correspond to an actual dose-response of the reaction.

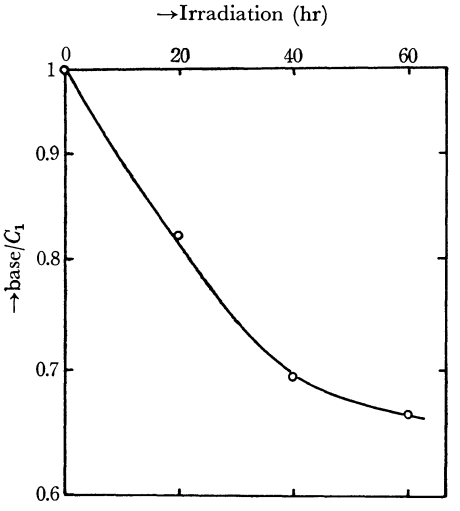

Fig. 6. Decrease of the ratio of NMR-signals, base to C_1, by the photosensitized reaction.
methylene blue, 3.3×10^{-4}M; deoxyguanylic acid, 5%.

Discussion

It was confirmed from spectral shifts that methylene blue interacts more strongly with purine nucleosides than with pyrimidine nucleosides. This is consistent with the results of Kodama *et al.*,[11] who observed that the spectral shifts of proflavine, acridine orange, and methylene blue are larger in the presence of apyrimidic acid than in the presence of apurinic acid, and who ascertained the base specificity of proflavine at the nucleoside level as well as at the polymer level on the basis of a measurement of the difference spectra. The specific destruction of deoxyguanosine, however, can not be accounted for by the specific interaction of methylene blue with deoxyguanosine, since deoxyadenosine was not destroyed by the present reaction and since the photosensitized reaction of deoxyguanosine was carried out at such a low concentration that the red shift was not observed.

Oster *et al.*[12] reported the photo-oxidation of 2,5-diaminotoluene using proflavine as a sensitizer, and postulated that the long-lived, electronically-excited (probably triplet) state of the dye reacted with oxygen to form some dye peroxide, which in turn oxidized the substrate. The reaction scheme for the present system can be built up in the same way:

$$D + h\nu \rightarrow D^* \quad (1)$$

$$D^* \rightarrow D + h\nu_f \quad (2)$$

$$D^* \rightarrow D' \quad (3)$$

11) M. Kodama, Y. Tagashira and C. Nagata, *J. Biochemistry.*, **64**, 167 (1968).

12) G. Oster, J. S. Bellin, R. W. Kimball and M. E. Schrader, *J. Amer. Chem. Soc.*, **81**, 5095 (1959).

$$D' \rightarrow D + h\nu_p \quad (4)$$

$$D' + D \rightarrow 2D \quad (5)$$

$$D' + P \rightarrow \text{product} \quad (5')$$

$$D' + O_2 \rightarrow DO_2 \quad (6)$$

$$DO_2 \rightarrow D + O_2 \quad (7)$$

$$DO_2 + D \rightarrow 2D + O_2 \quad (8)$$

$$DO_2 + P \rightarrow D + \text{product} \quad (8')$$

$$DO_2 + S \rightarrow D + SO_2 \quad (9)$$

where D is the ground state of the dye; D*, the singlet excited state of the dye; D′, the triplet excited state of the dye; P, phosphate; S, the substrate; $h\nu_f$, fluorescence and $h\nu_p$, phosphorescence. If the steady-state treatment is applied to each intermediate, namely, D*, D′, and DO_2, the rate formula may be expressed as follows;

$$-d[S]/dt = k_1 \cdot [D] \Big/ \left[\left(1 + \frac{k_7}{k_9 \cdot [S]} + \frac{k_8 \cdot [D] + k_{8'} \cdot [P]}{k_9 \cdot [S]} \right) \times \left(1 + \frac{k_4}{k_6 \cdot [O_2]} + \frac{k_5 \cdot [D] + k_{5'} \cdot [P]}{k_6 \cdot [O_2]} \right) \cdot \left(1 + \frac{k_2}{k_3} \right) \right]$$

where each k is the rate constant at the elementary process expressed by the subscript. This means that the plot of 1/rate *vs.* 1/[S] should be a straight line when [D], [O_2] and [P] are constant, while the plot of 1/rate *vs.* 1/[O_2] should be linear when [D], [S] and [P] are constant. The reciprocal plot of the experimental values approximately satisfied the above scheme.

Since the quantum yields of the fluorescence and the phosphorescence of methylene blue might be rather small, it may be postulated that $k_2 \ll k_3$ and $k_4 \ll k_6 \cdot [O_2]$. Furthermore, since the slope in the reciprocal plotting on the effect of the substrate concentration at $[P] = 1 \times 10^{-2}$M was nearly the same as that at $[P] = 1 \times 10^{-3}$M, the $k_{8'} \cdot [P] \ll k_7 + k_8 \cdot [D]$ relation is plausible. Thus, the following ratios of the rate constants could be roughly estimated. Comparing the above formula with the results on the effect of the oxygen concentration at different concentration of phosphate ions, we obtained $k_5/k_6 \approx 2.5$ and $k_5/k_{5'} \approx 4 \times 10^2$; that is, the difference between the probabilities of the deactivation of long-lived excited dye molecules (D′) by unexcited ones and of the reaction of D′ with molecular oxygen is not large, and the probability of reaction 5′ is very small. From the dependency on the substrate concentration at two concentrations of the dye, *i.e.*, 1×10^{-5} and 5×10^{-6}M, $k_7/k_8 \approx 2 \times 10^{-5}$M, $k_8/k_9 \approx 3 \times 10$, and $k_7/k_9 \approx 5 \times 10^{-4}$M.

In the reaction mechanism described above, the conception of the molecular complex (DO_2) was accepted as an intermediate on the basis of the reaction scheme proposed by Schenck.[13] However, even if one considers that the singlet excited state of the oxygen molecule, $O_2(^1\Delta_g)$[14,15] or $O_2(^1\sum_g)$,[15] is produced by process (6), the final formula for the kinetics is the same.

The results of the NMR measurements were not incompatible with the study of the kinetics. It may be concluded that, in the reaction of deoxyguanosine or deoxyguanylic acid with methylene blue, the guanine residue is preferentially subjected to the reaction, whereas the deoxyribose residue is rather stable.

According to Waskell *et al.*,[16] guanosine was decomposed by the sensitization of methylene blue to ribosyl urea, free ribose, guanidine, and traces of urea in the earlier stage of irradiation, while the ribose moiety disappeared in the latter stage. The preferential destruction the base component suggests that the secondary reaction of such intermediates as radicals, which may be formed in the primary process, with the sugar component is not appreciable.

The reaction kinetics of deoxyguanosine was studied as a sole solution in the present case. If its reaction is followed in the presence of the three other nucleosides, information about the reaction mechanism as a state closer to the actual system can be obtained. Furthermore, if a competitive reaction between DNA and deoxyguanosine is studied, the $k_{DNA}/k_{nucleoside}$ ratio must be estimated. The biological significance of the selective destruction of the guanine derivatives in DNA or RNA will be thus confirmed.

13) G. O. Schenck and E. Koch, *Z. Elektrochem.*, **64**, 170 (1960).

14) C. S. Foote and S. Wexler, *J. Amer. Chem. Soc.*, **86**, 3880 (1964).

15) D. D. Morgan and M. Orchin, Abstract for The 5th International Congress on Photobiology, New Hampshire, U.S.A. (1968), p. 30.

16) L. A. Waskell, K. S. Sastry and M. P. Gordon, *Biochim. Biophys. Acta*, **129**, 49 (1966).

BULLETIN OF THE CHEMICAL SOCIETY OF JAPAN VOL. 43 1182—1185 (1970)

Studies on the Baudisch Reaction. III. A Possible Intermediate in the Reaction[1)]

Iwao TANIMOTO

Faculty of Home Economics, Kyoto Women's University, Higashiyama-ku, Kyoto

(Received September 29, 1969)

The Baudisch reaction was applied to 1- and 2-naphthols, and 2-nitroso-1-naphthol was obtained as the sole product in both reactions. In a reinvestigation of the products obtained from phenols, it was also found that in some cases the nitroso group replaced the hydroxy group and a hydroxy group was newly introduced into the position *ortho* to the nitroso group. These results indicate that a copper(II)-hydroxylamine-catechol complex will be a possible intermediate of the reaction of phenol. The product studies on the reaction of catechols support the assumption. Kinetically, the formation of the complex seems to be the rate-determining step in the reaction of phenols.

Baudisch[2)] and Cronheim[3)] obtained various *o*-nitrosophenols from phenols by the reaction with hydroxylamine hydrochloride, hydrogen peroxide and copper(II) salt. At first we intended to extend this reaction to naphthols. However, the reaction of 2-naphthol gave an unexpected product, and it became necessary to reinvestigate the products from some substituted phenols. In the present paper, a possible intermediate of the Baudisch reaction is discussed on the basis of experimental results.

Results and Discussion

The Reactions of Naphthols. In methanol, 1- and 2-naphthols reacted with copper(II) nitrate, hydroxylamine hydrochloride and hydrogen peroxide at room temperature, though the reactions proceeded slower than that of phenol. The reaction mixture was poured into water, then the copper salt of the product precipitated. Nitrosonaphthol was liberated from precipitate by an acid. The product from 1-naphthol was 2-nitroso-1-naphthol. Unexpectedly, however, 2-naphthol also gave 2-nitroso-1-naphthol; the hydroxy group of 2-naphthol was replaced by the nitroso group and a hydroxy group was introduced into position 1. Identification of the products was carried out by means of elementary analysis, determination of mixed melting point with the authentic sample and measurement of the NMR spectrum.

Reexamination of the Products from Some Phenols. It was accepted without proof that the position of the hydroxy group does not change in the reactions of phenols.[2,3)] However, the results in the preceding section required reinvestigation of the configurations of *o*-nitrosophenols which were produced from substituted phenols. As *o*-nitrosophenols are volatile, *o*-nitrophenols obtained by oxidation of the products were identified. The results are tabulated in Table 1. Obviously the hydroxy groups of *p*-cresol and 3,5-dimethylphenol were replaced by nitroso groups.

Reactions of Catechols. It was demonstrated in a previous paper that catechol was found when the reaction of phenol was performed under higher pH and that the production of catechol would also be controlled by the copper-hydroxylamine complex.[1b)] However, the mechanistic relationship between the formation of catechol and that of *o*-nitrosophenol has not yet been established. A mixture of catechol, hydroxylamine hydrochloride and copper(II) nitrate in a buffered aqueous solution (pH 2.5) was blue and showed no change in color under a nitrogen atmosphere, but with the addition of a hydrogen peroxide solution the reaction started and proceeded very fast. The red reaction mixture was acidified and the product was extracted with petroleum ether. The product was oxidized and the resulting *o*-nitrophenol was identified. Thus it was confirmed that the reaction product from catechol under the Baudisch reaction conditions was *o*-nitrosophenol. Under the same conditions, 3,4-dihydroxytoluene selectively changed into 5-methyl-2-nitrosophenol which was the sole reaction product from both *m*- and *p*-cresols (Table 1).

Kinetic Measurements for Catechols. In Fig. 1, the kinetic plot for the reaction of catechol is shown, together with that for phenol. The concentration of catechol at any time was assumed

1) a) Part I: K. Maruyama, I. Tanimoto and R. Gotō, *J. Org. Chem.*, **32**, 2516 (1967); b) Part II: I. Tanimoto, This Bulletin, **43**, 139 (1970).

2) a) O. Baudisch and S. H. Smith, *Naturwissenschaften*, **27**, 769 (1939); b) O. Baudisch, *Science*, **92**, 336 (1940).

3) G. Cronheim, *J. Org. Chem.*, **12**, 7 (1947).

Table 1. Products from phenols in the baudisch reaction[a)]

Materials	Products	Oxidized products[b)]	Mp of Nitrophenols[c)] (lit, mp)(°C)
o-Cresol	6-Methyl-2-nitrosophenol	6-Methyl-2-nitrophenol	68[d)] (69—70)
m-Cresol	5-Methyl-2-nitrosophenol	5-Methyl-2-nitrophenol	54[e)] (56)
p-Cresol	5-Methyl-2-nitrosophenol	5-Methyl-2-nitrophenol	55[e)] (56)
2,4-Dimethylphenol	4,6-Dimethyl-2-nitrosophenol	4,6-Dimethyl-2-nitrophenol	70[f)] (71—72)
3,5-Dimethylphenol	4,6-Dimethyl-2-nitrosophenol	4,6-Dimethyl-2-nitrophenol	69[f)] (71—72)
Catechol	2-Nitrosophenol	2-Nitrophenol	46 (45)
3,4-Dihydroxytoluene	5-Methyl-2-nitrosophenol	5-Methyl-2-nitrophenol	54[e)] (56)

a) Conducted in aqueous medium at 30°C.
b) Oxidized by hydrogen peroxide in acetic acid.
c) Undepressed by admixture with authentic samples.
d) Depressed by admixture with authentic 3-methyl-2-nitrophenol (mp 41°C).
e) Depressed by admixture with authentic 4-methyl-2-nitrophenol (mp 32°C).
f) Depressed by admixture with authentic 3,5-dimethyl-2-nitrophenol(mp 63—64.5°C).

Table 2. Kinetic data for the baudisch reaction of catechol and phenol[a)]

	$k\times10^5$, sec^{-1}				E, kcal. mol^{-1}	$\Delta S^{\neq}$,[b)] e.u.
	0.0°C	10.0°C	20.0°C	30.0°C		
Catechol	4.09	7.54	32.3	50.0	14.8±1.5	−27.0
Phenol	2.39	3.56	14.0	29.8	14.9±1.5	−28.2

a) All reactions were conducted under a nitrogen atmosphere. Catechol (1×10^{-3} mol), copper(II) nitrate (1×10^{-3} mol) and hydroxylamine hydrochloride (2×10^{-3} mol) were stirred in 198 m*l* of a Walpole buffer (pH 2.50) after addition of a hydrogen peroxide solution (1.0M)(2 m*l*). Temperature was controlled within ±0.1°C.
b) Entropy of activation was calculated at10.0°C.
c) The data was taken from that shown in Part II of this series.[1b)]

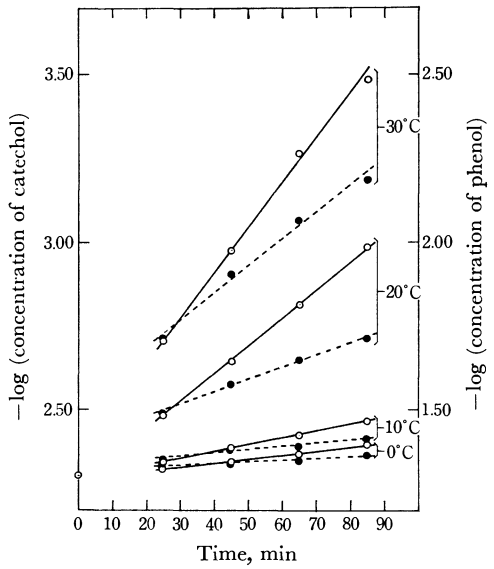

Fig. 1. First-order plots for the Baudisch reaction of catechol and of phenol.
The plot for the reaction of phenol was based on the data shown in the Part II of this series.[1b)]
Initial concentration of catechol (—○—): 5×10^{-3}M.
Initial concentration of phenol (—●—): 5×10^{-2}M.

to be given by the difference between its initial concentration and the concentration of *o*-nitrosophenol. Apparently the reaction of catechol is first-order in catechol, and from this plot the rate constants and thermodynamic quantities can be calculated. The results of the calculation are shown in Table 2, together with the data for the reaction of phenol. The rate constants for catechol are about twice those for phenol.

The reaction of 3,4-dihydroxytoluene proceeded much faster than that of both *m*- and *p*-cresols, but reliable kinetic data could not be obtained.

Discussion. The copper-hydroxylamine complex combined with the phenoxy group plays an important role in the reaction of phenol.[1b)] If the complex is responsible for the direct nitrosation of benzene ring, the position of the hydroxy group in the resulting *o*-nitrosophenol should not change from that of the hydroxy group in phenol. However, the formation of 5-methyl-2-nitrosophenol from 3,4-dihydroxytoluene, *m*- and *p*-cresols rejects this mechanism. A reasonable explanation for this may be given by the assumption that complex I is formed in each of the reactions as a common intermediate, because the isokinetic plots shown in the previous paper indicated a constant mechanism for the related series of reactions.[1b)] In Table 2, it is shown that catechol has a higher reaction rate

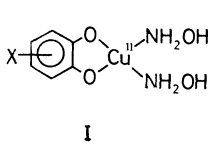

I

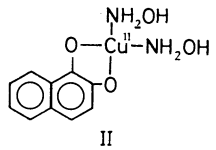

II

than phenol. Since catechol easily changes into complex I, it may be concluded that the kinetic data shown in Table 2 indicate the high reactivity of complex I. Thus the rate-determining step in the reaction of phenol would be the formation of complex I. In the reactions of naphthols, complex II will be formed as a common intermediate. This explains the production of 2-nitroso-1-naphthol from both 1- and 2-naphthols. There are two possible mechanisms by which complex I changes into *o*-nitrosophenol; the one involves the cleavage of the C–O bond and the attack of hydroxylamine moiety on the carbon atom, and the other the formation of *o*-quinone and subsequent oximation. Studies are in progress to establish the mechanism.

Experimental

Materials. Reagent grade 30% hydrogen peroxide solution and *p*- and *m*-cresols were the same as described.[1b] Other reagents were of the best available grade and, if necessary, were used after further purification. Some of the authentic samples were prepared according to directions in literature and others were of the best commercially available grade (Table 3).

TABLE 3. AUTHENTIC SAMPLES

Samples	Mp °C	Lit, mp °C
3-Methyl-2-nitrophenol[a]	41.0	41
4-Methyl -2-nitrophenol[b]	32.0	34
5-Methyl-2-nitrophenol[c]	55.0	56
6-Methyl-2-nitrophenol[d]	71.5—72.5	69—70
3,5-Dimethyl-2-nitrophenol[e]	63—64.5	66
4,6-Dimethyl-2-nitrophenol[b]	72	71—72
2-Nitrophenol[f]	45	45
2-Nitroso-1-naphthol[f]	160—162	162—164
1-Nitroso-2-naphthol[f]	109.5	109.5

a) G. P. Gibson, *J. Chem. Soc.*, **123**, 1269 (1923).
b) Obtained by the nitration of *p*-cresol and2, 4-dimethylphenol.
c) K. G. Blaikie and W. H.Perkin, *ibid.*, **125**, 307 (1924).
d) G. P. Gibson, *ibid.*,**127**, 42 (1925).
e) K. V. Auwers and E. Borsche, *Ber.* **48**, 1698 (1915).
f) Commercial guaranteed reagent.

2-Nitroso-1-naphthol. In a 1 *l* round-bottomed, threenecked flask provided with a stirrer, 12 g (0.05 mol) of copper(II) nitrate was dissolved with 100 m*l* of methanol, and the solution was mixed with a solution of 8 g (0.12 mol) of hydroxylamine hydrochloride in 100 m*l* of methanol. The flask was then well cooled with ice and stirred at 0°C under a nitrogen atmosphere. After 30 min, 4 g (0.028 mol) of 2-naphthol was added to the solution and stirring was continued for 10 min. A dilute solution of hydrogen peroxide which was obtained from 10 m*l* of 30% hydrogen peroxide solution and 30 m*l* of hydrochloric acid-sodium acetate buffer (pH 2.5) was added to the reaction mixture in about 1 hr. The mixture was then warmed to 20°C gradually and the reaction was continued for 4 hr. After the reaction was completed, the mixture was poured into 200 m*l* of water and allowed to stand in an ice-box overnight. The precipitate was filtered, washed twice with a small amount of ether, and suspended in a mixture of methanol (100 m*l*) and concentrated hydrochloric acid (100 m*l*). The suspension was added to chloroform in a 1 *l* separatory funnel, shaken well, and then separated into two layers by addition of water. The aqueous layer was repeatedly extracted with fresh chloroform. All of the chloroform extract was washed with 6N hydrochloric acid and twice-distilled water. The extract was dried over anhydrous sodium sulfate and the solvent was removed under reduced pressure. By recrystallization of the residue from ethanol-water, 1.6 g of 2-nitroso-1-naphthol of mp 160—162°C (lit, mp 162—164°C) was obtained. The yield was *ca.* 35% of the theoretical value.

Found: C, 69.64; H, 4.02; N, 7.84%. Calcd for $C_{10}H_7O_2N$: C, 69.36; H, 4.07; N, 8.09%.

With the same procedure 1-naphthol gave 0.3—0.4 g of 2-nitroso-1-naphthol, mp 166—167°C.

Found: C, 69.64; H, 4.07; N, 8.05%.

Nitrosophenols from Phenols and Catechols. As *o*-nitrosophenol is very volatile and difficult to identify, the product of the reaction was oxidized to nitrophenol and its identification was conducted. As a typical example of the procedure, the formation of 5-methyl-2-nitrosophenol from *p*-cresol will be described.

In a 1 *l* three-necked flask, equipped with a stirrer, was placed copper(II) nitrate (7.2 g, 0.03 mol) and 200 m*l* of hydrochloric acid-sodium acetate buffer (pH 2.5). To this was added a mixture of hydroxylamine hydrochloride (4.2 g, 0.06 mol) and *p*-cresol (3.24 g, 0.03 mol) dissolved in 400 m*l* of water. The solution was stirred for 6 hr at 30°C after the addition of 6 m*l* of hydrogen peroxide solution. The reaction mixture was acidified and extracted with petroleum ether. *o*-Nitrosophenol in the petroleum ether was extracted with aqueous solution of copper(II) sulfate as a copper salt. The red solution was acidified and extracted with petroleum ether. The petroleum ether solution of pure *o*-nitrosocresol was added with 40 m*l* of glacial acetic acid and evaporated at about 50°C. To the resulting acetic acid solution of *o*-nitrosocresol was added a mixture of glacial acetic acid (15 m*l*) and 30% hydrogen peroxide (15 m*l*) and the solution was allowed to stand at 70—80°C for about 20 min. Completion of oxidation was confirmed by observing that a drop of the acetic acid solution did not turn red with the addition of methanolic copper(II) nitrate solution. To the acetic acid solution was then added a large amount of ice-water and extraction was carried out with ethyl ether. The ether extract was washed with water and extracted with 2N sodium hydroxide solution. Steam distillation of the solution after acidification gave 75 mg of yellow crystalline needles with mp of

49.5—52°C. Recrystallization from aqueous ethanol gave 5-methyl-2-nitrophenol, mp 55°C (lit, mp 56°C), undepressed by admixture with an authentic sample.

Kinetic Studies. The general procedure for phenols was used.[1b)]

The work was supported in part by a Research Grant from Kyoto Women's University. The author wishes to express his gratitude to Professor Kazuhiro Maruyama, Kyoto University, for stimulating suggestions and discussions. The continued encouragement of Professor Ryōzō Gotō of Kyoto University is gratefully acknowledged.

BULLETIN OF THE CHEMICAL SOCIETY OF JAPAN VOL. 43 1185—1189 (1970)

A New Synthesis of Aziridines from β-Amino Alcohols with Triphenylphosphine Dibromide

Itaru OKADA, Kunihiro ICHIMURA and Rokuro SUDO

Laboratory of Organic Chemistry, Tokyo Institute of Technology, Ookayama, Meguro-ku, Tokyo

(Received September 29, 1969)

The reaction of β-amino alcohols with triphenylphosphine dibromide was found to give the corresponding aziridines in good yields. The reaction opened a new route to the synthesis of aziridine compounds which seems to be more convenient than the Gabriel and Wenker methods. In the ring closure of ephedrine, a Walden inversion was observed. A possible mechanism is suggested.

Aziridine derivatives are usually prepared from β-amino alcohols by the Gabriel method or by the Wenker method,[1] but both methods are inconvenient because they involve two-step syntheses *via* β-amino hydrogen sulfates or β-haloamines.

In the present paper, a new one-step method is reported; by means of this method β-amino alcohols were rapidly converted to aziridines by using triphenylphosphine dibromide under mild reaction conditions.

Results and Discussion

The amino alcohols (**1**) used were prepared by the reactions of amines with epoxides; the results are summarized in Table 1.

First, the reaction of β-amino alcohols (**1**) with phosphorus pentachloride in the presence of triethylamine was attempted, but the attempt to isolate aziridines (**2**) was unsuccessful.[2]

Triphenylphosphine dibromide (**3**), prepared by Horner and his co-workers, has a considerable advantage over phosphorus pentachloride in the preparation of alkyl and aryl halides from alcohols or phenols.[3]

By using this reagent (**3**), instead of phosphorus pentachloride, the expected aziridines (**2**) were readily obtained in good yields.

In the reaction of 1-phenyl-2-butylaminoethanol (**1a**) with triphenylphosphine dibromide (**3**) in the presence of two equivalents of triethylamine in dry acetonitrile at room temperature, 1-butyl-2-phenyl-aziridine (**2a**) was isolated in a 60% yield, along with 1,4-dibutyl-2,5-diphenylpiperazine (**4a**) as a by-product.

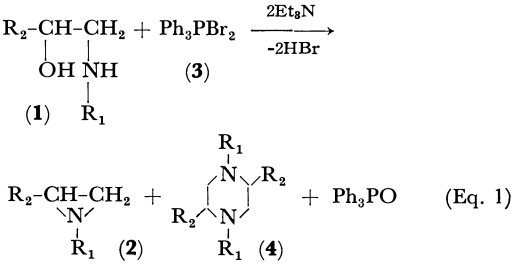

(Eq. 1)

(**a**) $R_1=n\text{-}C_4H_9$, $R_2=C_6H_5$
(**b**) $R_1=t\text{-}C_4H_9$, $R_2=C_6H_5$
(**c**) $R_1=C_6H_{11}$, $R_2=C_6H_5$
(**d**) $R_1=C_6H_5CH_2$, $R_2=C_6H_5$
(**e**) $R_1=C_6H_{11}$, $R_2=CH_3$
(**f**) $R_1=C_6H_5CH_2$, $R_2=CH_3$
(**g**) $R_1=C_6H_5CH_2$, $R_2=C_2H_5$

1) P. E. Fanta, "Heterocyclic Compounds with Three- and Four-Membered Rings," Part I, ed. by A. Weissberger, Interscience Publishers, Inc., New York, N. Y. (1964), p. 524.

2) Deyrup and Moyer reported that the reaction of β-amino alcohols with thionyl chloride in the presence of triethylamine gave not the expected aziridines but 2-oxo-1,2,3-oxathiazolidines.[5]

3) a) L. Horner, H. Oediger and H. Hoffmann, *Ann.*, **626**, 26 (1959); b) L. F. Fieser and M. Fieser, "Reagents for Organic Synthesis," John Wiley & Sons, Inc., New York, N. Y. (1967), p. 1247—1249.

TABLE 1. AMINO ALCOHOLS

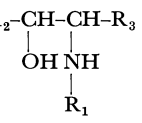

Compound	R_2	R_1	R_3	Mp, °C or Bp, °C/mmHg	Yield, %
1a	C_6H_5	n-C_4H_9	H	58—59[c,d]	62
1b	C_6H_5	t-C_4H_9	H	86—89[c,e]	81
1c	C_6H_5	C_6H_{11}	H	90—91.5[c]	78
1d	C_6H_5	$C_6H_5CH_2$	H	100—102[f]	68
1e	CH_3	C_6H_{11}	H	46—48[c]	75
1f	CH_3	$C_6H_5CH_2$	H	117.5—119.5/1.5	48
1g	C_2H_5	$C_6H_5CH_2$	H	126/2	61
1h	H	C_6H_{11}	H	91/1.5[h]	64
1i	H	$C_6H_5CH_2$	H	119—121/2[i]	50
1j	C_6H_5	CH_3	CH_3[a]	116—118[j]	42
1k	C_6H_5	CH_3	CH_3[b]	217—218[k]	

Compound	Formula	Elemental analysis					
		Calcd, %			Found, %		
		C	H	N	C	H	N
1c	$C_{14}H_{21}NO$	76.66	9.65	6.39	76.67	9.68	6.40
1d	$C_{15}H_{17}NO$	79.26	7.54	6.16	78.93	7.27	6.15
1e	$C_9H_{19}NO$	68.74	12.18	8.91	68.65	11.89	8.76
1g	$C_{11}H_{17}NO$	73.70	9.56	7.81	73.41	9.50	7.81

a) D(+)-*threo*- and L(−)-*erythro*-Ephedrine mixture.
b) L(−)-*erythro*-Ephedrine hydrochloride, commercial product.
c) Recrystallized from *n*-hexane.
d) Lit, mp 58—59°C, bp 164—179°C/18 mmHg.[4]
e) Lit, mp 86—87°C.[5]
f) Recrystallized from a benzene - *n*-hexane mixture.
g) Lit, bp 93—95°C/0.2 mmHg.[6]
h) Lit, bp 87—89°C/1 mmHg.[7]
i) Lit, bp 112—114°C/1 mmHg.[7]
j) Recrystallized from acetonitrile. Lit, mp 118°C.[8]
k) Lit, mp 216°C.[8]

2a was identified by elemental analysis and by means of a study of the NMR spectrum, and its IR spectrum shows neither NH or OH stretching vibrational absorption bands (3280, 1300 cm^{-1}). The structure of **4a** was established by the results of elemental analysis and by a comparison of its infrared spectrum with that of the authentic sample prepared by a procedure similar to that used in a previous paper.[9] A variety of 1,2-disubstituted aziridine derivatives (**2b**—**2g**) were prepared from β-amino alcohols (**1b**—**1g**) in the same way. The results are summarized in Table 2.

The application of this procedure to the synthesis of 1-monosubstituted aziridines was unsuccessful; in the case of 2-cyclohexyl-(**1h**) and 2-benzylamino-ethanol (**1i**), the products isolated were only the

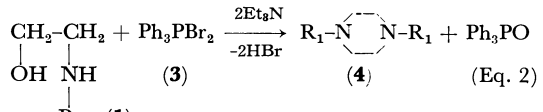

(Eq. 2)

(**h**) $R_1=C_6H_{11}$ (**i**) $R_1=C_6H_5CH_2$

4) W. S. Emerson, *J. Amer. Chem. Soc.*, **67**, 516 (1945).
5) J. A. Deyrup and C. L. Moyer, *J. Org. Chem.*, **34**, 175 (1969).
6) M. A. Stolberg, J. O'Neill and T. Wagner-Jauregg, *J. Amer. Chem. Soc.*, **75**, 5045 (1953).
7) A. T. Bottini and J. D. Roberts, *ibid.*, **80**, 5203 (1958).
8) K. Tanaka, *Yakugaku Zasshi*, **70**, 220 (1950).
9) I. Okada, N. Itoh and R. Sudo, This Bulletin, **42**, 547 (1969).

corresponding 1,4-disubstituted piperazines (**4h** and **4i**), which were identified by means of their melting points and their infrared spectra.

The stereochemical study of this ring-closure reaction (Eq. 1) was performed in the reaction of D(+)-*threo*-(**1j**) and L(−)-*erythro*-ephedrine (**1k**) with triphenylphosphine dibromide (**3**). In the case of *threo*-ephedrine (**1j**), L(−)-*cis*-1,2-dimethyl-3-phenylaziridine (**2j**) was prepared in a 74% yield. Although an analytically-pure sample was not

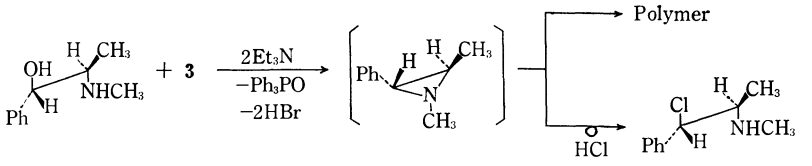

(**1k**) (**2k**) (**5k**)

Scheme 1

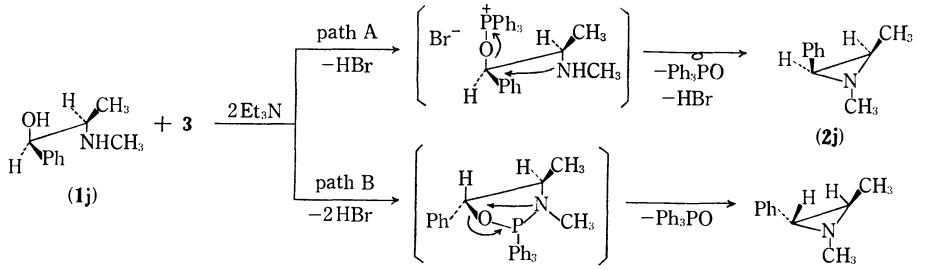

(**1j**) (**2j**) (**2k**)

Scheme 2

TABLE 2. REACTION OF β-AMINO ALCOHOLS WITH TRIPHENYLPHOSPHINE DIBROMIDE

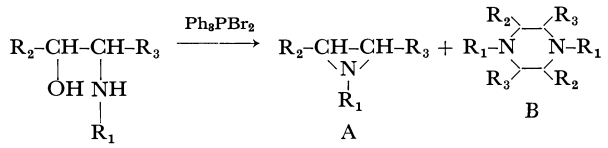

Compound	R_2	R_1	R_3	Product	Bp, °C/mmHg or Mp, °C	Yield, %	Formula	Calcd, % C	Calcd, % H	Calcd, % N	Found, % C	Found, % H	Found, % N
2a	C_6H_5	*n*-C_4H_9	H	A	80—81/1	60	$C_{12}H_{17}N$	82.23	9.78	7.99	82.13	9.52	8.26
4a				B	109.5—110.5[b]	12	$C_{24}H_{34}N_2$	82.23	9.78	7.99	82.16	9.51	8.18
2b	C_6H_5	*t*-C_4H_9	H	A	120/20[c]	66	$C_{12}H_{17}N$	82.23	9.78	7.99	82.22	9.95	7.87
4b				B	109—110[b]	9	$C_{24}H_{34}N_2$	82.23	9.78	7.99	82.61	9.96	8.14
2c	C_6H_5	C_6H_{11}	H	A	155—156/16	50	$C_{14}H_{19}N$	83.53	9.51	6.96	83.77	9.21	6.62
2d	C_6H_5	$C_6H_5CH_2$	H	A	138—139/1	54	$C_{15}H_{15}N$	86.08	7.22	6.69	85.83	6.98	6.85
2e	CH_3	C_6H_{11}	H	A	58—59/12	11	$C_9H_{17}N$	77.63	12.31	10.06	77.89	11.91	9.88
2f	CH_3	$C_6H_5CH_2$	H	A	57—58/1.5[d]	51	$C_{10}H_{13}N$	81.58	8.90	9.52	81.20	8.75	9.56
2g	C_2H_5	$C_6H_5CH_2$	H	A	102/13	51	$C_{11}H_{15}N$	81.93	9.37	8.69	81.56	8.99	8.62
4h	H	C_6H_{11}	H	B	117—118[b,e]	44	$C_{16}H_{30}N_2$	76.74	12.08	11.19	76.66	11.81	10.98
4i	H	$C_6H_5CH_2$	H	B	90—91[f,g]	28	$C_{18}H_{22}N_2$	81.16	8.33	10.52	81.01	8.70	10.35
2j	C_6H_5	CH_3	CH_3	A[a]	82/14[h]	74[h]							

a) See Experimental.
b) Recrystallized from acetonitrile.
c) Lit, bp 50°C/0.1 mmHg.[5]
d) Lit, bp 58°C/2 mmHg.[6]
e) Lit, mp 118°C[10]
f) Recrystallized from ethanol.
g) Lit, mp 92°C.[11]
h) Lit, 72°C/7 mmHg.[8]

10) C. N. Ionescu, *et al.*, *Acad. Rep. Populare Romine, Sutdii Cercetari Chim.*, **5**, No. 1, 7–15 (1957); *Chem. Abstr.*, **52**, 398i (1958).

11) Heilbron, "Dictionary of Organic Compounds," ed. by A. H. Cook and E. R. H. Jones, Oxford University Press, New York, N. Y. (1953), p. 216.

obtained, the structure was confirmed by a comparison of its NMR spectrum with that of the authentic sample reported in the literature.[10] The $[\alpha]_D^{28}-134°$ (EtOH), of the product (**2j**) indicates the occurrence of Walden inversion during the ring closure. On the other hand, in the reaction of *erythro*-ephedrine (**1k**) with **3**, the expected D(+)-*trans*-1,2-dimethyl-3-phenylaziridine (**2k**) was not isolated, and only a polymeric material was obtained. Taguchi and Kojima observed an analogous polymerization of the *trans*-isomer (**2k**) in the application of the Wenker synthesis to *erythro*-ephedrine (**1k**).[12] It seems probable that the *trans*-isomer (**2k**) is easily polymerized during the isolation. Therefore, immediately after the reaction was over, hydrogen chloride gas was introduced into the reaction mixture. The product isolated was the expected L(−)-*erythro*-1-chloro-1-phenyl-2-methylaminopropane hydrochloride (**5k**), which would suggest the formation of **2k**. Although the melting point of this product, 186—188°C, was slightly lower than the literature value,[8] 198°C, $[\alpha]_D^{23}-68.6°$ (EtOH), the infrared spectrum supported the structure.

On the basis of the results described above, in the cases of both *threo*- (**1j**) and *erythro*-ephedrine (**1k**), a Walden inversion should occur in the ring-closure process. This fact supports the idea of the 1,2-*trans*-elimination in path A postulated in Scheme 2; the five-membered ring intermediate shown in path B, which should afford a *cis*-isomer, can thus be eliminated.

Experimental

The acetonitrile used was distilled from phosphorus pentoxide and dried over calcium hydride. The triethylamine was distilled and dried over sodium. All the melting points and boiling points are uncorrected.

β-Amino Alcohols (1). These compounds were prepared by the methods of Emerson,[4] Stolberg,[6] and Bottini;[7] their physical constants are summarized in Table 1.

1-Butyl-2-phenylaziridine (2a). The general procedure for the reaction of β-amino alcohols (**1**) with triphenylphosphine dibromide (**3**) was as follows. To a solution of **3**, prepared from 10.48 g (0.04 mol) of triphenylphosphine in 100 m*l* of acetonitrile and 6.40 g (0.04 mol) of bromine in 40 m*l* of acetonitrile, 7.72 g (0.04 mol) of **1a** was added under ice cooling. A solution of 8.08 g (0.08 mol) of triethylamine in 10 m*l* of acetonitrile was then stirred, drop by drop, into the above mixture. After this mixture had stood overnight at room temperature, the precipitated triethylamine hydrobromide was filtered off (8.90 g, 62%). The filtrate was concentrated by rotary evaporation. The residue was extracted several times with *n*-hexane, and the extract was concentrated by rotary evaporation to about 5 m*l*. The triphenylphosphine oxide thus separated was removed by filtration, and the filtrate was further concentrated. The yellow residue (5.90 g) was distilled to give **2a**; bp 88—89.5°C/2 mmHg. Yield, 4.15 g (60%). The analytical sample was obtained by redistillation as a colorless liquid; bp 80—81°C/1 mmHg. IR (NaCl): 3030, 2920, 1600, 1495, 1450, 1205, 1080, 1025, 740, 720, and 690 cm^{-1}; NMR ($CDCl_3$): τ 2.8 (5H, singlet) due to aromatic protons, τ 7.5—7.9 (3H, multiplet) due to $>N-C\underline{H}_2-CH_2-$ and $C_6H_5-C\underline{H}$, τ 8.1—9.0 (6H, multiplet) due to $C_6H_5-CH-C\underline{H}_2$ and $CH_3-C\underline{H}_2-C\underline{H}_2-$, and τ 9.1 (3H, triplet) due to $-CH_3$. The oily, brown distillation residue was treated with a small quantity of ethanol to give 1,4-dibutyl-2,5-diphenylpiperazine (**4a**) as needle crystals. Yield, 0.85 g (12%). Recrystallization from acetonitrile afforded colorless needles; mp 109.5—110.5°C. Benzene and water were added to the residue resulting from *n*-hexane extraction. The organic layer was concentrated to give 10.60 g (96%) of triphenylphosphine oxide. The evaporation of the aqueous layer afforded 5.90 g (41%) of triethylamine hydrobromide. The total yield of this compound was 93%.

D(+)-*threo*-Ephedrine (1j). This compound was prepared from L(−)-*erythro*-ephedrine hydrochloride (**1k**) by the procedure of Tanaka.[8] The ratio of D(+)-*threo*- to L(−)-*erythro*-ephedrine in the product was 65 : 35.

L(−)-*cis*-1,2-Dimethyl-3-phenylaziridine (2j). 2j was prepared in a manner analogous to that described for the preparation of **2a**. Bp 82°C/14 mmHg. Yield, 74% $[\alpha]_D^{23}$ −134° (EtOH). (Lit, $[\alpha]_D^{11}$ −127°, EtOH). NMR ($CDCl_3$): τ 2.75 (5H, singlet) due to aromatic protons, τ 7.55 (3H, singlet) due to $>N-CH_3$, τ 7.65 (1H, doublet) due to $C_6H_5-C\underline{H}$, τ 8.4 (1H, quintet) due to $-C\underline{H}CH_3$, and τ 9.15 (3H, doublet) due to $-CH-C\underline{H}_3$. IR (NaCl): 2950, 1600, 1500, 1460, 1400, 1120, 730, and 700 cm^{-1}.

Reaction of L(−)-*erythro*-Ephedrine Hydrochloride (1k) with Triphenylphosphine Dibromide (3). 4.03 g (0.02 mol) of **1k** was added, under ice cooling, to a solution of **3** which had been prepared from 5.24 g (0.02 mol) of triphenylphosphine in 25 m*l* of acetonitrile and 3.20 g (0.02 mol) of bromine in 10 m*l* of acetonitrile. A solution of 6.06 g (0.06 mol) of triethylamine in 10 m*l* of acetonitrile was then stirred, drop by drop, into the mixture. After 0.5 hr, the triethylamine hydrobromide and hydrochloride thus precipitated were filtered off (7.50 g, 75%). This filtrate was treated with water or hydrogen chloride.

a) Treatment with Water. The filtrate was concentrated by rotary evaporation. The residue was treated with water, and the insoluble product was collected by filtration, washed with ethanol, and dried (1.30 g); mp 270—290°C. This compound could not be recrystallized from normal solvents. IR (KBr): 2950, 1600, 1490, 1450, 1025, 750, and 700 cm^{-1}.

b) Treatment with Hydrogen Chloride. Hydrogen chloride was introduced into the filtrate. The mixture was concentrated by rotary evaporation, and the residue was treated with 40 m*l* of benzene and 40 m*l* of water. The evaporation of the organic layer afforded 5.00 g (89%) of triphenylphosphine oxide. The aqueous layer was concentrated to give 2.90 g of L(−)-*erythro*-1-chloro-1-phenyl-2-methylaminopropane hydrochloride (**5k**). Recrystallization from ethanol gave colorless plates; mp

12) S. J. Brois and G. P. Beardsley, *Tetrahedron Lett.*, **42**, 5113 (1966).

13) T. Taguchi and M. Kojima, *Chem. Pharm. Bull.* (Tokyo), **7**, 103 (1959).

186—188°C, $[\alpha]_D^{28}$ −68.6° (EtOH). (Lit, $[\alpha]_D^{11}$ −65°, EtOH).[8] IR (KBr): 2950, 2750, 2400, 1600, 1450, 1400, 850, 760, and 700 cm^{-1}.

Found: C, 50.11; H, 6.24; N, 5.96%. Calcd for $C_{10}H_{15}NCl_2 \cdot H_2O$: C, 50.42; H, 6.30; N, 5.88%.

1,4-Dibutyl-2,5-diphenylpiperazine (4a). A mixture of 1.75 g (0.01 mol) of **2a**, a catalytic amount of aluminum chloride, and 20 m*l* of methanol was refluxed for 7 hr. The solvent was then evaporated, and the residue was treated with a slight excess of potassium hydroxide and water. The solution was then extracted several times by ether. The ether layer was dried over anhydrous potassium carbonate and evaporated. The crude product, 1.20 g (69%), was recrystallized from acetonitrile to give colorless needles; mp 109.5—110.5°C. IR (KBr): 2950, 2800, 1600, 1490, 1450, 1140, 1110, 750, and 700 cm^{-1}.

Found: C, 82.29; H, 9.59; N, 8.06%. Calcd for $C_{24}H_{34}N_2$: C, 82.23; H, 9.78; N, 7.99%.

BULLETIN OF THE CHEMICAL SOCIETY OF JAPAN VOL. 43 1189—1196 (1970)

Rearrangement of Aryl Sulfides in the Presence of Aluminum Chloride*1

Tamotsu FUJISAWA, Noriko OHTSUKA and Gen-ichi TSUCHIHASHI

Sagami Chemical Research Center, Ohnuma, Sagamihara-shi, Kanagawa

(Received October 1, 1969)

Aluminum chloride-catalyzed rearrangement of aryl sulfides leads to thermodynamically controlled equilibrium mixtures at room temperature. On treatment of *o*-, *m*- or *p*-tolyl phenyl sulfide without solvent, the isomer distribution converges to an equilibrium point, 17% *ortho*, 47% *meta* and 36% *para* isomer by intramolecular isomerization. Intermolecular disproportionation by methyl-group exchange to produce diphenyl sulfide and ditolyl sulfide accompanied isomerization. In addition, a new type of aromatic rearrangement, intermolecular disproportionation by exchange of the arylthio group, was found to occur simultaneously giving benzene, toluene and thianthrene derivatives. The rate of this reaction is slower than that of the methyl rearrangement. A similar treatment of α-naphthyl phenyl sulfide gave the β-isomer from intramolecular isomerization and diphenyl sulfide, naphthalene, thianthrene and benzene from intermolecular disproportionation. The mechanisms of the rearrangement of aryl sulfides are discussed.

In recent years, several kinds of aromatic rearrangement have been elucidated with the development of analytical methods such as gas chromatography and infrared spectroscopy. Various types are recorded in reports and monographs.[1] In particular, the acid-catalyzed rearrangements of alkyl groups in aromatic hydrocarbons and of halogen atoms in halogenoaromatic compounds, involving the Reverdin and Jacobsen rearrangements, have been discussed in detail. However, no rearrangement of aryl sulfides has yet been described.

Preceding communications on iron catalyzed aromatic sulfuration have shown that the direct sulfuration of the aromatic nucleus with sulfur chlorides in the presence of a trace amount of ironpowder provides a convenient method for the preparation of symmetrical sulfides, and the reaction proceeds through thiosulfenyl chloride and sulfenyl chloride as intermediates.[2-3]

$$ArH + S_xCl_2 \xrightarrow{Fe} ArSSCl \longrightarrow ArSCl \xrightarrow[Fe]{ArH} ArSAr$$

$x = 1$ or 2

Similarly the iron-catalyzed reaction with various types of sulfenyl chlorides as starting materials provides a facile synthetic route for unsymmetrical aryl sulfides.[4] During the course of an extensive study on aromatic sulfuration with various types of catalysts, methyl and arylthio substituents in tolyl

*1 This investigation was presented at the 22nd Annual Meeting of the Chemical Society of Japan, Tokyo, March, 1969.

1) a) H. J. Shine, "Aromatic Rearrangement," Elsevier, Amsterdam (1967); b) D. A. McCaulay, "Friedel-Crafts and Related Reactions," Vol. II, Part 2, ed. by G. A. Olah, Interscience, New York (1964), p. 1049; c) M. J. S. Dewar, "Molecular Rearrangement," Part 1, ed. by P. de Mayo, Interscience, New York (1963), p. 295; d) H. Suzuki, *Yuki Gosei Kagaku Kyokai Shi*, **23**, 713 (1965).

2) T. Fujisawa, N. Ohtsuka, T. Kobori and G. Tsuchihashi, *Tetrahedron Lett.*, **1968**, 4533.

3) T. Fujisawa, T. Kobori and G. Tsuchihashi, *ibid.*, **1969**, 4291.

4) T. Fujisawa, T. Kobori, N. Ohtsuka and G. Tsuchihashi, *ibid.*, **1968** 5071.

TABLE 1. REACTION OF BENZENESULFENYL CHLORIDE WITH TOLUENE

Catalyst	Wt %	Tolyl phenyl sulfide yield %	*ortho*	*meta* mol %	*para*	Diphenyl sulfide yield %
Fe	0.6	10	33	—	67	—
Fe	13.9	28	33	—	67	—
$FeCl_3$	0.6	10	33	—	67	—
$FeCl_3$	13.9	18	33	—	67	—
Al	1.4	—	—	—	—	—
Al	4.2	22	30	21	49	6
Al	13.9	22	26	26	48	4
Al_2Cl_6	1.4	16	36	—	64	—
Al_2Cl_6	4.2	20	31	8	61	2
Al_2Cl_6	13.9	43	22	35	43	17
Al_2Cl_6	27.8	42	17	41	42	16
Al-Hg	1.4	16	36	—	64	—
Al-Hg	4.2	26	34	21	45	5
Al-Hg	13.9	36	31	18	51	7

phenyl sulfides were found to rearrange in the presence of aluminum chloride. In the present experiments the rearrangement of aryl sulfides in the presence of aluminum chloride was investigated.

The products and isomer ratios from the reaction of toluene with benzenesulfenyl chloride depend on the kind and amount of the catalysts used. When iron catalysts such as iron powder or ferric chloride, are used, the products are *o*- and *p*-tolyl phenyl sulfides. The total yield increases with the increase of the amount of catalyst, and the *ortho-para* isomer ratio remains unchanged. On the other hand, in the case of aluminum catalysts such as aluminum metal, aluminum amalgam or aluminum chloride, the *meta* isomer is formed along with the other isomers, while the isomer ratios vary with the amount of the catalyst used. The formation of diphenyl sulfide in fair yield was simultaneously observed. The data for the reaction of toluene

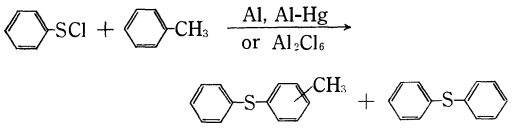

with benzenesulfenyl chloride in the presence of various types of catalysts are shown in Table 1. The product yields and isomer ratios were determined by glpc. The results suggest that intramolecular and intermolecular methyl group migration in the initially formed product mixture lead to the observed mixture of tolyl phenyl sulfide isomers and diphenyl sulfide. To confirm this hypothesis, each isomer of tolyl phenyl sulfide was chosen as a starting material and its rearrangement in the presence of aluminum chloride was studied.

Several common solvents were investigated under various conditions to determine how readily the dissolved tolyl phenyl sulfides undergo rearrangement. Representative runs are collected in Table 2. It is worth noting that no rearrangement took place in certain solvents under mild conditions (at room temperature).

Thus, *p*-tolyl phenyl sulfide was recovered after treatment in ether or acetonitrile and only very slowly changed in carbon tetrachloride or nitrobenzene. In petroleum ether, although the products after a 20 hr reaction time could be clearly distinguished by glpc analysis, other peaks appeared at the same region of the peaks of the tolyl phenyl sulfides in the glpc chart after a 40 hr reaction time and quantitative analysis became impossible. This seemed to be attributable to disproportionation between the sulfides and the petroleum ether. The intramolecular rearrangement was readily observed in diphenyl sulfide as solvent, but intermolecular rearrangement, disproportionation, could not be detected in this case. The equilibrium amounts of the sulfide isomers found after a 40 hr reaction time may characterize the equilibrium point when only the intramolecular isomerization took place. Since the tolyl phenyl sulfide isomer compositions were different when the disproportionation was occurring simultaneously, the rearrangements were carried out without solvent in order to observe both features of the reaction. Although the rearrangement occurred readily without solvent at room temperature, addition of a trace amount of water as cocatalyst resulted in an extremely rapid reaction lasting 30 min. After 2 hr, results were the same with or without the addition of water.

Thus, the tolyl phenyl sulfide isomer compositions were obtained by treating stirred mixtures of the sulfides with aluminum chloride (20 : 1 molar ratio) at room temperature in the presence of a drop of water, added by a microsyringe. The mixtures soon became homogeneous liquids and changed to viscous liquids after 72 hr making stirring by magnetic stirrer very difficult. At certain intervals, samples were withdrawn from the reaction mixtures,

Table 2. Solvent effect in rearrangement of *p*-tolyl phenyl sulfide with Al_2Cl_6 catalyst at room temperature

Solvent	Product wt% reaction time, 20 hr					Product wt% reaction time, 40 hr				
	Diphenyl sulfide	Tolyl phenyl sulfide *o-*	*m-*	*p-*	Ditolyl sulfide	Diphenyl sulfide	Tolyl phenyl sulfide *o-*	*m-*	*p-*	Ditolyl sulfide
Carbon disulfide	16	15	7	59	3	28	8	15	35	14
Benzene	26	3	11	57	4	36	7	16	32	9
Chloroform	20	4	12	52	12	24	4	14	46	12
Diphenyl sulfide	—	23	46	31	—	—	33	46	21	—
Petroleum ether	20	2	6	60	9					
Carbon tetrachloride	4	—	—	96	—	3	—	—	97	—
Nitrobenzene	1	—	1	98	—	1	—	1	98	—
Diethyl ether	—	—	—	100	—	—	—	—	100	—
Acetonitrile	—	—	—	100	—	—	—	—	100	—
Toluene	16	13	13	52	12					

Table 3. Isomerization of tolyl phenyl sulfides with $Al_2Cl_6 \cdot H_2O$ catalyst at room temperature

Isomer	Reaction time	% tolyl phenyl sulfide isomer distribution		
		ortho	*meta*	*para*
ortho	5 min	71	25	4
	10	66	29	5
	15	54	39	7
	30	33	58	9
	1 hr	18	69	13
	2	19	66	15
	6	16	61	23
	26	13	53	34
	48	15	49	36
	168	17	47	36
meta	5 min	14	82	4
	10	14	80	6
	15	15	78	7
	30	21	69	10
	1 hr	16	71	13
	2	16	67	17
	6	13	67	20
	26	12	51	37
	48	12	51	37
	168	17	47	36
para	5 min	0	1	99
	10	0	1	99
	15	0	2	98
	30	0	3	97
	1 hr	3	8	89
	2	4	13	83
	6	5	29	64
	26	12	48	40
	48	14	48	38
	168	17	47	36

hydrolyzed by addition of water and extracted with ether. The samples were then analyzed by glpc.

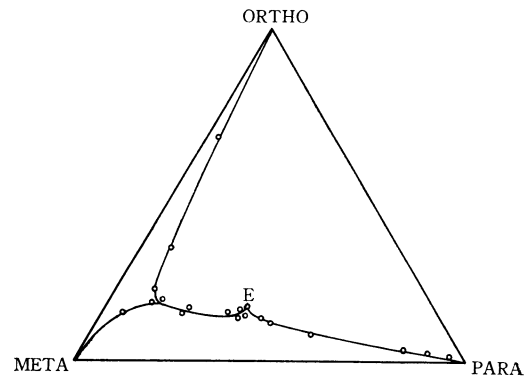

Fig. 1. *Ortho*, *meta* and *para* isomer equilibrations in isomerization of neat tolyl phenyl sulfides with $Al_2Cl_6 \cdot H_2O$ catalyst at room temperature.

The results are given in Table 3. Three runs are plotted in triangular coordinates[5] in Fig. 1.

The *ortho* isomer trajectory starts asymptotically to the 0% *para*-isomer side and the *meta* isomer trajectory starts asymptotically to the 0% *para* isomer side. Both trajectories combine after a 1-hr reaction time and then drift toward the *para* isomer side. After 168 hr, the joint trajectory meets the *para* trajectory at the thermodynamically controlled equilibrium point, in which the sulfide isomer compositions were *ortho* 17%, *meta* 47% and *para* 36%. This corresponds to a *meta*/*para* ratio of 1.3 and *ortho*/*para* ratio of 0.5. The most rapid rearrangement is shown to be the *ortho*→*meta* migration. The pattern of the triangular composition diagram resembles that for the acid-catalyzed isomerization of xylene[6] rather than that for isomerization of bromotoluene,[7] previously reported.

5) R. H. Allen, T. Alfrey, Jr., and L. D. Yats, *J. Amer. Chem. Soc.*, **81**, 42 (1959).
6) R. H. Allen and L. D. Yats, *ibid.*, **81**, 5289 (1959).
7) J. W. Crump and G. A. Gornowicz, *J. Org. Chem.*, **28**, 949 (1963).

Table 4. Equilibrium compositions of disubstituted benzenes

Substituents in ring		Reaction temperature	Catalyst	% Composition			Ratio *m/p*
				ortho	*meta*	*para*	
Me	PhS	room	$Al_2Cl_6 \cdot H_2O$	17	47	36	1.3
Me	Me	30	$Al_2Br_6 \cdot HBr$	12	72	16	4.5[a]
Me	Et	room	$Al_2Cl_6 \cdot HCl$	7	66	27	2.4[b]
Me	*i*-Pr	room	$Al_2Cl_6 \cdot HCl$	2	69	30	2.3[c]
Me	*t*-Bu	25	$Al_2Cl_6 \cdot H_2O$	0	64	36	1.8[d]
Et	Et	25	$Al_2Cl_6 \cdot H_2O$	3	69	28	2.5[e]
i-Pr	*i*-Pr	25	$Al_2Cl_6 \cdot H_2O$	0	67	33	2.1[f]
t-Bu	*t*-Bu	25	$Al_2Cl_6 \cdot H_2O$	0	52	48	1.1[g]
Br	Br	30	$Al_2Br_6 \cdot H_2O$	4	62	34	1.8[h]
Me	Br	30	$Al_2Cl_6 \cdot H_2O$	37	45	18	2.5[i]

a) K. S. Pitzer and D. W. Scott, *J. Amer. Chem. Soc.*, **65**, 803 (1943).
b) R. H. Allen, *ibid.*, **82**, 4853 (1960).
c) Ref. 5.
d) G. A. Olah, M. W. Meyer and N. A. Overchuck, *J. Org. Chem.*, **29**, 2310 (1964).
e) G. A. Olah, M. W. Meyer and N. A. Overchuck, *ibid.*, **29**, 2313 (1964).
f) G. A. Olah, M. W. Meyer and N. A. Overchuck, *ibid.*, **29**, 2315 (1964).
g) Ref. 8.
h) G. A. Olah, W. S. Tolgyesi and R. E. A. Dear, *J. Org. Chem.*, **27**, 3455 (1962).
i) Ref. 9.

The initial point at which the two *ortho* and *meta* trajectories become associated is considered to be close to the equilibrium point which would be observed if intramolecular rearrangement only took place.

A comparison of the rearrangement of tolyl phenyl sulfides to that of other disubstituted benzenes, which have been previously described, is summarized in Table 4.

The rearrangement of an alkyl group on the benzene nucleus in the presence of an acid-catalyst is well known: Xylenes are isomerized at room temperature and give a *meta/para* ratio of 4.5. This reaction has been shown to proceed by an intramolecular 1,2-shift mechanism.[6] Attachment of more bulky alkyl groups to the benzene nucleus gives a smaller *meta/para* ratio. Thus, the value became smaller in the order methyl, ethyl, isopropyl, *t*-butyl. When two *t*-butyl groups are substituted on the nucleus, the *meta/para* ratio is 1.1. In this case, the reaction is known to proceed by intermolecular rearrangement involving a π-complex at the transition state.[8] Halogen atoms can also move their position on the benzene nucleus in the presence of acid-catalysts by an electrophilic attack mechanism of halogen cation.[9] In the case of bromotoluene, the *meta/para* ratio is 2.5.

The value 1.3 for the *meta/para* ratio in the rearrangement of tolyl phenyl sulfides is fairly close to that for di-*t*-butylbenzenes mentioned above. This indicates that isomerization and disproportionation occur simultaneously in the rearrangement. The relative amounts of tolyl phenyl sulfide and of diphenyl sulfide and ditolyl sulfide, which are products of the intermolecular exchange of the methyl group, *versus* the reaction time (taking the sum of the amounts of the three compounds concerned as 100%) are summarized in Figs. 2—4.

The amount of diphenyl sulfide increases with reaction time, but the yield of the corresponding ditolyl sulfide is maximal at a 6-hr reaction time and thereafter diminishes. The ratio of diphenyl sulfide to tolyl phenyl sulfides converges to about 3.9. This failure in material balance of the methyl group

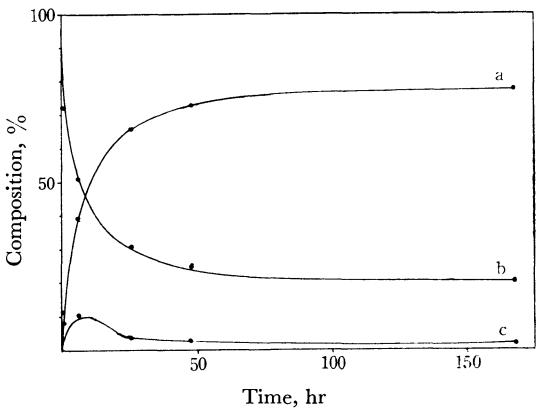

Fig. 2. Disproportionation of neat *o*-tolyl phenyl sulfide with $Al_2Cl_6 \cdot H_2O$ catalyst at room temperature.
a: diphenyl sulfide, b: tolyl phenyl sulfide, c: ditolyl sulfide

8) G. A. Olah, C. G. Carlson and J. C. Lapierre, *J. Org. Chem.*, **29**, 2687 (1964).
9) G. A. Olah and M. W. Meyer, *ibid.*, **27**, 3464 (1962).

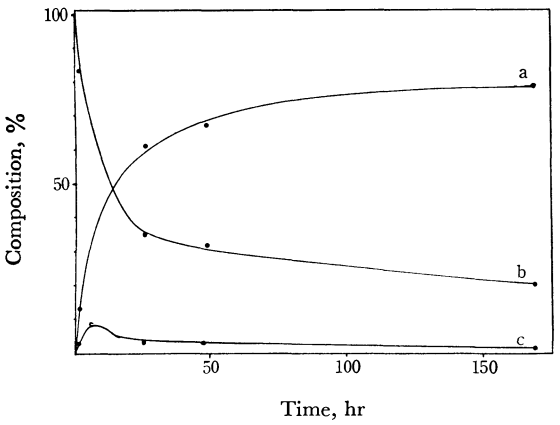

Fig. 3. Disproportionation of neat *m*-tolyl phenyl sulfide with $Al_2Cl_6 \cdot H_2O$ catalyst at room temperature.
a: diphenyl sulfide, b: tolyl phenyl sulfide, c: ditolyl sulfide

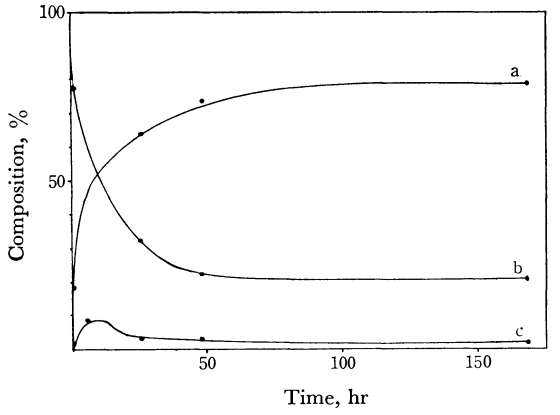

Fig. 4. Disproportionation of neat *p*-tolyl phenyl sulfide with $Al_2Cl_6 \cdot H_2O$ catalyst at room temperature.
a: diphenyl sulfide, b: tolyl phenyl sulfide, c: ditolyl sulfide

may be due to the formation of polymethyl derivatives of the sulfides, which also occurs in the case of the Jacobsen rearrangement.[10] In fact, the formation of trimethyldiphenyl sulfide and tetramethyldiphenyl sulfide could be observed on glpc analyses, but they also gradually diminished after a maximum at 6-hr reaction time.

The poor material balance for the methyl group might also suggest other products. Careful examination of the product analyses revealed bond fission between the aryl group and the sulfur atom of the sulfide as well as rearrangement of the methyl group: thianthrene, toluene and benzene were observed among the products from the tolyl phenyl sulfides. The relative amounts of these compounds are shown in Figs. 5—7.

Among the products, the proportion of polymethyl derivatives of thianthrene increased with long reaction times. Although these compounds were obtained by glpc separation, each isomer could not be isolated and the methyl-group positions could not be determined.

As mentioned above, the intermolecular methyl group rearrangement of tolyl phenyl sulfide gives diphenyl sulfide and ditolyl sulfide (Eq. (1)), while a similar arylthio group rearrangement affords benzene, toluene and thianthrene derivatives (Eq. (2)). Thus, in order to compare the rates of these two rearrangements, the ratio of the sum of mole fractions of benzene and toluene, which are formed by the arylthio migration, to the mole fraction of

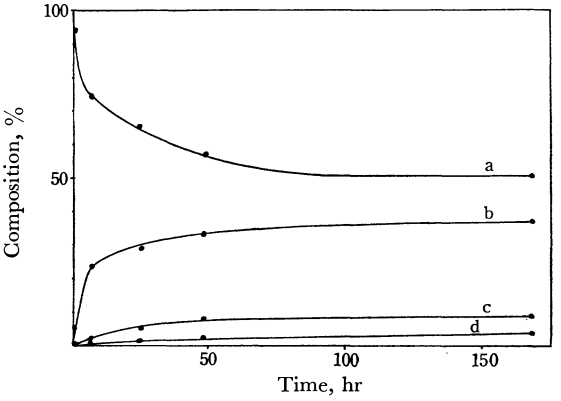

Fig. 5. Disproportionation of arylthio groups in neat *o*-tolyl phenyl sulfide with $Al_2Cl_6 \cdot H_2O$ catalyst at room temperature.
a: diaryl sulfides (diphenyl sulfide+tolyl phenyl sulfide+ditolyl sulfide), b: toluene, c: thianthrene, d: benzene

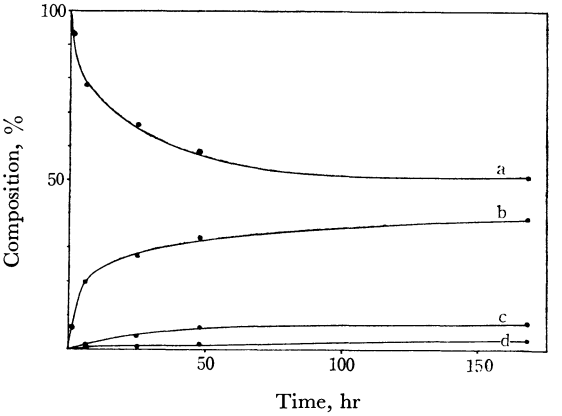

Fig. 6. Disproportionation of arylthio groups in neat *m*-tolyl phenyl sulfide with $Al_2Cl_6 \cdot H_2O$ catalyst at room temperature.
a: diaryl sulfides (diphenyl sulfide+tolyl phenyl sulfide+ditolyl sulfide), b: toluene, c: thianthrene, d: benzene

10) *e.g.*, R. Goto, *Kagaku to Kogyo*, **17**, 25 (1964).

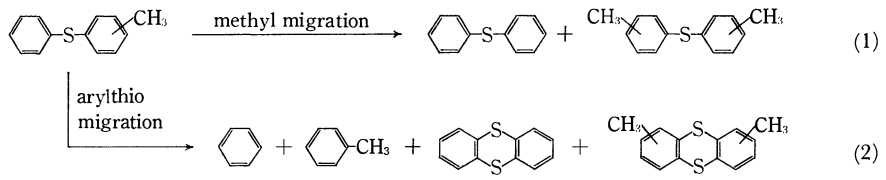

(1)

(2)

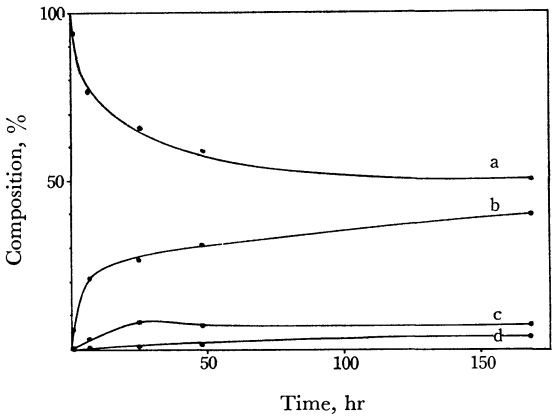

Fig. 7. Disproportionation of arylthio groups in neat *p*-tolyl phenyl sulfide with $Al_2Cl_6 \cdot H_2O$ catalyst at room temperature.
a: diaryl sulfides (diphenyl sulfide+tolyl phenyl sulfide+ditolyl sulfide), b: toluene, c: thianthrene, d: benzene

diphenyl sulfide, which results from the methyl migration, was calculated and is given in Table 5. The values of the ratio converge to about 0.9 after long reaction times in all cases, regardless of the choice of the isomer of tolyl phenyl sulfide as starting material. Table 5 also indicates that the amount

TABLE 5. RATIO OF THE SUM OF MOLE FRACTIONS OF BENZENE AND TOLUENE TO THE MOLE FRACTION OF DIPHENYL SULFIDE IN THE ALUMINUM CHLORIDE CATALYZED DISPROPORTIONATION OF TOLYL PHENYL SULFIDES

Reaction time	Tolyl phenyl sulfides		
	ortho	*meta*	*para*
10 min	0.2	—	0.3
30	0.3	0.1	0.4
1 hr	0.3	0.2	0.5
6	0.4	0.5	0.6
26	0.6	0.6	0.6
48	0.7	0.7	0.7
168	0.9	0.9	0.9

of diphenyl sulfide formed is larger than that of arenes in the initial stages of the reaction, which shows that the methyl rearrangement proceeds faster than the arylthio rearrangement in the disproportionation of tolyl phenyl sulfide.

This Lewis acid-catalyzed arylthio group rearrangement has not been reported and is thus a new type of aromatic rearrangement. The most striking characteristic of this rearrangement is that it proceeds at room temperature. In order to make a further study of it, the rearrangement of α-naphthyl phenyl sulfide in the presence of aluminum chloride at room temperature was tried. β-Naphthyl phenyl sulfide, the product of intramolecular rearrangement, increased rapidly at first (α/β=59/41 at 1 hr), then exceeded the amount of α isomer (11/89 at 24 hr), but the ratio of α and β isomers eventually approached 50 : 50 after about 72 hr (Table 6).

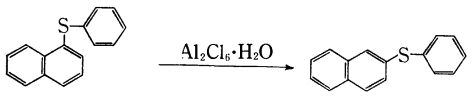

TABLE 6. ISOMERIZATION OF α-NAPHTHYL PHENYL SULFIDE WITH $Al_2Cl_6 \cdot H_2O$ CATALYST AT ROOM TEMPERATURE

Time, hr	0	1	6	24	72
α/β	100/0	59/41	15/85	11/89	50/50

As regards intermolecular rearrangement, the formation of diphenyl sulfide, naphthalene, thianthrene, diphenyl disulfide and benzene were ob-

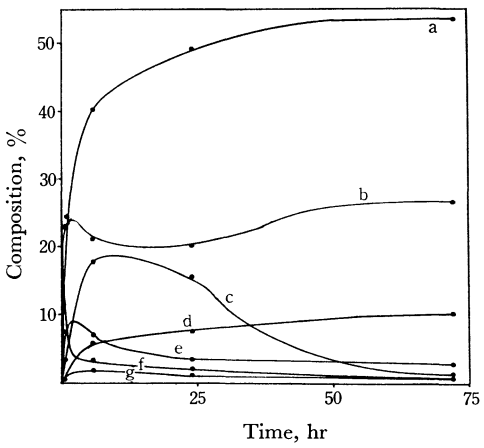

Fig. 8. Disproportionation of α-naphthyl phenyl sulfide with $Al_2Cl_6 \cdot H_2O$ catalyst at room temperature.
a: diphenyl sulfide, b: naphthalene, c: β-naphthyl phenyl sulfide, d: thianthrene, e: diphenyl disulfide, f: α-naphthyl phenyl sulfide, g: benzene

served, together with the decrease of naphthyl phenyl sulfide, as shown in Fig. 8. Other unidentified products observed by glpc, are probably thianthrene type products of naphthalene, and dinaphthyl sulfide, *etc.*

From the results, the isomerization and disproportionation of methyl and arylthio substituents were found to take place simultaneously on treatment of aryl sulfides with aluminum chloride. The mechanisms of the migrations may be as follows:

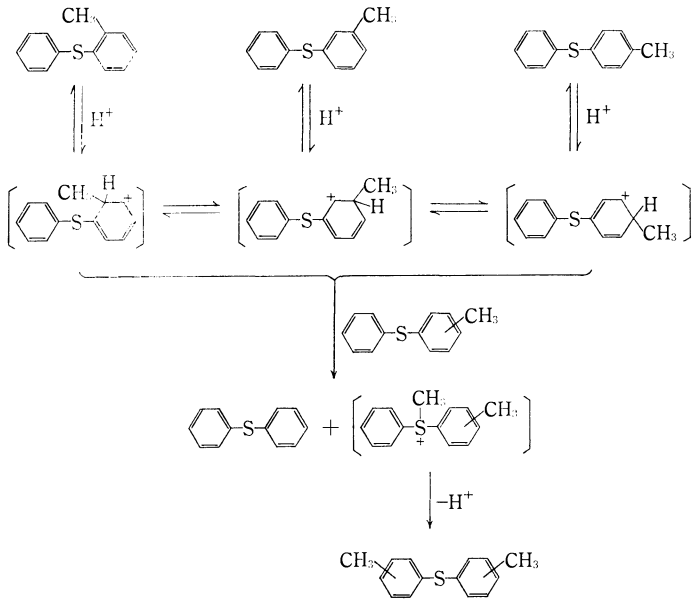

The proton attacks the position bonded to the methyl group of the aromatic nucleus to make σ-complexes, which are in equilibrium with each other *via* intramolecular 1,2-methyl shifts. In the case of intermolecular rearrangement, the complexes react with another tolyl phenyl sulfide to give diphenyl sulfide and ditolyl sulfide, which proceeds by way of a sulfonium-cation type intermediate.

On the other hand, the protonation at the position of the nucleus bonded to the sulfur atom may promote the intramolecular 1,2-arylthio shifts. The simultaneous bond fission between aryl group and

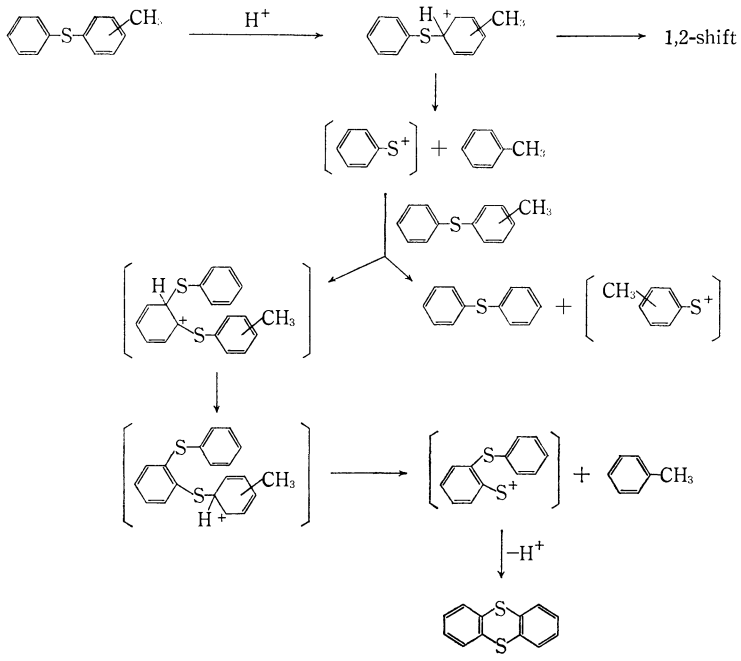

sulfur atom takes place yielding sulfenium cation.[11] This might be explained partly by the attack on a sulfur bearing carbon to yield another sulfenium cation and partly by the attack on the position *ortho* to the sulfur atom of another sulfide to give thianthrene derivatives, according to the above described routes.

The facility of the rearrangement is considered to be due to the easy protonation by electron-releasing effect of sulfur atom, and the sulfonium type intermediate through which the mobile substituents are able to migrate to the adjacent aromatic nucleus.

Experimental

Materials. Benzenesulfenyl chloride was prepared from thiophenol and chlorine according to the method of Lecher and Holschneider.[12] Most of the aryl sulfides, for reaction and for product analyses were prepared by the condensation of the aryl diazonium salt and the corresponding thiophenols, with modification of the procedure for diphenyl sulfide.[13] α-Naphthyl phenyl sulfide was prepared from α-bromonaphthalene and thiophenol.[14] Thianthrene was obtained as a by-product of the preparation of diphenyl sulfide.[15] The purity of all sulfides was determined by glpc. The following boiling points (melting points) for the sulfides are given: tolyl phenyl sulfides, *o*-, 104°C/0.15 mmHg; *m*-, 98°/0.1; *p*-, 99°/0.09; ditolyl sulfide, *p,p*-, (56—57°); *m,p*-, 114—124°/0.2; *o,p*-, 120—124°/0.15; *o,m*-, 118—124°/0.3; *m,m*-, 124—128°/0.2; naphthyl phenyl sulfides, α-, (42—43°); β-, (52—54°); thianthrene, (155—156°). Aluminum chloride was used as it was.

Reactions of Toluene with Benzenesulfenyl Chloride in the Presence of Various Types of Catalysts. To a solution of 46.0 g (0.5 mol) of toluene and 7.2 g (0.05 mol) of benzenesulfenyl chloride was added the catalyst given in Table 1. The reaction mixture was allowed to stand at room temperature with stirring for 7 hr. After removal of excess toluene, the residual oily product was fractionated by vacuum distillation and then analyzed by glpc (10% carbowax 20M, 1 m, 220°).

General Rearrangement Procedure. Aluminum chloride (0.0005 mol) was added to 0.01 mol of each isomer of tolyl phenyl sulfide in a flask equipped with magnetic stirrer and calcium chloride tube. One microliter of water was added as promoter. The reaction mixture was kept standing at room temperature with constant agitation. Samples were withdrawn periodically; the reaction was stopped by quenching with water. The organic materials were extracted with ether. The extracts were analyzed by glpc (10% carbowax 20M, 2m 220°). When a solvent was used, the concentration was 5×10^{-1}M and molar ratio of the sulfide to the catalyst 10 : 1.

In the case of rearrangement of α-naphthyl phenyl sulfide, carbon disulfide was used to obtain homogeneous liquid. Glpc analytical conditions were 10% QF-1, 1m, 180°.

Gas-liquid Partition Chromatographic Analysis. All analyses were carried out on a Hitachi Model K-53 Fractometer using a hydrogen flame-ionization detector. The accuracy of the gas-liquid partition chromatographic analytical method, as established from the analysis of isomer mixtures of known composition, was better than ±5 relative % for all products.

11) An alternative mechanism may involve an intermediate π-complex, analogous to that proposed for the migration of *t*-butyl group (Ref. 8).

12) H. Lecher and F. Holschneider, *Ber.*, **57**, 755 (1924).

13) "Methoden der Organischen Chemie," ed. by E. Müller, IX, Georg Thieme Verlag, Stuttgart (1955), p. 117.

14) R. G. R. Bacon and H. A. O. Hill, *J. Chem. Soc.*, **1964**, 1108.

15) G. Dougherty and P. D. Hammond, *J. Amer. Chem. Soc.*, **57**, 117 (1935).

BULLETIN OF THE CHEMICAL SOCIETY OF JAPAN VOL. 43 1197—1202 (1970)

Studies of Peptide Antibiotics. XVI. Analogs of Gramicidin S Containing β-Alanine in Place of L-Proline[1]

Shuji MATSUURA, Michinori WAKI, Satoru MAKISUMI and Nobuo IZUMIYA

Laboratory of Biochemistry, Faculty of Science, Kyushu University, Hakozaki, Fukuoka

(Received October 11, 1969)

5,5′-β-Alanine-gramicidin S having a larger ring size by two methylene groups than that of gramicidin S was synthesized to investigate the contribution of the ring size of gramicidin S to antibacterial activity. Cyclization of a protected linear decapeptide active ester in pyridine gave the protected 5,5′-β-alanine-gramicidin S in a good yield. The product obtained after the cyclization of a protected linear pentapeptide active ester consisted of the protected 5-β-alanine-cyclosemi- and 5,5′-β-alanine-gramicidin S. Pure compounds were obtained by column chromatographic separation of Sephadex LH-20. Hydrogenolysis of these protected cyclic peptides in the presence of hydrogen chloride afforded crystalline hydrochlorides of cyclic deca- and pentapeptide. These hydrochlorides exhibited no antibacterial activity against any of the microorganisms tested. Optical rotatory dispersion measurements of these peptides were also carried out.

For a study of the relationship between chemical structure and biological activity of gramicidin S, various analogs have been synthesized in this laboratory. Particularly in regard to ring size, a number of synthetic cyclic peptides, dipeptide anhydrides,[2] cyclo-L-valyl-L-ornithyl-L-leucyl-D-phenylalanyl-L-prolyl-glycyl,[3] cyclo-L-valyl-L-ornithyl-L-leucyl-D-phenylalanyl-L-prolyl-glycyl-glycyl[4] and cyclo-D-phenylalanyl-D-leucyl-L-ornithyl-L-valyl D-ornithyl-L-prolyl,[5] were found to be devoid of antibacterial activity. These results seemed to show that a certain minimum ring size and/or a specific amino acid sequence are necessary for the exhibition of antibacterial activity. On the other hand, 5,5′-glycine-gramicidin S[6] possessed activity five times higher than that of natural gramicidin S. Thus it is of interest to investigate the influence of a change in the ring size of gramicidin S or 5,5′-glycine-gramicidin S molecule on biological activity. Replacement of proline or glycine residues in gramicidin S or 5,5′-glycine-gramicidin S molecule by β-alanine residues, which results in the insertion of two methylene groups into the thirty-members ring structure of gramicidin S, may cause considerable change in the conformation and biological activity. The present paper will describe the synthesis, antibacterial properties and optical rotatory dispersion data of 5,5′-β-alanine-gramicidin S and 5-β-alanine-cyclosemigramicidin S.

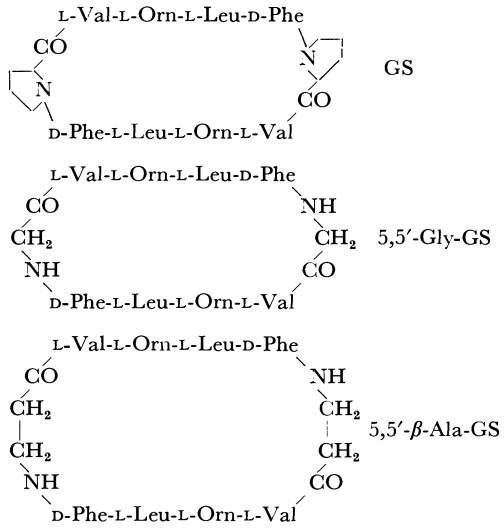

The sequence of reaction employed for the synthesis of XIII·2HCl is shown in Fig. 1. Acylpentapeptide acid (VIII) was prepared efficiently as follows. Acyltripeptide ester (IV) was prepared by stepwise elongation by means of the dicyclohexylcarbodiimide method. Saponification of IV gave acyltripeptide acid (V), which was then transformed into free tripeptide (VI). Condensation of azide (VII) with VI afforded the acylpentapeptide acid (VIII) in a good yield. Condensation of active ester (IX) derived from VIII with penta-

1) Presented at the 22nd Meeting of the Chemical Society of Japan, Tokyo, April, 1969.

2) N. Izumiya, T. Kato and Y. Fujita, This Bulletin, **37**, 1810 (1964).

3) T. Kato, M. Kondo, M. Ohno and N. Izumiya, *ibid.*, **38**, 1202 (1965).

4) O. Abe, K. Kuromizu, M. Kondo and N. Izumiya, *ibid.*, **43**, 1202 (1970).

5) T. Kato and N. Izumiya, *ibid.*, **39**, 2242 (1966).

6) H. Aoyagi, T. Kato, M. Ohno, M. Kondo and N. Izumiya, *J. Amer. Chem. Soc.*, **86**, 5700 (1964); This Bulletin, **38**, 2139 (1965).

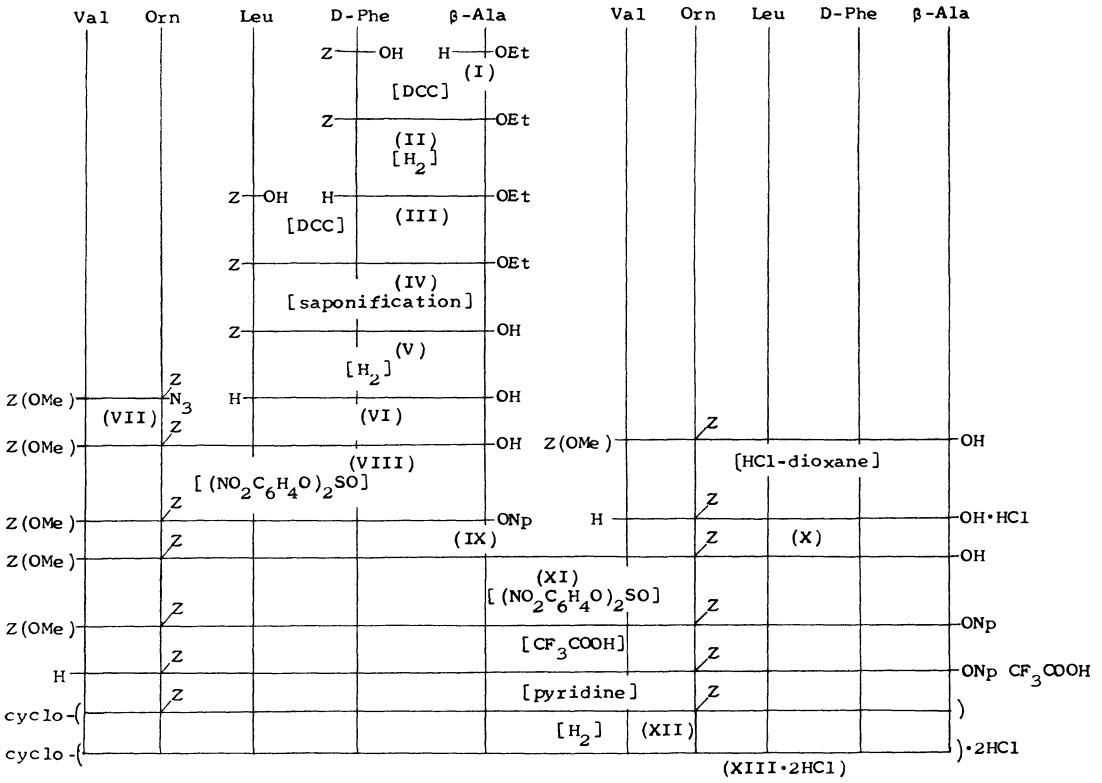

Fig. 1. Synthesis of 5,5′-β-alanine-gramicidin S.

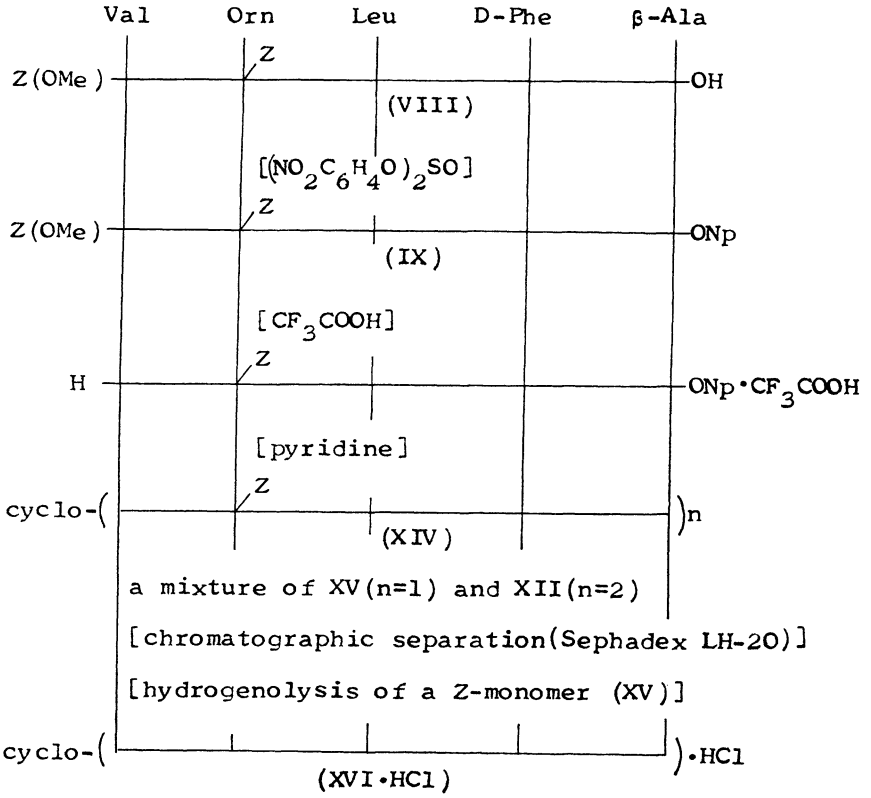

Fig. 2. Synthesis of 5-β-alanine-cyclosemigramicidin S.

peptide hydrochloride (X), which had been obtained from VIII by treatment with hydrogen chloride in dioxane, gave acyldecapeptide acid (XI). Successive treatment of XI with di-*p*-nitrophenyl sulfite, trifluoroacetic acid and excess pyridine afforded the benzyloxycarbonyl-substituted cyclic decapeptide (XII) in a good yield (42% from XI). Hydrogenation of XII in the presence of two equivalents of hydrogen chloride yielded the desired 5,5′-β-alanine-gramicidin S dihydrochloride. Synthesis of the protected cyclic decapeptide (XII) was also attempted by the possible dimerization reaction of acylpentapeptide active ester (IX) (Fig. 2). Active ester (IX) was treated successively with trifluoroacetic acid and excess pyridine. After evaporation, the reaction mixture was passed through Dowex 1 and 50 columns; the subsequent evaporation of the effluent yielded a semi solid residue. This was found to be a mixture of two components by analyzing the hydrogenated product of a small part of the residue (see, Figs. 3 and 4). The remains were subjected to a Sephadex LH-20 column to be separated into components; dimer (XII) was obtained in a yield of 3.7% and monomer (XV) obtained in 29.3%. Thus, the weight ratio of XII and XV is calculated as 11 : 89; the results indicate that the cyclization from acylpentapeptide active ester is favored for the formation of the cyclic monomer.

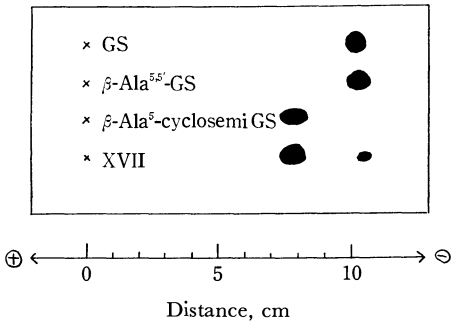

Fig. 3. Paper electrophoresis of the compounds. GS, gramicidin S; XVII; hydrogenated material after cyclization of pentapeptide ester.

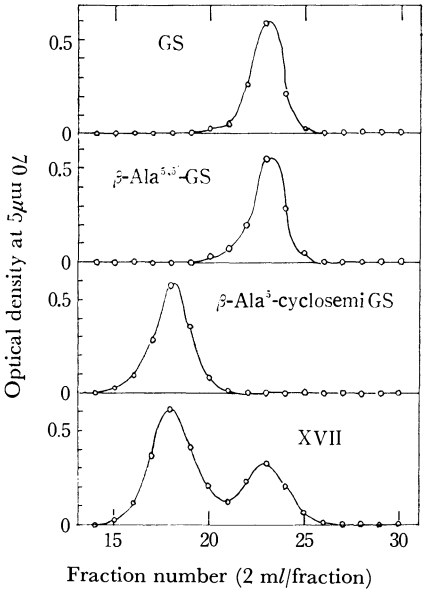

Fig. 4. Carboxymethylcellulose column chromatography of the compounds.

The antibacterial activity of gramicidin S, 5,5′-β-alanine-gramicidin S and 5-β-alanine-cyclosemi-gramicidin S toward several microorganisms was examined. Both monomer (XVI·HCl) and dimer (XIII·2HCl) showed no activity for any of the microorganisms even at 100 γ/ml of the assay medium, whereas minimum concentration of growth inhibition for *B. subtilis* was found to be 3 γ/ml with gramicidin S.

These results suggest that the replacement of proline or glycine residues in gramicidin S or 5,5′-glycine-gramicidin S molecule by β-alanine residues causes change in the conformation of the molecule. We measured the optical rotatory dispersion (ORD) of XIII·2HCl and XVI·HCl in ethanol for comparison with that of gramicidin S[7] (see Fig. 5). The result indicates that the conformation of XIII differs apparently from that of gramicidin S in ethanol. The relationship between ORD patterns and biological activity of gramicidin S analogs is now under investigation.

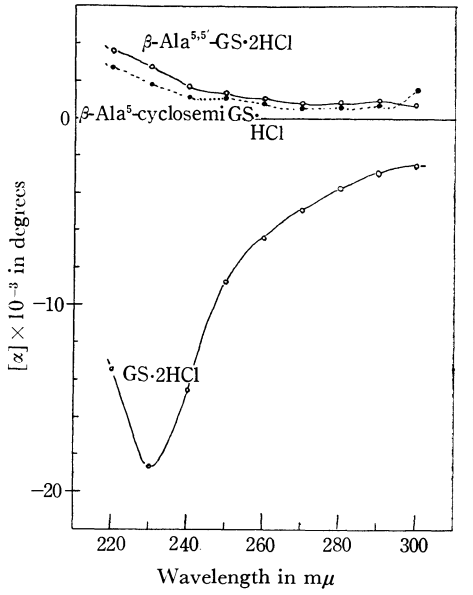

Fig. 5. Optical rotatory dispersion curves of the three compounds.

7) D. Balasubramanian, *J. Amer. Chem. Soc.*, **89**, 5445 (1967).

Experimental

All the melting points are uncorrected. Prior to analysis, the compounds were dried over phosphorus pentoxide to a constant weight at 80°C and 2 mmHg, except for the cyclic peptide hydrochlorides.

H-β-Ala-OEt·p-TsOH (I·p-TsOH).[8] This compound was prepared according to the general procedure of Kato *et al.*[9] A solution of β-alanine (4.45 g, 50 mmol) and *p*-toluenesulfonic acid monohydrate (9.51 g, 55 mmol) in a mixture of ethanol (40 m*l*) and carbon tetrachloride (200 m*l*) was refluxed azeotropically for 64 hr in an oil bath. The reaction mixture was concentrated *in vacuo*, and the residual oil was solidified by treatment with ether and petroleum ether. The hygroscopic product was collected by filtration in a cold room and dried. Recrystallization from hot acetone-ether gave 12.1 g (83.5%); mp 49—51°C; R_f 0.75.[10]

Found: C, 49.23; H, 6.61; N, 5.05%. Calcd for $C_{12}H_{19}O_5NS \cdot \frac{1}{4}H_2O$; C, 49.06; H, 6.69; N, 4.77%.

Z-D-Phe-β-Ala-OEt (II). Dicyclohexylcarbodiimide[11] (4.26 g, 20.6 mmol) was added to a solution of benzyloxycarbonyl-D-phenylalanine (6.18 g, 20.6 mmol) in anhydrous tetrahydrofuran (40 m*l*) with stirring at 0°C. After 30 min, to this mixture was added a solution of β-alanine ethyl ester *p*-toluenesulfonate (6.56 g, 22.7 mmol) and triethylamine (3.49 m*l*, 22.7 mmol) in chloroform (40 m*l*). The reaction mixture was stirred for 3 hr at 0°C and was then allowed to stand in a refrigerator overnight. The mixture was evaporated *in vacuo*, and ethyl acetate (60 m*l*) was added to the residue. The insoluble dicyclohexylurea was removed by filtration and the filtrate was washed successively with water, a 4% sodium bicarbonate solution, 2% hydrochloric acid and water. The organic layer was dried over anhydrous sodium sulfate and was then evaporated *in vacuo*. The residual oil was solidified by addition of ether and petroleum ether. The product was recrystallized from ethyl acetate-ether-petroleum ether; yield, 6.83 g (87%); mp 102—104°C; $[\alpha]_D^{20}$ +12.5° (*c* 1.04, DMF); R_f 0.98.[10]

Found: C, 66.40; H, 6.77; N, 7.35%. Calcd for $C_{22}H_{26}O_5N_2$: C, 66.31; H, 6.58; N, 7.03%.

HCl·H-D-Phe-β-Ala-OEt (III). A solution of II (3.38 g, 8.49 mmol) in methanol (30 m*l*) was subjected to hydrogenolysis in the presence of palladium black and 2.48N methanolic hydrogen chloride (4.13 m*l*) for 8 hr. The filtrate from the catalyst was evaporated to dryness *in vacuo*. The product was obtained as an oil; yield, 2.25 g (100%). R_f 0.82.[10]

Z-Leu-D-Phe-β-Ala-OEt (IV). Benzyloxycarbonyl-leucine dicyclohexylammonium salt (2.25 g, 5.04 mmol) was coupled with III (1.52 g, 5.04 mmol) by dicyclohexylcarbodiimide (1.04 g, 5.04 mmol) following the procedure employed for the preparation of II. Recrystallization from ethyl acetate-ether gave 1.32 g (81%); mp 130—132°C; $[\alpha]_D^{20}$ +15.8° (*c* 1.04, DMF); R_f 0.98.[10]

Found: C, 65.50; H, 7.47; N, 8.51%. Calcd for $C_{28}H_{37}O_6N_3$: C, 65.73; H, 7.29; N, 8.21%.

Z-Leu-D-Phe-β-Ala-OH (V). To a solution of IV (1.65 g, 3.21 mmol) in a mixture of methanol (10 m*l*) and dioxane (5 m*l*) was added 1.0N sodium hydroxide (4.05 m*l*), and the solution was allowed to stand for 4 hr at room temperature. After the addition of water (30 m*l*) and 1.0N hydrochloric acid (4.68 m*l*), the solution was concentrated *in vacuo* at a low temperature, and the residual oily product was extracted with ethyl acetate (50 m*l*). The organic layer was dried over anhydrous sodium sulfate and was then evaporated *in vacuo*. The residual foam weighed 1.7 g (100%). R_f 0.90.[10]

H-Leu-D-Phe-β-Ala-OH (VI). A solution of V (1.5 g, 3.22 mmol) in a mixture of methanol-water-acetic acid (3 : 1 : 6, v/v, 20 m*l*) was subjected to hydrogenolysis in the presence of palladium black for 6 hr. The filtrate from the catalyst was evaporated to dryness *in vacuo* and the oily residue was triturated with ether-petroleum ether. The crystals were collected by filtration in a cold room and dried *in vacuo*; yield, 1.17 g (95%); mp 189—191°C; $[\alpha]_D^{25}$ +57.7° (*c* 0.44, methanol); R_f 0.85.[10]

Found: C, 60.91; H, 7.84; N, 11.49%. Calcd for $C_{18}H_{27}O_4N_3 \cdot 1/3H_2O$: C, 60.82; H, 7.84; N, 11.82%.

Z(OMe)-Val-Orn(δ-Z)-Leu-D-Phe-β-Ala-OH (VIII). To a chilled solution of Z(OMe)-Val-Orn(δ-Z)-$NHNH_2$ (VII)[12] (1.68 g, 3.21 mmol) in glacial acetic acid (40 m*l*) were added successively with stirring 1.0N hydrochloric acid (6.42 m*l*) and sodium nitrite (265.8 mg) in 9 m*l* of water. After 6 min, cold water (520 m*l*) was added to the solution. The azide which precipitated as a white mass was collected by filtration and washed with cold water (200 m*l*), a 9% sodium bicarbonate solution (200 m*l*) and cold water (200 m*l*), and then dried in a vacuum in a desiccator. The azide was added to a solution of VI (1.35 g, 3.12 mmol) and triethylamine (0.87 m*l*) in dimethylformamide (25 m*l*), and the reaction mixture was stirred for 3 days at 0°C. The precipitate formed by the addition of 10% citric acid (15 m*l*) was collected, washed with 10% citric acid and water and then dried. Recrystallization from methanol-ether-petroleum ether gave 2.32 g (86%); mp 181—183°C; $[\alpha]_D^{20}$ +11.6° (*c* 0.53, DMF); R_f 0.87.[10]

Found: C, 62.52; H, 7.20; N, 9.68%. Calcd for $C_{45}H_{60}O_{11}N_6$: C, 62.77; H, 7.02; N, 9.76%.

Z(OMe)-Val-Orn(δ-Z)-Leu-D-Phe-β-Ala-ONp (IX). To a solution of VIII (600 mg, 0.69 mmol) in pyridine (10 m*l*) was added di-*p*-nitrophenyl sulfite[13] (2.25 g, 6.96 mmol), and the reaction mixture was allowed to

8) The following abbreviations are from *Biochemistry*, **5**, 2485 (1966); Z-, benzyloxycarbonyl; Z(OMe)-, *p*-methoxybenzyloxycarbonyl; -ONp, *p*-nitrophenoxy; DCHA, dicyclohexylammonium salt; DCC, dicyclohexylcarbodiimide; DMF, dimethylformamide. Amino acid symbols except D-Phe and β-Ala denote the L-configuration.

9) T. Kato, S. Makisumi, M. Ohno and N. Izumiya, *Nippon Kagaku Zasshi*, **83**, 1151 (1962).

10) The R_f value of thin-layer chromatography with Merck silica gel refers to a solvent system of *n*-butanol-acetic acid-pyridine-water (4 : 1 : 1 : 2, v/v). Spots of materials possessing a free amino group on a thin-layer plate were detected by spraying ninhydrin, and those of the amino group-blocked materials, by spraying 47% hydrobromic acid and then ninhydrin.

11) J. C. Sheehan and G. P. Hess, *J. Amer. Chem. Soc.*, **77**, 1067 (1955).

12) T. Kato, M. Kondo, M. Ohno and N. Izumiya, This Bulletin, **38**, 1202 (1965).

13) B. Iselin and R. Schwyzer, *Helv. Chim. Acta*, **43**, 1760 (1960).

stand for 24 hr at room temperature. After evaporation of the mixture to dryness, the oily product was triturated with petroleum ether and washed repeatedly with a mixture of ether-petroleum ether (1 : 1) by decantation until no yellow color could be discerned upon the addition of a sodium hydroxide solution to the washings. The resulting product was collected by filtration, washed with a mixture of ether-petroleum ether (1 : 1) and dried. The yield was 694 mg (108%); the *p*-nitrophenyl ester content in the product was estimated to be 95% spectrophotometrically by measuring the optical density of the solution of the compound in dimethylformamide - N sodium hydroxide (1 : 1) at 404 mμ.[14]

HCl·H-Val-Orn(δ-Z)-Leu-D-Phe-β-Ala-OH (X). To a solution of VIII (700 mg, 0.814 mmol) in dioxane (6 ml) were added anisole (0.6 ml) and 2.0N hydrogen chloride in dioxane (16.28 ml). The reaction mixture was allowed to stand for 7.5 hr at room temperature. After removal of the solvent *in vacuo*, the residue was triturated with ether. The product solidified was collected by filtration, washed with ether and dried in a vacuum in a desiccator; yield, 580 mg (97%); mp 144—146°C; $[\alpha]_D^{25}$ +22.4° (*c* 0.5, DMF); R_f 0.80.[10]

Found: C, 56.45; H, 7.50; N, 11.00%. Calcd for $C_{36}H_{53}O_8N_6Cl \cdot 2H_2O$: C, 56.20; H, 7.46; N, 10.93%.

Z(OMe)-Val-Orn(δ-Z)-Leu-D-Phe-β-Ala-Val-Orn-(δ-Z)-Leu-D-Phe-β-Ala-OH (XI). To a solution of X (273 mg, 0.37 mmol) and triethylamine (0.05 ml) in a mixture of pyridine (5 ml) and dimethylformamide (5 ml) was added IX (367 mg, 0.37 mmol), and the reaction mixture was stirred for 8 days at room temperature. The precipitate formed by the addition of 10% citric acid (30 ml) was collected, washed with 10% citric acid and water and then dried. Recrystallization from dimethylformamide-ether gave 464 mg (81%); mp 237—240°C; $[\alpha]_D^{20}$ +9.2° (*c* 0.5, DMF); R_f 0.99.[10]

Found: C, 62.53; H, 7.22; N, 10.41%. Calcd for $C_{81}H_{110}O_{27}N_{12} \cdot H_2O$: C, 62.45; H, 7.24; N, 10.79%.

***cyclo*-(Val-Orn(δ-Z)-Leu-D-Phe-β-Ala-)$_2$ (XII).** *From XI.* To a solution of XI (358 mg, 0.23 mmol) in pyridine (8 ml), di-*p*-nitrophenyl sulfite (3.01 g, 9.30 mmol) was added. After the mixture had been allowed to stand for 5 days at room temperature, it was evaporated *in vacuo*. The residual solid was collected by filtration with the aid of a mixture of ether and petroleum ether (1 : 1); yield, 476 mg. The *p*-nitrophenyl ester content for this product was estimated to be 100% by measuring the optical density of the compound at 404 mμ. To the active ester thus obtained, anisole (0.3 ml) and trifluoroacetic acid (4.5 ml) were added at 0°C. The solution was evaporated *in vacuo*, and the residual powder was collected by filtration with the aid of ether. This decapeptide *p*-nitrophenyl ester trifluoroacetate was dissolved in dimethylformamide (8 ml) and acetic acid (0.1 ml). The solution was added drop by drop over a period of 6 hr to pyridine (100 ml) which had been kept at 60°C; stirring was then continued for an additional 2 hr at the same temperature. After removal of the solvent by evaporation *in vacuo*, the residue was dissolved in a mixture of methanol (50 ml), dioxane (20 ml) and water (15 ml). The insoluble substance was removed by filtration, and the filtrate was successively passed through columns (1.8×15 cm, each) of Dowex 1 (OH^- form) and Dowex 50 (H^+ form). The columns were washed with the same solvent (400 ml), and the combined effluent was evaporated *in vacuo* to yield a crystalline product. The product was collected by filtration with the aid of water, and recrystallized from methanol-ether-petroleum ether; yield, 132 mg (42% from XI); mp 231—234°C (decomp); $[\alpha]_D^{25}$ −5.3° (*c* 0.6, acetic acid).

Found: C, 62.43; H, 7.44; N, 12.07%; mol wt, 1407.[15] Calcd for $C_{72}H_{100}O_{14}N_{12} \cdot 2H_2O$: C, 62.04; H, 7.53; N, 12.06%; mol wt, 1394.

From VIII. The acylpentapeptide VIII (1.82 g, 2.1 mmol) was converted to the pentapeptide *p*-nitrophenyl ester trifluoroacetate following the same procedure as described above, and then added to pyridine (300 ml). After the filtrate was passed through columns of Dowex 1 and Dowex 50 in the same way as described above, the effluent was evaporated to dryness, and the residual powder was collected by filtration with the aid of water; yield of the crude product (XIV), 482 mg. The solution of XIV (107 mg) in methanol (2 ml) was applied to a column (2.7×110 cm) of Sephadex LH-20, and development was continued with methanol. Elution was carried out at room temperature, and 3 ml fraction were collected under a flow rate 30 ml per hr. When the peptide content in the fractions was determined on a thin-layer plate, the peak of XII appeared from the test tube numbers 41 to 80 and the peak of XV from 90 to 130. The same chromatography was repeated further three times; thus, 430 mg of XIV was separated into two components. The four groups of the fractions of 41—80 were combined, evaporated *in vacuo* and the crystals (44 mg, 3.7% from VIII) of XII were obtained; yield after recrystallization, 40 mg; mp 230—233°C (decomp); $[\alpha]_D^{25}$ −5.0° (*c* 0.58, acetic acid).

***cylco*-(Val-Orn(δ-Z)-Leu-D-Phe-β-Ala-) (XV).** The four groups of the fractions of 90—130 obtained above were combined and evaporated *in vacuo* to afford the crystals (363 mg, 29.3% from VIII). It was recrystallized from methanol-ether-petroleum ether, yield, 358 mg; mp 213—215°C (decomp); $[\alpha]_D^{25}$ −12.5° (*c* 0.68, acetic acid).

Found: C, 61.00; H, 7.52; N, 11.34%; mol wt, 636.[15] Calcd for $C_{36}H_{50}O_7N_6 \cdot 3/2H_2O$: C, 61.16; H, 7.56; N, 11.80%; mol wt, 678.

5,5′-β-Alanine-gramicidin S, *cyclo*-(Val-Orn-Leu-D-Phe-β-Ala-)$_2$ (XIII). A solution of XII (51.6 mg, 0.038 mmol) in ethanol (6 ml) and 0.25N methanolic hydrogen chloride (0.37 ml), was subjected to hydrogenolysis in the presence of palladium black for 6 hr. The solution, after being filtered from the catalyst, was evaporated *in vacuo*. The residual product was recrystallized from methanol-ether-petroleum ether; yield of the air-dried product, 38 mg (86%); mp 280—282°C (decomp); $[\alpha]_D^{25}$ +43.2° (*c* 0.32, ethanol); R_f 0.77.[10]

Found: C, 52.46; H, 7.77; N, 12.66%. Calcd for $C_{56}H_{88}O_{10}N_{12} \cdot 2HCl \cdot 7H_2O$: C, 52.19; H, 8.12; N, 13.04%.

β-Alanine-cyclosemigramicidin S, *cylco*-(Val-Orn-Leu-D-Phe-β-Ala-) (XVI). XV (50.4 mg, 0.074 mmol) was treated as described for the preparation of XIII·2HCl; yield, 41 mg (95%); mp 250—252°C (dec.); $[\alpha]_D^{25}$ −13.4° (*c* 0.55, ethanol); R_f 0.70.[10]

Found: C, 51.61; H, 7.89; N, 12.60%. Calcd for

14) R. Schwyzer and P. Sieber, *ibid.*, **40**, 624 (1957).

15) Molecular weight was determined by a Hitachi Osmometer, type 115 (Solvent, methanol).

Table 1. Inhibitory activity of three compounds on microorganisms
Minimum inhibitory concentration, μg/ml

	Staphylococcus aureus 209P	*Bacillus subtilis ATCC 6633*	*Escherichia coli IAM 1253*	*Candida albicans IAM 4888*	*Proteus vulgaris IAM 1025*	*Shigella sonnei*	*Salmonella Paratyphi A*
Natural GS	6	3	50	13	100	50	100
5,5′-β-Alanine-GS	100	100	>100	>100	>100	>100	>100
5-β-Alanine-cyclosemi GS	>100	>100	>100	>100	>100	>100	>100

$C_{28}H_{44}O_5N_6 \cdot HCl \cdot 4H_2O$: C, 51.48; H, 8.17; N, 12.86%.

Electrophoresis and Carboxymethylcellulose (CMC) Chromatography. These experiments were carried out as previously described.[16] A part of the crude product (XIV), which was obtained after the cyclization reaction of the acylpentapeptide *p*-nitrophenyl ester (IX), was hydrogenated, and the product obtained was designated as XVII. As shown in Figs. 3 and 4, 5,5′-β-alanine-gramicidin S and 5-β-alanine-cyclosemigramicidin S were clearly separated in paper electrophoresis and in CMC chromatography.

Optical Rotatory Dispersion (ORD).[7,17] ORD measurements were performed with a Jasco Model ORD/UV5 spectropolarimeter. Cell of path length 1.0 cm was used and the runs were made at ambient temperature. As shown in Fig. 5, the ORD curve of gramicidin S is similar to that obtained by Balasubramanian,[7] and a trough is encountered at 230 mμ with a trough specific rotation of $-18560°$. 5,5′-β-Alanine-gramicidin S and 5-β-alanine-cyclosemigramicidin S showed the monotonic change toward positive at 230 mμ.

Microbiological Assays.[18] The microorganisms employed are listed in Table 1. Minimum amount of the compound necessary for the complete inhibition of growth was determined by the dilution method. As shown in Table 1, 5,5′-β-alanine-gramicidin S and 5-β-alanine-cyclosemigramicidin S were found to exhibit no antibacterial activity against the microorganisms tested, whereas gramicidin S exhibited activity against *Bacillus subtilis* and *Staphylococcus aureus*.

16) M. Waki and N. Izumiya, This Bulletin, **40**, 1687 (1967); *J. Amer. Chem. Soc.*, **89**, 1278 (1967).

17) We are indebted to Dr. K. Hayashi and Mr. T. Shimoda of Department of Biochemistry, Faculty of Agricalture, Kyushu University, for the ORD measurement.

18) We are indebted to Meiji Seika Co., Ltd., for the microbiological assays.

BULLETIN OF THE CHEMICAL SOCIETY OF JAPAN VOL. 43 1202—1207 (1970)

Studies of Peptide Antibiotics. XVII. Analogs of Gramicidin S Containing Glycine or Alanine in Place of Leucine

Okitoshi ABE[1] and Nobuo IZUMIYA[2]

Laboratory of Biochemistry, Faculty of Science, Kyushu University, Hakozaki, Fukuoka

(Received October 11, 1969)

In order to investigate the contribution to antibacterial activity of the leucine residues at 3- and 3′-position in gramicidin S, 3,3′-glycine- and 3,3′-L-alanine-gramicidin S (XII-G and XII-A) were prepared and tested for antibacterial properties. A crude product obtained after cyclization of a linear pentapeptide active ester consisted of a protected monomer and a dimer. The pure protected dimer was obtained by a Sephadex LH-20 column from the crude product. Hydrogenolysis of the pure protected dimer afforded the crystalline hydrochloride of XII-G or XII-A. It was found that XII-G showed no activity in any of the microorganisms tested, whereas XII-A exhibited substantial activity though weaker than that of gramicidin S.

Regarding the relationship between the chemical structure and the biological activity of gramicidin S (GS) (Fig. 1), it was reported in previous papers that 5,5′-glycine-GS[3] possessed higher activity than GS against several microorganisms, whereas 1,1′-

1) Present address: Institute for Muscle Disease, New York, N. Y., U.S.A.

2) To whom reprint requests should be addressed.

3) H. Aoyagi, T. Kato, M. Ohno, M. Kondo and N. Izumiya, *J. Amer. Chem. Soc.*, **86**, 5700 (1964); This Bulletin, **38**, 2139 (1965).

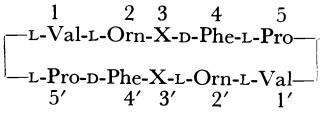

Fig. 1. Structure of gramicidin S (GS) and its analogs. X represents an amino acid residue such as L-Leu (GS), Gly (XII-G) or L-Ala (XII-A).

glycine-GS[4] and 4,4′-glycine-GS[5] exhibited no activity. Contrary to the inactivity of 1,1′-glycine-GS, it was found that 1,1′-L-alanine-GS was as active as GS.[4] These results indicate that the side chains, the isopropyls, of the valine residues in GS molecule can be replaced by smaller aliphatic side chains, the methyls, without influencing the activity, while glycine residues are too small to maintain it. In order to investigate to what extent the leucine residues in 3- and 3′-position of GS molecule contribute to the biological activity, we attempted to prepare several analogs of GS.

This paper deals with the syntheses and antibacterial properties of 3,3′-glycine- and 3,3′-L-alanine-GS besides the preparation of the cyclic pentapeptides, 3-glycine- and 3-L-alanine-cyclo-semiGS.

As shown in Fig. 2,[6] the acylpentapeptide ethyl ester (III-G or -A) was prepared by the coupling reaction of acyldipeptide azide derived from XIII with the tripeptide ester (II-G or -A). However, the ester (III-G or -A) showed considerable resistance to saponification. Hence, in the preparation of the acylpentapeptide acid (VI-G or -A), the azide from XIII was coupled with neutral free tripeptide (V-G or -A), as shown in Fig. 3.

Synthesis of the protected cyclic decapeptide (X-G or -A) was attempted by possible dimerization reaction of the pentapeptide active ester (VIII-G or -A) which was derived from the acylpentapeptide acid (VI-G or -A) (Fig. 3). Treatment of the active ester with a large amount of pyridine afforded a mixture of the protected monomer (IX-G or -A) and dimer (X-G or -A). Attempts to separate two components from the crude mixture by fractional recrystallization with methanol-ether failed because of no appreciable difference in solubility between the components. Separation of the components was achieved by the use of a Sephadex LH-20 column with methanol as an eluting solvent. The protected dimer was obtained from the faster eluting fraction, and the monomer from the slower fraction as shown in Fig. 4.

The weight of both components calculated are shown in Table 1 with the previous results. It is of interest to note that the ratio of formation of the protected monomer increased stepwise as 32→43→59 when the leucine residue in the active ester is replaced with alanine and glycine. The results indicate that a spacial conformation of a pentapep-

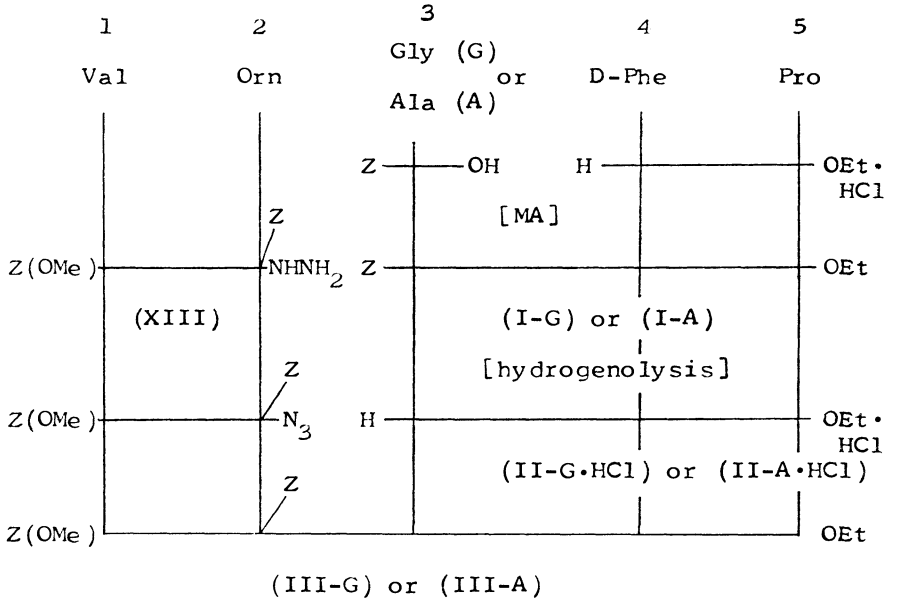

Fig. 2. Synthesis of acylpentapeptide ethyl ester.

4) M. Kondo and N. Izumiya, This Bulletin, **40**, 1975 (1967).

5) R. Nagata, M. Waki, M. Kondo, H. Aoyagi, T. Kato, S. Makisumi and N. Izumiya, *ibid.*, **40**, 963 (1967).

6) The following abbreviations are used; Z-, benzyloxycarbonyl; Z(OMe)-, *p*-methoxybenzyloxycarbonyl; -ONp, *p*-nitrophenoxy; -$NHNH_2$, hydrazide; -N_3, azide; MA, mixed anhydride method; DMF, dimethylformamide. Amino acid symbols except for D-Phe denote L-configuration.

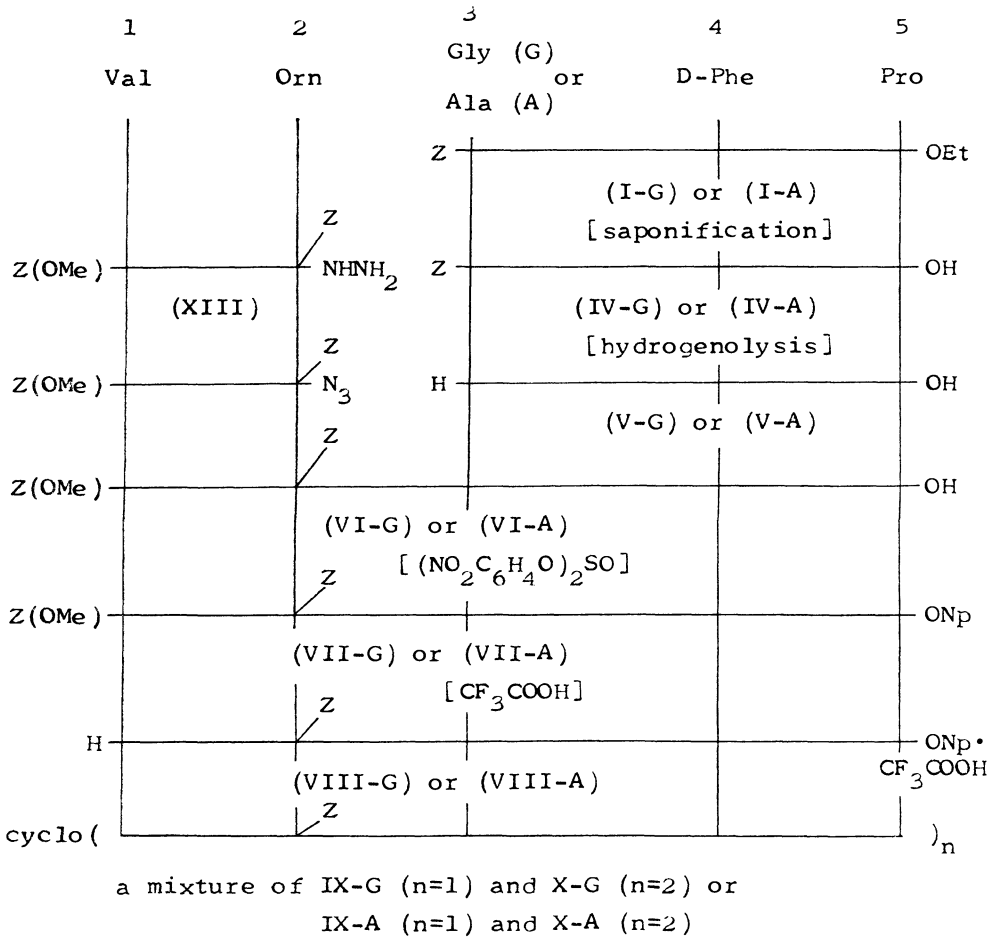

Fig. 3. Cyclization of linear pentapeptide active ester.

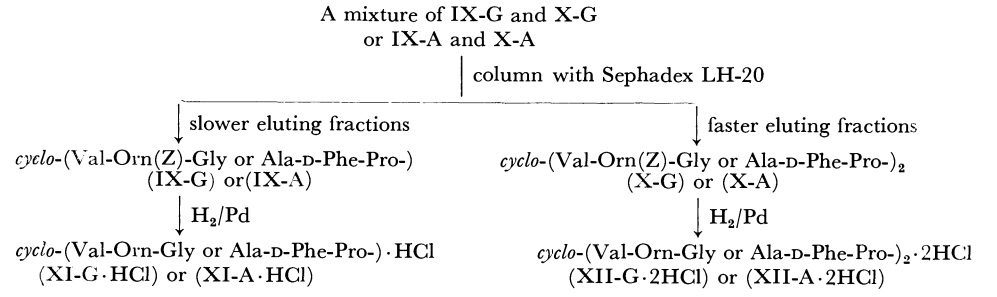

Fig. 4. Separation of the protected monomer and dimer, and preparation of the analogs of GS and cyclosemiGS.

tide active ester in pyridine is favorable for causing a monomerization reaction preferably when a small amino acid, glycine, occupies the third position in the pentapeptide active ester.

Hydrogenolysis of each of the protected cyclic peptides (IX and X) in the presence of hydrogen chloride yielded a crystalline hydrochloride of the required cyclic peptide (XI or XII). The antibacterial activities of these peptides toward several microorganisms were examined (Table 2). The two cyclosemiGS analogs (XI-G and -A) exhibited no activity as in the case of cyclosemiGS itself.[7] It was also found that 3,3′-glycine-GS (XII-G)

7) M. Waki and N. Izumiya, *J. Amer. Chem. Soc.*, **89**, 1278 (1967); This Bulletin, **40**, 1687 (1967).

Table 1. Ratio of protected monomer and dimer after cyclization of linear pentapeptide active esters

p-Nitrophenyl ester of[a]	Ratio of compounds in product[b]	
	Z-cyclic monomer	diZ-cyclic dimer
H-Val-Orn(δ-Z)-Leu-D-Phe-Pro-OH[7]	32	68
-Gly-[4]	100	0
-Ala-[4]	91	9
-Gly-	59	41
-Ala-	43	57
-Gly-[5]	0	100
-Gly-[3]	79	21

a) After H-Val-Orn(δ-Z)-Leu-D-Phe-Pro-OH listed, only variation of the residue is shown.
b) The concentrations of linear pentapeptide *p*-nitrophenyl esters in pyridine were of approximately 3×10^{-3}M.

exhibited no activity, whereas the alanine analog (XII-A) exhibited substantial activity toward two kinds of microorganisms though the degree of activity was weaker than that of GS (Table 2). These results indicate that the glycine residues which occupy the leucines are too small to maintain activity, while the alanines can replace the leucines without appreciable drop in activity.

Experimental

All melting points are uncorrected.

Z-Gly-D-Phe-Pro-OEt (I-G). To a solution of benzyloxycarbonyl-glycine (0.596 g, 2.85 mmol) and triethylamine (0.40 m*l*, 2.85 mmol) in tetrahydrofuran (5.8 m*l*), isobutyl chloroformate (0.37 m*l*, 2.85 mmol) was added at −5°C. After 15 min, a mixture of H-D-Phe-Pro-OEt·HCl[8] (0.932 g, 2.85 mmol) and triethylamine (0.40 m*l*, 2.85 mmol) in chloroform (5.8 m*l*) was added. The mixture was left to stand overnight at room temperature and then evaporated *in vacuo*. The oily residue was dissolved in ethyl acetate. The solution was washed successively with 4% sodium bicarbonate, 2% hydrochloric acid and water, and dried over sodium sulfate. The filtrate was evaporated *in vacuo*; yield of oil, 1.01 g (74%); R_f, 0.97.[9]

Z-Ala-D-Phe-Pro-OEt (I-A). This was obtained from benzyloxycarbonyl-alanine (3.21 g, 14.4 mmol) and H-D-Phe-Pro-OEt·HCl (4.70 g, 14.4 mmol) as described above; yield of oil, 6.48 g (91%); R_f, 0.97.[9]

H-Gly-D-Phe-Pro-OEt·HCl (II-G·HCl). A solution of I-G (2.54 g, 7.34 mmol) dissolved in 0.52N ethanolic hydrogen chloride (15.5 m*l*) was subjected to hydrogenolysis in the presence of palladium black. The filtrate from the catalyst was evaporated to dryness *in vacuo*; yield of oil, 1.82 g (100%); R_f, 0.73.[9]

Table 2. Inhibitory activity of the compounds on microorganisms

Minimum inhibitory concentration, μg/m*l*

	A. Synthetic medium[a]				
	Escherichia coli	*Proteus vulgaris*	*Staphylococcus aureus*	*Bacillus subtilis*	*Mycobacterium avium*
GS	>100	>100	10	10	>100
$Gly^{3,3'}$-GS (XII-G)	>100	>100	>100	>100	>100
$Ala^{3,3'}$-GS (XII-A)	>100	>100	100	20	>100
Gly^{3}-semiGS (XI-G)	>100	>100	>100	>100	>100
Ala^{3}-semiGS (XI-A)	>100	>100	>100	>100	>100
	B. Bouillon agar medium[b]				
	Escherichia coli	*Proteus vulgaris*	*Staphylococcus aureus*	*Bacillus subtilis*	*Mycobacterium avium*
GS	>100	>100	5	2—5	>100
$Gly^{3,3'}$-GS (XII-G)	>100	>100	>100	>100	>100
$Ala^{3,3'}$-GS (XII-A)	>100	>100	50	20	>100
Gly^{3}-semiGS (XI-G)	>100	>100	>100	>100	>100
Ala^{3}-semiGS (XI-A)	>100	>100	>100	>100	>100

a) Staphenson-Whetham's medium (modified), pH 7.0.
b) Usual bouillon agar medium, pH 7.0.

8) M. Ohno, T. Kato, S. Makisumi and N. Izumiya, This Bulletin, **39**, 1738 (1966).

9) The R_f values refer to the thin-layer chromatography with Merck silica gel G and to the *n*-butanol - acetic acid - pyridine - water (4 : 1 : 1 : 2, v/v) system. Compounds possessing a free amino group were detected by spraying them with ninhydrin, and those with blocked amino groups, by spraying them with 48% hydrobromic acid, and then with ninhydrin.

H-Ala-D-Phe-Pro-OEt·HCl (II-A·HCl). This was obtained from I-A (6.36 g, 12.8 mmol) as described above; yield of oil, 5.22 g (103%); R_f, 0.74.[9]

Z(OMe)-Val-Orn(δ-Z)-Gly-D-Phe-Pro-OEt (III-G). To a solution of Z(OMe)-Val-Orn(δ-Z)-$NHNH_2$ (XIII)[10] (1.71 g, 3.15 mmol) dissolved in a mixture of acetic acid (50 ml), DMF (10 ml) and 1.92N hydrochloric acid (4.1 ml) was added sodium nitrite (261 mg). After 15 min, cold water (300 ml) was added to the solution. The azide which precipitated was collected by filtration, washed with 4% sodium bicarbonate and water, and then dried *in vacuo*. The azide was added to a solution of II-A·HCl (0.781 g, 3.15 mmol) and triethylamine (0.44 ml) in DMF (25 ml). The mixture was stirred for 2 days at 0°C and evaporated *in vacuo*. The precipitate which formed upon the addition of water was collected, washed successively with 4% sodium bicarbonate, 10% citric acid and water. It was recrystallized from dioxane-methanol-ether; yield, 1.92 g (70%); mp 151—154°C; $[\alpha]_D^{20}$ −18.0° (*c* 1, DMF); R_f, 0.95.[9]

Found: C, 62.65; H, 6.80; N, 9.80%. Calcd for $C_{45}H_{58}O_{11}N_6$: C, 62.91; H, 6.82; N, 9.78% .

Z(OMe)-Val-Orn(δ-Z)-Ala-D-Phe-Pro-OEt (III-A). The azide derived from XIII (2.18 g, 4.0 mmol) was condensed with II-A·HCl (1.59 g, 4.0 mmol) and triethylamine (0.56 ml) as described above. The crude product was recrystallized from ethanol-dioxane-ether; yield, 3.16 g (91%); mp 165—170°C; $[\alpha]_D^{20}$ −14.0° (*c* 1, DMF); R_f, 0.95.[9]

Found: C, 63.51; H, 6.70; N, 9.86%. Calcd for $C_{46}H_{60}O_{11}N_6$: C, 63.27; H, 6.94; N, 9.63%.

Z-Gly-D-Phe-Pro-OH (IV-G). To a solution of I-G (1.88 g, 3.9 mmol) in a mixture of dioxane (8 ml) and methanol (8 ml), N sodium hydroxide (8.15 ml) was added; the solution was then allowed to stand for 1.5 hr at room temperature. After the addition of water, the solution was evaporated *in vacuo*. The residue was acidified with N hydrochloric acid and extracted with ethyl acetate. The extract was dried over sodium sulfate and evaporated *in vacuo*. The residual oil was solidified by the addition of ether; yield of powder, 1.23 g (69%); R_f, 0.79.[9]

Z-Ala-D-Phe-Pro-OH (IV-A). This was obtained from I-A (1.94 g, 3.9 mmol) as described for the preparation of IV-G; yield of powder, 1.31 g (72%); R_f, 0.84.[9]

H-Gly-D-Phe-Pro-OH (V-G). A solution of IV-G (0.722 g, 1.6 mmol) in a mixture of acetic acid (10.8 ml), methanol (5.4 ml) and water (1.8 ml) was treated with hydrogen in the presence of palladium black. The filtrate from the catalyst was evaporated *in vacuo* to dryness. The hygroscopic crystals were collected with the aid of ether; yield, 0.52 g (102%); R_f, 0.46.[9]

H-Ala-D-Phe-Pro-OH (V-A). This was obtained from IV-A (1.31 g, 2.8 mmol) as described for the preparation of V-G; yield, 0.71 g (76%); $[\alpha]_D^{20}$ −36.0° (*c* 1, DMF); R_f, 0.46.[9]

Z(OMe)-Val-Orn(δ-Z)-Gly-D-Phe-Pro-OH (VI-G). The azide derived from XIII (1.31 g, 2.4 mmol) was added to a solution of V-G (0.765 g, 2.4 mmol) and triethylamine (0.34 ml) in DMF (25 ml). The mixture was stirred for 2 days at 0°C and evaporated *in vacuo*. The residue was triturated with 0.5M citric acid, and the precipitate was collected by filtration and washed with water. It was recrystallized from dioxane-ethanol-ether; yield, 1.54 g (77%); mp 110—112°C; $[\alpha]_D^{20}$ −30.0° (*c* 1, DMF); R_f, 0.83.[9]

Found: C, 61.05; H, 6.80; N, 10.19%. Calcd for $C_{43}H_{54}O_{11}N_6 \cdot H_2O$: C, 60.83; H, 6.60; N, 9.90%.

Z(OMe)-Val-Orn(δ-Z)-Ala-D-Phe-Pro-OH (VI-A). The azide derived from XIII (0.936 g, 1.72 mmol) was condensed with V-A (0.570 g, 1.72 mmol) and triethylamine (0.24 ml) as described for the preparation of VI-G. The crude product was recrystallized from dioxane-methanol-ether; yield, 1.22 g (84%); mp 150—153°C; $[\alpha]_D^{20}$ −20.0° (*c* 1, DMF); R_f, 0.77.[9]

Found: C, 61.35; H, 6.69; N, 9.76%. Calcd for $C_{44}H_{56}O_{11}N_6$: C, 61.23; H, 6.79; N, 9.74%.

Z(OMe)-Val-Orn(δ-Z)-Gly-D-Phe-Pro-ONp (VII-G). To a solution of VI-G (1.08 g, 1.3 mmol) in pyridine (25 ml), di-*p*-nitrophenyl sulfite (4.21 g, 1.3 mmol) was added. After the mixture had been allowed to stand overnight at room temperature, it was evaporated *in vacuo*. The residual solid was collected with the aid of a mixture of ether and petroleum ether; yield, 1.50 g. The *p*-nitrophenyl ester content was estimated to be 91% by measuring the optical density at 412 mμ.

Z(OMe)-Val-Orn(δ-Z)-Ala-D-Phe-Pro-ONp (VII-A). The compound VI-A (0.423 g, 0.5 mmol) was converted to VII-A (0.663 g) as described above in which *p*-nitrophenyl ester content was estimated to be 107%.

Mixture of *cyclo*-(Val-Orn(δ-Z)-Gly-D-Phe-Pro-) (IX-G) and *cyclo*-(Val-Orn(δ-Z)-D-Phe-Pro-)$_2$ (X-G). The compound VII-G (1.49 g) was treated with anisole (1 ml) and trifluoroacetic acid (6 ml) at 0°C. After 40 min, the solution was evaporated, and the solid was collected with the aid of a mixture of ether and petroleum ether. The compound VIII-G·CF_3COOH thus obtained was dissolved in DMF (13 ml) and acetic acid (0.5 ml). The solution was added dropwise into pyridine (650 ml) at 55—60°C during 5 hr and the stirring was continued for additional 2 hr. The solution was evaporated, and the residue was dissolved in a mixture of methanol (150 ml) and water (30 ml). The solution was treated with column (1.8×15 cm) of Dowex 1 (OH^- form) and Dowex 50 (H^+ form). The columns were washed with the same solvent (450 ml), and the combined effluent was evaporated to dryness. The residual product was collected by filtration with the aid of water; yield, 0.51 g.[11] A part (0.1 g) of the product was dissolved in methanol (1.5 ml) and applied to a column (2.5×35 cm) with Sephadex LH-20, and the development continued with methanol. Elution was carried out at room temperature, at a flow rate of 30 ml per hour; a 2 ml fraction was collected. The peptide content in the fractions was determined as described previously.[7] The first peak appeared from tube number 31 to 51, and the second, from 56 to 70. The fractions 52 to 55 contained both components. The fractions were treated as follows.

***cyclo*-(Val-Orn(δ-Z)-Gly-D-Phe-Pro-) (IX-G).** The fractions 56—70 were combined and evaporated *in*

10) T. Kato, M. Kondo, M. Ohno and N. Izumiya, This Bulletin, **38**, 1202 (1965).

11) A few mg of this crude product was dissolved in methanol and subjected to hydrogenolysis. The paper electrophoresis of the hydrogenated material showed two spots.

vacuo, and the product was collected by filtration with the aid of water (yield, 39 mg). It was recrystallized from ethanol-ether; yield, 34 mg (20% from VI-G); mp 117—120°C; $[\alpha]_D^{20}$ −82.8° (*c* 0.5, MeOH); R_f, 0.98.[9]

Found: C, 62.03; H, 6.85; N, 12.90%; mol wt, 640.[12] Calcd for $C_{34}H_{44}O_7N_6 \cdot H_2O$: C, 62.07; H, 6.91; N, 12.78%; mol wt, 667.

***cyclo*-(Val-Orn(δ-Z)-Gly-D-Phe-Pro-)$_2$ (X-G).** The fractions 31—51 were treated as described above (yield, 27 mg). Recrystallization from ethanol-ether gave 25 mg (15% from VI-A); mp 208—210°C; $[\alpha]_D^{20}$ −232° (*c* 0.5, MeOH); R_f, 0.98.[9]

Found: C, 62.80; H, 6.83; N, 12.73%; mol wt, 1260. Calcd for $C_{68}H_{88}O_{14}N_{12}$: C, 62.93; H, 6.85; N, 12.96%; mol wt, 1298.

Mixture of *cyclo*-(Val-Orn(δ-Z)-Ala-D-Phe-Pro-) (IX-A) and *cyclo*-(Val-Orn(δ-Z)-Ala-D-Phe-Pro-)$_2$ (X-A). The compound VIII-A·CF_3COOH obtained from VII-A (0.662 g) was added to pyridine (250 ml) as described for the preparation of a mixture of IX-G and X-G. Yield of the crude product was 149 mg. A part (0.1 g) of the product was dissolved in methanol (2 ml) and applied to a column (2.5×35 cm) with Sephadex LH-20 as described. The first peak appeared from tube number 32 to 48, and the second 54 to 81. The fractions from 49 to 53 contained both components.

***cyclo*-(Val-Orn(δ-Z)-Ala-D-Phe-Pro-) (IX-A).** The fractions 54 to 81 were treated as described for the preparation of IX-G (yield, 26 mg). It was recrystallized from ethanol-ether; yield, 23 mg (10% from VI-B); mp 138—140°C; R_f, 0.98.[9]

Found: C, 61.62; H, 6.95; N, 12.30%; mol wt, 730.[12] Calcd for $C_{35}H_{46}O_7N_6 \cdot H_2O$: C, 61.74; H, 7.12; N, 12.35%; mol wt, 681.

***cyclo*-(Val-Orn(δ-Z)-Ala-D-Phe-Pro-)$_2$ (X-A).** The fractions 32 to 48 were treated as described above (yield, 35 mg). It was recrystallized from ethanol-ether; yield, 32 mg (15% from VI-B); mp 255—258°C; $[\alpha]_D^{20}$ −212° (*c* 0.5, MeOH); R_f, 0.98.[9]

Found: C, 61.38; H, 6.98; N, 11.97%; mol wt, 1320.[12] Calcd for $C_{70}H_{92}O_{14}N_{12} \cdot 2H_2O$: C, 61.74; H, 7.12; N, 12.35%; mol wt, 1362.

***cyclo*-(Val-Orn-Gly-D-Phe-Pro-)·HCl (XI-G·HCl).** A solution of IX-G (20 mg 0.03 mmol) dissolved in 0.01N methanolic hydrogen chloride (3.36 ml) was subjected to hydrogenolysis in the presence of palladium black. The filtrate was evaporated to dryness *in vacuo*. The crystals were collected with the aid of ether; yield of air-dried product, 16.0 mg (96%); mp 135—137°C (decomp); $[\alpha]_D^{20}$ −68.0° (*c* 0.5, MeOH); R_f, 0.84[9] and 0.76.[13]

Found: C, 51.30; H, 7.53; N, 13.86%. Calcd for $C_{26}H_{39}O_5N_6Cl \cdot 3H_2O$: C, 51.61; H, 7.50; N, 13.89%.

***cyclo*-(Val-Orn-Ala-D-Phe-Pro-)·HCl (XI-A·HCl).** The compound IX-A (20 mg 0.03 mmol) was converted to XI-A·HCl as described above; yield of air-dried product, 15.8 mg (95%); mp 140—142°C (decomp); $[\alpha]_D^{20}$ −55.3° (*c* 0.5, MeOH); R_f, 0.82[9] and 0.96.[13]

Found: C, 52.09; H, 7.68; N, 13.54%. Calcd for $C_{27}H_{41}O_5N_6Cl \cdot 3H_2O$; C, 52.37; H, 7.65; N, 13.57%.

***cyclo*-(Val-Orn-Gly-D-Phe-Pro-)$_2$·2HCl (XII-G·2HCl).** The compound X-G (20 mg; 0.015 mmol) was treated as described for the preparation of XI-G·HCl; yield of air-dried product, 15.4 mg (93%); mp 214—215°C (decomp); $[\alpha]_D^{20}$ −103° (*c* 0.5, MeOH); R_f, 0.86[9] and 0.97.[13]

Found: C, 51.44; H, 7.68; N, 13.76%. Calcd for $C_{52}H_{80}O_{10}N_{12}Cl_2 \cdot 6H_2O$: C, 51.51; H, 7.66; N, 13.87%.

***cyclo*-(Val-Orn-Ala-D-Phe-Pro-)$_2$·2HCl (XII-A·2HCl).** The compound X-A (20 mg, 0.015 mmol) was treated as described above; yield of air-dried product, 15.6 mg (92%); mp 260—263°C (decomp); $[\alpha]_D^{20}$ −101° (*c* 0.5, MeOH); *Rf*, 0.83[9] and 0.98.[13]

Found: C, 52.13; H, 8.00; N, 13.36%. Calcd for $C_{54}H_{84}O_{10}N_{12}Cl_2 \cdot 6H_2O$; C, 52.28; H, 7.82; N, 13.55%.

Electrophoresis. Electrophoresis on Toyo Roshi No. 52 paper was carried out with a solvent system, formic acid-acetic acid-methanol-water (1 : 3 : 6 : 10, v/v; pH 1.8) for 2 hr at 500 V/30 cm. Figure 5 shows

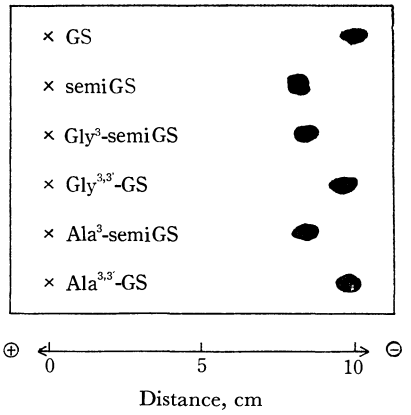

Fig. 5. Paper electrophoresis of the compounds.

that *cyclo*-decapeptides (XII-G and XII-A) migrate toward the cathode faster than *cyclo*-pentapeptides (XI-G and XI-A) and that mobilities of XII-G and XII-A are comparable with that of GS.

Microbiological Assays.[14] The minimum amount of the compounds necessary for the complete inhibition of growth was determined by a dilution method using a bouillon agar medium and a synthetic medium. As shown in Table 2, 3,3'-alanine-GS (XII-A) was found to exhibit weak antibacterial activity against *Staphylococcus aureus* and *Bacillus subtilis*, whereas 3,3'-glycine-GS (XII-G) and cyclosemiGS analogs (XI-G and XI-A) exhibited no activity against the microorganisms tested.

12) The molecular weight was determined on a Hitachi Osmometer, type 115, using methanol as the the solvent.

13) The R_f value of the paper chromatography with Toyo Roshi No. 52 refers to the *n*-butanol-acetic acid-pyridine-water (4 : 1 : 1 : 2, v/v) system.

14) We are indebted to Dr. M. Shibata of Takeda Chemical Industries, Ltd., for the assay.

BULLETIN OF THE CHEMICAL SOCIETY OF JAPAN VOL. 43 1208—1211 (1970)

The Graft Copolymerization of a Vinyl Monomer Containing a Glucose Residue onto Polypropylene Fiber

Yoshio IWAKURA, Keikichi UNO, Takakazu KOJIMA and Akihiko UENO

Department of Synthetic Chemistry, Faculty of Engineering, The University of Tokyo, Hongo, Bukyo-ku, Tokyo

(Received October 13, 1969)

The graft copolymerization of 3-*O*-methacryloyl 1,2; 5,6-diisopropylidene-α-D-glucofuranose (MDG) onto polypropylene fibers was carried out by the γ-ray pre-irradiation technique in the presence of oxygen. The isopropylidene groups of the glucose residue grafted on the copolymer were removed by hydrolysis in aqueous formic acid, and the hydroxyl and hemiacetal groups were regenerated. The deacetonated fibers exhibited a considerable affinity for water vapor and could be dyed with a reactive dye.

In our laboratory, several polymers containing sugar residues were synthesized and their graft copolymerizations onto polymers were studied in a series of studies of the reactive polymer,[1,2] because the polymers containing sugar residues was expected to have a high affinity for water vapor and chemical reactivities through the hydroxyl and hemiacetal groups of the sugar residue. Polypropylene is known to have no affinity for water vapor because it has no hygroscopic groups and little chemical reactivities through the lack of an active center such as hydroxyl groups except hydrogen atoms on the tertiary carbons in the main chain. If hydroxyl groups are introduced into polypropylene by grafting a vinyl monomer with a sugar residue, the physical and chemical character of the grafted polypropylene is modified.

In the present study, 3-*O*-methacryloyl 1,2;5,6-diisopropylidene-α-D-glucofuranose (MDG), prepared from 1,2;5,6-diisopropylidene-α-glucose (DG) and methacryloyl chloride as a vinyl monomer, was used to modify polypropylene. Graft copolymerization was carried out by means of a pre-irradiation process in air. It is well known that when a polymer is irradiated in air, hydroperoxides and peroxides are generally formed on the polymer chain. Therefore, the pre-irradiated polypropylene fiber was heated in MDG to give a MDG-grafted polypropylene fiber. The polypropylene fiber grafted with MDG was hydrolyzed by acid at the acetal linkages of its sugar residue in order to generate the hydroxyl group. The behavior of the hydrolyzed grafted fiber in reaction to water vapor and its dyeability were examined. The hydrolyzed grafted fiber could be dyed with a reactive dye through chemical bonding.

1) Y. Iwakura, Y. Imai and K. Yagi, *J. Polym. Sci.*, **A6**, 801 (1968).

2) Y. Iwakura, Y. Imai and K. Yagi, *ibid.*, **A6**, 1625 (1968).

Experimental

Preparation of 3-*O*-Methacryloyl-1,2;5,6-diisopropylidene-α-D-glucofuranose (MDG). MDG was prepared by the method described in the literature,[3,4] and was recrystallized from *n*-hexane at 0°C. Mp 40.5—41.5°C, $[\alpha]_D = -28.96°$ in benzene. ($[\alpha]_D = -28.8°$ in benzene[4]).

Graft Copolymerization. Unstretched polypropylene fiber, a product of the Chisso Co., was extracted with acetone for 5 hr in a Soxhlet apparatus and then irradiated by ^{60}Co in air at room temperature. An ampoule containing the irradiated fiber and the MDG-benzene solution was sealed, after having degassed by the freeze-and-thaw method under 10^{-4} mmHg. Graft copolymerization was carried out by heating the ampoule at a definite temperature. After the reaction, the resulting viscous solution was poured into a large amount of methanol, and the homopolymer thus precipitated was collected by filtration. The grafted fiber was extracted with benzene in a Soxhlet apparatus.

The percentage of grafting (G) and the grafting efficiency (F) were given by:

$$G = \frac{100(W_g - W_0)}{W_0}$$

$$F = \frac{100(W_g - W_0)}{(W_g - W_0) + H}$$

where W_0 is the initial weight of the polypropylene fiber, W_g is the weight of the grafted fiber, and H is the weight of the homopolymer produced during the graft copolymerization.

Hydrolysis.[5] The isopropylidene groups were removed from the MDG units of the grafted fiber by heating the fiber in aqueous formic acid (70 wt%) at

3) A. Chapiro, M. Magat and J. Sebban, French PV 690659, and PV 692736.

4) S. Kimura, K. Hirai and M. Imoto, *Kogyo Kagaku Zasshi*, **65**, 688 (1962).

5) T. P. Bird, W. A. P. Black, J. A. Colquhorn, E. T. Dewar and D. Rutherford, *J. Chem. Soc.*, **1966**, 1913.

65°C for 6 hr. After the reaction, the fiber was washed with water and acetone, and then dried *in vacuo* at 60°C. Through hydrolysis, two moles of acetone can be eliminated from the MDG (molecular wt 328) unit by the addition of two moles of water. Thus, the extent of deacetonation (D) can be calculated by the following equation:

$$D = \frac{W_g - W_d}{\frac{80}{328}(W_g - W_0)}$$

were W_d is the weight of the polypropylene fiber after hydrolysis.

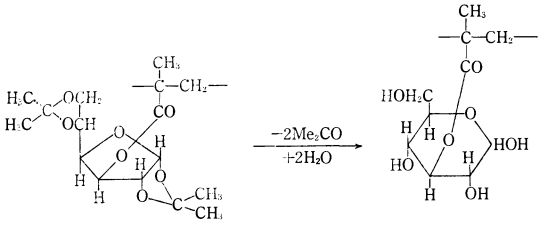

Dyeing. Mikacion Brilliant Red, a product of Mitsubishi Chemical Industries, Ltd., was used as the reactive dye. A solution of 0.3 g of the reactive dye, 1 g of sodium sulfate, 0.3 g of sodium carbonate, 2 m*l* of toluene, 1 m*l* of pyridine, a small amount of an emulsifier (Scourol 400), and 40 m*l* of water was prepared as the dyeing solution. Dyeing was carried out by dipping 0.1 g of the fiber into 3 m*l* of the above solution at room temperature. After standing overnight, the fiber was extracted with water in a Soxhlet apparatus.

Results and Discussion

In general, the variables which seemed to be important in a graft copolymerization carried out by the pre-irradiation method are the dose rate of irradiation, the total dose delivered to a polymer, the monomer concentration, the reaction temperature, the crystallinity of a polymer, and the time interval between irradiation and grafting. The effects of some of these variables on the pre-irradiation of the grafting of MDG to polypropylene were examined. The percentage of grafting and the grafting efficiency are plotted against the total doses in Fig. 1. It is well known that the characteristics of some polymers, such as polyethylene and polypropylene are changed by irradiation with γ-rays because of the formation of cross linkings.[6] It has also been reported that the monomer diffusion into the irradiated polymer is, in some cases, the rate-determining step in graft copolymerization by means of the pre-irradiated method.[7]

In this study, the fiber which was irradiated with a total dose of 3 Mrad was hard and brittle and was, further, not soluble in any solvent. This change in property was considered to be caused by cross-linking. As is shown in Fig. 1, the percentage of grafting increased with an increase in the total dose, whereas the grafting efficiency decreased.

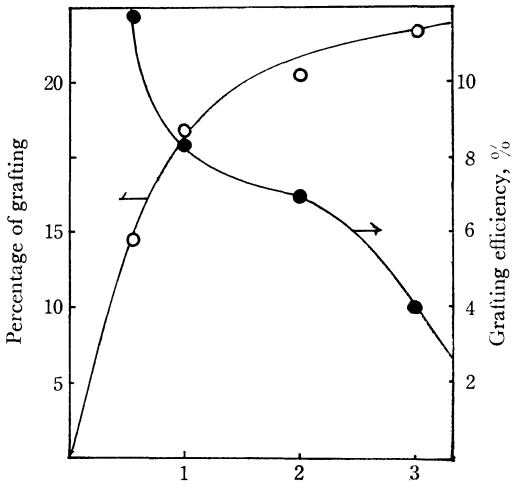

Fig. 1. Influence of irradiation total dose.
Dose rate: 2×10^5 r/hr; monomer concentration: 40 wt%; grafting temperature: 85°C; reaction time: 4 hr

The results obtained may be interpreted as follows. The cross-linked region of the fiber increased with an increased in the total dose, while the rate of the diffusion of the bulky monomer into the fiber decrease with an increase in the cross-linked region. On the other hand, the rate of the diffusion of the hydroxyl radical produced by the decomposition of hydroperoxide into the solution from cross-linked fiber is not much affected; as a result, a depression in grafting efficiency is observed.

Both the percentage of grafting and the grafting efficiency increased with an increase in the monomer concentration, as is shown in Fig. 2.

This fact can also be interpreted in terms of the diffusion of the monomer as follows. When the monomer concentration in the solution is high, the monomer concentration in the solid fiber will be high and the diffusion of the monomer from the solution into the fiber will also be high. This increases the propagation rate and results in the increase in the percentage of grafting. When the diffusion rate of the monomer from the solution into the fiber increases, the amount of homopolymer in the fiber which is polymerized by hydroxyl radical still in the fiber may be considered to increase also, because the diffusion rate of the hydroxide ion produced in the fiber into the solution is influenced by the monomer concentration in the solution. As the diffusion of the homopolymer produced in the fiber into the solution is usually very difficult, the result here obtained, the increase in the grafting

6) A. Chapiro, *J. Chim. Phys.*, **52**, 246 (1955).
7) A. Hoffman, E. R. Gillil, E. W. Merrill and W. H. Stockmayer, *J. Polym. Sci.*, **34**, 461 (1959).

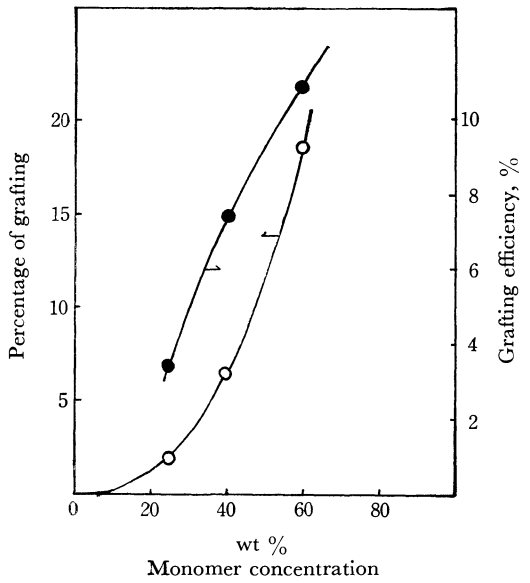

Fig. 2. Influence of monomer concentration.
Irradiation total dose: 2.0 Mrad; reaction condition: 85°C, 50 min
○ percentage of grafting
● grafting efficiency

efficiency, may be interpreted in the above terms.

The temperature dependency on the percentage of grafting is shown in Fig. 3.

The percentage of grafting increased with an increase in the temperature, whereas the grafting efficiency showed little change. These phenomena may indicate that the grafting is controlled by the diffusion of the monomer into the solid fiber. The diffusion rate of the monomer into the fiber from the solution, as well as that of the hydroxyl radical produced in the fiber, into the solution was accelerated by the increase in the reaction temperature. This results in an increase in the percentage of grafting for the reason described above, but it has almost no influence on the efficiency of the grafting.

The grafted fiber and the deacetonated fiber were

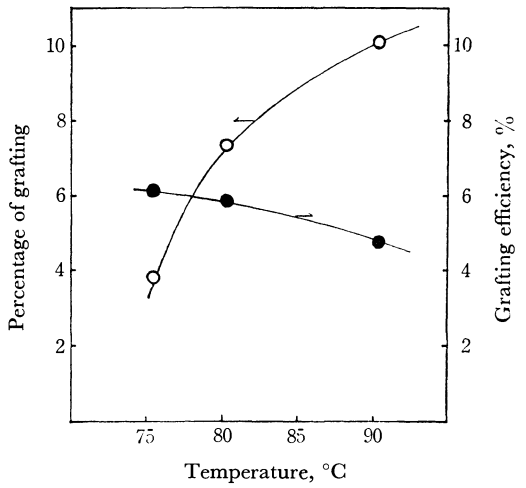

Fig. 3. Influence of reaction temperature.
Irradiation total dose: 2.0 Mrad; monomer concentration: 25 wt%; reaction time: 5 hr

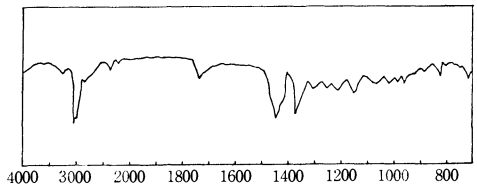

MDG-grafted polypropylene, percentage of grafting 13.

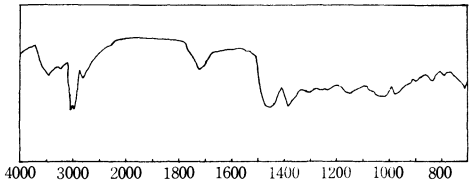

Deacetonated polypropylene, percentage of grafting 43.

Fig. 4. Infrared absorption spectra of MDG-grafted polypropylene.

TABLE 1. RESULT OF DEACETONATION

Grafting reaction					Deacetonation
Total irradiation Mrad	Monomer concentration wt %	Temperature °C	Time hr	Percentage of grafting %	Extent of deacetonation %
0.55	40	85	4	11.7	34
1.0	40	85	4	17.4	47
2.0	40	85	4	20.3	89
2.0	40	85	5/6	6.5	53
2.0	60	85	5/6	18.6	93
2.0	25	75	5	3.8	101
2.0	25	80	5	7.3	92
2.0	25	90	5	10.0	84

smashed to powder in liquid nitrogen and then analyzed by means of the infrared absorption spectra. The grafted polypropylene showed an absorption characteristic of the carbonyl group at 1730 cm^{-1} and a new absorption of the hydroxyl group at 3400 cm^{-1} after hydrolysis, as is shown in Fig. 4.

This indicates that the isopropylidene groups were removed. The results of the hydrolysis are summarized in Table 1.

The extent of deacetonation was calculated from the weight loss of the fiber.

The introduction of MDG units onto the polymer changed the physical properties of the fiber. A fiber grafted over 200% with MDG was obtained when the grafting reaction was carried out at 85°C for 9.5 hr. The fiber thus obtained was very brittle and was easily torn to pieces. The water-vapor adsorption aspect of the deacetonated homopolymer was also examined. The deacetonated homopolymer, when placed in air saturated with water vapor, adsorbed the water vapor in time and gradually became a viscous mass. The water adsorbed by a deacetonated grafted fiber placed in air saturated with water vapor increased with an increase in the percentage of grafting, as is shown in Fig. 5.

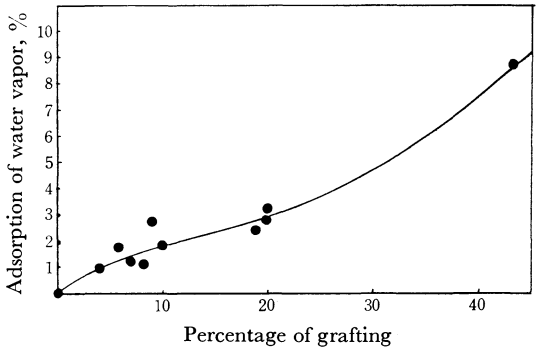

Fig. 5. Water vapor adsorption by the deacetonated grafted fiber at saturated vapor pressure

The amount of water adsorbed by the MDG units of the deacetonated grafted fiber is plotted against the percentage of grafting in Fig. 6.

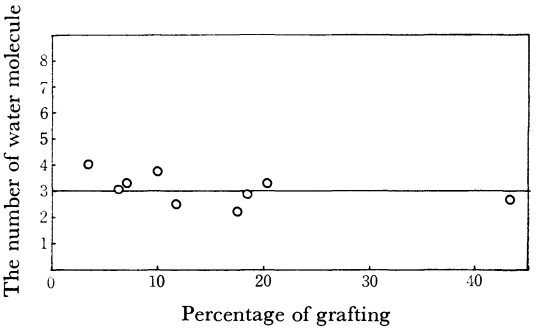

Fig. 6. The number of water molecule adsorbed by each MDG unit of deacetonated grafted fiber

Though no clear conclusion can be deduced from this figure, it can be pointed out that one MDG monomer unit adsorbs about three water molecules on the average.

Reactive dyes generally react with compounds containing hydroxyl groups, such as cellulose, by making covalent bond. The dyeability of the deacetonated fibers was examined with Mikacion Brilliant Red (MBR) as the reactive dye; this was the same kind of dye as Procion M. The shade of the colored fiber was responsible for the percentage of grafting. The observation of the cross-section of the dyed fiber by means of a microscope showed that the dyeing reaction occurred evenly in the fiber.

BULLETIN OF THE CHEMICAL SOCIETY OF JAPAN VOL. 43 1212—1218 (1970)

Studies on the Formation of Deoxy Sugars by Detosyloxylation with Lithium Aluminum Hydride*1

Sumio UMEZAWA, Tsutomu TSUCHIYA and Hirokuni HINENO

Department of Applied Chemistry, Faculty of Engineering, Keio University, Koganei-shi, Tokyo

(Received October 29, 1969)

The reduction of a number of tosylated, mesylated, sometimes further-benzoylated derivatives of methyl 4,6-*O*-benzylidene-α-D-glucopyranoside (I) with lithium aluminum hydride in tetrahydrofuran has been investigated; it has thus been found that methyl 4,6-*O*-benzylidene-2,3-di-*O*-tosyl-α-D-glucopyranoside (II) gave methyl 4,6-*O*-benzylidene-3-deoxy-α-D-*ribo*-hexopyranoside (III, major), methyl 4,6-*O*-benzylidene-2-deoxy-α-D-*arabino*-hexopyranoside (IV, minor), and methyl 4,6-*O*-benzylidene-2-deoxy-α-D-*ribo*-hexopyranoside (V, minor) as deoxy derivatives through two kinds of monotosyl derivatives (VIII and X), and that methyl 2-*O*-benzoyl-4,6-*O*-benzylidene-3-*O*-tosyl-α-D-glucopyranoside (VII) and methyl 3-*O*-benzoyl-4,6-*O*-benzylidene-2-*O*-tosyl-α-D-glucopyranoside (IX) gave VIII and X respectively, as intermediates. 2-*O*-Methyl-3-*O*-tosyl (XI) and 2-deoxy-3-*O*-tosyl derivatives (XIII) gave detosylated derivatives, (XII) and (IV) respectively. These and other results suggest, for detosyloxylation, a mechanism through the formation of an alkoxy-aluminum hydride.

The reduction of a secondary sulfonyl ester group with lithium aluminum hydride (hereafter abbreviated to LAH) sometimes provides a facile method for the synthesis of deoxysugars; in recent years, this kind of reaction has been studied fairly extensively. In connection with other work in progress in our laboratory, it became desirable to investigate further the scope and the mechanism of this kind of reaction. This report will deal with the reduction, with LAH in boiling tetrahydrofuran, of secondary sulfonyl groups in methyl 4,6-*O*-benzylidene-α-D-glucopyranoside (I).

In general, the reduction of a sulfonate of a secondary hydroxyl group with LAH causes desulfonylation, thus giving a corresponding secondary alcohol,[1] while a primary sulfonic ester is reduced to give a corresponding methyl group. In some cases,[2] however, a secondary sulfonyloxy group is eliminated to form a deoxy derivative, by the reduction with LAH, as in the usual case of a primary sulfonyloxy group.

Vis and Karrer[3] reported that the reduction of methyl 4,6-*O*-benzylidene-2,3-di-*O*-tosyl-α-D-glucopyranoside (II) with LAH in tetrahydrofuran caused both desulfonylation and desulfonyloxylation, thus giving a 3-deoxy sugar, namely, methyl 4,6-*O*-benzylidene-3-deoxy-α-D-*ribo*-hexopyranoside (III), apparently through a reaction intermediate epoxide, methyl 2,3-anhydro-4,6-*O*-benzylidene-α-D-allopyranoside (VI). However, the reduction[4] of VI with LAH in ether gave methyl 4,6-*O*-benzylidene-2-deoxy-α-D-*ribo*-hexopyranoside (V), indicating that the epoxide (VI) may not be the intermediate.

On the other hand, Allerton and Overend[5] observed that the reduction of methyl 2-*O*-tosyl-β-L-arabinopyranoside with LAH in ether afforded two kinds of deoxy derivatives, namely, methyl 2-deoxy-β-L-*erythro*-pentopyranoside and methyl 3-deoxy-β-L-*erythro*-pentopyranoside, and methyl 2,3-anhydro-β-L-riboside, the last epoxy-compound being considered to be the intermediate for the formation of 2-deoxy- and 3-deoxy-pentosides.

As has been mentioned above, the behavior of a sulfonate group towards the reduction with this hydride is critically dependent upon its position in, and the stereochemistry of, the carbohydrate molecule.

Experimental Results

A number of tosylated, mesylated, sometimes

*1 Presented at the 22nd Annual meeting of the Chemical Society of Japan, Tokyo, April, 1969. (see Abstracts of the Meeting, Vol. 3, p. 1897).

1) R. S. Tipson, *Advan. Carbohydrate Chem.*, **8**, 164 (1953); D. H. Ball and F. W. Parrish, *ibid.*, **23**, 275 (1968).

2) See a recent example: M. Strandtman, C. Puchalski and J. Shavel, Jr., *J. Org. Chem.*, **33**, 4015 (1968).

3) E. Vis and P. Karrer, *Helv. Chim. Acta*, **37**, 378 (1954).

4) D. A. Prins, *J. Amer. Chem. Soc.*, **70**, 3955 (1948). The lack of any formation of 3-deoxy-hexoside was further confirmed by a) E. J. Hedgley, W. G. Overend and R. A. C. Rennie, *J. Chem. Soc.*, **1963**, 4701, and by b) A. C. Richardson, *Carbohyd. Res.*, **4**, 422 (1967).

5) R. Allerton and W. G. Overend, *J. Chem. Soc.*, **1954**, 3629.

further-benzoylated derivatives of 4,6-*O*-benzylidene-α-D-glucopyranoside were caused to react with LAH in tetrahydrofuran. At the beginning, the structure of the 3-deoxy derivative (III) obtained from II (see Chart 1) by the method of Vis and Karrer[3] was confirmed by NMR spectroscopy. Then, a derivative, in which one of the tosyloxy groups of II is replaced by a benzoyloxy group, namely, methyl 2-*O*-benzoyl-4,6-*O*-benzylidene-3-*O*-tosyl-α-D-glucopyranoside (VII), was prepared and subjected to reduction with LAH for 20 hr. The separation of the resultant products by column chromatography with silica gel gave a mixture of deoxy products (A mixture, 73%) and a desulfonated product, methyl 4,6-*O*-benzylidene-α-D-glucopyranoside (I, 6.3%), which was expected to be produced by the desulfonylation typical for secondary sulfonyloxy groups. The examination of the A mixture by NMR spectroscopy (see Experimental) suggested that it was composed of a 3-deoxy derivative (III, about 93%) and a 2-deoxy derivative, methyl 4,6-*O*-benzylidene-2-deoxy-α-D-*ribo*-hexopyranoside (V, about 7%). When the reaction was pursued by thin-layer chromatography, it was found that the starting material (VII, R_f 0.95*[2]) disappeared rapidly and that, after 30 min, a product (R_f 0.8) became the main product; this was then gradually transformed to the above-mentioned three products constituting the A mixture, (III, V, and I). The intermediate proved to be methyl 4,6-*O*-benzylidene-3-*O*-tosyl-α-D-glucopyranoside (VIII); this pathway was supported by reducing VIII with LAH to give almost the same results as those obtained above.

Next, a positional isomer of VII, namely, methyl 3-*O*-benzoyl-4,6-*O*-benzylidene-2-*O*-tosyl-α-D-glucopyranoside (IX), was prepared and caused to react with LAH in the same manner. In this case, a 2-deoxy product, methyl 4,6-*O*-benzylidene-2-deoxy-α-D-*arabino*-hexopyranoside (IV), was produced in a 29% yield, together with compound I (54%). The structure of IV was confirmed by its melting point and by its NMR spectrum. In this reaction, contrary to the case of VII, the deoxy sugar (IV) was produced in a low yield but was not contaminated by the formation of other deoxy sugars, as in the case of the A mixture. Here again the formation of an epoxy intermediate was not likely.

Hereupon, we made a further investigation of the above-mentioned Vis and Karrer's experiment, and a similar pursuit of the reaction and the identification technique described above was carried out. In a 40-hr reaction, the ditosylated starting material (II) was changed into a mixture of deoxy products (B mixture, 61%) and compound I (15%).

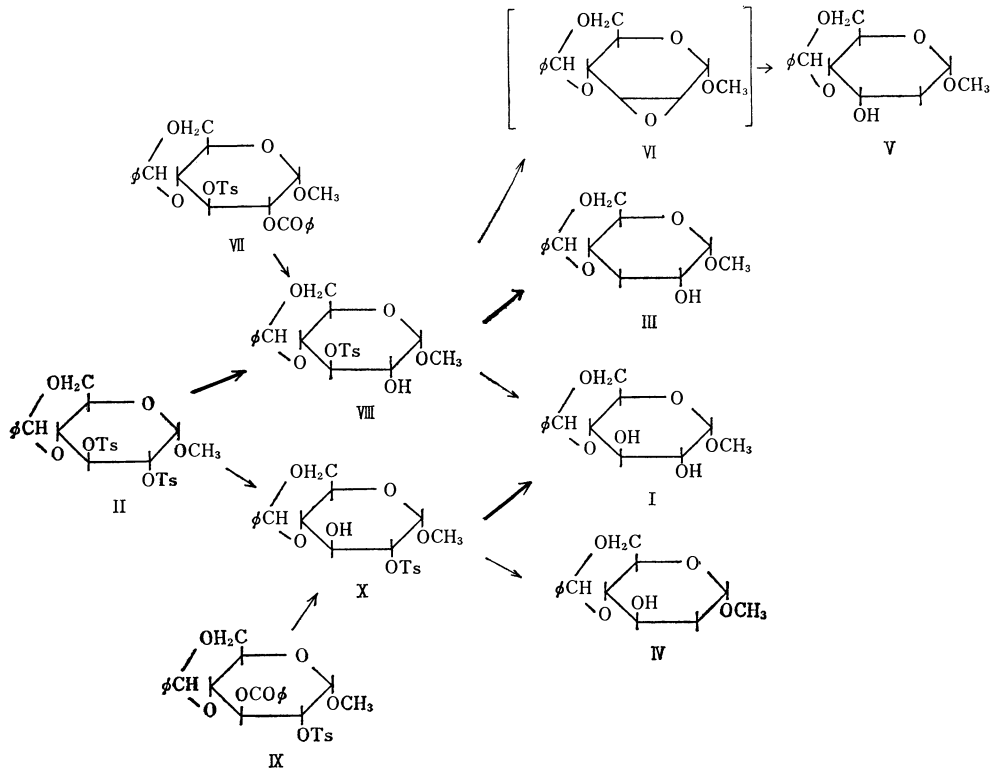

Chart 1

*[2] See Experimental.

An inspection of the NMR spectrum of the B mixture (see Experimental) indicated that the mixture was composed of three components: a 3-deoxy derivative (III, ~75%), a 2-deoxy derivative (V, ~12%), and another 2-deoxy derivative (IV, ~12%); the former two were identical with the components of the A mixture, while the latter was identical with the compound obtained from IX. When the reaction was stopped after 3.5 hr, the formation of two monotosylated products, namely, methyl 4,6-*O*-benylidene-3-*O*-tosyl and 2-*O*-tosyl-α-D-glucopyranoside (VIII and X, respectively), was revealed. Thus, it necessarily follows that the reaction of the ditosylated compound (II) with LAH may involve reactions of two kinds of monotosylated compounds (VIII and X) with LAH. The overall reaction pathway from II is depicted in Chart 1, as are those from VII and IX.

We then went on to prepare several compounds bearing methanesulfonyl (mesyl) groups instead of tosyl groups, namely, methyl 2-*O*-benzoyl-4,6-*O*-benzylidene-3-*O*-mesyl-[6] (XVII), 4,6-*O*-benzylidene-2,3-di-*O*-mesyl-[6,7] (XVIII), 4,6-*O*-benzylidene-2-*O*-mesyl-[6] (XIX), and 4,6-*O*-benzylidene-2-*O*-mesyl-3-*O*-tosyl-α-D-glucopyranoside (XX), and these compounds were caused to react with LAH under reaction conditions similar to those described above. It was found that, except for XX, the three compounds exclusively afforded the desulfonated compound I in high yields; on the contrary, XX gave a result analogous to that from VII. In conclusion, so far as this kind of reactions is concerned, a mesyloxy group acts similarly to that of a benzoyloxy group.

Preparation of the Samples

Methyl 2-*O*-benzoyl- and 3-*O*-benzoyl-4,6-*O*-benzylidene-α-D-glucopyranoside (XIV and XV respectively) were prepared from methyl 4,6-*O*-benzylidene-α-D-glucopyranoside (I) by modifying the method of Jeanloz[6]; the yield of XIV and XV was fairly well improved. The tosylation of XIV and XV was performed with tosyl chloride in pyridine, and the structural proofs of the products (VII and IX) were obtained from their NMR spectra. The debenzoylation of VII and IX were performed with sodium in methanol without the formation of any epoxy compounds to give methyl 4,6-*O*-benzylidene-3-*O*-tosyl- and 2-*O*-tosyl-α-D-glucopyranoside (VIII and X respectively). The methylation of VIII was performed by methyl iodide and silver oxide, thus giving methyl 4,6-*O*-benzylidene-2-*O*-methyl-3-*O*-tosyl-α-D-glucopyranoside (XI) in a high yield. The mesylation of I to methyl 4,6-*O*-benzylidene-2-*O*-mesyl-α-D-glucopyranoside (XIX) was performed by modifying the method of Jeanloz,[6] while XIX was tosylated to methyl 4,6-*O*-benzylidene-2-*O*-mesyl-3-*O*-tosyl-α-D-glucopyranoside (XX) in a good yield in a usual way. Methyl 4,6-*O*-benzylidene 2-deoxy-3-*O*-tosyl-α-D-*arabino*-hexopyranoside[8] (XIII) was prepared from methyl 4,6-*O*-benzylidene-2-deoxy-α-D-*arabino*-hexopyranoside (IV), which had itself been prepared from methyl 3-*O*-benzoyl-4,6-*O*-benzylidene-2-*O*-tosyl-α-D-glucopyranoside (IX) by reduction with LAH. The identification and the differentiation of methyl 4,6-*O*-benzylidene-2- or 3-deoxy-α-D-hexopyranosides (III, IV, and V), which all have the same R_f value in thin-layer chromatography, were conveniently performed by an inspection of their NMR spectra, which differ in τ-values and in the splitting patterns of anomeric, *O*-methyl, and benzylic hydrogens.

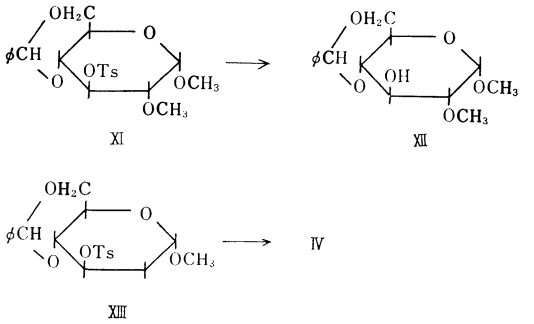

Chart 2

Discussion

In view of the above experimental results, it seems that any tosyl derivative desulfonyloxylated to a methylene-type deoxy compound by the action of LAH has a hydroxyl group, or a group easily changeable to a hydroxyl group by LAH, in the proximity of the secondary tosyloxy group in question. This suggests that the adjacent hydroxyl group may participate in this kind of reaction. To examine this point further, an *O*-methylated derivative (XI) of VIII was prepared and caused to react with LAH by the usual procedure; as expected, it has been found that this derivative was detosylated exclusively to give XII, while no trace of a detosyloxylated derivative was detected. Furthermore, a deoxy derivative of VIII, namely, methyl 4,6-*O*-benzylidene-2-deoxy-3-*O*-tosyl-α-D-*arabino*-hexopyranoside (XIII), was examined for this reaction; again, it has been found that no detosyloxylation, but rather detosylation, occurred to give IV. From these results, the important role of the adjacent

6) R. W. Jeanloz and D. A. Jeanloz, *J. Amer. Chem. Soc.*, **79**, 2579 (1957).

7) J. Honeyman and J. W. W. Morgan, *J. Chem. Soc.*, **1955**, 3660.

8) S. McNally and W. G. Overend, *J. Chem. Soc., C*, **1966**, 1978.

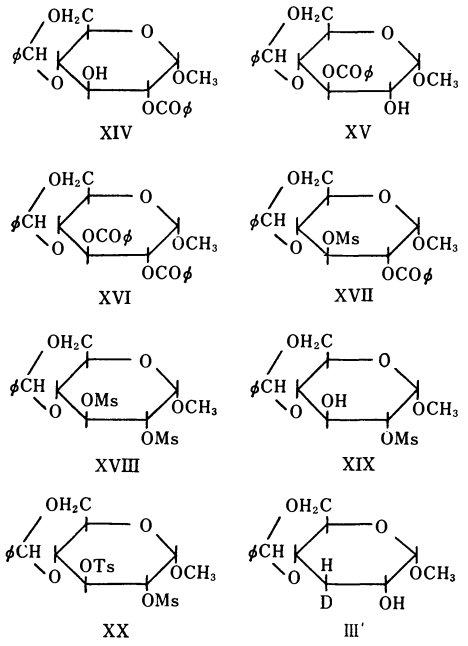

Chart 3. 4,6-*O*-Benzylidene derivatives used in this study other than those depicted in charts 1 and 2.

hydroxyl group in this kind of reaction became obvious. In this connection, Hedgley, Meresz, and Overend[9] found, in their synthesis of 5-deoxy-D-*xylo*-hexose, that 6-*O*-benzoyl-1,2-*O*-isopropylidene-5-*O*-tosyl-α-D-glucofuranose was converted mainly to 5-deoxy-1,2-*O*-isopropylidene-α-D-*xylo*-hexofuranose by the reaction with LAH in ether (or in tetrahydrofuran); they therefore suggested that the product might be formed favourably through a *C*-3-alkoxy-aluminum hydride intermediate. A similar kind of mechanism of desulfonyloxylation would be very likely in our experiments, though the conversion of compound II, VII, or VIII to III requires a higher reaction temperature (in boiling tetrahydrofuran) and a small volume of tetrahydrofuran; when the reaction is performed in ether, ether-tetrahydrofuran, benzene-tetrahydrofuran, or dioxane, the reaction is very slow or the ratio of the yield of III to I becomes small, while when a larger volume of tetrahydrofuran than such described in the Experimental section is used, the ratio of the yield of III to I is considerably decreased. The mechanism shown in the following chart may be reasonable for the conversion of VIII to III.

Conformational change will be required to force one of the hydrogens of the metal hydride part of the intermediate to come close to carbon-3; the proximity of the hydrogen will be the driving force of the reaction. The backside attack of the metal hydride was supported by the result obtained

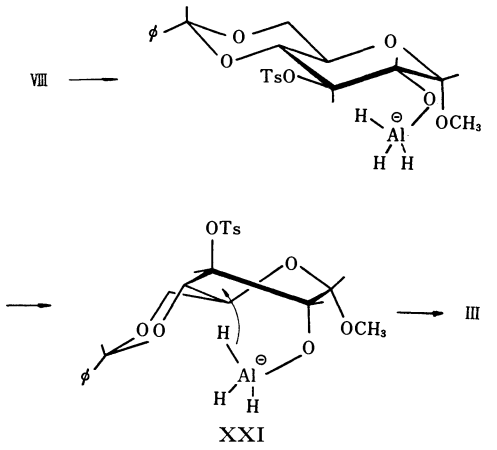

by means of lithium aluminum deuteride, which afforded methyl 3-deoxy-3-deuterio-4,6-*O*-benzylidene-α-D-allopyranoside (III').

In like manner, the formation of methyl 2-deoxy-β-L-*erythro*-pentopyranoside from methyl 2-*O*-tosyl-β-L-arabinopyranoside reported by Allerton and Overend[5] can be understood by the above-mentioned mechanism instead of that through an epoxy intermediate.

As for the mesyl derivatives (XVII, XVIII, and XIX), their desulfonylation may be ascribed to the fact that a mesyloxy group is more basic than a tosyloxy group and less functional as a leaving group in a transition state such as XXI.

Experimental

The NMR spectra were measured with a Varian A-60D spectrometer or a Japan Electron Optics 4H-100 spectrometer. Tetramethylsilane (τ 10.0) was used as the internal standard. The following abbreviations were used: p: proton, s: singlet, d: doublet, t: triplet, q: quartet, m: multiplet. Thin-layer chromatography (TLC) was carried out on microscope slides coated with silica gel, and the spots were visualized by spraying with 95% sulfuric acid and then heating at 110°C.

Methyl 2-*O*-Benzoyl-4,6-*O*-benzylidene-α-D-glucopyranoside (XIV) and Methyl 3-*O*-Benzoyl-4,6-*O*-benzylidene-α-D-glucopyranoside (XV). The method of Jeanloz and Jeanloz[6] was used; when the quantity of pyridine was increased about 20-fold, XIV was obtained in a higher yield as follows. To an ice-cold solution of I (5.0 g) in dry pyridine (100 m*l*) benzoyl chloride (2.1 m*l*) was gradually added; the mixture was allowed to stand under cooling for 4 hr and then at room temperature overnight. The reaction mixture was then treated as has been described in the literature[6] to give a crude syrup, which showed four spots on TLC (benzene-ethyl acetate 6 : 1): R_f 0.87 (XVI, a dibenzoylated derivative), 0.71 (XIV), 0.44 (XV), and 0.06 (I). The syrup was chromatographed on a silica-gel column (500 g, 4.7×54 cm) and then eluted with the same solvent system. After the first fraction (500 m*l*), the eluate was cut into 15-g portions. A dibenzoylated compound (XVI) was eluted between Nos. 12—20

9) E. J. Hedgley, O. Meresz and W. G. Overend, *J. Chem. Soc., C*, **1967**, 888.

(1.14 g, 13%); another, XIV, between Nos. 29—52 (3.47 g, 51%); a third, XV, between Nos. 110—154 (0.50 g, 7%). The starting material (I, 1.3 g, 26%) was eluted after the solvent had been changed to ethyl acetate. The dibenzoylated product (XVI) was recrystallized from benzene-*n*-hexane; mp 155°C (lit,[6] 154°C), $[\alpha]_D^{20}$ +97° (*c* 1, $CHCl_3$) (lit,[6] +94°); IR: 1725, 1275, 1095, 756, 707, 697 cm^{-1}.

Compound XIV was recrystallized from benzene-ether; mp 170—172°C (lit,[6] 169—170°C), $[\alpha]_D^{20}$ +112° (*c* 1, $CHCl_3$) (lit,[6] +111°); IR: 3450, 1735, 1270, 750, 713, 697 cm^{-1}; NMR (60 MHz, in pyridine-d_5): τ: 6.64 (3-p. s., OCH_3), 4.69 (1-p. d., H-1), 4.44 (1-p. q., H-2), 4.21 (1-p. s., benzylic); $J_{1,2}$ 3.5 Hz, $J_{2,3}$ 9.5 Hz.

Compound XV was recrystallized from benzene; mp 225—226°C (lit,[6] 219—220°), $[\alpha]_D^{20}$ +34° (*c* 1, $CHCl_3$) (lit,[6] +34°); IR: 3380, 1725, 1275, 750, 705, 695 cm^{-1}; NMR (60 MHz, in pyridine-d_5): τ: 6.62 (3-p. s., OCH_3), 4.89 (1-p. d., H-1), 4.23 (1-p. s., benzylic), 3.79 (1-p. t., H-3); $J_{1,2}$ 3.5 Hz, $J_{2,3}$—$J_{3,4}$ ~9.3 Hz.

Compound XIV was clearly differentiated from XV by comparing their NMR spectra. When $CDCl_3$ was used instead of pyridine-d_5, the separation of signals was indistinct.

Methyl 2-*O*-Benzoyl-4,6-*O*-benzylidene-3-*O*-tosyl-α-D-glucopyranoside (VII). Prepared by the usual method (yield 90%); mp 190°C (lit,[10] 188—189°C), $[\alpha]_D^{20}$ +89° (*c* 1, $CHCl_3$) (lit,[10] +88.5°); IR: 1730, 1600, 1365, 1270, 1175, 830, 750, 712 cm^{-1}; NMR (100 MHz, $CDCl_3$): τ: 7.87 (3-p. s., $TsCH_3$), 6.65 (3-p. s., OCH_3), 4.95—4.8 (2-p. m., H-1, H-2), 4.62 (1-p. s., benzylic), 4.58 (1-p. t., H-3); $J_{2,3}$—$J_{3,4}$ ~9.7 Hz.

Methyl 4,6-*O*-Benzylidene-3-*O*-tosyl-α-D-glucopyranoside (VIII). To a suspension of VII (594 mg) in dry methanol (60 m*l*) we added a piece of sodium metal; the mixture was then stirred at room temperature for several hours. If the suspension did not become clear, a little more of sodium was added and the mixture was treated as above. The resultant clear solution was neutralized with carbon dioxide and evaporated *in vacuo*. A chloroform solution of the residue was washed with water, dried over sodium sulfate, and evaporated to give a solid which contained a slight amount of an epoxy product (VI, R_f 0.55 on TLC) as a contaminant. Recrystallization from chloroform-*n*-hexane gave pure VIII; 398 mg (83%); R_f 0.30 (VII, R_f 0.72) by TLC (benzene-ethyl acetate 5 : 1); mp 164°C (lit,[7],*3 164°C), $[\alpha]_D^{22}$ +32° (*c* 1, $CHCl_3$) (lit,[7] +32.5°); NMR (60 MHz, $CDCl_3$): τ: 7.72 (3-p. s., $TsCH_3$), 6.55 (3-p. s., OCH_3), 5.18 (1-p. d., H-1), 5.10 (1-p. t., H-3), 4.67 (1-p. s., benzylic), 2.27 and 3.01 (4-proton AB quartet, *J* 8.3 Hz, Tosyl), ~2.65 (5-p., Ph.); $J_{1,2}$ 3.5 Hz, $J_{2,}$—$_3J_{3,4}$ ~9.5 Hz.

Methyl 4,6-*O*-Benzylidene-2-*O*-methyl-3-*O*-tosyl-α-D-glucopyranoside (XI). To a solution of VIII (586 mg) in dry acetone (6 m*l*) we added methyl iodide (1 m*l*), silver oxide (1.2 g), and freshly-prepared Drierite (1 g), after which the mixture was stirred overnight. The filtrate was evaporated, and the residue was dissolved in chloroform. The solution was then washed with water, dried over sodium sulfate, and evaporated. The residue was recrystallized from benzene-ethyl acetate (5 : 1), 591 mg (98%); mp 163—164°C, $[\alpha]_D^{20}$ +26° (*c* 1, $CHCl_3$); R_f 0.56 by TLC (benzene-ethyl acetate 5 : 1); IR: 2930, 1600, 1365, 1175, 1090, 975, 842, 750, 725, 700 cm^{-1}; NMR (60 MHz, $CDCl_3$): τ: 7.72 (3-p. s., $TsCH_3$), 6.63 (3-p. s., $O(2)CH_3$), 6.57 (3-p. s., $O(1)$-CH_3), 5.12 (1-p. d., H-1), 4.91 (1-p. t., H-3), 4.63 (1-p. s., benzylic), ~2.63 (5-p., Ph.), 2.27 and 2.99 (4-proton AB quartet, *J* 8.3 Hz, Tosyl); $J_{1,2}$ 3.5 Hz, $J_{2,3}$—$J_{3,4}$ ~9 Hz.

Found: C, 58.75; H, 5.75; S, 7.16%. Calcd for $C_{22}H_{26}O_8S$: C, 58.65; H, 5.82; S, 7.12%.

Methyl 4,6-*O*-Benzylidene-2-*O*-tosyl-α-D-glucopyranoside (X). Prepared from IX[10] in a manner similar to that described in VIII; yield 91%; mp 155°C (lit, 155°C,[7] 154°C[11]); $[\alpha]_D^{23}$ +63° (*c* 1, $CHCl_3$) (lit, +63.5°,[7] +62.9°[11]); NMR (60 MHz, $CDCl_3$): τ: 7.35 (1-p. broad singlet, disappeared on deuteration, OH), 7.58 (3-p. s., $TsCH_3$), 6.67 (3-p. s., OCH_3), 5.60 (1-p. q., H-2), 5.15 (1-p. d., H-1), 4.50 (1-p. s., benzylic); $J_{1,2}$ 3.2 Hz, $J_{2,3}$ 9.0 Hz.

Methyl 4,6-*O*-Benzylidene-2-*O*-mesyl-α-D-glucopyranoside (XIX). The method of Jeanloz and Jeanloz[6] was followed; when the quantity of pyridine was increased, a higher yield was obtained. To an ice-cold solution of I (2.82 g) in dry pyridine (56 m*l*), we added methanesulfonyl chloride (1.2 m*l*), after which the mixture was allowed to stand at 5°C overnight. A few drops of water were then added, and the solution was evaporated *in vacuo*. A chloroform solution of the resultant residue was washed successively with water, a potassium bisulfate solution, a saturated bicarbonate solution, and water again. After drying over sodium sulfate, the solution was evaporated to give a syrup; the syrup was chromatographed on a silica-gel column (250 g, 4.7×32 cm) and eluted with benzene-ethyl acetate (5 : 1). The dimesylated product (R_f 0.61 by TLC with the same solvent system; 0.81 g) was eluted from a portion between 700 and 800 m*l*, while XIX (R_f 0.47; 2.68 g, 74%) was eluted from a 850-m*l* portion with tailing. XIX was recrystallized from benzene-ethyl acetate (5 : 1); mp 134—135°C (lit, 135—136°C,[6] 132—133°C[7]), $[\alpha]_D^{20}$ +73° (*c* 1, $CHCl_3$) (lit, +73°,[6] +72°[7]); NMR (60 MHz, $CDCl_3$): τ: 5.54 (1-p. q., H-2), $J_{1,2}$ 3.5 Hz, $J_{2,3}$ 9.7 Hz, collapsed to a doublet when irradiated at H-1; 5.07 (1-p. d., H-1), 4.49 (1-p. s., benzylic).

Methyl 4,6-*O*-Benzylidene-2-*O*-mesyl-3-*O*-tosyl-α-D-glucopyranoside (XX). Prepared from XIX (5.08 g) by the usual method; yield 6.62 g (91%); mp 194—195°C, $[\alpha]_D^{20}$ +11° (*c* 1, $CHCl_3$), R_f 0.73 by TLC (benzene-ethyl acetate 5 : 1); IR: 1600, 1365, 1320, 1175, 1095, 1050, 985, 747, 720, 700 cm^{-1}; NMR (60 MHz, $CDCl_3$): τ: 7.76 (3-p. s., $TsCH_3$), 6.87 (3-p. s., SO_2CH_3), 6.50 (3-p. s., OCH_3), 5.40 (1-p. q., H-2), 4.95 (1-p. d., H-1), 4.80 (1-p. t., H-3), 4.71 (1-p. s., benzylic), 2.8—2.5 (5-p. m., Ph), 3.07 and 2.33 (4-p. AB quartet, Ts); $J_{1,2}$ 3.5 Hz, $J_{2,3}$ 9.7 Hz, $J_{3,4}$ ~9.3 Hz.

Found: C, 51.31; H, 5.13; S, 12.65%. Calcd for $C_{22}H_{26}O_{10}S$: C, 51.35; H, 5.09; S, 12.46%.

Methyl 4,6-*O*-Benzylidene-2-deoxy-α-D-*ribo*-hexopyranoside (V). Prepared from methyl 2,3-anhydro-4,6-*O*-benzylidene-α-D-allopyranoside[12] (VI) as has

10) E. J. Bourne, A. J. Huggard and J. C. Tatlow, *J. Chem. Soc.*, **1953**, 735.

*3 Honeyman and Morgan[7] made VIII and X by different routes.

11) K. S. Ennor and J. Honeyman, *J. Chem. Soc.*, **1958**, 2586.

12) "Methods in Carbohyd. Chem.", Vol. 1, Academic Press, New York (1962) p. 107.

been described by Richardson[4b]; mp 129—131°C (lit,[4b] 127—129°C), $[\alpha]_D^{20}$ +140° (*c* 1, $CHCl_3$) (lit,[4b] +140°); R_f 0.72 (VI: R_f 0.82) by TLC (benzene-ethyl acetate 1 : 2).

NMR (60 MHz, $CDCl_3$): τ: 8.3—7.6 (2-p. m., H-2, H-2′), 6.98 (1-p. d., disappeared on deuteration, OH), 6.61 (3-p. s., OCH_3), 5.23 (1-p. q., J 3.3 and 1.5 Hz, H-1), 4.38 (1-p. s., benzylic).

Methyl 4,6-*O*-Benzylidene-2-deoxy-3-*O*-tosyl-α-D-*arabino*-hexopyranoside (XIII). Prepared in the usual way from IV; mp 97°C (lit,[8] 95°C), $[\alpha]_D^{24}$ +46° (*c* 1, $CHCl_3$).

Treatment of Methyl 4,6-*O*-Benzylidene-2,3-di-*O*-tosyl-α-D-glucopyranoside (II) with Lithium Aluminum Hydride for 40 hr. The method of Vis and Karrer[3] was followed essentially. Lithium aluminum hydride (1.13 g) was refluxed in dry tetrahydrofuran (THF, 13 m*l*) for 2 hr, and then well-dried II (3.12 g) was added to the mixture. After refluxing for 40 hr, the reaction mixture was cooled and shaken with ethyl acetate (3 m*l*) for a while. Ether (400 m*l*) and an aqueous solution (150 m*l*) of Rochelle salt (15 g) were added under shaking. The aqueous layer was separated and extracted with ether (100 m*l*×5). The ethereal extract was dried over potassium carbonate and evaporated to give a solid (1.3 g), which was then chromatographed on a silica-gel column (150 g, 3.3×35 cm) with benzene-ethyl acetate (1 : 2). A mixture (0.2 g) of the starting material (II) and an unidentified substance (R_f 0.90 and 0.85 respectively, as determined by TLC with the same solvent system) was eluted in a portion between 200—250 m*l*; then a mixture of the products (the B mixture, all having the same R_f-value of 0.72) was eluted in a portion between 330—460 m*l*; 0.86 g; 61%; mp 168—173°C, $[\alpha]_D^{24}$ +128° (*c* 1, $CHCl_3$). Finally I was eluted in a portion between 820—1200 m*l*; 0.23 g (15%); mp 163—164°C (lit,[12] 163—164°C), $[\alpha]_D^{25}$ +109° (*c* 1, $CHCl_3$) (lit,[12] +110°), R_f 0.3 (the same value as that of the authentic I sample).

The fractional crystallization of the B mixture from ethyl acetate and petroleum ether gave pure III; mp 186°C (lit, 186.5—187.5°C,[3] 190—192°C[13]), $[\alpha]_D^{24}$ +126° (*c* 1, $CHCl_3$) (lit, +126.9°,[3] +116°[13]).

NMR (100 MHz, $CDCl_3$): τ: 8.16 (1-p. q., H_{ax}-3, $J_{3e,3a}$—$J_{2,3a}$—$J_{3a,4}$ ~11 Hz), 7.75 (1-proton doublet of triplets, H_{eq}-3; $J_{3e,3a}$ 11.0 Hz, $J_{2,3e}$—$J_{3e,4}$ ~4.5 Hz), 6.55 (3-p. s., OCH_3), 5.33 (1-p. d., $J_{1,2}$ 3.2 Hz, H-1), 4.49 (1-p. s., benzylic), 2.75—2.4 (5-p. m., Ph.). The results confirm the structure of III.

A comparison of the NMR spectrum of the intact A mixture with those of the standard substances (III, IV, and V) showed that the mixture was composed of three components: III (~75%), V (~12%), and another substance (IV, ~12%), the last of which has the same NMR pattern as the substance produced by the action of LAH on methyl 3-*O*-benzoyl-4,6-*O*-benzylidene-2-*O*-tosyl-α-D-glucopyranoside (IX), which will be described later. NMR (here, τ-values are indicated in the order of III (main), V, and IV): τ 6.55, 6.61, 6.68 (each singlet, OCH_3); τ 5.33 (d.), 5.24 (q.), 5.25 (q.)(H-1); τ 4.49, 4.38, 4.46 (each singlet, benzylic).

Treatment of II with Lithium Aluminum Hydride for 3.5 hr. Compound II (1.45 g) was caused to react with LAH in the same manner as has been described above, except that the time of reaction was 3.5 hr. The ethereal extracts thus obtained were evaporated to give a solid (0.85 g). On TLC (benzene-ether 5 : 1), the solid showed the presence of four components: the starting material (II, major, R_f 0.71), X (minor, R_f 0.51), a monotosylated (?) compound (minor, R_f 0.26), and III (major, R_f 0.28). The monotosylated compound had the same R_f-value and the same color-change as methyl 4,6-*O*-benzylidene-3-*O*-tosyl-α-D-glucopyranoside (VIII) when sprayed with sulfuric acid. The attempted isolation of VIII by preparative TLC[14] was, however, unsuccessful because of the concomitance of the 3-deoxy derivative (III). Another minor substance (R_f 0.51) was separated by preparative TLC[14] to give methyl 4,6-*O*-benzylidene-2-*O*-tosyl-α-D-glucopyranoside (X, 0.04 g, mp 154°C, $[\alpha]_D^{23}$ +63°). The identity was confirmed by the IR and NMR patterns.

Treatment of Methyl 2-*O*-Benzoyl-4,6-*O*-benzylidene-3-*O*-tosyl-α-D-glucopyranoside (VII) with Lithium Aluminum Hydride for 20 hr. Lithium aluminum hydride (1.04 g) was refluxed in dry THF (12 m*l*) for 2 hr; well-dried VII (3.04 g) was then added, and the mixture was refluxed for 20 hr. A crude solid (1.4 g) was obtained by the procedure described for the corresponding reaction of II. Column chromatography with silica gel (140 g) and benzene-ethyl acetate (1 : 2) gave a monotosylated product (VIII, R_f 0.8) in a fraction between 210—240 m*l* (0.09 g (3.7%), mp 163°C, $[\alpha]_D^{23}$ +33° (*c* 1, $CHCl_3$)), which showed IR and NMR patterns identical with those of authentic VIII. A mixture of deoxy derivatives (the A mixture, R_f 0.72) was eluted in a portion between 270—350 m*l* (1.09 g (73%); mp 180—184°C, $[\alpha]_D^{24}$ +121° (*c* 1, $CHCl_3$)), and compound I (R_f 0.3) in a portion between 550—850 m*l* (0.10 g (6.3%); mp 163—164°C, $[\alpha]_D^{25}$ +110° (*c* 1, $CHCl_3$)).

The fractional crystallization of the A mixture from ethyl acetate and petroleum ether gave pure III; mp 187°C, $[\alpha]_D^{24}$ +126°. A comparison of the NMR pattern of the intact A mixture with those of III and V in respect to *O*-methyl, anomeric, and benzylic hydrogens indicated that the mixture consisted of two components: III (~93%) and a 2-deoxy derivative (V, ~7%).

Treatment of VII with Lithium Aluminum Hydride for 30 min. A mixture of VII (206 mg) and LAH (78 mg) in dry THF (4 m*l*) was refluxed as has been described above. When the reaction was pursued by TLC (benzene-ethyl acetate 1 : 2), it was found that the starting material (R_f 0.95) disappeared fairly rapidly and that after 30 min of the reaction only the debenzoylated product (VIII, R_f 0.8) could be detected, the deoxy products (R_f 0.72) being then produced gradually. When the reaction was stopped after 30 min, the usual isolation procedure gave VIII (145 mg, 87%); mp 165°C, $[\alpha]_D^{22}$ +33° (*c* 1, $CHCl_3$). Its IR and NMR spectra were identical with those of an authentic sample.

Treatment of Methyl 2-*O*-Benzoyl-4,6-*O*-benzylidene-3-*O*-tosyl-α-D-glucopyranoside (VII) with Lithium Aluminum Deuteride. Formation of Methyl 3-Deoxy-3-deuterio-4,6-*O*-benzylidene-α-D-allopyranoside (III′). Lithium aluminum deuteride (0.46 g) was refluxed in dry THF (6 m*l*) for 2 hr, well-

13) D. A. Prins, *Helv. Chim. Acta*, **29**, 1 (1946).

14) D. Horton and T. Tsuchiya, *Carbohyd. Res.*, **5**, 426 (1967).

dried VII (1.49 g) was added, and then the mixture was refluxed for 20 hr. The reaction product was purified by a usual procedure. The crude product (0.73 g) obtained from the ethereal extract was chromatographed on a silica-gel column (100 g) with benzene-ethyl acetate (1 : 2). The monotosylated product (VIII), a mixture of deoxy derivatives and compound I were obtained in yields of 0.03 g (3%), 0.57 g (78%), and 0.05 g (6%) respectively. The recrystallization of the mixture of deoxy derivatives from ethyl acetate-petroleum ether gave pure III'; mp 186°C, $[\alpha]_D^{22}$ +125° (*c* 1, $CHCl_3$); NMR (60 MHz, $CDCl_3$): τ: 7.8—7.65 (1-proton broad singlet, H_{eq}-3); no signals corresponding to H_{ax}-3 were observed. The other signals were quite identical with those of III.

Treatment of Methyl 4,6-*O*-Benzylidene-3-*O*-tosyl-α-D-glucopyranoside (VIII) with Lithium Aluminum Hydride. A mixture of VIII (0.72 g) and LAH (0.27 g) in dry THF (2.8 m*l*) was refluxed for 20 hr. The extraction of the resultant products by a usual method was followed by column chromatography with silica gel and benzene-ethyl acetate (1 : 2) to give a mixture of deoxy derivatives (0.31 g, 71%; mp 180—183°C) and compound I (0.07 g, 15%). A comparison of the NMR spectrum of the former mixture with that of above-mentioned A mixture indicated that the former mixture consisted of III (major) and the 2-deoxy derivative (V, minor).

Treatment of Methyl 4,6-*O*-Benzylidene-2-*O*-methyl-3-*O*-tosyl-α-D-glucopyranoside (XI) with Lithium Aluminum Hydride. A mixture of XI (591 mg) and LAH (260 mg) in dry THF (3.1 m*l*) was refluxed for 40 hr, and the product was extracted as before. A crude solid (293 mg) thus obtained was passed through a short column of silica gel with benzene-ethyl acetate (1 : 2), and the product (XII) was recrystallized from the same solvent; 244 mg (63%); mp 170°C (lit, 166°C,[15] 168°C[10]), $[\alpha]_D^{22}$ +95° (*c* 1, $CHCl_3$) (lit, +95.4°[15] ($CHCl_3$), +74.5°[10] (ethanol)); NMR (60 MHz, $CDCl_3$) τ: 7.1 (1-p., disappeared on deuteration, OH), 6.57 (3-p. s., OCH_3), 6.49 (3-p. s., OCH_3), 5.13 (1-p. d., $J_{1,2}$ 3.5 Hz), 4.48 (1-p. s., benzylic).

Found: C, 60.40; H, 6.71%. Calcd for $C_{15}H_{20}O_6$: C, 60.80; H, 6.80%.

Treatment of Methyl 3-*O*-Benzoyl-4,6-*O*-benzylidene-2-*O*-tosyl-α-D-glucopyranoside[10] (IX) with Lithium Aluminum Hydride. A mixture of IX (1.10 g) and LAH (0.36 g) in dry THF (4 m*l*) was refluxed for 20 hr, and the resulting products were extracted by a usual procedure. The crude product (0.52 g) was chromatographed on silica gel (50 g) with benzene-ethyl acetate (1 : 2). Methyl 4,6-*O*-benzylidene-2-deoxy-α-D-*arabino*-hexopyranoside (IV) was eluted in a portion between 70—90 m*l* (R_f 0.72 by TLC with the same solvent mixture); 0.16 g (29%); mp 150—151°C (lit, 151—152°C,[16] 149—150°C[17]), $[\alpha]_D^{23}$ +95° (*c* 1, $CHCl_3$) (lit, +90°[16] (acetone), +83.8°[17] (ethanol)). Compound I was eluted in a portion between 150—270 m*l* (R_f 0.3, 0.31 g, 54%); mp 163—164°C, $[\alpha]_D^{24}$ +110° (*c* 1, $CHCl_3$).

NMR of IV (100 MHz, $CDCl_3$): τ: 8.23 (1-proton quartet of doublets, H_{ax}-2), 7.83 (1-proton quartet of small doublets, H_{eq}-2), 7.25 (1-proton broad singlet, disappeared on deuteration, OH), 6.69 (3-p. s., OCH_3), 6.58 (1-p. t., J~9.5 Hz, H-4), 6.28 (2-p. m., H-6, 6'?), 5.90 (1-p. m., H-3?), 5.77 (1-p. m., H-5?), 5.24 (1-proton doublet of small doublets, H-1), 4.47 (1-p. s., benzylic), 2.8—2.45 (5-p. m., Ph); $J_{1,2_a}$ 3.6 Hz, $J_{1,2_e}$~1.2Hz, $J_{2_a,2_e}$ 13 Hz, $J_{2_a,3}$ 11Hz, $J_{2_e,3}$ 5.5 Hz; irradiation at H-1 collapsed H_{ax}-2 to a quartet (J, 13 Hz and 11 Hz) and H_{eq}-2 to a quartet (J, 13 Hz and 5.5 Hz); irradiation at H_{ax}-2 collapsed H-1 to a singlet in appearance, and irradiation at H_{eq}-2 collapsed H-1 to a sharp doublet (J, 3.6 Hz). These values showed a fairly good agreement with those measured at 60 MHz by Coxon.[17]

Treatment of Methyl 4,6-*O*-Benzylidene-2,3-di-*O*-mesyl-α-D-glucopyranoside[6] (XVIII) with Lithium Aluminum Hydride. A mixture of XVIII (3.08 g) and LAH (1.17 g) in dry THF (12 m*l*) was refluxed for 20 hr, and then the product was extracted by a usual procedure. However, in this case, purification by column chromatography was not necessary. The crude product (1.9 g; R_f 0.3 by TLC with benzene-ethyl acetate 1 : 2) contained only a trace of the deoxy product (R_f 0.72). Recrystallization from chloroform-ether gave I (1.80 g, 91%); mp 163—164°C.

Treatment of Methyl 2-*O*-Benzoyl-4,6-*O*-benzylidene-3-*O*-mesyl-α-D-glucopyranoside[6] (XVII) with Lithium Aluminum Hydride. A mixture of XVII (2.93 g) and LAH (1.11 g) in dry THF (12 m*l*) was refluxed for 20 hr and then treated as above. The crude product (1.7 g), which was not contaminated by any deoxy product, was recrystallized from chloroform-ether to give I (1.16 g, 90%); mp 163—164°C.

Treatment of Methyl 4,6-*O*-Benzylidene-2-*O*-mesyl-3-*O*-tosyl-α-D-glucopyranoside (XX) with Lithium Aluminum Hydride. A mixture of XX (1.40 g) and LAH (0.47 g) in dry THF (6 m*l*) was refluxed for 20 hr, and then the reaction mixture was treated by a usual procedure. The crude product (0.70 g) obtained from the ethereal extract was chromatographed on silica gel (100 g) with benzene-ethyl acetate (1 : 2). At first, unidentified substances (0.08 g; TLC with benzene-ethyl acetate 5 : 1, R_f 0.59 and 0.49) were eluted, and then deoxy derivatives (R_f 0.72) were eluted, 0.43 g (59%); mp 172—175°C. Finally I was eluted (0.13 g (17%)). The deoxy derivatives were proved by a study of the NMR spectrum to be a mixture of the 3-deoxy compound (III, ~80%) and the 2-deoxy compound (V, ~20%).

The authors wish to thank Mr. Kohei Watanabe for his technical assistance.

15) R. Gigg and C. D. Warren, *J. Chem. Soc., C*, **1968**, 1903.

16) B. Flaherty, W. G. Overend and N. R. Williams, *J. Chem. Soc., C*, **1966**, 398.

17) B. Coxon, *Tetrahedron* **21**, 3481 (1965).

BULLETIN OF THE CHEMICAL SOCIETY OF JAPAN VOL. 43 1219—1223 (1970)

Proton Magnetic Resonance Studies on Specifically Deuterated Sucrose Acetates[1)]

Tetsuo SUAMI, Toshiki OTAKE,* Seiichiro OGAWA, Tadao SHOJI and Naoyuki KATO

Department of Applied Chemistry, Faculty of Engineering, Keio University, Koganei-shi, Tokyo

* *Nippon Electric Varian Co. Ltd., Azabu Iigura-cho, Minato-ku, Tokyo*

(Received October 31, 1969)

In the proton magnetic resonance spectrum of octa-*O*-acetylsucrose, an individual acetoxy group signal was assigned by direct comparisons of the spectra of specifically deuterated octa-*O*-acetylsucroses and that of nondeuterated one. The structures of 2,3,6,3′,4′-penta-*O*-acetylsucrose and 2,3,4,3′,4′-penta-*O*-acetylsucrose were further confirmed definitively by the present studies.

Penta-*O*-acetylsucrose of mp 156°C (II) was first prepared in a crystalline form by McKeown and his co-workers[2)] by detritylation of penta-*O*-acetyl-tri-*O*-tritylsucrose (I) in boiling aqueous acetic acid. The structure of I was assigned to be 2,3,4,3′,4′-penta-*O*-acetyl-6,1′,6′-tri-*O*-tritylsucrose[3)] by the relatively higher reactivity of the primary hydroxyl groups, compared with the secondary ones, towards trityl chloride,[2,4)] and soon after this structure was confirmed by methylation of tri-*O*-tritylsucrose.[5)]

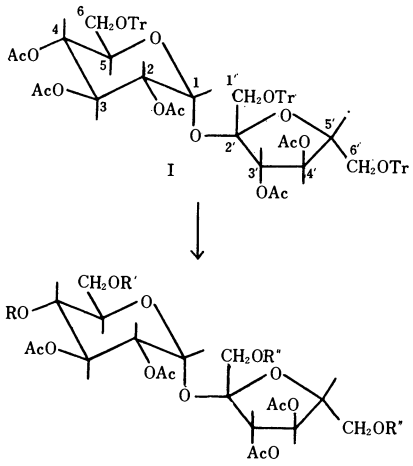

II R=H, R′=Ac, R″=H
III R=Ac, R′=R″=H
IV R=$COCD_3$, R′=Ac, R″=$COCD_3$
V R=Ac, R′=R″=$COCD_3$
Ac=$COCH_3$, Tr=$(C_6H_5)C$

Accordingly the structure of II was first supposed to be 2,3,4,3′,4′-penta-*O*-acetylsucrose,[2)] but on the way to establish the structure by methylation of its free hydroxyl groups, it was suspected that an acetyl migration from C-4 to C-6 might occur in a glucose moiety during the reaction leading to 2,3,6,3′,4′-penta-*O*-acetyl-4,1′,6′-tri-*O*-methylsucrose from II.[2,3)]

Later Lemieux and Barrette[6)] reexamined the structure of II and described that II seemed to be 2,3,6,3′,4′-penta-*O*-acetylsucrose, judging from the results of careful treatments of tritosylate of II with sodium iodide and sodium ethoxide.

While Bredereck and his co-workers[7)] prepared another penta-*O*-acetylsucrose of mp 122°C (III) by detritylation of I with hydrobromic acid in glacial acetic acid under ice cooling and described that III was 2,3,4,3′,4′-panta-*O*-acetylsucrose on the bases of its chemical behaviors.

The present authors wish to establish the structural differences between II and III by a definitive method and to open a new field for further synthetic works in sucrose chemistry.

Proton magnetic resonance (PMR) spectroscopy had been proved to be a powerful tool for structural studies of sugar derivatives,[8,9)] and so if it could be possible to distinguish an individual PMR signal arisen from each acetoxy group in octa-*O*-acetylsucrose, the structures of the two different penta-

1) Supported in part by a grant of the Japanese Ministry of Education.

2) G. E. McKeown, R. S. E. Serenius and L. D. Hayward, *Can. J. Chem.*, **35**, 28 (1957).

3) This numbering system for the position of sucrose molecule was proposed by Hockett and Zief: R. C. Hockett and M. Zief, *J. Amer. Chem. Soc.*, **72**, 1839 (1950).

4) B. Helferich, *Advan. Carbohydrate Chem.*, **3**, 79 (1948).

5) G. E. McKeown and L. D. Hayward, *Can. J. Chem.*, **35**, 992 (1957).

6) R. U. Lemieux and J. P. Barrette, *J. Amer. Chem. Soc.*, **80**, 2243 (1958).

7) H. Bredereck, H. Zinner, A. Wagner, G. Faber, W. Greider and W. Huber, *Chem. Ber.*, **91**, 2824 (1958).

8) R. U. Lemieux, R. K. Kullnig and R. Y. Moir, *J. Amer. Chem. Soc.*, **80**, 2237 (1958).

9) R. U. Lemieux, R. K. Kullnig, H. J. Bernstein and W. G. Schneider, *ibid.*, **80**, 6098 (1958).

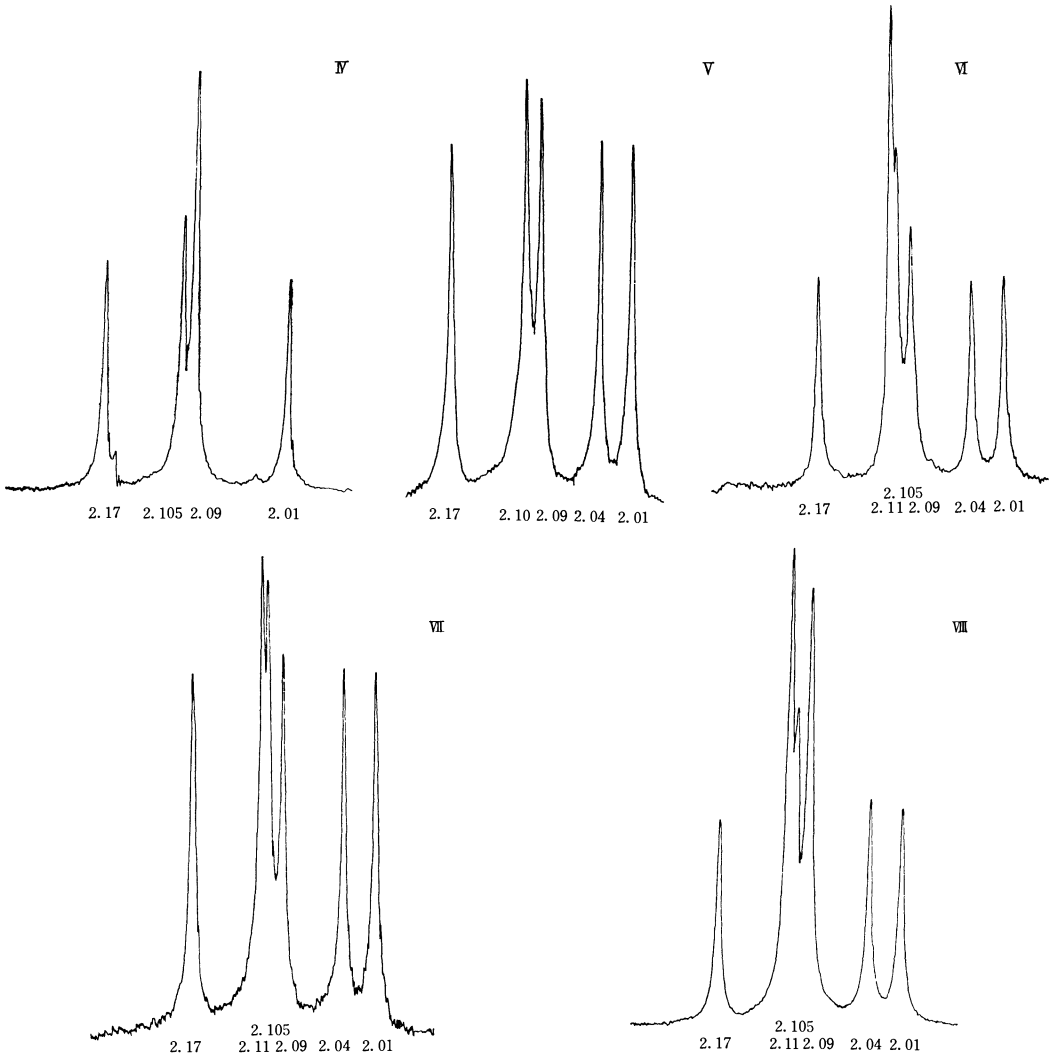

Fig. 1. The acetoxy group signals in the PMR spectra of specifically deuterated derivatives.

O-acetylsucroses would be established by PMR spectroscopy. For this aim, deuteration of an individual acetyl group seemed to be feasible, which had been used successfully by Horton and his co-workers for glucosamine derivatives[10,11] and by the present authors for diazabicyclo[3.2.1.]octanetetrol derivatives.[12]

In the present article, it will be described that some of the individual acetoxy group signals are assigned by the PMR (100 MHz) spectroscopic studies of specifically deuterated octa-*O*-acetylsucrose and it enables us to establish the structures of II and III unambiguously.

The compound II was prepared by the method of McKeown and his co-workers[2] and subsequently acylated with acetic anhydride-d_6 in pyridine, giving penta-*O*-acetyl-tri-*O*-trideuterioacetylsucrose (IV). The PMR spectrum of IV in deuteriochloroform revealed four sharp signals at δ 2.01 (3H), 2.09(6H), 2.105(3H) and 2.17(3H), which were attributed to the five acetoxy groups. When this spectrum was compared with the spectrum of nondeuterated octa-*O*-acetylsucrose (VIII)[13-15] which showed six sharp signals at δ 2.01(3H), 2.04(3H), 2.09(6H), 2.105(3H), 2.11(6H) and

10) D. Horton, J. B. Hughes, J. S. Jewell, K. D. Philips and W. N. Turner, *J. Org. Chem.*, **32**, 1073 (1967).
11) D. Horton, W. E. Mast and K. D. Philips, *ibid.*, **32**, 1471 (1967).
12) T. Suami, S. Ogawa, Y. Naito and H. Sano, *ibid.*, **33**, 2831 (1968).
13) W. W. Binkley, D. Horton and N. S. Bhacca, *Carbohyd. Res.*, **10**, 245 (1969).
14) A. Herzfeld, *Ber.*, **13**, 265 (1880).
15) C. S. Hudson and J. M. Johnson, *J. Amer. Chem. Soc.*, **37**, 2748 (1915).

2.17(3H), it was obvious to see that the two signals at δ 2.04(3H) and 2.11(6H) were missing in the former spectrum (Fig. 1).

Then the compound III was obtained by the method of Bredereck and his co-workers[7] and was acetylated analogously with acetic anhydride-d_6 in pyridine to give another penta-*O*-acetyl-tri-*O*-trideuterioacetylsucrose (V). In the spectrum of V in deuteriochloroform, the two signals at δ 2.09 (3H) and 2.11(6H) were missing, compared with the spectrum of VIII (Fig. 1).

In the two spectra of IV and V, the same acetoxy group signals at δ 2.11 with the same intensity of six protons were missing, and accordingly these signals should be arisen from the two acetoxy groups in the common positions. To find out these two acetoxy group, 2,3,4,1′,3′,4′,6′,-hepta-*O*-acetylsucrose[16] was acetylated with acetic anhydride-d_6 giving 2,3,4,1′,3′,4′,6′-hepta-*O*-acetyl-6-*O*-trideuterioacetylsucrose (VI). The PMR spectrum of VI showed a remarkable decrease of the intensity (1/2) of the signal at δ 2.09, compared with the spectrum of the nondeuterated octaacetate. Hence, the signal at δ 2.09 with an intensity of three protons was attributed to the acetoxy group at C-6 in the glucose moiety of sucrose. This assignment of the signal was agreeable with the fact that an acetoxy group at C-6 in methyl α-D-glucopyranoside tetraacetate revealed the signal at δ 2.09.[17]

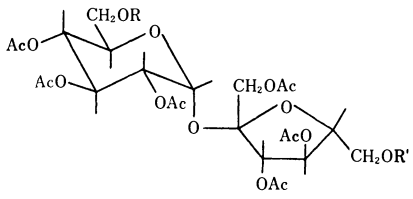

VI R=$COCD_3$, R′=Ac
VII R=R′=$COCD_3$
VIII R=R′=Ac

To substantiate the above mentioned assignment 2,3,4,1′,3′,4′-hexa-*O*-acetylsucrose[18] was analogously trideuterioacetylated to give 2,3,4,1′,3′,4′,-hexa-*O*-acetyl-6,6′-di-*O*-trideuterioacetylsucrose (VII). The spectrum of VII revealed the marked decreases of intensities of the signals at δ 2.09 (3H) and 2.11(3H), compared with the spectrum of VIII. Thus the signal of an intensity of three protons at δ 2.09 was ascribed to the acetoxy group at C-6 in the glucose moiety and the signal of an intensity of three protons at δ 2.11 was due to the acetoxy group at C-6′ in the fructose moiety.

Also, the signal patterns in a lower field in the spectrum of McKeown's penta-*O*-acetylsucrose II which were attributed to the ring protons gave a valuable information on its structure. The signal at δ 5.07 which was arisen from the ring proton at C-4[13] in octa-*O*-acetylsucrose was markedly shifted to a higher field (δ 3.5—4.2) in the spectrum of II (Fig. 2). This fact provided a strong evidence that an acetoxy group at C-4 was absent in the compound II.

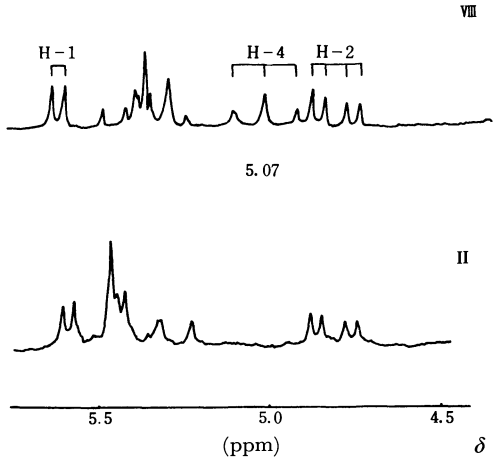

Fig. 2. Partial PMR spectra of II and VIII.

Accordingly the remaining half of the signal at δ 2.11 was due to the acetoxy group at C-4 or C-1′. So if it were arisen from C-4, the diminished signals in the spectrum of V were attributed to three acetoxy groups at C-4, C-6 and C-6′. This caused a big contradiction with the structure of I.

Therefore, the diminished signals at δ 2.11(6H) in the spectra of IV and V should be attributed to the two acetoxy groups at C-1′ and C-6′. Now the structure of V was established to be 2,3,4,3′,4′-penta-*O*-acetyl-6,1′,6′-tri-*O*-trideuterioacetylsucrose and consequently, III was assigned to be 2,3,4,3′4′-penta-*O*-acetylsucrose.

On the other hand, the signal at δ 2.04(3H) disappeared in the spectrum of IV from that of VIII, instead of the diminished signal at δ 2.09(3H) in the spectrum of V. Since Horton and his coworkers[17] described that the signal at δ 2.03 was attributed to the acetoxy group at C-4 of acetylated methyl glucoside, the signal at δ 2.04 in the spectrum of IV was reasonably attributed to the acetoxy group at C-4 of the glucose residue of sucrose. Thus, the structure of IV was assigned to be 2,3,6,3′,4′-penta-*O*-acetyl-4,1′,6′-tri-*O*-trideuterioacetylsucrose and accordingly the structure of II was established to be 2,3,6,3′,4′-penta-*O*-acetylsucrose.

Now four individual acetoxy group signals of the

16) T. Otake, unpublished data. The precursor of this compound: 2,3,4,1′,3′,4′,6′-hepta-*O*-acetyl-6-*O*-triphenylmethylsucrose has been described in the preprint of the 22nd Annual Meeting of the Japan Chemical Society, April (1969), p. 1895.

17) D. Horton and J. H. Lauterback, *J. Org. Chem.*, **34**, 86 (1969).

18) T. Otake and T. Suami, unpublished data.

TABLE 1. CHEMICAL SHIFTS OF ACETYL GROUPS OF SPECIFICALLY DEUTERATED DERIVATIVES

Compound		4-OAc	6-OAc		1′-OAc 6′-OAc	
IV	2.01(1)*	—	2.09(2)	2.105(1)	—	2.17(1)
V	2.01(1)	2.04(1)	2.09(1)	2.10(1)	—	2.17(1)
VI	2.01(1)	2.04(1)	2.09(1)	2.105(1)	2.11(2)	2.17(1)
VII	2.01(1)	2.04(1)	2.09(1)	2.105(1)	2.11(1)	2.17(1)
VIII	2.01(1)	2.04(1)	2.09(2)	2.105(1)	2.11(2)	2.17(1)

* Chemical shifts are expressed in δ-values. Values in parenthesis show number of acetyl groups.

eight ones were assigned in the PMR spectrum of VIII, and the assignments of other four ones are still under way.

But it was readily recognized that the acetoxy group at C-6 in the glucose moiety of sucrose revealed the signal at the same field as was shown by the acetoxy group at C-6 of methyl α-D-glucopyranoside tetraacetate[17] and this was true in the one at C-4. Therefore the two signals at δ 2.01 and 2.09 in the spectrum of VIII might be attributed to the acetoxy groups at C-3 and C-2 respectively in accordance with the Horton's assignment.[17]

The remaining two signals at δ 2.09 and 2.17 could be due to the two acetoxy groups in the fructose residue other than C-1′ and C-6′. The conformations of sucrose and sucrose sodium bromide dihydrate in crystalline states had been described by Brown and Levy,[19] but the conformation of sucrose in a solution is still unfamiliar. But the acetoxy group on C-4′ seemed to widely spread to an outside of the molecule and to be not affected by a deshielding effect of its environments. Therefore this acetoxy group might reveal its signal in a similar position as was shown by an acetyl group on a primary hydroxyl group.

In the low-field regions of the spectra of IV, V, VI, VII and VIII, the same pattern of the signals were observed, which were attributed to the methine and methylene protons[13] and a deuterium isotope effect on the chemical shifts of acetoxy, methine and methylene protons was not distinguished in these 100 MHz spectra.

Thus, Lemieux's[6] and Bredereck's structural assignments[7] of II and III were further confirmed definitively by the present studies.

Experimental

The melting points were determined on a Mitamura Riken micro hot stage. The PMR spectra were determined with a Varian HA-100D (100 MHz) instrument. All the spectra were measured in deuteriochloroform at a concentration of 10% (w/v) at 35°C with tetramethylsilane as an internal standard and the peak positions were expressed in δ-values. Thin layer chromatography (TLC) was run on a glass plate coated with silica gel (Wakogel B-10, Wako pure chemical industries Ltd.) in a solvent system with toluene-methyl ethyl ketone (4 : 1). The spots were detected by spraying a mixture of concd. H_2SO_4 and glacial acetic acid (1 : 1) and heating at 100°C for 30 min. Evaporations were accomplished under reduced pressure with a Tokyo Rikakikai rotary evaporator.

2,3,6,3′,4′-Penta-*O*-acetyl-4,1′,6′-tri-*O*-trideuterioacetylsucrose (IV). 2,3,6,3′,4′-Penta-*O*-acetylsucrose (II), mp 152.5—153.5°C, was prepared by the method of McKeown *et al.*[2] A 170 mg portion of II was acetylated with 0.4 m*l* of acetic anhydride-d_6 in 0.6 m*l* of pyridine and the solution was settled overnight at room temperature. The mixture was evaporated at 60—65°C. Crystallization of the residue from aqueous ethanol gave IV as fine needles, mp 83.5—87°C, yield, 52 mg. The mother liquor was evaporated and the residue was dissolved in chloroform. The chloroform solution was decolorized through a short column of active alumina and then evaporated. The residue was crystallized from aqueous ethanol giving a second crop of IV, mp 83.5—87°C, yield, 127 mg. Total yield was 179 mg (91%). TLC showed the product to be homogeneous with R_f 0.32 (R_f of octa-*O*-acetylsucrose=0.32).

2,3,4,3′,4′-Penta-*O*-acetyl-6,1′,6′-tri-*O*-trideuterioacetylsucrose (V). 2,3,4,3′,4′-Penta-*O*-acetylsucrose (III), mp 128°C, was prepared by the modified method of Bredereck *et al.*[7] A 2.0 g portion of 2,3,4,3′,4′-penta-*O*-acetyl-6,1′,6′-tri-*O*-tritylsucrose[2] was dissolved in a mixture of 7 m*l* of glacial acetic acid and 3 m*l* of chloroform. To the solution, 0.7 m*l* of glacial acetic acid previously saturated with hydrogen bromide was added under ice-cooling with an occasional shaking. After 10 min, the mixture was poured into ice-cold water. The aqueous solution was extracted two times with 10 m*l* of chloroform. The combined chloroform extract was washed with cold water, and evaporated. The residue was dissolved in 10 m*l* of toluene and chromatographed on a column of 10 g of silica gel (Kanto Chemical Co. Ltd. 60—80 mesh). The column was eluted with 150 m*l* of toluene, 200 m*l* of methyl ethyl ketone-toluene (1 : 5), 200 m*l* of methyl ethyl ketone-toluene (3 : 10) and 200 m*l* of methyl ethyl ketone-toluene (1 : 1). The fraction of the last solvent was evaporated to give 470 mg of the residue. The residue was dissolved in 3 m*l* of chloroform and 7 m*l* of ether was added to the solution. The mixture was kept in a refrigerator for 24 hr to give 362 mg of the crystalline product of III, mp 128°C. A 143 mg portion of III was acetylated with 0.2 m*l* of acetic anhydride-d_6 in 1 m*l* of pyridine by the procedure described for the preparation of IV, giving 85 mg of V, mp 83.5—87.5°C. TLC showed practically a single spot of R_f 0.32.

19) G. M. Brown and H. A. Levy, *Science*, **141**, 921 (1963): G. A. Jeffrey and R. D. Rosenstein, *Advan. Carbohydrate Chem.*, **19**, 11 (1964).

2,3,4,1′,3′,4′,6′-Hepta-*O*-acetyl-6-*O*-trideuterioacetylsucrose (VI). A 135 mg portion of 2,3,4,1′,3′,4′,6′-hepta-*O*-acetylsucrose[16] was acetylated with acetic anhydride-$_{f_6}$ in pyridine by an analogous procedure of the preparation of IV to give 95 mg of crystalline product of VI, mp 84.5—88°C. TLC showed a single spot of R_f 0.32.

2,3,4,1′,3′,4′-Hexa-*O*-acetyl-6,6′-di-*O*-trideuterioacetylsucrose (VII). To a solution of 2,3,4,1′,3′,4′-hexa-*O*-acetylsucrose (169 mg)[18] in 1 m*l* of pyridine, 0.12 m*l* of acetic anhydride-d_6 was added and the mixture was treated analogously as described in the preparation of IV to give 11.6 mg of the crystalline product, mp 83—87°C. TLC showed a single spot of R_f 0.32.

Octa-*O*-acetylsucrose (VIII). The product was prepared by the method of Hudson and Johnson[15] and recrystallized two times from aqueous ethanol, mp 84—88°C.

The authors wish to thank Professor Sumio Umezawa for his helpful advice, and Mr. Iwao Miura for determination of PMR spectra.

BULLETIN OF THE CHEMICAL SOCIETY OF JAPAN VOL. 43 1223—1229 (1970)

The Reaction of Sulfenyl Chlorides with Thioethers. I. The Scope of the Reactions

Michinori Ōki and Keiji Kobayashi

Department of Chemistry, Faculty of Science, The University of Tokyo, Hongo, Bunkyo-ku, Tokyo

(Received November 17, 1969)

It was found that thioethers reacted with sulfenyl chlorides to give four kinds of products. When the alkyl part of the thioether is capable of producing a rather stable carbonium ion, the thioether gives the chloride and an olefin, which are derived from the cation, the latter reacting also with the sulfenyl chloride to give adducts. There is another path to afford alkyl chloride; that is, an S_N2-type reaction takes place when the alkyl part gives a less stable carbonium ion. The third and fourth products are α-chloro sulfide and α,β-unsaturated sulfide, which are seemingly produced *via* a common intermediate. The latter may react further with the sulfenyl chloride to give enedithiol derivatives.

During the course of other investigations in this laboratory, a rather unexpected reaction was encountered.[1] Namely, when stilbene (I) and an excess of methanesulfenyl chloride were allowed to react, the product was not the one expected from the mere addition, but α-methylthio-α'-chlorostilbene (III). The treatment of 1,2-diphenyl-1-

$$C_6H_5CH{=}CHC_6H_5 \xrightarrow{CH_3SCl} C_6H_5\underset{\displaystyle CH_3S}{\underset{|}{C}}H-\underset{\displaystyle Cl}{\underset{|}{C}}HC_6H_5$$

(I) (II)

$$\xrightarrow{CH_3SCl} C_6H_5C{=}\underset{\displaystyle Cl}{\underset{|}{C}}C_6H_5$$

CH_3S (III)

methylthio-2-chloroethane (II) with methanesulfenyl chloride resulted in the formation of III. Thus, II seemed to be an intermediate in the formation of III when I was treated with methanesulfenyl chloride.

Since it is rather unusual for methanesulfenyl chloride to dehydrogenate, a series of reactions of sulfenyl chlorides with thioethers has been investigated in order to clarify the nature and the limitations of the reaction. A search of the literature at the outset indicated that, although there were some examples[2] of the reaction of disulfides with sulfenyl chlorides, there was only one paper concerning the reaction between thioethers and sulfenyl chloride;*1 Moor and Porter[3] reported the formation of alkyl chlorides as the major product when thioethers were treated with 2,4-dinitrobenzenesulfenyl chloride in acetic acid.

$$O_2N\text{-}C_6H_3(NO_2)\text{-}SCl + RSR' \rightarrow O_2N\text{-}C_6H_3(NO_2)\text{-}SSR + R'Cl$$

The purpose of this paper is to discuss the scope of the reaction, showing the various aspects of the reaction which result from the structural influences.

1) M. Ōki and A. Nakamura, unpublished work.

2) C. G. Moor and M. Porter, *J. Chem. Soc.*, **1958**, 2890.

*1 However, another paper was published concerning the reaction between sulfides and sulfenyl chlorides during the progress of this work. See Ref. 10.

3) C. G. Moor and M. Porter, *Tetrahedron*, **9**, 58 (1960).

Results and Discussion

Various unsymmetrical thioethers were allowed to react with *ca.* 2 mol benzenesulfenyl chloride (V) in carbon tetrachloride at room temperature. A spontaneous reaction set in, and the evolution of hydrogen chloride was observed. At the completion of the reaction, the red color of the solution of benzenesulfenyl chloride changed to a pale yellow and then did not change any more. The reaction products were analyzed, together with the yields based on the starting thioethers, by intergrating the NMR spectra and gas chromatography of the crude reaction mixture, the behavior of each reaction product being examined beforehand. When possible, the products were isolated by fractional distillation or column chromatography and were subjected to NMR, IR, and elementary analyses.

At the outset, it was expected that *t*-butyl phenyl sulfide (IV) might give the simpler results because of its structure, which would also make analyses by NMR easier. The treatment of *t*-butyl phenyl sulfide with benzenesulfenyl chloride gave 71% *t*-butyl chloride, as was anticipated from an earlier work,[3] and 29% *β*-chloro sulfides, VI and VII, in approximately 2 : 3 ratio. The formation of VI and VII may be expected if it is assumed that the reaction proceeds *via* the *t*-butyl cation, since the cation will give isobutylene together with the substitution product. The addition of benzenesulfenyl chloride to isobutylene will result in the formation of 2-chloro-2-methyl-1-phenylthiopropane (VI) and of 1-chloro-2-methyl-2-phenylthiopropane (VII).

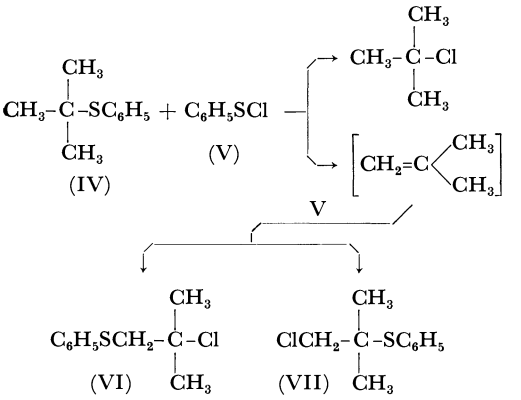

Indeed, the addition of benzenesulfenyl chloride to isobutylene in carbon tetrachloride at room temperature took place exothermally, and the resulting product distribution of VI and VII was in fair agreement with that of the products derived from the reaction of benzenesulfenyl chloride with *t*-butyl phenyl sulfide. The structures of the addition products, which were isomeric mixtures of Markownikoff and anti-Markownikoff adducts, were confirmed by the spectral evidence and by the treatment of the distilled product with potassium *t*-butoxide. On the distillation of the mixture under reduced pressure, isomerization took place and the only isolable compound was 2-chloro-2-methyl-1-phenylthiopropane (VI). Thus, treating the distillate with the base yielded pure 2-methyl-1-phenylthiopropene as a result of dehydrochlorination.

$$\text{VI} + \text{VII} \xrightarrow{\Delta} \text{VI} \xrightarrow{t\text{-BuOK}} C_6H_5SCH{=}C\begin{matrix}CH_3\\CH_3\end{matrix}$$

The facts suggest that the adduct VII is formed by the kinetic control and that VII then rearranges to the thermodynamically more stable VI, probably *via* the episulfonium ion intermediate, as has been suggested in an earlier paper,[4] although the reason for the stability of VI is not well understood at present.

The cleavage of the carbon-sulfur bond observed in the reaction of *t*-butyl phenyl sulfide with sulfenyl chloride should be generally observed if the reaction involves the formation of relatively stable carbonium ion. Thus, benzyl *t*-butyl sulfide (VIII) was treated with benzenesulfenyl chloride to give *t*-butyl chloride and the two adducts, VI and VII, in *ca.* 30% and 57% yields respectively. The stoichiometry of the reaction suggests that benzyl phenyl disulfide should be formed, and, indeed, the unsymmetric disulfide was isolated by column chromatography.

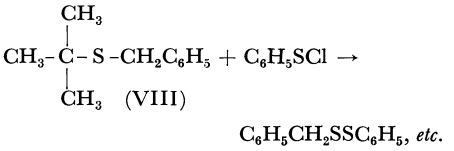

The carbon-sulfur cleavage in benzyl *t*-butyl sulfide occurs predominantly on the *t*-butyl side, giving only 8% benzyl chloride at most. The results conform with the other data on solvolysis,[5] which suggest that the *t*-butyl cation is more easily formed than the benzyl cation. Therefore, it seemed that it would be interesting to ascertain what happens with a sulfide having two alkyl groups which are both poor in giving stable carbonium ions. Benzyl methyl sulfide was, then, treated with benzenesulfenyl chloride. The result was the formation of 9% benzyl chloride and 30% *α*-chlorobenzyl methyl sulfide. A compound of the latter type is known to be a common product when sulfides are treated with chlorinating agents, such as chlorine,[6] sulfuryl chloride,[7] thionyl

4) W. H. Mueller and P. E. Butler, *J. Amer. Chem. Soc.*, **90**, 2075 (1968).
5) C. R. Strauss, H. G. Guay and H. J. Harwood, *J. Org. Chem.*, **29**, 1945 (1964).
6) H. Böhme and H. J. Gran, *Ann.*, **577**, 68 (1952).
7) F. G. Bordwell and B. M. Pitt, *J. Amer. Chem. Soc.*, **77**, 572 (1955).

chloride,[8] and *N*-chlorosuccinimide.[9]

$$C_6H_5CH_2\text{-}S\text{-}CH_3 + C_6H_5SCl \rightarrow C_6H_5CH_2Cl + C_6H_5\underset{\displaystyle Cl}{\underset{|}{C}}HSCH_3$$

When methanesulfenyl chloride was used in place of V, α-chlorobenzyl methyl sulfide was obtained in a better yield (78%) than in the case of V, and benzyl chloride was also obtained in a 10% yield. Oda and Hayashi have also reported similar results during the course of this study.[10]

The treatment of methyl α-phenethyl sulfide (IX) with V gave 55% α-phenethyl chloride (X). However, neither styrene nor α-chloro-β-phenylthioethylbenzene, which would be expected if styrene were formed and if the addition of V were to follow, was detected in the products. Instead, two unexpected olefins were found by NMR spectra: signals at τ 3.53 and τ 3.83 with relative intensities of *ca.* 3 : 1 and in a 45% yield. Since the elementary analyses of the mixture isolated by alumina chromatography agreed with the $C_{15}H_{14}S_2$ formula, it was assumed that this oily product was an isomeric mixture of the *cis* and *trans* olefinic compounds (XI). The NMR data (τ 3.53, 8.08 and τ 3.83, 8.02 besides the aromatic protons) also agreed with the above.

$$C_6H_5\underset{\displaystyle SCH_3}{\underset{|}{C}}HCH_3 + C_6H_5SCl \rightarrow$$

(IX)

$$C_6H_5\underset{\displaystyle Cl}{\underset{|}{C}}HCH_3 + CH_3SSC_6H_5 \quad (1)$$

(X) 55%

$$C_6H_5\underset{\displaystyle SCH_3}{\underset{|}{C}}HCH_3 + 3C_6H_5SCl \rightarrow C_6H_5\underset{\displaystyle SCH_3}{\underset{|}{C}}=CHSC_6H_5 + 3HCl + C_6H_5SSC_6H_5 \quad (2)$$

(XI) *cis* and *trans* 45%

The structure of XI was unambiguously determined by a comparison of the spectra with an authentic specimen prepared from α-phenylthioacetophenone dimethylmercaptal and dimethyl sulfate according to the published directions:[11]

$$C_6H_5\text{-}\underset{\displaystyle SCH_3}{\underset{|}{\overset{\displaystyle SCH_3}{\overset{|}{C}}}}\text{-}CH_2SC_6H_5 \xrightarrow{(CH_3O)_2SO_2} C_6H_5\underset{\displaystyle SCH_3}{\underset{|}{C}}=CHSC_6H_5 \quad (XI)$$

In order to examine the stoichiometry of this unusual olefin-forming reaction, the yields of the products were determined. Typical results from 0.030 mol of methyl α-phenethyl sulfide and 0.079 mol of benzenesulfenyl chloride are presented in Table 1. One point which warrants special attention is the formation of 149% of the hydrogen chloride. Since the formation of α-phenethyl chloride (Eq. (1)) does not need to liberate hydrogen chloride, the formation of 1 mol of the olefin should liberate 3 mol of hydrogen chloride. This treatment of the results also agrees with the distribution of the other products. Thus, Eq. (2) can be written for the formation of the olefin XI.

Table 1. Product distribution of the reaction between benzenesulfenyl chloride and methyl α-phenethyl sulfide in carbon tetrachloride at O°C

Compound	Yield[a] (%)
$C_6H_5CHClCH_3$	55 (b)
$CH_3SSC_6H_5$	55 (b)
HCl	149 (c)
$C_6H_5C(SCH_3):CHSC_6H_5$	45 (b)
$C_6H_5SSC_6H_5$	18 (d)

a) Yields based on methyl α-phenethyl sulfide.
b) NMR analysis.
c) Determined by titration.
d) Isolated yield based on benzenesulfenyl chloride. This does not have much significance, since excessive benzenesulfenyl chloride gives diphenyl disulfide during the work up.

Although the formation of the olefin XI may seem very curious, it can be explained by considering the process to involve the addition of the sulfenyl chloride or sulfenyl cation to α-methylthiostyrene, followed by dehydrochlorination or by the removal of a proton. In fact, the treatment of α-methylthiostyrene with equimolar benzenesulfenyl chloride in carbon tetrachloride at room temperature readily afforded a *cis* and *trans* mixture*[2] of the olefin XI, the distribution of which closely agreed with that formed in the reaction of methyl α-phenethyl sulfide. Hydrogen chloride was evolved during the course of the reaction. The above assumption can, then, be fairly well verified if the formation of α-methylthiostyrene during the reaction can be proved.

$$C_6H_5\underset{\displaystyle SCH_3}{\underset{|}{C}}=CH_2 + C_6H_5SCl \rightarrow C_6H_5\underset{\displaystyle SCH_3}{\underset{|}{C}}=CHSC_6H_5 + HCl \quad (XI)$$

The above discussion leads to the idea that some sulfides are dehydrogenated to form vinyl sulfide derivatives. This is in conformity with the observation in the reaction of stilbene and an excess of methanesulfenyl chloride[1] and suggests that the

8) W. E. Truce, G. Birum and E. T. McBee, *ibid.*, **74**, 3594 (1952).
9) D. L. Tuleen and T. B. Stephens, *J. Org. Chem.*, **34**, 31 (1969).
10) R. Oda and Y. Hayashi, *Tetrahedron Lett.*, **1967**, 3141.
11) J. Gosselck, L. Beress, H. Schenk and G. Schmidt, *Angew. Chem.*, **77**, 1140 (1965).

*2 As for the assignment of the configuration, see This Bulletin, **43**, 1234 (1970).

dehydrogenation of thioethers by sulfenyl chlorides is a fairly general reaction. However, in order to isolate the olefin intermediate, the olefin must be fairly inert toward the addition reaction of sulfenyl chloride. Thus, some other sulfides were treated with benzenesulfenyl chloride in an attempt to isolate the intermediate.

The olefinic linkage in an α,β-unsaturated carbonyl compound will be less reactive than the ordinary olefins toward the electrophilic attack because of the lower electron density. Thus, some α-methylthio ketone would give the α-methylthio-α,β-unsaturated ketone in the reaction with sulfenyl chloride. α-Methylthiocyclohexanone (XII) was treated with benzenesulfenyl chloride; as expected, 2-methylthio-2-cyclohexen-1-one (XIII) was isolated in a 40% yield. The structue of XIII was established on the basis of the spectral evidence and by the characterization of its 2,4-dinitrophenylhydrazone.

(XII) (XIII)

Other electron-deficient olefins, such as α-methylthioacrylonitrile and ethyl α-methylthioacrylate, were also detected when the corresponding nitrile and ester were treated with the sulfenyl chloride, although, in these cases, substitution by chlorine at the α-position was the main reaction.

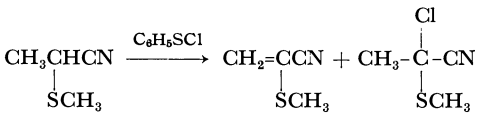

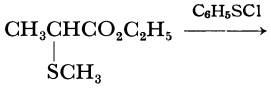

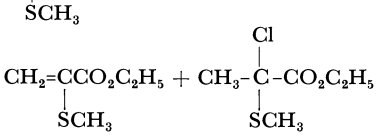

If 1,2-diphenylethyl methyl sulfide (XIV) is analogously dehydrogenated, it will give α-methylthiostilbene. However, XIV gave 30% corresponding chloride (XV) and 65% *cis*- and *trans*-α-methylthio-α'-phenylthiostilbene (XVI), the latter being formed by the addition of benzenesulfenyl chloride to α-methylthiostilbene, followed by dehydrochlorination (or by the addition of the sulfenyl cation, followed by the removal of the proton). These results indicate that the intermediate α-methylthiostilbene is too reactive to be isolated.

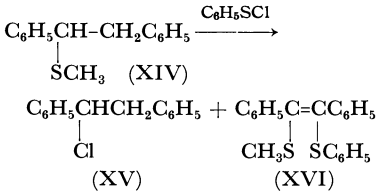

(XIV)

(XV) (XVI)

From these data it is now apparent that the vinyl sulfide derivative intervenes in these reactions and that the following equation, Eq. (3), can be written as a part of the reaction represented by Eq. (2):

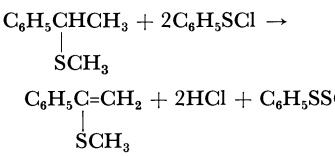

(3)

As to the oxidative chlorination of thioethers by sulfenyl chloride, there is another interesting example of the reaction. That is, α-methylthioacetophenone, which is not capable of undergoing dehydrogenation because of its structure, gives an almost quantitative yield of α-chloro-α-methylthioacetophenone. This is very interesting in that, while acetophenone gives α-phenylthioacetophenone when treated with benzenesulfenyl chloride, α-methylthioacetophenone does not give α-phenylthio-α-methylthioacetophenone. If only the enolization and addition are taken into account, α-methylthioacetophenone should have given α-phenylthio-α-methylthioacetophenone more easily. It seems that the sulfur atom in thioether is more vulnerable to attack in this case.

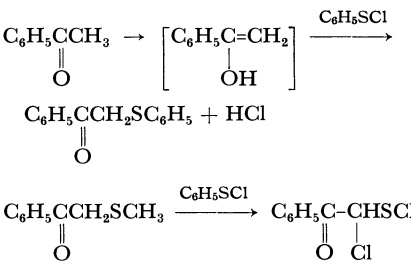

This oxidative chlorination may be classified as a Pummerer-type reaction,[12] which now seems to be a general term for a whole class of reactions involving the reduction of a sulfonium salt with the concomitant oxidation of the α-carbon.

It is thus established that three general types of reactions can occur for thioethers when they are treated with sulfenyl chlorides.

The first is an S_N1-type reaction on the sp^3 carbon atom where the cleavage of the carbon-sulfur bond takes place to produce the carbonium ion, followed by a nucleophilic attack by the chloride ion or by the removal of one of the α-hydrogens as a proton. This type of reaction was observed in the thioethers which carry alkyl groups which tend to give stable carbonium ions, such as the *t*-butyl cation. However, there is definitely another S_N2-type displacement of the alkylthio group by chlorine, for the treatment of optically active 1-phenyl-1-methylthiopropane with methanesulfenyl chloride gave

12) G. A. Russell and G. J. Mikol, "Mechanisms of Molecular Migrations," Vol. 1, Interscience Publishers, New York (1968), p. 157.

1-phenyl-1-chloropropane with an inverted configuration (see the Experimental part). The failure to detect styrene or its adduct in the reaction of methyl α-phenethyl sulfide could lend support to this proposition. This reaction seems to occur when the alkyl part gives a less stable carbonium ion.

$$C_6H_5\underset{\underset{SCH_3}{|}}{C}HC_2H_5 + CH_3SCl \rightarrow C_6H_5\underset{\underset{Cl}{|}}{C}HC_2H_5 + CH_3SSCH_3$$

inversion of configuration

The second type of reaction is the displacement of the α-hydrogen of the thioethers by chlorine to give α-chloro sulfide *i. e.*, oxidative chlorination. This reaction seems to take place when the carbonium ion alpha to sulfur is rather unstable and picks up the chloride anion before losing the proton. If the carbonium ion cannot lose the proton due to its inherent structure, this reaction takes place almost quantitatively.

The third type of reaction is the dehydrogenation which takes place competitively with the second type. It seems that dehydrogenation takes place preferentially when the carbonium ion alpha to sulfur is rather stable or when the product is stabilized by conjugation.

These three reactions may be summarized as in Eq. (4):

$$CH_3\text{-}\underset{|}{C}\text{-}SR \xrightarrow{R'SCl} \begin{cases} \rightarrow CH_3\text{-}\underset{|}{C}\text{-}Cl + CH_2{=}C\diagup \\ \rightarrow CH_3\text{-}\underset{|}{C}\text{-}Cl \\ \rightarrow CH_3\text{-}\underset{|}{\overset{Cl}{C}}\text{-}SR + CH_2{=}C\diagup\!\!\diagdown SR \end{cases} \quad (4)$$

It is not well understood what type of atom is necessary to induce these types of reactions with sulfenyl chlorides. However, the data accumulated in this laboratory indicate that chlorine and oxygen do not induce these reactions. That is, stilbene dichloride, α-phenethyl chloride, and benzyl ethyl ether failed to react with either benzene- or methanesulfenyl chloride.

Experimental

Starting Materials. Benzenesulfenyl chloride was prepared according to the published directions[13] and was always distilled prior to use. The thioethers, other than those indicated below, were prepared by methods that have already been described, and their physical constants were checked.

α-Methylthiostyrene. 1,2-Bis(methylthio)ethylbenzene[14] (45 g) was added to a solution of potassium *t*-butoxide prepared from 10 g of potassium and 400 m*l* of *t*-butyl alcohol, after which the mixture was heated under reflux for 3 hr. After the *t*-butyl alcohol had mostly been removed by distillation from the mixture, the remaining liquid was poured into 300 m*l* of water and extracted with ether. The ethereal extract was dried over anhydrous sodium sulfate and distilled to give 25 g of α-methylthiostyrene; bp 69—70°C/2 mmHg, n_D^{25} 1.5905 (lit,[14] n_D^{25} 1.5910). NMR (τ); 7.83 (3H, s), 5.16 (1H, s), 4.68 (1H, s), 2.5—2.9 (5H, m). IR (cm^{-1}); 1226, 1068, 1025, 848, 770, 699.

1,2-Diphenylethyl Methyl Sulfide. Methyl mercaptan (0.2 mol) was introduced at 0°C into a solution prepared from 4.6 g of sodium and 200 m*l* of ethanol. To this solution there was then added, drop by drop, 40 g of 1,2-diphenylethyl chloride in 100 m*l* of ethanol, after which the mixture was stirred under reflux for 10 min. The major portion of the solvent was removed under reduced pressure, and the residual mixture was extracted with ether after pouring it into 300 m*l* of water. The extract was dried over anhydrous sodium sulfate and distilled to afford 34 g of 1,2-diphenylethyl methyl sulfide; bp 151—152°C/3 mmHg, n_D^{28} 1.5938. NMR (τ); 8.29 (3H, s), 6.22 (1H) and 6.95 (2H) A_2X pattern, J_{AX}=8 Hz, 2.88 (5H, s), 3.0 (5H, m). IR (cm^{-1}); 1073, 1032, 768, 750, 730, 700, 543, 530. Found: C, 78.94; H, 7.06%. Calcd for $C_{15}H_{16}S$: C, 78.89; H, 7.07%.

General Procedure for the Reaction and the Product Analyses. To an approximately 0.2 M solution of the thioether in carbon tetrachloride, *ca.* 2 mol benzenesulfenyl chloride was added at room temperature under anhydrous conditions. After the reaction had been completed, the reaction mixture was poured into an aqueous solution of sodium bicarbonate and extracted with additional carbon tetrachloride. After the removal of most of the solvent under reduced pressure, the crude products were analyzed by NMR spectroscopy, and then any unknown products were isolated by distillation or by column chromatography. The reaction mixture before the removal of the solvent was examined by gas chromatography as required. An essentially quantitative consumption of the thioether was observed. Each product other than the known products was identified as will be described below.

Adducts of Benzenesulfenyl Chloride to Isobutylene. Isobutylene was slowly introduced into a carbon tetrachloride solution of benzenesulfenyl chloride at −10—0°C. The complete fading of the orange color indicated the completion of the reaction. After the solvent had then been removed under reduced pressure, the crude reaction mixture showed NMR signals for two isomers with a relative intensity of *ca.* 3 : 2; this was in fair agreement with that of the products from *t*-butyl phenyl sulfide and benzenesulfenyl chloride. In order to obtain analytical samples of the isomeric mixture, the adducts were distilled *in vacuo* when the distillate contained only one isomer. This isomer was found to be the Markownikoff adduct from the following data and from the dehydrochlorination to be described below. Bp 97°C/3 mmHg, n_D^{25} 1.5597 (lit,[15] bp 59—60°/3 mmHg, n_D^{28} 1.5661). NMR (τ); 8.45 (6H, s), 6.78 (2H, s), 2.7—3.1 (5H, m). IR (cm^{-1}); 1579, 1107, 1090, 740, 693, 615, 568. Found: C, 60.03; H, 6.24%. Calcd for

13) H. Lecher and F. Holschneider, *Chem. Ber.*, **57**, 755 (1924).

14) H. J. Schneider and J. J. Bargnell, *J. Org. Chem.*, **26**, 1984 (1961).

15) F. Montanari, *Tetrahedron Lett.*, **1964**, 2685.

$C_{10}H_{13}ClS$: C, 59.84; H, 6.53%.

The other product which disappeared on distillation had NMR signals at τ 8.62 (6H, s) and 6.48 (2H, s), the lower chemical shift of CH_2 supporting the assigned structure.

The distillate (9 g) was heated under reflux for 30 min with a solution prepared from 2 g potassium and 80 ml of *t*-butyl alcohol. After the usual work-up, the distillation of the product gave 5.1 g of 2-methyl-1-phenylthiopropene; bp 88°C/4 mmHg, n_D^{20} 1.5791 (lit,[16] n_D^{25} 1.5782). NMR (τ): 8.22 (3H, s), 8.20 (3H, d), 4.32 (1H, m), 3.05 (5H, m). IR (cm^{-1}): 1580, 803, 738, 690.

Benzyl Phenyl Disulfide. The crude mixture obtained from the reaction of benzyl *t*-butyl sulfide and benzenesulfenyl chloride was chromatographed on alumina to give the pure disulfide; $n_D^{28.5}$ 1.6409. NMR (τ): 6.32 (2H, s), 2.8—3.2 (10H, m). IR (cm^{-1}): 1070, 1027, 689, 567. Found: C, 67.19; H, 5.04%. Calcd for $C_{13}H_{12}S_2$: C, 67.17; H, 5.21%.

Methyl Phenyl Disulfide. The product from methyl α-phenethyl sulfide and benzenesulfenyl chloride was chromatographed on alumina. The disulfide was eluted as a yellow oil with petroleum ether; $n_D^{26.5}$ 1.6125. NMR (τ): 7.72 (3H, s), 2.7—3.2 (5H, m). IR (cm^{-1}): 1027, 955, 742, 693. Found: C, 53.75; H, 5.31%. Calcd for $C_7H_8S_2$: C, 53.80; H, 5.16%.

***cis*-and *trans*-α-Methylthio-β-phenylthiostyrenes.** This olefin was eluted with petroleum ether in a later fraction on the alumina chromatography of the product from the above-mentioned reaction. NMR (τ): 8.08 (3H, s), 3.53 (1H, s), 2.6—3.3 (10H, m) and 8.02 (3H, s), 3.83 (1H, s), 2.6—3.3 (10H, m). IR (cm^{-1}): 806, 758, 740, 698, 690. Found: C, 69.36; H, 5.33%. Calcd for $C_{15}H_{14}S_2$: C, 69.70; H, 5.46%.

***cis*-and *trans*-α-Methylthio-α′-phenylthiostilbenes.** An isomeric mixture of the olefin was isolated by alumina chromatography from the reaction mixture obtained from 1,2-diphenylethyl methyl sulfide and benzenesulfenyl chloride. NMR (τ): 8.17 (3H, s), 2.5—3.3 (15H, m) and 8.31 (3H, s), 2.5—3.3 (15H, m). IR (cm^{-1}): 1075, 1027, 738, 699, 582. Found: C, 75.41; H, 5.50%. Calcd for $C_{21}H_{18}S_2$: C, 75.41; H, 5.42%.

α-Chlorobenzyl Methyl Sulfide. Although this sulfide was not isolated, the NMR spectrum of the reaction mixture from benzyl methyl sulfide and benzenesulfenyl chloride showed the existence of the sulfide by the signals at τ 7.75 (3H, s) and 4.03 (1H, s); these signals were situated at the same positions as those of the chlorinated products of benzyl methyl sulfide with chlorine[6] or methanesulfenyl chloride.[10] When methanesulfenyl chloride was used, the reaction products were directly treated with 2,4-dinitrophenylhydrazine in acetic acid; the product was identified with the 2,4-dinitrophenylhydrazone of benzaldehyde (mp 237°C).

2-Methylthio-2-cyclohexen-1-one. The product from the reaction of α-methylthiocyclohexanone and benzenesulfenyl chloride was eluted with benzene through an alumina column to give crude 2-methylthio-2-cyclohexen-1-one, which showed an olefinic proton signal at τ 3.49 (triplet, J=4.5 Hz) in NMR and an absorption at 1679 cm^{-1} in IR.

When the crude product was treated with 2,4-dinitrophenylhydrazine, pure 2,4-dinitrophenylhydrazone of 2-methylthio-2-cyclohexen-1-one was obtained as dark red crystals; mp 222—224°C. NMR (τ): 7.66 (3H, s), 7.2—8.1 (6H, m), 3.78 (1H, t, J=4.5 Hz), aromatic protons (3H, m). IR (cm^{-1}): 3310, 848, 745. Found: C, 48.69; H, 4.65; N, 17.63%. Calcd for $C_{13}H_{14}O_4N_4S$: C, 48.44; H, 4.38; N, 17.38%.

α-Chloro-α-methylthiopropionitrile and α-Methylthioacrylonitrile. The NMR spectrum of the product from the reaction of α-methylthiopropionitrile showed two 1 : 1 singlets at τ 7.78 and 7.47 as the major component (90% yield). The formation of an olefinic compound in a small quantity (*ca.* 5%) was observed from the NMR signals at τ 3.99 (1H, d), 4.23 (1H, d), and 7.68 (3H, s); this compound was identified as α-methylthioacrylonitrile by comparing its NMR with that of an authentic sample prepared as described in the literature.[17] The major product was distilled under reduced pressure (29°C/4 mmHg); it was identified as α-chloro-α-methylthiopropionitrile from the spectroscopic data. IR (cm^{-1}): 2250, 720, 690. Treating this compound with 2,4-dinitrophenylhydrazine in ethanol and a small amount of sulfuric acid gave red crystalline hydrazone of pyruvonitrile; mp 185—186°C. NMR (τ): 7.61 (3H, s), aromatic proton (3H, m). IR (cm^{-1}): 3305, 2235, 850, 840, 745, 723, 600. Found: C, 43.41; H, 2.59; N, 28.35%. Calcd for $C_9H_7N_5O_4$: C, 43.38; H, 2.83; N, 28.10%.

Ethyl α-Chloro-α-methylthiopropionate and Ethyl α-Methylthioacrylate. The major component (40%) of the products was found to be ethyl α-chloro-α-methylthiopropionate by a study of the NMR spectrum of the crude reaction mixture (τ 8.02, τ 7.76, and ethyl protons). The ester was easily hydrolyzed to give ethyl pyruvate. The distillate (bp 28—43°C/5 mmHg), which contained the above product as the major component, was directly treated with 2,4-dinitrophenylhydrazine; the 2,4-dinitrophenylhydrazone of ethyl pyruvate was thus obtained; mp 155°C (lit,[18] mp 153°C). The structure of the olefinic product, which was obtained in a 15% yield, was assigned on the basis of a study of the NMR spectrum and from analogy with a previous example:[19] when the addition products of methanesulfenyl chloride to ethyl acrylate were dehydrochlorinated with an excess of triethylamine in carbon tetrachloride at 0°C, only the anti-Markownikoff adduct gave off hydrogen chloride to form ethyl α-methylthioacrylate, and the Markownikoff adduct was left intact. The NMR spectrum of the resulting products showed the signal of an olefinic compound at the same position as that of the product from the reaction of ethyl α-methylthiopropionate: τ 4.85 (s) and τ 3.75 (s).

α-Chloro-α-methylthioacetophenone. The NMR signals (τ 7.94, τ 3.65, and phenyl protons) of the product obtained from the reaction between α-methylthioacetophenone and benzenesulfenyl chloride agreed with those of the reaction product from α-methylsulfinylacetophenone and thionyl chloride,[20] and also with those

16) R. Adams and A. Ferretti, *J. Amer. Chem. Soc.*, **81**, 4927 (1959).

17) K. D. Grundermann and R. Thomas, *Chem. Ber.*, **89**, 1263 (1956).

18) W. W. Wisaksono and J. F. Arens, *Rec. Trav. Chim. Pays-Bas*, **80**, 846 (1961).

19) W. A. Thaler, W. H. Mueller and P. E. Butler, *J. Amer. Chem. Soc.*, **90**, 2069 (1968).

20) G. A. Russell and E. T. Sabourin, *J. Org. Chem.*, **34**, 2336 (1969).

of the product of the reaction between α-methylthioacetophenone and methanesulfenyl chloride.[21] The latter reaction was reported to give α-chloro-α-methylthioacetophenone.

Stereochemical Study of the Substitution Reaction. Optically active methyl 1-phenylpropyl sulfide was prepared from (−)-1-phenylpropyl chloride and methyl mercaptide. The stereochemical outcome must be inversion in this reaction. The treatment of the resulting (+)-sulfide with methanesulfenyl chloride afforded (−)-1-phenylpropyl chloride. Thus, the inversion of configuration must have taken place in this reaction, although racemization was observed to some extent.

$$C_6H_5\underset{\displaystyle Cl}{\underset{|}{C}}HC_2H_5 \xrightarrow{CH_3S^{\ominus}} C_6H_5\underset{\displaystyle SCH_3}{\underset{|}{C}}HC_2H_5 \xrightarrow{CH_3SCl} C_6H_5\underset{\displaystyle Cl}{\underset{|}{C}}HC_2H_5$$

(−)-1-Phenylpropyl Chloride. The racemic 1-phenylpropyl alcohol was resolved by the fractional crystallization of the strychnine salt of its hydrogen phthalate, $[\alpha]_{578}^{25}$ −25.53 (neat) (lit,[22] $[\alpha]_{578}^{25}$ −23.413 (neat)), and was treated with thionyl chloride as in the literature.[23] $[\alpha]_{365}^{25}$ −69.84, $[\alpha]_{436}^{25}$ −41.47 (ethanol) (lit,[23] $[\alpha]_{D}^{25}$ −28.9 (neat)).

(+)-Methyl 1-Phenylpropyl Sulfide. An ethanolic solution from 11.5 g of (−)-1-phenylpropyl chloride was treated with sodium methyl mercaptide from 0.075 mol of sodium in 130 m*l* of ethanol at 45°C for 20 min. The reaction mixture was then poured into an aqueous solution (200 m*l*) of sodium chloride and extracted with ether. The distillation of the extract after drying gave 9.3 g of (+)-methyl 1-phenylpropyl sulfide, bp 82°C/5 mmHg, $[\alpha]_{365}^{25}$ +108.49, $[\alpha]_{436}^{25}$ +64.70 (ethanol).

(−)-1-Phenylpropyl Chloride from (+)-Methyl 1-Phenylpropyl Sulfide and Methanesulfenyl Chloride. Methanesulfenyl chloride (3.8 g) was added to a solution of 7.5 g of (+)-methyl 1-phenylpropyl sulfide in 150 m*l* of carbon tetrachloride. After standing for 1 hr at 0°C, the mixture was decomposed with ice water. The organic part was then extracted with ether, dried over sodium sulfate, and distilled under reduced pressure to give 5.2 g of (−)-1-phenylpropyl chloride; $[\alpha]_{365}^{25}$ −47.97, $[\alpha]_{436}^{25}$ −27.61 (ethanol).

21) R. Oda and Y. Hayashi, *Tetrahedron Lett.*, **1967** 2181.

22) P. A. Levene and A. Rothen, *J. Biol. Chem.*, **127**, 237 (1939).

23) P. A. Levene, A. Rothen and M. Kuna, *J. Biol. Chem.*, **120**, 777 (1937).

BULLETIN OF THE CHEMICAL SOCIETY OF JAPAN VOL. 43 1229—1234 (1970)

The Reaction of Sulfenyl Chlorides with Thioethers. II. Kinetic Studies

Michinori Ōki and Keiji Kobayashi

Department of Chemistry, Faculty of Science, The University of Tokyo, Hongo, Bunkyo-ku, Tokyo

(Received November 17, 1969)

The rates of the reaction of methyl α-phenethyl sulfide with benzenesulfenyl chloride were measured by means of product analyses. It was found that the reaction was general-acid-catalyzed and autocatalyzed. The rate-determining step was suggested to be the formation of a sulfonium ion derived from the reactants. Mechanisms for the formations of the products are suggested.

In the preceding paper,[1] a general survey of the reactions of thioethers with sulfenyl chlorides has been presented. It has been established that three types of reactions occur, depending upon the structure of the thioethers: 1) the sulfur-carbon bond is cleaved to form a carbonium ion, which then undergoes nucleophilic substitution by chloride-ion and El-type elimination; 2) there is a cleavage of the C–S bond, with the simultaneous formation of a C–Cl bond, *i. e.*, an S_N2-type reaction takes place, and/or 3) there is oxidative chlorination at the alpha position, together with dehydrogenation, to form vinyl sulfide derivatives, probably *via* a common intermediate.

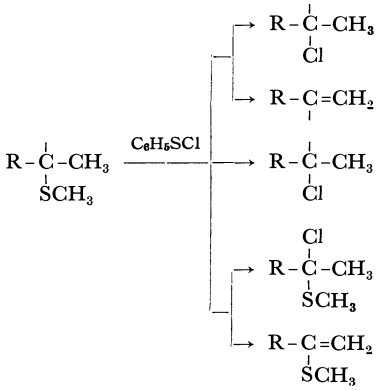

The purpose of this paper is to present kinetic data on the reaction between the thioether and the

1) M. Ōki and K. Kobayashi, This Bulletin, **43**, 1223 (1970).

sulfenyl chloride, and also to propose reaction mechanisms for the formation of products.

Results and Discussion

For the kinetic measurements, methyl α-phenethyl sulfide has been chosen as the sample because this compound has been shown to undergo two kinds of reactions of the possible three: the products are α-phenethyl chloride and a *cis-trans* mixture of α-methylthio-β-phenylthiostyrene. The stoichiometries of the formations of these compounds can be described as follows:[1]

$$C_6H_5\underset{\displaystyle SCH_3}{\underset{|}{C}}HCH_3 + C_6H_5SCl \rightarrow C_6H_5\underset{\displaystyle Cl}{\underset{|}{C}}HCH_3 + CH_3SSC_6H_5 \quad (1)$$

$$C_6H_5\underset{\displaystyle SCH_3}{\underset{|}{C}}HCH_3 + 3C_6H_5SCl \rightarrow C_6H_5\underset{\displaystyle SCH_3}{\underset{|}{C}}=CHSC_6H_5 + 3HCl + C_6H_5SSC_6H_5 \quad (2)$$

The rates of the reaction of 0.199M methyl α-phenethyl sulfide with 0.525M benzenesulfenyl chloride in carbon tetrachloride at 25°C were followed by analyzing the starting thioether and the products by means of the NMR spectra, after quenching a fraction of the reaction mixture by dilute alkali, at various time intervals. It was not hard to find signals which were suitable for analytical purposes; the product distribution was then computed from the relative intensities of the signals.

Characteristic kinetic curves are shown in Fig. 1, where the yields of the respective products are calculated on the basis of the starting methyl α-phenethyl sulfide. The olefinic isomer which is predominant at the completion of the reaction is named A, while the less populated isomer as B. The configuration of A is *cis*, as will be shown in a subsequent paper.[2]

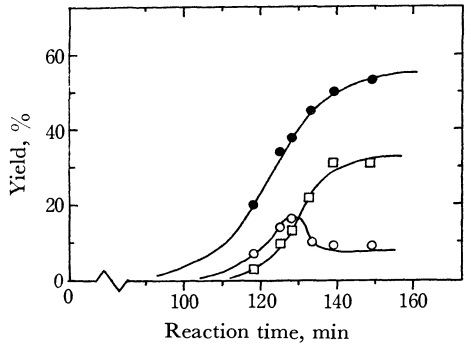

Fig. 1. Rate of the reaction of benzenesulfenyl chloride with methyl α-phenethyl sulfide at 25±0.1°C in carbon tetrachloride.
Initial concentration: benzenesulfenyl chloride 0.525M; methyl α-phenethyl sulfide 0.199M.

● : Yield of α-phenethyl chloride
□ : Yield of (A) ○ : Yield of (B)

The most remarkable feature of the kinetic curves is that each curve, not only of the olefin-forming reaction but of the chlorine-substitution reaction, shows the formation of the products with a definite induction period.

The addition of a small amount of trichloroacetic acid to the reaction mixture caused an increase in the rate of the formation of the products, whereas no decrease in the rate was observed upon the addition of a radical scavenger, 2,4,6-tri-*t*-butylphenol or *p*-benzoquinone, ruling out the possibility that these are radical reactions.

The appearance of the induction period, together with the rapid rise of the curve, suggests that some of the reaction products may be acting as catalysts; that is, these may be autocatalyzed reactions. None of the reaction products, except for the hydrogen chloride which was released by the reaction shown by Eq. (2), seemed to catalyze the reaction. Accordingly, a definite amount of trichloroacetic acid was added to the mixture, since, if this is a general acid-catalyzed reaction, the rate must be increased on the addition of this compound. The results, shown in Fig. 2, clearly indicate that the induction

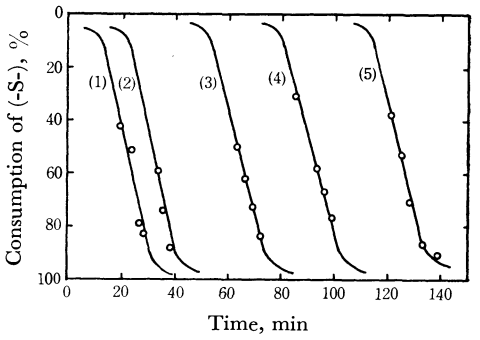

Fig. 2. The effect of added trichloroacetic acid on the rate of disappearance of methyl α-phenethyl sulfide.

Initial concentration of trichloroacetic acid:
(1) 4.11×10^{-3}M (2) 2.74×10^{-3}M
(3) 1.37×10^{-3}M (4) 0.69×10^{-3}M
(5) without trichloroacetic acid

period, characterized by the half-life period of the starting material, decreases with the increase in the concentration of added trichloracetic acid, providing a firm basis for the idea that the reaction is general-acid-catalyzed. Further support is obtained from the facts that Lewis acids such as alu-

2) M. Ōki and K. Kobayashi, This Bulletin **43**, 1234 (1970).

minum chloride and boron trifluoride also have the ability to catalyze the reaction.

Evidence that this reaction is autocatalyzed is obtained by plotting the logarithm of the initial concentration of acid *versus* the half-life period of methyl α-phenethyl sulfide. A good linear relation is obtained between these quantities, as is shown in Fig. 3. Since this behavior is characteristic

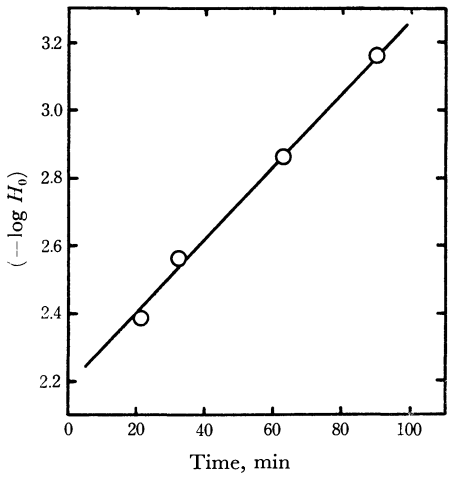

Fig. 3. Plot of the half-life period of methyl α-phenethyl sulfide *vs.* the logarithm of the concentration of added trichloroacetic acid (H_0).

of the autocatalyzed reactions, as will be discussed later, it is now established that the reaction between methyl α-phenethyl sulfide and benzenesulfenyl chloride is general-acid-catalyzed and autocatalyzed.

Under the conditions of a pseudo-first order, *i. e.*, high concentrations of acid and one of the reactants, the reaction was too fast to follow by conventional methods. Therefore, the following discussion has to rely upon the results of the product analyses.

The rates of the disappearance of the sulfide are affected by the initial concentrations of itself and of benzenesulfenyl chloride. As is shown in Fig. 4, the change in the initial concentration of benzenesulfenyl chloride, with the concentration of the sulfide kept constant, modified both the shape of the kinetic curves and the half-life period of methyl α-phenethyl sulfide. A similar dependence of the features of the curves on the initial concentration of methyl α-phenethyl sulfide was also observed, using the constant concentration of the sulfenyl chloride.

These results suggest that at least three molecules participate in the rate-determining step of the reaction: one molecule each of the sulfide, the sulfenyl chloride, and acid.* The existence of the induction period, not only in the formation of the olefins but also in the substitution reaction, suggests that there is a common intermediate from which two pathways are initiated to give chloride on the one hand and to give olefins on the other, and that the formation of the intermediate is the rate-determining step. Accordingly, the rates may be expressed by the following equation:

$$\text{rate} = k(\text{acid})(\text{sulfide})(\text{sulfenyl chloride})$$

A detailed observation of the rates of disappearance of *t*-butyl phenyl sulfide, on treatment with benzenesulfenyl chloride, shows the presence of the induction period here also. The same is true for the reactions of other sulfides, reported in the preceding paper, with benzenesulfenyl chloride. Thus, it is common for there to exist an induction period when sulfides are treated with sulfenyl chlorides.

The rates of the autocatalyzed three-molecular reaction can be expressed by,

$$\frac{dP}{dt} = k(R_0-P)(S_0-yP)(H_0+xP) \qquad (3)$$

where R, S, and P are the concentrations of methyl α-phenethyl sulfide, benzenesulfenyl chloride, and the products respectively, after t minutes. R_0, S_0, and H_0 denote the initial concentrations of the reactants, whereas x and y are the constants as determined by stoichiometry and represent the amount of hydrogen chloride formed by the reaction and the sulfenyl chloride consumed per mole of the consumed sulfide. Here it is assumed that, during the reaction, the ratio of the products from the two reactions is constant throughout. This assumption seems fair judging from the experimental results: a 55 : 45 ratio is observed at all times during the reaction. It is also assumed that the efficiency of hydrogen chloride as the catalyst is the same as that of trichloroacetic acid. Thus, H_0 is null when no trichloroacetic acid is added.

By integrating Eq. (3) when H_0 is negligible compared with R_0, S_0, and $P_{1/2}$, which is the concentration of products at the half-life period of the sulfide ($t_{1/2}$), the following relation between H_0 and $t_{1/2}$ is obtained:

$$t_{1/2} = -\frac{\ln H_0}{kxR_0S_0} + \text{"constant"} \qquad (4)$$

The term "constant" contains neither H_0 nor $t_{1/2}$. The observed relationship shown in Fig. 3 is in harmony with Eq. (4), since this equation shows that $t_{1/2}$ and (−log H_0) are related linearly. Equation (4) also implies that half-life period decreases with the increase in concentrations of either the sulfide or the sulfenyl chloride; it was found that this implication was really the case (for example, see Fig. 4).

Furthermore, it can be expected from Eq. (4) that kxR_0S_0 can be obtained as the slope in Fig. 3,

*1 It is not possible from these results to know how many molecules of the acid are participating. The authors assume that only one molecule of the acid is taking part in the reaction for the sake of convenience and simplicity of the analyses.

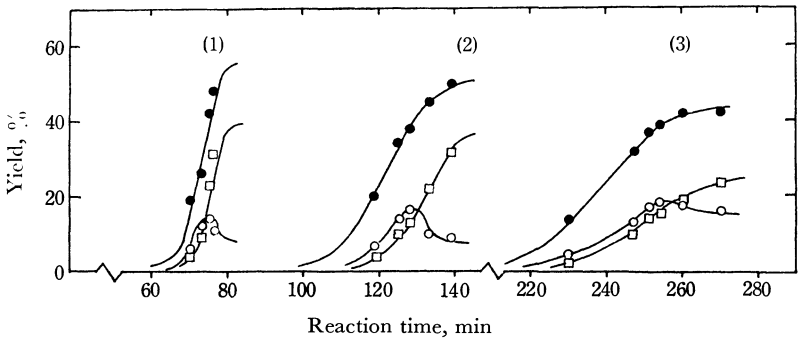

Fig. 4. The dependence of kinetic curves on the initial concentration of benzenesulfenyl chloride.
● : Yield of α-phenethyl chloride ○ : Yield of olefin (B)
□ : Yield of olefin (A)
Initial concentration; (1) (-S-): 0.199M, (PhSCl): 0.683M
(2) (-S-): 0.199M, (PhSCl): 0.525M
(3) (-S-): 0.199M, (PhSCl): 0.420M

since $t_{1/2}$ is now the abscissa and $(-\log H_0)$, the ordinate. Thus, various inclinations of the relationship between $(-\log H_0)$ and $t_{1/2}$ were obtained with various initial concentrations and plotted against R_0S_0. The good linear relation of these quantities implies that above treatment is fair (Fig. 5). These results also support the idea that

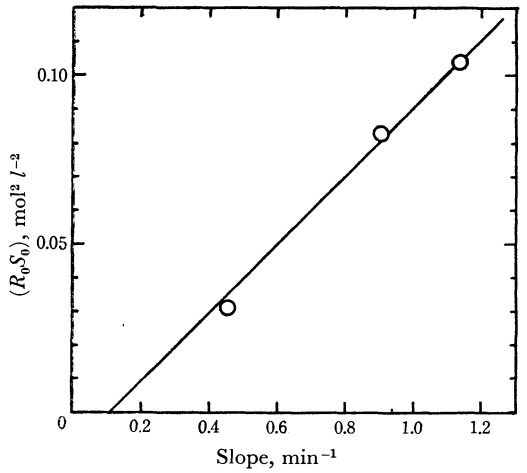

Fig. 5. Plot of the slope *vs.* R_0S_0.

the reaction is first-order in both the thioether and the sulfenyl chloride, since, if this were not the case, the linear relation would have been found between the slope and $(R_0S_0)^n$ instead of between the slope and R_0S_0.

From the discussions presented above, it appears that acid is necessary in order to promote the reaction of the thioether with the sulfenyl chloride, and that the formation of an intermediate from thioether, sulfenyl chloride, and acid is the rate-determining step. After the rate-determining step, there are several rapid reaction paths which could result in the formation of the products. A sulfonium ion resulting from the electrophilic attack by benzenesulfenyl chloride on the sulfur atom of the thioether is the most likely such intermediate, since the rate is proportional to the concentrations of both the thioether and the sulfenyl chloride.

Although there are many points to be clarified before we have a full understanding of the catalytic action of the acid, at present the authors choose to attribute it to the aid of acids in polarizing the sulfenyl chloride in an activated complex. That is, it is assumed that, although sulfenyl chlorides are polar enough to add to the olefinic bonds by second-order kinetics, they are too poorly electrophilic to attack the sulfur atom directly and that, subsequently, acids are necessary to assist the polarization. Thus, a kind of concerted mechanism can now be postulated:

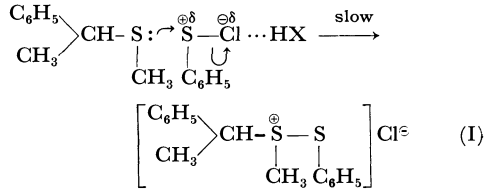

An analogy for this concerted reaction mechanism may be found in the electrophilic addition of hydrogen halide to olefins, which has been suggested[3] to proceed *via* an activated complex which involves a few extra molecules of hydrogen halide in addition to the actually-adding molecule of HX. The paticipation of the extra molecule has been attributed to assistance in the polarization of the attacking hydrogen halide, thus facilitating the ionic cleavage of the molecule.

The reactions involving the electrophilic attack

3) F. R. Mayo and J. J. Katz, *J. Amer. Chem. Soc.*, **69**, 1339 (1947).

by sulfenyl chloride are known to be accelerated by an acidic catalyst: the addition of sulfenyl chloride to the acetylenic bond[4] and electrophilic aromatic substitution[5] with arenesulfenyl chloride are catalyzed by Lewis acids. These examples, together with the results presented here, suggest that the sulfenium cation, RS^+, plays an important role in the electrophilic attack by the sulfenyl chlorides. Moreover, this idea is in conformity with the fact[6] that the solution of methanesulfenium 2,4,6-trinitrobenzenesulfonate generates dimethyl(methylthio)sulfonium salts in the presence of dimethyl sulfide.

It may be argued that the sulfonium ion (I) would be formed rather rapidly from the sulfenyl chloride and the sulfide, and that the decomposition of the sulfonium ion, I, would be the rate-determining step, because the data presented here are confined to product analyses and to the measurement of the half-life period, and because various S_N2 reactions of sulfonium ions are known. This argument can be worthwhile if it is assumed that the sulfonium ion from the disulfide gives back the starting sulfide upon the subsequent work-up. However, it is rather unlikely, since the measurements of the ultraviolet spectra ($\lambda_{max}=390$ mμ, $\varepsilon=470$) of benzenesulfenyl chloride, when mixed with the thioether, show an induction period in the decrease in the absorption coefficient, indicating that the sulfenyl chloride is not used until some time later, even in the presence of the thioether. The decrease in intensity might have been observed immediately after mixing if I were formed rapidly. Furthermore, this induction period corresponds to that of the decrease in the thioether.

After the unstable sulfonium ion intermediate is formed, the reaction may now take three different courses, according to the structure of the intermediate. One reaction path is the loss of the disulfide molecule to form a carbonium ion, which then undergoes nucleophilic substitution or the elimination of a proton to form the olefin. This occurs when a stable carbonium ion is to be formed; *t*-butyl phenyl sulfide[1] is an example. The second path is the S_N2 reaction by the chloride ion, which is evident from the inversion of the configuration in the reaction of methyl 1-phenylpropyl sulfide.[1] The third path is the elimination of α-hydrogen and the alkylthio (or arylthio) group. The mechanism of this last case has not been studied well enough to present the details here, but, by analogy from other Pummerer-type reactions, it can tentatively be postulated that a sulfur ylide is formed first by the elimination of α-hydrogen as the proton, followed by the elimination of the phenylthio group. In the latter step, probably another molecule of benzenesulfenyl chloride assists the removal by forming diphenyl disulfide. The carbonium ion thus formed will give α-chloro sulfide if it is not too stable, whereas it will give α,β-unsaturated sulfide if it can survive long enough to eliminate a proton from the β-carbon.

Although α,β-unsaturated sulfide is sometimes obtained[7] in the original Pummerer reaction, *i.e.*, the reaction of sulfoxide and acetic anhydride,

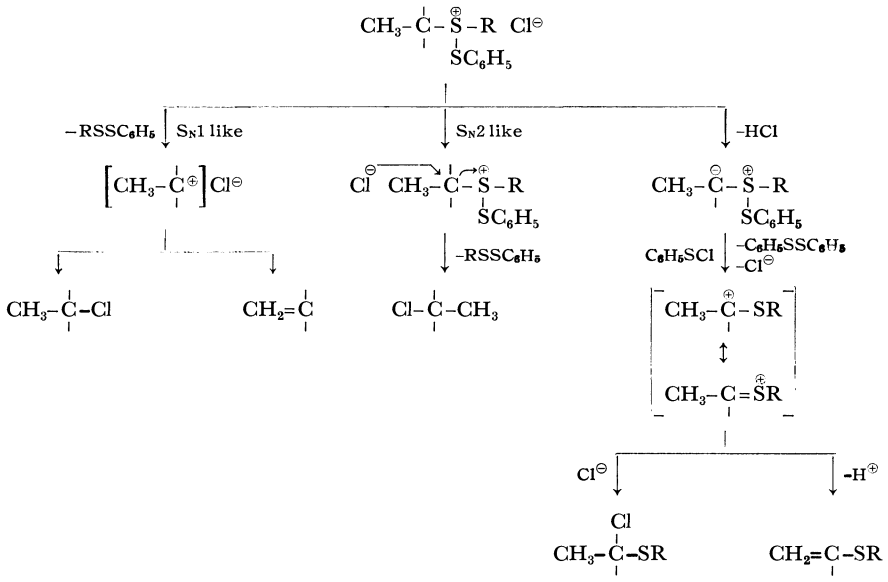

4) N. Kharasch and S. J. Assony, *ibid.*, **75**, 1081 (1953).

5) C. M. Buess and N. Kharasch, *J. Amer. Chem. Soc.*, **72**, 3529 (1950).

6) G. K. Helmkamp, D. C. Owsley, W. M. Barnes and H. N. Cassey, *ibid.*, **90**, 1635 (1968).

7) W. E. Parham and M. D. Bhavsar, *J. Org. Chem.*, **28**, 2686 (1963): R. B. Morin, D. O. Spry and R. A. Mueller, *Tetrahedron Lett.*, **1969** 849.

its formation can be explained if the thermal decomposition of an intermediate α-acetoxy sulfide is assumed. Therefore, there can be disagreement concerning the mechanism of the formation of α,β-unsaturated sulfide in the Pummerer reaction. The present authors feel that the discussions given above may throw light on the possibility of the presence of a carbonium ion intermediate in the formation of α,β-unsaturated sulfide.

Experimental

Starting Materials. Methyl α-phenethyl sulfide was prepared from α-phenethyl chloride and methyl mercaptan and was freshly distilled immediately before making the solution for experiments in every case; bp 67°C/3 mmHg, $n_D^{20.5}$ 1.5491 (lit,[8] n_D^{20} 1.5497).

Benzenesulfenyl chloride was prepared from diphenyl disulfide and chlorine, as in the literature,[9] and was always distilled prior to its use; bp 79°C/10 mmHg.

Carbon tetrachloride of a commercial source was purified by distillation.

Commercial trichloroacetic acid was distilled under reduced pressure in a dry atmosphere. Contact with moisture was carefully avoided.

Rate Measurements. Stock solutions of the sulfenyl chloride, methyl α-phenethyl sulfide, and trichloroacetic acid were prepared by weighing the proper amounts of the freshly-purified materials and by then making the solution up to the desired volume with dry carbon tetrachloride at 25°C. The solutions were then brought to a desired temperature (25±0.1°C) in a constant-temperature bath. The desired volume of each solution was pipeted and mixed. Although some change in volume may result from the mixing of three kinds of solutions, this effect was neglected in the calculation.

The reaction mixture was taken out with a pipet, *ca.* 20 m*l* at a time, and drained into a separately funnel containing 30 m*l* of aqueous sodium carbonate. The lower layer was dried over anhydrous sodium sulfate and then submitted to NMR analysis after filtration. In the NMR spectra of the reaction mixture, the signal of the methylthio protons of methyl α-phenethyl sulfide and the lower one of the doublet signal of methyl protons of α-phenethyl chloride coincided. However, the yields based on methyl α-phenethyl sulfide could be calculated by the integration of the other, non-overlapping signals.

8) W. E. Bacon and W. M. LeSuer, *J. Amer. Chem. Soc.*, **76**, 670 (1954).

9) H. Lecher and F. Holschneider, *Chem. Ber.*, **57**, 755 (1924).

BULLETIN OF THE CHEMICAL SOCIETY OF JAPAN VOL. 43 1234—1238 (1970)

The Reaction of Sulfenyl Chlorides with Thioethers. III. The Configuration and the Isomerization of *cis*- and *trans*-α-Methylthio-β-phenylthiostyrenes

Michinori Ōki and Keiji Kobayashi

Department of Chemistry, Faculty of Science, The University of Tokyo, Hongo, Bunkyo-ku, Tokyo

(Received November 17, 1969)

Various α-methylthio-β-arylthiostyrenes were prepared by the action of arenesulfenyl chloride on α-methylthiostyrene. The configuration of the stereoisomers of the styrene derivatives was determined by studying the nuclear Overhauser effect in the proton magnetic resonance. The relative stabilities of α-methylthio-β-phenylthiostyrene isomers were determined by equilibrating with the aid of hydrogen chloride at various temperatures.

It has been found that the treatment of methyl α-phenethyl sulfide with benzenesulfenyl chloride in carbon tetrachloride gives an isomeric mixture of *cis*- and *trans*-α-methylthio-β-phenylthiostyrenes in a 45% yield according to the following stoichiometry:

$$C_6H_5\underset{\displaystyle SCH_3}{\underset{|}{C}}HCH_3 + 3C_6H_5SCl \rightarrow C_6H_5\underset{\displaystyle SCH_3}{\underset{|}{C}}=CHSC_6H_5 + 3HCl + C_6H_5SSC_6H_5 \quad (I)$$

As has been shown in our previous papers,[1,2] one isomer which was predominant in the earlier stage of the reaction gradually decreased in quantity and another isomer became predominant in the later stage. That is, the formation of the olefins is kinetically-controlled, but these isomers are equilibrated even at room temperature under the present reaction conditions.

1) M. Ōki and K. Kobayashi, This Bulletin, **43**, 1223 (1970).
2) M. Ōki and K. Kobayashi, *ibid.*, **43**, 1229 (1970).

Since this phenomenon seemed interesting from the standpoints of stereochemistry and the reaction mechanism, an extensive study was made of the stereochemistry of the olefins. The purpose of this paper is to report the assignment of the configuration and some pertinent data on the geometrical isomers of α-methylthio-β-phenylthiostyrene.

Results and Discussion

Separation of Isomers. The NMR spectrum of the isomeric mixture of α-methylthio-β-phenylthiostyrene shows two sharp singlets for CH_3S protons at τ 8.08 and 8.02 and two singlets for olefinic protons at τ 3.53 and 3.85. From the integration of the peaks, the signals at τ 8.08 and 3.53 are assigned to one isomer and those at τ 8.02 and 3.85 to another. Hereafter, the isomer which is obtained in a higher yield at the equilibrium will be called the isomer A, and the other, the isomer B, for the sake of simplicity in discussion. The ratio of the formation of IA and IB is calculated from the NMR integration to be approximately 3 : 1 under the present reaction conditions.

All attempts at separating isomer IA and IB ended in failure. Therefore, we aimed to separate the corresponding isomers with a substituent at the *p*-position of the phenylthio group, since it seemed that the introduction of a substituent might help the separation owing to the change in intermolecular forces. Thus, α-methylthiostyrene was treated with *p*-nitrobenzene-, *p*-bromobenzene-, *p*-chlorobenzene-, *p*-methylbenzene-, and *p*-methoxybenzene-sulfenyl chlorides; the corresponding α-methylthio-β-arylthiostyrenes (II—VI) were thus obtained:

$$C_6H_5C(SCH_3)=CH_2 + ArSCl \rightarrow C_6H_5C(SCH_3)=CHSAr + HCl$$

II: Ar=*p*-$NO_2C_6H_4$ V: Ar=*p*-$CH_3C_6H_4$
III: Ar=*p*-BrC_6H_4 VI: Ar=*p*-$CH_3OC_6H_4$
IV: Ar=*p*-ClC_6H_4

The *p*-nitrophenylthio derivatives (IIA and IIB) could be separated by fractional recrystallization from ethanol. The less soluble isomer was found from its NMR spectrum to be the isomer IIA; the isomer which was richer at the equilibrium was found to be less soluble. Therefore the more soluble isomer was IIB. The less soluble isomers of the *p*-bromo derivative (IIIA) and the *p*-chloro derivative (IVA) were also isolated by recrystallization.

Assignment of the Configuration. Since we will not attempt to assign all the configurations of the olefins, but to use analogy in making assignments, it will be necessary to establish the general tendency of the physical and/or chemical characteristics of the A or B series and to confirm that the analogy holds in this series. The relative stabilities have already been established from the equilibration, and it will be safe to say that the introduction of a substituent at the *p*-position of the phenylthio group will not affect the stability to such an extent that the relative stability will be reversed, since this is rather a minor change in the whole molecule.

The second criterion is the chemical shifts of the olefinic and methylthio protons of the series. As is shown in Fig. 1, the more stable isomers, the series

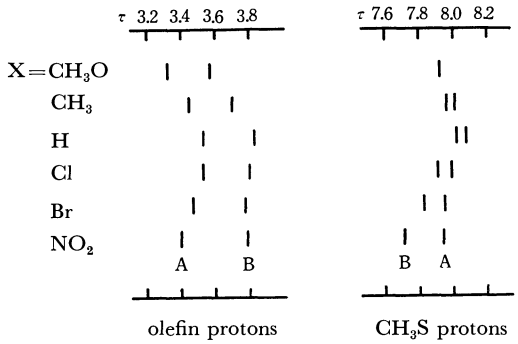

Fig. 1. Chemical shift data of the protons of α-methylthio-β-arylthiostyrenes in carbon tetrachloride solution (*ca.* 10%) except for the nitro derivative ($CDCl_3$).

A, always exhibit the methylthio signals at a higher field, and the olefinic proton signals, at a lower field, than the series B, except that the *p*-methoxy derivative (VI) happens to give signals of the methylthio protons of A and B at the same chemical shift. Here again, it may be assumed that the series A has the same configuration, since it is not usual to postulate that the introduction of a substituent may cause an abrupt anomaly in the chemical shifts of a series of compounds.

In spite of various attempts, we found it impossible to assign the configurations for the isolated isomers, IIA and IIB, on the basis of these chemical behavior: for example, attempted cyclization with ethylene iodide by heating ended only in the recovery of the starting material. The UV and the

Table 1. Spectroscopic data for the geometrical isomers of α-methylthio-β-*p*-nitrophenylthiostyrene (II)

	A more stable	B less stable
mp (°C)	134—135	88—89
NMR (τ)	7.94 (3H, s)	7.71 (3H, s)
in $CDCl_3$	3.40 (1H, s)	3.79 (1H, s)
	aromatic protons	
	(5H, m: 4H, m)	(5H, s: 4H, m)
UV in C_2H_5OH	231 (14800)	223 (16800)
mμ (ε)	289 (9500)	280 (8600)
	367 (13900)	364 (12700)
IR (cm^{-1})	1337, 1095, 840	1339, 1095, 833
	761, 742, 700	761, 735, 700

IR spectra of these isomers, shown in Table 1, do not help much in assigning the stereochemistry. Although the former does show some difference in the absorption maxima, the coplanarity of the molecule can not be assumed because of the steric effect of the other groups; this assumption is, however, essential to establishing the configuration from the UV spectra.

However, the NMR spectral data in Table 1 do give some clue for elucidating the structure of the isomers. If it is assumed that the additivity rule of the chemical shifts in substituted ethylenes holds in these cases, as has been reported by Pascual and his co-workers,[3] the chemical shift of the olefinic protons in the *cis* isomer will be at a lower field than in the corresponding *trans* isomer, since it is expected that a proton *cis* to the phenyl ring and *trans* to the methylthio group will give a signal at a lower field than the counterpart, which is *trans* to the phenyl and *cis* to the methylthio group. Thus, from the additivity rule, the compounds of the series A should be assigned to the *cis* isomers:

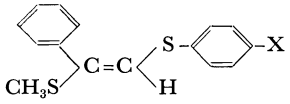

trans

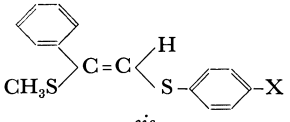

cis

It will not be safe, however, to rely too heavily on the additivity rule in the assignment, because the coplanarity of the molecule will not necessarily hold in these compounds. In order to confirm this tentative assignment, it will be necessary to use another technique in assigning the structure; the measurement of the intramolecular nuclear Overhauser effect (NOE) was chosen for this purpose.

The NOE has been increasingly used in assigning the stereochemistry of the organic compounds by identifying those protons which are in close proximity and which are coupled by dipole-dipole interaction. The transient method[4] was utilized for the NOE measurement with degassed solutions of IIA and IIB in deuteriochloroform. The magnetization of the methylthio protons was saturated by irradiating them at τ 7.94 for IIA and at τ 7.71 for IIB. After the irradiation, a transient recovery of the enhanced signal intensity of the olefinic proton to the thermal equilibrium was observed; IIB showed a definite enhancement in this process, while no change in signal intensity took place upon

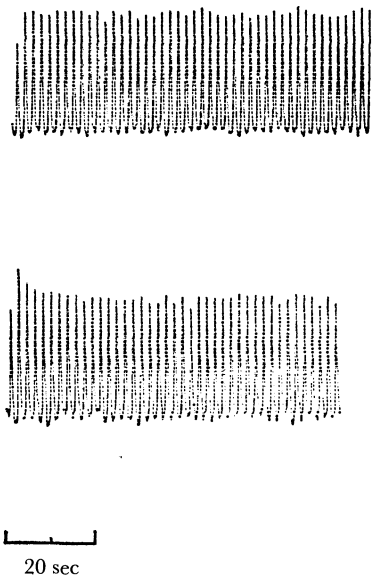

Fig. 2. Nuclear Overhauser enhancement and recovery to the thermal equilibrium of the olefinic proton.

this treatment in IIA. From Fig. 2, it can be estimated that a 25% Overhauser enhancement is associated with IIB, whereas IIA does not show any intramolecular NOE.

The spin-lattice relaxation time (T_1) of the olefin proton was also measured. The estimation of T_1 is necessary because the following correlation[4,5] should be used in comparing the internuclear distance between two protons in a pair of configurational or conformational isomers:

$$d \propto \left[\frac{T_1}{\eta}\right]^{1/6}$$

where η is the nuclear Overhauser enhancement parameter; d is, in this case, the internuclear distance between the methylthio and the olefinic protons. Namely, if the T_1 of one proton is much larger than the other, it may affect the observed enhancement.

T_1 was found to be 4.7 sec for the olefinic proton of the isomer IIB, which showed a 25% enhancement of the signal intensity, whereas that for IIA was 5.8 sec. These results establish that the distance between two kinds of protons in IIB is shorter than that in IIA, since the T_1 for the olefinic proton of IIB is the smaller; if it were T_1 that was affecting the enhancement, IIA would show more enhancement than IIB.

The distance between the olefinic proton and a closest proton in the methylthio group in the *trans* isomer is estimated to be 1.5 Å from the Dreiding model, if the molecule assumes a conformation which possesses these protons at the

3) U. E. Matter, C. Pascual, E. Pretsch, A. Pross, W. Simon and S. Sternhell, *Tetrahedron*, **25**, 691 (1969).

4) T. Fukumi, Y. Arata and S. Fujiwara, *J. Mol. Spectrosc.*, **27**, 443 (1968).

5) F. A. L. Anet and A. J. R. Bourn, *J. Amer. Chem. Soc.*, **87**, 5250 (1965).

closest approach, whereas the protons in the *cis* isomer are far apart. Thus, IIA is assigned to the *cis* isomer, and IIB, to the *trans*, confirming the results obtained by the use of the additivity rule.

The NOE of the *p*-methoxyphenylthio derivative (VI) was also examined by the usual stationary state method. Although the isomers could not be separated, and although they happened to give methylthio signals at the same chemical shift, τ 7.92, the situation was rather auspicious for the NOE measurements: simple irradiation at τ 7.92 and observation of the intensities at the olefinic proton region sufficed in comparing the isomers. A degassed sample of VI, which contained *ca.* 2 : 1 isomers of A and B, was irradiated. The olefinic signal due to VIB showed 21% NOE, the amount of which was estimated from the relative change in the intensities of the two singlets at τ 3.57 (VIB) and τ 3.32 (VIA). Thus, VIB can be assigned to the *trans* isomer, and VIA, to the *cis*.

At this stage, it has been established that the isomers of the A series, which are the more stable, have the *cis* configuration, while those of the series B have the *trans* configuration.

The observation of NOE enhancement for IIB and VIB indicates that the olefinic and methylthio protons are in close proximity, which would require that the carbon-sulfur bond in the methylthio group eclipse the carbon-carbon double bond (VII). If it were taking the S-*trans* conformation (VIII), the enhancement would be expected to be very small, since the distance between the two kinds of protons is estimated to be more than 4.6 Å from the Dreiding model, in contrast to 1.5 Å in the S-*cis* conformation.

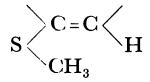

(VII)

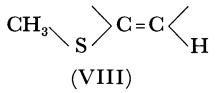

(VIII)

This conformation is supported by the analogy of the situation in methyl vinyl ether, which has been shown by microwave spectroscopy to possess the S-*cis* conformation.[6] There is also an example of NOE measurement with methyl vinyl ether derivatives in which NOE is observed between the *O*-methyl protons and the vinyl proton *cis* to each other.[7]

Relative Stabilities of the *cis-trans* Isomers. The *cis-trans* isomerization of the olefiins can be effected by the action of hydrogen chloride in carbon tetrachloride. The mechanism of the isomerization is assumed to proceed *via* a carbonium ion intermediate which is formed by addition of a proton and which forms olefins by the elimination of the proton. Incidentally, the intermediate is the same as that assumed in the addition of sulfenyl chloride to α-methylthiostyrene.

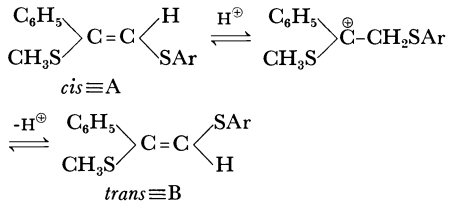

To estimate the thermodynamic parameters for the pair of *cis* and *trans* isomers, II was equilibrated with hydrogen chloride in carbon tetrachloride at four temperatures. The isomer distribution was calculated from the integration of the signal areas of the NMR spectra. The Arrhenius plot is shown in Fig. 3, while the parameters obtained therefrom are summarized in Table 2.

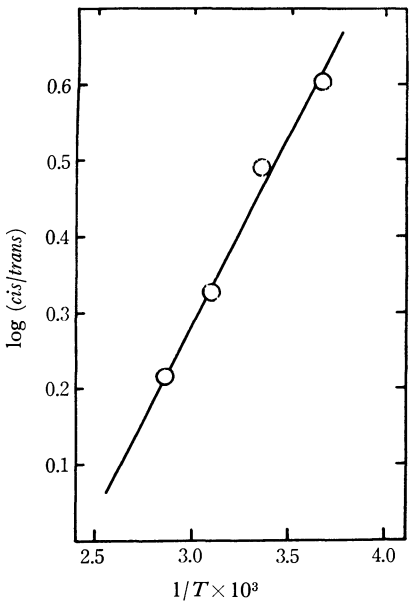

Fig. 3. Arrhenius plot for the *cis-trans* equilibration of α-methylthio-β-phenylthiostyrene.

Table 2. The thermodynamic parameters for the *cis-trans* equilibration of α-methylthio-β-phenylthiostyrene

ΔH	-2.2 ± 0.7 kcal/mol
ΔS	-5 ± 2 e.u.

Although the reasons for the stability of the *cis* isomer relative to the *trans* are not completely understood at the present time, two factors may be considered. The first factor may be of the steric origin. If it is assumed (and it is common to assume) that the steric effect in the olefinic compound is determined by the first atom which directly

6) P. Cahill, L. P. Gold and N. L. Owen, *J. Chem. Phys.*, **48**, 1620 (1968).

7) M. C. Woods, I. Miura, A. Ogiso, M. Kurabayashi and H. Mishima, *Tetrahedron Lett.*, **1968**, 2009.

Table 3. α-Methylthio-β-arylthiostyrenes ($C_6H_5C(SCH_3)$: $CHSC_6H_4X$-*p*)

X	NMR (τ)		Molecular formula	Analyses			
				calcd		found	
	SCH_3	=CH		C	H	C	H
OCH_3	A 7.92 B 7.92	3.32 3.57	$C_{16}H_{16}OS_2$	66.63	5.59	66.86	5.48
CH_3	A 8.01 B 7.96	3.45 3.70	$C_{16}H_{16}S_2$	70.54	5.92	70.34	6.18
Cl	A 7.99 B 7.91	3.53 3.80	$C_{15}H_{13}ClS_2$	61.51	4.47	61.42	4.21
Br	A 7.95 B 7.91	3.53 3.80	$C_{15}H_{13}BrS_2$	53.41	3.88	53.63	3.94
NO_2	A 7.94 B 7.71	3.40 3.79	$C_{15}H_{13}NO_2S_2$	59.38	4.32	59.18 59.45	4.52 4.21

attaches to the double bond, when there is freedom of rotation for the other part, sulfur must play the main role in determining the steric effect in the methylthio and arylthio groups; by appropriate rotation, methyl and aryl groups can take conformations in which these groups have little steric effect. Therefore, it is the van der Waals radius of the sulfur atom that should be taken into account; it is usually taken as 1.85 Å. The half-thickness of the benzene ring is also estimated to be 1.85 Å. Therefore, if the benzene ring is perpendicular with respect to the olefinic bond, the steric effect on the conformational energy will be almost the same in both isomers. However, due to the delocalization energy to be gained at the coplanar conformation, the benzene ring will come as close by as possible to the planar conformation. This, of course, increases the apparent van der Waals radius of the benzene ring; the steric interaction between the phenyl and the arylthio groups is then larger than that between the methylthio ant the arylthio groups. The steric factor, therefore, may favor the *cis* configuration.

There is another factor to be considered; it may be called the electrostatic interaction. It has been well known that the *cis* isomer is more stable than the *trans* in 1,2-dihaloethylenes,[8-10] although halogens are much larger than hydrogen. The cause for this phenomenon may be the dispersion force, and the same effect may be operating in the series of compounds discussed in this paper.

The separation of these factors is not at all possible at the present time and awaits further studies.

Experimental

The General Method for the Preparation of α-Methylthio-β-arylthiostyrenes. To a solution of 6 g (0.04 mol) of α-methylthiostyrene[2] in 50 m*l* of dry carbon tetrachloride, equimolar arenesulfenyl chloride in 25 m*l* of carbon tetrachloride was slowly added at 0°C; hydrogen chloride was then evolved. The solution was allowed to stand for another hour after the color of the sulfenyl chloride had essentially faded, and then poured into 100 m*l* of aqueous sodium carbonate. The organic layer was separated, and the aqueous layer was extracted with ether. The combined extracts were dried over anhydrous sodium sulfate and concentrated *in vacuo*. The residue was chromatographed on alumina to give 75—95% yields of α-methylthio-β-arylthiostyrene.

Isolation of Isomers. In the case of α-methylthio-β-*p*-nitrophenylthiostyrene, the remaining yellow solid was fractionally recrystallized from ethanol to give the *cis* isomer, mp 134—135°C, as a less soluble part and the *trans*, mp 88—89°C, as a more soluble part.

In the cases of α-methylthio-β-*p*-chlorophenylthiostyrene and α-methylthio-β-*p*-bromophenylthiostyrene, on long standing they gave crystals which were then separated from the oil and recrystallized from petroleum ether to give the *cis* isomers. The mp's of the chloro and bromo derivatives were 91°C and 92—93°C respectively.

Equilibration of *cis*- and *trans*-α-Methylthio-β-phenylthiostyrenes. The title isomers were equilibrated by maintaining a carbon tetrachloride solution, into which hydrogen chloride was introduced, at the specific temperature for 30 min. The temperatures at which the equilibration was carried out were 0, 25, 50, and 77°C. The products were analyzed by means of the NMR spectra of the reaction mixture after washing the solution with aqueous alkali and then drying it.

NOE Measurements. The NOE measurements were carried out with a Japan Electron Optics 4H-100 spectrometer operating at 100 MHz. The transient NOE was observed in the "HR mode," employing the usual double-resonance technique. In measuring the spin-lattice relaxation time, the magnetization of the olefin proton was inverted adiabatically and the recovery of the magnetization was observed by scanning through the resonance with a weak rf field.

The samples were dissolved in deuteriochloroform (in the case of II) or in carbon tetrachloride (in the case of VI) to make a *ca.* 15% solution, which was then degassed and sealed.

The authors are indebted to Mr. T. Fukumi for the NOE measurements.

8) H. Steinmetz and R. M. Noyes, *J. Amer. Chem. Soc.*, **74**, 4141 (1952).
9) K. S. Pitzer and J. L. Hollenberg, *ibid.*, **76**, 1493 (1954).
10) H. G. Viehe, *Chem. Ber.*, **93**, 1697 (1960).

BULLETIN OF THE CHEMICAL SOCIETY OF JAPAN VOL. 43 1239—1242 (1970)

Transformation of Progesterone by *Aspergillus niger* 100 and *Rhizopus nigricans* REF, 129

Lotfy SALLAM, Abdel-Monem EL-REFAI and Ismail EL-KADY

Microbiological Chemistry Research Lab., National Research Centre, Cairo, U.A.R.

(Received July 3, 1969)

The microbiological transformation of progesterone by the local moulds *Aspergillus niger* and *Rhizopus nigricans* was studied. To a 48 hr old culture, progesterone (0.4 g/*l* medium) dissolved in ethanol was added and the transformation was left to proceed for 72 hr. Thereafter, the different transformation products were resolved chromatographically. The identity of each product was established through the determination of mp, mixed mp, optical rotation and ultraviolet as well as infrared absorption spectra. A comparison of the R_f values of each product with that of the corresponding reference using different solvent systems as well as their colours with two spray reagents was used as a further proof for the identity of the isolated products. In case of *A. niger*, progesterone was converted to 17α-hydroxyprogesterone; 21-hydroxyprogesterone (cortexone); 11α-hydroxyprogesterone; 11α,17α-dihydroxyprogesterone; 6β,11α-dihydroxyprogesterone and 11α,17α, 21-trihydroxyprogesterone (epicortisol). These products together with 11α-hydroxy-5α-pregnane-3,20-dione were also identified in case of *R. nigricans*.

The microbiological oxidation of progesterone at one or more of the strategic carbon atoms 11, 17, and 21 was applied to the preparation of the cortical hormones. The introduction of a hydroxyl group at carbon 11 of progesterone was performed by many fungi, mostly Rhizopi and Aspergilli.[1,2] The 17α-hydroxyl group was introduced into steroids by *Trichothecium roseum*.[3,4] However, Meister *et al.*[5] announced that *Cephalothecium roseum* could accomplish this interesting tertiary hydroxylation along with simultaneous introduction of the biologically important oxygen at C-11. Meyster *et al.*[3] also found that *Ophiobolus herpotrichus* introduced a hydroxyl group at C-21. The microbial 21-hydroxylation of several susbtrates by *Aspergillus niger* was also reported.[6] Moreover, a strain of *A. niger* was able to introduce both 11α- and 21-hydroxyl groups simultaneously into progesterone.[7,8] Epicortisol (11α-,17α,21-trihydroxyprogesterone) was isolated by CIBA group[9] together with other transformation products when *R. nigricans* and *Cunninghamella blakesleeana* were acted on progesterone.

Many works have been carried out on hydroxylation for progesterone by *A. niger*, but in most work the strain ATCC 9142 was used, and hydroxylation occurred at C-6, 11 or 21. Screening of the ability of some microorganisms for the transformation of progesterone was carried out by the authors,[10] and some active moulds were found. Using the local strain *A. niger* 100, we observed that the hydroxylation of progesterone occurs at C-6, 11, 17 and 21. A similar hydroxylation was observed using the strain *R. nigricans* REF, 129. Qualitative as well as quantitative analyses were carried out on the different products which were obtained when these two active moulds were acted upon progesterone.

Experimental

Cultivation. The local strains; *Aspergillus niger* 100

1) D. H. Peterson, "Biochemistry of Industrial Microorganisms," ed. by Rainbow and Rose, Acad. Press, London and N. Y. (1963), Chap. 16, p. 537.

2) A. Capek, O. Hanc and M. Tadra, "Microbial Transformation of Steroids," W. Junk, publisher, Hague, Netherlands (1966).

3) Ch. Meystre, E. Vischer and A. Wettstein, *Helv. Chim. Acta*, **37**, 1548 (1954).

4) L. E. Dulaney, W. J. McAleer, M. Kozlowski, E. O. Stapley and J. Jaglom, *Appl. Microbiol.*, **3**, 372 (1955).

5) P. D. Meister, L. M. Reineke, R. C. Meeks, H. C. Murray, S. H. Eppstein, H. M. Leigh Osborn, A. Weintraub and D. H. Peterson, *J. Amer. Chem. Soc.*, **76**, 4050 (1954).

6) A. Zaffaroni, C. C. Campillo, F. Cordova and G. Rosenkranz, *Experientia*, **11**, 219 (1955).

7) E. Weisz, G. Wix and M. Bodanszky, *Naturwissenschaften*, **43**, 39 (1956).

8) G. Wix, M. Natonek and M. Kovacs, *Acta Microbiol. Sci. Hungary*, **6**, 197 (1959).

9) Ciba Ltd., Brit. 816922, July 22 (1959); *Chem. Abstr.*, **54**, 1659 (1960).

10) A. H. El-Refai, L. A. R. Sallam and I. A. El-Kady, *J. Gen. Appl. Microbiol* (Tokyo), **15**, 301 (1969)

and *Rhizopus nigricans* REF, 129 were collected from the Centre of culture of the Microbiological Chemistry Research Lab., National Research Centre, Cairo. The cultivation was performed in 250 m*l* Erlenmeyer flasks each containing 75 m*l* of the medium formulated by Capek *et al.*[11] The flasks were sterilized at 1 atm. for 20 min and inoculated with 2 m*l* inocula of a 48 hr culture of the pure organsim. The culture flasks were agitated on a reciprocal shaker (110 strokes/min, amplitude 7 cm) at 30±2°C for 48 hr. Thereafter, 30 mg of progesterone dissolved in 1 m*l* ethanol was added to each flask and fermentation was continued for another 72 hr.

Extraction. At the end of the fermentation periods, the contents of each flask (medium+mycelium) were homogenized in a blender (16000 rpm) with two volumes of chloroform (150 m*l*). The extraction was repeated 3 times in order to make sure that all the transformation products were extracted. The combined chloroform extracts were washed with half its volume 5% sodium bicarbonate, followed by an equal volume distilled water, dried over anhydrous sodium sulphate, filtered, then distilled to give a semi-solid residue.

Analysis of the Mixture of the Transformation Products. The semi-solid residue was dissolved in the minimal volume of benzene and then fractionated on standard activated alumina column (100 g). The following sequence of solvents was used: *n*-hexane : benzene (1 : 1); benzene containing different concentrations of chloroform and benzene containing different concentration of methanol. The fractions containing similar products were collected and crystallization from a suitable solvent was carried out whereby determination of mp; mixed mp; $[\alpha]_D$; IR and UV absorption spectra were made.

Further proof of the identity of each product was gained by the application of the thin-layer chromatographic technique.[12] The solvent systems used are: I: Cyclohexane : acetone : chloroform (75 : 25 : 20), II: Ethylene chloride : acetone (80 : 20), III: Benzene : ethyl acetate : acetone (60 : 20 : 20) and IV: Chloroform : cyclohexane : isopropanol (50 : 100 : 20).

The plates were then sprayed with two different colour reagents namely: I_2/KI,[13] and chlorosulphonic acid : acetic acid (3 : 1).[14]

Results and Discussion

Progesterone Bioconversion by *A. niger* 100. The chromatographic resolution of the mixture (1.3 g) containing the different transformation products obtained when *A. niger* was acted on progesterone (1 g) revealed the presence of unchanged progesterone (11%);*1 17α-hydroxyprogesterone (11.9%); 21-hydroxyprogesterone (cortexone) (13.3%); 11α-hydroxyprogesterone (22.4%); 11α,17α-dihydroxyprogesterone (13.1%); 6β,11α-dihydroxyprogesterone (10.8%) and 11α, 17α,21-trihydroxyprogesterone (epicortisol) (7.5%), respectively.

The fractions eluted with *n*-hexane : benzene (1 : 1) were evaporated and crystallized from methanol : chloroform to give crystals (110 mg), mp 128—129°C, $[\alpha]_D$+195°. This substance was found to be unchanged progesterone. The fraction eluted with 5% chloroform in benzene gave after repeated crystallization from chloroform: methanol crystals (119 mg), mp 218—220°C, $[\alpha]_D$ +120.3°, λ_{max}^{EtOH} 239 mμ (ε=12920). The material did not depress the mp of an authentic sample of 17α-hydroxyprogesterone. Reported[15] mp 210—214°C, identical IR spectra.

The solid residue eluted with 10% chloroform in benzene was repeatedly crystallized from methanol: chloroform to afford crystals (133 mg), mp 139—141°C, $[\alpha]_D$ +183°, λ_{max}^{EtOH} 241 mμ (ε=12700). This material was found to be 21-hydroxyprogesterone. Reported[6] mp 142—143°C, $[\alpha]_D$ +185°, identical IR spectra.

The combined fractions eluted with 20% chloroform in benzene on cyrstallization from chloroform: methanol gave crystals (224 mg), mp 165—168°C, $[\alpha]_D$ +177°, λ_{max}^{EtOH} 242 mμ (ε=12960). The material did not depress the mp of an authentic sample of 11α-hydroxyprogesterone. Reported[16] mp 166—168°C, $[\alpha]_D$ +176°, identical IR spectra.

The fifth product eluted with 5% methanol in benzene afforded after crystallization from methanol crystals (131 mg) mp 217—220°C, $[\alpha]_D$ +72°, λ_{max}^{EtOH} 242 mμ (ε=16100). This material was found to be 11α,17α-dihydroxyprogesterone. Reported[17] mp 220—222°C, $[\alpha]_D$ +76°, identical IR spectra.

The substance eluted with 10% methanol in benzene gave upon crystallization from methanol: water, crystals (180 mg), mp 244—246°C, $[\alpha]_D$ +140°, λ_{max}^{EtOH} 239 mμ (ε=13480). The material did not depress the mp of the authentic sample of 6β,11α-dihydroxyprogesterone. Reproted[16] mp 245—248°C, $[\alpha]_D$ +144°, identical IR spectra.

Final strip of the column with 25% methanol in benzene gave a solid material which yielded on repeated crystallization from methanol: water,

11) A. Capek, M. Tadra and J. Tuma, *Folia Microbiol. Prague*, **9**, 380 (1964).

12) L. A. R. Sallam, A. H. El-Refai and I. A. El-Kady, *J. Gen. Appl. Microbiol.* (Tokyo), **15**, 309 (1969).

13) E. Tumova, Z. O. Siblikova and O. Hanc, *Biochemika Oxydance Pregnaovych Steroidu*, **4**, 65 (1955).

14) D. Waldy, "Thin-Layer Chromatography, A Laboratory Handbook, Egon Stahl," Acad. Press. Inc., New York, London (1965). p. 249.

*1 Yields are represented by weight % based on added progesterone.

15) W. J. McAleer and E. L. Dulaney, *Arch. Biochem. Biophys.*, **62**, 111 (1956).

16) D. H. Peterson, H. C. Murray, S. H. Eppstein, L. M. Reineke, A. Weintraub, P. D. Meister and H. M. Leigh, *J. Amer. Chem. Soc.*, **74**, 5933 (1952).

17) P. D. Meister, D. H. Peterson, H. C. Murray, G. B. Spero, S. H. Eppstein, A. Weintraub, L. M. Reinke and H. M. Leigh, *ibid.*, **75**, 416 (1953).

Table 1. The R_f values and colours of the different transformation products obtained from progesterone bioconversion by *R. nigricans* and *A. niger*

	$R_f \times 100$ with solvent system				I_2/KI	Chlorosulphonic/acetic acid	
	I	II	III	IV		Day light	UV
17α-Hydroxyprogesterone	88	83	97	85	weak pink	brown	bluish violet
21-Hydroxyprogesterone (cortexone)	90	89	85	78	rust brown	deep blue	brilliant brick red
11α-Hydroxy-5α-pregnane-3,20-dione*	75	65	74	75	grey	brown	brilliant blue
11α-Hydrxoyprogesterone	75	61	74	72	deep blue	brown	greenish yellow
11α,17α-Dihydroxyprogesterone	48	46	67	57	deep blue	brown	yellow
6β,11α-Dihydroxyprogesterone	39	45	48	40	pale brown	brown	sky blue
11α,17α,21-Trihydroxyprogesterone (epicortisol)	17	12	33	28	deep blue	pale brown	yellow

* 11α-Hydroxy-5α-pregnane-3,20-dione was detected in case of *R. nigricans* only.

crystals (75 mg) mp 208—210°C, $[\alpha]_D$ 109°, λ_{max}^{EtOH} 241 mμ ($\varepsilon = 14700$). This substance did not depress the mp of an authentic sample of 11α, 17α,21-trihydroxyprogesterone (epicortisol). Reported,[18] mp 210—212°C, $[\alpha]_D$ +113°, identical IR spectra.

Futher proof of the identity of the different compounds produced from the bioconversion of progesterone by *A. niger* was made by application of thin-layer chromatographic analysis. The results of this study are presented in Table 1.

Progesterone Bioconversion by *R. nigricans* REF, 129. Inspection of the mixture (1.4 g) resulting from the bioconversion of progesterone (1 g) by *R. nigricans* revealed the presence of unchanged progesterone (6%), 17α-hydroxyprogesterone (8.2%), 21-hydroxyprogesterone (7.9%), 11α-hydroxy-5α-pregnane-3,20-dione (7.4%), 11α-hydroxyprogesterone (24.4%), 11α,17α-dihydroxyprogesterone (16.7%), 6β,11α-dihydroxyprogesterone (9.5%) and finally 11α,17α,21-trihydroxyprogesterone (epicortisol) (10.5%).

The first fraction eluted with *n*-hexane : benzene (1 : 1) gave upon crystallization from chloroform: methanol, crystals (60 mg) mp 126—128°C, $[\alpha]_D$ +194°. This was found to be unchanged progesterone. Evaporation of the fractions eluted with 5% chloroform in benzene followed by crystallization from chloroform : methanol gave crystals (82 mg), mp 209—212°C, $[\alpha]_D$ +120—123°, λ_{max}^{EtOH} 239 mμ ($\varepsilon = 12960$). This material did not depress the mp of an authentic sample of 17α-hydroxyprogesterone. Reported[15] mp 210—214°C, identical IR spectra.

The solid substance removed with 10% chloroform in benzene gave crystals (79 mg) mp 140—142°C, $[\alpha]_D$ +180°, λ_{max}^{EtOH} 241 mμ ($\varepsilon = 12700$). This substance was found to be 21-hydroxyprogesterone as no depression in the mp was observed upon admixture with an authentic sample of cortexone. Reported[14] mp 142—143°C, $[\alpha]_D$ +185°, identical IR spectra. The compound eluted with 15% chloroform in benzene gave on crystallization from chloroform : methanol crystals (74 mg) mp 194—196°C, $[\alpha]_D$ +81°. No depression in the mp of an authentic sample of 11α-hydroxy-5α-pregnane-3,20-dione with the isolated crystals. Reported[16] mp 198—200°C, $[\alpha]_D$ +84°, identical IR spectra. The fractions collected with 20% chloroform in benzene yield upon crystallization from methanol crystals (244 mg), mp 165—167°C, $[\alpha]_D$ +175°. This substance did not depress the mp of an authentic sample of 11αhydroxyprogesterone. Reported[16] mp 166—168°C, $[\alpha]_D$ +176°, identical IR spectra.

Elution with 5% methanol in benzene gave a compound which upon crystallization from methanol gave crystals (167 mg), mp 216—218°C, $[\alpha]_D$ +75°, λ_{max}^{EtOH} 243 mμ ($\varepsilon = 16200$). This compound is 11α,17α-dihydroxyprogesterone. Reported[17] mp 220—222°C, $[\alpha]_D$ +76°, identical IR spectra.

The fractions eluted with 10% methanol in benzene gave on crystallization from methanol : water crystal (95 mg), mp 242—245°C, $[\alpha]_D$ +139°, λ_{max}^{EtOH} 239 mμ ($\varepsilon = 13480$). This material was found to be 6β,11α-dihydroxyprogesterone. Reported[16] mp 245—248°C, $[\alpha]_D$ +144°, identical IR spectra.

The fractions collected with 25—50% methanol in benzene was crystallized from methanol: water to give crystals (105 mg), mp 208—210°C, $[\alpha]_D$ +105°, λ_{max}^{EtOH} 241 mμ ($\varepsilon = 14700$). This product did not depress the mp of an authentic sample of epicortisol. Reported[18] mp 210—212°C, $[\alpha]_D$ +113°, identical IR spectra.

Further establishment of these different products was made through thin-layer chromatographic analysis as presented in Table 1.

18) D. H. Peterson, S. H. Eppstein, P. D. Meister, B. J. Magerlin, H. C. Murray, H. M. Leigh, A. Weintraub and L. M. Reineke, *ibid.*, **75**, 412 (1953).

We are grateful to Professor Dr. M. Abdel-Aziz, Faculty of Science, Cairo University, Professor Dr. H. G. Osman, and Professor Dr. M. B. E. Fayez, National Research Centre, Cairo, for their encouragement and interest.

We are also very grateful to Professor Dr. Peterson, UpJohn Company, U. S. A., Dr. H. Azfasadour, Organon, Oss., Holland, and the Schering group, for the gifts of the steroids compounds.

NOTES

BULLETIN OF THE CHEMICAL SOCIETY OF JAPAN VOL. 43 1243—1244 (1970)

Formation of Acetals from Vinyl Chloride and Alcohols Catalyzed by Transition Metal Chlorides

Akira MISONO, Yasuzo UCHIDA and Ken-ichi FURUHATA

Department of Industrial Chemistry, Faculty of Engineering, The University of Tokyo, Hongo Bunkyo-ku, Tokyo

(Received March 31, 1969)

Recently, the formation of acetaldehyde dialkyl acetal from vinyl chloride and alcohol catalyzed by palladium chloride and a base was reported.[1,2]

In an attempt to oligomerize vinyl chloride by transition metal chlorides in alcohol, we have observed the formation of acetaldehyde dialkyl acetals instead of the oligomerization by ruthenium, rhodium and palladium chlorides. This reaction did not take place by iron, cobalt, chromium, zirconium and hafnium chlorides.

Results and Discussion

In a preliminary experiment, vinyl chloride and rhodium trichloride trihydrate (molar ratio; 150) were dissolved in methanol and the mixture was kept at 50°C for 48 hr. The only product isolated was acetaldehyde dimethyl acetal, no product corresponding to a dimer of vinyl chloride being detected on gaschromatography.

More detailed studies on the acetal formation reaction by rhodium trichloride trihydrate were carried out using ethanol. The time dependence of the formation of acetaldehyde diethyl acetal at 60°C is shown in Fig. 1. The selectivity for acetaldehyde diethyl acetal was about 70% and it decreased when the reaction time exceeded 25 hr. In the reaction at 80°C, vinyl chloride was consumed completely in 24 hr but the selectivity for acetaldehyde diethyl acetal was only 20.3%. Small amounts of vinyl ethyl ether and acetaldehyde were detected on gas chromatography (identified by comparing retention times with those of authentic samples), and the rest was higher boiling products. The formation of acetaldehyde is likely to be due to the reaction of vinyl chloride with water[3] and/or the oxidation of ethanol by rhodium(III). Higher boiling products were not studied further.

Ruthenium and palladium chlorides also catalyzed the formation of acetaldehyde diethyl acetal but iron, cobalt, chromium, zirconium and hafnium chlorides did not (Table 1). In the reaction using palladium dichloride as a catalyst, partial reduction to palladium metal was observed.

Recently, the formation of acetal from vinyl chloride and alcohol catalyzed by palladium chloride was reported, but those reactions require the presence of a strong base[1] or an alkoxide anion.[2]

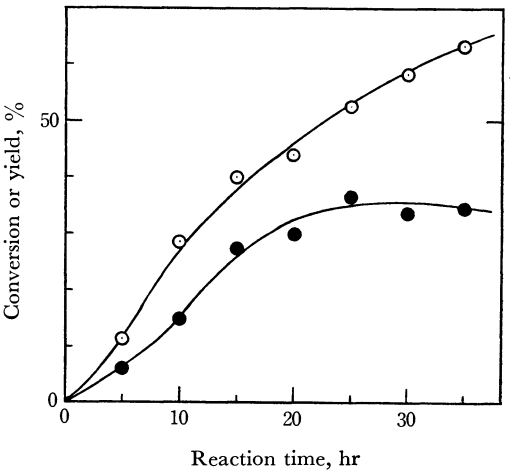

Fig. 1. Time dependence of the acetal formation.
—⊙—: Conversion of vinyl chloride, %
—●—: Yield of acetaldehyde diethyl acetal, %
Reaction conditions:
Vinyl chloride, 43 mmol; $RhCl_3.3H_2O$, 0.22 mmol; EtOH, 160 mmol; Reaction temperature, 60°C

1) E. W. Stern, M. L. Spector and H. P. Leftin, *J. Catal.*, **6**, 152 (1966).

2) C. F. Kohll and R. van Helden, *Rec. Trav. Chim. Pays-Bas*, **87**, 481 (1968).

3) J. Smidt, W. Hafner, R. Jira, J. Sedlmeier, R. Sieber, R. Ruttinger and H. Kojer, *Angew. Chem.*, **71**, 176 (1959).

Table 1. Reaction of vinyl chloride and ethanol

Catalyst	Reaction temp. (°C)	Reaction time (hr)	Conv.*	Yield**
$RhCl_3 \cdot 3H_2O$	60	5	12.3	6.3
	60	25	52.5	36.6
	80	24	100	20.3
$RhCl(PPh_3)_3$	60	6	5.3	3.2
$RuCl_3 \cdot 3H_2O$	80	24	41.5	21.9
$PdCl_2$	80	24	26.5	14.0
$FeCl_3$	60	48	no reaction	
$CoCl_2 \cdot 6H_2O$	60	48	no reaction	
$CrCl_3 \cdot 6H_2O$	80	24	no reaction	
$ZrCl_4$	80	24	no reaction	
$HfCl_4$	80	24	no reaction	

Reaction conditions: Vinyl chloride, 43 mmol; Catalyst, 0.2—0.4 mmol; Ethanol, 160 mmol

* Conversion of vinyl chloride, %

** Yield of acetaldehyde diethyl acetal based on vinyl chloride supplied, %

The reaction intermediate was considered to be vinyl ether which is formed by the nucleophilic attack of an alkoxide anion onto vinyl chloride coordinating to a palladium ion.

We believe that the coordination of vinyl chloride to ruthenium, rhodium or palladium is significant in the acetal formation reaction.

Experimental

Reagents. Vinyl chloride was passed through columns packed with calcium chloride and phosphorus pentoxide and then condensed into a pressure glass tube held at −78°C.

Methanol and ethanol were purified by conventional methods, and were distilled under a nitrogen stream.

Tris(triphenylphosphine)chlororhodium(I) was synthesized according to the reported method.[4]

Commercial metal chlorides were used without further purification.

Reaction Procedure. In a typical reaction, vinyl chloride (43 mmol) was charged into a glass ampule (20 m*l*) containing rhodium trichloride trihydrate (0.22 mmol) by a trap-to-trap distillation and then ethanol (160 mmol) was charged with a syringe under nitrogen stream. Then the solution was freezed with liquid nitrogen, and the ampoule was evacuated and was sealed. It was then kept at 60°C for 20 hr.

Analysis. The gas chromatography was carried out for the detection and the quantitative analysis of products using a 2 m stainless steel column, 4 mm in diameter, packed with bis(2-cyanoethyl) ether on Diasolid M. Operation conditions: column temperature, 68°C; flash evaporator, 200°C; carrier gas (helium) speed, 40 m*l*/min. Ethyl formate was used as the internal standard.

4) J. A. Osborn, F. H. Jardine, J. F. Young and G. Wilkinson, *J. Chem. Soc.*, *A*, **1966**, 1711.

BULLETIN OF THE CHEMICAL SOCIETY OF JAPAN VOL. 43 1244—1245 (1970)

Tantalum(V)-Schiff Base Complexes

Pramila PRASHAR and J. P. TANDON

Department of Chemistry, University of Rajasthan, Jaipur-4, India

(Received January 30, 1969)

Considerable amount of work has been reported on the stereochemically important and useful chelates of Schiff bases with bivalent metals[1-4] but only a few scattered references are available for similar complexes of tetravalent and pentavalent metals.[5,6] In earlier publications from this laboratory, a few titanium[7] and zirconium[8] compounds have been reported. In the present paper, the reactions of tantalum(V) alkoxides with Schiff bases have been studied and some of their important properties described.

Tantalum isopropoxides, prepared by the ammonia method[9] and Schiff bases, prepared by azeotropic condensation and vacuum distillation, are the starting materials for these reactions. The technique consists of the addition of stoichiometric quantity of the Schiff base to the anhydrous benzene solution of tantalum isopropoxide and refluxing the reac-

1) L. Sacconi and I. Bertini, *Inorg. Chem.*, **5**, 9 (1966).
2) M. Ciampolini and N. Nardi, *ibid.*, **5**, 41 (1966).
3) B. Kirson and H. Sechter, *Bull. Soc. Chim. Fr.*, **1966**, 2236.
4) S. Yamada, This Bulletin, **40**, 1864 (1967).
5) A. S. Kudravtsev and I. A. Savich, *Zh. Obshch, Khim.*, **33**, 3763 (1963).
6) Y.-Y. Chuang, I. A. Savich, A. V. Lapitskii, V. R. Samorokov and L. G. Titov, *Vestn, Mosk. Univ. Ser. II, Khim.*, 15, **3**, 40 (1960).
7) P. Prashar and J. P. Tandon, *J. Less-Common Metals*, **13**, 541 (1967).
8) P. Prashar and J. P. Tandon, *ibid.*, **15**, 219 (1968).
9) D. C. Bradley, W. Wardlaw and A. Whitley, *J. Chem. Soc.*, **1956**, 5, 1139, 2381.

TABLE 1

	Compound		Analysis Metal %	Analysis Nitrogen %	Molecular weights Found	Molecular weights Calcd	Molecular weights Molarity
1	$Ta(OPr^i)_3SB$ Pale yellow sticky solid	(a) (b)	35.09 34.70	2.78 2.68	622	521	1.2
2	$Ta(OPr^i)(SB)_2$ Yellow foamy solid	(a) (b)	32.19 31.96	4.80 4.94	795	566	1.4
3	$Ta(SB)_2(SBH)$ Yellow foamy solid	(a) (b)	25.78 26.95	6.12 6.25	707	671	1.1
4	$Ta(OPr^i)_3(S'B')$ Pale yellow semi-solid	(a) (b)	35.19 33.79	2.52 2.61	674	535	1.3
5	$Ta(OPr^i)(S'B')_2$ Yellow foamy solid	(a) (b)	29.75 30.44	4.60 4.71	787	594	1.3
6	$Ta(S'B')_2(S'B'H)$ Yellow foamy solid	(a) (b)	25.33 25.35	5.75 5.88	715	713	1.0
7	$Ta(OPr^i)_3(S_1B_1)$ Pale yellow semi-solid	(a) (b)	32.99 33.79	2.54 2.61	660	535	1.2
8	$Ta(OPr^i)(S_1B_1)_2$ Yellow foamy solid	(a) (b)	29.50 30.44	4.64 4.71	831	594	1.4
9	$Ta(S_1B_1)_2(S_1B_1H)$ Yellow foamy soild	(a) (b)	25.05 25.35	5.80 5.88	710	713	1.0
10	$Ta(OPr^i)_3(S_2B_2)$ Pale yellow viscous compound	(a) (b)	33.04 32.92	2.50 2.55	649	549	1.2
11	$Ta(OPr^i)(S_2B_2)_2$ Yellow foamy compound	(a) (b)	28.59 29.07	4.45 4.50	777	622	1.2
12	$Ta(S_2B_2)_2(S_2B_2H)$ Yellow foamy solid	(a) (b)	23.38 23.95	5.46 5.56	716	755	0.9

where -SB-=anion of salicylidene-2-hydroxyethylamine
-S'B'-=anion of salicylidene-2-hydroxy-*n*-propylamine
$-S_1B_1-$=anion of *o*-hydroxyacetophenone-2-hydroxyethylimine
$-S_2B_2-$=anion of *o*-hydroxyacetophenone-2-hydroxy-*n*-propylimine.
a=analysis of the compound, b=calcd for the formula

tion mixture on a fractionation column. The reaction is completed by the removal of the isopropanol produced azeotropically and drying the reaction mixture in a vacuum. These reactions in different molar ratios can be presented as

$$Ta(OPr^i)_5 + SBH_2 \longrightarrow Ta(OPr^i)_3(SB) + 2Pr^iOH,$$
$$Ta(OPr^i)_5 + 2SBH_2 \longrightarrow Ta(OPr^i)(SB)_2 + 4Pr^iOH,$$
$$Ta(OPr^i)_5 + 3SBH_2 \longrightarrow Ta(SB)_2(SBH) + 5Pr^iOH,$$

where SBH_2 represents the Schiff base and -SB- the corresponding anion of the Schiff base. The bases used in these reactions may be represented by the general formulae:

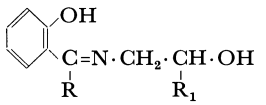

where in (I) R=H, R_1=H
(II) R=H, R_1=CH_3
(III) R=CH_3, R_1=H
and (IV) R=CH_3, R_1=CH_3.

These reactions take place quite easily and the resulting compounds could be isolated in quantitative yields. Tantalum (V) - Schiff-base chelates are pale-yellow to dark-yellow foamy solids (Table 1), soluble in benzene, parent alcohol and chloroform and are non-volatile. Their molecular weights have been determined ebullioscopically in benzene and they are almost monomers. Their probable structures may be indicated as follows:

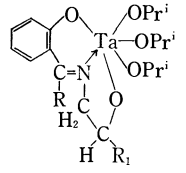

1:1 derivative

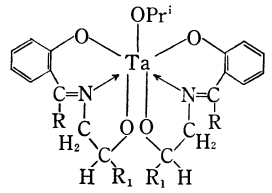

1:2 derivative

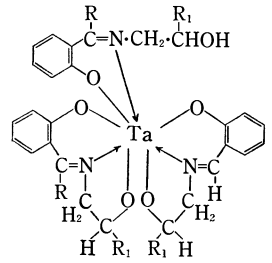

1:3 derivative

Analytical results and molecular weights of these derivatives are listed in the table.

One of us (P.P.) is grateful to the C. S. I. R., New Delhi for the award of a Research Fellowship. The authors are also grateful to Dr. R. C. Mehrotra, Professor and Head of the Chemistry Department, Rajasthan University, Jaipur, for providing research facilities.

BULLETIN OF THE CHEMICAL SOCIETY OF JAPAN VOL. 43 1246—1247 (1970)

Intramolecular Cyclization of *N*-(Phenylcarbamoyl)anthranilic Acid Derivatives

Shunroku TOHYAMA,*1 Masaru KURIHARA† and Naoya YODA†

Basic Research Laboratories, Toray Industries, Ltd., Tebiro, Kamakura

(Received May 16, 1969)

The thermal dissociation of urea derivatives under various conditions has been reported.[1,2] Iwakura and Nagakubo described the thermal decomposition of 1,3-di-*p*-phenetylurea in aliphatic alcohol solution to give *p*-phenetidine and phenyl isocyanate.[3] So far, no studies have been reported on the thermal dissociation of *ortho*-substituted *N*-(phenylcarbamoyl)aniline derivatives in polar organic solvents.

In connection with the study of cyclopolycondensation reactions[4] of aromatic diamino dicarboxylic acids with various active carbonyl compounds, we noted that several open-chain precursors of aromatic heterocyclic polymers such as polyurea acids[5] were sensitive to elevated temperatures in usual cyclodehydration. By the cyclodehydration reactions of *ortho*-substituted *N*-(phenylcarbamoyl)aniline derivatives, two condensation products, isatoic anhydride and 3-phenyl-2,4(1*H*,3*H*)-quinazoline-dione were isolated.

In this paper, we wish to report the new intramolecular cyclization reactions and the mechanism of the formation of isatoic anhydride (II) and 3-phenyl-2,4(1*H*,3*H*)-quinazolinedione (IV) from *N*-(phenylcarbamoyl)anthranilic acid derivatives (I). When *N*-(phenylcarbamoyl)anthranilic acid (Ia), its ammonium salts (Ib,c) and methyl ester (Ia) were treated either (A) in organic solvent such as *N*-methylpyrrolidone at 100°C or (B) in an inert gas at 220°C, the following two types of reactions were found to occur depending upon the reaction conditions.

The results of the cyclization reaction in *N*-methylpyrrolidone are summarized in Table 1.

The reaction product obtained in nitrogen was found to be solely 3-phenyl-2,4(1*H*,3*H*)-quinazoline-dione (IV). The yields of IV are shown in Table 2.

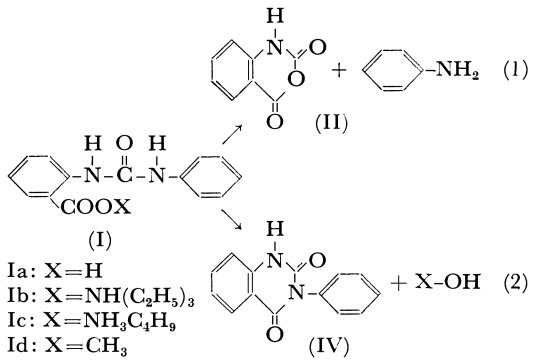

TABLE 1. PRODUCTS OF CYCLIZATION REACTION EN *N*-METHYLPYRROLIDONE (mol % yield)

Product	Compound			
	Ia	Ib	Ic	Id
II*	50	30	28	0
IV**	50	70	72	0
I (starting material recovered)	0	0	0	100

* mp 242°C. Found: C, 58.60; H, 3.12; N, 8.42%. Calcd for $C_{18}H_5O_2N_5$: C, 58.90; H, 3.09; N, 8.59%.

** mp 282°C. Found C, 70.36; H, 4.17; N, 11.45%. Calcd for $C_{14}H_{10}O_2N_2$: C, 70.58; H, 4.22; N, 11.48%.

TABLE 2. YIELD OF IV PRODUCED BY THE REACTION IN NITROGEN ATMOSPHERE

	Ia	Ib	Ic	Id
Yield of IV (mol%)	64	77	76	72

The formation of isatoic anhydride by the elimination of aniline is a new intramolecular cyclization reaction which has not been reported. For this cyclization reaction, two types of reaction mechanism are considered: (a) an intramolecular cyclization takes place directly by nucleophilic attack of carboxyl group on carbonyl group of ureido linkage to eliminate aniline as shown in Eq. (3),

*1 Present address: Nagoya Laboratory, Toray Industries, Ltd., Oe, Nagoya.

† Pioneering Research and Development Laboratories, Toray Industries, Ltd., Otsu, Shiga.

1) T. Mukaiyama, *Yuki Gosei Kagaku Kyokai Shi*, **16**, 55 (1958).

2) K. Taufel, C. Wagner and H. Dünwald, *Z. Electrochem.*, **34**, 115 (1928).

3) Y. Iwakura and K. Nagakubo, *Bull. Tokyo Inst. Technol.*, **18**, 25 (1948).

4) N. Yoda, *Kobunshi Kagaku*, **14**, 151 (1965).

5) S. Tohyama, M. Kurihara, K. Ikeda and N. Yoda, *J. Polym. Sci., Part, A*, **5**, 2523 (1967).

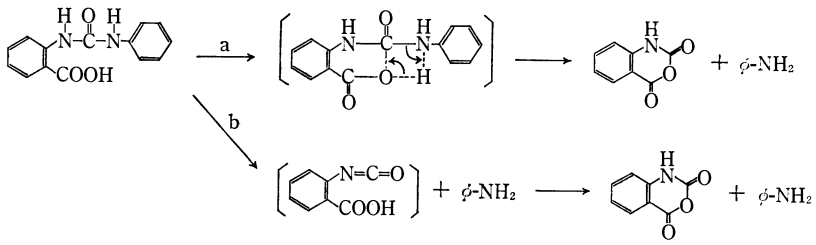

or (b) the dissociation of ureido group forms isocyanate as a reaction intermediate (Eq. (4)).

When *N*-methyl-*N*-(phenylcarbamoyl)anthranilic acid was treated in *N*-methylpyrrolidone under the same reaction conditions, *N*-methylisatoic anhydride was obtained. In this case the formation of isocyanate as an intermediate (Eq. (4)) is impossible, and it should inevitably involve the participation of carobxyl group in the reaction process. Furthermore, reaction path (a) is favored by the fact that *N*-(phenylcarbamoyl)anthranilic acid (Ia) and its ammonium salts (Ib,c) afforded isatoic anhydride, whereas methyl ester (Id) did not give isatoic anhydride in organic solvent as shown in Table 1. The fact suggests that only the species which easily dissociate to give carboxylate anion respond to path (a).

When methyl *N*-(phenylcarbamoyl)anthranilate was fused in nitrogen atmosphere, it affords quinazolinedione as a sole product by intramolecular cyclization.

Experimental

***N*-(phenylcarbamoyl)anthranilic Acid.** Phenyl isocyanate (4.0 g, 1/300 mol) dissolved in benzene (20 m*l*) was added slowly at 30°C into a solution of anthranilic acid (4.6 g, 1/300 mol) in benzene (40 m*l*). After stirring for 3 hr, the precipitate was collected and recrystallized from ethanol: mp 185—186°C. Found: C, 65.51; H, 4.65; N, 10.65%. Calcd for $C_{14}H_{12}O_3N_2$: C, 65.62; H, 4.72; N, 10.93%.

***N*-Methyl-*N*-(phenylcarbamoyl)anthranilic Acid.** A 3.02 g (0.02 mol) portion of *N*-methylanthranilic acid (mp 186—187°C, recrystallized from aqueous ethanol) was dissolved in 100 m*l* of benzene at 60°C. To this solution was added 2.38 g (0.02 mol) of phenyl isocyanate (bp 46—47°C/7 mmHg) in 10 m*l* of benzene, and the mixture was refluxed at 80°C for 2.5 hr. After the mixture had been allowed to cool to room temperature, the precipitate was filtered, washed several times with distilled water, and dried. It was then recrystallized twice from ethyl acetate to obtain colorless needles in a 43% yield. Mp 252—253°C. It was identified to be *N*-methyl-*N*-(phenylcarbamoyl)anthranilic acid on the basis of infrared spectrum and elemental analysis.

The infrared spectrum (KBr) shows absorption bands at 3300 cm^{-1} (N–H), and 1650 cm^{-1} (ureido carbonyl). Ultraviolet spectrum: λ_{max}=210 mμ (ε, 29200), 257 mμ (ε, 33600). Found: C, 66.87; H, 5.35; N, 10.41%. Calcd for $C_{15}H_{14}O_3N_2$: C, 66.81; H, 5.08; N, 10.58%.

Methyl *N*-(Phenylcarbamoyl)anthranilate. To a solution of methyl anthranilate (5.0 g, 1/300 mol) in 30 m*l* of benzene was added phenyl isocyanate (4.0 g, 1/300 mol) dissolved in 20 m*l* of benzene. After stirring for 3 hr at 30°C, benzene was removed and the residue was recrystallized from ethanol: mp 138—139°C. Found: C, 66.65; H, 5.22; N, 10.32%. Calcd for $C_{15}H_{14}O_3N_2$: C, 66.81; H, 5.08; N, 10.58%.

Cyclization Reaction in *N*-Methylpyrrolidone. A solution of *N*-(phenylcarbamoyl)anthranilic acid or its derivatives (1/300 mol) in 20 m*l* of *N*-methylpyrrolidone was kept at 100°C for 3 hr with stirring. After removal of the solvent under reduced pressure, the residue was separated by fractional recrystallization from ethanol.

Cyclization Reaction in Nitrogen Gas. *N*-(Phenylcarbamoyl) anthranilic acid derivative (0.1 g) was introduced into a test tube in a nitrogen atmosphere. The test tube was sealed and placed in an oven and heated at 220°C for 2 hr. In every case, the product was identified to be 3-phenyl-2,4(1*H*,3*H*)-quinazolinedione (IV) from its IR spectrum and melting point (282°C).

BULLETIN OF THE CHEMICAL SOCIETY OF JAPAN VOL. 43 1248—1249 (1970)

The Coupling Mode of Propargyl Undecynoate in a Cupric Acetate Monohydrate-Pyridine System

Ichiro WATANABE, Kunio KOGAMI, Shinichi ISAOKA and Ju KUMANOTANI

The Engineering Research Institute, The University of Tokyo, Yayoi-cho, Tokyo

(Received August 20, 1969)

It is well known that α,ω-diyne compounds are oxidatively coupled and that cyclic compounds containing α,γ-diyne units are formed in cupurous chloride-ammonia water[1] and cupric acetate-pyridine systems.[2]

However, the coupling mode of diyne esters into cyclic oligomers—whether diynes undergo the coupling in a head-to-head or in a tail-to-head manner—has not yet been established.

In the oxidative coupling reaction of propargyl undecynoate in a cupric acetate monohydrate-pyridine system,[3] we have found that, among the possible cyclic oligomers, the dimer results only from a head-to-head coupling reaction, and that linear oligomers are given in a head-to-tail coupling reaction. The structure of the dimer was identified according to the following scheme:

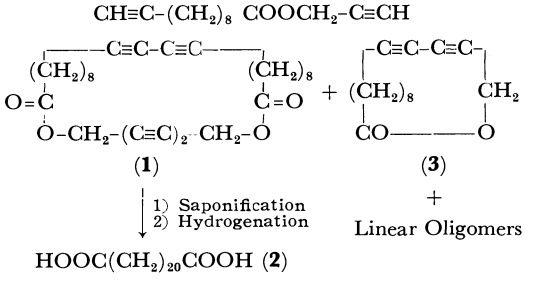

The yields of the dimer and monomer increased up to 20% (of the theoretical yield) with an increase in the dilution up to a pyridine : ester volume ratio of 200.

The linear oligomers were identified by the Ilosvay method[4] and they were derived into 14-hydroxy-tetradecanoic acid quantitatively.

The fact that the dimer (**1**) is formed in a head-to-head coupling manner, and not in a head-to-tail manner, can be explained by considering that, according to the Dale rule[5] concerning the conformational stability of macrocyclic compounds, the dimer (**1**), which has a strain-free conformation, can exist more stably than the other possible dimer, formed in a head-to-tail coupling manner.

The different formation modes of the cyclic dimer and the linear oligomer still remain to be elucidated.

Experimental*1

Propargyl Undecynoate. This was prepared by the esterification method of Black and Weedon[6]; bp 128—130°C/2 mmHg: d_{20}^{20} 0.9442; n_D^{20} 1.4624.

Oxidative Coupling of Propargyl Undecynoate. Into a mixture of cupric acetate monohydrate (30 g, 0.15 mol) and pyridine (1.4 *l*), a solution of the propargyl undecynoate (5 g, 0.023 mol) in 100 m*l* of pyridine was stirred, drop by drop, at 55—60°C over a 3-hr period. The reaction mixture was concentrated to *ca.* 300 m*l* at 55—60°C under a pressure of 20—30 mmHg and then cooled. Seven hundred m*l* of an aqueous solution of 15% hydrochloric acid previously cooled with ice were then added to the concentrated solution. The resulting solution was extracted with ether (100 m*l*×5). The ethereal solution was washed with 200 m*l* of an aqueous solution of 5% sodium carbonate and dried over Na_2SO_4. By the removal of the ether from the solution, an oily product (4.8 g) was obtained.

Separation of Products. The product showed three spots, with R_f values of 0.0, 0.47, and 0.77, by t.l.c. on a silica-gel layer (thickness, 0.25 mm) with a mixed

*1 The infrared (IR) spectra were obtained with a Nihon-Bunko IR-spectrometer, Model IR-S. The ultraviolet (UV) spectra were taken in ethanol with a Hitachi spectrometer, EPS-2. The nuclear magnetic resonance (NMR) spectra were determined in carbon tetrachloride and acetone at 60 Mc with a Nihon-Denshi. NMR spectrometer, JMN C-60. The chemical shifts are described in values relative to tetramethylsilane as the internal standard. The multiplicity of signals is indicated in abbreviated form; *s* for singlet, and *m* for multiplet. The molecular weight was measured in methyl ethyl ketone with a vapor-pressure osomometer, Model 301-A (Mechrolab, Inc.). The silica-gel layers used for the thin-layer chromatography(t.l.c.) were made from Silica Rider (silica-gel with 12—14% calcium sulfate, purchased from Daiichi Pure Chemicals) and were activated at 105°C for 1.5 hr.

1) F. Sondheimer and Y. Amiel, *J. Amer. Chem. Soc.*, **78**, 4178 (1956).

2) G. Eglinton and A. R. Galbraith, *Chem. Ind.* (London), **1956**, 737.

3) F. Sondheimer, Y. Amiel and R. Wolovsky, *J. Amer. Chem. Soc.*, **81**, 4600 (1959).

4) L. Ilosvay, *Ber.*, **32**, 2697 (1899).

5) J. Dale and A. J. Habert, *J. Chem. Soc.*, **1963**, 73.

6) H. K. Black and B. C. L. Weedon, *J. Chem. Soc.*, **1953**, 1785.

solvent of *n*-hexane and ether (7 : 3 v/v).

A suspension of silica-gel (100—200 mesh, 250 g) in *n*-hexane was poured in a tube (2.4 cm in diameter and 1200 cm long). Then, a solution of the product (4.8 g) in *n*-hexane was passed through the column and subsequently eluted with *n*-hexane-ether (7 : 3 v/v, 1.5 *l*). The effluent was divided into 25 m*l*×60 fractions using an auto-fraction collector. The elution speed was 100 m*l* per hour. Products with R_f value of 0.77 and 0.47 appeared in the fractions of Nos. 20—25 and Nos. 36—40 respectively; each of them gave 0.95 or 0.99 g of a white solid after the evaporation of the solvent *in vacuo*. A product with an R_f value of 0.0 remained in the column. After the elution, the silica-gel column was extracted with ether and then with acetone in a Soxhlet apparatus. Thus, by the removal of the solvent from the extract, ether- and acetone-soluble portions were obtained in yields of 2.4 g and 0.3 g respectively.

Identification. In order to collect a sufficient amount of aliquot for analysis, the above-described procedures were repeated twice within the limits of experimental error.

Cyclic Compounds Dimer (1). The dimer crystals had a melting point of 94.5—95.5°C. The IR spectrum, ν_{max} (KBr); 2190, 2280(–C≡C–C≡C–), and 1745 (>C=O) cm^{-1}. The UV spectrum, λ_{max} (CH_3OH) mμ (ε): 214(1272), 222(868), 233(1047), 245(1058), 258 (628), 267(185), 284(115). The NMR spectrum, τ (CCl_4): 5.25 (s, –C≡C–C≡C–CH_2–O–), 7.65 (m, –CH_2–C–O), 8.51 (m, –CH_2–). The saponification value was 256.9 (Calcd 256.8). Found: C, 76.94; H, 8.26%. Calcd for $C_{28}H_{36}O_4$: C, 77.03; H, 8.31%. The dimer (**1**) (a 1-g portion of the dimer separated by column chromatography) was saponified with 10 m*l* of an ethanolic 0.5N potassium hydroxide solution. The resultant solution was acidified with an aqueous solution of 10% hydrochloric acid, and then extracted with ether (20 m*l*×5). The ethereal solution was dried over Na_2SO_4 and then evaporated to give white crystals (1.2 g) as a residue. The crystals were hydrogenated in ethyl acetate (50 m*l*) at room temperature over 5% Pd-on-charcoal (100 mg) to give docosanedioic acid (**2**) (mp 126°C; acid value, 302.8 (theoretical value 302.7)), the identity of which was confirmed by observing no depression of the melting point when it was mixed with an authentic sample prepared from methyl undecynoate by the McCrae method,[7] further, the crystals were examined by t.l.c. (thickness of silica-gel layer, 0.25 mm; developing solvent, a mixture of *n*-hexane, ether and acetic acid (50 : 40 : 1 v/v); the chromatogram, after being sprayed with an aqueous sulfuric acid solution (1 : 1), was heated at 150°C for 30 min); they exhibited only one spot with the R_f value of 0.42 of docosanedioic acid, and not the spot with the R_f value of 0.24 of 14-hydroxytetradecanoic acid.

Monomer (3). The lactone (**3**) (1.0 g, 0.0045 mol) was recrystallized twice from *n*-hexane (5 m*l*) to give white crystals (500 mg); mp 41°C. The IR spectrum, ν_{max} (KBr): 2140, 2240(–C≡C–C≡C–), and 1750 (>C=O) cm^{-1}; the UV spectrum, λ_{max} (CH_3OH) mμ (ε): 219(897), 232(684), 245(624), 258(659), 273(601): the NMR spectrum, τ(CCl_4): 5.25(s, –C≡C–C≡C–CH_2–O–), 7.65(m, –CH_2–C=O), 8.51(m, –CH_2–). The saponification value was 257.0 (Calcd 256.8). Found: C, 76.76: H, 8.36%. Calcd for $C_{14}H_{18}O_2$: C, 77.03; H, 8.31%.

The crystals (200 mg) were hydrogenated over a 5% Pd-on-charcoal catalyst (50 mg) in ethyl acetate (50 m*l*) to yield cyclo-tetradecanolide (mp 28°C), the identity of which was confirmed by comparison with the IR spectrum and gaschromatogram of an authentic, commercially-available sample.

Linear Oligomer. A solution of a 0.3-g portion of the combined ether and acetone-soluble fraction in 40 m*l* of a mixed solvent of acetone-ether was shaken with a solution of the Ilosvay reagent,[4] consisting of cuprous chloride (1 g), ammonium carbonate (5 g), 28% ammonia water (5 m*l*), and water (20 m*l*). The precipitates thus formed were filtered off. The evaporation of the oily layer separated from the filtrate gave no product, indicating no contamination of cyclic oligomers in the products.

Upon the t.l.c. of the product obtained by the hydrolysis, followed by hydrogenation over the Pd-on-charcoal of the linear oligomer, only one spot, with a R_f value of 0.24, appeared; we may thus conclude that the linear oligomer is formed by a coupling of the esters only in a head-to-tail manner.

Moreover, the ether-soluble portion (2.3 g) was saponified with 50 m*l* of an ethanolic 1N potassium hydroxide solution. The resulting solution was acidified with an aqueous solution of 10% hydrochloric acid, and then extracted with ether (20 m*l*×4). The product (2.3 g) obtained by the removal of the solvent from the ether solution dried over Na_2SO_4 was hydrogenated at 10 kg/cm^2 of hydrogen over Pd-on-charcoal; 14-hydroxytetradecanoic acid, mp 95°C, was thus obtained in a 95% yield.

The IR spectrum, ν_{max} (KBr): 3300(HC≡C–), 2280 and 2150(–C≡C–C≡C–) and 1745(>C=O) cm^{-1}. The NMR spectrum, τ(acetone): 5.05(s, –C≡C–C≡C–CH_2–O–), 7.65(m, –CH_2–C=O) and 8.65(m, –$(CH_2)_8$–).

These spectral data were in good agreement with those of the linear oligomer prepared by the Sondheimer method.[8]

7) W. McCrae, *Tetrahedron*, **20**, 1773 (1964).

8) F. Sondheimer and Y. Amiel, *J. Amer. Chem. Soc.*, **81**, 6301 (1959).

BULLETIN OF THE CHEMICAL SOCIETY OF JAPAN VOL. 43 1250—1251 (1970)

Effects of Ditertiary Phosphine Ligands in Co-dimerization of Butadiene and Ethylene Catalyzed by Cobaltous Chloride —Ditertiary Phosphine— Triethylaluminum*1

Teruhiko KAGAWA, Yoshio INOUE and Harukichi HASHIMOTO

Department of Synthetic Chemistry, The University of Tokyo, Hongo, Bunkyo-ku, Tokyo

(Received September 8, 1969)

There are some reactions catalyzed by the transition metal catalyst in which the coordinated ligand plays an important role. This investigation has been carried out in order to find out the role of the ligand. The co-dimerization of butadiene and ethylene catalyzed by $CoCl_2$-ditertiary phosphine-$AlEt_3$[1a-e] was chosen for the study. Using ditertiary phosphine, $Ph_2P(CH_2)_nPPh_2$ ($n=1,2,3,4,5,10$) and $Ph_2P(CH_2)_mO(CH_2)_mPPh_2$ ($m=1,2$) as the ligand, the effects of the length of methylene chain between two phosphorus atoms and the ether bond have been investigated.

Experimental

Reagents. Toluene was purified by the usual method and distilled under an atmosphere of nitrogen. Triethylaluminum (Ethyl Corp., U.S.A.) was used without further purification. Butadiene was dried by passing through a column of anhydrous calcium chloride and condensed in a measuring vessel in a dry ice-methanol bath in order to measure its volume. Anhydrous cobaltous chloride and triphenylphosphine were obtained commercially. The preparation of ditertiary phosphines ($Ph_2P(CH_2)_nPPh_2$ and $Ph_2P(CH_2)_mO(CH_2)_mPPh_2$) were performed by the method described by Hewertson and Watson.[2] The purity was confirmed by elementary analysis and melting point. The cobalt complexes of ditertiary phosphine were obtained by the reaction of anhydrous cobaltous chloride with ditertiary phosphines in appropriate solvents, and used for experiments after recrystallization.[3]

Procedure. A 100 m*l* stainless steel autoclave equipped with a magnetic stirrer was charged with calculated amounts of cobalt complex, toluene, butadiene and triethylaluminum in this order under a nitrogen atmosphere. Temperature was then raised to 80—90°C, and ethylene was injected to a pressure of approximately 50 kg/cm² and the reaction was carried out with agitation under a constant ethylene pressure. After 2 or 3 hr, the autoclave was cooled to room temperature and the catalyst was quenched by adding a small amount of methanol. The reaction mixture was washed with water and dried with anhydrous sodium sulfate. The products were analyzed by gaschromatography.

Result snd Discussion

The co-dimerization products of butadiene and ethylene catalyzed by the cobalt catalyst are mainly 1,4-*cis*-hexadiene and a small amount of 1,3-hexadiene and 2,4-hexadiene. Among these products 2,4-hexadiene is formed by the isomerization of 1,4-hexadiene at higher temperature.[1f]

The effects of the length of methylene chain between two phosphorus atoms in the ditertiary phosphine are shown in Fig. 1. Complexes $CoCl_2$-($Ph_2P(CH_2)_nPPh_2$) ($n=3,4$) were found to show the most selective catalytic action for the formation of 1,4-*cis*-hexadiene. In the case of $n=1,5,10$,

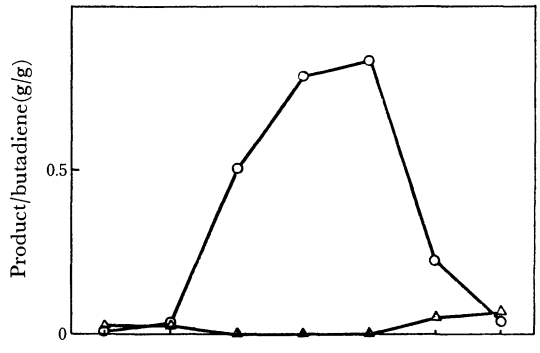

Fig. 1. Effect of the length of methylene chain in catalyst of $CoCl_2(Ph_2P(CH_2)_nPPh_2)$-$AlEt_3$ reaction condition: see footnote a) in Table 1, Al/Co=8—10
a) mixture ○ 1,3-hexadiene
△ 1,4-hexadiene

*1 Ligand Effects. I.

1) *e. g.* co-oligomerization of ethylene and butadiene. a) M. Iwamoto and S. Yuguchi, This Bulletin, **39**, 2001 (1966). b) M. Iwamoto and S. Yuguchi, *J. Org. Chem.*, **31**, 4290 (1966). c) M. Iwamoto and S. Yuguchi, This Bulletin, **41**, 150 (1968). d) M. Iwamoto and S. Yuguchi, *Kogyo Kagaku Zasshi*, **70**, 1221, 1505 (1967). e) M. Iwamoto and S. Yuguchi, *ibid.*, **71**, 133, 233, 237, (1968). f) G. Hata, This Bulletin, **41**, 2443, 2762 (1968).

2) W. Hewertson and H. R. Watson, *J. Chem. Soc.*, **1962**, 1490.

3) a) W. Dew. Horrockes, Jr., G. R. Van Hecke and D. Dew. Hall, *Inorg. Chem.*, **6**, 694 (1967). b) L. Sacconi and J. Gelsomini, *ibid.*, **7**, 291 (1968).

Table 1. Effect of Al/Co ratio[a)]

Complex mmol	Al/Co	Butadiene g	1,4-HD[b)] g	2,4-HD g	1,3-HD g
$CoCl_2$(DPP)	2.0	36.4	none	none	none
0.295	4.7	34.2	38.0	none	none
	8.9	32.4	38.3	none	none
	24.8	30.6	30.8	trace	none
$CoCl_2(DPE)_2$					
1.00	7.3	35.3	18.1	trace	none
$CoCl_2$(DPE)					
1.00	7.7	37.8	19.1	2.7	trace
0.50	11.0	31.2	4.0	trace	2.09[c)]

a) reaction temperature ~80°C,
reaction time 2 hr
$P_{C_2H_4}$=50 kg/cm²
b) HD=hexadiene
c) 8.3 g of 3-methyl-1,4,6-heptatriene was also produced.

the amount of 1,4-hexadiene decreased and that of 1,3-hexadiene increased and the products distribution became similar to that of $CoCl_2$-$AlEt_3$ catalyst. It seems that the above selectivity is partly due to the adequate stabilization of the active intermediate by the formation of six or seven membered chelate ring which consists of metal and ditertiary phosphine. However, the bulkiness of the ligand may also influence the selectivity of the products.

$CoCl_2$(DPE)*2 and $CoCl_2(DPE)_2$ had the same activity at a low concentration of triethylaluminum, but at the molar ratio of Al/Co=11, $CoCl_2$(DPE) lost the selectivity of 1,4-hexadiene as is given in Table 1. From a structural point of view, the complex $CoCl_2$(DPE) has a tetrahedral structure, and $CoCl_2(DPE)_2$ is considered to be five coordinated complex.[3a)] However, $CoCl_2$(DPP)*3 which has the same structure as $CoCl_2$(DPE)[3b)] was a good catalyst for 1,4-hexadiene formation in a wide range of the molar ratio of Al/Co.*4 It may be shown that the activity does not depend on the initial structure of the complex. The structure of reaction intermediates seems to be different. Further addition of DPE to $CoCl_2$DPE with molar ratio of DPE/$CoCl_2$(DPE)=1.0, did not change the yield of 1,4-hexadiene appreciably. When DPE was added to the $CoCl_2(DPE)_2$, the result was similar to that of $CoCl_2(DPE)_2$ alone. Thus the additional DPE may not disturb 1,4-hexadiene formation by occupying the active site of the metal

When $Ph_2P(CH_2)_mO(CH_2)_mPPh_2$ was used as a ligand, the selectivity of 1,4-hexadiene was small and the high boiling point products were produced. The product distribution depended on the reaction temperature; at lower temperatures 1,3-hexadiene and butadiene dimerization product *i. e.* 3-methyl-1,4,6-heptatriene were mainly formed, and at higher temperatures 1,4-hexadiene and 2,4-hexadiene. The catalyst $CoCl_2$DPMO*5 was active at 50°C. However, in the case of $CoCl_2$DPEO*6 the activity appeared over 120°C. If we compare the number of atoms between two phosphorus atoms of DPMO with that of DPP, the length of the ligand is of the same order, but the catalytic activity and the selectivity are extremely different. Thus the electronic effect of the oxygen atom in the ether bond can not be neglected.

*2 DPE=1,2-bis(diphenylphosphino)ethane
*3 DPP=1,3-bis(diphenylphosphino)propane
*4 see Table 1.
*5 DPMO=bis(1-diphenylphosphinomethyl) oxide
*6 DPEO=bis(2-diphenylphosphinoethyl) oxide

BULLETIN OF THE CHEMICAL SOCIETY OF JAPAN VOL. 43 1252—1254 (1970)

Studies on Reactions of Isoprenoids. XI.[1] Stereochemistry of the Ritter Reaction Products of Camphene with Unsaturated Nitriles

Tadashi SASAKI, Shoji EGUCHI and Takeshi OYOBE

Institute of Applied Organic Chemistry, Faculty of Engineering, Nagoya University, Chikusa-ku, Nagoya

(Received September 24, 1969)

The Ritter reactions of camphene (I) with various nitriles except unsaturated nitriles have been studied mainly from the interest in the pharmacological activities of the products.[2] We have recently reported the Ritter reactions of I with cyanoacetylene and chlorocyanoacetylene as the first examples of the Ritter reactions with acetylenic nitriles.[3] However, the stereochemistry of the corresponding products was not described in detail. This note describes the structural elucidation of the Ritter reaction products of I with cyanoacetylene and chlorocyanoacetylene as well as that with acrylonitrile on the basis of their analytical, IR and NMR data in comparison with the NMR data of *N*-acetylisobornylamine (IIId),[2a] and of their hydrolysis produdts.

The Ritter reactions were carried out with the ratio, I : nitrile : sulfuric acid = 1 : 2 : 4. The yields of IIIa from I and cyanoacetylene, and IIIb from I and chlorocyanoacetylene were both improved to 41 and 61% as compared with the previous values 15 and 40%. The Ritter reaction of I with acrylonitrile proceeded similarly to afford an unsaturated amide (IIIc) in 49% yield. The yields, mps and analyses of these products are summarized in Table 1.

In the NMR spectra (Table 2) of these products (IIIa—c), a common characteristic double triplet signal for one proton appeared in the range τ 6.00—6.08. A similar pattern signal was also observed at τ 6.07 in the spectrum of IIId,[2a] suggesting that IIIa—c have the same configuration as IIId at C-2 position. Thus, the structures of IIIa—c were assigned as *N*-propioloylisobornylamine, *N*-chloropropioloylisobornylamine, and *N*-acryloylisobornylamine respectively. These assignments were supported by hydrolyses of IIIa—c to afford the same isobornylamine (IV) in the yields

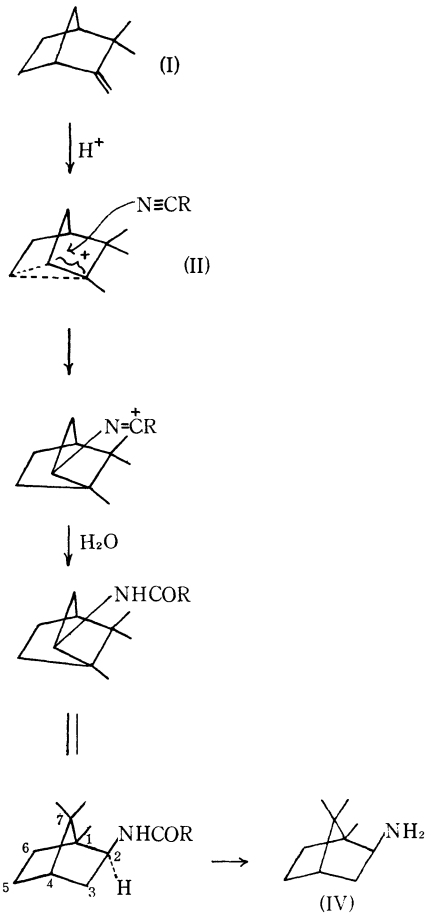

(IIIa) R = -C≡CH
(IIIb) R = -C≡CCl
(IIIc) R = -CH=CH$_2$

1) Part X of this series: T. Sasaki and S. Eguchi, This Bulletin, **42**, 2736 (1969).

2) a) J. J. Ritter and P. P. Minieri, *J. Amer. Chem. Soc.*, **70**, 4045 (1948); b) F. R. Benson and J. J. Ritter, *ibid.*, **71**, 4128 (1949); c) J. J. Ritter, U.S. 2573673 (1951); *Chem. Abstr.*, **46**, 9584h (1952); d) N. K. Kochetkov, A. Ya. Khorlin and K. I. Lopatina, *J. Gen. Chem. USSR (Eng. Transl.)*, **29**, 77 (1959); *Chem. Abstr.*, **53**, 22058i (1959); e) C. A. Stone, M. L. Torchiana, K. L. Meckelburg, J. Stavorski, M. Sletzinger, G. A. Stein, W. V. Ruyle, D. F. Reinhold, W. A. Gaines, H. Arnold and K. Pfister, III, *J. Med. Pharm. Chem.*, **5**, 665 (1962); *Chem. Abstr.*, **57**, 12341c (1962); f) P. L. de Bennevile, U.S. 2632766 (1953); *Chem. Abstr.*, **47**, 6686c (1953).

3) T. Sasaki, S. Eguchi and K. Shoji, *J. Chem. Soc., C*, **1969**, 406.

Table 1. The Ritter reactions of camphene (I) with unsaturated nitriles[a]

Nitrile	Product (Yield, %)	Mp (°C)	Analysis (%) Found C	Found H	Found N	Calcd[d] C	Calcd[d] H	Calcd[d] N
NC–C≡CH	IIIa (41)	142—143[b]						
NC–C≡CCl	IIIb (61)	131—132[c]	64.80	7.76	5.69	65.05	7.56	5.84
NC–CH=CH_2	IIIc[e] (49)	135—136	74.91	10.04	6.83	75.31	10.21	6.76

a) All reactions were carried out using 0.01 mol of I, 0.02 mol of nitrile, and 0.04 mol of concentrated sulfuric acid in 30 m*l* of acetic acid at *ca.* 30°C for 20 hr.
b) Lit,[3] mp 141°C.
c) Previous value, mp 106°C.[3] The compound seems still somewhat impure though its IR spectrum was superimposable on that of IIIb.
d) (IIIb): $C_{13}H_{18}NOCl$. (IIIc): $C_{13}H_{21}NO$.
e) The IR spectrum (KBr) had absorption bands at 3310, 1650, 1615, 1520, 960 and 903 cm^{-1}.

Table 2. NMR data of IIIa—d ($CDCl_3$, 60 MHz)

	IIIa τ	IIIb τ	IIIc τ	IIId τ
NH	4.10 (1H, broad s)	4.10 (1H, broad s)	4.15—4.55* (*ca.* 1H, broad s)	4.50 (1H, broad s)
C-2-*endo*-H	6.05 (1H, double t, J=5.5 and 9.0 Hz)	6.08 (1H, double t, J=5.5 and 9.0 Hz)	6.00 (1H, double t, J=5.5 and 9.0 Hz)	6.07 (1H, double t, J=5.5 and 9.0 Hz)
Isobornyl ring protons	7.88—8.95 (7H, m)	7.90—9.00 (7H, m)	7.80—8.92 (7H, m)	7.70—9.01 (7H, m)
Methyl protons	9.08, 9.13, 9.17 (9H, each s)	9.08, 9.13, 9.16 (9H, each s)	9.06, 9.17 (9H, each s)	9.08, 9.15 (9H, each s)
Other protons	7.21 (-C≡CH) (1H, s)		3.70—4.53($CH=CH_2$) (*ca.* 3H, ABX type m)	8.03 ($COCH_3$) (3H, s)

* This signal was overlapped with the signals of vinyl protons.

46, 10,[4] and 50%, respectively. This was identified as a phenylurea derivative with an authentic specimen[5] by means of mixed melting point determination and IR spectral comparison.

From the results it was concluded that the Ritter reactions of I with unsaturated nitriles at *ca.* 30°C afford the corresponding unsaturated amide derivatives after the Wagner-Meerwein rearrangement of I as observed in these reactions with certain saturated nitriles, though this type of rearrangement is known to be dependent on the reaction temperature as well as on nitriles (Scheme 1).[2d]

Experimental[6]

General Procedure for the Ritter Reactions. A mixture of 0.01 mol of I and 0.02 mol of nitrile was added to an ice-cooled mixture of 0.04 mol of concentrated sulfuric acid (sp. gr., *ca.* 1.84) and 30 m*l* of glacial acetic acid with stirring. Stirring was continued for 20 hr at room temperature (*ca.* 30°C) and the mixture was poured onto ice-water (200 g). The product was taken in chloroform and recrystallized from *n*-hexane or *n*-hexane-dichloromethane to give the corresponding amide derivatives (see Table 1).

General Procedure for the Hydrolyses of IIIa—c. *Ca.* 0.2 g of IIIa (or IIIb, and or IIIc) was heated in a mixture of 10 m*l* of ethanol and 20 m*l* of 6N hydrochloric acid under refluxing for 2 days.[4] After removal of ethanol under reduced pressure, the reaction mixture was washed with ether (30 m*l*×3). The water layer was made alkaline with 10% aqueous solution of sodium hydroxide and extracted several times with ether (30 m*l*×5). The combined ether extracts were dried over

4) IIIb was very stable to acidic hydrolysis; only 10% conversion to IV was observed together with an 80% recovery of IIIb after refluxing for 10 days under the conditions given in Experimental.

5) L. S. Luskin, A. J. McFaul and G. E. Geutest, *J. Org. Chem.*, **21**, 1430 (1956).

6) All melting points were determined on a Yanagimoto micromelting point apparatus and are uncorrected. Microanalyses were carried out on a Yanagimoto C. H. N. Corder Model MT-1. The IR spectra were recorded on a JASCO Model IR-S IR spectrophotometer and NMR spectra were obtained with a Varian A-60 spectrometer at 60 MHz using TMS as an internal reference.

sodium sulfate and the solvent was removed under reeduced pressure to give clorless solids of IV which were directly treated with phenyl isocyanate in dry benzene (10 m*l*) to afford a phenylurea derivative of IV, mp 255.5—258°C (dec.) (from aqueous ethanol, lit,[5] mp 252—255°C (dec.)).

BULLETIN OF THE CHEMICAL SOCIETY OF JAPAN VOL. 43 1254—1256 (1970)

Studies on Heteroaromaticity. XXXVII.[1] 1,3-Dipolar Cycloaddition of a Nitrilimine Possessing a Nitrofuran Ring

Tadashi SASAKI and Toshiyuki YOSHIOKA

Institute of Applied Organic Chemistry, Faculty of Engineering, Nagoya University, Chikusa-ku, Nagoya

(Received September 24, 1969)

In continuation of our previous reports concerning the 1,3-dipolar cycloaddition of nitril oxides,[2] nitrones,[3] and diazoalkanes[4] possessing a nitrofuran ring, this note deals with similar reactions of a nitrilimine also possessing a nitrofuran ring. Such a nitrilimine has not been reported yet.

Many procedures have been reported for the preparation of reactive nitrilimines.[5] Among them, the most probable access to nitrilimines is by the action of tertiary bases on hydrazidoyl halides as reported by Huisgen.[6] We treated 5-nitro-2-furoylhydrazide (I) with phosphorus pentachloride according to his procedure. However, the expected hydrazidoyl chloride (II) could not be isolated and intractable polymers were produced instead. Recently Gladstone[7] demonstrated the intermediate formation of nitrilimines in lead tetraacetate-oxidation of benzaldehyde arylhydrazones by the 1,3-dipolar cycloaddition to acrylonitrile.

We treated readily available 5-nitro-2-furfural phenylhydrazone (III) with lead tetraacetate in a tetrahydrofuran(THF)-benzene mixture in the presence of dipolarophilic acrylonitrile at room temperature. The crude product was purified on column chromatography to afford pale yellow crystals; the structure was assigned as 5-cyano-3-(5-nitro-2-furyl)-1-phenylpyrazole (IV) on the basis of analytical and spectral data. The structure was further confirmed by the treatment of III with cyanoacetylene under similar reaction conditions affording the same product IV. This indicates the initial formation of a pyrazoline (V) by the 1,3-dipolar cycloaddition of a nitrilimine (VI) to acrylonitrile followed by heteroaromatization[1] to afford IV. When acetic acid was used as the solvent in the above reactions, the yield was lowered to 10%. Attempts to isolate a sideproduced hydrazidic acetate were unsuccessful, though this type of compound is generally believed to be produced from nitrilimine and acetic acid.[6] Treatment with styrene instead of acrylonitrile in the above reactions afforded 3-(5-nitro-2-furyl)-1,5-diphenylpyrazole (VII), which could not be obtained, however, from phenylacetylene and III in the presence of lead tetraacetate; the reaction afforded intractable oils. Similar reactions with acrylic and methacrylic acid afforded 3-(5-nitro-2-furyl)-1-phenylpyrazole (VIII) and 5-methyl-3-(5-nitro-2-furyl)-1-phenylpyrazole (IX) respectively, in good yields. Their analytical and spectral data were compatible with the above structures. The results indicate that the above reactions involve decarboxylation of the initial 1 : 1 adducts (X) by radical mechanism of lead tetraacetate and its oxidative heteroaromatization.[1]

Contrary to this, when methyl acrylate, methacrylate and allyl bromide were used as dipolarophiles, deep-red colored products, XI, XII and XIII, respectively, were produced. Their analytical and spectral data supported their pyrazoline structures; especially in the UV spectra strong bathochromic shifts were observed in the pyrazoline derivatives compared with the corresponding pyrazole derivatives.

The direction of addition of nitrilimine VI in the formation of IV and VIII was concluded to be the same irrespective of the polarization of used dipolarophiles, and in good accordance with the results obtained from nitril oxides[2,8] and other

1) Part XXXVI of this series: T. Sasaki, T. Yoshioka and Y. Suzuki, *Yuki Gosei Kagaku Kyokai Shi*, **28**, 469 (1970).

2) a) T. Sasaki and T. Yoshioka, This Bulletin, **40**, 2608 (1967); b) T. Sasaki and T. Yoshioka, *ibid.*, **42**, 826 (1969).

3) T. Sasaki and T. Yoshioka, *ibid.*, **41**, 2964 (1968).

4) T. Sasaki and A. Kojima, *ibid.*, **41**, 1658 (1968); *J. Heterocycl. Chem.*, **5**, 243 (1968).

5) R. Huisgen, R. Grashey and J. Sauer, "Cycloaddition Reactions of Alkenes," in "The Chemistry of Alkenes," ed. by S. Patai, Interscience Publ., New York (1964), pp 812—822 and references cited therein.

6) R. Huisgen, M. Seidl, G. Wallvillich and H. Knupfer, Tetrahedron, **17**, 3 (1962).

7) W. A. F. Gladstone, *Chem. Commun.*, **1969**, 179.

8) R. A. Firestone, *J. Org. Chem.*, **33**, 2285 (1968), and references cited therein.

nitrilimines.[8] The same holds in the reactions with α,β-unsaturated acids, esters and olefins.

We reported the thermal 1,3-dipolar cycloaddition of aromatic hydroxamoyl chloride with indene and acenaphthylene affording the corresponding isoxazolidines.[9] Treatment of III with indene and acenaphthylene in the presence of lead tetraacetate at room temperature afforded indenopyrazole (XIV or XIV′) and acenaphthopyrazole (XV) after oxidative heteroaromatization of the expected pyrazolines. The pyrazole structure present in XIV or XIV′ and XV was demonstrated by their UV spectra and by the absence of C-4 and C-5 methine proton in the NMR spectra.[9] There are two possible structures for the indenopyrazole, either 3-(5-nitro-2-furyl)-1-phenylindeno[2,3-*d*]pyrazole (XIV) or its [3,2-*d*]pyrazole (XIV′). Assuming a similar trend in the direction of addition of nitrilimines to nitrile oxides,[9] we tentatively assigned XIV preferentially to XIV′.

However, no cycloaddition of VI to acetonitrile, benzonitrile, benzaldehyde and *m*-nitrobenzaldehyde was observed.

Experimental[10]

5-Cyano-3-(5-nitro-2-furyl)-1-phenylpyrazole (IV). *From Acrylonitrile.* To a solution of 1 g (4.5 mmol) of 5-nitrofurfural phenylhydrazone III[11] and 1.1 g (25 mmol) of acrylonitrile in 60 m*l* of a THF-benzene (1 : 5) mixture was added 4 g (9 mmol) of lead tetraacetate at room temperature with stirring. The reaction mixture was further stirred at room temperature for 3 days. After filtering off undissolved parts, the solvents were removed under reduced pressure. The residual crude product was purified on a silica-gel (Mallinckrodt, 100 mesh) column using chloroform as the eluent to afford 0.58 g (55%) of pale yellow crystals IV, mp 165—167°C (from ethanol). IR (KBr) cm^{-1}: 2260 (CN). UV λ_{max}^{EtOH} mμ (ε): 290 (shoulder, 8650) and 344 (18400). NMR ($CDCl_3$) τ: 2.59 (s, C-4-H of pyrazole ring).[12]

Found: C, 60.03; H, 2.53; N, 19.63%. Calcd for $C_{11}H_8N_4O_3$: C, 60.00; H, 2.88; N, 19.99%.

From Cyanoacetylene. Similar treatment of 1.6 g (25 mmol) of cyanoacetylene[13] instead of 1.1 g (25 mmol) of acrylonitrile in the above reaction afforded 0.57 g (55%) of IV.

3-(5-Nitro-2-furyl)-1,5-diphenylpyrazole (VII). Similar treatment of 2.0 g (25 mmol) of styrene instead of 1.1 g of acrylonitrile afforded 0.33 g (20%) of pale yellow crystals VII, mp 155—157°C (ethanol). UV λ_{max}^{EtOH} mμ (ε): 236(23600) and 358(18400). NMR ($CDCl_3$) τ: 3.01 (s, C-4-H of pyrazole ring).[12] Found: C, 69.19; H, 3.59; N, 12.67%. Calcd for $C_{19}H_{13}N_3O_3$: C, 68.87; H, 3.96; N, 12.68%.

3-(5-Nitro-2-furyl)-1-phenylpyrazole (VIII). Acrylic acid (2.0 g, 27 mmol) was dissolved in a mixture of 20 m*l* of THF and 30 m*l* of benzene. To this solution was added 1.0 g (4.5 mmol) of III and then a solution of 3.1 g (8.5 mmol) of lead tetraacetate in 30 m*l* of benzene with stirring at room temperature. Work up as above afforded 0.65 g (90%) of pale yellow crystals VIII, mp 124—126°C (ethanol). UV λ_{max}^{EtOH} mμ (ε): 264(13200) and 364(20600). NMR ($CDCl_3$) τ: 2.13 (d, 1H, J=3.0 Hz, C-5-H of pyrazole ring) and 3.20 (d, 1H, J=3.0 Hz, C-4-H of pyrazole ring).[12]

Found: C, 60.99; H, 3.41; N, 16.48%. Calcd for $C_{13}H_9N_3O_3$: C, 61.17; H, 3.55; N, 16.47%.

5-Methyl-3-(5-nitro-2-furyl)-1-phenylpyrazole. (IX). Similar treatment of 0.8 g of III, 1.5 g of methacrylic acid and 3.2 g of lead tetraacetate in 15 m*l* of THF and 60 m*l* of benzene afforded 0.62 g (88%) of pale yellow crystals IX, mp 121—123°C (ethanol). UV λ_{max}^{EtOH} mμ (ε): 252(17400) and 358(18200). NMR ($CDCl_3$) τ: 3.46 (s, C-4-H of pyrazole ring) and 7.65 (s, C–CH_3).

Found: C, 62.25; H, 3.99; N, 15.48%. Calcd for $C_{14}H_{11}N_3O_3$: C, 62.45; H, 4.12; N, 15.61%.

5-Methoxycarbonyl-3-(5-nitro-2-furyl)-1-phenyl-2-pyrazoline (XI). When 2 g of methyl acrylate was used instead of methacrylic acid in the above reaction, 40% yield of deep red colored crystals XI, mp 138—140°C (ethanol) was obtained. UV λ_{max}^{EtOH} mμ (ε): 245 (8700), 296(11700) and 452(19500). NMR ($CDCl_3$) τ: 5.18 (double d, J=8.0 and 10.0 Hz, C-5-H of pyrazoline ring),[14] 6.30 (s, $-COOCH_3$) and 6.45 (m, $-CH_2-$).[14]

Found: C, 57.51; H, 4.15; N, 13.28%. Calcd for $C_{15}H_{13}N_3O_5$: C, 57.14; H, 4.16; N, 13.33%.

5-Methyl-5-methoxycarbonyl-3-(5-nitro-2-furyl)-1-phenyl-2-pyrazoline (XII). Deep red colored crystals, mp 165—167°C (ethanol). Yield was 50%. UV λ_{max}^{EtOH} mμ (ε): 304(10000) and 450(19500). NMR ($CDCl_3$) τ: 6.35 (s, $-CH_2-$), 6.38 (s, $-COOCH_3$) and 8.18 (s, C-5-CH_3 of pyrazoline ring).[14]

Found: C, 58.23; H, 4.64; N, 12.70%. Calcd for $C_{16}H_{15}N_3O_5$: C, 58.35; H, 4.59; N, 12.76%.

5-Bromomethyl-3-(5-nitro-2-furyl)-1-phenyl-2-pyrazoline (XIII). Deep red colored crystals, mp 121—122°C (ethanol). Yield: 60%. UV λ_{max}^{EtOH} mμ (ε): 250(8800), 300(10800) and 460(20000). NMR ($CDCl_3$) τ: 5.15 (m, C-5-H of pyrazoline ring)[14] and 6.5 (m, $-CH_2-$ of pyrazoline ring and CH_2Br).

Found: C, 47.69; H, 3.12; N, 11.64%. Calcd for $C_{14}H_{12}N_3O_3Br$: C, 48.01; H, 3.45; N, 12.00%.

3-(5-Nitro-2-furyl)-1-phenyl-indeno[2,3-d]pyrazole (XIV). Pale yellow crystals, mp 238—240°C (ethanol). Yield: 15%. UV λ_{max}^{EtOH} mμ (ε): 270(23000) and 365 (21000). NMR (DMSO-d_6) τ: no signal due to methine

9) T. Sasaki, T. Yoshioka and Y. Suzuki, *Yuki Gosei Kagaku Kyokai Shi*, **27**, 998 (1969).

10) Melting points are uncorrected. Microanalyses were carried out with a Yanagimoto C.H.N. Corder MT-1 type. The ultraviolet absorption spectra (UV) were recorded on a Nippon Bunko optical rotary dispersion recorder, Model ORD/UV-5. The infrared spectra (IR) were obtained with a Nippon Bunko IR-S spectrophotometer. The NMR spectra were determined with a Varian A-60 spectrometer, using tetramethylsilane as the internal standard. The chemical shifts are recorded in τ-values.

11) T. Takahashi, H. Saikachi and S. Yoshina, *Yakugaku Zasshi*, **69**, 284 (1949).

12) I. L. Finar and D. M. Rackham, *J. Chem. Soc., B*, **1968**, 211.

13) French 1532848 (Cl. CO7c), 12, July, 1968. *Chem. Abstr.*, **71**, 229 (1969).

14) R. Sustman, R. Huisgen and H. Huber, *Chem. Ber.*, **100**, 1802 (1967).

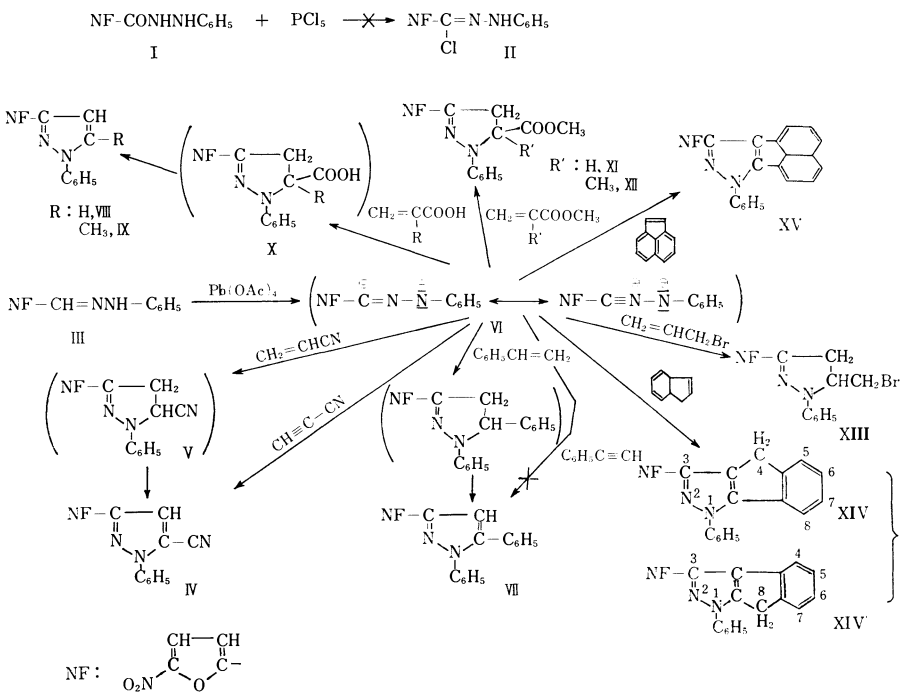

proton in a range of 3—5 τ.[9]

Found: C, 69.82; H, 3.76; N, 12.10%. Calcd for $C_{20}H_{13}N_3O_3$: C, 69.96; H, 3.83; N, 12.24%.

3-(5-Nitro-2-furyl)-1-phenylacenaphtho[1,2-*d*]pyrazole (XV). Pale yellow crystals, mp 284—286°C (ethanol). Yield: 13%. UV λ_{max}^{EtOH} mμ (ε): 320(18000) and 375(19000). NMR (DMSO-d_6) τ: no signal at 3—5 τ.[9]

Found: C, 73.07; H, 3.31; N, 10.86%. Calcd for $C_{23}H_{13}N_3O_3$: C, 72.81; H, 3.45; N, 11.08%.

BULLETIN OF THE CHEMICAL SOCIETY OF JAPAN VOL. 43 1256—1259 (1970)

The Reaction of α,α-Dichlorobenzyl Methyl Sulfone with Phenyllithium

Seiichi ASADA and Niichiro TOKURA

Department of Applied Chemistry, Faculty of Engineering, Osaka University, Suita-shi, Osaka

(Received September 24, 1969)

Few studies have been published on the intramolecular nucleophilic substitution of 1-halosulfones. Ramberg and Bäcklund[1] reported on how they formed *cis*-2-butene by reacting 1-bromoethyl ethyl sulfone with potassium hydroxide. Recently, Bordwell and Cooper[2] have elucidated the reaction mechanism as the formation of an episulfone, followed by decomposition to yield an olefin. It is worth noting here the predominant formation of *cis*-olefin:[3]

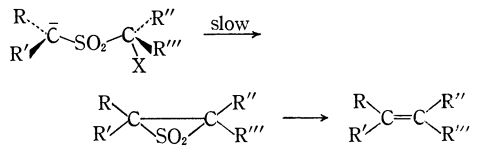

A similar reaction of 1,1-dihalosulfone with a base has been reported to yield an acetylenic compound and an olefinsulfonic acid, suggesting the

1) L. Ramberg and B. Bäcklund, *Chem. Abstr.*, **34**, 4725 (1940).

2) a) F. G. Bordwell and C. D. Cooper, *J. Amer. Chem. Soc.*, **73**, 5187 (1951). b) F. G. Bordwell, *J. Org. Chem.*, **33**, 1182 (1968).

3) a) L. A. Paquette, *J. Amer. Chem. Soc.*, **86**, 4383 (1964). b) L. A. Paquette, *ibid.*, **90**, 6783 (1968).

formation of thiirene dioxide as the intermediate:[4,5]

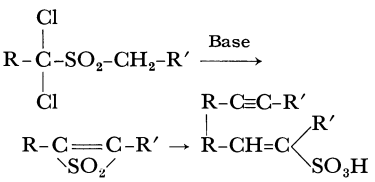

(2)

In the present communication, the results of the reaction of α,α-dichlorobenzyl methyl sulfone with phenylithium in tetrahydrofuran will be reported.

Results and Discussion

α,α-Dichlorobenzyl methyl sulfone (V) has been prepared from benzotrichloride (I). I was treated with *n*-butyllithium in tetrahydrofuran at −100°C to obtain a lithium compound (II). The insertion of sulfur dioxide into II has been found to be very easy, as is the carbon dioxide insertion into a similar compound,[6] which yields the α,α-dichlorobenzylsulfonyl lithium (III).

The reaction of III with methyl iodide resulted in the formation of α,α-dichlorobenzyl methyl sulfone (V) through the rearrangement of IV:

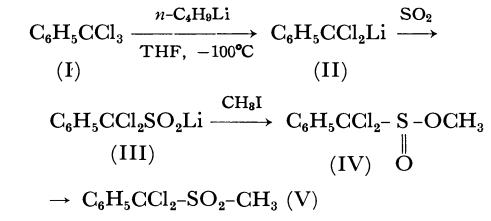

(3)

The reaction of the sulfone (V) with phenyllithium has been carried out in diethyl ether at 0°C for 3.5 hr. The products were then separated by alumina column chromatography. Several of the water-soluble products were treated with methyl iodide to convert the lithium salt to the methyl sulfone, and the products were eluted through a silica column in order to separate the methyl sulfones. The identified substances are listed in Table 1.

The following chart will account for the reaction paths for the various products from dichlorobenzyl methyl sulfone (V). (Chart 1).

The formation of *cis*- and *trans*-stilbenes (VI and VII), and the predominance of the *trans* compound over the *cis*, can be well reconciled with the fact that the addition of phenyllithium to 1-chloro-1-phenyl episulfone was followed by the elimination of sulfur dioxide. 1,1-Diphenyl episulfone was not found in the product. The difficulty of adding phenyl to the 1-position can be adequately explained by the steric reason and by the chlorine-lithium interaction.

The cleavage of 1-chloro-1-phenyl episulfone by phenyllithium leads to 1-chloro-1,2-diphenylethylsulfonyllithium, which then gives compound VIII by OLi-phenyl exchange and compound IX by the reaction with methyl iodide.

Experimental

α,α-Dichlorobenzyl Methyl Sulfone (V). To a solution of 58.7 g (0.3 mol) of benzotrichloride (I) in 600 m*l* of dehydrated tetrahydrofuran cooled at −100°C, freshly-prepared *n*-butyllithium (0.3 mol) in 150 m*l* of ether was slowly added under a nitrogen atmosphere for one hour, after which the mixture was stirred further at the same temperature for an additional half hour.

Sulfur dioxide (20 g) gas was streamed into the mixture at −100°C for 30 min, and then the solution was stirred for an additional hour and 50 m*l* of methyl iodide were added. The mixture was then slowly warmed and refluxed for fourteen hours.

After the mixture had been condensed to 1/3 its volume, water was added to the mixture and then it was extracted with ether. The ethereal solution was dried with sodium sulfate, condensed, and treated with 50 m*l* of petroleum ether to yield white crystals, which were then filtered and washed with chilled ether. Yield, 11.6 g (16.2%); mp 134.5—135.0°C. ν_{max}^{Nujol} 1155 and 1335 cm^{-1} (SO_2); 635 cm^{-1} (C–Cl). $\tau_{TMS}^{CCl_4}$, 6.80 (3H simple peak, SO_2CH_3), 2.4—2.7 (5H multiplet, phenyl).

Found: C, 39.96; H, 3.52%. Calcd for $C_8H_8Cl_2O_2S$: C, 40.18; H, 3.37%.

Reaction of α,α-Dichlorobenzyl Methyl Sulfone (V) with Phenyllithium. In a four-necked flask with

Table 1. The reaction of α,α-dichlorobenzyl methyl sulfone with phenyllithium

Product	Yield %
cis-Stilbene (VI)	2.7
trans-Stilbene (VII)	6.2
1,2-Diphenylethyl phenyl sulfoxide (VIII)	4.7
1,2-Diphenylethyl methyl sulfone (IX)	12.2
$C_6H_5CH{=}CHC(C_6H_5)CH_2C(C_6H_5)(OH){-}CH_2SO_2CH_3$ (X) SO_2CH_3	8.3
Phenyl methyl sulfone (XI)	24.6

4) a) L. A. Paquette, *J. Amer. Chem. Soc.* **86**, 4089 (1964). b) L. A. Paquette and L. S. Wittenbrook, *ibid.*, **89**, 4483 (1967).

5) L. A. Paquette, L. S. Wittenbrook and V. V. *Kane*, *ibid.*, **89**, 4487 (1967); *ibid.*, **90**, 5211 (1968).

6) D. F. Hoeg, D. I. Lusk and A. L. Crumbliss, *ibid.*, **87**, 4147 (1965).

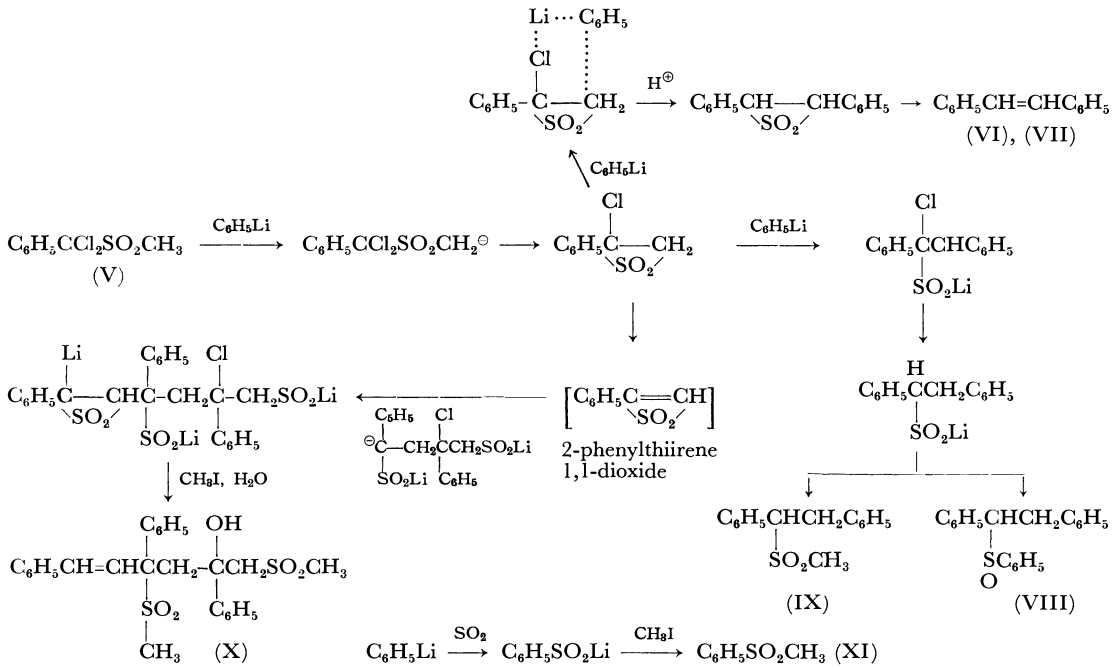

Chart 1

a capacity of 500 m*l*, 0.03 mol of phenyllithium in 70 m*l* of ether was cooled at 0°C; the mixture was stirred and then 2.0 g of α,α-dichlorobenzyl methyl sulfone dissolved in 250 m*l* of ether were added over a 1.5-hr period under a nitrogen atmosphere, with the temperature of the mixture kept at 0°C. The mixture was then stirred for an additional 3.5 hr at the same temperature.

After the reaction was over, the mixture was poured into ice water and the whole mixture was extracted with ether; the ether solution was then dried with sodium sulfate and condensed. The condensate was dissolved in petroleum ether and separated chromatographically using an alumina column. The solvents used as the eluants were in the following order: petroleum ether-benzene-ether-methanol. The aqueous layer was refluxed with 6.0 g of methyl iodide for 15 hr. The reaction mixture was then extracted with ether, and the extract was dried with sodium sulfate and evaporated. The residue was dissolved in benzene and eluted on a silica column.

***cis*- and *trans*-Stilbene.** The stilbenes were separated from the alumina column by elution with benzene and were then further separated and purified by preparative g.l.c. (45 m silicone D.C.) to *cis*- and *trans*-stilbenes. *cis*-Stilbene (VII), oil; yield 40.7 mg (2.7%); the results of the elemental analysis, the retention time, and the infrared and NMR spectra were consistnt with those of an authentic specimen. *trans*-Stilbene (VII), crystal; the mp and mixed mp with an authentic sample were 214—125.0°C; yield 11.28 mg (6.2%); the results of the elemental analysis, the retention time, and the IR and NMR spectra all supported the above identification.

1,2-Diphenylethyl Phenyl Sulfoxide (VIII). Elution by methanol gave the sulfoxide (VIII); yield, 122 mg (4.7%); mp 126.0—126.5°C. ν_{max}^{Nujol} 1050 cm^{-1} (SO), $\tau_{max}^{CCl_4}$, 2.5—3.4 (15H multiplet), 5.9—7.0 (3H ABC type multiplet). Found: C, 77.92; H, 5.75%. Calcd for $C_{20}H_{18}OS$: C, 78.39; H, 5.92%.

1,2-Diphenylethyl Methyl Sulfone (IX). An aqueous layer refluxed with methyl iodide was extracted with ether and then separated on a silica column. The fraction eluted with an ether-benzene mixture gave 1,2-diphenylethyl methyl sulfone (IX); yield 269 mg (12.2%); mp 124.5—125°C (from ethanol). ν_{max}^{KBr}, 1295 and 1130 cm^{-1} (SO_2). Mass., parent peak, 260 *m/e*, (Calcd 260). $\tau_{TMS}^{CDCl_3}$, 7.39 (3H, singlet, SO_2-$C\underline{H}_3$), 6.72 (1H quartet), 6.18 (1H quartet, C_6H_5-$C\underline{H}_A\underline{H}_B$), 5.72 (1H quartet, CH_2 - $C\underline{H}_X$), J_{BA}=13.8 Hz, J_{AX}=3.9 Hz, J_{AX}=10.6 Hz.

Found: C, 69.22; H, 6.24%. Calcd for $C_{15}H_{16}O_2S$: C, 69.21; H, 6.20%.

An authentic sample was prepared from benzylmagnesium bromide and benzaldehyde by the following route:

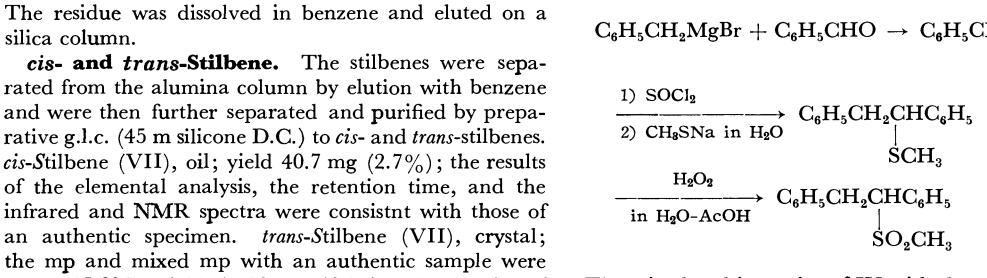

The mixed melting point of IX with the above specimen was not depressed: 124.5—125.0°C.

Disulfone (X). A fraction obtained from the silica column above mentioned (ether-benzene eluant) was condensed. Recrystallization of the residual substance from ethanol gave crystals of X; mp 182.0—182.5°C; yield 114 mg (8.3%). ν_{max}^{Nujol} 1290 and 1110 cm^{-1},

(=SO_2), 1645 cm^{-1}, (olefin). Mol. Wt. 480 (vapor) pressure osmometry) (calcd 484.5).

Found: C, 64.58; H, 5.97%. Calcd for $C_{26}H_{28}O_5S_2$: C, 64.43; H, 5.82%. $\tau_{max}^{CCl_4}$, 7.32 (3H singlet, SO_2CH_3), 7.41 (3H SO_2CH_3), 8.24 (1H singlet, OH), 5.80—7.00 (4H octet, $=CH_2$), 4.60 (1H doublet), 3.88 (1H doublet), 2.10—3.50 (15H multiplet).

Phenyl Methyl Sulfone (XI). This substance was obtained from a fraction eluted by benzene on the silica column; after the evaporation of the solvent this substance gave crystals. Yield, 251 mg (24.6%); mp 88.0—89.0°C (from ethanol); mixed mp with an authentic specimen, 88.0—89.0°C; Mass. parent peak, 156 *m/e*, (calcd 156). ν_{max}^{Nujol}, 1295 and 1150 cm^{-1}, (=SO_2). $\tau_{max}^{CCl_4}$, 6.92 (3H singlet, SO_2CH_3), 1.85—2.50 (5H multiplet, phenyl protons).

BULLETIN OF THE CHEMICAL SOCIETY OF JAPAN VOL. 43 1259—1261 (1970)

Molecular Orientation and Absorption Spectra of Quaterrylene Evaporated Film

Yusei MARUYAMA, Tohru IWAKI,*1 Takashi KAJIWARA, Ichimin SHIROTANI and Hiroo INOKUCHI

The Institute for Solid State Physics, The University of Tokyo, Roppongi, Tokyo

(Received October 4, 1969)

When, in 1963, experimental studies of the electrical and optical properties of quaterrylene evaporated films were carried out, interesting results were obtained.[1] In the optical absorption spectrum of the evaporated film, the large absorption peak in about the 540 mμ region, as is shown in Fig. 1, seems to be an anomalous one with respect to its position and absorbance in comparison with the spectrum of the crystalline state and also with the solution spectrum. It seems to be true that this peak appears only in the spectrum of the evaporated film, but not in that of the single crystal.

Therefore, the relation between the molecular orientation and the absorption spectra must be persued in order to analyze the structure of thin organic film.[2] The orientation of the molecules in the film was observed by the X-ray diffraction method, and its change was examined as a function of the deposited temperature, which was controlled by heating a glass plate substrate during the evaporation. The temperature dependence and pressure dependence of this absorption spectral peak were also measured.

Experimental

Quaterrylene evaporated films were prepared by the following method.[3] During the evaporation, the substrate was heated by a proper heater and a temperature gradient was set up along the substrate surface; the substrate temperature thus changed from 90°C to 300°C. The X-ray diffraction patterns and the optical absorption spectra of each part were observed. The structure of the highest-temperature part of the film was rather crystallized, and microcrystallites were deposited on the film. The absorption spectra produced by polarized light to the proper axis of the single crystal were measured by microscope-spectroscopy employing the micro-crystal thus obtained.

In order to ascertain the origin of the optical absorption bands, especially that of the 540 mμ band, of the evaporated film, the temperature dependence and pressure dependence of the optical absorption bands were observed. The former, the temperature dependence of the absorption bands, was observed down to 4.2°K using a liquid helium cryostat, while the latter, the pressure dependence, was measured up to 6.6 kbar using a high-pressure optical cell.[4]

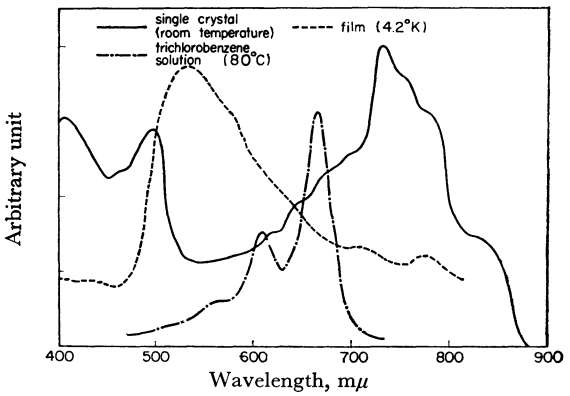

Fig. 1. The spectral response curve of absorption of quaterrylene.

*1 Department of Chemistry, Faculty of Science, Hiroshima University.

1) Y. Maruyama, H. Inokuchi and Y. Harada, This Bulletin, **36**, 1193 (1963).

2) H. Inokuchi, Y. Maruyama and H. Akamatu, *ibid.*, **34**, 1093 (1961).

3) Y. Maruyama and H. Inokuchi, *ibid.*, **39**, 1418 (1966).

4) T. Kajiwara, H. Inokuchi and S. Minomura, *ibid.*, **40**, 1055 (1967).

Results and Discussion

Figure 1 shows the absorption spectra of quaterrylene evaporated film, of its trichlorobenzene solution, and of the single crystal. The last is a polarized spectrum of a typical crystal axis. The absorption peaks in the 550—700 mμ region observed in the trichlorobenzene solution spectrum may be due to the lowest singlet excitation of the quaterrylene molecule. The 710 mμ and 780 mμ peaks in the film spectrum may correspond to an exciton band arising from this lowest molecular excitation. They are shifted in the direction of wavelengths longer than those of the solution spectrum because of intermolecular interaction in the solid state. These peaks also appear in the single crystal spectrum.

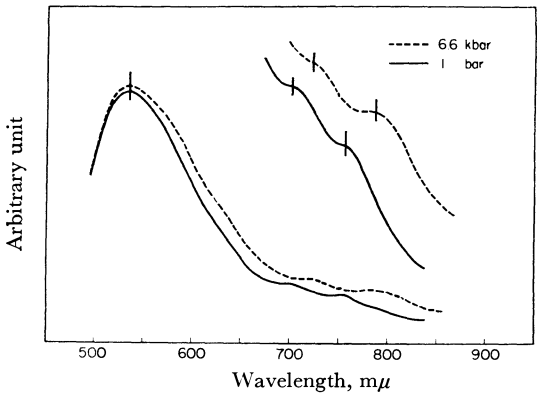

Fig. 2. The pressure induced red-shift of absorption spectral bands of quaterrylene.

This assignment is also supported by the fact that the pressure-induced red shift of these bands is about $-69\ cm^{-1}/kb$, as is illustrated in Fig. 2; this is a reasonable value for an exciton band.[5] These bands became rather sharper when the film was cooled to 4.2°K. This fact also suggests their exciton nature.

However, the 540-mμ band, found in the film spectrum, showed almost no change in its position and sharpness when it was cooled to 4.2°K or pressed to 6.6 kbar. This behavior is the most peculiar aspect of the band.

The relation between the spectra of the film and of the crystal was also strange, as is shown in Fig. 1. The effect of the molecular orientation on the absorption spectrum was studied next. The high temperature (~300°C)*2 part (1) appeared to be crystallized and micro-crystallites were deposited on the thin film. Part (2) (~150°C)*2 was bluish grey, Part (3) (~100°C)*2 was green, and the part (4) (room temperature),*2 violet.

Figure 3 shows the absorption spectra for the film specimens prepared at different substrate temperatures. The 540 mμ band in the spectrum deposited at room temperature seems to split to ~490 and ~630—680 mμ bands in the high-temperature specimens. The spectra of the (1)—(2)*3 and (2)—(3)*3 parts described above are rather similar to that of the single crystal (see Fig. 1).

The X-ray diffraction patterns of these different specimens deposited at various temperatures are shown in Fig. 4. The main diffraction lines of the high-temperature-part specimen (1) correspond to those from the (00n) planes, that is, the ab plane: The quaterrylene molecules are well oriented in

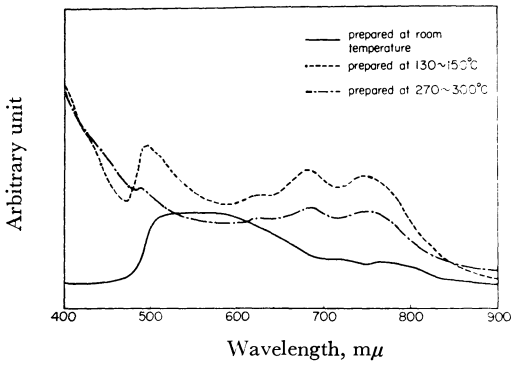

Fig. 3. The absorption spectral response curve of quaterrylene as a function of deposited temperature.

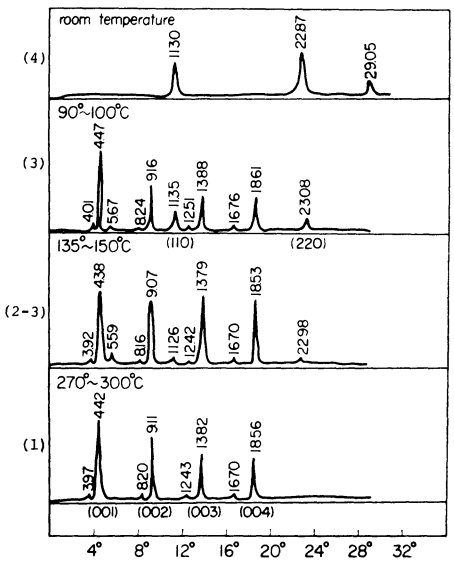

Fig. 4. The X-ray diffraction patterns of quaterrylene films deposited at various temperature: (1) is 270—300°C, (2—3) 135—150°C, (3) 90—100°C and (4) is room temperature.

5) I. Shirotani, H. Inokuchi and S. Akimoto, *ibid.*, **40**, 2277 (1967).

*2 The temperatures given in parentheses illustrate the substrate temperature.

*3 The (1)—(2) spectrum corresponds to the —·— line in Fig. 3, and (2)—(3), to the ------ line of Fig. 3.

this region.[2] In the patterns of (2)—(3) and (3), several diffraction lines other than (00n) appear. Among them, 11.30°, 22.87°, and 29.05° lines survive and grow in the region (4), as is the case with the substrate at room temperature.

The last three lines in (4) are not so sharp and large as the (00n) lines of (1) or (2)—(3), and no reasonable assignment of the crystal plane indices seems feasible. The possibility of crystal polymorphy cannot be perfectly denied, but the three lines in (4) may be, rather, due to an amorphous state judging from the appearance of these lines; that is, there is less sharpness and more weakness. Therefore, we assume that the existence of the 540 mμ band of the quaterrylene film is due to the plane ordering which is observable in the case of amorphous carbon.

BULLETIN OF THE CHEMICAL SOCIETY OF JAPAN VOL. 43 1261—1262 (1970)

The Copper(II) Complexes Distorted from a Planar Configuration

Takahiko INAZU and Takako INAZU

Department of Chemistry, Faculty of Science, Kyushu University, Hakozaki, Fukuoka

(Received October 11, 1969)

In the course of studies of the effects of bulky groups on the formation of dimeric copper(II) complexes with bridged alkoxy groups,[1] copper(II) complexes distorted from a planar configuration were synthesized.

With few exceptions, all X-ray analyses of the four coordinate copper(II) complexes have shown them to have a square planar arrangement of the donor atoms about the metal atom. We do not know of a purely tetrahedral copper(II) complex, but some distorted tetrahedral copper(II) complexes of Schiff bases from the substituted salicylaldehydes and the branched alkyl amines have been synthesized by Yamada and Nishikawa[2] and by Sacconi and Ciampolini.[3]

We synthesized the copper(II) complexes, I, II, and III, in which the bulky cyclohexyl or *t*-butyl groups are introduced not only in the amine component but also in the aldehyde portion. In these complexes, there must exist steric interactions between the bulky cyclohexyl or *t*-butyl group on the 3-position of the aldehyde portion and the bulky *t*-butyl group in the amine component. Two copper(II) complexes, I and III,[4] in chloroform showed a ligand-field band at 12200 cm^{-1}, while the complex II showed one at 12650 cm^{-1}. The square-planar copper(II) complexes of the Cu-$(N)_2(O)_2$ type show absorption in the 17700 cm^{-1}

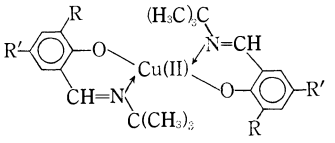

	R	R′
I	$C(CH_3)_3$	NO_2
II	cyclo-C_6H_{11}	CH_3
III	$C(CH_3)_3$	H

Fig. 1.

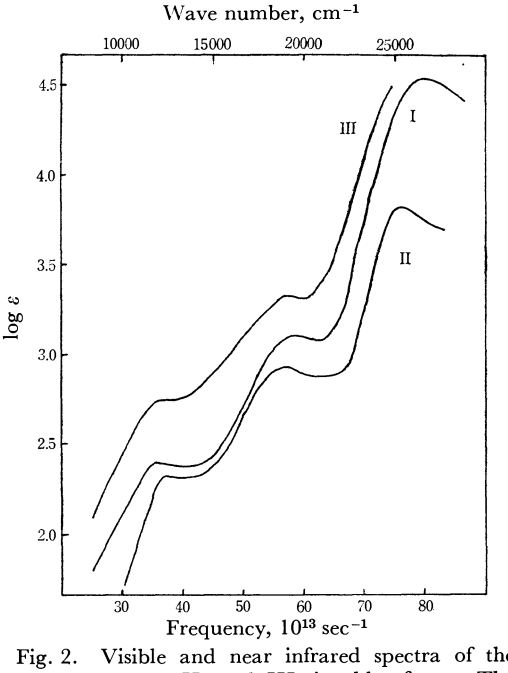

Fig. 2. Visible and near infrared spectra of the complexes, I, II, and III, in chloroform. The absorption curve of the complex, III, is arbitrarily plotted.

1) T. Inazu, H. Okawa, T. Inazu and T. Yoshino, This Bulletin, **42**, 2291 (1969).

2) S. Yamada and H. Nishikawa, *ibid.*, **36**, 755 (1963).

3) L. Sacconi and M. Ciampolini, *J. Chem. Soc.*, **1964**, 276.

4) The complex, III, was not isolated in a pure crystalline state.

region,[5] and it is known that a ligand-field band shifts to a lower-wave-number region as distortion from a planar configuration increases.[2] Bis(*N*-*t*-butylsalicylideneiminato)copper(II), IV, which was considered to have a distorted tetrahedral configuration,[6] shows absorption in the 13000 cm^{-1} region.[2]

From these facts, the copper(II) complexes obtained here can be though to have a configuration much more distorted from the square-plane than the complex IV.

Experimental

The melting point is uncorrected. The visible and near-infrared spectra in a chloroform solution were measured on a Hitachi EPS-3T spectrophotometer.

***N*-*t*-Butyl-3-*t*-butyl-5-nitrosalicylideneimine.** To 500 mg of 3-*t*-butylsalicylaldehyde[1] in 1 m*l* of acetic acid, we added 0.5 m*l* of nitric acid (sp gr 1.38) at room temperature. After standing for a few minutes, the mixture was poured into water. To the yellow crystals thus obtained we added excess *t*-butylamine in methanol and refluxed the mixture for a few minutes. The yellow crystals thus obtained were recrystallized from methanol. Yield, 180 mg, mp 150—151°C.

Found: C, 64.70; H, 8.00; N, 9.97%. Calcd for $C_{15}H_{22}N_2O_3$: C, 64.72; H, 7.97; N, 10.07%.

Bis(*N*-*t*-butyl-3-*t*-bultyl-5-nitrosalicylideneiminato)copper(II), I. To 37.3 mg of *N*-*t*-butyl-3-*t*-butyl-5-nitrosalicylideneimine in 2 m*l* of hot methanol, we added 13.6 mg of copper(II) acetate monohydrate in 5 m*l* of methanol. Immediately violet-black crystals were obtained. The crystals were filtered out and washed with methanol. Yield, 20 mg.

Found: C, 58.45; H, 7.04; N, 9.03; Cu, 9.42%. Calcd for $C_{30}H_{42}N_4O_6Cu$: C, 58.28; H, 6.85; N, 9.06; Cu, 10.28%.

Bis(*N*-*t*-butyl-3-cyclohexyl-5-methylsalicylideneiminato)copper(II), II. Black crystals.

Found: C, 70.83; H, 8.50; N, 4.85; Cu, 10.58%. Calcd for $C_{36}H_{52}N_2O_2Cu$: C, 71.08; H, 8.62; N, 4.60; Cu, 10.45%.

5) A. von Kiss, G. Bacskai and P. Csokan, *J. Prakt. Chem.*, **160**, 1 (1942).

6) In this complex, the angle between the planes containing the coordinating atoms of each chelate group and the copper atom is 54° instead of the 90° expected for a truly tetrahedral configuration.[7]

7) T. P. Cheeseman, D. Hall and T. N. Waters, *J. Chem. Soc., A*, **1966**, 685.

BULLETIN OF THE CHEMICAL SOCIETY OF JAPAN VOL. 43 1262—1265 (1970)

Intermolecular Interaction in Mixed Monolayers of *isotactic* and *syndiotactic* Poly(Methyl Methacrylate) at the Air-Water Interface

Akira TAKAHASHI, Shinji OHWAKI and Ikumi KAGAWA

Department of Applied Chemistry, Nagoya University, Chikusa-ku, Nagoya

(Received November 1, 1969)

Attention has recently been focussed on stereochemical interaction between *isotactic* and *syndiotactic* poly(methyl methacrylate)(PMMA). Various experimental methods have been utilized to clarify the nature of interaction. Beredjick *et al.*,[1,2] were the first not only to show that the film balance technique can differentiate two stereoisomers of PMMA but also that the pressure-area isotherm of 1 : 1 mixture of *synd*- and *iso*- PMMA was closer to that of stereoblock PMMA, thereby indicating strong cohesion between two isomers at the air-water interface. Watanabe *et al.*,[3] found that the mixing of dilute dimethylformamide solutions of two isomers resulted in instantaneous gelation. Liquori *et al.*,[4] reported that stereocomplex is formed between two isomers from their dimethylformamide solution, and the stoichiometry of the complex was 2/1 for the ratio of *synd*/*iso*. They proposed a structure of the complex in which extended *synd*-PMMA molecules are fitted between the grooves of 5_2 helix of *iso*-PMMA. Subsequent studies[5,6] also concluded the 2/1 complex formation. However, Chiang *et al.*,[7] concluded that the stoichio-

1) N. Beredjick, R. A. Ahlbeck, T. K. Kwei and H. E. Ries, Jr., *J. Polym. Sci.*, **46**, 268 (1960).

2) N. Beredjick and H. E. Ries, Jr., *ibid.*, **62**, S64 (1962).

3) W. H. Watanabe, C. F. Ryan, P. C. Fleisher and B. S. Garret, *J. Phys. Chem.*, **65**, 896 (1961).

4) A. M. Liquori, G. Anzuino, V. M. Corio, M. D'Alagni, P. DeSantis and M. Savino, *Nature*, **206**, 358 (1965).

5) H. Z. Liu and Kang-Jen Liu, *Macromolecules*, **1**, 157 (1968).

6) K. J. Liu, S. L. Lignowski and H. Z. Liu, IUPAC Symposium on Macromolecular Chem., Tronto, A2-2 (1968).

7) R. Chiang, J. J. Burke, J. O. Threlkeld and T. A. Orofino, *J. Phys. Chem.*, **70**, 3591 (1966).

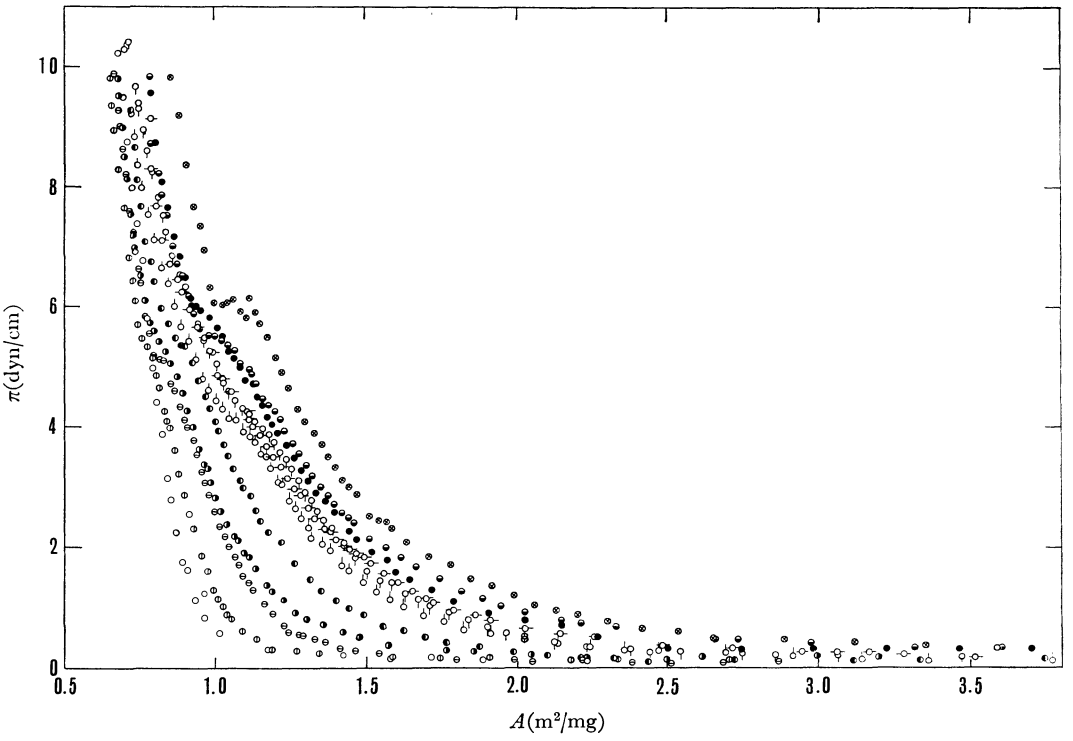

Fig. 1. Pressure-area isotherms for mixtures of *isotactic* and *syndiotactic* poly (methyl methacrylate) at the air-water interface at 25°C.
The ratio of *synd/iso*: ⊗ 0/1; ◒ 0.104/0.896; ● 0.178/0.822;-◯-0.286/0.714; ♀ 0.418/0.582; ♂ 0.468/0.532; ◐ 0.571/0.429; ◑ 0.717/0.289; ⊖ 0.783/0.217; ⓘ 0.915/0.085; ○ 1/0

metric ratio of *synd/iso* in the comlex formation was not as critical as reported by Liquori. Recently, Dayantis *et al.*,[8] determined an equilibrium curve of the concentration of the complex for each composition of *iso*- and *synd*-PMMA mixture in dimethylformamide-benzene solution. The curve has the maximum at the ratio 2/1 of *synd/iso*.

The measurement of the free energy of complex formation has not yet been reported, since its determination in bulk is cumbersome. In order to investigate the nature of interaction, we have carried out the measurements of pressure-area isotherms of mixtures of two stereoisomers of PMMA as a function of the ratio of *synd/iso*, and determined the molar excess free energy of mixing of monolayers of two stereoisomers at the air-water interface.

Experimental

Materials. The *isotactic* form was prepared by anionic polymerization, and purified by precipitation from a benzene solution into *n*-hexane and by freeze-drying from benzene. The *syndiotactic* form was synthesized by γ-irradiated polymerization at −70°C. Purification and drying were carried out in the same way as in the case of *isotactic* form. Viscosity average molecular weights were 1×10^6 for the *iso*-PMMA and 1×10^5 for the *synd*-PMMA, respectively. Tacticities were determined according to the NMR method of Bovey and Tiers.[9] The tacticity of *iso*-PMMA was *iso*=83.3%, *hetero*=8.2% and *synd*=10.5%; that of *synd*-PMMA was *iso*=0%, *hetero*=13.8% and *synd*=86.2%.

Film Balance. Teflon trough (20 cm × 120 cm) was used and surface pressures were measured at 25°C by a film balance similar in design to that of Inokuchi.[10] The spreading solvent was three times distilled benzene, and the substrate was three times distilled water. Benzene solutions of specified mixtures of two isomers were spread from an Agla microsyringe.

Results and Discussion

Pressure-area isotherms for specified mixtures are shown in Fig. 1. In the low pressure region, reproducibility was excellent. The isotherms obtained for both *iso*-PMMA and *synd*-PMMA are quite similar to that reported by Bereddjick *et al.*,[1,2] the *iso*-PMMA is more expanded, while the *synd*-PMMA is clearly condensed. The isotherm of *iso*-PMMA has distinct segments, and has a transition point at 6 dyn/cm; the extra-

8) J. Dayantis, C. Reiss and H. Benoit, *Makromol. Chem.*, **120**, 113 (1968).

9) F. A. Bovey and G. V. D. Tiers, *J. Polym. Sci.*, **44**, 173 (1960).

10) K. Inokuchi, This Bulletin, **26**, 471 (1953).

polated area is 18 and 15.5 Å²/monomer unit, respectively. The transition point at 6 dyn/cm could be attributed to conformational transformation involving 5_2 helices from extended form.[1] The monolayer of *synd*-PMMA is more tightly packed than that of *iso*-PMMA. The extrapolated area is 14 Å²/monomer unit.

Below surface pressure, $\pi=6$ dyn/cm, the isotherms for all mixtures fall in the region limited by that of two isomers, however, above $\pi=6$ dyn/cm, the isotherms shift to lower area with the increase of the composition of *synd*-PMMA. In particular, when the ratio of *synd/iso* exceeds 2/1, the isotherms lie on the left hand side as compared to that of *synd*-PMMA alone.

The molar excess free energy of mixing, $\Delta G^{\pi}_{xs,m}$, of two pure monolayers to forms as mixed monolayer at constant temperature and surface pressure was derived by Goodrich[11] and Gaines[12] and is given by

$$\Delta G^{\pi}_{xs,m} = \Delta G^{\pi}_{m} - \Delta G^{\circ}_{m} = \int_0^{\pi} (A_m - N_i A_i - N_s A_s) d\pi \quad (1)$$

where ΔG^{π}_{m} is the molar free enrgy of mixing at surface pressure π, and ΔG°_{m} is that at zero sufrace pressure. A_m is the molecular area measured in the mixed monolayer, N_i and N_s are the segment mol fractions of the *iso*- and *synd*-PMMA and A_i and A_s are the segment molar areas in the *iso*- and *synd*-PMMA monolayers at the same sufrace pressure. In evaluating the integral, we neglected the surface pressure of the polymer monoleyer in equilibrium with its surface vapor. If the mixed monolaryer behaves ideally, $\Delta G^{\pi}_{xs,m}$ vanishes so that the area of the mixed monolayer is the average of two isomer monolayers, thus

$$A_m = A_i N_i + A_s N_s \quad (2)$$

If A_m shows negative deviation from the average value, $\Delta G^{\pi}_{xs,m}$ will become negative. This indicates attractive interaction and compatibility. However, it is important to note that the linear additivity of areas holds also in the case of incompatibility.

The $\Delta G^{\pi}_{xs,m}$ values were calculated by Eq. (1) from the results shown in Fig. 1 using graphical integration. The results are shown in Fig. 2. In Fig. 3, areas of mixtures A_m at the specified surface pressures are plotted against isomer composition. Below 5 dyn/cm, $\Delta G^{\pi}_{xs,m}$ is almost zero and the additivity of areas holds as expected. Above 6 dyn/cm, $\Delta G^{\pi}_{sx,m}$ becomes negative, and at 10 dyn/cm it becomes minimum for the ratio 2/1 of *synd/iso*. At the same time, A_m shows negative deviation from the ideal behavior and has an inflexion point for the same ratio of *synd/iso*. These results indicate that, at the composition, *i. e.*, *synd/iso* is 2/1, the attractive interaction between two isomers is the strongest, and their efficient packing resulted under the surface pressure exceeding 6 dyn/cm.

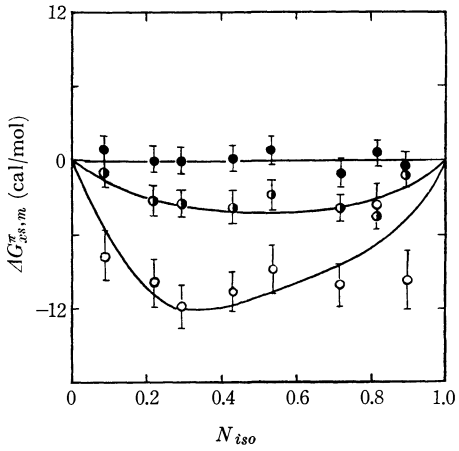

Fig. 2. Excess free energy of mixing of mixed monolayers of *iso*- and *synd*-PMMA at the surface pressures, ● 3; ◑ 6; O 10 dyn/cm (25°C).

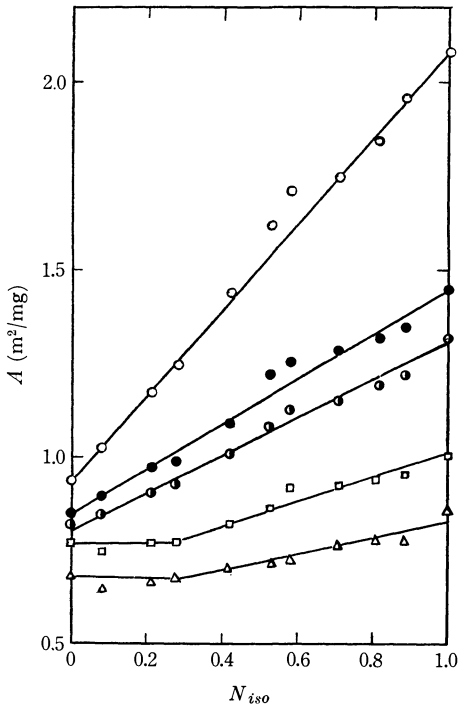

Fig. 3. Monolayer area *vs.* composition at the specified surface pressures for mixtures of *iso*- and *synd*-PMMA. π is, ○ 1; ● 3; ◑ 4; □ 6; △ 10 dyn/cm.

11) F. C. Goodrich, Proc. Intern. Congr. Surface Activity, 2nd, London, **1**, 85 (1957).

12) G. L. Gaines, Jr., "Insoluble Monolayers at Liquid Gas Interface," Interscience, New York, N.Y. (1966).

According to Crisp,[13] and Defay and Prigogine,[14] the surface phase rule is expressed as

$$F = C^B + C^S - P^B - q + 3 \quad (3)$$

where T, P and π are variables, F is the number of freedom, C^B is the number of components in the bulk phases, C^S is the number of componetns confined to the surface phase, P^B is the number of bulk phases, and q is the number of surface phases in equilibrium with one another. As is clear from Fig. 1, the transition point of surface pressures of mixtures, π_t, varies with the composition of monolayers; *viz.*, starting at $\pi_t=6$ dyn/cm for *synd/iso*=0/1, gradulally decreases with the increase of the ratio, reaches a minimum at 4 dyn/cm where the ratio is 0.468/0.532, and then increases with the increase of *synd.* content. Thus, we have one degree of freedom at T and P constant. We may consider four possible cases at the transition point with one degree of freedom.[15] (1) Compatible monolayer with phase transition ($C^B=2$, $C^S=2$, $P^B=2$ and $q=2$); (2) compatible monolayer with squeezing out of one component ($C^B=3$, $C^S=1$, $P^B=3$ and $q=1$); (3) compatible monolayer which becomes incompatible at π_t ($C^B=2$, $C^S=2$, $P^B=2$ and $q=2$); (4) incompatible monolayer which becomes compatible at π_t ($C^B=2^2$ $C^S=2$, $P^B=2$ and $q=2$). Of these four possibilities, case (3) may be discarded since the attractive interaction is shown to be above above π_t. Beredjick, *et al.*,[1] concluded that *iso*-PMMA is transformed to helical form from extended conformation at $\pi_t=6$ dyn/cm. Moreover, the isotherms of mixed monolayer with the ratio of *synd/iso* higher than 2/1 are almost superposed on those of the pure *synd*-PMMA monolayer above 5 dyn/cm. Thus, it is likely that an overlayer is formed. If we adopt a tentative layer model of the stereocomplex where *synd*-PMMA are snugly fitted between grooves of *iso*-PMMA helix as proposed by Liquori *et al.*,[4] case (1) is most likely, though no structural evidence such as an electron diffraction of built-up film of the mixed monolayer is present. It appears that the stereocomplementary molecular packing between two isomers at the air-water interface is promoted under pressure.

We are grateful to Dr. Tatsuo Matsuda, Government Industrial Research Institute, Nagoya and Dr. Masao Ishii for the supply of samples.

13) D. J. Crisp, *Research* (London) *Suppl. Surface Chem.*, **17**, 23 (1949).

14) R. Defay and I. Prigogine, "Surface Tension and Adsorption," Longmans, London (1966).

15) S. Wu and J. R. Huntsberger, *J. Colloid Interfac. Sci.*, **29**, 138 (1969).

BULLETIN OF THE CHEMICAL SOCIETY OF JAPAN VOL. 43 1265—1267 (1970)

Photoionization of Naphthalene

Jun-ichi AIHARA and Hiroo INOKUCHI

The Institute for Solid State Physics, The University of Tokyo, Roppongi, Minato-ku, Tokyo

(Received November 12, 1969)

Studies of the photoionization of aromatic hydrocarbons in the vapour phase play an important role in obtaining the direct information on the highly-excited states of these molecules. These results can also be used in the estimation of the exciton states in the molecular aggregates.

Recently, several articles concerning the ionization phenomena of naphthalene have been published. Various experimental values of the ionization potential have been obtained by an electron-impact method, by the spectroscopic method, and by photoelectron spectroscopy.[1-5] During the last decade, the theory of the ionization has also been improved.[6-9]

In this paper, we wish to report the ionization potentials of some aromatic hydrocarbons involving naphthalene and to compare the photoionization efficiency curve of naphthalene with the photoelectron spectrum obtained by Turner, and Dewar and Worley.[4,5]

1) M. E. Wacks and V. H. Dibeler, *J. Chem. Phys.*, **31**, 1557 (1959).
2) K. Watanabe, T. Nakayama and J. Mottl, *J. Quant. Spectrosc. Radiat. Transfer*, **2**, 369 (1962).
3) T. Kitagawa, *J. Mol. Spectrosc.*, **26**, 1 (1968).
4) D. W. Turner, *Chem. Brit.*, **5**, 435 (1969).
5) M. J. S. Dewar and S. D. Worley, *J. Chem. Phys.*, **50**, 654 (1969).
6) J. R. Hoyland and L. Goodman, *ibid.*, **36**, 12 (1962).
7) M. J. S. Dewar, J. A. Hashmall and C. G. Venier, *J. Amer. Chem. Soc.*, **90**, 1593 (1968).
8) R. J. Buenker and S. D. Peyerimhoff, *Chem. Phys. Lett.*, **3**, 37 (1969).
9) N. C. Baird and M. J. S. Dewar, *J. Chem. Phys.*, **50**, 1262 (1969).

Experimental

The photoionization efficiency curve obtained in this study was made by the method developed by Watanabe.[10] The experimental arrangements and the procedure were nearly the same as those described in Kitagawa's article.[3]

The apparatus employed consisted of a Seya-Namioka-type, 0.5-m vacuum ultraviolet monochromator. A spectral resolution of about 2 Å was obtained with the two slits set about 100 μ in width. The high-voltage discharge of hydrogen was used as the light source.

The photoionization cell was made of Pyrex glass, and LiF windows were attached. Non-magnetic stainless-steel electrodes were set in a cylindrical form 2 mm apart from each other.

The applied voltage of 10 V was sufficient to collect the electrons produced. The collected ionization current was measured on a Cary 31 vibrating-reed electrometer.

All the photoionization-yield measurements were made with a static pressure and at room temperature.

The naphthalene used was a zone-refined material; it was subjected to over 50 passes of the zone heater. Durene, acenaphthene, and indene were purified according to the usual procedures.

The ionization efficiency, Y, was obtained from the equation:

$$Y = \frac{Ki}{I - I_0} \qquad (1)$$

where K is an apparatus constant, i is the photocurrent, I is the intensity of the incident light, and I_0 is the intensity of the transmitted light through the gaseous specimen.

Results and Discussion

The photoionization efficiency of naphthalene is plotted as a function of the energy in electron volts in Fig. 1. The wavelength scale is also given. The lowest adiabatic ionization energy is denoted by I.P. The photoelectron spectrum of naphthalene is also shown in Fig. 1.[4]

In the region observed, the products caused by photolysis are considered to be small in amount. Therefore the ionization yield is mainly that of the naphthalene cation, $C_{10}H_8^+$.[11]

The photocurrent rapidly increased as the photon energy increased. Various structures exist in the ionization efficiency curve. In the first, this curve is a gradually varying-step function of the energy. The threshold is the first step: it corresponds to the first ionization potential, 8.12 eV. This value agrees well with that obtained by Watanabe *et al.*[2] The literature values of the ionization potential of naphthalene are summarized in Table 1.

In the region below the threshold energy, the yield exponentially increases forward the threshold energy. This exponential rise can be explained by the population of thermally-activated molecules in the ground state.

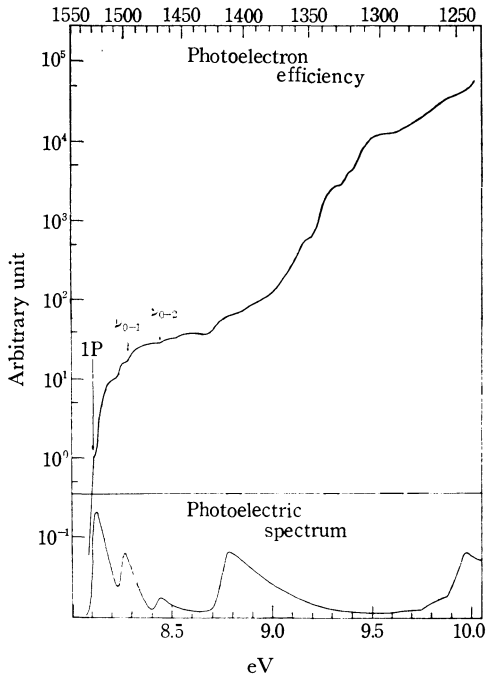

Fig. 1. Photoionization efficiency curve and photoelectron spectrum of naphthalene.*
* cited from Ref. 4.

Table 1. First ionization potential of naphthalene

Experimental	This work	8.12 eV
	Photoionization[2]	8.12
	The convergence limit of Rydberg series[3]	8.13
	Electron impact[1]	8.26
Theoretical	*Ab initio*[8]	9.20 eV
	Modified Koopman's theorem[6]	8.61
	Half-electron method[7]	8.30

In the first ionization region, three vibrational structures were observed. They were located at 1506, 1497, and 1466 Å. The origin of the first band is unknown. The second and the third bands correspond very well to the vibronic bands in the photoelectron spectrum.[4] Accordingly, these are interpreted as 0-1 and 0-2 bands. The vibrational spacings are around 0.17_5 eV.

The ratio of the contributions of the 0-0, 0-1, and 0-2 bands to the ionization yield is approximately 5 : 3 : 1. This trend is comparable to that of the integrated strengths of the vibrational structures in the photoelectron spectrum.

The ionization potential value, 8.26 eV, is that obtained by the electron-impact method.[1] It

10) K. Watanabe, *J. Chem. Phys.* **22**, 1564 (1954).
11) A. Terenin and F. Vilessov, "Advances in Photochemistry," Vol. 2, Interscience, New York (1964), p. 391.

was considered to be the vertical ionization potential. However, the strongest vibronic transition to the first ionization state is the 0-0 band, as is shown in Fig. 1. From this point of view, the vertical ionization potential should coincide with the adiabatic one; that is, the vertical ionization also takes place without any change in the molecular geometry. The observed difference in the measured ionization potentials, 0.14 eV, should be attributed not to the Franck-Condon factors, but to the experimental difficulties latent in the electron impact.

The higher ionization potentials have been reported to be located at 8.79, 9.96, and 10.90 eV.[5]

The electronic binding energies have also been calculated by the MINDO method in the energy range covering all the valence orbitals.[5] However, if we assume that the reorganization energy of an ion is the same in all the states, the higher ionization potentials can be estimated by means of the π-electron approximation by applying a constant correction. 1.15 was subtracted from the binding energies cited in the article of Baird and Dewar.[12] The results are entered in Table 2.

Table 2. Higher Ionization potentials of naphthalene

Experimental*	Theoretical	From the efficiency curve
8.11 eV	8.12 eV	8.12 eV
8.79	8.92	8.6—8.9
9.96	9.96	>9.6
10.90	10.89	
12.26	12.48	

* cited from Ref. 5.

When a radiation shorter than 1430 Å was used, there was a marked enhancement of the yield, mainly due to the second ionization by the resemblance to the photoelectron spectrum.

However, in the region concerned, the structure could not be observed distinctly. These phenomena are perhaps caused by the overlapping of possible vibrational modes. The Franck-Condon envelopes are smoothed. Consequently, the total ionization yield may become apparently continuous, or at least diffuse. These broad peaks, as well as the sub-step at 1506 Å, do not reflect on the photoelectron spectrum. In view of this the significance of such experiments is clear.

The efficiency curve shows a gradual rise again in the region shorter than 1250 Å; this is interpreted as the beginning of the third ionization region.

The approximate values of the ionization potentials estimated from the efficiency curve are also listed in Table 2. However, the exact potentials can not be obtained in this manner, since the efficiency in the higher-energy regions is closely related to the change in the molecular geometry and to such other effects as autoionization and predissociation.[13]

In spite of this, the spectral efficiency is well correlated with the photoelectron spectrum, as has been mentioned above. Further measurements in the higher-energy region are desirable: we are also preparing an apparatus for photoelectron spectroscopy.

In order to analyse the amount of the ionization yield, it is necessary to calculate the photoionization probability. Some theoretical formalisms have been reported using the hydrogenic continuum-wave function.[14,15] The probability of each ionization state depends on the wavelength of the exciting light, so no detailed analysis can be made between the efficiency curve and the photoelectron spectrum.

The behaviour of the experimental ionization cross-section is quite similar to the efficiency curve. The cross section in the first ionization region is of the order of 10^{-19} cm^2. It seems rather a reasonable value, judging from the calculated value of benzene, 10^{-19}—10^{-18} cm^2.[16]

We also measured the first ionization potentials of three compounds, durence, acenaphthene, and indene; they are 8.03 ± 0.02, 7.66 ± 0.03, and 8.08 ± 0.02 eV respectively.

The authors are very much indebted to Professor Taiji Kitagawa of Toyama University for giving them valuable advice and guidance throughout this work.

12) N. C. Baird and M. J. S. Dewar, *Theoret. Chim. Acta*, **9**, 1 (1967).

13) A. Russck, M. R. Patterson and R. L. Becker, *Phys. Rev.*, **167**, 17 (1968).

14) J. R. Hernandez, *ibid.*, **167**, 108 (1968).

15) P. M. Johnson and S. A. Rice, *J. Chem. Phys.*, **49**, 2734 (1968).

16) I. G. Kaplan and A. P. Markin, *Opt. Spectrosc.*, **24**, 275 (1968).

SHORT COMMUNICATIONS

Synthesis of Cinnamolide

Takeshi SUZUKI,*1 Mitsuru TANEMURA,*2 Tadahiro KATO and Yoshio KITAHARA*3

Department of Chemistry, Faculty of Science, Tohoku University, Sendai

(Received February 2, 1970)

Cinnamolide (I), a driman type sesquiterpene lactone isolated from *Cinnamosma fragrans*,[1] was reported to exhibit antifungal activity, which prompted us to synthesize I from drimenin II.

Reduction of II with lithium aluminum hydride afforded the corresponding diol (III), mp 75.5—77°C, which was subjected to oxidation with active manganese dioxide to give a mixture. Addition of *n*-hexane to the mixture afforded the crystalline (IVa), mp 95—97°C, IR (KBr) spectrum of IVa shows a strong band at 3300 cm^{-1} but no carbonyl absorption. In carbon tetrachloride IVa becomes an equilibrium mixture with IVb, the IR and NMR spectra of which show the presence of conjugated formyl group (1675 and 1628 cm^{-1} in IR (CCl_4) and 9.5 ppm in NMR).

The mixture of IVa and IVb was oxidized with chromic anhydride-pyridine complex in dichloromethane 2 to obtain a crystalline lactone (I), mp 88°C. Direct comparison of its IR and NMR spectra with those of natural cinnamolide, as well as conversion of I to diol (III) with lithium aluminum hydride indicate that the γ-lactone, thus obtained, is identical with (±)-cinnamolide.[3]

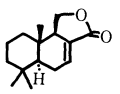

(I)

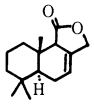

(II)

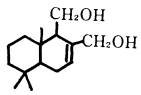

(III)

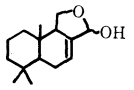

(IVa)

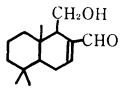

(IVb)

Since we have already carried out the synthesis of (±)-drimenin II based on biogenetic consideration,[4] the conversion of II to I demonstrates the synthesis of (±)-cinnamolide.

*1 Present address: Takasago Perfumery Co. 5-36-31, Kamata, Ota-ku, Tokyo.

*2 Present address: Chugai Central Laboratory, 3-41-8, Takada, Toshima-ku, Tokyo.

*3 To whom all correspondence regarding this paper should be addressed.

1) L. Canonica, A. Corbella, G. Jommi, J. Krepinsky, G. Ferrari and C. Casagrande, *Tetrahedron Lett.*, **1967**, 2137, see also *Tetrahedron*, **25**, 3895 (1969)

2) W. W. Hess, and F. J. Frank, *Tetrahderon Lett.*, **1968**, 3363.

3) The authors thank Prof. G. Jommi for his generous gift of natural cinnamolide.

4) Y. Kitahara, T. Kato, T. Suzuki, S. Kanno and T. Tanemura, *Chem. Commun.* **1969**, 342.

The Absolute Configuration of the $(-)_{589}$-$[Co(NCS)_2tn_2]$-$[Sb((+)\text{-tart})]\cdot 2H_2O$ Diastereoisomer

Keiji MATSUMOTO, Michitaka YONEZAWA, Hisao KUROYA
Hiroshi KAWAGUCHI and Shinichi KAWAGUCHI

Department of Chemistry, Faculty of Science, Osaka City University, Sugimoto-cho, Sumiyoshi-ku, Osaka

(Received November 17, 1969)

It has been shown by X-ray studies that the absolute configurations of $(+)_{589}$-$[Co(CN)_2en_2]^+$ [1] and $(-)_{589}$-$[Co\ ox\ en_2]^+$ [2] are of the *Λ*- and *Δ*- types respectively.[3] These results are consistent with the empirical predictions derived from CD or ORD measurements. Few investigations have, though, been made of the cobalt(III) complexes involving trimethylenediamine (=tn); with regard to the absolute configuration particularly, only that of $(-)_{589}$-$[Co\ tn_3]^{3+}$ [4] has been reported. We have now determined the crystal structure of $(-)_{589}$-$[Co(NCS)_2tn_2][Sb((+)\text{-tart})]\cdot 2H_2O$ as well as the absolute configuration of the complex cation.

Crystal data: orthorhombic, space group $P2_12_12$; $a=12.14$, $b=19.51$, $c=9.13$ Å; $Z=4$. Three-dimensional Fourier methods were used, the absolute configuration of the (+)-tartrate ion being referred to. The R value is 0.149 for 870 observed reflections.

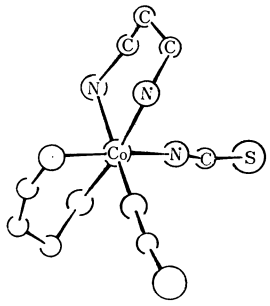

Fig. 1

Figure 1 is a perspective drawing of the complex cation, which has an approximately two-fold axis passing through the cobalt atom and bisecting the N(NCS)–Co–N(NCS) angle. Both of the two six-membered Co-tn rings are of the chair form. The absolute configuration of $(-)_{589}$-$[Co(NCS)_2tn_2]^+$ can be denoted as *Λ*, as is the case with $(-)_{589}$-$[Co\ tn_3]^{3+}$.

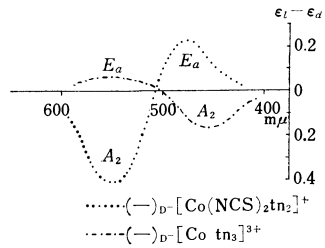

Fig. 2

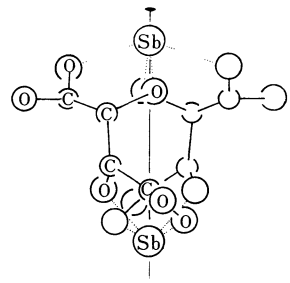

Fig. 3

The sign of the E_a component of the CD peaks in the first absorption-band region is regarded as diagnostic of the absolute configuration of the trigonal cobalt(III) complex ion.[5] The CD curve of $(-)_{589}$-$[Co\ tn_3]^{3+}$ [6,7] in this region shows a weak positive E_a peak in the longer-wavelength region and a strong negative A_2 peak on the shorter-wavelength side (Fig. 2). Therefore, the assignments indicated in Fig. 2 were made for the two components in the CD diagram of $(-)_{589}$-$[Co(NCS)_2tn_2]^+$ obtained in the present work.

In Fig. 3 the geometry of the (+)-tartrato-antimonate(III) ion is presented. A symmetric "dimerized" structure is built up of the two tetradentate tartrate ions bridging the two metal atoms lying on the two-fold axis of rotation.

1) K. Matsumoto, Y. Kushi, S. Ooi and H. Kuroya, This Bulletin, **40**, 2988 (1967).
2) T. Aoki, K. Matsumoto, S. Ooi and H. Kuroya, Proceedings of the 21st Annual Meeting of the Chemical Society of Japan (Osaka, 1968), p. 1122.
3) IUPAC Information Bull. No. **33**, p. 68 (1968).
4) Y. Saito, T. Nomura and F. Marumo, This Bulletin, **41**, 530 (1968).
5) A. J. McCaffery, S. F. Mason and R. E. Ballard, *J. Chem. Soc.*, **1965**, 2883.
6) F. Woldbye, ORD of transition metal complexes, European Research Office, U. S. Army, Frankfurt a. M. (1959); Record of Chemical Progress, **24**, 197 (1963).
7) P. G. Beddoe and S. F. Mason, *Inorg. Nucl. Chem. Lett.*, **4**, 433 (1968).

The Ring-size Effect in the Photoreaction of Phenylcycloalkenes

Masaru TADA and Hiraku SHINOZAKI

School of Science and Engineering, Waseda University, Shinjuku, Tokyo

(Received November 25, 1969)

We have been studying the ring-size effect in the photoreaction of phenylcycloalkenes, in which the double bonds are a part of the chromophore. A recent publication by Nozaki *et al.*[1] reporting the photo-induced addition of acetic acid to phenylcyclohexene and phenylcycloheptene has now prompted us to report the results from our independent work.*1

Methanolic solutions (0.1 M) of phenylcycloalkenes (I, II, III, and IV) containing a small amount (0.05% to methanol) of sulfuric acid were irradiated with a 100 W high pressure mercury lamp placed in a quartz cooling jacket for 6—24 hr (I, 10 hr; II, 6 hr; III, 7 hr: and IX, 24 hr). The reference solution was kept in the dark, and no change of phenylcycloalkenes was observed.

Phenylcyclopentene (I) gave a crystalline dimer, V-a (25%), mp 186°C, and an oily dimer V-b (12%) besides polymeric products. These two isomers were purified successively by alumina chromatography and preparative vapor-phase chromatography. The dimers have only phenyl-hydrogens and cycloparaffin-hydrogens in their NMR spectra. The mass spectrum of the V-a dimer has a strong peak at $m/e=144$ ($C_{11}H_{12}$) due to phenylcyclopentene, formed by the cleavage of the cyclobutane ring of the dimer upon electron impact, and no distinct peak over $m/e=144$. The V-b dimer has a molecular peak at $m/e=288$ ($C_{22}H_{24}$). Phenylcyclohexene (II) and phenylcycloheptene (III) gave methoxy-phenylcycloalkanes (VI, 54% and VII, 64%, after distillation) as the only isolable products besides the polymer. The structures of these adducts were characterized by a study of their mass spectra (M^+, $m/e=190$ for VI and 204 for VII) and by their NMR spectra, which have characteristic signals due to methoxy groups ($\delta=2.95$ for VI and 2.92 for VII in CCl_4). The irradiation of phenylcyclooctene (IV) gave phenylcyclooctane (VIII) (7%) and recovered phenylcyclooctene (15%) besides the polymer. The formation of the adduct between IV and methanol could be observed from the NMR spectrum of the crude product, but it was not present in an isolable amount.

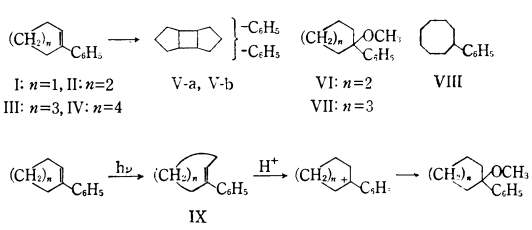

Cyclohexene and cycloheptene give adducts with alcohol upon irradiation in the presence of benzene, but no photo-addition of alcohol to cyclopentene and cyclooctene occurs.[2] This difference in the reactivity of cycloalkenes with a variation in the ring-size is also seen in our experimental results on phenylcycloalkenes. This similarity in the reactivity between cycloalkenes and phenylcycloalkenes indicates that the addition of methanol to phenylcycloalkenes (II and III) may be the thermal addition of methanol to the *trans*-phenylcycloalkenes (IX, $n=2,3$) formed through the orthogonal excited states of II and III.

The protonation to these *trans*-phenylcycloalknes with high energy contents is obviously the rate-determining step of the addition reaction, since the reaction without an acid catalyst is much slower. The steric requirements do not allow the formation of *trans*-phenylcyclopentene (IX, $n=1$) from the excited state, and the dimerization of phenylcyclopentene (I) takes place preferentially on irradiation. The formation of *trans*-phenylcyclooctene (IX, $n=4$) can be expected without difficulty. The *trans*-isomer, however, does not suffer much ring strain and the enrgy content is not high enough for the facile addition of methanol. Phenylcyclooctene (IV) gives no dimer, but abstracts hydrogen radicals from the solvent to give phenylcyclooctane (VIII).*2

1) S. Fujita, T. Nomi and H. Nozaki, *Tetrahedron Lett.*, **1969**, 3557.

*1 After the submission of our original manuscript, another paper dealing with the same subject has appeared: P. J. Kropp, *J. Amer. Chem. Soc.*, **91**, 5783 (1969).

2) a) P. J. Kropp, *J. Amer. Chem. Soc.*, **88**, 4091 (1966); **89**, 3651 (1967). b) J. A. Marshall, *Accounts Chem. Res.*, **2**, 33 (1969).

*2 The authors are indebted to the Kawakami Memorial Foundation for its financial support.

Peptide Synthesis *via* Oxidation-Reduction Condensation by the Use of Non-metallic Compound as a Mercaptan Scavenger

Teruaki MUKAIYAMA, Rei MATSUEDA and Hiroshi MARUYAMA

Laboratory of Organic Chemistry, Tokyo Institute of Technology, Ookayama, Meguro-ku, Tokyo

(Received January 16, 1970)

We have recently shown[1] that peptides with a high optical purity are produced in excellent yields (as determined by the Young test[2]) by the use of di-*p*-anisylmercury as a mercaptan scavenger *via* the following oxidation-reduction condensation reaction:

$$\text{Bz-L-Leu-OH} + \text{H-Gly-OEt} + \text{Ph}_3\text{P} + (o\text{-O}_2\text{NC}_6\text{H}_4\text{S})_2 + (p\text{-CH}_3\text{OC}_6\text{H}_4)_2\text{Hg} \longrightarrow \text{Bz-L-Leu-Gly-OEt} + \text{Ph}_3\text{P=O} + (o\text{-O}_2\text{NC}_6\text{H}_4\text{S})_2\text{Hg} + 2\,p\text{-CH}_3\text{OC}_6\text{H}_5 \quad (1)$$

In recent years, the potential utility of the solid phase method in peptide synthesis has been extended. With respect to this problem, various non-metallic mercaptan scavengers were investigated in an attempt to purge the insoluble metal mercaptide in the above equation.

First, the reaction was tried by the use of olefins as mercaptan scavengers; they yielded soluble sulfides instead of metal compounds (Eq. (1)), and good results were obtained. When the above reaction was carried out by using 2,3-dihydropyran and zinc chloride, the *N*-benzoyl-L-leucylglycine ethyl ester (Bz-L-Leu-Gly-OEt) was obtained in a 92% yield; mp 147—152°C $[\alpha]_D^{20}$ −32.9° (*c* 3.1, EtOH), L isomer 97%.[2] Another olefin, *n*-butyl vinyl ether, also gave a good result (90% yield, L isomer 95%).

Then, the reaction was carried out by using the sulfenate ester, which yields disulfide; a good result was obtained here also. When equimolar amounts of *N*-benzoyl-L-leucine, the *N*-*o*-nitrophenylsulfenylglycine ethyl ester, and triphenylphosphine were allowed to react in the presence of methyl 2,4-dinitrobenzenesulfenate in methylene chloride for 3 hr, Bz-L-Leu-Gly-OEt was obtained in a 92% yield; L isomer 92%.

Next, the reaction was tried in the absence of a mercaptan scavenger by using dipyridyl-2,2′-disulfide as a disulfide component, on the assumption that the 2-mercaptopyridine produced along with the peptide would isomerize to the stable thione form.[3] In a typical experiment, ethyl glycinate (5 mmol) and triphenylphosphine (5 mmol) in methylene chloride were added at room temperature to a stirred mixture of equimolar amounts of *N*-benzoyl-L-leucine and dipyridyl-2,2′-disulfide in methylene chloride. After stirring for 30 min, Bz-L-Leu-Gly-OEt was isolated by an ordinary procedure;[1] 1.46 g (91%); mp 148—152°C, $[\alpha]_D^{20}$ −32.6° (*c* 3.1, EtOH), L isomer 96%.

Finally, it was found that the third process could be successfully applied to the solid phase method and the dipeptide thus prepared in a high yield. For example, 0.644 mmol of *t*-amyloxycarbonylglycine estrified to 2 g of the supporting cross-linked polystyrene resin[4] was deprotected by 2N hydrogen chloride in acetic acid, and the general procedure[4] of the solid phase method was followed. Coupling was carried out using a threefold excess of *t*-butyloxycarbonyl-L-leucine monohydrate, triphenylphosphine, and dipyridyl-2,2′-disulfide in methylene chloride for 6 hr. The peptide was liberated from the resin by bubbling in hydrogen bromide in trifluoroacetic acid; after it had been evaporated to dryness and water had been added, the resin was filtered off. The amount of the peptide in the filtrate was determined by the aminoacid analyser to be 0.64 mmol of Leu-Gly (99% yield) (calculated from the authentic sample) and the glycine peak was not observed. This solution was desalted by DEAE cellulose, and the peptide was precipitated by adding ethanol after the water had been evaporated *in vacuo* to a very small amount. Ninety-one milligrams of H-L-Leu-Gly-OH (76% yield) were isolated after drying over phosphorus pentoxide at 100°C for 2 hr, mp 235—240°C (dec.), $[\alpha]_D^{20}$ 86.5 (*c* 2, H_2O). Found: C, 51.07; H, 8.48; N, 15.11%. Calcd for $C_8H_{16}N_2O_3$: C, 51.05; H, 8.57; N, 14.88%. [lit,[5] mp 235—242°C (dec.), $[\alpha]_D^{20}$ 85.99 (*c* 2, H_2O)]. The amino-acid analysis of a 24-hr 6N HCl hydrolysate gave: Leu, 0.92; Gly, 0.95.

1) T. Mukaiyama, R. Matsueda, H. Maruyama and M. Ueki, *J. Amer. Chem. Soc.*, **91**, 1554 (1969).

2) M. W. Williams and G. T. Young, *J. Chem. Soc.*, **1963**, 881. The L isomer % was calculated according to Young's equation.

3) R. A. Jones and A. R. Katritzky, *J. Chem. Soc.*, **1958**, 3610.

4) G. R. Marshall and R. B. Merrifield, *Biochemistry*, **4**, 2394 (1965).

5) E. Fischer, *Ber.*, **39**, 2893 (1906).

A New Route to Free Radical Aromatic Substitution

Atsuyoshi OHNO and Noboru KITO

Sagami Chemical Research Center, 3100 Onuma, Sagamihara-shi, Kanagawa

(Received February 2, 1970)

The mechanism of free radical aromatic substitution has been studied extensively[1-5] and shown to follow the scheme

$$\mathrm{ArH} + \mathrm{R}\cdot \longrightarrow \underset{\mathbf{1}}{\mathrm{RArH}\cdot} \xrightarrow{\mathrm{R'}\cdot} \mathrm{ArR} + \mathrm{R'H}$$

where R'· may be **1** or other radicals. The reactions of this type involve intermolecular hydrogen-transfer. We could expect a reaction involving intramolecular hydrogen-transfer if the composite radical **1** has an appropriate leaving group.

In this communication we wish to report a new example for free radical aromatic alkylation. A mixture of phenyl isopropyl ether (**2**) and di-*t*-butylperoxide (DTBP) (2 : 1 in mole ratio) was irradiated in a pyrex flask for 20 hr at 25°C with a high-pressure mercury lamp (Riko-kagakusangyo 400 W, principal wavelength 3150 and 3660 Å). Product analyses[6] showed the presence of a mixture of *o*- (predominant), *m*- and *p*-isomers of isopropoxycumene (**3**) (51.5%)[7] and phenol (**4**) (42.5%)[7] along with other minor products. Photolysis of a solution of azobis(2-phenoxy)-2-propane in **2** (0.25M) also resulted in the formation of **3** (21.3%) and **4** (15.3%).

The fact that neither dimer nor trimer of phenols could be detected from the reaction mixture, together with the absence of Pummerer's ketone in the products of photolysis of azobis(2-*p*-methylphenoxy)-2-propane, reveals that phenol is not produced from free phenoxy radical.[8,9] Furthermore, it is difficult to attribute the formation of **3** to carbene reaction because no information is obtained for the presence of propylene and 2-phenoxy-2,3-dimethylbutane that are expected from the reaction:[10]

$$(\mathrm{CH_3})_2\dot{\mathrm{C}}\mathrm{OPh} \longrightarrow \mathrm{PhO}\cdot$$
$$+ (\mathrm{CH_3})_2\mathrm{C}: \begin{cases} \nearrow \mathrm{CH_3{-}CH{=}CH_2} \\ \searrow (\mathrm{CH_3})_2\mathrm{C(OPh)CH(CH_3)_2} \end{cases}$$

Thus, the most probable mechanism for the formation of **3** is

$$(\mathrm{CH_3})_2\dot{\mathrm{C}}\mathrm{OPh} + \mathbf{2} \longrightarrow \mathrm{PhO{-}C(CH_3)_2{-}}\underset{\mathrm{H}}{\overset{\mathrm{OCH(CH_3)_2}}{\langle\bigcirc\rangle}} \xrightarrow{-\mathrm{PhOH}}$$
$$\left[(\mathrm{CH_3})_2\mathrm{C}{-}\langle\bigcirc\rangle{-}\mathrm{OCH(CH_3)_2} \longleftrightarrow (\mathrm{CH_3})_2\dot{\mathrm{C}}{-}\langle\bigcirc\rangle{-}\mathrm{OCH(CH_3)_2}\right] \xrightarrow{+\mathrm{H}\cdot} \mathbf{3}$$

where the driving force of the reaction may be the stability of phenol and aromatization of the composite radical.

Henbest and co-workers[11] obtained methylanisoles, phenoxymethylanisoles and phenol as products of the reaction of anisole with DTBP at 140°C. This clearly supports the first step of the above mechanism. Although they interpret the formation of methylanisoles as aromatic substitution with methyl radical, a part of it could be another example of intramolecular hydrogen abstraction.

1) a) D. H. Hey, M. J. Perkins and G. H. Williams, *Tetrahedron Lett.*, **1963**, 445; b) D. H. Hey, M. J. Perkins and G. H. Williams, *J. Chem. Soc.*, **1965**, 110.

2) D. F. DeTar and R. A. J. Long, *J. Amer. Chem. Soc.*, **80**, 4742 (1958).

3) a) E. L. Eliel, M. Eberhardt, O. Simamura and S. Meyerson, *Tetrahedron Lett.*, **1962**, 749; b) T. Inukai, K. Kimura, O. Simamura and T. Suehiro, This Bulletin, **35**, 129 (1960).

4) J. F. Garst and R. S. Cole, *Tetrahedron Lett.*, **1963**, 679.

5) T. Suehiro, A. Kanoya, T. Yamauchi, T. Komori and S. Igeta, *Tetrahedron*, **24**, 1551 (1968).

6) Identities with authentic samples were confirmed by VPC, NMR, IR, and mass spectra together with other evidence.

7) Based on consumed **2**.

8) See, for example, A. I. Scott, *Quart. Rev.* (London), **1965**, 1.

9) T. Matsuura and K. Omura, *Chem. Commun.*, **1966**, 127.

10) The sulfur analog of the radical undergoes this type of reaction.

11) H. B. Henbest, J. A. W. Reid and C. J. M. Stirling, *J. Chem. Soc.*, **1961**, 5239.

BULLETIN OF THE CHEMICAL SOCIETY OF JAPAN VOL. 43 1273—1275 (1970)

Determination of Magnetic Moments of Copper Ions in Water by the Viscometer Method

Toshio IKEDA

Department of Chemistry, Shizuoka University, Shizuoka

and Kazuo SUEOKA

Department of Chemistry, Johsai University, Sakado, Saitama

(Received May 10, 1969)

The viscometer method was applied to determine the magnetic susceptibilities of aqueous solutions of cupric salts. The effective magnetic moments of the cupric ions obtained were in agreement with values in literature, except for cupric nitrate and acetate. The former showed a relatively high value and the latter gave variable values, which suggest some dimerization effect occuring in aqueous solution with increasing concentration.

Recently, one of the authors reported the viscometer method[1] to determine the magnetic susceptibility of liquids by measuring the time of flow of liquids through the capillary of a viscometer in an external magnetic field. This method was applied to determine the magnetic moments of copper ions in aqueous solutions.

General Scheme

A capillary viscometer of the Ostwald type is placed in a magnetic field so that its bulb part is in the homogeneous part near the center of the pole gap of an electromagnet, while its capillary part extends vertically, through the inhomogeneous part, outside the field. In this case, the Hagen-Poiseuille expression for the time, t, of flow of a liquid of volume v through the capillary of the viscometer is reduced as follows ignoring the magnetostrictive effect.[1]

$$1/t_0 - 1/t = \kappa H^2/2\rho g h t_0 \qquad (1)$$

where t_0 is the time of flow in the absence of an external magnetic field; H denotes the local magnetic field in the liquid medium in the homogeneous magnetic field near the center of the pole gap of the magnet. This can be replaced by the intensity of an externally applied magnetic field; κ and ρ are the volume magnetic susceptibility and the density of the liquid, respectively; g is the gravity constant; h is the vertical height of the capillary part of the viscometer. We see from Eq. (1) that the liquid is identified as diamagnetic or paramagnetic according to whether time t is shorter or longer than t_0. A similar equation can be written also for water. Adopting water as a reference substance for calibration, we can calculate the mass magnetic susceptibility χ ($\kappa=\rho\chi$) of the solution in terms of the mass magnetic susceptibility of water χ_w as follows.

$$\chi = \frac{t_w(t-t_0)}{t(t_w-t_{w0})}\chi_w \qquad (2)$$

where t_w and t_{w0} are respectively the time of flow of water through the viscometer in the presence and absence of the magnetic field under the same field strength as applied in the solution.

Experimental

Materials. Aqueous solutions of cupric chloride, cupric nitrate, cupric sulfate, and cupric acetate were prepared by using Guaranteed Reagent grade chemicals obtained from Wakō Pure Chemicals and distilled oxygen-free water. Iron was found to be the only paramagnetic impurity involved in cupric chloride, cupric nitrate, and cupric sulfate in quantities below 0.0002, 0.02, and 0.005%, respectively. The content of copper in solutions was determined by electroanalysis.

Apparatus and Measurements. A Bitter type 500 kg electromagnet of Tokyo Denki Seiki Co. was used to produce a magnetic field of strength up to 20 kG with a relative fluctuation of 10^{-4} using a well stabilized d.c. source, where the pole pieces of the magnet were set at a distance 21 mm apart. A capillary viscometer of the Ostwald type, equipped with a thermostat water jacket, was inserted vertically between the pole gap of the magnet so as to have its upper reservoir (18 mm diameter) come within the homogeneous magnetic field formed in the central circular region (about 30 mm diameter) inside the 60 mm diameter pole pieces. The details of the apparatus were described previously.[1] The time of flow of liquids was measured with a stopwatch of 0.1 sec division, down to 0.01 sec by visual estimation, at 25°±0.05°C.

1) T. Ikeda and H. Yoshioka, *J. Phys. Chem.*, **72**, 4392 (1968).

Calculation. The mass magnetic susceptibility, χ_s, of cupric salts was calculated from the data of χ of the solution by means of the Wiedemann additivity law, $\chi = p\chi_s + (1-p)\chi_w$, where p is the weight fraction of cupric salt in aqueous solution. The value -0.722×10^{-6} emu/g was adopted for χ_w in the present work.[2] The molar magnetic susceptibility χ_+ of the cupric ion was obtained from the molar susceptibility of cupric salt, making correction for the diamagnetic contribution from the anion constituent in aqueous solution: *i.e.*, -28 for Cl^-, -23.5 for NO_3^-, -38 for SO_4^{2-} and $CH_3CO_2^-$ (in 10^{-6} emu/mol).[3] The effective Bohr magneton number, μ_{eff}, of copper(II) ion was calculated by using the Langevin equation as follows.

$$\mu_{eff} = 2.828\sqrt{\chi_+ T} \text{ B.M.}$$

where B.M. is the Bohr magneton unit, 0.9273×10^{-20} erg/G, and T is the absolute temperature. The diamagnetic correction for the cupric ion was not made.

Table 1. Time of flow of water through the capilllary of viscometer at different magnetic fields at 25°C

Magnetizing current (A)	Magnetic field[a] H (kG)	Time of flow[b] t_w (sec)
0	0	221.01
5	4.16	220.88
10	8.20	220.50
15	12.27	219.86
20	16.05	219.06
25	19.05	218.27
28	20.15	217.95

a) Measured with a TOSHIBA HM-3 Hall element magnetic field meter at the center of the pole gap of electromagnet.
b) Mean of seven measurements.

Results and Discussion

The results are shown in Tables 1, 2, and 3. When measurements are carried out with solutions of low concentration in a low magnetic field, the resulting magnetic moments might suffer an appreciable error, because a small difference between two large figures, t and t_0, and t_w and t_{w0}, seriously influences the value of magnetic susceptibility. This

Table 2. Effective magnetic moments of Cu^{2+} in aqueous solutions of copper salts at 25°C

Salt	$CuCl_2$				$Cu(NO_3)_2$				$CuSO_4$			
Wt%	23.80		40.36		20.98		35.15		14.89		18.00	
Current[a] (A)	t (sec)	μ_{eff} (B.M.)	t (sec)	μ_{eff} (B.M.)	t (sec)	μ_{eff} (B.M.)	t (sec)	μ_{eff} (B.M.)	t (sec)	μ_{eff} (B.M.)	t (sec)	μ_{eff} (B.M.)
0	371.40	—	655.52	—	353.66	—	743.76	—	374.54	—	432.01	—
5	372.18	2.1	658.07	2.1	354.12	2.2	746.03	2.3	374.90	2.2	432.19	1.6
10	373.97	1.94	664.31	1.94	355.62	2.2_3	751.82	2.2_3	375.58	1.9_7	433.69	1.9_7
15	377.22	1.94	675.77	1.94	358.14	2.24	761.90	2.21	376.70	1.92	435.57	1.93
20	381.34	1.93	690.39	1 93	361.33	2.23	775.73	2.23	378.40	1.94	438.01	1.92
25	385.59	1.93	705.85	1.93	364.63	2.24	788.42	2.20	379.68	1.91	440.82	1.94
28	387.41	1.93	712.10	1.93	365.66	2.22	795.04	2.22	380.30	1.91	441.59	1.93
μ_{eff} (B.M.)[b]	1.930				1.920—1.961				1.93—1.95			

a) The magnetizing current: refer to a) in Table 1.
b) Landolt-Börnstein, "Zahlenwerte und Funktionen aus Naturwissenschaften und Technik," New Series, Group II, Vol. 2, Springer Verlag, Berlin (1966).

Table 3. Effective magnetic moments of Cu^{2+} in aqueous solutions of cupric acetate at 25°C

Wt%	2.059		3.071		4.068		5.061		6.307		9.375	
Current[a] (A)	t (sec)	μ_{eff} (B.M.)	t (sec)	μ_{eff} (B.M.)	t (sec)	μ_{eff} (B. M.)	t (sec)	μ_{eff} (B.M.)	t (sec)	μ_{eff} (B.M)	t (sec)	μ_{eff} (B.M.)
0	247.96	—	253.68	—	263.39	—	273.66	—	278.15	—	277.40	—
15	247.00	1.9_4	252.86	1.9_4	262.61	1.7_9	272.92	1.6_8	277.69	1.8_1	—	—
20	246.37	2.01	252.31	1.96	262.14	1.85	272.41	1.69	277.13	1.67	276.81	1.5_5
25	245.69	1.97	251.72	1.93	261.59	1.83	272.06	1.78	276.68	1.65	—	—
28	245.41	1.95	251.51	1.95	231.33	1.80	271.85	1.77	276.50	1.65	276.43	1.54

a) The magnetizing current: refer to a) inTable 1.

2) H. Auer, *Ann. Phys.*, **18**, 593 (1933).
3) Landolt-Börnstein, "Zahlenwerte und Funktionen aus Physik, Chemie, Astrophysik, Geophysik und Techik," 6th Ed., Vol. I, Sect. 1, Springer Verlag, Berlin (1950), pp. 396—397.

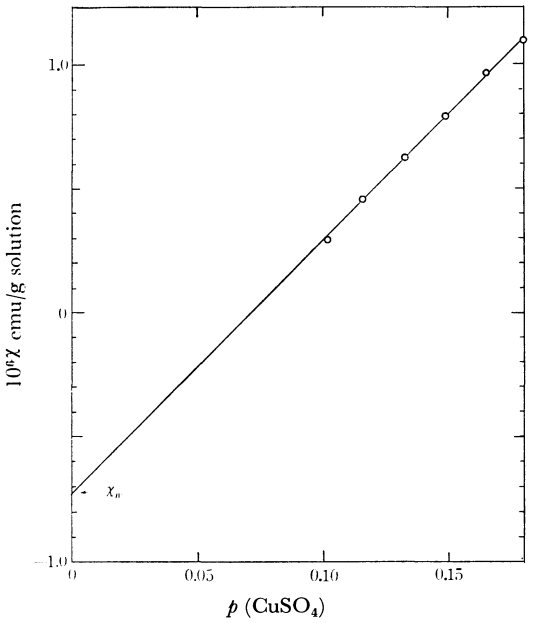

Fig. 1. The Wiedemann relation for aqueous solution of $CuSO_4$ at 25°C, representing the values measured at the magnetic field strength of 20.15 kG.

effect is actually seen in the Tables. Thus, in order to get reliable results, measurements should be carried out with solutions of higher concentration in as high a magnetic field as possible, particularly in the case of a solution involving a weak paramagnetic ion species such as Cu^{2+}: In the present method, a magnetic field of a strength higher than 12 kG gives results with tolerable accuracy.

Magnetic susceptibilities of aqueous solutions of cupric salts, except for cupric acetate, were found to obey the Wiedemann law. The Wiedemann relation for cupric sulfate was found to be perfectly linear, intersecting, on extrapolation to concentration zero, the ordinate at -0.725×10^{-6} emu/g. This is in close agreement with the susceptibility of water (Fig. 1). From the slope of the line in Fig. 1 we obtain the effective magnetic moment 1.92 B.M. for Cu^{2+}. The magnetic moments of copper(II) ion were found in good agreement with literature values,[4] except for cupric nitrate and cupric acetate (Tables 2 and 3). Cupric nitrate exhibited a value, about 15% higher than the

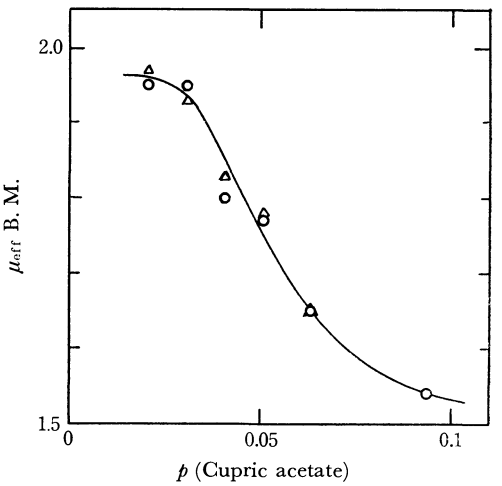

Fig. 2. Relation between the apparent magnetic moments of Cu^{2+} and the weight fraction, p, of cupric acetate in aqueous solutions at 25°C, Δ, measured at 19.05 kG; ○, measured at 20.15 kG.

literature values 1.92—1.96 B.M.[4] The magnetic moment we obtained seems to involve an error of 2—3%. The paramagnetic cation found as impurity in cupric nitrate was exclusively iron contained in such a minute quantity below 0.02% which can cause a deviation 0.15% at most from the accepted value of the magnetic moment of cupric ion. There might be some reason to cause such a large deviation of 15% in the case of cupric nitrate.

The apparent magnetic moments of Cu^{2+} observed in aqueous solutions of cupric acetate appeared to depend on the concentration (Table 3 and Fig. 2): A value of 1.95 B.M. found at lower concentration is in agreement with the literature value.[4] However, it decreased with increasing concentration towards a value 1.42 B.M. found in the crystalline state where the dimerization of cupric acetate through a weak copper-copper bond formation was concluded.[5] This fact suggests a similar association of cupric acetate occuring also in aqueous solution with increasing concentration.

4) Landolt-Börnstein, "Zahlenwerte und Funktionen aus Naturwissenschaften und Technik," New Series, Group II, Vol. 2. Springer Verlag, Berlin (1966).

5) B. N. Figgis and R. L. Martin, *J. Chem. Soc.*, **1956**, 3837.

BULLETIN OF THE CHEMICAL SOCIETY OF JAPAN VOL. 43 1276—1282 (1970)

Hot-Atom Chemistry of Bromine. IV. Chemical Effects of $^{81}Br(n,\gamma)^{82g}Br$, $^{81}Br(n,\gamma)^{82m}Br$ and $^{82m}Br(I.T.)^{82}Br$ Excitation in Antimony Tribromide and Benzene System[1,2]

Toshiaki KISHIKAWA, Yasuyuki ARATONO and Chiro SHINOMIYA

Department of Industrial Chemistry, Faculty of Engineering, Kumamoto University, Kumamoto

(Received July 19, 1969)

Antimony tribromide and a molecular compound between antimony tribromide and benzene (2 : 1) have been irradiated to provide ^{82m}Br sources. The results obtained by the dissolution of the irradiated molecular compound, by means of which technique the chemical effects of $^{81}Br(n,\gamma)^{82g}Br$ and $^{82m}Br(I.T.)^{82}Br$ were determined separately, had shown very low organic yields from either (n,γ) or (I.T.) excitation. The reaction of $^{82m}Br(I.T.)^{82}Br$ in benzene showed a growth in the organic yields. Moreover, the organic yield of ^{82}Br was lower when the system was frozen than when it was stored as a liquid. These results are explained by assuming that, in the frozen system, the antimony tribromide (^{82m}Br) forms a molecular compound with the benzene. The higher organic yields in the frozen systems than those in the molecular compound itself must be due to the formation of free bromine (^{82m}Br), which turns out to be an organic radiobromide. The hydrolytic behavior of the irradiated antimony tribromide and the molecular compound supports the idea of the presence of free bromine (^{82m}Br) at the end of the irradiation.

Since the discovery of the meta-stable-state bromine-82,[3] much work has been done on the chemical effects of the $^{82m}Br(I.T.)^{82}Br$ excitation in various liquid or solid organic media. The vertue of the subject transformation is that the experiment can be conducted in the absence of those transformations due to (n,γ) reactions and also of any possible influence of the accompanying gamma-radiation from a reactor. The major portion of the activity produced from the (n,γ) activation by ^{81}Br is the ^{82m}Br-activity, which undergoes the (I.T.) process (activation cross sections,[3a] $\sigma_m=3.0$ and $\sigma_g=0.3$ barns). The bromine-82m decays with a highly-converted transition[3a] of 46 keV (internal conversion coefficient, $\alpha_k=268$). This means that a large fraction of the ^{82}Br is produced with a positive charge. The ^{82m}Br source has thus far been prepared by two methods for the sake of experimental convenience: by irradiating molecular bromine,[4] and by irradiating an organic bromide.[5] A third method, to be proposed here, proceeds by irradiating an inorganic bromide.

The present work will deal with the chemical effects of radiative neutron capture by bromine-81 and of isomeric transition by bromine-82m in mixtures of antimony tribromide and benzene.

Experimental

Materials. Wako Pure Chemicals' JIS special-grade benzene was purified by the usual method. Tokyo Kasei JIS 1st-grade antimony tribromide was used after it has been purified by recrystallization (mp 96.6°C) from carbon disulfide. The other reagents used were all of a JIS special-grade, but were also further purified if necessary. The $2SbBr_3 \cdot C_6H_6$ molecular compound

1) Presented in parts at the 11th Symposium on Radiochemistry, Tokyo, October 1967, and at the 21st Annual Meeting of the Chemical Society of Japan, Suita, April, 1968.

2) C. Shinomiya, A. Oyoshi and T. Kishikawa, This Bulletin, **42**, 2040 (1969).

3) a) J. F. Emery, *J. Inorg. Nucl. Chem.*, **27**, 903 (1965). b) O. U. Anders, *Phys. Rev.*, **138**, B1 (1965).

4) a) R. M. Iyer and J. E. Willard, *J. Amer. Chem. Soc.*, **87**, 2494 (1965). b) N. A. Katsanos and M. I. Stamouli, *Z. Phys. Chem., Neue Folge*, **47**, 306 (1965). c) J. A. Merrigan and E. P. Rack, *J. Phys. Chem.*, **69**, 2795, 2806 (1965). d) J. A. Merrigan, W. K. Ellgren, Jr., and E.P. Rack, *J. Chem. Phys.*, **44**, 174 (1966). e) J. A. Merrigan, J. B. Nicholas and E. P. Rack, *Radiochim. Acta*, **6**, 94 (1966). f) R. M. Lambrecht and E. P. Rack, COO-1617-4 (1967). g) E. P. Rack, COO-1617-6 (1967); COO-1617-10 (1968). h) R. M. Lambrecht, N. J. Parks and E. P. Rack, COO-1617-7 (1967). i) N. A. Katsanos and M. I. Stamouli, *Radiochim. Acta*, **7**, 126, 177 (1967); *ibid.*, **9**, 13 (1968). j) C. Shinomiya and T. Kishikawa, This Bulletin, **41**, 3026 (1968).

5) a) N. A. Katsanos, "Proceedings of the Symposium on Chemical Effects of Nuclear Transformations," Vol. I, IAEA, Vienna (1965), p. 371; *J. Chem. Soc.*, **1965**, 4751. b) N. A. Katsanos and M. I. Stamouli, *Radiochim. Acta*, **5**, 148 (1966). c) I. L. Leontiadis and N. A. Katsanos, *Z. Phys. Chem.* (Frankfurt), **57**, 38 (1968).

($2SbBr_3Bz$) (mp 92.6°C, lit,[6] 92.5°C) was prepared[7] by adding antimony tribromide to hot benzene, followed by cooling and evaporating the excess benzene.

Neutron Irradiation. Samples sealed in a quartz ampule were irradiated in a pneumatic tube of KUR[8] at the temperature of dry ice or at the reactor temperature (*ca.* 40°C). The thermal neutron flux was 5×10^{12} n/cm²/sec, and the accompanying gamma-radiation flux was 2.7×10^{7} R/hr.

Procedure. *Dissolution Technique.* The ampule of the irradiated $2SbBr_3Bz$ molecular compound at the temperature of dry ice was immersed in a boiling-water bath immediately after it has been irradiated for 60 min; during the immersion almost all the ^{82m}Br isotopes produced by the radiative neutron capture decayed to the ^{82}Br ground state. The ampule was then cooled in a bath of dry ice and ethanol. The sample was extracted directly from the frozen state into a two-phase mixture of benzene containing a bromine carrier plus 0.5M aqueous sodium sulfite, after which hydrochloric acid (1 : 1) was added to the mixture.[9] The organic layer was then dried over calcium chloride.

Antimony Tribromide - Benzene System. The irradiated molecular compound or antimony tribromide was dissolved in benzene immediately after irradiation; it was then stored at room temperature (liquid) or at the temperature of dry ice (frozen). Aliquot portions were extracted after varying periods of time.

Counting and Analysis. A NaI(Tl) scintillation crystal and a multi-channel pulse height analyzer were used. By radiative neutron capture the activities of ^{122}Sb (half-life 2.75 day), ^{122m}Sb (4.2 min), ^{124}Sb (60 day), ^{124m}Sb (21 and 1.3 min), ^{80}Br (18.5 min), and ^{80m}Br (4.5 hr) as well as of ^{82}Br (36 hr) and ^{82m}Br (6.2 min[3]) were produced. Only the ^{82}Br activities were studied. After all, since the ^{82m}Br had dceayed to the ^{82}Br ground state, a 0.78 MeV gamma-ray photo peak was measured and used for the calculation.

Results and Discussion

Effects of the Time and Temperature of Irradiation and Those of Standing on the Organic Yields of the $2SbBr_3Bz$ Molecular Compound. To determine the effects of the accompanying gamma-ray and the temperature in the reactor, the molecular compound was irradiated for varying periods at different temperatures. Table 1 lists the overall organic yields (experimental error range, ±1%); these yields mean that it is not necessary to take the accompanying gamma dose in the reactor into consideration. Little dependency of the temperature of irradiation and standing was observed, as is shown in Fig. 1.

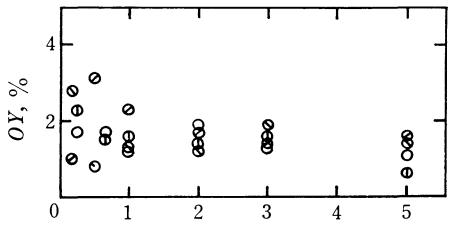

Fig. 1. Organic yields induced by $^{81}Br(n,\gamma)^{82}Br$, $^{81}Br(n,\gamma)^{82m}Br$ and $^{82m}Br(I.T.)^{82}Br$ processes at the molecular-compound $2SBr_3Bz$. Effects of temperature at time of these nuclear events.
Experimental error range is ±1%.

	Temp.	
	Irrad.	Standing
○	Dry ice	Dry ice
①	Dry ice	Room
⊘	Reactor	Dry ice
⊘	Reactor	Room

Table 1. The effects of the accompanying gamma-radiation and temperature in the reactor,[a] and the effects of tempfrature at time of standing on overall organic yields at the irradiated molecular-compound $2SbBr_3Bz$

Temp.		Overall organic yield,[b] %, at the irrad. period (sec) of							
Irrad.	Standing [c]	11	15	30	40	60	120	180	300
Dry ice	Dry ice		1.7	0.8	1.7	1.2	1.9	1.3	1.1
Dry ice	Room		2.3		1.5	1.6	1.4	1.6	0.6
Reactor [d]	Dry ice	1.0		3.1		2.3	1.7	1.9	1.6
Reactor	Room	2.8		0.8		1.3	1.2	1.4	1.4

a) Thermal neutron flux of 5×10^{12} n/cm²/sec and caccompanying gamma-dose rate of 2.7×10^{7} R/hr.
b) Experimental error range of ±1%.
c) During the time of standing (for 60 min) almost all the ^{82m}Br decayed to the ^{82}Br ground state.
d) *ca.* 40°C.

6) "International Critical Tables of Numerical Data," Vol. IV, ed. by E. W. Washburn, McGraw-Hill, New York (1933), p. 195; B. N. Menshutkin, *J. Phys. Chem. Soc. (Chem. Part)*, **43**, 393, 401, 425 (1911).

7) Procedure for the preparation of antimony trichloride-benzene (2 : 1) was applied; C. Shinomiya and T. Asahina, *Nippon Kwagaku Kwaishi*, **59**, 1165 (1939).

8) Kyoto University Reactor.

9) In dilute hydrochloric acid or in water a hydrolyzed product (white precipitate) of antimony tribromide can be produced, which interupts to separate the phases.

TABLE 2. THE EFFECTS OF DISSOLUTION ON OVERALL ORGANIC YIELDS INDUCED BY $^{81}Br(n,\gamma)^{82}Br$, $^{81}Br(n,\gamma)^{82m}Br$ AND $^{82m}Br(I.T.)^{82}Br$ PROCESSES AT THE MOLECULAR-COMPOUND $2SbBr_3Bz$ [a]

Major nucl. reaction	Standing		Overall organic yield, %, at the irrad. period (sec) of			
	Time min	Temp.	15	30	60	300
(n,γ)	60	100°C	0.7		0.4	0.5
(n,γ)+(I.T.)	6	Dry ice [b]	1.3	1.0	1.2	0.5
(n,γ)+(I.T.)	60	Dry ice	1.7	0.8	1.2	1.1
(I.T.)	60	Dry ice	1.0		0.8	0.6

a) Irradiation was carried out at the temperature of dry ice.
b) Temperature of dry ice/ethanol.

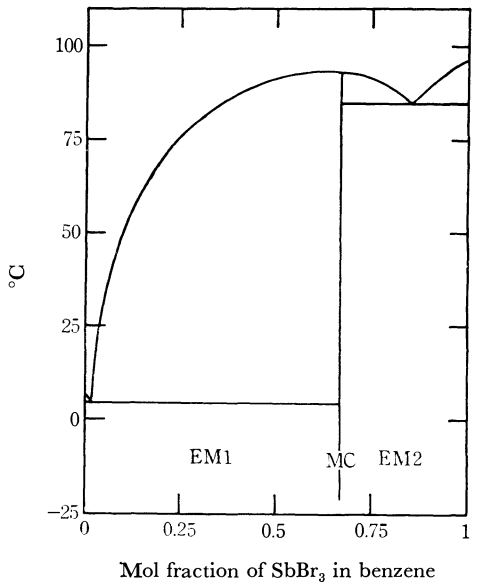

Fig. 2. Phase diagram of $SbBr_3$-C_6H_6.
EM1: Eutectic mixture ($C_6H_6+2SbBr_3\cdot C_6H_6$)
EM2: Eutectic mixture ($2SbBr_3\cdot C_6H_6+SbBr_3$)
MC: Molecular compound ($2SbBr_3\cdot C_6H_6$)

Dissolution of the Irradiated $2SbBr_3Bz$ Molecular Compound. The following experiments were performed in order to obtain information on the effects of the isomeric transition-induced process. Immediately after the irradiation, quartz ampules containing $2SbBr_3Bz$ were immersed in the boiling-water bath; the molecular compound in the ampule were thus decomposed into a two-phase mixture of its components - benzene (gas, bp 80.1°C) and antimony tribromide (liquid, mp 92.6°C), as may be seen in the phase diagram of the $SbBr_3$-C_6H_6 system[6] in Fig. 2.

After the completion of the (I.T.) process, the sample was resolidified in the bath of dry ice and ethanol and then extracted. The observed overall organic yields at the various irradiation periods are listed in Table 2. The results of standing at the temperature of dry ice are also listed in the table. If there were an organic radiobromide-(^{82m}Br) which had been produced by the (n,γ) activation and subsequent recoil bond-forming processes, the following (I.T.) process might cause the organic radiobromide to dissociate the ^{82}Br atom resulting from Coulombic repulsion. The overall organic yield value on the first line in each irradiation-time column in Table 2 may then be attributed, for the most part, to the organic radiobromides-(^{82g}Br) produced directly by the (n,γ) activation.

A slight increase in the organic yield with an increase in the standing time was observed (the values on the second and the third lines). The values on the last line, which are attributed to the fraction of the (I.T.)-excited reaction, are obtained by subtracting the value on the first line from that on the third line in each column.

Reaction of Bromine-82m Prepared by Irradiating Antimony Tribromide or the $2SbBr_3$-Bz Molecular Compound in Liquid and Solid Benzene. To ascertain whether or not the increase in the organic yield is affected by the (I.T.) depending process, the following rate determinations in liquid and solid benzene were carried out. As soon as the end of the irradiation of $SbBr_3$ or

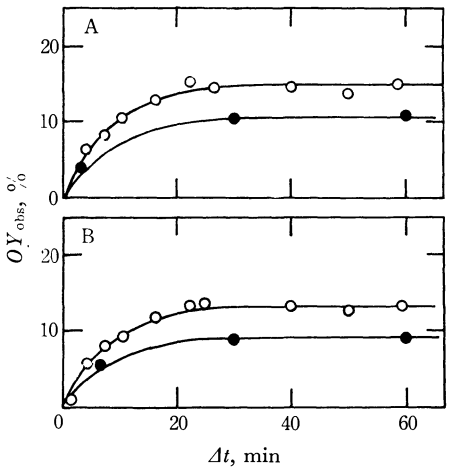

Fig. 3. Growths of ^{82}Br organic yields in benzene.
A) Irrad. $SbBr_3$. B) Irrad. $2SbBr_3Bz$.
○: Liquid, ●: Frozen

$2SbBr_3Bz$, the sample-benzene system (1.64×10^{-4} mol fraction of $SbBr_3$) was produced as is described in the Experimental section. The inorganic radiobromine in a portion of the system was separated by extraction at different time intervals. Figure 3 shows plots of the activities of the overall organic yield obtained from systems left to stand for various length of time, Δt, after the preparation of the systems. The curves increase with an increase in the standing time.

If the observed increase in the ^{82}Br organic yield is a result of chemical excitation by the (I.T.) alone, the rate of growth should be dependent only on the decay of the ^{82}Br and should be related to the half-life of the ^{82m}Br. Therefore, when OY^{∞}_{obs} represents the overall organic yield attained after all the ^{82m}Br has decayed to the ^{82}Br ground state, when OY^{0}_{obs} represents the organic yield present at the time the system is prepared (*viz.*, for the irradiated $SbBr_3$, $OY^{0}_{obs}=0$; for the irradiated $2SbBr_3Bz$, $OY^{0}_{obs}=$[the values listed on the first line of the irradiation-time column in Table 2 which are due to $^{81}Br(n,\gamma)^{82g}Br$]), and when $OY^{\Delta t}_{obs}$ represents the organic yield at any time before the ^{82m}Br has completely decayed, the growth of the ^{82}Br organic yield will be given[4d,4j] by:

$$(OY^{\Delta t}_{obs}-OY^{0}_{obs}) = (OY^{\infty}_{obs}-OY^{0}_{obs})(1-e^{-\lambda\Delta t}),$$

where λ is the decay constant of ^{82m}Br. By rearranging the equation, $\log(OY^{\infty}_{obs}-OY^{0}_{obs})-(OY^{\Delta t}_{obs}-OY^{0}_{obs})/(OY^{\infty}_{obs}-OY^{0}_{obs})$ *versus* Δt should yield a straight line (Fig. 4) with a slope of $-0.693/-2.303T_{1/2}$. The half-life of ^{82m}Br was determined to be 6.00 and 5.87 min from the yields of the liquid systems of the irradiated-$SbBr_3$ - C_6H_6 and of the irradiated-$2SbBr_3Bz$ - C_6H_6 respectively. The close relative rates of increase in the overall organic yields[10] in the different systems can be attributed to the ^{82m}Br(I.T.)-excited reaction. Similar phenomena have been reported in liquid and solid systems of irradiated-Br_2 - C_6H_6 by two of the present authors (C.S. and T.K.) in a previous paper.[4j]

Behavior of the ^{82}Br Produced by (n,γ)- and (I.T.)-activation at $SbBr_3$ and $2SbBr_3Bz$. If water is added to antimony tribromide, various antimony oxybromides are formed. An appropriate amount of water hydrolyzes it to form $Sb_4O_5Br_2$, the solubility of which in water is very low.[12]

$$4SbBr_3 + 5H_2O \longrightarrow Sb_4O_5Br_2 + 10HBr$$

Stoichiometrically speaking, five-sixths of all the bromine atoms are present in the aqueous solution,

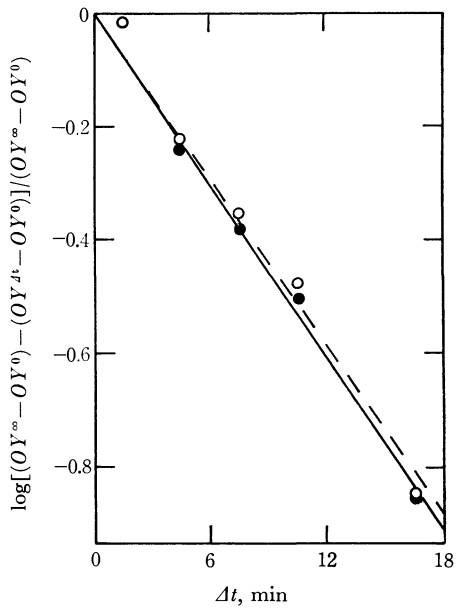

Fig. 4. Bromine-82 organic yields as a result of isomeric transition in benzene.
○: Irrad. $SbBr_3$, ●: Irrad. $2SbBr_3Bz$

and the rest in the precipitate. The hydrolysis of the compound provides a means to study the Szilard-Chalmers reaction,[13] in which a portion of the radiobromides produced by the (n,γ) reaction is found in an un-recombined form and thus can be extracted with water. The results of the hydrolysis are listed in Table 3. The higher bromide yield which was obtained by hydrolysis a short time after the irradiation can be attributed to the presence of the ^{82m}Br activities. When the irradiated sample was left standing for 90 min at the temperature of dry ice, the hydrolyzed yield of bromide was reduced nearly to the calculated value. The results of the hydrolysis coincide with those of dissolution.

Table 3. Hydrolytic behavior of ^{82}Br in irraditated $SbBr_3$ or $2SbBr_3Bz$

Irrad. sample	Standing[a] min	Yield, %	
		$Sb_4O_5Br_2$	Br^-
$SbBr_3$	2	3.9	96.1
$SbBr_3$	90	14.9	85.1
$2SbBr_3Bz$	90	15.8±1.2	84.2±1.2
$SbBr_3(^{82}Br)$[b]		18.4±1.6	81.6±1.6
Calculated		16.7	83.3

a) Time between the end of irradiation and hydrolysis.
b) Synthesized by using ^{82}Br as a tracer.[12]

10) Major products (see Ref. 11) was bromobenzene-(^{82}Br). The detailed report will be published in another paper.
11) Presented at the 13th Symposium on Radiochemistry, Nagoya, October 1969, Preprint, p. 98.
12) Detailed data will be submitted in another paper.
13) L. Szilard and T. A. Chalmers, *Nature*, **134**, 462 (1934).

TABLE 4. OVERALL ORGANIC YIELDS BY ^{82m}Br(I.T.)^{82}Br PROCESS

Irrad.		Standing[a]		OY^{∞}_{net}
Sample	Time min	Solvent	Phase	%
$2SbBr_3Bz$	0.25	No	Solid	1.0
$2SbBr_3Bz$	1	No	Solid	0.8
$2SbBr_3Bz$	5	No	Solid	0.6
$2SbBr_3Bz$	0.25	Benzene [b]	Liquid	17.2±2.2
$2SbBr_3Bz$	5	Benzene	Liquid	18.8±0.6
$2SbBr_3Bz$	1	Benzene	Frozen	12.9±0.6
$SbBr_3$	0.25	Benzene	Liquid	15.4±1.9
$SbBr_3$	5	Benzene	Liquid	20.1±1.4
$SrbB_3$	1	Benzene	Frozen	13.8±0.9

a) During the time of standing all the ^{82m}Br decayed to the ^{82}Br ground state.
b) $SbBr_3$ concentration was 1.64×10^{-4} mol fraction.

Determination of the ^{82}Br Organic Yield Resulting from the ^{82m}Br(I.T.)^{82}Br Process in the Liquid and Solid Systems. Correcting for the contributions of the activities of the ground-state ^{82}Br produced directly from the (n,γ) reaction and for those of the activities decayed from the ^{82m}Br before preparing the reaction systems, one can obtain the net organic yield values (OY^{∞}_{net}); these values are presented in Table 4.

As has been pointed out in the introduction, the decay of the ^{82m}Br goes through a 46 keV highly-converted transition; this suggests that a large fraction of the ^{82}Br is produced with a positive charge. It would appear that the chemical stabilization of the daughter ^{82}Br in the present liquid systems is due either to ion-molecule reactions of these charged atoms with the surrounding organic medium or to reaction of the neutralized hot atoms with the medium.

It is well known that molecular bromine is stable in benzene, forming a charge-transfer complex[14] (the charge-transfer energy is 4.25 eV[15]), and that aromatic bromination with molecular bromine proceeds quite gently in a non-polar organic medium such as benzene.[16] The electron acceptability of bromine in the charge-transfer complex depends on the state of bromine in the following order: $Br^+ > Br^0 > Br_2$. Also, the positively-charged ^{82}Br ion produced by the (I.T.) and the accompanying internal conversion processes is a much better electron-acceptor; the chance of its staying alive to form a charge-transfer complex with benzene may be small, since its electron affinity is high (the ionization potential of benzene is 9.25 eV,[17] lower than that of bromine by 2.59 eV). The fact that not all the bromines formed *via* the (I.T.) are found in the organic combination suggests that the ion-molecule reaction is less significant in the present systems. The ^{82}Br may, therefore, react by means of the energetic reaction. Some recent data[11] on the ^{82m}Br(I.T.)-induced reaction in alkyl benzenes indicate that the values of the overall organic yield follow the same order as the ionization potential of the benzenes. The charge-transfer complex may, then, act as a reaction intermediate. The small growth in the observed organic yield after 25 min (plateaus in Fig. 3) indicates that the simple free-radical reactions of the bromine atoms after complete thermalization are negligible.

On the other hand, in the resolidified systems, which are composed of polycrystalline mixtures[18] (eutectic mixture) of benzene plus the $2SbBr_3Bz$ molecular compound, the free bromine produced by the (n,γ) or (I.T.) reaction and remaining before resolidification may also be composed of a molecular compound ($^{82m}Br\cdot C_6H_6$ or $Br_2(^{82m}Br)\cdot C_6H_6$[4j,19]). Lambrecht and Rack,[4h] after a consideration[4d,20,21] of the clustering of bromine in an organic medium, put forward a scheme attempting to provide a better understanding of solid-state organic yields in polycrystalline systems. Their scheme can be rather satisfactorily applied to the present systems by replacing $(Br_2)_n$ by $(2SbBr_3Bz)_n$, because a very low organic yield has been observed in the irradiated molecular compound (the benzene in the molecular compound may be comparatively inert, since the ionization potential of antimony is 8.46 eV,[17] lower than that of benzene by 0.79 eV): That is, the ^{82}Br atoms formed by the (I.T.) process in the molecular-compound clusters mostly remained inorganically in the clusters, while those formed in the polycrystalline benzene reacted within the benzene, and while those formed on the surface of the molecular-compound clusters remained either organically or inorganically.

Distribution of Organic Radiobromides in the Irradiated Molecular Compound. The fractional distillation of the benzene layer of the

14) L. J. Andrews and R. M. Keefer, "Molecular Complex in Organic Chemistry," Holden-Day, San Francisco (1964).
15) R. M. Keefer and L. J. Andrews, *J. Amer. Chem. Soc.*, **72**, 4677 (1950).
16) For aromatic bromination with molecular bromine two theories have been proposed: a) R. M. Keefer and L. J. Andrews, *J. Amer. Chem. Soc.*, **78**, 255, 4549 (1956); b) P. B. D. de la Mare and J. T. Harvay, *J. Chem. Soc.*, **1956**, 36; *ibid.*, **1957**, 131, 923.
17) "Kagaku Binran, Kiso-hen. II," ed by S. Nagai, Maruzene, Tokyo (1966), p. 1124.
18) Examined concentration of antimony tribromide was below the eutectic point (mol fraction to give the eutectic point is 1.9×10^{-2}; see Fig. 2).
19) O. Hassel and K. O. Strømme, *Acta Chem. Scand.*, **12**, 1146 (1958).
20) R. M. H. Hahne and J. E. Willard, *J. Phys. Chem.*, **68**, 2582 (1964).
21) M. Milman, *J. Amer. Chem. Soc.*, **80**, 5592 (1958).

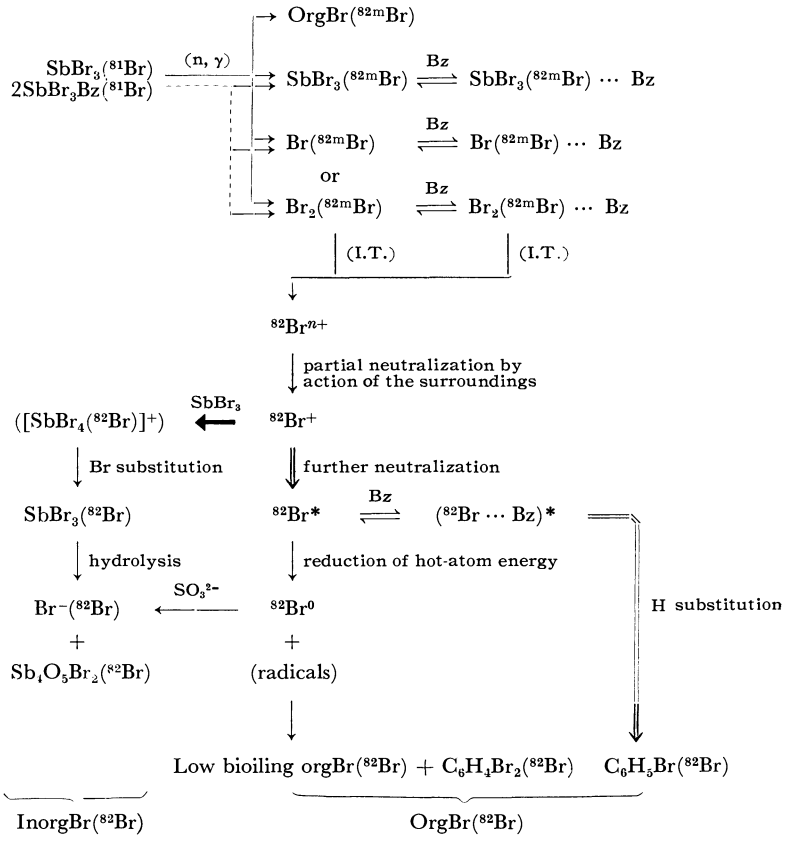

Fig. 5. Deactivation and organic-radiobromide formation process of the ^{82}Br atoms produced by the ^{82m}Br(I.T.) process in liquid or frozen systems of the irrad.-$SbBr_3$ - C_6H_6 and irrad.-$2SbBr_3Bz$ - C_6H_6.
⟹ Predominant path in the liquid system, or in or on the surface of the BrBz or Br_2Bz in the forzen system
⟶ Predominant path in the $(2SbBr_3Bz)_n$ clusters in the frozen system
^{82}Br* Energetically hot bromine atom

irradiated $2SbBr_3Bz$ after all the ^{82m}Br has decayed indicates the formation of low- and high-boiling products as well as of bromobenzene. Recrystallization with the addition of inactive *p*-dibromobenzene indicated its formation. The distributions (%) of (low bp fraction, bromobenzene and dibromobenzenes) in the benzene layers at the irradiation times of 1, 3, and 20 min were (24, 64, and 34), (21, 37, and 42) and (15, 46, and 39) respectively.

Contribution of Thermal Exchange and Substitution Reactions. To determine whether the organic yield built up after 60 min is due only to the (I.T.) process or whether a part of it is due to the thermal exchange and/or thermal substitution reactions of antimony tribromide(^{82}Br) with bromobenzene or with benzene, the following experiment was performed by synthesizing antimony tribromide-(^{82}Br).[12] It was dissolved in an organic medium (12.5×10^{-3} g-atom/*l* of $SbBr_3$(^{82}Br) and 3.54×10^{-3} g-atom/*l* of C_6H_5Br in benzene, or 20.0×10^{-3} g-atom/*l* of $SbBr_3$(^{82}Br) in bromobenzene). The reaction mixture was then stored at 25 or 19.5°C (±0.5°C reguration) and portions were extracted at regular intervals in the manner described above. The activities of both the organic and aqueous layers were then measured. After the conventional treatment of the isotopic exchange,[22] the apparent half-time values and the fractional exchange values at 60 min, after the preparation of the reaction mixture in all cases, were found to be 10^4 hr and 0.001 respectively; these value indicate no prominent role of either isotopic exchange or substitution reactions.

From these findings, the probable paths of the organic-radiobromide formation in the irradiated-$SbBr_3$ - benzene or the irradiated-S2bBr_3Bz - benzene systems due to the (I.T.) process by the ^{82m}Br may be assumed to be as is illustrated schemati-

22) O. E. Meyers and R. J. Prestwood, "Radioactivity Applied to Chemistry," ed. by A. C. Wahl and N. A. Bonner, 2nd Ed., John Wiley & Sons, New York (1958), p. 7.

cally in Fig. 5.

The authors are grateful to Dr. Akira Oyoshi of this University for his encouragement; to Drs. Shiro Iwata and Yoshiyuki Kiso, Mr. Kazuhisa Sasajima, and the personnel of the Research Reactor Institute, Kyoto University, for their assistance in the irradiation, and to the Institute for giving, under Contracts 42147 and 42211, the co-operative facilities which made this research possible.

BULLETIN OF THE CHEMICAL SOCIETY OF JAPAN VOL. 43 1282—1286 (1970)

Kinetics of Alkaline Hydrolysis of Esters. III. Acyl Acetals

R. C. SHARMA and M. M. SHARMA

Department of Chemical Technology, University of Bombay, Matunga Road, Bombay-19, India

(Received July 14, 1969)

The kinetics of the alkaline hydrolysis of some acyl acetals (liquid and solid) was studied in 90 parts (wt/wt) aqueous ethanol medium. Steric and inductive effects were found to play an important role. A straight line relationship was observed between the rate constants for the alkaline hydrolysis of benzylidene-, and *m*- and *p*-nitrobenzylidene diacetates and Hammett's substitution constant, σ. In the case of *n*-butylidene and benzylidene diacetates the theory of mass transfer accompanied by fast pseudo first-order reaction was employed for the determination of rate constants in an aqueous medium.

There is a limited information available in the literature on the kinetics of the alkaline hydrolysis of acyl acetals. The reaction can be written as:

$$R'CH(OAC)_2 + OH^- \xrightarrow[\text{slow}]{k_2} R'\underset{\displaystyle OH}{\underset{|}{C}}H(OAC) + CH_3COO^- \quad (1)$$

$$R'\underset{\displaystyle OH}{\underset{|}{C}}H(OAC) + OH^- \xrightarrow{\text{fast}} RCHO + H_2O + CH_3COO^- \quad (2)$$

The first step of the hydrolysis has been reported to be first order with respect to the ester and first order with respect to hydroxyl ions.[1,2] The second step is very fast.[3] There are some discrepancies in the data reported in the literature concerning the rate constants of the alkaline hydrolysis of acyl acetals. Skrabal and Schiffrer[1] and Skrabal and Belavic[2] have reported the value of the rate constant for the alkaline hydrolysis of methylene diacetate to be 18 and 16 $l/g \cdot mol \cdot sec$ at 25°C, respectively. Salmi and Kantola[3] have, however, reported a value of 5.3 $l/g \cdot mol \cdot sec$ for methylene diacetate and 2.33 $l/g \cdot mol \cdot sec$ for ethylidene diacetate. Most recently Euranto and Moisio[4] reported the rate constant for methylene diacetate as 5.85 $l/g \cdot mol \cdot sec$. It was thought desirable to study a series of typical acyl acetals like ethylidene-, *n*-butylidene- and benzylidene diacetates. The effect of an electronegative group, $-NO_2$, in the benzene ring of benzylidene diacetate was also studied in this work.

Mechanism

An acyl acetal is an acetic ester with the group $-OCOCH_3$ at the α-carbon atom of the alkyl part.

$$CH_3COO\underset{\displaystyle OCOCH_3}{\underset{|}{C}}H-R'$$

The alkaline hydrolysis of an acyl acetal probably involves acyl-oxygen fission ($B_{AC}2$)[5] and the following mechanism is likely to hold:

$$HO^- + \underset{\displaystyle CH_3}{\underset{|}{\overset{\displaystyle O}{\overset{\|}{C}}}}-O-\underset{\displaystyle R'}{\underset{|}{C}}-OCOCH_3 \underset{\text{I}}{\overset{\text{Slow}}{\rightleftharpoons}} \left[HO-\underset{\displaystyle CH_3}{\underset{|}{\overset{\displaystyle O}{\overset{|}{C}}}}-O-\underset{\displaystyle R'}{\underset{|}{C}}-OCOCH_3\right]^- \quad (3)$$

$$\left[\quad\right]^- \overset{\text{fast}}{\underset{\text{II}}{\uparrow\downarrow}}$$

1) A. Skrabal and A. Schiffrer, *Z. Phys. Chem.*, **99**, 290 (1921).

2) A. Skrabal and M. Belavic, *ibid.*, **103**, 451 (1923).

3) E. J. Salmi and K. K. Kantola, *Ann. Acad. Sci., Fennicae, Ser.* A, XLVI, No. 2 (1936).

4) E. K. Euranto and A. Moisio, Suomen Kemistilehti, **37B**, 92 (1964).

5) C. K. Ingold, "Structure and Mechanism in Organic Chemistry," Holt, Richard and Winston, N. Y., Chicago, San Francisco, Toronto, London (1964), p. 314.

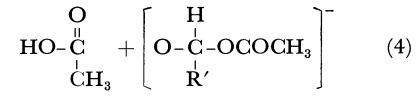

(4)

(5)

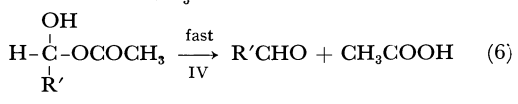

(6)

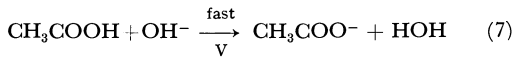

(7)

Materials

Ethylidene-, *n*-butylidene- and benzylidene diacetates were prepared by the reaction of the relevant aldehyde with acetic anhydride at a temperature of about 0 to 5°C in the presence of 0.5 per cent *ortho*-phosphoric acid as a catalyst.[6]

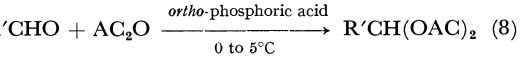

(8)

o-, *m*- and *p*-Nitrobenzylidene diacetates were synthesized by the method reported in the literature.[7]

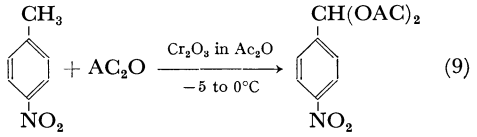

(9)

Ethylidene-, *n*-butylidene-, and benzylidene diacetates were purified by fractional distillation at a reduced pressure (10 to 50 mmHg). *o*-, *m*-, and *p*-Nitrobenzylidene diacetates were purified by recrystallization using 95 per cent ethanol as a solvent. For all the esters, studied in this work, except *n*-butylidene diacetate, the physical properties are reported in the literature. The boiling point of *n*-butylidene diacetate was 106°C at 25 mmHg.

Commercial ethanol was purified by the standard method. The amount of alcohol was estimated by the dichromate method.[8]

Kinetic Measurements

The kinetics of alkaline hydrolysis of acyl acetals was studied in 90 per cent (wt/wt) aqueous ethanol as some of the esters have very low solubility in water. Further, the rate constant of some of fast reacting acyl acetals can be conveniently studied in the alcoholic medium as rate constants in 90 per cent (wt/wt) aqueous ethanol medium are substantially lower than in water. In addition, experiments were carried out at lower temperatures so that the homogeneous method could be used.

Appropriate amounts of sodium hydroxide and ester solutions were taken separately in two conical flasks and brought to the experimental temperature in the thermostatic bath where temperature could be controlled to within ±0.05°C of the desired temperature. The reactants were mixed at a noted time and aliquots were withdrawn periodically into flasks containing a known excess of standard hydrochloric acid solution to arrest the reaction. The excess acid was back titrated with standard sodium hydroxide solution to a phenolphthalein end point. The following equation was used to calculate the rate constant:

$$k_2 = \frac{2.303}{t(2a-b)} \log_{10} \frac{b(a-x)}{a(b-2x)} \cdot \frac{V}{N} \qquad (10)$$

where, a and b are the initial concentrations of the ester and alkali, in terms of m*l* of sodium hydroxide of N normality used as titrant, respectively; $(a-x)$ and $(b-2x)$ are the concentrations of these reactants at time t. V is the volume of sample withdrawn from the reaction mixture, m*l*. A plot of $\log_{10}(a-x)/(b-2x)$ against t, should give a straight line with a slope of $k_2(2a-b)/2.303 \cdot N/V$ from which the value of the rate constant, k_2, can be calculated.

For fast reacting esters which are sparingly soluble in water, the theory of diffusion accompanied by fast pseudo first order reaction was employed for studying the kinetics. The details of this method have been reported in the previous paper.[9]

Results and Discussion

In Table 1 are reported the second order rate constants for the alkaline hydrolysis of some acyl acetals. The values are very much higher than that for simple acetic esters. The higher values are due to the presence of a highly electron attracting group, –O–C–CH_3, at the α-carbon atom of the alkyl part of the ester. The nature of R′ of an acyl acetal would also influence the rate of the reaction as it is also attached to the α-carbon atom of the alkyl part. The rate would increase with an increase in the electronegativity of R′ and decrease when R′ is a bulky group.

The most recent value of rate constant for alkaline hydrolysis of methylene diacetate, reported by Euranto and Moisio[4] is 5.85 *l*/g mol sec in water at 25°C. It would be expected that the rate constant for ethylidene diacetate would be about 4.0 *l*/g·mol·sec in water at 25°C as the rate constant decreases

6) W. Davy and B. R. Gwilt, *J. Chem. Soc.*, **1955**, 1385.

7) B. M. Nordlender and W. E. Cass, *J. Amer. Chem. Soc.*, **69**, 2679 (1947).

8) N. R. Kamath and M. M. Sharma, *J. Sci. Ind. Res.*, **20D**, 200 (1961).

9) R. C. Sharma and M. M. Sharma, *J. Appl. Chem.*, **19**, 162 (1969).

TABLE 1. RATE CONSTANTS FOR THE ALKALINE HYDROLYSIS OF ACYL ACETALS IN 90 PER CENT (wt/wt) AQUEOUS ETHANOL

No.	$R'CH(OAC)_2$ R′	k_2, l/g·mol·sec, temperature, °C							E kcal/g·mol
		−5.5	0.2	5	10	15	25	30	
1	$-CH_3$	0.118	0.166	0.256	0.328	0.495	1.08*	1.38*	11.0
2	$-CH_2CH_2CH_3$	0.089	0.128	0.182	0.301	0.372	0.75*	0.871*	10.3
3		0.275	0.357	0.479	0.76	—	2.51*	3.16*	12.1
4	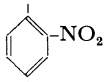	0.234	0.3	0.394	0.602	0.77	1.78*	2.2	11.2
5	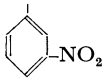	0.953	—	—	—	—	—	—	—
6		1.15	—	—	—	—	—	—	—

* Extrapolated

by a factor of about 1.5 when ethyl group is substituted at the alkyl portion instead of methyl group.[10] The value of the rate constant obtained in this work is 1.08 l/g·mol·sec in 90 per cent (wt/wt) aqueous ethanol at 25°C (extrapolated). It is likely that the rate constant increases by a factor of about 4 when water is used instead of 90 per cent (wt/wt) aqueous ethanol. Thus the estimated rate constant would be about 4.3 l/g·mol·sec.

n-Butylidene diacetate reacts at a rate lower than that of ethylidene diacetate because of the steric effect. The extrapolated value of the rate constant in 90 per cent (wt/wt) aqueous ethanol is 0.75 l/g·mol·sec at 25°C. The value of the ratio of the rate constants for ethyl and butyl acetates of about 1.35[11] may be compared with the ratio of rate constants for ethylidene and butylidene diacetates of about 1.4. Apparently the effect of steric factors for the alkaline hydrolysis of acetic esters and the corresponding acyl acetals is comparable.

The rate constant for the alkaline hydrolysis of benzylidene diacetate is nearly twice that of ethylidene diacetate. The higher rate is due to the electronegative nature of the phenyl group. The inductive effect is of the same order of magnitude as observed in the case of benzyl acetate.[12] The values of the rate constant for ethyl and benzyl acetates are 0.11 and 0.2 l/g·mol·sec, respectively, in water at 25°C.

It is obvious that substitution on the benzene ring of benzylidene diacetate would affect the value of the rate constant. Tommila and Hinshelwood[13] have studied the influence of substitution on the alkaline hydrolysis of benzoic, phenyl and benzyl esters.

The values of the rate constants for the alkaline hydrolysis of benzylidene diacetates were obtained at −5.5°C as these esters are relatively fast reacting. These values are 1.153 and 0.953 l/g·mol·sec

TABLE 2. RELATIVE INFLUENCE OF *m*- AND *p*-NITRO SUBSTITUENTS ON THE ALKALINE HYDROLYSIS OF ESTERS

No.	Ester	Solvent	Temperature °C	k_2, l/g·mol·sec			Ratio (m/p)	References
				Unsubstituted	*m*-Nitro substituted	*p*-Nitro substituted		
1	Ethyl benzoate	60% (wt/wt) aq. acetone	25	0.00289	0.1365	0.2465	0.554	13
2	Phenyl acetate	60% (wt/wt) aq. acetone	25	0.537	5.49	8.05	0.7	13
3	Benzyl acetate	60% (wt/wt) aq. acetone	25	0.0697	2.13	2.685	0.682	13
4	Benzylidene diacetate	90% (wt/wt) aq. ethanol	−5.5	0.275	0.953	1.15	0.828	This work

10) A. I. Kravchenko and U. E. Penzova, *Zh. Obsch. Khem.*, **20**, 2076 (1951); *Chem. Abstr.*, **45**, 1296 (1951).

11) M. M. Sharma and R. C. Sharma, unpublished work.

12) A. Skrabal and M. A. Hugetz, *Monatsh*, **47**, 17 (1926).

13) E. Tommila and C. N. Hinshelwood, *J. Chem. Soc.*, **1938**, 1801.

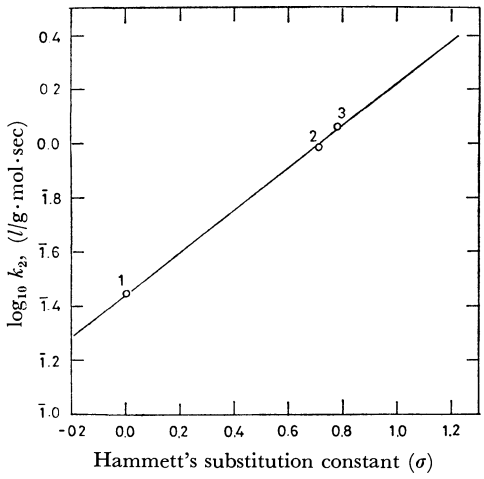

Fig. 1. Hammett's plot.
○(1) Benzylidene diacetate
○(2) *m*-Nitrobenzylidene diacetate
○(3) *p*-Nitrobenzylidene diacetate

for *p*- and *m*-nitrobenzylidene diacetates, respectively. The ratios of *m*- and *p*-substituted esters of different types are compared in Table 2.

A straight line relationship is obtained when the logarithms of the rate constants for the alkaline hydrolysis of benzylidene and *m*- and *p*-nitrobenzylidene diacetates in 90 per cent (wt/wt) aqueous ethanol at −5.5°C are plotted against the Hammett's substitution constant,[14] σ (Fig. 1). It would be necessary to investigate the kinetics of alkaline hydrolysis of some more related substituents, notably chloro- and bromo-, before it can be said that the Hammett's correlation is really applicable. Fife and Jao[15] have studied the acid catalyzed hydrolysis of acetals containing substituted benzene ring and found a straight line correlation between the logarithms of the rate cnstants and the substitution constant, σ.

Ortho Effect

It was thought desirable to investigate the effect of *ortho*-substitution on the kinetics of the alkaline hydrolysis of benzylidene diacetate. For this purpose, *o*-nitrobenzylidene diacetate was considered. *Ortho* effects arising from the proximity of the substituents to the reaction center vary with the reaction as well as with the substituents and this makes it almost impossible to represent the effect of *ortho*-substituents in the same manner as those of *m*- and *p*-substituents. The rate constant for the alkaline hydrolysis of *o*-nitro-benzylidene diacetate was found to be 0.23 *l*/g·mol·sec in 90 per cent (wt/wt) aqueous ethanol at −5.5°C which is lower than the value of 0.275 *l*/g·mol·sec for benzylidene diacetate.

Watkinson *et al.*[16] have investigated the *Ortho* effect in the alkaline hydrolysis of *Ortho* substituted ethyl phenyl acetate. The ratio of the rate constants of the unsubstituted and *o*-substituted benzylidene diacetates of 1.18, may be compared with that reported by Watkinson *et al.*[16] for unsubstituted and *o*-substituted ethyl phenyl acetates of 1.28.

Some of the acyl acetals satisfy the conditions for the applicability of the theory of mass transfer accompanied by fast pseudo first-order reaction for the determination of the rate constant for the alkaline hydrolysis of esters.[9] Solubilities of esters in water and aqueous solution of sodium chloride were determined experimentally in this work as such data are not available in literature. The results were correlated by the methods reported in the literature,[17-19] and are given in Table 3. Diffusivities of esters were estimated by the method of Wilke and Chang[20] and are reported in Table 4. The rate constants determined by the diffusion method are also reported in Table 4.

The rate constant for the alkaline hydrolysis of *n*-butylidene diacetate was found to be 2.58 *l*/g·mol·sec in the aqueous medium at 30°C (2M NaCl+1N NaOH). The value of the rate constant in alkaline solution at vanishing concentration of OH^- would be higher because of the negative salt effect. The value of the rate constant for the alkaline hydro-

Table 3. Solubilities of acyl acetals in water and aqueous sodium chloride solutions (1 to 4M)

No.	Acyl acetal	Temperature °C	Solubility, in water g·mol/cm³ $[E]_w \times 10^5$	K_s* (*l*/g ion)
1	Ethylidene diacetate	30	46	0.175
2	*n*-Butylidene diacetate	30	3.02	0.192
3	Benzylidene diacetate	30	0.139	0.265
		50	0.802	0.269
		60	1.026	0.266

* $\log_{10} \frac{[E]_w}{[E]} = K_s I$[9];
[E]=Solubility of the ester in aqueous sodium chloride solution, g·mol/cm³
I=Ionic strength, g·ion/*l*

14) R. W. Taft, Jr., "Steric Effect in Organic Chemistry," ed. by M.S. Newman John Wiley & Sons, Inc., N. Y. (1956), p. 556.
15) T. H. Fife and L. K. Jao, *J. Org. Chem.*, **30**, 1492 (1965).
16) J. K. Watkinson, W. Watson and B. L. Yates, *J. Chem. Soc.*, **1963**, 5437.
17) F. A. Long and W. F. McDevit, *Chem. Rev.*, **51**, 119 (1952).
18) D. W. Van Krevelen and P. J. Hoftizer, *Chem. Ind.* (London), **1948**, 168.
19) P. J. Kothari and M. M. Sharma, *Chem. Eng. Sci.*, **21**, 391 (1966).
20) C. R. Wilke and P. Chang, *A. I. Ch. E. J.*, **1**, 264 (1955).

TABLE 4. SPECIFIC RATES OF EXTRACTION, DIFFUSIVITIES AND RATE CONSTANTS FOR ALKALINE HYDROLYSIS OF ACYL ACETALS IN AQUEOUS SOLUTIONS

No.	Acyl acetal	Concentration of electrolytes, g·mol/l		Temp. °C	Specific rate of extraction, g·mol/cm²·sec ×10⁸	Diffusivity ×10⁶, cm²/sec	k_2 l/g·mol·sec
		NaCl	NaOH				
1	*n*-Butylidene diacetate	2	1	30	2.97	5.15	2.58
2	Benzylidene diacetate	0	0.5	30	2.94	6.46	11.5
		0	0.5	50	7.65	10.0	51.3
		0	0.5	60	14	12.1	93.6

lysis of *n*-butylidene diacetate at 30°C in 90% (wt/wt) aqueous ethanol is 0.87 *l*/g·mol·sec (Table 1). It would be expected that the rate constant in the aqueous medium would be about four times that in the aqueous medium containing 90% (wt/wt) alcohol. Thus the value of the rate constant in the aqueous medium would be expected to be about 3.5 *l*/g·mol·sec.

As the melting point of benzylidene diacetate is 46°C, the kinetics of alkaline hydrolysis was studied by the extraction of molten ester in the stirred cell at 50 and 60°C. Benzaldehyde, the hydrolysis product of benzylidene diacetate, may further react with sodium hydroxide (Cannizzaro's reaction).

$$2R'CHO + NaOH \rightarrow R'COONa + R'CH_2OH \quad (11)$$

Therefore, it was necessary to study the specific rate of extraction in aqueous sodium hydroxide for a short period (say 5 min) so that the possibility of the Cannizzaro's reaction was minimised. The rate constant was also determined at the room temperature (30°C) by the solid dissolution technique. The value of the rate constant for the alkaline hydrolysis of benzylidene diacetate was found to be 11.4 *l*/g·mol·sec at 30°C in water (Table 4). This value is about four times greater than the extrapolated value obtained by the conventional method in 90 per cent (wt/wt) aqueous ethanol at 30°C (3.16 *l*/g·mol·sec, Table 1). The energy of activation was found to be 13 kcal/g·mol.

Ethylidene diacetate did not satisfy the necessary conditions for the validity of the diffusion method as its solubility is relatively high. *o*-, *m*- and *p*-Nitrobenzylidene diacetates, on the other hand have too low a solubility to be determined accurately. In view of the above the diffusion method could not be used for these esters and conventional method was used employing 90 per cent (wt/wt) aqueous ethanol as the medium.

One of the authors (R.C.S.) wishes to thank the University Grants Commission for an award of scholarship which enabled this work to be carried out.

BULLETIN OF THE CHEMICAL SOCIETY OF JAPAN VOL. 43 1287—1292 (1970)

Studies of the Chemiluminescence of Several Xanthene Dyes. V. Blue Emission from an Excited State of a Reaction Product

Isao KAMIYA and Sadao KATO*1

Department of General Education, Nagoya University, Chikusa-ku, Nagoya

(Received July 26, 1969)

We have found that the chemiluminescence emission of several xanthene dyes with hydrogen peroxide is comprised of two emission components; one is a greenish-yellow emission whose spectral distribution is similar to that of the fluorescence of the dye, and the other is a blue emission similar to the fluorescence band which appears during the course of the reaction. Summarizing the results, we can conclude that the chemical formation of an excited species from the oxidation of a dye, and an energy-transfer process from the species to an unoxidized dye, are likely to be the mechanism for the luminescent reaction. Certain dyes, uranin, eosin Y, eosin R, erythrosin B, 2′,7′-dichlorofluorescein, mercurochrome, rhodamine B, rhodamine 6G, and rhodamine S, showed similar characteristic chemiluminescence emissions, whereas phloxine, rose bengale, 4-nitrofluorescein, 4,5,6,7-tetrachlorofluorescein, sulfonfluorescein, and pyronine G did not chemiluminesce under comparable conditions.

In the present study, we have found that the chemiluminescence emission from the reaction of several xanthene dyes with hydrogen peroxide in an alkaline solution is comprised of two emission components; one is a greenish-yellow emission whose spectral distribution is similar to that of the fluorescence of the dye, and the other is a blue emission similar to the fluorescence band which appears during the course of the reaction.

In our previous papers, though only the greenish-yellow emission component could be detected in a concentrated uranin or eosin Y system where appreciable self-absorption occurred,[1] the possibility of such a component as the blue emission from an excited product was considered[2] because the behavior of the emission (the kinetic data[3] and the enhancement effect with a foreign dye[4]) gave support to a reaction scheme; an excited species is produced by the reaction of a dye with a radical produced by the decomposition of hydrogen peroxide, and energy is transferred from the species to an unoxidized dye, thereby exciting the dye to emit fluorescence.

Eosin R, erythrosin B, 2′,7′-dichlorofluorescein, mercurochrome, rhodamine B, rhodamine 6G, and rhodamine S showed a similar characteristic chemiluminescence, whereas such dyes as phloxine, rose bengale, 4-nitrofluorescein, 4,5,6,7-tetrachlorofluorescein, sulfonfluorescein, and pyronine G did not chemiluminesce under comparable conditions.

This paper will describe our experimental results in detail and will present a discussion based on these results.

Experimental

The luminescent systems were prepared by a method essentially identical with that described previously.[3] The reaction was performed by adding 0.5 m*l* of a 20% aqueous solution of hydrogen peroxide to a mixture of 3 m*l* of an aqueous solution or a 50% dimethylsulfoxide solution of a dye (about 1.3×10^{-3} mol/*l*) and 1 m*l* of a 2N or 1/2N aqueous sodium hydroxide in a quartz cell ($10\times10\times45$ mm). The chemiluminescence spectra were measured with a Hitachi MPF-2A type fluorescence spectrophotometer (using a R-104 photomutiplier tube) equipped with a thermostatic cell assembly with water circulating at a constant temperature (40°C). The fluorescence spectra of the reaction systems were also measured by lowering the voltage of the photomultiplier, with the same apparatus with the exciting done at 380 mμ. The slit width for the chemiluminescence measurements was about 40 mμ, whereas that for the fluorescence measurements was about 10 mμ. The scan speed was 5 sec per 10 mμ, the recorded spectral curves were corrected if necessary by means of decay curves measured under the same experimental conditions.

Results

Figure 1 shows the chemiluminescence spectrum in an eosin Y system measured at several different reaction times. The results indicate that the spectrum varies during the course of the reaction. At

*1 Present address: Senior High School Attached to the Faculty of Education, Nagoya University, Chikusa-ku, Nagoya.

1) I. Kamiya and R. Iwaki, This Bulletin, **39**, 264 (1966).
2) I. Kamiya and R. Iwaki, *ibid.*, **39**, 277 (1966).
3) I. Kamiya and R. Iwaki, *ibid.*, **39**, 257 (1966).
4) I. Kamiya and R. Iwaki, *ibid.*, **39**, 269 (1966).

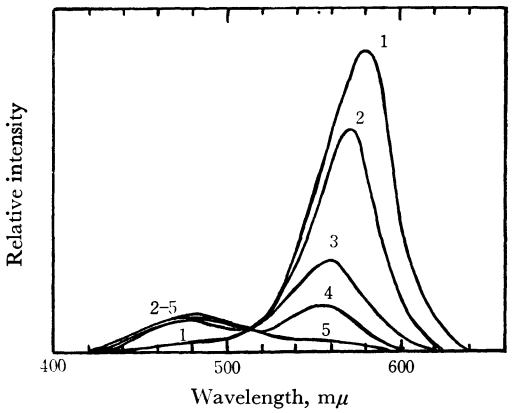

Fig. 1. Variation of the chemiluminescence emission spectrum in eosin Y system (aqueous solution) with reaction time.
1: after 2 min, 2: 4 min, 3: 6 min, 4: 9 min, 5: 15 min

the initial stage, the apparent emission is composed of one intense peak at about 580 mμ, as has been reported previously.[1] During the course of the reaction, however, the intensity of the peak gradually decreases with the blue shift, and simultaneously a new peak appears at about 480 mμ until only the blue emission is observed at the final stage.

The change in the fluoresence spectrum of the chemiluminescent eosin Y system after oxidation was measured*[2] with exciting at 380 mμ. The results are illustrated in Fig. 2. It is demonstrated that the fluorescence of the system shows the same spectral change with the reaction time as does the chemiluminescence emission. When we compare

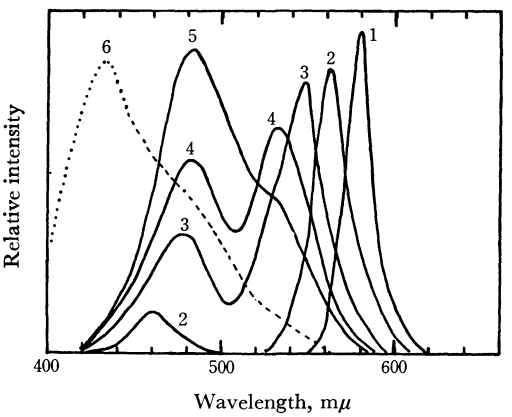

Fig. 2. Variation of the fluoresence emission spectrum in eosin Y system (aqueous solution).
1: before oxidation, 2: after 2 min, 3: 6 min, 4: 12 min, 5: 20 min, 6: 5 hr

*[2] In these measurements, no photocurrent caused by feeble chemiluminescence was detected at the photomutiplier-sensitivity at which the fluorescence was detected.

the spectral change in the chemiluminescence with that of the fluorescence, it is apparent that the greenish-yellow emission component is to be attributed to the fluorescence emission from an excited dye, and the blue-emission component to the emission from an excited species produced in the reaction.

The peak at 480 mμ of the blue-fluorescence emission was further blue-shifted to 430 mμ by successive oxidation, as is shown by the dashed line in Fig. 2, but no chemiluminescence emission appeared at this oxidation stage. Hence, it can be said that the primary excited species is an intermediate product.

The changes in both the chemiluminescence and the fluorescence spectra with the reaction time in a uranin system are shown in Figs. 3 and 4 respectively. In the system, the blue emission com-

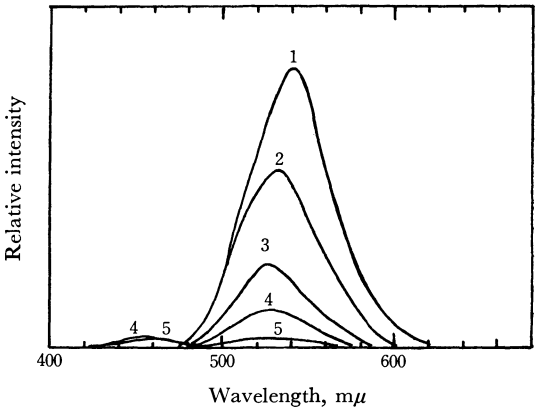

Fig. 3. Variation of the chemiluminescence emission spectrum in uranin system (aqueous solution) with reaction time.
1: after 2 min, 2: 4 min, 3: after 6 min, 4: 9 min, 5: 15 min

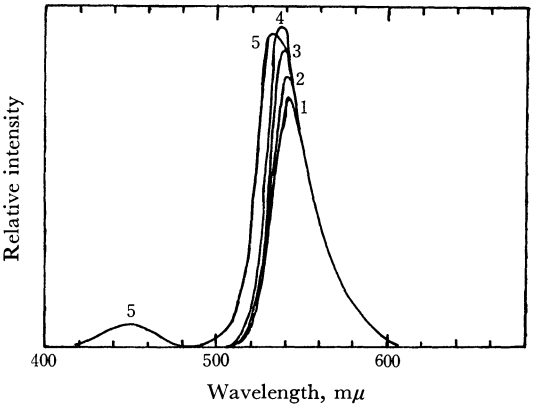

Fig. 4. Variation of the fluorescence emission spectrum in uranin system (aqueous solution) with reaction time.
1: after 2 min, 2: 4 min, 4: 6 min, 4: 12 min, 5: 20 min

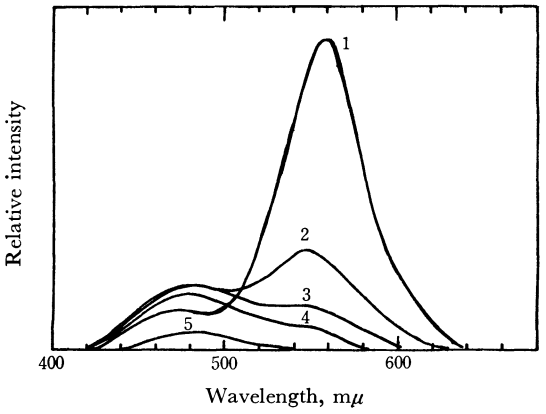

Fig. 5-a-1. Variation of the chmiluminescence emission spectra in the systems of several xanthene dyes with reaction time.
Eosin R system (aqueous solution)
1: after 2 min, 2: 4 min, 3: 6 min, 4: 9 min, 5: 15 min

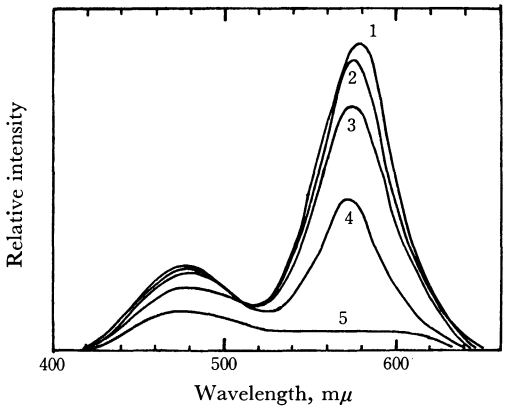

Fig. 5-a-2. Erythrosin B system (50% DMSO solution).
1: after 2 min, 2: 4 min, 3: 6 min, 4: 9 min, 5: 15 min

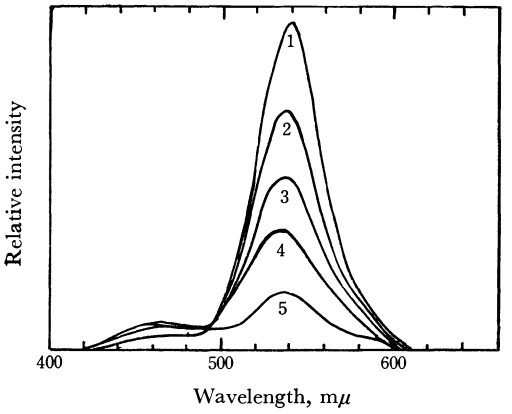

Fig. 5-a-3. 2′,7′-Dichlorofluorescein system (aqueous solution).
1: after 2 min, 2: 4 min, 3: 6 min, 4: 9 min, 5: 15 min

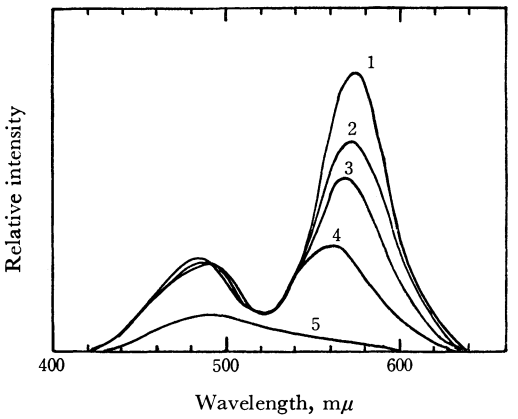

Fig. 5-a-4. Rhodamine B system (50% DMSO solution).
1: after 2 min, 2: 5 min, 3: 8 min, 4: 11 min, 5: 15 min

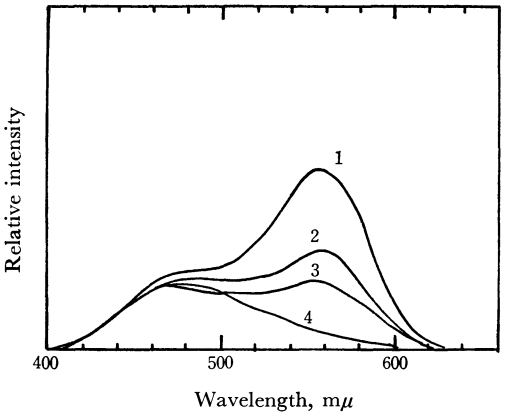

Fig. 5-a-5. Rhodamine S system (50% DMSO solution).
1: after 2 min, 2: 4 min, 3: 6 min, 4: 15 min

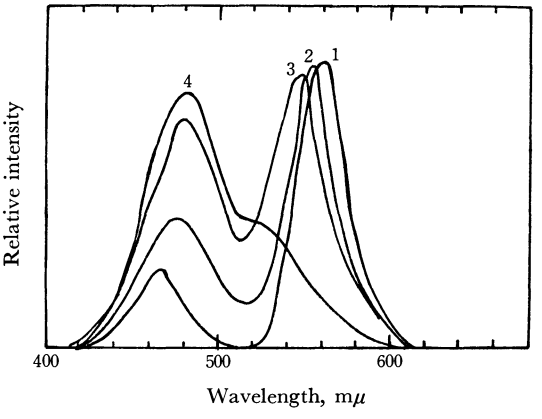

Fig. 5-b-1. Variation of the fluorescence emission spectra in the chemiluminescent systems of several xanthene dyes with reaction time.
Eosin R system (aqueous solution)
1: after 2 min, 2: 4 min, 3: 6 min, 4: 12 min, 5: 20 min

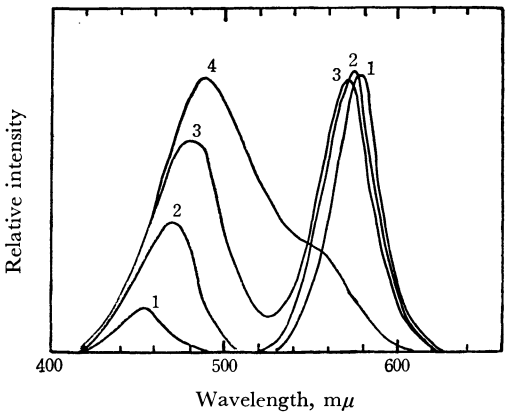

Fig. 5-b-2. Erythrosin B system (50% DMSO solution).
1: after 2 min, 2: 4 min, 3: 8 min, 4: 20 min

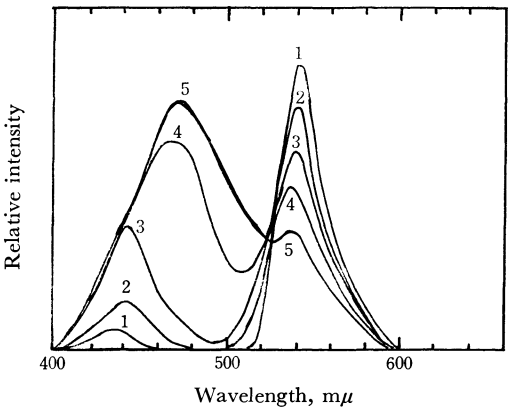

Fig. 5-b-3. 2′,7′-Dichlorofluorescein system (aqueous solution).
1: after 2 min, 2: 4 min, 3: 6 min, 4: 12 min, 5: 20 min

ponent was not very appreciable. However, with regard to the intense fluorescence of unoxidized uranin at the final stage, we may say that the self-absorption of the dye prevents any blue emission from the excited product.

Eosin R, erythrosin B, 2′,7′-dichlorofluorescein, mercurochrome, rhodamine B, rhodamine 6G, and rhodamine S chemiluminesced with the same two emission peaks as were observed in the eosin Y system. Typical examples of the results are illustrated in Fig. 5-a, where they are compared with the changes in the fluorescence spectra with the reaction time (Fig. 5-b). In each case, we can clearly find a spectral correspondence between the chemiluminescence and the fluorescence emissions.

On the other hand, such fluorescent dyes as phloxine, rose bengale, 4-nitrofluorescein, 4,5,6,7-tetrachlorofluorescein, sulfonfluorescein, and pyronine G did not actually chemiluminesce under comparable conditions. However, when one of

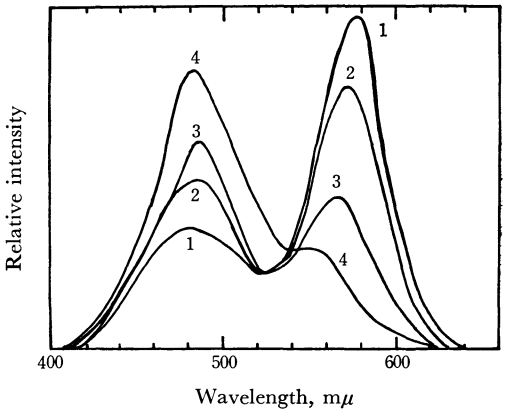

Fig. 5-b-4. Rhodamine B system (50% DMSO solution).
1: after 2 min, 2: 5 min, 3: 8 min, 4: 15 min

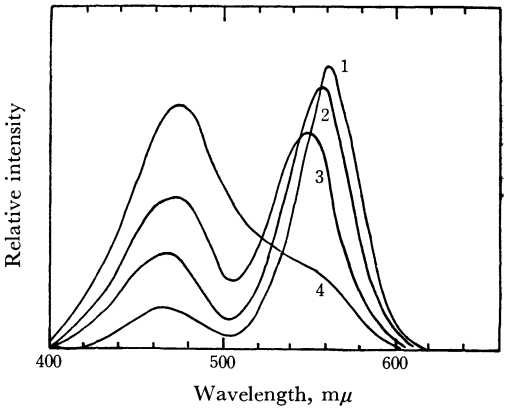

Fig. 5-b-5. Rhodamine S system (50% DMSO solution).
1: after 2 min, 2: 4 min, 3: 8 min, 4: 20 min

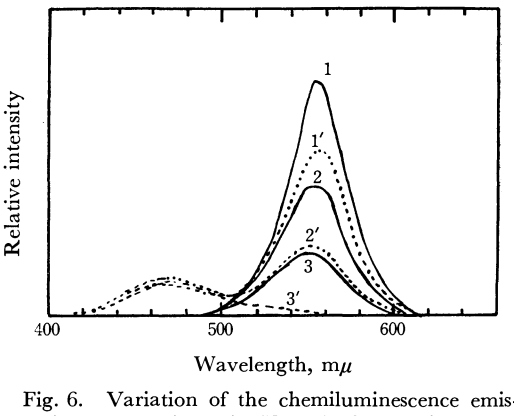

Fig. 6. Variation of the chemiluminescence emission spectra in eosin Y-sulfonfluorescein system (———) and eosin Y system (.....) with reaction time. eosin Y (4×10^{-4} mol/l), sulfonfluorescein (5×10^{-4} mol/l).
1, 1′: after 2 min, 2, 2′: 5 min, 3, 3′: 12 min

these dyes, such as sulfonfluorescein, was added to eosin Y, the emission corresponding to the fluorescence of the added dye appeared in place of the blue emission at the final stage, as is shown in Fig. 6. This experimental evidence can best be explained in terms of an energy-transfer process from an excited product to the added dye.

Discussion

All the findings presented above give support to the following reaction scheme, suggested in the previous paper; an excited species is produced from the reaction of the dye with a radical which is itself produced by the decomposition of hydrogen peroxide, and the energy is transferred from the species to the unoxidized dye, thereby exciting the dye to emit fluorescence.

An analogous mechanism has been proposed for the chemiluminescence of lucigenin.[5] The *N*-methylacridon produced is primary the emitting species because a blue emission corresponding to the fluorescence of *N*-methylacridon was observed in a hot dilute system, whereas a greenish-yellow emission whose major component was similar to that of the lucigenin fluorescence was observed in a cold, concentrated system.[6]

On the other hand, two different types of the chemiluminescence of several dyes have been reported. The first type is the induced-chemiluminescence of anthracene, acridine, eosin Y, fluorescein, quinoline sulfate, and aesculin, which is observed when these dyes are present in the reaction of alkaline hydrogen peroxide with chlorine gas or the hypochlorite ion.[7] The suggested mechanism involves the formation of excited (singlet) molecular oxygen, which then forms an excited dimer through collision, and an energy-transfer from the dimer to these added fluorescers.[8] The second type is the visible light emission, which builds up and decays over a period of microseconds, this emission is induced when deaerated solutions of certain dyes, rhodamine B, acriflavin, fluorescein, and eosin are electron-pulse radiolysed.[9] The emission corresponds to the fluorescence of each dye. The proposed mechanism involves the processes by which the OH-adduct, DOH, reacts with the hydrated electron, e^-, to give the excited dye, D*:[10]

$$DOH + e^- \longrightarrow D^* + OH^-$$

Neither of these two mechanism is likely, for if the excited dimer of oxygen and the blue-fluorescent product were involved, as a donor and an acceptor respectively, in an energy-transfer process, the intensity of the peak at 480 mμ would increase with the increase in the concentration of the fluorescent product.[11] (We can see from Figs. 1 and 2 that the intensity of the peak of the blue component of the chemiluminescence is kept almost constant, whereas that of the fluorescence increases with the increase in the concentration of the reaction product). Moreover, a significant emission would also be observed in the systems of such fluorescent dyes as 4-nitrofluorescein, 4,5,6,7-tetrachlorofluorescein, and sulfonfluorescein. Furthermore, if the dye were primarily excited, we would not observe a blue-emission component which changes to greenish-yellow emission when sulfonfluorescein or 4-nitrofluorescein is added.

In summarizing the above results, we can conclude that the chemical formation of an excited species from the oxidation of dye, and an energy-transfer process from the species to an unoxidized dye, are most likely to compose the mechanism for the chemiluminescent reaction. Reconsidering the present experimental findings, we can develop the previously-proposed reaction scheme:[2]

Radical ($R^\cdot$) formation:

$$H_2O_2 \longrightarrow R^\cdot (O_2H^\cdot \text{ or } OH^\cdot)$$

The production of an excited species (M_E^*) by the reaction of $R^\cdot$ with a dye, for example, eosin Y (E):

$$E + R^\cdot \longrightarrow M_E^* \quad \text{(reaction rate, } k_1\text{)}$$

An energy-transfer process:

$$M_E^* + E \longrightarrow M_E + E^* \qquad (k_2)$$

Blue fluorescence emission from M_E^*:

$$M_E^* \longrightarrow M_E + h\nu_1 \qquad (k_3)$$

Greenish-yellow fluorescence emission from E*:

$$E^* \longrightarrow E + h\nu_2 \qquad (k_4)$$

Self-quenching:

$$E^* + E \longrightarrow E + E \qquad (k_5)$$

According to the above scheme, the intensity of the chemiluminescence, I_E, is given by:

$$I_E = k_3[M_E^*] + k_4[E^*] \qquad (1)$$

Using the steady-state approximation, $d[M_E^*]/dt = 0$ and $d[E^*]/dt = 0$, I_E can be written as:

$$I_E = k_1k_3[E][R^\cdot]/(k_2[E]+k_3) + k_1k_2k_4[E]^2[R^\cdot]/(k_2[E]+k_3)(k_4+k_5[E]) \qquad (2)$$

The experimental results indicate that the intensity of blue emission is almost constant. This

5) H. Kautsky and K. H. Kaiser, *Z. Naturforsch.*, **56**, 353 (1950); A. Spruit van der Burg, *Rec. Trav. Chim. Pays. Bas*, **69**, 1526 (1950).

6) J. R. Totter, *Photochem. Photobiol.*, **3**, 231 (1964).

7) L. Mallet, *Compt. Rend.*, **185**, 352 (1927).

8) A. U. Khan and M. Kasha, *J. Amer. Chem. Soc.*, **88**, 1574 (1966).

9) W. Prutz, K. Sommermeyer and E. J. Land, *Nature*, **212**, 1045 (1966).

10) L. I. Grossweiner and A. F. Rodde, Jr., *J. Phys. Chem.*, **72**, 756 (1968).

11) E. A. Ogryzlo and A. E. Pearson, *ibid.*, **72**, 2913 (1968).

means that the first term of Eq. (2) can be reduced to (k_1k_3/k_2) [R·] by assuming that $k_2[E]>k_3$, since [E] decreases with the reaction time. On such an assumption, I_E is finally given by:

$$I_E = (k_1k_3/k_2)[R^\cdot] + k_1[E][R^\cdot]\phi_E \quad (3)$$

where ϕ_E is the fluorescence efficiency of E and is given by:

$$\phi_E = k_4/(k_4+k_5[E])$$

As has been shown, the greenish-yellow emission is so intense, compared to the blue emission, except for the final stage, that the I_E in the decay stage can be given as approximately:

$$I_E = k_1[E][R^\cdot]\phi_E \quad (4)$$

When a foreign dye such as sulfonfluorescein (S) is added to the eosin Y system, the following steps are also present: An energy-transfer process from M_E^* to S:

$$M_E^* + S \longrightarrow M_E + S^* \quad (k_6)$$

Fluorescence emission from S*:

$$S^* \longrightarrow S + h\nu_3 \quad (k_7)$$

Quenchings:

$$S^* + S \longrightarrow S + S \quad (k_8)$$

$$E^* + S \longrightarrow E + S \quad (k_9)$$

$$S^* + E \longrightarrow S + E \quad (k_{10})$$

Taking all of the steps into account, we can write the intensity of the emission in the eosin Y-sulfonfluorescein system as follows, since no blue emission appears:

$$I_{ES} = k_4[E]^* + k_7[S^*]$$

Under stationary conditions, we can write:

$$[E^*] = k_2[M_E^*][E]/(k_4+k_5[E]+k_9[S])$$

$$[S^*] = k_6[M_E^*][S]/(k_7+k_8[S]+k_{10}[S])$$

$$[M_E^*] = k_1[E][R^\cdot]/(k_2[E+k_6[S])$$

Assuming that the quenching with a foreign dye is not appreciable compared to the self-quenching, we can write that:

$$\phi_E = k_4/(k_4+k_5[E]) \fallingdotseq k_4/(k_4+k_5[E]+k_6[S])$$

Hence,

$$I_{ES} = k_1[E][R^\cdot](k_2[E]\phi_E+k_6[S]\phi_S)/(k_2[E]+k_6[S]) \quad (5)$$

where

$$\phi_S = k_7/(k_7+k_8[S]+k_{10}[E]).$$

From Eqs. (4) and (5), we obtain:

$$\Delta = \int (I_{ES}-I_E)dt$$

$$= k_1 \int \{[R^\cdot](k_2[E]^2\phi_E-k_6[E][S])\phi_S/$$

$$(k_2[E]+k_6[S])-[E]\phi_S\}dt \quad (6)$$

Since an intense fluorescence of the dye is observed in the reaction system, we prefer the approximations that $k_4 \gg k_5[E]+k_9[S]$ and that $k_7 \gg k_8[S]+k_{10}[E]$ to the approximation used previously. Using these approximations, and recalling the results that [R·] is independent of the reaction time and that $[E]=[E]_0 \exp(-K_E t)$, we can write:

$$I_E = k_1[R^\cdot][E]_0 \exp(-K_E t) \quad (7)$$

$$\Delta = (k_1k_6[R^\cdot](\phi_S-\phi_E)[S]/k_2K_E)$$

$$\times \ln(1+k_6[S]/k_2[E]_0) \quad (8)$$

We have already shown in the previous paper that the experimental results of I_E and Δ can be reasonably explained by Eqs. (7) and (8) respectively.

However, neither the exact nature of the emitting product nor the reason why some dyes produce chemiluminescence emission, whereas others do not, is at present known. Much further work, including the chemical identification of the blue-fluorescent product, is required.

BULLETIN OF THE CHEMICAL SOCIETY OF JAPAN VOL. 43 1293—1297 (1970)

The Reactions of ^{80}Br Activated by Isomeric Transition in the Gaseous Phase. The Isotopic Variation between CH_4 and CD_4

Enzo TACHIKAWA and Toshiki KAHARA*1

Japan Atomic Energy Research Institute, Tokai-Mura, Ibaraki

(Received September 13, 1969)

The roles of the excess kinetic energy and the thermal ionic processes in the reaction of the ^{80}Br from the isomeric transition of ^{80m}Br in gaseous CH_4 and CD_4 were investigated using a rare gas additive. A possible isotope effect has appeared on the substitution reaction of the energetic Br atom to form $CH_3{}^{80}Br$ or $CD_3{}^{80}Br$, but not on the thermal processes to form $CH_3{}^{80}Br$ and $CH_2{}^{80}BrBr$ or their isotopic alternatives. At a zero mole fraction of moderator, the $CH_3{}^{80}Br/CD_3{}^{80}Br$ ratio for the energetic process was found to be 2.7 ± 0.3. This is consistent with the moderator and/or probability integral isotope effects. However, in a highly moderated system the results indicated that the former effect is more important than the latter. Furthermore it can be inferred from the total pressure effects on the energetic reaction products that the excited primary products are able to decompose unimolecularly due to internal excitation.

Many investigations concerning the target isotope effect on the reactions of recoil atoms have been performed using the recoil tritium atom.[1,2] However, only a few papers have appeared on the recoil Br atom. Spicer and Gordus[3] observed the isotopic variations in the total organic yield between CH_4 and CD_4 in the reaction of ^{80}Br activated by the (I.T.) process. A different attitude was taken by Nicholas and Rack,[4] who concluded that there was same dependence in kinetic energy for (I.T.)-induced ^{82}Br reactions with CH_4 and CD_4.

Experimental evidence shows that both ^{80}Br and ^{82}Br react with CH_4 *via* the energetic process to form CH_3Br and *via* the thermal ionic process to form CH_3Br and CH_2Br_2.[5] These findings, along with the results on the target isotope effect between CH_4 and CD_4 using ^{82}Br reported in a previous paper,[6] have led to these tentative conclusions: a) a target isotope effect appears in the energetic process, but not in the thermal process. b) the yield from the energetic process is higher for ^{82}Br than for ^{80}Br, while the thermal ionic reaction yield is similar for the two species.

In this paper we will deal with the target isotope effect between CH_4 and CD_4 as well as with the pressure effect using ^{80}Br activated by the (I.T.) process, since a comparative study of ^{80}Br and ^{82}Br can provide further knowledge concerning the chemical consequences of the recoil Br atom.

Experimental

The general experimental procedure is the standard one for recoil Br atom reactions, involving the formation of the ^{80}Br atom from the ^{80m}Br(I.T.)^{80}Br and the analysis of the radioactive products by radio gaschromatography.[5] The neutron irradiations were carried out in the JRR-4 in JAERI under a neutron flux of $10^{13}n/cm^2/sec$. The total pressure was always kept at 51 ± 1 cmHg throughout the series of moderator experiments. The ratio of Br_2 as a scavenger, relative to CH_4 or CD_4 was 0.11 ± 0.01.

Materials. The CH_4 was supplied by the Takachiho Chemical Co., and CD_4, by the Merck Sharp and Dohm Co. Their nominal purities were 99.995 and 99.8% respectively, and they were used without further purification. The rare gas, xenon, was obtained from the Takachiho Chemical Co., its nominal purity was 99.995%.

Sample Processing. The inorganic bromides were isolated from the organic bromides by the insertion of a short glass column packed with potassium ferrocyanide into the gas stream ahead of the organic separation column. The gas-chromatographic separations were carried out in a column containing the celite and coated with dioctyl sebacate (15% by weight).

Correction and Experimental Error. All of the data obtained have been corrected using the half-lives 4.38 hr and 17.6 min for ^{80m}Br and ^{80}Br respectively. In most cases, the activity of the products was large enough to reduce the standard deviation of counting to

*1 On leave of absence from the Faculty of Engineering, Ibaraki University, Hitachi, Ibaraki.

1) E. K. C. Lee, J. W. Root and F. S. Rowland, "Chemical Effects of Nuclear Transformations," Vol. 1, IAEA, Vienna (1965), p. 55.

2) R. Wolfgang, *Progr. in Reaction Kinetics*, Vol. 3 (1965), p. 97.

3) L. D. Spicer and A. A. Gordus, "Chemical Effects of Nuclear Transformations," Vol. 1, IAEA, Vienna (1965), p. 185.

4) J. B. Nicholas and E. P. Rack, *J. Chem. Phys.*, **48**, 4085 (1968).

5) E. Tachikawa, This Bulletin, **43**, 63 (1970).

6) E. Tachikawa, *ibid.*, **42**, 2404 (1969).

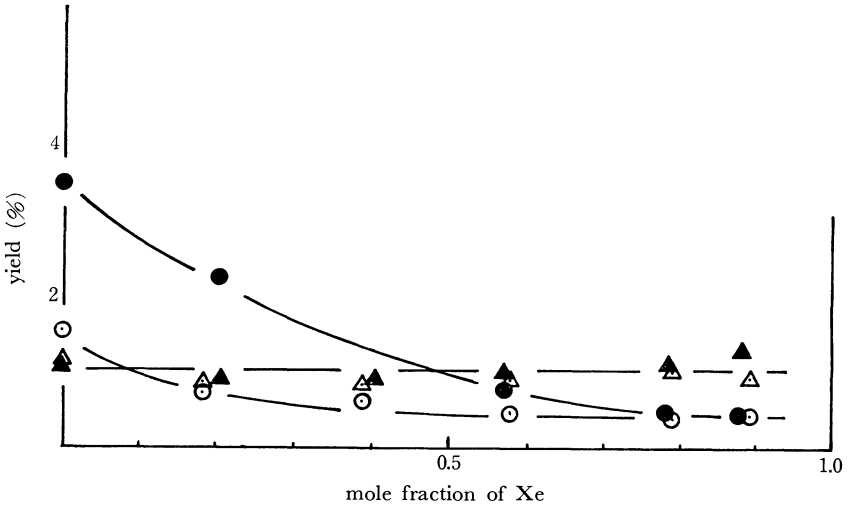

Fig. 1. Moderator curve at 50 cmHg total pressure for the reaction, $CH_4+{}^{80}Br$ and $CD_4+{}^{80}Br$, using xenon moderator.
● $CH_3{}^{80}Br$ ▲ $CH_2{}^{80}BrBr$ ⊙ $CD_3{}^{80}Br$ △ $CD_2{}^{80}BrBr$

a small percentage. The most serious error results from the correction of the results to the percentage yield, relative to the total activity. The product activities were measured in the flow system on radio gas chromatography. However, the total activities were measured under stationary conditions. The 17.6-min half-life is too short to obtain the correction factor between the different counting methods with a precision better than ±5%. Thus, the accuarcy of the present data is usually limited to ±5%. Moreover, in some cases where the total organic yield is relatively small, as in the case of the highly-moderated systems, the standard deviation of counting amounts to 15—20%.

Results and Discussion

Moderator Effect. The organic products observed in the reaction of gaseous CH_4 or CD_4 with the (I.T.)-activated ^{80}Br were $CH_3{}^{80}Br$ and $CH_2{}^{80}BrBr$ or their isotopic products. The moderator effects of Xe on these are graphically displayed in Fig. 1. The following things can be noticed in the figure. Firstly, both $CH_3{}^{80}Br$ and $CD_3{}^{80}Br$ are moderatorsensitive, although the effect of the additive is not the same, the former decreasing from 3.5±0.3% to 0.5±0.3%, and the latter, from 1.6±0.2% to 0.5±0.3%, with an increase in the mole fraction of Xe. Secondly, both $CH_2{}^{80}BrBr$ and $CD_2{}^{80}BrBr$ show a constant yield of 1.1±0.2% over the whole range of the mole fractions of the moderator. Under the present experimental conditions, the yield is 3.5−0.5=3.0% for $CH_3{}^{80}Br$ and 1.6−0.5=1.1% for $CD_3{}^{80}Br$ as formed *via* the energetic Br for H and Br for D processes respectively. Thus, the isotopic variation between them is obtained as 2.7±0.3, a value which is very consistent with the value, 2.8±0.2, found using ^{82}Br instead of ^{80}Br.[6] These results imply that the overall isotope effect between CH_4 and CD_4 is 2.7±0.3 for the energetic reaction of both ^{80}Br and ^{82}Br, although the absolute yield is always higher for ^{82}Br than for ^{80}Br by a factor of 1.5±0.2.[5]

In a previous paper[5] we attempted to ascribe the difference in the absolute yields between ^{82}Br and ^{80}Br to the difference in kinetic energies between them. The γ-transition of ^{82m}Br to the ground state is attained in a single transition, whereas ^{80m}Br is converted by two successive transitions. If the excited ^{80}Br resulting from the first transition enters into a chemical combination with the surrounding molecules within its lifetime, a kinetic energy achieved on ^{80}Br in the successive transition of the excited ^{80}Br is very much dependent upon the remainder of the molecule.[7,8]

From the results, the thermal yields are found to be 0.5±0.3% for $CH_3{}^{80}Br$ or $CD_3{}^{80}Br$ and 1.1±0.2% for $CH_2{}^{80}BrBr$ or $CD_2{}^{80}BrBr$. The ratio between them is 0.45±0.08. Again, these results are in good agreement with those found using ^{82}Br,[5] suggesting that the relative ionization potential of the reactant is the main factor controlling the thermal ionic reactions. Thus, as long as the difference in the ionization potentials between CH_4 (13.12 eV) and CD_4 (13.26 eV)[9] or between ^{80}Br and ^{82}Br is small enough to be ignored, compared to that between CH_4 and Br, it seems that no isotope effect appears as either a target or as a reacting one in the thermal ionic process.

7) A. A. Gordus and J. E. Willard, *J. Amer. Chem. Soc.*, **79**, 4609 (1967).
8) A. R. Kazanjian and W. F. Libby, *J. Chem. Phys.*, **42**, 2778 (1965).
9) F. H. Field and J. L. Franklin, "Electron Impact Phenomena and The Properties of Gaseous Ions," Appendix, Academic Press, New York (1957).

Spicer snd Gordus[3] observed the isotopic variations of the total organic yields between CH_4 and CD_4 as 1.4 ± 0.2. This value is not directly compared with the present value of $(3.5+1.1)/(1.6+1.1)=1.7\pm0.2$, since the amounts of Br_2 added as a scavenger are greatly different between their system and ours. However, the qualitative conclusion that the target isotope effect exists between CH_4 and CD_4 in the reaction of Br activated by the (I.T.) process can be drawn from both experiments. Contrarily, Nicholas and Rack observed no difference in the total organic yields from CH_4 and CD_4 using ^{82}Br, within the range of experimental uncertainty.[4] Unfortunately, it is not immediately possible to explain this contradiction.

Origin for the Isotope Effects. Extensive research into the isotope effects on the energetic reactions has been made using the recoil tritium atom. Several possible sources have been suggested for the variations in the yields measured for isotopic molecules.[10-12] If the energy losses in non-reacting collisions are not same for the two molecules, the isotopic variation can be observed. These differences are called "moderator isotope effects." On the other hand, the isotopic variation may still be expected if the reactivity integrals are not identical for the isotopic molecules. They can be grouped as "probability integral isotope effects." Another possible source is the "average-energy effect" resulting from the differences in the average energy for the reactions. All three effects may influence the energetic reaction of the Br atom and produce the observed differences in the yields from CH_4 and CD_4 molecules. However, the similar CH_3Br/CD_3Br ratios in the energetic processes for both ^{80}Br and ^{82}Br imply that the observed isotopic variations result from the same origins.

The "average-energy isotope effect" may be excluded, since it is only considered when the energetic *Br for H* and *Br for D* reactions compete with each other in the same reaction system. In such a system, the flux of the recoil Br atom surviving to lower energies can be noticeably diminished by a higher-energy reaction. Therefore, fewer energetic reaction may be observed with the lower-energy process than with the higher one.

Thus, the present results are consistent only with the "moderator isotope effect" and/or the "probability" one. One of the experimental approaches for distinguishing the "moderator isotope effect" from the "probability integral effect" is to use a single molecule containing both protium and deuterium. In this way, the same energy spectrum of the energetic Br atom can be used for both reactions; therefore, the "moderator isotope effect" is excluded. The second approach is to control the Br spectrum experimentally by the addition of a large excess of the third molecule.[13] In the limiting case of this type of approach, the reactant represents a negligible fraction of each sample. Therefore, the energetic reaction with a reactant would represent a negligible fraction of the total reaction and the non-reacting energetic Br collisions with the molecule would be completely unimportant. In such an ideal system, the reactant molecules would introduce only infinitely small perturbations to the total Br flux at each energy level, the total energetic yiels would, then, be a direct measure of the ease of the reactions.

Table 1. Yields of products from the reaction of ^{80}Br with CH_4 or CD_4 at high moderation with Xe

Br_2 (cmHg)	CH_4 (cmHg)	Xe (cmHg)	$CH_3{}^{80}Br$ (%)	$CH_2{}^{80}BrBr$ (%)
5.0	5.4	41.1	0.53 ± 0.03	0.71 ± 0.04
5.0	5.3	40.7	0.46 ± 0.02	0.65 ± 0.03
			av. 0.50 ± 0.04	0.68 ± 0.03
Br_2	CD_4	Xe	$CD_3{}^{80}Br$	$CD_2{}^{80}BrBr$
5.0	5.2	40.0	0.39 ± 0.02	0.71 ± 0.04
5.0	5.2	39.9	0.34 ± 0.02	0.68 ± 0.03
			av. 0.37 ± 0.03	0.70 ± 0.03

Table 1 shows the yields from the systems consisting of 0.8 m.f. of Xe, 0.1 m.f. of Br_2, and 0.1 m.f. of CH_4 or CD_4. The experiments are quite far from the ideal because the total reaction with a reactant is not negligible and the flux perturbation cannot be ignored. However, these conditions are the closest that we could attain experimentally. Thus, if the calculations are carried out as though the samples were actually of this ideal limiting type, a difference has been noticed between $CH_3{}^{80}Br$ and $CD_3{}^{80}Br$, but not between $CH_2{}^{80}BrBr$ and $CD_2{}^{80}BrBr$. By assuming that the $CH_3{}^{80}Br$ or $CD_3{}^{80}Br$ formed *via* the thermal ionic process is 45% of the total $CH_2{}^{80}BrBr$ or $CD_2{}^{80}BrBr$ (see Fig. 1), the thermal yield of the mono-substituted products can be extimated to be $0.69\times0.45=0.31$ (%). Thus, the yields of $0.50\%-0.31\%=0.19\%$ for $CH_3{}^{80}Br$ and of $0.37\%-0.31\%=0.06\%$ for $CD_3{}^{80}Br$ are assigned to the energetic process. The ratio between them is 3.2 ± 0.3; this is in the range of the value (2.7 ± 0.3) found in the system containing no moderator. Thus, it can be concluded that the isotope effect observed in the energetic reaction results mostly from the "probability integral isotope effect."

10) E. K. C. Lee and F. S. Rowland, *J. Amer. Chem. Soc.*, **85**, 2907 (1963).
11) H. C. Jurgeleit and R. Wolfgang, *ibid.*, **85**, 1057 (1963).
12) E. K. C. Lee, G. Miller and F. S. Rowland, *ibid.*, **87**, 190 (1965).
13) E. Tachikawa and F. S. Rowland, *ibid.*, **90**, 4767 (1968).

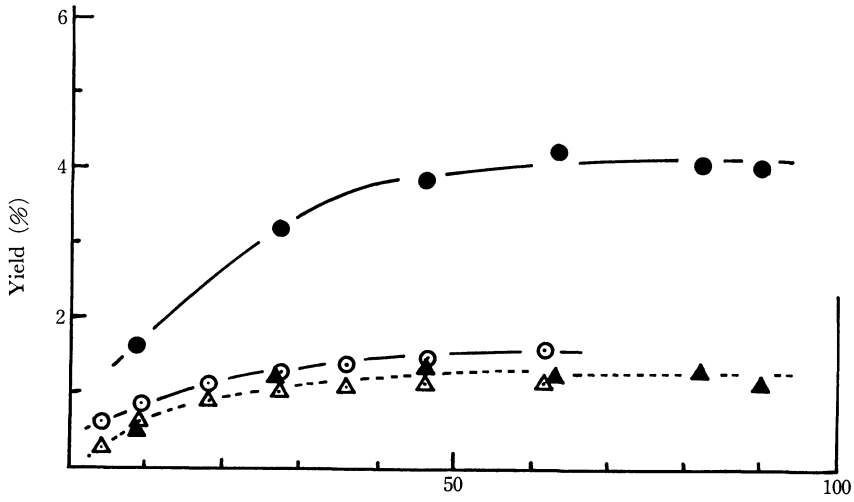

Fig. 2. Pressure dependence of the products from the reaction, $CH_4+^{80}Br$ and $CD_4+^{80}Br$.
● $CH_3{}^{80}Br$ ▲ $CH_2{}^{80}BrBr$ ⊙ $CD_3{}^{80}Br$ ◬ $CD_2{}^{80}BrBr$

Reaction Mechanisms Resulting in Isotopic Variations. The "probability integral isotope effect" observed in the replacement of the H or D atom by the Br atom could be either the result of the isotopic difference between the atoms replaced (the primary isotope effect) or between the CH_3 and CD_3 residues with which the Br atom then combines (the secondary isotope effect). The bond strength of C–H and C–D have been reported to be 4.45+0.02 eV and 4.56+0.03 eV respectively.[14] The C–H bond-dissociation energy has been shown to be correlated with the abstraction reaction of the recoil tritium atom,[13,15] but no definite correlation of it with the substitution reaction has yet been reported.[16] Instead, Rowland *et al.*[1] have suggested that the more rapid relaxation of the H atoms than D atoms into positions favorable for the successful bonding of the T atom is responsible for the observed isotopic variation in the recoil tritium substitution reactions. Moreover, the tendency in hot halogen reactions with alkanes for the reactivity of halogen atoms to decrease as the size of the halogen increases[17] has been ascribed to the ease with which the atoms can change direction in response to a newly-available chemical composition.[18] Thus, by analogy with this concept, it is possible that the fact the relaxation time for a new chemical bond is a controlling factor is also responsible for the present results. However, more work is required to clarify the reaction mechanisms of the substitution reaction of the energetic Br atom in detail.

Pressure Dependency of Products. The substitution of an energetic atom into a molecule is usually accompanied by a high excitation of the products. The excited molecule is able to undergo a secondary decomposition or isomerization, as detected by a pressure-dependent competition between the collisional stabilization and the secondary reaction, as in recoil tritium and other halogen experiments.[18-20] Recently, Spicer and Wolfgang[17]

TABLE 2. THE ESTIMATED YIELDS OF $CH_3{}^{80}Br$ AND $CD_3{}^{80}Br$ FROM THE ENERGETIC PROCESS IN THE REACTION OF ^{80}Br WITH CH_4 AND CD_4

Total Pressure (cmHg)	$CH_3{}^{80}Br$ (%)	$CD_3{}^{80}Br$ (%)
10	1.42±0.20	0.55±0.05
20	(1.97±0.20)*	0.69±0.07
30	2.61±0.20	0.82±0.08
40	(3.06±0.20)*	0.91±0.09
50	3.20±0.20	0.95±0.10
70	3.63±0.20	1.09±0.10
90	3.43±0.20	—
100	3.43±0.20	—

* Yields were estimated from the curve shown in Fig. 2.

14) J. Root, Ph. D. Thesis, The Univ. of Kansas, 1964.
15) J. Root, W. Breckenridge and F. S. Rowland, *J. Chem. Phys.*, **43**, 3694 (1965).
16) R. Cipollini and G. Stöcklin, *Radiochim. Acta*, **9**, 105 (1968).
17) L. Spicer and R. Wolfgang, *J. Chem. Phys.*, **50**, 3466 (1969).
18) C. M. Wai and F. S. Rowland, *J. Amer. Chem. Soc.*, **90**, 3638 (1968).
19) Y. N. Tang, E. K. C. Lee and F. S. Rowland, *ibid.*, **86**, 1280 (1964).
20) Y. N. Tang and F. S. Rowland, *J. Phys. Chem.*, **71**, 4576 (1967).

obtained negative evidence for a unimolecular decomposition of the $CH_3{}^{39}Cl$ and $CH_2{}^{39}Cl\cdot$ formed by the reaction of recoil ^{39}Cl with CH_4 and suggested that a collisional decomposition of hot molecules was involved.

Thus, it seemed that it would be very interesting to examine the pressure effects of the products from the present system. If a unimolecular decomposition of the excited $CH_3{}^{80}Br$ or $CD_3{}^{80}Br$ occurs, the splitting of the C–Br bond is most probable, since it is the weakest bond in the molecule (2.93 eV). However, in our radiochemical method of approach, a decomposition reaction is traced only through the fragment containing the radioactive atom. Under these conditions, no experimental procedures are available to trace the decomposition reaction of $CH_3{}^{80}Br$ or $CD_3{}^{80}Br$.

The results of a series of measurements of the yields *vs.* the total pressure is shown in Fig. 2. The results provide evidence for the pressure dependency of both $CH_3{}^{80}Br$ and $CD_3{}^{80}Br$. Pressure effects are also noticed on both $CH_2{}^{80}BrBr$ and $CD_2{}^{80}BrBr$. This suggests that the observed pressure dependency of $CH_3{}^{80}Br$ and $CD_3{}^{80}Br$ is partly due to the increase in the thermal ionic yields with an increase in the pressure. As an approximation, by assuming that the thermal ionic yields of these mono-substituted methanes are 45% of the $CH_2{}^{80}BrBr$ or $CD_2{}^{80}BrBr$ throughout the pressure range, $CH_3{}^{80}Br$ and $CD_3{}^{80}Br$ from the energetic process are estimated to be as is shown in Table 2. The yields increase with the pressure at the beginning and then tend to flatten out, suggesting that the excited $CH_3{}^{80}Br$ and $CD_3{}^{80}Br$ are stabilized through the collisional removal of the excitation energy. At low pressures, a considerable fraction of the energetic substitution products seems to decompose. The observed pressure dependency indicates the life-time of these species in the 10^{-8}—10^{-9} sec range. Furthermore, from the smaller significance of the pressure effect on the higher pressure side, it can be inferred that, at pressures of more than 50 cmHg, the excited $CH_3{}^{80}Br$ or $CD_3{}^{80}Br$ can be stabilized well. However, no highly-excited molecules having a life-time much shorter than 10^{-9} sec will be subjected to the present pressure effects.

On the other hand, the behavior of the thermal products in response to the pressure are consistent with either the increase in the collisional frequency of $CH_4Br^{+1}*$ and $CD_4Br^{+1}*$[21] the plausible primary reaction products ($Br^{+1}+CH_4$ or $CD_4=CH_4Br^{+1}*$ or $CD_4Br^{+1}*$), with their surroundings or the collisional stabilization of the products. Unfortunately, on the basis of the present experiments alone it is impossible to distinguish which process is involved here.

The authors are very grateful to Dr. K. Motojima and Dr. M. Koike for their encouragement during the course of the work.

21) E. Tachikawa and J. Okamoto, *Radiochim. Acta*, (in press).

BULLETIN OF THE CHEMICAL SOCIETY OF JAPAN VOL. 43 1298—1302 (1970)

The Anodic Oxidation of a Propionate-Propionic Acid Solution in the Presence of Several Organic Compounds

Akira KUNUGI, Toshiyuki SHIMIZU and Shigeo NAGAURA

Department of Applied Chemistry, Faculty of Engineering, Osaka City University, Sugimoto-cho, Sumiyoshi-ku, Osaka

(Received September 26, 1969)

The anodic oxidation of the propionate anion in aqueous solutions of propionic acid at a platinum electrode has been studied in the presence of several organic compounds in order to demonstrate the formation of both propionoxy and ethyl radicals as the reaction intermediates. One of the following organic compounds was added to each solution: two vinyl monomers (acrylic acid and acrylamide), two alkylbenzenes (toluene and cumene), and two aliphatic alcohols (methanol and isopropanol). The electrooxidation of sodium propionate in the presence of acrylamide resulted in polymerization, which was confirmed to be initiated by the ethyl radical. Acrylic acid, unlike acrylamide, gave no polymers. In this case, both the current efficiency for the formation of carbon dioxide and the yield ratio of ethylene to carbon dioxide were always less than those observed in the absence of acrylic acid. While the addition of alcohols gave no definite results, the addition of toluene or cumene resulted in an appreciable decrease in the yield ratio of ethylene to carbon dioxide, but affecting neither the ratio of ethane to carbon dioxide nor the current efficiency for the carbon-dioxide evolution. These results indicate that the anodic oxidation of the propionate anion proceeds through the consecutive formation of propionoxy and ethyl radicals as the reaction intermediates.

Although many studies have been made of the electrolytic Kolbe reaction, work has mainly been restricted to the acetic acid-acetate system. A few papers have been published on the propionate system.[1-4] The acetate system seems, however, somewhat exceptional in the series of straight-chain fatty acids, because, for instance, the yield efficiency of ethane is exceptionally high (90%) and no olefinic compound is found in the products. Putting aside the acetate system, the relative yield of alkenes increases and that of alkenes generally decreases with an increase in the carbon numbers in the series of straight-chain fatty acids.[5] Accordingly, it might be expected that the propionate system is more adequate for the Kolbe reaction than the acetate system.

The purpose of the present paper is to elucidate in detail the mechanism of the anodic oxidation of the propionate anion in aqueous solutions containing propionic acid. The effects of the presence of several organic compounds on the anodic oxidation of the propionate anion have been studied. Particular attention was paid to the current efficiency for the evolution of carbon dioxide and to the relative yield of ethane and ethylene to carbon dioxide.

1) P. Holeman and K. Clusius, *Ber.*, **70**, 819 (1937).
2) C. L. Willson and W. Lippincott, *J. Amer. Chem. Soc.*, **73**, 4290 (1950).
3) G. S. Pande and S. N. Shukla, *Electrochim. Acta*, **4**, 215 (1961).
4) K. Sasaki, K. Uneyama and S. Nagaura, *ibid.*, **11**, 891 (1966).
5) M. J. Allen, "Organic Electrode Processes," Reinhold Publishing Corp., New York, N. Y. (1958), p. 103.

Experimental

Reagents. Reagent-grade sodium propionate, methanol, toluene, and sodium hydroxide were used without further purification. Propionic acid, acrylic acid, cumene, and isopropanol were distilled under reduced pressure. The acrylic acid distilled was stocked in an ice box. Reagent-grade acrylamide was recrystallized from benzene and dride at about 60°C.

Solutions. An aqueous solution containing 2M propionic acid and 2M sodium propionate was used as the base solution (pH 4.8) for the experiments using acrylic compounds or alcohols. Each solution was made up to 1 or 0.5M. In the case of acrylic acid, sodium hydroxide was added to maintain the same pH as that of the base solution. Toluene and cumene were dissolved in 95% aqueous solutions of propionic acid containing 1M sodium propionate.

Apparatus. The electrolytic cell used in the present experiment was an H-shaped glass vessel having anode and cathode compartments separated by a sintered glass disk. The temperatures were 25 ± 0.3°C for the voltammetric experiments and 5—10°C for the macroscale electrolysis. The electrode used for the voltammetric measurements was a smooth platinum wire, 1.1 cm in

length and 0.03 cm in diameter, sealed at one end of a soft glass tube. The other end of the electrode was fused into a small glass bead to avoid any edge effect. The electrode was then subjected to repeated anodic and cathodic polarizations in a 10% sulfuric acid solution. The electrodes used for the macroscale electrolysis were cut from a sheet of platinum foil and spot-welded to a platinum wire.

Procedures. Cyclic voltammograms were obtained with a Nichia Keiki-type HE-Potentiostat in conjunction with a triangular sweep function generator and with an X–Y recorder, Model XYR–IA, of Toa Denpa, Ltd. Macroscale electrolysis were mainly using a Yanagimoto Model VE-3 controlled potential electrolyser. The current was recorded with a potentiometer-type recorder. The total quantity of electricity passed through was graphically determined.

In the polymerization experiment, the solution was agitated by bubbling in oxygen-free nitrogen gas before and during the electrolysis. The polymerization products were precipitated by adding a large amount of methanol. The precipitate was purified by repeated dissolution and precipitation, and was finally dried for weighing.

Gases evolved from the anodic chamber were collected in a gas buret. The first 60 cc portion of the gas was thrown away in order to avoid any error caused by air in the dead space. The composition of the sample gas was analysed by means of a Yanagimoto GCG-220 gas chromatograph equipped with an active charcoal column. The current efficiency for the formation of carbon dioxide was calculated by assuming that one mole of the gas corresponds to two faradays.

All the potential measurements are referred to the SCE with a salt bridge.

Results and Discussion

Cyclic Voltammetry. Shukla[3] reported that the current-potential curves for the propionate oxidation were monotonous and that the anode potential increased with an increase in the current density applied. This is in contrast with the curves observed with acetate, which exhibit a shoulder prior to the final rise of the current. The current-potential curve for the propionate oxidation has, therefore, been re-examined using the potential sweep method. When the anode potential was swept from 0.4 to 2.5 V (*vs.* SCE), the curve in the first sweep was monotonous, but a shoulder appeared at about 2.0 V in the succeeding sweeps. The critical potential*1 was dependent on both the sweep rate and propionate concentration, as in the case of the acetate oxidation.[6]

In Fig. 1, similar curves obtained with acrylic acid and acrylamide are shown by curves B and C respectively. It should be noted that the curve B, which was obtained in the presence of acrylic acid, exhibits a shoulder at a higher potential region than the curve A. Such a shoulder is not seen, however, in the curve C for the acrylamide solution. Similar behavior in acrylic compounds was observed in the acetic acid-acetate system,[7] although the reason why the critical potential shifted was uncertain.

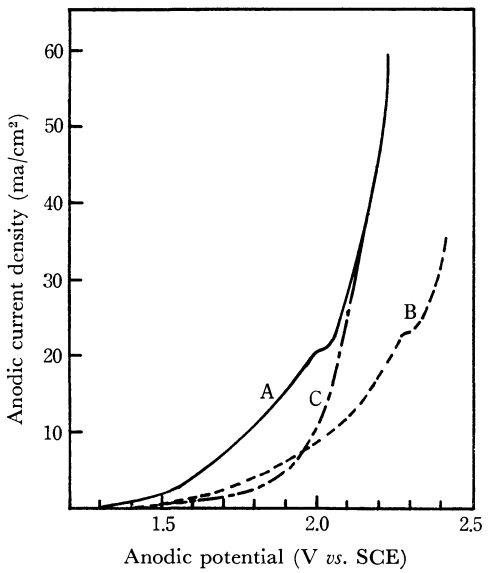

Fig. 1. Current-potential characteristics of aqueous propionate solutions with and without vinyl monomers.
A: 0.5M sodium propionate and 0.5M propionic acid with no additives
B: with 1.0M acrylic acid
C: with 1.0M acrylamide
pH of all solutions; 4.8, Potential sweep rate; 0.1 V/sec.

Electroinitiated Polymerization. In order to examine whether or not the anodic oxidation of propionate proceeds through the radical intermediate, a series of experiments on the electropolymerization of acrylic acid in aqueous propionate solutions has been carried out. The electrolysis of solutions containing 1M sodium propionate, 1M propionic acid, and 1.9M acrylic acid under constant-current conditions gave polymers in the cathodic chamber. No polymerization was observed in the anodic chamber, even when the anode potential was as high as 2.5 V (*vs.* SCE). When acetate was used in place of propionate, olygomers were obtained in the anodic chamber under similar conditions.[8] The reason why no polymer was obtained with propionate could be attributed to the fact that neither radical species was included in the anodic process of propionate, or to the fact

*1 The potential corresponding to the shoulder is called the "critical potential."

6) A. Kunugi, S. Iseki, K. Ohashi and S. Nagaura, *Denki Kagaku*, **36**, 237 (1968).

7) I. Izumi, A. Kunugi and S. Nagaura, to be published.

8) I. Izumi, A. Kunugi and S. Nagaura, *Mem. Fac. Eng. Osaka City Univ.*, **9**, 59 (1967).

TABLE 1. THE EFFECT OF VINYL MONOMERS ADDED ON THE COMPOSITION OF ANODIC GASES IN THE ELECTROLYSIS OF AN AQUEOUS SOLUTION OF 1.0M SODIUM PROPIONATE AND 1.0M PROPIONIC ACID AT 27 ma/cm²

Monomer added	Composition of gases (volume %)						Current efficiency for CO_2 evolution (%)*	Volume ratio of C_2H_4/CO_2
	O_2	CO	CO_2	C_2H_2	C_2H_4	C_2H_6		
None	1.1	trace	52.1	—	46.3	0.3	73.0	0.89
Acrylic acid** (1.3M)	36.8	trace	43.2	1.5	18.2	0.2	42.8	0.42
Acrylamide (1.3M)	0.1	trace	57.6	—	40.6	0.9	74.0	0.71

* Calculated as required two faradays for 1 mol of CO_2 evolved.
** pH was adjusted to 4.8 by adding NaOH solution

that the products formed were of a very low molecular weight, such as the dimer or the trimer.*2

In order to make this point clear, gases evolved from the anodic chamber were analysed. Table 1 summarizes the experimental results on the propionate solution with and without acrylic acid. It is evident from the table that there is a marked decrease in the current efficiency for the formation of carbon dioxide when acrylic acid is present. The yield ratio of ethylene to carbon dioxide also decreases in the presence of acrylic acid. This probably indicates that both propionoxy and ethyl radicals attack the acrylic acid molecule to form its dimers or trimers. It seems, therefore, probable to assume that acrylic acid itself does not participate in the charge-transfer reaction and that the propionate ion is the only species which is electroactive. Exploratory experiments showed that the anodic oxidation of acrylic acid (1.0M) at 2.6 V in a 0.5M sodium hydroxide solution at 25±3°C resulted in a minor formation of carbonaceous compounds, while gases consisting mainly of oxygen (more than 95%), plus minor portions of carbon dioxide, ethylene, acetylene, and carbon monoxide, were detected.

A series of studies of the electroinitiated polymerization was undertaken, using acrylamide as a monomer. With this substance, polymers were obtained in both the anodic and the cathodic chambers. The polymer yields at the anode electrode were found to increase linearly with increases in the concentrations of both propionate and acrylamide. When sodium sulfate and sulfuric acid were used in place of sodium propionate and propionic acid as electrolytes, the polymerization of acrylamide did not occur, suggesting that the presence of the propionate anion is essential for the polymerization. In addition, the presence of *p*-benzoquinone was found to inhibit the polymerization totally. This indicates that the polymerization of acrylamide under the present conditions was initiated by radicals originating from the propionate oxidation, while, on the other hand, *p*-benzoquinone trapped radicals to inhibit the polymerization.

The analysis of gases evolved from the propionate-acrylamide system showed that the addition of acrylamide resulted in a decrease in the yield ratio of ethylene to carbon dioxide. No appreciable change was observed in the current efficiency for the formation of carbon dioxide (see Table 1). On the basis of these findings, it can be concluded that the polymerization of acrylamide is initiated by the ethyl, not by propionoxy, radicals.

Effect of Aromatic Hydrocarbons. The base solution used in the experiment described here was composed of propionic acid containing 1M sodium propionate and 5% water. A desired quantity of the aromatic compounds was dissolved in this solution. Upon the electrolysis of the base solution, the anodic gases produced were almost entirely carbon dioxide and ethylene in a mole ratio of approximately 1 to 0.35. The formation of carbon dioxide required 2 F per mole. Other gaseous products (oxygen, ethane, and carbon monoxide) were also found (see Table 2). The addition of two aromatic hydrocarbons, toluene and cumene, to

TABLE 2. THE EFFECT OF ALKYLBENZENES ADDED ON THE COMPOSITION OF ANODIC GASES IN THE ELECTROLYSIS OF A SOLUTION OF 1.0M SODIUM PROPIONATE IN PROPIONIC ACID CONTAINING 5% WATER AT 14ma/cm²

Alkylbenzene added	Composition of gases (volume %)					Current efficiency for CO_2 evolution (%)	Volume ratio of C_2H_4/CO_2	Volume ratio of C_2H_6/CO_2
	O_2	CO	CO_2	C_2H_4	C_2H_6			
None	0.8	trace	70.2	24.2	4.7	85.0	0.35	0.07
Toluene (1.92M)	1.5	trace	77.5	14.9	6.0	86.0	0.19	0.08
Cumene (2.0M)	1.5	trace	71.5	20.6	6.4	82.6	0.29	0.09

*2 Neither a dimer nor a trimer is precipitated by the method used here.

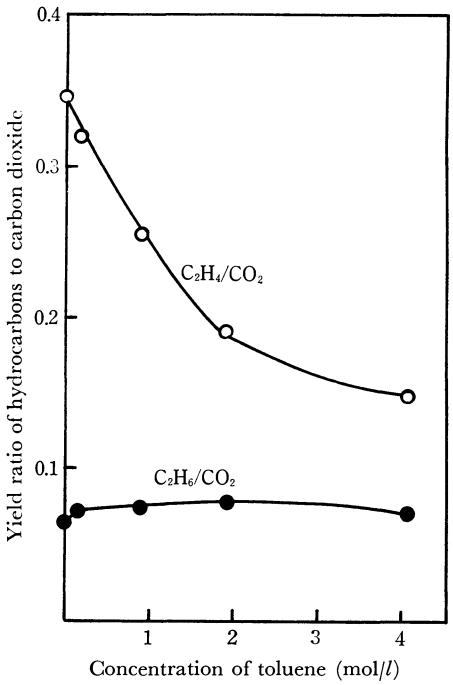

Fig. 2. The effect of the concentration of toluene added on the composition of gases evolved. Solution: 1.0M sodium propionate in propionic acid containing 5% water.

the solution resulted in profound changes in the composition of the gases produced during the electrolysis (see Table 2). The following discussion is based on the assumption that either the aromatic substrates examined in the present study are totally inactive to the electrooxidation or, even if they were oxidized, the oxidation is incomplete and no carbon dioxide is formed. If this assumption is acceptable, the determinations of the relative yields of the gases evolved, namely, ethane to carbon dioxide and ethylene to carbon dioxide, will serve as a sensitive means for the discussion of the mechanism of the reaction concerned. If the ethyl radical originating from propionate abstracts the hydrogen atom in the aromatic substrate, the ethane to carbon dioxide ratio will increase and the ethylene-to-carbon dioxide ratio will decrease. On the other hand, if the radical species effective in the hydrogen abstraction is propionoxy instead of the ethyl radical, the yield ratio of ethane to carbon dioxide will remain constant and the ratio of ethylene to carbon dioxide will vary with the type of termination reaction.

The experimental results are summarized in Table 2 and also in Fig. 2. It is evident from the table that the ethylene-to-carbon dioxide ratio is significantly decreased, while the ethane-to-carbon dioxide ratio was unchanged, when toluene or cumene was present. It should be noted that the ethan formation was not affected by changing the aromatic substrate from toluene to cumene, since it is accepted[9] that the rate of hydrogen abstraction is much greater in cumene than toluene. The current efficiency for the carbon dioxide evolution was found unaffected by the presence of the aromatic substrates. The results in Fig. 2 indicate that the ethylene-to-carbon dioxide ratio decreases and the ethane-to-carbon dioxide ratio increases, though slightly, with an increase in the concentration of toluene. Accordingly, two possibilities can be considered: (1) the hydrogen atom is abstracted from the side chain of aromatic substrates by the propionoxy radical, and the resultant benzyl radical combines with the ethyl radical, and (2) hydrogen abstraction occurs at the aromatic ring by means of the propionoxy radical and the aromatic radical so generated combines with the ethyl radical.

Ross and his co-workers[10] have reported that, when the acetic acid-acetate system was electrolyzed in the presence of ethylbenzene, the methylation occurred to both the side chain and the aromatic ring with greater ease than with the side-chain methylation. This indicates that the possibility (1) is the preferred reaction mode. The anodic oxidation of the propionate ion in the presence of an aromatic substrate, *e.g.*, toluene, can thus be considered to proceed in the following manner:

$$2C_2H_5CO_2^- \longrightarrow 2C_2H_5CO_2\cdot + 2e$$

$$C_2H_5CO_2\cdot \longrightarrow C_2H_5\cdot + CO_2$$

$$C_6H_5CH_3 + C_2H_5CO_2\cdot \longrightarrow C_6H_5CH_2\cdot + C_2H_5CO_2H$$

$$C_6H_5CH_2\cdot + C_2H_5\cdot \longrightarrow C_6H_5CH_2C_2H_5$$

Effect of Alcohols Added. Fioshin *et al.*,[11] have reported the effect of alcohol addititives on Kolbe's electrosynthesis. The addition of aliphatic alcohols up to hexanol to aqueous solutions of acetate or mono-methyl adipate increased the yields of ethane or di-methyl sebacate. In the present experiment, however, no such definite effects nor any others of alcohols were observed, as is shown in Table 3.

Mechanisms of the Anodic Oxidation of Propionate. The foregoing discussion revealed that both the propionoxy and ethyl radicals are involved in the anodic oxidation of the propionate anion. It was also confirmed that the yield ratio of ethylene to carbon dioxide was approximately unity, that the ratio of ethane to ethylene was very small (*ca.* 10^{-2}), and that a charge of 2 F was required for the formation of 1 mol of carbon

9) W. A. Pryor, "Free Radical," McGrow-Hill Book Co., New York (1966), p. 170.

10) S. D. Ross, M. Finkelstein and R. C. Petersen, *J. Amer. Chem. Soc.*, **86**, 4139 (1964).

11) M. Ya. Fioshin, G. P. Girina, Yu. B. Vasil'ev, M. V. Khrulev, M. K. Polievktov and A. G. Artem'ev, *Chem. Abstr.*, **56**, 12658 (1962).

TABLE 3. THE EFFECT OF ALCOHOLS ADDED ON THE COMPOSITION OF ANODIC GASES IN THE ELECTROLYSIS OF AN AQUEOUS SOLUTION OF 1.0M SODIUM PROPIONATE AND 1.0M PROPIONIC ACID AT 27 ma/cm²

Alcohol added	Composition of gases (volume %)					Current efficiency for CO_2 evolution(%)	Volume ratio of C_2H_4/CO_2
	O_2	CO	CO_2	C_2H_4	C_2H_6		
None	1.1	trace	52.1	46.3	0.3	73.0	0.89
Methanol (1.0M)	4.3	trace	51.0	44.3	0.3	68.0	0.86
Isopropanol (1.0M)	6.6	trace	51.4	41.4	0.5	70.2	0.81

dioxide. Therefore, two mechanisms can be considered for the formation of ethylene, *i.e.*:

I) Disproportionation reaction;

a) $2C_2H_5CO_2^- \longrightarrow 2C_2H_5CO_2\cdot + 2e$

b) $C_2H_5CO_2\cdot \longrightarrow C_2H_5\cdot + CO_2$

b′) $C_2H_5CO_2\cdot + C_2H_5\cdot \longrightarrow C_2H_4 + C_2H_5CO_2H$

II) Decomposition reaction;

$$C_2H_5CO_2^- \longrightarrow C_2H_5CO_2 + e$$
$$C_2H_5CO_2\cdot \longrightarrow C_2H_5\cdot + CO_2$$
$$C_2H_5\cdot \longrightarrow C_2H_4 + H$$
$$H \longrightarrow H^+ + e$$

or

$$C_2H_5\cdot \longrightarrow C_2H_4 + H^+ + e$$

At the present stage, it is impossible to differentiate the two mechanisms without ambiguity. Wilson and Lippincott[2] have suggested, though, that the anodic formation of ethylene proceeds through a second-order reaction with respect to the reaction intermediate. If this is the case, and if the intermediate with which they are concerned is the propionoxy radical, the mechanism I seems more likely.

On the other hand, the formation of ethane can be accounted for by the radical reactions shown below, where RH is the solvent or solute molecules:

III) $C_2H_5\cdot + C_2H_5\cdot \longrightarrow C_2H_6 + C_2H_4$

IV) $C_2H_5\cdot + RH \longrightarrow C_2H_6 + R\cdot$

Considering the fact that, in the electrolytic oxidation of anions of saturated aliphatic acids, the yield ratio of paraffins to olefines increases with an increase in the carbon numbers in the series of acids, the reaction III seems more favourable for the formation of ethane.

Although ethylene is formed in two ways, *i.e.*, disproportionation between two ethyl radicals (III) and disproportionation between propionoxy and ethyl radicals (I-b′), Reaction I-b′ might be concluded to be the dominant one because of the one-sided formation of ethylene *vs.* ethane.

BULLETIN OF THE CHEMICAL SOCIETY OF JAPAN VOL. 43 1303—1306 (1970)

The Solution Properties of Poly-*o*-methylstyrene

Kimiyoshi MATSUMURA

Department of Chemistry, Aichi Kyoiku University, Nagoya

(Received October 11, 1969)

The solution properties of poly-*o*-methylstyrene in toluene were measured by the light-scattering and viscosity methods, and the results were compared with those obtained from poly-*o*-chlorostyrene and other polystyrene derivatives. The dependencies of the intrinsic viscosity, the second virial coefficient, and the end-to-end distance of the polymer chain on the molecular weight are as follows:

$$[\eta] = 9.22 \times 10^{-5} \cdot M_w^{0.72} \text{ (dl/g)}, \quad A_2 = 3.89 \times 10^{-2} \cdot M_w^{-0.38} \text{ (mol·cc/g}^2\text{)}$$

and $\langle L^2 \rangle^{1/2} = 0.197 \times M_w^{0.62}$ (Å).

It was made clear that the unperturbed dimension of poly-*o*-methylstyrene was larger than that of poly-*p*-methylstyrene, and that the cause of this difference is the large steric repulsion between the side groups of the former. Moreover, the unperturbed dimension of poly-*o*-methylstyrene was smaller than that of poly-*o*-chlorostyrene. From these results, it is considered that the large extension of poly-*o*-chlorostyrene was affected by the electrostatic repulsion between the side groups.

Many authors have reported on the solution properties of polystyrene and its derivatives. These polystyrene derivatives are mainly *p*-substituted polymers, and the results of the experiments show that the unperturbed dimension of the polymer-chain skeleton is affected not by the electrostatic interaction between the substituents placed on the *p*-position of polystyrene, but by the volume of the side group, the *p*-substituted phenyl group, of the polymer.

In a preceeding paper[1] the present author reported his experimental results on poly-*o*-chlorostyrene, which showed that the unperturbed dimension is larger than that of poly-*p*-chlorostyrene. However, the reason for the difference between these two polymers was not made clear.

In this report, by means of light-scattering and viscosity measurements of the poly-*o*-methylstyrene solution, the effect of the substituent on the polymer-chain dimensions are compared with the findings for poly-*o*-chlorostyrene.

Experimental

Sample. The poly-*o*-methylstyrene was prepared from *o*-tolylmethylcarbinol, which had itself been obtained by the Grignard reaction of *o*-bromotoluene and acetaldehyde, by dehydration with potassium bisulfate; bp 34—36°C/4 mmHg.

The monomer was polymerized by heating it in a sealed tube at 90°C for 150 hr without any initiator. The conversion rate was about 60%. The polymer was a jelly-like substance. The polymer was dissolved in hot benzene (*ca.* 20 g/*l*), and the solution was fractionated at 30°C by subsequent precipitation with methanol. Twenty fractions were obtained. They were redissolved in benzene, reprecipitated with methanol, and dried under reduced pressure.

The toluene, used as the solvent, was purified by the method described in a previous paper.[1]

It seemed that poly-*o*-methylstyrene would dissolve in toluene at room temperature. However, the flow time of the solution in the viscometer decreased with the time of heating at 30°C, showing a constant value only after about 18 hr, as is shown in Fig. 1, in which the sample used for the test of the flow time was the fraction 1-1 and the concentration of the solution was about 0.5 g/dl. Therefore, the toluene solution used for the measurements were prepared by heating it at 35—40°C for about 20 hr.

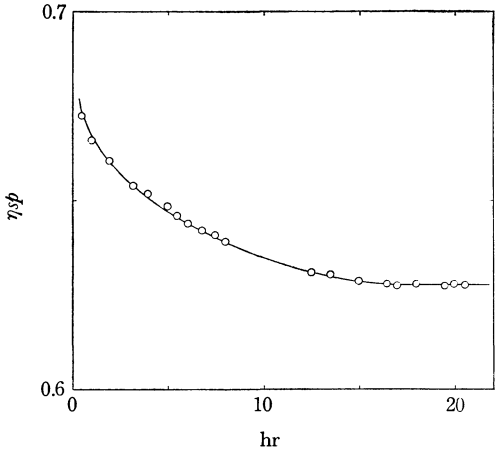

Fig. 1. Relation between the specific viscosity and time of heating at 30°C, for poly-*o*-methylstyrene (Frac. 1-1) in toluene (0.5 g/dl).

1) K. Matsumura, *Makromol. Chem.*, **124**, 204 (1969).

TABLE 1. THE EXPERIMENTAL RESULTS OF THE LIGHT-SCATTERING AND VISCOSITY MEASUREMENTS FOR POLY-*o*-METHYLSTYRENE IN TOLUENE AT 30°C

Fraction	$M_w \times 10^{-4}$	$A_2 \times 10^{-4}$ $(\frac{\text{mol ml}}{g^2})$	$\langle L^2 \rangle^{1/2}$ (Å)	$[\eta]$ $(\frac{dl}{g})$	k'	$\phi \times 10^{-21}$
1-2	43.0	2.64	616	1.047	0.31	1.9
1-3	42.2	2.90	613	1.023	0.32	1.9
2-1	32.0	3.17	494	0.867	0.34	2.3
2-2	22.2	3.85	416	0.651	0.31	2.0
3-2	17.6	3.86	355	0.564	0.36	2.2
4	14.6	4.25	311	0.476	0.38	2.3
5	10.2	4.80	251	0.368	0.38	2.4

Measurements. A Shimadzu photometer was used for the measurement of the light-scattering of the solutions. The measurements were carried out at 30°C by the use of the 436 mμ and 546 mμ of wavelengths and covering the angular range 40—140°. The increments of the refractive index of the solution with the concentration, dn/dc, were measured at 30°C with the wavelengths of 436 mμ and 546 mμ.

For the viscosity measurements of the solutions at 30°C, a modified Ubbelohde viscometer was used. At 30°C the flow time of toluene was 270.1 sec in this viscometer.

Results and Discussion

Results. By means of the light-scattering measurements, the weight-average molecular weight, M_w, the second virial coefficient, A_2, and the root-mean-square end-to-end distance of the polymer chain, $\langle L^2 \rangle^{1/2}$, were obtained according to the ordinary method by means of a Zimm plot for each fraction. The observed values of dn/dc were 0.120 ml/g for the 436 mμ wavelength and 0.116 ml/g for 546 mμ. An example of the Zimm plot, that for the fraction 1—3 of poly-*o*-methylstyrene in toluene at 30°C for 436 mμ, is shown in Fig. 2.

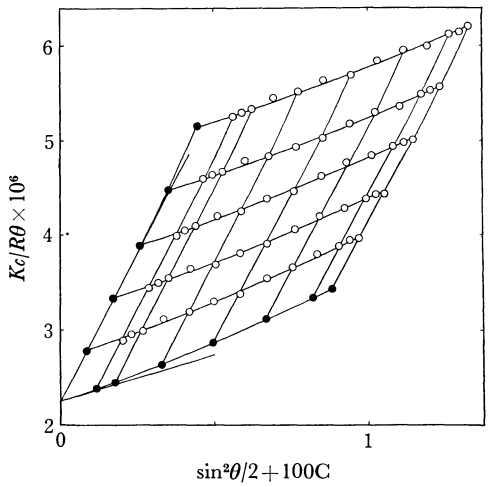

Fig. 2. Zimm plot for poly-*o*-methylstyrene 1—3 in toluene at 30°C for 436 mμ.

Through the viscosity measurements, the intrinsic viscosity, $[\eta]$, and the Huggins constant, k', shown in Fig. 3 are obtained.

These results are shown in Table 1.

The molecular-weight dependencies of $[\eta]$, A_2, and $\langle L^2 \rangle^{1/2}$ are obtained by means of the log–log relations between M_w and these values; they are shown in Figs. 4, 5, and 6 respectively. By the least-squares method, these relations are found to be as follows:

$$[\eta] = 9.22 \times 10^{-5} \cdot M_w^{0.72} \text{ (dl/g)},$$
$$A_2 = 3.89 \times 10^{-2} \cdot M_w^{-0.38} \text{ (mol·cc/g}^2\text{)},$$
$$\langle L^2 \rangle^{1/2} = 0.197 \times M_w^{0.62} \text{ (Å)}.$$

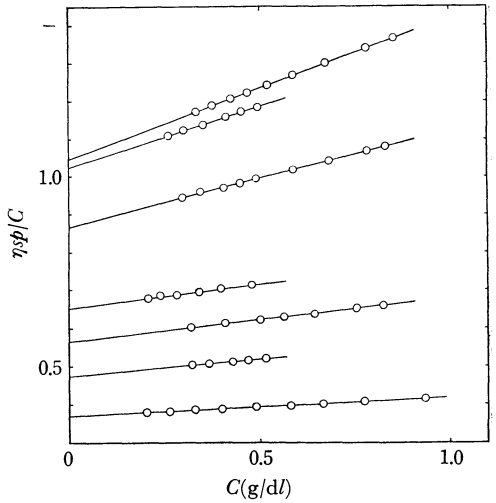

Fig. 3. Relation between reduced viscosity and concentration of poly-*o*-methylstyrene in toluene at 30°C.

TABLE 2. THE EFFECT OF TOLUENE ON THE EXPANSION OF POLY-*o*-METHYLSTYRENE AND POLYCHLOROSTYRENES P_w =4240

Polymer	Temp(°C)	$\{\langle L^2 \rangle / \langle L^2 \rangle_0\}^{1/2}$
Poly-*o*-methylstyrene	30	1.47
Poly-*o*-chlorostyrene	35	1.41
Poly-*m*-chlorostyrene	35	1.57
Poly-*p*-chlorostyrene	room temp.	1.48

Discussion. The dotted lines in Figs. 4—6 show the relations between M_w and $[\eta]$, A_2, and $\langle L^2\rangle^{1/2}$ of poly-*o*-chlorostyrene, in toluene at 30°C.[1] For the same molecular weight, these poly-*o*-methylstyrene values are larger than those of poly-*o*-chlorostyrene, as the figures show.

To ascertain the effect of the side group of poly-*o*-methylstyrene on the unperturbed dimension of the polymer-chain skeleton, the K_θ value was calculated by the Stockmayer-Fixman relation,[2] where $K_\theta=[\eta]_\theta/M^{1/2}=\Phi_0(\langle L^2\rangle_0/M)^{3/2}$, where $[\eta]_\theta$ is the intrinsic viscosity at the theta state, where $\langle L^2\rangle_0$ is the unperturbed dimension, and

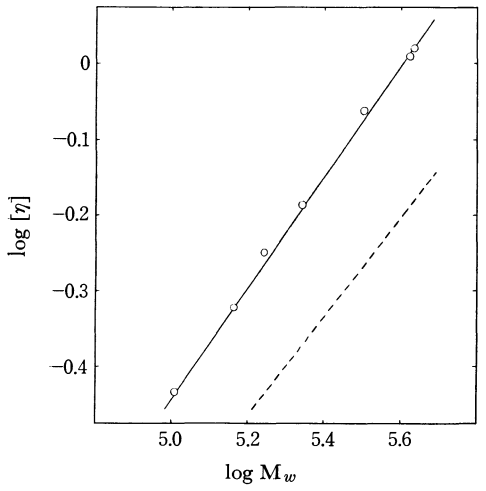

Fig. 4. Molecular weight dependencies of the intrinsic viscosities for poly-*o*-methylstyrene in toluene at 30°C. A dotted line is corresponding to poly-*o*-chlorostyrene.

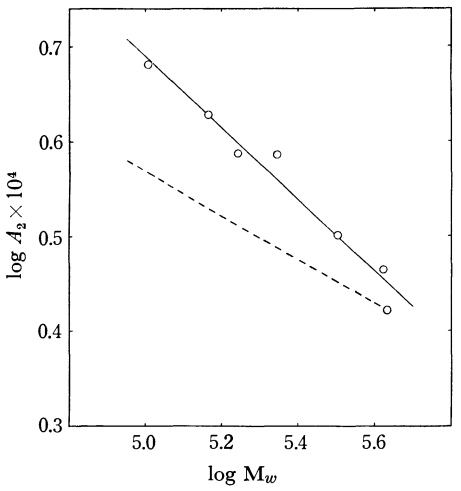

Fig. 5. Molecular weight dependencies of the second virial coefficients for poly-*o*-methylstyrene in toluene at 30°C.

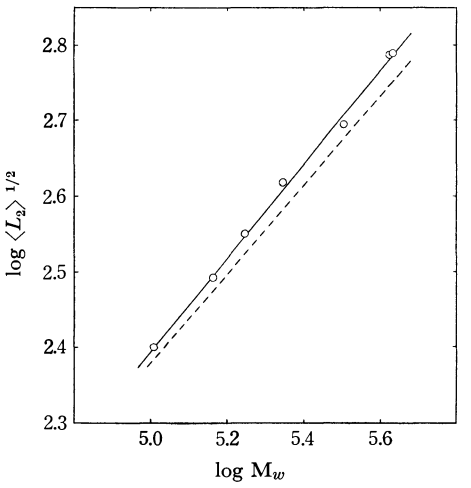

Fig. 6. Molecular weight dependencies of the end-to-end distances for poly-*o*-methylstyrene in toluene at 30°C.

where Φ_0 is the Flory parameter at the theta state, for which the value of 2.87×10^{21} is assumed in this paper.

As is shown in Fig. 7, K_θ was found as 7.75×10^{-4} by the least-squares method. By the use of this K_θ value, the value of $\{\langle L^2\rangle_0/M\}^{1/2}$ was calculated as 0.646 (Å), and the value of σ, $\{\langle L^2\rangle_0/\langle L^2\rangle_{0f}\}^{1/2}$, was obtained as 2.27, where $\langle L^2\rangle_{0f}$ is the mean-square end-to-end distance with the fixed valence angle of 109.5° for the carbon atom, but where there is a completely free internal rotation of the polymer-chain skeleton.

This σ value, 2.27, is slightly larger than that of poly-*p*-methylstyrene obtained by osmotic-pressure measurements at 30°C, 2.17.[3] It can, therefore,

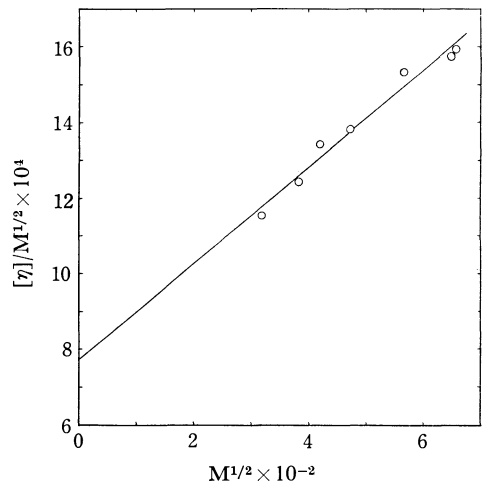

Fig. 7. Viscosity plots for poly-*o*-methylstyrene in toluene at 30°C.

2) W. H. Stockmayer and M. Fixman, *J. Polym. Sci., Part C*, **1**, 137 (1963).

3) N. Kuwahara, K. Ogino, A. Kasai, S. Ueno and M. Kaneko, *J. Polym. Sci., Part A*, **3**, 985 (1965).

be considered that the chain of poly-*o*-methylstyrene extends further than that of poly-*p*-methylstyrene. The difference between the σ values of these two polymers is caused by the steric repulsion between the neighboring side groups resulting from the difference in the substituted position of the methyl group on the phenyl group, as the strong electrostatic repulsions between the side groups for these polymers can not be considered.

The σ value, 2.27, for poly-*o*-methylstyrene is smaller than that for poly-*o*-chlorostyrene, 2.42.[1] Therefore, it can be considered that the extension of the poly-*o*-methylstyrene chain is smaller than that of the poly-*o*-chlorostyrene chain.

Kuwahara *et al.* concluded, from a comparison with the σ values for *p*-substituted polystyrene ($\sigma=$ 2.15 for poly-*p*-chlorostyrene, $\sigma=2.17$ for poly-*p*-methylstyrene, *etc.*) found by osmotic-pressure and viscosity measurements, that the chain conformations of these polymers are not so much affected by the electrostatic interaction between the polar side groups as by the molar volumes of the side groups, the effect of these on the polymer chain being the steric one.[3]

The molar volume of the side group of poly-*p*-methylstyrene and that of the side group of poly-*o*-methylstyrene are equal to that of toluene, 107.3 cc, and the molar volume of the side group of poly-*p*-chlorostyrene and that of the side group of poly-*o*-chlorostyrene are the same as that of chlorobenzene, 102.7 cc. Therefore, according to the findings for poly-*p*-substituted styrene, it can be considered that the difference between the σ value of poly-*o*-methylstyrene and that of poly-*o*-chlorostyrene must be a fairly small one as long as the steric effect of the side group on the chain conformation of these polymers is preferred to the electrostatic repulsion between the side groups. However, when we compare the findings for these polymers the difference between the σ values is fairly large.

From these considerations, it can be considered that the contribution of the electrostatic repulsion between the polar side groups, *o*-$Cl \cdot C_6H_4$, to the extension of the poly-*o*-chlorostyrene chain is fairly large.

The author wishes to thank Professor Akira Kotera for his kindly advice.

BULLETIN OF THE CHEMICAL SOCIETY OF JAPAN VOL. 43 1306—1312 (1970)

The Crystal Structure of 1-Ethyl-2-methylquinolinium Iodide, $[(C_{12}H_{14}N)^+ \cdot I^-]$

Seiki SAKANOUE,*1 Yasushi KAI, Noritake YASUOKA, Nobutami KASAI*2 and Masao KAKUDO

Department of Applied Chemistry, Faculty of Engineering, Osaka University, Yamadakami, Suita, Osaka

(Received November 11, 1969)

The crystal structure of an organic charge-transfer complex, 1-ethyl-2-methylquinolinium iodide, $[(C_{12}H_{14}N)^+ \cdot I^-]$, has been determined by means of three-dimensional X-ray data (Mo$K\alpha$). The crystals are monoclinic, space group $P2_1/c$, and have four formula units in a unit cell with the dimensions of $a=7.187\pm0.002$, $b=15.914\pm0.002$, $c=10.331\pm0.002$ Å, and $\beta=94.67\pm0.01°$. The structure is built up from an iodide anion and a planar 1-ethyl-2-methylquinolinium cation, which lie roughly on a plane. The cations are stacked approximately parallel to the a-plane, forming an endless column along the a axis; the interplanar spacings of these cations are alternately 3.4 and 3.6 Å. The iodide anions are located in the spaces between these columns and the ethyl groups of the cations. The closest distance between an iodide anion and the carbon atoms of a 1-ethyl-2-methylquinolinium ring is 3.93 Å.

The charge-transfer interaction of *N*-heteroaromatic iodide complexes in solution, in particular, the solvent effect and the effect of different cations on the transition energies, has been studied by Kosower[1] and by Mason.[2] The characteristic coloration of these complexes in the solid state seems to be due to the interaction between the *N*-heteroaromatic cation and the iodide anion.

It seemed that it would be interesting to obtain

*1 Present address: Research Laboratories, Ashigara, Fuji Photo Film Co. & Ltd., Minami-Ashigara, Kanagawa, 250-01.

*2 To whom any correspondence should be addressed.

1) E. M. Kosower, *J. Amer. Chem. Soc.*, **80**, 3253, 3261, and 3267 (1958).

2) S. F. Mason, *J. Chem. Soc.*, **1960**, 2437.

information on the crystal structure by which to elucidate the charge-transfer interaction. A series of crystal structure analyses of several organic charge-transfer complexes has thus been carried out, and some preliminary results have already been reported.[3,4] This paper will deal with the crystal structure determination of 1-ethyl-2-methylquinolinium iodide, $[(C_{12}H_{14}N)^+\cdot I^-]$.

Experimental

Yellowish-green crystals of 1-ethyl-2-methylquinolinium iodide, $[(C_{12}H_{14}N)^+\cdot I^-]$, were supplied by Professor Hiroshi Mikawa of this university. A small, regular-shaped crystal was selected for investigation. Although the approximate cell dimensions had previously been determined by Neuhaus,[5] they were redetermined accurately on a Rigaku on-line controlled four-circle diffractometer with Mo$K\alpha_1$ radiation (λ=0.70926 Å).

The crystals obtained by the recrystallization from an ethanol solution are monoclinic with unit cell dimensions of $a=7.187\pm0.002$, $b=15.914\pm0.002$, $c=10.331\pm0.002$ Å, and $\beta=94.67°\pm0.01$. The density, 1.689 g·cm^{-3}, was determined at 14°C by flotation in a carbon tetrachloride-methyl iodide mixture, while the calculated value is 1.687 g·cm^{-3}, assuming four formula units per unit cell.

The space group, $P2_1/c$, was uniquely determined from the systematic absences of reflections ($h0l$ with $l\neq2n$, $0k0$ with $k\neq2n$).

The intensity data were collected at room temperature on the diffractometer by the ω-2θ scan technique:

Range of ω-scan$=1.0°+0.35\tan\theta_c$ and

Starting angle of the scan$=\theta_s-0.5°$,

where θ_c is the calculated value of the Bragg angle of the reflection to be measured. At the end of each scan the background scattering was measured for 10 sec by the stationary-crystal stationary-counter technique. The intensity was then corrected for the background scattering and for the Lorentz-polarization effects on an Aicom-C2 computer attached to the diffractometer. All the reflections within a range of $(\sin\theta)/\lambda=0.57$ were measured; in all, 1841 independent non-zero reflections were obtained.

Determination of the Structure

The position of the iodide anion was readily deduced from a three-dimensional Patterson map; the positions of the remaining atoms were found on successive three-dimensional electron density maps based on the phases determined by the iodide anion. The calculation of the structure factors with an isotropic temperature factor, B, of 3.0 Å^2 for all non-hydrogen atoms gave a discrepancy factor, $R=\sum||F_o|-|F_c||/\sum|F_o|$, of 0.25.

The parameters of the I, N, and C atoms were then refined by the block-diagonal least-squares

Table 1. (a) The final atomic co-ordinates along with their estimated standard deviations within parentheses each multiplied by 10^2 (Å)

Atom	X	Y	Z
I	0.1650 (0.1)	0.1850 (0.1)	0.0238 (0.1)
N	0.7494 (1)	0.0861 (1)	0.3353 (1)
C (1)	0.6839 (2)	0.0609 (2)	0.0973 (2)
C (2)	0.7000 (1)	0.0363 (1)	0.2339 (2)
C (3)	0.6613 (2)	−0.0529 (2)	0.2635 (2)
C (4)	0.6808 (2)	−0.0827 (2)	0.3853 (2)
C (5)	0.7356 (1)	−0.0252 (2)	0.4909 (2)
C (6)	0.7644 (2)	−0.0601 (2)	0.6221 (2)
C (7)	0.8228 (2)	0.0009 (2)	0.7188 (2)
C (8)	0.8599 (2)	0.0793 (2)	0.6914 (2)
C (9)	0.8313 (2)	0.1168 (2)	0.5662 (2)
C (10)	0.7690 (1)	0.0582 (1)	0.4638 (1)
C (11)	0.7857 (2)	0.1785 (1)	0.3078 (2)
C (12)	0.6070 (2)	0.2284 (2)	0.3291 (2)

(b) The thermal parameters along with their estimated standard deviations each multiplied by 10^4

Atom	β_{11}	β_{22}	β_{33}	β_{12}	β_{13}	β_{23}
I	192 (2)	34(0.4)	107 (1)	18 (2)	28 (3)	5 (1)
N	125(23)	32 (5)	109(15)	−14(19)	55(30)	−10(14)
C(1)	272(47)	64 (11)	88(10)	−57(36)	−49(47)	−14(22)
C(2)	126(29)	26 (6)	134(20)	4(22)	4(38)	−36(18)
C(3)	143(34)	67 (11)	168(27)	−6(32)	44(48)	−37(28)
C(4)	138(32)	25 (6)	187(26)	0(23)	80(46)	−10(20)
C(5)	80(28)	54 (9)	159(23)	30(25)	84(40)	− 9(24)
C(6)	156(37)	71 (11)	166(26)	68(33)	82(49)	50(28)
C(7)	134(34)	75 (12)	147(24)	42(33)	65(46)	42(27)
C(8)	184(40)	92 (14)	130(23)	142(39)	105(49)	27(29)
C(9)	130(31)	64 (10)	99(18)	−9(29)	8(38)	−18(22)
C(10)	80(24)	25 (6)	104(16)	0(19)	50(32)	3(15)
C(11)	222(38)	12 (5)	144(21)	−10(23)	−1(45)	7(17)
C(12)	200(41)	38 (8)	218(32)	2(57)	−21(57)	0(26)

The expression used is: $\exp\{-(\beta_{11}h^2+\beta_{22}k^2+\beta_{33}l^2+\beta_{12}hk+\beta_{13}hl+\beta_{23}kl)\}$.

3) S. Sakanoue, Y. Kai, N. Yasuoka, N. Kasai, M. Kakudo and H. Mikawa, *Chem. Commun.*, **1968**, 176.

4) S. Sakanoue, N. Yasuoka, N. Kasai, M. Kakudo, S. Kusabayashi and H. Mikawa, This Bulletin, **42**, 2408 (1969).

5) A. Neuhaus, *Z. Kristallogr.*, **104**, 403 (1942).

TABLE 2. THE OBSERVED AND CALCULATED STRUCTURE FACTORS

K	FO	FC
H,L= 0 0		
2	36	-21
4	0	12
6	169	173
8	415	-411
10	140	134
12	37	56
14	142	-136
16	113	116
18	48	-41
H,L= 0 1		
1	36	-42
2	121	-103
3	389	-454
4	103	95
5	376	399
6	122	-112
7	45	-45
8	20	-19
9	141	-144
10	22	31
11	219	207
12	41	-32
13	151	-154
14	0	6
15	31	22
16	25	21
17	51	56
18	0	-16
H,L= 0 2		
0	315	335
1	80	-93
2	270	-309
3	60	-36
4	81	-71
5	71	56
6	248	249
7	65	-71
8	257	-264
9	73	63
10	127	125
11	27	-25
12	24	18
13	13	-19
14	111	-106
15	31	31
16	109	111
17	30	-26
H,L= 0 3		
1	213	217
2	144	-132
3	373	-387
4	77	85
5	249	254
6	135	-142
7	122	-132
8	0	-13
9	99	-103
10	100	102
11	210	219
12	36	-37
13	85	-85
14	49	53
15	16	8
16	0	8
17	59	51
H,L= 0 4		
0	306	313
1	266	-255
2	142	-146
3	64	76
4	28	47
5	106	103
6	267	257
7	115	-118
8	181	-180
9	117	122
10	82	80
11	41	-36
12	27	1
13	65	-67
14	109	-106
15	50	56
16	77	75
17	37	-41
H,L= 0 5		
1	27	18
2	108	-109
3	219	-218
4	184	184
5	145	137
6	121	-121
7	34	-32
8	20	-36
9	70	-64
10	104	100
11	96	103
12	86	-89
13	77	-80
14	49	51
15	17	8
16	20	10
H,L= 0 6		
0	159	159
1	176	-176
2	129	-133
3	48	48
4	19	-8
5	68	69
6	99	96
7	137	-136
8	107	-113
9	90	96
10	59	63
11	45	-39
12	34	35
13	43	-41
14	57	-50
15	70	61
H,L= 0 7		
1	39	36
2	135	-139
3	108	-111
4	171	172
5	80	80
6	99	-98
7	0	0
8	8	1
9	35	-26
10	95	100
11	59	66
12	80	-84
13	35	-36
14	30	33
H,L= 0 8		
0	52	53
1	117	-117
2	6	-15
3	83	88
4	24	16
5	87	94
6	43	45
7	117	-113
8	50	-47
9	77	80
10	0	6
11	0	-30
12	21	2
13	39	-44
H,L= 0 9		
1	31	20
2	95	-94
3	33	-35
4	104	102
5	24	8
6	68	-64
7	19	-14
8	14	-6
9	29	-15
10	63	59
11	14	10
H,L= 0 10		
0	0	12
1	94	-90
2	8	-2
3	37	35
4	0	0
5	40	36
6	3	8
7	79	-78
8	0	-10
9	56	58
H,L= 0 11		
1	18	2
2	55	-55
3	26	9
4	71	68
5	0	-7
6	43	-40
H,L= 1-11		
1	12	22
2	40	30
3	44	-50
4	34	-37
5	48	51
6	35	23
H,L= 1-10		
0	86	89
1	36	34
2	54	-58
3	12	-26
4	6	-9
5	29	-24
6	57	54
7	43	38
8	67	-66
9	31	-30
H,L= 1 -9		
1	25	32
2	74	69
3	132	-126
4	19	4
5	92	96
6	36	37
7	25	-24
8	0	-6
9	51	-46
10	27	-24
11	71	74
H,L= 1 -8		
0	190	191
1	0	1
2	88	-87
3	38	-36
4	13	5
5	15	-11
6	92	94
7	21	23
8	116	-122
9	7	-3
10	52	54
11	7	9
12	20	15
13	0	0
H,L= 1 -7		
1	95	97
2	12	4
3	170	-173
4	20	-13
5	148	151
6	11	-2
7	32	-38
8	16	13
9	64	-62
10	8	4
11	103	103
12	16	14
13	76	-78
14	22	-5
H,L= 1 -6		
0	266	267
1	12	-3
2	149	-149
3	25	25
4	0	-9
5	26	19
6	156	153
7	52	-57
8	224	-226
9	10	-24
10	57	59
11	29	-24
12	10	18
13	15	-6
14	82	-82
15	72	20
H,L= 1 -5		
1	79	83
2	146	-127
3	320	-313
4	48	49
5	202	202
6	41	-46
7	57	-53
8	8	17
9	47	-48
10	90	88
11	170	165
12	39	-35
13	86	-84
14	11	11
15	21	12
16	0	4
H,L= 1 -4		
0	291	296
1	154	-150
2	163	-162
3	62	65
4	16	29
5	30	35
6	208	202
7	87	-89
8	211	-208
9	84	79
10	92	99
11	26	-16
12	36	25
13	47	-35
14	70	-76
15	17	34
16	88	82
17	30	-26
H,L= 1 -3		
1	144	147
2	152	-146
3	320	-316
4	164	157
5	273	260
6	114	-107
7	39	-38
8	44	-41
9	126	-123
10	105	94
11	152	152
12	63	-64
13	148	-143
14	86	77
15	0	1
16	22	19
17	52	45
H,L= 1 -2		
0	335	365
1	297	-296
2	331	-304
3	81	76
4	13	-25
5	112	95
6	172	161
7	265	-258
8	242	-228
9	162	160
10	100	109
11	38	-43
12	43	43
13	91	-103
14	93	-94
15	67	71
16	65	67
17	56	-54
H,L= 1 -1		
1	27	-12
2	295	-313
3	238	-241
4	400	378
5	258	243
6	131	-143
7	22	10
8	44	20
9	48	-39
10	153	139
11	134	134
12	148	-139
13	81	-76
14	54	67
15	25	27
16	29	35
17	49	36
18	64	-59
H,L= 1 0		
0	228	225
1	235	-246
2	155	-150
3	167	192
4	80	-64
5	151	165
6	195	183
7	33	-285
8	145	-138
9	155	182
10	102	92
11	57	-53
12	23	28
13	67	-78
14	73	-70
15	106	91
16	65	65
17	76	-74
18	22	-15
H,L= 1 1		
1	133	135
2	295	-321
3	184	-186
4	451	441
5	149	142
6	174	-164
7	110	-109
8	13	-20
9	97	-90
10	218	208
11	74	82
12	189	-178
13	42	-46
14	95	91
15	0	-21
16	37	34
17	0	18
H,L= 1 2		
0	106	108
1	430	-454
2	10	-15
3	205	184
4	13	9
5	159	156
6	60	67
7	287	-291
8	54	-47
9	209	203
10	7	-12
11	75	-75
12	35	-33
8	83	81
9	84	81
10	32	-35
11	7	-2
12	0	-4
13	38	-34
H,L= 1 9		
1	21	-20
2	28	-36
3	90	85
4	96	97
5	77	-83
6	32	-29
7	57	21
8	0	-10
9	38	29
10	44	41
11	45	-51
H,L= 1 10		
0	67	-75
1	45	-43
2	48	49
3	10	15
4	18	11
5	21	24
6	37	-41
7	46	-38
8	59	57
9	13	26
H,L= 1 11		
1	36	-24
2	34	-25
3	54	52
4	25	32
5	47	-47
H,L= 2-11		
1	28	23
2	20	-25
3	58	-58
4	34	27
5	53	53
H,L= 2-10		
0	81	81
1	54	-47
2	54	-55
3	14	13
4	0	-11
5	29	20
6	39	41
7	39	-41
8	61	-55
9	21	-25
10	184	179
11	75	-74
12	101	-107
13	26	8
14	52	49
15	0	-7
16	30	23
H,L= 1 6		
0	84	-89
1	197	-194
2	77	81
3	59	58
4	0	-9
5	89	88
6	45	-53
7	170	-171
8	75	75
9	98	95
10	19	-20
11	41	-44
12	0	3
13	56	-53
14	10	25
15	73	73
H,L= 1 7		
1	24	-20
2	113	-107
3	69	72
4	150	148
5	72	-71
6	93	-97
7	32	22
8	26	-24
9	30	31
10	91	90
11	44	-39
12	78	-76
13	47	42
14	26	35
H,L= 1 8		
0	157	-156
1	143	-142
2	21	25
3	19	9
4	5	2
5	39	36
6	44	-41
7	88	-93
8	83	81
9	200	202
10	0	14
11	52	-49
12	31	31
13	109	-109
14	0	17
15	88	87
16	0	8
H,L= 2 -3		
1	54	-46
2	238	-232
3	14	1
4	317	319
5	27	-26
6	211	-212
7	21	24
8	39	-27
9	13	12
10	153	148
11	37	-39
12	127	-123
13	8	-2
14	80	81
15	10	0
16	46	28
17	17	2
H,L= 2 -2		
0	158	-152
1	344	-334
2	56	42
3	113	117
4	0	9
5	162	150
6	22	16
7	276	-273
8	36	23
9	219	205
10	34	-33
11	30	-35
12	0	2
13	82	-79
14	0	0
15	114	111
16	21	-19
17	66	-70
H,L= 2 -1		
1	295	263
2	471	-440
3	246	229
4	255	252
5	169	-148
6	228	-230
7	36	-39
8	49	-44
9	22	32
10	214	213
11	84	-72
12	186	-181
13	57	64
14	70	72
15	3	-11
16	26	31
17	23	-16
H,L= 2 0		
13	130	-127
14	42	-33
15	107	105
16	30	28
17	76	-68
H,L= 1 3		
1	45	38
2	240	-242
3	15	22
4	314	303
5	19	11
6	204	-202
7	0	-4
8	51	-47
9	18	-24
10	178	169
11	54	48
12	108	-143
13	28	15
14	97	91
15	20	14
16	17	21
17	0	6
H,L= 1 4		
0	39	32
1	300	-297
2	43	-45
3	128	118
4	60	-51
5	165	162
6	33	-33
7	241	-243
8	21	14
9	173	171
10	23	9
11	53	-52
12	22	28
13	87	-83
14	20	0
15	99	107
16	0	-5
H,L= 1 5		
1	0	-14
2	255	-253
3	103	97
4	221	233
5	23	-28
6	168	-175
7	15	5
8	0	6
9	26	29
H,L= 2 -9		
1	16	23
2	53	-64
3	68	-75
4	52	56
5	99	95
6	54	-56
7	0	-7
8	0	-7
9	38	-30
10	35	41
11	37	51
H,L= 2 -8		
0	99	98
1	101	-104
2	77	-76
3	54	58
4	25	-23
5	71	76
6	67	66
7	89	-86
8	76	-68
9	56	61
10	53	50
11	27	-25
12	0	19
H,L= 2 -7		
1	40	36
2	109	-110
3	91	-86
4	169	161
5	69	70
6	80	-82
7	31	-30
8	9	-4
9	33	-25
10	102	102
11	48	47
12	86	-81
13	35	-32
14	22	29
H,L= 2 -6		
0	56	62
1	206	-200
2	64	-74
3	77	76
4	0	-1
5	84	85
6	58	59
7	141	-139
8	74	-70
9	97	103
10	8	16
11	40	-40
12	0	-3
13	46	-48
14	21	-33
15	76	66
H,L= 2 -5		
1	102	95
2	169	-173
3	43	-42
4	248	245
5	82	80
6	164	-168
7	0	10
8	52	-54
9	27	-33
H,L= 2 1		
1	133	-116
2	265	-250
3	185	188
4	278	262
5	201	-202
6	123	-116
7	71	71
8	21	-11
9	45	44
10	151	142
11	99	-90
12	130	-129
13	71	75
14	66	59
15	15	-10
16	0	13
17	30	-23
H,L= 2 2		
0	190	-181
1	260	-256
2	181	184
3	30	38
4	13	7
5	101	100
6	187	-181
7	223	-219
8	202	196
9	174	182
10	75	-68
11	0	6
12	0	3
13	67	-71
14	70	71
15	84	86
16	85	-83
17	56	-50
H,L= 2 3		
1	123	-116
2	119	-118
3	345	334
4	249	249
5	146	-150
6	72	-73
7	98	93
8	24	-24
9	84	83
10	46	49
11	185	-188
12	111	-107
13	80	80
14	6	16
15	22	-19
16	32	24
H,L= 2 4		
0	312	-314
1	76	-80
2	142	144
3	67	63
4	76	-68
5	60	56
6	192	-186
7	105	-98
8	177	178
9	60	56
10	83	-79
11	0	-7
12	23	-7
13	20	-25
14	78	77
15	31	40
16	69	-71
H,L= 2 5		
1	89	-87
2	73	-77
3	219	216
4	70	71
5	181	-169
6	28	-28
7	39	39
8	28	-18
9	74	68
0	597	-582
1	301	-309
2	93	-75
3	247	232
4	0	-3
5	114	126
6	76	-73
7	264	-267
8	220	212
9	154	154
10	64	-57
11	34	-42
12	68	-21
13	82	-72
14	53	61
15	101	104
16	54	-56
17	50	-52
H,L= 2 6		
0	198	-194
1	50	-48
2	154	157
3	25	20
4	11	17
5	26	28
6	136	-137
7	24	-17
8	160	168
9	20	24
10	84	-81
11	0	8
12	31	-30
13	0	-17
14	73	73
H,L= 2 7		
1	39	-35
2	27	30
3	179	185
4	18	13
5	140	-141
6	7	1
7	34	20
8	16	-20
9	40	35
10	21	-8
11	99	-99
12	0	0
13	62	60
H,L= 2 8		
0	136	-140
1	0	0
2	66	71
3	45	-47
4	15	-3
5	13	-18
6	96	-91
7	10	9
8	95	95
9	8	-6
10	47	-49
11	0	14
12	0	-12
H,L= 2 9		
1	39	-42
2	2	19
3	93	96
4	14	-25
5	80	-81
6	0	9
7	28	23
8	6	-4
9	46	44
10	23	-7
H,L= 2 10		
0	81	-79
1	27	31
2	51	53
3	7	-17
4	14	6
5	2	-13
6	41	-50
7	36	26
H,L= 2 11		
1	17	-23
2	26	23
3	41	40
H,L= 3-11		
1	15	3
2	56	-52
3	13	-9
4	55	56
H,L= 3-10		
0	0	1
1	71	-68
2	0	5
3	55	53
4	12	-8
5	57	52
6	4	-10
7	66	-67
8	0	0
H,L= 3 -9		
1	0	-5
2	107	-108
3	37	37
4	69	64
5	3	-3
6	69	-69
7	0	8
8	15	-4
9	16	6
10	60	64

Table 2 (continued).

K	FO	FC	K	FO	FC	K	FO	FC	K	FO	FC	K	FO	FC	K	FO	FC	K	FO	FC	K	FO	FC
H,L= 3 -8			5	77	75	0	235	-230	4	50	46	7	127	129	9	103	-101	8	23	21	8	46	51	3	33	-29
0	32	-37	6	163	-162	1	117	119	5	84	-86	8	146	149	10	20	2	9	93	-91	9	27	-12	4	80	-83
1	113	-119	7	21	-22	2	156	146	6	0	0	9	92	-87	11	22	31	10	32	-26	10	51	-48	5	35	35
2	20	23	8	242	236	3	60	-57	7	19	10	10	70	-67	12	18	-13	11	27	14	11	99	94	6	44	43
3	45	46	9	50	44	4	67	60	8	0	1	11	19	26	13	51	44	H,L=	5	-5	12	95	94	7	0	1
4	20	-6	10	106	-105	5	95	-93	H,L=	4	-8	12	33	-23	14	7	12	1	34	-31	13	46	-42	H,L=	6	-6
5	44	48	11	0	-5	6	118	-125	0	113	-112	13	24	32	H,L=	4	5	2	98	95	14	38	-35	0	50	41
6	25	-26	12	22	-17	7	92	93	1	129	-14	14	71	84	1	26	27	3	38	37	H,L=	5	2	1	89	89
7	95	-97	13	0	-4	8	160	159	2	84	84	15	63	-57	2	125	121	4	134	-138	0	111	106	2	57	-55
8	38	39	14	105	104	9	70	-71	3	0	-2	H,L=	4	-1	3	0	-19	5	47	-52	1	138	142	3	27	-23
9	71	73	15	39	39	10	103	-103	4	0	8	1	228	-215	4	162	-165	6	80	86	2	86	-88	4	0	-6
10	21	-13	16	85	-78	11	54	49	5	9	1	2	287	275	5	31	31	7	0	-1	3	37	-37	5	13	-25
11	24	-15	H,L=	3	-1	12	64	-63	6	78	-78	3	60	67	6	93	96	8	13	16	4	0	-3	6	25	34
12	0	-4	1	39	-38	13	49	43	7	27	-15	4	101	-92	7	0	-16	9	27	20	5	36	-31	7	79	85
H,L=	3	-7	2	52	-41	14	54	63	8	92	87	5	135	-130	8	17	23	10	77	-77	6	75	72	8	65	-62
1	35	-33	3	295	295	15	43	-45	9	23	21	6	143	143	9	11	7	11	36	-23	7	107	113	9	41	-37
2	102	-100	4	68	61	H,L=	3	5	10	55	-50	7	48	56	10	94	-98	12	70	76	8	104	-103	H,L=	6	-5
3	67	71	5	307	-303	1	66	-67	H,L=	4	-7	8	12	2	11	0	2	H,L=	5	-4	9	90	-90	1	41	39
4	148	153	6	72	-47	2	108	105	1	61	-61	9	102	99	12	90	94	0	34	-33	10	32	36	2	59	65
5	67	-78	7	59	61	3	135	133	2	2	-5	10	130	-132	13	7	-18	1	182	184	11	22	-13	3	83	-81
6	95	-98	8	48	-28	4	129	-124	3	124	127	11	81	-88	H,L=	4	6	2	12	8	12	22	-14	4	73	-73
7	0	0	9	92	78	5	140	-133	4	0	7	12	108	102	0	69	67	3	65	-62	13	27	32	5	76	72
8	47	-41	10	28	35	6	93	93	5	102	-106	13	57	60	1	133	129	4	18	-3	H,L=	5	3	6	33	33
9	0	7	11	143	-150	7	36	38	6	0	-8	14	49	-49	2	26	-22	5	62	-70	1	64	64	7	8	-15
10	69	67	12	28	-32	8	17	-2	7	22	23	15	0	-10	3	39	-35	6	15	-20	2	90	92	8	17	-12
11	33	-37	13	101	97	9	76	70	8	15	-16	H,L=	4	0	4	25	-7	7	144	140	3	125	-124	9	13	-10
12	83	-80	14	8	-3	10	97	-98	9	35	37	0	119	-108	5	73	-72	8	16	18	4	107	-112	10	55	-59
13	22	35	15	28	-18	11	42	-47	10	0	-11	1	171	168	6	20	21	9	96	-102	5	138	137	H,L=	6	-4
H,L=	3	-6	16	26	7	12	45	54	11	81	-82	2	148	148	7	97	91	10	0	-7	6	34	31	0	91	98
0	178	-179	H,L=	3	0	13	67	65	12	0	-3	3	111	-103	8	47	-55	11	26	16	7	33	-30	1	71	72
1	171	-163	0	347	-344	14	44	-44	H,L=	4	-6	4	0	18	9	87	-86	12	23	-12	8	8	9	2	63	-62
2	40	47	1	6	-16	H,L=	3	6	0	145	-146	5	86	-86	10	23	25	13	19	34	9	35	-43	3	19	-18
3	13	21	2	265	258	0	113	-111	1	0	5	6	95	-92	11	19	14	H,L=	5	-3	10	59	-60	4	0	3
4	19	4	3	45	-43	1	130	132	2	143	146	7	192	184	12	0	1	1	8	10	11	56	55	5	48	-44
5	83	79	4	60	47	2	65	67	3	16	-15	8	67	67	H,L=	4	7	3	6	6	12	64	68	6	67	68
6	69	-61	5	31	24	3	46	-42	4	9	10	9	114	-111	1	27	-23	4	162	-161	13	71	-69	7	53	68
7	90	-89	6	263	-260	4	0	3	5	23	-18	10	56	-52	2	49	49	5	41	43	H,L=	5	4	8	81	-77
8	137	138	7	24	-32	5	35	-36	6	103	-104	11	43	44	3	70	-66	6	114	113	0	137	135	9	40	-39
9	133	131	8	215	207	6	77	-75	7	0	-5	12	14	-20	4	111	-112	7	0	-6	1	51	53	10	38	37
10	20	-25	9	36	26	7	96	94	8	137	138	13	46	45	5	46	50	8	21	22	2	93	-91	11	18	4
11	6	-4	10	158	-143	8	92	93	9	21	-10	14	43	44	6	52	56	9	0	7	3	5	-6	H,L=	6	-3
12	0	-10	11	25	23	9	70	-66	10	49	-50	15	68	-75	7	0	-3	10	96	-92	4	21	-16	1	59	64
13	38	-45	12	38	-39	10	29	-30	11	35	13	H,L=	4	1	8	14	16	11	0	9	5	18	-18	2	34	31
14	40	42	13	14	-11	11	34	31	12	21	-13	1	0	-9	9	6	-2	12	108	113	6	75	79	3	104	-101
H,L=	3	-5	14	105	106	12	30	-17	13	0	3	2	164	163	10	45	-42	13	24	0	7	68	69	4	92	-98
1	28	-37	15	20	21	13	34	25	H,L=	4	-5	3	127	128	H,L=	4	8	H,L=	5	-2	8	106	-108	5	104	108
2	89	-89	16	103	-109	H,L=	3	7	1	105	-104	4	246	-248	0	67	64	0	71	67	9	40	-42	6	34	41
3	182	179	H,L=	3	1	1	78	-78	2	31	30	5	93	-93	1	79	78	1	154	148	10	74	74	7	28	-31
4	160	163	1	141	-142	2	87	89	3	175	170	6	135	129	2	29	-35	2	10	1	11	10	-17	8	24	19
5	110	-108	2	31	25	3	74	69	4	61	-58	7	19	19	3	0	-10	3	98	-98	12	40	36	9	46	-49
6	101	-101	3	309	306	4	113	-109	5	174	-174	8	15	11	4	21	3	4	21	-24	H,L=	5	5	10	47	-41
7	38	35	4	65	-58	5	42	-46	6	60	62	9	63	64	5	35	-31	5	115	-114	1	44	53	11	71	74
8	28	-23	5	244	-241	6	71	74	7	21	16	10	102	-93	6	26	31	6	9	-6	2	40	39	H,L=	6	-2
9	45	42	6	13	10	7	14	18	8	34	29	11	65	-70	7	60	64	7	126	137	3	107	-106	0	128	127
10	57	62	7	80	82	8	0	12	9	47	59	12	107	104	8	20	-32	8	32	-34	4	39	-39	1	83	85
11	94	-97	8	4	-15	9	36	38	10	0	-6	13	29	30	9	55	-44	9	115	-113	5	90	91	2	142	-147
12	70	-73	9	126	118	10	67	-63	11	108	-107	14	57	-53	H,L=	4	9	10	30	17	6	22	26	3	62	63
13	61	63	10	57	-62	11	56	-57	12	0	16	15	0	1	1	30	20	11	21	22	7	39	-25	4	42	-37
14	18	29	11	200	-205	12	66	66	13	93	87	H,L=	4	2	2	52	40	12	14	-15	8	0	14	5	23	26
15	11	-12	12	19	16	H,L=	3	8	14	34	-30	0	48	-40	3	44	-45	13	38	40	9	24	-38	6	71	76
H,L=	3	-4	13	106	109	0	0	1	H,L=	4	-4	1	254	252	4	47	-46	14	0	-11	10	25	-16	7	45	46
0	235	-227	14	29	-26	1	104	110	0	209	-206	2	55	53	5	51	47	H,L=	5	-1	11	59	56	8	103	-103
1	168	-165	15	21	-2	2	72	61	1	92	88	3	28	-28	6	35	29	1	23	-7	H,L=	5	6	9	37	-38
2	160	153	16	21	3	3	28	-19	2	114	108	4	57	59	H,L=	5	-9	2	160	159	0	96	100	10	65	65
3	54	52	H,L=	3	2	4	0	0	3	14	-17	5	85	-82	1	26	-21	3	45	-50	1	34	30	11	0	-11
4	8	-19	0	310	-303	5	34	-30	4	0	11	6	48	-45	2	37	41	4	200	-205	2	85	-86	12	26	15
5	82	82	1	82	74	6	48	-46	5	51	-46	7	187	180	3	44	44	5	65	56	3	1	3	H,L=	6	-1
6	135	-133	2	216	215	7	92	93	6	118	-115	8	32	27	4	27	-31	6	110	105	4	0	4	1	95	93
7	145	-136	3	49	-50	8	27	18	7	53	50	9	186	-186	5	41	-56	7	23	-23	5	28	-18	2	24	-25
8	148	145	4	11	-10	9	66	-71	8	166	167	10	39	-40	6	6	37	8	25	15	6	69	70	3	92	-93
9	82	79	5	57	-60	10	20	-15	9	79	-79	11	0	1	H,L=	5	-8	9	32	-17	7	25	18	4	67	-71
10	73	-76	6	178	-175	11	0	9	10	74	-69	12	34	-29	0	77	-68	10	83	-93	8	91	-88	5	133	135
11	27	-15	7	51	53	H,L=	3	9	11	22	22	13	50	59	1	65	70	11	71	27	9	24	-17	6	0	-15
12	27	-20	8	208	199	1	10	-11	12	28	-31	14	21	29	2	54	47	12	105	104	10	32	34	7	42	-41
13	30	-33	9	34	-29	2	60	61	13	40	45	15	82	-81	3	0	-15	13	35	-30	H,L=	5	7	8	27	24
14	33	47	10	55	-58	3	14	24	14	48	50	H,L=	4	3	4	13	-1	14	35	-30	1	77	76	9	71	-67
15	80	74	11	55	54	4	84	-84	H,L=	4	-3	1	28	-29	5	29	-31	H,L=	5	0	2	6	-8	10	22	-7
H,L=	3	-3	12	21	17	5	23	-7	1	92	-96	2	147	144	6	61	-57	0	106	101	3	76	-74	11	70	69
1	146	-136	13	36	32	6	36	43	2	87	85	3	44	-34	7	48	48	1	176	175	4	17	-8	12	25	26
2	95	-94	14	105	99	7	27	1	3	211	206	4	219	-210	8	44	39	2	102	-101	5	56	64	H,L=	6	0
3	251	237	15	32	-21	8	0	0	4	113	-109	5	65	-68	H,L=	5	-7	3	44	-51	6	0	-4	0	158	160
4	135	130	16	89	-76	H,L=	3	10	5	152	-152	6	122	116	1	51	-49	4	18	8	7	35	-33	1	8	20
5	242	-239	H,L=	3	3	0	0	-7	6	58	57	7	6	-15	2	74	69	5	79	-74	8	13	10	2	93	-94
6	65	-68	1	123	-127	1	60	59	7	53	54	8	32	34	3	56	56	6	73	73	H,L=	5	8	3	0	-14
7	50	46	2	60	58	2	27	3	8	0	4	9	0	18	4	86	-90	7	140	144	0	51	51	4	0	-16
8	27	-24	3	218	208	3	31	-24	9	65	65	10	91	-94	5	20	-26	8	55	-59	1	0	-6	5	23	-18
9	99	100	4	82	-86	4	13	2	10	46	-47	11	20	15	6	81	81	9	132	-130	2	50	-57	6	95	106
10	85	81	5	211	-220	5	30	-27	11	108	-104	12	126	120	7	38	40	10	48	46	3	0	0	7	0	8
11	151	-150	6	95	96	H,L=	4	-10	12	63	56	13	17	6	8	22	28	11	0	0	4	0	-3	8	105	-105
12	92	-99	7	47	45	0	67	-69	13	67	66	14	53	-47	9	42	38	12	16	3	5	14	-7	9	0	-8
13	107	110	8	4	-6	1	23	-29	14	37	-44	H,L=	4	4	10	38	-42	13	43	50	H,L=	6	-8	10	59	61
14	23	-3	9	99	100	2	33	41	15	0	-9	0	0	1	H,L=	5	-6	14	0	-23	0	11	20	11	0	-16
15	0	-5	10	45	-37	3	0	17	H,L=	4	-2	1	184	182	0	25	-5	H,L=	5	1	1	58	66	12	26	12
16	0	-1	11	143	-141	4	12	12	0	141	-138	2	5	16	1	111	119	1	49	44	2	18	-20	H,L=	6	1
H,L=	3	-2	12	11	29	5	7	12	1	135	132	3	86	-89	2	58	60	2	106	103	3	15	-17	1	72	68
0	344	-346	13	90	88	6	27	-30	2	203	201	4	17	37	3	22	-33	3	118	-109	4	0	0	2	0	14
1	92	-87	14	36	-31	H,L=	4	-9	3	165	-157	5	84	-84	4	0	13	4	151	-148	5	27	-28	3	140	-141
2	196	196	15	15	-14	1	31	-29	4	31	33	6	6	4	5	56	-62	5	87	88	H,L=	6	-7	4	29	29
3	82	82	16	10	0	2	31	-21	5	94	-91	7	139	136	6	45	-52	6	75	76	1	29	21	5	122	126
4	69	67	H,L=	3	4	3	81	82	6	156	-155	8	21	-6	7	67	69	7	27	-20	2	49	51	6	16	-17

Table 2 (continued).

K	FO	FC	K	FO	FC	K	FO	FC	K	FO	FC	K	FO	FC	K	FO	FC	K	FO	FC	K	FO	FC
7	54	-54	4	31	30	3	76	-76	4	19	-8	3	86	-88	6	44	-39	8	25	-23	2	21	8	0	24	-27
8	14	-10	5	112	113	4	63	64	5	19	4	4	19	22	7	7	-12	9	50	-50	3	24	21	1	65	-56
9	65	-65	6	45	-41	5	47	48	H,L=	7	-5	5	57	56	8	7	-9	H,L=	7	2	4	24	-8	2	29	22
10	0	-11	7	0	-9	6	45	-50	1	36	36	6	47	-44	9	26	-28	0	51	46	5	22	30	3	0	29
11	83	85	8	0	-6	7	11	-16	2	10	-6	7	24	-22	H,L=	7	0	1	93	-88	6	0	8	H,L=	8	1
12	0	-11	9	41	-49	8	17	-1	3	83	-83	8	19	4	0	55	65	2	33	-22	H,L=	7	5	1	26	-38
H,L=	6	2	10	10	18	H,L=	6	6	4	31	21	H,L=	7	-2	1	91	-94	3	26	24	1	17	-6	2	51	-54
0	102	102	11	47	59	0	5	10	5	74	70	0	67	68	2	37	-32	4	0	-3	2	40	-45	3	22	25
1	61	-59	H,L=	6	4	1	53	-53	6	17	-11	1	49	-42	3	31	29	5	27	28	3	11	2			
2	116	-120	0	111	115	2	54	-54	7	30	-11	2	55	-65	4	15	-6	6	28	30	H,L=	8	-3			
3	11	1	1	55	-53	3	21	21	H,L=	7	-4	3	39	47	5	28	25	7	78	-89	1	0	-1			
4	38	-40	2	71	-72	4	0	-3	0	101	100	4	18	-12	6	41	43	8	10	-11	2	26	-28			
5	0	4	3	18	18	5	18	31	1	35	-32	5	38	35	7	47	-53	H,L=	7	3	H,L=	8	-2			
6	81	81	4	5	-6	6	47	53	2	60	-54	6	70	69	8	17	-31	1	0	1	0	21	-6			
7	17	-3	5	23	25	H,L=	6	7	3	22	18	7	45	-50	9	77	80	2	62	-69	1	79	-86			
8	86	-85	6	64	66	1	52	43	4	8	10	8	64	-64	H,L=	7	1	3	25	-9	2	8	22			
9	56	51	7	30	-35	2	35	-30	5	24	15	9	47	42	1	29	22	4	86	93	3	9	-12			
10	68	64	8	69	-73	3	31	-29	6	58	66	H,L=	7	-1	2	46	-54	5	15	0	H,L=	8	-1			
11	0	2	9	35	33	H,L=	7	-6	7	24	-31	1	39	32	3	26	-38	6	47	-41	1	23	-11			
H,L=	6	3	10	32	35	0	43	55	8	58	-62	2	58	-59	4	96	94	7	0	-5	2	45	-46			
1	56	55	H,L=	6	5	1	0	-7	H,L=	7	-3	3	74	-71	5	26	28	H,L=	7	4	3	0	7			
2	18	-23	1	33	31	2	62	-65	1	23	34	4	90	89	6	52	-50	0	9	2	4	71	79			
3	75	-78	2	33	-43	3	0	5	2	56	-63	5	58	68	7	0	-18	1	58	-70	H,L=	8	0			

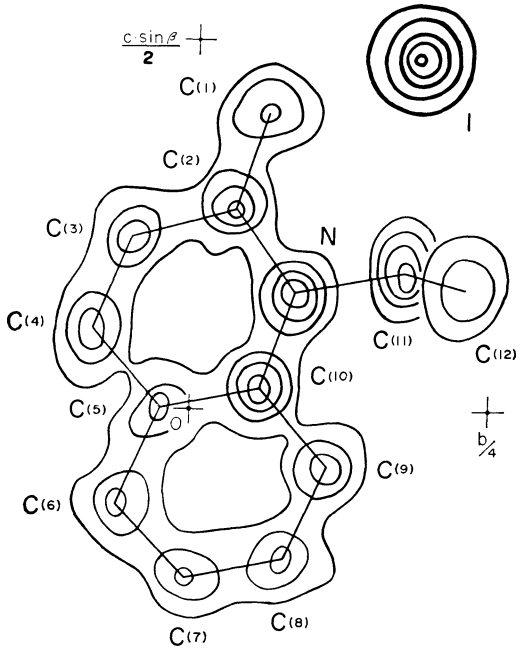

Fig. 1. A composite drawing of the electron density distribution, projected along the *a* axis. Contours at intervals of 1 eÅ^{-3} for the lighter atoms and of 10 eÅ^{-3} (thick lines) for the iodide ion.

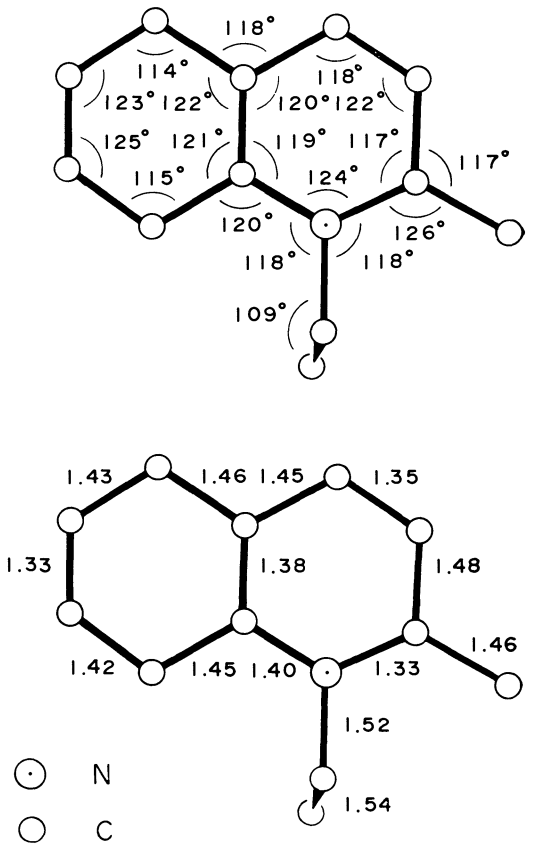

Fig. 2. Bond distances and angles in 1-ethyl-2-methylquinolinium cation. E.s.d.'s are about 0.028 Å and 1.6° respectively.

procedure, and anisotropic thermal parameters were considered. In the refinement, the function minimized was $\sum w(|F_o|-|F_c|)^2$, and the weight, w was taken as unity for all reflections. Using the HBLS IV (UNICS) program,[6] the calculation was done on a HITAC 5020E computer at the University of Tokyo. After 7 cycles of refinement, the R factor was reduced to 0.073 for non-zero reflections (R=0.082 for all reflections). The final atomic co-ordinates and thermal parameters, along with their estimated standard deviations, are listed in Table 1. The observed and calculated structure factors are listed in Table 2. In the calculation the neutral atomic scattering factors used were taken from those of Hanson and his co-workers.[7]

6) "Universal Crystallographic Computation Program System," ed. by Tosio Sakurai, Crystallographic Society of Japan, Tokyo (1967).

7) H. P. Hanson, F. Herman, J. D. Lea and S. Skillman, *Acta Cryst.*, **17**, 1040 (1964).

A composite diagram of the final electron density distributions along the a axis is shown in Fig. 1.

Description and Discussion of the Structure

The skeleton of the 1-ethyl-2-methylquinolinium cation, together with the bond distances and angles, is illustrated in Fig. 2. The estimated standard deviations of the bond distances and angles are about 0.028 Å and 1.6° respectively.

The quinoline ring is planar within the limit of experimental error. The mean plane of the ring is expressed by:

$$-0.9680X + 0.2188Y + 0.1228Z + 4.2243 = 0,$$

where

$$X = ax + cz \cdot \cos\beta,\ Y = by, \text{ and } Z = cz \cdot \sin\beta.$$

The views along the a and c axes of the crystal structure are both shown in Fig. 3. The main feature is that the iodide anions and the planar 1-ethyl-2-methylquinolinium cations lie roughly on a plane. Each iodide anion is surrounded by three cations. The planar cations are stacked approximately parallel to the a-plane, forming an endless column along the a axis. The interplanar spacings of these cations along the column are alternately 3.4 and 3.6 Å; there thus seem to be the usual van der Waals contacts. The iodide ions are located in the spaces between these columns and the ethyl groups of the cations. The closest contact between an iodide ion and the carbon atoms of

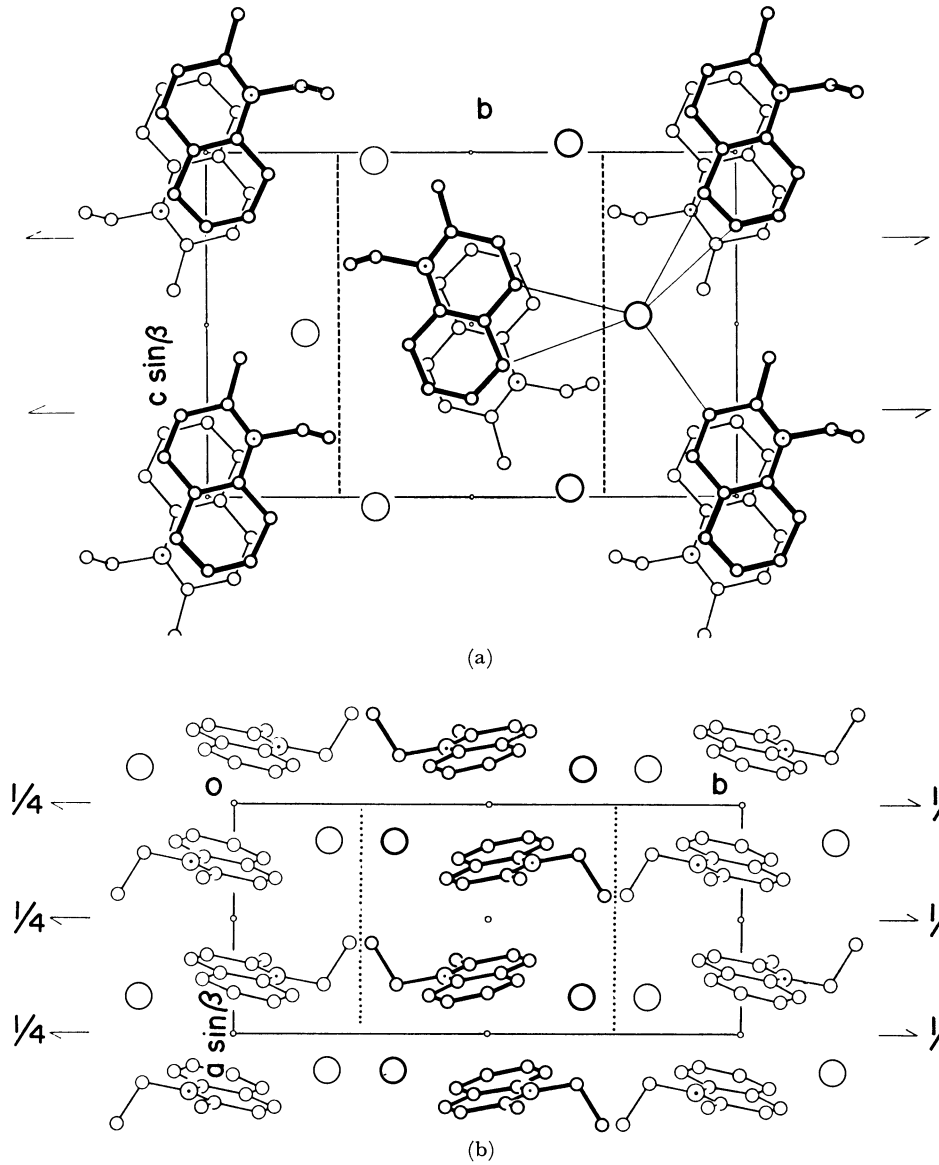

Fig. 3. The crystal structure viewed along the a axis (a) and the c axis (b).

TABLE 3. SHORT NON-BONDED DISTANCES LESS THAN 4.0 Å ALONG WITH THEIR ESTIMATED STANDARD DEVIATIONS WITHIN PARENTHESES EACH MULTIPLIED BY 10^2

C(5) ···C(5^{i})	3.50 (4) Å
C(7) ···C(3^{i})	3.59 (3)
C(3) ···C(7^{i})	3.59 (3)
C(4) ···C(8^{i})	3.45 (3)
C(6) ···C(10^{i})	3.54 (3)
C(4) ···C(9^{i})	3.54 (3)
C(2) ···C(7^{i})	3.47 (3)
C(10)···C(6^{i})	3.54 (3)
C(5) ···C(9^{i})	3.53 (3)
C(7) ···N	3.45 (3)
C(6) ···N	3.51 (3)
I ···C(9^{iii})	4.00 (2)
I ···C(3^{i})	3.93 (2)
I ···C(4^{ii})	3.95 (2)

Codes for superscripts:

i	$-x$,	$-y$,	$-z$;
ii	$-x$,	$0.5+y$,	$0.5-z$;
iii	x,	$0.5-y$,	$0.5+z$.

an 1-ethyl-2-methylquinolinium ring is 3.93 A (Fig. 3). Some close inter-ionic atomic contacts are shown in Table 3.

In the study of the solvent effects on the charge-transfer absorption band of 1-alkylpyridinium iodide complexes, Kosower[1] assumed that the complexes exist in the form of ion-pairs in non-polar solvents, and to explain the effects he proposed a model in which an iodide ion is in contact with a 1-alkylpyridinium ion, with the line joining the centers of charge perpendicular to the plane of the ring.

In the structure of the tropylium iodide crystal, it was found that the iodide ion is located on the center of the tropylium ring.[8] This finding gives evidence for a weak charge-transfer bond between the iodide ion and the tropylium ion, such a bond as might be expected to persist in an ion-pair.[9] In the *N*-methylacridinium iodide[10] and the quinolinium salt of 2-dicyanomethylene-1,1,3,3-tetracyanopropanediide,[4] it was again found that the crystal structures of these salts persist in having ion-pairs.

Unlike these, the obtained crystal structure of the present crystal (Fig. 3) seems not to be so useful in explaining the charge-transfer absorption band, although the yellowish-green color of the crystal may be due to weak interionic interaction. The differences in structure between the 1-ethyl-2-methylquinolinium iodide and the tropylium iodide may be due to the facts that the electron affinity of the tropylium ion is larger than that of the 1-ethyl-2-methylquinolinium ion and that the bulky ethyl and methyl groups of the 1-ethyl-2-methylquinolinium ion affect the packing of ions in the crystal.

The authors wish to express their deep thanks to Professor Hiroshi Mikawa of this University for supplying materials and for his continued interest.

8) A. I. Kitaigorodski, Yu. T. Struchkov, T. L. Khotsyanova, M. E. Vol'pin and D. N. Kursanov, *Izvest. Akad. Nauk S. S. S. R., Otdl. Khim. Nauk.*, **1**, 32 (1960).

9) K. M. Harmon, F. E. Cummings, D. A. Davis and D. J. Diestler, *J. Amer. Chem. Soc.*, **84**, 3349 (1962).

10) K. Nakamura, N. Yasuoka, N. Kasai and M. Kakudo, unpublished data.

BULLETIN OF THE CHEMICAL SOCIETY OF JAPAN VOL. 43 1313—1318 (1970)

Lattice Vibrations of Potassium Oxalate Monohydrate and the Bound State of Water of Crystallization

Kunio FUKUSHIMA

Department of Chemistry, Faculty of Science, Shizuoka University, Oya, Shizuoka

(Received November 19, 1969)

A normal coordinate treatment of the potassium oxalate monohydrate crystal as a whole was carried out. On the basis of the results of the calculation, the nature of the lattice vibrations and the bound state of the water of crystallization were discussed.

Recent investigations of the crystal structure of potassium oxalate monohydrate by Pedersen[1] and by Chidambaram *et al.*[2] have concluded that it is a monoclinic structure belonging to the $C2/c$ space group. The IR spectra of the substance have also been measured by Collman and Holtzclaw,[3] Schmelz *et al.*,[4] Pedersen,[5] and the present author.[6] In the region of 300—4000 cm^{-1}, no remarkable differences are not found among the spectra obtained by the various investigators except for the differences ascribed to the different resolving powers of the spectrometers. Pedersen measured a powder X-ray diagram for the sample used for the measurement of the IR spectra, and identified it with the sample which he had used for structural determination.[1] From these facts, it may be concluded that the samples used for the IR measurements by the other investigators have the same crystal structure as that of Pedersen's sample or that differences in IR spectra due to differences in crystal structure do not appear in the 300—4000 cm^{-1} region even if these are differences in crystal structure due to crystal modification among the samples. Therefore, in the present investigation, I calculated the lattice vibrations for the crystal structure obtained by Pedersen[1] and Chidambaram *et al.*,[2] using the observed frequencies,[6] in order to make clear the bound state of the water of crystallization and also to elucidate the nature of the lattice vibrations.

Normal Coordinate Treatment

A normal coordinate treatment was carried out for the crystal structure obtained by Chidambaram *et al.*;[2] the lattice parameters were $a=9.236$ Å, $b=6.190$ Å, $c=10.694$ Å, and $\beta=110°47'$. The Bravais unit lattice, which has a cell containig $2K_2C_2O_4\cdot H_2O$ and belonging to each lattice point, is the monoclinic lattice (C), and the cell-repeating vectors are $(\boldsymbol{a}+\boldsymbol{b})/2$, $(\boldsymbol{a}-\boldsymbol{b})/2$, and $(\boldsymbol{a}-\boldsymbol{c})$. The numbering of the atoms and ions in the chemical units and a part of the crystal lattice is shown in Fig. 1.

Optically-active lattice vibrations were calculated according to the $\boldsymbol{G}\boldsymbol{F}$ matrix method developed by

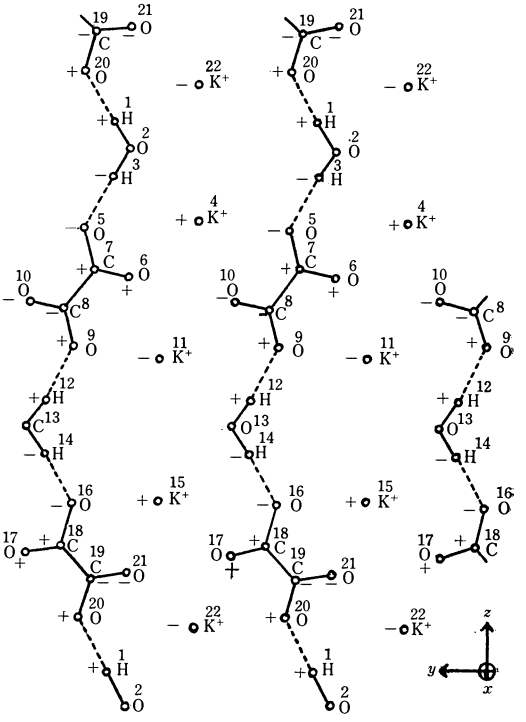

Fig. 1. A part of crystal lattice of potassium oxalate monohydrate (+and−represent "above the paper plane" and "below the plane," respectively)..

1) B.F. Pedersen, *Acta Chem. Scand.*, **18**, 1635 (1964).
2) R. Chidambaram, A. Sequeira and S.K. Sikka, *J. Chem. Phys.*, **41**, 3616 (1964).
3) J. P. Collman and H. F. Holtzclaw, Jr., *J. Amer. Chem. Soc.*, **80**, 2054 (1958).
4) M. J. Schmelz, T. Miyazawa, S. Mizushima, T.J. Lane and J.V. Quagliano, *Spectrochim. Acta*, **9**, 51 (1958).
5) B. F. Pedersen, *Acta Chem. Scand.*, **21**, 801 (1967).
6) K. Fukushima, This Bulletin, **43**, 39 (1970).

TABLE 1. CARTESIAN SYMMETRY COORDINATES (ELEMENTS OF THE VECTOR, $(X_s)^{i,j,k}_{\text{Bravais}}$)*

A_g

$x_{s1} = \Delta(x_1-x_3+x_{12}-x_{14})/2$
$x_{s2} = \Delta(y_1+y_3-y_{12}-y_{14})/2$
$x_{s3} = \Delta(z_1-z_3+z_{12}-z_{14})/2$
$x_{s4} = \Delta(y_2-y_{13})/\sqrt{2}$
$x_{s5} = \Delta(x_5-x_9+x_{16}-x_{20})/2$
$x_{s6} = \Delta(y_5-y_9-y_{16}+y_{20})/2$
$x_{s7} = \Delta(z_5-z_9+z_{16}-z_{20})/2$
$x_{s8} = \Delta(x_6-x_{10}+x_{17}-x_{21})/2$
$x_{s9} = \Delta(y_6-y_{10}-y_{17}+y_{21})/2$
$x_{s10} = \Delta(z_6-z_{10}+z_{17}-z_{21})/2$
$x_{s11} = \Delta(x_7-x_8+x_{18}-x_{19})/2$
$x_{s12} = \Delta(y_7-y_8-y_{18}+y_{19})/2$
$x_{s13} = \Delta(z_7-z_8+z_{18}-z_{19})/2$
$x_{s14} = \Delta(x_4-x_{11}+x_{15}-x_{22})/2$
$x_{s15} = \Delta(y_4-y_{11}-y_{15}+y_{22})/2$
$x_{s16} = \Delta(z_4-z_{11}+z_{15}-z_{22})/2$

A_u

$x_{s1} = \Delta(x_1-x_3-x_{12}+x_{14})/2$
$x_{s2} = \Delta(y_1+y_3+y_{12}+y_{14})/2$
$x_{s3} = \Delta(z_1-z_3-z_{12}+z_{14})/2$
$x_{s4} = \Delta(x_5+x_9-x_{16}-x_{20})/2$
$x_{s5} = \Delta(y_5+y_9+y_{16}+y_{20})/2$
$x_{s6} = \Delta(z_5+z_9-z_{16}-z_{20})/2$
$x_{s7} = \Delta(x_6+x_{10}-x_{17}-x_{21})/2$
$x_{s8} = \Delta(y_6+y_{10}+y_{17}+y_{21})/2$
$x_{s9} = \Delta(z_6+z_{10}-z_{17}-z_{21})/2$
$x_{s10} = \Delta(x_7+x_8-x_{18}-x_{19})/2$
$x_{s11} = \Delta(y_7+y_8+y_{18}+y_{19})/2$
$x_{s12} = \Delta(z_7+z_8-z_{18}-z_{19})/2$
$x_{s13} = \Delta(x_4+x_{11}-x_{15}-x_{22})/2$
$x_{s14} = \Delta(y_4+y_{11}+y_{15}+y_{22})/2$
$x_{s15} = \Delta(z_{12}+z_{11}-z_{15}-z_{22})/2$
$x_{s16} = \Delta(y_2+y_{13})/\sqrt{2}$

B_g

$x_{s1} = \Delta(x_1+x_3-x_{12}-x_{14})/2$
$x_{s2} = \Delta(y_1-y_3+y_{12}-y_{14})2$
$x_{s3} = \Delta(z_1+z_3-z_{12}-z_{14})/2$
$x_{s4} = \Delta(x_2-x_{13})/\sqrt{2}$
$x_{s5} = \Delta(z_2-z_{13})/\sqrt{2}$
$x_{s6} = \Delta(x_5-x_9-x_{16}+x_{20})/2$
$x_{s7} = \Delta(y_5-y_9+y_{16}-y_{20})/2$
$x_{s8} = \Delta(z_5-z_9-z_{16}+z_{20})/2$
$x_{s9} = \Delta(x_6-x_{10}-x_{17}+x_{21})/2$
$x_{s10} = \Delta(y_6-y_{10}+y_{17}-y_{21})/2$
$x_{s11} = \Delta(z_6-z_{10}-z_{17}+z_{21})/2$
$x_{s12} = \Delta(x_7-x_8-x_{18}+x_{19})/2$
$x_{s13} = \Delta(y_7-y_8+y_{18}-y_{19})/2$
$x_{s14} = \Delta(z_7-z_8-z_{18}+z_{19})/2$
$x_{s15} = \Delta(x_4-x_{11}-x_{15}+x_{22})/2$
$x_{s16} = \Delta(y_4-y_{11}+y_{15}-y_{22})/2$
$x_{s17} = \Delta(z_4-z_{11}-z_{15}+z_{22})/2$

B_u

$x_{s1} = \Delta(x_1+x_3+x_{12}+_{14})/2$
$x_{s2} = \Delta(y_1-y_3-y_{12}+y_{14})/2$
$x_{s3} = \Delta(z_1+z_3+z_{12}+z_{14})/2$
$x_{s4} = \Delta(x_5+x_9+x_{16}+x_{20})/2$
$x_{s5} = \Delta(y_5+y_9-y_{16}-y_{20})/2$
$x_{s6} = \Delta(z_5+z_9+z_{16}+z_{20})/2$
$x_{s7} = \Delta(x_6+x_{10}+x_{17}+x_{21})/2$
$x_{s8} = \Delta(y_6+y_{10}-y_{17}-y_{21})/2$
$x_{s9} = \Delta(z_6+z_{10}+z_{17}+z_{21})/2$
$x_{s10} = \Delta(x_7+x_8+x_{18}+x_{19})/2$
$x_{s11} = \Delta(y_7+y_8-y_{18}-y_{19})/2$
$x_{s12} = \Delta(z_7+z_8+z_{18}+z_{19})/2$
$x_{s13} = \Delta(x_4+x_{11}+x_{15}+x_{22})/2$
$x_{s14} = \Delta(y_4+y_{11}-y_{15}-y_{22})/2$
$x_{s15} = \Delta(z_4+z_{11}+z_{15}+z_{22})/2$
$x_{s16} = \Delta(x_2+x_{13})/\sqrt{2}$
$x_{s17} = \Delta(z_2+z_{13})/\sqrt{2}$

* Underscripts in the left side of the equations represent coordinate numbers, while those in the right side represent atom (or ion) numbers.

Shimanouchi *et al.*[7] The optically-active cartesian symmetry coordinate vector, X_{op}, and the optically-active internal symmetry coordinate vector, R_{op}, are expressed as follows.

$$X_{op} = \lim_{n_1, n_2, n_3 \to \infty} (n_1 n_2 n_3)^{1/2} \sum_{i=0}^{n_1} \sum_{j=0}^{n_2} \sum_{k=0}^{n_3} (X_s)^{i,j,k}_{\text{Bravais}}$$

$$R_{op} = \lim_{n_1, n_2, n_3 \to \infty} (n_1 n_2 n_3)^{1/2} \sum_{i=0}^{n_1} \sum_{j=0}^{n_2} \sum_{k=0}^{n_3} (R_s)^{i,j,k}_{\text{Bravais}}$$

In these equations, $(X_s)^{ijk}_{\text{Bravais}}$ and $(R_s)^{ijk}_{\text{Bravais}}$, respectively, are the cartesian and internal symmetry coordinate vectors associated with the three-dimensional Bravais cell, (i,j,k). The components of the vectors are shown in Tables 1 and 2. The optically-active B matrix, B_{op}, is defined as: $R_{op}=B_{op}X_{op}$.

The optically-active F matrix, F_{op}, constructed from the diagonal matrix with respect to each Bravais cell, F_{000}, and the interaction matrices, F_{100}, F_{010}, F_{001}, *etc.*, are as follows.

$$F_{op} = F_{000} + F_{100} + \tilde{F}_{100} + F_{010} + \tilde{F}_{010} + F_{001} + \tilde{F}_{001} + \cdots$$

The lattice vibration frequencies were calculated by the secular equation, $|M^{-1}F_{xs}-\lambda E|=0$. In this equation, M is the diagonal matrix constructed from the masses of the atoms and ions, and $F_{xs}=\tilde{B}_{op}F_{op}B_{op}$.

The following potential was assumed:

$$V = V^{2-}_{C_2O_4} + V_{H_2O} + V_{inter}$$

$V_{C_2O_4^{2-}}$ and V_{H_2O} represent the Urey-Bradley force fields associated with $C_2O_4^{2-}$ and H_2O respectively, and V_{inter} is the interaction potential of H_2O, $C_2O_4^{2-}$, and K^+. In the case of deuterated potassium oxalate monohydrate, the same potential function

7) T. Shimanouchi, M. Tsuboi and T. Miyazawa, *J. Chem. Phys.*, **35**, 1597 (1961).

Table 2. Internal symmetry coordinates (element of the vector, $(R_S)^{i,j,k}_{Bravais}$) *

A_g $\Delta R_{si} = \Delta(R_i^{I}+R_i^{II}+R_i^{III}+R_i^{IV})/2$
i = 1 to 36 excluding 5, 28, 34, 35
$\Delta(R_i^{I}+R_i^{III})/\sqrt{2}$
i = 5, 28, 34

A_u $\Delta R_{si} = \Delta(R_i^{I}-R_i^{II}-R_i^{III}+R_i^{IV})/2$
i = 1 to 36 excluding 5, 28, 34, 35
$\Delta(R_i^{I}-R_i^{III})/\sqrt{2}$
i = 28, 34, 35

B_g $\Delta R_{si} = \Delta(R_i^{I}+R_i^{II}-R_i^{III}-R_i^{IV})/2$
i = 1 to 36 excluding 5, 28, 34, 35
$\Delta(R_i^{I}-R_i^{III})/\sqrt{2}$
i = 5, 28, 34

B_u $\Delta R_{si} = \Delta(R_i^{I}-R_i^{II}+R_i^{III}-R_i^{IV})/2$
i = 1 to 36 excluding 5, 28, 34, 35
$\Delta(R_i^{I}+R_i^{III})/\sqrt{2}$
i = 28, 34, 35

$\Delta R_{28}^{I} = \Delta\alpha_{1\,(i,j,k)\,2\,(i,j,k)\,3\,(i,j,k)}$
$\Delta R_{29}^{I} = \Delta\alpha_{5\,(i,j,k)\,7\,(i,j,k)\,6\,(i,j,k)}$
$\Delta R_{30}^{I} = \Delta\alpha_{5\,(i,j,k)\,7\,(i,j,k)\,8\,(i,j,k)}$
$\Delta R_{31}^{I} = \Delta\alpha_{6\,(i,j,k)\,7\,(i,j,k)\,8\,(i,j,k)}$
$\Delta R_{32}^{I} = \Delta\alpha_{1\,(i,j,k)\,2\,(i,j,k)\,4\,(i,j,k)}$
$\Delta R_{33}^{I} = \Delta\alpha_{1\,(i,j,k)\,2\,(i,j,k)\,22\,(i,j,k+1)}$
$\Delta R_{34}^{I} = \Delta\alpha_{4\,(i,j,k)\,2\,(i,j,k)\,22\,(i,j,k+1)}$
$\Delta R_{35}^{I} = \Delta t$ (7–8) (internal rotation angle coordinate around the bond, 7–8)
$\Delta R_{36}^{I} = \Delta\pi$(7–568) (out- of -plane bending coordinate regarding the plane formed by atoms, 5,6,7 and 8)
$\Delta R_i^{II} = \mathbf{i}\,(\Delta R_i^{I})$, $\Delta R_i^{III} = \boldsymbol{\sigma}\,(\Delta R_i^{I})$, $\Delta R_i^{IV} = \mathbf{C}_2\,(\Delta R_i^{I})$

* In this table, ΔR_i^{I}'s for i=1 through 27 correspond to R_i's in Table 3. The symbols, **i**, $\boldsymbol{\sigma}$ and $\mathbf{C}_2$ represent symmetry operations associated with inversion, glide plane and 2-fold axis, respectively.

was assumed:

$$
\begin{aligned}
2V_{\text{inter}} = & \sum_i f_i(\text{O}\cdots\text{H})(\Delta q_i(\text{O}\cdots\text{H}))^2 \\
& + \sum_i f_i(\text{O}\cdots\text{K}^+)(\Delta q_i(\text{O}\cdots\text{K}^+))^2 \\
& + \sum_i f_i(\text{O}\cdots\text{O})(\Delta q_i(\text{O}\cdots\text{O}))^2 \\
& + \sum_i H_i(\text{H-O}\cdots\text{K}^+) r^i_{\text{O-H}} r^i_{\text{O}\cdots\text{K}^+} (\Delta\alpha^i_{\text{H-O}\cdots\text{K}^+})^2 \\
& + \sum_{(i,j)} 2a(\Delta\alpha^i_{\text{H-O}\cdots\text{K}^+})(\Delta\alpha^j_{\text{H-O}\cdots\text{K}^+}) \\
& + \sum_{(k,l)} 2b(\Delta\alpha^k_{\text{H-O}\cdots\text{K}^+})(\Delta\alpha^l_{\text{H-O}\cdots\text{K}^+})
\end{aligned}
$$

In the above potential, only those interactions between atoms and ions with an atom-ion or atom–atom distance of less than 4.5 Å were taken into account. The atom-ion and atom–atom distances are shown in Table 3. The force constant, a, is the interaction force constant between two bond angles, $\alpha^i_{\text{H-O}\cdots\text{K}^+}$ and $\alpha^j_{\text{H-O}\cdots\text{K}^+}$, which share a H–O bond, and the force constant, b, is the interaction force constant between two bond angles, $\alpha^k_{\text{H-O}\cdots\text{K}^+}$ and $\alpha^l_{\text{H-O}\cdots\text{K}^+}$, which share a O···K+ bond.

Table 3. atom-atom and atom-ion interactions *

	Atom or ion number		Atom-atom (atom-ion) distance (Å)
R_1	$2(i,j,k)$	$3(i,j,k)$	0.962 (O-H)
R_2	$3(i,j,k)$	$5(i,j,k)$	1.792 (H···O)
R_3	$5(i,j,k)$	$7(i,j,k)$	1.273 (C-O)
R_4	$6(i,j,k)$	$7(i,j,k)$	1.234 (C-O)
R_5	$7(i,j,k)$	$8(i,j,k)$	1.555 (C-C)
R_6	$2(i,j,k)$	$4(i,j,k)$	2.933 (O···K+)
R_7	$4(i,j,k)$	$5(i,j,k)$	2.762 (O···K+)
R_8	$4(i,j,k)$	$6(i,j,k)$	2.849 (O···K+)
R_9	$5(i,j,k)$	$4(i+1,j-1,k)$	3.486 (O···K+)
R_{10}	$6(i,j,k)$	$10(i-1,j+1,k)$	3.789 (O···O)
R_{11}	$6(i,j,k)$	$11(i-1,j+1,k)$	2.813 (O···K+)
R_{12}	$2(i,j,k)$	$5(i,j+1,k)$	3.699 (O···O)
R_{13}	$2(i,j,k)$	$10(i,j+1,k)$	3.792 (O···O)
R_{14}	$4(i,j,k)$	$9(i,j+1,k)$	2.795 (O···K+)
R_{15}	$2(i,j,k)$	$6(i+1,j,k)$	3.687 (O···O)
R_{16}	$5(i,j,k)$	$6(i+1,j,k)$	3.338 (O···O)
R_{17}	$5(i,j,k)$	$9(i+1,j,k)$	4.149 (O···O)
R_{18}	$6(i,j,k)$	$10(i-1,j,k)$	4.445 (O···O)
R_{19}	$2(i,j,k)$	$4(i+1,j,k)$	3.304 (O···K+)
R_{20}	$2(i,j,k)$	$6(i,j+1,k)$	3.592 (O···O)
R_{21}	$4(i,j,k)$	$6(i,j+1,k)$	2.966 (O···K+)
R_{22}	$4(i,j,k)$	$10(i+1,j+1,k)$	2.813 (O···K+)
R_{23}	$4(i,j,k)$	$20(i-1,j,k+1)$	3.025 (O···K+)
R_{24}	$4(i,j,k)$	$21(i-1,j,k+1)$	2.988 (O···K+)
R_{25}	$5(i,j,k)$	$6(i+1,j,k)$	3.338 (O···O)
R_{26}	$5(i,j,k)$	$9(i,j+1,k)$	3.721 (O···O)
R_{27}	$5(i,j,k)$	$10(i,j+1,k)$	4.138 (O···O)

* In this table $m(i,j,k)$ represents atom or ion, m, in the Bravais cell, (i,j,k). Regarding atom or ion number, m, refer to Fig. 1.

Table 4. Result of factor group analysis

$K_2C_2O_4\cdot H_2O$ (C^6_{2h}) or $K_2C_2O_4\,D_2O$ (C^6_{2h})					
	N	T	T'	R'	n
A_g	16	0	4	4	8
A_u	16	1	6	1	8
B_g	17	0	5	5	7
B_u	17	2	6	2	7

N; number of the total freedom,
T; number of the translations,
T'; number of the translational lattice vibrations,
R′; number of the rotational lattice vibrations,
n; number of intramolecular vibrations of $C_2O_4^{2-}$ and H_2O (orD_2O).

I also treated the optically-active lattice vibrations of A_g, A_u, B_g, and B_u species of potassium oxalate monohydrate and deuterated potassium oxalate monohydrate shown in Table 4. Based on the observed frequencies[6] of IR active vibrations (A_u and B_u species), the force constants marked

TABLE 5. FORCE CONSTANTS (in mdyn/Å)**

	Set I	Set II
K(O-H)*	5.640	5.839
K(O···H)*	0.150	0.122
K(C-O)*	7.200	7.500
K(C-C)	2.500	2.500
f(O···K$^+$)	$f=10.803\exp(-1.413r)(1.413-(2/r))$	
f(O···O)	$\ln f=7.070-2.820r$	
H(H-O-H)*	0.640	0.568
H(O-C-O)*	0.150	0.100
H(O-C-C)*	0.150	0.300
F(H-O-H)*	−0.100	−0.258
F(O-C-O)*	3.000	2.500
F (O-C-C)*	0.500	0.850
t (C-C)	0.250	0.250 mdyn.Å
H^1(H-O···K$^+$)*	0.040	0.125
H^2(H-O···K$^+$)*	0.040	0.102
H(K^+···O···K$^+$)*	0.000	0.026
F^1(H-O···K$^+$)	0.000	0.000
F^2(H-O···K$^+$)*	0.000	0.010
F(K$^+$···O···K$^+$)	0.000	0.000
a*	0.000	0.110 mdyn. Å
b*	0.000	−0.180 mdyn. Å

** H^1, F^1 relate to ΔR^{I}_{32} in Table 2, while H^2, F^2 relate to ΔR^{I}_{33} in the table.

with * in Table 5 were adjusted by the method of least squares.[8] The numerical computations were carried out by making use of the Computation Center, Tokyo University, and the programs, BGLZ and LSMB, set up at the Shimanouchi Laboratory, Department of Chemistry, Faculty of Science, University of Tokyo, and also a program made by the author. The force constants, Set I, in Table 5 were obtained by the following equations. The O···O force constant, f_i (O···O), was assumed to be $f_i=A\cdot\exp(-Br)$, and the parameters, A and B, were determined by the method of least squares, using seven values of the O···O force constant (5.14 mdyn/Å, 3.02 mdyn/Å, 3.03 mdyn/Å, 1.74 mdyn/Å, 1.05 mdyn/Å, 0.76 mdyn/Å, and 0.555 mdyn/Å, corresponding to the interatomic distances of 2.09 Å, 2.20 Å, 2.21 Å, 2.27 Å, 2.36 Å, 2.47 Å, and 2.48 Å),[9] while the K$^+$···O force constant, f_i(K$^+$—O), was assumed to be $f_i=C\cdot\exp(-Dr)$ $(D-(2/r))$ and the C and D parameters were determined using two values of the K$^+$···O force constant (0.11 mdyn/Å and 0.14 mdyn/Å, corresponding to the atom-ion distances of 3.05 Å and 2.83 Å).[10] In the above equations, represents the atom-atom or atom-ion distance.

Here, the expressions of the force constants, f_i(O···O) and f_i(K$^+$···O), were obtained from the second derivatives of an assumed repulsive potential, $a\cdot\exp(-br)$, and an electrostatic attractive potential, c/r. The potential for K$^+$···O was assumed to be $a\cdot\exp(-br)+(c/r)$, and the first derivative of the potential was set at zero, while the potential for O···O was assumed to be $a\cdot\exp(-br)$. The other force constants were transfered from related compounds. In Table 5, the force constants, Set II, are the force constants obtained by the method of least squares,[8] which gives the calculated frequencies shown in Tables 6, 7, 8 and 9.

Discussion

I. Assignment of IR Bands. Tables 6, 7, 8, and 9 show the significant terms of potential

TABLE 6. CALCULATED FREQUENCIES (in cm^{-1}) AND SIGNIFICANT TERMS OF POTENTIAL ENERGY DISTRIBUTIONS (A_u species)

$K_2C_2O_4\ H_2O$

ν_{obs}	ν_{calc}	Significant terms of p.e.d.
3200	3154	$R_1(97)$
1608	1638	$R_{28}(61)$, $R_{33}(19)$, $R_{32}(17)$
1580	1598	$R_3(65)$, $R_4(63)$
1303	1356	$R_4(47)$, $R_3(43)$
758	762	$R_{29}(71)$, $R_{31}(17)$
	520	$R_{32}(80)$, $R_{33}(15)$
524	518	$R_{36}(95)$
	309	$R_{31}(35)$, $R_{30}(29)$
	232	$R_{35}(34)$
210	224	$R_6(56)$, $R_2(11)$, $R_{20}(10)$
190	175	$R_9(32)$, $R_8(17)$, $R_7(11)$
	141	$R_{11}(20)$, $R_{14}(18)$, $R_{23}(13)$, $R_8(12)$
115	135	$R_{14}(29)$, $R_{23}(21)$, $R_{24}(14)$
92	95	$R_{23}(22)$, $R_{21}(12)$, $R_{11}(12)$
	79	$R_2(24)$, $R_6(17)$, $R_{22}(16)$

$K_2C_2O_4\ D_2O$

ν_{obs}	ν_{calc}	Significant terms of p.e.d.
	2286	$R_1(96)$
1595	1598	$R_3(65)$, $R_4(63)$
1305	1356	$R_4(47)$, $R_3(43)$
1225	1192	$R_{28}(61)$, $R_{33}(19)$, $R_{32}(17)$
760	762	$R_{29}(71)$,$R_{31}(17)$
505	518	$R_{36}(96)$
358	371	$R_{32}(79)$, $R_{33}(16)$
	309	$R_{31}(35)$,$R_{30}(29)$
	232	$R_{35}(34)$
215	215	$R_6(55)$, $R_2(10)$
165	174	$R_9(31)$,$R_8(17)$, $R_7(11)$
	141	$R_{11}(19)$, $R_{14}(18)$,$R_{23}(13)$,$R_8(11)$
125	135	$R_{14}(28)$,$R_{23}(21)$,$R_{24}(14)$
93	94	$R_{23}(22)$,$R_{21}(12)$,$R_{11}(11)$
	78	$R_2(24)$,$R_{22}(16)$,$R_6(16)$

8) D. E. Mann, T. Shimanouchi, J.H. Meal and L. Fano, *J. Chem. Phys.*, **27**, 43 (1957).
9) T. Shimanouchi, *Pure and Appl. Chem.*, **7**, 131 (1963).
10) I. Nakagawa, T. Shimanouchi and K. Yamasaki, *Inorg. Chem.*, **3**, 772 (1964).

Table 7. Calculated frequencies (in cm^{-1}) significant terms of potential energy distributions (B_u species)

$K_2C_2O_4\ H_2O$

ν_{obs}	ν_{calc}	Significant terms of p. e. d.
3370	3296	$R_1(98)$
1608	1600	$R_3(64),R_4(64)$
1303	1361	$R_3(45),R_4(45)$
758	789	$R_{29}(65),R_{31}(15),\ R_{30}(14)$
718	691	$R_{32}(133)$
614	601	$R_{33}(151),\ R_{32}(28)$
524	518	$R_{36}(96)$
351	351	$R_{30}(37),R_{31}(33)$
	232	$R_{35}(32),R_{22}(13),R_{11}(13),R_{24}(13)$
210	208	$R_2(32),R_6(31),R_{19}(14)$
190	199	$R_{23}(25),R_{14}(22)$
160	164	$R_8(28),R_{21}(22),R_{19}(12)$
129	144	$R_9(21),R_2(20),R_{14}(17)$
115	103	$R_{19}(48),R_{20}(22)$
56	56	$R_2(21),R_6(20),R_{24}(19),R_{20}(12)$

$K_2C_2O_4\cdot D_2O$

ν_{obs}	ν_{calc}	Significant terms of p.e.d.
2460	2417	$R_1(98)$
1595	1600	$R_3(64),R_4(64)$
1305	1361	$R_3(45),\ R_4(45)$
760	789	$R_{29}(65),R_{31}(15),R_{30}(14)$
	530	$R_{32}(119)$
505	518	$R_{36}(96)$
432	443	$R_{33}(154),R_{32}(40)$
358	351	$R_{30}(37),R_{31}(34)$
215	232	$R_{35}(32),\ R_{22}(13),\ R_{11}(13),R_{24}\ (13)$
	201	$R_6(22),R_9(17),R_2(14)$
195	197	$R_2(20),R_{14}(17),\ R_{23}(17)$
165	162	$R_8(24),R_{21}(22),R_{19}(14),R_6(11)$
...	142	$R_9(22),R_2(21),R_{14}(18),R_7(10)$
93	96	$R_{19}(50),R_{20}(22)$
54	56	$R_2(21),R_6(20),R_{24}(19),R_{20}(12)$

Table 8. Calculated frequencies (in cm^{-1}) and significant terms of potential energy distributions (A_g species)

$K_2C_2O_4\ H_2O$

ν_{obs}	ν_{calc}	Significant terms of p.e.d.
	3154	$R_1(97)$
	1701	$R_4(56),R_3(55),R_{30}(13),R_{31}(12)$
	1638	$R_{28}(61),R_{33}(19),R_{32}(17)$
	1408	$R_5(47),R_3(39),R_4(38),R_{29}(12)$
	992	$R_5(48),R_{29}(22)$
	805	$R_{36}(99)$
	575	$R_{30}(38),R_{31}(37)$
	520	$R_{32}(80),R_{33}(15)$
	484	$R_{29}(39),R_5(16)$
	232	$R_{11}(22),R_{22}(22),R_{24}(18),R_6(11)$
	207	$R_{14}(22),R_9(21),R_{26}(18),R_{23}(16)$
	179	$R_6(31)$
	166	$R_{21}(27),R_8(21),R_9(13),R_{14}(11)$
	131	$R_9(21)$
	87	$R_{26}(25),R_{20}(19),R_{19}(17),R_{24}(10)$
	57	$R_6(21),R_{20}(21),R_{26}(14),R_{27}(12)$

$K_2C_2O_4\cdot D_2O$

ν_{obs}	ν_{calc}	Significant terms of p.e.d.
	2286	$R_1(96)$
	1701	$R_4(56),R_3(55),R_{30}(13),R_{31}(12)$
	1408	$R_5(47),R_3(39),R_4(38),R_{29}(12)$
	1192	$R_{28}(61),R_{33}(19)R_{32}(17)$
	992	$R_5(48),R_{29}(22)$
	805	$R_{36}(99)$
	575	$R_{30}(38),R_{31}(37)$
	485	$R_{29}(39),R_5(16)$
	371	$R_{32}(80),R_{33}(16)$
	230	$R_{11}(23),R_{22}(23),R_{24}(19)$
	206	$R_{14}(23),R_9(21),R_{26}(19),R_{23}(18)$
	174	$R_6(33)$
	166	$R_{21}(29),R_8(22),R_9(12)$
	130	$R_9(20)$
	86	$R_{26}(24),R_{20}(20),R_{19}(17)$
	57	$R_6(21),R_{20}(21),R_{26}(14),R_{27}(12)$

energy distributions. From the terms, it is clear that the calculated frequencies, 691 cm^{-1} and 601 cm^{-1} (B_u species), are related to the R_{32} and R_{33} coordinates. Therefore, they are due to the rotational lattice vibrations of the water of crystallization and correspond to the bands at 718 cm^{-1} and 614 cm^{-1}. The vibration having the calculated frequency 520 cm^{-1} (A_u species) is also due to another lattice vibration associated with the water of crystallization, as the significant terms of the potential energy distributions show.

In the region below 250 cm^{-1}, it is interesting that the calculated frequencies correspond well with the observed frequencies despite the fact that the assumed potentials of $a\cdot\exp(-br)$ and $a\cdot\exp(-br)+(c/r)$ were used for the O···O and K^+···O interactions respectively.

II. Bound State of the Water of Crystallization. The potassium oxalate monohydrate crystal contains one kind of water of crystallization molecule. Each oxygen atom in the water of crystallization molecule is on the symmetry element, the 2-fold axis, of the Bravais cell of the crystal, and it is accompanied by two nearest neighbor potassium ions at a distance of 2.93 Å. Each water of crystallization molecule is bound to the oxygen atoms of $C_2O_4^{2-}$'s by hydrogen bonds. If we assume sp^3 orbitals for the oxygen atom of the water of crystallization molecule, as in the case of ice, the orbitals of the lone-pairs do not point to the potassium ions; therefore, we can not expect a simple σ-bond for O···K^+. In order to obtain information about the bound state of the water of crystallization molecule, the force constants of rotation about the principal axes of the moment of inertia, A, B and

TABLE 9. CALCULATED FREQUENCIES (in cm^{-1}) AND SIGNIFICANT TERMS OF POTENTIAL ENERGY DISTRIBUTIONS (B_g species)

$K_2C_2O_4H_2O$			$K_2C_2O_4D_2O$		
ν_{obs}	ν_{calc}	Significant terms of p.e.d.	ν_{obs}	ν_{calc}	Significant terms of p.e.d.
	3296	$R_1(98)$		2417	$R_1(98)$
	1701	$R_4(56),R_3(55),R_{30}(13),R_{31}(12)$		1701	$R_4(56),R_3(55),R_{30}(13),R_{31}(12)$
	1408	$R_5(47),R_3(39),R_4(38),R_{29}(12)$		1408	$R_5(47),R_3(39),R_4(38),R_{29}(12)$
	992	$R_5(48),R_{29}(22)$		992	$R_5(48),R_{29}(22)$
	805	$R_{36}(99)$		805	$R_{36}(99)$
	691	$R_{32}(133)$		575	$R_{30}(38),R_{31}(37)$
	602	$R_{33}(149),R_{32}(28)$		530	$R_{32}(119)$
	575	$R_{30}(38),R_{31}(37)$		484	$R_{29}(39),R_5(16)$
	484	$R_{29}(39),R_5(16)$		443	$R_{33}(154),R_{32}(40)$
	217	$R_6(20),R_{11}(13),R_{22}(13)$		214	$R_{11}(19),R_{22}(19),R_6(12)$
	201	$R_{11}(19),R_{22}(19),R_2(18)$		198	$R_9(18),R_2(14),R_{11}(13),R_{22}(13)$
	188	$R_{23}(18),R_{26}(17),R_9(14),R_{14}(12)$		185	$R_{23}(19),R_2(14),R_{21}(12),R_{14}(10)$
	165	$R_{21}(30),R_8(21)$		164	$R_{21}(25),R_8(18),R_6(13)$
	144	$R_{14}(37),R_{24}(26),R_{19}(14)$		143	$R_{14}(37),R_{24}(27),R_{19}(11)$
	112	$R_{19}(31),R_{20}(19),R_2(19),R_{24}(18)$		107	$R_{24}(23),R_{19}(19),R_{20}(14)$
	105	$R_9(20),R_7(14),R_{26}(12),R_8(12),$ $R_{23}(11),R_2(11)$		104	$R_2(28),R_9(15),R_{19}(12)$
	67	$R_{14}(26),R_{24}(21),R_{19}(14),R_{23}(12),$ $R_6(12)$		65	$R_{14}(25),R_{24}(20),R_{19}(17),R_6(12),$ $R_{23}(12)$

C, of the molecule were calculated.

Expressing the angle of rotation around the principal axis, m, and the force constant by $\Delta\theta_m$ and k_m respectively, we obtain the following equation:

$$k_m(\Delta\theta_m)^2 = \sum_n \tilde{\rho}_{mn}\tilde{B}FB\rho_{mn}$$

Here, ρ_{mn} represents the displacement of the atom, n, caused by the rotation around the axis, m, having an angle of rotation, $\Delta\theta_m$. B is the matrix transforming the displacements of the atoms in the water of crystallization molecule to the coordinates which change by the displacements, and F is the potential energy matrix having the coordinates as its bases. ρ_{mn} is expressed by the equation: $\rho_{mn}=e_m\times r_n\cdot\Delta\theta_m$. The vector, e_m, is a unit vector parallel to the principal axis, m, and r_n is a vector from the center of gravity of water molecule to the atom, n. The values of the k_m's obtained by the use of the force constants in Table 5 are as follows:

$$k_A=0.081 \text{ mdyn}\cdot\text{Å},\ k_B=0.237 \text{ mdyn}\cdot\text{Å},$$
$$k_C=1.886 \text{ mdyn}\cdot\text{Å}$$

From these values, it can be concluded that the water of crystallization molecule is more strongly bound around the C axis than around the A and B axes. The contributions of the hydrogen bonds to k_A, k_B, and k_C were calculated to be 0.001 mdyn·Å, 0.002 mdyn·Å, and 0.002 mdyn·Å respectively. As the $O\cdots K^+$ interactions make as little contributions to the k_m's as the $H\cdots O$ interactions, most contributions to the k_m's are considered to arise from the interaction between the nearest neighbor potassium ions and the lone-pair electrons of the water of crystallization molecule. Each of the potassium ions is on the side of the plane passing the oxygen atom of the water of crystallization molecule and perpendicular to H–O–H plane at the same distance, 2.02 Å, from the plane. The relatively small values of k_A suggest that the rotation around the axis, A, does not seriously change the degree of the interaction between the potassium ions and the lone-pair electrons; the small change in the degree of the interaction may be realized when we note that the lone-pair orbitals extend along the above-mentioned plane separating the two potassium ions. The large values of k_B and k_C also suggest this type of extension of the orbitals.

The author's thanks are due to Professor T. Shimanouchi of the University of Tokyo for allowing him to use the BGLZ and LSMB programs, and to Dr. I. Suzuki of Professor Shimanouchi's labolatory for his kind instruction on how to use the programs. He also wishes to express his gratitude to Professor S. Shibata of our Department for allowing him to use the IBM key-punch.

BULLETIN OF THE CHEMICAL SOCIETY OF JAPAN VOL. 43 1319—1322 (1970)

The Cadmium-photosensitized Decomposition of Acetone

Shin SATO, Chiharu TAKAHASHI and Shigeru TSUNASHIMA

Department of Applied Physics, Tokyo Institute of Technology, Ookayama, Meguro-ku, Tokyo

(Received November 22, 1969)

The cadmium-photosensitized decomposition of acetone has been studied and compared with the 3261 Å direct photolysis at 270±1°C. The data could be consistently explained by the following reaction mechanism:

$$Cd(^3P_1) + CH_3COCH_3 \longrightarrow Cd + {}^3A^* \quad (1)$$
$${}^3A^* \longrightarrow 2CH_3 + CO \quad (2)$$
$$CH_3 + CH_3COCH_3 \longrightarrow CH_4 + CH_3COCH_2 \quad (3)$$
$$2CH_3 \longrightarrow C_2H_6 \quad (4)$$
$$CH_3 + CH_3COCH_2 \longrightarrow C_2H_5COCH_3 \quad (5)$$
$$2CH_3COCH_3 \longrightarrow (CH_3COCH_2)_2 \quad (6)$$

The mechanism from (2) to (6) is exactly the same as that proposed for the 3130 Å direct photolysis at temperatures higher than 100°C. By using the *cis-trans* isomerization of 2-butene as the actinometer, the quantum yield of the photosensitized decomposition of acetone was estimated to be 0.3. Kinetic analysis showed that the energy-rich ethane produced by the recombination reaction (4) has the lifetime of 2×10^{-8} sec at 270°C.

In a previous series of papers,[1] we have reported the reactions of various hydrocarbons photosensitized by cadmium ($^3P_1$). Since the electronic energy tranferred in the cadmium photosensitization is only 87.7 kcal/mol, most of the hydrocarbons investigated did not decompose appreciably. The chemical changes observed thus far have been the *cis-trans* isomerizations of 2-butene and 2-pentene, the hydrogen-atom scrambling of dideuteroethylene, and the formations of vinylacetylene and benzene from acetylene.

In this paper, we have experimented with acetone as the reactant in the expectation that its decomposition may take place because of the low dissociation energy of the C–C bond attached to the carbonyl. The photochemistry of acetone has extensively been studied, and its reaction mechanism has almost been completely established.[2] Therefore, acetone was thought to be a suitable subject for the first application of the cadmium photosensitization of compounds containing oxygen atoms.

Experimental

Acetone (Koso Chemical Co.) was distilled bulb-to-bulb, with the middle third retained. Gas-chromatographic analysis showed no measurable impurities. Pure-grade *cis*-2-butene (Matheson Ltd.) was used as supplied.

The quartz reaction cell mounted in a furnace was 9.0 cm long and 4.8 cm in diameter, with a total volume, including acess tubing, of 175 m*l*. The cell was attached to the vacuum line through a greaseless stopcock equipped with a Viton diaphragm.

A home-made cadmium discharge lamp, with argon (2 mmHg) as the buffer gas, was used. The lamp was heated in another furnace which was kept at 270°C (within ±2°C) by an electric controller. The 2288 Å resonance line was filtered out by a UV-29 Toshiba glass filter, so that the emitting light was mainly the 3261 Å resonance line.

Products from the photolyses were analyzed by gas chromatography after removing the noncondensable gases at 77°K (carbon monoxide and methane) with a Toepler pump. The amounts of carbon monoxide and methane were measured using a gas buret attached to a cuprous oxide furnace at 280°C. In this furnace carbon monoxide is selectively oxidized to carbon dioxide, which is condensable at 77°K.

Since the extinction coefficient of acetone is strongly dependent on the temperature, it was measured using a combination of a set of slits, a photomultiplier (Toshiba MS-9SY), and a micro-ammeter. In the cadmium photosensitization, the light intensity absorbed by cadmium atoms was measured by using the *cis-trans* isomerization of 2-butene as the actinometer. The quantum yield was assumed to be 0.5.[1,3]

Results

Extinction Coefficients of Acetone. Since a monochromator was not used, the impinging light

1) S. Tsunashima and S. Sato, This Bulletin, **40**, 2987 (1967); **41**, 284, 2281 (1968); S. Tsunashima, S. Hirokami and S. Sato, *Can. J. Chem.*, **46**, 995 (1968); S. Tsunashima, S. Satoh and S. Sato, This Bulletin, **42**, 329, 1531 (1969).

2) E.W.R. Steacie, "Atomic and Free Radical Reactions," Reinhold Publishing Co., New York (1954).

3) H.E. Hunziker, *J. Chem. Phys.*, **50**, 1288, 1294 (1969).

was not only the 3261 Å resonance line, but was contaminated by the lights which were not absorbed by acetone. To estimate the molar extinction coefficient, therefore, the following equation was used:

$$I^{obs}-I=(I_0^{obs}-I)10^{-\varepsilon[A]l}$$

Here, I^{obs} and I_0^{obs} are the light intensities obtained in the presence and in the absence of acetone respectively. I is the intensity in the presence of a large amount of acetone. ε is the molar extinction coefficient, [A] is the concentration of acetone, and l is the length of the cell. Table 1 summarizes the obtained values. Although the 3261 Å resonance line is contaminated by weak lines at 3466 and 3613 Å,[4] which are in the absorption band of acetone, the extinction coefficients obtained are in fair agreement with the reported value[5] (about 0.6 $l\,mol^{-1}\,cm^{-1}$ at 3261 Å at 25°C).

TABLE 1. EXTINCTION COEFFICIENTS OF ACETONE AT 3261 Å.*

Temperature °C	Extinction Coefficient ε $l mol^{-1} cm^{-1}$
36	0.57
85	0.67
117	0.80
165	1.02
212	1.32
224	1.42
255	1.67
270	1.80
281	1.91

* The light is from a Cd resonance lamp through a Toshiba UV-D25 glass filter.

Direct Photolysis. The results are summarized in Table 2. The products observed were carbon monoxide, methane, ethane, methyl ethyl ketone, and a compound with a high melting point which was not identified. The formations of ethylene, hydrogen, ketene, and biacetyl were not observed. Since the quantum yield of carbon monoxide is believed to be unity above 100°C,[5] the light intensity at 3261 Å of this lamp was estimated using the data of Table 1 and those of Runs No. 2, 13, 12, 11 and 10 in Table 2, their acetone concentrations being almost constant in the cell ($3.02\pm0.02\times10^{-3}$ moll^{-1}). The estimated value was 0.55 ± 0.03 μEinstein min^{-1}.

Cadmium-sensitized Photolysis. In order to check the thermal reaction, a few mmHg of acetone were kept in the cell at 270°C for several hours in the presence of cadmium, but no decomposition was detected. The photolysis results are summarized in Table 3. The products observed were the same as those obtained in the direct photolysis. The light intensity absorbed by cadmium atoms was estimated to be 0.21 ± 0.01 μEinstein min^{-1}. Figure 1 shows the quantum yield of carbon monoxide as a function of the acetone pressure. The curve A was obtained from the data shown in Table 3. Obviously the quantum yield above 10 mmHg increases linearly with the increase in the pressure of acetone. The curve B shows the results of another series of experiments using a different lamp, the light intensity absorbed by cadmium being 0.12 μ-Einstein min^{-1}. In the latter case, the increase in the quantum yield of carbon monoxide was not appreciable. This discrepancy will be discussed in the next section.

TABLE 2. THE 3261 Å DIRECT PHOTOLYSIS OF ACETONE

Run No.	Acetone mmHg	Temperature °C	Products μmol $min^{-1}\times10^2$			
			CO	CH_4	C_2H_6	MEK*
6	2.46	270	0.25	0.26	0.06	0.05
4	5.11	270	0.40	0.55	0.06	0.12
8	7.68	270	0.59	0.88	0.10	0.14
3	10.1	270	0.74	1.07	0.08	0.20
9	15.1	270	1.20	1.42	0.11	0.31
1	19.1	270	1.27	1.90	0.22	0.25
5	47.7	270	2.63	4.47	0.19	0.58
7	62.3	270	3.48	5.96	0.15	n.d.
2	102	270	5.68	10.2	0.27	1.10
13	103	270	6.00	9.97	0.17	1.07
12	89.8	202	4.36	5.67	0.55	1.71
11	80.6	155	3.30	2.78	1.26	1.48
10	74.1	108	2.37	1.01	1.88	0.58

* Methyl ethyl ketone

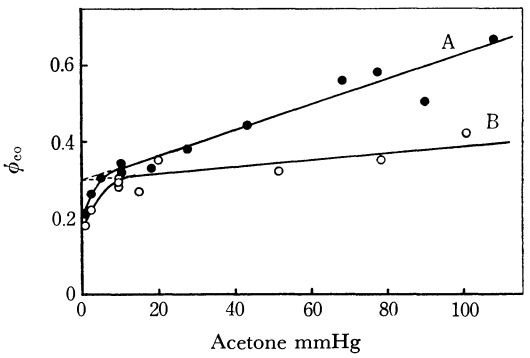

Fig. 1. The quantum yield of carbon monoxide in the cadmium photosensitized decomposition of acetone. For A and B, see the text.

4) S. Tsunashima, Ph. D. Thesis, Tokyo Institute of Technology (1968).

5) J. G. Calvert and J. N. Pitts, Jr., "Photochemistry," John Wiley & Sons, Inc., New York (1966).

6) S. W. Benson, "Advances in Photochemistry," Vol. 2 ed. by W. A. Noyes, Jr., G. S. Hammond and J. N. Pitts, Jr., Interscience Publishers, New York (1964).

Table 3. The cadmium-photosensitized decomposition of acetone at 270°C.

Run No.	Acetone mmHg	Products μmol min$^{-1}\times 10^2$			
		CO	CH_4	C_2H_6	MEK
25	1.14	4.44	1.87	2.36	0.3
23	2.38	5.38	2.68	3.62	1.10
18	4.90	6.20	4.00	3.28	1.59
21	10.1	7.14	6.86	2.57	2.82
29	10.1	6.65	6.00	2.14	2.50
26	18.6	6.89	7.50	1.77	2.51
22	27.4	7.90	9.48	1.35	3.16
20	43.0	9.33	12.0	1.32	2.94
27	68.3	11.8	17.5	1.03	3.65
19	77.5	12.2	17.2	0.67	2.95
28	89.9	10.4	16.5	0.52	n.d.
24	108	14.0	21.8	0.98	3.73

Discussion

The first absorption band of acetone extends from 3500 Å to 2200 Å. Therefore, if the broadening of the 3261 Å resonance line is large, direct photolysis will take place even in the presence of a large amount of cadmium vapor. The broadening of the resonance line is known to be very sensitive to the pressure of the buffer gas, the shape of the lamp, and the condition of discharge. In this experiment, we prepared two cadmium resonance lamps. The data presented here were obtained with the one of the higher intensity except for the curve B in Fig. 1. As has been stated in the Results section, the light intensity absorbed by acetone was 0.55 μEinstein min^{-1}, while that used for the cadmium photosensitization was 0.21 μEinstein min^{-1}. This difference may be attributed mainly to the broadening of the resonance line from the lamp. Thus, the increase in the quantum yield of carbon monoxide with the increase in the pressure of acetone can be interpreted in terms of the direct photolysis by the light which is not absorbed by cadmium. The difference in the slope between the curves A and B is explained by the difference in the broadening of the resonance line from the two lamps. The true quantum yield of carbon monoxide formed by the cadmium photosensitization is, therefore, obtained by extrapolating the curve obtained at higher pressures of acetone to zero pressure. Obviously the two curves point to the same value, 0.3.

The 3130 Å direct photolysis of acetone at temperatures higher than 100°C has been established to occur through the following reaction mechanism:[2]

$$CH_3COCH_3 + h\nu \longrightarrow {}^1A^* \quad (1)$$

$$^1A^* \longrightarrow {}^3A^* \quad (2)$$

$$^3A^* \longrightarrow 2CH_3 + CO \quad (3)$$

$$CH_3 + CH_3COCH_3 \longrightarrow CH_4 + CH_3COCH_2 \quad (4)$$

$$2CH_3 \longrightarrow C_2H_6 \quad (5)$$

$$CH_3 + CH_3COCH_2 \longrightarrow C_2H_5COCH_3 \quad (6)$$

$$2CH_3COCH_2 \longrightarrow (CH_3COCH_2)_2 \quad (7)$$

The quantum yield of the decomposition through the excited singlet state is known to be small.[5] The fluorescence and the phosphorescence, which are not shown in the above mechanism, are also known to be very small compared with the decomposition.[5] The quantum yield of carbon monoxide, therefore, is believed to be nearly unity. Although, in the present study of the 3261 Å direct photolysis, the quantum yields have not been measured, the products observed correspond well with the mechanism described above. In the cadmium photosensitization, the formation of the excited state of acetone may be written as follows:

$$CH_3COCH_3 + Cd(^3P_1) \longrightarrow {}^3A^* + Cd \quad (8)$$

The successive reactions will, then, be the same as has been described above from the reactions (3) to (7). We will show below that the data presented in the previous section can be consistently explained by this mechanism.

Since the quantum yields calculated from the data have some ambiguities, the relative yields will now be discussed. Figure 2 shows the relative rates of the formation of methane, ethane, and methyl ethyl ketone against that of carbon monoxide as a function of the pressure of acetone. The curves obtained in the two photolyses, direct and cadmium-photosensitized, are obviously different from each other. However, the material balance:

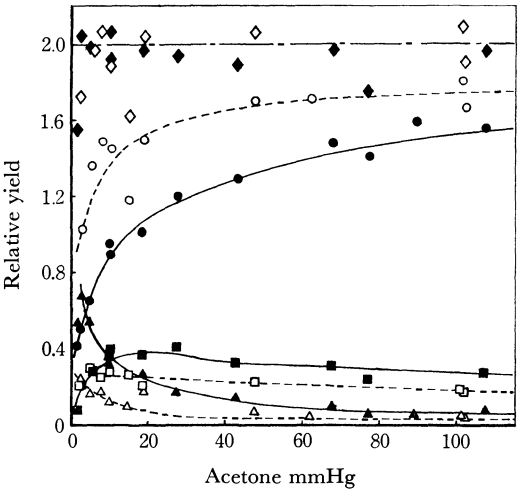

Fig. 2. Relative yields of products as a function of the pressure of acetone; open signs for the direct photolysis and filled signs for the cadmium photosensitization.
○, ● for CH_4
△, ▲ for C_2H_6
□, ■ for $C_2H_5COCH_3$
◇, ◆ for $[CH_4]+2[C_2H_6]+[C_2H_5COCH_3]$

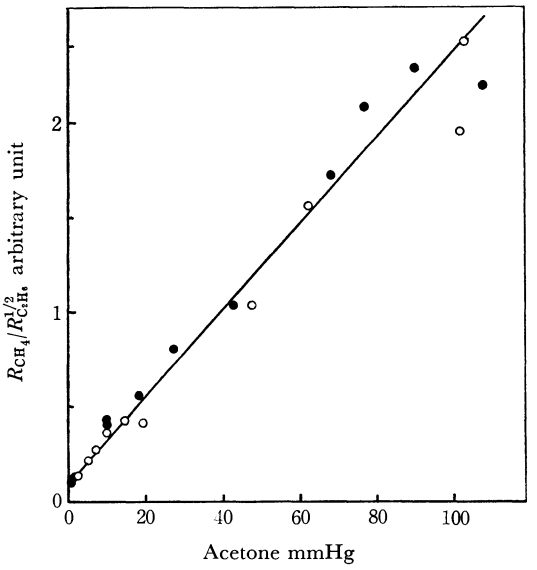

Fig. 3. The plots for $R_{CH_4}/R_{C_2H_6}^{1/2}$ against the pressure of acetone.
○ for the direct photolysis
● for the cadmium photosensitization

$$2[CO] = [CH_4] + 2[C_2H_6] + [C_6H_5COCH_3]$$

which is derived from the reaction mechanism proposed, holds rather nicely. This is also shown in Fig. 2. Moreover, the plots of the $[CH_4]/[C_2H_6]^{1/2}$ ratio against the pressure of acetone coincide with each other on a single straight line. This is shown in Fig. 3. The following equation is obtained by the steady-state treatment of the reaction mechanism proposed:

$$R_{CH_4}/R_{C_2H_6}^{1/2} = (k_4/k_5^{1/2})[A] \qquad [I]$$

Here, R_{CH_4} and $R_{C_2H_6}$ are the rates of the formation of methane and ethane, and k_4 and k_5 are the rate constants of the reactions (4) and (5). From the slope of the linear relationship in Fig. 3, the value for $(k_4/k_5^{1/2})$ is calculated to be 0.25 $l^{1/2}$ (mol sec)$^{-1/2}$. The literature values for k_4 and k_5 are $10^{8.88}\exp(-10.0/RT)$ and $10^{10.5}$ l (mol sec)$^{-1}$.[6] Therefore, the value for $(k_4/k_5^{1/2})$ at 270°C 0.58 $l^{1/2}$ (mol sec)$^{-1/2}$, a value which is in reasonable agreement with the value obtained in the present experiment. From the above discussion, it can be concluded that the apparent discrepancy between the two types of photolysis in the relative rate of the formation of the products is not essential, but is due to the difference in the concentrations of radicals in the steady states of the two photolyses. The light intensity used for the decomposition in the cadmium photosensitization is constant, while in the direct photolysis the intensity depends upon the pressure of acetone.

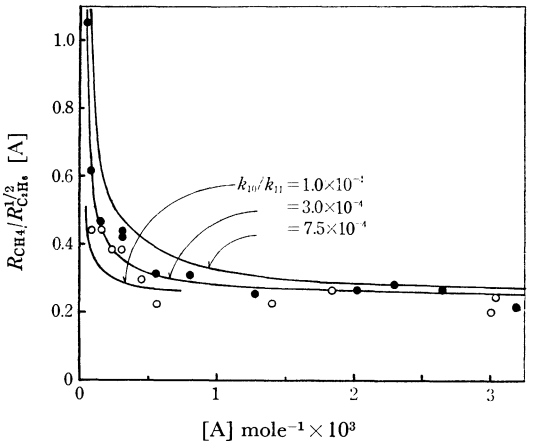

Fig. 4. The plots for the estimation of the lifetime of the energy-rich ethane molecule.
○ for the direct photolysis
● for the cadmium photosensitization

According to Eq. [I], the linear relationship in Fig. 3 should not have a definite intercept at the zero pressure of acetone. However, if the following mechanism:

$$2CH_3 \longrightarrow C_2H_6^* \qquad (9)$$

$$C_2H_6^* \longrightarrow 2CH_3 \qquad (10)$$

$$C_2H_6^* + CH_3COCH_3 \longrightarrow C_2H_6 + CH_3COCH_3 \qquad (11)$$

is assumed in place of the reaction (5), the existence of the intercept can be understood. Moreover, the lifetime of the energy-rich ethane formed in the reaction (9) can be estimated. If the reactions (9), (10) and (11) are included, the steady-state treatment gives Eq. [II] instead of [I]:

$$\frac{R_{CH_4}}{R_{C_2H_6}^{1/2}[A]} = \frac{k_4}{k_9^{1/2}}\left(1 + \frac{k_{10}}{k_{11}[A]}\right)^{1/2} \qquad [II]$$

In Fig. 4, the left-hand side of Eq. [II] is plotted against the concentration of acetone, [A]. Obviously at higher concentrations, the value of Eq. [II] remains around 0.25, but as the concentration of acetone decreases the value is rapidly increased. As is shown in Fig. 4, the best fit-curve is obtained by assuming the k_{10}/k_{11} ratio to be 3×10^{-4}. If every collision between energy-rich ethane and acetone is effective for the stabilization, then, by assuming the collision frequency to be $10^{11.3}$ $l$mol^{-1} sec^{-1},[6] the lifetime of energy-rich ethane molecules at 270°C can be calculated to be 2×10^{-8} sec.

BULLETIN OF THE CHEMICAL SOCIETY OF JAPAN VOL. 43 1323—1329 (1970)

NMR Study of Amino Acids and Peptides; Glycine and Valine Peptides

Makoto NAGAI and Atsuo NISHIOKA

Department of Polymer Chemistry, Faculty of Engineering, Tokyo Institute of Technology

and Juji YOSHIMURA

Laboratory of Chemistry for Natural Products, Faculty of Science, Tokyo Institute of Technology
Ookayama, Meguroku, Tokyo

(Received December 1, 1969)

The PMR spectra of 22 amino acids and peptides were measured in a D_2O solution. From the change in the NMR parameters in amino acids and their di- and tripeptides, it has been concluded that a tripeptide is a good model for polypeptides. The chemical shift of the α-proton of an amino-acid residue in tripeptide can be obtained from those of amino acid and dipeptide. The spin-spin coupling constant of an amino acid grows larger, and the population of a *trans* rotamer becomes larger, as its amino (or carboxyl) group forms a peptide bond. The PMR spectra of two diasteroisomers of valyl-valyl-valine were also measured, and the influences of the configuration of an amino-acid residue on the NMR parameters of its peptides were investigated.

The high-resolution NMR technique has been applied to the studies of oligopeptides and proteins. The PMR spectra of simple amino acids and dipeptides have been measured in an aqueous medium by Takeda and Jardetzky,[1] while Bovey and Tiers,[2] employing trifluoroacetic acid as the solvent, have investigated the relations between the NMR parameters and the peptide structures.

Several works[3-5] have also appeared trying to investigate the structures of proteins on the basis of the PMR spectra of amino acids and peptides. Spectrometers operating at 220 MHz have recently become available and have been used for this purpose.[4-5]

Sheinblatt[6] proposed a method for determing the sequence of amino acid residues in di- and tripeptides; he also measured[7] the rate of the exchange of the peptide hydrogen of glycylglycine. Morlino and Martin[8] reported glycylmethylene splitting due to a chemical-shift nonequivalence in amino acid-glycyl dipeptides. Kim and Martell[9] studied glycine dipeptides and their complexes with copper and nickel in an aqueous solution. Systematic analyses of the chemical shifts of the oligopeptides have also been reported by some workers. Gorkom[10] tried to distinguish a long-range shielding effect on the chemical shifts. For the chemical-shift calculation of an amino acid in a given polypeptide, a simple additive law has been found to hold by Nakamura and Jardetzky.[11-12] Beecham and Ham[13] reported the chemical-shift change of glycine and L-leucine residues in seversl peptides.

In this investigation, we have systematically investigated the changes in the NMR parameters (chemical shifts and spin-spin coupling constants) in amino acids and their di- and tri-peptides; we will here report a rather large difference in the vicinal coupling constants of amino-acid residues. From these changes, we deduced the structures of the peptides (the conformations of the side chains); we found that a tripeptide is a good model for polypeptides from the point of view of NMR parameters.

Experimental

The common amino acids and peptides were purchased

1) M. Takeda and O. Jardetzky, *J. Chem. Phys.*, **26**, 1346 (1957).
2) F. A. Bovey and G. V. D. Tiers, *J. Amer. Chem. Soc.*, **81**, 2870 (1958).
3) M. Mandel, *J. Biol. Chem.*, **240**, 1586 (1965).
4) B. Bak, C. Dambmann, F. Nicloaisen, E. J. Pedersen and N. S. Bhaccha, *J. Mol. Spect.*, **26**, 78 (1968).
5) C. C. McDonald and W. D. Phillips, *J. Amer. Chem. Soc.*, **91**, 1513 (1969).
6) M. Sheinblatt, *ibid.*, **88**, 2845 (1966).
7) M. Sheinblatt, *ibid.*, **87**, 572 (1965).
8) V. J. Morlino and R. B. Martin, *ibid.*, **89**, 3107 (1967).
9) M. K. Kim and A. E. Martell, *ibid.*, **91**, 872 (1969).
10) M. van Gorkom, *Tetrahedron Lett.*, **1966**, 5433.
11) A. Nakamura and O. Jardetzky, *Proc. Natl. Acad. Sci. U.S.*, **58**, 2212 (1967).
12) A. Nakamura and O. Jardetzky, *Biochem.*, **7**, 1226 (1968).
13) A. F. Beecham and N. S. Ham, *Tetrahedron*, **24**, 2773 (1968).

from Wako Pure Chemical Ind., Ltd. (Special Grade), or Tokyo Kasei Ind., Ltd. (GR). The L-valyl-L-valine, L-valyl-glycyl-glycine, L-valyl-L-valyl-D-valine, L-valyl-L-glutamic acid, L-valyl-L-valyl-L-glutamic acid, L-alanyl-glycine, and L-alanyl-glycyl-glycine were from the Ajinomoto Co., Ltd., while the glycyl-L-valyl-glycine, L-valyl-glycine, and L-valyl-L-valyl-L-valine were from the Institute for Protein Research, Osaka University; the D_2O was from E. Merck A.G. Darmstadt, "Solvent for NMR Spectroscopy" (99.75D%).

All the chemicals employed were PMR spectroscopically pure and were used without further purification.

The NMR spectra were obtained with samples prepared by dissolving 25 mg of the amino acids or peptides in 0.5 m*l* of D_2O, with 5 mg of sodium 2,2-dimethyl-2-silapentane 5-sulfonate(DSS) as a reference substance.

However, L-valyl-L-valine, L-valyl-L-valyl-L-valine, L-valyl-L-valyl-D-valine, L-valyl-L-valyl-L-glutamic acid, glycyl-glycine, and glycyl-glycyl-glycine were not soluble to that extent, and so about 2% D_2O solutions were prepared with these peptides. All the peptides are considered to have zwitter-ion forms in these solutions.

The NMR spectra were measured with a 60 MHz or a 100 MHz NMR spectrometer (JNM 3H-60 and JNM 4H-100) at a probe temperature of 29 ± 1°C. The chemical shift values were read from the frequency counter (Universal Counter MF-47 A, Anritsu Electric Co., Ltd.); the accuracy of the measurements is estimated to be within ± 0.05 Hz. All the chemical shifts were

TABLE 1. NMR PARAMETERS FOR AMINO ACIDS AND PEPTIDES MEASURED IN D_2O WITH DSS (60 MHz)

	J_{vic} (Hz)	δ_{CH_α} (Hz from DSS)	δ_{CH_3} (Hz from DSS)	δ_{CH_2} (Hz from DSS)
Glycine	—	—	—	213.6
Glycyl-glycine	—	—	—	(1) 231.4
(1) (3)	—	—	—	(3) 228.9
Glycyl-glycyl-glycine	—	—	—	(1) 235.4
(1) (2) (3)	—	—	—	(2) 243.7
	—	—	—	(3) 228.2
L-Alanine	7.2	227.8	88.9	—
Glycyl-L-alanine	7.2	251.3	81.9	230.6
L-Alanyl-glycine	7.2	248.5	93.6	227.5(q)
DL-Alanyl-DL-alanine	(1) 7.2	246.7	92.6	—
(1) (3)	(3) 7.2	250.8	82.8	—
DL-Analyl-glycyl-glycine	7.2	250.0	93.8	(2) 241.4
(2) (3)				(3) 226.8
L-Valine	4.3	215.8	57.7:60.9	—
Glycyl-L-valine	5.5	245.4	52.4:54.7	232.2
L-Valyl-glycine	6.1	228.1	61.2:62.4	228.0(q)
L-Valyl-L-valine	(1) 6.0	233.0	—	—
(1) (3)	(3) 6.5	244.5	—	—
L-Valyl-L-glutamic acid	5.8	230.6	—	—
Glycyl-L-valyl-glycine	6.6	254.6	55.3:56.4	(1) 234.2
(1) (3)				(3) 226.4
L-Valyl-glycyl-glycine	6.0	232.3	62.2	(2) 242.6(q)
(2) (3)				(3) 227.0
L-Valyl-L-valyl-L-valine	(1) 5.8	232.2	—	—
(1) (2) (3)	(2) 8.6	252.5	—	—
	(3) 6.4	242.6	—	—
L-Valyl-L-valyl-D-valine	(1) 5.8	232.7	—	—
(1) (2) (3)	(2) 7.5	257.1	—	—
	(3) 5.9	244.2	—	—
L-Valyl-L-valyl-	(1) 5.8	232.5	—	—
(1) (2)	(2) 8.3	249.7	—	—
L-glutamic acid				
L-Leucine	—	222.5	54.4:59.5	—
Glycyl-L-Leucine	—	251.1	—	229.6
L-Leucyl-glycine	—	241.2	54.7:60.1	227.6
L-Leucyl-glycyl-glycine	—	244.1	55.0:60.2	(2) 241.7
(2) (3)				(3) 230.6

where (q) denotes that it appears as AB quartet.

expressed in δ Hz from DSS at 60 MHz.

Results and Discussion

The results obtained for a series of peptides are presented in Table 1. For a given amino-acid residue in the peptides, the spin-spin coupling constants of the α-proton (H) with the β-H, and its chemical shifts, are designated as J_{vic} and δ_{CH_α} respectively. The chemical shifts of methyl groups for the valine and alanine residues, and the methylene group of glycine (δ_{CH_3} and δ_{CH_2}), are also presented when precise measurements were possible.

In this report, the amino-acid residues are numbered in the following way:

NH_2—A—COOH
(1, 3)

NH_2-A—A-COOH
(1) (3)

NH_2-A—A—A-COOH
(1) (2) (3)

where A denotes the amino-acid residue. Therefore, L-val(1,3) indicates L-valine. L-valyl-L-valine consists of two valine residues, L-val(1) and L-val(3).

1) Chemical Shifts. Generally speaking, the chemical shifts of amino-acid protons go to a lower field when peptide bonds are formed. Because an amino acid has both an amino and a carboxyl group, two types of dipeptides can exist; a rather distinct difference in NMR parameters is observable between them.

Let us now summarize the chemical shifts changes of the α-H of L-valine, paying special attention to the δ_{CH_α} of L-val(2) in tripeptides, in Fig. 1. The δ_{CH_α}'s of the amino-acid(1)(L-valine, L-leucine and L-alanine) residues in di- and tripeptides are shown in Fig. 2. Figure 3 shows the δ_{CH_2}'s of glycine peptides. From these figures, the δ_{CH_α} (or δ_{CH_2})'s of a given amino-acid residue in a certain position of the oligopeptides can be seen to have a tendency to cluster within a small range of chemical shift values. The mean values obtained for δ_{CH_α} and δ_{CH_2} are shown in Table 2. The difference, $\Delta\delta$, between the δ_{CH_α} of an amino acid residue in the peptide and that of the free amino acid is also presented in Table 2.

The δ_{CH_2}'s of glycine dipeptides have been reported to be 228.8, and 227.2 Hz from the DSS values for gly(1) and gly(3) respectively.[11] Our results agree fairly well.

A rather large discrepancy is found between

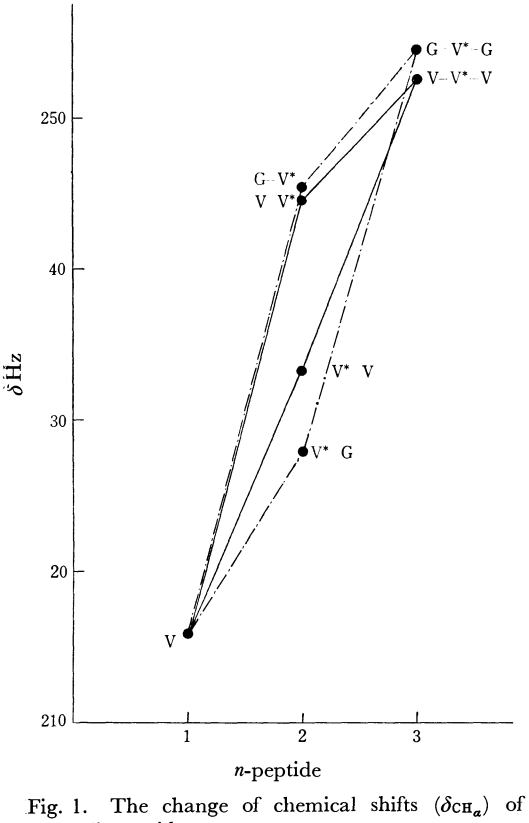

Fig. 1. The change of chemical shifts (δ_{CH_α}) of L-valine residues.
(δ_{CH_α} of the valine residue with an asterisk is shown. G; Glycine, V; Valine)

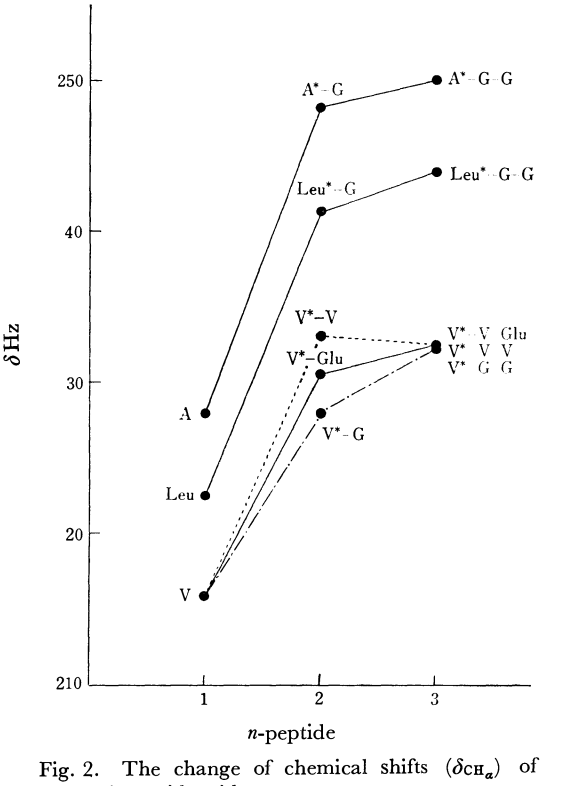

Fig. 2. The change of chemical shifts (δ_{CH_α}) of α-amino acid residues.
(δ_{CH_α} of the amino acid residue with an asterisk is shown. A; Alanine, G; Glycine, Glu; Glutamic acid, Leu; Leucine, V; Valine)

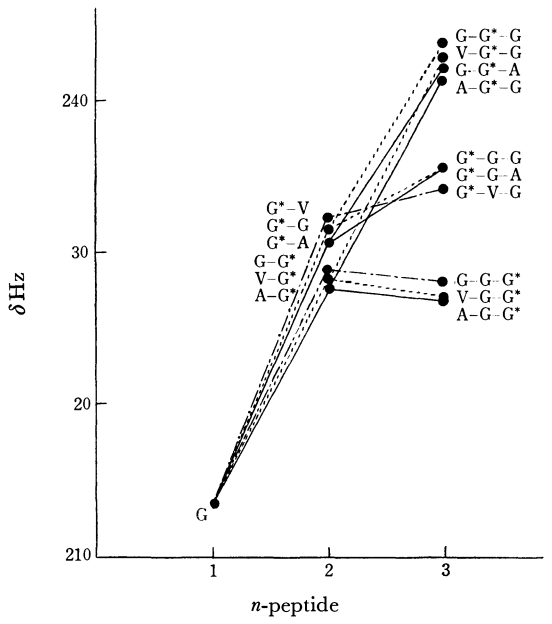

Fig. 3. The change of chemical shifts (δ_{CH_2}) of glycine residues.
(δ_{CH_2} of glycine residue with an asterisk is shown. A; Alanine, G; Glycine, V; Valine)
Values for glycyl-glycyl-alanine were from Ref. 10

TABLE 2. THE AVERAGE CHEMICAL SHIFT VALUES OF THE AMINO ACID RESIDUES IN *n*-PEPTIDES (δ_{CH_α} and δ_{CH_2}) AND THE DIFFERENCES IN THE CHEMICAL SHIFTS WITH RESPECT TO THE FREE AMINO ACID ($\Delta\delta$)

δ_{CH_α} of L-valine peptides

n-Peptides	Amino acid residue	δ_{CH_α} (Hz from DSS)	$\Delta\delta$ (Hz)	Number of cases
1	L-val (1,3)	215.8	0	1
2	L-val (1)	230.6	14.8	3
	L-val (3)	245.0	29.2	2
	L-val (1)	232.4	16.6	4
3	L-val (2)	253.5	37.7	4
	L-val (3)	242.6	27.6	1

δ_{CH_2} of glycine peptides

n-Peptides	Amino acid residue	δ_{CH_2} (Hz from DSS)	$\Delta\delta$ (Hz)	Number of cases
1	Gly (1,3)	213.6	0	1
2	Gly (1)	231.4	17.8	3
	Gly (3)	228.1	14.5	3
3	Gly (1)	234.8	21.2	2
	Gly (2)	242.6	29.0	3
	Gly (3)	227.1	13.5	4

δ_{CH_α} and δ_{CH_2}. That is, the δ_{CH_α} of L-val(3) does not agree with the δ_{CH_2} of gly(3), while the δ_{CH_α} of L-val(1,3) and the δ_{CH_2} of gly(1,3), and those of L-val(1) and gly(1), of dipeptides coincide. This discrepancy can not be explained in terms of the difference in electronegativity; this suggests that the electric field and the magnetic anisotropy effect play an important role in determining the chemical shifts of the peptides.

A rough correlation is found to exist between these chemical shift values; the δ_{CH_α} (or δ_{CH_2}) of the A(1) and A(3) of a given amino acid is almost unchanged through di- and tripeptide, and the δ_{CH_α} (or δ_{CH_2}) of A(2) can easily be estimated by adding the sum of the $\Delta\delta$'s of A(1) and A(3) to the δ_{CH_α} (or δ_{CH_2}) of A(1,3). From this observation, it may be concluded that a tripeptide can be a good model for polypeptides. This conclusion is supported by a comparison of the δ_{CH_2} of the central methylene group of triglycine (243.7 Hz) with the reported[12] δ_{CH_2} value of that of the pentaglycine (240.0 Hz).

2) Spin-spin Coupling Constants. The spin-spin coupling constants of L-valine change when it forms a peptide bond. Figures 4 and 5 show

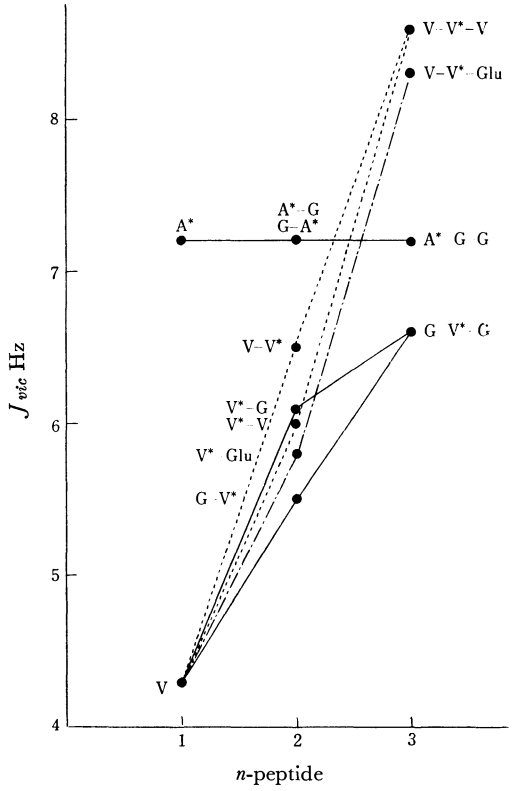

Fig. 4. The change of spin-spin coupling constants (J_{vic}) of L-valine and alanine residues.
(J_{vic} of amino acid residue with an asterisk is shown. A; Alanine, G; Glycine, Glu; Glutamic acid, V; Valine)

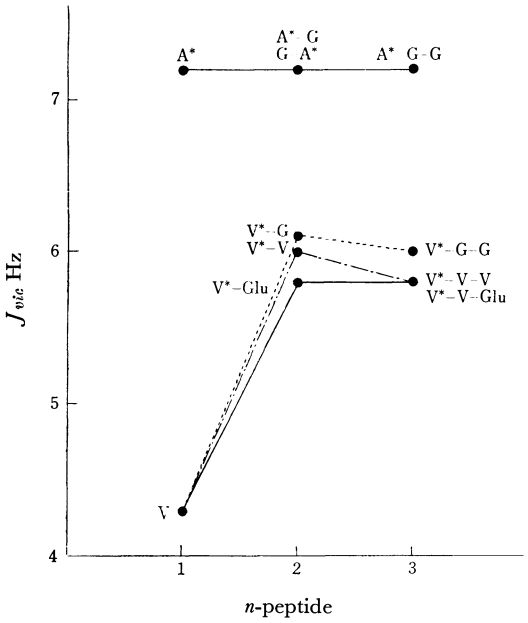

Fig. 5. The change of spin-spin coupling constants (J_{vic}) of L-valine and alanine residues.
(J_{vic} of amino acid residue with an asterisk is shown. A; Alanine, G; Glycine, Glu; Glutamic acid, V; Valine)

the J_{vic}'s of L-valine residues. From these figures, rather clear trends are observable; the J_{vic} for L-val(1,3) is 4.3 Hz. The averages of J_{vic} for L-val(1) and L-val(3) in dipeptides are 6.0 and 6.0 Hz respectively, while that for L-val(2) in tripeptides is 7.8 Hz. However, the J_{vic}'s for L-val(1) and L-val(3) hardly change from dipeptide to tripeptide; they are all about 6.0 Hz. That is, the J_{vic} for L-val(1,3) grows larger as its amino and carboxyl groups form peptide bonds. The difference in electronegativity between a free amino (or carboxyl) group and that which formed a peptide bond can not be considered[14] to have such a large effect on the J_{vic} of L-valine. Moreover, the J_{vic} of L-alanine is considered to be influenced by the difference in electronegativity alone and not by the population change in the rotamers,[15-16] because the three rotamers are equivalent. The observed J_{vic} of L-alanine is 7.2 Hz, and it does not change at all when it forms a peptide bond with glycine. From these considerations, it can be concluded that the difference in electronegativity between a free amino (or carboxyl) group and that which formed a peptide bond does not influence the J_{vic} of a given amino-acid residue. Therefore, the J_{vic} of L-valine residues in oligopeptides is mainly affected by the population change of the rotamers. Employing 13.6 and 2.6 Hz as the J_{vic} values of the *trans* and *gauche* rotamer (J_t and J_g)[17], we calculated the populations of the *trans* and *gauche* rotamers (P_t and P_g).

Table 3-1. The populations and the relative energies of the rotational isomers for L-valine derivatives

	J_{vic} (Hz)	P_t	P_g	ΔE (kcal/mol)
L-Val*	4.3	0.15	0.85	−0.63
L-Val*-Gly	6.1	0.31	0.69	−0.06
L-Val*-L-Val	6.0	0.31	0.69	−0.07
L-Val*-L-Glu	5.8	0.29	0.71	−0.11
L-Val*-Gly-Gly	6.0	0.31	0.69	−0.07
L-Val*-L-Val-L-Val	5.8	0.29	0.71	−0.11
L-Val*-L-Val-L-Glu	5.8	0.29	0.71	−0.11

Results for the valine residue with an asterisk are shown.

Table 3-2. The populations and the relative energies of the rotational isomers for L-valine derivatives

	J_{vic} (Hz)	P_t	P_g	ΔE (kcal/mol)
L-Val*	4.3	0.15	0.85	−0.63
Gly-L-Val*	5.5	0.26	0.74	−0.21
L-Val*-L-Val	6.0	0.31	0.69	−0.07
L-Val-L-Val*	6.5	0.36	0.64	0.07
Gly-L-Val*-Gly	6.6	0.36	0.64	0.07
L-Val-L-Val*-L-Val	8.6	0.55	0.45	0.53
L-Val-L-Val*-L-Glu	8.3	0.52	0.48	0.47

Results for the valine residue with an asterisk are shown.

The relative energies of *gauche* rotamers with respect to the *trans* rotamer (ΔE) were obtained, assuming that the two *gauche* rotamers have equal populations. The results are shown in Table 3. It can clearly be seen that the successive formations of peptide bonds to both ends of a valine (amino and carboxyl group) cause the population of the *trans* rotamer to grow larger, thus enlarging the dihedral angle. This phenomenon accords with the one observed hitherto[14] and may be explained in terms of the steric hindrance of the functional groups.

14) R. J. Abraham and K. G. R. Pachler, *Mol. Phys.*, **7**, 165 (1963).
15) H. Ogura, Y. Arata and S. Fujiwara, *J. Mol. Spect.*, **23**, 76 (1967).
16) J. W. Emsley, J. Feeney and L. H. Sutcliffe, "High Resolution Nuclear Magnetic Resonance Spectroscopy," Vol. 1, Pergamon Press, New York (1965), p. 561.
17) K. G. R. Pachler, *Spectrochim. Acta*, **20**, 581 (1964).

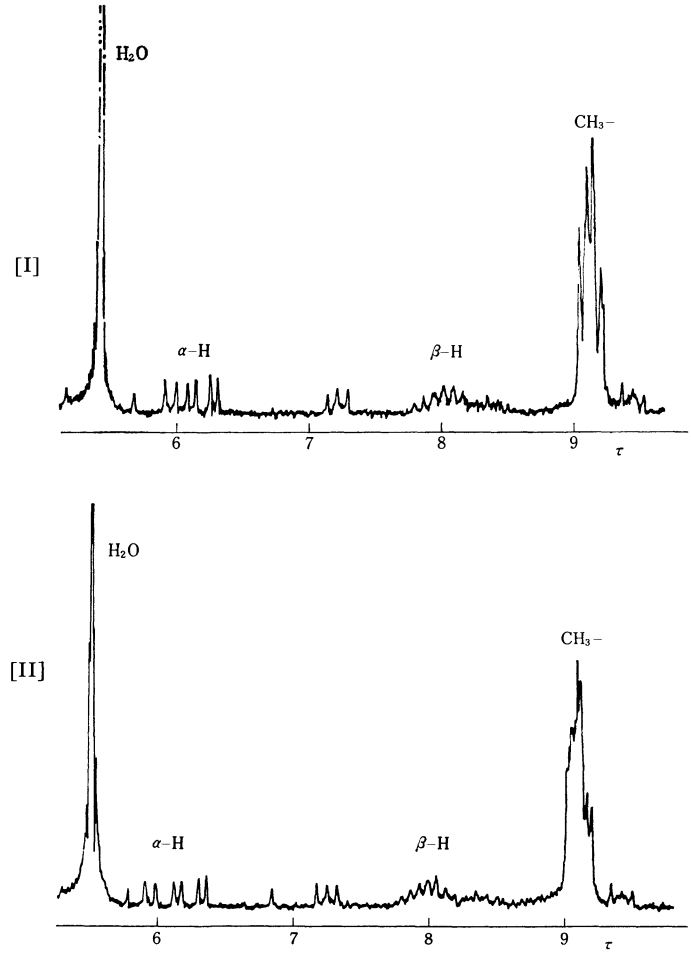

Fig. 6. NMR spectra of L-val-L-val-L-val [I] and L-val-L-val-D-val [II] in D_2O solution (100 MHz)

TABLE 4. THE NMR PARAMETERS, POPULATIONS AND THE RELATIVE ENERGIES OF ROTATIONAL ISOMERS FOR VALINE TRIPEPTIDES

	L-Val (1)	L-Val (2)	D-Val (3)
L-Val-L-Val-L-Val (1) (2) (3) [I]	δ_{CH_α} 232.2 (Hz from DSS)	δ_{CH_α} 252.5 (Hz from DSS)	δ_{CH_α} 242.6 (Hz from DSS)
	J_{vic} 5.8 (Hz)	J_{vic} 8.6 (Hz)	J_{vic} 6.4 (Hz)
	P_t 0.29	P_t 0.55	P_t 0.35
	P_g 0.71	P_g 0.45	P_g 0.65
	ΔE −0.12 (kcal/mol)	ΔE 0.53 (kcal/mol)	ΔE 0.03 (kcal/mol)
	L-Val (1)	L-Val (2)	D-Val (3)
L-Val-L-Val-D-Val (1) (2) (3) [II]	δ_{CH_α} 232.7 (Hz from DSS)	δ_{CH_α} 257.1 (Hz from DSS)	δ_{CH_α} 244.2 (Hz from DSS)
	J_{vic} 5.8 (Hz)	J_{vic} 7.5 (Hz)	J_{vic} 5.9 (Hz)
	P_t 0.29	P_t 0.45	P_t 0.30
	P_g 0.71	P_g 0.55	P_g 0.70
	ΔE −0.12 (kcal/mol)	ΔE 0.29 (kcal/mol)	ΔE −0.09 (kcal/mol)

In conclusion, the J_{vic} of a given amino acid residue is found to be influenced by the one with which it is combined directly; therefore, tripeptide is a good model for polypeptides.

3) The Influence of the Configuration of an Amino Acid Residue on the NMR Parameters of Peptides. Out of the eight diastereoisomers of valyl-valyl-valine, we have chosen two isomers, L-val-L-val-L-val [I] and L-val-L-val-D-val [II], and have studied the influence of optically active residues on the NMR parameters of these diastereoisomers. Figure 6 shows the NMR spectra of I and II at 100 MHz. The results, together with *Pt*, *Pg*, and the ΔE values calculated on the assumptions described above, are shown in Table 4. The influence of the configuration of val(3) is observable in the large differences between the NMR parameters of the val(2)'s of the two isomers.

With I, L-val(2) appears at a higher field and have a larger J_{vic} than L-val(2) of II. However, the NMR parameters of the L-val(1)'s of the two isomers agree very well. These facts show that the configuration of a given amino-acid residue influences its vicinal amino acid residues' NMR parameters and their conformations. However, the influence is very localized and change only the NMR parameters of the amino acid residues combined directly. Therefore, it can be concluded that tripeptide can be a good model compound for polypeptides, even when one considers the influence of the optical isomerism.

The authors are grateful to Professor Shizuo Fujiwara and to Dr's. Yoji Arata and Takeo Yamamoto of the University of Tokyo for stimulating and helpful discussions.

BULLETIN OF THE CHEMICAL SOCIETY OF JAPAN VOL. 43 1329—1336 (1970)

The Radiolysis and Photolysis of Methanolic Solutions of Eosin. I. The γ-Radiolysis of Neutral and Alkaline Solutions

Kazuie KIMURA, Takuji MIWA*1 and Masashi IMAMURA

The Institute of Physical and Chemical Research, Yamato-machi, Saitama

(Received December 1, 1969)

The γ-radiolysis of eosin has been studied in deaerated neutral and alkaline methanolic solutions. Eosin is reduced principally with CH_2OH radicals in dilute solutions. In neutral solutions, $G(-\text{eosin})$ is about 2 at the eosin concentration of 10^{-5}M and increases as the concentration of eosin is increased. The final products are leuco-eosin and an unidentified substance which has an absorption peak at 455 nm. In an alkaline solution (10^{-5}M), $G(-\text{eosin})$ is about 4 and the product is semireduced eosin, which is stable in the dark and which undergoes photo-debromination. The ESR spectrum of semireduced eosin has also been recorded. Comparative studies have also been made on uranin solutions.

The photochemistry of several xanthene dyes, eosin, erythrosin, and uranin in aqueous and alcoholic solutions was investigated by Imamura and Koizumi during the 1955—1958 period.[1-6] Thereafter, Koizumi and his co-workers have worked on the flash photolysis of these systems and have elucidated the primary processes in detail; the outlines have recently been reviewed by Koizumi.[7] The flash-photolysis technique has also been applied by Lindqvist[8,9] and by Grossweiner and Zwicker[10,11]

*1 Present address: Institute of Natural Color Technology, Chiba University, Yayoi-cho, Chiba.

1) M. Imamura and M. Koizumi, This Bulletin, **28**, 117 (1955).
2) M. Imamura and M. Koizumi, *ibid.*, **29**, 899 (1956).
3) M. Imamura and M. Koizumi, *ibid.*, **29**, 913 (1956).
4) M. Imamura, *ibid.*, **30**, 249 (1957).
5) M. Imamura, *ibid.*, **31**, 62 (1958).
6) M. Imamura, *ibid.*, **31**, 962 (1958).
7) M. Koizumi, *Nippon Kagaku Zasshi*, **90**, 117 (1969).
8) L. Lindqvist, *Ark. Kemi*, **16**, 79 (1960).
9) V. Kasche and L. Lindqvist, *Photochem. Photobiol.*, **4**, 923 (1965).
10) L. I. Grossweiner and E. F. Zwicker, *J. Chem. Phys.*, **31**, 1141 (1959); **34**, 1411 (1961); **39**, 2774 (1963).
11) E. F. Zwicker and L. I. Grossweiner, *J. Phys. Chem.*, **67**, 549 (1963).

to aqueous solutions of these dyes. The photochemical oxidation or reduction of these dyes is initiated by the reaction between the dye in the triplet state and the oxidizing or reducing substance or the dye in the ground state, depending upon the concentration of dye.

In the radiolysis of dilute solutions, however, dyes in the ground state are attacked by intermediates produced from the radiolyzed solvent. For aqueous solutions, the attacking species are principally hydrated electrons and hydroxyl radicals, and the products are semireduced and semioxidized dyes respectively.[12-14] Subsequent reactions seem similar to those in the photochemical systems. These intermediate products for uranin and eosin in aqueous solutions have been investigated by the pulse-radiolysis technique,[12,13] and the overall yields for the bleaching of eosin by γ-rays have been reported.[14] No corresponding studies have yet been reported on alcoholic solutions, however. As the radiolysis of alcohols has been investigated to a considerable extent,[15] it seemed that it would be interesting and worthwhile to compare the results for aqueous and alcoholic solutions. It seemed that it would be interesting also to observe if the dehalogenation of halogenated dyes occurred in the radiolysis; it has been observed but not fully explained in the photolysis of aqueous alcoholic solutions containing alkali.[3] The photochemical dehalogenation reaction will be described at length in the succeeding paper. In this paper the results obtained for the ^{60}Co-γ radiolysis of neutral and alkaline methanolic solutions of eosin, along with the ESR spectra of semireduced eosin and uranin produced in alkaline solutions, will be presented.

Experimental

Eosin (disodium salt of 2′,4′,5′,7′-tetrabromofluorescein) of Merck was recrystallized four times from a slightly alkaline methanol solution. Uranin (disodium salt of fluorescein) of Merck was also purified similarly. The molar extinction coefficient of the purified eosin was 1.17×10^{5}M^{-1}cm^{-1} in methanol at 521 nm, while that of uranin was 8.7×10^{4}M^{-1}cm^{-1} at 495 nm.

Methanol of a spectral quality (Dotite Spectrosol) was refluxed with sodium borohydride (1 g/400 m*l*) before distillation on a 40-theoretical-plate column. A middle fraction of the distillate was taken and was dried by refluxing it on magnesium methoxide prepared by dissolving 2—3 g of magnesium turnings in 150 m*l*. Purified methanol was kept *in vacuo*.

Nitrous oxide (standard gas of Takachiho Chem. Ind.; purity stated >99.9%) was further purified by distillation *in vacuo*. Extra-pure sodium and potassium hydroxides were used without further purification.

A concentrated eosin solution in methanol (stored in the dark) was diluted with purified methanol by distillation *in vacuo* and then degassed thoroughly by the microstill reflux method.[16] Nitrous oxide was added to the degassed solution manometrically; the concentration was calculated from the solubility data.[17]

Solutions were irradiated in the dark with 1.2 kCi ^{60}Co-γ rays at a dose rate in the vicinity of 1×10^{16} eV ml^{-1}min^{-1}. An irradiation ampoule made of Pyrex glass was provided with a quartz optical cell (10 or 1 mm thick). The optical cell was shielded from γ-rays with lead blocks during γ-irradiation. Dye solutions were kept in the dark throughout the experiment because some irradiation products were found to be particularly sensitive to light. The dose rate was determined by Fricke dosimetry on the basis of $G(Fe^{3+})=15.5$, with a correction for the electron density of the solvent used. The absorption spectra were recorded on a Shimadzu SV-50A spectrophotometer at room temperature.

The ESR spectra were recorded at room temperature with a JEOL 3B-X spectrometer with a 100 kHz-field modulation. A capillary cell (1 mm *i.d.*) attached to the irradiation ampoule was heated before use to remove any paramagnetism induced by γ-irradiation.

Results

Neutral Solutions. Upon the γ-irradiation of neutral eosin solutions in methanol in the concentration range of 9.38×10^{-6}—1.64×10^{-4}M, the absorption peak of eosin at the longest wavelength (521 nm) decreases with a slight shift (2—3 nm) to the shorter wavelength. Isosbestic points are observed in the vicinities of 242, 355, and 460 nm. A typical spectral change induced by γ-irradiation for the 7.64×10^{-5}M solution is shown in Fig. 1.

Close examination revealed that a small absorption band which was very sensitive to light appears between 360 and 450 nm. This absorption spectrum is shown more clearly in Fig. 2, which was obtained with the eosin solution (9.29×10^{-5}M) subjected to prolonged irradiation. Other product absorptions are observed at 289 and <260 nm.

The absorption spectra of irradiated eosin solutions did not change for at least one day so long as the solutions were kept in the dark. However, upon the absorption of light the 455 nm absorption band decreased, finally disappearing as the 521 nm band increased. The saturation by air or bubbling oxygen gas into the irradiated eosin solution caused a slight depression of both 455 and 521 nm absorption bands, but they were restored by bubbling nitrogen gas.

12) J. Chrysochoos, J. Ovadia and L. I. Grossweiner, *ibid.*, **71**, 1629 (1967).
13) P. Cordier and L. I. Grossweiner, *ibid.*, **72**, 2018 (1968).
14) A. F. Rodde, Jr., and L. I. Grossweiner, *ibid.*, **72**, 3337 (1968).
15) J. Teply, *Radiat. Res. Rev.*, **1**, 361 (1969).
16) L. M. Theard and M. Burton, *J. Phys. Chem.*, **67**, 59 (1963).
17) A. Seidell, "Solubilities of Inorganic and Metal Organic Compounds," 2, 4th Ed., American Chemical Society, Washington, D. C. (1965), p. 802.

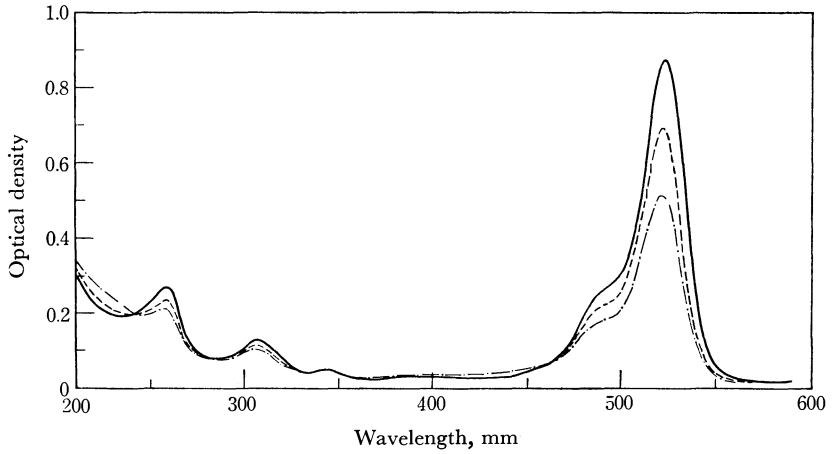

Fig. 1. Absorption spectra of 7.64×10^{-5}M eosin solution in MeOH before and after γ-irradiation (l=1 mm).
—— before irradiation, ------ after irradiation 6×10^{17} eV/ml, -·-·- 1.2×10^{18} eV/ml.

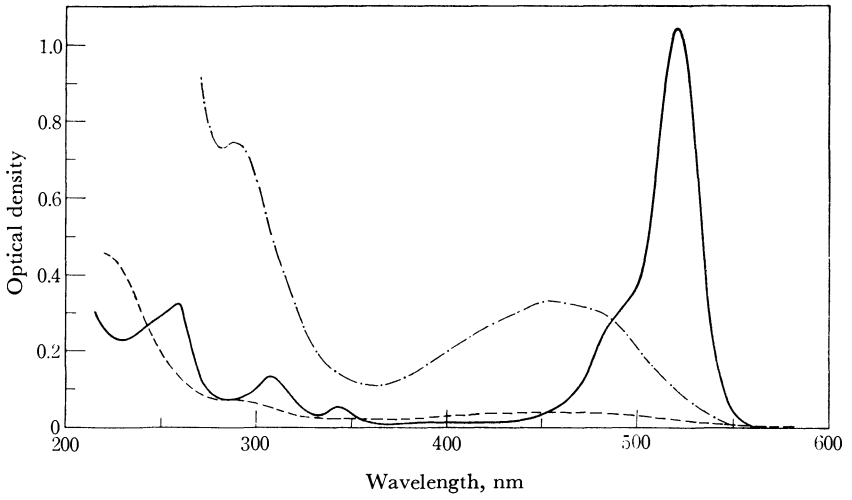

Fig. 2. Absorption spectra of 9.29×10^{-5}M eosin solution in MeOH before and after γ-irradiation.
—— before irradiation (l=1 mm), ------ afterirradiation 4.8×10^{18} eV/ml (l=1 mm), -·-·- (l=10 mm).

Similar absorption spectra were obtained with uranin solutions containing 2×10^{-3}M NaOH. Absorption peaks appear at 395, 280, 255, and $<$ 230 nm. The absorption at 395 nm probably corresponds to that for eosin at 455 nm; the latter was scarcely affected by light, however.

The radiation chemical yields for the disappearance of eosin can be obtained from the decrease in the optical density at 521 nm. The decrease in the optical density at 521 nm showed a good linear relationship with the radiation does. A typical example is shown in Fig. 3. The yields (G, the number of eosin molecules disappearing per 100 eV of energy absorbed) are plotted in Fig. 4 as a function of the initial concentration of eosin. The G(−eosin) rapidly increases to about 2 with an increase in the concentration from the initial 0 through 10^{-5}M; then it increases rather slowly. The scattered plots in the higher concentration range may be partly due to the effect of stray light, despite the meticulous care, and partly to some contamination in the eosin.

In Fig. 4 are also shown the yields for the solutions containing N_2O ($\sim10^{-2}$M), which is a solvated-electron scavenger. No substantial effect of N_2O on the G-value is observed within the range of

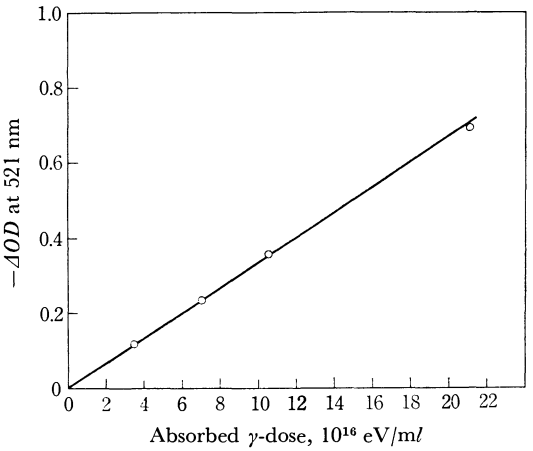

Fig. 3. A plot of $-\Delta OD$ at 521 nm *vs.* absorbed dose. Eosin 8.88×10^{-6}M in MeOH.

experimental error. The absorption spectra and the effects of light and oxygen on them were quite the same as in the case without N_2O.

Alkaline Solutions. Eosin disappears in an alkaline solution with $G(-\text{eosin})=4.0\pm0.3$ at 1.3×10^{-5}M eosin and 0.1—0.2M NaOH; this $G(-\text{eosin})$ is twice as large as in a neutral solution at the same concentration.

The absorption spectra of the irradiated eosin (10^{-5}—10^{-3}M) solutions in methanol containing 2 vol% H_2O and alkali hydroxide (NaOH or KOH 0.1—0.3M) were quite different from those of neutral solutions. The absorption spectrum obtained with a 1.29×10^{-5}M eosin solution containing about 0.2M NaOH is shown in Fig. 5. Figure 5 shows that a product with its absorption maximum at 408 nm forms as the eosin disappears. A similar absorption spectrum was obtained with uranin under the same conditions, the peak wavelength being 394 nm.

This product is considerably stable *in vacuo* and in the dark, but upon the addition of oxygen it converts rapidly and almost completely into the original eosin or uranin. Assuming a full conversion of the product into eosin or uranin by the addition of oxygen, which is reasonable when the amount of bleached dye is small, one can obtain the molar extinction coefficients for the products as $\varepsilon(408\text{ nm})=(6.28\pm0.05)\times10^4\text{M}^{-1}\text{cm}^{-1}$ for eosin and $\varepsilon(394\text{ nm})=(3.95\pm0.03)\times10^4\text{M}^{-1}\text{cm}^{-1}$ for uranin both in 98 vol% methanol containing 0.1M NaOH.

By comparing these results with the previous photochemical results,[6,9,11,18,19] one can assign this product to the basic form of the semireduced eosin or uranin. The absorption spectra of semireduced eosin and uranin produced by the prolonged γ-irradiation of eosin and uranin solutions containing NaOH are shown in Figs. 6 and 7 respectively. The ESR spectra could in fact be obtained as shown in Figs. 8 and 9 for semireduced eosin and uranin respectively.

Interestingly, upon excitation with 408 nm light, the absorption at 408 nm of the irradiated eosin solution showed a hypsochromic shift as its intensity was decreased. Consequently, the ESR spectrum grew more complex, until ultimately it was superimposable on the corresponding spectrum obtained with an irradiated uranin solution. This result has

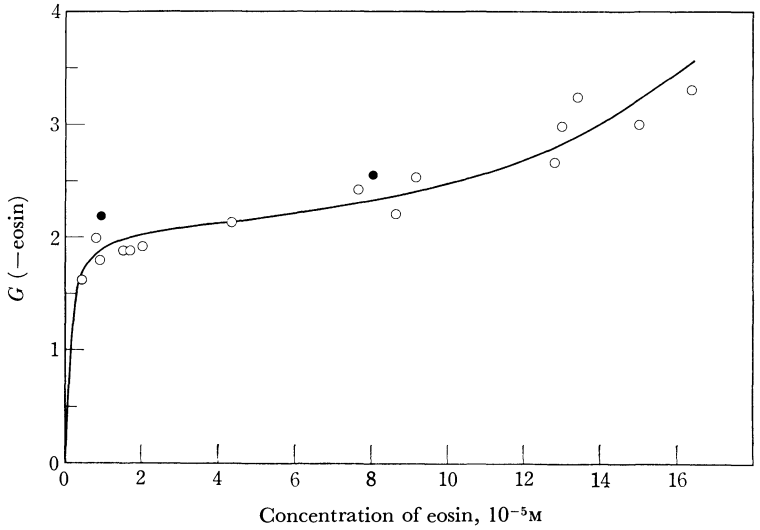

Fig. 4. $G(-\text{eosin})$ as a function of [eosin]. ○ in pure MeOH, ● in MeOH containing N_2O ($1.6-1.9\times10^{-2}$M).

18) A. Kira and S. Kato, *Sci, Rep., Tohoku Univ.*, **48**, 142 (1965).

19) T. Ohno, S. Kato and M. Koizumi, This Bulletin, **39**, 232 (1966).

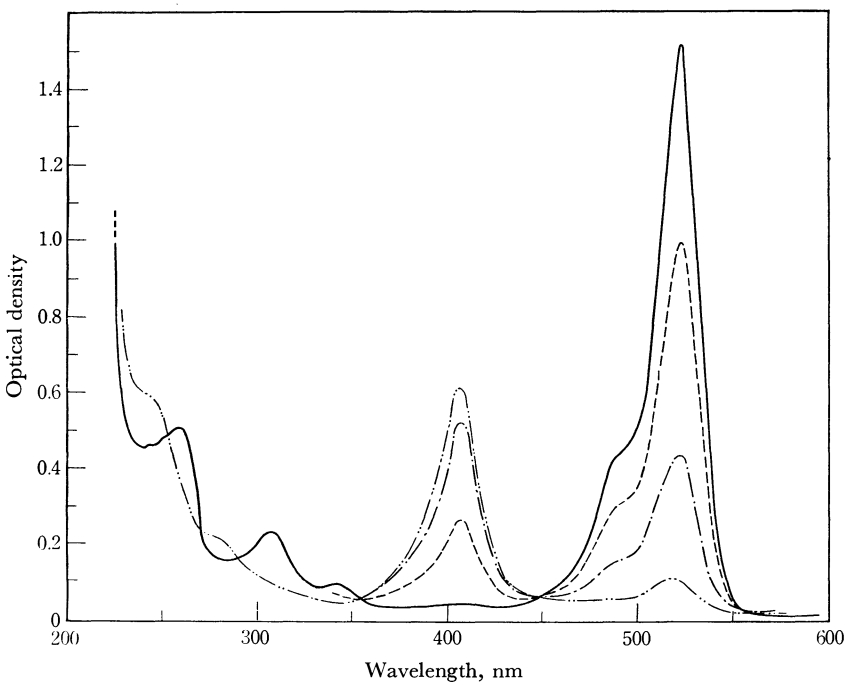

Fig. 5. Absorption spectra of 1.29×10^{-5}M eosin solution in 98% MeOH containing 0.2M NaOH before and after γ-irradiation (l=10 mm).
—— before irradiation, ------ after irradiation 7.5×10^{16} eV/ml,
-·-·- 1.5×10^{17} eV/ml, -··-··- 2.25×10^{17} eV/ml.

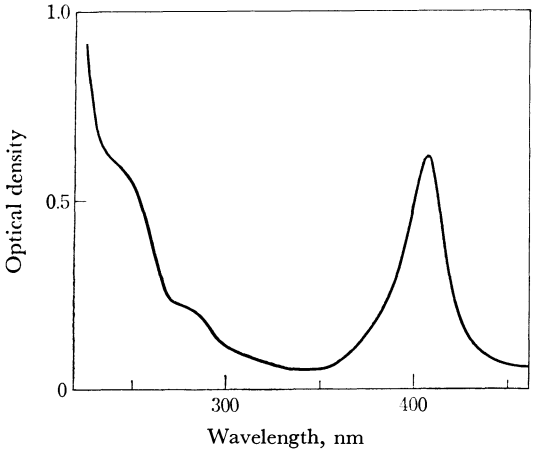

Fig. 6. Absorption spectrum of semireduced eosin prepared by prolonged γ-irradiation (2.8×10^{17} eV/ml) of 1.4×10^{-5}M eosin solution in 98% MeOH containing 0.3M NaOH.

been briefly communicated elsewhere;[20] a full account will be reported in the succeeding paper.

Discussion

Reactive Species in Aqueous and Methanolic Solutions. The radiolysis of methanol yields several primary free radicals:

$$CH_3OH \rightsquigarrow e^-_{solv}, \cdot H, \cdot CH_3O, \cdot CH_2OH, \cdot CH_3, \cdot OH, \text{ and molecular products} \quad (1)$$

In the radiolysis of a methanolic solution of eosin in the absence of oxygen, eosin will be reduced with some of these radicals. In an aqueous solution eosin is assumed to react with radicals by the following fast processes:[12,14]

$$D + e^-_{aq}(H) \rightarrow \cdot S \quad (2)$$

$$D + \cdot OH \rightarrow \cdot X + OH^- \quad (3)$$

$$D + \cdot OH \rightarrow \cdot DOH \quad (4)$$

where D, S, X, and DOH are eosin, semireduced eosin, semioxidized eosin, and OH adduct respectively. The rate constants of Reactions (2) and (3) have been determined by the pulse-radiolysis technique to be $k_2 \geq 5\times10^9 M^{-1}$ sec^{-1} and $k_3=(1.4\pm0.4)\times10^{10} M^{-1}$ sec^{-1}.[12]

In the γ-radiolysis of methanol, solvated electrons (G=2.0[21]) decay with a rate constant of the order of 10^5 sec^{-1}:[22,23]

20) K. Kimura, T. Miwa and M. Imamura, *Chem. Commun.*, **1968**, 1619.

21) H. Seki and M. Imamura, *J. Phys. Chem.*, **71**, 870 (1967).

22) H. Seki and M. Imamura, to be published.

23) a) I. A. Taub, D. A. Harter, M. C. Sauer, Jr., and L. M. Dorfman, *J. Chem. Phys.*, **41**, 979 (1964). b) F. S. Dainton, J. P. Keene, T. J. Kemp, G. A. Salmon and J. Teply, *Proc. Chem. Soc.*, **1964**, 265. c) K. N. Jha and G. R. Freeman, *J. Phys. Chem.*, **48**, 5480 (1968).

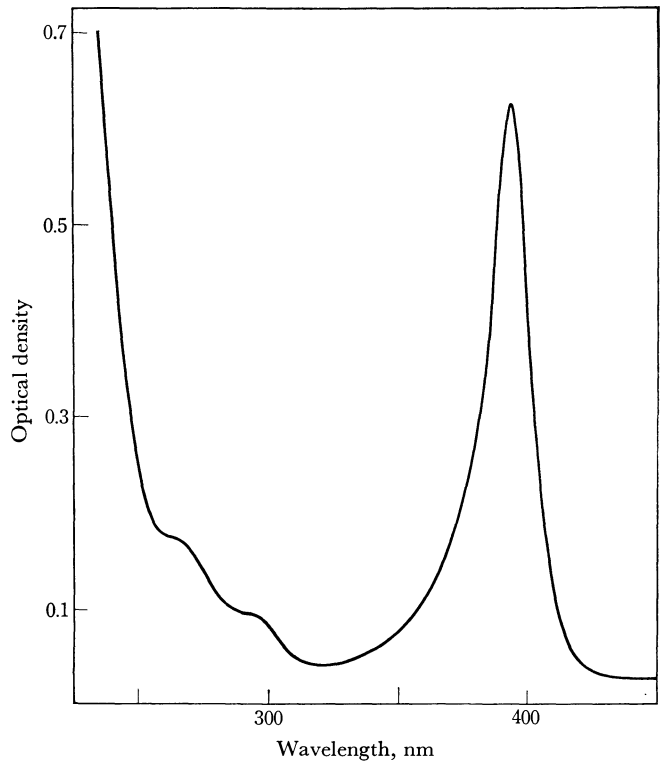

Fig. 7. Absorption spectrum of semireduced uranin prepared by prolonged γ-irradiation (1.4×10^{16} eV/ml) of 1.47×10^{-5}M uranin solution in 98% MeOH cantaining 0.1M KOH.

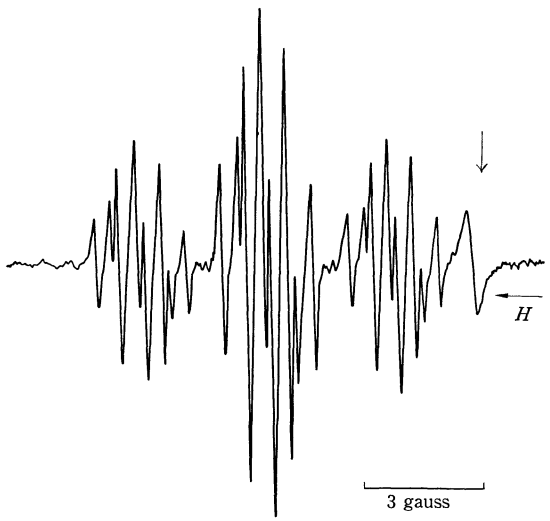

Fig. 8. ESR spectrum of semireduced eosin prepared by γ-irradiation (10^{18} eV/ml) of 1×10^{-4}M eosin solution in 70% MeOH cantaining 0.3M NaOH. The arrow indicates the standard signal of $K_2(SO_3)_2NO$.

$$e^-_{solv} \rightarrow CH_3O^- + \cdot H \qquad (5)$$

and H atoms ($G=1.7$[21]) react with methanol with $k_6=1.6\times10^6$M^{-1} sec^{-1} [24] to produce hydrogen and CH_2OH radicals:

$$\cdot H + CH_3OH \rightarrow H_2 + \cdot CH_2OH \qquad (6)$$

The other radicals produced by Reaction (1) also yield CH_2OH radicals by reactions with methanol, the total radical yield in the γ-radiolysis of methanol being determined to be 6.2.[25,26]

Reduction of Eosin in Methanolic Solutions. If the rate constant between the solvated electron and eosin in methanol is assumed to be the same as that in the aqueous solution,[27] $k_2[D]<k_5$ for the solution of 10^{-5}—10^{-4}M eosin. Figure 4 shows that $G(-\text{eosin})$ is about 2 at eosin concentrations as low as 10^{-5}M; above this point the rate of the increase in $G(-\text{eosin})$ is lower. This fact may indicate that eosin undergoes reduction principally by Reaction (7) to form semireduced eosin:

$$D + \cdot CH_2OH \rightarrow \cdot S + CH_2O \qquad (7)$$

24) P. Neta and L. M. Dorfman, *J. Phys. Chem.*, **73**, 413 (1969).
25) S. U. Choi and N. N. Lichtin, *J. Amer. Chem. Soc.*, **86**, 3948 (1964).
26) H. Seki, R. Nagai and M. Imamura, This Bulletin, **41**, 2877 (1968).
27) This assumption will be correct if reactions are diffusion-controlled.

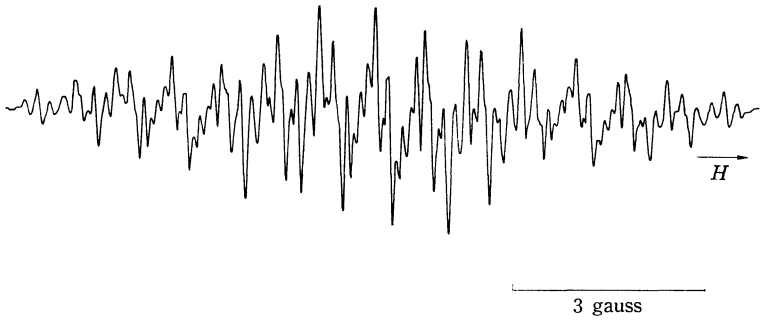

Fig. 9. ESR spectrum of semireduced uranin prepared by γ-irradiation (10^{18} eV/ml) of 1.4×10^{-4}M uranin solution in 80% MeOH containing 0.4M NaOH.

A similar reaction between eosin and C_2H_4OH radicals has been proved by Grossweiner *et al.* for aqueous eosin solutions containing 1 mM H_2O_2 and 10 mM C_2H_5OH; the rate constant of this reaction is $(1.1\pm0.2)\times10^{9}$M^{-1} sec^{-1}.[12]

Hydroxymethyl radicals combine with each other to form ethylene glycol:

$$\cdot CH_2OH + \cdot CH_2OH \rightarrow C_2H_6O_2 \qquad (8)$$

Reaction (8) is the principal reaction pathway of CH_2OH radicals in the radiolysis of methanol[26] and competes with Reaction (7) in the present systems. The rate constant of Reaction (8) has not been determined, but $2k=(1.4\pm0.4)\times10^{9}$M^{-1} sec^{-1} (23°) has been reported for C_2H_4OH radicals.[28]

Effect of Nitrous Oxide. The argument for Reaction (7) is obtained from the results with eosin solutions containing N_2O. Nitrous oxide scavenges solvated electrons in methanol completely at less than 5×10^{-3}M to form equivalent amounts of N_2 and OH radicals:[21,23c]

$$e^-_{solv} + N_2O \rightarrow N_2 + O^- (\rightarrow \cdot OH) \qquad (9)$$

The hydroxyl radicals produced by Reaction (9) react rapidly with the neighboring methanol to form CH_2OH radicals. If eosin is reduced with CH_2OH radicals, as has been mentioned above, the addition of N_2O to an eosin solution should not have any appreciable effect on $G(-\text{eosin})$; that is indeed the case, as may be seen from Fig. 4. As the concentration of eosin is increased, however, the reduction with solvated electrons may be of increasing importance.

Leuco-Dye Formation in Neutral Solutions. In deaerated aqueous solutions the reaction intermediates of eosin were assumed to decay predominantly by the back reaction:

$$\cdot S + \cdot X \rightarrow 2D \qquad (10)$$

accompanied by slower processes:

$$2X\cdot \rightarrow \text{products} \qquad (11)$$

$$2S\cdot \rightarrow D + L \qquad (12)$$

where L is the leuco-eosin.[14]

In dilute methanolic solutions, however, a principal intermediate is semireduced eosin, for the oxdizing radicals, CH_3O and OH, will rapidly disappear to form CH_2OH radicals by reactions with methanol. Thus, the semireduced eosin in methanol decays according solely to Reaction (12) to form leuco-eosin.

The absorption spectrum of the prolonged γ-irradiated eosin solution, Fig. 2, has three absorption peaks, at wavelengths of $<$230, 290 and 455 nm. For an irradiated uranin solution, four absorption peaks due to stable products were observed at $<$230, 255, 280, and 395 nm. The absorption spectrum of leuco-eosin has not been determined. However, Uchida *et al.*[29] have reported the absorption spectrum of leuco-uranin, which has two peaks at 210 and 280 nm ($\varepsilon=5\times10^{3}$M^{-1}cm^{-1}). We re-determined the absorption spectrum with leuco-uranin prepared chemically by a method similar to that employed by Uchida *et al.* and confirmed the existence of three absorption peaks, at $<$230, 255, and 280 nm. (We did not succeed in preparing leuco-eosin). Comparing the absorption spectra for the irradiated eosin and uranin with that for the chemically-prepared leuco-uranin, one may reasonably ascribe two of the three absorption peaks for eosin and three of the four for uranin to the formation of leuco-eosin and leuco-uranin by γ-irradiation.

Absorption at 455 nm Produced by γ-Irradiation. An absorption band at 455 nm produced in the γ-irradiated neutral eosin solution is sensitive to light, but is not affected by oxygen. A similar absorption appears in the uranin solution at 395 nm, but it is not sensitive at all to either light or oxygen. A free-radical nature can, therefore, be ruled out. The resumption of a complex between leuco-dye and one of the radiolysis products of methanol (say, formaldehyde) can also be ruled out, for no such absorption was observed for the leuco-dye solution containing formaldehyde. The experi-

28) L. M. Dorfman and I. A. Taub, *J. Amer. Chem. Soc.*, **85**, 2370 (1963).

29) K. Uchida, S. Kato and M. Koizumi, This Bulletin, **35**, 16 (1962).

mental facts that, upon light absorption, a simultaneous decrease in the 455 nm band and increase in the 521 nm band, with slight shifts to shorter wavelengths, were observed, and that no similar change was observed for uranin solutions, may indicate that the 455 nm absorption is due to an unidentified product which undergoes photo-debromination (see below).

Intermediate in Alkaline Solutions. The reaction intermediate produced in alkaline eosin solutions ($\lambda_{max}=408$ nm) can be identified with semireduced eosin. The semireduced eosin formation in aqueous media has been confirmed by the flash-photolysis technique;[9,11,18,19] the molar extinction coefficient at the peak wavelength has been reported as $\varepsilon=4\times10^4$ (405 nm),[9] 3.8×10^4 (405 nm),[11] and 2.5×10^4 M^{-1} cm^{-1} (408 nm).[19] For uranin $\varepsilon=5\times10^4$ M^{-1} cm^{-1} (394 nm) in an aqueous medium has been reported as well.[8] Imamura found that the semireduced uranin is produced photochemically in alcoholic solutions and that it is stable in the dark in the absence of oxygen.[6] Several semireduced quinones have been known to be stable in alkaline solutions as a result of the formation of symmetrical anions. In alkaline solutions $G(-\text{eosin})$ is about twice that for neutral solutions; this indicates that the semireduced eosin is stable and does not undergo Reaction (11).

Semireduced xanthene dyes may be represented as follows:

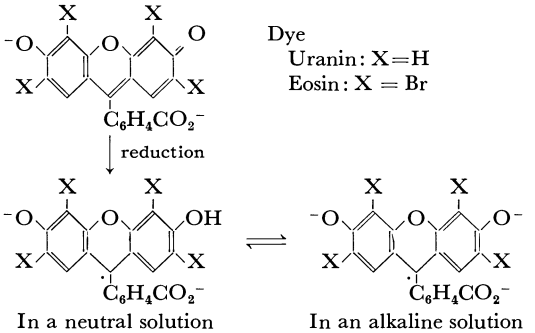

Semireduced forms

ESR Spectra of Simireduced Eosin and Uranin. The ESR spectrum for an irradiated eosin solution, Fig. 8, consists of three groups of lines with the intensity ratio of 1 : 2 : 1 and with the coupling constant of 3.16 gauss. Each group has hfs with the ratio of 1 : 1 : 3 : 3 : 3 : 1 : 1. The fact that the ESR spectrum for the uranin solution (Fig. 9) is more complex than for the eosin solution is apparent from the fact that four bromine atoms are replaced by hydrogen atoms for uranin. This result is in agreement with, and is evidence for, the conclusion that the product is the semireduced eosin. An ESR study of the semireduced uranin has been carried out by Okuda *et al.*;[30] the analysis of the ESR spectra for semireduced forms of xanthene dyes will be described in detail elsewhere.

30) M. Okuda, Y. Momose, S. Niizuma and M. Koizumi, *ibid.*, **40**, 1332 (1967).

BULLETIN OF THE CHEMICAL SOCIETY OF JAPAN VOL. 43 1337—1342 (1970)

The Radiolysis and Photolysis of Methanolic Solutions of Eosin. II. The Photo-Debromination of Eosin in an Alkaline Solution

Kazuie KIMURA, Takuji MIWA*1 and Masashi IMAMURA

The Institute of Physical and Chemical Research, Yamato-machi, Saitama

(Received December 1, 1969)

Semireduced eosin was found to undergo photo-debromination and was identified with a precursor in the photo-debromination of eosin in alkaline methanolic solutions. Semireduced eosin was prepared by the γ-irradiation of an eosin solution. The photolysis of semireduced eosin was investigated by the use of continuous and flash light. From the absorption spectral change and a study of the decay, the mechanism of the photo-debromination was proposed. The debromination process of the photo-excited semireduced eosin was explained satisfactorily by assuming the transient formation of the debrominated-eosin σ-radical as an intermediate. In addition, we found an electron-transfer reaction from semireduced debrominated eosin to eosin, which results in the formation of semireduced eosin and debrominated eosin in the dark. A general conclusion as to the photo-dehalogenation of xanthene dyes is also given.

The photochemical debromination of eosin was found by Imamura and Koizumi in alkaline alcoholic solutions.[1] Upon irradiation by light, the absorption peak of eosin shifts gradually to shorter wavelengths; this shift proceeds until it attains the wavelength corresponding to the peak wavelength of uranin. Other halogenated xanthene dyes, such as eosin-blue (dinitro-dibromo-fluorescein) and erythrosin (tetraiodofluorescein), have also been observed to undergo similar photochemical dehalogenation.[2]

The debromination of eosin has also been reported for aqueous solutions containing phenol[3] and tertiary amines.[4] Zwicker and Grossweiner[3] assumed that the debromination takes place from the semireduced eosin on the basis of the marked dependence on the acidity. Oster *et al.*[4] postulated the same intermediate, which decomposes spontaneously to yield the partially-dehalogenated species as well. No concrete evidence has, however, yet been presented for the precursor of the dehalogenation or for its reaction mechanism.

In the photochemical system of eosin solutions, there appear several reactive intermediates, either one of which might be the precursor of debromination. These are the triplet state and semioxidized and leuco-eosin as well as the semireduced eosin. In fact, leuco-anthraquinonoid dyes in alkaline aqueous ethanolic solutions have been reported to undergo photo-dehalogenation.[5] In the preceding paper of this series,[6] we have reported on the γ-radiolysis of the neutral and alkaline methanolic solutions of eosin. In both solutions, eosin is reduced with the CH_2OH radical to form semireduced eosin. The semireduced eosin becomes leuco-eosin by means of the disproportionation reaction in the neutral solution, whereas it is stable in the dark in the alkaline solution.

No debromination has been observed in the radiolysis in the dark. The stable semireduced eosin has, however, been found to undergo photo-debromination. We have, therefore, investigated in detail the photo-debromination of the semireduced eosin which had been prepared by γ-irradiation in alkaline methanolic solutions of eosin. The results having been briefly communicated,[7] the accounts will be presented in detail in this paper.

Experimental

The materials and the experimental procedures, except for the photolysis, were largely the same as those reported previously.[6]

Irradiation was carried out with a projector lamp (300 W) with the aid of a lense and several filters.

*1 Present address: Institute of Natural Color Technology, Chiba University, Yayoi-cho, Chiba.

1) M. Imamura and M. Koizumi, This Bulletin, **29**, 913 (1956).

2) M. Imamura, unpublished results.

3) E. F. Zwicker and L. I. Grossweiner, *J. Phys. Chem.*, **67**, 549 (1963).

4) G. Oster, G. K. Oster and G. Karg, *ibid.*, **66**, 2514 (1962).

5) J. J. Moran and H. I. Stonehill, *J. Chem. Soc.*, **1957**, 788; C. J. Cooper and H. I. Stonehill, *ibid.*, **1958**, 3353.

6) K. Kimura, T. Miwa and M. Imamura, This Bulletin, **43**, 1329 (6970).

7) K. Kimura, T. Miwa and M. Imamura, *Chem. Commun.*, **1968**, 1619.

Toshiba glass filters, VG-1, VY-450, and VV-40, and Bausch and Lomb filters, 7-3269-2, C, and C-1, were used independently or in combination. The absorption spectra were recorded on a Shimadzu SV-50A or a Cary 14R spectrophotometer.

Flash photolysis was carried out with semireduced eosin solutions by using an apparatus which has been described elsewhere.[8] Briefly, the photolysis flash consisted of two Ushio xenon lamps. The operating characteristics of the lamps were: energy per flash: 100 joule; flash duration, to 50% peak: 10 μsec. The reaction vessel was a quartz cylinder, 10 mm in *i.d.* and 10 cm in length, with flat plates sealed on either end. The apparatus had facilities for both flash spectroscopic and kinetic spectrophotometric measurements.

Results

Photo-Debromination of Eosin in Alkaline Solutions. The absorption spectral shift for eosin solutions in deaerated aqueous methanol containing alkali was observed when they were irradiated with white light or with light which had passed through a Toshiba glass filter VG-1[9] (Fig. 1). The spectral shift induced by light absorption is identical with that reported previously; it has been proved to be due to the debromination of eosin.[1] The absorption peak finall attains a wavelength corresponding to the peak wavelength (495 nm) of uranin (disodium salt of fluorescein), which has no bromine substitution. The absorption bands appearing between 521 and 495 nm are due to the formation of dyes in which there is a replacement of bromine by hydrogen; 4′,5′-dibromouranin has its absorption peak at 506 nm.[4]

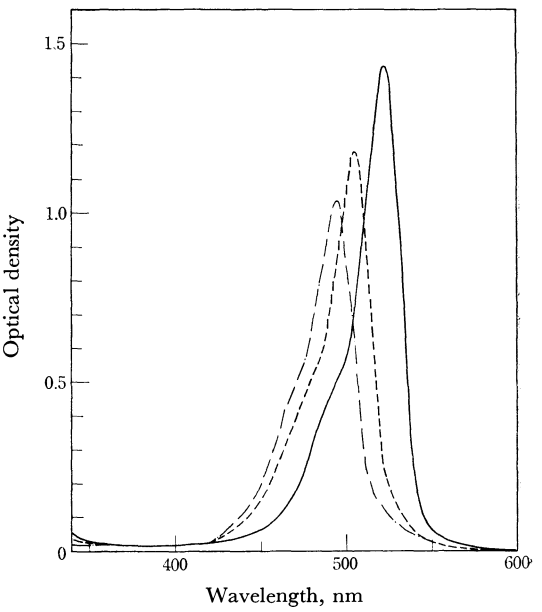

Fig. 1. Absorption spectra of 1.2×10^{-5}M eosin solution in 75% MeOH containing 1.2×10^{-2}M NaOH before and after light-irradiation.
—— before irradiation, ------, -·-·- after irradiation, filter VG-1.

Photolysis of Semireduced Eosin. If an interference filter which transmits a narrow band of light at 527 nm was used, irradiated eosin solutions showed merely the decrease at 521 nm and the increase at 408 nm (semireduced eosin[6]) in the intensity of the absorption peaks; they showed no

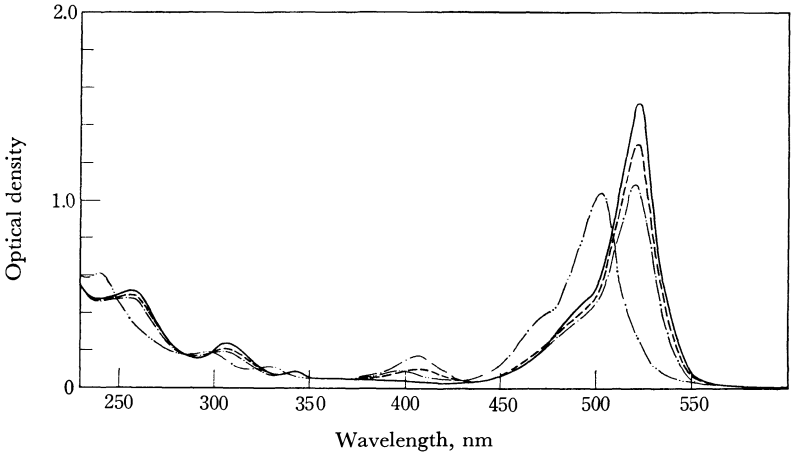

Fig. 2. Absorption spectra of 1.3×10^{-5}M eosin solution in 98% MeOH containing 0.2M NaOH before and after light-irradiation.
—— before irradiation, ------, -·-·- after irradiation by 527 nm light, filter combination C-1+7-3269-2+VY-450, -··-··- after irradiation of -·-·- by 402 nm light, filter combination 7-3269-2+C.

8) A. Kira and K. Nishi, *Rep. Inst. Phys. Chem. Res.*, **44**, 56 (1968).

9) The filter transmits light which is absorbed not only by eosin but also, to some extent, by semireduced eosin produced in alkaline solution.

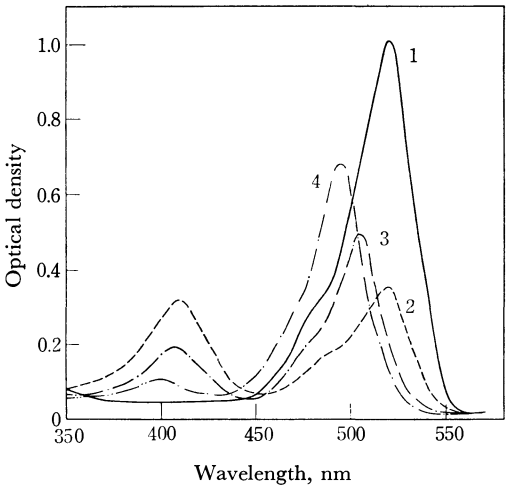

Fig. 3. Absorption spectra before and after irradiation.
1: 0.86×10^{-5}M eosin solution in 98% MeOH containing 0.2M NaOH before irradiation.
2: after γ-irradiation for 15 min at a dose rate of 1.13×10^{16} eV/m*l* min.
3 and 4: after irradiation of 2 by 402 nm light.

substantial spectral shift, as is shown in Fig. 2. These facts caused us promptly to carry out experiments to determine if the debromination would occur upon the photo-excitation of semireduced eosin. In fact, it took place, as is also shown in Fig. 2.

The photo-debromination of semireduced eosin was more clearly shown to take place for the solution of semireduced eosin which had been prepared by the γ-irradiation of an alkaline methanolic solution of eosin. In this solution, semireduced eosin is produced as quite a stable product, as has been reported previously.[6] Using an interference filter which transmits the light (402 nm) to be absorbed solely by semireduced eosin, we could observe the spectral change shown in Fig. 3; the change indicates that the photo-debromination of semireduced eosin is taking place.

As may be seen in Figs. 1, 2, and 3, the absorption bands developing in the course of the debromination process are as sharp as those for eosin or uranin, indicating that each intermediate absorption band may be due largely to a single compound and that, therefore, debromination may proceed in a step-by-step fashion. The above experimental results also indicate that the precursor of the photo-debromination of eosin is semireduced eosin.

ESR Spectrum Change Upon Light Irradiation. Figure 3 shows that the absorption peak of semireduced eosin also shifts to a shorter wavelength as its intensity is decreased. In a previous paper ESR spectra have been reported for semireduced eosin and uranin, prepared by the γ-irradiation of alkaline methanolic solutions of eosin

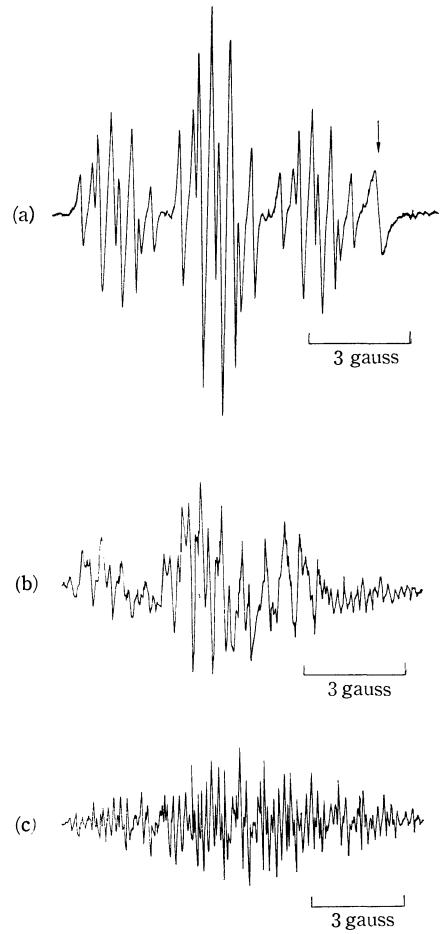

Fig. 4. Change of ESR spectrum of semireduced eosin caused by light-irradiation.
a: for semireduced eosin prepared by γ-irradiation of alkaline methanolic solution of eosin.
b and c: after irradiation by 402 nm light. ESR spectrum c is almost superimposable on that of semireduced uranin (see Ref. 6). The arrow indicates the standard signal of $K_2(SO_3)_2$-NO.

and uranin respectively.[6] Figure 4 shows the successive change in the ESR spectra for the semireduced-eosin solution which was subjected to light-irradiation for different periods. The ESR spectrum of semireduced eosin grows more complex until ultimately it is superimposable on that of semireduced uranin. These results indicate that semireduced forms of debrominated eosins are also produced as intermediate products.

Reaction of Eosin with Semireduced Uranin. Figure 3 implies another interesting feature. Upon the excitation of semireduced eosin (408 nm of the Absorption Spectrum 2), the absorption band of debrominated dye (505 nm of 3) developed and the original absorption band due to eosin (521 nm of 2) vanished. This result may be explained in terms of electron transfer from the semireduced

form of dehalogenated dye to eosin, the latter having an electron affinity higher than the former. By this electron-transfer reaction, semireduced debrominated-eosin is oxidized to debrominated eosin and the remaining eosin is reduced to semireduced eosin.

This reaction was demonstrated to take place by following experiment shown in Fig. 5. When semireduced uranin (2 in Fig. 5) prepared by the γ-irradiation of uranin (1) in an alkaline methanolic solution was mixed with eosin *in vacuo* and in the dark, the absorption peak of semireduced uranin (394 nm) shifted to a longer wavelength, the absorption band of eosin (521 nm) disappeared, and that of uranin (495 nm) increased (3). The results clearly show that uranin and semireduced eosin (408 nm) were produced by the electron-transfer reaction between semireduced uranin and eosin; this is in agreement with the assumption mentioned above.

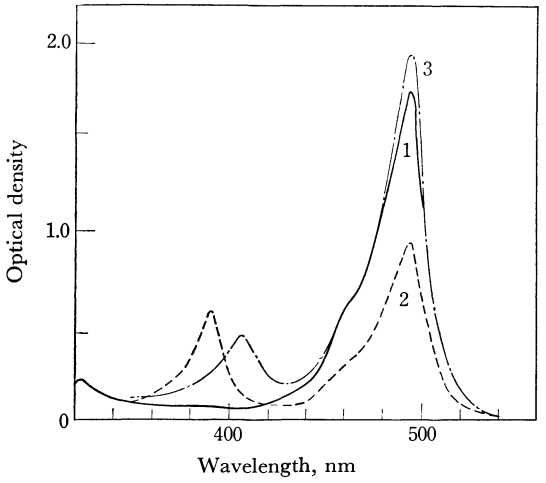

Fig. 5. Absorption spectra for (1) uranin, (2) semireduced uranin and (3) the mixed solution of semireduced uranin and eosin. All the solutions were in alkaline MeOH *in vacuo*. Note that the absorption of added eosin (521 nm) vanished.

Flash Photolysis of Semireduced Eosin. The primary processes of the photo-debromination of semireduced eosin were studied by flash photolysis. Semireduced eosin which had been prepared by the prolonged γ-irradiation of an alkaline methanolic solution of eosin, and which contained a negligible amount of unreacted eosin, was photolyzed by flash light through a VV-40 glass filter. The absorption spectra recorded 20 μsec and several minutes after the flash are given in Fig. 6. Upon the excitation of the semireduced eosin, a rapid development of the absorption band at 514 nm was observed; this development is due to the formation of partially-debrominated eosin. A decrease in the absorption intensity of the original semireduced eosin was observed at the same time. The absorption band at 514 nm then showed a decrease in intensity in the dark, along with a recovery of the absorption band at a shorter wavelength to an extent equivalent to the decrease in the intensity of the former band. The decay characteristics of semireduced eosin are given in Fig. 7, in which the oscillographic trace of the transmittance at 514 nm is also shown. These traces were recorded separately with semireduced eosin solutions which had been prepared in the same way by γ-irradiating solutions of equal eosin concentrations. Figure 7 shows that, upon flash-excitation, semireduced eosin rapidly converts during the duration of the flash to partially-debrominated eosin having its absorption peak at $\sim$514 nm.

The rapid processes are followed in the dark by

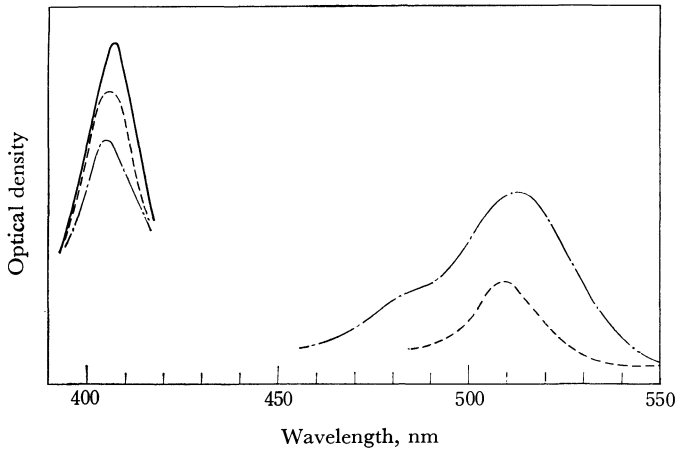

Fig. 6. Absorption spectra of semireduced eisoin solution after flash-irradiation.
—— before flash, practically no absorption of eosin (521 nm) is observed. -·-·- 20 μsec after flash, ------ several min after flash.

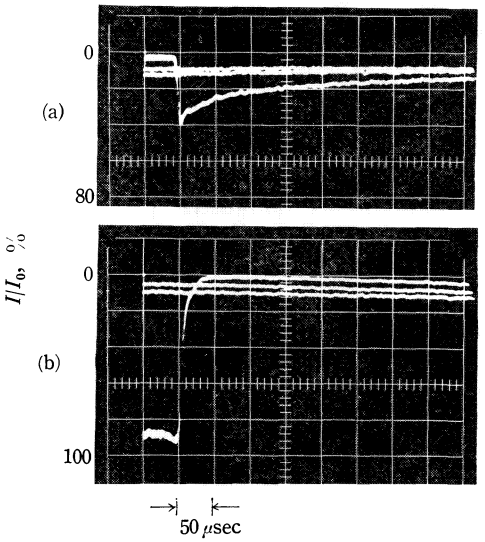

Fig. 7. Oscillographic traces of (a) semireduced eosin at 408 nm and (b) debrominated eosin at 514 nm.

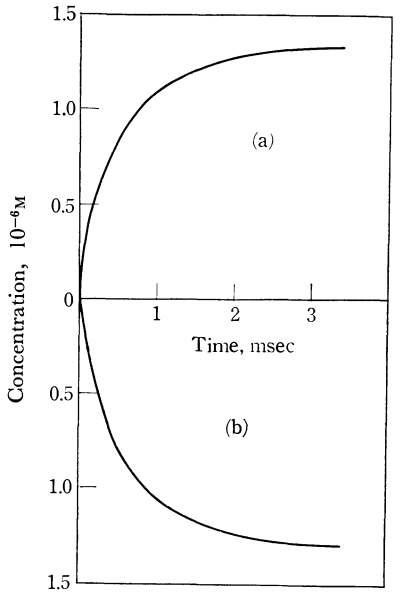

Fig. 8. Slow processes in the dark followed by flash photolysis of semireduced eosin.
(a) Increase in [semireduced eosin] at 408 nm.
(b) Decrease in [debrominated eosin] at 514 nm.

the slow processes. Figure 8 shows the slow processes more clearly by plotting the concentrations of semireduced and partially-debrominated eosin as a function of the time from 0.1 msec after the flash. The concentrations of both species were calculated by taking ε (514 nm) $= 1.08 \times 10^5 \text{M}^{-1}\,\text{cm}^{-1}$ and ε (408 nm) $= 5.67 \times 10^4 \text{M}^{-1}\,\text{cm}^{-1}$.[10] The two curves are apparently mirror images of each other, indicating that partially-debrominated eosin is reduced solely to its semireduced form in the dark.

Discussion

From the experimental results presented above, the following conclusions can be immediately drawn:

(1) The precursor of the photo-debromination is semireduced eosin, which is quite stable in deaerated alkaline methanolic solutions.

(2) Semireduced eosin is debrominated and oxidized, upon photo-excitation, to debrominated eosin.

(3) The photo-debromination of semireduced eosin takes place in a step-by-step fashion.

(4) Semireduced forms of debrominated eosin are successively produced as intermediates in the debromination process.

(5) The electron transfer from semireduced debrominated-eosin to eosin occurs in the dark.

Semireduced Eosin as a Precursor. The present results show clearly that the photo-debromination of eosin is actually initiated by the photo-excitation of semireduced eosin. Semireduced eosin is stable in alkaline media because of the symmetrical structure of its basic form.[6] In a neutral solution, however, semireduced eosin undergoes a disproportionation reaction to produce leuco-eosin and eosin.[6] These results provide an explanation of the fact that the photo-debromination of eosin is observed only in alkaline media in the presence of such reducing agents as alcohols and amines. This conclusion is in agreement with previous suggestions by other authors.[3,4]

All other reaction intermediates can be ruled out as the precursor of the photo-debromination. The experiment in which only eosin was photo-excited showed no debrominations, indicating that the excited eosin is not the precursor of the debromination. Semioxidized eosin, which has been proved to form in the radiolysis of aqueous solutions,[11-13] is not produced in alcoholic solutions.[6] Leuco-eosin, if any is present, might undergo debromina-

10) The molar extinction coefficients of debrominated eosins were estimated by assuming the linear relationship between the maximum ε's and the peak wavelengths of these dyes, those for eosin, dibromoeosin and uranin being known. The ε's for semireduced forms with different numbers of bromine were determined from the estimated ε's for their corresponding oxidized forms as mentioned above, where each semireduced form is assumed to be oxidized quantitatively by oxygen.

11) J. Chrysochoos, J. Ovadia and L. I. Grossweiner, *J. Phys. Chem.*, **71**, 1629 (1967).

12) P. Cordier and L. I. Grossweiner, *ibid.*, **72**, 2018 (1968).

13) A. F. Rodde, Jr., and L. I. Grossweiner, *ibid.*, **72**, 3337 (1968).

tion when it is oxidized, as has been observed for anthraquinonoid dyes,[5] because it probably produces semireduced eosin as a reaction intermediate. In the present system, however, no leuco-eosin was produced and no experiment has been carried out with leuco-eosin.

Debromination of Semireduced Eosin. The spectral change recorded in the flash photolysis of semireduced eosin (Fig. 6) seems to indicate that the replacement of bromine atoms by hydrogen atoms takes place one by one. Upon the flash irradiation of semireduced eosin, a new absorption band appeared with a peak at 514 nm. This absorption band is apparently due to the formation of debrominated eosin. The absorption peaks of eosin and uranin are at 521 and 495 nm respectively, while that of dibromouranin is between them (506 nm).[4] Insofar as the absorption band at 514 nm can be ascribed to any single debrominated product, this product (514 nm) may be assigned to the debrominated eosin, in which one bromine is replaced by one hydrogen. We have concluded in the "Results" section that each absorption band appearing in the course of the photo-debromination is due largely to a single debrominated product. The shape of the absorption spectra in Fig. 6 also supports this conclusion.

Figure 7 indicates that semireduced eosin is debrominated and simultaneously oxidized to debrominated eosin. The reaction is completed within the duration of the flash (10 μsec). Since no oxidizing species can be considered to be present in a concentration as to react rapidly with semireduced eosin, the reaction may reasonably be assumed to proceed by a first-order kinetics. No experimental evidence has been obtained for the reaction of excited semireduced eosin producing semireduced debrominated-eosin directly.

Proposed Mechanism of Debromination. The rapid formation of debrominated eosin caused by the photo-excitation of semireduced eosin and the ensuing slow process can be explained by assuming the following reactions:

$$\cdot S \xrightarrow{h\nu} \cdot S^* \longrightarrow \cdot D(-Br) + Br^- \quad (1)$$

$$\cdot D(-Br) + CH_3OH \longrightarrow D(-Br) + \cdot CH_2OH \quad (2)$$

$$D(-Br) + \cdot CH_2OH \longrightarrow \cdot S(-Br) + CH_2O \quad (3)$$

where D and S stand for eosin and semireduced eosin respectively.

Semireduced eosin exists in an alkaline solution in the basic symmetrical form.[6] The electron-rich semireduced eosin may easily release a bromide ion upon photo-excitation, thus forming the debrominated-eosin σ-radical, $\cdot D(-Br)$, Reaction (1). The exact position where the first bromine atom is released has not yet been established; $\cdot D(-Br)$ is, in any case, a free radical and will rapidly abstract hydrogen from the neighboring methanol to form debrominated eosin, $D(-Br)$, and the CH_2OH radical (Reaction (2)). The rapid process

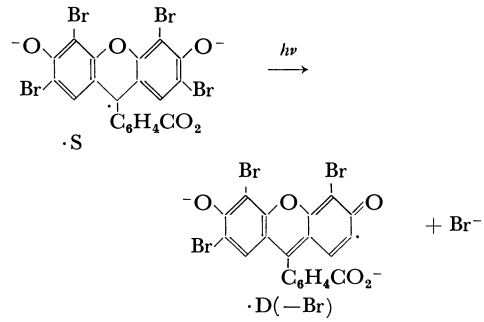

shown in Fig. 7 can thus be explained by the sequence of Reactions (1) and (2).

The ensuing slow process can be explained by Reaction (3), where debrominated eosin $D(-Br)$ is reduced with the CH_2OH radical produced by Reaction (2). The semireduced form of $D(-Br)$, $\cdot S(-Br)$, then replaces its bromine with hydrogen by a sequence similar to that of Reactions (1) and (2), and so on. Thus photo-debromination will continue until all the bromines are replaced with hydrogens, final product being nothing but uranin.

This mechanism can also explain the fact that semireduced forms of various debrominated eosins are successively produced in the course of the debromination process. It may be speculated that such an electron-transfer reaction as that observed between eosin and semireduced debrominated-eosin plays a role in making the intermediate products a single component.

Photo-debromination of Eosin. The overall mechanism of the photo-debromination of eosin can be understood on the basis of the results presented above. The photo-debromination does not take place unless semireduced eosin is photo-excited. In previous experiments,[1-4] solutions were exposed to the light, which is absorbed not only by eosin, but also by its semireduced form. Furthermore, the debromination is observable only in deaerated alkaline media containing appropriate reducing agents; every role of those agents is also clear from the present investigation. The dehalogenation of other xanthene dyes can be explained largely in the same manner.

Recently Sherman[14] has found another type of radiation-induced dehalogenation for some halogenated benzenes as well as for alkyl halides. Alkaline alcoholic solutions of these compounds have been reported to show chain dehalogenation. The reaction, however, is initiated by dissociative electron attachment to the halogens of these compounds; no indication of such a reaction has been observed with eosin solutions in the present study.

The authors wish to thank Dr. Akira Kira for his helpful advice in the flash-photolysis experiments.

14) W. V. Sherman, *J. Phys. Chem.* **72**, 2287 (1968).

BULLETIN OF THE CHEMICAL SOCIETY OF JAPAN VOL. 43 1343—1345 (1970)

Thermodynamic and X-Ray Studies of Solid Solutions of Silver Bromide and Lithium Bromide

Toshihide Tsuji,* Shunichi Murakoshi,** Kazuo Fueki and Takashi Mukaibo

Department of Industrial Chemistry, Faculty of Engineering, The University of Tokyo, Hongo, Tokyo

(Received December 2, 1969)

A miscibility gap in AgBr-LiBr solid solutions has been found by the high temperature X-ray diffraction method, and a new phase diagram is presented. Activity, partial molar free energy, enthalpy and entropy of AgBr in AgBr-LiBr solid solutions have been obtained at 350 and 400°C from the e.m.f. data of galvanic cells of the type Ag/AgBr-LiBr/Br_2. It has been found that the solid solution forms a regular solution difined by Hildebrand.

It was shown by Kiukkola and Wagner[1] that e.m.f. measurements on galvanic cells involving solid electrolytes can be used for the determination of standard free energies of formation of halides, oxides, sulfides and other compounds at elevated temperatures, and many e.m.f. studies have been carried out ever since.

The authors have determined the miscibility gap in AgBr-NaBr solid solutions by means of a high temperature X-ray diffraction method.[2] The authors have also measured the e.m.f. of solid electrolyte cells of the type Ag/AgBr-NaBr/Br_2 and calculated activities and partial molar quantities of AgBr in the AgBr-NaBr solid solution. It was found that the AgBr-NaBr system forms a regular solution above the critical temperature. This paper reports the results of similar studies on the AgBr-LiBr system.

Experimental

High purity lithium bromide and silver bromide, prepared by Yoneyama Chemical Industries Ltd. and Kojima Chemical Co., Ltd., respectively, were used.

Lithium bromide was dried *in vacuo* at about 300°C until the weight of the salt became constant. Lithium bromide and silver bromide were then mixed in a desired proportion, melted in a quartz tube in bromine atmosphere, and heated until the solution became clear. Subsequently, the solution was frozen, kept at about 400°C for several hours and quenched. After cooling, the sample was taken out from the quartz tube and ground in an agate mortar in a dry box.

The apparatus and the experimental procedures for the present work were the same as described in detail previously.[2]

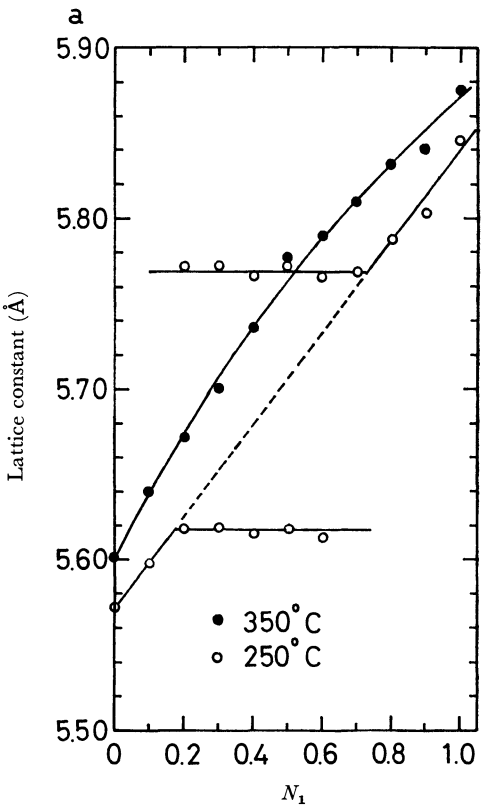

Fig. 1. Plot of lattice constant against the mole fraction of AgBr.

*Present address: Department of Nuclear Engineering, Faculty of Engineering, Nagoya University, Chikusa-Ku, Nagoya.

**Present address: Nippon Light Metal Company, Ltd., Kambara Works, Kambara, Shizuoka.

1) K. Kiukkola and C. Wagner, *J. Electrochem. Soc.*, **104**, 308, 379 (1957).

2) T. Tsuji, K. Fueki and T. Mukaibo, This Bulletin, **42**, 2193 (1969).

Results and Discussion

High Temperature X-Ray Diffraction Study. As reported previously, a miscibility gap exists in the AgBr-NaBr system.[2] Although Sandonnini and Scarpa[3] have reported that the AgBr-LiBr system forms a complete solid solution, a miscibility gap may exist in the system in view of the similarity between AgBr-NaBr and AgBr-LiBr systems.

In order to determine whether or not the solubility limit exists, a study by the high temperature X-ray diffraction method was carried out at temperatures between 50 to 350°C at an interval of 50°C. Lattice constants obtained from the reflections of (200), (220), (222), (422) and (600) planes are shown in Fig. 1 as plots against the mole fraction of silver bromide, N_1. We see that the lattice constant at 350°C increases continuously with the increase in mole fraction of silver bromide, but at lower temperatures such as 250°C, the discontinuities in lattice parameter exist.

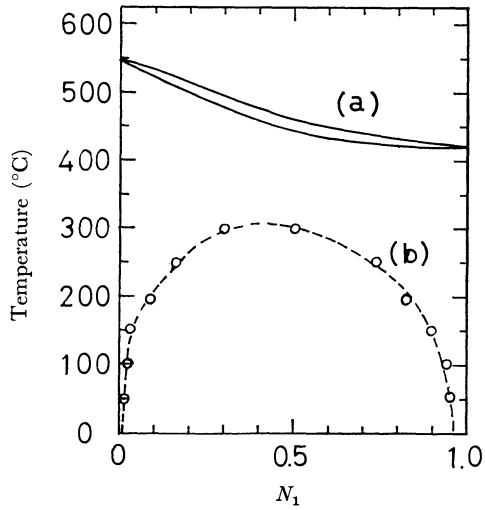

Fig. 2. Phase diagram of the AgBr-LiBr system. (a): Sandonnini and Scarpa, (b): this work

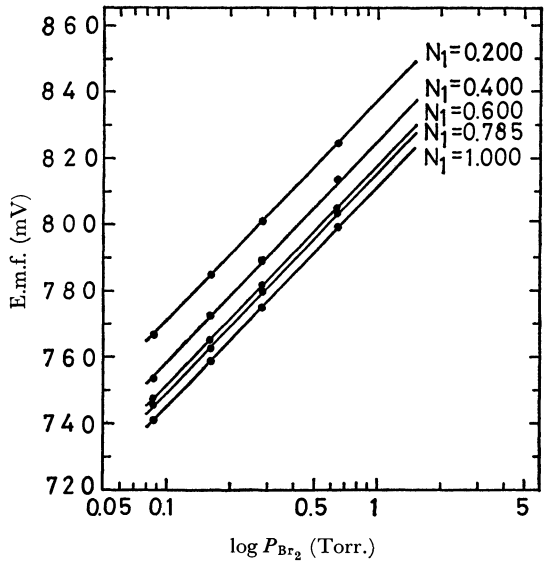

Fig. 3. Plot of E *vs.* log P_{Br_2} at 400°C.

3) C. Sandonnini and G. Scarpa, *At. reale accad. Lincei, Sez. II*, **22**, 517 (1913).

Table 1. Values of E_0 (mV)

N_1	°C 400	350
0.100	852.5	866.2
0.200	837.6	852.8
0.300	827.5	847.0
0.400	825.0	846.2
0.600	818.0	840.9
0.785	815.8	839.1
0.900	812.8	836.1
1.000	811.9	835.3

Figure 2 shows the phase diagram of the AgBr-LiBr system. The dotted line indicates the result of the present work and the liquidus and solidus lines the data by Sandonnini and Scarpa.[3]

E.m.f. Study. Figure 3 gives the plot of e.m.f. (E) *vs.* log P_{Br_2} for AgBr-LiBr solid solutions of various compositions. A good linearity holds between the logarithm of bromine vapor pressure and the e.m.f. in a pressure range, 0.0864 to 0.650 Torr. A similar linearity was obtained at temperatures from 250 to 400°C.

Table 2. Thermodynamic data of the AgBr-LiBr system at 350 and 400°C

N_1	ΔG_1 kcal	$\bar{G}_1$ kcal	$\bar{S}_1$ cal/°C	$\bar{H}_1$ kcal	a_1	a_2
400°C						
0.100	−19.66	−0.94	4.47	2.07	0.497	0.913
0.200	−19.32	−0.60	3.78	1.95	0.642	0.877
0.300	−19.08	−0.36	1.80	0.85	0.764	0.834
0.400	−19.03	−0.31	1.02	0.38	0.798	0.800
0.600	−18.86	−0.14	0.23	0.01	0.900	0.689
0.785	−18.81	−0.09	0.09	0.00	0.935	0.513
0.900	−18.74	−0.02	0.05	0.01	0.985	0.251
1.000	−18.72	0	0	0	1.000	0
350°C						
0.100	−19.98	−0.72	4.47	2.08	0.563	0.914
0.200	−19.67	−0.41	3.78	1.95	0.722	0.879
0.300	−19.53	−0.27	1.80	0.85	0.804	0.855
0.400	−19.51	−0.25	1.02	0.38	0.816	0.855
0.600	−19.39	−0.13	0.23	0.02	0.901	0.755
0.785	−19.35	−0.09	0.09	0.00	0.932	0.586
0.900	−19.28	−0.02	0.05	0.01	0.985	0.287
1.000	−19.26	0	0	0	1.000	0

The slope of the plot of E *vs.* $\log P_{Br_2}$ of AgBr-LiBr solid solutions with various compositions is the same as that of pure silver bromide. A similar relationship is found at 350°C. Since it was shown previously[2] that pure silver bromide is entirely ionic above 300°C, AgBr-LiBr solid solutions also seem to be an ionic conductor at 350 and 400°C.

Table 1 lists the value of E_0, the e.m.f. at a bromine pressure of 1 Torr., which was obtained by extrapolating the plot of E *vs.* $\log P_{Br_2}$.

If ΔG_1 and ΔG^0 denote the free energy changes of the reaction $Ag+\frac{1}{2}Br_2=(AgBr)$ in solid solution and in pure state, respectively, the partial molar free energy of silver bromide in solid solutions, $\bar{G}_1$, is obtained by the equation

$$\bar{G}_1 = \Delta G_i - \Delta G^\circ. \quad (1)$$

From the temperature dependenc of $\bar{G}_1$, the partial molar entropy and enthalpy of silver bromide in solid solutions are calculated. If pure silver bromide is chosen as the standard state, the activity of silver bromide in its solution is calculated by the relation

$$\bar{G}_1 = 2.303\,RT\log a_1. \quad (2)$$

The activity of lithium bromide, a_2, is obtained by the Gibbs-Duhem equation in the integrated form

$$\log(a_2/N_2) = -\int_0^{N_1}(N_1/N_2)\,d\log(a_1/N_1). \quad (3)$$

Thermodynamic data of the AgBr-LiBr system at 350 and 400°C are summarized in Table 2.

As seen in Fig. 4, the AgBr-LiBr system shows positive deviations from Raoult's law.

Figure 5 gives the plot of $(\bar{G}_1-\bar{G}_1^i)$ *vs.* N_2^2, where $\bar{G}_1^i$ is the partial molar free energy of component 1 in the ideal solution. Linearity holds between $(\bar{G}_1-\bar{G}_1^i)$ and N_2^2, and the two sets of points for 350 and 400°C lie on a single straight line. The result clearly shows that the AgBr-LiBr system above the critical temperature forms a regular solution defined by Hildebrand.[4] It is concluded from this result that the partial molar entropy is the same as it would be in the ideal solution, *i.e.*, $S_1=S_1^i=R\ln N_1$, and that two kinds of positive ions are distributed at random in the solid solution.

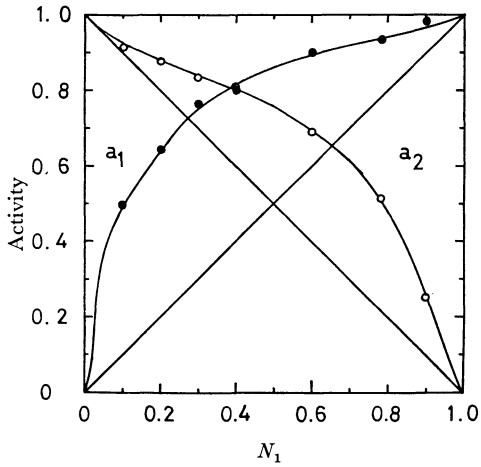

Fig. 4. Activity curves for AgBr-LiBr solid solutions at 400°C.

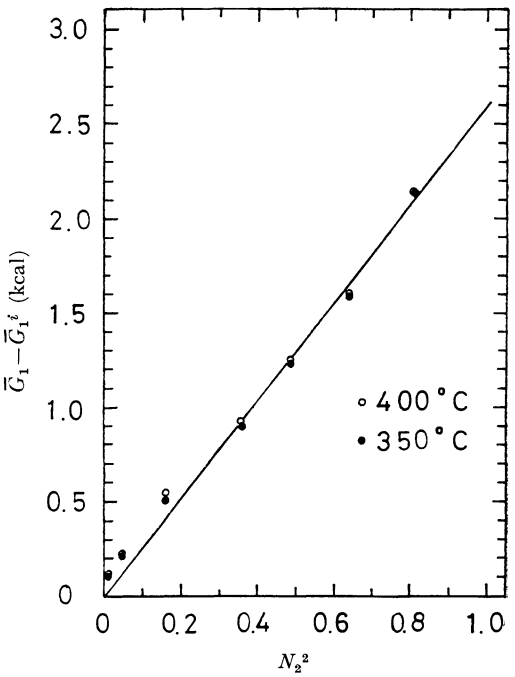

Fig. 5. Plot of $(\bar{G}_1-\bar{G}_1^i)$ against N_2^2.

Summary

1) The solubility limit in the AgBr-LiBr system was determined by means of the high temperature X-ray diffraction method and a new phase diagram of the system was presented.

2) The partial molar free energy of AgBr in the system was determined by the e.m.f. measurement for the galvanic cell, $Ag/AgBr\text{-}LiBr/Br_2$ at 350 and 400°C.

3) The partial molar entropy and the partial molar enthalpy of AgBr in the system were calculated.

4) The system was found to form a regular solution defined by Hildebrand.

4) J. H. Hildebrand, *J. Amer. Chem. Soc.*, **51**, 66 (1929).

BULLETIN OF THE CHEMICAL SOCIETY OF JAPAN VOL. 43 1346—1353 (1970)

Charge-Transfer Interaction in Linear Chain Molecular Crystals

Tadayoshi SAKATA and Saburo NAGAKURA

The Institute for Solid State Physics, The University of Tokyo, Roppongi, Minato-ku, Tokyo

(Received December 6, 1969)

The charge-transfer interaction is investigated theoretically for linear chain systems in molecular crystals. The charge-transfer excitation energy is shown to diverge in crystals by the usual configuration interaction method considering only one-molecule excitation. In order to overcome this difficulty, the second quantized Hamiltonian is solved with the Bose approximation for the charge-transfer exciton. Consequently, reasonable results are obtained for the stabilization of the ground state due to the contribution of many virtual excitons, for the electric dipole moment of the ground state, and for the transition moment of a charge-transfer excitation. The results correspond well to those by Mulliken's theory for an electron donor-acceptor pair. The second quantization model is also applied in the extended form to crystals of charge-transfer complexes and ionic radicals of complex stoichiometry. The lower excited states in these crystals are understood as the coupled ones of the one-site and two-site charge-transfer configurations.

Concerning the crystals of charge-transfer (abbreviated hereafter to CT) complexes and radical ion salts, the geometrical structures and also the electrical, magnetic and optical properties have been studied by many authors from the experimental point of view.[1-5] Consequently, some interesting phenomena have been found in relation with their electronic structures. For example, radical salt crystals such as (Quinolinium)$^+$(Tetracyano-*p*-quinodimethan)$_2^-$ and (*N*-Methylphenazinium)$^+$(Tetracyano-*p*-quinodimethan)$^-$ exhibit a large electrical conductivity up to $10^2\,\Omega^{-1}\mathrm{cm}^{-1}$.[3a,3c] Furthermore, some of radical salt crystals are known to show in the infrared region strong absorption bands characteristic of the interaction between electron donor and acceptor.[6-9] In contrast to a plenty of experimental studies, there are only a few literatures[10] about the theory of electronic structures of these crystals.

Concerning usual molecular crystals[11-15] as well as CT complex crystals, the CT interaction plays an important role in their electronic processes. For example, the absorption bands ascribed to no intramolecular excitations were found for the α-form crystals of perylene and 9,10-dichloroanthracene and were assigned reasonably to the CT band.[14,15]

Under these circumstances, we undertake to develop the theory in the second quantization form on the electronic structures of molecular crystals and also of crystals of CT complexes and radical ion salts. We propose a model Hamiltonian appropriate to the case where the Coulomb energy

1) For reviews of CT complexes, see R. S. Mulliken and W. B. Person, *Ann. Rev. Phys. Chem.*, **13**, 107 (1962), and G. Briegleb, "Elektronen-Donator-Acceptor-Komplexe," Springer-Verlag, Berlin (1961).

2) a) C. J. Fritchie, Jr., and P. Arthur, Jr., *Acta Crystallogr.*, **21**, 139 (1966). b) A. W. Hanson, *ibid.*, **B24**, 768 (1968). c) D. S. Brown, S. C. Wallwork and A. Wilson, *ibid.*, **17**, 168 (1964). d) H. Matsuda, K. Osaki and I. Nitta, This Bulletin, **31**, 611 (1958).

3) a) W. J. Siemons, P. E. Bierstedt and R. G. Kepler, *J. Chem. Phys.*, **39**, 3523 (1963). b) Y. Matsunaga, *ibid.*, **42**, 1982 (1965). c) L. R. Melby, *Can. J. Chem.*, **43**, 1448 (1965).

4) a) K. Nakamoto, *J. Amer. Chem. Soc.*, **74**, 1739 (1952). b) S. K. Lawer, R. M. Hochstrasser and C. Reid, *Mol. Phys.*, **4**, 162 (1961). c) J. Tanaka and K. Yoshihara, This Bulletin, **38**, 739 (1965). d) H. Kuroda, T. Kunii, S. Hiroma and H. Akamatu, *J. Mol. Spectry.*, **22**, 60 (1967). e) T. Amano, H. Kuroda and H. Akamatu, This Bulletin, **41**, 83 (1968). f) T. Sakata and S. Nagakura, *ibid.*, **42**, 1497 (1969). g) J. Tanaka and M. Mizuno, *ibid.*, **42**, 1841 (1969).

5) a) R. C. Hughes and Z. G. Soos, *J. Chem. Phsy.*, **48**, 1066 (1968). b) K. Siratori and T. Kondow, *J. Phys. Soc. Japan*, **27**, 301 (1969). c) R. G. Kepler, *J. Chem. Phys.*, **39**, 3528 (1963). d) D. B. Chesnut and P. Arthur, Jr., *ibid.*, **36**, 2969 (1962).

6) T. Kondow, K. Siratori and H. Inokuchi, *J. Phys. Soc. Japan*, **21**, 824 (1966).

7) T. Kondow, K. Siratori and H. Inokuchi, *ibid.*, **23**, 98 (1967).

8) Y. Iida, This Bulletin, **42**, 71 (1969).

9) Y. Iida, *ibid.*, **42**, 637 (1969).

10) J. I. Krugler, C. G. Montgomery and H. M. McConnell, *J. Chem. Phys.*, **41**, 2421 (1964).

11) L. E. Lyons, *J. Chem. Soc.*, **1957**, 5001.

12) J. Tanaka, *Progr. Theoret. Phys.* (Kyoto), Suppl. **12**, 183 (1959).

13) Sang-Il Choi, J. Jortner, S. A. Rice and R. Silbey, *J. Chem. Phys.*, **41**, 3294 (1964).

14) J. Tanaka, This Bulletin, **36**, 1237 (1963).

15) J. Tanaka and M. Shibata, *ibid.*, **41**, 34 (1968).

is larger than the transfer energy and discuss the CT electronic state. At first, the basic theory of the CT interaction in molecular crystals is presented. Thereafter the problem of some CT complexes and ionic radical crystals of complex stoichiometry, for example Et_3NH^+(Tetracyano-*p*-quinodimethan)$_2^-$ crystals, is treated by applying the basic theory in the extended form.

Theoretical

Wave Functions and Energy Levels. We consider a linear chain system consisting of N identical radicals or molecules and also that consisting of alternatively located N electron donors and N electron acceptors. In the former case, each component acts as both donor and acceptor. In the latter case, however, the electron donor and acceptor can be distinguished explicitly from each other. Furthermore, in these crystals the component molecules and radicals are assumed to be equally spaced. In actuality, the X-ray crystal analysis data show that there exists one-dimensional equivalent interaction along a chain in most of these crystals.[2a-d]

We can represent the ground configuration as $\psi(0,0)$ and one site CT configuration as $\psi(\pm 1,j)$ in which an electron on the jth site component transfers to the nearest neighbors.*1 Here + and − show the direction of electron migration. The numbering of j is made for identical molecules or radicals in the case of molecular or radical crystals, and for electron donors and for electron acceptors separately in the case of CT complexes.

Keeping the above-mentioned facts in mind, we construct the wave functions of crystals. In the case of usual molecular crystals and of weak CT complex crystals, the ground configurations $\psi(0,0)$ is singlet, and there are possibilities of singlet and triplet for the CT configurations. By considering only the highest occupied and lowest vacant orbitals, the wave functions of the ground and CT configurations can be represented by the following equations for usual molecular crystals:

$$\psi(0,0) = |\phi_1^0(1)\bar{\phi}_1^0(2)\cdots\phi_j^0(2j-1)\bar{\phi}_j^0(2j)\cdots \phi_N^0(2N-1)\bar{\phi}_N^0(2N)| \text{ (singlet)} \quad (1)$$

$$\psi(m,j) = \frac{1}{\sqrt{2}}\{|\phi_1^0(1)\bar{\phi}_1^0(2)\cdots\phi_j^0(2j-1)\bar{\phi}_{j+m}^v(2j)\cdots \phi_N^0(2N-1)\bar{\phi}_N^0(2N)| \pm |\phi_1^0(1)\bar{\phi}_1^0(2)\cdots \bar{\phi}_{j+m}^v(2j-1)\bar{\phi}_j^0(2j)\cdots\phi_N^0(2N-1)\bar{\phi}_N^0(2N)|\} \quad (2)$$

where $m=\pm 1$ (+ and − correspond to the singlet and triplet states, respectively), ϕ_j^0 is the highest occupied molecular orbital of the jth site component, and suffix v signifies the lowest vacant molecular orbital. They are orthonormalized like Wannier orbitals. The wave function for the CT configuration which satisfies the translational symmetry of crystals can be written as follows:

$$\Psi(m,k) = \frac{1}{\sqrt{N}}\sum_j e^{ikj}\psi(m,j),\ m = 1, -1 \quad (3)$$

where $k=2\pi/Nj$ ($j=1, 2, \cdots, N$) from the cyclic boundary condition and the unit length is taken to be equal to the distance between the neighbouring molecules for usual molecular crystals and that between the neighbouring donor (acceptor) molecules for CT complexes.

The above-mentioned two CT configurations $\Psi(1,k)$ and $\Psi(-1,k)$ mix with each other, and consequently the following two energy levels can be obtained.

$$\omega_{k+} = \omega + \sum_{l\neq 0} e^{-ikl}U_1(|l|) + |\sum_l e^{-ikl}U_2(l)|\cdot\tau$$
$$\omega_{k-} = \omega + \sum_{l\neq 0} e^{-ikl}U_1(|l|) - |\sum_l e^{-ikl}U_2(l)|\cdot\tau \quad (4)$$

where

$$U_1(|j-j'|) = \langle\psi(m,j)|H|\psi(m,j')\rangle$$
$$U_2(j-j') = \langle\psi(1,j)|H|\psi(-1,j')\rangle$$
$$\omega = \langle\psi(m,j)|H|\psi(m,j)\rangle;\ m=1,-1 \quad (5)$$
$$U_2(l)\neq U_2(-l)$$

and

$$\tau = \frac{\sum_l U_2(l)}{|\sum_l U_2(l)|}$$

The corresponding wave functions are

$$\Psi(1,k,\nu) = \frac{1}{\sqrt{2N}}\sum_j e^{ikj}\{\psi(1,j) + \nu e^{i\theta_k}\times\psi(-1,j)\} \quad (6)$$

where

$$e^{i\theta_k} = \frac{\sum_l e^{ikl}U_2(l)}{|\sum_l e^{ikl}U_2(l)|}\cdot\tau \quad (7)$$

and $\nu=\pm$.

The interaction between the ground configuration and the one site CT configuration with the spin multiplicity of singlet is rather large and can not be disregarded. For the evaluation of the matrix element necessary for the calculation of the interaction, the following two cases can be considered, when there is a center of symmetry of the point group between the neighbouring two molecules (or radicals).

Case A) When

$$\langle\psi(1,j)|H|\psi(0,0)\rangle = \langle\psi(-1,j)|H|\psi(0,0)\rangle$$

the matrix element is

$$\langle\Psi(1,k,\nu)|H|\psi(0,0)\rangle = \sqrt{2N}\,\beta\delta_{k0}\delta_{\nu+} \quad (8)$$

Case B) When

*1 In the case of CT complexes, $\psi(\pm 1,j)$ represents the configuration in which an electron on the jth donor molecule transfers to the nearest neighbouring acceptor molecule.

$$<\Psi(1,j)|\boldsymbol{H}|\psi(0,0)> = -<\psi(-1,j)|\boldsymbol{H}|\psi(0,0)>,$$

the matrix element is

$$<\Psi(1,k,\nu)|\boldsymbol{H}|\psi(0,0)> = \sqrt{2N}\,\beta\delta_{k0}\delta_{\nu-} \qquad (9)$$

where

$$\beta = <\phi(1,j)|\boldsymbol{H}|\psi(0,0)>$$

The quantity β corresponds to the transfer energy which determines the band width in the band model. As is seen in Eqs. (8) and (9), the only CT configurations of $k=0$, $\nu=+$ and $k=0$, $\nu=-$ mix with the ground configuration for cases A and B, respectively. Hereafter we consider only case A, since the similar discussion can be applied to case B. By taking the configuration interaction between the ground and CT configurations into account on the assumption of neglecting the contribution from the excited configurations in which many molecules are excited simultaneously in a crystal, the energy eigen values for the system can be obtained as follows:

$$E = \frac{\varepsilon_{0+}}{2} \pm \frac{1}{2}\sqrt{\varepsilon_{0+}{}^2+8N\beta^2} \qquad (10)$$

where

$$\varepsilon_{k\nu} = \omega_{k\nu} - <\psi(0,0)|\boldsymbol{H}|\psi(0,0)>$$

Therefore the excitation energy between these states is

$$E_{\text{exc.}} = \sqrt{\varepsilon_{0+}{}^2+8N\beta^2}$$

The obtained excitation energy depends on N and diverges with its increase.

$$E_{\text{exc.}} \to \infty \quad (N \to \infty)$$

This divergence arises from disregarding the configurations in which two or more than two molecules are excited simultaneously in a crystal. In the present paper, we undertake to overcome this difficulty by adopting second quantization formalism.

In the case of radical crystals and of strong CT complex crystals, each component has open shell structure and $S=1/2$. Since it is difficult to handle explicity the spin multiplicity of each electronic state of the crystal, we neglect the electron spin for simplicitly in these cases and represent the wave functions of the ground and CT configurations by the simple product of appropriate orbitals ϕ_j's. Then we can obtain the conclusion that the transition energy diverges with the increasing N also for this case.

Hamiltonian and the Bose Approximation. From the above discussion we can write a model Hamiltonian in the following second quantization form.[16]

$$\boldsymbol{H} = \boldsymbol{H}_1 + \boldsymbol{H}_2 + \boldsymbol{H}_3 \qquad (12)$$

$$\boldsymbol{H}_1 = \sum_{j,\sigma}\varepsilon\, a^+_{j\sigma}a_{j\sigma} \qquad (13)$$

$$\boldsymbol{H}_2 = \frac{1}{2}\sum_{\substack{j,j'\\ \sigma,\sigma'\\ (j\sigma)\neq(j'\sigma')}} U(j'\sigma',0;0,j\sigma)(a^+_{j'\sigma'}a_{j\sigma}+a^+_{j\sigma}a_{j'\sigma'}) + \frac{1}{2}\sum_{\substack{j,j'\\ \sigma,\sigma'\\ (j\sigma)\neq(j'\sigma')}} U(j'\sigma',j\sigma;0,0)(a^+_{j'\sigma'}a^+_{j\sigma}+a_{j\sigma}a_{j'\sigma'}) \qquad (14)$$

$$\boldsymbol{H}_3 = \sum_{j,\sigma}\beta(a^+_{j\sigma}+a_{j\sigma}) \qquad (15)$$

Here $a^+_{j\sigma}$ and $a_{j\sigma}$ are the creation and annihilation operators for an excitation which transfers an electron on the jth site, by one site, to $\sigma(\sigma=+,-)$ direction.

Hamiltonian $\boldsymbol{H}_1$ corresponds to the diagonal matrix element of $(j\sigma)$ excitation and $\varepsilon=<\psi(m,j)\cdot|\boldsymbol{H}|\psi(m,j)>-<\psi(0,0)|\boldsymbol{H}|\psi(0,0)>$; $m=1,-1$.

The first term of $\boldsymbol{H}_2$ signifies the process of the excitation transfer in which an excitation $(j\sigma)$ transfers to that of $(j'\sigma')$ and its inverse process. The coefficient $U(j'\sigma', 0;0, j\sigma)$ is the corresponding matrix element, satisfying the relations $U(j'\sigma, 0;0, j\sigma)=U_1(|\boldsymbol{j}-\boldsymbol{j}'|)$ and $U(j'-, 0;0, j+)=U_2(\boldsymbol{j}-\boldsymbol{j}')$. The second term of H_2 signifies the pair creation and the pair annihilation of two excitations $(j\sigma)$ and $(j'\sigma')$, $U(j'\sigma', j\sigma; 0,0)$ being its matrix element. The matrix elements $U(j'\sigma', 0;0, j\sigma)$ and $U(j'\sigma', j\sigma; 0,0)$ are considered to be small compared with the diagonal matrix element ε, since these quantities are proportional to the square of the intermolecular overlap integral.

Hamiltonian $\boldsymbol{H}_3$ represents the interaction between configurations which differ in the excitation number by one from each other and the interaction energy corresponds to the transfer (or resonance) energy β. This term represents the CT interaction.

Considering the diagonalization of the Hamiltonian $\boldsymbol{H}$, we disregard the second term of $\boldsymbol{H}_2$ for simplicity, since this term may give negligibly small influence when ε is large compared with $U(j'\sigma', j\sigma; 0,0)$.

We difine new operators which create and annihilate a one site CT exciton corresponding to Eq. (6).

$$b_{k+} = \frac{1}{\sqrt{2N}}\sum_j e^{-i\boldsymbol{kj}}(a_{j+}+e^{-i\theta_k}a_{j-})$$

$$b_{k-} = \frac{1}{\sqrt{2N}}\sum_j e^{-i\boldsymbol{kj}}(a_{j+}-e^{-i\theta_k}a_{j-}) \qquad (16)$$

The inverse transformation is,

$$a_{j+} = \frac{1}{\sqrt{2N}}\sum_k e^{i\boldsymbol{kj}}(b_{k+}+b_{k-})$$

$$a_{j-} = \frac{1}{\sqrt{2N}}\sum_k e^{i\boldsymbol{kj}+i\theta_k}(b_{k+}-b_{k-}) \qquad (17)$$

Operators $a^+_{j\sigma}$ and $a_{j\sigma}$ are essentially the Pauli operators.[10,16] However, we assume both $a^+_{j\sigma}$ and $a_{j\sigma}$ to be the Bose operators as usually done. Then $b^+_{k\nu}$ and $b_{k\nu}$ $(\nu=+,-)$ are also the Bose operators as can be shown easily. In this approximation the Hamiltonian can be diagonalized by the fol-

16) V. M. Agranovich, *J. Exptl. Theoret. Phys.* (U.S.S.R.), **37,** 430 (1959).

lowing procedures. From Eq. (16),

$$\sum_{j,\sigma} \varepsilon\, a^+_{j\sigma} a_{j\sigma} = \sum_{k,\nu} \varepsilon\, b^+_{k\nu} b_{k\nu}$$

$$\frac{1}{2}\sum_{\substack{j,j'\\ \sigma,\sigma}} U(j'\sigma', 0; 0, j\sigma)(a^+_{j'\sigma'} a_{j\sigma} + a^+_{j\sigma} a_{j'\sigma'}) \quad (j\sigma)\neq(j'\sigma')$$

$$= \sum_k \sum_l e^{-ikl} U_1(|l|)(b^+_{k+} b_{k+} + b^+_{k-} b_{k-}) + \sum_k \left|\sum_l e^{-ikl} U_2(l)\right| (b^+_{k+} b_{k+} - b^+_{k-} b_{k-})$$

$$\sum_{j,\sigma} \beta(a^+_{j\sigma} + a_{j\sigma}) = \sqrt{2N}\,\beta(b^+_{0+} + b_{0+}) \tag{18}$$

Therefore,

$$\boldsymbol{H} = \sum_{k,\nu} \varepsilon_{k\nu} b^+_{k\nu} b_{k\nu} + \sqrt{2N}\,\beta(b^+_{0+} + b_{0+}) \tag{19}$$

Furthermore, by introducing new Bose operators[17]

$$c_{0+} = b_{0+} + \frac{\sqrt{2N}\beta}{\varepsilon_{0+}} \tag{20}$$

$$c_{k\nu} = b_{k\nu} \qquad \text{expcept for } (k=0, \nu=+)$$

the Hamiltonian can be diagonalized as follows:

$$\boldsymbol{H} = \sum \varepsilon_{k\nu} c^+_{k\nu} c_{k\nu} - 2N\frac{\beta^2}{\varepsilon_{0+}} \tag{21}$$

Next we construct wave functions represented by the original representations which are applied prior to the diagonalization. For the ground state $|0\rangle$

$$|0\rangle = \sum_{n=0}^{\infty} \alpha_n |n\rangle_o \tag{22}$$

where $|n\rangle_o$ is the wave function of the original representation in which the number of virtual excitations of $(k=0, \nu=+)$ is n and no other excitation exists and suffix o means the original representation. Coefficient α_n can be obtained from

$$c_{0+}|0\rangle = 0 \tag{23}$$

$$\sum_n \alpha_n^2 = 1 \text{ (normalization condition)} \tag{24}$$

The final result is

$$\alpha_n = \frac{(-\gamma)^n}{\sqrt{n!}} e^{-\frac{1}{2}\gamma^2} \qquad (N\to\infty) \tag{25}$$

where

$$\gamma = \sqrt{2N}\frac{\beta}{\varepsilon_{0+}}$$

Extention of the Theory to Complex Radical Salt Crystals. As a model for complex radical salt, we take a closed linear chain of $2N$ acceptors (A) in which N excess electrons exist. The crystals of tetracyano-*p*-quinodimethan with various donor cations fit into this model. We take the above-mentioned localized model and neglect electron spin for simplicity. There are two ground configurations with excess electrons at odd and even number sites. They are represented by $\psi^o(0,0)$ and $\psi^e(0,0)$, respectively. The off diagonal matrix element between them is zero. Therefore the ground state is doubly degenerate unless there is an asymmetry concerning the locations of the cations. Hereafter we assume that N excess electrons locate at odd-number molecular sites even when the degeneracy is not removed. Then we can take $\psi^o(0,0)$ as the ground configuration of the system.

The CT configuration in which an electron on $(2j-1)$-th site migrates by m sites in the + (or −) direction is represented by $\psi^o(m, 2j-1)$ (or $\psi^o(-m, 2j-1)$), $m=1$ and 2 being assumed in the present paper. The excitation process corresponding to $m=1$ and 2 can be represented schematically by $\cdots$AA$^-$AA$^-\cdots \rightarrow \cdots$AAA$^-A^-\cdots$ and by $\cdots$ A$^-$AA$^-$A$\cdots \rightarrow \cdots$AAA$^=$A $\cdots$, respectively. Therefore these two kinds of excitations are different from each other in their characters.

By replacing $\phi(m,j)$ in Eq. (3) by $\psi^o(m, 2j-1)$, we can construct the wave function $\Psi^o(m,k)$ for the m site CT configuration which satisfies the translational symmetry of the crystal.*2 Furthermore, combining $\Psi^o(m,k)$'s corresponding to charge transfer in the + and − directions, we can obtain

$$\Psi^o(m,k,\nu) = \frac{1}{\sqrt{2N}} \sum_j e^{ikj}\{\psi^o(m,2j-1) + \nu\psi^o(-m,2j-1)\} \tag{26}$$

where $\nu=+,-$. We neglected for simplicity the small terms which correspond to $U_1(|l|)$ and $U_2(l)$ of Eq. (7). As in the case of usual molecular crystals and of crystals of CT complexes mentioned in the preceding chapter, the excitation energy calculated for complex radical salt crystals by this single excitation model diverges for $k=0$ and $\nu=+$.

The second quantization Hamiltonian may be written as

$$\boldsymbol{H} = \sum_{j,\sigma} \varepsilon a^+_{j\sigma} a_{j\sigma} + \sum_{j,\sigma} (\varepsilon+\Delta)\, b^+_{j\sigma} b_{j\sigma} + \sum_{j,\sigma} \beta\,(b^+_{j\sigma} a_{j\sigma} + a^+_{j\sigma} b_{j\sigma}) + \sum_{j,\sigma} \beta\,(a^+_{j\sigma} + a_{j\sigma}) \tag{27}$$

where ε, $\varepsilon+\Delta$ and β are defined as

$$\varepsilon = \langle\psi^o(m,2j-1)|\boldsymbol{H}|\psi^o(m,2j-1)\rangle - \langle\psi^o(0,0)|\boldsymbol{H}|\psi^o(0,0)\rangle \quad \text{for } m = \pm 1,$$

$$\varepsilon + \Delta = \langle\psi^o(m,2j-1)|\boldsymbol{H}|\psi^o(m,2j-1)\rangle - \langle\psi^o(0,0)|\boldsymbol{H}|\psi^o(0,0)\rangle \quad \text{for } \boldsymbol{m} = \pm 2$$

$$\beta = \langle\psi^o(2,2j-1)|\boldsymbol{H}|\psi^o(1,2j-1)\rangle = \langle\psi^o(1,2j-1)|\boldsymbol{H}|\psi^o(0,0)\rangle$$

$$\langle\psi^o(2,2j-1)|\boldsymbol{H}|\psi^o(0,0)\rangle = 0 \text{ (assumed)}$$

Operators $a^+_{j\sigma}$ and $a_{j\sigma}$ are the creation and the annihilation ones for an excitation which transfers an electron at $(2j-1)$th site, by one site, in the $\sigma(\sigma=+,-)$ direction. Operators $b^+_{j\sigma}$ and $b_{j\sigma}$ are the creation and the annihilation operators for an excitation which transfers an electron at the $(2j-1)$-

17) D. B. Chesnut, *Mol. Cryst.*, **1**, 351 (1966).

*2 By electron-phonon interaction the unit spacing of the crystal is twice that of the crystal without N excess electrons even if the chain is regular.

th site, by two sites, in the σ direction. The first and the second terms of Eq. (27) correspond to the diagonal matrix elements. The third terms represent the interactions between the one site CT configurations and the two site ones. The fourth terms represent the interaction between the ground configuration and the one site CT configurations. The usual Pauli commutation relations hold for the one-site and two-site CT operators. The one-site CT operators $a^+_{j\sigma}$ and $a_{j\sigma}$ commute with the two-sites ones $b^+_{j\sigma}$ and $b_{j\sigma}$, since the wave functions of the former are orthogonal to those of the latter when molecular orbitals in a crystal are orthonormalized.

The symmetry of translation is brought into the theory by transforming $a^+_{j\sigma}$, $a_{j\sigma}$, $b^+_{j\sigma}$ and $b_{j\sigma}$ to the wave operators $A_{k\nu}$ and $B_{k\nu}$;

$$A_{k+} = \frac{1}{\sqrt{2N}} \sum_{j=1}^{N} e^{-ikj}(a_{j+} + a_{j-})$$

$$A_{k-} = \frac{1}{\sqrt{2N}} \sum_{j=1}^{N} e^{-ikj}(a_{j+} - a_{j-}) \tag{28}$$

The operators $B_{k\nu}$ are defined in the same form as $A_{k\nu}$.

By the aid of the inverse transformation of Eq. (28), Eq. (27) is transformed as follows:

$$\boldsymbol{H} = \sum_{k,\nu} \varepsilon A^+_{k\nu} A_{k\nu} + \sum_{k,\nu} (\varepsilon + \Delta) B^+_{k\nu} B_{k\nu} + \sum_{k,\nu} \beta (A^+_{k\nu} B_{k\nu} + B^+_{k\nu} A_{k\nu}) + \sqrt{2N}\beta (A_{0+} + A_{0+}) \tag{29}$$

By assuming $a^+_{j\sigma}$, $a_{j\sigma}$, $b^+_{j\sigma}$ and $b_{j\sigma}$ to be the Bose operators as in the preceding section, the Hamiltonian can be diagonalized by the following transformation to new boson operators $C^+_{k\nu}$, $C_{k\nu}$, $D^+_{k\nu}$ and $D_{k\nu}$. The new operators are

$$C_{k\nu} = u_{k\nu} A_{k\nu} + v_{k\nu} B_{k\nu}$$
$$D_{k\nu} = u'_{k\nu} A_{k\nu} + v'_{k\nu} B_{k\nu} \tag{30}$$

for the k, ν states except for the $k=0$, $\nu=+$ state. For the $k=0$, $\nu=+$ state they are

$$C_{0+} = u_{0+} A_{0+} + v_{0+} B_{0+} + w$$
$$D_{0+} = u'_{0+} A_{0+} + v'_{0+} B_{0+} + w' \tag{31}$$

Here it may be assumed in general that coefficients $u_{k\nu}$, $v_{k\nu}$ $u'_{k\nu}$ and $v'_{k\nu}$ to be real.

The transformation is canonical when

$$u^2_{k\nu} + v^2_{k\nu} = 1,$$
$$u'^2_{k\nu} + v'^2_{k\nu} = 1, \quad u_{k\nu}u'_{k\nu} + v_{k\nu}v'_{k\nu} = 0 \tag{32}$$
$$\text{for all } k,\nu$$

Eq. (32) can be solved and the coefficients are represented by parameter $\chi_{k\nu}$ as follows:

$$u_{k\nu} = -\sin\chi_{k\nu}, \quad v_k = \cos\chi_{k\nu}$$
$$u'_{k\nu} = \cos\chi_{k\nu}, \quad v'_{k\nu} = \sin\chi_{k\nu}; \tag{33}$$
$$-\frac{\pi}{2} \leqq \chi_{k\nu} < \frac{\pi}{2}$$

where we neglect the trivial phase factor.

The parameter $\chi_{k\nu}$ is determined by the diagonalization of Hamiltonian. The Hamiltonian of Eq. (29) is reduced to the following diagonal forms:

$$[\boldsymbol{H}, C_{k\nu}] = -E_{k\nu} C_{k\nu}$$
$$[\boldsymbol{H}, D_{k\nu}] = -E'_{k\nu} D_{k\nu} \tag{34}$$

From Eqs. (30), (31) and (34)

$$(\varepsilon - E_{k\nu})u_{k\nu} + \beta v_{k\nu} = 0$$
$$\beta u_{k\nu} + (\varepsilon + \Delta - E_{k\nu})v_{k\nu} = 0$$
$$(\varepsilon - E'_{k\nu})u'_{k\nu} + \beta v'_{k\nu} = 0 \tag{35}$$
$$\beta u'_{k\nu} + (\varepsilon + \Delta - E'_{k\nu})v'_{k\nu} = 0$$

for all the k, ν. In particular, for the case of $k=0$, $\nu=+$

$$\sqrt{2N}\beta u_{0+} = E_{0+} w, \quad \sqrt{2N}\beta u'_{0+} = E'_{0+} w' \tag{36}$$

The solutions of Eq. (35) are

$$E_{k\nu} = \varepsilon + \frac{\Delta}{2} - \frac{1}{2}\sqrt{\Delta^2 + 4\beta^2}$$

$$E'_{k\nu} = \varepsilon + \frac{\Delta}{2} + \frac{1}{2}\sqrt{\Delta^2 + 4\beta^2} \tag{37}$$

where we tentatively assume $E_{k\nu} < E'_{k\nu}$. The energies $E_{k\nu}$ and $E'_{k\nu}$ and therefore also $u_{k\nu}$, $v_{k\nu}$, $u'_{k\nu}$ and $v'_{k\nu}$ are independent of k,ν. Therefore we remove the suffixes k,ν from these quantities.

The inverse transformation of Eq. (30) is

$$A_{k\nu} = u C_{k\nu} + v D_{k\nu}$$
$$B_{k\nu} = v C_{k\nu} - u D_{k\nu} \tag{38}$$

except for the case of $k=0$, $\nu=+$. For $k=+$, $\nu=+$

$$A_{0+} = u C_{0+} + v D_{0+} + (-uw - vw')$$
$$B_{0+} = v C_{0+} - u D_{0+} + (uw' - vw) \tag{39}$$

The transformation coefficients are

$$u = -v' = -\frac{|\beta|}{\beta}\left(\frac{1}{2} + \frac{\Delta}{2\sqrt{\Delta^2 + 4\beta^2}}\right)^{\frac{1}{2}}$$

$$v = u' = \left(\frac{1}{2} - \frac{\Delta}{2\sqrt{\Delta^2 + 4\beta^2}}\right)^{\frac{1}{2}} \tag{40}$$

where we assume Δ to be positive as reasonably expected. By this transformation, the Hamiltonian is diagonalized as,

$$\boldsymbol{H} = \sum_{k,\nu} E C^+_{k\nu} C_{k\nu} + \sum_{k,\nu} E' D^+_{k\nu} D_{k\nu} - (Ew^2 + E'w'^2) \tag{41}$$

The zero point energy is calculated from Eqs. (36), (37) and (40),

$$Ew^2 + E'w'^2 = 2N\beta^2 \frac{\varepsilon + \Delta}{\varepsilon^2 + \varepsilon\Delta - \beta^2} \tag{42}$$

The ground wave function $|0\rangle$ can be expanded by the original representations as

$$|0\rangle = \sum_{m,n} \alpha_{mn} |m,n\rangle_0 \tag{43}$$

Here $|m,n\rangle_0$ is the state function which contains

m one-site CT excitations of $k=0$, $v=+$ and n two-sites CT excitations of $k=0$, $v=+$. The suffix o signifies the original representations. The coefficient α_{mn} is determined from the following conditions.

$$\begin{aligned} &C_{0+}|0\rangle = 0 \\ &D_{0+}|0\rangle = 0 \\ &\sum_{m,n} \alpha_{mn}^2 = 1 \quad \text{(normalization condition)} \end{aligned} \tag{44}$$

The final result is

$$\alpha_{mn} = \frac{x^m y^n}{\sqrt{m!n!}} e^{-\frac{1}{2}(x^2+y^2)} \quad (N\to\infty) \tag{45}$$

and

$$x = -\frac{\varepsilon+\Delta}{EE'}\sqrt{2N}\beta \quad y = \frac{\beta}{EE'}\sqrt{2N}\beta \tag{46}$$

Discussion

First we consider the effect of the Bose approximation. The occupation number of $a_{j\sigma}^+ a_{j\sigma}$ is essentially 0 or 1. But the Bose approximation adopted in the present study takes off this restriction and consequently many excitations turn out to occupy the same crystals site. Therefore this approximation may be applicable only when the mean value $\langle a_{j\sigma}^+ a_{j\sigma}\rangle_{\text{av.}}$ for the concerned state is[16]

$$\langle a_{j\sigma}^+ a_{j\sigma}\rangle_{\text{av.}} \ll 1. \tag{47}$$

For the ground state represented by Eq. (21), the mean value is

$$\langle 0|a_{j\sigma}^+ a_{j\sigma}|0\rangle = \frac{\beta^2}{\varepsilon_{0+}^2} \tag{48}$$

Therefore under the restriction of $\beta^2/\varepsilon_{0+}^2 \ll 1$, the number of the virtual excitations in the ground state is small compared with N and the Bose approximation may not cause a large error. For most of the crystals which are treated here, this restriction seems to be satisfied.

The zero point energy $2N\beta^2/\varepsilon_{0+}$ in Eq. (20) represents the stabilization energy of the crystal due to the contribution of the CT configurations ($k=0$, $v=+$) to the ground state. This is twice as large as the simple sum of the CT stabilization energies of component pairs. The factor 2 comes from the fact that the charge transfer occurs in the two directions ($\sigma=+,-$).

From Eq. (21) the n-molecule excitation configuration is known to contribute to the ground state by α_n^2. As is seen in Eq. (25), the coefficient α_n^2 follows the Poisson distribution function. In Fig. 1 the relation between α_n^2 and n is shown for the case of $\gamma^2=10^6$. The number of virtual excitation $n_{\max}$ for the greatest α_n^2 and the average number of virtural excitations $\bar{n}$ are equal to each other, and they are evaluated form Eq. (24) as follows:

$$n_{\max} = \bar{n} = 2N\frac{\beta^2}{\varepsilon_{0+}^2} \tag{49}$$

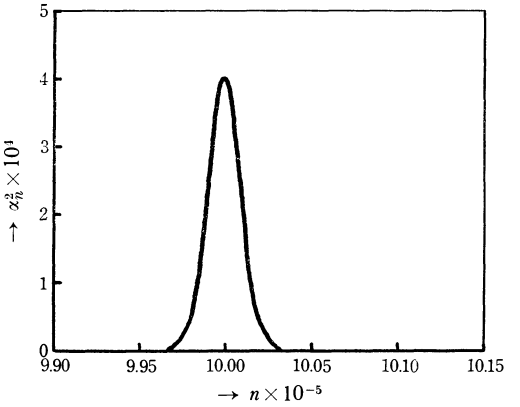

Fig. 1. The dependency of α_n^2 upon n for $\gamma^2=10^6$.

The $n_{\max}$ value is equal to N and $2N$ times the weight of the CT configuration in the corresponding component pairs for radical or molecular crystals and for CT complex crystals, respectively. The excitation density of the jth molecular site in the ground state is

$$\langle 0|\sum_\sigma a_{j\sigma}^+ a_{j\sigma}|0\rangle = 2\frac{\beta^2}{\varepsilon_{0+}^2} \tag{50}$$

Therefore weak CT complexes may be written schematically as $\cdots D^{+\delta}A^{-\delta}D^{+\delta}A^{-\delta}\cdots$ ($\delta=2\beta^2/\varepsilon_{0+}^2$).

According to the second quantization method combined with the Bose approximation the excitation energy between the ground and CT states is equal to ε_{kv} in Eq. (20). In this method, the transfer energy β does not affect the excitation energy.

One may calculate the matrix of operator $\hat{\boldsymbol{\mu}}=\sum_i e\boldsymbol{r}_i$. The operator $\hat{\boldsymbol{\mu}}$ can be expanded in the second quantization form for the following two cases.

Case 1, for usual molecular crystals, radical crystals and weak CT complexes;

$$\begin{aligned} \hat{\boldsymbol{\mu}} = \sum_i e\boldsymbol{r}_i &= \sum_j \{\boldsymbol{\mu}_{1+}(a_{j+}^+ + a_{j+}) + \boldsymbol{\mu}_{1-}(a_{j-}^+ + a_{j-})\} \\ &+ \sum_j \{\boldsymbol{\mu}_d(1)\, a_{j+}^+ a_{j+} + \boldsymbol{\mu}_d(-1) a_{j-}^+ a_{j-}\} \end{aligned} \tag{51}$$

Case 2, for strong CT complexes;

$$\begin{aligned} \hat{\boldsymbol{\mu}} = \sum_i e\boldsymbol{r}_i &= \sum_j \{\boldsymbol{\mu}_{1+}(a_{j+}^+ + a_{j+}) + \boldsymbol{\mu}_{1-}(a_{j-}^+ + a_{j-})\} \\ &- \sum_j \{\boldsymbol{\mu}_d(1)(1-a_{j+}^+ a_{j+}) + \boldsymbol{\mu}_d(-1)(1-a_{j-}^+ a_{j-})\} \end{aligned} \tag{52}$$

where

$$\boldsymbol{\mu}_{1+} = \langle \psi(1,j)|\sum_i e\boldsymbol{r}_i|\psi(0,0)\rangle$$

$$\boldsymbol{\mu}_{1-} = \langle \psi(-1,j)|\sum_i e\boldsymbol{r}_i|\psi(0,0)\rangle$$

$$\mu_{d(m)} = \langle(m,j,)|\sum_i e\boldsymbol{r}_i|\psi(m,j)\rangle - \langle\psi(0,0)|\sum_i e\boldsymbol{r}_i|\psi(0,0)\rangle \;;\; m=1,-1$$

$$\mu_{1//} = \frac{1}{2}(\mu_{1+}-\mu_{1-}), \quad \mu_{1\perp} = \frac{1}{2}(\mu_{1+}+\mu_{1-})$$

$$\mu_{d//} = \frac{1}{2}(\mu_d(1) - \mu_d(-1)),$$

$$\mu_{d\perp} = \frac{1}{2}(\mu_d(1) + \mu_d(-1)) \tag{53}$$

For case 1 every component molecule is assumed to have no dipole moment and $\langle\psi(0,0)|\sum_i e\boldsymbol{r}_i|\psi(0,0)\rangle=0$. The first term in Eqs. (51) and (52) comes from the off-diagonal matrix elements between the CT and ground configurations. The second terms signify the appearance and disappearance of the dipole with a CT excitation, respectively.

Equations (51) and (52) are transformed by the use of Eqs. (16) and (19) as follows:

Case 1,

$$\hat{\boldsymbol{\mu}} = \sqrt{2N}\left(\mu_{1\perp} - \frac{\beta}{\varepsilon_{0+}}\mu_{d\perp}\right)(c^+_{0+}+c_{0+}) + \sqrt{2N}\left(\mu_{1//} - \frac{\beta}{\varepsilon_{0+}}\mu_{d//}\right)(c^+_{0-}+c_{0-}) + \sum_k\{\mu_{d\perp}(c^+_{k+}c_{k+}+c^+_{k-}c_{k-}) + \mu_{d//}(c^+_{k-}c_{k+}+c^+_{k+}c_{k-})\} + 2N\left(-2\mu_{1\perp}\frac{\beta}{\varepsilon_{0+}} + \mu_{d\perp}\left(\frac{\beta}{\varepsilon_{0+}}\right)^2\right) \tag{54}$$

Case 2,

$$\hat{\boldsymbol{\mu}} = \sqrt{2N}\left(\mu_{1\perp} - \frac{\beta}{\varepsilon_{0+}}\mu_{d\perp}\right)(c^+_{0+}+c_{0+}) + \sqrt{2N}\left(\mu_{1//} - \frac{\beta}{\varepsilon_{0+}}\mu_{d//}\right)(c^+_{0-}+c_{0+}) + \sum_k\{\mu_{d\perp}(c^+_{k+}c_{k+}+c^+_{k-}c_{k-}) + \mu_{d//}(c^+_{k-}c_{k+}+c^+_{k-}c_{k-})\} + 2N\left(-2\,\mu_{1\perp}\frac{\beta}{\varepsilon_{0+}} - \mu_{d\perp}\left(1-\frac{\beta^2}{\varepsilon^2_{0+}}\right)\right) \tag{55}$$

As can be seen in the first and second terms of Eqs. (54) and (55), the optical transition from the ground state is allowed for the two kinds of states c_{0+} and c_{0-} within the approximation of electric dipole transition. Hereafter the corresponding state is abbreviatedly represented by the operator $c_{k\nu}$. Their transition moments are

$$\langle 0|c_{0+}\hat{\boldsymbol{\mu}}|0\rangle = \sqrt{2N}\left(\mu_{1\perp} - \frac{\beta}{\varepsilon_{0+}}\mu_{d\perp}\right)$$

$$\langle 0|c_{0-}\hat{\boldsymbol{\mu}}|0\rangle = \sqrt{2N}\left(\mu_{1//} - \frac{\beta}{\varepsilon_{0+}}\mu_{d//}\right) \tag{56}$$

for the both cases. According to Eq. (56), the absorption intensity of the transition to the $c_{0-}(c_{0+})$ state is $2N$ or N times larger in the component parallel (perpendicular) to the chain direction than that for a DA pair of the CT complex or that for a dimer of radicals and usual molecules, respectively.

Usually the second term on the right hand side of Eq. (56) is larger than the first term in their absolute values. Therefore the CT configurations mixing in the ground state contribute mainly to the intensity of optical absorption. In the one molecule excitation method where $\Psi(1,k,\nu)$ of Eq. (6) is taken as an excited state wave function and $\psi(0,0)$ as the ground state one, the optical transition is allowed for the two excited states of $(k=0, \nu=+)$ and $(k=0, \nu=-)$ and their transition moments are only the first term of Eq. (56). Therefore, the Hamiltonian $\boldsymbol{H}_3$ plays an essential role in the mechanism of optical transition.

The dipole moment of the ground state can be evaluated for cases 1 and 2.

Case 1,

$$\boldsymbol{\mu} = \langle 0|\hat{\boldsymbol{\mu}}|0\rangle = 2N\left(-2\mu_{1\perp}\frac{\beta}{\varepsilon_{0+}} + \mu_{d\perp}\frac{\beta^2}{\varepsilon^2_{0+}}\right)$$

Case 2,

$$\boldsymbol{\mu} = \langle 0|\hat{\boldsymbol{\mu}}|0\rangle = 2N\left(-2\mu_{1\perp}\frac{\beta}{\varepsilon_{0+}} - \mu_{d\perp}\left(1-\frac{\beta^2}{\varepsilon^2_{0+}}\right)\right) \tag{57}$$

Since in our model the CT complex has the translational symmetry, the CT complex of a zigzag chain has a dipole moment in the direction perpendicular to the chain. Its magnitude is $2N$ times larger than the component perpendicular to the chain direction of the dipole moment of a DA pair. Thus the zigzag chain of the CT complex is expected to have a large dipole moment, and therefore ferroelectricity is expected for crystals in which the component chain dipoles do not negate each other.

Next we discuss the results obtained in the case of complex radical crystals. The zero point energy $2N\beta^2(\varepsilon+\Delta)/(\varepsilon^2+\varepsilon\Delta-\beta^2)$ can be explained as the stabilization energy due to the mixing of the one-site and two-site CT configurations into the ground state. The main contribution to the zero point energy comes from the fourth term of Eq. (29) which is quite similar to the second terms of Eq. (18). The energy is larger than $2N\beta^2/\varepsilon$ which is the limiting value for $\beta/\varepsilon\to 0$.

The excitation energy E and E' are different from the respective diagonal matrix elements of the one-site and two-site CT states. As is seen in Eqs. (30) and (31), the excited state of the crystal can be understood as a coupled excited state of the one-site and two-site CT excitations. According to Eq. (40), the coupling strength between them becomes larger with the increase in β/Δ.

The configuration which contains m one-site and n two-site CT excitations contributes to the ground state by α^2_{mn}. The $m_{\max}$ and m values which are the m value for the greatest α^2_{mn} and the average number of m for a fixed n, respectively, are obtained from Eq. (45),

$$m_{\max} = \bar{m} = x^2 \tag{58}$$

In the similar way, for a fixed m,

$$n_{\max} = \bar{n} = y^2 \tag{59}$$

Then

$$\frac{n_{\max}}{m_{\max}} = \frac{\bar{n}}{\bar{m}} = \left(\frac{\beta}{\varepsilon+\Delta}\right)^2 \tag{60a}$$

$$\frac{m_{\max}}{N} = \frac{\bar{m}}{N} = 2\left\{\frac{(\varepsilon+\Delta)\beta}{\varepsilon^2+\varepsilon\Delta-\beta^2}\right\}^2 \tag{60b}$$

When $\beta/\varepsilon \to 0$, these quantities are

$$m_{\max} = \bar{m} \xrightarrow[\beta/\varepsilon\to 0]{} 2N\left(\frac{\beta}{\varepsilon}\right)^2 \tag{61a}$$

$$n_{\max} = \bar{n} \to 2N\left(\frac{\beta^2}{\varepsilon^2+\varepsilon\Delta}\right)^2 < 2N\left(\frac{\beta}{\varepsilon}\right)^4 \tag{61b}$$

$$\frac{m_{\max}}{N} = \frac{\bar{m}}{N} \to 2\left(\frac{\beta}{\varepsilon}\right)^2 \tag{61c}$$

Eq. (61a) corresponds to Eq. (49). The results shown by Eqs. (61a), (61b) and (61c) are reasonable.

The transition moment and the dipole moment of the system are obtained by using the equation similar to Eq. (51) except for the contribution from the two-sites CT excitation. The matrix element of transition moment is not zero only for C_{0+}, D_{0+}, C_{0-} and D_{0-}. The transition moments finally obtained are as follows:

$$\begin{aligned}\langle 0|C_{0+}\hat{\boldsymbol{\mu}}|0\rangle &= \boldsymbol{\mu}_{d\perp}(-uw-vw')u \\ &= -\sqrt{2N}\,\beta\,\frac{\varepsilon+\Delta}{E\,E'}\,u\,\boldsymbol{\mu}_{d\perp}\end{aligned}$$

$$\begin{aligned}\langle 0|D_{0+}\hat{\boldsymbol{\mu}}|0\rangle &= \boldsymbol{\mu}_{d\perp}(-uw-vw')v \\ &= -\sqrt{2N}\,\beta\,\frac{\varepsilon+\Delta}{E\,E'}\,v\,\boldsymbol{\mu}_{d\perp}\end{aligned}$$

$$\begin{aligned}\langle 0|C_{0-}\hat{\boldsymbol{\mu}}|0\rangle &= \boldsymbol{\mu}_{d//}(-u^2w+uvw'-2v^2w) \\ &= -\sqrt{2N}\,\beta\,\frac{\varepsilon+\sqrt{\Delta^2+4\beta^2}}{E\,E'}\,u\,\boldsymbol{\mu}_{d//}\end{aligned}$$

$$\begin{aligned}\langle 0|D_{0-}\hat{\boldsymbol{\mu}}|0\rangle &= \boldsymbol{\mu}_{d//}(-v^2w'+uvw-2u^2w') \\ &= -\sqrt{2N}\,\beta\,\frac{\varepsilon-\sqrt{\Delta^2+4\beta^2}}{E\,E'}\,v\,\boldsymbol{\mu}_{d//}\end{aligned} \tag{62}$$

The dipole moment of the ground state is

$$\begin{aligned}\langle 0|\hat{\boldsymbol{\mu}}|0\rangle &= \boldsymbol{\mu}_{d\perp}(-uw-vw')^2 = 2N\,\boldsymbol{\mu}_{d\perp} \\ &\times\left(\beta\,\frac{\varepsilon+\beta}{\varepsilon^2+\varepsilon\Delta-\beta^2}\right)^2\end{aligned} \tag{63}$$

where

$$\boldsymbol{\mu}_d(n) = \langle\psi^0(n,2j-1)|\sum_i e\boldsymbol{r}_i|\psi^0(n,2j-1)\rangle \;;$$

$$n = \pm 1, \pm 2.$$

$$\boldsymbol{\mu}_{d\perp} = \frac{1}{2}(\boldsymbol{\mu}_d(1)+\boldsymbol{\mu}_d(-1)),\quad \boldsymbol{\mu}_{d//} = \frac{1}{2}(\boldsymbol{\mu}_d(1)-\boldsymbol{\mu}_d(-1))$$

$$\langle\psi^0(n,2j-1)|\sum_i e\boldsymbol{r}_i|\psi^0(0,0)\rangle = 0 \quad \text{(assumed)};$$

$$n = \pm 1,\ \pm 2$$

As is seen in Eqs. (62) and (63), the regular chain has no transition dipole for C_{0+} and D_{0+} states and no dipole moment, because of $\mu_{d\perp}=0$ for the regular chain.

For $\beta/\varepsilon \to 0$, C_{0+} and C_{0-} states are mainly composed of the one-site CT state in which an electron transfers from an anion radical A^- to the nearest neighboring neutral molecule A, whereas D_{0+} and D_{0-} states are of the two-site CT state corresponding to an electron transfer between the two neighboring A^- ions. In this case the transition probability to D_{0+} and D_{0-} states become negligibly small, since $|u|\to 1$ and $v\to 0$. On the other hand, for the case where $|\beta|/\Delta$ is large, the transitions to D_{0+} and D_{0-} states turn out to have significant intensity and their excitation energies become lower, as is seen in Eqs. (37) and (40). These CT states become the strongly coupled ones of the one-site and two-sites CT configurations.

BULLETIN OF THE CHEMICAL SOCIETY OF JAPAN VOL. 43 1354—1359 (1970)

The Crystal Structure of *trans*-Dinitratobis(trimethylenediamine)-cobalt(III) Nitrate

Eeki YASAKI,*1 Isao OONISHI, Hiroshi KAWAGUCHI,* Shinichi KAWAGUCHI* and Yoshimichi KOMIYAMA*2

Department of Applied Chemistry, Faculty of Engineering, Yamanashi University, Kofu, Yamanashi
**Department of Chemistry, Faculty of Science, Osaka City University, Sumiyoshi-ku, Osaka*

(Received December 15, 1969)

The crystal structure of *trans*-$[Co(NO_3)_2(tn)_2]NO_3$ (tn: $H_2N-CH_2-CH_2-CH_2-NH_2$) has been determined from three-dimensional X-ray diffraction data. The dimensions of the monoclinic unit cell are: $a=8.62$ Å, $b=10.04$ Å, $c=9.61$ Å, $\beta=114.0°$, and $Z=2$. The space group is $P2_1/c$. The structure has been refined by the least-squares method to $R=0.114$. The complex ion has a slightly distorted octahedral coordination, with four N atoms of trimethylenediamine molecules at 1.990 ± 0.009 Å and two O atoms of nitrate ions at 1.898 ± 0.007 Å. The two six-membered cobalt-trimethylenediamine rings are identical, as is required by the center of symmetry, and take the chair form. The complex ions and nitrate ions are tightly bound together by N-H···O hydrogen bonds in the layers parallel to the (100) plane, but there exists no evidence for hydrogen bonding between the layers.

Only one investigation[1] has been made into the structure of a complex with trimethylenediamine chelate rings. It is, though, obviously important to obtain more information about the shape and size of the six-membered chelate ring. Several crystals of cobalt complexes of the type $[CoXY(tn)_2]Z$, where X, Y, and Z are Cl, NO_2, NO_3, and NCS, were previously prepared by two of the present authors.[2] We have now initiated a structure investigation of these complexes. This paper will report on the crystal structure of *trans*-$[Co(NO_3)_2(tn)_2]NO_3$.

Another point of interest in this work is how nitrate ions coordinate to the cobalt atom. The crystal structure of the α-form of $Cu(NO_3)_2$ has been studied by Wallwork and Addison,[3] that of $Cu(NO_3)_2\cdot CH_3NO_2$, by Duffin and Wallwork,[4] and that of $Cu(NO_3)_2\cdot 2CH_3CN$, by Duffin.[5] However, the nitrate ion coordinated to the cobalt atom has not yet been reported on. It seemed that it would be of interest to compare the results in our work with those of Cu(II) complexes.[3-5]

Experimental

The *trans*-$[Co(NO_3)_2(tn)_2]NO_3$ was prepared and purified according to the method described in a previous paper.[2] The final pure product appears as thin red-violet needles elongated along the *c*-axis. The unit-cell dimensions were determined from higher-order reflections of Weissenberg photographs (Ni$K\alpha$, $\lambda=1.6591$ Å). The systematic absences were: $h0l$ for l odd and $0k0$ for k odd. Hence, the space group was unequivocally determined. The crystal data are listed in Table 1. Sets of multiple-film, equi-inclination Weissenberg photographs were taken about the *c*-axis (0 to 7th layers), and the *a*- and *b*-axes (0th layer).

Ni$K\alpha$ radiation was used throughout. The intensities were estimated visually with a standard film strip and were converted to $|F_0(hkl)|^2$ and $|F_0(hkl)|$ by applying the usual Lorentz, polarization, and spot-shape corrections. No correction was made for absorption and extinction. The range of relative intensities was from 1 to 17000. 916 independent reflections fell within this range, whereas 207 others were too weak to be observed.

TABLE 1. CRYSTAL DATA *trans*-$[Co(NO_3)_2(tn)_2]NO_3$
tn: $H_2N-CH_2-CH_2-CH_2-NH_2$

Monoclinic
$a=8.62\pm0.01$ Å
$b=10.04\pm0.01$
$c=9.61\pm0.01$
$\beta=114.0\pm0.5°$
$Dx=1.72$ g·cm^{-3}
$Dm=1.72$ g·cm^{-3}
$Z=2$

Space group C_{2h}^5-$P2_1/c$
Linear absorption coefficient for Ni$K\alpha$, $\mu=33.3$ cm^{-1}

*1 Present address: Department of Synthetic Quartz, Toyo Communication Equipment Co., Ltd., Samukawa-cho, Koza-gun, Kanagawa.

*2 Deceased on Aug. 1, 1968.

1) T. Nomura, F. Marumo and Y. Saito, This Bulletin, **42**, 1016 (1969).

2) H. Kawaguchi, N. Yano and S. Kawaguchi, *ibid.*, **42**, 136 (1969).

3) S. C. Wallwork and W. E. Addison, *J. Chem. Soc.*, **1965**, 2925.

4) B. Duffin and S. C. Wallwork, *Acta Crystallogr*, **20**, 210 (1966).

5) B. Duffin, *ibid.*, **B24**, 396 (1968).

TABLE 2. ATOMIC PARAMETERS AND THEIR e.s.d.'s* ($\times 10^4$) The expression of the temperature factor is $\exp[-(h^2B_{11}+k^2B_{22}+l^2B_{33}+hkB_{12}+hlB_{13}+klB_{23})]$

Atom	x/a	y/b	z/c	B_{11}	B_{22}	B_{33}	B_{12}	B_{13}	B_{23}
Co	0000	0000	0000	140	65	86	−3	121	−7
O(1)	1536(8)	−391(6)	−906(7)	112	64	45	−11	135	−9
O(2)	2373(10)	1686(7)	−957(9)	175	67	105	27	161	−38
O(3)	3382(10)	76(10)	−1787(10)	167	171	158	7	281	11
O(4)	281(19)	−1072(14)	4267(17)	191	62	87	−7	199	−11
O(5)	880(19)	973(13)	4606(18)	167	48	134	−9	181	−9
O(6)	−661(20)	63(19)	5594(17)	182	159	48	−20	20	−4
N(1)	1013(10)	−1551(7)	1371(9)	118	43	43	−45	72	−47
N(2)	1570(10)	1159(8)	1640(9)	100	49	57	−17	60	−64
N(3)	2469(10)	511(9)	−1245(10)	99	99	47	−19	81	−51
N(4)	−142(46)	−15(35)	4643(31)	82	66	70	8	−377	−26
C(1)	2915(12)	−1705(10)	2034(13)	94	64	96	−55	43	−33
C(2)	3716(13)	−572(12)	3170(12)	112	101	56	−14	58	−23
C(3)	3449(12)	816(11)	2412(13)	79	77	97	−21	69	−54

*e.s.d.'s in parentheses

Structure Analysis

The presence of two formula units in a unit cell of the space group $P2_1/c$ requires the cobalt atoms to occupy one of the sets of two-fold positions. Without loss of generality they can be placed at 000 and $0\frac{1}{2}\frac{1}{2}$. On the other hand, nitrate ions have to take statistical configurations because they do not possess a center of symmetry.

At first, a three-dimensional Patterson synthesis was calculated. From the Patterson maps, the approximate positions of the lighter atoms of the complex ions were deduced, but those of the nitrate anion could not be fixed. Attempts were made to deduce the atomic parameters of the nitrate ions from two-dimensional Fourier and difference syntheses of electron density projected along the *b*- and *c*-axes, the signs of which were calculated from the parameter values of the atoms of the complex ion. From these maps, only two oxygens of the nitrate ion could be easily fixed; the others could not be fixed because of the overlapping of the electron density due to its particular statistical arrangement. Finally, the atomic parameters of the other atoms were assigned by assuming the nitrate ions to be triangular. After the inclusion of these parameters in the structure-factor calculation, these was a considerable improvement in the agreement between the observed and calculated structure factors. At this stage, the discrepancy factor, R, became 0.24 for all the observed reflections. The structure thus obtained was refined by three-dimensional Fourier and difference syntheses to $R=0.18$, and later by a block-diagonal least-squares method using a HBLS-4 program written by T. Ashida. In this least-squares method, anisotropic temperature factors were introduced and six cycles of refinement were carried out.

The weighting scheme employed was:

$w = 0.2$ if $F_0 \leqq F_{min.}$ $(=3.0)$

$w = 1.0$ if $F_{min.} < F_0 \leqq F_{max.}$ $(=90.0)$

$w = F_{max.}/F_0$ if $F_0 > F_{max.}$

The final discrepancy factor, $R=\sum||F_0|-|F_c||/\sum|F_0|$, was 0.114 for all the reflections. The atomic scattering factors were taken from the International Tables for X-ray Crystallography.[6] The final atomic parameters and their estimated standard deviations are summarized in Table 2. The observed and calculated structure factors are listed in Table 3.

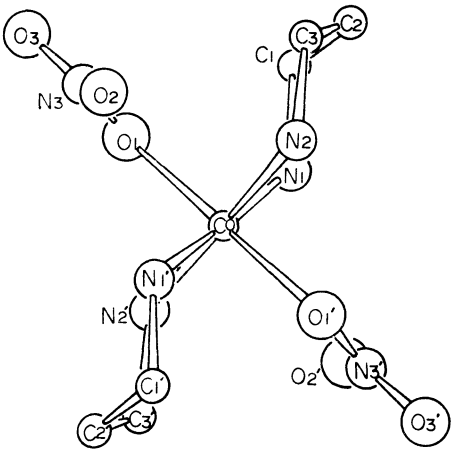

Fig. 1. A perspective drawing of the complex ion, *trans*-$[Co(NO_3)_2(tn)_2]^+$.

6) "International Tables for X-Ray Crystallography," Vol. III, Kynoch Press, Birmingham (1962), p. 202.

TABLE 3. OBSERVED AND CALCULATED STRUCTURE FACTORS

K	FO	FC
H,L= 0 0		
2	692	804
4	87	125
6	282	278
8	101	93
10	41	53
H,L= 1 0		
0	549	616
1	97	-99
2	274	315
3	146	-125
4	92	111
5	23	16
6	213	199
7	73	74
8	165	175
9	49	40
10	90	87
11	18	-15
H,L= 2 0		
0	92	-58
1	26	-12
2	248	237
3	18	12
4	196	202
5	47	46
6	78	92
7	90	78
8	180	185
9	40	36
10	130	112
11	23	-21
H,L= 3 0		
0	369	342
1	139	134
2	308	321
3	75	-81
4	248	248
5	18	7
6	135	140
7	106	100
8	106	83
9	49	40
10	104	91
11	33	-32
H,L= 4 0		
0	37	44
1	125	92
2	42	51
3	35	-32
4	168	156
5	137	-122
6	180	159
7	21	8
8	59	55
9	14	8
10	71	64
H,L= 5 0		
0	85	90
1	18	-13
2	170	169
3	21	-14
4	146	150
5	59	-60
6	54	47
7	101	-97
8	52	64
9	33	-31
10	61	56
H,L= 6 0		
0	154	144
1	42	-42
2	182	185
3	21	17
4	130	112
5	35	33
6	40	34
7	52	-51
8	87	86
9	11	-7
H,L= 7 0		
0	59	64
1	23	3
2	56	52
3	21	4
4	61	53
5	30	18
6	73	71
7	26	21
H,L= 8 0		
0	99	102
1	18	19
2	82	76
3	28	25
4	52	48
5	42	35
6	45	33
H,L= 9 0		
0	45	41
1	28	-27
2	40	37
3	11	-6
H,L= -9 1		
1	38	34
2	42	40
3	44	39
4	5	-6
H,L= -8 1		
1	87	83
2	38	36
3	36	34
4	9	12
5	75	68
6	22	-31
H,L= -7 1		
1	128	122
2	13	-7
3	75	64
4	40	-38
5	10	12
6	57	-55
7	22	25
8	28	-40
H,L= -6 1		
1	146	147
2	42	-44
3	209	232
4	11	-20
5	57	32
6	11	5
7	10	11
8	8	6
9	86	84
H,L= -5 1		
1	61	77
2	9	20
3	216	212
4	78	83
5	178	169
6	81	67
7	95	82
8	10	8
9	73	76
10	6	3
H,L= -4 1		
1	172	183
2	81	67
3	8	21
4	111	99
5	127	123
6	61	51
7	27	26
8	11	-3
9	20	-27
10	8	12
H,L= -3 1		
1	210	197
2	47	-52
3	97	130
4	67	65
5	131	131
6	10	4
7	103	94
8	11	-13
9	36	40
10	45	52
11	50	51
H,L= -2 1		
1	212	-143
2	156	-155
3	111	131
4	25	-19
5	134	138
6	126	-122
7	182	198
8	95	-98
9	155	143
10	29	33
11	42	35
H,L= -1 1		
1	221	177
2	112	93
3	178	-116
4	107	-94
5	8	18
6	46	-48
7	79	94
8	11	-7
9	23	26
10	27	-32
11	37	31
H,L= 0 1		
2	169	154
3	50	84
4	163	-153
5	286	271
6	50	48
7	158	155
8	128	108
9	11	-18
10	33	-46
11	22	18
H,L= 1 1		
1	112	147
2	88	-95
3	354	338
4	71	-52
5	323	308
6	38	-30
7	119	118
8	11	0
9	11	0
10	10	-8
11	7	-5
H,L= 2 1		
1	143	-128
2	22	35
3	232	217
4	165	137
5	90	98
6	10	2
7	12	-14
8	11	-9
9	11	14
10	25	24
11	33	31
H,L= 3 1		
1	200	-160
2	249	223
3	160	162
4	9	19
5	154	159
6	12	26
7	69	73
8	58	63
9	90	83
10	8	7
11	75	67
H,L= 4 1		
1	30	54
2	155	141
3	145	143
4	21	-27
5	100	90
6	23	-28
7	48	45
8	10	-14
9	75	66
10	7	-19
H,L= 5 1		
1	158	135
2	76	-72
3	50	49
4	30	33
5	11	-12
6	18	-29
7	10	11
8	71	-67
9	47	43
H,L= 6 1		
1	78	89
2	139	-137
3	44	50
4	18	-27
5	68	65
6	16	-19
7	80	80
8	34	-28
H,L= 7 1		
1	85	80
2	11	-9
3	83	82
4	10	-4
5	69	57
6	28	31
7	39	40
8	11	-3
9	59	50
10	27	29
11	21	21
H,L= -9 2		
0	12	-25
1	9	10
2	9	-4
3	8	12
4	31	29
5	27	21
H,L= -8 2		
1	85	-91
2	311	309
3	40	-27
4	241	236
5	21	20
6	103	107
7	14	-16
8	90	82
9	39	38
10	104	100
11	19	26
H,L= 3 2		
0	45	-18
1	77	50
2	159	178
3	10	13
4	102	176
5	12	0
6	59	59
7	45	44
8	154	150
9	10	21
10	117	116
H,L= 4 2		
0	255	239
1	17	33
2	247	234
3	62	70
4	103	103
5	90	88
6	39	42
7	46	45
8	125	120
9	9	-4
10	94	88
H,L= 5 2		
0	202	192
1	103	-97
2	57	59
3	85	-76
4	14	15
5	13	20
6	108	103
7	10	-7
8	75	72
9	6	5
H,L= 6 2		
0	116	106
1	62	-59
2	70	57
3	77	-69
4	73	66
5	12	20
6	113	99
7	9	-22
8	39	38
H,L= 7 2		
0	70	54
1	12	6
2	98	87
3	10	13
4	85	77
5	8	12
6	46	38
H,L= 8 2		
0	43	34
1	8	4
2	41	34
3	7	8
4	8	1
H,L= -10 3		
1	65	61
H,L= -9 3		
1	10	-22
2	9	7
3	9	7
4	8	1
5	18	23
H,L= -8 3		
1	58	61
2	14	30
3	54	51
4	12	1
5	12	23
6	18	28
7	20	21
H,L= -7 3		
1	95	104
2	62	-58
3	102	116
4	20	26
5	105	104
6	12	-5
7	66	63
8	16	-32
H,L= -6 3		
1	95	110
2	97	-96
3	87	88
4	13	20
5	98	94
6	83	-83
7	51	55
8	106	-116
9	8	15
H,L= -5 3		
1	320	320
2	83	84
3	169	186
4	12	-7
5	75	72
6	39	-39
7	14	-16
8	34	-36
9	49	51
10	7	0
H,L= -4 3		
1	334	327
2	201	195
3	145	163
4	10	-4
5	129	131
6	19	15
7	154	166
8	55	57
9	111	113
10	8	9
H,L= -3 3		
1	421	373
2	111	101
3	84	-61
4	99	117
5	54	58
6	36	32
7	111	113
8	39	34
9	30	34
10	28	24
11	37	40
H,L= -2 3		
1	388	397
2	44	-49
3	31	55
4	52	38
5	84	88
6	43	45
7	83	108
8	49	53
9	55	61
10	10	15
11	63	72
H,L= -1 3		
1	267	-198
2	105	-90
3	285	284
4	266	-244
5	169	175
6	57	-49
7	133	139
8	41	40
9	153	152
10	29	-29
11	58	55
H,L= 0 3		
1	254	-192
2	179	144
3	263	246
4	50	-63
5	116	115
6	39	-47
7	12	8
8	13	-15
9	49	52
10	20	-41
11	32	30
H,L= 1 3		
1	220	245
2	121	119
3	201	196
4	80	65
5	188	205
6	30	-29
7	38	39
8	14	-17
9	12	-7
10	16	17
11	43	50
H,L= 2 3		
1	195	188
2	14	-29
3	192	211
4	17	-13
5	176	180
6	70	-70
7	80	79
8	43	-44
9	37	33
10	36	37
11	3	3
H,L= -9 4		
1	10	-22
2	32	34
3	140	135
4	118	111
5	12	-4
6	20	16
7	25	28
8	40	-48
9	76	77
10	6	14
11	4	3
H,L= -8 4		
1	27	34
2	12	0
3	12	15
4	73	78
5	25	25
6	52	57
7	69	82
8	110	110
9	16	-22
10	91	-96
11	8	7
H,L= 0 4		
1	357	310
2	25	28
3	221	214
4	48	-34
5	52	62
6	18	-4
7	47	63
8	17	1
9	74	91
10	22	-37
11	38	-41
H,L= 1 4		
0	249	236
1	29	26
2	132	124
3	67	-53
4	72	100
5	65	-75
6	118	119
7	14	-6
8	79	78
9	13	-8
10	89	82
H,L= 2 4		
0	102	78
1	9	-21
2	80	69
H,L= -9 4		
0	68	59
1	13	-9
2	104	81
3	12	-13
4	68	55
5	9	16
H,L= -8 4		
0	65	-69
1	14	-8
2	14	2
3	14	-9
4	61	52
5	33	34
6	34	25
7	44	49
H,L= -7 4		
0	73	62
1	24	-35
2	38	37
3	14	0
4	135	114
5	37	31
6	143	147
7	12	-17
8	42	39
H,L= -6 4		
0	267	247
1	38	-37
2	147	125
3	22	-18
4	84	81
5	17	-19
6	106	108
7	59	-65
8	12	2
9	9	-21
H,L= -5 4		
0	13	33
1	18	-19
2	107	103
3	87	-88
4	89	94
5	81	-89
6	79	77
7	17	-17
8	23	24
9	12	10
10	25	19
H,L= -4 4		
0	200	191
1	61	55
2	243	237
3	10	-17
4	228	226
5	38	-47
6	161	173
7	34	42
8	139	125
9	13	18
10	47	35
H,L= -3 4		
0	376	399
1	128	113
2	153	158
3	115	114
4	138	125
5	76	81
6	173	171
7	142	127
8	24	19
9	28	28
10	26	19
11	40	-50
H,L= -2 4		
0	17	4
1	56	72
2	32	40
3	32	-32
4	167	167
5	34	32
6	159	149
7	87	95
8	52	49
9	42	43
10	48	44
11	9	-17
H,L= -1 4		
0	47	-46
1	320	293
2	93	-92
3	81	102
4	76	-91
5	18	13
6	98	-99
7	74	86
8	45	-43
9	80	92
H,L= -4 5		
0	52	52
1	99	95
2	14	-12
3	44	57
4	14	-20
5	52	62
6	18	-4
7	47	63
8	17	1
9	74	91
H,L= -6 5		
0	249	236
1	29	26
2	132	124
3	67	-53
4	72	100
5	65	-75
6	118	119
7	14	-6
8	79	78
9	13	-8
10	89	82
H,L= -5 5		
0	488	495
1	49	-55
2	345	354
3	14	-15
4	159	162
5	41	44
6	103	100
7	14	-15
8	77	78
9	18	-22
10	40	34
H,L= 3 4		
0	231	249
1	136	-133
2	186	196
3	52	-55
4	71	73
5	79	79
6	60	63
7	14	-15
8	94	99
9	9	0
H,L= 4 4		
0	83	83
1	45	-52
2	45	55
3	63	-63
4	57	63
5	14	14
6	107	114
7	42	48
8	71	73
H,L= 5 4		
0	95	95
1	42	56
2	71	69
3	44	47
4	84	83
5	21	26
6	87	88
7	59	63
H,L= 6 4		
0	48	50
1	13	3
2	49	47
3	32	-3
4	48	44
5	10	-17
6	18	23
H,L= 7 4		
0	52	42
1	9	-16
2	41	33
3	14	-25
H,L=-10 5		
1	54	86
2	10	-22
H,L= -9 5		
1	83	97
2	17	-36
3	100	119
4	13	14
5	42	53
H,L= -8 5		
1	51	-54
2	18	-16
3	17	27
4	17	7
5	54	63
6	13	6
7	39	57
H,L= -7 5		
1	81	95
2	97	99
3	20	-20
4	35	48
5	57	72
6	17	4
7	56	72
8	11	-6
H,L= -6 5		
1	258	250
2	47	49
3	49	43
4	18	-13
5	59	68
6	13	4
7	80	110
8	85	95
9	45	59
H,L= -5 5		
1	170	160
2	93	-92
3	81	102
4	76	-91
5	18	13
6	98	-99
7	74	86
8	45	-43
9	80	92
H,L= -4 5		
1	357	310
2	25	28
3	221	214
4	48	-34
5	52	62
6	18	-4
7	47	63
8	17	1
9	74	91
10	22	-37
11	38	-41
H,L= -3 5		
1	325	308
2	122	106
3	277	220
4	47	-63
5	195	175
6	61	67
7	107	100
8	102	97
9	81	90
10	11	-34
H,L= -2 5		
1	148	147
2	45	41
3	219	201
4	68	61
5	144	123
6	92	96
7	42	38
8	45	43
9	17	46
10	13	16
H,L= -1 5		
1	194	173
2	66	-73
3	127	118
4	73	-67
5	73	79
6	59	-62
7	119	114
8	28	-32
9	117	140
10	27	34
H,L= 1 5		
1	66	67
2	37	40
3	25	31
4	47	-48
5	49	46
6	18	-7
7	95	86
8	17	-3
9	73	70
10	15	-21
H,L= 2 5		
1	282	215
2	17	-14
3	56	59
4	57	73
5	59	64
6	20	30
7	69	81
8	15	-25
9	18	23
H,L= 3 5		
1	175	167
2	93	-109
3	66	65
4	18	-10
5	100	109
6	18	-20
7	78	65
8	11	-11
9	4	5
10	35	56
H,L= 4 5		
1	28	19
2	35	54
3	100	119
4	17	13
5	74	82
6	15	9
7	42	41
H,L= 5 5		
1	17	-8
2	80	97
3	35	43
4	17	27
5	25	32
6	10	9
H,L= 6 5		
1	37	40
2	11	18
3	18	22
4	8	-3
H,L=-10 6		
0	76	77
1	8	3
2	53	51
H,L= -9 6		
0	92	101
1	19	-26
2	129	111
3	28	-40
4	80	110
5	15	-2
6	45	59
H,L= -8 6		
0	115	110
1	14	24
2	100	90
3	15	34
4	76	69
5	99	3
6	63	59
7	11	-19
8	80	92
H,L= -7 6		
0	52	52
1	99	95
2	14	-12
3	44	57
4	14	-20
5	15	-17
6	18	-4
7	47	63
8	17	1
9	74	91
10	22	-37
11	38	-41
H,L= -2 6		
1	44	63
2	167	141
3	166	178
4	205	200
5	175	127
6	110	95
7	14	-1
8	15	9
9	11	-3
10	29	19
H,L= -1 6		
0	109	121
1	38	-44
2	75	57
3	51	58
4	59	60
5	73	90
6	90	82
7	28	-45
8	41	42
9	12	25
10	35	16
H,L= 0 6		
0	93	98
1	25	-45
2	119	116
3	42	-51
4	90	91
5	14	-12
6	93	89
7	14	-22
8	102	105
9	9	-5
10	15	7
H,L= 1 6		
0	36	26
1	12	9
2	59	45
3	12	-1
4	53	34
5	15	10
6	66	59
7	12	0
8	96	98
9	29	-43
H,L= 2 6		
0	143	144
1	35	-45
2	42	38
3	59	-59
4	32	26
5	14	-20
6	89	100
7	11	-4
8	29	40
H,L= 3 6		
0	196	195
1	14	-7
2	110	120
3	14	-17
4	100	110
5	12	-17
6	105	108
7	9	7
8	42	41
9	58	50
H,L= 4 6		
0	42	41
1	15	31
2	85	89
3	14	19
4	79	93
5	9	-20
6	31	31
H,L= 5 6		
0	25	13
1	11	7
2	58	50
3	9	-7
4	36	44
H,L= -9 7		
1	63	97
2	11	-7
3	27	56
4	20	27
5	18	66
H,L= -8 7		
1	146	167
2	30	36
3	97	106
4	13	7
5	29	59
6	10	12
H,L= -7 7		
1	17	-18
2	25	23
3	17	29
4	52	-68
5	15	24
6	13	13
7	44	50
H,L= -6 7		
1	42	27
2	37	-35
3	97	109
4	35	37
5	182	101
6	15	15
7	56	59
8	11	-16
9	27	48
H,L= -4 7		
1	27	62
2	145	-120
3	222	179
4	145	-106
5	58	60
6	63	-64
7	23	23
8	34	-49
9	58	66
H,L= -3 7		
1	152	148
2	17	14
3	254	239
4	13	3
5	52	73
6	17	-18
7	30	35
8	54	-50
9	80	90
H,L= -2 7		
1	273	292
2	32	29
3	124	107
4	59	64
5	83	93
6	17	22
7	88	97
8	13	-5
9	83	80
H,L= -1 7		
1	271	269
2	44	-46
3	22	21
4	23	34
5	51	59
6	47	50
7	93	95
8	42	42
9	35	35
H,L= 0 7		
1	155	157
2	35	-31
3	80	89
4	59	60
5	35	47
6	75	66
7	90	96
8	13	20
H,L= 1 7		
1	54	59
2	66	-61
3	54	59
4	44	-41
5	54	66
6	15	-5
7	92	98
8	10	6
H,L= 2 7		
1	44	46
2	15	21
3	17	17
4	42	-43
5	97	95
6	11	-8
7	59	59
H,L= 3 7		
1	58	69
2	63	64
3	73	72
4	15	15
5	73	77
6	8	-3
H,L= 4 7		
1	92	82
2	11	-2
3	116	97
4	10	-19

Table 4. Bond distances and angles and their e.s.d.'s*

Complex ion			
Co–O(1)	1.898(7) Å	N(1)–Co–N(2)	87.7(4)°
N(1)	1.997(9)	O(1)–Co–N(1)	86.7(3)
N(2)	1.983(9)	O(1)–Co–N(2)	96.2(3)
N(1)–C(1)	1.507(15)	Co–N(1)–C(1)	117.9(7)
N(2)–C(3)	1.522(15)	Co–N(2)–C(3)	120.1(7)
C(1)–C(2)	1.533(17)	N(1)–C(1)–C(2)	108.8(9)
C(2)–C(3)	1.546(17)	N(2)–C(3)–C(2)	111.0(9)
N(3)–O(1)	1.336(12)	C(1)–C(2)–C(3)	113.3(10)
O(2)	1.223(13)	Co–O(1)–N(3)	125.0(6)
O(3)	1.190(14)	O(1)–N(3)–O(2)	119.8(9)
	e.s.d. $\times 10^3$	O(1)–N(3)–O(3)	115.3(9)
		O(2)–N(3)–O(3)	124.9(10)
			e.s.d. $\times 10$
Nitrate ion			
N(4)–O(4)	1.22(4) Å	O(4)–N(4)–O(5)	111(3)°
O(5)	1.34(4)	O(4)–N(4)–O(6)	123(4)
O(6)	1.14(4)	O(5)–N(4)–O(6)	115(3)
	e.s.d. $\times 10^2$		e.s.d. $\times 1$

*e.s.d.'s in parentheses

Table 5. The other important interatomic distances in the complex ion and their e.s.d.'s*

O(1)–N(1)	2.674(11) Å	O(1)–C(1)	2.899(14) Å
N(1′)	2.834(11)	C(3)	3.174(14)
N(2)	2.890(11)	O(2)–N(1′)	2.784(12)
N(2′)	2.592(11)	N(2)	2.898(12)
N(1)–N(2)	2.757(12)	C(3)	3.109(15)
N(2′)	2.871(12)	O(1)–O(2)	2.214(11)
C(1)–C(3)	2.572(17)	O(3)	2.136(13)
		O(2)–O(3)	2.139(13)

The atom with an apostrophe indicates the atom related to the one without it by a center of symmetry at the cobalt atom.
*e.s.d.'s $\times 10^3$ in parentheses

Description of the Structure and Discussion

A perspective drawing of the complex ion, *trans*-$[Co(NO_3)_2(tn_2)]^+$, is illustrated in Fig. 1. The bond lengths and angles, with their e.s.d.'s as calculated on the basis of the atomic parameters in

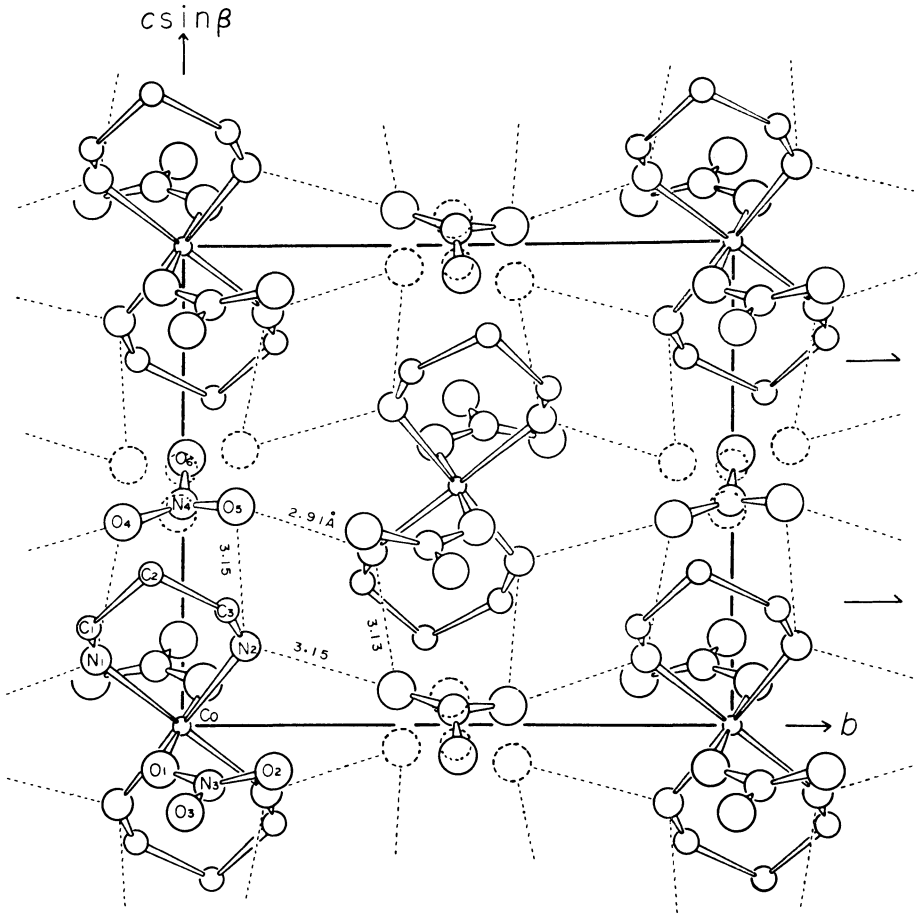

Fig. 2. The structure projected upon a plane normal to the *a*-axis.

TABLE 6. INTERMOLECULAR CONTACTS NOT EXCEEDING 3.5 Å

O(1)–O(4)(2)	3.306(18) Å	O(3)–C(3)(2′)	3.156(16) Å
O(5)(2)	3.361(19)	O(4)–N(1)(1)	3.131(19)
N(4)(2)	3.32 (4)	N(1)(3′)	3.024(19)
O(2)–O(4)(2)	3.132(18)	N(2)(4′)	3.147(19)
O(5)(3″)	2.836(20)	N(3)(2)	2.962(19)
N(2)(3″)	3.032(12)	O(5)–N(1)(4)	2.911(20)
C(3)(3″)	3.284(15)	N(2)(1)	3.145(20)
O(3)–O(3)(2′)	3.436(20)	N(2)(3)	3.394(20)
O(4)(2)	3.245(19)	O(6)–N(1)(2″)	3.418(20)
O(6)(2)	3.464(21)	N(2)(2″)	3.323(20)
N(4)(2)	3.02 (4)	C(2)(2″)	3.380(20)
C(2)(2′)	3.314(15)	N(3)–N(4)(2)	3.10 (4)

1) x, y, z
2) $-x, -y, -z$ 2′) $1-x, -y, -z$ 2″) $-x, -y, 1-z$
3) $x, \frac{1}{2}-y, \frac{1}{2}+z$ 3′) $x, -\frac{1}{2}-y, \frac{1}{2}+z$ 3″) $x, \frac{1}{2}-y, -\frac{1}{2}+z$
4) $-x, \frac{1}{2}+y, \frac{1}{2}-z$ 4′) $-x, -\frac{1}{2}+y, \frac{1}{2}-z$
e.s.d.'s $\times 10^3$ in parentheses

Table 2, are listed in Table 4, while the other important interatomic distances in the complex ion are listed in Table 5. The structure projected upon a plane normal to the *a*-axis is shown in Fig. 2. The important intermolecular contacts (*i.e.*, those less than 3.5 Å) are listed in Table 6. The interatomic distances and bond angles were calculated using a DAPH program written by T. Ashida.

The cobalt atoms are surrounded by two oxygen atoms of nitrate ions and four nitrogen atoms of trimethylenediamine molecules, which form a slightly distorted octahedron. Two nitrate ions are coordinated to a cobalt atom in *trans*-positions. The distortion of the coordinated octahedron is more marked than those in the nitroamminecobalt(III) complexes studied recently.[7,8] For example, the N(1)–Co–N(2), O(1)–Co–N(1), and O(1)–Co–N(2) angles are 87.7, 86.7, and 96.2° respectively. The N(1)–Co–N(2) angle of 87.7° in the Co–tn ring is less than those found in $[Co(tn)_3]Br_3 \cdot H_2O$[1] (96, 92, and 95°). Short contacts were found between O(2) and N(1′), and between O(2) and N(2), the distances being 2.898 and 2.784 Å respectively. A check on the angles (Co–N–O) at N(1′) and N(2) indicates that such short distances are not a intramolecular hydrogen bond: the angles are 75.4 and 78.0° respectively.

The Co–O (NO_3) distance of 1.897 Å agrees well with the corresponding values of 1.900 Å in ammonium ethylenediaminetetraacetatocobaltate(III) dihydrate.[9] The Co–N (tn) distances of 1.997 and 1.983 Å agree well with the values, 1.954—2.006 Å, in $[Co(tn)_3]Br_3 \cdot H_2O$ and nitroamminecobalt(III) complexes.[1,7,8]

The N–O (coordinated to the Co atom) distance in the nitrate ions of 1.336 Å is significantly longer than the other N–O distances of 1.223 and 1.190 Å. These values generally agree well with those found in the related compounds,[3,5] but the Co–O–N angle of 125.0° is larger than those of 110 and 113° in $Cu(NO_3)_2$,[3] and of 110 and 114° in $Cu(NO_3)_2 \cdot 2CH_3CN$.[5] This seems to be partly due to the short contacts described above. The plane of the nitrate ion coordinated to the cobalt atom is listed in Table 7. This plane makes an angle of 91.6° with the coordination plane and is approximately parallel to the direction of the N(1)—N(2) vector.

The shape and size of the trimethylenediamine chelate ring is illustrated in Fig. 3. Some least-squares and other important planes are listed in

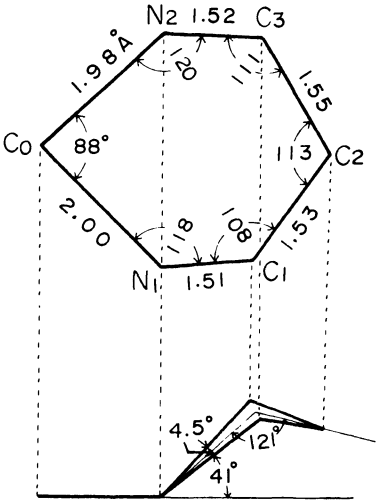

Fig. 3. The shape and size of the chelate ring.
tn: $H_2N-CH_2-CH_2-CH_2-NH_2$

7) I. Oonishi, F. Muto and Y. Komiyama, This Bulletin, **42**, 2791 (1969).
8) I. Oonishi, H. Fujimaki, F. Muto and Y. Komiyama, *ibid.*, **43**, 733 (1970).
9) H.A. Weakliem and J. L. Hoard, *J. Amer. Chem. Soc.*, **81**, 549 (1959).

TABLE 7. LEAST-SQUARES AND OTHER PLANES IN THE COMPLEX ION AND THE NITRATE ION

Coefficients of (least-squares) plane $AX+BY+CZ+D=0$

		A	B	C	D	($\times 10^3$)
Coordination plane	(α)	−921	94	379	0	
N(1), N(2), C(1), C(3)	(β)	427	41	−904	981	
C(1), C(2), C(3)	(γ)	−987	106	123	1656	
Nitrate ion coordinated to Co atom	(δ)	393	−120	912	18	
Nitrate ion	(η)	−541	219	−812	2506	

X (Å)$=ax+cz\cos\beta$ $Y=by$ $Z=cz\sin\beta$

Angles between the (least-squares) planes

	β	γ	δ (degree)
α	43.0	15.2	88.4
β		58.1	48.6
γ			73.2

Distances from the planes

	α	β	γ ($\times 10^3$)	δ ($\times 10^3$)		η ($\times 10^2$)	
Co	0	(981)	(1656)	Co	(18)	O(4)	0
N(1)	0	−26	(1307)	O(1)	0	O(5)	0
N(2)	0	32	(1254)	O(2)	0	O(6)	0
C(1)	(−1065)	30	0	O(3)	0	N(4)	(24)
C(2)	(−806)	(−719)	0	N(3)	(−12)		
C(3)	(−989)	−32	0				

( ) not included in the least-squares calculations

Table 7. The two six-membered Co-tn rings are identical, as is required by centrosymmetry, and take the chair form. They are nearly identical to those in $[Co(tn)_3]Br_3\cdot H_2O$[1] except for the bond lengths of N–C. The N–C distances of 1.522 and 1.507 Å are longer than the mean values of 1.47 Å in $[Co(tn)_3]Br_3\cdot H_2O$,[1] but not significantly so. The angle between the coordination plane (α) and the plane of N(1), N(2), C(3), and C(1) (β) is 43°, significantly larger than the values of 31°, 34°, and 38° in $[Co(tn)_3]Br_3\cdot H_2O$.[1] From these values it appears that the chelate rings in $[Co(tn)_3]Br_3\cdot H_2O$ are, as a result of non-bonded hydrogen interactions, rather more flattened out than those in *trans*-$[Co(NO_3)_2(tn)_2]NO_3$, where there exists no such repulsion, as the two chelate rings are in *trans*-positions. The angle between the β plane and the plane of C(1), C(2), and C(3) is 122°, which value agrees well with those in $[Co(tn)_3]Br_3\cdot H_2O$ (122°, 118°, and 122°). The Co–N–C bond angles of 117.9° and 120.1° are larger than the normal tetrahedral angle, but the mean value of the N–C–C and C–C–C angles is 111.0°, which is closer to the normal tetrahedral angle. The distortions of the chelate ring and of the octahedral coordination described above appear to make the complex less stable than that with five-membered chelate rings,[10] as in the case of $[Co(tn)_3]Br\cdot H_2O$.[1] The bond lengths and angles in the nitrate ion are different from those in *trans*-$[Co(NO_2)_2(NH_3)_4]NO_3\cdot H_2O$[7] and *cis*-$[Co(NO_2)_2(NH_3)_4]NO_3$.[8] The difference seems to be due to the presence of disorder in the arrangement of nitrate ions; at any rate, it is insignificant. The structure is built up of complex cations $[Co(NO_3)_2(tn)_2]^+$ and nitrate ions; thus, it is essentially ionic. A complex ion is surrounded by four nitrate ions in the layers parallel to the (100) plane. In these layers there are hydrogen bonds between complex ions and nitrate ions. They are indicated by dotted lines in Fig. 2. There exists no hydrogen bond between the layers.

The numerical calculations were carried out on the FACOM231 computer at this University and the HITAC5020E computer at the Computer Center, The Tokyo University.

Part of the cost of this investigation has been defrayed by a Scientific Research Grant of the Ministry of Education, to which the authors' thanks are due.

10) J. C. Bailar, Jr., and J. B. Work, *ibid.*, **68**, 232 (1946).

BULLETIN OF THE CHEMICAL SOCIETY OF JAPAN VOL. 43 1360—1364 (1970)

The Chemical Behavior of Low Valence Sulfur Compounds. II.[*1] Thin-layer Chromatographic Separation and Photometric Determination of Low Valence Sulfur Compounds

Kunishige NAITO, Shinsuke TAKEI[*2] and Taijiro OKABE

Department of Applied Chemistry, Faculty of Engineering, Tohoku University, Sendai

(Received May 21, 1969)

The quantitative determination of some low valence sulfur compounds, especially low polythionates, which appeared as intermediate products in the oxidation of elemental sulfur with compressed oxygen in aqueous ammonia was investigated by means of thin-layer chromatography and colorimetry with methylene blue to establish the mechanism of the oxidation of elemental sulfur. Thiosulfate and some low polythionates could be resolved clearly by thin-layer chromatography using silica gel as an absorbent. A suitable solvent for the development was a mixed solution of ethyl alcohol, *n*-butyl alcohol, aqueous ammonia, ammonium acetate and distilled water. The amount of sulfur in the developed spot of the thin-layer chromatogram was determined photometrically with precision of 10 to 20% using methylene blue as a color reagent. Sulfate, sulfite and thiosulfate could not be developed effectively by this method.

In a previous paper,[1] it was reported that ammonium sulfamate and ammonium sulfate were finally produced in the oxidation of elemental sulfur with compressed oxygen in aqueous ammonia solution. The reaction mechanism of the oxidation was not completely established, but its main course through some low polythionates has been disclosed. For the development of these serial studies, it is necessary to establish a rapid, reliable and simple analytical method for the mixture of polythionates in the presence of sulfite, sulfate and thiosulfate. Analytical methods have been proposed by many investigators. 1. A chemical method developed by Kurtenacker and Goldbach,[2] and Goehring[3] has generally been accepted for the detection and quantitative determination of polythionates. So far, this is the most reliable method. However, the skill and delicate operation required make it difficult to achieve reliable results. 2. A fractional precipitation method with benzidine was taken up by Spohn and Weitz[4] for the isolation of low polythionates, but the troublesome procedure prevents it from becoming popular. 3. A photometric method with ferric thiocyanate was proposed by Urban[5] and improved by Koh and Iwasaki.[6] As only a mean value of polythionate content is obtained, its application for the quantitative determination of polythionates is limited. 4. Recently, excellent works on the detection of polythionates using paper chromatography have been reported by Bighi and Trabanelli,[7] Scoffone and Carini,[8] and Pollard.[9] Two improved methods, in which radio-paper chromatography or thin-layer chromatography was used, were carried out by Blasius and his co-workers[10] and Seiler and Erlenmeyer,[11] respectively. These methods are superior in the effectiveness of qualitative separation of polythionates to any other

*1 Previous paper in series, M. C. Shieh, H. Otsubo and T. Okabe, This Bulletin, **38**, 1596 (1965).

*2 Present address: Department of Industrial Chemistry, Faculty of Engineering, Ibaragi University, Hitachi.

1) M. C. Shieh, H. Otsubo and T. Okabe, This Bulletin, **38**, 1596 (1965).

2) A. Kurtenacker and E. Goldbach, *Z. Anorg. Allg. Chem.*, **166**, 177 (1927); *ibid.*, **134**, 265 (1924).

3) M. Goehring, *Z. Anal. Chem.*, **128**, 6 (1948); *ibid.*, **129**, 346 (1949).

4) F. Weitz and K. Spohn, *Chem. Ber.*, **89**, 2332 (1956).

5) P. J. Urban, *Z. Anal. Chem.*, **179**, 415, 422 (1961); *ibid.*, **180**, 110, 116 (1961).

6) T. Koh and I. Iwasaki, This Bulletin, **39**, 352, 576, 703 (1966).

7) C. Bighi and G. Trabanelli, *Ann. Chim.* (Rome), **47**, 195 (1957); *Chem. Abstr.*, **51**, 9404a (1957); *Boll. Sci. Fac. Chim. Ind. Bologna*, **16**, 92 (1958); *Chem. Abstr.*, **53**, 4017g (1959).

8) E. Scoffone and E. Carini, *Ricerca Sci.*, **25**, 2109 (1956); *Chem. Abstr.*, **50**, 729e (1956).

9) F. H. Pollard, *J. Chromatogr.*, **15**, 393, 407, 518 (1964); *J. Chem. Soc.*, **1955**, 4377.

10) E. Blasius and W. Burmeister, *Z. Anal. Chem.*, **168**, 1 (1959); *Z. Anorg. Allg. Chem.*, **313**, 248 (1959); E. Blasius, W. Burmeister and G. Wermbter, *ibid.*, **313**, 254 (1959); E. Blasius and G. Werbmter, *ibid.*, **316**, 251 (1962); E. Blasius and R. Kramer, *ibid.*, **318**, 113 (1962); *ibid.*, **319**, 1 (1962).

11) H. Seiler and H. Erlenmeyer, *Helv. Chim. Acta*, **47**, 264 (1964).

method proposed previously.

In the present study, chromatographic separation and photometric determination of polythionates and some sulfur-oxy acids are examined by thin-layer chromatography and the colorimetric technique with methylene blue as a color reagent.

Experimental

Sample Compounds of Sulfur. Compounds of sulfur used in the present study were potassium salts of thiosulfate, sulfate, sulfite and tri-, tetra-, penta- and hexathionates. Potassium salts of thiosulfate, sulfate and sulfite were of E.C.P. grade from Kanto Chemical Co., Inc. Potassium tri- and tetrathoinates were prepared from potassium thiosulfate and sulfur dioxide gas and from potassium thiosulfate and ethyl alcoholic solution of iodine by Martin's method,[12] respectively. Potassium penta- and hexathionates were prepared from sodium thiosulfate, sulfur dichloride and alcoholic potassium hydroxide solution and from sodium thiosulfate, sulfur monochloride and alcoholic potassium hydroxide solution by Goehring's method,[13] respectively. Each polythionate was recrystallized from aqueous solution. Its purity is as follows: trithionate 98%, tetrathionate 99%, pentathionate 80% and hexathionate 96%.

Preparation of Thin-layer Plate. Before the application on a glass plate, silica gel, Wako gel B-O of Wako Pure Chemical Industries, Ltd., was washed with distilled water to be free from chloride ion, and soluble starch was also washed with ethyl alcohol for several hours. Washing soluble starch with ethyl alcohol prevents the back-ground of the thin-layer from being colored, and clearly colored spots were visualized when silver nitrate solution was sprayed. Developing time is shortened to one-half or one-third by adding a small quantity of aqueous ammonia to the paste before spreading it on a glass plate. Development takes more than five hours on the thin-layer without adding aqueous ammonia. Thin-layer plates were prepared as follows: Two grams of soluble starch was kneaded with 20 m*l* of about 1.6 mol/*l* solution of aqueous ammonia in a mortar. Twenty grams of silica gel and 20 m*l* of distilled water were added little by little to the mortar to obtain a uniform paste. The paste was spread in about 330 μ thickness on a $200\times200\times3$ mm of glass plate with an applicator. The plate was dried for 12 hr in air, and then activated by heating at 110 to 120°C for 2 to 3 hr and stored in a desiccator.

Development and Visualization. Two to five μ*l* of the sample solution was taken accurately with a 0.05 m*l* micro-pipet and applied along one side of the thin-layer plate at intervals of 2 cm. Then the plate was developed in a closed vessel under saturated vapor of the solvent by the ascending technique. After development, the plate was taken out, dried and sprayed with 0.1 mol/*l* solution of silver nitrate. By this operation, polythionates and thiosulfate were visualized as dark-brown spots of silver sulfide formed by the following reactions:

$$S_2O_3^{2-} + 2Ag^+ + H_2O = Ag_2S + H_2SO_4 \quad (1)$$

$$S_xO_6^{2-} + 2Ag^+ + 2H_2O = Ag_2S + 2H_2SO_4 + (x-3)S \quad (2)$$

Though sulfate and sulfite generally appear in the reaction of sulfur compounds, they cannot be detected with silver nitrate differing from thiosulfate and polythionates. In this case, before the detection of polythionates and thiosulfate, the thin-layer plate was first sprayed with barium chloride solution acidified with acetic acid and with sodium rhodizonate solution. Sulfate and sulfite appeared then as pale-yellow spots on a pink colored background. Visualization of polythionates and thiosulfate was attained by spraying the spots with a silver nitrate solution.

Procedure of Colorimetric Determination. Sulfur amounts in the visualized spot was determined colorimetrically by the technique proposed by Kiba and his co-workers[14] as follows: The visualized spot was scratched as completely as possible and removed into a reduction quartz tube. Two or three m*l* of barium solution and bromine water were added to oxidize sulfur compounds, such as sulfide and elemental sulfur, to barium sulfate.

After evaporation to dryness, 5 to 10 m*l* of strong phosphoric acid solution of stannous chloride was poured into the tube and nitrogen gas was passed through the tube vigorously for first 5 min and then reduced to the flow rate of one bubble per second. After heating the quartz tube at 300 to 320°C for 30 to 60 min to reduce barium sulfate to hydrogen sulfide, nitrogen gas was passed again through the tube vigorously for 5 min. The absorption tube of hydrogen sulfide was taken off from the quartz tube and 1.5 m*l* of 1 : 1 sulfuric acid solution of *p*-amino dimethyl aniline and 0.5 m*l* of ferric ammonium sulfate solution were added under vigorous shaking to form methylene blue coloration. The colored solution of methylene blue was removed into a measuring flask and was diluted to 50 m*l* with distilled water. After standing for 20 to 30 min at room temperature, the absorbance was measured at 662.5 mμ through 0.03 mm width of slit in a glass cell of 10 mm thickness.

Results and Discussion

Selection of Developing Solvent. As developing solvents for sulfur-oxy acids, the following mixtures were used.

Bighi and Trabanelli:[7] isopropyl alcohol, pyridine and water (5 : 3 : 5)

Scoffone and Carini:[8] *n*-butyl alcohol, aceto-acetic ester, acetic acid and water (10 : 2 : 1 : 7)

Pollard:[9] isopropyl alcohol, acetone and water (5 : 2 : 3)

Seiler and Erlenmeyer:[11] methyl alcohol, dioxane, aqueous ammonia and water (3 : 6 : 1 : 1)

The suitablity of mixed solvents of various alcohols given in literature was tested. From the results, it can be stated that no effective resolution of polythionates was obtained except for a case in

12) F. Martin and L. Metz, *Z. Anorg. Allg. Chem.*, **127**, 83 (1923).

13) M. Goehring and U. Feldmann, *ibid.*, **257**, 223 (1948).

14) T. Kiba, Y. Yoshimura, T. Takagi and I. Kishi, This Bulletin, **28**, 641 (1955); T. Kiba, I. Akaza and N. Sugishita, *ibid.*, **30**, 972 (1957).

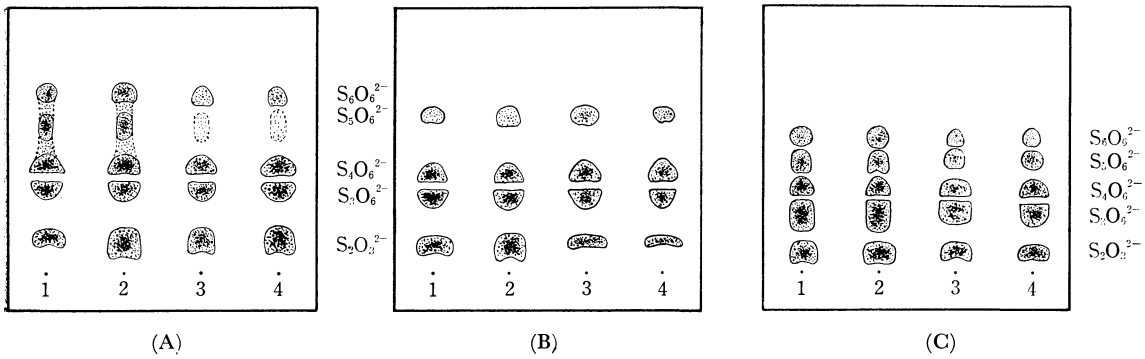

Fig. 1. Chromatograms obtained by varying the amount of aqueous ammonia.
Developing solvent: ethyl alcohol 75 m*l*, *n*-butyl alcohol 75 m*l* and aqueous ammonia
Developing time: 2 hr
Sample: a mixture of potassium thiosulfate, potassium tri- and tetrathionates
Amout of aqueous ammonia added
A: 4 m*l*, B: 8 m*l*, C: 12 m*l*

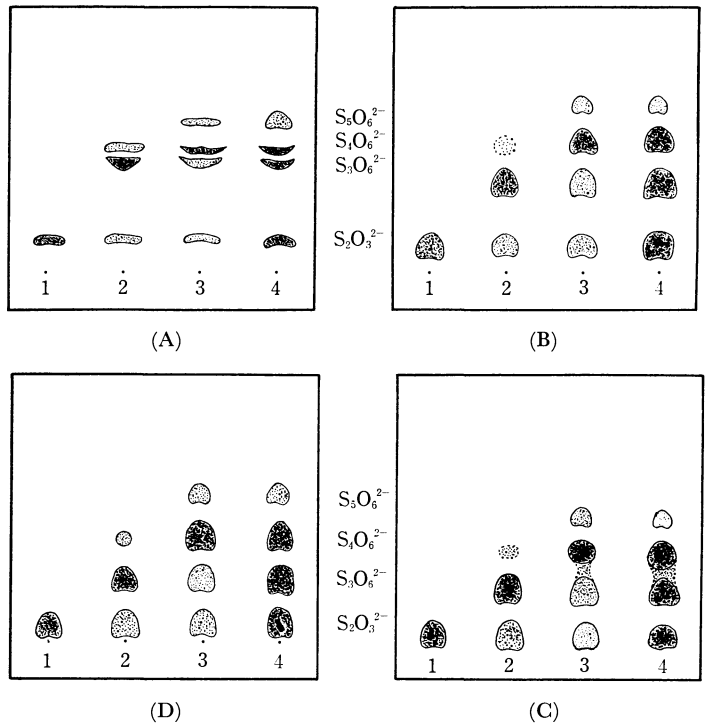

Fig. 2. Chromatograms obtained by addition of ammonium acetate.
Developing solvent: ethyl alcohol 75 m*l*, *n*-butyl alcohol 75 m*l*, aqueous ammonia 10 m*l*, ammonium acetate and distilled water
Developing time: 2.7 hr
Sample: 1. potassium thiosulfate 2. potassium trithionate
3. potassium tetrathionate 4. potassium pentathionate
Amount of 1 mol/*l* solution of ammonium acetate added
A: 0 m*l*, B: 10 m*l*, C: 20 m*l*, D: 40 m*l*

which a mixture of ethyl alcohol, *n*-butyl alcohol, aqueous ammonia and water or ethyl alcohol, methyl isobutyl ketone, aqueous ammonia and water was used. Therefore, the solvent system consisting of ethyl alcohol, *n*-butyl alcohol, aqueous ammonia and water was studied by varying the amounts

of aqueous ammonia. The results are shown in Fig. 1. The resolution of polythionates was almost independent of the amounts of aqueous ammonia.

Generally the addition of neutral salts affects activities of polythionates. It is expected that the resolution of polythionates might be improved. The addition of ammonium acetate to the solvent actually improved the resolution of the spots as shown in Fig. 2.

It is concluded that the following composition may be the most suitable as the developing solvent in the thin-layer chromatography of these sulfur compounds, *viz.* ethyl alcohol 75 m*l*, *n*-butyl alchol 75 m*l*, concentrated aqueous ammonia 8 to 10 m*l*, 1 mol/*l* solution of ammonium acetate 20 to 40 m*l* and distilled water 10 to 30 m*l*. Under these conditions, the R_s values of thiosulfate and some low polythionates obtained are shown in Table 1.

Table 1. The R_s values

Species	Present study	Pollard's results*
$S_2O_3^{2-}$	0.18—0.20	0.11
$S_3O_6^{2-}$	0.63—0.64	0.67
$S_4O_6^{2-}$	1.00	1.00
$S_5O_6^{2-}$	1.34—1.38	1.25

* Pollard's results were obtained by paper chromatography. R_s values: R_f values are normalized to that of tetrathionate.

The chromatographic separation of sulfate, sulfite and thiosulfate was studied by the same method using various mixed solvents, but a suitable solvent system for the resolution of these compounds was not found.

Colorimetric Determination of Sulfur in the Developed Spot. In the developed spot which was visualized by spraying silver nitrate solution, sulfur is contained as silver sulfide, sulfate and elemental sulfur. The amounts of sulfur can be roughly determined by comparing the color intensity of these spots with the standard color, but the accuracy is not satisfactory for quantitative determination of sulfur. Thus, the colorimetric technique proposed by Kiba and his co-workers[14] was chosen.

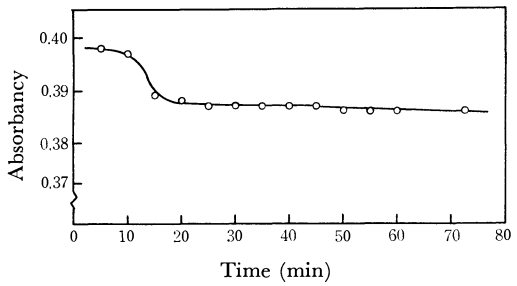

Fig. 4. The change of the absorbancy in the colored solution of methylene blue.

Reduction Time in Strong Phosphoric Acid. At the beginning, the detected amounts of sulfur fluctuated a great deal. The reduction time in strong phosphoric acid, one of the causes of fluctuation, was examined. The results are shown in Fig. 3. It was found that the sample should be heated for 20 to 30 min at 300°C to reduce sulfate to hydrogen sulfide completely.

Stability of the Color of Methylene Blue Solution. The stability of the color of methylene blue solution under room light, which has not been given in literature, was examined to simplify the analytical procedure. From the result, it is obvious that the absorbance has a constant value from 25 to 45 min after the color development. Thus the measurement should be carried out within 30 min after the solution was stood in room light at room temperature.

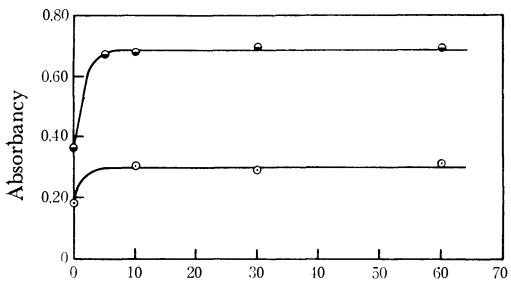

Fig. 3. The relation between absorbancy and heating time.
⊙ 0.5 m*l* of standard solution of sodium sulfate
◒ 1.0 m*l* of standard solution of sodium sulfate
The time when the temperature in the electric furnace reached 300°C is plotted as zero.

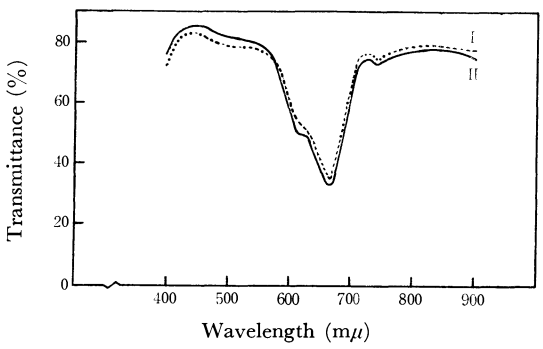

Fig. 5. The absorption spectrum curve of methylene blue solution.
I methylene blue solution prepared from a standard solution of sodium sulfide
II methylene blue solution prepared from a standard solution of sodium sulfate

Absorption Curve. Kiba and his co-workers[14] proposed that the absorbance of methylene blue solution should be measured at 655 mμ. Others[15] recommend 740 or 640 mμ as a proper wave length. Because of this uncertainty the absorption curve of methylene blue was reexamined with a Hitachi EPU-2A type spectrophotometer. The results are shown in Fig. 5. From the figure, it may be stated that the maximum absorption exists at 662.5 mμ rather than 655 mμ. Accordingly, the absorbance of methylene blue should be measured at 662.5 mμ.

Calibration curves were obtained by using sodium sulfide and sodium sulfate. These curves give linear relationship in the concentration range from 0 to 40 μg/50 ml. The molar absorptivity calculated from the slope of these calibration curves agreed well with the value reported by Johnson and Nishita.[16]

TABLE 2. THE MOLAR ABSORPTIVITY

Sulfur compounds	Molar absorptivity	
	present study	Johnson and Nishita
Sodium sulfide	34100	34000
Sodium sulfate	33800	—

Interference of nitrate on the absorbance was pointed out by Kiba and his co-workers.[14] Accordingly, the interference of silver nitrate used on the visualization of spots was examined by using potassium tetrathionate as a sample. No influence was found on the determination of sulfur. The sulfur derived from silica gel can be disregarded, because only 0.4 μg of sulfur is contained in about 20 mg of silica gel.

The Determination of Sulfur. The results obtained for the developed spots by the above procedure are shown in Table 3. Since the measured values are obtained 10 to 30% lower than the theoretical values, it is impossible to determine directly a minute amount of sulfur. Therefore, an internal standard method, in which the amount of polythionate sulfur is compared with that of thiosulfate sulfur determined iodimetrically, was examined by using a mixed solution containing

TABLE 3. RESULTS BY THE DIRECT METHOD

Sample volume added (μl)	Sulfur amounts(μg)		Concentration of sample (mol/l)
	added	detected	
1.94	13.6	9.4	0.0756
2.91	20.4	13.6	0.0730
3.40	23.9	16.5	0.0757
3.88	27.2	20.7	0.0834
4.37	30.7	24.2	0.0865
4.37	30.7	27.2	0.0974
4.37	30.7	26.4	0.0945
5.82	41.0	31.7	0.0850

sample solution: 0.1 mol/l (f=1.099) solution of sodium thiosulfate

TABLE 4. RESULTS BY THE INTERNAL STANDARD METHOD

Sample No.	Sulfur amounts detected (μg)			Mole ratios	
	S_2	S_3	S_4	S_3/S_2	S_4/S_2
I	16.2	6.4	5.3	0.205	0.164
	16.1	5.6	4.9	0.230	0.152
	11.2	4.8	—	0.288	—
	14.0	5.1	—	0.243	—
	12.8	—	4.5	—	0.176
II	9.2	10.6	7.1	0.738	0.386
	7.9	9.6	5.2	0.810	0.329
	8.5	9.2	6.7	0.722	0.394

Amount of sulfur added (μg) and theoretical mole ratios

	S_2	S_3	S_4	S_3/S_2	S_4/S_2
I	16.0	6.2	5.3	0.250	0.166
II	9.6	10.4	6.4	0.722	0.333

S_2, S_3 and S_5 represent thiosulfate, trithionate and tetrathionate, respectively.

an equal amount of potassium trithionate and tetrathionate. The results are shown in Table 4.

The measured values fluctuate within 10 to 20%. The cause of the fluctuation may be mainly due to the imperfect collection of visualized spots and could be diminished by careful technique. Thus this method may be applied to semi-quantitative determination of low valence sulfur compounds such as polythionates.

The authors wish to thank Professor Tsugio Sawaya of the Laboratory of Industrial Analytical Chemistry for very valuable advice and help.

15) D. F. Bolz, "Chemical Analysis" Vol. III; "Colorimetric Determination of Non-Metals," Interscience Publishers, New York (1958), p. 273.

16) C. M. Johnson and H. Nishita, *Anal. Chem.*, **24**, 736 (1952).

BULLETIN OF THE CHEMICAL SOCIETY OF JAPAN VOL. 43 1365—1372 (1970)

The Chemical Behavior of Low Valence Sulfur Compounds. III.*1 Production of Ammonium Sulfamate by the Oxidation of Ammonium Thiosulfate

Kunishige NAITO, Masahiro YOSHIDA,*2 Mu-Chang SHIEH and Taijiro OKABE

Department of Applied Chemistry, Faculty of Engineering, Tohoku University, Sendai

(Received August 1, 1969)

The oxidation of ammonium thiosulfate with compressed oxygen in aqueous ammonia solution was examined. It was found that ammonium sulfamate and ammonium sulfate are mainly produced and a small amount of nitrite and imidodisulfonate obtained in the final solution. The most suitable conditions to produce ammonium sulfamate from ammonium thiosulfate industrially are as follows: reaction temperature 100°C, oxygen pressure 50 kg/cm^2, concentration of ammonia 16 mol/*l*, concentration of cupric ion 0.1—0.2 mol/*l*. The electrolytic oxidation, hydrogen peroxide oxidation and ozone oxidation of ammonium thiosulfate were also examined.

The authors, in their studies on the chemical behavior of low valence sulfur compounds, have investigated the oxidation of elemental sulfur with compressed oxygen in aqueous ammonia solution.[1] It was found that oxidation proceeds through thiosulfate and some low polythionates as intermediates, and under a suitable condition, a large amount of ammonium sulfamate is formed by the oxidation. The oxidation of thiosulfate may be said to be the rate determining step of the overall reaction and has an important effect upon the yield of sulfamate.

The air-oxidation of thiosulfate is a very slow reaction under normal pressure. Under atmospheric pressure and normal temperature, a trace of sodium tetrathionate was detected in the air-oxidation of sodium thiosulfate by Schulek and Koros,[2] and ammonium thiosulfate was observed to be oxidized very little in a neutral or alkaline solution by Koseki.[3]

The oxidation of thiosulfate with compressed air or oxygen has been rarely investigated. In Gluud's work,[4] elemental sulfur and sodium sulfate were detected in a neutral solution, but only sodium sulfate in an alkaline solution at 100°C under an air-pressure of 10 kg/cm^2. The formation of ammonium trithionate was confirmed by Forward[5] in the oxidation of ammonium thiosulfate with compressed air. The oxidation of ammonium thiosulfate with compressed oxygen in aqueous ammonia solution has been investigated in the author's laboratory, and Kanematsu[6] found that the oxidation is almost a zero order reaction and that metal ions such as copper, nickel and cobalt extremely accelerate the oxidation reaction, although the products were not sufficiently confirmed.

In the present study, effort was made to clarify the chemical behavior of thiosulfate in oxidation and to obtain the most suitable conditions for industrial production of ammonium sulfamate from ammonium thiosulfate.

Experimental

Apparatus and Procedure. In the oxidation with oxygen, two autoclaves, one the same as shown in a previous paper,[1] and the other a Shin-Sakashita Seisakusho Model SR-100 with 1 *l* capacity lined with Hastelloy-F, were used for the reaction.

On addition of crystalline ammonium thiosulfate, aqueous ammonia and cupric sulfate as a catalyst, the autoclave was kept in a heated glycerine bath at temperatures regurated within 0.5°C. When the autoclave was heated to fixed temperature, oxygen was introduced and kept at a constant pressure. After the introduced oxygen showed the fixed pressure, 15 m*l* of the solution was withdrawn every few hours and was analyzed.

Electrolytic oxidation was carried out by keeping the anode potential constant with Yanagimoto Controlled Potential Electrolyser Model VE-3. The cell was a 300 m*l* closed glass vessel with platinum plates as electrodes and with a Soxlay filter paper (Toyo No. 84) as a diaphragm. A saturated calomel electrode (SCE) was used as a reference electrode, and concentrated aqueous ammonia was used as an intermediate solution and they were coupled with a salt bridge. The cell and electrode were kept at 0°C in an ice bath. Ammo-

*1 Preceding Paper: II. K. Naito, S. Takei and T. Okabe, This Bulletin, **43**, 1360 (1970).

*2 Present address: Idemitsu Kōsan Co., Ltd., Chiba.

1) M. C. Shieh, H. Otsubo and T. Okabe, This Bulletin, **38**, 1596 (1965).

2) E. Schulek and E. Koros, *Magy. Chem. Folyoirat*, **56**, 426 (1950); *Chem. Abstr.*, **46**, 1380 (1952).

3) K. Koseki, unpublished data.

4) W. Gluud, *Ber.*, **54**, 2425 (1921).

5) F. A. Forward, *Trans. Can. Inst. Min. Met.*, **66**, 191 (1957).

6) T. Okabe, and K. Kanematsu Lecture argument of the 4th Symposium on High Pressure, Japan (1962).

nium thiosulfate and aqueous ammonia were added into the cell and electrolyzed. The quantity of electricity was roughly calculated from the current and time.

Hydrogen peroxide oxidation was carried out by adding C.P. grade hydrogen peroxide solution to thiosulfate solution drop by drop from a buret at a constant temperature with constant stirring.

Analysis. The final solution contained sulfamate, sulfate, cupric ion, sometimes traces of nitrite and imidodisulfonate. When nitrite is present in the solution, it is necessary to determine these ions by avoiding the interference of nitrite, because nitrite decomposes sulfamate and imidodisulfonate to sulfate. The determination of sulfur compounds such as sulfamate, sulfate and imidodisulfonate was successfully carried out by the method proposed by Sisler and Audrieth,[7] and the determination of nitrite and cupric ion was performed by an improved iodimetric method proposed originally by Kolthoff and Abeledo.[8]

The sample solution was diluted to a suitable concentration and then analyzed.

SO_4^{2-}: After the addition of an equal volume of 4 mol/*l* aqueous ammonia to one portion of the sample solution, it was heated on a water bath. Barium salts of sulfate, imidodisulfonate and carbonate were precipitated by the addition of 0.5 mol/*l* solution of barium chlorid in excess. The precipitate was filtered and washed with 4 mol/*l* aqueous ammonia making the filtrate within 200 m*l*. It was washed with 4 mol/*l* acetic acid and a small amount of 0.1 mol/*l* hydrochloric acid to decompose and remove barium imidodisulfonate and barium carbonate making the filtrate within 200 m*l*, and was determined as barium sulfate by the usual method.

$SO_3NH_2^-$: The filtrate obtained by washing with aqueous ammonia was evaporated to 100 m*l*, and acidified with concentrated hydrochloric acid. Sulfamate was decomposed with sodium nitrite. The precipitate of barium sulfate was determined by the usual method.

$HN(SO_3)_2^{2-}$: The filtrate obtained by washing with acetic acid and hydrochloric acid was evaporated and acidified with 4 mol/*l* hydrochloric acid. Imidodisulfonate was decomposed with sodium nitrite as follows.

Imidodisulfonate was determined as barium sulfate

$$HN(SO_3)_2^{2-}+NaNO_2+HCl = 2HSO_4^-+N_2+NaCl$$

by the gravimetric method.

Total Amount of Sulfur: One portion of the sample solution was evaporated nearly to dryness. Potassium chlorate and concentrated hydrochloric acid were added in order to oxidize all sulfur compounds to sulfate. After evaporation to near dryness again, the sulfate in the solid was extracted with 4 mol/*l* hydrochloric acid and determined as barium sulfate.

Cu^{2+}: After the addition of potassium carbonate and urea, one portion of the sample solution was acidified with concentrated hydrochloric acid. When the generation of carbon dioxide ceased, potassium iodide was added and the iodine liberated was titrated with a standard solution of sodium thiosulfate.

NO_2^-: After addition of potassium carbonate and urea to one portion of the sample solution, nitrogen gas was passed through it for 15—20 min, and for additional 5—10 min after the addition of potassium iodide. It was acidified with hydrochloric acid and iodine liberated was titrated with a standard solution of sodium thiosulfate. The nitrite was obtained by subtraction of cupric ion from the total.

The solution taken out during the course of the reaction contains thiosulfate and traces of polythionates in addition to the above-mentioned compounds. For determination of thiosulfate by the iodimetric method, it is necessary to remove cupric ion previously added as a catalyst. When the concentration of cupric ion is low, it can be easily removed by passing the solution through ion-exchange resin column, but when the cupric ion concentration is higher than 0.1 mol/*l*, it is difficult to be removed with the resin because of the complex formation of cupric ion with thiosulfate. In this case, therefore, sulfate and sulfamate are determined as follows:

SO_4^{2-}: One portion of the sample solution was controlled at pH=5 with 4 mol/*l* acetic acid by using bromocresol purple. By adding iodine solution, thiosulfate in the sample solution was oxidized to tetrathionate. Sulfate was precipitated as barium sulfate by adding 0.02 mol/*l* solution of barium chloride and determined.

$SO_3NH_2^-$: By adding 1 mol/*l* solution of silver nitrate to one portion of the sample solution heated on a water bath, thiosulfate and some low polythionates in the solution were decomposed and converted into silver sulfide, sulfate and elemental sulfur. After the addition of barium chloride solution, insoluble matters such as silver sulfide, barium sulfate and silver chloride were removed by filtration. Sulfamate remained in the filtrate and was determined by the above method.

Results and Discussion

Oxidation of Ammonium Thiosulfate with Compressed Oxygen in Aqueous Ammonia Solution. In the present study, the formation of nitrite and imidodisulfonate were observed for the first time. Nitrite was ascertained by the Peter-Griess reaction, and imidodisulfonate was identified by X-ray diffraction of barium salt. During the cource of preliminary experiments, the composition of the products seemed to differ somewhat with autoclave made of SUS 32 stainless steel and that lined with Hastelloy-F alloy. In order to clarify the effect of reactor materials, several materials were tested for the reaction. However, no remarkable results were obtained as shown in Table 1.

The Effect of the Concentration of Cupric Ion. It has been found that cupric ion is the most suitable catalyst to increase the reaction rate and the yield of sulfamate in the oxidation of elemental sulfur. Although a similar effect was expected in the present study, the reaction was examined in the presence of 10^{-3} to 1.0 mol/*l* cupric ion.

7) H. H. Sisler and L. F. Audrieth, *J. Amer. Chem. Soc.*, **61**, 3392 (1931).

8) C. A. Abeledo and I. M. Kolthoff, *ibid.*, **53**, 2893 (1939).

Table 1. Effect of reactor material

Reactor material	Reaction time(hr)	$[Cu^{2+}]$ (mol/l)	Yield of products(mol%) $SO_3NH_2^-$	SO_4^{2-}	$NH(SO_3)_2^{2-}$	$[NO_2^-]$ (mol/l)
SUS 32	6.0—6.5	0.5	62.70	35.90	1.40	—
Ti	5.0—5.5	0.2	63.84	33.48	1.19	0.0549
	5.0—5.5	0.5	59.86	39.96	0.78	0.0137
	5.0—5.5	0.7	62.85	34.24	2.20	0.0183
10 g of* Hastelloy	6.0—6.5	0.5	63.86	35.81	trace	0.0194
20 g of* Hastelloy	6.0—6.5	0.5	60.47	42.37	2.48	0.0057
30 g of* Hastelloy	6.0—6.5	0.5	61.03	38.51	1.12	0.0034

Reaction temperature: 100°C
Oxygen pressure: 50 kg/cm²
Concn. of ammonia: 16 mol/l
Concn. of total sulfur: 2 S-g atom/l

* Small tip of Hastelloy-F was added into the autoclave made of SUS 32 stainless steel.

Table 2. Effect of cupric ion on the composition of the final solution

$[Cu^{2+}]$ (mol/l)	Yields of products (mol%) $SO_3NH_2^-$	SO_4^{2-}	$HN(SO_3)_2^{2-}$	$[NO_2^-]$ (mol/l)
0.0992	63.09	34.03	2.88	—
0.1873	67.60	37.85	1.76	0.0215
0.3003	64.96	37.04	3.86	0.0386
0.5022	62.69	35.88	—	0.0057
0.6189	60.64	39.16	—	0.0069
0.8225	60.57	40.39	—	0.0028

Reaction temperature: 100°C
Oxygen pressure: 50 kg/cm²
Ammonia concn.: 16 mol/l
Concn. of total sulfur: 2 S-g atom/l

The results obtained are shown in Table 2 and Figs. 1, 2 and 3. It is obvious that the reaction time is shortened with the increase of the concentration of cupric ion, but the yield of sulfamate has its maximum at 0.1—0.2 mol/l of cupric ion. The formation of sulfamate shows a zero order reaction in the concentration higher than 0.1 mol/l of cupric ion. The catlytic oxidation of thiosulfate has been explained by Abel[9] as

$$2Cu^{2+} + 2S_2O_3^{2-} = 2Cu^{+} + S_4O_6^{2-} \quad \text{(fast)}$$
$$2Cu^{+} + \tfrac{1}{2}O_2 = 2Cu^{2+} + O^{2-} \quad \text{(slow)}$$
$$O^{2-} + 2H^{+} = H_2O \quad \text{(fast)}$$

But it is supposed that cupric ion exists as an ammine complex in aqueous ammonia solution and in the presence of thiosulfate, forms further a thio-

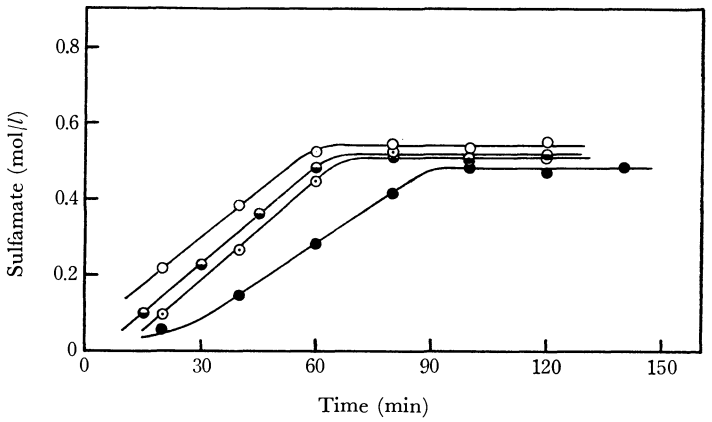

Fig. 1. Effect of the concentration of cupric ion with the yield of sulfamate on the oxidation of ammonium thiosulfate.
Reaction temp.: 100°C, Oxygen press.: 75 kg/cm², $(NH_4)_2S_2O_3$ concn.: 0.5 mol/l, NH_3 concn.: 16 mol/l
Cu^{2+} ion concn.: ○ 0.3 mol/l ◒ 0.1 ⊙ 0.01 ● 0.001

9) E. Abel, *Ber.*, **56**, 1076 (1923).

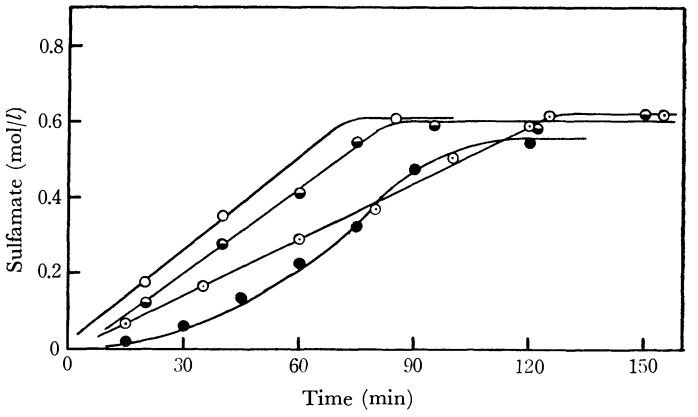

Fig. 2. Effect of the concentration of cupric ion with the yield of sulfamate on the oxidation of ammonium thiosulfate.
Reaction temp.: 100°C, Oxygen press.: 50 kg/cm^2,
$(NH_4)_2S_2O_3$ concn.: 0.5 mol/l, NH_3 concn.: 16 mol/l
Cu^{2+} ion concn.: ○ 0.5 mol/l ◒ 0.1 ⊙ 0.01 ● 0.001

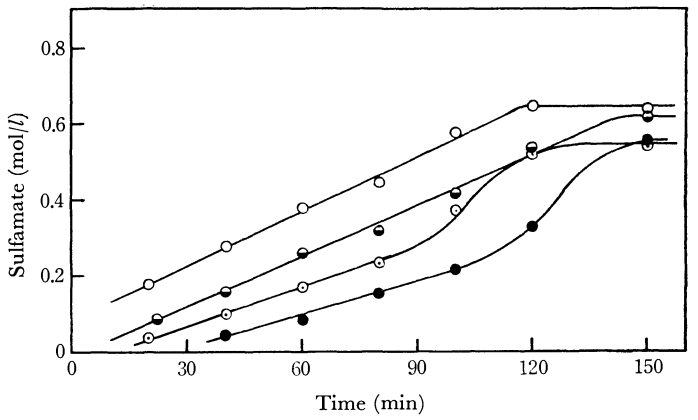

Fig. 3. Effect of the concentration of cupric ion with the yield of sulfamate on the oxidation of ammonium thiosulfate.
Reaction temp.: 100°C, Oxygen press.: 25 kg/cm^2,
$(NH_4)_2S_2O_3$ concn.: 0.5 mol/l, NH_3 concn. 16 mol/l,
Cu^{2+} ion concn.: ○ 0.5 mol/l ◒ 0.1 ⊙ 0.01 ● 0.001

sulfate complex. Abel's mechanism, therefore, can not be easily accepted. The formation of complexes between cobalt ammine[10] or cupric ethylenediamine[11] and thiosulfate has been actually known to take place.

The Effect of Oxygen Pressure. The effect of oxygen pressure, in which the vapor pressure of the solution was included, was examined in the range of 25—75 kg/cm^2. As shown in Figs. 4, 5 and 6, the reaction time is shortened with the increase of presure. The yield of sulfamate has its maximum at 50 kg/cm^2, while in the presence of 0.1 to 0.5 mol/l of cupric ion, it decreases with the increase of the pressure.

The Effect of the Ammonia Concentration. The ammonia concentration was varied from 4 to 16 mol/l. The results are shown in Fig. 7. An increase in the ammonia concentration improves the yield of sulfamate, and accelerates the reaction slightly. This tendency for the yield of sulfamate to increase in a high concentration of ammonia is quite similar to that of the oxidation of elemental sulfur and the decomposition of potassium trithionate in aqueous ammonia solution.

10) H. Yoneda, This Bulletin, **28**, 125 (1955). Y. Shimura and R. Tsuchida, *ibid.*, **28**, 572 (1955).
11) H. Yoneda, *ibid.*, **29**, 68 (1956).

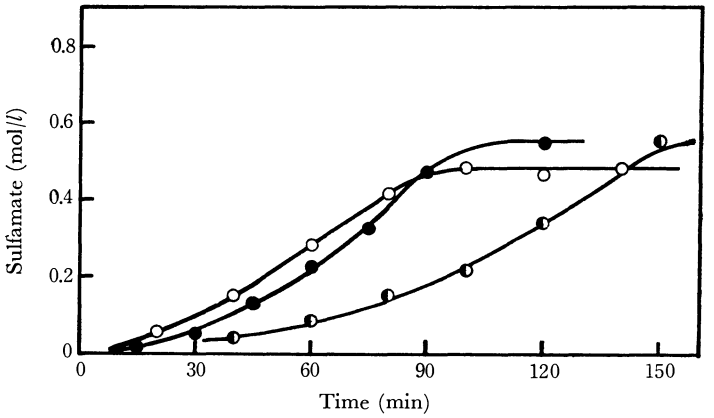

Fig. 4. Effect of the oxygen pressure with the yield of sulfamate in the oxidation of ammonium thiosulfate.
Reaction temp.: 100°C, Cu^{2+} concn.: 10^{-3} mol/*l*,
$(NH_4)_2S_2O_3$ concn.: 0.5 mol/*l*, NH_3 concn.: 16 mol/*l*,
Oxygen pressure: ○ 75 kg/cm² ● 50 ◐ 25

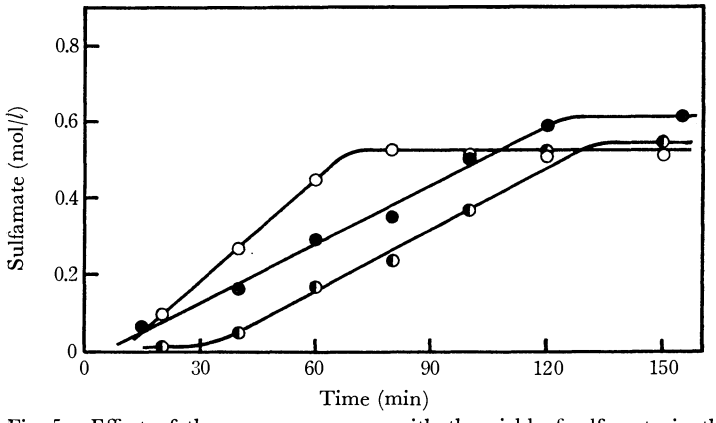

Fig. 5. Effect of the oxygen pressure with the yield of sulfamate in the oxidation of ammonium thiosulfate.
Reaction temp.: 100°C, Cu^{2+} concn.: 10^{-2} mol/*l*,
$(NH_4)_2S_2O_3$ concn.: 0.5 mol/*l*, NH_3 concn.: 16 mol/*l*,
Oxygen pressure: ○ 75 kg/cm² ● 50 ◐ 25

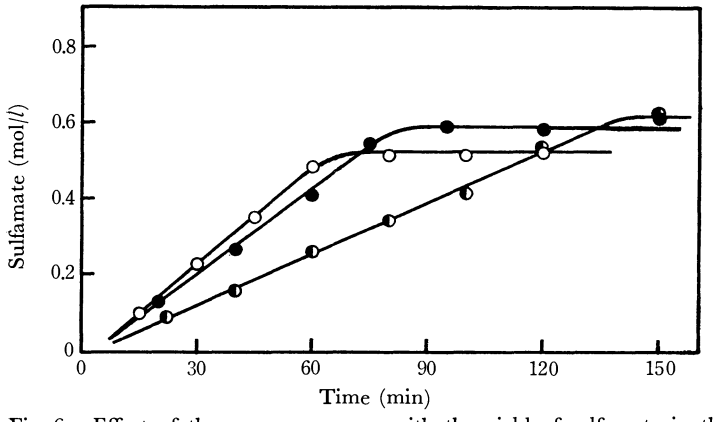

Fig. 6. Effect of the oxygen pressure with the yield of sulfamate in the oxidation of ammonium thiosulfate.
Reaction temp.: 100°C, Cu^{2+} concn.: 0.1 mol/*l*,
$(NH_4)_2S_2O_3$ concn.: 0.5 mol/*l*, NH_3 concn.: 16 mol/*l*,
Oxygen pressure: ○ 75 kg/cm² ● 50 ◐ 25

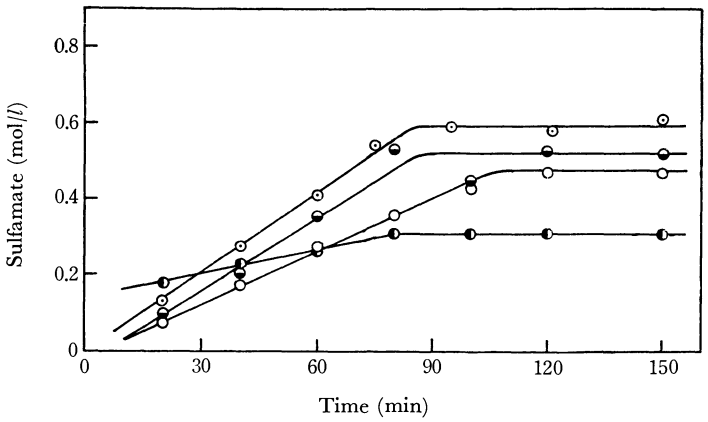

Fig. 7. Influence of the ammonia concentration with the yields of sulfamate in the oxidation of ammonium thiosulfate in aqueous ammonia.
Reaction temp.: 100°C, Oxygen press.: 50 kg/cm², $(NH_4)_2S_2O_3$ concn.: 0.5 mol/*l*, Cu^{2+} ion concn.: 0.1 mol/*l*,
$[NH_3]$: ⊙ 16 mol/*l* ◒ 12 ○ 8 ◐ 4

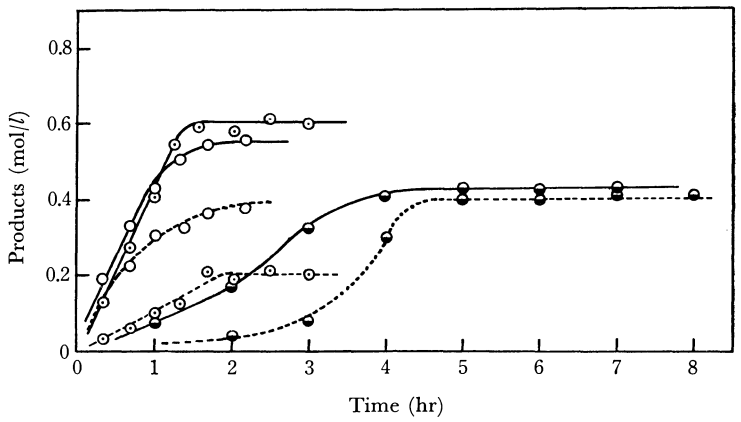

Fig. 8. Influence of the reaction temperature in the oxidation of thiosulfate in aqueous ammonia.
$(NH_4)_2S_2O_3$ concn.: 1 mol/*l*, Oxygen press.: 50 kg/cm², NH_3 conc.: 16 mol/*l*, Cu^{2+} ion concn.: 0.1 mol/*l*,
$SO_3NH_2^-$: ---○--- 120°C ---⊙--- 100 ---◒--- 80

TABLE 3. RESULTS OBTAINED IN THE ELECTROLYTIC OXIDATION OF AMMONIUM THIOSULFATE IN AQUEOUS AMMONIA SOLUTION

Quantity of electricity (C)	Concn. of reactant and products (S-g atom/*l*)					
	$S_2O_3^{2-}$	$S_2O_6^{2-}$	$S_3O_6^{2-}$	$S_4O_6^{2-}$	SO_4^{2-}	$SO_3NH_2^-$
0	1.052	0	0	0	0	0
10,500	0.428	0	0.481	0.054	0.036	0.034
19,800	0.013	0	0.748	0.096	0.079	0.091
36,700	0.018	0.108	0.747	0	0.152	0.108
77,000	0.021	0.284	0.446	0	0.306	0.184

Reaction temperature: 0°C
Ammonia concn.: 12.25 mol/*l*
Amounts of ammonium thiosulfate: 0.145 mol
Anode potential: 1.5 V (*vs.* SCE at 30°C)

The Effect of Reaction Temperature. The reaction temperature was varied from 80 to 120°C. The results are shown in Fig. 8. The reaction time is shortened with the rise in reaction temperature, while the yield of sulfamate has its maximum at 100°C. It seems that an induction period appears at 80°C in the beginning of the reaction.

From the above results, the suitable conditions to prepare ammonium sulfamate by the oxidation of ammonium thiosulfate with compressed oxygen in aqueous ammonia solution are as follows: the concentration of cupric ion 0.1—0.2 mol/*l*, the ammonia concentration 16 mol/*l*, oxygen pressure 50 kg/cm^2 and reaction temperature 100°C.

The Electrolytic Oxidation of Ammonium Thiosulfate in Aqueous Ammonia Solution. Ammonium thiosulfate was dissolved in 12.25 mol/*l* aqueous ammonia to make 0.145 mol/*l* solution, and oxidized by means of anodic oxidation at 0°C and 1.5 V of the anode potential (*vs.* SCE at 30°C). The results are shown in Table 3.

The oxidation was carried out in a high concentration solution of ammonia at a low temperature, because the yield of sulfamate increases with the increase of the concentration of ammonia and with the lowering of temperature. As the oxidation was carried out at a high potential to improve the reactivity, some known reactions took place simultaneously. From the results, it may be said that thiosulfate is oxidized to tetrathionate or trithionate and converted finally to sulfate, sulfamate and dithionate.

The electrolytic oxidation of sodium thiosulfate has been studied by several investigators.[12-14] It has found that the electrolytic oxidation of sodium thiosulfate proceeds as follows:

$$S_2O_3^{2-} = S_2O_3^{-} + e$$
$$2S_2O_3^{-} = S_4O_6^{2-}$$
$$S_2O_3^{2-} + H_2O = SO_4^{2-} + S + 2H^+ + 2e$$

The first reaction takes place mainly at the low voltage in a neutral solution. From the present results, it is not clear whether tetrathionate or trithionate is first formed from thiosulfate. However, it might be certain that the final products such as sulfamate and sulfate are formed from the low polythionates. The formation of sulfamate in the electrolytic oxidation of ammonium thiosulfate seems to be new.

The Oxidation of Ammonium Thiosulfate with Hydrogen Peroxide and Ozone in Aqueous Ammonia Solution. Hydrogen peroxide and ozone were tested as stronger oxidants than oxygen for the production of sulfamate. The results are shown in Tables 4 and 5. The oxidation of thiosulfate with hydrogen peroxide, an exothermic reaction, is one which accompanies simultaneous decomposition of hydrogen peroxide because of the alkalinity. Kurtenacker and Benson reported that thiosulfate is completely oxidized to sulfate with hydrogen peroxide in an alkaline solution and the oxidation is useful for the determination of thiosulfate.[15] The formation of sulfamate in this reaction is new information. As the presence of trithionate in the reaction solution was confirmed by thinlayer chromatography, the formation of sulfamate should proceed through the course of trithionate decomposition in an aqueous ammonia solution.

Table 4. Results obtained from the hydrogen peroxide oxidation of ammonium thiosulfate in aqueous ammonia

Sample No.	Concn. of the products (mol/*l*)	
	sulfamate	sulfate
1	0.0602	0.2107
2	0.0977	0.2176
3	0.0716	0.2208

Reaction temperature:	0—10°C
Concn. of ammonia:	12 mol/*l*
28% Solution of H_2O_2:	40 m*l*
3N (f=0.8740) solution of $Na_2S_2O_3$:	76 m*l*

Table 5. Results obtained from the ozone oxidation of ammonium thiosulfate in aqueous ammonia solution

Reaction time (hr)	Composition of the reaction solution (mol/*l*)			
	$S_2O_3^{2-}$	SO_3^{2-}	$SO_3NH_2^-$	SO_4^{2-}
0	0.900	0.103	0.049	0.044
2	0.641	0.245	0.044	0.505
7	0.003	0.000	0.084	2.001

Reaction temperature:	0—4°C
Ammonia concn.:	12 mol/*l*
flow rate of ozone:	5.02 g/hr

The ozone oxidation differes extremely from the above-mentioned oxidation in which the yield of sulfamate is very low, and, traces of sulfite and low polythionates appear. In a previous work by B. C. Brodie,[16] it was found that sodium thiosulfate is oxidized to dithionate, sulfate and sulfur

12) C. J. Thatcher, *Z. Phys. Chem.*, **47**, 641 (1904); *Trans. Electrochem. Soc.*, **45**, 157 (1924).

13) S. Glasstone and A. Hickling, "Electrolytic Oxidation and Reduction," Chapman & Hall, Ltd., London (1935), pp. 248—251.

14) W. D. Bancroft, *Trans. Electrochem. Soc.*, **71**, 195 (1937).

15) A. Kurtenacker, "Analytische Chemie der Sauerstoffsauren des Schwefels," Ferdinand Enke Verlag Stuttgart (1872), pp. 118; A. A. Besson, *Chem. Z.*, **37**, 926 (1913).

16) B. C. Brodie, *Phil. Trans.*, **162**, 435 (1872); A. Kotowski, "Gmelins Handbuch der Anorganischen Chemie," Schwefel Teil-B, Weinheim, Bergstrass (1960), p. 895.

dioxide with ozone in a weak alkaline solution according to the following schema.

$$Na_2S_2O_3 + O_3 = Na_2S_2O_3 \cdot O_3 \begin{cases} \nearrow Na_2S_2O_6 \\ \searrow Na_2SO_4 + SO_2 \end{cases}$$

Because of the presence of sulfite, which is not detected in the oxidation with oxygen, thiosulfate must be oxidized with ozone through a different mechanism from those of other oxidations.

Consequently, by the oxidation of ammonium thiosulfate with compressed oxygen in aqueous ammonia solution, 55—65 mol% of thiosulfate-sulfur is converted to sulfamate and the remainder to sulfate. The oxidation proceeds forming some low polythionates as intermediates.

Sulfamate and sulfate are formed by electrolytic oxidation or hydrogen peroxide oxidation, but the yield of sulfamate is lower than that by oxidation with compressed oxygen. By ozone oxidtaion, a large amount of sulfate is finally formed with sulfite as an intermediate, but the yield of sulfamate is extremely small.

BULLETIN OF THE CHEMICAL SOCIETY OF JAPAN VOL. 43 1372—1376 (1970)

The Chemical Behavior of Low Valence Sulfur Compounds. V. Decomposition and Oxidation of Tetrathionate in Aqueous Ammonia Solution

Kunishige NAITO, Mu-Chang SHIEH and Taijiro OKABE

Department of Applied Chemistry, Faculty of Engineering, Tohoku University, Sendai

(Received August 1, 1969)

The decomposition and oxygen oxidation of tetrathionate in aqueous ammonia solution have been investigated. In the decomposition, thiosulfate, sulfate and sulfamate were formed through penta- and trithionate as intermediate compounds. The molar ratio of the products $(SO_4^{2-}+SO_3NH_2^-)/S_2O_3^{2-}$ was roughly equal to 2/7, where 0.1N ammonia solution was used. The deficient use of ammonia made the solution neutral or weakly acidic and the precipitation of sulfur and the formation of higher polythionates were observed. The polythionate was detected by means of TLC (Thin Layer Chromatography). In the oxidation, tetrathionate was supposed to go through the following three sequent steps. 1) Decomposition of tetrathionate to form thiosulfate, tri- and pentathionate, and further decomposition of pentathionate to thiosulfate. 2) Oxidation of thiosulfate to tetrathionate and partly to sulfate. 3) Decomposition of trithionate to form sulfate, sulfamate and thiosulfate.

During the course of an investigation of the chemical behavior of low valence sulfur compounds, the oxidation of sulfur in aqueous ammonia was studied and the main process of the reaction was briefly proposed in the preceding paper.[1] It seemed reasonable to assume that tetrathionate is first formed as an intermediate in the oxidation of thiosulfate and disintergrates into pentathionate and trithionate as follows:

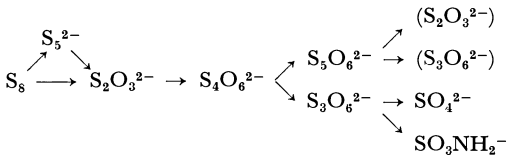

Kurtenacker and Goehring[2] have already reported that the decomposition of tetrathionate proceeds diversely, depending on the alkalinity of the solution as follows:[3-6]

pH = 8.9

$$2S_4O_6^{2-} = S_3O_6^{2-} + S_5O_6^{2-} \quad (1)$$

pH = 11.5

$$4S_4O_6^{2-} + 6OH^- = 2S_3O_6^{2-} + 5S_2O_3^{2-} + 3H_2O \quad (2)$$

1) Preliminary report: M. C. Shieh, H. Otsube and T. Okabe, This Bulletin, **38**, 1596 (1965).

2) M. Goehring, *Fortschr. Chem. Forsch.*, **2**, 444 (1952).

3) A. Kurtenacker and M. Kaufmann, *Z. Anorg. Allg. Chem.*, **148**, 43 (1925); A. Kurtenacker, A. Mutschin and F. Stastny, *ibid.*, **224**, 399 (1935).

4) F. Haber, *Naturwiss.*, **19**, 452 (1931); A. Kurtenacker and M. Kaufmann, *Z. Anorg. Allg. Chem.*, **148**, 369 (1925).

5) F. Foerster, *Z. Anorg. Allg. Chem.*, **144**, 337 (1925); A. Hornig, *ibid.*, **176**, 423 (1928).

6) J. Fordos and A. Gelis, *J. Prakt. Chem.*, **50**, 86 (1850); V. Lewes, *Ber.*, **15**, 2222 (1882); E. H. Riesenfeld, *Z. Anorg. Allg. Chem.*, **119**, 225 (1921).

pH = 12

$$S_3O_6^{2-} + 2OH^- = S_2O_3^{2-} + SO_4^{2-} + H_2O \quad (3)$$

pH = 13

$$2S_3O_6^{2-} + 6OH^- = S_2O_3^{2-} + 4SO_3^{2-} + 3H_2O \quad (4)$$

$$2S_5O_6^{2-} + 6OH^- = 5S_2O_3^{2-} + 3H_2O \quad (5)$$

When tetrathionate is stood for a long time in a strong alkaline solution, sulfite and thiosulfate are finally formed by the following reaction[7]

$$2S_4O_6^{2-} + 6OH^- = 3S_2O_3^{2-} + 2SO_3^{2-} + 3H_2O \quad (6)$$

In this reaction, sulfamate is not formed, but a great deal of sulfite is observed. The discrepancy of the products in each case is not due to the presence of compressed oxygen, but might dependent on the reaction medium which controls the first step of the decomposition of tetrathionate. In the present investigation, the decomposition and the oxidation of tetrathionate were studied to clarify the chemical behavior of sulfur compounds in aqueous ammonia solution.

Experimental

Materials. Potassium tetrathionate was prepared according to the method of Martin.[8] An alcoholic solution of iodine was added drop by drop into a potassium thiosulfate solution with stirring. The crude crystals of potassium tetrathionate obtained were then recrystallized from an alcoholic solution. Its purity was 99%, and was free from thiosulfate and sulfur.

Methods. The oxidation and decomposition reactions were carried out in the same autoclave and by the same procedure described in a previous paper.[1] The decomposition reaction in a diluted ammonia solution at low temperature was carried out in a 50 m*l* flask, which contained 20 m*l* of reactant. A portion of the solution in the flask was withdrawn at regular intervals and analyzed in the same manner as described previously, and chromatograph in ethanol-*n*-butanol-1 mol/*l* solution of NH_4Ac-conc. NH_4OH=75 : 75 : 40 : 10. The concentration of potassium tetrathionate in the decomposition and in the oxidation reaction were 0.02 and 0.25 mol/*l*, respectively.

Results

Decomposition of Tetrathionate. The decomposition of potassium tetrathionate was carried out in ammonia solution of various concentrations at 50—80°C. The results obtained are shown in Figs. 1—7. Under these conditions tetrathionate decomposed rapidly, and trithionate and thiosulfate were formed unless ammonia was deficiently used. Since trithionate also decomposed, thiosulfate remained in the final solution with small amounts of sulfate and sulfamate. The general view of the whole reaction is shown in Fig. 1.

The behavior of these sulfur compounds may be qualitatively supported from TLC as shown in Fig. 2. That is, the spots of tetrathionate, trithionate and thiosulfate appeared on the TLC plate at the beginning, but the first two faded away successively, the spot of thiosulfate remaining till the last.

The decomposition of tetrathionate was largely influenced by concentration of ammonia as shown in Figs. 3 and 4. The increase of ammonia concentration accelerated the decomposition. The largest amount of thiosulfate was produced in around 0.4N solution of ammonia. When an

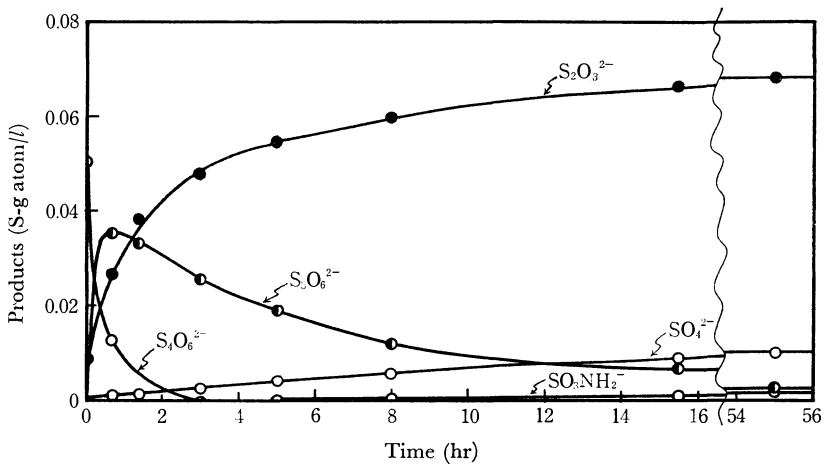

Fig. 1. The decomposition of tetrathionate in aqueous ammonia solution.
Reaction temp.: 60°C
Ammonia concn.: 0.416N
$K_2S_4O_6$ concn.: 0.020 mol/*l*

7) A. Gutmann, *Ber.*, **39**, 509 (1906); *ibid.*, **40**, 3614 (1907); E. H. Riesenfeld, *Z. Anorg. Allg. Chem.*, **141**, 109 (1924).

8) F. Martin and L. Metz, *Z. Anorg. Allg. Chem.*, **127**, 83 (1923).

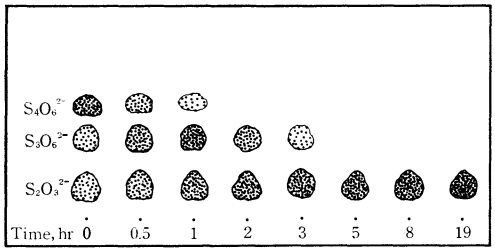

Fig. 2. TLC spot changes of $K_2S_4O_6$ on the aqueous ammonia solution with reaction time.
Reaction temp.: 80°C
Ammonia concn.: 1.64N
$K_2S_4O_6$ concn.: 0.020 mol/*l*
Solvent: Ethenol 75 m*l*, *n*-butanol 75 m*l*, 1 mol/*l*, of NH_4Ac 40 m*l*, concn. NH_4OH 10 m*l*

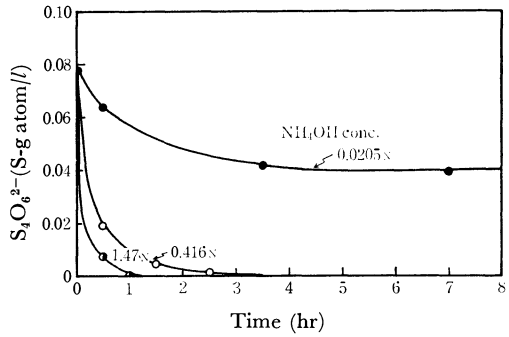

Fig. 3. Influence of ammonia concentration on the decomposition of $K_2S_4O_6$.
Reaction temp.: 60°C
$K_2S_4O_6$ concn.: 0.020 mol/*l*

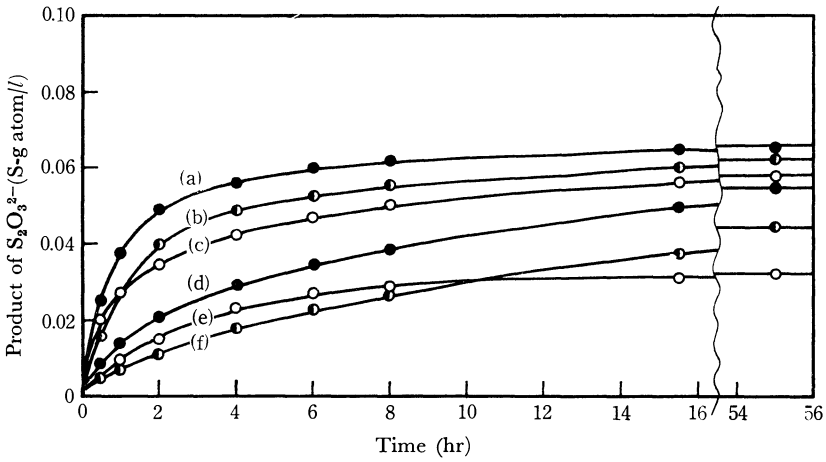

Fig. 4. Effect of ammonia concn. with the product of $S_2O_3^{2-}$ on the decomposition of $K_2S_4O_6$.
Reaction temp.: 60°C
$K_2S_4O_6$ concn.: 0.020 mol/*l*
NH_4OH concn.: (a) 0.416N (b) 0.105N (c) 2.057N (d) 5.120N (e) 0.0207N (f) 9.64N

extremely dilute ammonia such as 0.017N was used, the pH of the solution gradually decreased from 11.2 to 7.9, where elemental sulfur, pentathionate and hexathionate appeared as indicated by Figs. 5 and 6. The rise of temperature also accelerated the rate of decomposition as shown in Fig. 7.

Oxidation of Tetrathionate. The oxidation of potassium tetrathionate was carried out in 12N solution of ammonia at 90°C with compressed oxygen of 75 kg/cm². The results obtained are shown in Figs. 8 and 9. The difference of introduction time of oxygen made the reaction rate somewhat vary, but no remarkable change in the composition of the final solution was observed.

Discussion

It is apparent from this study that the mechanism of the decomposition of tetrathionate in aqueous ammonia solution is partly in conformity with Eqs. (1) and (2) suggested by the previous investigators. Therefore, the first products which depend on ammonia concentration are trithionate, pentathionate and thiosulfate. Then pentathionate and trithionate decompose as:

$$2S_5O_6^{2-} + 6OH^- = 5S_2O_3^{2-} + 3H_2O \quad (7)$$

$$S_3O_6^{2-} + 2OH^- = SO_4^{2-} + S_2O_3^{2-} + H_2O \quad (8)$$

$$S_3O_6^{2-} + NH_3 + OH^- = SO_3NH_2^- + S_2O_3^{2-} + H_2O \quad (9)$$

Equations (8) and (9) are in competition with each other. Sulfamate is formed through Eq. (9), which is different from tetrathionate decomposition in caustic soda solution.

It is obvious from the experiments that the yield of sulfamate depends on the ammonia concentration.

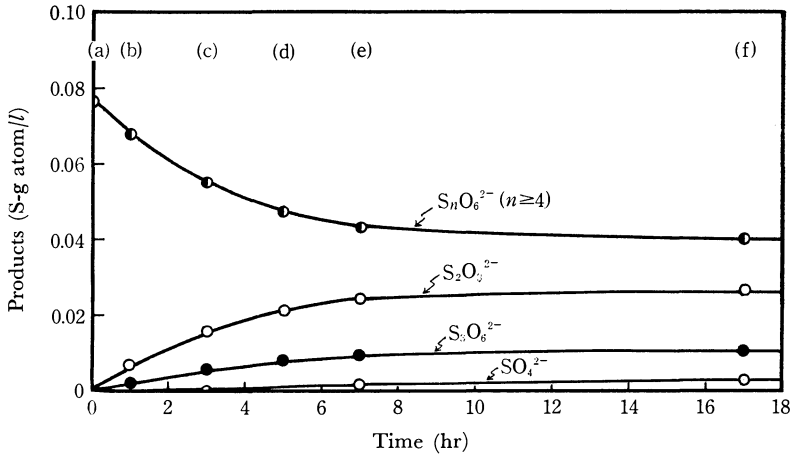

Fig. 5. The decomposition of $K_2S_4O_6$ on the dilute ammonia aqueous solution.
Reaction temp.: 50°C
Ammonia concn.: 0.017N
$K_2S_4O_6$ concn.: 0.020 mol/*l*
pH change with time:

	(a)	(b)	(c)	(d)	(e)	(f)
pH	11.19	10.48	10.12	9.71	9.52	7.92

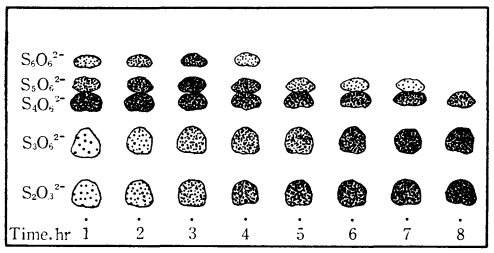

Fig. 6. TLC spot change of $K_2S_4O_6$ on the aqueous ammonia solution with reaction time.
Reaction temp.: 50°C
Ammonia concn.: 0.017N
$K_2S_4O_6$ concn.: 0.020 mol/*l*
Solvent: Ethenol 75 m*l*, *n*-butanol 75 m*l*,
1 mol/*l* of NH_4Ac 40 m*l*, conc. NH_4OH 10 m*l*

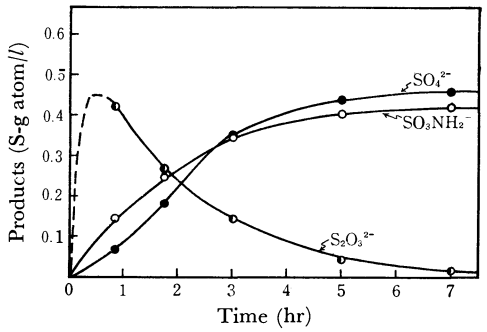

Fig. 8. Oxygen oxidation of $K_2S_4O_6$.
Oxygen was introduced at the beginning.
$K_2S_4O_6$ concn.: 0.25 mol/*l*, Oxygen pres.: 75 kg/cm², Ammonia concn.: 12N, Reaction temp.: 90°C

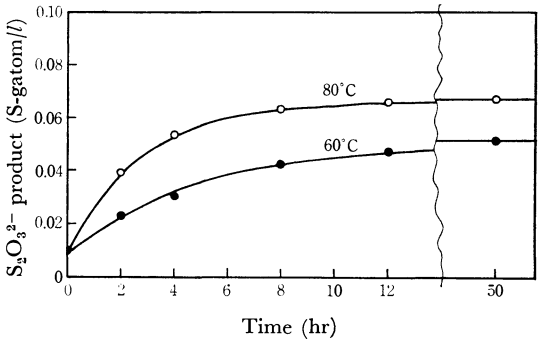

Fig. 7. Influence of the reaction temperature with $S_2O_3^{2-}$ yield on the decomposition of $K_2S_4O_6$.
Ammonia concn.: 5.0N
$K_2S_4O_6$ concn.: 0.020 mol/*l*

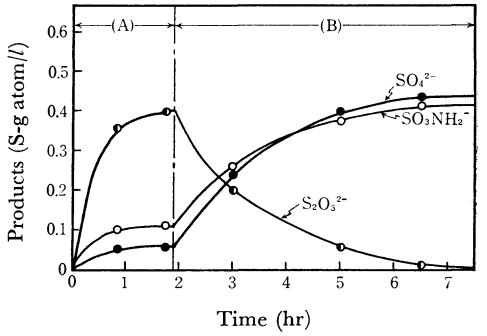

Fig. 9. Oxygen oxidation of $K_2S_4O_6$.
(A) Decomposition reaction
(B) Oxidation reaction under oxygen pressure
$K_2S_4O_6$ concn.: 0.25 mol/*l*, Oxygen press.: 75 kg/cm², Ammonia concn. 12N,: Reaction temp.: 90°C

TABLE 1. EFFECT OF AMMONIA CONCENTRATION ON THE DECOMPOSITION OF POTASSIUM TETRATHIONATE

Ammonia concn. (N)	$K_2S_2O_6$ concn. mol/l	Yield of product (S-g atom/l) molar ratio			
		$S_2O_3^{2-}$	SO_4^{2-}	$SO_3NH_2^-$	$(SO_4^{2-}+SO_3NH_2^-)/S_2O_3^{2-}$
0.11	0.020	0.0688	0.011	—	0.32
0.52	0.020	0.0658	0.0126	0.0013	0.42
1.92	0.020	0.0541	0.0208	0.0064	1.01
5.91	0.020	0.0525	0.0159	0.0113	1.04
9.65	0.020	0.0509	0.0153	0.0129	1.10

When the ammonia concentration is below 2N, sulfamate is hardly formed. If ammonia is deficiently used, the solution will become neutral or weakly acidic leading to the precipitation of sulfur and the formation of higher polythionates. In this case sulfite is also produced because trithionate and tetrathionate should react with excess thiosulfate to form higher polythionates, *viz*:

$$S_3O_6^{2-} + H^+ + S_2O_3^{2-} = S_4O_6^{2-} + HSO_3^- \quad (10)$$

$$S_4O_6^{2-} + H^+ + S_2O_3^{2-} = S_5O_6^{2-} + HSO_3^- \quad (11)$$

$$S_5O_6^{2-} = S_4O_6^{2-} + S \quad (12)$$

In the presence of excess free ammonia, the details of the reaction are not clear, but the overall reaction may be expressed as follows:

$$4S_4O_6^{2-} + 10OH^- = 7S_2O_3^{2-} + 2SO_4^{2-} + 5H_2O \quad (13)$$

$$4S_4O_6^{2-} + 2NH_3 + 8OH^- = 7S_2O_3^{2-} + 2SO_3NH_2^- + 5H_2O \quad (14)$$

The above equations indicate that the molar ratio of $(SO_4^{2-}+SO_3NH_2^-)/S_2O_3^{2-}$ should be equal to 2/7, even if the ammonia concentration or the temperature may change. When the ammonia concentration is about 0.1N, the experimental results obtained agree with the theoretical values within about 10% error. However, the molar ratio of $(SO_4^{2-}+SO_3NH_2^-)/S_2O_3^{2-}$ becomes about 1.01—1.10 in the ammonia concentration 2N or higher than 2N as shown in Table 1. This large discrepancy may be explained by the fact that tetrathionate is easily oxidized to sulfate in alkaline solution. That is, tetrathionate is easily oxidized to sulfate and sulfamate by air remaining in the flask. The overall equation may be considered as follows:

$$3S_4O_6^{2-} + 10OH^- + 2\tfrac{1}{2}O_2 = 4S_2O_3^{2-} + 4SO_4^{2-} + 5H_2O \quad (15)$$

$$3S_4O_6^{2-} + 4NH_3 + 6OH^- + 2\tfrac{1}{2}O_2 = 4S_2O_3^{2-} + 4SO_3NH_2^- + 5H_2O \quad (16)$$

Consequently, the oxidation of tetrathionate in the presence of excess free ammonia may be represented by the following three sequent steps.

1) At first, tetrathionate is decomposed to trithionate and pentathionate, or trithionate and thiosulfate according to Eq. (1) or (2), respectively. Pentathionate is further decomposed to thiosulfate.

2) Oxidation of thiosulfate occurs as:

$$2S_2O_3^{2-} + \tfrac{1}{2}O_2 + H_2O = S_4O_6^{2-} + 2OH^- \quad (17)$$

Decomposition of tetrathionate is repeated until all thiosulfate is consumed and, in these consecutive steps, this oxidation step of thiosulfate seems to be rate-determining. However, a small part of thiosulfate is considered to be oxidized to sulfate as:

$$S_2O_3^{2-} + 2O_2 + 2OH^- = 2SO_4^{2-} + H_2O \quad (18)$$

3) The final step is the decomposition of trithionate as shown in Eqs. (8) and (9).

From the above results, the oxidation of potassium tetrathionate in ammonia solution may be considered to proceed *via* the following course:

$$S_4O_6^{2-} \begin{cases} \nearrow (S_3O_6^{2-}) \\ \rightarrow S_5O_6^{2-} \rightarrow (S_2O_3^{2-}) \rightarrow (S_1O_6^{2-}) \\ \rightarrow S_3O_6^{2-} \rightarrow SO_4^{2-} \\ \searrow SO_3NH_2^- \end{cases}$$

BULLETIN OF THE CHEMICAL SOCIETY OF JAPAN VOL. 43 1377—1379 (1970)

Measurement of the Lyonium Ion Concentration in a H_2O-D_2O Mixed Solvent by Means of a Glass Electrode*1, *2

Hidetake KAKIHANA, Masunobu MAEDA and Toshihiko AMAYA

Research Laboratory of Nuclear Reactor, Tokyo Institute of Technology, Ookayama, Meguro-ku, Tokyo

(Received August 20, 1969)

In the present work, experiments were carried out for the systems of 20, 80 and 99.8% heavy water. It has turned out that the relationship between the emf and the lyonium ion concentration in a H_2O–D_2O mixed solvent can be expressed at 25°C by the so-called Nernst equation within the limits of experimental accuracy of ± 0.1 mV. This means that the lyonium ion concentration in a H_2O–D_2O mixed solvent can be measured with the same experimental accuracy (uncertainty of ± 0.1 mV) as that in light water by the use of a glass electrode.

The measurement of the lyonium ion concentration is of great importance to the studies of solution chemistry in a H_2O–D_2O mixed solvent. Thus far, the concentration of the lyonium ions has been measured with a H_2O–D_2O mixed gas electrode, a quinhydrone electrode, a glass electrode, and several other techniques.

It would, though, be very convenient for the studies of solution chemistry if the lyonium ion concentration in a H_2O–D_2O mixed solvent could be determined accurately with a glass electrode, which is rather cheap and easy to handle. The acidity in a H_2O–D_2O mixed solvent has been measured by several investigators.[1,2] They have standardized the pH meters with light water buffers and determined the values for pL by the addition of some experimental values to the readings of the pH meter. On the other hand, few determinations have been made by the direct measurement of emf with a glass electrode.[3] The determination of the lyonium ion concentration by the direct measurement of emf is of considerable importance to the investigation of complex ionic equilibria in a H_2O–D_2O mixed solvent containing background salt of a high concentration.[4-7]

This work has been undertaken to determine whether the electromotive-force-lyonium-ion dependence is the same as for the hydrogen ion and whether the lyonium-ion concentration can be determined with the same accuracy as the hydrogen-ion concentration by electromotive-force measurements employing a glass electrode.

Symbols

$[L_3O^+]$	concentration of free lyonium ions M (mol/l)
E, E_0, E_0', E_{og}	emf's (mV)
E_j	liquid junction potential
n	deuterium atom fraction
m	equilibrium constant of the following reaction: $1/3H_3O^+ + 1/2D_2O = 1/3D_3O^+ + 1/2H_2O$
$f_{L_3O^+}$	activity coefficient of the lyonium ion in a test solution
$f^g_{L_3O^+}$	activity coefficient of the lyonium ion in a gel layer of a glass electrode
C^g_0	total ion-exchange capacity of a gel layer of a glass electrode
$K_{L_3O^+}$	equilibrium constant of the following reaction: $H_2O(\text{glass}) + L_3O^+(\text{soln.}) = H_3O^+(\text{soln.}) + L_3O^+(\text{glass})$
V	volume of a test solution added (ml)
V_0	initial volume of a test solution (ml)
v	number of μF passed through a test solution
ω, C	constants

L will be used to mean H and D.

Experimental

Reagents and Apparatus. *All the reagents used* were prepared and analyzed by procedures similar to those described in Refs. 4 and 5.

A Wilhelm-type half cell[8] was used for the emf measurement, and a modified one for constant-current coulometry.

Glass electrodes of the Beckman type No. 40498 were employed.

*1 Ionic Equilibria in Heavy Water, Part IV.

*2 Part III: H. Kakihana and M. Maeda, This Bulletin, **43**, 1097 (1970).

1) P. K. Glasoe and F. A. Long, *J. Phys. Chem.*, **64**, 188 (1960).

2) P. Salomaa, L. L. Schaleger and F. A. Long, *J. Amer. Chem. Soc.*, **86**, 1 (1964).

3) R. S. Tobias and M. Yasuda, *J. Phys. Chem.*, **68**, 1820 (1964).

4) H. Kakihana and M. Maeda, This Bulletin, **42**, 1458 (1969).

5) H. Kakihana and M. Maeda, *ibid.*, **43**, 109 (1970).

6) M. Maeda and H. Kakihana, *ibid.*, **43**, 1097 (1970).

7) H. Kakihana, M. Maeda and T. Amaya, to be published.

8) W. Forsling, S. Hietanen and L. G. Sillén, *Acta Chem. Scand.*, **6**, 901 (1952).

Emf was measured with *a Radiometer PHM-4C(Copenhagen)*. The reading accuracy of this instrument is ± 0.1 mV.

Silver-silver chloride electrodes were used as references.

A coulometric analyzer(Leeds & Northrup Co., Philadelphia) was employed as a constant-current power source. In the present work, 6.43 mA was used as a constant current.

Procedures. All the measurements were carried out in a paraffin-oil thermostat kept at 25.00 ± 0.01°C and placed in a room thermostated at 25 ± 1°C. All the test solutions were made so as to contain 3M ClO_4^- as an ionic medium by the addition of $NaClO_4$.

The lyonium-ion concentration in a H_2O–D_2O mixed solvent was measured by means of the cell:

$$\text{Ref}|L\text{M } L^+, (3-L)\text{M } Na^+, 3\text{M } ClO_4^-|\text{GE} \qquad \text{(A)}$$

where GE denotes a glass electrode, and Ref, the reference half cell:

|3M $NaClO_4$ in a H_2O–D_2O mixed solvent|2.99M $NaClO_4$ and 0.01M $AgClO_4$ in light water|AgCl-Ag

The lyonium-ion concentration in the cell (A) was varied by two procedures; one was the technique of constant-current coulometry, whose experimental details are similar to those presented in Ref. 9, and the other was the technique of titration by the use of a buret.

A steady emf was usually attained within ten minutes. This means that the time required to reach equilibrium is the same as that for the system of light water. During the measurements, a test solution was stirred by a vigorous stream of nitrogen gas which had been purified by leading through a H_2O–D_2O mixed solvent and 3M $NaClO_4$ in a H_2O–D_2O mixed solvent.

Results

1) Relationship between the emf and the Lyonium-ion Concentration. The emf-lyonium-ion dependence was derived on the basis of the assumptions that a gel layer of a glass surface acts as a cation exchanger,[10,11] which adsorbs exclusively the ions of hydrogen isotopes when a glass electrode is brought into equilibrium with a H_2O–D_2O mixed solvent, that H^+ and D^+ ions are present in the forms of H_3O^+, H_2DO^+, HD_2O^+, and D_3O^+ in a H_2O–D_2O mixed solvent,[12,13] and that the rule of the geometric mean[14] is applicable as a first approximation to acid-base equilibria in a H_2O–D_2O mixed solvent. On the basis of the above assumptions, it was found that the emf of a glass electrode could be represented approximately by Eq. (1a):

$$E = E_0' - \boldsymbol{R}T/F(\ln C_0^g) + \boldsymbol{R}T/F\left(\ln\left(\frac{f_{H_2O^+}(1-n)^3}{f^g_{H_3O^+}(1-n+nm)^3} + \frac{f_{D_3O^+}K_{D_3O^+}n^3m^3}{f^g_{D_3O^+}(1-n+nm)^3} + \frac{3f_{HD_2O^+}K_{HD_2O^+}(1-n)n^2m^2}{f^g_{HD_2O^+}(1-n+nm)^3} + \frac{3f_{H_2DO^+}K_{H_2DO^+}(1-n)^2nm}{f^g_{H_2DO^+}(1-n+nm)^3}\right)\right) + \boldsymbol{R}T/F(\ln[L_3O^+]) \qquad \text{(1a)}$$

Since the first, second, and third terms on the right-hand side are constant provided that the temperature of the cell, the activity coefficients of the lyonium ions, and the deuterium atom fraction in a H_2O–D_2O mixed solvent are held constant, Eq. (1a) can be restated in this form:

$$E = E_0 + \boldsymbol{R}T/F(\ln[L_3O^+]) \qquad \text{(1b)}$$

On the other hand, the emf of a cell with a liquid-junction that corresponds to cell(A) is given by:

$$E = E_0 + \boldsymbol{R}T/F(\ln[L_3O^+]) + E_j \qquad \text{(2a)}$$

On the basis of the assumption that Henderson's equation for a continuous-mixture boundary and the rule of the geometric mean[14] are applicable as a first approximation to equilibria in which the ions of hydrogen isotopes take part, it was proved that the liquid-junction potential for the system of a 3M $NaClO_4$ solution of a H_2O–D_2O mixed solvent was approximated by a linear function of the lyonium-ion concentration. Therefore, the emf of a cell with a liquid-junction is given by:

$$E = E_0 + \boldsymbol{R}T/F(\ln[L_3O^+]) + \omega[L_3O^+] \qquad \text{(2b)}$$

Eq. (2b) is expressed at 25°C as follows:

$$E = E_0 + 59.15 \log [L_3O^+] + \omega[L_3O^+] \qquad \text{(3)}$$

2) Experimental Proof of the Reliability of Eq. (3). In this section, we will examine experimentally whether Eq.(3), which holds as a first approximation, is true within the limits of experimental error. 20, 80, and 99.8% heavy-water systems were used as the solvents. Since the liquid-junction potential for the system of light water containing 3M $NaClO_4$ has been found to be negligible in the acid region less than 0.01M[15] it was examined experimentally whether the $E = E_0 + 59.15 \log[L_3O^+]$ term in Eq.(3) held within the limits of experimental accuracy. It was then examined, at an acidity of more than 0.01M, whether the liquid-junction potential in the cell (A) had a linear dependence on the lyonium-ion concentration.

When the liquid-junction potential is negligible, Eq.(3) is transformed as follows:[16]

$$(V_0+V) \times 10^{E/59.15} = C(V_0(L)_0 - V(OL)) \qquad \text{(4)}$$

when an alkaline solution is added from a buret to a test solution, and

$$V_0 \times 10^{E/59.15} = C(V_0(L)_0 - \nu \times 10^{-3}) \qquad \text{(5)}$$

9) L. Ciavatta, *Ark. Kemi*, **20**, 417 (1962).
10) T. Okada, T. Nishi and H. Takahashi, *Kogyo Kagaku Zasshi*, **61**, 931 (1958).
11) N. Kishimoto, H. Matsushita, H. Hironaka and H. Maruyama, *Denki Kagaku*, **30**, 355 (1962).
12) V. Gold, *Proc. Chem. Soc.*, **1963**, 141.
13) K. Heinzinger and R. E. Weston, *J. Phys. Chem.*, **68**, 744 (1964).
14) J. Bigeleisen, *J. Chem. Phys.*, **23**, 2264 (1955).
15) G. Biedermann and L. G. Sillén, *Ark. Kemi*, **5**, 425 (1952).
16) G. Gran, *Analyst*, **77**, 661 (1952).

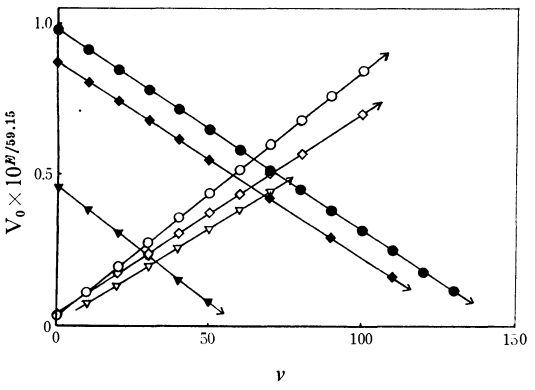

Fig. 1. $V_0 \times 10^{E/59.15}$ as a function of microfaraday.
▼, ●, ◆ generation of OL^- ion for the system of 99.8% heavy water, 80% heavy water and 20% heavy water, respectively.
▽, ○, ◇ generation of L_3O^+ ion for the system of 99.8% heavy water, 80% heavy water and 20% heavy water, respectively.

when an alkali is generated by constant-current coulometry.

A glass-electrode function in the higher acid region was investigated by the titration method, and one in the lower acid region was investigated by constant-current coulometry capable of generating a very small amount of acid or alkali.

If Eq. (3) is valid, plots of $(V_0+V)\times 10^{E/59.15}$ as a function of V, or of $V_0\times 10^{E/59.15}$ as a function of γ, should show straight lines.

The results obtained by means of constant-current coulometry for the systems of 20, 80 and 99.8% heavy water are visualized in Fig. 1.

From this figure, it is obvious that the experimental plots show straight lines. In addition, the values for E_0 calculated at each point were kept constant within the exprimental error of ± 0.1 mV, and there was no systematic error in the value of E_0. These things were also true for the results obtained by the titration method.

Next, it was examined experimentally, by plotting $(E-59.15\times\log [L_3O^+])$ as a function of $[L_3O^+]$, whether the liquid-junction potential could be approximated as a linear function of the lyonium-ion concentration. The experiments were carried out by the titration method. The results obtained thereby are pictured in Fig. 2. This figure shows that the liquid-junction potential for the system of a H_2O-D_2O mixed solvent is expressed approxi-

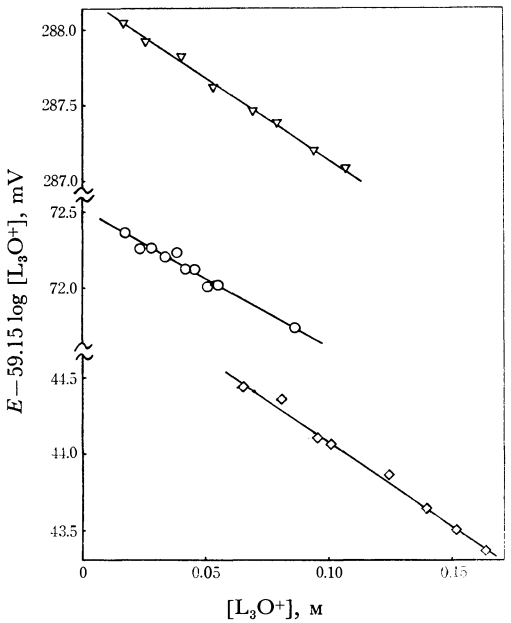

Fig. 2. $(E-59.15\log [L_3O^+])$ as a function of $[L_3O^+]$;
▽, for the system of 99.8% heavy water;
○, 80% heavy water; ◇, 20% heavy water

mately as a linear function of the lyonium-ion concentration.

From the slopes of the straight lines, the liquid-junction potentials for the systems of 20, 80 and 99.8% heavy water were found to be approximated by $-13._2\times[L_3O^+]$, $-8._4\times[L_3O^+]$, and $-10._9\times[L_3O^+]$mV respectively.

From the results described above, it has been found that Eq.(3) is valid within the experimental error of ± 0.1 mV.

Conclusion

In this work, it has been verified that the relationship between the emf of a glass electrode and the lyonium-ion concentration in a H_2O-D_2O mixed solvent is given at 25°C by the so-called Nernst equation with an experimental accuracy of ± 0.1 mV. This means that the lyonium-ion concentration in a H_2O-D_2O mixed solvent can be measured with the same experimental accuracy (an uncertainty of ± 0.1 mV) as that in light water by the use of a glass electrode.

BULLETIN OF THE CHEMICAL SOCIETY OF JAPAN VOL. 43 1380—1382 (1970)

Studies of the Behavior of Trivalent Uranium in an Aqueous Solution. III. Extraction from a Hydrochloric Acid Solution by Bis(*n*-butyl) Orthophosphoric Acid and by Bis-(2-ethylhexyl) Orthophosphoric Acid

Akiko Satō and Shin Suzuki

The Research Institute for Iron, Steel and Other Metals, Tohoku University, Katahira-cho, Sendai

(Received August 25, 1969)

The distribution of U(III) between hydrochloric acid solutions and benzene solutions of bis-(*n*-butyl) orthophosphoric acid or cyclohexane solutions of bis(2-ethylhexyl) orthophosphoric acid has been investigated by using the uranium-237 isotope as a tracer. It has been found that the log-log plot of the distribution ratio *vs.* the concentration of dimeric organophosphoric acids, and that of the distribution ratio *vs.* the hydrogen ion concentration, always show a good linearity, with a slope of 3. This indicates that the complex-forming reaction is as follows:

$$U^{3+} + 3(HA)_2 \rightleftarrows U(HA_2)_3 + 3H^+$$

where $(HA)_2$ represents the dimeric solvent, $(HDBP)_2$ or $(HDEHP)_2$. The above results are in agreement with the conclusions reached in the cases of other trivalent actinide and lanthanide elements by other investigators.

Several papers have been reported on U(III) because of its instability in aqueous solutions.[1-4] The present authors found that U(III) is fairly stable in aqueous solutions at low acid concentrations in the absence of atmospheric oxygen.[5] They studied the preparation, stability, absorption spectra, and ion-exchange behavior of U(III) in various acid solutions.[5,6] The reduction of U(VI) to U(III) with liquid zinc amalgam gives a high yield within a short period of time and with a good reproducibility. Particularly in a hydrochloric acid solution, the reduction is more complete than in other media, and the stability of U(III) is also high. Its stability increases with the decrease in the acid concentration.

In this paper, the solvent-extraction behavior of U(III) in hydrochloric acid solutions will be reported on; the investigations were done by using bis(*n*-butyl) orthophosphoric acid-benzene and bis-(2-ethylhexyl) orthophosphoric acid-cyclohexane.

Experimental

Reagents and Apparatus. *Uranium-237 and Hydrochloric Acid Solutions of U(VI).* The uranium-237 tracer was prepared by the conventional method[6,7] after natural uranium dioxide had been irradiated for about 2 hr with 20 or 50 MeV Bremsstrahlung from the Liniac, JAERI, or the Laboratory of Nuclear Science, Tohoku University.

Bis(2-ethylhexyl) Orthophosphoric Acid (HDEHP) and Bis(n-butyl) Orthophosphoric Acid (HDBP). The HDEHP and HDBP were purified by the method reported by Peppard *et al.*[8] The purified organophosphoric acids were dissolved with a purified solvent such as benzene or cyclohexane. The concentration of organophosphoric acid was determined by titrating it with a standard sodium hydroxide solution.

The liquid zinc amalgam was prepared by a method reported previously.[5] The benzene and the other solvents were purified before use in the usual manner. All the other chemicals, such as hydrochloric acid and lithium chloride, were of an analytical grade.

The reductor and radiation measurement instruments were those described in a previous report.[6]

Procedures. All the experiments were carried out in a plastic globe-box with an argon, nitrogen, or carbon dioxide atmosphere at 25±2°C.

Five milliliters of a uranyl chloride solution tagged with a uranium-237 tracer were taken into the reductor. A calculated quantity of lithium chloride solution was added to this to maintain the ionic strength of the total aqueous phase at 0.2, and then the total volume was adjusted to 10 m*l*. After about 10 m*l* of the liquid zinc amalgam had been added to the reductor, the U(VI) was reduced as has been described in a previous report.[5] After the liquid zinc amalgam had then been

1) K. Someya, *Z. Anorg. Allgem. Chem.*, **161**, 46 (1927).
2) C. K. Jørgensen, *Acta Chem. Scand.*, **10**, 1503 (1956).
3) D. C. Stewart, ANL-4812 (1952).
4) V. F. Peretrukhin, N. N. Krot and A. D. Gel'man, *Radiokhimiya*, **8**, 670 (1966).
5) A. Satō, This Bulletin, **40**, 2107 (1967).
6) A. Satō and S. Suzuki, *ibid.*, **41**, 2650 (1968).
7) E. Akatsu, T. Kuroyanagi and T. Ishimori, *Radiochim. Acta*, **2**, 1 (1963).
8) D. F. Peppard, J. R. Ferraro and G. W. Mason, *J. Inorg. Nucl. Chem.*, **7**, 231 (1958).

carefully removed from the reductor, 10 m*l* of a HDBP or HDEHP solution was added to it. Both phases were shaken with a mechanical shaker.

Pre-equilibration. Two portions of barren HDBP or HDEHP were, successively, placed in contact with two equal-volume portions of barren aqueous acid. The second portions of the solvent and aqueous phases were then used in the study.

Care was taken to ascertain the material balance in each case; the concentration of uranium in the aqueous phase was about 2×10^{-3}M.

After the separation of the two phases, a 1 m*l* aliquot of each phase was taken into a polyethylene tube. The γ-radioactivity was measured with a well-type scintillation counter, and the distribution ratio, D, was calculated.

Here, D is defined as:

$$D = \frac{\gamma\text{-activity per ml of the org. phase}}{\gamma\text{-activity per ml of the aq. phase}}$$

The hydrogen-ion concentration of the aqueous phase in equilibrium was determined by titration with a standard sodium hydroxide solution.

To an extent depending on the kind of mineral acid and its concentration, the reduction of U(VI) to U(III) does not proceed completely[5] and U(IV) is also present in the sample solution. Although an insoluble U(IV) compound forms between the two phases in the extraction with $(HDBP)_2$ below 0.10M, it can be easily separated by the centrifugal method. The solubility of this compound increases with an increase in the HDBP concentration; about 30% of the U(IV) is extracted with a 0.25M $(HDBP)_2$ - benzene solution. On the other hand, U(IV) is completely extracted into the HDEHP phase over a wide range of hydrochloric acid concentrations. Consequently, it was necessary to correct for this by the method reported previously.[6]

Results

Experimental Conditions. The equilibrium of the solvent extraction with HDBP or with HDEHP was reached within about 30 sec. Therefore, a shaking time of 60 sec is recommended.

Diluent. As is shown in Table 1, the relative extractability of U(III) increases in the following sequence: cyclohexane>xylene>isopropyl ether>toluene>benzene. Uranium(III) is extracted to a moderate extent with HDBP, while it is very poorly extracted with HDEHP from a weak hydrochloric acid solution. On the basis of these results, we used benzene as the diluent for the HDBP extraction and cyclohexane for the HDEHP extraction.

Table 1. Influence of the diluent for the U^{3+}-HDEHP and - HDBP system

Diluent	Distribution ratio*	
	U^{3+}-HDEHP	U^{3+}-HDBP
Cyclohexane	2.6	450
Xylene	0.8	36
Isopropyl ether	0.4	16
Toluene	0.03	9.8
Benzene	0	6.5

* HCl, 0.05M; $(HDEHP)_2$ or $(HDBP)_2$, 0.1M; U, 2×10^{-3}M

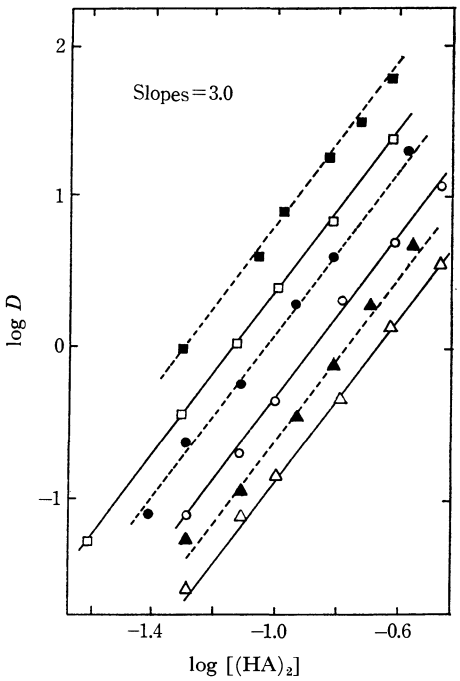

Fig. 1. Extractant dependency of the extraction o the U(III) into HDBP or HDEHP.
HDBP extraction;
---■---■---: 0.06M HCl ---●---●---: 0.1M HCl
---▲---▲---: 0.15M HCl
HDEHP extraction;
—□—□—: 0.06M HCl —○—○—: 0.1M HCl
—△—△—: 0.14M HCl

The extraction of U(IV) with HDEHP is practically complete over a wide range of hydrochloric acid concentrations. The back extraction into the aqueous phase is difficult even with high concentrations of hydrochloric acid. However, the back extraction of U(III) is complete in a hydrochloric acid solution of >2M. The above results are in good agreement with those of Peppard *et al.*,[9,10] who were concerned with the distribution coefficients of other actinide elements between HDEHP and hydrochloric acid.

Solvent Dependence of the Distribution Ratio. As is shown in Fig. 1, a good linear solvent dependency is seen to be directly third power over a wide range of HDBP and HDEHP concentrations for 0.06, 0.1, and 0.14M hydrochloric acid con-

9) D. F. Peppard, G. W. Mason, J. L. Maier and W. J. Driscoll, *ibid.*, **4**, 334 (1957).
10) D. F. Peppard, S. W. Molin and G. W. Mason, *ibid.*, **4**, 344 (1957).

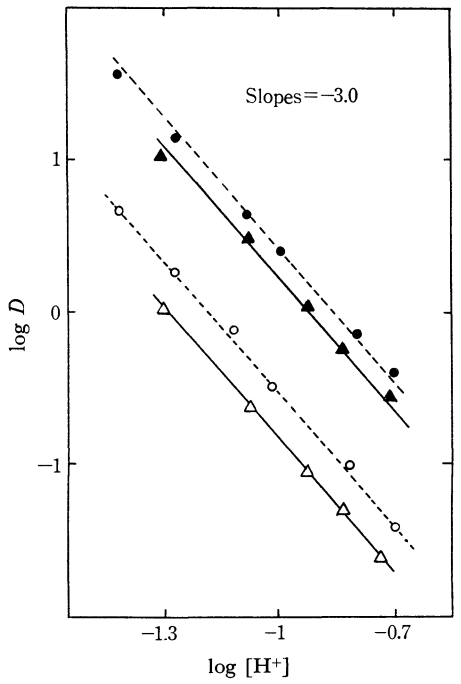

Fig. 2. Hydrogen ion dependency of the extraction of the U(III) into HDBP or HDEHP.
---○---○---: 0.05M $(HDBP)_2$, ---●---●---: 0.14M $(HDBP)_2$, —△—△—: 0.05M $(HDEHP)_2$, —▲—▲—: 0.15M $(HDEHP)_2$

centrations. Each point is the mean of six experiments, having the standard deviations of 2.3—3.8% for the HDEHP extraction and 1.7—4.2% for the HDBP extraction.

Acid Dependence of the Distribution Ratio in a Constant-ionic-strength Medium. The effect of the acidity of the aqueous phase was studied at the constant ionic strength of 0.2. Benzene solutions of 0.05 and 0.14M $(HDBP)_2$ and cyclohexane solutions of 0.05 and 0.15M $(HDEHP)_2$ were used for the extraction. It is clear from Fig. 2 that the log-log plot of the distribution ratio and the hydrogen ion concentration in the aqueous phase shows a linear relationship with a slope of an inversive third power. Each point is the mean of six experiments, having the standard deviations of 1.3—3.9% for the HDEHP extraction and 2.2—4.7% for the HDBP extraction.

Discussion

It should be noted that, in the present discussion, HA is a dimer.[8,11-15] Consequently, for HDBP or HDEHP, the ionization of the extractant and the composite equilibrium are written as:

$$(HA)_2(org) \rightleftarrows H^+(aq) + H(A)_2^-(org)$$

where the subscripts (aq) and (org) refer to the aqueous and the organic phase respectively and where HA represents the organophosphoric acid solvent, HDBP or HDEHP.

Thus, the above equation becomes:

$$M^{m+}(aq) + m(HA)_2(org) \rightleftarrows M[H(A)_2]_m(org) + mH^+(aq)$$

The expression for the distribution ratio, D, is written as:

$$D = K_E[(HA)_2]^m(org)/[H^+]^m(aq)$$

If the temperature and the concentration of HDBP or HDEHP, or the pH, are constant in the extraction, the following equations can be obtained from the above equation:

$$\log D = \log K_E[H^+]^{-m}(aq) + m \log [(HA)_2](org)$$

and:

$$\log D = \log K_E[(HA)_2]^m(org) + m \log [H^+]^{-1}(aq)$$

From the experimental results shown in Figs. 1 and 2, the plots of log D *vs.* the log of the HDBP or HDEHP concentration and the plots of log D *vs.* the pH show straight lines, with a slope of 3, so it can be considered that the species extracted into the organic phase have the form of $U[H(DBP)_2]_3$ or $U[H(DEHP)_2]_3$. This indicates that the complex-forming reaction is as follows:

$$U^{3+} + 3(HDBP)_2 \rightleftarrows U[H(DBP)_2]_3 + 3H^+$$

or:

$$U^{3+} + 3(HDEHP)_2 \rightleftarrows U[H(DEHP)_2]_3 + 3H^+$$

Here, a good agreement is seen with the conclusions reached in the cases of other trivalent actinide and lanthanide elements by other investigators.[15-21]

The authors wish to express their thanks to Mr. Mitsuyuki Takahashi for his technical assistance in the present experiments. Thanks are also due to the members of the Liniac laboratory of both JAERI and Tohoku University for their helpful operation of Liniac. Support by the Scientific Research Fund of the Ministry of Education is gratefully acknowledged.

11) D. F. Peppard, J. R. Ferraro and G. W. Mason, *J. Inorg. Nucl. Chem.* **4**, 371 (1957).
12) D. Dyrssen, *Acta Chem. Scand.*, **11**, 1771 (1957).
13) C. J. Hardy and D. Scargill, *ibid.*, **11**, 128 (1959).
14) D. Dyrssen and L. D. Hay, *ibid.*, **14**, 1091 (1960).
15) C. F. Baes, Jr., *J. Inorg. Nucl. Chem.*, **24**, 707 (1962).
16) D. Dyrssen, *Acta Chem. Scand.*, **11**, 1277 (1957).
17) D. F. Peppard, G. W. Mason, W. J. Driscoll and R. J. Sironen, *J. Inorg. Nucl. Chem.*, **7**, 276 (1958).
18) D. Dyrssen and L. D. Hay, *Acta Chem. Scand.*, **14**, 1100 (1960).
19) G. Duyckaerts, Ph. Dreze and A. Simon, *J. Inorg. Nucl. Chem.*, **13**, 332 (1960).
20) D. F. Peppard, G. W. Mason and I. Hucher, *ibid.*, **18**, 245 (1961).
21) G. W. Mason, S. Lewey and D. F. Peppard, *ibid.*, **26**, 2271 (1964).

BULLETIN OF THE CHEMICAL SOCIETY OF JAPAN VOL. 43 1383—1387 (1970)

Derivatographic Studies on Transition Metal Complexes. III.*1 The Thermal *trans-cis* Isomerization of $[CoCl_2pn_2](H_5O_2)Cl_2$ in Solid-Phase*2

Ryokichi Tsuchiya, Kiyoko Murai, Akira Uehara and Eishin Kyuno

Department of Chemistry, Faculty of Science, Kanazawa University, Kanazawa

(Received August 27, 1969)

The thermal decomposition of *trans*-$[CoCl_2pn_2](H_5O_2)Cl_2$ in solid-phase was measured by derivatography and the isothermal method with a thermobalance. It was found by the latter that dehydration and dehydrochlorination took place with partial isomerization below 170°C. The rate of isomerization gradually increased with temperature until it became equal to the rate of dehydration and dehydrochlorination above 170°C. The activation energies for dehydration and dehydrochlorination and for isomerization were calculated from the isothermal measurement below 170°C to be 10 kcal/mol and 23 kcal/mol, respectively. The activation energy obtained from DTA curve analysis at about 144°C in the derivatogram was 33 kcal/mol. The reaction was explained in terms of "aquation-anation" mechanism. Since the *trans-cis* isomerization in anhydrous state at 180°C gave a larger activation energy in DTA analysis, the "twisting" mechanism might be preferable to "aquation-anation" for the reaction.

Several examples of *cis* ↔ *trans* isomerization on transition metal complexes in solution[1] are known. However, the situation is different in solid-phase.[2] The complex, *trans*-$[CoCl_2(NH_3)_4]IO_3 \cdot 2H_2O$, undergoes a distinct color change on being heated in solid state.[3] A detailed study was reported.[4]

A complicated *trans-cis* isomerization involving both the thermal dehydration and the dehydrochlorination was also found for the complex, *trans*-$[CoCl_2pn_2](H_5O_2)Cl_2$.[5,6] It has been proposed that the *trans-cis* isomerization in the two complexes, *trans*-$[CoCl_2(NH_3)_4]IO_3 \cdot 2H_2O$ and *trans*-$[CoCl_2pn_2](H_5O_2)Cl_2$, occurred *via* an "aquation-anation" pathway on crystal surface when the water molecules are set free from the crystalline hydrates.[4,6]

It is of interest to note that the dehydration and dehydrochlorination of *trans*-$[CoCl_2en_2](H_5O_2)Cl_2$ are accompanied by no isomerization as in the corresponding pn-complex.[7]

A recent study on the dehydration and dehydrochlorination of *trans*-$[CoCl_2pn_2](H_5O_2)Cl_2$ and of the corresponding en-complex indicates that both chlorides exhibit the closely equal activation energies of 16.1 kcal/mol *in vacuo* regardless of the occurrence of *trans-cis* isomerization.[6,7] The activation energies in the thermal reaction of analogous bromo-complex bromides, *trans*-$[CoBr_2(A\text{–}A)_2](H_5O_2)Br_2$ (A–A: en or pn), were 24—29 kcal/mol. Only the corresponding pn-complex was found to undergo *trans-cis* isomerization such as the chloride.[8] The above difference of activation energies between the chloro- and the bromo-complexes is understood to be due to a somewhat more difficult diffusion of HBr and H_2O in the latter complex. In the present work, thermochemical and kinetic analysis of *trans*-$[CoCl_2pn_2](H_5O_2)Cl_2$ was carried out from derivatograms. They were also done by means of isothermal measurements. The mechanism is discussed in detail.

Experimental

Preparation of Complexes. Both *trans*-$[CoCl_2pn_2]$-

*1 Part II in this series: see R. Tsuchiya, A. Uehara and E. Kyuno, This Bulletin, **42**, 1886 (1969).

*2 Presented at the 18th Symposium on Coordination Chemistry, Kyoto, October, 1968.

1) F. Basolo and R. G. Pearson, "Mechanisms of Inorganic Reactions," 2nd Ed., John Wiley & Sons, Inc., New York, N. Y. (1967), pp. 274—291.

2) *Ibid.*, pp. 327—328.

3) N. I. Lobanov, *Zhur. Neorg. Khim.*, **4**, 151 (1959).

4) H. E. LeMay, Jr., and J. C. Bailar, Jr., *J. Amer. Chem. Soc.*, **89**, 5577 (1967).

5) This compound is frequently formulated as *trans*-$[CoCl_2pn_2]Cl \cdot HCl \cdot 2H_2O$. However, recent X-ray studies indicated that it contains $H_5O_2^+$ and Cl^- ions; Y. Saito and H. Iwasaki, This Bulletin, **35**, 1131 (1962). The same is true of *trans*-$[CoCl_2en_2](H_5O_2)Cl_2$; A. Nakahara, Y. Saito and H. Kuroya, *ibid.*, **25**, 331 (1952).

6) H. E. LeMay, Jr., *Inorg. Chem.*, **7**, 2531 (1968).

7) J. C. Bailar, Jr., *Inorg. Syn.*, **2**, 222 (1946).

8) H. E. LeMay, Jr., University of Nevada, Reno, Nevada, U. S. A., private communication (1969).

$(H_5O_2)Cl_2$[9] and *cis*-$[CoCl_2pn_2]Cl$[10] were prepared by the known method partly modified.*3 The corresponding *trans*-en-complex was prepared by the method in literature.[7] These compounds were confirmed by elemental analysis and spectrophotometric measurements.

Derivatographic Measurements. The derivatograms (the chart involves TGA, DTA and DTG curves) for these complexes were obtained with a MOM Derivatograph Typ-OD-102.[11,12] The activation energies (E^*) in the desired reaction steps were calculated by analysis of DTA curves in the derivatograms.[12,13] The enthalpy changes (ΔH) in the corresponding steps were estimated from the same DTA curves.[12,14] 0.5 g finely powdered samples were used in each run (100—200 mesh/inch) under a constant flow of nitrogen stream with the heating rate of 1°C min^{-1}.

Isothermal Measurements using a Thermobalance. Direct and isothermal determination of the dehydration and dehydrochlorination accompanied by isomerization were made by using a Shimadzu TM-1A Thermanobalance. Samples of 0.5 g in each run placed in a small platinum basket hung from one arm of the balance were heated at desired temperatures. The mass loss of each sample in a constant time interval at each temperature was recorded as a TGA curve, and the rates of dehydration and dehydrochlorination were determined. In the same experiment, a part of the products in the basket was dissolved in methanol and the *trans-cis* ratio was determined spectrophotometrically as follows. The visible and UV absorption spectra of the starting complex, *trans*-$[CoCl_2pn_2](H_5O_2)Cl_2$, and the final product, *cis*-$[CoCl_2pn_2]Cl$, were measured in methanol with a Hitachi R-3 Spectrophotometer, because the complexes are fairly soluble in methanol and the solutions do not undergo further isomerization within 20 min at room temperature. Their spectra are shown in Fig. 1. Since the pure *trans*- and *cis*-compounds have the absorption coefficients, 6.8 and 62.7, at 530 mμ, and, 40.8 and 51.6, at 600 mμ in methanol, respectively, the *trans/cis* ratios in the product in each step can be determined spectrophotometrically by means of the equations:

$$6.8X + 62.7Y = D_{530}$$

$$40.8X + 51.6Y = D_{600}$$

where X and Y are the concentrations (in mol^{-1}) of *trans*- and *cis*-compounds, and D_{530} and D_{600} are the absorbancies at 530 and 600 mμ with 1.0 cm cell, respectively. Thus, *trans/cis* ratios are given by X/Y.

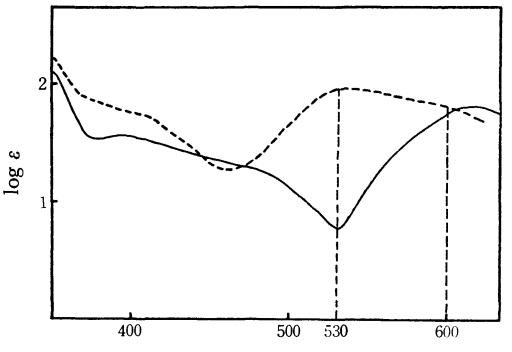

Fig. 1. The electronic absorption spectra of *trans*-$[CoCl_2pn_2](H_5O_2)Cl$ (———) and *cis*-$[CoCl_2pn_2]Cl$ (– – –) in methanol.

Results and Discussion

The derivatogram obtained for the thermal decomposition of *trans*-$[CoCl_2pn_2](H_5O_2)Cl_2$ is shown in Fig. 2, together with that of the corresponding en-complex.

In the case of the former pn-complex, as seen in Fig. 2, one molecule of hydrogen chloride and two molecules of water are simultaneously lost with partial isomerization at 144°C, where both DTA and DTG curves show a single peak. An apparently analogous decomposition reaction was observed for the corresponding en-complex by the appearance of a single endothermic peak in DTA due to the dehydration and dehydrochlorination as in the above pn-complex, but no isomerization occurred.

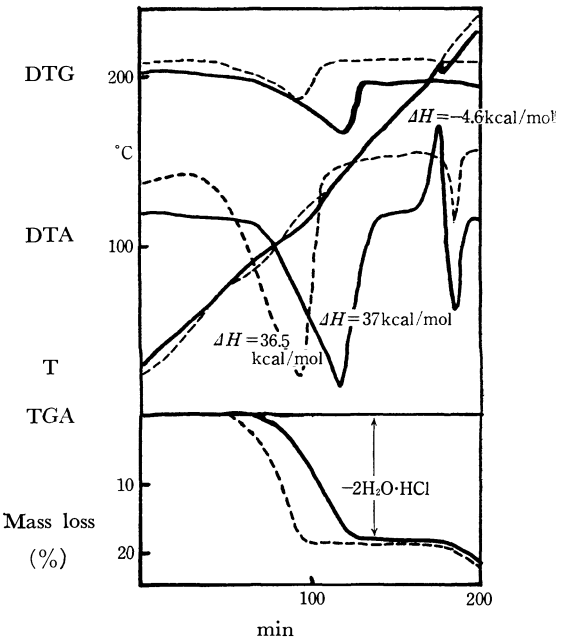

Fig. 2. The derivatograms for *trans*-$[CoCl_2pn_2](H_5O_2)Cl_2$ (———) and *trans*-$[CoCl_2en_2](H_5O_2)Cl_2$ (– – –).

9) A. Werner and A. Frohlich, *Ber.*, **40**, 2228 (1907).

10) J. C. Bailar, Jr., C. A. Stiegmen, J. H. Balthis and E. H. Huffman, *J. Amer. Chem. Soc.*, **61**, 2402 (1939).

*3 The details will be published elsewhere.

11) F. Paulik, J. Paulik and L. Erdey, *Talanta*, **13**, 1405 (1966).

12) R. Tsuchiya, Y. Kaji, A. Uehara and E. Kyuno, This Bulletin, **42**, 1881 (1969).

13) N. G. Dave and S. K. Chopra, *Z. Phys. Chem.*, **48**, 257 (1966).

14) H. G. Borchardt and F. Daniels, *J. Amer. Chem. Soc.*, **79**, 41 (1957).

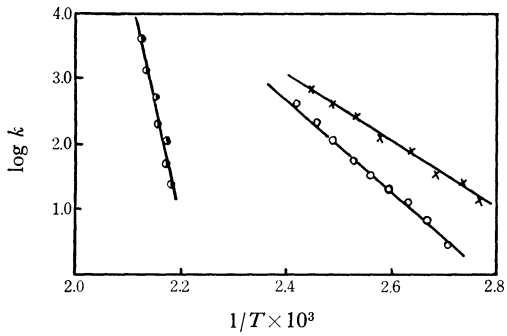

Fig. 3. The "Arrhenius plots" of the rate constants of the dehydration and dehydrochlorination and of the exothermic reaction without mass loss on *trans*-$[CoCl_2pn_2](H_5O_2)Cl_2$.
◑—◑: isomerization $E_i^* = 120 \pm 3$ kcal·M^{-1}
○—○: $-HCl \cdot 2H_2O$ reaction $E_{d(i)}^* = 33 \pm 2$ kcal·M^{-1} (DTA)
×—×: $-HCl \cdot 2H_2O$ reaction $E_{d(i)}^* = 31 \pm 2$ kcal·M^{-1} (DTG)

Dehydration and dehydrochlorination of the pn-complex begin to take place at a lower temperature than that of the corresponding en-complex as shown in Fig. 2.

Analysis of DTA curve for *trans*-$[CoCl_2pn_2](H_5O_2)Cl_2$ gave 36.5 kcal/mol as ΔH. The Arrhenius plots for the pn-complex, *viz.*, the relationships between the rate constants derived from the analysis of DTA and DTG curves and reciprocal absolute temperatures are shown in Fig. 3. The activation energies, E^*, are obtained to be 33 ± 2 and 31 ± 2 kcal/mol, respectively.

The values are larger than that for the dehydration and dehydrochlorination of the complex, *i. e.*, 16.1 kcal/mol given in literature.[6]

The second peak in DTA curve was found only for the pn-complex without any mass change in TGA, probably due to the occurrence of a small exothermic reaction at 180°C before complete decomposition. Since the corresponding en-complex did not show a similar peak, appearance of such a peak in the former complex is believed to be due to a certain constitutional change; *i e.*, *trans-cis* isomerization *trans*-$[CoCl_2pn_2]Cl$ in an anhydrous state partly remained after complete dehydration and dehydrochlorination. From the analysis of DTA curve, the enthalpy change was estimated to be -4.6 kcal/mol, and the activation energy in this step was calculated to be about 120 kcal/mol.

The relationship between mass losses and *trans/cis* ratios at various heating temperatures, obtained from the isothermal measurements with a thermobalance, are shown in Fig. 4.

From this figure, the *trans/cis* ratio at 140°C corresponding to the temperature of the first peak in the derivatogram of *trans*-complex is found to be 70 : 30. With stepwise elevation of temperature, the *trans/cis* ratio gradually increased. It should

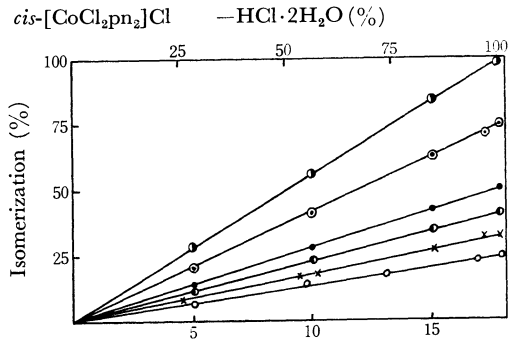

Fig. 4. The relationships between mass loss and *trans-cis* mixture ratio of various constant temperatures on *trans*-$[CoCl_2pn_2](H_5O_2)Cl_2$.
○—○: 110°C, ×—×: 130°C, ◐—◐: 140°C,
●—●: 150°C, ⊙—⊙: 160°C, ◑—◑: 170°C

be emphasized that, in other words, isomerization proceeds more slowly than dehydration and dehydrochlorination below 170°C, but it is completed as soon as dehydration and dehydrochlorination are finished above 170°C.

From the results, the rate constants for the mass loss (dehydration and dehydrochlorination), k_d, and those for the *trans-cis* isomerization, k_i, of the *trans* complex were calculated. They are listed in Table 1. At 110°C, the rate constant, k_d, is almost six times larger than that of isomerization, k_i. However, with the rise of temperature, the value of k_d gradually increases and approaches the value of k_i above 170°C.

The Arrhenius plots of the rate constants are shown in Fig. 5. The activation energies were obtained from these plots as 10 ± 2 and 23 ± 3 kcal/mol for the mass loss reaction and for isomerization, respectively. The activation energies for thermal dehydration and dehydrochlorination in this case may be considerably smaller than those in literature.[6] However, it can be accepted that the sum of the values of the activation energies for the mass loss reaction and isomerization is equal to the value 33 kcal/mol obtained from TDA analysis of the derivatogram.

Table 1. Rate constants for the mass loss k_d and isomerization k_i of *trans*-$[CoCl_2pn_2](H_5O_2)Cl_2$

Temp., °C	k_d, sec^{-1}	k_i, sec^{-1}
110	$(2.6 \pm 0.4) \times 10^{-4}$	$(4.4 \pm 0.4) \times 10^{-5}$
120	$(4.3 \pm 0.4) \times 10^{-4}$	$(1.2 \pm 0.4) \times 10^{-4}$
130	$(8.2 \pm 0.4) \times 10^{-4}$	$(1.8 \pm 0.4) \times 10^{-4}$
140	$(1.2 \pm 0.2) \times 10^{-3}$	$(3.8 \pm 0.4) \times 10^{-4}$
150	$(1.6 \pm 0.2) \times 10^{-3}$	$(7.3 \pm 0.2) \times 10^{-4}$
160	$(1.9 \pm 0.2) \times 10^{-3}$	$(1.3 \pm 0.2) \times 10^{-3}$
170	$(2.4 \pm 0.2) \times 10^{-3}$	$(2.4 \pm 0.2) \times 10^{-3}$
180	$(3.3 \pm 0.2) \times 10^{-3}$	$(3.3 \pm 0.2) \times 10^{-3}$
190	$(4.1 \pm 0.2) \times 10^{-3}$	$(4.1 \pm 0.2) \times 10^{-3}$

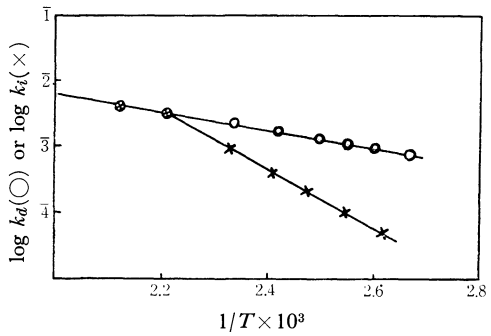

Fig. 5. The "Arrhenius plots" of k_d and k_i on *trans*-$[CoCl_2pn_2](H_5O_2)Cl_2$ in isothermal conditions by using a Shimadzu Thermobalance.
○—○: $-HCl\cdot2H_2O$ reaction $E_d^{\neq}=(10\pm2)$ kcal M^{-1}
×—×: Isomerization $E_i^{\neq}=(23\pm3)$ kcal M^{-1}.

The mechanism in the *trans*↔*cis* isomerization of the complex, $[CoCl_2en_2]Cl$, in polar solvents has been interpreted by solvation-anation reaction.[15,16] In a neutral solution, *trans*-isomer clearly changes to *cis*-isomer upon heating.[17] However, in an acidic solution, the inversed reaction occurs even at room temperature.[18] A similr isomerization has also been found with $[CoCl_2pn_2]^+$ in aqueous solution,[10] but the *trans*-complex undergoes more rapid acid hydrolysis than the corresponding en-complex under similar conditions.[8]

Isomerization with dehydration and dehydrochlorination in *trans*-$[CoCl_2pn_2](H_5O_2)Cl_2$ in the solid-phase is believed to occur by aquation-anation mechanism like that in aqueous solutions as follows:

LeMay, Jr., has found that the pn-complex shows a greater resistance to the loss of hydrogen chloride and water from the prominent (100) faces of the crystals than the corresponding en-complex.[6] Radioactive chloride-exchange studies[8] have indicated that the dehydration and dehydrochlorination of the pn-complex are accompanied by the almost complete scrambling of chloride ions in both inner and outer coordination spheres, but this is not the case for the corresponding en-complex under the same conditions. Considerable amounts of chloride ion were exchanged when the pn-complex was heated in solid phase at 120°C for 90 min in air.[8] However, in the corresponding en-complex only 1% exchange could be found upon heating at 125°C for 90 min.

Although the lack of examples for isomerization in solid-phase makes clarification of mechanism difficult, isomerization of *trans*-$[CoCl_2pn_2](H_5O_2)Cl_2$ to the *cis*-complex below 170°C might proceed through the aquation-anation pathway accelerated by the dehydration and dehydrochlorination on the faces except for (100).

All the pathways in the thermal decomposition of *trans*-$[CoCl_2pn_2](H_5O_2)Cl_2$ and the values of the thermochemical functions, ΔH and $E^{\neq}$, in each process are schematically summarized in Fig. 6.

The derivatogram for *trans*-$[CoCl_2pn_2](H_5O_2)Cl_2$ in Fig. 2 shows that the anhydrous *trans*-pn-complex remaining after dehydration and dehydrochlorination still undergoes *trans-cis* isomerization over 180°C. This indicates that the anhydrous *trans*-

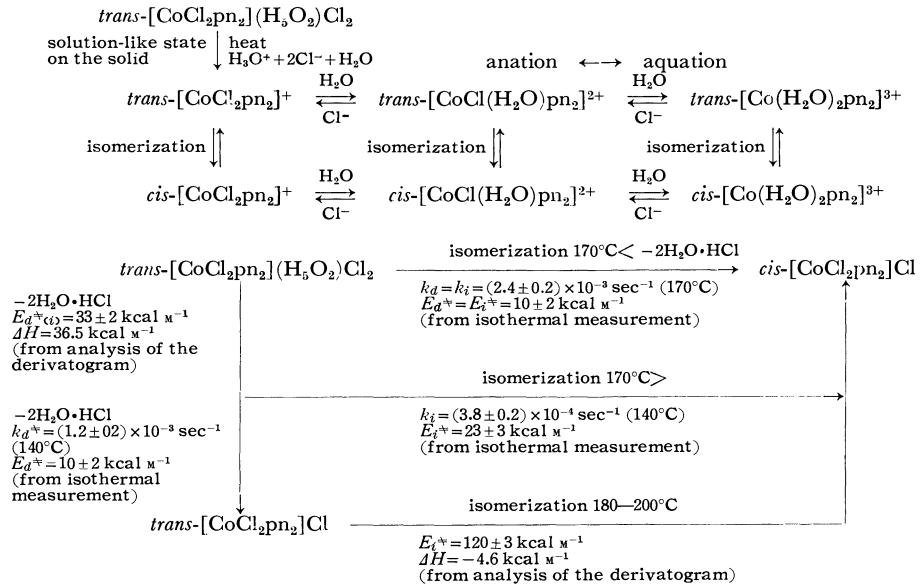

Fig. 6. Summary of results.

15) W. R. Fitzgerald and D. W. Watts, *J. Amer. Chem. Soc.*, **89**, 821 (1967).
16) M. L. Tobe and D. W. Watts, *J. Chem. Soc.*, **1964**, 2991.
17) J. C. Bailar, Jr., *J. Inorg. Nucl. Chem.*, **8**, 165 (1958).
18) S. M. Jφrgensen, *J. Prakt. Chem.*, **39**, 16 (1889).

complex is unstable and is changed to *cis*-complex. The mechanism may be explained by means of intramolecular isomerization, *e. g.*, "twisting"[17,19] or "chelate ring opening-closing"[20] because of a relatively large activation energy such as 120 kcal/mol. Although examples of activation energies calculated derivatographically on thermal *trans*↔*cis* isomerization are rare, the large value described above might be accepted as reasonable.

It should be noted that the activation energies calculated in a similar way by authors were 51.4 and 87 kcal/mol for the complexes, *cis*,*trans*-$[CoCl_2(NH_3)_2en]ClO_4$ and *trans*-$[CrBr(H_2O)(NH_3)_4]Br_2$, respectively. The details will be published elsewhere.

19) P. Pay and N. K. Dutt, *J. Indian Chem. Soc.*, **20**, 81 (1943).

20) H. D. K. Drew and N. H. Pratt, *J. Chem. Soc.*, **1937**, 506.

BULLETIN OF THE CHEMICAL SOCIETY OF JAPAN VOL. 43 1387—1389 (1970)

Studies on the Separation of Rare Earths. Determination of the Optimum Concentration of Ligand Ion Used in Electromigration

Emiko OHYOSHI

Department of Chemistry, Faculty of Science, Kumamoto University, Kumamoto

(Received September 20, 1969)

An attempt to determine the optimum concentration of ligand ion for the separation of adjacent pairs of rare earth elements by electromigration was made using the method employed for the determination of the stability constant of complex. To examine the theory, separation of lanthanum and cerium, and cerium and praseodymium was carried out using α-hydroxyisobutyric acid as a complexing agent. From the results, factors necessary for the separation of all kinds of rare earth elements were discussed.

Studies on the separation of rate earth elements by electromigration have been carried out. Successful results are obtained when α-hydroxyisobutyric acid[1-3] is used as a complexing agent. In most cases, however, the conditions for the separation are arbitrary.

In recent years, the theory of electromigration of metal and complex ions derived by Kiso[4] was applied to the separation of rare earth elements and justified experimentally.[5] Shvedov and Stepanov[6] proposed the method of determination of the stability constant of complex by electromigration. The results obtained were in good agreement with those by potentiometry.

In order to find the optimum condition for the separation based on the difference in the stability of complex of two elements, it is most important to choose a suitable concentration of ligand ion depending on the stability of complexes to be formed. In the present investigation, it is intended to determine the optimum concentration of ligand ion for the separation of rare earth elements using the method proposed by Shvedov and Stepanov which is simpler than that by Kiso. Factors affecting the separation are also discussed.

Determination of the Optimum Concentration of Ligand Ion. When a metal, M, forms a complex, ML, in solution the following equilibrium may be established (the charges are omitted for simplicity):

$$M + L = ML \quad (1)$$

The equilibrium constant of process (1), *i.e.*, stability constant, is expressed by

$$K = \frac{[ML]}{[M][L]} \quad (2)$$

According to Shvedov and Stepanov, when an electric field is applied to such solution, the over all migration of a metal can be expressed as the sum of two components one of which governs the

1) K. Buchtela, K. Aitzetmuller and F. Grass, *Atomkernenergie*, **10**, 264 (1965).

2) K. Aitzetmuller, K. Buchtela and F. Grass, *J. Chromatog.*, **22**, 431 (1966).

3) K. Aitzetmuller, K. Buchtela and F. Grass, *Anal. Chim. Acta*, **38**, 249 (1967).

4) Y. Kiso, *J. Sci. Hiroshima Univ.*, **27**, No. 1, 17 (1963).

5) Y. Kiso, I. Yamada, Y. Yamamoto and M. Shinagawa, This Bulletin, **38**, 695 (1965).

6) V. P. Shvedov and A. V. Stepanov, *Radiokhimiya*, **1**, No. 2, 62 (1959).

transfer in the form of metal ions and the other the transfer in the complex form.

$$u([M]+[ML]) = u_M[M] + u_{ML}[ML] \quad (3)$$

where u, u_M and u_{ML} are the mobilities of zone, of metal ion and of complex ion, respectively. Equation (3) can be brought into the form

$$[ML]/[M] = (u-u_M)/(u_{ML}-u) = K[L] \quad (4)$$

From Eq. (4), Shvedov and Stepanov determined the stability constant of the complex ML with measurements of u_M, u_{ML} and u. By rearrangement of Eq. (4), the zone mobility u is given as follows.

$$u = \frac{u_{ML}K[L] + u_M}{1 + K[L]} \quad (5)$$

To separate M_1 from M_2, in the first case where $u_{ML}>0$, *e.g.*, α-hydroxyisobutyric acid, lactic acid, *etc.*, the ratio of zone mobility of each metal u_1/u_2 can be taken as the separation factor S. Hence, it is important to find the condition under which S takes the maximum value. In the case of rare earth elements, the difference in mobility of metal or complex ions of two kinds of element is neglected. Thus we have

$$S = \frac{u_1}{u_2} = \frac{(1+K_2[L])(K_1[L]+u_M/u_{ML})}{(1+K_1[L])(K_2[L]+u_M/u_{ML})} \quad (6)$$

Differentiating with respect to [L], we get

$$\frac{dS}{d[L]} = \frac{(1-u_{ML}/u_M)(K_2-K_1)(1-u_{ML}/u_MK_1K_2[L]^2)}{\{(u_{ML}/u_MK_2[L]+1)(1+K_1[L])\}^2} \quad (7)$$

In the case of $K_2>K_1$, with an increase in [L], S increases and reaches maximum at $dS/d[L]=0$, and then decreases. At $dS/d[L]=0$, we have

$$[L] = \left(\frac{u_M/u_{ML}}{K_1K_2}\right)^{1/2} \quad (8)$$

S takes the maximum value. It can be seen that this concentration of ligand ion is the optimum one for separating M_1 from M_2.

In the second case, $u_{ML}\leqq 0$, *e.g.*, EDTA, NTA, *etc.*, S should be taken as the difference in the zone mobility of two metals. Thus we get

$$S = u_1-u_2 = \frac{u_{ML}K_1[L] + u_M}{1 + K_1[L]} - \frac{u_{ML}K_2[L] + u_M}{1 + K_2[L]} \quad (9)$$

Differentiation of this equation with respect to [L] leads to the expression

$$\frac{dS}{d[L]} = \frac{(u_M-u_{ML})(K_2-K_1)(1-K_1K_2[L]^2)}{\{(1+K_1[L])(1+K_2[L])\}^2} \quad (10)$$

At $dS/d[L]=0$, we obtain

$$[L] = \{1/(K_1K_2)\}^{1/2} \quad (11)$$

S becomes the maximum.

Comparing the two cases, $u_{ML}>0$ and $u_{ML}\leqq 0$, the optimum concentration of ligand ion in the former case is larger than that in the latter (since $u_M/u_{ML}>1$).

Experimental

Materials. Oxides of lanthanum (Mitsuwa Chemical Co. 99.99%) and praseodymium (Katayama Chemical Industries Co., Ltd. 99.9%) were dissolved in nitric acid. The solution of cerium was prepared by heating $Ce(NO_3)_3\cdot 6H_2O$ (Katayama Chemical Industries Co., Ltd. G. R. grade) with hydrogen peroxide in hydrochloric acid. Mixtures of lanthanum and cerium, and cerium and praseodymium at the same concentration of 10^{-3}M were used as samples. α-Hydroxyisobutyric acid (Tokyo Chemical Industry Co., Ltd. G. R. grade) in varying concentration at the constant ionic strength of 0.1 was used as electrolyte solution.

Procedures. A paper strip (Toyo Roshi No. 50 1×20 cm) was uniformly soaked in the electrolyte solution, and excess solution was removed by pressing between sheets of filter paper. The sample (0.005 m*l*) was then spotted at a point 6.5 cm from the end of the anodic side. The paper was set into a migration cell containing carbon tetrachloride as coolant. A potential gradient of 500 V(D.C.)/16 cm was applied for 15—25 min. After the current was switched off, the paper was dried rapidly under an infrared lamp. The migrating zone was detected by color reaction with Arsenazo III.

Results and Discussion

Measurements of u_M and u_{ML}. Equation (5) can be brought into the form

$$u = \frac{1}{K[L] + 1}(u_M-u_{ML}) + u_{ML} \quad (12)$$

Hence, the values of u_M and u_{ML} are obtained from the intercept and the slope of a plot of u *vs.* $1/(K[L]+1)$. Figure 1 gives the linear relationship of u to $1/(K[L]+1)$ for lanthanum and cerium using α-hydroxyisobutyric acid, where K[7] is the stability constant of complex LaL or CeL. The concentration of α-hydroxyisobutyrate ion [L] was

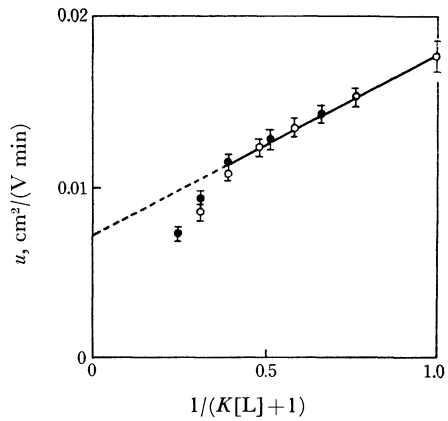

Fig. 1. A plot of u *vs.* $1/(K[L]+1)$ for La ○ and Ce ●.
L=α-hydroxyisobutyrate

7) W. R. Stagg and J. E. Powell, *Inorg. Chem.*, **3**, 242 (1964).

calculated from the equation $[L^-]=k_a([HL]_t-[L^-])/[H^+]$, where k_a is the dissociation constant of α-hydroxyisobutyric acid[8] and $[HL]_t$ is the total concentration of α-hydroxyisobutyrate. The deviation of the points from the linearity at high concentration of ligand suggests that the complexes formed are not only ML but also ML_2, ML_3,$\cdots ML_n$ with the increase of concentration of ligand ion. This also accounts for the fact that the zone mobilities of lanthanum are smaller than those of cerium at the same value of $1/(K[L]+1)$ in the range of high concentration of ligand ion (since the value of $k_{1(Ce)}/k_{1(La)}$ is larger than that of $k_{2(Ce)}/k_{2(La)}$, where k_1 and k_2 are the consecutive constants of complexes ML and ML_2). By extrapolation of the straight line in Fig. 1, u_M and u_{ML} are given as 0.0175 and 0.0070 cm^2/V min, respectively.

Separation of Lanthanum and Cerium, and Cerium and Praseodymium. From the values of u_M and u_{ML}, the optimum concentration of ligand ion for the separation of two kinds of rare earth elements can be calculated by Eq. (8). For example, the values for separation of lanthanum and cerium, and cerium and praseodymium are given as $(u_M/(u_{ML}k_{1(La)}k_{1(Ce)}))^{1/2}=8.04\times10^{-3}$M and $(u_M/(u_{ML}k_{1(Ce)}k_{1(Pr)}))^{1/2}=5.95\times10^{-3}$M. In the vicinity of these values of ligand concentration, the separation of lanthanum and cerium, and cerium and praseodynium was carried out to examine the theory. Figure 2 gives the separation factor S, the ratio of the zone mobility for two elements observed and calculated from Eq. (6) as a function of the concentration of ligand ion. It is found that the separation factor for the La–Ce pair is larger than that for the Ce–Pr pair at any concentration of ligand ion, indicating that the greater the difference of stability of the complex of two kinds of elements, the greater the effect on their separation. It is noted that at low concentration of ligand ion, both observed and calculated S values are close while with the increase of ligand concentration, a discrepancy between them becomes apparent, that is, the observed values do not decrease even after passing beyond the optimum concentration of ligand ion. The consecutive formation of complexes ML_2, ML_3,$\cdots ML_n$, might proceed with the increase of ligand concentration, though the calculated value from Eq. (6) is assumed to form only one complex ML. Thus, it can be seen that the formation of various complexes by the consecutive reaction makes the range of optimum concentration of ligand wider than cases in which only one kind of complex is possible. From this, the factor affecting the separation is not only the difference in the stability of complex but also the possibility to proceed a consecutive formation of complexes.

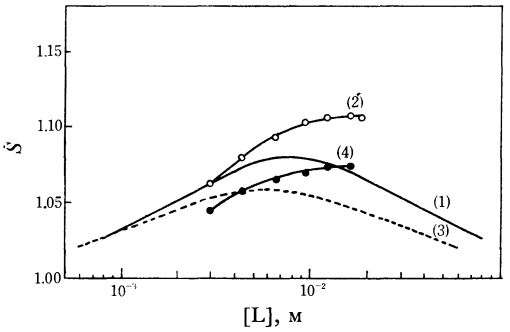

Fig. 2. The separation factor S calculated and observed for La–Ce and Ce–Pr as a function of ligand concentration. (1) calculated, (2) observed for La–Ce; (3) calculated, (4) observed for Ce–Pr.
L=α-hydroxyisobutyrate

In particular, in order to separate all kinds of rare earth elements, it is important to know whether consecutive formation of complexes is taking place or not. If only one complex ML can be formed, the ligand concentration optimum for a pair of light rare earths may greatly differ from that for a pair of heavy rare earths. For example, using the concentration of ligand ion suitable to separate light rare earths, heavy members can not be separated because of the complete formation of complex ML. On the other hand, the concentration suitable to separate the heavy members is so low that the light members remain almost as metal ions. In the case of the consecutive formation of complexes ML, ML_2, $\cdots$ ML_n, as illustrated in Fig. 2, the range of the ligand concentration suitable to separate an adjacent pair is extended toward the higher side because further transformation of ML to ML_2 or of ML_2 to ML_3 gives a different zone mobility to the respective element. Since this extension of the range is observed for any pair of adjacent elements it is probably that a higher part of the range for the last pair of the series (Yb–Lu) and a lower part of that for the first pair (La–Ce) overlap each other. Hence, choosing the ligand concentration at the position of overlapping, it is possible to separate all kinds of rare earths.

Thus, it seems reasonable that the use of α-hydroxyisobutyric acid for the separation of all rare earths gives more successful results as compared with EDTA.

8) J. E. Powell and Y. Suzuki, *Inorg. Chem.* **3**, 690 (1964).

BULLETIN OF THE CHEMICAL SOCIETY OF JAPAN VOL. 43 1390—1393 (1970)

Activity Measurements in Orthosilicate and Metasilicate Solid Solutions. II. $MgSiO_3$-$FeSiO_3$ at 1154, 1204, and 1250°C

Kenzo KITAYAMA

Department of Chemistry, Tokyo Institute of Technology, Ookayama, Meguro-ku, Tokyo

(Received October 18, 1969)

The activity-composition relation in the pyroxene solid solution, $MgSiO_3$–$FeSiO_3$, is determined by the quenching method in the atmosphere of a gas mixture of CO_2 and H_2 at 1154, 1204, and 1250°C. A non-ideality is found in the solution at these temperatures, and it increases with a decrease in the temperature. The standard free energy values of the formation of ferrosilite, $FeSiO_3$, from metallic iron, silica, and oxygen are -42.5 ± 0.3, -41.7 ± 0.2, and -41.3 ± 0.2 kcal per mole of $FeSiO_3$ at 1154, 1204, and 1250°C respectively. Using the data by Darken and Gurry, the standard free energies of the formation of ferrosilite from wüstite and silica are obtained as -1.8 ± 0.3, -1.5 ± 0.2, and -1.8 ± 0.2 kcal per mole of $FeSiO_3$ at 1154, 1204, 1250°C respectively.

In the previous paper[1] it was concluded that both olivine, Mg_2SiO_4–Fe_2SiO_4, and pyroxene, $MgSiO_3$–$FeSiO_3$, solid solutions showed significant deviations from ideality at 1204°C. The non-ideality in the olivine solid solution was also recognized by Nafziger and Muan,[2] but their results on the pyroxene solid solution are very different from ours; they found the pyroxene solid solution to be practically ideal in its activity-composition relation, though their data were from an experiment at 1250°C and the difference in temperature may have caused the difference in the deviations from ideality. The objectives of the present paper are to find the activity-composition relation in the pyroxene solid solution, to determine the standard free energy change in the formation of ferrosilite, and to confirm whether or not the deviations from ideality in the activity of $FeSiO_3$ in the pyroxene solid solution depend on the temperature. As has been described above, we have already reported data at 1204°C but the samples used in the present experiment are newly prepared by adding some silicon oxide to the previous samples in order to position, in the two-phase region, the silica+pyroxene solid solution. Therefore, the same experiment was repeated in order to check the first results.

Method of the Calculation of the Activity. The method of the calculation of the activity of the pyroxene solid solution has been described in the previous paper.[1] The activity of the $FeSiO_3$ in the pyroxene solid solution is represented by Eq. (1):

$$a_{(FeSiO_3)_{ss}} = (P_{O_2}/P_{O_2}^*)^{1/2} \quad (1)$$

The subscript ss means a solid solution. The P_{O_2} in Eq. (1) represents the oxygen partial pressures of the decomposition of pyroxene solid-solution samples with various compositions, and the equation:

$$(FeSiO_3)_{ss} = Fe + SiO_2 + \tfrac{1}{2}O_2 \quad (2)$$

indicates the corresponding chemical reaction. The $P_{O_2}^*$, which is used as the standard oxygen partial pressure, is the oxygen partial pressure corresponding to the reaction (2) of a pure ferrosilite that does not exist at ordinary temperatures and pressures but which is obtained at each temperature by extrapolating, by means of the α-function method, to $(1-N_{FeSiO_3})^2=0$ (Fig. 1).

Experimental

Preparation of Samples. The pyroxene solid solutions were prepared by the method of the previous paper.[1] It is very difficult to prepare one-phase samples with the desined composition. If the samples prepared had a lower silica content than that of the expected one-phase composition, the total composition of the samples would lie in the two-phase area of pyroxene and olivine solid solutions. Therefore, such samples must give a large oxygen partial pressure corresponding to the olivine solid solution. To avoid problems like this, the samples which contained excess silica were prepared.[3] The samples thus prepared were confirmed to be in the two-phase area, to be, that is, silica and pyroxene solid solution, by a chemical analysis of the iron and magnesium contents and by the use of an X-ray diffractometer. Excess silica does not participate the reaction (2), as can be seen from the phase diagram in the previous paper.[1] Table 1 shows the analytical values of the samples used in the present experiment in

1) K. Kitayama and T. Katsura, This Bulletin, **41**, 1146 (1968).

2) R. H. Nafziger and A. Muan, *Amer. Mineral.*, **52**, 1364 (1968).

3) K. Kitayama and T. Katsura, This Bulletin, **41**, 525 (1968).

Table 1. Analytical data of samples (mol%)

Sample No.	$N^*_{FeSiO_3}$	FeO	MgO	SiO_2
1	0.100	4.7	41.1	54.2
2	0.206	9.4	35.6	55.0
3	0.301	13.4	31.0	55.6
4	0.401	18.0	26.7	55.3
5	0.497	22.0	22.4	55.6
6	0.599	26.9	18.0	55.1

* The compositions of pyroxene solid solution are determined by the same method as in the case of Table 2.

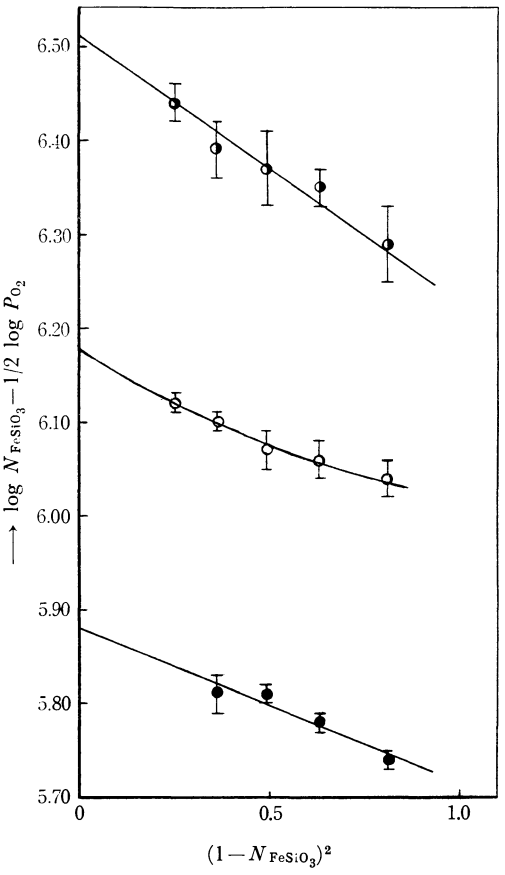

Fig. 1. Relationship between ($\log N_{FeSiO_3} - 1/2 \log P_{O_2}$) and $(1-N_{FeSiO_3})^2$ at 1154, 1204, and 1250°C.
◑ 1154°C ○ 1204°C ● 1250°C

mole percentages. The iron(II) was volumetrically determined with potassium permanganate, while the total iron was determined colorimetrically with α,α′-dipyridyl. The magnesium contents were gravimetrically determined by precipitating it as magnesium ammonium phosphate.

Apparatus. The vertical-type furnace, gas mixer, and other pieces of equipment were the same as those used in a previous paper.[4] Mixed gases of CO_2 and H_2 were used to obtain low oxygen partial pressures in the present experiment.

4) T. Katsura and S. Kimura, *ibid.*, **38**, 1664 (1965).

Table 2. Results of equilibrium experiments at 1154, 1204, and 1250°C

	N_{FeSiO_3}	$-\log P_{O_2}$	a_{FeSiO_3}	$\log N_{FeSiO_3} - 1/2 \log P_{O_2}$
1154°C	0.100Fs	14.57±0.07	0.17±0.03	6.29±0.04
	0.206	14.07±0.03	0.30±0.05	6.35±0.02
	0.301	13.78±0.08	0.42±0.07	6.37±0.04
	0.401	13.58±0.06	0.53±0.09	6.39±0.03
	0.497*	13.48±0.04	0.60±0.11	6.44±0.02
	0.599*	13.48±0.04		
1204°C	0.100	14.08±0.04	0.13±0.02	6.04±0.02
	0.206	13.49±0.03	0.27±0.02	6.06±0.02
	0.301	13.18±0.03	0.38±0.04	6.07±0.02
	0.401	12.97±0.02	0.49±0.03	6.10±0.01
	0.497	12.83±0.02	0.58±0.04	6.12±0.01
	0.599*	12.70±0.02		
1250°C	0.100	13.49±0.01	0.13±0.01	5.74±0.01
	0.206	12.94±0.02	0.26±0.01	5.78±0.01
	0.301	12.66±0.02	0.35±0.02	5.81±0.01
	0.401	12.42±0.03	0.47±0.03	5.81±0.02

* These values are determined assuming total composition were in the two-phases area as in the case of other samples.

Procedure. Mixed gases with various ratios of CO_2 and H_2 are introduced from the bottom to the top of the furnace tube. Then the samples are suspended by thin platinum wires at a definite position in the furnace controlled at the expected temperature. After 24 hr the suspended sample is quenched and a formation of iron metal corresponding to the reaction (2) is confirmed by dipping the sample into dilute hydrochloric acid. The details of the procedure are the same as those of the previous paper.[1] After determining the hydrogen-to-carbon dioxide ratio corresponding to that of the (2) reaction, the oxygen partial pressure is immediately measured by means of a solid electrolyte cell.[5]

Results and Discussion

The experimental results are listed in Table 2. In the second column, the compositions of the pyroxene solid solution are shown. It is found that the chemical compositions (Table 1) of the samples are in the two-phase area (SiO_2+pyroxene solid solution) of the phase diagram of the previous paper (Fig. 1).[1] Tie lines can then be drawn so as to pass through points of the sample composition in the two-phase area to the SiO_2 apex. The intersections of the tie lines and the pyroxene solid-solution line show the composition of the pyroxene solid solution. In the third column, the oxygen partial pressures corresponding to that of the reaction (2) are listed. The activities calculated with Eq. (1) are shown in the fourth column. The

5) T. Katsura and M. Hasegawa, *ibid.*, **40**, 561 (1967).

oxygen partial pressures of 0.599 Fs and 0.497 Fs samples at 1154°C have the same value. This fact suggests that the total compositions of both the samples may be situated within the three-phase area (SiO_2+pyroxene solid solution+olivine solid solution) at 1154°C. The data at 1204 and 1250°C are also shown in Table 2. At 1204°C the oxygen partial pressure of 0.599 Fs is different from that of 0.497 Fs. Therefore, the 0.497 Fs sample seems to be positioned in the two-phase area, while the 0.599 Fs sample in the three-phase area. Judging from the experimental results, the composition of 0.497 Fs seems to be near the boundary between the two- and three-phase areas. Moreover, the results presented above show that the boundary line between two- and three-phase areas must move toward the iron-rich side in the present subsolidus condition with an increase in the temperature. This result is in great contrast to those of Nafziger and Muan[2] and of Bowen and Schairer.[6]

In Fig. 1 the relationship between ($\log N_{FeSiO_3} - 1/2 \log P_{O_2}$) and $(1-N_{FeSiO_3})^2$ is shown at 1154, 1204, and 1250°C. Errors are given as the deviates of the results of three experiments. It may be concluded from Fig. 1 that α[1] is not zero, but 0.28, at 1154°C, that is, the pyroxene solid solution deviatives slightly from ideality. Extrapolating graphically to $(1-N_{FeSiO_3})^2=0$, $\log P_{O_2}=-13.03\pm 0.08$ atm is obtained as the value of the oxygen partial pressure of pure ferrosilite, corresponding to Eq. (2) at 1154°C. By substituting this value into the equation:

$$\Delta G^0 = 1/2RT \ln P_{O_2} \qquad (3)$$

-42.5 ± 0.3 kcal per mole is obtained as the standard free energy change of the formation of ferrosilite at 1154°C. The same relationships are shown at both 1204 and 1250°C. The values of 0.22 at 1204°C and 0.17 at 1250°C are obtained as the α values. They are smaller than that at 1154°C. That is, the higher the temperature becomes, the more ideal is the activity-composition relation. Nafziger and Muan's data show that α is nearly parallel to the abscissa at 1250°C. The present results show non-ideality even at 1250°C. The extrapolated values of $\log P_{O_2}$ for pure ferrosilite are determined to be -12.35 ± 0.04 and -11.76 ± 0.02 atm at 1204 and 1250°C respectively.

The $\log P_{O_2}$ value at 1204°C is in good agreement with the our previous result, -12.35 ± 0.03.[1]

It gives the standard free energy changes of the formation as -41.7 ± 0.2 and -41.3 ± 0.2 kcal/mol respectively. Those values are shown in Table 3 together with a previously determined value. At 1250°C Nafziger and Muan[2] reported -40.6 kcal/mol as the standard free energy change of the formation of ferrosilite. By combining the standard free energy change of the formation of ferrosilite corresponding to Eq. (2) with the value of that of wüstite obtained by Darken and Gurry,[7] the free energy changes of the formation of ferrosilite from wüstite and silica, followed by the reaction:

$$\text{"FeO"} + SiO_2 = FeSiO_3 \qquad (4)$$

are determined to be -1.8 ± 0.3, -1.5 ± 0.2, and -1.8 ± 0.2 kcal per mole at 1154, 1204, and 1250°C respectively. In the calculation of P_{CO_2}/P_{CO} ratios in Darken and Gurry's data to the oxygen partial pressure, the thermochemical data of Elliot and Gleiser[8] are used. The previous values relating to Eq. (4) are summarized in Table 4, together with the above present values. As may be seen from Table 4, the present values agree very well with the values of Akimoto *et al.*,[9] but they are smaller than those of the others. The relationship between the activity and the mole fraction of $FeSiO_3$ are represented in Fig. 2. As is shown in Fig. 2, and as can be expected from Fig. 1, the non-ideality is the largest at 1154°C, but the differences in the other values are small. It is also shown in Fig. 2 that nonideality increases with

Table 3. Results for the standard free energy change of formation of ferrosilite from iron, silica, and oxygen together with previous value

Temperature (°C)	ΔG° (kcal/mol)	
	Present values	Previous value
1154	-42.5 ± 0.3	
1204	-41.7 ± 0.2	
1250	-41.3 ± 0.2	-40.6[2]

Table 4. Present values for the standard free energy change of formation of ferrosilite from wüstite and silica together with previous values

Temperature (°C)	ΔG° (kcal/mol)	
	Present values	Previous values
1080		-1.1[12]
1150		-1.3 ± 0.3[11]
1154	-1.8 ± 0.3	-1.5[9]
1204	-1.5 ± 0.2	-1.4[9]
1250	-1.8 ± 0.2	-0.9 ± 0.5[2], -1.6[9]
1300		-1[a]

a) A. Muan, R. H. Nafziger and P. L. Roeder, *Nature*, **202**, 688 (1964).

6) N. L. Bowen and J. F. Schairer, *Amer. J. Sci.*, **29**, 151 (1935).

7) L. S. Darken and R. W. Gurry, *J. Amer. Chem. Soc.*, **67**, 1398 (1945).

8) J. E. Elliot and M. Gleiser, "Thermochemistry for Steelmaking," Addison-Wesley Pub. Co., Mass., U.S.A. (1960).

9) S. Akimoto, T. Katsura, Y. Syono, H. Fujisawa and E. Komada, *J. Geophy. Res.*, **70**, 5269 (1965).

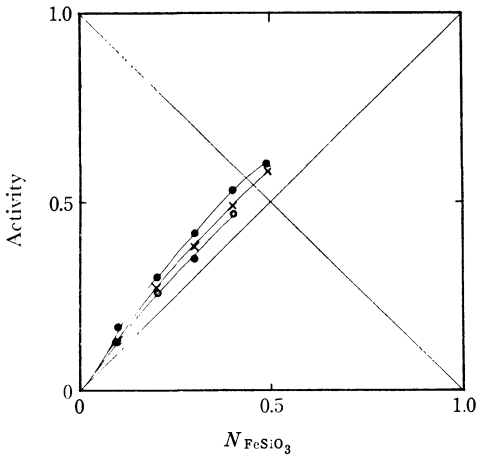

Fig. 2. Activity-composition relations in pyroxene solid solution at 1154, 1204, and 1250°C.
○ 1250°C × 1204°C ● 1154°C

a decrease in the temperature.

The variations in the activity with the temperature in other system have been reported by many investigator. In the MgO - FeO system[10] no apparent difference in activity between at 1100 and 1300°C is found. Aukrust and Muan[11] studied the activity-composition relations in the Co_3O_4-Mn_3O_4 system and did not find any differences in the activity in the 1100—1400°C temperature range.

Three metasilicate solid solutions, the Ca - Fe system[12] at 1080°C, the Mn - Co system[13] at from 1200 to 1250°C, and the Fe - Mn system[14] at 1154°C, are all ideal in their activity-composition relation, differing from the results obtained in the present experiment. In Fig. 3 the relation between the oxygen partial pressures of the formation of ferrosilite and the temperatures are shown. The abscissa represents a reciprocal of the absolute temperature. The log P_{O_2} is related to the standard free-energy change in the formation by the equation:

$$\Delta G^0 = 1/2RT \ln P_{O_2} = \Delta H^0 - T\Delta S^0 \quad (5)$$

Therefore, the gradient of the line in Fig. 3 indicates the $2\ \Delta H^0/R$ of the ferrosilite formation in the present experimental temperature ranges. The data for the fayalite formation:

$$2Fe + SiO_2 + O_2 = Fe_2SiO_4 \quad (6)$$

have already been reported.[3] The values are plotted in Fig. 3, as open circles, together with

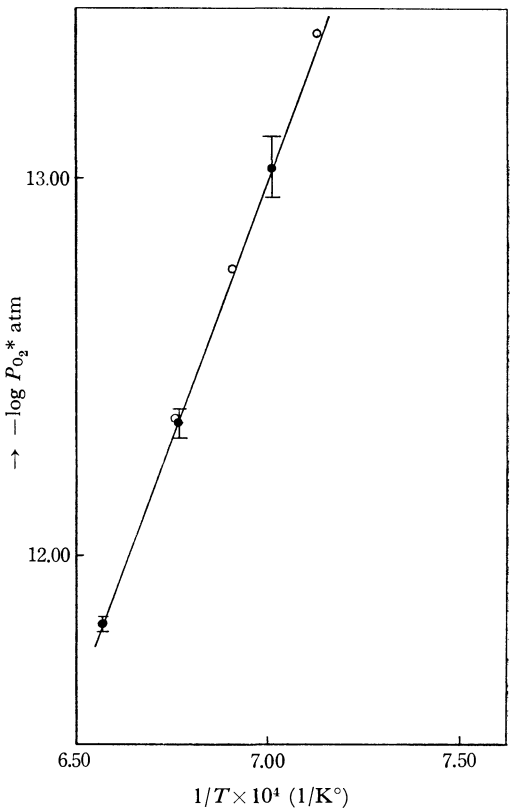

Fig. 3. Relationship between log P_{O_2}* and $1/T$ (K°)
○ $2Fe+SiO_2+O_2=Fe_2SiO_4$
● $Fe+SiO_2+\frac{1}{2}O_2=FeSiO_3$

the present ferrosilite results. The data for fayalite are plotted on just the present temperature-oxygen partial pressure line. That is, oxygen partial pressures of Eq. (2) for pure ferrosilite and Eq. (6) for fayalite are nearly equal. Strictly speaking, the oxygen partial pressure of the ferrosilite decomposition, shown in Eq. (2), should be lower than that of fayalite. The correspondence of the oxygen partial pressures in the two reaction may be due to the experimental technique. The difference is, however, so small that it can not be detected, and it may be due to the extrapolation done with the present, insufficient data. As has been described above, the difference in the changes in the free energy of formation is merely that of the factors of oxygen in the two equations. Therefore, the standard free-energy change in the formation of the ferrosilite must be one-half of that of fayalite.

The author wishes to express his hearty thanks to Dr. Takashi Katsura for encouraging him throughout the study, to Mr. Hiroshi Haramura to his kind chemical analysis of the samples, and to Dr. Yoshito Matsui to his kind discussion of the previous paper.

10) W.C. Hahn, Jr., and A. Muan, *Trans. Met. Soc. AIME (Amer. Inst. Minig., Met., Eng.)*, **224**, 416 (1962).
11) E. Aukrust and A. Muan, *ibid.*, **230**, 378 (1964).
12) R. E. Johnson and A. Muan, *ibid.*, **239**, 1931 (1967).
13) J. V. Biggers and A. Muan, *J. Amer. Chem. Soc.*, **50**, 230 (1967).
14) K. Schwerdtfeger and A. Muan, *Trans. Met. Soc. AIME (Amer. Inst. Mining, Met., Eng.)*, **236**, 201 (1966).

BULLETIN OF THE CHEMICAL SOCIETY OF JAPAN VOL. 43 1394—1397 (1970)

Bis-Type Cobalt(III) and Chromium(III) Complexes with Related Compounds of Iminodiacetic Acid*1

Akira UEHARA, Eishin KYUNO and Ryokichi TSUCHIYA

Department of Chemistry, Faculty of Science, Kanazawa University, Kanazawa

(Received November 11, 1969)

The geometrical structures and some properties of the following complexes were investigated: $K[Co(ida)_2]\cdot H_2O$ (I), $K[Co(ida)_2]\cdot 2H_2O$ (II), $K[Cr(ida)_2]\cdot 3H_2O$ (III), $Ba[Cr(ida)_2]_2\cdot 6H_2O$ (IV), $K[Co(mda)_2]$ (V), $K[Cr(mda)_2]$ (VI), $K[Co(eda)_2]\cdot H_2O$ (VII) and $K[Cr(eda)_2]\cdot H_2O$ (VIII), where ida, mda and eda are the abbreviations of iminodiacetate, methyliminodiacetate and ethyliminodiacetate ions, respectively. IV, VII and VIII are new compounds. On the basis of electronic spectra, it was found that VII and VIII have the *trans* form with respect to nitrogen atoms in the ligands, and IV, the *cis* form. Comparison of the properties and structures of the cobalt(III) complexes with those of the corresponding chromium(III) complexes were also made.

Although the stability constants[1,2] of the metal complexes with iminodiacetic acid(IDA) have been reported, no fundamental discussion on the coordinating structures, especially on geometrical isomerism, has been given, except for a few recent, preliminary works on the analysis of the isomerism of cobalt(III) and chromium(III) complexes with IDA or its derivative as methyliminodiacetic acid (MDA).[3-6]

There are three, geometrically possible isomers in the bis-type complexes with these ligands, their structures being depicted as (A), (B) and (C) in Fig. 1. So far as cobalt(III)-IDA complexes are concerned, the so-called "brown complex" was expected to have either (A) (*trans-fac*) or (B) (*trans-mer*),[4] whereas the "violet complex" was obviously assigned to have (C) structure (*cis-fac*).[3,4] On the other hand, a structural analysis of the complex species such as $[Co(ida)(dien)]^+$ (dien: diethylenetriamine) indicated that IDA prefers the *facial* to the *meridional* configuration.[5] The other works with respect to such configuration also supported the finding that (A) is more stable than (B) because of the more favorable angle ∠C–N–C in (A) than that in (B).[4,6]

Among chromium(III) complexes, $K[Cr(ida)_2]$ has been synthesized,[7,8] and is presumed to have the *cis* configuration (C) on the basis of its spectroscopic results.[9] The bis-type complexes of cobalt(III) and chromium(III) with MDA have also been reported,[5,6,9] where only the *trans-fac* configuration (A in Fig. 1) was assumed. The results that IDA can coordinate either in *cis* or *trans* form, but MDA can not coordinate in *cis* form suggest the presence of some steric hindrance between two methyl groups attached to nitorgen atoms in *cis* isomer.[5,6]

The present work was undertaken (1) to prepare

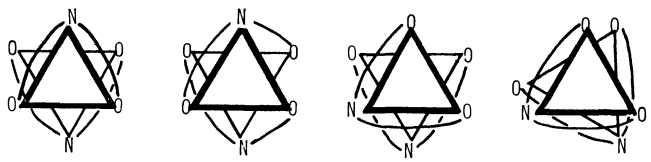

(A) *trans-fac* (B) *trans-mer* (C) *cis* (D) distorted *cis*

Fig. 1. Possible structures.

*1 Presented at the 19th Symposium on Coordination Compounds, Sendai, September, 1969.

1) G. Schwarzenbach, B. Kamptisch and R. Steiner, *Helv. Chim. Acta*, **28**, 1183 (1945).

2) S. Chaberek, Jr., and A. E. Martell, *J. Amer. Chem. Soc.*, **74**, 5052 (1952).

3) M. Mori, M. Shibata, E. Kyuno and F. Maruyama, This Bulletin, **35**, 75 (1962).

4) J. Hidaka, Y. Shimura and R. Tsuchida, *ibid.*, **35**, 567 (1962).

5) J. I. Legg and D. W. Cooke, *Inorg. Chem.*, **5**, 594 (1966).

6) D. W. Cooke, *ibid.*, **5**, 1141 (1966).

7) H. Mizuochi, S. Shirakata, E. Kyuno and R. Tsuchiya, This Bulletin, **43**, 397 (1970).

8) K. Yamasaki and S. Ito, *Proc. Japan. Acad.*, **42**, 1077 (1966).

9) J. A. Weyh and R. E. Hamm, *Inorg. Chem.*, **7**, 2431 (1968).

the bis-type complexes of cobalt(III) and chromium (III) with IDA, MDA or the alternative derivative as ethyliminodiacetic acid (EDA), and (2) to investigate systematically the coordinating structures and the properties of the complexes with the above three ligands.

Experimental

Preparation of Chelating Agents. *Methyliminodiacetic Acid.* $CH_3N(CH_2COOH)_2$. 190 g of monochloroacetic acid was dissolved in 300 m*l* of water, and the solution was neutralized by adding slowly 200 g of potassium hydrogen carbonate little by little. To this solution, 75 g of 40% methylamine solution was added, and the resulting solution was heated up to 50°C on a water bath. 200 m*l* of aqueous solution containing 110 g of potassium hydroxide was poured into the warm solution, and a violent reaction took place. Heating was continued for one hour to complete the reaction. After the solution was stood for a while at room temperature, 100 m*l* of concentrated hydrochloric acid was gradually added. At pH 3.5, the wall of the reaction vessel was scrubbed with a glass rod, and white powdered crystals were obtained. Recrystallization was carried out from water. Yield 67 g.

Found: N, 9.83; C, 40.63; H, 6.18%. Calcd for $C_5H_9O_4N$: N, 9.52; C, 40.81; H, 6.21%.

Ethyliminodiacetic Acid. $C_2H_5N(CH_2COOH)_2$. To 300 m*l* of aqueous solution containing 190 g of monochloroacetic acid, 200 g of potassium hydrogen carbonate was gradually added. 65 g of 70% ethylamine solution was added, and then the solution was heated up to 50°C on a water bath. As 200 m*l* of 50% potassium hydroxide solution was dropped little by little, the reaction gradually proceeded. After the solution was stood at room temperature, 100 m*l* of concentrated hydrochloric acid was added. The solution was gradually concentrated by evaporating on a water bath, and then the deposited potassium chloride was filtered off. The filtrate was concentrated to about 300 m*l*. From the solution stored in a refrigerator, white powdered crystals were obtained. Recrystallization was achieved from water. Yield about 60 g.

Found: N, 8.53; C, 44.36; H, 6.21%. Calcd for $C_6H_{11}O_4N$: N, 8.69; C, 44.63; H, 6.38%.

Iminodiacetic Acid. Special grade reagent of Wako Pure Chemical Co. was used.

Preparation of Complexes. 1) *trans-Potassium Bis-(iminodiacetato)cobaltate(III) Monohydrate, trans*-$K[Co(ida)_2]\cdot H_2O$ (I). The compound was prepared by the method as described in literature.[4]

2) *cis-Potassium Bis-(iminodiacetato)cobaltate(III) Dihydrate, cis*-$K[Co(ida)_2]\cdot 2H_2O$ (II). The preparation was carried out following the procedure given in literature.[3,4]

3) *Potassium Bis-(iminodiacetato)chromate(III) Trihydrate*, $K[Cr(ida)_2]\cdot 3H_2O$ (III). This was prepared by a method similar to that outlined in literature.[7,8]

4) *Barium Bis-(iminodiacetato)chromate(III) Hexahydrate*, $Ba[Cr(ida)_2]_2\cdot 6H_2O$ (IV). To 200 ml of aqueous solution containing 5 g of chromium(III) chloride hexahydrate, 5 g of iminodiacetic acid was added, and then 6.8 g of barium hydroxide octahydrate was added little by little under stirring. The mixed solution was evaporated on a water bath for one hour (to approximately 100 m*l*). After cooling, red needle-like crystals were obtained. The products were recrystallized from water.

Found: N, 6.32; C, 21.38; H, 3.49%. Calcd for $Ba[Cr(ida)_2]_2\cdot 6H_2O$: N, 6.41; C, 21.99; H, 3.66%.

5) *Potassium Bis-(methyliminodiacetato)cobaltate(III)*, $K[Co(mda)_2]$ (V). The preparation was carried out by the method in literature.[6]

6) *Potassium Bis-(methyliminodiacetato)chromate(III)*, $K[Cr(mda)_2]$ (VI). The crystals were prepared by the method already known.[9]

7) *Potassium Bis-(ethyliminodiacetato)cobaltate(III) Monohydrate*, $K[Co(eda)_2]\cdot H_2O$ (VII). To 200 m*l* of aqueous solution containing 5 g of cobalt(II) chloride hexahydrate, 6 g of EDA was added, and then 3 g of potassium hydrogen carbonate was gradually added. The mixed solution was heated on a water bath for one hour. After the pH of the solution was adjusted to 6—7, a few m*l* of hydrogen peroxide was added, and pink orange crystals were then obtained under cooling. Recrystallization was carried out from water. Yield about 2 g.

Found: N, 6.50; C, 32.98; H, 4.58%. Calcd for $K[Co(eda)_2]\cdot H_2O$: N, 6.45; C, 33.21; H, 4.61%.

8) *Potassium Bis-(ethyliminodiacetato)chromate(III) Monohydrate*, $K[Cr(eda)_2]\cdot H_2O$ (VIII). To 250 m*l* of aqueous solution containing 5 g of chromium(III) chloride hexahydrate, 6 g of EDA was added. The solution was heated on a water bath for one hour, and then 3 g of potassium hydrogen carbonate was added little by little to the solution. Heating was continued for one hour. After cooling, orange crystals were separated out. The crystals were recrystallized from water. Yield about 2.5 g.

Found: N, 6.57; C, 33.54; H, 4.52%. Calcd for $K[Cr(eda)_2]\cdot H_2O$: N, 6.55; C, 33.69; H, 4.68%.

Apparatus. Electronic and IR spectra, and molar conductivities were measured with a Hitachi EPS Spectrophotometer and a Nippon Bunko DS-301 Infrared Spectrophotometer and with a Yokogawa Universal Bridge BV-Z-13A, respectively.

Results and Discussion

IR Spectra. Infrared absorption spectra of the complexes were measured to confirm whether or not the carboxylate groups were coordinated.

It is well known that the characteristic band for the free carboxylic acid and that for the coordinated one in aminopolycarboxylic acid complexes appear at $\sim$1750 and $\sim$1640 cm^{-1}, respectively.[10]

Since all the complexes showed the bands near $\sim$1640 cm^{-1}, it is obvious that the carboxylate groups are all coordinated.

Molar Conductivities. The molar conductivities of the complexes in 10^{-3} mol/*l* aqueous solution were measured at 25°C in order to ascertain the valency-type of the complexes. All the complexes except for IV showed the values of 92—98 mho·cm^{-1}, indicating that they are 1 : 1 type electrolyte. The value of 183.1 mho·cm^{-1} for complex IV is fairly

10) D. H. Busch and J. C. Bailar, Jr., *J. Amer. Chem. Soc.*, **75**, 4574 (1953).

reasonable for 1 : 2 type electrolyte.

Electronic Spectra and Possible Structures. The electronic spectra of all the complexes were measured in aqueous solutions. The spectra for the cobalt(III) complexes are depicted in Fig. 2, and those for the chromium(III) complexes in Fig. 3. The absorption maxima are also listed up in Table 1, together with those of reference substances.

It has been discussed from MO treatments that, in the cobalt(III) complexes of N_2-O_4 type, the *trans* form with respect to the nitrogen atoms shows the splitting in the first band at the longer wavelength side.[11] The assignments of *trans*- or *cis*-K[Co(ida)$_2$] have been made from the above viewpoint.[4] The spectra for complexes V and VII show such a splitting in the first band as in the case of complex I, differing from that of II which shows no splitting. This indicates that the former two complexes are considered to have the *trans*-form. The frequencies of absorption maxima of the above three complexes in *trans*-form are seen from Fig. 2 and Table 1 to be raised in the order VII$<$V$<$I, suggesting that spectrochemical series of these ligands is concluded to follow the order, EDA$<$MDA$<$IDA. This is also in agreement with the fact that the stability of the complexes is lowered by *N*-alkyl substitution in the ligands.

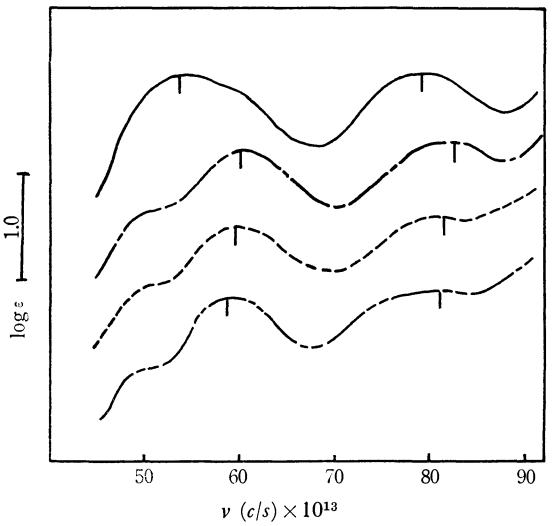

Fig. 2. Electronic spectra for *cis*-K[Co(ida)$_2$]·2H$_2$O (II) (———) *trans*-K[Co(ida)$_2$]·H$_2$O (I) (—·—), K[Co(mda)$_2$] (V) (– – – –) and K[Co(eda)$_2$]·H$_2$O (VII) (—··—).

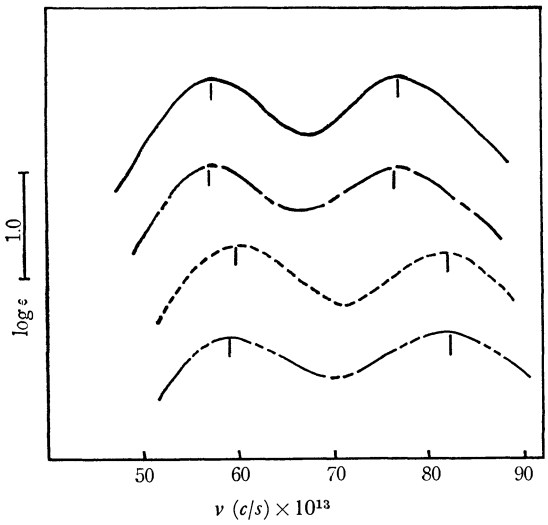

Fig. 3. Electronic spectra for K[Cr(ida)$_2$]·3H$_2$O (III) (———), Ba[Cr(ida)$_2$]$_2$·6H$_2$O (IV) (—·—), K[Cr(mda)$_2$] (VI) (– – – –) and K[Cr(eda)$_2$]·H$_2$O (VIII) (—··—).

TABLE 1. ABSORPTION MAXIMA

Complex	$m\mu_1(\nu_1 10^{-13}$/sec) log ε_1	$m\mu_2(\nu_2 10^{-13}$/sec) log ε_2
A. for the cobalt complexes		
I	500(60.00)1.70	365(82.19)1.74
II	566(53.00)2.03	380(78.95)2.04
V	509(58.94)1.74	367(81.74)1.84
VII	516(58.14)1.78	369(81.30)1.84
B. for the chromium complexes		
III	523(57.36)1.87	392(76.53)1.91
IV	524(57.25)1.85	393(76.34)1.92
VI	500(60.00)1.58	364(82.42)1.42
VIII	504(59.52)1.56	363(82.64)1.38
[Cr(edta)]$^-$ [12]	543	394
[Cr(tmta)]$^-$ [9,13]	509	385

Concerning *trans* configuration, two possible forms may be assumed; one is *trans-fac* (Fig. 1-A) and the other, *trans-mer* (Fig. 1-B). However, the former configuration seems to be reasonable in EDA complex of *trans* type, because the observation of the favorable angle of ∠C–N–C in the *trans* IDA and MDA complexes[4,6] suggested only the *trans-fac* configuration.

Preparation of the *cis*-isomer of the MDA or EDA complexes has not been successful probably because of the steric hindrance of methyl or ethyl groups, as reported by Weyh and Hamm.[9]

Although complexes VI and VIII do not show distinct splitting in the first band unlike cobalt complexes, it should be considered from the discussion of the corresponding cobalt complexes that they have also the same *trans-fac* configuration. As seen from Fig. 3, complex VIII has the absorption maxima at the longerwave length region than VI, as in the case of cobalt complexes.

Concerning the structures of complexes III and IV, if it is assumed that they have the *trans* configuration, their absorption maxima should be

11) H. Yamatera, This Bulletin, **31**, 95 (1958).

detected at ~500 and ~365 mμ, and their log ε_1 are expected to be 1.5—1.6. As can be seen from Table 1, however, the experimental results seem to be inconsistent with the above expectation. On the other hand, $[Cr(edta)]^-$ ion prepared by the method given in literature[12] shows the bands at 543 and 394 mμ. If III and IV are expected to have the same *cis*-form as $[Cr(edta)]^-$, the complexes should show the absorption maxima at 540—550 and 390—395 mμ.

The trimethylenediaminetetraacetatochromate (III) ion ($[Cr(tmta)]^-$),[13] which has six-membered chelate ring through two nitrogen atoms, shows the maxima at 509 and 385 mμ. These values are shorter than those of $[Cr(edta)]^-$ in spite of the fact that they have the same *cis*-configuration.

Studies of the metal chelate with diaminetetracarboxylic acids of the type $(HO_2CCH_2)_2N(CH_2)_n$-$N(CH_2CO_2H)_2$ indicated that the conformational strain becomes larger with the increase of n over 2,[14] when the octahedral coordination structure is assumed to be kept without any distortion. We thus consider that, in TMTA complex (TMTA: trimethylenediaminetetraacetic acid), the normal octahedral coordination form is somewhat distorted so as to diminish the strain due to the chelate ring through nitrogen atoms. It may be understood that complexes III and IV, like the chromium TMTA complex, take the *cis* configuration without much strain in the chelate ring structure as imagined by the sketch (D) in Fig. 1.

The authors wish to thank the Ministry of Education for the financial support granted for this research.

12) D. T. Sawyer and J. M. Mckinnie, *J. Amer. Chem. Soc.*, **82**, 4191 (1960).

13) R. Tsuchiya, A. Uehara and E. Kyuno, This Bulletin, **42**, 1886 (1969).

14) G. Schwarzenbach and G. Anderegg, *Z. Anorg. Allg. Chem.*, **282**, 286 (1955).

BULLETIN OF THE CHEMICAL SOCIETY OF JAPAN VOL. 43 1397—1402 (1970)

Bis-Type Cobalt(III) and Chromium(III) Complexes with Related Compounds of Nitrilotriacetic Acid*1

Akira UEHARA, Eishin KYUNO and Ryokichi TSUCHIYA

Department of Chemistry, Faculty of Science, Kanazawa University, Kanazawa

(Received November 17, 1969)

β-Amino-*n*-butyric-*N*,*N*-diacetic acid (β-ABDA) and γ-amino-*n*-butyric-*N*,*N*-diacetic acid (γ-ABDA) were prepared as compounds related to nitrilotriacetic acid (NTA). Bis-type cobalt (III) and chromium(III) complexes with these ligands, *viz.*, $K_3[Co(\beta\text{-abda})_2]$ (I), $K[Co(H\text{-}\gamma\text{-abda})_2]\cdot 2H_2O$ (II) and $K[Cr(H\text{-}\gamma\text{-abda})_2]\cdot 2H_2O$ (III), and the same type cobalt(III) complex with β-aminoethylsulfonic-*N*,*N*-diacetic acid (AEDA), *viz.*, $K_3[Co(aeda)_2]\cdot 4H_2O$ (IV), were also synthesized. Chemical properties of the above complexes were compared with those of the chromium (III) complex corresponding to IV and of the cobalt(III) and chromium(III) complexes with NTA and NPDA. From the analysis of electronic spectra, it was found that the new complexes, I, II, III and IV have the *trans* form with respect to the nitrogn atoms in the ligands. A spectrochemical series of these ligands, containing iminodiacetic acid (IDA), methyliminodiacetic acid (MDA) and ethyliminodiacetic acid (EDA), was determined to be:

IDA>MDA>NPDA>β-ABDA>EDA>AEDA>NTA>γ-ABDA.

Most active works on the aminetricarboxylic acid complexes may be classified into four categories. The first deals with the formation constants of the bivalent metal complex species, *e*,*g*., those with NTA[1,2] and nitrilopropionicdiacetic acid (NPDA).[3] The second deals with the reaction kinetics of

*1 Presented at 19th Symposium on Coordination Chemistry, Sendai, September, 1969.

1) G. Schwarzenbach, H. Ackermann and P. Ruckstul, *Helv. Chim. Acta*, **32**, 1175 (1949).

2) G. Schwarzenbach, E. Kampitish and R. Steiner, *ibid.*, **28**, 828 (1945).

3) S. Chaberek, Jr., and A. E. Martell, *J. Amer. Chem. Soc.*, **75**, 2888 (1950).

Table 1. Chelating agents and their abbreviations

A. Iminodiacetic Acid and Related Compounds

Rational formula	R	Name	Abbreviation
R–N(CH$_2$COOH)(CH$_2$COOH)	H	Iminodiacetic acid	IDA
	CH_3	Methyliminodiacetic acid	MDA
	C_2H_5	Ethyliminodiacetic acid	EDA

B. Nitrilotriacetic Acid and Related Compounds

Rational formula	R	R′	Name	Abbreviation
N(R′CH–R)(CH$_2$COOH)(CH$_2$COOH)	COOH	H	Nitrilotriacetic acid	NTA
	CH_2COOH	H	Nitrilopropionicdiacetic acid	NPDA
	CH_2SO_3H	H	β-Aminoethylsulfonic-*N*,*N*-diacetic acid	AEDA
	CH_2COOH	CH_3	β-Amino-*n*-butyric-*N*,*N*-diacetic acid	β-ABDA
	CH_2CH_2COOH	H	γ-Amino-*n*-butyric-*N*,*N*-diacetic acid	γ-ABDA

bivalent metals with NTA.[4,5] The third deals with the preparation of cobalt(III) and chromium(III) complexes containing NTA[6-8] or its related compounds, *e.g.*, NPDA,[9,10] AEDA,[11] nitriloisopropionicdiacetic acid (NIPDA),[12] and *l*-leucine-*N*,*N*-diacetic acid (LDA).[13] The fourth deals with the thermal reaction in the solid-state.[14] Study on the geometrical isomerism of the mixed cobalt(III) complexes with NTA and natural amino acids[15] might also be included.

In the previous paper,[16] the bis-type cobalt(III) and chromium(III) complexes with iminodiacetic acid (IDA) and its related compounds were reported from the viewpoint of geometrical isomerism. As a continuation of the work, investigations were carried out (1) to prepare bis-type cobalt(III) and chromium(III) complexes with nitrilotriacetic acid (NTA) or its related compounds, β-amino-*n*-butyric-*N*,*N*-diacetic acid (β-ABDA) and γ-amino-*n*-butyric-*N*,*N*-diacetic acid (γ-ABDA), the structures of these ligands being shown in Table 1, where those of IDA and its related compounds are also included, (2) to assign the geometrical structures of the complexes; *i. e.*, *cis* or *trans* with respect to the nitrogen atoms in ligands, (3) to inspect the difference in coordinating behaviors of these ligands, (4) to determine the spectrochemical series of all the ligands shown in Table 1, and (5) to compare the properties of cobalt(III) complexes with those of the corresponding chromium(III) ones.

Experimental

Preparation of Ligands. *β-Amino-n-butyric-N,N-diacetic Acid (β-ABDA)*, N(CH(CH$_3$)CH$_2$COOH)(CH$_2$COOH)$_2$. Five grams of β-amino-*n*-butyric acid was neutralized with 30 m*l* of water containing 3 g of potassium hydroxide. Fifty milliliters of water containing 10 g of monochloroacetic acid was gradually neutralized with 10 g of potassium hydrogen carbonate. The two solutions were mixed and heated on a water bath. When the temperature of solution was raised to *ca.* 70°C, 30 m*l* of water containing 6 g of potassium hydroxide was added, and heating was continued for 1—2 hr. The solution was cooled at room temperature. After potassium chloride deposited was filtered off, the pH of the solution was adjusted to *ca.* 5 by adding concentrated hydrochloric acid. The solution was then concentrated to about half its volume. After potassium chloride deposited was filtered off, the pH of the solution was adjusted to about 3. By scrubbing the wall of the reaction vessel with a glass rod, white powdered crystals were obtained. The crude products were recrystallized from water. Yield about 4 g.

Found: N, 6.31; C, 43.56; H, 5.82%. Calcd for $C_8H_{13}O_6N$: N, 6.39; C, 43.83; H, 5.98%.

γ-Amino-n-butyric-N,N-diacetic Acid (γ-ABDA), N(CH$_2$CH$_2$CH$_2$COOH)(CH$_2$COOH)$_2$. The preparative method closely resembles to that of β-ABDA; *i. e.*, in the preparation, γ-amino-*n*-butyric acid was used as a starting material in place of β-amino-*n*-butyric acid. Yield about 2 g.

4) N. Tanaka and M. Kimura, This Bulletin, **41**, 2375 (1968).
5) M. Kimura, *ibid.*, **42**, 407 (1969).
6) M. Mori, M. Shibata, E. Kyuno and Y. Okubo, *ibid.*, **31**, 940 (1958).
7) A. Uehara, E. Kyuno and R. Tsuchiya, *ibid.*, **40**, 2317 (1967).
8) A. Uehara, E. Kyuno and R. Tsuchiya, *ibid.*, **40**, 2322 (1967).
9) A. Uehara, E. Kyuno and R. Tsuchiya, *ibid.*, **41**, 2385 (1968).
10) M. Tachibana, A. Uehara, E. Kyuno and R. Tsuchiya, *ibid.*, **43**, 1061 (1970).
11) A. Uehara, E. Kyuno and R. Tsuchiya, *ibid.*, **42**, 2835 (1969).
12) A. Uehara, E. Kyuno and R. Tsuchiya, *ibid.*, **41**, 2393 (1968).
13) A. Uehara, E. Kyuno and R. Tsuchiya, *ibid.*, **43**, 414 (1970).
14) R. Tsuchiya, A. Uehara and E. Kyuno, *ibid.*, **42**, 1886 (1969).
15) N. Koine, N. Sakota, J. Hidaka and Y. Shimura, *ibid.*, **42**, 1583 (1969).
16) A. Uehara, E. Kyuno and R. Tsuchiya, *ibid.*, **43**, 1394 (1969).

Found: N, 6.29; C, 43.92; H, 5.73%. Calcd for $C_8H_{13}O_6N$: N, 6.39; C, 43.83; H, 5.98%.

Preparation of Complexes. *Potassium Bis-(β-amino-n-butyric-N,N-diacetato)cobaltate(III)*, $K_3[Co(\beta\text{-abda})_2]$ (I). Five grams of β-ABDA was added to 100 m*l* of aqueous solution containing 3 g of cobalt(II) chloride hexahydrate and the solution was then gradually neutralized with about 5 g of potassium hydrogen carbonate. After a few m*l* of 28% hydrogen peroxide solution was added, the solution was heated on a water bath and concentrated to about half its volume. After cooling pink crystals were obtained and recrystallized from water. Yield about 2 g.

Found: N, 4.74; C, 31.92; H, 3.31%. Calcd for $K_3[Co(\beta\text{-abda})_2]$: N, 4.60; C, 31.57; H, 3.29%.

Potassium Bis-(hydrogen-γ-amino-n-butyric-N, N-diacetato)-cobaltate(III) Dihydrate, $K[Co(H\text{-}\gamma\text{-abda})_2]\cdot 2H_2O$ (II). Five grams of γ-ABDA was added to 100 m*l* of aqueous solution containing 3 g of cobalt(II) chloride hexahydrate, and then about 3 g of potassium hydrogen carbonate was gradually added. A few m*l* of 28% hydrogen peroxide solution was dropped to oxidize the solution which was concentrated to half its volume on a water bath. After cooling pink crystals were obtained. The crude products were recrystallized from water. Yield about 1.5 g.

Found: N, 4.87; C, 33.42; H, 4.60%. Calcd for $K[Co(H\text{-}\gamma\text{-abda})_2]\cdot 2H_2O$: N, 4.93; C, 33.80; H, 4.61%.

Potassium Bis-(hydrogen-γ-amino-n-butyric-N, N-diacetato)-chromate(III) Dihydrate, $K[Cr(H\text{-}\gamma\text{-abda})_2]\cdot 2H_2O$ (III). To 100 m*l* of water containing 3 g of chromium(III) chloride hexahydrate, 5 g of γ-ABDA was added and 5 g of potassium hydrogen carbonate was then gradually added. The solution was heated on a water bath until the color of solution turned to pink from violet. From the solution pink crystals were obtained. Recrystallization was carried out from water. Yield about 3 g.

Found: N, 4.99; C, 33.85; H, 4.56%. Calcd for $K[Cr(H\text{-}\gamma\text{-abda})_2]\cdot 2H_2O$: N, 4.99; C, 34.22; H, 4.63%.

Potassium Bis-(β-aminoethylsulfonic-N,N-diacetato)cobaltate(III) Tetrahydrate, $K_3[Co(aeda)_2]\cdot 4H_2O$ (IV). 12 g of cobalt(II) chloride hexahydrate was dissolved in 200 m*l* of water and then 24 g of AEDA was added. 25 g of potassium hydrogen carbonate was gradually added to the mixture, which was then heated on a water bath until the solution turned from pink to red. After the solution was cooled to room temperature, about 5 m*l* of 28% hydrogen peroxide solution was added for oxidation. Reddish violet crystals were obtained from the cold solution. Recrystallization was carried out from water. Yield about 8 g.

Found: N, 3.83; C, 20.07; H, 3.27%. Calcd for $K_3[Co(aeda)_2]\cdot 4H_2O$: N, 3.86; C, 19.89; H. 3.31%.

Potassium Bis-(β-aminoethylsulfonic-N,N-diacetato) chromate(III) Tetrahydrate, $K_3[Cr(aeda)_2]\cdot 4H_2O$ (V),[11] *Potassium Bis(nitrilotriacetato)cobaltate(III) Trihydrate*, $K_3[Co(nta)_2]\cdot 3H_2O$ (VI),[10] *Potassium Bis-(hydrogennitrilotriacetato)cobaltate(III) Dihydrate*, $K[Co(Hnta)_2]\cdot 2H_2O$ (VII),[10] *Potassium Bis-(nitrilotriacetato)chromate(III) Tetrahydrate*, $K_3[Cr(nta)_2]\cdot 4H_2O$ (VIII),[7] *Potassium Bis-(hydrogennitrilotriacetato)chromate(III) Dihydrate*, $K[Cr(Hnta)_2]\cdot 2H_2O$ (IX),[7] *Potassium Bis(nitrilopropionic-diacetato)cobaltate(III) Dihydrate*, $K_3[Co(npda)_2]\cdot 2H_2O$ (X).[10] and *Potassium Bis-(nitrilopropionicdiacetato)chromate (III) Dihydrate*, $K_3[Cr(npda)_2]\cdot 2H_2O$ (XI)[9] were prepared by the similar method as in the corresponding ammonium salts given in literature and were identified by elemental analysis in order to compare their properties with those of complexes I, II, III and IV.

Apparatus. The same instruments as described previously were used.[16]

Results and Discussion

IR Spectra. Infrared absorption spectra were measured in Nujol mull state in order to see how carboxylate groups behave toward central metals. The band assignments with respect to carboxylate groups were carried out by the method of Busch and Bailar.[17] Numerical data of spectra arising from the free carboxylic acid (–COOH), the coordinated carboxylate (–COO–M) and the ionic carboxylate groups ($-COO^-$) are given in Table 2.

Complex IV shows the bands due to the coordinated carboxylate and the free sulfonate groups ($-SO_3^-$). The shoulder originating from the ionic carboxylate groups ($-COO^-$), besides the band assigned to a coordinated group, is also detected in the case of complex I. Complexes II and III give the bands assigned to the free carboxylate groups in addition to the coordinated groups.

Molar Conductivities. In order to examine to what kind of valency-type the new complexes belong, the molar conductivities were measured at 25°C in a 10^{-3} mol/*l* aqueous solution. The numerical values are given in Table 3.

The values of complexes I and IV fairly show that they are 1 : 3 type electrolytes. Complexes II and III show considerably high values which suggest partial dissociation of hydrogen ions in

Table 2. IR data (cm^{-1})

Complex	–COOH	–COO–M	–COO–	Complement
IV		1640 vs, br		1200 s, br*
V		1630 vs, br		1190 s, br*
I		1635 vs, br	1602 sh,	
II	1730 s	1655 vs, br		
III	1731 s	1660 vs, br		

* Absorptions arising from sulfonate groups (SO_3^-).
Abbreviations: s, strong; vs, very strong; br, broad; sh, shoulder.

Table 3. Molar conductivities (mho cm^{-1})

Complex	Molar conductivity* (mho cm^{-1})
IV	311.2
I	284.5
II	430.8
III	442.6

* 10^{-3} mol/*l* aqueous solution was used.

17) D. H. Busch and J. C. Bailar, Jr., *J. Amer. Chem. Soc.*, **75**, 4574 (1953).

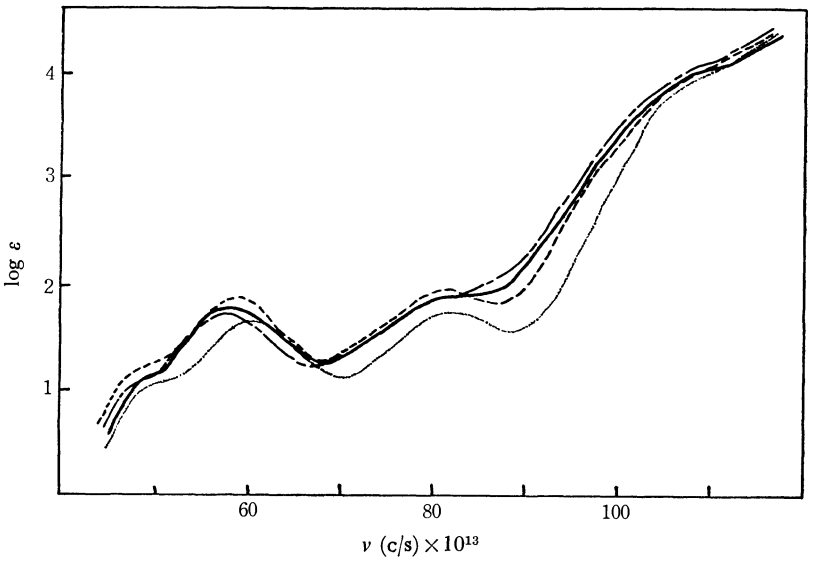

Fig. 1. Electronic spectra for complexes IV (———), I (– – –), II (—·—) and *trans*-K[Co(ida)$_2$]·H$_2$O (·····).

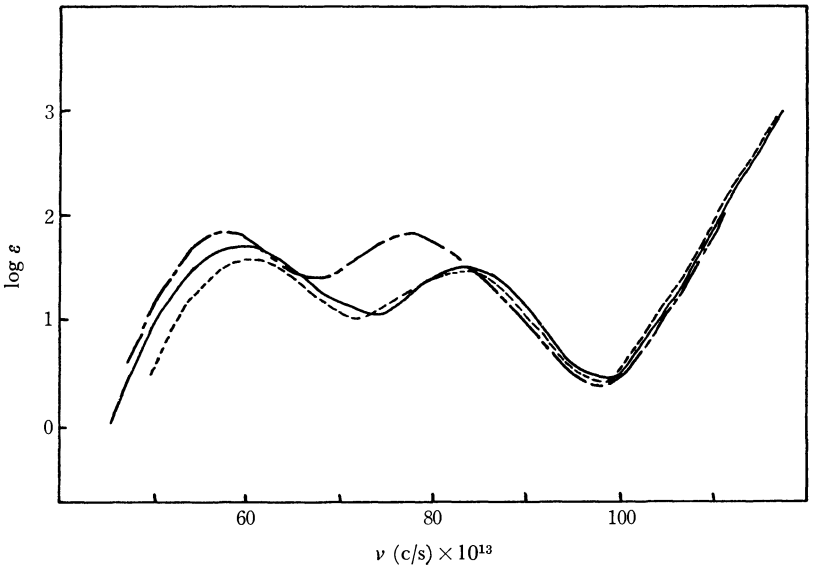

Fig. 2. Electronic spectra for complexes III (———), *trans*-[Cr(mda)$_2$] (------) and *cis*-K[Cr(ida)$_2$]·3H$_2$O (—·—).

TABLE 4. ABSORPTION MAXIMA FOR BIS COBALT(III) COMPLEXES

Complex	$m\mu_1$ ($\nu_1 10^{-13}$/sec)	log ε_1	$m\mu_2$ ($\nu_2 10^{-13}$/sec)	log ε_2
VI	521 (57.58)	1.83	366 (81.97)	2.27
VII	521 (57.58)	1.81	367 (81.74)	2.25
X	511 (58.71)	1.90	362 (82.87)	2.10
IV	520 (57.69)	1.77	367 (81.74)	1.87
I	515 (58.25)	1.85	370 (81.08)	1.93
II	525 (57.14)	1.75	367 (81.74)	1.86
trans-K[Co(eda)$_2$]·H$_2$O	516 (58.14)	1.78	369 (81.30)	1.84
trans-K[Co(mda)$_2$]	509 (58.94)	1.74	367 (81.74)	1.84
trans-K[Co(ida)$_2$]·H$_2$O	500 (60.00)	1.70	365 (82.19)	1.74
cis-K[Co(ida)$_2$]·2H$_2$O	566 (53.00)	2.03	380 (78.95)	2.04

Table 5. Absorption maxima for bis chromium(III) complexes

Complex	$m\mu_1$ ($\nu_1 10^{-13}$/sec)		log ε_1	$m\mu_2$ ($\nu_2 10^{-13}$/sec)		log ε_2
VIII	499	(60.12)	1.65	359	(83.57)	1.48
XI	492	(60.98)	1.62	362	(82.87)	1.43
V	500	(60.00)	1.54	360	(83.33)	1.39
III	508	(59.06)	1.66	363	(82.64)	1.47
trans-K[Cr(eda)$_2$]·H_2O	504	(59.52)	1.56	363	(82.64)	1.38
trans-K[Cr(mda)$_2$]	500	(60.00)	1.58	364	(82.42)	1.42
cis-K[Cr(ida)$_2$]·3H_2O	523	(57.36)	1.87	392	(76.53)	1.91

Abbreviations : eda, ethyliminodiacetate ion : mda, methyliminodiacetate ion.

the complex species.

Electronic Spectra and Coordinating Structures. The electronic absorption spectra for the complexes were measured in aqueous solutions. Those for complexes VIII and XI were measured in a buffer solution of pH 6—7 in order to prevent aquation. Figure 1 shows the spectra for complexes I, II, IV and *trans*-K[Co(ida)$_2$]·H_2O, and Fig. 2, those for complexes III, *trans*-K[Cr(mda)$_2$] and *cis*-K[Cr(ida)$_2$]·3H_2O. For the sake of comparison, the values of absorption maxima due to *d–d* transition for cobalt(III) and chromium(III) complexes are summarized in Tables 4 and 5 respectively, together with those for related complexes.

Appearance of splitting in the first band at longer wavelength in [Co N_2O_4] type complexes has been assigned to *trans* form from MO theory.[18] We see from Fig. 1 that complexes I, II and IV show the splitting in the first band at longer wavelength side which suggests that all the complexes have the *trans* configuration with respect to nitrogen atoms as in the case of *trans*-K[Co(ida)$_2$]·H_2O.[19]

It can be seen from Fig. 2 and Table 5 that complex III shows a spectrum similar to that of *trans*-K[Cr(mda)$_2$][16] rather than to that of *cis*-K[Cr(ida)$_2$]·3H_2O.[16] This suggests that complex III has a *trans* structure rather than *cis*. The possibility of the presence of *cis*-configuration in the bis complexes with aminetricarboxylic acids seems to be slight because the steric hindrance due to the methyl or ethyl groups prevents the formation of *cis* complexes even in the case of the MDA[20,21] and EDA[16] complexes.

With the *trans* isomer, two types of configuration can be assumed, one is *trans facial* and the other *trans meridional*. It has been mentioned that the former may be preferred because of the relevant bond angles of these ligands coordinated[22] as in the case of the bis-type complexes with IDA and the related compounds.[16] Thus the structures of complexes I, II, III and IV might belong to *trans-fac* type. In Fig. 3, two types of *trans-fac* are depicted, one of which has noncoordinating –COO$^-$ (A) and the other, –COOH (B). From IR and molar conductivity data, complexes I and IV may have (A) structure, and II and III (B) structure.

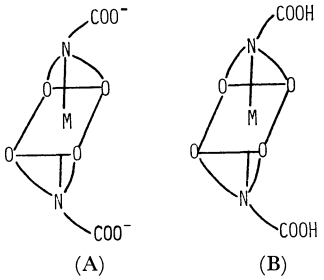

(A) (B)

Fig. 3. Possible structures. M: Co(III) or Cr(III).

From a comparison of the spectra in Figs. 1 and 2, it can be seen that the first and second bands clearly appear in the case of the chromium(III) complexes, while the second band of the cobalt(III) complexes is not so distinct owing to the overlap of CT bands. Such a difference has been detected in the case of acidopentaammine complexes of cobalt(III) and chromium(III).[23,24]

Spectrochemical Series of the Ligands. Although all the complexes obtained show a band pattern very similar to each other, a careful inspection of data in Tables 4 and 5 reveals a small but distinct difference in the wavelength of absorption bands. The differences in a series of cobalt(III) complexes are much remarkable in contrast with those in the chromium(III) ones. A spectrochemical series in the cobalt(III) complexes will be settled as follows according to the sequences of weavelength of the first band in Table 4;

IDA>MDA>NPDA>β-ABDA>EDA>AEDA>NTA>γ-ABDA

18) H. Yamatera, This Bulletin, **31**, 95 (1958).
19) J. Hidaka, Y. Shimura and R. Tsuchida, *ibid.*, **35**, 567 (1962)
20) J. I. Legg and D. W. Cooke, *Inorg. Chem.*, **5**, 594 (1966).
21) D. W. Cooke, *ibid.*, **5**, 1141 (1966).
22) J. A. Weyh and R. E. Hamm, *ibid.*, **7**, 2431 (1968).
23) M. Linhard and M. Weigel, *Z. Anorg. Allg. Chem.*, **266**, 49 (1951).
24) M. Linhard and M. Weigel, *ibid.*, **271**, 101 (1952).

TABLE 6. COORDINATING BEHAVIORS OF LIGANDS HAVING (5,5,5)-, (5,5,6)- OR (5,5,7)-MEMBERED CHELATE RINGS

Ligand	Chelate ring	Coordinating type	Coordination number	Cr(III)	Co(III)
NTA	5.5,5	N_1-O_3	4	○	○
		N_1-O_2	3	○	○
		O_3	3	○	×
NPDA	5,5,6	N_1-O_3	4	○	○
		N_1-O_2	3	○	○
		O_3	3	×	×
γ-ABDA	5,5,7	N_1-O_3	4	×	×
		N_1-O_2	3	○	○
		O_3	3	×	×

Difference in the Coordinating Behaviors of the Ligands. The relations between the coordinating behaviors in NTA, NPDA and γ-ABDA complexes which have three chelate rings consisting of (5,5,5)-, (5,5,6)-, (5,5,7)-members respectively are summarized in Table 6. Each complex is respectively classified into three groups owing to the possible coordinating types, N_1-O_3, N_1-O_2 and O_3, which represent the coordinating nitrogen and oxygen atoms and their number per one molecule of these ligands. The complexes which we succeeded in preparing are denoted by ○, and those in which we did not succeed by × in Table 6.

NTA could act as N_1-O_3, N_1-O_2 and O_3 types toward chromium(III), but not as O_3 type toward cobalt(III). This might be due to the smaller affinity of cobalt(III) to oxygen as compared with that of chromium(III).[10] NPDA could not behave as O_3 type to both metals.[9,10] It may be understood by empirical facts that the complexes with a ligand forming two five-membered and one six-membered chelate rings are more stable than those forming three five-membered rings.

γ-ABDA acted only as an N_1-O_2 type. In this case the butyric acid group may be uncoordinated, because the formation of a seven membered ring is difficult.

The authors wish to thank the Ministry of Education for the financial support granted for this research.

BULLETIN OF THE CHEMICAL SOCIETY OF JAPAN VOL. 43 1403—1407 (1970)

The Kinetics of the Aminolysis of Phenyl Phenoxyacetates with Benzylamine in Dioxane

Yoshiaki FURUYA* and Kazuo ITOHO**

*Department of Industrial Chemistry, Faculty of Engineering, Kumamoto University, Kumamoto
**Daiichi College of Pharmaceutical Sciences, Fukuoka

(Received May 30, 1969)

The rates of the reactions of *p*- and *m*-substituted phenyl phenoxyacetates with benzylamine in dioxane, thus forming *N*-benzylphenoxyacetamide and the corresponding phenols, were followed by the non-aqueous titration of benzylamine. The reaction satisfied the following general equation:

$$v = \{k_2' + k_3'[\text{Amine}]\}[\text{Amine}][\text{Ester}] + \{k_3'' + k_4[\text{Amine}]\}[\text{Amine}][\text{Ester}]^2.$$

The reaction was a neucleophilic substitution, and the Hammett plots gave straight lines with positive ρ values. A marked enhancement in the conductivity of the reaction mixtures in 50% dioxane was observed, it increasing with the reaction time. A probable mechanism was presented which involves an ion pair of the quaternary ammonium salt type somewhat similar to that discussed in a previous paper (Y. Furuya, S. Goto, K. Itoho, I. Urasaki and A. Morita, *Tetrahedron*, **24**, 2367 (1968)).

The mechanism for the aminolysis of carboxylates has been studied by many investigators.[1a-e] In our previous paper, we suggested that a probable mechanism of the triethylenediamine-catalyzed aminolysis of phenyl *N*-phenylcarbamates with aniline in dioxane involves an ion pair of quarternary ammonium salt as an incipient intermediate. Generally, a specific catalyst is not required for usual aminolyses because the reactant amine itself acts as a catalyst.

In the present paper, it will be shown that the non-catalyzed aminolysis also involves an ion pair of the ammonium salt type.

Experimental

Materials. The phenyl phenoxyacetates were prepared by the reaction of phenoxyacetyl chloride and the corresponding phenols in the presence of a catalytic amount of tertiary amine in dry benzene, and then the reaction mixtures were recrystallized from aqueous methanol. Phenyl phenoxyacetate, mp 54—55°C (lit,[2] 56—57°C). *p*-Tolyl phenoxyacetate, mp 86—86.5°C. Found: C, 74.55; H, 6.03%. Calcd for $C_{15}H_{14}O_3$: C, 74.36; H, 5.83%. *p*-Chlorophenyl phenoxyacetate, mp 101.5—102°C. Found: C, 64.35; H, 4.46%. Calcd for $C_{14}H_{11}O_3Cl$: C, 64.01; H, 4.22%. *m*-Nitrophenyl phenoxyacetate, mp 97°C. Found: C, 61.28; H, 3.94; N, 5.21%. Calcd for $C_{14}H_{11}O_5N$: C, 61.54; H, 4.06; N, 5.13%. The *N*-benzylphenoxyacetamide used as an authentic sample was obtained by the reaction of phenoxyacetyl chloride with benzylamine; mp 82—83°C (lit,[3] 85—86°C). The benzylamine was dried over anhydrous sodium sulfate and then distilled; bp 183°C. The dioxane was purified as has been described in a previous report;[4] bp 102°C. The N/100 glacial acetic acid solution of perchloric acid was prepared with glacial acetic acid and 70% perchloric acid (special grade), and then standardized with a N/100 sym.-diphenylguanidin benzene-monochlorobenzene solution, using a tetrahydrofuran (THF) solution saturated with methyl violet as the indicator. The benzene was distilled from metal sodium; bp 80.1°C.

Reaction Product Criterion. The crystal obtained in an almost quantitative yield by the reaction of phenyl phenoxyacetate with benzylamine in dioxane did not show any melting-point depression when the product was mixed with the authentic sample of *N*-benzylphenoxyacetamide; mp and mmp 82—83°C.

The Reaction Products in 50% Aqueous Dioxane. A mixture of phenyl phenoxyacetate (0.02 mol) and benzylamine (0.02 mol) in 200 m*l* of 50% aqueous dioxane was stirred for a few hours at room temperature (*ca.* 30°C) and then allowed to stand overnight. The reaction mixture was diluted with a 200 m*l* of cold water and subsequently extracted several times with a total of 200 m*l* of ether. The ether layer was dried on anhydrous sodium sulfate overnight and then was washed with cold water. The oily matter obtained by removing the ether was recrystallized from aqueous methanol.

1) a) R. L. Betts and L. P. Hammett, *J. Amer. Chem. Soc.*, **59**, 1568 (1937); b) J. F. Bunnett and G. T. Davis, *ibid.*, **82**, 665 (1960); c) W. P. Jencks and J. Carriuolo, *ibid.*, **82**, 675 (1960); d) T. C. Bruice and M. F. Mayahi, *ibid.*, **82**, 3067 (1960); e) M. F. Menger, *ibid.*, **88**, 3081 (1966), *etc.*

2) P. S. Bataev and Z. G. Vorob'eva, *Med. Prom. SSSR*, **17**(5), 13(1963); *Chem. Abstr.*, **59**, 8652a (1963).

3) S. Kushner, R. I. Cassell, J. Morton, II, and J. H. Williams, *J. Org. Chem.*, **16**, 1283 (1951).

4) Y. Furuya, S. Goto, K. Itoho, I. Urasaki and A. Morita, *Tetrahedron*, **24**, 2367 (1968).

The crystal of *N*-benzylphenoxyacetamide was thus obtained; mp and mmp, 82°C; yield, 64.2%. The aqueous layer was acidified with aqueous hydrogen chloride together with the washings, and then extracted several times with a total of 250 m*l* of ether. The extract was dried on anhydrous sodium sulfate overnight. When the ether was then removed, an acidic crystalline matter, phenoxyacetic acid, was obtained; mp and mmp, 96°C; yield, 33.5%.

The Calibration Curve in the Chemical Analysis of Benzylamine. The calibration curve gave a straight line in solutions with benzylamine concentrations ranging from 1×10^{-2} to 3×10^{-1}M. It was, moreover, not influenced at all by the presence of ester, amide, and phenol.

A Typical Run for the Rate Measurement. A 7.5-m*l* portion of a 0.2M dioxane solution of benzylamine was poured into a solution of 7.5 m*l* of 0.2M phenyl phenoxyacetate in dioxane to start the reaction after both solutions had attained temperature equilibrium. Aliquots (each 1.0 m*l*) were pipetted out at appropriate time intervals, and each one was diluted with cold benzene (50 m*l*). The solution was then titrated by a N/100 perchloric acid - glacial acetic acid solution, using a solution saturated with methyl violet (0.5—1.0 m*l*) as the indicator. The values of the second-order rate constants, k_{2obs}, were calculated from the conversions thus obtained.

A Typical Procedure for the Conductivity Measurement. A 25-m*l* portion of a 50% aqueous dioxane solution of 1×10^{-2}M benzylamine aged at 30 ± 0.2°C was added to a 25-m*l* portion of a 50% aqueous dioxane solution of 1×10^{-2}M phenyl phenoxyacetate; then the conductivity at 30 ± 0.2°C was measured by means of a Yokogawa-Hewlett-Packard universal bridge 4255A (BV-Z-13C) at appropriate intervals of time.

Results and Discussion

Typical rate data of the aminolysis at 20°C are shown in Fig. 1. Here, *a*, *b*, and *x* are the initial concentrations of the amine and the ester and the consumed concentration of the amine at time *t* respectively. The kinetics follows the second-order equation. The plots of the apparent second-order rate constant *vs.* the concentration of the ester gave a straight line which does not pass through the point of origin, as is illustrated in Fig. 2. Therefore, the k_{2obs} rate constant is given by the following equation:

$$k_{2obs} = k_2 + k_3[\text{Ester}] \quad (1)$$

The values of k_2 and k_3 varied with the concentration of benzylamine (Figs. 3 and 4). Hence, k_2 and k_3, the rate constants, should be expressed as follows:

$$k_2 = k_2' + k_3'[\text{Amine}] \quad (2)$$

$$k_3 = k_3'' + k_4[\text{Amine}] \quad (3)$$

The total kinetics is, therefore, given by the following equation:

$$v = \{k_2' + k_3'[\text{Amine}]\}[\text{Amine}][\text{Ester}] + \{k_3''+k_4[\text{Amine}]\}[\text{Amine}][\text{Ester}]^2 \quad (4)$$

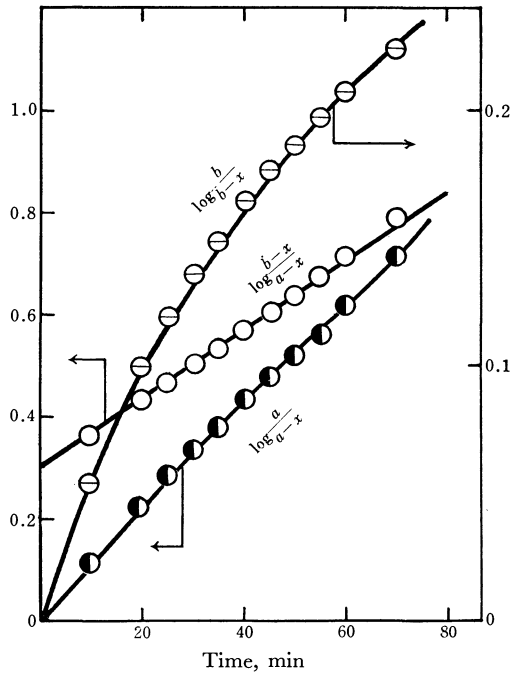

Fig. 1. Determination of reaction order of the aminolysis in dioxane at 20°C.
Concn. of phenyl phenoxyacetate: 0.20M
Concn. of benzylamine: 0.10M

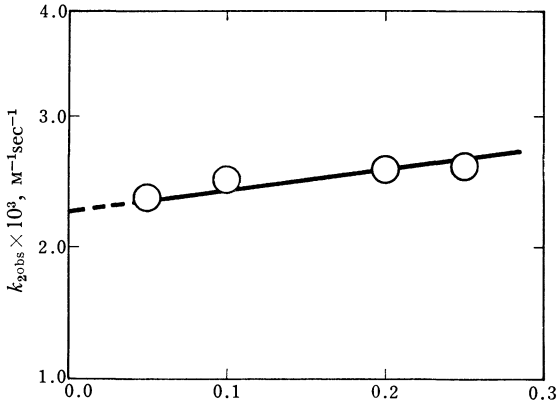

Fig. 2. The plots of k_{2obs} *vs.* the concentration of the ester for the aminolysis in dioxane at 20°C.
Concn. of benzylamine: 0.10M

The values of k_2', k_3', k_3'', and k_4 are tabulated in Table 1.

The reaction was retarded by the introduction of an electron-releasing group into the phenyl group of the ester. Thus, the plots of the logarithm of k_2', k_3', k_3'', and k_4 *vs.* Hammett's σ gave straight lines with slopes of $+1.13$, $+2.38$, $+2.42$, and $+2.45$ respectively. The reaction course represented by the first term of Eq. (4) is considered to be as follows:

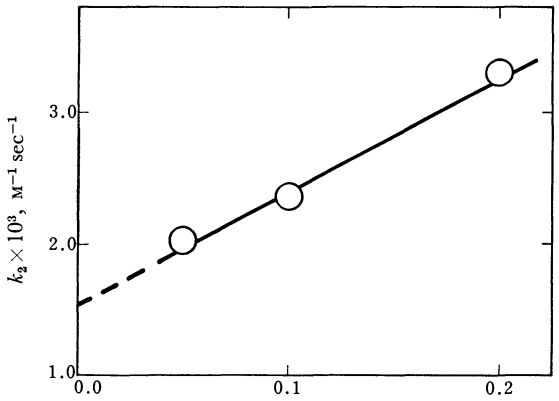

Fig. 3. The plots of k_2 *vs.* the concentration of the amine for the aminolysis in dioxane at 20°C.
Concn. of phenyl phenoxyacetate: 0.05—0.25M

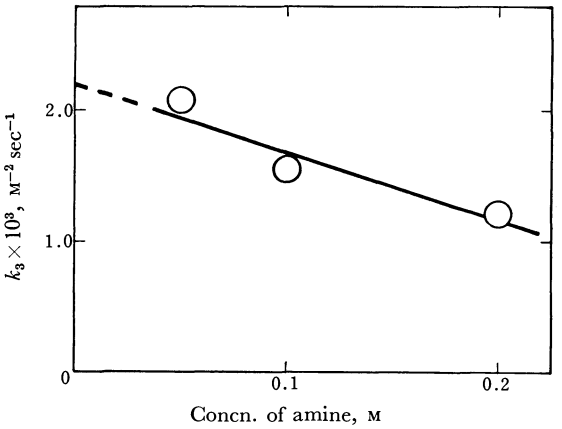

Fig. 4. The plots of k_3 *vs.* the concentration of the amine for the aminolysis in dioxane at 20°C.
Concn. of phenyl phenoxyacetate: 0.05—0.25M

TABLE 1. THE RATE DATA FOR THE AMINOLYSIS OF PHENYL PHENOXYACETATES WITH BENZYLAMINE IN DIOXANE AT 20°C
Initial concn. of the esters: 0.05—0.20 M
Initial concn. of benzylamine: 0.05—0.25 M

Esters	Rate constants			
	$k_2' \times 10^3$ M^{-1} sec^{-1}	$k_3' \times 10^3$ M^{-2} sec^{-1}	$k_3'' \times 10^3$ M^{-2} sec^{-1}	$k_4 \times 10^3$ M^{-3} sec^{-1}
p-Tolyl phenoxyacetate	0.95	6.29	0.61	6.38
Phenyl phenoxyacetate	1.53	8.55	2.20	−5.27
p-Chlorophenyl phenoxyacetate	2.65	67.0	5.70	−29.8
m-Nitrophenyl phenoxyacetate	9.65	430	91.5	−335

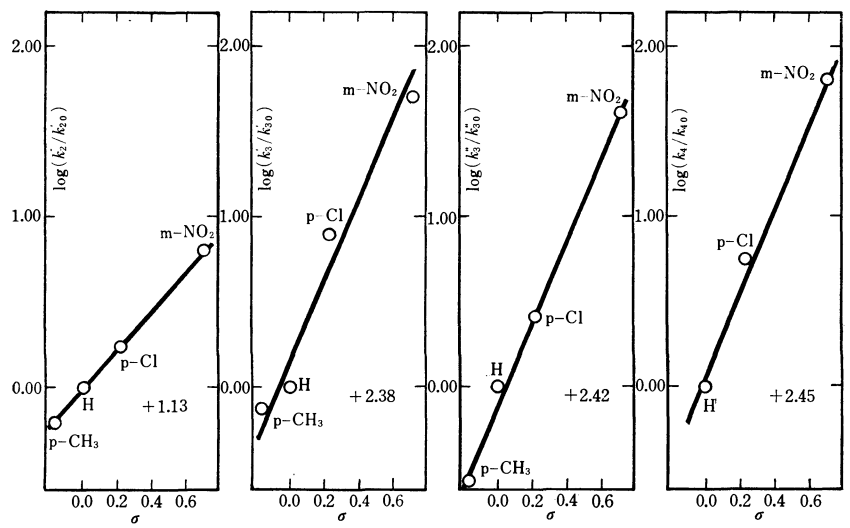

Fig. 5. Hammett's plots for k_2', k_3', k_3'' and k_4 rate constants of the aminolysis of the substituted esters at 20°C.
Initial concn. of phenyl phenoxyacetate: 0.025—0.25M
Initial concn. of benzylamine: 0.05—0.25M

$$PhOCH_2CO_2Ph + PhCH_2NH_2 \overset{k_2'}{\rightleftharpoons} \left[PhOCH_2\overset{\overset{O}{\|}}{C}\cdots OPh \;\; NH_2CH_2Ph \right]$$

[I]

As the ρ values of the reaction steps expressed by the second, third, and fourth terms all have plus signs and are nearly equal to each other, the rates must be controlled by similar steps. It is apparent from the calculation of the reaction order in the rate equation, however, that the rates of the two courses expressed by the second and third terms are not controlled by Step (7), but by Steps (5) and (6) respectively.

$$PhCH_2NH_2 + B \rightleftharpoons \left[PhCH_2\overset{\overset{H}{|}}{N}\cdots NHCH_2Ph \right]$$

[II]

$$\text{and/or} \left[PhOCH_2\overset{\overset{O}{\|}}{C}\cdots\overset{\overset{H}{|}}{N}\cdots NHCH_2Ph \right]$$

[III]

(B: Benzylamine or phenyl phenoxyacetate)

$$PhOCH_2CO_2Ph + II \overset{k_3', -\text{Amine}}{\rightleftharpoons} I \qquad (5)$$

$$PhOCH_2CO_2Ph + III \overset{k_3'', -\text{Ester}}{\rightleftharpoons} I \qquad (6)$$

$$I \longrightarrow \text{Prod.} + PhOH \qquad (7)$$

As the reaction indicated by the fourth term is very small under these concentration conditions, it might be negligible in the reaction of the non-substituted ester. However, if we make bold to suggest a probable mechanism for the reaction expressed by the fourth term, it can be written as follows:

$$PhCH_2NH_2 + PhOCH_2CO_2Ph \rightleftharpoons \left[PhOCH_2\overset{\overset{O}{\|}}{C}\cdots\overset{\overset{H}{|}}{N}\cdots NHCH_2Ph \right] \qquad (8)$$

[IV]

$$2\,IV \overset{k_4}{\rightleftharpoons} \left[PhCH_2\overset{\overset{H}{|}}{N}\cdots\overset{\overset{O}{\|}}{C}CH_2OPh \;\; \overset{\overset{H}{|}}{N}\cdots\overset{\overset{OPh}{|}}{C}\cdots NHCH_2Ph \right] \qquad (9)$$

[V]

$$V \longrightarrow \text{Prod.} + PhOH \qquad (10)$$

$$V \longrightarrow \text{Ester} + \text{Amine} \qquad (11)$$

Considering the reaction order obtained by the calculation, the rate-determining step is probably Step (9). When the phenoxy group has an electron-releasing group, phenol may be easily able to leave the ring complex, V. On the other hand, each bond in the carbophenoxy group, especially the bond between the carbonyl C-atom and the phenoxy O-atom, may be strengthened by the resonance effect in the carbophenoxy group when an electron-attracting group is introduced into the phenoxy group. This may be the reason why the Hammett plot of the k_4 rate constant has a positive ρ value.

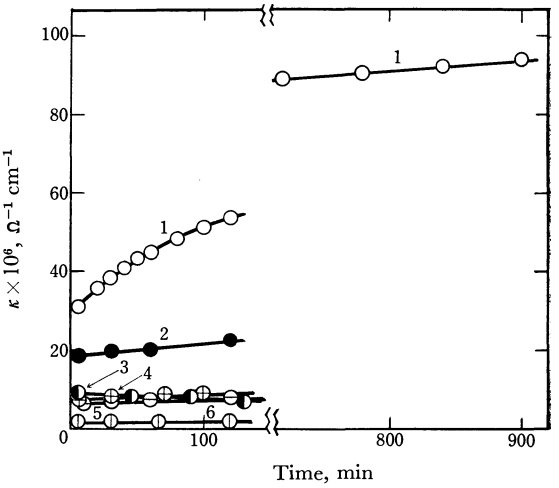

Fig. 6. Conductivity change with time for the each member and the couple of the aminolysis of phenyl phenoxyacetate with benzylamine in 50% aqueous dioxane at 30°C.
1, Concn. of the mixture of the ester and amine: each 5×10^{-3}M; 2, concn. of the mixture of the amine and phenol: each 5×10^{-3}M; 3, concn. of the mixture of the ester and amide: each 5×10^{-3}M; 4, concn. of the mixture of the amide and phenol: each 5×10^{-3}M; 5, concn. of the amine: 5×10^{-3}M; 6, concn. of the ester, amide and/or phenol: 5×10^{-3}M, respectively.

The conductivities of the [Ester+Amine], [Amine+PhOH] and [Amide+PhOH] couples are larger than the sums of the conductivities of the components, as is shown in Fig. 6 and Table 2. No initial large increase such as that in the conductivity of the [Ester+Amine] couple is observed in the conbinations of [Amine+PhOH] and [Amide+PhOH], as is shown in Fig. 6. The value of the conductivity on the heel of starting the actual reaction ($30\times10^{-6}\Omega^{-1}$cm^{-1}) is larger than the value of the sum of the ester and the amine ($10.4\times10^{-6}\Omega^{-1}$ cm^{-1}). It corresponds to the value in a 10% conversion of hydrolysis. Moreover, in the reaction in 50% aqueous dioxane at 30°C for 30 hr, the conversions of hydrolysis and aminolysis were 30 and 60% respectively. The conductivity of the model mixture, which has 30 and 60% conversions

Table 2. Specific conductivities of the reactants and products in 50% aqueous dioxane at 30±0.2°C
Initial reaction concn. of each component: 5×10^{-3}M
Measurement concn.: same concentration described above

Component	Specific conductivity $10^{-6}\Omega^{-1}cm^{-1}$	Couple of components	Specific[a] conductivity $10^{-6}\Omega^{-1}cm^{-1}$
Ester	1.3	Ester+Amine	31.1 (10.4)[b]
Amine	9.1	Amine+Phenol	18.5 (10.6)
Amide	1.4	Amide+Phenol	7.6 (2.9)
Phenol	1.5	Amide+Ester	8.6 (2.7)

a) The values measured on the heel of mixing the components of each couple.
b) The values in parentheses are the sums of an actual value of each component constituting each couple.

of hydrolysis and aminolysis respectively, was observed to be $69\times10^{-6}\Omega^{-1}$ cm^{-1}. This value is considerably smaller than the conductivity value ($94\times10^{-6}\Omega^{-1}$ cm^{-1}) obtained in the actual reaction at 30°C for 900 min. This suggests that another conductive matter is formed in addition to the formation of benzylammonium phenoxyacetate. It would be a quarternary ammonium salt like VI. Though the ion pair is perhaps formed, we can't

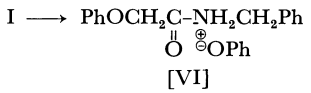

[VI]

decided that the salt is either an intermediate or a side reaction product. The amide formed by the reaction did not give benzylamine in either the presence or absence of phenol in dioxane at 70°C for 2 hr. From these findings, the following probable mechanism which involves I formed by the nucleophilic attack of the lone pair of the N-atom of amine on the carbonyl C-atom of the ester may be suggested:

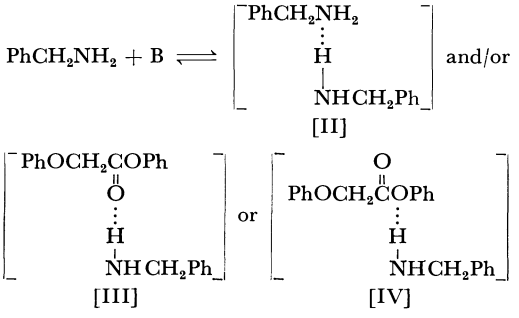

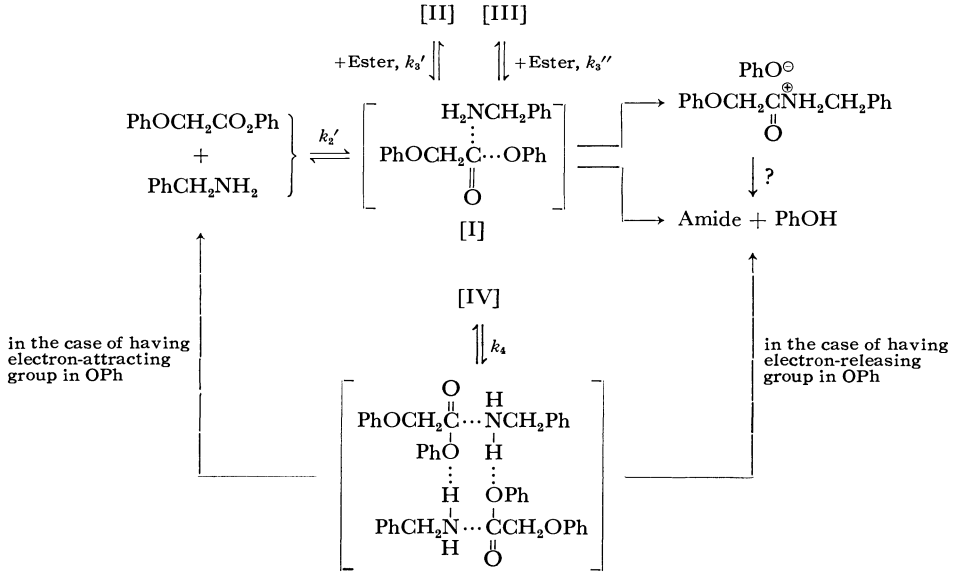

(B: Benzylamine, Phenyl Phenoxyacetate)

The authors are grateful to Mrs. N. Sato and Mr. T. Nishiyori for their aids in performing the work.

BULLETIN OF THE CHEMICAL SOCIETY OF JAPAN VOL. 43 1408—1411 (1970)

Mass Spectra of Phenyl *p*-Toluenesulfonates. Substituent Effect in Fragmentation

Seizi KOZUKA, Hideo TAKAHASHI, Seizo TAMAGAKI and Shigeru OAE

Department of Applied Chemistry, Faculty of Engineering, Osaka City University, Sugimoto-cho, Sumiyoshi-ku, Osaka

(Received June 30, 1969)

Mass spectra of substituted phenyl *p*-toluenesulfonates were analyzed with the aid of metastable peaks. Three steps in fragmentation were suggested as the main processes for these compounds *i.e.*, the initial S–O bond cleavage giving sulfonylcation, the second desulfonylation and the final loss of acetylene. Effect of substituent on the rate of the decomposition was observed in these three steps. The results are discussed in terms of various internal energies of the initial fragment ions. Apparently, the rates of the initial decomposition depend on the nature of the substituents.

Examination of mass-peak shifts by substituents is the usual method for clarifying the nature of electron impact decomposition. However, the effect of substituent on the rate of fragmentation has not been paid much attention till recently.[1] The substituent effects on the mass spectra hitherto being examined are those of acetophenones, benzophenones,[2–5] phenyl carbonates,[6,8] azobenzenes,[7] benzyl phenyl ethers,[9] dibenzyls,[10] methyl-4-phenyl butylate[11] and butyrophenones.[12] With most of these compounds, the relative peak heights (*Z*-values) of the first step of fragmentation, *i.e.*, the processes leading to the first fragment ions from the molecular ions, were nicely correlated with Hammett σ-values. In the case of substituted benzophenones, the effect of substituents was observed not only in the first step of fragmentation, *i.e.*, the formation of the benzoyl ions from the molecular ions, but also in the subsequent step, namely the decarboxylation of the benzoyl ions.[2]

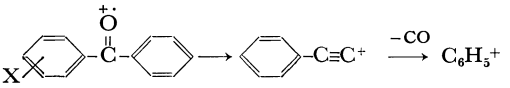

Recently we have reported the mass spectra of aromatic sulfur compounds having three different S–S bonds *i. e.*, disulfides, thiol sulfinates and thiol sulfonates.[13] As an extention of our previous work, we have examined the mass spectra of the following five diaryl sulfonates (I)

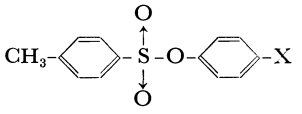

(I)

(X: NO_2, Cl, H, CH_3, OCH_3)

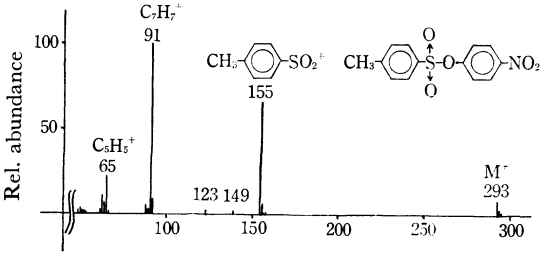

Fig. 1. The mass spectra of 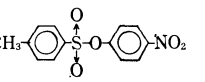 in 80 eV.

1) M. M. Bursey, *J. Org. Mass Spectrometry*, **1**, 31 (1968).
2) M. M. Bursey and F. W. McLafferty, *J. Amer. Chem. Soc.*, **88**, 529 (1966).
3) M. M. Bursey and F. W. McLafferty, *ibid.*, **88**, 4484 (1966).
4) M. M. Bursey and F. W. McLafferty, *ibid.*, **89**, 1 (1967).
5) M. L. Gross and F. W. McLafferty, *Chem. Commun.*, **1968**, 254.
6) P. Brown and C. Djerassi, *J. Amer. Chem. Soc.*, **89**, 2711 (1967).
7) J. H. Bowie, G. E. Lewis and R. G. Cooks, *J. Chem. Soc., B*, **1967**, 621.
8) P. Brown and C. Djerassi, *Angew Chem. Intern. Ed. Engl.*, **6**, 477 (1967).
9) P. Brown, *J. Amer. Chem. Soc.*, **90**, 2694 (1968).
10) F. W. McLafferty and M. M. Bursey, *ibid.*, **90**, 5299 (1968).
11) D. G. I. Kingston and H. P. Tannenbaum, *Chem. Commun.* **1968**, 444.
12) F. W. McLafferty, and T. Wacks, *J. Amer. Chem. Soc.*, **89**, 5043 (1967).
13) S. Kozuka, H. Takahashi and S. Oae, This Bulletin, **43**, 129 (1970).

Table 1. Relative intensities (80 eV)

Ion	Compd. NO_2	Cl	H	CH_3	OCH_3
M^+	8.5	13.5	25.0	27	15.5
CH_3-C$_6$H$_4$-SO_2^+	66	37.8	53.5	52	1.8
CH_3-C$_6$H$_4$-SO^+	1.7	1.2	1.7	1.5	0.4
CH_3-C$_6$H$_4$-S^+	1.9	—	1.1	—	—
$C_7H_7^+$	100	100	100	100	11.5
$C_5H_5^+$	21.5	22	28	16.6	8.7
X-C$_6$H$_4$-O^+	—	2.5	—	19.0	100
metastableble peak					
$M^+ \longrightarrow CH_3$-C$_6$H$_4$-SO_2^+	○*	○	○	○	○
CH_3-C$_6$H$_4$-$SO_2^+ \longrightarrow C_7H_7^+$	○	○	○	○	○
$C_7H_7^+ \longrightarrow C_5H_5^+$	○	○	○	○	○
$M^+ \longrightarrow O^+$-C$_6$H$_4$-X	—	—	—	—	○

* ○: metastable peak present

and found that the effects of substituents are clearly observed not only in the first step of the decomposition of the molecular ion but also in the second and third steps of fragmentation. In this paper, we wish to report the fragmentation scheme of diaryl sulfonates, the correlation of the decomposition rate with substituents and the energy states of the particular fragment ions.

Fragmentation. Five *p*-substituted phenyl *p*-toluenesulfonates were analyzed. An example of the mass spectrum is shown in Fig. 1. The intense peaks and metastable peaks of these compounds observed in their mass spectra are listed in Table 1.

All the compounds gave distinct molecular ions, and the subsequent fragment ions were formed by the loss of the phenoxy radicals from the molecular ions. Base peaks of most of these compounds appeared at the mass number of 91 which corresponds to tropylium ion.[9,10,14-17] However, in the case of *p*-methoxyphenyl toluenesulfonate, phenoxy cation was the base peak. This difference may be ascribed to the strong electron-releasing nature of the substituent, *i. e.*, methoxy group. Thus, the cleavage of the S–O bond of the molecular ion leaving a cationic center on the sulfur atom is less favored in the methoxy substituted compound and the heterolytic decomposition giving phenoxy cation would become the predominant process. This observation is in good accord with the previous observation of the mass fragmentation patterns of mono-substituted benzophenones in which similar two competing processes were suggested.[5]

All the patterns shown in Table 1 are similar to those of the thiol sulfonates.[13] A noticeable but minor difference may be the absence of oxygen migration which was presumed to occur from the sulfonyl sulfur to the sulfenyl sulfur atom at the initial stage of fragmentation of the thiol analogues.[13] The major fragmentation scheme suggested for the thiol sulfonates is applicable to the present compounds.

Substituent Effect. The relative peak heights

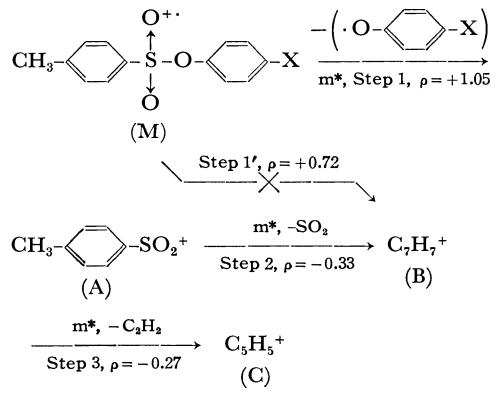

Scheme 1

14) F. W. McLafferty "Mass Spectrometry of Organic Ions," Academic Press, New York and London (1963), p. 488—506.

15) J. M. S. Tait, T. W. Shannon and A. G. Harrison, *J. Amer. Chem. Soc.*, **84**, 5 (1962).

16) S. Meyerson, H. Hart and L. C. Leitch, *ibid.*, **90**, 3419 (1968).

17) P. Brown, *ibid.*, **90**, 4461 (1968).

in mass spectra seem to be related to the rate of the decomposition.[1-5,18,19] The Hammett plots of the relative intensities of the peak heights corresponding to steps 1, 2 and 3 against σ^+ values are shown in Fig. 2. The ρ value of the individual steps calculated by the least square method is also given in Scheme 1.

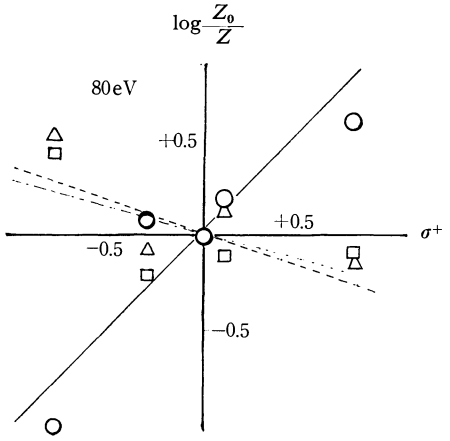

Fig. 2. Correlation of the relative intensities of the ions M^+, A^+, B^+ and C^+ with Hammett σ^+ constant (80 eV).

—○—○—: $Z=\frac{A}{M}$ (step 1)

--△--△--: $Z=\frac{B}{A}$ (step 2)

-·□-·□-·-: $Z=\frac{C}{B}$ (step 3)

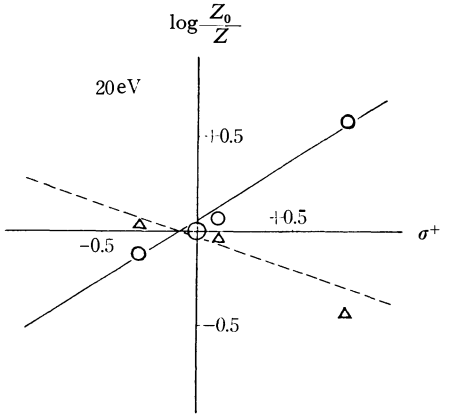

Fig. 3. Correlation of the relative intensities of the ions M^+, A^+ and B^+ with Hammett σ^+ constant (20 eV).

—○—○—: $Z=\frac{A}{M}$ --△--△--: $Z=\frac{B}{A}$

18) I. Howe and D. H. Williams, *J. Chem. Soc., B*, **1968**, 1213.

19) H. Budzikiewicz, C. Djerassi and D. H. Williams, "Mass Spectrometry of Organic Compounds," Holden-Day, Inc., San Francisco, Cambridge, London, and Amsterdam (1967), pp. 33—37.

The substituent effects hitherto reported in mass spectra have been correlated with σ values. However, in this particular case, a better correlation was attained with σ^+ values.

The low electron voltage mass spectroscopic determination was usually employed for obtaining a good Hammett plot in order to avoid various decompositions.[4] In this study, we have also examined the mass spectra of the compounds at 20 eV. The results are shown in Fig 3.

In this case, the decomposition of step 3 disappeared completely in all the compounds. The formation of the phenoxy cation in the methoxy compounds was observed more markedly since the formation of ions A and B was too small to be observed. Thus, the data obtained by 80 eV mass spectrometry will be discussed.

The effect of substituents observed at the first step of the decomposition is in good accord with electrostatic consideration. The electron-withdrawing substituent is expected to accelerate step 1 decomposition while the electron-donating substituent such as methoxy group retards the reaction accompanied by the fragmentation through the heterolysis of opposite orientation. The following considerations might help to explain the effect observed at the processes (steps 2 and 3) which do not actually deal with the fragment ions bearing substituents of the precursor ions.

One explanation is to assume the direct process leading to the fragment B from the molecular ion by the C–S bond fission or the concerted two bond fission. The stepwise reaction shown in Scheme 1 could not be neglected because of the existence of the metastable peaks. Thus the two competing processes must be included. The ρ-value obtained from the relative peak heights of the molecular ions and the ion B in the presumed direct process of step 1′ ($\rho=+0.72$) is identical with that of the sum of the ρ-values of steps 1 and 2. ($+0.72$). The hypothesis involving two competing processes is not in conflict with the additivity of the ρ-values. Therefore, the direct process from M to B is ruled out.

The only plausible explanation is to apply the statistical theory of mass spectra to the present system as was applied to the spectra of substituted benzophenones by Gross and McLafferty.[5] The two competing processes of the decomposition of the molecular ion in the series of substituted phenyl *p*-toluenesulfonates are the formation of *m/e* 155 $R\text{-}SO_2^+$ ion and substituted phenoxy cation. The pathway requiring less activation energy is the formation of the $R\text{-}SO_2^+$ ion when the substituent is electron-withdrawing group. The $R\text{-}SO_2^+$ ion thus formed would be recoiled with a less excess internal energy to accelerate the subsequent decomposition. When the substituent is an electron-donating group, the favored path gives rise to the formation of phenoxy cation. In this case, the

$R-SO_2^+$ ion formed in the minor path would be endowed with a larger internal energy, and the rate of the subsequent step (step 2) would be more accelerated than that of aryl *p*-toluenesulfonates having electron-withdrawing groups.

The positive and negative ρ-values of the first and the second steps of the decompositions are now rationalized. It is interesting to note that the absolute ρ-values decrease gradually ($1.05 \rightarrow 0.33 \rightarrow 0.27$). The deviation of the rate of the second step with the variation of substituents is ascribed to the various rates of the first step of decomposition. The negative ρ-value may result from the consumption of the excess energy of the $R-SO_2^+$ ion formed in the first step of fragmentation. If the consumption of the excess energy is enough, the ρ-value of the second step may have a magnitude similar to that of the first step but with opposite sign. If the excess internal energy of the $R-SO_2^+$ ion is retained even after the second step, the energy would be consumed by further decomposition processes. The magnitude of the absolute ρ-value of the second step would be smaller than that of the first step, and the ρ-value of the third and forth steps, if any, must have the same sign as that of the second step. The size of the ρ-values of these succeeding steps is considered to decrease to zero until any excess energy formed by the initial step completely disappears. The rates of the decomposition of the fragment ions A and B are influenced by the difference of the activation energies of the first step which depends on the substituent of the molecular ion.

In this connection, the result observed would suggest that the difference of the recoiled energy with the variation of the substituents is retained in the fragment ion even after step 3. The retained energy would be consumed by the succeeding fragmentation. Unfortunately, no clear fragmentation of ion C was observed except for a very small amount of loss of acetylene. However, the peak corresponding to $C_3H_3^+$ was too small to make any sensible plot of the fourth step.

The effect of substituent at the second and third steps of ion-fragmentations in mass spectroscopy is now being tested with other systems.

Experimental

The spectra were recorded with a Hitachi RMU-6E single focus mass spectrometer using 80 eV at the emission current 110 μA. Samples were introduced through an all glass inlet system kept at about 200°C.

The authors are grateful to Dr. K. Takeda of Shionogi Research Laboratory who enabled us to purchase a mass spectrometer.

BULLETIN OF THE CHEMICAL SOCIETY OF JAPAN VOL. 43 1411—1415 (1970)

Chlorinative Coupling of Thiophene by the Action of Sulfuryl Chloride and Iron Powder*1

Tyo SONE, Koji SAKAI and Kimio KURODA

Department of Applied Chemistry, Faculty of Engineering, Yamagata University, Yonezawa

(Received July 14, 1969)

In the presence of iron powder, thiophene reacted with sulfuryl chloride at room temperature to give a mixture of chlorinated 2,2′-dithienyls as the main product in yields of up to 42%, while the reaction without a catalyst gave chlorothiophenes. The yield of the coupling product and the chlorine content in the product increase with an increase in the molar ratio of sulfuryl chloride to thiophene. 5,5′-Dichloro-, 3,5,5′-trichloro-, and 3,3′,5,5′-tetrachloro-2,2′-dithienyls were isolated from the reaction products. The reaction was also catalysed by Friedel-Crafts-type catalysts, the efficiency of the catalysts decreasing in the order: $AlCl_3 > FeCl_3 > SnCl_4 > ZnCl_2$.

There have been several papers concerning the coupling of aromatic[1] and heteroaromatic compounds[2,3] with halogenating agents. In one of these papers, Töhl and Eberhard briefly and without structural elucidation described the forma-

*1 Presented at the 21st Annual Meeting of the Chemical Society of Japan, Osaka, April, 1968.

1) K. Bowden and C. H. Reece, *J. Chem. Soc.*, **1950**, 1686.

2) A. Töhl and O. Eberhard, *Ber.*, **26**, 2940 (1893).

3) a) M. Kunori, *Nippon Kagaku Zasshi*, **83**, 836 (1962); b) M. Kunori, *ibid.*, **83**, 839 (1962).

tion of chlorinated 2,2′-dithienyls by the reaction of thiophene with sulfuryl chloride and aluminum chloride.[2]

In the presence of iron powder as well as Friedel-Crafts-type catalysts, thiophene was found to react with sulfuryl chloride at room temperature to afford chlorinated 2,2′-dithienyls as the main product, while the reaction without a catalyst has been known to give 2-chloro- and 2,5-dichlorothiophene.[4] These facts are of interest not only from mechanistic but also from preparative points of view. Certain 2,2′-dithienyl derivatives, including 5,5′-dichloro-2,2′-dithienyl (II), have been shown to have a

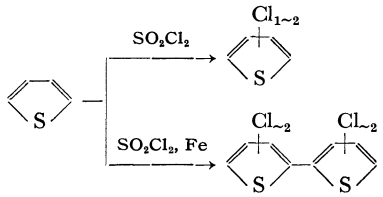

strong nematicidal activity.[5] Previous procedures of preparing 2,2′-dithienyls are based on the coupling of 2-halothiophene by the Ullmann or Grignard method. On the other hand, the present method may provide a convenient, one-step synthesis of those compounds.

The object of the present work is to ascertain the reaction conditions which favor the formation of the coupled products, to isolate the products, and to identify their structures.

Results and Discussion

The reaction of thiophene with sulfuryl chloride and iron powder afforded a crystalline product along with a small amount of liquid chlorothiophenes (less than 10%) and a polymeric material. The crystalline product melted over a rather wide temperature range (60—100°C); it has been suggested that it has a dithienyl structure on the basis of UV spectral and molecular-weight determination. In addition, the product gave a positive test for the Beilstein test. These facts indicate that the product is mainly a mixture of chlorine-substituted dithienyls, presumably chlorinated 2,2′-dithienyls. Although the separation of a pure chlorinated 2,2′-dithienyl from the others is not easy, as has been pointed out in connection with the preparation of 5-chloro-2,2′-dithienyl by the direct chlorination of 2,2′-dithienyl,[5,6] three chlorinated 2,2′-dithienyls, *i. e.*, II, 3,5,5′-trichloro-2,2′-dithienyl (III) and 3,3′,5,5′-tetrachloro-2,2′-dithienyl (IV), could be isolated by the fractional recrystallization of the reaction mixtures.

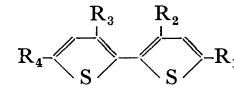

(I): $R_1=Cl$, $R_2=R_3=R_4=H$
(II): $R_1=R_4=Cl$, $R_2=R_3=H$
(III): $R_1=R_2=R_4=Cl$, $R_3=H$
(IV): $R_1=R_2=R_3=R_4=Cl$
(V): $R_1=R_2=R_3=Cl$, $R_4=H$

The product obtained from the reaction of thiophene with a large excess of sulfuryl chloride consisted principally of tetrachloro-2,2′-dithienyl. The positional assignment of chlorine atoms was based on the NMR spectrum of the dechlorination product of the tetrachloro-2,2′-dithienyl with zinc powder in an acetic acid solution. The spectrum of the trichloro-2,2′-dithienyl thus obtained shows a singlet and two doublets with a relative intensity of 1 : 1 : 1, as is shown in Table 1. The singlet at 6.84 ppm is due to the hydrogen at the β-position of one thiophen ring, and the doublets at 7.32 ppm and 6.95 ppm correspond to two hydrogens of the other ring in the trichloro-2,2′-dithienyl, coupling constant ($J=5.5$ Hz) being indicative of 2,3-disubstituted thiophene.[7] These results are in agreement with those to be expected for 3,3′,5-trichloro-2,2′-dithienyl (V), which in turn indicate that the original tetrachloro-2,2′-dithienyl is IV.

II and III were isolated from the products obtained by the reactions of thiophene with a one-half molar equivalent of sulfuryl chloride (Table 2, No. 3) and with an equimolar amount of sulfuryl chloride (Table 2, No. 4) respectively, but in low yields. II was identified by comparison with the authentic sample prepared from 2-chloro-5-iodothiophene by the Ullmann reaction. The structure of III was confirmed by means of NMR spectroscopy, as in the case of V.[7] The UV and NMR spectral data of the chlorinated 2,2′-dithienyls are summarized in Table 1.

The effects of the molar ratio of sulfuryl chloride to thiophene and catalysts on the composition of the product were studied in some detail. The crystalline products[8] obtained under various condi-

4) E. Campaigne and W. M. LeSuer, *J. Amer. Chem. Soc.*, **70**, 415 (1948).

5) J. H. Uhlenbroek and J. D. Bijloo, *Rec. Trav. Chim. Pays-Bas*, **79**, 1181 (1960).

6) W. Steinkopf, "Die Chemie des Thiophens," Steinkopf, Dresden and Leipzig (1941), p. 143.

7) S. Gronowitz, "Advances in Heterocyclic Chemistry," Vol. 1, ed. by A.R. Katritzky, Academic Press, New York (1963), p. 7. The coupling constants between two protons in disubstituted thiophenes are: $J_{35}=1.25$—1.70 Hz, $J_{25}=3.20$—3.65 Hz, $J_{34}=3.45$—4.35 Hz, and $J_{45}=4.90$—5.80 Hz.

8) The IR spectra of the crystalline products exhibit a moderate band other than those of the chlorinated 2,2′-dithienyls at about 710 cm^{-1}. It was also shown by vpc that the crystalline products usually consisted of 10—20% of unidentified materials in which one component predominated; when zinc chloride was used as the catalyst, the crystalline product, exceptionally, consisted of about 30% unidentified materials.

Table 1. Spectral data of chlorinated 2,2′-dithienyls

Compd.	UV λ_{max}^{MeOH} mμ (log ε)*1	NMR δ*2
2,2′-dithienyl	246 (3.80), 302 (4.09)	6.84 (4-H) 7.00 (5-H) 7.02 (3-H) } *3
2,3′-dithienyl	235 (3.92), 283 (4.07)*4	
I	247 (3.77), 311 (4.14)*5	
II	245 (3.76), 317 (4.22)	6.73 (d, 3-H or 4-H) 6.80 (d, 3-H or 4-H) } J=4.0 Hz
III	256 (3.75), 317sh (4.19) 326 (4.20)	6.78 (4-H) 6.83 (d, 3′-H or 4′-H) 7.02 (d, 3′-H or 4′-H) } J=4.0 Hz
IV	257 (3.99), 298 sh (4.00) 309 (4.04), 325 sh (4.00) 338 sh (3.79)	6.84 (4-H)
V	257 (3.99) 303 (3.96) 313 sh (3.92), 330sh (3.67)	6.84 (4-H) 6.95 (d, 4′-H or 5′-H) 7.32 (d, 4′-H or 5′-H) } J=5.5 Hz

*1 sh: shoulder
*2 Measured in carbon tetrachloride solution.
*3 K. Takahashi, private communication.
*4 H. Wynberg and A. Bantjes, *J. Org. Chem.*, **24**, 1421 (1959). Measured in ethanol solution.
*5 Data reported in Ref. 12. Measured in ethanol solution.

Table 2. Reaction of thiophene with sulfuryl chloride and iron powder
(Reaction temperature, room temperature; Reaction time, 3 hr)

No.	Thiophene g	Mol ratio thiophene/SO_2Cl_2	Catalyst	Chlorinated 2,2′-dithienyls Yield (Mol-%*1)			
				I	II	III	IV
1	21.0	1 : 1	none	2-chlorothiophene 39.8% 2,5-dichlorothiophene 4.7%			
2	21.0	1 : 0.1	Fe 0.5 g	0.2	2	0.2	—
3	21.0	1 : 0.5	Fe 0.5 g	trace	10	5	—
4	21.0	1 : 1	Fe 0.5 g	trace	9	13	1
5	21.0	1 : 2	Fe 0.5 g	—	2	25	11
6	10.5	1 : 5	Fe 0.5 g	—	—	—	42
7	21.0	1 : 1	Fe 5.0 g	trace	7	8	0.5
8	21.0	1 : 1	Fe 0.5 g $PhNO_2$ 20 ml	trace	7	12	1
9	21.0	1 : 1	Fe 0.5 g S 2 g	trace	9	14	1
10	16.8	1 : 1	$AlCl_3$ 0.45 g*2	trace	13	15	1
11	16.8	1 : 1	$FeCl_3$ 0.55 g*2	trace	11	14	1
12	16.8	1 : 1	$SnCl_4$ 0.88 g*2	trace	5	7	0.3
13	16.8	1 : 1	$ZnCl_2$ 0.46 g*2	trace	1	4	1

*1 Based on thiophene used.
*2 3.4 mmol.

tions were shown by vapor-phase chromatography (vpc) to consist mainly of a mixture of chlorinated 2,2′-dithienyls, the composition depending on the conditions employed. Table 2 shows the results. The yield of the coupling product, and at the same time the chlorine content in the product, increase with an increase in the molar ratio of sulfuryl chloride to thiophene. An increase in the amount of iron powder tends to increase the formation of the polymeric material. The presence of sulfur or nitrobenzene, which is known to retard free-radical reactions, did not essentially influence the composition of the product. The reaction was also catalyzed by Friedel-Crafts-type catalysts, the efficiency of the catalysts in the coupling reaction then decreasing in the order: $AlCl_3 > FeCl_3 > SnCl_4 > ZnCl_2$.[9] This

9) The use of zinc chloride as a catalyst particularly tends to increase the chlorine content in the product; the reason for this is not clear.

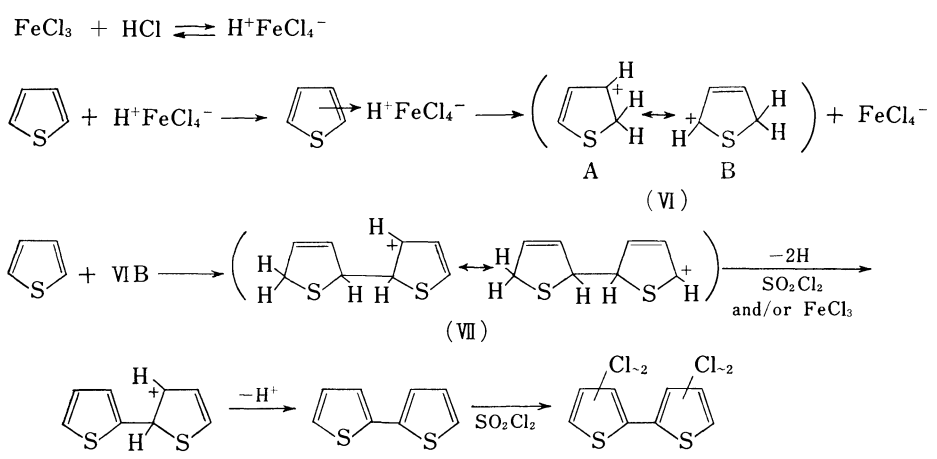

Scheme 1

order is substantially in agreement with that observed in the Friedel-Crafts reaction.[10] These results suggest that the chlorinative coupling of thiophene proceeds *via* an ionic mechanism.

Attempts to isolate 5-chloro-2,2′-dithienyl (I),[11] the presence of which was revealed by vpc, and the crystalline products other than I, II, III, and IV from the reaction mixtures were unsuccessful.

When another chlorinating agent, such as thionyl chloride or sulfur chloride, was used in place of sulfuryl chloride, not coupling but polymerization occurred.[13] The reaction of thiophene with bromine in the presence of iron powder gave only bromothiophenes. 2-Chlorothiophene and 2-methylthiophene, on the other hand, were merely chlorinated at the 5-position in the reaction with sulfuryl chloride and iron powder.

From the facts mentioned above, the following reaction path seems to be most probable for the chlorinative coupling of thiophene with sulfuryl chloride and iron powder (Scheme 1): The first step in the process is the protonation of thiophene by the hydrogen chloride and ferric chloride which were produced during the reaction, thus forming an ionic complex (VI) analogous to the Friedel-Crafts complex. The second step is the attack of the more stable cation, VIB, on the 2-position of a thiophene molecule, followed by the dehydrogenation of the so-formed carbonium ion intermediate (VII) with sulfuryl chloride and/or ferric chloride and then by the loss of a proton to yield 2,2′-dithienyl, although the stage at which dehydrogenation takes place is not yet clear. The chlorination of the resulting dithienyl produces chlorinated dithienyls. The repetition of the process will give polythienyls. In fact, a small amount of a polymeric material was formed in every run. The possibility of the formation of 2,3′-dithienyl derivatives (VIII) can not be ruled out, but VIII could not be isolated from the reaction mixtures. The reason why coupling does not take place with 2-chlorothiophene and with 2-methylthiophene may be expalined as follows. 2-Chlorothiophene is not basic enough to be protonated in the system, and even if it were, it is not susceptible to the attack of the so-formed cation analogous to VI in the next step. On the other hand, 2-methylthiophene is so reactive that chlorination occurs in preference to coupling.

Experimental[14]

Reaction of Thiophene with Sulfuryl Chloride in the Presence of Iron Powder. General Procedure. Sulfuryl chloride (34 g, 0.25 mol) was added to a stirred mixture of thiophene (21 g, 0.25 mol) and commercially-obtained reduced iron powder (0.5 g) at room temperature. Within several minutes the mixture darkened and sulfur dioxide and hydrogen chloride

10) L. F. Fieser and M. Fieser, "Advanced Organic Chemistry," Reinhold Publishing Corp., New York (1961), p. 651.

11) The authentic sample was prepared according to the method described in the literature.[12]

12) R. F. Curtis and G. T. Phillips, *J. Chem. Soc.*, **1965**, 5134.

13) Recently, Fujisawa *et al.* found that some aromatic compounds such as anisole reacted with sulfur chloride or sulfur dichloride in the presence of iron powder to give the corresponding diaryl sulfides in fair yields. T. Fujisawa, N. Kikuchi and G. Tsuchihashi, Preprints for the 21st Annual Meeting of the Chemical Society of Japan (April, 1968), pp. 1572, 1573.

14) All the melting points and boiling points are uncorrected. The infrared spectra were obtained on a Hitachi EPI-S2 spectrophotometer, and the ultraviolet spectra, on a Hitachi EPU-2A spectrophotometer. The NMR spectra were recorded with a Varian Associates A-60 spectrometer in carbon tetrachloride at 60 MHz, using tetramethylsilane as the internal reference. The vpc analyses were carried out on a Hitachi K23F instrument.

were evolved, but the temperature remained almost unchanged. After three hours chloroform (60 ml) and then water (100 ml) were stirred into the deep purple reaction mixture; when the mixture was stirred for an additional 10 min, the mixture turned brown. A small amount of the brown precipitate (0.5 g) was filtered and washed with chloroform. The chloroform layer was washed with water, a 5% sodium bicarbonate solution, and again with water, and then dried (Na_2SO_4). After the solvent and the unreacted thiophene (4.5 g, analyzed by vpc) had been removed, the residue was distilled under reduced pressure to give chlorothiophenes (2.4 g, bp 25—55°C/56 mmHg). The residual mass (12.2 g) was sublimed twice under reduced pressure (2—4 mmHg) at about 140°C; pale yellow crystals (8.7 g, mp 54—87°C) were thus separated from the tarry material.

The data for the various run are given in Table 2.

5,5′-Dichloro-2,2′-dithienyl (II). *a) Isolation of II from the Coupling Products.* II was isolated from the reaction mixture which had been obtained by the reaction of thiophene with a one-half molar equivalent of sulfuryl chloride (Table 2, No. 3) by fractional recrystallization from methanol; colorless leaflets; mp 107.5—109°C (lit, 109—110°C,[2] 109°C[5]).

Found: C, 41.16; H, 2.03%. Calcd for $C_8H_4Cl_2S_2$: C, 40.85; H, 1.71%.

b) Ullmann Reaction of 2-Chloro-5-iodothiophene (IX). The procedure was a modification of the method used for the preparation of 2-iodothiophene from thiophene.[15] Nitric acid (*d* 1.42; 20.6 g) was added to a stirred mixture of 2-chlorothiophene (20 g) and pulverized iodine (19.6 g) over a period of about 2 hr. During the addition, the temperature of the reaction mixture remained at 25—30°C and brown nitrogen oxides were evolved. After the addition was complete, the mixture was heated at 40—45°C for 1 hr and then at 80°C for 1 hr, after which it was treated as has been described for 2-iodothiophene. The yield was 35.5 g (86.6%); bp 94—97 °C/14 mmHg (lit, 95—96°C/14 mmHg[16]).

A mixture of IX (20 g) and copper-bronze (Cu 80%, 20 g) was heated with stirring at 210—215°C for 2 hr. The reaction mixture was then cooled and carefully extracted with chloroform (100 ml). The solvent was removed from the extract to leave a solid material, the recrystallization of which from methanol (300 ml) afforded almost pure II (4.8 g, mp 108—108.5°C). The concentration of the filtrate gave an additional crop (1.0 g, mp 106—107°C) and an oily material which was assumed to be recovered IX. The total yield of II was 5.8 g (60.3%). The sublimation of the crude product under reduced pressure raised the melting point to 108—109°C. This compound was proved to be identical with the II isolated from the coupling product by a comparison of their IR and NMR spectra and by a mixed-melting-point determination.

3,5,5′-Trichloro-2,2′-dithienyl (III). III was isolated from the product which had been obtained by the reaction of thiophene with an equimolar amount of sulfuryl chloride (Table 2, No. 4) by the repeated recrystallization from methanol: mp 102—103°C (lit, 103°C[2]).

Found: C, 35.36; H, 1.11%. Calcd for $C_8H_3Cl_3S_2$: C, 35.63; H, 1.12%.

3,3′,5,5′-Tetrachloro-2,2′-dithienyl (IV). The product obtained by the reaction of thiophene (10.5 g, 0.125 mol) with five molar equivalents of sulfuryl chloride (84.5 g, 0.625 mol) was sublimed at 2—4 mmHg and at 140°C; the sublimate (9.2 g, mp 118—126°C) was then recrystallized from chloroform (160 ml) to give almost pure IV (5.7 g) as colorless needles; mp 127—128°C (lit, 126.5—127°C[17]) (Table 2, No. 6).

Found: C, 31.21; H, 0.83%. Calcd for $C_8H_2Cl_4S_2$: C, 30.99; H, 0.65%.

The further chlorination of a mixture of the chlorodithienyls with excess sulfuryl chloride in carbon tetrachloride at the boiling temperature of the solvent also gave IV, along with a small amount of a resinous material.

Dechlorination of IV. A mixture of IV (0.62 g), zinc dust (2.5 g), acetic acid (20 ml), and water (10 ml) was gently refluxed for 30 hr. The reaction mixture was filtered while hot, and the solid material was washed with hot acetic acid (10 ml). The combined filtrates were cooled to room temperature, and the resultant crystals, which consisted of zinc acetate and recovered IV (0.25 g, mp 124—127°C), were filtered off. To this filtrate, water (100 ml) was added to give crystals (0.19 g, mp 52—56°C); the recrystallization of these crystals from methanol yielded 3,3′,5-trichloro-2,2′-dithienyl (V) as colorless needles; mp 56—57°C.

Found: C, 35.48; H, 0.71%. Calcd for $C_8H_3Cl_3S_2$: C, 35.63; H, 1.12%.

Vapor-phase Chromatographic Analysis. Vpc analyses were performed on a stainless steel column packed with 10% Silicone DC 44M on Chromosorb WAW (Gasukuro Kogyo Co., Ltd.; 60—80 mesh; 3 mmϕ × 1 m). The column temperature was programmed from 150° to 200°C at 5°C/min; the flow rate of nitrogen gas was 8 ml/min. Biphenyl was used as the internal standard.

The authors wish to express their gratitude to Professor Emeritus Yasuo Matsuki of Tohoku University for his continued interest in and support of this work. Thanks are also due to Mr. Fusaji Shoji for his help in many respects.

15) H. Y. Lew and C. R. Noller, "Organic Syntheses," Coll. Vol. IV, p. 545 (1963).

16) W. Steinkopf and W. Köhler, *Ann.*, **532**, 250 (1937).

17) O. Eberhard, *Ber.*, **28**, 2385 (1895)

BULLETIN OF THE CHEMICAL SOCIETY OF JAPAN VOL. 43 1416—1420 (1970)

Reaction of Sulfoxides with Acylating Reagents. I. Mechanism of Oxygen Exchange Reaction of Diaryl Sulfoxides with Acetic Anhydride[1)]

Shigeru OAE and Masahiro KISE

Department of Applied Chemistry, Faculty of Engineering, Osaka City University, Sugimoto-cho, Sumiyoshi-ku, Osaka

(Received July 21, 1969)

Racemization and oxygen exchange reactions were carried out by heating both optically active and ^{18}O-labeled diaryl sulfoxides in a large excess of acetic anhydride. The rate of racemization of *p*-tolyl phenyl sulfoxide was found to be twice the rate of oxygen exchange, suggesting the reaction to involve a Walden inversion at the rate-determining step. When the reaction was carried out in a mixture of acetic anhydride and chlorobenzene, the rate of racemization was found to be first order with respect to both the sulfoxide and acetic anhydride. The remarkably small substituent effect is also in keeping with the S_N2 type mechanism. The marked retardation of the rate of racemization by the addition of common salt is similar to well-known cases in the S_N2 reaction of alkyl halides, and the remarkably large acceleration of the rates of both racemization and oxygen exchange reactions by the addition of sodium perchlorate seems to be caused by a special salt effect.

The sulfur-oxygen linkage in sulfoxides has been considered to possess a semi-polar character,[2)] and unlike those in sulfone groups, the sulfur-oxygen links in sulfoxides are weak and readily cleaved. Another important feature is that optical isomerism can exist in sulfoxide compounds,[3)] and the stereochemical stability of sulfoxides is known greatly to exceed those of similar sulfonium compounds.[4)] Thus sulfoxides are utilizable for studying the nature of nucleophilic substitutions on sulfur atom.

Sulfoxides have been known to undergo concurrent oxygen exchange and racemization reactions in various acidic media, such as concentrated sulfuric acid,[5,6)] hydrochloric acid in aqueous dioxane,[7)] hydrobromic acid in acetic acid,[8)] dinitrogen tetraoxide[9)] and acetic anhydride.[10)] In a previous paper,[11)] we showed that sulfoxides undergo concurrent oxygen exchange and racemization reactions through an acid catalyzed S_N1-type process in weak carboxylic acids. In this paper we would like to report a detailed account of another oxygen exchange reaction of aromatic sulfoxides in acetic anhydride, which appears to proceed through an S_N2-type route.

We suggested[12)] on the basis of ^{18}O tracer experiments with ^{18}O-labeled acetic anhydride that the Pummerer reaction of dimethyl sulfoxide with acetic anhydride proceeds through an intermolecular nucleophilic attack of an acetate group on the methylene carbon of the ylide-ylene intermediate II.

$$CH_3SCH_3 + (CH_3CO)_2O \rightleftarrows CH_3-\overset{+}{S}(\overset{\downarrow}{O})-CH_3 + {}^-OAc \rightarrow CH_3-\overset{+}{S}(OAc)-CH_2OAc$$

(I)

$$\left[CH_3-\overset{+}{S}(OAc)-CH_2^- \leftrightarrow CH_3-S(OAc)=CH_2\right] \xrightarrow{HOAc} CH_3SCH_2OAc$$

(II)

However, the rather fast interchange of alkoxy groups in the following reactions, found recently by Johnson and Phillips,[13)] cast doubt on the

1) Paper XXVIII on Sulfoxides.

2) C.C. Price and S. Oae, "Sulfur Bonding," Ronald Press, New York (1962), Chapter 4.

3) K.K. Anderson, *Tetrahedron Lett.*, **1962**, 93.

4) a) D. Darwish and G. Tourigny, *J. Amer. Chem. Soc.*, **88**, 4303 (1966). *b*) R. Scartazzini and K. Mislow, *Tetrahedron Lett.*, **1967**, 2719.

5) S. Oae and N. Kunieda, This Bulletin, **41**, 696 (1968) and references cited in this paper.

6) H. J. Shine and D. R. Thompson, *Tetrahedron Lett.*, **1966**, 1591.

7) K. Mislow, T. Simmons, J. T. Mellillo and A. L. Ternay, Jr., *J. Amer. Chem. Soc.*, **86**, 1452 (1964).

8) W. Tagaki, K. Kikukawa, N. Kunieda and S. Oae, This Bulletin, **39**, 614 (1966).

9) a) C. R. Johnson and D. McCants, Jr., *J. Amer. Chem. Soc.*, **87**, 1109 (1965). b) S. Oae, N. Kunieda and W. Tagaki, *Chem. Ind.* (London), **1965**, 1790.

10) a) S. Oae and M. Kise, *Tetrahedron Lett.*, **1967**, 1409.

11) S. Oae. M. Yokoyama and M. Kise, This Bulletin, **41**, 1221 (1968).

12) S. Oae, T. Kitao, S. Kawamura and Y. Kitaoka, *Tetrahedron*, **19**, 817 (1963).

13) C. R. Johnson and W. G. Phillips, *Tetrahedron Lett.*, **1965**, 2101.

significance of our ^{18}O tracer experiments, since a facile acetoxy interchange could also take place within salt I.

$$^{14}CH_3O\text{-}\overset{+}{S}(CH_2Ph)(CH_2Ph) + CH_3O^- \rightleftharpoons$$

$$^{14}CH_3O^- + \overset{+}{S}(CH_2Ph)(CH_2Ph)\text{-}OCH_3$$

In fact, when an optically active diaryl sulfoxide labeled with ^{18}O was heated in acetic anhydride and the sulfoxide was quantitatively recovered by quenching the reaction mixture with cold water, the recovered sulfoxide was found to have lost its optical activity as well as the excess of ^{18}O. Thus the acetoxy interchange appears to take place readily. We have investigated this oxygen exchange reaction of diaryl sulfoxides extensively in order to understand the nature of the reaction, focusing our attention only on the acetoxy interchange, since with these sulfoxides other competing reactions such as Pummerer rearrangement and the heterolysis of carbon-sulfur linkage which will be discussed in a succeeding paper[14] can be avoided.

Results and Discussion

The oxygen exchange reaction was carried out by heating both optically active and ^{18}O-labeled diaryl sulfoxides in a large excess of acetic anhydride. The sulfoxides employed in this study were *p*-tolyl phenyl, *p*-chlorophenyl phenyl and diphenyl sulfoxides.

When the reaction of *p*-tolyl phenyl sulfoxide with acetic anhydride was carried out in an inert solvent, chlorobenzene, the rate was found to be correlated nicely with a second order kinetic equation, *i. e.* $v=k_2[p\text{-}CH_3C_6H_4SOC_6H_5][Ac_2O]$. (Table 1, Fig. 1). The rate of the reaction of *p*-tolyl benzyl sulfoxide with acetic anhydride was found to be correlated similarly with a second order equation in the same solvent.[14] However, when the reaction was carried out in dioxane, the rate was found not to be correlated by a second order equation. A similar anomaly was observed in the case of *p*-substituted phenyl benzyl sulfoxides with acetic anhydride. The plot of the second order rate constants against the concentration does not give a straight line of slope one in Fig. 2. In fact, the rate is apparently correlated by a 3rd order kinetic equation, namely second order with respect to the concentration of acetic anhydride and first order with the sulfoxide ($v=k_3[>S\rightarrow O][Ac_2O]^2$).

Probably this is due mainly to a special interaction between dioxane and acetic anhydride. Since dioxane is a nucleophilic solvent, it would interact with acetic anhydride to form a loose complex and this interaction may compete with the acetylation of the sulfoxide oxygen of low basicity ($pK_a=-4.40$),[15] thus reducing the rate of the reaction. Incidentally, the reaction between more basic α- or γ-alkylpyridine- or alkylquinoline *N*-oxide with

Table 1. Determination of the kinetic order of racemization reaction in chlorobenzene[a]

Run No.	Ac_2O (g)	Relative concn. Ac_2O	Relative rate
1	3.7565	1.00	1.00
2	6.5447	1.74	2.04
3	10.451	2.78	3.05

a) The reaction was carried out at 120°C in a sealed tube, with sulfoxide, 10^{-3} mol, dissolved in 10 m*l* of the reaction mixture of chlorobenzene and acetic anhydride.

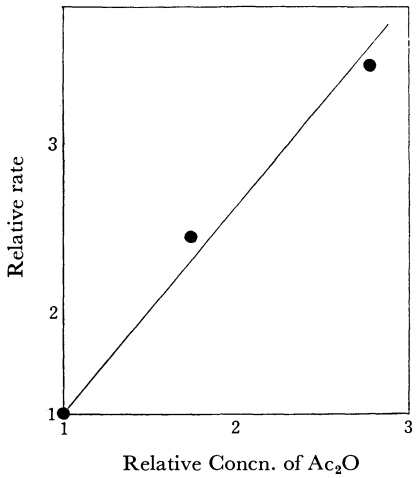

Fig. 1. Determination of the kinetic order of the racemization reaction in chlorobenzene. Plot of relative rate of racemization against concentration of acetic anhydride.

Table 2. Determination of the kinetic order of racemization reaction[a] in dioxane

Run No.	Ac_2O (g)	Relative concn. Ac_2O	Relative rate
4	4.042	1.00	1.00
5	5.033	1.25	1.33
6	8.027	1.99	4.20
7	8.965	2.22	8.83
8	10.451	2.59	11.3

a) The reaction was carried out at 120°C in a sealed tube, with sulfoxide, 10^{-3} mol, dissolved in 10 m*l* of the reaction mixture of dioxane and acetic anhydride.

14) M. Kise and S. Oae, This Bulletin, **43**, 1421, 1426 (1970).

15) a) K. K. Anderson, W. H. Edmonds, J. B. Biasotti and R. A. Strecker, *J. Org. Chem.*, **31**, 2859 (1966). b) K. Sakai, N. Kunieda and S. Oae, unpublished work in these laboratories.

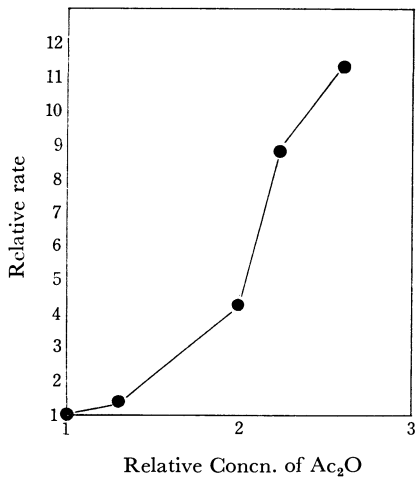

Fig. 2. Determination of the kinetic order of the racemization reaction in dioxane. Plot of relative rate of racemization against concentration of acetic anhydride.

acetic anhydride in dioxane is known to be correlated with the normal second order kinetic equation.[16] The oxygen exchange reaction is undoubtedly of ionic character and hence expected to be facilitated in a more polar solvent, acetic anhydride. A similar oxygen exchange reaction of aryl benzyl sulfoxides is accelerated markedly in a still more polar solvent, acetonitrile.[17]

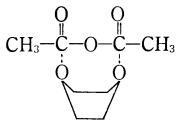

The rates of ^{18}O exchange and racemization in acetic anhydride, together with other pertinent data, are shown in Table 3.

Inspection of the kinetic data reveals that the rate of racemization, k(rac), of *p*-tolyl phenyl sulfoxides was twice that of oxygen exchange. This means that the reaction involves a Walden inversion at the rate determining step. The energy and the entropy (at 120°C) of activation for the reaction were found to be 19.2 kcal/mol and −28.6 e.u., respectively. The small value of the entropy of activation is also in keeping with the suggested mechanism. In the ^{18}O exchange reactions in both dinitrogen tetraoxide and highly concentrated sulfuric acid, k_{exch}/k_{rac} is unity, while the entropies of activation of both reactions are substantially large and positive. The oxygen exchange reaction in less concentraetd sulfuric acid (for example 75.4% H_2SO_4) is considered to be an S_N2-type process and gives a k_{exch}/k_{rac} value of roughly 1/2.[18] In this case the entropy of activation is quite small ($\Delta S^{\neq} = -18.9$ at 30°C).

The small substituent effects are also in accordance with the S_N2-type mechanism, since the reaction is expected to pass through an ideal transition state in which both the entering and the leaving group are identical. The polar effect of substituents should be considerably cancelled and reduced in many typical S_N2 reactions at the saturated carbon atom.[19] Thus, the over-all process of the reaction can be illustrated as shown in Fig. 3.

It is known that the acetate ion, once formed, undergoes a rapid interconversion with acetic anhydride as represented by the following equation.[20]

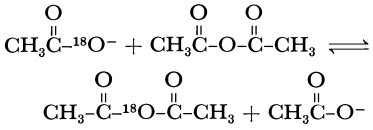

Table 3. Kinetic data on oxygen exchange and racemization reactions in acetic anhydride[a] at 120°C

Run No.	R in R-C$_6$H$_4$-S(=O)-C$_6$H$_5$	Added salt	k(rac) $\times 10^5$ (sec^{-1})	k(exch) $\times 10^5$ (sec^{-1})
9	CH_3		9.97±0.35	5.00±0.20
10	CH_3	CH_3COONa[b]	2.29±0.10	
11	CH_3	$NaClO_4$[c]	497±22	275±45
12	Cl			3.97±0.55
13	H			4.68±0.42

a) Sulfoxide, 5×10^{-3} mol, was treated with 0.5 mol of acetic anhydride.
b) NaOAc, 0.001 mol, in 0.5 mol Ac_2O
c) $NaClO_4$, 0.001 mol, 0.5 mol Ac_2O

16) S. Tamagaki, S. Kozuka and S. Oae, unpublished work in these laboratories.
17) M. Kise and S. Oae, This Bulletin, in press.
18) N. Kunieda and S. Oae, *ibid.*, **42**, 1324 (1969).
19) a) C. K. Ingold, "Structure and Mechanism in Organic Chemistry," Chapter 5 and 7, Cornell Univ. Press, Ithaca and London (1953). b) K. Akagi, S. Oae and M. Murakami, *J. Amer. Chem. Soc.*, **78**, 4034 (1956).
20) L. Ponticorvo and D. Rittenberg, *J. Amer. Chem. Soc.*, **76**, 1705 (1954).

Thus ^{18}O-containing acetate ion will be quickly diluted by rapid interchange with the bulk unlabeled acetic anhydride.

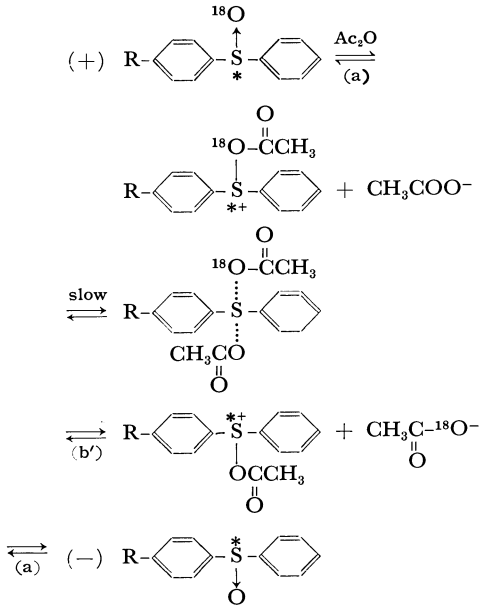

Fig. 3

The marked retardation of the rate of racemization by the addition of common salt is considered to be due to a similar retardation found in the S_N2 reactions of alkyl halides and related compounds.[21] A similar, though small, negative common salt effect was known in a few rearrangement reactions of heteroaromatic *N*-oxides and acetic anhydride.[22] The remarkably large acceleration of the rates of both racemization and oxygen exchange reactions by the addition of sodium perchlorate also seems to be caused by a special salt effect as in the well-known cases found by Winstein and his coworkers.[23] A similar rate acceleration by the addition of perchlorate ion was also observed in the reaction of quinaldine *N*-oxide and acetic anhydride.[24]

The addition of acetic acid also increases the rate of both the racemization[25] and the oxygen exchange. Racemization of sulfoxides in acetic anhydride is also known to be catalyzed markedly by a small amount of Lewis acid.[26]

21) S. Winstein, E. Clippinger, A. H. Fainberg, R. Heck and G. S. Robinson, *ibid.*, **78**, 328 (1956).
22) J. H. Markgraf, H. B. Brown, Jr., S. C. Mohr and R. G. Teterson, *ibid.*, **85**, 958 (1963).
23) C. A. Bunton, "Nucleophilic Substitution at Saturated Carbon Atom," Chapter, 5 Elsevier, Amsterdam (1963).
24) S. Oae, S. Tamagaki, T. Negoro, K. Ogino and S. Kozuka, *Tetrahedron Lett.*, **1968**, 917.
25) E. Jonsson, *Acta Chem. Scand.*, **21**, 1278 (1967).
26) E. Jonsson, *Tetrahedron Lett.*, **1967**, 3675.

Table 4. Influence of acetic acid on the racemization reaction of sulfoxides in acetic anhydride[a]

Run No.	AcOH	$k_{rac} \times 10^5$ (sec^{-1})	Rel rate
14	0	4.45	1
15	0.0663	6.25	1.40
16	0.1230	10.1	2.28
17	0.2492	16.7	3.75
18	1.0254	102.7	23.1
19	2.0484	231.7	52.1

a) The reaction was carried out at 120°C in a sealed tube. Sulfoxide, 10^{-3} mol, was treated with acetic anhydride. No solvent was used.

A question arises whether the acid catalyzed reactions would proceed through an S_N1-like path involving rate-determining S–O bond cleavage, as in the oxygen exchange reactions in carboxylic acids and concentrated sulfuric acid. When the reaction was carried out in the presence of a small amount of acetic acid, the ratio of the rate constants, k_{exch}/k_{rac} became unity. This may mean than the presence of Brönsted acid facilitates the cleavage of S–O bond by the easy protonation on the sulfoxide oxygen and the assistance of the nucleophilic attack by acetate becomes less important in the reaction.

The catalytic effect of both the Brönsted and Lewis acid is considered to be due to the acceleration of both the first acetylation step (a) and also the second slow step of S_N2 type process, since in both steps the leaving of acetate group will be facilitated by either protonation or co-ordination with a Lewis acid as shown below.

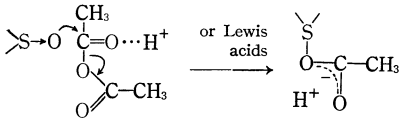

Phenol, albeit a weak Brönsted acid, was found to accelerate the rate of racemization of sulfoxides.

Experimental

Materials. *Optically Active p-Tolyl Phenyl Sulfoxide.* This sulfoxide was prepared by the method of Anderson[3] whereby (—)- menthyl (—)-*p*-toluenesulfinate was allowed to react with phenylmagnesium bromide in ether (mp 91—93°C $[\alpha]_D = +26.9°$ in ethanol).

^{18}O-Labeled p-Substituted Aryl Phenyl Sulfoxide. The corresponding sulfide was oxidized with bromine in the presence of pyridine in acetic acid and $H_2{}^{18}O$, according to the usual procedure.[27] All the sulfoxides had >S→O stretching bands in their infrared spectra at about 1050 cm^{-1}. Their melting points and ^{18}O-contents are shown below.

27) S. Oae, Y. Ohnishi, S. Kozuka and W. Tagaki, This Bulletin, **39**, 364 (1966).
28) G. Modena, *Gazz. Chim. Ital.*, **89**, 834 (1959).

p-CH_3; 69.8—71°C lit,[28] 71—72°C (1.09 atom%)
p-Cl; 45—46°C lit,[28] 45—46°C (1.05 atom%)
p-H; 71°C lit,[28] 71°C (0.89 atom%)

Dioxane, obtained commercially, was purified according to the usual procedure, thoroughly dried with sodium and distilled (bp 101.5°C).

Acetic Acid, obtained commercially, was treated with chromic oxide. After refluxing for several hours it was distilled (bp 117.5—118°C).

Acetic Anhydride, obtained commercially, was treated with anhydrous sodium acetate. After refluxing for several hours, it was distilled (bp 139.5—140°C).

Kinetic Procedure (I). Concurrent oxygen exchange and racemization reactions were carried out at 120±0.05°C (paraffin bath) while the molar ratio of sulfoxide to acid anhydride was kept at 1 : 100. Thus, a mixture of sulfoxide (5×10^{-3}) and acetic anhydride (5×10^{-1} mol) was allowed to react. From time to time, 5 m*l* of the reaction mixture was pippetted out and poured into an excess of water. The sulfoxide separated out, was then extracted with carbon tetrachloride, and dried with anhydrous magnesium sulfate. Carbon tetrachloride was distilled off and the resulting sulfoxide was recovered. The recovered sulfoxide was dried thoroughly and subjected to measurements of both specific rotation and ^{18}O-analysis. The specific rotation was measured in ethanol at c : 3.00, and ^{18}O-analysis of sulfoxide-oxygen was carried out as usual according to the modified Rittenberg-Porticorvo method.[5] The k values in Table 3 and the activation parameters were determined by this procedure. All the rate constants quoted were determined from the equations for racemization.

$$\log [\alpha]_{D0} - \log [\alpha]_{Dt} = \frac{kt}{2.303},$$

where $[\alpha]_{D0}$ and $[\alpha]_{Dt}$ are the rotatory powers at times 0 and t, respectively, and for oxygen exchange,

$$\log [\beta_0-\beta] - \log [\beta_t-\beta] = \frac{kt}{2.303},$$

where β_0 and β_t are the atom % ^{18}O at times 0 and t, respectively, and β is the atom % ^{18}O of natural CO_2. A typical kinetic run is shown below.

Kinetic Procedure II. The racemization reaction was carried out at 120±0.05°C in sealed tubes in which *p*-tolyl phenyl sulfoxide (10^{-3} mol) was dissolved in 10 m*l* of acetic anhydride containing no other solvent or solute. From time to time a sealed tube was taken out from the paraffin bath and placed in an ice bath in order to stop the reaction. Then the acetic anhydride solution containing the sulfoxide was immediately subjected to the measurement of specific rotation.

Polarimetric Run
No. 10 *p*-Tolyl phenyl sulfoxide, 10^{-3} mol, in 10^{-1} mol of Ac_2O

Time (min)	0	30	60	90	120	150	180
$[\alpha]_D$	23.7°	19.7°	16.9°	13.7°	12.2°	9.7°	7.5°

10^5k (sec^{-1}) = 9.98 ± 0.35

No. 11 *p*-Tolyl phenyl sulfoxide, 10^{-3} mol, in 10^{-1} mole of acetic anhydride contg. 2×10^{-4} mol NaOAc

Time (min)	0	25	55	85	115
$[\alpha]_D$	24.8	23.9	23.0	22.2	21.3

10^5k (sec^{-1}) = 2.29 ± 0.10

Exchange Run
No. 10 *p*-Tolyl phenyl sulfoxide, 10^{-3} mol, in 10^{-1} mol of Ac_2O

Time (min)	0	30	90	120	150	210
β_t	0.818	0.753	0.630	0.571	0.504	0.428

10^5k (sec^{-1}) = 5.00 ± 0.20

Determination of the Kinetic Order of Racemization Reaction in Dioxane. The reaction was carried out at 120°C in sealed tubes, each containing 10 m*l* of the reaction mixture, which was prepared from dioxane and acetic anhydride containing optically active *p*-tolyl phenyl sulfoxide (10^{-3} mol). From time to time, a sealed tube was taken out from the paraffin bath. Each kinetic run was carried out as in the above procedure.

Influence of Acetic Acid on Racemization. The reaction was carried out at 120°C in sealed tubes. A mixture af acetic anhydride and acetic acid containing an optically active sulfoxide (10^{-3} mol) was prepared and 10 m*l* of the reaction mixture was sealed in each tube and subjected to the usual kinetic measurements.

BULLETIN OF THE CHEMICAL SOCIETY OF JAPAN VOL. 43 1421—1426 (1970)

Reaction of Sulfoxides with Acylating Reagents. II. Mechanism of the Reactions of Aryl Benzyl Sulfoxides with Acetic Anhydride[1)]

Masahiro KISE and Shigeru OAE

Department of Applied Chemistry, Faculty of Engineering, Osaka City University, Sugimoto-cho, Sumiyoshi-ku, Osaka

(Received July 24, 1969)

Aryl benzyl sulfoxides undergo oxygen exchange and racemization reaction with acetic anhydride, and the rate is dependent on the concentration of both the sulfoxide and acetic anhydride. The reaction proceeds faster in a more polar solvent. Addition of sodium perchlorate or acetic acid accelerates the reaction. In this case, the rate of oxygen exchange is not exactly half of that of racemization. As an example, the ratio, k_{ex}/k_{rac}, is 0.36 when the reaction was carried out at 100°C. Under the same condition, both the Pummerer reaction and thermal racemization are negligible. Similar to diaryl sulfoxides the effects of phenyl group are small. Implication of the ratio is discussed.

In previous papers,[2)] dealing with the reaction of diaryl sulfoxides with acetic anhydride, we focused our attention only on the oxygen exchange. In this reaction with an optically active diaryl sulfoxide, the rate of racemization k_{rac}, was found to be twice that of oxygen exchange and the effect of polar substituents was rather small. Based on these and related observations, we suggested that the reaction proceeds through an S_N2 type Walden inversion at the rate determing step. As an extension of this oxygen exchange reaction with acetic anhydride, we have chosen aryl benzyl sulfoxides, with the intention of comparing the rate of the oxygen exchange with that of possible Pummerer rearrangement, since the rate-determining removal of proton from benzylic carbon in the Pummerer reaction is considered to be easier with these sulfoxides. Thus we have prepared a few *p*-substituted phenyl benzyl sulfoxides and subjected them to the reaction with acetic anhydride. This paper will describe detailed accounts of our kinetic experiments and the mechanistic implications of the data obtained.

Results and Discussion

When optically active *p*-tolyl benzyl sulfoxide was heated with a large excess of acetic anhydride at 100°C, the sulfoxide recovered from time to time was found to have lost its activity. The ^{18}O-labeled *p*-tolyl benzyl sulfoxide, under the same reaction condition, was found to undergo oxygen exchange reaction. The rate of the Pummerer rearrangement was quite small under the same reaction condition as compared to the rates of both oxygen exchange and racemization. The kinetic order of the racemization of *p*-tolyl benzyl sulfoxide was examined. When the reaction was carried out in chlorobenzene, the rate was found to be first order in each component *i. e.*, $v=k_2[>S\rightarrow O][Ac_2O]$ (Table 1, Fig. 1).

However, as in the case of diaryl sulfoxides, the kinetics of racemization did not follow the second order equation but satisfied the third order equation, $v=k_3[>S\rightarrow O][Ac_2O]^2$ when the reaction was

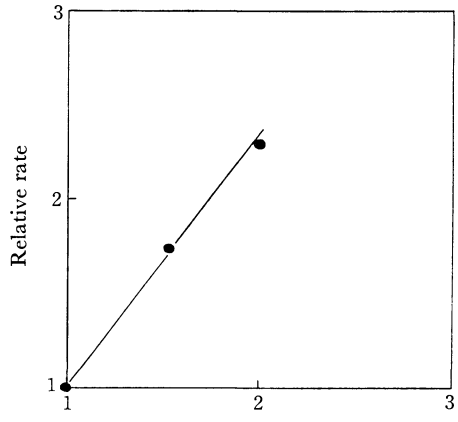

Fig. 1. The determination of kinetic order of racemization reaction in chlorobenzene. The relation between relative rate of racemization and concentration of acetic anhydride.

1) Paper XXIX on Sulfoxide, XXVIII on sulfoxide S. Oae and M. Kise, This Bulletin, **43**, 1416 (1970).

2) a) S. Oae and M. Kise, *Tetrahedron Lett.*, **1967**, 1409; b) S. Oae and M. Kise, This Bulletin, and related references cited in this paper.

Table 1. Determination of kinetic order of racemization reaction in chlorobenzene solvent[a)]

No.	Ac_2O(gr)	$k^{b)} \times 10^5$ (sec^{-1})	Rel. concn. $Ac_2O^{c)}$	Relative rate
1	10.7797	7.30	1	1
2	16.5660	12.0	1.53	1.74
3	21.5522	16.7	2.00	2.29

a) The reaction was carried out at 100°C in a sealed tube. Sulfoxide, 10^{-3} mol, was dissolved in 20 m*l* reaction mixture of chlorobenzene and acetic anhydride.
b) Pseudo lst order rate constant.[2)]
c) Relative concentration of acetic anhydride in 20 m*l* reaction mixture of acetic anhydride and chlorobenzene.

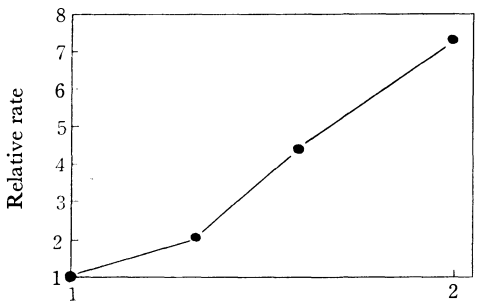

Fig. 2. The determination of kinetic order of racemization reaction in dioxane solvent. The relation between relative rate of racemization and concentration of acetic anhydride.

performed in dioxane (Table 2, Fig. 2). Since dioxane is a nucleophilic solvent, it would interact with acetic anhydride and the interaction might reduce the rate of the reaction notwithstanding the fact that the reaction is expected to be faster in a more polar solvent, acetic anhydride, than in nonpolar dioxane.

The effect of substituents on phenyl group in the oxygen exchange reaction of *p*-substituted phenyl benzyl sulfoxide was examined in acetic

Table 2. Determination of kinetic order of racemization reaction in dioxane solvent[a)]

No.	Ac_2O(gr)	$k \times 10^5$ (sec^{-1})	Rel. concn. Ac_2O	Rel. k rate
1	10.8228	2.30	1	1
2	14.3722	4.68	1.33	2.03
3	17.2515	10.1	1.60	4.39
4	21.5522	16.7	2.00	7.26

a) The reaction was carried out at 100°C in a sealed tube. Sulfoxide, 10^{-3} mol, was dissolved in 20 m*l* reaction mixture of dioxane and acetic anhydride.

Table 3. Kinetic data on oxygen exchange and racemization reaction on aryl benzyl sulfoxide[a)] 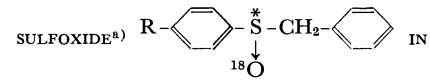 in acetic anhydride at 100°C

Substituent (R)	Added salt	$k_{ex} \times 10^5$	$k_{rac} \times 10^5$	k_{ex}/k_{rac}
OCH_3		4.70		
CH_3		4.75	13.4	0.36
CH_3	AcONa[b)]		3.58	
H		5.49		
Cl		4.28		
NO_2		6.01		

a) Sulfoxide 10^{-3} mol in Ac_2O 20 m*l* soln.
b) NaOAc 10^{-3} mol in Ac_2O 20 m*l* soln.

anhydride at 100°C and the results are tabulated in Table 3. (Table 3). As in the case of *p*-substituted diphenyl sulfoxides, the substituent effect is rather small, suggesting that the main path of the reaction is S_N2 type oxygen exchange process in which the effect of substituent is largely cancelled. We see, however, that the rate constant of racemization is more than two-fold that of oxygen exchange, *viz.*, the ratio, k_{ex}/k_{rac} was 0.36 when the reaction was carried out at 100°C. Apparently other processes cause additional racemization in addition to the main reaction of the oxygen exchange process of S_N2 type nucleophilic substitution which is the only path observed in the case of diaryl sulfoxides. Other processes responsible for the racemization may include thermal racemization of sulfoxide itself, nucleophilically assisted heterolysis of S–C bond of either non-acetylated or acetylated sulfoxide by acetate ion and Pummerer rearrangements. All these processes are illustrated as shown below (Fig. 3).

The first possibility, namely, the thermal racemization (path a), by either the direct inversion of the pyramidal structure of the sulfoxide[3,4)] or the double rearrangements involving the incipient formation of benzyl arylsulfenate as the intermediate, is quite unlikely, since these aryl benzyl sulfoxides undergo very little thermal racemization at this temperature (at 100°C) in any of the common solvents, chlorobenzene, acetonitrile, dioxane, and dimethyl sulfoxide without acetic anhydride.

The second possible path for racemization (path b) which does not necessarily accompany oxygen exchange, namely, the acetic acid-catalyzed racemization appears plausible but is not likely, since the

3) a) D. R. Rayner, E. D. Miller and K. Mislow, *J. Amer. Chem. Soc.*, **88**, 3138 (1966). b) D. R. Rayner, A. L. Gordon and K. Mislow, *ibid.*, **90**, 4854 (1968).
4) E. G. Miller, D. R. Rayner, H. T. Thomas and K. Mislow, *ibid.*, **90**, 4861 (1968).

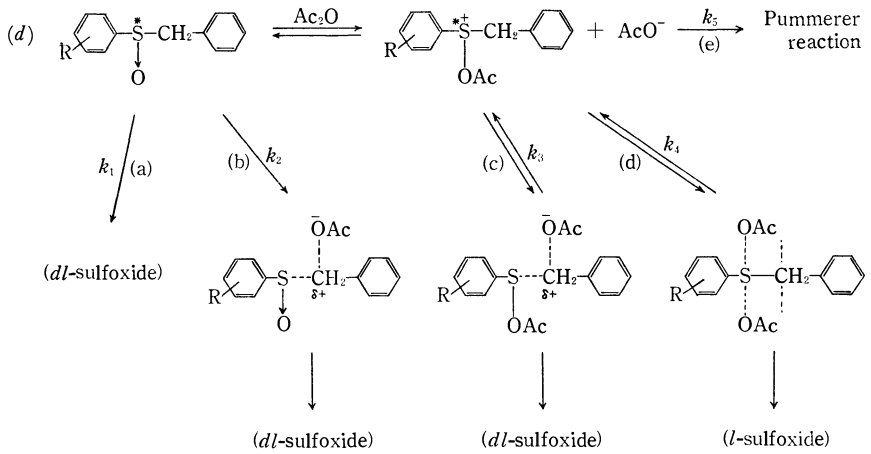

$$k_{rac} = k_1 + k_2 + k_3 + k_4 + k_5$$

Fig. 3

rate of racemization of any of aryl benzyl sulfoxides in acetic acid alone is negligible as compared to that in acetic anhydride ($k_{Ac_2O}/k_{AcOH} \gg 100$). Acetic anhydride undoubtedly takes part in facilitating the racemization.

The third possible path (path c) that takes the role of acetic anhydride into consideration is plausible. It involves the heterolysis of S–C bond following the prior acetylation of the sulfoxide function. Since benzylic sulfoxide compounds are known to undergo homolytic C–S bond cleavage in solvents of low polarities,[4] the heterolysis of benzyl acetoxysulfonium acetate would be more facile because of the substitution of more electronegative acetoxy group at the sulfur atom.

This path is very likely to contribute in the excess racemization during oxygen exchange. If the heterolysis always leads to a complete racemization, the contribution of path (c) in the racemization is calculated to be 29% from the value of 0.36 for k_{ex}/k_{rac}, and the rest of the racemization is ascribed to the S_N2 type process as illustrated by path (d).

Undoubtedly path (d) is the main reaction pathway for racemization, since the racemization is accompanied by a substantial oxygen exchange though not as completely as in the case of diaryl sulfoxides.

Another path which is responsible for reducing optical rotation of the original solution of the sulfoxide is the Pummerer rearrangement (path e) which eventually results in the conversion of the sulfoxide to α-acetoxybenzyl aryl sulfides. However, this reaction is negligible. Thus, the first two paths (a and b) can be ruled out and path (c) also appears to be negligible. The pathways (c) and (d) are the remaining possible paths for racemization and responsible for the apparent anomaly of the ratio of the rates of oxygen exchange and racemization, *i. e.* $k_{ex}/k_{rac}=0.36$. These reactions are interwoven to make the overall kinetic rates of the racemization complicated.

In order to clarify the relative importance of three different pathways at different temperatures, kinetic experiments were carried out in the range of temperatures between 60 and 120°C and the results are shown in Table 4. The Arrhenius plot of the kinetic data is shown in Fig. 4. The data

Table 4. Values of the rate constants of reaction at temperatures from 60 °C to 120 °C[a]

Temp. °C	T°K	$1/T\times10^3$	$k\times10^5$ (sec^{-1})	log k+5
60	333	3.003	0.50	−0.292
80	353	2.833	3.66	0.562
85	358	2.793	5.22	0.718
90	363	2.755	7.93	0.800
100	373	2.681	16.7	1.223
110	383	2.611	43.3	1.636
120	393	2.545	119	2.076

a) The reaction was carried out in a sealed tube.

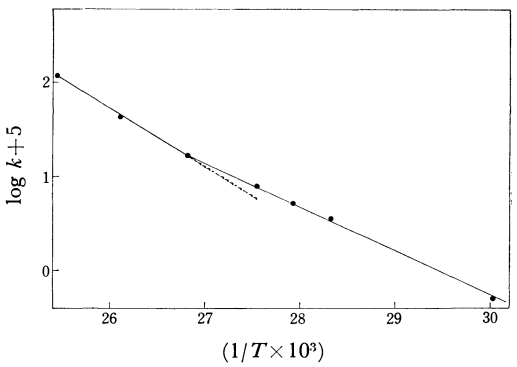

Fig. 4. The Arrhenius plot of the reaction between *p*-tolyl benzyl sulfoxides and acetic anhydride.

Table 5. Influences of acetic acid on the racemization reaction tolyl benzyl sulfoxides at 55°C

No.	AcOH (gr)	Ac_2O (gr)	$k_{rac} \times 10^5$ $(sec)^{-1}$	Relative rate
1	0		0.400	1
2	1.2898	9.4233	1.24	3.1
3	3.1357	7.5550	5.36	13.4
4	5.7052	4.9275	7.19	18.0
5	7.9020	2.5956	2.66	6.65
6	8.3702	2.2307	2.12	5.3

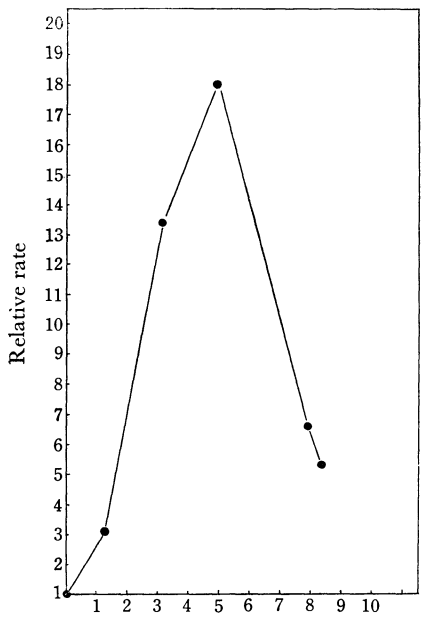

Fig. 5. The influences of acetic acid to the racemization reaction tolyl benzyl sulfoxides at 55°C.

in Table 4 and Fig. 4 reveal that the Arrhenius plot of the rate gives a curve instead of a straight line.

At 90°C the energy and entropy of activation of the overall racemization of the sulfoxide was estimated to be 21.8 kcal/mol and −17.24 e.u., while those at 110°C were calculated as 28.5 kcal/mol and 0.0 e.u. respectively. Apparently, there in a gradual change of mechanistic pathways around 100°C, where the curve of the Arrhenius plot makes a turn. We expected that the S_N2 type process would be the predominant path at a low temperature and the value of k_{ex}/k_{rac} would approach 0.5 while at a higher temperature other paths would participate giving rise to the reduction of the k_{ex}/k_{rac} value.

At a low temperature, *e. g.* 80°C, the Pummerer rearrangement is negligible. However, the value of k_{ex}/k_{rac} was found to be 0.35 suggesting that the S_N2 type oxygen-exchange process (path d) is not the only route but another path, very likely path (c), is participating in the racemization. The small activation energy and entropy factor suggest that the main reaction for the racemization is the nucleophilic substitution process (path d).

Table 6. Influence of mercuric chloride on the racemization reaction of tolyl benzyl sulfoxide at 25°C

No.	$HgCl_2$ (mg)	Relative concn. $HgCl_2$	$k_{rac} \times 10^4$ (sec^{-1})	Relative rate
1	0	0	0.0014	1
2	60.4	1	3.29	2350
3	115.4	1.91	4.73	3380
4	272.0	4.53	8.89	6350
5	447.7	7.41	13.8	9890

Table 7. Influence of sodium perchlorate on the racemization reaction of sulfoxide[a)]

No.	$NaClO_4$ (mg)	$[NaClO_4]$	$k_{rac} \times 10^5$ (sec^{-1})	Relative rate
1	8.8	0.00120	0.650±0.005	1
2	44.6	0.00607	2.31 ±0.04	3.31
3	89.3	0.01220	5.11 ±0.18	7.86
4	187.2	0.02550	10.7 ±0.1	16.5
5	307.5	0.04180	17.8 ±0.6	27.4
6	556.1	0.0757	24.1 ±0.7	37.1
7	961.7	0.1309	29.3 ±0.4	45.1
8	987.7	0.1344	31.3 ±1.2	48.2

a) The reaction was carried out at 55°C. The sulfoxide, 3×10^{-4} mol, was reacted in acetic anhydride of 6 ml soln. containing sodium perchlorate.

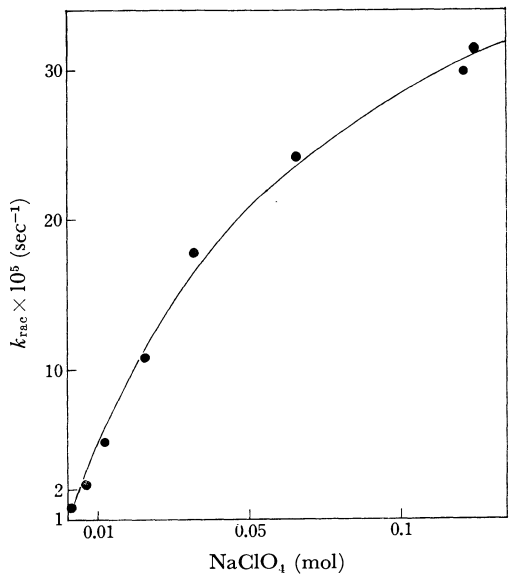

Fig. 6. The influences of sodium perchlorate to the racemization reaction of sulfoxides.

The racemization of the sulfoxide in this reaction was catalyzed markedly in the presence of acetic acid (Table 5, Fig. 5).

The rate of racemization increases remarkably with the increase of the concentration of acetic acid up to the concentration of acetic anhydride. It falls off gradually with further increase of the concentration. In a low concentration acetic acid it would solvate effectively only at the carbonyl groups of both acetic anhydride and the acetoxysulfonium intermediate, thus increasing the rate. Excess acetic acid would solvate sulfoxide oxygen either by hydrogen bonding or protonation and the initial acetylation would be retarded, though both the heterolysis of O–S and C–S bonds will be facilitated.

As in the case of diaryl sulfoxides, the addition of mercuric chloride or Lewis acid increases the rate of racemization remarkably (Table 6) as also is the case with sodium perchlorate (Table 7, Fig. 6).

Addition of the Lewis acid facilitates both the acetylation and heterolysis of both S–O and C–S bonds substantially while the addition of sodium perchlorate would increase the ionic strength of the medium and also shift the equilibrium of acetylation step to the right to increase the rate of racemization.

Table 8. Kinetic data of the racemization of *p*-tolyl benzyl sulfoxide with acetic anhydride in several solvents at 100°C[a)]

Run	Used solvent	$k_{rac} \times 10^5$ (sec^{-1}) at 100°C	Ac_2O (g)
1	C_6H_5Cl	7.20	10.7797
2	CH_3CN	17.2	10.7936
3		2.30	10.8228
4	$(CH_3)_2NCHO$	2.16	10.7573

a) Sulfoxide, 10^{-3} mol, was reacted with acetic anhydride in 20 ml reaction soln.

Solvent effect was examined with four different solvents and the results are summarized in Table 8. Apparently the reaction is slow in two nucleophilic solvents, dioxane and dimethyl formamide (DMF) but is faster in less nucleophilic and polar solvents, chlorobenzene and acetonitrile. Undoubtedly nucleophilic solvents interact with acetic anhydride to retard the initial acetylation of the sulfoxide group while both acetylation and the succeeding hetero lysis would be facilitated in less nucleophilic but polar media to result in the increase of the over-all rate of the racemization.

We might conclude that the apparent over-all racemization of aryl benzyl sulfoxides in acetic anhydride or acetic anhydride containing media is caused by two participating reactions, *i. e.*, pathways (c) and (d) in which (d) is the predominant route. At low temperatures below 100°C, the contribution of S–C bond cleavage pathway (c) is small but becomes substantial as the reaction temperature is raised.

Experimental

Material. *Optically Active p-Tolyl Benzyl Sulfoxide.* The sulfoxide was prepared by the method of Anderson[5)] in which (−)-menthyl (−)-*p*-toluenesulfinate was treated with benzylmagnesium chloride in ether. Mp 167°C $[\alpha]_D$ +250° (in ethanol), lit,[6)] mp 169—170°C $[\alpha]_D$ +252°.

p-Substituted Phenyl Benzyl Sulfoxides ^{18}O-Labeled.[7)] Each of the corresponding sulfide was oxidized with bromine in the presence of pyridine in acetic acid and $H_2{}^{18}O$, according to the usual procedure. All the sulfoxides had S–O stretching bonds in their infrared spectra at about 1050 cm^{-1}. Their melting points, ^{18}O-concentration (atom %) and chemical shift of methylene are summarized in Table 9.

Dioxane, obtained commercially, was purified according to the usual procedure, finally dried with sodium and distilled (bp 101.5°C).

Acetic Acid, obtained commercially was treated with chromic anhydride and after refluxing for several hours, was distilled (bp 117.5—118°C).

Table 9. Physical properties and ^{18}O-concentration of ^{18}O-labeled *p*-substituted aryl benzyl sulfoxides

R in R- -SO^{18}-CH_2-	Melting point (ref)	^{18}O-Concentration (atom%)	Chemical shift of methylene (ppm)
OCH_3	126C° (−)	1.08	3.99, 4.04
CH_3	140—141°C (140—141°C)[6)]	1.08	4.03
H	127°C (127°C)[8)]	1.06	4.03
Cl	135°C (135°C)[9)]	1.34	4.03
NO_2	168°C (168—169°C)[10)]	1.15	4.11

5) K. K. Anderson, *Tetrahedron Lett.*, **1962**, 93.
6) C. J. M. Stirling, *J. Chem. Soc.*, **1963**, 5741.
7) S. Oae, Y. Ohnishi, S. Kozuka and W. Tagaki, This Bulletin, **39**, 364 (1966).
8) M. Nishio and T. Ito, *Chem. Pharm. Bull.* (Tokyo), **13**, 1392 (1965).
9) J. D. M. Tiecco and A. Tundo, *Gazz. Chim. Ital.*, **1913**, 92.
10) G. L. A. Mangini and R. Passerini, *J. Chem. Soc.*, **1957**, 1386.

Acetic Anhydride, obtained commercially, was treated with anhydrous sodium acetate and after refluxing for several hours, was distilled (bp 139.5—140°C).

Kinetic Procedure I (Oxygen Exchange Reaction). The oxygen exchange reaction was carried out at 100±0.05°C in sealed tubes into which aliquotes of a solution containing *p*-substituted phenyl benzyl sulfoxide (10^{-3} mol) in 20 m*l* of acetic anhydride were placed. From time to time a sealed tube containing 5 m*l* of the solution of the reaction mixture was withdrawn and placed in an ice bath in order to stop the reaction. The sulfoxide separated out was extracted with carbon tetrachloride, then carbon tetrachloride was distilled off and the resulting sulfoxide was recovered. The recovered sulfoxide was dried throughly and subjected to ^{18}O-analysis.[11]

Kinetic Procedure II (Racemization Reaction). The racemization reaction was carried out at a set temperature ranging from 60 to 120°C in sealed tubes in each of which a portion of the reaction mixture containing optically active *p*-tolyl benzyl sulfoxide (10^{-3} mol) in 20 m*l* of acetic anhydride was placed without using other solvents. At suitable time intervals sealed tubes each containing 3 m*l* of reaction mixture were drawn out and placed into an ice bath to stop the reaction. 3 m*l* of dioxane was then added into the tube and the whole solution was subjected to the determination of specific rotation. The constants obtained are usually in good agreement with those obtained by isolating the product under kinetic procedure I.

11) S. Oae and N. Kunieda, This Bulletin, **41**, 696 (1968).

BULLETIN OF THE CHEMICAL SOCIETY OF JAPAN VOL. 43 1426—1430 (1970)

Reaction of Sulfoxides with Acylating Reagents. III. Mechanism of the Reactions of Phenyl Methyl Sulfoxide with Acetic Anhydride[1]

Masahiro KISE and Shigeru OAE

Department of Applied Chemistry, Faculty of Engineering, Osaka City University, Sugimoto-cho, Sumiyoshi-ku, Osaka

(Received July 29, 1969)

The Pummerer reaction, *viz.*, the reaction of sulfoxides having at least one methyl or methylene group with carboxylic acid anhydride gives α-acyloxy derivatives of the corresponding sulfide. Earlier, we suggested on the basis of ^{18}O tracer experiments with ^{18}O-labeled acetic anhydride that the Pummerer reaction of dimethyl sulfoxide with acetic anhydride proceeds through an intermolecular nucleophilic attack of acetoxy group on the methylene carbon of the ylide-ylene intermediate. Noticeable acetoxy interchange has been found to take place during a similar Pummerer reaction of aryl methyl sulfoxide. However, the Pummerer reaction is the main path when the reaction with acetic anhydride is performed at around 120°C. In the Pummerer reaction of aryl methyl sulfoxides, the substituent effect is large ($\rho = -1.6$) and the kinetic isotope effect (k_H/k_D) is also substantial, *i.e.*, 2.9. The reaction is assumed to involve the initial acetylation and the subsequent slow proton removal steps. Addition of sodium perchlorate or acetic acid accelerates the acetoxy exchange reaction rather than the Pummerer reaction.

The Pummerer Reaction[2] has been known for many years. When an alkyl (or aryl) methyl sulfoxide is treated with acetic anhydride, there is formed a rearranged ester (III) *i. e.* acetoxymethyl alkyl (or aryl) sulfide which upon hydrolysis results in the formation of alkyl (or aryl) mercaptan, formaldehyde and acetic acid. Among the mechanisms suggested for the Pummerer reaction[2-4]

$$\mathrm{R\text{-}S\text{-}CH_3} + (\mathrm{CH_3CO})_2\mathrm{O} \rightleftharpoons \underset{\mathrm{O}}{\mathrm{R\text{-}S\text{-}CH_3}} \rightarrow \underset{\text{(III)}}{\mathrm{R\text{-}S\text{-}CH_2O\overset{\overset{\mathrm{O}}{\|}}{C}CH_3}} + \mathrm{CH_3COOH} \xrightarrow{\mathrm{H_2O}} \mathrm{R\text{-}SH} + \mathrm{CH_2O} + \mathrm{CH_3COOH}$$

only the one by Bordwell and Pitt,[3] involving the

1) Paper XXX on Sulfoxides.

2) L. Horner and P. Kaiser, *Ann.*, **626**, 19 (1959), and references cited in this paper.

3) F. G. Bordwell and B. M. Pitt, *J. Amer. Chem. Soc.*, **77**, 572 (1955).

4) W. J. Kenney, J. A. Walsh and D. A. Davenport, *ibid.*, **83**, 4019 (1961).

ylide-ylene intermediate (II), appears reasonable. We suggested on the basis of ^{18}O tracer experiments with ^{18}O-labeled acetic anhydride that the Pummerer reaction of dimethyl sulfoxide with acetic anhydride proceeds through an intermolecular nucleophilic attack of acetoxy group on the methylene carbon of the ylide-ylene intermediate (II).[5]

$$CH_3SCH_3 + (CH_3CO)_2O \rightleftarrows CH_3-\overset{+}{S}(OAc)-CH_3 + \overset{+}{O}Ac \quad (I)$$

$$CH_3-\overset{+}{S}(OAc)-CH_2^- \longleftrightarrow CH_3-S(OAc)=CH_2 \xrightarrow{HOAc} CH_3SCH_2OAc$$

(II) (III)

However, the fast interchange of alkoxy group in the following reactions found by Johnson and Phillips[6] made the significance of our ^{18}O tracer experiments doubtful,

$$^{14}CH_3O-\overset{+}{S}(CH_2Ph)(CH_2Ph) + CH_3O^- \rightleftarrows$$

$$^{14}CH_3O^- + \overset{+}{S}(PhCH_2)(PhCH_2)-OCH_3$$

since a facile interchange could also take place within the salt (I) and the possible acetoxy interchange would also scramble the ^{18}O completely in the whole reaction system. We found that acetoxy interchange which causes both the oxygen exchange and the racemization does take place with diaryl sulfoxides in warm acetic anhydride. The rate of the racemization of *p*-tolyl phenyl sulfoxide was found to be twice that of the oxygen exchange suggesting that the reaction involves a Walden inversion at the rate-determining step.[7]

In the case of aryl methyl sulfoxides both concurrent oxygen exchange with racemization reactions and Pummerer reaction take place. As in the case of diaryl sulfoxides[8] racemization of aryl methyl sulfoxides with acetic anhydride is also catalyzed markedly by a small amount of Lewis acid. In order to clarify the over-all feature of the reaction, the kinetic investigation of the reaction is desirable. This paper describes a detailed account of the kinetic study of the Pummerer reaction and the concurrent oxygen exchange and racemization reactions of *p*-substituted phenyl methyl sulfoxide with acetic anhydrides.

5) S. Oae, T. Kitao, S. Kawamura and Y. Kitaoka, *Tetrahedron*, **19**, 820 (1963).

6) a) N. J. Leonald and C. R. Johnson, *J. Amer. Chem. Soc.*, **84**, 3701 (1962). b) C. R. Jonhson and W. G. Phillips, *Tetrahedron Lett.*, **1965**, 2101.

7) a) S. Oae and M. Kise, *Tetrahedron Lett.*, **1967**, 1409. b) S. Oae and M. Kise, *ibid.*, **1968**, 2261.

8) E. Jonsson, *ibid.*, **1967**, 3675.

Results and Discussion

A few *p*-substituted phenyl methyl sulfoxides and two α-trideuterated derivatives were synthesized and subjected to both the Pummerer reaction and the concurrent oxygen exchange and racemization reactions. The rate of the Pummerer reaction can be readily followed spectrophotometrically, taking an advantage of the difference of UV spectra of the starting sulfoxide and the final compounds, *i. e.*, aryl mercaptan obtained by quenching the reaction mixture with water.

The rate of racemization reaction of optically active *p*-tolyl methyl sulfoxide was determined by the usual procedure, measuring the optical rotation of the reaction solution. In this case, the rate constant of the racemization consisted of two rate constants, the one due to the oxygen exchange and the other caused by the Pummerer reaction. When the reaction was carried out in dioxane, the rate of the Pummerer rearrangement of *p*-tolyl methyl sulfoxide with acetic anhydride was found to be correlated by the second order equation, *i. e.*,

$$v = k_2[p\text{-}CH_3C_6H_4SOCH_3][Ac_2O]$$

Similarly, the rate of the racemization reaction was also found to be correlated by the second order

Table 1. The determination of kinetic order of the Pummerer reaction of *p*-tolyl methyl sulfoxide with acetic anhydride in dioxane[a]

Run No.	Ac_2O (g)	$k \times 10^5$ (sec^{-1})	Relative concn. Ac_2O	Relative rate
1	2.139	2.72	1	1
2	5.311	6.42	2.483	2.360
3	7.450	8.73	3.483	3.210
4	10.451	17.6	4.886	6.471

a) This reaction was carried out at 120°C in sealed tubes, and sulfoxide (*ca.* 0.5×10^{-4} mol) was dissolved in 10 m*l* reaction mixture of dioxane and acetic anhydride.

Table 2. Determination of kinetic order of racemization reaction of *p*-tolyl methyl sulfoxide with acetic anhydride in dioxane[a]

Run No.	Ac_2O (g)	$k \times 10^5$ (sec^{-1})	Relative concn. Ac_2O	Relative rate
5	2.1942	4.38	1	1
6	4.3416	9.08	1.98	2.07
7	6.1687	12.8	2.81	2.92
8	8.4894	19.8	3.87	4.52
9	10.4663	24.8	4.77	5.66

a) The reaction was carried out at 120°C in sealed tubes, and sulfoxide (10^{-3} mol) was dissolved in 10 m*l* relaction mixture of dioxane and acetic anhydride.

Table 3. Kinetic data of the Pummerer reaction in acetic anhydride[a)]

Run No.	R_1R_2 in R_1-C$_6$H$_4$-SO-R_2		k_H(sec^{-1})	k_D(sec^{-1})	k^H/k_D
	R_1	R_2			
10	CH_3	CH_3	2.07×10^{-4}	($\pm$0.10)	
11	H	CH_3	1.09×10^{-4}	($\pm$0.22)	2.9
12	H	CD_3		3.67×10^{-5}	($\pm$0.42)
13	Cl	CH_3	4.00×10^{-5}	($\pm$0.08)	
14	NO_2	CH_3	6.12×10^{-6}	($\pm$0.24)	2.8
15	NO_2	CD_3		2.15×10^{-6}	($\pm$0.11)

a) Sulfoxide (0.4—0.6×10^{-4} mol) was allowed to react with acetic anhydride. No solvent was used. Each kinetic run was carried out at 120°C.

equation.

However, in dioxane solutions containing acetic anhydride in high concentration, the plots of relative rates of both the Pummerer rearrangement and the racemization against the concentration give convex upward curves probably due to the solvent effect.[9)] Tables 1 and 2, reveal that the rate of racemization was the sum of the rates of the Pummerer and twice that of the oxygen exchange reaction, *i. e.*, $k_{rac}=k_P+2k_{ex}$

The over-all rates of the Pummerer reactions of a few *p*-substituted phenyl methyl sulfoxides were determined and the results are listed together with those of trideuterated compounds in Table 3.

The rates are in line with the Hammett equation, and a negative ρ value (for σ), -1.60, was obtained.

When only the rate variation of *p*-substituted phenyl methyl sulfoxides is considered as if the first step of the reaction, *i e.*, acetylation, is the rate-determining step. A large positive ρ-value obtained[10)] in the reaction of dimethyl sulfoxide and *p*-substituted benzoic anhydride seems to support this.

However, the kinetic isotope effect, $k_H/k_D=2.85$ indicates that the rate-determining step is the succeeding step of the reaction, namely the proton removal by acetate anion. Recently Johnson reported that acetoxy group migrates to the least substituted α-carbon in the Pummerer reaction of a few unsymmetrical dialkyl sulfoxide with acetic anhydride. The result is also undoubtedly a reflection of the difference in the acidities of α-protons of the two alkyl groups of the intermediate acetoxysulfonium salts, and the removal of the proton is the rate-determining step of the reaction.[11)] The relatively small value of kinetic isotope effect is due mainly to the fact that the first step of the reaction requires also a substantial energy of activation, as in the reaction between quinaldine *N*-oxide and acetic anhydride.[12)] The addition of sodium perchlorate or acetic acid[13)] was found to accelerate the over-all rates by 3 or 4 fold. Apparently the

Table 4. The influence of sodium perchlorate on the Pummerer reaction[a)]

Run No.	$NaClO_4$ (mg)	$k\times10^4$ (sec^{-1})	Relative rate
16	0	1.76	1
17	2.93	2.92	1.66
18	5.51	4.85	2.76
19	10.10	5.28	3.00

a) Each kinetic run was caried out at 120°C in sealed tubes and the sulfoxide (5×10^{-4} mol) was allowed to react with acetic anhydride. No solvent was used.

Table 5. Influence of acetic acid on the Pummererreaction[a)] of *p*-tolyl methyl sulfoxide

Run No.	AcOH (g)	$k\times10^{-4}$ (sec^{-1})	Relative rate
20	0	1.73	1
21	0.9561	4.97	2.87
22	1.9452	7.73	4.47
23	3.2010	7.73	4.47

a) Each kinetic run was carried out at 120°C in sealed tubes, and the sulfoxide (0.4—0.6×10^{-4}mol) was allowed to react with acetic anhydride. No solvent was used.

Table 6. Influence of acetic acid on the rate of racemization reaction[a)] of *p*-tolyl methyl sulfoxide

Run No.	AcOH (g)	$k\times10^4$ (sec^{-1})	Relative rate
24	0	0.720	1
25	1.0257	3.53	4.90
26	2.0533	8.29	11.5
27	3.7261	15.4	21.4

a) Each kinetic run was carried out at 100°C in sealed tubes, and the sulfoxide (10^{-3} mol), allowed to react with acetic anhydride. No solvent was used.

9) M. Kise and S. Oae, following paper in these series.

10) S. Arita, private communication.

11) a) C. R. Johnson, J. C. Sharp and W. G. Phillips, *Tetrahedron Lett.*, **1967**, 5299. b) C. R. Johnson and W. G. Phillips, *J. Amer. Chem. Soc.*, **91**, 682 (1969).

12) S. Oae, S. Tamagaki, K. Negoro, K. Ogino and S. Kozuka, *Tetrahedron Lett.*, **1968**, 917.

13) E. Jonsson, *Acta Chem. Scand.*, **21**, 1278 (1967).

Table 7. Kinetic data of the Pummerer and racemization reactions in acetic anhydride[a)]

Temp. (°C)	k_{obs} $\times 10^4$ $k_{racemization}$[b)] (sec^{-1})	$\times 10^4$ $k_{Pummerer}$ (sec^{-1})	$\times 10^4$ 2 $k_{exchange}$ (sec^{-1})	$\frac{k_{Pummerer}}{k_{exchange}}$
100	0.720±0.04			
110	1.25 ±0.19	0.853±0.12	0.397	4.3
120	2.53 ±0.06	1.77 ±0.12	0.610	5.8
130	4.48 ±0.09	3.53 ±0.05	0.905	7.4

a) Sulfoxide ($0.4-0.6\times10^{-4}$ moll^{-1}) was allowed to react with acetic anhydride. No solvent was used. This reaction was carried out at 120° C in a sealed tube.

b) The relation, $k_{racemization}=k_{pummerer}+2\ k_{exchange}$ is assumed. The rates of the oxygen exchange reaction were calculated from this equation.

addition of perchlorate tends to shift the equilibrium to the right to increase the concentration of the acetoxysulfonium salts, increasing the rate of the Pummerer reaction. The addition of both sodium perchlorate and acetic acid was found to increase the rate of the reaction of the acyloxy exchange markedly.

Racemization of sulfoxides in acetic anhydride is known to be catalyzed markedly by a small amount of Lewis acid.[8)]

In the oxygen exchange and racemization reactions, both Brönsted and Lewis acids will catalyze the first acetylation step and also the second slow step of S_N2 type process because the leaving of acetate group will be facilitated by either protonation or coordination of Lewis acids.[14)] But in the Pummerer reaction, the effect of the rate acceleration by the addition of acetic acid or sodium perchlorate was considerably smaller than that in oxygen exchange and racemization reaction. The over-all picture of the reaction can be depicted as follows. A mechanism similar to that of this reaction was recently suggested by Johnson.[11)] We have measured the rate of racemization of an optically active *p*-tolyl methyl sulfoxide in acetic anhydride in order to estimate the rate of concurrent oxygen exchange during the reaction. The results are listed together with the rates of the Pummerer reaction in Table 7.

Apparently, the rate of the Pummerer reaction increases markedly with the rise of reaction temperature. This can be seen from a comparison of the enthalpies and entropies of activation of the two reactions, *i. e.*, for O-exchange: E_a, 13.1 kcal/mol; $\Delta S^{\neq}$, −45.1 e. u., for the Pummerer reaction: E_a 21.2 kcal/mol; $\Delta S^{\neq}$, −20.7 e.u., respectively. Below 65°C, under which the Pummerer reaction is negligible, only the oxygen exchange proceeds slowly.

The Pummerer reaction involves the rate-determining proton removal and is accelerated slightly. However, the oxygen-exchange and racemization reactions are markedly accelerated by the addition of acid or sodium perchlorate as in the case of

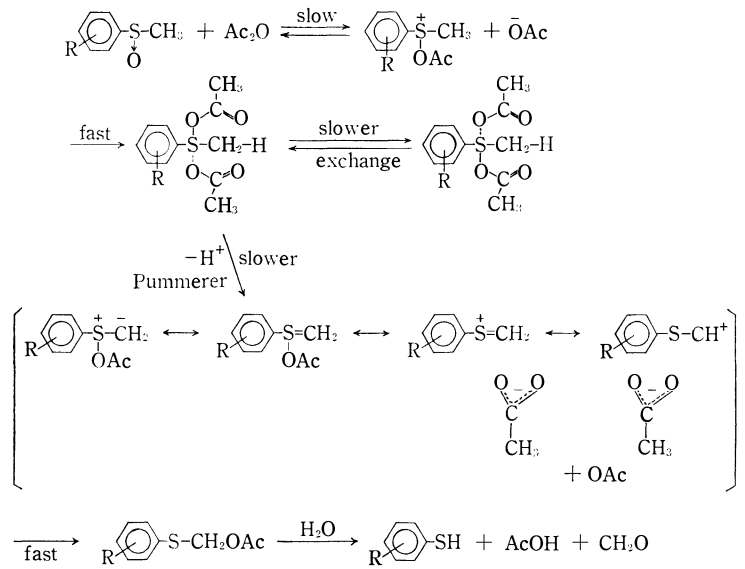

14) S. Oae and M. Kise, following paper in these series.

diaryl and aryl benzyl sulfoxides. The Pummerer reaction becomes significant and takes place faster than the possible oxygen exchange reaction at a high temperature. Our ^{18}O experiments may be still valid in the interpretation of the mechanism especially in connection with the rearrangement steps of the reaction. However, both the S–O bond cleavage and the succeeding formation of the ester are considered to be so fast that these steps cannot be significant in the energy profile of the over-all reaction.

Experimental

Materials. *Optically Active p-Tolyl Methyl Sulfoxide.* The sulfoxide was prepared by the method of Mislow[15] in which(−)-menthyl(−)-*p*-toluenesulfinate was allowed to react with methylmagnesium iodide in ether, (mp 75°C $[\alpha]_D$ +151° in ethanol), lit,[15] mp 73—74°C $[\alpha]_D$ +145.5° (*c* 2.0, acetone).

p-Substituted Phenyl Methyl Sulfoxides. The corresponding sulfide was oxidized with bromine in the presence of pyridine in acetic acid and water, according to the usual procedure.[16] All the sulfoxides has S–O stretching bands in the infrared region at about 1050 cm^{-1}. Thier melting points (boiling points where pressures are given) were *p*-CH_3: 42—43°C, lit,[16] 42—43°C. H: 110°C (1—2 mmHg), lit,[16] 84°C (0.25 mmHg). *p*-Cl: 46—47°C, lit,[16] 47—48°C. *p*-NO_2: 148—149°C, lit,[16] 148—147°C.

p-Substituted Phenyl Tridueterated Methyl Sulfoxide. Phenyl methyl sulfoxide (10^{-2} mol) was heated with deuterium oxide (5×10^{-1} mol) containing triethylamine (10^{-1} mol) for 20 hr at 100°C. After heating, triethylamine and deuterium oxide were distilled off and the residue was distilled *in vacuo* (105°C/1.5 mmHg, lit[16] 84°C/0.25 mmHg). From NMR spectrum the resulting phenyl methyl sulfoxide was found to contain only 85% deuterium at the methyl group. The above procedure was repeated until the resulting sulfoxide showed no methyl proton signal in the NMR spectrum. *p*-Nitro compound was also synthesized by the same procedure. (mp 149°C, lit,[17] 148—149°C).

Dioxane obtained commercially was purified according to the usual procedure and dried with sodium and distilled (bp 101.5°C).

Acetic Acid obtained commercially was treated with chromium trioxide, and was distilled (bp 117.5—118°C), after refluxing for several hours.

Acetic Anhydride obtained commercially was treated with anhydrous sodium acetate and was distilled (bp 139.5—140°C) after refluxing for several hours.

Kinetic Procedure I (The Rate of the Pummerer Reaction). The Pummerer reaction was carried out at 120±0.5°C in sealed tubes in which *p*-substituted phenyl methyl sulfoxide (5×10^{-5} mol) was dissolved without solvent in 10 m*l* of acetic anhydride. From time to time a sealed tube containing 1 m*l* solution of the above mixture was drawn out form the paraffin bath and cooled in an ice-bath to stop the reaction. The mixture was then hydrolyzed with 50 m*l* of alkaline solution (3%). The rates of the Pummerer reaction were readily followed spectrophotometrically, taking advantage of the difference of UV spectra of the starting and the final hydrolyzed compounds (*p*-substituted phenyl mercaptans). All the rate constants quoted in Table 2 were determined from the equation for the Pummerer reaction.

$$\log\frac{a-a_0}{a-a_t}=\frac{k\cdot t}{2.303},$$

where a = the intensity of the absorption due to resulting mercaptide.

Kinetic Procedure II (Racemization Reaction). Recemization reaction was carried out at 120±0.5°C in sealed tubes in which optically active *p*-tolyl phenyl sulfoxide (10^{-3} mol) was dissolved without any solvent in 20 m*l* acetic anhydride. From time to time a sealed tube containing 3 m*l* of the reaction mixture was drawn out from the paraffin bath and cooled in an ice bath to stop the reaction. After the reaction, 3 m*l* of dioxane was added into the sealed tube, and the acetic anhydride solution was subjected to measurement of specific rotation.

15) K. Mislow, M. Green, P. Laur, J. T. Mellio, T. Simmons and A. L. Ternay, Jr., *J. Amer. Chem. Soc.*, **87**, 1958 (1965).

16) S. Oae, Y. Ohnishi, S. Kozuka and W. Tagaki, This Bulletin, **39**, 364 (1966).

17) K. K. Anderson, W. H. Edmonds, J. B. Biasotti and R. A. Strecker, *J. Org. Chem.*, **31**, 2859 (1966).

BULLETIN OF THE CHEMICAL SOCIETY OF JAPAN VOL. 43 1431—1434 (1970)

The Photochromism, Thermochromism, and Piezochromism of Dimers of Tetraphenylpyrryl

Koko MAEDA, Akiko CHINONE*1 and Taro HAYASHI*2

Department of Chemistry, Faculty of Science, Ochanomizu University, Bunkyo-ku, Tokyo

(Received July 25, 1969)

By the oxidation of tetraphenylpyrrole, two types of dimers of tetraphenylpyrryl were obtained. One dimer showed piezochromism and thermochromism, while the other showed photochromism and thermochromism. These phenomena were found to correspond to those of the piezochromic and photochromic dimers of triphenylimidazolyl obtained from triphenylimidazole. The photochromism, thermochromism, and piezochromism of the dimers of tetraphenylpyrryl are determined to be due to the radical dissociation caused by irradiation, heating, and grinding, the same machanism as that in the case of the dimers of triphenylimidazolyl.

Kuhn and Kainer reported[1] that 2,3,4,5-tetraphenylpyrrole (I) was partially oxidized to the tetraphenylpyrryl radical (II) (about 4%). From spectroscopic and ESR studies Blinder *et al.* reported[2] that the oxidation product of I exhibits

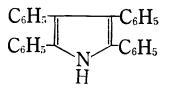

(I)

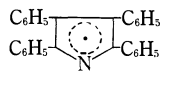

(II)

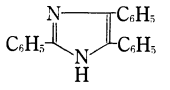

(III)

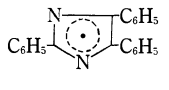

(IV)

photochromism and thermochromism in solutions and that the phenomena are due to the dissociation of the oxidation product into the radical II caused by irradiation and heating. These results corresponded to the photochromism and thermochromism of the photochromic dimer of triphenylimidazolyl (IV) obtained by the oxidation of triphenylimidazole (III).[3] The existence of the photochromic and piezochromic dimers for IV suggests the presence of similar dimers for II. This paper will deal with the preparation of two isomeric dimers of II and with the radical mechanism of photochromism, thermochromism, and piezochromism exhibited by these dimers.

Experimental

Materials. *Oxidation with Lead Dioxide.* A photochromic compound was obtained according to the method Kuhn and Kainer.[1] A solution of I (1 g) in benzene (50 m*l*) was refluxed with lead dioxide (10 g) for about 7 hr in a nitrogen atmosphere. The solution gradually turned pink. By the evaporation of the solvent in a dimmed room under reduced pressure in a nitrogen atmosphere, 0.7 g of a light pink powder (PH), mp 197—204°C, was obtained. PH was slightly soluble in benzene, ethanol, and *n*-hexane.

Found: C, 90.26; H, 5.62; N, 3.70%. Calcd for $C_{56}H_{40}N_2$ (dimer of II): C, 90.77; H, 5.44; N, 3.79%.

PH showed an infrared absorption spectrum similar to that of I. An almost colorless ethanolic solution of PH which was prepared in dim light at room temperature showed absorption maxima at 264 and 317 mμ, maxima which agreed with those of I. The solution turned pink on irradiation at room temperature. The pink solution showed new absorption maxima at 365, 525, and 563 mμ and an ESR signal (g=2.003). From these experimental results, PH was determined to be a mixture of I and a dimer of II. The dimer is called the photochromic dimer (photo-dimer). The concentration of the photo-dimer in PH was determined to be 13% by means of a hydroquinone titration according to the following reaction (1):

$$\underset{\text{(hydroquinone)}}{C_6H_4(OH)_2} + 2\underset{\text{(II)}}{C_{28}H_{20}N} \longrightarrow \underset{\text{(benzoquinone)}}{C_6H_4O_2} + 2\underset{\text{(I)}}{C_{28}H_{21}N} \qquad (1)$$

*1 Present address: Tokyo Institute of Technology, Ookayama, Meguro-ku, Tokyo.

*2 Present address: The Institute of Physical and Chemical Research, Yamato-machi, Kitaadachi-gun, Saitama.

1) R. Kuhn and H. Kainer, *Biochim. Biophys. Acta*, **12**, 325 (1953).

2) S. M. Blinder, M. L. Peller, N. W. Lord, L. C. Aamodt and N. S. Ivanchukov, *J. Chem. Phys.*, **36**, 540 (1962).

3) a) T. Hayashi, K. Maeda, S. Shida and K. Nakada, *ibid.*, **32**, 1568 (1960); b) T. Hayashi and K. Maeda, This Bulletin, **33**, 566 (1960); c) **38**, 685 (1965); d) **42**, 3509 (1969); e) T. Hayashi, K. Maeda and M. Morinaga, *ibid.*, **37**, 1563 (1964); f) T. Hayashi, K. Maeda and M. Takeuchi, *ibid.*, **37**, 1717 (1964); g) T. Hayashi, K. Maeda and T. Kanaji, *ibid.*, **38**, 957 (1965).

Oxidation with Potassium Ferricyanide. A piezochromic compound was obtained from I by means of a modification of the oxidation method of III.[3b] To a solution of I (1.5 g) in ethanol (280 m*l*), a 2% aqueous solution of potassium ferricyanide (400 m*l*) and a 5% ethanolic solution of potassium hydroxide (15 m*l*) were added[4] over about a 30-min period at about 50°C in a nitrogen atmosphere. The pink color of II first appeared, and then a light pink precipitate was formed. After the reaction mixture was cooled to room temperature, the precipitate was filtered in a nitrogen atmosphere, washed repeatedly with water, and dried at room temperature under reduced pressure. A light pink powder (PI) (1.3 g), mp 160—165°C, was thus obtained. PI is soluble in ethanol, benzene, and *n*-hexane.

Found: C, 90.16; H, 5.20; N, 3.67%. Calcd for $C_{56}H_{40}N_2$ (dimer of II): C, 90.77; H, 5.44; N, 3.79%.

The infrared absorption spectrum of PI was rather different from that of I, although it showed a weak N–H band at 3420 cm^{-1}, thus indicating the presence of I. PI showed a weak ESR absorption (g=2.00) and exhibited piezochromism which showed a pink color. A pink solution which was prepared by dissolving PI in ethanol at room temperature showed absorption maxima at 365, 525, and 563 mμ. From these experimental results, PI was determined to be a mixture of I, a dimer of the radical II, and a small amount of II. The dimer is called the piezochromic dimer (piezo-dimer). The concentration of the piezo-dimer in PI was determined to be 23% by means of hydroquinone titration according to Reaction (1).

PH and PI were used for the present study because I itself did not exhibit photochromism, thermochromism, and piezochromism and caused no disturbance in studies of these phenomena.

Spectroscopic Measurements. The absorption spectra were measured with a Hitachi EPS 2 recording spectrophotometer. The absorption spectra at temperatures from −196°C to room temperature were measured by the method described in a previous paper.[3d] The absorption spectrum in the solid state was measured by means of an opal-glass transmission method.

Electron Spin Resonance Absorption. The ESR measurements were carried out in a deaerated state with a Japan Electron Optics Laboratory JES-P-10-type ESR spectrometer (100 kc modulation) which had, as attachments, a 1D-2 integrator and a VT-2 variable temperature controller. The ESR spectra of the triplet state at −196°C were measured with a Japan Electron Optics Laboratory 3B-type ESR spectrometer (100 kc modulation).

Irradiation. The 365-mμ light of a high-pressure mercury lamp (Toshiba SHL-100 UV), filtered through a Toshiba UV-D1B glass filter, was used.

Results and Discussion

Structures of Photo-dimer and Piezo-dimer. The structures of the dimers of IV[5,6] suggest that two tetraphenylpyrryl radicals in the photo-dimer and the piezo-dimer combine at N, C2, or C3 of the pyrryl rings. The HMO calculation of the spin density of II (given in Fig. 1) shows a high probability of the dimerization of II to the piezo-dimer at C2.

The fact that 2,3,4,4-tetrachloro-1,4-dihydronaphthalene-1-one,[7] tetraphenylhydrazine,[8] and the photochromic dimer of IV exhibit photochromism due to a radical dissociation of C–Cl, N–N, and C–N respectively suggests a high probability of linking between the N of one pyrryl ring and the C of another ring in the photo-dimer.

Photochromism of PH in Solutions. An almost colorless solution of PH in benzene, ethanol,

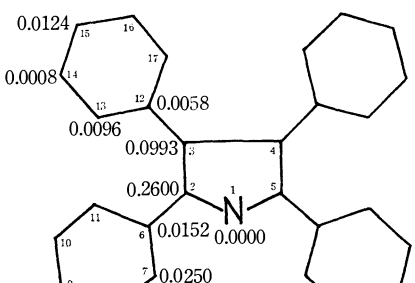

$\alpha_N=\alpha+0.5\beta$, $\beta_{2,6}=\beta_{3,12}=0.5\beta$

Fig. 1. Spin density of tetraphenylpyrryl radical.

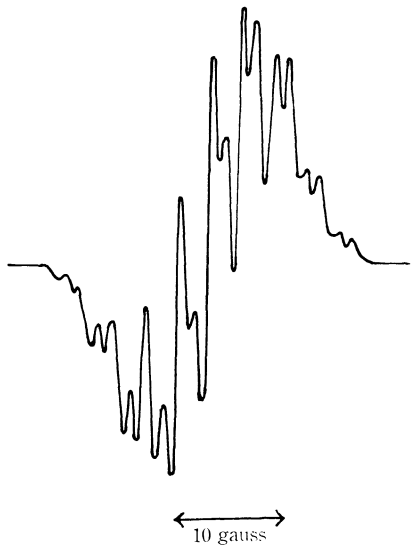

Fig. 2. ESR spectrum of PH in benzene.

4) When a larger amount of potassium hydroxide was added, a piezochromic compound which contained oxygen was obtained.

5) D. M. White and J. Sonnenberg, *J. Amer. Chem. Soc.*, **88**, 3825 (1966).

6) Presented by A. Fukuoka, H. Fukatsu, T. Kondo and T. Goto at the Annual Meeting of the Chemical Society of Japan (April, 1969, Tokyo); Preprint, p. 1379.

7) G. Scheibe and F. Feichtmayr, *J. Phys. Chem.*, **66**, 2449 (1962).

8) G. N. Lewis and D. Lipkin, *J. Amer. Chem. Soc.*, **64**, 2801 (1942); D. A. Wiersma and J. Kommandeur, *Mol. Phys.*, **13**, 241 (1967).

or another solvent, prepared in dim light and at room temperature, showed no ESR absorption. On irradiation at temperatures between room temperature and about −20°C, the benzene solution rapidly turned pink and showed a strong ESR signal (shown in Fig. 2) (g=2.003). The color and ESR hardly faded at all[9] over several days in the dark at room temperature. However, in solutions of PH in decaline and naphthalene, which turned pink on irradiation at 80—90°C, the color faded after the irradiation was cut off. This fact shows that PH exhibits photochromism at 80—90°C, above which exhibits thermochromism.

At temperatures between about −20°C and −100°C, the benzene solution showed no color change on irradiation. At temperatures lower than about −100°C, a purple color appeared on irradiation. The color became deeper with a decrease in the temperature. Such changes in the color were investigated by means of the absorption and the ESR spectra.

An EPA solution of PH, which turned purple on irradiation at −196°C, showed the absorption bands shown in Fig. 3. The bands corresponded to those of the pink solution obtained by irradiation at room temperature. The absorption maxima at −196°C showed a red shift of about 10 mμ compared with those of the pink solution. The change in the absorption spectra was measured at temperatures from −196°C to room temperature. The change corresponded to the dependence of the color change on the temperature.

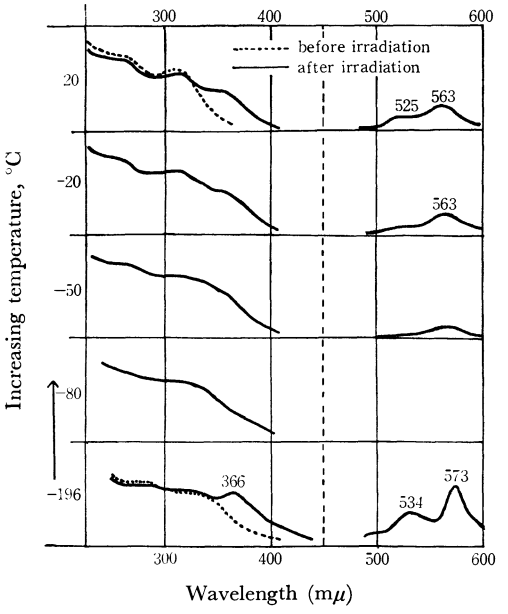

Fig. 3. Absorption spectra of PH in EPA at temperatures from −196°C to room temperature.

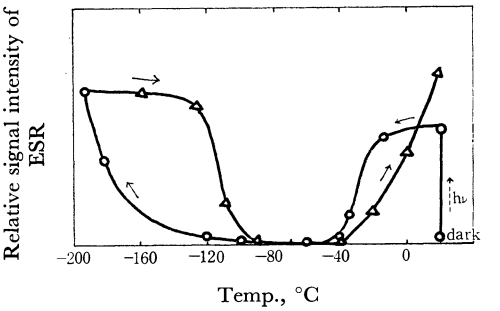

Fig. 4. Dependence of the ESR signal intensity on the temperature under irradiation in benzene.

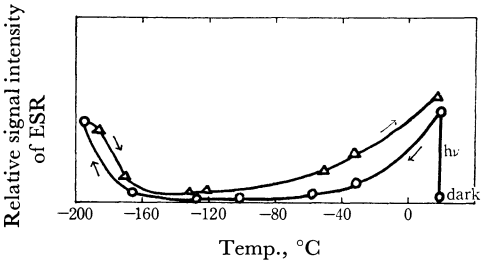

Fig. 5. Dependence of the ESR signal intensity on the temperature under irradiation in EPA.

The dependence of the relative signal intensity of ESR on the temperature under irradiation is shown in Figs. 4 and 5.

These experimental results can be interpreted by a mechanism similar to that used in the case of the dimer IV.[3,5,10]

$$R_2 \overset{h\nu}{\rightleftharpoons} R_2^* \underset{(a)}{\rightleftharpoons} 2R\cdot \underset{(b)}{\rightleftharpoons} R'_2$$

(photo-dimer) (radical II) (piezo-dimer)

The equilibrium (a) is likely to lie far to the side of R_2 at temperatures near room temperature. However, because the dimerization of R· produced by the photo-dissociation of R_2 is very slow, the photochromic color faded hardly at all at temperatures, near room temperature. With the elevation of the temperature, dimerization was accelerated and photochromism was exhibited at 80—90°C. At temperatures between about −20°C and −100°C the photochromic color does not appear, for the equilibrium (b) lies far to the side of R'_2 and the dimerization of R· is rapid. The purple color observed at temperatures lower than about −100°C is due to a tetraphenylpyrryl radical, which has more coplanarity than the pink radical. At low temperatures the equilibrium (b) lies far to the side

9) Blinder *et al.* reported[2] that a reversible, rapid color change was observed at room temperature in a benzene solution of the oxidation product of I. We could not observed such a reversible phenomenon at room temperature.

10) T. Shida, K. Maeda and T. Hayashi, This Bulletin, **42**, 3044 (1969).

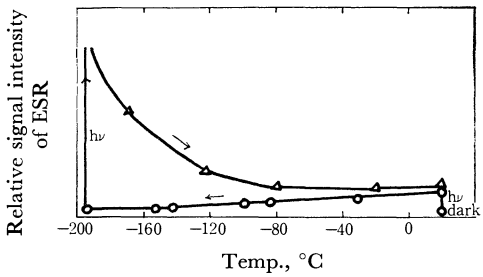

Fig. 6. Dependence of the ESR signal intensity of PH on the temperature in the solid state.
–○– in the dark

of R′$_2$. However, because the dimerization of the purple radical is slow at such low temperatures, the purple color was observed.

The ESR spectrum observed at −196°C showed a strong signal at 3296 gauss, three pairs of weak signals at 3358—3231 gauss, and a weak signal at 1762 gauss. These signals suggest the formation of a radical pair similar to that of the photochromic dimer of IV.[3d,10]

Photochromism of PH in the Solid State. PH exhibits photochromism in the solid state at temperatures near room temperature and near −196°C. With intense irradiation at room temperature, a pink color and a weak ESR signal were observed. On heating to about 50°C after irradiation was cut off, the color and ESR faded very slowly. On irradiation at −196°C, a deep bluish-purple color and a strong ESR signal were immediately observed. The color and ESR signal hardly faded at all at −196°C in the dark, but they rapidly faded on slight warming from −196°C, even under irradiation. The dependence of the signal intensity on the temperature was measured under irradiation, as is shown in Fig. 6.

These phenomena, which correspond to those shown by the photochromic dimer of IV in the solid state,[3g] suggest a radical mechanism similar to that of the photochromism of the latter. The ESR absorption at −196°C showed a strong signal at 3127 gauss and a weak signal at 1762 gauss which is likely to be due to the formation of a radical pair, as in solutions.

Thermochromism of PH and PI. PH and PI showed thermochromism in solutions and in the solid state. In solutions PH showed a thermochromic pink color and an ESR signal ($g=2.00$) when heated above 90°C without irradiation. In the solid state PH showed a pink color and an ESR signal ($g=2.00$) when heated to temperatures higher than about 180°C, and the deep pink melt formed on melting showed a strong ESR signal. When PH which had been heated to about 190°C in the solid state without irradiation was rapidly cooled to room temperature in the dark, the thermochromic color rapidly faded.

A benzene solution of PI prepared at room temperature showed a deep pink color due to the radical II (λ_{max} 365, 525 and 563 mμ) produced by the dissociation of the piezo-dimer present in PI. The color did not change with irradiation. When the pink solution was cooled, the color gradually faded until it disappeared at temperatures lower than about −20°C. The absorption and ESR spectra showed variations corresponding to the change in the color. In the solid state PI showed a thermochromic pink color on heating to about 130°C. PI heated in the solid state *in vacuo* at about 100°C for 1 hr showed photochromism both in solutions and in the solid state. This fact shows that the piezo-dimer isomerizes to the photodimer upon heating, probably through the radical II.

Piezochromism of PI. PI showed piezochromism in the solid state. PI, which turned pink with grinding, showed absorption maxima at 535 (sh) and 570 mμ; these maxima can be attributed to the radical II. The piezochromis of PI is due to a radical dissociation similar to that of the piezochromic dimer of IV.[3g] The change in the spin concentration caused by piezochromism was measured by means of ESR. The spin concentration increased from 7.8×10^{18} spin/g to 7.6×10^{19} spin/g when grinding was continued for about 1 min. The spin concentration of the PI ground gradually decreased at room temperature. It became about one third after 1 week.

The authors wish to express their hearty thanks to Dr. Hiroshi Midorikawa and Dr. Tadamasa Shida of the Institute of Physical and Chemical Research, and Professor Takeshi Nakajima of Tohoku University for their kind help, and to the Ministry of Education for the financial support granted this research.

BULLETIN OF THE CHEMICAL SOCIETY OF JAPAN VOL. 43 1435—1439 (1970)

β-Ferrocenyl-α,β-unsaturated Ketones. III.[1] The Conformational Study of β-Ferrocenyl-α,β-unsaturated Ketones by Means of IR Spectroscopy

Hiromichi KONO, Mikio SHIGA, Izumi MOTOYAMA and Kazuo HATA

Department of Chemistry, Faculty of Science, Tokyo Metropolitan University, Setagaya-ku, Tokyo

(Received July 26, 1969)

The geometrical and conformational isomerism of various β-ferrocenyl-α,β-unsaturated ketones, most of which had been reported in a previous paper, was discussed on the basis of their IR spectra in the 1700—1600 cm^{-1} range and their NMR spectra. An unusually strong IR absorption of the olefinic double bond was observed in comparison with that of the carbonyl group. Considering the IR and NMR data, it was concluded that 3-ferrocenyl-1-(*p*-substituted phenyl)-2-propen-1-ones may mostly exist in a *s-cis* conformation.

Generally, α,β-unsaturated ketones may exist in *s-cis* and *s-trans* forms. For the conformational study of such unsaturated ketones, UV and IR spectroscopic methods are very useful and a number of spectroscopic data concerning α,β-unsaturated carbonyl compounds have been reported.[2-5] Recently, Dimmock and his co-workers reported on their observation of carbonyl absorption bands due to *s-cis* and *s-trans* isomerism in the IR spectra of substituted 1-phenyl-1-hepten-3-ones and related compounds.[6] However, in such aryl-substituted α,β-unsaturated carbonyl compounds, the absorption bands near 1600 cm^{-1} due to the conjugated C=C stretching vibrations overlap unfavorably with the bands due to the C=C skeletal in-plane vibrations of the aromatic ring. On the other hand, the IR spectra of β-ferrocenyl-α,β-unsaturated ketones show a distinct absorption band due to the C=C bond conjugated with the ferrocenyl group, since the ferrocenyl group has no appreciable absorption in this region. Hence, they seem to be compounds favorable for such conformational study.

FcCH=CHCOR

(**1**)

1a: R=CH_3
1b: R=C_2H_5
1c: R=$CH_2CH(CH_3)_2$
1d: R=$C(CH_3)_3$

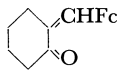

(**1e**)

FcCH=CHCO- -X

(**2**)

2a: X=H
2b: X=CH_3
2c: X=OCH_3
2d: X=Cl
2e: X=NO_2

FcCH=CHCOCH=CHFc

(**3**)

In this investigation, the IR spectra of five β-ferrocenyl-α,β-unsaturated ketones (**1**), which had been reported in a preceding paper,[7] and those of five 3-ferrocenyl-1-(*p*-substituted phenyl)-2-propen-1-ones (**2**) were measured in carbon tetrachloride and the assignment of bands near 1600 cm^{-1} to *s-cis* and *s-trans* isomers was discussed.

Results

The IR spectrum of 4-ferrocenyl-3-buten-2-one (**1a**) in a KBr disk shows two strong bands, at 1655 and 1619 cm^{-1}, due to the carbonyl and ethylenic stretching vibrations respectively. When it was observed in solution, a new band appeared near these bands, although its position and intensity varied with the nature of the solvent employed, as is shown in Fig. 1. These phenomena, also observed in all the other compounds studied here except **1e**, may be attributed to the presence of two rotational isomers, *s-cis* and *s-trans*, in the solution.

Table 1 summarizes the absorption maxima, ν_{max} and the extinction coefficients, ε' (for the definition of ε', see the Experimental part), of these bands, measured in CCl_4. According to the conformational study by Erskine and Waight[2] using α,β-unsaturated ketones which maintain their rigid conformations, the carbonyl stretching bands appear in the 1704—1684 cm^{-1} range (ε 250—333) for *s-cis* and the 1679—1669 cm^{-1} (ε 454—670) for *s-trans* isomers, while the ethylenic stretching bands

1) Part II: H. Kono, M. Ishige, K. Sakai, M. Shiga, I. Motoyama and K. Hata, This Bulletin **43**, 867 (1970).
2) R. L. Erskine and E. S. Waight, *J. Chem. Soc.*, **1960**, 3425.
3) R. D. Campbell and N. H. Cromwell, *J. Amer. Chem. Soc.*, **79**, 3456 (1957).
4) N. H. Cromwell and R. P. Cahoy, *ibid.*, **80**, 5524 (1958).
5) M. E. Kronenberg and E. Havinga, *Rec. Trav. Chim. Pays-Bas*, **84**, 17 (1965).
6) J. R. Dimmock, P. L. Carter and P. D. Ralph, *J. Chem. Soc., B*, **1968**, 698.
7) H. Kono, M. Shiga, I. Motoyama and K. Hata, This Bulletin, **42**, 3273 (1969).

TABLE 1. THE IR SPECTRA DATA OF β-FERROCENYL-α,β-UNSATURATED KETONES (in CCl_4)

Compound	Concentration (mol/l) 10^{-2}		$\nu_{max}(cm^{-1})$ s-cis C=O(ε')[b]	s-cis C=C(ε')	s-trans C=O(ε')	s-trans C=C(ε')
1a	1.654		1684(171)	1597(578)	1665(438)	1615(308)
1b	1.665		1688(218)	1604(568)	1663(246)	1621(216)
1c	1.442		1686(190)	1601(572)	1653(167)	1619(244)
1d			1685(0.717[c])	1600(0.164[c])	1663(0.095[c])	1617(0.248[c])
1e	1.527	*trans*[a]	1676(259)	1584(369)	—	—
		cis[a]	1684(sh)	1600(sh)	—	—
2a	1.285		1661(446)		1635(127)	
2b	1.813		1659(548)		1636(110)	
2c	1.365		1656(532)		—	
2d	1.073		1658(495)		1640(118)	
2e			1647		—	

Compound	$\Delta\nu_{max}(cm^{-1})$ (s-cis~s-trans) C=O	C=C	(C=O~C=C) s-cis	s-trans	ε's-cis/ε's-trans C=O	C=C	ε'c=o/ε'c=c s-cis	s-trans
1a	19	18	87	50	0.39	1.88	0.30	1.42
1b	25	17	84	42	0.89	2.63	0.38	1.14
1c	23	18	87	34	1.14	2.34	0.33	0.68
1d	22	17	85	46	2.38[d]	2.60[d]	2.89	1.72
1e	—	—	92					
	—	—	84					
2a	26				3.51			
2b	23				4.21			
2c	—							
2d	18				4.96			
2e	—							

a) Configuration with respect to C=C double bond.
b) Definition of ε': see Experimental part.
c) Absorbance $\log_{10} T_0/T$.
d) Calculated from absorbance values of *s-cis* and *s-trans* isomers.

TABLE 2. THE NMR SPECTRA OF 3-FERROCENYL-1-(*p*-SUBSTITUTED PHENYL)-2-PROPEN-1-ONE (**2**) (τ-value, in $CDCl_3$)

Compound α' β' FcCH=CHCO-(C6H4)-X β α		Cyclopentadienyl ring protons (Unsubst.)	(Subst.)	Vinyl protons α	β	Benzene ring protons β'	α'
2a	X=H	5.84(s)	5.55(t) 5.42(t) (J=2 Hz)	2.88(d) 2.23(d) ($J_{\alpha\beta}$=15 Hz)		2.44(m)	1.98(m)
2b	X=CH_3*	5.85(s)	5.54(t) 5.42(t) (J=2 Hz)	2.91(d) 2.23(d) ($J_{\alpha\beta}$=15 Hz)		2.71(d) ($J_{\alpha'\beta'}$=8 Hz)	2.08(d)
2c	X=OCH_3**	5.87(s)	5.56(t) 5.43(t) (J=2 Hz)	2.89(d) 2.24(d) ($J_{\alpha\beta}$=15 Hz)		3.05(d) ($J_{\alpha'\beta'}$=9 Hz)	1.99(d)
2d	X=Cl	5.84(s)	5.52(t) 5.42(t) (J=2 Hz)	2.95(d) 2.22(d) ($J_{\alpha\beta}$=15 Hz)		2.55(d) ($J_{\alpha'\beta'}$=9 Hz)	2.07(d)
2e	X=NO_2	5.83(s)	5.44 (broad)	2.97(d) 2.17(d) ($J_{\alpha\beta}$=15 Hz)		1.64(d) ($J_{\alpha'\beta'}$=9 Hz)	1.93(d)

* τ 7.58(s) ** τ 6.16

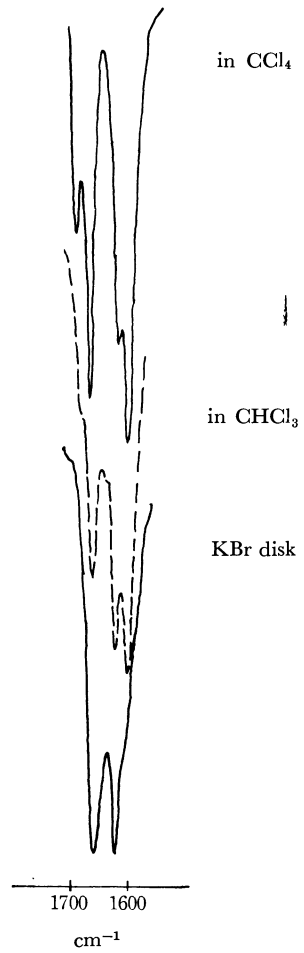

Fig. 1. IR spectra of 4-ferrocenyl-3-buten-2-one (**1a**) in various media.

are in the 1633—1613 cm^{-1} range for the *s-cis* and the 1639—1615 cm^{-1} range for the *s-trans* isomers. Following their observation, the carbonyl band with the higher frequency and the olefinic band with the lower frequency were identified as being due to *s-cis*, and the another pair were identified as being due to the *s-trans* isomer. Table 1 shows that the carbonyl bands for *s-cis* isomers are generally 19—25 cm^{-1} higher than those for *s-trans*, while the olefinic bands for *s-cis* isomers are 17—18 cm^{-1} lower than those for *s-trans*. The differences between the absorption maxima of the carbonyl and the olefinic bands were found to be 84—87 cm^{-1} and 34—50 cm^{-1} for *s-cis* and *s-trans* isomers respectively. These values are in accord with the observations of Braude and his co-workers.[8]

In the IR spectrum of 2-(ferrocenylmethylene)-cyclohexanone (**1e**), four bands were also observed in this region, in spite of its exclusive *s-cis* structure. This can, however, be explained by the presence of the geometric isomers with respect to the olefinic double bond. The bands at 1676 and 1584 cm^{-1} were assigned to the isomer in which ferrocenyl group lies *trans* to the carbonyl group, while those at 1684 and 1600 cm^{-1}, with lower intensities, were assigned to the *cis* isomer.

3-Ferrocenyl-1-(*p*-substituted phenyl)-2-propen-1-ones (**2**) were prepared by the base-catalyzed condensation[9] of formylferrocene with *p*-substituted acetophenones. It was proved, by means of their NMR spectra (Table 2), that their olefinic double bonds had *trans* configurations, as had previously been shown in the case of 4-ferrocenyl-3-buten-2-one and related compounds.[7]

In the IR spectra of the aryl ketones (**2**), the strong absorptions due to the carbonyl group of sterically-favored *s-cis* isomers appeared at about 1660 cm^{-1}, about 20 cm^{-1} lower than those of the corresponding alkyl ketones (**1**). In addition to the strong bands, weak bands were observed in the 1640—1635 cm^{-1} range in the spectra of **2a**, **2b**, and **2d**, the corresponding bands being absent in those of **2c** and **2e**. These bands are considered to be due to the carbonyl group of *s-trans* isomers. On the other hand, the band with several shoulders at about 1600 cm^{-1} could not be assigned because of the heavy overlapping of the olefinic band with the aromatic band.

Discussion

The main factors influencing the conformation of α,β-unsaturated ketones are the steric environment around the carbonyl group, especially the steric requirements of the substituent, and the nature of the solvent. It can be seen in Table 1 that the alteration of an alkyl group on the carbonyl group has a great influence on the extinction coefficients of both carbonyl and ethylenic absorption bands, whereas it does not very much affect the frequencies of these bands. The ratios of the extinction coefficient, $\varepsilon'_{C=O}/\varepsilon'_{C=C}$, were calculated to be 0.30—2.89 for *s-cis* isomers and 0.68—1.72 for *s-trans* isomers. These values are unusually small compared with those of the ordinary α,β-unsaturated ketones previously reported: $\varepsilon_{C=O}/\varepsilon_{C=C}$ for *s-cis*: 0.7—2.5; $\varepsilon_{C=O}/\varepsilon_{C=C}$ for *s-trans*: 6—9.[2] It is thus noticeable that the olefinic double bond in β-ferrocenyl-α,β-unsaturated ketones has an unusually strong absorption in this region. The enhanced olefinic absorption may be due to the conjugation of the double bond with the ferrocenyl group, a conjugation originating in the great electron-releasing ability of the ferrocenyl nucleus. In this connection, it must be mentioned that the ethylenic band of 1,5-diferrocenyl-1,4-pentadien-3-one (**3**) at

8) E. A. Braude and C. J. Timmons, *J. Chem. Soc.*, **1955**, 3766.

9) C. R. Hauser and J. K. Lindsay, *J. Org. Chem.*, **22**, 906 (1957).

1614 cm^{-1} was observed to be unusually stronger ($\varepsilon'=1740/2$) than the carbonyl band at 1649 cm^{-1} ($\varepsilon'=416$).[1]

The examination of the molecular structure of the *s-trans* conformation suggests that a bulky group on the carbonyl group may force the conjugated system of the unsaturated ketone out of coplanarity or force it to take the *s-cis* conformation. Although the estimation of the isomer ratio is impossible from the spectra data shown in Table 1, it is clear that the concentration of the *s-trans* isomer qualitatively decreases with an increase in the bulkiness of the alkyl group on the carbonyl group. The steric situation is especially emphasized in aryl ketones (**2**). An aryl substituent on the carbonyl group brings about a great decrease in the concentration of the *s-trans* isomer. If the whole conjugated system of the aryl-substituted unsaturated ketone with an *s-trans* conformation takes a coplanar arrangement, the ortho hydrogen atom of the phenyl group may overlap heavily with the β-vinyl hydrogen, as is shown in Fig. 2. Thus, the *s-cis* isomer,

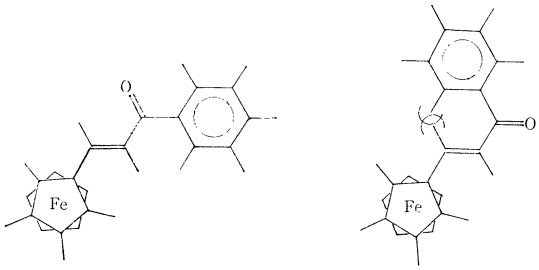

s-cis *s-trans*

Fig. 2.

which is free from this strain and which may be somewhat stabilized by holding the whole conjugated system of the molecule in a coplanar conformation, will be predominant in solution. This consideration is consistent with the observations that the $\varepsilon'_{s\text{-}cis}/\varepsilon'_{s\text{-}trans}$ ratios of carbonyl bands in the IR spectra of the aryl ketones (**2**) exhibited considerably larger values than those of the alkyl ketones (**1**), and that the chemical shift of the β-vinyl proton of the aryl ketones (**2**) appeared in a low field, as is shown in Table 2, probably due to the anisotropic effect of the carbonyl group.

The nature of the solvent used for the measurement will also affect the population of the isomers. In a polar solvent, solvation will take place so as to keep the positive and negative centers in the molecule very far apart from each other. Thus, *s-trans* would be a more favorable conformation than *s-cis* in a polar solvent. If the delocalization of the positive charge extended to the ferrocene ring because of the electron-releasing character of the ferrocene nucleus, the predominance of the *s-trans* conformation would be more promoted. However, contrary to expectation, no appreciable solvent effect was observed, probably because the steric effect overcomes the solvent effect.

Supposing a cyclopentadienyl ring in the ferrocene nucleus lies on a plane of the side-chain olefinic double bond, the other part of a ferrocene molecule stands out of this plane and the iron atom is situated so close to the π-orbital of the side chain that a certain anchimeric effect between them may be expected. Therefore, the conjugation of the π-electron system in the side chain with the ferrocene ring in β-ferrocenyl-α,β-unsaturated ketones may be somewhat different in nature from that with the benzene ring in β-phenyl analogs. Thus, such an anchimeric effect might contribute to some extent to the enhanced population of the *s-cis* isomer in β-ferrocenyl-α,β-unsaturated ketones, in addition to the prevailing steric effect.

Experimental

Spectral Measurements. The infrared spectra were measured in carbon tetrachloride with a Hitachi EPI-G2 grating spectrometer, using a rock salt cell 0.052 cm thick. The extinction coefficient, ε', employed in this study is defined as follows:

$$\varepsilon^{a}_{s\text{-}cis}=\frac{\log T_0/T_{s\text{-}cis}}{x_{s\text{-}cis}\cdot c\cdot l}=\frac{\varepsilon'_{s\text{-}cis}}{x_{s\text{-}cis}}$$

$$\varepsilon^{a}_{s\text{-}trans}=\frac{\log T_0/T_{s\text{-}trans}}{(1-x_{s\text{-}cis})\cdot c\cdot l}=\frac{\varepsilon'_{s\text{-}trans}}{1-x_{s\text{-}cis}}$$

where ε^a is a molar extinction coefficient, $x_{s\text{-}cis}$ is the molar ratio of the *s-cis* isomer, c is the molar concentration of the solution measured, l is the path length in cm, and T_0/T is the peak optical density.

The absorbances ($\log_{10} T_0/T$) of both the C=O and C=C absorption peaks were found to have a good linear relationship with the molar concentration of the unsaturated ketone.

The NMR spectra of **2** were measured in $CDCl_3$ with a Hitachi model H-60 spectrometer.

Materials: 4-Ferrocenyl-2-buten-2-one (**1a**), 1-ferrocenyl-1-penten-3-one (**1b**), 1-ferrocenyl-5-methyl-1-hexen-3-one (**1c**), 1-ferrocenyl-4,4-dimethyl-1-penten-3-one (**1d**), and 2-(ferrocenylmethylene)cyclohexanone (**1e**) were each prepared by the base-catalyzed condensation of formylferrocene with the corresponding ketones by means of a procedure reported previously.[7]

1-Ferrocenyl-4,4-dimethyl-1-penten-3-one (1d). Attempts at the chromatographic purification of **1d** were unsuccessful because it easily decomposed on alumina to give formylferrocene and pinacolone. When the crude material was left standing for several months, a small amount of long, dark red needles grew out of the crude solid. When collected, this was proved to be a pure substance by its sharp mp 91—92°C. It was identified as **1d** by means of its IR and UV spectra. λ_{max} (95% ethanol) 225, 260, 305, *ca.* 364(sh), and 480 mμ.

3-Ferrocenyl-1-(*p*-substituted phenyl)-2-propen-1-ones (2). These substances were prepared by the condensation of formylferrocene with *p*-substituted acetophenone in the manner used to prepare 3-ferrocenyl-1-phenyl-2-propen-1-one by Hauser and Lindsay.[9]

3-Ferrocenyl-1-phenyl-2-propen-1-one (2a). The crude product obtained by the condensation of formylferrocene and acetophenone was recrystallized from ethanol to afford violet needles; mp 142—145°C (lit.,[9] 138—140°C). Yield, 55%.

3-Ferrocenyl-1-(*p*-tolyl)-2-propen-1-one (2b). The crude product (92.4% yield) was recrystallized from ethanol to give violet needles; mp 138.5—139.5°C. λ_{max} (95% ethanol) 277.5, 326, 398(sh) and 514 mμ.

Found: C, 72.55; H, 5.59%. Calcd for $C_{20}H_{18}OFe$: C, 72.82; H, 5.46%.

3-Ferrocenyl-1-(*p*-anisyl)-2-propen-1-one (2c). The crude product (80.7% yield) was recrystallized from ethanol to afford purple needles; mp 154.5—155.5°C. λ_{max} (95% ethanol) 279, 327, 390 and 512 mμ.

Found: C, 69.40; H, 5.21%. Calcd for $C_{20}H_{18}O_2Fe$: C, 69.39; H, 5.20%.

3-Ferrocenyl-1-(*p*-chlorophenyl)-2-propen-1-one(2 d). The recrystallization of crude **2d** (88.2% yield) from ethanol gave reddish-orange needles; mp 167—168°C. λ_{max} (95% ethanol) 273, 330, 396 and 520 mμ.

Found: C, 65.08; H, 4.40%. Calcd for $C_{19}H_{15}OClFe$: C, 65.08; H, 4.28%.

3-Ferrocenyl-1-(*p*-nitrophenyl)-2-propen-1-one (2e). On the recrystallization of crude **2e** (8.47% yield) from chloroform – ether (2 : 1), violet needles were obtained; mp 228—230°C. λ_{max} (95% ethanol) 270, 337, 410(sh) and 546 mμ.

Found: C, 62.80; H, 4.28; N, 3.93%. Calcd for $C_{19}H_{15}O_3NFe$: C, 63.18; H, 4.16; N, 3.88%.

BULLETIN OF THE CHEMICAL SOCIETY OF JAPAN VOL. 43 1439—1443 (1970)

Liquid Phase Chlorination of Olefins with Cupric Chloride

Takashi KOYANO

Central Research Laboratory, Toa Nenryo Kogyo Co., Oi-machi, Iruma-gun, Saitama

(Received September 11, 1969)

Reactions of olefins with cupric chloride were studied in methanol at 100—140°C. The reactivity of olefins was in the order, ethylene>propylene>1-butene>2-butenes. A considerable amount of 1-chloro-2-methoxy compounds were found in the reaction products of 1-olefins. Competitive formation of dichloride and methoxychloride was suggested. Chlorination of 2-butenes leads to *meso*- and *dl*-2,3-dichlorobutanes, their ratio being invariable regardless of the starting material *cis*- or *trans*-2-butene. The mechanism is discussed in terms of ionic intermediates.

Although there are a number of investigations on the chlorination of unsaturated organic compounds by cupric chloride, the mechanism of the reaction is somewhat ambiguous. For the liquid phase chlorination of aromatic compounds a polar mechanism[1] or a mechanism involving homolytic decomposition of the π-complex between cupric chloride and the aromatic compound[2] has been proposed. Chlorination of alkenes in the vapor phase has been accepted to proceed through chloronium ion intermediates.[3] However, participation of both radical and ionic mechanisms has recently been demonstrated.[4]

Only a few reports have appeared on the chlorination of simple olefins in liquid phase. Although the photo-induced chlorination of olefinic compounds was noted earlier,[5] the thermal chlorination in aqueous phase was not reported until 1967.[6] Recently, the reaction in alcoholic media has been described in some detail.[7] However, efforts have been concentrated mostly on reaction with styrene and interpretation for the reaction with alkene is not conclusive.

We found that a considerable amount of methoxychloride is formed in addition to the anticipated dichlorides in the chlorination of alkenes in methanol. The object of this paper is to elucidate the mechanism of this type of reaction. A detailed description from the synthetic point of view will be presented later.

Results and Discussion

Several simple olefins were allowed to react with cupric chloride in methanol at 120°C (Table 1). The reactivity based on the conversion of cupric chloride was in the order, ethylene>propylene>

1) J. C. Ware and E. E. Borchert, *J. Org. Chem.*, **26**, 2263, 2267 (1961).
2) D. C. Nonhebel, *J. Chem. Soc.*, **1963**, 1216.
3) R. P. Arganbright and W. F. Yates, *J. Org. Chem.*, **27**, 1205 (1962)
4) P. P. Nicholas and R. T. Carroll, *ibid.*, **33**, 2345 (1968).
5) J. K. Kochi, *J. Amer. Chem. Soc.*, **84**, 2121 (1962).
6) M. L. Spector, H. Heinemann and K. D. Miller, *Ind. Eng. Chem., Process Des. Develop.*, **6**, 327 (1967).
7) K. Ichikawa, S. Uemura, T. Hiramoto and Y. Takagaki, *Kogyo Kagaku Zasshi*, **71**, 1657 (1968).

TABLE 1. REACTION OF OLEFINS

Olefin (mol)	$CuCl_2$ (mol)	Conversion ($CuCl_2$ %)	Product(mmol) A	B	C
C_2H_4	0.90	0.10 84.7	8.8	30.3	1.3
	1.47	0.20 98.5	33.6	57.3	1.6
	0.86	0.30 93.7	55.2	72.8	2.8
C_3H_6	0.92	0.20 90.0	31.8	34.9	trace
1-C_4H_8	0.65	0.20 72.1	27.6	19.5	trace
cis-2-C_4H_8	0.55	0.20 64.9	34.5*	0.9	0
trans-2-C_4H_8	0.67	0.20 57.0	42.6**	1.7	0

Ta autoclave reaction, MeOH 120 m*l*, 120°C, 3 hr
Product (RCHXCHYR′)
A: X=Cl, Y=Cl; B: X=Cl, Y=OMe;
C: X=OMe, Y=OMe
* *meso* 63.4%, *dl* 36.6%
** *meso* 65.5%, *dl* 34.5%

1-butene>2-butenes. This is in line with the facility of complex formation of the olefins with silver ion.[8] This suggests initial formation of olefin-copper complex such as acetylene-copper(II) complex speculated by Castro,[9] rather than olefin-chlorine complex deduced by Arganbright in the vapor phase reaction.[3]

Considerable amounts of methoxy compounds were found in the products. In the reaction of ethylene the ratio of 1,2-dichloroethane (I) to 2-chloroethyl methyl ether (II) increases with increase in the amount of cupric chloride present. This may be interpreted by assuming competitive reactions of the intermediate with chloride ion[10] and with methanol, in sharp contrast to the styrene chlorination reported by Ichikawa[7] where a consecutive reaction has been claimed. Although methanolysis of I is accelerated by the presence of cupric chloride (Table 2), the rate is too small to explain the present data. Since the rate of methanolysis of I is not greater than that of II (Table 3), a simple calculation for the consecutive first order reactions clearly shows that the formation of II by methanolysis should be much less than that actually obtained.[11] In accordance with this, a fairly large quantity of II was produced in the reaction at 100°C, whereas no 1,2-dimethoxyethane (III), which is presumed to be produced exclusively by methanolysis, was detected in the products (Table 4). This means that the methanolysis of I is negligible at this temperature and II is formed through a different route. As is expected, addition of chloride ion favors the formation of I significantly.

A tendency for the ratio of I/II to be larger in the lower temperature reaction may be ascribed to the lower conversion of cupric chloride, *viz.*, the products consist of only those formed at the higher cupric chloride concentration. The fact

TABLE 2. EFFECT OF $CuCl_2$ ON METHANOLYSIS OF I

$CuCl_2$ (mmol)	CuCl (mmol)	Yield (%) I	II	III
25	0	88.6	3.0	0
12	12	94.2	1.7	0
4	20	90.9	1.1	0
0	25	89.6	0.7	0

Test tube reaction, I 12 mmol, MeOH 10 m*l*, 140°C, 3 hr

TABLE 3. METHANOLYSIS OF I AND II

Reactant	Additive (mmol)	Yield (%) I	II	III
I	none	67.5	19.3	5.9
	ZnO 60	41.6	22.3	27.9
II	none	—	61.0	32.1
	ZnO 30	—	34.2	59.4

Sealed tube Reaction, I or II 50 mmol, MeOH 25 m*l*, 180°C, 6 hr

TABLE 4. REACTION OF ETHYLENE

Temp. (°C)	Additive	Conversion ($CuCl_2$ %)	Product (mmol) I	II	III
100		25.1	2.19	1.22	0
120		66.2	4.46	3.91	0.07
140		92.3	5.82	5.85	0.17
	Air*	72.7***	6.04	6.15	0.29
	LiCl**	84.4	7.29	3.17	0.09
160		98.0	5.45	5.21	0.65
180		100.0	4.18	3.54	1.45

Test tube reaction, C_2H_4 50 kg/cm², MeOH 10 m*l*, $CuCl_2$ 25 mmol, 3 hr
* 25 kg/cm²
** 20 mmol
*** Assuming that one mole of the product is formed by use of two moles of $CuCl_2$, the total selectivity of products based on $CuCl_2$ is 140%.

8) M. A. Bennet, *Chem. Rev.*, **62**, 612 (1962).
9) C. E. Castro, E. J. Gaughan and D. C. Owsley, *J. Org. Chem.*, **30**, 587 (1965).
10) Although the real attacking species on the intermediate to form I is not fully clear at this stage, its concentration should be higher with the higher cupric chloride concentration due to equilibria in the system.

$$Cu^{++} + Cl^- \rightleftharpoons CuCl^+$$
$$CuCl^+ + Cl^- \rightleftharpoons CuCl_2$$
$$CuCl_2 + Cl^- \rightleftharpoons CuCl_3^-$$

11) In the consecutive first order reactions,

$$A \xrightarrow{k_1} B \xrightarrow{k_1'} C$$

the equation $\ln([A]_0/[A]) = [B]/[A]$ can be derived when $k_1 = k_1'$. However, 0.37 $[A]_0$ is the largest possible solution of [B] for this equation, and [C] should be 0.27 $[A]_0$ in this case. When $k_1 < k_1'$, $[B] = 0.5\ [A]_0$ can not satisfy the equations given in literature.[12]

12) W. J. Moore, "Physical Chemistry," 3rd Ed., Prentice-Hall Inc., Englewood Cliffs, N. J. (1962), p. 266

Table 5. Effect of reaction time on products ratio

Time (hr)	Conversion ($CuCl_2$%)	Yield(mmol) I	Yield(mmol) II	Net Yield* (mmol) I	Net Yield* (mmol) II	II/I
0.5	24.8	12.1	12.2	12.1	12.2	1.01
1.0	40.5	18.3	21.3	6.2	9.1	1.47

Ta autoclave reaction, C_2H_4 0.55 mol (charged at the reaction temperature), MeOH 120 m*l*, $CuCl_2$ 0.20 mol, 100°C

* Yield of products during the initial and the following 30 min.

that the ratio is larger in the earlier stage of reaction at a temperature is also attributable to the same reason (Table 5).

These observations can be rationalized by the following mechanism.

$$C_2H_4 + CuCl_2 \rightleftharpoons [C_2H_4 \cdots CuCl_2 \rightarrow C_2H_4\overset{\delta+}{Cl} \cdots \overset{\delta-}{CuCl}]$$

$$\xrightarrow{CuCl_2} ClCH_2CH_2Cl + 2CuCl \quad (1)$$

$$\xrightarrow[MeOH]{} ClCH_2CH_2OMe + HCuCl \quad (2)$$

$$HCuCl + CuCl_2 \rightarrow 2CuCl + HCl \quad (3)$$

The olefin-copper complex initially formed is transformed into a cationic chlorine complex[13] which is the common intermediate for the formations of dichloride[14] and methoxychloride. Evidence for an ionic intermediate comes from the fact that the products from 1-butene consist of only both 1,2-dichlorobutane and 1-chloro-2-methoxybutane. No other compounds were detected. When methanol attacks the intermediate complex, the resulting HCuCl[15] is rapidly oxidized by another mole of cupric chloride to yield two moles of cuprous chloride and one mole of hydrogen chloride. Cupric chloride undergoes disproportionation only at high temperatures.[9,16] None of the present data suggests the participation of chlorine molecule.[17]

13) The structure of this complex is under investigation and will be discussed in succeeding papers.

14) Equation (1) does not necessarily mean that the attacking species is cupric chloride but it simply shows the stoichiometry on the dichloride side.

15) Existence of the cation CuH^+ and its reaction with cupric ion yielding cuprous ion have been demonstrated; J. Halpern, E. R. Mcgregor and E. Peters, *J. Phys. Chem.*, **60**, 1455 (1956).

16) M. C. Ball and R. F. M. Coultard, *J. Chem. Soc., A*, **1968**, 1417.

17) a) When methanol solution (10 m*l*) of cupric chloride (25 mmol) was heated at 140°C for 3 hr in a test tube, more than 90% of $CuCl_2$ was recovered unchanged. b) No substituted products were detected, *e. g.*, by gas chromatography (Condition *VI*). The products from 1-butene exhibited only two peaks (methoxychloride 9.0 min and dichloride 9.5 min) during 46 min running.

It should be noted that the presence of air reduces the apparent conversion of cupric chloride, regenerated from cuprous chloride and hydrogen chloride (produced according to equation (3)) by oxidation, to increase the total yield of products based on consumed cupric chloride as high as 140% (Table 4).

$$CuCl + HCl + \tfrac{1}{4}O_2 \rightarrow CuCl_2 + \tfrac{1}{2}H_2O \quad (4)$$

This furnishes a hint for a possible catalytic reaction analgous to usual oxychlorination.

Table 6. Reaction of 2-butenes

Reactant (%) *trans*	Reactant (%) *cis*	Recovered Gas (%) *trans*	Recovered Gas (%) *cis*	Product (mmol) A	Product (mmol) B
100.0	0	93.4	6.6	23.0*	1.1
4.5	95.5	6.8	93.2	12.9**	0.8***

Glasslined autoclave reaction, 2-C_4H_8 0.25 mol, MeOH 150 m*l*, $CuCl_2$ 0.10 mol, 140°C, 3 hr

A: 2,3-dichlorobutane

B: *erythro*-2-chloro-3-methoxybutane

* *meso* 62.5%, *dl* 37.5%

** *meso* 59.0%, *dl* 41.0%

*** A small amount of *threo* compound was also detected.

When *cis*- and *trans*-2-butenes were subjected to reaction, isomeric dichlorides were formed. However, the ratio of *meso*- to *dl*-dichlorides is almost independent of the starting material 2-butene (Tables 1 and 6). Although interconversion of 2-butenes has occurred slightly, the extent is by no means sufficient to account for the result. The stability of the dichlorides was examined to show that both the isomerization and the methanolysis do not take place significantly under the reaction condition. Therefore, the invariable *meso*/*dl* ratio must be determined during the course of reaction. A mechanism which accounts for the results is that the intermediate complex has considerable open-chain character[18] and is in equilibrium between two isomeric forms[20] by rotation around the central C–C bond faster than the attack of nucleophiles. Since the intermediate originally from *trans*-2-butene is less crowded than the one from the *cis* isomer by separating two methyl groups apart, it must be more stable. Thus, by

18) In this respect the intermediate is dissimilar to the strongly bridged chloronium ion intermediates in the chlorination of 2-butenes by chlorine molecule.[19]

19) R. C. Fahey and C. Schubert, *J. Amer. Chem. Soc.*, **87**, 5172 (1965).

20) Scheme of equilibrium:

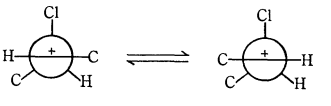

succesive *trans* addition of chloride ion, *meso*-dichloride predominates over *dl*-isomer. A σ-bonded complex, $Cl(CH_3)CHCH(CH_3)CuCl$, is unlikely to exist under the reaction conditions, although it can not be strictly ruled out.

Experimental

Materials. Olefins were commercially available. Ethylene, 99% pure grade (Nihon Sekiyu Kagaku Co.); propylene, pure grade (Takachiho Chemical Industrial Co.); 1-butene, 99.7% pure grade (Matheson Co.); *cis*- and *trans*-2-butenes, pure grade (Takachiho). Cupric chloride was anhydrous GR grade (Koso Chemical Co.). Methanol was GR grade (Koso), refluxed and distilled from magnesium methoxide[21] under N_2. 1,2-Dichloroethane, GR grade (Koso), and 2-chloroethyl methyl ether, chemical grade (Koso), were distilled after drying over $CaCl_2$. Other materials were the purest reagents commercially available.

Analytical Methods. *a*) Unchanged Cu(II) was determined by iodometry.[22] *b*) Reaction products were analyzed by gas chromatography. The conditions (apparatus, column, temperature, carrier gas) were as follows: *I.* Shimadzu GC-2C, dioctyl sebacate (plus sebacic acid) on Chromosorb W (DOS column), 100°C or 120°C, He; *II.* Shimadzu GC-2C, Triton X-305 on Diasolid L, 80°C, He; *III.* Shimadzu GC-1C, DOS column, 120°C; He; *IV.* Shimadzu GC-1C, Triton X-305 on Diasold L, 130°C, He; *V.* Shimadzu GC-1C, propylene carbonate plus glutaronitrile on Chromosorb W, room temp., He; *VI.* Shimadzu GC-4APT, DOS column, 100°C (program 4°C/min) max. 140°C, He; *VII.* Perkin-Elmer 226 (H_2 flame detector), Silicone DC-550 (300 ft capillary), 30°C (12 min, program 10°C/min) max. 120°C, N_2. *c*) IR spectra were measured by JASCO IR-G spectrophotometer. d) NMR spectra were measured by JEOL JNM-C-60H spectrometer.

Autoclave Reaction. Into a N_2 purged 300 m*l* Ta lined autoclave (with an agitator and a thermo-well made of Ta metal) were placed $CuCl_2$ and methanol, and the measured amount of olefin was added from a pressure bottle. The autoclave was heated with an electric oven with stirring. The reaction time was shown as the heating time after the autoclave reached the prescribed temperature (±1.0°C). After the reaction, the autoclave was immediately cooled with water to room temperature. Cuprous chloride was filtered off from the reaction solution, followed by extraction with methanol. The combined methanol solution was subjected to titration and gas chromatographic analysis (Conditions *I* and *II*, with toluene as the internal standard). The results are summarized in Table 1.

Test Tube Reaction. Since cupric chloride is very corrosive to steel, the methanol solution (10 m*l*)[23] was taken in a 45 m*l* glass test tube and placed in a 100 m*l* stainless steel autoclave. In the autoclave was placed 30 m*l* methanol in order to adjust partial pressure and minimize vaporization of the reactant methanol. After being flushed with N_2, ethylene was introduced, and the autoclave was heated (±1.0°C) for 3 hr with an oven without stirring. The reaction solution and the outside solution were taken out and analyzed separately. The combined results are shown in Table 4.

The same procedure was applied to methanolysis of I, in which N_2 (50 kg/cm^2) was used in place of ethylene (Table 2).

Methanolysis of I and II. The reaction was carried out in a 50 m*l* glass sealed tube, which was heated (±1.0°C) in a 500 m*l* autoclave with shaking (75/min). The products were analyzed by gas chromatography (Condition *I*). The results are listed in Table 3.

Reaction of 1-Butene. In a 500 m*l* glass lined autoclave (with a stirrer made of Ta metal) was placed cupric chloride (0.10 mol) in 150 m*l* of anhydrous methanol, followed by addition of 13.8 g (0.25 mol) of 1-butene. The autoclave was heated at 140°C in an oil bath for 3 hr with stirring. After cooling, the reaction solution was analyzed by gas chromatography (Condition *I*, 120°C). The products were 1,2-dimethoxybutane (trace, retention time 10.5 min), methoxychlorobutane (IV) (1.94 g (14.8 mmol), 13.5 min), and 1,2-dichlorobutane (1.42 g (11.2 mmol), 15.2 min), which were identified by comparing their retention times with those of the synthesized samples. No higher boiling products were detected by programmed gas chromatography.[17b] When the reaction mixture was heated with KOH in a sealed tube at 150°C for 1 hr, the peak at 10.5 min increased while the other two peaks disappeared. This shows that the peak at 10.5 min corresponds to 1,2-dimethoxybutane.

Product IV showed a single peak also in a capillary column gas chrotmaography (Condition *VII*), showing it consisted of a single product. The NMR and IR spectra of IV, which was separated by fractionation and preparative gas chromatography (Condition *III*), were identical with those of synthesized 1-chloro-2-methoxybutane. (NMR (CCl_4 solution): τ 9.05 (triplet, 3H), τ 8.37 (multiplet, 2H), τ 6.54 (singlet, 3H, τ 6.4—6.9 (multiplet, 3H)).

Synthesis of 1,2-Dichlorobutane. Chlorine gas was introduced slowly into 1-butene (10 m*l*) at −20°C with stirring. About 2 m*l* of pure (>99%) 1,2-dichlorobutane (confirmed by NMR and IR) was isolated from the higher substituted substances by fractionation using a spinning band column.

Synthesis of 1-Chloro-2-methoxybutane. This was carried out by modification of olefin chlorination with *t*-butyl hypochlorite[24] and the product was purified by preparative gas chromatography (Condition *III*).

Reaction of 2-Butenes. A methanol solution of cupric chloride was charged in a 500 m*l* glass lined autoclave, and 2-butene was then pressured in from a pressure bottle. The autoclave was heated at 140°C (±1.0°C) in an oil bath with stirring for 3 hr. After cooling to room temperature, gas chromatographic analysis was conducted on both gaseous (Condition *V*) and liquid (Condition *I*) products. The results are presented in

21) L. F. Fieser, "Experiments in Organic Chemistry," 3rd Ed., D. C Heath Co., Boston (1955), p. 289.

22) W. T. Elwell and D. Price, "Comprehensive Analytical Chemistry," Vol. Ic, ed. by C. L. Wilson and D. W. Wilson, Elsevier Publishing Co., Amsterdam (1962), p. 371.

23) If the volume exceeds 10 m*l*, the $CuCl_2$ solution might splash out into the autoclave on purging and on heating.

24) C. F. Irwin and G. F. Hennion, *J, Amer. Chem Soc.*, **63**, 858 (1941).

Table 6.

Synthesis of 2,3-Dichlorobutane.[25] 2-Butene was allowed to react with chlorine gas under a dry ice condenser. The products were purified by preparative gas chromatography (Condition *IV*). (NMR(CCl_4 solutions): *meso* (from *trans*), τ 8.39 (doublet, 3H), τ 6.01 (multiplet, 1H); *dl* (from *cis*), τ 8.45 (doublet, 3H), τ 5.82 (multiplet, 1H)). IR spectrum of *dl*-dichloride agreed with the standard chart (Sadtler No. 12165).

A mixture of 0.5 g (4 mmol) of *meso*- and *dl*-2,3-dichlorobutanes, 0.22 g (1.7 mmol) of $CuCl_2$, and 0.17 g (1.7 mmol) of CuCl in 5 m*l* of MeOH was heated in a 10 m*l* sealed glass tube at 140°C for 3.3 hr. Gas chromatographic analysis (Condition *I*) revealed that no isomerization and no detectable extent of methanolysis occurred under the reaction condition: a feed composed of *meso* 99.8% and *dl* 0.2% yielded a mixture of *meso* 99.7% and *dl* 0.3%, while a feed of *meso* 1.7% and *dl* 98.3% gave a mixture of *meso* 1.6% and *dl* 98.4%.

Synthesis of 2-Chloro-3-methoxybutane. The method of olefin chlorination with *t*-butyl hypochlorite[24] was applied to the synthesis. From *trans*-2-butene, the main product (assigned to *erythro*-2-chloro-3-methoxybutane) appeared at 16.3 min in the gas chromatogram (Condition *I*, 100°C) with a small amount of *meso*-dichloride at 18.2 min. On the other hand, *threo*-compound from *cis*-2-butene showed a peak at 17.3 min with *dl*-dichloride at 20.5 min.

The author is indebted to Professor Naoki Inamoto for valuable discussions. He also wishes to thank Mr. Katsumi Kaneko for his assistance in part of this work.

25) H. J. Lucas and C. W. Gould, Jr., *J. Amer. Chem. Soc.*, **63**, 2541 (1941).

BULLETIN OF THE CHEMICAL SOCIETY OF JAPAN VOL. 43 1443—1450 (1970)

Umwandlung von Aldehyden in 2-monosubstituierte Aziridine. Reduktion von α-Chlor, Brom- und Sulfonyloxynitilen mit Lithiumaluminiumhydrid

Kunihiro ICHIMURA*1 und Masaki OHTA

Laboratorium für Organische Chemie, Tokio Institut für Technologie, Tokio, Meguro-ku, Ookayama

(Eingegangen am 20. September, 1969)

The reductive cyclization of α-chloro, bromo- and sulfonyloxycarbonitriles are described. α-Chlorocarbonitriles were reduced by lithium aluminum hydride to afford aziridines in sufficient yields. The Walden inversion was found to take place in the cource of the reductive cyclization of *S*-α-chloroisocapronitrile. We have found the two-step conversion of aldehydes to 2-monosubstituted aziridines which consists of treating aldehydes with benzenesulfonyl chloride and alkali cyanide to form α-benzenesulfonyloxycarbonitriles which are reduced by lithium aluminum hydride to the corresponding aziridines. The reduction of α-bromocarbonitriles with the hydride yielded *prim.* amines together with the aziridines.

Die allgemeinen und bis jetzt benutzbarsten Darstellungmethoden der Aziridine wurde von Gabriel und Wenker entdeckt.[1] Im Nachteil sind jedoch in manchen Fällen diese beiden Verfahren, weil es sich dabei um die geringere Zugänglichkeit der Ausgangstoffe und um die unangenehm heftigen Reaktionsbedingungen handelt. In diesem Standpunkte ist es erforderlich, diese reaktionsfreudigen Heterocyclen, die zur Herstellung der stickstoffhaltigen Verbindungen als benutzbare Ausgangstoffe dienen können, unter milderen Bedingungen durch Umwandlungen der zugänglicheren funktionellen Gruppe darzustellen.

Vor kurzem sind einige modifizierten Verfahren zur Umwandlungen von Olefinen in Aziridine beschrieben, die auf den Anlagerung von Jodisocyanat,[2] Nitrosylchlorid[3] oder Dichlorurethan[4] an Olefine beruhen.

In dieser Arbeit sollen Umwandlungen der Aldehyde in 2-monosubstituierte Aziridine durch die Reduktion von α-Chlor, Brom- und Sulfonyloxynitrilen mit Lithiumaluminiumhydrid beschrieben werden, und die Stereospezifität des reduktiven Ringschlusses wird aus den folgenden ersichtlich.

*1 Neue Anschrift: Institut für Polymer- und Faserforschung, Yokohama, Kanagawa-ku, Sawatari 4.

1) P. E. Fanta, "Heterocyclic Compounds with Three- and Four-membered Rings, Part 1," Interscience, New York, London (1964), S. 524.

2) A. Hassner, M. E. Lober und C. Heathcock, *J. Org. Chem.*, **32**, 540 (1967).

3) G. L. Closs und S. J. Brois, *J. Amer. Chem. Soc.*, **82**, 6068 (1960).

4) T. A. Foglia und D. Swern, *J. Org. Chem.*, **31**, 3625 (1966); **32**, 75 (1967).

Tabelle 1. Aziridine durch reduktion der α-chlornitrile

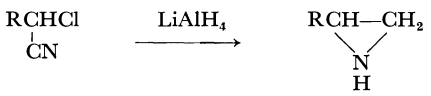

R	Molverhältnis LAH/Nitril	Ausbeute	Kp (°C/mmHg)	Analysenwert Gef N (Ber N)%
n-C_3H_7	1.3	82%	114—118	16.18 (16.45)*1
i-C_3H_7	1.0	72	103—105	16.54 (16.45)
n-C_6H_{13}	1.0	62	100/40	11.02 (11.02)
$C_6H_5CH_2$	1.0	58	117.5/22*2	
C_6H_5	1.0	46	97—99/13*3	
$(CH_2)_5CCH_2NH$*5	1.0	68	160*4	

*1 Gef (Ber) : C, 70.36 (70.52); H, 13.14 (13.02) %.
*2 Ber Kp: 78°C/3 mmHg. *N*-(*p*-Nitrobenzoyl)-Derivat: Schmp 86—90°C (Ber Schmp 85.5—86.5°C).[11]
*3 Ber Kp: 88—90°C/9 mmHg. [14b] 2-Chlor-2-phenyläthylamin-Pikrat: Schmp 147—148.5°C (Ber Schmp 147.5—148.5°C). [12]
*4 Ber. Kp: 158°C;[27] *N*-Phenylthiocarbamoyl-Derivat: Schmp 98—103°C (Ber Schmp 104.7°C).[13]
*5 1-Chlorcyclohexylcarbonitrile wurde reduziert.

Ergebnisse und Diskussion

Reduktion von α-Chlornitrilen mit Lithiumaluminiumhydrid.[5] Die nur wenig bekannte Bildungsweise der Aziridine hatten Booseré[6] und Theunis[7] mitgeteilt, die auf der Einwirkung des Äthylmagnesiumbromids auf einige α-Chlornitrile beruht.

Bei der Umsetzung von sonstigen α-Chlornitrilen mit Grignard-Reagenzien beobachtet man doch nicht immer die Entstehung der Aziridine. Beispielsweise bildet sich nur beträchtliche Menge der harzigen Substanz bei der Reaktion des Chloracetonitrils[8] wie des α-Chlorphenylacetonitriles[9] mit Phenylmagnesiumbromid neben der anderen wenigen Umsetzungsprodukte.

Auf Grund der verwandtschaftlichen Reaktionsweise von Grignard-Reagenzien mit Lithiumaluminiumhydrid (LAH) war mit dem letzteren ein analoger Reaktionsverlauf unter Bildung von Aziridinen zu erwarten.[10]

Bei der Reaktion von α-Chlorvaleronitril mit LAH in Äther bei −5—0°C erhält man, wie erwartet, 2-(*n*-Propyl)aziridin in 82%-iger Ausbeute. Andere 2-monosubstituierte Aziridine konnten in analoger Weise in den befriedigenden Ausbeuten erhalten werden, was in der Tabelle 1 angeführt ist.

Die analogen Ergebnisse hatte schon Krieger mitgeteilt,[14] worüber wir nach unseren Versuchen kennengelernt haben.*2

Er reduzierte mit Erfolg α-Chlornitrile des bicyclischen Heptens und Heptans mit LAH unter Bildung der *spiro*-Aziridine.

Im Gegensatz dazu hatte Wagner-Jauregg bei der LAH-Reduktion des 2-Chlor-3-cyclohexylaminopropionitril nur das entsprechende 1,3-Diamin isoliert.[15],*3

Was die Reaktionsmechanismen betrifft, kann man zwei Reaktionsfolgen zweckmäßig in Betracht

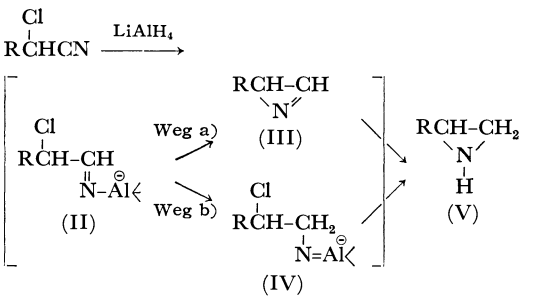

Fig. 1. Die mögliche Reaktionsfolge der reduktiven Cyclisierungsreaktion.

5) K. Ichimura und M. Ohta, Dieses Bulletin, **40**, 432 (1967).
6) O. de Booseré, *Bull. Soc. Chim. Belg.*, **32**, 26 (1923); *Chem. Zentr.*, **1928**, III. 1161.
7) M. Theunis, *Bull. Sci. Acad. Roy. Belg.*, **5**, 12, 786 (1926); *Chem. Zentr.*, **1927**, I 889.
8) L. Mathus, *Bull. Soc. Chim. Belg.*, **34**, 285 (1925); *Chem. Abstr.*, **20**, 739 (1926).
9) I. A. Smith, *Ber.*, **71B**, 634 (1938).
10) a) W. G. Brown, "Organic Reactions," Vol. 6, Wiley (1959), S. 469; b) N. G. Gaylord, "Reduction with Complex Metal Hydrides," Interscience, New York (1956).
11) D. V. Kashelikar und P. E. Fanta, *J. Amer. Chem. Soc.*, **82**, 4930 (1960).
12) F. Wolfheim, *Ber.*, **47**, 1440 (1914).
13) P. B. Tabular und P. E. Fanta, *J. Org. Chem.*, **24**, 526 (1959).
14) H. Krieger, *Suomen Kemistilhti*, **B 36**, 68 (1963).
*2 Wir sind Dr. H. Krieger für die Anweisung seines experimentellen Resultats[14] dankbar.
15) Th. Wagner-Jauregg, *Helv. Chim. Acta*, **44**, 1237 (1961).
*3 Wir danken Professor Th. Wagner-Jaüregg für die Anweisung seiner Arbeit.

ziehen.

Der Weg a) beruht auf dem Ringschluß des α-Chloraldimin-Derivates (II) in Azirin (III) und der anschließenden Reduktion mit dem Metallhydrid in Aziridin. Der alternative Weg b) besteht in der Reduktion vom α-Chlornitril unter Bildung des α-Chloramin-Derivates (IV), das dann in Aziridin zum Ringschluß gebracht würde.

Im Weg a) kommt es daher auf die Entstehung des ungesättigten Azirins als das Zwischenprodukt an, einige von welcher Klasse isolierbar[16] und in der Tat mit LAH in Aziridin übergeführt sind.[17] Um die Entstehung dieses Zwischenprodukts, Azirins, zu bestätigen, haben wir die Reduktion von α-Chlorisovaleronitril mit Unterschuß von LAH ausgeführt, aber die charakteristische infrarote Bande von Azirin bei etwa 1730—1780 cm^{-1} [16] keinesfalls beobachtet.

Brown und sein Mitarbeiter hatten eine wertvolle Umwandlung der Nitril-Gruppe in die entsprechenden Aldehyde mittels Lithiumtriäthoxyaluminohydrids mitgeteilt.[18] In der Umwandlung bildet sich offenbar das Aldimin-Derivat vor der Hydrolyse. Bei der Anwendung dieses Reagens an α-Chlornitril erwartet man also die Entstehung des α-Chloraldimin-Derivats, das nach der Reaktionsfolge a) Azirin liefern könnte.

Wenn man α-Chlorphenylacetonitril mit diesem Reduktionsmittel unterhalb 0°C behandelt, konnte man auch in diesem Fall keine Bildung des Azirins mittels des IR-Spektrums aufdecken, und *dl*-2,3-Diphenylbernsteinsäuredinitril selber wurde in geringer Ausbeute isoliert.

Diesen Ergebnissen nach mag die Cyclisierungsreaktion im Weg b) stattfinden und wird also als eine modifizierte Gabrielsche Reaktion bezeichnet.

Hinsichtlich des sonstigen Beispiels derartigen Cyclisierungsreaktion des Nitrils in Aziridin hatten Stork und seine Mitarbeiter beobachtet, daß bei der Einwirkung von LAH auf ein Glycidnitril neben einem Aminoalkohol ein Aziridinylcarbinol entsteht.[19] Bei der Umwandlung in Aziridinylcarbinol spielt die Epoxid-Gruppe als eine abspaltende Gruppe die Hauptrolle, gerade sowie Chloratom in der Reduktion der α-Chlornitrile. Sie hatten die Reaktionsfolge als intramolekulare *trans*-Eliminierung gezeichnet, ohne experimentellen Nachweis.

Beim Weg b) handelt es sich dann um die Frage, ob sich die Cyclisierungsreaktion der α-Chlornitrile wie in der Gabrielschen oder Wenkerschen Methode über die stereospezifische *trans*-1,3-Eliminierungsreaktion stattfinden würde.[20] Um diese Aufgabe zu lösen, haben wir optisch aktives α-Chlornitril synthetisiert und mit LAH reduziert.

Das optisch aktive α-Chlornitril, *S*-α-Chlorisocapronitril, wird wie in Fig. 2 dargestellt. Bekanntlich werden α-Aminosäure im allgemeinen mit Nitrosylhalogenid in die entsprechenden α-Halogencarbonsäure unter der Beibehaltung der sterischen Orientierung der Substituente übergeführt, mit Ausnahme von Valin und *iso*-Leucin.[21]

Die so erhaltene *S*-α-Chlorisocapronsäure wurde über das Säurechlorid ins Säureamid umgewandelt, das mittels Phosphorpentoxyds unter Bildung des *S*-α-Chlorisocapronsäurenitrils entwässert wurde.

Das so erhaltene α-Chlorisocapronitril, das sich mit Sicherheit in dem *R*-System befindet, wurde unterhalb 0°C mit LAH versetzt, und in 78%-iger Ausbeute entsteht 2-*iso*-Butylaziridin von $[\alpha]_D$

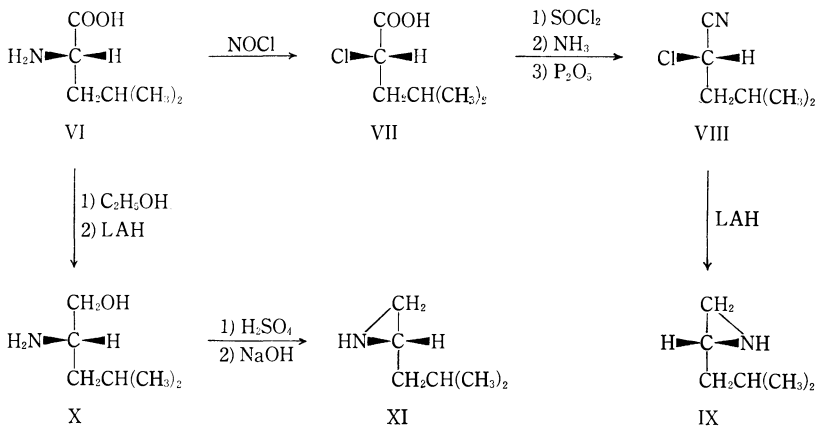

Fig. 2. LAH-Reduktion des optisch aktiven α-Chlornitrils.

16) G. Smolinsky, *J. Org. Chem.*, **27**, 3557 (1962).
17) a) D. J. Cram und M. J. Hatch, *J. Amer. Chem. Soc.*, **75**, 33 (1953); b) S. Eguchi und Y. Ishii, Dieses Bulletin, **36**, 1434 (1963).
18) H. C. Brown und C. P. Garz, *J. Amer. Chem. Soc.*, **86**, 1085 (1964).
19) G. Stork, W. S. Warrel und J. J. Pappas, *ebd.*, **82**, 4315 (1960).
20) A. Weissberger und H. Bach, *Ber.*, **64**, 1095 (1931); **65**, 631 (1932).
21) J. P. Greenstein und M. Winitz, "Chemistry of Amino Acids," Vol. I, Wiley, New York (1961), S. 152.

Tabelle 2. α-Benzolsulfonyloxynitrile (XII)

	R	Ar	M	Kp (°C/mmHg), [Schmp]	Ausb. %	Analysenwert Gef C	Gef H	Gef N	Ber C	Ber H	Ber N
a)	H	C_6H_5	K	191/12	72	49.35	3.88	7.11	48.72	3.58	7.10
b)	n-C_3H_7	C_6H_5	Na	172.5—173/3	79	55.57	5.47	6.13	55.21	5.47	5.86
c)	i-C_3H_7	C_6H_5	K	154—156.5/2	73	56.39	5.71	6.02	55.21	5.47	5.86
d)	t-C_4H_9	C_6H_5	Na	146—148/2	40	56.63	6.03	5.23	56.91	5.97	5.53
e)	$C_6H_5CH_2$	C_6H_5	K	56—57	57	62.93	4.84	4.82	62.70	4.88	4.88
f)	C_6H_5	C_6H_5	K	58—59*1	73						
g)	C_6H_5	p-$CH_3C_6H_4$	K	Öl*2	70						
h)	p-ClC_6H_4	C_6H_5	K	Öl	—						

*1 Ber Schmp 57.5—58.5°C.
*2 Umgewandelt in α-Chlorophenylacetonitrile bei der Umsetzung mit Lithiumchlorid.

+20.6°.

Um die absolute Konfiguration des Aziridins ins klare zu bringen, haben wir *S*-2-*iso*-Butylaziridin über L-Leucinol nach dem Verfahren von Tsuboyama synthetisiert,[22] und das so gebildete optisch aktive Aziridin zeigt $[\alpha]_D$ −26.4°.

Man kann auf dem Grunde dieser Ergebnisse schließen, daß das bei der Reduktion vom α-Chlornitril entstehende Aziridin die R-Chiralität hat, und daß also die Waldensche Umlagerung bei der Reduktionsstufe stattfindet.

Reduktion von α-Sulfonyloxynitrilen mit Lithiumaluminiumhydrid. Die synthetischen Anwendungen der oben beschriebenen reduktiven Cyclisierungsreaktion sind jedoch zur Synthese der Aziridin wegen der geringeren Ausbeuten an den α-Chlornitrilen und besonders wegen der heftigen Reaktionsbedingungen zur Herstellung der Nitrile so beschränkt, daß man die Verfahren zweckmäßig modifizieren sollte.

Wohlbekannt ist die Tatsache, daß sich Sulfonsäurealkylester sogleich wie Alkylhalogenid verhalten. Das veranläßt uns dazu, α-Sulfonyloxynitril mit LAH zu reduzieren, unter Erwartung der Bildung der Aziridine, indem die Hydrogenolyse des Sulfonsäureesters mittels LAH eine Prozedur ist, die Hydroxy-Gruppe mit Wasserstoff auszutauschen.[23]

Die Herstellung von α-Sulfonyloxynitril unter Benutzung des Sulfonylchlorids, Alkalicyanids und Aldehyds ist schon von einigen Arbeitern mitgeteilt.[24] Wir setzten die wäßrige Lösung des Alkalicyanids in Acetonitril-Lösung des Aldehyds und Chlorids unterhalb 0°C zu, und das α-Benzolsulfonyloxynitril wurde in befriedigenden Ausbeuten erhalten, was man in Tabelle 2 ersichtlich ist.

Im allgemeinen sind die von aromatischen Aldehyden ausgehenden α-Sulfonyloxynitrile bei Raumtemperatur zersetzlich. Beim Fall von Anisaldehyd beobachtete man jedoch bei erniedrigter Temperatur nach der flüchtigen Bildung der kristallinen Masse das beträchtliche Zerfließen und konnte das α-Sulfonyloxynitril keinesfalls isolieren.

Im Gegensazt dazu sind die von aliphatischen Aldehyden stammenden α-Sulfonyloxynitrile bei Raumtemperatur haltbar und unzersetzt destillierbar.

Interessant ist die Abwesenheit der Nitrilbande in den IR-Spektren der α-Sulfonyloxynitrile, gerade wie im Fall von α-Acyloxynitrilen.[25] Diese α-Sulfonyloxynitrile zeigen die charakteristischen Banden bei 1380, 1190, 1180, 1095, 930—1100, und 710—730 cm^{-1}.

Bei der Einwirkung von Alkalicyanid auf Benzolsulfonylchlorid und α,β-ungesättigte Aldehyde, Crotonaldehyd und Zimtaldehyd, konnte man keine gereinigten Verbindungen erhalten. Das Reaktionsgemisch zeigte keine Bande des Sulfonsäureesters.

Tabelle 3 Aziridine durch Reduktion von α-sulfonyloxynitrilen (XII)

R		Molverhältnis LAH/Nitril	Ausbeute %		Kp *2
a)	i-C_3H_7	1.0	20—40	(30)*1	100—108
b)	n-C_3H_7	1.0	0	(68)*1	—
c)	n-C_3H_7	1.5	61		113—116
d)	t-C_4H_9	1.5	68		113—116
e)	$C_6H_5CH_2$	1.0	0		—
f)	$C_6H_5CH_2$	1.5	53		113—115/18
g)	C_6H_5	1.5	59		95—98/13

*1 Polymeres Produkt.
*2 s Table 1.

22) S. Tsuboyama, Dieses Bulletin, **35**, 1004 (1962).
23) Ref. 10b, S. 855.
24) a) J. Lichtenberger und Ch. Franze, *Bull. Soc. Chim. Fr.*, **1948**, 995; b) R. M. Dadson und M. W. Turner, *J. Amer. Chem. Soc.*, **73**, 4517 (1951); c) E. C. Taylor, G. A. Berchtold, N. A. Geockner und F. G. Strohmann, *J. Org. Chem.*, **26**, 2715 (1961).
25) L. J. Bellamy, "The Infrared Spectra of Complex Molecules," Wiley, New York (1958), S. 226.

Methansulfonylchlorid kann zur Herstellung der entsprechenden α-Sulfonyloxynitrile nicht dienen.

Die Einwirkung des Alkalicyanids und Benzolsulfonylchlorids auf Cyclohexanon und Aceton wurde versagt.

Nach der Reduktion des α-Benzolsulfonyloxyvaleronitrils (XIIb) mit äquimolarem LAH polymerisiert das Reaktionsprodukt beim Erhitzen unter Bildung vom Polyäthylenimin, im Gegensatz zur Reduktion der α-Chlornitrile. Um diese Phänomena handelt es sich auch bei den Fallen von α-Sulfonyloxyisovaleronitril (XIIc) und 2-Phenylpropionitril (XIIe) bei Benutzung von äquimolarem LAH.

Die Polymerisierung der Aziridine verursachen bekanntlich mancherlei electrophile Reagenzien. Im vorliegenden Fall kann also α-Sulfonyloxynitril selbst als das Initiator dienen. Wenn man 2-*iso*-Butylaziridin in Gegenwart eines Tropfens des α-Benzolsulfonyloxyisovaleronitrils zu destillieren versucht, entsteht Polyäthylenimin, wie erwartet, und das Aziridin kann nicht mehr übergehen.

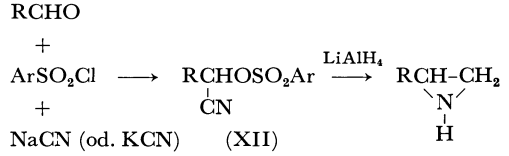

Diese unangenehmen Phänomena können bei Benutzung des anderthalbmolaren Metallhydrids vermieden werden, und 2-monosubstituierte Aziridine werden in befriedigenden Ausbeuten erhalten, was in Tabelle 3 angeführt ist.

Die Frage, ob sich die Hydroxy-Gruppe oder Acyloxy-Gruppe auch als die abspaltende Gruppe zur Bildung der Aziridine verhalten könnte, its für synthetische Anwendung interessant. Bekanntlich sind α-Cyanhydrin und Acyloxynitril nur in β-Aminoalkohol mittels LAH reduziert.[26] Wir haben auch diese Tatsache bei der Reduktion von α-Acetoxyisovaleronitril beobachtet, das nur den entsprechenden β-Aminoalkohol liefert.

Reduktion von α-Bromnitrilen mit Lithiumaluminiumhydrid. Unter Erwartung der Bildung der α-Chlornitril kocht man α-Benzolsulfonyloxyphenylacetonitril mit Lithiumchlorid in Aceton und erhält in guter Ausbeute α-Chlorphenylacetonitril. Diese Umwandlung kann man auf α-Benzolsulfonyloxyacetonitril anwenden.

Beim Erhitzen des α-Benzolsulfonyloxyisovaleronitril mit Lithiumchlorid in Aceton wurde das Ausgangsmaterial züruckgewonnen. Beim längeren Erhitzen des Nitrils in DMF mit Lithiumchlorid entsteht β-Methylcrotonitril in 53%-iger Ausbeute.

Durch Anwendung dieses Typs der Substitutionsreaction mittels Lithiumbromids gelang uns, die α-Sulfonyloxynitrile in α-Bromnitrile umzuwandeln. Die Ergebnisse werden in Tabelle 4 angeführt.

26) Ref. 10b, S. 742.

Tabelle 4 α-Halonitrile durch einwirkung von lithiumhalogenid auf α-sulfonyloxynitrile

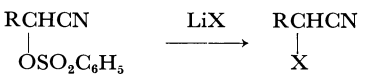

R	X	Ausb. (%)	Kp (°C/mmHg)	Reaktionsbedingungen
H	Cl	68	120—127	2 stdg. Rf.*3 in Aceton
C_6H_5	Cl	94	113—116/12	40 ming. Rf. in Aceton
i-Pr	Cl	Spur	—	2 stdg. Rf. in Aceton
n-Pr	Cl	Spur	—	2 stdg. Rf. in Aceton
i-Pr	Br	66	59—59.5/10*1	1.5 stdg. Rf. in MeCOEt
n-Pr	Br	71	72—73.5/13*2	1 stdg. Rf. in MeCOEt

*1 Gef (Ber): C, 38.89 (37.06); H, 5.34 (4.97); N, 8.57 (8.65) %.

*2 Gef (Ber): C, 37.83 (37.02); H, 5.28 (4.97); N, 8.27 (8.65) %.

*3 Rf.; Rückfluß.

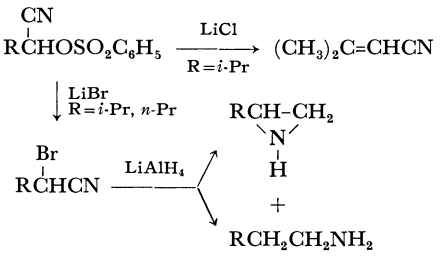

Wenn man α-Bromnitril mit äquimolarem LAH versetzt, beobachtet man bemerkenswerterweise die Entwicklung des Wasserstoffs und die Entstehung des Polyäthylenimins beim Erhitzen zur Destillieren. Wie im Fall der vorher erwähnten Reduktion der α-Benzolsulfonyloxynitrile werden α-Bromnitrile bei Benutzung von anderthalbmolarem LAH mit Erfolg in destillierbares Produkt umgewandelt. Nach der gaschromatographischen Analyse fanden wir, daß das Reaktionsprodukt aus dem 2-monosubstituierten Aziridin und dem entsprechenden *prim.* Amin besteht. Die Ergebnisse der gaschromatographischen Analyse bei der Reduktion der α-Chlor- und Sulfo-

Tabelle 5. Reduktionsprodukte

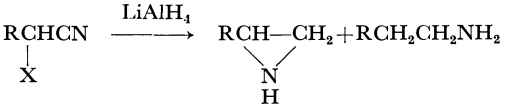

R	X	Produktsverhältnis Aziridin	*prim.* Amin
n-Pr	Cl	100	0
n-Pr	$OSO_2C_6H_5$	100	0
n-Pr	Br	43	57
i-Pr	Cl	97	3
i-Pr	$OSO_2C_6H_5$	100	0
i-Pr	Br	30	70
i-Bu	Br	34	64
t-Bu	$OSO_2C_6H_5$	100	0

nyloxynitrilen sind auch in Tabelle 5 angeführt.

Wie man in Tabelle 5 sehen kann, sind die Produktsverhältnisse von dem Substituente (R) und der abspaltenden Gruppe (X) abhängig, und im Fall des α-Bromnitrils entsteht das *prim.* Amin in größeren Mengen.

Das ist offenbar, daß bei der Bildung des *prim.* Amins es sich nicht um die hydrogenolytische Ringöffnung des Aziridins handelt. Denn bei der Reduktion des α-Sulfonyloxynitrils beobachtet man keine Bildung des *prim.* Amins.

Um die weiteren Kenntnisse der Reaktionsfolge zu gewinnen, haben wir die LAH-Reduktion des optisch aktiven α-Bromnitrils ausgeführt.

Wie im Fall des α-Chlornitrils wird *S*-α-Bromisocapronsäurenitril über die *S*-α-Bromsäure durch die Entwässerung des entsprecheden α-Bromamids hergestellt. Beim Zugeben des α-Bromnitrils auf die LAH-Aufschlämmung beobachtet man die Entwicklung des Wasserstoffs und isoliert die Reduktionsprodukte, die gaschromatographisch mit 2-*iso*-Butyaziridin und 4-Methylpentylamin identifiziert werden. Durch die präparativen Gaschromatographie fraktioniert man 2-*iso*-Butylaziridin, das $[\alpha]_D$ +25.5° zeigt.

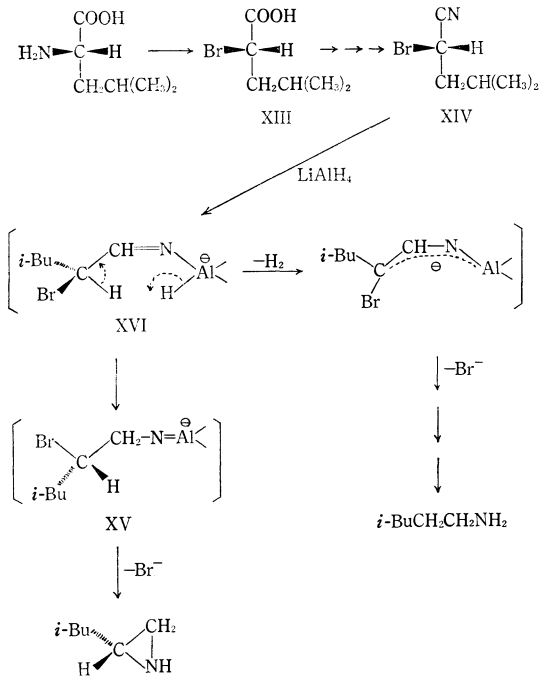

Fig. 3. LAH-Reduktion des optisch aktiven α-Bromnitrils.

Das *prim.* Amin bildet sich daher wahrscheinlich über die in Fig. 3 angegebene Zwischenstufe (XVI) unter Entwicklung des Wasserstoffs, während das Aziridin nach der Sättigung der Nitril-Gruppe so durch die *trans*-Eliminerung entsteht, wie im Fall des α-Chlornitrils.

Beschreibung der Versuche*4

Ausgangsmateriale. Die folgenden α-Chlornitrile wurden durch Chlorierung der entsprechenden Cyanhydrine hergestellet. α-Chlorvaleronitril vom Kp 158—161°C in 33%-iger Ausbeute (bezogen auf Butyraldehyd). α-Chlorisovaleronitril vom Kp 152—155.5°C in 57%-iger Ausbeute. α-Chlorcaprylnitril vom Kp 104.5—105°C/16 mmHg in 20%-iger Ausbeute. 1-Chlor-2-phenylpropionitril vom Kp 77.5—79.5°C/13 mmHg. 1-Chlorcyclohexancarbonitril wurde nach der Stevenschen Methode erhalten.[27]

Reduktion vom α-Chlornitril mit Lithiumaluminiumhydrid. *2-(n-Propyl)aziridin (eine typische Prozedur zur Herstellung der Aziridine).* Man setzt in die Suspension von 2.50 g (66 mmol) Lithiumaluminiumhydrid in 25 m*l* Äther 5.90 g α-Chlorvaleronitril in 10 m*l* Äther tropfenweise unter gutem Rühren und Eis-Kochsalzkühlung zu. Dabei riecht es schon nach dem charakteristischen Aziridin. Nach dem einigstündigen Rühren bei Raumtemperatur setzt man 0.5 g Natriumhydroxyd zu und zersetzt dann das Gemisch vorsichtig mit Wasser unter Eis-Kochsalzkühlung. Nach dem Filtrieren der anorganischen Absätze trocknet man die ätherische Lösung mit Kaliumcarbonat ab und entäthert mittels 20 cm Kolonne. Man destilliert den Rückstand und erhält 3.50 g 2-(*n*-Propyl)aziridin vom Kp 114—118°C. Alle Aziridine, die in analoger Weise hergestellt werden, zeigen die charakteristische Bande in IR-Spektren bei 3050 und 3200 cm^{-1}.

Reduktion des α-Chlorvaleronitrils mit Unterschuß von Lithiumaluminiumhydrid. Man setzt die Suspension von 0.45 g in 30 m*l* Äther teilweise in die ätherische Lösung von 5.00 g α-Chlorvaleronitril unter Eis-Kochsalzkühlung zu und rührt das Gemisch 2 Std bei Raumtemperatur. Nach vorsichtigem Zersetzen des Metallkomplexes und nach dem Freisetzen der anorganischen Absätze trocknet man die ätherische Lösung mit Natriumhydroxid ab und entäthert. Im IR-Spektrum dieses Rückstandes tritt weder die Absorptionsbande des Azirins (etwa 1740 cm^{-1}) noch die des Aziridins (3050 und 3200 cm^{-1}).

Reduktion von α-Chlorphenylacetonitril mit Lithiumtriäthoxyaluminohydrid. Man setzt 2.00 g Essigsäureäthylester in 8 m*l* Äther in die Suspension von 0.58 g Lithiumaluminiumhydrid in 12 m*l* Äther unterhalb 0°C zu. Danach tropft man 2.30 g α-Chlorphenylacetonitril in 8 m*l* Äther in das Reaktionsgemisch unterhalb 0°C ein, rührt 3 Std bei Raumtemperatur und läßt das Gemisch zwei Tage stehen. Man zersetzt das Reaktionsgemisch mit Wasser, trennt die ätherische Schicht ab und trocknet sie mit Kaliumhydroxyd ab. Nach dem Eindampfen des Lösungsmittels erhält man den braunen Rückstand, aus dem man 0.33 g farblose Kristalle des *dl*-α,β-Diphenylbernsteinsäuredinitrils vom Schmp. 163—164.5°C isoliert. Nach einmaligem Umkristallisieren aus Äthanol schemelzen sie bei 164.5—166°C. (Ber Schmp 164°C). Gef: C, 82.94; H, 4.57; N, 12.33%.

Der von Diphenylbernsteinsäuredinitril freigesetzte

*4 Die berichneten Kochpunkte und Schmelzpunkte sind aus Beilsteinschem Handbuch zitiert.

27) C. L. Stevens und T. H. Coffield, *J. Amer. Chem. Soc.*, **73**, 103 (1951).

Rückstand zeigt keine infrarote Absorption von Phenylazirin.

***S*-α-Chlorisocapronsäure.** Man löst 52.5 g L-Leucinol in 800 m*l* 6N HCl ein und setzt Natriumnitrit in kleinen Portionen in die Lösung unterhalb 0°C unter Eis-Kochsalzkühlung und gutem Rühren zu. Nach einhalbstündigem Rühren bei −8°C und dreistündigem Rühren bei Raumtemperatur sättigt man die gelbe Lösung mit Kochsalz ab und äthert die organische Schicht fünfmal aus. Nach Trocknen der ätherischen Lösung mit Natriumsulfat entäthert man sie unter verm. Druck. Man erhält 35.5 g *S*-α-Chlorisocapronsäure vom Kp 110—113°C/13 mmHg. Bei nochmaligem Destillieren siedet die Säure bei 112—114°C/10 mmHg. n_D^{20} 1.4412. $[\alpha]_D^{16}$ −24.6° (*c* 5, EtOH).

***S*-α-Chlorisocapronylchlorid.** Nach gelindem Rückfluß von 18.5 g α-Chlorisocapronsäure und 31.0 g Thionylchlorid erhält man 14.4 g α-Chlorisocapronylchlorid vom Kp 71°C/28 mmHg.

***S*-α-Chlorisocapronamid.** In 200 m*l* konz. Ammoniak tropft man Dioxan (20 m*l*)-Lösung von 14.4 g *S*-α-Chlorisocapronsäurechlorid bei 0——5°C unter Rühren und Eis-Kochsalzkühlung, rührt 30 Min das Gemisch bei 0°C und untscht die abgeschiedenen Kristalle ab. Man erhält 10.00 g *S*-α-Chlorisocapronamid vom Schmp 88—90°C. Nach Umkristallisieren der Kristalle aus wäßrig. Methanol schmelzen sie bei 91—91.5°C. $[\alpha]_D^{17}$ −46.9° (*c* 2, EtOH). Gef: C, 48.62; H, 7.99; N, 9.66%. Ber für $C_6H_{12}NOCl$: C, 48.16; H, 8.09; N, 9.36%.

***S*-α-Chlorisocapronitril.** Nach Mischen des verpulverten 5.0 g *S*-α-Chlorisocapronamid mit 7.2 g Phosphorpentoxyd erhitzt man das Gemisch unter vermindertem Druck über bloßer Falmme, und 3.6 g *S*-α-Chlorisocapronitril geht über und siedet bei 60.0°C/13 mmHg. n_D^{20} 1.4291. $[\alpha]_D^{17}$ −20.0° (*c* 2, EtOH). Gef: C, 54.96; H, 7.54; N, 10.41%. Ber für $C_6H_{10}NCl$: C, 54.76; H, 7.62; N, 10.65%.

***S*-2-Isobutylaziridin.** Man setzt 1.75 g *S*-α-Chlorisocapronitril in die Aufschlämmung von 0.52 g Lithiumaluminiumhydrid in 30 m*l* Äther unterhalb −5°C. Nach einstündigem Rühren bei Raumtemperatur fügt man 4 g Natriumhydroxyd zu, zersetzt das Metallkomplex mit 10 m*l* Wasser bei etwa 5°C unter gutem Rühren und Eis-Kochsalzkühlung. Man filtriert den Niederschlag ab und wäscht ihn dreimal mit Äther. Die vereinigte ätherische Lösung wird über Kaliumhydroxyd abgetrocknet, und nach Abdestillieren des Äthers bei gewöhnlichem Druck mittels 20 cm Kolonne erhält man 1.03 g rohes *S*-2-Isobutylaziridin, das bei nochmaligem Destillieren bei 130—131°C siedet. n_D^{20} 1.4267. $[\alpha]_D^{15}$ +20.6° (*c* 1.828, Bzl).

***R*-2-Isobutylaziridin.** Man versetzt 6.1 g L-Leucinol in 10 m*l* Wasser mit 5.7 g konz. Schwefelsäure und 10 m*l* Wasser und destilliert Wasser unter verm. Druck bei etwa 135°C ab. Das so gebildete Sulfonsäureester wird mit 10.5 g Natriumhydroxyd in 30 m*l* Wasser versetzt und erhitzt. Das Aziridin geht zusammen mit Wasser über. Die wäßrige Schicht wird mit Kaliumhydroxyd abgesättigt und dreimal mit Äther ausgezogen. Die Auszüge wird mit Kaliumhydroxyd abgetrocknet und entäthert. *R*-2-Isobutylaziridin siedet bei 130—134°C und beträgt 3.80 g. n_D^{20} 1.4270. $[\alpha]_D^{17}$ −26.4° (*c* 1.828, Bzl). (Ber, n_D^{28} 1.4242, $[\alpha]_D^{32}$ −24.6° (*c* 1.828, Bzl)).[22]

Allgemeine Vorschrift zur Herstellung der α-Sulfonyloxynitrile. Man versetzt äquimolares Benzolsulfonylchlorid und frisch destilliertes Aldehyd in Acetonitril und kühlt die Lösung bis auf −10°C ab. Unter gutem Rühren setzt man konz. wäßr. Lösung (30—40%) von 1.05 mol. Natrium- oder Kaliumcyanid unterhalb 0°C zu und rührt eine Stunde bei Raumtemperatur. Das Reaktionsgemisch wird anschließend mit Wasser versetzt. und das abgeschiedene Öl mit Methylenchlorid ausgezogen und mit Wasser gewaschen. Nach Abtrocken über Natriumsulfat und Eindampfen der Auszüge erhält man das α-Benzolsulfonyloxynitril als den Rückstand, der durch Vakuumdestillieren oder Umkristallisieren gereinigt wird.

Reduktion des α-Benzolsulfonyloxynitrils mit Lithiumaluminiumhydrid. Man reduziert α-Benzolsulfonyloxynitrile und arbeitet so gleich wie α-Chlornitrile auf. Für die in Äther nur schwer lösliche Sulfonyloxynitrile dient Tetrahydrofuran als besseres Lösungsmittel.

α-Acetoxyisovaleronitril. Man führt 12.5 g frisch destilliertes Isobutyraldehyd in das Cyanhydrin in gewöhnlicher Weise über, das mit 50 m*l* Acetanhydrid in der Gegenwart der katalytischer Mengen der *p*-Toluolsulfonsäure über Nacht umgesetzt. Ausbeute, 9.3 g, Kp 82°C/13 mmHg. n_D^{20} 1.4115. Gef: C, 60.80; H, 7.86; N, 10.45%. Ber für $C_7H_{11}NO_2$: C, 59.55; H, 7.86; N, 9.92%.

Reduktion des α-Acetoxyisovaleronitril mit Lithiumaluminiumhydrid. Man behandelt 7.0 g α-Acetoxyisovaleronitril mit 3.8 g Lithiumaluminiumhydrid in Äther in üblicher Weise und erhält 2.07 g 1-Amino-3-methylbutanol-2. Kp 101°C/44 mmHg. n_D^{20} 1.4447. Gef: C, 64.75; H, 8.07; N, 12.58%. Ber für $C_{12}H_{18}N_2O_2$: C, 64.84; H, 8.16; N, 12.61%.

α-Chlorphenylacetonitril. Man kocht 30 g α-Benzolsulfonyloxyphenylacetonitril und 7.6 g Lithiumchlorid 2 Std in 120 m*l* Wasser, extrahiert zweimal mit Äther und trocknet über Magnesiumsulfat ab. Ausbeute, 15.6 g. Kp 113.5—116.0°C/12 mmHg (Ber Kp 108—110°C/5 mmHg).

β-Methylcrotonitril. Man erhitzt 6.8 g α-Benzolsulfonyloxyisovaleronitril und 1.8 g Lithiumchlorid in Dimethylformamid 8 Std. bei 130—140°C. Die Lösung wird mit Wasser versetzt, und man zieht mit Äther aus und erhält 1.24 g β-Methylcrotonitril. Kp 142°C (Ber, Kp 140—142°C). (Gef: C, 73.88; H, 9.11; N, 16.50%).

α-Bromisovaleronitril. Man kocht 15.0 g α-Benzolsylfonuloxyisovaleronitril und 8.2 g Lithiumbromid 1.5 Std, in 50 m*l* wasserfreies Methyläthylketon unter Rückfluß und erhält nach üblichem Arbeiten 6.7 g α-Bromisovaleronitril vom Kp 59—59.5°C/13 mmHg. n_D^{20} 1.4595. Gef: C, 38.89; H, 5.34; N, 8.57%. Ber für C_5H_8NBr: C, 37.06; H, 4.97; N, 8.65%.

α-Bromvaleronitril. Man erhält das Bromnitril in oben beschriebener Weise in 71%-iger Ausbeute. Kp_{13} 72—73.5°C. n_D^{20} 1.4594. Gef: C, 37.83; H, 5.28; N, 8.27%. Ber für C_5H_8NBr: C, 37.06; H, 4.97; N, 8.65%.

Reduktion von α-Bromvaleronitril mit Lithiumaluminiumhydrid. Man setzt die ätherische Lösung von 7.94 g (0.045 mol) α-Brombutyronitril auf die Aufschlämmung des 2.80 g (0.067 mol) Lithiumaluminiumhydrids in 40 m*l* Äther zu, wobei sich 0.018 mol Wasserstoff entwickelt. Nach der üblichen Aufarbeitung destilliert man die ätherische Lösung mit 30 cm Kolonne und erhält das Reduktionsprodukt vom Kp 100—118°C die 2.67 g beträgt und gaschromatographisch analysiert.

Reduktion von α-Bromisovaleronitril mit Li-

thiumaluminiumhydrid. Gerade wie im Fall des α-Bromvaleronitrils erhält man 1.90 g Reduktionsprodukt von Kp 90—113°C aus 7.13 g α-Bromisovaleronitril und 2.52 g Lithiumaluminiumhydrid.

Gaschromatographische Analyse der Reduktionsprodukte. Die rohen Reduktionsprodukte werden gaschromatographisch analysiert und die Auftrennung der Aziridine und der entsprechenden Amine läßt sich mittels Carbowax-20M-Säule erzielen. Säulenlänge 1.5 m, Trägergas Helium, Strömungsgeschwindigkeit etwa 70 ml/min. Jedes Aziridin hat die längere Retentionszeit als das entsprechende Amin. Die gebildeten *prim.* Amine werden durch den Vergleich der Retentionszeit der authentischen Probe identifiziert.

***S*-α-Bromisocapronsäure.** Man löst 31.2 g L-Leucin und 85.8 g Kaliumnitrit unter gutem Rühren bei −5—0°C langsam zugesetzt wird. Nach einstündigem Rühren bei Raumtemperatur extrahiert man das abgeschiedene Öl viermals mit Äther. Nach Abtrocknen über Magnesiumsulfat der Auszüge destilliert man *S*-α-Bromisocapronsäure vom Kp 132—135°C/12 mmHg (Ber Kp 125—131°C/13 mmHg (der *dl*-Säure)). n_D^{19} 1.4665.

***S*-α-Bromisocapronsäurechlorid.** Man kocht 25 g *S*-α-Bromisocapronsäure und 40 ml Thionylchlorid 3 Std. Ausbeute, 20 g. Kp 75—78°C/15 mmHg.

***S*-α-Bromisocapronsäureamid.** Unter Eiskühlung und Rühren setzt man mit Dioxan verdünntes *S*-α-Bromisocapronsäurechlorid in konz. Ammoniak und rührt eine Std unter Eiskühlung. Man erhält das α-Bromamid vom Schmp 117—118°C, das aus Wasser Äthanol umkristallisiert wird. Gef: C, 37.30; H, 6.17: N, 7.17%. Ber für $C_6H_{12}NOBr$: C, 37.13; H, 6.23; N, 7.22%.

***S*-α-Bromisocapronitril.** Man erhitzt 9 g verpulvertes *S*-α-Bromisocapronsäureamid und 15 g Phosphorpentoxyd in vermindertem Druck und erhält man 7.3 g α-Bromnitril, das 80—81°C/13 mmHg siedet. n_D^{18} 1.4605. $[\alpha]_D^{20}$ −27.4° (*c* 1.950, Bzl). Gef: C, 41.37; H, 5.74: N, 7.75%. Ber für $C_6H_{10}NBr$: C, 40.95; H, 5.73: N, 7.96%.

Reduktion von *S*-α-Bromisocapronitril mit Lithiumaluminiumhydrid. Man setzt 5.98 g *S*-α-Bromisocapronitril und 2.20 g Lithiumaluminiumhydrid in Äther in üblicher Weise um und erhält 1.31 g Produkt von Kp 120—126°C, der durch die oben genannten Carbowax-20M-Säule gaschromatographisch in 4-Methylpentylamin und 2-Isobutylaziridin im Verhältnisse 66 : 34 fraktioniert wird. *N*-Phenylcarbamoyl-Derivat des 4-Methylpentylamins, Schmp 84°C (Ber Schmp 84°C). *R*-2-Isobutylaziridin, $[\alpha]_D^{20}$ +25.5° (*c* 1.035, Bzl).

BULLETIN OF THE CHEMICAL SOCIETY OF JAPAN VOL. 43 1450—1454 (1970)

Laser-induced Chemical Reactions. III. The Decomposition of Metal Salts of Carboxylic Acid and Selective Decomposition

Ko Taki, Pil Hyon Kim and Susumu Namba

The Institute of Physical and Chemical Research, Yamato-machi, Saitama

(Received September 24, 1969)

Various copper metal salts of organic acid were decomposed by laser heating and conventional heating methods. The product distributions were reasonably explained in terms of the expected reaction of the decarboxylated intermediates. Generally the yield percentage of products is higher in laser decomposition than in thermal decomposition. However, in maleate and fumarate the product distribution is quite different in thermal and laser decompositions. The main product is ethylene in the thermal decomposition, but acetylene in the laser decomposition. This difference may be the result of the heating rate. Since rapid heating and quenching are characteristic of laser heating, the formation of acetylene may be brought about by the simultaneous decarboxylation of two carboxyl groups, while the formation of ethylene may be brought about by successive decarboxylation. Selective decomposition by laser heating will also be discussed in binary systems, such as maleate and ethylene.

The chemical reaction induced by a laser beam (ruby laser) has been investigated previously. The reaction mechanism[1] has been considered to be: (1) photodissociation,[2,3] (2) direct heating of the solid, causing vaporization,[3,4] and (3) breakdown of gases.[5] The reaction of carbon vapor produced by the ruby laser and that caused by the breakdown of gases have been previously

1) J. F. Verdieck and A. W. H. Mau, *Chem. Commun.*, **1969**, 226.

2) I. Tanaka, Y. Mori, Y. Minagawa and E. Okutsu, *J. Phys. Chem.*, **72**, 2684 (1968).

3) W. B. Tiffany, *J. Chem. Phys.*, **48**, 3019 (1968).

4) R. Schaeffer and R. K. Pearson, *J. Amer. Chem. Soc.*, **91**, 2153 (1969).

5) A. H. Adelman, *J. Chem. Phys.*, **45**, 3152 (1966).

reported by the present authors.[6,7] As the ruby laser (photon energy: 1.8 eV) does not have enough energy to dissociate organic molecules, any photochemistry by the ruby laser is restricted and some of the reaction must be performed by multiphoton absorption processes. Therefore, the ruby laser may be most useful for the pyrolysis.

Organic carboxylic acids are well known to be decomposed by heating, resulting in decarboxylation in the presence of a copper catalyst.[8,9] Metal salts of carboxylic acid are also decomposed to produce organic radicals and ketones[10] under decarboxylation.[11] Acetic acid is decomposed at 530—762°C to give methane and ketene.[12]

By the absorption of the pulse ruby laser beam, the target surface is heated rapidly to about 600—800°C,*1 resulting in heat decomposition. As the copper salts of organic acids are blue and green, these salts may absorb the ruby laser beam efficiently and themselves be decomposed.

Among the copper salts of organic acids decomposed by laser heating (laser decomposition) and conventional heating (thermal decomposition), both maleate and fumarate give quite different results between the laser and thermal decompositions.

In this experiment the mechanism of laser decomposition has been studied; this paper will also discuss another possibility of the use of a laser beam.

Experimental

Copper maleate and fumarate were prepared by the reaction of maleic acid and copper carbonate, and of fumaric acid sodium salt and a copper sulfate solution, respectively. Each of them has crystal water,*2 and the decomposition temperature was checked by differential thermal analysis and thermal gravimetrical analysis.

The laser used was a pulse ruby laser, the output energy and pulse duration of which were about 3 J and 0.5 msec respectively. The sample target in the cell

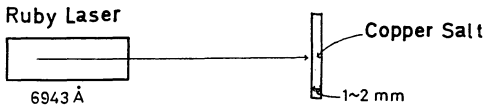

output energy 3 J
pulse duration 0.5 msec

Fig. 1. Experimental block diagram.

was irradiated by the laser beam as is shown in Fig. 1; after 2—7 pulse irradiations the gaseous products were analysed by gaschromatography using silica-gel, activated-charcoal, and squalane columns. Quantitative analysis was performed by the internal standard system.

The thermal decomposition (0.1 g salt) was carried out in a metal bath for 30—60 sec at various temperatures.

Results and Discussion

1) Decomposition of Metal Salt. Various copper salts (acetate, propionate, *n*-butyrate, isobutyrate, acrylate, malonate, benzoate, phthalate, succinate, adipate, maleate, and fumarate) were decomposed by both the thermal and laser decomposition methods. The results for several salts are shown in Table 1. Generally, the product distributions are almost the same in the two decomposition methods, but maleate and fumarate are exceptions. The gaseous products can be reasonably explained in terms of the expected reaction of the decarboxylated fragments. The amount of carbon dioxide may be considered to represent the fraction of the decomposed copper salt. For convenience, the product yield may be represented as per cent of carbon dioxide.

In the laser decomposition on both copper maleate and fumarate, the gaseous products consisted of

Table 1. Product yield from copper salts in thermal* and laser decomposition based on CO_2 produced

Substrate	Product	Yield (%) Thermal decomp. (at 400°C)	Laser decomp. (6 pulses)
Copper acrylate	CH_4	0.011	0.39
	C_2H_6	0.0011	0
	C_2H_4	6.7	15
	Butadiene	0.023	3.2
Copper Succinate	CH_4	0.05	0.37
	C_2H_6	0.014	0.07
	C_2H_4	2.3	14
	Propane	0	0.26
	C_2H_2	0	1.7
Copper maleate	C_2H_4	2.2	1.2
	C_2H_2	trace	8—12
Copper fumarate	C_2H_4	2.4—4.7	5.0
	C_2H_2	trace	10—12

* The yield percents of CO_2 for salts used were 80—90% in maleate and 45—50% in fumarate.

6) K. Taki, P. H. Kim and S. Namba, This Bulletin, **42**, 823 (1969).
7) K. Taki, P. H. Kim and S. Namba, *ibid.*, **42**, 2377 (1969).
8) D. M. Burness, "Organic Syntheses," Coll. Vol. IV. p. 628 (1963).
9) R. H. Wiley and N. R. Smith *ibid.*, Coll. Vol. IV. p. 731 (1963).
10) L. Ruzicka, W. Brugger, M. Pfeiffer, H. Schinz and M. Stoll, *Helv. Chim. Acta*, **9**, 514 (1926).
11) E. Piers and R. K. Brown, *Can. J. Chem.*, **40**, 559 (1962).
12) P. G. Blake and G. E. Jackson, *J. Chem. Soc., B*, **1969**, 94.

*1 The surface temperature was estimated by the ignition point of amorphous carbon and the melamine polymer.

*2 Copper maleate dried at 80°C has 1 mol crystal water (Found: C, 24.5; H, 2.16%, ($C_4H_2O_4Cu+H_2O$)).

Table 2. Product yield from copper maleate and fumarate in laser decomposition based on CO_2 produced

Product	Substrate	
	Maleate	Fumarate
Methane	0.5 %	2.2 %
Ethane	0.05	0.2
Ethylene	1.2	5.0
Acetylene	8—12	10—12

10—15% noncondensable gases at the temperature of liquid nitrogen; the products were methane and carbon monoxide, hydrogen not being detected. 65% of the condensable gases consisted of carbon dioxide, and the rest were hydrocarbon and water. The hydrocarbon consisted of acetylene, ethylene, and a small amount of C_3 and C_4 compounds, as is listed in Table 2. Acetylene is the main product, but the yield is only about 10% of the carbon dioxide (10^{-5}—10^{-6} mol). The decomposition processes are considered to be as follows:

$$\text{Maleate or fumarate} \xrightarrow[\text{irradiation}]{\text{laser}} \text{Decarboxylated intermediate } (-CH{=}CH-) \longrightarrow \text{Acetylene, } C_4 \text{ compounds, and nonvolatile products}$$

On the other hand, the thermal decomposition gives not acetylene but ethylene at 350°C. The high-temperature decomposition gives acetylene, but ethylene is still obtained in a high yield, as is listed in Table 3. In the laser decomposition, the ethylene yield increases as the laser power is lowered by using a copper-sulfate-solution filter, but acetylene is still the main product, as is shown in Table 4. From the above results, the difference between the laser and the thermal decomposition does not seem to depend only on the decomposition temperature. In the laser heating, the temperature rises very rapidly to decompose the salt in a moment, and then two decarboxylations are brought about at the same time to produce an intermediate (-CH=CH-). This intermediate forms acetylene intramolecularly. Therefore, the formation of acetylene seems to depend on the heating rate.

Table 3. The ratio of acetylene to ethylene from copper maleate and fumarate in thermal decomposition at various temperatures

Substrate	C_2H_2/C_2H_4			
	350°C	500°C	570°C	670°C
Copper maleate	0.0015	0.22	—	1.3
Copper fumarate	0.009	0.12	0.15	—

— Detection was not carried out.

Table 4. The ratio of acetylene to ethylene from copper maleate and fumarate in laser decomposition at various transmissions of laser beam by using $CuSO_4$ solution filter

Substrate	C_2H_2/C_2H_4		
	100 % trans.	50% trans.	25% trans.
Copper maleate	6—10	5.8	4.9
Copper fumarate	2—2.4	.2.0	1.3

In the thermal decomposition, the formation mechanism of ethylene and acetylene is not clear because the secondary decomposition may occur at a high temperature. However, on the basis of differential thermal analysis and thermal gravimetrical analysis data, the decomposition occurs over a wide temperature range in copper maleate (170—340°C) and fumarate (170—380°C). Therefore, it may be roughly presumed that the decarboxylation is brought about step by step, that the -CH=CH-COO-Cu- thus obtained may abstract hydrogen to produce an acrylic compound,[13] and that the secondary decarboxylation may give ethylene:

$$\text{Copper maleate or fumarate} \xrightarrow{\text{Decarboxylation}} -CH{=}CH-COOCu- \xrightarrow{\text{Hydrogen abstraction}} CH_2{=}CH-COOCu \xrightarrow{\text{Decarboxylation and hydrogen abstraction}} CH_2{=}CH_2$$

In fact, copper acrylate is decomposed to give ethylene in both the laser and thermal decompositions (Table 1).

The difference between the two types of decomposition may depend on whether or not the two decarboxylations occur at the same time. Moreover, it may be also decided by the property of the one-decarboxylated intermediate. In fact, no difference was found in copper succinate (decomposition temperature range: 280—380°C). In this case, the decarboxylated intermediate, $-CH_2-$

Table 5. Product yield from mixture of benzoate and other salts in laser decomposition based on CO_2 produced

Substrate (Copper salt)	Yield(%)			
	Benzene	Toluene	Ethyl-benzene	Isopropyl-benzene
Benzoate and Acetate	7.2	0.9	—	—
Benzoate and Propionate	6.0	0.02	0.08	—
Benzoate and Isobutyrate	6.5	0.05	—	0.03

— Not detected.

13) T. Voelker and H. Graefe, German 1195297. *Chem. Abstr.*, **63**, 8207[f] (1965).

Table 6. Product yield in selective decomposition of binary system by laser heating based on CO_2 produced

Substrate	Yield (%) C_3 compounds	C_4 compounds	C_5 compounds	C_6 compounds
Copper maleate and 760 Torr nitrogen	0.2	0.6	0.17	0
Copper maleate and 730 Torr ethylene	0.35	3.9	—	—
Copper maleate and 730 Torr propylene	—	—	0.45	—
Copper maleate and 730 Torr 1-butene	—	—	—	0.67
Copper fumarate and 760 Torr nitrogen	0.24	0.3	0.12	0
Copper fumarate and 730 Torr ethylene	—	1.8	—	—
Copper fumarate and 730 Torr propylene	—	—	0.46	—
Copper fumarate and 730 Torr 1-butene	—	—	—	0.82

— Detection was not carried out.

CH_2–COOCu–, may form ethylene intramolecularly in the thermal decomposition. The mechanism of decarboxylation in the laser decomposition may be supported by the following experimental fact. In the mixture of copper benzoate and acetate, benzoate and propionate, and benzoate and isobutyrate, the laser heating of the mixture gives toluene, ethylbenzene, and isopropylbenzene respectively, as is shown in Table 5. However, in the thermal decomposition at 400°C, toluene, ethylbenzene, and isopropylbenzene were not detected or were present in trace quantities only. The alkyl-substituted benzene may be formed by a recombination of the phenyl and alkyl radicals. Therefore, it is necessary for the decarboxylation of the two components to occur at the same time in a mixture of copper salts. The reaction mechanism may be considered to be as follows:

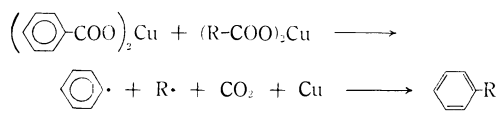

Each component is decomposed to produce R–R and biphenyl by both the laser and thermal decompositions. However, each component is decomposed in a different temperature range (acetate: 125—300°C; benzoate: 220—450°C; isobutyrate: 280—310°C, and propionate; 210—300°C). It is hard to obtain the product, 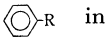 in thermal heating.

The above experimental results may be explained by the rapid heating and quenching by the laser heating. This type of pyrolysis is only possible in the laser heating.

2) Selective Decomposition. In a binary system, such as copper maleate and ethylene, the laser beam may decompose copper maleate only, and not ethylene, because the laser beam is absorbed on the copper maleate. If some intermediate in the decomposition of copper maleate is produced, the reaction with ethylene will be possible. Because copper maleate is decomposed by the laser heating to produce acetylene, the acetylene precursor, as has been mentioned before, may be the –CH=CH– intermediate. It is also dimerized to produce C_4 compounds. The determination of C_4 compounds was performed in the presence and in the absence of ethylene and acetylene. The data and the relative product yields in the binary system of copper salt and hydrocarbon gas are listed in Table 6. The (–CH=CH–) intermediate intramolecularly forms acetylene mainly, but a fraction reacts with ethylene and acetylene to produce C_4 compounds.

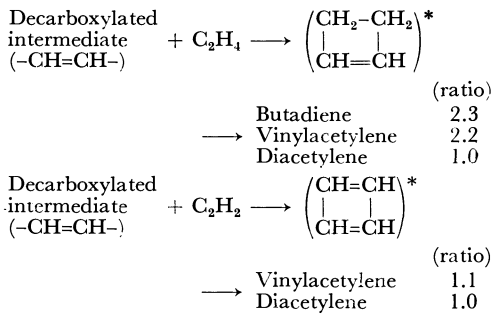

The decarboxylated intermediate (–CH=CH–) reacts with propylene and 1-butene to give C_5 and C_6 compounds respectively. Although C_5 compounds are produced in the laser decomposition of maleate itself, the yields of C_5 compounds in the mixture of maleate and propylene are higher than those in the decomposition of maleate itself.

It is worth noticing that the selective decom-

position and the above-mentioned reaction are only possible in the laser heating.

The authors wish to acknowledge the enthusiastic assistance of Miss K. Motegi in carrying out this work.

BULLETIN OF THE CHEMICAL SOCIETY OF JAPAN VOL. 43 1454—1459 (1970)

The Reaction of Cadalene and Eudalene with Sulfur

Shinji KUROKAWA

Department of Chemistry, Faculty of Education, Saga University, Honjyo-machi, Saga

(Received September 24, 1969)

The action of sulfur on two naphthalenes was investigated. Cadalene was heated with sulfur to give a new sulfur-containing naphthalene, 1,5,8-trimethylnaphtho[2,1-*b*]thiophene. It was formylated at the C_2-position of the thiophene moiety according to the Vilsmeier procedure, while an attempted acetylation according to this procedure was unsuccessful. Similarly, the reaction of eudalene with sulfur gave 3,9-dimethylnaphtho[1,2-*b*]thiophene, whose structure was determined by chromium trioxide oxidation, yielding *o*-quinone, and by a subsequent reaction with *o*-phenylenediamine, forming a quinoxaline derivative.

In a previous investigation of the reaction of azulene with sulfur, it was shown that 3,5,8-trimethylazuleno[6,5-*b*]thiophene and 3,5,9-trimethylazuleno[1,2-*b*]thiophene were, respectively, obtained from *S*-guaiazulene[1,2] and vetivazulene,[3] and that 6- and 7-acetyl-3,5,8-trimethylazuleno[6,5-*b*]thiophenes were yielded from 3-acetylguaiazulene, which was also isomerized to 2-acetylguaiazulene through the acetyl migration.[4] The sulfur-containing product in these reactions commonly contains a β-methylthiophene ring formed between an azulene-ring carbon atom and the isopropyl side chain of the azulenes.

The present investigation is concerned with how the action of sulfur on cadalene and eudalene, both naphthalene derivatives containing isopropyl groups, gives two new sulfur-containing naphthalenes. The compound thus obtained from cadalene (I) was determined to be 1,5,8-trimethylnaphtho[2,1-*b*]-thiophene (II), whose structure corresponds to that of furanocadinene[5] except that its oxygen atom of a hetero-ring is replaced with a sulfur atom. Formylation and acetylation by electrophilic substitution on the compound were attempted according to the Vilsmeier procedure.[6] On the other hand, the compound from eudalene (VI) was determined to be 3,9-dimethylnaphtho[1,2-*b*]thiophene (VIIa). Another compound (VIIb), which was also to be expected from the structure of eudalene (VI), could not be found in this reaction, however.

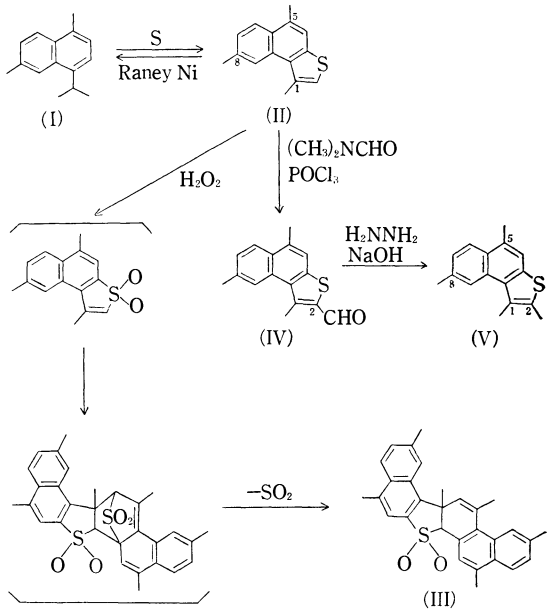

Chart 1

1) S. Hayashi, S. Kurokawa, M. Okano and T. Matsuura, *Tetrahedron Lett.*, **1967**, 3443.

2) S. Hayashi, M. Okano, S. Kurokawa and T. Matsuura, *J. Sci. Hiroshima Univ., Ser. A-II*, **31**, 79 (1967).

3) S. Hayashi, S. Kurokawa and T. Matsuura, This Bulletin, **42**, 1404 (1969).

4) S. Kurokawa, *ibid.*, **43**, 509 (1970).

5) H. Hikino, K. Agatsuma, C. Konno and T. Takemoto, *Tetrahedron Lett.*, **1968**, 4417.

6) M.-R. de Maheas, *Bull. Soc. Chim. France*, **1962**, 1989.

Results and Discussion

The Structure of the Sulfur-containing Cadalene: 1,5,8-Trimethylnaphtho[2,1-*b*]thiophene. The heating of cadalene with sulfur at 260°C for 10 hr produced colorless needles, mp 148—150°C, as the main product.

This compound had the molecular formula of $C_{15}H_{14}S$, and was desulfurized by heating it with Raney nickel catalyst (W-2 type), thus regenerating cadalene in a good yield. Hence, it is certain that the compound retains a cadalene skeleton in its molecule. The UV spectrum of this compound has an absorption maximum at 245.5 mμ; this maximum is 14 mμ more on the bathochromic side than that of the original cadalene. This fact shows the compound to have an elongated conjugate system, and it can be deduced that the compound has the structure of II, which consists of a fused ring system of naphthalene and β-methylthiophene.

This structure was confirmed mainly by the NMR spectrometry as follows. In IR and NMR spectra of this compound, isopropyl signals, which are clearly observed in those of cadalene, are absent; three aromatic methyl signals (2.86, 2.67, and 2.58 ppm, each 3H), corresponding to an increase of one methyl group from those of cadalene, are present in the NMR spectrum (Fig. 1B).

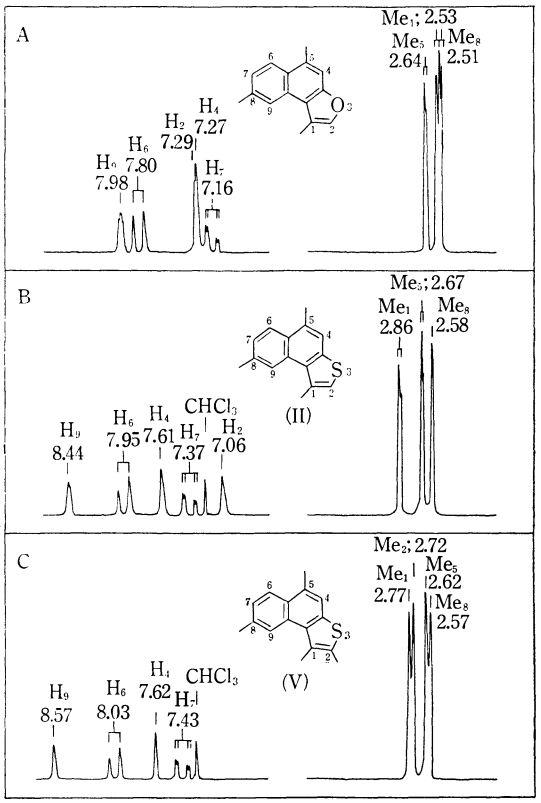

← ppm from TMS

Fig. 1. NMR spectra of furanocadinene (A), 1,5,8-trimethylnaphtho[2,1-*b*]thiophene (B) and 1,2,5,8-tetramethylnaphtho[2,1-*b*]thiophene (C).

In the aromatic-proton region of the NMR spectrum we observed three singlet-like signals at 8.44, 7.61, and 7.06 ppm (precisely, multiplets), one doublet at 7.95 ppm (J=8.8 Hz), and one double doublet at 7.37 ppm (J=8.8 and 1.5 Hz). These aromatic proton signals can be reasonably assigned to H_9, H_4, H_2, and H_6 and H_7 in the structure (II)*1 on the basis of comparisons with the spectra of 3-methylcadalene[7] and benz[*b*]thiophene,[8] and from the results of a double-resonance experiment: irradiation of the double doublet at 7.37 ppm decoupled the doublet at 7.95 ppm.

The methyl signals mentioned above could also be ascribed to methyl groups of the formula (II), as is shown in Fig. 1B, on the basis of a comparison with the spectra of 3-methylbenz[*b*]thiophene,[8] azulenothiophenes,[1-4] and naphthalenes,[7] and on the basis of the results of the irradiation experiment on H_2, which decoupled the doublet at 2.86 ppm.

In structure (II) the oxygen atom of furanocadinene is replaced with a sulfur atom. In fact, the NMR spectrum of the present compound (Fig. 1B) is very close to that of furanocadinene (Fig. 1A), except for the well-known fact regarding a thiophene ring, that an α-H is more shielded, while a β-methyl group is more deshielded than that of a furan ring.[9]

Oxidation of 1,5,8-Trimethylnaphtho[2,1-*b*]-thiophene with Hydrogen Peroxide. In order to clarify the presence of a thiophene nucleus, the sulfur-containing compound was oxidized with hydrogen peroxide. A sulfone was obtained as pale yellow needles, mp 178—179°C, which had sharp absorption bands characteristic to ν_{SO_2} at 1292, 1276, and 1124 cm^{-1} in the IR spectrum. On the other hand, the NMR spectrum (Fig. 2) exhibits the presence of two aliphatic methyl (1.77 ppm, 6H) and four aromatic methyl groups [2.30 (d), 2.67 (s), 2.84 (s) and 3.23 ppm (s), each 3H], and a tri-

*1 If the NMR data concerning the aromatic proton region are neglected, an alternative structure, 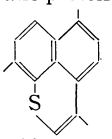 must be also taken into account. However, this structure can now be excluded, for one singlet and four doublets would be expected as the aromatic proton signals.

7) B. A. Nagasampagi, S. Dev, C. Rai and K. L. Murthy, *Tetrahedron*, **22**, 1949 (1966).
8) J. A. Elvidge and R. G. Foster, *J. Chem. Soc.*, **1964**, 981.
9) L. M. Jackman, "Application of Nuclear Magnetic Resonance Spectroscopy in Organic Chemistry," Pergamon Press, London (1959); Japanese translation by H. Shimizu, Tokyo-Kagaku-Dojin, Tokyo (1962), p. 95.

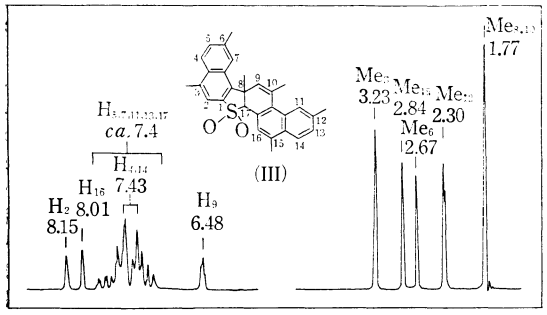

← ppm from TMS

Fig. 2. NMR spectrum of the sulfone dimer (III).

substituted olefinic proton [6.48 ppm (m), 1H], in addition to eight aromatic protons showing complicated signals. Thus, this spectrum cannot be explained in terms of the simple sulfone to be expected from naphthothiophene (II).

In the hydrogen-peroxide oxidation of thiophene, Davies and James have observed that the sulfone, supposed to be the primary oxidation product, was condensed through Diels-Alder addition accompanied by the loss of sulfur dioxide.[10] In the oxidation of 1,5,8-trimethylnaphtho[2,1-*b*]thiophene, also, if its sulfone is thought to be dimerized similarly, structure (III) is possible; it explains well the above spectrometric evidence. The absorption maximum (236 mμ) of the UV spectrum is rather closer to that of cadalene (I) (232 mμ) than to that of naphthothiophene (II) (245.5 mμ). This fact also supports structure (III), which contains a shorter conjugate system than the original trimethylnaphthothiophene.

Electrophilic Substitution of 1,5,8-Trimethylnaphtho[2,1-b]thiophene (II). We attempted to acetylate naphthothiophene (II) with *N,N*-dimethylacetamide in the presence of phosphorus oxychloride, according to the Vilsmeier procedure, but the trial resulted only in the recovery of the starting material. This result is different from the cases of 3,5,8-trimethylazuleno[6,5-*b*]thiophene[4] and 3,5,9-trimethylazuleno[1,2-*b*]thiophene.[3]

On the other hand, a Vilsmeier formylation of the trimethylnaphthothiophene proceeded almost quantitatively to give a pale yellow crystalline substance, mp *ca.* 108°C, which showed an absorption band due to an aldehyde group at 1650 cm^{-1} in the IR spectrum and which furnished semicarbazone, mp 210°C (decomposition).

The crystalline aldehyde, upon Wolff-Kishner reduction,[11] gave a pale yellow crystalline substance, mp 130—131°C, which had a molecular formula of $C_{16}H_{16}S$, representing the increase of one methyl group as compared with the original trimethylnaphthothiophene.

When the NMR spectrum (Fig. 1C) is compared with that of the original compound (Fig. 1B), an aromatic proton signal corresponding to the H_2 (7.06 ppm) of the original compound is absent, and four aromatic methyl signals [2.77, 2.72, 2.62 and 2.57 ppm, each (s) and 3H] are seen, equivalent to an increase of one methyl group from the original trimethylnaphthothiophene. Besides, the methyl signal (2.77 ppm) attributable to Me_1 becomes a singlet in this compound, while it is a doublet in the trimethylnaphthothiophene.

These facts indicate that the introduction of the fourth methyl group, namely, the Vilsmeier formylation, took place at the C_2 position of the trimethylnaphthothiophene.

The Structure of the Sulfur-containing Eudalene: 3,9-Dimethylnaphtho[1,2-*b*]thiophene. The reaction of eudalene with sulfur gave colorless needles, mp 41.5—42.5°C, having a molecular formula of $C_{14}H_{12}S$. This compound regenerated eudalene when it was submitted to reductive desulfurization with a Raney nickel catalyst and successively dehydrogenated with palladium on charcoal. Hence, the compound certainly retains the eudalene skeleton in the molecule.

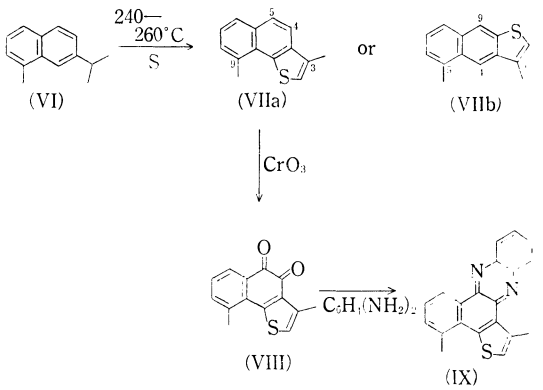

Chart 2

On the other hand, the participation of the isopropyl group of eudalene in the reaction with sulfur was indicated by the absence of splitting bands at 1382 and 1389 cm^{-1} in the IR spectrum and by the lack of NMR signals at 1.35 (doublet, 6H, J=6.7 Hz) and 3.05 ppm (multiplet, 1H) in Fig. 3A, as was seen in each spectrum of the starting material.

In the aromatic-methyl-proton region of the NMR spectrum (Fig. 3A), there is one more methyl doublet (2.52 ppm) than in the spectrum of the starting material, and the spin-coupling constant, J=1.0 Hz, of this newly-appeared doublet is in good agreement with the J value concerning the β-methyl group and the α-proton in 1,5,8-trimethylnaphtho[2,1-*b*]thiophene and in the other β-methyl-

10) W. Davies and F. C. James, *J. Chem. Soc.*, **1954**, 15.

11) H. Stetter and W. Dierichs, *Chem. Ber.*, **85**, 61 (1952).

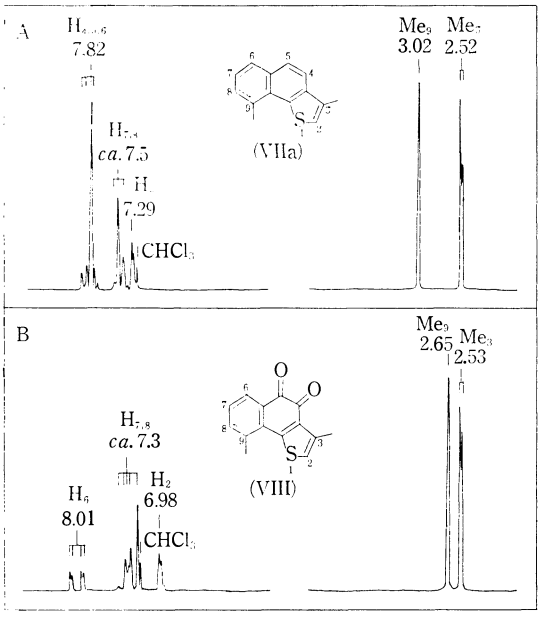

Fig. 3. NMR spectra of 3,9-dimethylnaphtho[1,2-*b*]thiophene (A) and its 4,5-quinone (B).

thiophenic compounds reported earlier.[1-4] Thus, this compound can also be concluded to be a naphthothiophene in which the isopropyl group and one of the aromatic-ring carbon atoms in eudalene forms a thiophene ring with sulfur, as in the reaction of cadalene or azulenes with sulfur. This deduction was powerfully supported by the prominent appearance of the $(M-1)^+$ ion (50.2%) in the mass spectrum of this compound, because the abundant formation of this ion is peculiar to methylthiophenes;[12] this ion can be described as a thiapyryrium ion formed through the expansion of a thiophene ring.

In this manner, two formulae, VIIa and VIIb become possible for the present compound. In order to determine the more reasonable structure of the two, the present compound was oxidized with chromium trioxide in glacial acetic acid to yield red needles, mp 206.5—207.5°C, as the main product. The red crystalline product exhibited $\nu_{C=O}$ bands at 1655 and 1667 cm^{-1} in the IR spectrum, showed two fewer proton signals in the aromatic-ring-proton region of the NMR spectrum (Fig. 3B) as compared with that of the dimethylnaphthothiophene (Fig. 3A), and had a molecular formula of $C_{14}H_{10}SO_2$ based on the parent ion ($M^+=242$) of the mass spectrum. This product is, therefore, a quinone yielded from the dimethylnaphthothiophene by the oxidation of one of two activated carbon positions, $C_{4,5}$ in VIIa or $C_{4,9}$ in VIIb. Besides, this red quinone had an intense absorption maximum at 466 mμ (log ε, 3.34) in the visible region, and in the NMR spectrum (Fig. 3B) the chemical shift between the two methyl groups ($\Delta Me_3 - Me_{9\text{ or }5}=0.12$ ppm) is much smaller than that of the dimethylnaphthothiophene (0.50 ppm) (Fig. 3A). From the latter fact, the quinone can be deduced to have a structure in which Me_3 is closer to the carbonyl group than the other methyl group, Me_9 or Me_5. Thus, these data suggest that the product is not the *p*-quinone expected from VIIb, but *o*-quinone (VIII) of a phenanthraquinone type derived from VIIa.

Supporting this suggestion is the fact that this quinone reacted with *o*-phenylenediamine to form a greenish yellow powder, mp 202—203°C, which was determined to be a quinoxaline derivative (IX) derived from *o*-quinone (VIII) by elementary analysis and by a study of its mass spectrum. From the above evidence, it can be concluded that the colorless needles obtained by the reaction of eudalene with sulfur are 3,9-dimethylnaphtho[1,2-*b*]thiophene of a phenanthrene type; all the data other than those mentioned here support this structure.

Experimental

All the melting points in this paper are uncorrected. The IR spectra were obtained using KBr disks, and the mass spectra, at 70 eV. The NMR spectra were taken at 60 MHz in deuteriochloroform. The thin-layer chromatography (TLC) was carried out by the use of silica gel-G (Merck); unless otherwise stated, all the spots were detected by spraying with a mixture of sulfuric acid and nitric acid (19 : 1).

Reaction of Cadalene (I) with Sulfur. A mixture of cadalene (3.0 g) and sulfur (1.5 g) was heated at 260°C for 10 hr under a nitrogen atmosphere. The reaction mixture, which solidified at room temperature, was crushed into small fragments and ground thoroughly in a mortar with *n*-hexane to give a viscous red oil (0.6 g). This oil was then repeatedly chromatographed on a silica-gel column with *n*-hexane; a colorless crystalline substance (40 mg) (1,5,8-trimethylnaphtho[2,1-*b*]thiophene) was thus isolated. After two recrystallizations from *n*-hexane, it afforded colorless needles, mp 148.0—150.0°C, which showed a single green spot (R_f, 1.81) in TLC with petroleum ether. Mass spectrum: *m/e* 226 (M^+, $C_{15}H_{14}S$), base peak; *m/e* 225 $(M-H)^+$, 22.9%. Relative intensities of isotope ions: Found; M^+ (100), $(M+1)^+$ (17.38), $(M+2)^+$ (5.29%). Calcd for $C_{15}H_{14}S$; M^+ (100), $(M+1)^+$ (17.23), $(M+2)^+$ (5.70%). UV (isooctane): mμ (log ε), 220 sh (4.22), 235 sh (4.49), 245.5 (4.62), 259.5 (4.44), 298.5 (4.02), 306 (4.01), 319.5 (3.58), 334.5 (3.47).

Found: S, 14.46%. Calcd for $C_{15}H_{14}S$: S, 14.17%.

Desulfurization of 1,5,8-Trimethylnaphtho[2,1-*b*]thiophene (II). Trimethylnaphthothiophene (40.8 mg) was dissolved into absolute methanol (20 m*l*); the solution, after the addition of a W-2 Raney nickel catalyst (0.2 g) prepared freshly, was refluxed on a water bath. After 40 min, trimethylnaphthothiophene;

12) H. Bujikiewicz, C. Djerassi and D. H. Williams, "Interpretation of Mass Spectra of Organic Compounds," Holden-Day, San Francisco (1964), p. 231.

the starting material, came to be hardly detected at all in TLC with *n*-hexane. Then the reaction mixture was filtered, washed with water, dried over anhydrous calcium chloride, and concentrated under reduced pressure to leave a colorless oil (50 mg). The oil exhibited a yellowish-green spot (R_f, 2.70) in TLC using *n*-hexane, together with a green spot (R_f, 1.62) attributable to unchanged trimethylnaphthothiophene. By means of preparative TLC, a colorless oil of R_f 2.70 was isolated; it was found to be identical with an authentic specimen of cadalene by UV and IR absorption spectrometry.

Hydrogen Peroxide Oxidation of 1,5,8-Trimethylnaphtho[2,1-b]thiophene (II). Formation of a Sulfone Dimer (III). A solution of trimethylnaphthothiophene (170 mg) in glacial acetic acid (1 m*l*) was mixed with 30% hydrogen peroxide (0.8 m*l*), and the mixture was refluxed on an oil bath for 20 min. The reaction mixture was then diluted with water (30 m*l*) and extracted with chloroform to give an orange, resinous material (200 mg). This material was chromatographed on a silica-gel column with chloroform; unchanged trimethylnaphthothiophene was recovered from a quickly-eluted fraction, and a yellow crystalline compound (71.1 mg) was obtained from the fraction next eluted. Further purification of the crystals by repeated elution chromatogaphy with mixed solvents of methylene chloride and chloroform (1 : 1 and 2 : 1) afforded a sulfone dimer (III) (26.2 mg) as pale yellow needles, mp 178—179°C. These crystals showed a single brown spot (R_f, 4.30) in TLC using a mixed solvent of methylene chloride and chloroform (7 : 3). UV (EtOH): mμ (log ε), 216 (4.82), 237.7 (4.95), 293 sh (4.09), 303 (4.13), 325 sh (3.81).

Vilsmeier Formylation of 1,5,8-Trimethylnaphtho[2,1-*b*]thiophene (II). To a solution of trimethylnaphthothiophene (125 mg) in *N*,*N*-dimethylformamide (4.2 m*l*), another solution of phosphorus oxychloride (0.42 g) in the same solvent (2.1 m*l*) was added under ice cooling. The mixture, after being allowed to stand at room temperature for 2 days, was heated at 60°C for 1 hr to complete the reaction, and then poured into water (160 m*l*). When the aqueous solution was made slightly alkaline by adding powdered sodium carbonate, followed by extraction with chloroform, a viscous yellow oil (255 mg) was obtained. Through the benzene-silica gel elution chromatography of the oil, 2-formyl-1,5,8-trimethylnaphtho[2,1-*b*]thiophene (114 mg) was separated as pale yellow needles, mp *ca.* 108°C, which showed a single reddish-orange spot (R_f, 5.40) in TLC with benzene when sprayed 2,4-dinitrophenylhydrazine.

Semicarbazone. From 2-formyl-1,5,8-trimethylnaphtho[2,1-*b*]thiophene, semicarbazone was obtained as a crystalline mass; this mass gave colorless needles. mp 210°C (decomposition), after being recrystallized from ethanol. IR: $\nu_{C=O}$ splitting band at 1726 and 1717 cm^{-1}, ν_{N-H} 3470 cm^{-1}.

Reduction of 2-Formyl-1,5,8-trimethylnaphtho[2,1-*b*]thiophene (IV). A mixture of formyltrimethylnaphthothiophene (211 mg), 100% hydrazine hydrate (160 mg), and powdered sodium hydroxide (377 mg) was heated at 200°C for 1.5 hr by which time the evolution of nitrogen gas had ceased. The reaction mixture, after being acidified with dilute hydrochloric acid, was extracted with chloroform; crude 1,2,5,8-tetramethylnaphtho[2,1-*b*]thiophene (V) (150 mg) was thus obtained as a reddish-orange crystalline mass, which was purified by means of benzene-silica gel elution chromatography. The purified pale yellow needles, mp 130—131°C (78 mg), showed a single green spot (R_f, 6.77) in TLC with benzene. Mass spectrum: *m/e* 240 (M^+, $C_{16}H_{16}S$), base peak; *m/e* 239 $(M-H)^+$, 22.8%; *m/e* 225 $(M-CH_3)^+$, 81.9%. Relative intensities of isotope ions: Found; M^+ (100), $(M+1)^+$ (17.96), $(M+2)^+$ (5.65%). Calcd for $C_{16}H_{16}S$; M^+ (100), $(M+1)^+$ (18.35), $(M+2)^+$ (5.70%).

Reaction of Eudalene (VI) with Sulfur. Eudalene (2.0 g) was heated with half as much powdered sulfur at 240—260°C for 6 hr. The reaction mixture was dissolved in hot benzene (100 m*l*) and poured into *n*-hexane (200 m*l*) to yield a brown precipitate. The solution, from which the precipitate had been filtered off, was then concentrated under reduced pressure to give a red oil (1.50 g). This oil was treated as has been described above for cadalene (I); a colorless crystalline substance (227.8 mg) was thus isolated. After recrystallization from methanol, dimethylnaphthothiophene (VIIa) was obtained as colorless needles, mp 41.5—42.5°C, which showed a single yellow spot (R_f, 5.8) in TLC with *n*-hexane. UV (EtOH): mμ (log ε), 238 sh (4.42), 245 (4.52), 259 sh (4.55), 266.2 (4.69), 283 (4.08), 294 (3.97), 305 (3.72).

Found: C, 79.19; H, 5.68; S, 15.04%. Calcd for $C_{14}H_{12}S$: C, 79.20; H, 5.70; S, 15.10%.

Desulfurization of 3,9-Dimethylnaphtho[1,2-*b*]thiophene (VIIa). The reaction of dimethylnaphthothiophene (15.07 mg) with a Raney nickel catalyst was carried out in a manner similar to that used in the experiment described for 1,5,8-trimethylnaphtho[2,1-*b*]thiophene (II). When the oil thus obtained (10 mg) was chromatographed on a silica-gel column with *n*-hexane, a colorless oil (7.6 mg) was separated in a pure state. It showed a single brown spot (R_f, 8.5) in TLC with *n*-hexane, and was clearly different from eudalene (R_f, 6.9). This substance may be concluded to be a partially hydrogenated eudalene on the basis of UV and the results of the following dehydrogenation experiment. UV (EtOH): mμ (log ε*[2]) 215.5 (4.02), 220 sh (3.99), 227 sh (3.66), 265 (2.62), 269.5 (2.71), 277.8 (2.70), 291 sh (1.96).

Dehydrogenation of the Desulfurized Product. The colorless oil (7.6 mg) obtained by the above desulfurization of dimethylnaphthothiophene (VIIa) was sealed in a glass tube with 5% palladium on charcoal (20 mg), and the tube was heated at 300°C for 10 min. After being cooled, the reaction mixture was dissolved in chloroform, the solution, from which the catalyst had been filtered off, was then concentrated under reduced pressure to give a colorless oil (50 mg). This oil was confirmed, by TLC with *n*-hexane, to be mainly composed of eudalene. A colorless oil purified by the use of preparative TLC was identical with eudalene (VI) in TLC and UV spectrometry.

Chromium Trioxide Oxidation of 3,9-Dimethylnaphtho[1,2-*b*]thiophene (VIIa). To a solution of the dimethylnaphthothiophene (209 mg) in glacial acetic acid (4.7 m*l*) we added, drop by drop another solution of chromium trioxide (350 mg) in 60% acetic acid (2.0 m*l*), after which the mixture was heated at 50—60°C for 1.5 hr. The reaction mixture was then poured into

*[2] These values were calculated on the assumption that MW=186.

water (53 m*l*) and extracted with chloroform. A viscous red material (250 mg) thus obtained was chromatographed on a silica-gel column with a mixed solvent of benzene-chloroform (2 : 1), a slightly yellow-colored, unchanged naphthothiophene (9.9 mg) fraction was eluted first, and then a red fraction. The red fraction gave, after the removal of the solvent, *o*-quinone (VIII) as red needles, mp 206.5—207.5°C (15.1 mg) which showed a single red spot (R_f, 2.5) in TLC (without any color reagent) when a benzene-chloroform (4 : 1) mixture was used. UV and visible absorption spectra (EtOH): mμ (log ε), 225 (4.39), 241 sh (4.13), 261 sh (4.19), 274 sh (4.33), 280 (4.37), 345.5 (3.71), 466 (3.34), 510 sh (3.17). Mass spectrum: *m/e* 242 (M^+, $C_{14}H_{10}SO_2$), 40.2%; *m/e* 214 $(M-CO)^+$ ($m^*=189.2$), base peak; *m/e* 186 $(M-2CO)^+$ ($m^*=161.7$), 10.4%; *m/e* 185 $(M-2CO-H)^+$, 33.1%.

Reaction of *o*-Quinone (VIII) with *o*-Phenylenediamine. *o*-Quinone (VIII) (8.1 mg) was heated with *o*-phenylenediamine (3.4 mg) on a steam bath for 10 min. At the end of this period, the reaction mixture was heated with ethanol (30 m*l*) and an insoluble part was filtered off. The hot ethanol solution was diluted with water (20 m*l*) and chilled overnight at −20°C; the precipitate of the quinoxaline derivative (IX) was obtained by filtration as a greenish-yellow powder, mp 202.0—203.0°C (2.9 mg). This powder showed a single yellow spot (R_f, 6.2) in TLC with a mixed solvent of chloroform-benzene (1 : 4). UV[*3]: mμ (log ε), 240 sh (4.57), 257 (4.83), 284.2 (4.49), 294.6 (4.52), 309 (4.46), 388 (4.22).

Found: N, 8.51%. Calcd for $C_{20}H_{14}SN_2$: N, 8.91%.

The author wishes to thank Professor Tamon Matsuura and Professor Shûichi Hayashi of Hiroshima University for their kind guidance and advice on this work. Thanks are also due to Professor Shô Itô of Tohoku University for his kind measurement of the NMR and mass spectra.

[*3] Ethanol containing 0.5% of chloroform was used as the solvent.

BULLETIN OF THE CHEMICAL SOCIETY OF JAPAN VOL. 43 1459—1472 (1970)

Substituent Effects on the NMR Chemical Shifts of Aromatic Side Chain Protons. I. The Effects of *meta*-Substituents

Hiroaki YAMADA

Department of Chemistry, Faculty of Science, Kobe University, Rokkodai-cho, Kobe

and Yuho TSUNO and Yasuhide YUKAWA

The Institute of Scientific and Industrial Research, Osaka University, Yamadakami, Suita, Osaka

(Received September 25, 1969)

The Hammett type treatment of the chemical shift of substituted aromatic side chain protons has not always been successful. The failure might be ascribed to the neglect of magnetic long-range effects. When the corrections were made both for the ring current diminution due to the contribution of polar resonance structure of the introduced substituent and for the substituent magnetic anisotropy effect, an excellent equation was obtained to relate the chemical shifts of *meta*-substituted aromatic side chain protons to the Hammett's constants.

Recent studies on the proton chemical shifts of substituted aromatic system have shown that Hammett type treatment[1a-i] of the substituent effects is not practically successful.[2a-i]

It is well established that the substituent effects on the proton chemical shifts can be divided into

1) a) L. P. Hammett, *J. Amer. Chem. Soc.*, **59**, 96 (1937); b) L. P. Hammett, "Physical Organic Chemistry," McGraw Hill, New York (1940), p. 184; c) H. H. Jaffé, *Chem. Rev.*, **53**, 191 (1953); d) P. R. Wells, *ibid.*, **63**, 171 (1963); e) R. W. Taft, Jr., and I. C. Lewis, *J. Amer. Chem. Soc.*, **80**, 2436 (1958); f) D. H. McDaniel and H. C. Brown, *J. Org. Chem.*, **23**, 420 (1958); g) Y. Yukawa, Y. Tsuno and M. Sawada, This Bulletin, **39**, 2274 (1966); h) Y. Yukawa and Y. Tsuno, *ibid.*, **32**, 965 (1959); i) Y. Yukawa and Y. Tsuno, *Nippon Kagaku Zasshi*, **86**, 873 (1965).

2) a) P. L. Corio and B. P. Dailey, *J. Amer. Chem. Soc.*, **78**, 3043 (1956); b) A. A. Bothner-By and R. E. Glick, *ibid.*, **78**, 1071 (1956); c) H. Spiesecke and W. G. Schneider, *J. Chem. Phys.*, **35**, 731 (1961); d) W. B. Smith and S. Chiranjeevi, *J. Phys. Chem.*, **70**, 3505 (1966); e) A. R. Katritzky, R. E. Reavill and F. J. Swinbourne, *J. Chem. Soc., B*, **1966**, 351; f) R. E. Klinck and J. B. Stothers, *Can. J. Chem.*, **40**, 1071 (1962); g) H. Güsten and M. Salzwedel, *Tetrahedron*, **23**, 173, 187 (1967); h) L. K. Dyall, *Aust. J. Chem.*, **17**, 419 (1964); i) T. Yonemoto, W. F. Reynolds, H. M. Hutton and T. Schäfer, *Can. J. Chem.*, **43**, 2668 (1965).

two main contributions;[3]

(1) Change of the electron density around the resonating proton.

(2) Change of the long range effect arising from the anisotropic magnetic susceptibility of the rest of the molecule.

Since the electron density can be altered by the substituent polar effect, proton chemical shift in aromatic system might be related to the Hammett σ constants[1a,b,f] or its modifications.[1e-i] This expectation will be realized as far as the chemical shifts are mainly determined by the electron density, as may be seen in the cases of the fluorine NMR chemical shifts of substituted fluorobenzenes[4] and ethynyl proton chemical shifts of substituted phenyl acetylenes[5a,b] where the contribution of factor (2) is relatively small.

General failure of the Hammett type treatment might thus be ascribed to the fact that both effects, (1) and (2), are often of equal magnitude and operate in a conflicting way.

The present paper deals mainly with the contribution of factor (2) and an attempt was made to obtain an excellent correlation between the chemical shifts of aromatic side chain protons as well as those of ring protons, and the Hammett's constant of the substituent.

In *para*-substituted aromatic side chain systems, an excess resonance interaction[6,1g,h] between substituent and a side chain can always result in the complication, leading to some difficulty in evaluating the substituent polar effects. For this reason, only the *meta*-substituent effect is considered in this paper and further studies on *para* system, which are now being undertaken, will appear in future.

Experimental

All the materials were purified by fractionation or by recrystallization and identified with their physical constants and elementary analyses.

1,1-Diphenylethylene[7] and most of substituted 1,1-diphenylethylenes were prepared by the dehydration of 1,1-diphenylethanols in 20% H_2SO_4 (Method a)[7] or by the dehydrochlorination of 1,1-diphenylethyl chlorides in pyridine (Method b).[8] The latter method was generally successful for *meta* halogeno derivatives. The 1,1-diphenylethanols were obtained by adding ethereal solution of ethyl acetate (Method A)[7] or of acetophenone (Method B)[9] to the Grignard solution of substituted bromobenzenes, or by adding ethereal solution of substituted benzophenones to the methylmagnesium bromide solution (Method C).[10]

1,1-Bis(cyanophenyl)ethylenes and 1-(cyanophenyl)-1-phenylethylenes were prepared by refluxing the corresponding bromophenylethylenes and cuprous cyanide in dry pyridine for 5—6 hr. (Method D).[10] The cyanides obtained were hydrolysed in alcoholic potassium hydroxide and the resulting carboxylic acids were esterified by dimethyl sulfates in methanolic potassium hydroxide media (Method E).

1,1-Bis(*m*-nitrophenyl)ethylene and 1-(nitrophenyl)-1-phenylethylenes were synthesized from the corresponding nitrobenzophenones through Wittig's reaction (Method F).[11]

1,1-Bis(*p*-nitrophenyl)ethylene was prepared by the dehydrobromination of 1-bromo-1,1-bis(*p*-nitrophenyl)-ethane in pyridine (Method G).[12] The bromide was prepared from 1,1-bis(*p*-nitrophenyl)ethane by bromination in carbon tetrachloride as usual with *N*-bromosuccinimide. In preparing 1,1-bis(*p*-nitrophenyl)ethane, 1,1-diphenylethane was nitrated by fuming nitric acid

TABLE 1-1. CHEMICAL SHIFTS OF METHYL PROTONS OF TOLUENES

Substituent	Observed [mp°C] or (bp°C/mmHg)	$\Delta\delta$/Hz*
p-OCH_3	(95/53,175)	+4.7
p-CH_3	(78.5—79.0/112)	+3.4
m-CH_3	(79.0—79.5/112)	+3.2
p-I	[34.9—35.0]	+2.6
p-Br	(105—106/69)	+2.2
m-I	(101—102/24)	+1.8
m-OCH_3	(108/96)	+1.8
p-F	(114)	+1.3
p-Cl	(87—87.5/70)	+1.2
H	(108.8—109.0)	τ=7.67
m-Br	(84—85/32)	0.0
m-Cl	(157—157.5)	−0.1
m-F	(112—113)	−1.3
m-CN	(118/30)	−4.0
p-Ac	(115—115.5/24)	−4.0
p-$CO_2C_2H_5$	(120—121/20)	−4.0
m-Ac	(108.5—109.5/19)	−4.5
p-CN	(103—103.5/20)	−5.4
p-NO_2	[52.8—53.1]	−8.2
m-NO_2	(108.9—109.2/15.2) [16.8—17.4]	−9.2

* Relative chemical shifts measured in 0.05 mol/*l* carbon tetrachloride solution.

3) J. A. Pople, W. G. Schneider and H. J. Bernstein, "High Resolution Nuclear Magnetic Resonance," McGraw Hill, New York (1959), p. 175.

4) R. W. Taft, Jr., *J. Phys., Chem.*, **64**, 1805 (1960).

5) a) C. D. Cook and S. S. Danyluk, *Tetrahedron*, **19**, 177 (1963); b) Y. Yukawa and H. Yamada, *Nippon Kagaku Zasshi*, **85**, 501 (1964).

6) H. C. Brown and Y. Okamoto, *J. Amer. Chem. Soc.*, **80**, 4979 (1958).

7) A. H. Blatt, "Organic Syntheses," Coll. Vol I, 226 (1956).

8) See Ref. 12.

9) S. N. Ege and K. W. Sherk, *J. Amer. Chem. Soc.*, **75**, 354 (1953).

10) J. N. Ashley, J. F. Grove and T. Henshnell, *J. Chem. Soc.*, **1948**, 261.

11) G. Wittig and U. Schöllkopf, *Chem. Ber.*, **87**, 1318 (1954).

12) H. H. Szmant and J. F. Deffner, *J. Amer. Chem. Soc.*, **81**, 958 (1959).

Table 1-2. Chemical shifts of methyl protons of anisoles and of acetophenones

Substituent	Anisoles		Acetophenones	
	Observed [mp°C] or (bp°C/mmHg)	$\Delta\delta$/Hz*	Observed [mp°C] or (bp°C/mmHg)	$\Delta\delta$/Hz*
p-OCH_3	[55.5—56]	+3.20	(154/32)	+4.14
p-CH_3	(95/53, 173—4)	+2.44	(115—115.5/24)	+2.47
m-CH_3	(108/96, 173—4)	+1.61	(108.5—109.5/19)	+1.57
m-OCH_3	(101/17.5)	+1.15	(129—130/17)	+1.01
p-Br	(102—102.5/17)	+0.50	[53.5—54.5]	+0.98
p-Cl	(87—87.5/17.5)	+0.30	—	—
H	(84—85/75)	τ=6.24	(118—119/62)	τ=7.47
m-Br	(98.5—99/17)	−1.01	(127.5—128.5/14.5)	−0.30
m-Cl	—	—	(108—109/11)	−0.51
p-CO_2CH_3	[49—50]	−4.16	—	—
p-$CO_2C_2H_5$	(136.5—137.0/12)	−4.27	[56.2—56.7]	−2.66
m-CN	(132—133/26)	−4.43	[97—98.5]	−3.68
p-Ac	(154/32)	−4.89	—	—
m-Ac	(129—130/17)	−4.95	—	—
p-CN	[60.5—61]	−5.24	[59.5—60]	−3.37
p-NO_2	[53.5—54]	−8.16	[80.5—81]	−5.55
m-NO_2	[38.2—38.5]	−8.46	[76—77]	−7.46

* Relative chemical shifts measured in 0.05 mol/*l* carbon tetrachloride solution.

Table 1-3. Chemical shifts of ethylenic protons of 1-(substituted phenyl)-1-phenylethylenes

Substituent	[mp°C] or (bp°C/mmHg)		Method†	$\Delta\delta$/Hz**
	Observed	Reported		
p-OCH_3	[76.5—76.8]	[75][a]	Ca	+7.2, +4.6***
p-CH_3	(121.5—122/6.5)	(90/0.3)[b]	Ca	+3.18
p-F	(112—114/6.2)	(105—110/0.3)[c]	Ca	+1.73
m-CH_3	(129—130/7)	(122—123/0.85)[d]	Ba	+1.84
m-OCH_3	(153.5—155/12.5)	(168/14)[e]	Bb	+0.39
H	(113—114/3.0)	(113/2)[f]	Aa	τ=4.61
p-Cl	(149.5—151/9.5)	(157/12)[g]	Ca	−0.3
p-Br	(167.0—167.4/10.0)[27—29]	(185/10)[25.5—26.0][g]	Ca	−0.5
m-Br	(155.5—156.2/7.2)	*	Bb	−2.18
m-F	(128—130/10.5)	*	Cb	−2.5
m-Cl	(144/7)	(152—153/14)[e]	Cb	−3.0
p-CO_2CH_3	[75—76]	*	E	−5.5
m-CN	(165—167/7)	*	D	−4.3, −7.7***
p-CN	[45.9—46.4]	*	D	−6.3, −8.9***
p-NO_2	[68.3—68.8]	[66—66.5][h]	F	−11.3, −8.8***
m-NO_2	[89.0—89.4]	*	F	−10.01

† Methods of preparation summarized in the experimental part.
* New compound.
** Relative chemical shifts measured in 0.10 mol/*l* carbon tetrachloride solution.
*** Calculated from observed AB-quartet signal in which J=1.0—1.3 Hz. The averaged relative shift, $\frac{1}{2}(\Delta\delta_A+\Delta\delta_B)$, was used for the Hammett type plotting.

a) D. C. Hurd and N. Webb, *J. Amer. Chem. Soc.*, **49** 546 (1927).
b) M.S. Kharasch, A. Fono, W. Nudenberg and C. Poshkus, *J. Org. Chem.*, **15**, 775 (1950).
c) F. Bergmann and J. Szmuszkowicz, *J. Amer. Chem. Soc.*, **70**, 2748 (1948).
d) W.E. McEwen and N.B. Mehta, *ibid.*, **74**, 526 (1952).
e) E. Bergmann and A. Bondi, *Chem. Ber.*, **64B**, 1455 (1931).
f) Ref. 7 in the text.
g) Ref. 22 in the text.
h) Ref. 11 in the text.

TABLE 1-4. CHEMICAL SHIFTS OF ETHYLENIC PROTONS OF 1,1-BIS(SUBSTITUTED PHENYL)ETHYLENES

Substituent	[mp°C] or (bp°C/mmHg) Observed	Reported	Method†	$\Delta\delta$/Hz**
p-OCH_3	[142.0—142.3]	[142—143][a]	Ba	+11.88
p-CH_3	[61.3—61.5]	[61][b]	Ba	+6.32
m-CH_3	(133—134/4.2)	(134—139/5)[c]	Aa	+3.92
p-F	[48.3—48.5]	[46.5—47.0][d]	Aa	+3.42
m-OCH_3	(167—168/9)	(190/10)[e]	Aa	+0.95
p-Cl	[86.3—86.8]	[86.2—86.5][d]	Ca	−0.58
p-Br	[86.9—87.1]	[85.8—86.2][d]	Ca	−1.23
m-Br	(170—175/6)	*	Bb	−4.57
m-F	(104/7)	*	Aa	−4.78
m-Cl	(155.6—156.0/4.0)	*	Aa	−4.85
p-CO_2CH_3	[131.6—131.9]	*	E	−11.04
m-CN	[87.6—87.9]	*	D	−12.42
p-CN	[157.3—158.1]	[158—158.5][f]	D	−14.67
p-NO_2	[174.1—174.6]	[175—176.5][g]	G	−19.6***
m-NO_2	[88.2—88.9]	*	F	−20.25

† Methods of preparation summarized in the experimental part.
* New compound.
** Relative chemical shifts measured in 0.05 mol/*l* carbon tetrachloride solution.
*** Because of the low solubility, the chemical shift was measured with a 0.03 mol/*l* solution at elevated temperatures (80, 67, 61 and 47°C) and these data were extrapolated to 23°C.
a) P. Pfeiffer and R. Wiziner, *Ann. Chem.*, **461**, 132 (1928).
b) R. Anschütz and A. Hilbert, *Chem. Ber.*, **57B**, 1697 (1924).
c) C.S. Marvel and V. E. Nichols, *J. Amer. Chem. Soc.*, **60**, 1455 (1938).
d) Ref. 22 in the text.
e) G. Wittig and W. Gauss, *Chem. Ber.*, **80**, 363 (1947).
f) H.H. Szmant and R. Yonkoskie, *J. Org. Chem.*, **21**, 78 (1956).
g) Ref. 12 in the text.

(d=1.5) at −15°C.[13]

The proton chemical shifts, δ_X, for the substituted aromatic side chains were measured at 60 MHz in dilute (0.05—0.10 mol/*l*) carbon tetrachloride solution using a JNM-3H-60 spectrometer. Prior to the measurements of the chemical shifts, an NMR sample tube fitted with a thermometer reaching into the liquid paraffin in the tube, was spinned in the probe and the temperatures were directly read on the thermometer scale. Thus, the temperature of the sample under the condition of NMR measurement was estimated to be 20—25°C. The line positions were determined by linear interpolation between known audio frequency side bands of internal TMS or by direct superposition of the side band on the proton signal. The audio frequencies were measured with a frequency counter. The estimated reproducibility of δ_X was ±0.1 Hz. The observed relative chemical shifts, $\Delta\delta=\delta_X-\delta_H$, and the physical constants of the materials are listed in Tables 1-1—1-4.

Results and Discussion

The plots of relative chemical shifts, $\Delta\delta_m$, against Hammett's σ_m[1f] are shown in Figs. 1-1—1-7.

In the case of phenylacetylenes,[5a,b] a satisfactorily linear relationship is observed between the chemical shifts and Hammett constants (Fig. 1.7) as given

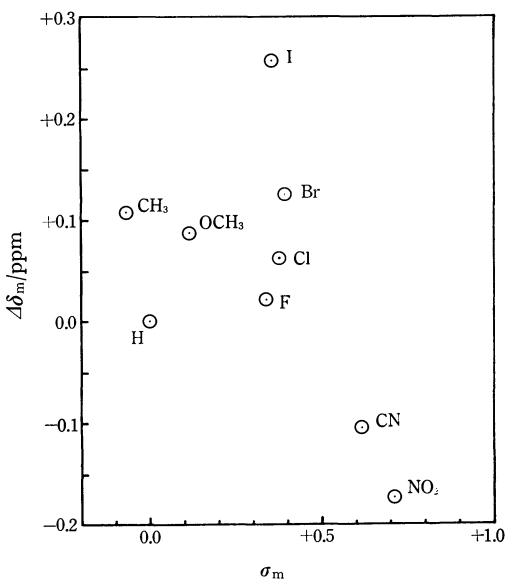

Fig. 1-1. Hammett plot for ring protons[14] *meta* from substituents.

13) I. P. Tsukervanik and M. D. Sokol'nikova, *Zh. Obshch. Khim.*, **24**, 1435 (1954).

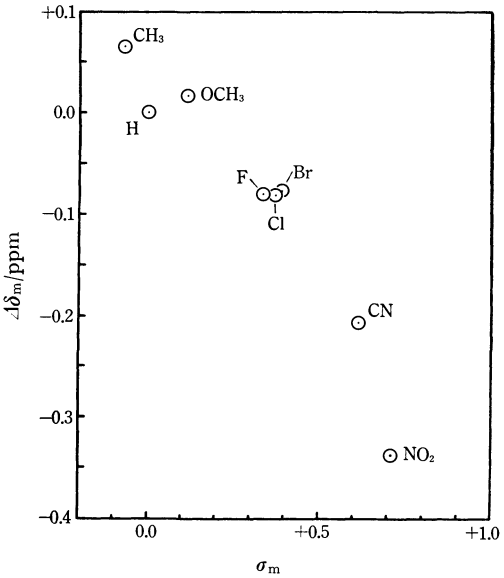

Fig. 1-2. Hammett plot for 1,1-di(*meta*-substituted phenyl)ethylenes.

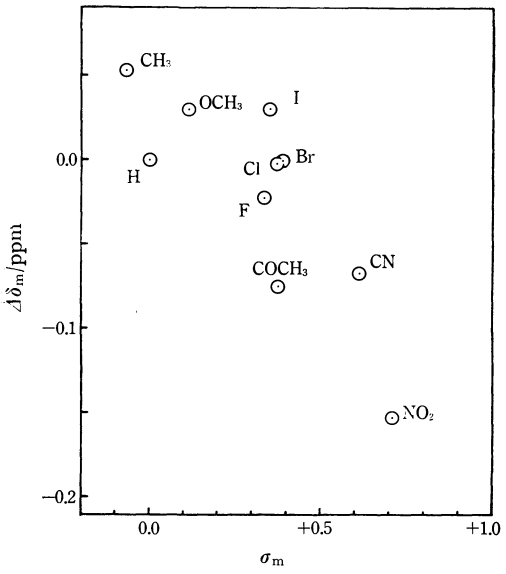

Fig. 1-3. Hammett plot for *meta*-substituted toluenes.

by the equation.

$$\Delta\delta_m = a_m\sigma_m \quad (1)$$

The relationship still roughly holds in the case of diphenylethylenes (Figs. 1-2 and 1-6). The ring protons[14] *meta* to the substituents, however, give no such correlation (Fig. 1-1), the points being scattered seriously. It is noted that the protons located far from the substituent generally give

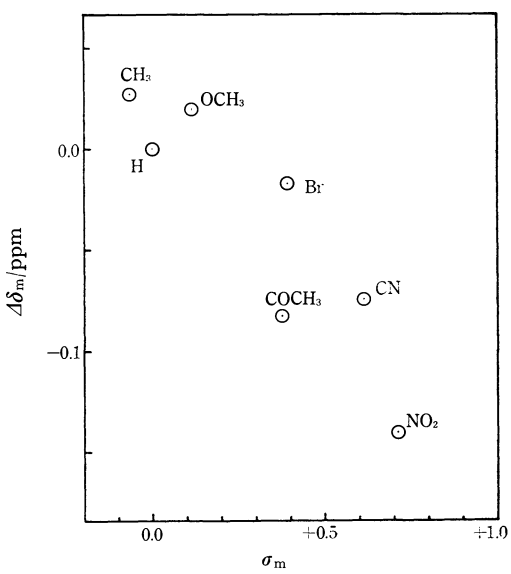

Fig. 1-4. Hammett plot for *meta*-substituted anisoles.

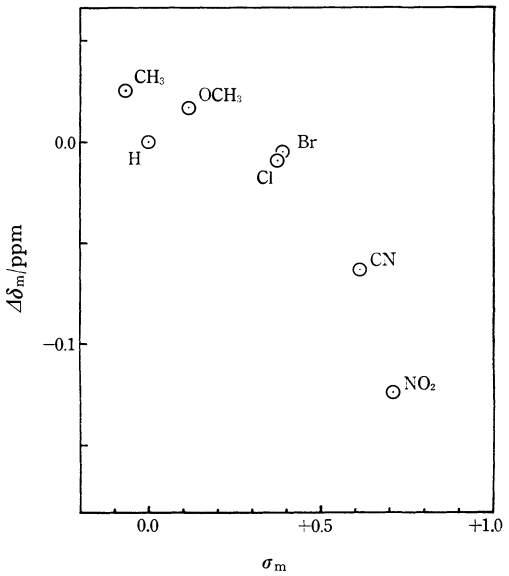

Fig. 1-5. Hammett plot for *meta*-substituted acetophenones.

better correlations.[15] Thus, the failure of correlation (1) could be mainly attributed to the long range effects of substituent magnetic anisotropy.[3,15]

Halogens and cyano group are known to have a large negative (shielding) magnetic anisotropy, $\Delta\chi$, along C-substituent axis.[3,16a-d] In fact, the

14) F. Langenbucher, E. D. Schmidt and R. Mecke, *J. Chem. Phys.*, **39**, 1901 (1963).

15) Y. Yukawa and Y. Tsuno, "Kagaku no Ryoiki," Nankodo, sp. ed. No. 85, Spectrochem. '**68B** (1969), Chap. 4, p. 87.

16) a) J. A. Pople, *Proc. Roy. Soc.*, **A239**, 549, 557 (1957); b) J. A. Pople, *J. Chem. Phys.*, **37**, 60 (1962); c) T. J. Flautt and W. F. Erman, *J. Amer. Chem. Soc.*, **85**, 3243 (1963); d) W. Zeil and H. Buchert, *Z. Phys. Chem.*, **38**, 47 (1963).

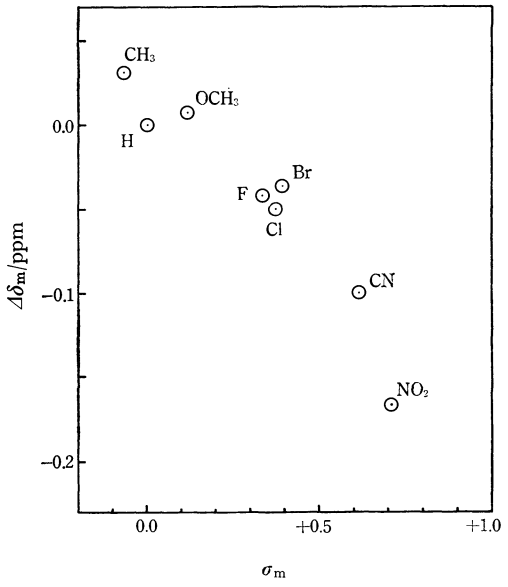

Fig. 1-6. Hammett plot for 1-phenyl-1-*meta*-substituted phenylethylenes.

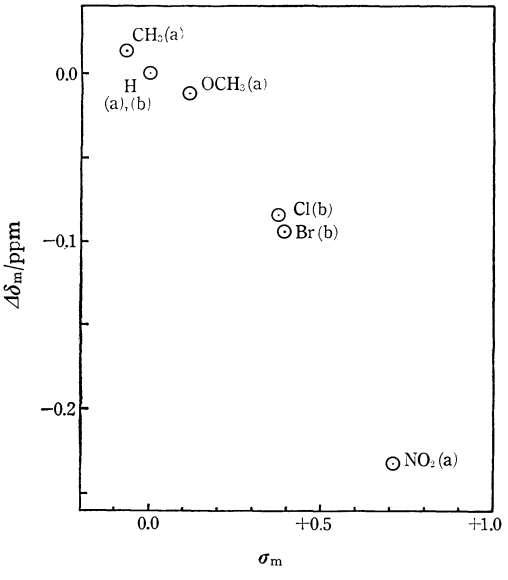

Fig. 1-7. Hammett plot for *meta*-substituted phenylacetylenes. (a) Ref. 5a, (b) Ref. 5b

remarkable deviations to the high field side are observed for these substituents (Figs. 1-1, 1-3, and 1-4). Methoxy, methyl, and nitro groups, on the other hand, show an interesting feature. Examination of Figs. 1-1—1-7 with these substituents indicates that each of the correlation line along the points of the three substituents does not pass through the origin of the coordinate but deviates remarkably to the high field side, in other words, the effect of electron attracting nitro group seems to be abnormally decreased, whereas the effect of electron releasing methyl and methoxy group, to be abnormally increased. It is important, however, to note that no significant anomaly has generally been observed in the Hammett type plotting of the aliphatic compounds[17a,b] with these three substituents as well as the hydrogen (unsubstituted compound). If we consider this observation as evidence suggesting the zero or negligibly small anisotropy of these four groups (hereafter referred to as the selected substituent), the high field deviations observed in the present experiments should not be ascribed to the substituent magnetic anisotropy effect. This suggestion is supported strongly by both theoretical and experimental evaluation of the anisotropy of the selected substituents as discussed below.

For methyl group anisotropy,[18a-d] even though there may still be many arguments about its magnitude (the positive $\Delta\chi$ along the C–CH_3 axis which should give a deshielding effect on the proton under discussion), an isotropic magnetic susceptibility ($\Delta\chi=0$) was proposed by Pople.[16b] Thus the high field deviation of methyl group can never be reduced but rather enlarged by the correction for the anisotropy effect. For hydrogen, such anisotropy can not be predicted theoretically.[16b] In methoxy group, magnitude and direction were calculated theoretically by Pople.[16b] By the use of Pople's $\Delta\chi$, it can be shown that the methoxy group exerts a shielding effect on the proton under investigation,*1 but the effects are negligibly small at the side chains. There has been no quantitative evaluation of nitro group anisotropy, but a negative $\Delta\chi$ could be supposed to exist along the axis perpendicular to O–N–O plane. This anisotropy, however, should give a low field shift of the protons. The situation for nitro group is therefore the same as for methyl group; the correction would result in the increased high field deviation.

In view of these facts, it can be concluded that the high field deviations observed for the three substituents (CH_3O, CH_3, NO_2) should be ascribed to the contribution of an unknown factor other than the substituent magnetic anisotropy effect.

One possible explanation for the high field deviation may be given by the different way of being

17) a) J. R. Cavanaugh and B. P. Dailey, *J. Chem. Phys.*, **34**, 1099 (1961); b) H. Spiesecke and W. G. Schneider, *ibid.*, **35**, 722 (1961).

18) a) R. F. Zürcher, *Discuss. Faraday Soc.*, **34**, 66 (1962); b) R. T. Narasimhan and M. T. Rogers, *J. Chem. Phys.*, **31**, 1302 (1959); c) J. Guy and J. Tillieu, *ibid.*, **24**, 1117 (1956); d) J. W. ApSimon, W. G. Craig, P. V. Demarco, D. W. Mathieson, L. Saunders and W. B. Whalley, *Tetrahedron*, **23**, 2339 (1967).

*1 The correction for the anisotropy effect would move the point of methoxy group somewhat downwards (−0.018 ppm in benzene series, −0.009 ppm on toluene series), but the improvement is clearly insufficient.

affected by the polar substituent between the chemical shift and chemical reactivity. According to Buckingham's theory,[19] the polar effect on the proton chemical shift can be given (neglecting the second order term) in terms of the electric field components along the C–H bond as shown in the equation

$$E_z = k_E \sum_i (q_i \cos\theta_i / \varepsilon r_i^2) \qquad (2)$$

where r_i denotes the distance between the resonating proton and the atom i carrying a point charge q_i, and θ_i is the angle between r_i and the C–H bond.

On the other hand, Hammett's σ_m constant, determined from a reactivity measurement, should approximately be related to a potential energy[20] arising from an interaction between the point charge induced at the reaction center and point charges, q_i, which are distributed over the rest of the molecule. Hammett's σ_m constant could thus be related to the term

$$\sum_i (q_i/\varepsilon R_i)$$

where R_i is the distance between the reaction center and the location of charges on the reacting molecule in transition or product state.

It is convenient to divide the electric field effect into two classes:

(a) An effect attributable to the charge distribution brought about in the side chain by a polar effect of substituted phenyl group.

(b) An effect attributable to the charge distribution arising from the C(phenyl)-substituent polarization and to the π-electron distribution affected by the polar resonance of the substituent.

Effect (a) on the chemical shift will be the same in character as that on the potential energy change. Then the effects may be expressed, in both cases, in terms of Hammett's σ_m. For effect (b), however, a somewhat larger contribution of the π-electronic charge in the case of chemical shift could be expected since the distance between the resonating proton and the π-electronic charge, r_π or R_π, will be generally shorter than that between the resonating proton and the charges distributed in the C(phenyl)-substituent dipole, r_μ or R_μ:

We have $r_\pi \ll r_\mu$ and $R_\pi \ll R_\mu$ as cited above and if $\cos\theta_\pi \fallingdotseq \cos\theta_\mu$ as might be expected in the molecule having a long side chain, then

$$\frac{\cos\theta_\pi / r_\pi^2}{\cos\theta_\mu / r_\mu^2} > \frac{1/R_\pi}{1/R_\mu}$$

If this is true, the polar effect on the chemical shift could be expressed in the following form by allowing the additional contribution of π-electronic effect, $k\sigma_\pi$,

$$\Delta\delta_m = a_m\sigma_m + k\sigma_\pi \qquad (3)$$

in which the σ_π is Yukawa-Tsuno's parameter[1i] measuring the resonance ability[4] of the substituent.*2

Another possible cause for high field deviation is a variation in the magnetic anisotropy of benzene ring due to π-electronic perturbation in the ring system brought about by the polar resonance of the substituent. There are two different aspects to interpret the effect of π-electronic perturbation. First of which predicts a decrease on the ring current by +R substituent[4] leading to a high field shift of the protons or an increase in the ring current by −R substituent[4] leading to a low field shift of the protons. If it is assumed that the variation of the π-electronic density on the benzene ring is proportional to the resonance ability, σ_π, of an introduced substituent, the correction for the ring current effect may be given in the same expression as (3).*3

By the use of Eq. (3), the deviations are somewhat reduced than before. However, the improvement is still not quite satisfactory, as may be seen in the case of ring protons and toluenes (Fig. 2). Failure of the additional π-electron contribution model is further verified by the fact that the evaluations of the geometric factors for the side chain systems under investigation show that the relative contributions of π-electronic effect in the chemical shift are generally equal to those in the reactivity and also that the contributions are independent of the nature of side chains at *meta* position.*4

$$\frac{\sum_i (\cos\theta_i/r_i^2)_\pi}{\sum_i (\cos\theta_i/r_i^2)_\mu} \fallingdotseq \frac{\sum_i (1/R_i)_\pi}{\sum_i (1/R_i)_\mu} \fallingdotseq \text{const.} \qquad (4)$$

It is well known that the olefinic protons of

19) A. D. Buckingham, *Can. J. Chem.*, **38**, 300 (1960).
20) T. Ri and H. Eyring, *J. Chem. Phys.*, **8**, 433 (1940).

*2 Yukawa and Tsuno separated the substituent effect into the sigma-inductive effect, σ_i, and pi-electronic effect, σ_π, and demonstrated the generality and utility of this separation.[1i] The success of this separation in explaining the polar effects justifies the use of σ_π here.

*3 Equation (3) is similar in form to the equation proposed by Taft

$$\Delta\delta_m = \alpha\sigma_I + \beta\sigma_R^0 = \alpha\sigma_m + (\beta-\alpha)\sigma_R^0$$

or to the equation[15]

$$\Delta\delta_m = \alpha\sigma_p^0 \fallingdotseq \alpha\sigma_m + \beta'\sigma_R^0$$

Although both these equations gave better correlations than in the simple Hammett relation, no detailed discussion was made about the correction term, $(\beta-\alpha)\sigma_R^0$ or $\beta'\sigma_R^0$.

*4 An exception for the generality (4) is noted in the case of ring protons at *para* position for which a large excess contribution of π-electronic effect to the chemical shift can be calculated from the examination of the geometric functions and this is consistent with the observation that the *para* ring protons[2c] are satisfactorily correlated to the σ_π constants[1i] rather than to the σ_p^0 constants.[4]

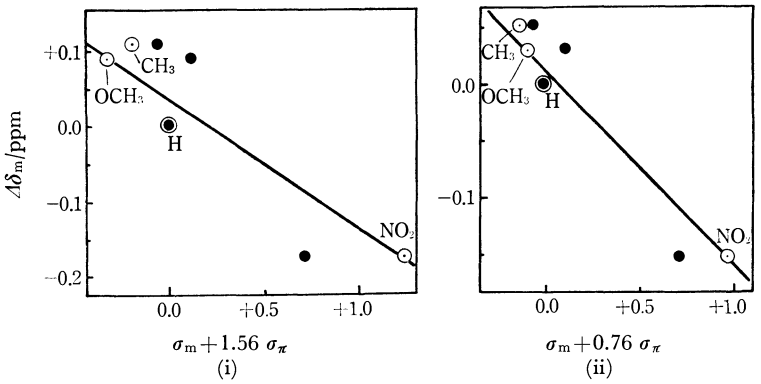

Fig. 2. Failure of the Eq. (3).
(i) Ring protons. (ii) Toluenes. Closed circle shows the original σ_m plot.

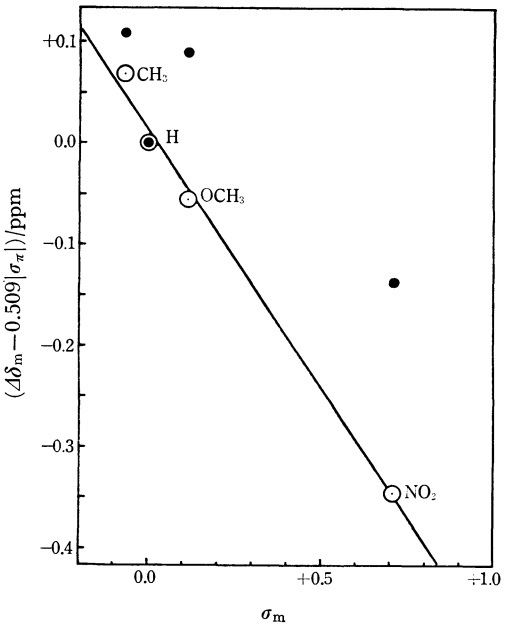

Fig. 3-1. Application of the Eq. (5) to ring protons *meta* from substituents.
Closed circle denotes the observed relative shift, $\Delta\delta_m$.

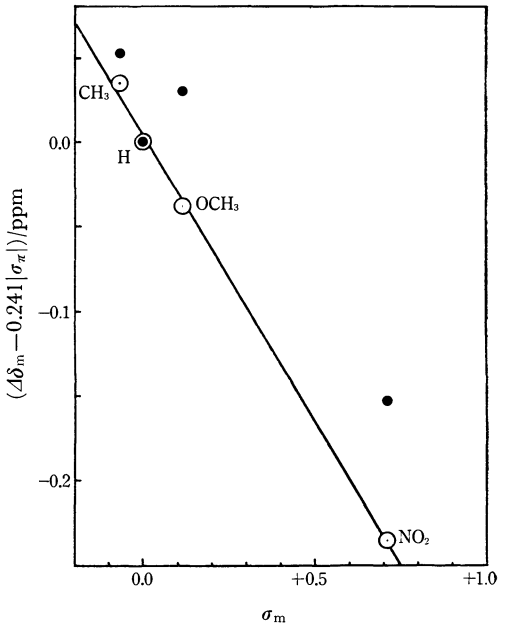

Fig. 3-2. Application of the Eq. (5) to *meta*-substituted toluenes.

TABLE 2. APPLICATION OF EQ. (5) AND JOHNSON-BOVEY'S RING CURRENT SHIFTS

Side chain system	Application of Eq. (5)				Ring current shift
	$-a_m$/ppm	K/ppm	r_c*	s/ppm**	$-f(\rho,z)$/ppm
X-$C_6H_4\underline{H}$	0.511	0.509	0.993	0.026	1.50
(X-$C_6H_4)_2C{=}C\underline{H}_2$	0.623	0.312	1.000	0.002	0.70
X-$C_6H_4C\underline{H}_3$	0.339	0.241	0.999	0.009	0.57
X-$C_6H_4O\underline{CH}_3$	0.283	0.187	0.999	0.006	0.40
X-$C_6H_4COC\underline{H}_3$	0.251	0.164	1.000	0.003	0.34
X-C_6H_4,$C_6H_5C{=}C\underline{H}_2$	0.305	0.149	1.000	0.002	0.35
X-$C_6H_4C{\equiv}C\underline{H}$	0.367	0.116	0.997	0.017	0.21

* Correlation coefficient.
** Standard deviation.

cycloolefin having localized double bonds show somewhat higher chemical shifts as compared with the normal aromatic ring protons. The feature has generally been explained in terms of the lack of ring current in those cyclic molecules.[21a,b] This suggests another possibility to interpret the effect of π-electronic perturbation due to introduced substituent. The introduction of substituent will result in an additional contribution of quinoidal structure (II) in the resonance hybrid and hence

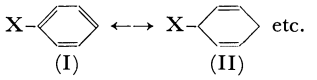

(I) (II)

lead to some decrease of the ring current. The extent of the contribution of structure (II), depending only on the resonating ability of the substituent but not on the direction of electronic displacement, could be estimated by the term, $|\sigma_\pi|$. Correcting for this term, we can express $\Delta\delta_m$ for the selected substituents at *meta* position as

$$\Delta\delta_m = a_m\sigma_m + K|\sigma_\pi| \qquad (5)$$

where K is a proportionality constant describing susceptibility to the contribution of quinoidal structure (II). Figures 3-1 and 3-2 show two examples of the plots of the relative chemical shifts corrected for the quinoidal effect, $\Delta\delta_m - K|\sigma_\pi|$, against Hammett's σ_m constants. The parameters, a_m and K, were determined using least squares method and are summarized in the first four columns of Table 2 where correlation coefficients, r_c and standard deviations, s, also are included. It is clear that the employment of treatment (5) for the given series yields significant improvements in the correlations. Additional evidence for the contribution of decreased ring current term, $K|\sigma_\pi|$, is provided by an examination of the variation of parameter K. Since K is a susceptibility coefficient to the diminution of ring current effect, it should depend only on the geometric relation between the resonating protons and the benzene ring. In order to testify this suggestion, the Johnson and Bovey's ring current shifts[21a] in ppm, $f(\rho,z)$, were utilized as a measure of the geometric factors for the resonating protons located at the usual cylindrical coordinates ρ and z.

In the last column of Table 2, the calculations of $f(\rho,z)$ were performed by averaging over all the reasonable orientations of the side chains; for the methyl protons, $f(\rho,z)$'s were calculated by assuming free rotation of the methyl group. In anisoles and acetophenones, the calculations were based on the planar *cis*- and *trans*-model of equal

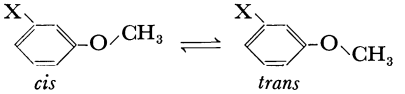

cis *trans*

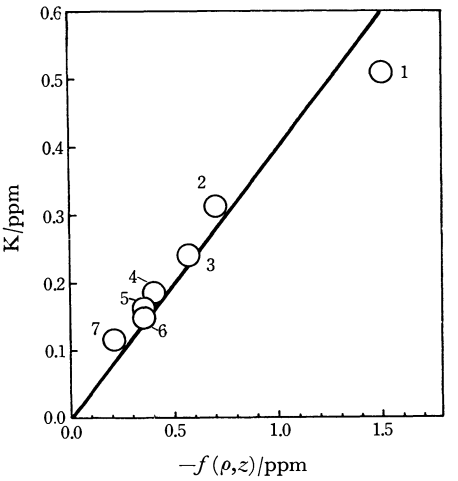

Fig. 4. Dependence of K in Eq. (5) on the Johnson-Bovey's ring current effect.
1. X-$C_6H_4\underline{H}$, 2. $(X\text{-}C_6H_4)_2C{=}C\underline{H}_2$, 3. X-$C_6H_4$-$C\underline{H}_3$, 4. X-$C_6H_4O\underline{CH}_3$, 5. X-$C_6H_4CO\underline{CH}_3$, 6. X-$C_6H_4$,$C_6H_5C{=}C\underline{H}_2$, 7. X-$C_6H_4C{\equiv}C\underline{H}$

populations. In diphenylethylenes, two benzene rings were twisted 30° out of $C{=}CH_2$ plane[22] and the equal populations of *cis*- and *trans*-form were assumed.

The result of closer examination of the relationship between K and $f(\rho,z)$ is shown in Fig. 4. A linear dependence of K on $f(\rho,z)$,

$$K = -0.4f(\rho, z) \qquad (6)$$

is consistent with the expectation that the effect of the ring current depression on the chemical shift will be nearly proportional to the strength of the ring current field to which the resonating proton is exposed. Using relation (6), we obtain, from (5),

$$\Delta\delta_m + 0.4f(\rho, z)|\sigma_\pi| = a_m\sigma_m \qquad (7)$$

which involves only one parameter, a_m. In applying Eq. (7) to the given side-chain systems, the agreement was quite satisfactory and no essential differ-

Table 3. Substituent constants in Eq. (10)

Substituent	σ_m	$-10^{23}A/(cm^3ppm)$	$\lvert\sigma_\pi\rvert$[11i]
OCH_3	+0.115	0.0	0.281
CH_3	−0.069	0.0	0.078
H	0.000	0.0	0.000
F	+0.337	1.1	0.118
Cl	+0.373	1.7	0.070
Br	+0.391	2.0	0.054
I	+0.352	~2.3	0.056
CN	+0.615	1.3	0.25
NO_2	+0.710	0.0	0.34

21) a) G. E. Johnson, Jr., and F. A. Bovey, *J. Chem. Phys.*, **29**, 1012 (1958); b) J. S. Waugh and R. W. Fessenden, *J. Amer. Chem. Soc.*, **79**, 846 (1957).

22) G. E. Cootes and L. E. Sutton, *J. Chem. Soc.*, **1942**, 567.

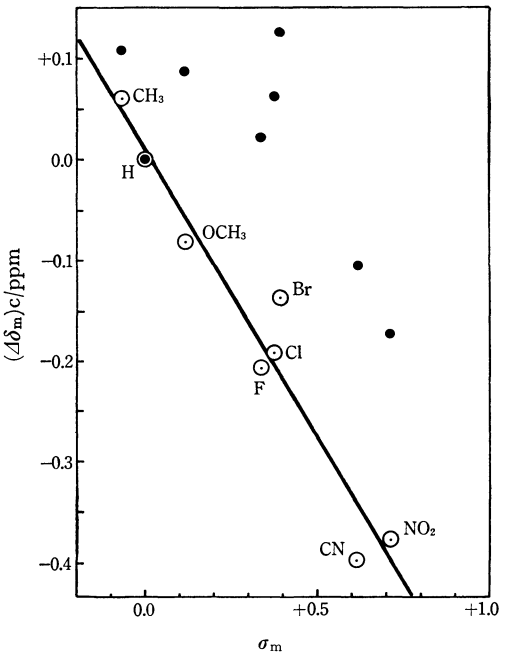

Fig. 5-1. Application of the Eq. (10) to ring protons *meta* from substituents.
Closed circle denotes the observed relative shift, $\Delta\delta_m$.

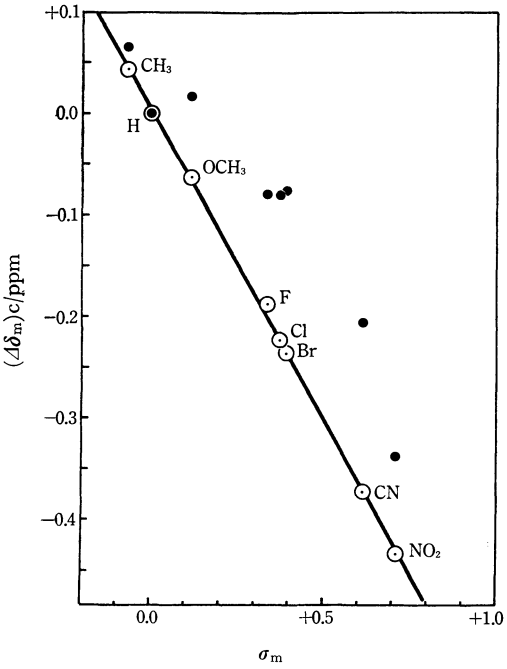

Fig. 5-2. Application of the Eq. (10) to 1,1-di (*meta*-substituted phenyl)ethylenes.

ence in results was noted as compared with the use of Eq. (5). While the present report was being written,[23a] Figeys and Flammang calculated theoretically the variation of ring current effect for the

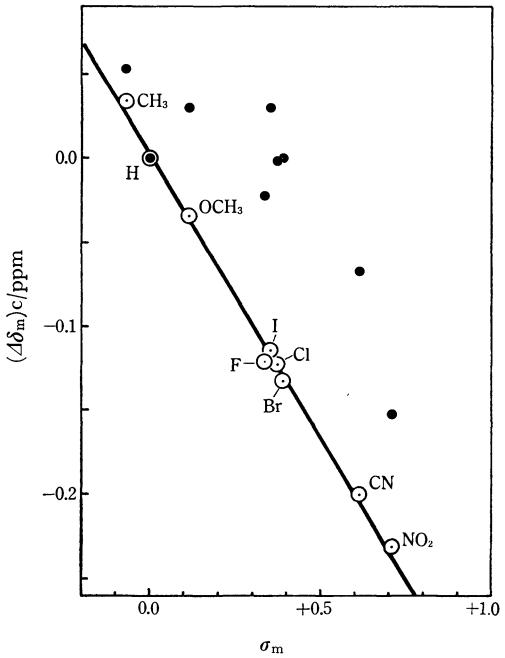

Fig. 5-3. Application of the Eq. (10) to *meta* substituted toluenes.

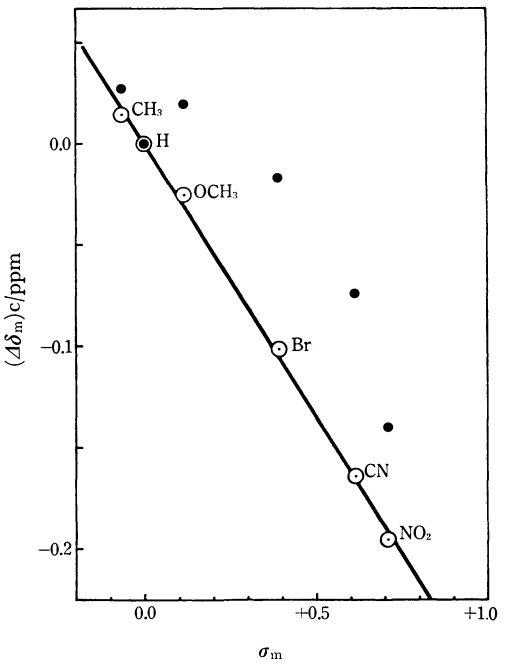

Fig. 5-4. Application of the Eq. (10) to *meta*-substituted anisoles.

ring protons at *para* position of mono-substituted benzenes.[23b] The calculated decreases of ring

23) a) H. Yamada, Dr. thesis, Osaka University (1968); b) H. P. Figeys and R. Flammang, *Mol. Phys.*, **12**, 581 (1967).

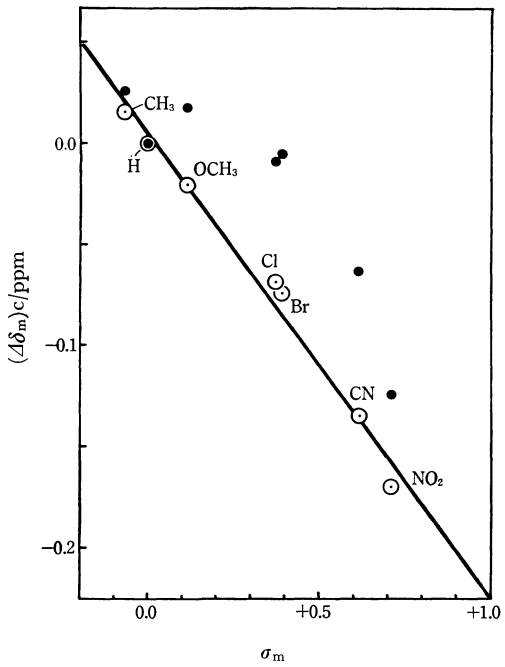

Fig. 5-5. Application of the Eq. (10) to *meta*-substituted acetophenones.

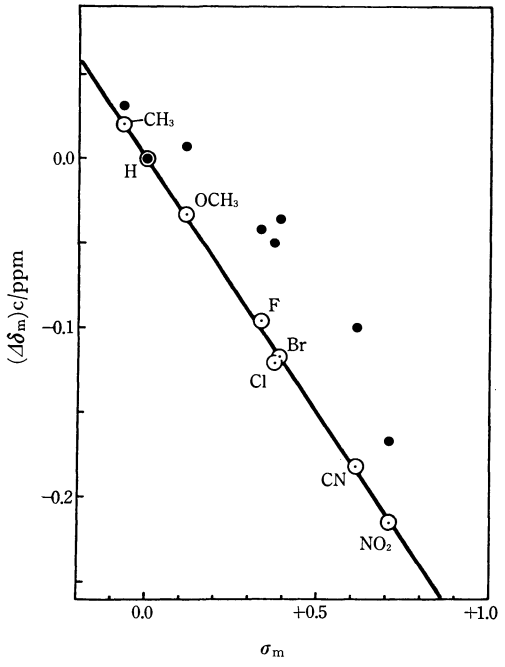

Fig. 5-6. Application of the Eq. (10) to 1-phenyl-1-*meta*-substituted phenylethylenes.

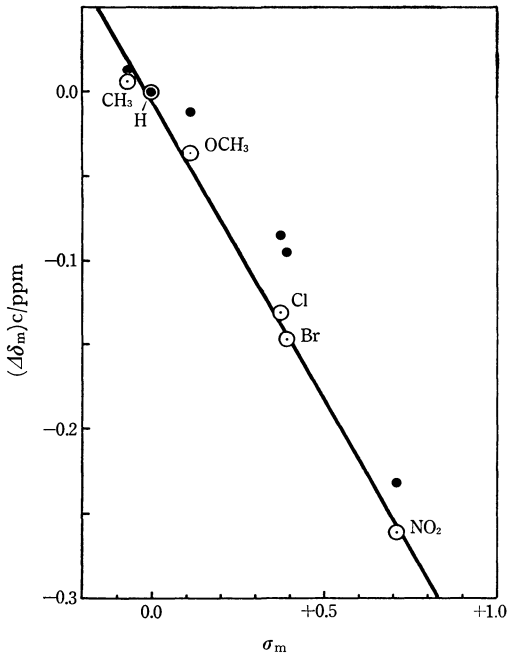

Fig. 5-7. Application of the Eq. (10) to *meta*-substituted phenylacetylenes.

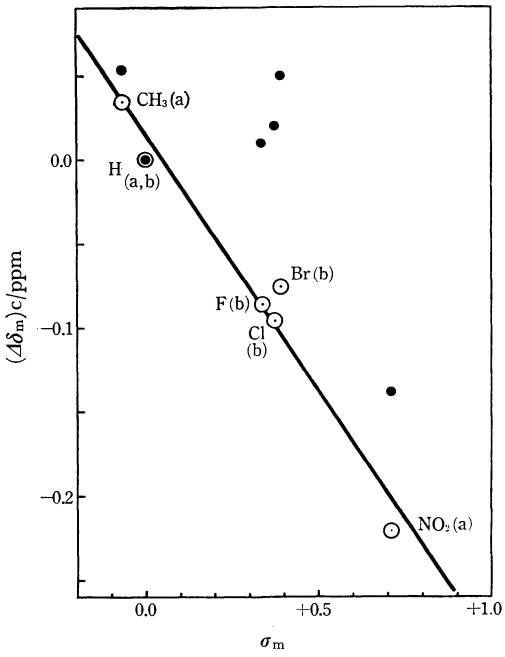

Fig. 5-8. Application of the Eq. (10) to *meta*-substituted benzaldehydes.
(a) T. Kinugasa, H. Yamada and S. Hamano, unpublished data. (b) Ref. 2f.

current effect were 0.15 ppm for NH_2, 0.08 ppm for OCH_3 and 0.06 ppm for $C\equiv N$. The values are in qualitative agreement with our estimations based on the term, $-0.4f(\rho,z)|\sigma_\pi|$ in Eq. (7). This fact, in addition to the success of correlation (6), suggests strongly that the observed high field deviations result from the decreased ring current due to introduced substituent.

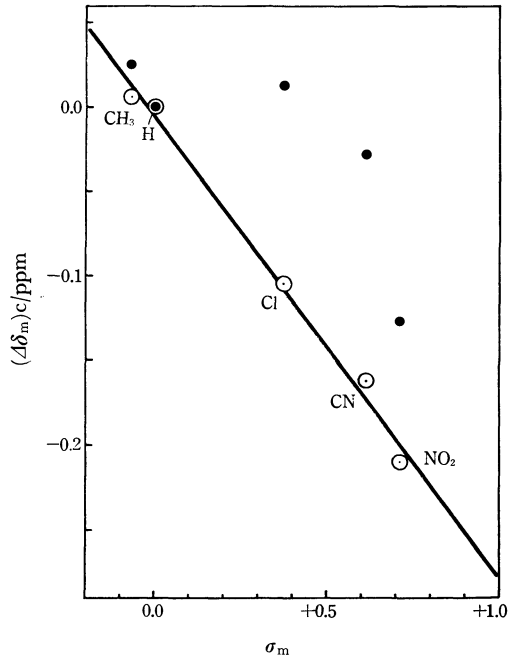

Fig. 5-9. Application of the Eq. (10) to α-protons of *meta*-substituted *trans*-cinnamic acids.[24]

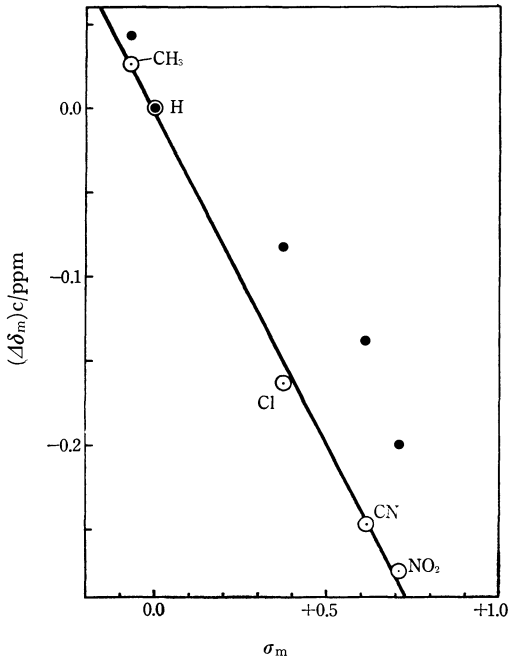

Fig. 5-10. Application of the Eq. (10) to β-protons of *meta*-substituted *trans*-cinnamic acids.[24]

The plot of the anisotropic substituents, however, still shows considerable deviations from the line required by Eq. (7). We may now consider the effect of the anisotropic substituents. If it is assumed that the observed deviation, Δ, is mainly ascribed

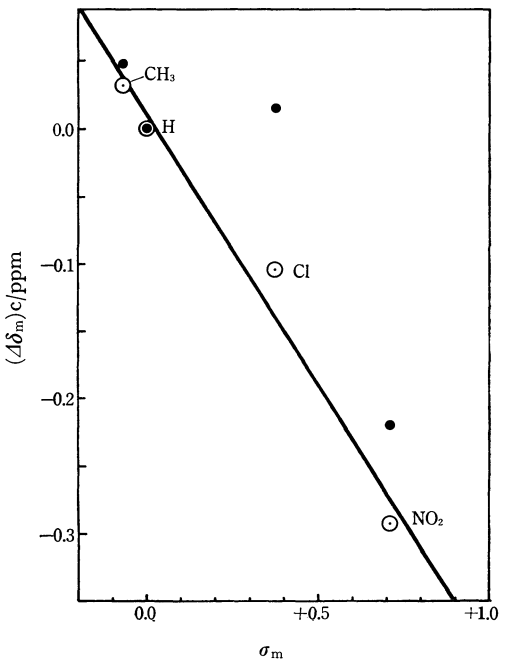

Fig. 5-11. Application of the Eq. (10) to α-protons of *meta*-substituted *cis*-cinnamic acids.[24]
The calculations of the geometric terms were based on the model in which the benzene ring was twisted 90° out of CH=CH plane.

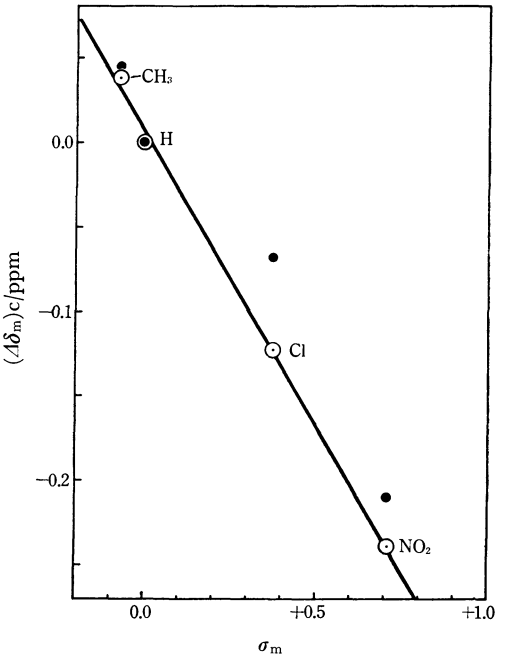

Fig. 5-12. Application of the Eq. (10) to β-protons of *meta*-substituted *cis*-cinnamic acids.[24]
The calculations of the geometric terms were based on the model in which the benzene ring was twisted 90° out of CH=CH plane.

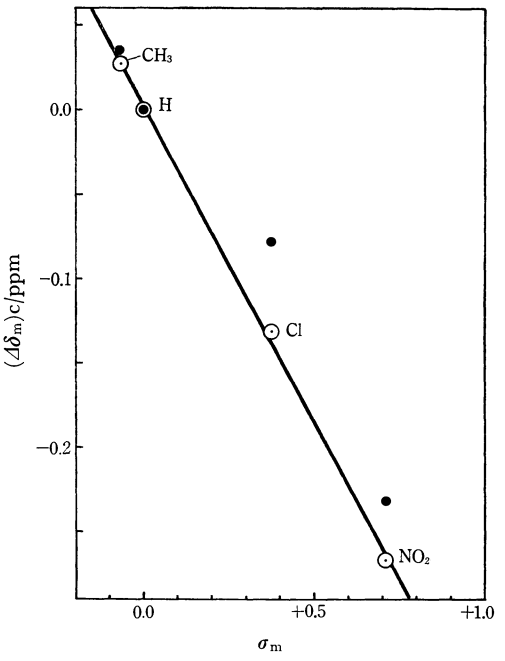

Fig. 5-13. Application of the Eq. (10) to *trans* protons of *meta*-substituted styrenes.[24]

to the anisotropy effect of the substituent, and also that the point dipole approximation[3] is applicable, the relative magnitude of the anisotropy effect between series A and B is given by

$$\frac{\Delta_B}{\Delta_A} = \frac{\Delta\chi(3\cos^2\theta_B - 1)3NR_A^3}{\Delta\chi(3\cos^2\theta_A - 1)3NR_B^3} = \frac{(3\cos^2\theta_B - 1)R_A^3}{(3\cos^2\theta_A - 1)R_B^3} \quad (8)$$

Equation (8) indicates that a magnetic anisotropy effect, Δ, in any side chain system can be calculated experimentally from Δ_A for a specified system A and geometric factors of the respective systems, even if the anisotropy of the substituent $\Delta\chi$ is not known:

$$\Delta = \Delta_A\frac{(3\cos^2\theta - 1)R_A^3}{(3\cos^2\theta_A - 1)R^3} \equiv \mathbf{A}\cdot\frac{3\cos^2\theta - 1}{R^3} \quad (9)$$

where **A** is a substituent anisotropy effect per unit geometric factor

$$\mathbf{A} = \Delta_A\frac{R_A^3}{3\cos^2\theta - 1},$$

and this can be calculated from a particular side chain system taken as the standard. In this study the values of **A** were evaluated by averaging two calculations based on toluenes and bis-(substituted phenyl)ethylenes (Table 3). For each of the halogen substituents, a magnetic point dipole μ_M, was assumed to be along the C(phenyl)-halogen bond, and located at the position of the halogen nucleus. For cyano group, the μ_M directed to the C≡N bond was located at the center of the bond. All the calculations were made on the basis of the same molecular model as that used in the estimation of ring current effect, $f(\rho,z)$.

Table 4. Application of Eq. (10)

Side chain system	$-a_m$/ppm	r_c*	s/ppm**
X-$C_6H_4\underline{H}$[a]	0.571	0.971	0.042
(X-$C_6H_4)_2C{=}C\underline{H}_2$	0.610	0.999	0.006
X-$C_6H_4C\underline{H}_3$	0.337	0.998	0.006
X-$C_6H_4OC\underline{H}_3$	0.270	0.999	0.004
X-$C_6H_4COC\underline{H}_3$	0.229	0.992	0.010
X-C_6H_4,$C_6H_5C{=}CH_2$	0.301	0.999	0.004
X-$C_6H_4C{\equiv}C\underline{H}$	0.355	0.997	0.009

a) $\Delta\delta_m$ for iodobenzene was omitted from the least squares calculation.
* Correlation coefficient.
** Standard deviation.

Introduction of the substituent anisotropy term (9) into Eq. (7) gives

$$\Delta\delta_m + 0.4f(\rho,z)|\sigma_\pi| + \mathbf{A}\cdot\frac{3\cos^2\theta - 1}{R_3} = a_m\sigma_m \quad (10)$$

which should be applicable to all the substituents including magnetically anisotropic ones. The left hand side of Eq. (10) represents the observed relative shifts corrected for the ring current variation and for the substituent magnetic anisotropy. This corrected value is regarded as an observable relative shift which depends only on the polar effects of the substituent. In Figs. 5-1—5-7, the corrected relative shifts, $(\Delta\delta_m)_c$, are plotted against Hammett's σ_m constants and the results are summarized in Table 4. The agreement is quite satisfactory. The applicability of Eq. (10) was further tested using data reported in literature.[2f,24] The successful results (Figs. 5-8—5-13) are collected in Table 5.

In view of the above results it may be concluded that Eq. (10) is fairly general in spite of the approximate nature of the derivation and useful, because of its simplicity, for estimating substituent chemical shifts and for examining the rotational conformation of the side chains.

It is pointed out that the variation of the susceptibility parameter to the polar effects, a_m, exhibits the same trend as that of ρ for the dissociation constants of corresponding carboxylic acid in a given solvent.[25] The lack of strict linear correlation between a_m and ρ might be attributed to the difference in the geometric functions for the chemical

24) T. A. Wittstruck and E. N. Trachtenberg, *J. Amer. Chem. Soc.*, **89**, 3803 (1967).
25) R. W. Taft, Jr., and I. C. Lewis, *ibid.*, **81**, 5343 (1959).

TABLE 5. APPLICATION OF EQ. (10) TO DATA OBTAINABLE FROM LITERATURE

Side chain system		$-f(\rho,z)$/ppm	$-a_m$/ppm	r_c*	s/ppm**	Ref.
X-C_6H_4C$\underline{H}$O		0.61	0.305	0.982	0.019	2f
X-C_6H_4 $\underline{H}_B$	A	0.62	0.272	0.995	0.011	24
$\underline{H}_A$ CO_2H	B	0.56	0.394	0.999	0.009	24
X-C_6H_4 CO_2H	A†	0.54	0.400	0.986	0.030	24
$\underline{H}_A$ $\underline{H}_C$	C†	0.21	0.348	0.999	0.007	24
X-C_6H_4 H		0.26	0.374	0.999	0.005	24
H $\underline{H}$						

* Correlation coefficient.
** Standard deviation.
† The calculations of the geometric terms were based on a model in which the benzene ring was twisted 90° out of CH=CH plane.

shift and for the reactivity. The quantitative explanation for this situation will require a precise knowledge of electronic distribution on the side chain.

Exceptions to the applicability of Eq. (10) are the iodo- and bromo-substituted benzene system. This might be partly due to the incorrect estimation of anisotropy effects for these substituents. The point dipole approximation may be no more valid in bromo- and iodobenzenes where the dimension of the anisotropic substituent seems to be too large as compared with the distance R. Nakagawa *et al.* suggested the importance of the spin polarization effects[26] particularly in the molecule possessing heavy atoms such as iodine and bromine. Such effects may also contribute to the relative chemical shifts of ring protons *meta* to the substituent since the transmittance of the spin coupling will be considerably larger than in other side chain systems in which the resonating protons are separated from the spin polarizable substituent by more than three atoms. An investigation of this possibility, in addition to the study on *para* systems, must be the subject of future research.

The authors wish to express their gratitude to Professor Toshio Kinugasa of Kobe University for his constant advice and encouragement and for making facilities available for carrying out the NMR measurements.

26) N. Nakagawa, M. Shinada and T. Ô-hinata, Preliminary Report of the 6th NMR Symp., Kyoto, p. 8 (1967).

BULLETIN OF THE CHEMICAL SOCIETY OF JAPAN VOL. 43 1473—1477 (1970)

The Photoreaction of *p*-Substituted *β*-Benzoylacrylic Acids

Noboru SUGIYAMA, Choji KASHIMA, Hiroshi KATAOKA and Keiko TANAKA

Department of Chemistry, Tokyo Kyoiku University, Otsuka, Bunkyo-ku, Tokyo

(Received October 3, 1969)

This paper will describe the photoreaction of *trans*-*β*-(*p*-ethylbenzoyl)acrylic acid (II) in methanol to give 5-(*p*-ethylphenyl)-5-methoxy-2-oxo-2,5-dihydrofuran (III), *β*-(*p*-ethylbenzoyl)-*α*-methoxypropionic acid (IV), and its methyl ester (V). The kinetic study of this reaction has revealed that II gives III and IV parallel by the first-order reaction and that IV then changes into V. Furthermore, the irradiation of *p*-substituted *β*-benzoylacrylic acids has been studied. From the product ratio and the substituent effects at the *para* position, the mechanism of the photoreactions of *γ*-oxoacrylic acids in methanol is proposed. This mechanism is also supported by the HMO calculations.

In our previous report[1] on the photoreaction of *β*-benzoylacrylic acid (I), a *γ*-oxoacrylic acid, in methanol, the formation of the methanol-addition product, *β*-benzoyl-*α*-methoxypropionic acid, and the reaction mechanism were described. However this mechanism is not sufficient to explain the photoreaction of *β*-acylacrylic acid, another *γ*-oxoacrylic acid, because *β*-acrylacylic acid is isomerized to 5-alkyl-5-hydroxy-2-oxo-2,5-dihydrofuran by irradiation.[2] Thus, we have examined the photoreaction of *p*-substituted *β*-benzoylacrylic acids in order to find a mechanism appropriate for all *γ*-oxo-acrylic acids.

Results and Discussion

Photoreaction of *β*-(*p*-Ethylbenzoyl)-acrylic Acid in Methanol. As a typical *p*-substituted *β*-benzoylacrylic acid, *β*-(*p*-ethylbenzoyl)acrylic acid (II) was chosen for the kinetic study. The structure of II was confirmed to be of the *trans* form by the coupling constant[1,2] of the olefinic protons (16.4 Hz) in the NMR spectrum. A methanol solution of II was irradiated with a 500-W high pressure mercury lamp for 105 hr at room temperature. From the reaction mixture after 80 hr irradiation, 5-methoxy-2-oxo-2,5-dihydrofuran (III), *β*-(*p*-ethylbenzoyl)-*α*-methoxy-propionic acid (IV) and the methyl ester (V) were obtained (Fig. 1). The yields of III, IV, and V were 27, 4, and 63% respectively.

The structures of these new photoproducts were determined as follows. The IR spectrum of III shows angelica lactone bands at 1820, 1780, and 1680 cm^{-1}, and the UV spectrum shows the absorption maximum at 243 nm. In the NMR spectrum the triplet signal at τ 8.77 was coupled with the quartet signal at τ 7.34 and the singlet signal

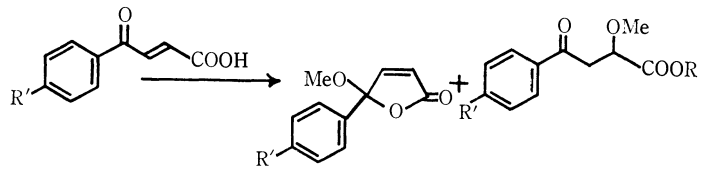

R′			R=H	R=Me
H	I			
Et	II	III	IV	V
Me	VII	XXI		XIV
i-Pr	VIII			XV
t-Bu	IX			XVI
MeO	X			XVII
EtO	XI			XVIII
Br	XII			XIX
Cl	XIII			XX

Fig. 1

1) N. Sugiyama, H. Kataoka, C. Kashima and K. Yamada, This Bulletin, **42**, 1353 (1969).

2) N. Sugiyama, H. Kataoka, C. Kashima and K. Yamada, *ibid.*, **42**, 1098 (1969).

corresponding to 3 protons appeared at τ 6.58. The signal at τ 3.91 was split to a doublet with a coupling constant of 6.0 Hz, and the multiplet of 5 protons appeared in the τ 2.36—3.16 region. From these spectral data and elemental analyses, the structure of III was deduced. The structure of V was determined by the IR, UV, and NMR spectra and by elemental analyses. These spectral data were then checked with the corresponding data of methyl β-benzoyl-α-methoxypropionate.[1] IV was methylated with diazomethane, and the product was identified with V.

For the sake of comparison, the reaction without any irradiation and the thermal reaction of II in methanol were carried out. When a methanol solution of II was placed in a dark place for 24 hr, it was found to be 12% methyl *trans*-β-(*p*-ethylbenzoyl)-acrylate (VI) and 88% II. When refluxed for 24 hr in methanol, II was converted into 36% V and 64% VI. Thus, it was recognized that the formation of III, IV, and V from II was induced by the irradiation. The formation of an angelica-lactone-type compound, III, by the irradiation of II suggested that this photoreaction is different from that of I or β-acylacrylic acid.[1,2]

In order to get some information on the reaction mechanism, the behavior of methyl *trans*-β-(*p*-ethylbenzoyl)acrylate (VI) was studied. By irradiation, VI was transformed into a *cis* isomer in a 87% yield, but when refluxed in methanol VI did not show any change. When the photoreaction of II in methanol was examined by means of the NMR spectra, it was observed that II was gradually converted into III and IV. The results are summarized in Fig. 2. The yield of IV reached its maximum after 20 hr, and then decreased. However the total yield of the alcohol adducts, IV and V, increased when the first-order reaction with $k_1 = 8.9 \times 10^{-6}$ sec^{-1}. The decrease curve of II showed a first-order reaction of II with $k = k_1 + k_3 = 13.3 \times 10^{-6}$ sec^{-1}, and the curve of III showed $k_3 = 4.4 \times 10^{-6}$ sec^{-1}. Moreover, III in methanol did not change upon irradiation or refluxing. From these results, it can be assumed that the irradiation of II produces two parallel photoproducts, III and IV, and that IV changes into V.

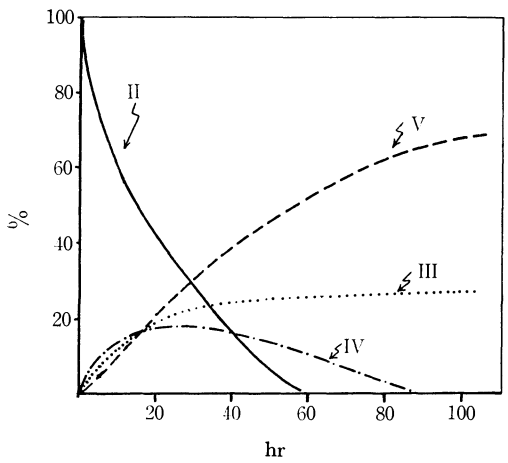

Fig. 2

On the other hand, it has been shown that the photoreaction of I does not occur in acidic or basic methanol, and that *cis*-β-benzoylacrylic acid (I′) is the intermediate of this reaction.[1] Also, it is well known that maleic acid has a partial grouping similar to that of I′ and that it has an intramolecular hydrogen bonding with a seven-membered cyclic ring between the γ-carbonyl and carboxyl groups.[3] From these facts, it can be assumed that the first step of the alcohol addition of *cis*-β-benzoylacrylic acids is the protonation on γ-carbonyl oxygen, and that γ-carbon becomes a carbonium ion, which makes it possible to represent by a resonance hybrid with a carbonium ion at the γ- or α-position. When a methanol molecule attacks the α-carbonium ion, the alcohol adducts will be formed, and when a methanol molecule attacks the γ-carbonium ion, the hemiketal of β-benzoylacrylic acids will be formed. These hemiketals can be cyclized to an angelica-lactone-type compound with ease. Consequently, the preponderance of the carbonium ion at the γ-position will result in the formation of an angelica-lactone-type compound, while that of the carbonium ion at the α-position will result in the formation of alcohol adducts.

Photoreaction of Other *p*-Substituted β-Benzoylacrylic Acids in Methanol. Since it is probable that the substituents at the *para* position of *p*-substituted β-benzoylacrylic acids will affect the preponderance of the carbonium ion at the γ- or α-position, the photoreactions of *p*-substituted derivatives of *trans*-β-benzoylacrylic acid were carried out in methanol. The derivatives used were *trans*-β-benzoylacrylic acid (I), *trans*-β-(*p*-toluoyl)acrylic acid (VII), *trans*-β-(*p*-isopropylbenzoyl)acrylic acid (VIII), *trans*-β-(*p*-*t*-butylbenzoyl)acrylic acid (IX),

Table 1. The NMR spectral signals of olefinic protons of *p*-substituted β-benzoylacrylic acid

Compd.	R′	$\tau_{H\alpha}$	$\tau_{H\beta}$	$J_{H\alpha H\beta}$
I	H	3.16	2.05	13.7 Hz
VII	Me	3.17	2.04	15.0
II	Et	3.20	2.04	16.4
VIII	*i*-Pr	3.19	2.06	15.2
IX	*t*-Bu	3.18	2.04	15.7
X	MeO	3.18	2.01	13.7
XI	EtO	3.18	2.03	16.1
XII	Br	3.26	2.14	13.7
XIII	Cl	3.18	2.06	15.7

3) F. H. Westheimer and O. T. Benfey, *J. Amer. Chem. Soc.*, **78**, 5309 (1956).

trans-*β*-(*p*-anisoyl)acrylic acid (X), *trans*-*β*-(*p*-ethoxybenzoyl)acrylic acid (XI), *trans*-*β*-(*p*-bromobenzoyl)-acrylic acid (XII), and *trans*-*β*-(*p*-chlorobenzoyl)-acrylic acid (XIII), all of them prepared by the method of Papa.[4] Their NMR spectra are shown in Table 1. The coupling constants[1,2] of the olefinic protons in the NMR spectra confirm that the structures of these *β*-benzoylacrylic acids have *trans* configurations.

The methanol solutions of these acids were irradiated with a 500-W high-pressure mercury lamp at room temperature. The reaction mixtures were separated by column chromatography, and the structures of these photoproducts were determined by a study of the IR, UV, and NMR spectra and by elemental analyses. The structure of each *p*-substituted *β*-benzoyl-*α*-methoxypropionic acid was determined to be that of the methyl ester obtained by treatment with diazomethane. Moreover, the yields of these photoproducts were determined by measuring the NMR spectra of the reaction mixtures (Fig. 1 and Table 2).

Table 2. The yield of the photoproducts from *p*-substituted *trans*-*β*-benzoylacrylic acid in methanol

Starting compd.	Material R′	Time (hr)	Photoproducts: Angelica lactone (%)	Alcohol adducts: Acid (%)	Alcohol adducts: Ester (%)
I	H	120	0	100	0
VII	Me	120	23	0	77
II	Et	168	17	4	76
VIII	*i*-Pr	168	10	70	15
IX	*t*-Bu	168	0	92	8
X	MeO	182	0	64	0
XI	EtO	168	0	89	11
XII	Br	168	trace	0	91
XIII	Cl	168	9	16	58

The methanol-addition reaction was observed in all cases. In the cases of the *p*-alkyl (except *t*-Bu) and *p*-halogeno *β*-benzoylacrylic acids, however 4-methoxy angelica-lactone-type compounds were produced.

From the results of the photo-reaction of *p*-alkyl *β*-benzoylacrylic acids, the hyperconjugation of alkyl groups at the *para* position appeared to have an effect on the yield of the angelica-lactone-type compounds. As is shown in Table 2, the stronger the hyperconjugation effect (Me>Et>*iso*-Pr>*t*-Bu), the higher was the yield of the angelica-lactone-type compound (VII>II>VIII>IX) observed.

4) D. Papa, E. Schwenk, F. Villani and E. Klingsberg, *ibid.*, **70**, 3356 (1948).

Table 3. The Sr^N values of *p*-substituted *β*-benzoylacrylic acids

Compd.	R′	$Sr^N(\alpha)$	$Sr^N(\gamma)$	$Sr^N(\gamma)/Sr^N(\alpha)$
VII	Me	6.3326	5.9856	0.9452
XII	Br	6.2731	5.9264	0.9449
XIII	Cl	6.2514	5.9044	0.9445
X	MeO	5.2183	4.8764	0.9345

The carbonium ion at the *γ*-position can be expected to be preponderant because of the hyperconjugation of the *para* substituents. Thus, the above assumption of the favored formation of angelica-lactone compounds by the preponderance of the carbonium ion at the *γ*-position seems to be reasonable.

Furthermore, in order to support this assumption, the Sr values for the nucleophilic reagent (Sr^N) of zwitter-ion-type intermediates from VII, X, XII, and XIII were calculated by means of the HMO method. These Sr^N values indicate the stability of the carbonium ion and its reactivity toward nucleophilic reagents. Thus, the ratios of the Sr^N for the *α*-position to that for the *γ*-position, $Sr^N(\alpha)/Sr^N(\gamma)$, which are listed in Table 3, are expected to be comparable with the production ratio between the angelica-lactone-type compound and the alcohol adduct. The $Sr^N(\alpha)/Sr^N(\gamma)$ ratio of VII is large, and that of X is small, while the yield of the angelica-lactone-type compound from VII was high and no angelica-lactone-type compound from X was detected. These results also supported the above assumption.

After all, the photoreaction mechanism of the *γ*-oxoacrylic acid system is concluded to be as is shown in Fig. 3. That is, *trans* acid is isomerized

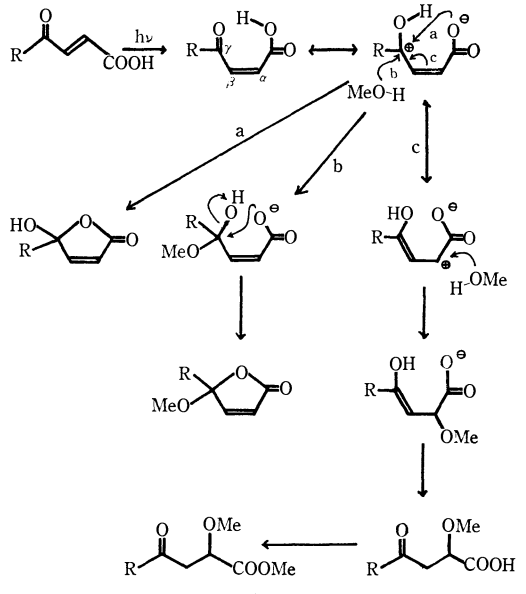

Fig. 3

to *cis* acid, which then undergoes protonation on γ-carbonyl oxygen through the seven-membered cyclic ring by means of intramolecular hydrogen bonding. By the protonation, the carboxyl group becomes the carboxylate anion and γ-carbon becomes the carbonium cation. In the case of β-aroylacrylic acids, this carbonium ion at the γ-position is dominated by the phenyl group and is attacked by the methanol molecule to give a hemiketal, which is then lactonized to 5-aryl-5-methoxy-2-oxo-2,5-dihydrofuran. At the same time, the carbon atom at the α-position can behave as a carbonium ion by means of resonance. The carbonium ion at the α-position is, then, attacked by a methanol molecule to give alcohol adducts. In the last step, the acid of the alcohol adduct is esterified.

In the case of β-acylacrylic acid, the carbonium ion at the γ-position is not stabilized and is attacked by the carboxylate anion. Thus, the production of 5-alkyl-5-hydroxy-2-oxo-2,5-dihydrofuran is also reasonable.

Experimental

Materials. *p*-Substituted *trans*-β-benzoylacrylic acids were prepared by the method of Papa.[4]

trans-β-Benzoylacrylic Acid (I). Mp 94—95.5°C (lit, 98—99°C). λ_{max}^{EtOH} (ε): 237 (10370), 268 (8080) and 357 nm (86). τ^{CDCl_3}: 1.31 (s, 1H), 2.05 (d, 1H), 1.8—2.7 (m, 5H) and 3.16 (d, 1H).

trans-β-(p-Ethylbenzoyl)acrylic Acid (II). Mp 104—106°C (lit, 105—106°C). λ_{max}^{EtOH} (ε): 233 (12460), 287 (10800) and 364 nm (125). τ^{CDCl_3}: 2.07 (d, 1H), 2.13 (d, 2H), 3.20 (d, 1H), 7.28 (q, 3H) and 8.67 (t, 2H).

trans-β-(p-Toluoyl)acrylic Acid (VII). Mp 137—139°C (lit, 137.5—138.5°C). λ_{max}^{EtOH} (ε): 237 (12300), 286.5 (11700) and 370 nm (104). τ^{CDCl_3}: 0.31 (s, 1H), 2.04 (d, 1H), 2.08 (d, 2H), 2.70 (d, 2H), 3.17 (d, 1H) and 7.53 (s, 3H).

trans-β-(p-Isopropylbenzoyl)acrylic Acid (VIII). Mp 100.5—102°C. λ_{max}^{EtOH} (ε): 234 (12700), 285.5 (11700) and 360 nm (127). τ^{CDCl_3}: 2.06 (d, 1H), 2.12 (d, 2H), 2.72 (d, 2H), 3.19 (d, 1H), 9.04 (sept, 1H) and 8.73 (d, 6H).

trans-β-(p-t-Butylbenzoyl)acrylic Acid (IX). Mp 122—124°C (lit, 123—125°C). λ_{max}^{EtOH} (ε): 234 (13200), 287 (12500) and 364 nm (124). τ^{CDCl_3}: 2.04 (d, 1H), 2.09 (d, 2H), 2.54 (d, 2H), 3.18 (d, 1H) and 8.64 (s, 9H).

trans-β-(p-Anisoyl)acrylic Acid (X). Mp 134°C (lit, 138—139°C). λ_{max}^{EtOH} (ε): 233 (17400) and 314 (13900). τ^{CDCl_3}: 1.60 (s, 1H), 2.01 (d, 1H), 2.01 (d, phenyl 2H), 3.07 (d, 1H), 3.18 (d, 1H) and 6.13 (s, 3H).

trans-β-(p-Ethoxybenzoyl)acrylic Acid (XI). Mp 142.5—145°C (lit, 145.5—146.5°C). λ_{max}^{EtOH} (ε): 235.5 (16800) and 315 nm (13200). τ^{CDCl_3}: 2.03 (d, 1H), 2.04 (d, 2H), 3.07 (d, 2H), 3.18 (d, 1H), 5.87 (q, 2H) and 8.55 (t, 3H).

trans-β-(p-Bromobenzoyl)acrylic Acid (XII). Mp 154—156°C (lit, 154—155°C). λ_{max}^{EtOH} (ε): 249 (10070), 278 (8390) and 362 nm (73). τ^{CDCl_3}: 2.06 (d, 2H), 2.17 (d, 1H), 2.54 (d, 2H) and 3.18 (d, 1H).

trans-β-(p-Chlorobenzoyl)acrylic Acid (XIII). Mp 157—159°C (lit, 159—160°C). λ_{max}^{EtOH} (ε): 230 (14500) and 282 nm (13000). τ^{CDCl_3}: 2.13 (d, 2H), 2.14 (d, 1H), 2.37 (d, 2H) and 3.26 (d, 1H).

Instrumentation. The infrared and ultraviolet spectra were recorded on a Hitachi EPI-2-type infrared spectrometer and a Hitachi EPS-3T-type spectrometer respectively. The NMR spectra were recorded on a Hitachi H-60 high-resolution NMR spectrometer, using TMS as the internal standard. A Taika 500-W hgih pressure mercury lamp was used as the irradiation source, and a Pyrex tube was used as the filter and reaction vessel in the reactions.

The Calculation of the Sr values by Means of the HMO Method. The Sr values in this work were calculated by means of the HMO method on a Hypac 103-type computer, using the following parameter:[5]

$$\alpha_x = \alpha + a\beta$$
$$\alpha_{adj} = \alpha + b\beta$$
$$\beta_{ex} = l\beta$$

X	*a*	*b*	*l*
OH	0.6	0	0.7
Me	3	−0.1	1
OMe	0.5	0	0.6
Br	1.4	0	0.7
Cl	1.8	0	0.8
C=O	1.3	0	1.1

Irradiation of *p*-Substituted *trans*-β-Benzoylacrylic Acid in Methanol. A solution of 1 g of *p*-substituted *trans*-β-benzoylacrylic acid in 20 m*l* of methanol in a Pyrex tube was irradiated at room temperature. After the reaction mixture had been worked up by the usual method, the yields of the products were estimated by the intensity of the NMR signals at τ 3.2 (d, olefinic proton of acrylic acid), 3.9 (d, α-olefinic proton of angelica lactone), 5.6 (t, methine proton of alcohol adducts), and 6.3 (s, ester methyl protons of the ester of the alcohol adducts). At the same time, the residue was methylated with diazomethane in ether. Then the reaction products were chromatographed on a silica-gel column with a benzene-ethyl acetate mixture.

Methyl β-(p-Ethylbenzoyl)-α-methoxypropionate (V). ν^{film}: 1745, 1675 and 1605 cm^{-1}. λ_{max}^{EtOH} (ε): 254.5 (17500) and 315.5 nm (117). τ^{CDCl_3}: 2.14 (d, 2H), 2.76 (d, 2H), 5.57 (t, 1H), 6.26 (s, 3H), 6.56 (s, 3H), 6.63 (d, 2H), 7.23 (q, 2H) and 8.78 (t, 3H).

Found: C, 67.18; H, 7.25%. Calcd for $C_{14}H_{18}O_4$: C, 67.18; H, 7.25%.

Methyl β-(p-Toluoyl)-α-methoxypropionate (XIV). ν^{film}: 1740, 1675, 1600 and 805 cm^{-1}. λ_{max}^{EtOH} (ε): 254 (19400), 290 (830) and 319 nm (107). τ^{CDCl_3}: 2.08 (d, 2H), 2.72 (d, 2H), 5.52 (t, 1H), 6.18 (s, 3H), 6.48 (s, 3H), 6.59 (d, 2H) and 7.56 (s, 3H).

Found: C, 65.86; H, 6.86%. Calcd for $C_{13}H_{16}O_4$:

5) a) L. E. Orgel, T. L. Cottrell, W. Dick and L. E. Sutton, *Trans. Faraday Soc.*, **47**, 113 (1951). b) H. H. Jaffé, *J. Chem. Phys.*, **20**, 279 (1952). c) A. Streiweisser, Jr., and P. M. Nair, "Conference of Hyperconjugation," Pergamon Press, London (1959).

C, 66.08; H, 6.83%.

Methyl β-(p-Isopropylbenzoyl)-α-methoxypropionate (XV). ν^{film}: 1755, 1685 and 1610 cm^{-1}. λ_{max}^{EtOH} (ε): 255 (20900) and 316 nm (123). τ^{CDCl_3}: 2.14 (d, 2H), 2.74 (d, 2H), 5.57 (t, 1H), 6.23 (s, 3H), 6.54 (s, 3H), 6.66 (d, 2H), 7.06 (sept, 1H) and 8.74 (d, 6H).

Found: C, 68.08; H, 7.67%. Calcd for $C_{15}H_{20}O_4$: C, 68.16; H, 7.63%.

Methyl β-(p-t-Butylbenzoyl)-α-methoxypropionate (XVI). ν^{film}: 1755, 1685 and 1610 cm^{-1}. λ_{max}^{EtOH} (ε): 254.5 (20000) and 315.5 nm (118). τ^{CDCl_3}: 2.13 (d, 2H), 2.57 (d, 2H), 5.57 (t, 1H), 6.24 (s, 3H), 6.56 (s, 3H). 6.66 (d, 2H) and 8.67 (s, 9H).

Found: C. 69.19; H. 8.07%. Calcd for $C_{16}H_{22}O_4$: C, 69.04; H, 7.97%.

Methyl β-(p-Anisoyl)-α-methoxypropionate (XVII). ν^{film}: 1760, 1685 and 1610 cm^{-1}. λ_{max}^{EtOH} (ε): 219 (6095) and 274 nm (9225). τ^{CDCl_3}: 2.03 (d, 2H), 3.09 (d, 2H), 5.57 (t, 1H), 6.16 (s, 3H), 6.22 (s, 3H), 6.68 (d, 2H) and 6.54 (s, 3H).

Found: C, 61.67; H, 6.58%. Calcd for $C_{13}H_{16}O_5$: C, 61.89; H, 6.39%.

Methyl β-(p-Ethoxybenzoyl)-α-methoxypropionate (XVIII). ν^{film}: 1750, 1675 and 1600 cm^{-1}. λ_{max}^{EtOH} (ε): 219 (11900) and 276 nm (18700). τ^{CDCl_3}: 2.14 (d, 2H), 3.14 (d, 2H), 5.58 (t, 1H), 5.94 (q, 2H), 6.25 (s, 3H), 6.59 (s, 3H), 6.67 (d, 2H) and 8.59 (t, 3H).

Found: C, 63.07; H, 6.96%. Calcd for $C_{14}H_{18}O_5$: C, 63.14; H, 6.81%.

Methyl β-(p-Bromobenzoyl)-α-methoxypropionate (XIX). ν^{film}: 1750, 1685, 1585 and 815 cm^{-1}. λ_{max}^{EtOH} (ε): 257 (20100) and 289.5 nm (944). τ^{CDCl_3}: 2.13 (d, 2H), 2.41 (d, 2H), 5.55 (t, 1H), 6.22 (s, 3H), 6.52 (s, 3H) and 6.63 (d, 2H).

Found: C, 48.01; H, 4.36%. Calcd for $C_{12}H_{13}O_4Br$: C, 47.85; H, 4.36%.

Methyl β-(p-Chlorobenzoyl)-α-methoxypropionate (XX). ν^{film}: 1745, 1685 and 1590 cm^{-1}. λ_{max}^{EtOH} (ε): 253.5 (19000) and 313 nm (89). τ^{CDCl_3}: 2.16 (d, 2H), 2.63 (d, 2H), 5.59 (t, 1H), 6.24 (s, 3H), 6.56 (s, 3H) and 6.66 (d, 2H).

Found: C, 56.09; H, 5.24%. Cacld for $C_{12}H_{13}O_4Cl$: C, 56.14; H, 5.11%.

5-(p-Ethylphenyl)-5-methoxy-2-oxo-2,5-dihydrofuran (III). ν^{film}: 1820, 1780, 1680 and 1605 cm^{-1}. λ_{max}^{EtOH} (ε): 243 nm (5000). τ^{CDCl_3}: 2.36—3.16 (m, 5H), 3.91 (d, 1H), 6.58 (s, 3H), 7.34 (q, 2H) and 8.77 (t, 3H).

Found: C, 71.57; H, 6.57%. Calcd for $C_{13}H_{14}O_3$: C, 69.88; H, 6.84%.

5-(p-Tolyl)-5-methoxy-2-oxo-2,5-dihdyrofuran (XXI). ν^{film}: 1810, 1775, 1670, 1610, 1200 and 815 cm^{-1}. λ_{max}^{EtOH} (ε): 203 (12000), 245 (5200), 263 (4100), 270 (3000) and 276 nm (3400). τ^{CDCl_3}: 2.61 (d, 2H), 2.68 (d, 1H), 2.79 (d, 2H), 3.86 (d, 1H), 6.64 (s, 3H) and 7.62 (s, 3H).

Found: C, 70.40; H, 5.89%. Calcd for $C_{12}H_{12}O_3$: C, 70.57; H, 5.92%.

A Kinetic Study of the Photoreaction of II. A solution of 250 mg of II in 5 m*l* of methanol was divided among 5 Pyrex tubes. These Pyrex tubes were then irradiated for 8, 24, 48, 72, and 96 hr respectively. The concentrations of III, II, IV, and V in each solution were estimated from the intensity of the NMR signals at τ 3.20 (d, olefinic proton of II), 3.91 (d, α-olefinic proton of III), 5.57 (t, methine proton of IV and V), and 6.26 (s, ester methyl protons of V). The results are plotted in Fig. 2.

The Dark Reaction of II in Methanol. A solution of 50 mg of II in 1 m*l* of methanol was left to stand in a dark place for 24 hr, this gave 12% of VI, which was identified by means of comparison with an authentic sample.

The Thermal Reaction of II in Methanol. A solution of 500 mg of II in 10 m*l* of methanol was refluxed for 24 hr, V and VI were thus obtained in 36 and 64% yields respectively.

The Irradiation of VI in Methanol. By irradiation for 120 hr through a Pyrex filter, a solution of 30 mg of VI in 1 m*l* of methanol gave 87% methyl *cis-β-*(*p*-ethylbenzoyl)acrylate.

However VI was recovered when the solution was refluxed for 24 hr in methanol.

The Reaction of III in Methanol. When irradiated for 96 hr through a Pyrex filter, or when refluxed for 24 hr, a solution of 30 mg of III in methanol was not changed.

We wish to thank Dr. O. Kikuchi, Department of Chemistry, Tokyo Kyoiku University, for kindly discussion of the calculations with us.

BULLETIN OF THE CHEMICAL SOCIETY OF JAPAN VOL. 43 1478—1484 (1970)

The Insertion Reaction of Isoprene into Metal-Ethyl Bonds in Various Transition-Metal Salt-Ethylaluminum Compound System

Yoshinobu TAKEGAMI, Toshimitsu SUZUKI and Takashi SHIRAI

Department of Hydrocarbon Chemistry, Faculty of Engineering, Kyoto University, Sakyo-ku, Kyoto

(Received October 3, 1969)

The insertion reaction of isoprene into metal-ethyl bonds in various transition-metal salt (VCl_4, $Fe(AA)_3$, $Co(AA)_2$, $CoCl_2$, $Ni(AA)_2$, or $NiCl_2$-ethylaluminum compound ($AlEt_2Cl$ or $AlEt_3$)) catalyst systems was studied. With the vanadium and the nickel catalysts, 2-methyl-2-hexene and 2-methyl-1-hexene were mainly formed by the methanolysis of the reaction mixture, showing that metal alkenyls, M–C(C)–C=C–C–Et and C=C(M)–C–C–Et respectively, are formed in the reaction system. However, in the iron catalyst, only 2-methyl-2,5-hexadiene and 3-methyl-2,5-hexadiene were formed from M–C(C)–C–C–C=C and M–C–C–C–C(C)=C–C respectively by the elimination reaction. These results suggest that the stability of metal alkenyls decreases in the order: V≫Ni>Co>Fe.

In a previous paper,[1] the insertion reactions of isoprene into metal-ethyl bonds in the $TiCl_4$-$AlEt_3$ catalyst system were studied, and the relation between the insertion products and the mechanism of the polymerization was discussed.

In the case of a Ziegler-type catalyst, it has been reported[2] that the micro structure of the polymer obtained was affected by the species of the transition metal compound and the organometallic compound. However, up to now the insertion processes of isoprene into a metal-carbon bond in a Ziegler-type catalyst system does not seem to have been discussed sufficiently.

The insertion processes of isoprene into metal-ethyl bonds may be formulated as follows:

1,4-addition:

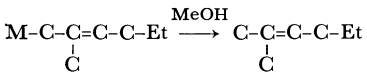

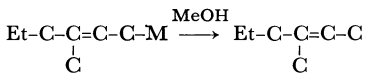

3,4-addition:

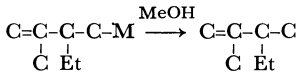

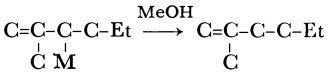

1,2-addition:

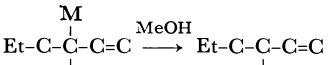

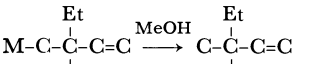

As has been reported in a previous paper,[1] isoprene inserts into metal-ethyl bonds in the $TiCl_4$-$AlEt_3$ catalyst system to give three metal alkenyls, I_m, III_m, and IV_m. In this paper, the insertion reaction of isoprene into metal-ethyl bonds in various transition-metal salt-ethylaluminum systems will be examined in order to establish the influence exerted by the species of the transition-metal compounds.

Experimental

Materials. The ethyl aluminum compounds were obtained from the Ethyl Corporation and were used without further purification.

The isoprene was distilled, deoxygenated by the freeze-thaw method with pumping, and later stored over calcium hydride. The solvent, toluene, was dried over sodium and distilled just before use.

The other reagents used were commercially-available materials.

1) Y. Takegami, T. Suzuki and T. Okazaki, *Kogyo Kagaku Zasshi*, **62**, 195 (1967).

2) C. E. H. Bawn and A. Ledwith, *Quart. Rev.*, **16**, 361 (1962).

Reaction Procedure. A three-necked flask (30 m*l*) was equipped with a magnetic stirrer, a gas inlet, a self-sealing rubber cap, and a gas outlet connected to a mercury manometer and a vacuum system. The gas inlet was connected with a line for argon. Certain amounts of a transition-metal salt, a solvent (toluene), an internal standard (methylcyclohexane), and an ethylaluminum compound were added, in this order, to the reaction flask in an atmosphere of dry argon. The catalyst mixture was aged for five minutes at a certain temperature, and then isoprene (10 mmol) was introduced to start the reaction. After a certain time, the reaction was stopped by adding an excess of methanol containing 10% hydrochloric acid to the reaction mixture. By this treatment the metal alkenyls formed in the system were converted to the corresponding olefinic hydrocarbons. The polymers, if formed. were filtered off, and the organic filtrate was subjected to gas-chromatographic analysis.

A Hitachi model-F6D gas-liquid chromatograph equipped with a hydrogen-flame ionization detector was employed for the quantitative and qualitative analyses of the products. The operating conditions are presented below:

Column	Golay Z45 (SE30)	Golay R45 (PEG)
Size	0.5 mmϕ × 45 m	0.25 mm × 45 m
Temperature	40°C	50°C
Carrier N_2	0.4 kg/cm^2	0.4 kg/cm^2
Sample size	2 μl	10 μl

Identification of the Products. As standard samples, three C_7 monoolefins, I, III, and IV, were obtained.[1] The isomerization products of 2-methyl-1,5-hexadiene and 3-methyl-1,5-hexadiene were also used for the identification of the C_7 diolefins. This isomerization reaction was carried out with the $Co(AA)_2$-$AlEt_3$ catalyst system.

In the VCl_4-$AlEt_3$ $AlEt_2Cl$ catalyst system, two products were found; they were identified as I and IV by gas-chromatographic analysis.

In the $Fe(AA)_3$ catalyst, two new products, VII and VIII, were found. The structural estimation of VII and VIII was carried out by gas chromatography as follows: a) The relative retention times of VII and VIII in the gas chromatogram were determined (Table 1) and found not to agree with those of the possible monoolefins (I—VI). With the Golay Z-45 column, the relative retention times of VII and VIII were between those of IV and I, but with the Golay R-45 column, those of VII and VIII were larger than those of IV and I.*1 b) After the hydrogenation of the reaction mix-

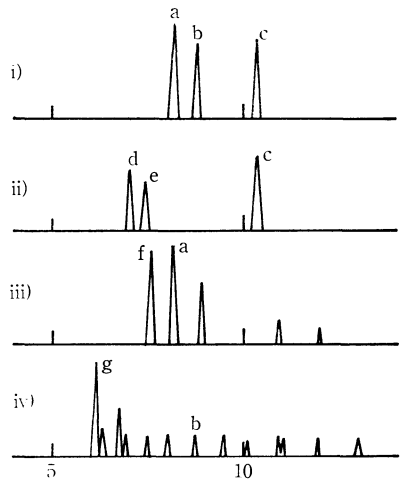

Fig. 1. Retention times of the products in the gas chromatogram.
i) The reaction products in the $Fe(AA)_3$-$AlEt_3$ catalyst system, ii) The hydrogenation products of i), iii) The isomerization products of 2-methyl-1,5-hexadiene, iv) The isomerization products of 3-methyl-1,5-hexadiene
a) 2-methyl-2,5-hexadiene, b) 3-methyl-2,5-hexadiene, c) methylcyclohexane, d) 2-methylhexane, e) 3-methylhexane, f) 2-methyl-1,5-hexadiene, g) 3-methyl-1,5-hexadiene

Table 1 Relative retention times of the products

Product	Bp (°C)	Relative retention times	
		Golay Z 45(40°C)	Golay R 45(50°C)
III=2,3-Dimethyl-1-pentene	84.3	0.66	0.84
2-Methylhexane	90.1	0.68	—
3-Methylhexane	91.9	0.73	—
XI=3-Methylhexadiene	—	0.75	0.90
IV=2-Methyl-1-hexene	92.0	0.78	0.91
VII=2-Methyl-2,5-hexadiene	91—92.5	0.80	0.95
VIII=3-Methyl-2,5-hexadiene	92.1—92.3[a]	0.83	0.98
I=2-Methyl-2-hexene	95.4	0.87	0.94
XII=3-Methylhexadiene	—	0.91	0.97
Methylcyclohexane	100.9	1.00	1.00
IX=3-Methylhexadiene	—	1.06	1.13
X=2-Methylhexadiene	—	1.13	1.18

a) at 752 mmHg

*1 Usually in the Golay R45 column a more polar substance elutes later than a less polar substance.

ture, the peaks of VII and VIII in the gas chromatogram disappeared and those of 2-methylhexane and 3-methylhexane appeared. The relative concentrations of VII and VIII were compared to those of the hydrogenation products, 2-methylhexane and 3-methylhexane (Fig. 1). c) The gas chromatogram of VII and VIII was compared with that of the isomerization products of 2-methyl-1,5-hexadiene or 3-methyl-1,5-hexadiene (Fig. 1). d) According to the literature[3] 2-methyl-2,5-hexadiene and 3-methyl 2,5-hexadiene were synthesized; the gas chromatograms of VII and VIII coincided with those of synthesized samples. From these analyses, and from the relation between the boiling point and the relative retention time, the structures of VII and VIII are considered to be 2-methyl-2,5-hexadiene and 3-methyl-2,5-hexadiene respectively.*2

In the cobalt catalyst, seven products were found; they were identified as I, IV, VII, 3-methylhexadienes (IX, XI, and XII), and 2-methylhexadiene (X) by the same method described above.*3 From their boiling points, IX and X seemed to be conjugated diolenfins.

The nickel catalyst gave four products, I, IV, XI, and XII.

The zirconium, the niobium, and the chronium catalysts gave two products, I and IV.

Results and Discussion

VCl_4-$AlEt_3$ or $AlEt_2Cl$ System. The results are summarized in Table 2 and Fig. 2. The catalyst system immediately became brown-black and homogeneous when $AlEt_3$ or $AlEt_2Cl$ was added to the VCl_4 solution. In this system, 2-methyl-2-hexene (I) and 2-methyl-1-hexene (IV) were formed, showing that two metal alkenyls, I_m and IV_m, are

TABLE 2 VCl_4-ALKYLALUMINUM SYSTEM[a]

Alkyl-aluminum	Temp. (°C)	Time (min)	Products (mol% of VCl_4) IV	I
$AlEt_2Cl$	−70	8	13.7	1.1
	−70	30	12.6	2.8
	−70	60	4.9	1.6
	−30	30	14.4	1.3
	0	30	4.8	2.4
$AlEt_3$	−70	6	4.2	6.0
	−70	30	4.5	3.5
	−70	90	3.3	2.7
	−30	30	2.5	6.0
	0	30	2.8	10.8

a) VCl_4: 1.0 mmol, Alkyl aluminum: 3.0 mmol, Toluene: 10 ml, Isoprene: 10 mmol, Catalyst was aged at −70°C for 5 min.

3) M. Iwamoto, Doctral thesis, to Kyoto University.

*2 These diolefins are considered to be elimination-reaction products from the metal alkenyls in the reaction system, as will be discussed below.

*3 The structures of the IX—XII diolefins could not be identified more precisely.

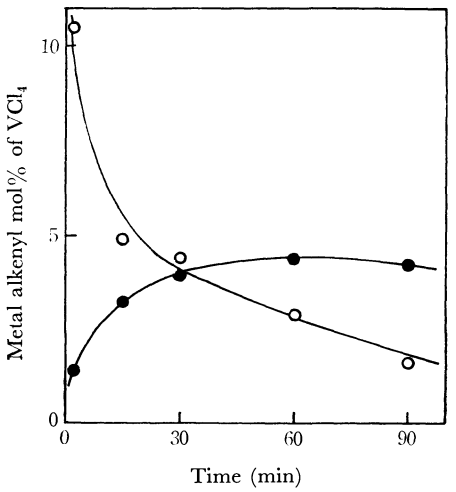

Fig. 2. Isomerization of metal alkenyl with the VCl_4-$AlEt_2Cl$ catalyst system.
Insertion reaction was carried out at −30°C for 10 min, then isoprene remained in the reaction system was pumped off and the reaction system was allowed to stand at 0°C.
○: C=C–C–Et (IV_m) ●: M–C–C=C–C–Et (I_m)
C M C

formed. The amounts of these products reached maxima at an early stage and thereafter gradually decreased with an increase in the reaction time.

With $AlEt_2Cl$, IV was predominant; this tendency was the more remarkable the lower the temperature. On the other hand, with $AlEt_3$, I was predominant; this tendency was the more remarkable the higher the temperature. Figure 2 shows that IV_m readily isomerizes to I_m at 0°C. This may show that an easy transformation of the $\sigma \rightarrow \pi \rightarrow \sigma$ allyl type has occurred. These results suggest that a lower valence state of vanadium is more favorable for the formation of I_m, and that at lower temperatures IV_m is stable, while at higher temperatures IV_m readily isomerizes to I_m. A small amount of a sticky polymer was always formed. In the vanadium catalyst,

TABLE 3 $Fe(AA)_3$-$AlEt_3$ SYSTEM[a]

Al/Fe	Reaction Temp. (°C)	Time (min)	Products (mol% of $Fe(AA)_3$) VII	VIII
1.0	30	10	2.4	1.7
1.0	30	60	11.5	8.4
1.0	30	120	15.7	11.2
2.0	30	60	8.2	5.3
2.0	0	60	2.0	1.0
5.0	30	120	0	0
2.0[b]	30	120	0	0

a) Aging temperature: the same temperature as reaction temperature Aging time: 5 min
$Fe(AA)_3$: 1.5 mmol
b) $AlEt_2Cl$

the mode of the insertion reaction was almost the same as that in the titanium catalyst reported on previously.[1]

$Fe(AA)_3$-$AlEt_3$ or $AlEt_2Cl$ System. The results are summarized in Table 3. The catalyst system immediately became brown-black and homogeneous when $AlEt_3$ was added. However, when $AlEt_2Cl$ was added it immediately became dark brown ($AlEt_2Cl/Fe(AA)_3=2$) or milk white ($AlEt_2Cl/Fe(AA)_3=5$) and heterogeneous.

In the case of $AlEt_3$, 2-methyl-2,5-hexadiene (VII) and 3-methyl-2,5-hexadiene (VIII) were formed. On the other hand, no monoolefins was detected in this system. These results suggest that, in the reaction system, the metal alkyls and/or alkenyls are not stable and that diolefins are formed.

One possible process for the formation of the diolefins from the metal alkenyls (I_m—VI_m) is a β-hydrogen transfer of them, with or without a hydride shift. However, this process is considered to give only conjugated and/or allene-type diolefins. Therefore, the selective formation of the isolated diolefins, VII and VIII, cannot be explained in terms of this process.

Hata[4] and Iwamoto[3] have reported that isoprene is co-dimerized with ethylene by the $Fe(AA)_3$-$AlEt_3$ catalyst system under a high pressure of ethylene to give 2-methyl-2,5-hexadiene and 3-methyl-2,5-hexadiene, and that this co-dimerization reaction is probably carried out by the metal hydride. The results obtained in this study are analogous to those obtained by them. However, in this study, even when the gaseous products in the aged mixture were pumped off (−70°C, 15 mmHg, 1 hr), VII and VIII were formed (0.030 and 0.017 mol/mol Fe), shownig that the ethylene is supplied by the iron and/or aluminum complexes having an ethyl bond. From these results, the process of the selective formation of VII and VIII may be formulated as follows:

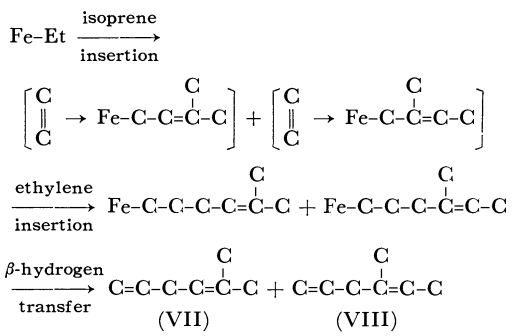

This insertion reaction is quite different from that in the VCl_4 catalyst.

With $AlEt_2Cl$, no products were detected. This may be because iron-ethyl bonds are not formed in this system, judging from the extraordinary color change.

As for the polymer, it was not formed in every case.

$Co(AA)_2$ or $CoCl_2$-$AlEt_3$ or $AlEt_2Cl$ System. The results are summarized in Table 4. The catalyst system became, either immediately ($Co(AA)_2$) or gradually ($CoCl_2$), brown-black and almost homogeneous when either $AlEt_3$ or $AlEt_2Cl$ was added.

With $AlEt_3$, the I and IV monoolefins and the VII, IX, X, XI, and XII diolefins were formed. The monoolefins are considered to be formed much as in the VCl_4 catalyst. For the formation of these diolefins, two processes are reasonable since, in this case, two conjugated diolefins, IX and X, were also formed. The process which forms the non-conjugated diolefins is the same as in the case of the $Fe(AA)_3$ catalyst. The other process, that which forms the conjugated diolefins, is a β-hydrogen transfer of the metal alkenyls (I_m-VI_m) with or without a hydride shift of them. Therefore, IX and X may be formed by the elimina-

Table 4. Co(AA) $CoCl_2$-$AlEt_3$ system[a]

Co salts mmol		Al/Co	Reaction temp. (°C)	Products (mol% of Co salt)						
				XI	IV	VII	I	XII	IX	X
$Co(AA)_2$	1.5	1.0	30[c]	0.4	0.4	1.3	0.6	0	0	1.6
	1.5	1.0	30	1.6	1.0	4.7	1.1	0	0.9	5.2
	1.5	1.0	30[d]	2.0	1.1	5.3	1.2	0.4	0.5	4.9
	1.5	2.0	30	0	0.4	0.7	1.5	0	0.5	1.0
	1.5	2.0	0[d]	0	0.5	0.4	2.2	0	0.6	1.9
	1.5	2.0[b]	30	0	0	0	0	0	0	0
$CoCl_2$	1.3	2.0	30	0	0	0	0	0	9.0	7.7
	1.5	2.0	0	0	0	0	0.3	0	0.8	1.0

a) The conditions are same as in Table 3, Reaction time: 60 min
b) $AlEt_2Cl$. c) Reaction time: 10 min. d) Reaction time: 120 min

4) G. Hata, *J. Amer. Chem. Soc.*, **86**, 3903 (1964).

TABLE 5 $Ni(AA)_2$ or $NiCl_2$-ALKYLALUMINUN SYSTEM[a]

Ni salt	Al/Ni		Reaction Temp. (°C)	Products (mol% of Ni salt) XI	IV	I	XII
$Ni(AA)_2$	1.0	$AlEt_3$	30[b]	0	1.1	1.1	0
	1.0		30	0	2.0	2.2	0
	1.0		30[c]	0	3.5	4.6	0
	2.0		30	0	1.0	1.1	0
	2.0		0	0.8	1.8	1.4	0
	2.0	$AlEt_2Cl$	30	0	1.7	3.2	0
	2.0		0	0	0.5	1.4	0
	5.0		30	0	0	0	0
$NiCl_2$	2.0	$AlEt_3$	30	0	0	0	0
	2.0		0[c]	0.4	0.3	2.6	1.0

a) The conditions are same as in Table 3, Reaction time: 60 min, Ni salt: 1.5 mmol.
b) Reaction time: 10 min. c) Reaction time: 120 min

tion reaction from II_m or V_m, and from I_m or IV_m, respectively.

Especially in the case of the $CoCl_2$ catalyst, the conjugated diolefins, IX and X, were selectively formed at the reaction temperature of 30°C. This result was quite different from that in the $Co(AA)_2$ catalyst, in which the I and IV monoolefins and the VII, XI, and XII diolefins were also formed. This may suggest that, in the $Co(AA)_2$ catalyst, the high reactivity of the metal alkenyls for the isomerization reaction give various products.

A very small amount of an oily yellow polymer was formed in several cases.

On the other hand, with $AlEt_2Cl$, no product was detected.

$Ni(AA)_2$ or $NiCl_2$-$AlEt_3$ or $AlEt_2Cl$ System. The results are summarized in Table 5. The catalyst system immediately became brown-black and homogeneous when either $AlEt_3$ or $AlEt_2Cl$ was added except in the case of $AlEt_2Cl$ ($AlEt_2Cl/Ni(AA)_2=2$), in which it immediately became dark green and homogeneous.

In this system, the I and IV monoolefins and the XI and XII diolefins were formed, with the monoolefins the main products in every case. Therefore, in this system, the metal alkenyls, I_m and IV_m, may be rather stable, as in the case of a titanium or vanadium catalyst.

A very small amount of an oily yellow polymer was formed in several cases.

Even with $AlEt_2Cl$, the I and IV monoolefins were formed at the $AlEt_2Cl/Ni(AA)_2$ molar ratio of 2. This result is different from that in the $Fe(AA)_3$ or the $Co(AA)_2$ catalyst.

The results obtained from the variation in the $AlEt_3/M(AA)_n$ ($M(AA)_n$: $Fe(AA)_3$, $Co(AA)_2$, or $Ni(AA)_2$) molar ratio showed that the amount of metal-ethyl bonds (or metal-hydrogen bonds) reaches a maximum at the molar ratio of a unit. This suggests that, with an increase in the $AlEt_3/M(AA)_n$ molar ratio, the valence state of transition metal is reduced to metal(0) and that the

TABLE 6. SEVERAL TRANSITION-METAL SALT-$AlEt_3$ SYSTEMS[a]

Transition-metal salt	mmol	Al/MX_n[d]	Reaction Temp (°C)	Time(min)	Products (mol% of MX_n) IV	I
$ZrCl_4$[b]	3.9	1	30	100	1.3	0.9
$ZrCl_4$[b]	4.0	1	0	100	0.2	0.1
$ZrCl_4$[b]	3.7	1	−30	150	0	0
$NbCl_5$[c]	3.4	1	30	60	0.2	0.3
$NbCl_5$[c]	3.3	1	0	60	0.7	0.6
$Cr(AA)_3$	1.5	2	30	60	0.1	0.1
$CrCl_3$	1.3	2	30	60	0	0.7
$CrCl_2$	1.5	2	30	60	0	0
$Mn(AA)_2$	1.5	2	0	120	0	0

a) The conditions are same as in Table 3
b) Aging temperature: 30°C, Aging time: 1 hr
c) Aging time: 15 min
d) $AlEt_3$/transition-metal salt molar ratio

amount of the metal-ethyl bonds effective for isoprene insertion decreases. The amount of the products in these systems gradually increased over the reaction time of 120 min, as is shown in Tables 3, 4, and 5.

Others. In the $ZrCl_4$-$AlEt_3$ catalyst system, the catalyst mixture remained heterogeneous; the liquid phase was dark brown, and the solid phase, dark orange.

In this system small amounts of monoolefins, I and IV, were formed. Increases in their amounts were observed when the reaction temperature was made higher.

The catalyst mixture became almost homogeneous after it had been aged for *ca.* 2 hr at 50°C, but when isoprene was introduced into the heterogeneous catalyst mixture at 30°C it became homogeneous and brown-red after 20 min. This shows that the state of the catalyst mixture was changed by adding isoprene. No such behavior was observed in the other systems, perhaps indicating the formation of a new complex participated with isoprene, but no further study was made.

In the $NbCl_5$-$AlEt_3$ catalyst system, the catalyst system became brown-black and homogeneous when $AlEt_3$ was added. In this system, small amounts of I and IV were formed.

In the $Cr(AA)_3$-$AlEt_3$ system, the aged mixture became brown-black and homogeneous, but in the $CrCl_3$ or $CrCl_2$-$AlEt_3$ system, the violet solid phase of $CrCl_3$ or $CrCl_2$ itself remained. In the $Cr(AA)_3$-$AlEt_3$ system, the I and IV monoolefins were formed, but they were present in very small amounts. Kapur *et al.*[5] have reported that the maximum activity of the $Cr(AA)_3$-$AlEt_3$ catalyst system in isoprene polymerization is obtained beyond the molar ratio of 4. In view of this, the insertion reaction was also carried out at the molar ratio of 5; the amounts of the monoolefins thereupon increased slightly. In the $CrCl_3$-$AlEt_3$ system, a small amount of I was formed, but in the $CrCl_2$-$AlEt_3$ system, no products were detected.

In the $Mn(AA)_2$-$AlEt_3$ system, the aged mixture became light brown but remained heterogeneous. In this system, no products were detected, either.

In the zirconium and niobium catalysts, a small amount of a sticky polymer was formed, but in the other systems no polymer was formed.

On the other hand, with $AlEt_2Cl$, no products at all were detected in these systems.

The Effects of Additives. The effects of the addition of a Lewis base to the several catalyst systems studied above were also examined. The catalyst mixture was prepared by adding materials in the following order: a transition-metal salt, a base, a solvent (toluene), an internal standard (methylcyclohexane), and an ethylaluminum compound. The state of the aged mixture was almost the same as that without an additive in every case.

Zambelli *et al.*[6] have reported that, in the polymerization of propylene to a syndiotactic polymer, the addition of a Lewis base such as anisole to the VCl_4-$AlEt_2Cl$ catalyst system (anisole/VCl_4 molar ratio = 1—2) makes the catalyst mixture active. The effect of the addition of anisole on the insertion reaction in this catalyst system was examined. The amounts of I and IV increased at the temperature of −70°C, but quite substantially decreased at 0°C. These findings agree with that obtained by Zambelli *et al.*[6]; the catalyst mixture is stable at temperatures lower than −40°C.

Misono *et al.*[7-9] have reported that a stable

Table 7. Effect of additives[a]

MX_n	Base	Base/MX_n[d]	Products (mol% of MX_n)							
			XI	IV	VII	VIII	I	XII	IX	X
VCl_4[b]	anisole	1.0	0	15.4	0	0	1.8	0	0	0
VCl_4[c]	anisole	1.0	0	1.4	0	0	0.4	0	0	0
$Fe(AA)_3$	PPh_3	1.0	0	1.0	0.4	0.7	0	0	0	0
$Fe(AA)_3$	$P(n\text{-}Bu)_3$	1.0	0	1.2	1.8	2.1	0	0	0	0
$Fe(AA)_3$	dipyridyl	0.5	0	0	26.1	28.2	4.2	0	1.2	0
$Co(AA)_2$	dipyridyl	0.5	0.1	2.5	0.6	0	1.5	0.1	0.6	0.8
$Ni(AA)_2$	dipyridyl	0.5	0.3	1.4	0	0	1.6	0.5	0	0

a) The conditions are same as in Table 3, Reaction temperature: 30°C Reaction time: 120 min M(AA): 1.5 mmol $AlEt_3$/M(AA) molar ratio: 2.0
b)c) Aging temperature: −70°C Aging time: 5 min VCl_4: 1.0 mmol $AlEt_2Cl/VCl_4$ molar ratio: 3.0
b) Reaction temperature: −70°C Reaction time: 30 min
c) Reaction temperature: 0°C Reaction time: 30 min
d) Base/transition-metal salt molar ratio

5) A. B. Deshpande, R. V. Subramanian and S. L. Kapur, *J. Polym. Sci.*, **A 5**, 761 (1967).
6) A. Zambelli, G. Natta and I. Pasquon, *ibid.*, **C 4**, 411 (1964).
7) T. Saito, Y. Uchida, A. Misono, A. Yamamoto, K. Morifuji and S. Ikeda, *J. Organometal. Chem.*, **6**, 572 (1966).
8) T. Saito, Y. Uchida, A. Misono, A. Yamamoto, K. Morifuji and S. Ikeda, *J. Amer. Chem. Soc.*, **88**, 5198 (1966).
9) A. Yamamoto, K. Morifuji, S. Ikeda, T. Saito, Y. Uchida and A. Misono, *ibid.*, **90**, 1878 (1968).

complex with a metal-ethyl bond can be isolated by adding α,α′-dipyridyl to the metal acetylacetonate (metal: Fe, Co, or Ni)-diethylaluminum monoethoxide system. The effects of the addition of α,α′-dipyridyl on the insertion reaction in the Fe(AA)$_3$, Co(AA)$_2$, or Ni(AA)$_2$-AlEt$_3$ catalyst system were also examined. In the iron catalyst, the amounts of VII and VIII increased markedly and XI were newly formed. This may be explained as follows: a) The amount of iron-ethyl bonds (or iron-hydrogen bonds) is increased by the α,α′-dipyridyl. b) The iron-ethyl bonds are slightly stabilized by the α,α′-dipyridyl and the monoolefin (I) is formed by the methanolysis of the corresponding metal alkenyl (I$_m$), which is also stabilized. On the other hand, the effects of the addition of α,α′-dipyridyl were not so pronounced for the cobalt or the nickel system. The difference between Fe and Co or Ni is considered to be due partly to the difference in their valence states.

The effects of the addition of PPh_3 or $P(n\text{-}C_4H_9)_3$ to the Fe(AA)$_3$-AlEt$_3$ catalyst system were also examined. In both cases, the amounts of VII and VIII decreased and IV was newly formed. This result indicates that PPh_3 and $P(n\text{-}C_4H_9)_3$ are more strongly coordinated to metal than α,α′-dipyridyl; therefore, it becomes difficult for the insertion reaction itself to occur, but the iron-ethyl bonds are rather stabilized and the monoolefin (IV) is formed.

From the above results, it can be concluded that the stabilities of the metal alkenyls formed by the insertion reaction decrease in the following order: Ti≅V$\gg$Ni$>$Co$>$Fe.

BULLETIN OF THE CHEMICAL SOCIETY OF JAPAN VOL. 43 1484—1489 (1970)

The Insertion Reactions of Olefins into Metal-Ethyl Bonds in the Vanadium Compounds-Ethyl Aluminum Ziegler Catalyst System. A Proposed Mechanism for the Syndiotactic Polymerization of α-Olefin

Toshimitsu SUZUKI and Yoshinobu TAKEGAMI

Department of Hydrocarbon Chemistry, Faculty of Engineering, Kyoto University, Kyoto

(Received October 21, 1969)

In order to clarify the mechanism of the syndiotactic polymerization of olefin, the insertion reaction of several olefins into metal-ethyl bonds in VCl_4-$AlEt_nCl_{3-n}$, $VOCl_3$-$AlEt_nCl_{3-n}$, and $V(AA)_3$-$AlEt_nCl_{3-n}$ systems were studied. Cyclohexene was easily inserted into metal-ethyl bonds in these catalysts to give a metal-ethylcyclohexyl bond at -70°C. Pentene-1 and 4-methylpentene-1 gave M–C–C–Et (I) and M–C–C–Et (II). At -70°C with VCl_4-$AlEt_2Cl$, where the syndiotactic polymerization of propylene proceeds, four times as much (II) as (I) was obtained. However, at 0°C or in the VCl_4-$AlEt_3$ catalyst system, the amount of (I) exceeded the amount of (II). With the $VOCl_3$-$AlEt_nCl_{3-n}$ or the $V(AA)_3$-$AlEt_3Cl_{3-n}$ system, the selectivity for the formation of metal-alkyl (II) was decreased. The above results lead to the conclusion that, in the course of syndiotactic polymerization, the secondary metal-alkyl bond (II) was an intermediate of the polymerization. By means of this mechanism every experimental result reported can be explained without difficulty.

A hypothesis for the mechanism of the syndiotactic polymerization of α-olefin was presented in a previous communication,[1] this hypothesis was based on the results of the insertion reactions of pentene-1 into metal-ethyl bonds in the VCl_4-$AlEt_2Cl$ catalyst system. In this paper, in order to generalize the hypothesis, the present authors will study the mode of the insertion reactions of several olefins into metal-ethyl bonds in various Ziegler-type catalysts containing certain vanadium compounds. Vanadium catalysts are known to be syndiospecific catalysts for propylene at low temperatures[2] and as good copolymerization catalysts for ethylene and propylene, producing random copolymers.[3] However,

1) Y. Takegami and T. Suzuki, This Bulletin, **42**, 848 (1969).

2) G. Natta, I. Pasquon and A. Zambelli, *J. Amer. Chem. Soc.*, **84**, 1488 (1962).

3) G. Natta, G. Mazzanti, A. Volvassori and G. Pajaro, *Chim. Ind.*, Milan), **39**, 733 (1957).

the reason for or the mechanism of the special properties of these catalyst systems has not yet been clarified.

Boor and Youngman[4] have suggested a mechanism for the syndiotactic polymerization of propylene, a mechanism in which the polymerization proceeds *via* a coordinate anionic mechanism and in which the steric interaction between substituents of the last-added monomer and the new monomer units plays a very important role in the stereo regulation. However, in this mechanism, in contrast to the isotactic polymerization, the necessity for the syndiotactic configuration is not satisfied.

Recently Zambelli *et al.*[5] have investigated the mode of the double-bond opening of deutero propylene in the course of the syndiotactic polymerization, and have demonstrated that the opening of the double-bond is *cis*, as in the case of the isotactic polymerization with the Natta catalyst.[6] They have also[7] suggested the use of bimetallic catalytic species for the polymerization.

In the course of the isotactic polymerization with a titanium catalyst ($TiCl_3$-$AlEt_3$), a primary metal-alkyl bond was predominantly formed as an insertion product of an α-olefin into metal-ethyl bonds in the catalyst.[8] It can be concluded that the primary metal-alkyl is the intermediate of the isotactic polymerization.

Experimental

Materials. Commercial vanadium tetrachloride and vanadium oxytrichloride were used without further purification and were diluted with olefin-free *n*-octane. Vanadium(III) acetylacetonate ($V(AA)_3$) was synthesized from VCl_3 and acetylacetone under a stream of dry NH_3 and was sublimed under reduced pressure; it was produced as a greenish-brown powder. Toluene, ethylbenzene, and *n*-octane were purified by distillation over dispersion sodium under an argon atmosphere. Commercial pentene-1 and 4-methylpentene-1 were dried by means of calcium hydride, and their purity was determined by gas chromatography.

Procedure. A three-necked flask equipped with a magnetic stirrer, a gas inlet, a gas outlet connected to an argon line and a vacuum line, and a self-sealing rubber cap was flushed with argon, and then a solvent, vanadium salt, an olefin, and an alkyl aluminum were introduced (in this order) at the reaction temperature. After a certain reaction time the reaction mixture was taken off with the use of a hypodermic syringe, quenched with cold methanolic hydrochloric acid, and washed with cold water to remove any methanol and hydrochrolic acid. The metal alkyls thus formed in the catalytic system were converted to the corresponding hydrocarbons and gas chromatographed.

A Hitachi model F6D gas liquid chromatograph with a Golay Z45 and an R45 column was employed for the qualitative and quantitative analyses.

Results and Discussion

Cyclohexene. It is well known that this olefin is not homopolymerized with a Ziegler-Natta-type catalyst, but, as has been shown in previous papers,[9] the insertion reaction into metal-ethyl bonds in the catalyst occurred and the amount of the insertion product is correlated with the amount of the metal-ethyl bond in the catalyst system.

To estimate the amount of the metal-ethyl bond in the vanadium catalyst, cyclohexene was reacted with the VCl_4-$AlEt_nCl_{3-n}$ catalyst system at various temperatures. The results are summarized in Table 1. The results show that, at −70°C, a relatively large amount of ethylcyclohexane was obtained; in the titanium catalyst systems, on the other hand, below 0°C a very small amount of ethylcyclohexane was obtained.*1

Table 1. Insertion reaction of cyclohexene in VCl_4-$AlEt_nCl_{3-n}$

AlR_3	Reaction Temp. (°C)	Reaction Time (min)	Et⟨H⟩ (mmol)	Remarks
$AlEt_2Cl$	−70	120	0.010	anisole 1.0 mmol added
		240	0.021	
		360	0.009	
	−70	60	0.091	
		120	0.124	
		240	0.082	
		360	0.027	
	−30	60	0.089	
	0	60	0.091	
$AlEt_3$	−70	60	0.040	
	0	60	0.095	
	30	60	0.146	

VCl_4 1.0 mmol solvent (*n*-heptane 15 ml)
AlR_3 3.0 mmol cyclohexene 10 mmol

In contrast to the titanium system, the amount of ethylcyclohexane was slightly affected by the reaction time, and it rather decreased with an increase in the reaction time. This may show that, in this catalyst, the formation of the metal-ethyl bond is very rapid at −70°C and that this metal-ethyl bond is very reactive toward the insertion reactions of an olefin. As the elimination of ethylcyclohexene or other decomposition products from metal-ethyl-cyclohexyl bond was not observed, the decrease in

4) J. Boor, Jr., and E. A. Youngman, *J. Polym. Sci., Part A-1*, **4**, 1861 (1966).
5) A. Zambelli, M. Giongo and G. Natta, *Makromol. Chem.*, **112**, 183 (1968).
6) T. Miyazawa and T. Ideguchi, *J. Polym. Sci., Part B-1*, 389 (1963).
7) A. Zambelli, I. Pasquon, R. Signorini and G. Natta, *Makromol. Chem.*, **112**, 160 (1968).
8) Y. Takegami, T. Suzuki and T. Okazaki, This Bulletin, **42**, 1060 (1969).
9) Y. Takegami, T. Suzuki and K. Hamada, *Kogyo Kagaku Zasshi*, **72**, 1720 (1969); *Shokubai (Catalyst)*, **7**, 11 (1965).
*1 0.2—0.5 mol % of $TiCl_3$.

the amount of ethylcyclohexane with an increase in the reaction time may be explained by the fact that cyclohexene is inserted into the metal-ethylcyclohexyl bond, on account of the high activity of the vanadium alkyl bond in the catalyst system. However, the formation of cyclohexylethylcyclohexane was not confirmed.

With $AlEt_2Cl$, the amount of ethylcyclohexane was not affected by an increase in the reaction temperature. On the other hand, in the case of the catalytic system containing $AlEt_3$ the amount of ethylcyclohexane increased with an increase in the reaction temperature. These results suggest that there are different types of metal-ethyl bonds in the $AlEt_2Cl$ and $AlEt_3$ systems, as will be descibed below. With $AlEt_2Cl$ a metal-ethyl bond which is relatively thermally unstable may be formed.

Pentene-1 and 4-Methylpentene-1. According to Zambelli *et al.*,[7] the mechanism of the anionic coordinated polymerization of propylene to the syndiotactic polymer can be explained by the fact that the bimetallic catalyst complex plays an important role. However, the bimetallic catalyst structure proposed by them has not well been elucidated, for the differences in the syndiotactic and the isotactic polymerizations remain unexplained.

As has been shown in a previous communication,[1] in the VCl_4-$AlEt_2Cl$ catalyst system at $-70°C$ pentene-1 was inserted into the metal-ethyl bond to give, predominantly, secondary metal alkyl (II). The insertion processes of an α-olefin into the metal-ethyl bond can be formulated as follows:

$$C{=}C{-}R \xrightarrow[M\text{-}Et]{}$$

$$\left.\begin{array}{l} -M{-}C(R){-}C{-}Et\ (I) \rightarrow M{-}C(R){-}C(R){-}C{-}Et\ (III) \\ -M{-}C(R){-}C{-}Et\ (II) \rightarrow M{-}C(R){-}C(R){-}C{-}Et\ (IV) \end{array}\right.$$

On the other hand, in the case of the isotactic polymerization catalyst systems, containing $TiCl_3$ or $TiCl_4$, only the insertion reactions occurred to give the primary metal alkyl (I) and (III); From the behavior of the primary metal alkyls (I) and (III), these substances were considered to be intermediates of the isotactic polymerization of the

Table 2. Insertion reaction of pentene-1 in VX_n-$AlEt_nCl_{3-n}$

Run No.	VX_n	AlR_3	Reaction Temp. (°C)	Reaction Time (min)	Products I (mmol)	Products II (mmol)	Olefin[a] (mmol)	Remarks
1	VCl_4	$AlEt_2Cl$	−70	5	0.0105	0.0422	0	
				10	0.0126	0.0392	0	
				360	0.0040	0.0142	0	
2	VCl_4	$AlEt_2Cl$	−70	10	0.0137	0.135	0	
				40	0.0150	0.115	0	anisole 1.0 mmol
				360	0.0022	0.103	0	
3	VCl_4	$AlEt_2Cl$	0	5	0.0289	0.0242	0	
				10	0.0284	0.0177	0	
				120	0.0360	0.0206	0	
4	VCl_4	$AlEt_3$	−70	5	0.0730	0.0502	0.037	
				40	0.0725	0.0505	0.048	
				120	0.0710	0.0505	0.033	
5	VCl_4	$AlEt_3$	0	5	0.0502	0.0232	0.032	
				30	0.0502	0.0233	0.033	
				60	0.0495	0.0208	0.034	
6	VCl_4	$AlEt_2Cl$	−70	5	0.0104	0.0431	0	
				5+5	0.0046	0.0191	0	C_3H_6 10 mmol
7	$V(AA)_3$	$AlEt_2Cl$	−70	120	~0	~0	0	
8	$V(AA)_3$	$AlEt_2Cl$	0	30	0.0502	0.0214	0.022	
9	$V(AA)_3$	$AlEt_3$	−70	10	0.0600	0.0061	0.025	
10	$V(AA)_3$	$AlEt_3$	0	10	0.0466	0.0050	0.020	
11	$VOCl_3$	$AlEt_2Cl$	−70	10	0.0199	0.0338		
				60	0.0237	0.0223		
12	$VOCl_3$	$AlEt_2Cl$	0	10	0.0393	0.0281		
13	$VOCl_3$	$AlEt_3$	−70	10	0.0910	0.0428	0.096	
14	$VOCl_3$	$AlEt_3$	0	10	0.0407	0.0292	0.021	

VX_n 1.00 mmol, AlR_3 3.00 mmol, Solvent: toluene 10 ml, pentene-1 5.0 mmol
I; 3-methylhexane, II; *n*-heptane, a) heptene-3

TABLE 3. INSERTION REACTION OF 4-METHYLPENTENE-1 IN VX_n-$AlEt_nCl_{3-n}$

Run No.	VX_n	AlR_3	Reaction Temp. (°C)	Reaction Time (min)	Products I (mmol)	Products II (mmol)	Remarks
15	VCl_4	$AlEt_2Cl$	−70	10	0.0158	0.0665	
				30	0.0179	0.0655	
				60	0.0044	0.0031	
16	VCl_4	$AlEt_2Cl$	−70	10	0.0165	0.0795	
				30	0.0162	0.0799	anisole 1.0 mmol
				60	0.0193	0.0805	
17	VCl_4	$AlEt_2Cl$	0	5	0.0223	0.0121	
				30	0.0199	0.0135	
				60	0.0225	0.0135	
18	VCl_4	$AlEt_3$	−70	10	0.0835	0.0565	
				30	0.0782	0.0503	a
				60	0.0800	0.0503	
19	VCl_4	$AlEt_3$	0	10	0.0640	0.0341	
				30	0.0582	0.0322	a
				60	0.0572	0.0325	
20	$V(AA)_3$	$AlEt_2Cl$	0	10	0.0801	0.0295	
				30	0.0845	0.0365	a
				60	0.0502	0.0203	
21	$V(AA)_3$	$AlEt_3$	−70	10	0.0504	0.0106	
				30	0.0500	0.0011	
22	$VOCl_3$	$AlEt_2Cl$	−70	10	0.0188	0.0186	
23	$VOCl_3$	$AlEt_2Cl$	0	10	0.0500	0.0691	
24	$VOCl_3$	$AlEt_3$	−70	10	0.0755	0.0330	
25	$VOCl_3$	$AlEt_3$	0	10	0.0870	0.0353	

VX_n 1.00 mmol; AlR_3 3.00 mmol; Solvent: ethylbenzene 10 ml, 4-methylpentene-1 5.0 mmol
a : olefins were formed. I: 2,4-dimethylhexane, II: 2-methylheptane

α-olefin.

When propylene was reacted with the VCl_4-$AlEt_2Cl$ catalyst at −70°C, the metal alkyls (I) and (II) were not detected after the methanolysis of the reaction mixture. However, at an elevated temperature a small amount of metal alkyl (I) was obtained and the polymer showed an IR absorption at 997 cm^{-1} which can be assigned to the isotactic band. These facts strongly support the idea that the formation of the primary metal-alkyl bond is connected with the isotactic polymerization. There are two possible reasons why, at −70°C metal, neither alkyl (I) or (II) was detected. One is that a steady-state concentration of the metal alkyls is very low; that is, the second step of the insertion process is very rapid. The other possibility is that the syndiotactic polymerization proceeds without any insertion process. However, the latter reason can be ruled out on the basis of Natta's experimental finding.*2 Therefore, in the case of propylene the concentration of any metal-alkyl bond formed by propylene insertion should be low.

As has been known, higher olefins, such as pentene-1 and 4-methylpentene-1, were not polymerized with the syndiospecific catalyst.[4] However, cyclohexene was inserted easily into the metal-ethyl bond in the catalyst. From the mode of the insertion reactions of these higher olefins, the insertion process of propylene can be guessed at. As has been shown in Tables 2 and 3, at −70°C these olefins gave the metal alkyls (I) and (II). However, no polymer was obtained at this temperature. The amount of the secondary metal alkyl (II) was larger than that of the primary metal alkyl (I) (runs 1, 2, 15, and 16); these facts are quite different from the results obtained in the case of titanium-containing catalyst systems.[8] On the other hand, at an elevated temperature (runs 3 and 17) or with $AlEt_3$ (runs 4, 5, 18 and 19), the amount of metal alkyl (I) increased and a small amount of a solid polymer containing an isotactic fraction was obtained. This means that, as has been described above in the case of propylene, at 0°C the polymerization proceeds *via* the primary metal alkyl (I), just as in the case of titanium-containing systems.[8] These results show that two types of vanadium-ethyl bonds can be produced; one has a tendency to form a secondary metal-alkyl bond, and the other has a tendency to form a primary metal-alkyl bond. At a low temperature the former vanadium-ethyl bond will be formed mainly. In the case of pentene-1 or 4-

*2 When radioactive $Al(^{14}C_2H_5)_2Cl$ is used, the polymer obtained also has radioactivity.

methylpentene-1, the secondary metal alkyl (II) has the bulky substituent closely attached to vanadium; this substituent causes steric hindrance between the next-coming monomer and the active center.

The vanadium-ethyl bond to form a primary metal-alkyl bond will be formed as a minor product and will be less reactive toward the insertion reaction of olefins. Thus, the polymerization of higher olefins does not occur at low temperatures.

On the contrary, in propylene, if the secondary metal alkyl (II) is formed, the steric hindrance between the growing chain and the next-coming monomer is not so large that propylene can attack the secondary metal alkyl (II) from the less hindered side of the active center. By this alternating-monomer attack on the secondary metal alkyl bond from the less hindered side, the syndiotactic configuration may be obtained. This mechanism is also supported by the results of the copolymerization experiment reported by Zambelli *et al.*[10] In their report, the alternate copolymers of ethylene and propylene, and of ethylene and butene-1, were obtained at the higher molar ratios of propylene or butene-1 to ethylene. These results can be explained by our mechanism thus: first, a higher olefin, which has a high concentration compared to that of ethylene, is inserted into a metal-ethyl bond, and the secondary metal-alkyl bond is formed. Into this secondary metal-alkyl bond ethylene can then be easily inserted, because higher olefin has much steric hindrance. Thus, the primary metal-alkyl bond is regenerated, and into this primary metal-alkyl bond a higher olefin can be inserted. The repetition of the above insertion reaction leads to the formation of the ethylene and α-olefin alternating copolymer.

This theory is also supported by run 6 of our experiment. In this experiment, after reacting pentene-1 with VCl_4-$AlEt_2Cl$ at $-70°C$, a small amount of propylene was introduced into the reaction mixture. The amounts of the metal alkyls (I) and (II) decreased compared with run 1, in which propylene was not introduced. This fact shows that propylene was inserted into the metal alkyls (I) and (II).

To elucidate the nature of the vanadium catalyst in the insertion reaction of olefin, the $VOCl_3$ and $V(AA)_3$-$AlEt_nCl_{3-n}$ systems were also investigated. With $VOCl_3$, even at $-70°C$ with $AlEt_2Cl$ (runs 11 and 22), the selectivity for the formation of the secondary metal alkyl (II) was not as high as in the case of VCl_4 in either olefin. With $V(AA)_3$-$AlEt_2Cl$ at $-70°C$ (run 7) very small amounts of the metal alkyls (I) and (II) were obtained and the tendency for the formation of the secondary metal-alkyl bond was not very large. With $V(AA)_3$-$AlEt_3$ (runs 9, 10 and 21) the formation of the primary metal-alkyl bond (I) is predominant, as in the titanium system. In the $V(AA)_3$ system at 0°C, even with the use of $AlEt_2Cl$, the formation of C_7 olefin is observed in the case of pentene-1 (run 8); the formation of olefin is also observed in the cases of VCl_4 and $VOCl_3$-$AlEt_3$ systems, even at $-70°C$. The structures of the olefins were not determined exactly, but judging from the retention time of the gas chromatogram they seemed to be heptene-3 (main) and 3-methylhexene-1. These olefins are eliminated from metal alkyls (I) and (II) by the β-hydrogen migration of the metal alkyl bond.

The elimination of olefin from a metal alkyl bond was observed in the case of the insertion reaction of cyclohexene into metal ethyl bonds in the $TiCl_4$-$AlEt_3$ and $AlEt_2Cl$ systems at a low Al/Ti molar ratio.[9] It was considered that the Ti(IV)-alkyl bond was unstable and that the elimination of the olefins was followed by a hydride shift. From the results obtained in vanadium systems, it may be shown that in rather lower valence states of vanadium, vanadium alkyl bonds will be more unstable than in titanium systems.

VCl_4, $V(AA)_3$, and $VOCl_3$-$AlEtCl_2$ systems were also investigated, but in these systems, on account of the strong cationic character of the catalyst, olefins were easily polymerized to a low-molecular-weight polymer and no insertion reactions were observed.

The addition of anisole is known to increase the syndiotacticity, but in the cases of the insertion reactions studied in this report, no remarkable changes were found. In the case of cyclohexene, the amount of the metal-ethylcyclohexyl bond decreased, in 4-methyl-pentene-1 no remarkable change was observed, and in pentene-1 the formation of the secondary metal-alkyl bond increased. However, in every case the stability of the metal-alkyl bond seemed to be increased.

From these results, it can be said that α-olefins are generally inserted into a vanadium-ethyl bond to form a secondary metal alkyl bond. Of the systems studied, the tendency to produce the secondary metal alkyl bond reaches its maximum with the catalytic system VCl_4-$AlEt_2Cl$ at $-70°C$. The hypothesis for the mechanism of the syndiotactic polymerization of α-olefin proposed in the previous communication,[1] that is, the secondary metal alkyl bond propagation mechanism, is strongly supported.

As has been reported by Natta,[11] V(III) species are present in the VCl_4-$AlEt_2Cl$ system at $-70°C$. Vanadium (III) has a $3d^2$ electronic structure and in the case of the titanium system the Ti(III) species has a $3d^1$ electronic structure. The difference between the electronic structure of the central

10) A. Zambelli, A. Lety, C. Tosi and I. Pasquon, *Makromol. Chem.*, **115**, 73 (1968).

11) G. Natta, A. Zambelli, G. Lanzi, I. Pasquon, E. R. Mongnashi, A. L. Segre and P. Centola, *ibid.*, **61**, 161 (1965).

metal is considered to cause the marked difference in the insertion reactions of an α-olefin into the metal ethyl bonds. At an elevated temperature or with $AlEt_3$, the valency state of vanadium was reduced to V(II) and a $3d^1$ electronic structure. In this case, the formation of the primary metal alkyl bond is most likely. Naturally, the differences in the ligands of the vanadium and the valency states of the starting vanadium play an important role, as do the differences among the vanadium salts.

The contribution of the configuration of the active center of the syndiospecific catalyst can not be ruled out, either.

BULLETIN OF THE CHEMICAL SOCIETY OF JAPAN VOL. 43 1489—1496 (1970)

Studies on Hydrogenolysis. LVI.[1] The Effect of Solvent and Additive on the Stereochemistry of Catalytic Hydrogenolysis of 2-Methyl-2-phenylaziridine Derivatives*[1]

Yoshihiro SUGI and Sekio MITSUI

Department of Applied Science, Faculty of Engineering, Tohoku University, Sendai

(Received October 9, 1969)

In order to assess the effects of solvent and additive on the stereochemical course of the catalytic hydrogenolysis of styrene imine derivatives, the hydrogenolysis of optically active 2-methyl-2-phenylaziridine (Ia), 1,2-dimethyl-2-phenylaziridine (Ib), and 1-acetyl-2-methyl-2-phenylaziridine (Ic) was carried out under various conditions. The hydrogenolysis of Ia and Ib over palladium hydroxide occurred preferentially with an inversion of the configuration in ethanol, but with a retention in benzene. Moreover, Ia was hydrogenolysed with a predominant inversion of the configuration in *n*-hexane, and the inverted product increased with a decrease in the adsorption strength of the hydrocarbon solvent. The hydrogenolysis of Ic, however, occurred with a significant inversion of the configuration in both ethanol and benzene. The addition of sodium hydroxide to the reaction mixture strongly promoted a retention of the configuration in the hydrogenolysis of Ia over palladium hydroxide, and finally Ia was hydrogenolysed with a stereospecific retention. In contrast, no such variations could be observed in the cases of Ib and Ic. The stereoselectivity was not affected significantly by the addition of sodium hydroxide in the Raney nickel-catalyzed hydrogenolysis of Ia. However, the addition of sodium hydroxide prompted a retention of the configuration in the case of Ib. These results can be explained consistently by the previously-proposed mechanism.

The mechanism of the hydrogenolysis of benzyl-type compounds at heterogenuous catalytic surfaces has been a subject of discussion for more than a decade.[1-9] Mitsui and his co-workers have reported the stereochemical course of this reaction.[1-6]

It seems established that the configurations of the products are responsible for the free-energy difference at the transition states leading to the π-benzyl intermediates. In a previous paper,[2] the present authors reported the hydrogenolysis of optically active 2-methyl-2-phenylaziridine with palladium, platinum, nickel, and cobalt catalysts. However, ethanol was used as the reaction solvent

*1 A part of this work was presented at the 24th Symposium on Catalysis, Tokyo, March, 1969 (*cf. Shokubai*, **11**, 54 P. (1969)) and has already been reported in a preliminary form: S. Mitsui and Y. Sugi, *Tetrahedron Lett.*, **1969**, 1291.

1) Part LV, S. Mitsui, M. Fujimoto, T. Sukegawa and Y. Nagahisa, *Kogyo Kagaku Zasshi*, **73**, 97 (1970).

2) S. Mitsui and Y. Sugi, *Tetrahedron Lett.*, **1969**, 1287; Y. Sugi and S. Mitsui, This Bulletin, **42**, 2984 (1969).

3) S. Mitsui and S. Imaizumi, *Nippon Kagaku Zasshi*, **77**, 1516 (1956); This Bulletin, **34**, 774 (1961); **36**, 855 (1963).

4) S. Mitsui, M. Fujimoto, Y. Nagahisa and T. Sukegawa, *Chem. Ind.* (London), **1969**, 241.

5) S. Mitsui, Y. Kudo and M. Kobayashi, *Tetrahedron*, **25**, 1921 (1969).

6) S. Mitsui, S. Imaizumi and Y. Esashi, This Bulletin, in press.

7) W. A. Bonner, *J. Amer. Chem. Soc.*, **74**, 1033, 3218 (1952); W. A. Bonner, J. A. Zderic and G. A. Caseletto, *ibid.*, **74**, 5086 (1952).

8) A. M. Khan, F. J. McQuillin and I. Jardine, *J. Chem. Soc. C*, **1967**, 136.

9) E. W. Garbisch, Jr., L. Schreader and J. J. Frankel, *J. Amer. Chem. Soc.*, **89**, 4233 (1967).

Table 1. Effect of the solvent on the stereochemistry of the catalytic hydrogenolysis of 2-methyl-2-phenylaziridine (Ia) and its derivatives (Ib and Ic)

Run	Reactant	Catalyst (g)	Solvent	Optical purity of I[b] (%)	Products (%)			II				
					II	III	IV	$[\alpha]_D$	Optical purity[b] (%)	Maintained optical activity (%)	Configuration: Retention (%)	Configuration: Inversion (%)
1	Ia	$Pd(OH)_2$ 0.05	Benzene	R 43.6	100	—	trace	−4.48	15	35	68	32
2	Ia	$Pd(OH)_2$ 0.05	Toluene	S 91.0	100	—	trace	−6.09	21	23	38	62
3	Ia	$Pd(OH)_2$ 0.05	*o*-Xylene	S 91.0	100	—	trace	−6.20	21	23	38	62
4	Ia	$Pd(OH)_2$ 0.05	*m*-Xylene	S 91.0	100	—	trace	−8.90	30	33	33	67
5	Ia	$Pd(OH)_2$ 0.05	*p*-Xylene	R 43.6	100	—	trace	+5.34	18	41	29	71
6	Ia	$Pd(OH)_2$ 0.05	*t*-Butylbenzene	R 43.6	100	—	?	+6.19	21	48	26	74
7	Ia	$Pd(OH)_2$ 0.05	*n*-Hexane	R 43.6	100	—	trace	+9.70	33	75	12	88
8[a]	Ia	$Pd(OH)_2$ 0.05	Ethanol	R 43.6	100	—	trace	+9.28	31	72	14	86
9	Ib	$Pd(OH)_2$ 0.05	Benzene	R 44.3	100	—	trace	−0.99	4	9	55	45
10	Ib	$Pd(OH)_2$ 0.05	Ethanol	R 44.3	97	—	3	+8.01	32	72	14	86
11	Ic	$Pd(OH)_2$ 0.05	Benzene	R 37.3	100	—	?	+15.05	32	85	7	93
12	Ic	$Pd(OH)_2$ 0.05	Ethanol	R 37.3	100	—	?	+13.23	28	75	12	88
13	Ia	Ra-Ni 1[c]	Benzene	S 91.0	88	11	1	+5.65	19	21	61	39
14	Ia	Ra-Ni 1[c]	*n*-Hexane	S 91.0	85	13	2	+4.67	16	17	59	41
15[a]	Ia	Ra-Ni 1[c]	Ethanol	S 91.0	93	7	trace	+6.26	21	23	62	38

I: 0.01 mol, Solvent: 20 m*l*, Under ordinary pressure and at room temperature.
a, Ref. 2, *b*, 100% optical rotation: S(+)-Ia, $[\alpha]_D$ +33.3°; S(+)-Ib, $[\alpha]_D$ +49.5°; S(+)-Ic, $[\alpha]_D$ +97.0°; R(+)-IIa, $[\alpha]_D$ +29.5°; R(+)-IIb, $[\alpha]_D$ +25.3°; R(+)-IIc, $[\alpha]_D$ +47.2°. All rotations were measured in ethanol, *c*, wet weight with ethanol.

Table 2. Effect of sodium hydroxide and potassium iodide on the stereochemistry of the catalytic hydrogenolysis of 2-methyl-2-phenylaziridine (Ia) and its derivatives (Ib and Ic)

Run	Reactant	Catalyst (g)	NaOH (1×10^{-4} mol)	Optical purity of I (%)	Products (%)			II				
					II	III	IV	$[\alpha]_D$	Optical purity (%)	Maintained optical activity (%)	Configuration	
											Retention (%)	Inversion (%)
8	Ia	$Pd(OH)_2$ 0.05	—	R 43.6	100	—	trace	+9.28	31	72	14	86
16	Ia	$Pd(OH)_2$ 0.05	1.0	R 43.6	100	—	trace	+5.98	20	46	27	73
17	Ia	$Pd(OH)_2$ 0.05	2.0	R 43.6	100	—	trace	−7.35	25	57	79	21
18	Ia	$Pd(OH)_2$ 0.05	5.0	R 43.6	100	—	trace	−10.10	34	79	90	10
19	Ia	$Pd(OH)_2$ 0.05	10	S 91.0	100	—	trace	+26.80	91	100	100	0
20	Ia	$Pd(OH)_2$ 0.05	KI 0.1	R 43.6	100	—	trace	+4.38	15	34	33	67
21	Ia	$Pd(OH)_2$ 0.05	KI 0.2	S 91.0	100	—	trace	−9.35	32	35	32	68
10	Ib	$Pd(OH)_2$ 0.05	—	R 44.3	97	—	3	+8.01	32	72	14	86
22	Ib	$Pd(OH)_2$ 0.05	5.0	R 44.3	100	—	trace	+7.26	29	65	17	83
23	Ib	$Pd(OH)_2$ 0.05	10	R 44.3	100	—	trace	+7.13	28	64	18	82
12	Ic	$Pd(OH)_2$ 0.05	—	R 37.3	100	—	?	+13.23	28	75	12	88
24	Ic	$Pd(OH)_2$ 0.05	5.0	R 37.3	100	—	?	+16.62	35	94	3	97
15	Ia	Ra-Ni 1	—	S 91.0	93	7	trace	+6·26	21	23	62	38
25	Ia	Ra-Ni 1	10	S 91.0	93	7	trace	+5.81	20	22	61	39
26	Ia	Ra-Ni 1	100	S 91.0	92	8	trace	+5.14	17	19	60	40
27	Ia	Ra-Ni 1	KI 10	S 91.0	90	10	trace	+4.27	15	16	58	42
28	Ib	Ra-Ni 1	—	S 89.0	78	—	22	+2.47	10	11	56	44
29	Ib	Ra-Ni 1	10	S 89.0	100	—	—	+10.22	40	45	73	27

I: 0.01 mol, Solvent: ethanol, 20 m*l*, Under ordinary pressure and at room temperature.

in all cases. In this work, we will attempt to assess the possible effects of solvent and additive on the stereochemical course of the catalytic hydrogenolysis of optically active 2-methyl-2-phenylaziridine (Ia), 1,2-dimethyl-2-phenylaziridine (Ib), and 1-acetyl-2-methyl-2-phenylaziridine (Ic) under ordinary pressure and at room temperature.

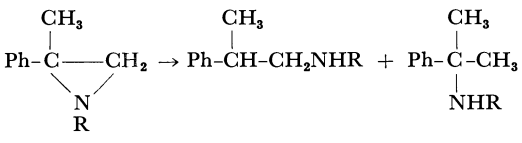

I II III

a) R=H, b) R=CH_3, c) R=$COCH_3$

Results

Effect of the Solvent on the Stereochemistry. The hydrogenolysis of Ia with palladium hydroxide was investigated in several kinds of solvents. The results are summarized in Table 1 (Runs 1—8). The hydrogenolysis in ethanol occurred preferentially with an inversion of the configuration, while the hydrogenolysis in benzene was accompanied by a retention. The inversion of the configuration occurred in several aromatic hydrocarbons other than benzene. In these cases, the inverted products increased in the order: benzene $<$ toluene $\fallingdotseq$ *o*-xylene $<$ *m*-xylene $<$ *p*-xylene $<$ *t*-butylbenzene; this order is associated with the adsorption strengths of these hydrocarbons under hydrogenation conditions.[10-12] The hydrogenolysis also proceeded with a significant inversion of the configuration in *n*-hexane. The stereochemical results of similar experiments on Ib and Ic are also summarized in Table 1 (Runs 9—12).*2 The hydrogenolysis of Ib occurred predominantly with an inversion of the configuration in ethanol, but with a retention in benzene; these results are in agreement with those in the case of Ia. The hydrogenolysis of Ic, however, proceeded with a significant inversion of the configuration in both ethanol and benzene.

On the other hand, no significant effect of the solvent on the stereochemical course was observed in the Raney nickel-catalyzed hydrogenolysis of Ia, in contrast with the case of palladium hydroxide (Runs 13—15).

Effects of Sodium Hydroxide and Potassium Iodide on the Stereochemistry. Table 2 shows the influence of sodium hydroxide on the stereochemical results in the hydrogenolysis of Ia, Ib, and Ic. The hydrogenolysis of Ia over palladium hydroxide occurred with a predominant inversion of the configuration in ethanol, as has been described previously.[2] However, the addition of sodium hydroxide to the reaction mixture strongly promoted a retention of the configuration, and finally Ia was hydrogenolysed with a stereospecific retention (Runs 8, 16—19). No such variations in the stereochemical results could be observed in the hydrogenolysis of Ib (Runs 10 and 23), and the stereoselectivity increases in the case of Ic (Runs 11 and 24).

The hydrogenolysis of Ia with Raney nickel was not seriously affected when sodium hydroxide was

TABLE 3. THE CATALYTIC HYDROGENOLYSIS OF 2-METHYL-2-PHENYLAZIRIDINE (Ia) AND 1,2-DIMETHYL-2-PHENYLAZIRIDINE (Ib) OVER PLATINUM CATALYSTS

Run	Reactant	Catalyst (g)	Optical purity of I (%)	Products (%) II	Products (%) IV	II $[\alpha]_D$	II Optical purity (%)	II Maintained optical activity (%)	II Configuration Retention (%)	II Configuration Inversion (%)
30[a]	Ia	PtO_2 0.1	R 37.3	92(4[b])	4	−10.36	35	94	97	3
31[a]	Ia	Pt-black 0.1[c]	S 91.0	94(3[b])	3	+19.60	67	73	87	13
32	Ia	Pt-black[d] 0.5[c]	S 91.0	93(5[b])	2	+13.78	47	51	76	24
33	Ib	PtO_2 0.1	S 89.0	94(4[e])	2	+19.30	78	87	94	6
34	Ib	Pt-black 0.1[c]	S 89.0	88(4[e])	8	+18.12	72	80	90	10

I: 0.01 mol, Solvent: ethanol, 20 m*l*, Under ordinary pressure and at room temperature.
a, Ref. 2, *b*, 2-cyclohexylpropylamine, *c*, weight as PtO_2, *d*, treated with concentrated nitric acid, see Experimental section, *e*, *N*-methyl-2-cyclohexylpropylamine.

10) C. P. Rader and H. A. Smith, *ibid.*, **84**, 1443 (1962).

11) H. A. Smith and W. E. Campbell, *Proc. Intern. Congr. Catalysis, 3rd., Amsterdam, 1964*, North Holland Publ. Co., Amsterdam, 1965, p. 1373.

12) J. L. Garnett and W. A. Sollich-Baumgartner, "Advances in Catalysis," Vol. 16, p. 95, Academic Press, London and New York (1966).

*2 The configurational relationships between the reactants and the products were established as has been described elsewhere.[13] (+)-Ia, (+)-Ib, and (+)Ic all have S configurations. However, (+)-IIa, (+)-IIb, and (+)-IIc all have R configurations.

13) Y. Sugi and S. Mitsui, This Bulletin, **43**, 564 (1970).

added to the reaction mixture (Runs 15, 25, and 26). A retention of the configuration occurred in the Raney nickel-catalyzed hydrogenolysis of Ib, although the maintained optical activity was only 10% (Run 28). However, the addition of sodium hydroxide to the reaction mixture prompted a retention of the configuration of IIb (Runs 28 and 29). Moreover, the following interesting results were also observed in the Raney nickel-catalyzed hydrogenolysis of Ib. *N*-Methyl-2-phenyl-2-propylamine (IIIb) was not obtained. 2-Phenylpropane (IV) was produced in the absence of sodium hydroxide, whereas IV was not formed in the presence of sodium hydroxide. These results are dissimilar to those in the case of Ia.[2]

The influence of potassium iodide on the stereochemistry in the hydrogenolysis of Ia is also shown in Table 2. The stereoselectivity decreased over palladium hydroxide (Runs 8, 20, and 21), but no significant variation was observed over Raney nickel (Runs 16 and 27).

Variation in the Stereoselectivity with Platinum Catalysts. Table 3 summarizes the influences of the alkaline substances present in platinum catalysts. The stereoselectivity with platinum black (Run 31) was lower than that with platinum oxide (Run 30) in the hydrogenolysis of Ia.[2] It is well known that platinum oxide contains a trace of alkaline substances. To remove them, platinum black, which had been prepared by the reduction of platinum oxide, was treated with concentrated nitric acid, as will be described in the Experimental Section. The maintained optical activity with this catalyst (Run 32) was lower than those with platinum oxide and platinum black (Runs 30 and 31). The hydrogenolysis of Ib occurred with a significant retention of the configuration with both platinum oxide and platinum black; no serious difference in the stereoselectivity was observed (Runs 33 and 34).

Discussion

It is generally considered[1-6] that the catalytic hydrogenolysis of benzyl-type compounds proceeds to form the π-benzyl intermediate, **5**, *via* different transition states, **2** and **3**, and that the π-benzyl intermediate, **5**, suffers an electrophilic substitution with *s*-type adsorbed hydrogen.[14] In this case, the configurations of the products are responsible for the free-energy difference at the transition states, **2** and **3**; this difference depends on the structure of the compound, the catalyst, the solvent, the additive, and other factors. If the substituent X has a very strong affinity for the catalyst, the radical cleavage reaction (iii) as well as the S*Ni*-type reaction (ii) participates in this hydrogenolysis.[2]

We have previously reported that the hydrogenolysis of Ia in ethanol occurred with a predominant inversion of the configuration over palladium catalysts, but with a predominant retention over platinum, Raney nickel, and Raney cobalt catalysts, although low stereoselectivities were observed over the latter two catalysts.[2] These results may depend on the affinity for the nitrogen lone-pair and the catalyst hindrance.[2] Since palladium does not have so strong affinity for the nitrogen lone-pair, Ia is more probably hydrogenolysed *via* **6** over the palladium catalyst. However, the hydrogenolysis over the platinum catalyst favors the path *via* **7**,

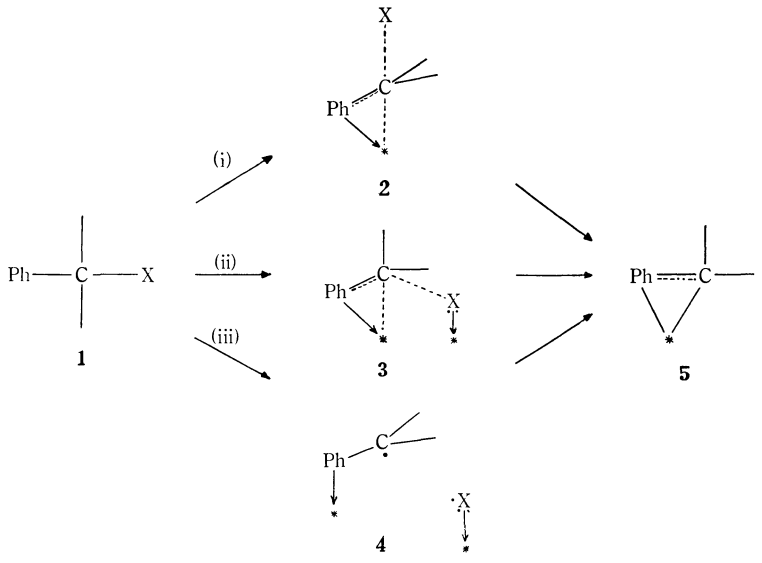

14) T. Toya, *J. Research Inst. Catalysis, Hokkaido Univ.*, **6**, 308 (1958), **8**, 209 (1960), **10**, 236 (1962); *Kinzoku Butsuri*, **10**, 147 (1964).

because platinum is less sensitive to the catalyst hindrance than are nickel and palladium. Nickel and cobalt have stronger affinities for the nitrogen lone-pair than have palladium and platinum. Therefore, the S_Ni-type reaction and the radical cleavage reaction occur competitively *via* **7** over Raney nickel and Raney cobalt catalysts.

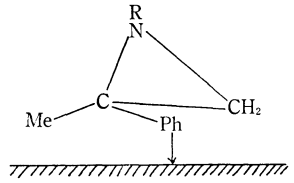

6

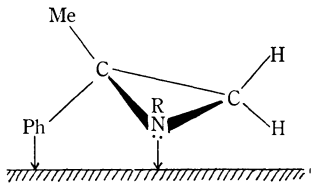

7

-R : a) -H, b) $-CH_3$, c) $-COCH_3$, d) Na

Effect of the Solvent on the Stereochemistry. The hydrogenolysis of Ia over palladium hydroxide in benzene occurred preferentially with a retention of the configuration, but with an inversion in several aromatic hydrocarbons other than benzene. In these cases, the inverted product increased with a decrease in the adsorption strengths of these hydrocarbons under hydrogenation conditions.[10-12] Furthermore, the hydrogenolysis proceeded with a significant inversion of the configuration in *n*-hexane and ethanol, which are considered not to be adsorbed so strongly on the catalyst. Similar variations were observed in the hydrogenolysis of Ib. However, the hydrogenolysis of Ic occurred with a significant inversion of the configuration in both ethanol and benzene.

This characteristic behavior of Ia and Ib in benzene suggests the following considerations. The adsorptions of the reactant and hydrogen decrease in benzene since benzene acts as a weak catalytic poison. It is known that the mobility of an electron in platinum foil diminishes upon the adsorption of benzene.[15] From these two reasons, we are led to consider that the nucleophilicity of the catalyst decreases when benzene is used as the reaction solvent. Therefore, the hydrogenolysis of Ia and Ib in benzene is retarded because the adsorption of the reactant and the nucleophilicity of the catalyst decrease as has been mentioned above. In this case, the hydrogenolysis *via* **7** is less inhibited than that *via* **6**, for the nitrogen is adsorbed on the catalyst in the former state, but directed away in the latter. Consequently, when benzene is used as the reaction solvent, the free-energy level of the transition state leading to the π-benzyl intermediate *via* **7** is lower than that *via* **6**, and the configuration of the product will be retained predominantly. However, in solvents other than benzene the free-energy level of the transition state *via* **6** becomes lower than that *via* **7** with a decrease in the adsorption strength of the solvent. Since potassium iodide acts as a catalytic poison, the decrease in the stereoselectivity in the hydrogenolysis of Ia upon the addition of potassium iodide may be explained consistently by the above arguments.

The nitrogen of Ic will be adsorbed less strongly on the catalyst than those of Ia and Ib, for the electron density of Ic becomes lower upon the withdrawal of the acetyl group. It seems, therefore, that the activation free-energy leading to the π-benzyl intermediate *via* **7** increases upon the adsorption of benzene. However, since the acetyl group withdraws the electrons of the benzylic-carbon-nitrogen bond of Ic, the stereoelectronic requirement of the transition state is fulfilled *via* **6**; the hydrogenolysis *via* this state is less inhibited by the adsorption of benzene. Consequently, the free-energy level of the transition state *via* **6** becomes lower than that *via* **7** in both ethanol and benzene; this is in contrast with the cases of Ia and Ib.

On the other hand, no such effect of the solvent and potsssium idodide was observed in the Raney nickel-catalyzed hydrogenolysis of Ia; this is in contrast with the case over palladium hydroxide. Since nickel has a very strong affinity for the nitrogen lone-pair, Ia will be hydrogenolysed without large inhibitions by the adsorption of benzene or potassium iodide.

Iijima and Mitsui[16] have reported similar solvent effects on the hydrogenolysis of 2-phenyl-2-butanol over a palladium catalyst. The retention of the configuration occurred preferentially in benzene, whereas the hydrogenolysis in ethanol, *n*-hexane, and toluene proceeded with a predominant inversion. Thus, these results are in accord with our present findings. Recently, Grimm and Bonner[17] have presented similar variations in the stereochemistry of the Raney nickel-catalyzed desulfuration of 2-phenyl-2-benzenesulfonylpropionamide. These authors have shown that this sulfone was hydrogenolysed with a predominant inversion of the configuration in ethanol, while the acetone treatment of the catalyst and the acetone solvent strongly prompted a retention of the configuration. However, they have not discussed the mechanistic details. These interesting observations can be interpreted consistently by the above arguments, for

15) V. M. Gryazow and V. I. Shimulis, *Kineti. Katal.*, **2**, 534 (1961).

16) K. Iijima and S. Mitsui, *Nippon Kagaku Zasshi*, **85**, 686 (1964).

17) R. A. Grimm and W. A. Bonner, *J. Org. Chem.*, **32**, 3470 (1967).

the nucleophilicity of the catalyst decreases upon treatment with acetone.

Effect of Sodium Hydroxide on the Stereochemistry. The hydrogenolysis of Ia in ethanol over palladium hydroxide occurred with a predominant inversion of the configuration in the absence of sodium hydroxide. However, the addition of sodium hydroxide promoted a retention of the configuration, and finally the hydrogenolysis proceeded with a stereospecific retention. On the other hand, no such variations in the stereochemistry were observed in the hydrogenolysis of Ib and Ic. These observations can be explained as follows. Ia and Id will establish an equilibirum as in Equation (1) in the presence of sodium hydroxide. It is difficult for Id to undergo hydrogenolysis *via* **6**, because

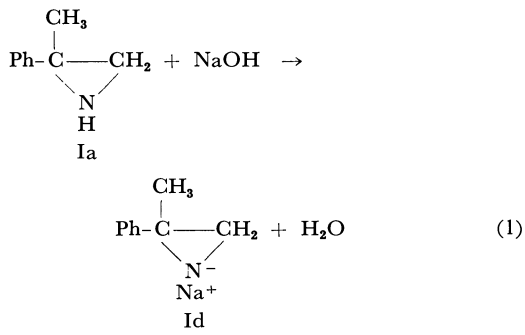

(1)

the nitrogen of Id acts as an electron-donor. However, the hydrogenolysis *via* **7** or **8** is less inhibited than that *via* **6**, since the nitrogen of **7** or **8** is absorbed on the catalyst. Therefore, Id participates in the hydrogenolysis of Ia in the presence of sodium hydroxide; consequently, the retained product will increase when sodium hydroxide is added to the reaction mixture. No such influences are observed in the hydrogenolysis of Ib and Ic, thus eliminating an equilibrium like that of Equation (1) and supporting the participation of Id in the hydrogenolysis of Ia in the presence of sodium hydroxide. The stereoselectivity in the hydrogenolysis of Ic over palladium hydroxide increased when sodium hydroxide was added to the reaction mixture; this variation is in accord with the hydrogenolysis of α-methylstyrene oxide with Raney nickel and palladium catalysts.[18] Adsorbed sodium hydroxide will retard the adsorption of the nitrogen lone-pair of Ic. Moreover,

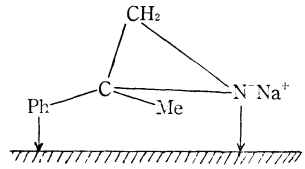

8

the stereoelectronic requirement of the transition state leading to the π-benzyl intermediate is fulfilled *via* the state **6**, since the acetyl group withdraws the electrons of the carbon-nitrogen bond. Therefore, the difference in the free-energies of the transition states *via* **6** and **7** becomes larger upon the adsorption of sodium hydroxide. The variation in the stereoselectivity with platinum catalysts can be explained similarly to that in the case with palladium hydroxide.

The hydrogenolysis of Ib over Raney nickel occurred with a predominant retention of the configuration, and the stereoselectivity increased when sodium hydroxide was added to the reaction mixture. This variation suggests that the radical-cleavage reaction decreases in the presence of sodium hydroxide because adsorbed sodium hdyroxide retards the adsorption of the nitrogen lone-pair of Ib. On the other hand, the hydrogenolysis of Ia with Raney nickel was not significantly affected by the addition of sodium hydroxide; this may be the result of alkaline substances present in the catalyst. We have previously reported the formation of 2-phenyl-2-propylamine (IIIa), in addition to IIa, in the Raney nickel-catalyzed hydrogenolysis of Ia, and have postulated that IIIa forms *via* the state **7**.[2] However, *N*-methyl-2-phenyl-2-propylamine (IIIb) was not formed in the case of Ib. This may be attributed to the inductomeric effect of the *N*-methyl group. Further, a considerable amount of 2-phenylpropane (IV) was produced in the Raney nickel-catalyzed hydrogenolysis of Ib, in contrast with the case of Ia.[2] It seems that the stability of $\cdot\ddot{N}CH_3$ and/or $\cdot\ddot{N}HCH_3$, which are formed according to the radical-cleavage reaction of Ib, is larger than that of $\cdot\ddot{N}H$ and/or $\cdot\ddot{N}H_2$, which are formed from Ia. However, IV was not obtained in the presence of sodium hydroxide. This is consistent with the decrease in the radical-cleavage reaction.

Experimental

Materials. S(+)- and R(−)-2-Methyl-2-phenylaziridines (Ia), S(+)- and R(−)-1,2-dimethyl-2-phenylaziridines (Ib), and R(−)-1-acetyl-2-methyl-2-phenylaziridine (Ic) were prepared by methods described previously.[2,14]

Catalysts. Palladium hydroxide ($Pd(OH)_2$) was prepared according to the literature.[19] Raney nickel (Ra-Ni) was prepared by the method used for W-4,[20] stored in ethanol, and used within a week. Except when ethanol was used as the reaction solvent, Raney nickel was dried in a hydrogen stream at 15—20 mmHg below 60°C just before use. Platinum oxide (PtO_2) was purchased from the Wako Pure Chem Co., Ltd., Osaka. Platinum black used in Runs 31 and 34 was obtained

18) S. Mitsui and S. Imaizumi, *Nippon Kagaku Zasshi*, **86**, 219 (1965).

19) Y. Takagi, T. Naito and S. Nishimura, This Bulletin, **38**, 2119 (1965).

20) H. Adkins and A. A. Pavlic, *J. Amer. Chem. Soc.*, **69**, 3039 (1947).

by the reduction of platinum oxide with hydrogen and was washed with water. However, platinum black used in Run 32 was prepared as follows. Platinum black which had been prepared from platinum oxide was boiled with concentrated nitric acid for 2 hr and then washed well with water. The resulting catalyst was reduced with hydrogen and washed with water. To remove any nitric acid present in the catalyst, this reduction-washing procedure was repeated three times.

Solvents. The aromatic solvent was purified by treatment with concentrated sulfuric acid and by subsequent distillation over sodium. *n*-Hexane was purified by treatment with Raney nickel under a hydrogen atmosphere and by subsequent distillation over sodium. Ethanol was obtained commercially.

Additives. Sodium hydroxide and potassium iodide were obtained commercially.

Catalytic Hydrogenolysis of Ia. The following general procedure was used.[2] After a definite amount of a catalyst and an additive in an solvent (10 *ml*) had been agitated under a hydrogen atmosphere for 1 hr, 0.01 mol (1. 33 g) of Ia in the solvent (10 *ml*) was added; the resulting suspension was agitated with hydrogen under ordinary pressure and at room temperature. After the theoretical amount of hydrogen had been absorbed, the catalyst was filtered off, and the reaction mixture was analyzed by gas chromatography (PEG 4000 dispersed on fire-brick at 150—180°C using helium as the carrier gas). It was then worked-up as has previously been described, ethanol, benzene, toluene, or *n*-hexane being used as the reaction solvent. However, when *o*-xylene, *m*-xlyene, *p*-xylene, or *t*-butylbenzene was used as the reaction solvent, the filtrate was treated with dilute hydrochloric acid, and the product IIa was obtained from the aqueous layer by treatment with aqueous ammonia. IIa was separated in the usual manner.

Catalytic Hydrogenolysis of Ib. The hydrogenolysis of Ib was carried out by a procedure similar to that used for Ia. However, Ib and IIb were unseparable under our gas-chromatographic conditions. After the evaporation of the solvent, the oily product was treatep with dilute hydrochloric acid and IIb was obtained from the apueous layer by treatment with aqueous ammonia. For the rotation of optically-pure IIb, we adopted $[\alpha]_D$ 25.3° (ethanol), a value calculated from the purity of IIa, as has been described elsewhere.[13]

Catalytic Hydrogenolysis of Ic. The hydrogenolysis of Ic was carried out by a procedure similar to that used for Ia. The reaction mixture was analyzed by gas chromatography (PEG 4000, Golay column (0.5 mm × 15 m), 180°C, using nitrogen as the carrier gas). In this case, Ic was decomposed during the gas-chromatographic analysis. Therefore, we considered the reaction to be complete when the decomposed product became undetectable. IIc was separated in the usual manner. For the rotation of optically-pure IIc, we adopted $[\alpha]_D$ 47.2° (ethanol), a value calculated from the purity of IIa.[13]

The authors are grateful to the Takeda Science Foundation for its financial support.

BULLETIN OF THE CHEMICAL SOCIETY OF JAPAN VOL. 43 1496—1500 (1970)

Oxidative Ring-contraction of Several 1,5-Benzodiazepines with Light

Masakatsu MATSUMOTO, Yoichi MATSUMURA, Akira IIO and Teijiro YONEZAWA

Department of Hydrocarbon Chemistry, Faculty of Engineering, Kyoto University, Kyoto

(Received October 14, 1969)

2,4-dimethyl- (I-a), 2-methyl-4-phenyl- (I-b), and 2,4-diphenyl-1,5-benzodiazepine (I-c) were irradiated with a high-pressure mercury arc under an oxygen atmosphere in benzene and in acetic acid. In all cases oxidative ring-contraction products, 2-acylquinoxalines (II), were obtained. It was found that there was a solvent effect in these reactions ; *e.g.*, in benzene the diazepine (II-d) leads to 2-benzoyl-3-methylquinoxaline (II-d), while in acetic acid it leads to 2-acetyl-3-phenylquinoxaline (II-b).

The oxidation reaction of 2,4-dimethyl-1,5-benzodiazepine (I-a : R, R′=CH_3) and 2-methyl-4-phenyl-1,5-benzodiazepine (I-b : R=CH_3, R′=Ph) with monopersulfuric acid or with peracetic acid has been reported by Barltrop *et al.* ;[1] the corresponding 3,6-diaza-4, 5-benzotropones, (III-a : R, R′=CH_3) and (III-b : R=CH_3, R=Ph), are not obtained, but the ring-contraction products, 2-acetyl-3-methylquinoxaline (II-a) and 2-acetyl-3-phenylquinoxaline (II-b) respectively, are obtained.

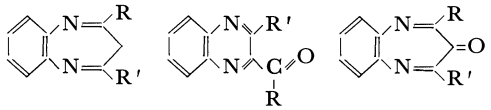

(I) (II) (III)

We have also studied the photooxidation of the dimethyl- (I-a) and the diphenylbenzodiazepine

1) J. A. Barltrop, C. G. Richards, D. M. Russel and G. Ryback, *J. Chem. Soc.*, **1959**, 1132.

(I-c) with a low-pressure mercury arc and have previously reported that the benzodiazepine (I-a) is oxidized to the quinoxaline (II-a) and that the photooxidation of the benzodiazepine (I-c) leads to a slight amount of the diazabenzotropone (III-c).[2] We suggested that, in the case of the benzodiazepine (I-a), the 6-oxo intermediate (III-a) may be subjected to a second photochemical reaction, thus forming a ring-contraction product (II-a). In this paper, we will report on the photooxidation reaction of the dimethyl-(I-a), the methylphenyl- (I-b), and the diphenyl-benzodiazepine (I-c) in benzene and in acetic acid employing a 200-W high-pressure mercury arc; the mechanism of the photooxidation reaction will also be discussed.

Results and Discussion

A benzene solution of the dimethylbenzodiazepine (I-a) was irradiated with a 200-w high-pressure mercury arc under an oxygen atmosphere; 2-acetyl-3-methylquinoxaline (II-a) and 3-methyl-2-quinoxalone (IV) were thus formed in yields of 29% and 8% respectively. When glacial acetic acid was used as the solvent, the reaction seemed to be promoted compared with that in benzene. When an 0.1 N sulfuric acid aqueous solution of diazepine (I-a) was irradiated under an oxygen atmosphere at 0-5 and 45–50°C, a slight amount of the quinoxaline (II-a) was formed; it and 2-methylbenziminazole (V-a) was obtained in yields of 5% and 75% respectively. The ring-contraction to 2-methylbenziminazole (V-a) may proceed thermally in an acidic aqueous solution, for it is known to be formed under acidic conditions in the dark.[1]

The auto-oxidation of the quinoxaline (II-a) under the action of light gave the quinoxalone (IV), so the product (IV) was probably formed *via* the second photooxidation of the quinoxaline (II-a) in the photooxidation of the diazepine (I-a).

When the methylphenylbenzodiazepine (I-b) in benzene was irradiated under an oxygen atmosphere, the photooxidation reaction proceeded smoothly and, surprisingly, 2-benzoyl-3-methyl-quinoxaline (II-d) was obtained in a yield of 25%, plus a small amount of 3-methylquinoxalone (IV); the oxidation of the benzodiazepine (I-b) with peracids leads to 2-acetyl-3-phenylquinoxaline (II-b). The abnormal ring-contraction product (II-d) was identified by means of its spectroscopic data, as is shown in Table 1 and Table 2.

Table 1. The spectroscopic data of 2-benzoyl-3-methylquinoxaline (II-d)

UV in ethanol	: $\lambda_{max}(\varepsilon)$	321(6460), 246(22900)
IR in KBr	: (cm^{-1})	1665($\nu_{C=O}$)
MS	: (m/e)	248(100), 233(10), 220(22), 219(62), 105(91)
NMR in $CDCl_3$:	(τ)	7.20 (3H, CH_3), 2.50–2.05 (9H, two Ph)

Table 2. The ultraviolet spectra of quinoxalines*

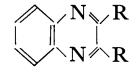

R	R′	$\lambda_{max}(m\mu)$	(ε)
H	H	233(28200)	315(6580) a)
CH_3	CH_3	237(23300)	316(6440) b)
CH_3	CH_3CO	245(32600)	304(6400)
CH_3	PhCO	246(32900)	321(6460)
Ph	CH_3CO	246(34300)	332(7400) b)
Ph	PhCO	252(38200)	340(9470)

* Measured in ethanol.
a) See Ref. 3.
b) See Ref. 1.

On the other hand, in acetic acid the photooxidation of the diazepine (I-b) leads to 2-acetyl-3-phenylquinoxaline (II-b), as in the case of oxidation with peracids. When the diphenylbenzodiazepine (II-c) was treated with peracetic acid, the ring-contraction product, 2-benzoyl-3-phenylquinoxaline (II-c), could not be obtained at all, but an amide (VI) was obtained.[4] On the other hand, in a benzene solution, the benzodiazepine (I-c) was photochemically oxidized very slowly with high-pressure mercury arc to give the corresponding oxidative ring-contraction product, 2-benzoyl-3-phenylquinoxaline (II-c). In the photooxidation of the diazepine (I-c), acetic acid highly promoted the oxidation reaction, and in acetic acid, 2-phenylbenziminazole (V-b), *N*,*N*′-dibenzoyl-*o*-phenylenediamine (VII), and an amide (VIII) were obtained as by-products. These results are shown in Table 3.

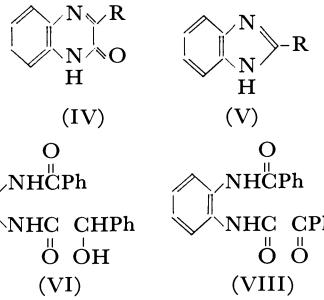

(IV) (V)

(VI) (VIII)

In the photooxidation of the benzodiazepine (I), the oxidative ring-contraction to the acylquinoxaline (II) seems to proceed in a different fashion from that in the oxidation with peracids, as has been mentioned above. Though the acylquinoxaline (II) may be produced through the 6-oxo intermediate (III) in the photooxidation of the diazepine (I), as in the oxidation of diazepine (I-a) and (I-b)

2) T. Yonezawa, M. Matsumoto and H. Kato, This Bulletin, **41**, 2543 (1968).

3) R. C. Hirt, *J. Chem. Phys.*, **25**, 574 (1956).

TABLE 3. OXIDATIVE RING-CONTRACTION OF THE BENZODIAZEPINES (I)

Benzodiazepine	Oxidation method	Solvent	Products (Yield, %)
(I-a)	$h\nu/O_2$	benzene	II-a(29), IV(8)
(I-a)	$h\nu/O_2$	acetic acid	II-a(31), IV(9)
(I-a)	$h\nu/O_2$ (at 0—5°C)	0.1 N H_2SO_4	II-a(2), V-a(5)
(I-a)	$h\nu/O_2$ (at 45—50°C)	0.1 N H_2SO_4	II-a(2), V-a(75)
(I-a)[a]	peracetic acid	acetic acid	II-a(27)
(I-b)	$h\nu/O_2$	benzene	II-d(25), IV(3)
(I-b)	$h\nu/O_2$	acetic acid	II-b(34)
(I-b)[a]	peracetic acid	acetic acid	II-b(35)
(I-c)	$h\nu/O_2$	benzene	II-c (trace)*
(I-c)	$h\nu/O_2$	acetic acid	II-c(14), V-b(16), VII, VIII (trace)
(I-c)[b]	peracetic acid	acetic acid	VI(44), (V-a)(9), VII(3)

* Oxidation was not completed within 40 hr.
a) See Ref. 1. b) See Ref. 4.

with peracids, diazabenzotropone (III) can not be expected to rearrange to the acylquinoxaline (II) in the case of the photooxidation, particularly in benzene, as in the case of the oxidation with peracids, for neither 2-benzoyl-3-phenylquinoxaline (II-c) nor 2-benzoyl-3-methylquinoxaline (II-d), but rather, the amide (VI) and 2-acetyl-3-phenylquinoxaline (II-b) were obtained upon treatment with peracetic acid. Thus, in the photooxidation of the diazepine (I) in benzene, the 6-oxo intermediate (III) is thought to undergo ring-contraction to the acylquinoxaline (II) photochemically. As is shown in Scheme II, we postulate that the diazabenzotropone (III) formed under the action of light may be subjected to the second photochemical reaction. In this point in Scheme I, as has been described in the work of Barltrop *et al.*,[1] the methylphenyldiazabenzotropone (III-b) rearranges to the acetylquinoxaline (II-b) through hydrolysis and successive dehydration ; in Scheme II, though diazatropone (III-b) rearranges to benzoylquinoxaline (II-d) photochemically.

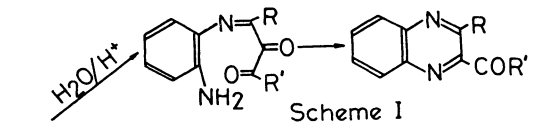

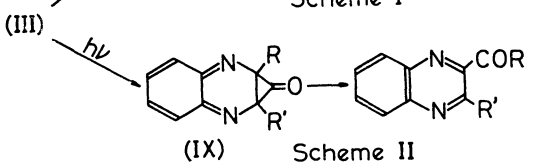

In Scheme II, Hückel calculation could give a reasonable result providing that this reaction occurred as a consequence of an n-π^* transition due the carbonyl group, as in the photochemical reactions of tropone[5] and tropolone,[6] and providing that the lowest vacant molecular orbital (LV) participates in that n-π^* transition.

Table 4 gives the characteristics of the lowest n-π^* excited state : the 1—3, 1—2, and 2—3 bonds show a tendency to be strengthened, while the 1—7 and 3—8 bonds become weak. The calculated results may support the idea that the photochemical reaction proceeds through a norcaradienone intermediate (IX), as shown in Scheme II. Therefore,

TABLE 4. CHANGES IN BOND ORDERS IN EXCITED DIAZABENSOTROPONE (III-b)

Atoms	Coefficients in LV π-MO	Bonds	Changes in bond orders
1	−0.123	1—2	+0.051
2	−0.419	2—3	+0.028
3	−0.195	1—3	+0.024
4	−0.023		
5	+0.272	2—6	−0.011
6	+0.027	2—4	+0.009
7	+0.418		
8	+0.476	1—7	−0.051
		3—8	−0.093

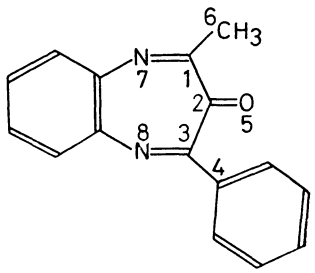

4) M. Matsumoto, A. Iio and T. Yonezawa, This Bulletin, **43**, 281 (1970).

5) W. G. Dauben, K. Koch, O. L. Chapman and S. L. Smith, *J. Amer. Chem. Soc.*, **83**, 1768 (1961).

6) *Cf.*, for example, P. de Mayo and R. W. Yip, *Proc. Chem. Soc.*, **1962**, 84.

the interaction between the phenyl group and the carbonyl group in (IX) may cause the bond fission of the 1—2 and 3—4 bonds. Thus, we can say that the tropone (III-b) in the excited state may rearrange to favor the formation of benzoylquinoxaline (II-d), but not acetylquinoxaline (II-b).

Experimental

2,4-Dimethyl-1,5-benzodiazepine (I-a). Acetylacetone (20 g) and *o*-phenylenediamine (20 g) were refluxed in dried benzene (100 m*l*) with *p*-toluene sulfonic acid (0.1 g) for 1 hr. Then the violet-coloured reaction mixture was filtered and condensed. The oily residue was chromatographed in benzene on silica gel (200 g). The diazepine (I-a) was then crystallized from 1: 1 benzene-cyclohexane; mp 131°C; yield, 70%.

Found: C, 76.39; H, 7.11; N, 16.14%. Calcd for $C_{11}H_{12}N_2$: C, 76.71; H, 7.02; N, 16.27%.

2-Methyl-4-phenyl-1,5-benzodiazepine (I-b). Benzoylacetone (40 g) and *o*-phenylenediamine (20 g) were reacted in xylene (200 m*l*) for an hour, as in the case of the diazepine (I-a). Then the crude product was chromatographed in petroleum ether on silica gel (200 g). Crystallization from aqueous ethanol gave yellow crystals of the diazepine (I-b) monohydrate which melted at 118°C. The IR spectrum showed ν_{N-H} and ν_{OH} at 3450–3300 cm^{-1}. The NMR spectrum in $CDCl_3$ showed three singlets, at $\tau=8.05$ (3H, 2-CH_3 protons), $\tau=6.25$ (2H, water of crystallization), and $\tau=4.10$ (1H, 3-methyne proton), and multiplets at $\tau=3.40$—2.00 (10H). The mass spectrum showed a parent peak at *m/e* 234.

Found: C, 75.84; H, 6.38; N, 11.06%. Calcd for $C_{16}H_{14}N_2\cdot H_2O$: C, 76.16; H, 6.39; N, 11.10%.

From these results, the diazepine (I-b) which melted at 118° was determined to have the 1-H form (I-b)′.

Veibel and Hromadko[7] give a mp of 87—88°C for the diazepine (I-b); we also obtained crystals which melted at 87°C. The NMR spectrum of the diazepine (I-b) which melted at 87°C in $CDCl_3$ showed two singlets, at $\tau=7.77$ (3H, CH_3 protons) and $\tau=6.83$ (2H, 3-methylene protons), and multiplets at $\tau=2.90$—1.85 (9H). Thus, the diazepine (I-b) which melted at 87°C was 3-H form (I-b)″.

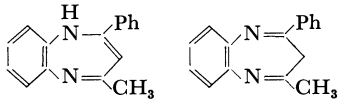

(I-b)′

(I-b)″

2,4-Diphenyl-1,5-benzodiazepine (I-c). The diazepine (I-c) was prepared from dibenzoylmethane and *o*-phenylenediamine as has been described by Barltrop *et al.*[1] The diazepine (I-c) was crystallized from methanol as colourless needles; mp 140°C.

Found: C, 85.20; H, 5.41; N, 9.51%. Calcd for $C_2H_{16}N_2$: C, 85.11; H, 5.44; N, 9.45%.

Photooxidation of the Diazepine (I-a) in Benzene. The diazepine (I-a) (3.0 g) in benzene (330 m*l*) was irradiated with a 200-W high-pressure mercury arc under an oxygen atmosphere for 8 hr. The irradiation was continued until the reaction mixture did not colour upon the addition of acetic acid. After irradiation, the reaction mixture was condensed *in vacuo*, and the oily residue was chromatographed in benzene on silica gel (200 g). 2-Acetyl-3-methylquinoxaline (II-a) was obtained as colourless needles which melted at 87°C by crystallization from aqueous ethanol yield 29%. Then 3-methyl-2-quinoxalone (IV) was obtained, mp 243°C from hot water as brown crystals; yield, 8%.

The quinoxaline (II-a): $\nu_{C=O}$ (in KBr) at 1689 cm^{-1}. Its phenylhydrazone, mp 174°C.

Found: C, 80.02; H, 5.46; N, 15.93%. Calcd for $C_{11}H_{10}ON_2$: C, 79.95; H 5.41; N, 15.95%.

The quinoxalone (IV); $\nu_{C=O}$ (in KBr) at 1668 cm^{-1}.

Found C: 67.49, H: 5.10, N: 17.40%, Calcd for $C_9H_8ON_2$ C: 67. 48, H: 5.03, N: 17.49%.

Photooxidation of the Diazepine (I-a) in Acetic Acid. After irradiation for 5 hr while an oxygen gas was being bubbled in, a violet-coloured acetic acid solution (330 m*l*) of the diazepine (I-a) (3.0 g) faded to a reddish brown. From the reaction mixture, acetic acid was removed *in vacuo*; the residue was treated as in previous experiments. The quinoxaline (II-a) and the quinoxalone (IV) were thus obtained in yields of 31 and 9% respectively.

Photooxidation of the Diazepine (I-a) in a 0.1 N H_2SO_4 Aqueous Solution. When a violet solution of the diazepine (I-a) (3.0 g) in a 0.1 N H_2SO_4 aqueous solution (330 m*l*) was irradiated for 5 hr at 0—5°C, the solution turned a reddish brown. After the solution had been neutralized by alkali and dried *in vacuo*, the dark brown oil was washed with chloroform. The washings, chromatographed on silica gel and eluted with benzene, gave, successively, the quinoxaline (II-a) and 2-methylbenziminazole (V-a) in yields of 2 and 5% respectively.

When the diazepine in a 0.1 N H_2SO_4 aqueous solution was photooxidized at 45—50°C, the quinoxaline (II-a) and the benziminazole (V-a) were obtained in yields of 2 and 75% respectively. 2-Methylbenziminazole (V-a): mp 175°C obtained as needles from ethanol.

Found: C, 72.81; H, 6.13; N, 21.13%. Calcd for $C_8H_8N_2$: C, 72.70; H, 6.10; N, 21.20%.

Photolysis of 2-Acetyl-3-methylquinoxaline (II-a). The quinoxaline (II-a) (0.5g) in benzene (100 m*l*) was irradiated with a 100-W high-pressure mercury arc, while oxygen gas was being bubbled in, for 5 hr. The product was chromatographed on silica gel in chloroform, giving, successively, the starting material (210 mg) and 3-methylquinoxalone (IV) (30 mg); mp 245°C (from hot water).

Photooxidation of the diazepine (I-b) in Benzene. The diazepine (3.5 g) in benzene (330 m*l*) was irradiated under an oxygen atmosphere for 6 hr. The mixture was concentrated to a small bulk and then chromatographed on silica gel in benzene; we thus obtained 2-benzoyl-3-methylquinoxaline (II-d) and the quinoxalone (IV) in yields of 25 and 3% respectively. The quinoxaline (II-d) was in the form of colourless needles which melted at 88—89°C. Upon crystallization from aqueous ethanol and which were identified as has been described above. The quinoxaline (II-d) oxime was obtained as needles, which melted at 208°C.

The quinoxaline (II-d): $\nu_{C=O}$ (in KBr) at 1665 cm^{-1}.

Found: C, 77.46; H, 4.92; N, 11.32%. Calcd for $C_{16}H_{12}ON_2$: C, 77.40; H, 4.87; N, 11.28%.

Photooxidation of the Diazepine (I-b) in Acetic Acid. The diazepine (3.5 g) was oxidized photo-

7) S. Veibel and S. F. Hromadko, *Chem. Ber.*, **93**, 2752 (1960).

chemically in acetic acid (330 ml) for 8 hr, after which the reaction mixture was condensed and chromatographed on silica gel in benzene. Then 2-acetyl-3-phenylquinoxaline (II–b) was isolated as needles, mp 110°C by crystallization from ethanol. Lutz and Stuart[8] give a mp 110—111°C. The quinoxaline (II–b): $\nu_{C=O}$ at 1698 cm^{-1}.

Found: C, 77.45; H, 4.92; N, 11.33%. Calcd for $C_{16}H_{12}ON_2$: C, 77.40; H, 4.87; N, 11.28%.

Photooxidation of the Diazepine (I-c) in Benzene. The diazepine (3.0 g) in benzene (330 ml) was irradiated for 40 hr under an oxygen atmosphere. Almost the only thing recovered was the starting material; the oxidation product, 2-benzoyl-3-phenylquinoxaline (II–c), was detected only by T. L. C.

Photooxidation of the Diazepine (I-c) in Acetic Acid. The diazepine (3.0 g) in acetic acid (330 ml) was irradiated under an oxygen atmosphere. After 36 hr, the violet solution was faded to a reddish brown. The reaction mixture was then concentrated *in vacuo*, chromatographed on silica gel, and eluted with chloroform; it thus gave, succesively, 2-benzoyl-3-phenylquinoxaline (II–c) (14%), the amide (VIII) (0.7%), *N,N'*-dibenzoyl-*o*-phenylenediamine (VII), and 2-phenylbenziminazole (V–b) (16%). The quinoxaline (II–c) was identified by comparing it with a specimen prepared from diphenyltriketone and *o*-phenylenediamine. Colourless needles; mp 153.5—154.5°C; crystallization from diethyl ether. $\nu_{C=O}$ (in KBr) at 1660 cm^{-1}.

Found: C, 81.33; H, 4.60; N, 9.00%. Calcd for $C_{21}H_{14}ON_2$: C, 81.27; H, 4.55; N, 9.03%.

The amide (VIII) was in the form of colourless needles which melted at 198°C and which were crystallized from benzene-petroleum ether. The mass spectrum showed a parent peak at *m/e* 344. The IR spectrum showed $\nu_{C=O}$ at 1670 and 1650 cm^{-1} in KBr.

Found: C, 73.27; H, 4.73; N, 8.19%. Calcd for $C_{21}H_{16}O_2N_2$: C, 73.24; H, 4.68; N, 8.14%.

The amide (VII) and *N,N'*-dibenzoyl-*o*-phenylenediamine prepared by the condensation of *o*-phenylenediamine and benzoyl chloride had identical infrared spectra. Mp 324°C, $\nu_{C=O}$ at 1664 cm^{-1}.

Found: C, 76.01; H, 5.13; N, 8.79%. Calcd for $C_{20}H_{16}O_2N_2$: C, 75.93; H, 5.10; N, 8.86%.

The iminazole (V–b) melted at 313—314°C.

Found: C, 80.45: H, 5.26; N, 14.50%. Calcd for $C_{13}H_{10}N_2$: C, 80.38; H, 5.19; N, 14.42%.

8) Lutz and Stuart, *J. Amer. Chem. Soc.*, **59**, 2316 (1937).

BULLETIN OF THE CHEMICAL SOCIETY OF JAPAN VOL. 43 1500—1505 (1970)

Reactions of Diazoketones in the Presence of Metal Chelates. III. Reactions with Carbonyl Compounds*[1]

Matsuji TAKEBAYASHI, Toshikazu IBATA and Kozaburo UEDA

Department of Chemistry, College of General Education, Osaka University, Toyonaka, Osaka

(Received October 18, 1969)

The reaction of α-diazoacetophenone with carbonyl compounds such as benzaldehyde, acetophenone and *p*-phenylacetophenone, has been studied in the presence of bis(acetylacetonato) copper (II). The reaction gave the corresponding tetrahydrofurans and dioxolanes accompanied by some by-products derived from benzoylcarbene. The mechanism of the reaction has been discussed in terms of an intermediate with a structure of betaine type, produced by the reaction of a ketocarbene-metal chelate complex with carbonyl compounds.

In previous papers,[1),2)] we reported that the reactivity of α-diazoacetophenone (I) toward alcohols could be modified by bis(acetylacetonato)copper (II) to give alkoxyacetophenones, instead of alkyl phenylacetate, and that the reaction with *cis*- and *trans*-stilbenes afforded the stereospecific addition products of benzoylcarbene to the double bond of these olefinic compounds. We also pointed out that the catalyzed reaction of α-diazoacetophenone with acetone gave mainly an enol-ether[3)] when copper powder was employed as a catalyst.[4)] The mechanism of these reactions could be explained by assuming the intermediacy of a ketocarbene-copper chelate complex (II).

This paper deals with the copper chelate-catalyzed reaction of α-diazoacetophenone with aromatic carbonyl compounds such as benzaldehyde, acetophenone and *p*-phenylacetophenone.

*1 Presented in part at the Symposium of Organic Reaction Mechanism, Yamagata, October, 1968.

1) M. Takebayashi, T. Ibata, H. Kohara and Bu H. Kim, This Bulletin, **40**, 2392 (1967).

2) M. Takebayashi, T. Ibata, H. Kohara and K. Ueda, *ibid.*, **42**, 2938 (1969).

3) M. Takebayashi, T. Ibata and H. Kohara, Symposium of Organic Reaction Mechanism, Tokyo, October, 1966.

4) M. S. Kharasch, T. Rudy, W. Nudenberg and G. Buchi, *J. Org. Chem.*, **18**, 1030 (1953).

Results and Discussion

The following two kinds of methods, A and B, were adopted for the copper chelate-catalyzed reaction of α-diazoacetophenone with carbonyl compounds. A. Dropwise addition method: A benzene solution of α-diazoacetophenone was added dropwise to a solution of a carbonyl compound and bis(acetylacetonato) copper (II) ($Cu(acac)_2$) in benzene at 80°C during the course of 2 hr under stirring. B. Mixed method: A mixture of α-diazoacetophenone, Cu $(acac)_2$ and a carbonyl compound was warmed gradually under an atmosphere of nitrogen.

Reaction of α-Diazoacetophenone with Acetophenones. In method A, 2-methyl-2-phenyl-3,4,5-tribenzoyltetrahydrofuran (III, 29%) and an oligomer (IVa, 44%) of benzoylcarbene were obtained as a by-product besides α-hydroxyacetophenone (V, 1%). In method B, however, 2,4-dimethyl-2,4-diphenyl-5-benzoyl-1,3-dioxolane (VIa, 7%) was produced accompanying small amounts of by-products such as V (1.7%), dibenzoylethane (VII, 1%) and a dilactone (VIII, 1%) in addition to III (8.3%) and IVa (10%).

The data of IR and NMR spectra indicate that the three benzoyl groups of III are oriented *trans* to each other, and that IVa is a linear oligomer consisting of 3—4 molecules of benzoylcarbene and one molecule of acetophenone.

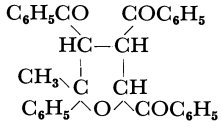

(III)

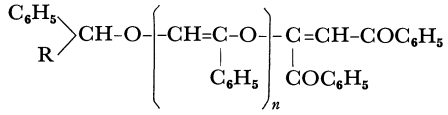

(IV)

n: 1—3 IVa: R=CH_3, IVb: R=H
IVc: R=OCH_3

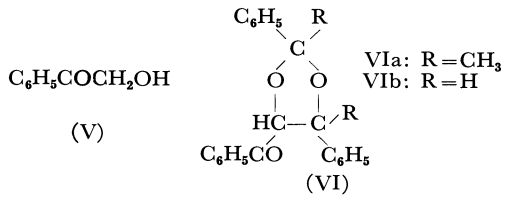

(V) (VI)

VIa: R=CH_3
VIb: R=H

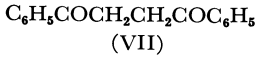

(VII)

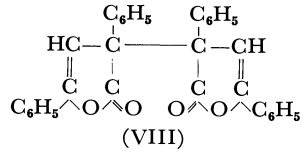

(VIII)

When *p*-phenylacetophenone was employed instead of acetophenone, the reaction (method B) gave *cis*- and *trans*-dibenzoylethylenes (IX, 1.2% and X, 6.2%), formal dimers of benzoylcarbene, and an oligomer (IVa, 12%) with a small amount (—1%) of an enol-ether (XI). However, neither dibenzoylethane, tetrahydrofuran nor dioxolane derivatives were obtained, in contrast to the case of acetophenone.

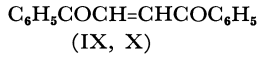

(IX, X)

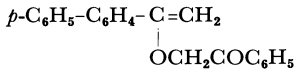

(XI)

The formation of enol-ether (XI) is noteworthy though the yield is very low, because such enol-ethers have been scarcely obtained in the reactions with aromatic ketones. Enol-ethers corresponding to XI have been obtained in the reactions with aliphatic and alicyclic ketones such as acetone and cyclohexanone.[3]

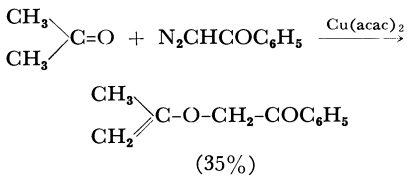

(35%)

The reaction with substituted acetophenones will be discussed elsewhere in connection with the results obtained above.

Reaction of α-Diazoacetophenone with Benzaldehyde. In method A, the reaction gave *trans*-dibenzoylethylene (X, 4.8%), an oligomer (IVb, 6.7%) and a copolymer (XIII) of benzaldehyde and benzoylcarbene.

In method B, the reaction, contrary to method A, yielded 2,5-diphenyl-4-benzoyl-1,3-dioxolane (VIb, 2.3%), an oligomer (IVb, 9%) and two kinds of copolymers (XII and XIII) of benzaldehyde and benzoylcarbene. IR and NMR spectra showed that XII, major product, and XIII were rich in benzaldehyde- and benzoylcarbene-moieties, respectively. Both copolymers have one benzyl group at one end of polymer chain and one benzoyl group at the other end.

Ried and Omran[5] observed that the thermal reaction of *p*-methyl- and *p*-methoxy-α-diazoacetophenones with substituted benzaldehydes gave dioxoles (XIV) in 25—33% yield. However, no dioxole was detected in our catalytic reaction products. The results suggest that the mechanism of copper chelate-catalyzed reaction between α-diazoacetophenone and benzaldehyde is quite different from that of purely thermal reaction.

5) W. Ried and J. Omran, *Ann. Chem.*, **673**, 120 (1964).

Table 1. Effects of the amount of methyl benzoate

Method	$C_6H_5COCHN_2$ (I) (mol)	$C_6H_5COOCH_3$ (ester) (mol)	[Ester]/[I]	Product (%) IX+X	IVc	VIII
A	0.034	0.17	5	1	89	0
	0.034	0.034	1	51	39	0
	0.034	0.007	1/5	83	12	0.16
	0.034	0	—	82	13	0.43
B	0.068	1.25	18	61	8.8	0

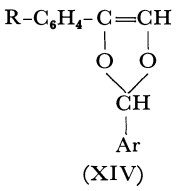

(XIV)

Reaction of α-Diazoacetophenone with Methyl Benzoate. In order to compare the behavior of esters to that of aldehydes and ketones, the reaction was carried out using methyl benzoate.

A large amount (89%) of oligomer (IVc) was produced accompanying a trace (1.1%) of *trans*-dibenzoylethylene (X) in method A, whereas dibenzoylethylenes (IX and X) (*cis*, 2.9%; *trans*, 58%) were obtained as main products with a small amount (8.8%) of oligomer (IVc) in method B. Neither tetrahydrofurans nor dioxolanes were obtained in both cases.

The effect of the amount of methyl benzoate on the yields of dimers (IX and X) and oligomer (IVc) was studied. The results are summarized in Table 1.

The data listed in Table 1 indicate that the yield of dimers (IX and X) of benzoylcarbene increases with decrease of the amount of methyl benzoate while that of oligomer decreases proportionally, and that dilactone (VIII) is produced when the ratio of the concentration of ester to I is low.

Mechanism

Diazoketone (I) reacts with the copper chelate to afford a ketocarbene-copper chelate complex (II).[1] The complex should react in two ways (path A and path B) according to the reactivity of carbonyl compounds employed.

In the case of acetophenone and benzaldehyde, the reaction of path A takes place in preference to that of path B to produce another intermediate (XV) with a structure of betaine type, from which tetrahydrofuran (III), oligomers (IV), dioxolanes (VI) and copolymers (XII and XIII) are derived. In the case of *p*-phenylacetophenone and methyl benzoate, however, the reaction of path B proceeds preferentially to give dimers (IX and X). The mechanism of the formation of these products is summaried in Scheme 1.

The fact that the yield of III increases by the addition of dibenzoylethylene (X) to the reaction mixture supports the reaction path to give III.

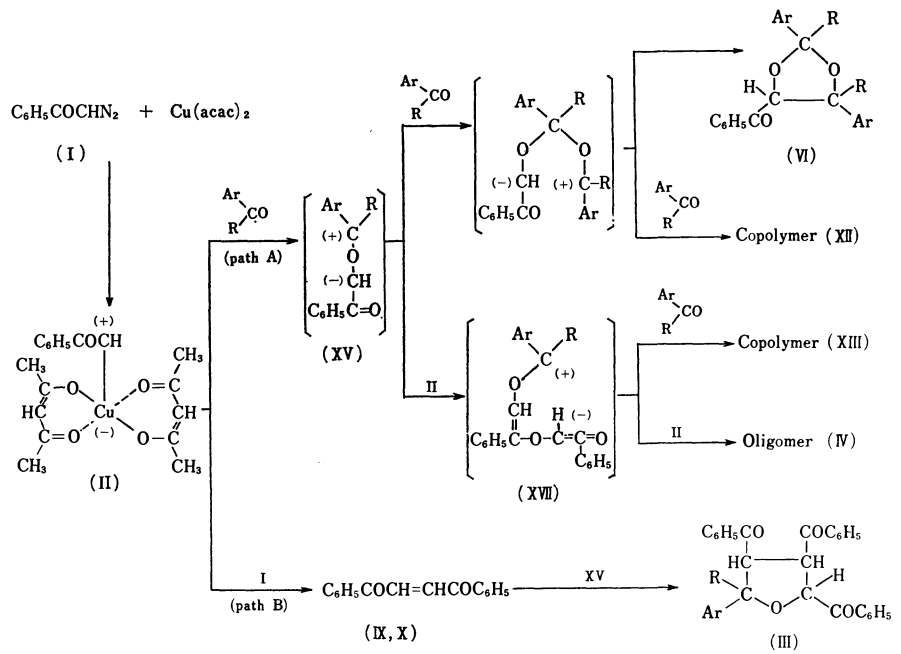

Scheme 1

The migration of proton in the intermediate (XV) will give XI.

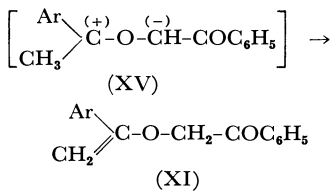

(XV)

(XI)

Generally, the proton migration hardly takes place in the intermediate from aromatic carbonyl compounds, since the intermediate (XV) is stabilized due to the resonance effect of aryl group.[6] However, the proton migration is expected to occur easily in the intermediate derived from aliphatic or alicyclic carbonyl compounds.

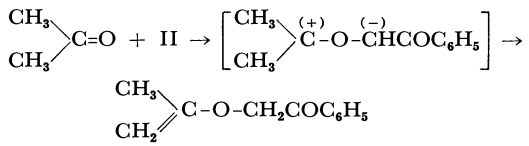

Apparently, the enol-ethers are produced by the insertion of benzoylcarbene to the O–H bond of enolated ketones. But this insertion mechanism can hardly explain the fact that the enol-ethers are obtained by the reactions with ketones having less enolic character such as acetone and cyclohexanone, and that no enol-ether is obtained by the reaction with more enolizable acetylacetone under the same conditions. Thus, the mechanism of the formation of enol-ethers can be explained by assuming an intermediate with the structure of betain type.

By-products such as α-hydroxyacetophenone (V), dibenzoylethane (VII) and dilactone (VIII), are derived from complex (II) as shown in Scheme 2. The formation of α-hydroxyacetophenone (V) arises from the reaction of complex (II) with a trace of water, because the yields of (V) vary from 1.7 to 10% according to the amount of water contained in the reaction mixture. If complex (II) abstracts a hydrogen atom from the solvent to give phenacyl radicals, recombination of the radicals takes place and affords dibenzoylethane (VII) as has been recognized in the cases of thermal[7] and copper chelate-catalyzed decomposition[3] of I in various solvents. When free benzoylcarbene is expelled from complex (II), the free carbene rearranges to the phenylketene and gives monolactone by reaction with I; the monolactone is easily oxidized to afford dilactone (VIII).[8,9]

Experimental

All melting and boiling points are uncorrected. The IR spectra were measured in potassium bromide disks for crystals and in liquid film for liquid samples, respectively, on a Hitachi Infrared Spectrometer, model EPI-S2. The NMR spectra were recorded at 60 Mc with a Varian Associates model A-60 Spectrometer, using tetramethylsilane as an internal standard. The UV spectra were taken on a Shimadzu Multipurpose Recording Spectrophotometer, model MPS-50L.

Material. *α-Diazoacetophenone* was prepared according to the method of Newman and Beal,[10] mp 47.5—48.0°C (lit,[10] mp 47.8—48.4°C).

Bis(acetylacetonato)copper (II) was prepared according to published directions.[11]

Benzaldehyde and *Acetophenone*. Commercial products were purified by distillation before use.

p-Phenylacetophenone,[12] mp 124.5—125.0°C (lit,[12] mp 121°C).

Reaction of I with Acetophenone (Method A). A solution of 5.0 g (0.034 mol) of I in 50 m*l* of benzene was added drop by drop to a solution of 20.4 g (0.17 mol) of acetophenone and 0.05 g (3.8×10^{-4} mol) of $Cu(acac)_2$ in 100 m*l* of benzene at 80°C under stirring. The color

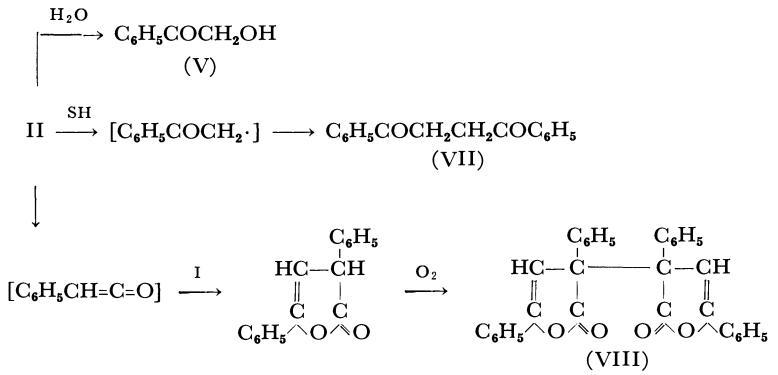

(VII)

(VIII)

Scheme 2

6) See also G. Heublein and P. Hallpap, *Tetrahedron Lett.*, **1968**, 340.

7) H. Staudinger, *Ann. Chem.*, **356**, 51 (1912).

8) M. Takebayashi, T. Ibata, H. Kohara and M. Hamaguchi, *Sci. Rep. Osaka Univ.*, **17**, 7 (1968).

9) P. Yates and T. J. Clark, *Tetrahedron Lett.*, **1961**, 435.

10) M. S. Newman and P. F. Beal, *J. Amer. Chem. Soc.*, **71**, 1506 (1949).

11) H. S. Booth, "Inorganic Syntheses," Vol. 2, McGraw-Hill, Inc., New York, N.Y., p. 14 (1946).

12) L. M. Long and H. R. Henze, *J. Amer. Chem. Soc.*, **63**, 1939 (1941).

of the reaction mixture turned dark brown with evolution of nitrogen. After the reaction was over, the reaction mixture was fractionated under a reduced pressure. The distillate (A) boiling at 60—90°C/1 mmHg crystallized at room temperature. The fractional recrystallization of A using light petroleum gave a trace of benzoic acid and 0.05 g (1%) of α-hydroxyacetophenone (V), mp 86.0—87.0°C (mp 86.0—87.0°C[13]).

Found: C, 69.99; H, 5.68%. Calcd for $C_8H_8O_2$: C,70.57; H, 5.92%. IR (KBr disk): 3380, 1685, 1405 and 1110 cm^{-1}.

The distillation residue (B) was dissolved in a mixture of benzene and *n*-heptane and allowed to stand for 2 days. A dark red solid (B-1) was isolated from the solution, and red oily substance (B-2) was separated from the filtrate by concentration. Recrystallization of B-1 from benzene-*n*-hexane gave 1.55 g (29%) of 2-methyl-2-phenyl-3,4,5-tribenzoyltetrahydrofuran (III), mp 167.0—168.0°C.

Found: C, 81.18; H, 5.44%. Calcd for $C_{32}H_{26}O_4$: C, 80.99; H, 5.52%. The NMR spectrum is shown in Fig. 1; UV: λ_{max}^{EtOH} 2683 Å (ε 1770) and 2734 Å (ε 5200). IR: 1685, 1450, 1280, 1245, 1215 and 985 cm^{-1}.

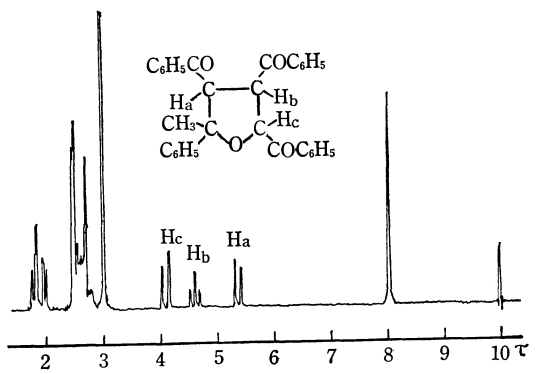

Fig. 1. NMR spectrum of III.

When a benzene solution of oily substance (B-2) was poured into *n*-hexane, a brown solid was obtained. This product did not crystallize from any solvents, but the data of IR and NMR spectra indicated that the product was an oligomer of benzoylcarbene with one molecule of acetophenone (IVa), and that the oligomer has a skeleton of vinyl ether. The yield of oligomer was 1.7 g (44%).

Found: C, 80.75; H, 5.38%. Calcd for $C_{32}H_{26}O_4$ ($C_6H_5COCH_3$+3 C_6H_5COCH:): C, 80.79; H, 5.52%. UV (in dichloromethane): λ_{max} 2480 Å (ε 14200) IR: 1640, 1445 and 1220 cm^{-1}. NMR: 2.65 τ (s, broad). Mol wt (Rast): Found, 490. Calcd for $C_{32}H_{26}O_4$, 474.5.

Reaction of I with Acetophenone (Method B). A solution of 5.0 g (0.034 mol) of I and 0.05 g (3.8×10^{-4} mol) of $Cu(acac)_2$ in 150 g of acetophenone was warmed gradually under an atmosphere of nitrogen. By distillation of the reaction mixture under a reduced pressure after removal of unreacted acetophenone, a distillate (C) boiling at 60—85°C/0.1 mmHg and a tarry residue (D) were obtained. Fractional recrystallization of C from light petroleum gave a trace of benzoic acid and 0.076 g (1.7%) of α-hydroxyacetophenone (V).*2

Besides, 0.04 g (1%) of dibenzoylethane (VII), mp 147.0—148.0°C (lit,[14] mp 140°C), was separated from the concentrated mother liquor after one week.

Found: C, 79.11; H, 5.85%. Calcd for $C_{16}H_{14}O_2$: C, 80.64; H, 5.92%. IR: 1687, 1225, 990, 743 and 698 cm^{-1}. The distillation residue D was treated with benzene. A small amount of precipitate was collected by filtration. This precipitate did not dissolve in usual organic solvents. The IR spectrum was completely superimposable with that of dilactone (VIII, 1%) prepared by the photolysis of I in benzene solution.[8,9]

From the benzene layer, 0.39 g (10%) of oligomer (IVa) was separated out by adding *n*-heptane. Moreover, 0.45 g (8.3%) of tetrahydrofuran (III) was obtained from the mother solution after being left to stand for several days at room temperature. Evaporation of the solvent gave a yellow oil. The oil could not be distilled, but the substance was deduced to be 2,4-dimethyl-2,4-diphenyl-5-benzoyl-1,3-dioxolane (VIa, 0.88 g, 7%) by means of IR spectra.

Found: C, 81.85; H, 6.44%. Calcd for $C_{24}H_{22}O_3$: C, 81.42; H, 6.19%.
IR: 1690, 1450, 1370, 1270, 1100, 1060 and 1020 cm^{-1}.

Reaction of I with *p*-Phenylacetophenone (Method B). The reaction of I (5.0 g, 0.034 mol) with *p*-phenylacetophenone (8.24 g, 0.024 mol) was carried out by the mixed method in benzene solution (150 g) in the presence of $Cu(acac)_2$ (0.05 g, 3.8×10^{-4}mol). Unreacted *p*-phenylacetophenone was separated by adding ligroin to the reaction products, and the solvent was removed by distillation. The residue was treated with light petroleum to separate insoluble part (E) from soluble part (F). The insoluble part E was dissolved in cyclohexane at the reflux temperature, and was kept standing overnight at room temperature. 0.48 g (12%) of oligomer (IVa) was separated out from the solution, and 0.1 g (1%) of yellow needles of enol-ether (XI), mp 91.0—92.0°C, precipitated from the filtrate after one week at 10°C.

Found: C, 83.65; H, 5.64%. Calcd for $C_{22}H_{18}O_2$: C, 84.05; H, 5.64%. IR: 1680, 1655, 1295, 1263, 1018 and 960 cm^{-1}.

The bromination of enol-ether (XI) in CCl_4 gave its dibromide, mp 117.0—119.0°C.

Found: C, 57.60; H, 3.53%. Calcd for $C_{22}H_{18}O_2Br_2$: C, 55.84; H, 3.62%. IR: 1685, 1290 and 990 cm^{-1}.

The soluble part F was allowed to stand for several days at room temperature. A yellow solid (F-1) precipitated in preference to solid (F-2). The solid F-1 was recrystallized from light petroleum, and was identified as *trans*-dibenzoylethylene (X) in a good agreement with elemental analyses and IR spectra with the authentic sample; mp 111.0—112.0°C, yield 0.25 g (6.2%).

Found: C, 81.84; H, 5.12%. Calcd for $C_{16}H_{12}O_2$: C, 81.34; H, 5.12%. UV: λ_{max}^{EtOH} 2608 Å (ε 19700).

13) L. Wolff, *Ann. Chem.*, **325**, 143 (1902).

*2 The yield of α-hydroxyacetophenone varied from 1.7 to 10% according to the amount of water contained in the acetophenone employed. When acetophenone was treated with anhydrous magnesium sulfate for one week at room temperature and then distilled, the yield was found to be 1.7%. If the treatment with anhydrous magnesium sulfate was omitted, the yield increased up to 10%.

14) C. Grundman and H. Trischmann, *Ann. Chem.*, **536**, 29 (1938).

IR: 1655, 1600, 1450, 1325, 1295, 1194 and 1023 cm^{-1}.

The solid F-2 was purified by recrystallization from benzene-*n*-hexane, and was identified as *cis*-dibenzoylethylene (IX) by elemental analyses and UV, IR and NMR spectra; mp 136.0—137.0°C, yield 0.05 g (1.2%).

Found: C, 81.43; H, 4.99%. Calcd for $C_{16}H_{12}O_2$: C, 81.34; H, 5.12%. IR: 1665, 1600, 1450, 1400, 1233 and 1015 cm^{-1}. UV: λ_{max}^{EtOH} 2608 Å (ε 26000). NMR (12 $CDCl_3$): 2.89 (s, 2H), 2.7—2.5 (m, 6H) and 2.2—2.0 τ (m, 4H).

Reaction of I with Benzaldehyde (method B). The reaction of I (5.0 g, 0.034 mol) with benzaldehyde (150 g, 1.42 mol) was carried out in the presence of $Cu(acac)_2$ (0.05 g, 3.8×10^{-4} mol) by the mixed method. After removal of unreacted benzaldehyde by distillation, the residue was dissolved in hot benzene under heating, and a small amount of ligroin was added to the solution. A white precipitate (G-1) was separated out from the solution. The precipitate G-1 was dissolved again in benzene and poured into *n*-hexane under stirring. When the mixture was let to stand overnight, a white substance precipitated from the solution. The precipitate was collected by filtration, and was confirmed to be copolymer (XII) of benzaldehyde-benzoylcarbene, 4.8 g, mp 127°C. IR: 1690, 1450, 1100 and 710 cm^{-1}. UV (in dichloromethane): λ_{max} 2500 Å. NMR (in $CDCl_3$): 3.3—3.1 (m, 2H), 5.5—4.0 (m, 15H) and 4.0—2.1 τ (m, 85H).

The copolymer (XII) is so stable that no change was observed during the treatment with hot concentrated hydrochloric acid or 10%-sodium hydroxide solution.

To the filtrate was added *n*-heptane under heating and allowed to stand overnight. A black oily substance (G-2) separated out, and then a brown oil (G-3) precipitated by concentrating the filtrate. After evaporation of the solvent, the residue was dissolved in benzene. The benzene solution was let to stand for 3 days to give yellow substance (G-4). The oil G-2 was confirmed to be oligomer of benzoylcarbene with one molecule of benzaldehyde (IVb) by means of IR spectrum; yield 0.29 g (6.7%). IR: 1675, 1600, 1445, 1215 and 1020 cm^{-1}.

The oil G-3 was dissolved in methyl alcohol, and the solution was allowed to stand at room temperature to give a brown precipitate. The IR spectrum indicates that the precipitate is another copolymer of benzaldehyde-benzoylcarbene (XIII) 0.38 g, mp 68—73°C. UV (in dichloromethane): λ_{max} 2500 Å. IR: 1675, 1600, 1450, 1240 and 1100 cm^{-1}.

Recrystallization of the product G-4 from methyl alcohol gave white needles. The crystalline product was identified to be dioxolane (VIb), yield 0.26 g (2.3%); mp 167.0—168.0°C.

Found: C, 80.41; H, 5.49%. Calcd for $C_{22}H_{18}O_3$: C, 79.98; H, 5.49%. The NMR spectrum is shown in Fig. 2. UV: λ_{max}^{EtOH} 2600 A (ε 10400). IR: 1690, 1450, 1410, 1215, 1090, 1052 and 1010 cm^{-1}.

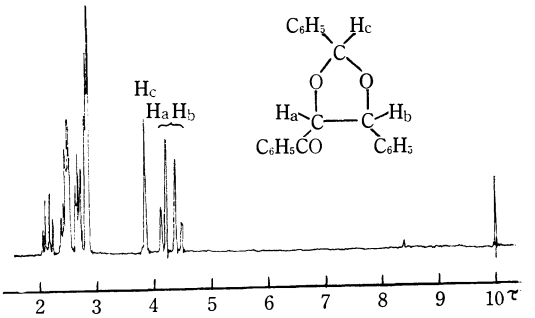

Fig. 2. NMR spectrum of VIb.

Reaction of I with Methyl Benzoate (Method B). The reaction of I (10.0 g, 0.068 mol) with methyl benzoate (150 g, 1.25 mol) in the presence of $Cu(acac)_2$ (0.05 g, 3.8×10^{-4} mol) was carried out by the mixed method. Unreacted methyl benzoate was removed by distillation. No distillate was obtained at 130°C under 0.1 mmHg. The fractional recrystallization of residue gave *cis*-dibenzoylethylene (IX) (0.5 g, 2.9%), *trans*-dibenzoylethylene (X) (4.8 g, 58%) and oligomer of benzoylcarbene with one molecule of methyl benzoate (IVc) (0.65 g, 8.8%).

Found: C, 78.30; H, 5.00%. Calcd for $C_{32}H_{26}O_6$: C, 78.35; H, 5.34%. IR: 1760, 1675, 1220 and 698 cm^{-1}.

The authors express their cordial thanks to Mr. Hiroyuki Kaburagi for his assistance in experiments, and also to the Ministry of Education for a grant-in-aid for Scientific Research.

BULLETIN OF THE CHEMICAL SOCIETY OF JAPAN VOL. 43 1506—1511 (1970)

Studies of Diazosulfides. II.*1 The Dissociation of *trans*- and *cis*-Diazosulfides and the Isolation of *cis*-Diaryldiazosulfides

Takashi YAMADA*2

Department of Chemistry, Faculty of Science, Kyoto University, Sakyo-ku, Kyoto

(Received October 20, 1969)

The reaction of *trans*- and *cis*-*N*-aryl-*S*-triphenylmethyldiazosulfides (I) with β-naphthol in alkaline ethanol was investigated. It was found that the dissociation of I occurs not only with the *cis* isomers, but also with the *trans* isomers, even in the dark. The kinetic study suggested that the *trans*-diazosulfides can dissociate not only through the *cis* form, but also directly, contrary to Zwet and Kooyman's suggestion. The dissociation of the *trans* isomer of diaryldiazosulfides (II) was also discussed analogously. Further, by a preparation at −78°C several *cis*-diaryldiazosulfides were isolated which had never before been isolated. The rate constant of the isomerization of *cis*-*N*-(*p*-cyanophenyl)-*S*-(*p*-tolyl)diazosulfide (IIf) was 2.55×10^{-3} sec^{-1} (at 0°C, in ethanol); this value is much larger than that for *cis*-I.

Recently, both *cis* and *trans* isomers of diazosulfides were isolated by Zwet and Kooyman.[1] In their paper, it was concluded that the ionization of diazosulfides can occur with only the *cis* isomers, whereas the *trans* isomer cannot dissociate unless it is first converted photochemically to the *cis* isomer. Similar behavior has been reported for diazocyanides and diazosulfonates.[2] However, the present author and his co-workers found previously that diaryldiazosulfides, which could be identified as having the *trans* form according to the UV spectral discussion,[1] dissociated at an appreciable rate and coupled with β-naphthol to afford azo-dyes in alkaline ethanol.[3] On the basis of the previous results,[3] it was suggested that the *trans* form of diazosulfides may generally dissociate, and that the *trans*-*N*-aryl-*S*-triphenylmethyldiazosulfides (I) treated by Zwet and Kooyman also dissociate, even though at a very low rate. In other to confirm this suggestion, the present author prepared both *trans* and *cis* forms of I and examined their reaction with β-naphthol. Further, in connection with the study of the dissociation of *trans*-diaryldiazosulfides (II), the author could successfully isolate the *cis* isomers of II, which had never before been isolated.

In the present paper, the author wishes to report the findings of his kinetic study of the reaction of *cis* and *trans* forms of diazosulfides (I) with β-naphthol in alkaline ethanol, and of his study of the isolation of *cis*-II isomers and their thermal isomerization.

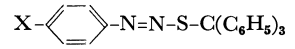

(I)

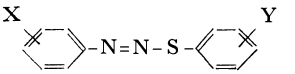

(II)

Results and Discussion

Reaction of *cis*- and *trans*-Diazosulfides (I) with β-Naphthol. The reaction of *trans*-*N*-aryl-*S*-triphenylmethyldiazosulfides (I) with β-naphthol was carried out in alkaline ethanol at 30.0°C. It was found that the *trans*-diazosulfides (Ia-c, X= OCH_3, CH_3 and H) reacted very slowly, but positively, to produce azo-dyes even in the dark, contrary to Zwet and Kooyman's observation.[1]

Table 1. Rate constants for the reaction of *N*-aryl-*S*-triphenylmethyl diazosulfides (I) with β-naphthol in alkaline ethanol*

	Substituent	$k\times10^6$ (sec^{-1})		
		cis-I	*trans*-I	
	X	35.0°C	35.0°C	45.0°C
Ia	OCH_3		1.9	6.5
Ib	CH_3	140	0.49	1.8
Ic	H	65	0.096	0.38
Id	Cl	16	—**	—**
Ie	NO_2	1.6	—**	—**

* [Diazosulfide] = 1.0×10^{-4} M, [β-Naphthol] = 1.0×10^{-3} M, [KOH] = 1.1×10^{-3} M.

** too slow to measure.

*1 Part I of this series: Ref. 3.

*2 Present address: Laboratory of Chemistry, Faculty of Science, Kōnan University, Okamoto, Higashinada-ku, Kobe.

1) H. van Zwet and E. C. Kooyman, *Rec. Trav. Chim. Pays-Bas*, **86**, 993 (1967).

2) H. Zollinger, "Azo and Diazo Chemistry," Interscience Publishers, New York (1961), pp. 66, 151.

3) T. Yamada, N. Tanaka, T. Morisawa, M. Nishikuri and A. Kaji, This Bulletin, **43**, 908 (1970).

The first-order rate constants of the reaction of *cis*-and *trans*-I are summarized in Table 1. The table shows that the *cis* isomer reacts much faster than the *trans* isomer, as is expected, and that the electron-donating substituents on the *N*-aryl part of both *cis*-I and *trans*-I promote the reaction. Hammett plots of the rate constants give good straight lines, the ρ-values being -2.05 for the *cis* isomers (ρ_{cis}) and -4.8 for the *trans* isomers (ρ_{trans}) (Fig. 1).

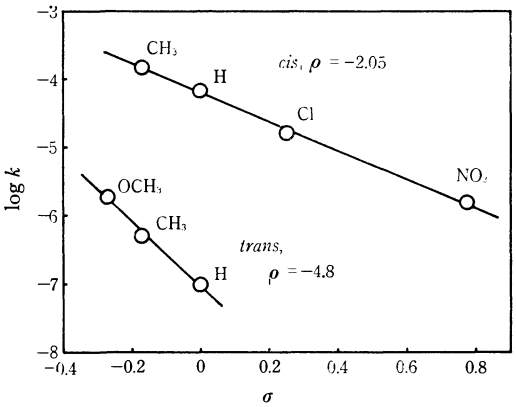

Fig. 1. Hammett plots for the reaction of *cis*- and *trans*-diazosulfides (I), *p*-X-C_6H_4-N=N-S-$C(C_6H_5)_3$, with β-naphthol in alkaline ethanol at 35.0°C.

Table 2. Activation parameters for the reaction of *trans*-diazosulfides (I) with β-naphthol in alkaline ethanol

Diazosulfide	Substituent X	E_a kcal/mol	$\Delta S^{\neq}$ (35°C) e. u.
Ia	OCH_3	24.0	−10.2
Ib	CH_3	25.4	−8.4
Ic	H	26.8	−7.2

Table 2 summarizes the activation parameters calculated from the values for the *trans* isomers listed Table 1. It is interesting that the values of the entropy of activation ($\Delta S^{\neq}$) are comparable with the values for diaryldiazosulfides, whereas the energies of activation (E_a) were considerably larger than that for diaryldiazosulfides; *e.g.*, the E_a value for *N*-(*p*-tolyl)-*S*-(*p*-chlorophenyl)diazosulfide is 10.2 kcal/mol.[3]

The negative ρ-values (Fig. 1) and the negative values of the entropy of activation (Table 2) suggest that the rate-determining step in this reaction is the dissociation of diazosulfides (I), just as in the case of diaryldiazosulfides (II).[3] Therefore, it seems reasonable that the following discussion of the dissociation of diazosulfides is based on the rate constants shown in Table 1.

The rate constants of the reaction of *cis*-I with β-naphthol at 30.0°C in alkaline ethanol are 10^{-4}—10^{-6} sec^{-1} (Table 1), whereas the isomerization rate constants of *cis*-I at 36.9°C in chloroform are 5×10^{-4} —7×10^{-4} sec^{-1}.[1] Therefore, even if the small solvent effect on the isomerization rate[1] is taken into account, it seems that the thermal *cis*→*trans* isomerization does not proceed through ionization and recombination, as Zwet and Kooyman suggested.

The present author observed the dissociation of the *trans*-diazosulfides. It is also a question whether this dissociation proceeds through the *cis* isomer analogously to Zwet and Kooyman's conclusion (Mechanism A), or whether it occurs directly from the *trans* isomer (Mechanism B). However, Mechanism A will be excluded by the following discussion.

The reaction was always carried out in the dark, and the solution of diazosulfides was quickly prepared in a room lighted as usual. No rate change was observed even for the solution prepared in the dark. Therefore, the photochemical *trans*→*cis* isomerization can be disregarded. We must, then, assume that the *trans*→*cis* isomerization occurs thermally in the course of the reaction of the *trans*-I with β-naphthol if the reaction proceeds by means of Mechanism A.

As has been described above, the rate-determining step of this reaction should be the dissociation of diazosulfides. Table 1 shows that the reaction of the *cis* isomer is much faster than that of the *trans* isomer. Therefore, even if the reaction of the *trans* isomer proceeds *via* the *cis* form, Step (iii) in Scheme 1 cannot be rate-determining.

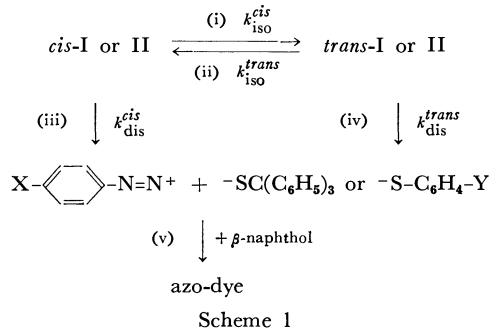

Scheme 1

On the other hand, Zwet and Kooyman showed that the substituent effect for the *cis*→*trans* isomerization (Step (i)) is negligible. Therefore, on the basis of the principle of the microscopic reversibility, it seems valid to say that the substituent effect on Step (ii) is negligible. This is not, however, in accord with the observed result ($\rho_{trans}=-4.8$). Therefore, it seems unreasonable to say that Step (ii) is the rate-determining step in the reaction of *trans*-I with β-naphthol.

Consequently, it seems reasonable to conclude that the *trans*-diazosulfides (I) dissociate directly, not through the *cis* forms. This may explain well the finding that ρ_{trans} is not the same as ρ_{cis}.

Although the rate data for the dissociation of the *cis* isomers are lacking, the same mechanism may

hold for the dissociation of the *trans*-diaryldiazosulfides (II) described in a previous paper ;[3] if *trans*-II cannot dissociate directly, *i.e.*, if $k_{dis}^{trans} \doteqdot 0$, then $k_{dis}^{cis} \ll k_{iso}^{trans}$ would be valid because the rate-determining step is the heterolytic rupture of the N-S bond of diazosulfide.[3] We shall suppose that the thermal equilibirum between the *cis* form and the *trans* is attained and that its equilibrium constant, $K(=k_{iso}^{cis}/k_{iso}^{trans})$ is larger than 10^{2}.[4] On the other hand, the isomerization rate constant for *cis*-IIf at 35°C (k_{iso}^{cis}), is estimated, by extrapolation from the data shown in Table 4, to be *ca.* 10^{-1} sec^{-1}. This figure gives $k_{iso}^{trans} \leqq 10^{-3}$ sec^{-1} (35°C) ; thus, $k_{dis}^{cis} \ll 10^{-3}$ sec^{-1}. If the substituent effect on the isomerization is neglected as in the case of diazosulfides (I), the rate constant for the net reaction, $k(=k_{dis}^{cis}/K)$, can be expected to be much smaller than 10^{-5} sec^{-1}. The actually-observed rate constants, however, are 4×10^{-3}—10^{-6} sec^{-1} (35°C). Therefore, the *trans* isomers of diaryldiazosulfides also seem to dissociate not through the *cis* form, but directly. In Scheme 1, Steps (iii) and (iv) are shown to be irreversible, because Step (v) may be much faster than those steps.

Isolation of *cis*-Diaryldiazosulfides (IV). Hantzsch and Freese[5] speculated that, in the preparation of diaryldiazosulfides, the *cis* form is first produced, but that it is immediately isomerized to the *trans* form. Similar examples have been reported for diazocyanides and diazosulfonates.[2]

As the bulky mercaptans (*e.g.*, triphenylmethylmercaptan and *t*-butylmercaptan) seemed, on the basis of Zwet and Kooyman's results, to prevent the *cis*→*trans* isomerization, the author first used 2,6-dimethylthiophenol to prepare diaryldiazosulfides (II) at −10—−5°C. However, they were all assigned to the *trans* isomer on the basis of the UV

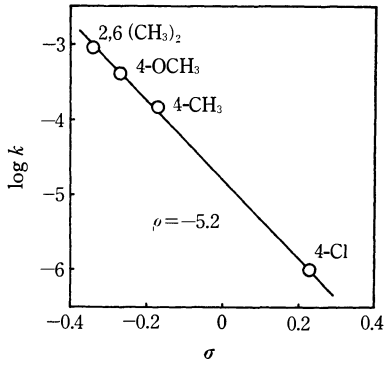

Fig. 2. Hammett plot for the reaction of diazosulfides (IIa-d), X-C_6H_4-N=N-S-$C_6H_3(CH_3)_2$-(2,6), with β-naphthol in alkaline ethanol at 35.0°C.

4) This assumption seems to be valid because the *cis* isomer could not be detected in the recrystallized *trans* isomer.

Table 3. Rate constants for the reaction of *N*-Aryl-*S*-(2,6-dimethylphenyl)diazosulfides (II) with β-naphthol in alkaline ethanol at 35.0°C*

	Substituent X	$k\times10^{4}$ sec^{-1}
IIa	2,6-$(CH_3)_2$	8.5
IIb	4-OCH_3	4.0
IIc	4-CH_3	1.5
IId	4-Cl	0.010

* [Diazosulfide] = 1.0×10^{-4} M, [β-Naphthol] = 1.0×10^{-3} M, [KOH] = 1.1×10^{-3} M.

spectra, *i.e.*, λ_{max} (Table 5) and the lack of spectral change. The Hammett plot of the rate constants for the reaction of II with β-naphthol in alkaline ethanol, summarized in Table 3, shows a straight line with a value of $\rho = -5.2$ (Fig. 2) ; this value is comparable with the value for the same reaction of the *trans*-I. It is interesting that the point for IIa falls on the line when the σ-value for the 2,6-dimethyl group is assumed to be equal to twice $\sigma_{p\text{-}CH_3}$ In other words, the steric effect by two *ortho*-methyl groups of mercaptan does not operate in this instance.

Further, the diazosulfides (IV and V), which have substituents in two *ortho*-positions of the *N*-aryl part, were also prepared. Although they do not have a λ_{max} beyond 320 mμ, they also seem to be *trans* isomers because no spectral change was observed at room temperature. The substituents in the *ortho*-positions of the *N*-aryl part, even in the *trans*

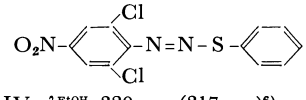

IV, λ_{max}^{EtOH} 320 mμ (317 mμ)[6]

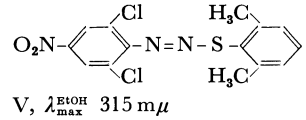

V, λ_{max}^{EtOH} 315 mμ

form, seem to make it difficult for the aromatic ring to be coplanar to the plane containing the N=N group.

Next, diazosulfides were prepared at −78°C. In this case, the diazonium salts with an electron-withdrawing substituent and the mercaptans with an electron-donating substituent were employed so that the *S*-coupling would proceed quickly, even at a low temperature. As a result, the *cis* isomers of five diaryldiazosulfides were isolated, as is shown in Figs. 3 and 4. Figure 5 shows the spectra of the *cis* isomers. These spectral changes cannot be ascribed to the transformations of the ionic dia-

5) A. Hantzsch and H. Freese, *Ber.*, **28**, 3237 (1895).

6) C. C. Price and S. Tsunawaki, *J. Org. Chem.*, **28**, 1867 (1963).

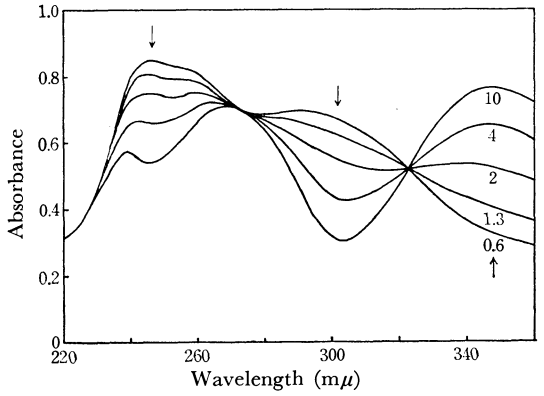

Fig. 3. The progressive spectral change in the *cis*→*trans* isomerization of *cis*-diazosulfide, *p*-O_2N-C_6H_4-N=N-S-C_6H_4-CH_3-(*p*), in ethanol. Numbers refer to time after sample was dissolved (in minutes).

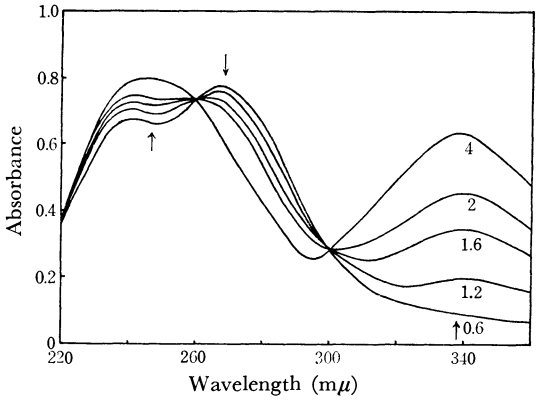

Fig. 4. The progressive spectral change in the *cis*→*trans* isomerization of *cis*-diazosulfide, *p*-NC-C_6H_4-N=N-S-C_6H_4-CH_3-(*p*), in ethanol. Numbers refer to time after sample was dissolved (in minutes).

zonium thiophenoxides into the covalent diazosulfides because of the following evidence: (i) The spectra shown in Fig. 5 have λ_{max} values different from those for the diazonium ions. (ii) *p*-cyanobenzenediazonium ion instantaneusly reacted with β-naphthol in alkaline ethanol to afford red azo-dye at −78°C, whereas diazosulfide (IIf), which was prepared at the same temperature and which was identified as a *cis* isomer, did not react under the same conditions.

The diazosulfides (IV and V) were also prepared at −78°C, but the products were still *trans* isomers. Accordingly, *ortho*-substituents seem to hinder the formation of the *cis* isomer or make the *cis*→*trans* isomerization occur more rapidly.

The rate constants of the thermal isomerization of *cis*-IIf were determined in ethanol (Table 4). It is noteworthy that the entropy of activation is fairly small compared with that for the *cis*-Ic ($\Delta S^{\ddagger}=18.6$ e.u.). The energy of activation for *cis*-IIf is comparable to other examples of the *cis*→*trans* isomerization (*e.g.*, Ic: 29.2 kcal/mol,[1] azonaphthalene: 22.0kcal/mol,[7] azobenzene: 23.0 kcal/mol,[8] diazocyanide: 21.5 kcal/mol,[9] and diazosulfonate: 14.7 kcal/mol[10]).

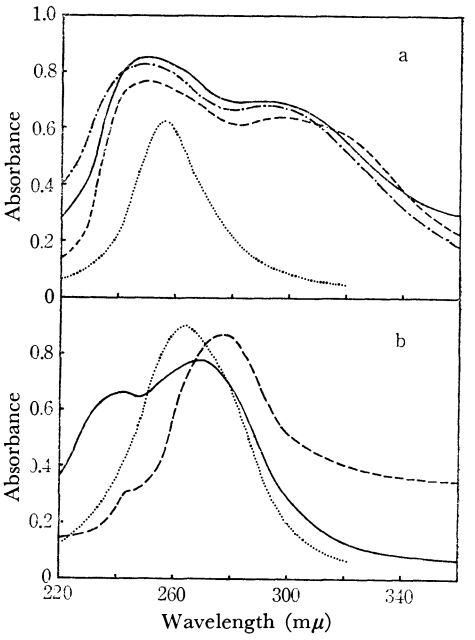

Fig. 5. Absorption spectra of *cis*-diaryldiazosulfides and diazonium ions in ethanol. a) *p*-O_2N-C_6H_4-N=N-S-Ar; ——: Ar=*p*-tolyl, —·—·: Ar=*p*-chlorophenyl, ----: Ar=2,6-dimethylphenyl. ·····: *p*-O_2N-C_6H_4-$N_2^+\cdot HSO_4^-$ b) *p*-NC-C_6H_4-N=N-S-Ar; ——: Ar=*p*-tolyl, ----: Ar=2,6-dimethylphenyl. ·····: *p*-NC-C_6H_4-$N_2^+\cdot Cl^-$.

Table 4. Rate constants and activation parameters for the isomerization of *cis*-*N*-(*p*-cyanophenyl)-*S*-(*p*-tolyl)diazosulfide(IIf) in ethanol

Temp. (°C)	$k\times10^4$ (sec^{-1})	
−20	1.28	E_a=20.5 kcal/mol
−10	6.08	$\Delta S^{\ddagger}$=2.9 e. u.
0	25.5	

Experimental

Preparation of Materials. All the *cis*- and *trans*-*N*-aryl-*S*-triphenylmethyldiazosulfides (I) were prepared

7) M. Frankel, R. Wolovsky and E. Fisher, *J. Chem. Soc.*, **1955**, 3441.
8) G. S. Hartley, *ibid.*, **1938**, 638.
9) R. J. W. Le Fèvre and H. Vine, *idib.*, **1938**, 431.
10) E. S. Lewis and H. Suhr, *Chem. Ber.*, **92**, 3031 (1959).

TABLE 5. THE PHYSICAL CONSTANTS AND ULTRAVIOLET SPECTRAL DATA OF DIAZOSULFIDES (I)

	Substituent X	*cis*-I		*trans*-I	
		mp (°C)	λ_{max} (mμ)*	mp (°C)	λ_{max} (mμ)*
Ia	OCH_3			112(dec.)	343
Ib	CH_3	88	318	117(dec.)	338
Ic	H	94	312	122(dec.)	335
Id	Cl	96	317	130(dec.)	340
Ie	NO_2	95	304	145(dec.)	359

* in benzene

TABLE 6. THE ANALYTICAL DATA AND ULTRAVIOLET SPECTRAL DATA OF DIAZOSULFIDES (II):

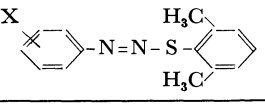

	Substituent X	Color	mp °C	λ_{max}^{EtOH} mμ	Analysis (calcd) C%	H%	N%
IIa	2,6-$(CH_3)_2$	Yellow	52	310*			
IIb	*p*-OCH_3	Yellow	67	345			
IIc	*p*-CH_3	Yellow	70	330	70.58	6.12	10.78
					(70.28)	(6.29)	(10.93)
IId	*p*-Cl	Yellow	95	332	60.46	4.85	9.84
					(60.75)	(4.73)	(10.12)
IIe	*p*-CN	Yellow	109—110	334	67.14	4.70	15.42
					(67.39)	(4.90)	(15.72)
IIg	*p*-NO_2	Orange	75— 76	345	56.92	3.81	15.27
					(57.14)	(4.06)	(15.38)

* shoulder

by the method of Zwet and Kooyman.[1] The physical constants and the UV spectral data of the I thus prepared are summarized in Table 6. The *trans*-*N*-aryl-*S*-(2,6-dimethylphenyl)diazosulfides (IIa–e, g) were prepared by the method described in a previous paper.[3] The analytical data, physical constants, and UV spectral data of II are summarized in Table 5. The α-(2,6-dimethylphenylazo)-β-naphthol was prepared by a method described previously.[3] Mp 147°C, λ_{max} 484 mμ ε 14300 (in alkaline ethanol).

Found: C, 78.44; H, 5.67; N, 10.16%. Calcd for $C_{18}H_{16}N_2O$: C, 78.24; H, 5.84; N, 10.14%.

The UV spectral data of the other azo-dyes were reported in the previous paper.[3]

Kinetic Measurements. The rate constants for the reaction of diazosulfides (I and II) with β-naphthol in alkaline ethanol were determined spectrophotometrically, as has been described previously.[3] The order of reaction with respect to β-naphthol could not be determined.[3] Accordingly, the rate was measured in the presence of excess β-naphthol. In most of the reactions, a rate depression with the time was observed; this may be ascribed to the competitive isomerization or decomposition of diazosulfides. Thus, the initial rates were measured; they are summarized in Tables 1 and 3.

Isolation of *cis*-Diaryldiazosulfides. The *cis*-diaryldiazosulfides were prepared as follows: a solution of 2 mmol of *p*-nitroaniline in 4 ml of 10% hydrochloric acid was diazotized with 2mmol of sodium nitrite in 1 ml of water at −5——10°C. The diazonium solution was then added to a stirred solution of 2 mmol of *p*-methylthiophenol in 50 ml of alkaline ethanol, while the mixture was being cooled by an acetone-dry ice bath. Yellow crystals of *cis*-diazosulfide were immediately formed. The yellow crystals were collected on a well-cooled filter, washed with cold ethanol (*ca.* −70°C), and preserved at

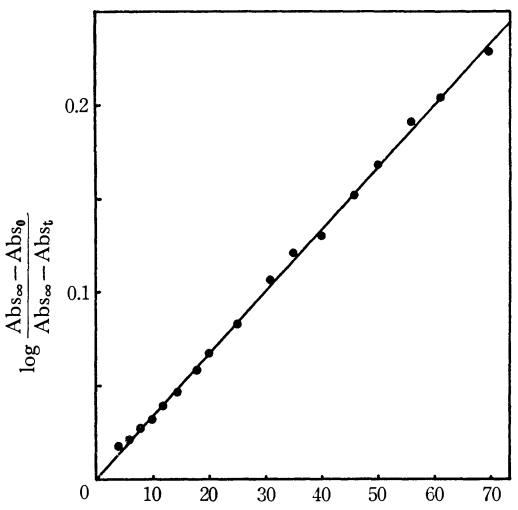

Fig. 6. First-order rate plot for the isomerization of *cis* isomer of diazosulfide (IIf), *p*-NC-C_6H_4-N=N-S-C_6H_4-CH_3-(*p*), in ethanol at −20.0°C.

about −70°C. At this temperature, no change was observed in the UV spectra for at least a day.

Isomerization of *cis*-Diaryldiazosulfides. The isomerization was followed spectrophotometrically using a Hitachi rapid scan spectrophotometer. Some of the *cis*-diazosulfide was dissolved in cold ethanol in a flask immersed in an acetone-dry ice bath. The solution was then quickly transferred into a well-cooled quartz cuvette set in the cell holder, and immediately the UV spectrum was recorded by an oscilloscope unit at appropriate intervals. Because an ambient temperature cell compartment was used, the solution in a cuvette rapidly warmed up, and then the isomerization proceeded acceleratively. Some examples of the spectral change with the time are shown in Figs. 3 and 4.

Kinetic Measurements of the Isomerization of *cis*-*N*-(*p*-Cyanophenyl)-*S*-(*p*-tolyl)diazosulfide (IIf). The rate constants of the isomerization of *cis*-IIf were determined spectrophotometrically. An appropriate amount of *cis*-IIf was dissolved in ethanol so that the concentration of the solution became suitable for the spectral measurements. The temperature was kept constant in a salt-ice bath using a thermos.

Aliquots were removed at intervals and put into a quartz cuvette set in a cell compartment, and the optical densities were immediately measured at 340 mμ (see Fig. 4), the absorption maximum of *trans*-IIf. The first-order rate constants were evaluated by the graphical method shown in Fig. 6 and are summarized in Table 4.

A solution of *cis*-IIf in ethanol can be stored without change for at least two hours at −78°C.

The author wishes to thank Professor Ryōzō Gotō for his encouragement of this work. He is also indebted to Professors Aritsune Kaji and Jun-ichi Hayami for their valuable discussions, and to Mr. Masao Nishikuri for his earnest assistance.

BULLETIN OF THE CHEMICAL SOCIETY OF JAPAN VOL. 43 1511—1516 (1970)

Effect of Carbonyl Compounds on Polymerization by Metal Acetylacetonates

Kyoji KAERIYAMA

Research Institute for Polymers and Textiles, Sawatari, Kanagawa-ku, Yokohama

(Received October 25, 1969)

Some ketones and aldehydes have an accelerative effect on the polymerization of various monomers by various metal chelates of acetylacetone. The conversion increases with an increase in the concentration of these additives in a correspondingly increasing polymerization time. A radical is formed by the equimolar reaction of cyclohexanone and manganese(III) acetylacetonate and by the reaction of two aldehyde molecules and a molecule of the chelate. The order with a monomer is lowered from 1.64 to 1.13 and to 1.07 by the addition of cyclohexanone and caproic aldehyde respectively. The relation between the polymerization rate and the square root of the chelate concentration is linear without any additive ; concave and convex curves are obtained for the systems containing cyclohexanone and caproic aldehyde respectively. The apparent activation energy is lowered from 19.9 kcal/mol to 13.9 and to 14.3 in the presence of cyclohexanone and caproic aldehyde respectively. The effectiveness of ketones is dependent on the nucleophilicity. A mechanism of the initiation reaction which interprets the molar ratio of reactants, the kinetical parameters, and the spectral data is proposed.

Metal acetylacetonates ($Macac_n$) have already been used as initiators for the polymerization of unsaturated compounds.[1-4] The polymerization proceeds *via* radical intermediates. The substituents on the acetylacetone ligand are shown to have an appreciable effect on the initiator activity of the chelate.[5-7] A solvent effect[7] and a high order with a monomer[6,7] are characteristic of a polymerization by $Macac_n$. This indicates the participation of monomers and solvents in the initiation reaction and suggests the presence of additives, a small amount of which accelerates the polymerization by the reaction of the additives with the chelate

1) E. M. Arnett and M. A. Mendelsohn, *J. Amer. Chem. Soc.*, **84**, 3821 (1962).

2) E. G. Kastning, H. Naarmann, H. Reis and C. Berding, *Angew. Chem.*, **77**, 313 (1965).

3) Y. Nishikawa and T. Otsu, *Kogyo Kagaku Zasshi*, **72**, 751 (1969).

4) K. Uehara, Y. Kataoka, K. Kamei, M. Tanaka and N. Murata, *ibid.*, **72**, 1831 (1969).

5) K. Uehara, T. Matsumura, Y. Murata, M. Tanaka and N. Murata, *ibid.*, **72**, 1825 (1969).

6) Y. Nishikawa and T. Otsu, *ibid.*, **72**, 1836 (1969).

7) C. H. Bamford and D. J. Lind, *Proc. Roy. Soc., Ser. A*, **302**, 145 (1968).

prior to that of monomers and solvents. In fact, the addition of pyridine has been found to accelerate the polymerization of styrene by the metal chelate of β-diketone.[8] The effect of carbon tetrachloride has also been discussed.[2,7,9]

The present author has previously shown that the addition of carbonyl compounds accelerates the polymerization of styrene by ceric salt in an organic solvent.[10] In the present study, the effect of ketone and aldehyde on polymerization by $Macac_n$ is investigated.

Experimental

Materials. The monomers, aldehydes, and ketones were distilled under reduced pressure just prior to use. The metal acetylacetonates were commercially obtained (Dotite Reagent) and were used without further purification.

Procedure. In a glass tube we placed a chelate solution in benzene, additives, monomers, and a solvent, in that order, under atmospheric conditions. After the tube had been degassed by repeated freezing, evacuating and thawing, it was sealed off. Polymerization was then carried out in the dark under a mild shaking. The polymer thus produced was precipitated in methyl alcohol containing hydroquinone and hydrogen chloride, filtered, and dried *in vacuo* to a constant weight.

The absorption spectra were measured by a Hitachi recording spectrophotometer, Model EPS-3T.

Results and Discussion

Effect of the Additive. The effects of various additives on the polymerization of styrene by $Mnacac_3$ are shown in Table 1. All the additives used have an accelerative effect. Since caproic aldehyde and cyclohexanone are the most effective of the additives examined, these two reagents will be mainly used as additives in the following parts of this paper.

Table 2 shows the effects of additives on the polymerization by various $Macac_n$. Accelerative effects can be seen in all the chelates used, but there is a large difference in the degree of the effects and in the conversions between the chelates.

The effects of additives on the polymerization of various monomers are shown in Table 3. Methyl

TABLE 1. EFFECTS OF ADDITIVES ON POLYMERIZATION OF STYRENE BY $Mnacac_3$

Additive	Conversion (%)
Cyclohexanone	18.6
Diethyl ketone	7.78
Benzophenone	4.34
Isobutyl methyl ketone	6.03
Caproic aldehyde	29.5
Benzaldehyde	12.9
Ethyl acetate	4.42
Diethyl ether	4.82
Tetrahydrofuran	6.50
Ethyl alcohol	8.95
Methyl alcohol	10.69
—	3.66

$[Mnacac_3]=1.42\times10^{-2}$ mol/l; [Additive]=0.483 mol/l; [styrene]=3.49 mol/l; solvent: benzene; at 60°C for 9.0 hr

TABLE 2. EFFECTS OF ADDITIVES ON POLYMERIZATION OF STYRENE BY VARIOUS $Macac_n$

Run	Chelate	Additive	Conversion (%)
A	$Mnacac_2$	Caproic aldehyde	3.33
A	$Mnacac_2$	Cyclohexanone	9.39
A	$Mnacac_2$	—	0.86
B	$Mnacac_3$	Caproic aldehyde	18.4
B	$Mnacac_3$	Cyclohexanone	13.1
B	$Mnacac_3$	—	2.69
C	$Coacac_2$	Caproic aldehyde	5.39
C	$Coacac_2$	Diethyl ketone	1.06
C	$Coacac_2$	Cyclohexanone	1.59
C	$Coacac_2$	—	1.00
D	$Feacac_3$	Caproic aldehyde	1.55
D	$Feacac_3$	Ethyl alcohol	1.11
D	$Feacac_3$	Cycloheptanone	0.86
D	$Feacac_3$	—	0.47

[additive]=0.483 mol/l; solvent: benzene; at 60°C for 6.0 hr

Run A: $[Mnacac_2]=1.98\times10^{-2}$ mol/l; [styrene]=3.49 mol/l

Run B: $[Mnacac_3]=1.42\times10^{-2}$ mol/l; [styrene]=3.49 mol/l

Run C: $[Coacac_2]=1.95\times10^{-2}$ mol/l; [styrene]=4.36 mol/l

Run D: $[Feacac_3]=1.42\times10^{-2}$ mol/l; [styrene]=3.49 mol/l

TABLE 3. EFFECT OF CARBONYL COMPOUNDS ON POLYMERIZATION OF VARIOUS MONOMERS

Monomer	(mol/l)	Additive	Conversion (%)
Methyl methacrylate	4.70	—	24.4
Methyl methacrylate	4.70	Cyclohexanone	70.9
Acrylonitrile	7.60	—	15.8
Acrylonitrile	7.60	Cyclohexanone	45.2
Acrylonitrile	7.60	Caproic aldehyde	88.0
Styrene	3.49	—	3.66
Styrene	3.49	Cyclohexanone	18.6
Styrene	3.49	Caproic aldehyde	29.5

$[Mnacac_3]=1.42\times10^{-2}$ mol/l; [additive]=0.483 mol/l; solvent: benzene; at 60°C for 9.0 hr

8) K. Uehara, Y. Kataoka, M. Tanaka, and N. Murata, *Kogyo Kagaku Zasshi*, **72**, 754 (1969).

9) T. Otsu, Y. Nishikawa and S. Aoki, *ibid.*, **71**, 1067 (1968).

10) K. Kaeriyama, This Bulletin, **41**, 722 (1968); *Polymer*, **10**, 11 (1969).

methacrylate and acrylonitrile are polymerized better than styrene. Accelerative effects are, thereby, observed in all the monomers used. It is apparent that some ketones and aldehydes have an accelerative effect on the polymerization of many unsaturated monomers by a variety of metal chelates.

The dependence of the conversion on the concentration of additives is shown in Fig. 1. The conversion increases monotonically with an increase in the concentration of the additive, and it is higher in the presence of caproic aldehyde than in the presence of cyclohexanone in all the concentrations examined. In the run with the highest concentration of caproic aldehyde, the polymerizing mixture lost its color at the end of the polymerization. This indicates the complete decomposition of the chelate. In the run with the second highest concentration of the aldehyde, the color faded. No color change could be observed in the other runs.

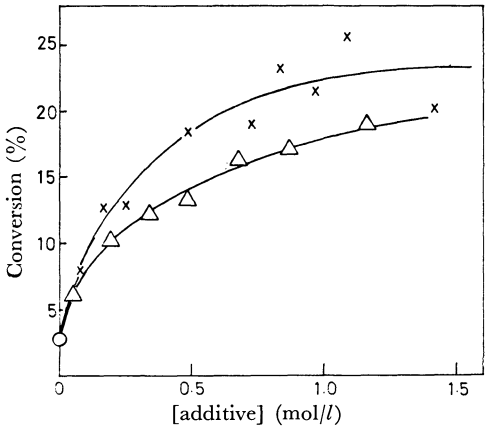

Fig. 1. Dependence of conversion on the concentration of additives.
[styrene]=3.49 mol/l; [$Mnacac_3$]=1.42×10^{-2} mol/l; solvent; benzene; at 60°C for 6.0 hr.
-△- cyclohexanone, -×- caproic aldehyde

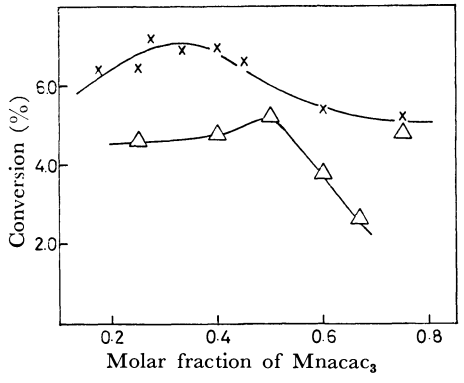

Fig. 2. Dependence of conversion on molar fraction of $Mnacac_3$.
[$Mnacac_3$]+[additive]=3.0×10^{-2} mol/l
[styrene]=3.49 mol/l; solvent: benzene; at 60°C for 7.0 hr.
-△- cyclohexanone, -×- caproic aldehyde

Figure 2 represents the conversion of styrene as a function of the mole fraction of $Mnacac_3$. The maxima do not appear sharp compared with those of other systems, for example, the amide-carbon tetrachloride system.[11] The maxima appear at the optimum fraction, which corresponds to the ratio of the reactants participating in the initiation reaction. In the case of cyclohexanone, the maximum is observed at the equimolar ratio. This implies that a chelate molecule and a cyclohexanone molecule participate in the initiation reaction. In the presence of caproic aldehyde, the maximum seems to be at the molar fraction of 0.33. This suggests that a radical is generated from one manganese tris-acetylacetonate molecule and two caproic aldehyde molecules.

Kinetics. Because a small deviation from a straight line is observed in time-conversion plots, the initial rates of polymerization can be evaluated by graphically determining a tangent at time 0. No change in or fading of the color of polymerizing mixture could be observed in the runs described here.

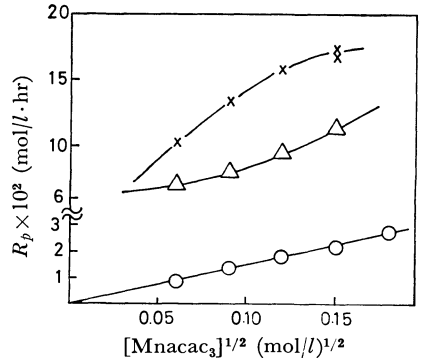

Fig. 3. Dependence of polymerization rate on [$Mnacac_3$]$^{1/2}$.
[styrene]=3.49 mol/l; solvent: benzene; at 60°C
-○- no additive, -△- [cyclohexanone]=0.483 mol/l, -×- [caproic aldehyde]=0.483 mol/l

The dependence of the initial rate of polymerization on the square root of the concentration of $Mnacac_3$ is shown in Fig. 3. In the absence of any additive, the rate is linearly dependent on the square root of the chelate concentration. The polymerization chain is terminated by the bimolecular reaction of polymer radicals. Bamford and Lind[7] have also reported that the polymerization rate of styrene and methyl methacrylate is proportional to the square root of the concentration of $Mnacac_3$. In the presence of cyclohexanone, the curve is concave. As is shown in Fig. 1, the polymerization rate increases with the concentration of cyclohexanone at a constant concentration of

11) K. Kaeriyama, This Bulletin, **42**, 3602 (1969).

$Mnacac_3$, because the ratio of cyclohexanone to the chelate increases. In the case of a constant concentration of cyclohexanone, the ratio of cyclohexanone to $Mnacac_3$ increases with a decrease in the concentration of the chelate. This is the reason why the rate is higher at low concentrations of the chelate than would be expected from the linear dependence on the square root of the chelate concentration. The possibility of the bimolecular termination can not be rejected. In the presence of caproic aldehyde, the curve is convex. If the termination is by the reaction of the polymer radical with the initiator, the polymerization rate is independent of the initiator concentration. In this case, both terminations, by the chelate and by bimolecular reaction of polymer radicals, take place. This is the reason why the curve is convex. Uehara *et al.* have described how the polymerization of acrylonitrile is terminated by copper chelates of β-diketones.[4]

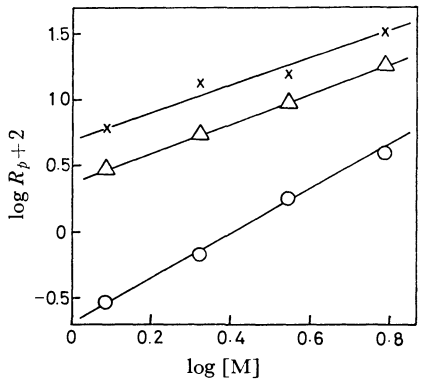

Fig. 4. Dependence of polymerization rate on styrene concentration.
$[Mnacac_3]=1.42\times10^{-2}$ mol/l
solvent: benzene; at 60°C
-○- no additive
-△- [cyclohexanonoe] = 0.483 mol/l
-×- [caproic aldehyde] = 0.483 mol/l

Figure 4 presents logarithmic plots of the initial rate of polymerization as a function of the monomer concentration at constant concentrations of $Mnacac_3$ and additives. The order with the monomer is 1.64 in the absence of any additive. This high order is attributable to the participation of the monomer in the initiation reaction. The order is lowered to 1.13 and 1.07 by the addition of cyclohexanone and caproic aldehyde respectively. This shows that the additive limits the participation of the monomer in the initiation reaction to a lesser extent. Bamford and Lind[7] have reported that the order with the monomer is dependent on the diluent, being 1.5 and 1.2 for toluene and ethyl acetate respectively. These findings are similar to those of present paper in the sense that the use of the carbonyl compound as the solvent lowers the order with the monomer. However, cyclanone is more effective than the ester. Uehara *et al.*[8] have also described that the addition of pyridine lowers the order with styrene from 1.9 to 1.2.

Arrhenius plots are shown in Fig. 5. The apparent activation energies and frequency factors are summarized in Table 4. The additives lower the apparent activation energy by *ca.* 6 kcal/mol. The frequency factors are very low, especially in the presence of cyclohexanone. This is characteristic of the polymerization by these initiator systems.

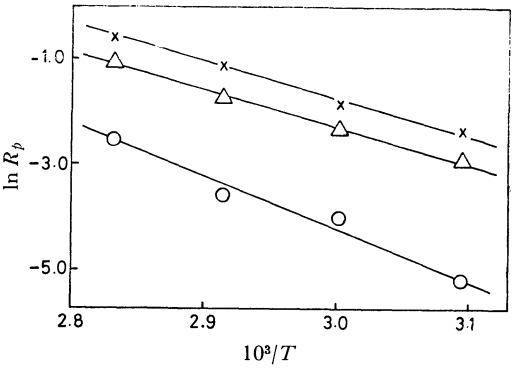

Fig. 5. Dependence of polymerization rate on temperature.
$[M]=3.49$ mol/l; $[Mnacac_3]=1.42\times10^{-2}$ mol/l
solvent: benzene; -○- no additive
-△- [cyclohexanone] = 0.483 mol/l
-×- [caproic aldehyde] = 0.483 mol/l

TABLE 4. SUMMARY OF PARAMETERS FOR Fig. 5

	No additive	Cyclo-hexanone	Caproic aldehyde
Activation energy (kcal/mol)	19.9	13.9	14.3
Frequency factor (mol/l·sec)	5.6×10^7	3.6×10^4	1.1×10^5

Spectra. The absorption spectra of $Mnacac_3$ in visible regions are shown in Fig. 6. Because the spectra in benzene and a benzene-styrene mixture (50 vol%) are completely identical, it can be said that styrene does not coordinate to $Mnacac_3$. The behavior of $Mnacac_3$ is different from that of the copper chelate.[6] The spectra in a cyclohexanone solution are essentially identical with those in a benzene solution, although a small deviation can be observed. The spectra in a caproic aldehyde solution are shifted to shorter wavelengths and show higher absorption coefficients. It is apparent that they are different from those in the benzene and cyclohexanone solutions. This can be attributed to the coordination of caproic aldehyde to $Mnacac_3$.

Initiation Mechanism. Although the coordination of cyclohexanone with $Mnacac_3$ can not be deduced from the spectral data, it is clear that

12) M. Tamres and S. Searles, *J. Amer. Chem. Soc.*, **81**, 2100 (1959).

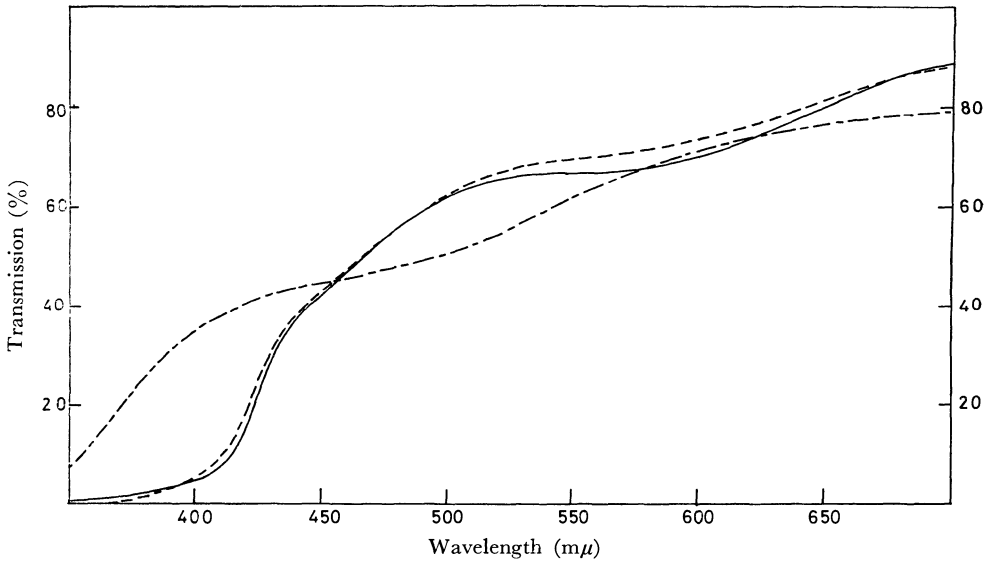

Fig. 6. Spectra of $Mnacac_3$.
$[Mnacac_3]=7.7\times10^{-4}$ mol/l
—— in benzen; ---- in cyclohexanone; ----- in caproic aldehyde

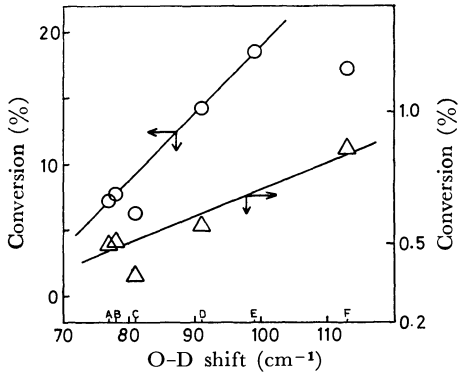

Fig. 7. Dependence of conversion on O-D shift.
[styrene]=3.49 mol/l; solvent: benzene: at 60°C
[additive]=0.483 mol/l
A : methyl ethyl ketone B : diethyl ketone
C : acetone D : cyclopentanone
E : cyclohexanone F : cycloheptanone
-○- $[Mnacac_3]=1.42\times10^{-2}$ mol/l, 9.0 hr
-△- $[Feacac_3]=1.42\times10^{-2}$ mol/l, 6.0 hr

ketone interacts with the chelate and accelerates the polymerization. Ketones are arranged in the order of nucleophilic tendency. Figure 7 shows the relation between the conversion and the O-D shift in IR spectra. The O-D shift of monodeuterated methanol, which is cited from the report of Tamres and Searles,[12] is due to a hydrogen bond with ketone and depends on the nucleophilicity of the ketone. Acetone deviates from the line. It also deviates from the linear relation between the O-D shift and the heat of mixing with chloroform because of association. The deviation of cycloheptanone can be interpreted in terms of the difference in bulkiness between methanol and the chelate molecule. Cycloheptanone deviates only in reaction with manganese chelate, which has a stronger interaction with the ketone. It appears from Fig. 7 that conversion is dependent on the nucleophilicity of ketone. These results and the spectral data suggest that ketone coordinates to the chelate in an activation state.

The initiation reactions can be summarized schematically as on the next page. Styrene does not coordinate to I judging from the spectra. I is activated into II, which reacts with the monomer to generate the radical IV. The mechanism shouldlead to an order of 1.5 with the monomer. The observed order of 1.64 can, therefore, not be explained. A possible explanation is to suppose another reaction in which II reacts with two molecules of monomer. In the presence of the ketone I reacts with the ketone to form an activated complex V, which in turn decomposes into VI and VII. The mechanism predicts the linear dependence on the monomer concentration. The observed order is attributable to the simultaneous reaction *via* II. The above explanation is consistent with the spectral data and the equimolar reaction of the chelate with ketone.

Otsu *et al.* reported that metal β-diketonates induced a coordination polymerization of aldehyde.[13] Chloral was most easily polymerized; when *n*-butyl aldehyde and chloral were copolymerized by Cu bis-(ethyl acetoacetate), a copolymer

13) T. Otsu, S. Watanuma and Y. Nishikawa, *Kogyo Kagaku Zasshi*, **72**, 1857 (1969); *Makromol. Chem.*, **115**, 278 (1968).

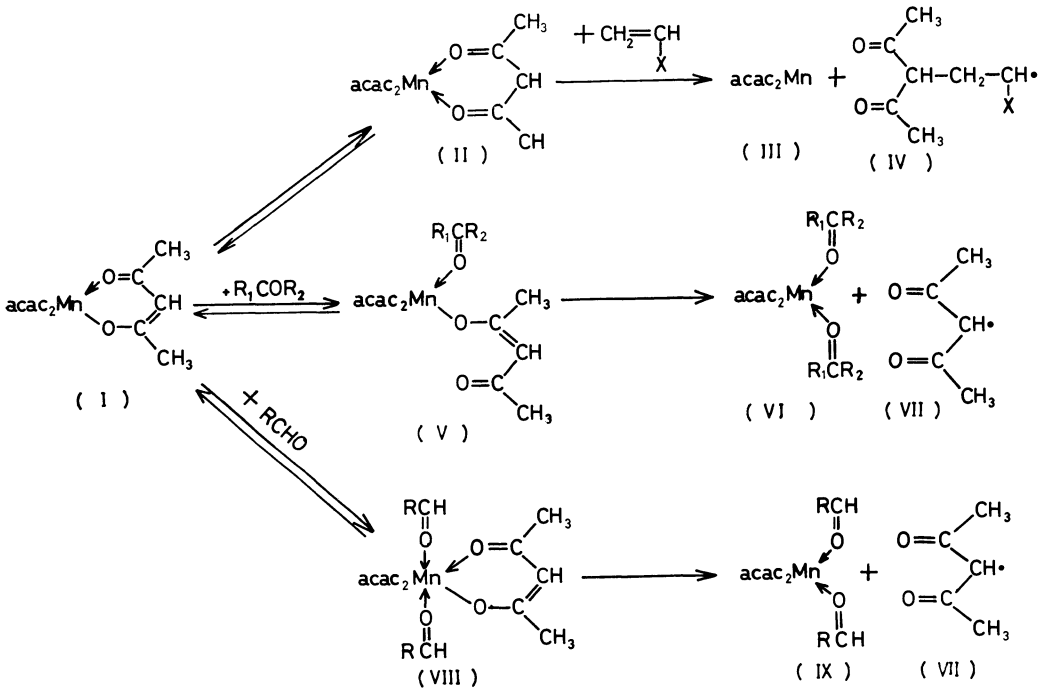

Scheme 1

containing a small amount of *n*-butyl aldehyde units was produced. They also reported that $Mnacac_3$ did not induce the polymerization of chloral. In the present study, no polymer of caproic aldehyde was detected by precipitation in benzene or methanol. No copolymerization of caproic aldehyde with styrene was deduced from the IR data. Although caproic aldehyde is not polymerized by $Mnacac_3$, it has a stronger interaction with the chelate than cyclohexanone. In the presence of caproic aldehyde, two aldehyde molecules coordinate to the chelate in the ground state and VIII is formed. The decomposition of VIII generates the radical VII. This route is compatible with the spectral data and with the optimum molar ratio of the reactants.

The bond between manganese and the acetylacetone ligand is weakened by the coordination of aldehyde, and a acetylacetone ligand in VIII reacts with the polymeric radical. This indicates that the chelate terminates the polymerization of styrene in the presence of caproic aldehyde, as has been described in the section on the dependence on the initiator concentration.

The polymers produced by the present initiator systems do not have stereoregularity, the IR data indicate.[14]

The author is grateful to Dr. M. Suzuki and Dr. A. Okada for their interest and encouragement during this work.

14) J. P. Luongo and R. Salovey, *J. Polym. Sci., Part A-3*, 2759 (1965).

BULLETIN OF THE CHEMICAL SOCIETY OF JAPAN VOL. 43 1517—1520 (1970)

Rhodium Tolane Complex and Cyclotrimerization of Substituted Acetylenes Catalyzed by Transition Metal Complexes

Yuji IWASHITA and Fumihide TAMURA

Central Research Laboratories, Ajinomoto Co., Inc., Suzuki-cho, Kawasaki

(Received October 25, 1969)

Cyclotrimerization of tolane and phenylacetylene has been studied from the viewpoint of the reaction intermediates and the composition of reaction products. $Rh_4(CO)_{12}$ and $Co_4(CO)_{12}$ have been found to catalyze the trimerization of tolane and phenylacetylene to yield some substituted benzenes. By the reaction of $Rh_4(CO)_{12}$ with tolane, an unknown complex was obtained. The triphenyl phosphine derivative of this complex has been determined to be $Rh_2(CO)_3$-$(C_6H_5C{\equiv}CC_6H_5)_2P(C_6H_5)_3$. From infrared spectroscopic study, it was concluded that the two tolane molecules in the complex are connected to rhodium atoms separately without completion of dimerization. On the basis of the ratio of 1,2,4-triphenylbenzene to 1,3,5-triphenylbenzene, the reaction course of trimerization is discussed.

Trimerization of acetylenes using transition metal catalysts has been studied by many investigators. Hübel and Krüerk[1] have described the cobalt complex in which three substituted acetylenes are involved. Hagihara and his coworker[2] have suggested a *cis*-butadiene type structure as an intermediate complex of cyclotrimerization reaction. However, evidence for the proposed structure of these intermediates does not seem to be conclusive. There remains the question whether acetylene completed trimerization in the complex or during the course of leaving the metal.

Rhodium Tolane Complex. Several rhodium complexes having acetylene as a ligand were obtained by the reaction of $Rh_4(CO)_{12}$ with acetylene in *n*-hexane. However, they were unstable even at low temperature and rapidly decomposed to give benzene. In order to obtain the stable complex, the reaction of $Rh_4(CO)_{12}$ with tolane was carried out at 50°C in *n*-hexane.

At the first stage of the reaction, the infrared spectrum of the solution (Fig. 1-I) was very similar to that of $CH{\equiv}CHCo_4(CO)_{10}$[1] (Fig. 2), and the formed complex is considered to be $(C_6H_5C{\equiv}CC_6H_5)$

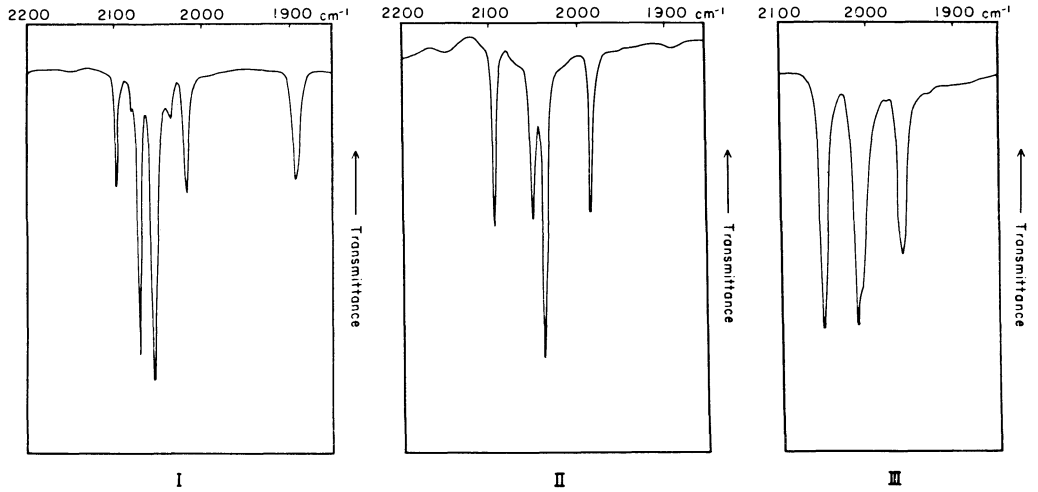

Fig. 1. Infrared spectra of reaction mixture: $Rh_4(CO)_{12}$ and tolane in *n*-hexane.

1) U. Krüerk und W. Hübel, *Chem. Ber.*, **95**, 2829 (1961).

2) H. Yamazaki and N. Hagihara, *J. Organometal. Chem.*, **7**, 22 (1967).

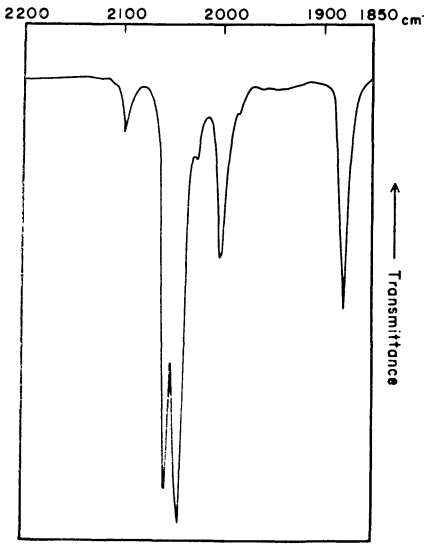

Fig. 2. Infrared spectrum of $CH{\equiv}CHCo_4(CO)_{10}$.

$Rh_4(CO)_{10}$.

After a while, the absorption due to the bridging carbonyls of the complex vanished (Fig. 1-II). When the reaction continued further at 50°C, the precipitation of hexaphenylbenzene was observed in the reaction vessel. Since the complex was too unstable to be isolated, it was transformed into a triphenylphosphine substituted complex. The same complex was also obtained from the reaction using aromatic solvents, although they show different powder X-ray patterns. When the formed complex was accompanied by some aromatic solvents such as benzene, toluene, *etc.*, the complex was washed by *n*-hexane, and recrystallized from ether. Thus, red-brown prisms decomposing at 115°C, were obtained.

The 100 MHz NMR spectrum of the complex shows the signals of triphenylphosphine protons[3] and tolane protons at separate positions in a perchloroethylene solution. The ratio of triphenylphos phine to tolane in the complex was then determined by the integration of spectrum. Molecular weight measurement failed because of decomposition. In the infrared spectrum of the complex, three strong bands at 2052.0, 2013.0 and 1954.5cm^{-1} were observed in terminal carbonyl stretching region (Fig. 1-III). The above-described spectroscopic data and elemental analysis are coincident with the molecular formula $Rh_2(CO)_3P(C_6H_5)_3(C_6H_5C{\equiv}CC_6H_5)_2$.

The course of the reaction may be expressed by the following equation :

$$Rh_4(CO)_{12} + C_6H_5C{\equiv}CC_6H_5 \rightarrow (C_6H_5C{\equiv}CC_6H_5)Rh_4(CO)_{10} + 2CO$$

$$(C_6H_5C{\equiv}CC_6H_5)Rh_4(CO)_{10} + 3C_6H_5C{\equiv}CC_6H_5 \rightarrow 2Rh_2(CO)_4(C_6H_5C{\equiv}CC_6H_5)_2 + 2CO$$

$$Rh_2(CO)_4(C_6H_5C{\equiv}CC_6H_5)_2 + P(C_6H_5)_3 \rightarrow Rh_2(CO)_3P(C_6H_5)_3(C_6H_5C{\equiv}CC_6H_5)_2 + CO$$

Infrared Spectra of the Coordinated Tolane. In order to separate the infrared absorption bands due to tolane from those due to triphenylphosphine moiety, the perdeuterio triphenylphosphine P-$(C_6D_5)_3$[4] substituted complex was prepared. Assignment of the infrared spectrum was done on the basis of a comparison with its deuterated compound (Table 1). In the region between 1600 cm^{-1} and 800 cm^{-1}, the bands attributed to the coordinated tolane have positions and intensities similar to those of free tolane molecule.

TABLE 1. VIBRATIONAL FREQUENCIES AND ASSIGNMENT OF $(C_6H_5C{\equiv}CC_6H_5)_2Rh_2(CO)_3{\cdot}P(C_6H_5)_3$

2052.0	v.s	C≡O		849	w	P	
2013.0	v.s	C≡O		803	w	N	
2007	sh			754	m	T	
1953.5	v.s	C≡O		749	m	P	
1598	v.w	T		729	s	N	
1591	w	P		702	s	P	
1570	w	P		699	sh	T	
1565	v.w	T		646	w	N	
1490	v.w	T		636	w	N	
1479	m	P		622	w	P	
1438	m	P	T	610	w	N	
1320	w	P		574	m	N	
1310	w	P	T	567	s	N	
1280	v.w	P	T	540	w	P	T
1186	m	P	T	520	s	P	
1159	w	P	T	507	m	T	
1118	w	N		501	m	P	
1089	m	P		483.0	w	N	
1071	m	P		469.0	w	T	
1028	m	P	T	444.0	w	P	
1000	m	P		430.0	w	P	
878	w	N					

N : The bands could not be assigned to tolane or triphenylphosphine. T : $C_6H_5C{\equiv}CC_6H_5$, P : $P(C_6H_5)_3$, v.s : very strong, s : strong, m : medium, w : weak, v.w : very weak, sh : shoulder

If the two coordinated tolane molecules take the form of *cis*-butadiene, the change of intensities and positions of absorptions should be observed.[5] Therefore, the two tolane molecules must be connected with the rhodium atoms independently. Several bands in far-infrared region which could not be assigned to tolane or triphenylphosphine may be due to rhodium-tolane[4] stretching, rhodium–(C≡O) stretching and Rh–(C≡O) bending vibrations. The

3) Y. Iwashita, F. Tamura and A. Nakamura, *Inorg. Chem.*, **8**, 1179 (1969).

4) Y. Iwashita and A. Hayata, *J. Amer. Chem. Soc.*, **91**, 2525 (1969).

5) W. Keim, *J. Organometal. Chem.*, **16**, 191 (1969).

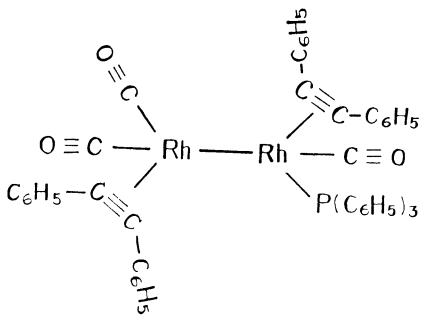

Fig. 3. The proposed structure of $(C_6H_5C{\equiv}CC_6H_5)_2Rh_2(CO)_3P(C_6H_5)_3$.

proposed structure of the complex is illustrated in Fig. 3.

Cyclotrimerization of Phenylacetylene. The $Rh_4(CO)_{12}$ or $Co_4(CO)_{12}$ catalyzed cyclotrimerization reaction of phenylacetylene was carried out in a benzene solution at 60°C. The products were identified by IR, E.A. and molecular weight measurements. The ratio of 1,2,4-triphenylbenzene to 1,3,5-triphenylbenzene was determined by gas chromatography. The results are given in Table 2. When $Co_4(CO)_{12}$ was used as a catalyst, the product was almost composed of 1,2,4-triphenylbenzene and when $Rh_4(CO)_{12}$ was used as a catalyst, the amount of 1,2,4-triphenylbenzene was twice as much as that of 1,3,5-triphenylbenzene.

In a transition state, three *cis*-butadiene type intermediates may be assumed (Fig. 4). Form III seems to be the most stable because of the lack of steric repulsion between phenyl groups and the metal carbonyl moiety. If the structure of the intermediate is supposed to be form III, the subsequent reaction to a phenylacetylene molecule should give 1,2,4-triphenylbenzene. In the $Rh_4(CO)_{12}$ catalyzed reaction, since rhodium atom has a larger covalent bond radii[6] than that of cobalt atom, the contribution of form II, which gives 1,3,5-triphenylbenzene, might be larger.

When the infrared spectra of the solution indicate the existence of $C_6H_5C{\equiv}CCHCo_4(CO)_{10}$ type complex only, half of triphenylbenzene is formed as a result of cyclotrimerization.

This means that not only $(C_6H_5C{\equiv}CH)_2M_2(CO)_4$ (M=Co or Rh) but also $(C_6H_5C{\equiv}CH)M_4(CO)_{10}$ has catalytic activity. Therefore these complexes must be transformed into *cis*-butadiene type structure in the transition state.

Experimental

Rhodium Tolane Complex. To a solution (50 m*l*) of $Rh_4(CO)_{12}$ (108 mg) in *n*-hexane, tolane (103 mg) was added and warmed at 50°C for 5 hr and then $P(C_6H_5)_3$ (62 mg) was added. The reaction product was chromatographed on alumina. From the eluted solution, red-brown prisms were obtained; yield 38%, mp 115°C (decomposed).

Found: C, 64.98; H, 4.36; Rh, 22.7%. Calcd for $C_{49}H_{35}O_3Rh_2P$: C, 64.77; H, 3.89; Rh, 22.65%.

The NMR spectrum was measured with a Varian HA-100 spectrometer in a tetrachloroethylene solution.

Table 2. Cyclotrimerization of phenylacetylene

Catalyst	$\frac{C_6H_5C{\equiv}CH(mM)}{Catalyst(mM)}$	1,2,4-TPB* (mM)	1,3,5-TPB (mM)	Total** yield	$\frac{1,2,4\text{-TPB}}{1,3,5\text{-TPB}}$
$Rh_4(CO)_{12}$	0.675/0.019=35.5	0.066	0.032	43%	2.2
	1.349/0.018=74.9	0.123	0.050	38%	2.4
$Co_4(CO)_{12}$	1.22/0.034=35.9	0.056	0.008	16%	7.0
	2.44/0.034=71.8	0.079	0.009	11%	8.9

* 1,2,4-Triphenylbenzene.
** Total yield for used phenylacetylene.

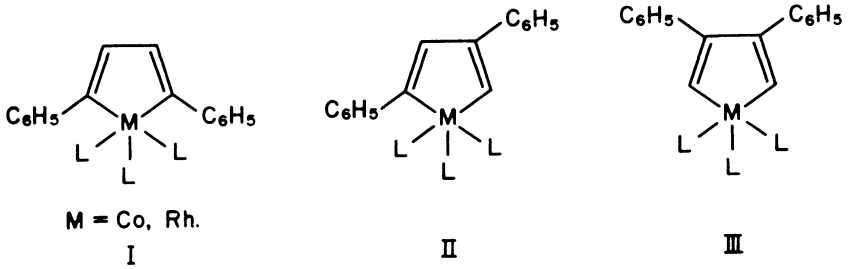

Fig. 4. The possible intermediates of cyclotrimerization.

6) L. Pauling, " The Nature of the Chemical Bonds," 3rd Ed., Cornell University Press, Ithaca, New York (1960).

TMS was used as an internal reference. The multiplet at 725 Hz was assigned to phenyl protons of $P(C_6H_5)_3$ and the multiplet at 676 Hz was assigned to phenyl protons of tolane, respectively. Integration of the spectrum showed that this complex contained one $P(C_6H_5)_3$ and two tolane molecules.

The infrared spectra were measured with a Hitachi-225 spectrometer as paste and KBr pellets. The absorption was corrected by the known absorption of standard polystyrene film.

Cyclotrimerization of Tolane. A 200 m*l* Schlenk tube was charged with 130 mg of $Rh_4(CO)_{12}$, 620 mg of tolane and 100 m*l* of degassed benzene, and then heated to 60°C for 10 hr. The reaction mixture was chromatographed on alumina, and the eluted solution was condensed to dryness. The product was recrystallized by methanol and identified by means of IR spectrum. (Yield 28%)

Cyclotrimerization of Phenylacetylene. The reaction was carried out in a Schlenk tube under a nitrogen stream at 60°C, for 4 hr. The ratio of 1,2,4-triphenylbenzene to 1,3,5-triphenylbenzene was determined with a Shimadzu GC-2 gas chromatograph, operated with a 3.0 m column packed with 4% OV-1 coated on Diatoport at 245°C.

The authors wish to thank Dr. Asao Nakamura and Dr. Ryoji Iwanaga for their discussions and encouragement.

BULLETIN OF THE CHEMICAL SOCIETY OF JAPAN VOL. 43 1520—1523 (1970)

Reaction of Cobalt Hydrotetracarbonyl with Acetylene

Yuji IWASHITA, Fumihide TAMURA and Hachiro WAKAMATSU

Central Research Laboratories, Ajinomoto Co., Inc., Suzuki-cho, Kawasaki

(Received October 25, 1969)

The reaction of cobalt hydrotetracarbonyl with acetylene was carried out in methanol as a model of the carboxylation of acetylene. The complexes formed in this reaction were identified by means of IR, NMR, EA and molecular weight measurement. The main product was acetylene dicobalt hexacarbonyl. From the decomposition reaction of this complex in ethanol, ethyl acrylate, ethyl propionate and diethyl succinate were obtained. The yield of ethyl acrylate increased in the presence of carbon monoxide. The reaction course from acetylene to acrylate was examined.

Natta and Pino[1] reported that the carboxylation of acetylene catalyzed by cobaltcarbonyl gives fumaric, acrylic and succinic esters in the presence of hydrogen and carbon monoxide in alcohol. It was found that the rate of acrylate formation is accelerated by the presence of hydrogen.[2] The authors have intended to throw light on the reaction course of carboxylation of acetylene by studying the nature of the complexes obtained from the reaction of cobalt carbonyl with acetylene.

Wender and his colleagues[3] reported that the reaction of cobalt hydrotetracarbonyl with acetylene in gas phase gives propanal and acetylene dicobalt hexacarbonyl. However, the reaction in solutions has not been studied yet.

Reaction of Cobalt Hydrotetracarbonyl with Acetylene. Cobalt carbonyl is known to take the form of hydrotetracarbonyl in alcoholic solution under high pressure of carbon monoxide and hydrogen.[3]

$$Co_2(CO)_8 + H_2 \xrightarrow[ROH]{} 2HCo(CO)_4$$

Thus, the reaction of cobalt hydrotetracarbonyl with acetylene in methanol has been carried out either at $-10°C$ or at 25°C, as a model of the first step of acrylic ester synthesis. In order to compare the reaction products in methanol with those in a non-polar solvent, the same reaction using *n*-hexane as a solvent has also been carried out at $-10°C$ and 25°C.

Triphenylphosphine was added to the reaction mixture. The resulting solution was concentrated and chromatographed on alumina. The products thus isolated are listed in Table 1. Ether-insoluble products I, III, VI and X were identified to be $Co_2(CO)_6[P(C_6H_5)_3]_2$[4a] (I, III, VI) and $[Co(CO)_3$-

1) G. Natta, and P. Pino, *Chim. Ind.* (Milan) **1952**, 34, 449.

2) H. Wakamatsu, J. Sato and M. Takesada, *Shokubai*, **9**, 14 (1967).

3) I. Wender, H. W. Sternberg, R. A. Friedel, S. J. Metlin and R. E. Markby, " The Chemistry and Catalytic Properties of Cobalt and Iron Carbonyls " (Bureau of Mines Bulletin 600), U. S. Dept. of Interior, Washington, (1962) p. 79.

4a) O. Vohler, *Chem. Ber.*, **91**, 1235 (1958).

Table 1. Complexes obtained from the reaction of acetylene with cobalt hydrotetracarbonyl

Solvent	Reaction temp.	Complex	
Methanol	−10°C	I	$Co_2(CO)_6[P(C_6H_5)_3]_2$
		II	$C_2H_2Co_2(CO)_5P(C_6H_5)_3$
	25°C	III	$Co_2(CO)_6[P(C_6H_5)_3]_2$
		IV	$C_2H_2Co_2(CO)_5P(C_6H_5)_3$
		V	$C_2H_2Co_2(CO)_4[P(C_6H_5)_3]_2$
n-Hexane	−10°C	VI	$Co_2(CO)_6[P(C_6H_5)_3]_2$
		VII	$C_2H_2Co_2(CO)_5P(C_6H_5)_3$
		VIII	$C_2H_2Co_4(CO)_8[P(C_6H_5)_3]_2$
		IX	$HCo(CO)_3P(C_6H_5)_3$
	25°C	X	$[Co(CO)_3(P(C_6H_5)_3)_2]^+[Co(CO)_4]^-$
		XI	$Co_2(CO)_6[P(C_6H_5)_3]_2$
		XII	$C_2H_2Co_2(CO)_5P(C_6H_5)_3$
		XIII	$C_2H_2Co_2(CO)_4[P(C_6H_5)_3]_2$

$(P(C_6H_5)_3)_2]^+[Co(CO)_4]^-$ (X) respectively, based on Vohler's studies.[4b] Complex IX, obtained from the reaction in *n*-hexane, was too unstable to be identified by means of IR and NMR, and rapidly decomposed to $Co_2(CO)_6[P(C_6H_5)_3]_2$. From the color and chemical behavior, complex IX was ascribed to $HCo(CO)_3P(C_6H_5)_3$, which Hieber has already reported.[5] Reddish brown crystals (II, IV, VII and XII) were obtained from the first eluted solution of *n*-hexane. All these components were proved to be identical, and this compound was the main product of the reaction not only in methanol but also in *n*-hexane. This complex shows four strong bands at 2065, 2011, 2001 and 1966 cm^{-1} in terminal carbonyl stretching region of the infrared spectrum. The NMR spectrum shows a doublet at $\delta = -5.03$ and a multiplet at $\delta = -7.3$ in a CS_2 solution. From elemental analysis and molecular weight measurement, the molecular formula was established to be $CH{\equiv}CHCo_2(CO)_5P(C_6H_5)_3$. The dark green complex (VIII) was obtained from the fraction eluted next to $CH{\equiv}CHCo_2(CO)_5P(C_6H_5)_3$. Complex VIII shows infrared bands at 2050.0 (s), 2015.0 (s), 1997.0 (m), 1982 (w), 1950 (m) and 1835.0 cm^{-1} in carbonyl stretching region. The NMR spectrum of complex VIII could not be observed, because of low solubility. The elemental analysis and molecular weight measurement have indicated the molecular formula of $C_2H_2Co_4(CO)_8[P(C_6H_5)_3]_2$. For the sake of comparison, the reaction of $Co_4(CO)_{12}$ with acetylene was carried out and the same complex as VIII was obtained.

The final component was isolated and determined to be $CH{\equiv}CHCo_2(CO)_4[P(C_6H_5)_3]_2$, from the infrared spectrum[6] and elemental analysis. The result is summarized in Table 1. The main product of the reaction of cobalt hydrotetracarbonyl with acetylene was established to be $CH{\equiv}CHCo_2(CO)_6$ in methanol and in *n*-hexane. The possibility of the association of cobalt hydrotetracarbonyl to form dicobalt octacarbonyl prior to the reaction was excluded for the reaction in methanol, because the former is considerably stable in methanol. The methanol solution of cobalt hydrotetracarbonyl shows only one broad infrared absorption at 1900 cm^{-1}, and this fact indicates that cobalt hydrotetracarbonyl dissociates into H^+ and $Co(CO)_4^-$. The reaction course is suggested as follows:

$$HCo(CO)_4 + CH{\equiv}CH \rightarrow HCo(CO)_3(CH{\equiv}CH) + CO$$

$$HCo(CO)_3(CH{\equiv}CH) + HCo(CO)_4 \rightarrow CH{\equiv}CHCo_2(CO)_6 + H_2 + CO$$

On the other hand, the reaction of sodium cobalt tetracarbonyl with acetylene has not given $CH{\equiv}CHCo_2(CO)_6$. This seems to be caused by the stability of $NaCo(CO)_4$ in a methanol solution. It is very interesting that all the complexes obtained from the reaction in methanol have the Co–Co covalent bond.

Decomposition Reaction of Acetylene Dicobalt Hexacarbonyl. Wender and his colleagues have reported that acetylene dicobalt hexacarbonyl catalyzes the polymerization of acetylene.[3] In order to investigate the role of $C_2H_2Co_2(CO)_6$ in acrylic ester formation, the decomposition reaction of this complex was carried out in the presence of ethanol and carbon monoxide.

4b) W. Hieber and W. Freyer, *ibid.*, **91**, 1230 (1958).
5) W. Hieber and E. Linder, *Z. Naturforsch.*, *B*, **16**, 137 (1961).
6) R. F. Heck, *J. Amer. Chem. Soc.*, **85**, 657 (1963).

Table 2. Products of decomposition reaction of $CH{\equiv}CHCo_2(CO)_6$

Complex (mM)	Temp. (°C)	CO (kg/cm^2)	Time (min)	Ethyl acrylate (%)	Ethyl propionate (%)	Diethyl succinate (%)
2.4	100	101	30	45	5	29
2.6	90	90	300	45	2	49
10.0	100	100	30	34	15	46
1.9	110	110	30	60	2	35
2.0	100	—	10	12	1	—
2.0	100	—	30	6	2	—
2.0	100	—	60	6	5	—
2.0	150	—	30	0	15	—

The reaction products were ethyl acrylate, ethyl propionate and diethyl succinate. In the absence of carbon monoxide the products were ethyl acrylate and ethyl propionate. The results are summarized in Table 2. The principal conclusions which emerge from a scrutiny of these data may be summarized as follows: (1) the presence of carbon monoxide increases the conversion ratio of $C_2H_2Co_2(CO)_6$ to ethyl acrylate, (2) diethyl succinate is not the secondary product from ethyl acrylate but is formed directly from $C_2H_2Co_2(CO)_6$, because the ratio of diethyl succinate to ethyl acrylate is almost constant during the course of reaction. (Table 2)

Reaction Course from Acetylene to Ethyl Acrylate. From the above-described experimental results and discussions, the following scheme can be suggested for the acrylate formation from acetylene under the pressure of carbon monoxide and hydrogen.

$$HC{\equiv}CH + 2HCo(CO)_4 \rightarrow HC{\equiv}CHCo_2(CO)_6 + H_2 + 2CO$$

$$HC{\equiv}CH + Co_2(CO)_8 \rightarrow HC{\equiv}CHCo_2(CO)_6 + 2CO$$

It has been suggested[7] that coordinated acetylene has C_{2v} symmetry and hybridization of this acetylene

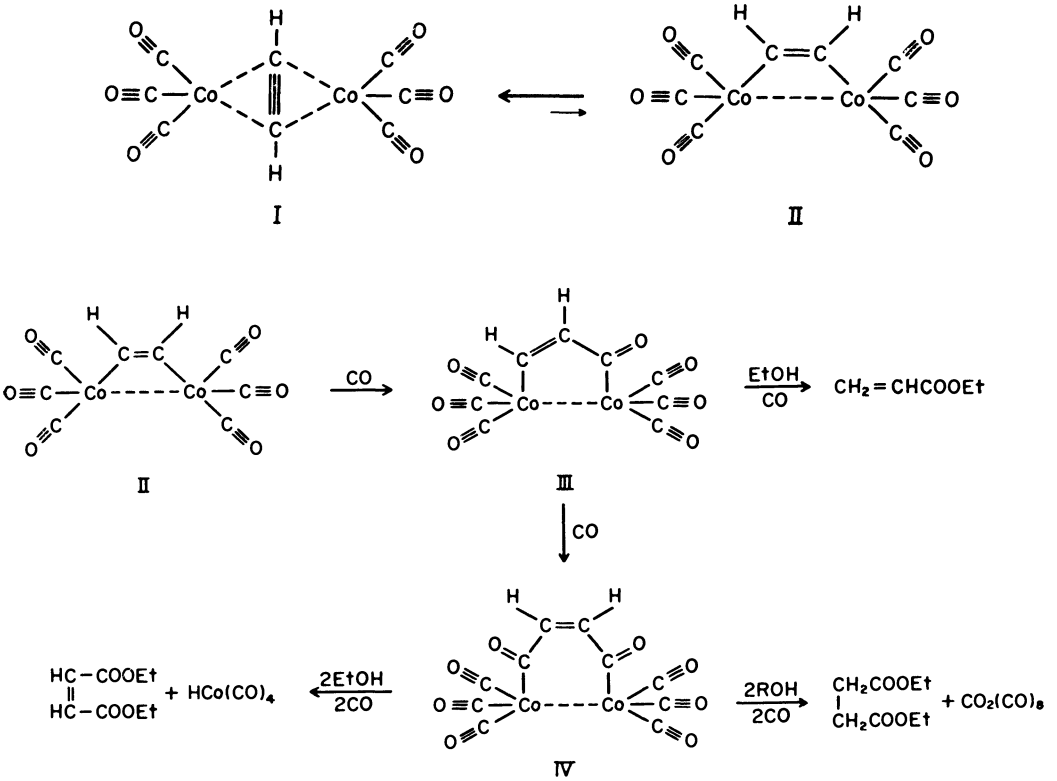

7) Y. Iwashita, F. Tamura and A. Nakamura, *Inorg. Chem.*, **8**, 1179 (1969).

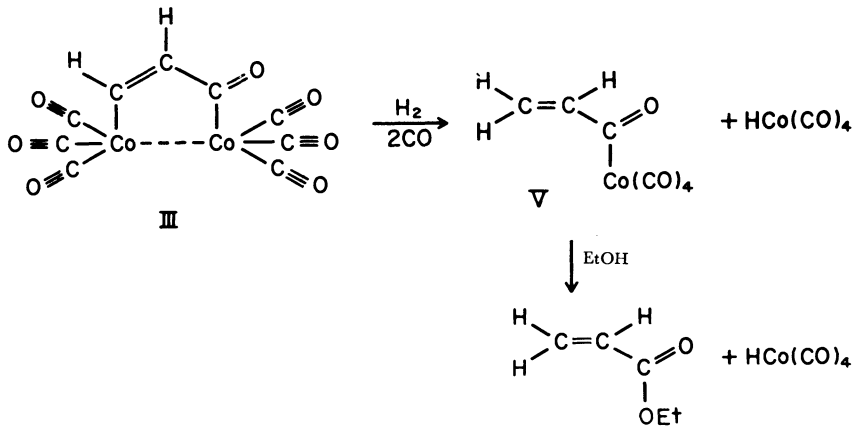

changes from *sp* to sp^2. The electrons in non-bonding orbital must occupy the two *cis*-positions of ethylene type structure. Therefore, the following isomerization may occur easily during the course of reaction. If the carbon monoxide or another Lewis base attacks isomer (II) the carbon monoxide can be inserted into the carbon-metal bond. This seems similar to the mechanism of butenolactone complex formation proposed by Heck.[8] The formation of other products (fumaric ester[1] and propanal) can be also explained on the basis of these assumed intermediates. Acetylene dicobalt hexacarbonyl has a considerable stability, and therefore, the rate determining step of acrylic ester formation from acetylene should be the transformation of this complex. The cobalt-carbon bond might be split by hydrogen as above. That the hydrogen can accelerate the rate of acrylate formation may be accounted for by these mechanisms.

Experimental

$HCo(CO)_4$ *n*-Hexane Solution. Thirteen grams of $Hg[Co(CO]_4]_2$ was dissolved into 200 m*l* of ether, and 200 g of Na-Hg was added to the solution. The ether solution was condensed after the color of $Hg[Co(CO)_4]_2$ had disappeared. $NaCo(CO)_4$ was obtained as white crystals. Five milliliters of concentrated hydrochloric acid was added to the aqueous $NaCo(CO)_4$ solution, and $HCo(CO)_4$ was extracted by *n*-hexane.

$HCo(CO)_4$ Methanol Solution. $HCo(CO)_4$ was generated from $Co(DMF)_6[Co(CO)_4]_2$ and concentrated HCl, and was absorbed by methanol.

Reaction of Acetylene with $HCo(CO)_4$. Acetylene purified by pyrogallol solution and dried by concentrated H_2SO_4, was admitted into $HCo(CO)_4$ solutions of methanol and *n*-hexane for 3 hr, and 10 g of $P(C_6H_5)_3$ was then added. The reaction mixture was condensed to dryness and extracted by ether. The ether layer was chromatographed on alumina. The main component of the ether soluble products was $C_2H_2Co_2(CO)_5P(C_6H_5)_3$ (yield about 45%). The yields of $C_2H_2Co_2(CO)_4[P(C_6H_5)_3]_2$ and $C_2H_2Co_4(CO)_8[P(C_6H_5)_3]_2$ were 5% and 3%, respectively (25°C, *n*-hexane solution). From ether-insoluble filtrate, $Co_2(CO)_6[P(C_6H_5)_3]_2$ and $[Co(CO)_3(P(C_6H_5)_3)_2]^+[Co(CO)_4]^-$ were obtained, but complete separation of these two species failed because of their sparing solubility in any solvent. (Yields of these two compounds were about 15%.)

Decomposition Reaction of $C_2H_2Co_2(CO)_6$ in Ethanol. $C_2H_2Co_2(CO)_6$ was thermally decomposed in ethanol under the pressure of CO in an autoclave. The reaction mixture was filtered and the filtrate was examined by gas chromatography (column PEG 400 with glycerine).

The authors wish to thank Dr. Asao Nakamura and Dr. Ryoji Iwanaga for their discussion and encouragement.

8) R. F. Heck, *J. Amer. Chem. Soc.*, **86**, 2819 (1964).

BULLETIN OF THE CHEMICAL SOCIETY OF JAPAN VOL. 43 1524—1529 (1970)

Synthetic Studies of the Flavone Derivatives. XVII.*[1] Synthesis of 5,7-Dihydroxy-6-methoxyflavone Derivatives[2]*

Kenji FUKUI and Mitsuru NAKAYAMA

Department of Chemistry, Faculty of Science, Hiroshima University, Higashisenda-machi, Hiroshima

and Tokunaru HORIE

Department of Applied Chemistry, Faculty of Engineering, University of Tokushima, Tokushima

(Received October 28, 1969)

2,4-Dibenzyloxy-6-hydroxy-3-methoxyacetophenone was esterified with 3,4-disubstituted benzoyl chlorides, and the resulting esters were converted into 7-benzyloxy-5-hydroxy-6-methoxyflavone derivatives *via* the corresponding diketones. The catalytic hydrogenolysis of the benzyloxyflavones gave the desired 5,7-dihydroxy-6-methoxyflavones. Ethyl ethers of these flavones were also prepared from 2,4-diethoxy-3-methoxy-6-hydroxyacetophenone by an unambiguous method. 6,3′-Dimethoxy-5,7,4′-trihydroxyflavone, desmethoxycentaureidin (6,4′-dimethoxy-5,7,3′-trihydroxyflavone), and 6-methoxyluteolin (6-methoxy-5,7,3′,4′-tetrahydroxyflavone) were thus prepared.

Recently 6,3′-dimethoxy-5,7,4′-trihydroxyflavone (Ia) has been isolated from *Digitalis lanata* L.,[1] *Helichrysum visocum* var. *bracteatum* DC.,[2] and *Helenium alternifolium* (Spreng) Cabrera,[3] desmethoxycentaureidin (6.4′-dimethoxy-5,7,3′-trihydroxyflavone) (Ib) has been isolated from *Centaurea nigrescens* Willd,[4] and 6-methoxyluteolin[5] (nepetin[6]) (6-methoxy-5,7,3′,4′-tetrahydroxyflavone*[3]) (Ic) has been isolated from *Rosmarinus officinalis* L.[5] and *Nepeta hindostana*.[6]

This paper will report on the syntheses of these 5,7-dihydroxy-6-methoxyflavone derivatives (Ia-c) and will attempt to confirm the structure.

2,4-Dibenzyloxy-6-hydroxy-3-methoxyacetophenone (II)[7] was prepared from 3-methoxy-2,4,6-trihydroxyacetophenone[8] by partial benzylation, it was then esterified with 3,4-disubstituted benzoyl chlorides, such as 4-benzyloxy-3-disubstituted benzyloxy-4-methoxy-(b), and 3,4-dibenzyloxy-(c)-chloride, in the presence of anhydrous pyridine. The resulting esters were converted into ω-(3,4-disubstituted benzoyl)-2,4-dibenzyloxy-6-hydroxy-3-methoxyacetophenones (IIIa-c) by Baker-Venkataraman transformation.[9] The cyclodehydration of the acetophenones (IIIa-c) with anhydrous sodium acetate in acetic acid afforded flavones (IVa-c). The UV spectra of the flavones (IVa-c) showed the bathochromic shift of Bands I and II in the presence of aluminum chloride (Table 3). The NMR spectra*[4] of IIIa-c indicated the presence of a chelated phenolic group. The spectra exhibit, further, reasonable signals of the aromatic-, benzyloxy-, and methoxy-protons (Table 1).

These facts indicate that IVa-c were obtained from IIIa-c by the cyclodehydration with anhydrous

---

*1 Part XVI of this series: K. Fukui, M. Nakayama and T. Horie, *J. Sci. Hiroshima Univ.*, A-II, **33**, 305 (1969).

*2 This paper was read before the 22th Annual Meeting of the Chemical Society of Japan, Tokyo, April, 1969. A part of this work has already been briefly communicated: *Experientia*, **25**, 355 (1969).

1) J. W. ApSimon, N. B. Haynes, K. Y. Sim and W. B. Whalley, *J. Chem. Soc.*, **1963**, 3780.

2) T. A. Geissman, R. Mukherjee and K. Y. Sim, *Phytochem.*, **6**, 1575 (1967).

3) W. Herz, C. M. Gast and P. S. Subramaniam, *J. Org. Chem.*, **33**, 2780 (1968).

4) F. Bohlmann and C. Zdero, *Tetrahedron Lett.*, **1967**, 3239.

5) C. H. Brieskorn and H. Michel, *ibid.*, **1968**, 3447.

6) N. R. Krishnaswamy, T. R. Seshadri and P. J. Tahir, *Indian J. Chem.*, **6**, 676 (1968).

*3 Pedalitin (from *Sesanum indicum*) was identified as 6-methoxy-5,7,3′,4′-tetrahydroxyflavone (N. Morita, *Chem. Pharm. Bull.* (Tokyo), **8**, 59, 66 (1960)). However, the revised structure has been postulated to be 7-methoxy-5,6,3′,4′-tetrahydroxyflavone by two groups of researchers (N. R. Krishnaswamy *et al.*[6] and K. Fukui, M. Nakayama, T. Matsui, M. Masumura and T. Horie, *Nippon Kagaku Zasshi*, **90**, 1270 (1969)).

7) K. Fukui, M. Nakayama and T. Horie, This Bulletin, **42**, 2327 (1969).

8) P. S. Phadke, A. V. Rama Rao and K. Venkataraman, *Indian J. Chem.*, **5**, 131 (1967).

9) W. Baker, *J. Chem. Soc.*, **1933**, 1381; K. Venkataraman and H. S. Mahal, *ibid.*, **1934**, 1767.

*4 The NMR spectra in this paper were measured with a Hitachi R-20 spectrometer (60 MHz), using tetramethylsilane as the internal standard (δ-value in $CDCl_3$); s, singlet; bs, broad singlet; d, doublet; t, triplet; q, quartet; m, multiplet.

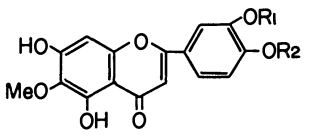

I

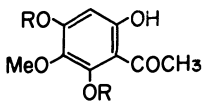

II R=$CH_2C_6H_5$
VII R=Et

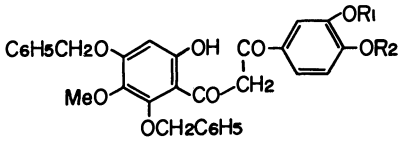

III

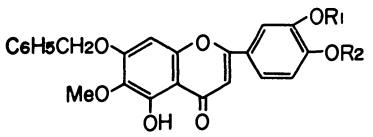

IV

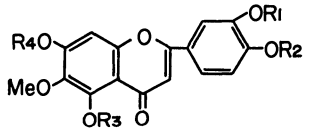

V R3=R4=Ac
VI R3=R4=Et
X R3=H, R4=Et

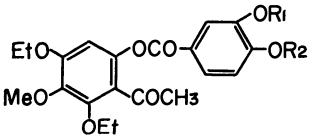

VIII

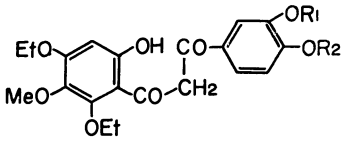

IX

I
a R_1=Me, R_2=H
b R_1=H, R_2=Me
c R_1=R_2=H

III, IV
a R_1=Me, R_2=$CH_2C_6H_5$
b R_1=$CH_2C_6H_5$, R_2=Me
c R_1=R_2=$CH_2C_6H_5$

V
a R_1=Me, R_2=Ac
b R_1=Ac, R_2=Me
c R_1=R_2=Ac

VI, VIII, IX, X
a R_1=Me, R_2=Et
b R_1=Et, R_2=Me
c R_1=R_2=Et

Table 1.*4 NMR Data of benzyloxyflavones (IVa-c)

	IVa	IVb	IVc
OH	12.78_s	12.87_s	12.87_s
Arom. H			
C-3 or C-8	6.57_s (2H)	6.53_s 6.57_s	6.56_s 6.60_s
C-5′	6.96_d J=9.0 Hz	7.01_d J=9.0 Hz	6.97_d J=9.0 Hz
others	$7.20—7.60_m$(12H)	$7.30—7.65_m$(12H)	$7.20—7.60_m$(17H)
$C_6H_5CH_2O$	5.25_s(4H)	5.27_s(4H)	5.30_s(6H)
CH_3O	3.97_s(3H) 3.94_s(3H)	3.97_s(6H)	3.97_s(3H)

sodium acetate and by the subsequent partial debenzylation. The flavones, IVa-c, can thus be formulated as 7-benzyloxy-5-hydroxy-6-methoxyflavone derivatives. The catalytic hydrogenolysis of IVa-c over palladium charcoal gave the desired flavones (Ia-c), which were then converted into the corresponding acetates (Va-c) by the conventional method. The hydroxyflavones (Ia, b) gave the corresponding ethyl ether derivatives (VIa, b) upon complete ethylation with diethyl sulfate and anhydrous potassium carbonate.

In order to establish the structure of the hydroxyflavones (Ia-c), the ethyl ether derivatives (VIb, c) were prepared by the following unambiguous method. The esterification of 2,4-diethoxy-6-hydroxy-3-methoxyacetophenone (VII)[10] with 3-ethoxy-4-methoxy- or 3,4-diethoxy-benzoyl chloride yielded 6-(3-ethoxy-4-methoxybenzoyloxy)- (VIIIb) or 6-(3,4-diethoxy benzoyloxy)- (VIIIc) -2,4-di-

10) L. Farkas, L. Hörhammer, H. Wagner, H. Rösler and R. Gurniak, *Chem. Ber.*, **97**, 610 (1964).

ethoxy-5-methoxyacetophenone. The esters (VIIIb and VIIIc) gave 6,4′-dimethoxy-5,7,3′-triethoxy-(VIb) and 6-methoxy-5,7,3′,4′-tetraethoxy-(VIc)-flavone *via* the corresponding diketones (IXb and IXc) by a method similar to that described above. These flavones (VIa, b) were identified by direct comparisons with the ethyl derivatives obtained by the ethylation of the hydroxy-flavones (Ia, b).*5 Furthermore, the partial ethylation of the hydroxy-flavones (Ib, c) gave the 5-hydroxyflavone derivatives (Xb, c), which were then easily converted into monoacetates. Xb, c were also prepared from VIb, c by partial deethylation with anhydrous aluminum chloride. The hydroxyflavones (Ia-c) were now established to be 5,7-dihydroxy-6-methoxy-flavone derivatives.

Ia and Va were shown to be identical with the natural pigment and its acetate*6 by a mixed-melting-point determination and by NMR, IR and UV spectral comparisons.*7

On the other hand, the natural desmethoxycentaureidin and 6-methoxyluteolin were, unfortunately, could not be compared directly, but the properties of the synthetic samples of Ib and Ic were superimposable upon those recorded in the literature.[4-6]

Experimental*8

ω-(4-Benzyloxy-3-methoxybenzoyl)-(IIIa), ω-(3-benzyloxy-4-methoxybenzoyl)- (IIIb), and ω-(3,4-dibenzyloxybenzoyl) - (IIIc) - 2,4 - dibenzyloxy-6-hydroxy-3-methoxyacetophenone. A mixture of the crude dibenzyloxyacetophenone (II)[7] (2—2.5 g) and 3,4-disubstituted benzoyl chloride (2.5—3.0 g) in anhydrous pyridine (8.0 m*l*) was heated at 120°C for 2 hr. The cooled reaction mixture was poured into diluted hydrochloric acid, and then extracted with ether (the insoluble material was filtered off). The ether layer was washed with a sodium carbonate solution and water. The removal of the solvent gave a semi-solid, which was then dried in a desiccator.

A mixture of the crude ester, freshly-powdered potassium hydroxide (2.5 g), and pyridine (15—20 m*l*) was heated at 60°C for 4 hr with stirring. The reaction mixture was acidified with diluted hydrochloric acid, and then extracted with ether. The ether layer was washed with a sodium carbonate solution. The solvent was evaporated to 2—5 m*l* and then allowed to stand overnight. The separated crystals were collected and recrystallized to give III (Table 2), which gave a green color with ferric chloride in ethanol.

7,4′-Dibenzyloxy-6,3′-dimethoxy- (IVa), 7,3′-dibenzyloxy-6,4′-dimethoxy- (IVb) and 7,3′,4-tribenzyloxy-6-methoxy- (IVc)-5-hydroxyflavone. A mixture of III (500—700 mg) and anhydrous sodium acetate (2—4 g) in acetic acid (20—40 m*l*) was heated at 140°C for 4—5 hr. The reaction mixture was then diluted with water and extracted with ether. The ether layer was washed with a sodium carbonate solution and then allowed to stand overnight in a refrigerator. The combined precipitates were crystallized to give IV (Table 3), which gave a dark brown or dark greenish brown color with ferric chloride in ethanol and a red color with magnesium and hydrochloric acid.

6,3′-Dimethoxy-5,7,4′-tribenzyloxyflavone (5-O-Benzylether of IVa). A mixture of IVa (30 mg), benzyl chloride (0.1 m*l*), and anhydrous potassium carbonate (300 mg) in dimethylformamide (1.0 m*l*) was gently refluxed for 2 hr. The cooled reaction mixture was diluted with water and then extracted with ether. The ether layer was washed with diluted hydrochloric acid and water, and then subjected to evaporation under a vacuum. The oily residue was triturated with hexane and then treated with ether at 20—30°C. The separated crystals were recrystallized from methanol to give tribenzyloxyflavone as colorless needles; mp 127°C (115—116°C sinter); yield, 25 mg (71%). IR: 1638 cm^{-1} ($CHCl_3$). UV: λ_{max} mμ (log ε); 240_{sh}*9 (4.40), 264 (4.20), 330 (4.47).

Found: C, 76.05; H, 5.30%. Calcd for $C_{38}H_{32}O_7$: C, 75.98; H, 5.37%.

6,3′-Dimethoxy-5,7,4′-trihydroxyflavone (Ia), 6,4′-dimethoxy-5,7,3′-trihydroxyflavone (desmethoxycentaureidin) (Ib) and 6-methoxy-5,7,3′,4′-tetrahydroxyflavone (6-methoxyluteolin) (Ic). A solution of IV (350—400 mg) dissolved in a mixture of methanol and ethyl acetate (1:2: 80—100 m*l*) was shaken with palladium charcoal (10%: 200 mg) in an atmosphere of hydrogen for 3—4 hr. After the catalyst had been filtered, the filtrate was evaporated and the residue was recrystallized to give I (Table 4), which gave a dark brown or dark greenish brown color with ferric chloride in ethanol.

Ia was identified with a natural pigment*6 by a mixed-melting-point determination and by IR and UV spectral comparisons.

Acetates (Va–c) of I were synthesized by a hot acetic anhydride-pyridine method (Table 5). The NMR spectra of V were assigned as is shown in Table 6.

Va was found to be identical with the triacetate of the natural pigment by a mixed-melting-point determination and by NMR, IR, and UV spectral comparisons.

6-(3-Ethoxy-4-methoxybenzoyloxy)-(VIIIb) and 6-(3,4 - diethoxybenzoyloxy) - (VIIIc) - 2,4 - diethoxy-3-methoxyacetophenone. A mixture of VII[10] (2.0 g) and 3-ethoxy-4-methoxybenzoyl chloride (2.0 g) (or 3,4-diethoxybenzoyl chloride (2.1 g)) in anhydrous pyridine (5.0 g) was heated at 120°C for 2 hr. The reaction mixture was then treated by the usual method, and the crude product was recrystallized (Table 7).

ω-(3-Ethoxy-4-methoxybenzoyl)- (IXb) and ω-(3,4-diethoxybenzoyl)- (IXc)-2,4-diethoxy-6-hydroxy-3-methoxy-acetophenone. A mixture of VIII (1.5 g) and freshly-powdered potassium hydroxide (3.0 g) in anhydrous pyridine (15 g) was heated at 60°C for 4 hr with stirring. The reaction mixture was then treated by the method described in the case of III, and the crude

*5 The synthesis of VIa was previously reported by the present authors (T. Horie, M. Masumura, K. Fukui and M. Nakayama, This Bulletin, **41**, 1460 (1968)).

*6 The natural pigment was kindly supplied by Professor W. B. Whalley, University of London.

*7 Recently, Ia has also been synthesized from 3-methoxy-2,4,6-trihydroxyacetophenone by Drs. K. Y. Sim and R. Mukherjee (private communications).

*8 All the melting points are uncorrected; the UV spectra were measured in ethanol.

*9 sh=shoulder.

Table 2. ω-(3,4-Disubstituted benzoyl)-2,4-dibenzyloxy-6-hydroxy-3-methoxyacetophenones (IIIa-c)

Compounds	Mp (°C) (From solvent)[a]	Cryst. form	Yield (%)	Formula	Found C%	Found H%	Calcd C%	Calcd H%
IIIa	124.5—125.5 (EA-E)	Yellow needles	9.5	$C_{38}H_{34}O_8$	73.90	5.40	73.77	5.54
IIIb	183—184 (MEK)	Yellow prisms	11	$C_{38}H_{34}O_8$	73.69	5.59	73.77	5.54
IIIc	136.5—137.5 (EA)	Yellow prisms	10	$C_{44}H_{38}O_8$	76.26	5.47	76.06	5.51
	135.5 (125 sinter) (E)	Yellow needles						

a) EA=Ethyl acetate, E=Ethanol, MEK=Methyl ethyl ketone.

Table 3. 7-Benzyloxy-5-hydroxy-6-methoxyflavones (IVa-c)

Compounds	Mp (°C) Cryst. form (From solvent)[a]	Yield (%)	IR (C=O) cm^{-1} (Nujol)	UV λ_{max} mμ (log ε) EtOH	UV λ_{max} mμ (log ε) EtOH-$AlCl_3$	Formula	Found C% H%	Calcd C% H%
IVa	166—167.5	71	1658	243.5(4.26)	260 (4.16)	$C_{31}H_{26}O_7$	72.73	72.93
	Colorless needles		1624	277.5(4.26)	292 (4.26)		5.35	5.13
	(E)			340 (4.42)	364 (4.41)			
IVb	145—146.5	71	1658	243.5(4.29)	261 (4.16)	$C_{31}H_{26}O_7$	72.84	72.93
	Pale yellow		1640	277 (4.24)	293 (4.25)		5.20	5.13
	needles (E)			339 (4.39)	364 (4.38)			
IVc	158—159 (143—145 sinter)	78	1655 (broad)	242.5(4.32)	258.5(4.21)	$C_{37}H_{30}O_7$	75.98	75.75
				277.5(4.25)	295 (4.28)		5.24	5.16
	Colorless needles			337 (4.43)	360 (4.38)			
	(E)							

a) E=Ethanol.

Table 4. 5,7-Dihydroxy-6-methoxyflavones (Ia-c)

Compounds	Mp (°C) Cryst. form (From solvent)[a]	Yield (%)	IR cm^{-1}	UV λ_{max} mμ (log ε) EtOH	UV λ_{max} mμ (log ε) EtOH-$AlCl_3$	Formula	Found C% H%	Calcd C% H%
Ia (Syn.)	226—227	82	3400, 1666[b]	275(4.19)	260 (4.12)	$C_{17}H_{14}O_7$	61.95	61.82
	Yellow needles		3200, 1624	346(4.41)	286 (4.18)		4.13	4.27
	(aq. E)		3100		370 (4.41)			
(Nat.)	226—227		3400, 1663[b]	275(4.20)	260 (4.14)			
	Yellow needles		3150, 1620	346(4.42)	286.5(4.20)			
	(aq. E)		3100		370 (4.42)			
Ib	262—263	83	3390(broad)[c]	245(4.24)	261.5(4.19)	$C_{17}H_{14}O_7$	61.56	61.82
	Yellow needles		1650	275(4.23)	289 (4.14)		4.05	4.27
	(E)		1615	344(4.40)	367 (4.39)			
(Lit.)[4]	269—272		3430(broad)					
			1670	273				
			1630	342	370			
Ic	264—266	78	3380(broad)[c]	255(4.21)	279 (4.28)	$C_{16}H_{12}O_7$	60.75	60.76
	Yellow needles		1658	273(4.21)	400 (4.38)		3.80	3.82
	(aq. M)		1615	350(4.42)				
(Lit.)[5]	258—262		3390(broad)	256	284			
			1655	273	365			
			1600	348				

a) aq.=aqueous; E=Ethanol; M=Methanol. b) Nujol. c) KBr.

TABLE 5. ACETATES (Va-c) OF 5,7-DIHYDROXY-6-METHOXYFLAVONES (I)

Compounds	Mp (°C) Cryst. form (From solvent)[a]	Yield (%)	IR (C=O) cm^{-1} (Nujol)	UV λ_{max}^{EtOH} mμ (log ε)	Formula	Found C% H%	Calcd C% H%
Va (Syn.)	217—218	95	1765	241.5(4.27)	$C_{23}H_{20}O_{10}$	60.52	60.52
	Colorless needles		1643	264.5(4.26)		4.26	4.42
	(E)			316 (4.32)			
(Nat.)	217—218						
	Colorless needles		1765	242 (4.31)			
	(E)		1643	264.5(4.30)			
				316 (4.38)			
Vb	186.5—187	92	1775	262 (4.17)	$C_{23}H_{20}O_{10}$	60.38	60.52
	Colorless needles		1640	320 (3.93)		4.29	4.42
	(E)						
(Lit.)[4]	189—190			261			
				319			
Vc	202.5—203 (180 sinter)	85	1776	265 (4.37)	$C_{24}H_{20}O_{11}$	59.25	59.50
	Colorless needles		1647	302 (4.39)		4.44	4.16
	(E)						
(Lit.)[6]	170—171						

a) E=Ethanol.

TABLE 6. NMR DATA OF Va-c*4

	Va	Vb	Vc
Arom. H			
C-3	6.57_s	6.55_s	6.60_s
C-8	7.28_s	7.28_s	7.27_s
C-2′	7.38_{bs}	7.57_d J=2.5 Hz	7.72_d J=2.5 Hz
C-5′	7.13_d J=9.0 Hz	7.07_d J=9.0 Hz	7.36_d J=9.0 Hz
C-6′	7.46_q J=9.0, 2.5 Hz	7.75_q J=9.0, 2.5 Hz	7.76_q J=9.0, 2.5 Hz
CH_3CO	2.33_s	2.36_s	2.34_s (6H)
	2.38_s	2.39_s	2.39_s
	2.48_s	2.49_s	2.50_s
CH_3O	3.87_s	3.87_s	3.87_s
	3.90_s	3.91_s	

TABLE 7. 6-(3,4-DISUBSTITUTED BENZOYLOXY)- (VIIIb, c) AND ω-(3,4-DISUBSTITUTED BENZOYL-)-(IXb, c)-2,4-DIETHOXY-6-HYDROXY-3-METHOXYACETOPHENONE

Compounds	Mp (°C) (From solvent)[a]	Cryst. form	Yield (%)	Formula	Found C%	Found H%	Calcd C%	Calcd H%
VIIIb	106—107 (M)	Colorless plates	59	$C_{23}H_{28}O_8$	63.92	6.81	63.88	6.53
VIIIc	106—107.5 (E)	Colorless prisms	57	$C_{24}H_{30}O_8$	64.71	6.71	64.56	6.77
IXb	107.5—108 (M)	Yellow needles	58	$C_{23}H_{28}O_8$	64.00	6.49	63.88	6.53
IXc	106—107.5 (M)	Yellow needles	45	$C_{24}H_{30}O_8$	64.39	6.58	64.56	6.77

a) M=Methanol; E=Ethanol.

Table 8. Some of ethoxyflavone derivatives

Compounds	Mp (°C) (From solvent)[a]	Cryst. form	Yield (%)	Formula	Found C%	Found H%	Calcd C%	Calcd H%
VIa	172—173 (E)	Pale yellow prisms	50[b]	$C_{23}H_{26}O_7$	66.50	6.19	66.65	6.32
VIb	154—155 (E)	Colorless needles	52[b] 93[c]	$C_{23}H_{26}O_7$	66.63	6.46	66.65	6.32
VIc	142—143.5 (E)	Colorless prisms	93[c]	$C_{24}H_{28}O_7$	67.27	6.44	67.27	6.59
Xb	170—171 (E)	Pale yellow needles	62[b] 70[d]	$C_{21}H_{22}O_7$	65.23	5.79	65.27	5.74
Xc	152.5—153.5 (E)	Pale yellow needles	68[b] 45[d]	$C_{22}H_{24}O_7$	65.69	5.86	65.99	6.04
Acetate of Xb	165—166.5 (M)	Colorless plates	90	$C_{23}H_{24}O_8$	64.69	5.57	64.48	5.65
Acetate of Xc	172—173.5 (aq. M)	Colorless needles	92	$C_{24}H_{26}O_8$	65.15	5.92	65.09	5.90

a) E=Ethanol; M=Methanol; aq.=aqueous.
b) Yield from I. c) Yield from VIII. d) Yield from VI.

product was recrystallized (Table 7).

5,7-Diethoxy-6-methoxyflavone Derivatives (VIa–c).

a) From I. A mixture of I (20—30 mg), diethyl sulfate (0.2—0.3 m*l*), and anhydrous potassium carbonate (0.5—1.0 g) in anhydrous acetone (15—20 m*l*) was refluxed for 20—24 hr and then treated with aqueous methanol (10%: 15 m*l*). The solvent was distilled off. The resulting precipitate was collected and recrystallized to give VIa, b (Table 8).

b) From IX. Concentrated sulfuric acid (0.7 m*l*) was added to a solution of IX (700 mg) in acetic acid (7.0 m*l*) after which the mixture was heated at 70°C for 3 min. The reaction mixture was treated with hot water (30 m*l*), and then the separated precipitate was collected and washed with water. The recrystallization of the precipitate afforded VI, which was undepressed in melting point on admixture with the sample of a).

7-Ethoxy-5-hydroxy-6-methoxyflavone Derivatives (X).

a) From I. A mixture of I (30 mg), diethyl sulfate (0.2 m*l*), and anhydrous potassium carbonate (0.4 g) in acetone was refluxed for 6 hr and then treated by the method described in the case of VI. The crude product was recrystallized to give Xb, c (Table 8).

b) From VI. To a solution of VI (500 mg) in anhydrous nitrobenzene (6.0 g), a solution of anhydrous aluminum chloride (5.0 g) in absolute ether (15 m*l*) was added, and the mixture was heated at 47°C for 5 hr. After the mixture had been poured into 1% hydrochloric acid (250 m*l*), the solution was concentrated to 100 m*l* in a vacuum. The resulting precipitate was collected, washed with water, and recrystallized to give Xb, c; the melting point was undepressed on admixture with the sample of a).

Acetate of X. The acetate was prepared by a hot acetic anhydride-pyridine method (Table 8).

The authors are grateful to Professor W. B. Whalley, University of London, for supplying the 6,3′-dimethoxy-5,7,4′-trihydroxyflavone.

BULLETIN OF THE CHEMICAL SOCIETY OF JAPAN VOL. 43 1530—1534 (1970)

Deamination of Methylenecyclopropylcarbinylamine. The Formation of a Vinyl Cation by Carbon–Carbon Bond Cleavage[1)]

Akio NISHIMURA and Masaki OHTA

Laboratory of Organic Chemistry, Tokyo Institute of Technology, Ookayama, Meguro-ku, Tokyo

and Hiroshi KATO[2)]

Department of Chemistry, Faculty of Science, Shinshu University, Asahi, Matsumoto

(Received October, 28, 1969)

The deamination of methylenecyclopropylcarbinylamine, prepared from ethyl methylenecyclopropanecarboxylate *via* the corresponding amide, gave acetylcyclopropane, methylenecyclopropylcarbinol, and 3-methylenecyclobutanol. On the basis of these results and the deuterium distribution of the deamination products of methylenecyclopropylcarbinylamine-α,α-d_2, the homoallylic (III) and cyclopropylvinyl (VIII) cations are proposed as intermediates.

The deamination reactions of cyclopropylcarbinylamine derivatives have been very scrupulously investigated in connection with the problem of the structure of the intermediate cation.[3)] The deamination reaction of methylenecyclopropylcarbinylamine (**1**), which we wish to report on here, merits even further investigation because the introduction of an *exo*-methylene group leads to some stereochemical features which are absent in the heretofore-investigated cyclopropylcarbinyl systems.

Two bicyclobutonium intermediates, I and II, are possible for this ring system; of them, I may be further stabilized by two allylic resonances with the *exo*-methylene group (I′), though the stabilization by such an interaction would be decreased by an unfavorable configuration of the *exo*-methylene group and the cationic center at the transition state. On the other hand, the formation of II requires the loosening of a relatively strong sp^2–sp^3 carbon bond and it involves a contribution from a vinyl cation, which is generally considered to be formed only with difficulty.

Another possible intermediate, II, which is a homoallylic-type intermediate, may exist. Although stabilization by homoallylic resonance has been calculated to be less than that by bicyclobutonium resonance,[4)] in the particular case of III the scale model indicates that the cationic center is ideally situated for an effective (p-π type) interaction with the *exo*-methylene π-electrons.

A tricyclobutonium intermediate, IV, may also be considered although the possibility of the intermediacy of such a species has been eliminated in the case of the cyclopropylcarbinyl cation.[5,6)]

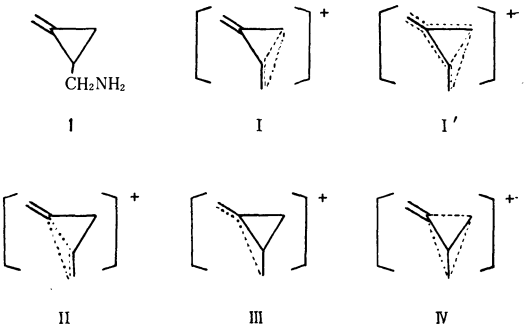

Results and Discussion

Methylenecyclopropylcarbinylamine (**1**) was prepared as is shown in Scheme 1. Ethyl methylenecyclopropanecarboxylate (**2**)[7)] was converted to methylenecyclopropanecarboxamide (**3**) by ammonolysis, or through the steps of the hydrolysis of

1) a) Taken from the Master of Science thesis of A. N. b) A part of this work has appeared in a preliminary communication: A. Nishimura, H. Kato and M. Ohta, *J. Amer. Chem. Soc.*, **89**, 5083 (1967).

2) To whom inquiries should be addressed.

3) See, for example, a) R. Breslow, "Molecular Rearrangements," Part I, ed. by P. de Mayo, Interscience Publishers, New York (1963), p. 254; b) P. D. Bartlett, "Nonclassical Ions," Benjamin Inc., New York (1965); c) G. D. Sargent, *Quart. Rev.* (London), **20**, 301 (1966).

4) M. E. H. Howden and J. D. Roberts, *Tetrahedron*, **19**, *Suppl.*, **2**, 403 (1963).

5) R. H. Mazur, W. N. White, D. A. Semenow, C. C. Lee, M. S. Silver and J. D. Roberts, *J. Amer. Chem. Soc.*, **81**, 4390 (1959). See, however, I. Lillien and L. Handloser, *Tetrahedron Lett.*, **1969**, 1035.

6) J. E. Baldwin and W. D. Foglesong, *J. Amer. Chem. Soc.*, **90**, 4311 (1968).

7) a) J. A. Carbon, W. B. Martin and L. R. Swett, *ibid.*, **80**, 1002 (1958). b) E. F. Ullman and W. J. Fanshawe, *ibid.*, **83**, 2379 (1961).

2 to the acid **4**, the conversion to acid chloride, **5**, with oxalyl chloride, and the treatment of **5** with ammonia. The amide, **3**, was converted to methylenecyclopropylcarbinylamine (**1**) by treatment with lithium aluminum hydride.

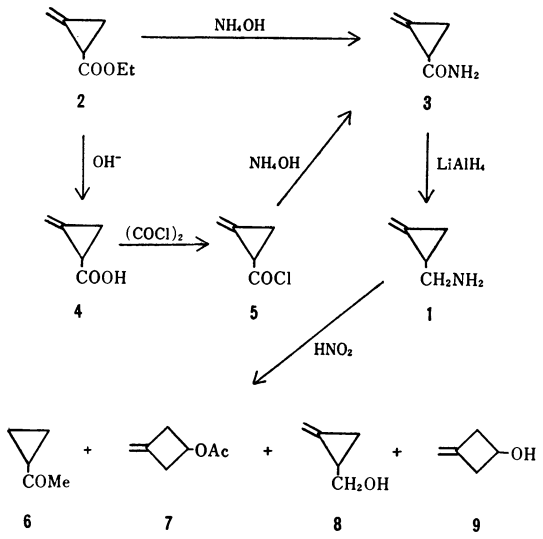

Scheme 1. Preparation and deamination of methylenecyclopropylcarbinylamine.

The deamination of **1** with nitrous acid in aqueous acetic acid gave four major products[8] (**A**—**D**) in a vpc-area ratio of 1.0 : 2.3 : 1.9 : 12.7 ; these products were separated by vpc and were identified as acetylcyclopropane (**6**), 3-methylenecyclobutyl acetate (**7**), methylenecyclopropylcarbinol (**8**), and 3-methylenecyclobutanol (**9**) respectively on the basis of the facts to be presented below.

The presence of an acetyl group in the component **A** could be detected by means of an NMR signal at τ 7.85 together with an infrared band at 1700 cm^{-1}, while a multiplet NMR signal at τ 9.0—9.4 was indicative of the presence of a cyclopropane ring. Its mass spectrum established its molecular weight and the presence of an acetyl group by peaks at *m/e* 84 and 43 (base peak). Its structure was confirmed to be **6** by a comparison of its spectral data and vpc retention times with those of authentic acetylcyclopropane.[9]

The infrared spectra of the component **C** suggested the presence of a hydroxyl group and of a terminal methylene group by bands at 3350, 3070, and 890 cm^{-1}. Its NMR spectrum displayed a broad two-proton singlet at τ 4.70 and a one-proton singlet at τ 7.09, supporting the idea of the presence of a terminal methylene group and of a hydroxyl group ; a two-proton doublet at τ 6.65 suggestive of a methylene group adjacent to the hydroxyl group, and a three-proton multiplet at τ 8.10—9.35 indicative of the presence of a cyclopropyl group. It was proved identical with methylenecyclopropylcarbinol, (**8**), prepared by the lithium aluminum hydride reduction of **2**.[7a]

The infrared spectrum of the component **D** showed absorption bands at 3320 and 1100 and at 3070, 1670, and 880 cm^{-1}, suggesting the presence of a secondary hydroxyl group and a terminal methylene group respectively. Its NMR spectrum indicated a terminal methylene proton by a two-proton quintet (J=2 Hz) at τ 5.23, a methine proton by a one-proton quintet (J=7 Hz) at τ 5.75, and a four-proton multiplet at τ 6.85—7.75. These spectral data are in accord with those of 3-methylenecyclobutanol (**9**).[10]

The NMR spectrum of the component **B** was similar to that of **9** except that the hydroxyl proton signal of **9** was replaced by a new three-proton singlet at τ 8.15,[11] and its infrared spectrum showed the bands of a terminal methylene group (3080, 1680 and 882 cm^{-1}) and bands at 1740 and 1240 cm^{-1} assignable to an ester group. These spectral data are consistent with 3-methylenecyclobutyl acetate (**7**) structure for the component **B**. This assignment was further corroborated by the fact that the acetylation of **9** gave **7**, and by the fact that the lithium aluminum hydride reduction converted **7** to **9**, as judged by their vpc retention times.

One of the components present in a minor proportion had, on a vpc column, a retention time identical with that of the acetylation product of methylenecyclopropylcarbinol, but it could neither be isolated nor further characterized.

The deamination, in aqueous acetic acid, of methylenecyclopropylcarbinylamine-α,α-d_2 (**1**-$\mathbf{d_2}$), itself prepared by the lithium aluminum deuteride reduction of **3**, gave α,α-dideuteriomethylenecyclopropylcarbinol and 2,2-dideuterio-3-methylenecyclobutanol (and its acetate). The quantity of deuterated acetylcyclopropane isolated in this experiment was too small to permit the determination of the position(s) of deuteration.

Among the reaction products, 3-methylenecyclobutanol (**9**) and acetylcyclopropane (**6**) deserve special consideration.

The bicyclobutonium intermediate I appears to be favored because of a possible stabilization of the cation I by allylic resonance (I′). Such an allylic resonance, however, should not be considered an efficacious one because the *exo*-methylene group cannot interact effectively with the cationic center at the transition state because of their unfavorable

8) These four components constituted 87% of the total products in the peak area, and most of other minor products had shorter retention times than those of **A**—**D**.

9) G. W. Cannon, R. C. Ellis and J. R. Leal, " Organic Syntheses," Coll. Vol. IV, p. 597 (1963).

10) D. E. Applequist and G. F. Fanta, *J. Amer. Chem. Soc.*, **82**, 6393 (1960).

11) Other NMR signals (τ): 5.12—5.50 (3 H, m; $=CH_2$+H-C-O), 6.8—7.5 (4 H, m; ring protons).

configurations. Moreover, neither 2-methylenecyclobutanol nor 2-methylene-3-buten-1-ol was found to be formed in a detectable quantity, as would be the case with a reaction product arising from the intermediate I. Appelquist,[10,12] on the basis of the results of the deamination of spiropentylamine, suggested the rearrangement of the 2-methylenecyclobutyl cation (V) to the 3-methylenecyclobutyl cation (VI) by a hydride migration. The possibility of the formation of **9** in the present experiment by this mechanism can, however, be eliminated since, if **1** first formed the cation V and it was then rearranged to VI, then the alcohol, **9**, formed should be deuterated equally on the 1- and 2-positions. The 3-methylenecyclobutanol isolated from the present experiment, however, had all the deuterium atoms solely on the 2-position.

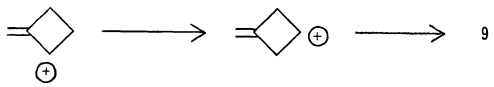

V VI

An alternative bicyclobutonium ion II[6] can structurally account for the formation of both methylenecyclopropylcarbinol (**8**) and 3-methylenecyclobutanol (**9**). However, methylenecyclopropylcarbinol was deuterated only on the α-methylene group. This means that the bicyclobutonium ion II is not in equilibrium with another bicyclobutonium ion of an identical structure. The presence of such an equilibirum has been established with the bicyclobutonium ion ;[5] thus, the intermediacy of II in this case is open to question.

Finally, the homoallylic intermediate, III, can be considered to be the precursor of the formation of both **8** and **9** if the isomerization of the intermediate III to VI is taken into account.

At present, it cannot be concluded whether or not the relief of strain in passing from the methylenecyclopropylcarbinyl to the 3-methylenecyclobutyl cation and the stabilization by conversion to a secondary cation is enough to compensate for the delocalization energy usually attainable by having a bicyclobutonium ion. Although it is generally accepted that a bicyclobutonium ion is, in general, capable of much more stabilization than a homoallyl cation, in the special case of III the conformation of III may favor the homoallylic cation by permitting an effective interaction of the cationic center with the *exo*-methylene π-electrons with a small entropy change, and/or the degree of stabilization of a bicyclobutonium ion may be lessened because of the extra strain imposed by the introduction of an *exo*-methylene group. In fact, the participation of the nitrogen atom to form an aza-bicyclobutonium ion, structurally analogous to III, in the solvolysis of both 1-*t*-butyl-3-azetidinyl- and 1-*t*-butyl-2-aziridinylcarbinyl derivatives has already been discussed.[13]

Considered in a classical way, the predominant formation of **9** rather than **8** may be considered to be a result of a vinyl group being a much better migrating group than a methyl group. Here, also, an intermediate similar to the homoallylic cation is considered to play an important role in creating this good migrating aptitude of a vinyl group.[14,15]

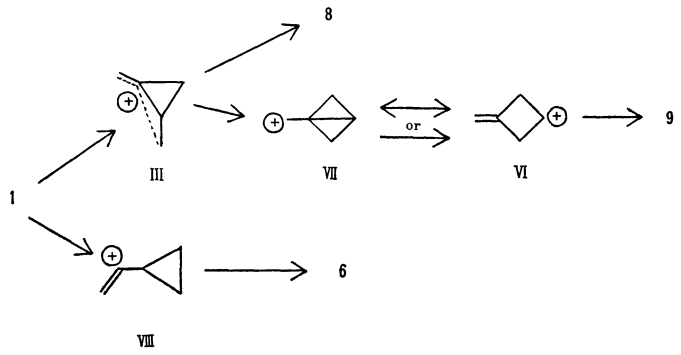

Scheme 2. Deamination pathway of methylenecyclopropylcarbinylamine.

12) This mechanism has been questioned: E. F. Kiefer and J. D. Roberts, *J. Amer. Chem. Soc.*, **84**, 784 (1962). See also: L. M. Konzelman and R. T. Conley, *J. Org. Chem.*, **33**, 3828 (1968).

13) V. R. Gaertner, *Tetrahedron Lett.*, **1968**, 5919; J. A. Deyrup and C. L. Moyer, *ibid.*, **1968**, 6179. An unpublished work of Martin and Anderson on the participation of sulfur atom in the solvolysis of 3-thietane derivative has been cited in these reports and in Ref. 10. These authors, however, also state that the ability of such a participation is poorer in the three-membered than in the four-membered ring, and absence of π-election participation in 3-methylene-cyclobutyl cation has been reported.[12]

14) W. Herz and G. Caple, *J. Org. Chem.*, **29**, 1691 (1964); R. S. Bly and R. T. Swindell, *ibid.*, **30**, 10 (1965), and references cited therein.

15) A completely different mode of ring cleavage has recently been reported with acid-catalyzed dehydration of phenyl-substituted methylenecyclopropylcarbinols. A. W. Herriott, E. P. Olavarria and W. M. Jones, *ibid.*, **33**, 3804 (1968).

The most unexpected result of the present work is the formation of acetylcyclopropane, albeit in a low yield. A tricyclobutonium intermediate, IV, may be considered to be an attractive candidate for the formation of **6**. The possibility of such a type of intermediate has, however, been denied with the cyclopropylcarbinyl system; also, the results of the labeling experiment with **1** is not in accord with this intermediate. The intermediate IV should give methylenecyclopropylcarbinol (**8**) with an equal deuterium distribution on the α-methylene and the cyclopropane ring.

Thus, the only remaining possible precursor for the formation of **6** is the cyclopropylvinyl cation (VIII). It is rather unexpected that a vinyl cation, which is generally believed to be obtainable only with difficulty, is formed even by the cleavage of a carbon-carbon bond, although there have recently been several examples of the formation of a vinyl cation intermediate by protonation and by π-electron migration.[16] The relief of strain in going from 1 to the cyclopropylvinyl cation, and the stabilization of the cationic center by the cyclopropane ring, probably accounts for this anomalous result.

To conclude, no adequate discussion is possible on the exact nature of the intermediate(s) or transition state(s) on the basis solely of the findings of a rather indiscriminate " hot cation " generated by deamination reaction. A solvolysis study of this and related systems would afford more fruitful information on this problem. Our preliminary attempt along this line, however, was unsuccessful because the reaction of methylenecyclopropylcarbinol with naphthalene-2-sulfonyl chloride gave a rearrangement product, 3-methylenecyclobutyl naphthalene-2-sulfonate.

Experimental[17]

Methylenecyclopropanecarboxylic Acid (4).[18] A solution of 5 g of ethyl methylenecyclopropanecarboxylate (**2**)[7] in 140 m*l* of methanol containing 4 g of potassium hydroxide was refluxed for one hour. The mixture was then diluted with 50 m*l* of water, acidified with hydrochloric acid, and extracted with ether. The extract was dried over magnesium sulfate and subsequently distilled to give 3.0 g (89% yield) of an acid, **4**, boiling at 101—103°C/17 mmHg; n_D^{25} 1.4660.

Methylenecyclopropanecarbonyl Chloride (5).[18] Oxalyl chloride (43 g) was added to 6.8 g of the acid, **4**, with external cooling, and then the resulting mixture was refluxed for two hours. Distillation gave 5.0 g (70% yield) of a liquid boiling at 42—43°C/19 mmHg; n_D^{25} 1.4695.

This substance, on treatment with methanol, was converted to methyl methylenecyclopropanecarboxylate.[19]

Methylenecyclopropanecarboxamide (3).

a). Into 10 m*l* of concentrated aqueous ammonia, 5 g of acid chloride **5** was added with stirring while the temperature was kept below 10°C. The mixture was concentrated under reduced pressure, and the residue was extracted with hot ethyl acetate. The extract, on cooling, afforded 2.4 g (62% yield) of **3** melting at 102.5—104°C. Its infrared spectrum was identical with, and its melting point was undepressed on admixture with, the specimen of **3** prepared by the procedure *b*.

b) A mixture of 14.2 g of the ester **2** and 50 m*l* of supersaturated aqueous ammonia was sealed in a pressure bottle and then allowed to stand for ten days. The residue which remained after the removal of the ammonia was recrystallized from benzene to give 7.8 g (71% yield) of **3** melting at 102—104°C.

Found: C, 62.16; H, 7.27; N, 14.16%. Calcd for C_5H_7NO: C, 61.84; H, 7.27; N, 14.42%.

Methylenecyclopropylcarbinylamine (1). To a stirred suspension of 4.5 g of lithium aluminum hydride in 120 m*l* of ether, 7.7 g of the amide **3** was added in portions, after which the resulting mixture was refluxed for eight hours. Aqueous sodium hydroxide (30%) was added to decompose the excess hydride, and the organic layer was decanted from the precipitate. The precipitate was washed with ether, and the combined extract was dried over magnesium sulfate and then distilled to give 2.8 g (42.5% yield) of a colorless liquid boiling at 105—115°C. Its purity was estimated to be *ca.* 90% by vpc (Carbo wax 20 M on Diasolid A). This crude product was used for the deamination study; the product composition was calibrated by the deamination of the vpc-purified sample of **1**. n_D^{25} 1.4725 (pure sample).

IR (cm^{-1}): 3360, 3295 (NH_2), 3065, 1745, 886 (=CH_2), 3040, 1019 (cyclopropane ring). NMR (τ): 4.90 (2H, m, =CH_2), 7.52 (2H, d, J=6 Hz; CH_2-N), 8.30—9.40 (3 H, m, ring protons), 9.02 (2 H, s, NH_2).

Phenyl isothiocyanate adduct: mp 70—71°C.

Found: C, 66.29; H, 6.68; N, 12.91%. Calcd for $C_{12}H_{14}N_2S$: C, 66.03; H, 6.47; N, 12.84%.

Methylenecyclopropylcarbinylamine-α,α-d_2 (1-d_2). This was prepared, by the method described above, from 3.0 g of the amide **3** and 2 g of lithium aluminum deuteride. A fraction distilling at 100—102°C was col-

16) M. Bertrand and M. Santelli, *Chem. Commun.*, **1968**, 718; D. S. Noyce and K. E. DeBruin, *J. Amer. Chem. Soc.*, **90**, 372 (1968); D. S. Noyce and M. D. Schiavelli, *ibid.*, **90**, 1020 (1968); M. Hanack, S. Bocher, K. Hummel and V. Vött, *Tetrahedron Lett.*, **1968**, 4613; M. Hanack and V. Vött, *ibid.*, **1968**, 4617; H. Fischer, K. Hummel, and M. Hanack, *ibid.*, **1969**, 2169; and references cited therein and in Ref. 1b.

17) All melting and boiling points are uncorrected, and the melting points were determined on a micro hot stage. The infrared spectra were recorded as neat liquid on a Hitachi model EPI-SII Spectrophotometer. The NMR spectra were determined using a JEOLCO C-60 (60 MHz) Spectrometer on solutions of carbon tetrachloride containing tetramethylsilane as internal standard, and the chemical shifts are reported by τ values. Mass spectra were taken on a Hitachi RMU-5 Spectrometer, and the vpc analyses were performed with a Shimadzu model GC-1B chromatograph.

18) For the preparation of **4** and **5**, *cf.* Ref. 7 b.

19) A. Nishimura, M. Ohta and H. Kato, This Bulletin, Manuscript under preparation. This compound was prepared by a base-catalyzed ester exchange of the corresponding ethyl ester **2**.

lected to give 1.0 g of **1-d_2**. The NMR peak at τ 7.52 of **1** completely vanished in this compound.

Deamination of the Amine 1. To a cooled and stirred solution of 2 g of **1** in 10 m*l* of 20% aqueous acetic acid, a solution of 3.6 g of sodium nitrite in 7 m*l* of water was added over a period of twenty minutes, after which the stirring was continued for seven hours. The mixture was then saturated with sodium chloride and extracted with ether. The extract was dried over sodium sulfate, and the ether was removed by fractional distillation. The residual oil was separated into four main components by vpc (Carbowax 20 M on Diasolid A). The product composition and pertinent spectral data, and the method used in identifying the products, have been described above.

Methylenecyclopropylcarbinol (8). To a stirred suspension of 3 g of lithium aluminum hydride in 100 m*l* of ether, 8.5 g of **2** was added slowly, and then the resulting mixture was stirred for three hours at room temperature. The mixture was decomposed by the addition of concentrated aqueous sodium hydroxide, the organic layer was separated, and the precipitate was washed with ether. The combined ether extract was dried over magnesium sulfate and subsequently distilled to give 3 g (45% yield) of a colorless liquid boiling at 142—146°C, n_D^{25} 1.4585.

Found: C, 71.06; H, 9.87%. Calcd for C_5H_8O: C, 71.39; H, 9.59%.

IR (cm^{-1}): 3340 (OH), 3070, 890 (=CH_2), 1015 (C–O). NMR (τ): 4.73 (2 H, m, =CH_2), 6.65 (2 H, d, J=7 Hz; -CH_2-O), 8.00 (1 H, s, -OH), 8.10—9.40 (3 H, m, ring protons).

p-Nitrobenzoate of **8:** mp 43.5—45°C.

Found: C, 61.57; H, 4.99; N, 6.29%. Calcd for $C_{12}H_{11}NO_4$: C, 61.80; H, 4.75; N, 6.01%.

Deamination of 1-d_2. The deuterated amine **1-d_2** (0.8 g) was treated with sodium nitrite by the method described above, and the products were separated by vpc.

The deuteriomethylenecyclopropylcarbinol obtained by this experiment showed no NMR peak at τ 6.6, and the NMR spectrum of deuteriomethylenecyclobutanol showed, among other signals, a two-proton triplet (J=2 Hz) at τ 5.28 and a two-proton multiplet centered at τ 7.3.

3-Methylenecyclobutyl Naphthalene-2-sulfonate. To a stirred solution of 1.0 g of **8** in 10 m*l* of 2,4,6-collidine, 3.0 g of 2-naphthalenesulfonyl chloride was added under cooling with an ice-salt bath; the mixture was kept at this temperature for two hours and then poured into 20 m*l* of 20% sulfuric acid containing ice. The resulting mixture was washed with aqueous sodium bicarbonate, dried over sodium sulfate, and concentrated under reduced pressure, and the residue was recrystallized from ether to give 1.0 g of crystals melting at 85—87°C.

Found: C, 65.86; H, 5.34%. Calcd for $C_{15}H_{14}O_3S$: C, 65.69; H, 5.15%.

NMR (τ; $CDCl_3$): 2.05 (1 H, m), 2.45—3.05 (6 H, m), 5.54 (1 H, t, J=6 Hz), 5.61 (2 H, pentuplet, J=2 Hz), 7.44 (4 H, d×t, J=6 and 2 Hz).

We are indebted to Miss Mizuko Yoshida for her measurement of the NMR spectra, to the microanalysis staff of this laboratory for the elemental analyses, and to Mr. Haruyoshi Sakurai for his measurement of the mass spectra.

BULLETIN OF THE CHEMICAL SOCIETY OF JAPAN VOL. 43 1535—1540 (1970)

Homolytic Chlorination of Aliphatic Compounds. IV.[1] Chlorination of Chloroalkanes by *t*-Butyl Hypochlorite

Masanori KOSUGI, Kohji TAKEUCHI and Toshihiko MIGITA

Department of Chemistry, Gunma University, Kiryu, Gunma

(Received November 7, 1969)

Chlorination of chloroalkanes by *t*-butyl hypochlorite was investigated by means of competitive experiment. Relative reactivities thus obtained were compared with those toward hydrogen abstraction by *t*-butoxy radicals derived from other sources. From the results it was concluded that a main chain carrier of this chlorination was a *t*-butoxy radical. Structure-reactivity relationships in *t*-butyl hypochlorite chlorination were also investigated. Linear free energy relationship was found to exist between the reactivities of methyl hydrogen of CH_3-X and Taft's σ^* constants for the substituent X, $\rho^* = -0.69$. α-Chlorine substituents were found always to enhance the rate of hydrogen abstraction of this position. Resonance effects of α-chlorine substituent is considered to be more important than in photochlorination with chlorine.

Chemistry of aliphatic chlorination by *t*-butyl hypochlorite has been extensively investigated by Walling and his co-workers.[2] They proposed a radical chain mechanism involving hydrogen abstraction by a *t*-butoxy radical, on the basis of the selectivity of the reaction being parallel to that of hydrogen abstraction by *t*-butoxy radicals derived from other sources.[3] Gilliom and Ward[4] reported ρ value (with σ) to be -0.75 for benzylic chlorination by *t*-butyl hypochlorite at 40°C. This value is quite different from that obtained by Sakurai and Hosomi[5] (with σ^+, -0.32 at 45°C) for benzylic hydrogen abstraction by *t*-butoxy radical derived from di-*t*-butyl peroxalate, and is rather similar to ρ value for chlorination by chlorine.[6] Thus it seems that benzylic chlorination by *t*-butyl hypochlorite involves a chlorine atom, rather than *t*-butoxy radical, as a chain carrier. Recently Walling and McGuiness[7] gave some evidence for the mechanism of benzylic chlorination by *t*-butyl hypochlorite.

We have been investigating substituent effects on the reactivities of aliphatic compound; toward a chlorine atom. A linear free energy relationship has been found to exist between the reactivity of CH_3-X and the σ^* value of X.[8] The study was extended to *t*-butyl hypochlorite chlorination. In this paper we wish to present an evidence which indicates that a main chain carrier of *t*-butyl hypochlorite chlorination of chloroalkanes is *t*-butoxy radical, in order to compare structure-reactivity relationship in this chlorination with that in photochlorination by chlorine.

Results and Discussion

t-Butoxy Radical as a Chain Carrier. Three possible chain carriers can be considered for the *t*-butyl hypochlorite chlorination.

scheme 1
$$t\text{-BuOCl} \xrightarrow{h\nu} t\text{-BuO}\cdot + \text{Cl}\cdot$$
$$t\text{-BuO}\cdot + \text{RH} \longrightarrow t\text{-BuOH} + \text{R}\cdot$$
$$\text{R}\cdot + t\text{-BuOCl} \longrightarrow \text{RCl} + t\text{-BuO}\cdot$$

scheme 2
$$t\text{-BuOCl} + \text{HCl} \rightleftharpoons \text{Cl}_2 + t\text{-BuOH}$$
$$\text{R}\cdot + \text{Cl}_2 \longrightarrow \text{RCl} + \text{Cl}\cdot$$
$$\text{Cl}\cdot + \text{RH} \longrightarrow \text{HCl} + \text{R}\cdot$$

scheme 3
$$t\text{-BuO}\cdot \longrightarrow \text{CH}_3\text{COCH}_3 + \text{CH}_3\cdot$$
$$\text{CH}_3\cdot + \text{RH} \longrightarrow \text{CH}_4 + \text{R}\cdot$$

Scheme 1 is a mechanism proposed originally by Walling,[2] which involves a *t*-butoxy radical as a chain carrier. In scheme 2, an actual chlorinating agent is chlorine molecule which is derived by a reversible reaction of *t*-butyl hypochlorite with hydrogen chloride formed through the subsequent chain steps involving a chlorine atom as a hydrogen abstracting species. The third possible chain carrier is a methyl radical which is formed by decomposition of *t*-butoxy radical (scheme 3). *t*-Butyl

1) Part III: M. Kosugi, K. Takeuchi and T. Migita, This Bulletin, **42**, 3354 (1969).

2) C. Walling and B. B. Jacknow, *J. Amer. Chem. Soc.*, **82**, 6108, 6113 (1960); C. Walling "Free Radicals in Solution," I. U. P. A. C. (1967), p. 69.

3) C. Walling and A. Padwa, *J. Org. Chem.*, **27**, 2979 (1962).

4) R. D. Gilliom and D. F. Ward Jr., *J. Amer. Chem. Soc.*, **87**, 3944 (1965).

5) H. Sakurai and A. Hosomi, *ibid.*, **89**, 458 (1967).

6) G. A. Russell and R. C. Williamson, *ibid.*, **86**, 2357 (1964).

7) C. Walling and J. A. McGuiness, *ibid.*, **91**, 2053 (1969).

8) T. Migita, M. Kosugi, Y. Tanaka and Y. Nagai, *Yuki Gosei Kagaku Kyokai Shi.*, **25**, 908 (1967).

hypochlorite reacted with chloroalkanes under irradiation by 500 W tungsten lamp, giving chlorinated products and *t*-butyl alcohol as main products. Relative amounts of these products are shown in Table 1. The results eliminate the possibility of scheme 3, since formation of *t*-butyl alcohol can not be expected from this mechanism.

Table 1. Ratio of chloride and *t*-butyl alcohol (40°)

(RH)	(RCl)/(*t*-BuOH)
CH_2ClCH_2Cl	1.05
$CHCl_3$	1.00
$(CH_3)_3CCl$	0.90
CH_2Cl_2	0.74
$(CH_3)_2CCl_2$	0.35

Table 1 shows that chlorination of 1,2-dichloroethane, chloroform gave the chlorinated product and *t*-butyl alcohol in equimolar amount. This is in agreement with the product pattern from the reaction schemes 1 and 2. However, less amounts of chlorinated products compared with *t*-butyl alcohol were formed from the chlorination of 2,2-dichloropropane and methylene chloride. In these cases, vapor-phase chromatographic analysis of the reaction mixtures showed the presence of considerable amounts of an additional common product, which was identified to be 1-chloro-2-methyl-2-propanol. Walling and Padwa[9] reported the formation of this compound in decomposition of *t*-butyl hypochlorite in carbon tetrachloride solution, and proposed the formation path way as follows:

$$t\text{-BuO}\cdot + Me_3COCl \longrightarrow t\text{-BuOH} + Me_2\overset{CH_2\cdot}{\overset{|}{C}}\text{-OCl}$$
$$\longrightarrow \quad \longrightarrow \quad Me_2\overset{OH}{\overset{|}{C}}\text{-}CH_2Cl$$

As will be seen later, while 1,2-dichloroethane and chloroform are relatively reactive substrates toward hydrogen abstraction by *t*-butoxy radical, 2,2-dichloropropane and methylene chloride are less reactive, so that *t*-butoxy radicals may abstract hydrogen atoms from *t*-butyl hypochlorite as well as from substrate molecules, forming *t*-butyl alcohol in a larger amount than chlorinated products.

In order to check the two possibilities of schemes 1 and 2, relative reactivities of several substrates towards the hypochlorite chlorination were compared with those towards hydrogen abstraction by *t*-butoxy radical derived from di-*t*-butyl peroxide.

Relative reactivities toward the chlorination were calculated from the relative yields of the chlorinated products from competitive reaction with binary mixtures of substrates. The relative reactivities towards *t*-butoxy radical formed by the photo-induced decomposition of di-*t*-butyl peroxide (high pressure mercury lamp) and *t*-butyl hypochlorite (tungsten lamp) were calculated from k_a/k_d derived from the relative yields of *t*-butyl alcohol and acetone formed by the following competition.[10]

$$t\text{-BuO}\cdot \begin{cases} \xrightarrow{k_d} CH_3COCH_3 + CH_3\cdot \longrightarrow CH_3Cl \\ \xrightarrow[k_a]{RH} t\text{-BuOH} + R\cdot \longrightarrow RCl \end{cases}$$

Relatively reactive chloroalkanes were chosen as substrates, in order to avoid the hydrogen abstraction from a *t*-butoxy radical sources, which would result in overestimation of the rates of hydrogen abstraction from substrate molecules. The results are shown in Table 2.

Apparently, relative reactivities obtained from competitive chlorination with *t*-butyl hypochlorite are very close to those from di-*t*-butyl peroxide and quite different from those for photochlorination by chlorine. We can conclude that *t*-butoxy radical is the most important chain carrier in *t*-butyl hypochlorite chlorination of chloroalkanes.

Relative Reactivities of Chloroalkanes. Relative reactivities of chloroalkanes toward *t*-butoxy radical were determined by competitive chlorination with *t*-butyl hypochlorite, and were formed as shown in Table 3.

As expected from the electron-seeking nature of *t*-butoxy radicals,[2] reaction rates are affected by the polar nature of the substituents in the substrates.

Table 2. Relative reactivities of chloroalkanes

Substrate	Reagents			
	t-BuOCl Competitive chlorination	*t*-BuOCl Relative value of k_a/k_d	*t*-BuOOBu-*t* Relative value of k_a/k_d	Cl_2[11] Competitive chlorination
CH_2ClCH_2Cl	1.00 standard	1.00 standard	1.00 standard	1.00 standard
CCl_3CH_2Cl	0.86	0.74	0.84	0.02
$CHCl_2CHCl_2$	3.5	2.4	2.1	0.04
	(40°)	(40°)	(20—23°)	(40°)

9) C. Walling and A. Padwa, *J. Amer. Chem. Soc.*, **85**, 1593 (1963).

10) A. L. Williams, E. A. Oberright and J. W. Brooks, *ibid.*, **78**, 1190 (1956).

Table 3. Relative reactivities of chloroalkanes (40°C)

Reaction site	Substituent	*t*-BuOCl	Cl_2
CH_3-	$-CH_2CMe_3$	10.7	44
	$-CH_2CH_2CH_2Cl$	12.7	—
	$-CH_2CH_2Cl$	9.0	21
	$-CMe_2Cl$	4.2	9.8
	$-CMeHCl$	3.6	9.9
	$-CMeClCH_2Cl$	2.1	3.4
	$-CHClCH_2Cl$	2.3	3.3
	$-CMeCl_2$	1.00 (standard)	1.00 (standard)
	$-CCl_3$	0.12	0.07
CH_2Cl-	$-CH_2CH_2CH_3$	43.2	—
	$-CH_2CH_3$	31.6	18
	$-CH_2CH_2CH_2Cl$	27.3	—
	$-CH_2CH_2Cl$	16.6	—
	$-CMe_2Cl$	21.0	—
	$-CH_2Cl$	16.1	3.0
	$-CCl_3$	13.9	0.24
$CHCl_2$-	$-CH_2CH_3$	124	6.3
	$-CH_2Cl$	74.2	0.78
	$-CHCl_2$	56.5	0.43

Logarithms of the relative reactivities for the methyl C–H bond are plotted against Taft's constants σ^* of the substituents in Fig. 1.

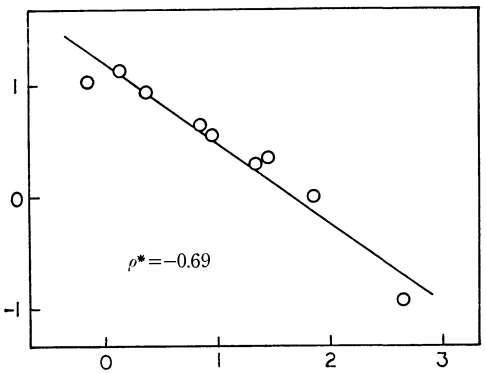

Fig. 1. Hammett plot for CH_3-*X*.

Good linear relationship was found to exist. The ρ^* value is −0.69, which is less negative than the value (−0.85) for chlorine atom reactions.[8] A similar trend of ρ values has been observed in the case of abstraction of benzylic hydrogen.[5,6] This indicates that *t*-butoxy radical is less electron-seeking than a chlorine atom.

Striking contrast to the chlorination with chlorine was observed in α-chlorine substituent effect. As was described previously,[11] a chlorine substituent will affect the reactivity of α-C–H bond in two ways. Its −I effect will deactivate the α-C–H bond. Contrarily the conjugative effect will accelerate the hydrogen abstraction from the C–H bond, since the stabilization of the incipient radical by the following resonance will diminish the dissociation energy of the C–H bond being reacted:

$$\dot{C}\text{-}\underline{\overline{Cl}}| \leftrightarrow \overset{(-)(+)}{\overline{C}\text{-}\dot{\underline{Cl}}}|$$

In photochlorination with chlorine, the following order of reactivities of C–H bonds were observed:

$H\text{-}CH_2CH_2Cl > H\text{-}CHClCH_2Cl > H\text{-}CCl_2CH_2Cl$

$H\text{-}CH_2CCl_3 > H\text{-}CHClCCl_3 < H\text{-}CCl_2CCl_3$

This indicates that the accelerating conjugative effect of α-chlorine substituent becomes more important than its inductive effect only when a strongly electron-withdrawing substituent like an trichloromethyl group is present in a substrate molecule.[11]

On the other hand, the present results for *t*-butyl hypochlorite chlorination show that an α-chlorine substituent always enhances the rate of hydrogen abstraction on this position. For example,

$H\text{-}CHClCH_2Cl < H\text{-}CCl_2CH_2Cl$

$H\text{-}CH_2CCl_3 < H\text{-}CHClCCl_3$

$H\text{-}CH_2CH_2CH_2Cl < H\text{-}CHClCH_2CH_2Cl$

This tendency indicates that electron-donating conjugative effect of a substituent is quite an important factor controlling the rate of hydrogen abstraction by a *t*-butoxy radical. It has been pointed out that concerning the radicals X which form the bond (X–H) of essentially equal bond energy, hydrogen abstraction from the side chains of toluenes by the less electron-seeking radical X· showed a less negative value of ρ and a greater isotope effect (k_H/k_D).[12] Thus compared with the reaction

11) T. Migita, M. Kosugi and Y. Nagai, This Bulletin, **40**, 908 (1967).

12) H. Sakurai and K. Tokumaru, "Chemistry of Free Radicals," Nankōdō, Tokyo (1967), Chap. 17, p. 355.

Table 4. Competitive experiments at 40°C

Molar ratio of substrates	Molar ratio of products	Relative reactivities*	v.p.c. column
$CH_3CH_2CMe_3$	$CH_2ClCH_2CMe_3$	CH_3-CH_2CMe_3	Apiezon L
t-BuCl	CH_2ClCMe_2Cl		2.5 m
0.598	0.54	2.73	102°C
0.598	0.38	1.92	
0.598	0.59	2.98	
$CH_3(CH_2)_2CH_2Cl$	$CH_2Cl(CH_2)_2CH_2Cl$	CH_3-$CH_2CH_2CH_2Cl$	P.E.G. 6000
CH_2ClCH_2Cl	$CHCl_2CH_2Cl$		1.5 m
1.01	0.60	0.78	100°C
1.01	0.61	0.80	
1.01	0.61	0.80	
$CH_3CH_2CH_2Cl$	$CH_2ClCH_2CH_2Cl$	CH_3-CH_2CH_2Cl	P.E.G. 6000
CH_2ClCH_2Cl	$CHCl_2CH_2Cl$		1.5 m
1.31	0.59	0.60	100°C
1.31	0.51	0.52	
1.31	0.56	0.57	
t-BuCl	CH_2ClCMe_2Cl	CH_3-CMe_2Cl	D.O.P
CH_2ClCH_2Cl	$CHCl_2CH_2Cl$		2 m
1.07	0.21	0.27	78°C
1.07	0.21	0.26	
1.07	0.27	0.26	
$CH_3CHClCH_3$	$CH_2ClCHClCH_3$	CH_3-$CHClCH_3$	Apiezon L
t-BuCl	CH_2ClCMe_2Cl		2.5 m
1.20	0.85	0.85	76°C
1.20	0.88	0.88	
$CH_3CMeClCH_2Cl$	$CH_2ClCMeClCH_2Cl$	CH_3-$CMeClCH_2Cl$	D.E.G.S.
CH_2ClCH_2Cl	$CHCl_2CH_2Cl$		2.3 m
1.20	0.12	0.13	56°C
1.20	0.11	0.12	
$CH_3CHClCH_2Cl$	$CH_2ClCHClCH_2Cl$	CH_3-$CHClCH_2Cl$	P.E.G. 6000
$CH_2Cl(CH_2)_2CH_2Cl$	$CHCl_2(CH_2)_2CH_2Cl$		1.5 m
2.26	0.15	0.086	105°C
2.26	0.14	0.082	
CH_3CMeCl_2	$CH_2ClCMeCl_2$	CH_3-$CMeCl_2$	Apiezon L
CH_2ClCH_2Cl	$CHCl_2CH_2Cl$		2.5 m
1.75	0.082	0.062	100°C
1.75	0.080	0.061	
1.75	0.082	0.062	
CH_3CCl_3	CH_2ClCCl_3	CH_3-CCl_3	D.O.S.
CH_3CMeCl_2	$CH_2ClCMeCl_2$		2 m
1.99	0.12	0.12	100°C
1.99	0.14	0.13	
1.99	0.12	0.12	
$CH_2Cl(CH_2)_2CH_3$	$CHCl_2(CH_2)_2CH_3$	CH_2Cl-$(CH_2)_2CH_3$	P.E.G. 6000
CH_2ClCH_2Cl	$CHCl_2CH_2Cl$		1.5 m
1.01	1.35	2.63	100°C
1.01	1.36	2.70	
1.01	1.36	2.70	

Table 4. (Continued)

Molar ratio of substrates	Molar ratio of products	Relative reactivities*	v.p.c. column
$CH_2ClCH_2CH_3$	$CHCl_2CH_2CH_3$	CH_2Cl-CH_2CH_3	P.E.G. 6000
CH_2ClCH_2Cl	$CHCl_2CH_2Cl$		1.5 m
1.31	1.38	2.09	100°C
1.31	1.21	1.81	
1.31	1.31	1.99	
$CH_2Cl(CH_2)_2CH_2Cl$	$CHCl_2(CH_2)_2CH_2Cl$	CH_2Cl-$(CH_2)_2CH_2Cl$	P.E.G. 6000
CH_2ClCH_2Cl	$CHCl_2CH_2Cl$		1.5 m
1.11	1.93	1.74	104°C
1.11	1.82	1.64	
1.11	1.89	1.70	
CH_2ClCMe_2Cl	$CHCl_2CMe_2Cl$	CH_2Cl-CMe_2Cl	D.E.G.S.
CH_2ClCH_2Cl	$CHCl_2CH_2Cl$		2.3 m
1.20	0.90	1.3	56°C
1.20	0.90	1.3	
CH_2ClCCl_3	$CHCl_2CCl_3$	CH_2Cl-CCl_3	K.F. 96
CH_2ClCH_2Cl	$CHCl_2CH_2Cl$		3 m
2.76	1.21	0.88	108°C
2.76	1.16	0.84	
$CHCl_2CH_2CH_3$	$CCl_3CH_2CH_3$	$CHCl_2$-Et	X.F. 1105
CH_2ClCH_2Cl	$CHCl_2CH_2Cl$		2.0 m
1.53	2.92	7.65	64°C
$CHCl_2CHCl_2$	CCl_3CHCl_2	$CHCl_2$-$CHCl_2$	Apiezon L
CH_2ClCH_2Cl	$CHCl_2CH_2Cl$		2.5 m
0.967	1.55	3.2	80°C
0.967	1.64	3.4	
0.967	1.74	3.5	
$CHCl_2CH_2Cl$	CCl_3CH_2Cl	$CHCl_2$-CH_2Cl	Apiezon L
t-BuCl	CH_2ClCMe_2Cl		2.5 m
0.483	0.97	18.0	80°C
0.483	0.97	18.3	
0.483	0.87	18.3	

Intramolecular reactivity pattern was found to be:

CH_2Cl-CH_2-CH_2Cl

1.79 1.00

Competitive chlorination with 1,4-dichlorobutane was carried out to find relative reactivity of 2-position of 1,3-dichloropropane.

$CH_2(CH_2Cl)_2$	$CHCl(CH_2Cl)_2$	$CH_2\langle^{CH_2Cl}_{CH_2Cl}$	P.E.G. 6000
$CH_2Cl(CH_2)_2CH_2Cl$	$CHCl_2(CH_2)_2CH_2Cl$		1.5 m
2.13	0.38	0.35	104°C
2.13	0.36	0.34	
2.13	0.34	0.33	

* Relative to that of a C–H bond of the other substrate.

of a chlorine atom, hydrogen abstraction by the less electron-seeking *t*-butoxy radical would be influenced by a polar factor in a less extent (less ρ^* value), and by bond dissociation energy of substrate C–H in a greater extent. The tendencies are in agreement with this generalization.

Experimental

Materials. *t*-Butyl hypochlorite and di-*t*-butyl peroxide were prepared by the method of Teeter and Bell,[13]

13) H. M. Teeter and E. W. Bell, "Org. Syn"., Vol. 32, 20 (1952).

and Milas and Surgenor,[14] respectively. Dichloromethane, chloroform, 1,2-dichloroethane, 1,1,1-trichloroethane, 1,1,2-trichloroethane, 1,1,2,2-tetrachloroethane, pentachloroethane, neohexane, propylene chloride, 1,3-dichloropropane and 1,4-dichlorobutane were purified by fractionating commercial materials, and their purities were checked by means of v.p.c.

t-Butyl chloride, 2,2-dichloropropane and *n*-propyl chloride were prepared by the method previously described.[8,11] *n*-Butyl chloride and isopropyl chloride were prepared by a method analogous to the synthesis of *n*-propyl chloride.[15] 1,2-Dichloro-2-methylpropane was obtained by the chlorination of *t*-butyl chloride, bp 106°C[16] Among the authentic samples of chlorination products, 1,2,2-trichloropropane and 1-chloro-3,3-dimethylbutane have been identified previously.[8,11] 1,1,2-Trichloro-2-methylpropane and 1,2,3-trichloro-2-methylpropane were collected by v.p.c. from the reaction mixtures of chlorination of 1,2-dichloro-2-methylpropane by *t*-butyl hypochlorite, and identified on the basis of their NMR spectrum. (τ values).

$(CH_3^1)_2CClCH^2Cl_2$ 8.21 (H^1 singlet)
4.23 (H^2 singlet)

$CH_3^1CCl(CH_2^2Cl)_2$ 8.28 (H^1 singlet)
6.22 (H^2 singlet)

1,2,3-Trichloropropane was prepared by adding a chlorine to allyl chloride, bp 155—158°C.[17] 1,1-Dichlorobutane was prepared by treating *n*-butyraldehyde with phosphorus pentachloride, bp 114°C.[18] 1,1,4-Trichlorobutane was collected by v.p.c. from the chlorination mixture of 1,4-dichlorobutane and identified with its NMR spectrum (τ values).

CH^1Cl_2-CH_2^2-CH_2^3-CH_2^4Cl 4.17 (H^1 triplet)
7.3—8.2 (H^2, H^3 multiplet) 6.41 (H^4 triplet)

$(CH_3^1)_2COHCH_2^2Cl$ 8.74 (H^1 singlet)
6.56 (H^2 singlet)

1-Chloro-2-methyl-2-propanol was collected by v.p.c. from the reaction mixture of chlorination of 2,2-dichloropropane by *t*-butyl hypochlorite, and identified by comparing its NMR spectrum and v.p.c. retention time (X.F. 1105, P.E.G. 6000 and D.O.S. column) with that of an authentic sample (τ values).[19]

Determination of the Ratio of Chloride and *t*-Butyl Alcohol. A mixture of chloride and *t*-butyl hypochlorite (*ca.* 10: 1 molar ratios) was placed in a reaction tube. After the mixture was degassed in a dark place, the tube was sealed and immersed in a thermostat (40°C $\pm$0.1) and irradiated with 500 W tungsten lamp until the color of chlorine in the mixture disappeared. Analysis of the products was carried out by v.p.c. method employing 1.5 m column of P.E.G. 6000.

Determination of Relative Reactivities. Reactions were carried out in sealed, degassed tubes as described above. For the decomposition of di-*t*-butyl peroxide, pyrex tubes were used and irradiated for 24 hr with 300 W high pressure mercury lamp. Analysis of the acetone and the *t*-butyl alcohol was carried out by v.p.c. method employing 2.0 m column of D.O.P. Relative values of k_a/k_d were calculated by the amounts of acetone and *t*-butyl alcohol.[10] Average values of three runs are presented in Table 2.

Competitive reactions were carried out with mixtures of two chloroalkanes and *t*-butyl hypochlorite (*ca.* 10: 1 molar ratios). Relative reactivities were calculated by the ratio of the chlorination products and the substrates. Analysis of the chlorination products was carried out by v.p.c. Table 4 shows the results. From these values, reactivities of C–H bonds of chloroalkanes relative to that of 2,2-dichloropropane were calculated as shown in Table 3.

This work was supported by the Scientific Research Fund of Ministry of Education, Japanese Government.

14) N. A. Milas and D. Surgenor, *J. Amer. Chem. Soc.*, **68**, 205 (1946).
15) J. E. Copenhaver and A. M. Whaley, Org. Syn., Coll. Vol. I, p. 142 (1956).
16) R. W. Taft Jr., and G. W. Stratton, *Ind. Eng. Chem.*, **40**, 1488 (1948).
17) M. S. Kharasch and H. C. Brown, *J. Amer. Chem. Soc.*, **61**, 2142 (1939).
18) H. C. Brown and A. B. Ash, *ibid.*, **77**, 4019 (1955).
19) The sample was supplied by Dr. S. Sekiguchi[20] of this university.
20) S. Sekiguchi, H. Inoue, M. Hayashi and K. Matsui, *Kagyo Kagaku Zasshi*, **71**, 1943 (1968).

BULLETIN OF THE CHEMICAL SOCIETY OF JAPAN VOL. 43 1541—1544 (1970)

New Method for the Separation of Diastereomeric Mixtures of β-Methylnorleucine and β-Methylleucine

Kazuo Ōkubo and Yoshiharu Izumi

Division of Organic Chemistry, Institute for Protein Research, Osaka University, Kita-ku, Osaka

(Received November 8, 1969)

β-Methylnorleucine and β-methylleucine were synthesized, separated into diastereomers and optically resolved. The configurational assignments of these isomers and the determinations of the optically active isomers were achieved by means of NMR spectroscopy and the enzymatic method respectively.

The present authors previously discovered the asymmetric hydrogenation catalyst, which is obtained by the modification of the Raney nickel catalyst with optically active α-amino or α-hydroxy acid, and found an experimental rule on the relation between the asymmetric activity of the catalyst and the structures of the modifying reagent.[1]

The syntheses, the separations in to diastereomers, and the optical resolutions of β-methylnorleucine and β-methylleucine were performed in order to study the effect of the β-asymmetric center of the α-amino acid on the asymmetric activity of the modified Raney nickel catalyst.

β-Methylnorleucine and β-methylleucine have β-asymmetric carbons in addition to α-asymmetric carbons and each has two diastereomers.

β-Methylnorleucine and β-methylleucine are not naturally occurring amino acids. For β-methylnorleucine, no descriptions of the synthesis, the diastereomers, or the optically active isomers have yet been published.

β-Methylleucine has been synthesized as the intermediate of the *N*,β-dimethylleucine, which is a component of antibiotic Ethamycin, and its four optically active isomers have been obtained by Kotake *et al.* and one of the present authors.[2]

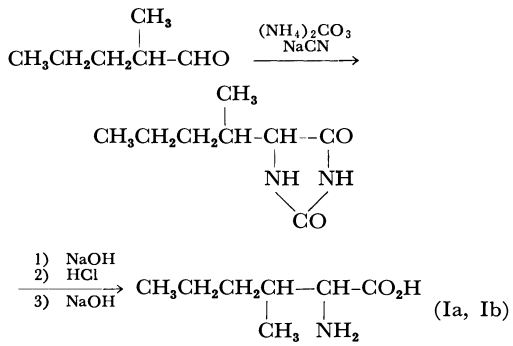

Scheme 1

In the present work, β-methylnorleucine was synthesized starting from α-methylvaleraldehyde by the general method developed by Bucherer and Steiner; it is described in Scheme 1.

The fine crystalline hydantoin derivative, obtained from the reaction of α-methylvaleraldehyde, ammonium carbonate, and sodium cyanide, was hydrolyzed with alkali in the autoclave; subsequent acidification with concentrated hydrochloric acid afforded an excellent yield of β-methylnorleucine hydrochloride.

β-Methylleucine was synthesized by a modification of the procedure developed by Kotake *et al.* The modification was based on catalytic hydrogenation with a Raney nickel catalyst of the α-methylisobutylidene derivative of the 2-benzyl-4-(5*H*)-imidazolone in a sodium hydroxide solution and successive treatment with concentrated hydrochloric acid.

By this method, β-methylleucine, which is a mixture of threo and erythro isomers in the molar ratio of 2 : 1, was directly obtained in a 87% yield (based on the α-methylisobutylidene derivative). (Scheme 2)

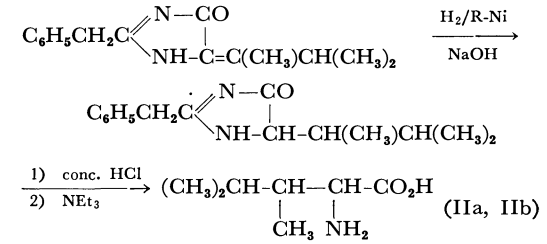

Scheme 2

Diastereomeric mixtures of β-methylnorleucine and β-methylleucine were crystallized from the concentrated hydrochloric acid, and the threo isomers (Ia and IIa) were obtained as the less soluble hydrochloride salts.

1) Part XII of the series: Y. Izumi, S. Tatsumi and M. Imaida, This Bulletin, **42**, 2373 (1969).

2) H. Kotake, T. Saito and K. Ōkubo, *ibid.*, **42**, 1367 (1969).

The erythro isomers (Ib and IIb) of these amino acids were purified as the less soluble copper salts in a hot 1% aqueous solution of cupric sulfate.

The extraction of the copper salt of the threo isomer with a hot 1% aqueous solution of cupric sulfate is a new, quite convenient method for the purification of the erythro isomers of these amino acids.

The relative configurational assignments of these amino acids were performed by the acylase resolution and the NMR spectroscopy. The stereochemically pure racemates, Ia, Ib, IIa, and IIb, were each *N*-acetylated and then resolved with acylase by the ordinary method to afford L-amino acids.

Recently Ōtsuka *et al.* introduced the use of NMR spectroscopy to elucidate the relative configurations at the α- aud β-carbon atoms of *N*,β-dimethylleucine diastereomers, which have $\rangle\underset{\alpha}{CH}-\underset{\beta}{CH}\langle$ structures, compared with the similar known compounds, the *N*-methylisoleucine diastereomers.[3] They proved that the threo form has a smaller coupling constant, $J_{\alpha,\beta}$.

Since the Karplud equation could be applied to β-methylnorleucine, (Ia and Ib) and β-methylleucine (IIa and IIb), although these amino acids were not *N*-methylated, we extended that theory, in the present work, to these amino acids. The observed coupling constants obtained from the doublet signals of the α-protons of the L-isoleucine, L-alloisoleucine, β-methyl-L-norleucine (Ia-L), β-methyl-L-norleucine (Ib-L), β-methyl-L-leucine (IIa-L), and β-methyl-L-leucine (IIb-L) are shown in Table 1.

Table 1. $J_{\alpha,\beta}$ Values obtained from the doublet signal of the α-proton

	$J_{\alpha,\beta}$ (Hz)
L-Alloisoleucine (*threo*)	3.6±0.1
L-Isoleucine (*erythro*)	4.1±0.1
β-Methyl-L-norleucine (Ia-L)	3.5±0.1
β-Methyl-L-norleucine (Ib-L)	4.0±0.1
β-Methyl-L-leucine (IIa-L)	3.5±0.1
β-Methyl-L-leucine (IIb-L)	5.2±0.1

As could be expected, L-alloisoleucine (*threo*) has a smaller coupling constant, $J_{\alpha,\beta}$, than L-isoleucine (*erythro*). For β-methylnorleucine and β-methylleucine, Ia and IIa have smaller coupling constants than Ib andIIb. From these results, Ia and IIa are said to be of the threo form, and Ib and IIb of the erythro form.

Additionally, this result coincides with the experimental rule that, in the asymmetric hydrogenation of methyl acetoacetate to methyl 3-hyoroxybutyrate, a Raney nickel catalyst modified with the optically active threo form has a stronger asymmetric activity than the optically active erythro form.*1

3) J. Shoji, K. Tori and H. Ōtsuka, *J. Org. Chem.*, **30**, 2772 (1965).

Experimental

Preparation of α-Methylvaleraldehyde (2-Methylpentanal). Two hundred and fifty-five grams of 2-methyl-2-pentenal were hydrogenated with a catalyst prepared from 4 g of $PdCl_3$ by Willstätter's method, at 90 atm and at 70°C. The hydrogenation product was distilled fractionally to yield 200 g (77.4%) of α-methylvaleraldehyde; bp 110—120°C.

Preparation of 5-(1-Methylbutyl)-hydantoin. A solution consisting of 125 g of sodium cyanide, 550 g of commercial ammonium carbonate, 1500 m*l* of methanol, and 1500 m*l* of water was placed in a 5-*l* four-necked, round-bottomed flask fitted with a mechanical stirrer, a dropping funnel, a reflux condenser, and a thermometer; the flask was then kept at 40°C in a water bath. Through the dropping funnel we stirred in 106 g of α-methylvaleraldehyde, drop by drop, where upon a vigorous reaction took place. After this vigorous reaction had ceased, the reaction mixture was stirred continuously at 55°C for 6 hr. When the resulting solution was concentrated to about one-half volume under reduced pressure, it became a sludge with crystals. The residual solution was boiled with 800 m*l* of concentrated hydrochloric acid for 1 hr in a draft chamber and then kept in a refrigerator. The precipitated crystals were collected, washed with water, and dried in air. The yield was 180 g (100%) of a practically pure material; mp 122°C.

Found: C, 56.25; H, 8.54; N, 16.55%. Calcd for $C_8H_{14}O_2N_2$: C, 56.45; H, 8.29; N, 16.46%.

Preparation of β-Methylnorleucine (Ia, Ib). In an autoclave, 170 g of 5-(1-methylbutyl)-hydantoin was hydrolyzed with 800 m*l* of aqueous sodium hydroxide containing 380 g of sodium hydroxide at 140°C for 5 hr. After removing the ammonia by boiling, the reaction mixture was neutralized with hydrochloric acid and treated with charcoal. Then, the solution was sufficiently acidified with hydrochloric acid and dried *in vacuo*, and the residue was extracted with 500 m*l* of methanol. The extract was dried *in vacuo*, and the residue was taken up with 300 m*l* of water and adjusted to pH 6.0 with aqueous sodium hydroxide to afford 136 g of β-methylnorleucine; another 9 g of the product were obtained from the mother liquid. Total yield, 145 g (100%).

A part of the product was recrystallized from 10% ethanol for the elemental analysis.

Separation and Purification of β-Methylnorleucine. One hundred and seventeen grams of the crude β-methylnorleucine (Ia+Ib) were recrystallized twice from 400 m*l* of concentrated hydrochloric acid; crystalline hydrochloride salt was collected and thoroughly washed with concentrated hydrochloric acid. Yield, 57 g (Ia·HCl).

The mother liquor obtained from the recrystallization was combined and concentrated to dryness under reduced pressure, and the residue was recrystallized twice from concentrated hydrochloric acid; another 17 g of β-

*1 These results will be reported fully in the near future in this Bulletin.

methylleucine hydrochloride were thus recovered. Yield, 74 g (50.8%).

The mother liquor and washings obtained by the above treatment were combined and evaporated to dryness, and the residue was taken up with 50 ml of water. The solution was neutralized to pH 6.5 with 20% sodium hydroxide to afford 32 g of crude β-methylnorleucine (Ib).

β-Methylnorleucine cupper salt was instantly precipitated from a solution containing 23 g of the crude β-methylnorleucine (Ib) and 6.5 g of sodium hydroxide in 300 ml of water, by the addition of 20 g of cupric sulfate. After heating the sluggish mixture, with occasional stirring, in a boiling-water bath for 1 hr, the precipitated cupper salt of β-methylnorleucine was collected from the hot, sluggish mixture and washed with methanol. The crude cupper salt was treated with 600 ml of a 1% cupric sulfate solution during heating on the water bath for 20 min with occasional stirring. An insoluble cupper salt was then collected from the hot mixture. This treatment with 1% cupric sulfate solution was repeated twice. The pure cupper salt obtained in this manner was dissolved in 10% hydrochloric acid and treated with hydrogen sulfide. After the cupric sulfide was filtered off, the filtrate was evaporated to dryness *in vacuo* to afford stereochemically pure β-methylnorleucine hydrochloride (Ib·HCl). The residue was recrystallized from hot acetone. Yield, 15 g (10.3%).

One portion of the hydrochloride salt was dissolved in a small amount of water and neutralized to pH 6.0 with aqueous hydroxide. The amino acid (Ib) thus precipitated was collected and washed with water.

Preparation of 2-Benzyl-5-(α-methylisobutylidene)-4-imidazolone. This material was prepared

Table 2. Derivatives of β-methylnorleucine and β-methylleucine (Formula I and II)

Compound	Mp (°C)	$[\alpha]_D$	Anal. (%) Calcd C	Calcd H	Calcd N	Found C	Found H	Found N
DL-Ia+Ib	275	—	57.90	10.41	9.65	57.32	11.07	9.61
DL-Ia	275	—	57.90	10.41	9.65	57.47	10.92	10.07
Acetyl-DL-Ia	151	—	57.73	9.15	7.48	57.74	9.35	7.76
DL-Ia·HCl	219	—	46.28	8.88	7.71	46.16	8.93	8.15
L-Ia	280	+46.7° (*c* 1.50, 6 N HCl)	57.90	10.41	9.65	57.50	10.48	9.38
Acetyl-D-Ia	151	−34.8° (*c* 2.07, EtOH)	57.73	9.15	7.48	57.00	9.59	7.87
D-Ia·HCl	253	−35.7° (*c* 35.7, 6N HCl)	46.28	8.88	7.71	46.09	9.16	7.71
D-Ia	280	−45.3° (*c* 1.50, 6N HCl)	57.90	10.41	9.65	57.59	10.59	9.36
DL-Ib	275	—	57.90	10.41	9.65	57.39	10.87	10.18
Acetyl-DL-Ib	131	—	57.73	9.15	7.48	57.80	9.60	7.53
DL-Ib·HCl	187	—	46.28	8.88	7.71	45.73	9.35	8.25
L-Ib	280	30.4 (*c* 1.51, 6N HCl)	57.90	10.41	9.65	57.42	10.56	9.44
Acetyl-D-Ib	146	−17.5° (*c* 2.12, EtOH)	57.73	9.15	7.48	56.57	9.41	7.01
D-Ib·HCl	203	−25.4° (*c* 2.44, 6N HCl)	46.28	8.88	7.71	45.72	9.11	7.56
D-Ib	280	−32.2° (*c* 1.55, 6N HCl)	57.90	10.41	9.65	57.32	10.54	9.37
DL-IIa+IIb	270		57.90	10.41	9.65	57.46	10.58	9.46
DL-IIa	270		57.90	10.41	9.65	57.21	10.71	9.45
Acetyl-DL-IIa	157—158		57.73	9.15	7.48	57.42	9.40	7.59
L-IIa	270	+40.6° (*c* 1.0, 6N HCl)	57.90	10.41	9.65	57.81	10.87	9.71
Acetyl-D-IIa	185—186	− 2.3° (*c* 8.3, EtOH)	57.73	9.15	7.48	57.31	9.54	7.48
D-IIa	270	−39.9° (*c* 1.2, 6N HCl)	57.90	10.41	9.65	57.64	10.74	9.63
DL-IIb	270		57.90	10.41	9.65	57.17	10.80	9.48
Acetyl-DL-IIb	169—170		57.73	9.15	7.48	57.42	9.55	7.47
L-IIb	270	+38.6° (*c* 1.2, 6N HCl)	57.90	10.41	9.65	57.59	10.84	9.62
Acetyl-D-IIb	199—200	− 2.8° (*c* 6.9, EtOH)	57.73	9.15	7.48	57.47	9.57	7.48
D-IIb	270	−39.4° (*c* 1.1, 6N HCl)	57.90	10.41	9.65	56.99	10.88	9.31

from 2-benzyl-5(*H*)-imidazolone and methylisopropylketone according to the procedure of Kotake *et al.* The crude product was recrystallized from ether-hexane for elemental analysis.

Found: C, 74.33; H, 7.49; N, 11.64%. Calcd for $C_{15}H_{20}ON_2$: C, 74.35; H, 7.49; N, 11.56%. Mp 134—136°C.

Preparation of β-Methylleucine (IIa, IIb). One hundred and ninety grams of an imidazolone derivative were dissolved in a solution of 80 g of sodium hydroxide in 100 m*l* of methanol and 220 m*l* of water; this was followed by hydrogenation in the presence of a Raney nickel catalysts from 25 g of the alloy at 100°C and at an initial pressure of 90 kg/cm².

After the removal of the catalyst by filtration, the filtrate was concentrated to about 200 m*l* *in vacuo* and then boiled with 100 m*l* of concentrated hydrochloric acid for 10 hr. After cooling, the phenyl acetic acid thus precipitated was removed by filtration; the filtrate was washed with ether and evaporated *in vacuo* to a syrup, and the residue was taken up in water and again evaporated. The residue was dissolved in 400 m*l* of ethanol, and the insoluble material was removed by filtration. Into the cooled ethanol solution, triethylamine was added cautiously with gentle stirring; then the resultant crystals were collected, washed with a large amount of ethanol, and dried in air. A small amount of the crude product was then recrystallized from water. Yield, 102 g (80%).

Found: C, 10.68; H, 57.46; N, 9.46%. Calcd for $C_7H_{15}O_2N$: C, 10.41; H, 57.90; N, 9.65%.

Separation and Purification of β-Methylleucine. The crude β-methylleucine (IIa+IIb), 102 g was recrystallized twice from 200 m*l* of concentrated hydrochloric acid. The crystalline hydrochloride salt (IIa·HCl) was collected by filtration and washed thoroughly with concentrated hydrochloric acid. Yield, 85 g (67%).

One portion of the hydrochloride salt was dissolved in ethanol and neutralized with triethylamine to afford an amino acid (IIa).

The mother liquor and washings were combined and adjusted to pH 6.8 with an aqueous hydroxide solution, and then 30 g of cupric sulfate were added to the solution. The resultant blue-purple solution was gently heated on the water bath, allowed to cool, and then carefully neutralized with 20 g of sodium bicarbonate. The crystalline cupper salt of the amino acid was collected by vacuum filtration and washed repeatedly with water and then with methanol. The crude cupper salt was suspended in a 1% solution of cupric sulfate, and the mixture was slightly heated. Insoluble crystals were collected by filtration under reduced pressure and then washed with methanol. This treatment was repeated twice, and then the crystals were dried in air. Yield, 56 g.

The pure copper salt obtained in this manner was dissolved in 10% hydrochloric acid and treated with hydrogen sulfide. The cupric sulfide thus precipitated was removed. The filtrate and washings were combined and evaporated *in vacuo* to afford stereochemically-pure β-methylleucine hydrochloride (IIb·HCl). Yield, 27 g (21.2%).

Resolution of the Amino Acid (Ia, Ib, IIa, IIb). IIa·HCl was acetylated with 2 N sodium hydroxide and acetic anhydride by the ordinary method. Fifty-six grams of the acetyl derivative of IIa were dissolved in 1.5 *l* of water, and the pH was adjusted to 6.8 with 2 N sodium hydroxide. To this solution, 3 g of prozyme acylase were then added, after which the mixture was allowed to stand for 50 hr at 42°C. After 50 hr, the pH of the solution was again adjusted to 6.8 with 2 N NaOH, and the hydrolysis was continued. Then, the solution was evaporated to 100 m*l* *in vacuo*; the crystals of the L-amino acid were subsequently collected by filtration and washed with a small amount of water. The crude L-amino acid was purified by recrystallization from the water by treatment with charcoal. Yield, 12 g (55.3%). $[\alpha]_D^{33}$ +40.6 (*c* 1, 6N HCl).

The mother liquor was acidified with 6 N hydrochloric acid. The *N*-acetyl-D-amino acid thus precipitated was collected and washed with dilute hydrochloric acid and then water. Yield, 24 g (85.7%). $[\alpha]_D^{25}$ −2.3 (*c* 8.3 EtOH).

One portion of the *N*-acetyl-D-amino acid was refluxed with 10% hydrochloric acid; the solution was then neutralized with triethylamine to afford, quantitatively, D-amino acid. $[\alpha]_D^{25}$ −39.9 (*c* 1.2, 6 N HCl).

The other amino acids, Ia, Ib, and IIb were resolved by a procedure similar to that used for IIa.

The authors wish to express their sincere thanks to Miss Kiku Koike and Miss Nobuko Ōya of this Institute for the elemental analyses. They are also indebted to the Kyowa Fermentation Co., Ltd., for the gift of PROZYME.

BULLETIN OF THE CHEMICAL SOCIETY OF JAPAN VOL. 43 1545—1553 (1970)

The Retentive Solvolysis. VII. Structural Effect of the Leaving Group on the Steric Course of the S_N1 Phenolysis of 1-Phenylethyl Systems*1

Kunio OKAMOTO, Tomomi KINOSHITA and Haruo SHINGU

Department of Hydrocarbon Chemistry, Faculty of Engineering, Kyoto University, Sakyo-ku, Kyoto

(Received November 12, 1969)

A series of optically active 1-phenylethyl systems with various leaving groups has been phenolyzed in the phenolic solvents. The 1-phenylethyl systems with a negative leaving group (*i.e.*, 1-phenylethyl chloride, bromide, 3,5-dinitrobenzoate, and tosylate) afforded 1-phenylethyl phenyl ether with a net retained configuration. In contrast, the 1-phenylethyl systems with a positively-charged leaving group (*i.e.*, the 1-phenylethyldiazonium ion, the diethyl-(1-phenylethyl)-oxonium ion, and the protonated 2,6-di-*t*-butyl-4-methyl-4-(1-phenylethyl)-cyclohexadien-1-one) gave the 1-phenylethyl phenyl ether with a net inverted configuration. These results provide further support for the view that the retentive S_N1 phenolysis proceeds *via* a four-center transition state between the phenol molecule and the ion-pair intermediate. Besides the phenolic ether, the *o*- and *p*-(1-phenylethyl)-phenols with net inverted configurations were obtained from all optically active substrates except 1-phenylethyl 3,5-dinitrobenzoate and the 1-phenylethyldiazonium ion. The 3,5-dinitrobenzoate gave the completely racemic *o*-alkylated phenol, along with the inverted *p*-alkylated phenol, whereas the diazonium ion afforded the *o*-alkylated phenol with a net retained configuration, together with the inverted *p*-alkylated phenol. The stereochemical and mechanistic implications of the *C*-alkylation are also discussed on the basis of the results of the acidic rearrangement of the phenolic ether under the S_N1 phenolysis conditions.

Some years ago investigations in this laboratory showed that the S_N1 phenolysis of optically active 1-phenylethyl chloride occurs with a net retention (20—50%) of configuration to give 1-phenylethyl phenyl ether in the presence of aniline or triethylamine;[1] in order to account for these results, we offered the explanation that the ether with the retained configuration was probably formed from an ion-pair and a phenol molecule *via* a four-centered transition state as follows:[1b,2]

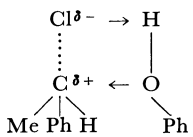

If this role of the phenol molecule were predominant in the retentive phenolysis of the chloride, we should observe the retention course in all 1-phenylethyl systems with a negative group such as the chlorine group. In contrast, for the case of the system with a positively-charged leaving group, the S_N1 phenolysis might proceed with a predominant inversion of configuration, as is typically observed in the other S_N1 solvolysis, since the positively-charged leaving group is conceivably unable to form such a specified transition state (*vide supura*) as the chlorine group does.

In order to ascertain these anticipations, we carried out the S_N1 phenolysis of several optically active 1-phenylethyl systems and examined the leaving-group influence. We chose 1-phenylethyl chloride, bromide, 3,5-dinitrobenzoate, and *p*-toluenesulfonate as the substrates with a negative leaving group; we also selected the 1-phenylethyldiazonium ion, the diethyl-(1-phenylethyl)-oxonium ion, and the protonated 2,6-di-*t*-butyl-4-methyl-4-(1-phenylethyl)-cyclohexan-1-one as the systems with a positively-charged leaving group.

Results

Phenolysis of the 1-Phenylethyl System with a Negative Leaving Group. The results of the phenolysis of a familiar set of substrates with a negative leaving group are presented in Table 1, along with the respective first-order rate constants.

*1 Presented at the 22nd Annual Meeting of the Chemical Society of Japan, Tokyo, April, 1969; Preprints for the Meeting, III, p. 1645. For the previous papers of this series, see K. Okamoto *et al.*, Ref. 1a (Part I); Ref. 1b (Part II); Ref. 2 (Part III); Ref. 10 (Part IV); Ref. 13 (Part V); This Bulletin, **40**, 1677 (1967) (Part VI).

1) a) K. Okamoto, K. Takeuchi and H. Shingu, *ibid.*, **35**, 525 (1962); b) K. Okamoto, H. Yamada, I. Nitta and H. Shingu, *ibid.*, **39**, 299 (1966).

2) K. Okamoto, M. Hayashi and H. Shingu, *ibid.*, **39**, 408 (1966).

Table 1. The formation of 1-phenylethyl phenyl ether in the phenolyses of the 1-phenylethyl systems with a negative leaving group

Solvent	RX M rotation	Base M	Temp. °C	Time hr	ROPh Yield %	Net steric course α%[a]	k_1 min^{-1}
PhOH-CH_3CN (1 : 1 by wt.)	RCl 0.143 α_D^{31} +22.1° (1 dm)	Et_3N 0.424	40	97	58.1	11.0 ret. (10.9 ret.[d])	1.42×10^{-3}[d]
PhOH-CH_3CN (1 : 1 by wt.)	RBr 0.142 α_D^{23} −33.2° (1 dm)	Et_3N 0.419	40	19	55.7	16.3 ret.	6.68×10^{-3}
PhOH	RODNB[a] 0.0933 $[\alpha]_D^{26}$ −21.0° (*c* 5.3, benz.)	PhONa 0.0933	150	4.3	40.0	28.2 ret.	3.45×10^{-2}
PhOH-CH_3CN (1 : 1 by wt.)	ROTs[b] 0.0914	$CO(NH_2)_2$ 0.234	20—35	2.2	20.5	>2.0[c] ret.	rapid

a) Calculated taking into account lack of optical purity of the starting substrate; the rotations of the optically pure materials are taken to be 125° (H. M. R. Hoffmann and E. D. Hughes, *J. Chem. Soc.*, **1964**, 1244) for R-(+)-1-phenylethyl chloride, 170° (H. M. R. Hoffmann and E. D. Hughes, *loc. cit.*) for R-(+)-1-phenylethyl bromide, 50.7° ($[\alpha]_D$, see Experimental section) for R-(+)-1-phenylethyl 3,5-dinitrobenzoate (RODNB), and 46.6° (Ref. 1b) for S-(+)-1-phenylethyl phenyl ether.

b) Prepared *in situ* from 1-phenylethyl chloride, α_D^{18} −57.1° (1 dm, neat), and silver *p*-toluenesulfonate (see text).

c) Calculated on the basis of the rotation of 1-phenylethyl chloride used for the preparation of the tosylate.

d) Cited from Ref. 1b.

Optically active 1-phenylethyl chloride and bromide were subjected to phenolysis in the presence of three molar equivalents of triethylamine in a 1 : 1 (by wt.) mixture of phenol and acetonitrile at 40.0°C. As anticipated, satisfactory first-order kinetic behavior was titrimetrically observed for each halide (Fig. 1); product analysis by chromatography showed that both halides gave 1-phenylethyl phenyl ether with a net retained configuration (Table 1),

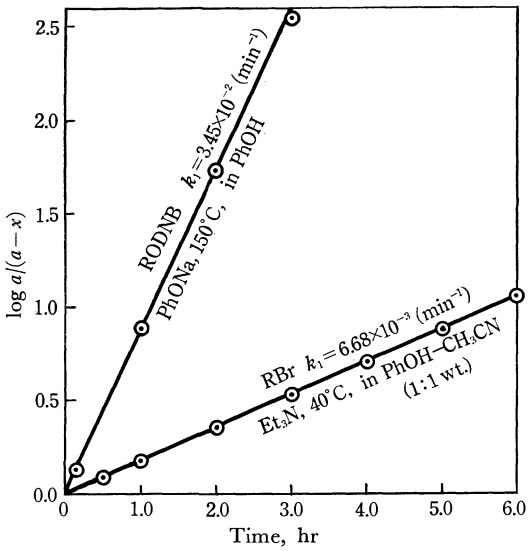

Fig. 1. The first-order plots for the phenolysis of the 1-phenylethyl system.

along with net inverted *o*- and *p*-(1-phenylethyl)-phenols (Table 3).

Optically active 1-phenylethyl 3,5-dinitrobenzoate was phenolized in the presence of one molar equivalent of sodium phenoxide in the phenol solvent. Because of the sluggishness of this phenolysis at the temperature (40°C) employed for the halides, the phenolysis was carried out at an elevated temperature (150°C). The decrease in the quantity of sodium phenoxide, followed titrimetrically, obeyed good first-order kinetics (Fig. 1). When chromatographed, the reaction mixture gave 1-phenylethyl phenyl ether with a 28% retained configuration (Table 1), along with completely racemized *o*-(1-phenylethyl)-phenol and 12% inverted *p*-(1-phenylethyl)-phenol (Table 3).

By modifying the method described by Hoffmann,[3] optically active 1-phenylethyl *p*-toluenesulfonate was prepared *in situ* from optically active S-(−)-1-phenylethyl chloride and silver *p*-toluenesulfonate in the acetonitrile solvent at 20°C. In order to determine the configuration of the tosylate thus formed, the concentrated solution of the tosylate was subjected to the reductive cleavage with sodium-naphthalene in tetrahydrofuran.[4] From the reaction mixture, R-(+)-1-phenylethyl alcohol was isolated by chromatography (see Experimental section). This indicates that the tosyl-

3) H. M. Hoffmann, *Chem. Ind.* (London), **1963**, 336.

4) W. D. Closson, P. Wriede and S. Bank, *J. Amer. Chem. Soc.*, **88**, 1581 (1966).

ate was formed with a net inversion of configuration, since it has been confirmed, for the other tosylates, that, in this reductive fission, no alkyl-oxygen bond, but only a sulfur-oxygen bond, is cleaved.[4]

$$\text{S-(}-\text{)-RCl} \xrightarrow[\text{in } CH_3CN]{\text{AgOTs}} \text{R-(?)-RO-Ts} \xrightarrow[\text{in THF}]{\text{Na-Naph.}} \text{R-(}+\text{)-RO-H}$$

When hydrolyzed, the tosylate gave S-(−)-1-phenylethyl alcohol, along with styrene (see Experimental section). This also indicates the inversive steric course for the formation of the tosylate, since, for the hydrolysis of the 1-phenylethyl system, a net inversion of configuration is typically observed.[5]

$$\text{S-(}-\text{)-RCl} \xrightarrow[\text{in } CH_3CN]{\text{AgOTs}} \text{R-(?)-ROTs} \xrightarrow{H_2O} \text{S-(}-\text{)-ROH}$$

To the acetonitrile solution of R-1-phenylethyl *p*-toluenesulfonate so prepared, we added a phenol solvent which contained about two molar equivalents of urea as a weak base.[6] After a rapid phenolysis at 20–35°C, R-(−)-1-phenylethyl phenyl ether, with a retained configuration, was isolated by chromatography, along with S-(−)-*o*-(1-phenylethyl)-phenol and S-(+)-*p*-(1-phenylethyl)-phenol (Tables 1 and 3).

Thus, in the phenolysis of the 1-phenylethyl system with a negative leaving group in the presence of a base, a net retention for the formation of the phenolic ether is the standard result, rather than a net inversion, this being shown in the following scheme:

$$\text{R-RCl} \xrightarrow[\text{in PhOH-CH}_3\text{CN}]{\text{Et}_3\text{N, 40°C}} \text{R-ROPh}$$

$$\text{S-RBr} \xrightarrow[\text{in PhOH-CH}_3\text{CN}_3]{\text{Et}_3\text{N, 40°C}} \text{S-ROPh}$$

$$\text{S-RODNB} \xrightarrow[\text{in PhOH}]{\text{PhONa, 150°C}} \text{S-ROPh}$$

(ODNB=3,5-dinitrobenzoate)

$$\text{R-ROTs} \xrightarrow[\text{in PhOH-CH}_3\text{CN}]{\text{CO(NH}_2\text{)}_2\text{, 20—35°C}} \text{R-ROPh}$$

The S_N1 Phenolysis of the 1-Phenylethyl System with a Positively-charged Leaving Group. The S_N1 phenolysis of this type can be classified as an S_N1 substitution of the missing-charge type.[7] As a representative S_N1 phenolysis of the missing-charge type, the phenolysis of the optically active 1-phenylethyldiazonium ion was conducted in a mixture of phenol and water. The diazonium was prepared *in situ* by adding concentrated hydrochloric acid to the mixture of optically active R-(+)-1-phenylethylamine and sodium nitrite in a 4 : 1 mixture of phenol and water at −8—+2°C. The diazotization and the succeeding nucleophilic reaction proceeded rapidly, with the evolution of nitrogen. From the reaction mixtures, a small amount of 1-phenylethyl phenyl ether with a net inverted configuration was isolated by chromatography (Table 2). In addition, *o*-(1-phenylethyl)-phenol with a net retained configuration and *p*-(1-phenylethyl)-phenol with a net inverted configuration were isolated (Table 3). In view of the poor yield (total 10.0%) of the substitution products and the 55% recovery of the starting amine, under these reaction conditions most of the nitrous acid was probably consumed by the phenol solvent to give the nitrosophenol. Besides the phenolic products, 1-phenylethyl alcohol with a 34.2% retained configuration was also isolated in a 5.30% yield. This retained alcohol seems to be formed from the diazonium hydroxide by a kind of S_Ni mechanism.[8]

As another example of the S_N1 phenolysis of a missing-charge type, we undertook the phenolysis of the diethyl-(1-phenylethyl)-oxonium ion. Optically active diethyl-(1-phenylethyl)-oxonium fluoroborate was prepared *in situ* in 1,2-dichloroethane from ethyl fluoroborate and S-(−)-1-phenylethyl ethyl ether.

$$\text{S-ROEt} + \text{EtBF}_4 \xrightarrow[\text{in ClCH}_2\text{CH}_2\text{Cl}]{} \text{S-R}\overset{+}{\text{O}}\text{Et}_2\text{BF}_4^-$$

The oxonium ion in 1,2-dichloroethane was subjected to phenolysis by addition of a mixture of phenol and 1,2-dichloroethane (*ca.* 10 : 1 by wt.) at 16—25°C. After the usual working-up, *o*- and *p*-(1-phenylethyl)-phenols with net inverted configurations were obtained (Tables 2 and 3); no phenolic ether was found in the products. This is most probably because of the rapid rearrangement of the *inverted* phenyl ether, initially formed, to the *inverted* *o*-(1-phenylethyl)-phenol, with a net retention of configuration, under the acidic reaction conditions. In fact, we confirmed that optically active 1-phenylethyl phenyl ether rapidly rearranges into *o*-(1-phenylethyl)-phenol, with a 35% retention of configuration, in the presence of hydrochloric acid in a 1 : 1 mixture of phenol and 1,2-dichloroethane (see Experimental section).

As has previously been reported,[9] the acidic cleavage of 2,6-di-*t*-butyl-4-methyl-4-(1-phenyl-

5) For an excellent summary of the solvolysis of 1-phenylethyl systems, see P. B. D. de la Mare, D. M. Hall and E. Mauger, *Rec. Trav. Chim. Pays-Bas*, **87**, 1394 (1968).

6) For the use of urea as a base, see W. S. Trahanovsky, M. P. Doyle and P. D. Bartlett, *J. Org. Chem.*, **32**, 150 (1967).

7) E. D. Hughes and D. J. Wittingham, *J. Chem. Soc.*, **1960**, 806.

8) For the mechanism of the formation of the retained alcohol from the diazohydroxide *via* the diazonium hydroxide, see E. H. White and D. J. Woodcock, "Cleavage of the Carbon-Nitrogen Bond," in "The Chemistry of the Amino Group," ed. by S. Patai, Interscience Publishers, New York (1968), pp. 407—498.

9) K. Okamato, I. Nitta and H. Shingu, This Bulletin, submitted for publication; to be published in the next issue.

Table 2. The formation of 1-phenylethyl phenyl ether in the phenolyses of the 1-phenylethyl systems with a positively-charged leaving group

Solvent	RX M	Temp. °C	Time hr	ROPh Yield %	Net steric course α% a)	
PhOH-H_2O b)	R-$RN_2^+Cl^-$ c) 1.80	−8—+2	2	0.152	8.36 inv.	This work f)
PhOH-$ClCH_2CH_2Cl$ (1 : 1 by wt.)	S-$R\overset{+}{O}Et_2$ d) 0.144	16—25	0.33	—	— (inv.)	This work
PhOH	S-RDBC+ e) 0.195 $[\alpha]_D^{19}$ +18.6°	75	1.5	12.2	13.5 inv.	Ref. 9

a) See the footnote a of Table 1.
b) The composition of the mixture was changed from 79 : 21 to 66 : 34 during the reaction (see Experimental section).
c) Prepared from 1-phenylethylamine, α_D^{17} +14.0° (1 dm, neat); the rotation of the optically pure amine was taken to be 38.88° (1 dm, neat) (W. Leithe, *Monatsh. Chem.*, **51**, 385 (1929)).
d) Prepared from 1-phenylethyl ethyl ether, $\alpha_D^{21.5}$ −7.18° (1 dm, neat), and ethyl fluoroborate; the rotation of the optically pure ether was taken to be 94.8° (1 dm. neat) (K. Mislow, *J. Amer. Chem. Soc.*, **73**, 4043 (1951)).
e) The protonated 2,6-di-*t*-butyl-4-methyl-4-(1-phenylethyl)-cyclohexan-1-one.
f) 1-Phenylethylamine (55.0%) was recovered; 1-phenylethyl alcohol (5.3% yield) with 34.2% retention of configuration was obtained besides the phenolic products, illustrated in Tables 2 and 3.

Table 3. The formation of (1-phenylethyl)-phenols in the phenolyses of 1-phenylethyl ststems

Solvent	RX a) M	Base M	Temp. °C	Time hr	*o*-RPhOH a) Yield %	*o*-RPhOH a) Net steric course, α% d)	*p*-RPhOH a) Yield %	*p*-RPhOH a) Net steric course, α% d)
PhOH-CH_3CN (1 : 1 by wt.)	RCl 0.143	Et_3N 0.424	40	97	17.0	41.2 inv.	12.6	48.5 inv.
PhOH-CH_3CN (1 : 1 by wt.)	RBr 0.142	Et_3N 0.419	40	19	16.2	53.6 inv.	11.1	50.6 inv.
PhOH	RODNB 0.0933	PhONa 0.0933	150	4.3	11.4	0.00 rac.	8.22	11.6 inv.
PhOH-CH_3CN (1 : 1 by wt.)	ROTs 0.0914	$CO(NH_2)_2$ 0.234	20—35	2.2	6.24	>8.67 c) inv.	12.3	>15.7 c) inv.
PhOH-H_2O a)	$RN_2^+Cl^-$ e) 1.80	—	−8—+2	2	1.19	1.30 c) ret.	3.24	29.2 c) inv.
PhOH-$ClCH_2CH_2Cl$ (1 : 1 by wt.)	$R\overset{+}{O}Et_2BF_4^-$ 0.144	—	16—25	0.33	34.8	9.00 c) inv.	55.2	4.33 c) inv.
PhOH b)	RDBC+ 0.195	—	75	1.5	18.6	10.2 inv.	48.6	15.9 inv.

a) See the footnotes in Tables 1 and 2.
b) Cited from Ref. 9.
c) Calculated on the basis of the rotations of the starting 1-phenylethyl chloride, amine, and ethyl ether, respectively; see the footnotes in Table 2.
d) The rotations of optically pure samples were taken to be 27.85° (1 dm, neat) for R-(+)-*o*-(1-phenylethyl)-phenol and 10.26° ($[\alpha]_D$) for S-(+)-*p*-(1-phenylethyl)-phenol (see Ref. 13).
e) See the footnote f in Table 1.

ethyl)-cyclohexadien-1-one into a 1-phenylethyl compound and 2,6-di-*t*-butyl-4-methylphenol is also considered to be a typical S_Ni reaction of the missing-charge type for the protonated dienone; this optically active dienone in the phenol solvent gives 1-phenylethyl phenyl ether with a net inverted configuration, along with *o*- and *p*-(1-phenylethyl)-phenols with net inverted configurations (Tables 2 and 3).

Thus, contrary to the cases of the negative leaving groups, in the phenolysis of the 1-phenylethyl system with a positively-charged leaving group, a net inversion of configuration is standard for the formation of the phenolic ether, as is typically observed in the usual S_Ni reactions. This is illustrated in the following scheme:

$$R\text{-}RN_2^+ \xrightarrow[\text{in PhOH-H}_2\text{O}]{-8—+2°C} S\text{-ROPh}$$

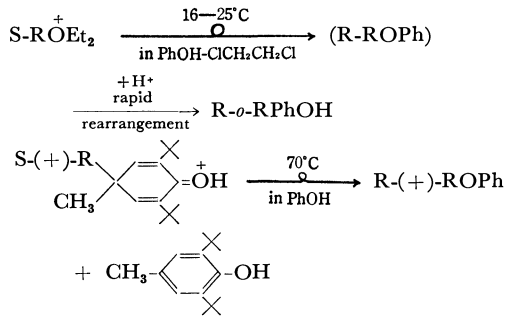

Discussion

The Steric Course of the Formation of the Phenyl Ether. All the results presented above are consistent with the expected results as regards the steric courses of the formation of the phenolic ether; consequently, they lend support to the previous suggestion that the phenol molecule acts as a component of the four-center transition state which leads to the retentive phenolysis.

However, it has been established that, in the acrylonitrile solvent which does not solvate the negative leaving group but the positively-charged carbonium ion, 1-phenylethyl chloride is hydrolyzed to the unusual retentive course when it is conducted in the 97% aqueous acrylonitrile solvent.[10] This most probably indicates that the specific solvation, or coordination,[5] of acrylonitrile on the back-side of the cationic component of the ion-pair intermediate can cause the retentive hydrolysis. In other words, a sort of back-side shielding[5,11] of the ion-pair intermediate may operate in the acrylonitrile solvent. Considering this factor, therefore, we can not exclude the possibility that the phenol molecule also acts as a back-side shielder just as the acrylonitrile molecule does, although its role may be minor in comparison with the concomitant front-side four-center attack of the phenol molecule.

The Steric Course of the Formation of the Alkylated Phenol. As illustrated in Table 3, in the phenol-acetonitrile solvent the formation of *o*- and *p*-(1-phenylethyl)-phenols proceeds with a predominant inversion of configuration; in the other phenolic solvents, inverted 1-phenylethylphenols are also obtained, irrespective of the charge-type of the leaving group (Table 3). These results can be explained as a consequence of the back-side attack of the phenoxide ion (or the phenol molecule) on the ion-pair intermediate.

10) K. Okamoto, K. Komatsu and H. Shingu, *ibid.*, **39**, 2785 (1966).

11) a) W. von E. Doering and H. H. Zeiss, *J. Amer. Chem. Soc.*, **75**, 4733 (1953); b) A. Streitwieser, Jr., and W. D. Schaeffer, *ibid.*, **79**, 6233 (1957); c) A. Streitwieser, Jr., and S. Andreades, *ibid.*, **80**, 6553 (1958); d) H. Weiner and R. A. Sneen, *ibid.*, **87**, 287, 292 (1965); e) N. Kornblum and D. E. Hardies, *ibid.*, **88**, 1707 (1966).

As an exception to the general trend, 1-phenylethyl 3,5-dinitrobenzoate afforded a racemic *o*-(1-phenylethyl)-phenol in the phenolic solvent. Since, in view of the facile acidic rearrangement with retention of configuration in the phenol-acetonitrile solvent at 40°C (see Experimental section), the retentive rearrangement of 1-phenylethyl phenyl ether to *o*-(1-phenylethyl)-phenol would proceed rather rapidly, even in the absence of a strong acid, at such an elevated temperature as 150°C, the formation of the racemic *o*-(1-phenylethyl)-phenol may be explained as the result of the fortuitous compensation of retention and inversion, caused by the concurrence of the retentive rearrangement and the inversive direct alkylations.

As another exceptional case of especial interest, the 1-phenylethyldiazonium ion gave a *retained* *o*-(1-phenylethyl)-phenol in the aqueous phenol solvent. Under similar acidic conditions, the rearrangement of 1-phenylethyl phenyl ether to *o*-(1-phenylethyl)-phenol was found to be comparatively slow (see Experimental section); moreover, any rearrangement should give an *inverted* *o*-(1-phenylethyl)-phenol, since, in the case of the diazonium ion, the *inverted* phenyl ether is formed and its rearrangement proceeds with a retention of configuration (*vide supra*) (Table 2). Therefore, the formation of the *o*-(1-phenylethyl)-phenol is probably caused by the "direct" and *retentive* *C*-alkylation of the phenol molecule; this is illustrated in the following scheme:

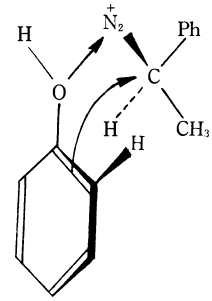

Hart and his collaborators[12] found that *o*-(1-phenylethyl)-phenol with a retained configuration is formed from 1-phenylethyl chloride in the phenol solvent in the absence of a base; they suggested that this is a direct and retentive alkylation with a four-center transition state. However, this result, at least partly, may stem from the rearrangement of the initially-formed phenyl ether with a retained configuration:

$$\text{R-RCl} + \text{PhOH} \xrightarrow[\text{in PhOH}]{} \text{(R-ROPh)} \xrightarrow[\text{rapid}]{\text{H}^+} \text{R-}o\text{-RPhOH}$$

$$\text{R-RCl} + \text{PhOH} \xrightarrow{\text{in the absence of a base}} \text{R-}o\text{-RPhOH (Hart } et\ al.^{12})$$

12) H. Hart, W. L. Spliethoff and H. S. Eleuterio, *ibid.*, **76**, 4547 (1954).

In fact, we confirmed that when the phenolysis of 1-phenylethyl chloride was conducted in the absence of the amine, no phenolic ether was obtained, while the retained *o*-(1-phenylethyl)-phenol, along with the inverted *p*-(1-phenylethyl)-phenol, was obtained in a 1 : 1 mixture of phenol and acetonitrile, and that under the same reaction conditions the phenolic ether undergoes a rapid rearrangement to give *o*-(1-phenylethyl)-phenol with a 74% retention of the configuration (see Experimental section).

Experimental

Materials. The R-(+)-1-phenylethyl chloride was prepared by the reaction of R-(+)-1-phenylethyl alcohol with thionyl chloride in a manner previously described.[13] The S-(−)-1-phenylethyl bromide was prepared by the reaction of R-(+)-1-phenylethyl alcohol with phosphorous tribromide after the method described by Hoffmann and Hughes.[14] The S-(−)-1-phenylethyl 3,5-dinitrobenzoate ($[\alpha]_D^{24}$ −23.7° (*c* 5.4, benzene), mp 101.5—103.4°C (corr.)) was synthesized by the reaction of S-(−)-1-phenylethyl alcohol, α_D^{22} +20.64° (1 dm, neat), with 3,5-dinitrobenzoyl chloride according to the method of Buckles and Maurer.[15] On the basis of this result, the value for the maximum rotation of the 3,5-dinitrobenzoate was calculated to be 50.7° ($[\alpha]_D$), using 44.2°[16] as the value for the maximum rotation of 1-phenylethyl alcohol. 1-Phenylethylamine was resolved according to the method of Theilacker and Winkler.[17] S-(−)-1-Phenylethyl ethyl ether, $\alpha_D^{21.5}$ −7.18° (1 dm, neat), was prepared by the reaction of R-(+)-1-phenylethyl chloride, α_D^{15} +22.3° (1 dm, neat), with potassium carbonate in ethanol after the method described by Kenyon and Phillips.[18] The silver *p*-toluenesulfonate was prepared from silver oxide and *p*-toluenesulfonic acid. All the other reagents employed were of an analytical reagent grade and were purified by fractional distillation.

The Isolation of the Reaction Products (General Procedure). A flask containing a reaction mixture was placed in a constant-temperature bath for at least ten half-lives. The reaction mixture was cooled at 0°C; then, after the addition of water (100 cc), the mixture was extracted with ether (4×100 cc). The combined extracts were washed successively with 10% aqueous sodium hydroxide (4×100 cc) and 10% aqueous sodium chloride (several 100-cc portions) until the washings became neutral to pH indicator paper. The ethereal solution, dried with anhydrous magnesium sulfate, was concentrated; the residual oil was chromatographed using an elution column packed with silica gel, 50-cc portions being taken out. The combined alkaline extracts were acidified with hydrochloric acid, and the resulting oil was extracted with ether; the dried ether extracts were concentrated and the residual oil was distilled *in vacuo* in order to recover some phenol. This residual oil was added to the sample (*vide supra*) for the chromatography.

The Phenolysis of Optically Active 1-Phenylethyl Chloride in the Phenol-Acetonitrile (1: 1 by Wt.) Solvent at 40°C. A mixture of phenol (42.8 g), acetonitrile (42.8 g), and triethylamine (6.09 cc; 0.424 M, as determined by titration) was prepared. To a 77.9-cc portion of the mixture, we added optically active 1-phenylethyl chloride (1.50 cc, 0.0113 mol; bp 56.0—58.0°C/4.0 mmHg; $\alpha_D^{31.2}$ +22.09±0.03°, 1 dm, neat). The reaction mixture so prepared was kept at 40.0±0.1°C for 97 hr. After the working-up described above, an oily material (2.12 g) was chromatographed over silica gel (80 g; Nakarai, No. 11-A, 100—200 mesh). The column was eluted successively with *n*-hexane-benzene (1: 1 by vol.), benzene, benzene-ether (97: 3 by vol.), ether, and ethanol, 50-cc portions being taken out. Fractions 4—9, obtained using *n*-hexane - benzene (1: 1 by vol.), gave 1-phenylethyl phenyl ether (1.284 g; 58.1% yield; the infrared spectrum was the same as that of an authentic sample; $\alpha_D^{27.5}$ −0.455±0.015°, 0.5 dm, neat). Fractions 15—21, obtained using benzene, gave *o*-(1-phenylethyl)-phenol (0.376 g; bp 140—145°C/4.0 mmHg; 17.0% yield; the infrared spectrum was the same as that of an authentic sample: $\alpha_D^{28.4}$ −1.015±0.015°, 0.5 dm, neat). Fractions 26—31, obtained using benzene-ether (97: 3 by vol.), gave *p*-(1-phenylethyl)-phenol (0.278 g; bp 150—156°C/4.0 mmHg; 12.6% yield; the infrared spectrum was the same as that of an authentic sample; $[\alpha]_D^{28.5}$ +0.12±0.02° (*c* 27.3, benzene)).

The Phenolysis of Optically Active 1-Phenylethyl Bromide in the Phenol-Acetonitrile (1: 1 by Wt.) Solvent at 40°C. A mixture of phenol (42.8 g), acetonitrile (42.8 g), and triethylamine (5.85-cc, 0.419 M) was prepared. To a 90.0-cc portion of the mixture, we added optically active 1-phenylethyl bromide (2.00 cc, 0.0145 mol; bp 48.0—53.8°C/0.7 mmHg; $\alpha_D^{23.2}$ −33.15±0.04°, 0.5 dm, neat). The reaction mixture so prepared was maintained at 40.0±0.1°C for 19 hr. After the working-up described above, an oily material (2.550 g) was chromatographed over silica gel (80 g). Fractions 7—15, obtained using *n*-hexane - benzene (1: 1 by vol.), gave 1-phenylethyl phenyl ether (1.448 g; 55.7% yield; the infrared spectrum was the same as that of an authentic sample; $\alpha_D^{22.6}$ −1.475±0.045°, 0.5 dm, neat). Fractions 19—29, obtained using benzene, gave *o*-(1-phenylethyl) phenol (0.420 g; bp 125—130°C/3.0 mmHg; 16.2% yield; the infrared spectrum was the same as that of an authentic sample; $\alpha_D^{25.6}$ +2.90±0.05°, 0.5 dm, neat). Fractions 35—45, obtained using benzene-ether (97: 3 by vol.), gave *p*-(1-phenylethyl)-phenol (0.288 g; bp 140—150°C/4.0 mmHg; 11.1% yield; the infrared spectrum was the same as that of an authentic sample; $[\alpha]_D^{22.4}$ −0.70±0.04° (*c* 69.4, benzene)).

The Phenolysis of Optically Active 1-Phenylethyl 3,5-Dinitrobenzoate in the Phenol Solvent at 150°C. To a mixture of phenol (40 cc) and sodium phenoxide (0.4490 g, 0.00386 mol; 0.0933 M), we added optically active 1-phenylethyl 3,5-dinitrobenzoate (1.0952 g, 0.00386 mol; mp 98.6—100.5°C (corr.); $[\alpha]_D^{25.9}$ −21.0±0.28° (*c* 5.32, benzene)). The reaction

13) K. Okamoto, M. Hayashi, K. Komatsu and H. Shingu, This Bulletin, **40**, 624 (1966).

14) H. M. R. Hoffmann and E. D. Hughes, *J. Chem. Soc.*, **1964**, 1244.

15) R. E. Buckles and J. E. Maurer, *J. Org. Chem.*, **18**, 1588 (1953).

16) D. J. Cram, K. R. Kopecky, F. Hauck and A. Langemann, *J. Amer. Chem. Soc.*, **81**, 5754 (1959).

17) W. Theilacker and H. G. Winkler, *Chem. Ber.*, **37**, 690 (1954).

18) J. Kenyon and H. Phillips, *J. Chem. Soc.*, **1930**, 1676.

mixture was kept at 150.0±0.1°C for 4.3 hr. After the working-up described above, an oily material (0.5067 g) was chromatographed over silica gel (40 g). Fractions 2—4, obtained using *n*-hexane - benzene (1: 1 by vol.), gave 1-phenylethyl phenyl ehter (0.305 g; bp 140—141°C/4.0 mmHg; 40.0% yield; the infrared spectrum was the same as that of an authentic sample; $\alpha_D^{26.7}$ −3.045±0.025°, 0.5 dm, heat). Fractions 8—11, obtained using benzene, gave *o*-(1-phenylethyl)-phenol (0.0872 g; bp 148—149°C/4.0 mmHg; 11.4% yield; the infrared spectrum was the same as that of an authentic sample; $[\alpha]_D^{26.7}$ 0.00±0.06° (*c* 23.6, benzene)). Fractions 16—19, obtained using benzene-ether (97: 3 by vol.), gave *p*-(1-phenylethyl)-phenol (0.0627 g; bp 150—155°C/4.0 mmHg; 8.22% yield; the infrared spectrum was the same as that of an authentic sample; $[\alpha]_D^{27.4}$ +0.554±0.262° (*c* 34.3, benzene)).

The Phenolysis of Optically Active 1-Phenylethyl *p*-Toluenesulfonate in the Phenol-Acetonitrile (1: 1 by Wt.) Solvent at from 20°C to 35°C. A solution (75 cc) of silver *p*-toluenesulfonate (4.221 g, 0.01508 mol in acetonitrile was prepared and kept at 20.0±0.1°C). When optically active 1-phenylethyl chloride (2.00 cc, 0.0148 mol; bp 45.0—46.1°C/1.0 mmHg; $\alpha_D^{18.2}$ −57.105±0.035°, 1 dm, neat) was then added to the solution, the precipitates of silver chloride appeared immediately. To the mixture, there was added a solution (85 cc) of urea (2.140 g, 0.0356 mol) in a mixture of phenol and acetonitrile (5.5: 1.0 by wt.). The reaction mixture so prepared was maintained at from 20.0°C to 35.0°C for 2.17 hr. The mixture was then cooled at 0°C and poured onto a mixture of ether and water (1: 1 by vol.; 200 cc). The precipitates of silver chloride were separated by filtration. After the working-up described above, an oily material (1.7820 g) was chromatographed over silica gel (50 g). Fractions 7—10, obtained using *n*-hexane - benzene (1: 1 by vol.), gave 1-phenylethyl phenyl ether (0.6008 g; 20.5% yield; the infrared spectrum was the same as that of an authentic sample; $[\alpha]_D^{19.6}$ −0.43±0.20° (*c* 42.1, benzene)). Fractions 14—17, obtained using benzene, gave *o*-(1-phenylethyl)-phenol (0.1831 g; bp 135—140°C/3.0 mmHg; 6.24% yield; the infrared spectrum was the same as that of an authentic sample; $[\alpha]_D^{20.4}$ −1.0;±0.85° (*c* 38.2, benzene)). Fractions 19—27, obtained using benzene and benzene-ether (97: 3 by vol.), gave *p*-(1-phenylethyl)-phenol (0.3604 g; bp 145—160°C/5.0 mmHg; 12.3% yield; the infrared spectrum was the same as that of an authentic sample; $[\alpha]_D^{24.1}$ +0.733±0.221° (*c* 58.7, benzene)).

The Reductive Cleavage of Optically Active 1-Phenylethyl *p*-Toluenesulfonate with Sodium-Naphthalene. Into a solution of silver *p*-toluenesulfonate (12.40 g, 0.0444 mol) in acetonitrile (32 cc), we added optically active 1-phenylethyl chloride (2.00 cc, 0.0148 mol; bp 45.0—46.1°C/1.0 mmHg; $\alpha_D^{18.2}$ −57.105±0.035°, 1 dm, neat). The flask was kept at 20.0±0.1°C for 3 hr. The reaction mixture was then cooled at 0°C, and burnt sodium chloride (5.50 g, 0.0942 mol) and ether (15 cc) were added successively. Precipitates of silver chloride (13.27 g) was separated by filtration. The filtrate was concentrated to about 20 cc by a rotary-evaporator at room temperature. To the concentrated solution, tetrahydrofuran (5 cc) was added. After the separation of the additional precipitates of silver chloride (2.08 g) by filtration, the filtrate was concentrated to about 10 cc. From the concentrated solution, 0.5 cc of an aliquot was pipetted, after which the solvent was removed by distillation *in vacuo* (at room temperature) to give white crystals, which rapidly became reddish violet when exposed to air. The crystals showed IR absorption (in CCl_4) at 3070, 2950, 1600, 1495, 1450, and 700 cm^{-1}. Following the method described by Closson *et al.*,[4] a concentrated solution of 1-phenylethyl *p*-toluenesulfonate was added, drop by drop, into a tetrahydrofuran solution (150 cc) of sodium (1.23 g, 0.0535 mol) and naphthalene (7.00 g, 0.0547 mol) at −3.0°C under nitrogen; the color of the mixture was dark green. After the addition of the tosylate, there was immediately added, drop by drop, a mixture of tetrahydrofuran (15 cc) and distilled water (5 cc) at from 4.0°C to 7.0°C; the color become grey. After the addition of distilled water (10 cc), the reaction mixture was poured onto water (150 cc); sodium chloride (50 g) was then added, and the mixture was extracted with ether (four 50-cc portions). After the combined extracts had then been dried with anhydrous magnesium sulfate, the solution was concentrated to about 10 cc. The white crystals were separated by filtration; the crystals were washed with ethanol (two 5-cc portions); the filtrate was combined with washings and concentrated to about 10 cc. The second crop was filtered and washed with ethanol. The procedure was repeated seven times. The combined white crystals were characterized as naphthalene (5.78 g, 82.6% recov.; the infrared spectrum was the same as that of an authentic sample; mp 79.0—79.8°C). The residual material (2.30 g), concentrated from the final filtrate, was chromatographed over silica gel (50 g). Fractions 1—8, obtained using *n*-hexane, gave naphthalene (0.7795 g; the infrared spectrum was the same as that of an authentic sample; mp 79.5—80.0°C). Fractions 9—13, obtained using benzene, gave slightly yellow crystals (0.3091 g). Fractions 19—28, obtained using successively benzene, benzene-ether (1: 1 by vol.), and ether, gave 1-phenylethyl alcohol (0.6184 g; bp 75.0—80.0°C/4.0 mmHg; 11.3% yield; the infrared spectrum was the same as that of an authentic sample; $\alpha_D^{19.8}$ +0.248±0.107°, 1 dm, neat).

The Hydrolysis of Optically Active 1-Phenylethyl *p*-Toluenesulfonate in the Aqueous Acetonitrile. A solution of silver *p*-toluenesulfonate (6.5226 g, 0.0234 mol) and optically active 1-phenylethyl chloride (2.00 cc, 0.0148 mol; bp 47.5—49.6°C/2.0 mmHg; $\alpha_D^{15.0}$ −56.42±0.04°, 1 dm, neat) in acetonitrile (70.0 cc) was kept at 19.8±0.1°C for 23.7 hr. Precipitates of silver chloride were separated by filtration. The filtrate was treated with water (10 cc), dried with anhydrous magnesium sulfate, and concentrated by distillation. The distillation of the residual material (0.7700 g) under reduced pressure afforded 1-phenylethyl alcohol (0.5121 g; bp 66.5—67.0°C/2.5 mmHg; 28.2% yield; the infrared spectrum was the same as that of an authentic sample; $\alpha_D^{19.2}$ −0.31±0.10°, 0.5 dm, neat), along with styrene (0.3070 g; 19.9% yield; the infrared spectrum was the same as that of an authentic sample).

The Phenolysis of Optically Active 1-Phenylethyldiazonium Salt in a Mixture of Phenol and Water (79: 21 to 66: 34 by Vol.) at from −8°C to +2°C. A mixture of phenol (44.20 g), distilled water (12.00 g), sodium nitrite (13.00 g, 0.1885 mol), and optically active 1-phenylethylamine (22.90 g, 0.1884 mol; bp 64.0—64.5°C/10.0 mmHg; $\alpha_D^{17.0}$ +13.96±

0.04°, 1 dm, neat) was prepared in a flask cooled in an ice-salt bath. To the mixture so prepared, we added concentrated hydrochloric acid (16.56 cc, 0.0113 mol), drop by drop, at from −8.0°C to +2.4°C. The reaction proceeded very fast, with the evolution of nitrogen. The volume of nitrogen was measured with a gas burette (708 cc). The reaction mixture was treated according to the above procedures; the unchanged amine was recovered from the acidic extracts. An oily material (7.5026 g) was chromatographed over silica gel (180 g). Fractions 10—13, obtained using *n*-hexane - benzene (1: 1 by vol.), gave an oily material (0.1961 g) containing 1-phenylethyl phenyl ether; this material was rechromatographed over basic alumina (15 g; Nakarai, Alumina Activated 200, *ca.* 200 mesh) to give 1-phenylethyl phenyl ether (0.0566 g; bp 141—146°C/4.0 mmHg; 0.152% yield; the infrared spectrum was the same as that of an authentic sample; $[\alpha]_D^{18.8}+1.40\pm0.22°$ (*c* 40.7, racemic 1-phenylethyl alcohol)). Fractions 18—25, obtained using benzene, gave an oily material (0.7125 g) containing *o*-(1-phenylethyl)-phenol; this material was rechromatographed over basic alumina (30 g) to give *o*-(1-phenylethyl)-phenol (0.4428 g; bp 145—150°C/4.0 mmHg; 1.19% yield; the infrared spectrum was the same as that of an authentic sample; $\alpha_D^{22.8}+0.065\pm0.015°$, 0.5 dm, neat). Fractions 28—43, obtained using benzene and benzene-ether (97: 3 by vol.), gave *p*-(1-phenylethyl)-phenol (1.2094 g; bp 150—155°C/4.0 mmHg; 3.24% yield; the infrared spectrum was the same as that of an authentic sample; $[\alpha]_D^{19.0}+1.07\pm0.09°$ (*c* 65.1, benzene)). Fractions 46—59, obtained using ether, gave 1-phenylethyl alcohol (1.2191 g; bp 90—95°C/10.0 mmHg; 5.30% yield; the infrared spectrum was the same as that of an authentic sample; $\alpha_D^{20.5}+2.69\pm0.02°$, 0.5 dm, neat). The combined acidic solution was made alkaline with 30% aqueous sodium hydroxide; the resulting oil was worked-up in the usual manner, and distilled under reduced pressure to give 1-phenylethylamine (12.60 g; bp 68.5—70.5°C/10.0 mmHg; 55.0% recov.; $\alpha_D^{20.7}+13.59\pm0.015°$, 1 dm, neat).

The Phenolysis of Optically Active Diethyl-(1-phenylethyl)-oxonium Fluoroborate in the Phenol-1,2-Dichloroethane (1: 1 by Wt.) Solvent at from 16°C to 25°C. Optically active diethyl-(1-phenylethyl)-oxonium fluoroborate was prepared by a modification of Meerwein's procedure;[19] all the operations were carried out under a nitrogen atmosphere. Silver fluoroborate (1.93 g, 0.00991 mol) was dissolved in 1,2-dichloroethane (20 cc); to the solution, ethyl iodide (1.54 g, 0.00991 mol) was then added. The yellow precipitate was filtered; to the filtrate, optically active 1-phenylethyl ethyl ether (1.49 g, 0.00991 mol; bp 71.0—73.2°C/10.0 mmHg; $\alpha_D^{21.5}-7.18\pm0.02°$, 1 dm, neat) was then added. To the mixture so prepared, a mixture of phenol (28.5 g) and 1,2-dichloroethane (3.44 g) was added. The mixture was kept at room temperature (16.0°C to 24.5°C) with stirring. After the working-up described above, an oily material (1.5921 g) was chromatographed over silica gel (70 g). Fractions 1—3, obtained using *n*-hexane - benzene (1: 1 by vol.), gave polystyrene (0.0437 g; 4.24% yield; the infrared spectrum was the same as that of an authentic sample). Fractions 6—9, obtained using benzene, gave *o*-(1-phenylethyl)-phenol (0.6834 g; bp 145—150°C/4.0 mmHg; 34.8% yield; the infrared spectrum was the same as that of an authentic sample; $[\alpha]_D^{17.5}+0.19\pm0.03°$ (*c* 58.0, benzene)). Fractions 11—19, obtained using benzene and benzene-ether (97: 3 by vol.), gave *p*-(1-phenylethyl)-phenol (1.0810 g; bp 150—153°C/4.0 mmHg; 55.2% yield; the infrared spectrum was the same as that of an authentic sample; $[\alpha]_D^{17.9}-0.146\pm0.048°$ (*c* 41.0, benzene)).

The Phenolysis of Optically Active 1-Phenylethyl Chloride in the Absence of a Base in the Phenol-Acetonitrile (1: 1 by Wt.) Solvent. A mixture of phenol (41.8 g) and acetonitrile (41.8 g) was prepared. To 78.4 cc of the mixture, we then added optically active 1-phenylethyl chloride (2.00 cc, 0.0148 mol; bp 39.8—40.2°C/2.5 mmHg; $\alpha_D^{16.8}-53.32\pm0.02°$, 1 dm, neat). The reaction mixture so prepared was kept at 40.0±0.1°C for 73 hr. After the working-up described above, an oily material (3.1180 g) was chromatographed over silica gel (90 g). Fractions 7—14, obtained using benzene, gave *o*-(1-phenylethyl)-phenol (1.0032 g; bp 145—150°C/4.0 mmHg; 34.9% yield; the infrared spectrum was the same as that of an authentic sample; $\alpha_D^{21.6}-0.455\pm0.045°$, 0.5 dm, neat). Fractions 17—24, obtained using benzene-ether (97: 3 by vol.), gave *p*-(1-phenylethyl-)phenol (1.8583 g; bp 151—158°C/4.0 mmHg; 62.8% yield; the infrared spectrum was the same as that of an authentic sample; $[\alpha]_D^{20.8}-0.532\pm0.223°$ (*c* 39.5, benzene)).

The Acidic Rearrangement of Optically Active 1-Phenylethyl Phenyl Ether in the Phenol-Acetonitrile (1: 1 by Wt.) Solvent at 40°C. Into 5 cc of a mixture containing phenol and acetonitrile (1: 1 ratio by wt.), anhydrous hydrogen chloride was bubbled for about 10 min. The acidic mixture was then diluted with the 1: 1 mixture of phenol and acetonitrile to make a solvent with the desired hydrogen chloride concentration. The exact normality (0.0234 N) was determined by titration with standard 0.05 N sodium acetate in acetic acid (crystal violet). A mixture of optically active 1-phenylethyl phenyl ether (0.8163 g, 0.00411 mol; bp 135—139°C/4.0 mmHg; $\alpha_D^{23.7}-6.41\pm0.02°$, 1 dm, neat) and the acidic solvent (41.7 cc) was maintained at 40.0±0.1°C for 5 hr. After the working-up described above, an oily material (1.2839 g) was chromatographed over basic alumina (40 g; Nakarai, Alumina Activated 200, *ca.* 200 mesh). Fractions 4—6, obtained using *n*-hexane - benzene (1: 1 by vol.), gave 2,3-diphenylbutane (0.0084 g; 1.94% yield). Fractions 8—11, obtained using *n*-hexane-benzene (1: 1 by vol.), gave *o*-(1-phenylethyl)-phenol (0.1908 g; bp 145—150°C/4.0 mmHg; 23.4% yield; the infrared spectrum was the same as that of an authentic sample; $[\alpha]_D^{22.4}+2.85\pm0.32°$ (*c* 53.1, benzene)). Fractions 14—20, obtained using benzene, gave *p*-(1-phenylethyl)-phenol (0.6163 g; bp 155—158°C/5.0 mmHg; 75.8% yield; the infrared spectrum was the same as that of an authentic sample; $[\alpha]_D^{22.3}+1.21\pm0.09°$ (*c* 73.6, benzene)).

The Acidic Rearrangement of Optically Active 1-Phenylethyl Phenyl Ether in the Phenol-1,2-Dichloroethane (1: 1 by Wt.) Solvent at 21°C. A mixture of phenol - 1,2-dichloroethane (1: 1 by wt.) containing the desired concentration of anhydrous hydrogen chloride (0.145 N, as determined by titration)

19) H. Meerwein, in Houben-Weyl, "Methoden der organischen Chemie," Georg Thieme Verlag, Stuttgart, (1965) Bd. VI/3, p. 338.

was prepared in a manner similar to that described above. To the acidic solvent (20.2 cc), optically active 1-phenylethyl phenyl ether (0.5871 g, 0.00298 mol; bp 140—145°C/4.0 mmHg; $\alpha_D^{19.2}$ −1.29±0.03°, 0.5 dm, neat) was added. The reaction mixture so prepared was allowed to stand at room temperature (21.0°C) for 0.5 hr. After the working-up described above, an oily material (0.5782 g) was chromatographed over silica gel (20 g). Fractions 2—5, obtained using *n*-hexane - benzene (1: 1 by vol.) and benzene, gave *o*-(1-phenylethyl)-phenol (0.2854 g; bp 145—151°C/4.0 mmHg; 48.6% yield; the infrared spectrum was the same as that of an authentic sample; $[\alpha]_D^{22.0}$ +0.54± 0.06° (*c* 66.4, benzene)). Fractions 7—11, obtained using benzene and benzene - ether (97: 3 by vol.), gave *p*-(1-phenylethyl)-phenol (0.2069 g; bp 155—158°C/4.0 mmHg; 35.3% yield; the infrared spectrum was the same as that of an authentic sample; $[\alpha]_D^{22.0}$ −0.91±0.066° (*c* 45.2, benzene)).

The Acidic Rearrangement of Racemic 1-Phenylethyl Phenyl Ether in a Mixture of Phenol and Water (79: 21 to 66: 34 by Wt.) at from −6°C to +2°C. A mixture of phenol (37.6 g) and distilled water (10.0 g) was prepared. To 30 cc of the mixture, racemic 1-phenylethyl phenyl ether (0.9731 g; bp 140—145°C/4.0 mHg) was added. To the stirred mixture, concentrated hydrochloric acid (6.90 cc; Nakarai, reagent-grade quality, min. 35.5%) was added, drop by drop, over a 2-hr period at from −6.0°C to +2.0°C. After the working-up described above, an oily material (0.8975 g) was chromatographed over silica gel (30 g). Fractions 1—4, obtained using *n*-hexane - benzene (1: 1 by vol.), gave 1-phenylethyl phenyl ether (0.8751 g; 90.0% recov.; the infrared spectrum was the same as that of an authentic sample). Fractions 9—11, obtained using benzene, gave *o*-(1-phenylethyl)-phenol (0.0124 g; 0.0128% yield; the infrared spectrum was the same as that of an authentic sample). Fractions 14—17, obtained using benzene-ether (97: 3 by vol.), gave *p*-(1-phenylethyl)-phenol (0.0139 g; 0.0143% yield; the infrared spectrum was the same as that of an authentic sample).

Kinetic Measurements. The previous procedure[1] was followed; the usual sealed-ampoule (1.000 cc) technique was employed. The diminution of base concentrations was followed by titration with standard perchloric acid (0.05 N) in acetic acid, using crystal violet as the indicator. All the data were treated graphically by a plot of log $a/(a-x)$ against the time. In each case, the reaction was followed to at least 80% conversion; a smooth linear relationship was thus obtained. Infinity titers were determined after at least ten half-lives. The rate data are shown in Fig. 1 and Table 1.

BULLETIN OF THE CHEMICAL SOCIETY OF JAPAN VOL. 43 1553—1556 (1970)

Reaction of *p*-Nitrophenyl Sulfate with Thiophenol

Takehiko KURUSU, Waichiro TAGAKI and Shigeru OAE

Department of Applied Chemistry, Faculty of Engineering Osaka City University, Sugimoto-cho, Sumiyoshiku, Osaka

(Received November 19, 1969)

The reaction of *p*-nitrophenyl sulfate with *p*-substituted thiophenols were carried out in aqueous dimethylformamide under varying conditions. The rate was found to be independent of the concentration of thiophenolate, and to vary very little with the change of substituent. The Hammett correlation with σ value gives $\rho=0.12$. There was no rate-change in the pH range 6—12. Those observations seem to suggest the reaction to be of A-1 type.

Oxidation and reduction of organic sulfur compounds are important reactions in the metabolic pathway of living organisms.[1] However, the chemistry of these enzymatic processes, especially the reduction process, has not been investigated thoroughly.

An interesting model reaction for this enzymic reduction is that between organic sulfates and thiols. Hilz and Kittler[2] studied the reduction of sulfate ion to sulfite ion by lipoic acid, and suggested the following mechanism.

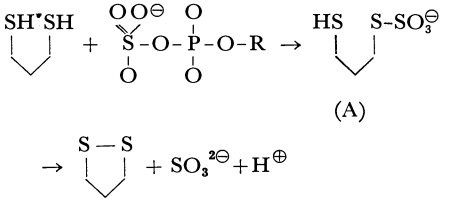

(A)

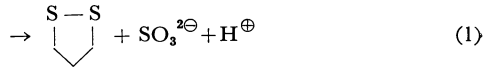

(1)

The reaction is actually a S_N2 type displacement reaction at a sulfur atom as shown by (A). It has to compete with the hydrolysis of the sulfate in aqueous media, especially in a high pH region,

1) F. Challenger, "Aspects of the Organic Chemistry of Sulfur," Academic Press, New York (1959). N. Kharasch, "The Chemistry of Organic Sulfur Compounds," Vol. 2, Pergamon Press, London, New York (1966).

2) H. Hilz. M. Kittler, *Biochem. Biophys. Res. Commun.*, **3**, 140 (1960).

since organic sulfates are considered to be hard acids[3] and hence would readily be attacked by hard bases, *i.e.*, $OH^{\ominus}$ ion in this case.

Thus, in order to understand the nature of oxidation and reduction on the sulfur atom of organic sulfur compounds, one should investigate the relative rates of alkaline hydrolysis and nucleophilic substitution of organic sulfates, as in the cases of aryl thiosulfonates,[4] aryl thiosulfate and aryl thiosulfonate.[5]

Hydrolysis of aryl sulfates has been studied considerably.[6] The mechanism suggested for the acid-catalyzed hydrolysis of alkyl sulfates involves the A-1 type cleavage of S–O bond.[7]

Kice and Anderson[8] studied the reaction in detail and concluded that the mechanism of the acid hydrolysis of sodium aryl sulfates is of A-1 type as shown by

$$ArOSO_3^{\ominus} + H^{\oplus} \overset{\text{fast}}{\rightleftarrows} Ar\text{-}\overset{\oplus}{O}(H)\text{-}SO_3^{\ominus} \xrightarrow{\text{slow}} ArOH + SO_3 \xrightarrow{\text{fast},\ H_2O} H_2SO_4 \qquad (2)$$

Benkovic[9] studied the pH-rate profile for the spontaneous hydrolysis of *p*-nitrophenyl sulfate and observed that the k_{obs} values are essentially independent of pH in the range 7—12, but change linearly with hydroxide ion concentration at higher pH values.

Thus, the spontaneous hydrolysis of *p*-nitrophenyl sulfate has been discussed in terms of a possible elimination of sulfur trioxide analogous to the monomeric metaphosphate formation in the hydrolysis of certain phosphate dianions. We have investigated the reaction of *p*-nitrophenyl sulfate with thiophenolate expecting it to result in the reduction of sulfate through nucleophilic substitution by thiol group.

Result and Discussion

An equimolar mixture of *p*-nitrophenyl sulfate and thiophenolate was heated in DMF in N_2 atmosphere in sealed tubes for 18 hr at 90°C. The products isolated were characterized by comparing the IR spectra, UV spectra and mps with those of the authentic samples. The products and yields are listed in Table 1.

Table 1. Product analysis of the reaction of *p*-nitrophenyl sulfate with thiophenolate[a]

Product		Yields[b] (%)
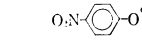	(I)	94
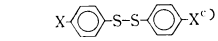	(II)	90
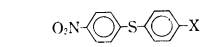	(III)	5

a) In DMF 90°C, 18 hr in sealed tubes under nitrogen atmosphere.
b) Based on the ester used.
c) X=H

Two conceivable mechanisms for the reaction obtained from analysis of products are shown below. According to the mechanism of A-1 type, Eq. (3), the initial step of the reaction is S–O bond fission. Sulfur trioxide thus formed reacts immediately with thiophenolate to yield a Bunte salt (IV). In this case, the rate-determining step appears to be the elimination of sulfur trioxide. This seems to be analogous to the mechanism suggested for the solvolysis of phosphate esters which proceeds by way of monomeric metaphosphate intermediate.[7,10]

Sulfur trioxide thus formed incipiently can function as the sulfate donor in the synthesis of various biologically important organic sulfates.[11] Another possible path, shown as A-2 type,. is essentially a SN2-type reaction involving the nucleophilic replacement of *p*-nitrophenyl sulfate by thiophenolate. Reaction (a) is a simple synchronous SN2-type displacement reaction on sulfur atom, while reaction (b) proceeds *via* the initial addition of nucleophile to the benzene ring (bond making), followed by the leaving of sulfate group (bond breaking) to give *p*-nitrophenyl aryl sulfide.

The kinetics of the reaction of *p*-nitrophenyl sulfate with thiophenolate was studied spectrophotometrically by following the rate of formation of *p*-nitrophenolate (I).

A-1 type

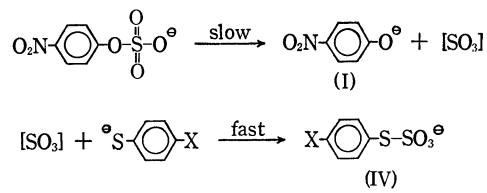

(3)

3) J. O. Edwards and R. G. Pearson, *J. Amer. Chem., Soc.*, **84**, 16 (1962); R. G. Pearson, *ibid.*, **85**, 3533 (1963). R. G. Pearson and J. Songstad, *ibid.*, **89**, 1827 (1967).
4) S. Oae, W. Tagaki and T. Kurusu, This Bulletin, **42**, 2894 (1969).
5) S. Oae, W. Tagaki, R. Nomura and Y. Yoshikawa, *ibid.*, **42**, 2903 (1969).
6) G. N. Burkhardt, W. G. K. Ford and E. Singleton, *J. Chem. Soc.*, **1936**, 17.
7) E. T. Kaiser, M. Panar and F. H. Westheimer, *J. Amer. Chem. Soc.*, **85**, 602 (1963); S. Burstein and S. Liberman, *ibid.*, **80**, 5235 (1958).
8) J. L. Kice and J. M. Anderson, *ibid.*, **88**, 5242 (1966).
9) S. J. Benkovic and P. A. Benkovic, *ibid.*, **88**, 5504 (1966).
10) G. Di. Sabato and W. P. Jencks, *ibid.*, **83**, 4393, 4400 (1961).
11) P. W. Robbins and F. Lipmann, *J. Biol. Chem.*, **229**, 837 (1957).

A-2 type

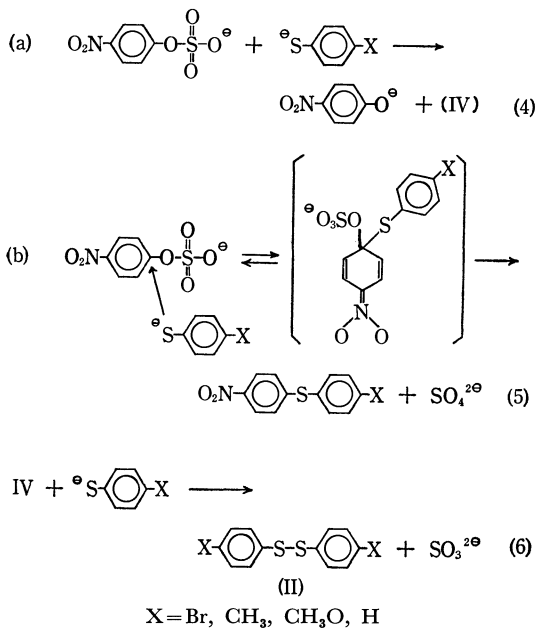

(4)

(5)

(6)

(II)

X=Br, CH_3, CH_3O, H

In order to avoid any complication due to possible side reactions, such as shown in Eq. (6), only the initial rate was used for calculation of the rate constants.

The pseudo-first-order constants of the reaction with substituted thiophenolate, k_{obs}, are listed in Table 2.

Table 2. Pseudo-first-order rate constants of the reaction of *p*-nitrophenyl sulfate with *p*-substituted thiophenols
(in DMF at 90°C)

X-	$k_{obs}\times10^6$ (sec^{-1})
p-Br	5.82
H	5.90
p-CH_3	6.14
p-CH_3O	6.40

It is apparent that the presence of electron-donor substituents in aromatic ring leads to only a very slight increase in the rate. From a good correlation with σ values, one can calculate the Hammett ρ value as +0.12. This means that the participation of nucleophilic attack by thiophenolate is very small at the transition state of the rate-determining step of this reaction. Therefore, the observed substituent effect seems to provide significant support for possible occurrence of an A-1 type pathway in (3).

The pH-rate profile for the reaction of *p*-nitrophenyl sulfate with thiophenol is shown in Fig. 1.

The k_{obs} values are independent of pH change in the range 6—12. Evidence supporting the A-1 type mechanism may be found in the pH-rate profile of the reaction, since the rate of A-2 type process varies with thiophilicity of thiophenol which in turn

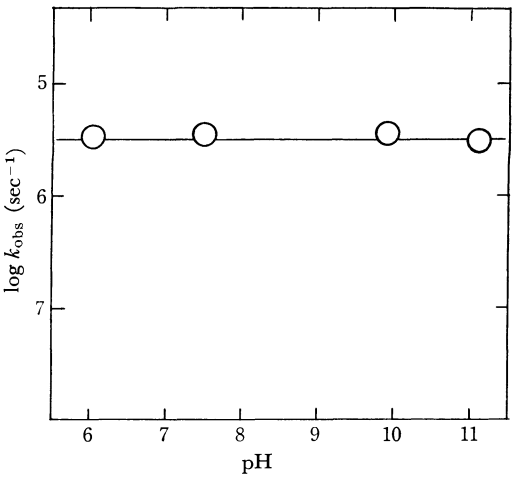

Fig. 1. The pH-rate profile for the reaction of *p*-nitrophenyl sulfate with thiophenyl (at 90°C, in 40% DMF-H_2O)

changes with pH of the reaction mixture. However, as Fig. 1 indicates, the difference in the rate is hardly discernible in the pH range 6—12. The mechanism of this reaction must be identical in this pH range and is very likely the A-1 type. Only at higher pH values or in the alkaline hydrolysis of *p*-nitrophenyl sulfate, the mechanism of A-1 type which depends on the first-power of hydroxide ion concentration may prevail. Thus, all these observations strongly suggest that the reaction of *p*-nitrophenyl sulfate with thiophenol proceeds by way of the A-1 type process.

Experimental

Reagents. *Potassium p-Nitrophenyl Sulfate.* This was prepared by a modification of procedure of Burkhardt and Lapworth.[12]

Chlorosulfonic acid (12 g) was slowly added pyridine (16 g) with stirring and cooling with ice-salt mixture. Benzene (100 cc) was then added, and the mixture was heated to 70°C. *p*-Nitrophenol (12 g) was then added, and the mixture was boiled for 4 hr, during which the pyridinium *p*-nitrophenyl sulfate crystallized out. The salt was then collected and poured into a slight excess of aqueous potassium hydroxide. After unchanged nitrophenol was extracted with ether, then water and pyridine were evaporated off *in vacuo*, potassium *p*-nitrophenol sulfate was obtained. It was purified by repeated recrystallization by dissolution in water and subsequent trituration with ethanol. The salt was dried under reduced pressure over calcium chloride, mp 203°C.

Found: C, 28.00; H, 1.60%. Calcd for $C_6H_4NO_6SK$: C, 28.01; H. 1.57%.

Solvent. *Buffer Solution.* 40% DMF-H_2O solvent was used in all pH solutions. At pH 6–8, KH_2PO_4–Na_2HPO_4 buffer was employed. pH~10 Na_2CO_3–$Na_2B_4O_7$ $10H_2O$, pH 11, NaOH (N/10)–Na_2HPO_4(M/

12) G. N. Burkhardt and A. Lapworth, *J. Chem. Soc.*, **1926**, 684.

10). The pH of the reaction mixtures were measured at 25°C by pH-meter (Horiba, Model-p, No. 17317).

Procedure for Kinetic Runs. Each kinetic run was carried out by monitoring the UV absorbance of *p*-nitrophenolate liberated during the reaction at 400 mμ. At first the solution of *p*-nitrophenyl sulfate (0.01 M 10 m*l*) in DMF was placed in a reaction vessel and immersed in a constant temperature bath which was kept at 90±0.05°C. 10 m*l* of thiophenoxide solution was then added to the ester solution. The reaction was followed by taking out 1 m*l* aliquots at suitable time intervals, diluting these aliquots with 25 m*l* of 0.01 N KOH–ethanol solution, and finally subjecting the solution for measurement of the optical density of the resulting solution at 400 mμ ($\varepsilon=18000$). The calculation of the rate constants was described in detail in earlier studies on the reaction of *p*-nitrophenyl benzenesulfonate with thiophenol.[3]

The Reaction of *p*-Nitrophenyl Sulfate with Thiophenolate. *p*-Nitrophenyl sulfate (4.8 g) and thiophenolate (2.6 g) were dissolved in DMF (20 cc) in an ampoule. The ampoule was sealed under N_2 atmosphere and then kept at 90°C for 18 hr. The solvent of the reaction mixture was evaporated off *in vacuo* and the residue was poured into water and extracted with ether. Work up of the ether layer gave (6.9 g) a mixture of *p*-nitrophenol, diphenyl disulfide and *p*-nitrophenyl phenyl sulfide. They were isolated by chromatography on alumina. The yield of *p*-nitrophenol could also be obtained spectrophotometrically in alkaline solution. The products and yields are listed in Table 1.

BULLETIN OF THE CHEMICAL SOCIETY OF JAPAN VOL. 43 1556—1560 (1970)

Ribonuclease T_1 Peptides. IV. Synthesis of a Protected Heptapeptide Corresponding to Sequence 17—23

Nobuo MITSUYASU, Michinori WAKI, Tetsuo KATO, Satoru MAKISUMI and Nobuo IZUMIYA

Laboratory of Biochemistry, Faculty of Science, Kyushu University, Hakozaki, Fukuoka

(Received December 8, 1969)

A protected heptapeptide corresponding to sequence 17—23 of ribonuclease T_1, namely benzyloxycarbonyl-L-seryl-L-threonyl-L-alanyl-L-glutaminyl-L-alanyl-L-alanyl-glycine ethyl ester (XIV), was synthesized by two routes. One consisted of the coupling of benzyloxycarbonyl-seryl-threonine azide with a pentapeptide ester, alanyl-glutaminyl-alanyl-alanyl-glycine ethyl ester. The other consisted of the coupling of benzyloxycarbonyl-seryl-threonyl-alanine azide with a tetrapeptide ester, glutaminyl-alanyl-alanyl-glycine ethyl ester. These four peptide segments were built up by the method of stepwise synthesis. Optical rotations, melting points and chromatographic behavior of XIV prepared by these two routes were found to be identical. Stereochemical homogeneity of the protected heptapeptide ester XIV was established by the digestion of the deblocked heptapeptide ester with leucine aminopeptidase.

Syntheses of the protected *N*-terminal undecapeptide (1—11) of ribonuclease T_1 containing asparagine residue in the 3rd position,[1] the protected pentapeptide (12—16)[2] and the heptapeptide (24—30)[3] were previously reported. In the present paper, we will describe the synthesis of the protected heptapeptide corresponding to the sequence 17—23, that is Z-Ser-Thr-Ala-Gln-Ala-Ala-Gly-OEt (XIV).[4] This heptapeptide sequence contains several functional groups, two hydroxys of serine and threonine and an acid amide of glutamine, in a rather short peptide, so the preparation of this compound seems to be interesting as an object of organic synthesis of a peptide.

The sequence of reaction for the synthesis of the desired compound XIV is shown in Fig. 1. The syntheses of the two C-terminal peptide segments, H-Gln-Ala-Ala-Gly-OEt·HCl (VI) and H-Ala-Gln-Ala-Ala-Gly-OEt·HCl (VIII), were achieved follows. Z-Ala-Ala-Gly-OEt (III) was prepared by coupling of H-Ala-Gly-OEt[5] with benzyloxycarbonyl-alanine *p*-nitrophenyl ester or a mixed

1) M. Ohno, T. Kato, N. Mitsuyasu, M. Waki, S. Makisumi and N. Izumiya, This Bulletin, **40**, 204 (1967).

2) M. Waki, N. Mitsuyasu, T. Kato, S. Makisumi and N. Izumiya, *ibid.*, **41**, 669 (1968).

3) T. Kato, N. Mitsuyasu, M. Waki, S. Makisumi and N. Izumiya, *ibid.*, **41**, 2480 (1968).

4) The following abbreviations are used; Z-, benzyloxycarbonyl; -OEt, ethyl ester; -ONp, *p*-nitrophenyl ester; -OBzl, benzyl ester; $-N_2H_3$, hydrazide; $-N_3$, azide; MA, mixed anhydride method; DMF, dimethylformamide; DMSO, dimethyl sulfoxide. Amino acid symbols donote the L-configuration.

5) W. Grassmann and E. Wünsch, *Chem. Ber.*, **91**, 449 (1958).

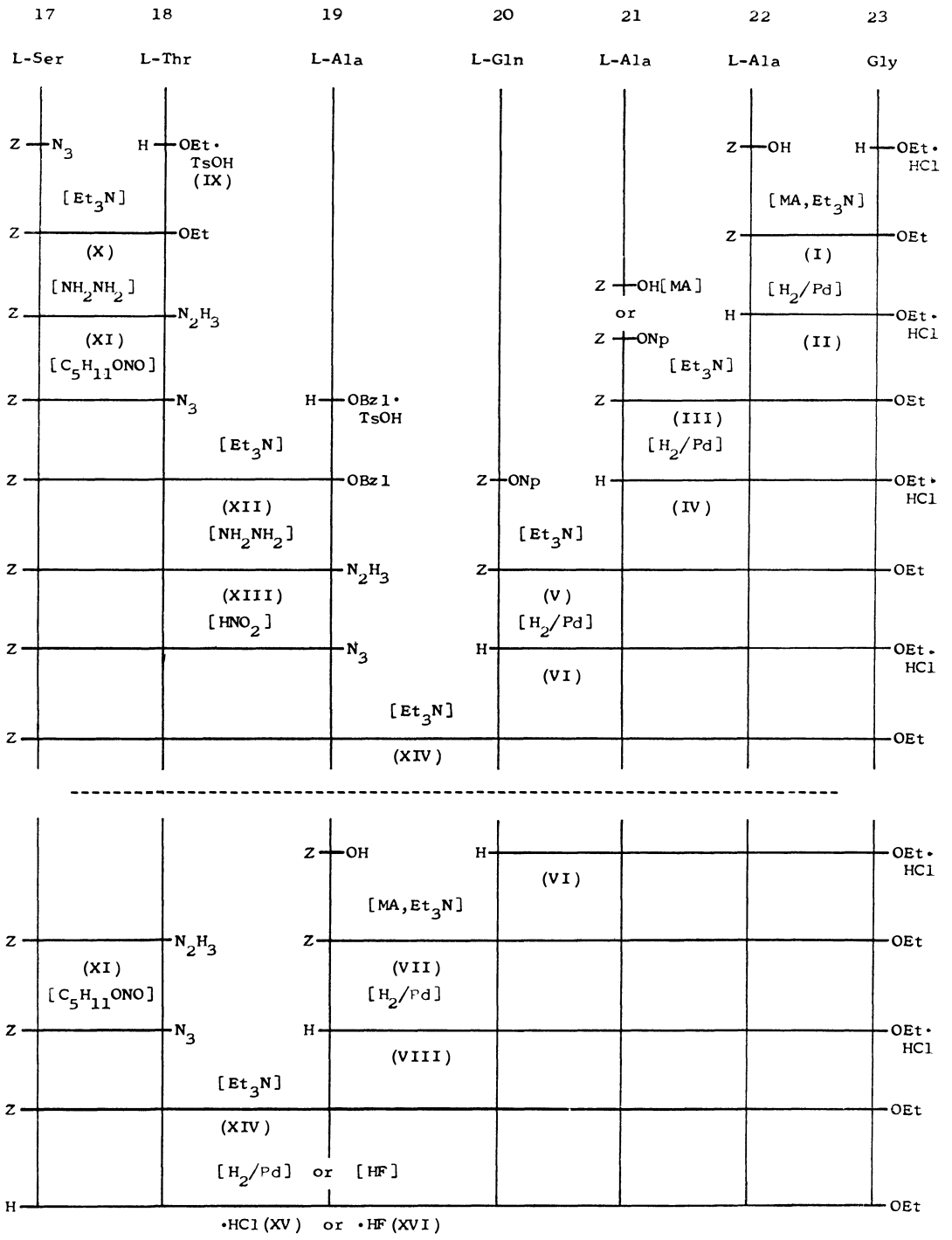

Fig. 1. Schematic diagram of synthesis of the heptapeptide ester.

anhydride[6] of benzyloxycarbonyl-alanine. The compound III was catalytically hydrogenated to yield the tripeptide ester hydrochloride (IV), which was then coupled with benzyloxycarbonyl-glutamine *p*-nitrophenyl ester. The protected tetrapeptide (V) obtained was suspended in methanol containing an equivalent hydrogen chloride and then hydrogenated to afford the tetrapeptide ester hydrochloride (VI) in a good yield. Z–Ala–Gln–

6) J. R. Vaughan, Jr. and R. L. Osato, *J. Amer. Chem. Soc.*, **73**, 5553 (1951).

Ala–Ala–Gly–OEt (VII) was prepared by coupling of benzyloxycarbonyl-alanine with VI by the mixed anhydride method in DMF because of poor solubility of VII. Compound VII thus obtained was hydrogenated as described for the preparation of VI to give the pentapeptide ester hydrochloride (VIII).

Synthesis of Z–Ser–Thr–N_2H_3 (XI) was reported previously.[7] Another *N*-terminal peptide segment, Z–Ser–Thr–Ala–N_2H_3 (XIII) was prepared as follows. The azide derived from the corresponding hydrazide XI was coupled with alanine benzyl ester to afford the acyl tripeptide ester, Z–Ser–Thr–Ala–OBzl (XII). The product obtained was converted to the hydrazide (XIII) by treatment with 2 equivalent of hydrazine.

For the synthesis of the desired protected heptapeptide ester, Z–Ser–Thr–Ala–Gln–Ala–Ala–Gly–OEt (XIV), two routes were developed (Fig. 1). The acyldipeptide azide derived from XI using isoamyl nitrite[8] was allowed to react with the pentapeptide ester (VIII) in DMF to give the desired protected heptapeptide ester (XIV) as a crystalline product. Compound XIV was obtained by condensation of the acyltripeptide azide derived from XIII with the tetrapeptide ester (VI) in a solvent of DMF. The optical rotation, melting point and chromatographic behavior of XIV prepared by these two routes were found to be identical.

For decarbobenzoxylation of the protected heptapeptide ester XIV, an attempt was made to perform catalytic hydrogenation of XIV in the presence of an equivalent of hydrogen chloride in methanol or DMF, but pure heptapeptide ester could not be obtained because of the insoluble character of XIV in an ordinary solvent. When XIV was subjected to hydrogenolysis in the presence of an equivalent of ethanolic hydrogen chloride in hexamethyl phosphoramide,[9] pure crystalline heptapeptide ester hydrochloride (XV) could be obtained. Thus, it was found that hexamethyl phosphoramide was a useful solvent for the hydrogenation of a sparingly soluble compound. The decarbobenzoxylation of XIV was performed by treatment of anhydrous hydrogen fluoride,[10] and pure crystalline heptapeptide ester hydrofluoride (XVI) was isolated. Homogeneity of the peptides, XV and XVI, was ascertained by thin-layer chromatography and by amino acid analysis on the acid hydrolysates of XV and XVI. Stereospecific homogeneity of the peptide XV was ascertained by digestion with leucine aminopeptidase.

Experimental

Melting points were uncorrected. Most of the optical rotations were measured on a Yanagimoto Photometric Polarimeter, OR-20 type, and some on a JASCO Model DIP–SL. Prior to analysis, samples were dried over phosphorus pentoxide at 60°C and 2 mmHg to a constant weight. Paper chromatography was carried out on Toyo Roshi No. 52 chromatography paper with the following solvent systems; R_f^1, *n*-butanol–acetic acid–pyridine–water, 4: 1: 1: 2 v/v. Thin-layer chromatography was carried out on Merck silica gel G with the following solvent systems; R_f^1, *n*-butanol–acetic acid–pyridine–water, 4: 1: 1: 2 v/v; R_f^2, *s*-butanol–formic acid–water, 75: 15: 10 v/v; R_f^3, chloroform–methanol, 5: 1 v/v; R_f^4, *n*-butanol–acetic acid–water, 4: 1: 2 v/v. Spots of materials possessing a free amino group on chromatograms were detected by spraying ninhydrin, and those of the amino group-blocked materials, by spraying 47% hydrobromic acid and then ninhydrin.

Z-Ala-Ala-Gly-OEt (III). (*a*) *Mixed Acid Anhydride Method.*[6] To a chilled solution of benzyloxycarbonyl-alanine (4.68 g, 21 mmol) and triethylamine (2.94 m*l*, 21 mmol) in tetrahydrofuran (40 m*l*), isobutyl chloroformate (2.75 m*l*, 21 mmol) was added. After 15 min, a chilled mixture of H–Ala–Gly–OEt·HCl[5] (II) (4.42 g, 21 mmol), triethylamine (2.94 m*l*, 21 mmol) and chloroform (40 m*l*) was added to the solution. The reaction mixture was stirred for one hour at 0°C, allowed to stand overnight at room temperature, and then evaporated to dryness *in vacuo*. The residual oil was extracted with ethyl acetate, and the solution was washed successively with a 3% sodium bicarbonate solution, 0.5 M citric acid and water, and dried over sodium sulfate. The filtered solution was concentrated *in vacuo* and the residual oil was crystallized after addition of ether and petroleum ether (5.0 g). It was recrystallized from ethanol–ether. Yield, 4.42 g (55%); mp 174—177°C; R_f^1 0.85; $[\alpha]_D^{15}$ −5.6° (*c* 2, DMF).

Found: C, 57.08; H, 6.43; N, 11.17%. Calcd for $C_{18}H_{25}O_6N_3$: C, 56.98; H, 6.64; N, 11.08%.

(*b*) *Active Ester Method.*[11] To a solution of II (0.84 g, 4 mmol) in a mixture of triethylamine (0.62 m*l*, 4 mmol) and DMF (5 m*l*), a solution of benzyloxycarbonyl-alanine *p*-nitrophenyl ester (1.38 g, 4 mmol) in DMF (5 m*l*) was added. The reaction mixture was allowed to stand overnight at room temperature, evaporated *in vacuo* and then extracted with ethyl acetate. The solution was treated by the same procedure as described above. Yield, 1.00 g (66%); mp 176—177°C; R_f^1 0.87; $[\alpha]_D^{15}$ −5.2° (*c* 2, DMF).

H-Ala-Ala-Gly-OEt·HCl (IV). A solution of III (2.66 g, 7 mmol) in a mixture of 0.52 N ethanolic hydrogen chloride (14.8 m*l*, 7.7 mmol) and ethanol (80 m*l*) was hydrogenated in the presence of palladium black. After 5 hr the filtrate from the catalyst was evaporated *in vacuo* and the residual oil was crystallized after addition

7) N. Mitsuyasu, M. Waki, S. Makisumi and N. Izumiya, *Memoirs of the Faculty of Science, Kyushu University, Ser. C. Chemistry*, **6**, 145 (1969).

8) J. Honzl and J. Rudinger, *Collect. Czech. Chem. Commun.*, **26**, 2333 (1961); E. Wünsch and A. Zwick, *Chem. Ber.*, **99**, 101 (1966).

9) U.S. 2487859 (1949), Eastman Kodak Co.; a product of Japan Oil Seal Industries Co. was used.

10) S. Sakakibara, Y. Shimonishi, M. Okada and Y. Kishida, "Peptides," Proc. 8th European Peptide Symp., ed. by H. C. Beyermann *et al.*, North Holland Publishing Co., Amsterdam (1967), p. 44; S. Sakakibara, Y. Shimonishi, Y. Kishida, M. Okada and H. Sugihara, This Bulletin, **40**, 2164 (1967).

11) M. Bodanszky, *Nature*, **175**, 685 (1955).

of ethyl acetate and ether. Yield, 1.88 g (95%); mp 187—188°C; R_f^1 0.57; R_f^I 0.70; $[\alpha]_D^{20}$ −2.8° (*c* 1, DMF).

Found: C, 42.58; H, 7.13; N, 14.60%. Calcd for $C_{10}H_{19}O_4N_3 \cdot HCl$: C, 42.63; H, 7.16; N, 14.91%.

Z-Gln-Ala-Ala-Gly-OEt (V). To a solution of IV (3.10 g, 11 mmol) in a mixture of triethylamine (1.68 m*l*, 12 mmol) and DMF (15 m*l*), was added a solution of benzyloxycarbonyl-glutamine *p*-nitrophenyl ester (4.42 g, 11 mmol) in DMF (5 m*l*). After it had been stood overnight at room temperature, the reaction mixture was diluted with 200 m*l* of water. The crystalline product deposited was collected by filtration and washed successively with a 3% sodium bicarbonate solution, 0.5 M citric acid and water (4.12 g). It was recrystallized from DMF-ethanol-ether. Yield, 4.04 g (73%); mp 223—225°C; R_f^1 0.75; $[\alpha]_D^{15}$ −18.0° (*c* 1, DMSO).

Found: C, 54.66; H, 6.64; N, 13.71%. Calcd for $C_{23}H_{33}O_8N_5$: C, 54.43; H, 6.55; N, 13.80%.

H-Gln-Ala-Ala-Gly-OEt·HCl (VI). A suspension of V (2.54 g, 5 mmol) in a mixture of methanol (75 m*l*) and 0.48 N methanolic hydrogen chloride (11.7 m*l*, 5.5 mmol) was hydrogenated in the presence of palladium black. After 7 hr the filtrate from the catalyst was concentrated *in vacuo* and the residual oil was crystallized after addition of ether. Yield, 1.82 g (89%); mp 176—179°C; R_f^1 0.56; R_f^I 0.58; $[\alpha]_D^{15}$ −6.3° (*c* 0.24, DMF).

Found: C, 43.44; H, 6.92; N, 16.62%. Calcd for $C_{15}H_{27}O_6N_5 \cdot HCl \cdot 1/2H_2O$: C, 43.01; H, 6.98; N, 16.72%.

Z-Ala-Gln-Ala-Ala-Gly-OEt (VII). To a chilled solution of benzyloxycarbonyl-alanine (0.89 g, 4 mmol) and triethylamine (0.56 m*l*) in tetrahydrofuran (5 m*l*), isobutyl chloroformate (0.52 m*l*, 4 mmol) was added. After 15 min, a precooled solution of VI (1.64 g, 4 mmol) in a mixture of triethylamine (0.56 m*l*) and DMF (25 m*l*) was added to the above solution. The reaction mixture was stirred for one hour at 0°C, allowed to stand overnight at room temperature and then concentrated *in vacuo*. Water (100 m*l*) was added to the residual oil and the crystalline product deposited was collected by filtration and washed as described for V (1.58 g). It was recrystallized from DMF-methanol-ether. Yield, 1.47 g (62%); mp 254—255°C; R_f^1 0.78; R_f^2 0.68; $[\alpha]_D^{15}$ −20.0° (*c* 1, DMSO).

Found: C, 53.38: H, 6.85; N, 14.50%. Calcd for $C_{26}H_{38}O_9N_6 \cdot 1/2H_2O$: C, 53.14; H, 6.69; N, 14.30%.

H-Ala-Gln-Ala-Ala-Gly-OEt·HCl (VIII). A suspension of VII (0.29 g, 0.5 mmol) in a mixture of DMF (10 m*l*) and 0.48 N methanolic hydrogen chloride (1.14 m*l*, 0.55 mmol) was hydrogenated in the presence of palladium black. After 6 hr the filtrate from the catalyst was evaporated *in vacuo* and the residual oil was crystallized after the addition of ethanol and ether. Yield, 0.23 g (97%); mp 206—208°C; R_f^1 0.52; $[\alpha]_D^{15}$ −17.0° (*c* 1, DMSO).

Found: C, 43.46; H, 7.16; N, 16.80%. Calcd for $C_{18}H_{32}O_7N_6 \cdot HCl \cdot H_2O$: C, 43.33; H, 7.07; N, 16.84%.

Z-Ser-Thr-Ala-OBzl (XII). To a chilled (−5°C) solution of Z-Ser-Thr-N_2H_3[7] (XI) (6.74 g, 19 mmol) in a mixture of 2 N hydrochloric acid (35 m*l*) and DMF (15 m*l*), N sodium nitrite (20 m*l*) was added. After it had been stood for 10 min, the precipitated azide was extracted with ethyl acetate (200 m*l*), washed with a 3% sodium bicarbonate solution and water, and then dried over sodium sulfate at 0°C. To the filtrate from the desiccant was added a precooled mixture of alanine benzyl ester *p*-toluenesulfonate[12] (8.08 g, 23 mmol) and triethylamine (3.22 m*l*, 23 mmol) in ethyl acetate (60 m*l*). After the reaction mixture had been stirred for 2 days at 0°C, it was washed successively with a 3% sodium bicarbonate solution, 0.5 M citric acid and water, dried over sodium sulfate, and then evaporated *in vacuo*. The residual oil was crystallized by the addition of ether and petroleum ether and the crystals were collected by filtration (5.11 g). It was recrystallized from ethanol-ether-petroleum ether. Yield, 4.82 g (51%); mp 149—150°C; R_f^1 0.87; R_f^3 0.49; R_f^4 0.95, $[\alpha]_D^{15}$ −7.0° (*c* 1, DMF).

Found: C, 59.47; H, 6.31; N, 8.28%. Calcd for $C_{25}H_{31}O_8N_3$: C, 59.84; H, 6.23; N, 8.38%.

Z-Ser-Thr-Ala-N_2H_3 (XIII). A solution of XII (2.50 g, 5 mmol) and hydrazine hydrate (0.485 m*l*, 10 mmol) in DMF (20 m*l*) was allowed to stand overnight at room temperature, and the reaction mixture was evaporated *in vacuo*. The residual oil was solidified by the addition of ether, and the crystals were collected by filtration (2.12 g). It was recrystallized from hot water. Yield, 1.17 g (60%); mp 212—214°C; R_f^1 0.77; R_f^3 0.36; R_f^4 0.77; $[\alpha]_D^{15}$ −9.5° (*c* 1, DMSO).

Found: C, 49.88; H, 6.48; N, 16.29%. Calcd for $C_{18}H_{27}O_7N_5 \cdot 1/2H_2O$: C, 49.76; H, 6.50; N, 16.12%.

Z-Ser-Thr-Ala-Gln-Ala-Ala-Gly-OEt (XIV). (*a*) *Condensation of Z-Ser-Thr-N_3 and H-Ala-Gln-Ala-Ala-Gly-OEt·HCl. (VIII).* To a chilled (−5°C) solution of XI (142 mg, 0.4 mmol) in a mixture of DMF (4 m*l*) and 0.45 N hydrogen chloride-tetrahydrofuran (1.79 m*l*) was added isoamyl nitrite[8] (0.054 m*l*, 0.4 mmol). After 10 min, triethylamine (0.112 m*l*, 0.8 mmol) was added. To the solution was added a precooled mixture of VIII (192 mg, 0.4 mmol), triethylamine (0.056 m*l*, 0.4 mmol) and DMF (10 m*l*). The reaction mixture was then stirred for 2 days at 0°C and then evaporated *in vacuo*. The residual oil was crystallized by the addition of water. The crystals were collected by filtration and washed as described for V (153 mg). It was recrystallized from DMSO-ethanol-ether. Yield, 138 mg (45%); mp 251—253°C; R_f^1 0.82; R_f^2 0.79; R_f^3 0.65; $[\alpha]_D^{20}$ −15.8° (*c* 1, DMSO).

Found: C, 50.46; H, 6.69; N, 14.15%. Calcd for $C_{33}H_{50}O_{13}N_8 \cdot H_2O$: C, 50.25; H, 6.55; N, 14.21%.

(*b*) *Condensation of Z-Ser-Thr-Ala-N_3 and H-Gln-Ala-Ala-Gly-OEt (VI).* To a chilled solution of XIII (213 mg, 0.5 mmol) in a mixture of acetic acid (0.5 m*l*), water (2 m*l*) and N hydrochloric acid (0.6 m*l*) was added N sodium nitrite (0.6 m*l*). After 10 min, the reaction mixture was diluted with water (20 m*l*). The precipitated azide was collected by filtration, washed with a 3% sodium bicarbonate solution and water, and then dried *in vacuo* at 0°C. To a chilled solution of VI (205 mg, 0.5 mmol) dissolved in a mixture of DMF (10 m*l*) and triethylamine (0.07 m*l*, 0.5 mmol) was added the azide prepared before. The solution was stirred for 2 days at 0°C and then diluted with water (30 m*l*). The precipitate was collected by filtration and washed as described for V (211 mg). It was recrystallized from DMSO-ethanol-ether. Yield, 196 mg (51%); mp 251—252°C; R_f^1 0.83; $[\alpha]_D^{20}$ −15.6° (*c* 1, DMSO).

Found: C, 50.34; H, 6.63; N, 14.11%. Calcd for $C_{33}H_{50}O_{13}N_8 \cdot H_2O$: C, 50.25; H, 6.65; N, 14.21%.

12) S. Makisumi and N. Izumiya, *Nippon Kagaku Zasshi*, **78**, 662 (1957).

H-Ser-Thr-Ala-Gln-Ala-Ala-Gly-OEt·HCl (XV). A solution of XIV (39 mg, 50 μmol) dissolved in hexamethyl phosphoramide[9] (6 ml) containing 3.4 N ethanolic hydrogen chloride (0.018 ml, 60 μmol) was hydrogenated in the presence of palladium black. After 24 hr, the solution was diluted with petroleum ether (50 ml) and an oil was precipitated. In order to remove hexamethyl phosphoramide completely, the resulting oil was washed twice with petroleum ether by decantation and then triturated with ethanol and ether to afford powder (32 mg). It was recrystallized from DMSO-ethanol-ether. Yield, 28 mg (83%); mp 220—225°C (decomp.); R_f^1 0.55; amino acid ratios in acid hydrolysate,[13] Thr 0.90, Ser 0.86, Glu 1.00, Gly 1.00, Ala, 3.33.

In order to establish the stereochemical homogeneity of XV, a small amount of XV was digested by leucine aminopeptidase following essentially the same procedure as that of Hofmann and Yajima;[14] amino acid ratios[13] in the digest, Thr+Gln 1.78, Ser 1.11, Gly 0.80, Ala 3.31.

H-Ser-Thr-Ala-Gln-Ala-Ala-Gly-OEt·HF (XVI). Compound XIV (39 mg, 50 μmol) was placed in a vessel together with a drop of anisole.[10] HF (1 ml) was added into the vessel using an HF-reaction apparatus,[10] and the mixture was allowed to react at 0°C for 1 hr with stirring. Excess HF was removed under reduced pressure at 0°C, and the residue was kept at reduced pressure (3 mmHg) for 5 hr at room temperature over calcium chloride and sodium hydroxide. The oily residue was washed with ethanol by decantation and then dissolved in DMSO. After the insoluble material in small amount was filtered off, the filtrate was evaporated *in vacuo*. The residual oil was crystallized with the addition of ethanol and the crystals were collected by filtration. Yield, 29 mg (92%); mp 235—240°C (decomp.); R_f^1 0.50; amino acid ratios in acid hydrolysate,[13] Thr 0.93, Ser 0.93, Glu 0.99, Gly 1.00, Ala 3.21.

13) We are indebted to Mr. K. Noda in this laboratory for the amino acid analysis.

14) K. Hofmann and H. Yajima, *J. Amer. Chem. Soc.*, **83**, 2289 (1961).

BULLETIN OF THE CHEMICAL SOCIETY OF JAPAN VOL. 43 1560—1563 (1970)

The Total Synthesis of (±)-Isoelliptone*1

Teruo HARANO

Department of Chemistry, Faculty of Science, Hiroshima University, Higashisenda-machi, Hiroshima

(Received December 10, 1969)

The condensation of 2′-hydroxy-4′,5′-dimethoxyfurano[3″,2″ : 6,7]isoflavone with ethyl bromoacetate in the presence of potassium carbonate gave the 2′-phenoxyacetate derivative. The subsequent treatment of this compound with dilute alkali gave isoelliptic acid. By the ring closure of the acid with acetic anhydride and anhydrous sodium acetate, or by the treatment of its ester with sodium methoxide, dehydroisoelliptone was obtained. The reduction of this compound with sodium borohydride, followed by Oppenauer oxidation, yielded isoelliptone, *via* a reduced compound, isoelliptol.

Isoelliptone[1] (erosone)[2] has been isolated, along with some rotenoids (*e.g.*, rotenone and pachyrrhizone), from yam beans (*Pachyrrhizus erosus*). Its chemical structure was shown to be an isomer of elliptone (I)[3] by Norton and Hansberry,[2] and has lately been identified as II on the basis of spectral studies by Ollis *et al.*[1,4] Derrisic acid derivatives are important intermediates in synthesizing some rotenoids (*e.g.*, munduserone,[5] rotenone,[6] deguelin[7] and elliptone[8]). These acids have been prepared from the corresponding phenols and ethyl (2-cyanomethyl-4,5-dimethoxyphenyl)acetate (III) by the Hoesch reaction. The preparation of the acetate III was, however, troublesome and did not give satisfactory results. Recntly, the present author has been reported a convenient method of synthesizing derrisic acid derivatives from the corresponding

*1 A part of this work had been preliminary communicated: *Experientia*, **25**, 789 (1969); presented at the Ube Local Meeting (June, 1969) of the Chemical Society of Japan.

1) W. D. Ollis, "Symposium on Phytochemistry," ed. by H. R. Arthur, Hong Kong Univ. Press, Hong Kong (1964), p. 128.

2) L. B. Norton and R. Hansberry, *J. Amer. Chem. Soc.*, **67**, 1909 (1945).

3) S. H. Harper, *J. Chem. Soc.*, **1939**, 1099, 1424; **1942**, 587, 593.

4) R. I. Reed and J. M. Wilson, *ibid.*, **1963**, 5949.

5) J. R. Herbert, W. D. Ollis and R. C. Russell, *Proc. Chem. Soc.*, **1960**, 176.

6) M. Miyano, A. Kobayashi and M. Matsui, *Bull. Agr. Chem. Soc. Jap.*, **24**, 540 (1960); **25**, 673 (1961).

7) H. Fukami, J. Oda, G. Sakata and M. Nakajima, *ibid.*, **24**, 327 (1960); **25**, 252 (1961).

8) H. Fukami, G. Sakata and M. Nakajima, *Agr. Biol. Chem.*, **29**, 82 (1965).

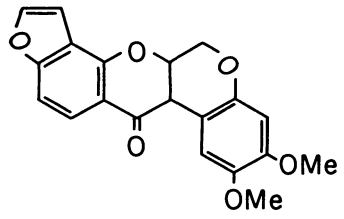

I

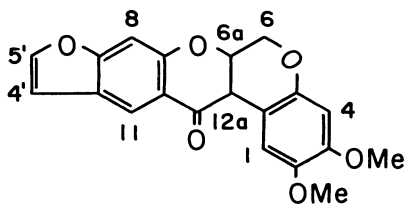

II

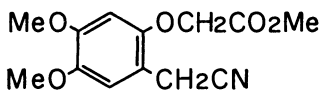

III

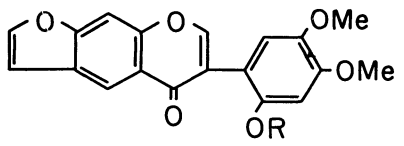

IV R=H
V R=CH_2CO_2Et

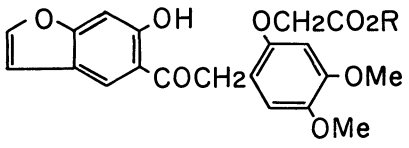

VI R=H
VII R=Me

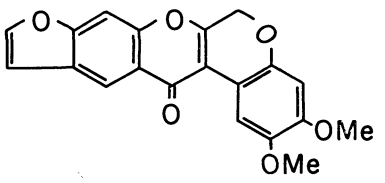

VIII

2′-hydroxyisoflavone derivatives.[9,10] The present paper will describe the total syntehsis of (±)-II from 2′-hydroxy-4′,5′-dimethoxyfurano[3″,2″ : 6,7]-isoflavone (IV),[11,12] *via* isoelliptic acid (VI) or its methyl ester (VII).

The reaction of the 2′-hydroxyisoflavone (IV) with ethyl bromoacetate in the presence of anhydrous potassium carbonate in acetone gave a 2′-phenoxyacetate (V), mp 180—181°C, in a good yield. The treatment of V with alcoholic potassium hydroxide afforded an acid (VI), mp 216—217°C, which yielded its methyl ester (VII), mp 134—135°C, when treated with diazomethane in dioxane. The NMR spectrum*[2] of VII indicates the presence of a phenolic group at δ 12.36 ; this group is located at the position *ortho* to the carbonyl group and forms an intramolecular hydrogen bonding. Further, the signals of two methylene groups appear at δ 4.40 and 4.60 (Fig. 1). On the basis of these facts, the structure of VII was identified as 5-ω-(2-methoxycarbonylmethoxy - 4,5 - dimethoxyphenyl)acetyl - 6-hydroxycoumarone. The cyclization of the VI acid with acetic anhydride containing sodium acetate and a trace of acetic acid[13] gave dehydroisoelliptone (VIII), mp 266—268°C, in a poor yield (*ca.* 20%). The treatment of VII with sodium methoxide[14] was, however, found to be a suitable way to prepare it (yield: *ca.* 80%). The NMR spectrum of VIII exhibits the signals of olefinic protons at δ 6.95(1H, q, J=2.0 and 1.0 Hz, $C_{4'}$–H) and 7.77 (1H, d, J= 2.0 Hz, $C_{5'}$–H) due to a disubstituted furan ring. In addition, the signals of methoxyl, methylene, and aromatic protons are observed at δ 3.90_s, 4.00_s (each 3H, $OC\underline{H}_3$); 5.07_s (2H, $-C\underline{H}_2O-$); 6.59_s (1H, C_4–H), 7.59_s (1H, C_8–H), and 8.52_s and 8.59_s (each 1H, C_1– and C_{11}–H). According to the method of Miyano and Matsui,[15] VIII was reduced

9) K. Fukui, M. Nakayama and T. Harano, *Experientia*, **23**, 613 (1967).

10) T. Harano, *J. Sci. Hiroshima Univ., Ser. A-II*, **33**, 63 (1969).

11) V. Chandrashkar, M. Krishnamurti and T. R. Seshadri, *Tetrahedron*, **23**, 2505 (1967).

12) K. Fukui, M. Nakayama and T. Harano, This Bulletin, **42**, 199 (1969).

*[2] The NMR spectra were measured with a Hitachi R-20 spectrometer, using tetramethylsilane as the internal standard (δ-values in $CDCl_3$); s, singlet; d, doublet; t, triplet; q, quartet.

13) S. Takei, S. Miyajima and M. Ono, *Ber.*, **65**, 1041 (1932).

14) N. Nakatani and M. Matsui, *Agr. Biol. Chem.*, **32**, 769 (1968).

15) M. Miyano and M. Matsui, *Bull. Agr. Chem. Soc. Jap.*, **22**, 128 (1958); *Chem. Ber.*, **91**, 2044 (1959).

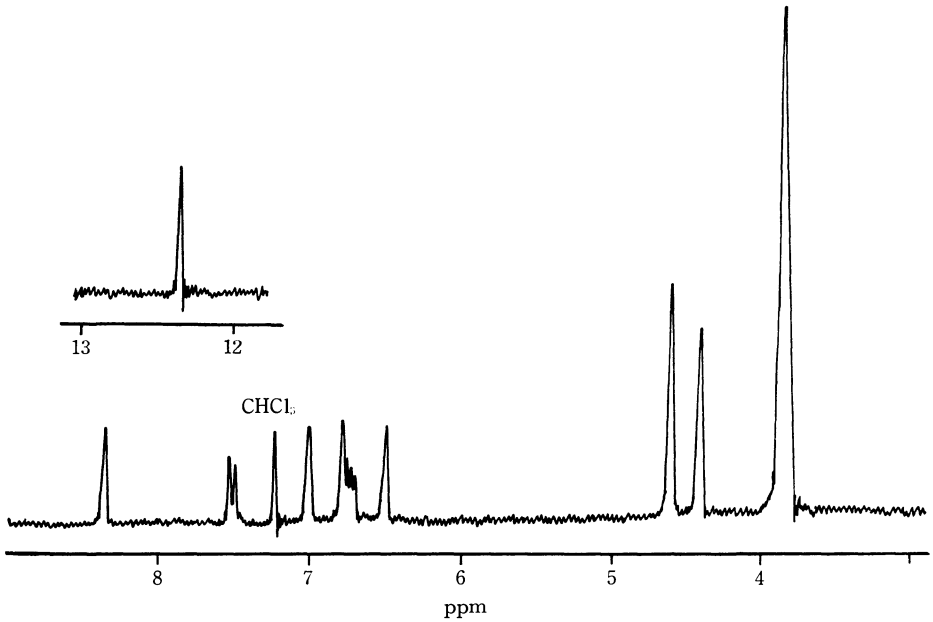

Fig. 1. The NMR spectrum of VII.

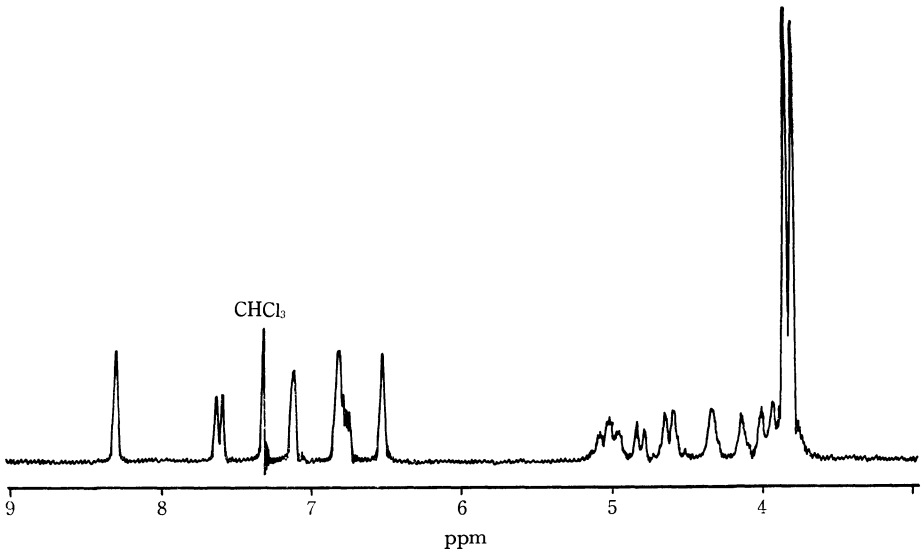

Fig. 2. The NMR spectrum of II.

with sodium borohydride in dioxane, subsequently, without any purification, Oppenauer oxidation gave (±)-isoelliptone (II), mp 215—216°C. The IR spectrum of II shows an absorption of the carbonyl at 1680 cm^{-1}. In the NMR spectrum of II, the signals due to the four protons in the positions 6, 6_a, and 12_a are observed at δ 3.9—5.2 as an ABCD system, and the signal of a proton in the position 1 shows an upper shift at δ 6.83 (Fig. 2).

These data are in accord with those reported by Ollis *et al.*[16] and by Crombie and Lown.[17] Furthermore, in the mass spectrum*3 of II the parent ion peak (M^+) appears at m/e=352 and the fragment ions are observed at 192, 191, 177, 161, 160, 149, 134, 131, 121, and 106. This mass spectrum is identical with that of natural isoelliptone, which has been previously reported by Reed and Wilson.[4]

16) W. D. Ollis, C. A. Rhodes and I. O. Sutherland, *Tetrahedron*, **23**, 4741 (1967).

17) L. Crombie and J. W. Lown, *J. Chem. Soc.*, **1962**, 775.

*3 The mass spectrum was measured by a Hitachi RMU-6E Mass Spectrometer.

Experimental*4

4′, 5′-Dimethoxy-2′-ethoxycarbonylmethoxyfurano[3″,2″: 6,7]isoflavone (V). A mixture of 4′,5′-dimethoxy-2′-hydroxyfurano[3″,2″:6,7]isoflavone (IV) (1.1 g), ethyl bromoacetate (700 mg), and anhydrous potassium carbonate (4.0 g) in acetone (80 m*l*) was refluxed for 24 hr. After the inorganic precipitates had been filtered off, the solvent was condensed to 10 m*l* and the residual solution was diluted with water. The separated solid was collected, washed with water, and then crystallized from ethanol to give V as colorless needless; mp 180—181°C; yield, 1.1 g. IR: 1725, 1653 cm^{-1} (C=O); UV: λ_{max}^{EtOH} mμ (log ε): 237 (4.54) 297 (4.10).

Found: C, 65.02; H, 4.70%. Calcd for $C_{23}H_{20}O_8$: C, 65.09; H, 4.75%.

Isoelliptic Acid (5-ω-(2-Carboxymethoxy-4,5-dimethoxyphenyl)acetyl-6-hydroxycoumarone) (VI). A mixture of V (1.0 g) and a 10% potassium hydroxide solution (40 m*l*) in ethanol (100 m*l*) was refluxed on an oil bath for 2 hr. The solvent was then removed as much as possible and acidified with 10% hydrochloric acid. After the separated solid had been extracted with ethyl acetate, the extract was washed with water and dried on sodium sulfate. The solvent was removed and the residual solid was crystallized from ethanol to give VI as yellow prisms; mp 216—217°C; yield, 800 mg. This substance gave a green color with alcoholic ferric chloride. IR: 3250 (OH), 1730, 1640 cm^{-1} (C=O); UV: λ_{max}^{EtOH} mμ (log ε): 233 (4.56), 278 (4.02), 340 (3.81).

Found: C, 62.04; H, 4.83%. Calcd for $C_{20}H_{18}O_8$: C, 62.17; H, 4.70%.

Methyl Ester (VII) of VI. To a solution of VI (1.0 g) in refreshed dioxane (100 m*l*), the ethereal diazomethane was added; the mixture was then allowed to stand overnight. The solvent was removed under reduced pressure to dryness, and the residue was crystallized from ethanol to give VII as light yellow needles; mp 134—135°C; yield, 950 mg. This substance gave a green color with alcoholic ferric chloride. IR: 1760, 1640 cm^{-1} (C=O); UV: λ_{max}^{EtOH} mμ (log ε): 236 (4.52), 264_i*5 (3.83), 281 (4.03), 334 (3.83). NMR: 383_s (9H), 6.51_s, 6.80_s, 7.01_s, 8.37_s (each 1 H), 6.75_q (1 H, J=2.0 and 1.0 Hz), 7.52_d (1 H, J=2.0 Hz).

Found: C, 62.96; H, 5.20%. Calcd for $C_{21}H_{20}O_8$: C, 62.99; H, 5.04%.

Dehydroisoelliptone (VIII). *a) With Acetic Anhydride-Anhydrous Sodium Acetate.* A mixture of VI (700 mg), acetic anhydride (15 m*l*), anhydrous sodium acetate (450 mg), and acetic acid (0.7 m*l*) was warmed at 120°C for 20 min. After the reaction mixture had been cooled, it was poured into ice water. The separated solid was then collected, washed with water, a large amount of a saturated sodium bicarbonate solution, and water again, and then dried under reduced pressure. The solid was chromatographed on silica gel (*ca.* 10 g) in dichloromethane and crystallized from dichloromethane-ethanol (1: 1 v/v) to give VIII as light yellow microneedles; mp 266—268°C; yield, 200 mg. IR: 1633 cm^{-1} (C=O); UV: λ_{max}^{EtOH} mμ (log ε): 237.5 (4.51), 273 (4.39), 307 (4.30).

Found: C, 68.40; H, 4.09%. Calcd for $C_{20}H_{14}O_6$: C, 68.57; H, 4.03%.

b) With Sodium Methoxide. To a refluxing solution of VII (0.9 g) in anhydrous methanol (90 m*l*), a sodium methoxide solution (prepared from 50 mg of Na and 5 m*l* of anhydrous methanol) was added dropwise for 30 min period. The mixture was refluxed for 3 hr and then allowed to stand overnight. The crystals which had been deposited were dissolved in dichloromethane, passed through a short column of silica gel (*ca.* 10 g), and crystallized from dichloromethane-ethanol (1: 1 v/v) to give VIII as light yellow needles; mp 265—267°C; yield, 750 mg. This compound was identical in all respects with the sample described above a).

Isoelliptone (II). A solution of sodium borohydride (100 mg) in absolute ethanol (10 m*l*) was added to a solution of VIII (200 mg) in dioxane (10 m*l*). The mixture was warmed at 50—60°C for 30 min and then allowed to stand overnight at room temperature. Acetone (20 m*l*) was added to the reaction mixture to decompose the excess reducing agent, and the solvent was removed under reduced pressure to dryness. The residual solid was dissolved in chloroform, washed with water, and dried on calcium chloride. The evaporation of chloroform under reduced pressure furnished crude isoelliptol; without any purification, this product was employed in the next reaction. Aluminum isopropoxide (4.0 g) was added to a solution of the crude isoelliptol in absolute benzene (40 m*l*) and refreshed acetone (30 m*l*), after which the mixture was gently refluxed for 12 hr. The reaction mixture was cooled, diluted with benzene (200 m*l*), washed with diluted sulfuric acid and water, and then dried on calcium chloride. After the solvent had then been removed under reduced pressure to dryness, the solid was chromatographed on silica gel (*ca.* 5 g) in dichloromethane and then crystallized from dichloromethane-ethanol (1: 1 v/v) to give II as colorless needles; mp 215—216°C; yield, 90 mg. IR: 1680 cm^{-1} (C=O); UV: λ_{max}^{EtOH} mμ (log ε): 236 (4.59), 254.5 (4.09), 276 (4.01), 300_s*6 (3.80), 335 (3.55); $\lambda_{max}^{CHCl_3}$ mμ (log ε): 280 (4.03), 344 (3.55). NMR: 3.78_s, 3.82_s (each 3 H), 6.54_s, 6.83_s, 7.12_s, 8.30_s (each 1 H), 6.80_q (1 H, J=2.0 and 1.0 Hz), 7.61_d (1 H, J=2.0 Hz).

Found: C, 68.14; H, 4.73%. Calcd for $C_{20}H_{16}O_6$: C, 68.18; H, 4.58%.

The author wishes to express his deep thanks to Professor Kenji Fukui, Hiroshima University, for his encouragement throughout the course of this work.

*4 All the melting points are uncorrected. The infrared spectra were measured in nujol, while the ultraviolet spectra were measured in an ethanol and a chloroform solution.

*5 i=inflection.

*6 s=shoulder.

BULLETIN OF THE CHEMICAL SOCIETY OF JAPAN VOL. 43 1564—1567 (1970)

Synthetic Studies of Bacitracin. VI.[1] Synthesis of Unprotected Thiazoline Peptides

Yoshihiro HIROTSU, Tetsuo SHIBA*1 and Takeo KANEKO*1

Department of Chemistry, Faculty of Science, Osaka University, Toyonaka, Osaka

(Received December 11, 1969)

For a total synthesis of bacitracian A, a synthetic method to secure unprotected thiazoline peptides must be established. 2-Aminomethyl-R-Δ^2-thiazoline-4-carboxamide, 2-aminomethyl-R-Δ^2-thiazoline-4-carboxylic acid, 2-aminomethyl-R-Δ^2-thiazoline-4-carbonyl-L-leucine were synthesized by either the iminoether coupling method or by the dehydration method using *N*-benzyloxycarbonyl group and benzyl ester as protecting groups.

In the previous papers,[1,2] the syntheses of protected thiazoline peptides by either the iminoether coupling method, or by dehydration of cysteine peptide in nonaqueous medium were described. Saponification of methyl or ethyl ester of thiazoline peptide was accompanied by racemization of cysteine residue and cleavage of thiazoline ring,[2] while the thiazoline ring was stable in strong acidic condition.[3] In order to obtain the unprotected thiazoline peptide, therefore, use of *N*-benzyloxycarbonyl group and benzyl ester group, both being cleavable by hydrogen bromide in acetic acid, is required. Based on this principle, a synthetic method of the unprotected thiazoline peptide was established.

A thiazoline derivative of a dipeptide derived from L-cysteinamide was prepared as shown in Fig. 1. *N,N'*-Bisbenzyloxycarbonyl-L-cystine[4] was converted to *N,N'*-bisbenzyloxycarbonyl-L-cystinyl dichloride[5] by treatment with phosphorus pentachloride. The acid chloride was treated with ammonia to afford *N,N'*-bisbenzyloxycarbonyl-L-cystine diamide (I), which was then reduced to benzyloxycarbonyl-L-cysteinamide (II) with zinc dust and hydrochloric acid. Amide II was treated with 30% hydrogen bromide in acetic acid to give L-cysteinamide hydrobromide (III).

Coupling of III with benzyloxycarbonylaminoacetimino ethyl ether[2] gave 2-benzyloxycarbonylaminomethyl-R-Δ^2-thiazoline-4-carboxamide (IV), which was then treated with 30% hydrogen bromide in acetic acid to afford 2-aminomethyl-R-Δ^2-thiazoline-4-carboxamide (V). Product V was very hygroscopic solid and gave L-cystine by hydrolysis with hydrochloric acid followed by oxidation.

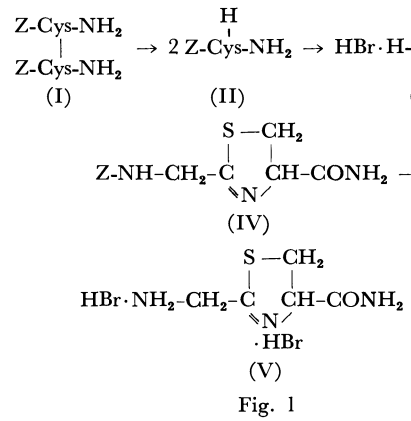

Fig. 1

$Z = C_6H_5CH_2OCO$

Cystine used is of L-configuration.

Unprotected thiazoline peptides were synthesized from di- or tripeptide involving cysteine residue by the dehydration method according to the scheme shown in Fig. 2. Coupling of benzyloxycarbonylglycine with dibenzyl L-cystinate dihydrochloride[6]

*1 This paper is dedicated to Emeritus Professor Munio Kotake in commemoration of his 75th birthday, November, 30, 1969.

1) Part V: Y. Hirotsu, T. Shiba and T. Kaneko, This Bulletin, **40**, 2950 (1967).

2) Y. Hirotsu, T. Shiba and T. Kaneko, *ibid.*, **40**, 2945 (1967).

3) H. T. Clark, J. R. Johnson and R. Robinson, "The Chemistry of Penicillin," Princeton Univ. Press. (1949), p. 470; J. C. Crawhall and D. F. Elliott, *J. Chem. Soc.*, **1952**, 3094; M. Calvin, "Glutathione," ed. by S. Colowick, Academic Press, New York, N. Y. (1954) p. 3; G. Preaux and R. Lontie, *Biochem. J.*, **66**, 26 p. (1957); O. Calvallini, B. Mondovi and C. de Marco, *Experientia*, **13**, 436 (1957); R. B. Martin and J. T. Edsall, *Bull. Soc. Chim. Biol.*, **40**, 1763 (1958); D. Garfinkel, *J. Amer. Chem. Soc.*, **80**, 4833 (1958); W. Stoffel, L. C. Craig, *ibid.*, **83**, 145 (1961); H. A. Smith and G. Gorin, *J. Org. Chem.*, **26**, 820 (1961).

4) M. Bergmann and L. Zervas, *Ber.*, **65**, 1192 (1932).

5) V. du Vigneaud and G. L. Miller, "Biochemical Preparations," Vol. 2, p. 76 (1952).

6) L. Zervas and I. Photaki, *J. Amer. Chem. Soc.*, **84**, 3887 (1962).

using *N,N'*-dicyclohexylcarbodiimide gave *N,N'*-bisbenzyloxycarbonylglycyl-L-cystine dibenzyl ester (IV), which was then converted to benzyloxycarbonylglycyl-L-cysteine benzyl ester (VII) by reduction with zinc dust and hydrochloric acid.

A ring closure of dipeptide VII through dehydration by hydrogen chloride in chloroform afforded benzyl 2-benzyloxycarbonylaminomethyl-R-Δ^2-thiazoline-4-carboxylate hydrochloride, from which the benzyloxycarbonyl thiazoline derivative (VIII) was obtained in crystalline state by removal of hydrogen chloride by treatment with an aqueous concentrated potassium carbonate solution.

Compound VIII was treated with 30% hydrogen bromide in acetic acid at 40°C for 3 hr to give a very hygroscopic solid of 2-aminomethyl-R-Δ^2-thiazoline-4-carboxylic acid dihydrobromide (IX).

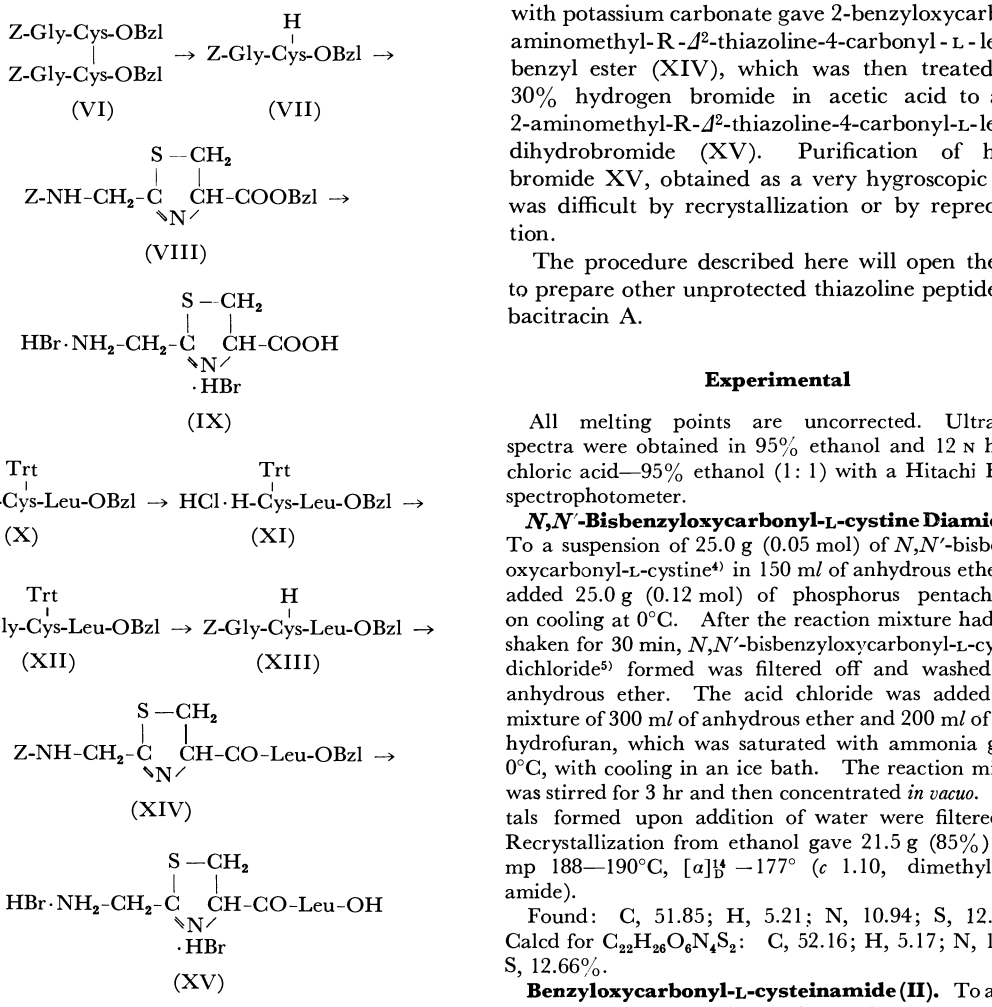

Fig. 2

Z=$C_6H_5CH_2OCO$
Bzl=$C_6H_5CH_2$
Trt=$(C_6H_5)_3C$
Cysteine and leucine used are of L-configuration.

A tripeptide containing the thiazoline ring was also prepared as follows. Condensation of *N,S*-ditrityl-L-cysteine diethylamine salt[7] with benzyl L-leucinate *p*-toluenesulfonate[8] by the carbodiimide method gave *N,S*-ditrityl-L-cysteinyl-L-leucine benzyl ester (X), which was then treated with hydrochloric acid in acetone to give benzyl *S*-trityl-L-cysteinyl-L-leucinate hydrochloride (XI). Coupling of XI with benzyloxycarbonylglycine by carbodiimide method gave benzyloxycarbonylglycyl-*S*-trityl-L-cysteinyl-L-leucine benzyl ester (XII). The *S*-trityl tripeptide XII was converted to the silver mercaptide by treatment with silver nitrate and pyridine. Removal of silver from the mercaptide by hydrochloric acid gave benzyloxycarbonylglycyl-L-cysteinyl-L-leucine benzyl ester (XIII). Compound XIII was cyclized to the thiazoline derivative by the action of hydrogen chloride in chloroform. Treatment of the product with potassium carbonate gave 2-benzyloxycarbonylaminomethyl-R-Δ^2-thiazoline-4-carbonyl-L-leucine benzyl ester (XIV), which was then treated with 30% hydrogen bromide in acetic acid to afford 2-aminomethyl-R-Δ^2-thiazoline-4-carbonyl-L-leucine dihydrobromide (XV). Purification of hydrobromide XV, obtained as a very hygroscopic solid, was difficult by recrystallization or by reprecipitation.

The procedure described here will open the way to prepare other unprotected thiazoline peptides like bacitracin A.

Experimental

All melting points are uncorrected. Ultraviolet spectra were obtained in 95% ethanol and 12 N hydrochloric acid—95% ethanol (1: 1) with a Hitachi EPS-3 spectrophotometer.

***N,N'*-Bisbenzyloxycarbonyl-L-cystine Diamide (I).** To a suspension of 25.0 g (0.05 mol) of *N,N'*-bisbenzyloxycarbonyl-L-cystine[4] in 150 m*l* of anhydrous ether was added 25.0 g (0.12 mol) of phosphorus pentachloride on cooling at 0°C. After the reaction mixture had been shaken for 30 min, *N,N'*-bisbenzyloxycarbonyl-L-cystinyl dichloride[5] formed was filtered off and washed with anhydrous ether. The acid chloride was added to a mixture of 300 m*l* of anhydrous ether and 200 m*l* of tetrahydrofuran, which was saturated with ammonia gas at 0°C, with cooling in an ice bath. The reaction mixture was stirred for 3 hr and then concentrated *in vacuo*. Crystals formed upon addition of water were filtered off. Recrystallization from ethanol gave 21.5 g (85%) of I; mp 188—190°C, $[\alpha]_D^{14}$ −177° (*c* 1.10, dimethylformamide).

Found: C, 51.85; H, 5.21; N, 10.94; S, 12.56%. Calcd for $C_{22}H_{26}O_6N_4S_2$: C, 52.16; H, 5.17; N, 11.06; S, 12.66%.

Benzyloxycarbonyl-L-cysteinamide (II). To a solution of 5.1 g (0.01 mol) of I in a mixture of 50 m*l* of

7) G. Amiard, R. Heymes and L. Velluz, *Bull. Soc. Chim. Fr.*, **1956**, 698.

8) N. Izumiya and S. Makisumi, *Nippon Kagaku Zasshi*, **78**, 662 (1957).

dimethylformamide and 6.5 m*l* of concentrated hydrochloric acid was added 3.0 g of zinc dust in small portions over a period of 15 min with vigorous stirring on cooling in an ice bath. The mixture was stirred for an additional 30 min at room temperature and then filtered. Precipitate was formed upon addition of water to the filtrate. It was filtered off and washed with water. Recrystallization from ethanol-water gave 4.1 g (80%) of II; mp 136—138°C, $[\alpha]_D^{14}$ +7.7° (*c* 2.28, dimethylformamide).

Found: C, 51.90; H, 5.55; N, 10.95; S, 12.56%. Calcd for $C_{11}H_{14}O_3N_2S$: C, 51.95; H, 5.55; N, 11.01; S, 12.61%.

L-Cysteinamide Hydrobromide (III). To a mixture of 10.0 g (0.04 mol) of II and 4.0 g of anisole was added 40 m*l* of 30% hydrogen bromide in acetic acid, and the reaction mixture was kept at room temperature for 3 hr with occasional swirling. To the reaction mixture was added 150 m*l* of anhydrous ether, and the precipitate formed was filtered off. Recrystallization from anhydrous methanol-anhydrous ether gave 6.5 g (81%) of III; mp 178—180°C (decomp.), $[\alpha]_D^{16}$ +8.2° (*c* 2.91, anhydrous methanol).

Found: C, 18.30; H, 4.59; N, 13.78%. Calcd for $C_3H_9ON_2SBr_2$: C, 17.92; H, 4.51; N, 13.93%.

2-Benzyloxycarbonylaminomethyl-R-Δ^2-thiazoline-4-carboxamide (IV). To a solution of 10.1 g (0.05 mol) of III in a mixture of 50 m*l* of anhydrous tetrahydrofuran and 10 m*l* of anhydrous methanol was added 11.8 g (0.05 mol) of benzyloxycarbonylaminoacetimino ethyl ether.[2] After the reaction mixture had been kept at room temperature for 3 hr, ammonium bromide was deposited. The reaction mixture was concentrated *in vacuo*. The residue obtained was dissolved in ethyl acetate. The solution was washed with water, dried with sodium sulfate, and then evaporated *in vacuo* to give crystals. Recrystallization from ethyl acetate-petroleum ether gave 13.0 g (89%) of IV; mp 110—112°C, $[\alpha]_D^{17}$ +46.5° (*c* 2.98, dimethylformamide), λ_{max}^{EtOH} 235 mμ (ε 2300), 252 mμ (ε 2800), $\lambda_{max}^{EtOH\cdot HCl}$ 268 mμ (ε 5900).

Found: C, 53.15; H, 5.19; N, 14.38; S, 10.67%. Calcd for $C_{13}H_{15}O_3N_3S$: C, 53.23; H, 5.15; N, 14.32; S, 10.93%.

2-Aminomethyl-R-Δ^2-thiazoline-4-carboxamide Dihydrobromide (V). To a solution of 11.6 g (0.04 mol) of IV in 100 m*l* of acetic acid was added 40 m*l* of 30% hydrogen bromide in acetic acid. The reaction mixture was kept at room temperature for 2 hr. To the mixture was added 200 m*l* of anhydrous ether. The precipitate formed was filtered off and washed with methylene chloride and acetone; wt of V: 10.8 g (84%), mp 100—105°C (decomp.), $[\alpha]_D^{25}$ +3.3° (*c* 1.05, anhydrous methanol), $\lambda_{max}^{abs\ MeOH}$ 234 mμ (ε 2400), 250 mμ (ε 2000). $\lambda_{max}^{12N\ HCl}$ 277 mμ (ε 3400). It was reprecipitated from anhydrous methanol—anhydrous ether; mp 100—105°C (decomp., sintered at 90°C).

Found: C, 20.25; H, 4.14; N, 11.99%. Calcd for $C_5H_{11}ON_3SBr\cdot CH_3OH$: C, 20.41; H, 4.28; N, 11.90%.

Isolation of L-Cystine from Acid Hydrolyzate of V. A solution of 3.1 g (0.01 mol) of V in 100 ml of 6 N hydrochloric acid was refluxed for 3 hr on addition of 1.1 g of anisole. The reaction mixture was cooled and then extracted with ether. The aqueous layer was concentrated *in vacuo* to dryness. The residue obtained was dissolved in 50 ml of water, and evaporation *in vacuo* was repeated. pH of a solution of the residue in 50 ml of water was adjusted to about 8.5 with 28% aqueous ammonia. Air was bubbled through the solution until the nitroprusside reaction became negative by a spot test. After the addition of a drop of acetic acid, the reaction mixture was allowed to stand at 0°C for 2 days. The precipitate thus formed was filtered off and then dissolved in 30 m*l* of N hydrochloric acid. Undissolved substance was removed by filtration and the filtrate was adjusted to pH 5.5—6.0 by the addition of an aqueous sodium acetate solution. After standing at 0°C for 2 days, the precipitate formed was filtered off and dried at 80°C *in vacuo* for 4 hr to give 0.78 g (65%) of L-cystine; $[\alpha]_D^{19}$ −217° (*c* 1.03, N HCl).

Found: C, 29.80; H, 5.02; N, 11.77; S, 26.42%. Calcd for $C_6H_{12}O_4N_2S_2$: C, 29.99; H, 5.04; N, 11.66; S, 26.69%.

***N,N'*-Bisbenzyloxycarbonylglycyl-L-cystine Dibenzyl Ester (VI).** To a suspension of 30.7 g (0.05 mol) of dibenzyl L-cystinate dihydrochloride[6] in 300 m*l* of methylene chloride was added 10.1 g (0.1 mol) of triethylamine. After the reaction mixture had been stirred for 1 hr, 100 ml of ether was added. The precipitate formed was filtered off, and the filtrate was concentrated *in vacuo*. To the solution of the residue thus obtained in 300 m*l* of tetrahydrofuran, 20.9 g (0.1 mol) of benzyloxycarbonylglycine and 22.7 g (0.11 mol) of *N,N'*-dicyclohexylcarbodiimide were added. After the reaction mixture had been stirred for several hours, 2 m*l* of acetic acid was added to it. *N,N'*-Dicyclohexylurea formed was filtered off, and the filtrate was evaporated *in vacuo* to dryness. The residue was dissolved in ethyl acetate and the solution was washed successively with 0.5 N hydrochloric acid, water, a 5% aqueous sodium hydrogencarbonate solution, and water. Upon evaporation *in vacuo* after drying with sodium sulfate and recrystallization of the residue from methanol—water, 35.0 g (78%) of crystals of VI were obtained; mp 118—119°C, $[\alpha]_D^{24}$ −45.5° (*c* 3.49, dimethylformamide).

Found: C, 59.91; H, 5.48; N, 6.99; S, 7.88%. Calcd for $C_{40}H_{42}O_{10}N_4S_2$: C, 59.83; H, 5.27; N, 6.98; S, 7.99%.

Benzyloxycarbonylglycyl-L-cysteine Benzyl Ester (VII). To a mixture of 10.0 g (0.0125 mol) of VI and 3.5 g of zinc dust in 200 m*l* of acetone was added 8.3 m*l* of concentrated hydrochloric acid with vigorous stirring on cooling at 0°C within a period of 20 min. The mixture was stirred for an additional 10 min, and then filtered. The filtrate was concentrated *in vacuo* at 30°C. An oily product separated out on addition of water was extracted with ethyl acetate. The extract was washed with water, dried with sodium sulfate and then evaporated *in vacuo*. Recrystallization of the residual solid from ethyl acetate—petroleum ether gave 7.5 g (75%) of crystals of VII; mp 76—77.5°C, $[\alpha]_D^{25}$ −13.5° (*c* 5.30, dimethylformamide).

Found: C, 59.87; H, 5.59; N, 6.97; S, 7.79%. Calcd for $C_{20}H_{22}O_5N_2S$: C, 59.68; H, 5.51; N, 6.96; S, 7.97%.

Benzyl 2-Benzyloxycarbonylaminomethyl-R-Δ^2-thiazoline-4-carboxylate (VIII). A solution of 4.0 g (0.01 mol) of VII in 50 m*l* of chloroform was saturated with dry hydrogen chloride gas on cooling in an ice bath. The mixture was allowed to stand at room temperature overnight, and then concentrated *in vacuo*. To the residue was added 100 m*l* of ethyl acetate, and the mixture

was treated with a concentrated potassium carbonate solution. The ethyl acetate layer was washed with water, dried with sodium sulfate and then evaporated to dryness to give crystals. Recrystallization from ethyl acetate—petroleum ether gave 2.1 g of VIII; mp 86—87.5°C, $[\alpha]_D^{19}$ +84.0° (*c* 2.13, dimethylformamide), λ_{max}^{EtOH} 235 mμ (ε 2300), 252 mμ (ε 3000), $\lambda_{max}^{EtOH\text{-}HCl}$ 264 mμ (ε 5000).

Found: C, 62.43; H, 5.31; N, 7.23; S, 8.29%. Calcd for $C_{20}H_{20}O_4N_2S$: C, 62.48; H, 5.24; N, 7.29; S, 8.34%.

2-Aminomethyl-R-Δ^2-thiazoline-4-carboxylic Acid Dihydrobromide (IX). To a mixture of 1.2 g (0.003 mol) of VIII and 1.0 g of anisole was added 20 m*l* of 30% hydrogen bromide in acetic acid, and the mixture was kept at 40°C for 3 hr with occasional swirling. To the reaction mixture was added 100 m*l* of anhydrous ether. The precipitate formed was filtered off, and washed with anhydrous ether; wt of IX: 0.70 g (73%), mp 177—182°C (decomp.), $[\alpha]_D^{14}$ +30.7° (*c* 1.01, anhydrous ethanol), $\lambda_{max}^{abs\ EtOH}$ 235 mμ (ε 2900), 250 mμ (ε 2600), $\lambda_{max}^{12N\ HCl}$ 276 mμ (ε 4100).

Found: C, 18.98; H, 3.38; N, 8.50%. Calcd for $C_5H_{10}O_2N_2SBr_2$: C, 18.65; H, 3.13; N, 8.70%.

***N*-*S*-Dityrityl-L-cysteinyl-L-leucine Benzyl Ester (X).** To a solution of 13.6 g (0.02 mol) of *N*,*S*-dityrityl-L-cysteine diethylamine salt[7] and 7.9 g (0.02 mol) of benzyl L-leucinate *p*-toluenesulfonate[8] in 150 m*l* of methylenechloride was added 4.6 g (0.022 mol) of *N*,*N'*-dicyclohexylcarbodiimide. After the reaction mixture had been stirred for several hours, 1 m*l* of acetic acid was added, and the urea derivative formed was filtered off. The filtrate was washed with water and dried with sodium sulfate. Upon concentration of the solution *in vacuo* an amorphous powder was obtained.

Benzyl *S*-Trity-L-cysteinyl-L-leucinate Hydrochloride (XI). To a solution of 16.2 g (0.02 mol) of X in 100 m*l* of acetone was added 10 m*l* of 6 N hydrochloric acid. After the reaction mixture was stirred for 1 hr, the resulting clear solution was evaporated to dryness at 30°C. The residue was triturated with ether. The precipitate was filtered off, and washed with ether. Recrystallization from ethyl acetate gave 6.8 g (56%) of crystals of XI; mp 182—184°C, $[\alpha]_D^{23}$ +13.3° (*c* 5.06, ethanol).

Found: C, 69.64; H, 6.51; N, 4.64%. Calcd for $C_{35}H_{39}O_3N_2SCl$: C, 69.69; H, 6.52; N, 4.65%.

Benzyloxycarbonylglycyl-*S*-trityl-L-cysteinyl-L-leucine Benzyl Ester (XII). To a suspension of 12.1 g (0.02 mol) of XI in 50 m*l* of chloroform was added 2.0 g (0.02 mol) of triethylamine. The precipitate formed on addition of 100 m*l* of ether was filtered off, and the filtrate was evaporated *in vacuo*. To the solution of the residue obtained in 100 m*l* of tetrahydrofuran, 4.2 g (0.02 mol) of benzyloxycarbonylglycine and 4.6 g (0.022 mol) of *N*,*N'*-dicyclohexylcarbodiimide were added. The mixture was stirred for several hours, and then 1 m*l* of acetic acid was added. The urea derivative precipitated was removed by filtration, and the filtrate was concentrated *in vacuo*. The residue was dissolved in ethyl acetate, and the solution was washed as usual. Evaporation of the solvent *in vacuo* and then recrystallization of the residue from ethanol—water gave 13.2 g (87%) of XII; mp 114—116°C, $[\alpha]_D^{23}$ −11.4° (*c* 4.30, dimethylformamide).

Found: C, 71.62; H, 6.26; N, 5.53; S, 4.16%. Calcd for $C_{45}H_{47}O_6N_3S$: C, 71.31; H, 6.25; N, 5.54; S, 4.23%.

Benzyloxycarbonylglycyl-L-cysteinyl-L-leucine Benzyl Ester (XIII). A hot solution of 1.7 g (0.01 mol) of silver nitrate and 0.95 m*l* of pyridine in 20 m*l* of ethanol was added to a warm solution of 7.6 g (0.01 mol) of XII in 40 m*l* of ethanol. After the mixture was refluxed for 30 min, the silver mercaptide of XIII was separated out; after standing for 2 hr at room temperature under nitrogen, it was filtered off and washed with ethanol and then dried; wt 5.6 g (90%).

To a suspension of 5.6 g of the mercaptide in 50 m*l* dimethylformamide, 1.3 m*l* of concentrated hydrochloric acid was added. The mixture was shaken for 2 hr at room temperature and then heated on a boiling water bath for 1 min. The precipitate of silver chloride formed was removed by filtration and washed with a small amount of dimethylformamide. After addition of chloroform to the filtrate, it was washed with water several times, dried with magnesium sulfate, and then evaporated *in vacuo*. Upon addition of water to the residue, crystals were separated out. Recrystallization from ethyl acetate—petroleum ether gave 4.0 g (78%) of XIII; mp 96—98°C, $[\alpha]_D^{26}$ −15.6° (*c* 4.24, dimethylformamide).

Found: C, 60.82; H, 6.59; N, 8.09; S, 5.95%. Calcd for $C_{26}H_{33}O_6N_3S$: C, 60.56; H, 6.45; N, 8.15; S, 6.22%.

Benzyl 2-Benzyloxycarbonylaminomethyl-R-Δ^2-thiazoline-4-carbonyl-L-leucinate (XIV). A solution of 5.2 g (0.01 mol) of XIII in 100 m*l* of chloroform was saturated with dry hydrogen chloride gas on cooling at 0°C. The mixture was allowed to stand at room temperature overnight, and then evaporated *in vacuo* to dryness. To the residue was added 100 ml of ether, and the mixture was treated with a concentrated potassium carbonate solution. The ether layer was separated, washed with water, dried with sodium sulfate and then evaporated to dryness to give a crude oil; wt 4.2 g. This was dissolved in a small amount of ether and subjected to the sillica gel column (Mallincrodt Chemical Works, 100 mesh, 50 g). Elution with petroleum ether—anhydrous ether gave 3.9 g (87%) of XIV; $[\alpha]_D^{26}$ +28.6° (*c* 2.70, ethanol), λ_{max}^{EtOH} 233 mμ (ε 2600), 252 mμ (ε 2700), $\lambda_{max}^{EtOH\text{-}HCl}$ 268 mμ (ε 4900).

Found: C, 62.26; H, 6.45; N, 8.37; S, 6.44%. Calcd for $C_{26}H_{31}O_5N_3S$: C, 62.75; H, 6.28; N, 8.44; S, 6.44%.

2-Aminomethyl-R-Δ^2-thiazoline-4-carbonyl-L-leucine Dihydrobromide (XV). To a mixture of 2.0 g (0.004 mol) of XIV and 1.0 g of anisole was added 30 m*l* of 30% hydrogen bromide in acetic acid and the reaction mixture was kept at 40°C for 3 hr with occasional swirling. To the mixture was added 100 m*l* of anhydrous ether, and the precipitate formed was filtered off and washed with anhydrous ether; wt of XV: 1.26 g (75%), mp 140—148°C (decomp.), $[\alpha]_D^{15}$ −4.1° (*c* 1.46, anhydrous ethanol), $\lambda_{max}^{abs\ EtOH}$ 230 mμ (ε 2900), 250 mμ (ε 2200), $\lambda_{max}^{12N\ HCl}$ 276 mμ (ε 3100).

Found: N, 9.56%. Calcd for $C_{11}H_{21}O_3N_3SBr_2$: N, 9.66%.

NOTES

BULLETIN OF THE CHEMICAL SOCIETY OF JAPAN VOL. 43 1568—1569 (1970)

The Chemical Behavior of Low Valence Sulfur Compounds. IV.*1 The Solubility of Ammonium Thiosulfate in Aqueous Ammonia

Kunishige NAITO, Masahito Yamada*2 and Taijiro Okabe

Department of Applied Chemistry, Faculty of Engineering, Tohoku University, Sendai

(Received August 1, 1969)

The solubility of ammonium thiosulfate in aqueous ammonia has been measured as an investigation concerning the preparation of ammonium sulfamate from ammonium thiosulfate by oxidation with compressed oxygen in aqueous ammonia solution. The solubility is not known except for the measurement at 15°C by E. Weitz.[1] The solubility in water has been measured by W. C. Zeise,[2] E. Terres and F. Overdick[3] and W. Klempt, F. Brodhobb and H. Erlbach,[4] but the data are fairly scanty.

Experimental

Crystals of ammonium thiosulfate recrystallized from a very diluted aqueous ammonia solution had a purity of 95.27 wt% with 4.17 wt% adhered water. The solubility was measured by cloud method as follows: The crystals was enclosed in a glass tube of 8 mmϕ × 150 mm with aqueous ammonia and a glass agitater. The tube was heated in a glass water bath to dissolve the crystals as a homogeneous solution. After the dissolution, it was carefully cooled, especially with the cooling speed of 0.05 to 0.1°C/min near the cloud point, and the temperature was measured at which the crystals appeared. When the cloud point was determined within 0.05 to 0.2°C after several measurements, it was decided as saturation temperature. A thermometer graduated at 0.01°C intervals was used. It was calibrated with a standard thermometer.

Results and Discussion

The solubility data measured are shown in Fig. 1. The isothermal curves shown in Fig. 2 were made by plotting the solubility against ammonia concentration in Fig. 1.

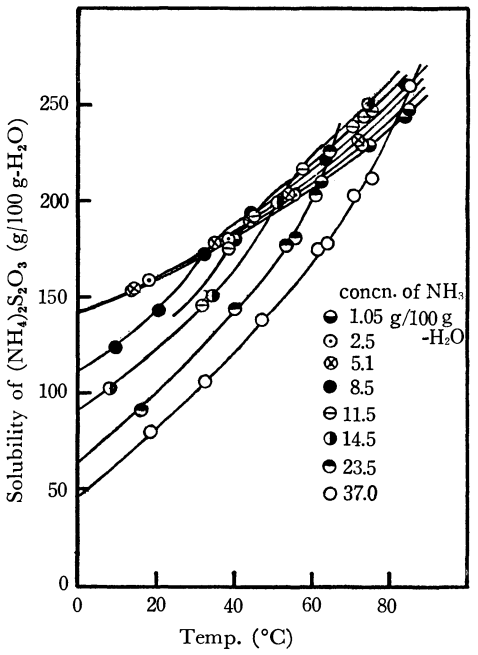

Fig. 1. Solubility of ammonium thiosulfate in aqueous ammonia (temperature-solubility curves).

As shown in Fig. 2, the solubility of ammonium thiosulfate increases with the increase of the ammonia concentration, reaches maximum and then decreases. The maximum point shifts toward the higher side of ammonia concentration with the rise in temperature. By means of X-ray diffraction it was observed that the bottom crystals in the low concentration of ammonia (undoubted ammonium thiosulfate) differ from those in the highly concentrated solution of aqueous ammonia should be an ammoniate of ammonium thiosulfate, because they decompose to ammonium thiosulfate on being stood in air for several hours.

*1 Preceding paper, III. K. Naito, M. Yoshida, M. C. Shieh and T. Okabe, This Bulletin, **43**, 1365 (1970).

*2 Present Address: Ministry of International Trade and Industry, Tokyo.

1) E. Weitz, *Z. Elektrochem.*, **31**, 546 (1925).

2) W. C. Zeise, *Schw. J.*, **41**, 183 (1824).

3. E. Terres and E. Overdick, *Gas-Wasserfach*, **71**, 83 (1928).

4) W. Klempt, F. Brodhobb and H. Erlbach, *Ber. Ges. Kohlentechn.*, **3**, 493 (1931).

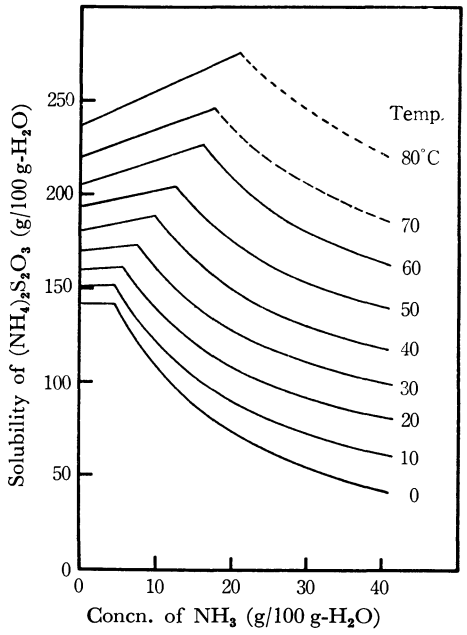

Fig. 2. Solubility of ammonium thiosulfate in aqueous ammonia (isothermal curves).

As elemental sulfur was liberated during the course of measurement at high temperature, the solubility of ammonium thiosulfate in pure water was estimated by extrapolating the solubility in aqueous ammonia to zero of ammonia concentration. The results are shown in Table 1 with those of the former investigators.

Table 1. The solubility of ammonium thiosulfate in water

Temperature	Solubility (g/100 g-H_2O)		
	Present work	Literature	
0°C	143.8	153.8[2)]	160.4[3)]
20	158	—	181.7
25	162	178.6	—
30	167	—	—
35	172	204.3	—
40	179	—	204.9
50	190	—	—
60	204	—	226.8

2), 3): see Reference

BULLETIN OF THE CHEMICAL SOCIETY OF JAPAN VOL. 43 1569—1571 (1970)

The Preparation of the Polyvinylmalachitegreen and Vinylcarbazole-Vinylmalachitegreen Copolymers and Their Absorption Spectra

Kenichi OKAMOTO, Yo HASEGAWA,*1) Shigekazu KUSABAYASHI and Hiroshi MIKAWA

Department of Chemical Technology, Faculty of Engineering, Osaka University, Suita, Osaka

(Received August 28, 1969)

It is well known that triphenylmethane dyes are photoconductive and that the photoconductivity of such polymers as poly-*N*-vinylcarbazole (PVCz) is sensitized by mixing the dyes. The present authors have previously reported on the sensitization of the photoconductivity in the PVCz film by copolymerized malachite green molecules.[1] This note will deal with the preparation of the polyvinylmalachitegreen (PVMG) and *N*-vinylcarbazole (VCz)-vinylmalachitegreen (VMG) copolymers and with their absorption spectra.

Preparation of PVMG. The VMG carbinol was prepared by the method reported by Manecke and Kosmehl[2] and was recrystallized three times from benzene-methanol under nitrogen stream. The VMG carbinol was polymerized by azobisisobutyronitrile (AIBN) in a vacuum-sealed tube at 80°C for 10 hr (Table 1). The resulting white PVMG carbinol was purified by repeated reprecipitation from the benzene solution by methanol. The molecular weight was 13000 (as ascertained by means of a vapor-pressure osmometer).

Found: C, 80.99; H, 7.35; N, 7.46%. Calcd for $(C_{25}H_{28}N_2)_n$: C, 80.61; H, 7.58; N, 7.56%.

The PVMG carbinol was transformed into the chloride (PVMG) as will be described below. An amount 1.7 times the calculated amount of a 0.3 N dry HCl-THF solution was stirred into the benzene solution of PVMG carbinol, and the resulting precipitate (PVMG) was reprecipitated three times from the methanol solution by Bz–THF (1 : 10 : 7 in vol. ratio). The potentiometric titration by a 0.01 N $AgNO_3$ aqueous solution showed that the PVMG thus obtained was monocationic (Cl^- ion content; Found: 9.26, Cacld for the monocation: 9.08%). It should be noticed that

*1 Present address: Research Laboratory, Wireless Division, Matsushita Electric Industrial Co. Ltd., Kadoma, Osaka.

1) K. Okamoto, Y. Hasegawa, S. Kusabayashi and H. Mikawa, This Bulletin, **41**, 2563 (1968).

2) G. Manecke and G. Kosmehl, *Chem. Ber.*, **93**, 1899 (1960); G. Manecke and G. Kosmehl, *Makromol. Chem.*, **80**, 22 (1964).

Table 1. Copolymerization of VCz with VMG carbinol[a)]

No.	Monomer mol% in feed		Conversion[b)] %	Fractionation %			VMG mol% in Fraction		
	VCz	VMG carb.		I	II	III	I	II	III
1	100	0	97.0		(100)			(0)	
2	99.9	0.1	92.0	0	100			0.073	
3	99.5	0.5	94.6	8.8	86.7	—	1.02	0.15	—
4	99.0	1.0	94.4	11.8	75.3	—	1.48	0.25	—
5	97.0	3.0	92.6	13.6	60.5	—	3.4	0.37	—
6	95.0	5.0	86.0	31.0	36.1	—	3.0	0.46	—
7	90.0	10.0	76.6	39.5	27.8	30.9	4.9	1.24	4.7
8	0	100	54.3	(100)			(100)		

a) Solvent: benzene, initiator: AIBN, Monomer conc.: 0.5 mol/l (in No. 1—7) or 0.25 mol/l (in No. 8), AIBN conc.: 0.01 in molar ratio to monomer.
b) This is the yield after the reprecipitations three times.

if a fairly large excess of a 0.3 N dry HCl–THF solution was added to the benzene solution of the PVMG carbinol, a fairly large proportion of the MG molecules were transformed into the dication.

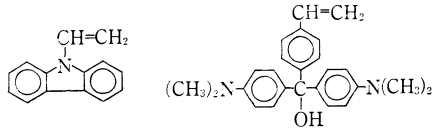

VCz VMG carbinol

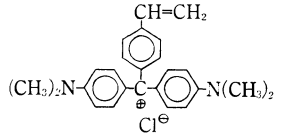

VMG

Preparation of the VCz-VMG Copolymer. The copolymerization of VCz with the VMG carbinol was carried out by means of AIBN in a vacuum-sealed tube at 80°C for 10 hr. The resultant VCz–VMG carbinol copolymer was purified by the repeated reprecipitation from the benzene solution by methanol. The VCz–VMG carbinol copolymer was then transformed into the VCz–VMG carbinol copolymer was then transformed into the VCz–VMG (HCl salt) copolymer and fractionated as follows. The 0.3 N dry HCl–THF solution (1.5-times the estimated MG dye content) was stirred into the benzene solution of the VCz–VMG carbinol copolymer, after which the precipitate was separated by the use of a centrifuge (Fraction I). A large amount of methanol was added to the filtrate, and the resultant precipitate was filtered (Fraction II). The filtrate was evaporated to dryness under reduced pressure (Fraction III). The VMG content of the copolymer was determined colorimetrically by use of the absorption maxima (626 and 452 mμ) of VMG, shown in Fig. 1. The results are shown in Table 1. The homopolymer of VCz is not contained in Fraction I, for PVCz is soluble in Bz–THF. Fraction II does not contain PVMG because of its insolubility in Bz–THF. Furthermore, Fraction I shows the same absorption spectrum as Fraction II and does not have the absorption peak characteristic

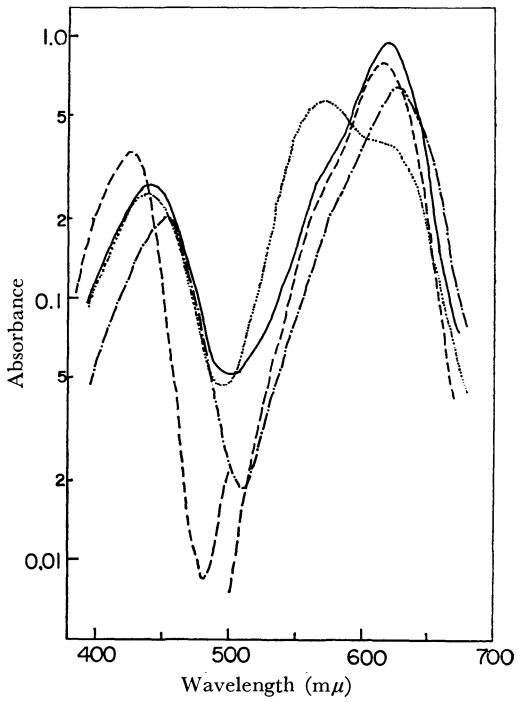

Fig. 1. Visible absorption spectra of MG dye derivatives in solution.
— — MG, 8.9×10^{-6} ($\lambda>500$ mμ) or 2.0×10^{-5} ($\lambda<500$ mμ) mol/l in 0.02 N HCl methanol.
—·— VMG, 9.0×10^{-6} mol/l in 0.01 N HCl THF-methanol (97 : 3 in volume ratio).
—— VCz-VMG copolymer (No. 4, Fraction II), 1.6×10^{-5} mol/l in 0.01 N HCl-THF-methanol (97 : 3 in volume ratio).
····· PVMG, 2.6×10^{-5} mol/l in 0.01 N HCl methanol.

Table 2. Visible absorption maxima λ_{max} and apparent extinction coefficient ε_{app} of MG dye derivatives[a)]

Dye	First				Second	
	λ_{max}	ε_{app}	λ_{max}	ε_{app}	λ_{max}	ε_{app}
MG[b)]	617.5	9.83			426	1.81
VMG[c)]	626	7.3			452	2.2
PVMG[b)]	620	1.5	570	2.1	440	0.94
VCz-VMG copolymer[c)]	620	5.6			440	1.6

a) λ_{max} [mμ], ε_{app} [$\times 10^4$ cm·l/mol]
b) in 1×10^{-2} N HCl-methanol solution
c) in 1×10^{-2} N HCl-THF-methanol solution (97 : 3 in volume ratio)

of PVMG at about 570 mμ. Fraction I, therefore, seems to consist of only the VCz–VMG copolymer. Fraction II will consist of the copolymer and PVCz (especially in the case of a low MG dye content). The molecular weight of the copolymer (Fraction II) is about 20000 (as determined by the use of the vapor pressure osmometer), a little lower than that of PVCz polymerized under the same conditions.

Absorption Spectra of the MG-dye Derivatives. Figure 1 shows the absorption spectra of PVMG, VMG, and the VCz–VMG copolymer in solution. The absorption maxima of these dye salts are listed in Table 2. The replacement of the 4-hydrogen of MG by the vinyl group or the main chain unit, $>CH-CH_2-$, causes the red shift of the visible absorption peaks.

It has been reported that MG has a small shoulder band at about 570 mμ in addition to its main peaks (426 and 618 mμ) and that this shoulder becomes larger with the increase in the concentration.[3)] Furthermore, Manabe *et al.*, have reported that the maximum extinction coefficient, ε_{max}, of the main peaks decrease with the increase in the dye concentration.[4)] These phenomena, which have also been observed in the spectra of such other cationic dyes as crystalviolet, have been attributed to the formation of the aggregate of the dye molecules, as is well known.[3-5)] A similar shoulder band was observed at about 570 mμ in the absorption spectra of VMG, the VCz–VMG copolymer and PVMG ;*2 it is also probably due to the formation of the aggregate. It should be noted that, in PVMG, the band attributed to the aggregation is larger than the main band and is not affected by either the temperature (0—50°C) or the concentration ($0.5—50\times10^{-5}$ mol/l). This suggests that the pendant MG group in the polymer chain aggregates much more easily than MG and VMG, and that most of the pendant dye molecules of PVMG exist in the aggregated form, even in a dilute solution.

It is well known that the aggregative cationic dyes show new peaks attributable to the aggregation, the so called methachromatic band, with the depression in the main band when they are adsorped on the anionic polymers and/or agar.[3)] In PVMG the distance between adjacent MG molecules is short, because each MG molecule is linked to a paraffinic polymer chain by a short covalent bond. The aggregation ability of the MG molecule will be enhanced by the short intermolecular distance in PVMG. No information on the aggregation state has been obtained for either MG or PVMG, however.

3) L. Michaelis and S. Granick, *J. Amer. Chem. Soc.*, **67**, 1212 (1945).
4) O. Manabe, K. Nanjo, S. Matsubara, M. Nakagaki and H. Hiyama, *Kagaku to Kogyo* (Osaka), **35**, 12 (1961).
5) M. Koizumi and N. Mataga, *Yuki Gosei Kagaku Kyokai Shi*, **14**, 181 (1956).
*2 It has been reported that the PVMG prepared from poly-*p*-lithiumstyrol has two peaks (590 and 630 mμ) at wave lengths longer than 500 mμ (D. Braun, *Makromol. Chem.*, **33**, 181 (1959).

BULLETIN OF THE CHEMICAL SOCIETY OF JAPAN VOL. 43 1572—1573 (1970)

p-Brombenzolsulfonyloxyacetonitril als Cyanmethylierungsmittel der Carbonsäure

Kunihiro ICHIMURA

Institut für Polymer- und Faserforschung, Yokohama, Kanagawa-ku, Sawatari 4

(Eingegangen am 20. September, 1969)

Schweyzer und seine Mitarbeiter haben mitgeteilt, daß Cyanmethylester der Carbonsäure als aktiviertes Ester zur Peptidkondensation zweckmäßig dienen kann.[1,2] Die Herstellung des Cyanmethylesters wird von ihnen mittels Chloracetonitrils durchgeführt. Taschner und andere haben vor kurzem mitgeteilt, daß Bromacetonitril hinsichtlich der Herstellungsbedingungen des aktivierten Esters nützlicher als Chloracetonitril ist.[3]

Im Zusammenhang mit Darstellung des Aziridins hat der Autor einige α-Sulfonyloxynitrile synthetisiert,[4] und in dieser Arbeit wird die Umsetzung der Cyanmethylester der Arensulfonsäure mit Carbonsäure durchgeführt.

Der vor kurzem beschriebenen Prozedur nach werden *p*-Toluolsulfonyloxy- und *p*-Brombenzolsulfonyloxyacetonitril von Sulfonylchlorid, Formalin und Natriumcyanid aus in guten Ausbeuten dargestellt.

Wenn man *p*-Toluolsulfonyloxyacetonitril mit äquivalentem Phthaloylglycin in Gegenwart des Triäthylamins bei Raumtemperatur reagieren läßt, vollendet sich die Reaktion in 20 Std, und das Cyanmethylester wird in 88%-iger Ausbeute erhalten. Unter Benutzung des *p*-Brombenzolsulfonyloxyacetonitrils ist doch das Cyanmethylester in 4.5 Std bei Raumtemperatur in 88%-iger Ausbeute erhältlich. Es ist also zweckmäßiger als im Fall des Chloracetonitrils und Bromacetonitrils im Hinsicht der Darstellungsbedingungen. Die einige Ergebnisse sind in Tabelle zusammengefaßt.

Beschreibung der Versuche

***p*-Brombenzolsulfonyloxyacetonitril.** Man setzt 25 g *p*-Brombenzolsulfonylchlorid und 11 m*l* Formalin (etwa 37%) in 50 m*l* Acetonitril zu und fügt die konz. wäßr. Lösung des 5.50 g Natriumcyanids in das Gemisch unter gutem Rühren bei etwa 10°C langsam zu. Man setzt Äther zu und trennt die org. Schicht, die nach Waschen mit Wasser über Magnesiumsulfat abgetrocknet wird. Nach Eindampfen des Lösungsmittels löst man sofort den Rückstand in 7.5 m*l* *n*-Butanol und läßt die

Tabelle 1. Cyanmethylester der carbonsäure

$RNHCH(R')COOH + p\text{-}X\text{-}C_6H_4SO_2OCH_2CN + NEt_3 \rightarrow RNHCH(R')COOCH_2CN$

R*1	R'	X	Reakt.-Zeit*2	Lösgsm.*3	Rohausb.	Schmp. (°C) (Umkrist.-Lösgsm.)
C_6H_5CO	H	CH_3	20 Std	EÄ	76%	98.5—100 (Äther)*4
C_6H_5CO	H	Br	4.5	EÄ	80	
p-$CH_3C_6H_4SO_2$	H	CH_3	24	AN	85	96—97 (Bzl)*5
p-$CH_3C_6H_4SO_2$	H	Br	5	EÄ	86	
p-$CH_3C_6H_4SO_2$	CH_3	CH_3	20	AN	76	97.5—99.5 (Bzl)*6
p-$CH_3C_6H_4SO_2$	CH_3	Br	5	EÄ	82	
Phth	H	CH_3	19	AN	77	132—133.5 (EtOH-EÄ)*7
Phth	H	Br	5	AN	80	
Phth	CH_3	CH_3	20	AN	88	87—90 (Bzl-Ligroin)*8
Phth	CH_3	Br	4.5	AN	88	
Cbo	H	Br	4.5	AN	87	69—70 (Bzl-Cyclohexan)*9

*1 Phth; Phthaloyl, Cbo; Carbobenzoxy. *2 Bei Raumtemp. *3 EÄ; Essigsäure-äthylester, AN; Acetonitril. *4 99—100°C.[1] *5 96—97°C, 94°C.[2] *6 Gef (Ber): C, 50.63 (51.08); H, 4.91 (5.00); N, 10.12 (9.01) %. *7 132—133.5°C.[5] *8 87—88°C.[3] *9 69—70°C.[2]

1) R. Schweyzer, M. Feurer, B. Iselin und H. Kägi, *Helv. Chim. Acta*, **38**, 80 (1955).

2) R. Schweyzer, B. Iselin und M. Feurer, ebd., **38**, 69 (1955).

3) E. Taschner, R. Rzeszotarska und A. Kuziel, *Acta Chem. Acad. Sci. Hung.*, **44**, 67 (1965); *Chem. Abstr.*, **63**, 13405 (1965).

4) K. Ichimura und M. Ohta, Dieses Bulletin, **43**, 1443 (1970).

5) B. Helfrich, P. Schellenberg und J. Ulbrich, *Chem. Ber.*, **90**, 700 (1957).

Lösung in Eisschrank über Nacht stehen. Die Kristalle werden abgenutscht und mit Ligroin nachgewaschen. Ausbeute, 21.66 g (80% d. Th.). Farblose Nadeln vom Schmp 58.5—60.0°C. Gef: C, 34.72; H, 2.14; N, 5.24%. Ber für $C_8H_6NO_3Br$: C, 34.92; H, 2.19; N, 5.65%. IR (KBr): 1380, 1190, 1095, 1000, 910, 720 cm^{-1}.

In der analogen Weise erhält man 28.65 g (52% d. Th.). *p*-Toluolsulfonyloxyacetonitril, von 50 g *p*-Toluolsulfonylchlorid, 30 m*l* Formalin und 14.9 g Natriumcyanid ausgehend. Die Kristalle vom Schmp 49—50°C werden aus *n*-Butanol unter Methanol-Trockeneiskühlung umkristallisiert. Gef: C, 51.79, H, 4.27; N, 6.63%. Ber für $C_9H_9NO_3S$: C, 51.19; H, 4.30; N, 6.63%. IR (KBr): 1380, 1190, 1180, 1090, 1050 910 cm^{-1}. NMR ($CDCl_3$): 2.50 (CH_3), 4.75 (OCH_2, 7.3—7.9 (arom.).

DL-Phthaloylalanincyanmethylester (eine typische Procedur zur Herstellung der Cyanmethylester). Man löst 2.19 g (10 mmol) DL-Phthaloylalanin, 2.76 g (10 mmol) *p*-Brombenzolsulfonyloxyacetonitril und 1.11 g (11 mmol) Triäthylamin in 10 m*l* wasserfreiem Acetonitril und rührt die Lösung bei Raumtemperatur 4.5 Std, wo man dünnschichtchromatographisch die Reaktion nachfolgt. Nach Versetzen mit Wasser und Ausziehen mit Äther wäscht man die äther. Lösung mit Wasser nach und eingedampft. 2.26 g (88% d. Th.) kristalliner Rückstand vom Schmp 80—88°C werden erhalten und aus Benzol/Ligroin umkristallisiert. Schmp 87—90°C (Ber Schmp[3] 87–88°C).

BULLETIN OF THE CHEMICAL SOCIETY OF JAPAN VOL. 43 1573—1574 (1970)

Rearrangements of Tertiary Amine *N*-Oxides. XXVI. Reactions of Arylnitrones with Lead Tetraacetate

Seizo TAMAGAKI and Shigeru OAE

Department of Applied Chemistry, Faculty of Engineering, Osaka City University, Sumiyoshi-ku, Osaka

(Received September 29, 1969)

Lead tetraacetate (LTA) has been used widely as a reagent for electron-oxidation of many organic compounds, for instance, the oxidation of alcohols or phenols to the corresponding ketones or quinones. An interesting example is the oxidation of quinoline *N*-oxide (I).[1] In this case, the heterocyclic carbon α to the *N*-oxide function is oxidized to afford the corresponding *N*-acetoxycarbostyril (III) which appears to be produced through the formation of α-acetoxyquinoline *N*-oxide(II) as shown below.

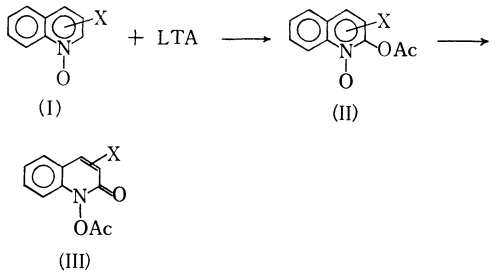

According to Ochiai and Ohta, electron-donating groups on the ring afford the corresponding carbostyrils in higher yields than electron-withdrawing groups.[1]

In extending this oxidation reaction by LTA to other tertiary amine *N*-oxides, we have examined the oxidation of arylnitrones which are considered to be the analogs of quinoline *N*-oxide.

When LTA was added portionwise into arylnitrones in dry benzene, the colorless powder precipitated immediately. When the precipitate was filtered off and benzene was removed from the filtrate by evaporation, either crystalline or oily products was obtained quantitatively irrespective of the nitrone employed. For instance, α,*N*-diphenylnitrone afforded *N*-acetoxy-*N*-benzoylaniline as the sole product.

Other examples of stoichiometries are tabulated in Table 1.

The structures of the products were determined by means of NMR, IR, elemental analysis as well as by chemical conversion to the corresponding *N*-hydroxybenzamides.

The reaction appears to proceed through the following scheme.

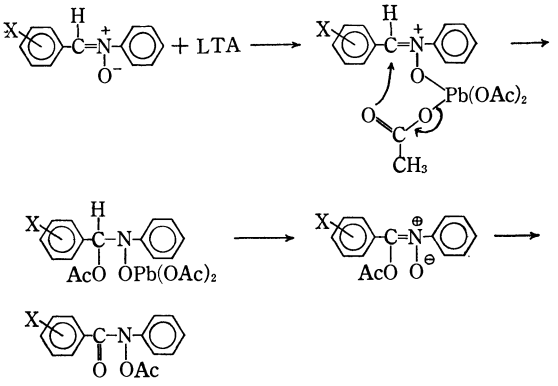

1) E. Ochiai and A. Ohta, *Chem. Pharm. Bull. (Tokyo)*, **10**, 1260 (1962). *ibid.*, **11**, 1586 (1963).

Table 1. Reaction of arylnitrones with lead tetraacetate in benzene

X-C6H4-C=N(O)-Ph	Mp (bp) (°C)	*N*-Oxide	Lead tetraacetate (g)	Product	Lead diacetate
p-Cl	108	2.0	4.0	2.15	2.17
H	(165—170/2 mmHg)	1.0	2.2	1.0	1.46
p-CH_3	95—96	0.75	1.6	0.90	1.12

The reaction of nitrones with LTA takes place very readily without heating the reaction mixture, whereas that of quinoline *N*-oxide requires refluxing of the solution. In the reaction with acylating agents also, nitrones are much more reactive than quinoline or pyridine *N*-oxide. Thus, we can conclude that nitrones are in general more reactive in oxidation than the aromatic *N*-oxides.

$$>C{=}N + LTA \xrightarrow[50°C]{CH_2Cl_2} >\overset{\overset{OAc^-}{\downarrow}}{C{=}N} \rightarrow >\overset{\overset{OAc}{|}}{C}{-}N{=}O$$
$$\quad\quad\quad

BULLETIN OF THE CHEMICAL SOCIETY OF JAPAN VOL. 43 1574—1577 (1970)

Studies of the Electric Discharge of Organic Compounds. I. The Decomposition of Toluene in 10-MHz and 2450-MHz Discharges

Ko Taki

The Institute of Physical and Chemical Research, Yamato-machi, Saitama

(Received October 16, 1969)

Extensive studies of the reactive species have been carried out with regard to the decomposition of inorganic and organic compounds in an electric discharge.[1-10]

In the present investigation, high-frequency electric discharges were used as the source for the formation of reactive species, and toluene was chosen as a representative substrate. Some comparisons of the reaction of toluene in a glow discharge produced by 10-MHz and by 2450-MHz fields will also be reported. The radical scavengers (such as NO, O_2, and C_2H_4) and the electron scavengers (such as N_2O) were used in both the discharges in order to ex-

1) G. Arnold, *Z. Naturforsch. A*, **20**, 435 (1965).
2) F. G. Vastola and J. P. Wightman, *J. App. Chem.* (London), **14**, 69 (1964).
3) F. Swift, Jr., R. L. Sung, J. Doyle and J. K. Stille, *J. Org. Chem.*, **30**, 3114 (1965).
4) J. K. Stille, R. L. Sung and J. V. Kooi, *ibid.*, **30**, 3116 (1965).
5) J. K. Stille and C. E. Rix, *ibid.*, **31**, 1591 (1966).
6) R. Mavrodineanu and R. C. Hughes, *Spectrochim. Acta*, **19**, 1309 (1963).
7) R. L. MacCarthy, *J. Chem. Phys.*, **22**, 1360 (1954).
8) A. Streitwieser, Jr., and H. R. Ward, *J. Amer. Chem. Soc.*, **85**, 539 (1963).
9) F. Le. Goff and B. Vuillermoz, *J. Chim. Phys.*, **66**, 403 (1969).
10) O. I. Zacharov-Nartsissov and N. G. Pilyugina, *Khim. Vysok. Energii*, **3**, 267 (1969).

amine the reaction mechanism. The mechanism is compared with that of the reactions by other energy sources (radiolysis,[11-15] photolysis,[16,17] and pyrolysis[18-20]). Also the formation of some reaction intermediates is discussed.

Experimental

All the runs were carried out in a flow system uing helium as the carried gas. The 10-MHz electric discharge was carried out in Pyrex tubing (1.3 cm od.) around which two 2.5-cm aluminum foil bands (3 cm apart) were fitted; the 10-MHz power of a few watts was generated by a hand-made Toshiba 2B29 valve generator. Microwave (2450-MHz) discharge was also carried out in Pyrex tubing (1.3 cm od.) using a cavity (2×1.4 cm); microwaves were fed into the cavity by means of a Raytheon PGM-10 magnetron (2450 MHz, 85 W). The experimental arrangement is shown in Fig. 1. All the products were analysed gas-chromatographically.

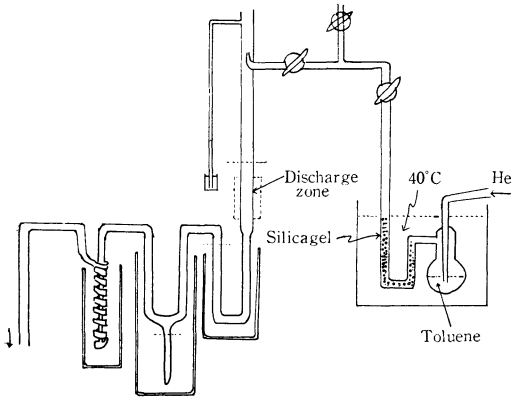

Fig. 1

Results and Discussion

The relative product yields are shown in Table 1. The eluting order*1 of C_6 and C_7 compounds in gas chromatography using a polyethylene glycol column is as follows:

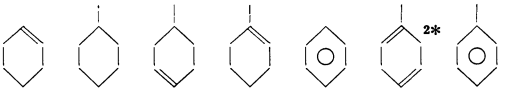

1-Methylcyclohexene and 4-methylcyclohexene, which are obtained in comparatively large yields, are the reduction products from toluene in the

Table 1. Relative product yields based on toluene consumed

	10-MHz discharge Toluene 6.7% in He (residence time 0.35 sec)	2450-MHz discharge Toluene 8.5% in He (residence time 0.008 sec)
Hydrogen	—	—
Methane	0.2	0.2
Ethane	1.0	0.7
Ethylene / Acetylene	0.3	0.4
Methylacetylene / Allene	0.2	1.0
Benzene	1.0	1.0
2,5-Dihydrotoluene	0.005	0.9
Ethylbenzene	0.8	1.5
Styrene	0.2	0.3
Phenylacetylene	—	0.7
Bibenzyl	0.04	0.09
Diphenylmethane	—	0.005
Polymer	9.6	1.5

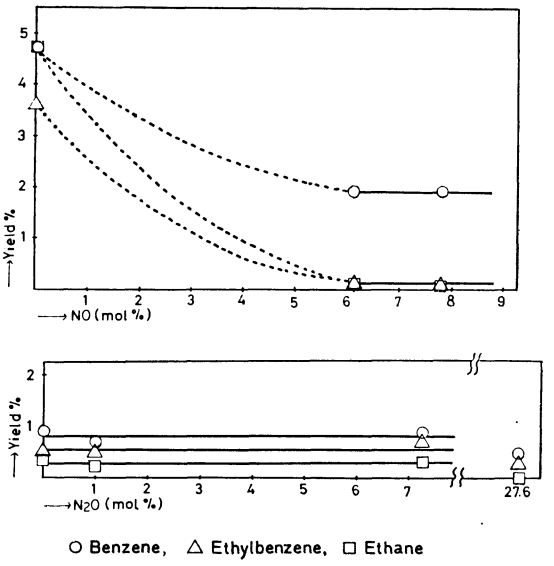

Fig. 2. 10-MHz discharge of toluene.

11) J. Hoigné and T. Gäumann, *Helv. Chim. Acta*, **44**, 2141 (1961).
12) J. Hoigné and T. Gäumann, *ibid.*, **46**, 365 (1963).
13) J. Hoigné, W. G. Burns, W. R. Marsh and T. Gäumann, *ibid.*, **47**, 247 (1964).
14) J. Weiss and C. H. Collins, *Radiat. Res.*, **28**, 1 (1966).
15) R. B. Ingalls, *J. Phys. Chem.*, **65**, 1605 (1961).
16) R. R. Hentz and M. Burton, *J. Amer. Chem. Soc.*, **73**, 552 (1951).
17) H. Schüller and M. Stockburger, *Spectrochim. Acta*, **15**, 841 (1959).
18) C. H. Leigh and M. Szwarc, *J. Chem. Phys.*, **20**, 403 (1952).
19) A. T. Blades and E. W. R. Steacie, *Can. J. Chem.*, **32**, 1142 (1954).
20) S. J. Price, *ibid.*, **40**, 1310 (1962).
*1 Professor M. Amagasa (Faculty of Engineering, Tohoku University) has been studying the reduction of toluene and related compounds. He kindly communicated the results of his gas-chromatographical analysis to Professor Murahashi.
*2 2,5-Dihydrotoluene was identified by comparison with an authentic sample prepared by the reduction of toluene.[21]
21) M. Amagasa, T. Yamaguchi and M. Tanaka, Brit. 1033760; *Chem. Abstr.*, **65**, 7075h (1966).

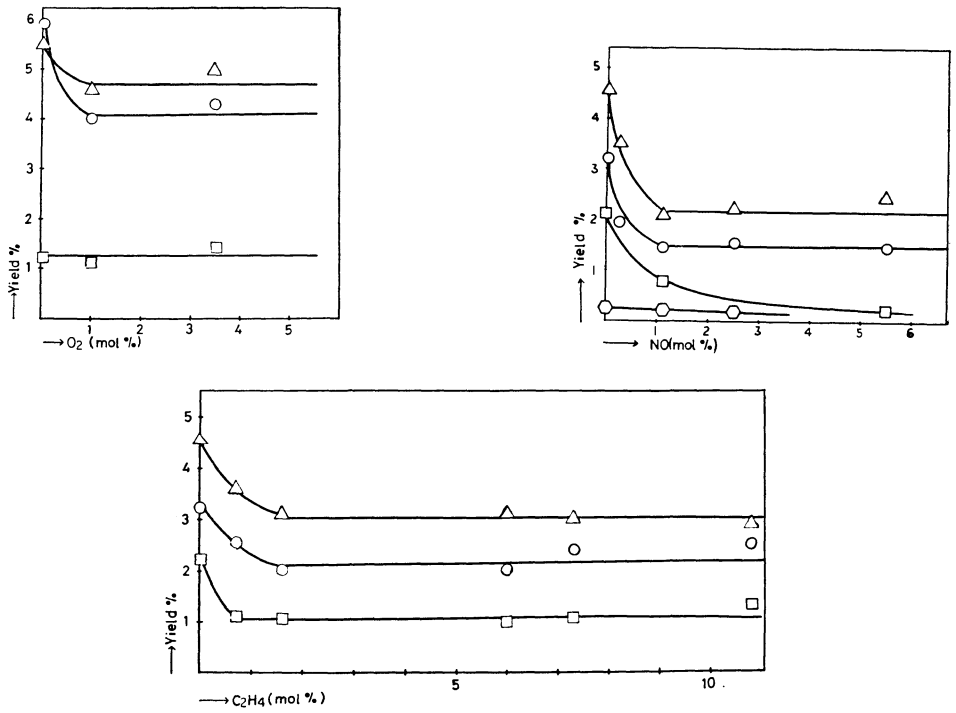

Fig. 3. 2450-MHz discharge of toluene.
△ Ethylbenzene, ○ Benzene, □ Ethane ⬡ 2,5-Dihydrotoluene

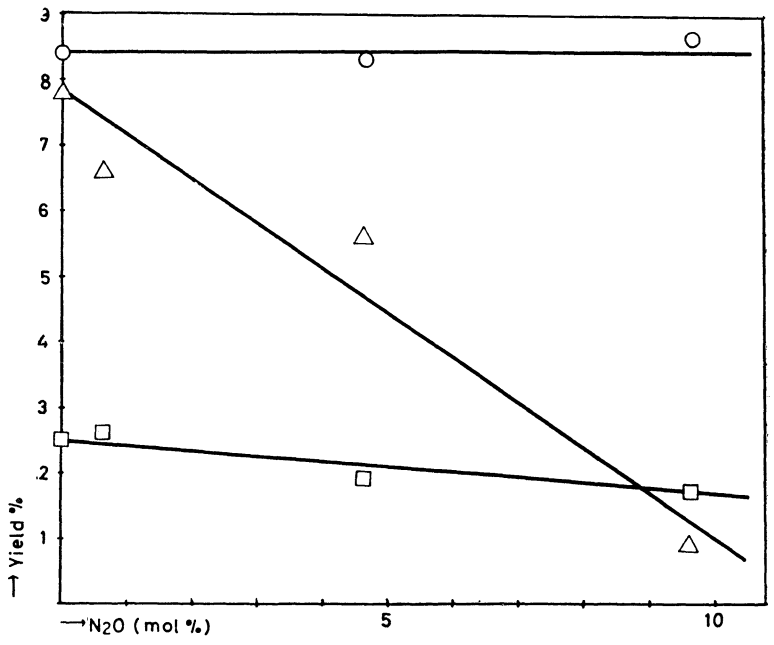

Fig. 4. 2450-MHz discharge of toluene.
△ Ethylbenzene, ○ Benzene, □ Ethane

electric discharge. Concerning the products, no difference in the reaction between 10 and 2450 MHz was found. Benzene and ethylbenzene were the main products in both the discharges. However, the variation in the product yields (based on the toluene consumed) with the concentration of the scavenger showed much difference between the 10- and 2450-MHz discharges, as is shown in Figs. 2, 3, and 4.

The Formation of Ethylbenzene. The main products are benzene and ethylbenzene. This experimental finding indicates that, in these discharges, phenyl radical are produced as well as benzyl radicals. Benzyl radicals have been reported to be commonly produced in the photolysis,[17] pyrolysis, and radiolysis of toluene. In the radiolysis[14] of liquid toluene, however, ethylbenzene is not the principal product. Cher[22] has found ethylbenzene, in the photolysis of gaseous toluene, to be a major non-gaseous product. Schüler and Stockburger[17] have also reported the formation of benzene and the benzyl radical in the discharge reaction of toluene and have pointed out, that in the electric discharge, the dissociation into H atoms is not a single process.

Effect of Scavenger. The fact that a small percentage of nitric oxide strongly inhibits the formation of ethylbenzene in the 10-MHz discharge, while nitrous oxide does not greatly inhibit it, suggests that the radical process is predominant in the reaction. On the other hand, in the 2450-MHz discharge about half of the ethylbenzene yield disappears in the presence of such radical scavengers as nitric oxide and ethylene. Moreover, the yield of ethylbenzene is also inhibited greatly in the presence of nitrous oxide. These experimental facts suggest that not only the radical but the ionic (not radical) process must be considered in the 2450-MHz discharge. This ionic process was also assumed by Streitwieser and Ward in the microwave discharge. However, these differences between the two discharge types are not yet clear.

Other Products. Benzaldehyde was found when nitric oxide and oxygen were used as scavengers in the 10-MHz discharge. One possible process of benzaldehyde formation may be shown as follows:

$$C_6H_5\text{-}CH_2\cdot + NO \rightarrow (C_6H_5\text{-}CH_2\text{-}NO) \rightarrow C_6H_5\text{-}COH + NH$$

In the 2450-MHz discharge, benzaldehyde was not detected in the presence of nitric oxide.

A small amount of nitrosobenzene was found in both the discharges; it may be produced by the reaction of the phenyl radical with nitric oxide. Phenylpropylene and phenylcyclopropane were not detected in these discharges when ethylene was used as a scavenger. Therefore, the formation of the benzal diradical[23] (C_6H_5-CH) was not confirmed. By using maleic anhydride, the formation of fulvene derivatives was not confirmed, either.

The author wishes to thank Professor S. Murahashi for his useful suggestions and encouragement, and Miss K. Motegi for her effort to the analyses of reaction products. He also thanks Dr. M. Imamura and Dr. M. Matsui for their helpful discussions and suggestions.

22) M. Cher, *J. Phys. Chem.*, **68**, 1316 (1964).

23) E. T. Roux, J. R. McNesby, W. M. Jackson and J. L. Faris, *ibid.*, **71**, 1531 (1967).

BULLETIN OF THE CHEMICAL SOCIETY OF JAPAN VOL. 43 1578—1580 (1970)

Studies of the Electric Discharge of Organic Compounds. II. The Decomposition of *o*-, *m*-, and *p*-Xylenes in 10-MHz and 2450-MHz Discharges

Ko Taki

The Institute of Physical and Chemical Research, Yamato-machi, Saitama

(Received October 16, 1969)

As has previously been shown[1] toluene gives benzene and ethylbenzene as the principal products in high-frequency electric discharges. The series of xylene isomers were chosen as the higher methyl-substituted benzene homologues in order to get further information on high-frequency electric discharges. Radical and electron scavengers were also used as additives in order to examine the reaction processes. The electric discharge assembly and the procedure of handling of the product were essentially the same as in previous studies. Product analyses were carried out by gas chromatography. The xylenes (Wako Pure Chemical Industries, Ltd.) were purified by repeated distillation or by recrystallization.

Table 1. The relative yields of the products based on *p*-xylene consumed

Residence time *p*-Xylene %	10-MHz discharge 0.15 sec 7.5% in He	2450-MHz discharge 0.009 sec 7.5% in He
Benzene	—	0.03
Toluene	1.00	1.00
2, 5-Dihydro-1,4-xylene	0.37	0.06
o-Xylene	—	0.03
4-Ethyltoluene	0.5	0.94
Styrene	0.05	0.05
1,2,4-Trimethylbenzene	0.13	0.03
Phenylacetylene		0.11
		5-Unidentified products
Methane	—	0.1
Ethane	0.19	0.14
Ethylene	—	0.02
Propane	—	0.01
Acetylene	—	0.04
Methylacetylene	0.04	0.06
Allene	0.02	0.01
Isobutane	0.01	0.11
1, 3-Butadiene	0.02	0.02
		3-Unidentified products
Polymer	17.7	0.41

1) K. Taki, This Bulletin, **43**, 1574 (1970).

Results and Discussion

The major products from *p*-xylene decomposition were benzene, toluene, 2,5-dihydroxylene,*1 and ethyltoluene. These products are similar to those from the toluene decomposition. The relative yields of these products are listed in Tables 1, 2, and 3.

Table 2. The relative yields of the products based on *m*-xylene consumed

Residence time *m*-Xylene %	10-MHz discharge 0.12 sec 9.5% in He	2450-MHz discharge 0.008 sec 9.2% in He
Benzene	0.05	0.1
Toluene	1.00	1.00
3-Ethyltoluene	0.6	0.7
Styrene	0.07	0.04
1, 2, 4-Trimethylbenzene	—	0.03
Phenylacetylene	—	0.04
Ethane	0.17	0.05
Polymer	14.6	1.8

Table 3. The relative yields of the products based on *o*-xylene consumed

Residence time *o*-Xylene %	10-MHz discharge 0.18 sec 3.1% in He	2450-MHz discharge 0.01 sec 3.5% in He
Benzene	0.2	0.1
Toluene	1.00	1.00
2-Ethyltoluene	1.8	1.0
Ethane	0.5	2.0
Polymer	12.6	2.3

The effects of the scavengers may be summarized as follows: the formations of ethyltoluene, toluene, and ethane are not affected by N_2O in the 10-MHz discharge, but the yields of toluene and ethyltoluene are inhibited to about half in the 2450-MHz discharge. On the other hand, while O_2 inhibits the

*1 2,5-Dihydroxylene was identified by comparison with an authentic sample prepared by the reduction of *p*-xylene in a liquid ammonia solution in the presence of sodium and water.

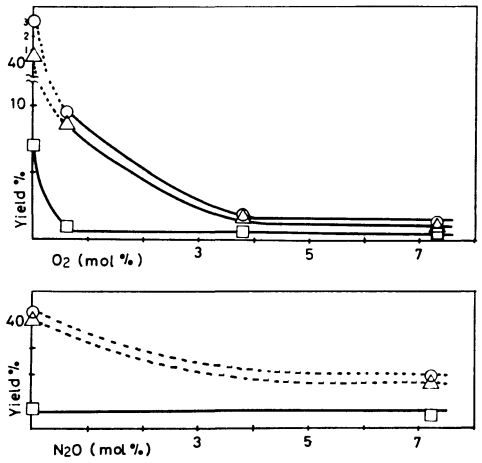

○ Toluene, △ Ethyltoluene, □ Ethane

Fig. 1 2450-MHz discharge of *p*-xylene.

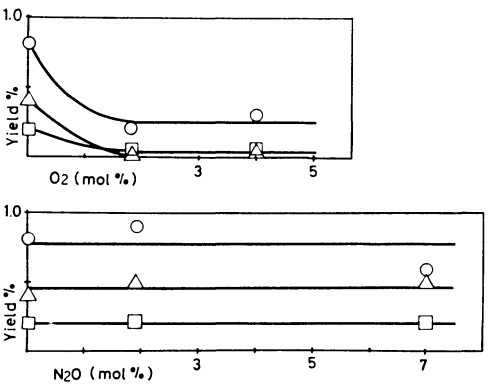

○ Toluene, △ Ethyltoluene, □ Ethane

Fig. 2. 10-MHz discharge of *p*-xylene.

yield of products in both the discharges, as is shown in Figs. 1 and 2. From the above results, both the radical and ionic (not radical) processes may be considered to be present in the 2450-MHz discharge and the radical process is predominant in the formation of products in the 10-MHz discharge as well as in the toluene decomposition.*2 In the 2450-MHz discharge, however, the inhibition of the product yields by O_2 is relatively higher in *p*-xylene than in toluene and the inhibition of the product by N_2O is smaller in *p*-xylene than in toluene. The difference in the effects of the scavengers between *p*-xylene and toluene may be considered to be the effects of the substituted methyl group. The ionic process is not more important than that of toluene decomposition. The process may be described as follows:

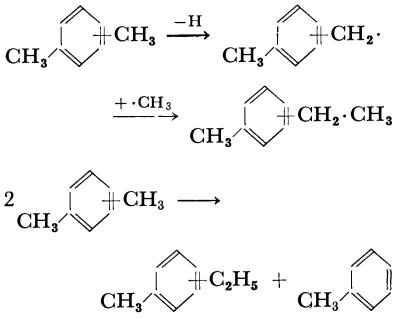

The High-boiling Fraction, Oligomer from *p*-Xylene. The IR spectra of the polymers from *p*-xylene showed the presence of an aliphatic methylene group at 2910 cm^{-1} and 2850 cm^{-1}, and a methyl group at 2950 cm^{-1} and 2875 cm^{-1}. The presence of the methylene group was also confirmed by another band at 1445 cm^{-1} (methylene skeleton vibration), and that of the *C*-methyl group, by a weak band at 1380 cm^{-1}. The presence of an aromatic ring was confirmed by the characteristic vibrations at 1510 cm^{-1} and 1605 cm^{-1}. In the 600—900 cm^{-1} region, the strong band at 815 cm^{-1} showed clearly the presence of *p*-substitution of the benzene ring. The band of double-bond stretching (1640 cm^{-1}) was not observed.

The NMR spectra of the polymers were determined in carbon tetrachloride, using tetramethylsilane (at τ value 10.0) as an internal standard. The chemical shifts were measured relative to the standard. The spectra involve three single bands, at τ 3.03, 7.15, and 7.67, having area ratios of 4.0 : 1.3 : 3.0 in both the 2450-MHz and 10-MHz discharge polymers. These protons are, respectively, those of *p*-substituted benzene, *p*-substituted methylene, and *p*-substituted methyl with IR data. From the area ratio of the protons, the number of *p*-substituted methylene ($\langle\bigcirc\rangle$-CH_2-CH_2-$\langle\bigcirc\rangle$) can be said to be small. However, it can not be monomethylene ($\langle\bigcirc\rangle$-CH_2-$\langle\bigcirc\rangle$) because the chemical shift of the proton of monomethylene is measured at τ 6.15. From these results, the structure of oligomer may be represented as:

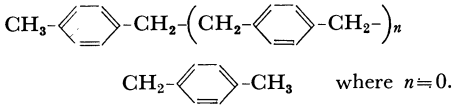

The presence of xylylene (CH_2=$\bigcirc$=CH_2) and its dimers could not be confirmed in these discharge reactions. The fraction of oligomers among the products was larger in the 10-MHz discharge than in the 2450-MHz, while the total conversion of *p*-xylene was higher in the 2450-MHz than in the 10-MHz discharge. The fraction of oligomer production may be considered to depend on the time of

*2 The photolysis of *o*-xylene gives ethyltoluene as the major product.[2]

2) H. R. Ward, *J. Amer. Chem. Soc.*, **89**, 2369 (1967).

residence in the discharge zone.*3

The author wishes to thank Professor S. Murahashi (Osaka University) for his useful suggestions and encouragement, Miss K. Motegi for her efforts in the analysis of the reaction products, and Dr. M. Imamura and Dr. M. Matsui for their helpful discussions and suggestions.

*3 Mr. K. Hiraoka[3] discussed the structure of the polymer obtained in the high-frequency electric discharge at the 20th and 21st Annual Meetings of The Chemical Society of Japan in 1967 and 1968.

3) K. Hiraoka, H. Kamada, and S. Hanai, *Nippon Kagaku Zasshi*, **90**, 1239 (1969).

BULLETIN OF THE CHEMICAL SOCIETY OF JAPAN VOL. 43 1580—1581 (1970)

Studies of the Electric Discharge of Organic Compounds. III. The Decomposition of Methylcyclohexane in 10-MHz and 2450-MHz Discharges

Ko Taki

The Institute of Physical and Chemical Research, Yamato-machi, Saitama

(Received October 16, 1969)

In the electric discharge of the methyl-substituted benzene homologue,[1,2] methyl migration has been found to be a main process. In this paper the methyl-group migration on methylcyclohexane in the high-frequency electric discharge was examined. Methylcyclohexane was chosen as a representative of saturated hydrocarbons. As has been shown previously,[1] radical and electron scavengers were used to investigate the reaction process, and the product distributions were described. Methylcyclohexane (Tokyo Kasei Kogyo Co., Ltd.) was purified by repeated distillation so as to make it gas-chromatographically pure.

Results and Discussion

The gaseous products were methane, ethane, ethylene, acetylene, propane, methylacetylene, allene, isobutane, butadiene, and seven unidentified products, while the liquid products were 1-methylcyclohexene, 4-methylcyclohexene, cyclohexane, and ten unidentified products. It was confirmed that ethylcyclohexane*1 is not formed in the present work, while in the case of toluene ethylbenzene is one of the major products. The yields of the products are shown in Table 1. Figures 1 and 2 show the effects of added oxygen and nitrous oxide on the yields of 1-methylcyclohexene and 4-methylcyclohexene.

From these data, the effects of additives can be summarized as follows: The yields of 1-methylcyclohexene and 4-methylcyclohexene decrease with an increase in the quantity of O_2 and N_2O scavengers in both the discharges, but the effect seems to be a little larger in the case of the O_2 scavenger. Moreover, the formation of ethane is inhibited by O_2, but not by N_2O, in both the discharges. The formation of cyclohexane is inhibited by both the scavengers; no striking difference in effect between the two additives is observed. The main products, 1- and 4-methylcyclohexenes, may be formed by the dehydrogenation, of the cyclohexane ring. Arnold[3] reported that the decomposition of cyclohexane in an electric discharge can be explained quantitatively by a radical mechanism.

The formation of cyclohexane and ethylcyclohexane involves the cleavage and recombination of the methyl group from methylcyclohexane, but ethylcyclohexane was not obtained in the discharges. The migration of the methyl group is quite different from that of toluene and xylene. The reason for this is not clear, but it may be explained by the stability of the benzene ring. Moreover, the fact that nitrous oxide does not inhibit the formation of 1- and 4-methylcyclohexenes so greatly as toluene decomposition[1] may be explained by assuming that the compounds having an electron network, such as toluene, behave differently from the saturated counterparts, such as methylcyclohexane, in the electron bombardment of an electric discharge.

The decomposition of methylcyclohexane gives many fragmented products in the discharges; this fact coincides with the result reported by Streitwieser and Ward.[4] The differences between the

1) K. Taki, This Bulletin, **43**, 1574 (1970).
2) K. Taki, *ibid.*, **43**, 1578 (1970).
*1 Authentic ethylcyclohexane was prepared by the reduction of ethylbenzene using a ruthenium carbon catalyser. The catalyser was kindly provided by Dr. Taya of this Institute.
3) G. Arnold, *Z. Naturforsch.*, *A*, **20**, 435 (1965).
4) A. Streitwieser, Jr., and H. R. Ward, *J. Amer. Chem. Soc.*, **85**, 539 (1963).

TABLE 1. THE YIELD % OF THE PRODUCTS BASED ON METHYLCYCLOHEXANE CONSUMED

	10-MHz discharge	2450-MHz dischage
Residence time	0.21 sec	0.009 sec
Methylcyclohexane %	9.1% in He	9.1% in He
Methane	0.39	2.1
Ethane	1.25	1.7
Ethylene	4.1	3.7
Acetylene	0.73	4.5
Propane	0.57	0.93
Methylacetylene + Allene	2.62	8.4
Isobutane + 1,3-Butadiene	0.08	2.3
	5-Unidentified products	7-Unidentified products
Cyclohexane	0.95	0.9
4-Methylcyclohexene	1.19	15.1
1-Methylcyclohexene	15.1	11.5
Benzene	—	0.2
Toluene	0.31	0.3
	6-Unidentified products	5-Unidentified products
Polymer	5.8	3.8

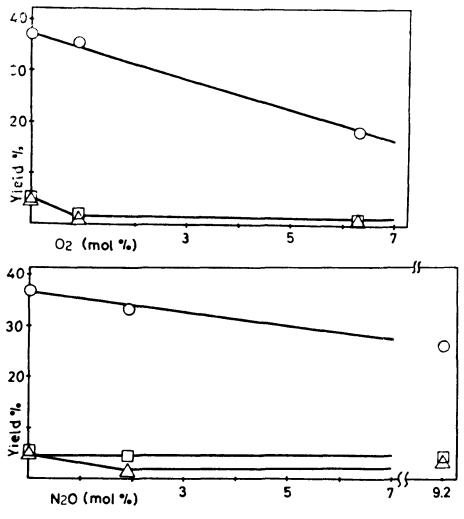

Fig. 1. 2450-MHz discharge of methylcyclohexane.
○ 1-Me-cyclohexene+4-Me-cyclohexene
△ Cyclohexane
□ Ethane

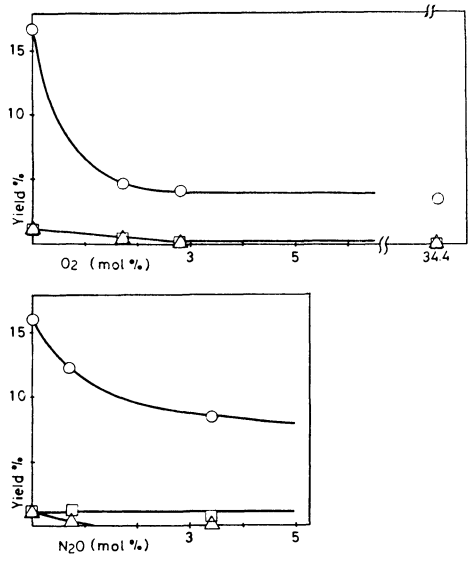

Fig. 2. 10-MHz discharge of methylcyclohexane.
○ 1-Me-cyclohexene+4-Me-cyclohexene
△ Cyclohexane
□ Ethane

two types of discharges, 10 and 2450 MHz, were not clear.

The author wishes to thank Professor S. Murahashi (Osaka University) for his useful suggestions and encouragement and Miss K. Motegi for her help with the analyses of the reaction products. He also wishes to thank Dr. M. Imamura and Dr. M. Matsui for their helpful discussions and suggestions.

BULLETIN OF THE CHEMICAL SOCIETY OF JAPAN VOL. 43 1582—1584 (1970)

Oxazolidone Derivatives of Hydroxyamino Acid. VI.[1] Reactions of Phosgene on *N*-Acylserine Esters

Toshishige INUI, Shigeo TANAKA and Masakatsu TAKINO

Institute of Chemistry, College of General Education, Osaka University, Toyonaka, Osaka

(Received October 20, 1969)

Treatment of *N*-(β-hydroxyethyl)-benzamide (I), *i.e.* *N*-benzoyl derivative of β-hydroxyethylamine, with phosgene and subsequent heating afforded *N*-(β-chloroethyl)-benzamide (II) through the corresponding *O*-chlorocarbonyl derivative. However, under the same condition, benzyl *N*-(β-hydroxyethyl)-carbamate (III) yielded only 3-benzyloxy-

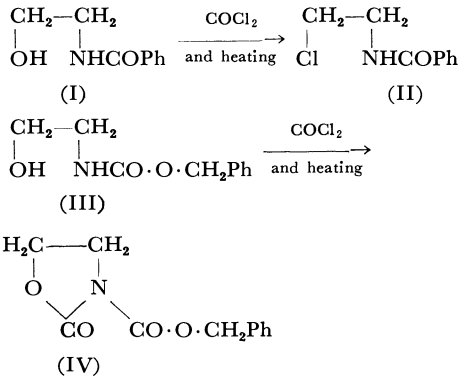

carbonyl(cbz)-2-oxo-oxazolidine (IV).[2] The present paper is concerned with the reactions of phosgene with *N*-benzoyl- and *N*-cbz-derivatives of methyl L-serinate (V and IX), having structures similar to those of I and III respectively.

Bergel reported that the reaction of benzyl *N*-cbz-DL-serinate with phosgene in benzene gave benzyl *N*-cbz-*O*-chlorocarbonyl-DL-serinate.[3] In the present study, methyl *N*-benzoyl-L-serinate (V), obtained from methyl L-serinate and benzoyl chloride, was converted with phosgene to the *O*-chlorocarbonyl derivative (VI). Reflux of VI in xylene provided a crystalline product, which was shown to be a mixture of methyl L-2-benzamido-3-chloropropionate (VII) and methyl 3-benzoyl-L-2-oxo-oxazolidine-4-carboxylate (VIII) by means of thin-layer chromatography with silica gel G (TLC). Separation of VII from VIII was achieved by using a column with silica gel, and by eluting it with a mixture of chloroform and ethyl acetate (9 : 1, v/v). The structures of compounds, VII and VIII, were

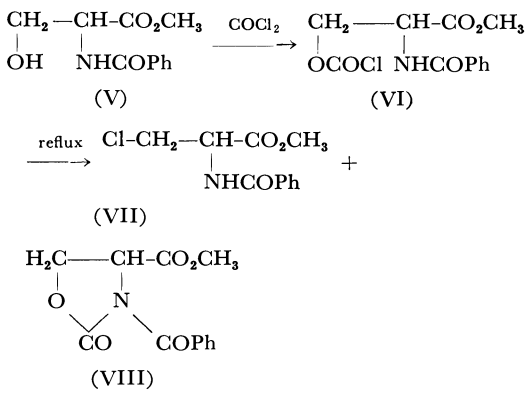

confirmed by their infrared spectra and nuclear magnetic resonance (NMR) spectra.

In a similar manner, the oily methyl *N*-cbz-L-serinate (IX) was converted with phosgene to the corresponding *O*-chlorocarbonyl compound (X). In this case, methyl 3-cbz-L-2-oxo-oxazolidine-4-carboxylate (XI) was obtained as the sole product by heating X in xylene. The structure of XI was also confirmed by elemental analysis and by a study of its

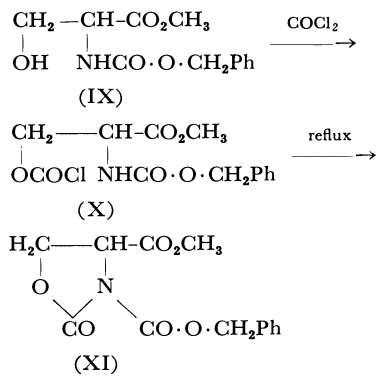

NMR spectra. Catalytic hydrogenation and subsequent hydrolysis of XI gave L-2-oxo-oxazolidine-4-carboxylic acid (XII). The properties tested on XII were identical with those of the authentic sample[4,5].

1) Part V: T. Inui, Y. Ohta, T. Ujike, H. Katsura and T. Kaneko, This Bulletin, **41**, 2148 (1968).
2) D. Ben-Ishai, *J. Amer. Chem. Soc.*, **78**, 4962 (1956).
3) F. Bergel and R. Wade, *J. Chem. Soc.*, **1959**, 941.
4) T. Kaneko, I. Takeuchi and T. Inui, This Bulletin, **41**, 974 (1968).
5) T. Saito, *ibid.*, **37**, 624 (1964).

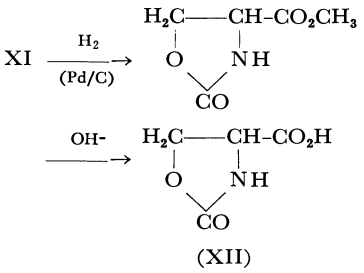

(XII)

Experimental*1

Methyl *N*-Benzoyl-L-serinate (V). To a cold solution of methyl L-serinate hydrochloride (15.6 g, 0.1 mol) in water (225 m*l*), sodium hydrogen carbonate (25.2 g, 0.3 mol) and benzoyl chloride (16.0 m*l*, 0.13 mol) were added in succession. The reaction mixture was stirred for 2—3 hr at room temperature, and the resulting clear solution was extracted twice with ethyl acetate. Evaporation of the dried extract provided V as crystals. Yield, 18.0 g (81%), mp 85—86°C after recrystallization from benzene, $[\alpha]_D^{20}$ +16.0° (*c* 1.25, 95% ethanol); lit,[6] mp 84—86°C, $[\alpha]_D^{26}$ +17.7° (*c* 1, 95% ethanol).

Found: C, 59.27; H, 5.95; N, 6.34%. Calcd for $C_{11}H_{13}NO_4$: C, 59.19; H, 5.87; N, 6.27%.

Methyl *N*-Benzoyl-*O*-chlorocarbonyl-L-serinate (VI). Phosgene was passed through a solution of V (13.4 g, 0.06 mol) and *N*,*N*-dimethylaniline (7.3 g, 0.06 mol) in benzene (240 m*l*) at 5—10°C for 20 min, and the mixture was stirred for 2—3 hr below 20°C. Nitrogen was passed through the solution to remove the excess phosgene. The benzene solution was washed with dilute hydrochloric acid. The dried solution was evaporated *in vacuo* to give VI. Yield, 15.1 g (88%), mp 95—96°C (decomp.) after recrystallization from benzene.

Found: C, 50.28; H, 3.86; N, 4.85%. Calcd for $C_{12}H_{12}NO_5Cl$: C, 50.46; H, 4.23; N, 4.90%.

Treatment of a solution of VI in benzene with an etheral solution of aniline gave methyl *N*-benzoyl-*O*-(*N*-phenylcarbamoyl)-L-serinate; mp 134°C, $[\alpha]_D^{20}$ −24.1° (*c* 2.36, *N*,*N*-dimethylformamide).

Found: C, 63.16; H, 5.22; N, 7.76%. Calcd for $C_{18}H_{18}N_2O_5$: C, 63.15; H, 5.30; N, 8.18%.

Methyl L-2-Benzamido-3-chloropropionate (VII) and Methyl 3-Benzoyl-L-2-oxo-oxazolidine-4-carboxylate (VIII). A solution of VI (2.86 g, 0.01 mol) in xylene (60 m*l*) was refluxed for 4.5 hr. The solution was evaporated *in vacuo* to give an oil which was solidified by seeding (wt, 2.44 g). It gave a strong positive Beilstein's test and exhibited two spots on TLC. The product in a minimum amount of chloroform was adsorbed on a column (diameter 1.6 cm) of silica gel (50 g) and eluted with a mixture of chloroform and ethyl acetate (9: 1, v/v). Aliquots of the effluent fractions were subjected to TLC.

The fractions, exhibiting a single spot (R_f~0.50)*2 on TLC, were combined and evaporated *in vacuo* to give VII as crystals. Yield, 0.62 g (25.6%) mp 112—114°C. Recrystallization from petroleum ether raised the melting point to 114—116°C, $[\alpha]_D^{20}$ −12.9° (*c* 1.67, 95% ethanol); lit,[6] mp 114—115.5°C,$[\alpha]_D^{23}$ −14° (*c* 1, 95% ethanol).

IR (Nujol mull): 3280, 1635, 1540 (–CONH– in the amide group), 1735 cm^{-1} (C=O in the ester group).

NMR (Deuterochloroform solution, 60 MHz): 3.84 (singlet, CH_3– peak in the ester group), 4.03 (doublet, J=3.2 Hz, $-CH_2-$ peak in the Cl–CH_2–CH group), 5.16 (quintet, >CH peak in the $-CH_2-CH-NH-$ group), 6.85—7.20 (broad, NH peak), 7.25—7.90 ppm (multiplet, C_6H_5– peak).

Found: C, 54.46; H, 4.70; N, 5.50%. Calcd for $C_{11}H_{12}NO_3Cl$: C, 54.67; H, 5.00; N, 5.80%.

The other fractions exhibiting a single spot (R_f~0.25)*2 on TLC, were also combined and evaporated *in vacuo* to obtain VIII as prisms. Yield, 0.25 g (10.0%), mp 123—124°C. For analysis, it was recrystallized from benzene-petroleum ether (2: 1), mp 124.0—124.5°C, $[\alpha]_D^{23}$ −10.6° (*c* 2.08, methanol).

IR (Nujol mull): 1790 (C=O in the oxazolidone ring), 1750, 1730 (C=O in the ester group), 1680 cm^{-1} (C=O in the benzoyl group).

NMR (Deuterochloroform solution, 60 MHz): 3.80 (singlet, CH_3– peak in the ester group), 4.17—5.15 (multiplet, $-CH_2-CH$ peak in the oxazolidone ring), 7.35—7.75 ppm (multiplet, C_6H_5– peak).

Found: C, 57.58; H, 4.40; N, 5.89%. Calcd for $C_{12}H_{11}NO_5$: C, 57.83; H, 4.45; N, 5.62%.

Methyl *N*-Cbz-L-serinate (IX). Applying the method for the preparation of dimethyl *N*,*N*′-biscbz-L-cystinate by Zervas[7], a solution of methyl L-serinate hydrochloride (3.1 g, 0.02 mol) in a mixture of 30% aqueous potassium hydrogen carbonate solution (30 m*l*) and chloroform (30 m*l*) was treated with cbz-chloride (4.0 m*l*) at 5°C for 1 hr. The chloroform layer was treated with pyridine (1.0 m*l*) at 5°C for 10 hr and then washed successively with dilute sulfric acid, water and dilute aqueous potassium hydrogen carbonate solution. Evaporation of the dried solution gave IX as syrup. Yield, 4.3 g (85%).

Methyl *N*-Cbz-*O*-chlorocarbonyl-L-serinate (X). In a way similar to that described for the preparation of VI, phosgene was passed through a solution of IX (5.0 g, 0.02 mol) and *N*,*N*-dimethylaniline (2.4 g, 0.02 mol) in benzene (80 m*l*) for 20 min at 5—10°C. From the reaction mixture, X was obtained as white crystals. Yield, 5.1 g (82%), mp 65—67°C.

Found: C, 49.98; H, 4.33; N, 3.85%. Calcd for $C_{13}H_{14}NO_6Cl$: C, 49.46; H, 4.47; N, 4.44%.

Methyl *N*-cbz-*O*-(*N*-phenylcarbamoyl)-L-serinate was obtained by treatment of aniline on X, mp 127—128°C and 128—129°C after recrystallization from benzene, $[\alpha]_D^{20}$ −23.6° (*c* 1.25, *N*,*N*-dimethylformamide).

Found: C, 61.08; H, 5.39; N, 7.40%. Calcd for $C_{19}H_{20}N_2O_6$: C, 61.28; H, 5.41; N, 7.52%.

Methyl 3-Cbz-L-2-oxo-oxazolidine-4-carboxylate (XI). A solution of X (2.5 g, 0.008 mol) in xylene (50 m*l*) was refluxed for 5 hr. The solution was evaporated *in vacuo* to leave crystals exhibiting a single spot (R_f~0.45)*2 on TLC. Yield, 1.6 g (72%), mp 63—64°C and 64—65°C after recrystallization from ether, $[\alpha]_D^{20}$ −80.1° (*c* 3.39, methanol).

IR (Nujol mull): 1810 (C=O in the oxazolidone ring), 1745 (C=O in the ester group), 1730 cm^{-1} (C=O in the cbz group).

*1 All melting points are uncorrected.

6) E. M. Fry, *J. Org. Chem.*, **15**, 438 (1950).

*2 The R_f values refer to TLC with the chloroform-ethyl acetate (9: 1, v/v) as solvent system.

7) L. Zervas and L. Photaki, *J. Amer. Chem. Soc.*, **84**, 3887 (1962).

NMR (Deuterochloroform solution, 60 MHz): 3.73 (singlet, CH_3– peak in the ester group), 4.14—4.94 (multiplet, $-CH_2-\underset{|}{CH}-$ peak in the oxazolidone ring), 5.30 (slightly split singlet, $-CH_2-$ peak in the cbz group) 7.35 ppm (singlet, C_6H_5– peak).

Found: C, 56.01; H, 4.62; N, 5.12%. Calcd for $C_{13}H_{13}NO_6$: C, 55.92; H, 4.69; N, 5.02%.

L-2-Oxo-oxazolidine-4-carboxylic Acid (XII). A stream of hydrogen was passed through a solution of XI (4.2 g, 0.015 mol) in a mixture of methanol (50 m*l*) and water (10 m*l*) for 3 hr in the presence of 10% palladium on carbon (1.0 g). After the catalysts had been removed by filtration, the filtrate was evaporated *in vacuo* to provide an oil (wt, 1.4 g). Into a solution of the oil in methanol (35 m*l*), 1 N potassium hydroxide (9.5 m*l*, 0.0095 mol) was added and the mixture was stirred for 1.5 hr at room temperature. The solvent was evaporated *in vacuo* to a small volume, and the residual solution was diluted with water. The aqueous solution was extracted with ethyl acetate and acidified with 1 N hydrochloric acid (10 m*l*). The acidic solution was evaporated *in vacuo* to dryness and the residue was extracted three times with hot ethyl acetate. The dried extract was evaporated *in vacuo* to give XII as crystals. Yield, 1.0 g (51%), mp 114—117°C and 118—119°C after recrystallization from ethyl acetate-petroleum ether, $[\alpha]_D^{20}$ −18.2° (*c* 2.23, water); lit,[4] mp 118.5—120°C, $[\alpha]_D^{22.5}$ −17.7° (*c* 3.44, water).

The mixed melting point with an authentic sample was not depressed. The results obtained by means of infrared spectra were also identical with those of an authentic sample.

The authors wish to express their thanks to Professor T. Kaneko of Faculty of Science, Osaka University, for his valuable discussions, and to the Ajinomoto Co., Inc., for supplying the amino acids.

BULLETIN OF THE CHEMICAL SOCIETY OF JAPAN VOL. 43 1584—1585 (1970)

Absolute Configuration of Menthenone Oxide

Jun KATSUHARA, Hisaichi YAMASAKI and Noriyuki YAMAMOTO

Sun Star Dentifrice Company, Research Laboratory, Takatsuki, Osaka

(Received October 25, 1969)

One[1] of the authors (J.K.) has recently discussed the epoxidation mechanism of endocyclic α,β-unsaturated terpene ketones, and, on the basis of orbital-overlap concept,[2] has concluded that the oxirane group is stereoselectively introduced to the double bond so as to sterically enable the most favored transition state conformation to be stabilized by an effective and concomitant orbital-overlap stabilization. When this generalization is applied to (1R)-4-menthene-3-one (II), the exclusive formation of 4-menthen-3-one oxide (III) having the (1R : 4R : 5R)-configuration may be predicted.

We wish in this paper to describe the determination of the absolute configuration of (+)-menthenone oxide (III) by an unequivocal chemical transformation into known derivative (+)-*trans*-menthenol (IV) of the well-defined configuration (1 S : 3 R) by the following scheme.

The results unambiguously demonstrate that the absolute configuration of (+)-menthenone oxide

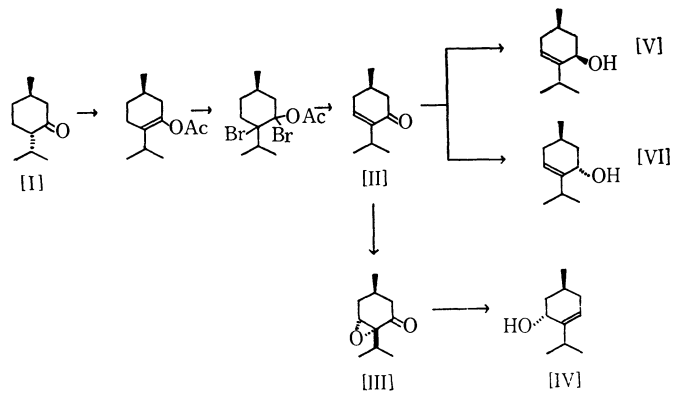

Scheme 1

1) J. Katsuhara, This Bulletin, **42**, 2391 (1969).
2) H. E. Zimmerman, L. Singer and B. S. Thyagaraja, *J. Amer. Chem. Soc.*, **81**, 108 (1959).

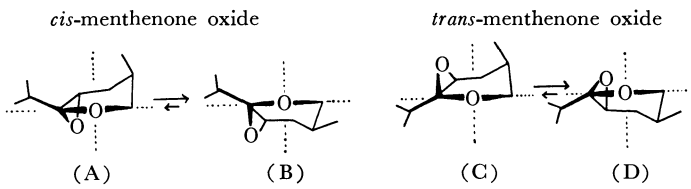

Scheme 2

(III) is *cis*-(1 R : 4 R : 5 R). This is what was predicted previously.[1]

Octant projection diagrams, when conformational generalization is applied to the present *cis*- and *trans*-menthenone oxide systems, are shown in Scheme 2. It can be seen that, of the four conceivable conformations A, B, C and D, B and D are conformationally more favored than the respective counterpart. The diagrams show that in the ORD-measurement, *cis*-menthenone oxide should exhibit a high positive [ϕ] value whereas the *trans*-oxide a low negative [ϕ] value. This is also in good agreement[3] with the ORD data found for the (+)-menthenone oxide (a=+25), cogently supporting the configuration of *cis*-(+)-III as assigned above.

Experimental

Preparation of Menthenone Oxide (III). (−)-Menthenone (II)[4] 7.0 g, $[\alpha]_D^{20}$ −52.2° (c 0.6, ethanol), UV; $\lambda_{max}^{methanol}$ 236 mμ (ε, 7240), II-2,4-dinitrophenylhydrazone mp 142°C (lit,[4] mp 143°C), yield 87.0%, derived from (−)-menthone (I), $[\alpha]_D^{20}$ −22.1° (c 0.6, ethanol) was epoxidized with 26 m*l* of 30% hydrogen peroxide and 3.5 g of sodium in 140 m*l* of methanol for 5 hr at −30°C to menthenone oxide (III). The crude III indicated a single product by VPC analysis. Further purification on a preparative VPC gave pure III, $[\alpha]_D^{20}$ +61.5° (c 1.0, methanol), UV; $\lambda_{max}^{methanol}$ 299 mμ (ε, 20), 288 mμ (ε, 19), CD; mμ ([θ]) in methanol, 350 (0), 308 (+2035), 245 (0), 205 (+6460), ORD; mμ ([ϕ]) in methanol, 400 (+392), 355 (+1632), 292 (−849), 250 (+554), 220 (+3589), 210 (+979), yield 63.5%.

Found: C, 71.26; H, 9.65%. Calcd for $C_{10}H_{16}O_2$: C, 71.44; H, 9.60%.

Preperation of (+)-*trans*-Menthenol. By means of the Wharton reaction[5] technique, the oxide III has been converted into crude (+)-*trans*-menthenol (IV), $[\alpha]_D^{20}$ +69.1° (c 0.6, ethanol), yield 87.0%, IV-*p*-nitrobenzoate mp 54°C (lit,[6] mp 55°C), $[\alpha]_D^{20}$ −197° (c 0.1, chloroform).

Reduction of Menthenone (II). (−)-Menthenone (II) was reduced with lithium aluminum hydride in ether to give a mixture (yield 80.0%) of (−)-*cis*-menthenol (V), $[\alpha]_D^{24}$ −32.0° (c 1.0, ethanol), V-*p*-nitrobenzoate mp 38°C, $[\alpha]_D^{24}$ −10.4° (c 0.1, chloroform), and (−)-*trans*-menthenol (VI), the ratio of formation V: VI was 93: 7 as determined by VPC analysis. The epimeric (−)-VI was identified to be (+)-IV by comparison of each R_t of VPC.

The author wishes to thank Professor Tamon Matsuura of Hiroshima University, Professor Yuzo Inouye of Kyoto University, and Dr. Hitoshi Minato and Dr. Kaoru Kuriyama of Shionogi Research Laboratory for many helpful discussions during the course of this work.

3) C. Djerassi, W. Klyne, T. Norin, G. Ohloff and E. Klein, *Tetrahedron*, **21**, 163 (1965).

4) W. Treibs and H. Albrecht, *J. Prakt. Chem.*, **13**, 291 (1961).

5) P. S. Wharton and D. H. Bohlen, *J. Org. Chem.*, **26**, 3615 (1961).

6) D. Malcolm and J. Read, *J. Chem. Soc.*, **1939**, 1037.

BULLETIN OF THE CHEMICAL SOCIETY OF JAPAN VOL. 43 1586—1588 (1970)

Preparation of Some α,β-Unsaturated Aldehydes

Sadayoshi SATSUMABAYASHI, Kiyoshi NAKAJO, Ryuichi SONEDA and Shinichi MOTOKI

Department of Chemistry, Science University of Tokyo, Kagurazaka, Shinjuku-ku, Tokyo

(Received November 5, 1969)

Copenhaver[1] and Hoaglin[2] reported that α,β-unsaturated ethers reacted with saturated aldehydes to form unsaturated aldehydes having two more carbon atoms than the starting aldehydes. However, the works were limited to the reactions of vinyl alkyl ethers with aldehydes except for the reaction of 1-butenyl methyl ether with butyraldehyde. If β-substituted vinyl alkyl ethers were used in addition to vinyl alkyl ethers in these reactions, they could be generalized as a preparative method for α,β-unsaturated aldehydes.

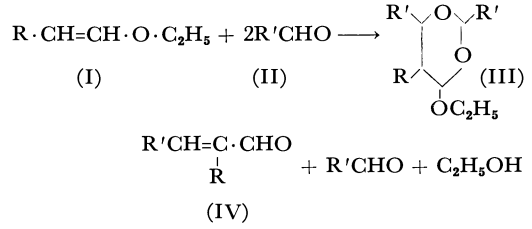

(I) (II) (III)

(IV)

In the present study, 1-propenyl ethyl ether (Ia), 1-butenyl ethyl ether (Ib) and 3-cyano-1-propenyl ethyl ether (Ic) were used as the alkenyl alkyl ether component (I), and acetaldehyde (IIa), propionaldehyde (IIb), butyraldehyde (IIc), benzaldehyde (IId) and β-cyanopropionaldehyde (IIe) were used as the aldehyde component (II). All the reactions of I with II were carried out according to Hoaglin's method, and the results obtained are presented in Table 1.

Hoaglin and Hirsch reported that the intermediate of the reaction was 1,3-dioxane (III), an addition product of one molecule of I and two of II, but gave no experimental details on the isolation and identification of III.[2]

When the catalyst was neutralized with sodium carbonate prior to hydrolysis, a colorless compound was isolated by distillation in a fairly good yield. The analytical values and molecular weight of this compound were very close to those of III, and the IR spectrum exhibited strong doublet peaks in the region 1150—1080 corresponding to those of 1,3-dioxane. This compound was readily converted to the unsaturated aldehyde (IV) by means of hydrolysis with dilute acid. From these facts, it may be concluded that the product is III. The results are summarized in Table 2.

The reaction was also extended to ketones. In a similar manner to that with aldehydes, the reaction of I with acetone (Va) as well as methyl ethyl ketone (Vb) was carried out. Although the yields of VI were lower than those of IV, the expected α,β-unsaturated aldehydes (VI) were also obtained as shown in Table 3. The intermediates were not isolated in this case.

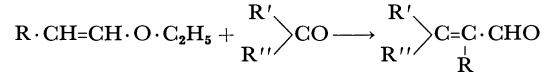

(I) (V) (VI)

The advantage of this method, in comparison with aldol condensation, lies in the preparation of the optional α-substituted-α,β-unsaturated aldehydes and the ease of isolation of the product. Condensation of aldehyde with ketone has a significant limitation. Self-condensation of aldehyde or condensation at the α-carbon atom of ketone takes place and ketone does not condense at the α-carbon atom of aldehyde to form unsaturated aldehyde with simple basic or acid catalysts. Thus, the present reaction to yield VI is regarded as a reaction of wide utility.

Experimental

Materials. 1-Propenyl ethyl ether (Ia) and 1-butenyl ethyl ether (Ib) were obtained by catalytic decomposition of the corresponding aldehyde diethyl acetals.[3]

3-Cyano-1-propenyl ethyl ether (Ic) was prepared from β-cyanopropionaldehyde diethyl acetal.[4]

α-Substituted-α,β-unsaturated Aldehydes (IV). To a mixture of 0.1 mol of unsaturated ether (I) and 0.3 mol of aldehyde (II), 0.5 g of boron trifluoride etherate in 5 m*l* of diethyl ether was added with good agitation under an anhydrous condition. The temperature of the content was maintained at about 30°C by regulating the rate of addition of catalyst and by external cooling with water. After the mixture was stirred for 4 hr at room temperature, the reaction mixture was directly hydrolyzed by refluxing with 50 m*l* of 10% hydrochloric acid for 6 hr. The oily product was ex-

1) J. W. Copenhaver, U. S. 2543312 (1951).

2) R. I. Hoaglin and D. H. Hirsh, *ibid.* 2628257 (1953).

3) W. Rottig and O. Liethen, German 1019090 (1957).

4) S. Satsumabayashi and S. Motoki, This Bulletin, **41**, 2538 (1968).

TABLE 1. $R\cdot CH{=}CH\cdot O\cdot C_2H_5$ (I) + $R'CHO$ (II) ⟶ $R'CH{=}\overset{R}{\overset{|}{C}}\cdot CHO$ (IV)

Ether	Aldehyde	R	R′	Product
Ia	IIa	CH_3	CH_3	IVa: 2-methyl-2-butenal-(1)
Ia	IIb	CH_3	C_2H_5	IVb: 2-methyl-2-pentenal-(1)
Ia	IIc	CH_3	n-C_3H_7	IVc: 2-methyl-2-hexenal-(1)
Ia	IId	CH_3	C_6H_5	IVd: 2-methyl-3-phenyl-2-propenal-(1)
Ia	IIe	CH_3	$NC\cdot CH_2CH_2$	IVe: 5-cyano-2-methyl-2-pentenal-(1)
Ib	IIa	C_2H_5	CH_3	IVf: 2-ethyl-2-butenal-(1)
Ib	IIb	C_2H_5	C_2H_5	IVg: 2-ethyl-2-pentenal-(1)
Ib	IIc	C_2H_5	n-C_3H_7	IVh: 2-ethyl-2-hexenal-(1)
Ib	IId	C_2H_5	C_6H_5	IVi: 2-ethyl-3-phenyl-2-propenal-(1)
Ib	IIe	C_2H_5	$NC\cdot CH_2CH_2$	IVj: 5-cyano-2-ethyl-2-pentenal-(1)
Ic	IIa	$NC\cdot CH_2$	CH_3	IVk: 2-cyanomethyl-2-butenal-(1)
Ic	IIb	$NC\cdot CH_2$	C_2H_5	IVl: 2-cyanomethyl-2-pentenal-(1)

	Bp	Yield	IR(cm^{-1})		Analysis: Calcd		Found	
	(°C/ mmHg)	(%)	-CHO	C=C	C%	H%	C%	H%
IVa	117—118	50.5	2725, 1692	1645	71.39	9.59	71.10	9.82
IVb	51— 52/4	91.5	2720, 1685	1640	73.43	10.27	73.35	10.47
IVc	55— 57/11	67.5	2710, 1680	1639	74.95	10.78	75.11	10.57
IVd	97— 99/4	52.8	2725, 1685	1629	82.16	6.90	81.98	7.13
IVe	118—120/5	29.0	2730, 1692	1641	68.27	7.37	68.20	7.62
IVf	57— 59/55	55.1	2725, 1692	1648	73.43	10.27	73.21	9.99
IVg	58— 59/25	67.9	2700, 1680	1637	74.95	10.78	74.79	10.93
IVh	54— 55/7	54.9	2710, 1682	1640	76.14	11.18	75.85	11.24
IVi	102—104/3	64.1	2730, 1690	1635	82.46	7.55	82.39	7.80
IVj	122—123/4	33.4	2725, 1679	1639	70.04	8.08	69.78	8.31
IVk	87— 89/4	30.8	2720, 1681	1650	66.03	6.47	65.81	6.70
IVl	115—117/4	25.0	2710, 1688	1645	68.27	7.37	67.99	7.45

TABLE 2. $R\cdot CH{=}CH\cdot O\cdot C_2H_5 + 2R'CHO$ ⟶ 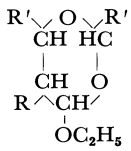

(I) (II) (III)

Ether	Aldehyde	R	R′	Product
Ib	IIa	C_2H_5	CH_3	IIIa: 4-ethoxy-5-ethyl-2,6-dimethyl-1,3-dioxane
Ib	IIc	C_2H_5	n-C_3H_7	IIIb: 4-ethoxy-5-ethyl-2,6-dipropyl-1,3-dioxane
Ib	IId	C_2H_5	C_6H_5	IIIc: 4-ethoxy-5-ethyl-2,6-diphenyl-1,3-dioxane

	Bp	Yield	IR(cm^{-1})	Analysis: Calcd	Found	Molecular weight: Calcd	Found
	(°C/ mmHg)	(%)	-C-O-C-O-C-	(%)	(%)		
IIIa	64- 65/6	57.2	1145, 1105	C: 63.79 H: 10.71	63.57 10.99	188.3	183.2
IIIb	127-129/2	58·8	1145, 1100	C: 68.81 H: 11.55	68.64 11.81	244.4	238.5
IIIc	175-177/2	70.1	1130, 1090	C: 76.89 H: 7.74	76.78 7.53	312.4	320.2

TABLE 3. $R\cdot CH{=}CH\cdot O\cdot C_2H_5 + \begin{matrix}R'\\R''\end{matrix}\!\!>\!CO \longrightarrow \begin{matrix}R'\\R''\end{matrix}\!\!>\!C{=}C\cdot CHO$ (R)

(I) (V) (VI)

Ether	Ketone	R	R′	R″	Product
Ia	Va	CH_2	CH_3	CH_3	VIa: 2,3-dimethyl-2-butenal-(1)
Ia	Vb	CH_3	CH_3	C_2H_5	VIb: 2,3-dimethyl-2-pentenal-(1)
Ib	Va	C_2H_5	CH_3	CH_3	VIc: 2-ethyl-3-methyl-2-butenal-(1)
Ib	Vb	C_2H_5	CH_3	C_2H_5	VId: 2-ethyl-3-methyl-2-pentenal-(1)

	Bp	Yield	IR(cm^{-1})			Analysis Calcd		Analysis Found	
	(°C/mmHg)	(%)	-CHO		C=C	C%	H%	C%	H%
VIa	43-45/16	36.8	2705,	1693	1637	73.43	10·27	73.61	10.55
VIb	84-86/30	33.0	2702,	1690	1636	74·95	10·78	74·73	10·84
VIc	55-57/14	27.7	2710,	1692	1640	74·95	10.78	74.68	11.01
VId	64-65/14	29·4	2705,	1692	1638	76·14	11.18	75·91	11.46

tracted with ether and dried over anhydrous sodium sulfate. Distillation of the extract gave the results shown in Table 1.

In the case of the use of acetaldehyde, the reaction temperature was maintained at about 10°C on account of the low boiling point of the aldehyde.

1,3-Dioxane Derivatives (III). After stirring the reaction mixture of I and II for 4 hr as in the preceding experiment, 5 g of powdered anhydrous sodium carbonate was added to the mixture in order to neutralyze the catalyst. The mixture was well agitated for 3 hr and then filtered. Fractional distillation of the filtrate gave III. The results are summarized in Table 2.

Hydrolysis of III with 10% hydrochloric acid gave IV, yield *ca.* 90%.

2-Ethyl-2-butenal-(1) (IVf) was obtained from IIIa. bp 55—56°C/50 mmHg. Found: C, 73.14; H, 10.31%, Calcd for $C_6H_{10}O$: C, 73.43; H, 10.27%.

2-Ethyl-2-hexenal-(1) (IVh) from IIIb, bp 54—56°C/7 mmHg. Found: C, 76.28; H, 11.10%. Calcd for $C_8H_{14}O$: C, 76.14; H, 11.18%.

2-Ethyl-3-phenyl-2-propenal-(1) (IVi) from IIIc, bp 102—104°C/3 mmHg. Found: C, 82.20; H, 7.78%. Calcd for $C_{11}H_{12}O$: C, 82.46; H, 7.55%.

α-Substituted-α,β-unsaturated Aldehydes (VI). A mixture of 0.1 mol of I and 0.3 mol of the ketone (V) was treated with boron trifluoride in the same manner as for IV. After stirring for 6 hr, the mixture was hydrolyzed for 10 hr. The results are summarized in Table 3.

The authors wish to thank Professor Yojiro Tsuzuki for his helpful advice and encouragement.

BULLETIN OF THE CHEMICAL SOCIETY OF JAPAN VOL. 43 1588—1589 (1970)

Preparation of Tricarbonyliron-μ-Carbonyl-μ-Diphenylphosphido-π-Cyclopentadienylnickel*[1]

Katsutoshi YASUFUKU and Hiroshi YAMAZAKI

The Institute of Physical and Chemical Research, Yamato-machi, Saitama

(Received November 17, 1969)

Since hexacarbonyl-π-cyclopentadienylmolybdenum-π-cyclopentadienyltungsten was reported by Abel,[1] many efforts have been made for the preparation of mixed transition-metal complexes with metal-metal bond.[2] The complexes were mostly mixed metal carbonyls in which metals are bonded only with a metal-metal bond. Tricarbonyl-π-cyclopentadienyliron-π-cyclopentadienylnickel[3] and monocarbonyl-π-cyclopentadienyliron-μ-dicarbonyl-tricarbonylcobalt[4] belong to a few complexes which consist of a metal-metal bond and

*1 Paper I in a series of "Chemistry of Mixed Transition-Metal Complexes."

1) E. W. Abel, Apar Singh and G. Wilkinson, *J. Chem. Soc.*, **1960**, 1321.

2) N. S. Vyazankin, C. A. Razuvaev and O. A. Kruglaya, *Organometal. Chem. Rev.*, **A3**, 323 (1968).

3) J. F. Tilney-Bassett, *J. Chem. Soc.*, **1963**, 4784.

4) J. K. Joshi and P. L. Pauson, *Z. Naturforsch.*, *B*, **17**, 565 (1962).

bridged carbonyls. Recently, Thompson[5] reported the synthesis of a new class of heterodinuclear transition-metal complexes joined by a metal-metal bond and a single phosphorus bridge by the reaction of tetracarbonyldiphenylphosphineiron with π-allyltricarbonylmanganese, -cobalt and π-allylpalladium chloride dimer.

In the present paper, we wish to report the preparation of a new mixed transition-metal complex consisting of iron and nickel which are bonded with a metal-metal bond, and with a bridged phosphido and a bridged carbonyl groups.

Experimental and Results

π-Cyclopentadienyltriphenylphosphinenickel chloride (1 g)[6] and 0.8 g of tetracarbonyldiphenylphosphineiron (I)[7] were allowed to react with excess diethylamine in methylene chloride at room temperature for two days. The reaction mixture was concentrated and subjected to chromatography on alumina with hexane-methylene chloride mixture as an eluent. Concentration of the brown eluate gave 0.41 g of brown cyrstals, mp*2 150—152°C, (Yield 45%. Found: C, 52.93; 3.30%. Calcd for $C_{21}H_{15}O_4PFeNi$: C, 52.90; H, 3.17%) The X-ray emission spectrum*3 indicated bands corresponding to NiKα at 51°34′, to FeKα at 61°08′ and PKα at 54°54′.

The same product was obtained in 25% yield by a similar treatment from π-cyclopentadienylcarbonylnickel iodide (prepared by method of Schropp[8]) and I in benzene with excess diethylamine at 0°C for four hours and at room temperature for two days.

$$\pi\text{-}C_5H_5Ni(PPh_3)Cl \text{ or } \pi\text{-}C_5H_5Ni(CO)I + HPh_2PFe(CO)_4 \rightarrow C_{21}H_{15}O_4PFeNi \quad (I)$$
$$\text{or } (\pi\text{-}C_5H_5)_2Ni$$

IR spectrum of the product showed the presence of terminal carbonyls and a bridged carbonyl both in KBr disk and in solutions as shown in Table 1. NMR spectrum (in $CDCl_3$) indicated signals of phenyl protons at 2.2—2.8τ and of cyclopentadienyl protons at 4.58τ. In mass spectrum,*4 the molecular peak consisting of ^{58}Ni and ^{56}Fe (which are the most abundant isotopic combination) appeared at m/e 476 (Calcd Mol Wt, 476) followed by peaks corresponding to successive loss of carbonyls as shown in Table 2. The peak at m/e 364 ($C_5H_5NiPPh_2Fe^+$) was the most abundant.

Table 1. IR spectrum of II in the ν_{CO} region

Solvent	ν_{CO} cm^{-1} terminal CO				bridged CO
KBr	2025	2018 s	1977 s	1956 s	1814 s
Hexane	2035 s	1990 s	1978 s		1840 s
CH_2Cl_2	2030 s	1985 s	1970 s		1820 s
CS_2	2032 s	1986 s	1972 s		1830 s
THF	2030 s	1965 s	broad		1825 s

Table 2. Mass spectrum of II
(only peaks consisting of ^{58}Ni and ^{56}Fe)

Fragment	m/e	Relative intensity
M^+	476	24
$(M-2CO)^+$	420	22
$(M-3CO)^+$	392	11
$(M-4CO)^+$	364	100
$(M-4CO-C_6H_6)^+$	286	22
$(M-4CO-C_6H_6-H_2)^+$	284	20

These spectral data suggest structure II for the present complex. It had been noted that the infrared spectra of octacarbonyldicobalt[9] and dicarbonyl-π-cyclopentadienyliron dimer[10] are markedly dependent on solvent in the ν_{CO} region and the structure in solution differs from that in crystalline state. Although the other structure III seems to be plausible as seen in the complexes obtained by Thompson,[5] the IR spectra in various solvents indicated no serious transformation in the ν_{CO} region showing the absence of any contribution of structure III even in solution.

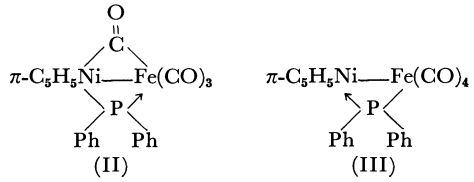

II was also obtained in 35% yield by the reaction of I with nickelocene in tetrahydrofuran at room temperature for a week. The reaction did not occur in benzene or in methylene chloride solutions. In contrast to the high reactivity of the π-allyl complexes of cobalt, manganese and palladium with I,[5] π-allyl-π-cyclopentadienylnickel was much less reactive and gave II only in a low yield (<2%).

II is very stable in air, especially in solid state and is soluble in most organic solvents.

We thank Dr. Yasuo Takahashi and Mr. Sakae Satooka for measurement of the X-ray emission spectrum and the mass spectrum.

5) B. C. Benson, R. Jackson, K. K. Joshi and D. T. Thompson, *Chem. Commun.*, **1968**, 1506.

6) H. Yamazaki, T. Nishido, Y. Matsumoto, S. Sumida and N. Hagihara, *J. Organometal. Chem.*, **6**, 86 (1966).

7) J. G. Smith and D. T. Thompson, *J. Chem. Soc., A*, **1967**, 1694.

*2 Measured on hot-stage apparatus.

*3 Measured by JEOL Primary X-ray Analyzer Type JPX-3 with KAP.

8) W. K. Schropp, *J. Inorg. Nucl. Chem.*, **24**, 1690 (1962).

*4 Measured by JEOL Mass Spectrometer Type JPS-1S at 75eV.

9) K. Noack, *Spectrochim. Acta*, **19**, 1925 (1963).

10) F. A. Cotton, H. Stammreich and G. Wilkinson, *J. Inorg. Nucl. Chem.*, **9**, 3 (1959).

BULLTEIN OF THE CHEMICAL SOCIETY OF JAPAN VOL. 43 1590—1591 (1970)

Coumarin-4-carboxylic Acids from Coumaran-2,3-diones

Masao KAWAI, Teruo MATSUURA and Ruka NAKASHIMA

Department of Synthetic Chemistry, Faculty of Engineering, Kyoto University, Kyoto

(Received November 18, 1969)

The synthesis of coumarin-4-carboxylic acids (I) reported so far consists of condensation of phenols with phenols with oxalacetic acid or its equivalent.[1-3] During the course of our studies[4] on the structure and reactions of 4,7-dimethyl-5-ethylcoumaran-2,3-dione (IIg), a pyrolysis product of tetrahydrophysalin A,[5] we found that coumaran-2,3-diones (II) gave coumarin-4-carboxylic acids (I) under reflux in acetic anhydride containing catalytic amount of pyridine. The results are given in Table 1. This reaction is considered useful for the preparation of I with $R_1=R_4=CH_3$, because, by the earlier method, condensation of 2,5-xylenol with oxalacetate occurred mainly at 4-position of xylenol, affording the maleic acid derivative (III).

Table 1. Results of the formation of I from II

Starting material	Coumarin-4-carboxylic acids obtained (Yield %)	Recovery (%)
IIa[6]	Ia (12)	5
IIb[4]	Ib (14)	20
IIc[7]	Ic (7)	45
IId[7]	Id (8)	8
IIe[4]	Ie (12)	43
IIf[4]	If (19)	50

The mass spectra of I are summarized in Table 2. Compounds I with $R_1=CH_3$ gave a strong peak at *m/e* *M*-18 as well as at *m/e* *M*-44 and *m/e* *M*-45. In contrast to this, I with $R_1=H$ showed no significant peak at *m/e* *M*-18, suggesting that in the case of I with $R_1=CH_3$ the ion corresponding to *m/e* *M*-18 has mainly structure IV. From this observation, the mass spectra of various monomethyl derivatives of 1-naphthoic acid were examined. As expected only 8-methyl derivative gave a strong peak at *m/e* 168 (*M*-18). In other cases the peak at *m/e* 169 (*M*–OH) was stronger than that at *m/e* 168 (*M*-H_2O). The results are summarized in Table 3.

Table 2. Relative peak heights of the mass spectra of coumarin-4-carboxylic acids

Compound	*M*	*M*-18	*M*-44	*M*-45
Ia	100	0	6	14
Ib	100	1	25	120
Ic	100	130	105	39
Id	100	170	300	70
Ie	100	180	155	27
If	100	200	155	50

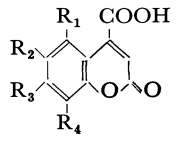

(I)

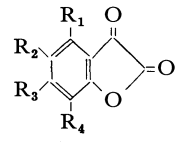

(II)

	R_1	R_2	R_3	R_4
a	H	H	H	H
b	H	Me	H	Me
c	Me	H	H	Me
d	Me	H	Me	H
e	Me	H	Me	Me
f	Me	Me	H	Me
g	Me	H	Et	Me

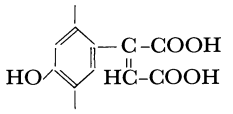

(III)

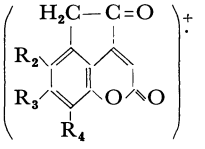

(IV)

Experimental

Melting points were uncorrected. IR spectra were measured in KBr. Mass spectra were obtained using a Hitachi RMS-4 mass spectrometer with ionizing voltage of 70 eV.

General Procedure. Coumaran-2,3-dione (II) (*ca.* 400 mg) was refluxed in acetic anhydride (40 ml) containing a few drops of pyridine for 7—8 hr. The reaction mixture was evaporated *in vacuo* and the residual mass was triturated with water. The crude product was chromatographed on silica gel (3.0 g). First, elution with 5% acetone-light petroleum gave starting material (II), and then with 15% acetone-light petroleum, mainly cou-

1) H. V. Pechmann and E. V. Krafft, *Ber.*, **34**, 421 (1901).

2) B. B. Day, *J. Chem. Soc.*, **107**, 1606 (1915).

3) R. V. Smith and M. D. Bealor, *J. Org. Chem.*, **27**, 3092 (1962).

4) T. Matsuura, M. Kawai and Y. Butsugan, unpublished work.

5) T. Matsuura, M. Kawai, R. Nakashima and Y. Butsugan, *Tetrahedron Lett.*, **1969**, 1083.

6) E. H. Huntress and W. M. Hearon, *J. Amer. Chem. Soc.*, **63**, 2762 (1941).

7) R. Stollé and E. Knebei, *Ber.*, **54B**, 1213 (1921).

Table 3. Relative peak heights of the mass spectra of various monomethyl derivatives of 1-naphthoic acid

Position of methyl	*M* (186)	*M*-17 (169)	*M*-18 (168)	*M*-44 (142)	*M*-45 (141)	*M*-46 (140)
3	100	37	5	7	19	7
4	100	21	4	8	20	8
5	100	21	7	10	21	19
6	100	23	8	11	19	17
7	100	32	15	15	31	25
8	100	76	98	17	81	91

Table 4. Analytical data of I

Compound	mp (°C) (Solvent of recrystallization)	Formula	Found		Calcd	
			C%	H%	C%	H%
Ia	183—187 (acetone-benzene)	$C_{10}H_6O_4$	62.98	3.05	63.16	3.18
Ib	255—256 (acetone)	$C_{12}H_{10}O_4$	66.07	4.56	66.05	4.62
Ic	188—198 (benzene)	$C_{12}H_{10}O_4$	65.75	4.72	66.05	4.62
Id	219—224 (acetone-light petroleum)	$C_{12}H_{10}O_4$	66.05	4.86	66.05	4.62
Ie	219—223 (benzene)	$C_{13}H_{12}O_4$	66.95	5.18	67.23	5.21
If	226—228 (benzene)	$C_{13}H_{12}O_4$	66.96	5.25	67.23	5.21

marin-4-carboxylic acid (I). When necessary, this fraction was rechromatographed on silica gel (2.0 g) using 10% ether-light petroleum as eluent. Melting points and the results of elementary analysis of I are given in Table 4. The IR spectra of Ia and Ib were identical with those of authentic samples synthesized.[1,3]

Condensation of 2,5-Xylenol with Sodium Diethyl Oxalacetate. Intimate mixture of 2,5-xylenol (3.97 g) and sodium diethyl oxalacetate (5.25 g) was added into the ice-cooled concd. H_2SO_4 (25 m*l*). After 7 hr the reaction mixture was poured into ice-water. The solid separated was dissolved in NaOH aq. solution and carbon dioxide was introduced into it to remove unreacted xylenol by filtration. HCl aq. solution was added to the filtrate and the crude product separated was recrystallized from acetone giving 650 mg of III, mp 165—70°C.

IR spectrum: 1730, 1690, 1620 and 1575 cm^{-1}.

Found: C, 60.73; H, 5.20%. Calcd for $C_{12}H_{12}O_5$: C, 61.01; H, 5.12%.

Sublimation of III gave an anhydride (mp 169°C). IR spectrum: 1820, 1750, 1615 and 1565 cm^{-1}. (Found: C, 65.87; H, 4.68%).

On thin layer chromatography the mother liquor of III showed no spot corresponding to Ic.

The authors wish to thank Drs. T. Fujita and M. Utaka for the supply of 3-, 4-, 5-, 6-, 7- and 8-methyl-1-naphathoic acids.

BULLETIN OF THE CHEMICAL SOCIETY OF JAPAN VOL. 43 1592—1593 (1970)

Polymeric Structure in *N*-Picolinoyl-1,3-propanolaminatocopper(II) Dihydrate

Motomichi INOUE,* Heijirō OJIMA,** Kiyoko YAMADA,** and Masaji KUBO*

* *Department of Chemistry, Nagoya University, Chikusa, Nagoya*

** *Department of Chemistry, Aichi University of Education, Okazaki*

(Received November 19, 1969)

A number of copper(II) complexes have been synthesized with terdentate ligands. Magnetic measurements have indicated the presence of dimeric molecules in the crystals of these compounds.[1] Subsequently, the binuclear structure of acetylacetonemono(*o*-hydroxyanil)copper(II) has been established by X-ray crystal analysis.[2] The compound presents a typical example of binuclear structure in which copper atoms are bridged by two oxygen atoms. Its magnetic susceptibility conforms to the Bleaney-Bowers equation. On the other hand, the magnetic property of *N*-[2-(2-hydroxyethylthio) phenyl] arenesulfoamidatocopper-(II) obeys a theoretical equation for isolated ternuclear rings.[3] Ojima[4] has synthesized *N*-picolinoyl-1,3-propanolaminatocopper(II) dihydrate, which presents a new type of copper (II) complexes having terdentate ligands. Since the complex is prepared in basic solutions as described below, the nitrogen atom of the amide group coordinates to the metal ion as shown in Fig. 1.[5] In order to obtain some information about the structure of the copper(II) complex, we have determined the magnetic susceptibility in a temperature range of 80–300°K, using a Gouy magnetic balance described in previous papers.[3,6]

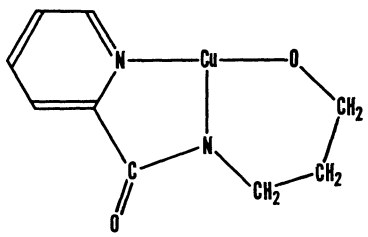

Fig. 1. Coordination of *N*-picolinoyl-1,3-propanolamine to a copper ion.

The material was prepared by a method described in a previous paper.[4] A mixture of methyl picolinate (1 mol) and 1,3-propanolamine (1 mol) was heated at 180—200°C for 8 hr. When the reaction product was diluted with water (1 : 2) and a saturated solution of copper(II) sulfate (1/2 mol) was added to it, the solution turned deep blue with heat evolution. On adding ethanol to the hot solution, blue crystals separated on cooling. When the crystals were left to stand in a desiccator over calcium chloride, $Cu(C_9H_{12}N_2O_2)_2SO_4 \cdot 2.5H_2O$ was obtained. Found: Cu, 11.45; N, 9.70; H_2O, 7.91%. Calcd for $Cu(C_9H_{12}N_2O_2)_2SO_4 \cdot 2.5H_2O$: Cu, 11.25; N, 9.92; H_2O, 7.97%. On adding sodium hydroxide solution (2 mol) to a concentrated aqueous solution of $Cu(C_9H_{12}N_2O_2)_2SO_4 \cdot 2.5H_2O$ (1 mol), *N*-picolinoylpropanolaminatocopper(II) dihydrate was obtained. It was recyrstallized from hot water. Found: Cu, 22.86; C, 38.86; H, 5.20; N, 10.20; H_2O, 12.99%. Calcd for $CuC_9H_{10}N_2O_2 \cdot 2H_2O$: Cu, 22.87; C, 38.92; H, 5.08; N, 10.09; H_2O, 12.97%.

The dihydrate was dehydrated in a vacuum desiccator over phosphorus pentoxide at about 100°C. Found: Cu, 26.28; C, 44,56; H, 4.22; N, 11.44%. Calcd for $CuC_9H_{10}N_2O_2$: Cu, 26.45; C, 44.72; H, 4.18; N, 11.59%.

The molar magnetic susceptibilities of the dihydrate and the anhydrous complex were determined as $0.77_8 \times 10^{-3}$ emu/mol (25°C) and 0.254×10^{-3} emu/mol (31°C), respectively. Corrections were made for diamagnetic contributions (in 10^{-6} emu/mol) from *N*-picolinoylpropanolamine (−120), water (−13),[7] and copper(II) ions (−11).[8] The value for the ligand was calculated from Pascal's constants.[7] The corrected molar susceptibilities are shown in Fig. 2 as functions of temperature.

Bleaney and Bowers[9] have proposed a theoretical

1) M. Kishita, Y. Muto and M. Kubo, *Aust. J. Chem.*, **10**, 386 (1957); **11**, 309 (1958).

2) G. A. Barclay, C. M. Harris, B. F. Hoskins and E. Kokot, *Proc. Chem. Soc.*, **1961**, 264.

3) S. Emori, M. Inoue, M. Kishita, M. Kubo, S. Mizukami and M. Kono, *Inorg. Chem.*, **7**, 2419 (1968).

4) H. Ojima, *Nippon Kagaku Zasshi*, **88**, 44 (1965).

5) K. Yamasaki and M. Sekizaki, This Bulletin, **38**, 2206 (1965).

6) M. Inoue, M. Kishita and M. Kubo, *Inorg. Chem.*, **6**, 900 (1967); M. Inoue, S. Emori and M. Kubo, *ibid.*, **7**, 1427 (1968).

7) G. Foëx, "Constantes Sélectionnées, Diamagnétisme et Paramagnétisme," Masson, Paris (1957).

8) P. W. Selwood, "Magnetochemistry," 2nd Ed., Interscience Publishers, Inc., New York, N. Y. (1956).

9) B. Bleaney and K. D. Bowers, *Proc. Roy. Soc., Ser. A*, **214**, 451 (1952).

equation for the susceptibility, χ, of copper(II) complexes having a binuclear structure.

$$\chi = \frac{Ng^2\beta^2}{3kT}\left(1+\frac{1}{3}e^{2J/kT}\right)^{-1} + N\alpha \qquad (1)$$

where apart from obvious notations, J is the exchange integral and $N\alpha$ is the temperature-independent paramagnetism assumed to be equal to 60×10^{-6} emu/mol.[10] As shown in Fig. 2, the observed susceptibility of the anhydrous salt agrees well with the theoretical curve ($J/k=400$°K, $g=2.14$) above about 150°K, indicating the existence of dimer molecules in crystals. Presumably, the paramagnetic behavior below about 100°K is due to the presence of impurities and/or magnetically isolated copper(II) ions in small quantities.

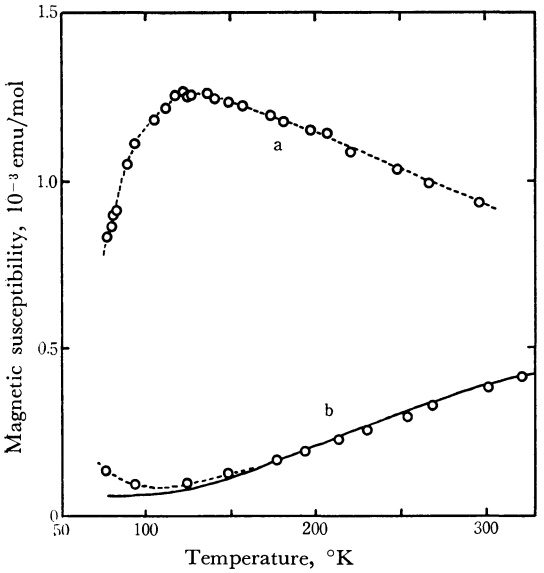

Fig. 2. Magnetic susceptibilities of *N*-picolinoyl-1,3-propanolaminatocopper(II) dihydrate (a) and the anhydrous salt (b). The solid curve represents the Bleaney-Bowers equation.

The magnetic susceptibility of the dihydrate cannot be fitted to the theoretical equation for isolated binuclear clusters. The magnetic susceptibilities for polymeric rings of spins have been calculated numerically by Bonner and Fisher[11] by use of the following Hamiltonian.

$$\mathcal{H} = -2J\sum_{i=1}^{n}\left(\boldsymbol{S}_i\boldsymbol{S}_{i+1}-\frac{1}{4}\right) \qquad (2)$$

where J is the exchange integral and $\boldsymbol{S}$ is the spin angular momentum ($\boldsymbol{S}_{n+1}=\boldsymbol{S}_1$). The theoretical curves are shown in Fig. 3. The observed susceptibility apparently fits the curve for a ring composed of even number of spins, especially that for a four-membered ring. The exchange integral, J, and g value were estimated as $|J|/k=92$°K and $g=2.08$, respectively. However, the observed values do not agree perfectly with the theoretical curve in the whole temperature range investigated. A conceivable reason for the discrepancy is the presence of two kinds of magnetic interaction in the cluster. Alternatively magnetic interaction might exist between clusters. In any case, polymeric structural units mostly containing even number of spins are formed in the crystal. The polymeric molecules in the dihydrate change to the binuclear clusters on dehydration. The important role of water molecules is open to speculation.

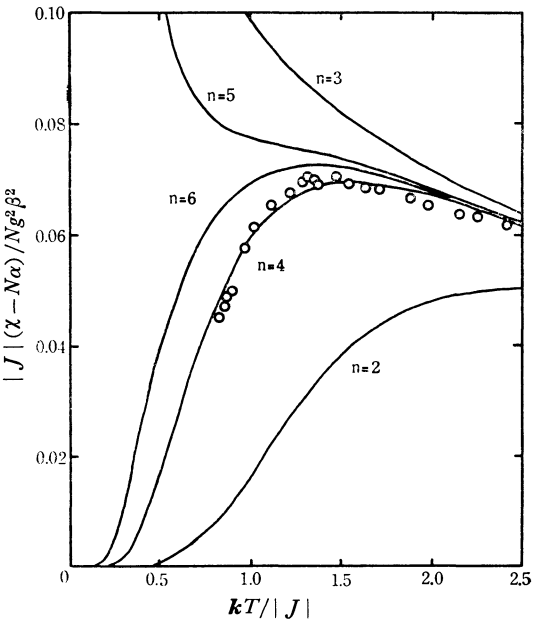

Fig. 3. Observed magnetic susceptibility of *N*-picolinoyl-1,3-propanolaminatocopper(II) dihydrate and theoretical curves calculated by Bonner and Fisher with Eq. (2). For a binuclear cluster ($n=2$), the exchange integral is equal to one fourth of the energy separation between the singlet and triplet states.

10) B. N. Figgis and R. L. Martin, *J. Chem. Soc.*, **1956**, 3837.

11) J. C. Bonner and M. E. Fisher, *Phys. Rev.*, **135A**, 640 (1964).

BULLETIN OF THE CHEMICAL SOCIETY OF JAPAN VOL. 43 1594—1596 (1970)

The Kinetics of the Electrophilic Substitution Reaction of the *trans*-1,2-Cyclohexanediaminetetraacetatocadmate(II) Complex with Copper(II) Ion

Masaru KIMURA*[1]

Department of Applied Chemistry, Yamagata University, Yonezawa

(Received May 29, 1969)

The kinetics and the mechanisms of the electrophilic substitution reaction of the metal-ethylenediaminetetraacetate(EDTA) complex have been studied for several different reaction systems.[1-9] These metal-ion exchange reactions are all shown to proceed through the reaction of the entering metal ion with the EDTA complex and through that of the dissociated EDTA anion with the entering metal ion. Recently, similar electrophilic substitution reactions have been studied with *trans*-1,2-cyclohexanediaminetetraacetic acid (CyDTA) in place of EDTA.[2,10-12] In this case, there was no direct reaction between the entering metal ion and the CyDTA complex. This behavior was confirmed in the present study. In most cases, a metal-CyDTA complex has a larger stability constant (from 1 to 3 larger in the logarithm scale) than the corresponding EDTA complex.[13] Therefore, the dissociation reaction of CyDTA complexes may be expected to be considerably slower than that of the corresponding EDTA complexes. This expectation was also examined in this study.

Experimental

The solutions of disodium CyDTA and copper(II) nitrate were the same as those described in previous papers.[14,15] The cadmium(II) nitrate solution was prepared by dissolving pure cadmium metal in nitric acid: it was standardized against a standard CyDTA solution by amperometric titration.

The apparatus and procedure were also the same in principle as those described in the previous papers.[14,15]

Results

The overall reaction in acetate media is represented by:

$$\left\{\begin{matrix}Cu^{2+}\\ \uparrow\downarrow\\ CuOAc^{+}\\ \uparrow\downarrow\\ Cu(OAc)_2\end{matrix}\right\} + CdCy^{2-} \overset{V_i^+}{\rightleftharpoons} CuCy^{2-} + \left\{\begin{matrix}CdOAc^{+}\\ \uparrow\downarrow\\ Cd^{2+}\end{matrix}\right\} \quad (1)$$

Where Cy^{4-} denotes a tetravalent CyDTA anion. The forward reaction rate was obtained by the polarographic measurements of the copper(II)-ion concentration with the time. The copper-ion concentration that can be determined is an apparent concentration, *i.e.*, $[Cu^{2+}]_{app}=[Cu^{2+}]+[CuOAc^{+}]+[Cu(OAc)_2]$. Under the present experimental conditions, the forward reaction of Eq. (1) was so sluggish that the initial rate could be determined accurately. When the copper ion is present in a large excess over the cadmium ion, the initial rate was independent of the copper-ion concentrations, but it was proportional to the concentrations of the Cd(II)-CyDTA complex and the hydrogen ion (see Figs. 1, 2, and 3) On the other hand, when the cadmium ion is present in a large excess over the copper ion, the rate

*1 Correspondence to be addressed to: School of Chemistry, University of Minnesota, Minneapolis, Minn. 55455 U.S.A.

1) M. Kimura, This Bulletin, **42**, 404 (1969).
2) J. R. Kuempel and W. B. Schaap, *Inorg. Chem.*, **7**, 2435 (1968).
3) a) N. Tanaka, H. Osawa and M. Kamada, This Bulletin, **26**, 67 (1963); b) N. Tanaka and H. Ogino, *ibid.*, **36**, 175 (1962). c) N. Tanaka and M. Kamada, *ibid.*, **35**, 1596 (1962). d) K. Kato, *ibid.*, **33**, 600, (1960). e) N. Tanaka and K. Kato, *ibid.*, **32**, 1376 (1959). f) N. Tanaka, K. Kato and R. Tamamushi, *ibid.*, **31**, 283 (1958).
4) H. Ackermann and G. Schwarzenbach, *J. Phys. Chem.*, **35**, 485 (1952).
5) K. Bril, S. Bril and P. Krumholz, *ibid.*, **59**, 596 (1955); **60**, 251 (1956).
6) a) S. Jones and F. A. Long, *ibid.*, **56**, 25 (1952). b) C. M. Cook, Jr., and F. A. Long, *J. Amer. Chem. Soc.*, **80**, 33 (1958).
7) R. J. Day and C. N. Reilley, *Anal. Chem.*, **36**, 1073 (1964).
8) R. J. Kula and G. H. Reed, *ibid.*, **38**, 697 (1966).
9) a) T. J. Bydalek and D. W. Margerum, *J. Amer. Chem. Soc.*, **83**, 4326 (1961); *Inorg. Chem.*, **1**, 852 (1962); **2**, 678 (1963). b) D. W. Margerum, D. B. Rorabacher and J. F. G. Clarke, Jr., *ibid.* **2**, 667 (1963). c) D. B. Rorabacher and D. W. Margerum, *ibid.*, **3**, 382 (1964).
10) D. W. Margerum and T. J. Bydalek, *Inorg. Chem.*, **2**, 683 (1963).
11) D. L. Janes and D. W. Margerum, *ibid.*, **5**, 1135 (1966).
12) G. F. Smith and D. W. Margerum, *ibid.*, **8**, 135 (1969).
13) L. G. Sillen and A. E. Martell, "Stability Constants," Chemical Society, London (1964).
14) M. Kimura, *Nippon Kagaku Zasshi*, **89**, 1209 (1968).
15) M. Kimura, This Bulletin, **42**, 3588 (1969).

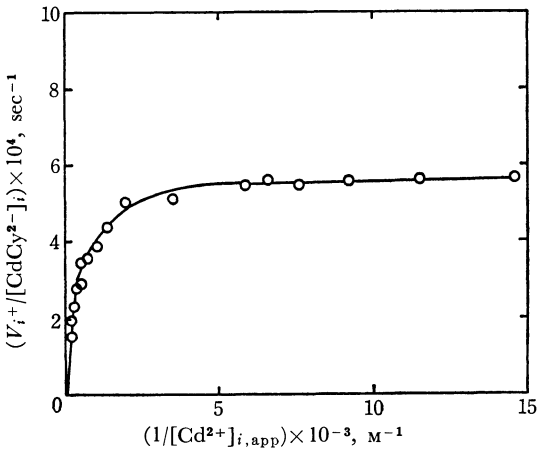

Fig. 1. $V_i^+/[CdCy^{2-}]_i$ as a function of the reciprocal cadmium concentration at ionic strength 0.2 and 25°C.
Initial concentrations are 1.12 mM and 5.03×10^{-1} mM for $[CdCy^{2-}]_i$ and $[Cu^{2+}]_{i,app}$ respectively, pH 4.90.

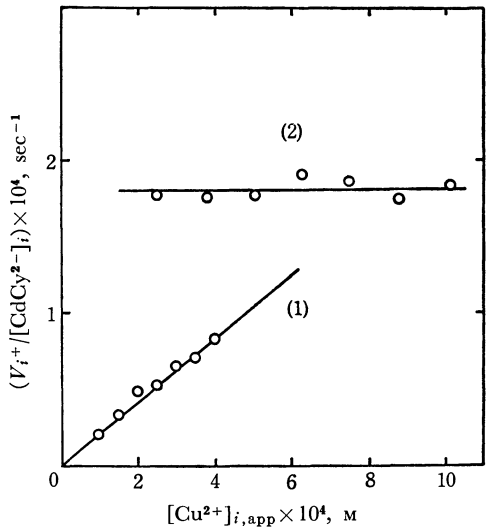

Fig. 2. $V_i^+/[CdCy^{2-}]_i$ as a function of the concentration of copper ion at ionic strength 0.2 and 25°C.
Initial concentrations are $[CdCy^{2-}]_i=2.25$ mM, $[Cd^{2+}]_{i,app}=6.3$ mM and pH 4.95 for curve 1, and $[CdCy^{2-}]_i=1.12$ mM, $[Cd^{2+}]_{i,app}=3.3\times 10^{-2}$ mM and pH 5.42 for curve 2.

was proportional to the concentrations of the copper ion as well as those of the Cd(II)-CyDTA complex and the hydrogen ion, and the rate was inversely proportional to the concentrations of the cadmium ion (Figs. 1, 2, and 4). These results indicate that the reaction between the copper(II) ion and the cadmium(II)-CyDTA complex proceeds through the following reaction paths;

$$CdCy^{2-} + H^+ \underset{k^{HCy}_{Cd}}{\overset{k^{H}_{CdCy}}{\rightleftharpoons}} HCy^{3-} + Cd^{2+} \qquad (2)$$

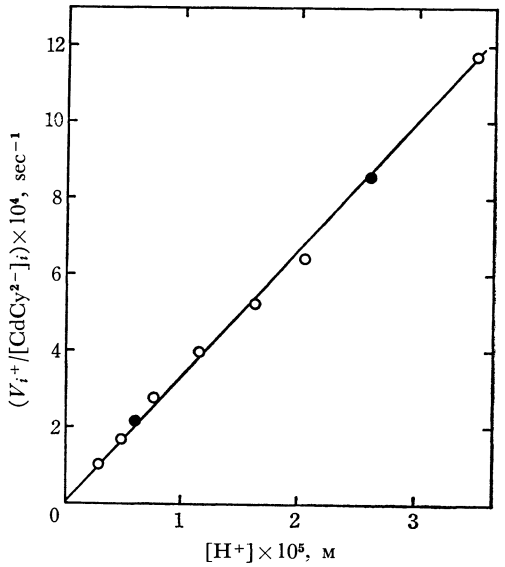

Fig. 3. $V_i^+/[CdCy^{2-}]_i$ as a function of the hydrogen ion concentration at ionic strength 0.2 and 25°C.
Initial concentrations are $[CdCy^{2-}]_i=1.12$ mM and $[Cd^{2+}]_{i,app}=3.3\times 10^{-2}$ mM for ○, $[CdCy^{2-}]_i=2.25$ mM and $[Cd^{2+}]_{i,app}=6.6\times 10^{-2}$ mM for ●, and $[Cu^{2+}]_{i,app}=5.03\times 10^{-1}$ mM for ○ and ●.

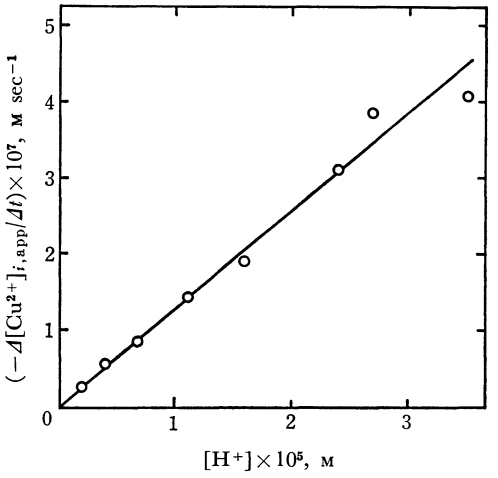

Fig. 4. Initial rate as a function of the hydrogen ion concentration at ionic strength 0.2 and 25°C.
Initial concentrations are 2.25 mM, 5.38 mM and 2.50×10^{-1} mM for $[CdCy^{2-}]_i$, $[Cd^{2+}]_{i,app}$ and $[Cu^{2+}]_{i,app}$ respectively.

$$Cu^{2+} + HCy^{3-} \underset{k^{H}_{CuCy}}{\overset{k^{HCy}_{Cu}}{\rightleftharpoons}} CuCy^{2-} + H^+ \qquad (3)$$

Determination of the Rate Constant of the Dissociation Reaction of the Cadmium(II)-CyDTA Complex. When the copper ion is present in a large excess over the cadmium ion, the

Table 1. Rate constants of the reaction (at 25°C)

$$M^{2+} + HY^{3-} \underset{k_b}{\overset{k_f}{\rightleftharpoons}} MY^{2-} + H^+$$

Reaction system	μ	Rate constant, $l\ mol^{-1}\ sec^{-1}$ k_f	k_b	Method	Researcher
Cd-EDTA	0.1	6.4×10^9	3×10^3*	$E_{1/2}$	Aylward, Hayes[16a]
Cd-EDTA	0.5	2.3×10^9	1×10^3	ϕ	Matsuda, Tamamushi[16b]
Cd-EDTA	1.6	1×10^9	7.6×10^3	NMR	Sudmeier, Reilley[16c]
Cu-EDTA	0.2	3.0×10^9	7.1*	Pol	Tanaka, Kato[3f]
Cd-CyDTA	0.1	1.4×10^9	41.4	Sp	Smith, Magerum[12]
Cd-CyDTA	0.2	1.1×10^9*	32.8	Pol	The present study
Cu-CyDTA	0.2	3.3×10^9	2.1*	Pol	The present study

* Calculated by the author using the relation of $k_f/k_b=K_{MY}K_{HY}$.
$E_{1/2}$ refers to the analysis of the half wave potential of polarograph, ϕ, the phase angle behavior, NMR, to the nuclear magnetic resonance, Pol, to the polarographic diffusion current measurement, and Sp, to the spectrophotometry.

rate-determining step is the dissociation reaction of the Cd(II)-CyDTA complex. Therefore, the rate is expressed as Eq. (4);

$$-\frac{\Delta[Cu^{2+}]_{i,app}}{\Delta t} = V_i^+ = k^H_{CdCy}[CdCy^{2-}]_i[H^+] \quad (4)$$

where the i subscript indicates the initial state. The initial rate was obtained as a function of the hydrogen-ion concentration at two different concentrations of both the cadmium-CyDTA complex and the cadmium ion. The results are given in Fig. 3. Figure 3 clearly indicates that the value of k^H_{CdCy} can be determined from the slope. The value of k^H_{CdCy} was 32.8 l mol^{-1}sec^{-1}.

Determination of the Rate Constant of the Complex-forming Reaction between the Hydrated Copper(II) Ion and the CyDTA Anion. When the cadmium ion is present in a large excess over the copper ion, the relation of $k^{HCy}_{Cu}[Cu^{2+}] \ll k^{HCy}_{Cd}[Cd^{2+}]$ is satisfied. The following rate equation can then be deduced:

$$-\frac{\Delta[Cu^{2+}]_{i,app}}{\Delta t} = V_i^+ = k^{HCy}_{Cu}[Cu^{2+}]_i[HCy^{3-}]_i$$
$$= k_1\frac{[CdCy^{2-}]_i[Cu^{2+}]_{i,app}}{[Cd^{2+}]_{i,app}}[H^+] \quad (5)$$

$$k_1 = k^{HCy}_{Cu} \times \frac{1+\beta_{CdOAc}[OAc^-]}{K_{CdCy}K_{HCy}(1+\beta_{CuOAc}[OAc^-]+\beta_{Cu(OAc)_2}[OAc^-]^2)}$$
$$= k^{HCy}_{Cu}\frac{1+16\times0.04}{10^{19.23}\times10^{-11.70}(1+52\times0.04+93\times0.04^2)}$$
$$= k^{HCy}_{Cu}\times1.37\times10^{-8} \quad (5')$$

The initial rate was obtained as a function of the hydrogen-ion concentration(Fig. 4) and also as a function of the concentrations of the copper ion (Curve 1 in Fig. 2). The rate constant, k^{HCy}_{Cu}, was determined to be 8.0×10^9 l mol^{-1}sec^{-1} from Fig. 2, and to be 8.7×10^9 l mol^{-1}sec^{-1} from Fig. 4.

Discussion

Several workers have studied the kinetics of the dissociation or formation reactions of copper-EDTA[3a,c,d,f] and cadmium-EDTA[16] complexes. A few of their representative data are given in Table 1, together with the present results on the CyDTA complexes. The rate constant of the complex-forming reaction does not show any large differences between EDTA and CyDTA, nor between cadmium and copper. However, the dissociation reactions of CyDTA complexes are much slower than those of the corresponding EDTA complexes, and the dissociation-rate constants of the cadmium-CyDTA and -EDTA complexes are, respectively, 16 and about 1000 times larger than those of the copper-CyDTA and EDTA complexes. These facts indicate that the rate of the dissociation of these complexes is dependent on the stability of the complex. In the present case, the ratios of the stability constants are;

$$K_{Cu(cydta)}/K_{Cu(edta)} = 10^{21.3}/10^{18.7} = 10^{1.6} \text{ and}$$
$$K_{Cd(cydta)}/K_{Cd(edta)} = 10^{19.2}/10^{16.4} = 10^{2.8}$$

There were two noticeable conclusions for comparing the kinetic behavior of the CyDTA complex with that of the EDTA complex; (1) although are direct reactions between the copper ion and EDTA complex, there were on appreciable direct reactions between the copper ion and the CyDTA complex, and (2) there was a close similarity between the hydrogen-ion reaction with the two complexes. This kinetic behavior is consistent with that of the other metal-CyDTA and -EDTA complexes.

16) a) G. H. Aylward and J. W. Hayes, *Anal. Chem.*, **37**, (1965). b) K. Matsuda and R. Tamamushi, This Bulletin, **41**, 1563 (1968). c) J. L. Sudmeier and C. N. Reilley, *Inorg. Chem.*, **5**, 1047 (1966). d) J. Koryta and Z. Zabransky, *Collect. Czech. Chem. Commun.*, **25**, 3153 (1960). e) T. Fujisawa and N. Tanaka, *Nippon Kagaku Zasshi*, **87**, 965 (1966). f) N. Tanaka, R. Tamamushi and M. Kodama, *Z. Phys. Chem.* (Frankfurt am Main), **41**, 141 (1958).

BULLETIN OF THE CHEMICAL SOCIETY OF JAPAN VOL. 43 1597—1598 (1970)

On the Valence State Energy of the Carbon and Nitrogen Atoms

Hideyuki NARUMI and Kimio OHNO

Department of Chemistry, Faculty of Science, Hokkaido University, Sapporo

(Received December 5, 1969)

Several years ago, one of the present authors (K.O.) reported calculations on the energies of the carbon and nitrogen atoms in their valence states.[1] The valence state energies were those defined by Van Vleck.[2] A single Slater-type orbital (STO) was used for each atomic orbital (AO) and orbital exponents δ of the $1s$, $2s$, $2p\sigma$, and $2p\pi$ AO's were varied to make the energy minimum. It turned out that this approximation is especially inadequate for negative ions. Calculated electron affinities for carbon and pyridine-type nitrogen were -4.3 and -5.2 eV, respectively. A semi-empirical estimate[3] gives the value of 0.03 eV for C and 1.8 eV for N. The reason for this failure is probably that a single STO is not adequate for describing the long tail of the charge distribution of a negative ion, especially of the $2p\pi$ orbital.

In this note, results obtained by using two STO's to express the $2p\pi$ AO, instead of one STO, are reported. A very similar calculation was carried out on C by Silverstone and Joy,[4] namely Basis III calculation given in their Table III. However, their valence state was defined for hydrocarbon whose π-electrons were described in terms of molecular orbitals. Thus their energies differ from ours by an extra term, that is one fourth of the π Coulomb integral. Orloff and Sinanoğlu[5] have performed very extensive calculations on the valence state of C. Although their sets of basic orbitals are much bigger than ours, our calculations differ from theirs in that the $2p\sigma$ and $2p\pi$ AO's are allowed to differ. On pyridine-type and pyrrole-type nitrogens, there seems to be no calculation more detailed than our previous one.[1]

Results and Discussion

The numerical results are collected in Table 1. The coefficients and orbital exponents of the two STO's in the $2p\pi$ orbital are denoted as C_1, C_2, δ_1 $(2p\pi)$ and $\delta_2(2p\pi)$. The π one-electron energy W is defined by

$$W(n, q) \equiv \langle 2p\pi(q)\left|-\frac{1}{2}\Delta+V(n, q)\right|2p\pi(q)\rangle,$$

where V is the potential due to the σ-core, n is the

Table 1. Valence state energy of C, pyridine-type N, and pyrrole-type N (eV)

	C			Pyridine-type N			Pyrrole-type N		
	C^+	C	C^-	N^+	N	N^-	N^{++}	N^+	N
Electron config.	$(sp^2)^3$	$(sp^2)^3\pi$	$(sp^2)^3\pi^2$	$(sp^2)^4$	$(sp^2)^4\pi$	$(sp^2)^4\pi^2$	$(sp^2)^3$	$(sp^2)^3\pi$	$(sp^2)^3\pi^2$
$\delta(1s)$	5.66	5.66	5.67	6.65	6.66	6.66	6.65	6.65	6.65
$\delta(2s)$	1.75	1.65	1.62	2.04	1.95	1.90	2.17	2.06	1.98
$\delta(2p\sigma)$	1.75	1.58	1.53	2.07	1.89	1.80	2.27	2.09	1.94
$\delta_1(2p\pi)$	—	2.17	1.86	—	2.71	2.42	—	2.67	2.72
$\delta_2(2p\pi)$	—	1.03	0.56	—	1.26	0.78	—	1.44	1.19
C_1	—	0.466	0.488	—	0.462	0.492	—	0.532	0.450
C_2	—	0.614	0.691	—	0.622	0.670	—	0.525	0.644
Total energy	−1007.98	−1017.27	−1015.25	−1454.68	−1466.55	−1464.42	−1428.05	−1455.04	−1464.57
σ-Core energy	−1007.98	−1007.05	−1006.52	−1454.68	−1453.33	−1451.73	−1428.05	−1427.02	−1424.71
W	—	−10.22	−9.04	—	−13.22	−12.85	—	−28.02	−28.75
$(\pi\pi\|\pi\pi)$	—	15.05	9.35	—	18.47	13.00	—	21.05	17.64

1) K. Ohno, *Theor. Chim. Acta*, **2**, 219 (1964). Unfortunately there was an error in the calculation and the corrected results will be published as an erratum in the same journal shortly.

2) J. H. Van Vleck, *J. Chem. Phys.*, **2**, 20 (1934).

3) J. Hinze and H. H. Jaffé, *J. Amer. Chem. Soc.*, **84**, 540 (1962).

4) H. J. Silverstone and H. W. Joy, *J. Chem. Phys.*, **47**, 1384 (1967).

5) M. K. Orloff and O. Sinanoğlu, *ibid.*, **43**, 49 (1965).

Table 2. Pi-electron ionization potential (in eV)

	C	Pyridine-type N	Pyrrole-type N	
			First	Second
Calculated with one STO for π AO	8.69	10.87	7.62	26.43
Calculated with two STO for π AO	9.29	11.87	9.52	27.00
Semi-empirical estimate[3,6]	11.16	14.12	11.96	28.71

difference between the nuclear charge and the number of σ-electrons (*e.g.* $n=1$ for C and pyridine-type N, and $n=2$ for pyrrole-type N) and q is the π-electon charge on the atom ($q=1$ for C, 2 for C^-).

These results show that the effect of q on W is not very big, less than 1.2 eV. The usual assumption in the Pariser-Parr-Pople method

$$W(n, 1)=W(n, 2)=-I_n$$

is valid within an error of about 2 eV. These general conclusions were reached in the previous treatment[1] and do not change under the extended calculations.

On the other hand, the use of two STO's for the π orbital improved somewhat the calculated π-electron affinities. They are -2.0 eV for C and -2.1 eV for pyridine-type N. The errors were reduced to about one half but still the correct sign could not be obtained.

The calculated and semi-empirically estimated π-ionization potentials are compared in Table 2. Here again, by using a better approximation, the calculated values come closer to the semi-empirical estimate but the differences could still be as large as 2.5 eV.

In conclusion, these simple variational calculations of valence state energies show that the deformation of the σ and π orbitals due to the change in the number of π electrons is considerable, but their effects on W apparently cancel each other and the net effect is not large. On the other hand, using two STO's for the π orbital is not good enough for calculating the π-electron ionization potentials and electron affinities for C and N more accurately than 2—3 eV.

The authors are grateful to Dr. J. H. Gallagher and Professor R. McWeeny for reading the manuscript.

6) J. Hinze and H. H. Jaffé, *J. Phys. Chem.*, **67**, 1501 (1963).

SHORT COMMUNICATIONS

trans- and *cis*-Yabunikkeol, New Monoterpene Alcohols Isolated from the Essential Oils of *Cinnamomum japonicum* Sieb.

Yasuji FUJITA, Shin-ichi FUJITA and Hisashi YOSHIKAWA

Government Industrial Research Institute, Osaka; Midorigaoka, Ikeda-shi, Osaka

(Received February 23, 1970)

We have examined the essential oils of *Cinnamomum japonicum* Sieb. (Japanese name, "Yabunikkei"); we could isolate two new monoterpene alcohols, named *trans*-yabunikkeol (I) and *cis*-yabunikkeol (II).

The essential oil was obtained by the steam distillation of twigs (yield: 0.75% of the fresh material as a case). The monoterpene alcohols were separated by activated-alumina-column chromatography using the fraction with a bp of 129—132°C/20 mmHg which resulted from the fractional distillation of the oil; they well purified finally by preparative GLC. (Yields: I, 1.0%, and II, 1.5% of the original oil).

These alcohols all have the same molecular formula, $C_{10}H_{16}O$ (mol. wt 152 by MS spectra). The IR and UV spectra show the presence of a secondary hydroxy group, terminal methylene linkage, an isopropyl group, and conjugated double bonds. The UV spectra show a close resemblance to that of β-phellandrene.[1]

On dehydrogenation with selenium, both alcohols gave small amounts of carvacrol. Furthermore, by isomerization with sulfuric acid in an ethanol solution, they were converted to carvotanacetone easily. The IR spectrum of the carvotanacetone obtained was quite identical with that of an authentic sample[2] prepared from carvone.

These evidences show that both alcohols are *p*-mentha-1(7),5-dien-2-ol. The *cis-trans* assignments were made chiefly by means of comparing the retention times of the GLC and IR spectra with those of *cis*- and *trans-p*-menth-1(7)-en-2-ol.[3,4]

trans-Yabunikkeol (I) (*trans-p*-mentha-1(7),5-dien-2-ol) is a colorless oil; bp 226°C/760 mmHg, d_4^{30} 0.9335, n_D^{30} 1.4988, α_D^{22} −17.80°. UV spectrum: λ_{max}^{EtOH} 232 mμ (ε=15700), 239 mμ (ε=11200). The IR spectrum is shown in Fig. 1.

cis-Yabunikkeol (II) (*cis-p*-mentha-1(7),5-dien-2-ol) has the following properties: mp 34°C, bp 228°C/760 mmHg, d_4^{30} 0.9503, n_D^{30} 1.5036, α_D^{22} +41.20°. UV spectrum: λ_{max}^{EtOH} 230 mμ (ε=16400), 238 mμ (ε=11000). The IR spectrum is shown in Fig. 2.

The specific retention times of GLC against α-terpineol (PEG 6000, 175°C) are 1.53 for I and 2.10 for II.

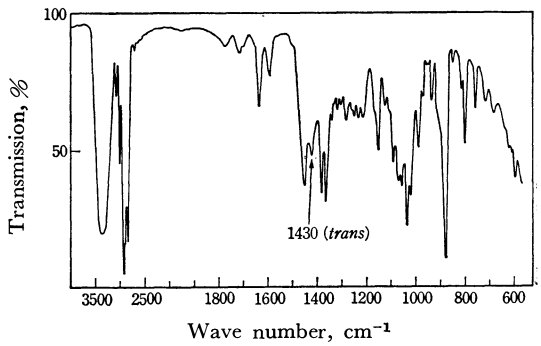

Fig. 1 IR spectrum of I.

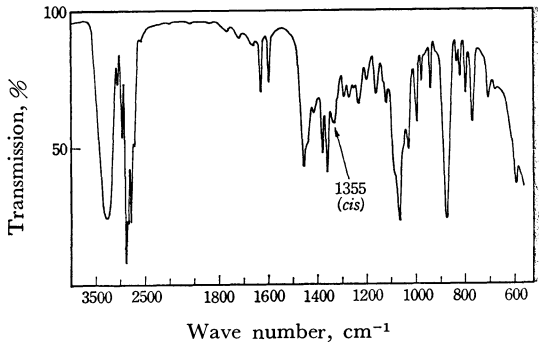

Fig. 2 IR spectrum of II.

1) H. Booker, L. K. Evans and A. E. Gillam, *J. Chem. Soc.*, **1940**, 1453.

2) B. M. Mitzner and V. J. Mancini, *Amer. Perf. Cosm.*, **84**, 37 (1969).

4) R. L. Kenney and C. S. Fisher, *J. Org. Chem.*, **28**, 3509 (1963).

4) B. M. Mitzner, V. J. Mancini, S. Lemberg and E. T. Theimer, *Appl. Spectrosc.*, **22**, 34 (1968).

Polymorphism of Inosine

Yoshihisa SUZUKI and Nobuya NAGASHIMA

Central Research Laboratories, Ajinomoto Co., Inc., Suzuki-cho, Kawasaki

(Received December 2, 1969)

Two different forms of anhydrous inosine crystals have been found during the course of studies on the crystallization and purification of inosine. The crystal data of inosine dihydrate were reported by Bugg, Thewalt and Marsh,[1] but there is no report on the crystal data of anhydrous inosine. One inosine in orthorhombic system is usually crystallized with ease from aqueous solution above 20°C, as needles or long prisms elongated along the *b* axis. The other in the monoclinic system is crystallized as plates from the aqueous dimethylsulfoxide solution (about 70 v/v%). We call the former modification the α-form, and the latter the β-form.

X-ray diffraction studies were carried out on the two crystalline forms with CuK_α radiation. The space groups were obtained from equi-inclination Weissenberg photographs of zero and first layers about axes *a* and *b*. The unit-cell dimensions determined from precession photographs are shown in Table 1, with other data. Density was measured by flotation in a chloroform-tetrabromoethane mixture.

An interesting feature of the polymorphism is relatively large difference in density. A larger difference in density in the polymorphs was reported by Bugg & Marsh[2] in cytydilic acid b.

TABLE 1. CRYSTALLOGRAPHIC DATA OF ANHYDROUS INOSINE CRYSTALS

	α-Form	β-Form
System	Orthorhombic	Monoclinic
Space group	$P2_12_12_1$	$P2_1$
Unit-cell parameters	a=21.26 Å	a=10.925 Å
	b=8.09	b=4.84
	c=13.22	c=10.44
		β=90.6°
Density obsd	1.576 g·cm^{-3}	1.61 3 g·cm^{-3}
calcd	1.568	1.614
Number of molecules per unit cell	8	2
Melting point	218—220°C	212—214°C

TABLE 2. X-RAY POWDER DIFFRACTION DATA OF ANHYDROUS INOSINE CRYSTALS

α-Form			β-Form		
d (Å)	I/I_1[a]	hkl	d (Å)	I/I_1[a]	hkl
11.33	5	101	10.95	10	100
10.72	20	200	7.59	80	101, $\bar{1}$01
8.37	100	201	5.50	15	200
7.63	5	110	5.24	5	002
6.66	30	002	4.87	100	201, $\bar{2}$01
6.50	20	210	4.74	15	102, $\bar{1}$02
6.37	60	102	4.46	30	110
6.30	60	301	4.41	30	011
5.83	30	211	4.11	70	111, $\bar{1}$11
5.67	5	202	3.81	5	202, $\bar{2}$02
5.00	40	112, 311, 401	3.66	10	300
4.87	20	302	3.62	20	210
4.65	20	212	3.56	10	012
4.34	10	103	3.46	60	003, 301, $\bar{3}$01
4.24	20	411	3.42	10	211, $\bar{2}$11
4.08	20	501, 020	3.40	15	112, $\bar{1}$12
3.88	10	021	3.34	10	103, 103
3.83	20	121, 113	3.00	10	{302, $\bar{3}$02
3.79	20	510, 303			{212, $\bar{2}$12
3.66	30	221, 511, 213			
3.59	20	502			
3.56	20	600			
3.53	20	320			
3.41	30	403, 321, 122			
3.31	20	222			
3.29	20	104, 512			
3.23	20	420			
3.16	30	602, 413			

a) The scale is so chosen as to make the most intense line have the value 100.

The X-ray powder diffraction data of these two forms are shown in Table 2. The infrared spectra differ from each other in certain points.

The solubility data of inosine reported by Suzuki[3] were of α-form. Details of solubility data and crystallizing conditions of the β-form will be reported in the future.

1) C. E. Bugg, U. T. Thewalt and R. E. Marsh, *Biochem. Biophys. Res. Commun.*, **33**, 436 (1968).

2) C. E. Bugg and R. E. Marsh, *J. Mol. Biol.*, **25**, 67 (1967).

3) Y. Suzuki, T. Toki and T. Nakamura, Presented at 18th Annual Meeting of the Chemical Society of Japan, Osaka, 1965.

New-Type of Copper(II) Complexes with a Subnormal Magnetic Moment Derived from *N,N'*-Bis(2-carboxyethyl)oxamide

Heijiro OJIMA and Kiyoko YAMADA

Department of Chemistry, Aichi Kyoiku University, Kariya, Aichi

(Received February 12, 1970)

The present authors are continuing their syntheses and characterization of metal complexes coordinating negative amide nitrogen.[1] This paper will report that the *N,N'*-bis-substituted-oxamidato copper(II) acts as a bidentate ligand to afford new-type copper(II) complexes with a subnormal magnetic moment: that is, a new ligand, *N,N'*-bis(2-carboxyethyl)oxamide, has been synthesized, and then three kinds of copper(II) complexes with this ligand (abbreviated, Na_2[Cu–CEoxd], [Cu–CEoxd–Cu–bipy], and [Cu(CEoxdH)(OH)]$_2$) have been isolated.

The [Cu–CEoxd–Cu-bipy] was obtained as yellowish-green fine crystals by mixing one mole of the Na_2[Cu–CEoxd] and one mole of mono-(2,2'-bipyridyl)-copper(II) nitrate in a water solution in which the pH value had been adjusted at 9. Found for the tetra-hydrate, Cu, 21.50%; N, 9.99%; H_2O, 12.66%. Calcd for $C_{18}H_{16}O_6N_4Cu_2 \cdot 4H_2O$, Cu, 21.78%; N, 9.60%; H_2O, 12.35%. Found for the anhydrous salt, Cu, 24.85%. Calcd for anhydrous salt, Cu, 24.85%.

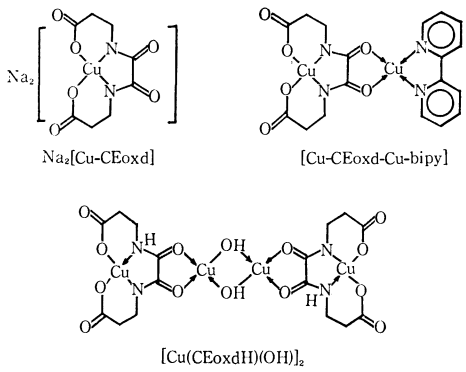

Na_2[Cu-CEoxd] [Cu-CEoxd-Cu-bipy]

[Cu(CEoxdH)(OH)]$_2$

Fig. 1. Copper (II) complexes isolated.

The [Cu(CEoxdH)(OH)]$_2$ was obtained as green fine crystals by the reaction of one mole of Na_2[Cu–CEoxd] with one mole of copper(II) salt in a water solution at room temperature. Found for deca-hydrate, Cu, 27.38%; N, 6.18%; H_2O, 19.59%. Calcd for $C_{16}H_{20}O_{14}N_4Cu_4 \cdot 10H_2O$, Cu, 27.43%; N, 6.05%; H_2O, 19.44%. Found for anhydrous salt, Cu, 34.12%; N, 7.59%. Calcd for anhydrous salt, Cu, 34.05%; N, 7.51%.

The values of the magnetic moment for the [Cu–CEoxd–Cu-bipy] and [Cu(CEoxdH)(OH)]$_2$ are obviously subnormal. This suggests that the mutual interaction between the two copper(II) ions must take place through the partial structure:

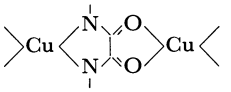

and that they belong to the category of "super exchange interaction."[2] Putting it concretely, the interaction may take place through a π-path way (Cu–N–C–C–O–Cu) set up by using $3d_{yz}$ (or $3d_{xz}$) orbitals of the cupric ions and $2p_\pi$ orbitals of the bridging oxamide group. These two complexes are new-type complexes with a subnormal magnetic moment.

TABLE 1. SOME PROPERTIES OF COPPER (II) COMPLEXES ISOLATED.

Ligand and its complex	Magnetic data				IR-spectra[c]			
	$10^6\chi_g$	$10^6\chi_M$	μ_{eff} (BM)	T°K	ν_{N-H}	COOH	COO–Cu	amide I
Ligand $CE_{oxd}H_4$	—	—	—	—	3310	1700	d)	1645
Na_2[Cu-CE_{oxd}]·$4H_2O$	2.86	1173.5	1.78	287				
anhydrous salt	3.44	1160.6	1.79	300	d)	d)	1630	1585[b]
[Cu-CE_{oxd}-Cu-bipy]·$4H_2O$	1.32	385.4	1.10	287				
anhydrous salt	1.73	442.4	1.13	287	d)	d)	1654	1619
[Cu(CE_{oxd}H)(OH)]$_2$·$10H_2O$	2.61	605.3	1.27	286				
anhydrous salt[a]	3.28	612.7	1.25	287	3350[b]	d)	1650	1635

a) The band which is due to the ν_{O-H} (bridged OH group) was observed at 3230 cm^{-1}.
b) Broad band. c) Anhydrous salts were used for the determinations. d) Disappeared.

1) H. Ojima, and K. Yamada, *Nippon Kagaku Zasshi*, **88**, 329, 333, 952, 1056 (1967); *ibid.*, **89**, 490 (1968); *ibid.*, **91**, 49 (1970).

2) M. Kato, H. B. Jonassen and J. C. Fanning, *Chem. Rev.*, **64**, 99 (1964).

A New Method for the Protection of *trans*-Diequatorial Amino and Hydroxyl Groups in Aminosugars and Aminocyclitols

Sumio UMEZAWA, Tsutomu TSUCHIYA and Yasushi TAKAGI

Department of Applied Chemistry, Faculty of Engineering, Keio University, Koganei-shi Tokyo

(Received March 16, 1970)

The combined protection of vicinally situated *trans*-diequatorial amino and hydroxyl groups of pyranoside type aminosugars or inosamines is sometimes necessary in preparing their derivatives. However, contrary to the case of *cis* amino and hydroxyl groups, this kind of protection has not been achieved satisfactorily. Very recently, Miyai and Gross[1] prepared the 2,3-carbamate derivative of benzyl 2-amino-4,6-*O*-benzylidene-2-deoxy-β-D-glucopyranoside with the use of *N,N'*-carbonyldiimidazole in absolute tetrahydrofuran.

We wish to report that the protection was successfully performed by utilizing *p*-nitrophenoxycarbonyl chloride; a characteristic feature of this method is that the products are prepared by a one-step procedure in good yields and the reaction proceeds in a medium containing water, which is necessary in dealing with water-soluble compounds. As an example, the preparation of 2-deoxystreptamine 1,6;3,4-dicarbamate (I) and methyl 2-amino-2-deoxy-α-D-glucopyranoside 2,3-carbamate (II) is described.

To an aqueous solution of 2-deoxystreptamine (DST), Dowex 1×2 resin (OH form) was added, and an excess *p*-nitrophenoxycarbonyl chloride in acetone was added with stirring. A cyclic dicarbamate I was obtained in 73% yield; mp >285°C; IR spectrum: 1760 and 1735 cm^{-1} (C=O); no peak near 1550 cm^{-1} (amide II) was observed indicating I to be a cyclic amide. The 5-*O*-acetyl derivative of I was prepared from I with pyridine-acetic anhydride; mp 276°C (decomp.); molecular weight: 256 (mass spectrum); IR spectrum: 3300 (NH), 1770, 1735 cm^{-1}; NMR (dimethyl sulfoxide-d_6): τ: 4.45 (1-proton triplet, J 9.4 Hz, H-5), 5.91 (2-proton quartet, $J_{4,5}=J_{5,6}$ 9.4 Hz, $J_{3,4}=J_{1,6}$ 11.2 Hz, H-4,6), 6.30 (2-proton double triplets, $J_{3,4}=J_{1,6}$ $J_{1,2_a}=J_{3,2_a}$ 11.2 Hz, $J_{1,2_e}=J_{3,2_e}$ 3.2 Hz, H-1,3), 7.85 (1-proton double triplets, J 3.2 and 11 Hz, H-2_e), 8.40 (1-proton quartet, J 11 Hz, H-2_a). The results support the structure for I.

On alkaline hydrolysis I gave DST, and on ethanolysis in the presence of sodium ethoxide, I gave *N,N'*-diethoxycarbonyldeoxystreptamine (III); mp 225°C (decomp.); IR spectrum: 1695 (NH*COO*), 1545 (amide II) cm^{-1}.

Methyl 2-amino-2-deoxy-α-D-glucopyranoside was treated similarly to give the corresponding 2,3-carbamate derivative (II) in 70% yield; hygroscopic solid, $[\alpha]_D^{21}$ +110° (*c* 0.5, water); IR spectrum: 1760 cm^{-1} (C=O); NMR (deuterium oxide): τ: 4.86 (1-proton doublet, $J_{1,2}$ 3 Hz, H-1), 5.40 (1-proton quartet, $J_{2,3}$ 12 Hz, $J_{3,4}$ 9.3 Hz, H-3), 5.93 (1-proton triplet, $J\sim9$ Hz, H-4), 6.22 (1-proton quartet, J 3 and 12 Hz, H-2), 6.5 (3-proton singlet, OMe). A similar acetylation of II gave the 4,6-di-*O*-acetyl derivative; amorphous solid, $[\alpha]_D^{21}$ +94° (*c* 0.5, chloroform); NMR (deuteriochloroform): τ: 4.67 (1-proton quartet, $J_{4,5}$ 9.2, $J_{3,4}$ 10 Hz, H-4), 4.96 (1-proton doublet, $J_{1,2}$ 3 Hz, H-1), 5.33 (1-proton quartet, $J_{3,4}$ 10, $J_{2,3}$ 11.8 Hz, H-3), 6.5 (3-proton singlet, OMe), 7.88 and 7.90 (each 3-proton singlet, OAc). These results indicate the CI conformation of II.

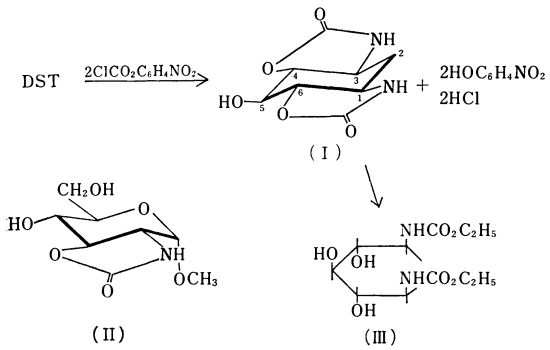

1) K. Miyai and P. H. Gross, *J. Org. Chem.*, **34**, 1638 (1969).

BULLETIN OF THE CHEMICAL SOCIETY OF JAPAN VOL. 43 1603—1607 (1970)

Redox Reactions on the Lithiated Nickel Oxide Electrode

Hiroshi YONEYAMA and Hideo TAMURA

Department of Chemical Technology, Faculty of Engineering, Osaka University, Yamadakami, Suita, Osaka

(Received April 14, 1969)

The redox reactions of the Ce^{3+}/Ce^{4+}, Fe^{2+}/Fe^{3+} and $Fe(CN)_6^{4-}/Fe(CN)_6^{3-}$ systems on lithiated nickel oxide electrodes in a H_2SO_4 medium were studied. For the Fe^{2+}/Fe^{3+} and $Fe(CN)_6^{4-}/Fe(CN)_6^{3-}$ systems, the reactions were controlled by an activation process when the electrode was polarized anodically, while the current tended to saturation as the current was increased in the cathodic direction. The apparent exchange current densities of these systems were distinctly dependent on the resistivity of the electrode. These phenomena were discussed qualitatively from a consideration of the energy states of the charge carriers in the electrode and redox systems, and it was concluded that all the reactions had proceeded through only hole transfer.

A large number of metallic oxides exhibit semiconductivity. For a catalytic reaction which proceeds in the presence of such kinds of oxides, it has often been found that the reactivity is affected by their semiconducting character. In such a case, the chemical reaction is supposed to be controlled by the behavior of the charge carriers in the oxides. More particularly, for the electrode of a semiconductor such as Ge it has been found that the behavior of the charge carriers clearly controls an electrochemical reaction.[1,2] Recently, studies of electrode reactions on semiconductors have been developed to cover oxide semiconductors.[3,4] Almost all of the semiconductors on which electrode reactions have been studied have, though, been ones with a clear energy-band scheme. In these electrodes, the current-potential curves are often affected by the behavior of the minority carrier in the electrode, and from these curves it is possible to estimate which carrier, electron or hole, participates in the reaction. This estimation is also possible from the study of the reactions of redox systems having various standard electrode potentials,[5,6] because the density of the electron or hole in the electrode-surface region is adjusted in accordance with the redox potential of the redox system.

In contrast to a usual band-type semiconductor such as Ge and ZnO, a hopping-type semiconductor is normally considered to have a different energy-band structure,[7] although this question has not yet been completely clarified. However, the kind of charge carrier participating in an electrode reaction on a hopping-type semiconductor electrode may be estimated by means of the experimental technique used in the study of the electrode reaction on usual band-type semiconductors, because a reaction should also proceed when the energy state of the charge carrier in the semiconductor almost coincides with that of ions in an electrolyte. Recently, Yohe and his co-workers studied the redox reactions on a lithiated nickel oxide electrode[8], which is classified as a typical hopping-type semiconductor.[7,9] However, they examined the behavior of the electrode over a wide pH range, and so the condition of the electrode surface may not have been always the same[10]; moreover, the effect of the resistivity of the electrode on the reactivity is not clear, either. Therefore, we studied the reactivity of the redox reactions on this electrode as a function of its resistivity. Experiments were carried out in an acid medium so as always to establish the same surface condition of the electrode.

Experimental

Electrode. High-purity Ni powder (99.99%) was dissolved in a H_2SO_4 solution, and $NiCO_3$ was precipitated by the addition of $NaHCO_3$ to the solution.

1) F. Beck and H. Gerisher, *Z. Elektrochem.*, **63**, 500 (1959).
2) D. R. Turner, *J. Electrochem. Soc.*, **103**, 252 (1956).
3) S. R. Morrison and T. Freund, *Electrochim. Acta*, **13**, 1343 (1968).
4) F. Lohman, *Ber. Bunsenges. Phys. Chem.*, **70**, 438 (1966).
5) F. Beck and H. Gerisher, *Z. Elektrochem.*, **63**, 943 (1959).
6) H. Gerisher, *Ber. Bunsenges. Phys. Chem.*, **69**, 578 (1965).
7) F. J. Morrin, *Bell System Tech. J.*, **37**, 1047 (1958).
8) D. Yohe, A. Riga, R. Greef and E. Yeager, *Electrochim. Acta*, **13**, 1351 (1968).
9) D. P. Snoden and H. Saltsburg, *Phys. Rev. Lett.*, **14**, 497 (1965).
10) M. Pourbaix, "Atlas of Electrochemical Equilibra in Aqueous Solution," Pergamon Press, New York (1966), p. 330.

After several decantations, the precipitate was filtrated, washed thoroughly by de-ionized water, and then evaporated to dryness. It was finally decomposed to NiO by heating at 600°C for 4 hr in the air. The NiO powder prepared in this way was spectroscopically pure. Using this NiO powder, an electode was prepared by a method descirbed previously.[11] This electrode showed P-type semiconductivity when examined by the thermo-electromotive-force measurements.

Specific Resistivity. The specific resistivity of the electrode was measured by the four-probe method[12] at 25°C after completing the measurements of the polarization curves in various redox solutions. The electrode had a specific resistivity of 1.9—193 Ω-cm. The electrodes had the Li contents shown in Table 1. The Li contents in Table 1 were estimated from the relationship between the Li content and the resistivity, which had been obtained beforehand for various NiO's. In the previous investigation we estimated the resistivity from the voltage drop between platinum contacts on both faces of a disk-shaped electrode. The value estimated before was somewhat larger than that obtained by the four-probe method. Even if this difference had been caused by bringing Pt into contact with the lithiated NiO, Pt contact on the lithiated NiO did not have any serious effect on the electric conduction as will be discussed below.

TABLE 1. Li CONTENT IN TEST ELECTRODES

Resistivity at 25°C (Ω-cm)	1.9	5.0	13.3	44.0	192
Li content (atom %)	7.0	2.4	0.80	0.23	0.054

Electrode Area. The effective area of the electrode was estimated by a method described previously.[11] The area was fixed in a small part of the face of the disk-shaped electrode by covering it with epoxy resin in order to eliminate the voltage drop in the electrode, which would make the current-potential curves more complex. In the estimation of the surface area, the resistivity estimated by the method reported previously[11] was used, because the electrode always had Pt contact on the lithiated NiO.

Cell Equipment. Connection between the reference electrode (SCE) and the solution was made by an agar bridge containing a saturated KCl solution, but the agar bridge was not inserted directly into the electrolytic cell. The cell was convered with aluminum foils so as to shut off the light.

Current-potential Relation. Steady-state current-potential (*I-V*) curves were obtained potentiostatically by means of an electronic potentiostat. Electrodes were conditioned by successive pre-electrolysis in 0.1N H_2SO_4 at 1.6 V and −1.2 V each 10 min and finally at 0V for 5 min. Before and during measurements N_2 gas was bubbled into the electrolyte so as to remove any dissolved oxygen and stir the solution. All the measurements were carried out at 25±0.5°C.

Chemicals. All the chemicals used in this study were of a G.R. grade. Three kinds of redox systems were used in this study. They are indicated in Table 2. The concentrations of the ions were determined by analysis, if necessary. The Fe^{2+}/Fe^{3+} and Ce^{3+}/Ce^{4+} systems were prepared by their sulfates, while potassium salts were used to prepare the $Fe(CN)_6^{4-}/Fe(CN)_6^{3-}$ system.

TABLE 2. REDOX SYSTEMS STUDIED

System	Medium
5 mM Ce^{3+} 5 mM Ce^{4+}	0.17N H_2SO_4
5 mM Fe^{2+} 5 mM Fe^{3+}	0.1N H_2SO_4
5 mM $Fe(CN)_6^{4-}$ 5 mM $Fe(CN)_6^{3-}$	0.1N H_2SO_4

Results

Steady-state *I-V* curves in 0.1N H_2SO_4 are shown in Fig. 1 for 1.9, 5.0, 13.3, 44, and 192Ω-cm electrodes. *I-V* curves for $Fe(CN)_6^{4-}/Fe(CN)_6^{3-}$, Fe^{2+}/Fe^{3+}, and Ce^{3+}/Ce^{4+} systems are shown in Figs. 2, 3, and 4 respectively. For the Ce^{3+}/Ce^{4+} system, a saturation current was observed when the anodic

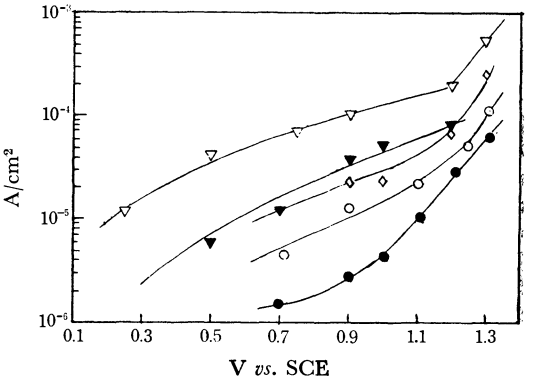

Fig. 1. *I-V* curves for lithiated NiO electrodes in 0.1N H_2SO_4.
—▽— 1.9Ω-cm, —▼— 5.0Ω-cm, —◇— 13.3Ω-cm, —○— 44Ω-cm, —●— 192Ω-cm

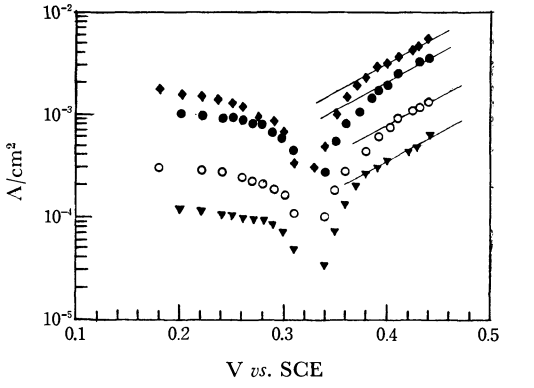

Fig. 2. *I-V* curves in the $Fe(CN)_6^{4-}/Fe(CN)_6^{3-}$ system.
—◆— 1.9 Ω-cm, —●— 5.0 Ω-cm, —○— 13.3 Ω-cm, —▼— 44 Ω-cm

11) H. Yoneyama and H. Tamura, This Bulletin, **42**, 1795 (1969).
12) L. B. Valdes, *Proc. IRE*, **42**, 420 (1954).

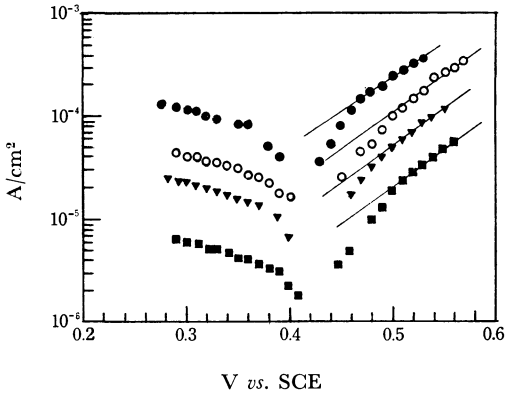

Fig. 3. *I-V* curves in the Fe^{2+}/Fe^{3+} system.
—●— 5.0 Ω-cm —○— 13.3 Ω-cm
—▼— 44 Ω-cm —■— 192 Ω-cm

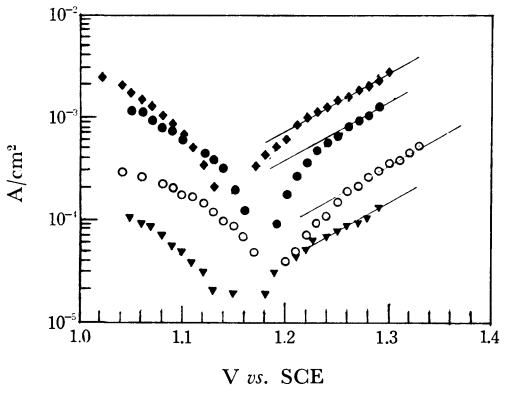

Fig. 4. *I-V* curves in the Ce^{3+}/Ce^{4+} system.
—◆— 1.9 Ω-cm, —●— 5.0 Ω-cm,
—○— 13.3 Ω-cm, —▼— 44 Ω-cm

polarization was increased to about 1.5 V, and with a further increase in polarization beyond 1.6 V the current increased again, supposedly because of commencement of the oxygen-evolution reaction. In these figures, the following facts can be noticed: (a) In a cathodic polarization the current tends to become saturated in the $Fe(CN)_6^{4-}/Fe(CN)_6^{3-}$ and Fe^{2+}/Fe^{3+} systems, this phenomena appearing more distinctly in the former. (b) In the anodic polarization, the electrode reaction seems to proceed by an activation process. (c) The current in Figs. 2—4 is considered to be related to the reaction of the redox system itself, since this current is over 10 times that in Fig. 1. (d) The reactivity of the redox system was much influenced by the resistivity of the electrode. To make clear the nature of the cathodic current for the $Fe(CN)_6^{4-}/Fe(CN)_6^{3-}$ and Fe^{2+}/Fe^{3+} systems, which showed a tendency toward saturation, the dependence of this current on the concentration of the oxidant was obtained. One typical result is shown in Fig. 5 for the reduction of Fe^{3+}.

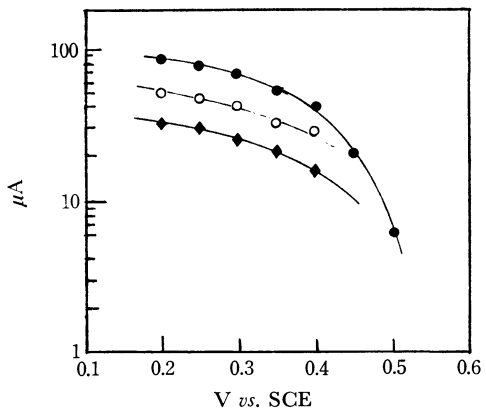

Fig. 5. *I-V* curves for the 192 Ω-cm electrode in Fe^{3+} solutions
Electrode area: 0.65 cm²
—●— 0.1M Fe^{3+} —○— 0.05M Fe^{3+}
—◆— 0.025M Fe^{3+}

Discussion

When a metal comes in contact with a P-type semiconductor, a barrier layer may be formed on the contact surface between them. If this layer exists, the current is hindered by this layer when a metal is biased positively against the P-type semiconductor. As is shown above, however, the current flowed more easily in the anodic polarization and a Tafel slope was observed. Therefore, the contact between the Pt and the lithiated NiO can be considered not to have caused any serious problem if it existed at all.

The (a) fact in the previous section conceivably does not indicate the character of the redox system itself, but that of the redox reaction restricted by the behavior of the charge carrier participating in the reaction, because the *I-V* curves of the same redox system were quite different on an N-type semiconductor electrode of αFe_2O_3 doped with titanium.[13] Therefore, the *I-V* curves of the various redox systems can be reasonably explained if it is assumed that the flow of the cathodic current was hindered by the potential barrier formed on the electrode surface as a result of the polarization. As the flat-band potential of the lithiated NiO is 0.65 V *vs.* SCE in 0.1N H_2SO_4 and 0.76 V in 0.17N H_2SO_4,[14] the energy levels of the electron and positive hole of the electrode were lowered in the electrode surface region for the $Fe(CN)_6^{4-}/Fe(CN)_6^{3-}$ and Fe^{2+}/Fe^{3+} systems because the redox potentials of these systems are lower than the flat-band potential; hence, the Fermi level of the

13) H. Yoneyama, S. Hamamatsu and H. Tamura, This Bulletin, to be published.
14) T. O. Rouse and J. L. Weininger, *J. Electrochem. Soc.*, **113**, 184 (1966).

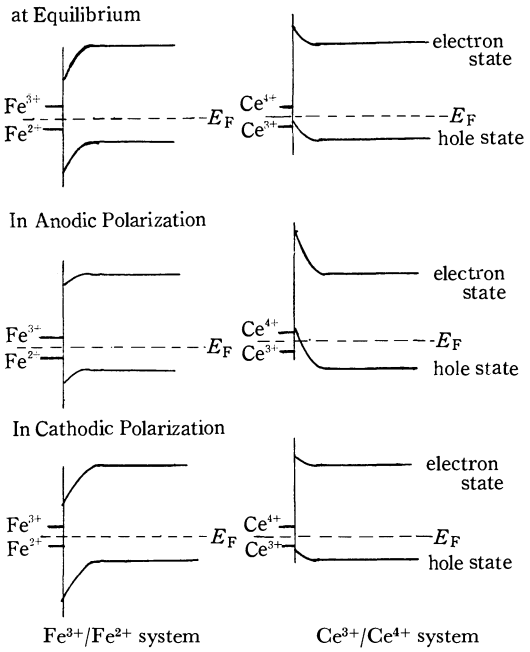

Fig. 6. Schematic representation of energy profile at the interface of electrode and redox electrolyte.

electrode surface is apparently shifted toward a higher energy state compared to the inside of the electrode. The hole concentration in the surface region of the electrode will then decrease, while electron density will increase if it is present at all. This situation is strengthened by the cathodic polarization. Such a energy scheme of the electrode and the electrolyte is represented in Fig. 6 using a band model, though it may not precisely represent the energy structure of 3*d* transition metal oxide.[15] In Fig. 6, each energy state pictured by a solid line in the electrode part indicate the localized energy level at which a positive hole and a localized free electron exist. According to Fig. 6, the electron exchange may occur in the cathodic polarization if the energy state of the electron in the electrode is higher than that of the oxidant of the redox system, that is, $Fe(CN)_6^{3-}$ or Fe^{3+}. However, if electron transfer had occurred, the tendency of the current toward saturation with an increase in the cathodic polarization would not have been observed because the electron transfer from the electrode into the electrolyte could not possibly have been hindered. The only exceptional case is when the current had been hindered by the deficiency of the electron on the electrode surface, but if this were true in this case, no dependence of the cathodic current on the Fe^{3+} concentration would have been observed. The electron transfer mechanism can be eliminated from such a consideration, though Bosman and Crevecouer[16] reported the existence of an electron in the lithiated NiO. On the contrary, the hole-transfer mechanism is reasonable for the following reasons. The height of the potential barrier over which the hole should jump into the electrode under the reaction increases with an increase in the cathodic polarization. The cathodic current would then show a tendency toward saturation. The dependence of the cathodic current on the concentration of Fe^{3+} shown in Fig. 5 means that the probability function of the electron state in the electrolyte[17] was almost proportional to the concentration of Fe^{3+}. In the anodic polarization of $Fe(CN)_6^{4-}/Fe(CN)_6^{3-}$ and Fe^{2+}/Fe^{3+} systems, hole transfer would more easily occur, since the barrier height for the hole transfer into the electrode decreases with a rise in the anodic potential; thus the Tafel slope was observed. One possible explanation[18] for the mechanism in which the reaction proceeds only through hole transfer is that the energy state of the electron is separate from that of the hole state even if free electron exists in the lithiated NiO.[16] According to Houten's calculation,[19] the energy level of the electron denoted as Ni^+ is located about 5.4 eV above the acceptor level of Ni^{3+} next to a substitutional Li^+.

The situation is very different for the Ce^{3+}/Ce^{4+} system, which has a higher redox potential, that is, 1.36 V *vs.* SCE.[20] The energy levels occupied by charge carriers are raised; this causes the hole concentration in the electrode surface to increase. Such a situation is also represented in Fig. 6. The potential barrier for hole transfer into the electrode will decrease with polarization in the cathodic direction. Thus, the cathodic current would apparently not be suppressed by this potential barrier. On the other hand, hole transfer from the electrode into the electrolyte would occur in the anodic polarization, and no potential barrier would exist in this pathway. The Tafel relation conceivably appears because of such a condition. The *I-V* curves of the Ce^{3+}/Ce^{4+} system possibly indicate

15) F. J. Morin, *Phys. Rev.*, **93**, 1195 (1954); *ibid.*, **93**, 1204 (1954). Bosman *et al.* claimed that application of band model is larther erasonable (see Ref. 16). Yu. M. Ksendzov and I. A. Darbkin also support existence of a band for the energy state of Ni^+ (*Soviet Physics-Solid State*, **7**, 1519 (1965)).

16) A. Bosman and C. Crevecouer, *Phys. Rev.*, **144**, 763 (1966). If N_D and N_A denote concentration of donors and acceptors $(N_A-N_D)/N_D \sim 10$ and density of states at 300°K is about 3.5×10^{20}.

17) H. Gerisher, "Advance in Electorchemistry and Electrochemical Engineering," Vol. 1, ed. by P. Delahey and C. W. Tobias, Interscience Publishers, New York (1961), p. 193.

18) H. Gerisher, *ibid.*, p. 201.

19) S. van Houten, *J. Phys. Chem. Solid*, **17**, 7 (1960).

20) W. M. Latimer, "Oxidation Potential," 2nd ed. Prentice-Hall, Inc., Englewood Cliffs, N. J. (1952), p. 339.

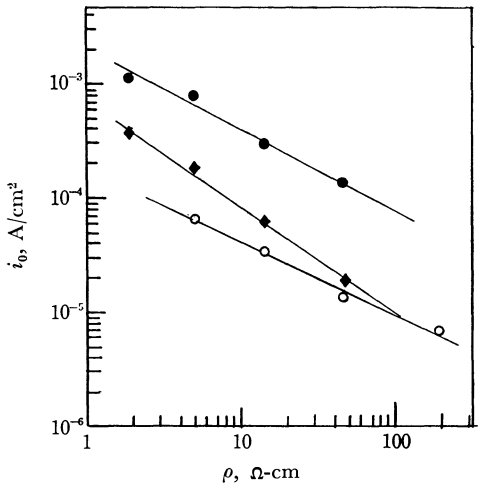

Fig. 7. Relationship between i_0 and resistivity of electrodes.
—●— $Fe(CN)_6^{4-}/Fe(CN)_6^{3-}$
—○— Fe^{2+}/Fe^{3+}
—◆— Ce^{3+}/Ce^{4+}

the reaction patterns of this redox system itself.

The apparent exchange current density, i_0, was estimated by extraporation of the anodic Tafel slope to the measured open-circuited potential of each redox system; it is plotted against the resistivity of the electrode in Fig. 7. The i_0 value increases with a lowering of the resistivity of the electrode, and nearly a linear relationship exists between these two values. From this result, it is obvious that i_0, and, accordingly, the rate of the electrochemical reaction is determined by the charge carrier density in the electrode. This is a reasonable result, since the charge carrier density on the surface of the electrode is larger for the electrode with the lower resistivity.

In conclusion, we can state that the charge carrier density in the lithiated NiO is the most important factor in determining the reaction rate for the electrochemical reaction which proceeds on this electrode. The reaction potential is another important factor in controlling the reaction rate in either oxidation or reduction. The present studies may give instructive information on the rate of some electrochemical reactions on the Ni electrode, since the Ni electrode in solution usually forms a passivated or oxide film in the specified potential region and the flat-band potential of this film coincides with that of the lithiated NiO.[21]

21) S. Toshima, *Denki Kagaku*, **34**, 564 (1966).

BULLETIN OF THE CHEMICAL SOCIETY OF JAPAN VOL. 43 1607—1610 (1970)

Magnetic Susceptibilities of Chloroform Mixtures

R. GOPALAKRISHNAN

Sri Venkateswara University, College of Engineering, Tirupati, India

(Received January 7, 1969)

Magnetic susceptibilities of nine typical liquid mixtures were determined as a function of concentration. Deviations from an additive law were observed for these mixtures of chloroform with triethylamine, aniline, pyridine, α-picoline, 2,4-lutidine, diphenyl ether, toluene, nitrobenzene and chlorobenzene. The observed deviations are explained on the basis of hydrogen bond formation.

Early experimental work regarding the effect of hydrogen bond formation on magnetic susceptibility has been done by Angus and Hill,[1] Venkataramaiah,[2] Varadachari,[3] and Rumpf and Seguin.[4] Milligan and Whitehurst[5] reviewed the work up to 1952, and interpreted their own measurements of magnetic properties of hydrogen-bonding substances namely, water, propanol and acetic acid absorbed on silica gel with the assumption that hydrogen bonding decreases diamagnetism. Recent studies of Venkateswarlu and Sriraman[6] and

1) W. R. Angus and W. K. Hill, *Trans. Faraday Soc.*, **36**, 923 (1940).

2) H. S. Venkataramaiah, *J. Mysore Univ. Sect. B.*, Contrib. 10, in Phys. 3, Part 4, 19 (1942).

3) S. V. Ananthakrishnan and P. S. Varadachari, *Proc. Indian Acad. Sci., Sect. A*, **20**, 128 (1944).

4) P. Rumpf and M. Seguin, *Bull. Soc. Chim. Fr.*, **1949**, D 366; **1950**, 177, 542.

5) W. O. Milligan and H. B. Whitehurst, *J. Phys. Chem.*, **56**, 1073 (1952).

6) K. Venkateswarlu and S. Sriraman, *Trans. Faraday Soc.*, **53**, 433 (1957).

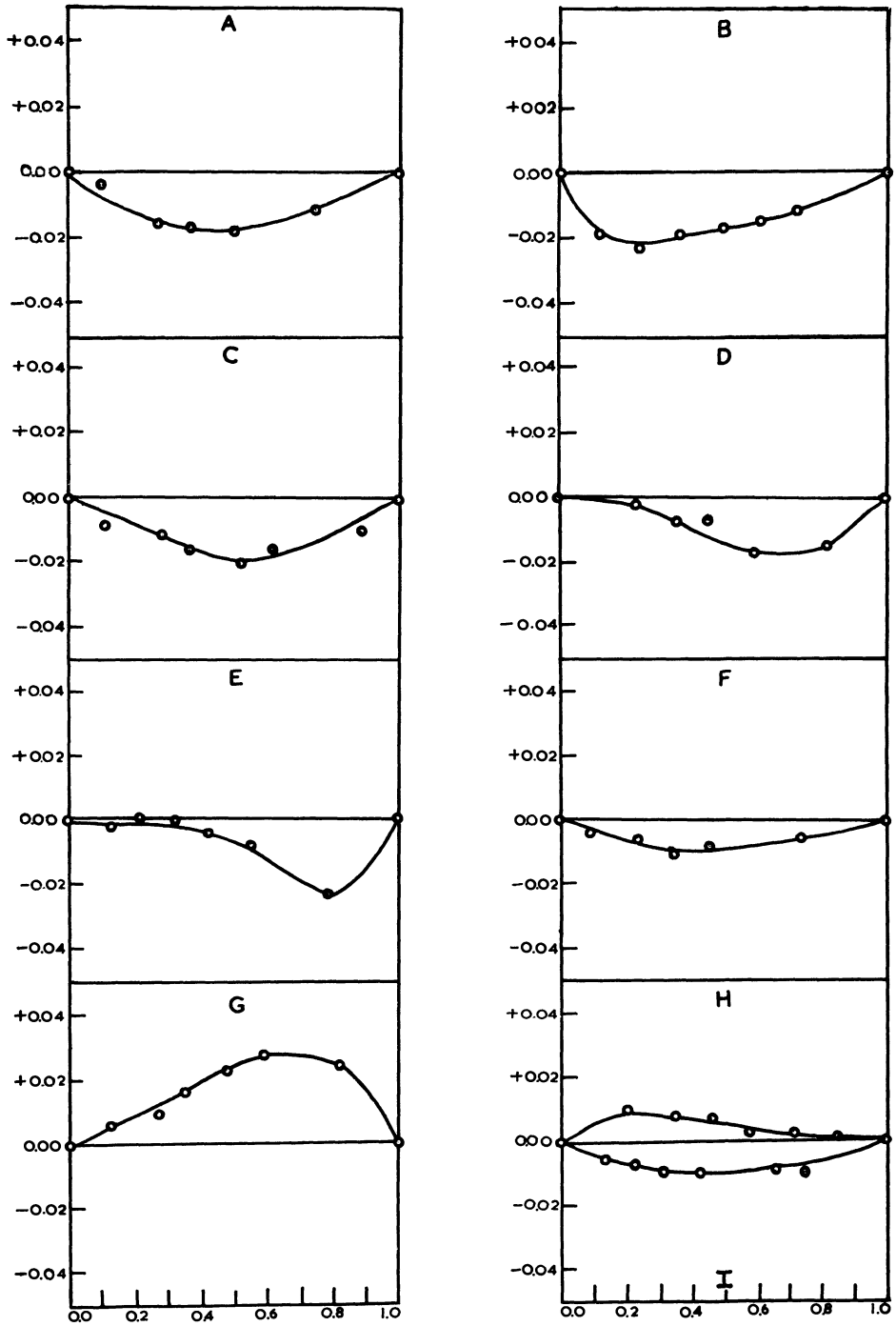

Fig. 1. Excess susceptibility, χ^E *vs.* Mole fraction of second component, x_B.

A, triethylamine	B, aniline	C, pyridine
D, α-picoline	E, 2,4-lutidine	F, diphenyl ether
G, toluene	H, nitrobenzene	I, chlorobenzene

Deshpande and Pathki[7] confirm the above view.

Experimental

Mixtures were prepared by mixing weighed amounts of pure components. Pure components were previously distilled in an all-glass apparatus. The specific susceptibilities were measured using a standard Gouy balance. The Gouy force ranged from 20 to 30 mg and the accuracy of its determination was estimated to be 0.05 mg. The magnetic susceptibilities of standard liquids were determined as a check and results were in good agreement with the accepted values. Water was used as a reference liquid in all measurements with $\chi=-0.720\times10^{-6}$. Densities were determined by the pycnometer method.

Results and Discussion

The results are presented in the figure where the excess susceptibility, χ^E, defined as the difference between the experimental value and linear law value, is represented as a function of molecular concentration x_B of the second component, the concentration of the first component (chloroform) being x_A.

Before a discussion of the results in the light of hydrogen bond formation it is necessary to find whether there would be any effect of hydrogen bond on susceptibility. For this, we use the explanations given by Pople, Bernstein and Schneider.[8]

In the electrostatic picture of hydrogen bond[9] of the type X–H---Y, Y system is superposed on the X–H bond to produce a strong electric field which attracts the partially screened proton of the X–H bond. Consequently, the proton of the hydrogen bond will be drawn away from its own bonding electrons. This produces a distortion in the charge distribution round H. The screening, not being spherically symmetrical, has to be expressed in terms of an appropriate tensor. The components of this tensor will then affect the values of magnetic susceptibility of the hydrogen and endow it with an anisotropic character. The principal components of susceptibility parallel and perpendicular to the bond can be written as

$$\chi_{\parallel}=\chi_0+\eta_{\parallel}E^2$$
$$\chi_{\perp}=\chi_0+\eta_{\perp}E^2$$

where χ_0 is the value of the susceptibility in the free state, E is the electric field at the hydrogen due to the donor electrons. The values of η's are given by

$$\eta_{\parallel}=-\frac{159a^6}{16mc^2};\quad \eta_{\perp}=-\frac{797a^6}{48mc^2}$$

where a is the radius of the Bohr orbit. The mean susceptibility value is given by

$$\chi=\chi_0+\frac{1}{3}(\eta_{\parallel}+2\eta_{\perp})E^2$$

Therefore, the fractional change in susceptibility per hydrogen atom is

$$\left|\frac{\chi-\chi_0}{\chi_0}\right|=\left|\frac{\Delta\chi_0}{\chi_0}\right|=28.76\ \frac{a^4}{c^2}E^2=28.76\times E_{au}^2$$

where E_{au} is the value of electric field expressed in atomic units. A rough estimate of this change can be made by considering a O–H---O bond. Calculations carried out by Pople[10] show that $E=4\times10^5$ e.s.u. or 0.024 au. It therefore leads to a value of (-0.017) for $\left|\frac{\Delta\chi}{\chi_0}\right|$ *i. e.*, a lowering of roughly 2%. In the present investigations, values of χ^E of this order of magnitude have been observed.

There is still another aspect of the hydrogen bonding refered to as "ring effect" which arises in the case of mixtures of chloroform with certain aromatic compounds (Pople,[11] Reeves and Schneider[12]).

The mixtures of chloroform with different liquids are discussed one by one. In the case of triethylamine the electronegative 'N' leads to the formation of C–H---N bond with chloroform. There is considerable evidence in support of this based on PMR and infrared absorption[13,14] studies of these mixtures. Such a hydrogen bond formation usually results in large negative excess function. Our observations are consistent with this.

The nitrogen in aniline has two attached hydrogen atoms and by itself is an electron donor. There is a possibility of bonding between N and C–H bond of the chloroform. This is consistent with evidence from infrared absorption studies.[15,16] Our measurements show a large negative value for χ^E.

Consider the solution of chloroform with pyridine. There is evidence for hydrogen bond formation between chloroform and this strong base.[17] The nitrogen is highly electronegative. Consistent with

7) V. T. Deshpande and S. Pathki, *ibid.*, **58**, 2134 (1962).

8) J. A. Pople, W. G. Schneider and H. J. Bernstein, "High Resolution Nuclear Magnetic Resonance," McGraw Hill, New York (1959).

9) J. A. Pople, "Hydrogen Bonding" Symposium on Hydrogen Bonding at Lubljana, ed. by D. Hadzi, Pergamon Press, London (1959), p. 73.

10) J. A. Pople, *ibid.*, p. 74.

11) J. A. Pople, *J. Chem. Phys.*, **24**, 1111 (1956).

12) L. W. Reeves and W. G. Schneider, *Can. J. Chem.*, **35**, 251 (1957).

13) G. M. Barrow and E. A. Yerger, *J. Amer. Chem. Soc.*, **76**, 5247 (1954).

14) C. M. Huggins, G. C. Pimental and J. N. Schoolery, *J. Chem. Phys.*, **23**, 1244 (1955).

15) J. Landauer and H. McConnell, *J. Amer. Chem. Soc.*, **74**, 1221 (1952).

16) K. C. Medhi and G. S. Kastha, *Indian J. Phys.*, **37**, 139 (1963).

17) G. C. Pimental and A. L. McClellan, "Hydrogen Bond," Freeman and Coy, San Francisco (1960), p. 199.

this we obtain a large negative value for χ^E.

α-Picoline molecule can be considered to be arising out of the attachment of a methyl group to the pyridine ring in its α-position. In this case also there is evidence from IR studies[18] in favour of hydrogen bonding. The excess value, χ^E is small in our studies, which does not enable us to lay any great stress on it.

Similar is the case with 2,4-lutidine. There seems to be no chemical or other evidence in support of hydrogen bonding. The possibility of such a bonding is small because of disubstitution by methyl groups in 2 and 4 positions of the pyridine ring. In our studies, we find very small, irregular positive and negative values of χ^E.

In diphenyl ether solutions, we find small progressive deviation and this is attributable to hydrogen bonding. The ether oxygen is highly electronegative and because of this there is a possibility of hydrogen bond formation (type C–H---O). Deviations, however, are small. In the absence of any conclusive evidence, we feel that this may be taken to be a case where there is a large dipolar interaction.

The small negative value of χ^E in the case of 2,4-lutidine, and diphenyl ether mixtures can be explained by invoking a relaxation mechanism associated with hydrogen bonding as has been done by Reddy.[19] Hydrogen bonds are formed and broken in such quick succession that on a macroscopic scale their effect is not perceptible particularly, if the effect is sought to be measured employing a static method of measurement.

Toluene mixtures show a positive deviation, nitrobenzene an almost zero or slight positive deviation, and chlorobenzene a negative deviation. These substances are built round the benzene ring. NMR studies[12] of their mixtures with chloroform show evidence of "ring effect". Taking this "ring effect" into account it is possible to explain the observed trends in χ^E.

The electrons circulating in the aromatic ring have a donor character. The hydrogen in chloroform has an acceptor character. In the mixtures of chloroform with aromatic compounds, chloroform attaches itself to the aromatic ring and forms a bonded complex. There are two positions for such a bonding. The C–H bond in chloroform standing perpendicular to the plane of the ring is called π-bonding and its orientation parallel to the plane of the ring leads to the formation of *n*-bonding.

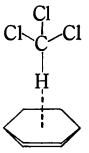

(π-type)

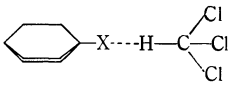

(*n*-type)

The aromatic ring, unless hindered, orients itself with its plane perpendicular to an external magnetic field. Therefore, the π bonding produces a paramagnetic effect and an *n*-bond which is a normal hydrogen bond produces a diamagnetic effect. The effects of these bondings contribute a corresponding term to the diamagnetic susceptibility of the mixture. The NMR studies cited above show that there is a strong π interaction with toluene, a relatively weak π interaction nitrobenzene and a still weaker one with chlorobenzene.

In the case of toluene mixtures, there is only π interaction and no *n*-interaction because of preferential orientation of chloroform proton above or below the ring. This introduces a paramagnetic contribution and therefore leads to a positive χ^E as observed in these investigations.

Nitrobenzene is a relatively poor π donor and a better *n*-donor. As a result the net deviation (χ^E) is almost zero in the case of nitrobenzene. In the case of chlorobenzene the *n*-interactions are preponderant leading to a negative χ^E.

I thank Professor J. Bhimasenachar for his guidance and inspiration throughout the progress of this work. Thanks are also due to the authorities of Sri Venkateswara University for offering me the facilities to carry out the present invesgitation.

18) W. Gordy, *J. Chem. Phys.*, **7**, 163 (1939).
19) K. C. Reddy, Ph. D., Thesis, Sri Venkateswara University (1964).

BULLETIN OF THE CHEMICAL SOCIETY OF JAPAN VOL. 43 1611—1614 (1970)

Charge Transfer Interaction between 2,3-Dichloro-5,6-dicyano-*p*-benzoquinone and Substituted Benzenes

R. D. SRIVASTAVA and G. PRASAD

Chemical Laboratories, University of Lucknow, Lucknow, India

(Received February 21, 1969)

Charge transfer complexes between 2,3-dichloro-5,6-dicyano-*p*-benzoquinone and various methyl and phenyl substituted benzenes have been studied. The spectral characteristics and equilibrium constants of *o*-, *m*-, and *p*-xylenes and those of *o*-, *m*-, and *p*- terphenyls are reported. The results have been interpreted in terms of Mulliken's charge transfer theory. From the spectral data, the electron affinity of 2,3-dichloro-5,6-dicyano-*p*-benzoquinone has been estimated to be 1.974 eV. The energy of the first CT band has been found to be related to the ionization potential of the donors by the expression $h\vartheta_{CT}=0.7I_D-3.86$.

In a previous communication[1] we have reported some of the studies on the charge transfer complexes of 2,3-dichloro-5,6-dicyano-*p*-benzoquinone (DDQ) with aromatic hydrocarbons. The studies have now been extended to substituted benzenes with a view to get a more clear picture of the interactions and to test the characteristic regularities of the charge transfer complexes. The reported results have been used in estimating the electron affinity of DDQ.

Experimental

Pure 2,3-dichloro-5,6-dicyano-*p*-benzoquinone (DDQ) was obtained from Light & Co. It was further purified by crystallizing from chloroform. Xylenes (B.D.H.) were distilled before use while terphenyls (Light & Co.) were crystallized from carbon tetrachloride or chloroform.

Spectrophotometric studies were carried out on a Unicam SP-500 spectrophotometer using 1.00 cm matched silica cells. The measurements were made at room temperature 25°C±2.0. Stock solutions for each of the donors were prepared separately which were mixed and diluted to required concentrations just before use. Optical density measurements have a maximum error of 1 percent. Equilibrium constants K_c (l mol^{-1}) and extinction coefficient, ε (l mol$^{-1}\cdot$cm^{-1}) were calculated graphically, using the appropriate forms of the Ketelaar's equation.[2] The following two equations served the purpose:

$$\frac{q}{A-A_q}=\frac{1}{(\varepsilon-\varepsilon_q)K_c}\cdot\frac{1}{D}+\frac{1}{\varepsilon-\varepsilon_q} \quad (1)$$

$$\frac{q}{A}=\frac{1}{\varepsilon K_c}\cdot\frac{1}{D}+\frac{1}{\varepsilon} \quad (2)$$

Equation (1) was used in cases where the absorption due to the acceptor molecules could not be neglected, while Eq. (2) was used when the acceptor and donor molecules did not have appreciable absorption at the λ_{max}. In the above equations, q represents the acceptor concentration, D the concentration of the donor, both in mol/l. A is the optical density, ε is the extinction coefficient at the maximum of the charge transfer band λ_{max}, and the subscript q represents the contribution in the property due to the presence of the acceptor in the system. In cases where the optical density of the quinone could not be neglected, its appropriate concentration was taken in the reference cell.

Results and Discussion

The yellow colour of DDQ turned to deep red on addition of xylenes and to amethyst or apple green on addition of terphenyls. Spectroscopic investigations in the region 400 to 700 mμ revealed in each case band characteristics of charge transfer complexes of the stoichiometric ratio of 1 : 1. In the case of xylenes one charge transfer band was obtained, but in the case of terphenyls two charge transfer bands were noted. It may be pointed out that xylenes are expected to show two bands but these could not be resolved in our experiments. Hammond[3] using 10 cm silica cells isolated the second CT band of *o*- and *m*-xylenses in dichloromethane, which are found to occur at 452 mμ and 451 mμ respectively. From the shape of the curves it is apparent that second CT and of *p*-xylene should appear somewhere around 460 and 470 mμ.

Ionization Potential and Energy of CT Band. The energy of the CT band is approximately related to the parameters of the components by the equation

$$h\vartheta_{CT}=I_D-E_A-W \quad (3)$$

1) R. D. Srivastava and G. Prasad, *Spectrochim. Acta*, **22**, 1969 (1966).

2) J. A. A. Ketelaar, C. van De Stolpe, A. Goudsmit and W. Dzcubass, *Rec. Trav. Chim. Pays-Bas*, **71**, 1104 (1952).

3) P. Hammond, *J. Chem. Soc.*, **1963**, 3113.

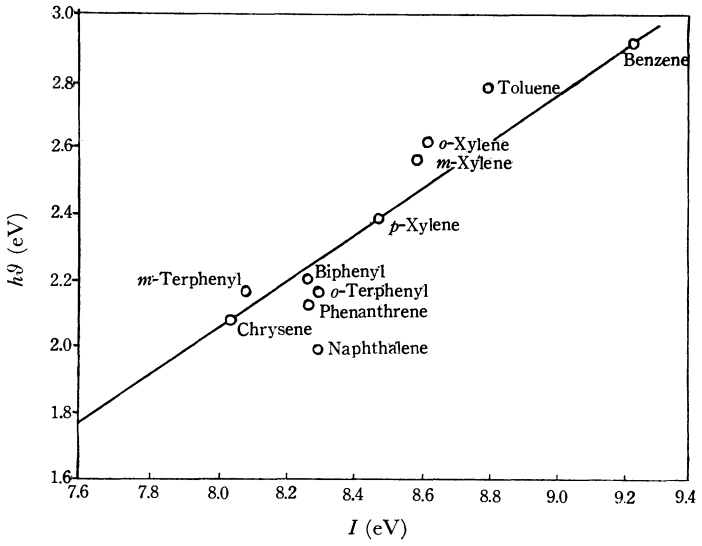

Fig. 1. Relationship between ionization potential (I) and energy of the charge-transfer band ($h\vartheta_{CT}$)

TABLE 1. EQUILIBRIUM CONSTANTS OF THE COMPLEXES WITH DDQ

Donor	$q\times10^3$ mol/l	D range mol/l	λ_{max} mμ	($1\ mol^{-1}\ cm^{-1}$) ε_c	K_c ($1\ mol^{-1}$)
o-Xylene	0.348	0.248 to 2.08	480	3480	2.60
m-Xylene	0.351	0.245 to 1.75	480	3636	2.50
p-Xylene	3.810	0.245 to 1.65	520	3540	3.00
o-Terphenyl	1.960	0.213 to 0.48	580	1000	0.83
m-Terphenyl	1.870	0.068 to 0.18	574	900	2.70
p-Terphenyl	6.000	0.019 to 0.05	635	1000	5.00

where ϑ_{CT} is the frequency of the CT band, I_D is the ionization potential of the donor, E_A is the electron affinity of the acceptor and W is the difference in the stablization energy of the ground and excited state. From the data given in Tables 1 and 2 we find that a plot of $h\vartheta_{CT}$ *versus* I_D gives a straight line of the form (see Fig. 1)

$$h\vartheta_{CT} = 0.7I_D - 3.86 \quad (4)$$

Orgel[4] explains the appearance of more than one CT band in the substituted benzenes on the basis that degeneracy of $^2E_{1g}$ ground state of benzene positive ion is removed by suitably arranged substitution. The two orbitals now split to an extent depending on the number of substituents, their nature and relative positions on the ring. The resultant two electronic states have two different ionization energies. The following are the expressions for the energy difference between the ionisation potential, I_B of benzene itself and the two ionisation potentials, I_1 and I_{11} of the substituted molecules.

$$I_1 = I_B - n\vartheta_s - p_1\varepsilon_s \quad (5)$$
$$I_{11} = I_B - n\vartheta_s - p_{11}\varepsilon_s \quad (6)$$

Here n is the number of the substituents S in the benzene ring; ε_S and ϑ_S are parameters arising from perturbation by S and depend on the nature of the substituent. ε_S relates to the total interaction of S with the π-electron system of the ring, while ϑ_S describes the interaction of S with the σ-system of the ring. p_1 and p_{11} are constants depending on both n and the relative position of the substituents; these values were calculated by Orgel,[4] which are shown below for 0, 1, 1-2, 1-3, and 1-4, substituents.

Position substituent	0	1	1-2	1-3	1-4
p_1	0	1	3/2	3/2	2
p_{11}	0	0	1/2	1/2	0

If $p_1 \neq p_{11}$, two charge transfer bands will result for all substitutions; for $p_1 = p_{11}$ only one band will be observed. When $p_1 = p_{11} = 0$, the charge-transfer energy will be fairly close to that of the benzene complex, since ϑ_S turns out to be rather small compared to ε_S. The band separation $h\vartheta_{11,1} \simeq I_{11} - I_1 = \Delta p_{11,1}\varepsilon_S$ will be very significant in the case of *p*-disubstituted and symmetrically tetra substituted benzenes. Therefore for *o*- and *m*-substituents of benzene, the two ionization potentials would be

4) L. E. Orgel, *J. Chem. Phys.*, **23**, 1352 (1955).

Table 2. Spectral characteristics of DDQ complexes

Donor	λ_{max} in mμ	$h\vartheta_{CT}$ in eV	I_d in eV	f	K_c (1 mol^{-1})
Benzene	427	2.906	9.24	0.0995	0.47
Toluene	450	2.760	8.82	0.1076	0.92
o-Xylene	480	2.585	8.58	0.1520	2.60
m-Xylene	480	2.585	8.60	0.1528	2.50
p-Xylene	520	2.385	8.48	0.1240	3.00
Biphenyl	564	2.200	8.27	0.0653	0.95
	440	2.816	—	—	—
o-Terphenyl	580	2.140	8.25	—	0.83
	458	2.710	—	—	—
m-Terphenyl	574	2.160	8.09	—	2.70
	444	2.794	—	—	—
p-Terphenyl	635	1.954	8.30	—	5.00
	425	2.920	—	—	—

Table 3. Separation of the first CT band of methyl derivatives with respect to benzene

Separation in	Calculated	Observed $\Delta\vartheta_{max}$
Benzene and toluene	$\vartheta_s+\varepsilon_s$	1200cm^{-1}
Benzene and *o*-xylene	$2\vartheta_s+3/2\ \varepsilon_s$	2600cm^{-1}
Benzene and *m*-xylene	$2\vartheta_s+3/2\ \varepsilon_s$	2600cm^{-1}
Benzene and *p*-xylene	$2\vartheta_s+2\ \varepsilon_s$	4200cm^{-1}

Table 4. Separation of the first CT band of phenyl derivatives with respect to benzene

Separation in	Calculated	Observed $\Delta\vartheta_{max}$
Benzene and biphenyl	$\vartheta_s+\varepsilon_s$	5700cm^{-1}
Benzene and *o*-terphenyl	$2\vartheta_s+3/2\ \varepsilon_s$	6100cm^{-1}
Benzene and *m*-terphenyl	$2\vartheta_s+3/2\ \varepsilon_s$	6000cm^{-1}
Benzene and *p*-terphenyl	$2\vartheta_s+2\ \varepsilon_s$	7700cm^{-1}

equal to each other. This would mean that corresponding CT bands should occur with equal energy and in fact this has been found to be the case in the present investigations. (Tables 3 and 4).

The band separations, $\Delta\vartheta_{max}$ (11-1) observed on varying the number and positions of donor substitutent are *p*-disubstituted$>$*o*- and *m*-disubstituted donors$\geq$mono substituted donor. Again this agreed with what is predicted from the difference Δp (11-1): *p*-disubstituted$>$*o*- and *m*-disubstituted$=$mono substituted donor.

In fact, numerically, the charge-transfer band for a *p*-(1-4) substituted isomer corresponding to a fixed arbitrary value of ϑ_S and ε_S has to be separated from the bands of benzene with an energy interval twice that of corresponding separation between the

Table 5. Separation of the second CT band of phenyl derivatives with respect to benzene

Separation in	Calculated	Observed $\Delta\vartheta_{max}$
Benzene and biphenyl	ϑ_s	600cm^{-1}
Benzene and *p*-terphenyl	$2\vartheta_s$	≈000cm^{-1}

second CT bands of mono substituted benzenes. This has not been found to be true. The reported separations as given in Tables 3—5 do not support the above prediction.

Electron Affinity of DDQ. Another consequence of Eq. (3) is that the CT spectra of a single donor with various closely related acceptors should be displaced with an energy interval corresponding to the difference in the electron affinities of the two acceptors. Also if the electron affinity of one of the acceptors is known and the spectra shift is studied, the electron affinity of an acceptor can be estimated from this shift. As pointed out in Ref. 1, the CT band of DDQ complexes with various hydrocarbons shifts to the red region with respect to the corresponding CT band of chloranil. This shift is 4870 cm^{-1} or equivalent to 0.604 eV.

The electron affinity of chloranil is 1.37 eV.[5] Hence the electron affinity of DDQ should be

$$h\vartheta_{CT}(\text{chloranil}) - h\vartheta_{CT}(\text{DDQ})$$

$$= E_A(\text{DDQ}) - E_A(\text{chloranil}) = 0.604\ \text{eV}$$

$$\therefore\ E_A(\text{DDQ}) = 1.37 + 0.604 = 1.974\ \text{eV}$$

Stability of the Complex and the Ionization Potential. The main stablization energy[6] for the charge transfer complex arises from the resonance energy between the no bond state (A–D) and the ionic stage (A^-D^+) of the complex configurations. Thus, the lower the ionization potential, the higher should be the stability of the complex. This preposition has been found to be true. If the K_c values of Ref. 1 and of the present investigations are considered, it is seen that in general the complexes of donors of comparatively lower ionisation potentials have greater values of equilibrium constants than the complexes of donors of comparatively higher ionization potentials. One must however be careful to choose donors which are similar. For instance, the three separate groups of methyl substituted, the phenyl substituted and the polynuclear hydrocarbon donors should be considered separately. When this is done regularity in regard to complex stability is observed.

5) G. Briegleb and J. Czekalla, *Angew. Chem.*, **72**, 401 (1960); G. Briegleb, *ibid.*, **76**, 617 (1964).

6) R. S. Mulliken, *J. Amer. Chem. Soc.*, **74**, 811 (1952).

Benzene $<$ toluene $<$ xylene

Benzene $<$ biphenyl $<$ terphenyl

Benzene $<$ naphthalene $<$ phenanthrene $<$ chrysene $<$ pyrene

Intensity and Stability. According to Mulliken[6] the intensity of the charge transfer band μ_{1n} should be directly proportional to the stability or the equilibrium constant of the complex. The intensity is related to oscillator strength by the equation

$$f = 4.704 \times 10^{-7} \vartheta_{mesc} \times \mu_{1n} \quad (7)$$

The oscillator strength has been calculated using the equation of Briegleb[7] and is recorded in Table 2. The present investigations do not conform to the predicted relationship.

One of us (G. Prasad) is grateful to the Ministry of Education for the grant of research training Scholarship.

7) G. Briegleb and J. Czekalla, *Z. Phys. Chem.* (Frankfurt), **24**, 37 (1960).

BULLETIN OF THE CHEMICAL SOCIETY OF JAPAN VOL. 43 1614—1617 (1970)

Solvent Effect on the Dielectric Properties of Nitroalkanes

Suresh CHANDRA*[1] and Dina NATH

Physics Department, Allahabad University, Allahabad-2, India

(Received June 2, 1969)

Permittivity and dielectric loss of four nitroalkanes have been measured in solution in three solvents *viz.*, *n*-heptane, benzene and cyclohexane at 9.8 GHz and 30°C. The variation of the relaxation time calculated from the data, with the viscosity of the solutions has been discussed. It has been found that the results cannot be explained on the basis of known relations between relaxation time and viscosity. It is expected that some other interactions such as proton-proton interaction are responsible for the relaxation time in cyclohexane lower than in benzene. The loss tangents are found to vary linearly with the concentration of the solution. Dipole moments have also been evaluated in all the three solvents and are in good agreement with the values in literature within experimental error.

The measurement of dielectric relaxation time provides a means of studying the molecular interaction and intermolecular forces. Many papers have appeared in which the authors have given the relaxation time of polar molecules in non-polar solvents. They have tried to correlate the relaxation time with some molecular model but with only partial success. Most of the work has been done to prove or disprove the theory given by Debye.[1] The Debye theory considers the molecule as a sphere embedded in a continuous viscous fluid with inner friction coefficient ζ which is related to the relaxation time τ by

$$\tau = \zeta/2kT.$$

Using Stokes' law, Debye identifies the inner friction coefficient with the viscosity η of the fluid by

$$\zeta = 8\pi\eta a^3,$$

where a is the radius of the sphere. Thus the Debye equation becomes

$$\tau = \frac{4\pi\eta a^3}{kT}.$$

Several empirical and semi-empirical formulae have been suggested to modify the Debye equation. On the basis of the present theories, it is expected that the relation between ln τ and ln η will be linear. It has been found that this is not true for the case of nitroalkanes when τ is measured in solvents of different viscosity *viz.*, *n*-heptane, benzene and cyclohexane.

Experimental

Measurements have been made at 9.8 GHz and at 30°C. The permittivity and dielectric loss (ε' and ε'') have been determined using Smyth's method[2] and short wave technique. The relaxation time τ and the dipole moment μ were then determined by the Gopal

*1 Physics Department, Gorakhpur University, Gorakhpur, India.

1) P. Debye, "Polar Molecules," Dover Publications, New York (1949).

2) W. M. Heston, Jr., A. D. Franklin, E. J. Hennelly and C. P. Smyth, *J. Amer. Chem. Soc.*, **72**, 3443 (1950).

TABLE 1. PERMITTIVITY AND DIELECTRIC LOSS OF NITRO ALKANES IN SOLUTIONS

a) Nitromethane

Concentration in mol/cc × 10^4	ε'	ε''	tan δ	X	Y
Solvent: *n*-Heptane			Viscosity=0.390 cp		
0.937	1.970	0.010	0.0050	0.2471	0.0018
1.945	2.046	0.013	0.0063	0.2585	0.0024
2.817	2.087	0.016	0.0076	0.2659	0.0028
3.864	2.114	0.017	0.0080	0.2708	0.0030
4.864	2.155	0.020	0.0092	0.2779	0.0034
Solvent: Benzene			Viscosity=0.564 cp		
0.857	2.388	0.023	0.0096	0.3174	0.0036
1.913	2.503	0.036	0.0143	0.3355	0.0053
2.905	2.621	0.048	0.0183	0.3530	0.0068
3.931	2.699	0.055	0.0203	0.3639	0.0074
4.896	2.813	0.063	0.0223	0.3794	0.0080
Solvent: Cyclohexane			Viscosity=0.808 cp		
0.988	2.100	0.010	0.0048	0.2683	0.0019
1.895	2.198	0.017	0.0077	0.2853	0.0030
2.764	2.248	0.022	0.0098	0.2938	0.0037
3.838	2.281	0.028	0.0122	0.2991	0.0046
4.966	2.313	0.030	0.0129	0.3045	0.0048

c) 1-Nitropropane

Concentration in mol/cc × 10^4	ε'	ε''	tan δ	X	Y
Solvent: *n*-Heptane			Viscosity=0.390 cp		
1.034	2.025	0.023	0.0113	0.2547	0.0042
1.921	2.114	0.041	0.0193	0.2709	0.0074
2.885	2.213	0.058	0.0262	0.2880	0.0098
3.809	2.313	0.073	0.0315	0.3046	0.0118
4.857	2.425	0.094	0.0387	0.3223	0.0144
Solvent: Benzene			Viscosity=0.564 cp		
0.854	2.394	0.041	0.0169	0.3172	0.0063
1.829	2.503	0.064	0.0255	0.3339	0.0094
2.825	2.621	0.099	0.0378	0.3511	0.0139
3.778	2.750	0.144	0.0526	0.3691	0.0192
4.763	2.808	0.164	0.0583	0.3767	0.0212
Solvent: Cyclohexane			Viscosity=0.808 cp		
0.393	2.100	0.024	0.0114	0.2683	0.0043
1.227	2.209	0.048	0.0217	0.2874	0.0081
2.510	2.313	0.069	0.0298	0.3046	0.0113
3.575	2.412	0.088	0.0364	0.3203	0.0136
4.410	2.530	0.114	0.0450	0.3382	0.0167

d) 2-Nitropropane

Concentration in mol/cc × 10^4	ε'	ε''	tan δ	X	Y
Solvent: *n*-Heptane			Viscosity=0.390 cp		
0.982	2.020	0.018	0.0089	0.2538	0.0034
1.910	2.129	0.032	0.0150	0.2734	0.0055
2.822	2.260	0.047	0.0207	0.2958	0.0078
3.586	2.370	0.073	0.0308	0.3136	0.0115
4.780	2.486	0.097	0.0390	0.3316	0.0145
Solvent: Benzene			Viscosity=0.564 cp		
0.948	2.429	0.031	0.0128	0.3276	0.0048
1.848	2.554	0.052	0.0205	0.3414	0.0076
2.875	2.728	0.091	0.0334	0.3657	0.0122
3.748	2.773	0.103	0.0372	0.3717	0.0136
4.679	3.006	0.163	0.0544	0.4014	0.0196
Solvent: Cyclohexane			Viscosity=0.808 cp		
0.981	2.057	0.023	0.0111	0.2605	0.0041
1.681	2.233	0.041	0.0183	0.2913	0.0068
2.800	2.347	0.065	0.0276	0.3101	0.0103
3.611	2.436	0.082	0.0336	0.3238	0.0124
4.482	2.571	0.111	0.0431	0.3440	0.0159

b) Nitroethane

Concentration in mol/cc × 10^4	ε'	ε''	tan δ	X	Y
Solvent: *n*-Heptane			Viscosity=0.390 cp		
0.770	1.982	0.011	0.0056	0.2466	0.0020
1.728	2.124	0.019	0.0089	0.2726	0.0033
3.013	2.223	0.043	0.0193	0.2897	0.0072
3.903	2.314	0.061	0.0263	0.3046	0.0099
5.043	2.418	0.073	0.0310	0.3210	0.0113
Solvent: Benzene			Viscosity=0.564 cp		
0.911	2.388	0.041	0.0173	0.3163	0.0064
2.839	2.706	0.091	0.0337	0.3627	0.0123
4.788	2.891	0.125	0.0434	0.3871	0.0157
6.813	2.993	0.149	0.0496	0.3997	0.0179
8.820	3.387	0.220	0.0650	0.4440	0.0227
Solvent: Cyclohexane			Viscosity=0.808 cp		
1.002	2.120	0.019	0.0089	0.2718	0.0034
1.886	2.217	0.029	0.0130	0.2886	0.0048
2.851	2.327	0.047	0.0201	0.3076	0.0075
3.988	2.445	0.068	0.0278	0.3252	0.0103
5.005	2.550	0.081	0.0317	0.3409	0.0117

TABLE 2. RELAXATION TIMES AND DIPOLE MOMENTS OF NITROALKANES IN SOLUTION

λ=3.1 cm Temperature, 30°C

Solvent	Nitromethane	Nitroethane	1-Nitropropane	2-Nitropropane
n-Heptane	$\tau=1.1\times10^{-12}$ sec	$\tau=1.8\times10^{-12}$ sec	$\tau=2.5\times10^{-12}$ sec	$\tau=2.2\times10^{-12}$ sec
η=0.390 cp	μ=2.06 D	μ=2.91 D	μ=2.97 D	μ=3.31 D
	Δ (tan δ)/c=0.0012	Δ (tan δ)/c=0.0060	Δ (tan δ)/c=0.0079	Δ (tan δ)/c=0.0074
Benzene	$\tau=1.3\times10^{-12}$ sec	$\tau=2.2\times10^{-12}$ sec	$\tau=4.7\times10^{-12}$ sec	$\tau=3.3\times10^{-12}$ sec
η=0.564 cp	μ=2.79 D	μ=2.75 D	μ=2.69 D	μ=3.22 D
	Δ (tan δ)/c=0.0039	Δ (tan δ)/c=0.0061	Δ (tan δ)/c=0.0114	Δ (tan δ)/c=0.0107
Cyclohexane	$\tau=1.3\times10^{-12}$ sec	$\tau=1.9\times10^{-12}$ sec	$\tau=2.7\times10^{-12}$ sec	$\tau=2.7\times10^{-12}$ sec
η=0.808 cp	μ=2.44 D	μ=2.95 D	μ=3.06 D	μ=3.11 D
	Δ (tan δ)/c=0.0028	Δ (tan δ)/c=0.0060	Δ (tan δ)/c=0.0107	Δ (tan δ)/c=0.0080

Krishna method.[3] Viscosities of the solutions were determined by an Ostwald viscometer. All the chemicals were distilled twice before use.

Results

The experimental data and results are presented in Tables 1 and 2 respectively.

Discussion

The relaxation times τ for nitroalkanes have been determined from the data obtained with dilute solution of these compounds in *n*-heptane, benzene and cyclohexane. The values of relaxation times obtained in solutions are lower than the values obtained in pure liquids. In *n*-heptane the lower values of relaxation time can be explained on the basis of the low viscosity value of the solvent because the viscosity of *n*-heptane at 30°C is 0.390 cp whereas the viscosities of the nitro compounds are 0.617, 0.644, 0.759 and 0.718 cp respectively. The viscosity of benzene is 0.564 cp which is again less than the viscosities of the solute molecules at the same temperature. The values of relaxation times in benzene are greater than the values obtained in *n*-heptane. This seems reasonable due to the difference in viscosities of the two solvents. The other reason is the hindrance of molecular rotation by dipole-dipole interaction which is present in the pure liquid and mostly absent in dilute solutions. Since the polar molecules used in the present investigation are not quite spherical, viscosity of the surrounding medium should have considerable effect on the dielectric relaxation time. Such results have already been reported by others.[4,5] However, in the case of cyclohexane the values of τ obtained are smaller than the values of relaxation time in benzene, although the viscosity of cyclohexane is about one and a half times that of benzene and three times that of *n*-heptane. This cannot be explained on the basis of the effect of viscosity. The relation between τ and η given recently by Krishnaji and Mansingh[6,7] requires that at constant temperature the plots of $\ln\tau$ *vs.* $\ln\eta$ should be linear. Such plots for four nitroalkanes have been made, but the curves are not linear, the values of relaxation time in cyclohexane being less than the values obtained in benzene. Data of other workers[8-11] give straight lines for $\ln\tau$ *vs.* $\ln\eta$ because they have used a single solvent and have changed the viscosity by varying the temperature. By varying the temperature the viscosity changes but the interactions of solute and the solvent molecules remain the same. They used the same concentration at a single frequency, but in the present investigation the concentration variation at a single frequency method has been used. The viscosity has been varied by using different solvents. The behaviour of $\ln\tau$ *vs.* $\ln\eta$ plots in this case cannot be explained in the light of existing theories. The dependence of $\ln\tau$ upon $\ln\eta$ cannot be explained on the basis of the viscoelastic relaxation time. Such results, however, giving smaller relaxation times in solvents of higher viscosity than in the solvent of lower viscosity have been reported by Higasi[12,13] and Walker *et al.*[14] Walker has also obtained lower values of relaxation time in benzene and carbon tetrachloride for chloroform and has suggested that this might be due to hydrogen bonding of the hydrogen atom in chloroform to the π-electrons. Higasi,[12] on the other hand, has explained the difference in relaxation times as due to the solvent effect. The relaxation time is a physical quantity which is easily affected by the surroundings. The relaxation times and the dipole moments in aromatic solvents are greater than those in aliphatic solvents. There is a possibility of complex formation due to hydrogen bonding or a large interaction energy due to proton-proton interactions. It is possible that the molecule goes into a different isomeric configuration because of these short range interactions. Such an effect has been observed by Higasi[13] in 1,2-dichloroethane.

The relaxation times in each solvent increase with the increase in the number of carbon atoms and molecular size. This is in accordance with the Debye relationship relating the relaxation time τ with the molecular radius, a. The dependence of relaxation time τ on the chain length can be explained on the basis of Fröhlich's equation[15]

$$\tau = AE^{nH/kT}$$

where H is the energy required to lift a link of the

3) K. V. Gopal Krishna, *Trans. Faraday Soc.*, **53**, 767 (1957).

4) A. D. Franklin, W. M. Heston, Jr., E. J. Hennelly and C. P. Smyth, *J. Amer. Chem. Soc.*, **72**, 3447 (1950).

5) A. J. Curtis, P. L. Mc Geer, G. B. Rathmann and C. P. Smyth, *ibid.*, **74**, 644 (1952).

6) K. Chitoku and K. Higasi, This Bulletin, **36**, 1064 (1963).

7) K. Krishnaji and A. Mansingh, *Indian J. Pure Appl. Phys.*, **2**, 176 (1964).

8) B. Sinha, S. B. Roy and G. S. Kastha, *Indian J. Phys.*, **40**, 101 (1966).

9) J. Bhattacharya, B. Sinha, S. B. Roy and G. S. Kastha, *ibid.*, **38**, 413 (1964).

10) D. H. Whiffen and H. W. Thompson, *Trans. Faraday Soc.*, **42A**, 122 (1946).

11) J. Sobhanadri, *Indian J. Phys.*, **33**, 511 (1959).

12) K. Higasi, "Dielectric Relaxation and Molecular Structure," Research Institute of Applied Electricity, Hokkaido University, Sapporo (1961).

13) K. Chitoku and K. Higasi, This Bulletin, **40**, 773 (1967).

14) W. F. Hassell, M. D. Magee (Miss), S. W. Tucker and S. Walker, *Tetrahedron*, **20**, 2137 (1964).

15) H. Fröhlich, "Theory of Dielectrics," Oxford University Press, London (1949).

chain over the potential barrier. Experimental values of log τ have been plotted against the number of carbon atoms and they are found to be straight lines satisfying the above relationship.

From the plots of $\tan\delta$ *vs.* concentration it is seen that the loss tangent varies linearly with concentration for all the four liquids in all the three solvents. The rates of variation of the loss tangents, $\tan\delta$, with concentration, c, are given in Table 2 and it is found that the rate of variation of $\tan\delta$ with c in a particular solvent increases with increase in the number of carbon atoms.

The dipole moment values obtained are in agreement, within experimental error, with the solution values given in literature. The values are slightly lower than those reported, and this is in agreement with the apparent tendency to obtain slightly lower moments by the microwave method.

The authors are grateful to Professor Krishnaji for his valuable suggestions and kind interest in the present work.

BULLETIN OF THE CHEMICAL SOCIETY OF JAPAN VOL. 43 1617—1621 (1970)

Reaction Intermediates in γ-Irradiated Mercaptans at 77°K

Ayako TORIKAI, Shuzo SAWADA, Kenji FUEKI and Zen-ichiro KURI

Department of Synthetic Chemistry, Faculty of Engineering, Nagoya University, Chikusa-ku, Nagoya

(Received September 11, 1969)

Elementary processes in the radiolysis of ethyl mercaptan has been investigated by both spectrophotometric and electron spin resonance (ESR) methods. Ethyl mercaptan (C_2H_5SH) forms a glassy solid at 77°K, and when irradiated with γ-rays from Co-60, it develops a deep orange color; this color fades upon illumination with visible light, leaving a clear yellow color. The ESR spectrum of γ-irradiated C_2H_5SH at 77°K consists of two components; one is a complex spectrum which has been identified with the spectrum of $C_2H_5S\cdot$, while the other is a photo-bleachable broad singlet which has been assigned to the ionic species. The $C_2H_5S\cdot$ radical shows an absorption spectrum with $\lambda_{max}=405$ nm. The *G*-values for the formation of the radicals and the ionic species were 0.5 and 2.9 respectively. Studies of 2-methyltetrahydrofuran and butyl chloride solutions of C_2H_5SH were performed to identify these ionic species. Some significant elementary processes will be discussed on the basis of these results.

The reaction intermediates in the radiolysis of organic compounds have recently been studied in order to elucidate the elementary processes in the radiation chemistry using spectrophotometric and ESR methods. Much information about the ionic species and radicals produced by the γ-irradiation of organic glasses has been given by these techniques.

Ethyl mercaptan forms a clear glass at 77°K, so it is easy to measure the reaction intermediates by an optical method. In the case of sulfur-containing compounds, molecular ions have been expected as intermediates of γ-radiolysis.[1-3] Hitherto, there have been only a few ESR studies of the intermediates in the radiolysis of mercaptans and other organic compounds containing sulfur atoms in the solid state.[4-9] The assignment of free radicals has been established in these studies, while the broad ESR singlet observed in ethyl mercaptan has been attributed to ionic species without conclusive evidence.[5,8,9]

In the present study, the ionic intermediates and radicals produced by the γ-irradiation of pure ethyl mercaptan and by those in 2-methyltetrahydrofuran (MTHF) or butyl chloride glasses at 77°K have been investigated in detail by both spectrophoto-

1) F. K. Truby, D. C. Wallace and J. E. Hesse, *J. Chem. Phys.*, **42**, 3845 (1965).
2) S. B. Milliken, K. Morgan and R. H. Johnson, *J. Phys. Chem.*, **71**, 3238 (1967).
3) T. Shida, *ibid.*, **72**, 2597 (1968).
4) C. F. Luck and W. Gordy, *J. Amer. Chem. Soc.*, **78**, 3240 (1956).
5) K. Akasaka, S. Ohnishi and H. Hatano, *Kogyo Kagaku Zasshi*, **68**, 1548 (1965).
6) H. Shields and W. Gordy, *J. Phys. Chem.*, **62**, 789 (1958).
7) Y. Kurita and W. Gordy, *J. Chem. Phys.*, **34**, 282 (1961).
8) J. J. Myron and R. H. Johnson, *J. Phys. Chem.*, **70**, 2951 (1966).
9) S. B. Milliken, K. Morgan and R. H. Johnson, *ibid.*, **71**, 3238 (1967).

metric and ESR methods. Studies of several alkyl mercaptans have also been performed.

Experimental

Materials. Extra-pure-grade ethyl, *n*-propyl, isopropyl, and *n*-butyl mercaptans were distilled several times on a vacuum line and then stored in a vessel containing calcium hydride. MTHF (supplied by K & K Co.) was purified by passing it through an alumina column after having been fractionally distilled and dried with calcium hydride. Butyl chloride was purified by passing it through a silica gel column, after which it was distilled under vacuum and stored in a vessel containing calcium hydride.

Procedure. Sample tubes for ESR measurements were 4 mm in i.d. and were made of high-purity quartz; the quartz cells with a rectangular cross-section ($1\times 1\times 4$ cm) were used for spectrophotometric measurements. The degassing of the purified samples was accomplished by repeated freeze-pump-thaw cycles. Irradiations were made with γ-rays from Co-60 at 77°K, and in most cases at a dose rate of 6.3×10^{18} eV/g·hr. After γ-irradiation, ESR and optical absorption spectra measurements were carried out at 77°K on a Japan Electron JES-3BX spectrometer and a Hitachi EPU-2-type or Hitachi-Perkin Elmer 139 type spectrophotometer respectively.

Results

Pure Ethyl Mercaptan. Ethyl mercaptan is a glassy solid at 77°K; when irradiated with γ-rays, it develops a deep orange color and gives the ESR spectrum shown in Fig. 1a. This spectrum consists of two components. When γ-irradiated ethyl mercaptan glass is photobleached with visible light ($\lambda>325$ nm), the broad singlet ($\Delta H_{msl}=30$ gauss) centered at $g=2.010$ gradually decreases and there remains a complicated radical spectrum (Fig. 1c).

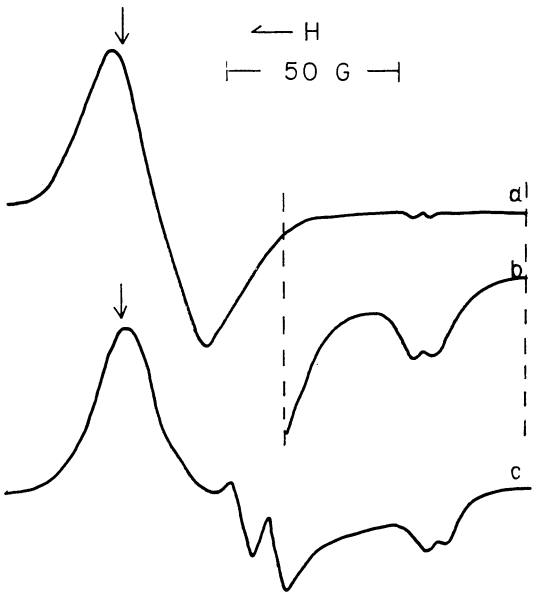

Fig. 1. ESR spectra of γ-irradiated ethyl mercaptan at 77°K.
a: before photobleaching (40db), b: the same spectrum with a greater sensitivity (80db), c: after photobleaching with light of $\lambda>325$ nm (80db) irradiation dose: 3.7×10^{19} eV/g

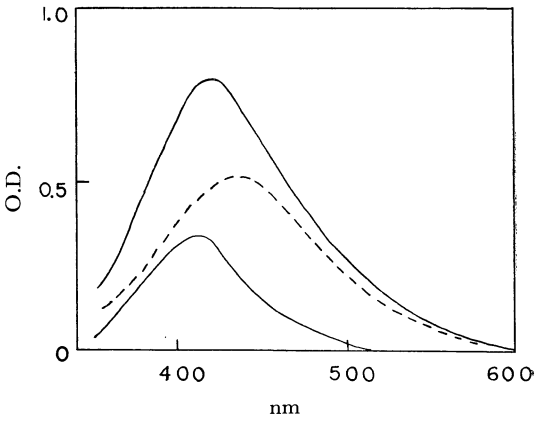

Fig. 2. Absorption spectra of γ-irradiated ethyl mercaptan at 77°K.
a: before photobleaching, b: after photobleaching with light of $\lambda>325$ nm, c: photobleached species, irradiation dose: 2.5×10^{18} eV/g

The absorption spectrum of a glassy ethyl mercaptan at 77°K is shown in Fig. 2. γ-Irradiation produces a broad band centered about 430 nm. This band is bleached with visible light and is responsible for the deep orange color. When bleached with visible light, there remains a band centered at 405 nm which is responsible for the yellow color.

When pure ethyl mercaptan is irradiated with light from a low-pressure mercury lamp at 77°K, it develops a clear yellow color and gives an absorption spectrum with $\lambda_{max}=405$ nm (Fig. 3). The ESR spectrum of UV-irradiated pure ethyl mercaptan is shown in Fig. 4. This spectrum is identical with that in Fig. 1c and is assigned to the $C_2H_5S\cdot$ radical, because its g-tensor agrees with

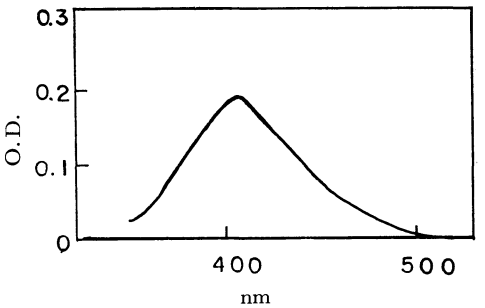

Fig. 3. Absorption spectrum of UV-irradiated ethyl mercaptan at 77°K.

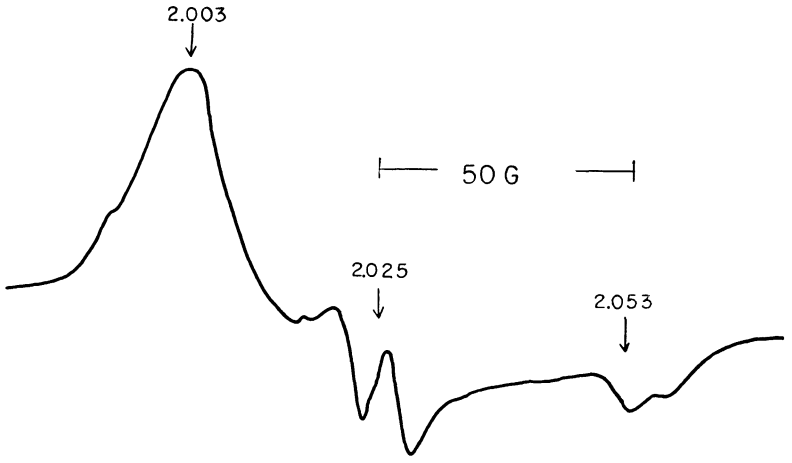

Fig. 4. ESR spectrum of UV-irradiated ethyl mercaptan at 77°K.

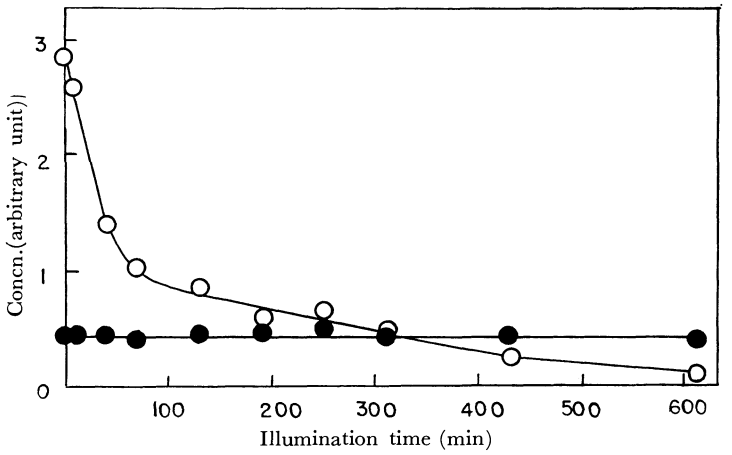

Fig. 5. Photobleaching of ionic species in γ-irradiated ethyl mercaptan at 77°K.
○: ionic species, ●: $C_2H_5S\cdot$ radicals

that of the cystein radical,[4] $HOOC(NH_2)CHCH_2S\cdot$.

The broad singlet which gives $\lambda_{max}=430$ nm is tentatively assigned to an ionic species, and the complicated ESR spectrum which gives $\lambda_{max}=405$ nm is assigned to the $C_2H_5S\cdot$ radical.

The effect of the time of photobleaching on the ionic species and the radicals is shown in Fig. 5. The ionic species decayed rapidly in the initial period and then slowly at 77°K, while the amounts of $C_2H_5S\cdot$ radicals did not change significantly between before and after photobleaching. It was also confirmed that the ionic species decayed relatively rapidly in the initial stage and then very slowly at 77°K in the dark, and no increase was observed in the quantity of $C_2H_5S\cdot$ radicals.

The concentrations of ionic species and of $C_2H_5S\cdot$ radicals increases with an increase in the irradiation dose in the range studied.

The *G*-values for the formation of the ionic species and the radicals were 2.9 and 0.5 respectively. The latter value agrees with the radical yield of hexyl mercaptan, $G(\text{radical})=0.4$ at -150°C,[10] within the limits of experimental error.

Ethyl Mercaptan in MTHF. When a MTHF solution containing 5 mol% of ethyl mercaptan is irradiated at 77°K with γ-rays, it develops a yellowish green color. The ESR spectrum is shown in Fig. 6, superimposed on the seven-line spectrum due to the MTHF radical. This broad singlet spectrum is the same as that observed in γ-irradiated pure ethyl mercaptan. Small amounts of the ethyl radical are also seen in Fig. 6. The narrow singlet due to the trapped electron of MTHF was not observed in this case.

The optical absorption spectrum of the MTHF solution of ethyl mercaptan is essentially the same as that of Fig. 2, although some shift in λ_{max} is

10) V. I. Trofimov, I. I. Chkheidze, L. I. Bellen'kii and N. Ya. Buben, *Kinetika i Katalyz*, **7**, 540 (1966).

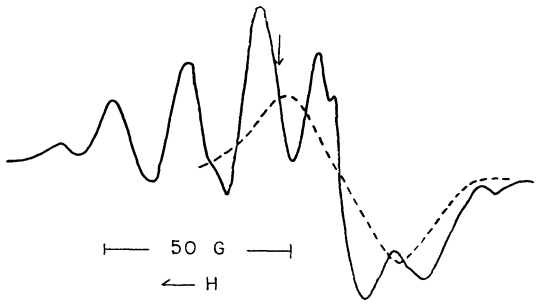

Fig. 6. ESR spectra of γ-irradiated MTHF solutions containing 5 mol% of ethyl mercaptan at 77°K.
irradiation dose: 8.7×10^{18} eV/g

seen in this case. Upon the illumination of this sample with light of $\lambda>325$ nm, the band centered at 410 nm was bleached. This band is also reduced by the addition of carbon tetrachloride as an electron scavenger.

Ethyl Mercaptan in Butyl Chloride. The ESR spectrum of γ-irradiated butyl chloride containing 5 mol% of ethyl mercaptan consists of two components; one is assigned to the butyl radicals, and the other is the same broad singlet as that observed in γ-irradiated pure ethyl mercaptan.

The general features of the optical absorption spectrum of γ-irradiated BuCl solution of ethyl mercaptan are like those of γ-irradiated pure ethyl mercaptan.

Other Alkyl Mercaptans in MTHF. The optical absorption spectra of γ-irradiated MTHF solutions of *n*-propyl, isopropyl, and *n*-butyl mercaptans give broad bands centered at about 410 nm and develop a deep orange color. They are also photobleached with visible light ($\lambda>325$ nm) leaving a yellow color.

Discussion

The species responsible for the ESR singlet and the 430 nm band observed in γ-irradiated ethyl mercaptan may be attributable to ionic species, because they can be photobleached and considerably reduced in the presence of iodine.

Truby *et al.*[1] have extensively studied the intermediates in the solid state radiolysis of disulfides and have concluded that electron ejected by the radiation are captured by the sulfur group of disulfide, that positive charges are also localized at the sulfur group, and that these processes do not lead to molecular dissociation. In the case of the solid state radiolysis of ethyl mercaptan, it also seems reasonable to consider that the mercaptan positive ion remains in the form of $C_2H_5SH^+$ and that ejected electrons are captured to form a molecular anion, $C_2H_5SH^-$. The results obtained from the ESR and optical absorption spectra of γ-irradiated ethyl mercaptan in MTHF solutions essentially coincide with those of γ-irradiated pure ethyl mercaptan. The bond dissociation energy of $C_2H_5{}^-SH$ (69 ± 5 kcal/mol) is greater than its electron affinity (60 kcal/mol); the dissociative electron capture, $C_2H_5SH+e^-\rightarrow C_2H_5\cdot+SH^-$, can, therefore, not be expected in this case. These facts indicate that $C_2H_5SH^-$ is involved in the spectrum of γ-irradiated pure ethyl mercaptan.

The ethyl radicals observed in γ-irradiated ethyl mercaptan in MTHF solutions may arise from the decomposition of directly excited C_2H_5SH. The fact that the ethyl radical was not observed in an appreciable amount in pure ethyl mercaptan can be explained by assuming that the $C_2H_5\cdot+C_2H_5$-$SH\rightarrow C_2H_6+C_2H_5S\cdot$ reaction takes place in this case, although the activation energy of this reaction has not been established. This assumption seems reasonable, because diethyl disulfide has been found among the radiolysis products of liquid ethyl mercaptan.[8]

The following interpretations of the broad ESR singlet and the optical absorption band in the 430 nm region observed in γ-irradiated ethyl mercaptan in BuCl glasses may be derived from the experimental results:

It is well known that butyl chloride forms a glass at 77°K and that radiation ejected electrons in the chloride are scavenged by the matrix itself,

$$BuCl + e^- \rightarrow Bu\cdot + Cl^-{}^{11)} \quad (1)$$

The positive hole is mobile at an early stage but is then trapped by the matrix, giving rise to a broad band at 400—600 nm.

In the case of the γ-irradiated ethyl mercaptan in BuCl glasses, the BuCl cation band disappeared. The 430 nm band is similar to that of the anion band in its position, but considering the efficient scavenging reaction (1), this species may be attributable to the $C_2H_5SH^+$ produced instead of $BuCl^+$.

Another possible species is $C_2H_5SH^-$, which is produced by the competivie reaction between (1) and

$$C_2H_5SH + e^- \longrightarrow C_2H_5SH^- \quad (2)$$

for the following reasons: 1) The rate constants of hydrated electrons at room temperature are of the order of $\sim5\times10^{18}M^{-1}\,sec^{-1}$ for butyl chloride and of $\sim2\times10^{10}M^{-1}$ for methyl mercaptan. The efficiency of the electron capture of mercaptan in an aqueous solution is roughly 40 times that of BuCl, so the competition between (1) and (2) seems conceivable under the present experimental conditions (the concentration of ethyl mercaptan in BuCl is 5 mol% in this case) and 2) The fact that $C_2H_5SH^+$ and $C_2H_5SH^-$ have the same posi-

11) a) T. Shida and W. H. Hamill, *J. Chem. Phys.*, **44**, 4372 (1966). b) *J. Amer. Chem. Soc.*, **88**, 3683 (1966). c) *Ibid.*, **88**, 5371 (1966). d) *Ibid.*, **88**, 5376 (1966).

tion in λ_{max} is not acceptable in view of the general features of the optical absorption measurements of many other linear organic compounds.

If the 430 nm band or the broad ESR singlet is assigned to an anionic species, $C_2H_5SH^+$ should be found, because the BuCl cation band disappears upon the addition of ethyl mercaptan.

The cationic species of disulfides have been found to have absorption maxima between 700—900 nm.[3,12] The absorption spectra of ethyl mercaptan in the BuCl matrix and the 3-methylpentane matrix were measured over the range of 700—1000 nm in order to identify $C_2H_5SH^+$. However, no species other than the 430 nm band was found in this case. This fact seems to indicate that $C_2H_5SH^+$ has an absorption maximum at a wavelength longer than 1000 nm or that the extinction coefficient of C_2H_5-SH^+ band is too small to be found in the visible region of the absorption spectrum under the present experimental conditions. Another possibility is that the 430 nm band includes some cationic species other than $C_2H_5SH^+$.

It is difficult to identify the 430 nm band in the BuCl matrix with either cationic or anionic ones. Further study is required to establish the assignment of this band.

The following elementary processes for γ-irradiated ethyl mercaptan can be considered on the basis of these results, although cationic species have not yet been clearly identified:

$$C_2H_5SH \rightsquigarrow \begin{cases} C_2H_5SH^+ + e^- \\ C_2H_5SH^* \end{cases}$$

$$C_2H_5SH + e^- \longrightarrow C_2H_5SH^-$$

$$C_2H_5SH^* \longrightarrow C_2H_5S\cdot + H$$

$$\searrow \text{ or } C_2H_5\cdot + \cdot SH$$

$$C_2H_5\cdot + C_2H_5SH \longrightarrow C_2H_6 + C_2H_5S\cdot$$

Photobleaching

$$C_2H_5SH^- \longrightarrow C_2H_5SH + e^-$$

$$C_2H_5SH^+ + e^- \longrightarrow C_2H_5SH$$

The optical absorption spectra of γ-irradiated MTHF solutions of *n*-propyl, isopropyl, and *n*-butyl mercaptans give broad bands centered about 410 nm and develop a deep orange color. They are also photobleached with visible light ($\lambda > 325$ nm) leaving a yellow color. The photobleachable species may be attributable to a molecular anion, RSH^-, and unbleachable parts, to the radicals, RS··.

12) J. Wendenburg, H. Mockel, A. Granzow and A. Henglein, *Z. Naturforsch.*, **21b**, 632 (1966).

BULLETIN OF THE CHEMICAL SOCIETY OF JAPAN VOL. 43 1622—1634 (1970)

Hydrogen-bonding Effects on the Electron Spin Resonance Spectra of the Anion Radicals of Several Aromatic Amine *N*-Oxides

Tanekazu KUBOTA, Yoshiko ŌISHI, Koichi NISHIKIDA and Hiroshi MIYAZAKI

Shionogi Research Laboratory, Shionogi & Co., Ltd., Fukushima-ku, Osaka

(Received November 10, 1969)

The hydrogen-bonding effects of ethanol, phenol, and water on the electron-spin-resonance spectra of the anion radicals of 4-nitro- and 4-cyano-pyridine *N*-oxides, pyrazine mono- and di-*N*-oxides, and 4-nitropyridine electrochemically generated in dimethylformamide have been studied quantitatively. The equilibrium constant, *K*, pertinent to the hydrogen-bonding systems was determined on the basis of analyses of the variation in the hyperfine coupling constant caused by the addition of a proton donor. The active site in a radical anion participating in the hydrogen-bonding interaction and the *K* values were then discussed on the basis of the theoretical calculation of the spin density and the coupling constant of the radicals in the hydrogen-bonding interaction. It has been pointed out that this sort of experiment in hydrogen bonding interaction is also useful for assigning the hyperfine coupling constant to a definite atom in a radical. Last, these *K* values are used to explain the mechanism of radical formation by the controlled potential electrolysis at different reduction potentials of pyrazine mono- and di-*N*-oxides in dimethylformamide-ethanol mixed solvents.

Since the first finding in 1962 by Deguchi,[1] Stone and Maki,[2] Piette *et al.*,[3] and other workers[4] regarding the quite large solvent dependence of the isotropic hyperfine coupling (hfc) constant of some organic free radicals, the study of the mechanism of solvent effects on electron spin resonance (ESR) spectra has attracted the attention of many workers. The theoretical considerations for explaining these solvent effects have been presented by Gendell, Freed, and Fraenkel (GFF),[5] who applied the mass-action-law, which describes the solvent dependence in terms of radical-solvent of molecular-complex formation, and who pointed out that the change in hfc constant arises from the redistribution of an unpaired electron due to the variation in the electronic state of free radicals with the complex formation. Later, this GFF theory was supported by experimental studies,[6,7] where mixed solvents consisting of water or alcohol and acetonitrile (AN) or dimethylformamide were frequently used. However, a successful quantitative examination of the GFF theory has been reported only by Stone and Maki.[8] In those studies, however, one component in the mixed solvents was a well-known proton donor, water, appearing in hydrogen-bonding complexes which seem to play an important role in the solvent effects.

Aside from the studies mentioned above, Deguchi *et al.*[1,9,10] also studied in detail the solvent effects on the ESR spectra of several organic free radicals; they showed that electrostatic interaction and charge transfer (CT) interaction, such as hydrogen bonding[9] or usual CT complex formation,[10,11] are the two main factors in the solvent effects. Including the studies mentioned above, a survey of the investigations reported thus far of solvent effects on the hfc constant or on the *g*-value of ESR spec-

1) Y. Deguchi, This Bulletin, **35**, 260 (1962).
2) E. W. Stone and A. H. Maki, *J. Chem. Phys.*, **36**, 1944 (1962).
3) L. H. Piette, P. Ludwig and R. N. Adams, *J. Amer. Chem. Soc.*, **84**, 4212 (1962).
4) a) A. W. Iljasav, *Zh. Strukt. Khim.*, **3**, 95 (1962); b) F. W. Heineken, M. Bruin and F. Bruin, *J. Chem. Phys.*, **37**, 452 (1962); c) A. J. Tench and P. Coppens, *J. Phys. Chem.*, **67**, 1378 (1963); d) P. L. Kolker and W. A. Water, *Proc. Chem. Soc.*, **1963**, 55.
5) J. Gendell, J. H. Freed and G. K. Fraenkel, *J. Chem. Phys.*, **37**, 2832 (1962).
6) P. Ludwig, T. Layloff and R. N. Adams, *J. Amer. Chem. Soc.*, **86**, 4568 (1964).
7) J. Pannell, *Mol. Phys.*, **7**, 317 (1964).
8) E. W. Stone and A. H. Maki, *J. Amer. Chem. Soc.*, **87**, 454 (1965). See also Ref. 7.
9) K. Mukai, H. Nishiguchi, K. Ishizu, Y. Deguchi and H. Takaki, This Bulletin, **40**, 2731 (1967).
10) Y. Ōishi, K. Mukai, H. Nishiguchi, Y. Deguchi and H. Takaki, *Tetrahedron Lett.*, **46**, 4773 (1968). See also J. Yamauchi, H. Nishiguchi, K. Mukai, Y. Deguchi and H. Takaki, This Bulletin, **40**, 2512 (1967).
11) S. Aono and M. Suhara, This Bulletin, **41**, 2553 (1968). Refer also to F. Gerson and W. B. Martin, Jr., *J. Amer. Chem. Soc.*, **91**, 1883 (1969); A. Ishitani and S. Nagakura, *Mol. Phys.*, **12**, 1 (1967).

tra[12],*1 clearly tells us that the hydrogen-bonding effect plays an important role in the case of solvents having O–H or N–H groups. However, only a few quantitative studies of the equilibrium system have been reported thus far.

In the foregoing paper[13] we reported in detail on the ESR spectra the anion radicals of many heterocyclic amine *N*-oxides, and also on the polarographic behavior of these radicals. During our studies we found that the hfc constants (absolute value) due to the nitrogen atom $|a_N|$ or ring hydrogen $|a_H|$ show quite a large solvent dependence with the addition of a proton donor. In this paper quantitative data on the equilibrium constant, K, for the hydrogen-bonding systems composed of some heterocyclic amine *N*-oxide anion radicals and several proton donors will be reported on the basis of the different formulation in GFF's concept.[5] These K values, as well as the change in the hfc constants with hydrogen-bonding interaction, are then discussed theoretically from the viewpoint of the electronic structures of these radical anions, and are also used to explain the mechanism of radical formation by controlled potential electrolysis at the different reduction potentials observed in non-aqueous polarograms of some amine *N*-oxides.

Experimental

Methods and Measurements. Anion radicals were generated electrochemically using the controlled-potential electrolysis cell reported in a previous paper.[13] The potential for the electrolysis was determined by using the polarographic data. The electrolysis cell for nonaqueous polarography has also been previously reported in detail.[13] The ESR spectra were measured under almost the same conditions as in the polarographic measurement. A 0.1M solution of tetra-*n*-propylammonium perchlorate was employed as a supporting electrolyte throughout the experiments. It has been reported[14] that this kind of bulky ammonium salt has almost no concentration effect on the hfc constants of free radicals. The instruments used for recording the ESR spectra were a Varian V-4502-15 X-band spectrometer with a 100 KHz magnetic field modulation, the magnetic field being monitored with a Varian F-8 nuclear fluxmeter and a Takeda Riken TR-5578 frequency counter. A Yanagimoto polarograph, Model PA-102, was used to record the DC and AC polarograms. The experimental conditions for operating these instruments and the cautions taken in obtaining the accurate observed values have already been described elsewhere.[13] All the measurements were made at ~25°C.

Samples and Solvent. 4-Nitropyridine *N*-oxide (4NPO), 4-cyanopyridine *N*-oxide (4CNPO), pyrazine mono- and di-*N*-oxides, and 4-nitropyridine (4NP) were adopted as the mother substances for producing the anion radicals. The methods of syntheses and purifications of these compounds, and also the ESR spectra, except for those of 4NP,[15] in a dimethylformamide (DMF) solvent have been reported in previous papers.[13,16] 4NP was yielded by the deoxygenation of the *N*-oxide-group oxygen atom of 4NPO by using the method reported by Hamana and Yoshimura,[15] it being repeatedly recrystallized from petroleum ether (mp 47.0—47.2°C). As to the proton donors, ethyl alcohol, water, and phenol were used. On the other hand, ethyl ether was used as a reference substance. 99.5% special-grade ethyl alcohol and special-grade ethyl ether were, respectively, dried sufficiently with $CuSO_4 \cdot H_2O$ (alcohol) or a molecular sieve (ether), and then rectified carefully. Phenol of a special pure grade was distilled two times under reduced pressure. The solvent DMF and the supporting electrolyte, tetra-*n*-propylammonium perchlorate, were of the same quality as in a previous report.[13]

Results

Behavior of ESR Spectra and Polarograms upon the Addition of Proton Donors. Since the polarographic reduction potential, $E_{1/2}$, of the

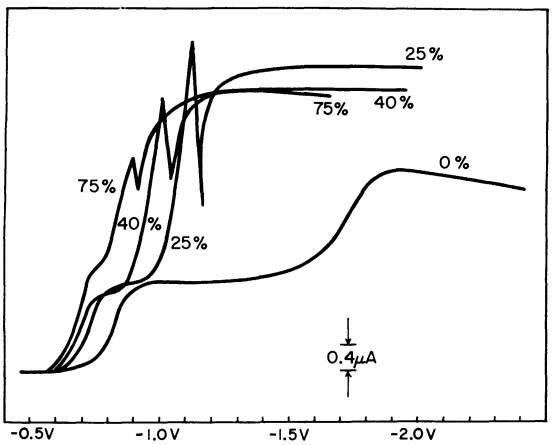

Fig. 1. Variation of the polarogram of 4-nitropyridine *N*-oxide (5.28×10^{-4} mol/*l*) in dimethylformamide with the addition of ethanol (vol%).

12) T. Kawamura, S. Matsunami, T. Yonezawa and K. Fukui, This Bulletin, **40**, 1111 (1967); *ibid.*, **38**, 1935 (1965).

*1 It was also reported that the visible spectrum of nitrobenzene anion radical in acetonitrile is blue shifted by the addition of proton donor (water). J. Q. Chambers and R. N. Adams, *Mol. Phys.*, **9**, 413 (1965).

13) T. Kubota, K. Nishikida, H. Miyazaki, K. Iwatani and Y. Ōishi, *J. Amer. Chem. Soc.*, **90**, 5080 (1968).

14) a) T. Kitagawa, *Rev. Polarog.* (Kyoto), **12**, 11 (1964); b) T. Kitagawa, T. Layoff and R. N. Adams, *Anal. Chem.*, **36**, 925 (1964); c) J. Burgess and M. C. R. Symons, *Quart. Rev.* (London), **22**, 276 (1968).

15) a) M. Hamana and H. Yoshimura, *J. Pharm. Soc. Japan*, **72**, 1051 (1952); b) K. Ezumi, H. Miyazaki and T. Kubota, *J. Phys. Chem.*, in press. See also K. Ezumi *et al.*, Preprints for the 21st Annual Meeting of the Chemical Society of Japan, Osaka (April 1968), No. 20114.

16) T. Kubota, H. Miyazaki and Y. Mori, *Rev. Polarog.* (Kyoto), **14**, 313 (1967). See also previous literature given in Refs. 13 and 15b.

compounds studied here moves toward a positive value (*i. e.*, these are a positive shift) upon the addition of proton donors into the DMF or acetonitrile solvent, the set potential for controlled potential electrolysis is also shifted to a positive potential. When the first and the second waves are obviously separated in the DMF solvent alone, just like the reduction wave of 4NPO,[13] as is shown in Fig. 1, the above-mentioned positive shift of $E_{1/2}$ is remarkable for the second wave. As a result, the coalescence of the first and the second waves occurs with an increase in the proton donor concentration, while the radical formed by the electrolysis simultaneously becomes unstable. Of

TABLE 1. SOLVENT EFFECTS ON HYPERFINE COUPLING CONSTANTS (ABSOLUTE VALUE) OF SOME AROMATIC AMINE OXIDE ANION RADICALS

[A] 4-Nitropyridine *N*-oxide[a]

Proton donor	Concentrtation mol/*l*	Concentrtation vol%	$a_{N(NO_2)}$	$a_{N(N\rightarrow O)}$	a_{3H}	a_{2H}
Ethanol	0	0	6.040	4.730	3.320	1.260
	0.853	5	6.272	4.720	3.276	1.204
	1.705	10	6.492	4.703	3.324	1.196
	3.410	20	6.669	4.618	3.351	1.190
	5.115	30	6.913	—	—	—
	6.820	40	6.849	4.635	3.337	1.162
	10.230	60	7.326	4.577	3.337	1.143
	11.935	70	7.405	4.440	3.331	1.113
Water	2.770	5	6.495	4.716	3.309	1.187
	5.540	10	7.031	4.559	3.324	1.155
	8.310	15	7.404	4.491	3.332	1.153
	11.080	20	7.707	4.424	—	1.190
	13.850	25	7.955	4.514	3.305	1.116
	16.620	30	8.057	4.366	3.254	1.107
Phenol	1.306×10^{-2}	—	6.169	4.751	3.333	1.243
	3.094×10^{-2}	—	6.225	4.736	3.327	1.234
	5.092×10^{-2}	—	6.261	4.750	3.363	1.238
	5.834×10^{-2}	—	6.329	4.717	3.332	1.212
	13.44×10^{-2}	—	6.489	4.713	3.324	1.220

[B] 4-Cyanopyridine *N*-oxide[a]

Proton donor	Concentration mol/*l*	Concentration vol%	$a_{N(N\rightarrow O)}$	$a_{N(C\equiv N)}$	a_{3H}	a_{2H}
Ethanol	0	0	9.610	1.760	2.360	0.610
	0.171	1	9.512	1.787	2.144	0.912
	0.341	2	9.651	1.813	2.131	1.072
	0.682	4	9.642	1.824	2.059	1.143
	1.023	6	9.514	1.818	2.018	1.207
	1.705	10	9.620	1.830	1.999	1.255
	2.728	16	9.630	1.820	2.015	1.202

[C] Pyrazine mono-*N*-oxide[a]

Proton donor	Concentration mol/*l*	Concentration vol%	$a_{N(N\rightarrow O)}$	$a_{N(\rangle N)}$	a_{3H}	a_{2H}
Ethanol	0	0	12.050	5.493	2.132	1.542
	0.017	0.1	12.134	5.589	2.122	1.640
	0.051	0.3	12.122	5.643	2.126	1.732
	0.102	0.6	12.121	5.742	2.135	1.796
	0.171	1.0	12.179	5.727	2.136	1.866
	0.341	2.0	12.184	5.804	2.141	1.844
	0.682	4.0	12.188	5.842	—	1.874

TABLE 1. (continued)

[D] 4-Nitropyridine[a)]

Proton donor	Concentration mol/l	Concentration vol%	$a_{N(NO_2)}$	$a_{N(\rangle N)}$	a_{3H}	a_{2H}
Ethanol	0	0	7.257	2.622	3.021	0.398
	0.341	2	7.538	2.590	3.037	0.434
	0.682	4	7.763	2.563	3.052	0.440
	0.853	5	7.830	2.577	3.064	0.443
	1.194	7	7.861	2.560	3.029	0.447
	1.705	10	8.016	2.550	3.052	0.454
	2.558	15	8.141	2.528	3.084	0.449
	3.410	20	8.344	2.496	3.023	0.453
	5.115	30	8.553	2.511	3.075	0.472
	6.820	40	8.818	2.469	3.082	0.484
	8.525	50	9.011	2.453	3.085	0.504
	10.230	60	9.189	2.442	3.078	0.508

[E] Pyrazine di-*N*-oxide[a)]

Proton donor	Concentration mol/l	Concentration vol%	a_H	$a_{N(N\to O)}$
Ethanol	0	0	1.362	9.441
	0.341	2	1.496	9.775
	0.682	4	1.531	9.749
	1.023	6	1.546	9.727
	1.364	8	1.552	9.884
	1.705	10	1.565	—
	2.387	14	1.591	9.846
	3.069	18	1.616	—

a) Numbering of each ring atom in the radicalas is as follows:

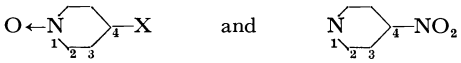

course, the selection of the set-potential becomes difficult because of the above-mentioned coalescence of the first and the second reduction waves, the former being due to the anion-radical formation of mother compounds. Our hydrogen-bonding experiments were, thus, restricted within some limited concentrations of proton donors, as is shown in Table 1. Nevertheless, the anion radical of 4NPO was most stable, and it was possible to use some proton donors in making the hydrogen-bonding study. It should be now noted that even though ethyl ether of, for example, about 20% is added in a DMF solvent instead of ethyl alcohol, we observed almost no change in the polarogram of 4NPO or in the ESR spectrum of the 4NPO anion radical compared with those recorded in the DMF solvent alone, but that when ethyl alcohol is added the ESR spectra and polarograms undergo considerable change. These facts may support the evidence that the hydrogen-bonding effect is an important factor in bringing about the change in the ESR spectra and in the polarograms. As examples, the ESR spectral change in 4NPO and 4CNPO anion radicals arising from the addition of proton donors is shown in Figs. 2 and 3 respectively. Figures 4A and 4B show the variation in the hfc constants caused most predominantly by the addition of proton donors.

Evaluation of the Equilibrium Constant, *K*. According to the GFF concept, let us consider this hydrogen-bonding equilibrium:

$$RS + D \rightleftarrows RD + S \quad (1)$$

Here, RS, D, and RD stand for the assumed radical-solvent complex, the proton donor, and the radical-proton donor complex respectively. On the other hand, if no radical-solvent complex is assumed, the equilibrium may be written as:

$$R + D \rightleftarrows RD \quad (2)$$

this sort of expression being usually employed for the equilibrium study of various charge-transfer (CT) complexes, including hydrogen-bonding complexes. If the equilibrium in Eqs. (1) and (2) is

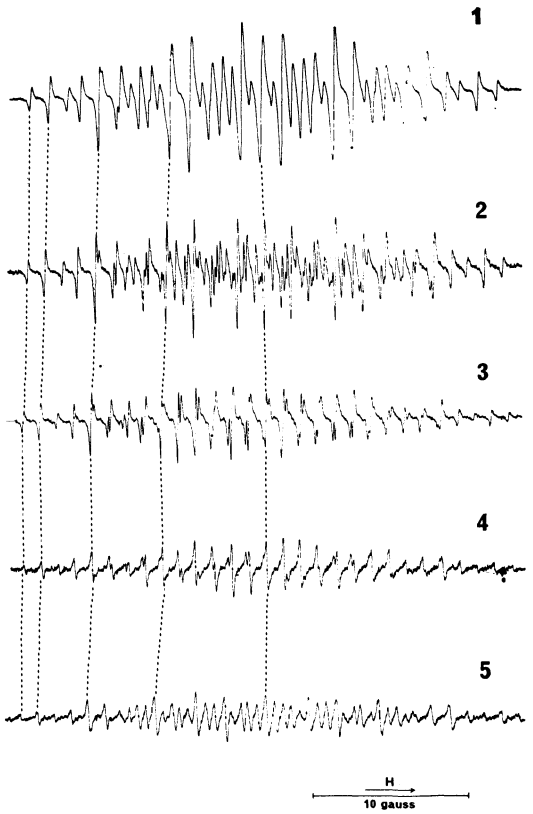

Fig. 2. ESR spectral change of 4-nitropyridine *N*-oxide anion radical in dimethylformamide with the addition of ethanol, the concentration of which is 0, 10, 30, 40 and 60 vol% for spectral No. 1, 2, 3, 4 and 5, respectively.

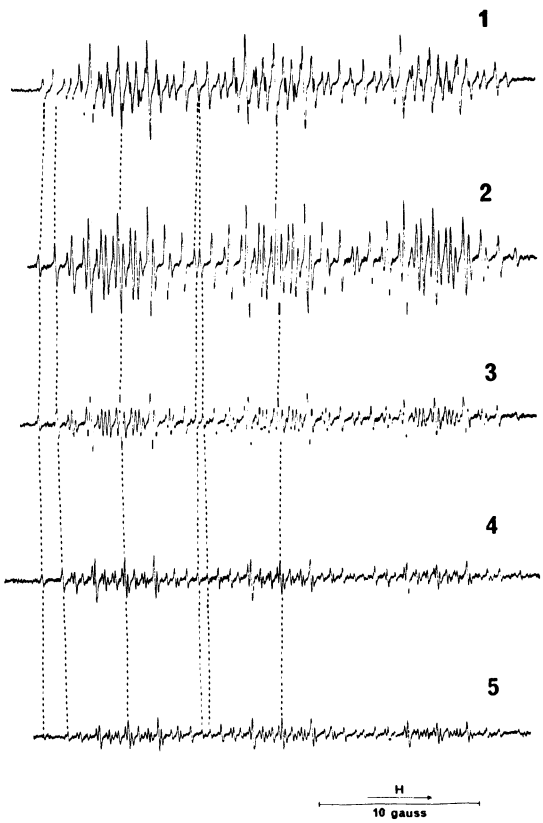

Fig. 3. ESR spectral change of 4-cyanopyridine *N*-oxide anion radical in dimethylformamide with the addition of ethanol, whose concentration is ~0, 2, 4, 10 and 16 vol% for spectral No. 1, 2, 3, 4 and 5, respectively.

very rapid,*2 the observable hfc constant, $\bar{a}$, is easily given by $\bar{a}=P_{RS}a_{RS}$(or P_Ra_R)$+P_{RD}a_{RD}$; for the case of hydrogen-bonding interaction, this expression for $\bar{a}$ would be correct because it is well known that the hydrogen-bonding equilibrium is very rapid.*2 Using the definition of $K=$(RD)·(S)/(RS)(D) for Eq. (1), P_{RS} and P_{RD} are now written as $P_{RS}=1/(1+K\alpha)$, $P_{RD}=K\alpha/(1+K\alpha)$, and $P_{RS}+P_{RD}=1$. Here, $\alpha=$(D)/(S). If Eq. (2) is applied, $K=$(RD)/(R)(D), $P_R=1/(1+K$(D)), and $P_{RD}=K$(D)$/(1+K$(D)). Now, by combining those equations we can get:

$$\bar{a} = a_{RD} - (1/K)(\bar{a}-a_{RS})/\alpha \quad (3)$$

and

$$\bar{a} = a_{RD} - (1/K)(\bar{a}-a_R)/(D) \quad (4)$$

from Eqs. (1) and (2) respectively. The concentrations (D) and (S) in Eqs. (3) and (4) are those in the equilibrium state, but the radical concentration is very small ($<10^{-4}$ mol/l), so that, in good approximation, (D)$\approx$(D)$_0$ and $\alpha\approx$(D)$_0$/(S)$_0$. The zero subscript means the initial concentration. It can easily be understood that the plot of $\bar{a}$ against $(\bar{a}-a_{RS})/\alpha$ or $(\bar{a}-a_R)/$(D) should satisfy the linear relation if Eq. (1) or (2) holds. Thus, from the slope and the intersection at the ordinate the $1/K$ (then K) and a_{RD} values can be directly obtained.*3

For the equilibrium system where 1 (radical) : 2 (proton donor) complex formation, such as

$$SRD + D \rightleftarrows DRD + S \quad (5)$$

has to be taken into consideration in addition to the 1 : 1 form (Eq. (1)), Stone and Maki[8] derived the equation:

*2 The recombination rate process in usual hydrogen bonding or proton addition equilibriums was reported to be in the order of $\sim 10^{10}$ (mol/l)$^{-1}$(sec)$^{-1}$. N. Mataga, Y. Torihashi and Y. Kaifu, *Z. Phys. Chem. N. F.*, **34**, 379 (1962); A. Weissberger (Editor), Technique of Organic Chemistry, Vol. 8, Part II, Chapters XV—XX "Very Rapid Reactions in Solution," p. 793, Interscience Publishers Inc., New York (1963).

*3 From this viewpoint Eq. (3) seems to be more convenient than the equation, $\bar{a}=(1/2)(a_{RS}+a_{RD})+(1/2)[(a_{RD}-a_{RS})\times(K\alpha-1)]/(K\alpha+1)$, given in the GFF paper.[5]

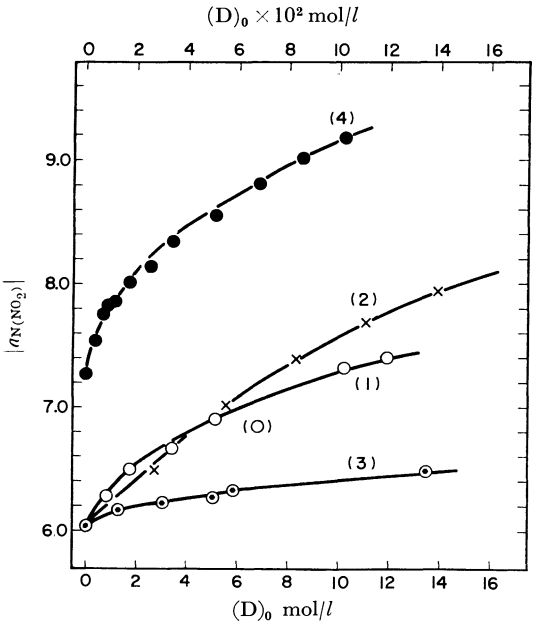

Fig. 4A. Variation of hfc constant due to the nitro group nitrogen atom of 4-nitropyridine *N*-oxide (curves 1, 2 and 3) and 4-nitropyridine (curve 4) with the addition of proton donor. Added proton donors are ethanol, water, and phenol for curves 1 and 4, 2, and 3, respectively. Upper abscissa should be referred only to curve 3. Here note that each curve is obtained theoretically by the method written in the text, but each point is the experimental value.

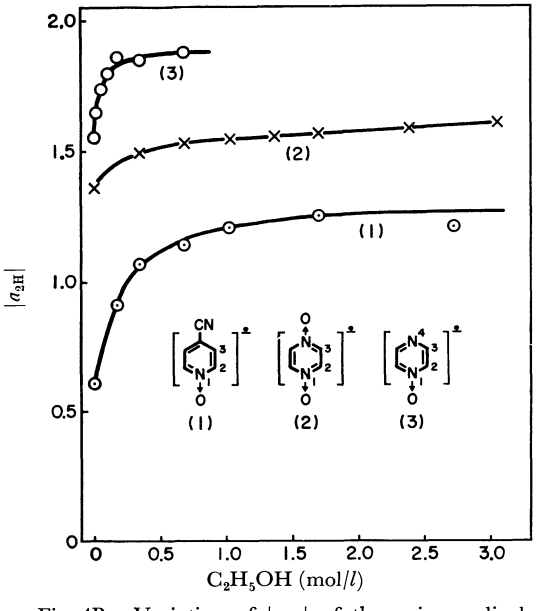

Fig. 4B. Variation of $|a_{2H}|$ of the anion radicals given in this figure with the addition of ethanol. Each curve is obtained theoretically (see text), but each point is the observed one.

$$a = \frac{a_{SRS} + K\alpha a_{SRD} + KK'\alpha^2 a_{DRD}}{1 + K\alpha + KK'\alpha^2} \quad (6)$$

K' represents the equilibrium constant corresponding to Eq. (5), while a_{SRS}, a_{SRD}, and a_{DRD} are, respectively, the hfc constants pertinent to the SRS, SRD, and DRD complexes. Note that, in this case, the radical has two or more effective active sites in a molecule for hydrogen-bonding interaction. Usually $K' < K$, and K is not so large in the present experiment (see Table 2). In addition, if the experiment is made under the conditions where $\alpha \ll 1$, if, that is, the concentration of the proton donor (D) is much smaller than that (S) of the solvent, the $KK'\alpha^2$ and $KK'\alpha^2 a_{DRD}$ terms may be neglected in Eq. (6). Then, Eq. (6) is easily reduced to Eq. (3), from which the values of K and a_{SRD} are determined. Eq. (6) is now modified as follows:

$$\bar{a} = a_{DRD} - \frac{1}{K'}\left[\frac{(\bar{a} - a_{SRS}) + K\alpha(\bar{a} - a_{SRD})}{K\alpha^2}\right] \quad (7)$$

The plotting of $\bar{a}$ *vs.* "the quantity in the brackets" on the right-hand side of Eq. (7) makes it possible to evaluate the values of K' and a_{DRD} separately. Thus, we tried the above-mentioned linear plots using Eqs. (3), (4), and (7), and also using the

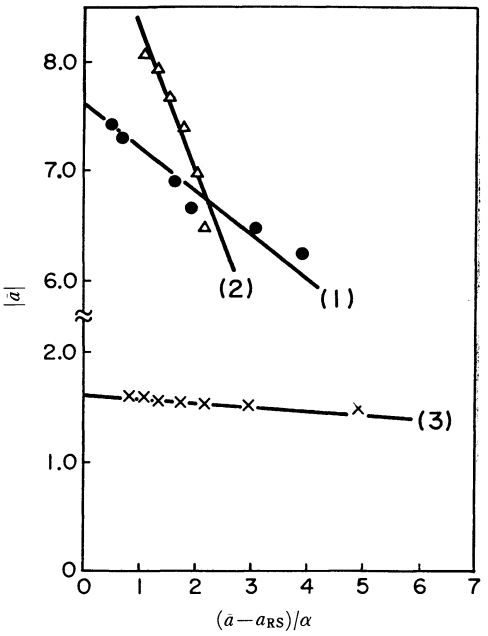

Fig. 5. Some examples of the linear relation of Eq. (3) (see text). The straight lines 1 and 2 are for the change of $|a_{N(NO_2)}|$ of 4-nitropyridine *N*-oxide anion radical with the addition of ethanol (line 1) and water (line 2), respectively. Line 3 is for the $|a_H|$ of the system: pyrazine di-*N*-oxide anion radical + ethanol. Solvent is dimethylformamide.

TABLE 2. EQUILIBRIUM CONSTANTS K'S AND HYPERFINE COUPLING CONSTANTS a'S (absolute value) PERTINENT TO THE HYDROGEN BONDING SYSTEMS OF THE ANION RADICALS STUDIED HERE

Anion radical of	Proton donor	K (dimensionless) by Eq. (3)	a_{RD}* by Eq. (3)	K (l/mol) by Eq. (4)	a_{RD}* by Eq. (4)
4 NPO	Water	0.72 ± 0.16	9.75 ± 0.54[a]	0.043 ± 0.016	10.96 ± 1.33[a]
4 NPO	Ethanol	3.39 ± 0.59	7.37 ± 0.11[a]	0.18 ± 0.04	7.83 ± 0.25[a]
4 NPO	Phenol	—	—	25.95 ± 11.56	6.51 ± 0.11[a]
4 CNPO	Ethanol	66.97 ± 10.18	1.29 ± 0.03[b]	5.05 ± 0.82	1.30 ± 0.03[b]
Pyrazine di-*N*-oxide	Ethanol	39.00 ± 7.02	1.61 ± 0.01[c]	3.00 ± 0.58	1.62 ± 0.01[c]
Pyrazine mono-*N*-oxide	Ethanol	301.57 ± 13.25	1.89 ± 0.01[b]	23.25 ± 1.03	1.89 ± 0.01[b]
4-Nitropyridine	Ethanol	$K=10.0\pm1.5$ $a_{SRD}=8.50\pm0.2$[a] $K'=0.49\pm0.02$ $a_{DRD}=10.00\pm0.05$[a] with Eqs. (5), (6) and (7).		—	—

* The value of hyperfine coupling constant is that of $a_{N(NO_2)}$, a_{2H} and a_H for the superscript a, b and c, respectively.

experimental data listed in Tables 1A—1E. Assuming the 1 : 1 interaction model, quite a good linear relation for Eq. (3) or (4) was then yielded for each system except for the case of the 4NP anion radical plus ethanol, where the 1 : 2 model was much better (see below). In Fig. 5 these linear plottings for Eq. (3) are illustrated as examples.

The values of the equilibrium constant, K, and the hfc constants in the hydrogen-bonding state thus evaluated are shown in Table 2. Also, the solid curves given in Figs. 4A—4B were theoretically obtained using the values listed in Table 2. We see that there is quite a good agreement of the proton-donor dependence of $\bar{a}$ yielded experimentally with the corresponding curve obtained theoretically. The behaviour of the $|a_N|$ of the 4NP anion radical upon the addition of ethanol may be interpreted by assuming the 1 : 2 model. In small ethanol concentrations Eq. (3) or (4) is well satisfied, but the linear relation of Eq. (7) is again fulfilled in the region of relatively high ethanol concentrations. The values of K, K', a_{SRD}, and a_{DRD} were thus determined; they are included in Table 2. As may be seen in Fig. 4A, the experimental values of $\bar{a}$ were reproduced by the theoretical $\bar{a}$ curve drawn by employing the above-mentioned K and K' values.

Discussion

Active Site for Hydrogen-bonding Interaction. The compounds used in this study have, in a molecule, more active atoms than the one for hydrogen-bonding interaction. From the viewpoint of the electronic structures of the present anion radicals, it is important and interesting to examine which atom in a molecule enters into hydrogen-bond formation with proton donors. The studies reported thus far suggest that the intermolecular charge transfer of a lone-pair electron, belonging to the active-atom, non-bonding orbital which enters into hydrogen bonding to, for example, the O–H antibonding orbital of proton donors, is the most important mechanism in hydrogen-bond formation.[17] Of course, there is also electrostatic force. Now, note that the charge-transfer mechanism and the electrostatic interaction both bring about an increase in electronegativity at the atom in question. In other words, the Coulomb integral concerning the π-AO at the atom increases in magnitude in the HMO calculation, as was suggested by Frankel *et al.*[5] The change in the spin-density distribution arising from the perturbation due to hydrogen bonding can then be calculated. The parameter values in the HMO calculation, as modified by McLachlan's treatment (MHMO calculation),[18] have already been given for heterocyclic amine *N*-oxides and their derivatives, having NO_2, CN groups *etc.*, in order to interpret the hfc constants and, thus, the spin densities of these anion radicals in the free state.[13] The results agree well with the observed values.*4 Assuming some active sites,

17) S. Nagakura, *J. Chim. Phys.*, **61**, 217 (1964); K. Nukazawa, J. Tanaka and S. Nagakura, *J. Phys. Soc. Japan*, **8**, 792 (1953); R. S. Mulliken, *J. Chim. Phys.*, **61**, 20 (1964).

18) A. D. McLachlan, *Mol. Phys.*, **3**, 233 (1960).

*4 Parameter values for the MHMO calculation of the anion radicals of *N*-oxide compounds are: $k_N^{\delta+}=1.0$ with inductive effect$=0.1$, $k_O=0.6$, and $\beta_{NO}=0.8$ for $\rangle N^{\delta+}\rightarrow O^{\delta-}$ group. See Fig. 7 in Ref. 13 for the parameter sets and their literature on the substituents NO_2 and C≡N, and ring nitrogen atom ($\rangle$N:). The hfc constants were theoretically calculated using the following equations[13] connecting spin density and σ-π interaction term: $a_{N(NO_2)}=99.0\rho_N-35.8(\rho_O+\rho_{O'})$; $a_{N(N\rightarrow O)}=42.57\rho_N-18.98\rho_O-6.66(\rho_C+\rho_{C'})$; $a_H=-25.67\rho_C$; $a_{N(C\equiv N)}=23.1\rho_N-6.8\rho_C$; $a_{N(\rangle N\cdot)}=27.3\rho_N-1.7$ $(\rho_C+\rho_{C'})$.

the spin density and the hfc constant in the hydrogen-bonding state can be calculated using many parameter sets which are reasonably selected by referring to the ones in the free state, and the calculated values are compared with the behavior of the hfc constants observed upon the addition of proton donors (see Table 1 and Fig. 4). This comparison may lead to the acceptable conclusion as to which atom in an anion radical mainly participates in the hydrogen-bond formation.

First, let us discuss the 4NPO anion radical. This radical has two active groups in the molecule; one is the NO_2 group, while the other is the *N*-oxide group. If the lone-pair orbital of the *N*-oxide-group oxygen atom enters into hydrogen bonding, the Coulomb integral of the oxygen atom in the MHMO calculation becomes larger than the standard value, $\delta\alpha_0=0.6\beta$.[13],*4 The hfc constants*4 obtained using the spin densities led from the calculation under the above boundary conditions are illustrated in Fig. 6. On the other hand, in Fig. 7 are shown the calculation results assuming that the nitro-group oxygen atom makes a hydrogen bond with the proton donors.*5,[19,20] Since the ESR spectrum in the hydrogen-bonding interaction of the 4NPO anion radical can be well interpreted as the radical is in C_{2v} molecular symmetry, the hydrogen-bonded hydrogen atom of proton donors should be rapidly exchanged between two oxygen atoms in the NO_2 group (*vide infra*). The same circumstances would also hold in the 1 : 1 hydrogen bonding system, consisting of a proton donor and pyrazine di-*N*-oxide, as will be discussed later.

Now, when we compare the theoretical values shown in Figs. 6 and 7 with the experimental results seen in Table 1A and Fig. 2, it seems certain that the active center partaining to the hydrogen-bonding interaction of the 4NPO anion radical with proton donors is the nitro group in the molecule, since the experimental and theoretical results are in quite good agreement in this case. This conclusion is in agreement with the conclusion that the hydrogen-bonding or alkali metal-complexing center of the anion radicals of nitrobenzene and related nitro-compounds is in the nitro group,[6,14,21]

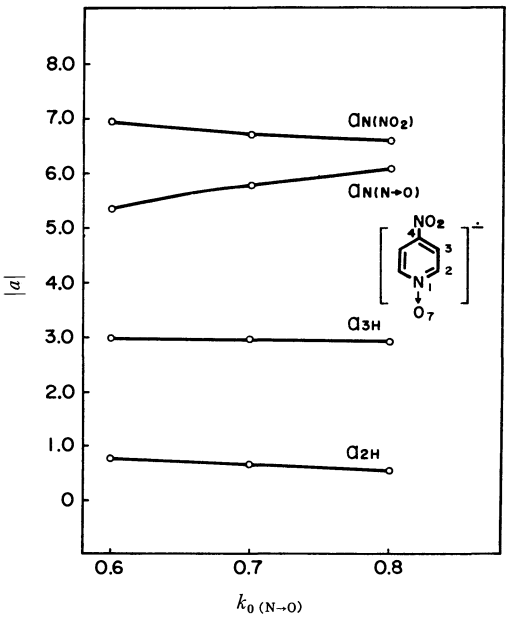

Fig. 6. The behavior of hfc constants theoretically estimated (see text for the method) assuming that the *N*-oxide oxygen atom of 4-nitropyridine *N*-oxide anion radical is the active site for hydrogen bonding interaction.

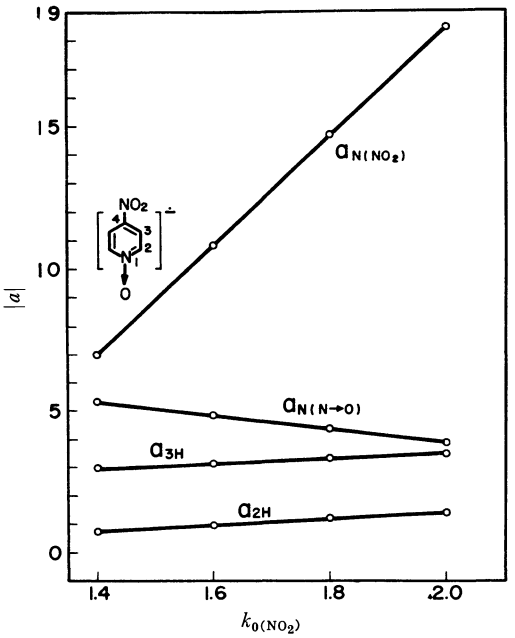

Fig. 7. The behavior of hfc constants theoretically estimated (see text for the method) assuming that the nitrogroup oxygen atom of 4-nitropyridine *N*-oxide anion radical is the active site for hydrogen bonding interaction.

*5 It should be noted that the MO calculation[13,15,19] leads to the conclusion that the $\rangle C{=}NO_2$ bond order in the anion radicals of 4NPO, nitrobenzene, *etc.* becomes larger than in the corresponding neutral molecules. The possibility of the twisting around the C–N bond due to the hydrogen bonding effect would be then rejected from the consideration unless bulky substituent at ortho position brings about the steric hidrance against the nitro group. This argument seems to be experimentally supported.[15b,6,20]

19) a) D. H. Geske, J. L. Ragle, M. A. Bambenek and A. L. Balch, *J. Amer. Chem. Soc.*, **86**, 987 (1964); b) T. E. Peacock, *Proc. Phys. Soc.*, **78**, 460 (1961).
20) Y. Nakai, This Bulletin, **39**, 1372 (1966).
21) R. L. Ward, *J. Amer. Chem. Soc.*, **83**, 1296 (1961); C. Ling and J. Gendell, *J. Chem. Phys.*, **47**, 3475 (1967).

whose complexing ability is not so small in the anion radical. However, it should be recalled[22] that the protonation of the 4NPO neutral molecule in an aqueous solution occurs at the *N*-oxide group oxygen atom, and that the pK_a value is -1.7.[22] Therefore, we can say that the active center for the hydrogen-bonding or protoantion interaction of 4NPO is exactly reversed between the neutral molecule and the anion radical. There is much evidence supporting the idea that the intramolecular charge transfer (CT) from a *N*-oxide-group oxygen atom to a nitro group is an important factor in describing the nature of the ground state as well as the excited state of 4NPO, 4-nitroquinoline *N*-oxide, *etc.**6,22,23) For example, the $pK_a = -1.7$ of 4NPO is much smaller than the correspoding value, 0.78, of pyridine *N*-oxide.[22] The theoretical MO considerations[13,15,19] reported thus far on various aromatic nitro compounds including 4NPO suggest that the lowest vacant MO (LVMO) is mainly localized on the NO_2 group and that, thus, the unpaired π electron densitie on that group are very large. Also, an intramolecular CT absorption band pertinent to nitrobenzene, 4NPO, *etc.* may appear in the near ultraviolet region.[23,24] This result implies that the nitro-group oxygen lone-pair electrons become quite active for n-σ type intermolecular interaction when the species is in an anion radical or in an intramolecular CT excited state, although the above interaction is weak in the case of the neutral nitro compounds.[25] Our aforementioned conclusion on the active site of the 4NPO anion radical for hydrogen-bonding interaction seems, therefore, to be reasonable.

Next, let us discuss the hydrogen-bonding active site of the 4CNPO anion radical, which is of interest in comparison with that of the 4NPO anion radical discussed above. It is well known that the nitrile-group lone-pair electrons show a very weak n-σ-type intermolecular interaction ability,[26] so that the hydrogen-bonding power is also weak, and that the nitrogen hfc constant, $|a_N|$, due to the cyano group in the aromatic nitrile anion radicals is found only within 1—3 gauss.[13] In addition, the cyano group is a weak π substituent[27] and affects the near-UV spectra of aromatic substances weakly, and the intramolecular CT band partinent to benzonitrile has been reported not to be exhibited in the near-UV region.[27] In view of these facts, we may expect that the hydrogen-bonding ability of the nitrile group in π anion radicals is not large. In fact, MHMO spin-density calculations according to the procedure used in the case of 4NPO led to the finding that the stronger active site for the hydrogen-bond formation of the 4CNPO anion radical is the *N*-oxide group and not the cyano group, for, if we assume the latter case, the change in the calculated spin densities and hfc constants arising from hydrogen bonding does not reproduce the experimental results so well; however, the agreement between experiment and theory is good for the former case. Here, note that the hfc constant due to the hydrogen atom at the position 2, $|a_{2H}|$ (see Fig. 4B for numbering), increases in magnitude in the hydrogen-bonding complex, while $|a_{3H}|$ is relatively insensitive. These results are in good agreement with the calculation results. Conversely, this type of experiment on the solvent effect seems to be a useful technique for determining the assignment of the hfc constants.[13,16]

The calculation was next carried out on the anion radicals of pyrazine mono *N*-oxide and 4-nitropyridine. It was clearly concluded that, in the case of the former radical, the hydrogen-bonding interaction ability of the *N*-oxide group is stronger than that of the ring-nitrogen atom, but that the stronger active atom in the 4NP anion radical is, of course, the nitro-group oxygen atom, with the ring-nitrogen atom next. As may be understood from Table 1, the experimental values of $|a_{N(ring)}|$[13] and $|a_{2H}|$[13] for the case of the pyrazine mono-*N*-oxide anion radical are quite increased by the addition of ethanol, but the increase is small for the $|a_{N(N\to O)}|$ and $|a_{3H}|$ values. These results are satisfied by assuming the active site to be the *N*-oxide-group oxygen atom, and have confirmed the assignment of $|a_{3H}| > |a_{2H}|$ which was preferred in the previous paper.[13] In Fig. 8 are shown these calculated results. The calculation on the assumption that both the *N*-oxide-group oxygen atoms are the active centers of the hydrogen-bonding interaction for the pyrazine di-*N*-oxide anion radical

22) See many experimental data given in the Chapter 4 of the book: E. Ochiai, "Aromatic Amine Oxides," Elsevier Publishing Co., Amsterdam (1967).

*6 In resonance structures these circumstances will be written as follows:

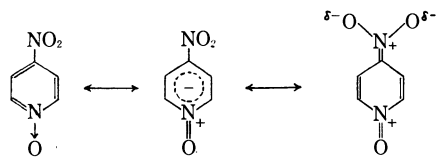

23) M. Yamakawa, T. Kubota and H. Akazawa, *Theor. Chim. Acta*, **15**, 244 (1969); T. Kubota and M. Yamakawa, This Bulletin, **35**, 555 (1962); S. Kobinata and S. Nagakura, *Theor. Chim. Acta*, **14**, 415 (1969).

24) S. Nagakura and J. Tanaka, *J. Chem. Phys.*, **22**, 236 (1954); S. Nagakura, *ibid.*, **23**, 1441 (1955); J. Tanaka and S. Nagakura, *ibid.*, **24**, 1274 (1956), *etc.*

25) S. Nagakura and M. Gouterman, *J. Chem. Phys.*, **26**, 881 (1957).

26) N. Mataga and Y. Kaifu, *Mol. Phys.*, **7**, 137 (1963); T. Kubota, M. Yamakawa, M. Takasuka, K. Iwatani, H. Akazawa and I. Tanaka, *J. Phys. Chem.*, **71**, 3597 (1967) and other papers given therein.

27) K. Kimura and S. Nagakura, *Theor. Chim. Acta*, **3**, 164 (1965); *Nippon Kagaku Zasshi*, **86**, 1 (1965).

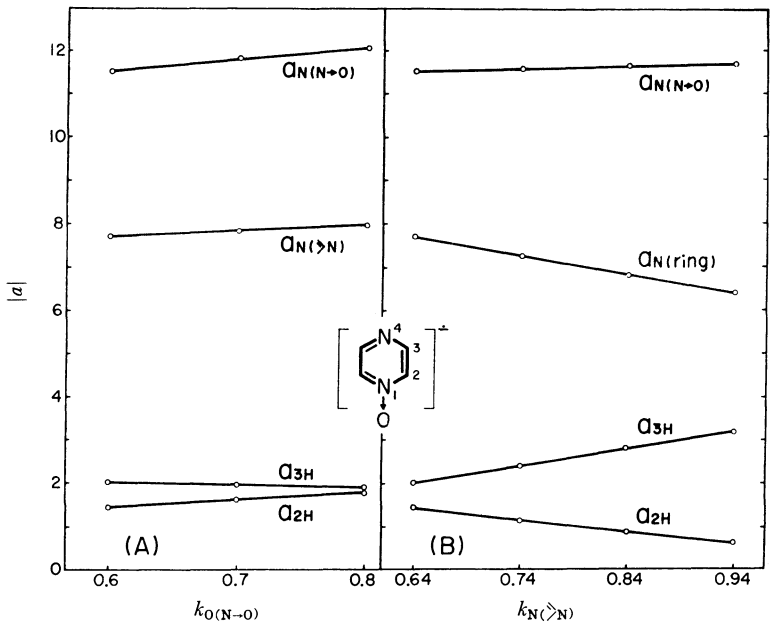

Fig. 8. The behavior of hfc constants theoretically estimated (see text) assuming that the active site entering into hydrogen bonding interaction is the *N*-oxide group oxygen atom (case A) or ring nitrogen atom (case B).

results in a good agreement with the experimental values listed in Table 1. Note also that the ESR spectrum observed in DMF-ethanol mixed solvents has a pattern corresponding to the V_h symmetry of the anion radical. This may be attributed to the rapid exchange of hydrogen-bonding interaction at the two oxygen atoms, just as in the case of the *p*-benzosemiquinone- 1-^{13}C molecule.[8]

Equilibrium Constants of Hydrogen Bond Formation. Let us first examine the values of the equilibrium constant, *K*, which are listed in Table 2. It is deemed that, except for pyrazine mono-*N*-oxide, the *K* values are not very large considering that the species are anion radicals; they are comparable to the corresponding *K* values of neutral pyridine *N*-oxide, quinoline *N*-oxide, *etc.*[28] However, it should be remembered that the compounds whose π-anion radicals are relatively stable are those which have electron-drawing substituents, like CN, COOR, NO_2, *etc.*, in a molecule and that these are conjugated with π-electron systems. In the present case, these substituents cause the decrease in the electron densities at the *N*-oxide oxygen atom, even in the anion radicals, as the calculation[13] of the spin densities shows. In turn, the nitro group in, for example, nitrobenzene is essentially a weak base. Pyrazine di-*N*-oxide may be also a weak base, as may be understood from the pK_a value (−1.62)[22] of phenazine di-*N*-oxide. This weak basicity of the above-mentioned functional groups might be one of reasons for the present, perhaps, small *K* values, except for the case of the pyrazine mono-*N*-oxide anion radical, which has rather large *K* value compared with those of the other radicals (see Table 2). The basicity of neutral pyrazine-mono-*N*-oxide may be not so different from, or only a little weaker than, that of pyridine *N*-oxide. This may be inferred from the fact[22] that the pK_a value (1.57) of acridine *N*-oxide is almost the same as that (1.32) of phena-

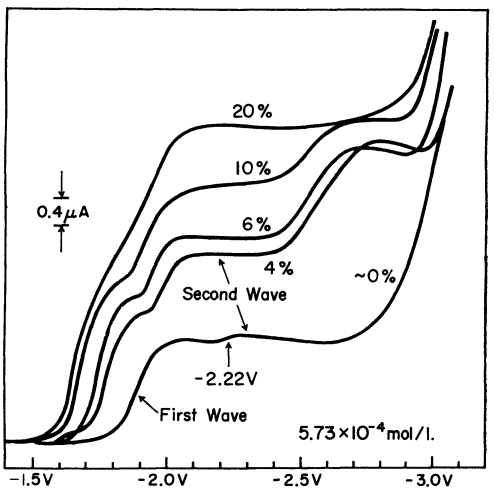

Fig. 9. Observed polarograms of pyrazine mono-*N*-oxide in the mixed solvents: dimethylformamide+ethanol (vol%).

28) T. Kubota, *J. Spectroscopical Soc. Japan*, **10**, 83 (1962).

TABLE 3. ANION RADICALS PRODUCED BY THE CONTROLLED POTENTIAL ELECTROLYSIS OF PYRAZINE MONO- AND DI-*N*-OXIDES AT DIFFERENT POLAROGRAPHIC REDUCTION WAVES AND UNDER DIFFERENT ETHANOL CONCENTRATIONS ADDED IN DMF SOLVENT

Mother compound	Ethanol concentration	Anion radical species[a] (observed ESR spectra) produced at		
		First wave	Second wave	Third wave
Pyrazine mono-	~0	PMNO	Pyrazine	—
N-oxide	0.1	PMNO	Pyrazine	—
(PMNO)	0.3	PMNO	PMNO	—
	1.0	PMNO	PMNO	—
	>2.0	PMNO	PMNO	—
Pyrazine di-	~0	PDNO	PMNO	Pyrazine
N-oxide	<0.5	PDNO	PMNO	Pyrazine
(PDNO)	1.0	PDNO	PMNO	PMNO
	>2.0	PDNO	PDNO	PDNO

a) ESR spectum observed at the second or third reduction wave is sometimes contaminated more or less by the other spectra, but the main spectrum is the one shown in this Table.

zine mono-*N*-oxide. Keeping in mind this fact, we may expect that the *K* value (the active site is the *N*-oxide group) of the pyrazine mono-*N*-oxide anion radical for the hydrogen bonding with alcohol is larger than that (~15 *l*/mol in *n*-heptane, ~6—7 in CCl_4) of the corresponding equilibrium in the pyridine *N*-oxide, quinoline *N*-oxide, and acridine *N*-oxide neutral molecules, because the former is the anion radical with an extra electron in the molecule. In fact, this is actually the case, the *K* value (23.3 *l*/mol) obtained here being larger than that just mentioned above for the neutral species.

Now let us consider the hydrogen-bonding equilibrium constant, *K*'s, formed between the 4NPO anion radical and water, ethanol, and phenol. As Table 2 indicates, the *K* values are increased in the following order of proton donors: water<ethanol <phenol. This order seems to be in agreement with that of the proton-donating power for 1:1 hydrogen-bond formation studied by infrared spectral measurements.[29] In relation to these results, it is thought that, for the same hydrogen-bonding systems as the above, the $|a_{RD}^{N}|$ value (see Eqs. (3) and (4), and Table 2) of the 4NPO anion radical is in an order just the reverse of that of the *K* value, namely, water>ethanol>phenol. Remember that the *K* value for the 4NPO anion radical-water system is quite small. Much water is necessary to bring about the change in the hfc constant $|a_N|$, as may be seen in Table 1. In these mixed solvents with high values of $\alpha=(D)/(S)$ (see Eq. (3)), the nature of the mixed solvents is never the same as that of DMF itself in the present experiments. The dielectric constant of water is very large. The effect of electrostatic interaction, that is, the effect of the reaction field of the mixed solvent on the electronic state of radicals can not be ignored in these cases. In view of this, the thermodynamic and ESR data for the case of phenol as the proton donor might be attributed to the fact that the data are closer to hydrogen binding itself; since phenol is a strong donor, the phenol concentration added in the solvent system is small. The solvent character may be unchanged with the addition of such a small phenol concentration.*[7]

Relation of Equilibrium Constant Data to the Radical Species Produced by Controlled Potential Electrolysis. In the course of this experimental study, we observed that the polarograms of pyrazine di- and mono-*N*-oxides in a DMF solvent exhibit a slight increase in wave height at about −1.98 and −2.24 V for the former and the latter respectively (abbreviated henceforth as "the second wave; see Fig. 9). This observation seems to be attributable to the presence of a slight quantity of water[13] introduced into the solvent during the process to remove the dissolved oxygen with N_2 gas. The result in the case of pyrazine mono-*N*-oxide is illustrated in Fig. 9 as an example. The second wave obviously increases in wave height with the addition of a proton donor, ethanol. When controlled-potential electrolysis is carried out at the first and the second reduction waves, the recorded ESR spectra, *i.e.*, the anion radicals produced, are different and depend on the concentration of the proton donor. At any rate, the second wave would be due to the electrode reaction of radical species produced at the first wave, and the reaction is dependent on the proton-donor concentration. These

29) M. Tuboi, *Kagaku no Ryoiki* (in Japanese), **7** (No. 10), 611 (1953).

*7 The presence of supporting electrolyte, tetra-*n*-propylammonium perchlorate 0.1 mol/*l*, would render the system somewhat complicated.

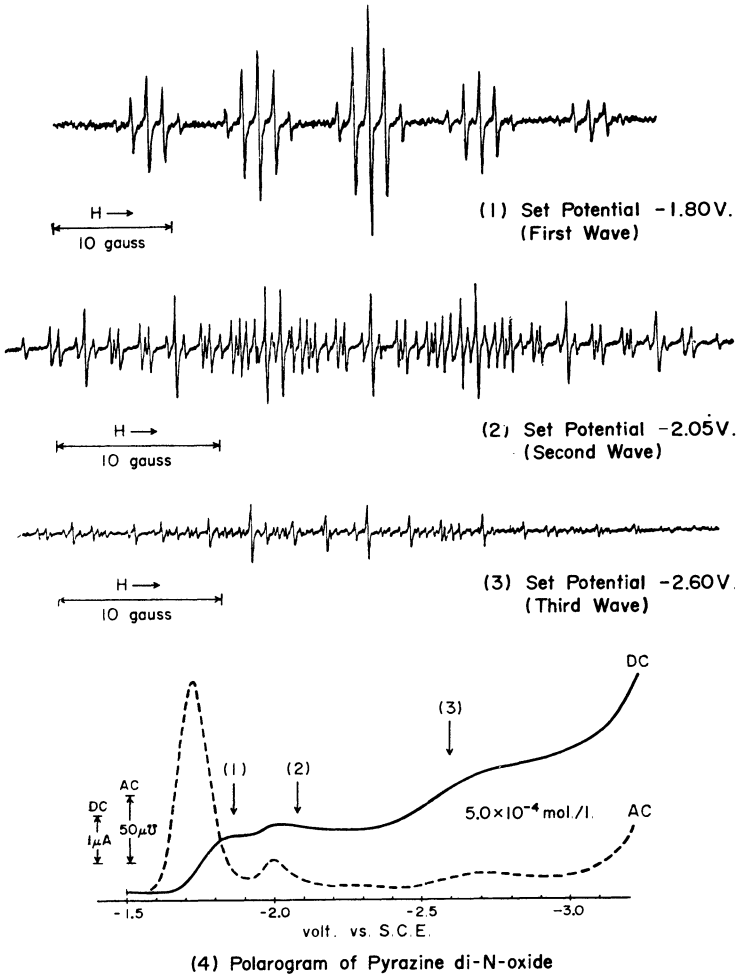

Fig. 10. ESR spectra observed by the controlled potential electrolysis of pyrazine di-*N*-oxide at the three different potentials shown in the polarogram (4) in this figure. ESR spectra (1), (2) and (3) are easily identified to the anion radical of pyrazine di-*N*-oxide, pyrazine mono-*N*-oxide, and pyrazine, respectively, by comparing with the data given in our foregoing paper.[13] But, note that the spectrum (3) is contaminated to some extent by the spectrum (2) of pyrazine mono *N*-oxide anion radical (see footnote of Table 3).

experimental results have been summarized in Table 3, while the ESR spectra observed at three different potentials, corresponding to the first, second, and third reduction waves, are exhibited in Fig. 10 for the case of pyrazine di-*N*-oxide itself without any proton donor. The identification of these spectra is easy,[13] as may be understood from the figure caption. It is understood that incresing the ethanol concentration makes the deoxygenation process of the *N*-oxides more difficult, and that, when the quantity of ethanol added is more than a suitable critical concentration, the ESR spectrum of the pyrazine mono- or di-*N*-oxide anion radical occures even in electrolysis at a more negative potential than that of the first reduction wave. This relation is depicted in Fig. 11, in which the C (~0.3%) and C′ (~2.6%) points, respectively, correspond to the above-mentioned critical concentrations of pyrazine mono- and di-*N*-oxides. These concentrations are almost in agreement with those where hydrogen-bonded and free species exist in an equal molar ratio. In other words, there is an intimate correlation between the hydrogen-bonding equilibrium constant, *K*, and the experimental results shown in Table 3 and Fig. 11. We also note that when ethyl ether instead of ethanol is added to the DMF system, the phenomenon seen in Fig. 11 and Table 3 is not observed. This result

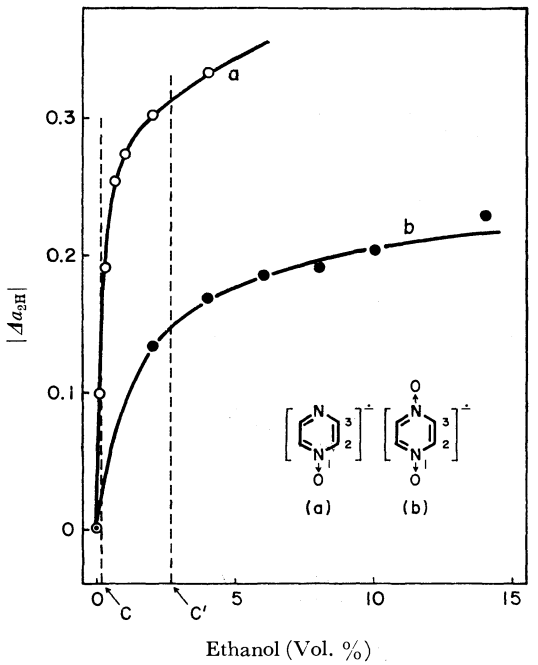

Fig. 11. Change (Δa_{2H}) in $|a_{2H}|$ of the anion radicals shown in this figure upon the addition of ethanol. See text for the meaning of the points C and C'. Solvent: dimethylformamide

suggests the importance of hydrogen-bonding interaction in relation to the experimental results presented above.

The reason for this phenomenon is not completely clear. One possibility is that the anion radical in hydrogen-bonding interaction is more stabilized than in the free radical itself, if no side chemical reaction occurs. Dianion or similar unstable chemical species of the mother compounds produced by the electrolysis at the second or third reduction waves*8 easily bring about electron transfer to the neutral molecule. Thus, the anion radical stabilized by hydrogen bonding has been observed at all reduction waves. If the anion radical is not stabilized, the deoxygenation reaction of the mother compound occurs in the higher-potential electrolysis. The ESR spectra corresponding to that of the anion radical of deoxygenated species have thus been observed.

The authors wish to express their thanks to Professor Saburo Nagakura of the Institute for Solid State Physics, the University of Tokyo and to Professor Yasuo Deguchi of the Department of Chemistry, the University of Kyoto for useful discussions.

*8 In this connection it is noted that the ESR spectrum of 4NPO anion radical is always observed by the electrolysis at the second reduction wave as well as the first wave regardless of the addition of ethanol in DMF solvent. 4NPO anion radical is quite stable, so that the equilibrium such as $(4NPO)^{=}+(4NPO) \leftrightarrows (4NPO)^{-}$ may occur easily whether or not the species is hydrogen bonded. That dianion $(4NPO)^{=}$ is formed at the second reduction wave was experimentally confirmed from the polarographic measurement of 4NPO anion radical itself.[30]

30) H. Miyazaki, K. Nishikida and T. Kubota, presented at the 14th Symposium of Polarography, Hiroshima, Oct. 7, 1968. Abstract No. 7.

BULLETIN OF THE CHEMICAL SOCIETY OF JAPAN VOL. 43 1634—1642 (1970)

Studies on Associated Solutions. I. Excess Volume of Binary Systems of Alcohols with Various Organic Liquids

Koichiro NAKANISHI and Hideko SHIRAI*

Department of Industrial Chemistry, Kyoto University, Sakyo-ku, Kyoto

(Received November 13, 1969)

Excess volumes of mixing have been determined at 25.00°C by pycnometry for eleven binary solutions of methanol and two binary solutions of ethanol with organic liquids. The second components include three aliphatic amines, *n*-butyraldehyde, ethyl acetate, isopropyl ether, anisol, chlorobenzene, acetonitrile, pyridine and nitromethane. The excess volumes of binary solutions containing aliphatic alcohols, which are evaluated from the available density data, were critically reviewed and compared with the present results.

The specific interaction due to the hydrogen bond between the polar groups of different components is primarily responsible for the non-ideal behaviors of binary associated solutions. In binary solutions containing alcohols, for example, the hydrogen bond energy between the hydroxyl group in the alcohol

* Tokyo College of Pharmacy, Shinjuku-ku, Tokyo.

molecules and the proton acceptor group in the other component is estimated to be more than 2 kcal/mol, while the interactions between the inert groups such as the aliphatic hydrocarbon portion of the molecules are almost negligible. This is why the simple lattice theory as proposed by Barker[1] proved considerably successful in interpreting the behavior of the excess functions of associated solutions such as benzene + methanol or chloroform + acetone.

When an alcohol is mixed with other organic compounds, part of alcohol molecules will tend to dissociate from the polymeric aggregates through the hydrogen bond to form other kinds of hydrogen bonds with different kinds of molecules. The degree of dissociation from polymeric species would be dependent on the proton accepting ability of the functional group in the molecule. As a rough first approximation, this may be the most decisive factor in determining the sign and magnitude of the deviation from the ideal solution law.[2]

It is the purpose of the present studies to investigate in detail the dependence of each thermodynamic property of the mixtures of polar and associated liquids including alcohols on the nature of component liquids. The present paper deals with the volume of mixing for thirteen binary solutions containing methanol or ethanol as one component. The results are discussed with available data.

Experimental

Purification of Liquids. Samples of alcohols and other organic liquids were the same as in our recent vapor-liquid equilibrium studies.[3,4] They were prepared as follows. Available reagents of the best grade were dried, whenever necessary, over dehydrating agents such as CaO, and then distilled with a 30 plates fractionating column under atmospheric or reduced nitrogen pressure. Only the middle fraction was used. When the liquids are highly hygroscopic, they are re-distilled immediately before use.

Density Measurement. The densities of pure liquids and solutions were determined with a bicapillary-type pycnometer.[5-7] The capacity of the pycnometer was 10 m*l*. All the measurements were carried out at 25.00°C in a thermostat. The temperature was controlled to ±0.005°C. The present density data seems to be accurate within ±0.00005 g/m*l*.

1) J. A. Barker, *J. Chem. Phys.*, **20**, 1526 (1952).
2) K. Nakanishi, S. Ichinose and H. Shirai, *Ind. Eng. Chem. Fundamentals*, **7**, 381 (1968).
3) K. Nakanishi, H. Shirai and K. Nakasato, *J. Chem. Eng. Data*, **13**, 188 (1968).
4) K. Nakanishi, R. Toba and H. Shirai, *J. Chem. Eng. Japan*, **2**, 4 (1969).
5) K. Nakanishi, This Bulletin, **33**, 793 (1960).
6) K. Nakanishi, N. Kato and M. Maruyama, *J. Phys. Chem.*, **71**, 814 (1967).
7) K. Nakanishi, H. Touhara, K. Sato and M. Nagao, This Bulletin, **41**, 2536 (1968).

Results and Discussion

Density and Excess Volume Data. The density data d_{12} were converted to the excess volumes of mixing V^E by means of

$$V^E = \frac{x_1M_1 + x_2M_2}{d_{12}} - \left(x_1\frac{M_1}{d_1^0} + x_2\frac{M_2}{d_2^0}\right) \quad (1)$$

where x is mole fraction, M is molecular weight, d^0 is density of pure liquid, and subscript 1 refers to alcohols. V^E values for each solution were then fitted to the equation

$$V^E = x_1(1-x_1)\sum_{n=0}^{2}A_n(1-2x_1)^n \quad (2)$$

where constants A_n were determined by the method of least squares.*1

The density and excess volume data are presented in Table 1 and the latter is plotted in Fig. 1. The constants in Eq. (2) and the excess volume for equimolar mixture, $(V^E)_{x_1=x_2}$, are listed in Table 2. As is evident from Eq. (2), the values $(A_0+A_1+A_2)$ and $(A_0-A_1+A_2)$ represent the terminal values of V^E/x_1x_2 at $x_1=0.0$ and $x_1=1.0$. Thus, they are equivalent to $\bar{v}_1-v_1^0$, the difference between the molar volume of pure liquid and the partial molar volume of the same liquid at infinite dilution. They are also shown in Table 2.

The excess volumes of all the systems investigated are negative for the whole composition ranges. The only exception is the nitromethane-rich region of ethanol+nitromethane systems. As seen in Table 2, the largest volume contraction in methanol solutions is observed with *n*-butyraldehyde, which is followed by aliphatic amines (Et_2NH, Et_3N, and *n*-$BuNH_2$), isopropyl ether, pyridine in this order. Other polar liquids show smaller volume contraction. The volume contraction in ethanol solutions is smaller than that in corresponding methanol solutions. It should be remarked that constant A_1 is always negative, which means $\bar{v}_1-v_1^0$ is more positive than $\bar{v}_2-v_2^0$.

Literature Survey. In order to interpret the present data, we found it necessary to compare them with available data. Therefore, we have made an extensive literature survey and analyzed the density data of binary solutions containing methanol, ethanol, propanols, or butanols as a component. The results are summarized in Table A (see Appendix) by listing the value of $(V^E)_{x_1=x_2}$ $(=0.25\,A_0)$ for each system. Most of the data published be-

*1 As seen in Table 1 and Fig. 1, the precision with which the V^E values are established is sometimes not enough for evaluating three constants in Eq. (2). This is the case especially for the systems having small absolute values of V^E. However, it is revealed that the V^E/x_1x_2 *vs.* x_1 plot, though not shown here, cannot be approximated by a straight line. Thus, it is necessary to assign three constants for each system as in Table 1.

TABLE 1. DENSITIES AND EXCESS VOLUMES OF BINARY SOLUTIONS AT 25.00°C

Mole fraction of alcohols x_1	Density d_{12} (g/ml)	Excess volume V^E (ml/mol)
MeOH (1)+*n*-Butyraldehyde (2)		
0.0000	0.80025	0.0
0.2007	0.82740	−2.770
0.3232	0.84534	−4.174
0.4763	0.86369	−5.207
0.5759	0.86627	−5.081
0.6259	0.86393	−4.779
0.6875	0.85793	−4.234
0.7248	0.85309	−3.851
0.7691	0.84531	−3.299
0.8416	0.83057	−2.352
0.9012	0.81609	−1.516
1.0000	0.78624	0.0
MeOH (1)+Ethyl acetate (2)		
0.0000	0.89407	0.0
0.1719	0.88604	−0.050
0.3219	0.87713	−0.069
0.4856	0.86468	−0.072
0.5810	0.85574	−0.074
0.6871	0.84378	−0.072
0.7433	0.83633	−0.068
0.7871	0.82975	−0.056
0.8362	0.82184	−0.058
0.9175	0.80605	−0.031
0.9686	0.79431	−0.012
MeOH (1)+Isopropyl ether (2)		
0.0000	0.71838	0.0
0.1546	0.72511	−0.585
0.2011	0.72719	−0.711
0.3295	0.73316	−0.950
0.5117	0.74237	−1.012
0.6782	0.75302	−0.886
0.7347	0.75760	−0.822
0.7783	0.76128	−0.737
0.8200	0.76570	−0.686
0.8543	0.76866	−0.559
0.8962	0.77383	−0.472
0.9443	0.77975	−0.303
MeOH (1)+Anisol (2)		
0.0000	0.98938	0.0
0.1770	0.97532	−0.099
0.2279	0.97050	−0.118
0.3950	0.95192	−0.194
0.6643	0.90637	−0.218
0.8632	0.84977	−0.161
MeOH (1)+Chlorobenzene (2)		
0.0000	1.10103	0.0
0.1239	1.08507	−0.073
0.4908	1.01618	−0.180
0.5908	0.98895	−0.194
0.6551	0.96859	−0.205
0.7514	0.93219	−0.192
0.8559	0.88235	−0.149
0.9183	0.84541	−0.094
0.9605	0.81654	−0.046
MeOH (1)+*n*-Butylamine (2)		
0.0000	0.73514	0.0
0.1876	0.74477	−0.619
0.3679	0.75723	−1.260
0.4694	0.76426	−1.461
0.5472	0.76924	−1.504
0.7049	0.77818	−1.326
0.8295	0.78310	−0.903
0.9084	0.78532	−0.539
0.9487	0.78606	−0.322
MeOH (1)+Diethylamine (2)		
0.0000	0.69893	0.0
0.0775	0.70593	−0.598
0.1202	0.70970	−0.869
0.1736	0.71467	−1.196
0.2366	0.72072	−1.539
0.2682	0.72380	−1.688
0.3381	0.73071	−1.965
0.4144	0.73867	−2.209
0.4950	0.74625	−2.270
0.5953	0.75574	−2.204
0.6652	0.76186	−2.026
0.7128	0.76575	−1.845
0.7534	0.76903	−1.665
0.8046	0.77268	−1.376
0.8519	0.77596	−1.079
0.9272	0.78137	−0.568
0.9402	0.78238	−0.478
MeOH (1)+Triethylamine (2)		
0.0000	0.72284	0.0
0.0567	0.72608	−0.398
0.1288	0.73028	−0.840
0.1873	0.73383	−1.158
0.2514	0.73770	−1.435
0.2991	0.74094	−1.650
0.3438	0.74400	−1.815
0.4196	0.74939	−2.035
0.4989	0.75538	−2.189
0.5543	0.75965	−2.230
0.5996	0.76337	−2.241
0.6454	0.76658	−2.154
0.6942	0.77035	−2.052
0.7520	0.77491	−1.880
0.8525	0.78135	−1.323
0.9506	0.78561	−0.515
MeOH (1)+Acetonitrile (2)		
0.0000	0.77700	0.0
0.0786	0.77800	−0.027
0.0819	0.77801	−0.026
0.1095	0.77843	−0.039
0.2007	0.77952	−0.062

Table 1 (Continued)

Mole fraction of alcohols x_1	Density d_{12} (g/ml)	Excess volume V^E (ml/mol)
0.3391	0.78147	−0.109
0.5060	0.78386	−0.156
0.5124	0.78377	−0.146
0.5472	0.78417	−0.149
0.6176	0.78513	−0.161
0.6779	0.78586	−0.165
0.7488	0.78627	−0.142
0.8735	0.78703	−0.103
0.8970	0.78712	−0.093
0.9146	0.78714	−0.082
MeOH (1)+Pyridine (2)		
0.0000	0.97810	0.0
0.0407	0.97488	−0.065
0.1874	0.96085	−0.207
0.2638	0.95286	−0.301
0.3736	0.93954	−0.403
0.4491	0.92910	−0.462
0.5012	0.92138	−0.510
0.5497	0.91270	−0.491
0.6109	0.90163	−0.514
0.7608	0.86771	−0.445
0.8276	0.84890	−0.362
0.8919	0.82842	−0.266
0.9491	0.80727	−0.130
MeOH (1)+Nitromethane (2)		
0.0000	1.13117	0.0
0.1427	1.09411	−0.067
0.4616	0.99930	−0.170
0.5797	0.95920	−0.185
0.7157	0.90909	−0.183
0.7941	0.87805	−0.169
0.8704	0.84596	−0.133
EtOH (1)+Diethylamine (2)		
0.0000	0.69893	0.0
0.0419	0.70243	−0.239
0.1206	0.71067	−0.806
0.1734	0.71583	−1.083
0.2309	0.72119	−1.307
0.3121	0.72888	−1.566
0.4199	0.73998	−1.883
0.4808	0.74591	−1.956
0.5638	0.75351	−1.933
0.6485	0.76157	−1.861
0.7240	0.76767	−1.631
0.8098	0.77335	−1.200
0.9131	0.78062	−0.648
1.0000	0.78507	0.0
EtOH (1)+Nitromethane (2)		
0.0000	1.13090	0.0
0.1000	1.09261	0.052
0.1961	1.05727	0.060
0.3436	1.00457	0.051
0.4043	0.98333	0.043
0.4393	0.97138	0.026
0.4734	0.95973	0.015
0.5033	0.94953	0.006
0.6077	0.91429	−0.023
0.7005	0.88359	−0.058
0.7567	0.86497	−0.064
0.8039	0.84989	−0.098
0.8386	0.83838	−0.089
0.9039	0.81709	−0.086

fore 1956 have been collected by Timmermans.[8] We have used his data and also the more recent ones as shown in the footnote of the table.

Dependence of V^E on Various Factors. We call attention to the following evidence obtained from the present work and literature survey.

1. As Fig. 2 illustrates, $(V^E)_{x_1=x_2}$ increases generally with the molar volume of primary normal alcohol. For *c*-C_6H_{12}, Et_2O, $CHCl_3$, and Et_3N, the dependence is somewhat irregular. Since the molar volume of the second component chosen is generally larger than 80 ml/mol, the results indicate that the empirical congruent principle proposed by Brönsted[9] cannot be applied to alcohol solutions.

2. As was shown by Brown,[10] the $(V^E)_{x_1=x_2}$ values for secondary and tertiary alcohols are larger than those for the corresponding normal alcohol. This can also be verified from the cases with acetone and *n*-heptane.

3. The $(V^E)_{x_1=x_2}$ value increases generally with tepmerature. There are some exceptional cases. An inverse dependence is observed with phenol, aniline, and formamide. Note that they are all associated liquids.

4. As regards to the symmetricity of the excess function, it appears that highly a symmetric V^E *vs.* x relation is observed for definite type of second component (*e. g.*, $CHCl_3$, CCl_4, toluene, *etc.*). As was discussed by Rowlinson[11] and van Ness,[12] these liquids have very weak interactions with hydroxyl group and break the alcohol hydrogen bond only insufficiently. However, such high asymmetry

8) J. Timmermans, "Physico-Chemical Constants of Binary Systems in Concentrated Solutions, "Interscience, New York (1959).

9) J. N. Brönsted and J. K. Koeford, *danske vidensk Selsk (Mat. fys. Medd)*, No. 17, 22 (1946).

10) I. Brown and F. Smith, *Aust. J. Chem.*, **15**, 1 (1962).

11) J. S. Rowlison, "Liquids and Liquids Mixtures," 2nd Ed. Butterworths, London (1969).

12) F. Pardo and H. C. van Ness, *J. Chem. Eng. Data*, **10**, 163 (1965).

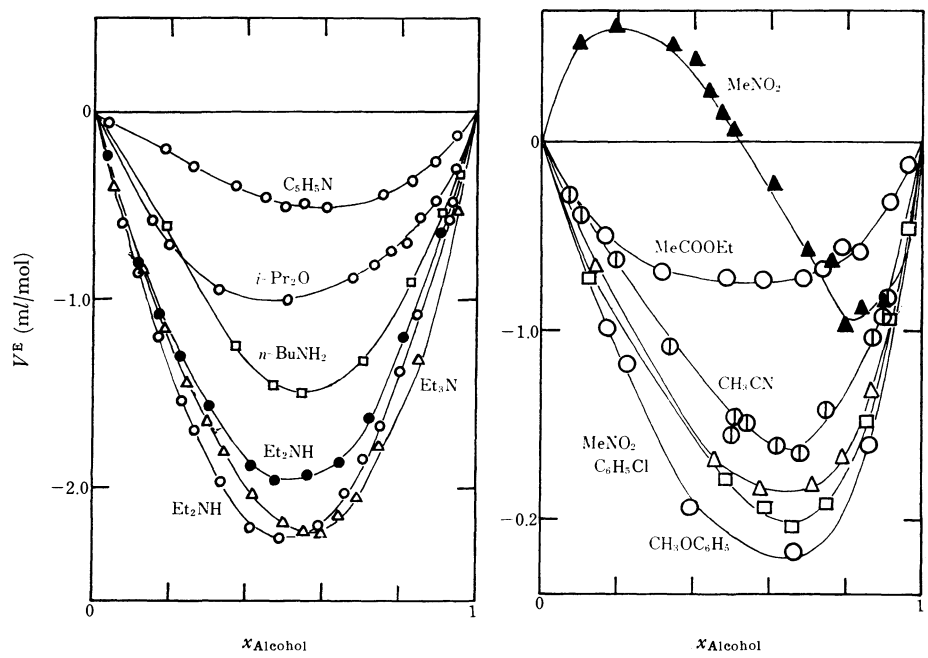

Fig. 1. Excess volumes of 13 binary solutions containing methanol or ethanol at 25°C. Filled marks indicate the data for ethanol solutions.

TABLE 2. CONSTANTS FOR EXCESS VOLUME EQUATION AND DERIVED QUANTITIES

Second component	Constants of Eq. (2)			Excess volume for equimolar mixture	Partial molar volume at infinite dilution	
	A_0	A_1	A_2	$(V^E)_{x_1=x_2}$ [a]	$\bar{v}_1-v_1^0$ [a]	$\bar{v}_2-v_2^0$ [a]
MeOH solutions						
n-Butyraldehyde	−20.553	−1.007	+7.387	−5.138	−12.159	−14.173
Ethyl acetate	− 0.305	−0.021	−0.122	−0.076	− 0.406	− 0.448
Isopropyl ether	− 3.851	−0.092	−1.816	−0.963	− 5.576	− 5.759
Anisol	− 0.840	−0.452	−0.325	−0.210	− 0.713	− 1.618
Chlorobenzene	− 0.766	−0.332	−0.256	−0.192	− 0.690	− 1.355
n-Butylamine	− 5.909	−1.912	+1.449	−1.477	− 2.549	− 6.373
Diethylamine	− 9.063	−3.281	+1.218	−2.266	− 7.517	− 8.173
Triethylamine	− 8.773	−2.094	−0.491	−2.183	− 7.130	−11.317
Acetonitrile	− 0.579	−0.389	−0.167	−0.145	− 0.357	− 1.135
Pyridine	− 1.931	−0.876	−0.176	−0.483	− 1.231	− 2.981
Nitromethane	− 0.691	−0.410	−0.310	−0.173	− 0.590	− 1.411
EtOH solutions						
Diethylamine	− 7.736	−0.585	+0.154	−1.934	− 6.997	− 8.167
Nitromethane	+ 0.044	−0.771	−0.450	+0.011	+ 0.366	− 1.176

[a] ml/mol

is not limited to the cases of practically nonpolar liquids. As an example, EtOH+dioxan or EtOH+nitromethane shows a similar trend. In the cases where the excess volume changes sign, there is always a volume contraction in alcohol-rich region.

5. There exists a sequence in the values of excess volumes of binaries with a given alcohol. The excess volume has an exceptionally large negative value of −2 to 5 ml/mol for the combination of alcohols with the liquids in which a chemical reaction might take place. Binary systems with aldehydes or acids are typical examples. Another group of binary systems which exhibit a large negative V^E is the mixture, aliphatic amine and alcohol. The V^E values are between −0.5 and −2.5 ml/mol. On the other hand, the V^E

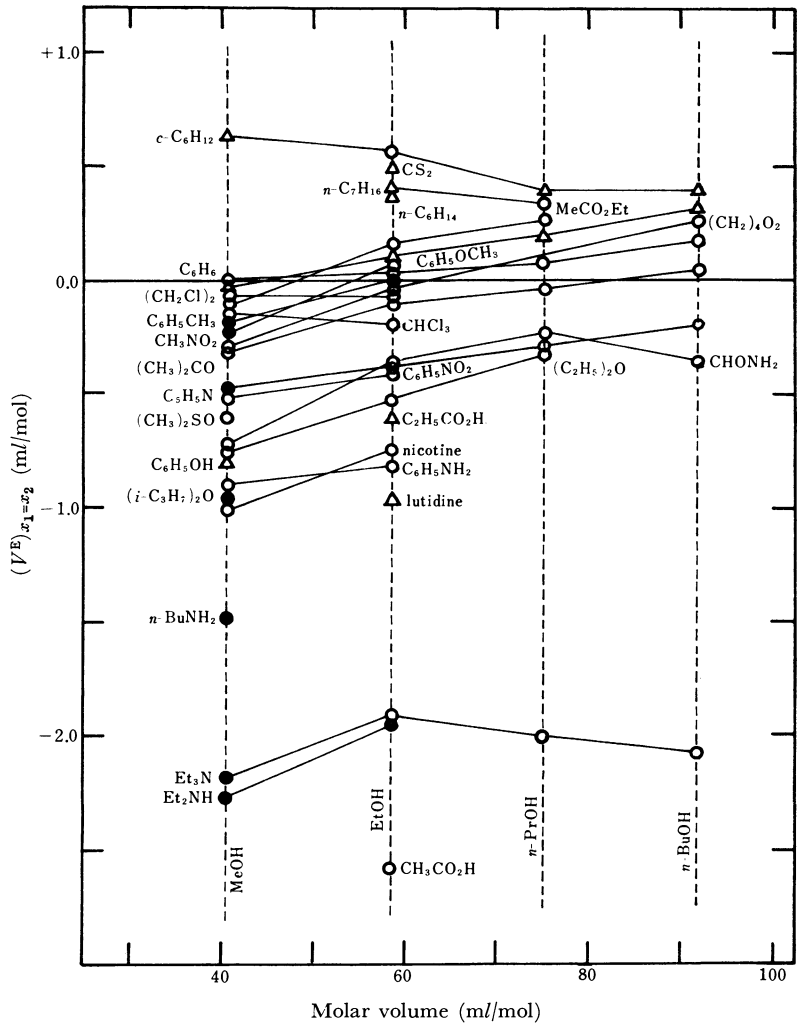

Fig. 2. Relation between excess volume at equimolar mixture and molar volume of alcohol. ● this work, ○ literature value, △ indicates the values at other temperatures than 25°C

values for the systems with paraffin hydrocarbons such as *c*-C_6H_{12}, *n*-C_6H_{14}, *etc.* are positive and usually larger than +0.3 ml/mol. The V^E values for aromatic hydrocarbons and weakly polar liquids are nearly equal to zero or slightly negative. Thus, an obvious relationship between the V^E and the proton affinity of the functional group in the second component is now widely confirmed. This sequence is also parallel with that observed in spectroscopic studies.[2,13] The variation in the values of V^E for aliphatic amines deserves attention. We will compare them with the heat of mixing data in a succeeding paper.[14]

Part of the above observations has been discussed by Brown *et al.*,[10,15] Paraskevopoulos and Missen[16] and Copp and Findlay.[17] The systems alcohol +nonpolar liquid were discussed extensively by Brown *et al.* in their recent paper.[15] We were able to reveal the V^E behaviors for a wide variety of binary solutions. Figure 1 of Ref, 15 shows the behaviors with higher alcohols in certain cases.

Qualitative Interpretation. In view of the present status of solution theories, our analysis is limited to a qualitative description, since the speci-

13) W. Gordy and S. C. Stanford, *J. Chem. Phys.*, **8**, 170 (1940).

14) K. Nakanishi, H. Touhara and N. Watanabe, submitted to This Bulletin, in press.

15) I. Brown, W. Fock and F. Smith, *J. Chem. Thermodynamics*, **1**, 273 (1969).

16) G. C. Paraskevopoulos and R. W. Missen, *Trans. Faraday Soc.*, **58**, 869 (1962).

17) J. L. Copp and T. J. V. Findlay, *ibid.*, **56**, 13 (1960).

fic interactions in alcohol solutions are too complicated. Paraskevopoulos and Missen[16] have concluded in their analysis of V^E data for alcohol+CCl_4 solutions that there are two contributions to the total volume change on mixing, *viz*, the break-up of the alcohol structures and the geometrical fitting of the second component into the remaining alcohol structure. Since the alcohol structure has open cavities, the first contribution should be positive. On the other hand, the geometrical fitting leads to a negative contribution, as it is a process of co-operative accommodation of the second component into the alcohol structure which is accompanied by an interstitial dissolution. This interpretation seems to be valid also for various types of binary alcohol solutions. The fact that the V^E values are generally negative indicates that the second contribution is more important in determining the sign of V^E values. For the co-operative accommodation of the second component to be effective, the molecules should have higher proton accepting ability. The second contribution may then be roughly proportional to the proton accepting ability, though the geometrical characteristics of each molecule will produce an additional effect. A comparison of the V^E data with the spectroscopic data such as "hydrogen bond shift" indicates that this is the case for binary methanol solutions. Existence of a positive contribution reflects on the positive temperature coefficient of V^E. Relative easiness of the break-up of alcohol structure may be responsible for less negative value of secondary and tertiary alcohols than primary alcohols. This will be verified by a comparison with V^E data for alcohol-alcohol mixtures, which are positive with a combination of primary and secondary alcohols. The available data are as follows; The $(V^E)_{x_1=x_2}$ value is +0.005 for MeOH +EtOH (15°C), +0.045 for MeOH+*n*-PrOH (15°C), +0.07 for MeOH+*n*-BuOH (25°C), +0.09 for MeOH+*i*-BuOH (15°C), +0.01 for EtOH+*n*-BuOH (25°C), +0.045 for EtOH+*i*-BuOH (15°C) and 0.00 for *n*-PrOH+*n*-BuOH (15°C).[8,18]

In conclusion, the present data comprise a new and important addition to our knowlegde of excess volume behavior of binary methanol solutions, for which there are less data than for ethanol.

The authors thank K. Nakasato, S. Ichinose, R. Toba and T. Minamiyama for their assistance in experimental work. They also wish to thank Professor N. Watanabe and Mr. H. Touhara for their interest and discussions.

Appendix

The density data are available in literature. We summarize the present information on V^E for binary solutions containing five lower aliphatic alcohols in Table A by listing $(V^E)_{x_1=x_2}$ value.

TABLE A. LITERATURE VALUES OF EXCESS VOLUME FOR EQUIMOLAR MIXTURE OF BINARY SOLUTIONS CONTAINING SOME ALIPHATIC ALCOHOLS

Second component	Excess volume for equimolar mixture $(V^E)_{x_1=x_2}$ (ml/mol)					Reference
	MeOH	EtOH	*n*-PrOH	*i*-PrOH	*n*-BuOH	
n-Hexane		+0.41(25)*				
		+0.41(30)	+0.18(25)	+0.48(22)	+0.08(25)	a, b
		+0.33(6)				
n-Heptane		+0.58(50)	+0.85(30)	+0.58(25)		a, c, d
		+0.42(30)	+0.31(25)			
		+0.32(10)				
i-Octane		+0.59(50)				a
		+0.40(25)				
		+0.29(0)				
Cyclohexane	+0.69(40)	+0.58(30)	+0.40(22)		+0.39(22)	a, e, f, g, h
		+0.49(6)	+0.65(70)			
		+0.58(30)	+0.50(60)			
		+0.58(27)	+0.35(50)			
		+0.58(25)				
		+0.67(45)				
Benzene	0.0 (25)	+0.03(25)	+0.09(25)	+0.27(25)	+0.18(25)	i
Toluene	−0.06(20)	−0.06(25)		+0.26(25)		a, g
	−0.11(25)	−0.07(25)				

18) J. Singh and G. C. Benson, *Can. J. Chem.*, **46**, 1249, 2065 (1968).

TABLE A (Continued)

Second component	Excess volume for equimolar mixture $(V^E)_{x_1=x_2}$ (ml/mol)					Reference
	MeOH	EtOH	*n*-PrOH	*i*-PrOH	*n*-BuOH	
		−0.13(17) −0.07(25) +0.03(45)				
o-Xylene		−0.04(25)				g
m-Xylene		+0.02(25) +0.12(45)				g
p-Xylene		−0.03(25) +0.07(45)				g
Acetone	−0.35(25) −0.40(25)	−0.05(25)	−0.04(20)	+0.24(25) +0.29(25)	+0.06(25)	a, j
Acetic acid		−2.57(25)				a
n-Butyric acid		−0.61(−)				a
Ethyl acetate	−0.08(25)	+0.13(25) +0.19(25) +0.09(0)	+0.24(25)			a, k
Diethyl ether	−0.76(25)	−0.51(25) −0.59(0) −0.55(0)	−0.62(25)			a
Isopropyl ether				−0.51(25)		a
Dioxane	−0.27(22) −0.28(25)	−0.02(30) −0.03(25)			+0.29(25)	a
Phenol	−0.73(20) −0.79(30) −0.83(40)					a, l
Anisol	−0.20(25)	+0.10(25)				a
Chloroform	−0.15(25)	−0.19(25)		+0.02(25)		a, k
Carbon tetrachloride	−0.04(25)	−0.05(25)	−0.10(25)		−0.07(25)	a, m
Methyl iodide		+0.38(25)	+0.42(25)			a
Ethylene dichloride	0.0 (30) 0.0 (40)	+0.10(30) +0.18(40)	+0.32(30) +0.22(40)		+0.4 (30) +0.3 (40)	a
Carbon disulfide		+0.49(30) +0.38(6)				a
Dimethylsulfoxide	−0.60(25)					n
Isopropylamine				−1.32(25)		j
Triethylamine	−2.23(25)	−1.92(25)	−2.02(25)		−2.06(25)	o
Acetonitrile		−0.15(20) −0.01(25)				a, j
Propionitrile				+0.26(25)		j
Aniline	−0.92(20) −1.07(30) −1.34(40) −0.89(25)	−0.51(16.3) −0.75(25) −0.83(25)				a, l

TABLE A (Continued)

Second component	Excess volume for equimolar mixture $(V^E)_{x_1=x_2}$ (ml/mol)					Reference
	MeOH	EtOH	*n*-PrOH	*i*-PrOH	*n*-BuOH	
Pyridine		−0.37(25)				a, p
		−1.31(25)	−0.29(25)		−0.19(25)	
2,4-Lutidine		−0.96(25)				a
Quinoline		−0.5 (25)				a
Nicotine	−1.0 (20)	−0.8 (20)				a
Ethylene chlorohydrin		−0.17(20)			−0.07(25)	a
		−0.18(60)				
Formamide	−0.73(25)	−0.41(25)	−0.23(25)		−0.36(25)	a
	−0.85(40)					
Nitrobenzene	−0.4 (25)	−0.5 (25)				a

* Figures in parentheses indicate the temperature in °C.

a) Ref. 8. b) Ref. 15.
c) S. M. K. A. Gurukul and B. N. Raju, *J. Chem. Eng. Data.* **11**, 501 (1966).
d) H. C. van Ness, C. A. Soczek, G. L. Peloquin and R. L. Machado, *J. Chem. Eng. Data.* **12**, 217 (1967).
e) I. Klesper, *Z, Phys. Chem.* (Frankfurt), **51**, 1 (1966).
f) G. Scatchard and F. G. Satkiewicz., *J. Amer. Chem. Soc.*, **86**, 130 (1964).
g) Ref. 12. h) W. Brzostowski and T. M. Hardman, *Bull. Acad. Pol. Sci.*, **11**, 545 (1963).
i) Ref. 10. j) R. Thacker and J. S. Rowlinson, *Trans. Faraday Soc.*, **50**, 1036 (1954).
k) I. Nagata, Thesis, Kyoto University, 1962.
l) K.M. Sumer and A. R. Thompson, *J. Chem. Eng. Data.*, **12**, 489 (1967).
m) Ref. 16. n) R. J. Fort and W. R. Moore, *Trans. Faraday Soc.*, **61**, 2102 (1965).
o) Ref. 17. p) T. J. V. Findlay and J. L. Copp, *Trans. Faraday Soc.*, **65**, 1463 (1969).

BULLETIN OF THE CHEMICAL SOCIETY OF JAPAN VOL. 43 1642—1649 (1970)

Semi-Empirical SCF MO Method for Systems Including All Valence Electrons

Fumihiko HIROTA and Saburo NAGAKURA

The Institute for Solid State Physics, The University of Tokyo, Roppongi, Minato-ku, Tokyo

(Received November 18, 1969)

For the purpose of evaluating approximate SCF-MO's for systems including all valence electrons, two semi-empirical methods are presented. One of them (method I) uses non-empirical Coulomb integrals and the other (method II) empirical ones. The orbital energies, charge distributions, and excitation energies are calculated for ethylene, acetylene formaldehyde, carbon monoxide and hydrogen cyanide, and are compared with those obtained by the other semi-empirical and non-empirical calculations and also with the corresponding experimental values. The present methods are found to give rather satisfactory results. The calculated orbital energies are improved by the present methods compared with those by the CNDO type calculation. Calculated charge distributions are well coincident with those of the non-empirical SCF calculation. Calculated dipole moments change in parallel with experimental values from a molecule to another, though the former values are generally larger than the latter.

It is desirable to develop a theoretical method convenient for the quantitative or semi-quantitative treatment of all valence electrons of complex molecules. Yoshizumi[1] and also Hoffman[2] extended the simple Hückel method to σ-electron systems

1) H. Yoshizumi, *Trans. Faraday Soc.*, **53**, 125 (1957).

2) R. Hoffman, *J. Chem. Phys.*, **39**, 1397 (1963).

in spite of several difficulties[3] inherent to the method. More quantitative theories for all valence electrons analogous to the Pariser-Parr-Pople[4] method for π-electrons were developed.[5-13]

One of them is the CNDO (Complete Neglect of Differential Overlap) method developed by Pople, Santry and Segal.[8,9] This method, in spite of its simplicity, brought about much success in explaining several points such as the charge distributions of diatomic molecules and the bending force constants of AH_2 and AH_3 type molecules (A; C, N and O). It failed, however, in explaining several problems, for example, the streching force constants[9] or the charge densities at hydrogen atoms for a series of CH_4, C_2H_6, C_2H_4 and C_2H_2.[10]

Several other methods[14-16] are presented along the lines of considering all valence electrons and of evaluating semiempirically Coulomb integrals. Yonezawa *et al.*[16] obtained rather satisfactory results for charge distributions, ionization potentials and excitation energies by the aid of the method (called hereafter the Y-Y-K method) developed on this line. But in details there are still several difficulties; for example, the orbital energy separation is usually too small compared with those obtained by the exact non-empirical SCF calculation. This seems to be mainly due to the use of empirical Coulomb integrals. In this connection, the following points may be pointed out as the problem of the CNDO and Y-Y-K method. It may be expected[17] that σ-orbitals are more closely packed than π-orbitals and therefore that the Coulomb integrals are larger for σ-electrons than for π-electrons. In the CNDO method all one-center Coulomb integrals are taken to be equal to one another and two-center Coulomb integrals are independent of the character of atomic orbitals. In the Y-Y-K method, one-center Coulomb integrals are evaluated differently for s and p orbitals but the individuality of two-center Coulomb integrals is not considered except for the cases where one-center integrals are different. This effect is expected to be especially great for the molecules which have both σ- and π-electrons.

In this paper, we present improved semi-empirical methods suitable to the theoretical treatment of systems including all valence electrons and compare the results obtained for some small molecules with those by the other methods.

Theoretical

Roothaan's equation of LCAO SCF[18] is employed, the atomic integrals necessary for the calculation being evaluated by the following two methods. In method I, the integrals are evaluated approximately but non-empirically except for off-diagonal core integrals; in method II, the integrals are evaluated empirically. The essential points of our calculation are described below.

1. Molecular orbitals are expressed as linear combinations of all the valence atomic orbitals (AO's) centered on each atom except for the 1s orbitals of carbon, nitrogen and oxygen which are pushed into the cores. The Slater type AO's are taken, if necessary, the orbital exponent being determined by Slater's rule except for the hydrogen 1s AO, the effective nuclear charge of which is taken to be 1.2.

2. In Roothaan's equation,[18] the overlap integrals and two-electron integrals including two-center differential overlap are disregarded. This means that all the one-center integrals and the Coulomb type two-center integrals are taken into account in the present calculation.

3. The one-center core integrals are calculated non-empirically in method I with the core Hamiltonian H^{core};

$$H^{\text{core}} = \sum_{\mu} H_{\mu}^{\text{core}} = \sum_{\mu}\left[-\frac{1}{2}\Delta_{\mu} - \sum_{A}\frac{Z_A}{R_{A\mu}} \right] \qquad (1)$$

where Z_A is taken as the number of valence electrons in atom A and $R_{A\mu}$ is the distance between the μth electron and atom A. But for 2s orbital, a different method based on the experimental ionization potentials (I.P.) are used as follows;

$$\langle 2s|H^{\text{core}}|2s\rangle = \langle 2p|H^{\text{core}}|2p\rangle + (\text{I.P.}(2s) - \text{I.P.}(2p)) \qquad (2)$$

In method II, this integral for AO x is evaluated

3) K. Morokuma, H. Kato, T. Yonezawa and K. Fukui, This Bulletin, **38**, 1263 (1965).

4) R. Pariser and R. G. Parr, *J. Chem. Phys.*, **21**, 416 (1953), J. A. Pople, *Trans. Faraday Soc.*, **49**, 1375 (1953).

5) H. A. Pohl, R. Rein and K. Appel, *J. Chem. Phys.*, **41**, 3385 (1964).

6) N. L. Allinger and J. C. Tai, *J. Amer. Chem. Soc.*, **87**, 1227 (1965).

7) S. Katagiri and C. Sandorfy, *Theor. Chim. Acta*, **4**, 203 (1966).

8) J. A. Pople, D. P. Santry and G. A. Segal, *J. Chem. Phys.*, **43**, s129 (1965).

9) J. A. Pople and G. A. Segal, *ibid.*, **43**, s136 (1965); *ibid.*, **44**, 3289 (1966).

10) J. A. Pople and M. Gordon, *J. Amer. Chem. Soc.*, **89**, 4253 (1967).

11) D. W. Davis, *Chem. Phys. Lett.*, **2**, 173 (1968).

12) J. M. Sichel and M. A. Whitehead, *Theor. Chim. Acta*, **11**, 239 (1968).

13) J. M. Sichel and M. A. Whitehead, *ibid.*, **11**, 254 (1968).

14) G. Klopman, *J. Amer. Chem. Soc.*, **86**, 4550 (1964).

15) M. J. S. Dewar and G. Klopman, *ibid.*, **89**, 3089 (1967); **89**, 3966 (1967).

16) T. Yonezawa, K. Yamaguchi and H. Kato, This Bulletin, **40**, 536 (1967).

17) See, for example, B. J. Ransil, *Rev. Mod. Phys.*, **32**, 245 (1960).

18) C. C. J. Roothaan, *ibid.*, **23**, 69 (1951).

$$\langle x|H^{\text{core}}|x\rangle = -\text{I.P.}(x) - \sum_{i\neq x} n_i\left\{(xx|ii) - \frac{1}{2}(ix|ix)\right\} \quad (3)$$

where n_i is the occupation number of the ith orbital and the summation is taken over all valence orbitals.

4. One-center Coulomb integrals are estimated non-empirically in method I by using the Slater type functions.

In method II, the Pariser approximation[19] is used for (pp|pp) type integral. Since the valence states of atoms, particularly of hetero-atoms can not be determined exactly, we assume the following valence states:*1 sp^3 for carbon, sp^4 for nitrogen and s^2p^4 for oxygen. The other one-center Coulomb integrals are estimated by making use of the Slater-Condon parameters[20] F_2^{pp} and G_1^{sp} obtained from atomic spectra of neutral atoms:*2

$$\begin{aligned}(pp|p'p') &= F_0^{pp} - 2F_2^{pp}\\ (sp|sp) &= G_1^{sp}\\ (pp'|pp') &= 3F_2^{pp}\end{aligned} \quad (4)$$

where p and p′ are orthogonal to each other and F_0^{pp} is estimated by using the Pariser approximation. The integral (ss|pp) is taken as the arithmetic mean of (ss|ss) and (pp|pp).

5. Two-center Coulomb integrals are evaluated by using the following approximate formulas of Roothaan's exact ones[21] for several sub-integrals.*3

$$\begin{aligned}[3S|3S] &= \frac{1}{\rho}\left[1 - S^2/\{(1-\tau^2)^7\cdot(1+0.465\rho)\}\right]\\ [3S|1S] &= \frac{1}{\rho}\left[1 - \frac{S^2}{-0.2 + (1-1.66\tau)\rho}\right]\\ [3S|3D\Sigma] &= \frac{1}{(1-\tau)^2\rho^3}[1-S^2\cdot(1+0.5\rho)]\\ [3S|3P\Sigma] &= \frac{1}{(1-\tau)\rho^2}[1-S\cdot(1+0.12\rho)]\end{aligned} \quad (5)$$

Here S means the overlap integral between two s type AO's, $\tau=(\zeta_a-\zeta_b)/(\zeta_a+\zeta_b)$, ζ_a and ζ_b being taken as the orbital exponents of two AO's, and $\rho=R_{AB}(\zeta_a+\zeta_b)/2$, R_{AB} being the distance between atoms A and B. The following more approximate formulas are employed for other smaller sub-integrals.

$$\begin{aligned}[3P\Sigma|3P\Sigma] &= \frac{2}{\rho^3}(1-2S^2)\\ [3P\pi|3P\pi] &= \frac{1}{\rho^3}\left(1-\frac{16}{\rho^3}\right)\\ [3D\Sigma|3D\Sigma] &= \frac{6}{\rho^5}\left(1-\frac{3.76}{\rho^4}\right)\\ [3D\Delta|3D\Delta] &= \frac{1}{\rho^5}\left(1-\frac{7.5}{\rho^2}\right)\end{aligned} \quad (6)$$

In method II, the semi-empirical values for these integrals are evaluated from the corresponding non-empirical values in method I by using the following formulas:

$$\begin{aligned}(s_As_A|p_Bp_B)^{emp} &= (s_As_A|p_Bp_B)^n\\ &\quad - \Big[\frac{1}{2}(s_A|s_B)^2\{(s_Bs_B|p_Bp_B)^n - (s_Bs_B|p_Bp_B)^{emp}\}\\ &\quad + (p_A|p_B)^2\{(s_As_A|p_Ap_A)^n - (s_As_A|p_Ap_A)^{emp}\}\\ &\quad + (s_A|p_B)^2\{(p_Bp_B|p_Bp_B)^n - (p_Bp_B|p_Bp_B)^{emp}\}\\ &\quad + (s_A|p_B)^2\{(s_As_A|s_As_A)^n - (s_As_A|s_As_A)^{emp}\}\Big]\\ (s_Ap_A|p_Bp_B)^{emp} &= (s_Ap_A|p_Bp_B)^n\\ &\quad - \Big[\frac{1}{2}(s_A|s_B)(p_A|s_B)\{(s_Bs_B|p_Bp_B)^n\\ &\quad - (s_Bs_B|p_Bp_B)^{emp}\}\\ &\quad + (s_A|p_B)(p_A|p_B)\{(p_Bp_B|p_Bp_B)^n\\ &\quad - (p_Bp_B|p_Bp_B)^{emp}\}\Big]\end{aligned} \quad (7)$$

Here superfixes emp and n mean empirical and non-empirical values, respectively. These formulas are obtained by expanding the AO of atom A with regard to the position of atom B.*4

6. The off-diagonal core integral (β_{ab}) between AO's a and b is evaluated by the following formula;

$$\beta_{ab} = C\cdot S_{ab}\left\{\left(a\left|\frac{Z_A}{R_{A\mu}}\right|a\right) + \left(b\left|\frac{Z_B}{R_{B\mu}}\right|b\right) - \left(a\left|\frac{Z_B}{R_{B\mu}}\right|a\right) - \left(b\left|\frac{Z_A}{R_{A\mu}}\right|b\right)\right\}\Big/4 \quad (8)$$

where C is an empirical parameter and is commonly taken $C=0.92$ for all molecules. S_{ab} is the overlap integral between AO's a and b. β_{ab} is taken for both neighboring and non-neighboring AO's.

Our treatment is similar to the NDDO (Neglect of Diatomic Differential Overlap) method of Pople *et al.*,[8] in the sense that the overlap integrals and the two-center differential overlaps are disregarded. The integrals of these two types may be expected to be cancelled out when Löwdin's orthogonalized

*1 The (pp|pp) type integrals are not so sensitive to the valence state of each atom.

*2 The use of F_2^{pp} and G_1^{sp} for neutral atoms seems to be incompatible with the fact that F_0 evaluated by the Pariser approximation is that of the corresponding anion. But F_2 and G_1 are so small that the difference between the neutral and anionic values may be safely disregarded.

19) R. Pariser, *J. Chem. Phys.*, **21**, 568 (1953).

20) Concerning the use of this parameter, see for example, T. Anno, *ibid.*, **29**, 1161 (1958).

*3 The meaning of symbols like [3S|3S], [3S|3S], — are the same as described in Ref. 21.

21) C. C. J. Roothaan, *J. Chem. Phys.*, **19**, 1445 (1951).

*4 The formulas of this type were first used by Matsushita for the theoretical study of π-electron systems. T. Matsushita, private communication.

Table 1. One-center and two-center integrals calculated by the aid of the Slater AO's and the Löwdin OAO's

Type	AO integrals	OAO integrals
$(h\|H^{core}\|h)^0$*	−13.60	−12.45
$(p\|H^{core}\|p)^0$	−54.28	−51.40
$(hh\|hh)^0$	17.01	19.22
$(\sigma\sigma\|\sigma\sigma)^0$	16.93	18.42
$(\pi\pi\|\pi\pi)^0$	16.93	17.62
(hh|ss)	10.32	9.85
$(\sigma\sigma\|\sigma\sigma)$	11.92	11.30
$(\sigma\sigma\|\pi\pi)$	10.35	10.01
$(\pi\pi\|\pi\pi)$	9.35	9.13

* The estimation is made for the case of C_2H_4, the 1s orbital exponent of hydrogen being taken to be 1.0, and 2s and 2p orbital exponents for carbon to be 1.59. Superscript 0 means the one-center integrals.

orbitals (OAO's)[22] are taken as the basis AO's as was pointed out by Fischer-Hjalmars[23] for π-electron systems. This cancellation may be expected to be less perfect for σ-orbitals than for π-orbitals, but this approximation is essential for the simplification of the calculation. Furthermore, we neglect the changes of the remaining integrals (except for β) caused by the transformation of the basis set from the Slater AO's to the OAO's.*5 According to our estimation, they are larger for σ-orbitals than for π-orbitals, but are not fatal as is shown in Table 1.

Since the Slater type 2s orbital is not orthogonal to the inner 1s orbital, the direct calculation leads to a too large absolute value of the one-center core integral for this orbital. The ionization potential for an electron in orbital x can be obtained by Koopmans' theorem[24] as the sum of the core integrals and electron repulsion part. Therefore, if the repulsive part is considered to be equal to each other for 2s and 2p electrons, the difference in the core integrals for these orbitals may be thought to be equal to that in the ionization potentials. Thus we obtain Eq. (2).

The approximations adopted to the evaluation of the two-center Coulomb integrals are not always necessary. In view of computational convenience, however, the present formulas are satisfactory from the practical point of view. The present approximate formulas are applicable to the rather small region of orbital exponents and atomic distances. In the sub-integrals of Roothaan's formulas which are

Table 2. Comparison between approximate and exact integral values

Type[a]	Approximate values	Exact values
For Ethylene		
(ss|ss)	9.99 eV	9.98 eV
$(ss\|\pi\pi)$	9.56	9.47
$(\sigma\sigma\|\sigma\sigma)$	11.71	11.86
$(\pi\pi\|\pi\pi)$	9.14	9.42
$(\sigma\sigma\|\pi\pi)$	10.42	10.41
$(ss\|s\sigma)$	1.89	1.86
For CO of Formaldehyde		
(ss|ss)	11.23	11.22
$(ss\|\sigma\sigma)$	11.93	11.84
$(\sigma\sigma\|ss)$	12.61	12.56
$(\sigma\sigma\|\sigma\sigma)$	13.56	13.57
$(\pi\pi\|\pi\pi)$	10.28	10.40
$(\pi\pi\|\pi'\pi')$	10.03	10.10

a) Here, s, σ, π and π' mean 2s, $2p\sigma$, $2p\pi$ and $2p_y$ (y-axis is in the molecular plane) AO's, whose orbital exponents are determined following Slater's rule.

common to several atomic integrals, the term including $\exp(-2\rho)$ is approximated by the term including the square of overlap integrals for the first four formulas. For other small sub-integrals, the more approximate formulas are employed. These formulas give the resultant integrals different by less than 6% from the exact values as is shown in Table 2.

In the evaluation of the semi-empirical two-center Coulomb integrals in method II, the following three factors are considered. First the correlation effect discussed by many researchers,[25] second the effect of the reorganization of orbitals caused by the one-electron ionization or excitation,[26] and third the expansion of the excited orbitals.[27] These effects may affect two-center Coulomb integrals, even when overlap integrals are zero. By considering these effects we evaluated the integrals by Eq. (7) obtained by expanding the AO of atom A with regard to the position of atom B. When the same method is applied to π-electron systems, the evaluated values are somewhat larger than those obtained by the uniformly charged sphere model or by the Ohno approximation.[28]

The formula for the off-diagonal core integral is obtained by adopting the Mulliken approximation and by considering the effect of the orthogonalization to the first order of overlap integrals between

22) P. O. Löwdin, *ibid.*, **18**, 365 (1950).
23) I. Fischer-Hjalmars, *ibid.*, **42**, 1962 (1965).
*5 Cook, Hollis and McWeeny used the hybrid orbitals as basis AO's to avoid this difficulty, but their method is more complicated than ours (D. B. Cook, P. C. Hollis and R. McWeeny, *Mol. Phys.*, **13**, 553 (1967)).
24) T. Koopmans, *Physica*, **1**, 104 (1933).
25) See, for example, O. Sinanoglu, "Advances in Chemical Physics," Vol. VI, ed. by I. Prigogine, Interscience Publishers, London (1964), p. 315.
26) M. K. Orloff and O. Sinanoglu, *J. Chem. Phys.*, **43**, 49 (1965).
27) S. Huzinaga, *ibid.*, **36**, 453 (1962).
28) K. Ohno, *Theor. Chim. Acta* (Berl.), **2**, 219 (1964).

the nearest neighbouring atoms. The value of parameter C is optimized for the orbital energies of ethylene.

The computation is carried out by a HITAC 5020E electronic computer located at the Computer Center of the University of Tokyo. Several quantities are calculated with the aid of the evaluated orbital wavefunctions and energies. The atomic

TABLE 3. ORBITAL ENERGIES (eV) OF C_2H_4

Symmetry[a]	Method I	Method II	CNDO[b]	Y-Y-K[c]	Non-empirical[d]	Inoization[e] potential (eV)
$b_{1u}(\pi)$	−10.96	−11.85	−10.93	−12.24	−10.17	10.48
b_{1g}	−12.59	−13.39	−10.98	−13.98	−14.00	12.51
a_g	−15.00	−14.06	−13.01	−13.75	−15.81	14.9
b_{2u}	−18.90	−18.41	−17.15	−15.65	−17.81	15.63
b_{3u}	−22.62	−20.42	−19.48	−19.70	−21.66	19.13
a_g	−30.60	−25.07	−26.01	−24.09	−28.29	—

a) The molecular plane is taken to be xy plane and x axis is parallel to the C=C bond.
b) Ref. 13.
c) Ref. 16.
d) J. M. Schulman, J. W. Moskowitz and C. Hollister, *J. Chem. Phys.*, **46**, 2759 (1967).
e) Ref. 30.

TABLE 4. ORBITAL ENERGIES (eV) OF H_2CO

Symmetry[a]	Method I	Method II	Y-Y-K[b]	Non-empirical[c]	Ionization[d] potential (eV)
$b_1(n)$	−11.99	−11.71	−13.36	−10.76	10.86
$b_2(\pi)$	−14.07	−13.91	−14.28	−13.53	14.4
a_1	−15.44	−16.10	−14.85	−16.14	16.0
b_1	−18.85	−20.03	−21.84	−18.40	16.9
a_1	−23.31	−24.21	−22.15	−22.62	21
a_1	−36.80	−37.82	−34.06	−38.07	—

a) The molecular plane is taken to be xy plane and x axis is parallel to the C=O bond.
b) Ref. 16.
c) M. D. Newton and W. E. Palke, *J. Chem. Phys.*, **45**, 2329 (1966).
d) Ref. 31.

TABLE 5. ORBITAL ENERGIES OF CO

Character	Method I	Method II	Y-Y-K[a]	Non-empirical[b]	Ionization[c] potential (eV)
σ	−14.50	−14.09	−14.43	−15.08	14.01
π	−16.33	−15.42	−15.32	−17.40	16.51
σ	−21.11	−22.14	−20.50	−21.87	19.72
σ	−42.73	−40.03	−35.17	−41.39	—

a) Ref. 16.
b) A. D. McLean and M. Yoshimine, "Table of Linear Molecule Wavefunctions," *IBM J. Research and Development* (1967).
c) Ref. 30.

TABLE 6. ORBITAL ENERGIES OF HCN

Character	Method I	Method II	CNDO[a]	Non-empirical[b]	Ionization[c] potential (eV)
π	−14.52	−13.42	−13.33	−13.48	13.91
σ	−15.80	−15.31	−13.72	−15.83	
σ	−22.93	−21.63	−20.69	−22.69	
σ	−35.73	−34.81	−27.60	−33.60	

a) Ref. 12.
b) Ref. b in Table 5.
c) J. D. Morrison and A. J. C.Nicholson, *J. Chem. Phys.*, **20**, 1021 (1952).

population of a certain AO is calculated as the sum of the square of the coefficients of the corresponding AO in the occupied MO's. This definition coincides with Mulliken's gross or net atomic population in this case in which overlap integrals are disregarded. Dipole moments are calculated by the method proposed by Pople and Segal.[9] Excitation energies are calculated by considering the configuration interaction among several singly excited configurations of lower energy.

Results and Discussion

In this section, we present the results obtained by applying the above-mentioned two methods to several small molecules and compare them with those of other calculations and also with the experimental results.

Orbital Energies. In Tables 3—6 are shown the occupied orbital energies calculated by the present authors. In these tables the results calculated by other theoretical methods are also shown for the purpose of comparison, together with the observed ionization potentials which correspond to the absolute values of orbital energies according to Koopmans' theorem.[24] Recently, the ionization potentials higher than the first one are measured by the photo-electron spectroscopy technique for various molecules.[29,30]

Concerning ethylene (Table 3), the original CNDO/2 parameters failed in giving the orbital energies in correct order. Modifying the parameters, Sichel and Whitehead[13] obtained by the CNDO method the results which are fairly in good agreement with the observed ionization potentials, but the separation between the highest and second highest occupied orbitals is still too small. In the result of the Y-Y-K method, the order of the second highest and third highest occupied orbitals is reverse to that obtained by the other methods. Either of the present results obtained by methods I and II is generally in rather good agreement with the result obtained by the non-empirical calculation and with the observed ionization potentials. In particular, it may be noticed that the present methods lead to better agreement with the ionization potentials for the higher three orbital energies than the other non-empirical or semi-empirical methods.

The result of ethylene obtained by method II shows rather smaller orbital energy separations compared with that of method I. This tendency holds for formaldehyde, carbon monoxide and hydrogen cyanide, too. Anyhow, from the results in Tables 3—6, it is revealed that both the empirical and non-empirical Coulomb integrals in the present methods are applicable to the theoretical prediction of ionization potentials.

Charge Density. The charge density on the hydrogen atom in several molecules are listed in Table 7. The present results as well as those by the other methods show that the positive charge on hydrogen increases in the order of $CH_4 < C_2H_4 < C_2H_2$. This is coincident with the fact that the hydrogen atom of acetylene is rather easily replaced by metal and also with the fact that the dipole moments of C–H bonds in these molecules estimated from the absolute intensities of the infrared absorption spectra[31] increase in the same order. Comparing the results of methods I and II with each other, the former gives a little smaller values for all molecules under consideration than the latter. The results of INDO[32] calculation give considerably large values compared with those by other methods.

In Table 8, the calculated atomic population of ethylene is shown. Our results show rather good agreement with those of the non-empirical calculation except for the population on the 2p orbital. The value calculated by the present method is smaller than that by the non-empirical one, but

Table 7. Charge density on H

	Method I	Method II	CNDO[a]	Non-empirical	INDO[d]
CH_4	0.941	0.988	0.987	0.87[b]	1.009
C_2H_4	0.891	0.920	0.985	0.86	1.001
C_2H_2	0.887	0.901	0.937	0.81	0.947
HCN	0.876	0.904	0.928	0.78	—
H_2CO	0.917	0.931	1.001	0.90[c]	—

a) Ref. 10.
b) W. Palke and W. Lipscomb., *J. Amer. Chem. Soc.*, **88**, 2384 (1966).
c) P. L. Goodfriend, F.W. Birss and A.B.F. Duncan, *Rev. Mod. Phys.*, **32**, 307 (1960).
d) W. J. Hehre and J. A. Pople, *Chem. Phys, Lett.*, **2**, 379 (1968).

Table 8. Atomic population of ethylene

	Method I	Method II	PNDDO[a]	Non-empirical[b]
H	0.899	0.920	0.985	0.860
C_{2s}	1.194	1.149	1.243	1.197
$C_{2\sigma}$	1.017	1.008	0.844	1.013
C_{2y}	0.990	1.002	0.845	1.072

a) Ref. 15 (PNDDO means Partial Neglect of Diatomic Differential Overalp).
b) Ref. b in Table 7.

29) M. I. AL-Joboury and D. W. Turner, *J. Chem. Soc.*, **1964**, 4434.
30) G. R. Brundle and D. W. Turner, *Chem. Commun.*, **7**, 314 (1967).
31) L. A. Gribov and V. N. Smirnov, *Soviet Physics Uspekhi*, **4**, 919 (1962).
32) J. A. Pople, D. L. Beveridge and P. A. Dobosh, *J. Chem. Phys.*, **47**, 2026 (1967).

TABLE 9. ATOMIC POPULATION OF H_2CO

	Method I	Method II	CNDO[a]	Non-empirical[b]
H	0.917	0.931	0.958	0.90
s_c	1.230	1.230	1.184	1.42
σ_c	0.819	0.837	0.958	0.63
y_c[c]	0.980	0.985	0.990	1.01
s_o	1.862	1.853	1.731	1.97
σ_o	1.300	1.336	1.348	1.08
y_o[c]	1.963	1.932	1.926	1.98
π_c	0.990	0.981	0.978	1.04
π_o	1.010	1.019	1.022	0.96

a) Ref. 9.
b) Ref. c in Table 7.
c) The direction of y is prependicular to the C=O bond in the molecular plane.

TABLE 10. ATOMIC POPULATION OF CO

AO	Method I	Method II	CNDO[a]	Non-empirical[b]
s_c	1.59	1.63	1.70	1.68
σ_c	0.96	0.97	1.08	0.96
s_o	1.84	1.80	1.70	1.85
σ_o	1.69	1.52	1.51	1.51
π_c	0.65	0.69	0.65	0.63
π_o	1.31	1.35	1.35	1.37

a) Ref. 9.
b) R. Ransil, *J. Chem. Phys.*, **30**, 1113 (1959).

not so extremely small as the result by Dewar and Klopman.[15]

In Table 9, the atomic population of formaldehyde is shown. According to our results the population on the $p\pi$ orbital is larger for oxygen than for carbon. This is reverse to the results by the non-empirical calculation. In the other points, the atomic populations of formaldehyde calculated by the present method are well coincident with those by the non-empirical calculation.

TABLE 11. DIPOLE MOMENTS OF SOME SIMPLE MOLECULES

Molecule	Method I	Method II	CNDO[a]	Exp.[b]
CO	−1.40	−1.56	−1.28	−0.13
NH_3	3.01	1.80	1.99	1.47
H_2CO	3.22	2.97	1.27	2.30
HCN	4.10	3.10	2.07	2.95

a) Ref. 9.
b) A.L. McClellan, "Tables of Experimental Dipole Moments," W. H. Freeman & Co., San Francisco, California (1963).

Now let us turn to the atomic population of carbon monoxide shown in Table 10. According to our calculation, the oxygen atom is negatively charged in accordence with the non-empirical calculation, while the CNDO method leads to the reverse result. Concerning the total electron density on the oxygen atom, the result of method I (6.15) is well coincident with that of the non-empirical calculation (6.10) and method II gives a little smaller value (6.02). Since the same tendency is also found for the result by the Y-Y-K method, this seems to be an intrinsic to the use of the empirical integral values.

As a general tendency found for the calculated atomic populations, method II gives the smaller value for the population of 2s orbital than the non-empirical calculation. This is probably because the diagonal core integrals for 2s are a little underestimated (in absolute values) in method II.

The calculated dipole moments of several mo-

TABLE 12. EXCITATION ENERGIES (eV)

	Symmetry of excited state	Character of transition	Method I	Method II	Number of configuration**	Exp.
C_2H_4	$^3B_{3u}$	π-π^*	6.70	4.45	(4)	4.6[a]
	$^1B_{3u}$	π-π^*	10.80	7.84	(4)	7.6[b]
H_2CO	$^3A_2$	n-π^*	4.98	4.17	(4)	3.0[c]
	$^1A_2$	n-π^*	8.46	5.32	(4)	4.2[d]
	$^1A_1$	π-π^*	11.38	9.86	(3)	8.0[d]
CO	$^3\Pi$	n-π^*	8.73	7.10	(4)	6.22[e]
	$^1\Pi$	n-π^*	11.57	8.90	(4)	8.74[e]
	$^3\Sigma^+$	π-π^*	11.55	7.60	(3)	8.25[e]
	$^1\Sigma^+$	π-π^*	13.92	9.41	(3)	10.8[e]

** The number of configurations taken in the configuration interaction calculation is shown in parentheses.
a) D. F. Evans, *J. Chem. Soc.*, **1960**, 1735.
b) P. G. Wilkinson and R. S. Mulliken, *J. Chem. Phys.*, **23**, 1895 (1955).
c) A. D. Cohen and C. Reid, *ibid.*, **24**, 85 (1956).
d) H. Sponer and E. Teller, *Rev. Mod. Phys.*, **13**, 75 (1941).
e) H. Brion and C. Moser, *J. Chem. Phys.*, **32**, 1194 (1960).

lecules are shown in Table 11 compared with the experimental values. We can find a parallelism between the calculated and experimental values, though the former values are generally larger than the latter. Generally speaking, the dipole moment values calculated by method I are better coincident with experimental ones than those by method I.

Excitation Energies. In Table 12, the excitation energies calculated for ethylene, formaldehyde and carbon monoxide are listed. In the both methods the calculated energies are too high compared with the experimental results. This point may be improved by selecting the optimum β_{ab} value for the calculation of excited state quantities.

According to method I, the lowest singlet and triplet excited states of ethylene include σ—σ^* excited configurations by 30 and 22%, respectively, and the separation between them is a little improved by the configuration interaction compared with the single configuration picture. The separation is evaluated to be 4.16 and 3.39 eV by methods I and II, respectively. The latter is well coincident with the observed value (3.0 eV). The situation is the same for the separation between the singlet and triplet $n\rightarrow\pi^*$ states of formaldehyde. That is to say, the value calculated by method II agrees well with the observed one, though the value evaluated by method I is somewhat larger than the experimental value.

Concerning the orbital energies and atomic populations, the both methods give similarly good results, while method II is better for the excitation energies than method I. It may be noticed that method I gives fairly satisfactory results for the quantities of the ground state, in spite of its simplicity and the great reduction in the calculation time compared with the non-empirical calculation.

BULLETIN OF THE CHEMICAL SOCIETY OF JAPAN VOL. 43 1649—1656 (1970)

Measurement of Negative Ions Formed by Electron Impact. VI. Negative Ion Mass Spectra and Ionization Efficiency Curves of Negative Ion of *m/e* 35 from Alkyl Chlorides

Satoru TSUDA, Akira YOKOHATA and Michihiro KAWAI

Department of Chemistry, Faculty of Engineering, University of Hiroshima, Senda-machi, Hiroshima

(Received November 20, 1969)

The negative ion mass spectra of alkyl (methyl, ethyl, *n*- and *iso*-propyl) chlorides, with emphasis on their relative abundance to the positive ions under 80, 40, 20 and 15 eV electron energies, and the ionization efficiency (IE) curves of Cl^- ions to the extent of 30 eV electron energies were measured. In every sample, the electron impacts of 80 eV and 40 eV gave almost the same distribution of *m/e* for negative ion mass spectra, in which, besides the intense peaks of *m/e* 35 and 37 (Cl^-), a relatively strong peak of *m/e* 25 (C_2H^-) in ethyl chloride and *n*- and iso-propyl chlorides was characteristic. For 20 eV and 15 eV, Cl^- ions predominated other negative ions. The ratio of the abundance of negative ions to positive ions was the order 10^2—10^3 for CH_3Cl^+/Cl^-, $C_2H_5Cl^+/Cl^-$, $C_3H_6^+/Cl^-$ and $C_3H_7^+/Cl^-$ throughout the range of electron energies. Each onset value observed in IE curves was interpreted to correspond to the appearance of the following reactions, the reaction scheme for second process being tentative. For the first process $RCl+e^-\rightarrow R+Cl^-$, for the second process $CH_3Cl+e^-\rightarrow H+CH_2+Cl^-$, $C_2H_5Cl+e^-\rightarrow H_2+H+C_2H_2+Cl^-$, C_3H_7Cl(*n*- or iso-)$+e^-\rightarrow H+C_2H_4+CH_2+Cl^-$. For the third process the possibility of ion pair formation was pointed out. For the fourth process in ethyl chloride a brief discussion was made in view of the overlapping phenomena of a complicated dissociative electron capture process with an ion pair formation.

When molecules are bombarded with electrons in the ion source of a mass spectrometer, both positive and negative ions may be formed, the latter often several orders of magnitude less abundantly. If the energy of the ionizing electrons is greater than about 30 eV the relative abundance of the positive ions produced is generally independent of electron energy, and positive-ion mass spectral

data for many molecules are available.[1-3] However, only a few data have been reported[4-8] regarding the identity and distribution of the negative-ion species produced when molecules of chemical interest undergo electron bombardment. Data on the ionization efficiency (IE) curves of negative ions are very limited.[9-12]

There are mainly three mechanisms by which ion formation for negative ions may occur; at low electron energies by electron capture, at intermediate energies by a dissociative resonance process and at higher electron energies by ion-pair formation. Hence the ions observed and their abundance are markedly energy-dependent.

In the present stage when information on negative ion mass spectra is lacking, further work is needed. This work was extended to alkyl chlorides, emphasis being placed on the relative abundance of negative ions to the positive ions in relation to the electron energies and on the measurement of IE curves of Cl^- ions.*1

Experimental

Experiments were performed on a Hitachi RMU-6D mass spectrometer equipped with a T-2M ion source having a rhenium filament. The ion detection circuit consisted of a ten stage electron multiplier having Ag-Mg dynode and of a Faraday collector. All the spectra were measured with a total emission current of 20 μA, accelerating voltage of 3.6 kV and electron multiplier voltage 2.5 kV, under the ionizing energies of 80, 40, 20 and 15 eV and pressure $\sim 10^{-6}$ mmHg in the source. Ionizing current varied from 10.5 to 6.4 μA in the range from 10 to 3 eV, while it was constant in the range higher than 10 eV (Fig. 1).

The electron energy was always calibrated in every measurement by the vanishing current method as compared to the ionization potential of argon for the positive ions and to the appearance potential of *m/e* 16 (O^-) from carbon monoxide, carbon dioxide and oxygen[13] for the negative ions.[8] Repeller voltage was adjusted to the best condition to collect the ions for positive and negative ions. The chemicals used were of research grade.

Results and Discussion

Negative Ion Mass Spectra. *Methyl Chloride.* In 80 eV electron impact experiment, negative ions of *m/e* 35(Cl^-) and *m/e* 37(Cl^-) besides a small peak of *m/e* 12(C^-) ion have mainly been observed (Fig. 2a), the most intense peak *m/e* being 35 (Cl^-) ion. The relative abundance of *m/e* 37 ion shows an isotope ratio of chlorine atom. Comparison of the yield of Cl^- ion (*m/e* 35) with that of CH_3Cl^+ ion (*m/e* 50, the most intense peak among the positive ions) gave $\sim 2.7 \times 10^2$ for CH_3Cl^+/Cl^-.

For 40 eV electron energies (Fig. 2b) the pattern of the negative ions was the same as that for 80 eV except for a small change in the yield of minor ions, and the ratio of CH_3Cl^+ to Cl^- was $\sim 4.5 \times 10^2$.

For 20 and 15 eV electron energies (Fig. 2c and 2d) Cl^- ions predominated other negative ions. The values $CH_3Cl^+/Cl^- \simeq 5.1 \times 10^2$ and 4.1×10^3 were obtained.

Table 1 shows the yield of minor negative ions for 80, 40, 20 and 15 eV. For 80 and 40 eV, *m/e* 12 (C^-), *m/e* 13 (CH^-), *m/e* 14 (CH_2^-), *m/e* 47 (CCl^-), *m/e* 48 ($CHCl^-$), *m/e* 49 (CH_2Cl^- or CCl^-), *m/e* 50($CHCl^-$) and *m/e* 51 (CH_2Cl^-) ions were found. The result for 40 eV was almost consistent with

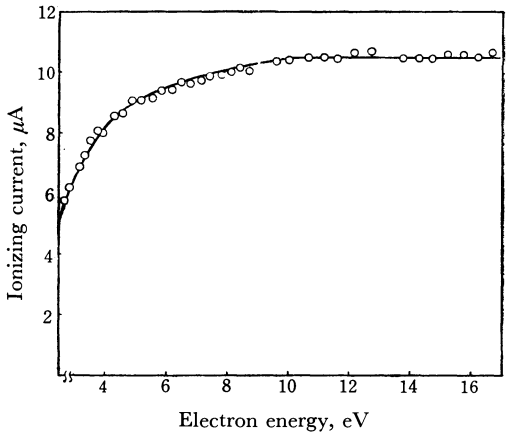

Fig. 1. The relation between ionizing current and electron energy (total emission current, 20 μA).

1) Amer. Petrol. Inst. Research Project 44, Mass Spectral Tables.
2) ASTM Committee E-14, Unclassified Mass Spectral Data.
3) Uncertified Mass Spectral Data, (The Dow Chemical Company, Midland Michigan, U. S. A.).
4) C. E. Melton, "Mass Spectrometry of Organic Ions," ed. F. W. McLafferty, Academic Press, New York, N. Y. (1963), p. 163.
5) R. T. Aplin, H. Budzikieweiz and C. Djerassi, *J. Amer. Chem. Soc.*, **87**, 3180 (1965).
6) D. F. Munro, J. E. Ahnell and W. S. Koski, *J. Phys, Chem.*, **72**, 2682 (1968).
7) K. A. G. MacNeil and J. C. J. Thynne, *Trans. Faraday Soc.*, **64**, 2112 (1968).
8) S. Tsuda, A. Yokohata and M. Kawai, This Bulletin, **42**, 607 (1969).
9) E. W. MacDaniel, "Collision Phenomena in Ionized Gases," John Wiley & Sons, Inc., New York (1964), p. 368.
10) L. G. Christophorou, R. N. Compton, G. S. Hurst and P. W. Reinhardt, *J. Chem. Phys.*, **45**, 536 (1966).
11) L. G. Christophorou and R. N. Compton, *Health Physics*, **13**, 1277 (1967).
12) S. Tsuda, A. Yokohata and M. Kawai, This Bulletin, **42**, 614 (1969).
*1 Recently, the measurement of ethyl chloride was reported. However, the method is different, and no detailed discussions were given (refer 10).
13) G. J. Schulz, *Phys. Rev.*, **128**, 178 (1962).

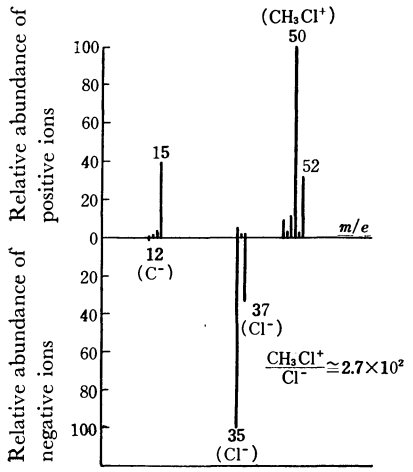

Fig. 2-a

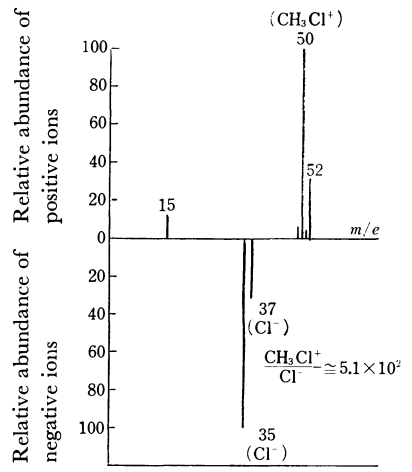

Fig. 2-c

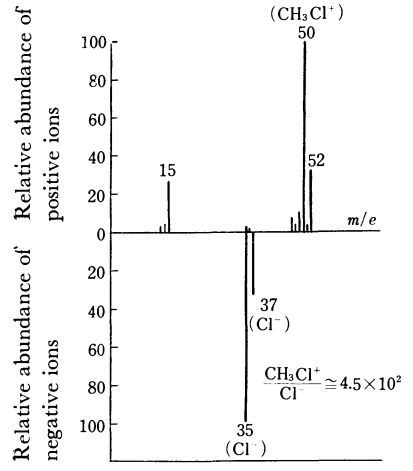

Fig. 2-b

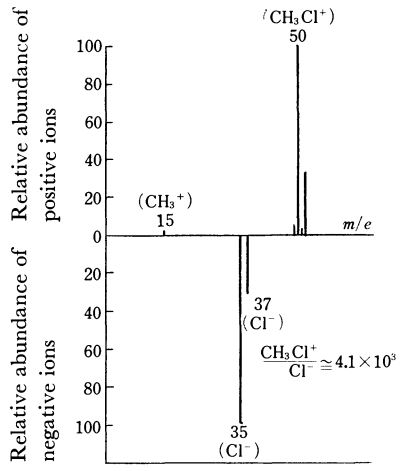

Fig. 2-d

Fig. 2. Positive and negative ion mass spectra of methyl chloride (source pressure: $\sim 10^{-6}$mmHg).
a 80 eV b 40 eV c 20 eV d 15 eV

Table 1. Minor negative ions from CH_3Cl
(Normalized to [*m/e* 35 (Cl^-)]=100)

m/e (ions)	Relative abundances for electron energies of			
	80 eV	40 eV	20 eV	15 eV
12 (C^-)	1.86	0.42		
13 (CH^-)	0.93	0.20		
14 (CH_2^-)	0.07	0.28		
35 (Cl^-)	100	100	100	100
47 (CCl^-)	1.1	0.2		
48 ($CHCl^-$)	0.19	0.36		
49 (CH_2Cl^-, CCl^-)	0.43	0.38	0.46	
50 ($CHCl^-$)	0.06	0.12		
51 (CH_2Cl^-)	0.14	0.12	0.14	

that of MacNeil *et al.*[7] except that the relative intensity of *m/e* 12 (C^-) ion to *m/e* 14 (CH_2^-) ion was reversed. It is probable that differences in the source pressure and in the geometry of the ion source are responsible for the discrepancy, which emphasizes the much greater sensitivity of negative ion mass spectrometry toward the change in experimental conditions as compared with positive ion mass spectrometry.

Molecular ion (CH_3Cl^-) was not observed, contrary to the formation of $CH_3NO_2^-$ ion from nitromethane at 80 eV and 40 eV electron impacts.

Ethyl Chloride. For the electron impact of 80 eV (Fig. 3a) negative ions of *m/e* 13 (CH^-), *m/e* 24 (C_2^-), 25 (C_2H^-), 35 (Cl^-) and 37 (Cl^-) have been mainly observed. The peak of molecular ion ($C_2H_5Cl^-$) was not found. When the yield of Cl^- ion (*m/e* 35) is compared with that of $C_2H_5Cl^+$ ion (*m/e* 64, the most intense peak among the positive ions),

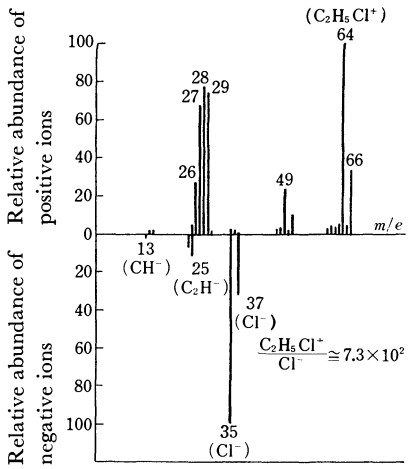

Fig. 3-a

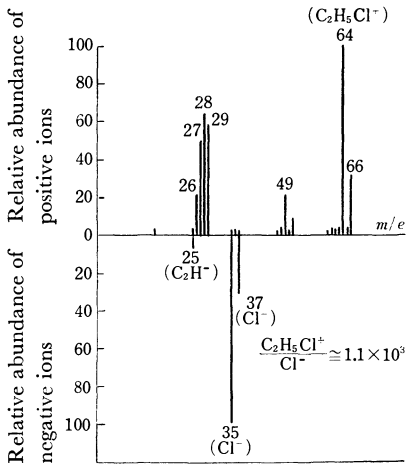

Fig. 3-b

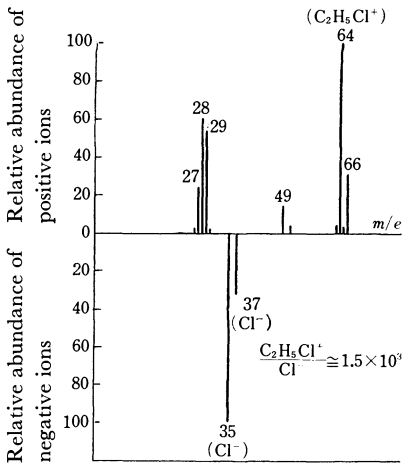

Fig. 3-c

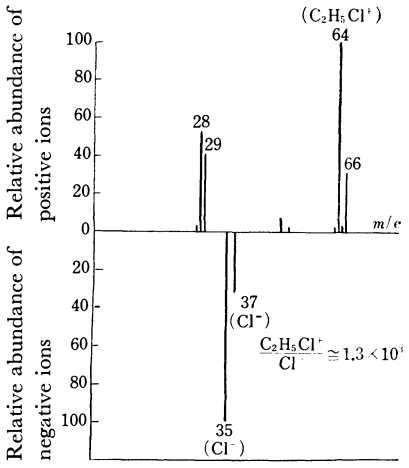

Fig. 3-d

Fig. 3. Positive and negative ion mass spectra of ethyl chloride (source pressure: $\sim10^{-6}$ mmHg).
a 80 eV b 40 eV c 20 eV d 15 eV

$C_2H_5Cl^+/Cl^-$ gave $\sim7.3\times10^2$. A relatively large peak of *m/e* 25 (C_2H^-) ion among the negative ions arising from the ethyl group is quite similar to the situations in ethane,[4] ethyl alcohol[4] and nitroethane.[8]

TABLE 2. MINOR NEGATIVE IONS FROM C_2H_5Cl
(Normalized to [*m/e* 35 (Cl^-)] = 100)

m/e (ions)	Relative abundances for electron energies of			
	80 eV	40 eV	20 eV	15 eV
12 (C^-)	0.71	trace		
13 (CH^-)	1.29	0.7		
14 (CH_2^-)		trace		
24 (C_2^-)	7.15	0.7		
25 (C_2H^-)	10.62	6.3		
35 (Cl^-)	100	100	100	100

Mass spectra for 40 eV (Fig. 3b) did not differ so much from those for 80 eV except for the decrement of peaks of *m/e* 13 (CH^-), 24 (C_2^-) and 25 (C_2H^-) ions. The ratio of $C_2H_5Cl^+/Cl^-$ gave $\sim1.1\times10^3$.

For 20 and 15 eV (Fig. 3c and 3d), *m/e* 35 (Cl^-) and 37 (Cl^-) ions predominated other negative ions. The values $\sim1.5\times10^3$ and $\sim1.3\times10^3$ for $C_2H_5Cl^+/Cl^-$ were obtained respectively.

Table 2 shows the yield of the minor negative ions in relation to electron energies. It should be noted that no ion is formed containing carbon, hydrogen and chlorine atoms, or carbon and chlorine atoms.

n- and Iso-propyl Chlorides. For the electron impacts of 80 eV and 40 eV, both samples gave almost the same negative ions except for a small change of minor ions (Figs. 4a, 5a and 4b, 5b). It is of great interest that a relatively strong peak of *m/e* 25 (C_2H^-) ion has been observed as one

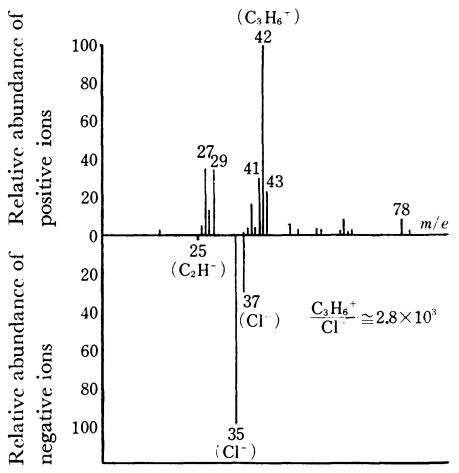

Fig. 4-a

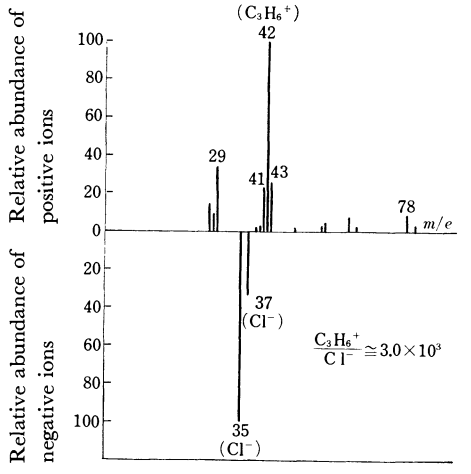

Fig. 4-c

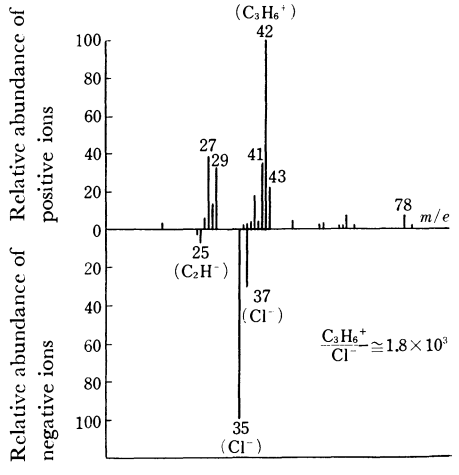

Fig. 4-b

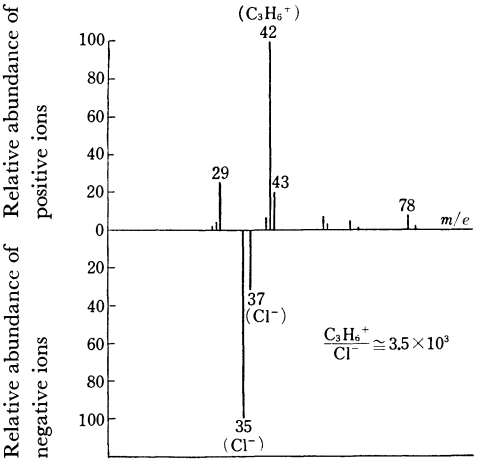

Fig. 4-d

Fig. 4. Positive and negative ion mass spectra of *n*-propyl chloride (source pressure: $\sim10^{-6}$mmHg).
a 80 eV b 40 eV c 20 eV d 15 eV

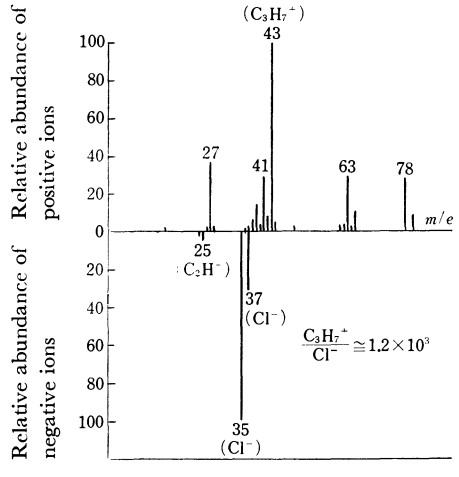

Fig. 5-a

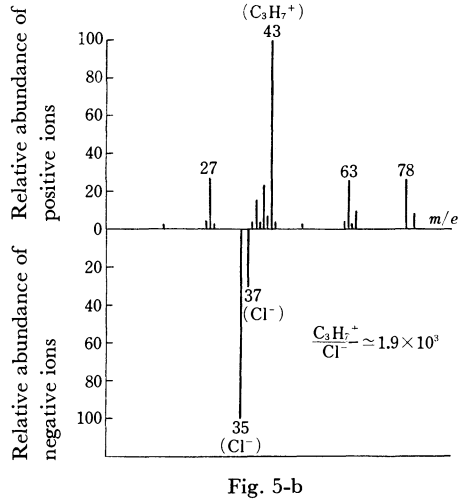

Fig. 5-b

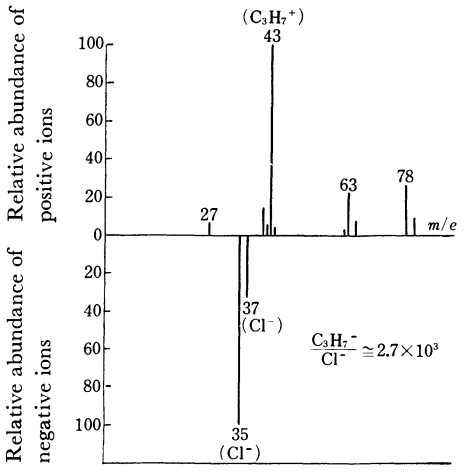

Fig. 5-c

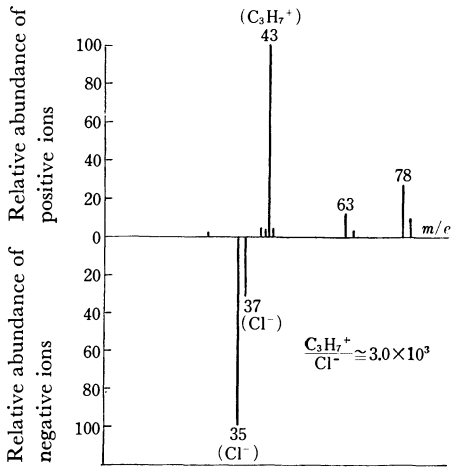

Fig. 5-d

Fig. 5. Positive and negative ion mass spectra of isopropyl chloride (source pressure: $\sim10^{-6}$mmHg).
a 80 eV b 40 eV c 20 eV d 15 eV

TABLE 3. MINOR NEGATIVE IONS FROM n-C_3H_7Cl
(Normalized to [m/e 35 (Cl^-)]=100)

m/e (ions)	Relative abundances for electron energies of			
	80 eV	40 eV	20 eV	15 eV
13(CH^-)	trace	0.91		
14(CH_2^-)	trace	0.23		
24(C_2^-)	3.01	0.23		
25(C_2H^-)	6.60	1.71		
26($C_2H_2^-$)	0.19			
35(Cl^-)	100	100	100	100
36(HCl^-)	0.68			

TABLE 4. MINOR NEGATIVE IONS FROM iso-C_3H_7Cl
(Normalized to [m/e 35 (Cl^-)]=100)

m/e (ions)	Relative abundances for electron energies of			
	80 eV	40 eV	20 eV	15 eV
13(CH^-)	0.94	0.4		
14(CH_2^-)		0.06		
24(C_2^-)	2.34			
25(C_2H^-)	4.53			
35(Cl^-)	100	100	100	100
36(HCl^-)	1.04			

of negative ions arising from the propyl group. This was consistent with the results in propyl alcohol[4] and nitropropane.[8]

Patterns obtained for 20 eV and 15 eV were quite similar in both samples (Figs. 4c, 5c and 4d, 5d). The most intense peak was always of Cl^- ions.

The values of $C_3H_6^+/Cl^-$ were $\sim1.8\times10^3$ at 80 eV, $\sim2.8\times10^3$ at 40 eV, $\sim3.0\times10^3$ at 20 eV and $\sim3.5\times10^3$ at 15 eV for n-propyl chloride and those of $C_3H_7^+/Cl^-$ were $\sim1.2\times10^3$, $\sim1.9\times10^3$, $\sim2.7\times10^3$ and $\sim3.0\times10^3$ for isopropyl chloride, respectively.

Tables 3 and 4 show the yield of minor negative ions for n- and iso-propyl chlorides in relation to the electron energies. It should be noted that neither ions containing carbon, hydrogen and chlorine, nor ions containing carbon and chlorine are observed. This is in sharp contrast with the observations for methyl chloride. This may be explained on the basis of the size, symmetry and bonding of the molecule or of the electron affinity of the radical,[7] but a quantitative explanation is not so easy in the present stage. Ferguson *et al.*[11] gave geometrical considerations for negative ion processes, but their discussions are limited to a few simple molecules.

IE Curves of Cl^- Ions. Figs. 6A-a, 6B-a, 6C-a and 6D-a show the ionization efficiency curves of Cl^- ions from methyl chloride, ethyl chloride, n- and iso-propyl chlorides, respectively. Figs. 6A-b, 6B-b, 6C-b and 6D-b show the same curves to the extent of electron energies of 30 eV on an enlarged scale. The result for ethyl chloride was consistent with that obtained by using the combined swarm-beam method by Christophorou *et al.*[10] In the three compounds except for ethyl chlrodie, the contributions of at least three processes can be observed. The first process appears at a considerably lower energy*[2] for all compounds, the second process at $\sim$3.2 eV for methyl chloride, at $\sim$3.5 eV for ethyl chloride, at $\sim$4.1 eV for

14) E. E. Ferguson, F. C. Fehsenfeld and A. L. Schmeltekopf, *J. Chem. Phys.*, **47**, 3085 (1967).

*2 Reliability of this work is restricted to electron energies above $\sim$3 eV because of instrumental difficulty.

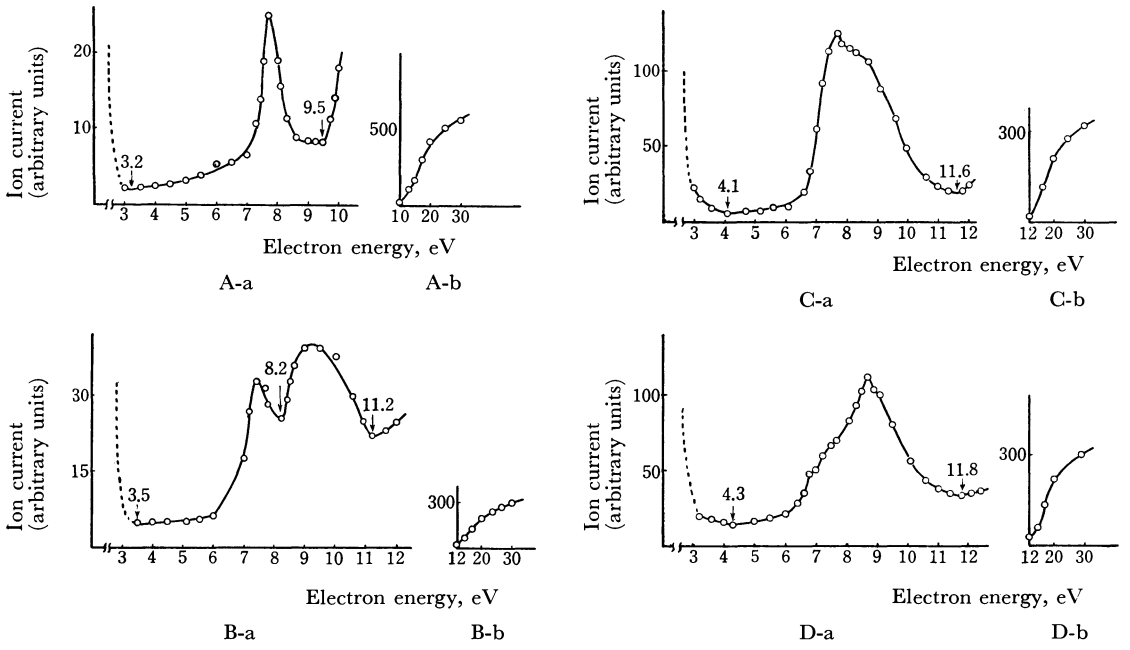

Fig. 6. Ionization efficiency curves of Cl^- from alkyl chlorides.
A CH_3Cl B C_2H_5Cl C *n*-C_3H_7Cl D *iso*-C_3H_7Cl

n-propyl chloride and at ~4.3 eV for isopropyl chloride, and the third process at ~9.5, ~8.2, ~11.6 and ~11.8 respectively.*3

In ethyl chloride, the fourth process was observed at ~11.2 eV.*4 As discussed later, this may not correspond to a simple reaction but an overlapping of two different reactions.

The plausible reaction schemes expected to occur at each onset value observed were sought on the basis of appearance potentials calculated by using $\Delta H_f(CH_3Cl) = -0.90$ eV, $\Delta H_f(C_2H_5Cl) = -1.16$ eV, $\Delta H_f(n\text{-}C_3H_7Cl) = -1.38$ eV, $\Delta H_f(iso\text{-}C_3H_7Cl) = -1.50$ eV,[15] $\Delta H_f(Cl^-) = -2.35$ eV,*5 $\Delta H_f(CH_3) = 1.39$ eV, $\Delta H_f(CH_2) = 2.5$ eV, $\Delta H_f(CH) = 6.16$ eV, $\Delta H_f(C_2H_2) = 2.35$ eV, $\Delta H_f(H) = 2.26$ eV, $\Delta H_f(C_2H_5) = 1.1$ eV, $\Delta H_f(C_2H_4) = 0.54$ eV, $\Delta H_f(C_2H_3) = 2.8$ eV, $\Delta H_f(n\text{-}C_3H_7) = 0.96$ eV, $\Delta H_f(iso\text{-}C_3H_7) = 0.73$ eV, $\Delta H_f(CH_3^+) = 11.23$ eV, $\Delta H_f(C_2H_5^+) = 9.88$ eV, $\Delta H_f(n\text{-}C_3H_7^+) = 9.65$ eV and $\Delta H_f(iso\text{-}C_3H_7^+) = 8.65$ eV.[16]

For the first process

		AP_{calc} (eV)*6
$CH_3Cl + e^- \longrightarrow CH_3 + Cl^-$	(1)	(−0.06)
$C_2H_5Cl + e^- \longrightarrow C_2H_5 + Cl^-$	(2)	(−0.09)
$n\text{-}C_3H_7Cl + e^- \longrightarrow n\text{-}C_3H_7 + Cl^-$	(3)	(0.01)
$iso\text{-}C_3H_7Cl + e^- \longrightarrow iso\text{-}C_3H_7 + Cl^-$	(4)	(−0.12)

For the second process

		AP_{calc} (eV)
$CH_3Cl + e^- \longrightarrow H + CH_2 + Cl^-$	(5)	(3.31)
$\longrightarrow H_2 + CH + Cl^-$	(6)	(4.71)
$C_2H_5Cl + e^-$		
$\longrightarrow H_2 + C_2H_2 + H + Cl^-$	(7)	(3.42)
$\longrightarrow 2H + C_2H_3 + Cl^-$	(8)	(6.13)
$n\text{-}C_3H_7Cl + e^-$		
$\longrightarrow H + C_2H_4 + CH_2 + Cl^-$	(9)	(4.33)
$\longrightarrow CH_3 + 2CH_2 + Cl^-$	(10)	(5.42)
$iso\text{-}C_3H_7Cl + e^-$		
$\longrightarrow H + C_2H_4 + CH_2 + Cl^-$	(11)	(4.45)
$\longrightarrow H + C_2H_3 + CH_3 + Cl^-$	(12)	(5.6)

For the third process

		AP_{calc} (eV)
$CH_3Cl + e^- \longrightarrow CH_3^+ + Cl^- + e^-$	(13)	(9.78)
$C_2H_5Cl + e^- \longrightarrow C_2H_5^+ + Cl^- + e^-$	(14)	(8.69)

*3 Since the tailing due to the 1st or 2nd process might be overlapped with the appearance of the 2nd or 3rd process, the exact determination of appearance potential of the 2nd or 3rd process is difficult. In this work, the minimum values in IE curves were taken as the subject of discussion. (G. J. Schulz, *Phys. Rev.*, **113**, 816 (1959)).

*4 The situation is the same as *3.

15) J. A. Kerr, *Chem. Rev.*, **66**, 465 (1966).

*5 To be estimated from $\Delta H_f(Cl) = 1.25$ eV (Refer 9) and $EA(Cl) = 3.6$ eV (J. M. Williams and W. H. Hamill, *J. Chem. Phys.*, **49**, 4467 (1968)).

16) R. R. Bernecker and F. A. Long, *J. Phys. Chem.*, **65**, 1565 (1961).

*6 For the estimation of AP_{calc}, the kinetic energies of fragment ions are ignored, and the ions are assumed to be formed in ground state.

n-$C_3H_7Cl + e^-$

$\longrightarrow n$-$C_3H_7^+ + Cl^- + e^-$ (15) (8.68)

$\longrightarrow C_2H_5^+ + CH_2 + Cl^- + e^-$ (16)(11.41)

iso-$C_3H_7Cl + e^-$

$\longrightarrow iso$-$C_3H_7^+ + Cl^- + e^-$ (17) (7.8)

$\longrightarrow C_2H_5^+ + CH_2 + Cl^- + e^-$ (18)(11.53)

The first process observed in a lower energy than $\sim$3 eV appears to correspond to the reactions (1)—(4) (the dissociative electron capture). The situation is similar to the reaction, $RNO_2 + e^- \rightarrow R + NO_2^-$ in nitroalkanes.[12]

As evident from Figs. 6A-a—6D-a, the second processes extend over the relatively broad range of electron energies and their dependence on electron energies is very small, especially near the onset. Although this makes it difficult to determine exactly each onset value, reactions (5), (7), (9) or (11) are likely to be assigned for each onset.

The third process seems to be more complicated. Although the simple ion pair formations such as (13), (14), (15) and (17) are expected, consistency of AP_{calc} with AP_{obs} is not so good. This is probably due to overlapping. In n- and iso-propyl chlorides, the possibility of reaction (16) or (18) is stronger than that of (15) or (17).

The fourth process in ethyl chloride might be also interpreted in terms of the overlapping of a complicated dissociative electron capture (for example, reaction (19)) and an ion pair formation (reaction (14)).

$C_2H_5Cl + e^- \rightarrow 3H + C_2H_2 + Cl^-$ (19) $AP_{calc} = 8.39$ eV

If each IE curve of reaction (19) and reaction (14) is expressed by curves (A) and (B) in Fig. 7, they would result in curve (C) which consists qualitatively of the last part (the part higher than 8.8 eV of IE curves in Fig. 6B-a). This is a tentative interpretation.

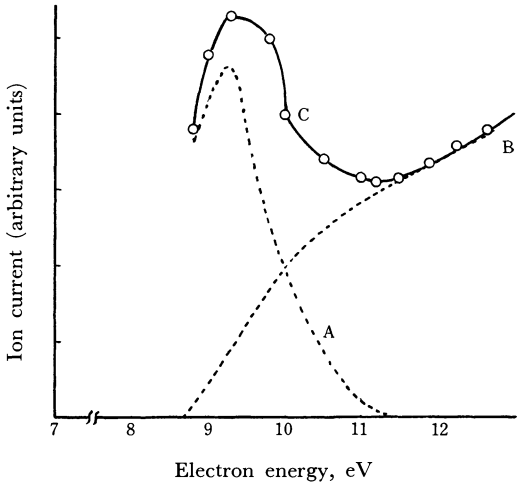

Fig. 7. An interpretation diagram for the fourth process in ethyl chloride.

It should be emphasized that (1) for ethyl chloride and n- or iso-propyl chlorides, neither ions containing carbon, hydrogen and chloride, nor ions containing carbon and chlorine are observed, (2) for all compounds the negative ions observed at electron energies lower than 20 eV are only Cl^- ion, and (3) for the Cl^- ion formation in the range of electron energies lower than about 12 eV the contribution of at least three different mechanisms are considered. The Cl^- ion yield increases monotonically with increasing electron energies in the range higher than about 12 eV.

BULLETIN OF THE CHEMICAL SOCIETY OF JAPAN VOL. 43 1657—1661 (1970)

Hydrogen Formation in the Radiolysis of Saturated Hydrocarbons in the Liquid and Solid Phases. Effect of Temperature

Toyoaki KIMURA, Kenji FUEKI and Zen-ichiro KURI

Department of Synthetic Chemistry, Faculty of Engineering, Nagoya University, Chikusa-ku, Nagoya

(Received November 24, 1969)

Hydrogen yields have been determined for thirteen saturated hydrocarbons (*n*-pentane, cyclopentane, methylcyclopentane, 3-methylpentane, *n*-hexane, cyclohexane, methylcyclohexane, *n*-heptane, *n*-octane, 2,2,4-trimethylpentane, *n*-nonane, *n*-decane and polyethylene) γ-irradiated at 20°C, −72°C and −196°C. The decrease in hydrogen yield with decreasing temperature from 20°C to −196°C has been correlated with the yield of thermal hydrogen atoms, which was obtained by adding ethylene as a scavenger at 20°C; the decrease in most cases was nearly equal to a half of the thermal hydrogen atom yield. Evidence of thermal hydrogen atom production at −196°C has also been demonstrated by ESR measurement. It has been concluded that thermal hydrogen atoms abstract hydrogen atoms from solvent molecules at 20°C, but they mostly recombine with each other to form hydrogen molecules at −196°C. An empirical formula based on the C–H bond parameter has been presented which is adapted for the hydrogen yield from normal alkanes.

One of the major products from γ-irradiated hydrocarbons is hydrogen and in most cases its yield depends upon the irradiation temperature. Dewhurst showed in the 800 Kvp electron radiolysis of *n*-hexane that the hydrogen yield was 5.0 (*G* unit) at 30°C and 3.0 (*G* unit) at −196°C.[1]

Recently we reported the hydrogen yield from γ-irradiated methylcyclohexane in the temperature range from 20°C to −196°C.[2] In contrast to Dewhurst's result, the decrease in hydrogen yield in our case was only 0.5 (*G* unit). Several workers[3-5] also reported results similar to those obtained by us; the decrements of hydrogen yield were lower than 1.0 (*G* unit). Only the result by Dewhurst is significantly different from the others. In this paper, we will report the hydrogen yields from thirteen γ-irradiated saturated hydrocarbons at 20°C, −72°C and −196°C and attempt to give a semiquantitative explanation for the yields.

A few studies have been made to explain the yields of products in the radiolysis of hydrocarbons from the view point of their chemical structure.[6-8] We will propose an empirical formula from which the hydrogen yield from *n*-alkanes can be evaluated fairly well.

Experimental

The experimental procedure was almost the same as that described earlier.[2] *n*-Pentane, cyclopentane, methylcyclopentane, *n*-hexane, cyclohexane, methylcyclohexane, *n*-heptane, and 2,2,4-trimethylpentane were Tokyo Kagaku Seiki 99.9% standard pure materials and used as received. Tokyo Kagaku Seiki 99.0% 3-methylpentane was shaken with concentrated sulfuric acid in a separating flask, washed with distillated water and dried over Galuber's salt. Passing through a silica gel column, 3-methylpentane was fractionally distillated. *n*-Octane, *n*-nonane and *n*-decane were Nakarai Kagaku 99% guaranteed reagents and purified in the same procedure as for 3-methylpentane. Polyethylene was "Takasen" made by ^{60}Co γ-irradiation at the Japan Atomic Energy Research Institute (Takasaki) and used without further purification.

Irradiations at −196°C were performed in a Dewar filled with liquid nitrogen and the absorbed dose was determined by correcting for the shielding effect of Dewar and liquid nitrogen. This shielding effect was measured with two Fricke dosimeters; one was settled in a position in the radiating field and the other in a Dewar filled with liquid ethanol, which has almost the same density as liquid nitrogen, in the same position as the first one. This shielding effect was 11.1%; the dose rate at −196°C decreased to 88.9% of that at 20°C.

1) H. A. Dewhurst, *J. Phys. Chem.*, **62**, 15 (1958).
2) T. Kimura, T. Miyazaki, K. Fueki and Z. Kuri, This Bulletin, **41**, 2861 (1968).
3) W. H. Taylor, S. Mori and M. Burton, *J. Amer. Chem. Soc.*, **82**, 5817 (1960).
4) N. H. Sagert, *Can. J. Chem.*, **46**, 89 (1968).
5) V. G. Berezkin, I. M. Kustanovich and N. Y. Chernyak, *Dokl. Akad. Nauk SSSR*, **129**, 1042 (1959).
6) K. L. Hall, R. O. Bolt and J. G. Carroll, "Radiation Effects on Organic Materials," ed. by R. O. Bolt and J. G. Carroll, Academic Press, New York (1963).
7) K. Fueki and K. Hirota, *Nippon Kagaku Zasshi*, **81**, 1402 (1960).
8) H. Yamazaki and S. Shida, *J. Chem. Phys.*, **32**, 950 (1960).

The dose absorbed at −72°C was estimated assuming that the shielding effect of dry-ice is proportional to its density.

ESR measurements were performed using a JES 3BX ESR spectrometer.

Results

The hydrogen yields from thirteen hydrocarbons irradiated at 20°C, −72°C and −196°C are listed in Table 1. The doses were 2.28×10^{19}, 1.43×10^{20} and 1.62×10^{20} eV/g at the irradiation temperatures of 20, −72 and −196°C, respectively. From Table 1, the following three features can be pointed out: (1) the decrease in hydrogen yield $\{G(H_2)_{20°C}-G(H_2)_{-196°C}\}$ is low in the cases of *n*-pentane, methylcyclopentane and 3-methylpentane, (2) the hydrogen yield from 2,2,4-trimethylpentane increases at −196°C, although it decreases at −72°C, and (3) the decrease in hydrogen yield from the other hydrocarbons is $\lesssim 1$. The results differ considerably from those of Dewhurst.[1)]

Table 1. Hydrogen yields at each irradiation temperature

Substance	Temperature		
	20°C	−72°C	−196°C
n-Pentane	5.13	4.58	4.70
Cyclopentane	5.60	5.30	4.46
Methylcyclopentane	4.18	4.40	4.10
3-Methylpentane	4.25	4.40	3.90
n-Hexane	5.50	5.00	4.30
Cyclohexane	5.60	5.60	5.00
Methylcyclohexane	4.85	4.50	4.40
n-Heptane	5.45	4.70	4.40
n-Octane	5.36	5.26	4.36
2,2,4-Trimethylpentane	2.72	2.34	2.87
n-Nonane	5.30	4.80	4.40
n-Decane	5.20	5.20	4.25
Polyethylene	4.40	4.20	3.40

It seemed that the decrease in hydrogen yield could be explained in terms of "thermal" hydrogen atom, so we measured the yields of thermal hydrogen atoms from hydrocarbons excepting polyethylene. For this purpose, ethylene was added to the hydrocarbons, which were γ-irradiated at 20°C at a dose of 2.74×10^{20} eV/g. Figure 1 shows the effect of ethylene on the hydrogen yield from *n*-pentane. The curve was drawn to fit the experimental data. The hydrogen decrease is almost completed at about 0.3M. The limiting value of the decrement in hydrogen yield in Fig. 1 can be taken as the yield of thermal hydrogen atoms, $G(H_{thermal})$. In the same manner as for *n*-pentane, the yields

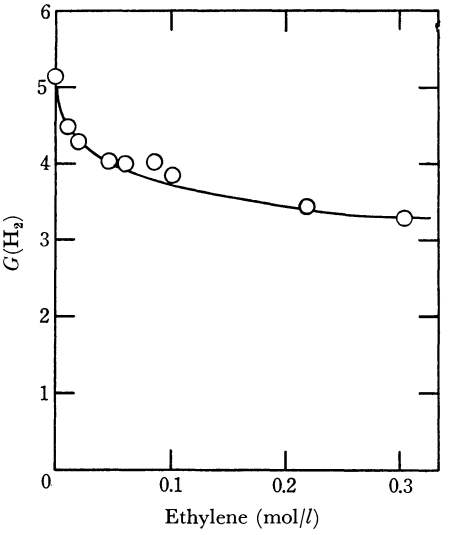

Fig. 1. Effect of ethylene on the hydrogen formation from γ-irradiated *n*-pentane at 20°C.

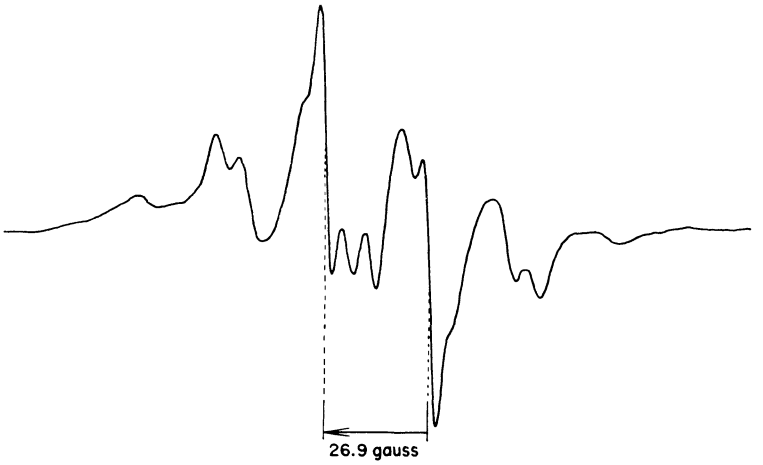

Fig. 2. ESR spectrum of γ-irradiated 3-methylpentane glass containing 3.73 mol% of ethylene at −196°C.

of thermal hydrogen atoms from the other hydrocarbons were obtained and are listed in Table 2. These thermal hydrogen atom yields are between 1 and 2 (G unit).

To ascertain whether thermal hydrogen atoms are produced at -196°C, ESR measurements were performed for γ-irradiated 3-methylpentane glass which contains 3.74 mol% of ethylene. In Fig. 2, we can see 3-methylphentyl radicals mixed with ethyl radicals the splitting constant of which is 26.9 gauss.

Discussion

The mechanism of hydrogen formation from γ-irradiated hydrocarbons has been investigated by many workers and are described as follows:

$$RH \rightsquigarrow \begin{cases} -RH^+ + e^- & (1) \\ -RH^* & (2) \end{cases}$$

$$\left.\begin{matrix} RH^+ + e^- \longrightarrow \\ RH^* \longrightarrow \end{matrix}\right\} \begin{cases} -H\ (\text{thermal}) + R\cdot & (3) \\ -H\ (\text{hot}) + R\cdot & (4) \\ -H_2 + \text{Olefin} & (5) \end{cases}$$

The molecular hydrogen detachment (Eq. (5)) needs a lower energy than that of atomic hydrogen detachment (Eqs. (3) and (4)).[9] Thus the molecular detachment process does not seem to be affected by temperature. Hot H atoms abstract hydrogen atoms from solvent molecules to form H_2 molecules and solvent radicals both at 20°C and -196°C.

$$H(\text{hot}) + RH \longrightarrow H_2 + R\cdot \quad (6)$$

Thermal H atoms abstract H atoms from solvent molecules to produce H_2 molecules at room temperature, but in the presence of an H atom scavenger such as olefin, they are scavenged and the total hydrogen yield decreases.[10-12]

$$H(\text{thermal}) + RH \longrightarrow H_2 + R\cdot \quad (7)$$

$$H(\text{thermal}) + C_2H_4 \longrightarrow C_2H_5\cdot \quad (8)$$

However, up to the present, the formation of thermal H atom in solid hydrocarbons at -196°C has not been confirmed.

We have reported the effect of ethylene on the hydrogen formation from γ-irradiated methylcyclohexane at -196°C as well as 20°C[13] and ascribed it to thermal H atom scavenging.

On the other hand, Timm *et al.*[14] have shown in the ESR measurements at 4°K that no thermal H atom can be observed in solid hydrocarbons except methane. However, as is shown in Fig. 2, H atoms are captured by ethylene to form ethyl radicals. Therefore it can be said that thermal H atoms are probably produced not only at room temperature, but also at liquid nitrogen temperature. The reason for the absence of H atoms in the ESR spectra may be that thermal H atoms cannot be trapped by solid hydrocarbons except methane, but recombine with each other to form hydrogen molecules, as was suggested previously.[13]

$$2H(\text{thermal}) \longrightarrow H_2 \quad (9)$$

Molecularly detached hydrogen and hot H atoms do not affect the total hydrogen yield when the irradiation temperature decreases from 20°C to -196°C. Only thermal H atoms can affect the total hydrogen yield. From Eqs. (7) and (9), it seems that the total hydrogen yield decreases by $0.5\,G(H_{thermal})$ when the irradiation temperature decreases from 20°C to -196°C. Thus we can describe the hydrogen yields at 20°C and -196°C as follows:

$$G(H_2)_{20°C} = G(H_2)_{molecular} + G(H)_{hot} + G(H)_{thermal} \quad (10)$$

$$G(H)_{-196°C} = G(H_2)_{molecular} + G(H)_{hot} + 0.5G(H)_{thermal} \quad (11)$$

Table 2. Yields of thermal H atoms in hydrocarbons irradiated at 20°C

	$G(H_{thermal})$
n-Pentane	1.8
Cyclopentane	1.6
Methylcyclopentane	1.1
3-Methylpentane	1.3
n-Hexane	2.0
Cyclohexane	1.0
Methylcyclohexane	1.0
n-Heptane	1.7
n-Octane	1.8
2,2,4-trimethylpentane	1.1
n-Nonane	1.7
n-Decane	1.4

Substracting Eq. (11) from Eq. (10), we obtain

$$\Delta G(H)_2 = G(H_2)_{20°C} - G(H_2)_{-196°C} = 0.5G(H)_{thermal} \quad (12)$$

To see if Eq. (12) holds for our results or not, we compared $\Delta G(H_2)$, obtained from Table 1, with $0.5\,G(H_{thermal})$ from Table 2. The results are listed in Table 3. Although $\Delta G(H_2)$ is not exactly equal to $0.5\,G(H_{thermal})$ because thermal H atoms cannot be completely scavenged by ethylene, the results shown in Table 3 illustrate the validity of Eq. (12) except in the cases of *n*-pentane, methyl-

9) L. M. Dorfman, *J. Phys. Chem.*, **60**, 826 (1956).
10) W. A. Cramer and G. J. Piet, *Trans. Faraday Soc.*, **63**, 1402 (1967).
11) J. L. McCrum and R. H. Schuler, *J. Phys. Chem.*, **71**, 1953 (1967).
12) M. C. Sauer, Jr., and I. Mani, *ibid.*, **72**, 3865 (1968).
13) T. Kimura, K. Fueki and Z. Kuri, This Bulletin, **42**, 3088 (1969).
14) D. Timm and J. E. Willard, *J. Phys. Chem.*, **73**, 2403 (1969).

TABLE 3. COMPARISON BETWEEN $\Delta G(H_2)$ AND $0.5G$ ($H_{thermal}$).
$\Delta G(H_2)=G(H_2)_{20°C}-G(H_2)_{-196°C}$

	$\Delta G(H_2)$	$0.5\,G$-($H_{thermal}$)
n-Pentane	0.43	0.9
Cyclopentane	1.14	0.8
Methylcyclopentane	0.08	0.6
3-Methylpentane	0.35	0.6
n-Hexane	1.20	1.0
Cyclohexane	0.60	0.8
Methylcyclohexane	0.50	0.5
n-Heptane	1.05	0.9
n-Octane	1.00	0.9
2,2,4-Trimethylpentane	−0.15	0.6
n-Nonane	0.90	0.9
n-Decane	0.95	0.7

cyclopentane, 3-methylpentane and 2,2,4-trimethylpentane. In the case of these four hydrocarbons, Eq. (12) does not hold and $\Delta G(H_2)$ is considerably less than $0.5\,G(H_{thermal})$ (2,2,4-trimethylpentane gives a negative value of $\Delta G(H_2)$).

It is not easy to explain the exceptions, but we might consider the difference in intramolecular energy partition in the liquid and solid states, which may change the relative contribution of the C–C and C–H bond cleavage.

To investigate the relation between the hydrogen yield and the chemical structure, we have made the following calculation. Denoting the number of hydrogen molecules formed per unit absorbed energy (eV), per 1 g of hydrocarbon, by P_i, we can express the G value of hydrogen as

$$G(H_2) = 100P_i \tag{13}$$

Denoting the number of hydrogen molecules formed per 1 eV energy absorbed, per 1 molecule of hydrocarbon, by p_i, we can write as

$$p_i = P_i(M/N) \tag{14}$$

where M is the molecular weight of a hydrocarbon and N is the Avogadro number. Combining Eqs. (13) and (14), we obtain p_i as a function of $G(H_2)$;

$$p_i = \frac{M}{100N}G(H)_2 \tag{15}$$

Here we restrict our discussion to normal alkanes and make the following assumption; the number of hydrogen molecules per 1 eV, per 1 molecule of normal alkane is given by

$$p_i = n_pX_p + n_sX_s, \tag{16}$$

where n_p and n_s are the number of primary and secondary hydrogen atoms, respectively, and X_p X_s are parameters associated with the primary and secondary C–H bonds, respectively. From Eqs. (15) and (16), the hydrogen yield from each normal alkane is expressed as

$$G(H_2) = 100N\left(\frac{n_p}{M}X_p + \frac{n_s}{M}X_s\right) \tag{17}$$

If Eq. (17) holds, the hydrogen yield from a normal alkane can be calculated substituting the numbers of primary and secondary hydrogen atoms and the molecular weight into Eq. (17).

Using the data in Table 1, we obtain the values of X_p and X_s; $X_p=5.40\times10^{-25}$ and $X_s=5.78\times10^{-25}$ at 20°C, and $X_p=X_s=4.57\times10^{-25}$ at −196°C. Using these values, we calculated the hydrogen yields for normal alkanes. The calculated and observed yields at 20°C and −196°C are listed in Tables 4 and 5, respectively. The calculated values at

TABLE 4. CALCULATED AND OBSERVED HYDROGEN YIELDS AT 20°C

	Calcd. $G(H_2)$	Obs. $G(H_2)$
n-Pentane	5.60	5.13
n-Hexane	5.49	5.50
n-Heptane	5.42	5.45
n-Octane	5.36	5.36
n-Nonane	5.32	5.30
n-Decane	5.28	5.25

$X_p=5.40\times10^{-25}$ $X_s=5.78\times10^{-25}$

TABLE 5. CALCULATED AND OBSERVED HYDROGEN YIELDS AT −196°C

	Calcd. $G(H_2)$	Obsd. $G(H_2)$
n-Pentane	4.57	4.70
n-Hexane	4.46	4 30
n-Heptane	4.39	4 40
n-Octane	4.33	4.36
n-Nonane	4.29	4.40
n-Decane	4.25	4.25

$X_p=X_s=4.57\times10^{-25}$

20°C (Table 4) are in good agreement with the observed values except for *n*-pentane. The observed hydrogen yield for *n*-pentane is somewhat lower than the calculated one. A possible reason for this is that the C–C bond cleavage in *n*-pentane is more favorable than that in higher normal alkanes, resulting in suppression of hydrogen formation to some extent. Equation (17) appears to be valid for normal alkanes which are larger than *n*-pentane. We also calculated the hydrogen yield from the normal alkane, whose C–C chain is infinitely long, which was 4.97 (G unit). The observed hydrogen yield from polyethylene was 4.40 (G unit). This difference between the calculated and the observed yield may be due to terminal double bonds or branching methyl (or other) groups in polyethylene which reduce the hydrogen yield.

Equation (17) also holds for non-branching cyclic alkanes, if we use $X_s=6.51\times10^{-25}$ which is higher than that for normal alkanes. We need more data

for further investigation on this class of hydrocarbons. Equation (17) does not hold for branching alkanes which involve the tertiary C–H bond. Taking 3-methylpentane as an example, Eq. (17) must be changed to

$$G(H_2) = 100N\left(\frac{n_p}{M}X_p + \frac{n_s}{M}X_s + \frac{n_t}{M}X_t\right) \qquad (17')$$

where subscript t is associated with the tertiary C–H bond.

Even if we use $X_t=0$, the calculated value is higher than the observed one.

It should be noted that the branching methyl group decreases the hydrogen yield which is easily recognizable if we compare the yield from cyclopentane with that from methylcyclopentane, and the yield from cyclohexane with that from methylcyclohexane.

The effect of this branching methyl group on the hydrogen yield will not be due to the increase in the fraction of primary H atoms, but the branching methyl group itself, which would affect the decomposition pattern of the molecule.

Polyethylene used in the present work has 2.1 methyl groups per 1000 units of $-CH_2-$, and the deviation of the hydrogen yield from the expected value may partly be due to these branching methyl groups.

We now consider the physical meaning of the parameters, X_p and X_s. These are interpreted as representing contributions of a hydrogen atom at a specified position to the total hydrogen yield. In other words, these parameters indicate the overall probability of C–H bond cleavage, including detachment of H atom, H atom abstraction by the detached H atom, and molecular H_2 detachment. Since X_p and X_s do not differ very much from one another, the C–H bond cleavage seems to occur almost equally at the primary and secondary C–H bonds for normal alkanes. However, our results are not consistent with those of Gäumann,[15] who used isotopic compounds to determine the scission probability of bonds. This discrepancy might be ascribed to the isotope effect.

15) T. Gäumann, "Aspect of Hydrocarbon Radiolysis," ed, by T. Gäumann and J. Hoigné, Academic Press, London (1968) p. 226.

BULLETIN OF THE CHEMICAL SOCIETY OF JAPAN VOL. 43 1661—1667 (1970)

The Crystal and Molecular Structure of Dimethyltin Chloride *N,N*-Dimethyldithiocarbamate

Kenji FURUE, Toshihide KIMURA, Noritake YASUOKA, Nobutami KASAI*1 and Masao KAKUDO

Department of Applied Chemistry, Faculty of Engineering, Osaka University, Yamadakami, Suita, Osaka

(Received November 29, 1969)

The molecular structure of dimethyltin chloride *N,N*-dimethyldithiocarbamate, $[(CH_3)_2SnCl(S_2CN(CH_3)_2)]$, has been determined from three-dimensional X-ray diffraction data. The unit-cell dimensions are $a=12.67$, $b=7.64$, $c=12.11$ Å, and $\beta=110.3°$. The space group is $P2_1/c$. Four formula units are contained in a unit-cell. The structure was established by the heavy-atom method. The coordination around the tin atom is a distorted trigonal bipyramid with the following bond distances: Sn–C, 2.17(5) and 2.20(5) Å; Sn–Cl, 2.46(1) Å, and Sn–S, 2.48(1) and 2.79(1) Å. Two methyl groups are both in equatorial positions.

Recently, numerous studies have been reported on transition metal complexes of dialkyldithiocarbamates. The crystal structures of several complexes have also been determined; however, few structures of non-transition metal complexes have yet been reported.

Tanaka and his co-workers[1] reported on the preparation and properties of some organotin *N,N*-dimethyldithiocarbamates. According to the spectroscopic studies, the three configurations shown in Fig. 1 were proposed for a penta-coordinated complex, dimethyltin chloride *N,N*-dimethyldithio-

*1 To whom any correspondence should be addressed.

1) M. Honda, M. Komura, Y. Kawasaki, T. Tanaka and R. Okawara, *J. Inorg. Nucl. Chem.*, **30**, 3231 (1968).

carbamate, $[(CH_3)_2SnCl(S_2CN(CH_3)_2)]$ (to be abbreviated as $Me_2SnCl(dtc)$ hereafter). Among these configurations, (3) is considered to be most likely; in it the two methyl groups are both in equatorial positions.

To determine the exact configuration, the crystal structure analysis has now been undertaken by means of X-ray diffraction.

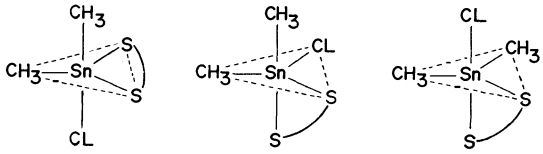

Fig. 1. Three possible configurations of Me_2SnCl-(dtc) molecule.

The purpose of this study is also to contribute to the understanding of the bonding nature of the tin atom in penta- and hexa-coordinated dimethyltin complexes, among which the crystal structures and molecular configurations of $[(CH_3)_2SnCl_2((CH_3)_2SO)_2]$,[2] $[(CH_3)_2Sn(C_9H_6NO)_2]$,[3] and $[((CH_3)_2$-SnCl, terpyridil)$^+\cdot((CH_3)_2SnCl_3)^-]$[4] have already been determined.

Experimental

The crystals of $Me_2SnCl(dtc)$ were recrystallized from a chloroform-ethanol solution. They belong to the monoclinic system, and the unit-cell dimensions are: $a=12.67\pm0.07$, $b=7.64\pm0.01$, $c=12.11\pm0.06$ Å, and $\beta=110.3\pm0.4°$. The unit-cell dimensions were determined from Weissenberg photographs taken around the b and c axes, on which Debye lines of aluminum were superposed for calibration. The observed density is 1.86 $g\cdot cm^{-3}$, while the calculated density, assuming four formula units per unit-cell, is 1.84 $g\cdot cm^{-3}$. From the systematic absences of reflections (l: odd for $h0l$ and k: odd for $0k0$), the space group was determined to be $P2_1/c$.

A set of three-dimensional intensity data was collected on multiple-film equi-inclination Weissenberg photographs with nickel-filtered Cu$K\alpha$ radiation. Layers from 0 through 5 were recorded around the b axis; layers from 0 through 5 around the c axis were also recorded, mainly for the purpose of inter-layer scaling. The intensities of 1968 independent reflections were estimated visually by using a calibrated standard scale. The intensities were corrected for the usual Lorentz and polarization factors. No absorption correction was made.

Determination and Refinement of the Structure

A three-dimensional Patterson function was computed; from it the location of the tin atom was easily determined. The chlorine and two sulfur atoms could also be located from the Patterson function, but the chlorine atom could not be distinguished from the sulfur atoms. Therefore, the first Fourier synthesis was computed with the phases based on the tin atom only, while the chlorine and two sulfur atoms were identified at the positions which had been suggested from the Patterson synthesis. The nitrogen and three carbon atoms were also found in the Fourier map. The remaining two carbon atoms were found in another Fourier map, with phases based on all the atoms which had already been located.

The structure factor calculation after a cycle of least-squares refinement gave a discrepancy factor, $R=\sum||F_o|-|F_c||/\sum|F_o|$, of 0.27. Successive block-diagonal least-squares refinement was carried out on a HITAC 5020E computer at the University of Tokyo. In the refinement, the weight was taken as unity for all reflections. After five cycles of

TABLE 1

(a) The final atomic coordinates along with their estimated standard deviations (in fraction of cell edges) in parentheses (each multiplied by 10^3)

Atom	x	y	z
Sn	0.1818(0.2)	0.1041(0.3)	0.1625(0.2)
Cl	0.1452(0.7)	−0.0682(1.8)	−0.0191(1.0)
S(1)	0.3851(0.6)	0.0557(1.2)	0.1995(0.8)
S(2)	0.3191(0.7)	0.2627(1.5)	0.3720(0.8)
N	0.528(2)	0.168(4)	0.400(3)
C(1)	0.421(2)	0.158(5)	0.330(3)
C(2)	0.621(3)	0.088(6)	0.365(4)
C(3)	0.596(3)	0.260(6)	0.524(3)
C(4)	0.113(4)	−0.075(7)	0.259(4)
C(5)	0.111(3)	0.355(5)	0.981(4)

(b) The anisotropic thermal parameters (each multiplied by 10^4) of the form: $\exp\{-(\beta_{11}h^2+\beta_{22}k^2+\beta_{33}l^2+\beta_{12}hk+\beta_{13}hl+\beta_{23}kl)\}$.

Atom	β_{11}	β_{22}	β_{33}	β_{12}	β_{13}	β_{23}
Sn	16	66	44	3	17	20
Cl	27	228	70	13	12	−104
S(1)	21	85	41	13	15	−38
S(2)	25	151	48	17	27	−63
N	39	44	44	25	15	−45
C(1)	7	99	53	59	10	−12
C(2)	13	99	109	17	−1	11
C(3)	42	163	32	108	−4	92
C(4)	50	234	62	268	−60	125
C(5)	25	9	140	105	2	147

2) N. W. Isaacs, C. H. L. Kennard and W. Kitching, *Chem. Commun.*, **1968**, 820.

3) E. O. Schlemper, *Inorg. Chem.*, **6**, 2021 (1967).

4) F. W. B. Einshtein and B. R. Penfold, *J. Chem. Soc.*, *A*, **1968**, 3019.

TABLE 2. THE OBSERVED AND CALCULATED STRUCTURE FACTORS

K FO FC	K FO FC	K FO FC	K FO FC	K FO FC	K FO FC	K FO FC	K FO FC	K FO FC	K FO FC
H,L= 0 0	4 26 -22	2 149 188	2 0 -4	0 181-176	H,L= 3 7	4 49 -40	2 25 23	H,L= 5 1	2 33 -16
2 68 46	5 65 62	3 58 52	3 76 74	1 44 -38	1 75 -65	5 49 -45	3 0 22	1 122 116	3 126-145
4 127-107	6 69 58	4 93 127	4 76 -70	2 56 -50	2 101 97	H,L= 3-11	H,L= 4 12	2 127-122	4 36 27
6 105-102	7 0 7	5 33 29	5 0 12	3 42 -28	3 0 7	1 0 10	0 0 -18	3 50 -38	5 36 -18
H,L= 0 1	8 57 62	6 0 -18	6 74 -62	4 53 44	4 62 60	2 62 57	1 38 42	4 77 -62	6 0 0
1 84 114	H,L= 1 2	7 0 -8	7 0 21	5 0 -1	5 40 45	3 0 15	2 0 2	5 103 -87	7 66 66
2 191-185	0 126-108	8 70 -62	8 50 43	H,L= 2 -7	H,L= 3 8	4 36 28	3 0 32	6 0 7	H,L= 5 -5
3 18 11	1 30 -22	9 0 -16	H,L= 2 5	1 54 -40	0 83 73	5 0 -6	H,L= 4 -1	H,L= 5 2	1 116 115
4 67 -84	2 59 -50	H,L= 1 -4	1 77 63	2 113-106	1 86 80	H,L= 3-12	1 124-109	0 37 -26	2 85 -77
5 66 -64	3 49 44	0 131-127	2 81 -74	3 0 -15	2 0 -17	0 85 -73	2 36 29	1 120-110	3 30 5
6 63 42	4 94 132	1 100 87	3 31 -20	4 54 -46	3 79 84	1 0 20	3 52 47	2 0 9	4 50 -39
7 43 -35	5 45 41	2 79 -71	4 0 0	5 0 -6	4 0 -18	2 0 5	4 30 -17	3 121-123	5 89 -88
8 45 36	6 63 50	3 97 84	5 38 -29	H,L= 2 -8	5 0 23	3 0 37	5 114 93	4 0 -16	6 40 27
9 38 29	7 0 6	4 80 80	6 78 74	0 95 83	H,L= 3 9	4 31 26	6 59 -52	5 44 -39	7 42 -25
H,L= 0 2	8 44 -33	5 52 38	7 0 -13	1 0 0	1 76 73	5 0 5	7 42 28	6 0 -7	8 51 46
0 74 -69	H,L= 1 3	6 69 68	8 38 40	2 30 22	2 0 1	H,L= 3-13	8 0 -16	7 40 60	H,L= 5 -6
1 44 -34	1 40 27	7 0 -15	H,L= 2 6	3 82 -64	3 0 -13	1 53 -48	9 50 -38	H,L= 5 3	0 134 129
2 52 -42	2 137 177	8 0 -24	0 0 -12	4 71 -64	4 0 17	2 0 -19	H,L= 4 -2	1 115-120	1 0 0
3 131-176	3 59 51	H,L= 1 -5	1 31 -28	5 0 -6	5 49 -49	3 0 9	0 134-168	2 98 -99	2 62 60
4 51 48	4 55 51	1 105 -99	2 0 5	H,L= 2 -9	H,L= 3 10	4 0 -10	1 103-109	3 0 2	3 71 68
5 0 5	5 44 39	2 87 -81	3 85 -68	1 84 70	0 32 33	5 26 36	2 0 10	4 48 -39	4 96-102
6 40 28	6 59 -49	3 27 16	4 69 67	2 68 59	1 0 -15	H,L= 3-14	3 98-113	5 94 87	5 0 3
7 68 54	7 0 -19	4 43 -34	5 0 14	3 0 -22	2 0 24	0 0 -16	4 70 63	6 0 28	H,L= 5 -7
8 0 -6	8 49 -49	5 73 62	H,L= 2 7	4 0 14	3 52 -60	1 0 -20	5 0 -8	7 0 18	1 0 -5
H,L= 0 3	H,L= 1 4	6 46 37	1 54 -45	5 56 -52	4 0 -14	2 0 -7	6 79 68	8 33 38	2 106 105
1 82-103	0 161 158	7 0 11	2 0 7	H,L= 2-10	5 0 12	3 43 -54	7 0 24	H,L= 5 4	3 0 -5
2 31 -22	1 106 120	8 41 27	3 51 42	0 0 -1	H,L= 3 11	4 0 1	8 42 -37	0 116-116	4 0 18
3 40 38	2 61 47	H,L= 1 -6	4 0 -9	1 75 66	1 0 -22	H,L= 4 0	H,L= 4 -3	1 0 5	5 0 -13
4 0 -6	3 61 57	0 63 44	5 62 63	2 39 -30	2 37 -38	0 173-160	1 0 7	2 78 -77	H,L= 5 -8
5 89 89	4 61 -44	1 119-104	H,L= 2 8	3 76 69	3 0 6	1 40 30	2 114-136	3 56 46	0 125-112
6 0 7	5 0 0	2 0 -13	0 88 -72	4 0 21	4 25 -20	2 80 -64	3 0 1	4 87 97	1 50 40
7 0 18	6 66 -48	3 92 -86	1 60 52	5 0 15	5 0 18	3 156 162	4 103 -97	5 0 0	2 0 10
8 0 9	7 89 -86	4 0 -4	2 0 3	H,L= 3 12	H,L= 3-12	4 31 20	5 0 2	6 0 44	3 0 2
9 41 -46	H,L= 1 5	5 0 -5	3 65 54	1 79 -74	0 63 -67	5 53 -36	6 71 62	7 0 -13	4 57 46
H,L= 0 4	1 100 97	H,L= 1 -7	4 0 15	2 39 34	1 0 -5	6 56 40	7 0 0	H,L= 5 5	5 0 -8
0 104 -95	2 0 2	1 126 116	5 0 -8	3 0 10	2 0 -12	7 60 -59	8 63 65	1 0 -3	H,L= 5 -9
1 65 61	3 54 -47	2 0 -8	H,L= 2 9	4 35 25	H,L= 3 -1	H,L= 4 1	9 0 -8	2 103 99	1 44 -30
2 58 44	4 0 -13	3 51 -34	1 0 10	5 52 53	1 77 -88	1 70 65	H,L= 4 -4	3 0 10	2 53 -46
3 102 115	5 98 -97	4 0 10	2 81 81	H,L= 2-12	2 65 -77	2 87 94	0 112 109	4 37 29	3 43 33
4 53 48	6 0 0	5 86 -84	3 0 -9	0 63 -56	3 32 28	3 66 -61	1 35 -29	5 0 14	4 38 -25
5 0 6	7 42 4	H,L= 1 -8	4 43 41	1 36 -32	4 23 -17	4 71 64	2 22 15	6 38 -44	5 69 65
6 0 29	8 39 -12	0 63 51	5 0 -27	2 45 -34	5 99 98	5 73 -73	3 72 -73	7 35 -12	H,L= 5-10
7 57 -48	H,L= 1 6	1 53 35	H,L= 2 10	3 0 -20	6 44 40	6 0 -27	4 77 -73	H,L= 5 6	0 41 25
H,L= 0 5	0 47 33	2 53 40	0 86 78	4 40 41	7 0 3	7 0 5	5 44 40	0 101 109	1 32 -22
1 119 113	1 41 -30	3 113 115	1 0 9	5 0 -6	8 50 41	8 0 -24	6 62 -57	1 48 40	2 0 7
2 124 124	2 59 44	4 72 -64	2 43 37	H,L= 2-13	9 50 -46	H,L= 4 2	7 0 32	2 0 -4	3 76 -80
3 28 -13	3 82 -77	5 0 2	3 46 37	1 0 -4	H,L= 3 -2	0 184 184	8 40 36	3 0 6	4 0 20
4 56 50	4 80 -64	H,L= 1 -9	4 52 -60	2 51 -50	0 0 0	1 54 -48	H,L= 4 -5	4 49 -45	5 0 16
5 58 -51	5 39 29	1 51 -39	5 0 13	3 0 3	1 101-111	2 0 13	1 63 57	5 0 -3	H,L= 5-11
6 73 -67	H,L= 1 7	2 102 98	H,L= 2 11	4 31 -36	2 17 -17	3 39 -30	2 66 56	H,L= 5 7	1 60 47
7 0 -12	1 28 -1	3 0 -5	1 50 49	5 17 2	3 83 -85	4 61 -62	3 72 -66	1 33 25	2 55 -48
8 50 -40	2 85 -81	4 58 50	2 35 -37	H,L= 2-14	4 28 -22	5 0 -1	4 31 26	2 39 -38	3 0 -20
H,L= 0 6	3 45 33	5 0 7	3 0 9	0 30 28	5 0 14	6 73 -73	5 59 -52	3 0 -22	4 0 -4
0 162 156	4 0 -15	H,L= 1-10	4 0 -6	1 0 -17	6 0 -9	7 41 32	6 46 -37	4 0 -22	5 40 -42
1 70 -57	5 40 20	0 128-118	5 29 -31	H,L= 3 0	7 110 102	H,L= 4 3	7 0 0	5 60 -58	H,L= 5-12
2 48 39	H,L= 1 8	1 0 20	H,L= 2 12	0 152-173	8 0 13	1 0 4	8 0 -29	H,L= 5 8	0 67 60
3 0 5	0 60 -49	2 0 -15	0 0 4	1 55 49	H,L= 3 -3	2 133-137	H,L= 4 -6	0 32 -24	1 0 1
4 83 -78	1 0 -6	3 0 18	1 30 -31	2 72 -74	1 19 4	3 0 -1	0 23 16	1 38 -36	2 0 0
5 54 -46	2 0 12	4 37 33	2 0 0	3 21 14	2 59 -51	4 71 -65	1 60 54	2 0 -9	3 0 20
H,L= 0 7	3 0 11	5 0 5	3 30 -32	4 110 148	3 53 -51	5 0 -9	2 52 -46	3 73 -74	4 37 -36
1 68 54	4 62 57	H,L= 1-11	4 0 17	5 0 6	4 0 7	6 56 50	3 71 65	4 34 -23	5 0 -8
2 110-106	5 0 -18	H,L= 2 13	5 0 -6	6 51 43	5 87 -92	7 0 -6	4 38 27	5 0 9	H,L= 5-13
3 59 -59	H,L= 1 9	2 38 -33	1 28 -32	7 56 -39	6 0 20	8 37 35	5 76 -65	H,L= 5 9	1 0 11
4 63 -59	1 0 -16	3 0 9	2 21 -10	H,L= 3 1	7 0 15	H,L= 4 4	H,L= 4 -7	1 54 -46	2 37 35
5 52 -46	2 55 40	4 0 -20	3 0 10	1 95 -98	8 0 16	0 137-140	1 80 -69	2 48 -46	H,L= 5 0
H,L= 0 8	3 0 13	5 46 47	H,L= 2 -1	2 115 142	9 52 61	1 29 -21	2 0 0	3 0 12	0 175 138
0 0 -5	4 0 15	H,L= 1-12	1 12 -18	3 30 -27	H,L= 3 -4	2 63 -51	3 60 54	4 0 -5	1 78 -86
1 71 -59	5 38 37	0 0 22	2 50 -62	4 26 20	0 29 25	3 103-108	4 0 9	5 38 35	2 0 13
2 44 -33	H,L= 1 10	1 0 -20	3 18 -14	5 53 47	1 63 53	4 60 53	5 72 67	H,L= 5 10	3 127-107
3 87 -69	0 42 37	2 0 0	4 42 -40	6 67 -66	2 21 14	5 0 -8	H,L= 4 -8	0 63 -58	4 79 -63
4 43 35	1 42 36	3 46 -47	5 44 -35	7 42 24	3 64 53	6 63 50	0 86 -64	1 0 -2	5 0 -18
5 0 6	2 0 -13	4 0 0	6 88 79	8 54 -54	4 104-115	7 38 36	1 66 -57	2 0 -6	6 67 -63
H,L= 0 9	3 43 37	5 0 10	7 0 -2	H,L= 3 2	5 42 -35	H,L= 4 5	2 0 -12	3 28 28	7 0 16
1 63 -54	4 0 -10	H,L= 1-13	8 51 53	0 18 -2	6 0 7	1 139-146	3 0 -17	4 42 44	H,L= 6 1
2 0 -8	5 0 -25	1 31 31	9 42 36	1 121 134	7 53 -53	2 0 5	4 68 68	5 0 -5	1 0 -2
3 0 31	H,L= 1 11	H,L= 2 0	H,L= 2 -2	2 0 -9	H,L= 3 -5	3 34 23	5 0 -12	H,L= 5 11	2 154-139
4 0 -12	1 52 48	0 100-112	0 142 172	3 84 78	1 32 -26	4 0 13	H,L= 4 -9	1 0 -11	3 0 -5
5 64 54	2 0 15	1 32 -41	1 52 -41	4 69 -71	2 115 120	5 84 86	1 0 -9	2 0 34	4 100 -86
H,L= 0 10	3 34 -33	2 29 -23	2 75 -64	5 50 35	3 53 41	6 0 -2	2 90 -78	3 0 -2	5 0 -9
0 37 -28	4 0 6	3 53 -58	3 53 -54	6 0 -20	4 0 10	7 38 32	3 0 14	4 0 12	6 56 61
1 50 38	5 37 -40	4 52 51	4 80 -89	7 69 -65	5 0 1	H,L= 4 6	4 38 -34	H,L= 5 12	7 0 1
2 0 0	H,L= 1 12	5 73 72	5 31 21	8 41 37	6 65 -66	0 96 -91	5 0 -3	0 17 20	H,L= 6 2
3 37 20	0 47 49	6 82 64	6 63 -53	H,L= 3 3	7 0 -9	1 80 77	H,L= 4-10	1 0 4	0 128-115
4 36 31	1 0 -7	7 69 68	7 0 -5	1 106 111	8 63 -58	2 55 11	0 41 34	H,L= 5 -1	1 0 -10
5 0 -8	2 8 13	H,L= 2 1	8 67 58	2 30 21	H,L= 3 -6	3 105 108	1 37 -30	1 0 -1	2 0 -7
H,L= 0 11	3 33 -34	1 109-130	H,L= 2 -3	3 55 -53	0 125-126	4 0 1	2 0 16	2 148 159	3 84 -63
1 0 15	4 0 -18	2 73 71	1 88 92	4 46 33	1 67 56	5 0 5	3 62 -50	3 0 -11	4 58 52
2 38 34	5 21 28	3 78 87	2 104 119	5 94 -97	2 25 -13	H,L= 4 7	4 62 -58	4 78 67	5 39 25
3 0 3	H,L= 1 13	4 57 54	3 51 -51	6 45 46	3 30 17	1 55 54	5 0 -1	5 0 6	6 56 64
4 0 5	1 0 4	5 92 99	4 24 23	7 0 2	4 81 72	2 72 75	H,L= 4-11	6 45 -42	7 38 33
5 31 -26	2 29 -33	6 0 -4	5 59 -55	H,L= 3 4	5 32 23	3 0 -19	1 54 43	7 0 9	H,L= 6 3
H,L= 0 12	3 0 15	7 0 9	6 66 -59	0 0 5	H,L= 3 -7	4 49 47	2 0 10	8 69 -56	1 76 -66
0 43 32	4 0 -25	8 0 -9	7 0 -19	1 71 -65	1 102 -98	5 39 -40	3 37 -25	9 0 -1	2 54 42
1 0 -1	H,L= 1-11	H,L= 2 2	8 43 -31	2 66 49	2 56 -48	H,L= 4 8	4 36 -24	H,L= 5 -2	3 78 69
2 0 13	1 0 207	0 78 -70	9 40 33	3 76 -68	3 0 12	0 68 58	5 35 -35	0 133-156	4 36 27
3 0 4	2 59 -62	1 53 52	H,L= 2 -4	4 38 -30	4 0 -17	1 46 -43	H,L= 4-12	1 77 76	5 57 56
4 51 -58	3 40 -43	2 42 32	0 24 4	5 37 29	5 82 83	2 0 22	0 37 31	2 78 -77	6 0 -20
5 0 -14	4 18 -15	3 119 146	1 92 85	6 0 -11	H,L= 3 -8	3 0 -3	1 41 39	3 0 -1	H,L= 6 4
H,L= 0 13	5 93-125	4 29 29	2 23 -14	7 69 63	0 48 -32	4 47 -52	2 0 10	4 109 111	0 0 7
1 0 15	6 0 -6	5 90 -43	3 160 194	H,L= 3 5	1 68 -52	5 0 -5	3 0 17	5 0 1	1 49 41
2 32 -34	7 0 -15	6 0 22	4 67 56	1 74 -64	2 52 -40	H,L= 4 9	4 0 9	6 61 50	2 44 37
3 0 -16	8 0 2	7 74 -66	5 0 -11	2 86 -85	3 82 -80	1 0 0	5 34 -8	7 54 -47	3 67 54
4 0 0	9 37 33	8 43 -27	6 0 -16	3 46 32	4 0 14	2 57 -56	H,L= 4-13	8 0 -16	4 37 -28
H,L= 1 0	H,L= 1 -2	H,L= 2 3	7 63 -63	4 54 -39	5 0 12	3 0 -10	1 0 -9	H,L= 5 -3	5 62 -55
1 69-142	0 122 142	1 76 67	8 0 -8	5 64 58	H,L= 3 -9	4 38 -39	2 29 27	1 89 -97	6 0 12
2 47 62	1 129 178	2 105 104	H,L= 2 -5	6 0 26	1 53 39	5 0 -14	3 0 19	2 117-122	7 46 -48
3 59 -80	2 120 126	3 59 -51	1 119-121	7 0 8	2 76 -65	H,L= 4 10	H,L= 5 0	3 44 29	H,L= 6 5
4 57 -67	3 88 128	4 69 58	2 59 50	8 35 35	3 48 -40	0 43 -39	0 143 120	4 73 -75	1 68 59
5 0 2	4 84-111	5 61 -56	3 38 29	H,L= 3 6	4 44 -32	1 30 -27	1 85 69	5 99 88	2 0 11
6 35 -23	5 0 -1	6 63 -64	4 79 73	0 109 -97	5 44 -41	2 35 -33	2 98 77	6 0 3	3 48 -35
7 73 71	6 44 -38	7 0 10	5 92 91	1 0 -12	H,L= 3-10	3 36 -34	3 27 15	7 0 6	4 0 2
H,L= 1 1	7 66 -54	8 41 -38	6 0 0	2 68 -66	0 78 63	4 33 31	4 101 -91	8 0 21	5 60 -57
1 67 -76	8 0 -4	H,L= 2 4	7 0 14	3 0 19	1 0 -6	5 28 13	5 0 0	H,L= 5 -4	6 46 -46
2 43 -48	H,L= 1 -3	0 139 128	8 0 -16	4 80 73	H,L= 4 11	6 34 25	6 57 -53	0 74 65	H,L= 6 6
3 0 8	1 75 -63	1 0 -10	H,L= 2 -6	5 40 -22	3 0 18	1 48 -51	7 50 -36	1 114-124	0 67 61

TABLE 2. (continued)

K	FO	FC
1	50	-41
2	0	3
3	44	-25
4	57	-54
5	0	-6
H,L=	6	7
1	0	2
2	70	-65
3	0	-15
4	40	-38
5	0	-1
H,L=	6	8
0	52	-35
1	31	-23
2	0	-13
3	52	-54
4	48	48
5	0	14
H,L=	6	9
1	41	-31
2	0	11
3	0	23
4	26	-21
5	28	32
H,L=	6	10
0	35	-31
1	28	34
2	0	-5
3	0	15
H,L=	6	11
1	0	5
2	0	20
H,L=	6	-1
1	154	152
2	0	13
3	57	-37
4	0	-6
5	94	-79
6	46	-34
7	0	-19
8	37	-18
H,L=	6	-2
0	88	97
1	54	46
2	58	49
3	146	149
4	0	3
5	0	-22
6	52	-41
7	53	-54
8	0	-14
H,L=	6	-3
1	69	-63
2	94	94
3	48	37
4	59	54
5	71	61
6	39	-32
7	0	8
8	0	-17
H,L=	6	-4
0	183	-187
1	78	-77
2	0	-4
3	55	-42
4	69	61
5	0	-1
6	63	62
7	39	38
H,L=	6	-5
1	0	4
2	123	-126
3	0	5
4	81	-72
5	0	8
6	46	42
7	0	14
8	43	41
H,L=	6	-6
0	131	121
1	34	-27
2	75	70
3	100	-96
4	68	-63
5	0	0
H,L=	6	-7
1	122	130
2	34	22
3	0	-19
4	0	18
5	81	-84
H,L=	6	-8
0	95	80
1	85	75
2	0	-15
3	99	96
4	0	-14
5	0	13
H,L=	6	-9
1	77	-63
2	66	60
3	37	26
4	44	40
5	46	45
H,L=	6	-10
0	62	-52
1	53	-46
2	34	-24
3	0	-2
4	61	56
5	0	-11
H,L=	6	-11
1	0	4
2	62	-61
3	0	12
K	FO	FC
4	41	-33
5	0	6
H,L=	6	-12
0	41	39
1	45	-32
2	41	34
3	34	-24
4	41	-37
5	0	7
H,L=	6	-13
1	48	44
2	0	20
3	0	-23
4	0	14
5	34	-43
H,L=	7	0
0	44	20
1	109	-84
2	0	-7
3	84	-63
4	0	10
5	0	-2
H,L=	7	1
1	52	-30
2	61	-45
3	66	49
4	0	17
5	93	77
6	0	23
H,L=	7	2
0	0	-9
1	66	44
2	0	-11
3	50	39
4	92	90
5	0	-22
6	0	3
7	35	-38
H,L=	7	3
1	30	14
2	101	83
3	0	-12
4	0	6
5	0	2
6	51	-60
H,L=	7	4
0	107	94
1	41	30
2	0	14
3	0	11
4	76	-72
5	0	14
6	39	-41
7	28	-40
H,L=	7	5
1	83	71
2	34	-24
3	0	-9
4	0	-13
5	68	-73
6	32	26
H,L=	7	6
0	0	20
1	66	-57
2	39	29
3	60	-55
4	0	-8
5	0	14
H,L=	7	7
1	32	-24
2	53	-54
3	34	34
4	32	-28
5	29	30
H,L=	7	8
0	49	-45
1	0	-10
2	0	-18
3	0	12
4	41	41
5	38	-40
H,L=	7	9
1	0	-8
2	41	45
3	0	-12
4	0	19
H,L=	7	10
0	0	46
1	19	18
2	0	-3
3	0	31
H,L=	7	-1
1	88	75
2	104	-89
3	37	-34
4	35	-15
5	103	-83
6	39	37
7	0	1
8	34	31
H,L=	7	-2
0	128	116
1	38	28
2	75	62
3	41	31
4	111	-96
5	0	-18
6	46	-42
7	39	-32
8	0	15
H,L=	7	-3
1	83	86
2	110	112
K	FO	FC
3	0	7
4	40	30
5	50	-38
6	51	-50
7	0	-16
8	53	-52
H,L=	7	-4
0	38	-31
1	95	101
2	0	7
3	75	68
4	70	60
5	45	34
6	0	14
7	49	-48
8	34	-38
H,L=	7	-5
0	0	0
1	48	47
2	0	7
3	33	28
4	35	20
5	89	87
H,L=	7	-6
1	69	63
2	72	-62
3	36	-30
4	53	-40
5	52	-50
H,L=	7	-7
0	91	69
1	0	2
2	29	17
3	75	-52
4	67	-56
5	66	47
6	55	-43
7	52	52
H,L=	7	-8
1	58	49
2	93	89
3	0	-4
4	58	54
5	45	-37
H,L=	7	-9
0	86	-71
1	76	64
2	0	5
3	79	78
4	0	14
5	0	16
H,L=	7	-11
1	76	-69
2	0	-1
3	0	14
4	0	7
5	47	45
H,L=	7	-12
0	0	-22
1	0	-12
2	0	-17
3	41	28
4	57	46
5	52	38
6	51	-45
7	0	1
H,L=	7	-13
1	32	27
2	46	-38
3	0	-7
0	113	-116
1	0	-17
2	0	-1
3	59	50
4	69	69
5	0	16
H,L=	7	-14
0	58	-51
1	0	10
2	59	-55
3	0	7
4	0	-4
5	0	17
H,L=	8	-1
1	80	-65
2	100	77
3	67	50
4	0	14
5	62	53
6	47	-46
7	0	8
H,L=	8	2
0	0	13
1	59	50
2	0	-4
3	128	119
4	0	-15
5	0	-8
H,L=	8	3
1	50	47
2	0	7
3	53	42
4	0	-19
5	0	4
H,L=	8	-4
1	0	-16
2	74	71
3	0	9
4	43	39
5	0	25
H,L=	8	-5
0	74	-65
1	0	-5
2	40	-35
3	0	27
4	45	48
5	0	12
K	FO	FC
3	0	10
4	40	-34
5	0	2
H,L=	8	6
3	0	-5
H,L=	9	0
5	72	77
H,L=	9	-8
1	0	-5
2	0	-8
3	60	-58
4	52	55
5	37	39
H,L=	8	8
0	0	0
1	51	-47
2	42	37
3	0	8
4	0	1
5	39	33
6	46	37
7	44	-47
H,L=	9	1
1	32	13
2	135	123
3	37	-36
4	0	-14
5	0	-18
H,L=	9	-10
0	0	10
1	44	33
2	0	18
3	57	57
4	0	-15
H,L=	9	2
0	100	75
1	49	32
2	62	46
3	58	35
4	75	-67
H,L=	9	4
1	0	2
2	0	11
3	0	22
4	66	-62
5	0	-14
H,L=	9	5
1	80	-75
2	0	-9
3	0	23
4	0	-1
5	60	58
H,L=	9	6
0	45	-47
1	34	25
2	34	-30
3	71	75
4	44	47
H,L=	9	7
0	68	75
1	21	23
H,L=	9	-1
1	113	-108
2	49	-38
3	64	40
4	0	-10
5	93	84
H,L=	9	-2
0	41	39
1	84	-77
2	34	-32
3	74	-54
4	62	41
H,L=	10	5
1	41	-33
2	57	64
3	0	14
4	28	3
5	0	-11
H,L=	10	-1
1	87	-74
2	109	104
3	0	3
4	62	51
5	42	-36
H,L=	10	-2
0	210	-200
1	0	-7
2	51	-34
3	0	-6
4	69	56
5	0	-12
6	68	74
7	0	3
H,L=	10	-3
1	66	-60
2	113	-109
3	0	14
4	66	-54
K	FO	FC
5	56	46
6	34	36
7	0	14
8	0	7
H,L=	10	-4
0	57	47
1	0	-13
2	38	28
3	102	-96
4	54	-40
5	0	4
6	0	-14
7	37	38
8	4	7
H,L=	10	-5
1	78	70
2	0	-2
3	38	-33
4	0	2
5	71	-66
6	0	10
7	0	-18
H,L=	10	-6
0	49	44
1	65	59
2	33	-27
3	73	66
4	0	-24
5	0	4
6	0	-16
7	41	35
H,L=	10	-7
1	68	-63
2	62	68
3	0	2
4	37	30
5	0	-8
6	0	-17
7	0	10
H,L=	10	-8
1	33	-27
2	34	-25
3	0	2
4	63	69
5	36	-33
6	0	-9
7	0	7
H,L=	10	-9
1	38	-29
2	67	-67
3	0	27
4	40	-37
5	33	29
6	0	-10
7	0	5
H,L=	10	-10
0	0	5
1	49	-44
2	0	25
3	0	-14
4	32	-32
5	0	8
H,L=	10	-11
1	40	33
2	0	1
3	0	-23
4	0	-11
5	63	-56
6	0	6
H,L=	10	-12
0	76	67
1	47	-36
2	0	-19
3	83	-80
4	35	-31
5	0	8
H,L=	11	0
1	63	54
2	39	36
3	0	-16
4	76	-73
5	0	-22
H,L=	11	1
0	1	2
1	92	-86
2	39	-30
3	43	-43
4	0	16
5	31	-31
H,L=	11	2
0	84	-85
1	71	-69
2	32	-29
3	39	-37
4	36	32
5	28	3
H,L=	11	3
1	63	-55
2	0	7
3	0	21
4	0	5
5	54	54
H,L=	11	4
0	28	-30
1	32	28
2	27	-19
3	43	45
4	39	46
5	0	-11
H,L=	11	5
1	62	61
2	0	-17
3	49	-41
4	32	-32
5	59	-57
H,L=	11	-1
0	79	74
1	0	15
2	0	4
3	0	17
4	0	0
5	0	-2
H,L=	11	-2
1	76	65
2	0	-19
3	69	48
4	36	21
5	0	7
6	30	27
H,L=	11	-3
1	109	-109
2	0	18
3	0	31
4	0	7
5	82	81
6	0	2
H,L=	11	-4
0	88	-63
1	78	-71
2	71	-57
3	36	30
4	71	60
5	32	37
6	0	-16
7	61	-60
H,L=	11	-5
1	42	32
2	43	10
3	90	-100
4	39	-37
5	0	-3
H,L=	11	-6
0	49	44
1	0	10
2	59	48
3	73	66
4	0	-8
5	0	4
H,L=	11	-7
1	68	-63
2	55	50
3	0	2
4	37	30
5	0	-5
H,L=	11	-8
1	30	13
2	56	61
3	0	-5
4	0	3
5	0	8
H,L=	11	-9
1	64	-68
2	0	6
3	0	19
4	0	-10
5	0	3
H,L=	11	-10
0	40	-37
1	0	25
2	0	-14
3	68	-77
4	38	43
5	0	0
H,L=	11	-11
1	33	30
2	58	-64
3	0	-2
4	26	-31
5	20	-3
H,L=	11	-12
0	71	78
1	0	-10
2	0	4
3	40	-44
4	40	49
5	0	-7
H,L=	13	1
1	43	-40
2	0	-12
3	0	20
H,L=	13	2
0	0	-17
1	39	41
2	23	-17
3	25	33
H,L=	13	-1
1	42	38
2	64	-62
3	0	2
4	0	-13
5	22	-26
H,L=	13	-2
0	61	65
1	35	-25
2	35	31
3	0	-6
4	64	-74
5	0	-3
H,L=	13	-3
1	44	41
2	50	47
3	0	-11
4	0	6
5	48	-56
H,L=	13	-4
0	0	-7
1	40	43
2	0	17
3	33	36
4	0	6
5	0	-2
H,L=	13	-5
1	31	-22
2	31	26
3	38	36
4	0	0
5	48	53
H,L=	13	-6
0	31	-22
1	0	-17
2	0	-11
3	0	-32
4	48	48
5	26	24
H,L=	13	-7
1	0	6
2	63	-69
K	FO	FC
0	80	-72
1	0	4
2	0	4
3	0	31
4	0	7
5	56	52
6	0	-6
7	32	38
H,L=	12	-5
1	68	-59
2	61	-60
3	36	30
4	0	-16
5	32	37
6	0	-3
H,L=	12	-6
0	0	7
1	48	-43
2	43	10
3	90	-100
4	39	-37
5	0	-3
H,L=	12	-7
0	82	88
1	48	38
2	32	27
3	0	18
4	31	-23
5	0	3
H,L=	12	-8
1	30	13
2	56	61
3	0	-5
4	37	36
5	0	8
H,L=	12	-9
0	53	-51
1	0	6
2	28	-24
3	29	31
4	47	47
5	0	3
H,L=	12	-10
0	40	-37
1	31	-25
2	0	-14
3	68	-77
4	43	43
5	0	0
H,L=	12	-11
1	33	30
2	58	-64
3	0	-2
4	26	-31
5	20	-3
H,L=	12	-12
0	0	5
1	38	-46
2	22	17
3	37	-46
4	0	-9
5	0	-7
H,L=	13	1
1	43	-40
2	0	-12
3	0	20
H,L=	13	2
0	0	-17
1	39	41
2	23	-17
3	25	33
H,L=	13	-1
1	42	38
2	64	-62
3	0	2
4	0	-13
5	22	-26
H,L=	13	-2
0	61	65
1	35	-25
2	35	31
3	0	-6
4	64	-74
5	0	-3
H,L=	13	-3
1	44	41
2	50	47
3	0	-11
4	0	6
5	48	-56
H,L=	13	-4
0	0	-7
1	40	43
2	0	17
3	33	36
4	0	6
5	0	-2
H,L=	13	-5
1	31	-22
2	31	26
3	38	36
4	0	0
5	48	53
H,L=	13	-6
0	31	-22
1	0	-17
2	0	-11
3	0	-32
4	48	48
5	26	24
H,L=	13	-7
1	0	6
2	63	-69
K	FO	FC
3	0	-17
4	0	-10
5	0	-4
H,L=	13	-8
0	68	72
1	29	-28
2	0	4
3	0	-13
4	37	-41
5	21	-18
H,L=	13	-9
1	48	51
2	27	23
3	0	-2
4	0	13
5	24	-49
H,L=	13	-10
0	0	8
1	24	26
2	25	24
3	46	56
H,L=	13	-11
1	70	72
2	42	-33
3	0	-17
4	46	-41
5	49	-54
H,L=	13	-12
0	45	-50
H,L=	14	0
0	72	-81
1	0	9
2	0	-6
H,L=	14	2
0	42	59
H,L=	14	-1
1	0	-23
2	42	-48
3	0	26
4	0	-34
H,L=	14	-2
0	44	46
1	0	-26
2	33	29
3	54	-68
4	0	-6
H,L=	14	-3
1	65	73
2	0	-3
3	31	-33
4	0	3
H,L=	14	-4
0	69	70
1	39	38
2	0	-8
3	42	44
4	27	-31
H,L=	14	-5
1	0	-9
2	55	63
3	0	2
4	39	42
H,L=	14	-6
0	32	-38
1	27	3
2	0	-13
3	27	33
4	41	44
H,L=	14	-7
1	27	-28
2	26	-27
3	31	35
4	0	-10
H,L=	14	-8
0	0	-3
1	30	-33
2	0	15
3	25	-32
4	0	-20
H,L=	14	-9
1	34	32
2	0	-8
3	22	-29
H,L=	14	-10
0	36	35
1	31	34
H,L=	15	0
0	16	-3
1	0	57
2	0	0
H,L=	15	-1
1	37	-49
2	0	38
3	0	6
H,L=	15	-2
0	44	-57
1	0	-20
2	0	-30
3	0	-19
H,L=	15	-3
1	0	12
2	48	-67
3	0	1
H,L=	15	-4
0	63	72
1	22	-31
2	28	29
3	0	-2
H,L=	15	-5
1	40	40
2	44	59
3	49	-16
H,L=	15	-6
0	27	-34
1	42	46
H,L=	15	-7
1	40	-52
H,L=	15	-8
0	41	-51
H,L=	15	-10
0	37	55

isotropic refinement for all the atoms except hydrogen, the R factor was reduced to 0.156 non-zero reflections. Anisotropic temperature factors for all atoms were introduced at this stage and the refinement was continued; four subsequent cycles of refinement gave $R=0.137$. The atomic scattering factors used in the refinement were taken from those of Hanson and his co-workers.[5]

The final positional and thermal parameters are given in Table 1. The observed and calculated structure factors are given in Table 2.

Result and Discussion

The Geometry around the Tin Atom. The molecular structure and the numbering system of $Me_2SnCl(dtc)$ are shown in Fig. 2. The bond distances and angles in the environment of the tin atom are listed in Table 3. As can be seen in Fig. 2 and Table 3, the configuration about the tin atom is a penta-coordinated distorted trigonal bipyramid. The four atoms, S(1), C(4), C(5), and Sn, lie on the same plane, the equatorial plane of the bipyramid. The Cl and S(2) are at the tops of the bipyramid; the Sn–Cl and the Sn–S(2) bonds cross the equatorial plane at angles of 81.8° and 72.7° respectively. The methyl groups attached to the tin atom are both in the equatorial positions. This configuration

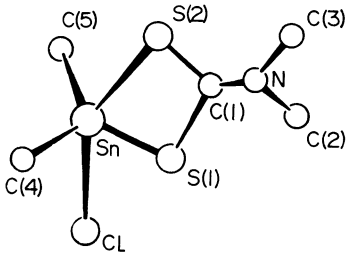

Fig. 2. The molecular structure and the numbering system of $Me_2SnCl(dtc)$.

Table 3. Geometry around the tin atom

(a) Bond distances and angles along with their estimated standard deviations in parentheses.

Bond distance (Å)		Bond angle (°)	
Sn-Cl	2.46 (1)	Cl-Sn-S (1)	86.4 (0.4)
Sn-S (1)	2.48 (1)	Cl-Sn-S (2)	154.5 (0.4)
Sn-S (2)	2.79 (1)	Cl-Sn-C(4)	99 (1)
Sn-C(4)	2.17 (5)	Cl-Sn-C(5)	98 (1)
Sn-C(5)	2.20 (5)	S (1)-Sn-S (2)	68.2 (0.3)
		S (1)-Sn-C(4)	113 (1)
		S (1)-Sn-C(5)	116 (1)
		S (2)-Sn-C(4)	91 (1)
		S (2)-Sn-C(5)	93 (1)
		C(4)-Sn-C(5)	128 (2)

b) The least-squares plane of four atoms, Sn, S (1), C(4), and C(5):

$-0.01339x - 0.52110y - 0.85339z + 2.15929\text{Å} = 0$,

Deviations from the least-squares plane(Å): Sn 0.15
S(1) −0.04
C(4) −0.05
C(5) −0.05

Angle between the least-squares plane and the Sn–Cl bond: 81.8°,

Angle between the least-squares plane and the Sn–S(2) bond: 72.7°.

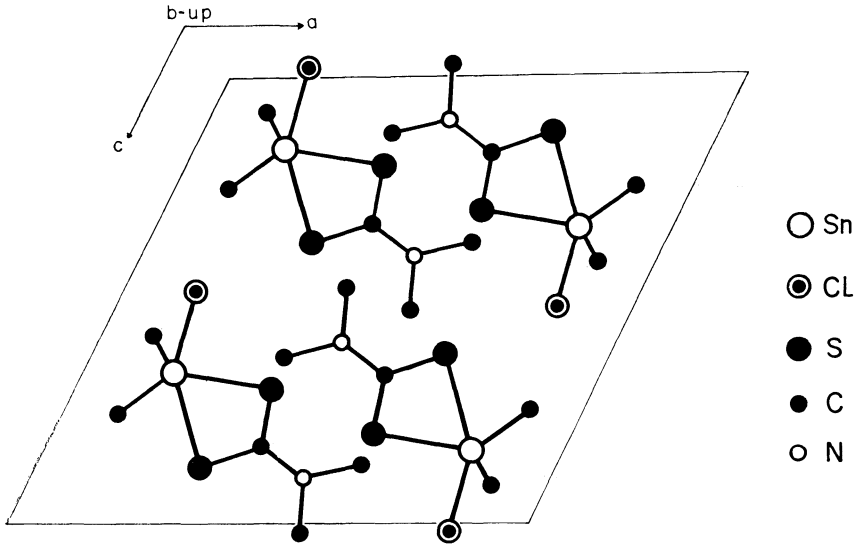

Fig. 3. The crystal structure of $Me_2SnCl(dtc)$ projected onto the (010) plane.

5) H. P. Hanson, F. Herman, J. D. Lea and S. S. Skillman, *Acta Crystallogr.*, **17**, 1040 (1964).

is in good agreement with the model (3) proposed in Fig. 1.

In tin compounds with coordination numbers greater than four, a qualitative MO approach to the bonding nature of the tin atom has been postulated in which no contribution of the 5*d*-orbital of a tin atom is considered.[6,7] In the case of the present complex, it may be assumed, in a way similar to that postulated by Schlemper,[3] that the bonding could also involve the sp^3 hybrid orbitals on the tin atom participating in normal covalent bonds with the two methyl groups and with the chlorine atom and in a three-centered bond with the ligand group. The M–Sn–C(4), M–Sn–C(5), and M–Sn–Cl angles, where M is the midpoint of the line connecting S(1) and S(2), are 104°, 107°, and 122° respectively. The C(4)–Sn–C(5) angle of 128(2°) is, however, considerably larger than the tetrahedral angle. Furthermore, as will be described later, the difference between the two Sn–S bond distances is significant (Table 3); it may be due to the difference in nature between the axial and equatorial bonds. From these facts and from the other angles around the tin atom listed in Table 3, it is better to consider that the configuration about the tin atom in the present complex is a distorted trigonal bipyramid similar to that of the $[(CH_3)_2SnCl_3]^-$ anion.[4]

The Sn–C bond distances, (2.17(5) and 2.20(5) Å), are in good agreement with the sum of the covalent radii of Sn and C, 2.17 Å. These observed values are, within the limits of experimental error, equal to those in $[(CH_3)_2SnCN]$,[8] $[CH_3SnH_3]$[9], and $[(CH_3)_2Sn(C_9H_6NO)_2]$;[3] in the first compound the tin atom takes a trigonal bipyramidal configuration, in the second, a tetrahedral one, and in the third, a hexa-coordination. On the other hand in $[(CH_3)_2SnF_2]$[10] a slightly shorter Sn–C distance (2.06 Å) is obtained.

The Sn–Cl distance, 2.46(1) Å, is slightly longer than the sum of the covalent radii, 2.39 Å. In the $[(CH_3)_2SnCl_3]^-$ ion,[3] the tin atom takes a pentacoordination, and the equatorial Sn–Cl bond distance, 2.32 Å, is shorter than the observed one, while the axial distance, 2.54 Å, is longer.

In the Sn–S distances, the equatorial one (Sn–S(1), 2.48(1) Å), is slightly longer than the sum of the covalent radii, 2.44 Å, but the axial one (Sn–S(2), 2.79(1) Å), is considerably longer. This may suggest that the Sn–S(2) is a weak coordination bond. Such a weak metal-sulfur bond as Sn–S(2) is also found in $[(C_6H_5)As(S_2CN(C_2H_5))_2]$[11] and in $[As(S_2CN(C_2H_5))_3]$.[12]

Table 4. Geometry of the ligand, *N,N*-dimethyldithiocarbamate group

a) Bond distances and angles along with their estimated standard deviations in parentheses.

Bond distance (Å)		Bond angle (°)	
S(1)-C(1)	1.68 (4)	Sn-S(1)-C(1)	91 (1)
S(2)-C(1)	1.74 (4)	Sn-S(2)-C(1)	80 (1)
C(1)-N	1.32 (5)	S(1)-C(1)-S(2)	120 (2)
N-C(2)	1.51 (6)	S(1)-C(1)-N	121 (3)
N-C(3)	1.57 (6)	S(2)-C(1)-N	119 (3)
		C(1)-N-C(2)	122 (3)
		C(1)-N-C(3)	124 (3)
		C(2)-N-C(3)	114 (3)

b) The lest-squares plane of the ligand $-0.27960x-0.85166y+0.4367z+0.5562=0$, Deviations from the least-squares plane (Å):

S(1)	0.02,
S(2)	−0.02,
N	0.00,
C(1)	0.02,
C(2)	−0.03,
C(3)	0.01,

Table 5. The short intermolecular atomic contacts less than 4.0 Å.

From the unit No. 1,			
To the unit No. 2			
Sn-Cl	3.90 Å	Cl-C(4)	3.69 Å
To the unit No. 3			
S(2)-C(3)	3.95		
To the unit No. 4			
N-S(1)	3.52	C(1)-S(1)	3.99
C(1)-C(2)	3.97	C(2)-Cl	3.90
C(2)-S(1)	3.96	C(3)-Cl	3.87
C(3)-S(1)	3.72	C(5)-C(2)	3.68
To the unit No. 5			
S(2)-Cl	3.76	C(3)-S(1)	3.94

Key			
No. 1	x,	y,	z
2	$-x$,	$-y$,	$-z$
3	$1-x$,	$1-y$,	$1-z$
4	$1-x$,	$1/2+y$,	$1/2-z$
5	x,	$1/2-y$,	$1/2+z$

The Geometry of the Ligand Group. The bond distances and angles in the ligand group, *N,N*-dimethyldithiocarbamate, are listed in Table 4(a). The S(1)–C(1) and S(2)–C(1) bond distances are

6) I. R. Beattie and G. P. McQuillan, *J. Chem. Soc.*, **1963**, 1519.

7) M. M. McGrady and R. S. Tobias, *J. Amer. Chem. Soc.*, **87**, 1909 (1965).

8) E. O. Schlemper and D. Britton, *Inorg. Chem.*, **5**, 507 (1966).

9) L. E. Sutton, Ed., "Tables of Interatomic Distances and Configuration in Molecules and Ions," The Chemical Society, London (1958).

10) E. O. Schlemper and W. C. Hamilton, *Inorg. Chem.*, **5**, 995 (1966).

11) R. Bally, *Acta Crystallogr.*, **23**, 295 (1967).

12) M. Colapietro, A. Domenicano, L. Scaramuzza and A. Vaciago, *Chem. Commun.*, **1968**, 302.

1.68(4) and 1.74(4) Å respectively, but the difference is not significant. The C(1)–N distance, 1.32(5) Å, is equal to those found *in other* dialkyldithiocarbamates;[11–19] this fact suggests that the carbon(sp^2)-nitrogen(sp^2) bond has a high double-bond character, as was to be expected on the basis of the IR studies. The N–C(2) and N–C(3) distances, 1.51(6) and 1.57(6) Å are equal; they are close to the N–C single bond distance (1.48 Å) within the limits of experimental error.

The ligand group is planar within ± 0.03 Å. Deviations from the least-squares plane are listed in Table 4(b).

Crystal Structure. The crystal structure projected along the *b* axis is shown in Fig. 3. The short intermolecular atomic contacts, less than 4.0 Å, are summarized in Table 5. None of them is short enough to suggest any significant deviation from the normal van der Waals interaction.

The authors wish to express their deep thanks to Professor Toshio Tanaka and to Professor Rokuro Okawara of this university for their kindness in supplying crystals and in engaging in helpful discussions.

13) M. Bonamico, Mazzone, A. Vaciago and L. Zambonelli, *Acta Crystallogr.*, **19**, 898 (9165).
14) M. Colapietro, A. Domenicano and A. Vaciago, *Chem. Commun.*, **1968**, 572.
15) G. Peyronel and A. Pignedori, *Acta Crystallogr.*, **23**, 398 (1967).
16) M. Bonamico, G. Dessy, A. Mugnoli, A. Vaciago and L. Zambonelli, *ibid.*, **19**, 886 (1965).
17) M. Bonamico, G. Dessy, C. Mariani, A. Vaciago and L. Zambonelli, *ibid.*, **19**, 619 (1965).
18) K. Bowman and Z. Dori, *Chem. Commun.*, **1968**, 636.
19) A. Domenicano, L. Torelli, A. Vaciago and L. Zambonelli, *J. Chem. Soc., A*, **1968**, 1352.

BULLETIN OF THE CHEMICAL SOCIETY OF JAPAN VOL. 43 1667—1670 (1970)

The Visible Spectra of Alizarine Saphirol SE in Water-Dioxane Mixtures

Masaru MITSUISHI, Mieko HASHIZUME, Akira KATAYAMA*1 and Nobuhiko KUROKI*1

Faculty of Textile Science and Technology, Shinshu University, Ueda, Nagano

(Received December 2, 1969)

The visible absorption spectra of Alizarine Saphirol SE in water-dioxane mixtures were obtained, and the spectral changes were considered on the basis of the results of the conductance measurements of the dye. In the spectra of the dye in the mixtures containing less than 60% dioxane, the absorption was found to increase with an increase in the dioxane content. This spectral change was attributed to the decrease in the tendency of the dye to aggregate. In the spectra of the dye in the mixtures containing more than 70% dioxane, however, the absorption found to decrease with an increase in the dioxane content, *i.e.*, with a reduction in the dielectric constant of the solvent. This spectral change was considered to be characteristic of the increase in the electrostatic interaction between the dye ion and the counter ion.

In a previous paper,[1] the ion-association constants were determined by means of Shedlovsky's treatment from the conductance behavior of Alizarine Saphirol SE in water-dioxane mixtures, and they were found to become enormously larger with an increase in the dioxane content of the mixtures, *i.e.*, with a lowering of the dielectric constant. In a solvent with a low dielectric constant, a spectrum characteristic of the ion association between the dye ion and the counter ion can be expected.

In water-organic solvent mixtures having a medium (*ca.* 20) or a low dielectric constant (*ca.* 5), however, no spectrum characteristic of the ion association of the aromatic sulfonate ion with the sodium ion has yet been reported. Therefore, it seems that it would be valuable to examine whether a characteristic spectrum of the interaction between the dye ion and the counter ion is found in the spectrum of Alizarine Saphirol in water-dioxane mixtures.

Experimental

The Alizarine Saphirol SE (sodium salt of 1,5-dihydroxy-4,8-diaminoanthraquinone-2-sulfonic acid) was

*1 College of Engineering, University of Osaka Prefecture, Sakai, Osaka.

1) M. Mitsuishi, Y. Funatsu and N. Kuroki, This Bulletin, **42**, 2384 (1969).

a laboratory stock used in a previous work.[2]

The dioxane was purified by the method described in the previous work.[1]

The visible absorption spectra of the dye were measured by the procedures described in another previous work.[2]

Results and Discussion

The spectra of Alizarine Saphirol in water-dioxane mixtures are shown in Figs. 1 and 2. The spectra of the dye in water and in water-dioxane mixtures containing less than 60% dioxane in Fig. 1 are quite similar to those in water-ethanol mixtures.[2]

The spectrum of Alizarine Saphirol in water is characterized by a prominent peak at about 590 mμ (α-band) and a shoulder at about 620 mμ (β-band). Both the α- and β- bands are intensified by increasing the dioxane content, the β -band is more intensified than the α-band in the solvents containing more than 10% dioxane, and the β-band becomes a prominent peak. The wavelengths of maximal absorption are found to shift towards longer wavelengths. This spectral behaviour is similar to that found in the spectra of the dye in water-ethanol mixtures.[2] The curves from III to VI in Fig. 1 and all of the curves in Fig. 2 have doublet peaks at about 590 and 630 mμ.

These doublet peaks in the main band are known to be characteristic of a monomeric dye with two electron-donating groups, such as hydroxyl or amino groups, in the 1- and 4- positions of an anthraquinone nucleus.[3,4] From the conductance data reported in a previous paper,[1] Alizarine Saphirol was supposed to be monomeric in mixtures containing more than 60% dioxane. Therefore, the spectral changes produced by increasing the dioxane in the mixtures containing less than 60% dioxane (in Fig. 1) may be supposed to come from the decrease in the tendency of the dye to aggregate.

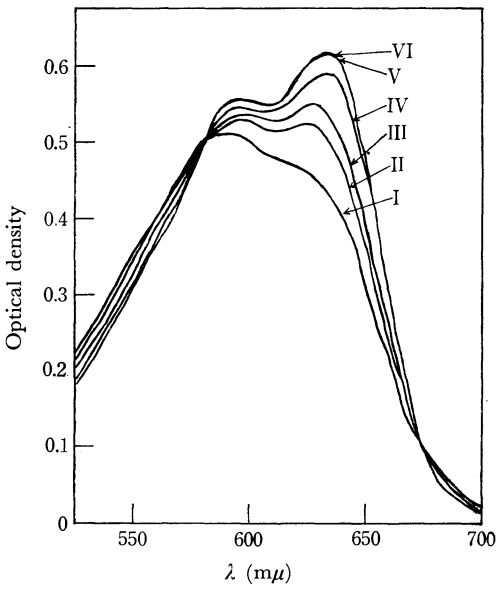

Fig. 1. Spectra of Alizarine Saphirol SE in water-dioxane mixtures at 25°C (3.79×10^{-5} mol/l, 10 mm cell), dioxane concentration; I, 0; II, 10%; III, 20%, IV, 45%; V, 60%; VI, 70%.

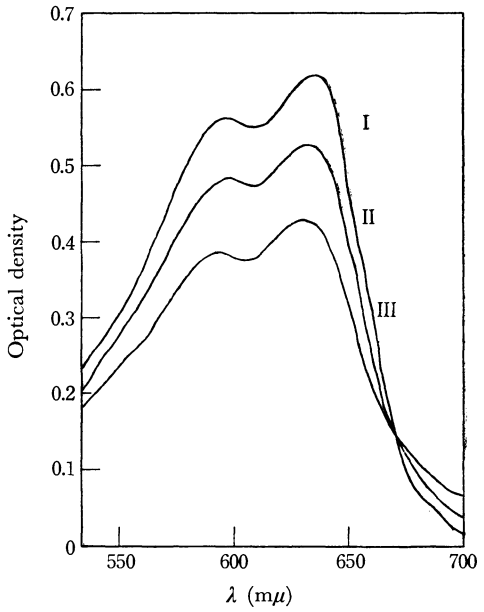

Fig. 2. Spectra of Alizarine Saphirol SE in water-dioxane mixtures at 25°C (3.79×10^{-5} mol/l, 10 mm cell), dioxane concentration; I, 70%; II, 82%; III, 85%.

In Fig. 2, the intensities of both the α- and β-bands are found to decrease progressively with an increase in the dioxane content in the mixtures containing more than 70% dioxane, and an isosbestic point is found at about 670 mμ. As no such spectral change in Alizarine Saphirol is found in water-ethanol mixtures, the spectral changes induced by an increase in the content may be supposed to be caused by the reduction of the dielectric constant of the mixtures to values lower than those of the water-ethanol mixtures.*2

The presence of an isosbestic point at about 670 mμ suggests that a certain equilibrium is set up in the mixtures.

Next, let us examine the cause of the spectral changes induced by increasing the dioxane content

2) M. Mitsuishi and G. Aida, This Bulletin, **39**, 246 (1966).

3) C. H. Allen, C. V. Wilson and C. F. Frame, *J. Org. Chem.*, **7**, 169 (1942).

4) G. S. Egerton and A. G. Roach, *J. Soc. Dyers Colour.*, **74**, 401 (1958).

*2 The dielectric constants of ethanol and of 70, 82, and 85% dioxane are 24.3, 17.7, 9.5, and 8.2 respectively.

in the mixtures. In previous papers,[1,5] the following equilibrium among the dye ion, the sodium ion, and the ionic associate of the dye was established in water-dioxane mixtures with a low dielectric constant;

$$D^- + Na^+ \rightleftarrows (D^-Na^+)^0 \quad (1)$$

where, D^- and $(D^- Na^+)^0$ are the dye ion and the ionic associate respectively.

The ion-association constant, K_A, was obtained by the equation;

$$K_A = \frac{1-2}{c\alpha^2 f_\pm^2} \quad (2)$$

where, α and $f_\pm$ are the degree of dissociation of the ionic associate and the mean activity coefficient of the ion at the dye concentration, C.

The electrostatic interaction between the dye ion and the counter ion was found to increase enormously with an increase in the dioxane content in the mixtures.[1],*3 Accordingly, the spectral changes seen in Fig. 2 may be produced when the ion-association constant of the dye increases enormously with an increase in the dioxane contents of the mixtures.

If the spectral changes in Alizarine Saphirol induced by an increase in the dioxane content are caused by the increase in the electrostatic interaction between the dye ion and the counter ion, *i.e.*, by the increase in the concentration of the ionic associate, spectral changes similar to those shown in Fig. 2 must be observed under any condition that cause the equilibrium constant, K_A, of Eq. (2) to vary.

The ion-association constants of the dye in water-dioxane mixtures with a low dielectric constant and a constant composition were found to increase with a rise in the temperature of the solution.[5],*4 In water-dioxane mixtures of a constant composition, the degree of dissociation of the ionic associate obviously decreases with an increase in the dye concentration; that is the concentration of the ionic associate increase with an increase in the dye concentration.*5

Therefore, if the spectral changes induced by an increase in the dioxane content (Fig. 2) are similar to those spectral changes induced by raising the temperature of the solution and by increasing the dye concentration in the mixtures with a constant composition, the spectral changes shown in Fig. 2 may be concluded to be induced by the increase in the interaction between the dye ion and the counter ion.

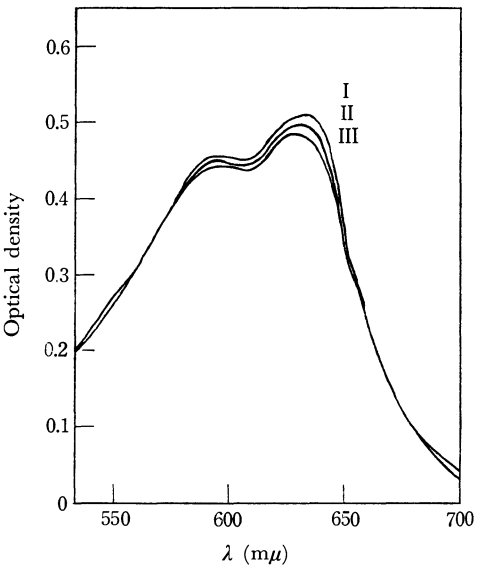

Fig. 3. Spectra of Alizarine Saphirol SE in 82% dioxane at various temperatures (3.79×10^{-5} mol/l, 10 mm cell); I at 16°C; II, 24°C; III, 35°C.

The effect of raising the temperature of the solution on the visible spectrum of Alizarine Saphirol in 82% dioxane is shown in Fig. 3. The intensities of both the α- and β-bands are found to decrease with a rise in the temperature of the solution, *i.e.*, with an increase in the ion-association constant, and an isosbestic point is found at about 670 mμ. The spectral change seen in Fig. 3 is found to be less than that seen in Fig. 2, but these spectral changes can be explained reasonably by taking into consideration the fact that the effect of the increase of dioxane content is larger than that of the elevation of the temperature of the solvent with a constant composition on the ion-association constant of the dye.*6

The visible spectrum of Alizarine Saphirol in 70% dioxane is shown in Fig. 4. The intensities of both the α and β-bands are found to decrease with an increase in the dye concentration, and an isosbestic point is found at about 670 mμ. The decrease in the intensities seen in Fig. 4 may be supposed to be induced by the decrease in the degree of dissociation of the ionic associate. The spectral change shown in Fig. 4 is less than that shown in Fig. 2, but these changes can be explained reasonably by taking into consideration the fact that the effect of the increase in the dioxane content is larger than that of the increase in the dye concentration in the solvent

5) M. Mitsuishi, M. Hashizume, A. Katayama and N. Kuroki, This Bulletin, **43**, 960 (1970).

*3 The ion association constants of the dye in 70, 82, and 85% dioxane at 25°C are 1.88×10^3, 9.86×10^3, and 3.46×10^4 respectively.

*4 For example, the ion association constants at 15, 25, and 35°C in 82% dioxane are 8.67×10^3, 9.86×10^3, and 1.30×10^4 respectively.

*5 For example, the degrees of the dissociation of the ionic associate at dye concentration of 0.79, 2.34, and 5.64×10^{-5} mol/l in 70% dioxane are estimated to be about 0.990, 0.970, and 0.935 respectively.

*6 *Cf.* footnotes *4 and *3.

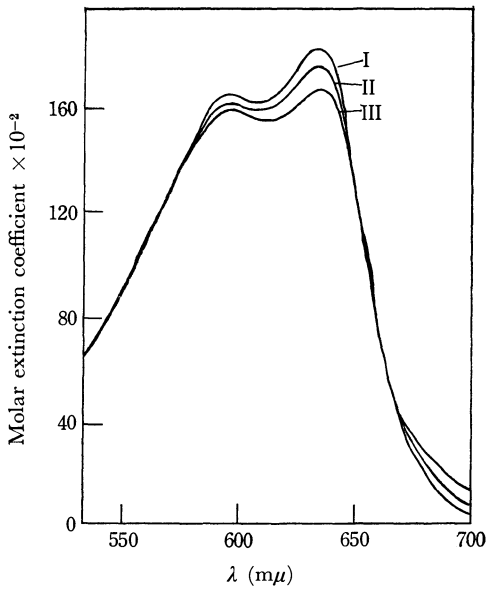

Fig. 4. Spectra of Alizarine Saphirol SE in 70% dioxane at 25°C, dye concentration; I, 0.179×10^{-5} mol/l; II, 2.34×10^{-5} mol/l; III, 5.64×10^{-5} mol/l.

of a constant composition on the degree of dissociation of the ion associate.*7

From the results noted above, the spectral changes in Alizarine Saphirol induced by increasing the dioxane content in mixtures containing more than 70% dioxane (Fig. 2) has been found to be quite similar to those changes induced by raising the temperature of the solution (Fig. 3) and those induced by increasing the dye concentration in mixtures with a constant composition (Fig. 4). That is to say, the intensities of the main band of the visible spectra of Alizarine Saphirol in water-dioxane mixtures with low dielectric constants are invariably found to decrease under any conditions where the interaction between the dye ion and the counter ion increases in the mixtures.

As has been described above, we can conclude that the changes in the spectra of Alizarine Saphirol induced by increasing the dioxane content in mixtures containing more than 70% dioxane are to be attributed to the increase in the interaction between the dye ion and the counter ion, and that such spectral changes are characteristic of the increase in the electrostatic interaction between the two ions.

The authors wish to thank Professor Haruo Gotoh for his helpful discussions.

*7 The values of α at a concentration of 3.79×10^{-5} mol/l in 70, 82, and 85% dioxane are estimated to be about 0.945, 0.750, and 0.640 respectively.

BULLETIN OF THE CHEMICAL SOCIETY OF JAPAN VOL. 43 1670—1675 (1970)

Photo-Ionization of Molecules in Solutions. VI. Studies on the Photocurrent Arising from the Flash-Excitation of Aromatics in Solutions

Takeshi IMURA,* Naoto YAMAMOTO and Hiroshi TSUBOMURA

Department of Chemistry, Faculty of Engineering Science, Osaka University, Toyonaka, Osaka

(Received December 13, 1969)

A technique is described for the study of the photocurrent due to the transient ionic species produced by the flash photolysis of aromatics in solutions at room temperature. The technique has proved to give valuable information in a way complementary to conventional flash spectrometry. The photo-ionization of *N,N,N′,N′*-tetramethyl-*p*-phenylenediamine was studied by this method in polar and non-polar solvents. The photocurrents of the solutions of some electron donor-acceptor systems were also measured, and the results were compared with that obtained from flash spectrometry. The recombination rate constants of the ionic species were estimated from the decay of transient photocurrents.

Flash spectroscopy is a powerful tool for studies of chemical reaction intermediates, including unstable ionic species.

The photo-ionization of *N,N,N′,N′*-tetramethyl-*p*-phenylenediamine (TMPD) has been studied extensively by steady state illumination in low-temperature matrices and by flash spectroscopy at room temperature. The photo-ionization was shown to

*1 Present address: Faculty of Engineering, Osaka University, Suita, Osaka

take place by the two-step process, with the triplet state as the intermediate.[1-5]

By flash spectrometry for the intermolecular electron-transfer processes between an electron donor (D) and acceptor (A), Leonhardt and Weller found that the cation (D^+) from a donor molecule and the anion (A^-) from an acceptor molecule were formed momentarily by photo-excitation in a polar solvent, and disappeared immediately by the recombination process.[6,7] This process is closely related with the mechanisms of fluorescence quenching in polar solutions. More evidence on the formation of ionic intermediates has been obtained recently by photo-excitation of donor-acceptor systems in polar solutions.[8]

However, the flash-spectroscopic technique has limitations: 1) Measurement of the spectra of the intermediates is difficult when they lie in the same region as that of the solvent or the original solute molecules. 2) It is often difficult to make the assignment of the transient spectrum. 3) The spectroscopic data cannot give information on whether there are loose associations between cations and anions (or solvated electrons).

We have attempted to extend information on the ionic intermediates formed by flash-illumination of aromatics in solutions at room temperature by measuring the transient photocurrent arising from these intermediates. In the present paper, some of the results are reported.

As an earlier photoconductivity work of the same kind, Jarnagin *et al.*,[9-11] studied photocurrents caused by the flash illumination of aromatic hydrocarbons in solutions which they attributed to a result of bimolecular triplet-triplet interaction of the aromatics. Recently, Pilloff and Albrecht have measured the photocurrent appearing in a non-polar solvent containing TMPD,[4] and found the photocurrent signal to be proportional to the square of the total intensity of flash light.

Experimental

Commercially-available TMPD dihydrochloride was neutralized in an aqueous solution with a little excess of ammonia. The precipitate of TMPD was washed slightly with water, dried, and sublimed twice in a vacuum. Anthracene and maleic anhydride were recrystallized from a benzene and a chloroform solution. *p*-Dimethoxybenzene and 1,3,5-trinitrobenzene were recrystallized from ethanol solutions and sublimed twice in a vacuum. Acetonitrile and ethanol were purified by methods described in an earlier paper.[1] G. P. grade formamide and spectro-grade dimethylformamide were used without further purification.

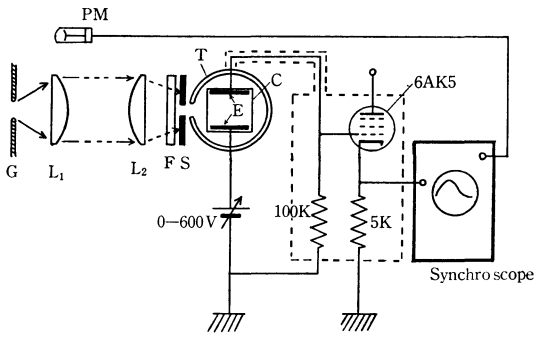

Fig. 1. Schematic diagram of the apparatus. G: tungsten gap. L_1 and L_2: quartz lenses (ϕ=100 mm). F: filter. S: slit. T: copper shield tube. C: quartz sample cell. E: electrodes. PM: photomultiplier.

In Fig. 1, a schematic diagram of the apparatus is shown. Flash light was generated from the condenser discharge through a tungsten gap (G), initiated with a high voltage trigger pulse. In order to decrease the electrical noises due to the flash discharge, a distance of about 5 m was taken between quartz lenses L_1 and L_2. The quartz sample cell was put into a copper shield tube (T). The light comes into the cell through a slit 2 mm in width, so that direct irradiation on the two electrodes (spaced by approximately 9 mm) was avoided. The electrode was a plate having the dimensions 1 cm × 4 cm. Aluminum, nickel and platinum electrodes were tested and no substantial difference in the photocurrent response was found by use of any electrode, although the first two electrodes were somewhat stained gradually in the course of experiments. The photocurrents for the acetonitrile solutions containing TMPD were measured by the above mentioned procedure. As photocurrents were very weak in all other cases, the light source (G) was placed directly before the filter so as to increase the light intensity. The tungsten gap (G) used as the light source was fired at 250J (5 μF, 10 kV) in the case of the acetonitrile solution of TMPD and at 125J (2.5 μF, 10 kV) in other cases. The duration of the flash was less than 3 μsec.

The upper part of the sample cell (C) can be sealed with a ground glass stopper. Before each of the experiments a fine Teflon tube was inserted into the cell and commercial high-purity nitrogen was bubbled

1) Y. Nakato, N. Yamamoto and H. Tsubomura, This Bulletin, **40**, 2480 (1967).
2) N. Yamamoto, Y. Nakato and H. Tsubomura, *ibid.*, **40**, 451 (1967).
3) N. Yamamoto, Y. Nakato and H. Tsubomura, *ibid.*, **39**, 2603 (1966).
4) H. S. Pilloff and A. C. Albrecht, *J. Chem. Phys.*, **49**, 4891 (1968).
5) G. E. Johnson and A. C. Albrecht, *ibid.*, **44**, 3162, 3179 (1966).
6) H. Leonhardt and A. Weller, *Z. Physik. Chem. N. F.*, **29**, 277 (1961).
7) H. Leonhardt and A. Weller, *Ber. Bunsenges. Physik. Chem.*, **67**, 791 (1963).
8) K. Kawai, N. Yamamoto and H. Tsubomura, This Bulletin, **42**, 369 (1969).
9) A. Kawada and R. C. Jarnagin, *J. Chem. Phys.*, **44**, 1919 (1966).
10) K. deGroot, L.P. Gary and R.C. Jarnagin, *ibid.*, **48**, 5280 (1968).
11) L. P. Gary, K. deGroot and R. C. Jarnagin, *ibid.*, **49**, 1577 (1968).

through the solution.

The circuit rise time was less than 0.4 μsec. The d.c. dark current in the case of polar solvents was of the order of 10^{-4} A. An Iwasaki SS-5302 type synchroscope was used for measurements of the currents. A part of the flash light was received by a photomultiplier(PM) and the signal was used to trigger the synchroscope. Electrical noise resulting from flash-firing on the photocurrent signal disappeared within 20 μsec after the flash.

Results

Flash-excitation of TMPD. In Fig. 2 are shown the synchroscope tracings of the photocurrents produced by the flash irradiation of deoxygenated solutions containing TMPD. The lower straight lines indicate the dark current. Two maxima of the photocurrent were found for the acetonitrile solution. The first one appeared at about 0.2 msec, more accurately 170 μsec as found by magnifying the sweep velocity of the synchroscope. The second maximum was at about 50 msec under this applied electric field.

Flash light intensity was so weak in this experiment that the characteristic color of TMPD cation (Würster's blue) did not appear. But under the condition of very strong flash intensity the irradiated TMPD solution was colored and exhibited a large photocurrent signal having a prolonged tail measurable even at 60—90 sec after the flash.

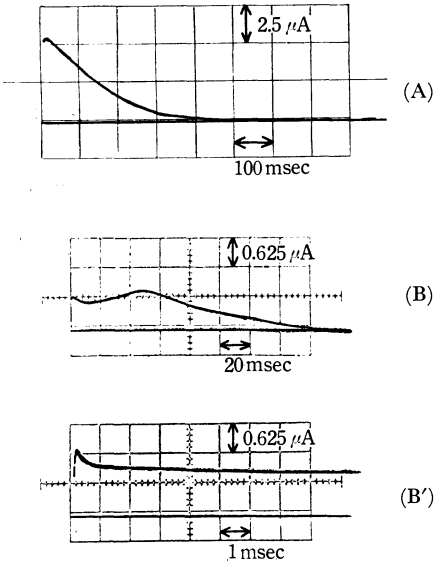

Fig. 2. The photocurrent of TMPD solution.
(A) In dimethylformamide, 1.5×10^{-4}M. Applied field: *ca.* 100 V cm^{-1}. 2.5×10^{-6} A/div, 100 msec/div.
(B), (B′) In acetonitrile, 3.7×10^{-3}M. Applied field: *ca.* 700 V cm^{-1}. 6.25×10^{-7} A/div., (B) 20 msec/div, (B′) 1 msec/div.

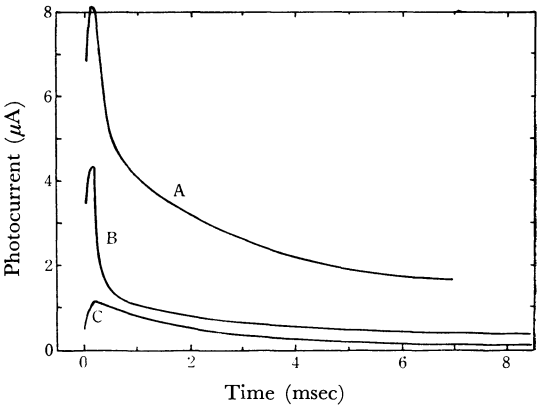

Fig. 3. The photocurrent of solution of DMB and TNB in acetonitrile. Applied field: *ca.* 100 V cm^{-1}. Concentration of DMB and TNB: both 1.5×10^{-3}M.
A: Deoxygenated. B: Not deoxygenated. C: Deoxygenated, and a 0.1M DMB solution was used as a filter.

Flash-excitation of Donor-Acceptor System. Figure 3 shows the photocurrent signals in an acetonitrile solution of *p*-dimethoxybenzene (DMB) and 1,3,5-trinitrobenzene (TNB). Curve A is the transient photocurrent signal for a deoxygenated solution, and curve B for an aerated solution. The difference between curve A and B indicates the effect of dissolved oxygen which seems to reduce the formation of charge carriers. Curve C indicates the photocurrent for the case where only 1,3,5-trinitrobenzene (acceptor) was selectively excited by the flash light through a filter solution of *p*-dimethoxybenzene (0.1M, 10 mm) in front of the sample cell. The photocurrents observed for these samples indicate only one maximum at 140 μsec. There is no such a maximum for the absorbance of the ionic species in the flash spectroscopic measurement of the same solution.[8] Assuming that the decay is second order, the rate constant is derived from curve C of Fig. 3 to be 9.2×10^{8}M^{-1}sec^{-1}. The value is about the same as that of the decay rate constant of *p*-dimethoxybenzene cation reported in a previous paper,[8] by taking the molar extinction coefficient of the cation to be about 3×10^{3}. The initial concentration of the ions interpolated to zero time becomes $\sim10^{-5}$M.

The photocurrent of a dimethylformamide solution containing *p*-dimethoxybenzene and 1,3,5-trinitrobenzene (both 1.4×10^{-3}M) was also measured. Its shape was essentially the same as that of the acetonitrile solution, but the photocurrent at the maximum was only one half. The maximum comes later and the decay is slower than for the acetonitrile solution.

In Fig. 4, curve A shows the photocurrent of an acetonitrile solution containing 1.1×10^{-3}M anthracence and 1.4×10^{-3}M maleic anhydride. Curve

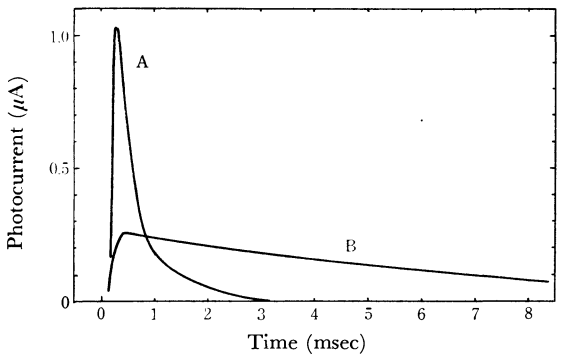

Fig. 4. The photocurrent of solution of anthracene and maleic anhydride in acetonitrile. Filter: UV-35.
A: anthracene (1.1×10^{-3}M), maleic anhydride (1.4×10^{-3}M). Applied field: *ca.* 100 V cm^{-1}.
B: anthracene alone (1.1×10^{-3}M). Applied field: *ca.* 600 V cm^{-1}.

B shows the photocurrent of anthracene alone (1.1×10^{-3}M) in the same solvent. A filter (Toshiba UV-35) was used to excite selectively the first bands (^1L_a) of anthracene. The recombination rate constants were calculated from the decay of the photocurrents to be $\sim10^{10}$M^{-1} sec^{-1} from both curves A and B, if the effective volume where the ions were generated was taken to be 0.1 cm^3. The schematic aspect of curve B resembles that obtained by Kawada and Jarnagin.[9] When dissolved oxygen was not removed by bubbling with pure nitrogen gas, the photocurrent for curve B was so weak that the measurements were almost impossible.

After more than ten flashes, it was found that the ^1L_a absorption bands of anthracene in the sample solution decreased, indicating that the concentration of anthrancene was reduced. This seems to be most probably due to the Diels-Alder type addition reaction between anthracene and maleic anhydride. Attempts to detect the absorption spectra of intermediates from this donor-acceptor system by means of the flash spectrometry[12] were made. But no spectrum of ionic species was obtained in the wavelength range from 300 to 650 mμ, though transient T–T′ absorption bands of anthracene were found near 420 mμ.

Discussion

The photocurrent density is given by

$$i(t) = \sum_j Z_j e n_j(t) \mu_j E,$$

in which e represents the charge of the electron, E the applied electric field and μ_j the carrier mobility. $n_j(t)$ represents the number of positive and negative charge carriers in unit volume which changes with time by reactions between the carrier and solvent (or impurities), by the recombination reaction, or by the electrical discharge at the electrodes when E or μ is very large.

The lower limit C_l (mol/l) of the concentration of ions produced by a flash irradiation in the sample solution, is expressed by

$$C_l \sim (1/VF)\int_0^\infty i(t)\mathrm{d}t,$$

where V is the volume of the sample solution in liter and F Faraday constant. C_l is calculated to be less than 10^{-9}M for the acetonitrile solution of TMPD. Lower values, 10^{-10}M, are obtained for the donor-acceptor systems.

The behavior of the photocurrents may be classified into three types as shown below, where τ is the lifetime of charge carriers or ionic species, and t_t the time required for the charge carriers produced near the center of two electrodes to arrive at the electrode, *i. e.* the 'transit time' which depends upon E and μ:

(1) $t_t \gg \tau$: In this case, the velocity of the charge carriers in the electric field is negligibly small, and the behavior of the photocurrent may be explained only by taking account of the reactions of the ionic species, *i. e.*, the charge neutralization or the electron transfer reactions;

(2) $t_t \ll \tau$: In this case, the ionic species remain stable enough until they arrive at the electrodes. This case is suitable for the study of the electrical transfer phenomena in solutions;

(3) $t_t \simeq \tau$: This is an intermediate case of the former two.

It is generally stated that the mobilities of inorganic ions in aqueous solutions are of the order of 10^{-4} cm^2 V^{-1} sec^{-1}, and those of organic ions in organic solutions may also be roughly estimated at the same order.[6,7] Taking the mobility to be this order of magnitude, the distance between the electrodes to be 1 cm, and the applied electric field to be 10^2 V cm^{-1}, the drift velocity of ions and the transit time become the order of 10^{-2} cm sec^{-1} and 50 sec, respectively. As all samples, except TMPD solution, examined in the present work have decay times of the order of 1 msec to 10 msec, they fall into the above-mentioned case (1). As the lifetime of TMPD cation is exceptionally long, estimated at 10^2—10^3 sec from the decay of its absorption spectrum in flash photolysis,[1] the photocurrent for this case falls into case (3).

Without exception, the photocurrent measured showed an initial rise to a maximum, which is attained at about 100 μsec. This behavior is contrary to the results of transient absorption spectra obtained from the flash spectrometry of donor-acceptor systems.[8] This delayed photocurrent was also found for the flash illumination of anthracene *etc.* in tetrahydrofuran by Jarnagin *et al.*[9–11] who regarded it as evidence for the 'delayed

12) The apparatus used here was the same as described in Ref. 3.

ionization' through the triplet-triplet interaction of the aromatics. Our results in an acetonitrile solution of anthracene closely resembled theirs. This interpretation does not apply, however, to the donor-acceptor systems or to the photo-ionization of TMPD in solutions. The fact that the rise time of the photocurrent gets longer for the more viscous solvent favors the interpretation that the photochemically produced ions initially exist in the form of loose ion-pairs,[13,14] which do not contribute to the electric current, and then seperate into free ions by the thermal motion of surrounding solvent molecules. The fact that the photocurrents reach maxima at about 100 μsec, however, seems too long for such diffusional processes.[15] Therefore, the explanation for the appearance of the maxima of the photocurrents is difficult at present.

TMPD Solutions. In previous papers,[1-3] it was found by means of flash spectrometry that TMPD in polar solvents is photo-ionized by biphotonic process *via* the triplet state as the intermediate. The fact that photocurrent has been detected for the irradiated solution certainly indicates that ions are generated and are present rather as separate positive and negative ions (or solvated electrons) than in the form of ion-pairs.

It has already been stated in the early part of this paper that the photocurrent in an acetonitrile solution of TMPD has two maxima (at 170 μsec and at about 50 msec). This behavior of the photocurrent was not found in formamide, dimethylformamide and *n*-hexane and for all other solutes examined in this work. Kawada and Jarnagin had found two maxima in a tetrahydrofuran solution of anthracene or phenanthrene and considered the second maximum to be due to impurities.[9] The second maximum of the photocurrent in this work suggests the existence of a different kind of charge carrier (Q_2). If the recombination rate of the charge carrier corresponding to the first maximum (Q_1) is larger than that of Q_2 and the mobility of Q_2 is larger than that of Q_1, it is possible that the photocurrent has double maxima. The dark reaction of Q_1 with the surrounding solvent molecules or impurities might form Q_2. The carrier, Q_2 might be cyanide anion (CN^-), methylene cyanide anion (CH_2CN^-) or $CH_3\underset{\displaystyle CH_2CN}{\underset{|}{C}}=N^-$ as conjectured from the reaction of acetonitrile with sodium metal. Cationic intermediates will not be concerned with the second maximum, since TMPD cation is rather stable.

The position of the second maximum was found to be proportional to the reciprocal of the applied voltage. This fact suggests that the time of the appearance of the maximum, t_m is of the same order of magnitude as t_t, because if t_m is much smaller than t_t, t_m should be determined mainly by the charge annihilation processes in the solution and not by the change with applied voltage.

The influence of some macroscopic properties of solvents on the photocurrent for TMPD is listed in Table 1. In ethanol the photocurrent was hardly detectable though the transient electronic spectrum of the TMPD cation appeared after flash illumination. This seems to imply that the ionic species produced by the photo-ionization in ethanol is in the form of ion-pairs.[16] In *n*-hexane a weak photocurrent (less than 6×10^{-8} A) having the decay time of a few milli-seconds was observed. Further, it appears from Table 1 that the photocurrent depends both on the dielectric constant and on the viscosity, and not on the refractive index. This is a reasonable result, because (1) the ion-pair may be

TABLE 1. PHOTOCURRENT OF TMPD SOLUTION

($\sim10^{-4}$M. Applied field: *ca.* 100 V cm^{-1}. A glass plate (5 mm thick) was used as a filter.)

Solvent	Dielectric constant (25°)	Square of refractive index	Viscosity (centipoise)	Peak of photocurrent (10^{-7}A)	Appearance of TMPD cation spectrum
n-Hexane	1.9	1.890	0.324 (15°C)	<0.6	—
Ethanol	24.3	1.856	1.08 (20°C)	very weak	+
Dimethylformamide	36.7	2.015	0.908 (25°C)	3.75	+
Acetonitrile	37.5	1.812	0.375 (15°C)	43.8*	+
Formamide	109.5	2.089	3.76 (20°C)	10.0	+

* At the first peak. The light source was placed directly before the filter, as was done in all other solutions.

13) G. S. Hooper and C. A. Kraus, *J. Amer. Chem. Soc.*, **56**, 2265 (1934). R. M. Fuoss and C. A. Kraus, *ibid.*, **57**, 1 (1935).
14) T. E. Hogen-Esch and J. Smid, *ibid.*, **88**, 307, 318 (1966).
15) H. Knibbe, D. Rehm and A. Weller, *Ber. Bunsenges. Physik. Chem.*, **72**, 257 (1968).
16) M. Koizumi and H. Yamashita, *Z. Physik. Chem. N. F.*, **57**, 103 (1968).

dissociated into free ions the more easily, the higher the dielectric constant, and (2) the mobility of the charge carrier becomes the smaller, the more viscous the solvent.

Donor-Acceptor Systems. It has been fairly well established by means of the flash spectrometry that the flash excitation of a donor-acceptor system in polar solvents produces transient cations and anions through excited charge transfer states, as described below,[6-8]

$$A+D+h\nu \longrightarrow A^*+D \text{ (or } A+D^*) \rightleftarrows (A\cdots D)^*$$
$$(A\cdots D)^* \longrightarrow (A^-\cdots D^+)_{solv} \longrightarrow A^-_{solv}+D^+_{solv} \longrightarrow A+D,$$

where $(A\cdots D)^*$ means the charge transfer state and $(A^-\cdots D^+)_{solv}$ the ion-pair. The existence of the photocurrent for the system of *p*-dimethoxybenzene-1,3,5-trinitrobenzene in acetonitrile as revealed in the present research confirmed the formation of free ions in the solution. This may be taken as a supplementary evidence for the electron transfer process of the same system observed by flash spectroscopy.[8]

For the system of anthracene-maleic anhydride-acetonitrile, no flash-spectrum of the ionic species was found. The reason for this may probably be the insensitivity of the photographic film used here at the near infrared region where the anthracene cation is expected to have the absorption spectrum. The weak absorption bands of this cation to be present in the visible and ultraviolet region should also overlap with those of the orginal solutes. The observation of photocurrent in this system, therefore, shows the superiority in the sensitivity of detection of ionic species by the present photocurrent method over the spectroscopic method.

As described in the Results, the flash irradiation of an acetonitrile solution of anthracene alone showed a photocurrent. But the intensity of the photocurrent was much weaker than that for the solution containing both anthracene and maleic anhydride. It seems reasonable, therefore, to attribute the photocurrent for anthracene (An)-maleic anhydride (Ma) system to the formation of An^+ and Ma^- through the charge transfer excited state, similar to the *p*-dimethoxybenzene-1,3,5-trinitrobenzene system. The photocurrent observed for the former is much weaker compared with that for the latter, although the experimental conditions for both cases are about the same. The main reason for this may be attributed to the difference in the strengths of the acceptors. Thus, 1,3,5-trinitrobenzene, with larger electron affinity than maleic anhydride may produce more free ionic species in the course of the reaction

$$(D^+\cdots A^-)_{solv} \longrightarrow D^+_{solv}+A^-_{solv}.$$

As is well known, anthracene and maleic anhydride form Diels-Alder type adducts by the effect of ultra-violet light. The quantum yield of this reaction in dioxane was determined to be 0.02.[17] This low value of the quantum yield seems to show that most of the 'encounter complex' of excited anthracene and maleic anhydride ($An^*\cdots Ma$) will transfer to the charge transfer state $(An\cdots Ma)^*$ which should be lower in energy than the former, and then to free ions and a small part of the encounter complex will undergo addition reaction.

$$\begin{array}{ccccc} {}^1An^* + Ma & \longrightarrow & (An^* \cdots Ma) & \dashrightarrow & \text{adduct} \\ \uparrow & & \downarrow & & \\ h\nu & & (An \cdots Ma)^*_{solv} & & \\ \downarrow & & \downarrow & & \\ An + Ma & & An^+_{solv} + Ma^-_{solv} & & \end{array}$$

17) J. P. Simons, *Trans. Faraday Soc.*, **56**, 391 (1960).

BULLETIN OF THE CHEMICAL SOCIETY OF JAPAN VOL. 43 1676—1682 (1970)

Some Semi-Empirical SCF MO Calculations on Norbornadiene, Norbornene, and Their 7-Cations

Hideyuki KONISHI, Hiroshi KATO*1 and Teijiro YONEZAWA

Department of Hydrocarbon Chemistry, Faculty of Engineering, Kyoto University, Kyoto

(Received December 13, 1969)

Using a semi-empirical SCF MO method for valence electron systems proposed previously by the present authors, the electronic structures of norbornadiene (NBD), norbornene (NBE), and their 7-cations are discussed, together with the configurational problem of the 7-cations. In NBE and NBD, the interaction between the π AO's in the double bond and the AO's of the other parts of the molecules is made clear by the charge densities and the bond orders. For the first electronic transition assigned to a π–σ^* or σ–π^* in NBD, the present calcuation gives a rather larger excitation energy than does the experiment. For 7-norbornenyl and 7-norbornadienyl cations, the presence of structures distorted from NBE and NBD respectively can theoretically be concluded. The delocalization of the positive charge and the bonding interaction between the bridged carbon atom and the double bond carbon atoms support the concept of the so-called non-classical carbonium ions.

Norbornadiene (NBD), norbornene (NBE), and related compounds have been investigated from many points of view, such as reaction mechanisms,[1] electronic transitions,[2,3] and other physicochemical properties.[1] The first electronic band of NBD, which was identified as a forbidden π–π^* one,[4-6] has recently been pointed out to be a π–σ^* or σ–π^* one by Robin and Kuebler.[3] It seems interesting to include σ electrons in our theoretical studies in order to compare the electronic structures of NBD with earlier π-electron calculations.[4-6] An investigation of the σ electronic structures of NBD as well as of the π electronic structures is an aim of the present calculations, made by the semi-empirical SCF MO method for valence electron systems previously presented by the present authors.[7]

The carbonium ions of NBD and NBE have been discussed as so called non-classical carbonium ions.[1] In our study of the 7-carbonium ions of NBD and NBE, we have focussed our attention on the following four points: the distortion of the valence angle and the alternation of the bond length with reference to the neutral molecules, the migration of charges, and the non-bonding interactions in these ions.

Method and Parameters

The present calculations were performed by means of our previously-reported semi-empirical SCF MO method, using the zero-differential overlap approximation except for the one-center exchange integrals.[7] All the core-resonance integrals are taken into account in estimating the non-bonding interactions of atoms as:

$$H_{rs} = -KS_{rs}(I_r+I_s)$$

where K is a constant which will be described in a later part of this section, where S_{rs} is the overlap integral between the rth and the sth atomic orbitals (AO's), and where I_r denotes the valence-state ionization potential of the rth AO. The other parts of the present method and the basic integral values are the same as in our previous paper.[7]

For the geometry of NBD, the gas-electron diffraction datum reported by Morino *et al.*[8] is adopted. (All the skeletal carbon atoms for the compounds treated in the present paper are numbered as is shown in Fig. 1.) For the 5- and 6-carbon skeletal structures of NBE, the datum of norbornane[8] is used, while for the residual part,

*1 Present address: Department of General Education, Nagoya University, Nagoya.

1) P. D. Bartlett, "Nonclassical Ions," Benjamin, N. Y. (1965).

2) S. Stokes and L. W. Pickett, *J. Chem. Phys.*, **23**, 258 (1955).

3) M. B. Robin and N. A. Kuebler, *ibid.*, **44**, 2664 (1966).

4) C. F. Wilcox, Jr., S. Winstein and W. G. McMillan, *J. Amer. Chem. Soc.*, **82**, 5450 (1960).

5) R. B. Hermann, *J. Org. Chem.*, **27**, 441 (1962).

6) N. L. Allinger and M. A. Miller, *J. Amer. Chem. Soc.*, **86**, 2811 (1964).

7) T. Yonezawa, H. Konishi and H. Kato, This Bulletin, **42**, 933 (1969).

8) Y. Morino, K. Kuchitsu and A. Yokozeki, *ibid.*, **40**, 1522 (1967).

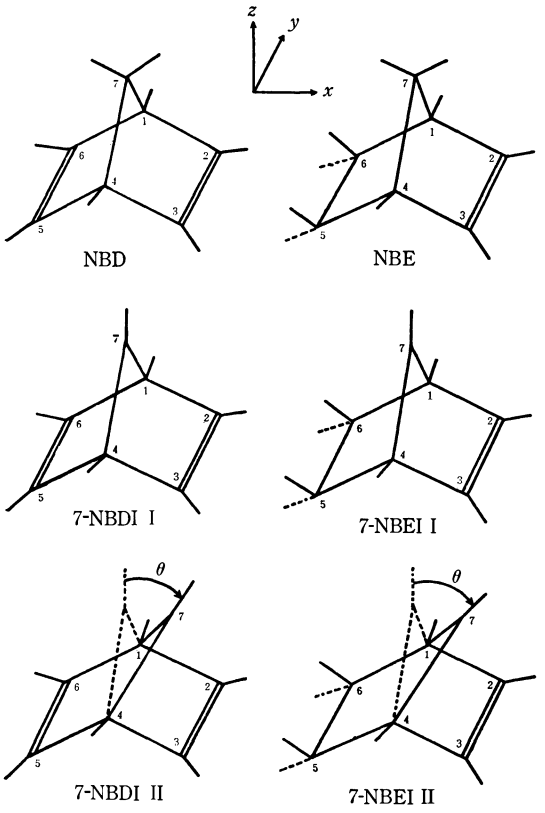

Fig. 1. Structures of NBD, NBE and their 7-cations.

that of NBD is adopted. In the 7-Norbornenyl and 7-norbornadienyl cations (7-NBEI and 7-NBDI), the sp^2 hybridization of the 7-carbon atoms is assumed, along with the same C–H bond distances as in the neutral molecules. The distortion of 7-NBEI and 7-NBDI is also investigated by moving the C_5, C_6, and C_7's, with their hydrogens, on arcs determined by fixing the plane formed by C_1, C_2, C_3, and C_4 carbon atoms and by keeping the C_s symmetry of the compounds and all the bond lengths unchanged. The distortion is indicated by the θ angle (illustrated in Fig. 1), which represents the displacement of the C_1, C_7, C_4-plane from its positions in the parent neutral molecule. The displacement of the C_1, C_4, C_5, C_6-plane is also tentatively taken to be $\theta/2$ in the same direction as the C_1, C_7, C_4-plane so as to reduce the strain on the compound.

The parameter, K, is taken to be 1.05, so that the calculated value of the lowest singlet transition energy of NBE may fit the observed value. The parameter dependence of several calculated quantities is presented in Table 1, together with the observed values. From this table, it may be noticed that the transition energies depend remarkably on the values of K, while the ionization potentials and the charge distributions are almost independent of the K values.

Table 1. Dependence of K values for the calculated quantities of NBE[a)]

K	1.00	1.05	1.10	obs.
I_p eV	9.84	9.87	9.91	9.05[b)]
V eV	6.13	6.35	6.56	6.33[c)]
Q_{c1}	+0.006	+0.004	+0.003	—
Q_{c2}	−0.124	−0.126	−0.128	—
Q_{c7}	−0.135	−0.136	−0.138	—

a) K, parameter in the equation of the core resonance integral; I_p, ionization potential; V, singlet $^1A' \rightarrow {}^1A''$ transition energy; Q_{cN}, net charge of the Nth carbon atom.
b) T. McAllister, Z. Dolešek, F.P. Lossing, R. Gleiter and P. R. Schleyer, *J. Amer. Chem. Soc.*, **89**, 5982 (1967).
c) Ref. 11.

Results and Discussions

NBE and NBD. The charge distribution of NBE and NBD is recorded in Table 2. The π-charge densities on the unsaturated carbons are also shown, together with the other AO's.[10] The calculated charge densities on the π AO's of NBE and NBD are larger than unity. This indicates the presence of electron delocalization due to interaction between the π AO's and the residual parts of the molecules. This can also be seen in the fact that the values of the π-bond orders, such as the $P_{\pi_2\pi_3}$ in both NBE and NBD, are less than unity.

The π AO coefficients[10] of some of the MO's of NBE and NBD in Table 3 represent a measure of the localization of the MO's in the π AO's. For this purpose, the D quantity is defined as:

$$D(\text{NBE}) = 2\{C(\pi_2)\}^2$$
$$D(\text{7-NBEI}) = 2\{C(\pi_2)\}^2 + \{C(\pi_7)\}^2$$
$$D(\text{NBD}) = 4\{C(\pi_2)\}^2$$
$$D(\text{7-NBDI}) = 2\{C(\pi_2)\}^2 + 2\{C(\pi_5)\}^2 + \{C(\pi_7)\}^2$$

where $C(\pi)$ is the transformed π-AO coefficient of an MO. A large D value denotes the localization of electrons occupying the MO. The highest occupied (HO) MO's of NBE and NBD are least localized, as is indicated by the D values in Table 3.

The transition energies of NBE are presented in Table 4, together with the experimental values measured in an ultraviolet vacuum by Stokes and Pickett.[2] The calculated values are obtained

9) R. Hoffmann, *J. Chem. Phys.*, **40**, 2480 (1964); *J. Amer. Chem. Soc.*, **86**, 1259 (1964).

10) The π-AO coefficients can be defined at every sp^2 carbon atom by transforming the MO coefficients to those of the p AO perpendicular to a local molecular plane. Therefore, in 7-NBDI the π AO's of the 2,5 and 7 carbon atoms are not parallel to one another.

Table 2. Charge distribution of NBE, NBD and their 7-cations

		NBE	7-NBEI		NBD	7-NBDI	
			I	II		I	II
C_1		3.996	4.002	3.992	4.002	4.006	4.000
C_2	π[a]	1.029	1.005	0.936	1.032	1.004	0.960
	π'	0.987	0.953	0.970	0.977	0.948	0.954
	σ	1.039	1.045	1.054	1.037	1.044	1.050
	s	1.030	1.026	1.024	1.029	1.026	1.025
	total	4.085	4.028	3.984	4.075	4.024	3.989
C_5		4.126	4.110	4.126	4.075	4.024	4.046[b]
C_7	π	—	0.278	0.430	—	0.243	0.346
	total	4.136	3.648	3.730	4.107	3.621	3.666
H_1		0.963	0.908	0.907	0.962	0.905	0.905
H_2		0.951	0.898	0.896	0.947	0.895	0.893
H_5		0.937 exo 0.935 endo	0.900 exo 0.889 endo	0.898 exo 0.894 endo	0.947	0.895	0.896
H_7		0.937 syn 0.942 anti	0.881	0.875	0.938	0.879	0.874
$P_{\pi_2\pi_3}$		0.959	0.940	0.866	0.958	0.940	0.891
$P_{\pi_5\pi_6}$		—	—	—	—	—	0.958
$P_{\pi_2\pi_7}$		—	0.163	0.379	—	0.189	0.316

a) π, $2p_\pi$ AO; π', 2p AO which is orthogonal to π and σ AO's; σ, $2p$ AO directed to the double bond axis; s, $2s$ AO.
b) π, 1.019; π', 0.957; σ, 1.042; s, 1.028.

Table 3. AO Coefficients of some MO's of NBE, NBD and their 7-cations

		Sym-metry	Orbital energy (eV)	C_2[a]				C_7[a]	D
				π	π'	σ	s	π	
NBE	LV[b]	a″	2.27	0.6731	0.0047	−0.0028	−0.0004	—	0.91
	HO	a′	−9.87	0.5388	−0.0641	0.0101	0.0338	—	0.58
7-NBEI I	NLV	a″	−3.45	0.6535	0.0008	−0.0057	0.0064	—	0.85
	LV	a′	−7.00	0.1065	−0.1385	−0.0388	0.0844	−0.9255	0.88
	HO	a′	−15.77	0.5669	−0.0095	0.0328	0.0012	0.0596	0.65
NBD	NLV	a_2	2.52	0.4841	0.0842	−0.0545	−0.0456	—	0.94
	LV	b_2	1.74	0.4704	−0.0788	0.0457	0.0443	—	0.89
	HO	a_1	−9.87	0.3277	−0.1533	0.0709	0.0717	—	0.43
	NHO	b_1	−10.20	0.4727	0.1001	−0.0756	−0.0407	—	0.89
7-NBDI I	TV	a_2	−3.03	0.4831	0.0863	−0.0525	−0.0431	—	0.93
	NLV	b_2	−4.05	0.4522	−0.0809	0.0375	0.0476	—	0.82
	LV	b_1	−7.00	0.1075	−0.1197	0.0316	0.0738	−0.9286	0.91
	HO	a_1	−15.89	0.3000	−0.1566	0.1329	0.0631	—	0.36
	NHO	b_1	−15.91	0.4960	0.1196	−0.0722	−0.0517	0.0710	0.98

a) π, π', σ and s are the same AO's that are represented in Table 2.
b) LV, the lowest vacant; HO, the highest occupied; NLV, the next lowest vacant; NHO, the next highest occupied; TV, the third vacant from the occupied.

by taking account of the configuration interactions among a limited number of singly-excited configurations. The notation, f_π, is the oscillator strength contributed by all kinds of π AO's. The difference between f_{total} and f_π for the lowest transition of NBE can be attributed to the σ AO's participation.

All previous theoretical treatments of the electronic transition of NBD have been carried out for π-electrons.[4-6] In these treatments the first transition is forbidden, whereas the second one is

Table 4. Calculated transition energies (ΔE) of NBE and NBD

(a) NBE

State	Calcd[a]			Obsd[c]	
	ΔE_{ev}	f_{total}	f_{π}[b]	ΔE_{ev}	f
$^1A''$	6.29	0.270	0.239	6.33	0.15
$^1A''$	6.75	0.001	0.003	7.40	0.15
$^1A'$	6.36	0.031	0.008		
$^1A'$	8.18	0.020	0.006		

(b) NBD

State	Calcd[a]			Obsd[d]	
	ΔE_{ev}	f_{total}	f_{π}[b]	ΔE_{ev}	$\log \varepsilon$
$^1B_2$	5.92	0.133	0.126	6.70	~3.7
$^1B_2$	6.92	0.108	0.163		
$^1A_2$	5.83	0	0	—	
$^1B_1$	6.52	0.027	0.005	—	
$^1A_1$	6.93	0.002	0.001	5.95	~3.3
$^1A_1$	7.91	0.022	0.001	—	

a) The number of configurations in CI treatment are 13 for NBE and 22 for NBD.
b) oscillator strength contributed from π AO's.
c) Ref. 11.
d) Ref. 3.

allowed. Robin and Kuebler,[3] however, assigned the first transition to a $^1A_1 \rightarrow {}^1A_1$ species (corresponding to a π–σ^* or σ–π^* transition) on the basis of a vibrational analysis in the vapor phase.

The $^1A_1 \rightarrow {}^1A_1$ transition energy calculated by the present method (in Table 4 (b)) is considerably larger than the experimental energy. For the $^1A_1 \rightarrow {}^1B_2$ transition energy, the calculated value does not agree with the experimental finding. In view of these defects, there seems to be some room for improvements in the present theory.[11]

7-NBEI and -NBDI. The non-classical structures of the carbonium ions derived from NBE and NBD have been discussed previously.[1] The electron delocalization of the 5-norbornenyl cation by means of Hückel MO calculations was made by Simonetta and Winstein.[12] 7-NBEI was treated as a bishomocyclopropenyl cation by Woods, Carboni, and Roberts.[13] These treatments shows the stabilizing energies of the non-classical models due to electron delocalization, though they are estimated by means of Hückel MO calculations and empirical calculations of the strain energy. All the valence electrons of NBEI and NBDI were treated with an extended Hückel theory by Hoffmann,[9] who also discussed the charge distribution and the stable conformation of NBEI and NBDI. Recently, a more quantitative treatment for NBEI has been performed by Ohorodnyk and Santry using the CNDO method.[14]

The experimental evidence on 7-NBDI was obtained from the NMR spectra by Story *et al.*,[15] The signals for four kinds of protons in 7-NBDI show a structure with a C_s, not a C_{2v}, symmetry. Recently, the bridge flipping of 7-NBDI was detected also from the NMR spectra by Brookhart, Lustgarten, and Winstein.[16] Further, the existence of 7-NBEI was proposed by Winstein *et al.*[17] on the basis of the unusual reactivity and complete retention of configuration in the acetolysis of aniti-7-norbornenyl tosylate. In the present paper, the configuration and the electronic structures of 7-NBEI and 7-NBDI will be discussed.

To deal with a configurational problem, the total energy is obtained as a sum of the total electronic energy of the valence electrons and the repulsion energy between cores:

$$E_{total} = E_{electronic} + E_{core}$$

The E_{core} is approximated by a point-charge model as follows:[18]

$$E_{core} = \sum_{A<B} \sum Z_A Z_B e^2 / R_{AB}$$

where Z_A is the core charge of the atom A and where R_{AB} is the internuclear distance between the atoms A and B.

The calculated potential energy curves are plotted in Fig. 2 for 7-NBDI and 7-NBEI using the distortion described in the previous section. In 7-NBEI, the positive θ corresponds to the motion of the C_7 toward the double bond. The existence of the calculated potential minima at the angles different from zero for 7-NBDI and 7-NBEI in Fig. 2 supports

11) In the present paper, the parameter, K, in the equation of the core-resonance integral is taken to be 1.05, whereas the value of 0.8 for benzene, pyridine, and so on (Ref. 7), and that of 0.9 for ethylene, have been adopted. The different values taken for K may suggest defects in the evaluation of the integrals, *e.g.*, the core-resonance integral and the Coulomb repulsion integrals.

12) M. Simonetta and S. Winstein, *J. Amer. Chem. Soc.*, **76**, 18 (1954).

13) W. G. Woods, R. A. Carboni and J. D. Roberts, *ibid.*, **78**, 5653 (1956).

14) H. O. Ohorodnyk and D. P. Santry, *ibid.*, **91**, 4711 (1969).

15) P. R. Story and M. Saunders, *ibid.*, **84**, 4876 (1962); P. R. Story, L. C. Synder, D. C. Douglass, E. W. Anderson and R. L. Kornegay, *ibid.*, **85**, 3630 (1963).

16) M. Brookhart, R. K. Lustgarten and S. Winstein, *ibid.*, **89**, 6352 (1967).

17) S. Winstein, M. Shatavsky, C. Norton and R. B. Woodward, *ibid.*, **77**, 4183 (1955).

18) If the total energy difference between a neutral molecule and its dehydrated cation (or between a neutral molecule and its protonated cation) is calculated on the basis of the point-charge model, the ionization energy (or proton affinity) becomes too small. In the present paper, where the E_{core} is used mainly in the distortion problem, this approximation can be used.

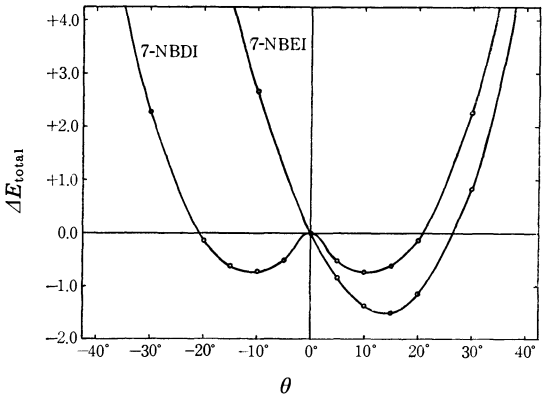

Fig. 2. Potential energy curves for distortion of the bridge in 7-NBEI and 7-NBDI.

the idea of non-classical structures of them. These results are also supported by Hoffmann[9,19] and Ohorodnyk and Santry,[14] though the angles of the potential minima differ among these treatments. The conclusion of Story *et al.*[15] obtained by means of NMR is also substantiated. The calculated potential minimum for 7-NBDI is obtained at $\theta=10°$, with the stabilization energy of 0.75 eV referred to the energy at $\theta=0°$. The present value of the stabilization energy is close to the values estimated by Brookhart, Lustgarten, and Winstein[16] by means of NMR spectroscopy ($\geq$0.85 eV). The calculated energy minimum for 7-NBEI is found at $\theta=15°$. In order to discuss the electronic structures of these ions with variable θ angles, we will hereafter use the following abbreviations: 7-NBDI I ($\theta=0°$), 7-NBDI II ($\theta=10°$), 7-NBEI I ($\theta=0°$), and 7-NBEI II ($\theta=15°$).

The charge distribution of the cations is presented in Table 2. The remarkable migration of the positive charge in the molecule may be a characteristic of a non-classical structure. The positive charge on C_7 is not so large as those found by Hoffmann using the extended Hückel method.[9] In 7-NBEI II and 7-NBDI II, the $2p_\pi$ AO's of the C_2's lost a little charge compared with those in their neutral molecules, whereas the $2p_\pi$ AO's of the C_7's gained somewhat. This trend and the fairly large values of the $P_{\pi_2\pi_7}$'s support our ideas as to the features of the nonclassical carbonium ion. (A more detailed discussion will be given below.)

In our previous paper,[7,20] we used a semiempirical relation between the bond length and the E_{AB}^1 value of the AB bond, which corresponds to the bond energy, in estimating unknown bond lengths. In the

Table 5. Changes of the values of E_{AB}^1 and E_{AB}^2 for 7-NBEI and 7-NBDI (eV unit)

Bond[a]	NBE		7-NBEI			
			I		II	
	E_{AB}^1	E_{AB}^2	ΔE_{AB}^1	ΔE_{AB}^2	ΔE_{AB}^1	ΔE_{AB}^2
2—3	−41.17	47.90	+0.61	−0.05	+2.02	−0.06
5—6	−24.66	34.86	+0.29	−0.03	+0.14	±0
1—2	−25.98	35.31	+0.65	−0.03	+0.97	−0.03
1—6	−24.53	34.74	+0.45	+0.01	−0.28	±0
1—7	−23.58	33.20	−1.43	±0	−0.88	−0.01
(2—7)	−0.07	12.22	−1.03	−0.11	−3.39	+2.57
Bond[a]	NBD		7-NBDI			
			I		II	
	E_{AB}^1	E_{AB}^2	ΔE_{AB}^1	ΔE_{AB}^2	ΔE_{AB}^1	ΔE_{AB}^2
2—3	−41.32	47.89	+0.49	−0.04	+1.48	−0.04
5—6					+0.12	−0.03
1—2	−25.73	35.29	+0.55	±0	+0.87	±0
1—6					+0.01	±0
1—7	−23.38	33.20	−1.43	±0	−1.18	±0
(2—6)	−0.30	10.67	−0.10	−0.03	+0.08	−0.76
(2—7)	−0.10	12.21	−0.80	−0.10	−2.45	+1.58
(5—7)					−0.05	−0.68

a) the pair in the parenthesis is non-bonding one.

19) The extended Hückel theory, which is not recklessly applicable to charged compounds,[9] can probably be applied to the distortion problem in the present case because the main contribution is by the electronic terms rather than by the Coulombic terms, as will be discussed later in terms of E_{AB}^1 and E_{AB}^2.

20) In Ref. 7, the E_{AB} notation is adopted instead of E_{AB}^1 in the present paper.

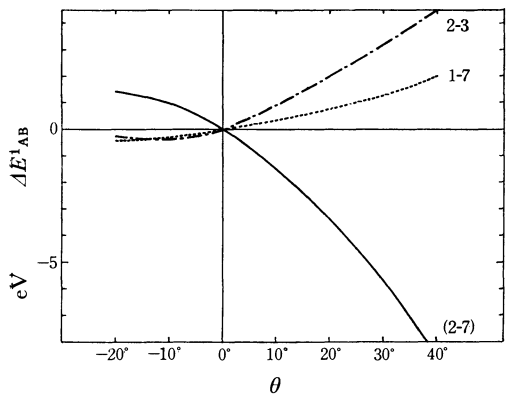

Fig. 3. Variation of E^1_{AB} values for 7-NBEI according to the distortion.

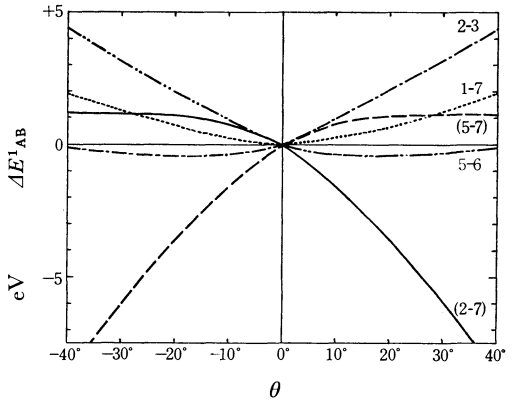

Fig. 4. Variation of E^1_{AB} values for 7-NBDI according to the distortion.

present paper, another index, $E_{AB}{}^2$, is introduced to discuss the strength of the heteropolan bond. The value of E_{AB}, which consists of $E_{AB}{}^1$ and $E_{AB}{}^2$ terms, can be used as a measure of the strength of a bond, where a stronger bond has a smaller value (see Appendix).[21]

In Table 5, the changes in the values of $E_{AB}{}^1$ and $E_{AB}{}^2$ for 7-NBEI and 7-NBDI, referred to NBE and NBD respectively, are tabulated. Based on these values for 7-NBEI I, which is assumed to have the same carbon skeleton as NBE, the trend of the alternation of the bond length can be confirmed. That is, all of the bonds in NBEI I, except for the 1–7 and 4–7 bonds, must be longer than those of NBE. Moreover, the non-bonding atomic distance between C_2 and C_7 (C_3 and C_7) can be predicted to become shorter than that of the neutral molecule. A similar trend can also be pointed out for 7-NBDI I. The $\Delta E_{AB}{}^1$'s of the non-bonding pairs of C_2 and C_7 for 7-NBEI II and 7-NBDI II have quite large absolute values, with a minus sign, though their $\Delta E_{AB}{}^2$'s also have large positive values. These facts indicate a partial bond characteristic of the so-called non-classical carbonium ions.

The variation in $E_{AB}{}^1$ values for 7-NBEI and 7-NBDI according to their distortion is illustrated in Figs. 3 and 4. For both cations, the interaction between C_2 and C_7 becomes stronger as θ increases, whereas the double bond (2–3) becomes weaker. The course of yielding the tricyclo-isomers[22] through

Table 6. Calculated transition energies (ΔE) of 7-NBEI and 7-NBDI

(a) 7-NBEI

I				II			
State	ΔE	f_{total}	f_π	State	ΔE	f_{total}	f_π
$^1A''$	2.98	0.004	0.000	$^1A''$	3.50	0.175	0.003
$^1A''$	3.93	0.002	0.001	$^1A''$	4.89	0.000	0.003
$^1A''$	4.58	0.007	0.001	$^1A''$	5.40	0.000	0.001
$^1A''$	6.47	0.262	0.227	$^1A''$	6.44	0.069	0.042
$^1A'$	2.92	0.043	0.018	$^1A'$	4.16	0.130	0.055
$^1A'$	4.23	0.003	0.010	$^1A'$	4.87	0.013	0.002
$^1A'$	5.42	0.013	0.006	$^1A'$	5.94	0.020	0.001

(b) 7-NBDI

I				II			
State	ΔE	f_{total}	f_π	State	ΔE	f_{total}	f_π
$^1B_2$	4.08	0.005	0.007	$^1A''$	4.10	0.003	0.004
$^1B_2$	5.99	0.083	0.033	$^1A''$	6.00	0.096	0.075
$^1A_2$	4.03	0	0	$^1A''$	4.50	0.001	0.006
$^1A_2$	5.61	0	0	$^1A''$	5.75	0.001	0.003
$^1B_1$	2.85	0.054	0.006	$^1A'$	2.98	0.053	0.017
$^1B_1$	4.66	0.006	0.006	$^1A'$	4.77	0.041	0.060
$^1A_1$	3.33	0.005	0.031	$^1A'$	4.02	0.009	0.002

21) This point is connected with the relation between the values of E_{AB} and the experimental bonding energy attributed to the AB bond of a molecule (*cf.* a paper to be published).

22) H. C. Brown and H. M. Bell, *J. Org. Chem.*, **27**, 1928 (1962); *J. Amer. Chem. Soc.*, **85**, 2324 (1963).

the carbonium ions can theoretically be expected, though there is a high potential barrier, accompanied by an alternation in the bond length and a variation in the valence angle.

The absorption spectra of these cations have been reported on only a little. The absorption band at 350 mμ (3.54 eV), which is assigned to an electronic transition in 7-NBDI by Winstein and Ordronneau,[23] is not compatible with the finding of Stofy and Saunders,[15] who found no absorption sbove 330 mμ (3.76 eV). The transition energies characteristic of the carbonium ions[24] are calculated to be slightly less than 3 eV for 7-NBDI (2.85 eV for I and 2.98 eV for II): these and the other results are presented in Table 6. Since we lack experimental data comparable with the present results, further experiments on the present problem must be undertaken.

In conclusion, the distorted configurations of 7-NBEI and 7-NBDI have been theoretically indicated. The delocalization of the positive charge and the bonding interaction between the bridged carbon atom and the double-bond carbon atoms, measured with E^1_{AB} and E^2_{AB} values, have been pointed out as the features of the so-called non-classical carbonium ions.

The calculations were carried out at the computation centers of both Tokyo University (HITAC 5020E) and Kyoto University (HITAC 5020).

Appendix

The total electronic energy of the valence electrons is:

$$E_{\text{electoronic}} = \frac{1}{2}\sum_r\sum_s P_{rs}(H_{rs}+F_{rs}) \qquad \text{(A-1)}$$

where $\sum_r$ denotes the summation of all the valence AO's considered, and where P_{rs}, H_{rs}, and F_{rs} are, respectively, the bond order, the core-resonance integral, and Fock's operator between the rth and sth AO's. With the choice of a point-charge model for the repulsion energy between cores, the total energy of the molecule can be represented as follows:
where I_r is the valence-state ionization potential of the

$$E_{\text{total}} = \frac{1}{2}\sum_r\sum_s P_{rs}(H_{rs}+F_{rs}) + \sum_{A<B}\sum Z_A Z_B e^2/R_{AB} \qquad \text{(A-2)}$$

The substitution of the one-center integrals presented in our previous paper[7] into Eq. (A-2) leads to the following expression:

$$E_{\text{total}} = \sum_A E_A + \sum_{A<B}\sum E_{AB}$$
$$= \sum_A E_A + \sum_{A<B}\sum (E^1_{AB}+E^2_{AB}) \qquad \text{(A-3)}$$

Here, the monoatomic part, E_A, and the diatomic parts, E^1_{AB} and E^2_{AB}, are:

$$E_A = \sum_r^{\text{on A}} P_{rr}\left[-I_r-\left(N_r-1-\frac{1}{4}P_{rr}\right)(rr|rr)\right]$$
$$-\sum_r^{\text{on A}}\sum_{r'<r}^{\text{on A}}\left[P_{rr}(2N_{r'}-P_{r'r'})\left\{(rr|r'r')-\frac{1}{2}(rr'|rr')\right\}\right.$$
$$\left.+\frac{1}{2}P^2_{rr'}\{(rr|r'r')-3(rr'|rr')\}\right] \qquad \text{(A-4)}$$

$$E^1_{AB} = \sum_r^{\text{on A}}\sum_s^{\text{on B}} P_{rs}(H_{rs}+F_{rs}) \qquad \text{(A-5)}$$

$$E^2_{AB} = \sum_r^{\text{on A}}\sum_s^{\text{on B}}(P_{rr}P_{ss}-P_{rr}N_s-P_{ss}N_r)(rr|ss)$$
$$+ Z_A Z_B e^2/R_{AB} \qquad \text{(A-6)}$$

rth AO, where N_r is the number of valence electrons occupying the rth AO in the valence state, and where $(rr|ss)$ and $(rr'|rr')$ are the two-center Coulomb and one-center exchange repulsion integrals respectively. The relation between the E_{AB} and the experimental bonding energy attributed to the AB bond of a molecule is shown graphically. This will be presented in detail in a following paper. By the use of the positive hole approximation[25,26] instead of the point-charge model for the repulison energy between cores, E^2_{AB} can be expressed as follows:

$$E^2_{AB} = \sum_r^{\text{on A}}\sum_s^{\text{on B}}(N_r-P_{rr})(N_s-P_{ss})(rr|ss) \qquad \text{(A-7)}$$

Thus, for two neutral atoms with P_{rr} equal to N_r, E_{AB} consists of only E^1_{AB}. However for charged species, it should be necessary to take into account E^2_{AB} terms because of their large contributions, as is shown in Table 5.

23) S. Winstein and C. Ordronneau, *ibid.*, **82**, 2084 (1960).

24) For a carbonium ion, we generally noticed a small energy transition toward the lowest vacant MO, which lies very low.

25) G. del Re and R. G. Parr, *Rev. Mod. Phys.*, **35**, 604 (1963).

26) R. G. Parr and R. Pariser, *J. Chem. Phys.*, **23**, 711 (1955).

BULLETIN OF THE CHEMICAL SOCIETY OF JAPAN VOL. 43 1683—1686 (1970)

Temperature Dependence of the Heats of Solution of Poly(ethylene glycol) and of Related Compounds

Haruo NAKAYAMA

Department of Chemistry, Faculty of Engineering, Yokohama National University, Ooka-machi, Minami-ku, Yokohama

(Received December 18, 1969)

The heats of solution of poly(ethylene glycol) and of related compounds (1,4-dioxane, tetrahydrofuran, ethylene glycol, diethylene glycol, and several ethyl ethers of ethylene glycol and of diethylene glycol) have been measured as a function of the temperature. The change in the partial molar heat capacity of the solute molecule in the dissolution process, $\Delta\bar{C}_{p2}$, is obtained from the temperature coefficient of the heat of solution. The $\Delta\bar{C}_{p2}$ for poly(ethylene glycol) is 15 cal/deg per $-CH_2CH_2O-$ chain unit. This value is in good agreement with those obtained for other low-molecular-weight compounds. The effect of the polar groups (the ethereal oxygen atom and the hydroxyl group) on the iceberg formation around the nonpolar residues has been discussed. From the results obtained, it seems likely that the iceberg formation around the $-CH_2-CH_2O-$ group is somewhat suppressed by the orientation-dependent interactions (hydrogen bond formation) between the ethereal oxygen atom and the water molecule.

As a typical solvent, water has many unique properties which depend on the nature of the molecules dissolved in it. When a compound containing a nonpolar group only (such as hydrocarbon) is introduced into an aqueous solution, an ice-like structure is stabilized in the neighborhood of the solute (the iceberg formation[1]). On the other hand, in aqueous solutions of substances having not only nonpolar residues, but also functional groups which may participate in hydrogen bonding, the situation becomes much more complex and their thermodynamic functions are apparently governed to a considerable extent by the relative strengths of the two types of interactions: nonpolar group-water (such as the iceberg formation) and polar group-water (such as the hydrogen-bond formation).

In the present investigation, we have been concerned with the aqueous-solution properties of the latter compounds, that is, the molecules having both nonpolar residues and polar groups, in order to ascertain how the hydrogen-bond formation influences the water structure around the nonpolar groups which are located near or adjacent to the functional groups. It is obvious from several investigations[2-6] that the ions with large nonpolar groups promote the water structure by increasing its likeness to ice. However, so far little is known about the structure-making effect of relatively small nonpolar residues which are directly connected with the functional groups. As a typical example of such a characteristic compound, we have chosen poly(ethylene glycol), in which each ethylene group is hemmed in by ethereal oxygen atoms.

The partial molar heat capacities of solutes in aqueous solutions make them suitable for studying the influence of the solutes on the structural modifications of water.[6] Therefore, we have determined the change in the heat capacity for the dissolution process by measuring the temperature dependence of the heats of solution. The heats of solution at infinite dilution, ΔH_s°, are simply expressed as:

$$\Delta H_s^\circ = n_2(\bar{H}_2^\circ - H_2), \tag{1}$$

where $\bar{H}_2^\circ$ is the partial molar-heat content of the solute at an infinite dilution, $\bar{H}_2$ is the molar-heat content of the pure solute, and n_2 is the number of moles of the solute. The temperature coefficient of Eq. (1) gives the change in the heat capacity for the dissolution process, $\Delta\bar{C}_{p2}$:

$$\frac{\mathrm{d}(\Delta H_s^0)}{\mathrm{d}T} = n_2(\bar{C}_{p2}^0 - C_{p2}) = n_2\Delta\bar{C}_{p2} \tag{2}$$

in which $\bar{C}_{p2}$ is the partial molar-heat capacity of the solute at an infinite dilution, while C_{p2} is the molar-heat capacity of the pure solute.

1) H. S. Frank and M. W. Evans, *J. Chem. Phys.*, **13**, 507 (1945).
2) R. L. Kay, T. Vituccio, C. Zawoyski and D. F. Evans, *J. Phys. Chem.*, **70**, 2336 (1966).
3) S. Lindenbaum and G. E. Boyd, *ibid.*, **68**, 911 (1964).
4) W. Y. Wen and S. Saito, *ibid.*, **68**, 2639 (1964).
5) R. L. Ray and D. F. Evans, *ibid.*, **70**, 2325 (1966).
6) S. Subramanian and J. C. Ahluwalia, *ibid.*, **72**, 2525 (1968).

Experimental

Materials. The poly(ethylene glycol) was obtained from the Wako Pure Chemicals Company and was purified by recrystallization from a hot methyl-ethyl ketone solution. The melting point was 61.5—62.3°C, and its molecular weight was about 1.4×10^4, as was estimated from the intrinsic viscosity measurements (0.224 cc/g in water at 25°C). The ethylene glycol, the diethylene glycol, the mono- and di-ethyl ethers of these glycols, the 1,4-dioxane, and the tetrahydrofuran were of a reagent grade and were purified by vacuum distillation just before use. The 1,4-butanediol was of a reagent grade and was used without further purification.

Calorimetric Measurements. The calorimeter employed in this study was a twin-type micro-calorimeter manufactured by Oyodenki Kenkyujo (CM-502).[7] Each sample (about 0.5 g or less), sealed in an ampoule, was dissolved into 50 m*l* of redistilled water whose temperature was kept constant. The measured values of the heat of solution may be in error by as much as 4% at worst. The results shown in Figs. 1 and 2 and tabulated in Table 1 are averages of three or four determinations.

TABLE 1. HEATS OF SOLUTION AND $\Delta\bar{C}_{p_2}$'s FOR PEG AND RELATED COMPOUNDS

Substance	Heat of solution (kcal/mol) 25°C	40°C	$\Delta\bar{C}_{p_2}$ (cal/deg·mol)
$-(CH_2CH_2O)_n-$	+0.07	+0.29	15
$(CH_2CH_2O)_2$	−2.58	−2.21	25
$CH_2CH_2\rangle O$ (1,4-dioxane)	−3.96	−3.09	58
$HOCH_2CH_2OH$	−1.74	−1.76	0 (0)*
$HOCH_2CH_2OC_2H_5$	−4.38	−4.05	22 (22)
$C_2H_5OCH_2CH_2OC_2H_5$	−6.94	−6.30	43 (44)
$HO(CH_2CH_2O)_2H$	−3.81	−3.58	15 (15)
$HO(CH_2CH_2O)_2C_2H_5$	−6.91	−6.37	36 (37)
$C_2H_5O(CH_2CH_2O)_2C_2H_5$	−9.05	−8.17	59 (59)
$HO(CH_2)_4OH$	−2.53	−2.22	21

* See text.

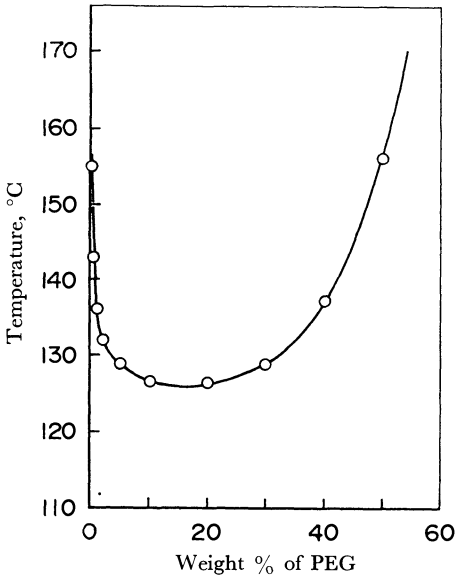

Fig. 1. The liquid-liquid phase diagram for the H_2O-PEG system.

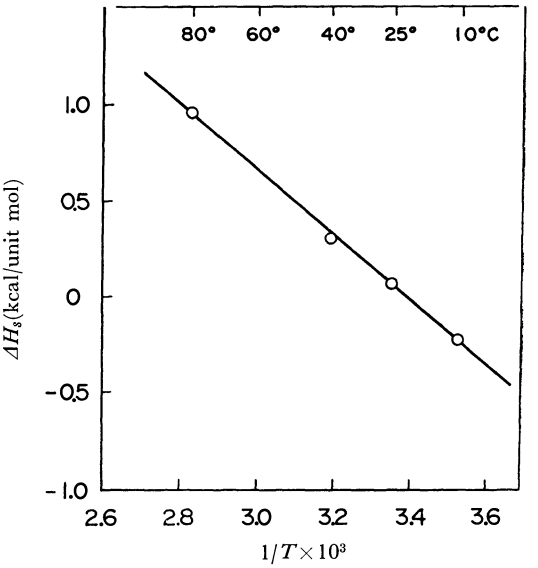

Fig. 2. Temperature dependence of the heats of solution of PEG in H_2O.

Results

The liquid-liquid phase diagram for the water-poly(ethylene glycol) (which we will denote by PEG hereafter) system is shown in Fig. 1. This system has a lower critical solution temperature. The critical solution temperature and critical concentration are about 126°C and 15 wt% respectively. At 160°C, for example, a very dilute solution (less than 0.1%) is in equilibrium with a fairly concentrated solution (*ca.* 50%); the latter corresponds to the solution in which there are 2.5 water molecules per $-CH_2CH_2O-$ group.

The temperature dependence of the heats of solution of solid PEG, ΔH_s, is shown in Fig. 2. The final concentration is about 1%. The heat of solution at 80.3°C (which is higher than the melting point) is obtained by adding the heat of fusion of PEG (2.07 kcal/unit mol[8,9]) to the heat of soultion of liquid PEG at 80.3°C, which has been measured by Rowlinson *et al.*[10] It may be seen from Fig. 2

7) K. Amaya, *Bussei*, **4**, 588 (1963); M. Koishi, This Bulletin, **39**, 2406 (1966).

8) R. H. Beaumont, B. Clegg, G. Gee, J. B. M. Herbert, D. J. Markes, R. C. Roberts and D. Smis, *Polymer*, **7**, 401 (1966).

9) W. Braun, K.-H. Hellwege and W. Knappe, *Kolloid Z.*, **215**, 10 (1967).

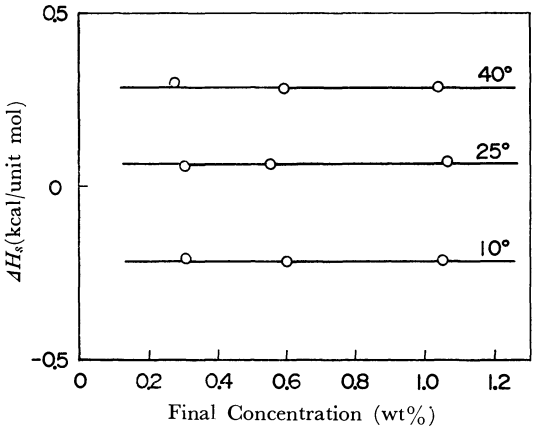

Fig. 3. Concentration dependence of the heats of solution of PEG in H_2O.

that, over the temperature intervals examined, the heat of solution of PEG is approximately a linear function of the reciprocal of the absolute temperature. Obviously, the decrease in exothermicity with rise in the temperature causes phase separation at high temperatures, as is shown in Fig. 1.

In Fig. 3 the concentration dependence of the heats of solution of PEG in dilute regions is shown. As is evident from this figure, the heat of solution is almost independent of the concentration if the final concentration is less than 1%. Therefore, we may safely conclude that the observed heats of solution of PEG (in about a 1% solution, Fig. 2) may be regarded as the heats of solution at an infinite dilution. Thus, from Eq. (2) and Fig. 2, the $\Delta\bar{C}_{p2}$ for PEG can be calculated to be 15 cal/deg. unit-mol around 25°C.

The heats of solution of various low-molecular-weight compounds containing an ethereal oxygen atom and/or a hydroxyl group at 25 and 40°C are listed in Table 1. The final concentration is about 1% or less. For these compounds the values of $\Delta\bar{C}_{p2}$, which are calculated from the temperature coefficients over the 25—40°C temperature range, are also included in Table 1.

Discussion

The heat of solution of solid PEG is slightly endothermic at 25°C (0.07 kcal/unit-mol, as is seen from Fig. 2 or Table 1). This means that the heat of fusion of solid PEG (2.07 kcal/unit-mol[8,9]) is almost canceled out by the exothermic heat of solution of liquid PEG (2.00 kcal/unit-mol). The fact that the introduction of liquid PEG into water leads to a large evolution of heat indicates that the exothermic heat of solution due to a specific interaction between PEG and water exceeds the endothermic heat of solution due to the difference in the cohesive energy densities of the two substances.[11]

The main factors which lead to an exothermic heat of mixing are, presumably: (1) the hydrogen-bond formation between the ethereal oxygen atom of PEG and the hydrogen atom of water, and (2) the structural modifications (the iceberg formation) of water around the hydrocarbon portions of PEG. These interactions will also be reflected in the temperature dependence of the heat of solution. However, we have no quantitative information concerning the effect of the hydrogen-bond formation upon the value of $\Delta\bar{C}_{p2}$. Regarding the latter effect, however, it has been established that the $\Delta\bar{C}_{p2}$ increases about 10 cal/deg·mol[12,13] per $-CH_2-$ group. In any case, we may reasonably expect a value of more than 20 cal/deg-mol for the $\Delta\bar{C}_{p2}$ of the $-CH_2CH_2O-$ group if a stable, ice-like structure is formed in the immediate neighborhood of the $-CH_2CH_2O-$ chain. However, the observed value of $\Delta\bar{C}_{p2}$ for the $-CH_2CH_2O-$ group is 15 cal/deg·mol, as has been mentioned above. This suggests, convincingly but not conclusively, that the iceberg formation around the $-CH_2CH_2O-$ chain is somewhat suppressed by the orientation-dependent interactions (*i. e.*, the hydrogen-bond formation) between ethereal oxygen atoms and water molecules. We believe much more work needs to be done before anything can be said conclusively about the behavior of water molecules in the neighborhood of the $-CH_2CH_2O-$ group.

In Table 1 we may derive some interesting observations about the $\Delta\bar{C}_{p2}$ in relation to the molecular structure:

(1) The $\Delta\bar{C}_{p2}$ for 1,4-dioxane, which is a cyclic dimer of the $-CH_2CH_2O-$ group, is somewhat smaller than twice the $\Delta\bar{C}_{p2}$ for the $-CH_2CH_2O-$ group. On the other hand, for tetrahydrofuran the $\Delta\bar{C}_{p2}$ value is considerably greater than that to be expected from the values of $\Delta\bar{C}_{p2}$ for one $-CH_2-CH_2O-$ group and two methylene groups. These discrepancies are probably due to the difference in structure-making ability between the small cyclic molecule and the linear molecule.

(2) The heat of solution of ethylene glycol is almost independent of the temperature around 25°C. This fact suggests that the strong hydrogen-bond formation between the hydroxyl group and the water molecule causes a disruption of the water structure so striking that the structure-making capacity of the methylene group adjacent to the hydroxyl group is considerably lowered. As has

10) G. N. Malcolm and J. S. Rowlinson, *Trans. Faraday Soc.*, **53**, 921 (1957).

11) K. Shinoda and M. Fujihira, This Bulletin, **41**, 2612 (1968).

12) P. White and G. C. Benson, *J. Phys. Chem.*, **64**, 599 (1960).

13) G. Nemethy and H. A. Scheraga, *J. Chem. Phys.*, **36**, 3401 (1962).

been mentioned above, the occurrence of a similar phenomenon can also be expected in the case of poly (ethylene glycol), though the effect there is not so marked. However, as the $\Delta\bar{C}_{p2}$ of 1,4-butanediol shows (Table 1), the structural modifications of water occur around the methylene groups, remote from the hydroxyl group. An analogous effect has also been observed in the aqueous solutions of alkylhexaoxyethylene glycol monoethers.[14]

(3) The differences in the $\Delta\bar{C}_{p2}$'s between diethylene glycol and ethylene glycol, between diethylene glycol monomethyl ether and ethylene glycol monoethyl ether, and between diethylene glycol diethyl ether and ethylene glycol diethyl ether are 15, 14, and 16 cal/deg·mol respectively. These differences may be ascribed to the cntribution of the $-CH_2CH_2O-$ group to the $\Delta\bar{C}_{p2}$. It is interesting that they are in very good agreement with the $\Delta\bar{C}_{p2}$ observed for the $-CH_2CH_2O-$ group in PEG (15 cal/deg·mol).

(4) If we assign 15 cal/deg·mol to the $\Delta\bar{C}_{p2}$ for the $-CH_2CH_2O-$ group, 22 cal/deg·mol to that for the $-CH_2OC_2H_5$ group, and 0 cal/deg·mol to that for the $-CH_2OH$ group, the $\Delta\bar{C}_{p2}$ values for ethylene glycol, diethylene glycol, and their various ethyl ethers can be reasonably estimated. In Table 1, these calculated values are also listed (in parentheses). They are in good agreement with the observed values.

The author wishes to thank Dr. Kōzō Shinoda for his helpful criticisms and suggestions.

14) J. M. Corkill, J. F. Goodman and J. R. Tate, *Trans. Faraday Soc.*, **63**, 773 (1967).

BULLETIN OF THE CHEMICAL SOCIETY OF JAPAN VOL. 43 1686—1692 (1970)

Hydrogen Ion Titration of Poly-S-carboxymethyl-L-cysteine

Shoichi IKEDA*1

Department of Biology, Osaka University, Toyonaka and Department of Chemistry, Nagoya University, Nagoya

(Received December 25, 1969)

Potentiometric titration curves have been determined for aqueous solutions of poly-S-carboxymethyl-L-cysteine. A pH-induced transition of the polymer conformation is manifest from the occurrence of a transition region around pH 5, where the solution has an essentially infinite buffer action. The titration curve at higher ionization corresponds to that of a random coil. At lower ionization the polymer is associated to form a β-structure and its titration behavior is qualitatively accounted for by the Gouy model for a uniformly charged sheet. Deviation from the model would partly be ascribed to the aggregation of sheets in the β-form. The standard free energy of transition from random coil to β-form has been estimated for the unchanged polymer and is found to depend on the molecular weight of polymer. It is suggested that fine structure of the β-form and its mode of aggregation vary with polymer chain length.

It has been accepted that some synthetic polypeptides, which exist as the β-conformation in solid, can retain the β-structure even in solution, if some specific solvent systems are chosen,[1-3] However, most of these polypeptides are insoluble in aqueous media and thus have been examined in mixtures of organic solvents. A conformational transition takes place from random coil to β-form at a certain solvent composition, as the solvent mixture becomes less polar. Evidence for the coil-β transition and the formation of the β-form was mainly derived from measurements of optical rotation and infrared spectrum. However, thermally induced formation of β-form of poyl-L-lysine in water was elaborated by two groups of workers.[4-6]

*1 Present address: Department of Chemistry, Faculty of Science, Nagoya University, Nagoya.

1) G. D. Fasman and E. R. Blout, *J. Amer. Chem. Soc.*, **82**, 2262 (1960).

2) E. M. Bradbury, A. Elliott and W. E. Hanby, *J. Mol. Biol.*, **5**, 487 (1962).

3) S. Ikeda, H. Maeda and T. Isemura, *ibid.*, **10**, 223 (1964).

4) P. K. Sarker and P. Doty, *Proc. Nat. Acad. Sci., U.S.*, **55**, 981 (1966).

5) a) B. Davidson, N. Tooney and G. D. Fasman, *Biochem. Biophys. Res. Commun.*, **23**, 156 (1966); b) R. Townend, T. F. Kumosinsky, S. N. Timasheff, G. D. Fasman and B. Davidson, *ibid.*, **23**, 163 (1966).

6) B. Davidson and G. D. Fasman, *Biochemistry*, **6**, 1616 (1967).

Recently, pH-induced coil-β transition was found for a water-soluble polypeptide, poly-S-carboxymethyl-L-cysteine.[7,8] The transition was observed as large changes in optical rotation, intrinsic viscosity and infrared spectrum around pH 5. The polymer is associated into an intermolecular β-conformation upon lowering pH, while it is in a random coil conformation at higher pH. Its ultraviolet rotatory properties were also investigated as a function of pH and correlated with the conformational transition.[9] .Is can be expected that the transition is also observed on potentiometric titration curves of the polymer, provided that ionized carboxyl groups in the β-form have different affinity or electrostatic interaction with hydrogen ions from those in the random coil. The pH titration method would provide another useful approach to elucidate the detailed structure of the β-form and its transition to random coil. Preliminary titration curves have already published.[7,8]

The helix-coil transition of poly-L-glutamic acid in aqueous meida was successfully investigated by means of the titration method.[10-13] The results clearly showed the presence of three regions on a titration curve, each corresponding to the pure helix, the pure coil and the intervened transition region, and made it possible to estimate the standard free energy of transition.

Experimental

Materials. Poly-S-carboxymethyl-L-cysteine used was the same samples as described previously.[8] The intrinsic viscosities (in $dl\ g^{-1}$) of the three samples were 0.230 for E602, 0.089 for E527 and 0.041 for E515, in 0.2M NaCl at pH 7, 25°C. Most experiments were performed on the highest molecular weight sample, E602.

Carbonate-free 1N NaOH was standardized against potassium acid phthalate, and 1N HCl was standardized against Na_2CO_3 and checked against the NaOH. Glass-redistilled CO_2-free water was used to make up all the solutions.

pH Measurements. A Horiba Model P pH-meter of a potentiometric type, accurate to ± 0.003 pH unit, was used with a Horiba standard buffer (pH 6.86 at 25°C).

Hydrogen Ion Titration. Titrants were delivered from calibrated micrometer syringes with 0.5 ml capacities. All the measurements were carried out under nitrogen flushing. Temperature was 25°C, unless otherwise stated. A specially designed titration vessel with three necks, two of which were installed with a glass electrode and a reference electrode, respectively, and the other was fitted with a syringe, thermometer and nitrogen inlet, was placed on a magnetic stirrer which was grounded to the earth.

To a weighed amount of sample was added 10 ml of solvent with appropriate ionic strength of NaCl. The suspension was first titrated with 1N NaOH up to pH 11.5, when the sample had been in solution at about pH 6. Then the alkaline solution was back-titrated with 1N HCl. Each addition of HCl yielded white gel upon the tip of the syringe needle but the gel redissolved within a few minutes. However, below about pH 4, the solution was so viscous and turbid that observed pH values were unreliable.

The degree of ionization, α, was calculated from the difference between total and free concentrations of hydrogen ions. Free hydrogen ion concentration was computed by assuming that liquid junction potentials and mean activity coefficients of the solution were the same as those of solution containing no polymer.

Results

The titration curves in a forward direction, *i. e.*, from acid to alkaline, and those in a backward direction were not necessarily conicident with each other. The forward curve generally shifted to slightly more alkaline side than the backward curve. This would be caused mostly by the different rates of reactions in suspension and in homogeneous solution. The suspension became clear when its pH was raised to 5 or higher. The homogeneous solution could be kept clear down to pH 4 or even lower during the beckward titration, which was more reproducible. The backward titration may be regarded as closer to the equilibrium titration

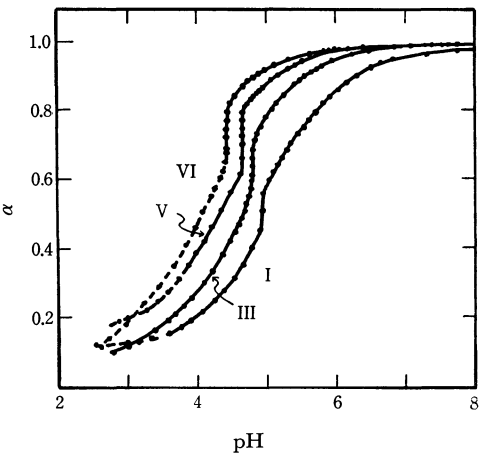

Fig. 1. Potentiometric titration curves at different ionic strengths.
Initial NaCl concentration: I, 0.00M NaCl; III, 0.05M; V, 0.20M; VI, 1.00M. Dashed parts indicate the region where turbidity was manifest.

7) N. G. Illiarionova, I. A. Bolotina, B. Z. Volchek, V. I. Kalichevich, U. V. Mitin, O. B. Ptitsin and A. V. Purkina, *Biofizika*, **11**, 762 (1966).
8) S. Ikeda, *Biopolymers*, **5**, 359 (1967).
9) S. Ikeda and G. D. Fasman, *J. Mol. Biol.*, **30**, 491 (1967).
10) B. H. Zimm and S. A. Rice, *Mol. Phys.*, **3**, 391 (1960).
11) A. Wada, *ibid.*, **3**, 409 (1960).
12) M. Nagasawa and A. Holtzer, *J. Amer. Chem. Soc.*, **86**, 531 (1964).
13) M. Nagasawa and A. Holtzer, *ibid.*, **86**, 538 (1964).

behavior of the system. All the results presented below are concerned with those of the backward titration process, which moves from the alkaline to the acid side, using acid titer.

A characteristic feature common to all the titration curves should be noted. As the titration proceeds from alkaline to acid side, a region always appears where the solution exhibits an essentially infinite buffer action or where the pH of solution remains unaltered upon addition of some amount of acid. This is illustrated in Fig. 1. The location of this particular region is slightly dependent on polymer concentration and temperature and is markedly dependent on ionic strength. The characteristic region is located around pH 5 or slightly lower. Previous results[7-9] have shown that various properties suddenly change around pH 5 and conformational change from coil to β-from takes place here. Thus the characteristic pH titration curve may be reasonably identified with the pH where the polymer undergoes a conformational change. In this sense, the specific pH region will be referred to as the transition pH or the transition region. At pH higher than this, the polymer is in a randomly coiled form, but at lower pH it is in an intermolceular β-conformation. Occurrence of such a transition region during the titration would imply that the affinity of hydrogen ions with ionized carboxyl groups is higher in the coil form than in the β-form. The observed sharpness of the transition would be related to the cooperative formation of hydrogen bonds upon lowering pH.

The titration curve slightly shifted to higher pH with increasing polymer concentration. The transition pH in 0.2M NaCl was 4.64 for 0.154 g dl^{-1}, 4.68 for 0.295 g dl^{-1} and 4.72 for 0.608 g dl^{-1}. The last pH value is in complete agreement with that found previously[8] for the titration. As the concentration was as high as 0.5 g dl^{-1}, gelation occurred at the transition pH and made it difficult to obtain reliable values at lower pH. The concentration dependence would be ascribed to stronger electrostatic interaction between ionized groups at higher concentrations or in larger aggregates. Most experiments were, therefore, performed at polymer concentrations around 0.150 g·dl^{-1} or 0.0093N.

Typical titration curves at different ionic strengths are shown in Fig. 1. As the ionic strength is higher, more carboxyl groups are ionized at a given pH, and the transition pH is more acid but the degree of ionization is higher. The latter indicates that the β-form is stabilized by the ionic atmosphere formed around charged groups, which is in accord with the previous results.[8,9]

The effect of temperature on the titration in 0.2M NaCl is shown in Fig. 2. The observed shift of the titration curve indicates that at higher temperature the β-form is less stable owing to the increased ionization.

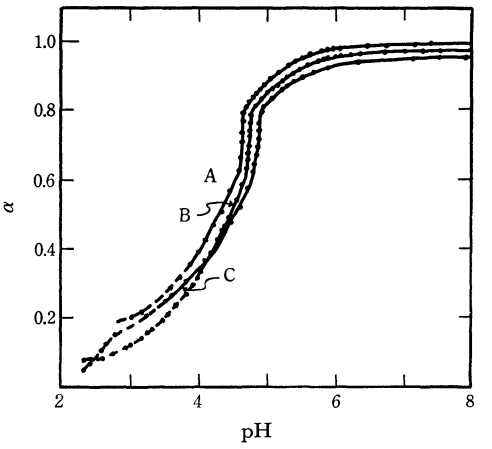

Fig. 2. Titration curves in 0.2M NaCl at different temperatures.
A, 25°C; B, 16°C; C, 3°C. Dashed parts indicate the region where turbidity was manifest.

Discussion

Electrostatic Free Energy and Polymer Conformation. Potentiometric titration of polyelectrolytes having a uniform distribution of ionizable groups can be described by the expression[14-16]

$$\mathrm{pH} - \log \frac{\alpha}{1-\alpha} = \mathrm{p}K_{\mathrm{int}} + \frac{0.434}{ZkT}\frac{\partial G_{\mathrm{el}}}{\partial \alpha} \qquad (1)$$

where $\mathrm{p}K_{\mathrm{int}}$ is the negative logarithm of intrinsic dissociation constant, Z the total number of ionizable groups in a molecule (or its associated from), and G_{el} is the electrostatic free energy of the molecule (or its associated form) with $Z\alpha$ ionized groups. Since the last term, $\partial G_{\mathrm{el}}/\partial(Z\alpha)$, represents the work necessary to remove a hydrogen ion from the molecule (or its associated form) with $Z\alpha$ charges, Eq. 1 may be written[17,18]

$$\mathrm{pH} - \log \frac{\alpha}{1-\alpha} = \mathrm{p}K_{\mathrm{int}} - 0.434\frac{\varepsilon\psi_0}{kT} \qquad (2)$$

where ε is the elementary charge and ψ_0 is the electrostatic potential at the molecular surface.

Figure 3 shows the modified plots, $\mathrm{pH} - \log \alpha/(1-\alpha)$ *vs.* α, at various ionic strengths. As was also noted in Fig. 1, each of the curves in Fig. 3 can be separated into at least three regions, corresponding to the random coil at higher α, the β-

14) A. Katchalsky and J. Gillis, *Rec. Trav. Chim. Pays-Bas*, **68**, 879 (1949).
15) A. Arnold and J. Th. G. Overbeek, *ibid.*, **69**, 192 (1950).
16) F. E. Harris and S. A. Rice, *J. Phys. Chem.*, **58**, 725 (1954).
17) G. S. Hartley and J. W. Roe, *Trans. Faraday Soc.*, **36**, 101 (1940).
18) A. Katchalsky, N. Shavit and H. Eisenberg, *J. Polym. Sci.*, **13**, 69 (1954).

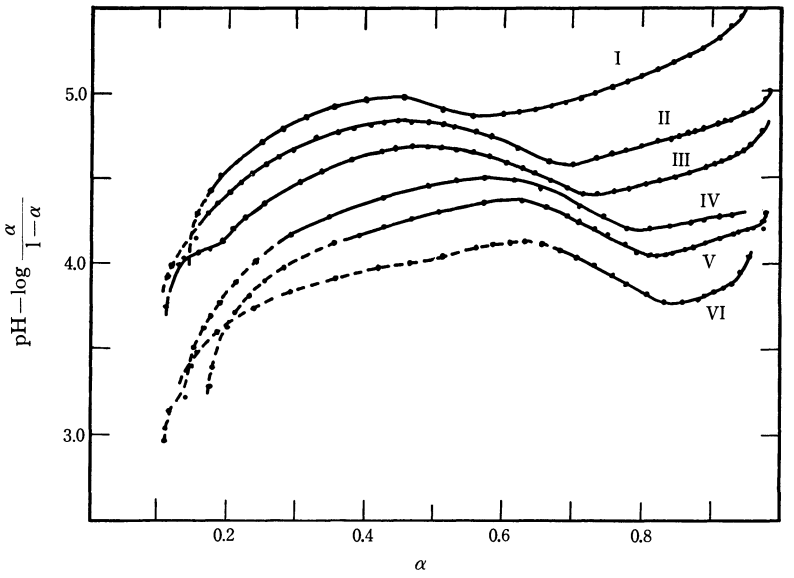

Fig. 3. Modified titration curves at different ionic strengths.
Initial NaCl concentration: I, 0.00M; II, 0.01M; III, 0.05M; IV, 0.10M; V, 0.20M; VI, 1.00M. Dashed parts indicate the region where turbidity was manifest.

form at lower, α, and the intermediate transition region. The portion of curves at very low α could not be traced down to $\alpha=0$, owing to its large curvature, to determine the pK_{int} value. However, the pK_{int} value seems to be considerably lower than that ($pK_{int}=4.5$) for poly-L-glutamic acid.[12,13] In fact, the δ-carboxyl group of the monomer, S-carboxymethyl-L-cysteine, has a pK value, 3.12, in 0.2M NaCl, as will be seen in Fig. 6 below. As there is no way for the extrapolation to $\alpha=0$, the pK_{int} value is assumed to be 3.00 for both random coil and β-form, irrespective of the ionic strength. Then the specific titration behavior of the polymer in each region may be accounted for by different electrostatic interactions, each characteristic of the conformation in that region. The electrostatic interaction or the electrostatic free energy has been evaluated for various systems, either analytically or numerically, using idealized model appropriate to the system.

Although a detailed structure of the β-form in solution is not known yet, its fundamental structure may be sheet-like, as in the solid, in which polypeptide chains are aligned and held together by inter- or intra-molecular hydrogen bonds. The two-dimensional hydrogen bonded structure can stack together through side chain interactions to form intersheet aggregates. To the first approximation or at some stage of its formation, the β-structure would have the sheet-like structure in solution. Then the β-form of ionized polypeptides in solution would be most adequately represented by a uniformyl charged plane, *i. e.*, by the Gouy model. The electrostatic potential at a charged plane dipped in an electrolyte solution is given by[19,20]

$$\psi_0 = \frac{2kT}{\varepsilon}\sinh^{-1}\frac{\kappa\sigma}{4n\varepsilon} \tag{3}$$

where σ is the surface charge density, n is the number concentration of salt, and κ is the Debye-Hückel parameter.

Charged groups in the present polymer are side chain carboxyls and they are directed to both sides of the molecular sheet alternately along with polypeptide chains or hydrogen bonds in the β-structure. Thus an electric double layer is formed at each side of the molecular sheet, and the area assigned to a charge should be twice as large as the area occupied by an amino acid residue, A_0. The surface charge density may be given by

$$\sigma = -(\varepsilon/2A_0)\,\alpha \tag{4}$$

Substitution of Eq. (4) into Eq. (3) leads to an expression for the surface potential of a charged β-form

$$\psi_0 = -\frac{2kT}{\varepsilon}\sinh^{-1}\frac{125\pi}{DN_AkT}\frac{\varepsilon\alpha}{A_0\sqrt{C_s}} \tag{5}$$

where C_s is the molar concentration of salt, D the dielectric constant of solvent, and N_A the Avog-

19) a) G. Gouy, *J. Phys.* (Paris), IV, **9**, 457 (1910); *Ann. Phys.* (Paris), IX, **7**, 129 (1910); b) D. L. Chapman, *Phil. Mag.*, VI, **25**, 475 (1913)

20) E J. W. Verwey and J. Th. G. Overbeek, "Theory of the Stability of Lyophobic Colloids," Elsevier Publishing Co., Inc., New York (1948).

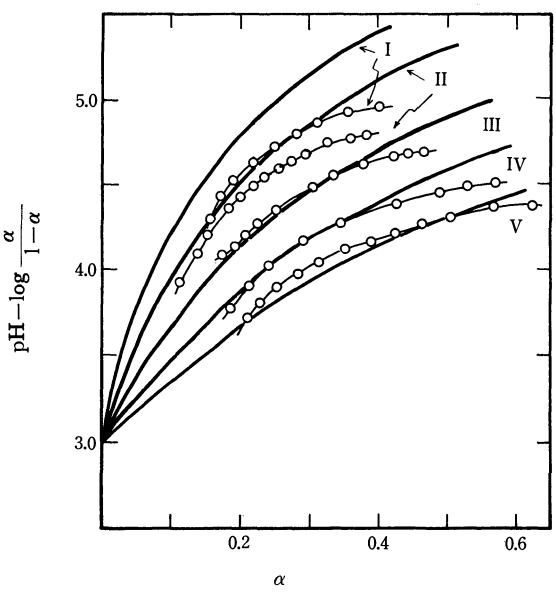

Fig. 4. Calculated and experimental titration curves of the β-form.
Thick curves are calculated by Eq. (6) with $pK_{int}=3.00$ and $A_0=16.8$ A². Circles show experimental values. NaCl concentrations (in M) are:

	I	II	III	IV	V	
C_s	0.01	0.02	0.05	0.10	0.20	(Calcd)
Initial	0.00	0.01	0.05	0.10	0.20	(Exp.)

adro number.

Thus the potentiometric equation for the charged β-form is obtained as

$$\mathrm{pH}-\log\frac{\alpha}{1-\alpha}=\mathrm{p}K_{\mathrm{int}}+0.868\sinh^{-1}\frac{125\pi}{DN_AkT}\frac{\varepsilon\alpha}{A_0\sqrt{C_s}} \quad (6)$$

This can be brought to direct comparison with experimental results. Assuming that pK_{int} is 3.00 and the area per residue, A_0, is 16.8 A², theoretical curves can be obtained for different C_s values. Figure 4 shows the calculated curves together with the experimental plots in the region of the β-form.

Agreement is rather good, except for the lowest ionic strength, if the use of the idealized model and the assumed values for the parameters are taken into account. At low ionic strengths, the effect of increase in ionic strength during the titration is considerably high. While the β-structure has not been well defined, the sheet-like structure postulated above would stack into a larger aggregate owing to the side-chain interaction. Only at the initial stage of its formation, *i. e.*, at pH far from the transition pH, the β-structure would be more like a sheet. Upon lowering pH, the intersheet aggregation would become predominant and cause the β-form to deviate from the sheet-like structure. In this sense, the agreement mentioned above appears to be fortuitous, and in fact, deviation is noticed in different curvatures between experimental and calculated curves.

Randomly coiled polyelectrolytes have been treated on the basis of various models, and the Poisson-Boltzmann equations have been solved by means of the Debye-Hückel approximation or electronic computors. Among them, Kotin and Nasasawa[21] obtained computor solutions, postulating a rod-like model for a charged random coil, and found that the titration data of polyacrylic acid and polymethacrylic acid could be described by these solutions.[21,22] Although no precise comparison has been made, the present titration data at higher ionization appear to conform to the Kotin-Nagasawa solution, if the pK_{int} value is assumed to be 3.00 and the molecular dimension is properly chosen.

Standard Free Energy for the Coil-β Transition. The pH-induced transition of the polymer is of electrostatic one, and the process bringing polymer molecules from an uncharged β-form to fully charged random coils can be divided into two steps: first, transforming the uncharged molecules from β-form to random coils and secondly, charging up the random coil molecules. More significant in the discussion of conformational change is the free energy charge accompanying the first step, *i. e.*, the charge-independent part, which will be denoted by $-\Delta G^0_{c\to\beta}$ per residue.

The second step, during which random coils are being charged, yields a free energy change per residue

$$dG^{(c)}=2.30\,kT\left(pK^{(c)}-pH^{(c)}+\log\frac{\alpha}{1-\alpha}\right)d\alpha \quad (7)$$

where $pK^{(C)}$ is the pK in the random coil form and $pH^{(C)}$ is the pH of the hypothetical random coil solution. The free energy change per residue accompanying the ionization process through the actual titration course can be expressed by

$$dG=2.30kT\left(pK-pH+\log\frac{\alpha}{1-\alpha}\right)d\alpha \quad (8)$$

where pK is the apparent pK in the actual polymer. In equilibria, Eqs. (7) and (8) lead to the Henderson–Hasselbach equations, respectively, which permit the calculation of the pK values from titration data.

It follows from an earlier statement that a thermodynamic relation

$$\Delta G=-\Delta G^0_{c\to\beta}+\Delta G^{(c)} \quad (9)$$

holds for integrated values of the above quantities. Equation (9) can be written as

21) L. Kotin and M. Nagasawa, *J. Chem. Phys.*, **36**, 873 (1962).
22) M. Nagasawa, T. Murase and K. Kondo, *J. Phys. Chem.*, **69**, 4005 (1965).

$$\Delta G^0_{c\to\beta} = 2.30\,kT\int_0^1 (pK^{(c)} - pK)\,d\alpha \qquad (10)$$

$$= 2.30\,kT\int_0^1 (pH^{(c)} - pH)\,d\alpha \qquad (11)$$

Equations (10) and (11) provide methods of evaluating charge-independent part of the free energy of transition.

The methods of evaluating the transition free energy have been presented by Zimm and Rice,[11] Nagasawa and Holtzer,[14] and Leyte and Mandel.[23] The helix-coil transitions of poly-L-glutaimc acid,[14,14-26] poly-L-lysine,[25] and copolymers of L-leucine and L-glutamic acid[24] were treated by these methods, and an undefined conformational transition of polymethacrylic acid[23] was also examined in the same way. From the method of derivation it is clear that Eqs. (10) and (11) have a general validity for any conformational change, even if it accompanies an association-dissociation equilibrium.

Equation (10) was applied to the present coil-β transition to estimate the charge-independent part of transition free energy. Graphical integration was performed on the modified titration curve such as shown in Fig. 3, after both coil and β-form regions, drawn in solid curves, were extrapolated to lower ionization in such a way to give an identical pK_{int} value (3.00) at $\alpha=0$. The values of $\Delta G^0_{c\to\beta}$ obtained

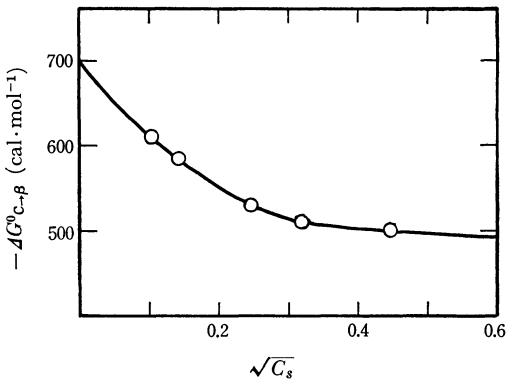

Fig. 5. Dependence of $-\Delta G^0_{c\to\beta}$ on the square root of ionic strength.

are plotted against the square root of ionic strength in Fig. 5. The charge-independent part of transition free energy is still dependent on the ionic strength, as was also observed in the helix-coil of transition, of poly-L-glutamic acid,[14] and varies from -700 cal mol^{-1} in water to -480 cal mol^{-1} at higher ionic strength. These values suggest that the β-form of unionized poly-S-carboxymethyl-L-cysteine is generally much more stable than the

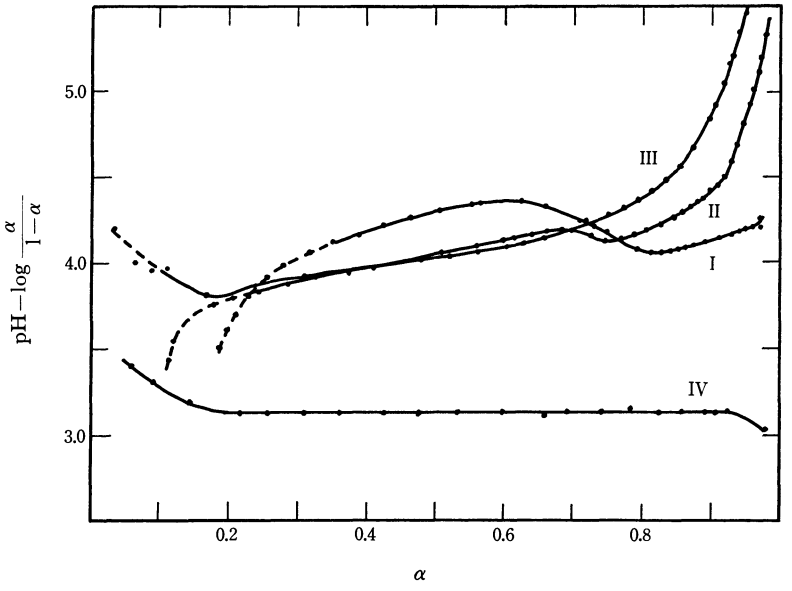

Fig. 6. Modified titration curves for different samples in 0.2M NaCl.
I, E602, $[\eta]=0.230$; II, E527, $[\eta]=0.089$; III, E515, $[\eta]=0.041$, IV, δ-carboxyl group of S-carboxymethyl-L-cysteine. ($[\eta]$: dl g^{-1} in 0.2M NaCl at pH 7, 25°C). Dashed parts indicate the region where turbidity was manifest.

23) J. C. Leyte and M. Mandel, *J. Polymer Sci., Part A-2*, **1964**, 1879.
24) W. G. Miller and R. E. Nylund, *J. Amer. Chem. Soc.*, **87**, 3542 (1965).
25) J. Hermans, Jr., *J. Phys. Chem.*, **70**, 510 (1966).
26) J. Hermans, Jr., *J. Amer. Chem. Soc.*, **88**, 2418 (1966).

α-helix of unionized poly-L-glutamic acid,[14,24-26] relative to their random coil forms. However, this conclusion can not be extended to the other poly-S-carboxymethyl-L-cysteine samples, because of marked molecular weight dependence of $\Delta G^{2}_{C\to\beta}$, as will be shown below.

The coil-β transition of the polymer in 0.2M NaCl was also examined at different temperatures, as illustrated in Fig. 2, and the charge-independent transition free energy was estimated at each temperature. Rough estimates lead to a corresponding transition enthalpy of about -2.4 kcal mol^{-1} and a transtion entropy of -6.5 e.u., giving a transition temperature around 100°C. Both negative values obtained would reflect the nature of hydrogen bonding and hydrophobic interaction.

The Effect of Molecular Weight upon the Titration Behavior. Figure 6 shows modified plots of titration curves for three samples of poly-S-carboxymethyl-L-cysteine in 0.2M NaCl, together with that for δ-carboxyl group of its monomer, S-carboxymethyl-L-cysteine, in 0.2M NaCl. The three polymer samples differ from one another in their molecular weight, as revealed in their intrinsic viscosity of random coil form.

It can be seen that the δ-carboxyl group of the monomer has a constant pK value, 3.12, reasonably close to the pK_{int} value assumed for the polymers. The lowest molecular weight sample, E515, does not show any sharp transition region on its titration curve. Its rotatory properties have shown only trivial changes with pH,[9,10] in accordance with the titration result. Berger, Noguchi and Katchalski[27] have reported that titration curves of poly-S-carboxymethylcysteine prepared by other synthetic methods can be described by the Linderstrøm-Lang equation, suggesting the absence of clear transition region.

With increasing molecular weight, the transition region becomes more distinct. The molecular weight dependence of titration behavior is considerably stronger at higher ionization, where random coil forms are predominant. At lower ionization, however, no such regular dependence is observed. If the charged β-form could be represented by the Gouy model, in which hydrogen-bonded polypeptide chains would form an infinitely extended sheet, its titration behavior would not depend on the molecular weight of constituent polymer. Thus the observed molecular weight dependence indicates deviation of the β-structure from an infintely extended sheet model. The sheet structure of the β-form would have a finite size with appreciable edge effect, which would depend on the chain length of polymer. More possibly, the sheet-like structures would form a globular aggregate by side chain interaction.

The charge-independent transition free energy of these three polymer samples was estimated by Eq. (10) and found to be -80 ± 80 cal mol^{-1} for E515, -180 cal mol^{-1} for E527, and -500 cal mol^{-1} for E602, in 0.2M NaCl at 25°C. The uncharged β-form is less stable as the molecular weight becomes smaller. It is not yet known whether such dependence of stability of β-form is extended to a higher molecular weight range. However, it is conceivable that the dependence reflects variations of a detailed structure of the β-form and its mode of aggregation with polymer chain length and is closely related with the intermolecularly associated structure of the β-form.

27) A. Berger, J. Noguchi and E. Katchalski, *J. Amer. Chem. Soc.*, **78**, 4483 (1956).

BULLETIN OF THE CHEMICAL SOCIETY OF JAPAN VOL. 43 1693—1703 (1970)

Determination of the Molecular Structures of AsF_3 and $AsCl_3$ by Gas Electron Diffraction*1

Shigehiro KONAKA and Masao KIMURA

Department of Chemistry, Faculty of Science, Hokkaido University, Sapporo

(Received January 8, 1970)

The thermal-average distances and mean amplitudes of $AsCl_3$ and AsF_3 have been determined by gas electron diffraction. The sources of experimental errors have been discussed in detail. The observed molecular parameters are r_g(As–Cl)$=2.1621\pm0.0033$ Å, θ_g(ClAsCl)$=98°\ 34'\pm34'$, l(As–Cl)$=0.0470\pm0.0024$ Å, l(Cl–Cl)$=0.0945\pm0.0063$ Å, r_g(As–F)$=1.7089\pm0.0016$ Å, θ_g(FAsF)$=95°53'\pm22'$, l(As–F)$=0.0433\pm0.0022$ Å, and l(F–F)$=0.0689\pm0.0044$ Å. The results have been compared with the structures of other trihalides of the Vb-group elements.

The interatomic distances of AsF_3 and $AsCl_3$ were first observed by the visual method of electron diffraction. Those previous results are summarized in Table 1. The bond angle of AsF_3 was not determined. Kisliuk and Townes[4] measured the rotational constants of $As^{35}Cl_3$ and $As^{37}Cl_3$ by microwave spectroscopy and obtained the r_s(As–Cl) distance of 2.161 ± 0.004 Å and the bond angle of $98°25'\pm30'$.

TABLE 1. MOLECULAR STRUCTURES OF $AsCl_3$ AND AsF_3 DETERMINED BY THE VISUAL METHOD OF ELECTRON DIFFRACTION

r (As–Cl)	∠ ClAsCl	r (As–F)	Ref.
2.18 ± 0.03 Å	$101°\pm40'$		1
2.16 ± 0.03 Å	$103°\pm3°$	1.72 ± 0.02 Å	2
2.17 ± 0.02 Å	$99°\pm2°$		3

The molecular structure of AsF_3, however, could not be determined uniquely from the rotational constant observed in the microwave study of Kisliuk and Geschwind,[5] for no isotope of the fluorine atom was present. They estimated the bond angle of AsF_3 to be $102\pm2°$ by a comparison of the observed quadrupole interaction constant of AsF_3 with that of $AsCl_3$, and determined the r_0(As–F) distance to be 1.712 ± 0.005 Å.

Recently, Mirri[6] obtained the centrifugal distortion constants, D_j and D_{jk}, as well as the rotational constant, B_0, his values agreeing with the results of Kisliuk and Geschwind, by an analysis of the millimeter-wave rotational spectrum of AsF_3. She determined the quadratic potential constants of AsF_3 from the observed centrifugal distortion constants and the four observed vibrational frequencies. Then, she calculated the Coriolis coupling constant, ζ_4, from the potential constants and compared it with those determined by studies of the band envelope of infrared spectra.[7,8] It was found that the calculated and the observed values of ζ_4 did not agree well unless the bond angle of AsF_3 was in the range of $99\pm1°$. Mirri assumed the angle to be 98° by referring to the 98.5° of $AsCl_3$,[4] and she obtained 1.708 Å for the As–F distance. However, it is most desirable to determine the molecular structure of AsF_3 directly; her method is still indirect.

The molecular structures derived directly from the observed rotational constants, B_0, include the effect of the interaction of the vibration and the rotation, so they have no definite physical meaning. Although this effect is not large, it can not be neglected in determining molecular structures in the order of one-thousandth of an Angstrom. On the other hand, the interatomic distances obtained by gas electron diffraction are the thermal averages of instantaneous interatomic distances. It is the principal purpose of the present study to determine the accurate structures of AsF_3 and $AsCl_3$ by gas electron diffraction.

*1 Part of this report was included in the doctoral thesis presented by one of the authors (S. K.) to the Faculty of Science, Hokkaido University.

1) L. O. Brockway and F. T. Wall, *J. Amer. Chem. Soc.*, **56**, 2373 (1934).

2) L. Pauling and L. O. Brockway, *ibid.*, **57**, 2684 (1935).

3) S. M. Swingle, quoted by P. W. Allen and L. E. Sutton, *Acta Crystallogr.*, **3**, pt. 1, 46 (1950).

4) P. Kisliuk and C. H. Townes, *J. Chem. Phys.*, **18**, 1109 (1950).

5) P. Kisliuk and S. Geschwind, *ibid.*, **21**, 828 (1953).

6) A. M. Mirri, *ibid.*, **47**, 2823 (1967).

7) I. W. Levin and S. Abramowitz, *ibid.*, **44**, 2562 (1966).

8) L. C. Hoskins, *ibid.*, **45**, 4594 (1966).

Experimental

The diffraction apparatus used in the present study was designed and constructed by Murata, Kuchitsu, and Kimura.[9] The camera length was fixed at 10.930 cm. In order to measure the accurate value of the scale factor, the diffraction patterns of CS_2 molecules, the precise structure of which had been given by spectroscopy,[10,11] were taken just before or after those of the samples.

Research-grade arsenic trichloride (above 99% pure) obtained from the Yamanaka Chemical Industry, Inc., was used as the sample. The experimental conditions were as follows: accelerating voltage, about 45 kV; sample pressure, about 4 mmHg; exposure time, 3—4 minutes; electron-beam current, about 0.15 μA, and nozzle temperature, about 18°C. The vacuum in the diffraction chamber was about 6×10^{-5} mmHg during exposures.

A sample of arsenic trifluoride in a polyethylene bottle was obtained from the K and K Laboratories, Inc., of the United States. It was transferred into a sample holder made of glass just before taking photographs. Since arsenic trifluoride (mp −6°C) reacts to some extent with glass, the sample was solidified at about −10°C and evacuated by a rotary pump to eliminate any possible impurities such as SiF_4 (mp −90°C). The experimental conditions were as follows; accelerating voltage, about 52.5 kV; sample pressure, about 10mmHg; exposure time, 70—100 sec; electron-beam current, about 0.15 μA, and nozzle temperature, about 19°C. The vacuum pressure was about 8×10^{-5} mmHg during exposures.

Photographs taken on Fuji-Process Hard plates were developed at 20°C for five minutes with an FD-131 developer diluted twice in volume.

The plates were spun rapidly about the centers of the diffraction patterns, while optical densities were measured with an NLM-VII microphotometer. In the case of $AsCl_3$, the densities were read out at integral q values from 20 to 130 from the density curves recorded on charts. A value taken from one side and the corresponding value from the other side were averaged, point by point, in order to diminish the errors due to the uncertainty as to the center position of the chart.

In the case of AsF_3, the densities were measured with a digital microphotometer*2 at intervals of $\Delta R=1/3$ mm along the diameters of the concentric patterns. The q value corresponding to the distance, R, on a plate from its center was calculated as:

$$q = \left(\frac{40}{\lambda}\right)\sin\left(\frac{1}{2}\tan^{-1}\left(\frac{R}{L}\right)\right) \qquad (1)$$

where λ is the wavelength of the incident electron beam and where L is the camera length. The two sides of the photometer curve were analyzed independently.

The relation between the optical densities and the scattering intensities of the electrons was investigated by the use of two selected plates of AsF_3. The ratio of the densities for the same q value of the two plates was about 1.5. The density-intensity curve obtained by Karle's method[13] fit the $E=D\ (1+0.03D)$ relation with a good approximation. A linear relation between the density and the intensity was assumed for the case of $AsCl_3$. The systematic errors caused by this assumption will be discussed in a later section.

The intensities were corrected for the deviation of the rotating sector from the ideal r^3-shape.

Five plates for $AsCl_3$ and six plates for AsF_3 were selected for analysis. The number of CS_2 plates used for determination of the scale factors were four and five for $AsCl_3$ and AsF_3 respectively.

Analysis of Data

The intensities were levelled by smooth functions based on the theoretical backgrounds. Smooth background curves, I_B, were first drawn arbitrarily through the total intensity curves, I_T, thus obtained. The molecular intensities, $qM(q)$, were calculated as $q(I_T-I_B)/I_B$. The theoretical expression of $qM(q)$ may be written, with notations of the usual significance,[14] as follows:

$$qM(q) = k\sum_{i\neq j} A_{ij}\mu_{ij}\cos\Delta\eta_{ij} \times\sin\left\{\frac{\pi}{10}q\left(r_{aij}-\left(\frac{\pi}{10}q\right)^2\kappa_{ij}\right)\right\} \times\exp\left\{-\frac{1}{2}\left(\frac{\pi}{10}q\right)^2 l_{ij}^2\right\}. \qquad (2)$$

The r_a distance is an apparent interatomic distance; it can easily be converted into the thermal-average distance, r_g, as follows:[15]

$$r_g = r_a + \frac{l^2}{r_a}. \qquad (3)$$

The elastic scattering factors were calculated by the partial-waves method from the Hartree-Fock potentials.[16] The inelastic scattering factors, also based on the Hartree-Fock potentials, were taken from the table presented by Tavard *et al.*[17] They were used to compute $\mu_{ij}\cos\Delta\eta_{ij}$ and the theoretical

9) Y. Murata, K. Kuchitsu and M. Kimura, *Japan. J. Appl. Phys.*, to be published.

10) B. P. Stoicheff, *Can. J. Phys.*, **36**, 218 (1958).

11) Y. Morino and T. Iijima, This Bulletin, **35**, 1661 (1962).

*2 Recently, an integrating digital voltmeter (TR-65A15) has been combined with the microphotometer in order to speed up the measurement of the densities and to improve the precision. The intensities of light passing through a plate are recorded on a tape and easily converted to optical densities by using a FACOM 270-20 electronic computer.[12]

12) T. Iijima, H. Fujii and M. Kimura, unpublished.

13) J. Karle and I. L. Karle, *J. Chem. Phys.*, **18**, 957 (1950).

14) S. Konaka, Y. Murata, K. Kuchitsu and Y. Morino, This Bulletin, **39**, 1134 (1966).

15) K. Kuchitsu and L. S. Bartell, *J. Chem. Phys.*, **35**, 1945 (1961).

16) M. Kimura, S. Konaka and M. Ogasawara, *ibid.*, **46**, 2599 (1967).

17) C. Tavard, D. Nicolas and M. Rouault, *J. Chim. Phys.*, **64**, 540 (1967).

backgrounds. In order to revise the background curves, radial distribution curves (RD curves) were calculated as the following Fourier integral:

$$f(r) = \int_0^{q_{max}} (qM(q)_{obs} + \Delta qM(q)) \sin\left(\frac{\pi}{10} qr\right) \times \exp(-bq^2)\, dq. \quad (4)$$

The correction, $\Delta qM(q)$, was added to use the non-negativity criterion of the RD curves as:[13,18]

$$\Delta qM(q) = k \sum_{i \neq j} A_{ij}(g_{ij} - \mu_{ij} \cos \Delta\eta_{ij}) \times \sin\left\{\frac{\pi}{10} q \left(r_{aij} - \left(\frac{\pi}{10} q\right)^2 \kappa_{ij}\right)\right\} \times \exp\left\{-\frac{1}{2}\left(\frac{\pi}{10} q\right)^2 l_{ij}^2\right\}, \quad (5)$$

$$\begin{aligned} g_{As-Cl} &= \cos(0.0072\, q), \\ g_{Cl-Cl} &= 1.11, \\ g_{As-F} &= 0.7 \cos(0.0095q) + 0.5 \exp(-5 \times 10^{-4} q^2), \\ g_{F-F} &= 1.25 \exp(-3 \times 10^{-6} q^2) + 0.65 \exp(-10^{-3} q^2). \end{aligned} \quad (6)$$

The g functions were so chosen that the correction terms, $\Delta qM(q)$, were small compared with $qM(q)_{obs}$. In practice, the background curves were revised by the inverse Fourier transformation of $f(r)$ in the range of r ($r \leqq 1$ Å). At small q values where $qM(q)$ could not be observed, theoretical values were used. The artificial damping factor, b, was so chosen as to reduce the molecular intensity to one-tenth of the original value at q_{max}.

One of the I_T curves and its I_B curve thus obtained are shown in Fig. 1 for both $AsCl_3$ and AsF_3. The values of I_B express approximately the ratio between the observed and the theoretical background intensities. At small scattering angles, the ratio is smaller than unity. This is mainly due to the errors in the sector correction curve, and it has no effect on the molecular parameters. The gradual increase in the ratio at large scattering angles ($q \geqq 90$) is due to extraneous scattering. This may cause a slight increase in the observed values of mean amplitudes. The molecular intensities, $qM(q)_{obs}$, were then multiplied by the ratio in order to eliminate errors caused by the extraneous scattering.

The index of resolution, k, and the molecular parameters, r_{ij} and l_{ij}, were determined by the least-squares fitting of the observed $qM(q)$ to its theoretical expression. The anharmonicity parameters were fixed. The anharmonicity parameters for bonded pairs were estimated in the diatomic approximation as;[19]

$$\kappa_{As-Y} = \left(\frac{1}{6}\right) a_3 \left(1 + \frac{8\kappa}{(1+\kappa)^2}\right) l_{As-Y}^4, \quad (7)$$

where:

$$\chi = \exp\left(\frac{h\nu_{As-Y}}{kT}\right). \quad (8)$$

Here, the anharmonicity parameter of the Morse function, a_3, was assumed to be 2.0 Å^{-1} and the characteristic frequencies, ν_{As-Y}, were taken to be 400 and 721 cm^{-1} for $AsCl_3$ and AsF_3 respectively.[20,7] The estimated values were 3.6×10^{-6}

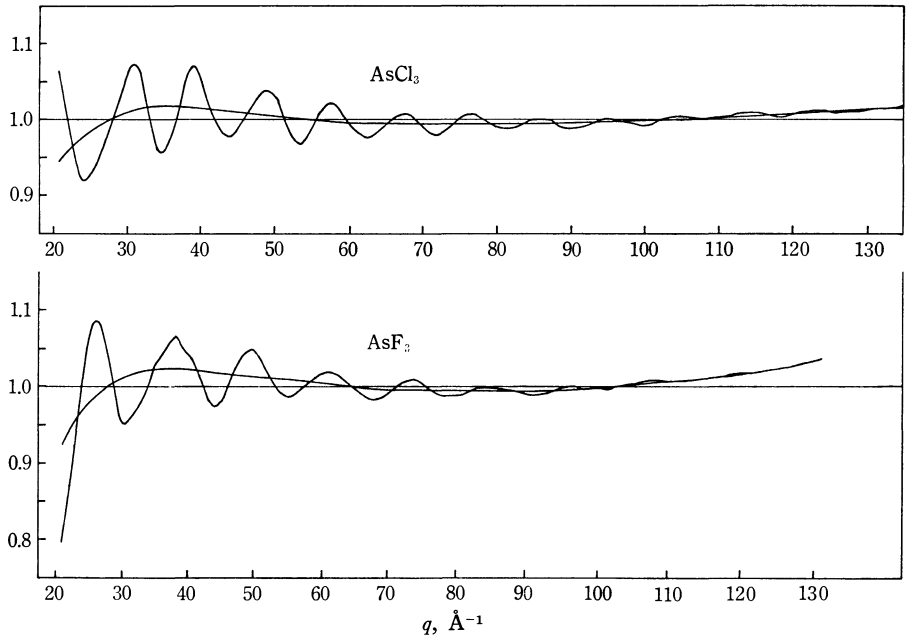

Fig. 1. Levelled intensities and backgrounds.

18) R. A. Bonham and L. S. Bartell, *J. Chem. Phys.*, **31**, 702 (1959).
19) K. Kuchitsu, This Bulletin, **40**, 505 (1967).
20) P. W. Davis and R. A. Oetjen, *J. Mol. Spectrosc.*, **2**, 253 (1958); *ibid.*, **3**, 581 (1959).

and 1.2×10^{-6} Å^3 for κ_{As-Cl} and κ_{As-F} respectively. The anharmonicity parameters, κ_{Y-Y}, for non-bonded paris were assumed to be zero, since no simple method of estimating them was available and since their values could be expected to be of the same order as κ_{As-Y} or less.

The weights of the observed values for least-squares fitting were reduced at small scattering angles because of the uncertainty in the correction curve for the sector shape; those at large scattering angles were also taken to be small because of extraneous scattering. The following from was assumed for AsF_3:

$$\begin{aligned} P(N) &= \exp(-a(N-N_1)^2), & 1\leqq N\leqq N_1 \\ P(N) &= 1.0, & N_1\leqq N\leqq N_2 \\ P(N) &= \exp(-b(N-N_2)^2), & N_2\leqq N \end{aligned} \quad (9)$$

where N shows the numbering of the observed data.

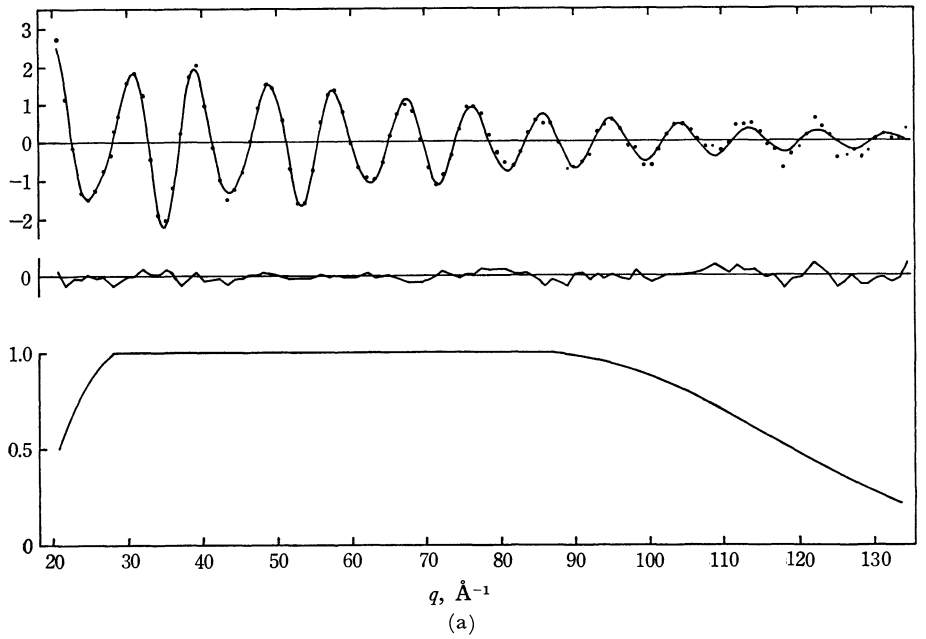

(a)

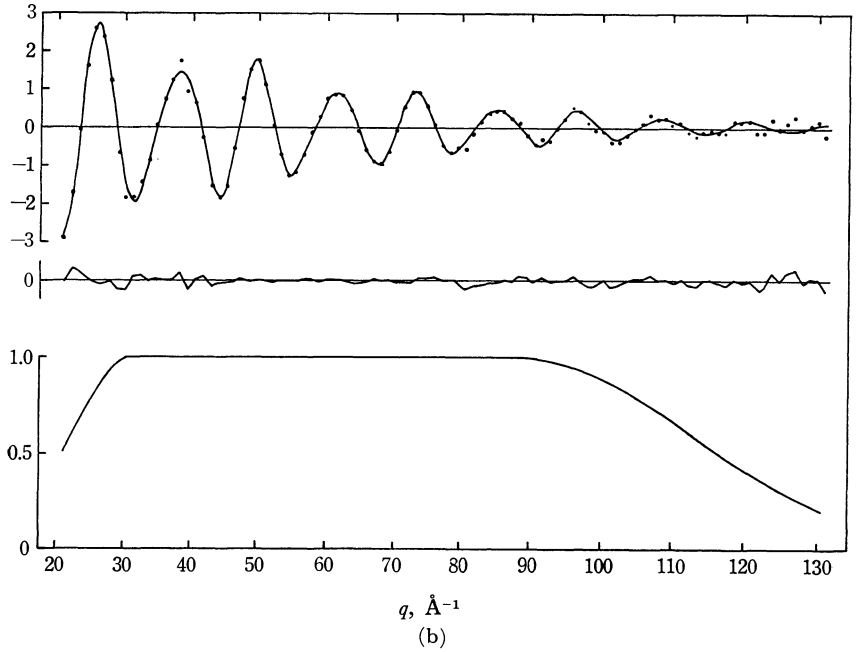

(b)

Fig. 2. Molecular intensities (dots for observed values and the solid curve for the best-fit theoretical intensity), the residuals and the weight function used.
(a) $AsCl_3$ and (b) AsF_3.

Errors due to the arbitrariness of the weights were estimated by using several sets of weight functions which had been obtained by changing the parameters, a, b, N_1, and N_2, in the least-squares treatment.

In the case of AsF_3, the analysis was repeated by correcting the positions of the centers of the photometer curves until the interatomic distances obtained from the two sides of each curve showed satisfactory agreement.

A program for the HITAC 5020E electronic computer was written which allowed for automatic computation from the density-intensity transformation to the least-squares fittings. The analysis for AsF_3 was made by using this program. The average time needed for one computation was about 7 sec. The theoretical values of the μ factors and the levelling function were calculated for the observed points by interpolation of the input data, which had been calculated beforehand for the integral values of q by another program.

Examples of the observed molecular intensities and their best-fit curves are shown in Fig. 2, along with the weight function used.

The analysis of the diffraction patterns for CS_2 was made according to the same procedure as that employed for the samples. Five plates for $AsCl_3$ were numbered from I to V, and six plates for AsF_3 were numbered from I to VI. The wavelength for each plate and the number of CS_2 plates employed were as follows: 0.05539 ± 0.00007 Å for the $AsCl_3$ plates I and II, two CS_2 plates; 0.05626 ± 0.00005 Å for the $AsCl_3$ plates from III to V, two CS_2 plates; 0.05217 ± 0.00003 Å for the AsF_3 plates from I to III, three CS_2 plates; 0.05214 ± 0.00004 Å for the AsF_3 plates from IV to VI, two CS_2 plates.

The above values of the wavelengths for the sample plates had, however, to be corrected if the accelerating voltage had drifted during the experimental sequence. The drift of the accelerating voltage was monitored throughout the experiment. Such corrections for the wavelengths were found unnecessary for the $AsCl_3$ plates I, II and IV, but those of about 0.26% and −0.05% were found necessary for the plates III and V respectively by measuring the load current of the high-voltage source. The drift for AsF_3 was confirmed to be less than 0.01% by measuring the voltage drops of the standard resistance in the high-voltage source by the use of a digital voltmeter. The results of the least-squares analyses, corrected for scale factors, are shown in Table 2, along with the averages of standard deviations, $\bar{\sigma}$.

The mean amplitudes and the shrinkage, δ_g, which is defined as $\delta_g=2r_g(\text{C-S})-r_g(\text{S-S})$,[21] observed for CS_2 are shown in Table 3, along with the errors. The method of estimating the errors will be described in a later section. The observed values are close to those calculated from the spectroscopic data.[11]

Table 2. Least-squares results (r and l in Å unit)

(a) $AsCl_3$

plate	r_a (As-Cl)	r_a (Cl-Cl)	l (As-Cl)	l (Cl-Cl)	k
I	2.1612	3.2822	0.0478	0.0930	0.890
II	2.1611	3.2729	0.0474	0.0901	0.915
III	2.1631	3.2797	0.0452	0.0993	0.818
IV	2.1601	3.2662	0.0478	0.0957	0.863
V	2.1598	3.2685	0.0486	0.0975	0.862
Average	2.1611	3.2739	0.0474	0.0951	0.870
$\bar{\sigma}$	0.0011	0.0069	0.0017	0.0054	0.023
σ_1	0.0005	0.0031	0.0008	0.0024	0.011
σ_2	0.0006	0.0031	0.0006	0.0016	0.016

(b) AsF_3

plate	r_a (As-F)	r_a (F-F)	l (As-F)	l (F-F)	k
I	1.7078	2.5370	0.0457	0.0685	0.963
II	1.7084	2.5361	0.0431	0.0710	0.932
III	1.7077	2.5315	0.0436	0.0689	0.908
IV	1.7094	2.5371	0.0439	0.0711	0.919
V	1.7082	2.5343	0.0437	0.0699	0.913
VI	1.7060	2.5353	0.0431	0.0696	0.920
Average	1.7079	2.5352	0.0439	0.0698	0.926
$\bar{\sigma}$	0.0009	0.0045	0.0017	0.0037	0.022
σ_1	0.0004	0.0018	0.0007	0.0015	0.009
σ_2	0.0005	0.0009	0.0004	0.0004	0.008

Table 3. Mean amplitudes, shrinkage, and index of CS_2 (l and δ_g in Å unit)

	Obsd[a]	Obsd[b]	Calcd[c]
l (C-S)	0.0378 ± 0.0030	0.0366 ± 0.0026	0.0391
l (S-S)	0.0426 ± 0.0036	0.0403 ± 0.0030	0.0421
δ_g	0.0061 ± 0.0049	0.0073 ± 0.0031	0.0070
k	0.90 ± 0.05	0.92 ± 0.05	

a) Results of four CS_2 plates used for determining the scale factors for $AsCl_3$.
b) Results of five CS_2 plates used for determining the scale factors for AsF_3.
c) Ref. 11.

Error Analysis

1) Estimation of Random Errors. Experimental random errors are introduced mainly in the process of photographing, development, and photometry. Random errors can be estimated from the standard deviations in the least-squares treatment (σ_1) and from the fluctuation among the results on several plates (σ_2).[22] The standard deviations, σ_1,

21) Y. Morino, J. Nakamura and P. W. Moore, *J. Chem. Phys.*, **36**, 1050 (1962).

22) Y. Morino, K. Kuchitsu and Y. Murata, *Acta Crystallogr.*, **18**, 549 (1965).

associated with the average values in Table 2 were estimated to be $\bar{\sigma}/\sqrt{N}$, where N is the number of plates, since the individual standard deviations for all the plates were nearly equal. The standard deviations, σ_2, are defined by $\sqrt{\sum_{i=1}^{N}(x_i-\bar{x})^2/N(N-1)}$. Random errors corresponding to a 99% confidence interval have so far been taken to be 2.5 times the larger of σ_1 and σ_2.[14,22] It seems, however, more reasonable to estimate them from either 2.58 times σ_1, or 4.60 ($N=5$) or 4.03 ($N=6$) times σ_2, according to Student's t-distribution.[23] If σ_1 and σ_2 are of nearly equal magnitude, 2.58 σ_1 can be taken as the confidence interval, because all the observations on N plates are considered to belong to a single statistical population, as has been discussed by Morino *et al.*[22] When σ_2 is considerably larger than σ_1, the confidence interval should be estimated from σ_2 and the t-value depending on N. Since σ_2 is equal to, or slightly smaller than, σ_1 for almost all the parameters in the present analysis, 2.58 σ_1 was chosen as the random error corresponding to the 99% confidence interval.

2) Estimation of Systematic Errors for Interatomic Distances. The sources of systematic errors taken into consideration were as follows:

a) The Uncertainty in the Camera Length.

b) The Uncertainty in the Scale-magnification Ratio on the Microphotometer Trace.[24] The above two errors are, however, negligible because of the use of the reference sample (CS_2).

c) Errors in the Determination of the Center of the Microphotometer Trace. These errors are also negligible since, in the case of AsF_3, both sides of the photometer trace were analyzed and the results from both sides averaged, and in the case of $AsCl_3$ the corresponding densities of both sides were averaged.

d) The Finite Size of the Light Beam on Microphotometry. This effect was discussed by Kuchitsu.[24] In the present experiment, the size of the light beam was 0.03 mm × 0.1 mm. The inward shift of the halo of the radius, R (mm), is about $(0.1)^2/24R$ in mm units, which is about 0.001% of R even at $R=6$ mm. Thus, this effect is completely negligible.

e) Errors Due to Averaging Densities over a Scanning Length of About 0.1 mm on the Plate on Microphotometry. In the case of AsF_3, the optical density obtained on microphotometry is the average of densities over a range of about 0.1 mm on the plate.*3 The effect of such an averaging process on molecular-parameter values may be estimated as follows. The average of the molecular intensity is given by the following integration:

$$M=\frac{1}{2\Delta R}\int_{R_0-\Delta R}^{R_0+\Delta R}\exp\left(-\frac{1}{2}l^2s^2\right)\frac{\sin sr}{sr}\,dR \qquad (10)$$

Here s is a function of the scanning length, R, measured from the center of the photographic plate and ΔR is half of the range over which the average is taken. By noting that s is proportional to R in a good approximation, Eq. (10) can be transformed into the following equation by neglecting higher-order terms than $(\Delta R/R_0)^2$:

$$M=\exp\left(-\frac{1}{2}l^2s_0^2\right)\frac{\sin s_0r}{s_0r}\left[1+\frac{1}{6}\left(\frac{\Delta R}{R_0}\right)^2\times\{(ls_0)^4-(rs_0)^2-2(l^2s_0^2+1)s_0r\cot s_0r\}\right] \qquad (11)$$

This can be rewritten in the same order of approximation as follows:

$$M=(1+\Delta k)\exp\left\{-\frac{1}{2}(l+\Delta l)^2s_0^2\right\}\frac{\sin s_0(r+\Delta r)}{s_0(r+\Delta r)} \qquad (12)$$

where:

$$\Delta k=-\frac{1}{6}\left(\frac{\Delta R}{R_0}\right)^2(s_0r)^2, \qquad (13)$$

$$\frac{\Delta l}{l}=\frac{1}{6}\left(\frac{\Delta R}{R_0}\right)^2(s_0l)^2, \qquad (14)$$

and:

$$\frac{\Delta r}{r}=-\frac{1}{3}\left(\frac{\Delta R}{R_0}\right)^2((s_0l)^2+1). \qquad (15)$$

Since the value of $\Delta Rs_0/R_0(=\Delta s)$ is about 0.05 Å^{-1} for the accelerating voltage of 52.5 kV, the apparent decreases of interatomic distances are about 0.001% for both As–F and F–F distances; both are negligible.

f) Errors Involved in the Determination of the Scale Factors. They were estimated to be 0.14% and 0.07% for $AsCl_3$ and AsF_3 respectively from the standard errors corresponding to the 99% confidence interval of the C–S and S–S distances in the least-squares treatment of CS_2 and from the drift of the accelerating voltage while taking photographs of CS_2 and the samples.

g) Errors Due to Uncertainty in the Parameter, κ. The uncertainties for the κ values were estimated to be 1, 8, 0.6, and 4×10^{-6} Å^3 for As–Cl, Cl–Cl, As–F, and F–F respectively, values which correspond to uncertainties of 0.0004, 0.0016, 0.0002, and 0.0014 Å in the respective distances.

h) Errors Due to Uncertainty in the Correction Curve for the Sector Shape. They include errors due to small pieces of dust which might have been at the edge of the sector during the experiment. They were estimated by changing the sector correction curve over the range of small scattering angles ($q\leqq40$).

i) Errors Due to the Delocalization of the Sample

23) J. Bass, "Elements of Probability Theory," Academic Press Inc., New York (1966), p. 214.

24) K. Kuchitsu, This Bulletin, **32**, 748 (1959).

*3 In the microphotometry of AsF_3, photographing plates were moved at the speed of about 0.025 mm/sec, while the intensities of light passing through the plates were integrated for 4 seconds by using a digital voltmeter.[12]

Gas. Scattering from unlocalized gas causes an apparent increase in the interatomic distances.[25] If the decrease in the index of resolution from unity is assumed to be due completely to the samlpe delocalization in the diffraction chamber, the apparent increase in interatomic distances can be estimated as follows:[25]

$$\frac{\Delta r}{r} = \frac{[3(1-k)/k]}{[20+(sr)^2]} \tag{16}$$

By taking the effective value of s to be 15 $Å^{-1}$, the values listed in Table 4 were obtained for $AsCl_3$ and CS_2, and for AsF_3 and CS_2. The corrections for r_a distrances were estimated to be as shown in Table 9. The errors associated with this correction were taken to be 0.02%.

Table 4. Apparent increases of the interatomic distances ($\Delta r/r$) due to the delocalization of sample gas for $AsCl_3$ and CS_2, and AsF_3 and CS_2

r(As-Cl)	r(Cl-Cl)	r(C-S)	r(S-S)
0.04%	0.02%	0.06%	0.02%

r(As-F)	r(F-F)	r(C-S)	r(S-S)
0.04%	0.02%	0.05%	0.01%

Table 5. Estimation of errors for r_a distances (in 10^{-4} Å unit)

Source of errors	As-Cl	Cl-Cl	As-F	F-F
Random errors (2.58 σ_1)	13	80	10	47
Scale factor	30	46	12	18
Uncertainty of κ	4	16	2	14
Sector correction curve	2	8	1	10
Delocalization of sample gas	4	6	3	5
Arbitrariness of background	2	3	2	2
Arbitrariness of weight	3	4	2	13
Total errors	33	94	16	55

j) Errors Due to Arbitrariness of the Background Curves. The errors were estimated by changing the artificial damping factor and the range of the inverse Fourier transformation.

k) Errors Due to Arbitrariness of the Weight Function. They were estimated by changing weight functions.

The errors for interatomic distances are summarized, along with the total errors, in Table 5.

3) Estimation of Systematic Errors for Mean Amplitudes. *a) Effect of the Finite Sample Size.* The finite sample size causes an apparent increase in the mean amplitudes.[26] The distribution of gaseous molecules spouted from the nozzle depends mainly on the distance, a, from the top of the nozzle to the main beam, the diameter, b, of the nozzle aperture and the viscosity of the gas.

The distribution of silicon tetrachloride molecules jetted from the needle-type nozzle (a=0.41 mm and b=0.55 mm) was investigated by Morino and Murata.[26] The distribution function obtained by their experiments was:

$$f(x) = \left(\frac{2.74}{2}\right) \exp(-2.74\,|x|) \tag{17a}$$

for $|x| \leqq 0.7$, and:

$$f(x) = 0.356 \exp(-1.59x) \tag{17b}$$

for $|x| \geqq 0.7$, where x is the distance in millimeters measured from the center of the nozzle inlet along the direction of the beam. Since the nozzle type with a diameter of 0.2 mm was used at a=0.4 mm in the present experiment, more localization of gas molecules may be expected than in their experiment. The following distribution function was, therefore, tentatively assumed:

$$f(x) = 1.5 \exp(-3\,|x|). \tag{18}$$

The apparent increase in the mean amplitudes estimated from this distribution is:

$$\Delta l_{ij} = \frac{r_{ij}^2}{l_{ij}} \frac{1}{(3L)^2} \tag{19}$$

where L is the camera distance in millimeters. Numerical values of Δl_{ij} for $AsCl_3$, AsF_3, and CS_2 are tabulated in Table 6. The errors associated with this correction were taken to be 70% of the correction. The values of CS_2 corrected for this effect are shown in Table 3.

b) Errors for Density-Intensity Calibration. For AsF_3, they were estimated by changing the parameter c from 0 to 0.5 in the relation, $E/D=(1+cD)$.

Table 6. Apparent increases in the mean amplitudes caused by the finite sample size (in Å unit)

l(As-Cl)	l(Cl-Cl)	l(As-F)	l(F-F)	l(C-S)	l(S-S)
0.0009	0.0010	0.0006	0.0009	0.0006	0.0021

Table 7. Estimation of errors for mean amplitudes (in 10^{-4} Å unit)

Source of errors	As-Cl	Cl-Cl	As-F	F-F
Random errors (2.58 σ_1)	21	62	18	39
Sample size	6	7	4	6
E-D calibration	2	1	4	3
Extraneous scattering	2	2	2	2
Atomic scattering factors	5	9	8	14
Sector correction curve	4	6	6	11
Arbitrariness of background	2	2	1	2
Arbitrariness of weight	6	4	1	7
Total errors	24	63	22	44

25) L. S. Bartell, *J. Appl. Phys.*, **31**, 252 (1960).
26) Y. Morino and Y. Murata, This Bulletin, **38**, 114 (1965).

Because a linear relation ($c=0$) was assumed in the analysis of the $AsCl_3$ data, the effect of the parameter c on the mean amplitudes was examined by the reanalysis of the densest plate ($D_{max}=0.8$) of $AsCl_3$. By taking 70% of the correction for this plate as the average values of the mean amplitudes, they were estimated to be 0.0002 Å and 0.0001 Å for As–Cl and Cl–Cl respectively. The uncertainties of this correction were estimated to be as is shown in Table 7.

c) Errors for Averaging Densities over a Scanning Length of About 0.1 mm on the Plate on Microphotometry. This effect was considered in the previous section. The apparent increase in the mean amplitudes of AsF_3 is smaller than 0.0005%; this effect is thus found to be completely negligible.

d) Corrections for Extraneous Scattering. The correction was made in the analysis. The errors for this correction were estimated to be 70% of the correction.

e) Errors Due to the Uncertainty of the Atomic Scattering Factors. Since the complex scattering factors based on the Hartree-Fock atomic potentials were used, these errors would be small. Their estimated values are shown in Table 7.

f) The Drift of the Wavelength of the Incident Electron during Exposure for One Plate. For the plates III, IV, and V of $AsCl_3$, a slight drift of accelerating voltage was observed; its effect on the molecular parameters must be investigated. If the wavelength is assumed to have drifted from $\lambda_0-\Delta\lambda$ to $\lambda_0+\Delta\lambda$ during one exposure, the observed molecular intensity is given by;

$$M=\frac{1}{2\Delta\lambda}\int_{\lambda_0-\Delta\lambda}^{\lambda_0+\Delta\lambda}\exp\left(-\frac{1}{2}l^2s^2\right)\frac{\sin sr}{sr}\,d\lambda \qquad (20)$$

where s is a function of λ. By expanding this equation into the power series of $(\Delta\lambda/\lambda_0)$ and by neglecting the higher order terms than $(\Delta\lambda/\lambda_0)^2$, it can be rewritten in the following form;

TABLE 8. ESTIMATION OF ERRORS FOR INDICES

Source of errors	$AsCl_3$	AsF_3
Random errors ($2.58\,\sigma_1$)	0.02_8	0.02_3
E-D calibration	0.02	0.02
Atomic scattering factors	0.03	0.03
Sector correction curve	0.02	0.02
Arbitrariness of background curve	0.00_5	0.00_5
Arbitrariness of weight	0.02	0.02
Total errors	0.05	0.05

TABLE 9. CORRECTIONS FOR INTERATOMIC DISTANCES (in 10^{-4} Å unit)

	As–Cl	Cl–Cl	As–F	F–F
Delocalization of sample gas	0	6	−1	3
r_g-r_a	10	28	11	19

TABLE 10. FINAL RESULTS FOR $AsCl_3$ AND AsF_3

	$AsCl_3$	AsF_3
r_g(As-Y)	2.1621±0.0033	1.7089±0.0016
r_g(Y-Y)	3.2773±0.0094	2.5374±0.0055
θ_g(YAsY)	98°34′ ±34′	95°53′ ±22′
l(As-Y)	0.0470±0.0024	0.0433±0.0022
l(Y-Y)	0.0945±0.0063	0.0689±0.0044
k	0.87 ±0.05	0.93 ±0.05

TABLE 11. MOLECULAR STRUCTURES OF GROUP Vb TRIHALIDES

(a) Bond distances (in Å unit)

	F	Cl	Br	I
N	1.365 ±0.002[a]			
p	1.570_6±0.001_2[b]	2.039 ±0.0014[c]	2.18 ±0.03[e]	2.43 ±0.04[e]
		2.043 ±0.003[d]		
As	1.708_9±0.001_6[f]	2.162_1±0.003_3[f]	2.329±0.002[g]	2.557±0.005[h]
Sb	1.876 ±0.005[i]	2.325 ±0.005[k]	2.51 ±0.02[e]	2.719±0.0015[l]
	1.879 ±0.004[j]	(2.37 ±0.02[e])		

(b) Bond angles (in degrees)

	F	Cl	Br	I
N	102.37±0.04[a]			
P	97.8 ±0.2[b]	100.27±0.09[c]	101.5±1.5[e]	102 ±2[e]
		100.1 ±0.3[d]		
As	95.9 ±0.4[f]	98.6 ±0.6[f]	99.7±0.3[g]	100.2±0.4[h]
Sb	94 ±2.5[i]	99.5 ±1.5[k]	97 ±2[e]	99.1[l]
	95.0 ±0.8[j]	96 ±4[e]		

a) Ref. 28 b) Ref. 29 c) Ref. 30 d) Ref. 4 e) Ref. 3 f) Present results
g) Ref. 31 h) Ref. 32 i) Ref. 33 j) Ref. 34 k) Ref. 35 l) Ref. 36

$$M = \exp\left(-\frac{1}{2}l^2s_0^2\right)\frac{\sin s_0 r}{s_0 r}\left[1-\frac{1}{6}\left(\frac{\Delta\lambda}{\lambda_0}\right)^2 \times \{(s_0 l)^2+(s_0 l)^2\cot s_0 r+(s_0 r)^2-(s_0 l)^4\}\right] \quad (21)$$

Therefore, an apparent increase in the mean amplitude is given approximately as:

$$\Delta l = \frac{1}{6}\left(\frac{\Delta\lambda}{\lambda_0}\right)^2\frac{r^2}{l}. \quad (22)$$

Since the value of $\Delta\lambda/\lambda_0$ was 0.2% at most, the corrections for the mean amplitudes of $AsCl_3$ are 0.0001 Å or less. The effects on interatomic distances can also be completely ignored.

The following three kinds of systematic errors were estimated in the same way as has been described for the case of interatomic distances:

g) Errors Due to the imperfection of the correction curve for the sector shape.

h) Errors Due to the arbitrariness of the backgrounds.

i) Errors Due to the arbitrariness of the weight func-

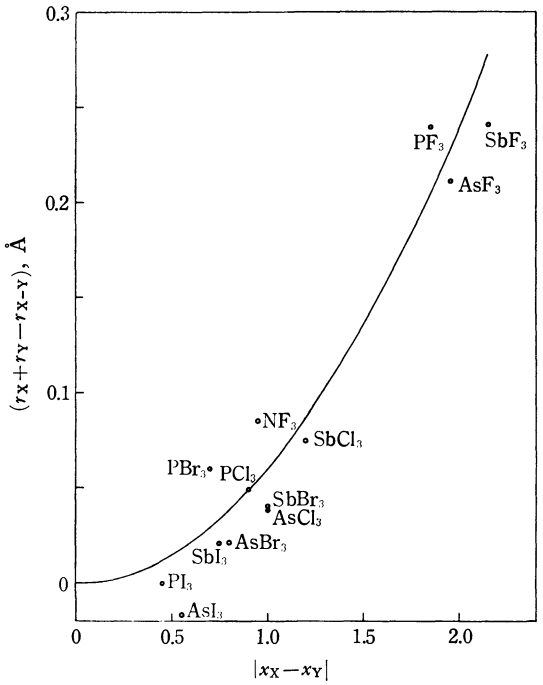

Fig. 3. Plot of the shortenings of bond distances from the sum of the covalent radii *versus* the differences of electronegativities. The solid curve represents a relation $(r_X+r_Y-r_{X-Y})=0.06\ (x_X-x_Y)^2$.

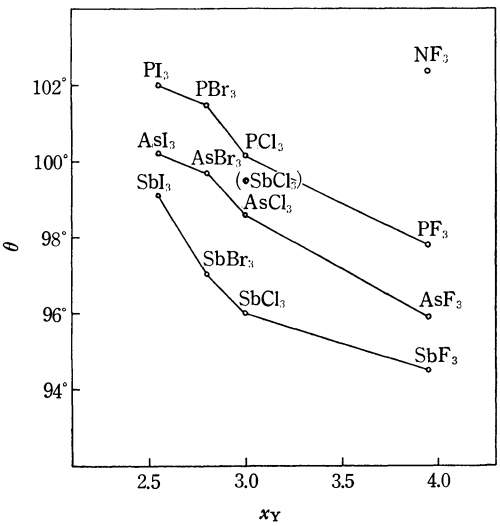

Fig. 4. Variation of bond angles θ with the electronegativities of halogens x_Y.

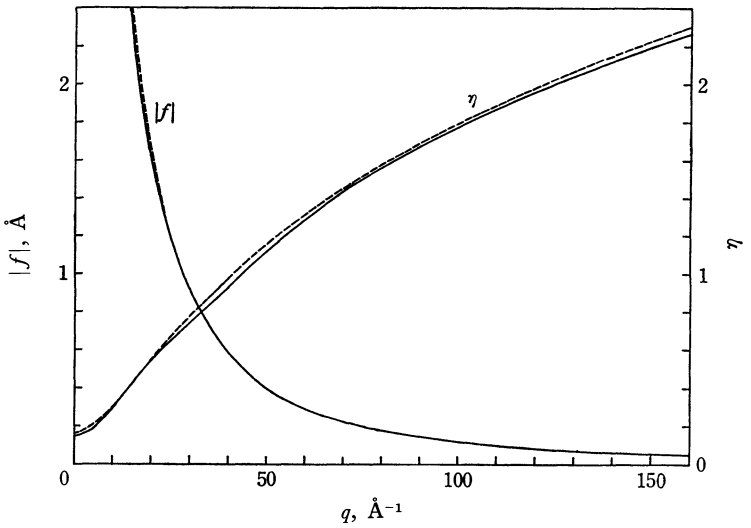

Fig. 5. Scattering factors of arsenic calculated from the H. F. and T. F. D. potentials for 52.5 keV electrons.
—— H. F., ------ T. F. D.

tion. The systematic errors for the mean amplitudes are summarized in Table 7, together with the total errors.

The systematic errors for the index of resolution were estimated to be as shown in Table 8. The deviation of the indices of resolution from unity is considered to be due mainly to the extraneous scattering, which raises the background intensities uniformly over the whole observed range of scattering angles. This extraneous scattering is certainly caused partly by the delocalization of the sample gas in the diffraction chamber and partly by the reflection of scattered electrons by the chamber walls.

Results and Discussion

The corrections necessary for obtaining thermal average distances from the interatomic distances given in Table 2 are listed in Table 9. The final values of the r_g distances, the mean amplitudes, and the indices of resolution are tabulated in Table 10. The θ_g(YAsY) bond angles were calculated by the relation:*4

$$\sin\left(\frac{\theta_g}{2}\right) = \frac{r_g(\text{Y-Y})}{2r_g(\text{As-Y})} \tag{23}$$

The bond angle of $AsCl_3$ is close to the microwave value, but that of AsF_3 is about 6° smaller than Kisliuk's value and 2° smaller than Mirri's value.*5 The molecular structures are compared with those of other arsenic trihalides in Table 11.[28-36] They vary gradually with the atomic numbers of halogens.

The molecular structures of the other trihalides of the Vb-group elements XY_3 are also shown in Table 11. The bond distances, r_{X-Y}, are shorter than the sum of the covalent radii*6 (r_X+r_Y) in almost all cases. Figure 3 shows the shortenings $(r_X+r_Y-r_{X-Y})$ plotted against the differences in electronegativities $|x_X-x_Y|$ taken from the literature.[38] The curve can be roughly expressed by the $(r_X+r_Y-r_{X-Y})=0.06\,(x_X-x_Y)^2$ relation. Aside from the causes of these bond shortenings, this relation shows that the bond shortening varies rather regularly with the difference in electronegativity.

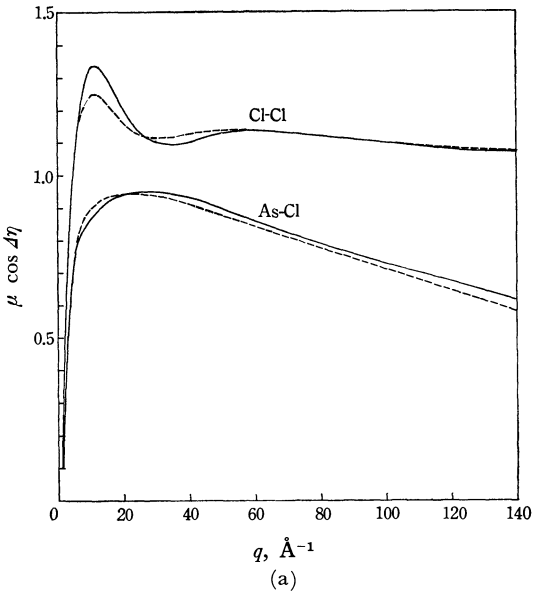

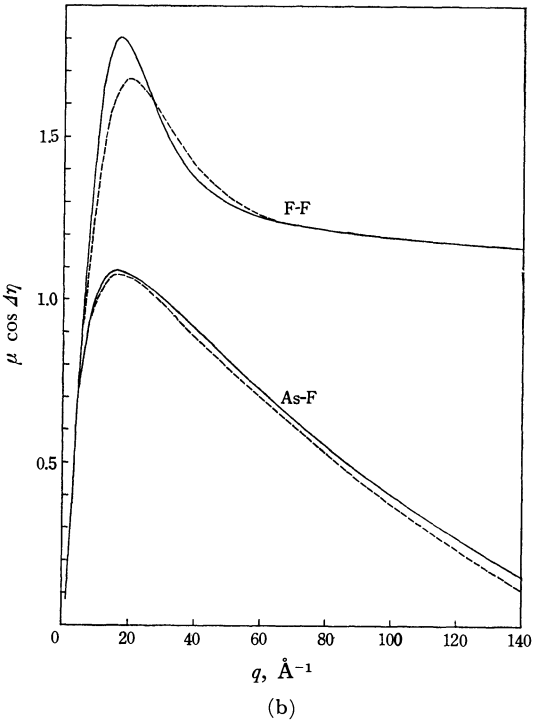

Fig. 6. The μ factors calculated by using the H. F. scattering factors (——) and those obtained by replacing the elastic scattering factors for arsenic by the T. F. D. scattering factors (------).
(a) $AsCl_3$ 45 keV and (b) AsF_3 52.5 keV.

*4 Strictly speaking, the bond angles thus obtained are not necessarily equal to the thermal average of the bond angles. It is likely, however, that the difference is, in the present case, much smaller than the experimental uncertainty. K. Kuchitsu, private communication.

*5 The present finding for the structure of AsF_3 is consistent with the recent gas electron diffraction finding obtained independently by Clippard and Bartell.[27]

27) F. B. Clippard and L. S. Bartell, "Symposium on Molecular Structure and Spectroscopy," Columbus, Ohio, September, 1968, E9.

*6 The covalent radii were taken from the literature.[37]

28) M. Otake, C. Matsumura and Y. Morino, *J. Mol. Spectrosc.*, **28**, 316 (1968).

29) Y. Morino, K. Kuchitsu and T. Moritani, *Inorg. Chem.*, **8**, 867 (1969).

TABLE 12. CHANGE OF PARAMETERS (X) AND STANDARD DEVIATIONS ($\bar{\sigma}$) IN THE LEAST-SQUARES FITTING WHEN $f_{T.F.D.}$ IS USED FOR ARSENIC (r and l in 10^{-4} Å unit)

X	$AsCl_3$		AsF_3	
	ΔX	$\Delta\bar{\sigma}$	ΔX	$\Delta\bar{\sigma}$
r_a(As-Y)	2	0	−5	1
r_a(Y-Y)	−6	1	−5	5
l(As-Y)	−5	0	3	1
l(Y-Y)	16	2	27	4
k	0.014	0.001	0.036	0.003

30) K. Hedberg and M. Iwasaki, *J. Chem. Phys.*, **36**, 589 (1962).
31) K. Hedberg, *Trans. Amer. Cryst. Association*, **2**, 79 (1966).
32) Y. Morino, T. Ukaji and T. Ito, This Bulletin, **39**, 71 (1966).
33) T. Ukaji and H. Uchimura, presented at the 22nd Annual Meeting of the Chemical Society of Japan, Tokyo, March, 1969.
34) C. Matsumura and H. Takeo, "Symposium on Molecular Structure," Fukuoka, Oct., 15, 1969.
35) P. Kisliuk and C. H. Townes, *Phys. Rev.*, **83**, 210 (1951).
36) A. Almenningen and T. Bjorvatten, *Acta Chem. Scand.*, **17**, 2573 (1963).
37) W. Gordy, W. V. Smith and R. F. Trambarulo, "Microwave Spectroscopy," John Wiley & Sons, Inc., New York (1953), p. 309.
38) W. Gordy and W. J. O. Thomas, *J. Chem. Phys.*, **24**, 439 (1956).

The bond angles decrease with the increase in the electronegativity of halogens relative to Vb-group atoms as is shown in Fig. 4. This is in accordance with the valence-shell electron-pair repulsion theory of Gillespie,[39] as discussed by Morino *et al.*[29]

The values of the parameters listed in Table 10 were obtained by using the Hartree-Fock scattering factors ($f_{H.F.}$), which are better than the Thomas-Fermi-Dirac scattering factors ($f_{T.F.D}$).[16] Since $f_{H.F.}$ factors are not available for atoms heavier than krypton, it is worthwhile looking at the changes in the results given rise to by the use of $f_{T.F.D}$ factors instead of $f_{H.F.}$ factors for arsenic. The two scattering factors are compared in Fig. 5, while the corresponding μ factors are shown in Fig. 6. Table 12 shows that, although the changes in parameter values are apparent, they are smaller than the experimental errors. Slight increases in the standard deviations were found, as was expected.

The molecular structures and mean amplitudes obtained here will be combined with the spectroscopic data to determine harmonic potential constants and more accurate molecular structures in a succeeding paper.[40]

We wish to thank the Computing Center of the University of Tokyo for providing their facilities. Our thanks are also due to Dr. Takao Iijima for his helpful discussions.

39) R. J. Gillespie, *J. Chem. Educ.*, **40**, 295 (1963).
40) S. Konaka, This Bulletin, to be published.

BULLETIN OF THE CHEMICAL SOCIETY OF JAPAN VOL. 43 1703—1707 (1970)

Location of Gadolinium Ions in Hydrated Oxalate by ESR

Hsiu CHI

Department of Chemistry, New Asia College, The Chinese University of Hong Kong, Hong Kong

(Received April 30, 1969)

Gadolinium oxalate hydrate crystallizes isomorphously as $La_2(C_2O_4)_3 \cdot 10H_2O$, with two molecules in a unit cell of dimensions: $a_0 = 11.61 + 0.05$, $b_0 = 9.656 + 0.020$, $c_0 = 10.22 + 0.05$ Å and $\beta = 119.0 + 0.1°$. A detailed study of the *d*-spacings for the coprecipitates of varying composition in the La-Gd oxalate system was made, and 46 nearest-neighbor pairs were selected for Van Vleck second moment calculation. Agreement of the results of the calculation with those of the experiment justifies the suggested model representing the location of the gadolinium ions in the hydrated oxalate salt.

During the course of investigation of the coprecipitated phases of calcium-gadolinium oxalate system[1] the author found it desirable to know the relative positions of gadolinium ions in the lattice of the hydrated salt. However, no such information is available in literature. In the work of Gilpin and

1) H. Chi and K. Nagashima, This Bulletin, **41**, 2054 (1968).

McCrone[2,3] concerning the crystallographic data of hydrated lanthanum oxalate, the authors did not seem to pay attention to the structural refinements or to the location of ions in such a specified lattice. Studies on the single crystal X-ray data of oxalates of rare-earths other than lanthanum cannot be carried out easily. This is because most of these salts, prepared from their aqueous solutions, can be obtained only in the form of a fine powder.

In this article a new result is presented. Even when direct crystallographic data are lacking or a well-resolved Fourier projection has not been examined, recent refinements of ESR measurements enable one to obtain detailed information for the distribution of paramagnetic ions in solids.[4,5] In favorable cases, we can solve problems concerning the exact location of each kind of paramagnetic ions in their respective crystals.

Since the gadolinium ion has no resultant orbital momentum, it is very active to ESR at room temperature.[6] The author has therefore worked on the following presumption: ESR may offer excellent opportunities of providing exact knowledge of the location of lanthanide ions in crystals. The only necessary condition is that they are similarly located to gadolinium ions in their respective crystals. Thus, gadolinium ions may be regarded as a guide in ESR experiments for determining the exact positions of other allied lanthanide ions, either less active to ESR or perfectly inert, in many kinds of isomorphous salts.

The Van Vleck calculation of the magnetic second moment for a polycrystalline sample usually gives good results which are valuable for the verification of ESR experimental data.[7] However, in order to use the Van Vleck equation for this purpose, we need a fixed model in which the distances between the nearest neighboring paramagnetic ions are precisely known. In the present study, the process is reversed. The Van Vleck calculation is used as an independent means to determine whether or not the positions of the paramagnetic ions are crystallographically well fitted.

Experimental

Reagents and Procedure. Lanthanum oxide was dissolved in nitric acid and heated on a water bath until crystallization took place. The resulting lanthanum nitrate was dissolved and diluted. Gadolinium oxide was treated in the same way. The two solutions were then mixed in various proportions. A total of 200 m*l* each of the resulting solutions contained 1.25 mM of tripositive ions. The pH value of the solutions was adjusted to near 1.5. Three series of the specimens were prepared. To each of them was added 50 m*l* of water containing 1 g of oxalic acid or dimethyl oxalate, the latter being used to effect homogeneous precipitation. In the first series, oxalic acid was added as a precipitant at room temperature. In the second, dimethyl oxalate was added at room temperature. In the last, dimethyl oxalate was added and the temperature was held at about 80°C. In the first instance, the mixtures turned turbid at once. However, in the case of homogeneous precipitation, the reaction proceeded very slowly and lasted from 8 to 16 hr. Generally, the smaller the content of gadolinium in the solution, the slower was the rate of precipitation. All the precipitates were allowed to settle overnight, filtered, washed and air-dried. One part from each of the precipitates was taken for X-ray powder study, and the remaining was used for ESR spectrometry.

Apparatus. Measurement for electron spin resonance was carried out at room temperature swept both increasingly from 250 up to 10000 gauss and decreasingly from 10000 down to 250 gauss with a JES-3BS-X ESR spectrometer, manufactured by the Japan Electron Optics Laboratory. The X-ray measurement was carried out with a Rigaku-Denki X-ray diffractometer operated at 30 KV and 15 mA, using a copper target.

Results and Discussion

A. X-Ray Diffractometry. The author studied carefully the *d*-spacings for each of the coprecipitates of varying composition in the lanthanum-gadolinium oxalate system. The coprecipitates were prepared by three different procedures. It was observed that in each case the *d*-spacings, except for d_{020}, changed slightly and regularly with composition. Three typical and strong diffraction data together with the corresponding axial lengths were selected. They are listed in Table 1 for comparison.

In Table 1, the values of each of the cell dimensions were calculated from the general relation: Monoclinic: $a : 1 : c$, $\alpha=\gamma=90°$, $\beta \neq 90°$

TABLE 1. SHRINKAGE ALONG *a* AND *c* AXES OF LANTHANUM OXALATE DECAHYDRATE

Spacing and Axis	Alteration of the lattice of Hydrated La-Gd Oxalate (Å) Mole Fraction of Gadolinium					
	0	0.20	0.40	0.60	0.80	1.00
(1) d_{100}	10.40	10.36	10.30	10.25	10.20	10.16
a_0	11.91	11.86	11.78	11.72	11.66	11.61
(2) d_{011}	6.66	6.63	6.60	6.58	6.57	6.56
c_0	10.47	10.41	10.35	10.30	10.26	10.22
(3) d_{020}	4.84	4.84	4.84	4.84	4.83	4.83
b_0	9.68	9.68	9.68	9.68	9.66	9.66

2) V. Gilpin and W. C. McCrone, *Anal. Chem.*, **24**, 225 (1952).

3) Fink, Inorganic Index to the Powder Diffraction File, **14**, 775, ASTM Publication (1965).

4) S. Fujiwara, *Anal. Chem.*, **36**, 2259 (1964).

5) S. Fujiwara and K. Nagashima, *ibid.*, **38**, 1464 (1967).

6) F. W. Lancaster and W. Gordy, *J. Chem. Phys.*, **19**, 1181 (1951).

7) G. E. Pake and E. M. Purcell, *Phys. Rev.*, **74**, 1184 (1948).

$$d_{hkl} = \frac{b_0}{\sqrt{\dfrac{(h/a)^2 + (1/c)^2 - \dfrac{2hl}{ac}\cos\beta}{\sin^2\beta} + k^2}} \quad (1)$$

where $a=a_0/b_0$, $c=c_0/b_0$.

The results indicate that with the replacement of lanthanum ions by smaller gadolinium ions, the angle β remains unchanged in all cases, and most of the shrinkage occurs along a and c axes in the proportion of 1 : 0.88 which is approximately equal to the axial ratio of pure lanthanum oxalate decahydrate. Although a_0 and c_0 in this coprecipitated system vary linearly with the mole fraction of gadolinium, the shortest b-axis only shows little variation to the extent of 0.02 Å with change of composition.

In order to ascertain whether the mole number of hydration was altered the author analyzed both the pure precipitates and the coprecipitates. All gave the same result, with the mole number lying around 10. Analysis of pure lanthanum oxalate and pure gadolinium oxalate precipitated by the three procedures described above, gave the average mole number as 10.58 and 10.49, respectively. The calculated density of the latter 2.514 g/cm^3 for the two formula weights in a unit cell agreed with that obtained (2.49±0.01 g/cm^3 at 28°) by means of flotation and pyconometry.

B. Validity of the Van Vleck Equation. The Van Vleck equation in a general form[8] is expressed as

$$\langle \Delta\nu^2 \rangle = \frac{3}{4} g^4 \mu_B^4 h^{-2} s(s+1) \sum_j r_{jk}^{-6} (3\cos^2\theta - 1)^2 \quad (2)$$

Under the present experimental conditions of varying external magnetic field for a fixed frequency, an equivalent magnetic field second moment $\langle \Delta H^2 \rangle$ is conveniently computed instead of $\langle \Delta\nu^2 \rangle$ for very fine polycrystalline specimens, like those used in this experiment, the powers of the direction cosines can be replaced by their average over a sphere. Neglecting surface effect, equation (2) may be transformed into a precise and useful equation as

$$\langle \Delta H^2 \rangle_{calc} = \frac{3}{5} g^2 \mu_B^2 s(s+1) \sum_j r_{jk}^{-6} \quad (3)$$

The theoretical values can be readily calculated by means of (3) on the basis of X-ray diffraction data. For the present purpose, g is taken to be 2.0023 and s to be 7/2 for free Gd^{3+}. The Bohr magneton μ_B has its usual value 9.2732×10^{-21} erg/gauss. The Van Vleck equation may be rewritten for this special case in a very simple form:

$$\langle \Delta H^2 \rangle_{calc} = 3.258 \times 10^9 \sum_j r_{jk}^{-6} \quad (4)$$

In this equation r and $\langle \Delta H^2 \rangle_{calc}$ are given in Ångstroms and gauss^2 respectively.

We come now to the point in question: How will gadolinium ions orient themselves so as to provide a proper summation term as shown in Eq. (4). In this summation term, every r-value must satisfy theoretically probable conditions; the total amount of the negative sixth power of every r-value must also give a correct answer for the $\langle \Delta H^2 \rangle_{calc}$ in coincidence with the result obtained from the ESR measurements.

The theoretically probable conditions are not restricted to the verification based on d-spacing data. The following aspects have also been noted.

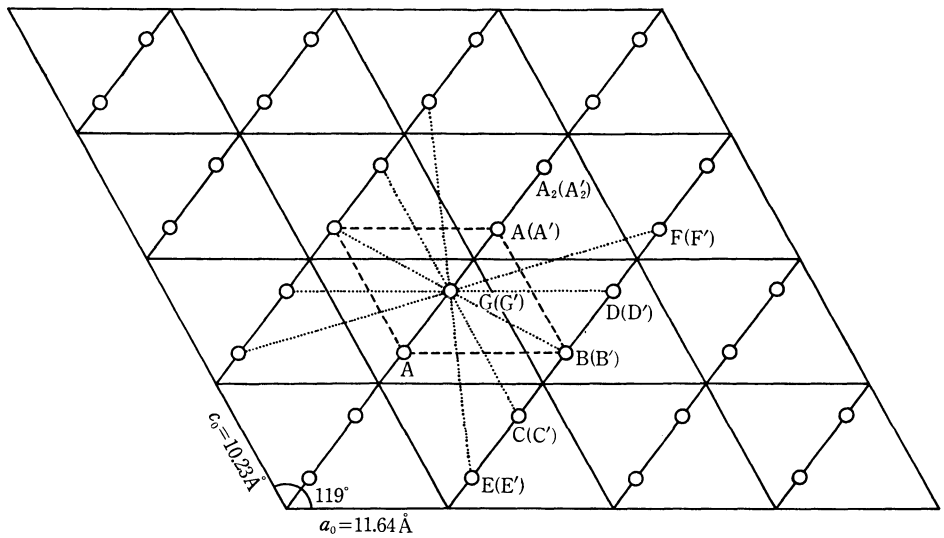

Fig. 1. Location of Gadolinium Ions on the a—c Plane.

8) J. H. Van Vleck, *Phys. Rev.*, **74**, 1168 (1948).

Table 2. Distances assumed for the nearest neighboring gadolinium ion in the lattice of hydrated oxalate

Symbol**	r-Value* Å	$10^6 r^{-6}$	n	$10^6 n r^{-6}$
r_1 (GG′)	4.828	78.958	2	157.916
r_2 (GA)	5.577	33.235	2	66.470
r_3 (GA′)	7.376	6.210	4	24.840
r_4 (GB)	9.411	1.439	2	2.878
r_5 (GB′)	10.58	0.713	4	2.852
r_6 (GC)	10.23	0.878	2	1.756
r_7 (GC′)	11.30	0.480	4	1.920
r_8 (GD)	11.61	0.408	2	0.816
r_9 (GD′)	12.57	0.254	4	1.016
r_{10} (GA″)	11.15	0.520	4	2.080
r_{11} (GA$_2$′)	12.15	0.311	4	1.244
r_{12} (GE)	13.80	0.145	2	0.290
r_{13} (GE′)	14.62	0.102	4	0.408
r_{14} (GF)	15.12	0.084	2	0.168
r_{15} (GF′)	15.85	0.063	4	0.252
		Total	46	264.906

* $r_1 = b_0/2$
$r_2 = \frac{1}{2}(r_6^2 + r_8^2 - 0.9696\, r_6 r_8)^{1/2}$
$r_3 = (r_1^2 + r_2^2)^{1/2}$
$r_4 = \frac{1}{2}(r_6^2 + r_8^2 + 0.9696\, r_6 r_8)^{1/2}$
$r_5 = (r_1^2 + r_4^2)^{1/2}$
$r_6 = c_0$
$r_7 = (r_1^2 + r_6^2)^{1/2}$
$r_8 = a_0$
$r_9 = (r_1^2 + r_8^2)^{1/2}$
$r_{10} = (4r_1^2 + r_2^2)^{1/2}$
$r_{11} = (r_1^2 + 4r_2^2)^{1/2}$
$r_{12} = (r_2^2 + r_6^2 + 0.9696\, r_2 r_6)^{1/2}$
$r_{13} = (r_2^2 + r_{12}^2)^{1/2}$
$r_{14} = (r_2^2 + r_8^2 + 0.9696\, r_2 r_8)^{1/2}$
$r_{15} = (r_1^2 + r_{14}^2)^{1/2}$

** Every single primed letter indicates the same position of Gd^{3+} on the upper or lower adjoining plane, and the double primed letter indicates the plane next to the adjoining plane. GA$_2$′ represents a distance twice as long as GA′.

Firstly, every tripositive ion should settle in an electrostatic balancing position. Secondly, the closest arrangement of the heaviest gadolinium ion should reflect the most intensive X-ray diffraction. Lastly, the hydrogen bonding between oxalate ions and water molecules would as usual have a habit of forming the framework of a monoclinic cell.[9,10] The locations of 46 nearest neighboring ion pairs of gadolinium are shown in Figure 1, and the r-values of each of the ion pairs are summarized in Table 2. In providing these locations and r-values, due consideration has been given and a geometrical allowance has also been made.

The sum of the summation terms in Eq. (4) gives the value 264.9×10^{-6}, from which the theoretical value $\langle \Delta H^2 \rangle$ is calculated to be 8.630×10^5 gauss^2.

$$\langle \Delta H^2 \rangle_{\text{calc}} = 3.258 \times 10^9 \times 264.9 \times 10^{-6} = 8.630 \times 10^5 \text{ gauss}^2$$

The experimental value of the equivalent magnetic field second moment is computed by referring to the corresponding ESR differential curve. The width between the points of maximum slope is measured and calculated to be 1850 gauss (average). The value for $\langle \Delta H^2 \rangle$ thus obtained is 8.626×10^5 gauss^2. Since a good agreement exists between the observed second moment and that calculated theoretically, the validity of the suggested model representing the location of gadolinium ions in the hydrated gadolinium oxalate is well justified.

C. Location Diagram. Referring to Fig. 1, we see that each pair of the gadolinium ions lies on the diagonal of a parallelogram in the a—c plane. Each ion rides on the head of the other, and a total of four gadolinium ions in a unit cell with the coordinates (¼ 0 ¼), (¾ 0 ¾), (¼ ½ ¼), and (¾ ½ ¾) constitute the $\bar{1}01$ plane. One of the densest packed planes with gadolinium ions is 020 plane, which gives rise to the strongest diffractions throughout the experiment. Another characteristic of the packing is that each gadolinium ion is located at the center of gravity of a parallelogram. Both the upper and lower planes are similarly packed, hence the ions coexist centrosymmetrically around G.

The method for locating ions in salts in this experiment has one great advantage, *viz.*, exchange interactions contribute nothing to the second moment. Moreover, this method reveals immediately whether the assumption is correct. Decision is very easy owing to the extreme sensitiveness of the summation term of r^{-6}. If 1 per cent error was made in estimating the smallest r-value, such as r_1 in Table 2, the error of the result would be over 5 per cent. If an incorrect position was so assigned that in the unit cell of gadolinium oxalate decahydrate two Gd^{3+} ions were located on the longer diagonal at (¼ 0 ¾) and (¾ 0 ¼), and the other two on the shorter at (¼ ½ ¼) and (¾ ½ ¾), the calculated second moment compared with the experimental result would have been too low, with a discrepancy of more than 30 per cent. Another remarkable feature of this method is that the smallest r-value has a decisive influence on the second moment. It is readily seen from Table 2: the shortest distance r_1 (2 ions) has an effect as much as 60 per cent; the next two distances r_2 and r_3 (6 ions) 34 per cent; whereas all the others, from r_4 to r_{15} (38 ions), only 6 per cent of the grand total. Such a characteristic may serve as a convenient guide leading to the right assignment of location of ions in a crystal.

9) F. R. Ahmed and D. W. J. Cruickshank, *Acta Crystallgr.*, **6**, 385 (1953).
10) G. A. Jeffrey and G. S. Parry, *J. Amer. Chem. Soc.*, **76**, 5283 (1954).

The author expresses his sincere thanks to Professor Kozo Nagashima, Tokyo Kyoiku University, and Professor Shizuo Fujiwara, the University of Tokyo, for their constructive guidance and advice throughout this study. Professor Nagashima made all facilities of his research laboratory available for three successive summers since 1966, where all the fundamental work, including sample preparation and X-ray diffraction measurement, was successfully performed. The important data for the computation of magnetic second moment could not have been obtained without the high precision JES-3BS-X ESR spectrometer, which was made available by Professor Fujiwara from the summer of 1967 onward. During the same period, the author benifited from stimulating discussion with Mr. Yoshinori Sugitani, Tokyo Kyoiku University. The author is also indebted to Dr. Tokuko Watanabe, the University of Tokyo, for her skilled technical assistance in the ESR spectrometry.

This research was supported in part by a grant from The Chinese University of Hong Kong through the recommendation of New Asia College, for which the author expresses his appreciation.

BULLETIN OF THE CHEMICAL SOCIETY OF JAPAN VOL. 43 1707—1714 (1970)

Polarography of Halides in Dimethylformamide. II. The Iodide Ion, the Triiodomercurate Ion, and Mercuric Iodide

Yoshihisa MATSUI, Yukio KUROSAKI*1 and Yoshio DATE

Department of Agricultural Chemistry, Faculty of Agriculture, Shimane University, Nishikawazu-cho, Matsue

(Received July 28, 1969)

The polarographic behavior of the iodide ion, the triiodomercurate ion, and mercuric iodide at the dropping mercury electrode was investigated in dimethylformamide, using d.c. polarography, controlled potential electrolysis, and oscillographic polarography with a multi-triangular voltage sweep. The iodide ion gives two well-defined anodic waves: the first wave corresponds to the reversible oxidation of mercury to the triiodomercurate ion, and the second, to the reversible oxidation of mercury to mercuric iodide. A maximum arises on the reduction wave of the triiodomercurate ion, but it is suppressed by the addition of a small amount of polyvinyl chloride. The oscillographic polarograms and electrocapillary curves suggested that the iodide ion, like the triiodomercurate ion and mercuric iodide, is strongly adsorbed on the dropping mercury electrode. The maximum on the wave due to the reduction of the triiodomercurate ion to mercury and the iodide ion was ascribed to the convection of the mercury drop, which was itself probably caused by the abrupt desorption of the iodide ion formed successively with an increase in the negative potentials. The adsorption phenomena of the corresponding bromides and chlorides are also discussed.

In a previous paper,[1] the electrode reaction mechanism of the bromide ion, the tribromomercurate ion, and mercuric bromide in dimethylformamide (DMF) was studied with the dropping mercury electrode. The results of d.c. polarography and large-scale electrolysis at a controlled potential indicated that two well-defined anodic waves given by the bromide ion can be attributed to the formation of the tribromomercurate ion and mercuric bromide by this reaction sequence:

$$2Hg + 6Br^- \rightleftharpoons 2HgBr_3^- + 4e \quad (1)$$

$$Hg + 2HgBr_3^- \rightleftharpoons 3HgBr_2 + 2e \quad (2)$$

The present study was undertaken in order to extend the previous study of the bromides to the corresponding iodides, namely, the iodide ion, the triiodomercurate ion, and mercuric iodide. Also, the adsorption phenomena of these depolarizers on the electrode surface were studied by the measurements of the oscillographic polarograms with a multi-triangular voltage sweep and of the electrocapillary curves. The adsorption phenomena of halide ions on the surface of the dropping mercury electrode have been extensively studied in aqueous

*1 Present address: Matsue Technical High School, Koshibara-cho, Matsue.

1) Y. Matsui, R. Kawakado and Y. Date, This Bulletin, **41**, 2913 (1968).

solution,[2-6] but scarecely studied at all in non-aqueous solutions. The adsorption of the bromide ion on the electrode surface has been suggested[1] on the basis of the partial deviation from linearity of the log plot of the more negative wave, but the phenomenon has not been studied in detail.

Experimental

Materials. The DMF was purified as has been described previously,[1] except that distillation was carried out in the presence of a few lumps of calcium hydride. The tetraethylammonium perchlorate, used as a supporting electrolyte, was prepared as has been described by Fujinaga *et al.*[7] The tetraethylammonium iodide was prepared according to the directions of Given, Peover, and Schoen.[8] The tetraethylammonium bromide was prepared as has been described in a previous paper.[1] The tetraethylammonium chloride was prepared by neutralizing an aqueous solution of tetraethylammonium hydroxide with an equivalent quantity of hydrochloric acid. Mercuric iodide, bromide, and chloride obtained commercially were purified by recrystallizing them from ethanol. The polyvinyl chloride (PVC), used as a maximum suppressor, was obtained commercially. The degree of polymerization was about 1000.

Apparatus. D.c. polarography, large-scale electrolysis at a controlled potential, and conductivity measurements were carried out as have been described previously.[1] Likewise, all the potential measurements were referred to the aqueous saturated calomel electrode connected with the test solution by a DMF-agar salt bridge.[9] The dropping mercury electrodes used had the following characteristics in a 0.10M solution of tetraethylammonium perchlorate in DMF (open circuit): (1) $m=1.165$ mg/sec, $t=5.60$ sec for $h=66.0$ cm, (2) $m=1.540$ mg/sec, $t=4.50$ sec for $h=66.0$ cm.

The oscillographic polarograms were obtained using an apparatus similar in construction to that of Shinagawa *et al.*[10] An isosceles triangular voltage sweep obtained by integrating a square-wave voltage was amplified and then applied to the electrode alternatively. The polarographic cell used was the same as that used for d.c. polarography. In order to minimize the iR drop yielded across the cell, a fairly concentrated electrolyte solution (0.50M of tetraethylammonium perchlorate) was used. No test solutions were degassed. The two-electrode system with the dropping mercury electrode and the mercury pool electrode was used. The mercury pool electrode in 0.50M of tetraethylammonium perchlorate did not always provide a stable reference potential, but the variation in the reference potential was so small that it did not prevent us from observing electrochemical phenomena. The current-potential curves were observed on a dual-beam cathode-ray oscilloscope VC-6 of the Nihon Kohden Kogyo Co., which had a relatively high sensitivity up to 1.0 mV/cm. The horizontal sweep of the cathode-ray oscilloscope was synchronized with the frequency of an applied potential. The vertical deflection was proportional to the current flowing through the polarographic cell, so that the resulting trace had an i-E relationship. The oscillographic pattern of the trace was recorded on Fuji Neopan SS film using a Canon Pellix camera. The sweep frequency used for the oscillographic polarography was kept constant at 20 Hz.

Results and Discussion

Complex Formation between Tetraethylammonium Iodide and Mercuric Iodide in DMF. In order to elucidate the anodic dissolution mechanism of mercury in the presence of the halide ion, it is necessary to know what kinds of mercury complexes are formed between the mercuric or mercurous cation and the halide ion in solution. For example, it has been reported that, in an aqueous solution, the bromide ion depolarizes the dropping mercury electrode with the formation of mercurous bromide,[11] which is the most stable species in water. In DMF, however, mercurous bromide is less stable than either the tribromomercurate ion or mercuric bromide, so in DMF the bromide ion gives two anodic waves which correspond to the formation of the latter.[1]

Mercuric iodide is extremely soluble in DMF (*ca.* 4M at 20°C[12]) and stable in the solution. On the other hand, mercurous iodide is essentially insoluble in DMF and decomposes in part to mercury and mercuric iodide. Accordingly, when a dilute solution of the iodide ion is polarographically studied in DMF, it is not necessary to consider the formation of mercurous iodide.

Mercuric iodide has been reported to form a complex ion with the iodide ion in DMF.[12,13] The resulting complex ion has been thought to be the tetraiodomercurate ion (HgI_4^{2-}), formed from one mole of mercuric iodide and two moles of the iodide ion. However, in the case of the corresponding bromides it has been shown,[1] by means of conductometric titration, that the complex ion formed

2) B. Breyer and S. Hacobian, *Aust. J. Sci. Res.*, **A4**, 610 (1951).
3) B. Breyer and S. Hacobian, *Aust. J. Chem.*, **6**, 186 (1953).
4) A. A. Vlcek, *Collect. Czech. Chem. Commun.*, **19**, 221 (1954).
5) Y. Takemori and I. Tachi, This Bulletin, **28**, 151 (1955).
6) T. Biegler, *J. Electroanal. Chem.*, **6**, 357, 365, 373 (1963).
7) T. Fujinaga, K. Izutsu, K. Umemoto, T. Arai and K. Takaoka, *Nippon Kagaku Zasshi*, **89**, 105 (1968).
8) P. H. Given, M. E. Peover and J. Schoen, *J. Chem. Soc.*, **1958**, 2674.
9) K. Takaoka, *Rev. Polarography*, **14**, 63 (1966).
10) M. Shinagawa, H. Imai and S. Chaki, *J. Electrochem. Soc. Japan*, **23**, 132 (1955).
11) I. M. Kolthoff and C. S. Miller, *J. Amer. Chem. Soc.*, **63**, 1045 (1941).
12) P. H. Given and M. E. Peover, *J. Chem. Soc.*, **1959**, 1602.
13) S. Wawzonek, E. W. Blaha, R. Berkey and M. E. Runner, *J. Electrochem. Soc.*, **102**, 236 (1955).

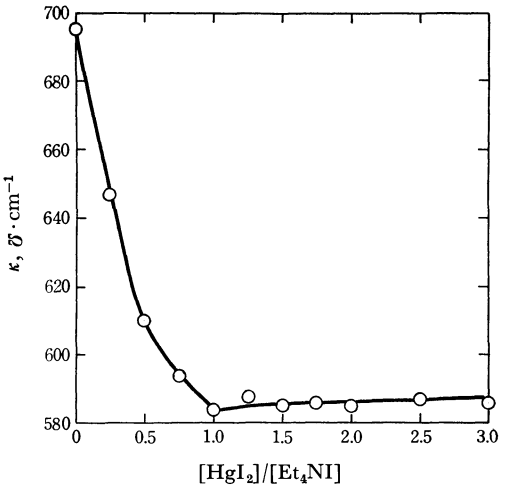

Fig. 1. Effect of HgI_2 on specific conductance of 10 mM Et_4NI in DMF at 25°C.

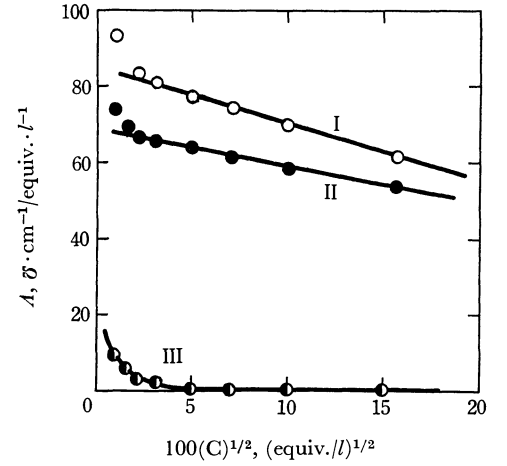

Fig. 2. Equivalent conductivities of Et_4NI (I), Et_4NHgI_3 (II), and HgI_2 (III) *vs.* square root of concentration in DMF at 25°C.

from mercuric bromide and the bromide ion was the tribromomercurate ion ($HgBr_3^-$) rather than the tetrabromomercurate ion ($HgBr_4^{2-}$). Consequently, the composition of the complex ion between mercuric iodide and the iodide ion was reexamined by the same method. The results are given in Fig. 1.

The addition of mercuric iodide to the solution of tetraethylammonium iodide in DMF lowered the specific conductivity, which reached the minimum value when the mole-ratio became equal to one. This obviously suggests that the complex formation occurs in solution and that the resulting complex ion is the triiodomercurate ion (HgI_3^-). The line in Fig. 1 curves also at the point where the mole-ratio is equal to 0.5. This suggests that the tetraiodomercurate ion may be formed in solution when the concentration of the iodide ion is more than double that of mercuric iodide.

The complex formation between mercuric iodide and the iodide ion can be confirmed by the data from the UV spectrum, too. The spectrum of the mixture of the iodide ion and the mercuric iodide equivalent in concentration has a strong absorption maximum at 304 mμ ($\varepsilon = 1.1 \times 10^5$), while neither mercuric iodide nor tetraethylammonium iodide shows such a maximum in the same wavelength region.

The equivalent conductivities of tetraethylammonium iodide, tetraethylammonium triiodomercurate, and mercuric iodide are plotted as a function of the square root of the concentration in Fig. 2. The data for tetraethylammonium iodide and tetraethylammonium triiodomercurate fit the Onsager equation, indicating that these salts behave as strong electrolytes in DMF. The equivalent conductivity of mercuric iodide is very low and does not fit the Onsager equation, showing that it is a weak electrolyte in DMF.

D. c. Polarography. A. Tetraethylammonium Iodide as Depolarizer. Using anhydrous DMF as a solvent, with 0.10M tetraethylammonium perchlorate as a supporting electrolyte, the d.c. polarographic behavior of tetraethylammonium iodide was investigated. This depolarizer gave two well-defined anodic waves (Fig. 3). The ratio between the heights of these waves was approximately 2 : 1, as was observed for tetraethylammonium bromide. The half-wave potentials ($E_{1/2}$) and the diffusion current constants (I_d) in various concentrations are given in Table 1. The I_d's of both the waves were practically constant over the concentration range studied. The limiting currents

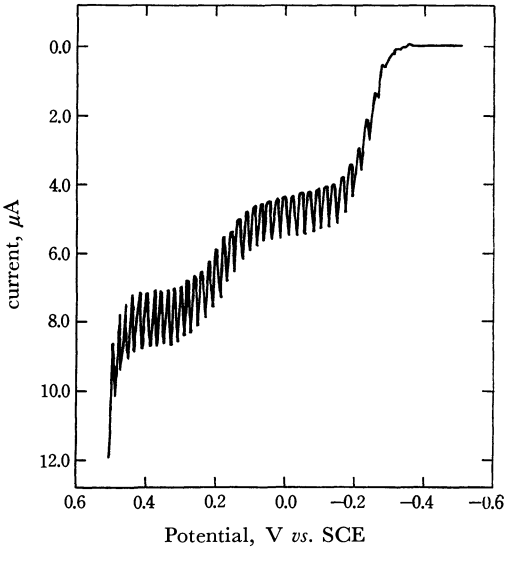

Fig. 3. Polarogram of 2.50 mM Et_4NI in DMF.

Table 1. Polarographic behavior of tetraethylammonium iodide in DMF at 25±0.1°C

Concn. (mM)	$E_{1/2}$ (V *vs.* SCE)		I_d	
	more pos.	more neg.	more pos.	more neg.
0.10	+0.130	−0.183	0.61	1.22
0.25	+0.135	−0.189	0.76	1.19
0.50	+0.153	−0.202	0.57	1.28
1.00	+0.155	−0.225	0.68	1.30
2.50	+0.168	−0.250	0.68	1.29
5.00	+0.175	−0.278	0.58	1.26

Table 2. Relation between the limiting current (i_d) of 0.50 mM of tetraethylammonium iodide and the effective pressure ($h_{corr.}$) on the dropping mercury electrode

$h_{corr.}$ (cm)	i_d (μA)		$i_d/(h_{corr.})^{1/2}$	
	more pos.	more neg.	more pos.	more neg.
84.3	0.450	1.14	0.049	0.124
74.3	0.430	1.06	0.050	0.123
64.3	0.425	1.01	0.053	0.126
54.3	0.395	0.90	0.053	0.122
44.3	0.345	0.83	0.052	0.123
38.3	0.325	0.77	0.052	0.124

for 0.50 mM of the depolarizer were found to be proportional to the square root of the effective pressure of mercury applied to the dropping mercury electrode (Table 2). These results indicate that the limiting currents of the two waves are diffusion-controlled.

The polarographic waves of the iodide ion are so similar to those of the bromide ion that the electrode-reaction mechanism proposed for the latter may also be presumed to hold for the former (Eqs. (3) and (4)):

$$2Hg + 6I^- \rightleftharpoons 2HgI_3^- + 4e \quad (3)$$

$$Hg + 2HgI_3^- \rightleftharpoons 3HgI_2 + 2e \quad (4)$$

This mechanism was substantiated by analyzing the polarographic waves as follows. If the electrode reactions (3) and (4) are reversible, the equations of the waves are expressed by:

$$E_n = C_n + (\boldsymbol{RT}/2\boldsymbol{F}) \ln i/(i_d - i)^3 \quad (5)$$

$$E_p = C_p + (\boldsymbol{RT}/2\boldsymbol{F}) \ln i^3/(i_d - i)^2 \quad (6)$$

where E_n and E_p denote the potential of the electrode for the more negative and the more positive waves respectively, and where C_n and C_p are constant. These equations show that the half-wave potentials should change with i_d or with the concentration of the iodide ion according to:

$$E_{n,1/2} = C'_n - (\boldsymbol{RT}/\boldsymbol{F}) \ln i_d \quad (7)$$

$$E_{p,1/2} = C'_p + (\boldsymbol{RT}/2\boldsymbol{F}) \ln i_d \quad (8)$$

The results of the analysis of the waves are given in Fig. 4. The log plot for the more positive wave was a fairly good straight line, with a slope equal to 0.032 V, which is in fair agreement with the theoretical value of 0.030 V. The log plot for the more negative wave was also linear, with a slope equal to 0.030 V, over the greater part of the potential range. However, it became somewhat curved in the more negative region of potential, just as was observed in the case of the bromide ion.[1] As was suggested in the previous paper, this is probably due to the adsorption of the iodide ion on the surface of the dropping mercury electrode before depolarizing. The deviation can also be considered to be due in part to the formation of the tetraiodomercurate ion in the more negative part of the wave, where the concentration of the iodide ion on the mercury drop is much higher than that of mercuric

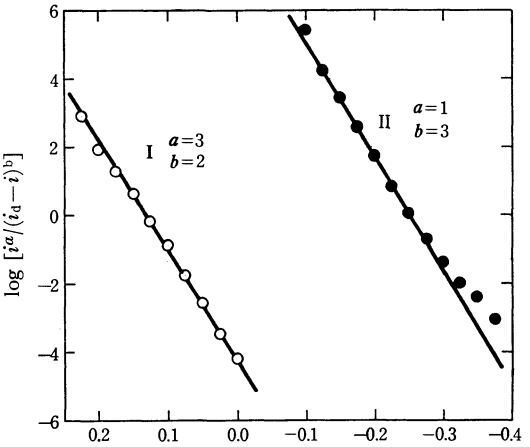

Fig. 4. Analysis of the waves of 0.50 mM Et_4NI.
Slope: (I) 0.032; (II) 0.030

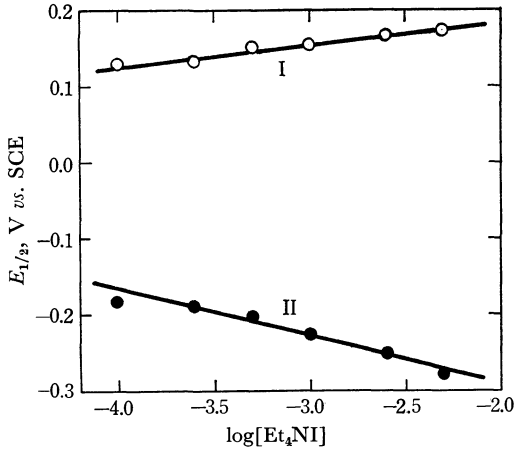

Fig. 5. Effect of concentration of Et_4NI on its half-wave potential.
Slope: (I), 0.030; (II), −0.060

ion dissolved.

The relation between the half-wave potential and the concentration of the depolarizer is plotted in Fig. 5. Straight-line relations were obtained for the waves with slopes equal to −0.060 V for the more negative wave (calculated for Eq. (7): −0.059 V) and 0.030 V for the more positive wave (calculated for Eq. (8): 0.030 V). All these results indicate that Eqs. (3) and (4) are both valid.

B. Mercuric Iodide. If Eqs. (3) and (4) are both valid, mercuric iodide should give two cathodic waves according to the following reactions:

$$3HgI_2 + 2e \rightleftharpoons Hg + 2HgI_3^- \quad (9)$$

$$2HgI_3^- + 4e \rightleftharpoons 2Hg + 6I^- \quad (10)$$

Actually, mercuric iodide gave two cathodic waves, though a maximum appeared on the more negative one (Fig. 6-I). In order to suppress the maximum, a small amount of PVC was dissolved in the test solution. PVC was reported to suppress all the maximum waves of thallium(I), lead(II), cadmium(II), and zinc(II) in *N*,*N*-dimethylacetamide.[14] As is shown in Fig. 6-II, PVC was found to suppress the maximum of mercuric iodide very effectively. In the concentration range from 0.003 to 0.007%, PVC acted as a satisfactory suppressor and had no effect on either the half-wave potential or the diffusion-current constant. At concentrations lower than 0.002% as well as higher than 0.010%, the effect of PVC became weak.

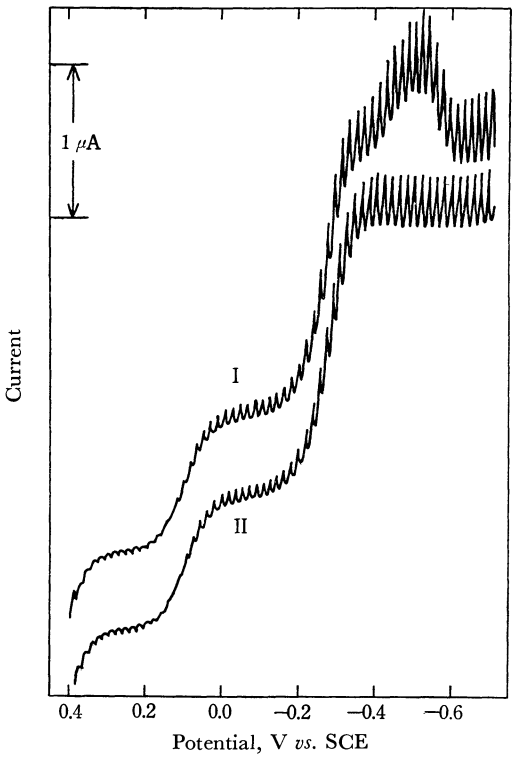

Fig. 6. Polarograms of 0.50 mM HgI_2 in DMF; (I) without PVC and (II) with 0.005% PVC.

14) S. Musha, T. Wasa and K. Tani, *Rev. Polarography*, **11**, 169 (1963).

Table 3. Polarographic behavior of mercuric iodide in DMF containing 0.005% of PVC at 25±0.1°C

Concn. (mM)	$E_{1/2}$ (V *vs.* SCE)		I_d	
	more pos.	more neg.	more pos.	more neg.
0.10	+0.121	−0.210	1.05	2.29
0.25	+0.124	−0.231	0.73	2.40
0.50	+0.128	−0.242	1.08	2.36
1.00	+0.142	−0.260	1.10	2.34
2.50	+0.144	−0.279	1.14	2.39

Table 4. Relation between i_d of 0.50 mM of mercuric iodide and $h_{corr.}$

$h_{corr.}$ (cm)	i_d (μA)		$i_d/(h_{corr.})^{1/2}$	
	more pos.	more neg.	more pos.	more neg.
84.3	0.90	2.10	0.098	0.228
74.3	0.84	1.98	0.098	0.230
64.3	0.75	1.80	0.094	0.226
54.3	0.73	1.70	0.099	0.230
44.3	0.65	1.50	0.097	0.224
38.3	0.58	1.40	0.094	0.226

The polarographic characteristics of mercuric iodide at various concentrations in the presence of 0.005% of PVC are given in Table 3. The limiting currents of both the waves were proportional to the concentration and to the square root of the effective pressure of mercury applied to the dropping mercury electrode (Table 4), indicating that they are diffusion-controlled.

The waves of mercuric iodide were analyzed in the same way as those of tetraethylammonium iodide. The results showed that the waves are in fair agreement with those given theoretically by Eqs. (11) and (12).

$$E'_p = C''_p - (\boldsymbol{R}T/2\boldsymbol{F}) \ln i^2/(i_d - i)^3 \quad (11)$$

$$E'_n = C''_n - (\boldsymbol{R}T/2\boldsymbol{F}) \ln i^3/(i_d - i) \quad (12)$$

The shift of the half-wave potential with i_d is given by Eqs. (7) and (8), which were accepted to hold as is shown by the results in Table 3.

C. Tetraethylammonium Triiodomercurate. As was to be expected from Eqs. (4) and (10), tetraethylammonium triiodomercurate gives two waves, anodic and cathodic, and on the latter a maximum arises (Fig. 7-I). The maximum was also suppressed by the addition of 0.005% of PVC (Fig. 7-II). The polarographic behavior is summarized in Table 5. Analysis of the current-voltage curves showed that the anodic wave is ex-

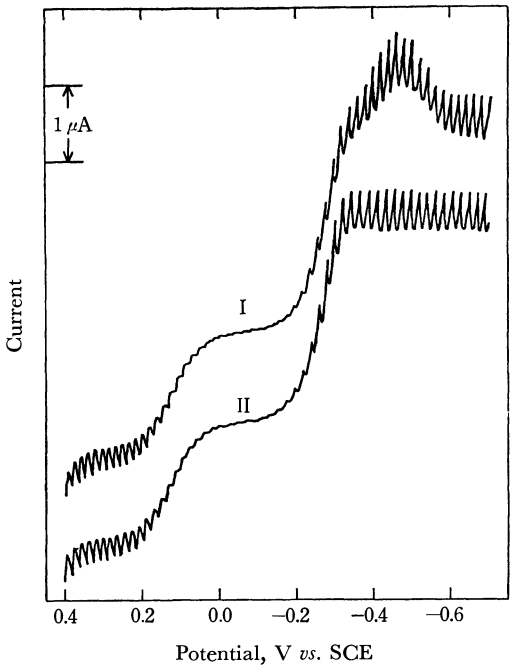

Fig. 7. Polarograms of 0.50 mM Et_4NHgI_3 in DMF, (I) without PVC and (II) with 0.005% PVC.

Table 5. Polarographic behavior of tetraethylammonium triiodomercurate in DMF containing 0.005% of PVC at 25±0.1°C

Concn. (mM)	$E_{1/2}$ (V vs. SCE)		I_d	
	more pos.	more neg.	more pos.	more neg.
0.10	+0.107	−0.226	0.91	3.32
0.25	+0.126	−0.246	1.87	3.56
0.50	+0.129	−0.264	1.70	3.46
1.00	+0.149	−0.269	1.72	3.42
2.50	+0.169	−0.282	1.63	3.06

pressed by Eq. (6), and the cathodic wave, by Eq. (12).

Controlled Potential Electrolysis of Mercuric Iodide. Further evidence for the electrode-reaction mechanism postulated above was obtained by a large-scale electrolysis of mercuric iodide at a mercury pool cathode with a controlled potential. Electrolytic reduction at a potential of the plateau of the more positive wave yielded tetraethylammonium triiodomercurate, the formation of which was confirmed by measuring the polarogram and the UV spectrum of the catholyte. The quantity of electricity transferred per mole of the depolarizer (n=0.64 F) virtually agreed with that calculated for Eq. (9) (n=0.67 F). As was expected from Eq. (10), tetraethylammonium iodide, identified by the polarogram of the catholyte, was obtained by the electroreduction of mercuric iodide at a potential of the plateau of the more negative wave. The value of n (n=2.21 F) also agreed with that calculated for Eqs. (9) and (10) (n=2.00 F).

Oscillographic Polarography of Tetraethylammonium Iodide. In order to investigate the polarographic behavior of tetraethylammonium iodide in more detail, an isosceles-triangular voltage sweep was applied to polarize the dropping mercury electrode alternatively. A current-potential curve obtained on a cathode-ray oscilloscope is shown in Fig. 8-I. It may be inferred at sight that the anodic peaks, A and B, are due to the step-by-step oxidation of mercury to the triiodomercurate ion and to mercuric iodide respectively. The cathodic peaks, C and D, probably correspond to the step-by-step re-reduction of mercuric iodide to the triiodomercurate ion and to the iodide ion respectively.

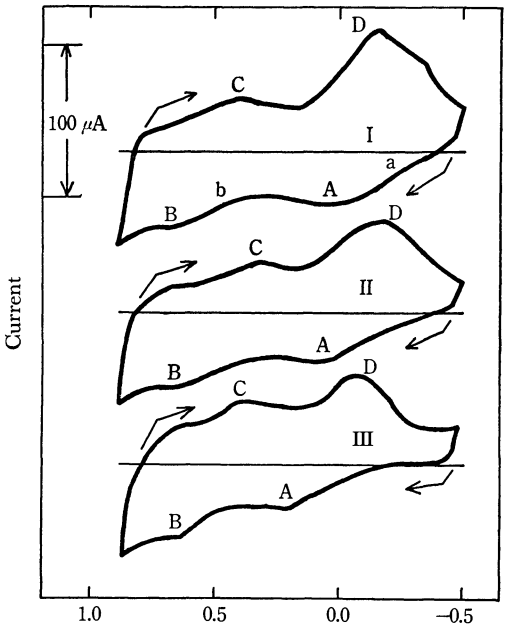

Fig. 8. Oscillographic polarograms of Et_4NI (I), Et_4NBr (II), and Et_4NCl (III) in DMF.

It is noticeable that the base line of the anodic peaks goes down as the positive potential increases, whereas that of the cathodic peaks remains essentially the same. Furthermore, it is remarkable that the peak D is exceptionally higher than the other peaks, A, B, and C. The peak D is so high that it cannot be considered that the whole current is due only to the re-reduction of the triiodomercurate ion formed in the preceeding electrooxidation and re-reduction processes. These results indicate that not only the electron transfer process, but also the adsorption-desorption process, occurs on the electrode surface.

The species which can be adsorbed on the elec-

trode are the iodide ion, the triiodomercurate ion, and mercuric iodide. In the anodic scan, the adsorption of these depolarizers may cause the increase in the anodic charging current. Since the iodide ion is the only depolarizer existing in the solution before electrolysis, the moderate increase in the charging current shown by the curve a may be due to the successive adsorption of the iodide ion on the electrode surface. At the potential close to the peak A, the iodide ion adsorbed is converted into the triiodomercurate ion as a result of its reaction with the mercuric ion formed by the electrooxidation of mercury. The resulting triiodomercurate ion may also be adsorbed on the electrode surface, so the double-layer capacity may gradually increase with an increase in the amount of the adsorbate during electrolysis (curve b). At the potential near the peak B, the triiodomercurate ion adsorbed is further converted into mercuric iodide, which may also be adsorbed on the electrode surface, and a considerable charging current flows consecutively.

In the cathodic scan, on the other hand, the desorption of the depolarizers can cause an increase in the cathodic charging current. However, when mercuric iodide is re-reduced to mercury and the triiodomercurate ion at the potential close to the peak C, both mercuric iodide and the triiodomercurate ion may be strongly adsorbed on the electrode surface. Consequently, the double-layer capacity may scarcely change, and the base line of the cathodic scan remains essentially the same. At the potential near the peak D, the triiodomercurate ion is reduced to mercury and the iodide ion. The resulting iodide ion may be abruptly desorbed from the electrode surface with an increase in the negative potential. As a result, a large quantity of charging current flows (the peak D).

Considering that the potential of the maximum, which arises on the reduction wave of the triiodomercurate ion, is close to that at which the iodide ion is abruptly desorbed, we might be able to relate the desorption phenomena to the appearance of the polarographic maximum as follows. It has been confirmed that the current density at the bottom of the mercury drop is greater than that at the top as a result of the screaning effect of the tip of the capillary.[15] If the iodide ion, which is formed by the reduction of the triiodomercurate ion adsorbed on the electrode surface, is abruptly desorbed from the electrode surface, the difference in current density must cause an unequal distribution of the triiodomercurate ion in the double layer at the bottom and at the top of the mercury drop, which may also cause a tangental potential gradient in the double layer around the mercury drop, as well as the difference in surface tension between that at the bottom and that at the top of the drop. Consequently, the interface is pulled from top to bottom. The resulting streaming of the double layer and mercury in the drop may be responsible for the polarographic maximum. The maximum may not disappear until the potential of the mercury electrode becomes too negative for the triiodomercurate ion to adsorb on the electrode surface. The PVC added to the solution as a maximum suppressor may be adsorbed on the electrode surface with the formation of a thin film, which may prevent the iodide ion from being abruptly desorbed from the electrode surface. In the case of the electrooxidation of mercury in the presence of the iodide ion, the iodide ion may be supplied to the electrode surface by diffusion, and so no convection of the electrode can occur. Although the above description of the cause of the polarographic maximum is plausible, it is no more than a speculation; further experimental data are necessary before we can discuss it conclusively.

The oscillographic polarograms of tetraethylammonium bromide and chloride (Fig. 8-II and -III) were very similar to those of the corresponding iodide, but with some differences. The most remarkable difference was that the heights of the peaks D of I^-, Br^-, and Cl^- decrease in that order. This clearly indicates that the peak D is due not only to the electron-transfer process, but also to the nonfaradic desorption process. Furthermore, it was ascertained that the adsorptive activities of the triiodomercurate ion, the tribromomercurate ion, and the trichloromercurate ion decrease in that order.

Electrocapillary Curve. The adsorption phenomena of the halides were also studied by the measurement of the electrocapillary curves. The

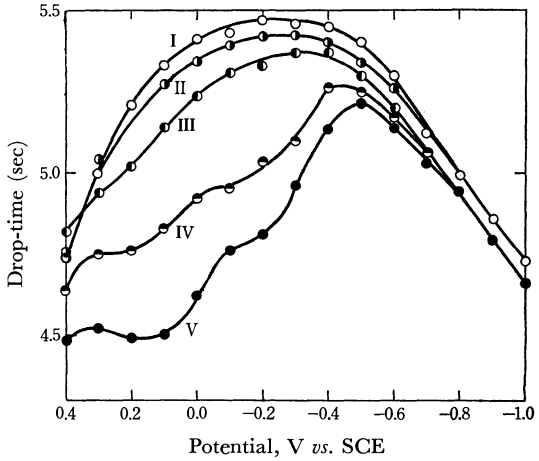

Fig. 9. Electrocapillary curves: (I), 0.1M Et_4NClO_4; (II), (I)+0.005% PVC; (III), (II)+1.0 mM $HgCl_2$; (IV), (II)+1.0 mM $HgBr_2$; (V), (II)+1.0 mM HgI_2.

15) I. M. Kolthoff and J. J. Lingane, "Polarography," 2nd ed., Vol. I, Interscience Publishers, New York (1952), p. 176.

effect of 1.0 mM of mercuric halide on the shape of the electrocapillary curve is shown in Fig. 9. The electrocapillary curve in the presence of 2.0 mM of tetraethylammonium iodide was essentially identical with that in the presence of 1.0 mM of mercuric iodide.

In the presence of mercuric iodide, a marked decrease in the surface tension was observed in the potential region between +0.4 and −0.8 V *vs.* SCE. Considering the electrode reaction mechanism elucidated above, it can be presumed that the decrease in the drop time in the potential region between +0.4 and +0.2 V *vs.* SCE is due to the adsorption of mercuric iodide. Similarly, the decrease in the surface tension in the potential range between +0.1 and −0.1 V *vs.* SCE and that between −0.3 and −0.8 V *vs.* SCE may correspond to the adsorption of the triiodomercurate ion and the iodide ion respectively on the electrode surface.

The results in Fig. 9 also reveal that the iodide ion and its mercuric complexes are the most capillary-active. The bromide ion and its mercuric complexes are less strongly adsorbed on the electrode surface. The chloride ion and its mercuric complexes are only slightly capillary-active.

The effect of PVC on the shape of the electrocapillary curve is also shown in Fig. 9. The addition of a small amount of PVC caused a slight decrease in the drop time of the mercury in the potential region more positive than −0.7 V *vs.* SCE. It is apparent that the adsorption of PVC on the electrode surface occurs, this may prevent the convection of the mercury drop and, consequently, the appearance of the maximum. All the results mentioned here are in fair agreement with those obtained by oscillographic polarography.

BULLETIN OF THE CHEMICAL SOCIETY OF JAPAN VOL. 43 1714—1718 (1970)

Lattice Constants of Tetragonal Sodium Potassium Tungsten Bronzes

Seiichiro UTSUMI and Shuko FUJIEDA*1

Department of Chemistry, Faculty of Science, Ochanomizu University, Bunkyo-ku, Tokyo

(Received October 30, 1969)

Sodium potassium tungsten bronzes, $Na_xK_yWO_3$, having various values of x and y were prepared by electrolytically treating a fused mixture of carbonates of the two alkali metals and tungsten-(VI) oxide. Lattice constants, a and c, of the tetragonal crystals were estimated by the X-ray powder method. Similarity of the crystal lattice of these bronzes to that of potassium tungsten bronzes, instead of to that of sodium tungsten bronzes, suggests that the lattice constants of the sodium potassium bronzes are by far more influenced by the potassium content than by the sodium content.

Tungsten bronzes are nonstoichiometric crystalline compounds represented by a general formula, Na_xWO_3, in which M is a metal ion and x has a value less than unity. Among them, sodium tungsten bronzes*2 Na_xWO_3 and potassium tungsten bronzes K_yWO_3, especially the former, are the most popular.

Sodium bronzes have been prepared with relative ease over a wide range of x value. Their color and crystal system vary with values of x, and the crystal surfaces exhibit a characteristic metallic luster. On the other hand, the crystals of the potassium bronzes show neither variety in color nor metallic luster as in of sodium bronzes.

The marked difference in appearance between the two series of bronzes might be clarified by investigating the crystals of sodium potassium bronzes, intermediate or mixed bronzes having a general formula $Na_xK_yWO_3$ where the sum of x and y is less than unity. Also the role of metal ions could be revealed by determining the color and structure of the crystals.

Several kinds of sodium potassium bronzes have been prepared and their crystals investigated,[1-3] but with little information. We prepared sodium potassium bronzes with a wider range of composition and higher purity. Tetragonal crystals were

*1 Responsible co-author.

*2 Hereinafter, the tungsten bronze is designated as bronze.

1) G. von Knorre, *J. Prakt. Chem.*, [2]**27**, 49 (1883).
2) W. Feit, *Ber.*, **21**, 134 (1888).
3) E. O. Brimm, J. C. Brantley, J. H. Lorenz and M. H. Jellinek, *J. Amer. Chem. Soc.*, **73**, 5427 (1951).

subjected to X-ray diffraction in order to obtain their lattice constants.

Experimental

Materials. All chemicals used were of reagent grade. Tungsten rods supplied by Tokyo Tungsten Co., Ltd. were 2 mm in diameter and specified to be 99.98% pure.

Preparation. A powdered mixture consisting of anhydrous sodium, potassium carbonates and tungsten(VI) oxide $WO_3 \cdot H_2O$ (Table 1), was thoroughly melted in a porcelain crucible by heating at 800 ± 15°C in an electric furnace. Two tungsten rods were placed in the crucible as electrodes with one end of each rod immersed in the melted mixture. An electric voltage was applied between the two electrodes so that the voltage drop across the electrodes was 1.0—1.2 V. A direct current, 2—5 A, was supplied. Crystals were soon formed at the cathode. After carrying out electrolysis for several hours, the current was switched off and the electrodes were removed. The melted mixture, along with the crystals, was allowed to cool to room temperature, and the remaining mass was treated first with boiling water, then with a hot nitric acid solution and finally with a hot sodium hydroxide solution. Thus the remaining crystals could be obtained.

Analytical Procedure. A powdered and weighed sample was fused in a nickel crucible together with a mixture of sodium carbonate and sodium nitrate in the ratio of 1 to 3 by weight,[4] and the fused product was dissolved in water. In the first place, potassium was determined gravimetrically as potassium tetraphenylborate precipitate $KB(C_6H_5)_4$. Subsequently tungsten was oxidized completely to sexivalent state with nitric acid, precipitated with hydrochloric acid and cinchonine, and the precipitate was ignited and weighed as WO_3. If the two procedures of precipitation were carried out in reverse order, an erroneous value for the potassium content would result from to the presence of excessive cinchonine in the solution which is used for the determination of potassium. Values of x and y for sodium potassium bronzes were estimated assuming that the ratio of tungsten to oxygen was 1 : 3[5] in bronzes, and also that the remainder which was obtained by subtracting the contents of potassium, tungsten and oxygen from the initial weight of the sample was estimated as sodium content.

Lattice Constants. The diffraction pattern of the powder was obtained with an X-ray diffractometer, compact type from Rigaku Denki Co., Ltd., Tokyo, using Cu-Kα radiation, $\lambda = 1.5418$ Å. Values of lattice distance, d, calculated from the pattern of each sample were then used to determine the appropriate lattice constants a and c by the usual procedure. The values of a and c were accurate within the error ± 0.01 Å.

Density. The density of crystals was measured with a pycnometer using water as the immersion liquid. The values of density were reproducible within ± 0.03 g/cm^3. The accuracy of the data was proved by the density of metallic cadmium which was observed by the same procedure, the value 8.61 g/cm^3 being sufficiently close to the value 8.642 g/cm^3.[6]

Results and Discussion

Brimm *et al.*[3] prepared sodium potassium bronzes by merely fusing a mixture of Na_2WO_4, K_2WO_4, WO_3 and metallic tungsten. In the present work, however, carbonates were preferred to tungstates as starting materials on account of lower melting point and easier access. The bronzes produced by the process of Brimm *et al.* were by no means free from contamination, presumably of fine particles of metallic tungsten and some compounds of tungsten of lower oxidation states, as demonstrated by X-ray powder photography.[3,7] Thus we employed the electrolytic process of Knorre.[1] Sienko and Mazumder[8,9] prepared tungsten bronzes in an atmosphere of argon. In the present work materials were kept open to atmosphere without any difficulties. Crystals having uniform color and metallic luster were obtained.

The tetragonal crystals in square prisms of the sodium potassium bronzes are listed in Table 1. They are not exhaustive, but only those whose values of x and y and lattice constants were determined are shown. In Table 1 are shown, in successive columns, compositions of the starting materials, colors, compositions and the lattice constants a and c. Twenty one species of bronzes are arranged in the table in decreasing order of the alkali metal contents of the starting materials.

Crystals of tetragonal sodium bronzes were more or less bluish purple, probably because the tetragonal structure was limited to a narrow region of x. In the case of potassium bronzes, however, blue and reddish purple crystals were formed independent of the composition of the starting materials. In contrast, a variety of colors ranging from reddish purple to blue is covered by the group of tetragonal sodium potassium bronzes, as seen in the table. The crystal shown as No. 12 in Table 1 was the most reddish.

The ratios of Na to K in the bronzes were very nearly equal to the ratios of sodium carbonate to potassium carbonate in the composition of starting materials. But there were some exceptions. For instance, when the starting materials contained approximately ten times as much Na as K (Nos. 7, 8 and 9, Table 1), the product was a mixture of a small amount of needle-shaped blue crystals of

4) L. E. Conroy and M. J. Sienko, *J. Amer. Chem. Soc.*, **74**, 3520 (1952).

5) B. A. Raby and C. V. Banks, *Anal. Chem.*, **36**, 1106 (1964).

6) "CRC Handbook of Chemistry and Physics," 47th Ed., Chemical Rubber Co. (1966), B-161.

7) W. R. Gardner and G. C. Danielson, *Phys. Rev.*, **93**, 46 (1954).

8) M. J. Sienko, *J. Amer. Chem. Soc.*, **81**, 5556 (1959).

9) M. J. Sienko and B. R. Mazumder, *ibid.*, **82**, 3508 (1960).

TABLE 1. COMPOSITION AND LATTICE CONSTANTS OF TETRAGONAL SODIUM POTASSIUM BRONZES

No.	Composition* of materials for preparation	Color** of product	Composition					
			Content (% wt)		$Na_xK_yWO_3$		Lattice constant	
	$Na_2CO_3 : K_2CO_3 : WO_3$		K	WO_3	x	y	a (Å)	c (Å)
1	2 : 1 : 4.5	p	4.640	90.38	0.56	0.30	12.28	3.83
2	1 : 2 : 4.5	rp	5.901	90.73	0.37	0.39	12.29	3.84
3	3 : 1 : 7	p	3.772	93.55	0.29	0.24	12.26	3.83
4	2 : 1 : 5.25	rp	4.515	93.59	0.20	0.29	12.30	3.83
5	1 : 1 : 3.5	rp	6.117	91.15	0.30	0.40	12.30	3.83
6	1 : 2 : 5.25	rp	5.395	93.63	0.10	0.34	12.30	3.84
7	15 : 1 : 32	b	1.094	94.89	0.43	0.07	12.17	3.78
8	10 : 1 : 22	b	1.639	92.97	0.58	0.10	12.18	3.79
9	6 : 1 : 14	bp	2.027	94.05	0.42	0.13	12.21	3.80
10	3 : 1 : 8	p	3.621	93.88	0.27	0.23	12.27	3.82
11	2 : 1 : 6	p	4.497	93.37	0.23	0.29	12.28	3.83
12	1 : 1 : 4	rp	4.858	92.37	0.30	0.31	12.29	3.83
13	1 : 2 : 6	p	5.465	91.61	0.32	0.35	12.28	3.83
14	1 : 5 : 12	p	5.934	92.08	0.22	0.38	12.28	3.83
15	1 : 20 : 42	p	6.763	92.18	0.12	0.43	12.28	3.83
16	2 : 1 : 6.75	p	3.350	92.69	0.43	0.21	12.24	3.82
17	1 : 1 : 4.5	p	4.676	93.50	0.20	0.30	12.28	3.83
18	1 : 2 : 6.75	p	5.120	93.58	0.14	0.32	12.26	3.83
19	1 : 5 : 13.5	p	6.215	91.83	0.21	0.40	12.27	3.83
20	2 : 1 : 7.5	bp	3.215	92.92	0.42	0.21	12.22	3.81
21	1 : 1 : 5	bp	4.500	94.32	0.13	0.28	12.26	3.82

* expressed in molar ratio ** rp: reddish purple, p: purple, bp: bluish purple, b: blue

sodium potassium bronze and a large amount of cubic sodium bronze.

It is noteworthy that the color of crystals varies from blue to reddish purple in accordance with the increase of the y values instead of the sum of x and y. In other words, the color of the crystal with a small y value was blue and that with a large y value was reddish.

Magnéli[10] stated that the tungsten-oxygen octahedra in tetragonal tungsten bronzes join each other by sharing oxygen atoms at the corners so as to form a framework with the formula WO_3, where the lattice contains empty tunnels which run right through the structure whose projections on the 001 plane consist of triangle, square and pentagon. Alkali metal atoms in bronzes are considered to be accomodated in either of the square and pentagonal empty tunnels. Particularly, in the crystal structure of the bronzes $Na_xK_yWO_3$, the potassium ions which are larger than the sodium ions would be accomodated more easily in the pentagonal interstices. On the other hand, dimensional consideration concerning the W–O bond length in comparison with the ionic size of K suggests that the square tunnels, as well as the triangular ones, would be too small to accomodate potassium ions. Thus it seems that the potassium ions should exist only in pentagonal spaces. Referring to the structure of sodium potassium bronzes, Wadsley[11] proposed that the interstitial ions are assorted according to their size. The present interpretation is consistent with the opinion of Magnéli and Wadsley, and is further supported by the following experimental facts.

Current efficiency in the electrolytic preparation was much lower for preparing potassium bronzes than for sodium bronzes. The process in which potassium bronzes were formed from a starting material consisting of potassium carbonate and tungsten(VI) oxide hardly proceeded, but the presence of only a twentieth part of sodium carbonate in one part of potassium carbonate remarkably facilitated the preparation of bronze, a sodium potassium bronze in this case instead of a potassium bronze. For example, from a starting material mixture consisting of potassium carbonate and tungsten(VI) oxide in the ratio of 1 : 2 a potassium bronze $K_{0.41}WO_3$ was produced, while from a starting material containing potassium salt and tungsten oxide in approximately the same ratio as above and additional sodium carbonate in such a small amount as a twentieth of the amount of potassium

10) A. Magnéli, *Ark. Kemi.*, **1**, 213 (1949).

11) A. D. Wadsley, "Nonstoichiometric Compounds," ed. by L. Mandelcon, Academic Press, New York (1964), p. 98.

salt (No. 15, Table 1) a sodium potassium bronze $Na_{0.12}K_{0.43}WO_3$ was prepared in preference to the tetragonal potassium bronze. Brimm *et al.* similarly found that incorporation of any potassium into the structure of cubic sodium bronzes led exclusively to tetragonal bronzes. Therefore, it might be presumed that sodium ions were inserted into the K_yWO_3 host lattice which belonged to the tetragonal system, so that incorporation of sodium in the interstitial spaces existing in the host lattice stabilized the tetragonal crystal structure.

The lattice constant a of cubic sodium bronzes Na_xWO_3 is known to be linearly proportional to the x value as expressed by $a=0.0819x+3.7846$.[12] In other words, the WO_3 host lattice was expanded in accordance with the increase of the sodium concentration in the lattice. A similar result was observed with respect to potassium bronzes, because the reported y values of some tetragonal potassium bronzes K_yWO_3 proved to be in a parallel relation to the lattice constants of their crystals.[10,13]

It may be reasonable to presume that the potassium ions, larger than the sodium ions, in the crystal would influence more decisively the host lattice and might determine the size. The lattice constants, a and c, measured by the X-ray powder method are shown in Table 1. The value of c/a was unequivocally 0.312, so that, for the sake of simplicity, plotting in Fig. 1 was only for the constant a.

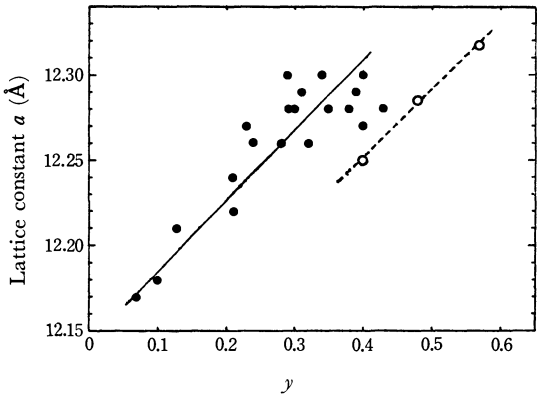

Fig. 1. Lattice constant a as a function of y.
● of tetragonal $Na_xK_yWO_3$
○ of tetragonal K_yWO_3[13,14]

The variation of the lattice constant a for $Na_xK_yWO_3$ crystal is shown as a function of y in Fig. 1. The lattice constant a reported of tetragonal potassium bronzes, K_yWO_3, for $y=0.40-0.57$[10,13] is also shown by open circles. The lattice constant for sodium potassium bronzes represented by solid circles, though it diverges more for larger values of y, seems to vary in the linear relation to y within the range in which measurement was made, as shown by the full line. The inclination of the line is approximately parallel to that of the broken line which shows the linear variation concerning potassium bronzes. For the same value of y, the lattice constant of a sodium potassium bronze is larger than that of a potassium bronze, presumably due to the sodium ions which are incorporated in the corresponding potassium bronze. Extrapolation of the full line to $y=0$ suggests that the extremity of sodium potassium bronze, where the potassium content diminishes to null, would have the lattice constant 12.14 Å. This value may be considered to be not inconsistent with 12.1 Å reported by Magnéli[14] for the lattice constant of a tetragonal sodium bronze because of larger error involved.

Although a linear relationship exists as stated above between the lattice constant a and y of the sodium potassium bronzes, no correlation was found between the lattice constant a and x. Therefore it may be concluded that, in determining the structure of sodium potassium bronzes, the role of y, or of the potassium content, is more important than that of x, or of the sodium content.

Crystals of tetragonal potassium bronzes K_yWO_3 are stable for y values larger than 0.14.[3] The y values with which crystals of sodium potassium bronzes are stable extend from over 0.4 to less than 0.1. In other words, a tetragonal form of potassium bronze crystals has been made stable for smaller y values by introducing sodium ions into the structure.

The color of crystals of sodium potassium bronzes can be related to their lattice constants. Thus, as seen in Table 1, it varies from reddish to bluish as the lattice constant a is decreased. The same inclination was observed with sodium bronzes, including cubic and tetragonal.[15,16] Color referred to in this paper involves the relevant regular reflectance spectrum, which will be discussed elsewhere in the near future.

The density of eleven samples of sodium potassium bronzes, whose x and y values varied from 0.22 to 0.58 and from 0.07 to 0.39, respectively, was 7.15 g/cm^3 within an error of 0.03. This value argees with the density of tetragonal potassium bronze, 7.18 ± 0.03 g /cm^3 for $K_{0.40}WO_3$, by Sienko and Morehouse.[13]

The number of $Na_xK_yWO_3$ unit included in a unit cell of the crystal can be calculated from the observed density and lattice constants. The calculated value of the number for eleven different sodium potassium bronzes was 10, which agrees with

12) B. W. Brown and E. Banks, *J. Amer. Chem. Soc.*, **76**, 963 (1954).
13) M. J. Sienko and S. M. Morehouse, *Inorg. Chem.*, **2**, 485 (1963).
14) A. Magnéli, *Ark. Kemi.*, **1**, 269 (1949).
15) M. E. Straumanis, *J. Amer. Chem. Soc.*, **71**, 679 (1949).
16) G. Hägg, *Z. Phys. Chem.* (Leipzig), **B29**, 192 (1935).

that of the tetragonal potassium bronzes published by Magnéli[10] and by Brimm *et al.*[3]

In conclusion, the close resemblance of tetragonal sodium potassium bronzes as a whole to tetragonal potassium bronzes, instead of to sodium bronzes, with respect to color, lattice constants, density and the related quantity, has convenced us that the crystal lattices of the sodium potassium bronzes are mainly decided by the lattices of the corresponding potassium bronzes, and that the sodium ions are incorporated and play a less important role in determining the structure of the crystal.

The authors wish to thank Professor Masaki Nakanishi of Ochanomizu University for his kind advice.

BULLETIN OF THE CHEMICAL SOCIETY OF JAPAN VOL. 43 1718—1722 (1970)

Studies of the Alkaline Earth Complexes in Various Solutions. V. Calcium(II) and Strontium(II) Complexes with Carbonate Ions in 1M Sodium Chloride Media

Yuko HASEGAWA, Hiroshi KAWASHIMA and Tatsuya SEKINE

Department of Chemistry, Science University of Tokyo, Kagurazaka, Shinjuku-ku, Tokyo

(Received November 28, 1969)

The complex formation of calcium(II) and strontium(II) with carbonate ions in 1M sodium chloride media at 25°C has been determined by a liquid-liquid distribution method. The metal ions in the aqueous phase were extracted with a mixture of benzoylacetone and tributylphosphate in hexane as adduct chelate complexes. The distribution ratio was determined by radiometry as a function of the carbonate-ion concentration in the aqueous phase. The decrease in the metal distribution caused by the addition of carbonate ions to the aqueous phase has been explained in terms of the complex formation, and the stability constants have been determined from these data by a "curve-fitting" method. It has been concluded from the results that the stabilities of these complexes are about the same magnitude of those of the sulfate complexes of these metal ions and that the concentration of the carbonate complexes in usual natural waters is probably negligibly small.

The formation of calcium(II) and strontium(II) complexes with carbonate ions may influence the chemical behavior of these metal ions in various aqueous solutions in equilibrium with atmospheric carbon dioxide, such as in the sea or in living bodies. Since the chemical behavior of these ions, especially of calcium(II), has attracted the attention of many chemists for many years, the solubility or solubility products of these metal carbonates have been reported repeatedly by many authors, but only few of these investigators have determined the stability constants of carbonate complexes in aqueous solutions.[1] The present authors have studied the solvent extraction of calcium(II) and strontium(II) in 1 M sodium chloride media containing various amounts of carbonate ions, and have determined the distribution ratio as a function of the carbonate concentration.

For the solvent extraction of calcium(II) and strontium(II), 8-hydroxy-quinoline has very often been used.[2-4] However, the solvent extraction method with this reagent seems to be unsuitable for the determination of complexes in aqueous solutions because the distribution behavior of the 8-hydroxyquinolinates of these metal ions is complicated due to the formation of an aqueous chelate with this extractant.[4] The use of thenoyltrifluoroacetone (TTA) in methylisobutylketone(MIBK) has been also suggested for the extraction of these metal ions.[5-6] The extraction equilibria of calcium(II)

1) L. G. Sillén and A. E. Martell, "Stability Constants," The Chemical Society, Spec. pub. 17, London (1964).

2) G. H. Morrison, H. Freiser, "Solvent Extraction in Analytical Chemistry," John Wiley & Sons., New York (1957).

3) J. Stary, "The Solvent Extraction of Metal Chelates", Pergamon Press, Oxford (1964).

4) D. Dyrssen, *Svensk Kem. Tidskr.*, **67**, 311 (1955).

5) T. Kiba and S. Mizukami, This Bulletin, **31**, 1007 (1958).

6) T. Kiba and M. Kametani, *ibid.*, **31**, 1013 (1958).

or strontium(II) with TTA in carbon tetrachloride containing MIBK, tributylphosphate(TBP), or trioctylphosphine oxide (TOPO) have been studied in detail,[7] and these adduct-chelate extraction systems have been used for the study of the oxalate and sulfate complexes of alkaline earth metal ions in previous papers of this series.[8-11]

In the present study, the hydrogen-ion concentration of the aqueous phase had to be kept much lower than in the previous studies because carbonic acid is a weaker acid (the pK_{a_1} and pK_{a_2} in 1M $Na(ClO_4)$ are 6.04 and 9.57 respectively[12]) than sulfuric or oxalic acid; thus, it was necessary to keep the $-\log[H^+]$ above 8.5 in order to prevent the dinegative carbonate ions from associating with protons.

However, if the $-\log[H^+]$ is kept high, a chelating acid of a higher dissociation constant, such as TTA (pK_a is 6.23[7]), in the organic phase will be distributed into the aqueous phase due to the acid dissociation;[7] it was, therefore, concluded that the use of TTA as the extractant was unsuitable for the present purpose. For this reason, benzoylacetone (BZA) (pK_a is 8.96[3]) was employed in conjunction with TBP, which was found to form adduct complexes with the BZA chelates in hexane and which enhances the extraction considerably. The ionic media used in the previous studies were 1M $Na(ClO_4)$. These media, however, were found to be unsuitable for the present work because of the extraction of the mixed chelate or the metal perchlorate at higher TBP concentrations, as has been pointed out previously,[13] and so the 1M Na(Cl) media were employed throughout this study instead of the perchlorate media. The distribution ratio was determined from the radioactivity in the two phases. A decrease in the distribution ratio of the metal ions was caused by the addition of carbonate ions to the aqueous phase; this decrease was explained in terms of the complex formation. The stability constants were determined graphically from these data by using a curve-fitting method. These complexes were then discussed.

Experimental

Tracers. The calcium-45 was obtained from the Nuclear Science and Engineering Co., U. S. A., as a hydrochloric acid solution. The strontium-85 was obtained from the New England Nuclear Corp. as a hydrochloric acid solution. They were both diluted with a 1M sodium chloride solution. The calcium stock solution thus prepared contained 1.5×10^{-5}M calcium, while the strontium stock solution contained 7.5×10^{-6}M strontium.

Reagents. All the reagents were of an analytical grade. The TBP and MIBK were obtained from the Tokyo Kasei Co. In order to remove impurities, they were washed successively with 0.1M perchloric acid, water, and a 0.1M sodium hydroxide solution, and then several more times with water. The other reagents were used without further purification.

Procedures. All the procedures were carried out in a thermostatted room at 25 ± 0.5°C. Hexane containing BZA and 0.6M TBP was used as the organic solvent. The concentrations of BZA were 0.1M and 0.2M for the calcium and the strontium extractions respectively. The two phases were equilibrated in stoppered glass tubes (volume 20 m*l*). Various amounts of a 0.5M sodium carbonate solution and/or a 1M sodium acid carbonate solution were placed in the tubes. When it was necessary, a small amount of sodium borate (0.0025M at initial) was added to the aqueous phase as a buffer. The tracer (calcium-45 or strontium-85) was then added to this solution, and finally the aqueous phase was made up to 5 m*l* with a 1M sodium chloride solution. A 5-m*l* portion of the organic phase was then placed in the tubes, and the two phases were agitated mechanically for 30 min and then centrifuged. After the two phases had then been separated, a small portion of the aqueous phases was transferred into a glass vessel and the hydrogen ion concentration was determined potentiometrically by using 1M sodium chloride containing 1.00×10^{-2}M hydrochloric acid as the standard of $-\log[H^+]$ 2.00.

The radioactivity in the two phases was determined as follows. Calcium: A 2-m*l* portion of the aqueous phase was transferred into another stoppered glass tube and agitated with 2 m*l* of MIBK containing 0.2M TTA in order to extract the calcium into the MIBK phase. A 1-milliliter portion of this MIBK solution was pipetted out, placed on a stainless steel dish, and then decomposed gradually on a hot plate under controlled heating. The β-radioactivity of the sample in the dish was measured with an end-window-type G. M. counter. The calcium in the organic phase containing TBP was first back-extracted into 4m*l* of 0.1M nitric acid, and then a 2-m*l* portion of this aqueous phase was transferred into another tube and 2-m*l* of 0.1M sodium hydroxide were added. The calcium in this aqueous solution was treated just as has been described above.

Strontium. A two-milliliter portion was pipetted from each phase; these portions were then transferred into small test tubes. The γ-radioactivity of the samples was then measured with a well-type (NaI) scintillation counter.

Statistical Treatment

The complex formation of a dipositive metal

7) T. Sekine and D. Dyrssen, *Anal. Chim Acta*, **37**, 217 (1967).
8) T. Sekine, M. Sakairi and Y. Hasegawa, This Bulletin, **39**, 2141 (1966).
9) T. Sekine and M. Sakairi, *ibid.*, **40**, 261 (1967).
10) Y. Hasegawa, M. Maki and T. Sekine, *ibid.*, **40**, 1845 (1967).
11) T. Sekine, Y. Kawashima, T. Unnai and M. Sakairi, *ibid.*, **41**, 3013 (1968).
12) M. Frydman, G. Nilsson, T. Rengemo and L. G. Sillén, *Acta Chem. Scand.*, **12**, 878 (1958).
13) T. Sekine and Y. Hasegawa, Proceedings of 5th International Conference of Solvent Extraction Chemistry, Jerusalm, September 1968. The full paper will be published from John Wiley & Sons.

ion, M^{2+}, with dinegative ligand ions, L^{2-}, in the aqueous phase may be described as:

$$M^{2+} + nL^{2-} \rightleftarrows ML_n^{2-2n} \quad (1)$$

$$\beta_n = [ML_n^{2-2n}]/[M^{2+}][L^{2-}]^n \quad (2)$$

The extraction of this metal ion into an organic phase containing a chelating acid, HA, and an adduct-forming ligand, E, may be described as follows:

$$M^{2+} + 2HA(org) + eE(org) \rightleftarrows MA_2E_e(org) + 2H^+ \quad (3)$$

$$K = [MA_2E_e]_{org}[H^+]^2/[M^{2+}][HA]_{org}^2[E]_{org}^e \quad (4)$$

In the present study, the concentration of the adduct-forming ligand (TBP) is kept constant (0.6M) throughout the experiments, and so the terms of this adduct-forming ligand will not be presented in the equations. Thus, the organic metal species will be denoted by MA_2, and the extraction constant, K_{ex} will be defined and described as;

$$K_{ex} = [MA_2]_{org}[H^+]^2/[M^{2+}][HA]_{org}^2 \quad (5)$$

When no ligand exists in the aqueous phase, the distribution ratio is:

$$D_0 = [MA_2]_{org}/[M^{2+}] \quad (6)$$

Then, the K_{ex} in Eq. (4) can be described as:

$$K_{ex} = D_0[H^+]^2[HA]_{org}^{-2} \quad (7)$$

Here, this K_{ex} should give a constant value at a certain temperature.

When the complex-forming ligand is present in the aqueous phase and when the concentration is $[L^{2-}]$, the distribution ratio may be described from Eqs. (2) and (5) as:

$$D = [MA_2]_{org}/([M^{2+}] + [ML] + [ML_2^{2-}] + \cdots) = D_0/(1+\sum\beta_n[L^{2-}]^n) \quad (8)$$

From Eqs. (7) and (8), the following can be described:

$$D[H^+]^2[HA]_{org}^{-2}/K_{ex} = (1+\sum\beta_n[L^{2-}]^n)^{-1} \quad (9)$$

The dissociation constants of carbonic acid are described as follows:

$$H_2CO_3 \rightleftarrows H^+ + HCO_3^-$$

$$K_{a_1} = \frac{[H^+][HCO_3^-]}{[H_2CO_3]}$$

$$HCO_3^- \rightleftarrows H^+ + CO_3^{2-}$$

$$K_{a_2} = \frac{[H^+][CO_3^{2-}]}{[HCO_3^-]}$$

The values in 1M $NaClO_4$ at 25°C are 9.12×10^{-7} and 2.70×10^{-10} respectively for K_{a_1} and K_{a_2}.[12]

The total concentration of carbonate ions is, then;

$$[\text{carbonate}]_{\text{total}} = [H_2CO_3] + [HCO_3^-] + [CO_3^{2-}] = [CO_3^{2-}]\left(1 + \frac{[H^+]}{K_{a_2}} + \frac{[H^+]^2}{K_{a_1}\cdot K_{a_2}}\right) \quad (10)$$

The concentration of the dinegative carbonate ions at a certain hydrogen-ion and a certain total carbonate concentration can be calculated from Eq. (10), while the stability constants, β_n, can be determined from the distribution data by a curve-fitting method[7-10] using Eq. (9).

Results

Dependence of D on the Hydrogen-ion Concentration. In order to determine the extraction constant, K_{ex}, in Eq. (5), the distribution ratio of the metal ions between 1M NaCl containing no carbonate ions and hexane containing 0.6M TBP and 0.1M BZA (extraction of Ca(II)) or 0.2M BZA (extraction of Sr(II)) was determined as a function of $-\log[H^+]$. The results are shown in Fig. 1. We can see from Fig. 1 that the plots of both the calcium(II) and strontium(II) extractions have a slope of +2. Thus, the extraction equilibria can be represented by Eq. (4); that is, neither the aqueous chelate formation nor the decrease in the $[HA]_{org}$ occurs in the hydrogen-ion concentration

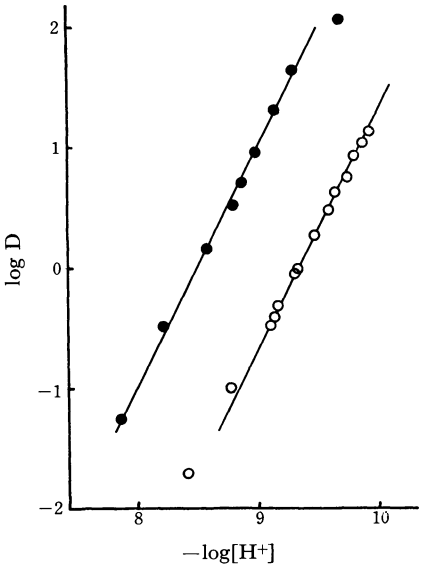

Fig. 1. Distribution ratio of calcium(II) (closed circles) and strontium(II) (open circles) as a function of the hydrogen ion concentrations.
Aqueous phase: 1M Na(Cl).
Organic phase: Ca(II), 0.1M BZA+0.6M TBP in hexane.
Sr(II), 0.2M BZA+0.6M TBP in hexane.
The straight lines give $\log D = -2\log[H^+] - 17.04$ ··· (Ca(II)) and $\log D = -2\log[H^+] - 18.75$ ··· (Sr(II))

Table 1. The stability constants of alkaline earth complexes

	CO_3^{2-}*			SO_4^{2-}**			$C_2O_4^{2-}$**	
	$\log \beta_1$	$\log \beta_2$	$\log \beta_3$	$\log \beta_1$	$\log \beta_2$	$\log \beta_3$	$\log \beta_1$	$\log \beta_2$
Be(II)	—	—	—	—	1.78	2.08	3.55	5.40
Ca(II)	1.22	1.38	—	1.10	1.36	—	1.64	2.68
Sr(II)	1.28	1.60	1.70	0.72	1.29	—	1.25	1.90
Ba(II)	—	—	—	0.66	1.42	—	0.58	2.20

* In 1 M Na(Cl) data are taken from the present work.

** In 1 M $Na(ClO_4)$ data are taken from Ref. 8 (Ba(II)), Ref.9 (Be(II)) and Ref. 10 (Ca(II) and Sr(II)).

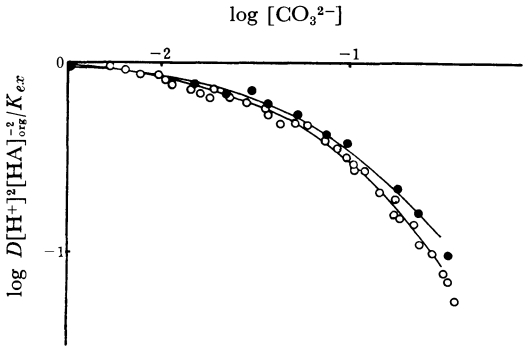

Fig. 2. Decrease in the calcium(II) (closed circles) and strontium(II) (open circles) extraction as a function of the carbonate ion concentration. The solid lines represent the followings;

$Ca(II): \log D[H^+]^2[HA]_{org}^{-2}/K_{ex} = -\log(1+10^{1.22}[CO_3^{2-}]+10^{1.38}[CO_3^{2-}]^2)$

$Sr(II): \log D[H^+]^2[HA]_{org}^{-2}/K_{ex} = -\log(1+10^{1.28}[CO_3^{2-}]+10^{1.60}[CO_3^{2-}]^2+10^{1.70}[CO_3^{2-}]^3)$

range studied in Fig. 1. The decrease in the extraction of metal ions by the addition of carbonate ions into the aqueous phase is given in Fig. 2. The results in Fig. 2 were analyzed by the curve-fitting method. The extraction curve of calcium(II) (closed circles) was found to fit with a standard curve by assuming the first and the second complexes. From the parameters of this best-fit standard curve, the stability constants were obtained as shown in Table 1. The extraction curve of strontium(II) (open circles), on the other hand, could be fitted to none of the standard curves drawn by assuming the formation of the first and the second complexes. Therefore, the curve-fitting was further carried out by assuming the formation of the third complex, and finally the best-fit standard curve was found. The three stability constants determined from the parameters of the standard curve for the strontium extraction are given in Table 1. Table 1 also gives the stability constants previously obtained in this series to facilitate comparison with the present results.

Discussion

From the present results, it may be concluded that the complexes containing the acid carbonate ion, HCO_3^-, are negligible within the limits of experimental accuracy. The data in Fig. 2 were plotted against the carbonate concentration disregarding the acid carbonate ions, but this seems to have caused no systematic deviation.

The stability constants of calcium(II) and strontium(II) carbonate complexes in Table 1 are rather similar to each other, except for the third complex of strontium(II), which has not been observed in calcium(II). Such similarity in the magnitude of the constants——in other words, the small difference in the stability constants among the complexes of metal ions of different ionic sizes——can also be seen in the sulfate complexes of alkaline earth ions given in Table 1. Although no direct evidence showing the nature of the interactions between the metal and the ligand ion could be obtained from only these distribution data, we might assume the following. Among these, the oxalate complexes should be the inner-sphere chelate complexes. On the other hand, the sulfate complexes should be mainly outer-sphere complexes (ion-pairs), as has been suggested by the kinetic data.[14] The similarity in the stabilities of sulfate and carbonate complexes can be explained if we assume that the carbonate complexes are also outer-sphere complexes.

The stability constants of carbonate complexes in Table 1 seem to show that the contribution of carbonate complexes to the total concentrations of these metal ions in usual natural water is negligibly small. For example, in a 1 M aqueous sodium chloride solution at pH 8, the total carbonate concentration necessary to convert a 1% portion of the total calcium(II) into carbonate complexes can be calculated from these data as about 2×10^{-2} M; this is about ten times larger than the carbonate con-

14) M. Eigen and K. Tamm, *Z. Elektrochem.*, **66**, 107 (1962).

centration in sea water (0.6M NaCl, pH 8.1 and $[HCO_3^-]=2.3\times10^{-3}$M.[15,16]).

15) G. Atkinson and S. K. Kor, *J. Phys. Chem.*, **69**, 128 (1965).

16) H. U. Sverdrup, M. W. Johnson, R. H. Fleming: "The Oceans," Prentice-Hall, Inc., New York (1946), p. 173.

Part of this work has been carried out in the Laboratory of Nuclear Chemistry, Institute of Physical and Chemical Research. The authors are grateful to Professor Nobufusa Saito, the head of the Laboratory. They are also grateful to Messrs. Nobukazu Isogai and Hiroshi Takeuchi of the present laboratory for their experimental aid.

BULLETIN OF THE CHEMICAL SOCIETY OF JAPAN VOL. 43 1722—1728 (1970)

An NMR Study of Metal Complexes Containing Acetylacetone and Related Compounds. I. The Preparation, Halogenation and NMR Spectra of Cobalt(III) Complexes Containing Acetylacetone and Bis(acetylacetone)ethylenediimine

Yuki Fujii

Department of Chemistry, Ibaraki University, Bunkyo-cho, Mito, Ibaraki

(Received December 1, 1969)

A mixed cobalt(III) complex containing both bis(acetylacetone)ethylenediimine and acetylacetone anions, [Co(bean)(acac)] (bean=dianion of bis(acetylacetone)ethylenediimine, acac=anion of acetylacetone), was newly prepared and its electrophilic substitution reaction at the chelate ring protone was studied by means of NCS, NBS, and NIS (NCS, NBS and NIS are the abbreviated forms of *N*-chloro-, *N*-bromo- and *N*-iodosuccinimide). The structures of this complex, [Co(baen)-(acac)], and of the halogenated complex were both determined to be of the β-form (*cis* with respect to the coordinated two oxygen atoms of baen) on the basis of their NMR spectra. The ring protons of the imine chelates were found to be more reactive than that of the acetylacetone chelate in the chlorination reaction. Then, a bi-substituted complex, [Co(baen-Cl_2)(acac)], in which two chlorine atomes were attached to the two imine chelate rings, was prepared. Tri-substituted complexes, [Co(baen-X_2)(acac-X)] (X=Cl, Br and I), were also prepared. The quasiaromaticity of both the acetylacetone and imine rings was considered on the basis of their NMR spectra. A new complex, [Co(baen)(OH)(H_2O)], was also prepared in order to assign the NMR spectrum of the complex, [Co(baen)(acac)]. The IR, UV, and visible absorption spectra were also considered.

The quasiaromaticity of the metal-acetylacetonate is quite interesting and has been discussed by several authors. On the basis of their reactivity for the electrophilic substitution reaction, characteristic of aromatic compounds, Collman pointed out that metal-acetylacetonates had an aromatic character.[1,2] He also pointed out that imine complexes of β-diketone underwent electrophilic substitution reactions at the chelate-ring protons, as did acetylacetone complexes.[3] For the imine chelate, however, not such a large benzenoid resonance is expected as for the acetylacetone chelate because of the asymmetric property of the imine chelate.[4] Therefore, the quasiaromaticity of the imine chelate is quite an interesting question.

Under these circumstances, it seemed that it would be worthwhile to study the reactivity of the imine chelate ring towards the electrophilic substitution reaction and to compare the reactivity of the imine chelate ring with that of the acetylacetone chelate ring. Mixed cobalt(III) complex containing both the bis(acetylacetone)ethylenediimine anion (baen) and the acetylacetone anion (acac) was prepared and the halogenation reaction on the chelate ring was examined.

1) J. P. Collman, *Advan. Chem. Ser.*, No. 37, 78 (1963).
2) J. P. Collman, *Angew. Chem.*, **77**, 154 (1965).
3) J. P. Collman and E. T. Kittelman, *Inorg. Chem.*, **1**, 499 (1962).
4) P. J. McCarthy and A. E. Martell, *ibid.*, **6**, 781 (1967).

Experimental

Preparation of the Complexes. *1) Bis(acetylacetone)ethylenediiminatohydroxoaquocobalt(III)*, [Co(baen)(OH)(H_2O)] (I). Bis(acetylacetone)ethylenediiminatodiaquocobalt(II)[5] (12.5 g, 0.04 mol) was dissolved in 200 m*l* of methanol, 4.0 g of potassium hydroxide in 20 m*l* of water was then added, and the resulting solution was oxidized by sucking air through the solution for 4 to 5 hr. When the solution was allowed to stand overnight, reddish crystals were separated out in a low yield. They were subsequently recrystallized from methanol. Found: C, 45.69; H, 6.34; N, 8.65%. Calcd for $C_{12}H_{21}CoN_2O_4$: C, 45.58; H, 6.70; N, 8.86%.

When the filtrate of the complex I was further concentrated by allowing it to stand for 2 or 3 days in an atmosphere, dark green crystals were separated out. They were subsequently recrystallized from methanol. This dark green complex was assigned to the complex II on the basis of its NMR spectrum.

2) Bis(acetylacetone)ethylenediiminatoacetylacetonatocobalt(III), [Co(baen)(acac)] (II). Bis(acetylacetone)ethylenediiminatodiaquocobalt(II) (25 g, 0.079 mol) was dissolved in 200 m*l* of methanol. Acetylacetone (7.8 g, 0.078 mol) neutralized with potassium hydroxide (10 g) in 100 m*l* of water was then added. The resulting solution was oxidized by sucking air through the solution for 4 to 5 hr. After oxidation was completed, the solution was concentrated under a reduced pressure to a volume of about 200 m*l*. During the course of the concentration, a small amount of bisacetylacetonatocobalt(II) was isolated and filtered off. When the solution was allowed to stand for two days, dark green crystals were separated out. They were subsequently recrystallized from methanol. The yield was about 55%. Found: C, 53.68; H, 6.80; N, 7.36%. Calcd for $C_{17}H_{25}CoN_2O_4$: C, 53.55; H, 6.63; N, 7.35%.

Halogenation of the Complex II. *1) Bis(3-chloroacetylacetone)ethylenediiminatoacetylacetonatocobalt(III)*, [Co(baen-Cl_2)(acac)] (III). The methanol solution (40 m*l*) of NCS (2.0 g, 0.015 mol) was added slowly to the methanol solution (40 m*l*) of the complex II (3.8 g, 0.01 mol) at 40°C. After five minutes' stirring, about 100 m*l* of water was added. When the resulting solution was allowed to stand for a day at room temperature, light green crystals were separated out. They were subsequently recrystallized from methanol-water. Yield, about 1.2 g (27%). Found: C, 45.55; H, 5.25; N, 6.25%. Calcd for $C_{17}H_{23}CoCl_2N_2O_4$: C, 45.45; H, 5.16; N, 6.24%.

2) Bis(3-chloroacetylacetone)ethylenediiminato-3-chloroacetylacetonatocobalt(III), [Co(baen-Cl_2)(acac-Cl)] (IV). Method 1. A methanol solution (40 m*l*) of NCS (4.0 g, 0.03 mol) was slowly added to a methanol solution (40 m*l*) of the complex II (3.8 g, 0.01 mol) at about 50°C. The solution was stirred for five minutes and then treated with about 100 m*l* of water, and allowed to stand for a day at room temperature. This gave light green crystals and they were then washed with methanol. Yield, about 3.8 g (79%). Found: C, 42.65; H, 4.54; N, 5.44%. Calcd for $C_{17}H_{22}CoCl_3N_2O_4$: C, 42.22; H, 4.58; N, 5.79%.

Method 2. To a methanol solution (20 m*l*) of the complex III (0.54 g, 0.0012 mol), a methanol solution (10 m*l*) of NCS (0.2 g, 0.0015 mol) was added at 50°C. After five minutes, 50 m*l* of water were added and the solution was allowed to stand for a day. This gave light green crystals, which were subsequently washed with methanol. Yield, about 0.4 g (70%). Found: C, 42.36; H, 4.38; N, 5.52%. Calcd for $C_{17}H_{22}CoCl_3N_2O_4$: C, 42.22; H, 4.58; N, 5.79%.

3) Bis(3-chloroacetylacetone)ethylenediiminato-3-bromoacetylacetonatocobalt(III), [Co(baen-Cl_2)(acac-Br)] (V). To a methanol solution (20 m*l*) of the complex III (0.54 g, 0.0012 mol), a methanol solution (10 m*l*) of NBS (0.3 g, 0.0017 mol) was added at 50°C. After five minutes' stirring, about 50 m*l* of water was added to it. The resulting solution was allowed to stand for a day to give light green crystals, which were subsequently washed with methanol. Yield, about 0.4 g (63%). Found: C, 38.55; H, 4.36; N, 5.29%. Calcd for $C_{17}H_{22}CoBrCl_2N_2O_4$: C, 38.66; H, 4.20; N, 5.30%.

4) Bis(3-bromoacetylacetone)ethylenediiminatoacetylacetonatocobalt(III), [Co(baen-Br_2)(acac)] (VI). This compound was prepared from the complex II and NBS in methanol by the same method as in the case of the dichlorination described in *1)*. Yield, about 4.0 g (71%). Found: C, 36.88; H, 4.24; N, 5.07%. Calcd for $C_{17}H_{23}CoBr_2N_2O_4$: C, 37.94; H, 4.31; N, 5.21%.

5) Bis(3-bromoacetylacetone)ethylenediiminato-3-bromoacetylacetonatocobalt(III), [Co(baen-Br_2)(acac-Br)] (VII). This compound was prepared from the complex II (or the complex VI) and NBS in methanol in the way as described above *2)*. Yield, about 4.5 g (74%) for the method 1 and about 0.5 g (82%) for the method 2. Found for the method 1: C, 33.94; H, 3.55; N, 4.73%. Found for the method 2: C, 33.88; H, 3.47; N, 4.69%. Calcd for $C_{17}H_{22}CoBr_3N_2O_4$: C, 33.64; H, 3.65; N, 4.61%.

6) Bis(3-iodoacetylacetone)ethylenediiminato-3-iodoacetylacetonatocobalt(III), [Co(baen-I_2)(acac-I)] (VIII). This compound was prepared from the complex II and NIS in methanol by the method used in the case of trichlorination. Yield, about 5.0 g (65%). Found: C, 27.21; H, 3.05; N, 3.58%. Calcd for $C_{17}H_{22}CoI_3N_2O_4$: C, 26.94; H, 2.93; N, 3.70%.

Measurements. All the NMR spectra were recorded with a Hitachi R-20 spectrometer (60 MHz) at 35°C. The spectra were measured with about a 5—10% solution of deuterochloroform and/or carbontetrachloride. As the internal reference, chloroform (2.74 τ) (when deuterochloroform was used as the solvent) and tetramethylsilane (when carbontetrachloride was used as the solvent) were used. The infrared absorption spectra were taken on potassium bromide disks with a Hitachi EPI-S2 spectrophotometer. All the visible and ultraviolet absorption spectra were recorded by a Hitachi EPS-3 spectrophotometer, with methanol as the solvent.

Results and Discussion

Synthesis and Halogenation Reaction. The complex II was successfully prepared in a yield of about 55% by oxidizing an alkaline methanol solution containing both bis(acetylacetone)ethylenediiminatodiaquocobalt(II), [Co(baen)(H_2O)$_2$], and acetylacetone. Although the yield was low, it could also be prepared by oxidizing an alkaline

5) G. T. Morgan and J. D. Smith, *J. Chem. Soc.*, **127**, 2030 (1925).

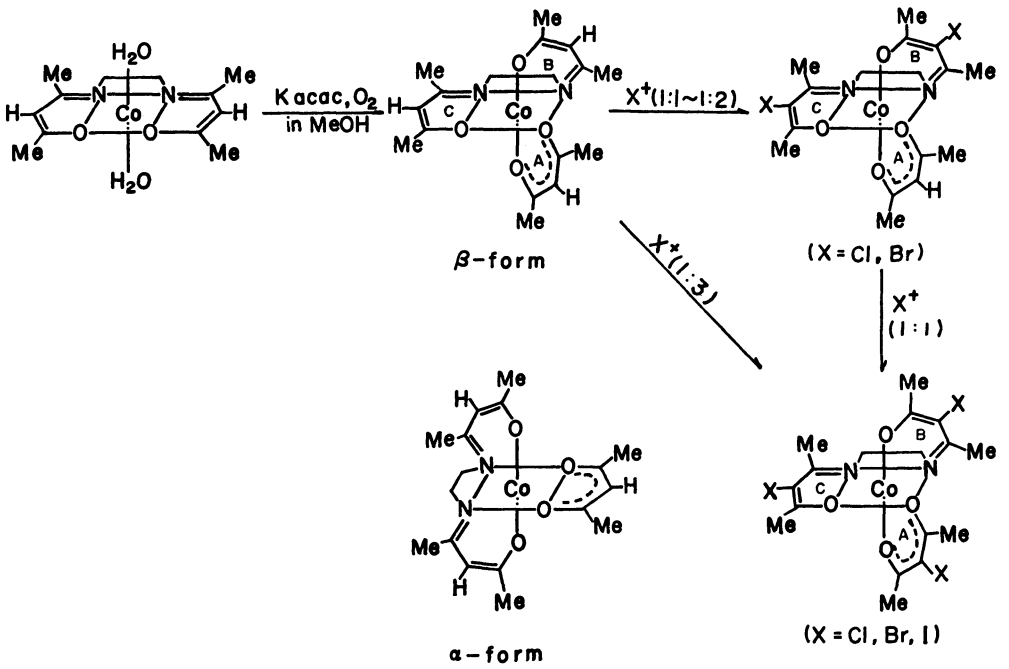

Fig. 1. The preparative scheme and the two geometrical isomers of the complex, [Co(baen)(acac)].

methanol solution containing only the complex, [Co(baen)$(H_2O)_2$]. With both procedures, only the β-form complex was isolated. Therefore, it may be presumed that the β-form may be preferred in this reaction, for the starting material, [Co(baen)-$(H_2O)_2$], takes a planer structure with respect to the two nitrogen atoms and the two oxygen atoms of the coordinated baen. Then, for the two oxygen atoms of baen to coordinate *trans* (α-form), two oxygen atoms of baen should move from the *cis* position to the *trans* position. However, only one oxygen atom should move when the β-form is taken.

Two dihalogenated complexes, III and VI, were obtained whenever the complex II was treated with NCS and NBS in a molar ratio of the reactants of 1 : 1 or 1 : 2. However, no diiodinated complex could be isolated because of the contamination of the complex VIII. When iodine monochloride (ICl) was used as the iodinating reagent, the complex II decomposed instantaneously.

The trichloro- and tribromo-substituted complexes were obtained by the two methods shown in the preparative scheme (Fig. 1).

NMR Spectrum of the Complex I. The NMR spectra of the new complexes are shown in Figs. 2, 3, and 4. The numerical data are summarized in Table 1.

The NMR spectrum of the complex I in deuterochloroform exhibits three types of protons, at τ 5.10, 6.97, and 8.15, with the area ratio of 1 : 2 : 6. On the other hand, in carbon tetrachloride I exhibits four types of protons, at τ 5.26, 7.02, 8.20, and 8.25, with the area ratio of 1 : 2 : 3 : 3. Since these spectra resemble that of bis(acetylacetone)ethylenediiminatonickel(II), [Ni(baen)],[4] the peaks were assigned as is shown in Table 1. The difference between the methyl signals in deuterochloroform and in carbon tetrachloride is thought to be due to the difference in the solvation effect; a similar

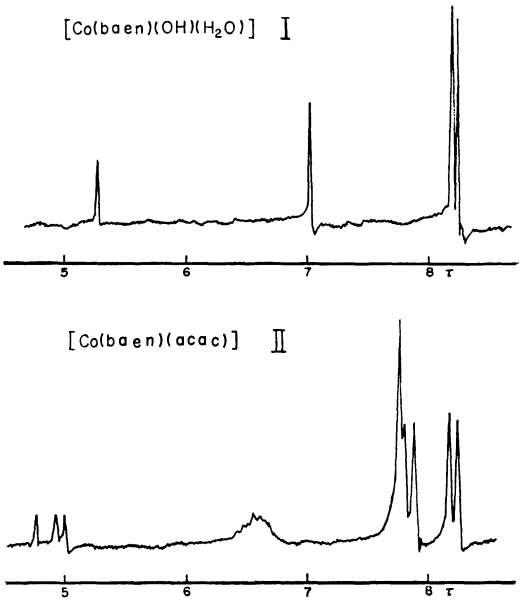

Fig. 2. The NMR spectra of the complexes I and II in CCl_4.

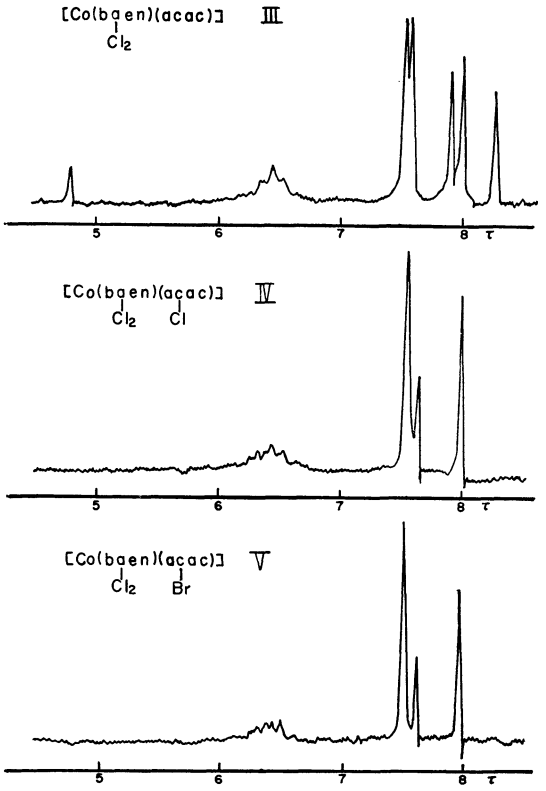

Fig. 3. The NMR spectra of the complexes III, IV, and V in CCl_4.

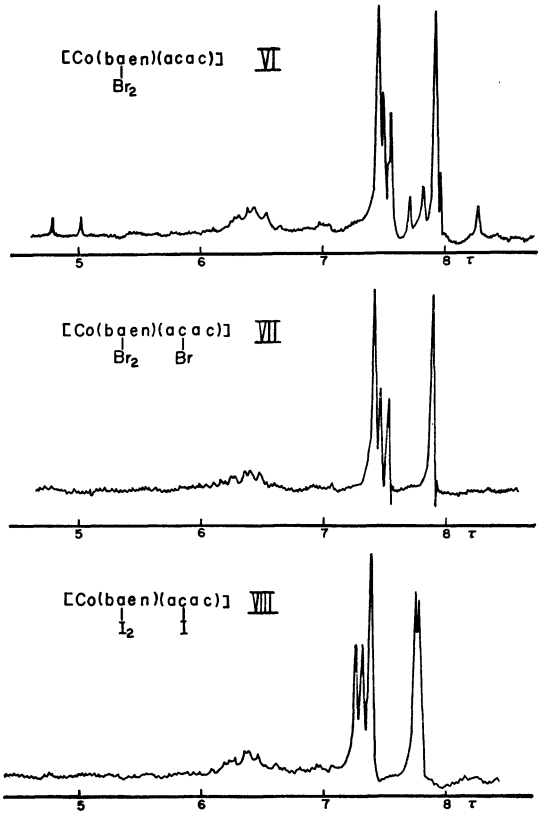

Fig. 4. The NMR spectra of the complexes VI, VII, and VIII in CCl_4.

Table 1. NMR Spectra of the complexes (in τ)

Complex	CH=C (acac)	CH=C (imine)	CH_2	CH_3 B,C_{C-O}	B_{C-N}	C_{C-N}	A_{C-O}	
(I)		5.26 (5.10)	7.02 (6.97)	8.20 (8.15)		8.25		
(II)	4.76 (4.64)	4.92 5.00 (4.79) (4.81)	6.54* (6.64)	7.77 (7.75)	7.79 (7.68)	8.16 (8.12)	7.89 (7.88)	8.25 (8.23)
(III)	4.76 (4.61)		6.43* (6.38)	7.52 (7.47)	7.57 (7.54)	7.99 (7.93)	7.89 (7.85)	8.25 (8.20)
(IV)			6.41*	7.52	7.52	7.98	7.62	7.98
(V)			6.43*	7.52	7.52	7.97	7.61	7.97
(VI)	4.76	5.00	6.39*	7.43, 7.47, 7.51, 7.54, 7.69, 7.79, 7.91, 7.93, 8.25				
(VII)			6.41*	7.44	7.47	7.91	7.55	7.91
(VIII)			6.36*	7.26 7.32	7.38	7.76	7.38	7.78

( ) represents the spectra in $CDCl_3$. * shows the complicated band.

phenomenon has been reported for the NMR spectrum of [Ni(baen)].[4] The assignment of the methyl signals in carbon tetrachloride is as follows: the lower-field signal is due to the methyls adjacent to the C–O groups, and the higher-field signal, to the methyls near the C–N groups,[4] since the methyls adjacent to the C–O groups would be slightly less shielded than those near the C–N groups because of the lower electronegativity of nitrogen than of oxygen.

The peak positions of all the protons were scarcely changed by replacing the metal ion from Ni^{2+} to Co^{3+}. This may be due to the nearly identical ionic radii of the two metal ions.

Though there are four possible geometrical isomers for the complex I, the probable structure may be (a) or (b) in Fig. 5, since the resonance of the ethylene protons shows a single peak.

The coordinated OH and H_2O protons in the complex I did not appear in this measurement ($\tau - 10.0 \sim 10.0$), perhaps because of the broadening.

NMR Spectrum of the Complex II. The

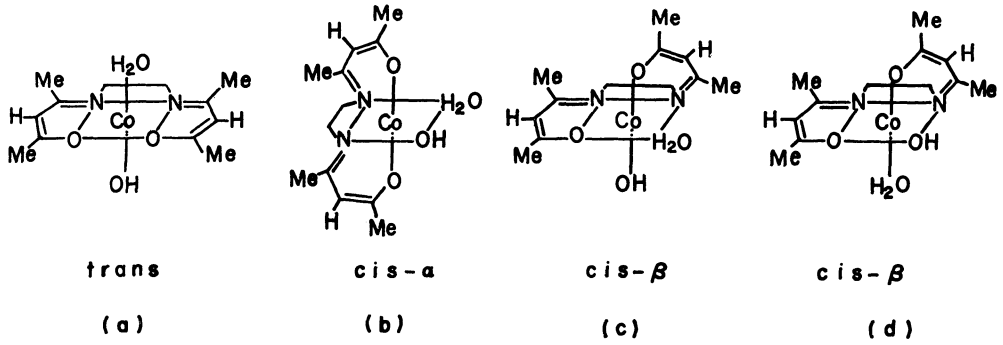

Fig. 5. The possible structures of the complex, [Co(baen)(OH)(H_2O)].

NMR spectrum of the complex II shows a rather more complex pattern than that of the complex I. Though two geometrical isomers are possible, as is shown in Fig. 1, this complicated pattern can be safely assigned to that of the β-form, for nine peaks with the area ratio of 1 : 1 : 1 : 4 : 6 : 3 : 3 : 3 : 3, in which the ethylene peak is splitted into the complex pattern, were observed in carbon tetrachloride. If the complex II took the α-form, six peaks, of which the ethylene peak consists of only one signal, should be observed. On the other hand, the β-form would give ten peaks, of which the ethylene peak would consist of more than one signal.

It is known that the signal of the ring proton of the trisacetylacetonatocobalt(II) complex appears at τ 4.63.[1] This position is apparently located at a field lower than that of the ring protons of imine chelates, such as are seen in the complex I. Therefore, the peak of τ 4.76 in carbon tetrachloride of the complex II may be assigned to the ring proton of the acetylacetone chelate, and the two peaks at τ 4.92 and 5.00 to the ring protons of the two imine chelates. The separation between the chemical shifts of the two imine ring protons is thought to be due to the differences in the solvation and ion-pair effects of the imine rings rather than to the differences in the diamagnetic shielding of the two imine ring protons by the ring-current of the acetylacetone chelate ring, for, from the molecular model, it is known that the ring proton of the B-ring in Fig. 1 is closer to the ethylene bridge than of the C-ring and only very small ring-current, if any, can be expected for the β-diketone complexes.[6] The separation between the chemical shifts of the ring protons of the acetylacetone ring (A-ring) and the ring protons of the imine rings (B- and C-rings) suggests that the electron density of the γ-position of the A-ring is a little smaller than those of the B- and C-rings and/or that the paramagnetic shielding for the A-ring proton by the ring-current of its own A-ring is a little larger than those in the case of the B- and C-rings. Experimentally, these separations were found to be due mainly to the differences in the electron density at the γ-position between the A-ring and the B- and C-rings, for the chlorination reaction at the imine ring (B- and C-rings) proton precedes the chlorination of the acetylacetone ring (A-ring). The details will be discussed in the next paragraph.

The peak of the ethylene-bridge protons is very complicated; such a complex pattern suggests that the configuration of the complex II is of a β-form, since only one peak is expected for that of the α-form on the basis of the symmetrical property.

The methyl protons show five peaks, with an area ratio of 6 : 3 : 3 : 3 : 3, but evidently the signal at τ 7.77 represents two methyl groups which have not been resolved.

The methyl signals of the complex II were assigned as follows, with the aid of the NMR spectra of the dichlorinated complex, III, and the trichlorinated complex, IV. The signals at τ 7.89 and 8.25 in the complex II were not shifted to the lower field even when the complex II was dichlorinated; they were shifted only when it was trichlorinated. Since the methyl signal of the acetylacetone chelate[1,2] and the imine chelate of β-diketone*1 is shifted to the lower field when the ring proton is halogenated, the two signals at τ 7.89 and 8.25 can be assigned to the two methyl groups of the acetylacetone ring. The two peaks, τ 7.79 and 8.18, can be assigned to the two methyl groups near the C–N groups, and the peak at τ 7.77, to the two methyl groups adjacent to the C–O groups of the imine rings, for the methyl protons near the C–N groups will appear at a higher field than that near the C–O groups.[4] The separation of the chemical shifts between the two methyl groups near the C–N groups is thought to be due to the difference in the steric strain between the two $-CH_2-N=$ groups. Since the steric strain in the C-ring is a little larger than that in the B-ring because of their steric requirement,[7] since, that is,

6) R. J. York, W. D. Bonds, B. P. Cotsoradis and R. D. Archer, *Inorg. Chem.*, **8**, 789 (1969).

*1 This report will be published elsewhere.

7) J. Hidaka, Y. Shimura and R. Tsuchida, This Bulletin, **35**, 567 (1962).

the C-ring takes the meridional form with respect to the two nitrogen atoms and one oxygen atom, while the B-ring takes the facial form, the signal at τ 7.79 can be assigned to the methyl group near the C–N group of the B-ring, and the signal at τ 8.18, to that of the C-ring.

If the ring-current of the β-diketone chelate compounds could be expected to be large enough to be detectable in the NMR spectra, the signals of the methyl groups of acetylacetone chelate should appear at a further lower field than those of the imine chelate of acetylacetone, for the benzenoid resonance of the imine chelate ring can be expected to be smaller than that of the β-diketone chelate ring because of the asymmetric property of the imine ring.[4] Therefore, the paramagnetic shielding of the methyl groups of the imine ring by the ring-current of its own ring is not expected to be larger than that of the acetylacetone ring. However, the peaks of the methyl groups of the acetylacetone ring evidently appear at a higher field than those of the imine rings in the complex II. Therefore, it may be concluded that the ring-current for the β-diketone chelate, if any, is very small, and that the ring-current for the imine chelate of β-diketone, if any, is very small, also. Here, again, the separation of the chemical shifts of the ring protons between the A-ring and the B- and C-ring is confirmed to be due mainly to the difference in the electron density at the γ-positions of the chelate rings.

NMR Spectra of the Complexes III, IV, and V. The dichlorinated complex, III, gives signals at τ 4.76, 6.34, 7.52, 7.57, 7.89, 7.99, and 8.25, with the area ratio of 1 : 4 : 6 : 3 : 3 : 3 : 3 in carbontetrachloride. Evidently, the two ring protons of the imine rings disappears upon dichlorination and only one peak, to be assigned to the ring protons of acetylacetone ring, remains at the same position as the ring proton of acetylacetone ring of the complex II. Therefore, it is clear that the dichlorination occurs at the two imine chelate rings. This means that the two imine-ring protons are more reactive than the acetylacetone-ring proton. This fact also indicates that the electron density at the γ-positions of the imine rings is slightly larger than that of the acetylacetone ring. Therefore, the difference in the chemical shifts of the ring protons between the imine and the acetylacetone rings can be concluded to be due mainly to the difference in the electron density of the carbon atoms (γ-position) where the ring proton is attached.

The methyl signals of the complex III are shifted to a lower field than those of the complex II except the two peaks at τ 7.89 and 8.25. As has been mentioned above, the shift of the methyl signals to the lower field is due to the halogen substitution at the γ-positions of their rings. Therefore, the methyl signals shifted to the lower field by dichlorination can be assigned to the methyl groups of the two imine rings, and the two peaks at τ 7.89 and 8.25, to the two methyl groups of the acetylacetone ring. These assignments are further supported by the NMR data of the trichlorinated complex, IV. The two peaks at τ 7.89 and 8.25 in the complex III are shifted to a lower field by trichlorination and the signal at τ 4.76 assigned to the ring proton of acetylacetone ring disappears.

The methyl protons of the imine rings of the complexes III and IV were also assigned in the same way described above for the complex II. Although the signal at τ 7.57 of the complex III in Fig. 3 seems to have the same intensity as that at τ 7.52, the integration of these peaks indicates that the intensity of the peak at τ 7.57 is half that of the peak at τ 7.52. This is due to the overlap of the skirts of these two peaks. The complex IV shows three methyl peaks, at τ 7.52, 7.62, and 7.98, with an area ratio of 9 : 3 : 6. It is estimated that the signal at τ 7.98 consists of the protons of the two methyl groups, of which one is the methyl group of the acetylacetone ring, and the other, the methyl group near the C–N group of the C-ring. Also, the signal at τ 7.52 is estimated to consist of three methyl groups; two of them are the methyl groups adjacent to the C–O groups of B- and C-rings, while the third is the methyl group near the C–N group of the B-ring.

In the NMR spectra of both complexes, III and IV, the signals of the ethylene-bridge protons are still complicated, as are those of the complex II. This indicates that the configuration of the β-form in the complex II holds also in the chlorinated complexes, III and IV.

The NMR spectrum of the complex V is nearly the same as that of the complex IV. This fact suggests that the substitution of the ring proton by chlorine or bromine atoms does not cause any remarkable change in their NMR spectra.

NMR Spectra of the Complexes VI, VII, and VIII. The NMR spectrum of the complex VI shows a very complicated pattern which is obviously different from that of the complex III. In spite of the dibromination, the signal at τ 5.00 remains, together with the peak at τ 4.76, in the complex VI, while the peak area also remains the same. Furthermore, many elemental analyses of the complex VI invariably showed that the complex VI has two bromines per mole. The possibility of the contamination of the tribrominated complex, VII, to the complex VI during the preparative procedure could thus be ruled out, since the former is less soluble in methanol than the latter and is easily separated from the reaction mixture. Since it has been reported that NBS is stronger than NCS as a halogenating reagent in methanol,[8] it is probable that the bromination occurs at the A-ring proton as well as the B- and

8) Y. Fujii, E. Kyuno and R. Tsuchiya, This Bulletin, **42**, 1301 (1969).

C-rings protons. Therefore, it can be estimated that the complex VI is a mixture of the three dibrominated compounds. This estimation is supported by the complicated methyl signals, that is, the peaks at τ 7.91 and 8.25 which are assigned to the two methyl groups of the unsubstituted acetylacetone ring exist together with the two peaks, at τ 7.54 and 7.91, which are assigned to the two methyl groups of the brominated acetylacetone ring by the aid of the NMR spectrum of the complex VII.

The tribrominated complex VII shows a spectrum very similar to that of the complex IV, though the positions of the peaks in the complex VII are shifted to a slightly lower field. Tribromination at γ-positions was confirmed by the disappearance of the three ring protons. The methyl peaks were assigned as in the case of the complex IV.

The triiodinated complex VIII showed a spectrum similar to those of the IV and VII complexes. Triiodination at the γ-positions is also confirmed by the disappearance of the signals of three ring protons. The peaks were assigned as in the case of the complexes IV and VII.

Table 2. IR spectra (in cm^{-1})

Complex	asym. $\nu_{C=C}$	asym. $\nu_{C=O}$ and $\nu_{C=N}$
(I)	1589	1511
(II)	1589	1515
(III)	1579	1520
(IV)	1570	—
(V)	1570	—
(VI)	1564	1515
(VII)	1561	—
(VIII)	1548	—

Infrared, Ultraviolet, and Visible Absorption Spectra. It has been established that the $\nu_{C=C}$ and $\nu_{C=O}$ bands in the region from 1600 to 1500 cm^{-1} of the trisacetylacetonatocobalt(III) complex are shifted to lower-energy site by the substitution at the γ-position and that only one band assigned to the $\nu_{C=C}$ remains in this region.[9]

The complex I shows two bands between 1600 and 1500 cm^{-1}, as is shown in Table 2. The band at the higher-energy site can be assigned to the $\nu_{C=C}$ band, and that at the lower-energy site, to the $\nu_{C=N}$ band.[10]

The complex II also shows two bands in this region. The band at 1589 cm^{-1} can be assigned to the $\nu_{C=C}$ bands of the acetylacetone ring and the imine ring, which overlap, and the band at 1515 cm^{-1}, to the overlapping bands of $\nu_{C=O}$ and $\nu_{C=N}$. The dihalogenated complexes, III and VI, show two bands in this region, though the intensity of the band at the lower-energy site is small. On the other hand, the trihalogenated complexes show only one band in this region. These bands were assigned as in the case of the trisacetylacetonatocobalt(III), as has been mentioned above. These IR spectra give strong evidence that the complex VI is a mixture of three dibrominated complexes.

The numerical data of the ultraviolet and visible absorption spectra of the new complexes are summarized in Table 3.

The first absorption band is shifted only a little by halogenation. On the other hand, the band near 340 mμ in the complex II is shifted to the lower-energy site by halogenation. The order of this red-shift is Cl<Br<I; this order is that expected for the order of the elongation of the π-system by introducing the halogen atom to the acetylacetone ring and its imine ring.[11]

The author wishes to express his deep thanks to Professor K. Yamamoto and Dr. M. Kodama of Ibaraki University for their encouragement. The author wishes also to express his deep thanks to Dr. M. Hirayama of Ibraraki University for his kind help in the measurements of the NMR spectra and to Professor S. Ito and his coworkers of Tohoku University for their kind help in the elemental analysis. He also wishes to thank Mr. A. Okada for his helpful assistance in the measurements.

Table 3. The ultraviolet and visible absorption spectra (in c/s$\times 10^{-13}$)

Complex	ν (log ε)	ν (log ε)	ν (log ε)	ν (log ε)	ν (log ε)
(I)	52.8 (1.88)	66.7 (2.43)	82.2 (3.65) 87.2 (3.67) 100.0 (3.61)	111.1 (4.08)	127.7 (4.53)
(II)	47.6 (2.19)	65.2 (2.50)	88.2 (3.47)	111.1 (3.98)*	122.5 (4.08)
(III)	47.2 (2.30)	63.8 (2.71)	85.7 (3.85)	111.1 (4.27)*	120.0 (4.44)
(IV)	47.2 (2.61)	63.8 (3.04)	84.5 (4.12)	111.1 (4.48)*	125.0 (4.68)
(V)	47.6 (2.61)	63.8 (3.07)	88.2 (4.17)	111.1 (4.46)*	125.0 (4.66)
(VI)	47.2 (2.27)	63.8 (2.71)	87.0 (3.77)	111.1 (4.14)*	125.0 (4.34)
(VII)	47.2 (2.52)	63.8 (2.91)	83.3 (3.95)	111.1 (4.27)*	125.0 (4.49)
(VIII)	47.2 (2.32)	63.8 (2.91)	82.6 (3.80)	111.1 (4.32)*	125.0 (4.62)

* represents the shoulder.

9) K. Nakamoto, P. J. MacCarthy, A. Ruby and A. E. Martell, *J. Amer. Chem. Soc.*, **83**, 1066 (1961).
10) K. Ueno and A. E. Martell, *J. Phys. Chem.*, **59**, 998 (1955).
11) J. P. Collman, R. A. Moss, H. Martz and C. C. Heindel, *J. Amer. Chem. Soc.*, **83**, 531 (1961).

BULLETIN OF THE CHEMICAL SOCIETY OF JAPAN VOL. 43 1729—1733 (1970)

Macro Chelate Rings. III.*1 Syntheses and Configurations of Complexes of New Ligands, 4,4′-Dimethyl-2,2′-bis(salicylideneaminomethyl)-diphenyl Ether and 4,4′-Dimethyl-2,2′-bis(salicylidene-aminomethyl)diphenylamine

Hisashi Okawa, Hiroyuki Koyama, Takahiko Inazu and Tamotsu Yoshino

Department of Chemistry, Faculty of Science, Kyushu University, Hakozaki, Fukuoka

(Received December 3, 1969)

Two quadridentate chelating agents, 4,4′-dimethyl-2,2′-bis(salicylideneaminomethyl)diphenyl ether and 4,4′-dimethyl-2,2′-bis(salicylideneaminomethyl)diphenylamine, which may form a metal complex with a ten-membered chelate ring, were synthesized by a sequence of steps. The cobalt(II), nickel(II), copper(II), and zinc(II) complexes could be derived from the ligands. Their configurations around the central divalent metal ion were explored on the basis of the absorption in the ligand field in a solution. A tetrahedral configuration for cobalt(II) complexes as well as the zinc(II) complexes, and a pseudo-tetrahedral configuration for the nickel(II) and copper(II) complexes, were concluded.

There have already been reports upon complexes derived from 2,7-dimethyl-4,5-bis(salicylideneaminomethyl)acridone[1] and 2,7-dimethyl-4,5-bis(salicylideneaminomethyl)xanthone,[2] which are sterically-controlled ligands and which form a non-planar metal complex with a ten-membered chelate ring with a divalent metal ion. They are rather favorable for a complex formation in that the two salicylideneaminomethyl groups are oriented in the same direction. If the carbonyl group in the acridone or the xanthone nucleus is eliminated from the ligand in each case, the new ligands thus made, which are 4,4′-dimethyl-2,2′-bis(salicylideneaminomethyl)diphenylamine and 4,4′-dimethyl-2,2′-bis(salicylideneaminomethyl)diphenyl ether (Fig. 1)

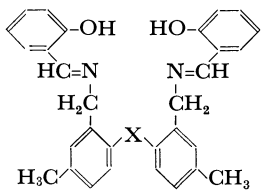

(X = O and NH)

I

Fig. 1. Structures of the ligands.
X=O: 4,4′-Dimethyl-2,2′-bis(salicylideneaminomethyl)diphenyl ether
X=NH: 4,4′-Dimethyl-2,2′-bis(salicylideneaminomethyl)diphenylamine

respectively, may be quite flexible and may form a metal complex different from the complex of the parent ligands. Out of our interest in the configuration of the complex with a macro chelate ring, we attempted to prepare the new chelating agents 4,4′-dimethyl-2,2′-bis(salicylideneaminomethyl)diphenyl ether and 4,4′-dimethyl-2,2′-bis(salicylideneaminomethyl)diphenylamine, shown in Fig. 1. It is, of course, one of the objects of this work to determine if a stable monomeric complex can be made from these ligands.

Experimental

Syntheses of Ligands. The synthetic schemes of the ligands are shown in Fig. 2. All the melting points are uncorrected.

2,2′-Dibromo-4,4′-dimethyldiphenyl Ether (II, X=O). To a solution of 4,4′-dimethyldiphenyl ether (40 g) in chloroform (100 m*l*), bromine (66.2 g) was added in the course of an hour's stirring, while the temperature was maintained at 60°C. The reaction mixture was then poured into water to give a pale-colored mass, which was collected and crystallized from alcohol as colorless prisms with a mp of 79—80°C. The yield was above 80%.

Found: C, 47.28; H, 3.51%. Calcd for $C_{14}H_{12}OBr_2$: C, 47.23; H, 3.68%.

2,2′-Dicyano-4,4′-dimethyldiphenyl Ether (III, X=O). A mixture of 2,2′-dibromo-4,4′-dimethyldiphenyl ether (30 g) and cuprous cyanide (15 g) in *N,N*-dimethylformamide (200 m*l*) was refluxed on an oil bath for six hours. Cuprous cyanide was then dissolved into a solution gradually. The reaction mixture was once filtered when hot and then poured into a hot solution of ferric chloride ($FeCl_3 \cdot 6H_2O$ 50 g, water 200 m*l*) to give a pale-colored mass of the nitrile, which

*1 Part II: Ref. 2.

1) H. Okawa and T. Yoshino, This Bulletin, **42**, 1934 (1969).

2) H. Okawa and T. Yoshino, *ibid.*, **43**, 805 (1970).

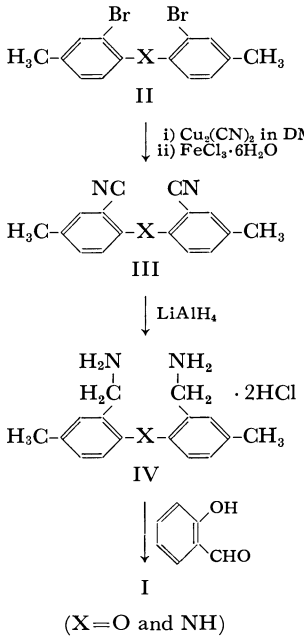

Fig. 2. The synthetic scheme of the ligands.

was collected, washed with water, and crystallized from ethanol as colorless needles with a mp of 131—132°C. The weight of the pure product was 16 g.

Found: C, 77.22; H, 4.77; N, 11.29%. Calcd for $C_{16}H_{12}N_2O$: C, 77.40; H, 4.87; N, 11.28%.

2,2′-Di(aminomethyl)-4,4′-dimethyldiphenyl Ether Dihydrochloride (IV, X=O). 2,2′-Dicyano-4,4′-dimethyldiphenyl ether (2.0 g) was reduced with lithium aluminum hydride (1 g) in tetrahydrofuran (50 m*l*). The mixture was then stirred for 5 hr at the boiling point of the solvent. After the reaction mixture had been decomposed with water (20 m*l*), the pH of the solution was adjusted to 8 and the inorganic substance which separated out was eliminated by filtration. The pale brown, oily substance which remained after the evaporation of the solvent was suspended in ether (150 m*l*), and to it we introduced a dry hydrogen chloride gas to give colorless needles of the diamine dihydrochloride. It was recrystallized from 95% ethanol.

Found: C, 58.31; H, 6.83; N, 8.33%. Calcd for $C_{16}H_{22}N_2OCl_2$: C, 58.26; H, 6.73; N, 8.51%.

4,4′-Dimethyl-2,2′-bis(salicylideneaminomethyl)-diphenyl Ether (I, X=O). 2,2′-Di(aminomethyl)-4,4′-dimethyldiphenyl ether dihydrochloride (0.6 g) and salicylaldehyde (1 g) were dissolved into 50% ethanol (150 m*l*), and then to the solution was added a 10% sodium bicarbonate solution until it was neutralized to give yellow needles; these needles were collected and recrystallized from ethanol as yellow needles with a mp of 92°C.

Found: C, 77.53; H, 6.03; N, 6.14%. Calcd for $C_{30}H_{28}N_2O_3$: C, 77.56; H, 6.08; N, 6.03%.

2, 2′-Dibromo-4, 4′-dimethyldiphenylamine (II, X=NH). To a solution of 4,4′-dimethyldiphenylamine (39.4 g) in chloroform (200 m*l*) we added bromine (35 g) over the course of one hour. After all of the bromine had been added, the stirring was continued for one more hour at the boiling point of chloroform. The reaction mixture was poured into water, and the organic layer was separated, washed with water, and dried over calcium chloride. When the solvent was evaporated, there remained an oily liquid, which soon solidified. It was crystallized from methanol as colorless needles with a mp of 61—63°C. The yield was 76%.

Found: C, 47.22; H, 3.66; N, 3.99%. Calcd for $C_{14}H_{13}NBr_2$: C, 47.36; H, 3.69; N, 3.94%.

2, 2′-Dicyano-4, 4′-dimethyldiphenylamine (III, X=NH). A solution of 2,2′-dibromo-4,4′-dimethyldiphenylamine (35.5 g) and cuprous cyanide (19.0 g) in *N,N*-dimethylformamide (200 m*l*) was heated on an oil bath for five hours. The reaction mixture was once filtered when hot, and then poured into a hot ferric chloride solution ($FeCl_3 \cdot 6H_2O$ 50 g, water 200 m*l*), to give a dark-colored, oily substance which solidified when cooled. It was collected, washed with water, and crystallized from methanol as colorless needles (17 g) with a mp of 151°C.

Found: C, 77.48; H, 5.26; N, 16.78%. Calcd for $C_{16}H_{13}N_3$: C, 77.71; H, 5.30; N, 16.99%.

2,2′-Di(aminomethyl)-4,4′-dimethyldiphenylamine Dihydrochloride (IV, X=NH). To a solution of 2,2′-dicyano-4,4′-dimethyldiphenylamine (2 g) in tetrahydrofuran (50 m*l*), we added powdered lithium aluminum hydride (1 g). After the mixture had then been heated at the boiling point of the solvent for seven hours under stirring, the reaction mixture was decomposed with water and the pH of the solution was adjusted to 8. After any inorganic substances had been eliminated by filtration, the solvent was evaporated. There remained a viscous oily liquid. It was then treated in the same way as 2,2′-di(aminomethyl)-4,4′-dimethyldiphenyl ether, and the reduced product was isolated as dihydrochloride in the solid state. It was recrystallized from 95% ethanol as colorless needles.

Found: C, 55.83; H, 7.35; N, 12.36%. Calcd for $C_{16}H_{23}N_3Cl_2 \cdot H_2O$: C, 55.49; H, 7.28; N, 12.13%.

4,4′-Dimethyl-2,2′-bis(salicylideneaminomethyl)-diphenylamine (I, X=NH). To a solution of 2,2′-di(aminomethyl)-4,4′-dimethyldiphenylamine dihydrochloride (0.6 g) and salicylaldehyde (1 g) in 50% ethanol (150 m*l*), we added a 10% sodium bicarbonate solution until neutralization had been effected. A yellow precipitate which separated was collected and crystallized from ethanol as yellow prisms or needles with a mp of 130—131°C. The yield was quantitative.

Found: C, 77.70; H, 6.32; N, 8.97%. Calcd for $C_{30}H_{29}N_3O_2$: C, 77.73; H, 6.31; N, 9.06%.

Syntheses of Complexes. Cobalt(II), nickel(II), copper(II), and zinc(II) complexes could be made from the ligands. However, we were not successful in preparing palladium(II) and platinum(II) complexes. The methods of synthesizing the complexes were almost all the same; a typical procedure is given below. A slight excess of a metal acetate and a ligand (Schiff base) were treated in warm ethanol. The solution was kept at 60—70°C for about half an hour and then allowed to stand until its temperature went down to room temperature. The product which separated was collected and washed with a small amount of ethanol.

The cobalt(II) complexes are orange prisms, and the nickel(II) and copper(II) complexes were green and black prisms respectively. On the other hand, the zinc(II) complexes were almost colorless prisms. Although the molecular weights of these complexes are not

Table 1. Analyses of complexes*

		Found(%)				Calcd(%)			
		C	H	N	M	C	H	N	M
X=O	M=Co	68.80	4.98	5.57		69.10	5.03	5.37	
X=O	M=Ni	69.19	5.13	5.34		69.13	5.03	5.37	
X=O	M=Cu	67.25	5.07	5.41	12.23	67.35	5.09	5.24	11.87**
X=O	M=Zn	68.20	5.14	5.20		68.26	4.96	5.31	
X=NH	M=Co	69.33	5.39	8.09		69.25	5.23	8.07	
X=NH	M=Ni	69.05	5.42	7.96		69.26	5.23	8.08	
X=NH	M=Cu	68.38	5.17	7.83	11.86	68.62	5.18	8.00	12.10
X=NH	M=Zn	68.34	5.27	7.93		68.38	5.16	7.97	

* See Fig. 1 about X=O and X=NH.
** It contains a half molecule of water.

measured, they are surely monomeric. The results of elementary analyses of these complexes are given in Table 1.

Measurements. The electronic absorption spectra of the complexes in solution were determined with a Hitachi EPS-3T spectrophotometer in the near-infrared and visible regions at room temperature. Wako spectrograde pyridine was used in some measurements. The infrared spectra were measured with a Hitachi EPI-S2 spectophotometer in the region from 4000—650 cm^{-1} on a KBr disk.

Results and Discussion

Infrared Spectra of Complexes. Some main infrared absorption bands of complexes of 4,4′-dimethyl-2,2′-bis(salicylideneaminomethyl)diphenyl ether are given in Table 2. When a complex was formed, a red shift of from 10 to 25 cm^{-1} in the C=N stretching vibration was observed and a new absorption band appeared at 1535 cm^{-1}; this band being constant when the metal was changed. On the other hand, the C–O stretching vibration due to diphenyl ether did not appreciably shift upon complex formation; this demonstrates that the possibility of interaction as well as of bonding between the central metal ion and the oxygen in diphenyl ether can be eliminated and that the ligand acts as a quadridentate chelating agent, forming a metal complex with a ten-membered chelate ring.

Table 2. IR absorption bands of complexes of 4,4′-dimethyl-2,2′-bis(salicylideneaminomethyl)diphenyl ether(cm^{-1})

	C=N	New band	Ar–O–Ar	
Ligand	1635	—	1220	1250
M=Co	1612	1535	1228	1253
Ni	1610	1535	1225	1250
Cu	1620	1535	1225	1255
Zn	1625	1535	1225	1255

Table 3. IR absorption bands of complexes of 4,4′-dimethyl-2,2′-bis(salicylideneaminomethyl)diphenylamine(cm^{-1})

	N-H	C=N	New band	C-N
Ligand	3400	1630	—	1310
M=Co	3325	1612	1535	1317
Ni	3350	1610	1535	1325
Cu	3370	1615	1535	1325
Zn	3325	1620	1535	1320

Data from the infrared absorption spectra of the complexes derived from 4,4′-dimethyl-2,2′-bis(salicylideneaminomethyl)diphenylamine are given in Table 3. By a complex formation, a red shift by 10 to 20 cm^{-1} in the C=N stretching vibration was found and a new absorption band appeared at 1535 cm^{-1}; this band remained constant even when the metal was exchanged. Although the N–H stretching vibration shifted toward a lower wave number, the possibility of a direct interaction or bonding between the metal ion and the nitrogen atom in diphenylamine was also eliminated by the fact that the C–N stretching vibration of diphenylamine did not considerably shift upon complex formation. Thus, it can also be concluded that this compound is a quadridentate ligand which forms a complex with a ten-membered chelate ring.

The Electronic Absorption Spectra and Configurations of Complexes. The electronic absorption spectra of the cobalt(II) complex of 4, 4′-dimethyl-2, 2′-bis (salicylideneaminomethyl) diphenyl ether clearly showed that the configuration of the complex was always tetrahedral in chloroform as well as in pyridine (Fig. 3). As it is well known that a tetrahedral cobalt(II) complex, which is made from *N*-substituted salicylideneimine, changes to an octahedral complex in a donor solvent pyridine,[3] the steric condition of 4,4′-dimethyl-2,2′-

3) H. Nishikawa and S. Yamada, This Bulletin, **37**, 8 (1964); **38**, 1506 (1965); E. Yoshida and S. Yamada, *ibid.*, **40**, 1395 (1967).

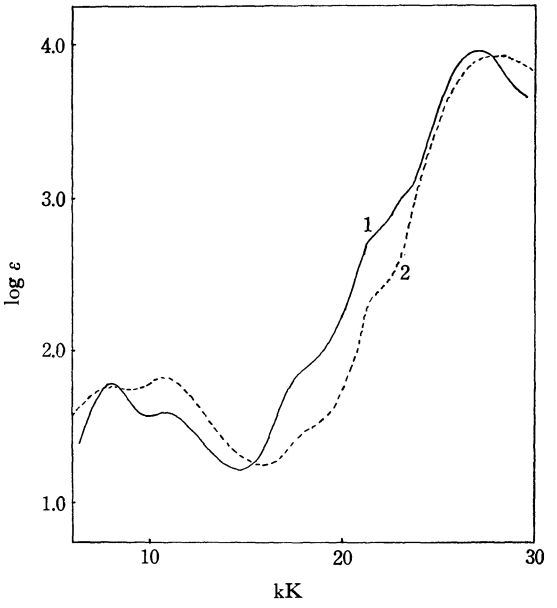

Fig. 3. Electronic absorption spectra of the cobalt(II) complex of 4,4′-dimethyl-2,2′-bis(salicylideneaminomethyl)diphenyl ether in chloroform (1) and pyridine(2).

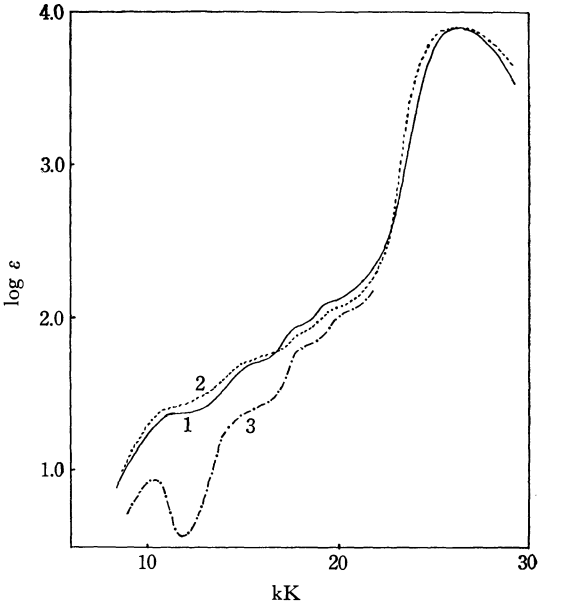

Fig. 4. Electronic absorption spectra of the nickel(II) complexes of 4,4′-dimethyl-2,2′-bis(salicylideneaminomethyl)diphenyl ether (1) and 4,4′-dimethyl-2,2′-bis(salicylideneaminomethyl)diphenylamine (2) in pyridine, and bis(*N*-isopropylsalicylideneiminato)nickel(II) in chloroform (3).

bis(salicylideneaminomethyl)diphenyl ether may be quite unfavorable for an octahedral configuration around the cobalt(II) ion. On the other hand, the cobalt(II) complex of 4,4′-dimethyl-2,2′-bis(salicylideneaminomethyl)diphenylamine was very unstable in solution, and we were unsuccessful in measuring the ligand-field band of the complex. However, it was supposed that the complex also had a tetrahedral structure because of the close resemblance of its infrared spectrum to that of the zinc(II) complex of 4,4′-dimethyl-2,2′-bis(salicylideneaminomethyl)diphenylamine.

The ligand-field bands of the nickel(II) complexes were measured in pyridine. They are given in Fig. 4. The appearance of the d-d transition bands in the region from 10—15 kK precluded a planar configuration around the nickel(II) ion, as it had been well established that a square-planar configurational nickel(II) complex of *N*-substituted salicylideneimine showed two d-d transition bands at 16—18 and 20—24 kK.[4] Although the measurements were done in pyridine, the possibility of an octahedral configuration around the nickel(II) ion could also be rejected; two d-d transition bands, at 9—10 and at 15—17 kK, were found in an octahedral nickel(II) complex of *N*-substituted salicylideneimines.[4,5] Judging from these facts and from the resemblance of the spectra of the nickel(II) complexes to that of a nearly tetrahedral nickel(II) complex bis(*N*-isopropylsalicylideneiminato)nickel(II), in which the angle between the planes containing the coordinating atoms of the chelate group and the nickel(II) atom is 81°,[6] it is quite natural to say that these nickel(II) complexes possess a tetrahedral configuration. The small shift in the ligand-field bands of our complexes from bis(*N*-isopropylsalicylideneiminato)nickel(II) may be caused by a distortion of a configuration around the nickel(II) ion.

The electronic absorption spectra of the copper(II) complexes measured in chloroform are given in Fig. 5. The d-d transition bands of the complexes shifted toward a considerably lower wave number than with a normal square-planar copper(II) complex, which had a d-d transition band at 17.5—17.7 kK. As it has been well established that this shift is caused by the distortion of the configuration around the copper(II) ion from coplanarity,[7] our complexes can be effected to be fairly much distorted. Yamada and Nishikawa[8] measured

4) S. Yamada, A. Takeuchi, K. Yamanouchi and K. Iwasaki, This Bulletin, **42**, 131 (1969).

5) S. Yamada and K. Yamanouchi, *ibid.*, **42**, 2562 (1969).

6) M. R. Fox, E. C. Lingafelter, P. L. Orioli and L. Sacconi, *Nature*, **197**, 1104 (1963).

7) M. Honda and G. Schwarzenbach, *Helv. Chim. Acta*, **40**, 27 (1957); R. L. Belford and T. S. Piper, *Mol. Phys.*, **5**, 251 (1962).

8) S. Yamada and H. Nishikawa, This Bulletin, **36**, 755 (1963).

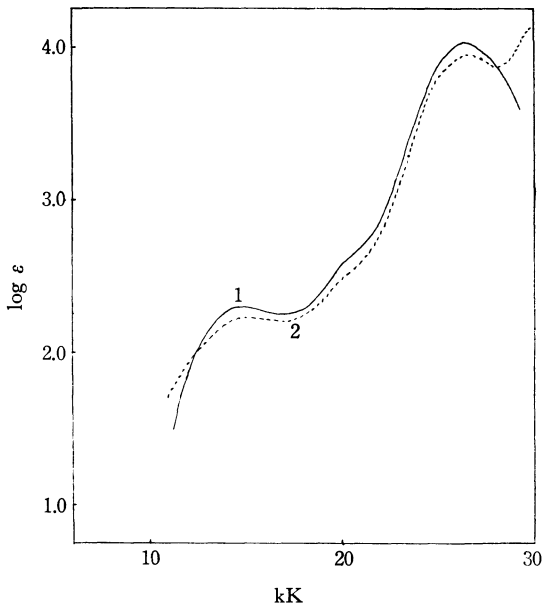

Fig. 5. Electronic absorption spectra of the copper(II) complexes of 4,4′-dimethyl-2,2′-bis(salicylideneaminomethyl)diphenyl ether (1) and 4,4′-dimethyl-2,2′-bis(salicylideneaminomethyl)diphenylamine (2) in chloroform.

the ligand-field bands of copper(II) complexes of *N*-R-substituted salicylideneimines in chloroform and found a band at 13 kK for R=*t*-butyl and one at 15.7 kK for R=isopropyl, *s*-butyl, 1-ethylpropyl or cyclohexyl; They decided that all of these are not planar but tetrahedral. On the other hand, Cheesemann *et al.*[9] studied several copper(II) complexes by X-ray analyses and found that the angle between the planes containing the coordinating atoms in the ligand and the central copper(II) ion in bis(*N*-*t*-butylsalicylideneiminato)copper(II) was only 54°. They also found that the angle in bis(*N*-ethylsalicylideneiminato)copper(II), which had been thought, from its absorption spectrum in solution, to be a planar complex, was unexpectedly, 36°. The drastic red shift in the d-d transition was, thus, caused by the fact that the angle between the planes containing the coordinating atoms and the central copper atom altered by only 18°. As the copper(II) complexes in this work had a ligand-field band at 14.7 kK, they must have an intermediate configuration. Insofar as their spectra are concerned, it is, however, reasonable to interpret the copper(II) complexes as exhibiting a pseudo-tetrahedral configuration.

The zinc(II) complexes must also have a tetrahedral configuration, judging from the steric requirements of the ligands, which inhibit a square-planar configuration, as well as from the tendency for a zinc(II) ion to take a tetrahedral configuration.

9) T. P. Cheesemann, D. Hall and T. N. Waters, *J. Chem. Soc.*, **1966**, 694.

BULLETIN OF THE CHEMICAL SOCIETY OF JAPAN VOL. 43 1733—1736 (1970)

Metal Halide Complexes with Trimethylstibine Sulfide

Takayuki SAITO, Junzo OTERA and Rokuro OKAWARA

Department of Applied Chemistry, Osaka University, Yamadakami, Suita, Osaka

(Received December 23, 1969)

2:1 complexes of trimethylstibine sulfide (TMSS) with zinc(II), cadmium(II), mercury(II) and cobalt(II) halides were prepared. 1:1 complexes were also obtained with cadmium bromide and mercuric iodide. On the basis of infrared spectra, it was found that TMSS coordinates to the metal through the sulfur atom and that $Hg(TMSS)I_2$ has a sulfur-bridged structure. The electronic spectral parameters of the tetrahedral $Co(TMSS)_2X_2$ (X=Cl, Br and I) complexes are quite close to those of trimethyl-phosphine and -arsine sulfide complexes. These results indicate that for Co–S interactions, polarizability of the thioxo ligand is more important than polarity.

In previous papers, we reported the electronic character of the Sb–S bond in tertiary stibine sulfide[1] and the unique behavior of the bond towards organotin halides.[2]

Recently, various metal complexes with tertiary

1) J. Otera and R. Okawara, *J. Organometal. Chem.*, **16**, 335 (1969).

2) M. Shindo, Y. Matsumura and R. Okawara, *ibid.*, **11**, 299 (1968): This Bulletin, **42**, 265 (1969).

phosphine[3-10] and arsine[11-14] sulfide were prepared and their properties were discussed in relation to the nature of the P–S or As–S bond. However, only a few investigations have been reported[2,8] on the metal complexes of tertiary stibine sulfide.

In the present paper, we describe the preparation and properties of the complexes of zinc(II), cadmium(II), mercury(II) and cobalt(II) halides with trimethylstibine sulfide (TMSS).

Experimental

Preparation of the Complexes. *Zinc and Cadmium Complexes.* These complexes were obtained by mixing the methanol solutions of the ligand and metal halides in stoichiometric ratios, followed by evaporation of the solvent. The complexes obtained were washed with methanol and dichloromethane. In the treatment of the ligand with cadmium bromide, the 1 : 1 complex was precipitated from the solution (yield 38%) and the 2 : 1 complex was obtained from the filtrate after evaporating the solvent under reduced pressure (yield 60%). When a large excess of the ligand was employed, only the 2 : 1 complex was obtained in a good yield.

$Hg(TMSS)_2Br_2$. On adding methanol solution of the ligand to mercuric bromide in methanol, yellow powder precipitated, which soon decomposed after separation from the solvent and could not be confirmed. From the filtrate the 2 : 1 complex was obtained. This complex decomposes slowly by heating and on exposure to light.

$Hg(TMSS)I_2$ and $Hg(TMSS)_2I_2$. To a suspension of mercuric iodide in methanol was added a slight excess of the ligand. The color of mercuric iodide gradually changed to pale yellow. Washing the obtained powder with dichloromethane gave the 1 : 1 complex. When a large excess of the ligand and mercuric iodide in chloroform were stirred until the color of mercuric iodide disappeared, white precipitates of the 2:1 complex were obtained.

$Co(TMSS)_2X_2$. The methanol solutions of trimethylstibine sulfide and cobalt halides were combined in 2:1 molar ratio. Evaporation of methanol under reduced pressure and washing the resulting precipitates with methanol and dichloromethane gave the corresponding complexes. The chloride complex, however was contaminated with a small amount of black precipitates which seemed to be CoS. The precipitates obtained by evaporating methanol were therefore quickly recrystallized from a large amount of dichloromethane-

Table 1. Analytical data and molar conductivities of trimethylstibine sulfide complexes

Compound	C% Found	C% Calcd	H% Found	H% Calcd	Λ_M cm²/ohm·mol
$Zn(TMSS)_2X_2$					
X=Cl	13.45	13.49	3.25	3.39	14.8[a]
Br	11.24	11.56	2.70	2.91	8.6[a]
I	10.37	10.04	2.55	2.53	16.5[a]
$Cd(TMSS)_2X_2$					
X=Cl	12.82	12.40	2.98	3.12	10.2[a]
Br	10.70	10.75	2.78	2.70	8.3[a]
I	8.83	9.43	2.25	2.37	[b]
$Hg(TMSS)_2X_2$					
X=Br	9.77	9.50	2.49	2.39	[b]
I	8.79	8.45	2.15	2.11	[b]
$Co(TMSS)_2X_2$					
X=Cl	13.58	13.66	3.54	3.44	<1[c]
Br	11.39	11.69	2.95	2.94	<1[c]
I	10.45	10.14	2.67	2.55	1.3[c]
$Cd(TMSS)Br_2$	7.55	7.64	2.01	1.92	22.2[d]
$Hg(TMSS)I_2$	5.78	5.51	1.50	1.30	[b]

a) 10^{-3} mol/*l* in acetonitrile. b) Not sufficiently soluble for measurement. c) 3×10^{-3} mol/*l* in dichloromethane. d) 10^{-4} mol/*l* in acetonitrile.

3) E. Bannister and F. A. Cotton, *J. Chem. Soc.*, **1960**, 1959.
4) H. Teichmann, *Angew. Chem.*, **77**, 809 (1965).
5) D. W. Meek and P. Nicpon, *J. Amer. Chem. Soc.*, **87**, 4951 (1965).
6) A. L. Allred and R. A. Potts, *J. Inorg. Nucl. Chem.*, **28**, 1479 (1966).
7) J. A. W. Dalziel, A. F. leC. Holding and B. E. Watts, *J. Chem. Soc., A*, **1967**, 358.
8) M.G. King and G.P. McQuillan, *ibid.*, **1967**, 898.
9) A. M. Brodie, S. H. Hunter, G. A. Rodley and C. J. Wilkins, *ibid.*, **1968**, 2039.
10) W. E. Slinkard and D. W. Meek, *Inorg. Chem.*, **8**, 1811 (1969).
11) A. Merijanian and R. Zingaro, *ibid.*, **5**, 187 (1966).
12) P. Nicpon and D. W. Meek, *Chem. Commun.*, **1966**, 389.
13) A. M. Brodie, S. H. Hunter, G. A. Rodley and C. J. Wilkins, *J. Chem. Soc., A*, **1968**, 987.
14) A. M. Brodie, J. E. Douglas and C. J. Wilkins, *ibid.*, **1969**, 1931.

methanol. The complexes decompose slowly in air in the solid state, and a little more rapidly in solution.

Sulfur-halogen Exchange Reaction. Trimethylstibine sulfide in methanol was added to an equimolar amount of mercuric chloride in the same solvent at room temperature. Black powder of mercuric sulfide was filtered off, and the filtrate gave trimethylantimony dichloride almost quantitatively. When trimethylstibine sulfide and mercuric bromide were mixed in hot methanol, a similar exchange reaction occurred, yielding trimethylantimony dibromide.

Analytical data of these complexes, together with their molar conductivities, are summarized in Table 1.

Physical Measurements. The infrared spectra in Nujol mulls were recorded with a Hitachi EPI-L grating spectrophotometer. Measurements of the electronic spectra were carried out by a Hitachi EPS-3 spectrophotometer. Molar conductivities were measured using a Yokogawa Universal Bridge (Bv-Z 13 C).

Results and Discussion

As shown in Table 1, trimethylstibine sulfide usually forms 2 : 1 complexes with the metal halides employed and also 1 : 1 complexes with cadmium bromide and mercuric iodide. No complex*1 can be obtained with mercuric chloride. However, sulfur-halogen exchange reaction (1) takes place, similar to that reported[2] for some organotin halides.

$$(CH_3)_3SbS + HgCl_2 \longrightarrow (CH_3)_3SbCl_2 + HgS \quad (1)$$

The infrared frequency of the ν(Sb–S) band in all the complexes, as listed in Table 2, shifts to a lower frequency by 25—55 cm^{-1} from that of the free ligand, indicating coordination through the sulfur atom. These ν(Sb–S) frequencies are comparable with, or a little higher than those (357—381 cm^{-1}) in trimethylantimony halide thiocarboxylates.[15] Thus, the Sb–S bond in the complexes seems to exist almost in the form of the semipolar structure, [I], although slight $d\pi$-$p\pi$ bonding might still remain in this bond.

Table 2. Relevant infrared frequencies (cm^{-1}) of trimethylstibine sulfide complexes
(Nujol mulls)

Compound	ν(Sb–S)	ν(M–S)	ν(M–X)
TMSS	433		
$Zn(TMSS)_2Cl_2$	403	280	300
$Zn(TMSS)_2Br_2$	403	278	210
$Zn(TMSS)_2I_2$	408	277	
$Cd(TMSS)_2Cl_2$	406	254	262
$Cd(TMSS)_2Br_2$	403	257	
$Cd(TMSS)_2I_2$	406,385	255	
$Hg(TMSS)_2Br_2$	397	250	
$Hg(TMSS)_2I_2$	406		
$Co(TMSS)_2Cl_2$	402	303,282	313
$Co(TMSS)_2Br_2$	399	295,280	236
$Co(TMSS)_2I_2$	404	305,280	
$Cd(TMSS)Br_2$	397	214	
$Hg(TMSS)I_2$	387,383		

$$[(CH_3)_3\overset{+}{S}b\text{–}\overset{-}{S}]_2\cdot MX_2$$
[I]

The molar conductivities (Table 1) suggest weak dissociation of the halide anion in the zinc and cadmium complexes in acetonitrile. However, both ν(M–S) and ν(M–Cl) (or ν(M–Br)) bands can be observed in some of their infrared spectra in Nujol mulls so that the complexes appear to have a non-ionic tetrahedral structure in the solid state.

The 1 : 1 complex, $Cd(TMSS)Br_2$, is less soluble than the corresponding 2 : 1 complex, $Cd(TMSS)_2Br_2$. The molar conductivity (22.2 cm^2/ohm·mol) seems to be too small to assume the ionic structure, $[Cd(TMSS)Br]^+Br^-$. The associated structure may be presumed in the solid state for the tetrahedral arrangement around the cadmium atom, but the present data are not sufficient to give a more detailed structure. The 1 : 1 complex, $Hg(TMSS)I_2$, shows the marked lower shift of the ν(Sb–S) frequency as compared with the 2 : 1 complex, $Hg(TMSS)_2I_2$. This is interpreted as suggesting that the sulfur-bridged structure [II] or [III] is more probable than the halogen-bridged structure. The latter

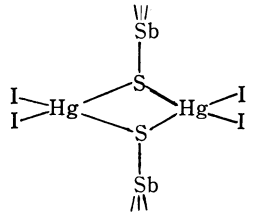

(II)

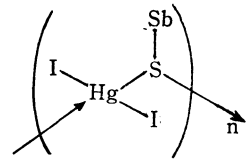

(III)

structure is suggested for the 1 : 1 complex of mercuric bromide with tris(dimethylamino)phosphine sulfide on the basis of the infrared spectrum.[10]

From the low molar conductivities as given in Table 1, ionic formulations are ruled out for the cobalt complexes in dichloromethane. In accordance with these results, the electronic spectra of the complexes (Table 3) give two structured bands characteristic of tetrahedral coordination (ν_3, $^4A_2$–$^4T_1$(P) and ν_2, $^4A_2$–$^4T_1$(F)). As presented in Table 4, the ligand field splitting energies, Δ, and the β values calculated from the above data fall in quite

*1 It has been reported[5,7] that with mercuric chloride, trimethyl- and triphenyl-phosphine sulfide give 2 : 1 and 1 : 1 complexes, respectively.

15) J. Otera and R. Okawara, *J. Organometal. Chem.*, **17**, 353 (1969).

16) F. A. Cotton and M. Goodgame, *J. Amer. Chem. Soc.*, **83**, 1777 (1961).

Table 3. Electronic spectral date for the cobalt complexes[a] (cm^{-1})

Compound	ν_3	ν_2
$Co(TMSS)_2Cl_2$	15870(475)[b]	6760(95)
	14710(519)	5950(30)
	13420(400)	5200(122)
$Co(TMSS)_2Br_2$	15150(492)	6560(95)
	14080(539)	5860(47)
	13160(522)	5000(125)
$Co(TMSS)_2I_2$	14490(570)	6250(126)
	13510(733)	5530(37)
	12500(701)	4830(126)

a) $2—3\times10^{-3}$ mol/l in dichloromethane
b) Molar extinction coefficients given in parentheses.

close values to those obtained for trimethyl-phosphine and -arsine sulfide complexes. In the series of these three ligands, the basicity of the sulfur atom is likely to increase from phosphorus to antimony, because the size difference between the central atom and the sulfur atom becomes larger and the extent of $d\pi$-$p\pi$ bonding should decrease in this order. The close similarity of the electronic spectral parameters of the cobalt complexes indicates that the interaction of the cobalt atom with ligand is not affected by polarity of the ligand. It is apparent from the low β values that a considerably large covalency is implied in the Co–S bond. Thus, polarizability (or covalent-bonding character) of the ligand seems to have a primary effect on Co–S interactions. This is consistent with the results reported for the relations between the trimethylphosphine and -arsine sulfide complexes.[9]

Table 4. Electronic spectral parameters of the cobalt complexes

Compound	ν_3[c] (cm^{-1})	ν_2[c] (cm^{-1})	Δ[d] (cm^{-1})	β[e]	References
$Co(TMSS)_2Cl_2$	14740	5890	3400	0.72	f
$Co(TMPS)_2Cl_2$[a]	14990	5810	3340	0.74	g
$Co(TMAS)_2Cl_2$[b]	14920	5900	3390	0.73	h
$Co(TMSS)_2Br_2$	14110	5710	3300	0.69	f
$Co(TMPS)_2Br_2$	14540	5700	3280	0.72	g
$Co(TMAS)_2Br_2$	14580	5750	3310	0.72	h
$Co(TMSS)_2I_2$	13440	5540	3200	0.65	f
$Co(TMPS)_2I_2$	13710	5650	3260	0.66	g
$Co(TMAS)_2I_2$	13760	5770	3340	0.66	h

a) TMPS; trimethylphosphine sulfide.
b) TMAS; trimethylarsine sulfide.
c) Evaluated from the center of gravity of the intensities.
d) Calculated according to Ref. 16; Values are ±100 cm^{-1}.
e) β=B(complex)/967 (free ion).
f) This work.
g) See Ref. 9.
h) See Ref. 13.

The authors wish to thank Dr. Y. Kawasaki for his helpful discussions.

BULLETIN OF THE CHEMICAL SOCIETY OF JAPAN VOL. 43 1737—1743 (1970)

Preparation and Circular Dichroism of *trans*(*N*) and *cis*(*N*) Isomers of (L- or D-Alaninate-*N,N*-diacetato) (amino-acidato)-cobaltate(III) Complexes

Norio KOINE,* Naokazu SAKOTA,* Jinsai HIDAKA** and Yoichi SHIMURA**

* *Department of Industrial Chemistry, Faculty of Engineering, Ehime University, Bunkyo-cho, Matsuyama*

** *Department of Chemistry, Faculty of Science, Osaka University, Toyonaka, Osaka*

(Received January 8, 1970)

Eight new complexes, *trans*(*N*) or *cis*(*N*) isomers of (L- or D-alaninate-*N,N*-diacetato) (amino-acidato)cobaltate(III) ions, have been synthesized as their potassium salts, where the amino acids are glycine, L-alanine and L-proline. Stereoselective formation of a limited number of the isomers with respect to the geometrical arrangement of the coordinated nitrogen and oxygen atoms and with respect to the position of the chelate ring containing the methyl group of the coodinated alaninate-*N,N*-diacetate ion, were confirmd from the results of the studies by ion-exchange column chromatography, proton magnetic resonance and circular dichroism spectra. The additivity of vicinal circular dichroism contributions from the two different optically active ligands in a complex has been discussed for the complexes without the configurational chirality.

There have been many studies[1,2] concerning the so-called vicinal contribution to circular dichroism (CD) spectra of Co(III) complexes containing optically active ligands; in most of these complexes,[1] however, the "vicinal" effect is combined with the "configurational" CD contribution due to a chiral configuration around the central Co(III) ion. Therefore, it was inevitable to separate the two kinds of contribution from each other on the CD curves. In a previous paper,[3] we reported the CD spectra of *trans*(*N*)- and *cis*(*N*)-(ammoniatriacetato)(L-amino-acidato)cobaltate(III) ions, [Co(ata)(L-am)]$^-$, in which the configuration around the central Co(III) ion is not chiral, and the coordinated chelate ligand has a chiral configuration. In the present paper,*1 the preparation and the CD curves of *trans*(*N*)- and *cis*(*N*)-(L- or D-alaninate-*N,N*-diacetato) (L-amino-acidato) cobaltate(III), [Co(L- or D-alada)(L-am)]$^-$, will be reported. These have no chiral configuration around the central Co(III) ion in a first approximation but have two kinds of optically active ligand in their coordination sphere, the one being bidentate and the other quadridentate. The electronic absorption spectra, CD and PMR spectra of these complexes will be discussed mainly in relation to their geometrical structures.

Experimental

Preparation of L- or D-Alanine-*N,N*-diacetic Acid. To a solution of 8.9 g of L- or D-alanine in 25 m*l* of 4N lithium hydroxide, a solution of 20.8 g of monochloroacetic acid in 30 m*l* of 4N lithium hydroxide and 80 m*l* of 4N lithium hydroxide were added simultaneously over a period of about 2 hr with vigorous stirring at 70°C, the pH of the reaction mixture being adjusted in a range of 9—10 all over the reaction time. At the end of the reaction, the mixture was heated at 90°C for about 10 min. After the reaction mixture had been cooled to room temperature, 25 m*l* of concentrated hydrochloric acid was added to it. The solution was concentrated as far as possible in a vacuum evaporator. When about 300 m*l* of absolute ethanol was added to the residue, insoluble crystals separated out, which were collected by filtration and then washed well warm ethanol. The white crystals were lithium salt of the desired acid, which was contaminated with a small amount of lithium chloride. It was recrystallized from 35 m*l* of 2N hydrochloric acid and then from 50 m*l* of 0.2N hydrochloric acid. The yield was approximately 10 g. L-aladaH$_3$: mp 199—200°C (decomp.), $[\alpha]_D^{25}$ −41.5° (*c* 4.0, water).

Found: C, 40.66; H, 5.42; N, 6.71%. Calcd for $C_7H_{11}O_6N$: C, 40.97; H, 5.41; N, 6.83%. D-aladaH$_3$:

1) C. T. Liu and B. E. Douglas, *Inorg. Chem.*, **3**, 1356 (1964); B. E. Douglas and S. Yamada, *ibid.*, **4**, 1561 (1965); S. K. Hall and B. E. Douglas, *ibid.*, **8**, 372 (1969); K. Yamasaki, J. Hidaka and Y. Shimura, This Bulletin, **42**, 119 (1969); N. Matsuoka, J. Hidaka and Y. Shimura, *Inorg. Chem.*, **9**, 719 (1970).

2) T. Yasui, J. Hidaka and Y. Shimura, This Bulletin, **39**, 2417 (1966); T. Yasui, J. Fujita and Y. Shimura, *ibid.*, **42**, 2081 (1969).

3) N. Koine, N. Sakota, J. Hidaka and Y. Shimura, *ibid.*, **42**, 1583 (1969).

*1 The following abbreviations are used for the ligands: "gly" for glycinate ion, "L-ala" L-alaninate, "L-pro" L-prolinate, "ata" ammoniatriacetate and "L- or D-alada" L- or D-alaninate-*N,N*-diacetate ion.

TABLE 1. ANALYTICAL RESULTS (amounts in %)

Complex	C		H		N	
	Found	Calcd	Found	Calcd	Found	Calcd
trans(*N*)-K[Co(L-alada)(gly)]·H_2O	27.76	27.55	3.50	3.60	7.06	7.14
trans(*N*)-K[Co(L-alada)(L-ala)]·$2H_2O$	28.52	28.30	4.24	4.28	6.91	6.60
trans(*N*)-K[Co(D-alada)(L-ala)]·$2H_2O$	28.00	28.30	4.50	4.28	6.84	6.60
trans(*N*)-K[Co(L-alada)(L-pro)]·H_2O	33.30	33.33	4.37	4.20	6.29	6.48
trans(*N*)-K[Co(D-alada)(L-pro)]·$2H_2O$	31.89	32.00	4.63	4.49	6.08	6.22
cis(*N*)-K[Co(L-alada)(gly)]·$3H_2O$	25.12	25.24	4.23	4.24	6.48	6.54
cis(*N*)-K[Co(L-alada)(L-ala)]·$3H_2O$	27.34	27.15	4.55	4.57	6.37	6.33
cis(*N*)-K[Co(D-alada)(L-ala)]·$3H_2O$	27.60	27.15	4.48	4.57	6.34	6.33

mp 198—199°C (decomp.), $[\alpha]_D^{25}$ +41.4° (*c* 4.0, water). Found: C, 40.53; H, 5.42; N, 6.74%.

Preparation and Separation of Potassium (L- or D-Alaninate-*N*,*N*-diacetato)(amino-acidato)-cobaltate(III). *1) Trans(N)- and cis(N)-K[Co(L-alada)(gly)].* A solution of 7.5 g of cobalt(II) acetate tetrahydrate in 20 m*l* of water was added to a solution containing 6.2 g of L-aladaH$_3$ in 15 m*l* of 2N potassium hydroxide. To this solution was added gradually 4.0 g of lead dioxide and the mixture was warmed at 60°C on a water bath for about 40 min. After the mixture had been filtered, 2.3 g of glycine was dissolved in the blue-violet filtrate. When the solution was concentrated almost to dryness at 60°C on a water bath, the color of the reaction mixture changed from blue-violet to red-violet. To the residue was added a saturated aqueous solution of 2.6 g of potassium sulfate in order to eliminate the lead ion. The precipitate was filtered off. The filtrate was evaporated in a vacuum evaporator to a fourth of its original volume. When about 30 m*l* of methanol was added to the concentrated solution, the crude *trans*(*N*) isomer crystallized out. After cooling in an ice bath, the crude product was filtered out and recrystallized from water-methanol (1 : 2) mixture. This isomer was confirmed to be pure *trans*(*N*) isomer by ion-exchange column chromatography.[3] To the filtrate was added a large amount of ethanol and ether. The precipitated crude *cis*(*N*) isomer was filtered off and purified by ion-exchange column chromatographic method.[3] Recrystallization was achieved from water-methanol (1 : 1).

2) Trans(N)- and cis(N)-K[Co(L- or D-alada)(L-ala)]. The L-alada complexes were prepared and separated by a similar procedure to that of the corresponding glycinato complexes, using L-alanine instead of glycine. The D-alada complexes were prepared by the same way as that of L-alada complexes, using D-alada instead of L-alada.

In preparation 1) and 2), the *trans*(*N*) isomer can be also easily separated and purified from the original reaction mixture by ion-exchange column chromatography as in preparation 3) of L-prolinato complex.

3) Trans(N)-K[Co(L-alada)(L-pro)]·H_2O. To a solution containing 8.2 g of L-aladaH$_3$ in 20 m*l* of 2N potassium hydroxide was added a solution of 10.0 g of cobalt(II) acetate tetrahydrate in 30 m*l* of water. To the solution 5.3 g of lead dioxide was gradually added and the resulting mixture was warmed at 60°C on a water bath for 40 min. After the insoluble materials had been filtered off, 4.6 g of L-proline was dissolved in the filtrate and the solution was added to a saturated aqueous solution containing 3.5 g of potassium sulfate and the resulting precipitate was filtered off. A large amount of ethanol and ether was added to the filtrate. The crude product precipitated was purified by ion-exchange column chromatographic method.[3] The complex was recrystallized from water-methanol (1 : 5). The column chromatographic investigation indicated that no *cis*(*N*) isomer arose in this preparation.

4) Trans(N)-K[Co(D-alada)(L-pro)]·$2H_2O$. This complex was prepared and separated in a similar way to that of L-alada complex, using D-alada instead of L-alada. The *cis*(*N*) isomer was not formed in this preparation. Recrystallization was achieved from methanol containing a small amount of water.

In the preparation of each isomer, the solid complex finally isolated was more than 80% of the isomer separated by column chromatography.

The results of the chemical analysis for the complexes obtained are shown in Table 1.

Measurements. The electronic absorption spectra of the complexes were measured with a Shimadzu QV-50 spectrophotometer. The CD spectra were recorded with a Rousel-Jouan dichrograph. All the measurements were made in aqueous solution at room temperature.

The proton magnetic resonance (PMR) spectra of the complexes were recorded with a Japan Electron Optics JNM-4H-100 spectrometer operating at 100 MHz, in D_2O solutions. The spectra for the *trans*(*N*) complexes were measured after adding a few drops of 20% DCl to the D_2O solution to avoid the overlap of the signals of the complex and of HOD. No significant variation of the general pattern on the spectra was observed by the addition of the acid. Measurements were carried out using *t*-butanol as an internal standard. All the signals lie at a lower field than that of the standard. The chemical shifts are referred to NaTMS (sodium trimethylsilylpropanesulfonate) as zero; *t*-butanol resonates at 1.234 ppm downfield of NaTMS.

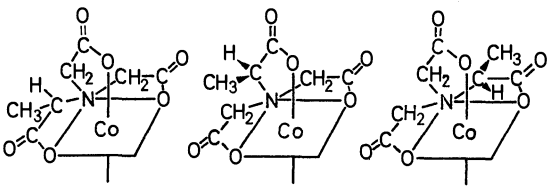

Fig. 1. Three geometrical isomers with respect to the methyl group of the coordinated L-alada.

Results and Discussion

Stereoselectivity. Complete stereoselective formation of the *trans*(*N*) isomer was observed in the preparation of (L- or D-alanine-*N*,*N*-diacetato)(L-prolinato)cobaltate(III) ion as in the case of (ammoniatriacetato)(L-prolinato)cobaltate(III) ion.[3] On the column chromatographic investigation of the reacted solutions, it was confirmed that for all of the present complexes the *trans*(*N*) isomers are dominantly formed in comparison with the corresponding *cis*(*N*) ones. This fact coincides with the results of the corresponding ata complexes.[3]

In the case of L- or D-alada complexes, three geometrical isomers due to the difference in the position of the chelate ring containing a methyl group are possible for each of the *trans*(*N*) and *cis*(*N*) isomer as shown in Fig. 1. It is reasonable to expect that these isomers concerning the methyl group are separable by ion-exchange column chromatographic method. For each of the present complexes, however, all the fractions by solubility difference or by ion-exchange chromatography showed a constant CD spectrum. All the *trans*(*N*) and *cis*(*N*) isomers were obtained in good isolation yields (more than 80% of the yields estimated by absorbance measurements). These results suggest that each of the complexes obtained is not a mixture of the isomers concerning the methyl group but only one type of isomer, and that the present complexes were stereoselectively formed. This consideration is strongly supported from the results of PMR and CD spectra of the complexes.

Proton Magnetic Resonance Spectra. It can

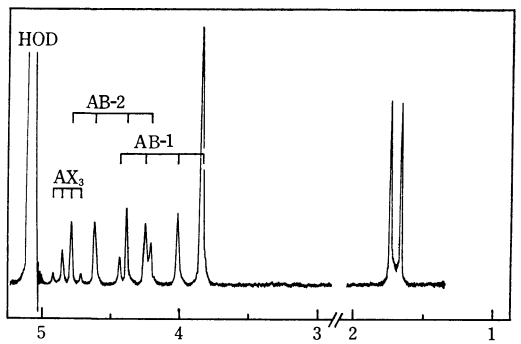

Fig. 2. PMR spectrum of *trans*(*N*)-K[Co(L-alada)-(gly)]·H_2O in acid D_2O solution.

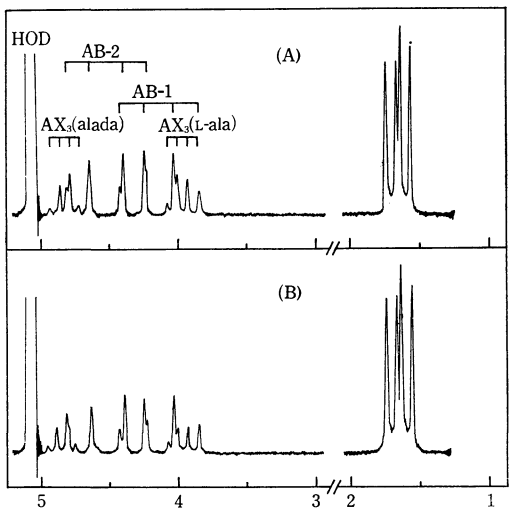

Fig. 3. PMR spectra of (A) *trans*(*N*)-K[Co(L-alada)-(L-ala)]·$2H_2O$ and (B) *trans*(*N*)-K[Co(D-alada)-(L-ala)]·$2H_2O$ in acid D_2O solution.

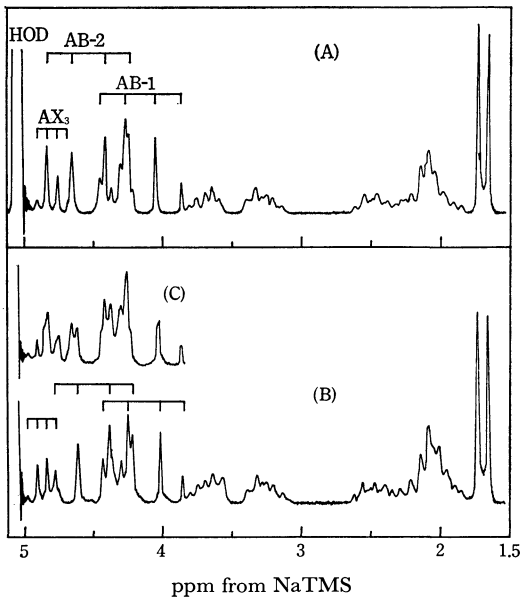

Fig. 4. PMR spectra of (A) *trans*(*N*)-K[Co(L-alada)-(L-pro)]·H_2O, (B) *trans*(*N*)-K[Co(D-alada)(L-pro)]·$2H_2O$ and (C) *trans*(*N*)-K[Co(DL-alada)(L-pro)]*2 in acid D_2O solution.

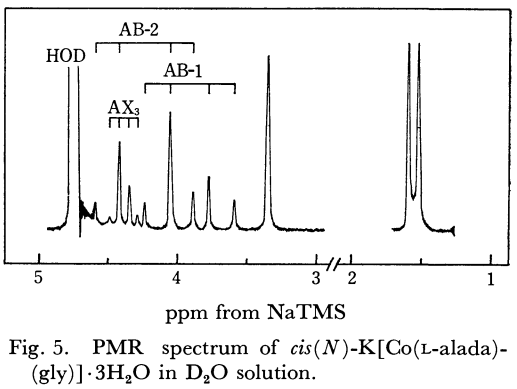

Fig. 5. PMR spectrum of *cis*(*N*)-K[Co(L-alada)-(gly)]·$3H_2O$ in D_2O solution.

*2 This complex was prepared by mixing equivalent amounts of (L-alada)- and (D-alada)-complexes.

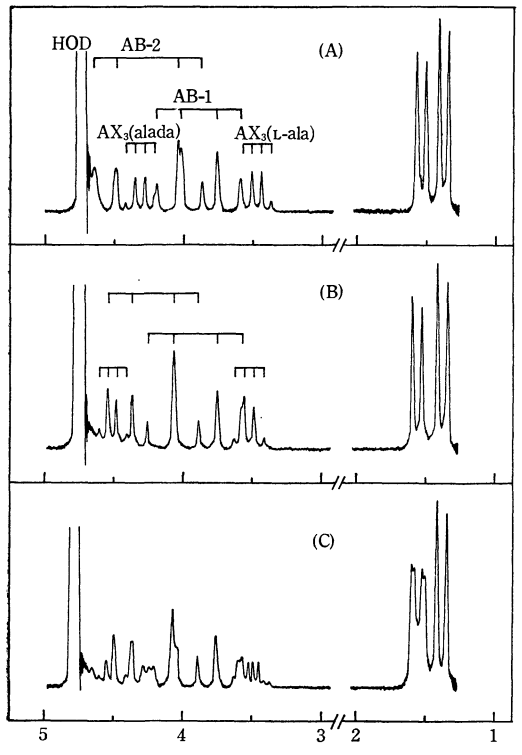

Fig. 6 PMR spectra of (A) *cis*(*N*)-K[Co(L-alada)(L-ala)]·$3H_2O$, (B) *cis*(*N*)-K[Co(D-alada)(L-ala)]·$3H_2O$ and (C) *cis*(*N*)-K[Co(DL-alada)(L-ala)]*[2] in D_2O solution.

be expected that the three geometrical isomers concerning the methyl group show a difference in their PMR spectra due to the protons of the coordinated alada or amino acid.

The PMR spectra of the complexes are shown in Figs. 2—6 and the assignments of the signals are summarized in Tables 2 and 3 with the coupling constants. For all the complexes, the signals for the protons of the alada consist of one AX_3 pattern due to the $>CH-CH_3$ and two AB pattern (AB-1 and AB-2) of equal intensities due to the two $-CH_2-$ groups. The molecular model indicates that the two $-CH_2-$ groups of the alada are in different environments; furthermore, the geminate protons in each the group are also in different environments. The appearance of two AB patterns due to the protons of L-alada coincides well with this topological consideration. This result indicates that the complexes obtained here are just one of the three isomers concerning the methyl group of alada.

The spectra of the alada complexes with L-alaninate exhibit another AX_3 pattern due to the metal-L-alaninate ring protons; the doublet and the quartet are at a fairly higher field than that of the protons of alada (Tables 2 and 3). This is justified by the chemical shifts of the corresponding ata complexes. Namely, the chemical shifts of the signals assigned to AX_3 pattern of L-alaninate protons in *trans*(*N*)-[Co(L- or D-alada)(L-ala)]$^-$ ion are quite similar to those (1.59 ppm for the doublet and 3.90 ppm for the quartet) of L-alaninate protons in *trans*(*N*)-[Co(ata)(L-ala)]$^-$ ion.*[3]

The complexes with L-prolinato ligand show very complicated spectra because of the many spin-spin couplings between the protons in pyrrolidine ring. Judging from the integrations and chemical shifts, however, it is possible to point out that the multiple signals at the region from 1.83—2.73 ppm are assigned to four ethylenic protons ($-CH_2CH_2-$) which are not adjacent to nitrogen atom and the

TABLE 2. PMR SPECTRAL DATA OF *trans*(*N*)-K[Co(L- or D-alada)(am)] COMPLEXES IN ACID D_2O SOLUTION

Assignment	Chemical shifts(ppm from NaTMS) (L-alada)-(gly)	(L-alada)-(L-ala)	(D-alada)-(L-ala)	(L-alada)-(L-pro)	(D-alada)-(L-pro)	Coupling constant(Hz)*
gly, $-CH_2-$	3.83					
L-ala, $-CH_3$ (AX_3)		1.60	1.60			7
$>CH-$		3.96	3.96			
alada, $-CH_3$ (AX_3)	1.69	1.70	1.70	1.70	1.70	7
$>CH-$	4.81	4.82	4.86	4.80	4.87	
$-CH_2-$(AB-1)	3.94	3.95	3.96	3.97	3.96	18
	4.32	4.31	4.32	4.34	4.32	
$-CH_2-$(AB-2)	4.31	4.34	4.33	4.34	4.32	16
	4.68	4.71	4.72	4.73	4.68	

* The values are common for all of the complexes.

*[3] Only one AB pattern and one singlet for the protons of the coordinated ata was observed in the spectrum of *trans*(*N*)-[Co(ata)(L-ala)]$^-$ ion.[3] From more detailed measurements, however, it was confirmed that the AB pattern splits into two as expected theoretically. Thus the two signals at the lower field in the AB quartet are somewhat broad, while each one at the higher field splits further into two signals of equal intensities separated by 1.0 Hz.

TABLE 3. PMR SPECTRAL DATA OF *cis*(*N*)-K[Co(L- or D-alada)(am)] COMPLEXES IN D_2O SOLUTION

Assignment	Chemical shifts (ppm from NaTMS) (L-alada)-(gly)	(L-alada)-(L-ala)	(D-alada)-(L-ala)	Coupling constant (Hz)*
gly, $-CH_2-$	3.35			
L-ala, $-CH_3$ (AX_3)		1.37	1.38	7
>CH–		3.68	3.52	
alada, $-CH_3$ (AX_3)	1.56	1.54	1.56	7
>CH–	4.38	4.31	4.51	
$-CH_2-$(AB-1)	3.70	3.69	3.68	18
	4.12	4.09	4.14	
$-CH_2-$(AB-2)	3.97	3.96	3.99	17
	4.49	4.56	4.44	

* The values are common for all of the complexes.

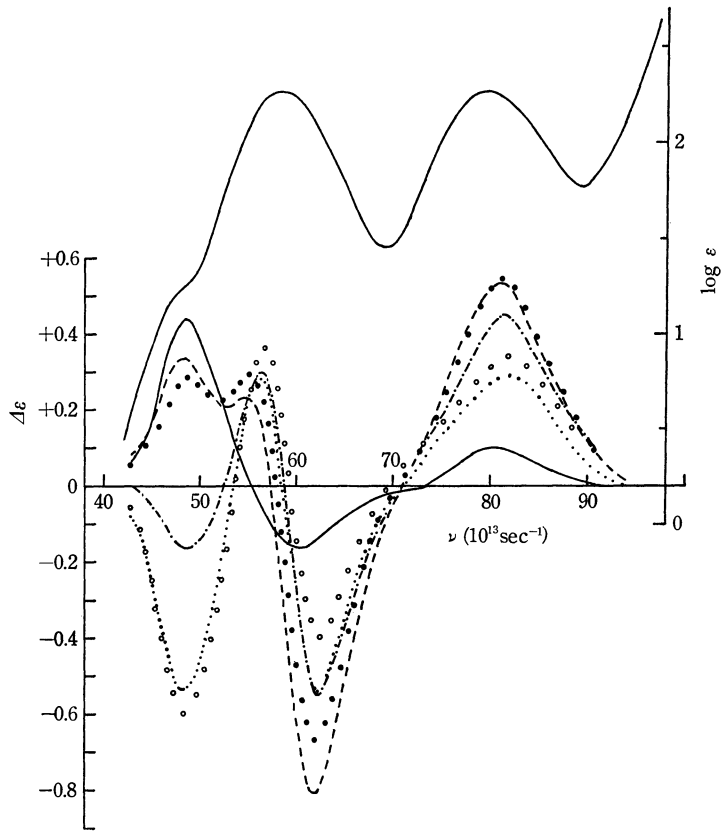

Fig. 7. Absorption and CD curves of *trans*(*N*)-[$Co(O)_4(N)_2$] type complexes.
Absorption curve: ——, [Co(L-alada)(L-pro)]⁻, CD curves: (1) –·–·–, [Co(ata)(L-pro)]⁻; (2) ——, [Co(L-alada)(gly)]⁻; (3) – – –, [Co(L-alada)(L-pro)]⁻; (4) ····, [Co(D-alada)(L-pro)]⁻; (5) ••••, calculated curve, (1)+(2); (6) ○○○○, calculated curve, (1)−(2).

TABLE 4. ABSORPTION MAXIMA OF [Co(L- or D-alada)(am)]$^-$ IONS

Complex ion	I Band		II Band	
	ν max	(log εmax)	ν max	(log εmax)
trans(*N*)-[Co(L-alada)(gly)]$^-$	*ca.* 48	(1.3)	80.2	(2.23)
	58.9	(2.26)		
trans(*N*)-[Co(L-alada)(L-ala)]$^-$	*ca.* 48	(1.3)	80.2	(2.23)
	58.9	(2.27)		
trans(*N*)-[Co(D-alada)(L-ala)]$^-$	*ca.* 48	(1.3)	80.2	(2.23)
	58.9	(2.27)		
trans(*N*)-[Co(L-alada)(L-pro)]$^-$	*ca.* 48	(1.2)	80.0	(2.26)
	58.6	(2.26)		
trans(*N*)-[Co(D-alada)(D-pro)]$^-$	*ca.* 48	(1.3)	80.0	(2.25)
	58.6	(2.25)		
cis(*N*)-[Co(L-alada)(gly)]$^-$	52.8	(2.37)	77.7	(2.24)
cis(*N*)-[Co(L-alada)(L-ala)]$^-$	52.8	(2.37)	77.9	(2.22)
cis(N)-[Co(D-alada)(L-ala)]$^-$	52.8	(2.36)	77.8	(2.23)

The frequencies, ν_{max}, are given in 10^{13} sec^{-1}.

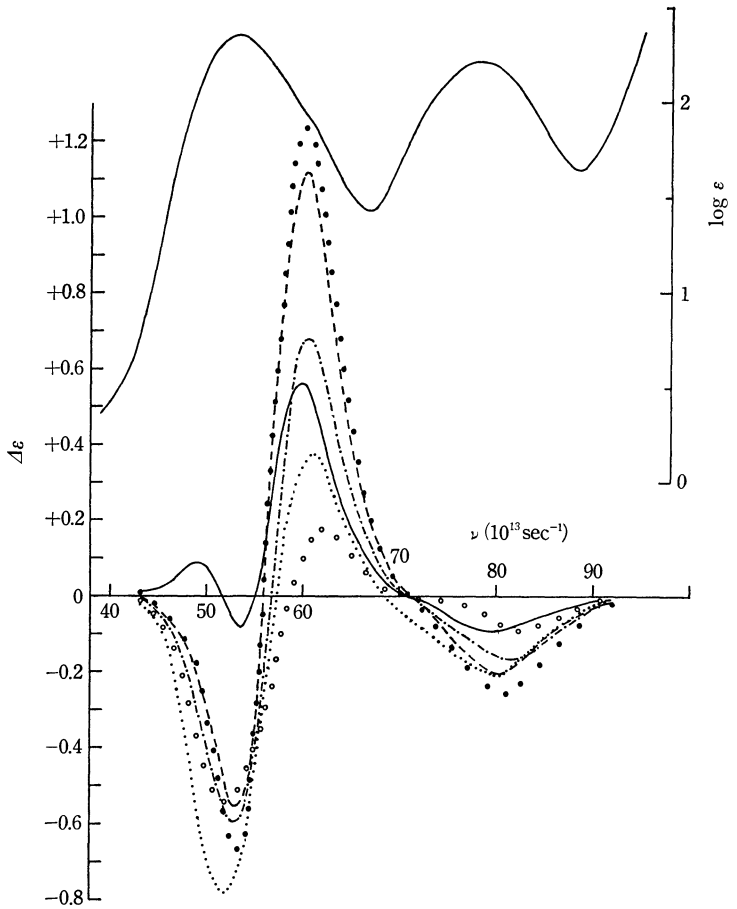

Fig. 8. Absorption and CD curves of *cis*(*N*)-[Co(O)$_4$(N)$_2$] type complexes.
Absorption curve: ——, [Co(D-alada)(L-ala)]$^-$, CD curves: (1) -·-·-, [Co(ata)(L-ala)]$^-$; (2) ——, [Co(L-alada)(gly)]$^-$; (3) ----, [Co(L-alada)(L-ala)]$^-$; (4) ····, [Co(D-alada)(L-ala)]$^-$; (5) ••••, calculated curve, (1)+(2); (6) ○○○○, calculated curve, (1)−(2).

TABLE 5. CD DATA OF [Co(L- or D-alada)(am)]$^-$ IONS

Complex ion	I Band		II Band	
	ν_{ext}	$(\Delta\varepsilon_{ext})$	ν_{ext}	$(\Delta\varepsilon_{ext})$
trans(*N*)-[Co(L-alada)(gly)]$^-$	48.6	(+0.44)	81.3	(+0.10)
	60.1	(−0.16)		
trans(*N*)-[Co(L-alada)(L-ala)]$^-$	48.5	(+0.35)	81.3	(+0.44)
	61.7	(−1.00)		
trans(*N*)-[Co(D-alada)(L-ala)]$^-$	48.3	(−0.54)	81.7	(+0.20)
	56.3	(+0.12)		
	62.4	(−0.68)		
trans(*N*)-[Co(L-alada)(L-pro)]$^-$	48.3	(+0.34)	81.3	(+0.35)
	55.3	(+0.23)		
	62.0	(−0.81)		
trans(*N*)-[Co(D-alada)(L-pro)]$^-$	48.5	(−0.54)	82.2	(+0.29)
	56.5	(+0.28)		
	62.4	(−0.55)		
cis(*N*)-[Co(L-alada)(gly)]$^-$	49.2	(+0.09)	78.5	(−0.09)
	53.8	(−0.09)		
	60.0	(+0.57)		
cis(*N*)-[Co(L-alada)(L-ala)]$^-$	53.1	(−0.56)	78.1	(−0.20)
	60.5	(+1.12)		
cis(*N*)-[Co(D-alada)(L-ala)]$^-$	51.9	(−0.79)	79.6	(−0.26)
	61.0	(+0.37)		

The frequencies, ν_{ext}, are given in 10^{13} sec^{-1}.

signals at 3.03—3.93 ppm to the remaining two protons ($-CH_2-$). Consequently, the weak signals at 4.22, 4.30 and 4.37 ppm for the L-alada complex and the signals at 4.30 and 4.37 ppm for the D-alada complex will be assigned to the methine protons.

In conclusion, all the signals observed for each of the present complexes can be assigned without considering the existence of more than one isomer. Therefore, it is reasonable to consider that each of the complexes obtained consists of only one species of the three possible isomers concerning the methyl group of alada.

Circular Dichroism and Absorption Spectra. The visible absorption data of the complex ions are summarized in Table 4 and the representative curves are shown in Figs. 7 and 8. The absorption spectra are very similar to those of the corresponding ata complexes.[3] The geometrical structures with respect to the two coordinated nitrogen atoms were confirmed from the splitting pattern of the so-called first absorption band and from the ion-exchange column chromatographic behavior.[3-5] The CD data and curves of the complexes are shown in Table 5, and Figs. 7 and 8. The observed CD curve of the *trans*(*N*)-[Co(L-alada)(L-ala)]$^-$ and the *trans*(*N*)-[Co(D-alada)(L-ala)]$^-$ ion agrees quite well with the CD curve calculated from those of the *trans*(*N*)-[Co(ata)(L-ala)]$^-$ and *trans*(*N*)-[Co(L-alada)(gly)]$^-$ ions, on the basis of the following additivity formulas;[4]

$$\text{CD(L-alada, L-ala)} = \text{CD(L-alada, gly)} + \text{CD(ata, L-ala)} \quad (1)$$

$$\text{CD(D-alada, L-ala)} = \text{CD(D-alada, gly)} + \text{CD(ata, L-ala)} = -\text{CD(L-alada, gly)} + \text{CD(ata, L-ala)} \quad (2)$$

Similar good agreement of the observed CD curves with the calculated ones is also realized for the two *trans*(*N*) complexes with L-prolinate and for one of the two *cis*(*N*) complexes, *cis*(*N*)-[Co(L-alada)-(L-ala)]$^-$ (Figs. 7 and 8). These facts indicate that the additivity of the two vicinal contributions is perfect and each of the asymmetric carbon atoms of the two optically active ligands in a complex contribute independently to the optical activity of the complex ion. This agreement will show that the complexes obtained have commonly only one type of geometrical structure concerning the methyl group of the quadridentate ligand alada.

As an exception, the observed CD curve of *cis*(*N*)-[Co(D-alada)(L-ala)]$^-$ deviates considerably from the calculated one derived from the observed CD curves of *cis*(*N*)-[Co(L-alada)(gly)]$^-$ and *cis*(*N*)-[Co(ata)(L-ala)]$^-$ (Fig. 8). This deviation suggests that the position of the chelate ring containing the methyl group of the D-alada in this *cis*(*N*)-[Co(D-alada)(L-ala)]$^-$ complex obtained here differs from that of the other complexes, since from their PMR data we confirmed that the complex obtained is not a mixture of the possible isomers.

4) N. Koine, N. Sakota, J. Hidaka and Y. Shimura, This Bulletin, **42**, 1779 (1969).

5) N. Matsuoka, J. Hidaka and Y. Shimura, This *ibid.*, **40**, 1868 (1967).

BULLETIN OF THE CHEMICAL SOCIETY OF JAPAN VOL. 43 1744—1746 (1970)

Gold Complexes of Schiff Bases obtained from Salicylaldehyde Derivatives and Alkyl Amines*1

Shoichiro YAMADA and Kuniko YAMANOUCHI

Institute of Chemistry, College of General Education, Osaka University, Toyonaka, Osaka

(Received January 16, 1970)

Gold complexes (abbreviated as $[Au^{III}(X\text{-}SAL\cdot alkyl)_2][Au^{I}Cl_2]$) with salicylideneimine derivatives were prepared as red-brown crystals, where X denotes H, 5,6-benzo and 5-Cl. Since all these complexes are diamagnetic and exhibit similar electronic absorption spectra, the complexes of the $[Au(X\text{-}SAL\cdot R)_2]^+$ type are considered to have a similar configuration, namely a square-planar one. It should be noted that the complexes of the $[Au(X\text{-}SAL\cdot i\text{-}C_3H_7)_2]^+$ type are also planar. The result is found to be similar to that for the palladium(II) and platinum(II) complexes, but different from that for the nickel(II) complexes.

In previous papers, we reported palladium(II) and platinum(II) complexes with salicylideneimine derivatives,[1-3] in order to compare the results with those of the corresponding nickel(II) complexes, which had been studied extensively.[4,5] It seems to be of interest to extend a similar study to gold(III) having a $5d^8$ configuration and to compare the results with those of the corresponding complexes of nickel(II), palladium(II) and platinum(II), which also have a d^8 configuration. No systematic study has ever been carried out on the gold(III) complexes (Fig. 1)*2 with the Schiff bases, except for a small number of examples.[6] The present paper deals with the results of a study on these gold(III) complexes.

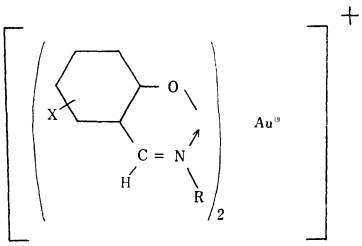

Fig. 1. $[Au^{III}(X\text{-}SAL\cdot R)_2]^+$.

Experimental

Materials. The complexes of the type $[Au^{III}(X\text{-}SAL\cdot R)_2][Au^{I}Cl_2]$ were prepared as red-brown crystals according to the following method.

To an aqueous solution of sodium tetrachloroaurate(III) dihydrate (0.01 mol) were added a solution of salicylaldehyde or its derivative (0.018 mol) in ethanol and a solution of an appropriate amine (0.02 mol) in ethanol. The resulting solution was warmed at about 40°C for about one hour. A brown precipitate formed in the solution was filtered off and recrystallized from suitable organic solvents.

Analytical data of the gold complexes obtained are shown in Table 1. Any attempt to isolate the complexes of the $[Au(X\text{-}SAL\cdot t\text{-}C_4H_9)_2][AuCl_2]$ type according to the method described above has so far been unsuccessful. In this case, the colour change of the solution immediately

TABLE 1. ANALYTICAL DATA OF GOLD COMPLEXES OF THE $[Au(X\text{-}SAL\cdot R)_2][AuCl_2]$

Compound		Calcd, %			Found, %		
X	R	C	H	N	C	H	N
H	C_2H_5	28.40	2.65	3.68	28.35	2.27	3.39
	$n\text{-}C_3H_7$	30.44	3.07	3.55	30.46	2.86	3.50
	$i\text{-}C_3H_7$	30.44	3.07	3.55	30.02	2.97	3.63
	$n\text{-}C_4H_9$	32.33	3.45	3.43	31.46	3.37	3.27
5,6-Benzo	C_2H_5	36.34	2.82	3.26	35.77	2.63	3.15
	$n\text{-}C_3H_7$	37.81	3.17	3.15	36.85	2.84	2.96
	$i\text{-}C_3H_7$	37.81	3.17	3.15	36.97	3.02	3.11
	$n\text{-}C_4H_9$	39.28	3.52	3.05	38.82	3.21	3.09
5-Cl	CH_3	23.96	1.76	3.49	23.84	1.69	3.51

*1 Presented, in part, at the 19th Symposium on Coordination Chemistry, Sendai, September, 1969.

1) S. Yamada, H. Nishikawa and K. Yamasaki, This Bulletin, **36**, 483 (1963).

2) S. Yamada and E. Yoshida, *ibid.*, **38**, 2179 (1965).

3) S. Yamada and K. Yamanouchi, *ibid.*, **42**, 2543 (1969).

4) S. Yamada, *Coord. Chem. Rev.*, **1**, 415 (1966).

5) R. H. Holm, G.W. Everett, Jr., and A. Chakravorty, "Progress in Inorganic Chemistry," Vol. VII, ed. by F. A. Cotton, Interscience Publishers, New York, N. Y. (1966), p. 83.

*2 These metal complexes are abbreviated as $[Au(X\text{-}SAL\cdot R)_2]^+$ in this paper.

6) T. Inazu, This Bulletin, **39**, 1065 (1966).

took place, but crystals of the desirable complexes could not be isolated from the solution.

These gold complexes are soluble in acetone, chloroform and ethanol, but insoluble in water. The solubility, however, varies from compound to compound and from solvent to solvent. They are stable to the atmosphere, and do not undergo decomposition when stored in an ordinary sample-tube.

Measurements. Electronic absorption spectra of the gold complexes were determined with a Shimadzu MPS-50L spectrophotometer and a Shimadzu QR-50 spectrophotometer. The solution spectra were determined with ethanol or acetone as a solvent according to the solubility of the complex. The spectrum of the ethanolic solution was found to be nearly the same as that of the acetone solution, when the determination of the spectrum was possible with both solvents.

Diamagnetism of the complexes was detected by the Gouy method.

Electric conductivities of the complexes in acetone were determined with a Toadempakogyo CM-1 conductance bridge.

Results and Discussion

The gold complexes, $[Au(X\text{-}SAL\cdot R)_2][AuCl_2]$, obtained in the present work, which are shown in Table 1, are found to correspond to the empirical formula, Au(X-SAL·R)Cl. The oxidation state of gold in this formula might apparently be plus two. This, however, proves to be incorrect, since these complexes are all diamagnetic; the gold(II) complex, having a d^9 configuration, would be expected to be paramagnetic with one spin-free electron. Thus, we might assume that the complex with the composition Au(X-SAL·R)Cl be formulated as $[Au^{III}(X\text{-}SAL\cdot R)_2][Au^{I}Cl_2]$, which involves one gold ion in the tervalent and the other in the univalent state. It seems difficult to tell exactly how the reduction of gold(III) to gold(I) has taken place. However, gold complexes of this sort, containing $[Au^{I}Cl_2]^-$ or $[Au^{III}Cl_4]^-$ as a counter-anion, have often been reported in literature;[6,7] the syntheses of the complexes in these reports were also carried out using reactions of a type somewhat similar to those employed in the present work. Electric conductivities of some of the complexes in solution were determined. The values for the acetone solutions, which are shown in Table 2, seem to correspond to the values expected for uni-uni-electrolytes, in agreement with the formulation proposed above for these gold complexes.[7]

Since it is known that the gold(III) ion generally requires a quadri-coordinate planar configuration, the complexes of the $[Au(X\text{-}SAL\cdot n\text{-}alkyl)_2]^+$ may reasonably be considered to be planar, no steric hindrance being expected, in this case, against the planar configuration.

7) C. M. Harris, *J. Chem. Soc.*, **1959**, 682; C. M. Harris and T. N. Lockyer, *ibid.*, **1959**, 3083.

Table 2. Molecular conductivities(Λ) of gold complexes of the $[Au(X\text{-}SAL\cdot R)_2]\cdot[AuCl_2]$ type in acetone at 25°C

Compound		Conc.(mol/l)	Λ (mho)
H	n-C_3H_7	5.15×10^{-4}	144
	i-C_3H_7	6.12×10^{-4}	134
5,6-Benzo	i-C_3H_7	6.50×10^{-4}	132
	n-C_4H_9	7.75×10^{-4}	131
5-Cl	CH_3	5.91×10^{-4}	126

The complexes of the $[Au(X\text{-}SAL\cdot n\text{-}alkyl)_2][AuCl_2]$ type in solution show electronic spectra which are similar to each other. Some of the representative spectra are shown in Fig. 2.*3 In the region shown in Fig. 2, the ion $[AuCl_2]^-$ exhibits almost no absorption, so that the spectra in Fig. 2 may be considered to represent those due to the complexes $[Au(X\text{-}SAL\cdot n\text{-}alkyl)_2]^+$. That the spectra are similar to each other indicates that the complexes of the $[Au(X\text{-}SAL\cdot n\text{-}alkyl)_2]^+$ type have a similar configuration, namely a square-planar one. The broad absorption band which appears in the region between about 17 and 24 kK may be considered to arise principally from spin-allowed *d-d* transitions in the planar complexes $[Au(X\text{-}SAL\cdot n\text{-}alkyl)_2]^+$. The broadness of the band indicates that this band consists of a few components. The intensity of this band seems to be a little too high for the transitions of the pure *d-d* origin, but this finding may be interpreted as due to the considerably high mixing-in of the ligand π-orbitals with the metal *d*-orbitals, as has often been observed with most transition metal complexes with Schiff bases of a similar type. An intense absorption band with its maximum at about 26.7 kK may be considered as due to the internal transitions within the ligands under the influence of the gold(III) ion.

Since Beer's law holds for all these complexes in solution, no association of the planar gold(III) complexes is found to take place. This result is similar to that for the corresponding palladium(II) or platinum(II) complexes,[1-3] but different from that for the nickel(II) complexes, in agreement with the current view that the gold(III) ion, like the palladium(II) or platinum(II) ion, has a high tendency to take a quadri-coordinate planar configuration.

For the complexes of the $[Au(X\text{-}SAL\cdot i\text{-}C_3H_7)_2]^+$ type, steric hindrance may be expected to be considerably high against the planar configuration of the complexes. It should be remembered that the corresponding nickel(II) and copper(II) complexes of the $[M(X\text{-}SAL\cdot i\text{-}C_3H_7)_2]$ type were previously

*3 It was confirmed that the spectra of these complexes in the solid state are essentially similar to their solution spectra.

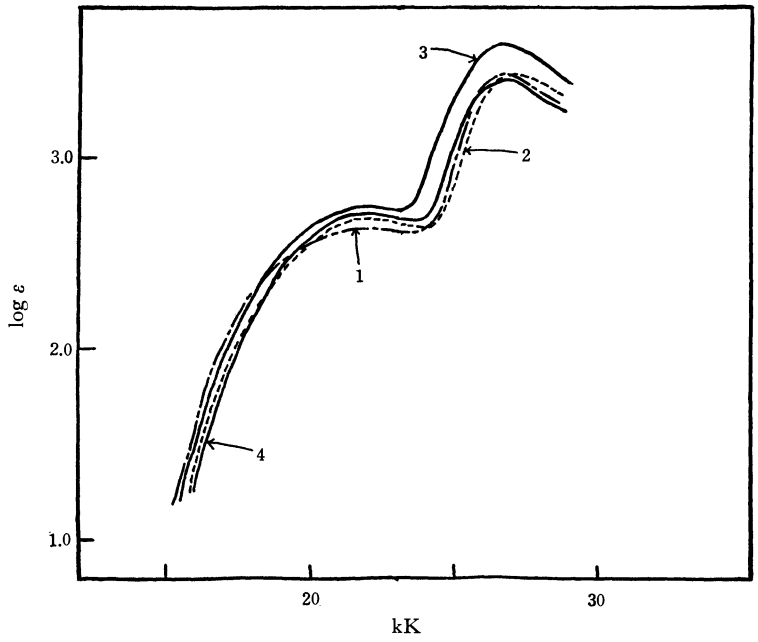

Fig. 2. Electronic absorption spectra of $[Au(X\text{-}SAL\cdot R)_2][AuCl_2]$. 1, X=H, R=*n*-$C_3H_7$, in chloroform; 2, X=H, R=*i*-C_3H_7, in acetone; 3, X=5,6-benzo, R=*i*-C_3H_7, in acetone; 4, X=5-Cl, R=CH_3, in acetone.

concluded to be tetrahedral or planar, depending upon X; they are tetrahedral for X=H[8,9] and planar for X=5-Cl and 5,6-benzo.[9] It is considered that the gold(III) complexes of the $[Au(X\text{-}SAL\cdot i\text{-}C_3H_7)_2]^+$ type have a planar configuration, since their spectra are similar to those of the complexes of the $[Au(X\text{-}SAL\cdot n\text{-alkyl})_2]^+$ type. This result with the gold(III) complexes is evidently different from that with the corresponding nickel(II) complexes, both metal ions having a d^8 configuration. This difference between the gold(III) and the nickel(II) complexes may be ascribed principally to the two factors, which are related with the bonding nature and the size of the metal ions, in quite the same way as was previously discussed in the case of the corresponding palladium(II) and platinum(II) complexes.[1-3]

8) L. Sacconi, "Essays in Coordination Chemistry," ed. W. Schneider, G. Anderegg and R. Gut, Birkhauser Verlag, Basel (1964), p. 148.

9) S. Yamada and H. Nishikawa, This Bulletin, **36**, 755 (1963).

Financial support of this work by the Ministry of Education is gratefully acknowledged.

BULLETIN OF THE CHEMICAL SOCIETY OF JAPAN VOL. 43 1747—1751 (1970)

The Transformation of the Triphenylmethyl Radical into the Triphenylmethyl Cation in the Sulfur Dioxide - Oxygen System

Hiroshi TAKEUCHI, Toshikazu NAGAI and Niichiro TOKURA

Department of Applied Chemistry, Faculty of Engineering, Osaka University, Suita, Osaka

(Received May 10, 1969)

The decomposition of phenylazotriphenylmethane (I) in the presence of SO_2 and O_2 in benzene at 60°C gives *p*-hydroxytetraphenylmethane (II) by the reaction of the trityl cation and the phenol formed in the reaction system. However, in the absence of O_2 or SO_2, the above-mentioned reaction produces trityl phenyl sulfone (III) or bistrityl peroxide (IV), without forming any II. Also, 1-diphenylmethylene-4-trityl-2,5-cyclohexadiene (Gomberg's trityl) (V) has been chosen as the trityl radical source, and reacted with phenol in the presence of SO_2 and O_2 to give II as the product. However, in the absence of SO_2, IV and a trace of II are formed. Moreover, in the absence of O_2 in the above system, *p*-benzhydryltetraphenylmethane (VI) and a small amount of II are formed. The benzene solution of VI is stable on exposure to air at 60°C. Further, the UV spectrum of V in the liquid SO_2-O_2 system shows λ_{max} at 405 mμ (log ε 4.1) and 434 mμ (log ε 4.1) (trityl chloride in 98% H_2SO_4: λ_{max} 430 mμ (log ε 4.58)). However, the UV spectrum of VI in the liquid SO_2-O_2 system has no absorption in this range. The NMR spectrum in the liquid SO_2-O_2 system of V exhibits only aromatic protons (2.6—3.1 τ). These facts indicate that the trityl radical generated from V is transformed into the trityl cation in the SO_2-O_2 system at room temperature, whereas VI does not dissociate into the trityl radical even at 60°C in benzene.

We have previously established[1] the reaction of SO_2 with a radical source such as phenylazotriphenylmethane (I) which is able to liberate both the π- and the σ-character radicals[2,3] (the trityl and phenyl radicals). The nearly-quantitative formation of trityl phenyl sulfone (III) in the above reaction could be considered to be the result of the intramolecular radical recombination of the radical pairs (the phenylsulfonyl and trityl radicals) surrounded by SO_2 molecules.

On the other hand, the reaction of I with SO_2 in the presence of O_2 gave *p*-hydroxytetraphenylmethane (II) and benzenesulfonic acid, but neither III nor bistrityl peroxide (IV). Busch and Knoll have reported[4] the formation of II from the ionic reaction of Ph_3CCl with PhOH. Therefore, the formation of II from I in the presence of SO_2 and O_2 was expected to result by means of the trityl cation formed from the trityl radical. The thermal electron-transfer reaction[5] in the presence of SO_2 and O_2 has been recongnized as reasonable in the polymerization of *N*-vinylcarbazole.

The present study was concerned with the ionic behavior of the trityl radical in the SO_2-O_2 system by using I and using 1-diphenylmethylene-4-trityl-2,5-cyclohexadiene (V) as the trityl radical source. Phenol was used as a trapping reagent of the trityl cation.

Further, the transformation of the trityl radical into the tritvl cation in the liquid SO_2-O_2 system was proved by a study of the UV and NMR spectra. This fact arouses our interest in the field of polymerization.

Results and Discussion

The Effect of Oxygen - Sulfur Dioxide in the Reaction of Phenylazotriphenylmethane (I) with Phenol. In a previous paper,[1] we reported that the reaction of I with SO_2 in benzene or *n*-heptane gave trityl phenyl sulfone (III) in a good yield:

$$\underset{\text{(I)}}{Ph\text{-}N{=}N\text{-}CPh_3} + SO_2 \xrightarrow[\text{in benzene or } n\text{-heptane}]{-N_2} \underset{\text{(III)}}{Ph\text{-}SO_2\text{-}CPh_3}$$

In the presence of O_2, the above reaction gave *p*-hydroxytetraphenylmethane (II), benzenesulfonic acid, and a small amount of phenol, but neither III nor bistrityl peroxide (IV) was found, although the reaction of I with only O_2 gave IV, without

1) H. Takeuchi, T. Nagai and N. Tokura, *Tetrahedron*, **25**, 2987 (1969).
2) H. Takeuchi, T. Nagai and N. Tokura, *ibid.*, **23**, 1783 (1967).
3) H. Takeuchi, T. Nagai and N. Tokura, This Bulletin, **40**, 2375 (1967).
4) M. Busch and R. Knoll, *Ber.*, **60**, 2240 (1927).
5) T. Nagai, T. Miyazaki and N. Tokura, *J. Polym. Sci., Part B*, **6**, 346 (1968).

any II. These facts suggest that the reaction in the presence of SO_2 and O_2 is ionic. Actually, Busch and Knoll[4] reported a 98% yield of II from the reaction of Ph_3CCl with PhOH. Therefore, it was expected that II was formed by the reaction of the trityl cation with phenol.

Then, phenol (five equivalents to I) was added to the system (Exp. 1). In this reaction, the yield (58%) of II increased in comparison with the yield (18—24%) of II in the reaction without phenol. However, in the absence of O_2 in Exp. 1, III was formed without giving II (*cf.* Exp. 2). These facts suggest the formation of II by the reaction of the trityl cation with phenol, as in Scheme 1:

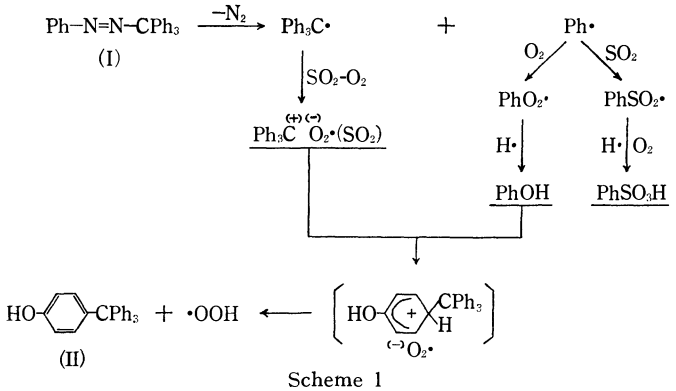

Scheme 1

The Effect of Oxygen - Sulfur Dioxide in the Reaction of 1-Diphenylmethylene-4-trityl-2,5-cyclohexadiene (V) with Phenol. The reaction of V with phenol in the presence of SO_2 and O_2 in benzene at 60°C gave II (52%) (*cf.* Exp. 3). However, in the absence of SO_2, IV (41%) and II (trace) were formed in Exp. 4. Moreover, in the absence of the O_2 of Exp. 3, *p*-benzhydryltetraphenylmethane (VI) (45%) and a small amount of II were formed (*cf.* Exp. 5).

These observations support the idea that the transformation of the trityl radical into the trityl cation in the SO_2-O_2 system occurs as Scheme 1 shows.

The Formation of *p*-Benzhydryltetraphenylmethane (VI). As is indicated in Exp. 6, VI was obtained by the reaction of V with phenol under Ar gas. When HCl was used in place of phenol, VI was also produced (Exp. 7).

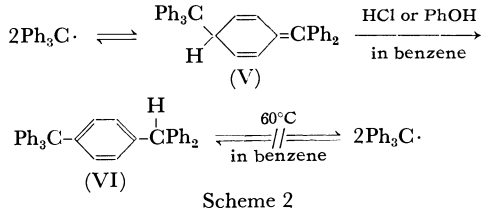

Scheme 2

It has been reported by Lankamp, Nauta and MacLean[6] that Gomberg's trityl has a cyclohexadiene structure, as is shown in Scheme 2. Gomberg *et al.*[7,8] have reported that the reaction of V with HCl or CH_3COOH gives hexaphenylethane. However, it was found that the product was not hexaphenylethane, but VI, on the basis of the IR, NMR and mass spectral data (*cf.* Exp. 5). The details of the reaction mechanism of the formation of VI will be reported in the near future.*1

The UV spectrum of VI has $\lambda_{max}^{cyclohexane}$ at 263 mμ (log ε 3.11). The NMR spectrum of VI shows aromatic protons (2.6—3.1 τ) and a methine proton (4.6 τ) in CCl_4. The mp (225—227°C) of VI is higher than the mp (145—147°C) of V. Further,

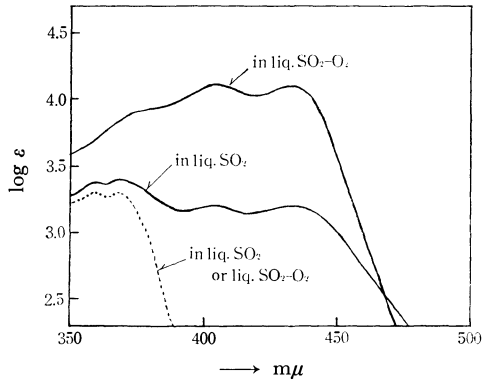

Fig. 1. The electronic spectra of Gomberg's trityl (V).
—— Gomberg's trityl (V)
---- *p*-Benzhydryltetraphenylmethane (VI)

6) H. Lankamp, W. Th. Nauta and C. MacLean, *Tetrahedron Lett.*, **1968**, 249.
7) M. Gomberg, *Ber.*, **35**, 2877 (1902).
8) F. Ullmann and W. Borsum, *ibid.*, **35**, 3914 (1902).

*1 In the experiment using I in place of the V of Exp. 3, VI was never found. Similarly, the treatment of 1-(phenyl-*p*-tolylmethylene)-4-(diphenyl-*p*-tolylmethyl)-2,5-cyclohexadiene with HCl in benzene afforded α,α,α′-triphenyl-α,α′-ditolyl-*p*-xylene by the isomerization of the cyclohexadiene structure.

Table 1. The UV spectra of V in liquid SO_2 and liquid SO_2-O_2

Number	log ε in liquid SO_2				log ε in liquid SO_2-O_2		
	360 mμ *max*	368 mμ *max*	405 mμ *max*	434 mμ *max*	374 mμ shoulder	405 mμ *max*	434 mμ *max*
1	3.26	3.25	3.0	3.0	3.91	4.11	4.10
2	3.36	3.37	3.3	3.3	3.94	4.01	4.0
3	3.44	3.44	3.3	3.3	—	—	—
Average	3.4	3.4	3.2	3.2	3.9	4.1	4.1

This transformation is shown as Fig. 1.

the benzene solution of VI is stable on exposure to air, even at 60°C.

The Transformation of the Trityl Radical into the Trityl Cation in the Liquid SO_2-O_2 System. The UV spectra of Compound V were measured in liquid SO_2 and liquid SO_2-O_2 systems at room temperature. The results are summarized in Table 1.

This transformation is shown as Fig. 1.

In the liquid SO_2-O_2 system, no absorption corresponding to the trityl radical[9] appears. The values of log ε at 405 and at 434 mμ in liquid SO_2 were 3.2,*2 whereas those in the liquid SO_2-O_2 system were 4.1. The UV spectra of the trityl cation have been established to be as follows:

Trityl chloride[10]: $\lambda_{max}^{98\%\ H_2SO_4}$ 430 mμ (log ε 4.58).

Compound V[11]: $\lambda_{max}^{H_3PO_4}$ 400 mμ and 440 mμ (log ε 4.5).

Compound V[11]: $\lambda_{max}^{POCl_3}$ 420 mμ and 440 mμ (log ε 4.2).

Therefore, the peaks at 405 and 434 mμ in the liquid SO_2-O_2 system may be said to correspond to the absorptions of the trityl cation.

The absorption with $\lambda_{max}^{SO_2}$ at 360 and 368 mμ is observed characteristically in liquid SO_2. Also, the UV spectrum of VI was measured as: $\lambda_{max}^{SO_2\ or\ SO_2\text{-}O_2}$ 360 mμ (log ε 3.3) and 368 mμ (log ε 3.3). The UV spectrum of VI does not have the absorption corresponding to the trityl cation in the liquid SO_2-O_2 system, indicating that the dissociation of VI into the trityl radical does not occur as in Scheme 2, since the trityl radical is transformed into the trityl cation in this system. This finding is in fair agreement with the chemical evidence. In a cyclohexane solution, the absorption with λ_{max}= 360 and 368 mμ did not appear in the case of either V or VI.

These observations indicate that the absorption with λ_{max}=360 and 368 mμ is attributable to a C–T complex of SO_2 with V (*cf.* A in Scheme 3).

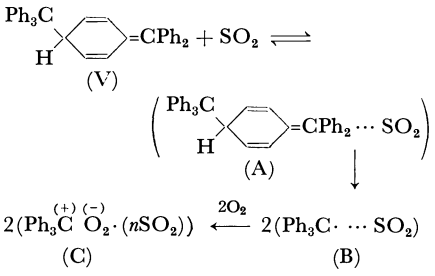

Scheme 3

Therefore, the transformation of V into C may be assumed to proceed *via* an A complex. The oxygen counter anion is stabilized by a solvated SO_2 such as $\overset{(-)}{O}_2\cdot(nSO_2)$.

The NMR spectrum shows that the cation formed from V in this system is not the 1-diphenylmethylene-2,5-cyclohexadienyl cation, but the trityl cation having only aromatic protons (2.6—3.1 τ).

Although the electron affinity of SO_2 (0.2—0.3 eV)[5] is larger than that of O_2 (0.15 eV),[5] the promotion*3 of the transformation of the trityl radical into the trityl cation in SO_2-O_2 rather than SO_2 may be expected to proceed as follows:

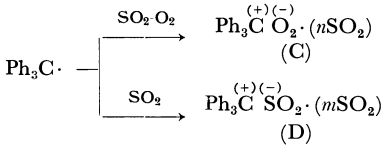

Scheme 4

The interaction energy between an anion and solvated SO_2 molecules with a dipole moment may

9) W. Theilacker and M. L. W. Ewald, *Ann.*, **594**, 214 (1955).

*2 The dissolved oxygen in liquid SO_2 was eliminated by the method described in the Experimental section. However, this absorption may arise from a very small amount of oxygen, or else from the trityl cation already generated in liquid SO_2.

10) A. G. Evans, J. A. G. Jones and G. O. Osborne, *J. Chem. Soc.*, **1954**, 383.

11) T. L. Chu and S. I. Weissman, *J. Chem. Phys.*, **22**, 21 (1954).

*3 Because of the following reasons, it seems feasible that a trityl cation such as D is formed even in the liquid SO_2 system, as is shown in Scheme 4. The UV spectrum of V even in liquid SO_2 shows peaks corresponding to those of the trityl cation, as Fig. 1 shows. Further, the reaction of V with phenol in the presence of SO_2 and Ar gas, as in Exp. 5, gives II (11%) and thus corresponds to the reaction of the trityl cation with phenol.

be represented by the following formula:

$$\overset{(-)}{O_2}\cdot \underset{r_i}{\longleftrightarrow} SO_2 \quad E_1 = \sum_{i=1}^{n}\{N(-e)\mu_{SO_2}\cos\theta_i/r_i^2\}$$

$$\overset{(-)}{SO_2}\cdot \underset{r_j}{\longleftrightarrow} SO_2 \quad E_2 = \sum_{j=1}^{m}\{N(-e)\mu_{SO_2}\cos\theta_j/r_j^2\}$$

$-e$: electric charge.
μ_{SO_2}: dipole moment of SO_2 (1.61 debye).
r: distance between dipole and ionic center.
θ: angle between the direction of r and that of μ_{SO_2}.
N: Avogadro number.

Since $\overset{(-)}{SO_2}\cdot$ is bulkier than $\overset{(-)}{O_2}\cdot$, the value of r_i is smaller than r_j. Therefore, the absolute value of the interaction energy between $\overset{(-)}{O_2}\cdot$ and SO_2, E_1, becomes greater than that between $\overset{(-)}{SO_2}\cdot$ and SO_2, E_2, so that the difference between the above interaction energies appears to compensate sufficiently for the electron affinity difference between SO_2 and O_2. Also, the Coulombic enregy stabilization by $\overset{(+)}{Ph_3C}$ and $\overset{(-)}{O_2}\cdot$ is greater than that by $\overset{(+)}{Ph_3C}$ and $\overset{(-)}{SO_2}\cdot$. These stabilization energies of the trityl-cation formation due to the oxygen counter anion, $\overset{(-)}{O_2}\cdot(nSO_2)$, may act as the driving force to transform the trityl radical into the trityl cation in the SO_2-O_2 system.

Experimental

Apparatus. The IR spectra were run on an EPI-S2-type Hitachi IR spectrometer. The NMR spectra were obtained with a Japan Electron Optics Lab. spectrometer (JNM3H-60). The UV spectra were taken on an EPS-3 Hitachi recording spectrometer.

Materials. The liquid SO_2 was dehydrated with P_2O_5 and distilled. The benzene was purified by an ordinary method. The phenol was obtained commercially. The phenylazotriphenylmethane (I) (mp 111°C dec.) was synthesized by the method of Cohen and Wang.[12] The 1-diphenylmethylene-4-trityl-2,5-cyclohexadiene (V) was synthesized by the method of Gomberg and Cone.[13]

Experiment 1. Compound I (4.7 mmol) and phenol (23.5 mmol) were dissolved in 95 m*l* benzene; the solution was then heated at 60°C for 2 hr with stirring while 70 g of gaseous SO_2 and O_2 were being passed through. The benzene was distilled under reduced pressure. The residue was chromatographed over silica gel, using benzene as the eluent; we then isolated and identified the *p*-hydroxytetraphenylmethane compound (58%), showed no depression of mp in a mixed-melting-point determination and which had an IR spectrum identical with that of an authentic sample.[4]

Experiment 2. Compound I (8.6 mmol) and phenol (43 mmol) were dissolved in 60 m*l* benzene; the solution was then heated at 60°C for 2 hr while 30 g of gaseous SO_2 were being passed through. The benzene was distilled under reduced pressure. The residue was crystallized from MeOH - ether, and trityl phenyl sulfone (55%) was isolated and identified. This compound showed no depression of mp in a mixed-melting-point determination with an authentic sample,[1] and the IR spectra were identical.

Experiment 3. Compound V (4.7 mmol) and phenol (47 mmol) were dissolved in 65 m*l* benzene; the solution was then heated at 60°C for 2 hr with stirring while 32 g of gaseous SO_2 and O_2 were being passed through. *p*-Hydroxytetraphenylmethane (52%) was confirmed as has been described above.

Experiment 4. In this experiment, SO_2 was eliminated from the system of Exp. 3. The residue obtained after the evaporation of the benzene was chromatographed over silica gel, using a petroleum ether - benzene mixture as the eluent by changing the polarity of the eluting medium. Bistrityl peroxide (IV) was isolated and identified, along with a small amount (3%) of *p*-hydroxytetraphenylmethane.

Bistrityl Peroxide (IV). Mp 183°C (recrystallized from toluene), 41%. This compound showed no depression of mp in a mixed-melting-point depression with an authentic sample[14] and had an identical IR spectrum.

Experiment 5. This experiment was carried out much as in Exp. 3, but Ar gas was used in place of O_2. The residue after the distillation of the benzene was chromatographed over silica gel, using a petroleum ether - benzene mixture as the eluent by changing the polarity of the eluting medium. The following compounds were isolated and identified (*p*-hydroxytetraphenylmethane (11%) was also confirmed, as has been described above):

***p*-Benzhydryltetraphenylmethane (VI).**[15] Mp 225—227°C (recrystallized from benzene - acetic acid), 45%, IR: 2880 (ν_{C-H}), 840 cm^{-1} (*p*-substituted phenyl). $\lambda_{max}^{cyclohexane}$ 263 mμ (log ε 3.11), shoulder; 255 mμ (log ε 3.15), 269 mμ (log ε 2.99) and 272 mμ (log ε 2.67). NMR (in CCl_4): τ; 2.6—3.1 (aromatic, multiplet, 29H), 4.6 (methine, singlet, 1H). Mass spectrum: *m/e*; 486, 409, 243 and 167.

Found: C, 93.71; H, 6.41%. Calcd for $C_{38}H_{30}$: C, 93.79; H, 6.21%.

Triphenylmethane. Mp 92°C (recrystallized from MeOH), 6%. This compound showed no mixed-mp depression.

Experiment 6. In this experiment, Ar gas was used in place of the SO_2 and O_2 of Exp. 3. *p*-Benzhydryltetraphenylmethane (68%), *p*-hydroxytetraphenylmethane (3%), and triphenylmethane (3%) were confirmed as has been described above.

Triphenylcarbinol. Mp 164°C, 5%. The IR spectrum of this compound coincided with that of a specimen synthesized by another method; this compound was confirmed by a mixed-mp determination.

Experiment 7. Compound V (2.9 mmol) was dissolved in 15 m*l* of benzene saturated with HCl; the solution was then allowed to stand at room temperature for half an hour. The benzene was distilled by reduced

12) S. G. Cohen and C. H. Wang, *J. Amer. Chem. Soc.*, **75**, 5504 (1953).
13) M. Gomberg and L. H. Cone, *Ber.*, **37**, 2034 (1904).
14) M. Gomberg and L. H. Cone, *ibid.*, **37**, 3538 (1904).
15) M. Gomberg, *ibid.*, **36**, 376 (1903).

pressure, and 25 ml of ether was added to this residue. *p*-Benzhydryltetraphenylmethane (82%) was confirmed as has been described above.

Measurement of the UV and NMR Spectra. The dissolved oxygen in liquid SO_2 was eliminated by the following method. The dehydrated and distilled liquid SO_2 was frozen by liquid N_2 and evacuated at about 10^{-3} mmHg. Subsequently, this solvent was melted at room temperature by introducing Ar gas. This operation was repeated six times. This liquid SO_2 was used in the measurement of the UV and NMR spectra at room temperature.

BULLETIN OF THE CHEMICAL SOCIETY OF JAPAN VOL. 43 1751—1762 (1970)

Kinetics for Reversible Menschutkin Reactions. The Effects of Variations in Reactant Structures on the Sensitivity of the Reaction Rate to Solvent Variations

Takeki MATSUI and Niichiro TOKURA

Department of Applied Chemistry, Faculty of Engineering, Osaka University, Suita, Osaka

(Received June 5, 1969)

The reaction rates and equilibrium constants for quaternization of *N,N*-dimethylaniline and its derivatives with methyl iodide have been measured in acetonitrile, acetone, tetrahydrofuran, nitrobenzene, benzene, benzyl alcohol, and methanol at various temperatures. There is an approximate tendency for the solvent dependence of the reaction rates to diminish linearly with increasing reactivity of nucleophile. This could be interpreted in terms of the theory of an absolute reaction rate and of the concept of the rise of interaction term. In this connection it was proposed that such a problem must be considered in terms of the unitary term of rates. Using the data of rates of the reaction between pyridine and methyl iodide in various solvents, the activity coefficients of dimethylaniline and its derivatives in methanol relative to that of pyridine are estimated. Some inferences have been drawn concerning the nature of S_N2 transition state from effects of solvents on both rates and equilibria.

The nucleophilic tendency for S_N2 reactions seems to be affected by the nature of electrophiles and of solvents, and also by temperature and pressure. The effects of variations in substrates on nucleophilic tendency have the subject of some authors.

However, the subject is not so simple as Swain and Scott considered.[1] From the study of Hine and Weimar on carbon basicity, correlation of nucleophilicity of bases with the hydrogen basicity is not always good.[2] Qualitatively the priciple of hard and soft acids and bases (HSAB) seems to be an explanation for this problem. Pearson *et al.*[3] explained qualitatively the fact that no good correlation exists for the difference between methyl iodide and *trans*-$[Pt(py)_2Cl_2]$ in the variations of rates of reactions with charged and uncharged bases in terms of this principle. It seems, however, unlikely that there is no systematic tendency at all. For one thing it has been reported that there is a relatively simple linear relation between the nucleophilic tendency and the polarizability of leaving group.[4]

It should be noted that most experiments on these problems were carried out using the most complicating medium, water as solvent. It is yet uncertain whether the specificity of water as solvent contributes to the nucleophilic tendency in any way.

Thus it is of importance to examine the effects of solvents on nucleophilic tendency. For the Finkelstein or S_NAr reactions, Parker and his collaborators have tried to settle these effects on nucleophilic tendency by comparing the S_N2 reactivity in each solvent-solvent pair.[5] It remains to be proved whether the compilation of both charged

1) C. G. Swain and C. B. Scott, *J. Amer. Chem. Soc.*, **75**, 141 (1953).

2) J. Hine and R. D. Weimar, Jr., *ibid.*, **87**, 3387 (1965).

3) R. G. Pearson, H. Sobel and J. Songstad, *ibid.*, **90**, 319 (1968).

4) a) R. E. Davis, *ibid.*, **87**, 3010 (1965); b) R. G. Pearson and J. Songstad, *ibid.*, **89**, 1827 (1967); c) G. Bartoli and P. E. Todesco, *Tetrahedron Lett.*, **1968**, 4867.

5) R. Alexander, E. C. F. Ko, A. J. Parker and T. J. Broxton, *J. Amer. Chem. Soc.*, **90**, 5049 (1968) and references cited in this literature.

and uncharged nucleophiles should be made after due consideration of the solvent used. We have studied this type of problem within the linear free energy relationship framework of unchanged nucleophiles.[6] It has been proposed that the effects of solvents on the measure of sensitivity to the variations in nucleophiles (as an example, Hammett's ρ value) and the effects of variations in nucleophiles on the measure of sensitivity to the variations in solvents (denoted by ζ) are two aspects of the phenomenon. Therefore, the subject can be discussed as the factors influencing the value of ζ. The present paper reports a study of some factors influencing the dependence of the reaction rates of the quaternization of a base $R \cdot C_6H_4N(CH_3)_2$ with methyl iodide on solvent variations. The effects of R on ζ, the comparison of pyridine with dimethylaniline as a nucleophile, and the difference of ζ of the reaction based on methyl iodide and 2,4,6-trinitro-anisole or methyl picrate are reported here.

The reaction of dimethylaniline or its derivatives with methyl iodide have been followed in various solvents.[7] This reaction is of interest with respects to the occurrence of a reverse decomposition reaction at relatively low temperature. Rossell[7a] has made use of data for the series of this reaction to throw a doubt upon earlier views expressed by Glasstone *et al.*[8] of the resemblance of the transition state to quaternary ammonium salt produced. In this respect the present paper supports his view: The transition state is not as highly ionic as the quaternary ammonium salt.

Experimental

Materials. *N,N*-Dimethylaniline and its derivatives were prepared and purified as in our earlier work.[6] The purity was checked by glc in which only a single peak was observed. Methyl iodide was purified by the method of Cowley and Partington.[9] The purification procedure was repeated once a month. Various solvents used except acetonitrile were purified as in the previous paper. Acetonitrile was purified by the method of Coetzee *et al.*[10] The purification procedure was repeated once a week. The density of these solvents which were measured at a certain temperature agreed with the earlier values[11] within $\pm 0.2\%$. Glc chart for solvents showed sufficient purity.

Apparatus and Kinetic Procedure. Pipettes were calibrated both with water and with each solvent, and burettes were calibrated with water. The experimental procedure of Rossell[7a] was used with the following modifications; (1) Aliquot portions withdrawn were analyzed for iodide by potentiometric titration with 0.005N to 0.01N silver nitrate and not with 0.02N silver nitrate as in the Volhard method. (2) Prevention of further reaction during the extraction was done by dilution with cold benzene rather than with light petroleum. (3) The reaction vessels were pyrex glass tubes which could be closed with a polyethylene plate in place of ampoules. Sealing could be omitted. Initial concentration of each reactant was 0.02—0.1M.

a) The Simple Kinetic Runs. The kinetics except for noted in the later section gave good second order rate constants in which the rate law is the simplest. When comparison was made of results obtained with independently prepared solutions, the reproducibility was within $\pm 2\%$ even in the worst case. Examples of the results are given in Fig. 1.

b) Kinetics Accompanying the Methanolysis of Methyl Iodide. Quaternization based on *N,N*-dimethylanilines in methanol gave good second order rate constants. The use of *N,N*-dimethyl-*m*-nitro aniline makes the kinetic run complicated, not because of the reverse decomposition reaction, but because of the slow rate of quaternization relative to the concurrent methanolysis of methyl iodide.[7b] However, analysis of the kinetic data through a way similar to our earlier paper[6] gave the rate constant with reasonable accuracy. The rate law used is

$$(dx/dt)_0 = k \cdot a \cdot b + k_M \cdot a, \quad (1)$$

where a and b are the initial concentrations of methyl iodide and *N,N*-dimethyl-*m*-nitroaniline, respectively, k is the second order rate constant, k_M is the first order rate constant of methanolysis of methyl iodide, and $(dx/dt)_0$ is the initial rate of the production of salt. Modification of equation (1) shows the linear relation between the term on the left hand side and b, *viz.*,

$$(dx/dt)_0/a = k \cdot b + k_M \quad (2)$$

Therefore k is given by the slope of this linear plot and

Table 1. The reaction rate for the quaternization based upon *N,N*-dimethyl-*m*-nitroaniline in methanol and the concurrent methanolysis rate constant of methyl iodide

	40°C	50°C	60°C
k, $M^{-1}\,hr^{-1}$	0.0107	0.0273	0.0632
k_M, hr^{-1}	4.96×10^{-4}	1.40×10^{-3}	3.51×10^{-3}

6) Y. Kondo, T. Matsui and N. Tokura, This Bulletin, **42**, 1037 (1969).

7) a) In nitrobenzene, J. B. Rossell, *J. Chem. Soc.*, **1963**, 5183; H. Essex and O. Gelormini, *J. Amer. Chem. Soc.*, **48**, 882 (1926); b) In methanol, D. P. Evans, H. B. Watson and R. Williams, *J. Chem. Soc.*, **1939**, 1345; *ibid.*, **1939**, 1348; A. D. Harris and K. E. Weale, *ibid.*, **1961**, 146; c) In other solvents, W. C. Davies, *ibid.*, **1938**, 1865; R. A. Benkeser, C. E. DeBoer, R. E. Robinson and D.M. Sauve, *J. Amer. Chem. Soc.*, **78**, 682 (1956); W. C. Davies and R. G. Cox, *J. Chem. Soc.*, **1937**, 614.

8) S. Glasstone, K. J. Laidler and H. Eyring, "The Theory of Rate Processes," McGraw-Hill, New York (1941), p. 419.

9) E. G. Cowley and J. R. Partington, *J. Chem. Soc.*, **1938**, 977.

10) J.F. Coetzee, G. P. Cunningham, D. K. McGuire and G. R. Padmanafhan, *Anal. Chem.*, **34**, 1139 (1962).

11) J. Timmermans, "Physico - Chemical Constants of Pure Organic Compounds," Elsevier Publishing Com., Inc., Amsterdam (1950).

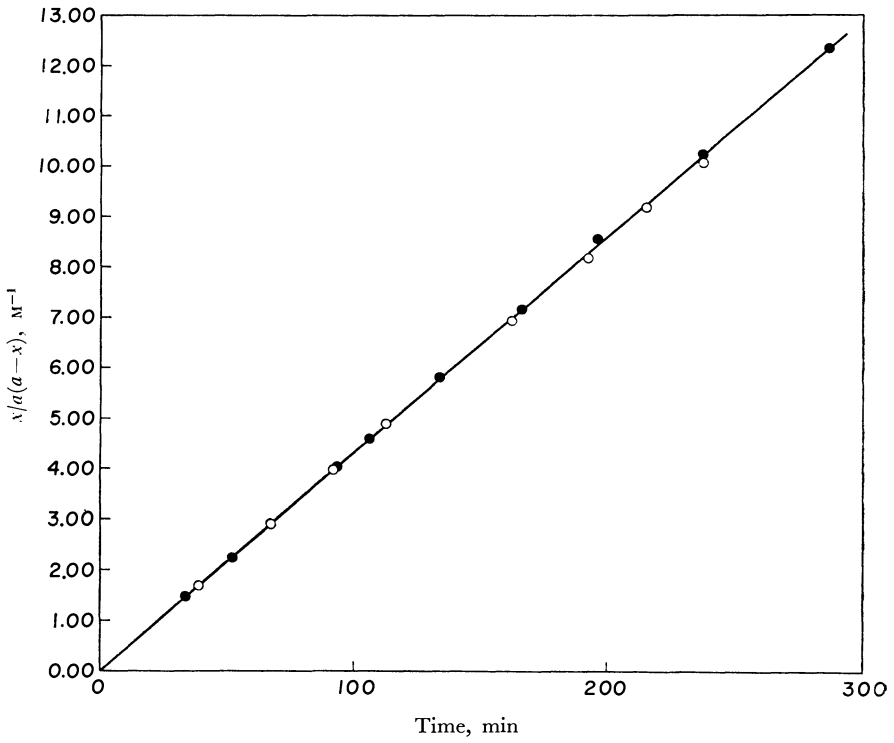

Fig. 1. Typical run for the reaction of *N,N*-dimethyl-*m*-toluidine with methyl iodide in acetonitrile at 40±0.1°C, ●: a=0.0945M, ○: a=0.02713M.

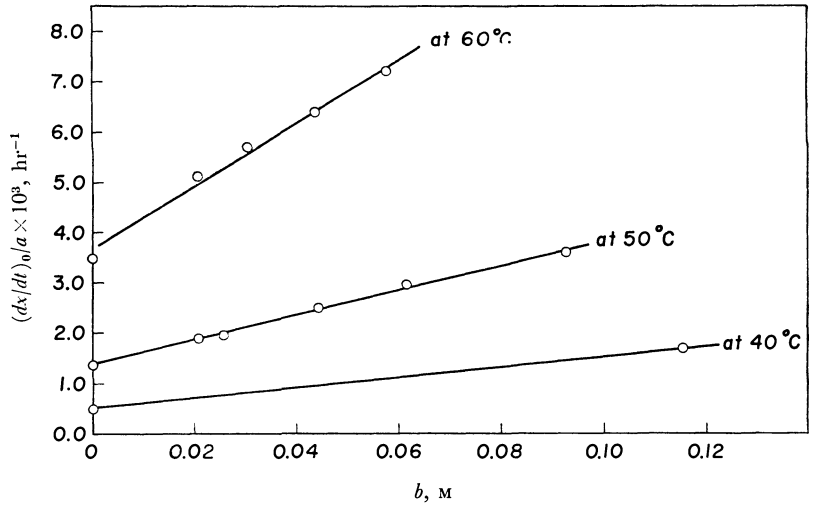

Fig. 2. The treatment of kinetic data for the reaction of *N,N*-dimethyl-*m*-nitroaniline with methyl iodide in methanol. See in text.

k_M by the intercept. Fig. 2 shows such plots. The results of k and k_M are given in Table 1. We believe that the accuracy of k by this method is no less than that of other methods. Both k and k_M show the Arrhenius relationship over the temperature range of experimental condition.

This type of correction was also made for the reaction of *N,N*-dimethyl-*m*-chloroaniline with methyl iodide. The reverse decomposition reaction might give a further complication, but it did not occur in methanol even at 70°C. The concentration of iodide at 20 half-lives period showed 100.3% completion for the reaction of *N,N*-dimethyl-*m*-toluidine with methyl iodide.

c) Kinetics Accompanying the Reverse Decomposition Reactions. Most of the present reactions show a rapid fall of the second order rate constants as the reaction proceeds. The higher the temperature and the more nonpolar the solvent is, the larger the decrease becomes.

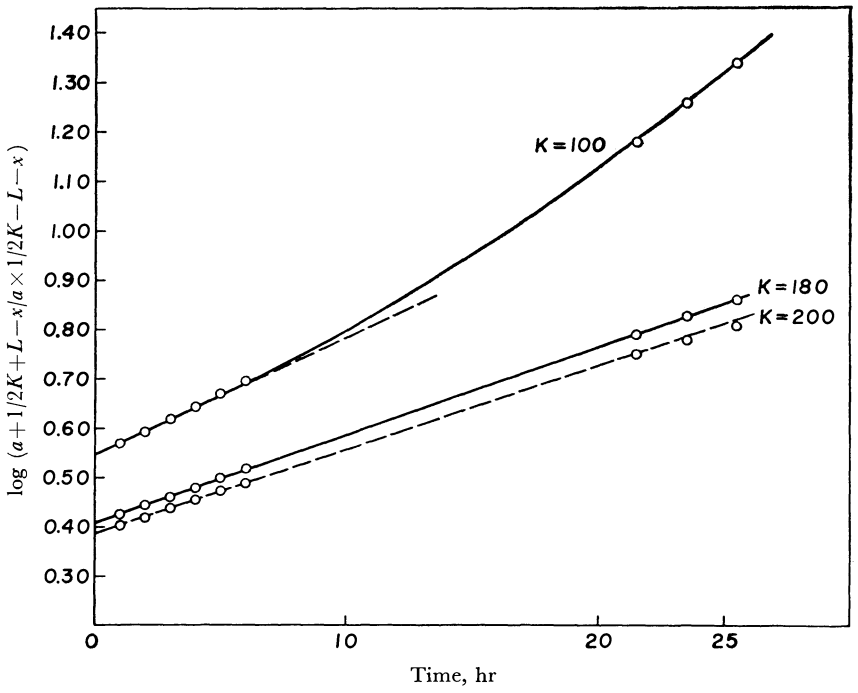

Fig. 3. Typical trial and error procedures of the treatment of kinetic data for the Menschutkin reaction containing the reverse decomposition of the salt. The reaction of dimethyl aniline with methyl iodide in nitrobenzene at 50°C.

The rate law is

$$dx/dt = k(a-x)^2 - k_d x \quad (3)$$

where k_d is the first order rate constant for the reverse reaction based on ion-pair decomposition. The hypothetical equilibrium constant is

$$K = k/k_d. \quad (4)$$

The use of Eqs. (3) and (4) gives

$$k \cdot t = 2.303/2L \log \{a+(1/2K)+L-x/a+(1/2K) -L-x\} \times \{a+(1/2K)-L/a+(1/2K)+L\}, \quad (5)$$

where L is the parameter given by

$$L = \sqrt{1+4Ka} \,/\, 2K. \quad (6)$$

The hypothesis used in the derivation might be proved to be right in terms of the linear relation between $\log\{a+(1/2K)+L-x/a+(1/2K)-L-x\}$ and time and the agreement of k obtained by the slope of this plot with k obtained from the initial slope of second order plot. The calculation for K was essentially the trial and error method, in which parameter K was adjusted so that the linear relation was obtained. The successive procedures are shown in Fig. 3. We could experimentally obtain the equilibrium point for some cases and show that the values obtained from the equilibrium point were in fair agreement with that from the hypothetical procedure. In the case of the reaction of *N,N*-dimethylaniline with methyl iodide in tetrahydrofuran (THF) at 50°C, for example, K through the former procedure is 0.432 and the latter value is 0.436. Even in acetonitrile, the most polar solvent in the present work, at 50°C, the decomposition of quaternary ammonium salt of *N,N*-dimethylaniline occurred, but in this case the degree of decomposition was *ca.* 2% after 100 hr and was too slow to obtain the value of K from the deviation of second order plot described above.

It is of interest that the rate of formation of iodide increases rapidly as soon as iodide precipitates and equilibrium is destroyed. These examples were observed in such solvents as benzene and THF. Measurement of k in the precipitation range was made on solutions ranging in concentration from *ca.* 0.08M to *ca.* 0.8M, but disagreement of each k value was over the experimental error as shown in Table 2. Thus the comparison for some nucleophiles in this solvent, was made with the same initial concentration.

TABLE 2. DEPENDENCE OF k FOR A QUATERNIZATION BASED ON DIMETHYLANILINE IN BENZENE AT 50°C UPON THE INITIAL CONCENTRATIONS OF REACTANTS (k in M^{-1} hr^{-1})

a	0.123	0.0890	0.820	0.194	0.0815	0.122
b	0.0459	0.0992	0.0862	0.194	0.768	0.0786
k	0.0260	0.0397	0.0612	0.0609	0.0778	0.0400

Results and Discussion

Tables 3 and 4 give results for reactions in various solvents at three to four temperatures. All reaction rate constants and equilibrium constants were calculated by the method of least squares and were corrected for the thermal expansion of the

Table 3. Summary of rate constants (k, in $l\ mol^{-1}\ hr^{-1}$) at different temperatures in various solvents for quaternization of a base $R\cdot C_6H_4N(CH_3)_2$ with CH_3I

No.	R	30°C	40°C	50°C	60°C
		In CH_3CN			
1	*p*-CH_3	2.64	4.90	8.46	15.8
2	*m*-CH_3	1.345	2.57	4.66	8.24
3	H	0.913	1.725	3.12	5.83
4	*m*-Cl	0.105	0.208	0.396	0.772
5	*m*-NO_2	0.0180	0.0379	0.0767	0.143
		In $C_6H_5NO_2$			—
6	*p*-CH_3	1.62	3.06	5.60	9.79
7	*m*-CH_3	0.715	1.40	2.69	4.82
8	H	0.451	0.883	1.74	
9	*m*-Cl	0.0375	0.0809	0.176	0.365
10	*m*-NO_2	4.85×10^{-3}	0.0133	—	—
		In CH_3COCH_3			
11	*p*-CH_3	1.38	2.53	4.37	7.36
12	*m*-CH_3	0.731	1.325	2.30	4.16
13	H	0.492	0.925	1.58	2.81
14	*m*-Cl	0.0556	0.118	0.214	0.433
15	*m*-NO_2	9.78×10^{-3}	0.0177	0.0406	0.0674
		In CH_3OH			
16	*m*-CH_3	—	0.874	1.96	—
17	H	—	0.647	1.42	—
18	*m*-Cl	0.0265	0.0752	0.175	—
19	*m*-NO_2		0.0107	0.0273	0.0632
		In $C_6H_5CH_2OH$			
20	*m*-CH_3	0.833	1.79	3.72	7.13
21	H	0.644	1.32	2.76	5.36
22	*m*-NO_2	—	0.022	0.0499	—
		In THF			
23	*p*-CH_3	—	0.466	0.85	1.60
24	*m*-CH_3	0.158	0.304	0.493	0.714
25	H	—	0.168	0.327	0.528
26	*m*-Cl	—	0.0121	—	—
		In C_6H_6			
27	*p*-CH_3	—	0.099	—	—
28	*m*-CH_3	—	0.039	0.059	0.10
29	H	0.015	0.028	0.040	—
		In $CH_3COC_2H_5$			
30	*p*-CH_3	0.870	1.57	—	—
31	*m*-CH_3	0.464	0.852	1.55	—
32	H	—	0.560	1.03	—
		In C_6H_5Br			
33	*m*-CH_3	—	—	0.229	0.44

Table 4. Summary of equilibrium constants (K in $l\ mol^{-1}$) for quaternization of a base $R\cdot C_6H_4\cdot N(CH_3)_2$

Temperature	*p*-CH_3	*m*-CH_3	H	*m*-Cl	*m*-NO_2
		In CH_3CN			
60°	—	~1000	~1000	~50	3.7
		In $C_6H_5NO_2$			
30°	—	—	—	8.9	1.0
40°	—	—	—	5.0	0.44
50°	2000	450	180	2.3	—
60°	1000	200	66.7	1.7	0.22
		In CH_3COCH_3			
40°	—	—	—	5.2	—
50°	—	360	180	2.8	0.165
60°	~200	80	40	1.36	0.1
		In THF			
30°	—	2.66	—	—	—
40°	~4	1.84	1.00	0.041	—
50°	~2	1.17	0.434	—	—
60°	0.98	0.494	0.254	—	—
		In C_6H_6			
50°	—	0.40	—	—	—
60°	—	0.089	—	—	—
		In C_6H_5Br			
50°	—	0.75	~0.29	—	—
60°	—	0.33	—	—	—

solvent. The values of the equilibrium constants K were unfortunately the apparent values for the following reactions.

$$R\cdot C_6H_4\cdot N(CH_3)_2 + CH_3I \overset{K}{\rightleftharpoons} R\cdot C_6H_4\cdot N(CH_3)_3^+\cdot I^-(\text{ion-pair})$$

But the conclusion drawn from the relation based upon K may be the same.

The Unitary Term of k or K. It is necessary to compare the so-called unitary terms[12] of k or K, k_u or K_u when the effects of solvents on k or K and ζ are discussed in detail. The unitary part of k for the reactions under consideration is represented by

$$k_u = k\times 1000 d_{solv}/M_{solv} \quad (7)$$

where k is the rate constant in common use whose dimension is M^{-1} time^{-1}, and d_{solv} and M_{solv} are the density of the solvent and the molecular weight of the solvent, respectively. The relation between k_u in Eq. (7) and the representation of k through the theory of absolute reaction rate,[13] given by the equation

$$k = k_g'\times r_A\cdot r_B/r_{M^{\neq}}\times V_{solv.}/RT \quad (8)$$

is self-evident, *viz.*,

$$k_u = k_g''\times r_A\cdot r_B/r_{M^{\neq}} \quad (9)$$

In these equations r_A, r_B, and $r_{M^{\neq}}$ are the activity coefficients, based upon the solvent standard state, of reactant amine, of methyl iodide, and of the activated complex of the transition state, respectively.

12) D. W. Gurney, "Ionic Processes in Solution," Dover Publication Inc., New York (1953), Chapter 6.
13) Y. Kondo and N. Tokura, This Bulletin, **40**, 1433 (1967).

The unitary values of the activation parameters, $\Delta H_u^{\neq 0}$ and $\Delta S_u^{\neq 0}$ are given by

$$\Delta H_u^{\neq 0} = -RT - R\partial \ln k/\partial(1/T) - R\partial \ln d/\partial(1/T) \quad (10)$$

$$\Delta S_u^{\neq 0} = -R - \frac{R}{T}\partial \ln k \cdot d/\partial(1/T) + R \ln k_u - R \ln \frac{\kappa T}{h} \quad (11)$$

where κ and h are Boltzman and Planck constants respectively, k_u being independent of the composition of the solution.[12] This correction for k mainly contributes to the change of entropy.

The essential point of the correction is in the choice of the standard state. The appropriate value for k is one mole per liter of solvent and that for k_u one mole per one mole of solvent. By comparing k_u for one solvent with that for others, the effects of solvents on the reaction rates and ζ may be discussed in terms of the commonly used activity coefficients through Eq. (9). All of the data will, therefore, be treated by using k_u in place of k. The above treatment is of course applied for the equilibrium constant K. The expression of K_u is

$$K_u = K_g' \times r_A \cdot r_B / r_{A^+ \cdot B^-} \quad (12)$$

The Effects of Variations in Uncharged Nucleophiles on the Measure of k_u to Solvent Variations, ζ. The treatment is essentially the same as given previously.[6] The difference of ζ among nucleophiles arises from interaction term of the substituent variable and the solvent variable. Existence of the linear free energy relationship concerning the substituent change is necessary in order to treat the data in terms of this method. It is shown in Fig. 4. The expression of ζ for substituted dimethylanilines is defined by

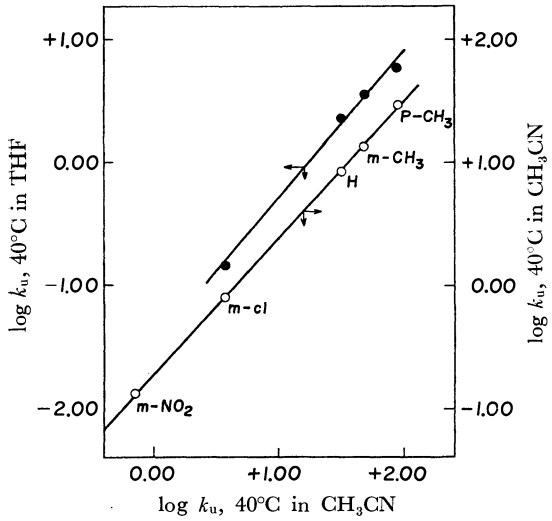

Fig. 4. The representation of the linear free energy relationships with respect to substituents.

$$\zeta = \delta_S \log k_u^X / \delta_S \log k_u^H \quad (13)$$

where δ_S means the differential with respect to the variations in solvents. The plot for this treatment is shown in Fig. 5, in which the slope gives the value of ζ. Deviation from this plot in some solvents is over the experimental error. But there is an approximate tendency for the dependence of ζ on the substituent. When the substituent is more electron donating, the value of ζ become smaller. This is illustrated in Fig. 6. The rate of reaction obtained by using a reactant with electron withdrawing substituent is more sensitive to solvent changes than others. In other words, the interaction constant between substituent variable and solvent variable has a positive value. The reason for the interaction between substituent variable and solvent variable might be interpreted in the following way. Equation (9) shows that these differences in ζ are not attributed to the effects of solvents on r_B, but to those on r_A or $r_{M^{\neq}}$, because by the first approximation the dependence of r_B on solvent change does not affect such a slope. Thus the substituent effect on the activity coefficients of either the reactant nucleophiles or of the activated complexes is somewhat modified by the nature of the solvent. The behavior is attributed to the latter for the following reasons. Firstly the modified Brϕnsted plot of $\delta_R \log k_u$ *versus* $\delta_R \log K_u$ has a relatively smaller slope than 1.00. Secondly the substituent effect in solvents with greater slopes is larger (see later section).

In terms of the solvent dependence of the Hammett's ρ value this explanation may be more clarified. That the slope of ζ *versus* σ has in general a positive value means that the value of ρ in more nonpolar solvent (in which the rate is slower) is more negative than that in polar solvent. There is a clear example of such a case; the difference of ρ in acetonitrile and that in methanol. The following equation which is derived from Eq. (9) will be applied.

$$\rho^{CH_3CN} \cdot \sigma_X = \rho^{CH_3OH} \cdot \sigma_X + \log ({}^{CH_3CN}r_{AX}^{CH_3OH} / {}^{CH_3CN}r_{AH}^{CH_3OH}) - \log ({}^{CH_3CN}r_{M^{\neq}X}^{CH_3OH} / {}^{CH_3CN}r_{M^{\neq}H}^{CH_3OH}) \quad (14)$$

In this equation ρ^{CH_3CN}, ρ^{CH_3OH}, and σ_X show Hammett's ρ in acetonitrile, in methanol, and substituent constant respectively. ${}^{CH_3CN}r_{AX}^{CH_3OH}$, ${}^{CH_3CN}r_{AH}^{CH_3OH}$, ${}^{CH_3CN}r_{M^{\neq}X}^{CH_3OH}$, and ${}^{CH_3CN}r_{M^{\neq}H}^{CH_3OH}$ denote the relative activity coefficient of the reactant, substituted amine and unsubstituted amine, and that of the activated complex with and without substituent, respectively. If the difference in quantity between ρ^{CH_3CN} and ρ^{CH_3OH} is attributed to the second term in Eq. (14), the relation of $|\rho|^{CH_3OH} < |\rho|^{CH_3CN}$ would be obtained because the solvation by methanol through hydrogen bonding will be diminished by the substitution

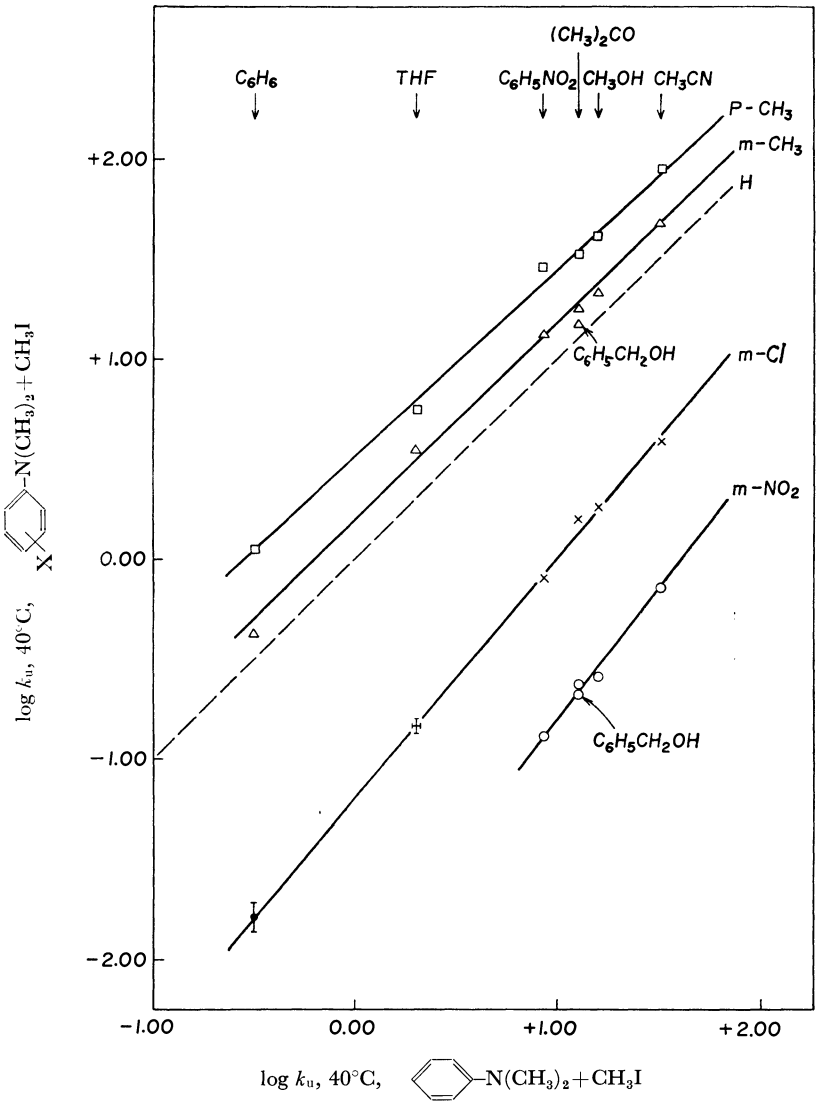

Fig. 5. The dependence of ζ on a few substituted nucleophiles at 40°C.

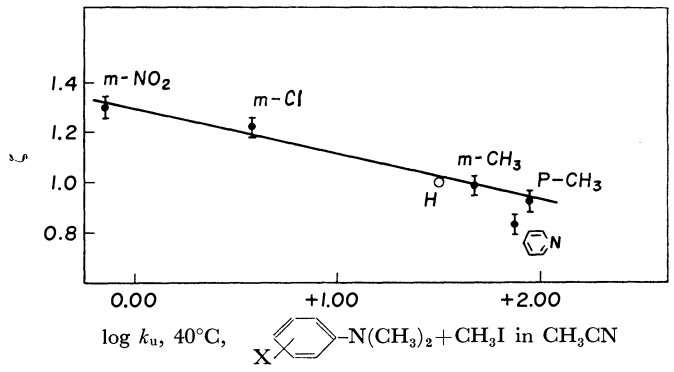

Fig. 6. The relationship between ζ and substituent variable.

of electron withdrawing group. The data show that this is not true unless the electron donating group (m-CH_3, p-CH_3) is introduced where a little downward deviation is observed (Fig. 5). The levelling off through the factor as expressed by the second factor in the right hand side of equation (14) was observed in liq. SO_2 which has strong solvation with amine bases.[14] A similar levelling off behavior is reported in ionizations of phosphines.[15]

Thus the substituent effect on ζ (Fig. 6) should result from the dependence of $\delta_R \log r_{M^*}$ on the solvent changes, and the deviation from these plots (Fig. 5) should be attributed to the dependence of $\delta_R \log r_A$ on the solvent changes. When pyridine is used as a nucleophile, the large deviation with regard to methanol (Fig. 7) clearly shows the existence of hydrogen bonding between pyridine and methanol.[16] The degree of divation expresses the difference between r_{Py} and r_{DMA} in methanol. For example, the relation of $\log r_{DMA}^{CH_3OH}/r_{Py}^{CH_3OH} = 0.70$ exists at 40°C.

It is of interest to examine the substituent effects on $\delta_S \Delta S_u^{\neq}$, the differences in $\Delta S_u^{\neq}$ among solvents. From the above explanation for ζ-δ relationship $\delta_S \Delta S_u^{\neq}$ must be larger by using the more electron withdrawing substituent. This is illustrated by the data in Table 5. Thus it also accounts for the fact that the interaction constant has positive value.

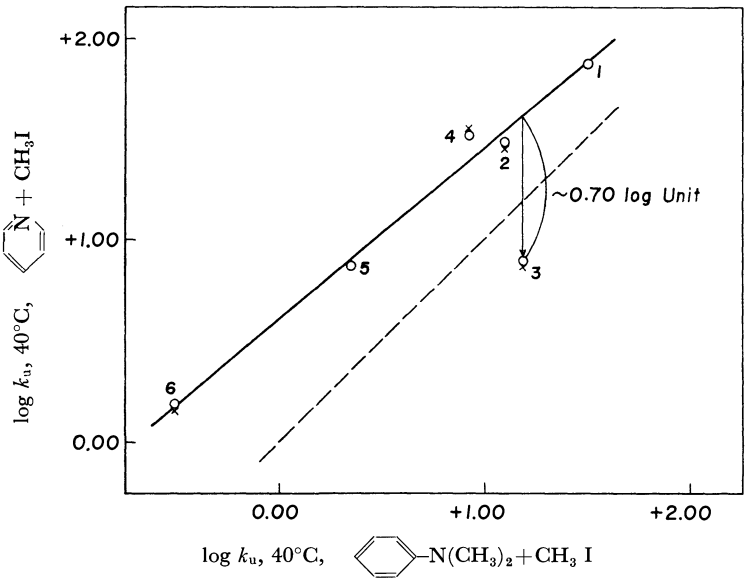

Fig. 7. The difference in ζ value detween pyridine and dimethylaniline. The data of quaternization of pyridine are taken from the two previous reports. ○ is from N. Tokura and Y. Kondo, This Bulletin, **36**, 400 (1963), × is from H. Hartmann, H. Kelm and G. Rinck, *Z. Phys. Chem.*, **44**, 335 (1965). (1) CH_3CN, (2) $(CH_3)_2CO$, (3) CH_3OH, (4) $C_6H_5NO_2$, (5) THF, (6) C_6H_6.

TABLE 5. DIFFERENCE IN δ_s $\Delta Su^{\neq}$, 50°C AMONG SOME SUBSTITUTED DIMETHYLANILINES

	p-CH_3	m-CH_3	H	m-Cl	m-NO_2
CH_3CN	0.00(−31.12)[a]	0.00(−31.56)[a]	0.00(−31.61)[a]	0.00(32.68)[a]	0.00(−33.84)[a]
$(CH_3)_2CO$	−3.58	− 3.78	− 4.51	−1.25	− 4.19
$C_6H_5NO_2$	−1.18	+ 0.15	+ 0.37	+3.44	+ 2.81
CH_3OH	+6.76[b]	+ 7.75[c]	+ 7.90[c]	+14.68	+14.22
THF	−2.9	−11.5	−10.5	+11.3	—

a) Values in parentheses represent the unitary term of the activation entropy in acetonitrile.
b) From the data given by Evans *et al.*, Ref. 7b.
c) Our data for m-CH_3 and H presented in Table 3 in this solvent are in fair agreement with the data by Evans *et al.* The activation parameters were calculated from both our data and theirs.

14) N. Tokura and Y. Kondo, This Bulletin, **37**, 133 (1964).
15) W. A. Henderson, Jr., and S. A. Buckler, *J. Amer. Chem. Soc.*, **82**, 5794 (1960).
16) E. Becker, *Spectrochim. Acta*, **17**, 436 (1961).

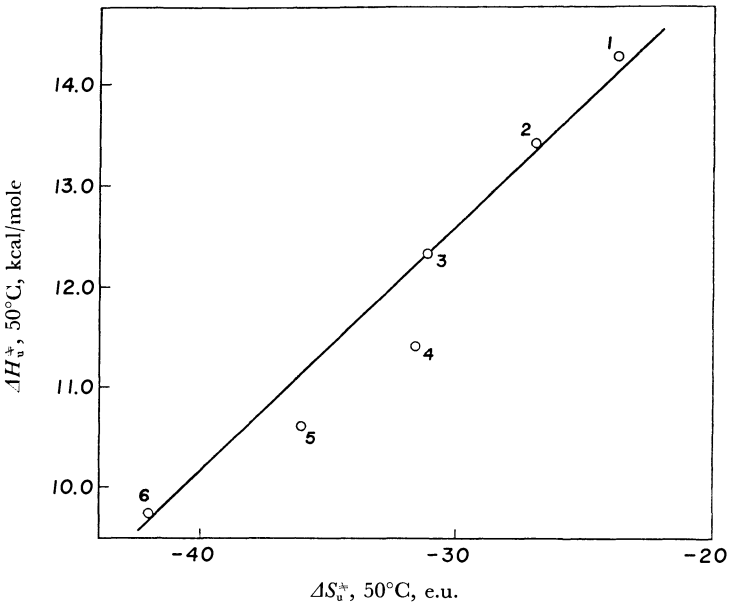

Fig. 8. The plot of $\Delta H_u^{\ddagger}$ *versus* $\Delta S_u^{\ddagger}$ for a reaction of *N,N*-dimethylaniline with methyl iodide.

There is another reason why the above tendency is denoted as the only "approximate" tendency at all. The order of the relative rates with respect to the solvent will be modified by the change of temperature. The degree of this modification is illustrated in the plot of $\Delta H_u^{\ddagger}$ *versus* $\Delta S_u^{\ddagger}$. Unless the so-called isokinetic linear relationship between these values exists, this relative order is modified. Figure 8 shows the approximate linearity between these two values.

The dependence of ζ on substituents which was explained on the basis of the above electrostriction theory will predict the variation of the pressure dependence of rates with the substitution of nucleophile. The substitution by the electron withdrawing groups will influence the pressure effect of rate by larger amount. In other words, the dependence of the volumes of activations on nucleophiles will be larger in so-called nonpolar solvents than in polar solvents. The solvent dependence of Hammett's ρ for the equilibria of a series of benzoic acids has been attributed to the activity coefficients of the carbonium ions.[6] For this type of equilibrium the pressure effect will be decreased by using the acids substituted by electron withdrawing groups. This was experimentally proved by Fischer *et al.*[17]

There is a case where the solvent effects of the nucleophilic tendency are mainly attributed to the relative activity coefficients of charged species *i*, $\delta_S \log r_i$. That is the Finkelstein reaction.[18] Thus the difference between charged and uncharged nucleophiles in the solvent dependence of the rate is clear. For the fomer the relative activity coefficients of the reactant bases are the main factor in determining the solvent dependence of ζ, but for the latter those of the activated complexes mainly affect the relative order of rates with solvent changes. Thus the compilation of both charged and uncharged reactants as nucleophiles is questionable, if the solvent used is taken into consideration.

Difference in the Factor Influencing the ζ between Methyl Iodide and Methyl Picrate. According to the compilation by Reinheimer *et al.*[19] the modification of the sensitivity of the rates to solvent changes caused by using EtI in place of EtBr for quaternization of pyridine may be made by a negligible amount at least in aromatic solvent. However, comparison of the present data with our previous data[6] shows that the ζ are markedly influenced by

17) A. Fischer, B. R. Mann and J. Vaughan, *J. Chem. Soc.*, **1961**, 1093.

18) N. Tokura, preprint at the Symposium of Oxidation-Reduction in Non-Aqueous Solvent Systems, Kyoto, Oct., 1968, from the data of A. J. Parker in "Advances in Physical Organic Chemistry," Vol. 5, ed. by V. Gold, Academic Press, London, New York (1967), p. 173. Table 3 in this print is based on the reliable fact that the levelling off on anion solvation exists in these solvents, and not on the fact that in dipolar aprotic solvents the desolvation occurs with respect to small anion. *Cf.* R. F. Rodewald, K. Mahendran and R. Fuchs, *J. Amer. Chem. Soc.*, **90**, 6698 (1968).

19) J. D. Reinheimer, J. D. Harley and W. W. Meyers, *J. Org. Chem.*, **28**, 1575 (1963).

the change of $CH_3Pic.$ to CH_3I. Figure 9 illustrates this situation. It is observed that the quaternization of *N,N*-dimethylaniline with methyl picrate is less sensitive to the variations in solvents than that with methyl iodide. The relation of $\zeta < 1.0$ is observed for methyl picrate. According to the interpretation of rate by the transition state theory (Eq.(9)) such a diffence should be attributed to the difference in the dependence on solvent variations between r_{CH_3I} and r_{CH_3Pic} or between $r_{M^+,I}$ and

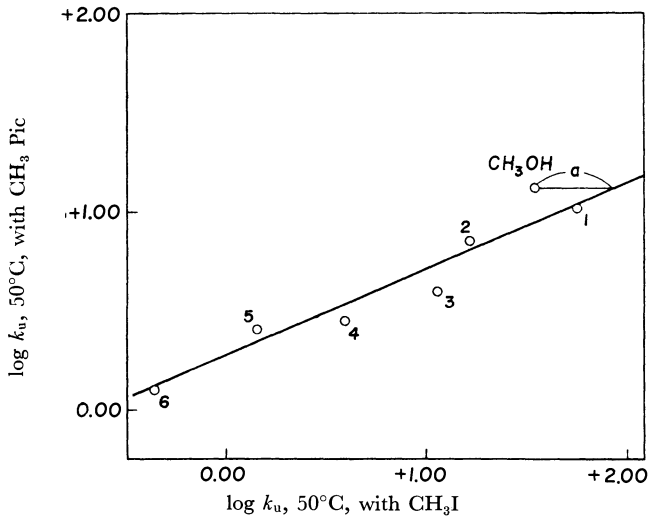

Fig. 9. The difference in ζ between the reaction of *N,N*-dimethylaniline with methyl iodide and that with methyl picrate. (1) CH_3CN, (2) $C_6H_5NO_2$, (3) $CH_3COC_2H_5$, (4) THF, (5) C_6H_5Br, (6) C_6H_6.

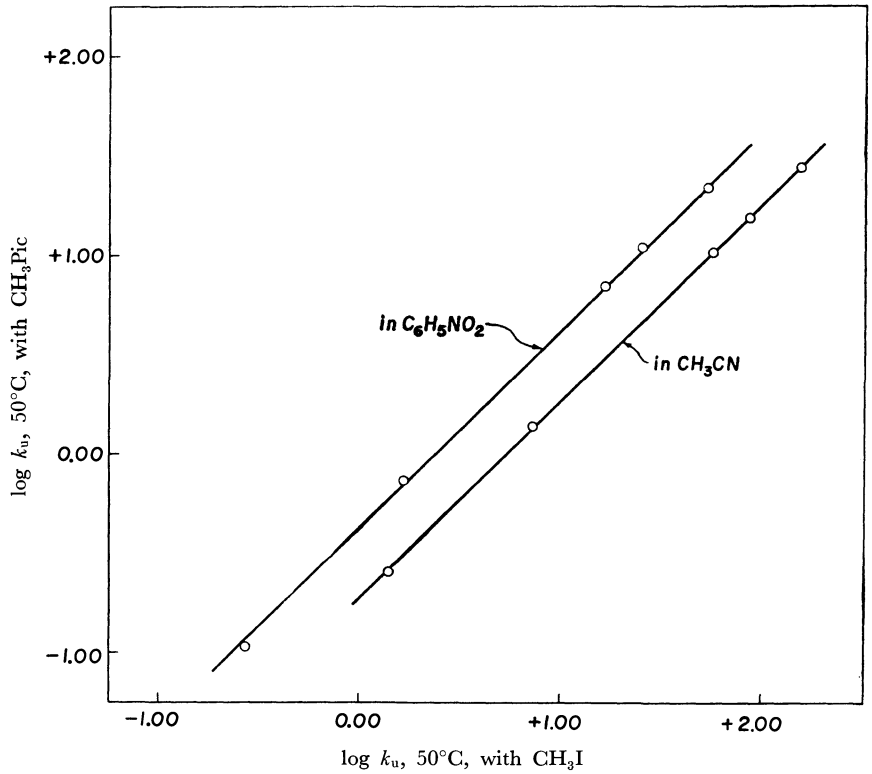

Fig. 10. The small difference in the substituent effects between the reactions with CH_3I and those with CH_3Pic both in $C_6H_5NO_2$ and in CH_3CN.

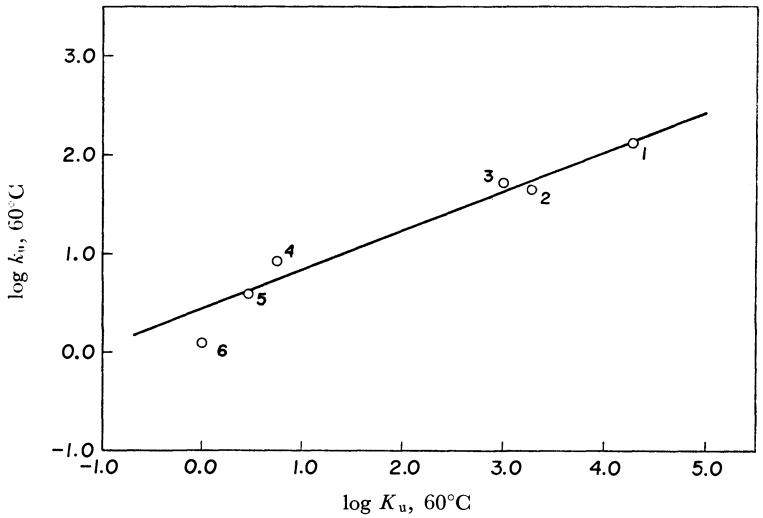

Fig. 11. The relationship between δ_S log k_u and δ_S log K_u for the relation of *m*-methyl-*N*,*N*-dimethylaniline with methyl iodide.
(1) CH_3CN, (2) $C_6H_5NO_2$, (3) $(CH_3)_2CO$, (4) THF, (5) C_6H_5Br, (6) C_6H_6.

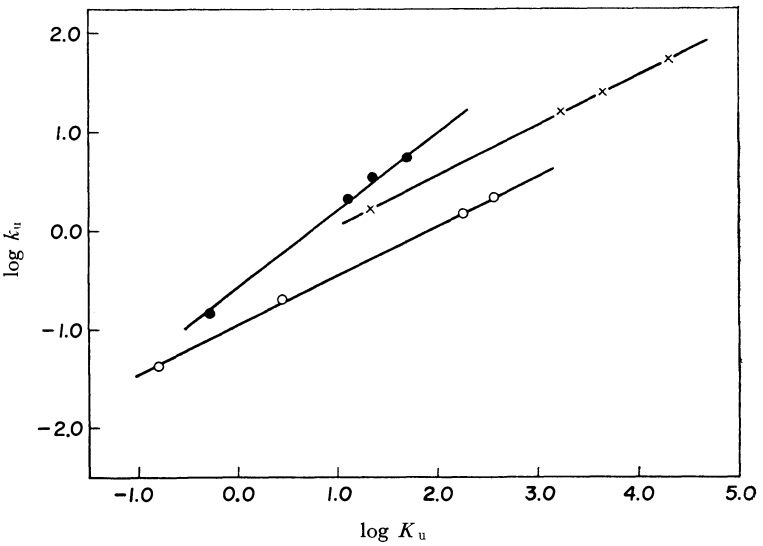

Fig. 12. Some of the modified Brønsted plots.
○ in $(CH_3)_2CO$ at 50°C
● in THF at 40°C
× in $C_6H_5NO_2$ at 50°C

$r_{M^{\neq},Pic}$. Although we have no data on r_{CH_3I} and r_{CH_3Pic} in various solvents, the existence of an approximately linear relationship as shown in Fig. 9 explains this behavior in terms of the difference in solvent dependence between $r_{M^{\neq},I}$ and $r_{M^{\neq},Pic}$. Our explanation is further supported by the fact that in the picrate there is large negative charge distribution and no net charge at any one atom.[20] The combination of this fact with the electrostriction theory leads to the following explanation; in the case of the transition state for the reaction with methyl picrate the negative charge distribution may be large. Thus, $r_{M^{\neq},Pic}$ may not become smaller even in polar solvents as $r_{M^{\neq},I}$ does, while in non-polar solvents the reverse relation may be true. There is less entropy loss accompanied with the electrostriction of solvent molecules along the reaction coordinate.

That the "completely" linear relation does not exist means that there is the difference in solvent effects between r_{CH_3I} and r_{CH_3Pic}. A large devia-

20) E. Grunwald and E. Price, *J. Amer. Chem. Soc.*, **86**, 4517 (1964).

tion is observed in methanol. The experimental error of reaction rate was less than 0.02 log unit. The data of r_{CH_3I} in acetonitrile and in methanol at 25°C,[3] $\log r_{CH_3I}^{CH_3CN} - \log r_{CH_3I}^{CH_3OH} \simeq 0.35$ is in accordance with this deviation 0.35 which is given as the distance, a in Fig. 9. This shows that the relation of $\log r_{CH_3Pic}^{CH_3CN} \simeq \log r_{CH_3Pic}^{CH_3OH}$ exists.

For both cases of CH_3Pic and CH_3I the relation of $|\rho|^{C_6H_5NO_2} > |\rho|^{CH_3CN}$ exists and in each solvent the differences in the substituent effects between CH_3I and CH_3Pic is apparently equal, as shown in Fig. 10. This seems to be inconsistent with the above discussion. But we can explain the relation similarly as in the previous section, if we assume that the substituent effects on the stability of each activated complex are almost independent of the leaving group.

The Nature of the S_N2 Transition State. The concept of Glasstone *et al.*[8] about the stereochemistry of the S_N2 transition complex has been criticized by Rossell[7a] and by Weale.[21] Weale *et al.* studied the volume of activation for a reversible Menschutkin reaction, $CH_3I + C_6H_5\text{–}N(CH_3)\cdot(C_2H_5) \rightleftarrows C_6H_5\text{–}N(CH_3)_2^{\delta+}\cdot C_2H_5\cdots I^{\delta-}$ in acetone and showed that in absolute value the volume of activation is less than the change of volume accompanied with an equilibrium between reactant and product as ion-pair. Rossell criticized the relevance of the view of Glasstone *et al.* which was concluded from the similarity of ΔS° and $\Delta S^\ddagger$ found in the reaction of dimethylaniline with methyl iodide in nitrobenzene. According to Rossell, "such a similarity is the exception rather than the rule."

If the solvent effects on the reaction rates are mainly attributed to the differences in the activity coefficients of the activated complexes among the variations of solvents, the dependence of k on the variations in solvents should be correlated with the dependence of K on those variations, and the slope of $\delta_S \log k_u$ *versus* $\delta_S \log K_u$ must show the degree of charge separation in the transition state. For the reaction of *m*-CH_3-DMA with CH_3I at 60°C Fig. 11 shows the approximate linear relation between $\delta_S \log k_u$ and $\delta_S \log K_u$ which has a relatively small slope. It can be considered that the nature of the transition state for the reactions is not very similar to that of the final product, quaternally ammonium salt. This result should be correlated with any relationship between $\delta_R \log k_u$ and $\delta_R \log K_u$ in each solvent. Figure 12 which shows a nearly linear relation[22] among these values reflects the fact[23] that the equilibrium between ions and ion-pairs is quite insensitive to the substituent effects. Figure 12 also shows the insensitivity of the reaction rate to substituent changes relative to that of the equilibrium constant.

21) K .E. Weale, "Chemical Reactions at High Pressures," E. F. N. Spon Ltd., London (1967), p. 143.

22) The modified Brønsted type. This is an example for usually accepted generalization where relatively good correlation of carbon nucleophilicity exists in a series of bases with their carbon basicity, instead of with hydrogen basicity. See Ref. 2.

23) T. T. Denison and J. B. Ramsey, *J. Amer. Chem. Soc.*, **77**, 2615 (1955); G. W. Ceska and E. Grunwald, *ibid.*, **89**, 1371 (1967); N. N. Lichtin and P. D. Bartlett, *ibid.*, **73**, 5530 (1951).

BULLETIN OF THE CHEMICAL SOCIETY OF JAPAN VOL. 43 1763—1768 (1970)

Mechanism of the Ullmann Condensation. I.*1 Kinetic and Thermodynamic Studies

Tran Dinh TUONG and Mitsuhiko HIDA

Department of Synthetic Chemistry, Faculty of Engineering, The University of Tokyo, Hongo, Bunkyo-ku, Tokyo

(Received September 3, 1969)

Kinetic studies of the Ullmann condensation of an aryl halide, sodium 1-amino-4-bromoanthraquinone-2-sulfonate and an amine, aniline, were undertaken. Cupric copper was used as the catalyst. The reaction was found to be first order in monomeric aryl halide and first order in amine, and to depend hyperbolically on the concentration of the catalyst. It was shown by ESR measurements that the copper catalyst exists largely as cupric species. The experimental results were discussed mechanistically.

A large number of patents and papers have been written on the condensation reaction of aryl halides with amines or phenoxides in the presence of a copper catalyst. This reaction is known as the Ullmann condensation reaction[1] and has been an important tool in, for example, the synthesis of dyes, drugs and compounds of biochemical interest. On the other hand, the reaction has been classified as an unknown mechanism[2,3] since the mechanism has not yet been well established in spite of the efforts of several investigators.[4-10]

Particularly it is noticeable that little information is availahle as to what the real catalytic species is. Mechanistic studies are difficult for the following reasons:

a) The reaction must often be carried out under vigorous conditions, *i.e.*, at temperatures higher than 150°C and sometimes under high pressure.

b) Since homogeneous systems are rarely obtained, kinetic studies are hampered.

Because the mechanism is not yet known in detail, the improvement of this industrially important reaction has been attempted[11-14] empirically rather than from the theoretical point of view. Thus, in order to use this reaction in synthetic chemistry more efficiently, more investigations must be undertaken in connection with the mechanism of this reaction. This necessity prompted the present study. The preliminary results will be reported in this paper.

Results and Discussion

A kinetic study was made of the condensation of sodium 1-amino-4-bromoanthraquinone-2-sulfonate (I) with aniline in an aqueous buffer solution. Cupric sulfate was selected as the catalyst because of its large solubility in water and because of the weak coordinating ability of the sulfate ion to the metal ion. The reaction is known to proceed under comparatively mild conditions.[15,16]

When aniline was used in large excess compared with I, a homogeneous system could be attained and kinetic measurements with a good reproducibility were possible.

Reaction Products. Paper chromatography revealed that the reaction products were bromamic

*1 Presented in part at the Annual Meetings of the Chemical Society of Japan, March, 1968 (Osaka), and April, 1969 (Tokyo).

1) J. E. Gowan and T. S. Wheeler, "Name Index of Organic Reactions," Williams Clowes & Sons, London (1962).

2) J. F. Bunnett and R. E. Zahler, *Chem. Rev.*, **49**, 297 (1951).

3) J. F. Bunnett, *Quart. Rev.* (London), **12**, 1 (1959).

4) P. W. Weston and H. Adkins, *J. Amer. Chem. Soc.*, **50**, 859 (1928).

5) A. A. Goldberg, *J. Chem. Soc.*, **1952**, 4368.

6) W. Mayer and R. Fikentscher, *Chem. Ber.*, **91**, 1536 (1958).

7) R. G. R. Bacon and O. J. Stewart, *J. Chem. Soc.*, **1965**, 4953.

8) H. Weingarten, *J. Org. Chem.*, **29**, 977 (1964).

9) H. Weingarten, *ibid.*, **29**, 3624 (1964).

10) A. L. Williams, R. E. Kinney and F. R. Bridger, *J. Org. Chem.*, **32**, 2501 (1967).

11) R. Robinson and S. Sugasawa, *J. Chem. Soc.*, **1931**, 3173.

12) T. Kametani, K. Fukumoto and T. Takano, *Yakugaku Zasshi*, **82**, 1307 (1961).

13) Y. K. Sawa, N. Tsuji and S. Maeda, *Tetrahedron*, **15**, 144 (1961).

14) Y. K. Sawa, N. Tsuji and S. Maeda, *ibid.*, **20**, 2255 (1964).

15) T. Maki, Annual Reports of The Committee on Chemistry of Aromatics, Japan Society for Promotion of Science, **4**, 98 (1951).

16) T. Maki, *ibid.*, **5**, 162 (1952).

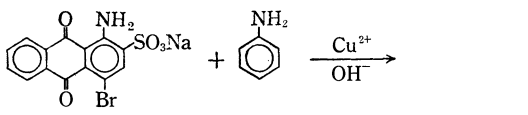

I

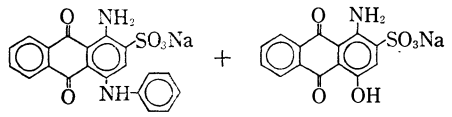

II III

acid (I), sodium 1-amino-4-anilinoanthraquinone-2-sulfonate (II), and sodium 1-amino-4-hydroxyanthraquinone-2-sulfonate (III).

Their amounts were determined spectrophotometrically.

Compared with the main product, II, III was found to be formed in a negligibly small quantity (less than 3% of the total concentration) and so it was neglected in the calculation of the reaction rates. This by-product was also formed in the reaction carried out in the absence of aniline, but it was not produced by treating II in an alkaline solution. These facts show without doubt that III was the condensation product of I with the alkaline aqueous solvent. Other side reactions, such as dehalogenation and biaryl formation which are known often to accompany the Ullmann condensation reaction,[17] were not observed.

Kinetics. As is shown in Fig. 1, the initial rate, v_0, was not proportional to the concentration of I.

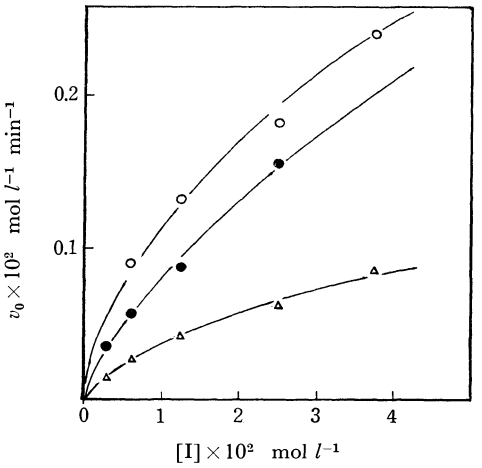

Fig. 1. Dependence of the initial rate on the concentration of I.
pH=9.94, T=343°K
$[PhNH_2]_0$=0.30 mol l^{-1}
$[Cu^{2+}]_0=2.5\times10^{-4}$ mol l^{-1} (△)
12.5×10^{-4} mol l^{-1} (●)
50.0×10^{-4} mol l^{-1} (○)

These results can be understood as follows.

The spectrum of bromamic acid (I) in an aqueous solution was observed to change bathochromically and hypochromically with an increase in the concentration. This fact suggests that I aggregates in an aqueous solution. The degree of aggregation and the aggregation constant at 70°C and at pH 9.94 were found to be 2 and about 200 respectively by the maximum slope method.[18] Thus, the monomeric and dimeric species are equilibrated in the reaction system. If the initial rate is assumed to be proportional to the concentrations of the monomer and the dimer (c_1 and c_2), the initial rate may be expressed by Eq. (1):

$$v_0 = k_1c_1 + k_2c_2 \quad (1)$$

where k_1 and k_2 are rate constants associated with the monomer and the dimer respectively.

If the analytical amount of I is denoted as c_0, we have:

$$c_0 = c_1 + 2c_2 \quad (2)$$

By combining Eq. (1) with Eq. (2), we obtain Eq. (3):

$$v_0 = \left(k_1 - \frac{k_2}{2}\right)c_1 + \frac{k_2}{2}c_0 \quad (3)$$

Therefore,

$$\frac{v_0}{c_0} = \left(k_1 - \frac{k_2}{2}\right)f_1 + \frac{k_2}{2} \quad (4)$$

where f_1 is the fraction of the monomer.

The concentration, c_1, of the monomeric species

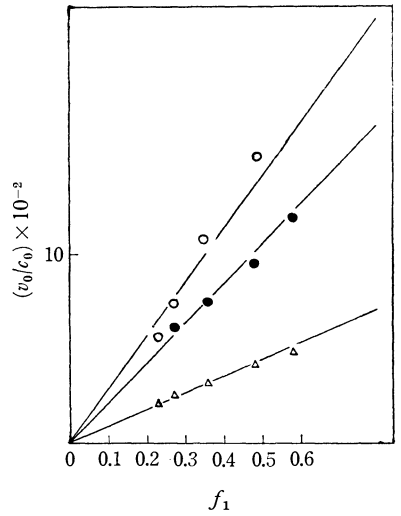

Fig. 2. Linear relationsnip between v_0/c_0 and the monomer fraction f_1.
pH=9.94, T=343°K
$[PhNH_2]_0$=0.30 mol l^{-1}
$[Cu^{2+}]_0=2.5\times10^{-4}$ mol l^{-1} (△)
12.5×10^{-4} mol l^{-1} (●)
50.0×10^{-4} mol l^{-1} (○)

17) R. G. R. Bacon and H. A. O. Hill, *Quart. Rev.*, **19**, 95 (1965).

18) M. Hida, A. Yabe, H. Murayama and M. Hayashi, This Bulletin, **41**, 1776 (1968).

is obtained by solving Eq. (5):

$$400c_1^2 + c_1 - c_0 = 0 \quad (5)$$

Figure 2 shows the linear plot of v_0/c_0 against f_1. The values of k_1 and k_2 can be determined from the slope ($=k_1-k_2/2$) and the intercept ($=k_2/2$) of the straight lines.

These results suggest that only the monomeric species was active and that the reaction was first order with respect to the monomer of I.

The unimolecularity of the aryl halide in the Ullmann condensation reaction has been reported by several workers.[9,10]

Figure 3, where the initial rate is plotted against the initial concentration of aniline, shows that the first order can be assigned to the amine.

The rate law is, therefore, given by:

$$\text{rate} = k_0 f_1 c_0[\text{PhNH}_2] = k_{app} c_0[\text{PhNH}_2] \quad (6)$$

where k_{app} is a function of the reaction conditions (pH, temperature and the atmosphere) and of the concentration of the copper ion.

The dependence of the apparent rate constant, k_{app}, on the concentration of the catalyst is shown by the data tabulated in Table 1. The experimental data can be satisfied by the following three relations:

a) $$k_{app} = k[\text{Cu}^{2+}]^m \quad (7)$$

where k and m are constants.

The value of m varied over the range from 0.48 to 0.70, according to the conditions of the reaction (pH and temperature). The fact that the value of m varied around 0.50 is interesting, but attempts to devise mechanisms which could fit the above relation were unsuccessful.

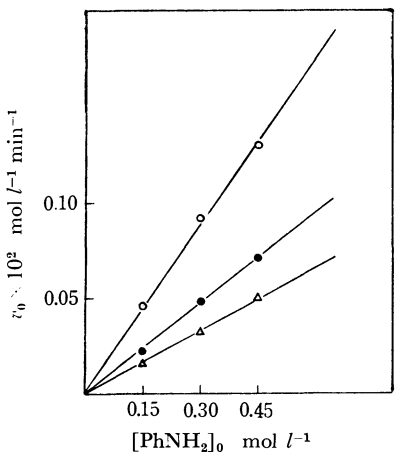

Fig. 3. Linear relationship between the initial rate and the concentration of aniline.
pH=9.94, T=343°K
$[I]_0=1.25\times10^{-2}$ mole l^{-1}
$[Cu^{2+}]_0=2.50\times10^{-4}$ mol l^{-1} (△)
5.00×10^{-4} mol l^{-1} (●)
100.00×10^{-4} mol l^{-1} (○)

Table 1.[a] Dependence of the apparent rate constant k_{app} on the catalyst concentration

No	pH	T, °K	$Cu^{2+}\times10^4$ mol l^{-1}	$k_{app}\times10^2$, l mol^{-1} min^{-1}
1	9.46	343	2.62	3.23
2	9.46	343	5.81	4.68
3	9.46	343	8.32	5.61
4	9.46	343	12.87	7.07
5	9.46	243	16.64	7.53
6	9.94	343	2.50	8.46
7	9.94	343	2.80	9.22
8	9.94	343	5.02	15.74
9	9.94	343	8.12	19.58
10	9.94	343	12.50	24.96
11	9.94	343	50.00	28.72
12	10.57	343	2.74	9.06
13	10.57	343	5.54	13.67
14	10.57	343	8.11	16.90
15	10.57	343	12.88	17.82
16	9.94	333	2.72	5.76
17	9.94	333	5.50	9.91
18	9.94	333	8.29	12.29
19	9.94	333	13.08	13.98
20	9.94	353	2.72	14.21
21	9.94	353	5.35	22.89
22	9.94	353	8.17	31.72
23	9.94	353	12.84	36.86
24	9.94	363	2.69	18.05
25	9.94	363	5.54	32.33
26	9.94	363	8.22	42.55
27	9.94	363	12.77	46.69

a) Experiments under nitrogen atmosphere, $[I]_0=1.25\times10^{-2}$ mol l^{-1}, $[PhNH_2]_0=0.30$ mol l^{-1}.

b) $$k_{app} = k\frac{[\text{Cu}^{2+}]}{[\text{Cu}^{2+}] + \alpha} \quad (8)$$

where k and α are constants, their values depending on the pH and the temperature.

The energies and entropies associated with k and α were found to be as follows:

$$\Delta E^*(k) = 12.37 \text{ kcal}\cdot\text{mol}^{-1}$$
$$\Delta S^*(k) = -19.80 \text{ eu } (T=343°\text{K})$$
$$\Delta E^*(\alpha) = 4.12 \text{ kcal}\cdot\text{mol}^{-1}$$
$$\Delta S^*(\alpha) = -60.30 \text{ eu } (T=343°\text{K})$$

This hyperbolic relation could be derived from the following mechanism (I is denoted as ArBr):

$$\text{Cu}^{2+} \overset{K_1}{\rightleftarrows} \text{Cu}^{+} \quad (9)$$

$$\text{Cu}^{+} + \text{ArBr} \overset{K_2}{\rightleftarrows} \text{Cu}^{+}\cdot\text{BrAr} \quad (10)$$

$$\text{Cu}^{2+} + \text{Cu}^{+} \overset{K_3}{\rightleftarrows} \text{Cu}^{2+}\cdot\text{Cu}^{+} \quad (11)$$

$$Cu^{+}\cdot BrAr + PhNH_2 + OH^- \xrightarrow{k} Cu^{+} + ArNHPh + Br^- + (ArOH) \quad (12)$$

If the values of both K_2 and K_3 are sufficiently small, we can derive Eq. (13) from Eqs. (9)—(12):

$$\text{rate} = (kK_1K_2/2K_3)[ArBr][PhNH_2][Cu^{2+}]/([Cu^{2+}]+K_1+1/2K_3) \quad (13)$$

Equation (13) is identical with Eq. (8) provided that:

$$k_0 = kK_1K_2/2K_3$$

and

$$\alpha = K_1 + 1/2K_3$$

In proposing this mechanism, an equilibrium between cuprous and cupric species, the activity of cuprous[19] copper and the deactivating effect of the cupric ion were postulated.

c) The dependence of the reaction rates on the catalyst concentration could also be interpreted on the assumption of the formation of clusters. Thus, the catalyst is assumed to exist in the reaction system as a monomer and as a cluster of the n-th degree, so that:

$$n\text{Cu} \underset{}{\overset{K}{\rightleftharpoons}} \text{Cu}_n \quad (14)$$

By designating the initial concentration of the catalyst as $[Cu^{2+}]_0$, we obtain Eq. (15):

$$[Cu^{2+}]_0 = [Cu] + n[Cu_n] \quad (15)$$

Further, it is assumed that the apparent rate constant, k_{app} $(=k_0f_1)$, can be written as follows:

$$k_{app} = k_1[Cu] + n\bar{k}_n[Cu_n] \quad (16)$$

where k_1 is the rate constant of the reaction of the monomeric species and where $\bar{k}_n$ $(=k_n/n)$ is the rate constant of the clusters (per molecule).

By combining Eq. (15) with Eq. (16), we get Eq. (17):

$$k_1[Cu^{2+}]_0 - k_{app} = n(k_1-\bar{k}_n)Cu_n \quad (17)$$

and:

$$k_{app} - \bar{k}_n[Cu^{2+}]_0 = (k_1-\bar{k}_n)[Cu] \quad (18)$$

By inserting Eq. (18) into Eq. (14):

$$\frac{k_1[Cu^{2+}]_0 - k_{app}}{n(k_1-\bar{k}_n)} = \frac{K}{(k_1-\bar{k}_n)^n}(k_{app}-\bar{k}_n[Cu^{2+}]_0)^n \quad (19)$$

or

$$\log (k_1[Cu^{2+}]_0-k_{app}) = n \log (k_{app}-\bar{k}_n[Cu^{2+}]_0) + \log \frac{nK}{(k_1-\bar{k}_n)^{n-1}} \quad (19')$$

where K is the equilibrium constant.

19) The addition of reducing agents, such as $NaHSO_3$, $SnCl_2$, $FeSO_4$, $TiCl_3$, *etc.*, to the reaction system, was observed to enhance markedly the reaction rate. Detailed results will be reported and discussed in a later paper of the series.

If the cluster is assumed to be inactive, we can rewrite Eq. (19′) as Eq. (20):

$$\log (k_1[Cu^{2+}]_0-k_{app}) = n \log k_{app} + \log \frac{nK}{k_1^{n-1}} \quad (20)$$

The value of k_1 is given by Eq. (21):

$$k_1 = \lim_{[Cu^{2+}]_0 \to 0} \frac{dk_{app}}{d[Cu^{2+}]_0} \quad (21)$$

The value of k_1 was determined graphically from the slope of the tangent of the plot of k_{app} *vs.* $[Cu^{2+}]_0$ at $[Cu^{2+}]_0=0$, and then $\log (k_1[Cu^{2+}]_0-k_{app})$ was plotted against $\log k_{app}$ (Fig. 4). The values of n and K were determined from the slope and the intercept; their values are summarized in Table 2. It was found that n was independent of the reaction conditions and that it has a constant value of 3.

The activation parameters associated with k_1 were determined from the Arrhenius plot:

$$\Delta E^{\ddagger}(k_1) = 9.91 \text{ kcal}\cdot\text{mol}^{-1}$$

$$\Delta S^{\ddagger}(k_2) = -18.33 \text{ eu } (T=343^{\circ}\text{K})$$

The apparent energy of activation associated with k_{app} was also determined to be 9.14 kcal mol^{-1}. As is shown in Fig. 5, the apparent energy of activation is independent of the concentration of the cupric ion. Since:

$$k_{app} = k_1f_1F_1[Cu^{2+}]_0$$

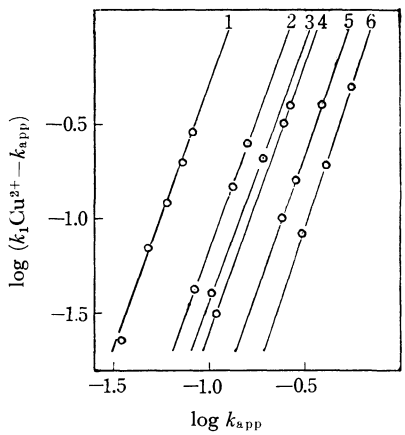

Fig. 4. Linear relationship between $\log(k_1Cu^{2+}-k_{app})$ and $\log k_{app}$.

	1	2	3	4	5	6
pH	9.46	9.94	10.57	9.94	9.94	9.94
T°K	343	343	343	333	353	363

Table 2
The aggregation of copper catalyst

pH	T°K	$k_1\times10^{-2}$	n	$k\times10^{-6}$
9.46	343	1.85	3	5.85
9.94	343	4.05	3	1.70
10.57	343	4.75	3	3.60
9.94	333	2.40	3	8.39
9.94	353	5.75	3	5.65
9.94	363	8.00	3	8.53

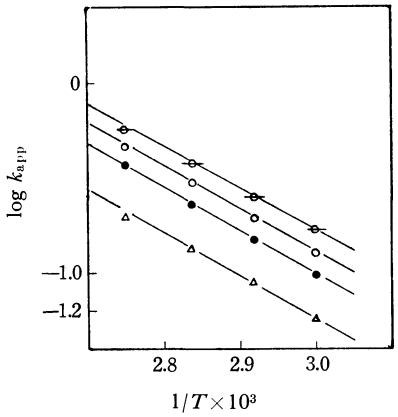

Fig. 5. Arrhenius plots.
pH=9.94, $[I]_0=1.25\times10^{-2}$ mole l^{-1}
$[PhNH_2]_0=0.30$ mole l^{-1}
$[Cu^{2+}]_0=2.5\times10^{-4}$ mol l^{-1} (△)
5.0×10^{-4} mol l^{-1} (●)
8.1×10^{-4} mol l^{-1} (○)
13.0×10^{-4} mol l^{-1} (-⊖-)

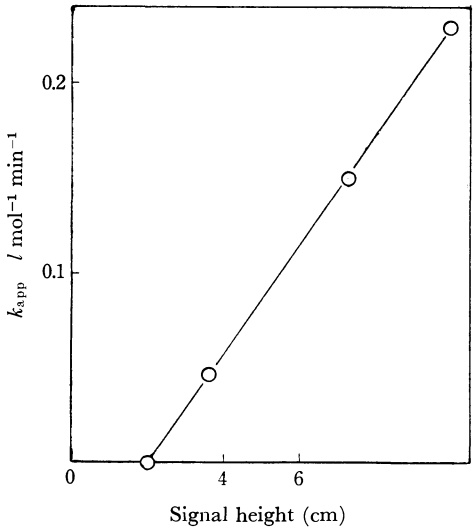

Fig. 6. Linear relationship between the apparent rate constant k_{app} and ESR absorption intensity.

where F_1 is the fraction of the monomeric catalyst, the apparent enthalpy of activation, H_{app}, is given by Eq. (22):

$$\Delta H^{\ddagger}_{app} = \Delta H^{\ddagger}_0 + \frac{1-f_1}{2-f_1}\Delta H_1 + \frac{1-F_1}{3-2F_1}\Delta H_2 \quad (22)$$

In Eq. (22), the enthalpy of activation for k_1 and the enthalpies of the aggregation of bromamic acid and the catalyst are designated as $\Delta H_0^{\ddagger}$, ΔH_1 and ΔH_2 respectively.

The second and third terms are negligibly small, compared with the first term. Therefore, the apparent energy of activation is near to $\Delta E^{\ddagger}(k_1)$ and independent of the concentration of the catalyst.

In order to obtain more information as to the nature of the catalyst species in the reaction solution, we examined the ESR spectra of the reaction system.[20] The results showed that the catalyst exists mostly in the divalent form, and a good proportionality was observed between the apparent rate constant, k_{app}, and the intensity (height) of the signal (Fig. 6). The intercept on the abcissa axis corresponds to the absorption due to the solvent water.

The kinetic data and the results of ESR measurements can be correlated if we assume that the copper clusters are inactive towards both the reaction and the electron-spin-resonance absorption. The monomeric cupric species can thus be postulated to be responsible for the promotion of the condensation reaction, but the possibility that this species exhibits the catalytic activity only after being reduced to a lower oxidation state[19] cannot be excluded.

Further studies are in progress to elucidate the nature of the "true" catalytic species and to obtain more information as to the elementary processes of the reaction.

20) Detailed results will be reported later. The authors are indebted to Dr. K. Hirasawa of The University of Tokyo for ESR measurements and helpful discussions.

Experimental

Materials. Commercial sodium 1-amino-4-bromoanthraquinone-2-sulfonate (I) was purified by repeatedly salting out with sodium acetate until the absorbance became constant. The purity was confirmed by paper chromatography (R_f=0.72), by elemental analysis (Found: N, 3.51%. Calcd: 3.47%), and by the conversion into its salts (*p*-toluidine salt : mp(corr) 241—241.2°C, Found: N, 5.82%. Calcd: 5.67%. *S*-benzylthiuronium salt: mp (corr) 202.9—203.4°C, Found: N, 7.64. Calcd: 7.66%). The visible spectrum shows a maximum at 485 mμ.[21]

Sodium 1-amino-4-anilinoanthraquinone-2-sulfonate (II) was synthesized by the reaction of I with aniline. Purification was carried out by salting out with sodium chloride. R_f=0.86. Found: N, 6.69%. Calcd 6.73%. λ_{max}=604 mμ.[21]

Sodium 1-amino-4-hydroxyanthraquinone-2-sulfonate (III) was obtained from the reaction of I and boric acid in 4% oleum, in yield of 85% (based on I). R_f=0.66. Found: N, 4.11%. Calcd: 4.54%. λ_{max}=540 mμ[21]

G.R. aniline was used after having been distilled under reduced pressure in the presence of zinc powder.

The cupric sulfate (pentahydrate) was of a reagent grade. The copper content was determined by iodometry.

The solvent was prepared by combining aqueous solutions of sodium carbonate (0.2M) and borax (0.15M) at an appropriate volumetric ratio.

21) T. Tokumitsu, M. Okamoto and T. Hayashi, *Kogyo Kagaku Zasshi*, **67**, 201 (1964).

Analytical Procedures. Paper chromatography was accomplished on Toyo Paper No. 5 at room temperature, using the *n*-BuOH - EtOH - 2% aqueous ammonia (6 : 2 : 3) solution as the solvent.[22]

The concentrations of the reaction products were determined by the usual spectrometrical method, in which the absorbances at 485, 540, and 604 mμ were used.

It was also confirmed that copper salts did not influence the spectrum of the reaction mixture.

Apparatus and Operation. Experiments were carried out in an apparatus devised to shut out the air. The nitrogen was purified of contaminating oxygen by passing it through pyrogallol.

A typical kinetic measurement was as follows:

Aniline, bromamic acid (I) and the solvent were mixed in a flask. A nitrogen stream was then introduced and allowed to bubble into the solution at room temperature for 2.5 hr. The solution was subsequently brought to the reaction temperature and the catalyst (in an aqueous solution) was added with the help of a syringe. This instant was taken to be time 0.

At 3-min intervals, 0.05-cc portions of the reaction solution were taken out with the micropipette, diluted in 50 or 25 cc of water, and subjected to spectroscopic measurements.

This research was supported financially in part by the Asahi Glass Foundation for the Contribution to Industrial Technology.

22) T. Tokumitsu, M. Okamoto and T. Hayashi, *Kogyo Kagaku Zasshi*, **67**, 197 (1964).

BULLETIN OF THE CHEMICAL SOCIETY OF JAPAN VOL. 43 1768—1777 (1970)

The Acid-catalyzed Cleavage of 2,6-Di-*t*-butyl-4-methyl-4-(1-phenylethyl)-cyclohexadien-1-one in the Hydroxylic Solvent. The Solvolysis of a Protonated Dienone*1

Kunio Okamoto, Issei Nitta and Haruo Shingu

Department of Hydrocarbon Chemistry, Faculty of Engineering, Kyoto University, Sakyo-ku, Kyoto

(Received September 6, 1969)

In acetic acid, aqueous methanol, and phenol solvents, 2,6-di-*t*-butyl-4-methyl-4-(1-phenylethyl)-cyclohexadien-1-one (I) did not undergo a typical dienone-phenol rearrangement in the presence of sulfuric or perchloric acid, but yielded the solvolysis products, *viz.*, 1-phenylethyl acetate, 1-phenylethyl methyl ether, and 1-phenylethyl phenyl ether, in the respective solvents, along with 2,6-di-*t*-butyl-4-methylphenol (II). The reactions carried out with the optically-active dienone (Ia) yielded solvolysis products which were predominantly racemized, but accompanied by a net inversion of the configuration. The polarimetric rate constant of racemization, measured in acetic acid containing sulfuric acid at 25°C, is in agreement with the spectrophotometric rate constants for the decrease in the dienone Ia and for the increase in the phenol II, essentially within the limits of experimental error. These stereochemical results can be accomodated by a typical S_N1 mechanism, in which the dienone I, protonated on the carbonyl-oxygen, acts as a substrate, and the phenol II, as a leaving group.

Transformations of *p*-cyclohexadienones to phenols in the presence of acidic catalysts have been known for many years; recently Miller and Margulies[1] have observed some interesting 1,2- or 1,3-allyl migration rearrangements of 2,6-di-*t*-butyl cyclohexadienones (III), accompanied by the loss of the *t*-butyl group.

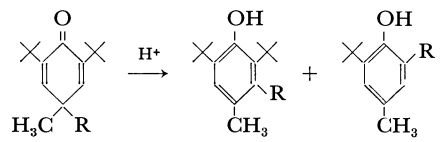

(III) R=Allyl

They have also observed the loss of a migrating group R, *e.g*, crotyl and isopropyl, under the conditions of such a dienone-phenol rearrangement:

*1 Presented at the 22nd Annual Meeting of the Chemical Society of Japan, Tokyo, April, 1969; Preprints, III, p. 1643.

1) B. Miller and H. Margulies, *Tetrahedron Lett.*, **1965**, 1727; *J. Amer. Chem. Soc.*, **87**,5106 (1965).

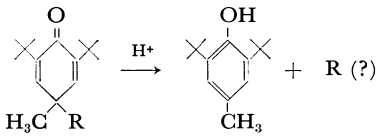

R=Crotyl and Isopropyl (II)

However, little study has been made of the fate of the eliminated group.

We have now prepared 2,6-di-*t*-butyl-4-methyl-4-(1-phenylethyl)-cyclohexadien-1-one (I) in connection with our study of the solvolysis mechanism of 1-phenylethyl halide, and have confirmed, in the course of its structural assignment, that this dienone I loses its 1-phenylethyl group in acidic hydroxylic solvents and gives 2,6-di-*t*-butyl-4-methylphenol (II) in a fashion similar to the above-mentioned case for the crotyl and isopropyl dienone (III).[1]

In this paper, we will report on the results of our examinations of the fate of the 1-phenylethyl group so eliminated and of its stereochemical course. Our results show that the 1-phenylethyl group is converted into a racemized solvolysis product, with a net inversion of configuration, and that this transformation of the dienone I into the phenol II and a 1-phenylethyl derivative may be considered to be a typical S_N1 reaction of the protonated dienone I, containing the phenol II as a leaving group.

Results and Discussion

Preparation of 2,6-Di-*t*-butyl-4-methyl-4-(1-phenylethyl)-cyclohexadien-1-one (I). This dienone I was synthesized from 1-phenylethyl halide and potassium 2,6-di-*t*-butyl-4-methylphenoxide according to the method of Kornblum and Seltzer.[2] For example, the reaction of 1-phenylethyl bromide and potassium 2,6-di-*t*-butyl-4-methylphenoxide, prepared *in situ* from potassium and the phenol II, was carried out in a *t*-butanol-tetraethylene glycol dimethyl ether solvent (1.7 : 1.0 by vol.) for 20 min at 20°C; the dienone I, bp 113—118°C/0.21—0.24 mmHg, was thus obtained in an 87% yield. The structure of I was deduced from its elemental composition and from the IR, UV, and NMR spectra (see Experimental section). This assignment was confirmed by the ozonolysis of I, which is shown in the following scheme (see also Experimental section):

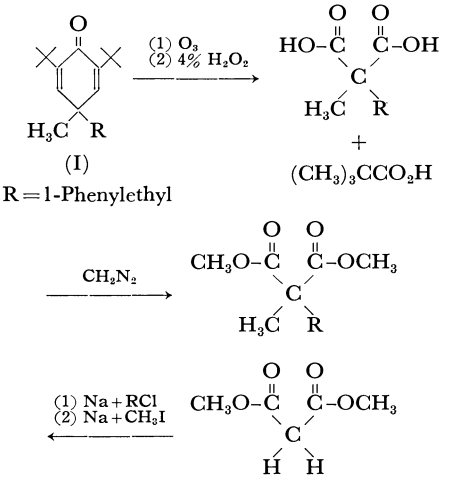

(I)

R=1-Phenylethyl

The optically active S-(+)-2,6-di-*t*-butyl-4-methyl-4-(1-phenylethyl)-cyclohexadien-1-one (Ia) was prepared from R-(+)-1-phenylethyl chloride and potassium 2,6-di-*t*-butyl-4-methylphenoxide in a fashion similar to that used in the reaction with a

Table 1. Preparation of optically active 2,6-di-*t*-butyl-4-methyl-4-(1-phenylethyl)-cyclohexadien-1-one (Ia)

t-BuOK M	DBC[a] M	R-(+)-RCl[b] M	R-(+)-RCl[b] α_D[c]	Solvent *t*-BuOH: TGDM[e]	Temp. °C	Time hr	S-(+)-Dienone Ia Yield[f]	S-(+)-Dienone Ia $[\alpha]_D$[g]	S-(+)-Dienone Ia Max. $[\alpha]_D$[h]
0.505	0.474	0.474	+26.26°[d]	1:1 vol.	20	13.5	78.0%	+18.6°	+88.5°
0.436	0.415	0.442	+16.15°	1:2.6 vol.	25	8.5	68.8%	+11.2°	+86.6°
0.236	0.225	0.241	+16.15°	1:2.6 vol.	25	9.5	52.7%	+10.63°	+82.5°
0.164	0.156	0.167	+16.15°	1:2.6 vol.	25	9.5	52.5%	+11.1°	+86.0°

a) DBC=2,6-Di-*t*-butyl-4-methylphenol.
b) RCl=1-Phenylethyl chloride.
c) Neat, 1 dm, at 13.5°C.
d) Measured at 23.0°C.
e) TGDM=Tetraethylene glycol dimethyl ether.
f) Based on DBC.
g) *c* 16.4—27.1, benzene, at 19—21°C.
h) The maximum rotation of R-(+)-1-phenylethyl chloride was taken to be 125° (1 dm, neat; H.M.R. Hoffmann and E.D. Hughes, *J. Chem Soc.*, **1964**, 1244).

2) N. Kornblum and R. Seltzer, *ibid.*, **83**, 3668 (1961).

Table 2. Acid-catalyzed cleavage of 2,6-di-*t*-butyl-4-methyl-4-(1-phenylethyl)-cyclohexadien-1-one in hydroxylic solvents

Solvent	Acid M	Dienone M	Temp. °C	Time hr	Product	Yield %
CH_3CO_2H[a]	H_2SO_4, 3.94×10^{-3}	5.00×10^{-1}	25	20	DBC[b]	90.9
					ROAc[c]	92.2
					Styrene	0.0
MeOH-H_2O (85.9:14.1 by vol.)	$HClO_4$, 2.16	9.65×10^{-2}	25	6	DBC	94.8
					ROMe	80.0
					ROH	7.6
$ClCH_2CH_2Cl$	CF_3CO_2H, 5.82×10^{-2}	3.23×10^{-2}	25	22	DBC	77.4
					CF_3CO_2R	61.9
					Styrene	1.4
					Others[d]	14
PhOH	—	1.95×10^{-1}	75	1.5	DBC	91.5
					ROPh	12.2
					p-R-PhOH	48.6
					o-R-PhOH	30.0

a) Containing 1.5×10^{-3} wt% of water.
b) DBC=2,6-Di-*t*-butyl-4-methylphenol.
c) R=1-Phenylethyl.
d) Substituted phenols.

racemic 1-phenylethyl bromide. The results are summarized in Table 1.

The maximum rotation for the optically active dienone, Ia, was calculated from the rotation of the dienone obtained from R-(+)-1-phenylethyl chloride and potassium 2,6-di-*t*-butyl-4-methylphenoxide. The initial concentrations of the chloride and of the phenoxide were varied over the range from 0.1 to 0.5M. Despite such a wide range of variation in the initial concentration, the calculated values for the maximum rotation of the dienone I seem to be little affected (see Table 1). This indicates that the racemization of 1-phenylethyl chloride during this S_N2 reaction, if any, is slight. Considering this, we took the highest value among those cited in Table 1, *i.e.*, +88.5°, as the maximum rotation of the optically active dienone I with the S-configuration.

Products of the Acidic Cleavage of 2,6-Di-*t*-butyl-4-methyl-4-(1-phenylethyl)-cyclohexadien-1-one (I) in Hydroxylic Solvents. The acidic cleavage of the dienone I was carried out in wet acetic acid (containing *ca.* 1.5×10^{-3} wt% of water), aqueous methanol (14.1 vol% of water), 1,2-dichloroethane, and phenol. Sulfuric acid (*ca.* 10^{-3}M), perchloric acid (*ca.* 2M), and trifluoroacetic acid (*ca.* 10^{-2}M) were used as the acid catalyst in acetic acid, aqueous methanol, and 1,2-dichloroethane solvents respectively. In the case of the phenol solvent, no acid catalyst was added. The results are summarized in Table 2.

For each reaction, the substitution products and the phenol II were obtained in fairly good yields; in acetic acid, 1-phenylethyl acetate was obtained in a 92% yield and no elimination product was isolated from the products; in aqueous methanol, 1-phenylethyl methyl ether and 1-phenylethyl alcohol were obtained in 80 and 8% yields respectively; in phenol, 1-phenylethyl phenyl ether, *p*-1-phenylethylphenol, and *o*-1-phenylethylphenol were obtained in 12, 49, and 30% yields respectively; even in 1,2-dichloroethane containing a catalytic amount of trifluoroacetic acid, 1-phenylethyl trifluoroacetate was obtained in a 62% yield.

Rates of the Acid-catalyzed Cleavage of 2,6-Di-*t*-butyl-4-methyl-4-(1-phenylethyl)-cyclohexadien-1-one (I). The rates of the cleavage of the dienone I were followed spectrophotometrically; the change in the optical density at 249 mμ (or 352 mμ for the reaction in aqueous methanol) was followed with the reaction mixture placed in an absorption cell. The decrease in the optical density corresponding to the dienone I obeyed good first-order kinetics. The results for wet acetic acid,[3] aqueous methanol (15.1 vol% of water), and 1,2-dichloroethane solvents are summarized in Table 6 (see Experimental section).

In Fig. 1 the logarithm of the first-order rate constant is plotted against the logarithmic concentration of perchloric acid (or trifluoroacetic acid). From the graphical presentation in Fig. 1, the ability of cleavage for these acidic media is seemingly in the sequence: perchloric acid in wet

3) The water arose from the 70% perchloric acid used as the catalyst.

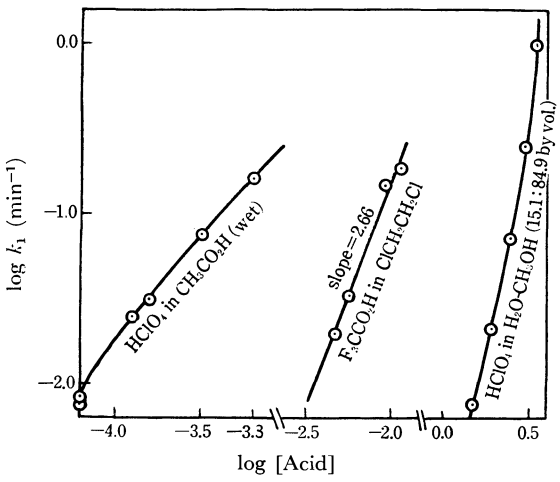

Fig. 1. Rates of acid-catalyzed cleavage of dienone I in various solvents at 25.0°C.

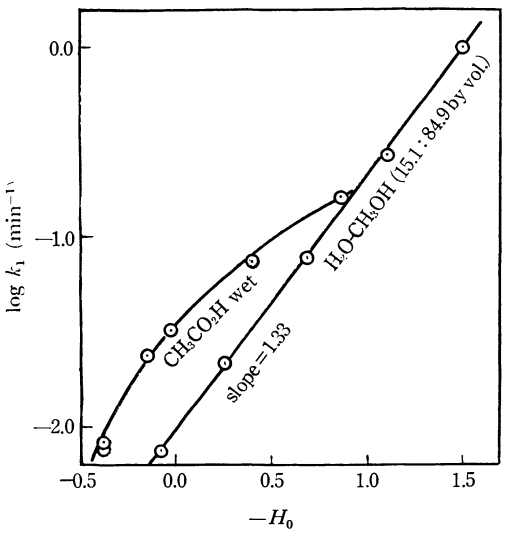

Fig. 2. Rates of cleavage of dienone I in the presence of perchloric acid at 25°C.

acetic acid (containing about 10^{-4} wt% of water)> trifluoroacetic acid in 1,2-dichloroethane>perchloric acid in aqueous methanol (15.1 vol% H_2O).

However, as is shown in Fig. 2, when the logarithm of the rate constant is plotted against the acidity function, H_0, of the acidic medium, the curve for the acetic acid solvent is not far over the line for the aqueous methanolic solvent. Consequently, the medium composed of perchloric acid and acetic acid is not so efficient as it seems in Fig. 1. In this connection, if the H_0 of these media is a measure of the ability of proton donation to the dienone I, the gap between the two in Fig. 2 may be attributed to the difference in the solvent effect on the intrinsic cleavage rate of the protonated dienone I.

The $-H_0$ value for 1,2-dichloroethane containing about 10^{-2}M trifluoroacetic acid is estimated to be −3.3——4.0 by extrapolation from the date (see Table 7) on the medium with higher concentrations of trifluoroacetic acid. These H_0 values are too small to be plotted in Fig. 2. However, it is obvious that 1,2-dichloroethane containing trifluoroacetic acid is the most effective medium among the media shown in Figs. 1 and 2 for the cleavage of the protonated dienone I. In other words, the solvent effect for the cleavage of the protonated dienone I is in the sequence: 1,2-dichloroethane>acetic acid>aqueous methanol.

In Figs. 1 and 2, the plots of $\log k$ are linear against neither log [Acid] nor $-H_0$, except in the cases of aqueous methanol in Fig. 2 and of 1,2-dichloroethane in Fig. 1. Even in these cases, the linear plots have a slope different from 1. Consequently, for these acid-catalyzed reactions the Hammett-Zucker hypothesis,[4] which discusses the details of the mechanism on the basis of the proportionality of $\log k$ to H_0 or to log [Acid], seems to be invalid. This discrepancy can probably be ascribed to the deviation of the dienone I from a group of normal Hammett bases.[5]

The Steric Course of the Acid-catalyzed Cleavage of Optically Active 2,6-Di-*t*-butyl-4-methyl-4-(1-phenylethyl)-cyclohexadien-1-one (Ia). The optically active dienone Ia was subjected to acid-catalyzed cleavage in wet acetic acid (10^{-3}—10^{-4} wt% H_2O) containing perchloric acid or sulfuric acid, in aqueous methanol (13 vol% H_2O) containing perchloric acid and in phenol. The results are summarized in Table 3.

On the basis of the absolute configuration and of the maximum rotation for the relevant solvolysis products (see Table 3, Footnote i), it is confirmed that the cleavage of the dienone Ia gives predominantly racemized solvolysis products, with some net inversion of the configuration in wet acetic acid and also in phenol; in aqueous methanol, the cleavage affords the methyl ether with a predominant inversion of configuration. These are the stereochemical characteristics of an S_N1 type reaction.

As is shown in Table 4, one of the solvolysis products, 1-phenylethyl acetate, was found to racemize about 10% in the presence of acid under the same reaction conditions as those of the cleavage reaction. Therefore, in the calculation of the extent of racemization (or inversion) for 1-phenylethyl acetate, we made a correction for the racemization of the acetate during the course of the acidic cleavage. The rotation of 1-phenylethyl methyl ether was not affected in aqueous methanol, even at higher perchloric acid concentrations than in the

4) L. Zucker and L. P. Hammett, *J. Amer. Chem. Soc.*, **61**, 2791 (1939).

5) This problem is now being examined in these laboratories.

Table 3. Acid-catalyzed cleavage of optically active 2,6-di-*t*-butyl-4-methyl-4-(1-phenylethyl)-cyclohexadien-1-one at 25°C

Solvent	Acid M	Dienone M	Dienone $[\alpha]_D$[d]	Time hr	RY[c]	Yield	α_D[d]	α_D[h]	Net steric course[i]
CH_3CO_2H (10^{-3}—10^{-4} wt% H_2O)	$HClO_4$ 1.38×10^{-4}	0.148	+10.88°	5	ROAc	51%	+0.935°[e]	+1.02°	6.4% inv.
	$HClO_4$ 6.90×10^{-4}	0.148	+10.88°	1	ROAc	45%	+0.72°[f]	+0.79°	5.0% inv.
	H_2SO_4 3.94×10^{-3}	0.500	+18.6°	20	ROAc	92.2%	+2.63°[f]	+3.04°	11.2% inv.
	H_2SO_4 4.26×10^{-3}	0.156	+11.2°	6	ROAc	69%	+1.52°[f]	+1.76°	10.5% inv.
H_2O-MeOH (13:87 by vol.)	$HClO_4$ 2.24	0.182	+10.28°	3.5	ROMe	71.5%	+8.02°[f]	—	57% inv.
PhOH[a]	—	0.195	+11.2°	1.5	ROPh	12.2%	−1.33°[f]	—	13.5% inv.
					p-RPhOH	48.6%	−0.344°[g]	—	15.9% inv.
					o-RPhOH	30.0%	+0.65°[f]	—	10.2% inv.

a) The reaction was conducted at 75°C
b) Benzene, *c* 15—17, at 20—21°C.
c) R=1-Phenylethyl.
d) Measured at 19—21°C.
e) α_D for 1 dm, calculated from the value for the neat liquid composed of ROAc and 2,6-di-*t*-butyl-4-methylphenol (*ca.* 2:3 by wt.).
f) α_D for 1 dm, measured with a neat sample.
g) $[\alpha]_D$, *c* 68.3, benzene.
h) Corrected for the racemization of ROAc during the course of the reaction.
i) The rotations of the optically pure materials are taken to be 88.5° for the titled S-(+)-dienone (see text), 129° for R-(+)-ROAc (determined in these laboratories), 120° for R-(+)-ROMe (K. Mislow, *J. Amer. Chem. Soc.*, **73**, 4043 (1951)), 46.6° for S-(+)-ROPh (K. Okamoto *et al.*, This Bulletin, **39**, 299 (1966)), 10.26° for S-(+)-*p*-RPhOH (K. Okamoto *et al.*, *loc. cit.*), and 27.85° for R-(+)-*o*-RPhOH (K. Okamoto *et al.*, *loc. cit.*).

Table 4. Racemization of 1-phenylethyl acetate and of 1-phenylethyl methyl ether in the presence of strong acids in hydroxylic solvents at 25°C

Substrate M	Substrate α_D	Acid M	Solvent	Time hr	Substrate recovered α_D	Substrate recovered Racemization %
ROAc 0.152	+67.4°[a]	$HClO_4$ 6.90×10^{-4}	HOAc[c]	1	+61.02°[a]	9.4
ROAc 0.152	+67.4°[a]	$HClO_4$ 1.38×10^{-4}	HOAc[c]	5.2	+61.12°[a]	9.4
ROAc 0.589	+6.23°[b]	H_2SO_4 3.68×10^{-3}	HOAc[c]	24	+ 5.38°[b]	13.6
ROMe 0.564	−7.17°[a]	$HClO_4$ 1.81	H_2O-MeOH (12.3:87.7 by vol.)	3.2	− 7.18°	0.0

a) 1 dm, neat, at 20°C for ROAc and at 15°C for ROMe.
b) $[\alpha]_D^{23}$ *c* 9.6, HOAc.
c) Containing 10^{-3} wt% of water.
d) Containing 10^{-4} wt% of water.

case of 1-phenylethyl acetate.

Mechanism of the Acid-catalyzed Cleavage of 2,6-Di-*t*-butyl-4-(1-phenylethyl)-4-methylcyclohexadien-1-one (I). Polarimetric rate measurements were carried out with an acetic acid solution of the dienone Ia (0.500M) at 25°C, using 3.94×10^{-3}M sulfuric acid as the acid catalyst. For purposes of comparison, the spectrophotometric rate measurements were conducted by the use of the same reaction mixture as that used for the polarimetric run; the decrease in the dienone I and the increase in the phenol II were followed at

the characteristic bands of 249 and 284 mμ respectively.

The polarimetric rate constant, k_P, the rate constant for the decrease in the dienone I, k_D, and the rate constant for the increase in the phenol II, k_{DBC}, were graphically calculated; as is illustrated in Figs. 3,4, and 5, the observed values for the three k's are all essentially the same within the limits of experimental error.

All the results, *i.e.*, steric and kinetic, are most readily accomodated by an S_N1 solvolysis mechanism of the protonated dienone I; this is illustrated by the following scheme:

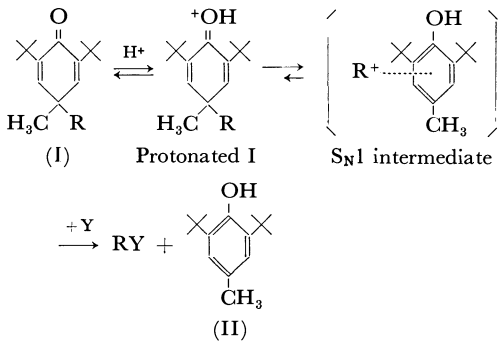

The protonation of a dienone with a structure similar to that of the dienone I has been confirmed in the case of 2,6-di-*t*-butyl-4-dichloromethyl-4-methylcyclohexadien-1-one by the use of the spectrophotometric method.[6]

Since the k_P is equal to k_D or to k_{DBC}, the rate for the return of the S_N1 intermediate to the protonated dienone would be negligibly small as compared with rate for the attack of the solvent nucleophile, Y, on the S_N1 intermediate.

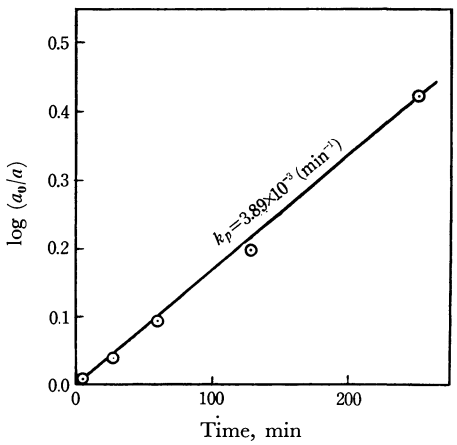

Fig. 3. Polarimetric rate constant for the conversion of optically active dienone Ia in wet acetic acid at 25°C.
[Dienone]$_0$=0.500M
[H_2SO_4]=3.94×10^{-3}M

6) H. Budzikiewicz, *Tetrahedron Lett.*, **1960**, 12.

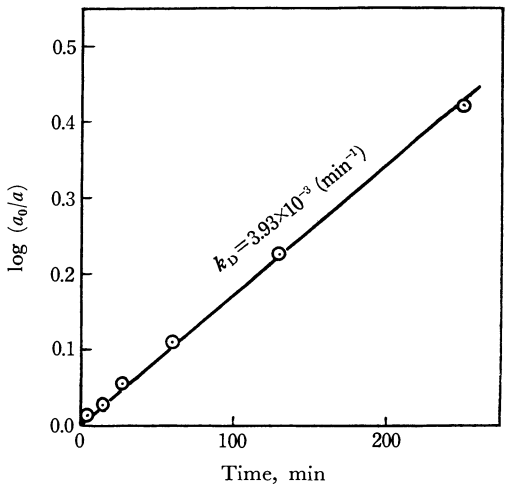

Fig. 4. Rate of decrease of the dienone I in wet acetic acid at 25.0°C.
[Dienone]$_0$=0.500M
[H_2SO_4]=3.94×10^{-3}M

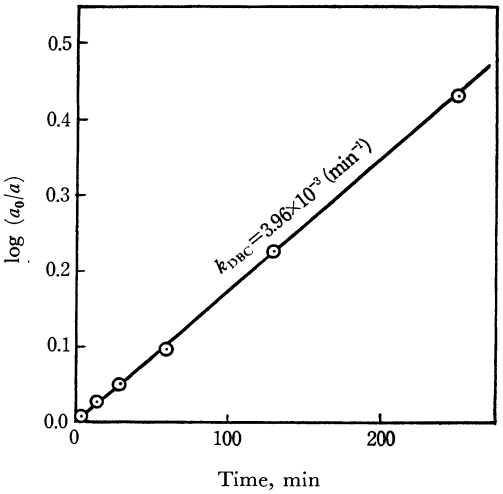

Fig. 5. Rate of increase of the phenol II in wet acetic acid at 25.0°C.
[Dienone]$_0$=0.500M
[H_2SO_4]=3.94×10^{-3}M

In view of the existence of carbonium ion-aromatic hydrocarbon charge-transfer complexes in various solvents,[7] the S_N1 intermediate would be close to a charge-transfer complex between the 1-phenylethyl cation and the phenol II.

This reaction of the protonated dienone I is considered to be an example of the S_N1 reaction of the "missing-charge" type;[8] a phenol molecule,

7) a) M. Feldman and S. Winstein, *J. Amer. Chem. Soc.*, **83**, 3338 (1961); b) H. J. Dauben, Jr., and J. D. Wilson, *Chem. Commun.*, **1968**, 1629.

8) E. D. Hughes and D. J. Whittingham, *J. Chem. Soc.*, **1960**, 806.

Table 5. Preparation of 2,6-di-*t*-butyl-4-methyl-4-(1-phenylethyl)cyclohexadien-1-one (I)

Substrate	Reagent		Solvent	Temp.	Time	Dienone I
RBr[a] 0.50 M	DBC[b] 0.455 M	*t*-BuOK 0.455 N	*t*-BuOH: TGDM[c] 26:15[d]	20°C	20 min	87%
RCl 0.54 M	DBC 0.54 M	*t*-BuOK 0.54 N	*t*-BuOH: TGDM 32:35	30°C	6 hr	79%
RCl 0.57 M	DBC 0.57 M	*t*-BuOK 0.59 N	*t*-BuOH: DGM[e] 28:20	60°C	3 hr	59%[g]
RBr 0.035 M	KDBC[f] 0.039 N		CH_3CN	82°C	17.5 hr	79%[h]

a) R=1-Phenylethyl.
b) DBC=2,6-di-*t*-butyl-4-methylphenol.
c) TGDM=tetraethylene glycol dimethyl ether.
d) m*l*: m*l*
e) DGM=diethylenglycol dimethyl ether.
f) KDBC=potassium 2,6-di-*t*-butyl-4-methylphenoxide.
g) Unchanged RCl (23%) was recovered.
h) Styrene (11%)was obtained.

II, acts as a leaving group of the charged substrate, *i.e.*, the protonated dienone I. The observed solvent effect (*vide supra*) for the cleavage of the protonated dienone is consistent with that observed for such S_N1 reactions of the "missing-charge" type as the solvolyses of *t*-butyldimethylsulfonium ion[9] and of cyclohexylmercuric perchlorate.[10]

Experimental[11]

2,6-Di-*t*-butyl-4-methyl-4-(1-phenylethyl)-cyclohexadien-1-one (I). The dienones, racemic and optically active, were prepared under various conditions, according to the method of Kornblum and Seltzer.[2] The results are tabulated in Tables 1 and 5. The details of a representative run will now be described.

To a mixture of a *t*-butanol solution (22.4 m*l*) of potassium *t*-butoxide (0.87N), tetraethylene glycol dimethyl ether (15 m*l*), *t*-butanol (4 m*l*), and 2,6-di-*t*-butyl-4-methylphenol (II) (4.41 g, 0.02 mol), 1-phenylethyl bromide (3.0 m*l*, 0.022 mol) was added in one portion at 20°C. The titration analysis of an aliquot showed that the reaction was 87.5% complete within 20 min. After the mixture had stood overnight at room temperature, benzene (50 m*l*) was added; the benzene solution was then washed with water and condensed to leave an oily material (8.47 g), which was chromatographed over alumina (146 g, 200—300 mesh). The dienone I (5.25 g and 0.37 g; total yield 86.7%) was eluted successively by *n*-hexane (400 m*l*) and benzene (80 m*l*).

Found: C, 85.43; H, 10.07%; mol. wt, 322.0 (cryoscopic, benzene). Calcd for $C_{23}H_{32}O$: C, 85.13; H, 9.94%; mol. wt, 324.5.

The IR spectrum for the dienone I shows a doublet carbonyl absorption at 1640 and 1655 cm^{-1}, corresponding to a conjugated dienone; the UV maximum appears at 249 mμ (ε=10650, methanol), showing a cross structure for the conjugated dienone I. In the NMR spectrum (60 MHz) of the dienone I, five phenyl protons appear as a multiplet centered at τ 2.9; two vinyl protons, as a quartet showing an AB pattern (ν_A τ 3.55, ν_B τ 3.73, J_{AB}=3 Hz); a methine proton, as a quartet centered at τ 7.16 (J=7.5 Hz); 18 *t*-butyl protons, as two singlets (nine for each) at τ 8.78 and 8.87; three protons on a methyl group, attached to a quaternary carbon, as a singlet at τ 8.89. Three methyl protons of the 1-phenylethyl group appear in the range of τ 8.7—9.0, but they could not be well characterized because of the overlapping of the other methyl proton signals. The magnetic non-equivalence for two vinyl protons and for the protons of two *t*-butyl groups may be attributed to the asymmetric structure of the 1-phenylethyl group.

Ozonolysis of the Dienone I. A solution of the dienone I (2.32 g) in a mixture of acetic acid (150 m*l*) and ethyl acetate (90 m*l*) was treated with ozonized oxygen at 0°C. A stream of ozonized oxygen (1.6 mmol of ozone/*l*) was passed into the solution at a rate of 80 m*l*/min. The amount of unchanged ozone was determined every 20 or 30 min by collecting it in a potassium iodide trap and titrating the liberated iodine. After an uptake of 30 mmol of ozone in 7 hr, the mixture was treated with a mixture of 30% hydrogen peroxide (6 m*l*) and water (40 m*l*). After it had stood overnight and ether (500 m*l*) had subsequently been added, the resulting mixture was washed with 5% aqueous sodium chloride (6×50 m*l*), condensed to 100 m*l*, and washed with additional 5% aqueous sodium chloride (8×25 m*l*). From the alkaline extracts of the organic layer, an acidic oily material (1.869 g) was recovered by the usual working-up. The oil was distilled *in vacuo* to give a mixture of acetic acid and tri-

9) C. G. Swain, L. E. Kaiser and T. E. C. Knee, *J. Amer. Chem. Soc.*, **80**, 4092 (1958).
10) F. R. Jensen and R. J. Ouellette, *ibid.*, **83**, 4478 (1961).
11) The melting points are uncorrected. Rotations were measured with a Zeiss-Winkel "Kreis-Polarimeter 0.01°." The infrared spectra and ultraviolet spectra were obtained on Shimadzu spectrometers models IR-27 and UV-50M. The gas-liquid chromatograms were obtained with a Shimadzu model GC2B apparatus. The microanalyses were performed by the Microanalysis Center, Kyoto University.

methylacetic acid (bp *ca.* 50°C/5 mmHg, 0.810 g), leaving a residual oil (the acid equivalent: 150±10, 1.059 g). The residual oil (1.000 g) was dissolved in ether (6 m*l*), and treated with diazomethane (11.4 mmol) in ether (24 m*l*). After the usual working-up, the methylated products were distillated *in vacuo* to afford a fraction with bp of 77—91°C/0.3 mmHg. This fraction was analyzed on a 2 m×4 mm copper tubing packed with high vacuum silicone grease on Celite under the following conditions: column temperature, 175°C; hydrogen flow rate, 70 m*l*/min. The fraction contained component with the retention time of 5.1 min (26%) and dimethyl α-methyl-α-(α-phenylethyl)malonate (68%; retention time, 14.6 min). After several injections, the dimethyl ester was collected as eluted (51% of recovery; 102 mg; the IR spectrum was identical with that of the authentic sample).

Preparation of the Authentic Dimethyl α-Methyl-α-(α-phenylethyl)-malonate. To a solution of sodium (1.13 g, 49.1 mmol) in a mixture of methanol (8 m*l*) and diglyme (15 m*l*), we added dimethyl α-(α-phenylethyl)-malonate (9.03 g, 40.3 mmol), which had been prepared according to the method of Snyder and Brewster.[12] To the cooled mixture, methyl iodide (9.17 g, 64.6 mmol) was added drop by drop; after 1.5 hr, the mixture was diluted with benzene (100 m*l*), washed with 10% aqueous sodium chloride, and condensed to give a viscous oil. The vacuum distillation of the oil gave a fraction with a bp of 102—116°C/0.3 mmHg (7.1 g); this fraction was a mixture of dimethyl α-(α-phenylethyl)-malonate (27%) and dimethyl α-methyl-α-(α-phenylethyl)-malonate (73%). The composition analysis was performed by means of GLC under the above-mentioned conditions; the retention time for dimethyl α-(α-phenylethyl)-malonate was 10.9 min. The pure dimethyl α-methyl-α-(α-phenylethyl)-malonate was collected as eluted by GLC.

Prepration of 1-Phenylethyl Trifluoroacetate. A mixture of trifluoroacetic anhydride (1.00 m*l*), 1-phenylethyl alcohol (0.50 m*l*, 4.17 mmol), and a drop of pyridine was kept at 0°C overnight. After the evaporation of the low-boiling materials *in vacuo*, distillation gave 1-phenylethyl trifluoroacetate; bp 63.0—63.2°C/5 mmHg; 0.80 g, 88% yield; IR: 1700 (C=O) and 1220 (C–O–C) cm^{-1}.

Product Analysis for the Cleavage Reaction of the Racemic (I) and Optically Active (Ia) Dienones. The results are summarized in Tables 2 and 3. The details of the experimental procedure for representative runs, which were carried out in various solvents, will be described below.

The Acidic Cleavage Reaction of the Optically Active Dienone Ia in Acetic Acid (Product Analysis and Rate Measurements). To a solution of the dienone Ia (1.6226 g, 5.00 mmol, $[\alpha]_D^{19}$ +18.6°, benzene, *c* 16.4) in acetic acid (3 m*l*), a solution of sulfuric acid *ca.* 9×10^{-3}M) in acetic acid was added to make 10 m*l* of a reaction mixture (3.94×10^{-3}M sulfuric acid). After a specified length of time at 25.0°C, an aliquot (1 m*l*) was withdrawn and neutralized with a solution (0.10 m*l*) of sodium acetate (0.10N) in acetic acid. From the neutralized aliquot (1.10 m*l*), an aliquot of 0.100 m*l* was then withdrawn and diluted to 34 times its volume with methanol; the optical density at 249 mμ (the dienone Ia) and 284 mμ (the phenol II) was measured using an absorption cell 10 mm thick. The rest of the neutralized acetic acid solution was used for the rotation measurements employing a tube 1 dm long. Six aliquots (1 m*l* for each) were withdrawn from the reaction mixture in a period of 4 hr. The results of the graphical calculation of the respective rate constants are illustrated in Figs. 3, 4, and 5.

After 24 hr at 25°C, an aliquot of 1.50 m*l* was pipetted out from the reaction mixture and added to ether (30 m*l*). The resulting ethereal solution was washed with 10% aqueous sodium bicarbonate (5 m*l*) and 10% aqueous sodium chloride (2×10 m*l*) and then evaporated to give an oily material (0.265 g) which was composed of 1-phenylethyl acetate (92.2% yield, based on the dienone Ia) and the phenol II (90.9% yield, based on the dienone Ia). The analysis was performed on a 2 m×4 mm copper tubing column packed with 20% Apiezon grease L on Neosorb N under the following conditions: column temperature, 122°C for 1-phenylethyl acetate and 169°C for the phenol II; hydrogen flow rate, 80 m*l*/min; retention times: 1-phenylethyl acetate, 10.3 min (122°C); the phenol II, 14.9 min (169°C).

The rest of the reaction mixture was chromatographed over alumina. The phenol II (124.9 mg, 84.6% yield, based on the dienone Ia) and 1-phenylethyl acetate (86 mg, the IR spectrum was identical with that of the authentic sample) were eluted with *n*-hexane (150 m*l*) and with benzene (45 m*l*) respectively. The latter was distilled *in vacuo* to give a purified, optically active sample (74.3 mg); this sample was then diluted with racemic 1-phenylethyl acetate (87.3 mg) to give α_D+1.21° (1 dm, neat, at 22°C). The rotation of the original sample was calculated to be α_D+2.63° (1 dm, neat, at 22°C).

The Acidic Cleavage Reaction of the Optically Active Dienone Ia in Phenol. A mixture of the dienone Ia (3.9765 g, 12.25 mmol, $[\alpha]_D^{19}$ +18.6°, benzene, *c* 16.4) and phenol (57.0 g) was kept at 75°C for 1.5 hr. After the addition of ether (100 m*l*) the ethereal solution was washed with 10% aqueous sodium hydroxide (5×50 m*l*) and 10% aqueous sodium chloride (3×100 m*l*), and then concentrated to give an oily material (4.356 g). The oil was then subjected to chromatography on silica gel (100 g). The phenol II (2.460 g, 91.2% based on the dienone Ia) was eluted with *n*-hexane-benzene (15: 1 by vol., 50 m*l*); 1-phenylethyl phenyl ether (containing a hydroxylic compound), with *n*-hexane-benzene (15: 1 by vol., 500 m*l*); *o*-1-phenylethylphenol (743 mg, 30.0% yield), with benzene (600 m*l*), and finally *p*-1-phenylethylphenol (812 mg), with benzene-ether (4 : 1 by vol., 150 m*l*).

From the alkaline extracts additional amounts of *p*-1-phenylethylphenol (369 mg; the total yield was 48.6%) were recovered by the usual working-up and by subsequent distillation *in vacuo* (bp 120°C/4 mmHg, bath temp.).

1-Phenylethyl phenyl ether was rechromatographed over alumina with *n*-hexane as an eluent to give a pure sample (272 mg, 12.2% yield) and a hydroxylic compound (43.5 mg). The latter was not identified.

Each compound so isolated gave a sole spot in TLC on silica gel and exhibited the same IR spectrum as the corresponding authentic sample;[13] the isolated com-

12) H. R. Snyder and J. H. Brewster, *J. Amer. Chem. Soc.*, **71**, 291 (1949).

13) For the authentic samples, see K. Okamoto, M. Hayashi, K. Komatsu and H. Shingu, This Bulletin, **40**, 624 (1967).

Table 6. Rates of acid-catalyzed cleavage of the dienone I in various solvents at 25.0°C

Solvent-Acid	Dienone M	Acid M	k_1 min^{-1}	$-H_0$	H_2O
Wet acetic acid-Perchloric acid	2.59×10^{-2}	6.25×10^{-4}	1.64×10^{-1}	0.86	1.49×10^{-3}M
	2.59×10^{-2}	3.13×10^{-4}	7.50×10^{-2}	0.39	7.46×10^{-4}M
	2.77×10^{-2}	3.14×10^{-4}	7.51×10^{-2}	0.39	7.46×10^{-4}M
	2.77×10^{-2}	1.57×10^{-4}	3.19×10^{-2}	−0.03	3.98×10^{-4}M
	2.59×10^{-2}	1.25×10^{-4}	2.30×10^{-2}	−0.14	2.98×10^{-4}M
	2.59×10^{-2}	6.25×10^{-5}	7.27×10^{-3}	−0.37	1.49×10^{-4}M
	2.77×10^{-2}	6.27×10^{-5}	8.50×10^{-3}	−0.37	1.49×10^{-4}M
Aqueous methanol-Perchloric acid	1.02×10^{-4}	3.44	1.02	1.50	15.1 vol%
	1.02×10^{-4}	2.94	2.69×10^{-1}	1.10	14.3 vol%
	1.02×10^{-4}	2.94	2.47×10^{-1}	—	15.6 vol%
			(2.54×10^{-1})[a]	(1.09)[a]	(15.1 vol%)
	1.02×10^{-4}	2.45	7.55×10^{-2}	0.73	13.4 vol%
	1.02×10^{-4}	2.45	6.82×10^{-2}	—	16.0 vol%
			(7.06×10^{-2})[a]	(0.69)[a]	(15.1 vol%)
	1.02×10^{-4}	1.96	2.16×10^{-2}	0.37	12.5 vol%
	1.02×10^{-4}	1.96	2.23×10^{-2}	—	16.5 vol%
			(2.20×10^{-2})[a]	(0.26)[a]	(15.1 vol%)
	7.64×10^{-5}	1.47	1.32×10^{-2}	0.14	6.5 vol%
	1.02×10^{-4}	1.47	5.32×10^{-3}	—	17.0 vol%
			(6.70×10^{-3})[a]	(−0.08)[a]	(15.1 vol%)
1,2-Dichloroethane-Trifluoroacetic acid	9.18×10^{-5}	1.12×10^{-2}	1.88×10^{-1}	(−3.3)[a]	
	7.83×10^{-5}	9.22×10^{-3}	1.48×10^{-1}		
	9.13×10^{-5}	5.60×10^{-3}	3.36×10^{-2}		
	7.83×10^{-5}	4.61×10^{-3}	1.94×10^{-2}		
	7.83×10^{-5}	2.31×10^{-3}	3.47×10^{-3}		
	7.83×10^{-5}	2.31×10^{-3}	3.34×10^{-3}		
	7.83×10^{-5}	1.15×10^{-3}	8.89×10^{-4}		
	7.83×10^{-5}	5.75×10^{-4}	3.06×10^{-4}	(−5.9)[a]	

a) Extrapolated or interpolated values.

pounds were redistilled *in vacuo* and then the optical rotation was measured: 1-phenylethyl phenyl ether, 235 mg, bp 100°C/0.05 mmHg (bath temp.), α_D^{20} −1.33± 0.08° (1 dm, neat); *p*-1-phenylethylphenol, 731 mg, bp 150°C/0.05 mmHg (bath temp.), $[\alpha]_D^{19}$ −0.344° (benzene, *c* 68.3); *o*-1-phenylethylphenol, bp 140°C/ 0.05 mmHg (bath temp.), α_D^{19} +0.65±0.04° (1 dm, neat).

The Acidic Cleavage Reaction of the Racemic Dienone I in 86% Aqueous Methanol. In a 10-m*l* volumetric flask we placed the dienone I (313 mg, 0.965 mmol) and a solution (7.7 m*l*) of perchloric acid in aqueous methanol ($[HClO_4]=2.80$N, $[H_2O]=18.8$ vol%); then some methanol was added to bring the volume of the reaction mixture to 10 m*l*. After standing for 6 hr at 25.0°C, the mixture was poured into 50 m*l* of benzene; the benzene solution was then washed successively with 10% aqueous sodium chloride (3× 20 m*l*), 10% aqueous sodium hydroxide (2×20 m*l*), and 10% aqueous sodium chloride (2×20 m*l*). The dried benzene layer was concentrated to about 3 m*l* and made to a 5-m*l* solution in a 5-m*l* volumetric flask by adding some benzene. The composition of the products was determined by GLC using the same column as that employed in the analysis for 1-phenylethyl acetate (at 122°C and the hydrogen flow rate 48.4 m*l*/ min): 1-phenylethyl methyl ether, 6.85 min (retention time)(80.0% yield, based on the dienone I); 1-phenylethyl alcohol, 9.1 min (7.6% yield); the phenol II, 22.8 min (at 165°C)(94.8% yield).

The Acidic Cleavage Reaction of the Racemic Dienone I in the Presence of Trifluoroacetic Acid in 1,2-Dichloroethane. The dienone I (574 mg, 1.615 mmol) and a 0.1455M solution (20 m*l*) of trifluoroacetic acid in 1,2-dichloroethane were placed in a 50-m*l* volumetric flask; some 1,2-dichloroethane was then added to bring the volume of the reaction mixture to 50 m*l*. After 22 hr of standing at 25.0°C, a portion of the reaction mixture was subjected to GLC on the Apiezon column described above under the following conditions: column temperature, 140°C; the hydrogen flow rate, 44.3 m*l*/min; retention time for 1-phenylethyl trifluoroacetate, 2.25 min (61.9% yield, based on the dienone I). An aliquot, withdrawn from the reaction mixture, was titrated with 0.1N aqueous sodium hydroxide, and the amount of trifluoroacetic acid consumed was calculated to be 60.2% of the dienone I. Another aliquot was subjected to UV spectroscopy; it was confirmed that the amount of styrene (λ_{max} 248 mμ, $\varepsilon=1.101\times10^4$) produced during the reaction was less than

1.4% of the dienone I.

The rest of the reaction mixture (46 ml) was concentrated and distilled *in vacuo* to give 1-phenylethyl trifluoroacetate (101 mg, bp 80°C/2 mmHg (bath temp.); the IR spectrum was identical with that of the authentic sample). The residual oil (485 mg) was subjected to chromatography on alumina (20 g). The phenol II (385 mg, 77.4% yield) was eluted with *n*-hexane (150 ml), and some phenolic materials (72 mg) were eluted with benzene and with ethanol. The phenolic materials were characterized by IR analysis.

Racemization of 1-Phenylethyl Acetate and of 1-Phenylethyl Methyl Ether in the Acidic Media. Optically active samples of 1-phenylethyl acetate and of 1-phenylethyl methyl ether were dissolved in the acidic solvents indicated in Table 4. After a specified length of time, the ester or the ether was recovered, purified by distillation *in vacuo*, and subjected to rotation measurements. In the case of the acetic-acid solvent containing sulfuric acid, the solution of 1-phenylethyl acetate was placed in a 1-dm tube; the change in the rotation was followed polarimetrically. The results are summarized in Table 4.

Kinetic Procedure. The rate measurement for the optically active dienone Ia was performed as has been described above. The results are illustrated in Figs. 3,4, and 5. The rate measurement for the racemic dienone I was carried out spectrophotometrically. A glass-stoppered 1-cm quartz cell was placed in a cell-compartment with circulating water thermostated at 25.0°C. Appropriate amounts of a temperature-equilibrated dienone solution was mixed with a temperature-equilibrated acid solution in the cell; the absorbance was followed at a specified wavelength. The first-order rate constants were calculated graphically. The results are summarized in Table 6.

The Measurement of the Acidity Function. The acidity function for each acidic medium measured according to the method of Braude and Stern.[14] For the mixtures of perchloric acid and aqueous methanol, of perchloric acid and acetic acid, and of trifluoroacetic acid and methanol, *o*-nitroaniline (indicator constant, −0.29[15]) was used as the Hammett base; for the mixture of trifluoroacetic acid and 1,2-dichloroethane, *p*-nitroaniline (indicator constant, +0.99[15]) was so employed. The absorbance of *o*-nitroaniline decreased in acetic acid in the course of the measurements; the value of absorbance at time zero was extrapolated from the observed data. The results are illustrated in Table 6, while the H_0 values for trifluoroacetic acid in 1,2-dichloroethane are tabulated in Table 7.

Table 7. Acidity function for trifluoroacetic acid in 1,2-dichloroethane at 25°C

CF_3CO_2H M	0.432	0.259	0.155	0.109	0.076
H_0	0.107	0.592	0.810	0.964	1.119

14) E. A. Braude and E. S. Stern, *J. Chem. Soc.*, **1948**, 1976.

15) M. A. Paul and F. A. Long, *Chem. Revs.*, **57**, 1 (1957).

BULLETIN OF THE CHEMICAL SOCIETY OF JAPAN VOL. 43 1778—1782 (1970)

3,4-Benzotropolone and Related Compounds. VIII.[1] Azo, Nitro and Amino Derivatives of 6-Hydroxy-2,3-benzotropone

Masamatsu Hoshino and Seiji Ebine

Department of Chemistry, Saitama University, Urawa, Saitama

(Received September 29, 1969)

On diazo coupling and nitration, 6-hydroxy-2,3-benzotropone (I) and its 5-bromo derivative (II) gave their 7-azo (V and VI) and 7-nitro substitution products (VII and VIII), respectively. In the same reactions, 7-bromo-6-hydroxy- (III) and 5,7-dibromo-6-hydroxy-2,3-benzotropones (IV) replaced their 7-bromo substituent to give the same 7-azo and 7-nitro substitution products as above. On nitration of III and IV, 2,2-dibromo- (IX) and 2,2,7-tribromo-4,5-benzocyclohepta-4,6-diene-1,3-diones (X) were also formed. Hydrogenation of V, VI, VII and VIII gave 7-amino-6-hydroxy-2,3-benzotropone (XI), diazotization of which gave 2-diazo-4,5-benzocyclohepta-4,6-diene-1,3-dione (XII). 7-Chloro-6-hydroxy-2,3-benzotropone (XV) was brominated to 2-bromo-2-chloro-4,5-benzocyclohepta-4,6-diene-1,3-dione (XVII) at room temperature, to 5-bromo-7-chloro-2,3-benzotropone (XVI) at 100°C, and to 2-chloro-2,7-dibromo-4,5-benzocyclohepta-4,6-diene-1,3-dione (XVIII) with excess bromine at 100°C. XVII and XVIII were easily debrominated to XV and XVI, respectively, on heating with hydrochloric or hydrobromic acid. XV changed into a mixture of I and II on heating with hydrobromic acid.

Nitration, azo coupling and related reactions of 6-hydroxy-2,3-benzotropone (I)[2],*1 have been investigated as a series of benzotroponoid studies.[1-3]

I and its 5-bromo derivative (II),[2] like tropolone[4,5] and its benzologs,[6-8] underwent coupling with diazotized *p*-toluidine in a pyridine solution to give the corresponding 7-*p*-tolylazo derivatives (V and VI). 7-Bromo (III)[3] and 5,7-dibromo (IV)[3] derivatives of I also reacted with diazotized *p*-toluidine, expelling their 7-bromo substituent, to give the same products (V and VI) as above.

Nitration of I and II, like that of tropolone[5] and its benzologs,[7,9] was not successful in concentrated sulfuric acid but successful in acetic acid solution to give 6-hydroxy-7-nitro-2,3-benzotropone (VII) and its 5-bromo derivative (VIII), respectively, in good yields. On nitration of III, the 7-bromo substituent was replaced with a nitro group to give VII and the liberated bromo cation attacked an unreacted III to give 2,2-dibromo-4,5-benzocyclohepta-4,6-diene-1,3-dione (IX) (infrared absorption spectrum in KBr disk: 1690 and 1653 cm^{-1} for two carbonyls). Intermediate formation of the bromo cation, however, has no experimental evidence. A similar nitration of IV gave a tribromo diketone (X),[3] a possible product (VIII) not being isolated. X was also obtained by bromination of IV and IX.

7-Amino-6-hydroxy-2,3-benzotropone (XI) was produced by hydrogenation of azo compounds (V and VI) or nitro compounds (VII and VIII). Treatment of XI with nitrous acid at 0—5°C resulted in the formation of 2-diazo-4,5-benzocyclohepta-4,6-diene-1,3-dione (XII), which would be produced *via* an intermediate diazonium salt. The structure of XII was confirmed by intense infrared absorption at 2178 cm^{-1} characteristic to diazoketone[10] and by Wolff rearrangement reaction to 1-hydroxy-2-naphthoic acid along with a small amount of α-naphthol on heating in aqueous solution, and to

1) Part VII. M. C. Woods, S. Ebine, M. Hoshino, K. Takahashi and I. Miura, *Tetrahedron Lett.*, **1969**, 2879.

2) S. Ebine, M. Hoshino and K. Takahashi, This Bulletin, **41**, 2942 (1968).

*1 6-Hydroxy-2,3-benzotropone is tautomeric with 3-hydroxy-4,5-benzotropone. Since it is not clear which form predominates in the tautomeric mixture, the former form is tentatively employed in this paper.

3) M. Hoshino and S. Ebine, *ibid.*, **41**, 2949 (1968).

4) T. Nozoe, E. Sebe and S. Ebine, *Proc. Japan Acad.*, **26** (8), 24 (1950).

5) W. von E. Doering and L. H. Knox, *J. Amer. Chem. Soc.*, **73**, 828 (1951); J. W. Cook, J. D. Loudon and D. K. V. Steel, *J. Chem. Soc.*, **1954**, 530.

6) D. S. Tarbell and J. C. Bill, *J. Amer. Chem. Soc.*, **74**, 1234 (1952).

7) G. A. Nicholls and D. S. Tarbell, *ibid.*, **74**, 4935 (1952).

8) S. Ebine, This Bulletin, **38**, 2029 (1965).

9) S. Ebine, *ibid.*, **35**, 122 (1962).

10) M. P. Cava, R. L. Litle and D. R. Napier, *J. Amer. Chem. Soc.*, **80**, 2258 (1958).

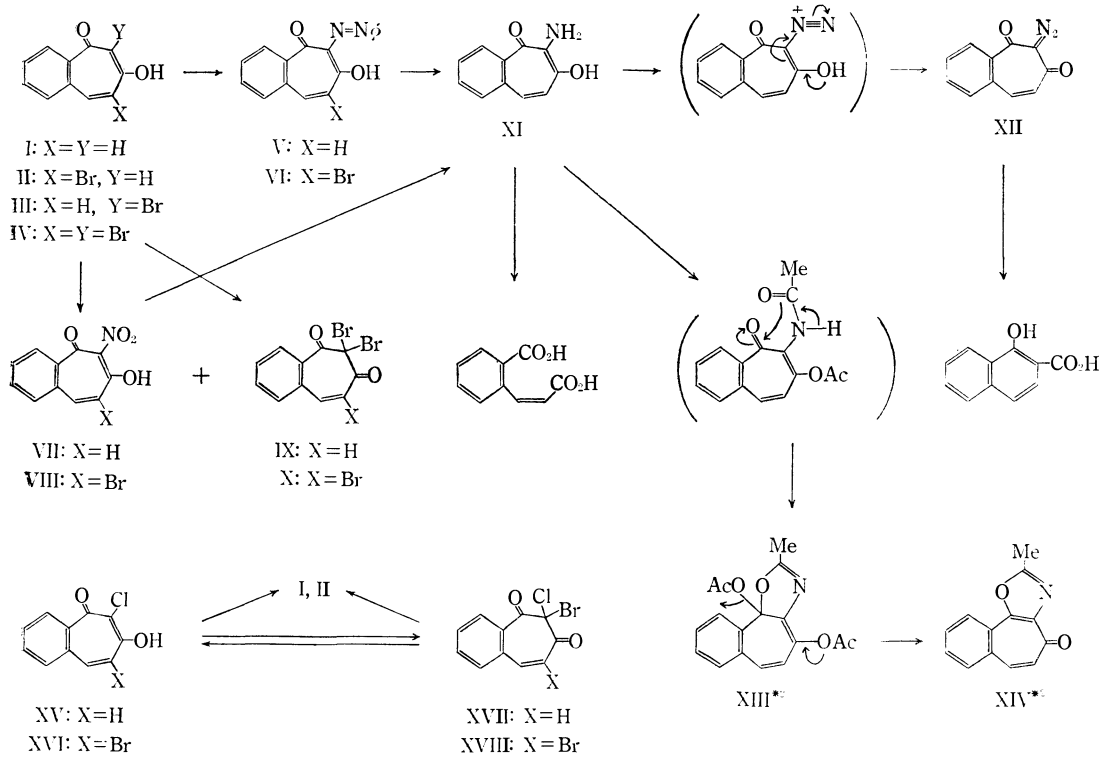

1-hydroxy-2-naphtho-*p*-toluidide on heating with *p*-toluidine in xylene solution. Acetylation of XI gave an unusual product (XIII), hydrolysis of which gave a compound (XIV). XIV is assumed to be an oxazolobenzotropone based on its infrared absorption spectrum (KBr): 1620, 1590, 1548 and 1130 cm^{-1} for C=O, C=N, C=C and C–O–C, no absorption for acetoxyl and acetamide carbonyls. The structure of XIII is also assumed as given in the chart due to infrared absorption at 1770 and 1710 cm^{-1} for two acetyl carbonyls. A similar reaction has been reported in the case of acetylation of 3-amino-4,5-benzotropolone[7] and 3-aminotropolone.[11]

By analogy to the case of III and IV, 7-chloro-6-hydroxy-2,3-benzotropone (XV) was subjected to halogenation and dehalogenation. Bromination of XV at 100°C gave 5-bromo-7-chloro-6-hydroxy-2,3-benzotropone (XVI).[3] Bromination of XV and XVI at room temperature gave the corresponding bromo chloro diones (XVII and XVIII) which, on treatment with alkali or hydrochloric acid, turned back to the original XV and XVI, respectively. Bromination of III at room temperature gave III-bromine adduct[3] instead of IX.

XV remained unchanged on heating with hydrochloric acid but changed to give both I and II on heating with hydrobromic acid. A similar treatment of XVI, XVII and XVIII with hydrobromic acid liberated one of their halogen substituents to afford II in good yield. III and XV also liberated with difficulty their halogen substituent to give I on heating with sulfuric acid. The diones (IX, XVII and XVIII) were dehalogenated under mild condition to the tropones (III, XV and XVI, respectively). Halogenation and dehalogenation of these chloro derivatives are analogous to those of the corresponding bromo derivatives.[3]

Experimental*3

Azo Coupling of 6-Hydroxy-2,3-benzotropone (I)[2] and Its Bromo Derivatives (II[2], III[3] and IV[3]). *6-Hydroxy-7-p-tolylazo-2,3-benzotropone (V).* To a solution of 300 mg of I in 5 m*l* of pyridine was added a diazotized *p*-toluidine solution prepared from 243 mg of *p*-toluidine, 132 mg of sodium nitrite and 3.14 m*l* of 2.4N hydrochloric acid. After standing overnight in an ice-chest, the precipitate formed was filtered and recrystallized from ethanol, giving 480 mg (95%) of V, reddish orange needles, mp 153—154°C, infrared

*2 Alternative structures XIII′ and XIV′ are conceivable. It is not clear which pair of structures are more correct.

XIII′ 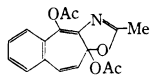 XIV′ 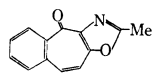

11) Y. Kitahara, *Sci. Rep. Tohoku Univ., Ser. I*, **40**, 87 (1956).

*3 Thanks are due to the Department of Chemistry, Tohoku University, for the microanalyses.

spectrum above 1500 cm^{-1} (KBr, cm^{-1}): 3406, 1638, 1591, 1556, ultraviolet spectrum (MeOH), mμ (log ε): 229 (4.44), 265 (4.38), 455 (4.46).

Found: C, 74.17; H, 4.77; N, 9.43%. Calcd for $C_{18}H_{14}N_2O_2$: C, 74.47; H, 4.86; N, 9.65%.

Coupling of 200 mg of 7-bromo-6-hydroxy-2,3-benzotropone (III) with diazotized *p*-toluidine gave 30 mg (13%) of the same product (V) as above.

5-Bromo-6-hydroxy-7-p-tolylazo-2,3-benzotropone (VI). Coupling of 200 mg of 5-bromo-6-hydroxy-2,3-benzotropone (II) and 300 mg of 5,7-dibromo-6-hydroxy-2,3-benzotropone (IV) with diazotized *p*-toluidine gave 230 mg (78%) and 130 mg (39%), respectively, of the same VI, orange needles (from ethanol), mp 181—182°C, infrared spectrum above 1500 cm^{-1} (KBr, cm^{-1}): 3420, 1647, 1590, 1565, ultraviolet spectrum (MeOH), mμ (log ε): 257 (4.67), 460 (4.45).

Found: C, 58.36; H, 4.05; N, 7.34%. Calcd for $C_{18}H_{13}N_2O_2Br$: C, 58.55; H, 3.55; N, 7.59%.

4-Bromo-6-hydroxy-7-p-tolylazo-2,3-benzotropone.[2] Coupling of 4-bromo-6-hydroxy-2,3-benzotropone with diazotized *p*-toluidine gave 4-bromo-6-hydroxy-7-*p*-tolylazo-2,3-benzotropone, reddish orange needles, mp 152—153°C, in 70% yield, infrared spectrum above 1500 cm^{-1} (KBr, cm^{-1}): 3420, 1655, 1608, 1588, 1560, ultraviolet spectrum (MeOH), mμ (log ε): 230 (4.28), 265 (4.27), 450 (4.45).

Found: C, 58.50; H, 3.45; N, 7.56%. Calcd for $C_{18}H_{13}N_2O_2Br$: C, 58.55; H, 3.55; N, 7.59%.

Nitration of I, II, III and IV. *6-Hydroxy-7-nitro-2,3-benzotropone (VII).* To a stirred suspension of 400 mg of I in 10 m*l* of glacial acetic acid was dropped at 10—15°C 0.174 m*l* of concentrated nitric acid (sp. gr. 1.38), diluted with an equal volume of glacial acetic acid in the course of one and a half hours. The mixture was stirred for further 4 hr and then allowed to stand at room temperature overnight. A precipitate formed was collected and recrystallized from ethanol to give 440 mg (87%) of pale yellow, granular crystals, mp 203°C (dec), infrared spectrum above 1500 cm^{-1} (KBr, cm^{-1}): *ca.* 3388, 3026, 1640, 1600, 1560, 1515, ultraviolet spectrum (MeOH), mμ (log ε): 258 (4.63), 335 (3.89).

Found: C, 60.77; H, 3.20; N, 6.14%. Calcd for $C_{11}H_7NO_4$: C, 60.83; H, 3.25; N, 6.45%.

5-Bromo-6-hydroxy-7-nitro-2,3-benzotropone (VIII). A similar nitration of 300 mg of 5-bromo-6-hydroxy-2,3-benzotropone (II) gave 280 mg (79%) of VIII, pale yellow, granular crystals, mp 103—105°C (dec), infrared spectrum above 1500 cm^{-1} (KBr, cm^{-1}): *ca.* 3440, 3026 (shoulder), 1605, 1573, 1548, ultraviolet spectrum (MeOH), mμ (log ε): 273 (4.66).

Found: C, 44.86; H, 2.04; N, 4.31%. Calcd for $C_{11}H_6NO_4Br$: C, 44.62; H, 2.04; N, 4.73%.

2,2-Dibromo-4,5-benzocyclohepta-4,6-diene-1,3-dione (IX). III (300 mg) was nitrated in the same way as above and the crude product was fractionally recrystallized from dilute methanol to give 46 mg (18%) of VII and 127 mg (32%) of IX, intensely yellow, granular crystals, mp 110—111°C, infrared spectrum (KBr, cm^{-1}): 1690 and 1653 for two carbonyls, ultraviolet spectrum (MeOH), mμ (log ε): 243 (3.89).

Found: C, 40.10; H, 1.94%. Calcd for $C_{11}H_6O_2Br_2$: C, 40.03; H, 1.83%.

2,2,7-Tribromo-4,5-benzocyclohepta-4,6-diene-1,3-dione (X).[3] a) Nitration of 300 mg of IV in acetic acid or acetic anhydride solution gave 105 mg (28%) of X, mp 131—132°C. (Found: C, 32.91; H, 1.38%. Calcd for $C_{11}H_5O_2Br_3$: C, 32.81; H, 1.23%).

b) A solution of 30 mg of bromine in 0.2 m*l* of acetic acid was added to a solution of 50 mg of IV in 3 m*l* of acetic acid, and the resulting solution was allowed to stand at room temperature for 2 hr. The solvent was removed *in vacuo* and the residue was extracted with warm petroleum ether. After standing in an ice-chest, the precipitate formed was collected and recrystallized from ethanol to give 17 mg (27%) of X, mp 132—133°C.

The products obtained in the above two ways were identified by mixture mp determination and infrared comparison with an authentic sample.[3]

7-Amino-6-hydroxy-2,3-benzotropone (XI) and Its Derivatives. *7-Amino-6-hydroxy-2,3-benzotropone (XI).* A solution of 300 mg of V or 400 mg of VII in 50—100 m*l* of ethanol was hydrogenated with a theoretical amount of hydrogen in the presence of 100 mg of 5% palladium chloride-charcoal catalyst. After completion of the reaction, the catalyst was filtered, the solution was evaporated and the product was recrystallized from ethanol giving 160 mg (83%) or 255 mg (74%) of XI, yellow needles, mp 192—193°C (dec). A similar hydrogenation of 400 mg of VI, VIII or 4-bromo-6-hydroxy-7-*p*-tolylazo-2,3-benzotropone in ethanol in the presence of 100 mg of 5% palladium chloride-charcoal and 400 mg of fused sodium acetate gave XI in around 80% yield. Infrared spectrum above 1500 cm^{-1} (KBr, cm^{-1}): *ca.* 3386, 3046, 1638, 1573, 1538, ultraviolet spectrum (MeOH), mμ (log ε): 254 (4.51), 410 (4.05).

Found: C, 70.71; H, 5.05; N, 7.16%. Calcd for $C_{11}H_9NO_2$: C, 70.58; H, 4.85; N, 7.48%.

Hydrochloride. Colorless needles, mp 223—225°C (dec).

Found: C, 59.15; H, 4.46; N, 6.00%. Calcd for $C_{11}H_{10}O_2NCl$: C, 59.07; H, 4.51; N, 6.26%.

Sulfate. Pale yellow crystals, mp 208—210°C (dec).

Found: C, 46.23; H, 4.14; N, 4.64%. Calcd for $C_{11}H_{11}O_6NS$: C, 46.31; H, 3.89; N, 4.91%.

Picrate. Yellow needles, mp 172°C (dec).

Found: C, 55.73; H, 3.59; N, 11.16%. Calcd for $C_{28}H_{21}O_{11}N_5$: C, 55.72; H, 3.51; N, 11.61%.

Reaction of XI with Acetic Anhydride. A mixture of 400 mg of XI, 400 mg of fused sodium acetate and 12 m*l* of acetic anhydride was heated at 100°C for 30 min. After cooling the mixture was poured on ice and the precipitate which separated was collected by filtration. The precipitate (A) and the filtrate (B) were worked up as follows. Recrystallization of A from ethanol gave 304 mg (45%) of a compound (XIII), colorless prisms, mp 146°C, infrared spectrum (KBr, cm^{-1}): 1770, 1710, 1635 (shoulder), 1623, 1593, 1580, *etc.*, ultraviolet spectrum (MeOH), mμ (log ε): 236 (4.45), 325 (3.91).

Found: C, 65.14; H, 4.83; N, 4.43%. Calcd for $C_{17}H_{15}NO_5$: C, 65.17; H, 4.82; N, 4.47%.

Extraction of B with ethyl acetate, evaporation of the solvent from the organic layer and recrystallization of the residue from ethanol gave 87 mg (19%) of oxazole derivative (XIV), colorless needles, mp 192—193°C (dec), infrared spectrum (KBr, cm^{-1}): 1628 (shoulder), 1620, 1590, 1548, *etc.*, ultraviolet spectrum (MeOH), mμ (log ε): 237 (4.31), 270 (4.71).

Found: C, 73.70; H, 4.13; N, 6.14%. Calcd for

$C_{13}H_9NO_2$: C, 73.92; H, 4.30; N, 6.63%.

Heating of XIII with concentrated hydrochloric acid at 100°C for 20 min gave XIV in 83% yield.

Oxidation of XI to o-Carboxycinnamic Acid. To a solution of 200 mg of XI in 20 m*l* of 0.5N sodium hydroxide was added 5 m*l* of 35% hydrogen peroxide. After standing for 2 hr at room temperature, the solution was acidified with 6N hydrochloric acid to give 70 mg (34%) of *o*-carboxycinnamic acid, mp and mixed mp 186—188°C.

2-Diazo-4,5-benzocyclohepta-4,6-diene-1,3-dione (XII) and Its Wolff Rearrangement. *Diazoketone (XII).* To a stirred suspension of 500 mg of XI in 12.5 m*l* of 42% borofluoric acid (HBF_4) was dropped a solution of 204 mg of sodium nitrite in 1 m*l* of water and the reaction mixture was set aside for 1 hr at 0—5°C. The precipitate (A) was collected by filtration. The filtrate was set aside for several days, giving a precipitate (B) of unknown compound (mp>240°C, 149 mg). The precipitate (A) was recrystallized from methanol to afford 314 mg (59%) of XII, yellow needles, mp 118—119°C, infrared spectrum (KBr, cm^{-1}): *ca.* 2178, 1636, 1579(shoulder), 1578, 1560, *etc.*, ultraviolet spectrum (MeOH), mμ (log ε): 255 (4.61), 330 (3.90), NMR spectrum ($CDCl_3$, ppm): 8.84 (an aromatic H), 7.64 (multiplet, three aromatic H), 7.21 and 6.45 (AB pattern, 6-H and 7-H, J=13.1 Hz).

Found: C, 66.70; H, 3.30; N, 14.35%. Calcd for $C_{11}H_6N_2O_2$: C, 66.66; H, 3.05; N, 14.14%.

XII (147 mg, 69%) as well as a trace (4 mg, 2%) of 1-hydroxy-2-naphthoic acid were formed when a solution of 82 mg of sodium nitrite in 2 m*l* of water was added to a suspension of 200 mg of XI in 10 m*l* of 6N sulfuric acid, and the resulting mixture was allowed to stand at 0—5°C for 1 hr and then refluxed for 5 min.

Wolff Rearrangement of XII. a) A suspension of 100 mg of XII in 40 m*l* of water was refluxed for 4.5 hr, during which time the suspended mixture became homogeneous. After cooling, the solution was extracted with ethyl acetate and then the organic layer was shaken with aqueous sodium bicarbonate. The organic layer was evaporated and the residue was recrystallized from petroleum ether to give 12 mg (14%) of α-naphthol, mp and mixed mp 91—93°C. The aqueous sodium bicarbonate layer was acidified with dilute hydrochloric acid and then extracted with ethyl acetate. The extract was evaporated and the residue was recrystallized from benzene to give 55 mg (59%) of 1-hydroxy-2-naphthoic acid, mp and mixed mp 188.5—190.5°C, which was identified by infrared comparison with an authentic sample.

A solution of 200 mg of 1-hydroxy-2-naphthoic acid in 50 m*l* of water was refluxed for 2.5 hr to give 150 mg of α-naphthol, proving that a part of 1-hydroxy-2-naphthoic acid was decarboxylated to α-naphthol during the above Wolff rearrangement.

b) A solution of 120 mg of XII and 500 mg of *p*-toluidine in 15 m*l* of xylene was refluxed for 3 hr. The solution was washed with dilute hydrochloric acid to remove excess *p*-toluidine and the organic layer was evaporated. Recrystallization of the residue from cyclohexane gave 125 mg (74%) of 1-hydroxy-2-naphtho-*p*-toluidide, mp and mixed mp 149—151°C (Found: C, 78.17; H, 5.47; N, 5.06%. Calcd for $C_{18}H_{15}NO_2$: C, 77.96; H, 5.45; N, 5.05%).

Derivatives of 7-Bromo-6-hydroxy-2,3-benzotropone (III)[3] and 7-Chloro-6-hydroxy-2,3-benzotropone (XV)[3]. *Acetate of III.* Colorless granular crystals (from ether-petroleum ether), mp 139—140°C.

Found: C, 53.18; H, 3.30%. Calcd for $C_{13}H_9O_3Br$: C, 53.27; H, 3.09%.

Methyl Ether of III. Colorless prisms (from methanol), mp 138—139°C.

Found: C, 54.48; H, 3.58%. Calcd for $C_{12}H_9O_2Br$: C, 54.36; H, 3.42%.

Acetate of XV. Colorless plates (from methanol), mp 141—142°C.

Found: C, 62.37; H, 3.70%. Calcd for $C_{13}H_9O_3Cl$: C, 62.79; H, 3.65%.

Methyl Ether of XV. Colorless needles (from methanol), mp 137—137.5°C.

Found: C, 64.88; H, 4.15%. Calcd for $C_{12}H_9O_2Cl$: C, 65.32; H, 4.11%.

Bromination of XV.[3] *5-Bromo-7-chloro-6-hydroxy-2,3-benzotropone (XVI).* A solution of 52.5 mg of bromine in 2 m*l* of acetic acid was added to a solution of 50 mg of XV[9] in 2 m*l* of acetic acid and the resulting solution was heated at 100°C for 1 hr. On evaporation of the solvent *in vacuo*, recrystallization of the residue from ethanol gave 53.5 mg (77%) of XVI, yellow needles, mp and mixed mp 213—214°C (dec), whose infrared spectrum coincided with that of a sample prepared by a different method.[3]

2-Bromo-2-chloro-4,5-benzocyclohepta-4,6-diene-1,3-dione (XVII). Bromination of 100 mg of XV with 80 mg of bromine and 60 mg of fused sodium acetate in 10 m*l* of acetic acid at room temperature (18°C) gave 135 mg (98%) of XVII, yellow plates (from methanol), mp 121—122°C (dec), infrared spectrum (KBr, cm^{-1}): 1698 and 1663 for two carbonyls, ultraviolet spectrum (MeOH), mμ (log ε): 247 (4.10), 334 (3.65).

Found: C, 46.06; H, 2.17%. Calcd for $C_{11}H_6O_2BrCl$: C, 46.27; H, 2.12%.

2-Chloro-2,7-dibromo-4,5-benzocyclohepta-4,6-diene-1,3-dione (XVIII). a) Bromination of 100 mg of XV with 184 mg of bromine and 105 mg of fused sodium acetate in 10 m*l* of acetic acid at 60—70°C gave 119 mg (67%) of XVIII, yellow prisms (from methanol), mp 140—141°C (dec), infrared spectrum (KBr, cm^{-1}): 1706 and 1691 for two carbonyls, ultraviolet spectrum (MeOH), mμ (log ε): 270 (3.86), 277 (3.86).

Found: C, 36.39; H, 1.51%. Calcd for $C_{11}H_5O_2Br_2Cl$: C, 36.25; H, 1.38%.

b) A similar treatment of 200 mg of XVI with 150 mg of bromine and 150 mg of fused sodium acetate in 70 m*l* of acetic acid gave 230 mg (90%) of XVIII.

Dehalogenation of Halo-6-hydroxy-2,3-benzotropones (III[3], XV[3], XVI[3]) and Halo-4,5-benzocyclohepta-4,6-diene-1,3-diones (IX, XVII, XVIII). *From III and XV to I (and II).* a) A solution of 150 mg of XV in 20 m*l* of acetic acid and 20 m*l* of 47% hydrobromic acid was refluxed for 2 hr. Evaporation of the solvent and fractional recrystallization of the residue from dilute alcohol gave 44 mg (35%) of I, 208°C (dec) and 72 mg (40%) of II, mp 234°C (dec).

XV remained unchanged on heating with hydrochloric acid.

b) A solution of 100 mg of III in 15 m*l* of acetic acid and 10 m*l* of 6N sulfuric acid was refluxed for 2 hr. Concentration of the reaction mixture and dilution with 50 m*l* of water gave 76.2 mg of a precipitate of unchanged III. After filtration the filtrate was extracted

with ethyl acetate and the extract was evaporated to give 13 mg (19%) of I, mp 208°C (dec).

Heating of III with hydrobromic acid gave I (4%) and II (29%).[9]

c) A similar treatment of 100 mg of XV with 6N sulfuric acid gave 4.2 mg (5%) of I, a greater part of XV remained unreacted.

From XVI, XVII, and XVIII to II. A 50-mg sample of XVI, XVII or XVIII, dissolved in 5 m*l* of acetic acid and 5 m*l* of 47% of hydrobromic acid, was heated for 2 hr. Evaporation of the solvent and recrystallization of the residue from methanol gave II, mp 234°C (dec), in over 90% yield.

From IX, XVII and XVIII to III, XV and XVI, respectively. a) A solution of 50 mg of IX in 6 m*l* of N sodium hydroxide was set aside at room temperature for 1 hr. The solution was acidified with dilute hydrochloric acid and the precipitate which separated was recrystallized from ethanol to give 20 mg (52%) of III, mp 173.5°C (dec).

b) XVII (50 mg), 5 m*l* of 6N hydrochloric acid and 8 m*l* of acetic acid were heated under reflux for 1 hr. The solution was evaporated and the residue was recrystallized from methanol to give 24 mg (66%) of XV, mp 173°C.

c) XVIII (50 mg), 5 m*l* of 47% hydrobromic acid and 8 m*l* of acetic acid were set aside at room temperature for 2 days. Concentration of the solution gave 31 mg (79%) of XVI, mp 214°C (dec).

XVIII (50 mg), 5 m*l* of 6N hydrochloric acid and 8 m*l* of acetic acid were refluxed for 1 hr, yielding 20 mg (52%) of XVI.

XVIII (100 mg) and 20 drops of 2N potassium hydroxide in 20 m*l* of methanol were allowed to stand at room temperature for 1 hr. Removal of methanol, acidification with dilute hydrochloric acid, extraction with chloroform, and evaporation of the solvent from the extract gave 21 mg (27%) of XVI.

The above products I, II, III, XV and XVI were identified by elemental analyses, mixture mp determinations and infrared comparisons with authentic samples.[3]

The present work has been supported in part by a Grant for Scientific Research from the Ministry of Education.

BULLETIN OF THE CHEMICAL SOCIETY OF JAPAN VOL. 43 1782—1788 (1970)

Pyrolytic and Photolytic Reactions. I. Thermal Rearrangement of 1-Acetyl- and 1-Isopropenyl-3-methylenecyclobutane[1)]

Shigehiro Ooba and Masaki Ohta

Laboratory of Organic Chemistry, Tokyo Institute of Technology, Ookayama, Meguro-ku, Tokyo

and Hiroshi Kato[2)]

Department of Chemistry, Faculty of Science, Shinshu University, Asahi, Matsumoto

(Received October 28, 1969)

1-Acetyl- and 1-isopropenyl-3-methylenecyclobutane (I and II) were prepared and then subjected to pyrolysis. The pyrolysis of I at 304—340°C gave 2-methyl-5-methylene-Δ^2-dihydropyrane, which was then converted to 4-methylenecyclohexanone at this temperature. The pyrolysis of II at 255—340°C gave 1-methyl-4-methylenecyclohexene, which was disproportionated at this temperature to *p*-xylene and 1,4-dimethylcyclohexene. In neither case was fragmentation to olefins observed. These results were interpreted by a two-step biradical mechanism.

There have been ample examples of the thermal fragmentation of a cyclobutane derivative into two molecules of olefins.[3)] For example, cyclobutane is pyrolyzed into two molecules of ethylene, and methylenecyclobutane is likewise pyrolyzed into ethylene and allene. The comparison of these two reactions reveals that the activation energy (63.3 kcal/mol)[4)] required for the pyrolysis of methylenecyclobutane is slightly higher than, or almost equal to, that (61.5—63.2 kcal/mol)[5)] required for

1) a) Taken from the Master of Science thesis of S. O. b) Presented at the 20th Annual Meeting of The Chemical Society of Japan, Tokyo, April, 1967.

2) To whom inquiries should be addressed.

3) See for example, a) R. Breslow, "Molecular Rearrangements," Part I, ed. by P. de Mayo, Interscience Publishers, New York (1963), p. 245; b) H. Kato, *Yuki Gosei Kagaku Kyokai Shi*, **24**, 265 (1966).

4) J. P. Chesick, *J. Phys. Chem.*, **65**, 2170 (1961).

5) R. L. Brandauer, S. Short and S. M. Kellner, *ibid.*, **65**, 2269 (1961); R. W. Vreeland and D. F. Swinehart, *J. Amer. Chem. Soc.*, **85**, 3349 (1963); J. N. Butler and R. B. Ogawa, *ibid.*, **85**, 3346 (1963); C. T. Genaux, F. Kern and W. D. Walters, *ibid.*, **75**, 6196 (1953). A value of 61.2 kcal/mol is reported as the activation energy for the fragmentation of methylcyclobutane: M. N. Das and W. D. Walters, *Z. Phys. Chem.*, **15**, 22 (1958).

cyclobutane. This result may appear contrary to the expectation that the presence of an exocyclic methylene group would reduce the activation energy of pyrolytic fragmentation as a result of the extra strain (*ca.* 2.5 kcal/mol)[6] imposed by the introduction of a methylene group. It was thought of interest to learn if this seemingly anomalous value corresponds, not to the initial ring-cleavage step to give a biradical, but, rather, to the final stage of producing the fragmentation products.[4] Such distinction would be possible by a study of the pyrolysis of deliberately chosen compounds in which a second reaction path exists in preference to, or in competition with, fragmentation.

With this in mind, we studied the thermal behavior of 1-acetyl-3-methylenecyclobutane (I) and 1-isopropenyl-3-methylenecyclobutane (II). These compounds will give fragmentation and/or ring-enlargement products depending on the heights of the energy barriers existing in the two reaction paths.

During the course of this investigation, Doering and Gilbert[8] have unequivocally shown with 1,1-dideuteriomethylenecyclobutane that the fragmentation step indeed requires a higher activation energy than that of the initial ring cleavage to a biradical.

Results and Discussion

The reaction of 3-methylenecyclobutanecarbonitrile[9] and methylmagnesium iodide, followed by hydrolysis, gave 1-acetyl-3-methylenecyclobutane (I). The NMR spectrum of I, in complete agreement with the assigned structure, showed a three-proton singlet at τ 8.05 for the acetyl group, a four-proton multiplet and a one-proton multiplet at τ 7.27 and 7.25 for the two methylene and the methine groups, and a two-proton pentuplet (J=2.5 Hz) for the exocyclic methylene group. Its infrared spectrum confirmed the presence of the acetyl (1720, 1370 cm^{-1}) and the exocyclic methylene (3080, 1680, 1410, 880 cm^{-1}) groups. The mass spectrum of I showed a parent peak at *m/e* 110, in accord with the molecular formula of $C_7H_{10}O$, and major fragment peaks at *m/e* 95 $(P-Me)^+$, 67 $(P-Ac)^+$, and 43 $(Ac)^+$.

The treatment of I with methylenetriphenylphosphorane afforded 1-isopropenyl-3-methylenecyclobutane (II), the structure of which was established by the spectral data described below. The NMR spectrum of II consisted of three poorly-resolved multiplets at τ 8.32 (3H), 7.30 (5H), and 5.33 (4H), corresponding to the methyl group on the double bond, the ring protons, and the two terminal methylene groups respectively. The infrared spectrum of II had bands of the terminal methylene groups at 3100, 1680, 1650, 1420, 1380, 885, and 875 cm^{-1}.

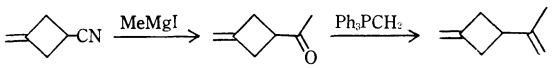

I II

Pyrolysis of 1-Acetyl-3-methylenecyclobutane. The pyrolysis of 1-acetyl-3-methylenecyclobutane (I), as a neat liquid or as a toluene solution and in a sealed tube at 304 and 340°C, gave two products besides the starting material, which were considered as 2-methyl-5-methylene-Δ^2-dihydropyrane (III) and 4-methylenecyclohexanone (IV) on the basis of the following spectral data.

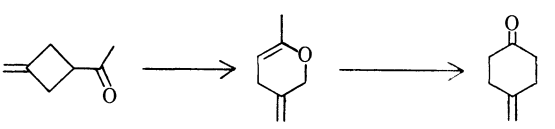

I III IV

The NMR spectrum of III consisted of a three-proton singlet (with fine splittings) at τ 8.35 corresponding to the methyl group on the double bond, a two-proton multiplet at τ 7.35 corresponding to the methylene group between the two double bonds, a two-proton singlet (with fine splittings) at τ 5.80 corresponding to the methylene group between the double bond and the oxygen atom, a one-proton triplet (J=5 Hz, with fine splittings) at τ 5.69 corresponding to the proton on the double bond, and a two-proton singlet (with fine splittings) at τ 5.10 corresponding to the terminal methylene protons. Its infrared spectrum showed bands of a terminal methylene and olefinic groups at 3100, 1680, 1430, and 900 cm^{-1} and characteristic bands of a vinyl ether at 1240 and 1050 cm^{-1}. Its mass spectrum showed a parent peak at *m/e* 110 and prominent framgent peaks at 95 $(P-Me)^+$, 67 $(P-Ac)^+$, 43 $(Ac)^+$, and 39 $(CH_2-C\equiv CH\ ?)^+$.

The NMR spectrum of the ketone IV displayed only two broad peaks, at τ 7.60 (8H) and 5.15 (2H), which are attributable to the ring protons and the exocyclic methylene groups respectively. The infrared spectrum of IV supported the presence of the exocyclic methylene (3080, 1650, 1430 and 900 cm^{-1}) and the carbonyl (1710 cm^{-1}) groups. Further support for structure IV was provided by its mass spectrum which, in addition to a parent peak at *m/e* 110, showed a fragment peak at 82 (P—

6) R. B. Turner, "Theoretical Organic Chemistry—Papers Presented to the Kekulé Symposium," Butterworths Sci. Pub., London (1959), p. 67. This value may now be regarded as an overestimation.[7]

7) R. B. Turner, P. Goebel, B. J. Mallon, W. von E. Doering, J. F. Coburn, Jr., and M. Pomerantz, *J. Amer. Chem. Soc.*, **90**, 4315 (1968).

8) W. von E. Doering and J. C. Gilbert, *Tetrahedron*, Supplement No. 7, 397 (1966).

9) H. N. Cripps, J. K. Williams and W. H. Sharkey, *J. Amer. Chem. Soc.*, **80**, 751 (1958).

CO)$^{\cdot+}$, characteristic of a cyclic ketone, and peaks at 81 (P−CO−H)$^+$, 67 (P−Ac)$^+$, 54 ($\overline{CH_2CH_2C}$=CH_2 or $\overline{CH{=}CHC}$=O ?)$^{\cdot+}$, and 39 (CH_2–C≡CH ?)$^+$.

The results of a kinetic study of this rearrangment are shown in Fig. 1. The figure clearly shows that III is the initial product of the pyrolysis of I and that III rearranges further to IV at the reaction temperature.

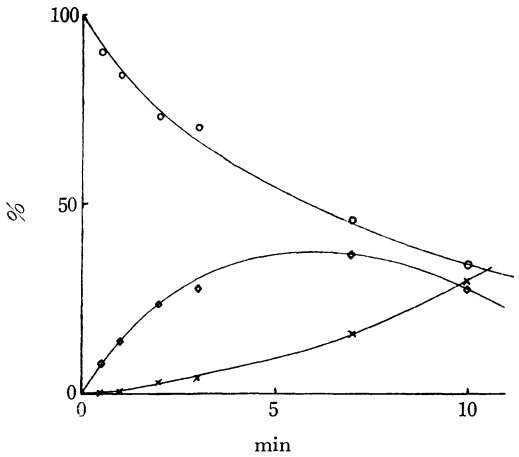

Fig. 1. Pyrolysis of 1-acetyl-3-methylenecyclobutane.
○—○ 1-Acetyl-3-methylenecyclobutane
◇—◇ 2-Methyl-5-methylene-Δ^2-dihydropyrane
×—× 4-Methylenecyclohexanone

Neither allene nor methyl vinyl ketone, which is the expected fragmentation product of I, was found to be formed by the pyrolysis of I. However, it may be reasonable to assume that the observed product, III, was formed by the cycloaddition reaction of the fragmentation products. To check on this possibility, a mixture of allene and methyl vinyl ketone was heated to 220°C for two hours in an autoclave. A resinous product resulted, and from it a small amount of a distillable component could be isolated. The distillate consisted of I (1 part) and a compound (20 parts) tentatively thought to be 2-methyl-6-acetyl-Δ^2-dihydropyrane (V), a dimer of methyl vinyl ketone but neither III nor IV could be detected. This must mean that the pyrolysis of I does not proceed through the fragmentation-recombination pathway considered earlier.

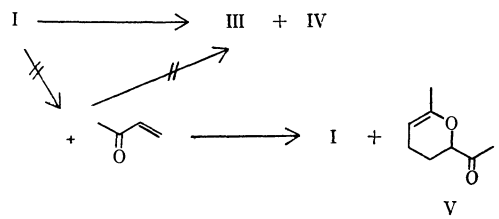

V

The assignment of structure V to the addition product follows from the NMR spectrum, which showed a three-proton doublet (J=1.5 Hz) and a three-proton singlet at τ 8.25 and 7.75 for the two methyl groups, a four-proton broad multiplet centered at τ 8.10 for the ring methylene protons, a one-proton multiplet at τ 5.87 for the proton between the acetyl group and the oxygen atom, and a one-proton multiplet at τ 5.55 for the proton on the double bond. Its infrared spectrum, showing bands of an acetyl group at 1720 and 1360 cm^{-1}, and bands of a vinyl ether at 1238 and 1070 cm^{-1}, is consistent with the indicated structure.

Pyrolysis of 1-Isopropenyl-3-methylenecyclobutane. The pyrolysis of 1-isopropenyl-3-methylenecyclobutane (II) as a neat liquid or as a toluene solution, at 255—340°C and in a sealed tube, gave 1,4-dimethylcyclohexene (VI),[10] *p*-xylene (VII), and 1-methyl-4-methylenecyclohexene (VIII).

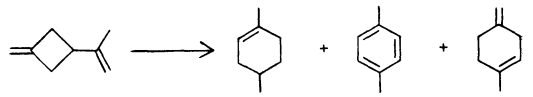

II VI VII VIII

The NMR spectrum of VIII had a three-proton singlet (with fine splittings) at τ 8.38 for the methyl group on the double bond, two overlapping two-proton multiplets at τ 7.90 and 7.78 for the two methylene groups adjacent to a double bond, a two-proton multiplet at τ 7.35 for the methylene group between the two double bonds, a slightly-broadened two-proton singlet at τ 5.38 for the terminal methylene group, and a one-proton multiplet at τ 4.75 for the hydrogen atom on the double bond. Its infrared spectrum exhibited bands of a terminal methylene group and an olefinic group at 3075, 1655, 1445, 1435, and 884 cm^{-1}. Conclusive evidence for the structure assignment could be obtained by an independent synthesis of VIII by the route to be described below.

1-Methylcyclohexene-4-carboxylic acid (IX)[11]

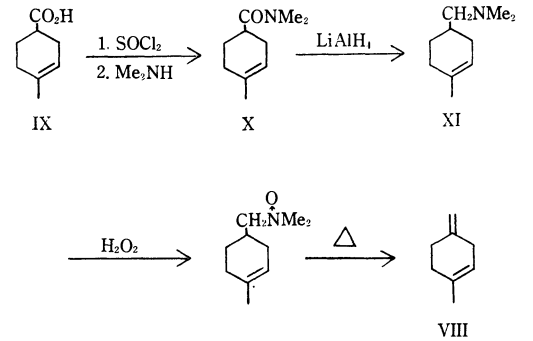

10) J. -F. Sauvage, R. H. Baker and A. S. Hussey, *J. Amer. Chem. Soc.*, **82**, 6090 (1960).
11) E. Lehmann and W. Paasche, *Ber.*, **68**, 1068 (1935).

was converted to the corresponding dimethylamide, X, through its acid chloride. The amide X was then reduced with lithium aluminum hydride to 1-methyl-(4-dimethylaminomethyl)cyclohexene (XI), which was subsequently converted to the corresponding *N*-oxide with hydrogen peroxide. The pyrolysis of the *N*-oxide afforded 1-methyl-4-methylenecyclohexene (VIII), which proved identical with the sample obtained by the pyrolysis of II.

When 1-methyl-4-methylenecyclohexene (VIII) was heated at 340°C in a sealed tube, three new products were formed in a vpc peak area ratio of 3:1:10, of which the two major products were identified as 1,4-dimethylcyclohexene (VI) (3 parts) and *p*-xylene (10 parts) respectively by comparison with authentic samples. Such a conversion of VIII may be considered to proceed through an initial isomerization to 1,4-dimethylcyclohexa-1,3-diene (XII) and its intermolecular hydrogen transfer and, in part, dehydrogenation.[12]

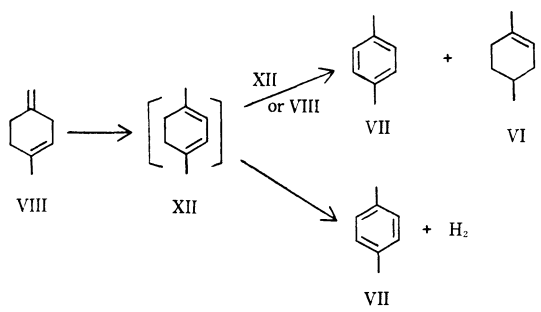

It was observed that no fragmentation product, allene or isoprene, was formed by the pyrolysis of II. In this case, the possibility of the fragmentation of II and recombination to VIII should also be considered. If the addition of allene and isoprene proceeds by a stepwise radical mechanism, then the reaction may be expected to proceed through pathway b to give a slightly more stabilized biradical intermediate, XIIIb, than the biradical XIIIa.

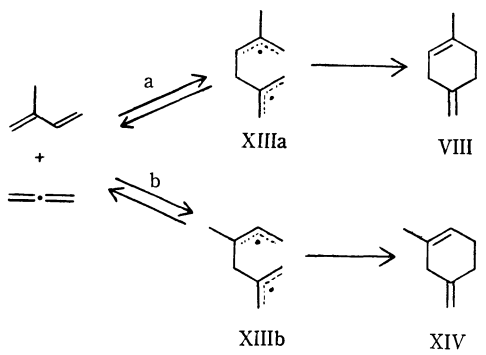

12) A similar disproportionation reaction has recently been reported with cyclohexa-1,3-diene: S. W. Benson and R. Shaw, *J. Amer. Chem. Soc.*, **89**, 5351 (1967).

The reaction of allene and isoprene at 300°C in an autoclave afforded, besides a large quantity of unreacted starting materials and polymeric substances, a small quantity of distillable products, which consisted of five components in a ratio of 7.5:4:8:1:1.5 (in the increasing order of their retention times). The vpc retention times of none of these components corresponded to *p*-xylene. The vpc retention time of the component with the shortest retention time was identical with that of VIII, and its infrared and NMR spectra were very similar to those of VIII except that the multiplet at τ 7.78 of VIII was shifted to a slightly higher magnetic field to give a poorly-resolved four-proton multiplet centered at τ 7.85. When it was subjected to the same pyrolysis conditions as those for VIII described earlier, it was converted to two products in a ratio of 1:1.3, though much more sluggishly than VIII. This isomerization could be effectively accelerated by the addition of a catalytic amount of alumina. The major product of the isomerization was identified as *m*-xylene by comparison with an authentic sample. From the above experiment, it may now be concluded that allene and isoprene react regiospecifically to give 1-methyl-5-methylenecyclohexene (XIV). This fact, as well as the absence of XIII and *m*-xylene in the pyrolysis products of II, gives conclusive evidence that no fragmentation occurred in the pyrolysis of 1-isopropenyl-3-methylenecyclobutane (II).

Interpretation of the Results. An arresting feature of the pyrolyses of I and II described above is that no fragmentation products could thus be detected. The pyrolysis of acetylcyclobutane gives ethylene and methyl vinyl ketone,[13] while the pyrolysis of isopropenylcyclobutane gives ethylene, isoprene, and 1-methylcyclohexene.[14] The activation energies of these reactions (54.5 kcal/mol and 51.0 kcal/mol respectively) clearly demonstrate the contribution of allylic resonance at the ring-cleavage step.

For steric reasons, the ring-enlargement reaction of II cannot proceed concertedly through a transition state similar to that of the Cope rearrangement,[15] to which it bears a formal analogy, nor can it be regarded as a concerted sigmatropic rearrangement.[16] The same holds true of the ring-enlargement reaction of I. Thus, it appears most reasonable to assume that the reaction proceeds by a stepwise biradical mechanism. The seem-

13) L. G. Daignault and W. D. Walters, *ibid.*, **80**, 541 (1958).

14) R. J. Ellis and H. M. Frey, *Trans. Faraday Soc.*, **59**, 2076 (1963).

15) W. von E. Doering and W. R. Roth, *Tetrahedron*, **18**, 67 (1962).

16) R. B. Woodward and R. Hoffmann, *J. Amer. Chem. Soc.*, **87**, 2511 (1965); R. Hoffmann and R. B. Woodward, *Accounts Chem. Res.*, **1**, 17 (1968).

ingly anomalous rearrangements of I and II can, then, readily be explained on the basis of the results of the degenerate rearrangement of methylenecyclobutane, elegantly studied by Doering and Gilbert.[8]

The pyrolysis of II (or I) gives a biradical intermediate, XIIIc, in which a full delocalization of the two radical sites have been attained (Chart 1). The biradical XIIIc may regenerate II (or I) *via* a transition state, XIIId, in which one allylic delocalization is completely, and the other, partially, retained,[17] but in order for the biradical XIIIc to give fragmentation products, one of the allylic stabilizations have to be nearly completely lost at the transition state XIIIe, since the two planes occupied by the two H–C–H groups in the allyl group should be almost perpendicular to each other.

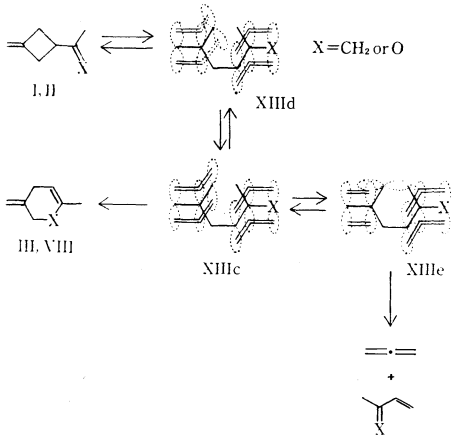

Chart 1. Pyrolytic path of 1-acetyl- and 1-isopropenyl-3-methylenecyclobutane.

Thus, the energetically most preferred path for the biradical XIIIc is ring enlargement, because, in this case, the biradical XIIIc can give a ring-enlargement product simply by rotation about a single bond, which can rotate freely with virtually no loss of stabilization energy.

In the cases of 1-acetyl- and 1-isopropenylcyclobutane, there is no such conformational preference of the biradical intermediates to warrant one of the two reaction paths (ring enlargement *vs.* fragmentation), and in the case of methylenecyclobutane, only a recombination to the starting material or fragmentation is possible.

17) It has been established that the ring-opening of (and thus recombination to) methylenecyclobutane is markedly assisted by allylic delocalization. For further discussion on the transition states and intermediates of this system, see Ref. 8.

Experimental[18]

1-Acetyl-3-methylenecyclobutane (I). A solution of 20 g (0.26 mol) of 3-methylenecyclobutanecarbonitrile[9] in 30 m*l* of ether was added, with cooling and stirring, to a solution of methymagnesium iodide, prepared from 8.7 g (0.36 g atom) of magnesium and 51.1 g (0.36 mol) of methyl iodide, in 50 m*l* of ether. The mixture was stirred for three hours at room temperature and was then hydrolyzed by the addition of dilute sulfuric acid; the organic layer was separated, and the aqueous layer was extracted repeatedly with ether. The ether extract was washed with aqueous sodium bicarbonate and then with water, and dried over sodium sulfate. Distillation gave 16.3 g (60% yield) of I boiling at 53—54°C/14 mmHg. n_D^{25} 1.4543.

Found: C, 76.45; H, 9.15%. Calcd for $C_7H_{10}O$: C, 76.32; H, 9.15%.

Semicarbazone of I: mp 146—148°C.

Found: C, 57.33; H, 7.81%. Calcd for $C_8H_{13}N_3O$: C, 57.46; H, 7.84%.

2,4-Dinitrophenylhydrazone of I: mp 142—143°C.

Found: C, 53.86; H, 5.10; N, 19.54%. Calcd for $C_{13}H_{14}N_4O_4$: C, 53.79; H, 4.86; N, 19.30%.

1-Isopropenyl-3-methylenecyclobutane (II). A solution of 8 g (0.07 mol) of 1-acetyl-3-methylenecyclobutane in 20 m*l* of ether was added, under an atmosphere of nitrogen and with cooling and stirring, to a solution of methylenetriphenylphosphorane in 300 m*l* of ether, prepared *in situ* from 35.7 g (0.1 mol) of triphenylmethylphosphonium bromide and *n*-butyllithium, and the resulting mixture was refluxed for ten hours. The precipitate was then filtered off, and the filtrate was dried over calcium chloride. The fraction distilling between 80—130°C and consisting of II and benzene was collected and subsequently purified by vpc (Carbowax 20M on Diasolid A). Bp 98—100°C, n_D^{25} 1.4531.

Found: C, 88.64; H, 10.44%. Calcd for C_8H_{12}: C, 88.82; H, 11.18%.[19]

Thermal Rearrangement of I. Samples of I (10—100 μl) were sealed in Pyrex tubes under an atmosphere of nitrogen, and were placed in an atmosphere of refluxing acetanilide (bp 304°C) or anthracene (bp 340°C) for periods of time, and then quenched by immersion in an ice bath. Vpc analysis showed the presence of three components, which were fractionated by vpc (Carbowax 20M on Diazolid A) to afford I, 2-methyl-5-methylene-Δ^2-dihydropyrane (III), and 4-methylenecyclohexanone (IV).

18) The melting points were determined on a micro hot stage, and all melting and boiling points are not corrected. The infrared spectra were recorded on a Hitachi model EPI-SII spectrophotmeter as neat liquid. The NMR spectra were determined using a Jeolco C-60 model (60MHz) spectrometer on solutions of carbon tetrachloride and the chemical shifts are represented by τ values. The vpc analyses were performed with a Shimadzu model GC-1B chromatograph. The spectral data discussed in the text are not reproduced in this section.

19) Some compounds, especially low boiling liquid, did not give satisfactory analytical values although they were proved homogeneous by vpc, and showed quite satisfactory spectra.

Samples of I containing 20% of toluene as an internal standard were heated at the refluxing temperature (340°C) of anthracene, and the concentration of the components, I, III, and IV, as evaluated by the ratio of their vpc peak areas to those of toluene, were plotted against the time. The results are shown in Fig. 1.

Reaction of Allene and Methyl Vinyl Ketone. A solution of 5 g (0.07 mol) of methyl vinyl ketone, 5 m*l* (*ca.* 0.08 mol) of allene, and 0.5 g of hydroquinone in 50 m*l* of toluene was heated at 220°C for two hours in a 100-m*l* autoclave under autogeneous pressure (20 atm). The reddish-brown product was concentrated and distilled under reduced pressure to give 0.9 g of a colorless liquid boiling at 88—90°C/50 mmHg. The residue of the distillation consisted of a large amount of a polymeric material. The distillate was separated into two components (A and B) in a ratio of 1 : 20 (Carbowax 20M on Diasolid A).

Component A had the same infrared spectrum and vpc retention time as those of an authentic sample of I.

The spectral data of component B are given in the text above.

Thermal Rearrangement of II. Samples of II were heated as has been described above at the refluxing temperature of biphenyl (bp 255°C), acetanilide or anthracene, and the product mixture was separated by vpc (Silicone DC 550 on Shimalite) giving II, *p*-xylene, 1-methyl-4-methylenecyclohexene (VIII), and a component with identical vpc retention times with those of an authentic sample of 1,4-dimethylcyclohexene (VI).[10] The infrared spectra and the vpc retention times of VIII and *p*-xylene were identical with those of authentic samples of VIII and *p*-xylene respectively.

1-Methylcyclohexene-4-carbodimethylamide (X). Into an ice-cooled, saturated solution of dimethylamine in 100 m*l* of ether, there was added with stirring, 31.7 g (0.2 mol) of 1-methylcyclohexene-4-carbonyl chloride,[11] and the resulting mixture was allowed to stand overnight at room temperature. The mixture was washed with water and then with a saturated aqueous solution of sodium chloride, and was dried over magnesium sulfate. Distillation afforded 24 g (72% yield) of X boiling at 147—153°C/23 mmHg.

Found: C, 71.70; H, 10.31; N, 8.57%. Calcd for $C_{10}H_{17}NO$: C, 71.81; H, 10.25; N, 8.38%.

1-Methyl-4-dimethylaminomethylcyclohexene (XI). Into a suspension of 5 g (0.14 mol) of lithium aluminum hydride in 100 m*l* of ether, 19 g (0.11 mol) of 1-methylcyclohexene-4-carbodimethylamide (X) was slowly added with stirring, after which the mixture was stirred for another three hours at room temperature. The excess hydride was decomposed by the addition of 5% aqueous sodium hydroxide, and the organic layer was separated, washed with aqueous sodium chloride, and dried over sodium sulfate. Distillation gave 14.2 g (80% yield) of 1-methyl-4-dimethylaminomethylcyclohexene boiling at 74—76°C/11 mmHg, n_D^{25} 1.4628.

This product was characterized by conversion to its methiodide; mp 209—210°C.

Found: C, 45.03; H, 7.58; N, 4.99%. Calcd for $C_{11}H_{22}NI$: C, 44.76; H, 7.51; N, 4.74%.

1-Methyl-4-dimethylaminomethylcyclohexene *N*-Oxide. Compound XI (10 g, 0.034 mol) was slowly added to a stirred and cooled solution of 50 m*l* of 10% aqueous hydrogen peroxide. The mixture was then stirred at room temperature for twenty hours, and the excess peroxide was decomposed by catalase. The mixture was subsequently filtered, and the water was removed under reduced pressure, and the yellow, viscous residue which remained was used for the pyrolysis reaction without further purification.

1-Methyl-4-methylenecyclohexene (VIII). The crude *N*-oxide prepared by the above-described method was decomposed at 200°C on an oil bath under reduced pressure; the distillate was collected in a trap which was cooled by a Dry Ice-acetone bath. The condensate was dissolved in 40 m*l* of ether, washed successively with dilute hydrochloric acid, water, and a saturated aqueous solution of sodium chloride, and dried over sodium sulfate. Distillation gave 2.5 g of VIII boiling at 113—114°C. The infrared spectrum and the vpc retention times of this material were identical with those of the sample of VIII isolated from the pyrolysis of II, n_D^{25} 1.4690.

Found: C, 87.97; H, 10.87%. Calcd for C_8H_{12}: C, 88.82; H, 11.18%.[19]

Thermal Rearrangement of 1-Methyl-4-methylenecyclohexene (VIII). Compound VIII (100 μl) was sealed in a Pyrex tube under an atmosphere of nitrogen and heated at 340°C for seven minutes. The product consisted of three components in a vpc peak area ratio of 3 : 1 : 10, of which the two major components (C and D) were collected by vpc (Carbowax 20M on Diasolid A).

Component C had the same infrared spectrum and vpc retention times as those of an authentic sample of 1,4-dimethylcyclohexene (VI).[10]

Component D had the same NMR and infrared spectra and vpc retention times as those of *p*-xylene.

The Reaction of Allene and Isoprene. A mixture of 5 g (0.07 mol) of isoprene, 5 m*l* (*ca.* 0.08 mol) of allene, 0.5 g of hydroquinone, and 50 m*l* of *n*-hexane was slowly heated to 300°C for seven hours in an autoclave and under autogeneous pressure (maximum, 50 atm). The product was distilled to give 1.5 g of a product boiling at 78—80°C/40 mmHg. Considerable amounts of allene and isoprene were recovered, and a transparent polymeric material was formed on the wall of the autoclave. The distillate consisted of five components in a vpc peak area ratio of 7.5 : 4 : 8 : 1 : 1.5 (Carbowax 20M on Diasolid A), none of which had the same vpc retention time as that of *p*-xylene. The first three major components (E, F, G) were collected by vpc.

Component E (1-Methyl-5-methylenecyclohexene, XIV): NMR: 8.35 (3H, s), 7.85 (4H, m), 7.38 (2H, m), 5.34 (2H, s) and 4.75 (1H, m). IR: 3075, 1660, 1445, 1440 and 885 cm^{-1}. Its vpc retention times (Carbowax 20M and Silicone DC 550) were identical with those of 1-methyl-4-methylenecyclohexene (VIII).

Component F was found to be a mixture of 1,4-dimethyl-4-vinylcyclohexene and 2,4-dimethyl-4-vinylcyclohexene by comparison of its NMR and infrared spectra with the reported values.[20]

Component G was identified as 1-methyl-5-isopropenylcyclohexene by comparison of its infrared spectrum with a previously reported chart.[21] NMR: 8.39 (3H, s), 8.29 (3H, s), 8.08 (7H, m), 5.35 (2H, s)

20) G. S. Hammond, N. J. Turro and R. S. H. Liu, *J. Org. Chem.*, **28**, 3297 (1963).

21) J. I. Binder, K. C. Eberly and G. E. P. Smith, Jr., *J. Polym. Sci.*, **38**, 229 (1959).

and 4.68 (1H, m).

Thermal Rearrangement of 1-Methyl-5-methylenecyclohexene (XIV). Compound XIV was sealed, under an atmosphere of nitrogen, in a Pyrex tube in the presence of a small amount of alumina, and then heated at 540°C for one hour. The product consisted of two components in a vpc area ratio of 1 : 1.3; the latter, major component was collected by vpc (Carbowax 20M on Diasolid A) and identified as *m*-xylene by a comparison of its NMR and infrared spectra and vpc retention times.

We are indebted to Miss Mizuko Yoshida for the measurement of NMR spectra, to the staffs of microanalysis in this laboratory for the elemental analyses, and to Takeda Chemical Industries, Ltd, for the measurement of mass spectra.

BULLETIN OF THE CHEMICAL SOCIETY OF JAPAN VOL. 43 1788—1791 (1970)

The Polymerization of α-Amino Acid *N*-Carboxy Anhydride (4-Alkyl-oxazolidine-dione). IV. A Novel Synthesis of a Block Copolypeptide

Masanao Oya

College of Techonology, University of Gunma, Tenjin-cho, Kiryu, Gunma

and Keikichi Uno and Yoshio Iwakura

Department of Synthetic Chemistry, Faculty of Engineering, The University of Tokyo, Hongo, Bunkyo-ku, Tokyo

(Received November 5, 1969)

It has been found that, when the polymerization of NCA is initiated with *n*-butylamine in acetonitrile, the amino end group in the polymer produced which is insoluble in the solvent is active (Y. Iwakura, K. Uno and M. Oya, *J. Polym. Sci., Part A-1*, **8**, 2165 (1968)). The amino end group in the polymer isolated without drying could initiate the polymerization of NCA in acetonitrile. By using this characteristic of the polymer, block copolypeptides consisting of various kinds of α-amino acid and of various chain lengths were synthesized. The solubility of the block copolypeptides in a solvent was different from that of the random copolypeptides obtained by the usual copolymerization of a mixture of NCA in acetonitrile. Sometimes the infrared spectra of the block copolypeptides were different from those of the random copolypeptides.

A block copolypeptide has been synthesized by polymerizing α-amino acid *N*-carboxy anhydride, with a soluble, low-molecular weight polypeptide, *i.e.*, polysarcosine dimethylamide, poly-γ-benzyl-L-glutamate, or poly-DL-lysine, as the initiator.[1-3] Because an insoluble polypeptide in an inert solvent for NCA's, *i.e.*, polyglycine and poly-L-alanine, could not initiate the polymerization of NCA, it has generally been considered that a block copolypeptide consisting of insoluble polypeptides would be difficult to synthesize. Therefore, the kind of block copolypeptides would be limited when this method was used.

It has been considered that the polymerization of NCA's initiated with primary amine in dioxane and tetrahydrofuran proceeds by both route by nucleophilic attack and by proton abstraction from the nitrogen of the NCA's.[4] When the polymerization is initiated with the amino end group of polypeptide by proton abstraction from 3N on NCA, a block copolypeptide containing the initiator polymer would not be produced. Further, it is very difficult to synthesize block copolypeptides consisting of three kinds of α-amino acids.

When the polymerization of NCA was carried out in acetonitrile, with *n*-butylamine as an initiator, we found that the polymer formed existed in the precipitation state that the initiator was consumed completely in the earlier stage of the polymeriza-

1) C. H. Bamford, *Proc. Roy. Soc., Ser. A*, **223**, 495 (1957).

2) P. Doty, *J. Amer. Chem. Soc.*, **79**, 3961 (1957).

3) R. T. Ingwall and H. A. Scheraga, *Biopolymers*, **6**, 331 (1968).

4) M. Goodman and J. Hutchinson., *J. Amer. Chem. Soc.*, **88**, 3627 (1966).

tion, that further propagation was performed by the attack of the amino end group of the precipitated polymer on the C-5 carbonyl carbon of NCA in acetonitrile, with almost no termination, and that the degree of polymerization increased with an increase in the reaction period in the precipitation state.[1] These case, it was found that the amino end group of the polymer was active in the precipitation state in acetonitrile. Such a consideration indicated the possibility of preparing various kinds of block copolypeptides which are insoluble in an inert solvent for NCA's.

In this paper the preparation of block copolypeptides containing an insoluble polypeptide in an inert solvent for NCA's and more than two kinds of α-amino acid will be described.

Results

The polypeptide obtained by the polymerization of the first α-amino acid NCA with *n*-butylamine in acetonitrile was isolated by filtration and washed well with absolute acetonitrile in order to remove any residual NCA. The isolated polypeptide was without drying put into a second NCA solution in acetonitrile. The polymerization was initiated by the attack of the amino end group of the first polymer on the C-5 carbonyl of the second NCA; a block copolypeptide consisting of two kinds of α-amino acid was thus produced. This block copolypeptide was isolated again by filtration, washed well with absolute acetonitrile, and put into a third NCA solution in acetonitrile. Block copolypeptides consisting of three kinds of α-amino acid were thus produced. The polypeptides obtained at the first or second step became inactive upon drying. The polypeptides obtained were extracted in solvents consisting of homopolypeptides in order to remove any coexisting homopolymer. As the polymerization was carried out in a heterogeneous system, there was no need to use the first polypeptide (initiator polymer) which is soluble in the polymerization solvent, acetonitrile. Any α-amino acid NCA could be used for this synthesis.

The average sequence length of each component in the block copolypeptides could be controlled by changing the polymerization period, the temperature and the monomer concentration for each step.

By this method, various kinds of block copolypeptides were synthesized. The block copolypeptides thus obtained are shown in Tables 1 and 2. The solubility of the block copolypeptides obtained was different in several solvents compared with those of the homopolypeptides consisting of the α-amino acids in the block copolypeptides. For example, the block copolypeptide consisting of L-leucine and DL-alanine (B-1) was soluble in formic acid in spite of the insolubility of poly-L-leucine in this solvent. However, the solubility of the block copolypeptide was essentially dependent on the sequence length of each component. Copolypeptide (B-2), which was constructed of a chain of L-leucine rather longer than that of B-1, became insoluble in formic acid and was still insoluble in hot benzene. The solubility of the block copolypeptide was different from that of the corresponding random copolypeptide obtained by the polymerization of the mixture of two or three kinds of NCA's. For example, the B-2 block copolypeptide in Table 1 was insoluble in dichloroacetic acid, while the corresponding random copolypeptide, R-1, was soluble in dichloroacetic acid and highly swelled in ether. Moreover, the solubility of the B-4 and B-5 block copolypeptides is different from that of the corresponding random copolypeptides, R-2 and R-3

Table 1. Block and random copolypeptides consisted of two components

No.	N%	$\eta_{sp/c}$	Component (wt% ratio)	Solvent of polymer	Non solvent of polymer
Block					
B-1	17.88	0.68	L-Leu 15 DL-Ala 85	Formic acid	Hot benzene
B-2	16.50	0.96	L-Leu 35 DL-Ala 65	Trifluoroacetic acid	Formic acid, dichloro acetic acid, hot benzene
B-3	11.80	0.55#	γ-Me-L-Glu 73 DL-Ala 27	Dichloroacetic acid	Formic acid, hot chloroform
B-4	13.77	0.56#	γ-Me-L-Glu 54 DL-Ala 46	Dichloroacetic acid	Formic acid, hot chloroform
B-5	20.14	0.68	L-Ala 68 Gly 32	Trifluoroacetic acid	Dichloroacetic acid
Random					
R-1	16.50	0.67	L-Leu 35 DL-Ala 65	Dichloroacetic acid Ether (Highly swelled)	Benzene
R-2	14.00	0.25	γ-Me-L-Glu 55 DL-Ala 45	Formic acid	
R-3	20.41	0.44	L-Ala 55 Gly 45	Dichloroacetic acid	

#: $\eta_{sp/c}$ in DCA.

Table 2. Block copolypeptides consisted of three components

No.	N%	$\eta_{sp/c}$	Component	Solvent	Nonsolvent
B-6	18.23	0.34	γ-Bz-L-Glu DL-Ala Gly	Trifluoroacetic acid	Formic acid, dichloroethane, tetrahydrofuran
B-7	16.95	0.24	γ-Bz-L-Glu L-Leu Gly	Trifluoroacetic acid	Formic acid, hot dichloroethane
B-8	11.24	0.99	L-Ala γ-Bz-L-Glu L-Leu	Trifluoroacetic acid	Dichloroethane, hot benzene tetrahydrofuran

N% (found) of homopolymers: Polyglycine 22.45%, Poly-DL-alanine 18.99%, Poly-L-leucine 10.99%, Poly-L-alanine 18.81%, Poly-γ-methyl-L-glutamate 9.7%.

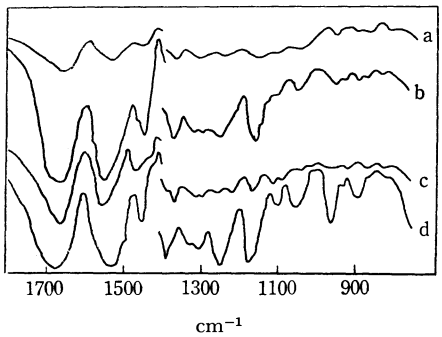

Fig. 1. Infrared spectra of block copolymer and random copolymer consisted of DL-alanine and L-leucine.
a. Block copolypeptide B-2 shown in Table 1.
b. Random copolypeptide R-1 shown in Table 1.
c. Poly-L-leucine obtained in acetonitrile.
d. Poly-DL-alanine obtained in acetonitrile.

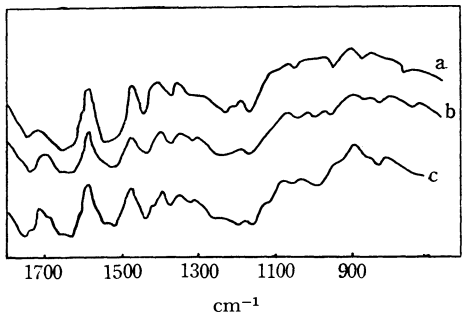

Fig. 2. Infrared spectra of block copolymer and random copolymer consisted of DL-alanine and γ-methyl L-glutamate.
a. Random copolypeptide R-2 in Table 1.
b. Block copolypeptide B-3 in Table 1.
c. Poly-γ-methyl-L-glutamate.

respectively. Such behavior supports the theory that the copolypeptide obtained is of the block type. The infrared spectra of the block copolypeptides described in Tables 1 and 2 are shown in Fig. 1—4. Sometimes, the spectra of the block

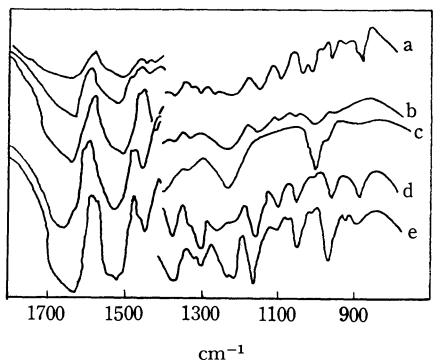

Fig. 3. Infrared spectra of block copolymer and random copolymer consisted of L-alanine and glycine.
a. Block copolypeptide B-5 in Table 1.
b. Random copolypeptide R-3 in Table 1.
c. Polyglycine.
d. α-Forms poly-L-alanine.
e. β-Forms poly-L-alanine.

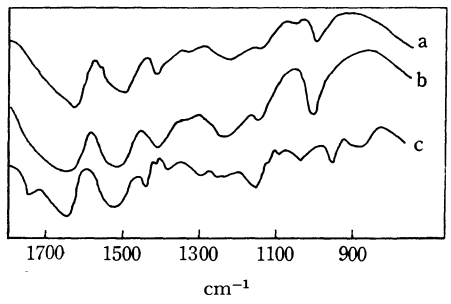

Fig. 4. Infrared spectra of block copolymer consisted of three kinds of α-amino acid.
a. Block copolypeptide B-6 in Table 2.
b. Block copolypeptide B-7 in Table 2.
c. Block copolypeptide B-8 in Table 2.

copolypeptides were clearly different from those of the random copolypeptide with the same components. For example, the spectra of the block copolypeptide consisting of L-alanine (68 mol%) and glycine (32 mol%) showed the spectra of both poly-L-alanine and polyglycine (an absorption at

1305 cm^{-1} which is characteristic of the α-helix of poly-L-alanine), but it was different from that of the random copolypeptide with the same component no absorption appeared at 1305 cm^{-1} (Fig. 3).

Experimental

The NCA's used in this study were prepared in a high degree of purity by methods reported previously.[5]

Synthesis of Block Copolypeptides. (L-Leu)$_m$-(DL-Ala)$_n$: First, L-leucine NCA (0.5 g) was polymerized in acetonitrile (10 m*l*), using 1.0 mol% of *n*-butylamine (to NCA) as the catalyst, for 1.7 hr at 30°C. The polymer precipitated thus was isolated by filtration and washed with absolute acetonitrile. The polymer isolated without drying was added to 10 m*l* of a DL-alanine NCA solution in acetonitrile (0.05 g/m*l*), after which the mixture was kept standing for 120 hr at 30°C. The polymer thus formed was washed with hot benzene in order to remove the coexisting homopolymer. The B-1 block copolymer (0.384 g) was thus obtained. When the polymerization was stopped at the first step, the specific viscosity ($\eta_{sp/c}$) of the poly-L-leucine obtained was 0.20 (in TFA), and its yield was 0.048 g.

The first and second steps of the polymerization described above lengthed 18 and 120 hr respectively, and the polymer isolated was washed with formic acid and hot benzene. A block copolymer (B-2) (0.376 g) was thus obtained. When the polymerization was stopped at the first step, the $\eta_{sp/c}$ value of the poly-L-leucine obtained was 0.68, and its yield was 0.20 g.

(γ-Me-L-Glu)$_m$-(DL-Ala)$_n$: First, γ-methyl-L-glutamate NCA (0.5 g) was polymerized in acetonitrile (10 m*l*), with 1.0 mol% of *n*-butylamine as catalyst, for 57 hr at 30°C. The polymer thus precipitated was isolated by filtration and washed well with absolute acetonitrile. The polymer isolated without drying was added to 20 m*l* of a DL-alanine NCA solution in acetonitrile (0.025 g/m*l*), and the mixture was left to stand for 207 hr at 30°C. The polymer thus obtained was washed with hot chloroform and formic acid to remove the homopolymers. The B-3 copolymer (0.294 g) was thus obtained. When the polymerization was stopped at the first step, the $\eta_{sp/c}$ value of the poly-γ-methyl-L-glutamate obtained was 0.46 g, and its yield was 0.205 g.

Under the polymerization conditions described above, the concentration of the γ-methyl-L-glutamate NCA was reduced to 0.45 g/10 m*l*, the other conditions were the same as those described above. The B-4 polymer (0.129 g) was thus produced. When the polymerization was stopped at the first step, $\eta_{sp/c}$ value of the poly-γ-methyl-L-glutamate obtained was 0.44, and its yield was 0.189 g.

(L-Ala)$_m$-(Gly)$_n$: L-Alanine NCA (0.65 g) was polymerized in acetonitrile (13 m*l*), with 0.5 mol% of *n*-butylamine as an initiator, for 1.7 hr at 30°C. The polymer isolated without drying was added to 10 m*l* of a glycine NCA solution (0.044 g/m*l*) after which the mixture was kept standing for 12 hr at 30°C. The B-5 polymer (0.207 g) was thus obtained. In this case, the $\eta_{sp/c}$ value of the poly-L-alanine obtained at the first step was 0.45 (in TFA).

(γ-Bz-L-Glu)$_k$-(DL-Ala)$_m$-(Gly)$_n$: γ-Benzyl-L-glutamate NCA (0.5 g) was polymerized in acetonitrile (10 m*l*), with 1.0 mol% of *n*-butylamine as an initiator, for 4 hr at 20°C. The polymer thus precipitated was isolated by filtration and washed well with absolute acetonitrile. The polymer isolated without drying was added to 10 m*l* of a DL-alanine NCA solution in acetonitrile (0.05 g/m*l*), after which the mixture was kept standing for 16 hr at 20°C. The copolymer was isolated by filtration and washed sufficiently with absolute acetonitrile, and then the copolymer was again added to 10 m*l* of a glycine NCA solution in acetonitrile (0.05 g/m*l*) and the resulting mixture was kept for 23 hr at 20°C. The polymer thus isolated was washed with hot dichloroethane and formic acid to remove the homopolymer. The B-6 block copolymer (0.15 g) was thus produced. When the polymerization was stopped at the first or second step, the specific viscosities of the polymers thus obtained were 0.107 and 0.243, and their yields were 0.045 g and 0.088 g respectively.

(γ-Bz-L-Glu)$_k$-(L-Leu)$_m$-(Gly)$_n$: The first step of the polymerization was carried out under the same conditions as were used for B-6, while the second and third steps of the polymerization were carried out by using 10 m*l* of an L-leucine NCA solution in acetonitrile (0.05 g/m*l*) for 18 hr at 20°C, and by using 10 m*l* of a glycine NCA solution (0.05 g/m*l*) for 23 hr at 20°C respectively. The B-7 copolypeptide (0.118 g) was thus obtained. The polymer obtained in the second step of the polymerization had a specific viscosity of 0.118.

(L-Ala)$_k$-(γ-Bz-L-Glu)$_m$-(L-Leu)$_n$: The first, second, and third steps of the polymerization were carried out by using 10 m*l* of an L-alanine NCA solution in acetonitrile (0.05 g/m*l*) for 3 hr at 20°C, 10 m*l* of a γ-benzyl-L-glutamate NCA solution (0.05 g/m*l*) for 10 hr at 20°C, and 10 m*l* of an L-luecine solution (0.05 g/m*l*) for 10 hr at 20°C, respectively. The copolypeptide was washed with hot dichloroethane and hot benzene. The B-8 block copolypeptide (0.185 g) was thus obtained. The specific viscosities of the polymer obtained at first and second steps were 0.69 (in TFA) and 0.83 (in TFA) respectively.

Analysis of Copolypeptides. The compositions of the copolypeptides were determined by the analysis of the nitrogen in the polymer: the results are presented in Tables 1 and 2.

Further, paper-chromatographic analysis for the hydrolyzate of these copolymers with hydrochloric acid gave two or three spots for the corresponding α-amino acids in the copolymers.

The viscosity of the polymer was measured at a concentration of 0.25 g/100 m*l* in trifluoroacetic acid (no mark or TFA) or dichloroacetic acid (DCA), using an Ostwald viscometer and at 25°C.

5) M. Oya, K. Uno and Y. Iwakura, *Kogyo Kagaku Zasshi*, **69**, 741 (1966).

BULLETIN OF THE CHEMICAL SOCIETY OF JAPAN VOL. 43 1792—1795 (1970)

Asymmetric Hydrogenation of C=N Double Bond with Modified Raney Nickel 1.*1 New Determination Method for the Reaction Mechanism Using Asymmetric Catalyst

Yoshiharu IZUMI, Hidemitsu TAKIZAWA,*2 Kunio NAKAGAWA,*3 Ryushichi IMAMURA,*4 Masami IMAIDA,*5 Toshio NINOMIYA and Shinichi YAJIMA*2

Division of Organic Chemistry, Institute for Protein Research, Osaka University, Kita-ku, Osaka

(Received November 8, 1969)

The hydrogenation process of ethyl 2-acetoximinopropionate was investigated by means of a novel technique using asymmetric hydrogenation with an asymmetrically modified R–Ni catalyst. It was found that the hydrogenation of ethyl 2-acetoximinopropionate to ethyl alaninate proceeded in two steps through ethyl acetoxyalaninate, and that the asymmetric hydrogenation was performed in the step of the formation of ethyl acetoxyalaninate from ethyl 2-acetoximinopropionate. Besides, the asymmetric reductive amination of ethyl pyruvate was tested with an asymmetrically modified R–Ni catalyst.

The most impressive characteristics of the enzyme reactions are their high catalytic reactivities and their substrate- and stereo-specificities. The catalytic reactivities of the enzyme are promoted by the extreme approach of the reacting molecules to the enzyme, due to the binding of the reacting molecule with the active site of the enzyme. The substrate- and stereo-specificities are performed by the steric interaction between the protein molecule surrounding the active site and the substrate molecule. In the earlier works on catalytic asymmetric hydrogenation done by our research group, silk-palladium was used as the asymmetric catalyst; it had been prepared by the dispersion of palladium metal on silk fibroin.[1] It was expected in the investigation of the silk-palladium catalyst that the palladium and the silk fibroin molecule would act as the active site and the protein molecule surrounding the active site of the enzyme respectively. After the fundamental investigation of the silk-noble metal-type catalyst, we intended to substitute the metal catalyst surface for the active site and most of the protein molecule, which takes part in hardening the environment around the active site of the enzyme, and to give the substrate-specificity and the stereospecific environment to the catalyst by means of the adsorption of the optically active molecule on the catalyst surface.

On the basis of the fundamental considerations mentioned above, the asymmetrically-modified Raney nickel (R–Ni) catalyst was prepared by the treatment of R–Ni catalyst with an aqueous solution of the optically active α-amino or α-hydroxy acid, or other compounds. On the surface of the R–Ni catalyst, the reacting molecules, active hydrogen and the substrate, are placed in close contact, as in the enzyme reaction. As, according to the established theory, the hydrogen attacks the double bond to form a *cis*-addition product, the catalyst modified with an optically active compound would have an asymmetric hydrogenation ability if the catalyst surface could control the adsorption style of the substrate molecule. That is, the asymmetric site of the modified R–Ni catalyst would act as the protein molecule surrounding the active site of the enzyme.

The fundamental investigation of the asymmetric hydrogenation of the C=O double bond with a modified R–Ni catalyst, using methyl acetoacetate as the substrate, has been previously reported in a series of reports by our research group.[2] The experimental rules of the relation between the asymmetric hydrogenation activity of the modified R–Ni catalyst for methyl acetoacetate and the structure of the modifying reagent have been made clear.

The asymmetric hydrogenation of the C=N double bond is very useful and important in the syntheses

*1 Presented at the 24th Meeting on Catalysis, Tokyo, March, 1964.

*2 Present address: Kawaken Fine Chemical Co., Ltd., Kawagoe, Saitama.

*3 Present address: Central Research Laboratory of Nisshin Flour Milling Co., Ltd., Fukuoka, Saitama.

*4 Present address: Saito Shozo Co., Ltd., Chiba.

*5 Present address: The Osaka Prefectural Institute of Public Health, Osaka.

1) S. Akabori, Y. Izumi and Y. Fujii, *Nature*, **178**, 323 (1956). S. Akabori, Y. Izumi, Y. Fujii and S. Sakurai, *Nippon Kagaku Zasshi*, **77**, 1374 (1956). S. Akabori, Y. Izumi and Y. Fujii, *ibid.*, **78**, 886 (1957).

2) Part XII of the series; Y. Izumi, S. Tatsumi and M. Imaida, This Bulletin, **42**, 2373 (1969).

of the natural products, especially in the syntheses of amino acids and alkaloids. To date, however, only three reports on the asymmetric hydrogenation of the C=N double bond in the presence of an asymmetric catalyst have been published.[1,3,4] The first success was accomplished by our research group using the silk-palladium catalyst on the hydrogenation of ethyl 2-acetoximino-3-phenylpropionate, benzil dioxime, and diethyl 2-acetoiminoglutarate.[1] Subsequently, Isoda *et al.* performed the asymmetric hydrogenation of diethyl 2-oximinoglutarate and 2-acetoiminoglutaric acid with a palladium catalyst and a R–Ni catalyst which had been treated with optically-active amino acids.[3] Recently, acetophenone oxime was asymmetrically hydrogenated with a modified R–Ni catalyst by Petrov *et al.*[4] However, no systematic investigation of the asymmetric hydrogenation of the C=N double bond has been done, in spite of its scientific and economical importance.

New efforts to obtain an effective asymmetric hydrogenation catalyst, one which has an asymmetric hydrogenation activity for the C=N double bond to the optically-active amine, have been made by the present authors. The present paper will deal with our preliminary and basic research into the asymmetric hydrogenation of the C=N double bond.

Acetoximino compounds may be suitable as a substrate for the asymmetric hydrogenation of the C=N double bond. However, three hydrogenation route for acetoximino compounds to amino compounds can be expected when two moles of hydrogen are taken up in two steps during the hydrogenation. The supposed hydrogenation routes of ethyl 2-acetoximinopropionate (I) are shown schematically in Fig. 1. Ethyl alaninate (IV) can be obtained through three pathways; I-II-IV, I-III-IV, and I-II-III-IV; the A and D processes give a chance of asymmetric hydrogenation. Consequently, for the investigation of asymmetric hydrogenation, it is very important to elucidate the main route of the hydrogenation.

An asymmetrically-modified R–Ni catalyst was used in the present work in order to elucidate the reaction path of the hydrogenation of I; this is a novel technique for the investigation of the reaction mechanism. The authors proved that I-II-IV is the main route of the hydrogenation of an acetoximino compound and that the asymmetric hydrogenation occurs in the A process.

Independently of the investigation described above, the asymmetric reductive amination of ethyl pyruvate was performed.

Results and Discussion

Hydrogenation of Ethyl 2-Acetoiminopropionate (I). The hydrogenation of I was performed in alcohol and in ethyl acetate; the results are shown in Fig. 2. Depending on the solvent used for the hydrogenation, different hydrogenation products were obtained.

In methanol, ethyl alaninate (IV) was obtained by the hydrogenation with a hydrogen uptake of two moles. On the other hand, in ethyl acetate I took up only one mole hydrogen to give ethyl acetoxyalaninate (II), and at this point the hydrogen uptake was over; II was identified by elemental analysis and by gas chromatography.

The results of the gas chromatography of the hydrogenation products in methanol are shown in Fig. 3. Figure 3-a and 3-b show the analytical results for the partial hydrogenation products,

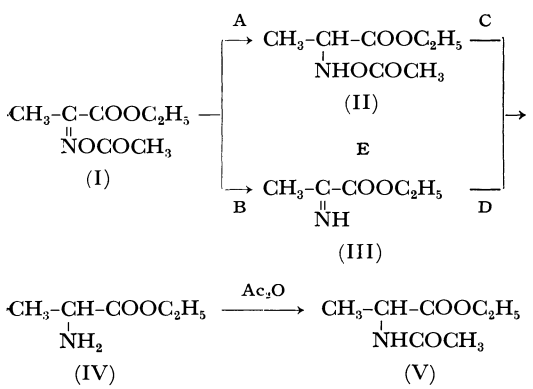

Fig. 1. Hydrogenation routes of ethyl 2-acetoximinopropionate.

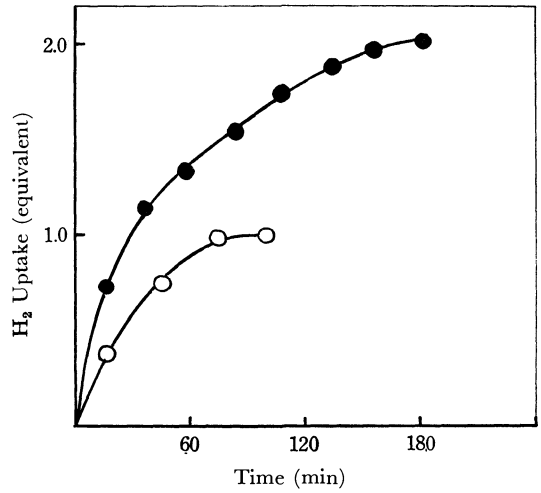

Fig. 2. Effect of solvent on the hydrogenation of I.
—○— In ethyl acetate or ether
—●— In methyl alcohol or ethyl alcohol

3) T. Isoda, A. Ichikawa and T. Shimamoto, *Riken Hokoku*, **34**, 134, 143 (1958).

4) Yu. I. Petrov, E. I. Klabnovskii and A. A. Balandin, *Kinetika i Kataliz*, **8**, 814 (1967).

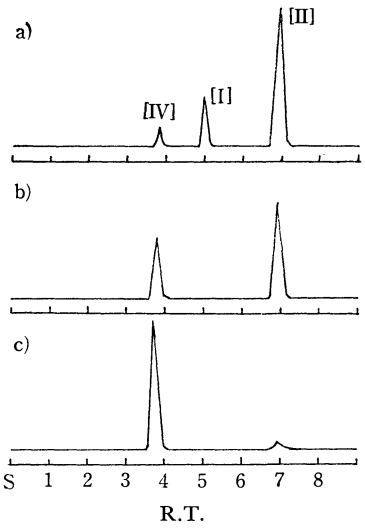

Fig. 3. Relation between products and H_2 uptake of ethyl 2-acetoximinopropionate.
Shimadzu GC-4A P.E.G. 20M 3 m
Column temp. 130°C
a; 28% of theoretical H_2 uptake
b; 68% of theoretical H_2 uptake
c; 98% of theoretical H_2 uptake

which were obtained at 28, 64, and 98% of the theoretical value of the hydrogen uptake.

From the findings that the ratio of II to IV decreases with the increase in the hydrogen uptake, it is clear that II occupies the intermediate position in the hydrogenation of I to IV in methanol.

Asymmetric Hydrogenation of I. The optically-active II and IV were, respectively, obtained by the hydrogenation of I in alcohol and in a nonpolar solvent in the presence of a R–Ni catalyst modified with optically-active histidine, as is shown in Table 1. The asymmetric direction of the product depends on the absolute configuration of the histidine used as a modifying reagent. That is, the catalyst modified with D-histidine gave (−)-II or ethyl (−)-acetylalaninate ((−)-V),*2,*3) and that modified with L-histidine gave (+)-II or (+)-V, while that, with DL-histidine gave (±)-II or (±)-V.

Hydrogenation of II. As is shown in Table 2, the optical purity of the hydrogenation product depends only on the optical purity of the substrate, II, and not on the absolute configuration of the modifying reagent; that is, II with $[\alpha]_D^{20}=-0.25$ gave V with $[\alpha]_{20}^{D}=-0.25$ upon hydrogenation in the presence of a R–Ni catalyst modified with L-histidine, D-histidine, or DL-histidine and upon N-acetylation with acetic anhydride. From these results, it is clear that the asymmetric hydrogenation does not occur in this process and that the hydrogenation of II to IV does not proceed through ethyl 2-imino-propionate (III).

As is shown in Table 2, by the hydrogenation of (−)-II with the catalyst modified with L-, D-, or DL-histidine, L-IV, which gives (−)-V, was obtained. Since this reaction proceeds with a retention of the configuration of II, (−)-II can be said to have an L-configuration.

TABLE 2. HYDROGENATION OF ETHYL ACETOXYALANINATE (II)

$[\alpha]_D^{20}$ of II	Modifying reagent	Solvent	$[\alpha]_D^{20}$ of ethyl acetylalaninate (V)*	Yield (%)
−0.25	DL-His	CH_3OH	−0.25	58
−0.25	L-His	CH_3OH	−0.25	60
−0.25	D-His	CH_3OH	−0.25	60
±0.00	L-His	CH_3OH	±0.00	51

* Ethyl alaninate, the hydrogenation product, was acetylated for the measurement of the optical rotation.

TABLE 1. ASYMMETRIC HYDROGENATION OF ETHYL 2-ACETOXIMINOPROPIONATE (I)

	Modifying reagent	Solvent	Product	$[\alpha]_D^{20}$**	Yield (%)
1	L-His	—	Ethyl acetylalaninate (V)*	+0.25	38
2	L-His	CH_3OH	Ethyl acetylalaninate	+0.25	45
3	D-His	CH_3OH	Ethyl acetylalaninate	−0.25	43
4	DL-His	CH_3OH	Ethyl acetylalaninate	±0.00	48
5	L-His	C_2H_5OH	Ethyl acetylalaninate	+0.25	43
6	L-His	$CH_3COOC_2H_5$	Ethyl acetoxyalaninate (II)	+0.25	60
7	D-His	$CH_3COOC_2H_5$	Ethyl acetoxyalaninate	−0.25	57
8	DL-His	$CH_3COOC_2H_5$	Ethyl acetoxyalaninate	±0.00	63
9	L-His	$C_2H_5OC_2H_5$	Ethyl acetoxyalaninate	+0.25	46

* Ethyl alaninate, the hydrogenation product, was acetylated for the measurement of the optical rotation.
** Measured without dilution.

*2 The hydrogenation product is ethyl alaninate, and its optically rotatory power was measured after the acetylation.

*3 Ethyl (−)-acetylalaninate has an L-configuration.

Table 3. Reductive amination of ethyl pyruvate

Modifying reagent	Solvent	Product	$[\alpha]_D^{20}$ of V	Yield (%)
L-His	Ammonia-methanol	Ethyl acetyl-alaninate (V)*	+0.09	21

* Ethyl alaninate, the hydrogenation product, was acetylated for the measurement of the optical rotation.

Asymmetric Reductive Amination of Ethyl Pyruvate. The possibility of the asymmetric hydrogenation of III is confirmed by the results of the asymmetric reductive amination of ethyl pyruvate, as is shown in Table 3.

Experimental

1) Preparation of Asymmetric Catalysts. a) Preparation of the R–Ni Catalyst. Into 60 m*l* of 20% aqueous sodium hydroxide solution, 4.5 g of the R–Ni alloy (Ni : Al=40 : 60) were added in small portions without cooling. After the reaction mixture had then been maintained at 100°C for 1 hr, the aqueous solution was removed by decantation and the R–Ni catalyst was washed with deionized water.

b) Modification of the Catalyst. Onto the R–Ni catalyst obtained from 4.5 g of an alloy we poured, as soon as possible 200 m*l* of a 2% aqueous solution of histidine, which had been cooled at 0°C. The mixture was then allowed to stand, with occasional shaking, at 0°C for 1.5 hr. After the removal of the modifying solution by decantation, the catalyst was washed twice with 50-m*l* portions of water and twice with 50-m*l* portions methanol.

2) Hydrogenation of Ethyl 2-Acetoximinopropionate. *a) Hydrogenation to Ethyl Alaninate (IV) in Methanol.* Twenty grams of I in 20 m*l* of methanol were hydrogenated with the R–Ni catalyst, or with the modified R–Ni catalyst obtained from 4.5 g of an alloy, at room temperature under an initial hydrogen pressure of 90 kg/cm² and in shaking 100-m*l* autoclave. After the hydrogen uptake ceased, the reaction product, IV, was separated from the catalyst and treated with 20 m*l* of acetic anhydride at 5°C for 2 hr. The acetylated product, V, was distilled under reduced pressure, and a fraction with a bp of 100—102°C/3 mmHg was collected. The purity of the distillate was checked by means of gas chromatography and the optical rotation measured without dilution.

Found: C, 53.06; H, 8.26; N, 8.41%. Calcd for $C_7H_{13}O_3N$: C, 52.81; H, 8.23; N, 8.80%.

b) Hydrogenation to Ethyl Acetoxyalaninate (II) in Ethyl Acetate. The product obtained by the hydrogenation in ethyl acetate was distilled; a distillate boiling at 100—102°C/3 mmHg was thus collected.

Found: C, 48.30; H, 7.96; N, 7.76%. Calcd for $C_7H_{13}O_4N$: C, 47.99; H, 7.48; N, 8.00%.

3) Asymmetric Hydrogenation of II. The optically-active or racemic II prepared by the hydrogenation of I in ethyl acetate was hydrogenated in methanol with a modified R–Ni catalyst under the conditions described above. The hydrogenation product, IV, was acetylated and distilled, and its optical rotation was measured without dilution.

4) Ethyl Acetyl-L-alaninate (L-V). L-IV prepared by the esterification of L-alanine with alcohol and hydrogen chloride, and by subsequent neutralization with triethylamine, was acetylated by acetic anhydride and triethylamine in chloroform.

A fraction of bp 100—102°C/3 mmHg was collected. The optical rotatory power of the product was $[\alpha]_D^{20}$ −56° (without dilution): lit.,[5] $[\alpha]_D^{20}$ −46.4° (without dilution).

5) Reductive Amination of Ethyl Pyruvate. Twenty grams of ethyl pyruvate (0.085 mol) in 50 m*l* of a 5.4N ammonia methanol solution (0.25 mol) were hydrogenated with the modified R–Ni at 60°C under an initial hydrogen pressure of 90 kg/cm² in a shaking 100-m*l* autoclave. When the hydrogenated product was acetylated by the method described above and distilled under reduced pressure, a fraction with a bp of 100—102°/3 mmHg was collected. Yield, 2.1 g. The purity of the distillate was checked by means of gas chromatography and elemental analyses.

Found: C, 52.69; H, 8.45; N, 8.45%. Calcd for $C_7H_{13}O_3N$: C, 52.81; H, 8.23; N, 8.80%.

The authors wish to express their thanks to Misses Kiku Koike and Nobuko Ohya for their elemental analyses. This research was supported by the Kawaken Fine Chemicals Co., Ltd., Tokyo. Part of the expenses of this work has also been defrayed by a grant from the Ministry of Education.

5) K. Freunenberg, F. Rhino, *Ber.*, **57**, 1554 (1924).

BULLETIN OF THE CHEMICAL SOCIETY OF JAPAN VOL. 43 1796—1803 (1970)

The Migration of the Alkyl Groups of 6-Acetyl and 6-Methoxycarbonyl Derivatives of 2,3-Dimethyl-5-alkylbenzofurans*[1]

Yoshiyuki KAWASE, Setsuko TAKATA and Toshio MIWA*

Department of Chemistry, Faculty of Literature and Science, Toyama University, Gofuku, Toyama
**Department of Chemistry, Faculty of Science, Osaka City University, Sumiyoshi-ku, Osaka*

(Received November 10, 1969)

The migration of the 5-alkyl groups of 2,3-dimethyl-5-alkyl-6-benzofuranyl methyl ketones by aluminum chloride was studied further, and an analogous migration was observed in the cases of methyl 2,3-dimethyl-5-alkyl-6-benzofurancarboxylates. The 5-ethyl-, 5-*n*-propyl-, and 5-isopropyl-ketones were converted to the corresponding carboxylic acids by the bromoform reaction and then, further, to the esters. The action of aluminum chloride on the 5-*n*-propyl-ketone and the esters in carbon disulfide at room temperature afforded the corresponding 4-alkyl-compounds as a result of the migration of the 5-alkyl groups to the 4-position, analogously to the way in which the 5-ethyl- and 5-isopropyl-ketones had afforded two 4-alkyl-ketones. The structures of the compounds were confirmed by converting both the ketones and the esters to the same carboxylic acids and from the data of their IR, UV and NMR spectra and gas chromatograms. It was found that the 5-alkyl groups were less likely to migrate in the cases of the esters than the corresponding alkyl groups in the cases of the ketones, while the *n*-propyl groups of the ketone and the ester were less likely to migrate than the other alkyl groups, and that the migration seemed to be intramolecular, as the *n*-propyl group was not isomerized to an isopropyl group during the migration.

It has previously been reported that the action of aluminum chloride on *o*-alkylphenyl methyl ketones at 100—170°C,[1,2] and in some cases at room temperature[2] also, caused the migration of the *o*-alkyl groups to the *m*-position; moreover, one of the present authors and others[3,4] have recently reported that 2,3-dimethyl-5-ethyl- and 5-isopropyl-6-benzofuranyl methyl ketones (**3**a and c) afforded the corresponding 4-alkyl-ketones (**4**a and c) by the analogous migration of the 5-alkyl group to the 4-position.

Now in the present experiments, the migration of the alkyl groups of the benzofuranyl ketones (**3**), especially that of the *n*-propyl-ketone (**3**b), was studied further, and an analogous migration was observed also in the cases of the related methyl 2,3-dimethyl-5-alkyl-6-benzofurancarboxylates (**7**a, b, and c).

2,3-Dimethyl-5-*n*-propyl-6-benzofuranyl methyl ketone (**3**b) was prepared much as in the cases of the 5-ethyl-[5] and 5-isopropyl-ketones[4] (**3**a and c) by the action of acetyl chloride and aluminum chloride or stannic chloride on 2,3-dimethyl-5-*n*-propylbenzofuran (**2**b), which had, in turn, been prepared by the cyclo-dehydration of 3-(*p*-*n*-propylphenoxy)-butanone (**1**b). The ketones (**3**a, b, and c) were converted to the corresponding carboxylic acids (**5**a,b, and c) by the bromoform reaction,[6] and then to the methyl esters (**7**a,b, and c).

The ketone (**3**b) and the esters (**7**a,b, and c) were treated with aluminum chloride in carbon disulfide at room temperature to afford the corresponding 4-alkyl-ketone (**4**b) and -esters (**8**a,b, and c) as a result of the migration of the 5-alkyl groups to the 4-position, just as the 5-ethyl- and 5-isopropyl-ketones (**3**a and c) afforded the 4-alkyl-ketones[3,4] (**4**a and c) (see Table 1). The products were purified by distillation and then by crystallization from petroleum ether, except for the ketone (**4**b), which was purified by chromatography on alumina, with benzene as the solvent. The yields of the esters (**8**a,b, and c) were poorer than those of the

*1 A major part of this paper was presented at the 20th Annual Meeting of the Chemical Society of Japan, Tokyo, April, 1967.

1) G. Baddeley, *J. Chem. Soc.*, **1944**, 232; G. Baddeley and A. G. Pendleton, *ibid.*, **1952**, 807; G. Baddeley and S. Varma, *ibid.*, **1957**, 2727; M. Lukin and B. B. Carson, *J. Org. Chem.*, **23**, 1007 (1958).

2) G. Baddeley, G. Holt and W. Pickles, *J. Chem. Soc.*, **1952**, 4162.

3) Y. Kawase, M. Hubert-Habart, J.-P. Buisson and R. Royer, *Compt. Rend.*, **258**, 5007 (1964).

4) Y. Kawase, R. Royer, M. Hubert-Habart, A. Cheutin, L. René and J.-P. Buisson, *Bull. Soc. Chim. Fr.*, **1964**, 3131.

5) R. Royer, M. Hubert-Habart, L. René and A. Cheutin, *ibid.*, **1964**, 1259.

6) Y. Kawase and M. Takashima, This Bulletin, **40**, 1224 (1967).

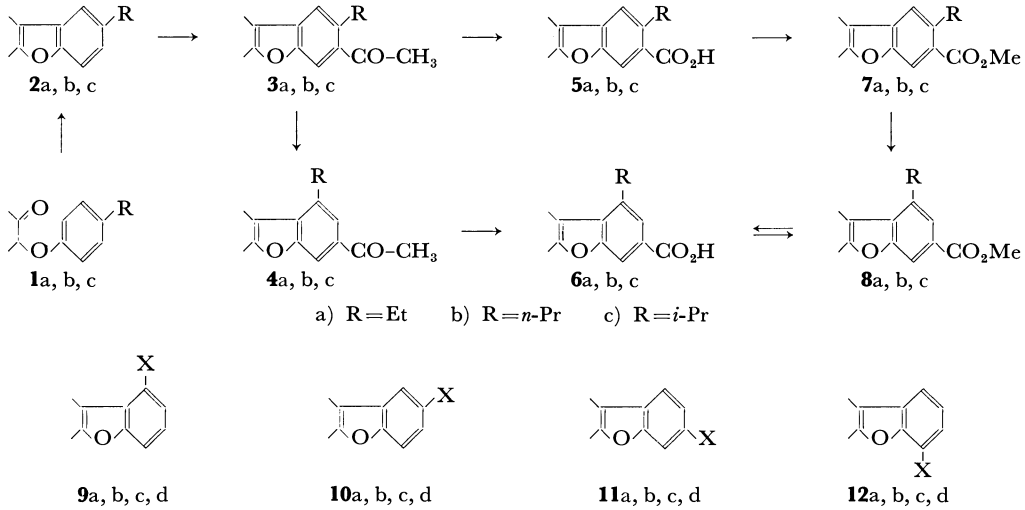

Chart 1

corresponding ketones (**4**a,b, and c), while those of the *n*-propyl-ketone (**4**b) and -ester (**8**b) were poorer than those of the other alkyl-compounds. The structures of the compounds were confirmed by converting both the ketones (**4**a,b, and c) and the esters (**8**a, b, and c) to the respective carboxylic acids (**6**a, b, and c) by bromoform reaction or hydrolysis; they were confirmed also by comparing their IR, UV, NMR, and gas chromatographical data with each other and with those of the compounds without *bz*-alkyl groups.

In the UV spectra, the absorption curves of the ketones (**3** and **4**), acids (**5** and **6**), and esters (**7** and **8**) are almost identical with each other and with those of the ketone (**11**b), acid (**11**c), and ester (**11**d) without the *bz*-alkyl group, except for a slight variation in the 210—230 mμ region according to the position of the *bz*-alkyl groups, and

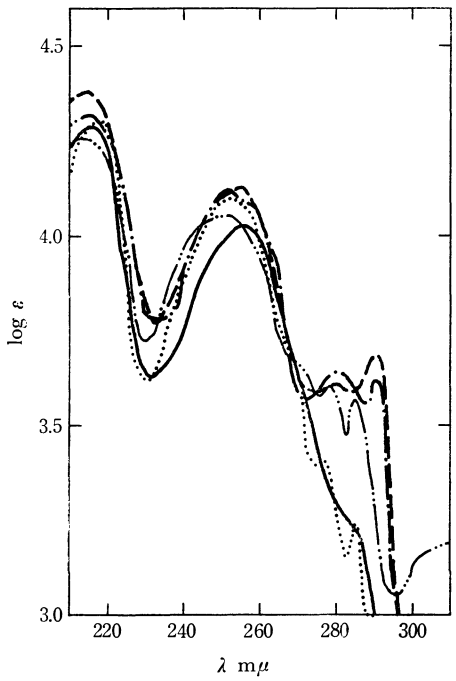

Fig. 1. The UV spectra of alkylbenzofurans. -·-· **2** (R=H), —— **9**a, ---- **10**a (=**2**a), -·-· **11**a, ···· **12**a

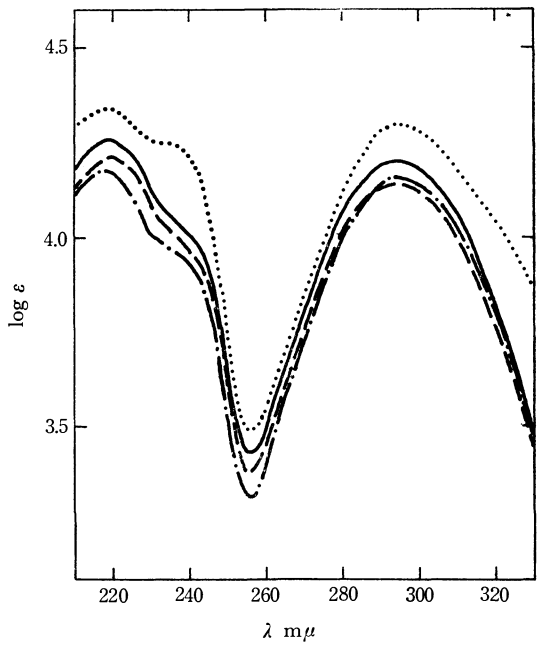

Fig. 2. The UV spectra of benzofuranyl ketones. -·-· **3** (R=Me), —— **3**a, ---- **3**b, ···· **3**c

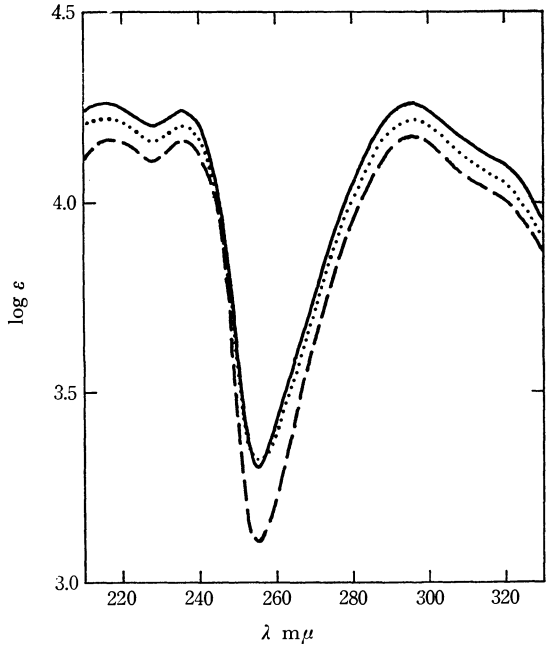

Fig. 3. The UV spectra of benzofuranyl ketones.
—— **4**a, ---- **4**b, ···· **4**c

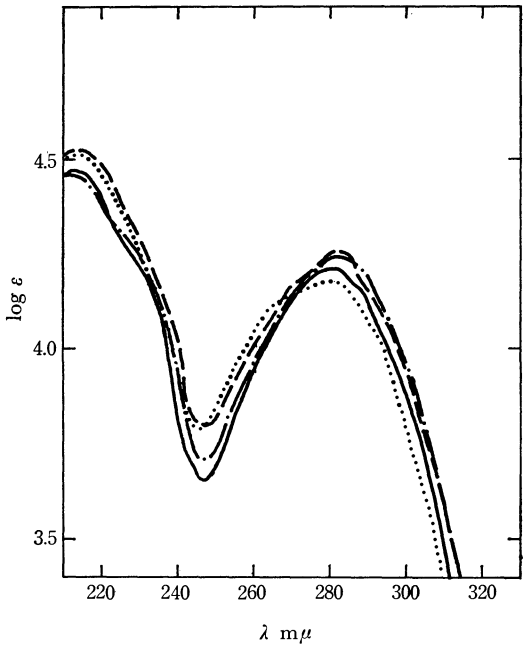

Fig. 5. The UV spectra of benzofurancarboxylic acids.
-·-· **5** (R=Me), —— **5**a, ---- **5**b, ····**5**c

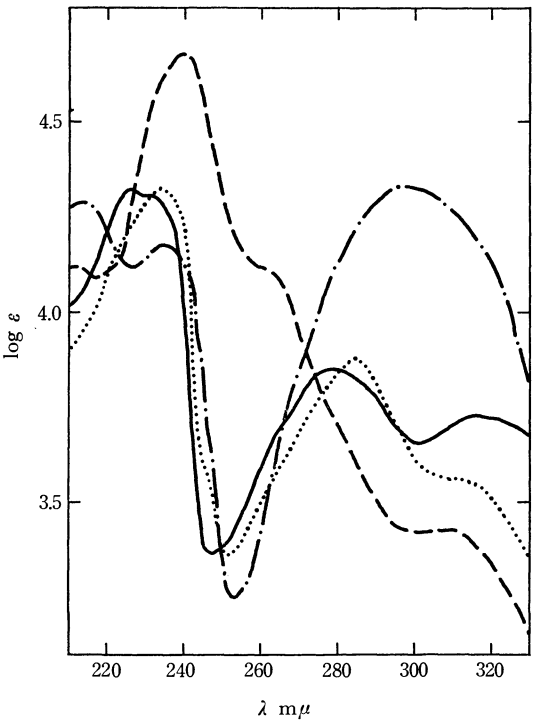

Fig. 4. The UV spectra of benzofuranyl ketones.
—— **9**b, ---- **10**b, -·-· **11**b, ···· **12**b

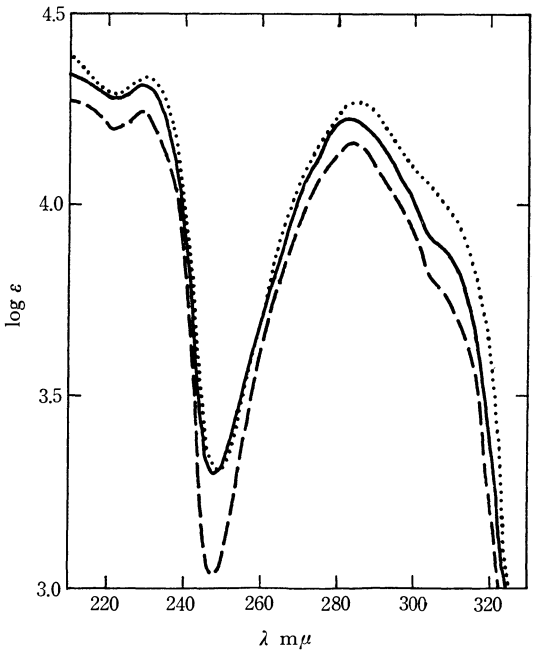

Fig. 6. The UV spectra of benzofurancarboxylic acids.
—— **6**a, ---- **6**b, ···· **6**c

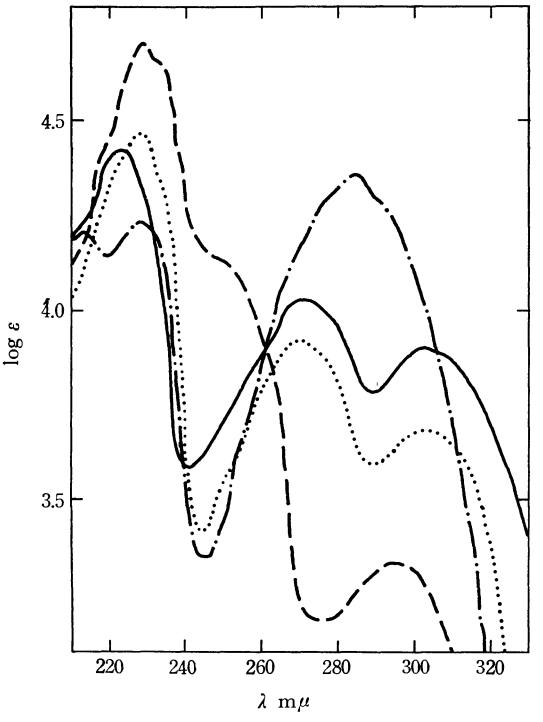

Fig. 7. The UV spectra of benzofurancarboxylic acids.
—— **9**c, ---- **10**c, -·-· **11**c, ···· **12**c

except for a slight shift of peaks by 1—5 mμ or 4—9 mμ in the cases of the esters and ketones, respectively, from those in the cases of the acids. Moreover, the absorption curves of the 6-acetyl-, 6-carboxyl-, and 6-methoxycarbonyl-2,3-dimethylbenzofurans (**11**b,c, and d) are quite different from those of the isomeric 4-, 5-, and 7-substituted compounds (**9**, **10**, and **12**); the absorption curves of the 4- and 7-isomers (**9** and **12**) are very similar to each other, having three peaks at 225—235 mμ, 270—285 mμ, and 300—315 mμ, while those of the 5-isomers (**10**) have remarkably high peaks at around 240 mμ, while those of the 6-isomers (**11**) have higher and broader peaks at 285—295 mμ (see the figures and Table 4).

In the NMR spectra, it was found that the peaks corresponding to the 3-methyl protons appeared at δ=2.04—2.14 ppm in the cases of the 5-alkyl-ketones and -esters (**3** and **7**), while they appeared at a field lower by about 0.13—0.26 ppm in the cases of the 4-alkyl-compounds (**4** and **8**); these differences are comparable to the cases of 2,3-dimethylbenzofurans substituted by electron-donating methoxyl, amino, ethyl, and chloro groups.[7] The peaks corresponding to the aromatic protons appeared as two singlets in the cases of **3**a,b, and c and **7**a,b, and c, while they appeared as two doublets (J=2 Hz) in the cases of **4**a,b, and c and **8**a,b, and c, indicating that the hydrogens are in the *para* and *meta* positions to each other respectively (see Table 5).

In the gas chromatograms, the peaks corresponding to the 4-alkyl-ketones (**4**) and -esters (**8**) appeared at 200—205°C, and those of the 5-alkyl-compounds (**3** and **7**) appeared at temperatures higher by about 5°C, while those of the 6-ketone and the 6-ester (**11**b and **11**d) appeared at 195 and 198°C respectively.

On the basis of these measurements, the ratio of the 5- and 4-alkyl-compounds (**3** and **4**, or **7** and **8**) in the crude rearrangement products of 5-alkyl-ketones or -esters (**3** or **7**) was determined by estimating the area of the peaks corresponding to the 5- and 4-alkyl-compounds in the gas chromatograms and that of the peaks corresponding to the 3-methyl protons of 5- and 4-alkyl-compounds in the NMR spectra (see Table 1). It seems that the 5-alkyl groups migrate less easily in the cases of the 5-alkyl-6-esters (**7**) than do the corresponding alkyl groups in the cases of the 5-alkyl-ketones (**3**), that the *n*-propyl group migrates less easily than the other alkyl groups, and that the migration is intramolecular, for the *n*-propyl group is not isomerized to an isopropyl group during the migration.

In conclusion, it seems that the migration of the 5-alkyl groups of 5-alkyl-6-ketones and -esters (**3** and **7**) by aluminum chloride occurs through the cationic cleavage of the alkyl group caused by the electron-attracting effect of the carbonyl group and by the steric hindrance of the aluminum chloride co-ordinated to the carbonyl group, followed by the synchronous attack of the split cationic alkyl group at the adjacent 4-position.

Experimental

All the boiling points and melting points are uncorrected. The IR spectra were measured in the form of KBr disks, the UV spectra were measured in an ethanol solution, the NMR spectra were measured on a Nihon Denshi 60 MHz spectrometer in a CCl_4 solution (5—10%), with TMS as the internal standard, and the gas chromatography was carried out on a Hitachi K23 apparatus, with Silicone DC-11 on Chamelite as the stationary phase, a flow rate of 46 ml/min (0.7 kg/cm^2), and a temperature rise of 5°C/min from 180°C. The detailed data are summarized in the tables and figures.

Materials. a) Alkylbenzofurans. 2,3-Dimethylbenzofuran[8] (**2** R=H), 2,3,5-trimethylbenzofuran[5] (**2** R=Me), 2,3-dimethyl-5-ethyl-[8] and -5-isopropylbenzofurans[3,4] (**2**a and c) and 2,3-dimethyl-6- and -7-ethylbenzofurans[8] (**11**a and **12**a) were prepared following the methods in the respective references. 2,3-Dimethyl-5-*n*-propylbenzofuran (**2**b) and 2,3-dimethyl-4-ethylbenzofuran (**9**a) were prepared much as were **2**a and **11**a respectively.

7) Y. Kawase, *Chem. Ind.* (London), to be published.

8) E. Bisagni and R. Royer, *Bull. Soc. Chim. Fr.*, **1962**, 925.

TABLE 1. MIGRATION OF THE ALKYL GROUPS OF KETONES (**3**a, b, and c) AND ESTERS (**7**a, b, and c) BY $AlCl_3$ IN CS_2 AT ROOM TEMPERATURE

Starting compd.	Crude products				Purified product,[b] Yield %
	Bp °C/mmHg	Yield %	Composition[a] Recovery %	Composition[a] Migrated %	
3a	186—193/17	75	10	90	**4**a, 60
3b	185—195/19	70	60	40	**4**b, 12[c]
3c	187—192/20	75	10	90	**4**c, 60
7a	187—191/19	75	40	60	**8**a, 17
7b	195—200/19	60	60	40	**8**b, 9
7c	186—192/21	90	10	90	**8**c, 40

a) The composition of the crude products were determined by gas chromatography and NMR spectra, and small amounts (about 1%) of the dealkylated compounds were detected in all cases by gas chromatography.
b) Crystallized from petroleum ether.
c) Purified by chromatography with alumina and benzene as a solvent furnishing also the 30% of recovery **3**b.

TABLE 2. RESULTS OF THE REACTIONS OTHER THAN THE MIGRATION

Starting compd.	Product	Method[a]	Yield %
b)	**1**b	A	79
1b	**2**b	B	74
2b	**3**b	C	48
2b	**3**b	D	46
3a	**5**a	E	78
3b	**5**b	E	80
3c	**5**c	E	62
4a	**6**a	E	74
4b	**6**b	E	67
4c	**6**c	E	83
5a	**7**a	F	78
5b	**7**b	F	77
5c	**7**c	F	67
6a	**8**a	F	69
8a	**6**a	G	62
8b	**6**b	G	70
8c	**6**c	G	55
9b	**9**a	H	51

a) A: 3-Chlorobutanone and K_2CO_3 in acetone, B: Cyclo-dehydration by H_2SO_4, C: Acetyl chloride and $AlCl_3$, D: Acetyl chloride and $SnCl_4$, E: Bromoform reaction, F: Esterification, G: Hydrolysis, and H: Reduction.
b) *p-n*-Propylphenol.

*3-(p-n-Propylphenoxy)butanone (**1**b).* Anhydrous potassium carbonate (98 g) was added to a solution of *p-n*-propylphenol (32 g) and 3-chlorobutanone (27.6 g) in acetone (200 m*l*), after which the mixture was refluxed for 9 hr. Most of the acetone was then distilled off, and the residue was dissolved in water and extracted with ether. The residual product obtained from the ethereal solution was distilled to give **1**b; bp 139—145°C/17 mmHg; 38.2 g (79%).

*2,3-Dimethyl-5-n-propylbenzofuran (**2**b).* Concentrated sulfuric acid (38 g) was stirred, drop by drop, into the butanone **1**b (38 g) with cooling below 30°C, and then the solution was allowed to stand at that temperature for 1 hr. The mixture was poured into ice water and extracted with ether. The ethereal solution was washed with an aqueous sodium hydroxide solution and dried, and then the ether was distilled off. The residual product from the ethereal solution was distilled to give **2**b; bp 138—140°C/18 mmHg; 25.7 g (74%).

*2,4-Dimethyl-4-ethylbenzofuran (**9**a).* A mixture of 2,3-dimethyl-4-benzofuranyl methyl ketone[6] (**9**b) (1.9 g), hydrazine hydrate (0.8 g), and diethylene glycol (30 m*l*) was heated gently for 1.5 hr in a distillation apparatus to distill off the water formed. Potassium hydroxide (2.9 g) was then gradually added to the slightly-cooled mixture in the same apparatus, and the mixture was heated gently for 1 hr to complete the development of nitrogen. The hot mixture was poured into water, acidified with dilute hydrochloric acid, and extracted with ether. After the ether was then distilled off, the residue was distilled to give **9**a; bp 127—131°C/17 mmHg; 0.9 g (51%).

b) Benzofuranyl Ketones. 2,3,5-Trimethyl-6-benzofuranyl methyl ketone[5] (**3** (R=Me)), 2,3-dimethyl-5-ethyl-[5] and -5-*i*-propyl-6-benzofuranyl methyl ketones[3,4] (**3**a and c) and 2,3-dimethyl-4-,[6] -5-,[9] -6-,[8] and -7-benzofuranyl methyl ketones[10] (**9**b, **10**b, **11**b, and **12**b) were prepared following the methods of the respective references. 2,3-Dimethyl-5-*n*-propyl-6-benzofuranyl methyl ketone (**3**b) was prepared much as were **3**a and c, as follows:

*2,3-Dimethyl-5-n-propyl-6-benzofuranyl Methyl Ketone (**3**b).*
i) By Aluminum Chloride. Powdered anhydrous aluminum chloride (15.4 g, 1.2 mol equivalents) was gradually added, with stirring and cooling, to a solution of the benzofuran **2**b (18 g) and acetyl chloride (8.3 g, 1.1 mol equivalents) in carbon disulfide (100 m*l*); the mixture was stirred at room temperature for 4 hr and then allowed to stand overnight. The mixture was poured into ice water and extracted with chloroform. The organic layer was washed with an aqueous sodium hydroxide solution and dried, and then the solvent was distilled off. The residual product was distilled, bp 187—200°C/22 mmHg, and then crystallized from petroleum ether to give **3**b; mp 45—47°C; 10.5 g (48%).

ii) By Stannic Chloride. Anhydrous stannic chloride (11.5 g, 1.5 mol equivalents) was gradually added, with stirring and cooling, to a solution of **2**b (5.5 g) and acetyl chloride (3 g, 1.3 mol equivalents) in carbon disulfide (50 m*l*); the mixture was then treated much as has been described in the case of aluminum chloride.

c) Benzofurancarboxylic Acids. 2,3,5-Trimethyl-6-benzofurancarboxylic acid[6] (**5** R=Me) and 2,3-dimethyl-4-,[6] -5-,[6] -6-,[6] and -7-benzofurancarboxylic

9) E. Bisagni, J.-P. Marquet, A. Cheutin, R. Royer and M. L. Desvoye, *Bull. Soc. Chim. Fr.*, **1965**, 1466.
10) C. Pène, P. Demerseman, A. Cheutin and R Royer, *ibid.*, **1966**, 586.

Table 3. The Mp, Bp, IR and analyses of the new compounds

Compd.	Mp °C (solv[a])) or bp °C/mmHg n (°C)	ν_{CO}^{KBr} cm^{-1}	Formula	Found C%	Found H%	Calcd C%	Calcd H%
			Aryloxybutanone				
1b	139—145/17 1.5030 (22)	1720	$C_{13}H_{18}O_2$	75.50	8.55	75.69	8.80
			Alkylbenzofurans				
2b	138—140/18 1.5360 (24)		$C_{13}H_{16}O$	82.85	8.77	82.93	8.57
9b	127—131/17 1.5512 (20.5)		$C_{12}H_{14}O$	82.61	8.05	82.72	8.10
			Benzofuranyl ketones				
3b	45—47[b]) (P)	1680[c])	$C_{15}H_{18}O_2$	78.35	8.16	78.23	7.88
4b	44—45[d]) (P)	1680[e])	$C_{15}H_{18}O_2$	78.08	8.06	78.23	7.88
			Benzofurancarboxylic acids				
5a	186—187.5 (E)	1685	$C_{13}H_{14}O_3$	71.12	6.50	71.54	6.47
5b	187—188 (E)	1685	$C_{14}H_{16}O_3$	72.19	7.16	72.39	6.94
5c	194—195.5 (E)	1685	$C_{14}H_{16}O_3$	72.50	7.39	72.39	6.94
6a	198—199 (E)	1670	$C_{13}H_{14}O_3$	71.25	6.48	71.54	6.47
6b	187—188 (E)	1670	$C_{14}H_{16}O_3$	71.99	7.08	72.39	6.94
6c	239—240 (E)	1670	$C_{14}H_{16}O_3$	71.98	6.74	72.39	6.94
			Methyl benzofurancarboxylates				
7a	177—180/20 1.5593 (22.5)	1710	$C_{14}H_{16}O_3$	72.11	7.08	72.39	6.94
7b	189—190/19 1.5572 (13)	1715	$C_{15}H_{18}O_3$	72.45	7.39	73.14	7.37
7c	182—184/20 1.5580 (9)	1725	$C_{15}H_{18}O_3$	72.91	7.47	73.14	7.37
8a	60—61.5 (P)	1710	$C_{14}H_{16}O_3$	72.55	7.06	72.39	6.94
8b	63—65 (P)	1710	$C_{15}H_{18}O_3$	73.22	7.52	73.14	7.37
8c	55—57 (P)	1710	$C_{15}H_{18}O_3$	73.22	7.60	73.14	7.37

a) E: Ethanol, P: Petroleum ether.
b) 2,4-Dinitrophenylhydrazone, mp 188—189°C (AcOEt). Found: C, 61.25; H, 5.15; N, 14.34%. Calcd for $C_{21}H_{22}O_5N_4$: C, 61.45; H, 5.40; N, 13.65%.
c) ν_{CO}^{KBr} of **3**a and **3**c are 1670 and 1685 cm^{-1}, respectively.
d) 2,4-Dinitrophenylhydrazone, mp 223—224°C (AcOEt). Found: C, 61.88; H, 5.41; N, 13.22%. Calcd for $C_{21}H_{22}O_5N_4$: C, 61.45; H, 5.40; N, 13.65%.
e) ν_{CO}^{KBr} of **4**a and **4**c are 1670 and 1680 cm^{-1}, respectively.

Table 4. The UV spectra

Compd.	λ_{max}^{EtOH} mμ[a]) (log ε)	Compd.	λ_{max}^{EtOH} mμ[a]) (log ε)
	Alkylbenzofurans	**5**c	215(4.51), 281(4.18)
2(R=H)	214(4.26), 251(4.05), 278(3.60), 285(3.56)	**6**a	229(4.31), 282(4.22)
9a	216(4.29), 256(4.03), 285[s](3.25)	**6**b	229(4.24), 284(4.16)
2a(=**10**a)	214(4.37), 254(4.13), 280(3.61), 291(3.69)	**6**c	230(4.23), 285(4.27)
11a	216(4.32), 252(4.12), 280(3.64), 291(3.62)	**9**c	224(4.42), 271(4.03), 304(3.90)
12a	218(4.30), 253(4.10), 276(3.41), 285(3.24)	**10**c	229(4.70), 252[s](4.10), 295(3.33)
	Benzofuranyl ketones	**11**c	212(4.22), 228(4.24), 285(4.35)
3(R=Me)	218(4.10), 240[s](3.48), 296(4.09)	**12**c	228(4.46), 270(3.92), 303(3.69)
3a	219.5(4.13), 240[s](4.01), 294(4.10)		**Methyl benzofurancarboxylates**
3b	220(4.11), 240[s](3.48), 294(4.07)	**7**(R=Me)	214(4.12), 230[s](4.06), 285(4.10)
3c	219(4.17), 235[s](4.13), 295(4.15)	**7**a	215.5(4.19), 230[s](4.13), 284(4.14)
4a	215.5(4.13), 235.5(4.10), 296(4.13)	**7**b	215(4.19), 230[s](4.15), 284(4.15)
4b	216(4.11), 236[s](3.49), 293(4.01)	**7**c	215(4.18), 230[s](4.10), 282(4.12)
4c	215(4.11), 236(4.10), 295(4.11)	**8**a	211(4.12), 229.5(4.13), 284.5(4.11)
9b	226(4.32), 232[s](4.30), 279(3.85), 316(3.73)	**8**b	212.5(4.13), 230(4.15), 284.5(4.13)
10b	213(4.13), 240(4.68), 261[s](4.12), 310(3.43)	**8**c	211(4.11), 229.5(4.13), 284(4.11)
11b	213(4.29), 235(4.18), 296(4.33)	**9**d	226(4.39), 274(3.94), 307(3.83)
12b	233(4.32), 285(3.88), 315[s](3.55)	**10**d	233(4.77), 254[s](4.11), 290(3.42), 301(3.40), 329[s](3.11)
	Benzofurancarboxylic acids	**11**d	229(4.26), 288(4.34)
5(R=Me)	211(4.46), 282(4.35)	**12**d	229(4.45), 275(3.92), 306(3.70)
5a	213(4.67), 281(4.18)		
5b	214(4.52), 282(4.23)		

a) s: Shoulder.

TABLE 5. THE NMR SPECTRA[a)]

Compd.	Ph-H		Ph-CH<	CO-Me or CO_2Me	2-Me	3-Me	Ph-C-CH<	Ph-C-C-Me
			Aklylbenzofurans					
2(R=H)					2.13	1.91		
2(R=Me)			2.40		2.31	2.08		
2a(=**10a**)			2.64(q)		2.25	2.02	1.26(t)	
2b			2.54(t)		2.28	2.07	1.57(m)	0.90(t)
2c			2.94(m)		2.26	2.06	1.28(d)	
9a			2.82(q)		2.17	2.12	1.20(t)	
11a			2.61(q)		2.17	1.94	1.19(t)	
12a			2.82(q)		2.27	2.03	1.29(t)	
			Benzofuranyl ketones					
3(R=Me)	7.50	6.96	2.50	2.47	2.32	2.05		
3a	7.56	7.09	2.94(q)	2.51	2.34	2.10	1.19(t)	
3b	7.64	7.14	2.90(t)	2.54	2.37	2.12	1.52(m)	0.98(t)
3c	7.46	7.36	3.72(m)	2.49	2.28	2.06	1.25(d)	
4a	7.57(d)	7.43(d)	2.91(q)	2.47	2.33	2.23	1.26(t)	
	J=2 Hz							
4b	7.68(d)	7.48(d)	2.88(t)	2.49	2.35	2.26	1.60(m)	1.00(t)
	J=2 Hz							
4c	7.65(d)	7.65(d)	3.57(m)	2.53	2.37	2.31	1.36(d)	
	J=1 Hz							
9b				2.49	2.27	2.11		
10b				2.55	2.39	2.18		
11b				2.50	2.37	2.14		
12b				2.68	2.37	2.12		
			Methyl benzofurancarboxylates					
7(R=Me)	7.82	7.01	2.58	3.82	2.30	2.02		
7a	7.80	7.09	3.03(q)	3.82	2.31	2.06	1.22(t)	
7b	7.75	7.01	2.95(t)	3.78	2.30	2.04	1.51(m)	0.96(t)
7c	7.66	7.31	3.91(m)	3.81	2.28	2.06	1.30(d)	
8a	7.70(d)	7.49(d)	2.90(q)	3.79	2.32	2.24	1.29(t)	
	J=2 Hz							
8b	7.68(d)	7.47(d)	2.85(t)	3.81	2.35	2.26	1.63(m)	1.01(t)
	J=2 Hz							
8c	7.63(d)	7.55(d)	3.63(m)	3.89	2.37	2.32	1.35(d)	
	J=2 Hz							
9d				3.85	2.32	2.21		
10d				3.89	2.35	2.18		
11d				3.79	2.30	2.00		
12d				3.89	2.36	2.06		

a) δ (ppm) values determined on a Nihon Denshi 60 MHz spectrometer in CCl_4 (5—10% solution) with TMS as the internal standard and (d)=doublet, (t)=triplet, (q)=quartet, and (m)=multiplet.

acids[11)] (**9c**, **10c**, **11c**, and **12c**) were prepared following the methods of the respective references.

d) Methyl Benzofurancarboxylates. Methyl 2,3,5-Trimethyl-5-benzofurancarboxylate[6)] (**7** R=Me) and methyl 2,3-dimethyl-4-,[11)] -5-,[6)] -6-,[6)] and -7-benzofurancarboxylates[11)] (**9d**, **10d**, **11d**, and **12d**) were prepared following the methods of the respective references.

Migration of the Alkyl Groups of the Ketones (3) and the Esters (7). Powdered anhydrous aluminum chloride (4.7 g, 2 mol equivalents) was gradually added, with stirring and cooling, to a solution of the ketone **3b** (4 g) in carbon disulfide (50 m*l*), after which the mixture was stirred for 4 hr at room temperature and then allowed to stand overnight. The mixture was

11) Y. Kawase, T. Okada and T. Miwa, to be published.

then poured into ice water and extracted with chloroform. The organic layer was washed with an aqueous sodium hydroxide solution and dried, and then the solvent was distilled off. The residual product was distilled to give the crude product; bp 185—195°C/19 mmHg; 2.8 g (70%). By the same procedure, the ketone **3**a and c and the esters **7**a, b, and c afforded the crude products; their compositions were determined by gas chromatography and by NMR spectroscopy. The crystallization of the crude products from petroleum ether furnished the pure crystalline products except in the case of **3**b. The crystallization in the case of **3**b furnished only the crystalline-recovery ketone (0.2 g); a part (0.5 g) of the residual oil was purified, by chromatography with alumina and benzene as a solvent, to give the recovery ketone (0.2 g) and the rearranged ketone **4**b; mp 44—45°C, 0.1 g (total 12%).

2,3-Dimethyl-5- and -4-alkyl-6-benzofurancarboxylic Acids (5a,b, and c and 6a,b, and c). *a) by the Bromoform Reaction of the Ketones (3a,b, and c and 4a, b, and c).* A solution of **3**a (8 g) in dioxane (50 m*l*) was added, with cooling and stirring, to an aqueous sodium hypobromide solution, which had been prepared by adding bromine (23 g, 3.8 mol equivalents) with cooling to a mixture of sodium hydroxide (14.5 g, 9 mol equivalents), water (45 m*l*), and ice (45 g). Stirring was continued for 30 min and then for another 1.5 hr at 45°C. The cooled mixture was diluted with water and washed with ether, and the aqueous layer was acidified after the addition of a small amount of sodium bisulfite. The crystalline precipitates thus formed were collected and recrystallized from ethanol to give 2,3-dimethyl-5-ethyl-6-benzofurancarboxylic acid (**5**a); mp 186—187.5°C; 6.3 g (78%).

2,3-Dimethyl-5-*n*-propyl- and -5-isopropyl-6-benzofurancarboxylic acids (**5**b and c) and 2,3-dimethyl-4-ethyl-, -4-*n*-propyl- and -4-isopropyl-6-benzofurancarboxylic acids (**6**a,b, and c) were also obtained by this procedure.

b) By the Hydrolysis of the Esters (8a, b, and c). An aqueous potassium hydroxide solution (1 g in 4 m*l* of water) was added to a solution of **8**a (1 g) in ethanol (5 m*l*), and then the mixture was refluxed for 3 hr. The cooled solution was diluted with water, washed with ether, and then acidified to give the crystalline product (**6**a), which was then recrystallized from ethanol; mp 198—199°C; 0.6 g (62%).

2,3-Dimethyl-4-*n*-propyl- and -4-isopropyl-6-benzofurancarboxylic acid (**6**b and c) were also obtained by this procedure.

Methyl 2,3-Dimethyl-5- and -4-alkyl-6-benzofurancarboxylates (7a,b, and c and 8a). Powdered potassium carbonate (43 g, 6 mol equivalents) was added to a solution of **5**a (11.3 g) and dimethyl sulfate (13.2 g, 2 mol equivalents) in acetone (200 m*l*), after which the mixture was refluxed for 8 hr. Most of the acetone was distilled off, and the residue was treated with water and extracted with ether. The ethereal layer was washed with a dilute aqueous sodium hyroxide solution, and then the ether was distilled off. The residual product was distilled to give methyl 2,3-dimethyl-5-ethyl-6-benzofurancarboxylate (**7**a); bp 177—180°C/20 mmHg; 9.4 g (78%).

Methyl 2,3-dimethyl-5-*n*-propyl- and -5-isopropyl-6-benzofurancarboxylates (**7**b and c) and methyl 2,3-dimethyl-4-ethyl-6-benzofurancarboxylate (**8**a) were also obtained by this procedure.

The authors are grateful to the members of the Laboratory of Microanalysis, Faculty of Pharmacology of this University, for their microanalyses.

This paper is dedicated to Emeritus Professor Munio Katake in Commemoration of the 75th birthday, november, 30, 1969.

BULLETIN OF THE CHEMICAL SOCIETY OF JAPAN VOL. 43 1804—1808 (1970)

Reaction of Sulfoxides with Acylating Reagents. IV.[1] The Catalytic Effect of Both the Brönsted and Lewis Acids in the Oxygen Exchange Reaction of Diaryl Sulfoxides with Acetic Anhydride

Masahiro KISE and Shigeru OAE

Department of Applied Chemistry, Faculty of Engineering, Osaka City University, Sumiyoshiku, Osaka

(Received November 12, 1969)

Diaryl sulfoxides undergo oxygen exchange and racemization reaction with acetic anhydide. The rate of racemization of *p*-tolyl phenyl sulfoxide was found to be twice that of oxygen exchange. The remarkably small substituents effect is also in keeping with the S_N2 type mechanism. Addition of acetic acid increases the rate of both the racemization and oxygen exchange. Racemization of sulfoxides is also known to be catalyzed markedly by a small amount of Lewis acid. When the reaction was carried out in the presence of a small amount of both acetic acid and Lewis acid, the ratio of the rate constants, k_{ex}/k_{rac} becomes unity. This may mean that the presence of both Brönsted and Lewis acids facilitates the cleavage of S–O bond by easy protonation (or hydrogen-bonding) or coordination on the sulfoxide oxygen, and the assistance of the nucleophilic attack by acetate becomes less important in the reaction. The larger substituent effect is also in keeping with the S_N1 type mechanism.

In a previous paper,[2] dealing with the reaction of diaryl sulfoxides with acetic anhydride, we suggested on the basis of our kinetic investigations (such as the value of $k_{ex}/k_{rac}=1/2$, rather small substituent effect, *etc.*,) that the reaction proceeds through an S_N2 type Walden inversion process at the rate-determining step as shown below. (Fig. 1).

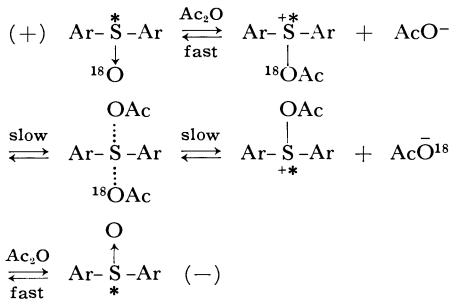

Fig. 1

The addition of acetic acid increases the rate of both the racemization[3] and oxygen exchange. Racemization of aryl benzyl sulfoxides in acetic anhydride is also known to be catalyzed markedly by a small amount of Lewis acid[4] such as mercuric chloride. In the racemization reaction of *p*-tolyl methyl sulfoxide with acetic anhydride, the large catalytic effect was reported by Jonsson[5] on the addition of metal halide such as mercuric chloride, zinc chloride or acetylating reagents. Jonsson proposed that in the racemization reaction of sulfoxide the acetylium ion formed reacts with the sulfoxide giving an acetoxysulfonium ion, and racemization was then brought about by exchange of acetate groups through a symmetrical transition state as proposed earlier.[2,3] The mechanism of the reaction is illustrated in Fig. 2.

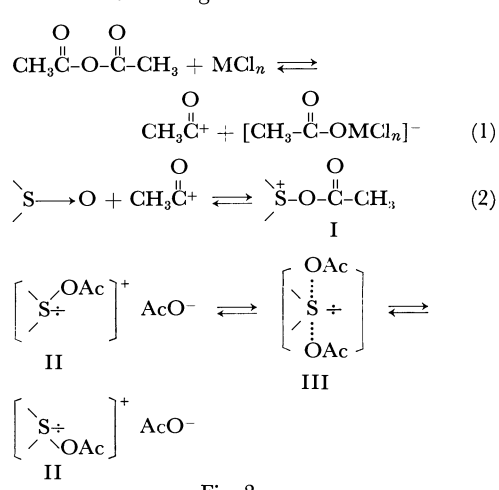

Fig. 2

1) Paper XXXIII on Sulfoxides.

2) S. Oae and M. Kise, *Tetrahedron Lett.*, **1967**, 1409.

3) E. Jonsson, *Acta Chem. Scand.*, **21**, 1278 (1967).

4) M. Kise and S. Oae, This Bulletin, **43**, 1421 (1970).

5) E. Jonsson, *Tetrahedron Lett.*, **1967**, 3675.

Since intermediate III is symmetrical the recovered sulfoxide should be racemized while the ratio of the rates, k_{ex}/k_{rac}, is expected to be 1/2.

We suggested,[2] on the basis of the ratio of the rate, $k_{ex}/k_{rac}=1$, in the oxygen exchange and racemization reaction of diaryl sulfoxide with acetic anhydride containing small amounts of acetic acid that the presence of Brönsted acid and acetic acid may facilitate the cleavage of S–O bond by the easy protonation or hydrogen bonding on the sulfoxide oxygen, and that the assistance of the nucleophilic attack by acetate becomes less important.

Sulfoxides bearing at least one methyl or methylene group directly attached to the sulfur atom undergo "Pummerer Rearrangement" in the reaction with acetic anhydrides as shown below[6] (Fig. 3).

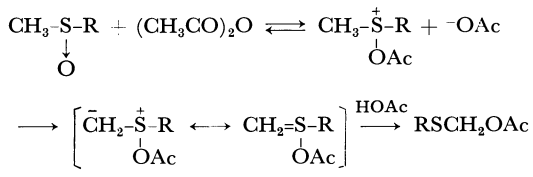

Fig. 3

We suggested on the basis of ^{18}O tracer experiments with ^{18}O-labeled acetic anhydride that the Pummerer reaction of dimethyl sulfoxide with acetic anhydride proceeds through an intermolecular nucleophilic attack of acetoxy group on the methylene carbon of the ylide-ylene intermediate. Noticeable acetoxy interchange has been found to take place during a similar Pummerer reaction of aryl methyl sulfoxide. In the reaction of *p*-tolyl methyl sulfoxide with acetic anhydride, below 65°C, under which the Pummerer reaction is minor, only the oxygen exchange proceeds slowly. But the addition of Lewis acids accelerates both the reaction of acetoxy interchange and Pummerer rearrangement.[6] We have investigated this catalyzed oxygen exchange reaction of diaryl sulfoxides by Lewis acids extensively in order to understand the nature of the reaction. With diaryl sulfoxides, our attention is focused only on the acetoxy interchange, since the other competing reactions such as Pummerer rearrangement and the heterolysis of carbon-sulfur linkage do not take place with these sulfoxides. In fact, when an optically active diaryl sulfoxide labeled with ^{18}O- atom was reacted with acetic anhydride containing Lewis acid, the sulfoxide was recovered quantitatively by quenching the reaction mixture with an excess cold water.

Results and Discussion

When the reaction were carried out at 120°C with both optically active and ^{18}O-labeled diaryl sulfoxides in a large excess of acetic anhydride, the rate of racemization of *p*-tolyl phenyl sulfoxide was twice that of oxygen exchange. This suggests that the reaction involves a Walden inversion at the rate-determining step. Sulfoxides are known to undergo concurrent oxygen exchange and racemization reactions through an acid catalyzed S_N1 type process in weak carboxylic acids such as acetic, chloroacetic, dichloroacetic and trichloroacetic acids.[7]

Table 1. Activation parameters and k_{ex}/k_{rac} values of (+) *p*-tolyl phenyl sulfoxides

Reagents	*Ea.* (kcal/mol)	$\Delta S^{\neq}$ (e.u.)	k_{ex}/k_{rac}	Temp. °C
Trichloroacetic acid[a]	18.6	−32.9	1.09	120
Acetic anhydride[b]	19.2	−28.6	0.50	120
Acetic anhydride-AcOH[c]	21.9	−17.0	1.11	90
Acetic anhydride-$HgCl_2$[d]	15.2	−23.1	1.02	10

a) Sulfoxide 0.001 mol, acid 0.25 mol in dioxane
b) Sulfoxide 0.005 mol, acetic anhydride 0.5 mol
c) Sulfoxide=0.05M Ac_2O/AcOH=9 AcOH 10% solution
d) Sulfoxide=0.05M $HgCl_2$=0.018M

Activation parameters and k_{ex}/k_{rac} values of the reaction of (+) *p*-tolyl phenyl sulfoxide with trichloroacetic acid,[7] acetic anhydride,[2] acetic anhydride containing a small amount of acetic acid and mercuric chloride are summarized in Table 1.

The small value of entropy of activation in the reaction of *p*-tolyl phenyl sulfoxide with trichloroacetic acid was assumed to be due to the solvation by the acid in the transition state.[7] However, in the reaction with acetic anhydride, the addition of acetic acid or mercuric chloride resulted in the increase of the entropy of activation and also in a probable change from the S_N2 process to the S_N1 in the transition state.

The small change of the entropy is perhaps due

Table 2. Rate constants of ^{18}O-exchange and racemization of *p*-tolyl phenyl sulfoxide in acetic anhydride containing a small amount of acetic acid and ratio of the rate k_{ex}/k_{rac}

Temp. °C	k_{rac} (sec^{-1})	k_{ex} (sec^{-1})	k_{ex}/k_{rac}
90	$(9.08\pm0.22)\times10^{-5}$	$(10.05\pm0.30)\times10^{-5}$	1.11
100	$(2.18\pm0.20)\times10^{-4}$	$(2.32\pm0.30)\times10^{-4}$	1.06
110	$(4.74\pm0.20)\times10^{-4}$	$(4.52\pm0.19)\times10^{-4}$	0.95

$\Delta S^{\neq}$ = −17.0 e.u. (90°C)
E_a = 21.9 kcal/mol.

6) a) S. Oae and M. Kise, *ibid.*, **1968**, 2261; b) M. Kise and S. Oae, This Bulletin, **43**, 1426 (1970).

7) S. Oae and M. Yokoyama and M. Kise, This Bulletin, **41**, 1221 (1968).

TABLE 3. RATE OF ^{18}O-EXCHANGE AND RACEMIZATION OF *p*-TOLYL PHENYL SULFOXIDE IN ACETIC ANHYDRIDE CONTAINING A SMALL AMOUNT OF MERCURIC CHLORIDE AND RATIO OF THE RATE k_{ex}/k_{rac}

Temp. °C	k_{ex} (sec^{-1})	k_{rac} (sec^{-1})	k_{ex}/k_{rac}
10	$(10.3\pm0.31)\times10^{-5}$	$(10.1\pm0.23)\times10^{-5}$	1.02
15		$(1.65\pm0.05)\times10^{-4}$	
20	$(2.49\pm0.30)\times10^{-4}$	$(2.54\pm0.08)\times10^{-4}$	0.98
25		$(3.94\pm0.11)\times10^{-4}$	

$\Delta S^{\neq} = -23.1$ e.u. (10°C)
$E_a = 15.2$ kcal/mol

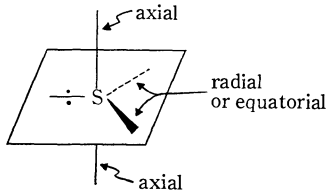

to the solvation or participation of these acids in the transition state of the reaction with a weak acid such as trichloroacetic acid. Actually the ratios of the rate, k_{ex}/k_{rac}, became unity as shown in Tables 2 and 3 in the reactions of *p*-tolyl phenyl sulfoxide with acetic anhydride containing a small amount of Brönsted acid or Lewis acid. If the reaction proceeds through the path shown in Fig. 2, the ratio of the rate, k_{ex}/k_{rac}, would become 1/2.

Thus the mechanism shown in Fig. 2 cannot account for the observation.

When an intermediate or an incipient activated complex at the transition state of the nucleophilic substitution reaction assumes a typical bipyramidal structure, two possible stereochemical consequences will arise depending upon the steric arrangement of both incoming and outgoing groups.[8]

When both the entering and leaving groups assume axial positions, the process is similar or identical to S_N2 reaction on carbon atom, and the net result is the inversion of configuration. A typical example of the reaction at the axial positions in trigonal bipyramidal might be the reaction of (+) *p*-tolyl phenyl sulfoxide with acetic anhydride.[2] Another example may be both the oxygen exchange and racemization reactions of (+) *p*-tolyl phenyl sulfoxide in less concentrated sulfuric acid (75.4%).[9] A similar net inversion would result also when both incoming and outgoing groups assume radial positions as shown below.

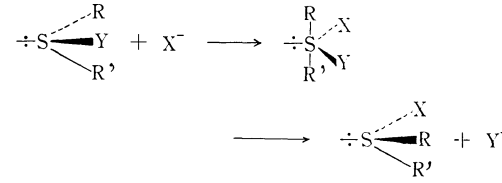

A possible example is the recent work of Day and Cram who showed that the formation of sulfilimine from the corresponding sulfoxide resulted in net inversion.[10] When the leaving and entering groups assume axial and radial arrangement with each other around the central sulfur atom of the trigonal bipyramidal structure, the displacement will lead to the retention of configuration at the sulfur atom. An example of this type was found for the first time in the oxygen exchange reaction between *p*-tolyl methyl sulfoxide and DMSO.[8]

Another reaction on the sulfur atom is similar to the S_N1 type reaction on sp^3 carbon atom, where the cleavage of S–O bond takes place in the initial slow step followed by a rapid recombination with solvent or a reagent, resulting in racemization. In this reaction, the ratio k_{ex}/k_{rac}, becomes unity.

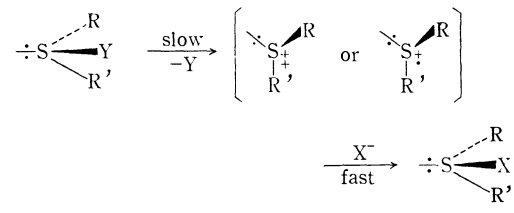

Thus, in both the reactions in concentrated sulfuric acid (95.5%), the ratio of the rate k_{ex}/k_{rac} is unity.[11] This shift of mechanism resulting from the change of the concentration of H_2SO_4 from 95% to 75%, is caused by the change of the nature of sulfuric acid solution, namely, the protonating ability of the solution diminishes steadily as acid concentration decreases while the activity of water increases. If the S_N1-like cleavage of the S–O bond of the sulfoxides takes place through the diprotonated species $>S-OH_2$ in the rate determining step, formation of this diprotonated species will decrease with the decrease of acid concentration. Other examples of this S_N1 type reaction are concurrent oxygen exchange and racemization reaction of sulfoxides in phosphoric acid[12] and dinitrogen tetroxide.[13]

Such a change in mechanism may be assumed to

8) a) S. Oae, M. Yokoyama and M. Kise, *Tetrahedron Lett.*, **1968**, 4131; b) K. Kimura and S. H. Bauer, *J. Chem. Phys.*, **39**, 3172 (1963).

9) N. Kunieda and S. Oae, This Bulletin, **42**, 1324 (1969).

10) a) J. Day and D. J. Cram, *J. Amer. Chem. Soc.*, **87**, 4398 (1965); b) D. R. Rayner, D. M. von Schriltz, J. Day and D. J. Cram, *ibid.*, **90**, 2721 (1968).

11) S. Oae and N. Kunieda, This Bulletin, **41**, 696 (1968).

12) N. Kunieda and S. Oae, *ibid.*, **41**, 1025 (1968).

13) N. Kunieda, K. Sakai and S. Oae, *ibid.*, **42**, 1090 (1969).

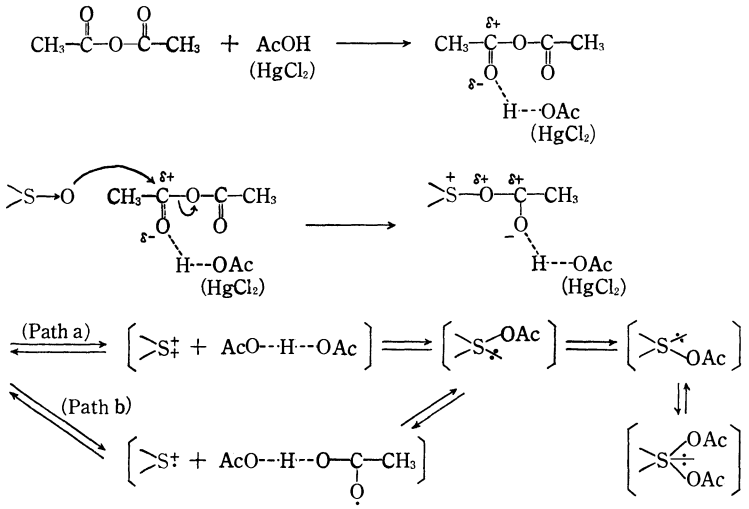

Fig. 4

take place also in the reaction of sulfoxides with acetic anhydride containing a small amount of acid. The transition state in these reactions may be assumed to be S_N1 type as in concentrated sulfuric acid. The change of transition state of this reaction may depend on the hydrogen bonding (protonating) or co-ordination on the oxygen atom of sulfoxide by these acids. The protonation or hydrogen bonding to the carbonyl oxygen of acetic anhydride of these acids can also enhance the initial acetylating step of these reaction (Fig. 4).

Table 4. Effect of aging at 10°C. Rate of ^{18}O-exchange and racemization of *p*-tolyl phenyl sulfoxide in acetic anhydride containing a small amount of mercuric chloride and ratio of the rate, k_{ex}/k_{rac}

Period	k_{ex} (sec^{-1})	k_{rac} (sec^{-1})	k_{ex}/k_{rac}
0	$(1.06\pm0.07)\times10^{-4}$	$(1.34\pm0.02)\times10^{-4}$	1.19
3 days	$(2.56\pm0.35)\times10^{-4}$	$(2.91\pm0.09)\times10^{-4}$	0.90

Jonsson[5] suggested that the rate enhancement by the acids in this reaction depends only on the formation of acetylium ion in the initial step. According to this mechanism, formation of acetylium ion would bring about an increased conductivity of the acetic acid solution. However, a careful measurement of conductivity of the reaction solution revealed no increase of conductivity. Ion separation did not take place in these solutions as shown in Table 4.

This effect may be due to the gradual formation of acylinium ion species which would react with sulfoxides so rapidly that measurement of conductivity becomes impossible.

The large enhancement of the rate, however, does not seem to be due to the discrete formation of a small amount of acetylium ion, but to the hydrogen bonding or participation of these acids in the initial acetylating step and also in the suc-

Table 5. Rate constants of ^{18}O-exchange of R-C$_6$H$_4$-S^{18}O-C$_6$H$_5$ in acetic anhydride containing a small amount of mercuric chloride at 10°C[a]

R in R-C$_6$H$_4$-S^{18}O-C$_6$H$_5$	k_{ex} (sec^{-1})
CH_3	$(10.3\pm0.31)\times10^{-5}$
H	$(11.2\pm0.03)\times10^{-5}$
Cl	$(3.85\pm0.42)\times10^{-5}$
NO_2	very slow

a) Sulfoxide=0.05M $HgCl_2$=0.018M

Table 6. Rate constants of ^{18}O-exchange R-C$_6$H$_4$-S^{18}O-C$_6$H$_5$ in acetic anhydride containing small amounts of acetic acid at 90°C[a]

R in R-C$_6$H$_4$-S^{18}O-C$_6$H$_5$	k_{ex} (sec^{-1})
CH_3	$(10.05\pm0.30)\times10^{-5}$
H	$(10.3\ \pm0.02)\times10^{-5}$
Cl	$(\ 5.37\pm0.25)\times10^{-5}$
NO_2	$(\ 6.84\pm0.20)\times10^{-6}$

a) Sulfoxide=0.05M $Ac_2O/AcOH$=9 AcOH 10% solution

ceeding fission of S–O bond. The over-all scheme of the oxygen exchange reaction of diaryl sulfoxides in acetic anhydride containing some acids may be formulated as in Fig. 4.

In order to confirm the S_N1-like character of this reaction, the oxygen exchage reaction of *p*-substituted diphenyl sulfoxides in acetic anhydride was carried out in the presence of a few acids. The results obtained with Lewis acids are shown in Table 5, while those with acetic acid are summarized in Table 6.

Kinetic data clearly reveal that the polar effect of substituents on the rate of oxygen exchange is markedly larger in this reaction than that in a typical S_N2 type reaction, such as reaction of sulfoxide with acetic anhydride[2] or with less concentrated sulfuric acid.[10] Two different mechanisms are conceivable, one in which the heterolysis of S–O bond involves the rate determining formation of the doubly charged "sulfidonium ion" intermediate (path a in Fig. 4), and the other in which the homolysis forms a radical cation intermediate (path b in Fig. 4). The relatively small polar effect ($\rho \fallingdotseq 1$) seems to favor the homolytic path for this reaction.

Experimental

Materials. *^{18}O-Labeled Diaryl Sulfoxides* were prepared by the bromine oxidation of the corresponding sulfides using ^{18}O-enriched water.[14]

An aryl sulfide (0.1 mol) was dissolved (0.2—0.5 mol) in a mixture of ^{18}O-enriched water (1.63 atom%), pyridine (0.12 mol) and small amount of acetic acid, and the solution was cooled down to 0°C, and an acetic acid solution of bromine (0.1 mol) was then added dropwise over a period of 1 hour. After one hour of stirring, the reaction mixture was poured into a large excess of ice-water, and the aqueous solution was neutralized with sodium bicarbonate. The precipitate formed was extracted with ether and the ether solution was washed with 10% sodium thiosulfate to remove both bromine and water, respectively, and dried over anhydrous sodium sulfate. After the solvent was distilled off thoroughly, the ^{18}O-labeled sulfoxide obtained was recrystallized three times from *n*-hexane-ether solution. The yields, melting points and ^{18}O-concentrations of the sulfoxides obtained are listed in Table 7.

TABLE 7. ^{18}O-LABELED ARYL SULFOXIDES

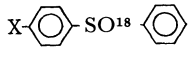

X	Mp (°C) (lit[15])	Yield (%)	^{18}O-concn. (atom %)
H	71 (71)	85	0.89
CH_3	69.8—71 (71—72)	80	1.09
Cl	45—46 (45—46)	70	1.05
NO_2	107 (106—107)	70	0.996*

* Prepared from 3.50 atom %-H_2O^{18}

Optically Active p-Tolyl Phenyl Sulfoxide. This sulfoxide was prepared by the method of Anderson[16] in which (−)-menthyl (−)-*p*-toluenesulfinate was allowed to react with phenylmagnesium bromide in ether (mp 91—93°C $[\alpha]_D = +27°$ in EtOH).

Acetic Acid obtained commercially was treated with chromic anhydride and after refluxing for several hours, it was distilled (bp 117.5—118°C).

Acetic Anhydride obtained commercially was treated with anhydrous sodium acetate and then distilled (bp 139.5—140°C).

Kinetic Procedure I (Oxygen Exchange Reaction). The oxygen exchange reaction was carried out in sealed tubes at a set temperature, ranging from 90 to 110°C in acetic anhydride containing a small amount of acetic acid, or from 10 to 20°C in acetic anhydride containing a small amount of mercuric chloride. In the sealed tubes were placed aliquots of the reaction mixture containing optically active *p*-tolyl phenyl sulfoxide (1.25×10^{-3} mol) in 25 m*l* acetic anhydride-acetic acid solution (Ac_2O/AcOH 9/1 (v/v)) or in the same acetic anhydride solution containg $HgCl_2$ (2.4353 g $HgCl_2$/500 m*l* Ac_2O) without other solvents. From time to time a sealed tube containing 4 m*l* of the reaction mixture was drawn out from the bath and quenched with ice water. The sulfoxide separated out was extracted with carbon tetrachloride, carbon tetrachloride was then distilled off and the resulting sulfoxide was recovered. The recovered sulfoxide was dried thoroughly and subjected to ^{18}O-analysis.[11]

Kinetic Procedure II (Racemization Reaction). The racemization reaction was carried out under the same conditions as for the oxygen exchange reaction. From time to time a sealed tube containing 4 m*l* of reaction mixture was drawn out from the paraffin bath and poured into an ice bath to stop the reaction of *p*-tolyl phenyl sulfoxide with acetic anhydride-acetic acid. In the reaction of *p*-tolylphenyl sulfoxide with acetic anhydride-mercuric chloride, the rates were measured directly by checking the polarimeter which was set at a desired temperature by connecting it with a constant temperature bath. The rate constants obtained by these methods are usually in good agreement with those obtained by isolating the product under kinetic procedure I.

Measurement of Conductivity. The electric conductivity of the solutions was measured by a universal bridge. At first the conductivity of acetic anhydride solution was measured by using a regular cell with platinum plates, and the value 40 MΩ was obtained. The conductivity of 25 m*l* acetic anhydride containing 136 mg mercuric chloride was found to be also 40 MΩ. The same value was obtained after 3 days and also after a week.

14) S. Oae, Y. Ohnishi, S. Kozuka and W. Tagaki, This Bulletin, **39**, 364 (1966).

15) G. Modena, *Gazz. Chim. Ital.*, **89**, 834 (1959).

16) K. K. Anderson, *Tetrahedron Lett.*, **1962**, 93.

BULLETIN OF THE CHEMICAL SOCIETY OF JAPAN VOL. 43 1809—1811 (1970)

Chromatographic Resolution of Several Racemates by Means of Optically Active Acidic Polymers Derived from α-Amino Acids

Tetsushi YAMASHITA and Nobuo NAKAMURA

Faculty of Science, Osaka City University, Sumiyoshi-ku, Osaka

(Received November 20, 1969)

The chromatographic resolution of several racemic amines was investigated by using three types of copolymers composed by *N*-acroylated α-amino acid and *N,N'*-dimethacroylhexamethylenediamine. The anilides of DL-phenylalanine and DL-valine, and of DL-phenylglycine and DL-1,2-diphenylethylamine, were partially resolved. The combination of substrate and sorbent giving the most efficient resolution was anilide of phenylglycine and the copolymer involving L-phenylalanine.

There have been a number of reports[1-11] concerning the use of synthetic optically active polymers as adsorbents for the chromatographic resolution of racemate.

Most such polymers have been synthesized by either one of the following two methods. The first is the method in which an optically active group is introduced into an optically inactive "reactive polymer"[7] (*e.g.*, chloromethylated polystyrene[4,5,7-9] and polymethacryl chloride[3]). The second method[1,2,6,11] includes the homogeneous copolymerization of an optically active monomer with some suitable crosslinking agent.

In a previous paper,[1] the syntheses of three types of optically active polymers by the second method and some of the results on the chromatographic resolution of racemate were reported.

This article will describe some more successful examples of resolution with DL-1,2-diphenylethylamine and with the anilides of DL-phenylalanine, DL-phenylglycine, and of DL-valine as substrates. In practice, these substrates were transformed into the corresponding acetates before the runs for resolution. The polymer sorbents used were the same as have been reported earlier[1,12] [crosslinking agent (CA): *N,N'*-dimethacroylhexamethylenediamine; copolymers A (acroyl phenylalanine-CA), B (acroyl valine-CA), and C (acroyl tryptophan-CA)].

Results and Discussion

Of course, the fraction with the highest specific rotation came out at the earliest stage of the elution

TABLE 1. OPTICAL RESOLUTION OF RACEMATES BY MEANS OF SYNTHESIZED POLYMERS

Acetates of racemic amines		Copolymer A	Copolymer B	Copolymer C
1,2-Diphenylethylamine	$[\alpha]_D$(°)	−11	0	−5
	C	0.1N	0.1N	0.1N
	O.P.(%)	16	0	7
Phenylalanine anilide	$[\alpha]_D$(°)	−49	0	−5
	C	0.1N	0.1N	0.1N
	O.P.(%)	52	0	5
Phenylglycine anilide	$[\alpha]_D$(°)	−85	−1	—
	C	0.01N	0.01N	—
	O.P.(%)	63	0.7	—
Valine anilide	$[\alpha]_D$(°C)	−15	0	—
	C	0.001N	0.1N	—
	O.P.(%)	21	0	—

C, acid concentration of eluent. O.P., Optical purity.

1) N. Nakamura, T. Yamashita and T. Uemura, *Nippon Kagaku Zasshi*, **88**, 1238 (1967).
2) J. F. Bunnet and J. L. Mark, *J. Amer. Chem. Soc.*, **74**, 5893 (1952).
3) N. Grubhofer and L. Schleith, *Z. Phys. Chem.*, **296**, 262 (1954).
4) S. Tsuboyama and M. Yanagita, *Sci. Papers Inst. Phys. Chem. Res.*, **53**, 245 (1959).
5) H. Suda and R. Oda, *Kanazawa Daigaku Kiyo*, **2**, 215 (1960).
6) G. Losse, H. Jeschkeit and H. Robe, *Z. Naturforsch.*, **176**, 419 (1962).
7) C. W. Roberts and D. H. Haigh., *J. Org. Chem.*, **27**, 3375 (1962).
8) J. A. Lott and W. Rieman, *ibid.*, **31**, 561 (1966).
9) G. Maneck and W. Lamer, *Naturwissenschaften*, **52**, 539 (1965); *ibid.*, **54**, 140 (1967).
10) D. R. Buss and T. Vermeulen, *Ind. Eng. Chem.*, **60**, 12 (1968).
11) H. Shimazaki and H. Ono, *Chem. Abstr.*, **68**, 3469 (1967).
12) R. K. Kulkurni and H. Morawetz, *J. Polym. Sci.*, **54**, 496 (1961).

TABLE 2. RESULT OF RESOLUTION OF ACETATE OF DL-PHENYLALANINE ANILIDE (200 mg) WITH COPOLYMER A

Fraction No.	Weight (mg)	c	α_D	$[\alpha]_D(°)$	α_{Hg}	$[\alpha]_{Hg}(°)$
1— 20	3	0.10	−0.049	−49	−0.063	−63
21— 40	10	0.33	−0.068	−20	−0.092	−27
41— 60	10.4	0.34	−0.039	−11	−0.060	−18
61— 90	15	0.50	−0.029	− 6	−0.036	− 7
91—200	50	1.66	0.000	0	0.000	0
201—300	26	0.86	+0.023	+ 2	+0.027	+ 3
301—400	20	0.66	+0.026	+ 4	+0.031	+ 4
401—500	15	0.50	+0.035	+ 7	+0.038	+ 8
501—600	11	0.33	+0.034	+10	+0.039	+11
601—700	8	0.26	+0.031	+11	+0.026	+10
701—800	3	0.10	+0.018	+18	+0.026	+26
last fractions	12	0.40	+0.101	+25	+0.127	+32

The wavelength of Hg-line is 546 mμ.

of the resolved substrate. However, 20—60 fractions had to be combined to obtain a sufficient amount of eluted substrate for the observation of specific rotation. Table 1 illustrates the observed values of specific rotation for the earliest combined fractions, along with those of the optical purity and the acid concentration of the eluent solvent.

In the case of copolymer A, the anilides of DL-phenylalanine and DL- phenylglycine were satisfactorily separated into their antipodes, whereas the resolutions of DL-1,2-diphenylethylamine and DL-valine anilide were rather poor. Only DL-phenylglycine anilide was resolved by copolymer B under similar conditions. Copolymer C, which is of interest because of its structure, with three adsorption centers per monomer unit, resolved DL-1,2-diphenylethylamine and DL-phenylalanine anilide with efficiencies next to those of copolymer A. The resolution ability was not examined extensively for this sorbent, since it was instable under acidic conditions. The results of the resolution of DL-phenylalanine anilide with copolymer A are given in detail in Table 2.

In order to investigate the dependence of the degree of optical resolution on the acid concentration of the eluent solvent, several resolutions of DL-valine anilide on copolymer A were carried out by changing the molarity of acetic acid from 0.1N to 0.001N (Table 3).

TBBLE 3. THE DEPENDENCE OF THE DEGREE OF OPTICAL RESOLUTION ON ACID CONCENTRATION OF THE ELUENT SOLVENT

Acid concentration	$[\alpha]_D(°)$	$[\alpha]_{Hg}(°)$	Optical purity (%)
0.1N	0	0	0
0.01N	−9	−13	13—15
0.001N	−15	−17	20—22

The data may be interpreted as follows. In the case of a low acid concentration, the racemate would be more strongly adsorbed on the surface of the sorbent, and hence one antipode would be more susceptible to influences from the asymmetric field of the sorbent than the other. A higher acid concentration would cause a more insufficient resolution.

It may be useful to discuss the interrelation between the substrate-sorbent and the degree of optical resolution on the basis of the results shown in Table I.

1) Roberts and Haigh[7] examined the partial resolution (22%) of DL-methionine on poly-[S-(ar-vinylbenzyl)-L-cysteine], a method which was employed on the basis of the assumption that the structual similarity between a substrate and the asymmetric site of a polymer must be a potent factor in efficient resolution.

Although a much higher resolution (52%) of DL-phenylalanine anilide on copolymer A seems to give an additional example of how their principle actually works in the adsorption process, the failure of the resolution (0%) of valine anilide on copolymer B suggests that some other factors also govern the resolution efficiency.

2*a*) Remarkable differences in optical purity are noticed between the resolved acetate of valine anilide and those of phenylalanine and phenylglycine anilides. These differences may be principally attributed to the difference in the bulkiness of the substituents on the asymmetric carbon atom of the molecule. The difference in the electronic characters of the substituents may also play a role.

2*b*) In comparing the data for the acetate of phenylglycine anilide with those for the acetate of 1,2-diphenylethylamine, it may be pointed out that the racemate involving the –CO·NH– group is much more efficiently resolved than is that having the $-CH_2-$ group in the corresponding moiety of the molecule. This is apparently due to the higher

adsorption suitability of the former group.

2*c*) The resolution ability of copolymer A with an asymmetric carbon atom carrying a benzyl group, is also higher than that of copolymer B which carries an isopropyl group, and which gave, at the highest of four examples, only a 0.7% resolution.

These results (2a—2c) are in accord with the general rules on asymmetric adsorption proposed by Krebs[13] and Dalgliesh,[14] both of whom studied sorbent polymers with some polysaccharides.

Experimental

The Syntheses of Optically Active Acidic Polymers. The optically active polymers were synthesized according to the method reported earlier.[1]

The Syntheses of the Acetates of α-Amino Acid Anilides. *N*-phthaloyl-α-amino acid anilides obtained by the ordinary method[15-17] were treated with hydrazine hydrate to give α-amino acid anilides.[15] When acetic acid was added to the ether solution of these anilides, white precipitates were formed. The recrystallization of the filtrated precipitates from ethanol or ethyl acetate gave the pure acetates of anilides. The specific rotations of these salts were determined in 0.1N-*aqueous* acetic acid.

The physical and analytical data of the several new racemates thus obtained are:

Acetate of DL-phenylalanine anilide. Mp 110—113°C. $[\alpha]_D = +93°$, $[\alpha]_{Hg} = +155°$ (*c* 1) in L-form. Found: C, 68.35; H, 6.89; N, 9.37%. Calcd for $C_{17}H_{20}N_2O_3$: C, 68.00; H, 6.66; N, 9.33%.

Acetate of DL-phenylglycine anilide. Mp 100—105°C. $[\alpha]_D = +133°$, $[\alpha]_{Hg} = +166°$ (*c* 0.56) in L-form. Found: C, 67.13; H, 6.35; N, 9.68%. Calcd for $C_{16}H_{18}N_2O_3$: C, 67.11; H, 6.34; N, 9.78%.

Acetate of DL-valine anilide. Mp 139—141°C. $[\alpha]_D = +74°$, $[\alpha]_{Hg} = +90°$ (*c* 1) in L-form. Found: C, 61.87; H, 8.06; N, 11.09%. Calcd for $C_{13}H_{20}N_2O_3$: C, 61.90; H, 7.93; N, 11.19%.

Acetate of DL-1,2-diphenylethylamine. Mp 125—130°C. $[\alpha]_D = -68°$, $[\alpha]_{Hg} = -83°$ (*c* 0.5) in L-form. Found: C, 74.91; H, 7.56; N, 5.88%. Calcd for $C_{16}H_{19}NO_2$: C, 74.68; H, 7.44; N, 5.44%.

Column Chromatography. An Example with Copolymer A. Copolymer A (80 g) suspended in a sufficient volume of *aqueous* acetic acid was poured into a column (2.5 cm in diameter; 150 cm in length; *ca.* 100 cm, the final length of the packed polymer).

Racemate (200—500 mg) dissolved in a suitable volume (*ca.* 10 m*l*) of *aqueous* acetic acid (0.1, 0.01, or 0.001N) was adsorbed on the upper zone of the sorbent and then eluted with the same solvent at room temperature. The flow rate of the solvent was *ca.* 6 m*l*/hr under atmospheric pressure. 8 m*l* portions of the eluent were collected automatically, and the concentration of the sample in each fraction was estimated by UV absorption by using a Hitachi EPS-2-spectrometer. 20—60 consecutive fractions were combined when the observed concentration was too low to determine the optical rotation. The optical rotation of the evaporated residue was determined in 0.1N *aqueous* acetic acid by a Rex-automatic polarimeter.

The chromatographic resolution of racemates on copolymers B and C were also carried out by a procedure similar to that described above.

13) H. Krebs, L. Diewald and J. A. Wagner, *Chem. Ber.*, **89**, 1875 (1956).

14) C. E. Dalgliesh, *J. Chem. Soc.*, **1952**, 3940.

15) J. C. Sheehan, D. W. Chapman and R. W. Roth, *J. Amer. Chem. Soc.*, **74**, 3822 (1952).

16) J. C. Sheehan and V. S. Franck, *ibid.*, **71**, 1856 (1949).

17) E. F. Schallenberg and M. J. Calvin, *ibid.*, **77**, 2779 (1955).

BULLETIN OF THE CHEMICAL SOCIETY OF JAPAN VOL. 43 1812—1816 (1970)

Chlorofluorination of Carbon Disulfide and Sulfur*1

Takashi ABE, Shunji NAGASE, Kazuo KODAIRA and Hajime BABA

Government Industrial Research Institute, Nagoya, Kita-ku, Nagoya

(Received November 24, 1969)

Chlorofluoromethanes and sulfur hexafluoride were obtained in good yields by the electrochemical fluorination of carbon disulfide in the presence of chlorine. The yields and compositions of the products were altered by the amount of chlorine fed in during electrolysis and also by the concentration of sulfur or carbon tetrachloride dissolved in carbon disulfide. Tetrafluoromethane, trifluoromethylsulfur pentafluoride, difluoromethylene bis-(sulfur pentafluoride), bistrifluoromethyl disulfide, and chlorodifluoromethylsulfur pentafluoride were also among the products. Further, the electrochemical fluorination of elementary sulfur was accomplished by the application of the technique of chlorofluorination, and sulfur hexafluoride was obtained in a reasonable yield. The chlorofluorinations of methyl sulfide and methyl disulfide were also attempted, but they afforded only chlorotrifluoromethane in poor yields.

Much attention has been paid to the fluorination of carbon disulfide with various fluorinating agents,[1] *e.g.*, fluorine, iodine pentafluoride, cobalt trifluoride and silver fluoride. The electrochemical fluorination of carbon disulfide has also been investigated by several workers.[2] On the other hand, the treatment of carbon disulfied with, *e.g.*, antimony pentachloride in the presence of hydrogen fluoride has been established to produce chlorofluoromethanes.[3]

In the present paper, we wish to report on the chlorofluorination of carbon disulfide and sulfur by the electrochemical process, which was found to proceed quite smoothly by a method similar to one described previously.[4]

We attempted initially to fluorinate the perchloroorganosulfur compounds, including trichloromethanesulfenyl chloride.*2 However, it was found that, upon electrochemical fluorination, these samples afforded mainly chlorofluoromethanes and sulfur hexafluoride as the cleaved products. This suggested the possible electrochemical fluorination of carbon disulfide in the presence of chlorine to obtain chlorofluoromethanes and sulfur hexafluoride. As expected, these products were obtained in good yields. In addition, their yields and compositions could be controlled satisfyingly by changing the chlorine feed rate and also by changing the composition of the substrate which was subjected to chlorofluorination.

An important feature of this halogenation is that chlorofluoromethanes and sulfur hexafluoride were simultaneously obtained in good yields from carbon disulfide. This process was applied successfully to the electrochemical fluorination of elementary sulfur. The fluorination of sulfur has previously been carried out with fluorine,[5] chlorine trifluoride,[6] and chlorine monofluoride.[7]

Results and Discussion

The electrochemical fluorination of perhalogenoorganosulfur compounds yielded, not the expected derivatives of sulfur hexafluoride, but the cleaved products, as is indicated in the following scheme:

*1 Presented in part at the 22nd Annual Meeting of the Chemical Society of Japan, Tokyo, April, 1969.

1) a) E. A. Tyczkowski and L. A. Bigelow, *J. Amer. Chem. Soc.*, **75**, 3523 (1953); b) G. A. Silvey and G. H. Cady, *ibid.*, **72**, 3624 (1950); c) R. N. Haszeldine and J. M. Kidd, *J. Chem. Soc.*, **1953**, 3219; d) H. J. Emeléus and D. E. MacDuffie, *ibid.*, **1961**, 2597.

2) G. A. Silvey and G. H. Cady, *J. Amer. Chem. Soc.*, **74**, 5792 (1952); A. F. Clifford, H. K. El-Shamy, H. J. Emeléus and R. N. Haszeldine, *J. Chem. Soc.*, **1953**, 2372.

3) Kinetic Chemical Co., Inc., U. S. 2004932 (1935); Imperial Chemical Industries Co., Ltd., Brit. 463970 (1937).

4) S. Nagase, H. Baba and T. Abe, This Bulletin, **40**, 2358 (1967).

*2 Trichloromethanesulfenyl chloride is generally synthesized by the reaction of carbon disulfide with chlorine in the presence of iodine as a catalyst at 0°C (P. Klason, *Ber.*, **20**, 2376 (1887)).

5) K. G. Dinbich and R. W. Ray, *J. Chem. Soc.*, **1934**, 1346; B. Cohen and A. G. MacDiarmid, *Inorg. Chem.*, **1**, 754 (1962).

6) F. Nyman and H. L. Roberts, *J. Chem. Soc.*, **1962**, 3180.

7) J. J. Pitts and A. W. Jach, *Inorg. Chem.*, **7**, 1661 (1968).

Sample*3	Products*4
CCl_3SCl	$\longrightarrow$ CCl_2F_2, $CClF_3$, CCl_3F, CF_4, SF_6 and CHF_3
CCl_2S	$\longrightarrow$ SF_6, CCl_2F_2, $CClF_3$, CF_4, CHF_3 and CF_3SF_5
$(CCl_2S)_2$	$\longrightarrow$ SF_6, $CClF_3$, CCl_2F_2, CF_4, CHF_3, $CHClF_2$ and CF_3SF_5
$(CF_2S)_2$	$\longrightarrow$ CF_4, SF_6, CHF_3, CF_3SF_5 and $(CF_3)_2SF_4$
CCl_3SO_2Cl	$\longrightarrow$ SO_2F_2, CF_4, $CClF_3$, CF_3SO_2F, CCl_3F and CCl_2F_2

As contrasted with the behavior of the carbon-oxygen double bond upon electrochemical fluorination, the carbon-sulfur double bond is easier to cleave. For example, phosgene afforded the trifluoromethyl hypofluorite in about a 7% yield,[8] but from thiophosgene, the corresponding product, trifluoromethylsulfur pentafluoride was obtained in only a 1% yield, and there was no trace of thiocarbonyl fluoride. It seems that the cleavage of the carbon - sulfur bond, especially in such compounds as perhalogenoorganosulfur derivatives, occurs extensively on electrochemical fluorination and that the yields of products which retain the carbon-sulfur bond are poor.

The reaction conditions for the chlorofluorination of carbon disulfide, and for that of carbon disulfide and sulfur, are presented in Tables 1 and 2 respectively.

The results obtained with carbon disulfide and those obtained with carbon disulfide and sulfur are summarized in Table 3.

While chlorine was being absorbed in carbon disulfide, the fluorination of the resulting chlorinated compounds as well as that of unchanged carbon disulfide led to the formation of chlorofluoromethanes and sulfur hexafluoride, together with trifluoromethylsulfur pentafluoride and difluoromethylene bis(sulfur pentafluoride).

Table 1. Conditions for the chlorofluorination of carbon disulfide

Anodic current density, 2.7 A/dm²; cell voltage, 6.5—7.5 V; cell temperature, 5—6°C; He, 45 ml/min; carbon disulfide containing catalytic amount of iodine (0.1% by wt), 0.2 mol

Run No.	Chlorine*a feed rate (ml/min)	Total amount of chlorine fed (mol)	Electricity passed (A·hr)
1	15	0.22	129
2	30	0.44	132
3*b	30	0.42	129
4	60	0.85	131
5*c			132

*a Gas volume is expressed in normal condition.
*b Sodium fluoride (10 g) was added.
*c Carbon tetrachloride (30.8 g) was added.

Under the reaction conditions applied, chlorofluoromethanes were obtained in the highest yield (33.9%) in Run 3, in which sulfur hexafluoride was produced in a 52.8% yield. The yield of sulfur hexafluoride is a little lower than that from the electrochemical fluorination of sulfur mono- or dichloride.[9] In Run 3, the addition of sodium fluoride can be considered to have an effect on the solubilities of the fluorinated products and to result in increased amounts of the products obtained. By increasing the molar ratios (chlorine to carbon disulfide) from approximately 1 to 2, the yield of chlorofluoromethanes is increased from 5.1 to 31.7%, but a further increase in the molar ratio has no effect on the yield.

The chlorofluorination proceeded also by the

Table 2. Conditions for the chlorofluorination of carbon disulfide and sulfur

Anodic current density, 2.7 A/dm²; cell voltage, 5.1—7.1 V; cell temperature, 5—6°C; He, 45 ml/min; sodium fluoride, 10 g

Run No.	Carbon disulfide*a fed (mol)	Sulfur fed (g)	Chlorine*b feed rate (ml/min)	Total amount of chlorine fed (mol)	Electricity passed (A·hr)
6	0.20	6.4	30	0.43	129
7	0.20	6.4	60	0.86	129
8		12.8	30	0.43	129
9		12.8	60	0.86	131

*a Iodine was dissolved in it by 0.1% (by wt).
*b Gas volume is expressed in normal condition.

*3 These samples except trichloromethanesulfenyl chloride are sparingly soluble in anhydrous hydrogen fluoride, so the addition of sodium fluoride was required in order to obtain an electrical conducting solution.

*4 The components are arranged in order of the decrease in the product composition (mol%).

8) To be published.

9) S. Nagase, T. Abe and H. Baba, This Bulletin, **42**, 2062 (1969).

Table 3. Results with chlorofluorination

Run No.	Product obtained (g)	Total*a yield (%)	Cl-F*b methanes (%)	SF_6*c yield (%)	Product composition, mol%							
					CF_4	$CClF_3$	CCl_2F_2	CCl_3F	SF_6	CF_3SF_5	CF_3SSCF_3	Others
1	41.9	170.0	5.1	39.6	29.3	1.7	1.0	0.3	46.5	19.9	0.3	CHF_3(0.8), $CF_2(SF_5)_2$(0.2)
2	46.0	181.7	31.7	43.5	29.3	7.1	7.5	2.8	47.9	3.9	1.3	CF_2ClSF_5(0.1), CHF_3(0.1)
3	49.0	191.4	33.9	52.8	17.6	8.8	4.6	4.3	55.2	6.2	2.5	CHF_3(0.6), CF_2ClSF_5(0.2)
4	43.8	176.8	29.0	43.5	20.9	6.6	7.2	2.7	49.2	9.3	1.9	CHF_3(1.8), CF_2ClSF_5(0.2), $CF_2(SF_5)_2$(0.2)
5	65.4	130.0	44.3	45.4	23.1	5.8	12.2	16.2	31.6	8.0		$CF_2(SF_5)_2$(1.7), CHF_3(1.0), $CHClF_2$ (0.3), CF_2ClSF_5(0.1)
6	47.7		7.5	38.4	17.0	2.5	1.2	0.4	65.9	9.4	2.1	CHF_3(1.5)
7	47.7		18.7	38.2	11.4	4.0	2.7	3.4	66.2	8.0	3.4	CHF_3(0.9)

	SF_6*d yield (%)	Current*e efficiency (%)
8	37.5	3.3
9	43.2	8.4

*a The total yield={(the total moles of the products including fragmented ones)/[(the mole of carbon disulfide consumed)+(the mole of carbon tetrachloride fed)]}×100

*b Total yield of chlorofluorinated methanes; the total yield of chlorofluoromethanes={(the total moles of the chlorofluoromethanes)/[(the mole of carbon disulfide consumed)+(the mole of carbon tetrachloride fed)]}×100

*c The yield of sulfur hexafluoride={(the mole of sulfur hexafluoride)/[2×(the mole of carbon disulfide consumed)+(g·atom of sulfur fed)]}×100

*d The yield of sulfur hexafluoride={(the mole of sulfur hexafluoride)/(g·atom of sulfur consumed)}×100

*e The calculation of current efficiency was based on the amount of current assumed to be required to form fluorine with a discharging fluoride ion which would react with sulfur according to the following equation. $S+6F=SF_6$

non-electrochemical mechanism to a certain extent in anhydrous hydrogen fluoride. For example, without a passing current, chlorine was fed into anhydrous hydrogen fluoride containing carbon disulfide at the feed rate of 30 ml/min for 320 min (reaction conditions; CS_2 fed, 0.2 mol; total amount of Cl_2 fed, 0.43 mol; cell temp., 5—6°C); a product with the following composition (mol %) was obtained in a 40.4% yield of chlorofluoromethanes: chlorotrifluoromethane (2.0), dichlorodifluoromethane (82.0), trichlorofluoromethane (14.3), and bistrifluoromethyl disulfide (1.7).

It is interesting to note that bistrifluoromethyl disulfide was produced in these experiments. It has been reported that the fluorination of carbon disulfide with iodine pentafluoride led to the formation of bistrifluoromethyl disulfide in a good yield;[1c] however, in the present experiment, it was derived from the hydrolytic reaction of trifluoromethanesulfenyl chloride[10] in gas-washing bottles which is easy to produce, even without a passing current.

An increased amount of sulfur hexafluoride was obtained when carbon disulfide containing sulfur was subjected to chlorofluorination, and the yield of chlorofluoromethanes (in Runs 6 and 7) was reduced. Similarly, the co-fluorination of carbon disulfide and carbon tetrachloride yielded an increased amount of chlorofluoromethanes in Run 5, which might be considered to result in the chlorination of carbon disulfide by means of chlorine liberated from the carbon tetrachloride attacked by fluorine radical during electrolysis.

The electrochemical fluorination of elementary sulfur feeding chlorine yielded mainly sulfur hexafluoride, together with a trace of sulfur chloridepentafluoride. The conversion of sulfur hexafluoride, however, was low, and most of the starting material (finely powdered sulfur) was recovered in an aggregated state. The composition of the reaction product was nearly constant throughout the electrolysis. For example, the composition (mol%) of the products (direct analysis by G.C.) was as follows (in Run 9): SF_6 77.5, SO_2F_2 18.0, and $SClF_5$ 4.5. It is not clear why sulfuryl fluoride was detected in the above experiment.

The chlorofluorination of methyl sulfide and methyl disulfide was also conducted in a similar manner. The yields of chlorofluorinated compounds were, however, low, giving chlorotrifluoromethane only in yields of 0.6% and 1.1% respectively. In order to make this point clear, the fluorinations of chloromethyl sulfides were subsequently attempted. The instability of all chloromethyl sulfides, except one having a trichloromethyl group, when treated with antimony trifluoride has been reported.[14]

10) R. N. Haszeldine and J. M. Kidd, *J. Chem. Soc.*, **1955**, 2901.

In this electrochemical fluorination, similarly, α,α-dichloromethyl sulfide gave no appreciable quantities of the corresponding fluorinated products. When α,α-dichloromethyl sulfide was subjected to electrochemical fluorination (reaction conditions: sample, 0.2 mol; helium, 45 ml/min; anodic current density, 2.7 A/dm²; electricity passed, 99.2 A·hr; cell voltage, 6—7 V; cell temp., 5—6°C), the product consisted of chlorotrifluoromethane (8.6 mol %), dichlorodifluoromethane (1.3), chlorodifluoromethane (0.6), tetrafluoromethane (31.9), trifluoromethane (11.8), sulfur hexafluoride (13.6), trifluoromethylsulfur pentafluoride (26.9), bis(trifluoromethyl)sulfur tetrafluoride (4.4), pentafluoroethylsulfur pentafluoride (0.2), and hexafluoroethane (0.7). The yield of chlorofluoromethanes was 15.7%.

When α,α,α-trichloromethyl sulfide, which shows a facile halogen exchange with hydrogen fluoride, affording α,α,α-trifluoromethyl sulfide, was fluorinated under the conditions described above (electricity passed, 48.3 A·hr), the composition (mol%) of the product was as follows; chlorotrifluoromethane (1.9), dichlorodifluoromethane (2.5), tetrafluoromethane (23.6), trifluoromethane (4.6), sulfur hexafluoride (5.7), trifluoromethylsulfur pentafluoride (11.3), bis(trifluoromethyl)sulfur tetrafluoride (14.9), and α,α,α-trifluoromethyl sulfide (35.5). The yield of chlorofluoromethanes was 5.3%. Notably, bis(trifluoromethyl)sulfur tetrafluoride was obtained in better yields, 6.6% from α,α-dichloromethyl sulfide and 18.0% from α,α,α-trichloromethyl sulfide respectively, compared to the yield (3.8%) from dimethyl sulfide.

The results may suggest that, in the chlorofluorination of methyl sulfide, the fluorination takes place with a priority to chlorination, at least at the monochloro-form stage, before chlorination proceeds further.

Thus, carbon disulfide is chlorinated by chlorine in anhydrous hydrogen fluoride, affording trichloromethanesulfenyl chloride and sulfur mono- or dichloride. The former might then proceed further to carbon tetrachloride and sulfur mono- or dichloride, or to trifluoromethanesulfenyl chloride, as a result of the easy replacement of the chlorine of the trichloromethyl group in anhydrous hydrogen fluoride, then, upon the electrochemical fluorination of part of it, carbon - sulfur bond fission occurs to give tetrafluoromethane and sulfur hexafluoride.

Sulfur is considered to be converted into a divalent state (S_2Cl_2 or SCl_2) by chlorine in the cell; subsequent fluorination yields hexavalent sulfur (SF_6 and $SClF_5$).

Experimental

Materials. The carbon disulfide, sulfur (finely

powdered, guaranteed reagent), trichloromethanesulfonyl chloride, methyl sulfide, and methyl disulfide were purchased from commercial sources, while the trichloromethanesulfenyl chloride, thiophosgene,[11] thiophosgene dimer,[12] 2,2,4,4-tetrafluoro-1,3-dithietane,[13] α,α-dichloromethyl sulfide, and α,α,α-trichloromethyl sulfide[14] were synthesisted by the methods described in the literature.

All these chemicals except sulfur were purified by conventional methods; their purity was confirmed before use by gas chromatography using a Shimadzu GC - 1C model Chromatograph and by mass spectroscopy using a Hitachi Model RMU-7.

The purity of anhydrous hydrogen fluoride was better than 99%.

Apparatus. The electrochemical fluorination apparatus used was almost the same as that described in previous papers.[4,15] The cell capacity was 1 *l*. The nickel electrodes consisted of a pack of alternate anodes (8 sheets) and cathodes (7 sheets). The effective surface area of the anodes was 9.2 dm^2. For charging the liquid samples precisely, a so-called "sample injector" was devised. It was fastened on the top of the cell with a fluoroelastomer rubber stopper. It consisted of a small tube (inlet) [8 mm od. × 5 mm id. × 3 cm length; poly(tetrafluoroethylene) resin] connected with an even smaller tube (outlet) [2 mm od. × 1 mm id. × 50 cm length; poly(chlorotrifluoroethylene) resin] which was inserted into the cell so as to reach its bottom. The inlet of the tube was covered with a silicone rubber stopper. A weighed liquid sample was led into the cell through the sample injector. The sampling valve was fitted with the line next to a sodium fluoride pellet tube for the direct analysis by GC of the evolving gaseous products from the cell.

Trap-to-trap distillation was carried out by a vacuum line technique using a series of traps (100 m*l* capacity) which were a part of a low-temperature distillation unit.

IR spectrum measurements was accomplished with a Hitachi EPI-S2 recording spectrometer, using a 6-cm gas cell equipped with two NaCl windows.

Procedures. As a typical example, the procedures for the chlorofluorination of carbon disulfide containing sulfur (Run 6) will be described.

Sulfur (6.4 g) was dissolved in carbon disulfide (15.2 g) while being warmed slightly, and then 15 mg of iodine was added. This mixture was introduced into anhydrous hydrogen fluoride (1 *l*) which had been purified by electrolysis. The carbon disulfide solution and anhydrous hydrogen fluoride formed two layers. The lower layer (the carbon disulfide solution) covered the bubbler located at the bottom of the cell.

Then sodium fluoride (10 g) was added in anhydrous hydrogen fluoride, and chlorine (30 m*l*/min) diluted by helium (45 m*l*/min) was directed through the bubbler into the carbon disulfide layer; the electrolysis of the solution was then carried out with an anodic current density of 2.7 A/dm^2, at a cell voltage of 5.9—7.1 V, and with a cell temperature of 5—6°C. The electrolysis was conducted for 129 A·hr.

The gases evolved from the cell were passed through a reflux condenser kept at −30°C, and over sodium fluoride (hydrogen fluoride absorber), and then bubbled through an aqueous solution of sodium sulfite containing a small amount of potassium iodide in consecutive Ichinose gas washers in order to eliminate oxygen difluoride, chlorine, derivatives of sulfur tetrafluoride, and sulfur chloridepentafluoride, passed through a trap cooled in ice, and finally condensed in two consecutive traps immersed in liquid nitrogen.

At regular intervals, gas was sampled from the sampling valve and was analysed directly by gas chromatography (columns and conditions: Kel F 3*[5] 30% on Chromosorb PAW, 3 m, 0°C; FC 43*[5] 66% on Celite 545 SK, 6 m, 0°C: carrier gas; He).

The composition (peak area %) of the evolved gas was, for example, $CF_4+CClF_3+CHF_3$ (47), SF_6 (6), CF_3SF_5 (8), CCl_2F_2 (2), CF_3SCl (32), CS_2+CCl_3F (5) after 60 A·hr electrolysis.

The reaction products (47.7 g) condensed in the cold traps were carefully divided into five fractions by trap-to-trap distillation.

The subsequent identification and the analysis of individual species, was accomplished by gas chromatography (column: silica gel; carrier gas : He) and IR spectrum measurements, as has been described previously.[4,9]

11) See *[2].

12) A. Schönberg and A. Stephenson, *Ber.*, **66B**, 567 (1933).

13) W. J. Middleton, E. G. Howard and W. H. Sharkey, *J. Org. Chem.*, **30**, 1375 (1965).

14) W. E. Truce, G. H. Birum and E. T. McBee, *J. Amer. Chem. Soc.*, **74**, 3594 (1952).

15) Preceding paper: T. Abe, S. Nagase and K. Kodaira, This Bulletin, **43**, 957 (1970).

*[5] Minnesota Mining and Manufacturing Co., Ltd.,

*[6] Trifluoromethanesulfenyl chloride (bp −1°C) was identified by employing authentic samples prepared by the reaction of bistrifluoromethyl disulfide with chlorine under the irradiation of UV light.[2c] The infrared spectrum of trifluoromethanesulfenyl chloride exhibited strong characteristic absorbtion bands (CF_3 stretch) at 1190 cm^{-1} and 1135 cm^{-1}.

BULLETIN OF THE CHEMICAL SOCIETY OF JAPAN VOL. 43 1817—1820 (1970)

On the Mechanism of the Vinyl Transetherification Reaction Catalyzed by Mercuric Acetate

Heimei YUKI, Koichi HATADA and Kazuhiko NAGATA

Department of Chemistry, Faculty of Engineering Science, Osaka University, Toyonaka, Osaka

(Received November 26, 1969)

The vinyl interchange reaction of methyl vinyl ether and methanol, methanol-d_4, or ethanol catalyzed by mercuric acetate has been studied. Some organomercuric compounds have been isolated from the reaction mixture, and their catalytic activity for the interchange reaction has been examined. From these results, the mechanism proposed by Watanabe and Conlon (*J. Amer. Chem. Soc.*, **79**, 2828 (1957)) has been confirmed and further details of the reaction mechanism are discussed.

The vinyl transetherification catalyzed by mercuric salt is known to be of wide utility for the preparation of various vinyl ethers.

$$ROCH{=}CH_2 + R'OH \rightleftharpoons ROH + R'OCH{=}CH_2$$

In a previous work[1,2] we studied this transetherification reaction using methyl vinyl ether (MVE) as a starting vinyl ether and a mercuric acetate ($Hg(OAc)_2$) catalyst, and found that the reaction could be smoothly shifted toward the product by the selective absorption of the produced methanol on the molecular sieves. Although a probable mechanism of the reaction[3] has been proposed, sufficient evidence has not yet been obtained. In the present work we investigated the reaction of MVE and methanol, methanol-d_4, or ethanol in the presence of $Hg(OAc)_2$ to clarify the mechanism of the reaction.

Experimental

Materials. MVE was purified in a gas phase by being passed through a saturated aqueous solution of potassium hydroxide and a column packed with potassium hydroxide pellets successively; then it was collected over calcium hydride in a cold trap cooled at −78°C. It was subsequently distilled under reduced pressure and stored over lithium aluminum hydride. The MVE thus purified was redistilled under a vacuum just before use.

The methanol and ethanol were purified by refluxing them over calcium oxide and by subsequent distillation, and these were stored under a nitrogen atmosphere. The methanol-d_4 and mercuric acetate were commercially obtained and were used without further purification.

The 2-acetoxymercuri-1,1-dimethoxyethane was prepared from sodium methoxide, mercuric acetate, and methyl vinyl ether.[3] Mp 64.0—65.0°C.

Reaction of MVE and Alcohol in the Presence of $Hg(OAc)_2$. A two-necked flask, equipped with a special reflux condenser for low-boiling liquid[4] and a thermometer, was flushed with dry nitrogen and then charged with an equimolar mixture of MVE and the alcohol, and a mercuric acetate catalyst. The reaction was carried out at 30°C for 1 hr under a nitrogen atmosphere. The reaction mixture was then flash-distilled under a high vacuum, and the distillate was analyzed by gas-liquid chromatography or NMR spectroscopy. The remaining solid residue was recrystallized from ether and was identified by means of analyses.

In another experiment, the reaction mixture was treated with potassium carbonate before flash-distillation under a high vacuum.

Analytical Procedure. Gas-liquid chromatographic analysis was carried out using a Shimadzu Seisakusho gas-liquid chromatograph equipped with a column (2 m long, 4 mm I.D.) containing 30% dioctyl phthalate on Shimalite B (a kind of kieselguhr). The apparatus was operated at 80°C with a helium-carrier gas stream of 68 ml/min, while toluene was employed as the intensity standard for the determination of the product composition.

The NMR spectra were taken on a JNM-4H-100 spectrometer (JEOL) at 100 MHz in CCl_4 at 22.5°C. Tetramethylsilane was used as the internal reference.

The molecular weight was determined on a Mechrolab Vapor Pressure Osmometer (Model 310A) in carbon tetrachloride at 37.0°C.

Analysis for mercury was carried out by the decomposition of a sample with concentrated sulfuric acid and by subsequent titration with ammonium thiocyanate, according to the method of Hirai.[5]

1) H. Yuki, K. Hatada and K. Nagata, This Bulletin, **42**, 3546 (1969).

2) H. Yuki, K. Hatada and K. Nagata, *Kogyo Kagaku Zasshi*, **73**, 715 (1970).

3) W. H. Watanabe and L. E. Conlon, *J. Amer. Chem. Soc.*, **79**, 2828 (1957).

4) R. P. Linstead, J. A. Elvidge and M. Whalley, "A Course in Modern Techniques of Organic Chemistry," Butterworths Scientific Publications, London, (1955), p. 82.

5) M. Hirai and R. Hayatsu, *Yakugaku Zasshi*, **70**, 670 (1950).

TABLE 1. REACTION OF METHYL VINYL ETHER AND METHANOL AT 30°C FOR 1 hr IN THE PRESENCE OF $Hg(OAc)_2$

Reaction Conditions: MVE 0.1 mole, MeOH 0.1 mole, $Hg(OAc)_2$ 0.0016 mole.

No.	K_2CO_3 (g)	Reaction product (g) I[b]	II[c]	Mp (°C)	Mol wt Found	Calcd	Elementary analysis[d] (%) C	H	Hg
123	0	0 6	0	64~5°C	352	348	20.76	3.29	57.4
117	1.0	0	0.5	liquid	367	378	25.89	4.88	51.7
118[a]	1.0	0	0.4	liquid	377	378	25.02	4.64	52.1

a) Reaction temp. 0°C.

b) CH_3O, CH_3O > $CHCH_2HgOAc$

c) $\left(\begin{matrix}CH_3O\\CH_3O\end{matrix}\!>\!CHCH_2-\right)_2 Hg$

d) Calcd for I ($C_6H_{12}O_4Hg$): C, 20.66; H, 3.47; Hg, 57.52%. Calcd for II ($C_8H_{18}O_4Hg$) C, 25.36; H, 4.79; Hg, 52.95%.

Results

Reaction of MVE and Methanol or Methanol-d_4 in the Presence of $Hg(OAc)_2$. An equimolar reaction of MVE and methanol in the presence of $Hg(OAc)_2$ was carried out at 30°C for 1 hr under a nitrogen atmosphere. The vacuum distillation of the reaction mixture gave a recovery of 93% of the equimolar mixture of MVE and methanol, leaving a solid residue. The recrystallization of this residue from ether gave 2-acetoxymercuri-1,1-dimethoxy-ethane (I), which was identified by an NMR spectral comparison with an authentic sample. This identification was also supported by the measurements of its melting point and molecular weight, and by the results of an elementary analysis (Table 1).

When the reaction mixture was treated with potassium carbonate before vacuum distillation and the residue was extracted with diethyl ether, a viscous liquid with a high boiling temperature was obtained after the removal of ether from the extract. This compound was found by NMR spectroscopy to be bis-2,2-dimethoxyethylmercury (II) (Fig. 1). This structure was also established by the measurements of the molecular weight and by the results of an elementary analysis (Table 1).

In order to examine the catalytic activity of these two compounds for transetherification, equimolar reactions of MVE and methanol-d_4 were performed in the presence of these compounds at 30°C for 1 hr, and the reaction mixtures were analyzed by NMR spectroscopy. The NMR spectrum of the reaction mixture of MVE, methanol-d_4 and

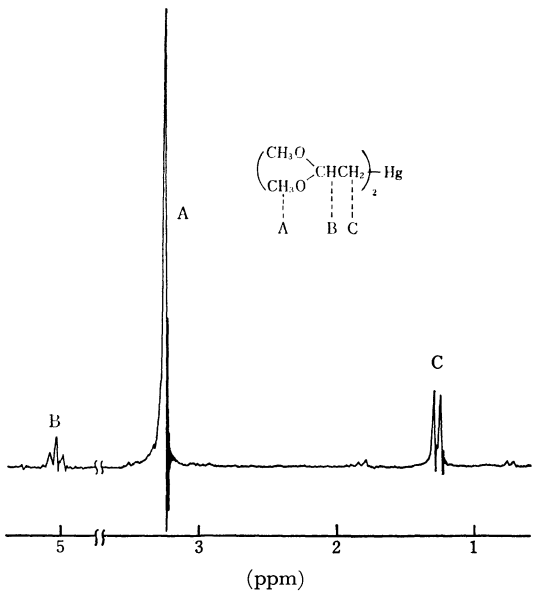

Fig. 1. NMR spectrum of bis-2,2-dimethoxyethylmercury. Intensity ratio of the signals: A : B : C=6.00 : 0.90 : 2.06.

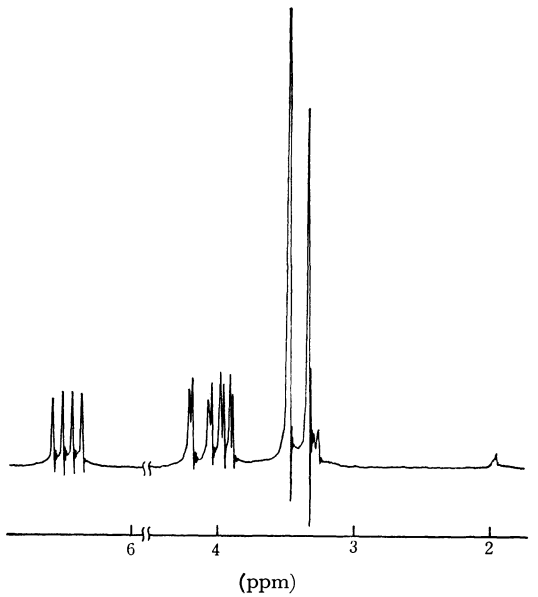

Fig. 2. NMR spectrum of the reaction mixture of MVE and methanol-d_4 in the presence of 2-acetoxymercuri-1,1-dimethoxyethane.

the compound I showed a sharp singlet

$$CH_3OCH=CH_2 + CD_3OD \rightleftharpoons CD_3OCH=CH_2 + CH_3OD$$

at 3.35 ppm due to the methyl protons of CH_3OD produced (Fig. 2). From the intensity ratio of this signal to the methoxy proton signal of MVE, the conversion of MVE to MVE-d_3 was calculated to be 44%. On the other hand, the compound II showed no catalytic activity in the interchange reaction. However, in the presence of a small amount of acetic acid, this compound catalyzed the reaction quite well and 50% of MVE-d_3 was produced.

Reaction of MVE and Ethanol in the Presence of $Hg(OAc)_2$. To prove that mercurial compounds such as I are formed in the interchange reaction of a combination of MVE and another alcohol, a mixture of 0.1 mol of MVE, 0.1 mol of ethanol, and 0.0016 mol of $Hg(OAc)_2$ was reacted at 30°C for 1 hr under a nitrogen atmosphere. From the reaction mixture the volatile component was then distilled off under a high vacuum. The residue was extracted with diethyl ether, the ether was then distilled off under a high vacuum. The NMR spectrum (Fig. 3) of the remaining liquid

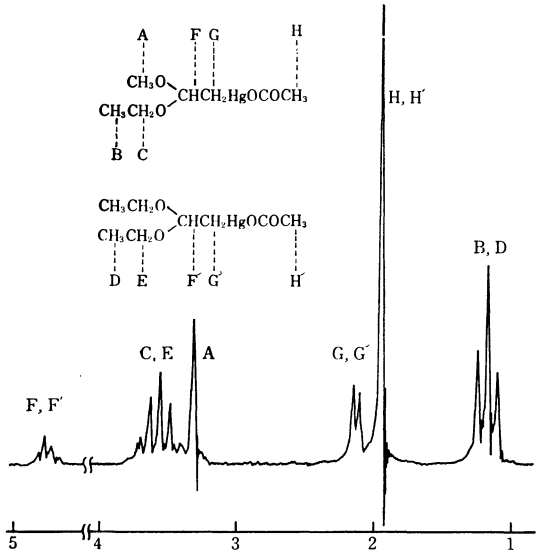

Fig. 3

with a high boiling temperature (0.6 g) shows that the product is a mixture of 2-acetoxymercuri-1-methoxy-1-ethoxyethane (III) and 2-acetoxymercuri-1,1-diethoxyethane (IV). The ratio of the compounds III and IV was roughly estimated to be 1 : 1 by the intensity measurement of the NMR signals.

When the reaction mixture was treated with potassium carbonate before vacuum distillation,

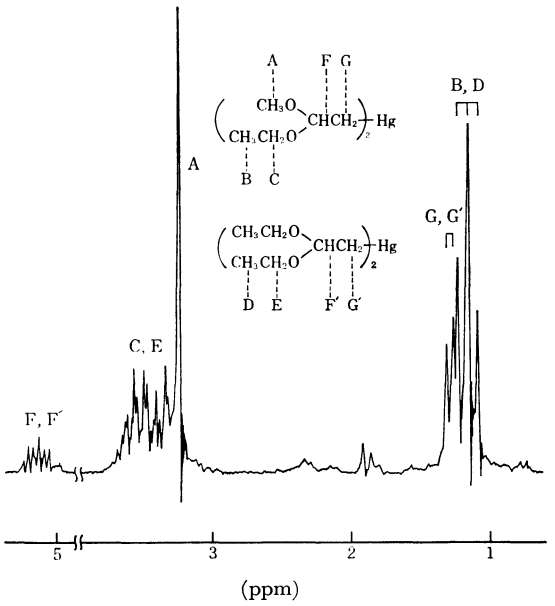

Fig. 4

0.6 g of a liquid with a high boiling temperature was also obtained. The NMR spectrum (Fig. 4) shows that the product formed is probably a mixture of bis-2-methoxy-2-ethoxyethylmercury (V), bis-2,2-diethoxyethylmercury (VI), and a small quantity of acetoxymercuric compounds.

Discussion

In 1957 Watanabe and Conlon[3] proposed a mechanism of the transetherification reaction on the basis of the fact that the 2-acetoxymercuri-1,1-diethoxyethane was decomposed readily by acetic acid to ethyl vinyl ether and ethyl alcohol. According to their proposal, the mechanism of the reaction starting with MVE can be illustrated as follows:

$$Hg(OAc)_2 \rightleftharpoons HgOAc^+ + AcO^-$$

$$HgOAc^+ + CH_3OCH=CH_2 + ROH \rightleftharpoons \underset{\text{A}}{\overset{CH_3O}{\underset{RO}{}}\!\!>\!CHCH_2HgOAc} + H^+$$

$$A + CH_3OCH=CH_2 + ROH \rightleftharpoons \underset{\text{B}}{\left(\overset{CH_3O}{\underset{RO}{}}\!\!>\!CH\text{-}CH_2\right)_2\!\!-Hg} + HOAc$$

$$\Downarrow$$

$$A + ROCH=CH_2 + CH_3OH$$

In the present work we have been able to isolate the intermediate A(R=CH_3) directly from an equilibrium mixture of MVE, methanol, and mercuric acetate; and we found this intermediate to be

catalytically active for the transetherification reaction of MVE and methanol-d_4. The intermediate B ($R=CH_3$), which was found to be catalytically inactive but become active in the presence of a small amount of acetic acid, was scarcely formed in the mixture. After the treatment of the equilibrium mixture with potassium carbonate, the intermediate A vanished and the intermediate B was formed. The formations of analogous intermediates were proved in the reaction of MVE and ethanol catalyzed by $Hg(OAc)_2$.

These results clearly confirm the mechanism proposed by Watanabe and Conlon. No direct evidence can be found for the existence of an intermediate of the type B in the reaction mixture. However, this must exist to a very small extent in equilibrium with other species. The addition of an excess of potassium carbonate to the reaction mixture causes the equilibrium to shift toward the intermediate B as a result of the salt formation with acetic acid; consequently, this inactivates the catalyst.

If a proton from the acetic acid attacks the oxygen atom of the CH_3O group in the intermediate B, the resulting oxonium ion decomposes to A and the desired vinyl ether, while the methanol is expelled. On the other hand, if the attack of a proton takes place on the oxygen atom of the RO group, the reaction proceeds to the left and the starting vinyl ether and alcohol are recovered. Therefore, it is expected that the larger the electron-repelling power of the R group, the greater the tendency for a proton attack to occur on the oxygen of the RO group and the less the tendency for the desired vinyl ether to be formed. The equilibrium constant of the transetherification reaction of MVE and alcohol (ROH) decreases in the order of; $R=C_2H_5>n\text{-}C_3H_7>i\text{-}C_3H_7>t\text{-}C_4H_9$.[2)]

$$CH_3OCH{=}CH_2 + ROH \overset{K}{\rightleftharpoons} ROCH{=}CH_2 + CH_3OH$$

This result exactly coincides with the above explanations and also supports the idea of the existence of the intermediate B.

The authors wish to express their thanks to Mr. K. Kajiyama for his help in the laboratory work and to Mrs. F. Yano for her clerical assistance in preparing the manuscript.

BULLETIN OF THE CHEMICAL SOCIETY OF JAPAN VOL. 43 1820—1824 (1970)

Synthesis of Adamantane Derivatives. IX.[1] The Ritter Reaction of 1-Hydroxymethyladamantane with Acetonitrile

Tadashi SASAKI, Shoji EGUCHI, Takeshi TORU and Katsumi ITO

Institute of Applied Organic Chemistry, Faculty of Engineering, Nagoya University, Chikusa-ku, Nagoya

(Received November 27, 1969)

The Ritter reactions of 1-hydroxymethyladamantane (**1**) and 3-homoadamantanol (**14**) with acetonitrile in concd. sulfuric acid were investigated. Two products, *N*-3-homoadamantyl acetamide (**2**) and *N*-1-adamantylmethyl acetamide (**3**) were isolated. Their total- and relative yields were determined in various reaction conditions by GLC analysis, indicating the facile conversion of *N*-3-homoadamantyl acetonitrilium cation (**12**) into *N*-1-adamantylmethyl acetonitrilium cation (**13**).

In contrast with numerous examples of the Ritter reactions of tertiary, secondary alcohols and their corresponding derivatives, there seem to be no reports concerning a similar reaction of aliphatic primary alcohols.[2] We wish to describe the results of the Ritter reaction of 1-hydroxymethyladamantane (**1**), regarded as one of the primary alcohols, and 3-homoadamantanol (**14**) in various conditions.

1) Preceding paper of this series: T. Sasaki, S. Eguchi and T. Toru, *J. Amer. Chem. Soc.*, **91**, 3390 (1969).

2) a) L. I. Krimen and D. J. Cota, "The Ritter Reaction," in "Organic Reactions," Vol. 17, John Wiley & Sons, Inc., New York (1969), pp. 213—325; b) F. Johnson, "Heterocyclic Syntheses Involving Nitrilium Salts and Nitriles under Acidic Conditions," in "Advances in Heterocyclic Chemistry," Vol. 6, ed. by A. R. Katritzky and A. J. Boulton, Academic Press Inc., New York, N. Y. (1966), pp. 95—146; c) H. Stetter, J. Mayer, M. Schwarz and K. Wulff, *Chem. Ber.*, **93**, 226 (1960); T. Sasaki, S. Eguchi and T. Toru, This Bulletin, **41**, 236 (1968).

Stetter and his coworkers[3,4] have reported that both the Koch-Haaf carboxylation of **1** and the Demjanov reaction of 1-aminomethyladamantane afford the ring-expanded homoadamantyl derivatives at the sacrifice of the strain-free ring structure. On the contrary, the ring-contraction of homoadamantane to the strain-free adamantane ring system has also been described in the reaction of 3-homoadamantanol with hydrogen halide in acetic acid at 150°C to 1-hydroxymethyladamantane, though the simple bridgehead substitutions have been accomplished under the milder reaction conditions or with some other reagents, in the maintenance of the skeletal integrity of homoadamantane ring.[4] This delicate change in the reaction products might be effected by the presence of equilibrium between the primary adamantylcarbinyl cation and the tertiary homoadamantyl cation under the given reaction conditions. These problems in the solvolytic conditions have been extensively studied by Nordlander and Schleyer.[5] The Ritter reaction of **1** might provide a new synthetic method for *N*-3-homoadamantyl amide derivatives if the corresponding nitrilium cations are stable in the reaction conditions.

Results and Discussion

The Ritter reaction of **1** with acetonitrile in concd. sulfuric acid proceeded smoothly. However, the ring-expanded *N*-3-homoadamantyl acetamide **2** was produced only in low yields and the major product was *N*-1-adamantylmethyl acetamide **3**. The total yields and relative yields of the two prodcuts were dependent on reaction temperature and time (see Table 1).

$$\mathbf{1} \longrightarrow \mathbf{2} + \mathbf{3}$$

Product Analysis. The crude amide product obtained by the reaction of **1** with acetonitrile in sulfuric acid, followed by hydrolysis was purified on a silica-gel column to afford two kinds of crystalline amides, mp 138—139°C and 126—127°C to which the structures **2** and **3** were assigned respectively based on the following data. Both compounds gave satisfactory analytical results as that of $C_{13}H_{21}ON$. The IR absorption bands at 3330 (NH), 1640 (amide-I) and 1570 (amide-II) cm^{-1} for **2**, and 3300 (NH), 1640 (amide-I) and 1570 (amide-II) cm^{-1} for **3** indicate both compounds to be secondary amides. In the NMR spectrum of **2**, a signal assignable to methyl protons of acetamide moiety appeared at τ 8.05 superimposed to those of homoadamantane ring protons. However, in the NMR spectrum of **3**, a signal assignable to $N-CH_2-$ protons appeared at τ 6.97 (2H) in a doublet with $J=6.75$ Hz and also the typical signals at τ 7.95, 8.22, and 8.41 due to 1-adamantyl ring protons besides that of $-NHCOCH_3$ protons at τ 7.93. The structures of **2** and **3** were further verified by comparison with specimens prepared by the following reaction sequences, **2** *via* 3-homoadamantylamine **7**[6] and **3** *via* 1-adamantylmethylamine **9**:[4]

Table 1. Reaction of **1** with acetonitrile in sulfuric acid*

Reaction temp.	Reaction time hr	Total yields of amides** %	Relative yields of **2** and **3**	
			2, %	**3**, %
room temp.	1	20	66	34
(*ca.* 15°C)	5	20	35	65
	12	50	15	85
	24	42	10	90
	48	51	16	84
50°C	1	40	2.9	97.1
	5	95	1.3	98.7
	12	92	1.9	98.1
	24	92	0.2	99.8

* A mixture of **1** (1.2 mmol) and acetonitrile (76.5 mmole) was added to stirred sulfuric acid (1.5 m*l*).
** Most of the other products were recovered **1**.

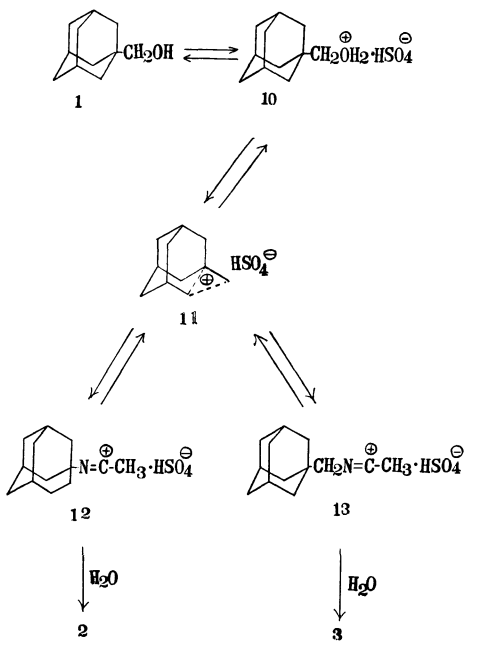

Chart I.

3) H. Stetter, M. Schwarz and A. Hirshhorn, *Chem. Ber.*, **92**, 1629 (1959).
4) H. Stetter and P. Goebel, *ibid.*, **96**, 550 (1963).
5) a) J. E. Nordlander, S. P. Jindal, P. von R. Schleyer, R. C. Fort, Jr., J. J. Harper and R. D. Nicholas, *J. Amer. Chem. Soc.*, **88**, 4475 (1966); b) S. H. Liggere, R. Sustmann, P. von R. Schleyer, *ibid.*, **91**, 4571 (1969).
6) J. R. Geigh A.-G., Belg. 661640 (1955); *Chem. Abstr.*, **65**, 10515d (1966).

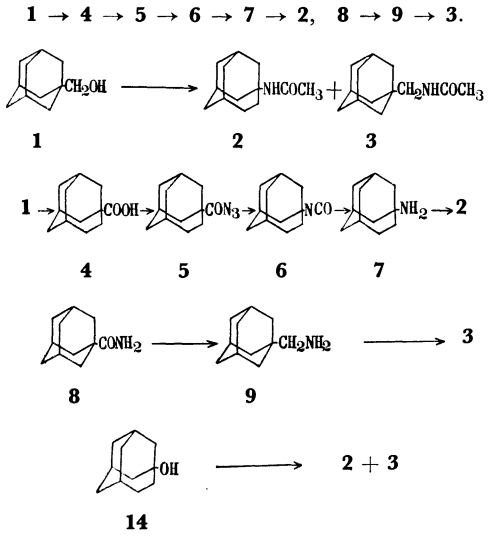

Equilibrium Problem. As summarized in Table 1, the total and relative yields of **2** and **3** were much influenced by the reaction time and temperature even in the presence of excess acetonitriles. From these data, it can be concluded that with the prolonged reaction time, the total yields of amides increase but the relative amounts of **2** to **3** decrease rapidly. This tendency was also observed at 50°C and the total and relative yields at both temperatures reached approximately constant values after 12 and 5 hr respectively.

Formation of **2** and **3** could be visualized as shown in Chart I: the practical isolation of **2** and **3** indicates the formation of nitrilium cations **12** and **13**. However, there are two possibilities that **12** and **13** can be produced by the addition of acetonitrile to the corresponding carbonium ions, 1-adamantylcarbinyl- and 3-homoadamantyl cations respectively, which are derivable from **1** *via* **10**, and/or **12** and **13** by addition of acetonitrile to a bridged- or nonclassical cation. This was recently demonstrated to be an intermediate in solvolytic rearrangements of 1-adamantylcarbinyl tosylate and 3-homoadamantyl bromide.[5b] Nonclassical form (**11**) is tentatively depicted in Chart 1. Our results indicate that the *N*-3-homoadamantyl acetonitrilium cation **12** is a kinetically controlled product and is converted gradually to the more stable *N*-1-admantylmethyl acetonitrilium cation **13**. The relative stability between 1-adamantylcarbinyl- and 3-homoadamantyl derivatives seems to be very much dependent on the substituents.[7] In the Ritter reaction, the ring strain of **12** could not be compensated by the stabilizing effect of the tertiary carbon.

Another aspect of this Ritter reaction is manifested by the lower yields of the amides compared to higher yields of those for the typical tertiary adamantyl bromide in similar reaction conditions.[2c] The reaction of 3-homoadamantanol **14** as the tertiary alcohol with excess acetonitrile in sulfuric acid was examined, the results of which are summarized in Table 2. Obviously, under the same conditions, **14**→**2**+**3**, higher total yields than those in the reaction of **1** were obtained, indicating the formation of the carbonium ion from **14** was more facile than from **1**.

Table 2. Reaction of **14** with acetonitrile in sulfuric acid*

Reaction temp.	Reaction time hr	Total yields of amides %	Relative yields of **2** and **3**	
			2, %	**3**, %
room temp. (*ca.* 15°C)	24	93	16.5	83.5
50°C	24	98	10	90

* A mixture of **14** (1.2 mmol) and acetonitrile (76.5 mmol) was added to stirred sulfuric acid (1.5 m*l*).

Effects of Addition of Other Lewis Acids. The results of the Ritter reactions of **1** and **14** in the presence of aluminum trichloride and/or boron trifluoride etherate in concd. sulfuric acid are summarized in Tables 3, 4 and 5. In the reaction of **1** using sulfuric acid-aluminum trichloride system, the relative yield of **2** to **3** was much higher than those in sulfuric acid after 24 hr.

It required about 4 days to obtain an approximately constant yield. The total and relative yields of amides were almost similar to those in sulfuric acid (Table 1). These results could be explained by weaker reactivity of the catalyst-system in which an acidic calcide like aluminum sulfate might be produced.[8] Such supression of

Table 3. Reaction of **1** with acetonitrile in aluminum trichloride - sulfuric acid*

React. temp.	React. time hr	Total yields of amides %	Relative yields of **2** and **3**	
			2, %	**3**, %
room temp.	24	23	92	8
(*ca.* 15°C)	52	25	45	55
	96	42	17	83
50°C	12	52	13.5	86.5
	24	32	12	88
	48	45	9	91

* A mixture of **1** (1.2 mmol) and acetonitrile (76.5 mmol) was added to a stirred mixture of aluminum trichloride (0.6 g) and sulfuric acid (1.5 m*l*).

7) R. C. Fort, Jr., and P. von R. Schleyer, *Chem. Rev.*, **64**, 277 (1964).

8) G. A. Olah, "Catalysts and Solvents," in "Friedel-Crafts and Related Reactions," Vol. I, ed. by G. A. Olah, Interscience Publishers, Inc., New York, N. Y. (1963), pp. 201—366.

Table 4. Reaction of **1** with acetonitrile in boron trifluoride etherate - sulfuric acid*

React. temp.	React. time hr	Total yields of amides %	Relative yields of **2** and **3**	
			2,%	**3**,%
room temp.	24	24	12	88
(*ca.* 15°C)	48	44	8.5	91.5

* A mixture of **1** (1.2 mmol) and acetonitrile (76.5 mmole) was added to a stirred mixture of boron trifluoride etherate (1.5 m*l*) and sulfuric acid (1.5 m*l*).

Table 5. Reaction of **14** with acetonitrile in aluminum trichloride - sulfuric acid and boron trifluoride etherate - sulfuric acid at room temperature (*ca.* 15°C)

Catalyst system	React. time hr	Total yields of amides %	Relative yields of **2** and **3**	
			2,%	**3**,%
$AlCl_3$(0.6 g)-H_2SO_4(1.5 m*l*)	24	72	31	69
BF_3 etherate (1.5 m*l*)-H_2SO_4 (1.5 m*l*)	24	76	3	97

* A mixture of **14** (1.2 mmol) and acetonitrile (76.5 mmol) was added to the respective catalyst-system with stirring.

the rearrangement of **12** to **13** is interesting from the view point of preparation. The effects of addition of boron trifluoride etherate were different from those of the above system. The total yields were similarly as low as 24% after 24 hr at room temperature, but an extreme inclination of the products to **3** was observed. A mixture of boron trifluoride - sulfuric acid known as an effective mixed catalyst system for the Friedel-Crafts alkylation seems to have an ionized form.[8] Therefore, the observed rapid establishment of the equilibrium could be ascribed to the increased dielectric property of the reaction system. Similar effects of addition of aluminum trichloride and boron trifluoride etherate were observed in the reactions of **14** (Table 5).

The reaction of **1** with acetonitrile in sulfuric acid-acetic acid afforded 1-adamantylcarbinyl acetate (52%), **2** (9%) and **3** (trace), but no trace of 3-homoadamantyl acetate could be detected by GLC analysis.

Other fuctionalized 1-adamantylmethyl systems like tosylate and bromide were stable in acetonitrile - sulfuric acid at room temperature, indicating the lower reactivity of adamantylcarbinyl system than that of 1-adamantyl system[2c] in the Ritter reactions.

It should be mentioned that the Ritter reactions of **1** and **14** with acetonitrile afford both *N*-3-homoadamantyl acetamide (**2**) and *N*-1-adamantylmethyl acetamide (**3**) in contrast with the Koch-Haaf carboxylation of **1**, in which the exclusive formation of 3-homoadamantanecarboxylic acid is known,[3] even though both reactions are performed in sulfuric acid. Interesting effects of aluminum trichloride for the Ritter reaction were observed, in which the kinetically controlled product **2** was obtained in 21—23% yields compared to *ca.* 10% yields in the reactions without aluminum trichloride.

Experimental

Melting points were determined on a Yanagimoto micro-melting point apparatus (hot-stage type) and are uncorrected. NMR spectra were determined on a JEOLCO MINMAR spectrometer at 60 MHz using TMS as an internal standard and infrared spectra, on a JASCO Model IR-S infrared spectrophotometer. GLC analysis was carried out on a Yanagimoto Gas Chromatograph Model GCG-220 and a Hitachi Gas Chromatograph Model K-23 using 2 m column packed with Apiezon-L and/or Silicone SE-30. Percentage composition of the products was estimated by relative peak area (uncorrected). For microanalyses a Yanagimoto Automatic C.H.N. Corder Model MT-1 was used.

General Procedure for the Ritter Reactions. A mixture of 1-adamantylmethyl alcohol **1**[3] (0.2 g, 1.2 mmol) and/or 3-homoadamantanol **14**[5a] (0.2 g, 1.2 mmol) and acetonitrile (4 m*l*, 76.5 mmol) was added slowly to stirred concd. sulfuric acid (sp. gr., *ca.* 1.84, 1.5 m*l*). After stirring was continued for an appropriate time, the reaction mixture was poured onto ice-water (*ca.* 300 g) and the resulting mixture was neutralized with 10% aqueous sodium hydroxide, extracted with ether (100 m*l*×4) and the ether extracts were washed with water (100 m*l*×2) and dried (Na_2SO_4). Removal of the solvent afforded crude amides as a mixture of **2** and **3**. The crude products were analyzed by GLC. The results are summarized in Tables 1—4.

Isolation of 3-Homoadamantyl Acetamide (2) and *N*-1-Adamantylmethyl Acetamide (3). Crude amides obtained from the reactions of **1** (0.5 g, 3.0 mmol) with acetonitrile (10 m*l*, 191 mmol) in concd. sulfuric acid (3.5 g) at room temperature (*ca.* 15°C) for 40 hr, were purified on a silica-gel (Mallinckrodt, 100 mesh) column eluting with chloroform. From the first fractions, 45 mg (7.7%) of **2** was obtained as colorless crystals, mp 138—139°C (*n*-hexane - acetone).

Found: C, 75.38; H, 9.95; N, 6.65%. Calcd for $C_{12}H_{21}NO$: C, 75.31; H, 10.21; N, 6.76%.

From the second fractions, 215 mg (36.7%) of **3** was obtained as colorless crystals, mp 126—127°C (*n*-hexane - acetone).

Found: C, 75.61; H, 10.51; N, 6.78%. Calcd for $C_{12}H_{21}NO$: C, 75.31; H, 10.21; N, 6.76%.

Both **2** and **3** were identified by mixed-melting points determination and by the complete superposition of their IR spectra on those of authentic samples.

Preparation of 3-Homoadamantylamine (7). Preparation of this amine has been described in a Patent[6] *via* 3-homoadamantyl isocyanate (**6**) by using the Hofmann reaction of 3-homoadamantylcarboxamide. We prepared the amine similarly *via* **6**, though **6** was

prepared by the Curtius reaction of 3-homoadamantylcarbonyl azide **5**, since the Hofmann reaction caused considerable side reactions lowering the yield of **7** in our experiments. A solution of sodium azide (5.5 g, 0.085 mol) in 14 m*l* of water was added to a stirred ice-cooled solution of 3-homoadamantylcarbonyl chloride[9] prepared from 1.7 g (8.75 mmol) of 3-homoadamantylcarboxylic acid **4** and thionyl chloride. After stirring was continued overnight at room temperature, the mixture was diluted with water and extracted with ether (100 m*l*×3). The combined ether extracts were washed with water (30 m*l*×2) and dried (Na_2SO_4), which gave crude azide **5** (1.7 g) as an oil after removal of the solvent under reduced pressure. **5** had strong IR absorption bands at 2150 ($-N_3$) and 1705 (C=O) cm^{-1}, and it was directly decomposed by heating under reflux in 50 m*l* of dry benzene for 2 hr. Removal of the solvent afforded 1.4 g (95%) of **6** as colorless crystals, mp 150—152°C (lit,[6] 144—146°C), which had strong IR absorption at 2280 (-N=C=O) cm^{-1}.

A mixture of 1.15 g (6.0 mmol) of **6**, 10 m*l* of dioxane and 20 m*l* of 2N hydrochloric acid was heated under reflux overnight. The cooled reaction mixture was made alkaline with 10% aqueous sodium hydroxide and extracted with ether. The work-up gave colorless crystals of **7** (0.9 g, 91%), mp 193—194°C (lit,[6] 191—193°C).

Acetylation of *N*-3-Homoadamantylamine (7). A mixture of **7** (0.2 g, 1.21 mmol), dry pyridine (2 m*l*) and acetic anhydride (0.2 g, 1.96 mmol) was stirred at room temperature overnight. Addition of water resulted in the precipitation of crystals of **2**, which were filtered and recrystallized from *n*-hexane to give 0.2 g (80%) of pure **2**, mp 138—139°C.

Preparation of *N*-1-Adamantylmethyl Acetamide (3). This was prepared similarly as above by acetylation of 1-adamantylmethylamine[4] with acetic anhydride in pyridine as colorless crystals, mp 126—127°C (*n*-hexane) in 70% yield.

The Ritter Reaction of 1 with Acetonitrile in Sulfuric Acid - Acetic Acid. A mixture of **1** (0.2 g, 1.2 mmol) and acetonitrile (4 m*l*, 76.5 mmol) was added to a stirred mixture of acetic acid (1.5 m*l*) and sulfuric acid (1.5 m*l*). The mixture was stirred for 48 hr at room temperature (*ca.* 15°C) and the work-up product was analyzed on GLC. For the analysis authentic specimens of 1-adamantylcarbinyl acetate and 3-homoadamantyl acetate[5a] were used.

BULLETIN OF THE CHEMICAL SOCIETY OF JAPAN VOL. 43 1824—1828 (1970)

The Rearrangement of Chromanone Oximes with Lithium Aluminum Hydride

Shoei Ito[1]

College of General Education, Tohoku University, Kawauchi, Sendai

(Received November 28, 1969)

The lithium aluminum hydride reduction of 7-methoxychromanone oxime (I) and 7-methoxy-3-methylchromamone oxime (II) gave only the rearrangement product (the 2,3,4,5-tetrahydro-1,5-benzoxazepine derivative). 7-Methoxy-2-methylchromanone oxime (III) and 7-methoxy-2-isopropylchromanone oxime (IV) gave a mixture of the rearrangement product (secondary amine) and the normal reduction product (primary amine). 7-Methoxy-2-*t*-butylchromanone oxime (V) gave only the normal reduction product. The main conclusions to be drawn from these results are as follows: (1) The chromanone oximes without a C_2 substituent give only the rearrangement product. (2) The chromanone oximes with a C_2 substituent give a mixture of the normal reduction product and the rearrangement product. (3) The more bulky substituent at C_2 gives the more normal reduction product and the smaller quantity of the rearrangement product.

The reduction of ketoximes and aldoximes with lithium aluminum hydride has been reported, in numerous instances, to give the corresponding primary amine.[2] However, in the reduction of certain arylketoximes[3] and aldoximes[4], the pri-

1) Present address: Department of Chemistry, Faculty of Science, Hirosaki University, Hirosaki.

2) N. G. Gaylord, "Reduction with Complex Metal Hydrides," Interscience Publishers Inc., New York (1956), p. 751.

3) a) D. R. Smith, M. Maienthal and J. Tipton, *J. Org. Chem.*, **17**, 294(1952); b) R. E. Lyle and H. J. Troscianiec, *ibid.*, **20**, 1757(1955); c) M. N. Rerick, C. H. Trottier, R. A. Daignault and J. D. DeFoe, *Tetrahedron Lett.*, **1963**, 629; b) S. H. Graham and A. J. S. Williams, *Tetrahedron*, **21**, 3263(1965).

4) A. E. Petrarca and E. M. Emery, *Tetrahedron Lett.*, **1963**, 635.

mary amine was accompanied by an isomeric secondary amine which was produced by the migration of the aryl group. It has also been reported that the addition of aluminum chloride to lithium aluminum hydride increased the yield of the secondary amine.[3]

In most of the systems investigated, the secondary amine has been a minor product of the reduction, but in special cases of highly-substituted arylketoximes where the aryl group is part of the phenoxazine ring system, the exclusive product has been the secondary amine.[5]

In the reduction of tetramethylbenzocyclobutenone oxime with lithium aluminum hydride, the sole product is the secondary amine, and the primary amine has not been detected.[6] The lithium aluminum hydride reduction of tetramethylcyclobutenone oxime gave only the rearrangement product,[7] while the same reaction of cyclopentanone oxime gave the primary amine accompanied by the secondary amine.[3] Recently it has been reported that the reduction of benzylketoximes with lithium aluminum hydride in refluxing tetrahydrofuran gave the aziridine derivatives, together with primary amine.[8]

Inoue and his co-workers reported the rearrangement in the reduction of isoflavanone oximes with lithium aluminum hydride.[9] The reduction of isoflavanone oxime, 7-methoxyisoflavanone oxime, and 7,4′-dimethoxyisoflavanone oxime with lithium aluminum hydride in refluxing ether afforded the corresponding tetrahydro-1,5-benzoxazepine derivatives. The same reaction of flavanone oximes gave no rearrangement product, but only the normal reduction product (4-aminoflavan).

From these results it was considered that the position (C_2 or C_3) and the size of a substituent in the chromanone oxime may exert a remarkable influence on the reaction between the chromanone oximes, with or without a C_2 or C_3 alkyl substituent, and lithium aluminum hydride.

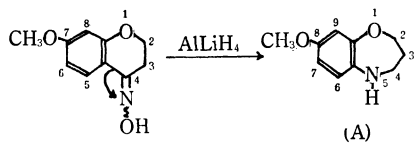

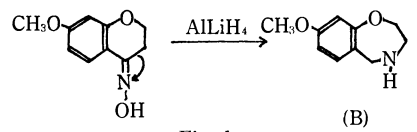

Fig. 1

The reaction of 7-methoxychromanone oxime (I) and 7-methoxy-3-methylchromanone oxime (II) with lithium aluminum hydride in refluxing ether and subsequent treatment with hydrochloric acid gave the amine hydrochlorides, X (mp 208—209°C) and XI (mp 182—183°C) respectively.

In both cases no by-product was found, and the X and XI were not identical with the 7-methoxy-4-aminochroman hydrochloride VI (mp 206—207°C) and the 7-methoxy-3-methyl-4-aminochroman hydrochloride VII (mp 205—206°C) which were obtained by the catalytic hydrogenation of I and II respectively.

The same reaction of 7-methoxy-2-methylchromanone oxime (III) gave two amine hydrochlorides, XII (mp 214—215°C) and VIII (mp 204—205°C). 7-Methoxy-2-isopropyl chromanone oxime (IV) also gave two amine hydrochlorides, XIII (mp 161—163°C) and IX (mp 196—197°C), by the same reaction. The VIII and IX were found to be identical with the 7-methoxy-2-methyl-4-aminochroman hydrochloride which were obtained by the catalytic hydrogenation of III and IV respectively.

The lithium aluminum hydride reduction of 7-methoxy-2-*t*-butylchromanone oxime (V) and subsequent treatment with hydrochloric acid gave only amine hydrochloride with a mp of 230—231°C (XIV); this was identical with the hydrochloride of the catalytic hydrogenation product of V.

The infrared spectra of X,XI, XII, and XIII all show a broad band at 3000—2400 cm^{-1} which is a characteristic absorption of secondary amine hydrochloride (ν^{+}_{NH}). On the other hand, the infrared spectra of VI, VII, VIII, IX, and XIV all show a broad band of $\nu^{+}_{NH_2}$ (primary amine salt) at 3200—2700 cm^{-1}.

The treatment of X, XI, XII, and XIII with acetic anhydride and pyridine gave acetamido derivatives, XV (mp 98—100°C), XVI (bp 160°C/2mmHg), XVII (mp 106—107°C), and XVIII (mp 95—96°C) respectively. The infrared spectra of XV, XVI, XVII, and XVIII all showed a characteristic band at 1660 cm^{-1} (ν_{CO} of CH_3CON) and no band of ν_{NH}.

The same treatment of the 4-aminochroman hydrochlorides, VI, VII, VIII, IX, and XIV, gave acetamido derivatives, XIX (mp 170—171°C), XX (mp 150—151°C), XXI (mp 184—185°C), XXII (mp 151—152°C), and XXIII (mp 177—178°C) respectively. The infrared spectra of XIX, XX, XXI, XXII, and XXIII all showed absorption bands of 3260 cm^{-1} (ν_{NH}) and 1640 cm^{-1} (ν_{CO}).

A comparison of the infrared spectra of these two series of acetamido derivatives shows that X, XI, XII, and XIII are secondary amine hydrochlorides.

The molecular weights of XV, XVI, XVII, and

5) M. Farfenist and E. Magnieu, *J. Amer. Chem. Soc.*, **80,** 6080 (1958).

6) H. Hart, J. A. Hartlege, R. W. Fish and R. R. Rafos, *J. Org. Chem.*, **31**, 2244 (1966).

7) F. Lautenshlaeyer and G. F. Wright, *Can. J. Chem.*, **41**, 863 (1963).

8) a) K. Kitahonoki, K. Kotera, Y. Matsukawa, S. Miyazaki, T. Okada, H. Takahashi and Y. Takano, *Tetrahedron Lett.*, **1965**, 1059. b) K. Kotera, T. Okada and S. Miyazaki, *ibid.*, **1967**, 841.

9) N. Inoue, S. Yamaguchi and S. Ito, This Bulletin, **41**, 2078 (1968).

Table 1. pK_a values of tetrahydrobenzoxazepines and 4-aminochromans

Compound (a)	pK_a	Compound (b)	pK_a
VI	8.62	X	5.05
VII	8.60	XI	5.05
VIII	8.65	XII	5.10
IX	8.60	XIII	5.35
XIV	8.55		

(a) Determined by UV method using Britton-Robinson's buffer solution.[12]
(b) Determined by titration using 1/100 N NaOH solution.

XVIII, as observed by mass spectrometry, were the same as those of XIX, XX, XXI, and XXII respectively.[10]

Accordingly, it may be considered that the X, XI, XII, and XIII compounds possess an A- or B-type structure which is derived by the ring enlargement of the chroman ring involving the migration of the phenyl group (A) or C_3 (B) to the nitrogen atom of the oximino group. (Fig. 1)

Since A is a monoalkylaniline derivative and B is a benzylamine derivative, there must be a remarkable difference between their pK_a values. The pK_a values of X, XI, XII, and XIII are shown in Table 1, along with those of the 4-aminochroman hydrochlorides, VI, VII, VIII, IX, and XIV.

From the data shown in Table 2 it may reasonably be concluded that the free amines of X, XI, XII, and XIII possess the A-type structure, which is a derivative of tetrahydrobenzoxazepine.

The summarized results of the lithium aluminum hydride reduction of the chromanone oximes are shown in Table 2. The reduction of flavanone oximes (2-phenylchromanone oximes) with lithium aluminum hydride gave only the corresponding 4-aminoflavans, not the rearrangement product (the secondary amine). On the other hand, the same reaction of isoflavanone oximes (3-phenylchromanone oximes) gave the rerrangement products, exclusively, not the corresponding 4-aminoisoflavan.[9]

As is shown in Table 1, 7-methoxychromanone oxime (I) and 7-methoxy-3-methylchromanone oxime (II) give the rearrangement products exclusively.

It is clear that the substituent on C_2 or C_3 exerts a remarkable influence on the yield of the rearrangement product in this reaction.

7-Methoxy-2-methylchromanone oxime (III) gives the rearrangement product in a 50% yield and the 4-amino compound in a 10% yield. 7-Methoxy-2-isopropylchromanone oxime (IV) gives the rerrangement product in a 35% yield and the 4-amino compound in a 50% yield. 7-Methoxy-2-*t*-butylchromanone oxime (V) does not give the rearrangement product, but only the corresponding 4-amino compound.

Thus, it is evident that the more bulky substituent at C_2 gives the more normal reduction product (4-aminochroman) and the smaller quantity of the rearrangement product. The chromanone oxime with a substituent at C_3 and the unsubstituted chromanone oxime give only the rearrangement product and no 4-aminochroman derivative.

The mechanism involved in the rearrangement reaction of chromanone oxime with lithium aluminum hydride will be reported by Kitahara and his co-workers in the near future.

Experimental

All the melting points are uncorrected. The infrared spectra were recorded with a Hitachi EPI-510 infrared spectrophotometer.

7-Methoxychromanone Oxime (I), 7-Methoxy-3-methylchromanone Oxime (II), 7-Methoxy-2-methylchromanone Oxime (III), 7-Methoxy-2-isopropylchromanone Oxime (IV), and 7-Methoxy-2-*t*-butylchromanone Oxime (V). *General Procedure.* The chromanone (1 g)[11] was refluxed for 10 hr with hydroxylamine hydrochloride (1 g), anhydrous ethanol (10 ml), and pyridine (10 ml). After cooling, the reaction mixture was poured into water; the precipitate was then recrystallized from dilute ethanol to give the

Table 2. Reduction of chromanone oximes

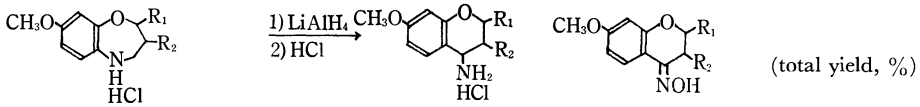

		(yield, %)	(yield, %)	(total yield, %)
$R_1=R_2=H$;	I	VI (0)	X (70)	(70)
$R_1=H$, $R_2=CH_3$;	II	VII (0)	XI (85)	(85)
$R_1=CH_3$, $R_2=H$;	III	VIII (10)	XII (50)	(60)
$R_1=CH(CH_3)_2$, $R_2=H$;	IV	IX (50)	XIII (35)	(85)
$R_1=C(CH_3)_3$, $R_2=H$;	V	XIV (80)	(0)	(80)

10) The details will be reported elsewhere.
11) The synthesis of these chromanones will be reported elsewhere by N. Inoue and his co-workers.
12) H. T. S. Britton and R. A. Robinson, *J. Chem. Soc.*, **1931**, 1456.

oxime almost quantitatively. The analytical data of chromanone oximes and their melting points are reported in Table 3.

Table 3. Chromanone oximes

Chromanone oxime	Mp (°C)	Formula	Analysis % Found N	Calcd N
I	135—136	$C_{10}H_{11}O_3N$	7.42	7.25
II	115—116	$C_{11}H_{13}O_3N$	6.67	6.76
III	161—163	$C_{11}H_{13}O_3N$	6.72	6.76
IV	94—95	$C_{13}H_{17}O_3N$	5.89	5.95
V	158—159	$C_{14}H_{19}O_3N$	5.72	5.62

7-Methoxy-4-aminochroman Hydrochloride (VI), 7-Methoxy-3-methyl-4-aminochroman Hydrochloride (VII), 7-Methoxy-2-methyl-4-aminochroman Hydrochloride (VIII), 7-Methoxy-2-isopropyl-4-aminochroman Hydrochloride (IX), and 7-Methoxy-2-*t*-butyl-4-aminochroman Hydrochloride (XIV). *General Procedure.* The oxime (1 g) in acetic acid (50 m*l*) containing 0.5 m*l* of 70% perchloric acid was hydrogenated by the usual manner at ordinary pressure and temperature in the presence of 1 g of 5% palladium on carbon.[13] The catalyst was then filtered off, and the acetic acid solution was concentrated under reduced pressure. To the residue, 6N hydrochloric acid was added to give crystals, which were then recrystallized from a suitable solvent. All the experimental results are summarized in Table 4.

By the usual method, the hydrochloride was acetylated with acetic anhydride in the presence of pyridine. The analytical data of these acetamido derivatives and their melting points are reported in Table 5.

Reduction of 7-Methoxychromanone Oxime (I) with Lithium Aluminum Hydride. To a swirling suspension of 1.9 g of lithium aluminum hydride in 100 m*l* of ether, there was added, drop by drop and at room temperature, a solution of 1.9 g of I in 150 m*l* of ether. After it had been refluxed for 24 hr, the reaction mixture was decomposed with water under cooling with ice. The ether layer was washed with 1N sodium hydroxide and water, and then dried over anhydrous sodium sulfate. After the removal of the solvent, 6N hydrochloric acid was added to give 1.4 g of crude crystals (90% yield). Recrystallization from ethanol gave 0.9 g of 8-methoxy-2,3,4,5-tetrahydro-1,5-benzoxazepine hydrochloride (X); mp 208—210°C. ν_{NH}^{+} 3000—2400 cm^{-1}.

Found: C, 55.43; H, 6.28; N, 6.38%. Calcd for $C_{10}H_{14}O_2NCl$: C, 55.60; H, 6.55; N, 6.49%.

By the usual method, the hydrochloride (X) was acetylated with pyridine-acetic anhydride to give a viscous liquid; bp 160—180°C/2 mmHg. On standing at room temperature the liquid gradually deposited crystals of an amide; mp 98—100°C. ν_{COCH_3} 1660 cm^{-1}.

Found: C, 64.63; H, 6.51; N, 5.93%. Calcd for $C_{12}H_{15}O_3N$: C, 65.14; H, 6.83; N, 6.33%.

Reduction of 7-Methoxy-3-methylchromanone Oxime (II) with Lithium Aluminum Hydride. A solution of 1 g of II in 100 m*l* of ether was added, drop by drop and at room temperature, to a swirling suspension of lithium aluminum hydride in 80 m*l* of ether. After it had been allowed to reflux for 24 hr, the reaction mixture was decomposed with water under cooling with ice. The layer was washed with 1N sodium

Table 5. 4-Acetamidochromans

Compound	Mp (°C)	Formula	Analysis % Found (Calcd) C	H	N
XIX	170—171	$C_{12}H_{15}O_3N$	65.28 (65.14)	6.71 (6.83)	6.25 (6.33)
XX	150—151	$C_{13}H_{17}O_3N$	66.27 (66.36)	7.04 (7.28)	5.96 (5.95)
XXI	184—185	$C_{13}H_{17}O_3N$	66.62 (66.36)	7.13 (7.28)	5.96 (5.95)
XXII	151—152	$C_{15}H_{21}O_3N$	68.12 (68.41)	7.98 (8.04)	5.36 (5.32)
XXIII	177—178	$C_{16}H_{23}O_3N$	69.32 (69.28)	8.24 (8.36)	5.12 (5.05)

Table 4. 4-Aminochroman hydrochlorides

Compound	Yield %	Mp (°C)	Recryst. solvent	Formula	Analysis % Found (Cacld) C	H	N
VI	70	206—207	Ethanol	$C_{10}H_{14}O_2NCl$	55.41 (55.60)	6.32 (6.55)	6.43 (6.49)
VII	85	205—206	Ethanol	$C_{11}H_{16}O_2NCl$	57.62 (57.45)	7.18 (7.04)	6.07 (6.09)
VIII	80	204—205	Ethanol	$C_{11}H_{16}O_2NCl$	57.21 (57.45)	7.02 (7.04)	6.08 (6.09)
IX	72	195—196	Ethyl acetate	$C_{13}H_{20}O_2NCl$	60.48 (60.57)	7.65 (7.82)	5.28 (5.44)
XIV	70	230—231	Ethyl acetate	$C_{14}H_{22}O_2NCl$	61.66 (61.86)	8.07 (8.16)	5.13 (5.15)

13) Five percent palladium on carbon, obtained from the Kawakami Research Institute, was used in the experimental.

hydroxide and water, and then dried over sodium sulfate. After the removal of the ether, 6N hydrochloric acid was added to give a solid (870 mg, 85% yield). Recrystallization from chloroform-benzene gave 500 mg of 8-methoxy-3-methyl-2,3,4,5-tetrahydro-1,5-benzoxazepine hydrochloride (XI); mp 182—183°C. ν^{+}_{NH} 3000—2400 cm^{-1}.

Found: C, 57.67; H, 7.01; N, 6.10%. Calcd for $C_{11}H_{16}O_2NCl$: C, 57.45; H, 7.04; N, 6.09%.

By the usual method, the hydrochloride (XI) was acetylated with pyridine-acetic anhydride to give a liquid; bp 160—180°C/2 mmHg. ν_{COCH_3} 1660 cm^{-1}.

Found: C, 66.02; H, 6.95; N, 5.65%. Calcd for $C_{13}H_{17}O_3N$: C, 66.36; H, 7.28; N, 5.95%.

Reduction of 7-Methoxy-2-methylchromanone Oxime (III) with Lithium Aluminum Hydride. A solution of III in 130 m*l* of ether was added, drop by drop and at room temperature, to a swirling suspension of 1 g of lithium aluminum hydride in 130 m*l* of ether. After it had been refluxed for 24 hr, the reaction mixture was decomposed with water under cooling with ice. The ether layer was washed with 1N sodium hydroxide and water, and then dried over anhydrous sodium sulfate. After the removal of the solvent, 6N hydrochloric acid was added; it was then allowed to stand overnight at room temperature, and the solid which separated (530 mg, 50%) was recrystallized from ethanol to give 400 mg of 8-methoxy-2-methyl-2,3,4,5-tetrahydro-1,5-benzoxazepine hydrochloride (XII); mp 214—215°C, ν^{+}_{NH} 3000—2400 cm^{-1}.

Found: C, 57.20; H, 7.25; N, 6.05%. Calcd for $C_{11}H_{16}O_2NCl$: C, 57.45; H, 7.04; N, 6.09%.

The filtrate was allowed to stand overnight under cooling with ice; the solid which thus separated (110 mg, 10%) was identical with 7-methoxy-2-methyl-4-aminochroman hydrochloride (VIII).

By the usual method, the hydrochloride (XII) was acetylated with pyridine-acetic anhydride; this gave crystals which were then recrystallized from benzene-petroleum ether to give an amide; mp 106—107°C, ν_{COCH_3} 1660 cm^{-1}.

Found: C, 66.58; H, 7.21; N, 5.72%. Calcd for $C_{13}H_{17}O_3N$: C, 66.36; H, 7.28; N, 5.95%.

Reduction of 7-Methoxy-2-isopropylchromanone Oxime (IV) with Lithium Aluminum Hydride. To a swirling suspension of 2 g of lithium aluminum hydride in 100 m*l* of ether, there was added, drop by drop at room temperature, a solution of 2 g of IV in 150 m*l* of ether. The reaction mixture was then treated as above. After the removal of the solvent, 6N hydrochloric acid was added; the solution was subsequently allowed to stand overnight at room temperature. The solid which separated (1.03 g, 50%) was filtered and recrystallized from chloroform to give colorless crystals which were identical with 7-methoxy-2-isopropyl-4-aminochroman hydrochloride (IX). After filtrate had been allowed to stand overnight under cooling with ice, the solid which separated (720 mg, 35%) was filtered and recrystallized from ethyl acetate to give 8-methoxy-2-isopropyl-2,3,4,5-tetrahydro-1,5-benzoxazepine hydrochloride (XIII); mp 161—163°C, ν^{+}_{NH} 3000—2400 cm^{-1}.

Found: C, 61.65; H, 8.02; N, 5.05%. Calcd for $C_{14}H_{22}O_2NCl$: C, 61.86; H, 8.16; N, 5.32%.

By the usual manner, the hydrochloride (XIII) was acetylated with pyridine-acetic anhydride. Recrystallization from dilute methanol then gave an amide; mp 95—96°C, ν_{COCH_3} 1660 cm^{-1}.

Found: C, 68.12; H, 7.93; N, 5.35%. Calcd for $C_{15}H_{21}O_3N$: C, 68.41; H, 8.04; N, 5.32%.

Reduction of 7-Methoxy-2-*t*-butylchromanone Oxime (V) with Lithium Aluminum Hydride. To a swirling suspension of 1.5 g of lithium aluminum hydride in 100 m*l* of ether, there was added, drop by drop and at room temperature, a solution of 1.5 g of V in 100 m*l* of ether. The solid (1.32 g, 80%) obtained by the usual treatment was recrystallized from ethyl acetate to give colorless crystals which were identical with 7-methoxy-2-*t*-butyl-4-aminochroman hydrochloride (XIV).

Methods of the pK_a Determination of Amines. *(A) Determination by the Titration Method.* The values of pK_a in Table 1 (Compounds VI, VII, VIII, IX, and XIV) were taken as the values of the amines at the mid-points of the titration curves, plotting the volume of 1/100 N aqueous sodium hydroxide against pH.

(B) Determination by the UV Method. The ultraviolet spectra were recorded with a Hitachi EPI-032 ultraviolet spectrophotometer. The values of pK_a in Table 1 (Compounds X, XI, XII, and XIII) were taken as the pH values of the amines in the Britton-Robinson buffer solution at the mid-points of the titration curves, plotting the absorbance at λ_{max} of the free amines against pH. The concentrations and the λ_{max} values of these amines are shown in Table 6.

Table 6.

Amine	Concentration (mol/*l*)	λ_{max} (mμ)
X	2.71×10^{-4}	292.5
XI	2.43×10^{-4}	292
XII	2.71×10^{-4}	292.5
XIII	2.89×10^{-4}	293.5

The author wishes to express his gratitude to Professor Naoto Inoue and Professor Shozo Yamaguchi for their helpful discussions and encouragement throughout the course of this work.

BULLETIN OF THE CHEMICAL SOCIETY OF JAPAN VOL. 43 1829—1834 (1970)

Studies of Peptide Antibiotics. XVIII. The Synthesis of Tyrocidine E[1,2]

Nobuo MITSUYASU, Shuji MATSUURA, Michinori WAKI, Motonori OHNO,[3] Satoru MAKISUMI and Nobuo IZUMIYA

Laboratory of Biochemistry, Faculty of Science, Kyushu University, Hakozaki, Fukuoka

(Received December 1, 1969)

The synthesis of cyclic decapeptide, *cyclo*-L-phenylalanyl-D-phenylalanyl-L-asparaginyl-L-glutaminyl-L-phenylalanyl-L-valyl-L-ornithyl-L-leucyl-D-phenylalanyl-L-prolyl, which has the amino acid sequence designated as tyrocidine E by Kurahashi, and the chemical and biological properties of the synthetic product, have been described. The degree of the activity of the synthetic product toward the Gram positive microorganisms is nearly the same as that of tyrocidine A. The results indicate that the L-tyrosine residue in the molecule of tyrocidine A can be replaced by L-phenylalanine without influencing activity.

Tyrocidine E is a new basic polypeptide isolated by Kurahashi and his coworkers[4] from an incubation mixture in a cell-free enzyme system of *Bacillus brevis* ATCC 8185 when both tryptophan and tyrosine were subtracted from the standard culture mixture for the biosynthesis of tyrocidine A, B and C. They have suggested the structure of tyrocidine E to be a cyclic decapeptide shown as XVI[4] in Fig. 1 by comparison of the amino acid composition of a sample designated as tyrocidine E with that of tyrocidine A, since the amino acid sequence of tyrocidine A has been already established.[5,6] However, they did not mention the property of an antibacterial activity of tyrocidine E and data such as melting point, specific rotation and elemental analysis.

We reported previously the synthesis of tyrocidine A[6] and B,[7] and have been attempting to synthesize other tyrocidines. This paper describes the synthesis of cyclic decapeptide hydrochloride (XVI·HCl) having the amino acid sequence of tyrocidine E (Fig. 1), and the chemical and biological properties of the synthetic product.

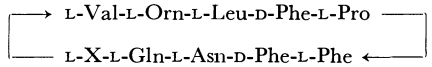

Fig. 1. Structure of tyrocidine E (XVI) and A (XVII).
X represents an amino acid residue such as Phe (XVI) and Tyr (XVII).

The synthesis of the pentapeptide derivative, Z(OMe)-Phe-D-Phe-Asn-Gln-Phe-$NHNH_2$ (VI), was achieved as follows (Fig. 2). The tripeptide derivative (III) of the C-terminal moiety was built up by stepwise elongation from the carboxyl toward the amino end to minimize racemization. The condensation of benzyloxycarbonyl-glutamine *p*-nitrophenyl ester with phenylalanine ethyl ester gave dipeptide derivative (I). This was hydrogenated in the presence of palladium black in a mixture of methanol and dimethylformamide containing an equivalent of hydrogen chloride to give dipeptide ester hydrochloride (II). The condensation of benzyloxycarbonyl-asparagine *p*-nitrophenyl ester with II gave acyl tripeptide ester (III) which was converted to tripeptide ester hydrochloride (IV) by the catalytic hydrogenation as described for II. In a previous study[6] the decarbobenzoxylation of the protected di- and tripeptide stages was performed by treatment with hydrogen bromide in acetic acid and the oily products obtained were contaminated by a small amount of impurities. However, the decarbobenzoxylation step in the

1) A part of this work was presented at the 21st Annual Meeting of Chemical Society of Japan, Osaka, April, 1968 (Preprints, Vol. 3, p. 2242), and communicated briefly; N. Mitsuyasu and N. Izumiya, *Experientia*, **26**, in press (1970).

2) The following abbreviations are used; Z-, benzyloxycarbonyl; Z(OMe)-, *p*-methoxybenzyloxycarbonyl; -ONp, *p*-nitrophenyl ester; -OEt, ethyl ester; $-NHNH_2$, hydrazide; $-N_3$, azide; TEA, triethylamine; DMF, dimethylformamide. Amino acid symbols except for D-Phe denote L-configuration.

3) Present address: Department of Chemistry, College of General Education, Kyushu University, Fukuoka.

4) K. Fujikawa, Y. Sakamoto, T. Suzuki and K. Kurahashi, *Biochim. Biophys. Acta*, **169**, 520 (1968).

5) A. Paladini and L. C. Craig, *J. Amer. Chem. Soc.*, **76**, 688 (1954).

6) M. Ohno and N. Izumiya, *ibid.*, **88**, 376 (1966); M. Ohno, T. Kato, S. Makisumi and N. Izumiya, This Bulletin, **39**, 1738 (1966).

7) K. Kuromizu and N. Izumiya, presented at the 7th Symposium on Peptide Chemistry at Tokyo University, Tokyo, Nov. 21, 1969; submitted for publication in *Experientia*.

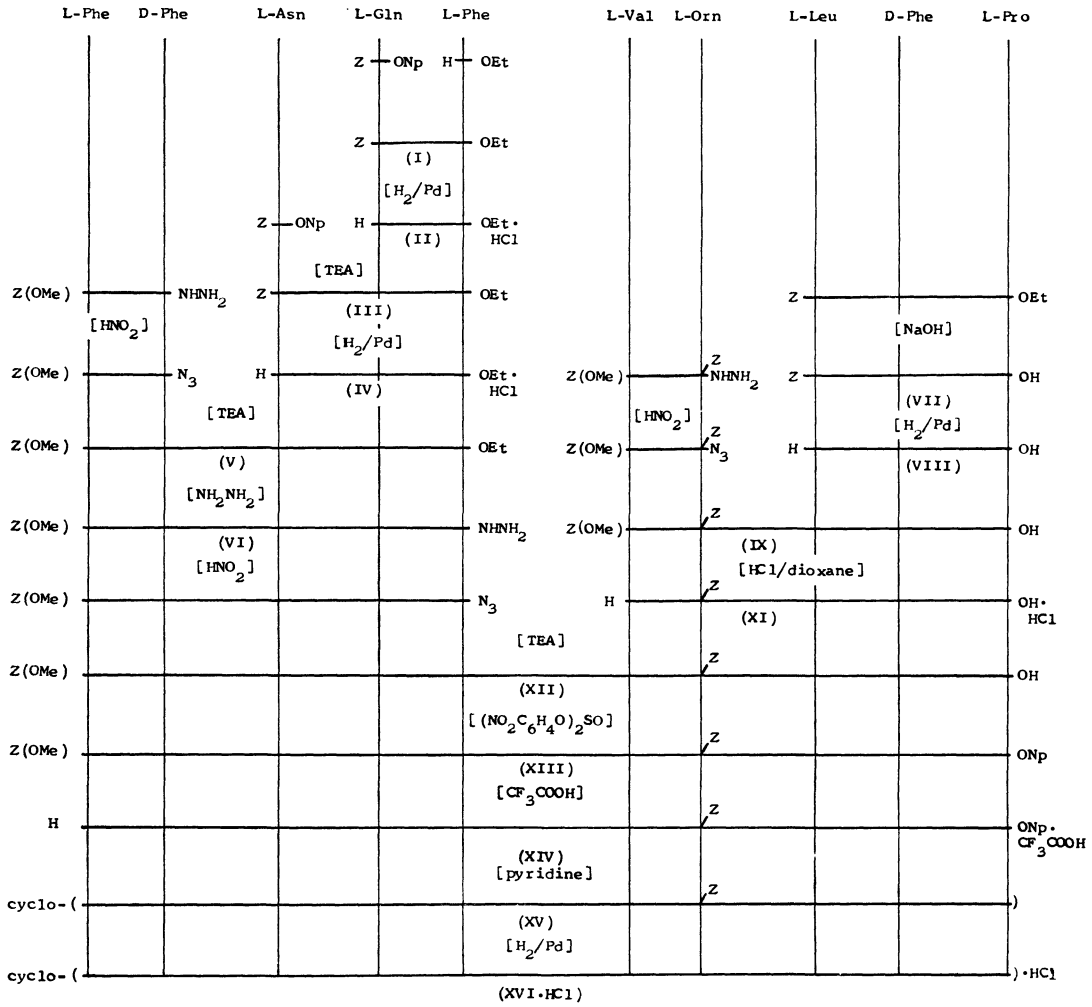

Fig. 2. Synthesis of tyrocidine E.

present study was much improved by this catalytic hydrogenation procedure which afforded pure crystalline products. The azide derived from Z(OMe)-Phe-D-Phe-$NHNH_2$[6] was allowed to react with tripeptide ester (IV) to afford acylpentapeptide ester (V) in a 73% yield. Compound V was converted to the corresponding hydrazide (VI) in a 97% yield by treatment with hydrazine.

Another pentapeptide derivative, H-Val-Orn-(δ-Z)-Leu-D-Phe-Pro-OH·HCl (XI), was prepared as follows (Fig. 2). The free tripeptide (VIII) was prepared from Z-Leu-D-Phe-Pro-OEt by saponification and successive hydrogenation in a mixture of methanol, acetic acid and water. The azide derived from Z(OMe)-Val-Orn(δ-Z)-$NHNH_2$[8] was allowed to react with VIII in the presence of an equivalent amount of triethylamine to yield crystalline protected pentapeptide (IX)[9] in a 73% yield. Treatment of IX with twenty equivalents of hydrogen chloride in dioxane afforded pure crystalline pentapeptide hydrochloride (XI)[10] in a yield of 90%.

Subsequent synthesis of the cyclic decapeptide hydrochloride (XVI·HCl) was achieved as follows (Fig. 2). Condensation of the azide derived from VI with XI in the presence of two equivalents of triethylamine gave amorphous protected decapeptide (XII) in a yield of 80%. XII was converted

8) T. Kato, M. Kondo, M. Ohno and N. Izumiya, This Bulletin, **38**, 1202 (1965).

9) Acylpentapeptide acid (IX) was prepared previously by saponification of Z(OMe)-Val-Orn(δ-Z)-Leu-D-Phe-Pro-OEt; M. Waki and N. Izumiya, *J. Amer. Chem. Soc.*, **89**, 1278 (1967); This Bulletin, **40**, 1687 (1967).

10) Hydrochloride (XI) of the neutral pentapeptide was prepared by the action of hydrogen chloride on BOC-Val-Orn(δ-Z)-Leu-D-Phe-Pro-OH: see Ref. 6.

to the corresponding decapeptide *p*-nitrophenyl ester (XIII) with the action of twenty equivalents of di-*p*-nitrophenyl sulfite in the presence of pyridine. Removal of the *p*-methoxybenzyloxycarbonyl group from XIII by the action of trifluoroacetic acid yielded amorphous decapeptide *p*-nitrophenyl ester trifluoroacetate (XIV). Cyclization reaction of XIV in a large amount of hot pyridine gave crude benzyloxycarbonyl-substituted cyclic decapeptide (XV), which was then purified by passing its aqueous dioxane - methanol solution through columns of cation and anion exchangers. The yield of XV from XII was 40% after recrystallization. The homogeneity of XV was established by the criteria of thin-layer chromatography and by elemental analysis. Molecular weight determination using a vapor pressure osmometer demonstrated that the molecular weight of XV corresponded to that of cyclic decapeptide. The hydrogenation of XV in the presence of an equivalent amount of hydrogen chloride in methanol afforded cyclic decapeptide hydrochloride (XVI·HCl) in an 84% yield. The homogeneity of hydrochloride (XVI·HCl) was confirmed by thin-layer and paper chromatography, paper electrophoresis, elemental analysis and amino acid analysis.

Antibacterial activity toward several microorganisms was examined[11] (Table 1). In addition to synthetic XVI, synthetic tyrocidine A[6] and natural gramicidin S[12] were examined as reference compounds. It was found that the degree of the activities of synthetic XVI toward the Gram positive microorganisms was nearly the same as that of tyrocidine A, indicating that the L-tyrosine residue in the molecule of tyrocidine A can be replaced by the L-phenylalanine without influencing activity.

Syntheses of the cyclic decapeptides corresponding to the proposed structures for tyrocidine C[13] and D[14] is in progress in this laboratory.

Experimental

Melting points were uncorrected. The optical rotations were determined with a Yanagimoto Photometric Polarimeter, OR-20 type. Paper chromatography was performed on Toyo Roshi No. 52 with the following solvent systems: R_f^{I}, *n*-butanol - acetic acid - pyridine - water, 4 : 1 : 1 : 2 v/v; R_f^{II}, *n*-butanol - acetic acid - water, 4 : 1 : 2 v/v. Thin layer chromatography was performed on Merck silica gel G with the following solvent systems: R_f^1, *n*-butanol - acetic acid - pyridine - water 4 : 1 : 1 : 2 v/v; R_f^2, chloroform-methanol, 5 : 1 v/v; R_f^3, *n*-butanol - acetic acid - water, 4 : 1 : 2 v/v; R_f^4, *s*-butanol - pyridine - water, 75 : 15 : 10 v/v; R_f^5, chloroform - benzene - methanol, 6 : 3 : 1 v/v. Spots of materials possessing a free amino group on a thin layer plate were detected by spraying ninhydrin, and those of the amino group-blocked materials, by spraying 47% hydrobromic acid and then ninhydrin. Prior to analysis, the compounds were dried over phosphorus pentoxide at 60°C and 2 mmHg to a constant weight unless otherwise described.

Z-Gln-Phe-OEt (I). To a solution of phenylalanine ethyl ester hydrochloride (1.37 g, 6 mmol) dissolved in a mixture of TEA (0.84 m*l*, 6 mmol) and DMF (10 m*l*), a solution of benzyloxycarbonyl-glutamine *p*-nitrophenyl ester (2.0 g, 5 mmol) in DMF (5 m*l*) was added. After the solution had been allowed to stand for 6 hr at room temperature, it was diluted with water (250 m*l*). The crystalline precipitate was collected by filtration and washed successively with N hydrochloric acid, a 3% sodium bicarbonate solution and water. It was recrystallized from methanol-ether. Yield, 2.12 g (93%); mp 167—169°C; R_f^1 0.86; R_f^2 0.61; $[\alpha]_D^{15}$ −4.0° (*c* 1.0, DMF).

Found: C, 63.28; H, 6.40; N, 8.83%. Calcd for $C_{24}H_{29}O_6N_3$: C, 63.28; H, 6.42; N, 9.23%.

H-Gln-Phe-OEt·HCl (II). A solution of I (1.28 g, 2.8 mmol) dissolved in a mixture of 2.53N hydrogen chloride in methanol (1.23 m*l*) and DMF (10 m*l*) was hydrogenated in the presence of palladium black. After 6 hr the filtrate from the catalyst was concentrated to a small volume *in vacuo* and then ether was added. The resulting crystals were collected by filtration. Yield, 0.99 g (99%); mp 178—182°C; R_f^1 0.79; R_f^2 0.16; $[\alpha]_D^{15}$ +17.0° (*c* 1.0, DMF).

Found: C, 52.55; H, 6.69; N, 11.58%. Calcd for $C_{16}H_{23}O_4N_3 \cdot HCl \cdot \frac{1}{2}H_2O$: C, 52.38; H, 6.87; N, 11.46%.

Z-Asn-Gln-Phe-OEt (III). To a solution of II (0.54 g, 1.5 mmol) dissolved in a mixture of TEA (0.224 m*l*, 1.6 mmol) and DMF (10 m*l*), a solution of benzyloxycarbonyl-asparagine *p*-nitrophenyl ester (0.58 g, 1.5 mmol) in DMF (5 m*l*) was added. After the solution had been stood overnight at room temperature, it was diluted with water (150 m*l*). The crystalline product deposited was collected by filtration and washed successively with N hydrochloric acid, a 3% sodium bicarbonate solution and water (0.69 g). It was recrystallized from DMF-ethanol-ethyl acetate. Yield, 0.66 g (77%); mp 225—227°C; R_f^1 0.82; R_f^2 0.28; $[\alpha]_D^{15}$ −16.0° (*c* 0.5, DMF).

Found: C, 58.76; H, 6.25; N, 12.10%. Calcd for $C_{28}H_{35}O_8N_5$: C, 59.04; H, 6.19; N, 12.30%.

H-Asn-Gln-Phe-OEt·HCl (IV). This compound was prepared by the same procedure as for II. Hydrogenolysis of III (0.62 g, 1.09 mmol) in the presence of a 1.1 equivalent of hydrogen chloride afforded IV as amorphous solid. Yield, 0.50 g (97%); mp 199—202°C; R_f^1 0.73; R_f^2 0.05; $[\alpha]_D^{15}$ −8.0° (*c* 0.3, DMF).

Found: C, 49.08; H, 6.88; N, 14.10%. Calcd for $C_{20}H_{29}O_6N_5 \cdot HCl \cdot H_2O$: C, 49.03; H, 6.58; N, 14.30%.

Z(OMe)-Phe-D-Phe-Asn-Gln-Phe-OEt (V). A solution of Z(OMe)-Phe-D-Phe-$NHNH_2$[6] (0.44 g, 0.9 mmol) dissolved in a mixture of DMF (9 m*l*) and acetic acid (6 m*l*) was cooled to −5°C. To this solution, N hydrochloric acid (2.0 m*l*) was added, followed by N sodium nitrite (1.0 m*l*). After it had been stood for 5 min at

11) We are indebted to Dr. M. Shibata of Takeda Chemical Industries for the bioassay.

12) We wish to express our thanks to Mr. I. Kitazato of Meiji Seika Co. for the generous gift of crystalline gramicidin S dihydrochloride.

13) M. A. Ruttenberg, J. P. King and L. C. Craig, *Biochemistry*, **4**, 11 (1965).

14) M. A. Ruttenberg and B. Mach, *ibid.*, **5**, 2864 (1966).

this temperature, the solution was diluted with cold water (50 ml). The azide deposited was collected by filtration, washed with a 3% sodium bicarbonate solution and water, and then dried *in vacuo* at 0°C. To a chilled (−5°C) solution of IV (0.45 g, 0.9 mmol) dissolved in a mixture of TEA (0.14 ml, 1.0 mmol) and DMF (15 ml), the azide was added. The solution was stirred for 2 days at 0°C and then diluted with water (200 ml). The precipitate formed was collected by filtration and washed successively with 0.5M citric acid, a 3% sodium bicarbonate solution and water. Yield, 0.59 g (73%); R_f^1 0.88; R_f^2 0.57; R_f^3 0.76.

For analysis 80 mg of the product was recrystallized from DMF-ethanol-ether (60 mg); mp 212—215°C; $[\alpha]_D^{15}$ −16.4° (*c* 0.5, DMF).

Found: C, 62.78; H, 6.19; N, 10.86%. Calcd for $C_{47}H_{55}O_{11}N_7$: C, 63.14; H, 6.20; N, 10.97%.

Z(OMe)-Phe-D-Phe-Asn-Gln-Phe-NHNH$_2$ (VI). A solution of V (0.49 g, 0.55 mmol) and hydrazine hydrate (0.53 ml, 11 mmol) in DMF (15 ml) was allowed to stand at room temperature. After 24 hr hydrazine hydrate (0.27 ml, 5.5 mmol) was added to allow the reaction to proceed completely and the reaction mixture was stood at room temperature for another 24 hr. The solution was then evaporated *in vacuo* to remove the excess hydrazine, after which water (200 ml) was added to the residual solution; the gelatinous product deposited was collected by filtration. Yield, 0.47 g (97%); R_f^1 0.78; R_f^2 0.10; R_f^3 0.66.

For analysis 48 mg of the product was recrystallized from DMF-ether (36 mg); mp 218—221°C; $[\alpha]_D^{15}$ −23.5° (*c* 0.5, dimethylsulfoxide).

Found: C, 60.59; H, 6.27; N, 14.12%. Calcd for $C_{45}H_{53}O_{10}N_9 \cdot \frac{1}{2}H_2O$: C, 60.80; H, 6.12; N, 14.18%.

Z-Leu-D-Phe-Pro-OH (VII). To a solution of Z-Leu-D-Phe-Pro-OEt[6] (1.07 g, 2 mmol) dissolved in a mixture of methanol (15 ml) and dioxane (10 ml), N sodium hydroxide (4 ml) was added. Saponification was carried out at 0°C for 2 hr and then at room temperature for 2 hr. The progress of the reaction was followed by thin-layer chromatography. The solution was evaporated *in vacuo*, after which the residual solution was diluted with water (20 ml) and then acidified to pH 3 with N hydrochloric acid. The resulting oil was taken up twice with each 20 ml of ethyl acetate. The combined ethyl acetate solutions were washed with water, dried over sodium sulfate, and then evaporated *in vacuo*. Yield of an oily product, 0.91 g (89%); R_f^1 0.84; R_f^2 0.72.

H-Leu-D-Phe-Pro-OH (VIII). A solution of VII (0.52 g) dissolved in a mixture of methanol (3 ml), water (1 ml) and acetic acid (6 ml) was hydrogenated in the presence of palladium black. After 3 hr the filtrate from the catalyst was concentrated *in vacuo* and then a mixture of ether and petroleum ether (1 : 1) was added. The resulting amorphous powder was collected by filtration. Yield, 0.36 g (73%); R_f^1 0.75; R_f^2 0.00; R_f^I 0.68.

Z(OMe)-Val-Orn(δ-Z)-Leu-D-Phe-Pro-OH (IX). A solution of Z(OMe)-Val-Orn(δ-Z)-NHNH$_2$[8] (0.50 g, 0.95 mmol) in acetic acid (15 ml) was cooled to −5°C. To this, N hydrochloric acid (2.1 ml) was added, followed by N sodium nitrite (1.0 ml). After it had been stirred for 5 min at this temperature, the solution was diluted with cold water (150 ml). The azide precipitated was treated as for the preparation of V. The dried azide was added to a chilled solution of VIII (0.36 g, 0.95 mmol) dissolved in a mixture of TEA (0.133 ml, 0.95 mmol) and DMF (10 ml). After the solution had been stirred for 2 days at 0°C, it was concentrated to a small volume and then acidified with cold 0.5M citric acid. The resulting crystals were collected by filtration, washed with 0.5M citric acid and water. It was recrystallized from methanol-ether-petroleum ether. Yield, 0.62 g (73%); mp 138—140°C; R_f^1 0.83; R_f^2 0.54; $[\alpha]_D^{17}$ −20.1° (*c* 1.0, DMF). In order to confirm the homogeneity of the product a small portion was hydrogenated; a single ninhydrin positive spot was observed on a thin-layer chromatogram, R_f^1 0.65.

We prepared compound (IX) by saponification of the corresponding acyl-pentapeptide ethyl ester; $[\alpha]_D^{20}$ −18.2° (*c* 1.0, DMF).[9]

H-Val-Orn(δ-Z)-Leu-D-Phe-Pro-OH·HCl(XI). To a solution of IX (0.53 g, 0.6 mmol) in dioxane (10 ml), 2.57N dry hydrogen chloride in dioxane (4.67 ml, 12 mmol) and anisole (0.1 ml) were added. The solution was then allowed to stand at room temperature and the reaction was followed by thin layer chromatography. After 9 hr the solution was concentrated to a small volume *in vacuo* and ether was added. The crystals precipitated were collected by filtration and washed thoroughly with ether. Yield, 0.41 g (90%); mp 139—142°C (decomp.); R_f^1 0.73; R_f^2 0.11; R_f^3 0.56; $[\alpha]_D^{15}$ −19.8° (*c* 0.5, DMF).

Found: C, 58.29; H, 7.41; N, 10.54%. Calcd for $C_{38}H_{54}O_8N_6 \cdot HCl \cdot \frac{3}{2}H_2O$: C, 58.04; H, 7.43; N, 10.69%.

We prepared compound (X) by the treatment with hydrogen chloride of the corresponding BOC-pentapeptide acid; $[\alpha]_D^{20}$ −22.5° (*c* 2.12, DMF).[10]

Z(OMe)-Phe-D-Phe-Asn-Gln-Phe-Val-Orn(δ-Z)-Leu-D-Phe-Pro-OH (XII). A solution of VI (0.42 g, 0.475 mmol) dissolved in DMF (6 ml) was treated with N hydrochloric acid (0.6 ml) and N sodium nitrite (0.52 ml). After it had been stood for 5 min, the solution was diluted with cold water (50 ml). The azide deposited was treated as described previously. The dried azide was added to a chilled solution of XI (0.38 g, 0.5 mmol) dissolved in a mixture of TEA (0.14 ml, 1.0 mmol) and DMF (8 ml). The solution was stirred for 2 days at 0°C, and then diluted with 0.25M citric acid (30 ml). The resulting product was collected by filtration and washed with water. Yield, 0.65 g (80%); R_f^1 0.82; R_f^2 0.00; R_f^3 0.90; R_f^4 0.81; R_f^5 0.77. In order to establish further the homogeneity of the product, a small portion was hydrogenated; R_f^1 0.26; R_f^5 0.07; a single ninhydrin-positive spot was observed on paper electrophoresis with pH 1.8 buffer:[6] relative mobility to gramicidin S[12] 0.89.

For analysis 100 mg of the product was recrystallized from DMF-ether (61 mg); mp 236—239°C; $[\alpha]_D^{15}$ −31.8° (*c* 0.5, dimethyl sulfoxide).

Found: C, 61.98; H, 6.73; N, 11.30%. Calcd for $C_{83}H_{103}N_{13}O_{18} \cdot 2H_2O$: C, 62.04; H, 6.71; N, 11.33%.

Z(OMe)-Phe-D-Phe-Asn-Gln-Phe-Val-Orn(δ-Z)-Leu-D-Phe-Pro-ONp(XIII). To a suspension of XII (196 mg, 0.125 mol) in anhydrous pyridine (5 ml) was added di-*p*-nitrophenyl sulfite (810 mg, 25 mmol) The mixture was stirred for 2 days at room temperature and then evaporated *in vacuo*. The oily residue was triturated with a mixture of ether and petroleum ether (1 : 1). The solid mass was collected by filtration and

washed with a mixture of ether and petroleum ether (1 : 1) until yellow color could not be discerned upon the addition of N sodium hydroxide to the filtrate. A faintly yellow product was thus obtained (179 mg); R_f^1 0.98; R_f^2 0.74. The *p*-nitrophenyl ester content of this product was estimated to be 104% by means of the method described by Schwyzer and Sieber,[15] except that a mixture of DMF and N sodium hydroxide (1 : 1) was used as the solvent and the absorption measurements were performed at the wavelength of 412 mμ. This product was used for the next reaction without further purification.

H-Phe-D-Phe-Asn-Gln-Phe-Val-Orn(δ-Z)-Leu-D-Phe-Pro-ONp·CF_3COOH (XIV). To a mixture of XIII (179 mg) and anisole (0.2 m*l*), anhydrous trifluoroacetic acid (2.3 m*l*) was added at −5°C. When swirled, the reaction mixture formed a solution after 10 min. The solution was then evaporated *in vacuo* at 0°C, and the resulting oily residue was triturated with ether. The product was collected by filtration and washed with ether: yield, 199 mg; R_f^1 0.87.

***cyclo*-(Phe-D-Phe-Asn-Gln-Phe-Val-Orn(δ-Z)-Leu-D-Phe-Pro) (XV).** A solution of XIV (199 mg) dissolved in a mixture of acetic acid (0.3 m*l*) and DMF (10 m*l*) was stirred, drop by drop, into anhydrous pyridine (60 m*l*) kept at 65—70°C over a 3.5 hr period. The solution was further stirred for 1.5 hr at this temperature, and then evaporated to dryness *in vacuo*. The resulting residue was collected by filtration with the aid of water, dried *in vacuo* (131 mg), and then dissolved in 15 m*l* of a mixture of dioxane, methanol and water (1 : 3 : 1). This solution was passed successively through columns (2×6.5 cm) of Dowex −50 (H^+ form) and Dowex-1 (OH^- form) which had been washed with a mixture of dioxane, methanol and water (1 : 3 : 1). The columns were then washed with the same solvent. The filtrate and washings were combined (total 150 m*l*) and evaporated *in vacuo*. The oily residue crystallized upon the addition of water (76 mg). It was recrystallized from dioxane-water. Yield, 68 mg (40% from XII); mp 252—255°C (decomp.); R_f^1 0.92; R_f^2 0.57; $[\alpha]_D^{23}$ −129° (*c* 0.5, methanol).

Found: C, 62.66; H, 6.80; N, 12.32%. Calcd for $C_{74}H_{93}O_{14}N_{13}\cdot 2H_2O$: C, 62.39; H, 6.86; N, 12.78%.

The molecular weight was determined on a Hitachi Osmometer, type 115, using methanol as the solvent. Found: 1435. Calcd for the benzyloxycarbonyl-substituted cyclic decapeptide dihydrate: 1425.

***cyclo*-(Phe-D-Phe-Asn-Gln-Phe-Val-Orn-Leu-D-Phe-Pro)·HCl (XVI·HCl).** A solution of XV(51 mg, 0.036 mmol) dissolved in a mixture of 0.046 N dry methanolic hydrogen chloride (0.87 m*l*, 0.041 mmol) and methanol (3.5 m*l*) was hydrogenated in the presence of palladium black. The progress of the reaction was followed by thin-layer chromatography. After 3 hr the filtrate from the catalyst was concentrated to a small volume (0.1 m*l*), and 2 m*l* of ether was added to give crystals. The crystals were collected by filtration and washed with ether. Yield, 39 mg (84%); mp 265—267°C (decomp.); $[\alpha]_D^{23}$ −126° (*c* 0.2, methanol). Homogeneity of the compound was ascertained as follows.

a) Paper chromatography: R_f^I 0.96; R_f^{II} 0.95.

b) Thin-layer chromatography: R_f^1 0.78; R_f^2 0.40.

c) Paper Electrophoresis: Paper, Toyo Roshi No. 52; solvent, formic acid-acetic acid-methanol-water (1 : 3 : 6 : 10 v/v) (pH 1.8); voltage gradient, 17 V/cm; charged period, 2.5 hr. Gramicidin S dihydrochloride[12] was used as the reference compound. Figure 3 shows

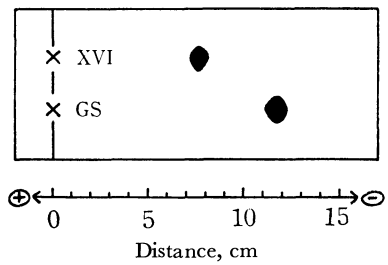

Fig. 3. Paper electrophoresis of synthetic cyclic decapeptide hydrochloride (XVI·HCl) and natural gramicidin S (GS) dihydrochloride.[12]

Table 1. Inhibitory activity of the three compounds on microorganisms

Minimum inhibitory concentration, μg/m*l*

A. Bouillon agar medium[a]

	Escherichia coli	*Proteus vulgaris*	*Staphylococcus aureus*	*Bacillus subtilis*	*Mycobacterium avium*
Synthetic XVI	>100	>100	10	5	>100
Tyrocidine A	>100	>100	8	8	>100
Gramicidin S	>100	>100	2	2	>100

B. Synthetic medium

	Escherichia coli	*Proteus vulgaris*	*Staphylococcus aureus*	*Bacillus subtilis*	*Mycobacterium avium*
Synthetic XVI	>100	>100	10	10	>100
Tyrocidine A	>100	>100	10	8	>100
Gramicidin S	>100	>100	2	2	>100

a) Usual bouillon agar medium, pH 7.0.

b) Stephenson-Whetham's medium (modified).

15) R. Schwyzer and P. Sieber, *Helv. Chim. Acta*, **40**, 624 (1957).

that XVI migrates more slowly toward the cathode than gramicidin S as observed for tyrocidine A.[6]

d) Elemental Analysis: The elemental analysis was carried out using a sample which had been dried over anhydrous phosphorus pentoxide at room temperature and 2 mmHg.

Found: C, 58.81; H, 6.96; N, 13.32%. Calcd for $C_{66}H_{87}O_{12}N_{13}\cdot HCl\cdot 3H_2O$: C, 58.94; H, 7.04; N, 13.54%.

e) Amino Acid ratios in the acid hydrolysate: Phe 3.90, Asp 1.00, Glu 1.03, Val 0.92, Orn 1.03, Leu 1.03, Pro 1.00, NH_3 1.89.[16]

Microbiological Assays.[11] The microorganisms employed are listed in Table 1. The minimum amount of the compound necessary for the complete inhibition of growth was determined by a dilution method with a bouillon agar medium and with a synthetic medium. In addition to the synthetic XVI·HCl, synthetic tyrocidine A hydrochloride[6] and natural gramicidin S dihydrochloride[12] were examined as reference compounds. Table 1 shows that the degree of the activities of synthetic XVI toward the Gram positive microorganisms was nearly the same as that of tyrocidine A.

16) We are indebted to Mr. K. Noda in this laboratory for the amino acid analysis.

The authors wish to express their thanks to Professor Kiyoshi Kurahashi of Osaka University for his interest throughout this work.

BULLETIN OF THE CHEMICAL SOCIETY OF JAPAN VOL. 43 1834—1839 (1970)

Reaction of Glycylglycine with Formaldehyde in the Presence of Cupric Ion[1]

Kosaku NODA, Motoaki BESSHO,[2] Tetsuo KATO and Nobuo IZUMIYA

Laboratory of Biochemistry, Faculty of Science, Kyushu University, Hakozaki, Fukuoka

(Received December 8, 1969)

The reaction mixture of glycylglycine with formaldehyde in an alkaline aqueous solution containing cupric ion at 100°C gave seven ninhydrin positive components which were identified as follows; α-hydroxymethylserine, serine, glycine, 3-carboxymethyl-4-imidazolidone, α-hydroxymethylseryl-glycine, serylglycine and glycylglycine. The yield of serylglycine increased in proportion to the amount of cupric ion, whereas the yield of 3-carboxymethyl-4-imidazolidone was maximum when no cupric ion was added. A single-step synthesis in preparative scale of serylglycine or 3-carboxymethyl-4-imidazolidone under the best condition was achieved in a good yield.

Sato, Okawa and Akabori[3] reported the synthesis of a diastereomeric mixture of threonine and allothreonine by the reaction of an aqueous alkaline solution of copper glycinate with acetaldehyde. Benoiton *et al.*[4] described a general preparation of β-hydroxy-α-amino acid by the condensation of copper glycinate with various aldehydes, ketones and α-keto acids under comparable conditions. Akabori *et al.*[5] observed that the reaction of glycine with formaldehyde in the presence of cupric ion caused formation of serine and an unidentified ninhydrin reactive substance. Later Otani and Winitz characterized the unidentified substance as α-hydroxymethylserine, and they indicated that this amino acid could be derived from the interaction of serine and formaldehyde with cupric ion.[6]

Regarding the reaction of glycyl peptide with aldehyde, Akabori *et al.*[7] attempted to introduce side-chains into polyglycine, which had been dispersed on a clay, with formaldehyde or acetaldehyde in an alkaline medium; they observed that 0.4—3.1% or 1.4—1.5% of glycine residues were converted to serine or threonine residues. Furuyama *et al.*[8] treated polyglycine with acetaldehyde in

1) Presented at the 17th and 21st Annual Meeting of the Chemical Society of Japan, Tokyo, April, 1964 and Osaka, April, 1968.

2) Present address: Eisai Research Laboratories, Eisai Co. Ltd., Bunkyo-ku, Tokyo.

3) M. Sato, K. Okawa and S. Akabori, This Bulletin, **30**, 937 (1957).

4) L. Benoiton, M. Winitz, R. F. Colman, S. M. Birnbaum and J. P. Greenstein, *J. Amer. Chem. Soc.*, **81**, 1726 (1959).

5) S. Akabori, T. T. Otani, R. Marshall, M. Winitz and J. P. Greenstein, *Arch. Biochem. Biophys.*, **83**, 1 (1959).

6) T. T. Otani and M. Winitz, *ibid.*, **90**, 254 (1960).

7) S. Akabori, K. Okawa and M. Sato, This Bulletin, **29**, 608 (1956).

8) T. Furuyama, F. Sakiyama and K. Narita, *ibid.*, **36**, 903 (1963).

liquid ammonia in the presence of metallic sodium; 7—8% of glycine residues were shown to be converted to threonines.

This paper will describe the isolation and characterization of several components from a reaction mixture of glycylglycine with formaldehyde in the presence of cupric ion. Convenient single-step synthesis of serylglycine, which was conceived as a consequence of these studies, will also be described.

We assumed the formation of either serylglycine or glycylserine as a major product when glycylglycine is subjected to the reaction with formaldehyde in the presence of cupric ion. The methylene group in copper glycylglycinate might be more active than that in free glycylglycine and the amino group in copper salt might be protected from unfavorable side reactions. This supposition suggested the possibility for such a reaction sequence shown in Fig. 1.

$$NH_2CH_2CO\text{-}NHCH_2COOH \xrightarrow[OH^-,\ Cu^{2+}]{HCHO}$$

$$NH_2CH(CH_2OH)CO\text{-}NHCH_2COOH$$

or $$NH_2CH_2CO\text{-}NHCH(CH_2OH)COOH$$

Fig. 1. Assumed reaction sequence.

In this investigation, several dipeptides such as serylglycine, glycylserine and α-hydroxymethylserylglycine were prepared in a conventional manner as the first step of the experiment. These dipeptides were to be used as authentic samples. For example, α-hydroxymethylserylglycine was synthesized as follows.[9]

$$\text{Z-HMSer} + \text{Gly-OBzl} \xrightarrow{DCC} \text{Z-HMSer-Gly-OBzl} \xrightarrow{H_2/Pd} \text{HMSer-Gly}$$

Fig. 2. Synthesis of a dipeptide.

We observed that a reaction mixture of glycylglycine and formaldehyde with cupric ion in an alkaline medium gave seven ninhydrin positive components which were identified by the use of an amino acid analyzer (Fig. 4-B). We could easily identify six components to be α-hydroxymethylserine, serine, glycine, α-hydroxymethylserylglycine, serylglycine and glycylglycine by means of paper chromatography and an amino acid analyzer. However, one component which emerged at the fourth peak in the chromatogram by the amino acid analyzer (Fig. 4-B) could not be characterized at this stage. Therefore, the reaction mixture was prepared on a large scale, and was fractionated with a column (1.8×110 cm) of Dowex 50 (NH_4^+ form) using 0.2M ammonium acetate buffer as a solvent.[10] Thus, the unidentified component emerging at the fourth peak could be isolated as crystals, and finally its structure was characterized as 3-carboxymethyl-4-imidazolidone (Cm-Iz) shown in Fig. 3, by means of elemental analysis, molecular weight determination and IR and NMR

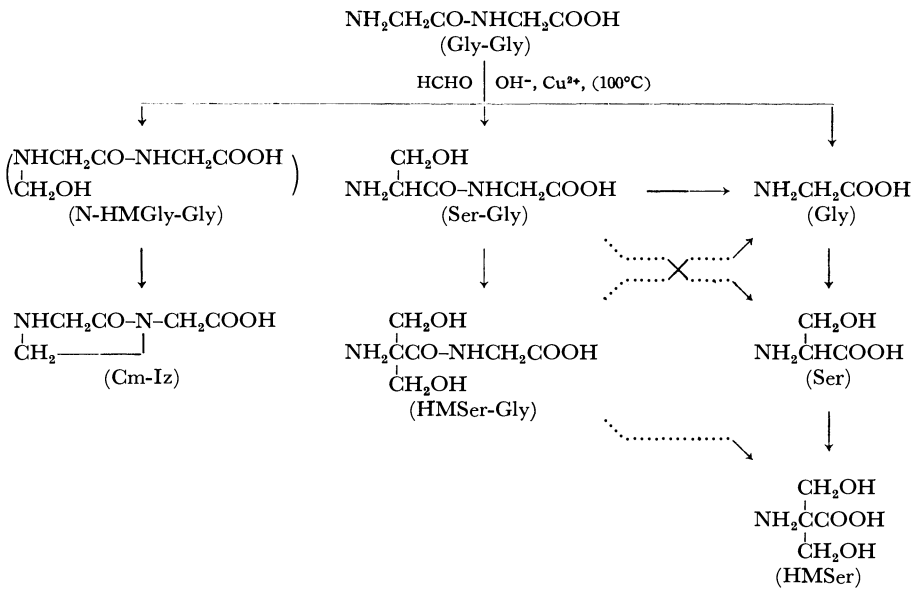

Fig. 3. Summary of the reaction of Gly-Gly and formaldehyde with cupric ion.

9) Abbreviations: Z-, benzyloxycarbonyl; -OBzl, benzyl ester; HMSer, α-hydroxymethyl-DL-serine; Cm-Iz, 3-carboxymethyl-4-imidazolidone. Amino acid symbols except Gly denote the DL-configuration.

10) K. Noda, H. Okai, T. Kato and N. Izumiya, This Bulletin, **41**, 401 (1968).

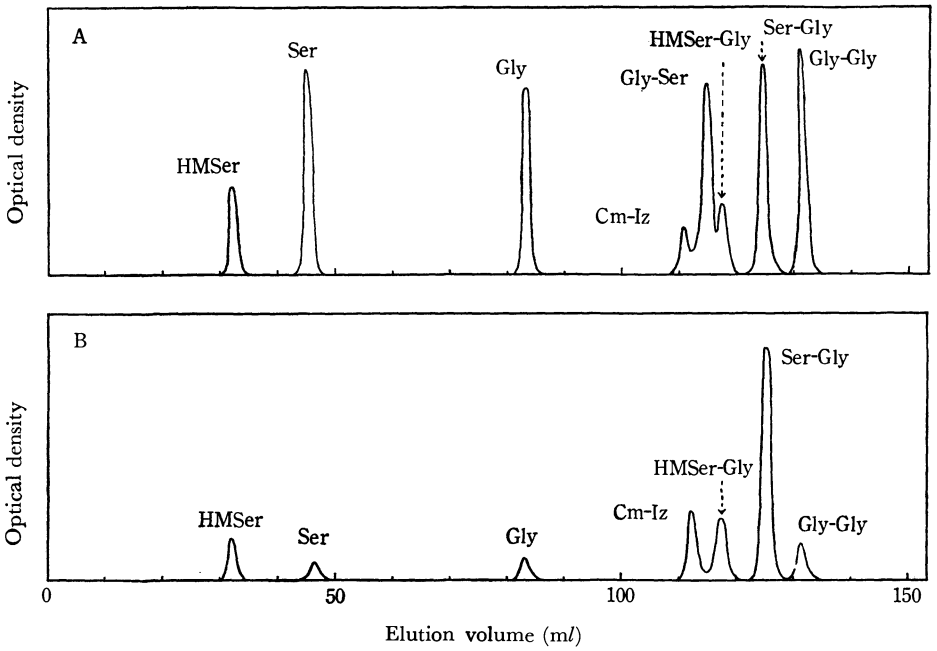

Fig. 4. Elution pattern of a model mixture (A) and a reaction mixture (B) by amino acid analyzer.

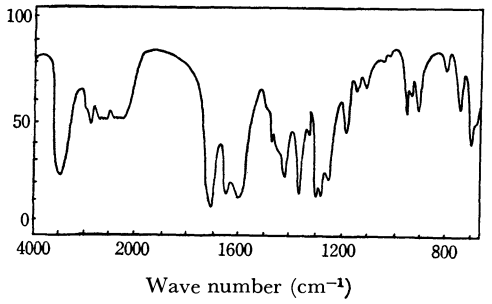

Fig. 5. Infrared spectrum of 3-carboxymethyl-4-imidazolidone in KBr disk.

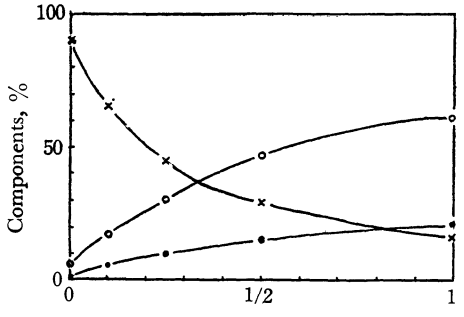

Fig. 6. Effects of cupric ion concentration.
—○—, Ser-Gly; —×—, Cm-Iz; —●—, HMSer-Gly

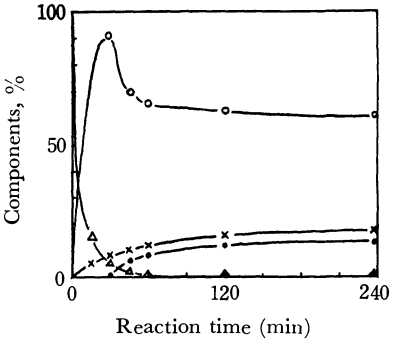

Fig. 7. Effects of reaction time.
—○—, Ser-Gly; —×—, Cm-Iz; —●—, HMSer-Gly; —△—, Gly-Gly

spectra. Later it was found that this substance, Cm-Iz, was isolated easily in a good yield from the reaction mixture of glycylglycine and formaldehyde without cupric ion (see Fig. 6).

Figure 3 indicates the reaction sequence of glycylglycine and formaldehyde with cupric ion. Kim and Martell[11] have reported the structure of copper glycylglycinate in aqueous solution in detail. They have indicated that the amino group in copper salt in sodium carbonate is protected by cupric ion. It is therefore considered that the methylene group is more active than that of free glycylglycine. We have already described the formation of serylglycine and α-hydroxymethylserylglycine. However, it should be mentioned that not even a trace of glycylserine could be found, contrary to our ex-

11) M. K. Kim and A. E. Martell, *Biochemistry*, **3**, 1169 (1964).

pectation indicated in Fig. 1. When the amount of cupric ion is decreased, the amino group in free glycylglycine is apt to react with formaldehyde to produce 3-carboxymethyl-4-imidazolidone (Cm-Iz); Cm-Iz may be produced *via* a possible intermediate, *N*-HMGly-Gly (Fig. 3). It is considered that the components of amino acid were derived by an alkaline hydrolysis at peptide bond, and some amino acid such as glycine was converted further to serine and hydroxymethylserine as Otani and Winitz reported.[6]

The effects of variations of concentration of cupric ion and reaction time were studied by using the amino acid analyzer in order to find optimal condition for the serylglycine formation. The experiments revealed that the formation of serylglycine was favored when the ratio of copper to glycylglycine increased, and no serylglycine was formed in the absence of cupric ion (Fig. 6). Within the conditions we studied, the maximum formation of serylglycine was observed when the molar ratio of copper to glycylglycine was 1 : 1 and the reaction mixture was heated at 100°C for 30 min (Fig. 7).

As an experiment on a preparative scale, we tried to prepare serylglycine under the best conditions described above. Thus, a practicable one-step synthesis of serylglycine has been achieved in a good yield of 70%. The method of synthesis of serylglycine developed in these studies has merits of simplicity, convenience and inexpensive starting materials.

Experimental

The melting points were uncorrected. Paper chromatography was run on Toyo Roshi No. 52 in 80% pyridine. The infrared spectra were measured on a Hitachi EPI-S2 spectrophotometer. The NMR spectra were recorded on a Varian Associates A-60 model, using tetramethylsilane as the internal standard and acetic acid as solvent.

Gly-Ser. This peptide was prepared by the hydrogenolysis of Z-Gly-Ser-OBzl;[12] 85%, mp 197—199°C (decomp.), R_f 0.36.

Ser-Gly. This was also prepared from Z-Ser-Gly-OBzl;[12] 82%, mp 204—206°C (decomp.); R_f 0.45.

Z-HMSer. To a solution of α-hydroxymethylserine[6] (1.62 g, 12 mmol) and sodium bicarbonate (2.52 g) in water (50 m*l*) was added benzyloxycarbonyl chloride (1.82 m*l*, 14.4 mmol) portionwise under stirring at room temperature. Stirring was continued for 4 hr and the solution was extracted with ether. After the aqueous layer was acidified with hydrochloric acid, it was extracted with ethyl acetate (4 times, each 50 m*l*). The combined extracts were dried over sodium sulfate and evaporated *in vacuo*. The residual syrup was solidified by the addition of petroleum ether. It was recrystallized from ethyl acetate-petroleum ether; yield, 1.64 g (51%); mp 109—110°C.

Found: C, 53.50; H, 5.78; N, 5.19%. Calcd for $C_{12}H_{15}O_6N$: C, 53.53; H, 5.62; N, 5.20%.

Z-HMSer-Gly-OBzl. To a solution of Z-HMSer (0.7 g, 3 mmol) and glycine benzyl ester *p*-toluenesulfonate (1.01 g, 3 mmol) in chloroform (15 m*l*) with triethylamine (0.42 m*l*) was added DCC (0.62 g, 3 mmol) at room temperature. The mixture was left to stand overnight, and evaporated *in vacuo*. To the residue was added ethyl acetate, and dicyclohexylurea was filtered off. The filtrate was washed with a 4% sodium bicarbonate solution, 2% hydrochloric acid and water, and dried over sodium sulfate. The filtered solution was evaporated and the oily residue was solidified by the addition of petroleum ether. It was recrystallized from ethyl acetate-petroleum ether; yield, 0.75 g (61%); mp 91—93°C.

Found: C, 60.48; H, 5.89; N, 6.70%. Calcd for $C_{21}H_{24}O_7N_2$: C, 60.56; H, 5.81; N, 6.73%.

HMSer-Gly. A solution of Z-HMSer-Gly-OBzl (0.42 g, 1 mmol) in a mixture of acetic acid (5 m*l*), *t*-butanol (3 m*l*) and water (1 m*l*) was treated with hydrogen in the presence of palladium black. The filtrate from the catalyst was evaporated *in vacuo* to dryness. The residual crystals were recrystallized from water-ethanol; yield, 0.154 g (80%); mp 190—192°C (decomp.); R_f 0.56.

Found: C, 37.26; H, 6.38; N, 14.70%. Calcd for $C_6H_{12}O_5N_2$: C, 37.50; H, 6.29; N, 14.58%.

3-Carboxymethyl-4-imidazolidone (Cm-Iz). A solution of Gly-Gly (1.32 g, 10 mmol), sodium carbonate (4.24 g, 40 mmol) and 37% aqueous formaldehyde (6 m*l*, 80 mmol) in water (200 m*l*) was kept at 100°C for 1 hr, and evaporated to a small volume (about 10 m*l*) *in vacuo*. It was put on a column of Dowex 50×8 (1.8×30 cm, 100—200 mesh, H^+ form). After the column was washed with water, it was treated with 2N ammonium hydroxide. The eluate was evaporated *in vacuo* and the residual crystals were recrystallized from water-ethanol; yield, 1.18 g (82%); mp 200°C (decomp.); R_f 0.42.

Calcd for $C_5H_8O_3N_2$: C, 41.66; H, 5.59; N, 19.44%. Found: C, 41.64; H, 5.67; N, 19.43%.

A definite amount of the product was hydrolyzed with 6N hydrochloric acid at 110°C for 12 hr; the hydrolysate indicated the value of $Gly_{2.03}$ by the amino acid analysis and the presence of formaldehyde qualitatively by a reagent of chromotropic acid.[13] The following observations confirm the structure of the product to be Cm-Iz. The molecular weight was determined on a Hitachi Osmometer, type 115, using methanol as a solvent. Calcd, 141.1; Found, 141.5. Infrared spectrum was shown in Fig. 5: ν_{max} 3400 (>N–H); 2750—2350 (this series is not seen in amino acid and acyldipeptide acid); 1718 (C=O in δ-lactam); 1647 (–CO–N<), 1590, 1314, 1302, 1012 (C–N–C) cm^{-1}. The NMR spectra were in accord with that assumed for Cm-Iz: δ=4.10 (singlet, methylene protons, 2H); 4.23 (singlet, methylene protons, 2H); 4.98 (singlet, methylene protons, 2H).

Chromatography of Model Mixture by Amino Acid Analyzer. We tried to obtain sufficient separation of each component of an artifical mixture by an amino acid analyzer, and found the following conditions to satisfy this purpose. A mixture of each one μmole of eight compounds listed in Table 1 was treated with a Hitachi amino acid analyzer, model KLA-3B, using

12) G. Fölsch, *Acta Chem. Scand.*, **12**, 561 (1958).

13) E. Eegriwe, *Z. Anal. Chem.*, **110**, 22 (1937).

TABLE 1. VALUES OF COMPOUNDS IN A MODEL MIXTURE

Compound	Effluent volume (ml)	Color constant[a]
HMSer	45	3.74
Ser	57	11.90
Gly	86	11.50
Cm-Iz	114	3.07
Gly-Ser	117	11.63
HMSer-Gly	119	2.71
Ser-Gly	129	11.00
Gly-Gly	135	12.15

a) Observed constants for the integration of peaks obtained from each 1 μmol of peptides and amino acids (see D. H. Spackman, W. H. Stein and S. Moore, *Anal. Chem.*, **30**, 1190 (1958)).

a 0.9×50 cm column with spherical resin under the conditions of flow rate 60 ml/hr and jacket temperature 55°C. The 0.2M sodium citrate buffer at pH 3.25 was applied until 70 ml, and then the system was changed to the pH 4.25 buffer. The effluent volumes and color yields of the compounds are summarized in Table 1, and the pattern of elution is shown in Fig. 4-A.

Isolation of Components in Reaction Mixture of Gly-Gly and Formaldehyde with Cupric Ion. *a) Preparation of Reaction Mixture.* A solution of Gly-Gly (1.32 g, 10 mmol), sodium carbonate (4.24 g, 40 mmol), cupric sulfate pentahydrate (1.25 g, 5 mmol) and 37% formaldehyde (6 ml, 80 mmol) in water (200 ml), was kept 100°C for 1 hr. The mixture was cooled with tap water and insoluble material in a small amount was filtered off. After the filtrate was acidified with acetic acid, the solution was evaporated *in vacuo*. The residue was dissolved in water, then the solution was treated with a column of Dowex 50×8 (1.8×30 cm, H^+ form). The column was washed with water and eluted with 2N ammonium hydroxide. The eluate was evaporated *in vacuo*, the residue was dissolved in water (1 ml), and the solution (about 1 ml) was used for the separation experiment as described in the following section. Approximately 1/2000 part of the solution was analyzed with the amino acid analyzer under the conditions described before, the pattern indicating the presence of seven components (Fig. 4-B).

b) Isolation and Characterization of Components. After several runs under various conditions, we found the following conditions to be satisfactory for separating the reaction mixture into each component. The solution (about 1 ml) was put on a column (1.8×110 cm) of Dowex 50×8 (200—400 mesh, NH_4^+ form), and the column was eluted with 0.2M ammonium acetate buffer of pH 4.0 with a flow rate of 30 ml/hr. An aliquot of each fraction (3 ml) was tested on a paper strip with ninhydrin, and the strip demonstrated that the reaction mixture was also separated into seven portions. The fractions containing each component were combined and evaporated to dryness *in vacuo* for removal of most of the ammonium acetate. The residue was dissolved in water and treated with a column of Dowex 50×8 (H^+ form) to remove the remaining acetate ion. After washing with water, the column was eluted with 2N ammonium hydroxide and the eluate was evaporated *in vacuo*. A residual solid was recrystallized from water-ethanol. The amount obtained is shown in Table 2 together with methods of characterization of the product isolated.

TABLE 2. ISOLATION AND CHARACTERIZATION OF COMPONENTS IN A REACTIION MIXTURE[a]

Component	Numbers of test tubes treated (tube, 3 ml)	Amount isolated and yield mg (%)	Method of characterization
HMSer	55—65	71(5)	PPC
Ser	67—80	5(0.5)	PPC
Gly	95—115	8(1)	PPC
Cm-Iz	117—145	353(25)	PPC, EA, AAA
HMSer-Gly	155—170	195(10)	PPC, EA, AAA
Ser-Gly	180—250	605(37)	PPC, EA, AAA
Gly-Gly	250—270	12(1)	PPC, AAA

a) The reaction mixture was prepared from Gly-Gly (1.32 g), formaldehyde (6 ml), sodium carbonate (4.24 g) and cupric sulfate (1.25 g) (for details, see Experimental).

b) PPC, paper chromatography compared with authentic sample. EA, elemental analysis (C, H and N). AAA, analysis by amino acid analyzer on hydrolysate derived from the component with 6N hydrochloric acid at 110°C for 12 hr.

As an example, a procedure for identification of Cm-Iz is described below. The fractions from tube number 117 to 145 were treated as described above, and the crude product obtained was recrystallized from water-ethanol; yield, 353 mg (25%); mp 200°C (decomp.); R_f 0.42; amino acid analysis, $Gly_{2.05}$.

Calcd for $C_5H_8O_3N_2$: C, 41.66; H, 5.59; N, 19.44%. Found: C, 41.59; H, 5.71; N, 19.33%.

Effect of Cupric Ion and Reaction Time on Formation of Dipeptides. *a) Effect of Cupric Ion.* Effect of variation in concentration of cupric ion was examined. A solution of Gly-Gly (132 mg, 1 mmol), sodium carbonate (424 mg, 4 mmol), 37% formaldehyde (0.6 ml, 8 mmol) and an appropriate amount of cupric sulfate (0 to 1 mmol) in water (20 ml) was heated at 100° for 1 hr, and treated as described before. The residue was dissolved in 0.2M citrate buffer (20 ml) of pH 2.2, and 0.1 ml of the solution was applied to the amino acid analyzer. The results obtained were shown in Fig. 6.

b) Effect of Reaction Time. Effect of variation in reaction time was examined. A solution of Gly-Gly (1 mmol), sodium carbonate (4 mmol), cupric sulfate (1 mmol) and 37% formaldehyde (8 mmol) in water (20 ml), was heated at 100°C. After various time intervals a portion of the solution was treated as described before. Each solution in citrate buffer at pH 2.2 was applied to the amino acid analyzer, the results being shown in Fig. 7.

Preparation of Ser-Gly from Gly-Gly. A solution of Gly-Gly (5.28 g, 0.04 mol), sodium carbonate (17 g, 0.1 mol), cupric sulfate (1.0 g, 0.04 mol) and 37% formaldehyde (24 ml) in water (800 ml) was heated at 100°C for 30 min. The reaction mixture was treated with a Dowex 50×8 column (2.5×60 cm, 100—200 mesh, H^+ form). It was washed with water and eluted

with 2N ammonium hydroxide. The eluate was evaporated *in vacuo*, and the residual crystals were recrystallized from water-ethanol; yield, 4.42 g (70%); mp 203—205° (decomp.); R_f 0.45.

Found: C, 37.15; H, 6.11; N, 17.29%. Calcd for $C_5H_{10}O_4N_2$: C, 37.03; H, 6.62; N, 17.28%.

The authors wish to thank Miss Isako Saeki, Faculty of Agriculture, Kyushu University, for her valuable technical assistance and Prof. Taku Matsuo and Mr. Yasushi Kodera, Faculty of Engineering, Kyushu University, for the NMR determination.

BULLETIN OF THE CHEMICAL SOCIETY OF JAPAN VOL. 43 1839—1843 (1970)

Reaction of 2-Aminobenzophenones with Aliphatic Acids in the Presence of Polyphosphoric Acid*1

Takumi ISHIWAKA, Mitsuo YONEMOTO, Kakuzo ISAGAWA and Yasaburo FUSHIZAKI

Department of Applied Chemistry, Faculty of Engineering, University of Osaka Prefecture, Sakai, Osaka

(Received December 15, 1969)

The reaction of 2-aminobenzophenones with aliphatic acids, such as acetic acid, propionic acid, *n*-butyric acid, and bromoacetic acid, in the presence of polyphosphoric acid afforded 6-substituted 2-anilino-4-phenylquinoline derivatives in fairly good yields. Some of these quinolines were acetylated in the usual way, and the products, 2-(*N*-acetylanilino)quinolines, were treated with sodium ethoxide to give 1-quinolyl-2(1*H*)-quinolone derivatives. 2-Amino-5-chlorobenzophenone (Ic) reacted with an equimolar amount of 2-acetamido-5-methylbenzophenone to give 2-(2-benzoyl-4-methylanilino)-6-chloro-4-phenylquinoline, which was also obtained from the reaction of 2,6-dichloro-4-phenylquinoline with Ib in the presence of copper powder. It was found that the reaction mechanism in the formation of 2-anilinoquinolines is similar in type to that in Friedländer's reaction. Furthermore, the structures of the 2-anilinoquinolines are discussed on the basis of our NMR spectral study.

In an earlier paper,[1] 2-aminobenzophenones (I) were treated with zinc chloride to afford the rearrangment products, benzanilides, together with dibenzo-[*b*,*f*]-1,5-diazocines and 9-acridones. On the other hand, it has been reported by Dippy *et al.*[2,3] that, on the treatment of *N*-monoacyl- or *N*,*N*-diacylaniline with anhydrous aluminum chloride or zinc chloride, a migration of their acyl groups occurred.

Then, 2-acetamido-5-chlorobenzophenone (IIIc), which has two acyl groups, was treated with zinc chloride at 190—200°C for 10 hr as the basis for a discussion of the rearrangement of the acyl groups. However, this reaction gave no rearrangement products. It did, though, afford intermolecular condensation product, 2-(2-benzoyl-4-chroroanilino)-6-chloro-4-phenylquinoline (IIc), in a 54% yield; it had already prepared in a 90% yield by Drukker and Judd[4] by the treatment of IIIc with polyphosphoric acid (PPA) at 130—140°C for 2 hr. The present authors found that this compound could easily be obained by slightly modifying Drukker's method.

Now, this paper will report the direct syntheses of 2-anilinoquinolines (II) from I and the syntheses of 1-quinolyl-2(1*H*)-quinolones (IX), and will des-

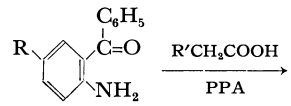

Ia : R=H
b : R=CH_3
c : R=Cl

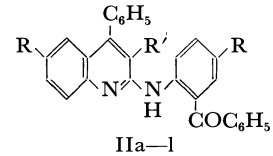

IIa—l

IIa—l: R and R′ are shown in Table 1

Scheme 1

*1 Part VIII, "*o*-Aminobenzophenone Derivatives." This study was presented at the 22nd Annual Meeting of the Chemical Society of Japan, Tokyo, April, 1969. Part VII: T. Ishiwaka, M. Sano, K. Isagawa and Y. Fushizaki, This Bulletin, **43**, 135 (1970).

1) K. Isagawa, T. Ishiwaka, M. Kawai (the late) and Y. Fushizaki, This Bulletin, **42**, 2066 (1969).

2) J. F. J. Dippy and J. H. Wood, *J. Chem. Soc.*, **1949**, 2719.

3) J. F. J. Dippy and V. Moss, *ibid.*, **1952**, 2205.

4) A. E. Drukker and C. I. Judd, *J. Heterocycl. Chem.*, **3**, 359 (1966); *Chem. Abstr.*, **65**, 20096 (1966).

Table 1. 2-Anilinoquinolines (II)

Compound			Reaction conditions		Yield	Mp	Elementary analysis (%)					
							Calcd			Found		
II	R	R′	Temp. °C	Time min	%	°C	C	H	N	C	H	N
a	H	H	140—145	30	80	140—142	83.98	4.96	6.93	84.22	5.03	7.00
b	CH_3	H	150—155	20	72	179—181	84.08	5.65	6.54	84.32	5.81	6.83
c	Cl	H	140—145	15	89	188—190	71.65	3.87	5.97	71.80	4.04	5.97
d	H	CH_3	110—115	10	90	191—192	84.03	5.35	6.76	84.25	5.56	7.05
e	CH_3	CH_3	125—130	15	91	194—196	84.13	5.92	6.33	84.03	6.20	6.60
f	Cl	CH_3	125—130	15	94	222—224	72.06	4.17	5.80	72.03	4.40	5.77
g	H	C_2H_5	110—115	15	85	162—164	84.09	5.66	6.54	83.79	5.71	6.50
h	CH_3	C_2H_5	110—115	15	81	216—218	84.18	6.18	6.14	84.45	6.30	6.04
i	Cl	C_2H_5	110—115	15	92	229—230	72.44	4.46	5.63	72.68	4.46	5.78
j	H	Br	105—110	15	71	210—211	70.16	4.00	5.84	70.35	4.07	5.61
k	CH_3	Br	105—110	15	72	216—217	71.01	4.57	5.52	71.30	4.62	5.56
l	Cl	Br	105—110	15	82	228—230	61.33	3.13	5.11	61.62	3.31	5.20
m[a]			135—140	30	83	191—192	77.58	4.71	6.24	77.44	4.95	6.18
n[a]			155—160	60	94	183—185	77.58	4.71	6.24	77.40	4.66	6.14
n[b]			175—180	300	24							

Compound			NMR[c] δ(ppm)			
II	R	R′	NH	Arom H	R′	R
a	H	H	11.08(b)	9.43—7.08(m)	6.96(s)	—
b	CH_3	H	10.74(b)	9.24—7.21(m)	6.89(s)	2.40(s), 2.28(s)
c	Cl	H	10.90(b)	9.38—7.28(m)	6.95(s)	—
d	H	CH_3	11.14(b)	9.50—6.82(m)	2.32(s)	—
e	CH_3	CH_3	10.95(b)	9.48—6.98(m)	2.30(s)	2.30(s), 2.30(s)
f	Cl	CH_3	11.02(b)	9.43—7.18(m)	2.28(s)	—
g	H	C_2H_5	11.28(b)	9.64—7.06(m)	2.78(q), 1.26(t)	—
h	CH_3	C_2H_5	11.09(b)	9.40—6.94(m)	2.74(q), 1.23(t)	2.33(s), 2.33(s)
i	Cl	C_2H_5	11.10(b)	9.52—7.12(m)	2.74(q), 1.23(t)	—
j	H	Br	11.34(b)	9.47—7.00(m)	—	—
k	CH_3	Br	11.16(b)	9.22—7.00(m)	—	2.35(s), 2.35(s)
l	Cl	Br	11.21(b)	9.33—7.22(m)	—	—
m[a]			10.88(b)	9.40—7.30(m)	6.88(s)	2.41(s)
n[a]			10.86(b)	9.20—7.33(m)	6.90(s)	2.28(s)
n[b]						

a) From the reactions of Ib with IIIc and of Ic with IIIb.
b) From the reaction of Ib with V in the presence of copper powder.
c) Measured in $CDCl_3$, using tetramethylsilane as the internal standard. b: broad, m: multiplet, s: singlet, t: triplet, q: quartet.

cribe the reaction mechanism in the formation of II.

When I was reacted with various aliphatic acids in the presence of PPA at the temperature shown in Table 1 for 10—30 min, the corresponding 2-anilinoquinolines were obtained in fairly good yields. By using this method, the reaction time could be very much shortened (Scheme 1).

The yields, physical properties, and results of the elemental analyses of II are summarized in Table 1.

In order to discuss the reaction mechanism in the formation of II, the reaction of 2-acetamido-5-chlorobenzophenone (IIIc) with Ib and that of 2-acetamido-5-methylbenzophenone (IIIb) with Ic were carried out in the presence of PPA. 2-(2-Benzoyl-4-chloroanilino)-6-methyl-4-phenylquinoline (IIm) was formed from the former reaction. On the other hand, the latter reaction afforded 2-(2-benzoyl-4-methylanilino)-6-chloro-4-phenylquinoline (IIn), which was also obtained from the reaction of 2,6-dichloro-4-phenylquinoline (V) with Ib, using copper powder as the catalyst. The formations of IIn in the former reaction and of IIm in the latter reaction were not detected (Scheme 2).

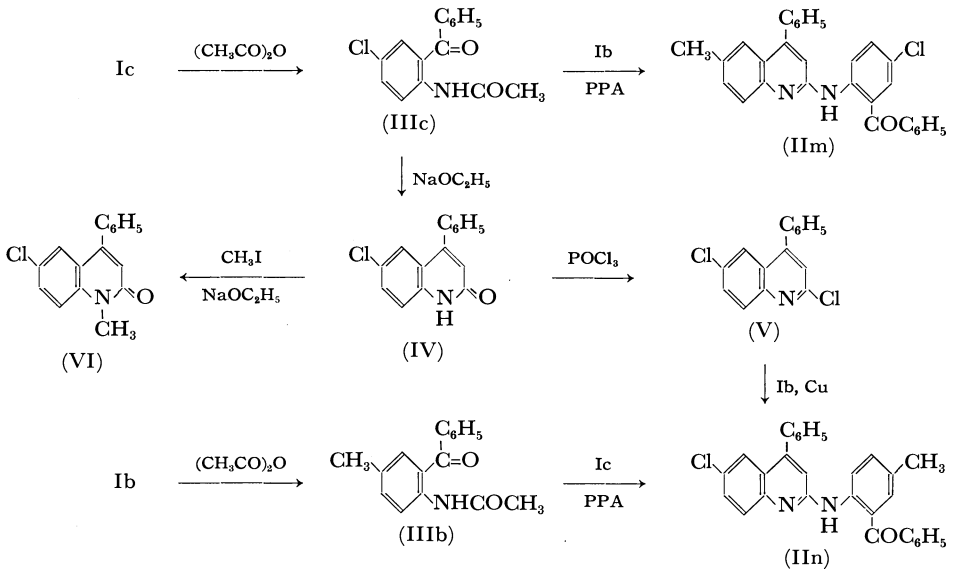

Scheme 2

It may be suggested from these facts that this reaction involves the preliminary acylation of I by aliphatic acids to give 2-acylaminobenzophenone derivatives, which subsequently react with other 2-aminobenzophenones in a manner presumably analogous to the mechanism of the Friedländer process.

In the case of the reaction described by Drukker and Judd, Kanaoka[5] has suggested that Ic, resulting from the deacylation of IIIc, condensed with other IIIc to give IIc. Although he has not described the mechanism of this condensation in detail, it is probably analogous to that of the Friedländer process.

Drukker and Judd have reported that, in the NMR spectrum*[2] of IIc, the sharp peak at δ 6.86 ppm is due to NH (1H). On treatment with deuterium oxide, however, this peak remains and the broad peak at δ 10.90 ppm (1H) disappears. As is shown in Table 1, the other 3-nonsubstituted anilinoquinolines, such as IIa, IIb, IIm, and IIn, also reveal peaks at δ 6.88—6.96 ppm, while the 3-substituted compounds, IId—III, show no peaks in this range.

The above observations indicate that the peaks at δ 6.96 ppm and at δ 10.90 ppm in IIc are to be assigned to CH at the 3-position and to NH respectively.

On the other hand, the methine-proton signals at the 3-position of 6-chloro-4-phenyl-2(1*H*)-quinolone (IV)*[3] and its 1-methyl derivative (VI)*[2] appear at δ 6.56 ppm and at δ 6.76 ppm respectively.

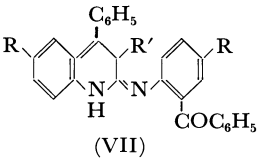

(VII)

Fig. 1

The complex multiplets at δ 7.44—7.86 ppm and at δ 7.43—7.73 ppm in them correspond to aromatic proton signals. In the case of 2,6-dichloro-4-phenylquinoline (V),*[2] however, there is only the peak of the aromatic proton at δ 7.48—8.14 ppm (multiplet), not the peak of methine-proton at δ 6.5—6.9 ppm.

The differences may be successfully explained in terms of the non-aromaticity of the methine-protons in IV and VI, and the aromaticity in V.

Considering the above observations, it may be

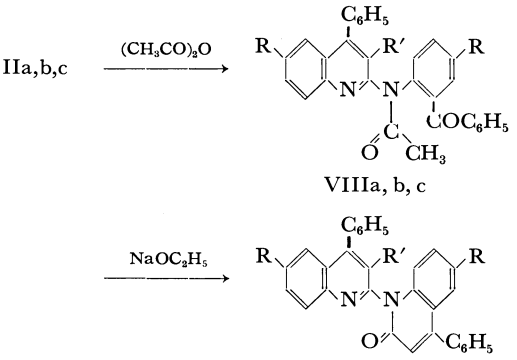

a: R=R′=H b: R=CH_3, R′=H c: R=Cl, R′=H

Scheme 3

5) Y. Kanaoka, *Kagaku*, Vol. 24, No. 3, Kagaku Dojin, Kyoto (1969), p. 42.

*[2] Measured in $CDCl_3$.

*[3] Measured in $CDCl_3$–DMSO-d_6 (3 : 2).

Table 2. 2-(*N*-Acetylanilino)quinolines and 1-quinolyl-2(1*H*)-quinolones

Compound		Yield %	Mp °C	Elementary analysis (%) Calcd C	H	N	Found C	H	N	NMR[c] δ (ppm) Arom H	CH[d]	CH_3
VIII[a]	a	72	146—147	81.43	5.01	6.33	81.13	4.85	6.14	7.84—7.36(m)	—	2.20(s)
	b	91	173—174	81.68	5.57	5.95	81.43	5.87	5.77	7.89—7.30(m)	—	2.40(s), 2.40(s), 2.17(s)
	c	94	187—188	70.46	3.94	5.48	70.47	3.64	5.19	7.80—7.39(m)	—	2.19(s)
IX[b]	a	87	290	84.88	4.75	6.60	84.63	4.66	6.42	8.30—7.26(m)	6.75(s)	—
	b	79	196—198	84.93	5.35	6.19	84.84	5.54	6.14	8.18—7.27(m)	6.72(s)	2.52(s), 2.28(s)
	c	86	251—252	73.03	3.68	5.68	73.21	3.39	5.67	8.22—7.32(m)	6.77(s)	—

a) Reaction conditions: temp. 75—80°C, time 60 min.
b) Reaction conditions: temp. 75—80°C, time 30 min.
c) Measured in $CDCl_3$, using tetramethylsilane as the internal standard. m:multiplet, s: singlet.
d) Methine-proton at 3-position of quinoline ring or quinolone ring.

deduced that the 2-anilinoquinolines II exist as imino-type VII, as is shown in Fig. 1.

6-Substituted 2-(4-substituted *N*-acetylanilino)-4-phenylquinolines (VIII) which had been obtained by the acetylation of the quinolines II with acetic anhydride were treated with sodium ethoxide to afford 6-substituted 1-(6-substituted 4-phenyl-2-quinolyl)-4-phenyl-2(1*H*)-quinolone derivatives (IX).

The yields, physical properties, and results of the elemental analyses of VIII and IX are listed in Table 2.

Whereas the NMR spectra of the acetyl quinolines, VIII, in deuteriochloroform reveal no peaks at δ 6.5—6.9 ppm, those of the 1-quinolyl-2(1*H*)-quinolones, IX, show the peaks at δ 6.72—6.77 ppm which are assigned to CH at the 3-position of the quinolone ring.

Experimental

All the melting points are uncorrected. The NMR spectra were determined on a Hitachi R-20 spectrometer.

Materials. The 2-aminobenzophenone (Ia) was prepared according to the method of Scheifele and DeTar;[6] mp 104—105°C (lit,[6] mp 105—106°C). The 2-amino-5-methylbenzophenone (Ib) was prepared by the method of Staskun;[7] mp 66—67°C (lit,[7] mp 66—67°C). The 2-amino-5-chlorobenzophenone (Ic) was prepared by the method of Sternbach *et al.*;[8] mp 100—101°C (lit,[7] mp 100—101°C).

The 2,6-dichloro-4-phenylquinoline (V) was prepared in the following way. 2-Acetamido-5-chlorobenzophenone (IIIc), which had been obtained by the acetylation of Ic, was treated with sodium ethoxide to give 6-chloro-4-phenyl-2(1*H*)-quinolone (IV). The treatment of IV with phosphorus oxychloride in the presence of dry pyridine at 130—140°C gave V; mp 111—112°C (lit,[9] mp 114—115°C).

The PPA was obtained from the Wako Pure Chemical Industries Co., Ltd.

The Reaction of 2-Aminobenzophenones (I) with Aliphatic Acids. Only a typical reaction will be described here. All of these reactions were carried out by a method similar to that described below.

A mixture of 2-amino-5-chlorobenzophenone (5 mmol), acetic acid (15 mmol), and PPA (20 g) was heated to 140—145°C for 15 min. After cooling, the reaction mixture was poured into ice water (*ca.* 100 m*l*), neutralized with 28% ammonia water, and extracted with methylene chloride (*ca.* 100 m*l*). The extract was then washed with water and dried over anhydrous magnesium sulfate. The solution was concentrated to 30 m*l* and chromatographed on silica gel with the same solvent. The first eluate (*ca.* 100 m*l*) was evaporated to dryness, and the resulting solid was recrystallized from a mixture of methylene chloride and methanol to afford IIc as yellow needles.

2-(2-Benzoyl-4-chloroanilino)-6-methyl-4-phenylquinoline (IIm). A mixture of Ib (4 mmol), IIIc (4 mmol), and PPA (20 g) was heated to 135—140°C for 30 min. The reaction mixture was worked up according to the procedure described for the preparation of IIc. Recrystallization from a mixture of methylene chloride and methanol afforded IIm as yellow needles.

2-(2-Benzoyl-4-methylanilino)-6-chloro-4-phenylquinoline (IIn). *i) From IIIb.* A mixture of Ic (4 mmol), IIIb (4 mmol), and PPA (20 g) was heated to 155—160°C for 1 hr. The reaction mixture was then worked up according to the procedure described for the preparation of IIc. Recrystallization from a mixture of methylene chloride and methanol afforded IIn as yellow needles.

ii) From V. A mixture of Ib (4 mmol), V (4 mmol), and copper powder (20 mg) was sealed into a glass ampoule and then heated at 175—180°C for 5 hr. After the ampoule had been cooled and opened, the reaction mixture was dissolved in methylene chloride (*ca.* 20 m*l*) and filtered to remove the catalyst. The

6) H. J. Scheifele, Jr., and D. F. DeTar, "Organic Syntheses," Coll. Vol. IV, p. 34 (1962).
7) B. Staskun, *J. Org. Chem.*, **29**, 2856 (1964).
8) L. H. Sternbach, E. Reeder, O. Keller and W. Metlesics, *ibid.*, **26**, 4488 (1961).
9) G. A. Reynolds and C. R. Hauser, *J. Amer. Chem. Soc.*, **72**, 1852 (1950).

solution was then chromatographed on silica gel with the same solvent. The first eluate (*ca.* 100 m*l*) was evaporated to dryness, and the resulting solid was recrystallized from a mixture of methylene chloride and methanol to afford IIn as yellow needles.

The product was identified by means of mixed-melting-point measurements and by a comparison of its IR and NMR spectra with those of the sample obtained from *i*.

Acetylation of IIa, IIb, and IIc. A typical experiment will be described below.

A solution of IIc (2 mmol) in acetic anhydride (25 m*l*) was heated at 75—80°C in the presence of sodium acetate (2 g). After 1 hr, the mixture was cooled to room temperature and kept overnight. Then the solution was poured into ice water and extracted with chloroform. The extract was successively washed with water, a 5% sodium hydrogencarbonate solution, and water. The solution was dried over anhydrous magnesium sulfate and then evaporated to dryness. The residual oil was solidified by adding a small amount of methylene chloride, and the resulting solid was recrystallized from a mixture of methylene chloride and methanol to afford VIIIc as white prisms.

VIIIa and VIIIb were also obtained according to methods similar to that described above.

General Procedure for the Preparation of 1-Quinolyl-2(1*H*)-quinolone (IX). Into a solution of VIII (1.5 mmol) in absolute ethanol (120 m*l*), a sodium ethoxide solution [from sodium (0.1 g) and absolute ethanol (20 m*l*)] was stirred, drop by drop, at 75—80°C over a 15 min period. After having been stirred for an additional 15-min, the reaction mixture was poured into water. The crude product was collected by filtration and washed with warm water. Recrystallization from carbon tetrachloride afforded 6-substituted 1-(6-substituted 4-phenyl-2-quinolyl)-4-phenyl-2(1*H*)-quinolones (IX) as white prisms.

The authors wish to express their thanks to Miss N. Morimoto for her assistance in the experimental work.

BULLETIN OF THE CHEMICAL SOCIETY OF JAPAN VOL. 43 1843—1846 (1970)

Aminocyclitols. XXII. A Synthesis of Actinamine and Hyosamine[1]

Tetsuo SUAMI, Seiichiro OGAWA and Hiroshi SANO

Department of Applied Chemistry, Faculty of Engineering, Keio University, Koganei-shi, Tokyo

(Received December 16, 1969)

Hydrazinolysis of 2,4,5,6-tetra-*O*-acetyl-1,3-di-*O*-*p*-toluenesulfonyl-*myo*-inositol, followed by catalytic hydrogenation afforded *myo*-inosadiamine-1,3 *via* an intermediary 6,7-diazabicyclo[3.2.1]-octane-2,3,4,8-tetrol. In this reaction, the use of *N,N'*-dimethylhydrazine and *N*-methylhydrazine, instead of hydrazine, gave actinamine: a component of an antibiotic spectinomycin, and *N*-methyl-*myo*-inosadiamine-1,3: an important intermediary compound for a synthesis of DL-hyosamine, respectively. Details of the convenient syntheses of actinamine and DL-hyosamine are described.

Actinamine has been found in the antibiotic spectinomycin[2,3] as its component and its structure has been established to be *N,N'*-dimethyl-*myo*-inosadiamine-1,3.[4-6] The synthesis has been done by several authors[7-10] in laborious procedures.

While hyosamine has been discovered in the antibiotic hyosamine B[11] and later in destomycin A[12] as their components. The structure has been established to be *N*-methyl-2-deoxy-streptamine[11,12] and the synthesis has been described by Nakajima and his coworkers.[13]

In the present papers, the authors wish to report

1) For a preliminary account see T. Suami and H. Sano, *Tetrahedron Lett.*, **1968**, 2655; *ibid.*, **1969**, 1795.

2) D. J. Mason, A. Dietz and R. M. Smith, *Antibioti. Chemotherapy*, **11**, 118 (1961).

3) T. J. Oliver, A. Goldstein, R. R. Bower, J. C. Holper and R. H. Otto, *ibid.*, **11**, 495 (1961).

4) G. Slomp and F. A. MacKellar, *Tetrahedron Lett.*, **1962**, 521.

5) P. F. Wiley, *J. Amer. Chem. Soc.*, **84**, 1514 (1962).

6) A. L. Johnson, R. H. Gourlay, D. S. Tarbell and R. L. Autrey, *J. Org. Chem.*, **28**, 300 (1963).

7) M. Nakajima, N. Kurihara, A. Hasegawa and T. Kurokawa, *Ann. Chem.*, **689**, 243 (1965).

8) F. W. Lichtenthaler, H. Leinert and T. Suami, *Chem. Ber.*, **100**, 2383 (1967).

9) T. Suami and S. Ogawa, This Bulletin, **40**, 1295 (1967).

10) S. Ogawa, T. Abe, H. Sano, K. Kotera and T. Suami, *ibid.*, **40**, 2405 (1967).

11) P. Wiley, M. V. Sigal, Jr., and O. Weaver, *J. Org. Chem.*, **27**, 2793 (1962).

12) S. Kondo, M. Sezaki, M. Koike and E. Akita, *J. Antibiotics*, **A18**, 192 (1965).

13) M. Nakajima, A. Hasegawa and N. Kurihara, *Ann. Chem.*, **689**, 235 (1965).

a detail of a convenient synthesis of actinamine and DL-hyosamine.

myo-Inosadiamine-1,3 has been readily prepared from 1,3-di-*O*-*p*-toluenesulfonyl-*myo*-inositol (I)[14] by the reaction with hydrazine,[15] and hence, actinamine and DL-*N*-methyl-*myo*-inosadiamine-1,3 could be prepared from I by the reactions with *N*,*N*′-dimethylhydrazine and *N*-methylhydrazine.

From the latter compound, DL-hyosamine could be prepared by analogous reaction procedures in which 2-deoxystreptamine had been successfully synthesized from *myo*-inosadiamine-1,3.[16,17]

When I was heated under reflux in a mixture of *N*,*N*′-di-methylhydrazine and 2-methoxyethanol for 19 hr, an oily product was obtained upon evaporation of the solvent, which was hydrogenated in the presence of the Raney nickel catalyst under 3.4 kg/cm^2 of an initial hydrogen pressure for 22 hr at 40°C. The reduction product was acylated with acetic anhydride in pyridine to give crystalline hexaacetyl-actinamine (II) in a yield of 36%, which was identified with an authentic sample[18] by a mixed melting point determination and a comparison of IR spectra.

While I was heated under reflux in a mixture of *N*-methylhydrazine and 2-methoxyethanol for 20 hr and the product was hydrogenated in the presence of Raney nickel, followed by a conventional acetylation, hexaacetyl DL-*N*-methyl-*myo*-inosadiamine-1,3 (III) was obtained in 43% yield. A selective de-*O*-acetylation of III afforded di-*N*,*N*′-acetyl-DL-*N*-methyl-*myo*-inosadiamine-1,3 (IV) in 98% yield, and a hydrolysis of III in 6N hydrochloric acid gave DL-*N*-methyl-*myo*-inosadiamine-1,3 dihydrochloride (V) in 86% yield.

The hydroxyl groups vicinal and in a *cis* position to an amino or acetamido group in aminocyclitols are preferentially displaced by halogen in a mixture of acetyl halide and acetic anhydride.[17,19] Since there is an axial hydroxyl group on C-2 in a *cis*-disposition to the vicinal amino groups in the compound V, the hydroxyl group should be displaced by halogen in a mixture of acetyl halide and acetic anhydride with an inversion of the configuration on C-2.

When V was heated in the mixture of acetyl bromide and acetic anhydride in a sealed tube at 130—135°C for 13 hr, the bromination product was obtained in 22% yield, which was identified to be pentaacetyl-DL-2-bromo-2-deoxy-*N*-methyl-*scyllo*-inosadiamine-1,3 (VI) by analogy with a bromination product of *myo*-inosadiamine-1,3 dihydrochloride in an analogous reaction condition.

Catalytic debromination of VI with Raney nickel and Amberlite IR-4B (OH^-) under a hydrogen stream of 3.4 kg/cm^2 for 20 hr afforded pentaacetyl DL-hyosamine (VII) in a yield of 87%, which was identified with an authentic sample obtained from antibiotic destomycin A[12] with an exception of an optical activity.

To elucidate the reaction mechanism of the present hydrazinolysis, an attempt to isolate an inter-

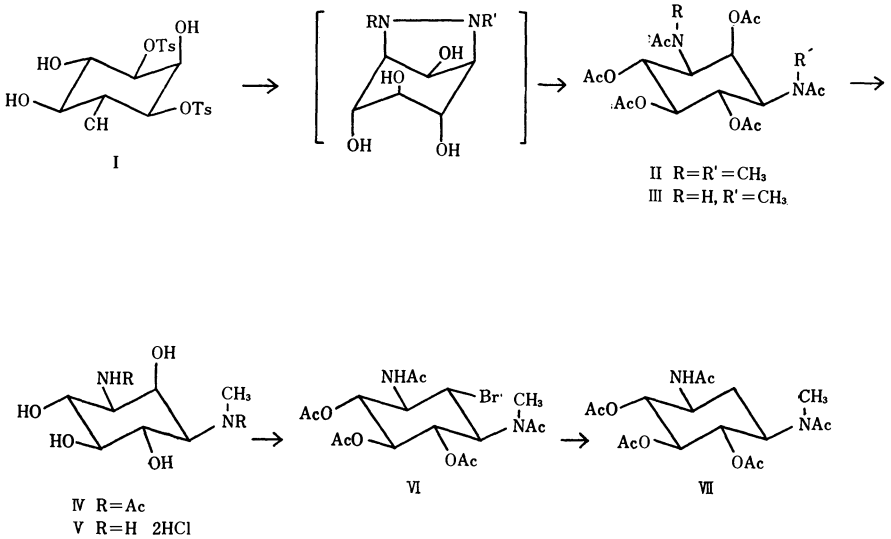

14) T. Suami, F. W. Lichtenthaler and S. Ogawa, This Bulletin, **40**, 1488 (1967).

15) T. Suami, S. Ogawa, S. Naito and H. Sano, *J. Org. Chem.*, **33**, 2831 (1968).

16) T. Suami, S. Ogawa and H. Sano, *Tetrahedron Lett.*, **1967**, 2671.

17) T. Suami, F. W. Lichtenthaler, S. Ogawa, Y. Nakashima and H. Sano, This Bulletin, **41**, 1014 (1968).

18) The authors thank Dr. P. F. Wiley (Upjohn Co., Kalamazoo, Mich., U. S. A.) for supplying an authentic sample of hexaacetyl-actinamine.

19) T. Suami, S. Ogawa, Y. Nakashima and H. Sano, This Bulletin, **40**, 2958 (1967).

mediate in a crystalline state failed. But it seemed quite sure that these hydrazinolyses might proceed through intermediary bicyclic compounds, because II or III was obtained in a considerably good yield as a sole product, and formations of II and III were reasonably explained only by assuming an existence of bicyclic intermediates.

Experimental

The melting points reported were determined on a Mitamura Riken micro hot stage and uncorrected. The PMR spectra of the samples were measured on Varian Associate A-60D spectrometer at the frequency of 60 MHz at a concentration of 10% in deuteriochloroform, deuteriodimethylsulfoxide (d_6-DMSO) or deuterium oxide with tetramethylsilane or sodium trimethylsilylpropanesulfonate as an internal standard. The peak positions are given in τ-values.

Hexaacetyl Actinamine (II). A suspension of 2.18 g of *N,N'*-dimethylhydrazine sulfate in 50 m*l* of 2-methoxyethanol was treated with 1.31 g of sodium hydroxide in 1.5 m*l* of water. A 1.48 g portion of 1,3-di-*O*-*p*-toluenesulfonyl-*myo*-inositol (I) was added to the resulting solution and refluxed for 20 hr. An insoluble material was filtered off and the filtrate was evaporated *in vacuo* to give an oily residue. A solution of the residue in 35 m*l* of water was hydrogenated in the presence of Raney nickel catalyst (two spatula) in a Parr shaker type apparatus at room temperature in the initial hydrogen pressure of 3.4 kg/cm^2. After shaking for 22 hr, the reaction mixture was filtered to remove the catalyst and evaporated to dryness. The glassy residue was treated with a mixture of 15 m*l* of acetic anhydride and 15 m*l* of pyridine at room temperature overnight. Evaporation of excess reagent *in vacuo* gave an oily product, which was chromatographed on active aluminum oxide and eluted with chloroform to afford 507 mg of colorless plates (36.3%), mp 202—203°C. One recrystallization from methanol gave a pure sample of II, mp 205—206°C, which was identified with the authentic sample derived from antibiotic spectinomycin by mixed melting point determination and comparing with IR spectra.

Hexaacetyl DL-*N*-Methyl-*myo*-inosadiamine-1,3 (III). A suspension of 6.63 g of *N*-methylhydrazine sulfate in 50 m*l* of 2-methoxyethanol was treated with 3.69 g of sodium hydroxide in 5 m*l* of water and a precipitated sodium sulfate was removed by filtration. An 1.50 g portion of I was added to the filtrate and the mixture was refluxed for 20 hr under nitrogen. The reaction mixture was evaporated *in vacuo* to dryness and a solution of the residue in 20 m*l* of water was hydrogenated in the presence of Raney nickel catalyst (two spatula) in a Parr shaker type apparatus at 40—50°C in the initial hydrogen pressure of 3.4 kg/cm^2 for 22 hr. Filtering off the catalyst, the solution was evaporated *in vacuo* to dryness. Then the oily product was treated with a mixture of 15 m*l* of acetic anhydride and 15 m*l* of pyridine at room temperature overnight. The reaction mixture was evaporated *in vacuo* to remove excess reagent and the residue was chromatographed on active aluminum oxide. Elution with chloroform gave a colorless oil which crystallized upon addition of ethanol and ether. Recrystallization from ethanol gave colorless rhombic crystals weighing 582 mg (42.7%), mp 229—230°C. IR (KBr): 1750 (OAc), 1694, 1642 and 1525 cm^{-1} (amide). PMR ($CDCl_3$): τ 7.12 (NCH_3), 7.79 (3), 7.95 (6), 7.99 (6) and 8.12 (3)*1 (OAc and NAc).

Found: C, 51.39; H, 6.85; N, 6.17%. Calcd for $C_{19}H_{28}N_2O_{10}$: C, 51.34; H, 6.35; N, 6.30%.

Di-*N,N'*-acetyl-DL-*N*-methyl-*myo*-inosadiamine-1,3 (IV). A 203 mg portion of III was treated with 20 m*l* of methanol saturated with ammonia (at 5°C) overnight at room temperature. The solution was evaporated *in vacuo* to yield an oily residue which crystallized upon trituration by ethyl acetate. Crude crystals were recrystallized from 80% methanol to afford 113 mg of colorless needles (89.3%), mp 253—254°C. PMR (D_2O): τ 6.95, 7.00 (NCH_3), 7.82 (3) and 7.95 (3) (NAc).

Found: C, 48.16; H, 7.82; N, 9.77%. Calcd for $C_{11}H_{20}N_2O_6$: C, 47.82; H, 7.30; N, 10.14%.

DL-*N*-Methyl-*myo*-inosadiamine-1,3 Dihydrochloride (V). A 239 mg portion of III was refluxed with 10 m*l* of 6N hydrochloric acid for 2 hr. The reaction mixture was evaporated *in vacuo* and the crystallization was induced by addition of aqueous ethanol. Colorless needles were obtained by recrystallization from aqueous ethanol, 122 mg (85.5%), mp 300°C (dec.). PMR (D_2O): τ 7.16 (NCH_3).

Found: C, 31.64; H, 6.98; N, 10.45; Cl, 26.52%. Calcd for $C_7H_{16}N_2O_4 \cdot 2HCl$: C, 31.71; H, 6.84; N, 10.56; Cl, 26.75%.

Pentaacetyl-DL-2-bromo-2-deoxy-*N*-methyl-*scyllo*-inosadiamine-1,3 (VI). A mixture of 359 mg of powdered V (dried *in vacuo* P_2O_5 at 100°C), 0.43 m*l* of acetyl bromide and 0.94 m*l* of acetic anhydride was heated in a sealed tube at 130—135°C for 13 hr. After cooling to room temperature, the sealed tube was opened carefully, to which 25 m*l* of ethanol was added dropwise under ice cooling. The reaction mixture was allowed to stand in a refrigerator overnight, and then treated with 20 m*l* of Amberlite IRA-400 (OH^-). The solution was evaporated *in vacuo* to drynesss and the residue was acetylated with a mixture of 25 m*l* of acetic anhydride and 25 m*l* of pyridine at room temperature overnight. The mixture was evaporated *in vacuo* to remove excess reagent and the residue was dissolved in a small amount of chloroform. The solution was chromatographed on active aluminum oxide and eluted with chloroform afforded an oil which crystallized upon trituration by a mixture of ethanol and ether. Crude crystals (233 mg) showed mp 165—175°C and a small amount of III was shown to be contained by TLC (silica gel, chloroform-ethanol=8 : 2). Fractional crystallization from ethanol and ether afforded 80 mg of III and 120 mg of VI, mp 168—180°C (dec.). The yield of VI was 22.0% based on V consumed. Recrystallization from ethanol and ether gave analytical pure crystals of VI, mp 179—183°C (dec.). PMR ($CDCl_3$): τ 6.85, 7.10, 7.20 (NCH_3), 7.79, 7.88, 7.92 and 7.98 (OAc and NAc).

Found: C, 44.19; H, 5.52; N, 6.03; Br, 16.76%. Calcd for $C_{17}H_{25}N_2O_8Br$; C, 43.88; H, 5.42; N, 6.02; Br, 17.18%.

Pentaacetyl-DL-hyosamine (VII). A solution of 106 mg of VI in 8 ml of 50% aqueous ethanol was

*1 In parentheses, proton numbers are indicated.

hydrogenated in the presence of Raney nickel catalyst (one spatula) and 1.2 m*l* of Amberlite IR-4B (OH^-) in a Parr shaker type apparatus in the initial pressure of 3.4 kg/cm^2 at room temperature. After shaking for 20 hr, the catalyst and resin were filtered off and the filtrate was evaporated *in vacuo* to give a colorless oil. Trituration by chloroform and ether gave 76 mg of colorless crystals (86.6%), mp 201—202.5°C (with transition at 143—165°C). Recrystallization from chloroform and ether afforded colorless crystals, mp 202—203°C after melting and resolidified at 162—165°C. This product was identified with an authentic active material derived from antibiotic destomycin A by comparing with IR (in chloroform) and PMR (in $CDCl_3$) spectra.

Found: C, 52.50; H, 7.00; N, 7.37%. Calcd for $C_{17}H_{26}N_2O_8$: C, 52.84; H, 6.78; N, 7.25%.

The authors are grateful to Professor Sumio Umezawa for his kind advice, to Mr. Saburo Nakada for his elementary analyses and to Mr. Naoyuki Kato for his assistance in the preparative experiments. The financial support from the Ministry of Education for this work is gratefully acknowledged.

BULLETIN OF THE CHEMICAL SOCIETY OF JAPAN VOL. 43 1846—1849 (1970)

Yields of Methylcyclohexanone Intermediates in the Hydrogenation of Isomeric Cresols over Ruthenium and Palladium Catalysts[1]

Yuzuru TAKAGI, Shigeo NISHIMURA and Kozo HIROTA

The Institute of Physical and Chemical Research, Yamato-machi, Saitama, Department of Industrial Chemistry, Tokyo University of Agriculture and Technology, Koganei, Tokyo, and Department of Chemistry, Faculty of Science, Osaka University, Toyonaka, Osaka

(Received December 24, 1969)

Isomeric cresols have been hydrogenated over ruthenium and palladium catalysts at elevated temperature and pressure. The yields of the methylcyclohexanone intermediates formed were estimated by application of a kinetic method. Hydrogenation with ruthenium catalyst gave 77, 61 and 60% of the ketone as the intermediate for *o*-, *m*- and *p*-cresol, respectively, while with palladium catalyst all isomeric cresols yielded the ketone intermediates quantitatively. The hydrogenation pathways leading to the formation of methylcyclohexanones were discussed. The stereochemistry of hydrogenation of isomeric cresols and methylcyclohexanones were also studied, and the results were interpreted on the basis of the estimated yields of the ketone intermediates.

It is known that cyclohexanones are produced as intermediates in the catalytic hydrogenation of phenols and the ketones produced often accumulate in considerable amounts in the course of hydrogenation.[2-4] Cresols may give stereoisomeric methylcyclohexanols on hydrogenation and the stereochemistry of the hydrogenation is closely related to the production and subsequent hydrogenation of the corresponding methylcyclohexanones formed as intermediates. Although some studies on the hydrogenation of isomeric cresols have recently been reported with rhodium and ruthenium catalysts,[5] and with a rhodium-platinum catalyst,[6] a more detailed study will be required for the quantitative interpretation of the results.

In previous papers,[7,8] we estimated quantitatively the yields of the methylcyclohexanone intermediates formed in the rhodium-catalyzed hydrogenation of isomeric cresols by application of the following three methods: (a) the stereochemistry of the hydrogenation of a cresol and the corresponding methylcyclohexanone, (b) initial yield method, (c) a kinetic interpretation of the product change

1) Presented at the Research Meeting of the Catalysis Society of Japan, Sendai, October, 1968.

2) G. Vavon and A. L. Berton, *Bull. Soc. Chim. Fr.*, [**4**]**37**, 296 (1925).

3) F. Coussemant and J. C. Jungers, *Bull. Soc. Chim. Belges*, **59**, 295 (1950).

4) H. A. Smith and B. L. Stump, *J. Amer. Chem. Soc.*, **83**, 2739 (1961).

5) P. N. Rylander and D. R. Steele, *Engelhard Ind. Tech. Bull.*, **3**, 125 (1964).

6) F. Zymarkowsky and G. Strippel, *Arch. Pharm.*, **297**, 727 (1964).

7) Y. Takagi, S. Nishimura, K. Taya and K. Hirota, *J. Catalysis*, **8**, 100 (1966).

8) Y. Takagi, S. Nishimura and K. Hirota, *ibid.*, **12**, 214 (1968).

during hydrogenation. Although the results obtained by the three methods did not differ much from each other and were in some cases in excellent accord, the kinetic method mentioned above seemed to be the most reliable and widely applicable to the estimation of the ketone intermediates, because of the quantitative nature of the method. In this study, therefore, the yields of the ketone intermediates formed in the ruthenium- and palladium-catalyzed hydrogenations of isomeric cresols have been determined by the kinetic method and the results compared with those obtained previously with rhodium catalyst. Stereochemistry of the hydrogenation has also been studied and interpreted on the basis of the estimated yields of the ketone intermediates.

Experimental

Materials. Cresols and methylcyclohexanones of G. R. grade of the Tokyo Kasei Kogyo Co. were used after fresh distillation through a 30 cm Vigreux column under reduced pressure. The cresols and methylcyclohexanones were sufficiently pure for the present purpose (more than 99% purity as judged from the analysis by gas chromatography of the hydrogenation products).

Catalysts. Ruthenium hydroxide used for hydrogenation was prepared by adding a slight excess of 10% sodium hydroxide solution to a 1% hot aqueous solution of ruthenium chloride.[9] The hydroxide catalyst was used without being prereduced to metals. For the palladium catalyst, 5% palladium-on-carbon of a commercial preparation (obtained from the Nippon Engelhard Co.) was used, since unsupported palladium was easily deactivated during hydrogenation under the present reaction conditions.

Hydrogenation. Hydrogenation was carried out without solvent at 80°C for ruthenium catalyst and at 120°C for palladium catalyst under a hydrogen pressure of 80—100 kg/cm². Cresol (0.1 mol) was hydrogenated with 20 mg of ruthenium hydroxide or with 300 mg of supported palladium in a 100 m*l* bomb equipped with an agitator driven up and down.

Analysis of Products. The reaction mixture was analyzed directly by gas chromatography (detector: hydrogen flame ionization type; column dimension: 3 m by 0.4 cm OD; stationary phase: 10 wt% diglycerol on 60 mesh firebrick; temperature: column 80—95°C, detector 80—95°C; carrier gas: nitrogen at 90—100 m*l*/min).

Results

The hydrogenation of cresol to methylcyclohexanol will proceed through two simultaneous reaction pathways: one *via* methylcyclohexanone and the other not *via* the ketone as indicated below.

As shown in a previous paper on the rhodium-catalyzed hydrogenation,[8] concentration of the ketone (C_2) varying during hydrogenation may be given by Eq. (1) in which C_1 is the concentration of cresol, k_i's are the rate constants for the respective reaction pathways in Scheme 1, and $K=k_2b_2/(k_1+k_3)b_1$ where b_1 and b_2 represent the adsorption coefficients of cresol and methylcyclohexanone, respectively. The yields of the ketone intermediates and the values of K were obtained by finding the most suitable values of $k_1/(k_1+k_3)$ and K in such a way that the following equation, when these values are substituted into it, may represent the actual variation of the concentration of the ketone with the least deviation.

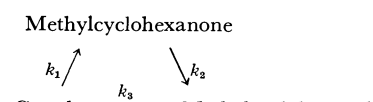

Scheme 1

$$C_2 = \frac{k_1/(k_1+k_3)}{K-1}(C_1 - C_1^K) \qquad (1)$$

The yields of the methylcyclohexanone intermediates and the values of K thus obtained are summarized in Table 1, along with those for the rhodium-catalyzed hydrogenation obtained previously. The theoretical curves given by Eq. (1) showing the variation in the concentration of the ketone are compared with a set of experimental values in Figs. 1,2 and 3 for the hydrogenation of *o*-, *m*- and *p*-cresol, respectively. The data for the rhodium-catalyzed hydrogenation are reproduced in the figures for comparison. The ratios of the adsorption coefficients (b_2/b_1) can be evaluated from the values of K and the ratios of the rate constants of methylcyclohexanone and cresol $[k_2/(k_1+k_3)]$.*1

Table 1. Estimation of methylcyclohexanone intermediate by kinetic method in hydrogenation of cresol with platinum metal catalysts of group $VIII_2$

Cresol	Catalyst	Yield of the ketone intermediate, mol%[a]	K	$\frac{k_2}{k_1+k_3}$	$\frac{b_2}{b_1}$
Ortho	Ru	77	0.98	0.14	6.9
Meta	Ru	61	2.25	3.05	0.74
Para	Ru	60	3.50	1.54	2.3
Ortho	Pd/C	100	0.94	1.71	0.57
Meta	Pd/C	100	1.07	1.50	0.65
Para	Pd/C	110	1.60	2.31	0.50
Ortho	Rh[b]	55	0.07	0.09	0.78
Meta	Rh[b]	52	0.25	0.53	0.47
Para	Rh[b]	54	0.30	0.39	0.77

a) Given by $100k_1/(k_1+k_3)$.
b) Reproduced from Ref. 8.

*1 These were obtained from the initial rates of hydrogenation of methylcyclohexanone and cresol under the same conditions.

9) Y. Takagi, T. Naito and S. Nishimura, This Bulletin, **38**, 2119 (1965).

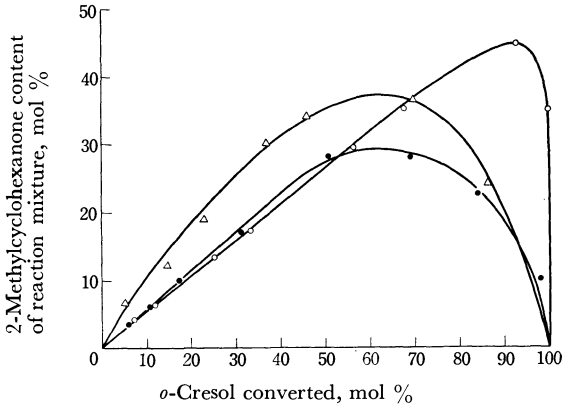

Fig. 1. 2-Methylcyclohexanone intermediate formed in hydrogenation of *o*-cresol over Ru, Rh and Pd/C catalysts as a function of the conversion of the cresol; temp., 80°C for Ru and Rh; 120°C for Rd/C; hydrogen press., 80—100 kg/cm². Experimental values in the Figure are a set of results obtained by separate experiments in each hydrogenation:
● Ru; ○ Rh; △ Pd/C. ——: Theoretical curve given by Eq. (1).

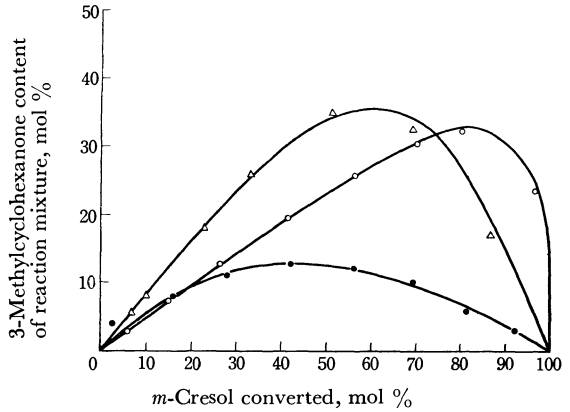

Fig. 2. 3-Methylcyclohexanone intermediate formed in hydrogenation of *m*-cresol over Ru, Rh and Pd/C catalysts as a function of the conversion of the cresol. For other indications see Fig. 1.

They are also listed in Table 1. The stereoisomeric compositions of the methylcyclohexanols produced by hydrogenation of cresols and methylcyclohexanones under comparable conditions are summarized in Table 2, along with those for the rhodium-catalyzed hydrogenation.

Discussion

It has been shown by the kinetic method that the rhodium-catalyzed hydrogenation of isomeric cresols yielded 52—55% of methylcyclohexanones as intermediates.[8] The yields obtained by the other two methods ranged between 43—66%. For the formation of the ketone intermediates in large amounts, we have suggested an explanation which is based on the assumptions that all dihydrocresols are produced from parent cresols in equal probability and that unsaturated ketones or their enols formed

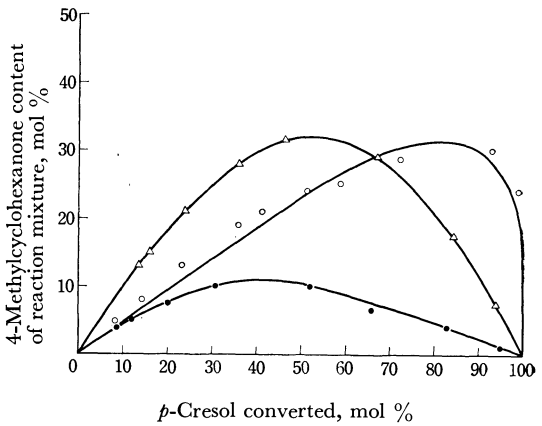

Fig. 3. 4-Methylcyclohexanone intermediate formed in hydrogenation of *p*-cresol over Ru, Rh and Pd/C catalysts as a function of the conversion of the cresol. For other indications see Fig. 1.

Table 2. Stereochemistry of hydrogenation of cresol and methylcyclohexanone with platinum metal catalysts of group VIII[2]

Catalyst	Cresol or cyclohexanone	Composition of methylcyclohexanol, %			
		From cresol		From ketone[a]	
		cis	*trans*	*cis*	*trans*
Ru	Ortho or 2-methyl	60	40	58	42
Ru	Meta or 3-methyl	56.5	43.5	51	49
Ru	Para or 4-methyl	59.5	40.5	53	47
Pd/C	Ortho or 2-methyl	54	46	54	46
Pd/C	Meta or 3-methyl	62	38	62	38
Pd/C	Para or 4-methyl	46	54	45	55
Rh[b]	Ortho or 2-methyl	78	22	64	36
Rh[b]	Meta or 3-methyl	64	36	49	51
Rh[b]	Para or 4-methyl	73	27	70	30

a) The mean of the values obtained by hydrogenating the respective ketone in phenol and cyclohexanol solutions under the same conditions as used for the hydrogenation of the corresponding cresol.
b) Reproduced from Ref. 7.

are preferentially converted to saturated ketones on further hydrogenation. According to these assumptions, all isomeric cresols should give the ketone intermediates in 67% yield. It was pointed out that the yields estimated on the rhodium-catalyzed hydrogenation were close to this value and that they were nearly the same for *o*-, *m*- and *p*-cresol. As seen from Table 1, the yields of the ketone intermediates obtained with ruthenium catalyst are even more close to the value 67%, and the assumptions mentioned above also appear to hold for the ruthenium-catalyzed hydrogenation. It is to be noted that *o*-cresol gave a considerably greater yield of the ketone (77%) than *m*- and *p*-cresol (60—61%) over ruthenium. In the palladium-catalyzed hydrogenation all isomeric cresols gave quantitative yields of the ketone intermediates.*2 Obviously the assumption that all dihydrocresols are produced in equal probability does not hold with this metal. It might be possible that over palladium cresol is hydrogenated in the keto form (I) rather than in the enol form (II) or it is hydrogenated through the selective formation of the dihydro intermediate (III). The hydrogenation of I or III is expected to give the saturated ketone

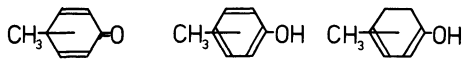

(I) (II) (III)

quantitatively.*3

From Table 1 it will also be seen that the values of K are in the order with respect to catalyst metals, rhodium<palladium<ruthenium for every isomeric cresol. With respect to the three isomers of cresol the values of K decrease in the order, para>meta>ortho for any catalyst metal. The ratio b_2/b_1 is not always in the same order as K. It is of interest that the ratio is the smallest for hydrogenation of *m*-cresol both on rhodium and ruthenium catalysts.

A rather large yield of the ketone intermediate obtained in hydrogenation of *o*-cresol with ruthenium catalyst is supported by a small difference in the stereoisomeric compositions of the methylcyclohexanols formed from *o*-cresol and from 2-methylcyclohexanone (see Table 2). The results in Table 2 also indicate that the ketone intermediates are produced quantitatively in hydrogenation with palladium catalyst, because the methylcyclohexanols of the same stereoisomeric composition were obtained in the hydrogenation of cresols and the corresponding methylcyclohexanones, and thus support the conclusion deduced by the kinetic method. The results also indicate that the adsorption-desorption equilibrium was completely established in the formation and hydrogenation of the ketone intermediate on the surface of the palladium catalyst.

*2 Nearly quantitative formation of cyclohexanone has also been reported recently on the hydrogenation of phenol with a palladium-carbon catalyst in acetic acid at 50°C under the hydrogen pressure of 1 atm [M. Matsumoto, T. Suzuki and S. Suzuki, *Kogyo Kagaku Zasshi*, **72**, 881 (1969)].

*3 The possibility that the methylcyclohexanone intermediates are formed through the production of allyl type alcohols, followed by isomerization to the ketones, is excluded, because the hydrogenolysis product (methylcyclohexane), which would result from the allyl type alcohols, was not found in the products of the palladium-catalyzed hydrogenation.

BULLETIN OF THE CHEMICAL SOCIETY OF JAPAN VOL. 43 1850—1854 (1970)

Studies of Peptide Antibiotics. XIX. Syntheses of 1,1′-Leucine-gramicidin S and 1-Leucine-cyclosemigramicidin S

Michio KONDO* and Nobuo IZUMIYA**

*Department of Chemistry, Faculty of Science and Engineering, Saga University, Saga
**Laboratory of Biochemistry, Faculty of Science, Kyushu University, Fukuoka

(Received December 25, 1969)

Analogs of gramicidin S, 1,1′-L-leucine-gramicidin S (XI) and 1-L-leucine-cyclosemigramicidin S (XII), have been synthesized and tested for antibacterial properties. The cyclization reaction of a linear decapeptide active ester, in which δ-amino functions of ornithine residues were protected with benzyloxycarbonyl groups, yielded exclusively a protected cyclic decapeptide which was hydrogenated to afford the dihydrochloride of XI. A linear pentapeptide active ester afforded a mixture of protected cyclic penta and decapeptide. The pure protected cyclic pentapeptide was obtained with the use of a Sephadex LH-20 column, and the hydrogenolysis of the product afforded the hydrochloride of XII. The decapeptide analog (XI) was as active as natural gramicidin S, whereas the pentapeptide (XII) showed no activity toward any of the microorganisms tested.

We reported that 1,1′-L-alanine gramicidin S was as active as natural gramicidin S (GS) (Fig. 1) toward several microorganisms.[1] The result indicated that the side chains of valine residues, the isopropyls, in a GS molecule can be replaced by smaller aliphatic side chains, the methyls, without a decrease in the antibacterial activity. From this finding, it seemed of interest to investigate the antibacterial properties of an analog of GS with larger side chains than the isopropyls of the valines.

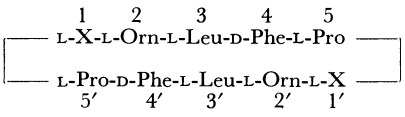

Fig. 1. Structure of GS and its analog.
X represents amino acid residue such Val (GS) or Leu (XI).

This paper will describe the synthesis and antibacterial properties of 1,1′-L-leucine-GS besides the preparation of the cyclic pentapeptide, 1-L-leucine-cyclosemiGS.

Figure 2 indicates the route for the synthesis of the desired cyclic decapeptide (XI).[2] Condensation of the azide derived from *p*-methoxybenzyloxycarbonyl pentapeptide hydrazide (V) with the corresponding neutral pentapeptide (VII) gave an acyldecapeptide acid (VIII). Acid VIII was transformed to an acyldecapeptide nitrophenyl ester, and its *p*-methoxybenzyloxycarbonyl group was removed by means of trifluoroacetic acid.

TABLE 1. RATIO OF PROTECTED CYCLIC MONOMER AND DIMER AFTER CYCLIZATION OF LINEAR PENTAPEPTIDE ACTIVE ESTERS

p-Nitrophenyl ester of[a]	Ratio of compounds in product[b]	
	Z-cyclic monomer	di-Z-cyclic dimer
H-Gly-Orn(Z)-Leu-D-Phe-Pro-OH[1]	100	0
-Ala-[1]	91	9
-Leu-	78	22
-Val-[3]	32	68
-Gly-Lys(Z)-[c]	100	0
-Val-Lys(Z)-[d]	29	71

a) The first compound is listed and only variations of the residue are shown.
b) The concentration of pentapeptide nitrophenyl esters in pyridine was 3×10^{-3} M.
c) M. Kondo and N. Izumiya, to be published.
d) M. Waki, O. Abe, R. Okawa, T. Kato, S. Makisumi and N. Izumiya, This Bulletin, **40**, 2904 (1967).

1) M. Kondo and N. Izumiya, This Bulletin, **40**, 1975 (1967).

2) Abreviations: GS, gramicidin S; Z-, benzyloxycarbonyl; Z(OMe)-, *p*-methoxybenzyloxycarbonyl; -ONp, *p*-nitrophenoxy; CMC, carboxymethyl cellulose; DMF, dimethylformamide; MA, mixed anhydride; TLC, thin-layer chromatography. Amino acid symbols except D-Phe denote the L-configuration.

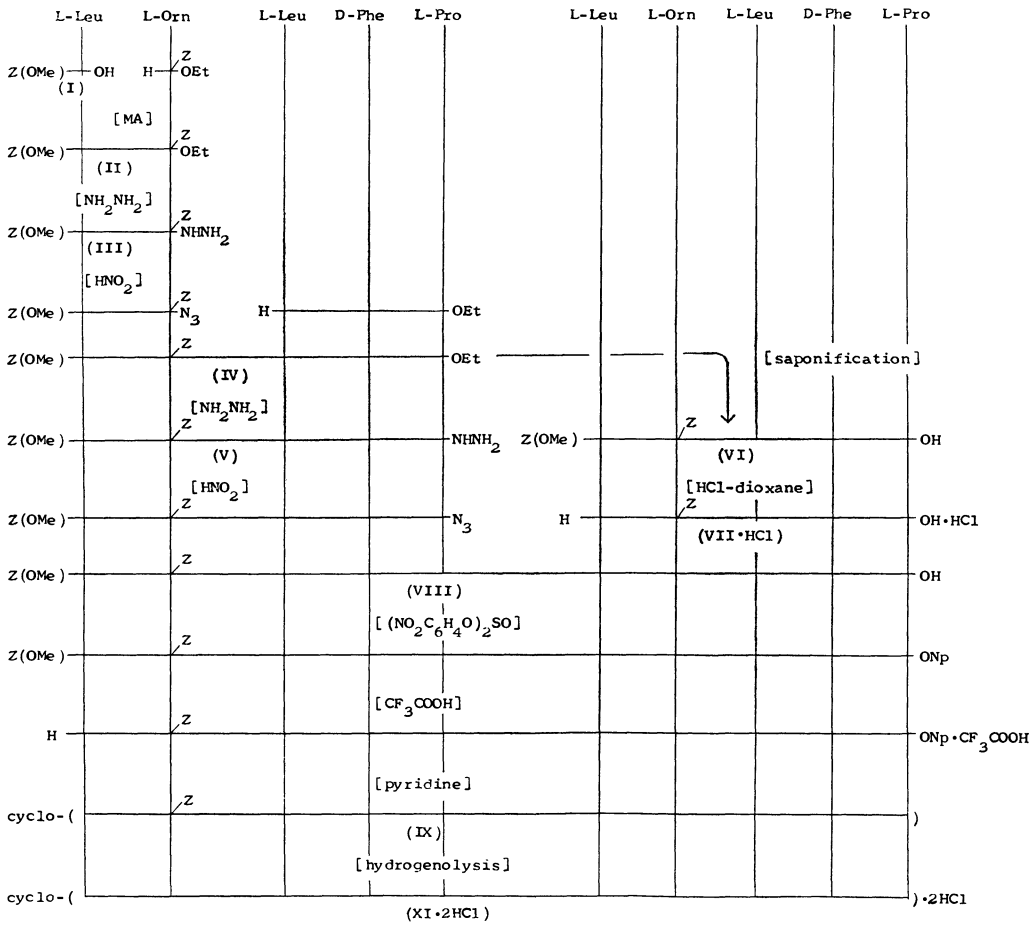

Fig. 2. Cyclization of linear decapeptide active ester.

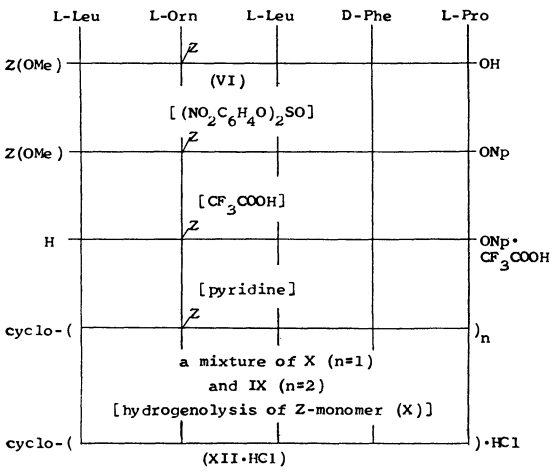

Fig. 3. Cyclization of linear pentapeptide active ester.

Decapeptide ester trifluoroacetate thus obtained was treated with pyridine for the cyclization reaction. The reaction mixture yielded a pure benzyloxycarbonyl-substituted cyclic decapeptide (IX) which was hydrogenated to afford the desired cyclic decapeptide (XI) as a crystalline dihydrochloride.

Synthesis of the protected cyclic decapeptide (IX) was attempted by possible dimerization reaction of the linear pentapeptide active ester which was derived from *p*-methoxybenzyloxycarbonyl pentapeptide acid (VI) (Fig. 3). Treatment of the active ester with pyridine afforded a mixture of the protected monomer (X) and dimer (IX); the ratio in weight of X and IX in the mixture was found to be approximately 78 : 22. Separation of the components was achieved with the use of a Sephadex LH-20 column with methanol as an eluting solvent, the protected monomer (X) being obtained as a pure crystalline material. Hydrogenolysis of X in the presence of hydrogen chloride yielded a crystalline hydrochloride of the cyclic pentapeptide (XII).

The weight ratios of the protected cyclic monomer and dimer in the crude product after the cyclization reaction of the linear pentapeptide active ester are shown in Table 1 with the previous results related to the present paper. It is recognized that the

Table 2. Amount of compound necessary for complete inhibition of growth, $\mu g/ml$

	A. Bouillon agar medium, pH 7.0				
	B. subtilis	*St. aureus*	*E. coli*	*Pr. vulgaris*	*M. avium*
GS	5	5	>100	>100	>100
Leu-GS (XI)	10	5	>100	>100	>100
Leu-semiGS (XII)	>100	>100	>100	>100	>100
	B. Synthetic medium, pH 7.0				
	B. subtilis	*St. aureus*	*E. coli*	*Pr. vulgaris*	*M. avium*
GS	2	5	>100	>100	>100
Leu-GS (XI)	5	10	>100	>100	>100
Leu-semiGS (XII)	>100	>100	>100	>100	>100

pentapeptide sequence with the alanine or leucine residue as N-terminus is more favorable for the intramolecular cyclization reaction compared with that with the valine residue.[3] This means that the degree of the monomer formation is influenced more profoundly by the shape of the side chain of the N-terminus in the pentapeptide active ester than its size; the side chain of valine is indicated as R–CH(R)– (R, methyl), whereas that of alanine or leucine as R–CH_2– (R, H or isopropyl). In this connection, the syntheses of 1,1′-L-isoleucine-GS and several related compounds are in progress.

The antibacterial activities of the synthetic cyclic peptides toward several microorganisms are listed in Table 2. It was observed that 1-leucine-cyclo-semiGS (XII) exhibited no antibacterial activity similar to those of 1-glycine and 1-alanine-cyclosemi-GS,[1] whereas 1,1′-leucine-GS was as active as natural GS against several microorganisms. The results indicate that the side chains of the valine residues in a GS molecule can be replaced with larger aliphatic side chains, the isobutyls, without influencing antibacterial activity.

Experimental

Melting points were not corrected. Prior to analysis, the compounds were dried to a constant weight over phosphorus pentoxide at 60°C and 2 mmHg, except in the case of the cyclic peptide hydrochlorides (XI·2HCl and XII·HCl).

Z(OMe)-Leu-OH (I). The general procedure[4] to prepare Z(OMe)-amino acid was modified as follows. A mixture of L-leucine (3.93 g, 30 mmol), water (90 m*l*), dioxane (90 m*l*), sodium bicarbonate (6.05 g) and *p*-methoxybenzyloxycarbonyl azide (7.46 g, 36 mmol) was stirred at room temperature for 60 hr, the reaction being followed by TLC. The solution was evaporated *in vacuo* to a small volume, extracted with ether, acidified with 0.5M citric acid, and then extracted with ethyl acetate. The organic layer was dried over sodium sulfate and evaporated to dryness. The product was obtained as an oil; yield, 6.55 g (74%). Reported yield for the oil, 28%.[4] A part of the oily product was converted to crystalline dicyclohexylamine salt; yield 85%; mp 163°C; $[\alpha]_D^{15}$ −6.8° (*c* 2, methanol). Reported value for the salt; mp 162°C; $[\alpha]_D^{24}$ −6.67° (methanol).[4]

Z(OMe)-Leu-Orn(δ-Z)-OEt (II). To a chilled solution of I (5.02 g) and triethylamine (1.99 m*l*) in tetrahydrofuran (28 m*l*), isobutylchloroformate (1.86 m*l*) was added. After 15 min, a mixture of H-Orn(δ-Z)-OEt·TsOH,[5] triethylamine (1.99 m*l*) and chloroform (38 m*l*) was added to the chilled solution. The reaction mixture was allowed to stand overnight, evaporated *in vacuo*, and the residue was dissolved in ethyl acetate (100 m*l*). The solution was washed with 0.5M citric acid, 4% sodium bicarbonate and water, dried over sodium sulfate and then evaporated *in vacuo*. The oily residue was crystallized by the addition of a mixture of ether and petroleum ether. It was recrystallized from ethyl acetate-ether-petroleum ether; yield, 5.97 g (81%); mp 109—110°C; $[\alpha]_D^{15}$ −6.3° (*c* 2, DMF).

Found: C, 62.74; H, 7.12; N, 7.41%. Calcd for $C_{30}H_{41}O_8N_3$: C, 63.03; H, 7.23; N, 7.35%.

Z(OMe)-Leu-Orn-(δ-Z)-NHNH$_2$ (III). A solution of II (5.15 g) and hydrazine hydrate (9 m*l*) in DMF (35 m*l*) was allowed to stand for 2 days at 30°C. The solution was concentrated *in vacuo* to a small volume. The hydrazide which precipitated upon the addition of water was collected; yield, 4.70 g (94%); mp 147—148°C; $[\alpha]_D^{15}$ −7.4° (*c* 1, DMF).

Found: C, 58.41; H, 7.17; N, 12.19%. Calcd for $C_{28}H_{39}O_7N_5 \cdot H_2O$: C, 58.42; H, 7.18; N, 12.17%.

Z(OMe)-Leu-Orn(δ-Z)-Leu-D-Phe-Pro-OEt (IV). To III (4.47 g, 8 mmol) dissolved in acetic acid (35 m*l*) and N hydrochloric acid (16 m*l*) was added sodium nitrite (0.66 g) in water (5 m*l*) at −5°C. After 10 min, the solution was diluted with water (120 m*l*). The azide precipitated was extracted with ethyl acetate (150 m*l*), and the organic layer was washed with 4% sodium bicarbonate and water. After being dried over sodium sulfate for 15 min at 0°C, the filtrate was added to a solution of H-Leu-D-Phe-Pro-OEt·HCl (3.87 g, 8.8 mmol)[6] dissolved in triethylamine (1.24 m*l*) and DMF (50 m*l*). The mixture was stirred for 3 days at

3) M. Waki and N. Izumiya, *J. Amer. Chem. Soc.*, **89**, 1278 (1967); This Bulletin, **40**, 1687 (1967).

4) F. Weygand and K. Hunger, *Chem. Ber.*, **95**, 1 (1962).

5) N. Izumiya, T. Kato, Y. Fujita, M. Ohno and M. Kondo, This Bulletin, **37**, 1807 (1964).

6) M. Ohno, T. Kato, S. Makisumi and N. Izumiya, *ibid.*, **39**, 1738 (1966).

0°C, and then evaporated *in vacuo*. The precipitate formed upon the addition of water was collected, and washed with 4% sodium bicarbonate, 0.5M citric acid and water. The product was recrystallized from methanol-ether-petroleum ether; yield, 5.81 g (78%); mp 147—148°C; $[\alpha]_D^{15}$ −31.0° (*c* 1, DMF); R_f 0.98;[7] R_f of hydrogenated product of IV, 0.77[7] and 0.91.[8]

Found: C, 64.44; H, 7.62; N, 8.96%. Calcd for $C_{50}H_{68}O_{11}N_6$: C, 64.63; H, 7.38; N, 9.05%.

Z(OMe)-Leu-Orn(δ-Z)-Leu-D-Phe-Pro-NHNH$_2$ (V). A solution of IV (0.929 g, 1 mmol) and hydrazine hydrate (2 m*l*) in DMF (10 m*l*) was allowed to stand for 3 days at 30°C. The solution was then evaporated *in vacuo* in order to remove the excess hydrazine. The product which precipitated upon the addition of water was collected by filtration; yield, 0.851 g (93%); mp 144—147°C; $[\alpha]_D^{15}$ −38.2° (*c* 1, DMF); R_f of hydrogenated product of V, 0.77.[8]

Found: C, 62.24; H, 7.36; N, 11.89%. Calcd for $C_{48}H_{67}O_{10}N_8 \cdot \frac{1}{2}H_2O$: C, 62.32; H, 7.41; N, 12.11%.

Z(OMe)-Leu-Orn(δ-Z)-Leu-D-Phe-Pro-OH (VI). To a solution of IV (0.929 g, 1 mmol) in methanol (15 m*l*) and dioxane (15 m*l*), 0.46N sodium hydroxide (2.3 m*l*) was added at 0°C. The solution was allowed to stand overnight at room temperature and then concentrated *in vacuo* at 10—15°C. To the residue was added water (20 m*l*), and the mixture was extracted with ether. The aqueous layer was diluted with dioxane (10 m*l*) and acidified with N hydrochloric acid (1.07 m*l*) at 0°C. The mixture was evaporated to remove dioxane *in vacuo* at 0°C, and the crystals produced were collected by filtration. It was recrystallized from dioxane-ether-petroleum ether; yield, 0.692 g (77%); mp 109—112°C; $[\alpha]_D^{15}$ −33.6° (*c* 0.5, DMF); R_f 0.82.[7]

Found: C, 63.21; H, 7.40; N, 9.20%. Calcd for $C_{48}H_{64}O_{11}N_6 \cdot \frac{1}{2}H_2O$: C, 63.35; H, 7.20; N, 9.24%.

H-Leu-Orn(δ-Z)-Leu-D-Phe-Pro-OH·HCl (VII·HCl). To a mixture of VI (0.70 g, 0.77 mmol) and anisole (0.1 m*l*), 3.4N hydrogen chloride in dioxane (4.5 m*l*) was added at room temperature. After 2 hr, the solution was evaporated to dryness, and the residue was triturated with ether. The crystals were collected with the aid of ether; yield, 0.584 g (97%); mp 142—144°C; $[\alpha]_D^{15}$ −28.0° (*c* 1, DMF); R_f 0.79[7] and 0.81.[8]

Found: C, 60.05; H, 7.44; N, 10.55%. Calcd for $C_{39}H_{56}O_8N_6 \cdot HCl \cdot \frac{1}{2}H_2O$: C, 59.87; H, 7.47; N, 10.74%.

Z(OMe)-Leu-Orn(δ-Z)-Leu-D-Phe-Pro-Leu-Orn(δ-Z)-Leu-D-Phe-Pro-OH (VIII). To V (0.601 g) dissolved in DMF (8 m*l*) and N hydrochloric acid (2 m*l*) was added sodium nitrite (0.052 g) in water at −5°C. After 15 min, cold water was added to the solution. The azide precipitated was collected by filtration and washed with 4% sodium bicarbonate and water, and then dried in a vacuum in a desiccator. The azide was added to a solution of VII (0.507 g) and triethylamine (0.18 m*l*) in DMF (12 m*l*). The mixture was stirred for 3 days at 0°C and then evaporated *in vacuo*. The precipitate formed upon the addition of water was collected, washed with 0.5M citric acid and water, and dried. The product was recrystallized from dioxane-ether-petroleum ether; yield, 0.968 g (89%); mp 119—121°C; $[\alpha]_D^{15}$ −50.0° (*c* 1, DMF); R_f 0.90;[7] R_f of hydrogenated product of VIII, 0.60.[7]

Found: C, 63.08; H, 7.56; N, 10.13%. Calcd for $C_{87}H_{118}O_{18}N_{12} \cdot 2H_2O$: C, 63.10; H, 7.43; N, 10.15%.

***cyclo*-(Leu-Orn(δ-Z)-Leu-D-Phe-Pro-)$_2$ (IX).** To a solution of VIII (0.662 g, 0.4 mmol) in pyridine (5 m*l*) was added di-*p*-nitrophenyl sulfite at room temperature. After 20 hr, the solution was evaporated and the residue was collected with the aid of a mixture of ether and petroleum ether. The yield of acyldecapeptide *p*-nitrophenyl ester was 0.655 g, and the *p*-nitrophenyl ester content was estimated to be 99% by measuring the optical density at 412 mμ.[9] This was treated with anisole (0.2 m*l*) and trifluoroacetic acid (4 m*l*) at −5°C. After 30 min, the solution was evaporated *in vacuo* at 0°C, and the residue was collected with ether. The decapeptide *p*-nitrophenyl ester trifluoroacetate so obtained was dissolved in DMF (8 m*l*) and acetic acid (0.1 m*l*). The solution was added dropwise into pyridine (150 m*l*) at 60°C for 4 hr and the stirring was continued for additional 2 hr. The solution was evaporated, and the residue was dissolved in a mixture of methanol (40 m*l*) and water (15 m*l*). After the insoluble substance in small amount was filtered off, the filtrate was passed through columns (1.8×10 cm) of Dowex 1 (OH^- form) and Dowex 50 (H^+ form). The columns were then washed with the same solvent, the combined effluents (400 m*l*) were evaporated, and the product was collected by filtration with the aid of water (yield, 0.235 g). It was recrystallized from methanol-ether-petroleum ether; yield, 0.222 g (39% from VIII); mp 138—140°C; $[\alpha]_D^{15}$ −188° (*c* 0.25, acetic acid); R_f 0.93.[7]

Found: C, 64.34; H, 8.04; N, 11.89%; mol wt, 1482.[10] Calcd for $C_{78}H_{108}O_{14}N_{12} \cdot H_2O$: C, 64.35; H, 7.62; N, 11.55%; mol wt, 1456.

***cyclo*-(Leu-Orn(δ-Z)-Leu-D-Phe-Pro-) (X).** Compound VI (0.586 g, 0.65 mmol) was treated with di-*p*-nitrophenyl sulfite (1.68 g) in pyridine (4.5 m*l*) as described for the preparation of acyldecapeptide ester, and acylpentapeptide *p*-nitrophenyl ester (0.66 g) was obtained as an amorphous powder; its *p*-nitrophenyl ester content was estimated to be 96%. The substance was treated with trifluoroacetic acid, and the pentapeptide *p*-nitrophenyl ester trifluoroacetate was added to pyridine (180 m*l*) as described above. The effluent from the ion-exchangers was evaporated to yield a powdery residue (0.186 g); the residue was designated as XIII. Two mg of XIII was hydrogenated, and the CMC column chromatography of the hydrogenated material (XIV) showed two peaks (Fig. 5-XIV). It was determined that the faster peak contained the cyclic pentapeptide (XII), the slower peak the cyclic decapeptide (XI), and the ratio of the integrated areas of the

7) The R_f of TLC with Merck Silica Gel G refers to the *n*-butanol-acetic acid-pyridine-water (4 : 1 : 1 : 2, v/v) system. Compounds possessing a free amino group were detected by spraying with ninhydrin, and those with blocked amino groups, by spraying with 47% hydrobromic acid and then ninhydrin.

8) The R_f of the paper chromatography with Toyo Roshi No. 52 refers to the *n*-butanol-acetic acid-pyridine-water (4 : 1 : 1 : 2, v/v) system.

9) R. Schwyzer and P. Sieber, *Helv. Chim. Acta*, **43**, 1760 (1960).

10) The molecular weight was determined on a Hitachi Osmometer, type 115, using methanol as the solvent.

two peaks was calculated to be 78 : 22. If the color intensities resulting from ninhydrin between XII (molar base as an unit) and XI (a half molar base as an unit)[1] are assumed to be same, the ratio in weight of X and IX in the residue (XIII) is calculated to be 78 : 22. A half (0.092 g) of the residue (XIII) was dissolved in methanol (1 m*l*), and the solution was applied to a column (1.7×40 cm) with Sephadex LH-20, and the development continued with methanol. Elution was carried out at room temperature, at flow rate of 50 m*l* per 1 hr; a 1.5 m*l* fraction was collected.[3] The main peak appeared from tube number 32 to 42. The other half of the residue (XIII) was chromatographed similarly. The combined fractions were evaporated, and the product was recrystallized from methanol-ether-petroleum ether; yield, 0.121 g (26% from VI); mp 101—104°C; $[\alpha]_D^{15}$ −112° (*c* 0.25, acetic acid); R_f 0.93.[7]

Found: C, 63.40; H, 7.91; N, 11.20%; mol wt, 757.[10] Calcd for $C_{39}H_{54}O_7N_6 \cdot H_2O$: C, 63.56; H, 7.66; N, 11.41%; mol wt, 737.

***cyclo*-(Leu-Orn-Leu-D-Phe-Pro-)$_2$·2HCl(XI·2HCl).** A solution of IX (102 mg, 0.07 mmol) in 0.04N methanolic hydrogen chloride (2 m*l*) was subjected to hydrogenolysis in the presence of palladium black. The filtrate was evaporated, and the crystals were collected with the aid of ether; yield of the air dried product, 78 mg (81%); mp 242—244°C (decomp.); $[\alpha]_D^{15}$ −197° (*c* 0.3, acetic acid); R_f 0.97;[8] amino acid ratios in acid hydrolysate; Leu 2.0, Orn 1.0, Phe 0.9, Pro 1.0.

Found: C, 55.26; H, 7.96; N, 12.42%. Calcd for $C_{62}H_{96}O_{10}N_{12} \cdot 2HCl \cdot 6H_2O$: C, 55.14; H, 8.21; N, 12.45%. The air-dried product lost 6.14% of its weight after it had been dried over phosphorus pentoxide at 80°C (2 mmHg) to a constant weight. Calcd for $5H_2O$: 6.74%.

***cyclo*-(Leu-Orn-Leu-D-Phe-Pro-)·HCl (XII·HCl).** Compound X (74 mg, 0.1 mmol) was treated as described above; yield of the air-dried product, 58 mg (84%); mp 200—201°C (decomp.); $[\alpha]_D^{15}$ −143° (*c* 0.3, acetic acid); R_f 0.92;[8] amino acid ratios in acid hydrolysate; Leu 2.0, Orn 1.0, Phe 1.0, Pro 0.9.

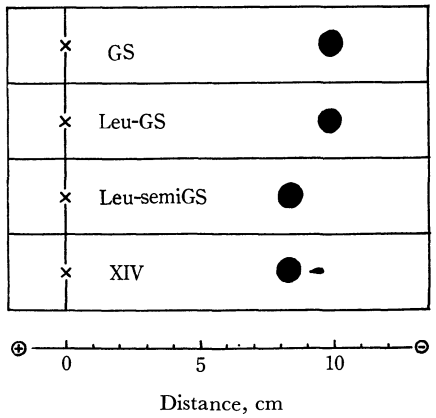

Fig. 4. Paper electrophoresis of GS, Leu-GS (XI), Leu-semiGS (XII) and the hydrogenated material (XIV) after cyclization of pentapeptide ester.

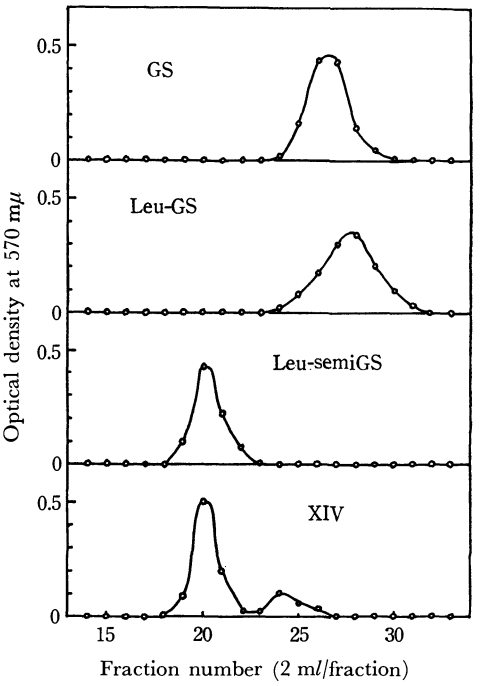

Fig. 5. CMC column chatography of the compounds.

Found: C, 55.29; H, 8.01; N, 12.50%. Calcd for $C_{31}H_{48}O_5N_6 \cdot HCl \cdot 3H_3O$: C, 55.13; H, 8.21; N, 12.45%. The air-dried product lost 5.84% of its weight after being dried. Calcd for $2H_2O$: 5.49%.

Electrophoresis and CMC Chromatography. Electrophoresis on Toyo Roshi No. 52 paper was carried out at pH 1.8 (formic acid-acetic acid-methanol-water, 1 : 3 : 6 : 10, v/v) at 500 V/30 cm for 3 hr. Figure 4 shows that XI migrates toward the cathode faster than XII and that the mobility of XI was similar to that of GS. In CMC column chromatography, a sample (0.5—1 mg) was dissolved in 0.2 m*l* of 0.2M pyridinium acetate containing 30% methanol (pH 5.0), the solution was applied to a column (0.9×50 cm) with CMC (Eastman No. 7796), and development was continued with the same solvent. Two-m*l* fractions were collected at a flow rate of 20 m*l* per 1 hr. The peptide content in the fractions was determined by the ninhydrin method, and the results are shown in Fig. 5.

Microbiological Assays.[11] The minimum amount of compounds necessary for the complete inhibition of growth was determined by a dilution method with a bouillon agar medium and with a synthetic medium. As is shown in Table 2, 1,1′-Leu-GS (XI) was found to be as active as natural GS against *B. subtilis* and *St. aureus*, whereas the cyclic pentapeptide (XII) exhibited no antibacterial activity against the microorganisms tested.

11) We are indebted to Dr. M. Shibata of Takeda Chemical Industries, Ltd. for the biological assay.

BULLETIN OF THE CHEMICAL SOCIETY OF JAPAN VOL. 43 1855—1860 (1970)

Poly-β-Amino Acids. I. The Preparation of Phenyl Substituted β-Amino Acid Polymers

Heimei YUKI, Yutaka TAKETANI, Shuzo YAMASHITA, Hiroshi OKUNO and Hiromichi TANAKA

Department of Chemistry, Faculty of Engineering Science, Osaka University, Toyonaka, Osaka

(Received January 12, 1970)

α-Phenyl-, β-phenyl-, and α,β-diphenyl-β-aminopropionic acid were synthesized. Their polymers were obtained in good yields when the *p*-nitrophenyl esters of β-amino acids were polymerized at 60°C. The ethyl esters gave low-molecular-weight polymers in poor yields at 150°C *in vacuo*. By the thermal polycondensation of β-amino acids themselves at 250°C, polymers were not obtained, but the corresponding cinnamic acid derivatives were obtained by the intramolecular β-elimination reaction. Poly(α-phenyl-β-amino acid), and poly(β-phenyl-β-amino acid) were soluble in trifluoroacetic acid, and chloroform containing a small amount of dichloroacetic acid. On the other hand, poly(α,β-diphenyl-β-amino acid) was soluble only in conc. sulfuric acid, while it was insoluble in usual organic solvents. The DP of poly(β-phenyl-β-amino acid) was about 18. None of the polymers showed any melting point below 300°C.

Many reports and discussions have been published on the syntheses and the properties of poly-α-amino acids. On the other hand, only a few investigations have been reported on poly-β-amino acids, which have only one additional methylene group per residue compared with poly-α-amino acids and which may be expected to have properties as interesting as those of the α-isomers.

Poly(β-alanine) was obtained by Noguchi and Hayakawa[1] *via* the *N*-carbothiophenyl derivative of the amino acid. Breslow and his co-workers[2] prepared the polymer by the polymerization of acrylamide with base catalysts, a process which is called a proton transfer polymerization. Birkofer and Modic[3] also polymerized β-methyl-β-alanine through its *N*-carboxyanhydride. Poly(α,α-dimethyl-β-alanine) was obtained by the thermal polycondensation of β-amino pivalic acid.[4] These polymers seem not to have large molecular weights. Recently, Bestian[5] has obtained high-molecular-weight polymers by the ring-opening polymerization of some substituted β-lactams.

In order to investigate the properties of the polymer, it is necessary that the polymer have a high molecular weight and good solubilities in suitable organic solvents, the solubilities of which may be expected to be brought by a proper substituent in the monomeric unit. In this work, the syntheses of the polymers of α-, β-phenyl-, and α,β-diphenyl-β-aminopropionic acid were investigated. Thermal polycondensations were attempted on the amino acids themselves and their ethyl esters, the latter of which gave only small amounts of the polymers. The *p*-nitrophenyl esters gave the poly-β-amino acids in good yields. The ester is known as an active ester reagent in peptide syntheses. Poly(α-phenyl-β-amino acid) and poly (β-phenyl-β-amino acid) were soluble in trifluoroacetic acid, dichloroacetic acid, and chloroform containing a small amount of dichloroacetic acid. Poly(α,β-diphenyl-β-amino acid) was soluble only in conc. sulfuric acid, while it was insoluble in usual organic solvents. None of the polymers showed any melting point below 300°C.

Experimental and Results

Syntheses of β-Amino Acids. The amino acids were prepared according to the methods of Rodinow and his co-workers[6] and of Steiger.[7] All are racemic forms.

α-Phenyl-β-aminopropionic Acid (α-PA). A hot solution of hydroxylamine hydrochloride (11.0 g) in 100 m*l* of water was added, in one portion, to a solution of sodium ethoxide prepared from 3.5 g of sodium

1) J. Noguchi and T. Hayakawa, *J. Amer. Chem. Soc.*, **76**, 2846 (1954).
2) D. S. Breslow, G. E. Hulse and A. S. Matlack, *ibid.*, **79**, 3760 (1957).
3) L. Birkofer and R. Modic, *Ann. Chem.*, **628**, 162 (1959).
4) J. Linkoln, U.S. 2500317 (1946).
5) H. Bestian, *Angew. Chem.*, **80**, 304 (1968).
6) W. M. Rodinow and W. E. Th. Malewinskaja, *Ber.*, **59**, 2952 (1926).
7) R. E. Steiger, "Organic Syntheses," Coll. Vol. III, p. 91 (1955).

and 105 m*l* of ethanol. The sodium chloride thus precipitated was filtered out; ethyl atropate (11.5 g) was added to the resulting solution, and the resulting mixture was boiled under reflux for 1 day. White precipitates were filtered out, washed with absolute ethanol, and recrystallized from water and ethanol.

β-Phenyl-β-aminopropionic Acid (β-PA). Benzaldehyde (36.9 g) and malonic acid (40.7 g) were added to 120 m*l* of absolute ethanol saturated with dry ammonia, after which the mixture was boiled on a steam bath for 8 hr. After cooling, white precipitates were collected by filtration and recrystallized from water and ethanol.

α,β-Diphenyl-β-aminopropionic Acid (α,β-DPA). α-Phenylcinnamic acid (78.4 g) was added to a solution of hydroxylamine prepared from its hydrochloride (49.0 g) in 35 m*l* of water and sodium ethoxide (0.7 mol) in 350 m*l* of absolute alcohol, and the mixture was boiled under reflux for 8 hr. White precipitates were collected and recrystallized from water and ethanol.

The yields and the analytical data of the amino acids are listed in Table 1.

TABLE 1. β-AMINO ACIDS $H_2NCHR_1CHR_2COOH$

R_1	R_2	Mp (dec) °C	Yield %	Found (Calcd) C%	H%	N%
H	C_6H_5	228	31.6	65.20	6.67	8.28
				(65.44	6.71	8.48)
C_6H_5	H	215	67.8	65.39	6.68	8.67
				(65.44	6.71	8.48)
C_6H_5	C_6H_5	205	30.0	74.43	6.29	5.69
				(74.65	6.28	5.81)

Ethyl Esters of β-Amino Acids. β-Amino acid was suspended in 300 m*l* of dry ethanol, after which dry hydrogen chloride was passed through the mixture until it became homogeneous. The solution was evaporated *in vacuo* at 60°C. Dry ethanol (100 m*l*) was added to the residue and evaporated *in vacuo*. This operation was repeated twice, and then the residue was allowed to stand in a refrigerator overnight. The crude product was recrystallized from ethanol and ether. The results are shown in Table 2.

Into the ethyl ester hydrochloride covered with ether, a 150 m*l* portion of a saturated aqueous solution of sodium carbonate was stirred. The ether layer was separated and the aqueous layer was extracted with ether. The ether solutions were combined and the solvent was distilled off. The vacuum distillation of the residue gave the ethyl esters of amino acid, except for the ester of α,β-DPA which was crystalline and was purified by recrystallization from ethanol and water to give colorless needles. The results are listed in Table 3.

***N*-Carbobenzyloxy-β-amino Acids.** β-Amino acid (30 mmol) was dissolved in 33 m*l* of a 1N aqueous sodium hydroxide solution. The solution was cooled to −3—0°C, and then 33 m*l* of 2N aqueous sodium hydroxide solution and carbobenzoxy chloride (6.1 g) was vigorously stirred into it alternately, portion by portion. After the addition, stirring was continued for 2 hr at 0°C. Then, the solution was acidified to pH 3 with 15 m*l* of 6N hydrochloric acid. The precipitates thus formed were extracted with ether. The extract was dried with anhydrous sodium sulfate, and the ether was evaporated. The residual carbobenzyloxyamino acid was recrystallized from ethanol and water. The results are shown in Table 4.

TABLE 2. β-AMINO ACID ETHYL ESTER HYDROCHLORIDES $HCl\cdot H_2NCHR_1CHR_2COOC_2H_5$

R_1	R_2	Mp °C	Yield %	Found (Calcd) C%	H%	N%	Cl%
H	C_6H_5	162 —163	90.2	57.50	6.97	5.87	15.68
				(57.51	7.02	6.10	15.43)
C_6H_5	H	138.5—139.5	92.0	57.91	7.06	6.16	15.63
				(57.51	7.02	6.10	15.43)
C_6H_5	C_6H_5	194 —197	81.5	66.89	6.67	4.45	11.59
				(66.79	6.60	4.58	11.59)

TABLE 3. β-AMINO ACID ETHYL ESTERS $H_2NCHR_1CHR_2COOC_2H_5$

R_1	R_2	Bp (°C/mmHg) [Mp (°C)]	Yield[a] %	Found (Calcd) C%	H%	N%
H	C_6H_5	96— 96.5/0.5	56.8	68.35	7.87	7.23
				(68.37	7.92	7.25)
C_6H_5	H	100—101.5/1.0	60.0	68.32	7.82	7.22
				(68.37	7.92	7.25)
C_6H_5	C_6H_5	[65—67.5]	73.4	76.16	7.10	5.06
				(75.79	7.12	5.24)

a) Based on amino acid.

Table 4. *N*-Carbobenzyloxyamino acids
$C_6H_5CH_2OCONHCHR_1CHR_2COOH$

R_1	R_2	Mp °C	Yield %	Found (Calcd) C%	H%	N%
H	C_6H_5	122—123	92.9	68.10	5.68	4.71
				(68.21	5.72	4.68)
C_6H_5	H	124	84.9	68.17	5.85	4.71
				(68.21	5.72	4.68)
C_6H_5	C_6H_5	184—186	60.2	73.38	5.68	3.75
				(73.58	5.64	3.73)

p-Nitrophenyl Esters of *N*-Carbobenzyloxyamino Acids. *N*-Carbobenzyloxy-β-amino acid (20 mmol) and *p*-nitrophenol (2.8 g) were dissolved in 90 m*l* of anhydrous ethyl acetate. Into the solution, dicyclohexylcarbodiimide (6.0 g) was stirred at room temperature. After stirring for 20 hr, the precipitated dicyclohexyl urea (4.4 g) was filtered and the filtrate concentrated at reduced pressure. The residue was recrystallized from ethyl acetate and *n*-hexane to give the *p*-nitrophenyl ester of *N*-carbobenzyloxyamino acid. The results are shown in Table 5.

p-Nitrophenyl Ester Hydrobromides of β-Amino Acids. The *p*-nitrophenyl ester of *N*-carbobenzyloxyamino acid (27 mmol) was dissolved in a saturated solution of hydrogen bromide in 33 m*l* of acetic acid at room temperature. After the solution had stood for 1 hr, 200 m*l* of ether were added; the solution was then kept overnight in a refrigerator. The precipitates thus formed were filtered and recrystallized from ethanol and ether. The results are listed in Table 6.

Thermal Polymerization of β-Amino Acids. β-Amino acid (*ca.* 1 g) was placed in a glass ampoule and the ampoule was sealed *in vacuo*. After the ampoule had been heated at 250°C for 24 hr, 10 m*l* of ethanol was added and an insoluble solid was filtered out. The filtrate was then concentrated under reduced pressure, and the residue was recrystallized from ethanol and water. Table 7 shows the results of the thermal polycondensations of the β-amino acids. From α-PA and β-PA, polymeric materials were obtained as solid materials insoluble in ethanol, but the yields were too low for the characteristics to be investigated. The amino acid, α,β-DPA, gave no products insoluble in ethanol. The ethanol-soluble materials were found to be phenyl-substituted acrylic acids, *i. e.*, cinnamic acid from β-PA, and α-phenyl cinnamic acid from α,β-DPA. The material obtained from α-PA was found from the IR spectrum to contain the polymer of atropic acid.

Thermal Polycondensation of Ethyl Esters of β-Amino Acids. The ethyl ester (1—2 g) was placed in an ampoule and sealed *in vacuo*. After it had then been heated at 150°C for 10 days, 20 m*l* of ethanol was added. An insoluble solid was separated by filtration, and the filtrate was concentrated *in vacuo*. The residue was extracted with 50 m*l* of ether, and an ether-insoluble solid was filtered out. When the ether solution was then concentrated, only a syrupy residue was obtained. The results are shown in Table 8. The thermal polycondensations of the ethyl esters gave the ethanol-insoluble polymers in appreciable yields not only *in vacuo*, but also at an ordinary nitrogen pressure. These polymers were insoluble in water, ethanol, acetone, dimethylformamide, and dimethyl sulfoxide, partially soluble in formic acid and *m*-cresol, and soluble in dichloroacetic acid. From the ethanol-soluble parts, lower-molecular-weight polymers were obtained as frac-

Table 6. β-Amino acid *p*-nitrophenyl ester hydrobromides
$HBr\cdot H_2NCHR_1CHR_2COOC_6H_4NO_2$ (*p*)

R_1	R_2	Mp (dec) °C	Yield %	Found (Calcd) C%	H%	N%	Br%
H	C_6H_5	138	96.0	49.20	4.50	7.34	21.68
				(49.06	4.12	7.63	21.76)
C_6H_5	H	175.5	72.3	49.08	4.28	7.74	21.60
				(49.06	4.12	7.63	21.76)
C_6H_5	C_6H_5	199	79.6	56.47	4.38	6.25	18.17
				(56.89	4.32	6.30	18.03)

Table 7. Thermal polycondensation of β-amino acids
Temp. 250°C, Time 2 hr, Pressure 7mmHg

Amino Acid mg		EtOH Insol. mg	Yield %	EtOH Sol. mg	Yield %
α-PA	256	3.5	1.3	—	—
β-PA	836	6.0	0.8	664	86.8[a]
α,β-DPA	1020	0	0	260	25.0[b]

a) Cinnamic acid
b) α-Phenyl cinnamic acid

Table 5. *N*-Carbobenzyloxyamino acid *p*-nitrophenyl esters
$C_6H_5CH_2OCO\text{–}NHCHR_1CHR_2\text{–}COOC_6H_4NO_2$(*p*)

R_1	R_2	Mp °C	Yield %	Found (Calcd) C%	H%	N%
H	C_6H_5	74 — 76	72.8	65.65	4.82	6.65
				(65.70	4.80	6.66)
C_6H_5	H	116.5—117.5	77.6	65.98	4.84	6.62
				(65.70	4.80	6.66)
C_6H_5	C_6H_5	144 —146	55.0	69.73	4.93	5.56
				(70.15	4.87	5.64)

TABLE 8. THERMAL POLYMERIZATION OF β-AMINO ACID ETHYL ESTERS
Temp. 150°C, Time 10 days, pressure 7mmHg

Et Ester		Polymer							
		EtOH Insol.	Anal.[a]			Ether Insol.			
	g	%	C%	H%	N%	%	C%	H%	N%
α-PA-Et	1.345	1.6	—	—	—	3.2	—	—	—
β-PA-Et	1.137[b]	3.1	73.1	6.4	7.8	17.3	71.4	6.5	7.3
	1.166	8.2	73.1	6.3	8.0	22.3	72.4	6.5	7.4
α,β-DPA-Et	2.000	1.4	78.9	5.2	9.1	7.4	—	—	—

a) Calcd for $C_6H_5CH{=}CHCO[NHCH(C_6H_5)CH_2CO]OC_2H_5$
$n=6$ C, 73.7; H, 6.3; N, 7.9%
$n=4$ C, 73.8; H, 6.3; N, 7.3%
Calcd for $H[NHCH(C_6H_5)CH(C_6H_5)CO]_3NH_2$
C, 78.7; H, 6.1; N, 8.2%
b) Pressure 760 mmHg

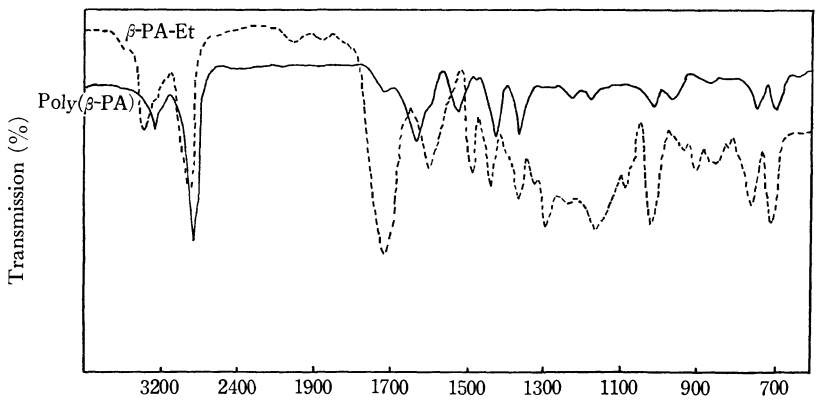

Fig. 1. Infrared spectra of ethyl β-phenyl-β-aminopropionate and polymer. The spectra were taken with JASCO IR-S spectrophotometer with nujol mulls method.

tions insoluble in ether. Figure 1 shows the IR spectra of the monomeric ethyl ester of β-PA and the polymer which was insoluble in ethanol. In the spectrum of the polymer, there are absorptions of polyamide (3240, 1650 and 1530 cm^{-1}), the free ester (1730 cm^{-1}), and α,β-disubstituted C=C double bond (1620 and 960 cm^{-1}). From these absorptions, the probable structure of the polymer may be presented as follows:

$$C_6H_5\text{–}CH{=}CH\text{–}CO(NH\text{–}\underset{\displaystyle C_6H_5}{\underset{|}{CH}}\text{–}CH_2\text{–}CO)_n\text{–}OC_2H_5$$

Polycondensation of *p*-Nitrophenyl Esters of β-Amino Acids. The *p*-nitrophenyl ester (PNP) hydrobromide (2 g) was suspended in 15 m*l* of a purified solvent in an ampoule, which was then flushed with dry nitrogen. In all the solvents used except dimethylformamide, the ester hydrobromides were insoluble. A slight excess of triethylamine was then added to the suspension by means of a hypodermic syringe. Triethylamine hydrobromide was thus separated, and the reaction mixture turned pale yellow. In dimethylformamide the monomer hydrobromides were dissolved completely, but massive precipitates soon appeared when triethylamine was added. The ampoule was left to stand for 72 hr at 60°C with occasional shaking. The reaction proceeded in a heterogeneous state, and the precipitates solidified after 30 minutes. The solid was crushed, filtered, and washed three times with ethanol by applying centrifugration. The resultant pale yellow powder was washed with ether and dried *in vacuo*. No insoluble material was obtained by adding ethanol.

TABLE 9. POLYCONDENSATION OF β-AMINO ACID *p*-NITROPHENYL ESTERS
Monomer HBr 2 g (5.4 mmol) Et_3N 0.658 g (6.5 mmol) Solvent 15 m*l*, Temp. 60°C, Time 72 hr

Solv.	α-PA-PNP[a]		αβ-PA-PNP[a]		α,β-DPA-PNP[b]	
	Yield %	η_{sp}/c (d*l*/g)	Yield %	η_{sp}/c (d*l*/g)	Yield %	η_{sp}/c (d*l*/g)
Tol	98.5	0.10	91.3	0.12	51.8	0.05
Cl-Bz	87.3	0.11	89.6	0.12	54.4	0.03
THF	90.0	0.09	93.6	0.11	3.2	—
Diox	86.9	0.09	84.8	0.10	21.0	0.03
DMF	56.9	0.12	72.0	0.09	0.0	—

Viscosity of the polymer was measured a) in trifluoroacetic acid solution (c=1.0 g/d*l*) at 30.0°C and b) in conc. sulfuric acid solution (c=0.5 g/d*l*) at 30.0°C.

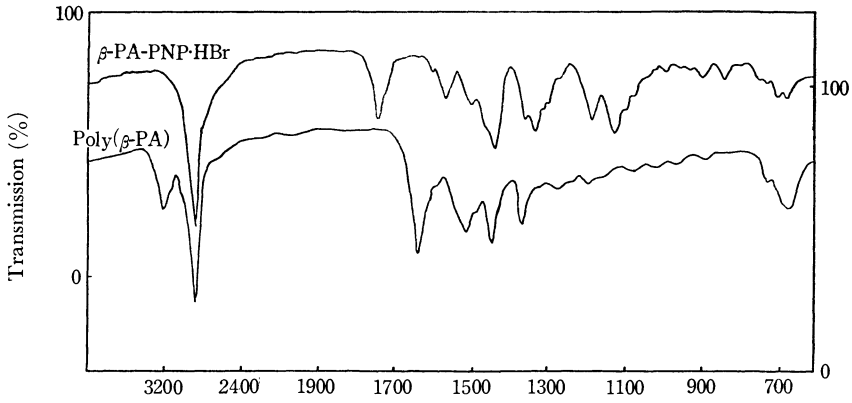

Fig. 2. Infrared spectra of *p*-nitrophenyl β-phenyl-β-aminopropionate hydrobromide and polymer. The spectra were taken with JASCO IR-S spectrophotometer with nujol mulls method.

to supernatant liquid of the reaction mixture. The results of the polymerization reaction are shown in Table 9. The polymers from α-PA-PNP and β-PA-PNP were soluble in dichloroacetic acid and trifluoroacetic acid, partially soluble in *m*-cresol, and insoluble in other usual organic solvents. They were also soluble in the mixture of dichloroacetic acid and chloroform. On the other hand, the polymer from α,β-DPA-PNP was insoluble not only in usual solvents but also in trifluoroacetic acid and dichloroacetic acid. It was soluble only in concentrated sulfuric acid, in which the solution viscosity of the polymer showed no change for a long time. All the polymers were crystalline, and none showed a melting point below 300°C. The IR spectra of β-PA-PNP·HBr and poly(β-PA) are shown in Fig. 2. The degree of polymerization was estimated from the content of the *p*-nitrophenyl group, which was analyzed as the end group by means of UV spectroscopy. The measurements were made on the polymer solution in dichloroacetic acid using the absorption band at 300 mμ and the molar extinction coefficient of the monomeric ester hydrobromide ($\varepsilon=6390$). The degree of polymerization was found to be about 18, with the polymer having a η_{sp}/c value of 0.15.

Viscosity of the Poly(β-Phenyl-β-aminopropionic Acid) *p*-Nitrophenyl Ester in a Chloroform-Dichloroacetic Acid Mixture. The polymer prepared from β-PA-PNP was dissolved in dichloroacetic acid at a given concentration. The solution was then diluted with chloroform and dichloroacetic acid in such a way that the resulting solution had a constant polymer concentration at 0.5 g/d*l* and a known composition of the solvents, the ratios of chloroform to dichloroacetic acid ranging from 0/100 to 90/10 (vol/vol). The viscosity of the solution was measured at 30°C. The results are shown in Fig. 3. No precipitation of the polymer was observed even in the mixed solvent consisting 90% of chloroform. The viscosity was almost constant over the whole range of solvent compositions measured.

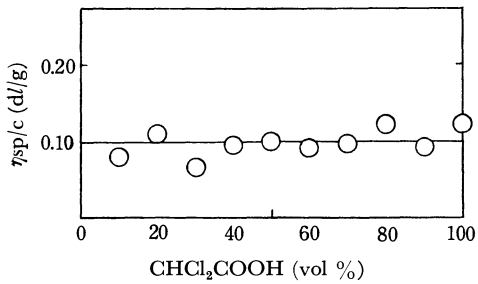

Fig. 3. Viscosity of poly(β-PA) in chloroform-dichloroacetic acid mixture at 30.0°C ($c=0.5$ g/d*l*).

Discussion

Contrary to the polycondensation of β-amino pivalic acid by Linkoln,[4] the polycondensation of the phenyl-substituted β-amino acids used here was not successful because of the removal of ammonia by β-elimination reaction. The removal of ammonia took place intramolecularly much faster than the intermolecular dehydration of β-amino acid.

$$\mathrm{NH_2\text{–}\underset{R_1}{\underset{|}{CH}}\text{–}\underset{R_2}{\underset{|}{CH}}\text{–}COOH} \longrightarrow \mathrm{\underset{R_1}{\underset{|}{CH}}{=}\underset{R_2}{\underset{|}{C}}\text{–}COOH} + \mathrm{NH_3}$$

From α-PA, atropic acid would be obtained, but the acid polymerized easily to poly (α-phenylacrylic acid) above 200°C, so it was difficult to isolate it in a monomeric form.

In the thermal reaction of the ethyl ester of β-amino acid, the polycondensation reaction can compete, although only slightly, with the intramolecular elimination of ammonia, and the polymer was obtained in a low yield. However, the elimination reaction also took place in the polymer thus produced and terminated the further growth of the polymer, forming a double bond in its molecule. By the elementary analysis, the degree of polymerization was roughly estimated to be 4—6 for the polymer derived from the β-PA ethyl ester. The large N content in the polymer obtained from the α,β-DPA ethyl ester may be due to the amide group formed by the reaction between the ester group and the ammonia produced during the polymerization.

The polycondensation of the *p*-nitrophenyl ester seemed to proceed very fast, judging from the observation of the polymer deposit in the reaction mixture. The IR spectrum of the polymer showed an absorption due to NH stretching at 3240 cm^{-1} and no absorption band in the region of the C=C double bond, suggesting that no β-elimination reaction occurred under the reaction conditions empolyed. However, the degree of polymerization of the obtained polymer did not exceed twenty and was almost constant independently of the solvent used in the reaction, as was shown by the viscosity of the polymer in solution. The low degree of polymerization may be attributed to the precipitation of the polymer during polymerization because of its insolubility in the reaction mixture.

In all the polycondensation reactions, α,β-diphenyl-β-amino acid and its esters gave the polymers in low yields and with a low degree of polymerization compared with the other two amino acids and their esters. This must be caused by the steric hindrance due to the bulky substituents occupying both the α and β positions.

Contrary to our expectation, none of the polymers exhibited any solubilities in non-polar organic solvents. The poly(β-phenyl-β-aminopropionic acid) *p*-nitrophenyl ester could be dissolved in chloroform-dichloroacetic acid mixtures, but no distinct changes corresponding to the "helix-coil" transformation such as that found in poly-α-amino acid were observed in the polymer viscosity with the variation in the solvent composition.

BULLETIN OF THE CHEMICAL SOCIETY OF JAPAN VOL. 43 1860—1863 (1970)

Reactions of Haloferrocenes. II.[1] Kinetic Studies of the Reaction of Haloferrocene with Copper(I) Chloride - Pyridine Complex

Masaru SATO, Izumi MOTOYAMA and Kazuo HATA

Department of Chemistry, Faculty of Science, Tokyo Metropolitan University, Setagaya-ku, Tokyo

(Received January 16, 1970)

The reaction of bromoferrocene with copper(I) chloride - pyridine complex was found to be second-order, that is, first-order in each of bromoferrocene and copper(I) chloride - pyridine complex. The results obtained from the competitive reactions between bromoferrocene and bromobenzene indicated that bromoferrocene was 10^3 times more reactive than bromobenzene in the halogen-exchange reaction. The effects of the pyridine bases on the halogen-exchange reaction of bromoferrocene were examined, and the trend of the results was found to be different from that of bromobenzene. The reason for this was discussed on the basis of the reaction mechanism.

In a previous paper,[1] we reported that, when haloferrocene was treated with copper(I) salt in boiling pyridine, a halogen-exchange reaction easily occurred. According to this procedure, chloro-, bromo-, and cyanoferrocene were prepared in high yields by treating iodoferrocene with copper(I) chloride, bromide, and cyanide respectively. Since the reaction of *p*-substituted halobenzene with copper(I) salt is facilitated by an electron-withdrawing group,[2,3] this reaction is generally regarded as a nucleophilic substitution.[4] In contrast with halobenzene, the reaction of haloferrocene with copper(I) salt was markedly retarded by a hetero-annularly-substituted electron-withdrawing group. This interesting observation, along with the unusually high reactivity of haloferrocene in this reaction, prompted us to a kinetic study of this reaction in the hope of getting some information concerning the reaction mechanism.

Results

As was reported in an earlier paper,[2] the heterogeneous reaction mixture of bromobenzene and copper(I) cyanide in nitrobenzene was turned into a homogeneous solution by the addition of an organic base such as pyridine at 120°C, and the halogen-exchange reaction then took place at 160—180°C. When pyridine was added to the copper(I) chloride in chlorobenzene, a homogeneous solution similarly obtained at 100°C. The subsequent addition of bromoferrocene to the homogeneous solution gave rise to a considerably rapid halogen-

1) Part I: M. Sato, T. Ito, I. Motoyama, K. Watanabe and K. Hata, This Bulletin, **42**, 1976 (1969).
2) T. Ito and K. Watanabe, *ibid.*, **41**, 419 (1968).
3) R. G. R. Bacon and H. A. O. Hill, *J. Chem. Soc.*, **1964**, 1097.
4) J. F. Bunnett and R. E. Zahler, *Chem. Rev.*, **49**, 273 (1951).

exchange reaction of the bromoferrocene. During this procedure, chlorobenzene used as a solvent did not react with copper(I) bromide which arose from the reaction of bromoferrocene with copper(I) chloride. Hence, this procedure was employed for the kinetic study of the exchange reaction of haloferrocene. The effect of the base/Cu-salt ratio on the reaction rate was investigated by Ito and Watanabe.[2] It was found that, in comparison with the reaction rate when equimolar amounts of the base and the Cu-salt were used, the reaction rate stayed unchanged even if the base/Cu-salt ratio exceeded 1. However, when the base/Cu-salt ratio was less than 1, the reaction rate diminished in proportion to the base/Cu-salt ratio. Therefore, a little excess of pyridine over the copper(I) salt was used in the present experiment. When an excess of copper(I) chloride over bromoferrocene was used, a linear relationship was observed between the yield of chloroferrocene and the reaction time. When the initial concentration of bromoferrocene was kept constant and that of copper(I) chloride was varied, a linear relationship was generally found between the initial rate and the initial concentration of copper(I) chloride, although some deviations were observed. These observations clearly indicate that this reaction is second-order, that is, first-order in each of bromoferrocene and copper(I) chloride. Copper(I) salt and pyridine have been supposed to form a 1 : 1 complex in the reaction mixture.[2] Accordingly, the reaction rate may be represented as follows:

$$d[\mathrm{FcCl}]/dt = k[\mathrm{FcBr}][\mathrm{CuCl\text{-}Pyridine\ Complex}]$$

When a pyridine base was added to a heterogeneous mixture of copper(I) chloride and bromobenzene, a homogeneous solution was obtained at 102°C, and the reaction of bromobenzene with copper(I) chloride was observed to occur at this temperature. When bromoferrocene was added to this reaction system, together with bromobenzene, a competitive halogen-exchange reaction between bromoferrocene and bromobenzene was observed. The ratio of the reaction rates of the two halides was determined in such a competitive reaction using α-picoline, γ-picoline, methyl isonicotinate, or pyridine as the pyridine base. On the other hand, when the reactions of bromobenzene with copper(I) chloride in the presence of the cited pyridine bases were carried out using bromobenzene as the solvent and under conditions similar to those used in the competitive reaction, the pseudo first-order rate constants of the reaction were determined. The results of these kinetic studies are shown in Table 1, where k^2_{FcBr} and k^2_{PhBr} represent the second-order rate constants of bromoferrocene and bromobenzene respectively in the competitive reaction, and where k^1_{PhBr} stands for the pseudo first-order rate constant of the reaction of bromobenzene with copper(I) chloride in bromobenzene.

It is clear from Table 1 that bromoferrocene reacts 10^3 times or more faster than does bromobenzene in the reaction using any of these pyridine bases. This observations is qualitatively consistent with the results reported in a previous paper.[1]

In order to see the effect of the pyridine base on the halogen-exchange reaction of bromoferrocene, the k^2_{FcBr} values were calculated on the assumption that the coexistence of bromoferrocene will not affect the reaction rate of bromobenzene.*1 The ratios of the rate constants, k^2_{FcBr}, thus obtained for pyridine, α-picoline, γ-picoline, and methyl isonicotinate are 1.00, 1.47, 1.22, and 1.57 respectively.

The solvent effect on the halogen-exchange reactions was examined using three kinds of aprotic polar solvents, that is, nitrobenzene, nitromethane, and acetonitrile. These solvents gave a homogeneous solution with copper(I) chloride, even at a lower temperature (30—50°C), in the presence of an equimolar amount of pyridine. However, in the observation of the kinetics on the reaction of bromoferrocene with copper(I) chloride in these solvents,

Table 1. Rate constants of the reactions between bromoferrocene or bromobenzene and copper(I) chloride in the presence of various pyridine bases

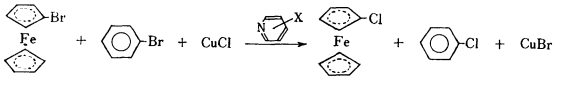

Exp. No.	Pyridine base	$k^2_{\mathrm{FcBr}}/k^2_{\mathrm{PhBr}}$	k^1_{PhBr} (min^{-1})	k^2_{FcBr}* ($l/\mathrm{mol}\cdot\mathrm{min}$)
1	γ-Picoline	1.02×10^3	8.10×10^{-3}	8.3
2	α-Picoline	9.4×10^3	1.06×10^{-3}	10.0
3	Pyridine	1.15×10^3	5.87×10^{-3}	6.8
4	Methyl isonicotinate	3.10×10^3	3.45×10^{-3}	10.7

* Calculated from the values of $k^2_{\mathrm{FcBr}}/k^2_{\mathrm{PhBr}}$ and k^1_{PhBr}.

*1 No appreciable change in the reaction rate was observed on the addition of ferrocene instead of bromoferrocene to the reaction mixture.

TABLE 2. SOLVENT EFFECT ON THE REACTION BETWEEN BROMOFERROCENE AND COPPER(I) CHLORIDE-PYRIDINE COMPLEX AT 50.0°C

Solvent	Dielectric constants[a] (20°C)	Initial rate (mol/l·min)
Nitrobenzene	35.7	5.1×10^{-2}
Nitromethane	37.5	5.7×10^{-2}
Acetonitrile	37.5	6×10^{-4}

a) J. Hine, "Physical Organic Chemistry," 2nd Ed., McGraw-Hill, Inc., New York (1960), p. 39.

the plots of the rate constant gradually deviated from the second-order relation, unlike as in the reaction using bromobenzene or chlorobenzene as a solvent. Hence, the solvent effects were compared with each other by the initial reaction rates observed in these three solvents, as is shown in Table 2. These results clearly indicate that a remarkable solvent effect is present in the halogen-exchange reaction of bromoferrocene, but no significant correlation was observed between the relative rates and the dielectric constants of these solvents.

Discussion

When iodoferrocene and copper(I) iodide were refluxed in pyridine, iodoferrocene was recovered quantitatively; neither ferrocene nor biferrocenyl, both of which had been expected as the dehalogenation or coupling products, could be detected in the reaction mixture. This is consistent with the observation by Bacon and Hill,[3] who investigated the reaction of chlorobenzene with copper(I) chloride carried out by refluxing in pyridine using an isotopic chloride. The Ullmann coupling reaction of chlorobenzene was also reported not to occur at the boiling temperature of pyridine.[5] On the other hand, when iodoferrocene was treated with activated copper in boiling pyridine, both the coupling product (biferrocenyl) and the dehalogenated product (ferrocene) were isolated.[6] In view of the above facts, the most reasonable conclusion is that neither the ferrocenyl radical nor ferrocenylcopper,[7] which would give biferrocenyl and ferrocene, may be involved as the intermediate in the reaction between haloferrocene and copper(I) salts.

The reaction of bromoferrocene with copper(I) chloride-pyridine complex in chlorobenzene was confirmed to be a second-order reaction, in just the same manner as the reaction of aryl halides with copper(I) salts.[2,3] This fact strongly suggests that the reaction of haloferrocene with copper(I) chloride-pyridine complex proceeds through a process similar to that previously proposed in the benzene series.[2,3] Probably, the halogen atom in haloferrocene coordinates to the copper(I) chloride-pyridine complex (**1**) to form a metastable, reactive intermediate (**2**), which then provides a final product *via* the four-center-type transition state (**3**).

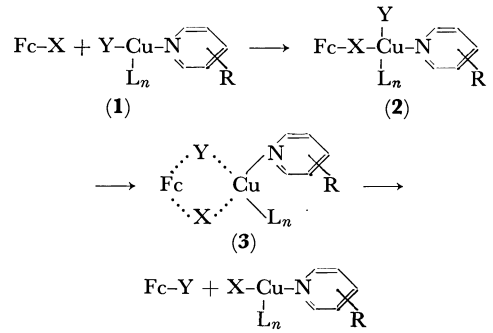

L = Pyridine base or solvent

The above reaction mechanism was strongly supported by a remarkable solvent effect found in this reaction. As is shown in Table 2, the reaction proceeds quickly in nitrobenzene and nitromethane, but slowly in acetonitrile. The observed difference seems to arise from their coordinating ability to produce a copper complex, because there is no significant correlation between the reaction rates and the dielectric constants of the solvents used. The slow reaction rate in acetonitrile may be interpreted as follows: the vacant coordination site of copper(I) chloride will be almost entirely occupied by acetonitrile because of its large affinity for copper(I) ion;[8] thus, the coordination of haloferrocene to copper(I) atom suffers a considerable hindrance, which brings about the fall in the reaction rate. An example of such a solvent effect in the reaction of a metal complex was found in the reaction between *trans*-dichlorobis(pyridine)platinum and the isotopic chloride ion in various solvents.[9] It has been shown that this halogen-exchange reaction proceeds more rapidly in nitromethane as a solvent than in acetonitrile, much as with the present result shown in Table 2.

5) P. E. Fanta, *Chem. Rev.*, **38**, 139 (1946).
6) M. Sato, I. Motoyama and K. Hata, to be published in the subsequent paper.
7) A. H. Lewin and T. Cohen, *Tetrahedron Lett.*, **1965**, 4531.
8) I. M. Kolthoff and J. F. Coetzee, *J. Amer. Chem. Soc.*, **79**, 1852 (1957).
9) R. G. Pearson, H. B. Gray and F. Basolo, *ibid.*, **82**, 787 (1960).

Recently it was suggested[2] that the structure of the pyridine base coordinated in the copper(I) complex exerted a definite influence on the reaction of halobenzene with copper(I) salt. The reexamination of this reaction led to the conclusion that the more strongly the nitrogen atom of the pyridine base is coordinated to the copper atom, the more the reaction is accelerated.[10] The acceleration of the reaction of bromobenzene with copper(I) chloride by γ-picoline, and the retardation of the reaction by methyl isonicotinate, each in comparison with pyridine, were explained by means of studying the electronic effect of the substituent upon the electron density on the nitrogen atom of the base, which might affect the coordination of the base to copper(I) chloride. On the other hand, the retardation by α-picoline was attributed to the steric hindrance to the coordination of the base to copper(I) chloride. A similar trend was also observed in the substituent effect expressed by k^1_{PhBr} in Table 1.

On the contrary, no such trend of the substituent effect was observed in the reactions of bromoferrocene with copper(I) chloride-pyridinebase complexes. Those reactions were accelerated by any of the substituted pyridines examined. However, it is interesting that the trend is the opposite of that of the benzene series. As an exception, γ-picoline accelerates both the reaction of bromobenzene and that of bromoferrocene, but the acceleration in the latter is not so marked as by α-picoline or methyl isonicotinate. The equivocal behavior of the substituted pyridines might be explained by a very delicate and complicated balance among the following factors: (1) the stability of the intermediate (**2**); (2) the ease of the attack of the halogen atom in haloferrocene on the copper atom (X→Cu attack), and (3) the nucleophilicity of the halogen atom of the complex (**2**) toward the carbon atom in the ferrocene ring (Y→C attack). The results of the experiments (Table 1) suggest that the reaction of bromoferrocene with copper(I) chloride-pyridine base complex might be governed rather by the ease of the X→Cu attack in (2) than by the Y→C attack in (3), unlike the similar reaction of bromobenzene.[10]

The discussion presented above is useful in explaining most of the facts observed in the reaction of bromoferrocene with the copper(I) chloride-pyridine complex, but some difficulties still remain in explaining the fact that bromoferrocene is 10^3 times or more reactive than bromobenzene in this reaction and that heteroannular substituents on bromoferrocene exert a marked electrophilic effect upon this reaction.[1] It is necessary to consider additional factors specific to the ferrocene series in order to elucidate the mechanism of this reaction further.

10) M. Sato, I. Motoyama and K. Hata, to be published in the subsequent paper.

Experimental

All of the reactions were operated under an atmosphere of nitrogen.

Procedure for a Competitive Reaction (Table 1, Exp. 3). In a 100-m*l*, three-necked flask fitted with a sealed stirrer, a thermometer, a gas-inlet tube, and a reflux condenser, were placed 1.20 g (4.5 mmol) of bromoferrocene, 0.50 m*l* (5.0 mmol) of pyridine, 30 m*l* of bromobenzene, 0.25 m*l* (2.0 mmol) of ethylbenzene, and 0.70 g (4.5 mmol) of biphenyl. The last two substances were added as the internal standard for gas chromatography, by which process the products were analyzed. The contents were then heated to 102°C on an oil bath. When the temperature was regulated to be constant (102.7±0.1°C), 0.45 g (4.5 mmol) of copper(I) chloride was quickly added to the solution. A small quantity of the reaction mixture was taken out every two minutes and quenched with dilute hydrochloric acid. The organic layer was analyzed by gas chromatography. From the results of these measurements, the ratio of the rate constants (k^2_{FcBr}/k^2_{PhBr}) was calculated by the following equation:

$$-\frac{d(\mathrm{FcBr})}{d(\mathrm{PhCl})} = \frac{k^2_{FcBr}}{k^2_{PhBr}} \times \frac{(\mathrm{FcBr})}{a}$$

$$\text{or} \quad -\ln\frac{(\mathrm{FcBr})}{(\mathrm{FcBr})_0} = \frac{k^2_{FcBr}}{k^2_{PhBr} \times a} \times (\mathrm{PhCl})$$

where a and $(\mathrm{FcBr})_0$ are the initial concentrations of bromobenzene and bromoferrocene respectively.

Analytical Conditions for Gas Chromatography. Apparatus: OHKURA Model 1100. Column: a 2 m× 6 mm stainless-steel column packed with 5% Silicone Grease on Diachrom A (60—80 meshes). Temperature: 165°C. Carrier gas: H_2. Flow rate: 80 m*l*/min. Relative retention times: Ferrocene (0.88). Biphenyl (1.00), Chloroferrocene (1.39), Bromoferrocene (1.88), and Iodoferrocene (2.59).

BULLETIN OF THE CHEMICAL SOCIETY OF JAPAN VOL. 43 1864—1869 (1970)

Tri(hetero)substituted Carbonium Ions. II. 2-Dialkylamino-1,3-dithiolanylium Ions. Reactions with Nucleophiles and Ambident Behaviors[1,2]

Takeshi NAKAI and Makoto OKAWARA

Research Laboratory of Resources Utilization, Tokyo Institute of Technology, Ookayama, Meguro-ku, Tokyo

(Received January 17, 1970)

The reactions of 2-dialkylamino-1,3-dithiolanylium perchlorates with a variety of nucleophilic species including oxygen, sulfur and nitrogen nucleophiles have been investigated. Examination of the isolated products reveals that these trihetrosubstituted carbonium ions behave as ambident electrophiles toward nucleophiles with two reactive sites, *i.e.*, the electron-deficient centered carbon (a) and the ring-methylene carbon atom (b), and that the nature of nucleophiles greatly affects the reaction course in a straightforward manner. The reaction course may be classified as follows. If the nucleophile is basic, the reaction at the site (a) (mode A) is favored, but if it has large substituents, the initial proton abstraction reaction (mode C) is predominant, while if the nucleophile is polarizable, the reaction at the site (b) (mode B) is favored. The major factor deciding the reaction course is discussed in terms of the schematic energy profile of the overall reaction.

Stabilization of carbonium ions is usually done by electron-donating conjugation with a hetero atom adjacent to the electron-deficient carbon atom. Stabilization is more manifest when two or three electron-donating groups coordinate their nonbonding electron pairs with the cationic center.[3]

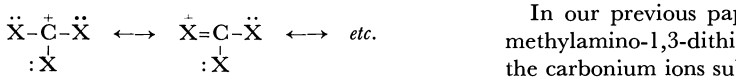

X = S, N, O, Cl, *etc.*

Carbonium ions stabilized through two hetero atoms are of great significance from preparative and theoretical points of view, since they are readily isolated under an ordinary condition and behave toward nucleophiles as ambident electrophiles having two reactive sites.[4] Among them dialkoxycarbonium salts are the most important as facile alkylating agents.[5] However, very little systematic investigation has been carried out as regards carbonium ions stabilized through three α-hetero atoms although reactions of trialkoxy-[6] and trialkylthiocarbonium ions[7] have been reported.

In our previous paper[2] it was shown that 2-dimethylamino-1,3-dithiolanylium ion (Ia),[8] one of the carbonium ions substituted by one nitrogen and two sulfur atoms, is isolated as perchlorate or tetraphenylborate, and that Ia reacts with hydroxide and *N,N*-dimethyldithiocarbamate ions to give, respectively, β-mercaptoethyl *N, N*-dimethylthiolcarbamate and ethylene bis(*N,N*-dimethyldithiocarbamate). These observations suggest that Ia may behave as an ambident electrophile with two reactive sites, (a) and (b), as shown below.

1) T. Nakai and M. Okawara, *Tetrahedron Lett.*, **1967**, 3835. A preliminary communication.

2) Part I: T. Nakai, Y. Ueno and M. Okawara, This Bulletin, **43**, 156 (1970).

3) To what extent one is justified in considering such a cation a carbonium ion rather than an onium ion, depends upon the extent of contribution to the resonance hybrid of the structure carrying the positive charge on carbon and on the electron-donating tendency of the hetero atom X. Other factors, *e. g.*, steric ones which enhance or diminish the internal dissipation of charge, are also important: *cf.* C. D. Nenitzescu, "Carbonium Ions," ed. by G. A. Olah and P. von R. Schleyer, Vol. 1, Interscience Publ., New York, N. Y. (1968), p. 20. In our studies these cations are regarded as triheterosubstituted carbonium ions only for a systematic nomenclature.

4) For a review, see S. Hünig, *Angew. Chem. Intern. Ed.*, **3**, 548 (1964).

5) S. Kabuss, *ibid.*, **5**, 675 (1966); K. Dimroth and D. Heinrich, *ibid.*, **5**, 676 (1966).

6) H. Meerwein, K. Bodenbenner, P. Borner, F. Kunnert and K. Wunderlich, *Ann. Chem.*, **632**, 38 (1960); H. Meerwein, V. Hederick, J. Morschel and K. Wunderlich, *ibid.*, **635**, 1 (1960); H. Meerwein, "Houben-Weyl: Methoden der Organischen Chemie," Vol. VI/3, Georg Thieme Verlag, Stuttgart (1965), p. 346.

7) R. Gompper and E. Kutter, *Chem. Ber.*, **98**, 1365 (1965); W. P. Tucker and G. L. Roof, *Tetrahedron Lett.*, **1967**, 2747.

8) This carbonium ion is more exactly termed 2-dimethylamino-1,3-dithiolan-2-ylium ion. In our papers the word 1,3-dithiolanylium is used only for the sake of convenience. The carbonium ion is also termed 2-dimethylamino-1,3-dithiolenium ion: J. L. Richards, D. S. Tarbell and E. H. Hoffmeister, *Tetrahedron*, **24**, 6485 (1968).

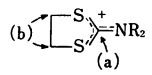

Ia, R=CH_3 b, R=C_2H_5

In general, the relative reactivities at the two reactive sites of such ambident electrophiles should depend upon three factors: the nature of the nucleophile, the structure of the carbonium ion, and the reaction conditions. Thus a systematic investigation of the effects of these factors on the reactivities of carbonium ions stabilized through one nitrogen and two sulfur atoms was initiated.

The present paper describes the effect of the nature of nucleophile on the reactivity and reaction course of 2-dialkylamino-1,3-dithiolanylium ions. The subsequent paper[9] is concerned with structural effect on reactivities of this type of ambident electrophiles.

Results and Discussion

2-Dialkylamino-1,3-dithiolanylium ions (Ia, R=CH_3; Ib, R=C_2H_5) were isolated as perchlorate from the equimolar reaction of 1,2-dichloroethane with the corresponding sodium *N,N*-dialkyldithiocarbamate in ethanol.[2] These carbonium salts were recrystallized from aqueous solutions. In order to investigate the effect of the nature of nucleophile on reactivities of these carbonium ions, reactions of I with a variety of nucleophilic reagents including oxygen nucleophilies (hydroxide and ethoxide), sulfur nucleophiles (alkyl and aryl mercaptides, and dithiocarbamates), nitrogen nucleophiles (anilines and triethylamine) and carbon nucleophile (cyanide) were studied.

A wide spectrum of reactivity is shown by 2-dialkylamino-1,3-dithiolanylium ions (Chart 1). Reaction conditions and products obtained are summarized in Table 1. Identification of products is based upon elemental analyses, physical properties, spectral data and chemical transformations (Experimental section),

It can be said, on the whole, that these two carbonium ions behave toward nucleophiles in a similar manner, although the dimethylamino compound (Ia) seems to be more reactive than diethylamino Ib. Significant differences between the two carbonium ions were observed in reactions with aniline and with sodium cyanide. Carbonium ion Ia reacted with aniline to give 2-phenylimino-1,3-dithiolane (IVa) in a good yield, while Ib did not afford (IVa) but a small amount of *N,N'*-diphenylthiourea. With cyanide ion, Ia afforded 2-cyano-2-dimethylamino-1,3-dithiolane (IXa), while Ib did not produce diethylamino derivative (IXb) but a complex mixture.

Examination of stuructures of products reveals the following facts: (i) as expected, 2-dialkylamino-1,3-dithiolanylium ions (I) are ambident electrophiles with two reactive sites, *i.e.*, the electron-deficient centered carbon atom (a) and the ring-methylene neutral carbon atoms (b); (ii) in contrast to behaviors of ambident nucleophiles toward electrophilic reagents,[10] reactions between these ambident electrophiles and the nucleophilic reagents proceed in a more straightforward manner; (iii) the nature of nucleophile (Nu^-) greatly affects the reaction course, which may be classified into three modes (Chart 2).

Mode A involves initial attack of the nucleophile at the site (a) with the retention of the ring structure to yield adduct X, which, in turn, undergoes various subsequent reactions. Nucleophiles which react *via* mode A are oxygen nucleophiles, aryl amines and cyanide ion. The proton transfer from

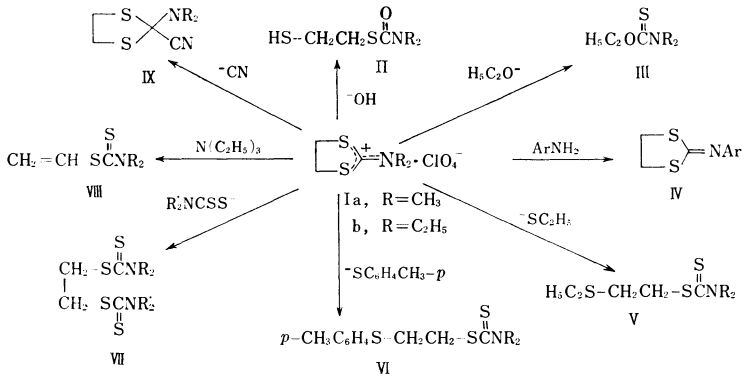

Chart 1. Reactions of I with various nucleophiles.

9) T. Nakai, Y. Ueno and M. Okawara, Abstracts of papers presented at the 18th Symposium on Organic Reaction Mechanisms, Kyoto (October, 1967), p. 77.

10) For ambident anions, *e. g.*, see N. Kornblum, R. A. Smiley, R. K. Blackwood and D. C. Iffland, *J. Amer. Chem. Soc.*, **77**, 6269 (1955); R. Gompper, *Angew. Chem. Intern., Ed.*, **3**, 560 (1964).

Table 1. Reactions of I with nucleophiles

Starting materials: Perchlorate	Starting materials: Nuleophile (mol ratio)	Conditions: Solvent	Conditions: Temp. °C	Conditions: Time hr	Product [a]	Yield [b] (%)
Ia	H_2O/NEt_3 (2.0)	DMF	80	3	IIa, R=CH_3	30
Ib	H_2O/NEt_3 (2.0)	DMF	80	3	IIb, R=C_2H_5	28
Ia	$NaOC_2H_5$ (3.0)	Dioxane	reflux	2	IIIa, R=CH_3	52
Ib	$NaOC_2H_5$ (3.0)	Dioxane	reflux	6	IIIb, R=C_2H_5	82
Ia	$C_6H_5NH_2$ (2.0)	DMSO	80	4	IVa, Ar=C_6H_5	70
Ia	*p*-$CH_3C_6H_5NH_2$ (2.0)	DMSO	80	4	IVb, Ar=*p*-$CH_3C_6H_4$	77
Ib	$C_6H_5NH_2$ (2.0)	DMSO	80	4	*N,N'*-diphenylthiourea[c]	8
Ia	$NaSC_2H_5$ (1.0)	DMF	60	4	Va, R=CH_3	36
Ib	$NaSC_2H_5$ (1.0)	DMF	60	4	Vb, R=C_2H_5	(38)[d]
Ia	$NaSC_6H_4CH_3$-*p* (1.0)	DMF	60	4	VIa, R=CH_3	77
Ib	$NaSC_6H_4CH_3$-*p* (1.0)	DMF	60	4	VIab, R=C_2H_5	59
Ia	$NaSCSN(CH_3)_2$ (1.0)	DMF	60	4	VIIa, R=CH_3, R'=CH_3	95
Ia	$NaSCSN(C_2H_5)_2$ (1.0)	DMF	60	4	VIIb, R=CH_3, R'=C_2H_5	90
Ib	$NaSCSN(CH_3)_2$ (1.0)	DMF	60	4	VIIb	92
Ib	$NaSCSN(C_2H_5)_2$ (1.0)	DMF	60	4	VIIc, R=C_2H_5, R'=C_2H_5	85
Ia	$N(C_2H_5)_3$ (2.0)	DMSO/Diox.	75	2	VIIIa, R=CH_3	65
Ib	$N(C_2H_5)_3$(2.0)	DMSO/Diox.	70	3	VIIIb, R=C_2H_5	63
Ia	NaCN(3.0)	DMF	60	4	IXa, R=CH_3	64
Ib	NaCN (3.0)	DMF	60	4	e)	

a) Numbers refer to compounds in Chart 1.
b) Based upon Ia or Ib. No attempt was made to maximize conditions.
c) In contrast to Ia, Ib did not produce IVa at all.
d) Both UV and IR spectra suggested that this fraction was contaiminated with *S*-vinyl dithiocarbamate (VIIIb).
e) In contrast to Ia, Ib did not afford IXb (R=C_2H_5), but a complex mixture.

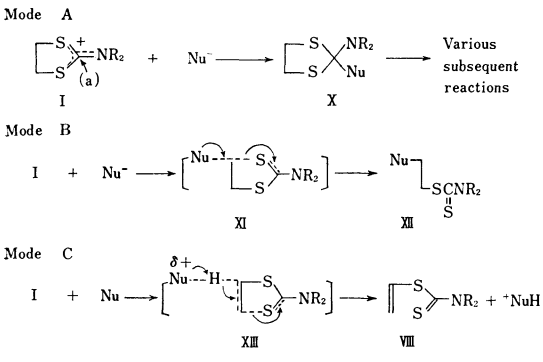

Chart 2. Reaction modes.

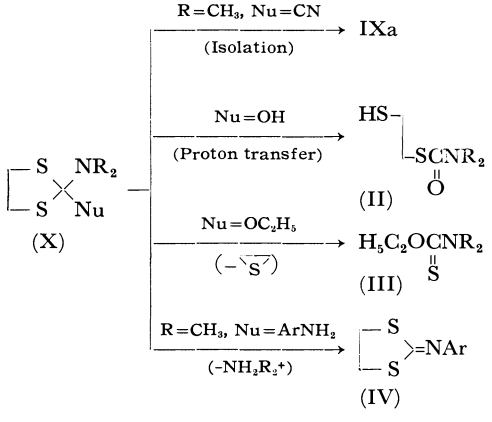

Chart 3. Subsequent reaction of X.

X (Nu=OH) results in the formation of VI, while loss of episulfide from X (Nu=OEt) can account for the formation of thioncarbamate (III).[11] Formation of IV from Ia and aniline can be interpreted by deamination of adduct X (Nu=$ArNH_2$) (Chart 3).

Mode B involves initial attack of the nucleophile at the site (b) to give β-substituted ethyl dithiocarbamate (XI). Nucleophiles which react *via* mode B are all sulfur nucleophiles examined. Attack of the nucleophiles to (b) might proceed through the S_N2-type mechanism, *i.e.*, *via* transition state XI,

11) For elimination of episulfide from sulfur-containing heterocyclics, see R. Feinaer, *Angew. Chem. Intern., Ed.*, **5**, 894 (1966). We have also observed that ethylene oxide cyclo-adds to the thiocarbonyl group to give the corresponding carbonyl compound involving loss of episulfide from the cyclo-adduct: Y. Ueno, T. Nakai and M. Okawara, This Bulletin, **43**, 168 (1970).

which has been kinetically verified with the reaction of Ia with sodium *N,N*-dimethyldithiocarbamate.[2] This fact is also supported by the observation that the yield of XII under similar conditions (see Table 1) increases with an increase in nucleophilicity of the attacking reagent, being in the order: $C_2H_5S^- < p\text{-}CH_3C_6H_4S^- < R'_2NCSS^-$[12] for both carbonium ions.

Finally, there are two possible mechanisms for the formation of *S*-vinyl dithiocarbamates (VIII) from I and triethylamine. The first mechanism involves the Hofmann elimination of tetraalkylammonium salt XII ($Nu = NEt_3$) formed *via* mode B. The other consists of mode C which involves initial abstraction of the proton of the ring-methylene followed by the ring scission through the well-known concerted mechanism accepted for the general E2 reaction. It seems reasonable to assume that mode C is operative since triethylamine is basic and so combines more preferentially with the proton that the neutral carbon atom bearing the proton.

It may be roughly summarized that if the nucelophile is basic, *e.g.*, OH^- or RO^-, mode A is favored, but if it has large substituents, *e.g.*, NEt_3, the initial proton abstraction (mode C) is predominant. On the other hand, if the nucleophile is polarizable, *e.g.*, RS^- or R_2NCSS^-, mode B is favored. According to the concept of soft and hard acids and bases,[13] it can also be said that hard bases react *via* mode A while soft bases react *via* mode B, and that, with respect to the carbonium ion, the reactive site (a) is hard and (b) is soft.

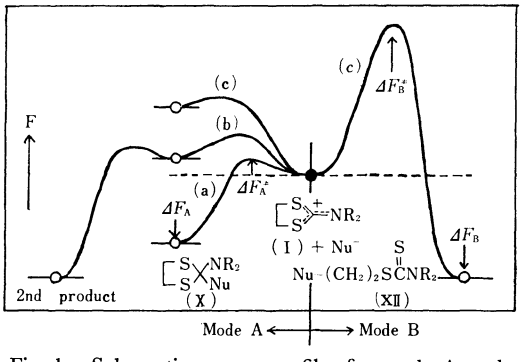

Fig. 1. Schematic energy profiles for mode A and B: curve (a), $Nu^- = e.g.$, ^-CN; (b), $Nu^- = e.g.$, ^-OH; (c), $Nu^- = e.g.$, $^-SCSNR_2$. Strictly speaking, the energy content of the initial system, I^+ and Nu^-, depends upon the nature of Nu^-.

We might conclude that the nature of the nucleophile largely changes the reaction course, though the factors deciding the reaction course remain unknown. To clarify this point, the schematic energy profile of the overall reaction was considered tentatively (Fig. 1).[14]

Since the primary process of mode A corresponds to a simple association between the cation and the anion, the free activation energy ($\Delta F_A^{\neq}$) is always less than that for mode B ($\Delta F_B^{\neq}$). It may be assumed that the position of the equilibrium between cation I and adduct X in mode A should depend upon the difference in ΔF_A between I and X, *i.e.*, upon their relative position in the energy diagram, except for steric factors. On the other hand, since the transformation of I into XII in mode B results in release of the mesomeric energy of XII as well as the energy of charge neutralization, product XII must be a thermodynamically stable product, *i.e.*, $\Delta F_B > \Delta F_A$. Both ΔF_B and $\Delta F_B^{\neq}$ may be assumed to be very large since mode B is irreversible. In short, it can approximately be said that the primary reaction of mode A is kinetically controlled, while mode B is thermodynamically controlled. These discussions substantially lead to the hypothesis that the major factor deciding the reaction course is the relative position of the kinetically controlled product (X) in the energy diagram, *i.e.*, the magnitude of ΔF_A (Fig. 1). Since the small free activation energy ($\Delta F_A^{\neq}$) changes only slightly with the nature of nucleophile, kinetic adduct (X) can be isolated only when a strong nucleophile such as CN^- was used (Table 1). In the case where the primary adduct is not so stable, if the adduct may be readily converted into the more stable second product by various irreversible reactions (Chart 3), the reaction will be also directed to mode A, while if adduct (X) cannot undergo such second irreversible reactions, the reaction will be directed to mode B, as has been observed in the reactions with sulfur nucleophiles. Naturally $\Delta F_B^{\neq}$ depends upon the nucleophilicity of the attacking reagent; this accounts for the difference in yield of product XII with a series of sulfur nucleophiles.

This may qualitatively explain behaviors of all nucleophiles except triethylamine toward the ambident electrophiles (Table 1). The fact that triethylamine reacts with I *via* mode C, not *via* mode A, might be expained by the steric factor, *i.e.*, both by an increase of $\Delta F_A^{\neq}$ and a decrease of ΔF_A. In all cases, from these qualitative results it is difficult to determine whether the major factor deciding the reaction course is the stability of kinetic adduct (X) or the steric factor. Further quantitative data based upon kinetic studies are required to ascertain this point.

12) Dithiocarbamate anions are ranked with the strongest nucleophiles in aqueous solutions: R. E. Davis, "Survey of Progess in Chemistry," ed. by A. Scott, Vol. 2, Academic Press Inc., New York, N. Y. (1964), p. 189; R. E. Davis, H. Nakshbendi and A. Ohno, *J. Org. Chem.*, **31**, 2702 (1966).

13) R. G. Pearson, *J. Amer. Chem. Soc.*, **85**, 3533 (1963).

14) For analogous considerations, see Ref. 4; S. Winstein and E. M. Kosower, *J. Amer. Chem. Soc.*, **81**, 4399 (1959); J. Miller, *ibid.*, **85**, 1628 (1963).

Experimental

General. Melting and boiling points are uncorrected. The infrared spectra were recorded with a Hitachi EPI-S2 spectrometer. Ultraviolet spectra were recorded with a Hitachi EPS-2 spectrometer. Nuclear magnetic resonance spectra were determined with either a Varian Associates A-60 or a Japan Electron Optics C-60 spectrometers. Chemical shifts are given in a parts per million (ppm) from tetramethylsilane as an internal standard. All nucleophilic reagents employed were either commercially available materials or prepared by a standard method.

2-Dimethylamino-1,3-dithiolanylium Perchlorate (Ia). To a solution of 39.0 g (0.40 mol) of 1,2-dichloroethane in 80 m*l* of ethanol, was added a solution of sodium *N,N*-dimethyldithiocarbamate (72.0 g, 0.40 mol) in 120 m*l* of ethanol. The mixture was stirred at 55°C for 3 hr. Sodium chloride formed was filtered off and the filtrate was concentrated under reduced pressure. The mixture was poured into 300 m*l* of cold water to give 4.2 g of white precipitates, ethylene bis(*N,N*-dimethyldithiocarbamate): mp 187—189°C. To the resulting aqueous solution was added sodium perchlorate (45 g) to give 62.0 g (62%) of white precipitates (Ia): mp 179—180°C (acetone) (lit,[2] 179—180°C); UV: λ_{max} (H_2O) 249 mμ ($\varepsilon=1.31\times10^4$).

2-Diethylamino-1,3-dithiolanylium Perchlorate (Ib). In a similar fashion the reaction of sodium *N,N*-diethyldithiocarbamate with 1,2-dichloroethane gave perchlorate Ib in 44% yield; mp 89—90°C (water); UV: λ_{max} (H_2O) 255 mμ.

Found: C, 30.62; H, 5.15; N, 5.01%. Calcd for $C_7H_{14}ClNO_4S_2$: C, 30.38; H, 5.12; N, 5.08%.

Hydrolyses of Salt I. Salt Ia (6.2 g, 0.025 mol) was added to a solution of 1.0 g (0.01 mol) of triethylamine and 1.0 g (0.05 mol) of water in 15 m*l* of dimethylformamide (DMF). The reaction mixture was stirred at 100°C for 3 hr, then poured into cold water. The mixture was extracted several times with ether. The ether layer was dried over sodium sulfate and the solvent evaporated *in vacuo*. Distillation of the residue gave 1.2 g of β-mercaptoethyl *N,N*-dimethylthiolcarbamate (IIa): bp 85—87°C/2 mmHg; n_D(25°C) 1.6038; IR (neat): 1650 (C=O) and 1490 cm^{-1} (N–CO). The physical properties and spectral data of this distillate were in agreement with those of the authentic sample.[2]

Hydrolysis of salt Ib carried out as in the case of Ia yielded 2.0 g of thiolcarbamate IIb: bp 116—118°C/2 mmHg; n_D(20°C) 1.5800; IR (neat): 1650 and 1495 cm^{-1}.

Both these products discolored an aqueous solution of iodine and gave mercury mercaptide on treatment with mercuric chloride indicating the presence of a mercapto group.

Reactions of Salt I with Sodium Ethoxide. Salt Ia (12.5 g, 0.05 mol) was added to a suspension of 10.2 g (0.15 mol) of sodium ethoxide in 70 m*l* of dioxane. The mixture was stirred at 100°C for 2 hr in a nitrogen atmosphere, then poured into water. The ether layer was dried over sodium sulfate and the solvent was evaporated. Distillation of the residue gave 3.5 g (52%) of ethyl *N,N*-dimethylthioncarbamate (IIIa): bp 81—82°C/10 mmHg; n_D(25°C) 1.5082; UV (EtOH): 250 and 285 mμ (shoulder) (lit, bp 82.6°C/10 mmHg;[15] n_D(20°C) 1.5075;[16] UV: 250 and 285 mμ (shoulder)[17]).

The reaction of Ib with sodium ethoxide carried out as in the case of Ia gave ethyl *N,N*-diethylthioncarbamate (IIIb) in 82% yield; bp 99—101°C/13 mmHg; n_D(23°C) 1.4968 (lit, bp 114°C/20 mmHg;[18] n_D(15°C) 1.5021[19]); UV (EtOH): 250.5 and 290 mμ (shoulder). The infrared spectrum of IIIb was in agreement with that of the authentic sample.[20]

Reactions of Salt I with Anilines. Salt Ia (6.2 g, 0.025 mol) was added to a solution of 5.0 g (0.05 mol) in aniline in 40 m*l* of dimethylsuldefoxide (DMSO). The reaction mixture was stirred at 80°C for 3.5 hr, then poured into water. The ether layer was dried over sodium sulfate and the solvent and unreacted aniline were removed *in vacuo*. Recrystallization of the residue from ethanol gave 3.6 g (73%) of 2-phenylimino-1,3-dithiolane (IVa): mp 47—48°C; IR (KBr): 1570 cm^{-1} (C=N); NMR (CCl_4): δ 3.32 (s, CH_2S) and 6.55—7.10 ppm (m, aromatic protons).

Found: C, 55.48; H, 4.89; N, 7.00%. Calcd for $C_9H_9NS_2$: C, 55.38; H, 4.65; N, 7.18%.

Imino-dithiolane IVa reacted with hydroxylamine in ethanol giving 2-hydroxyimino-1,3-dithiolane: mp 122—124°C (lit,[21] 124—127°C); IR (KBr): 3100 (OH) and 1590 cm^{-1} (C=N).

The reaction of Ia with *p*-toluidine was carried out as in the case of aniline. Salt Ia (6.2 g, 0.025 mol) and *p*-toluidine (5.0 g, 0.05 mol) gave 4.8 g (77%) of a yellowish oil (IVb); IR (neat): 1580 cm^{-1} (C=N). The oil was treated with a 6N alcoholic solution of hydrogen chloride to give white precipitates of the hydrochloride: mp 209—211°C (lit,[22] 190—192°C).

Found: C, 48.52; H, 4.99; N, 5.62%. Calcd for $C_{11}H_{11}ClNS_2$: C, 48.89; H, 4.92; N, 5.73%.

By the same procedure the reaction of Ib (7.0 g, 0.025 mol) with aniline (5.0 g, 0.05 mol) gave 0.5 g of *N,N'*-diphenylthiourea as only ether-soluble product.

Reactions of Salt I with Sodium Ethylmercaptide. Salt Ia (12.5 g, 0.05 mol) was added to a solution of 4.2 g (0.05 mol) of sodium ethylmercaptide in 40 m*l* of DMF. The reaction mixture was stirred at 70°C for 5 hr, then poured into cold water. The carbon tetrachloride layer was dried over sodium sulfate and the solvent evaporated *in vacuo*. Distillation of the residue gave 3.6 g (36%) of a pale oil, β-(ethylthio)ethyl *N,N*-dimethyldithiocarbamate (Va): bp 67—68°C/0.14 mmHg; n_D(22°C) 1.5819; IR (neat): 1500 cm^{-1} (N–CS);[23] UV (EtOH): 250 and 278 mμ.[24]

---

15) O. Billeter, *Ber.*, **43**, 1853 (1910).
16) B. Holmberg, *Svensk. Kim. Tids.*, **41**, 249 (1929).
17) M. J. Janssen, *Rec. Trav. Chim.*, **79**, 454 (1960).
18) A. Hantzsch, *Ber.*, **64**, 661 (1931).
19) M. Delepine, *Ann. Chim. Phys.*, (8)**25**, 529 (1912).
20) E. E. Reid, "Organic Chemistry of Bivalent Sulfur," Vol. IV, Chemical Publ. Inc., New York, N. Y. (1962), p. 202.
21) R. W. Addor, U. S. 3193561 (1965); *Chem. Abstr.*, **63**, 11577 (1965).
22) A. Miolati, *Ann. Chem.*, **262**, 61 (1891).
23) The thioureisd band of dithiocarbamates: H. M. Randall, R. G. Fowler, N. Fuson and J. Dangl, "Infrared Determination of Organic Structure," Van Nostrand, New York, N. Y. (1949).

Found: C, 39.82; H, 7.53; N, 6.99%. Calcd for $C_7H_{15}NS_3$: C, 40.19; H, 7.53; N, 6.99%.

By the same procedure the reaction of salt Ib (14.0 g, 0.05 mol) with sodium ethylmercaptide (4.2 g, 0.05 mol) gave 4.5 g of a pale-yellowish oil: bp 84—86°C/0.4 mmHg; UV (EtOH): λ_{max} 250 and 280 mμ.[24] The IR spectrum of the distillate showed an absorption band at 1600 cm^{-1} (C=C) as well as bands presumably due to β-(ethylthio)ethyl *N,N*-diethyldithiocarbamate (Vb). In comparison with the IR spectrum of *S*-vinyl *N,N*-diethyldithiocarbamate (VIIIb), the spectrum indicates that the distillate was contaimnated with a small amount of VIIIb.

Reactions of Salt I with Sodium *p*-Tolylmercaptide. Salt Ia (6.3 g, 0.025 mol) was added to a solution of 4.0 g (0.027 mol) of sodium *p*-tolylmercaptide in 40 m*l* of DMF. The reaction mixture was stirred at 70°C for 5 hr, then poured into cold water. The carbon tetrachloride layer was dried over sodium sulfate and the solvent evaporated. Recrystallization of the residue from ethanol gave 5.7 g (77%) of β-(*p*-tolylthio)ethyl *N,N*-dimethyldithiocarbamate (VIa): mp 48—49°C; IR (KBr): 1495 cm^{-1} (N–CS);[23] UV (EtOH): λ_{max} 257 and 278 (shoulder);[24] NMR (CCl_4): δ 2.30 (s, $C\underline{H}_3C_6H_4$), 3.42 (s, CH_3–N), 3.10—3.80 (m, S–$C\underline{H}_2$–$C\underline{H}_2$–S–CS) and 6.80—7.40 ppm (m, aromatic protons).

Found: C, 52.86; H, 6.25; N, 4.95%. Calcd for $C_{12}H_{17}NS_3$: C, 53.13; H, 6.32; N, 5.16%.

In a similar fashion the reaction of salt Ib (10.4 g, 0.042 mol) with sodium *p*-tolylmercaptide (5.5 g, 0.037 mol) was carried out. Distillation of the oily residue gave 6.5 g (59%) of β-(*p*-tolyl)ethyl *N,N*-diethyldithiocarbamate (VIb): bp 165—170°C/0.6 mmHg; n_D(20°C) 1.6426; UV (EtOH): λ_{max} 257 and 278 mμ (shoulder).[24]

Found: N, 4.82%. Calcd for $C_{14}H_{21}NS_3$: N, 4.68%.

Reactions of Salt I with Sodium Dithiocarbamates. Salt Ia (2.5 g, 0.01 mol) was added to a solution of 1.8 g (0.01 mol) of sodium *N,N*-dimethyldithiocarbamate in 25 m*l* of DMF. The mixture was stirred at 60°C for 4 hr, then poured into cold water giving 2.4 g (96%) of white precipitates, ethylene bis(*N,N*-dimethyldithiocarbamate) (VIIa): mp 188—189°C (DMF) (lit,[25] 188—190°C).

By the same procedure salt Ib (2.8 g, 0.01 mol) and the same dithiocarbamate salt (1.8 g, 0.01 mol) gave 2.5 g (92%) of ethylene bis(*N,N*-dimethyl-*N',N'*-diethyldithiocarbamate) (VIIb): mp 102—103°C (ethanol); UV (EtOH): 253 and 279 mμ.[24]

Found: C, 40.42; H, 6.92; N, 9.11%. Calcd for $C_{10}H_{20}N_2S_4$: C, 40.54; H, 6.80; N, 9.46%.

Similarly the reaction of salt Ia with sodium *N,N*-diethyldithiocarbamate yielded VIIb in 90% yield. On the other hand, the reaction of salt Ib with the same dithiocarbamate salt gave ethylene bis(*N,N*-diethyldithiocarbamate) (VIIc): mp 93—94°C (ethanol) (lit,[26] 94—95°C); UV (EtOH): λ_{max} 254 and 280 mμ.[24]

Reactions of Salt I with Triethylamine. Salt Ia (12.5 g, 0.05 mol) was added to a solution of 6.0 g (0.06 mol) of triethylamine in a mixture of DMSO (30 m*l*) and dioxane (20 m*l*). The reaction mixture was stirred at 60°C for 5 hr, then poured into water. The ether layer was dried and the solvent evaporated. Distillation of the residue gave 2.0 g (65%) of a pale-yellowish oil, *S*-vinyl *N,N*-dimethyldithiocarbamate (VIIIa): bp 87—90°C/2 mmHg; n_D(25°C) 1.5907 (lit,[27] bp 82—83°C/1 mmHg; n_D(20°C) 1.6025); IR (neat): 1590 cm^{-1} (C=C); UV (EtOH): 253 and 280 mμ (shoulder).

By the same procedure the reaction of salt Ib with triethylamine gave *S*-vinyl *N,N*-diethyldithiocarbamate (VIIIb) in 63% yield: bp 80—84°C/0.1 mmHg (lit,[28] 92—94°C/2 mmHg); n_D(25°C) 1.5942; IR (neat): 1600 cm^{-1} (C=C); UV (EtOH): 258 and 280 mμ (shoulder).

Found: C, 48.23; H, 7.86; N, 7.96%. Calcd for $C_7H_{13}NS_2$: C, 47.99; H, 7.48; N, 8.00%.

The IR spectra of these products were identical with those of the authentic samples.[27]

Reactions of Salt I with Sodium Cyanide. Salt Ia (12.5 g, 0.05 mol) was added to a solution of 7.5 g (0.15 mol) of sodium cyanide in 50 m*l* of DMF. The reaction mixture was stirred at 60°C for 4 hr, then poured into water. The ether layer was dried and the solvent evaporated. Distillation of the residue gave 5.2 g (64%) of a yellowish oil, 2-cyano-2-dimethylamino-1,3-dithiolane (IXa): bp 114—116°C/3 mmHg; n_D(27°C) 1.5633; IR (neat): 2250 cm^{-1} (C=N); NMR (CCl_4): δ 2.47 (s, CH_3–N) and 3.37 ppm (s, CH_2–S).

Found: N, 15.69%. Calcd for $C_6H_{10}N_2S_2$: N, 16.09%.

By the same procedure the reaction of salt Ib (14.0 g, 0.05 mol) and sodium cyanide (7.5 g, 0.15 mol) gave 4.8 g of a yellowish oil: bp 83—85°C/0.2 mmHg. This distillate was proved to be not 2-cyano-2-diethylamino-1,3-dithiolane, but a complex mixture by the IR spectrum (neat) exhibiting several absorption bands due to the –S–CS–N< structure as well as C=C and C=N groups.

24) The characteristic bands due to the –S–CS–N< structure. The higher wavelength band is associated with transition to the imminium state (*N*-conjugation) while the lower wavelength feature arises from transition to the sulfonium state (*S*-conjugation): M. J. Janssen, *Rec. Trav. Chim.*, **79**, 454, 464 (1960).

25) A. W. Campbell and P. F. Tryan, *Ind. Eng. Chem.*, **45**, 125 (1953).

26) K. Pilgram, D. Phillips and F. Korte, *J. Org. Chem.*, **29**, 1848 (1964).

27) T. Nakai, K. Shioya and M. Okawara, *Makromol. Chem.*, **108**, 95 (1967).

28) J. C. Sauer, *J. Org. Chem.*, **24**, 1592 (1959).

BULLETIN OF THE CHEMICAL SOCIETY OF JAPAN VOL. 43 1870—1873 (1970)

Synthetic Studies on Bacitracin. VII.[1] Isomerization of Amino Acid Components of Thiazoline Peptides*1

Yoshihiro HIROTSU, Tetsuo SHIBA and Takeo KANEKO

Department of Chemistry, Faculty of Science, Osaka University, Toyonaka, Osaka

(Received February 2, 1970)

Ethyl 2-(1-benzyloxycarbonylaminoethyl)-R-Δ^2-thiazoline-4-carboxylate (III), ethyl 2-(1-benzyloxycarbonylamino-2-methyl-*n*-butyl)-R-Δ^2-thiazoline-4-carboxylate (VI) and their acid amide derivatives (V, VII and VIII) were prepared by either the iminoether coupling method or the dehydration method. As a general character of thiazoline peptide, it was found that the amino acid residue connected to thiazoline ring at *N*-terminal side is completely racemized at the stage of thiazoline ring formation, and further epimerized, in the case of isoleucine, by treatment with the basic reagent.

In earlier works on an amino acid composition of bacitracin A, the ambiguity of isoleucine content made the final conclusion of the molecular formula difficult.[2-6] Amino acid analysis of the hydrolyzate of somewhat impure bacitracin A showed often less than one mole of D-alloisoleucine which compensates the loss of L-isoleucine from three mole value in pure peptide.[2,5,6] The inactivation of the antibiotic activity of bacitracin A is closely related to isomerization of *N*-terminal isoleucine residue of the peptide.[7,8] Konigsberg *et al.* separated the high and low potency forms of bacitracin A by carbomethoxy cellulose chromatography after exposure in acidic medium, and showed that the high potency forms has L-isoleucine as *N*-terminal residue which is changed to D-alloisoleucine in the low potency one.[8]

In the present investigation, optical properties of the amino acid components of thiazoline ring of the various model peptides were studied in order to clarify the basic character of the isomerization of *N*-terminal amino acid of bacitracin A and to gain fundamental knowledge of its total synthesis.

General procedure used for the syntheses of thiazoline peptides were described previously.[9-10] Measurement of optical purity of the amino acid was performed by gaschromatography after conversion into trifluoroacetyl amino acid menthyl ester[11] for alanine and by amino acid analysis for isoleucine.

Acid hydrolysis of ethyl 2-(1-benzyloxycarbonylaminoethyl)-R-Δ^2-thiazoline-4-carboxylate (III) which was obtained by imino ether coupling method[9] from L-2-benzyloxycarbonylamino-propioimino ethyl ether (IV) and ethyl L-cysteinate hydrochloride gave completely racemized DL-alanine and L-cystine, while optically pure L-alanine was recovered from an acid hydrolyzate of IV. This fact indicates that racemization occurred during ring closure of thiazoline ring through the imino ether procedure. In order to know whether racemization depends on the method of ring closure or is an essential nature characteristic to thiazoline ring, the same thiazoline peptide III was prepared by dehydration method[10] as follows.

Benzyloxycarbonyl-L-alanyl-L-cysteine ethyl ester (II) was synthesized by coupling of benzyloxycarbonyl-L-alanine with diethyl L-cystinate dihydro chloride[12] using *N,N'*-dicyclohexylcarbodiimide followed by reduction of the product, *N,N'*-bisbenzyloxycarbonyl-L-alanyl-L-cystine diethyl ester (I), with zinc dust and hydrochloric acid. Cyclization of II to the thiazoline derivative was carried out with hydrogen chloride in chloroform. Neutralization

*1 This paper is dedicated to Emeritus Professor Munio Kotake in commemoration of his 75th birthday, November 30, 1969.

1) Part VI of this series: This Bulletin, **43**, 1564 (1970).
2) J. Porath, *Acta Chem. Scand.*, **6**, 1237 (1952).
3) L. C. Craig, W. Hausmann and J. R. Weisiger, *J. Biol. Chem.*, **199**, 865 (1952).
4) G. G. F. Newton and E. P. Abraham, *Biochem. J.*, **53**, 597 (1953).
5) W. Hausmann, J. R. Weisiger and L. C. Craig, *J. Amer. Chem. Soc.*, **77**, 721 (1955).
6) I. M. Lockhart, E. P. Abraham and G. G. F. Newton, *Biochem. J.*, **61**, 534 (1955).
7) W. Konigsberg and L. C. Craig, *J. Amer. Chem. Soc.*, **81**, 3452 (1959).
8) W. Konigsberg, R. J. Hill and L. C. Craig, *J. Org. Chem.*, **26**, 3867 (1961).
9) Y. Hirotsu, T. Shiba and T. Kaneko, This Bulletin, **40**, 2945 (1967).
10) Y. Hirotsu, T. Shiba and T. Kaneko, *ibid.*, **40**, 2950 (1967).
11) S. V. Vitt, M. B. Saporovskaya, I. P. Gudkova and V. M. Belikov, *Tetrahedron Lett.*, **39**, 2575 (1965).
12) E. Abderhalden and E. Eybert, *Ber.*, **49**, 2449 (1916).

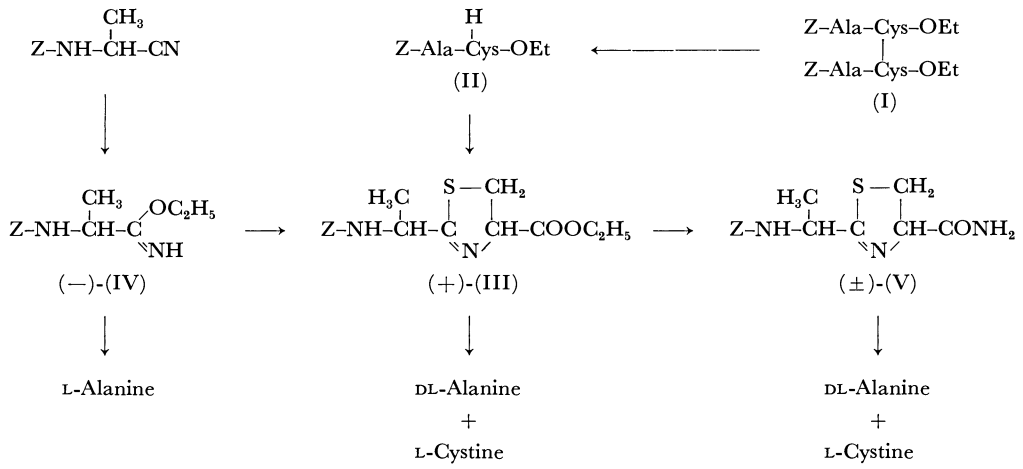

Fig. 1

$Z = C_6H_5CH_2OCO$

Cystine and alanine used are of L-configurations.

of the product with aqueous potassium carbonate afforded compound III. Thiazoline peptide III thus obtained was hydrolyzed with hydrochloric acid to give DL-alanine as well as L-cystine. Acid amide derivative V derived from compound III by treatment with ammonia in ethyl alcohol gave DL-alanine and DL-cystine on acid hydrolysis.[9]

From the results, it is concluded that *N*-terminal amino acid of the thiazoline peptide III is completely racemized during the stage of ring closure regardless of the method employed for the ring formation. Cysteine residue does not change in optical property at the ring closure but is also racemized under basic condition.

A similar result was observed in hydrolyzate of the other thiazoline peptide in which isoleucine is linked at the *N*-terminal side. 2-(1-Benzyloxycarbonylamino-2-methyl-*n*-butyl)-R-Δ^2-thiazoline-4-carboxamide (VIII) was synthesized by coupling of L-2-benzyloxycarbonylamino-3-methylvaleroimino

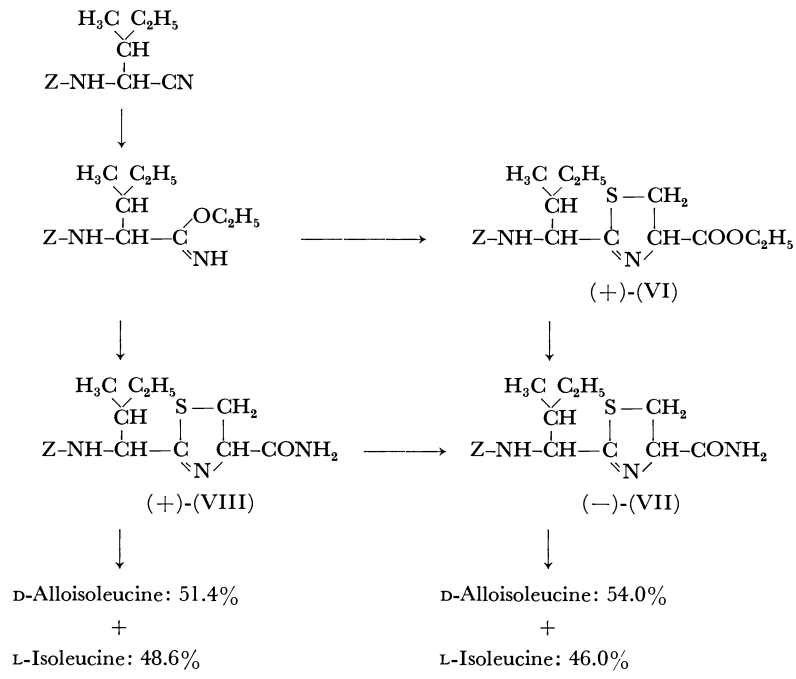

Fig. 2

$Z = C_6H_5CH_2OCO$

Cystine and isoleucine used are of L-configurations.

ethyl ether[9] and L-cysteinamide hydrobromide[1] as shown in Fig. 2. On amino acid analysis, hydrolysis of this thiazoline compound with hydrochloric acid gave a mixture of exactly the same amounts of L-isoleucine and D-alloisoleucine. This indicates that the racemization of the amino acid residue at *N*-terminal side of thiazoline ring is not limited to alanine derivative but is probably a general character based on thiazoline ring structure.

However, after a basic treatment of the thiazoline peptide, for instance, conversion of ethyl 2-(1-benzyloxycarbonylamino-2-methyl-*n*-butyl)-R-Δ^3-thiazoline-4-carboxylate (VI)[9] into carboxamide derivative (VII) with ammonia in ethyl alcohol or keeping of VIII in ethyl alcohol saturated with ammonia at room temperature for 3 days, a ratio of L-isoleucine and D-alloisoleucine in acid hydrolyzate changed to 46 : 54. Deviation from the ratio 50 : 50 seems to be significant in consideration of the accuracy of the analytical method. This means that the isoleucine residue connected to thiazoline ring at *N*-terminal side is racemized instantly on ring closure and further epimerized under basic condition. Epimerization of α-asymmetric carbon of isoleucine might progress under the steric influence of β-asymmetric carbon atom of isoleucine.

Konigsberg *et al.* demonstrated that the high potency form of bacitracin A isomerized to a low potency form on standing in 3% acetic acid, and the amount of the two forms becomes nearly equal after two days. Interconversion of the two isomers occurs even at pH 5.45. This isomerization can be well understood as the general character of thiazoline peptide. However, it is supposed that in comparison with rapid racemization of the model thiazoline peptide, the rate of isomerization of natural bacitracin A slows down because of a peculiar structural factor like the cyclol structure in the intact molecule of bacitracin A.

For the total synthesis of bacitracin A, it is expected that the racemization of the *N*-terminal isoleucine residue can not be avoided whatever method is applied for closure of the thiazoline ring, and the product must be purified by the fractional method based on the principle of separation of diasteromers to secure pure bacitracin A.

Experimental

All melting points are uncorrected. Ultraviolet spectra were obtained in 95% ethanol and 12N hydrochloric acid - 95% ethanol (1 : 1) with a Hitachi EPS-3 spectrophotometer. For gas chromatography a Shimazu GC-4APF was used. Amino acid analysis was carried out by a Hitachi Amino Acid Analyzer LKA-3.

N,N'-Bisbenzyloxycarbonyl-L-alanyl-L-cystine Diethyl Ester (I). To a suspension of 11.0 g (0.03 mol) of diethyl L-cystinate dihydrochloride[12] in 100 m*l* of chloroform was added 6.0 g (0.06 mole) of triethylamine. After the mixture was stirred for 1 hr, 100 m*l* of ether was added. The precipitate formed was filtered off, and the filtrate was concentrated *in vacuo*. To a solution of the residue thus obtained in 150 m*l* of dioxane, 13.4 g (0.060 mol) of benzyloxycarbonyl-L-alanine and 13.6 g (0.066 mol) of *N,N'*-dicyclohexylcarbodiimide were added. After the reaction mixture had been stirred for several hours, 1 m*l* of acetic acid was added. *N,N'*-Dicyclohexylurea formed was filtered off, and the filtrate was diluted with water. The precipitate formed was filtered off and washed with water. Recrystallization from ethanol gave 18.6 g (82%) of I; mp 165—167°C, $[\alpha]_D^{15}$ −74.0° (*c* 2.00, dimethylformamide).

Found: C, 54.48; H, 6.02; N, 7.88; S, 9.05%. Calcd for $C_{32}H_{42}O_{10}N_4S_2$: C, 54.38; H, 5.99; N, 7.93; S, 9.07%.

Benzyloxycarbonyl-L-alanyl-L-cysteine Ethyl Ester (II). To a suspension of 17.7 g (0.025 mol) of I in 200 m*l* of dioxane and 16.5 m*l* of concentrated hydrochloric acid was added 7.5 g of zinc dust in many portions over a period of 15 min with vigorous stirring at 30—40°C. The mixture was stirred for additional 30 min, and then filtered. The filtrate was concentrated *in vacuo*. An oily product separated out on addition of water was extracted with ethyl acetate. The extract was washed with water, dried with magnesium sulfate and then evaporated *in vacuo*. Recrystallization of the residual solid from ethyl acetate-petroleum ether gave 11.5 g (65%) of II; mp 106—109°C, $[\alpha]_D^{15}$ −14.1° (*c* 2.18, dimethylformamide).

Found: C, 54.17; H, 6.26; N, 7.91; S, 8.86%. Calcd for $C_{10}H_{22}O_5N_2S$: C, 54.22; H, 6.26; N, 7.91; S, 9.05%.

Ethyl 2-(1-Benzyloxycarbonylaminoethyl)-R-Δ^2-thiazoline-4-carboxylate (III). A solution of 10.6 g (0.03 mol) of II in 500 m*l* of chloroform was saturated with dry hydrogen chloride gas on cooling in an ice bath. The mixture was allowed to stand at room temperature overnight and then concentrated *in vacuo*. To the residue was added 300 m*l* of ether, and the mixture was treated with a concentrated aqueous potassium carbonate. The ether layer was washed with water, dried with sodium sulfate and then concentrated *in vacuo* to give a crude oil of 7.5 g: this was dissolved in a small amount of ether and subjected to silica gel column chromatography (Mallincrodt Chemical Worker, 100 mesh, 100 g). Elution with petroleum ether - anhydrous ether gave 5.8 g (57%) of III, $[\alpha]_{25}^{D}$ +59.4° (*c* 3.26, ethanol).

Found: C, 57.06; H, 5.97; N, 8.29; S, 9.40%. Calcd for $C_{16}H_{20}O_4N_2S$: C, 57.12; H, 5.99; N, 8.33; S, 9.53%.

2-(1-Benzyloxycarbonylamino-2-methyl-*n*-butyl)-Δ^2-thiazoline-4-carboxamide (VII). A solution of 1.9 g (0.005 mole) of ethyl 2-(1-benzyloxycarbonylamino-2-methyl-*n*-butyl)-R-Δ^2-thiazoline-4-carboxylate (VI)[9] in 20 m*l* of anhydrous ethanol was saturated with ammonia at 0°C, and the mixture was kept at room temperature for 3 days. The solution was concentrated *in vacuo* below 40°C. The residue thus obtained was recrystallized from ethanol-water to give 1.4 g (82%) of VII, mp 131—133°C, $[\alpha]_D^{25}$ −5.8° (*c* 1.25, dimethylformamide), λ_{max}^{EtOH} 235 mμ (ε 2300), 252 mμ (ε 2800), $\lambda_{max}^{EtOH\text{-}HCl}$ 269 mμ (ε 4800).

Found: C, 58.36; H, 6.63; N, 12.00; S, 8.94%. Calcd for $C_{17}H_{23}O_3N_3S$: C, 58.43; H, 6.63; N, 12.03; S, 9.18%.

2-(1-Benzyloxycarbonylamino-2-methyl-*n*-butyl)-R-Δ^2-thiazoline-4-carboxamide (VIII). To a solution of 5.7 g (0.026 mol) of L-cysteinamide hydrobromide[1]

in tetrahydrofuran and 10 m*l* of anhydrous methanol was added 7.5 g (0.026 mole) of L-2-benzyloxy-carbonylamino-3-methylvaleroimino ethyl ether.[9] After the reaction mixture had been kept at room temperature for 3 hr, ammonium bromide was deposited. The reaction mixture was concentrated *in vacuo*, and the residue obtained was dissolved in ethyl acetate. The ethyl acetate solution was washed with water, dried with sodium sulfate, and then evaporated *in vacuo*. The residue obtained was recrystallized from ethyl acetate - petroleum ether gave 2.8 g (35%) of VIII; mp; 138—140°C, $[\alpha]_D^{24}$ +26.7° (*c* 2.20, dimethylformamide).

Found: C, 58.40; H, 6.69; N, 11.82; S, 8.89%.

Isolation of L-Alanine from Hydrolyzate of IV. Hydrolysis of 5.0 g (0.02 mole) of IV was carried out by refluxing in 100 m*l* of 6N hydrochloric acid for 3 hr. After cooling, the reaction mixture was extracted with ether. An aqueous layer was evaporated *in vacuo*. The residue obtained was dissolved in 30 m*l* of water, subjected to Dowex-50 column (W×8, H^+ form, 200—400 mesh, 30 m*l*) and eluted with 50 m*l* of N ammonium hydroxide. The eluate was evaporated *in vacuo* and the residue obtained was then crystallized from water - ethyl alcohol; wt. 1.45 g (81%), $[\alpha]_D^{25}$ +14.3° (*c* 2.58, N HCl).

Found: C, 40.42; H, 7.97; N, 15.61%. Calcd for $C_3H_7O_2N_2$: C, 40.44; H, 7.92; N, 15.72%.

Gaschromatography of Menthyl Trifluoroacetylalaninate obtained from Hydrolyzates of III and V. Hydrolysis of 0.3 g each of III, which was synthesized by either the imino ether or the dehydration method, and of V, was carried out by refluxing in 20 m*l* of 6N hydrochloric acid with 0.3 g of anisole for 3 hr. After cooling, the reaction mixture was extracted with ether. An aqueous layer was evaporated *in vacuo*. The residue was dissolved in 10 m*l* of water and evaporation was repeated. The residue thus obtained was dissolved in 5 m*l* of water and subjected to Dowex-50 column (W×8, H^+ form, 200—400 mesh, 10 m*l*). Eluate with 20 m*l* of N ammonium hydroxide was evaporated *in vacuo* to yield alanine. Three mg each of the samples of alanine were mixed with 0.7 g of menthol. Hydrogen chloride gas was passed through the melted mixture at 110°C for one and a half hour.[11] Excess of menthol was removed by sublimation at 100°C under reduced pressure of 3 mmHg. To the residue thus obtained, a few m*l* of trifluoroacetic anhydride was added. After the mixture had been allowed to stand at room temperature overnight, excess of trifluoroacetic anhydride was removed by evaporation *in vacuo*. The residue was dissolved in 1 m*l* of acetone and subjected to gaschromatography. Gas chromatography was carried out on a column of 3m-length packed with 1.5% NPGS on 60—80 mesh Chromosorb W at column temperature of 150°C under excess pressure of 1.8 atm, and at detector temperature of 180°C and injection temperature of 250°C. All the three samples of menthyl trifluoroacetylalaninate were shown to be of complete DL-form.

Isolation of L-Cystine from Acid Hydrolyzate of III. Hydrolisys of 1.7 g each (0.05 mol) of III, which was synthesized by either the imino ether or dehydration method, was carried out by refluxing in 50 m*l* of 6N hydrochloric acid with 0.5 g of anisole for 3 hr. The reaction mixture was cooled and extracted with ether. The aqueous layer was concentrated *in vacuo* to dryness. A solution of the residue in 30 m*l* of water was adjusted to pH about 8.5 with 28% aqueous ammonia. Air was bubbled through the solution until the nitroprusside reaction became negative by a spot test. The reaction mixture was allowed to stand at 0°C for 2 days. The precipitate thus formed was filtered off and then dissolved in 15 m*l* of N hydrochloric acid. The solution was adjusted to pH 5.5—6.0 with an aqueous sodium acetate solution. After standing at 0°C for 2 days, the precipitate formed was filtered off and dried at 80°C *in vacuo* for 4 hr to give 0.33 g (55%) and 0.37 g (62%) of L-cystine respectively; $[\alpha]_D^{20}$ −218° (*c* 1.00, N HCl).

Found: N, 11.51 and 11.62; S, 26.09 and 26.38%. Calcd for $C_6H_{12}O_4N_2S_2$: N, 11.66; S, 26.69%.

Amino Acid Analysis of L-Isoleucine and D-Alloisoleucine in Acid Hydrolyzate of VII and VIII. *a)* A suspension of 0.05 g of VIII in 10 m*l* of 6N hydrochloric acid was refluxed for 2 hr. The hydrolyzate was extracted with ether. An aqueous layer was used for amino acid analysis. The ratio of D-alloisoleucine and L-isoleucine was found to be 51.4 : 48.6.

b) In a similar way, 0.1 g each of VII and VIII, which was treated with ammonia in ethanol at room temperature for 3 days, was hydrolyzed by refluxing in 10 m*l* of 6N hydrochloric acid for 3 hr, and the hydrolyzate was applied to amino acid analysis. Ratios of D-alloisoleucine and L-isoleucine for both compounds were found to be 54.7 : 45.3 and 54.0 : 46.0% respectively.

NOTES

BULLETIN OF THE CHEMICAL SOCIETY OF JAPAN VOL. 43 1874—1875 (1970)

Notiz zur Umsetzung des Ketenimins

Kunihiro ICHIMURA*1 und Masaki OHTA

Laboratorium für Organische Chemie, Tokyo Institut für Technologie, Tokyo, Meguro-ku, Ookayama

(Eingegangen am 20. September, 1969)

Bekanntlich ist, daß das Ketenimin sich als so starkes Elektrophil wie andere Heteroallene verhält, und vor kurzem haben wir die Addition der aktiven Methylenverbindungen an Ketenimin beschrieben.[1] In dieser Arbeit wollen wir einige Beispiele der nucleophilen Addition an Ketenimine angeben.

Wenn man Schwefelwasserstoff in die benzolische Lösung des *N*-(*p*-Tolyl)diphenylketenimin in Gegenwart des Triäthylamins einleitet, so wird *N*-(*p*-Tolyl)diphenylthioacetamid erhalten. In Abwesenheit der Base war die Reaktion beträchtlich langsam.

Im Zusammenhang der Entschwefelung des Thioharnstoffs zu Carbodiimid[2] haben wir dann das Zurückgewinnen des Ketenimins durch die Einwirkung des Quecksilberoxyds auf das Thioamid versucht, und jedoch nur ein strukturunbekanntes entschwefeltes Produkt erhalten.

Dieartige Bildung der kummulierten Doppelbindungen wurde ja bei der Umsetzung des *N*-Methyldiphenylthioacetamids mit Quecksilberoxyd beobachtet, während Effenberger nur das entsprechende Säureamid bei der Einwirkung des Quecksilberoxyds auf *N*-Phenyl-bis(äthoxycarbonyl)thioacetamid isoliert hatte.[3]

Nach den Ergebnissen der Anlagerung der aktiven Methylenverbindungen an Ketenimin könnte man die Entstehung des Diphenylmethylenaziridins durch die Addition-Elimination-Reaktion erwarten, wenn man das Ketenimin mit der aktiven α-Halomethylenverbindung in Gegenwart der Base reagieren läßt. Bei Benutzung des Phenacylbromids, Chloressigsäureesters sowie Benzylpyridiniumsalzes konnte man aber keine einheitliche Substanz isolieren.

Bei der Umsetzung des (*p*-Chlorphenyl)diphenylketenimin mit Chloroform in Gegenwart von Natrium-*t*-butoxyd wurde α-(*p*-Chlorphenylimino)-β,β-diphenylpropionsäure-*t*-butylester in geringer Ausbeute erhalten, dessen Struktur auf der Elementaranalyse und dem infraroten Spektrum beruht. Das *t*-Butylester III liefert durch säure Hydrolyse-*p*-Chloranilin, und die Umwandlung des Esters in 2,4-Dinitrophenylhydrazon des Diphenylacetaldehyds (IV) stützt weiter dessen Struktur. Das *t*-Butylester bildet sich vermutlich über Diphenylmethylendichloraziridin V, das nach der Bildung vom Laktamacetal VI durch Abspaltung des C–N-Bindung des Dreirings in das isolierte Produckt umgewandelt würde.

Dieartige Umsetzung in Gegenwart des Natriummethylats liefert nicht das entsprechende Methylester, sondern *N*-(*p*-Chlorphenyl)diphenylacetimidat-methylester.

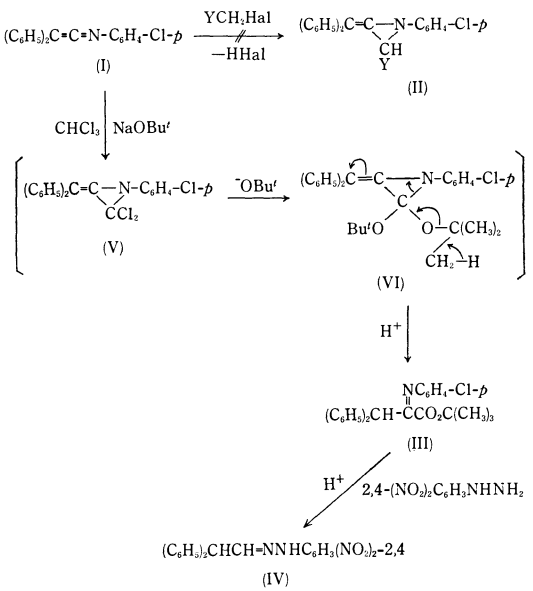

Beschreibung der Versuche

***N*-(*p*-Tolyl)diphenylthioacetamid.** Man leitet 20 min Schwefelwasserstoff in die benzolische Lösung

*1 Neue Anschrift: Institut für Polymer- und Faserforschung, Yokohama, Kanagawa-ku, Sawatari 4.

1) K. Ichimura und M. Ohta, Dieses Bulletin, **40**, 2135 (1967).

2) R. Herbeck und M. Pezzati, *Ber.*, **71**, 1933 (1938).

3) F. Effenberger, *Angew. Chem.*, **75**, 496 (1962).

ein, die 0.50 g *N*-(*p*-Tolyl)diphenylketenimin und 2 m*l* Triäthylamin enthält. Nach Eindampfen des Lösungsmittels erhält man 0.45 g Kristalle, die aus Methanol umkristallisiert werden. *N*-(*p*-Tolyl)diphenylthioacetamid als gelbe Prismen schmilzt zuerst bei 135—140°C und nach der anschließenden Erstarrung schließlich bei 190—191°C. Gef: C, 79.46; H, 6.67; N, 4.74%. Ber für $C_{21}H_{19}NS$: C, 79.47; H, 6.03; N, 4.41%.

Das Thioamid liefert die strukturunbekannten entschwefelten farblosen Nadeln vom Schmp 184—185°C bei Einwirkung des Quecksilberoxyds in Benzol. Gef: C, 60.84; H, 4.76; N, 3.64%.

Einwirkung des Quecksilberoxyds auf *N*-Methyldiphenylthioacetamid. Man kocht die benzolische Lösung von 0.50 g *N*-Methyldiphenylthioacetamid und 1.00 g Quecksilberoxyd, macht sie vom Niederschlag frei und erhält den glassartigen Rückstand, der ja bei 2100 cm^{-1} die starke charakteristische Bande des Ketenimins zeigt.

Umsetzung des *N*-(*p*-Chlorphenyl)diphenylketenimins mit Chloroform. In das Gemisch von 1.52 g *N*-(*p*-Chlorphenyl)diphenylketenimin (I) und aus 0.28 g Natrium erhaltenem verpulvertem Natrium-*t*-butoxyd in 20 m*l* Benzol und 20 m*l* *n*-Hexan setzt man 1.44 g Chloroform in 10 m*l* *n*-Hexan unter gutem Rühren und Eis-Kochsalzkühlung bei −17——15°C langsam zu, rührt weiter bei Raumtemperatur und läßt das Gemisch über Nacht stehen. Nach Behandlung mit der aktiven Kohle und Filtrieren dampft man die Filtrat unter vermindertem Druck ein und erhält 0.50 g kristallinen Rückstand, der aus *n*-Hexan umgelöst wird. Farblose Nadeln vom Schmp 111—113°C. Gef: C, 73.42; H, 6.04; N, 3.19.% Ber für $C_{25}H_{24}NO_4Cl$: C, 73.97; H, 5.96; N, 3.45%. IR (KBr): 1710 (s), 1615 (m), 1390 (schw), 1370 (schw), 1155 (s), 1090 (m) cm^{-1}.

Man kocht 0.28 g oben erhaltene Kristalle in 2N-Salzsäure-Methanol während 50 min, neutralisiert mit Natriumhydroxyd und extrahiert mit Äther. 0.02 g Kristalle vom Schmp 69—71.5°C werden erhalten und durch Mischprobe mit *p*-Chloranilin identifiziert.

Wenn man die Kristalle vom Schmp. 111—113°C mit 2,4-Dinitrophenylhydrazin in Äthanol in Gegenwart der katalytischen Mengen Schwefelsäure behandelt, so bildet sich das Hydrazon des Diphenylacetaldehyds (IV) vom Schmp 151°C (Ber. Schmp 150—151°C).[4] Gef: C, 63.82; H, 4.42; N, 15.38%. Ber für $C_{20}H_{16}N_4O_4$: C, 63.82; H, 4.29; N, 14.89%. IR (KBr): 3270 (m), 1620 (s), 1520 (s), 1340 (s) cm^{-1}.

Versuche zur Umsetzung des *N*-(*p*-Chlorphenyl)-diphenylketenimins mit Chloroform in Gegenwart von Natriummethylat. In der analogen Weise versetzt man das *N*-(*p*-Chlorphenyl)diphenylketenimin mit Chloroform in Gegenwart des trocknen Natriummethylats in Benzol-*n*-Hexan bei −11—18°C. Nach gleicher Aufarbeitung sind die farblosen Kristalle vom Schmp 111—112.5°C erhältlich, die sich mittels IR-Spektrums mit *N*-(*p*-Chlorphenyl)diphenylacetimidatmethylester identifizieren, das bei Einwirkung des Natriummethylats auf das Ketenimin in Methanol hergestellt wird. Gef: C, 74.53; H, 6.16; N, 4.19%. Ber für $C_{21}H_{18}NOCl$: C, 75.10; H, 5.40; N, 4.17%.

4) H. O. House, *J. Amer. Chem. Soc.*, **77**, 3070 (1955).

BULLETIN OF THE CHEMICAL SOCIETY OF JAPAN VOL. 43 1875—1877 (1970)

The Photoreaction of 1,2-Dibenzoylethylene in Acidic Methanol

Noboru SUGIYAMA and Choji KASHIMA

Department of Chemistry, Tokyo Kyoiku University, Otsuka, Tokyo

(Received October 20, 1969)

We have previously reported that the photoreaction of β-aroylacrylic acids in methanol produced the methanol adducts, β-aroyl-α-methoxypropionic acids.[1] β-Aroylacrylic acids have the structure of an α,β-unsaturated γ-ketoacid. As an analogy, 1,2-dibenzoylethylene (I), an α,β-unsaturated γ-diketones, is expected to give the methanol adduct upon irradiation. On the other hand, Griffin[2] and Zimmerman[3] reported that the irradiation of I in methanol gave only the rearrangement product, methyl 4-phenyl-4-phenoxy-3-butenoate (II), unlike as in the methanol addition reaction. Thus, it is interesting to re-examine the irradiation of I in methanol.

Results and Discussion

We found that the irradiation of I in methanol gave II as the main product, as well as a methanol adduct, 1,2-dibenzoyl-1-methoxyethane (III), as the minor product. The structure of III was determined by the spectral data and by identification with an authentic sample.[4] The yields

1) N. Sugiyama, H. Kataoka, C. Kashima and K. Yamada, This Bulletin, **42**, 1353 (1969).

2) G. W. Griffin and E. J. O'Connell, *J. Amer. Chem. Soc.*, **84**, 4148 (1962).

3) H. E. Zimmerman, H. G. C. Dürr, R. G. Lewis and S. Bram, *ibid.*, **84**, 4149 (1962); H. E. Zimmerman, H. G. Dürr, R. S. Givens and R. G. Lewis, *ibid.*, **89**, 1863 (1967).

4) R. E. Lutz and C-K. Dien, *J. Org. Chem.*, **21**, 551 (1956).

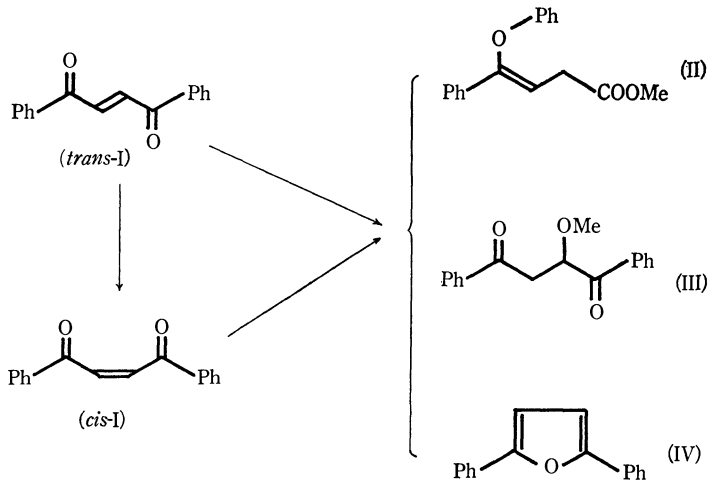

Fig. 1

Table 1. The photoproducts from *trans*-1,2-dibenzoylethylene in acidic methanol

Concn. of HCl mol/*l*	Product Total %	Products		
		II%	III%	IV%
0	68.6	95	5	0
9.9×10^{-6}	79.5	90	10	0
9.5×10^{-5}	70.0	95	5	0
9.9×10^{-5}	77.6	94	4	2
1.9×10^{-4}	57.6	78	19	4
4.7×10^{-4}	45.6	29	47	24
9.5×10^{-4}	52.1	15	56	28
9.9×10^{-4}	49.0	5	40	55

of II and III were estimated by means of the intensity of the NMR signals, which appeared as triplets at δ 6.01 and 5.43 ppm, and which were assigned to the olefinic proton of II and the methine proton of III respectively. The mechanism of the formation of III seems to be similar to that of the photoaddition of β-benzoylacrylic acids.

Considering that the addition of methanol to β-benzoylacrylic acids was initiated by protonation on carbonyl oxygen,[5] the yield of III from I was expected to increase in acidic methanol. Thus, the photoreaction of I was examined in methanol containing various amounts of hydrochloric acid. As is shown in Table 1, when the concentration of hydrochloric acid was 9.9×10^{-5} mol/*l* or less, the

Table 2. The photoproducts from *trans*- or *cis*-1,2-dibenzoylethylene in methanol or in acidic methanol

Structure of I	Concn. of HCl (mol/*l*)	Filter	Total product %	Products		
				II%	III%	IV%
trans	0	Py[a]	68.6	95	5	0
trans	0	Py+Ni[b]	13.2	100	0	0
trans	0	Py+Cu[c]	90.6	100	0	0
cis	0	Py[a]	57.1	100	0	0
cis	0	Py+Ni[b]	26.7	100	0	0
cis	0	Py+Cu[c]	85.1	100	0	0
trans	4.7×10^{-4}	Py[a]	45.6	29	47	24
trans	4.7×10^{-4}	Py+Ni[b]	30.1	18	73	9
trans	4.7×10^{-4}	Py+Cu[c]	69.2	33	47	21
cis	4.7×10^{-4}	Py[a]	51.4	49	49	3
cis	4.7×10^{-4}	Py+Ni[b]	21.1	25	75	0
cis	4.7×10^{-4}	Py+Cu[c]	68.6	26	65	10

a) Pyrex filter.
b) Pyrex filter and aqueous solution filter of $NiSO_4$ and $CoSO_4$.
c) Pyrex filter and aqueous solution filter of $CuSO_4$ and NH_4OH.

5) C. Kashima, H. Kataoka, K. Tanaka and N. Sugiyama, This Bulletin, **43**, 1473 (1970).

effect of the acid was not observed in the photoreaction of I. At more than 1.9×10^{-4} mol/*l*, the yield of II decreased and that of III increased.

Moreover, in methanol containing more than 1.9×10^{-4} mol/*l* of hydrochloric acid, 2,5-diphenylfuran (IV) was obtained as one of the photoproducts. The structure of IV was determined by the spectral data and by identification with an authentic sample.[6] The yield of IV was estimated by means of the singlet signal of the NMR spectrum at δ 6.68 ppm assigned to two methine protons on the furan ring. In the presence of 4.7×10^{-4} mol/*l* of hydrochloric acid in methanol, the reaction mixture was shown to contain 29% of II, 47% of III, and 24% of IV. Then, the influence of the light source on the photoreaction of I was examined (Table 2). In the absence of acid, the main product is II, even when the light is filtered through an aqueous solution of nickel sulfate and a cobalt sulfate mixture or ammoniac copper sulfate. However, in the presence of 4.7×10^{-4} mol/*l* of acid, the yield of III increased when the light came through a filter of nickel sulfate and a cobalt sulfate solution. In acidic methanol, *cis*-1,2-dibenzoylethylene also gave II and III photoproducts.

Table 3. The photoproducts from *trans*-1,2-dibenzoylethylene in acidic alcohols
(5×10^{-4} mol/*l* HCl)

Alcohol	Total product %	Rearrangement product %	Alcohol adduct %	Diphenyl furan %
MeOH	70.4	29	52	19
EtOH	67.4	80	20	0
n-PrOH	53.9	75	25	0
iso-PrOH	30.8	100	0	0
t-BuOH	36.8	100	0	0

Furthermore, the photoreaction of I in alcohols other than methanol was examined in the presence of 5×10^{-4} mol/*l* of hydrochloric acid; the results are listed in Table 3. In ethanol or *n*-propanol, both the alcohol adduct and the rearrangement product were obtained, but in the sterically-hindered alcohols, such as isopropanol or *t*-butanol, only the rearrangement product was obtained. In case of alcohols other than methanol, IV was not obtained.

By the facts that the addition occurs by the irradiation in acidic methanol or ethanol, and that the *cis* isomer gives the addition product in acidic methanol, it can be deduced that the mechanism of this reaction is similar to that of the photoaddition of methanol to β-benzoylacrylic acids.[1,5]

6) S. Skraup and S. Guggenheimer, *Ber.*, **58**, 2488 (1925).

Experimental

Materials. *trans*-1,2-Dibenzoylethylene was prepared from fumaroyl chloride by a Friedel-Crafts reaction and was recrystallized from ethanol; mp 110.5°C (lit,[7] 109—110°C). λ^{EtOH} (ε): 268 (18400) and 360 nm (sh, 257). δ^{CDCl_3}: 7.97 (s, 2H), 7.9—8.15 (m, 6H) and 7.4—7.7 ppm (m, 4H). *cis*-1,2-Dibenzoylethylene was prepared by the irradiation of I in ethanol;[8] mp 135.5°C. λ^{EtOH} (ε): 260 (17800) and 340 nm (sh, 210). δ^{CDCl_3}: 7.16 (s, 2H), 7.4—7.7 (m, 6H) and 7.8—8.1 ppm (m, 4H).

Instrumentation. The infrared and ultraviolet spectra were measured with a Hitachi EPI-2-type infrared spectrometer and a Hitachi EPS-3T-type spectrometer respectively. The NMR spectra were recorded with a Hitachi H-60 high-resolution NMR spectrometer, with TMS as the internal standard. An Ushio 450 W high-pressure mercury lamp was used as the irradiation source.

Filter. The light from the high-pressure mercury lamp was filtered by three types of filters:

1) Pyrex filter; transparent at wavelengths longer than 310 nm.

2) Aqueous solution (3 *l*) of nickel sulfate (1350 g) and cobalt sulfate (320 g) and a Pyrex filter; thickness 1 cm; transparent from 290 to 370 nm; 290 nm, 5% T; 310 nm, 50% T; 330 nm, 70% T; 350 nm, 25% T; with a maximum at 320 nm, 85% T.

3) Aqueous solution (2 *l*) of copper sulfate (100 g) and aqueous ammonia (400 m*l*); thickness 1 cm; transparent from 320 to 480 nm; 330 nm, 15% T; 350 nm, 47% T; 370 nm, 68% T; 390 nm, 80% T; 410 nm, 82% T; 430 nm, 69% T; 450 nm, 40% T; 470 nm, 8% T; with a maximum at 404 nm, 82.5% T.

Irradiation of I. A solution of 100 mg of I in 5 m*l* of the methanol was irradiated at room temperature. After the solvent had been removed, the residue was analyzed by means of the intensity of the NMR signals at δ 5.43 (t, methine proton of III), 6.01 (t, olefinic proton of II), and 6.68 ppm (s, methine protons of IV). The residue was chromatographed on a silica-gel (Merck 7734) column with a benzene-ethyl acetate mixture, we thus obtained II, III, and IV in a pure state.

Methyl 4-Phenyl-4-phenoxy-3-butenoate (II). ν^{film}: 1735, 1600, 1485, 1220, 750 and 690 cm^{-1}. δ^{CDCl_3}: 3.26 (d, 2H), 3.60 (s, 3H), 6.01 (t, 1H) and 6.7—7.6 ppm (m, 10H).

1,2-Dibenzoyl-1-methoxyethane (III). ν^{film}: 1680, 1595, 1450, 1110, 1090, 755 and 685 cm^{-1}. δ^{CDCl_3}: 3.37 (s, 3H), 3.41 (d, 2H), 5.43 (t, 1H), 7.2—7.6 (m, 6H) and 7.8—8.2 ppm (m, 4H).

2,5-Diphenylfuran (IV). mp 85°C. ν^{KBr}: 1600, 1020, 920, 910, 795, 760 and 690 cm^{-1}. δ^{CDCl_3}: 6.68 (s, 2H) and 7.1—7.9 ppm (m, 10H).

7) R.E. Lutz, "Organic Syntheses", Col. Vol. III, p. 248 (1955).

8) H. Keller, R. Pasternak and H. V. Halban, *Helv. Chim. Acta*, **29**, 512 (1946).

BULLETIN OF THE CHEMICAL SOCIETY OF JAPAN VOL. 43 1878—1879 (1970)

The Photoreaction of 3-Hexene-2,5-dione in Methanol

Noboru SUGIYAMA and Choji KASHIMA

Department of Chemistry, Tokyo Kyoiku University, Otsuka, Tokyo

(Received October 25, 1969)

We have investigated the photoreactions of α,β-unsaturated γ-dicarbonyl compounds, such as 1,2-dibenzoylethylene,[1] β-aroylacrylic acids,[2,3] β-acylacrylic acids,[4] and their esters. The photoproducts of these systems in methanol are the *cis* isomers, 4-hydroxy- and 4-methoxy angelica lactones, and methanol adducts. As a part of these investigations, we have now examined the photoreaction of 3-hexene-2,5-dione, one of the α,β-unsaturated γ-diketones, in methanol.

Results and Discussion

By the irradiation of a filtered light through a Pyrex filter in methanol for 6 hr, *trans*-3-hexene-2,5-dione (I), which shows absorption maxima at 228 (ε 14000) and 331 mμ (ε 69), gave the *cis* isomer (II). The structure of II was deduced by means of the spectral data and by identification with an authentic sample.[5] Upon continuous irradiation for 22 hr, I gave two products, III and IV, which were separated by vapor-phase chromatography. In the NMR spectra, III showed singlet signals at δ 5.78, 3.20, and 1.40 ppm, while IV showed them at δ 5.77, 3.10, and 1.48 ppm. From these results and from other spectral and elemental analysis data, the structures of III and IV were deduced to be *cis*- and *trans*-2,5-dimethoxy-2,5-dimethyl-2,5-dihydrofuran respectively. Although the stereo isomers were not separated, the preparation of 2,5-dimethoxy-2,5-dimethyl-2,5-dihydrofuran from 2,5-dimethylfuran has been reported by Levisalles.[5] Thus, we also prepared III and IV by the method of Levisalles, and identified them with the photoproducts.

For the purpose of clarifying the reaction mechanism from I to II, III, and IV, kinetic studies were carried out. The concentrations of I, II, III, and IV in the reaction mixture were measured by means of the NMR spectra and by vapor-phase chromatography. The changes in the concentration with the time are shown in Fig. 1. The curve for II showed a maximum at 5 hr, and those for III and IV, a gradual increase. Also, it was confirmed

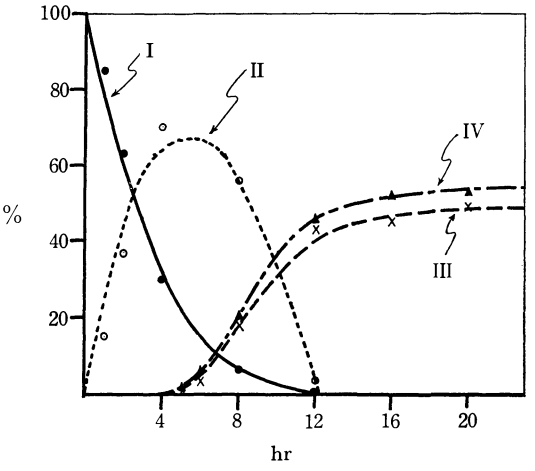

Fig. 1

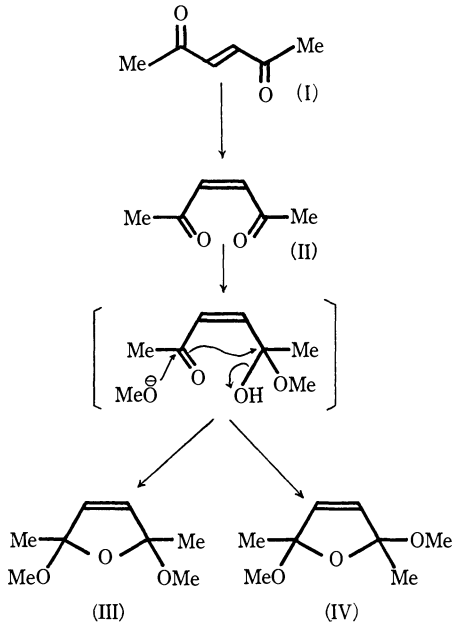

Fig. 2

1) C. Kashima and N. Sugiyama, This Bulletin, **43**, 1875 (1970).

2) N. Sugiyama, H. Kataoka, C. Kashima and K. Yamada, *ibid.*, **42**, 1353 (1969).

3) C. Kashima, H. Kataoka, K. Tanaka and N. Sugiyama, *ibid.*, **43**, 1473 (1970).

4) N. Sugiyama, H. Kataoka, C. Kashima and K. Yamada, *ibid.*, **42**, 1098 (1969).

5) J. Levisalles, *Bull. Soc. Chim. Fr.*, (**5**) **24**, 997 (1957).

that II does not react with methanol at room temperature without irradiation.

Thus, a probable reaction mechanism for the formation of III and IV from I may be proposed (Fig. 2). That is, I is isomerized to II, the excited species of which is attacked by methanol to produce the hemiacetal intermediate. This intermediate is immediately cyclized to III and IV in parallel.

From these results, it seems that the photoreaction from I to III and IV is similar to the formation of 4-methoxy angelica lactone.

Experimental

Material. *trans*-3-Hexene-2,5-dione was prepared from 2,5-hexanedione by oxidation with selenium dioxide, and then recrystallized from *n*-hexane; mp 73°C (lit,[6] 78°C). λ^{EtOH} (ε): 228 (14000) and 331 mμ (69). δ^{CDCl_3}: 6.78 (s, 2H) and 2.38 ppm (s, 6H).

Instrumentation. The infrared and ultraviolet spectra were measured with a Hitachi EPI-2-type infrared spectrometer and a Hitachi EPS-3T-type spectrometer respectively. The NMR spectra were recorded with a Hitachi A-60 high-resolution NMR spectrometer, with TMS as the internal standard. A Hitachi KGL-2A-type gas-chromatograph analyzer was used with 10% PEG-adipate at 104°C. The light from a Ushio 450-W high-pressure mercury lamp was irradiated on the sample through the Pyrex filter.

***cis*-3-Hexene-2,5-dione (II).** A solution of 100 mg of I in 5 m*l* of methanol was irradiated at room temperature. After 2 hr, the solvent was removed; we then measured the spectra and chromatographed them on a silica-gel thin layer. λ^{EtOH} (ε): 224 mμ (8600). ν^{KBr}: 1675, 1610, 1415, 1390, 1355, 1255, 1215, 1170 and 985 cm^{-1}. δ^{CDCl_3}: 6.30 (s, 2H) and 2.29 ppm (s, 6H).

The photoproduct was identified with the *cis*-3-hexene-2,5-dione prepared from 2,5-dimethoxy-2,5-dimethyl-2,5-dihydrofuran.[5]

***trans*- and *cis*-2,5-Dimethoxy-2,5-dimethyl-2,5-dihydrofuran (III and IV).** A methanol solution of I was irradiated for 22 hr, and then the solvent was removed. The residual oil was passed through preparative vaporphase chromatography. The first fraction, with Rt 9.5 min, was collected as III. λ^{EtOH} (ε): 251 mμ (342). ν^{film}: 1450, 1370, 1350, 1285, 1170, 1125, 1090, 1050, 945, 890 and 770 cm^{-1}. δ^{CDCl_3}: 5.78 (s, 2H), 3.20 (s, 6H) and 1.40 ppm (s, 6H).

Found: C, 60.59; H, 9.17%. Calcd for $C_8H_{14}O_3$: C, 60.74; H, 8.92%. The second fraction, with Rt 12.0 min, was collected as IV. λ^{EtOH} (ε): 224 (sh, 179) and 253 mμ (sh, 104). ν^{film}: 1450, 1370, 1350, 1170, 1095, 1050, 945, 890 and 770 cm^{-1}. δ^{CDCl_3}: 5.76 (s, 2H), 3.10 (s, 6H) and 1.48 ppm (s, 6H).

Found: C, 60.36; H, 8.89%. Calcd for $C_8H_{14}O_3$: C, 60.74; H, 8.92%. Both III and IV were identical with the mixture of *trans*- and *cis*-2,5-dimethoxy-2,5-dimethyl-2,5-dihydrofuran previously prepared from 2,5-dimethylfuran[5] by vapor-phase chromatography.

Kinetic Studies. A solution of 1 g of I in 50 m*l* of methanol was divided into 10 aliquots, which were irradiated at 30°C for 1, 2, 4, 5, 6, 8, 12, 16, 20, and 22 hr, respectively. Each portion was then concentrated, and the concentrations of I, II, III and IV were measured by means of intensity of the NMR signals at δ 6.78 (s, olefinic protons of I) and 6.30 ppm (s, olefinic protons of II), and by means of those of a vapor-phase chromatogram at Rt 9.5 min (III) and 12.0 min (IV).

6) M. W. Goldberg and P. Müller, *Helv. Chim. Acta*, **21**, 1699 (1938).

BULLETIN OF THE CHEMICAL SOCIETY OF JAPAN VOL. 43 1879—1880 (1970)

Photochemical Reactions of Bridged Polycyclic Ketones

Noboru SUGIYAMA, Takehiko NISHIO, Kazutoshi YAMADA and Hiromu AOYAMA

Department of Chemistry, Tokyo Kyoiku University, Otsuka, Bunkyo-ku, Tokyo

(Received October 31, 1969)

By photochemical reactions, the non-conjugated cyclic ketones which have hydrogens close to the carbonyl group undergo internal hydrogen transfer, thus giving cyclic tertiary alcohols.*1,1)

In this paper, we wish to report the results of our photochemical reactions of bridged polycyclic ketones (**1**, **2** and **3**),[2,3] where the hydrogen extremely close to the carbonyl oxygen was not

*1 In these reactions, the hydrogen to be abstracted is usually γ-hydrogen. However, if by virtue of structure other hydrogens are closer to the excited carbonyl group, they will be transferred to the carbonyl group.[1f)]

1) a) H. Wehrli, M. S. Heller, K. Schaffner and O. Jeger, *Helv. Chim. Acta*, **44**, 2162 (1961). b) I. Iriarte, K. Schaffner and O. Jeger, *ibid.*, **46**, 1599 (1963). c) J. Fried and J. Brown, *Tetrahedron Lett.*, **1966**, 1677. d) E. Altenburger, H. Wehrli and K. Schaffner, *Helv. Chim. Acta*, **48**, 704 (1965). e) N. Sugiyama, K. Yamada and H. Aoyama, *Chem. Commun.*, **1968**, 1254. f) M. Barnard and N. C. Yang, *Proc. Chem. Soc.*, **1958**,302.

2) P. Bruck, D. Thompson and S. Winstein, *Chem. Ind.* (London), **1960**, 405.

3) R. B. Woodward, T. Fukunaga and R. C. Kelly, *J. Amer. Chem. Soc.*, **86**, 3162 (1964).

abstracted.

When **1** in ethanol was irradiated in the n–π^* region of the carbonyl group, an unsaturated aldehyde (**4**) (α-cleavage product) was obtained. The structure of **4** was established by elemental analysis and by a study of its physical data. The NMR spectrum showed a triplet (1H) at δ 9.82 (the aldehyde proton) and a complex multiplet (2H) at δ 5.40 (the olefinic protons).

The irradiation of **2** under the same conditions also gave an α-cleavage product (**5**). On the other hand, **3** did not show any changes upon irradiation, but was recovered almost quantitatively.

In any one of these three cases, no internal hydrogen transfer product could be detected. This may result from the stereoelectronic requirements for the hydrogen-abstraction step.*[2]

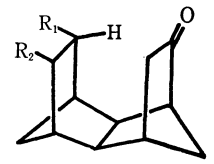

1: $R_1=R_2=H$

2: R_1, R_2=–O–

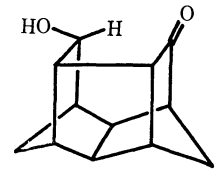

3

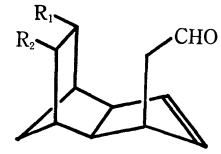

4: $R_1=R_2=H$

5: R_1, R_2=–O–

Fig. 1

Experimental

Irradiation of 1. A solution of 700 mg of **1** in 50 m*l* of ethanol was irradiated for 6 hours under a nitrogen atmosphere. The light source was a 500-W high-pressure mercury lamp with a Pyrex filter. After the solvent had been removed, the residue was chromatographed on silica gel (70 g). Elution with benzene-*n*-hexane (8 : 2) gave the unreacted ketone (250 mg) and **4** (420 mg), which was distilled to give a colorless oil; bp 90°C/20 mmHg.

IR: (cm^{-1}, liq. film) 3040, 1608, 740 (*cis* –CH=CH–), 2750, 1720 (–CHO).

NMR: (δ, in $CDCl_3$) 5.40 (m, 2H, –CH=CH–), 9.84 (t, 1H, –CHO).

Dimedone derivative of **4**: mp 170—173°C. Found: C, 76.71; H, 8.77%. Calcd for $C_{28}H_{38}O_4$: C, 76.67; H, 8.73%.

Irradiation of 2. A solution of 500 mg of **2** in 50 m*l* of ethanol was irradiated as above for 10 hr. The product was isolated by chromatography on silica gel and distilled to give a colorless oil (260 mg); b 130°C/5 mmHg.

IR: (cm^{-1}, liq. film) 3050, 1610, 733 (*cis* –CH=CH–), 2740, 1720 (–CHO).

NMR: (δ, $CDCl_3$) 5.39 (m, 2H, –CH=CH–), 9.85 (t, 1H, –CHO).

Dimedone derivative of **5**: mp 167—170°C. Found: C, 74.30; H, 8.03%. Calcd for $C_{28}H_{36}O_5$: C, 74.30; H, 8.02%.

Irradiation of 3. A solution of 100 mg of **3** in 20 m*l* of ethanol was irradiated as above for 20 hr. No detectable quantities of products were found in the reaction mixture.

*[2] Turror and Weiss have stated that, in the transition state of the photochemical hydrogen transfer reaction of alkyl ketones, the hydrogen to be abstracted needs to approach the halfvacant nonbonding orbital of the carbonyl oxygen atom.[4] However, these ketones, **1**, **2**, and **3**, cannot achieve the required transition state.

4) N.J. Turro and D.W. Weiss, *J. Amer. Chem. Soc.*, **90**, 2185 (1968). See also A. Padwa, E. Alexander and M. Niemcyzk, *ibid.*, **91**, 456 (1969) and F.P. Boer, T.W. Shannon and F. W. McLafferty, *ibid.*, **90**, 7239 (1968).

BULLETIN OF THE CHEMICAL SOCIETY OF JAPAN VOL. 43 1881—1883 (1970)

Unperturbed Dimensions of Poly-*p*-chlorostyrene

Kimiyoshi MATSUMURA, Masamichi FUKAYA and Keisuke MIZUNO

Department of Chemistry, Aichi Kyoiku University, Nagoya

(Received November 4, 1969)

The unperturbed dimensions of various polymers have been studied by light-scattering measurements of polymers in a theta solvent, or from results of viscosity measurements in a good solvent by the use of the Kurata-Stockmayer[1] or the Stockmayer-Fixman[2] relation.

In this paper, the temperature dependence of the unperturbed dimensions of poly-*p*-chlorostyrene was obtained by the viscosity measurements of poly-*p*-chlorostyrene in critical consolute solvents, which were mixtures of benzene (solvent) - cyclohexane (nonsolvent) at various ratios of mixing.

Experimental

Polymer. Poly-*p*-chlorostyrene was prepared by heating *p*-chlorostyrene in a sealed tube at 95°C without any initiator. A benzene solution of the polymer was fractionated at 30°C by successive precipitation with methanol. The obtained fractions were redissolved in benzene, reprecipitated with methanol, and dried under reduced pressure. Five fractions were used for the measurements.

The molecular weights of these fractions were determined by viscosity measurements of the toluene solutions at 30°C with an intrinsic viscosity - molecular weight relationship of $[\eta]=1.28\times10^{-4}\cdot M^{0.64}$.[3] The molecular weights were 100.9×10^4 (fraction 1-1), 76.8×10^4 (1-3), 49.9×10^4 (2-2), 41.2×10^4 (3), and 26.7×10^4 (4) respectively.

Solvent. The benzene and the toluene was washed successively with sulfuric acid, water, a solution of sodium hydroxide, and water, and refluxed with metallic sodium and distilled. Cyclohexane was washed with a mixture of sulfuric acid and nitric acid, and then treated in the same way as benzene.

The critical consolute solvent mixtures were prepared by mixing benzene and cyclohexane by volumes at 25°C.

Measurements. For the determination of the theta temperature, the method of Mandelkern and Flory[4] was used.

For the measurements of the viscosity of the solutions, the viscometer described in a preceding paper[5] was used.

Results and Discussion

The Determination of the Theta Temperature. The ratios of benzene *vs.* cyclohexane used for the measurements were (A) 1.8/1, (B) 1.4/1, and (C) 1.1/1 at 25°C. By the method of Mandelkern and Flory, the theta temperatures for poly-*p*-chlorostyrene in the above critical consolute solvent mixtures, (A), (B), and (C), were determined to be 28 ± 2°C, 43 ± 2°C, and 60 ± 3°C respectively. An example of the measurements of the precipitation temperature and the determination of the theta temperature for poly-*p*-chlorostyrene in one critical consolute solvent mixture, (A), is shown in Fig. 1.

Viscosity. The results of the viscosity measurements of poly-*p*-chlorostyrene in the critical consolute solvents and in toluene are shown in Table 1. As is shown in Fig. 2, from the data of the toluene solutions the following relations were obtained: $[\eta]=1.72\times10^{-4}\cdot M^{0.62}$ (dl/g) (28°C), $[\eta]=1.35\times10^{-4}\cdot M^{0.64}$ (43°C), and $[\eta]=1.07\times10^{-4}\cdot M^{0.66}$ (60°C).

Discussion. The relations between $[\eta]/M^{1/2}$ and $M^{1/2}$ at each temperature, as obtained by the

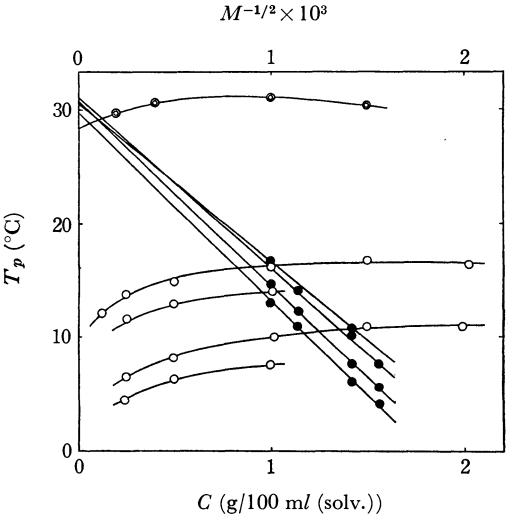

Fig. 1. The determination of the theta temperature for poly-*p*-chlorostyrene in solvent (A): open circle, T_p-C for each fraction; double circle, T_p-C for $M=\infty$; closed circle, T_p-$M^{-1/2}$ for several concentrations.

1) M. Kurata and W. H. Stockmayer, *Fortschr. Hochpolymer. Forsch.*, **3**, 196 (1963).

2) W. H. Stockmayer and M. Fixman, *J. Polym. Sci., Part C*, **1**, 137 (1963).

3) T. Saito, This Bulletin, **35**, 1580 (1962).

4) L. Mandelkern and P. J. Flory, *J. Amer. Chem. Soc.*, **74**, 2517 (1952).

5) K. Matsumura, This Bulletin, **42**, 1874 (1969).

Table 1. The experimental results of the viscosity measurements for poly-*p*-chlorostyrene in the critical consolute solvent mixtures and in toluene

Fraction	$M\times10^{-4}$	$[\eta]_\theta$(dl/g) solvent (A) 28°C	(B) 43°C	(C) 60°C	$[\eta]$ (dl/g) solvent (toluene) 28°C	43°C	60°C
1-1	100.9	0.649	0.640	0.629	0.915	0.951	0.986
1-3	76.8	0.565	0.555	0.530	0.760	0.782	0.808
2-2	49.9	0.461	0.448	—	0.584	0.597	0.612
3	41.2	—	—	0.398	—	—	—
4	26.7	0.334	0.332	0.325	0.398	0.404	0.409

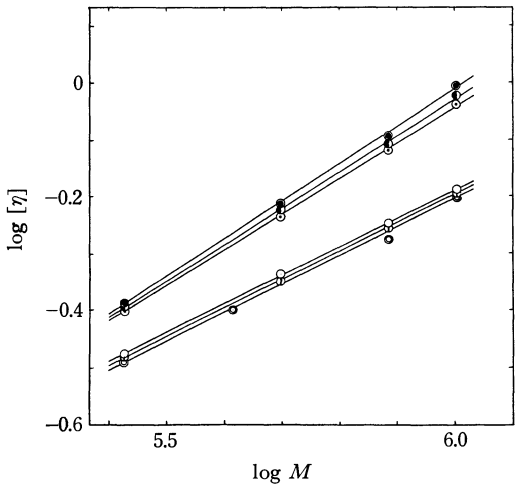

Fig. 2. Molecular weight dependencies of the intrinsic viscosities for poly-*p*-chlorostyrene: critical consolute solution, ○ (28°C), ⓘ (43°C), ◎ (60°C); toluene solution, ⊙ (28°C), ◐ (43°C), ◉ (60°C).

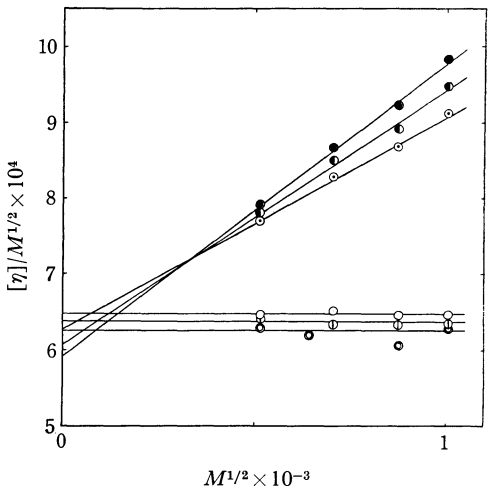

Fig. 3. Viscosity plots for poly-*p*-chlorostyrene: critical consolute solution, ○ (28°C), ⓘ (43°C), ◎ (60°C); toluene solution, ⊙ (28°C), ◐ (43°C), ◉ (60°C).

Table 2. The K_θ values and the σ values of poly-*p*- chlorostyrene: the results in this paper (upper table), and in the reference (lower table)

Solvent	Temp. (°C)	$K_\theta\times10^4$	$\left\{\frac{\langle L^2\rangle_0}{M}\right\}^{1/2}$ (Å)	σ	Ref.
(A) (θ)	28	6.48	0.609	2.32	
(B) (θ)	43	6.37	0.605	2.31	
(C) (θ)	60	6.25	0.602	2.30	
Toluene	28	6.26	0.602	2.30	
	43	6.09	0.596	2.28	
	60	5.93	0.591	2.26	
(θ)	13.4	5.88	0.590	2.26	6)
(θ)	58.9	5.44	0.574	2.20	
	30	5.67	0.585	2.23	3)
	30	5.2	0.565	2.16	7)
	30	6.1	0.600	2.30	8)

Stockmayer-Fixman equation,[2] are shown in Fig. 3. The determined K_θ values are shown in Table 2. Here $K_\theta=[\eta]_\theta/M^{1/2}$ and $[\eta]_\theta$ is the intrinsic viscosity in the theta state. The K_θ values of the toluene solutions are in fairly good agreement with those of the critical consolute solutions at each temperature. The temperature dependence of the K_θ values of poly-*p*-chlorostyrene in the critical consolute solvents gives a linear relation, in which the K_θ values is smaller the higher the temperature, similar as with the temperature dependence of K_θ for polystyrene and for poly-*p*-chlorostyrene.[6]

The K_θ values obtained from the viscosity measurements for the critical consolute solutions are slightly larger than those values by many authors.[3,6-8] From the results for polystyrene in the theta solvents, cyclohexane and diethylmalonate, at about 35°C, it can be seen that the K_θ values of a polymer in different solvents show a fairly large disagreement at the same temperature.[9] Therefore, it can be considered that the difference between the K_θ values of poly-*p*-chlorostyrene in the theta solvents in this paper and those in the previous paper[6] is a result of the solvent effect.

On the basis of the K_θ values, the values of $\{\langle L^2\rangle_0/M\}^{1/2}=(K_\theta/\Phi_0)^{1/3}$ ($\Phi_0=2.87\times10^{21}$) and $\sigma=\{\langle L^2\rangle_0/\langle L^2\rangle_{of}\}^{1/2}$, were found; here $\langle L^2\rangle_0$ is the unperturbed dimension, and $\langle L^2\rangle_{of}$ is the mean-square end-to-end distance of the polymer chain for the free rotation model. The results are shown in Table 2. The obtained σ values are slightly larger than those obtained by other authors. However, as the difference is very small, it is considered our results confirm the conclusion by many authors,[8,10] that the effect of the chlorine atom on the unperturbed dimension of poly-*p*-chlorostyrene is not very large.

6) K. Kubo, K. Ogino and T. Nakagawa, *Nippon Kagaku Zasshi*, **88**, 1254 (1967)

7) N. Kuwahara, K. Ogino, A. Kasai, S. Ueno and M. Kaneko, *J. Polym. Sci., Part A*, **3**, 985 (1965).

8) K. Takamizawa, This Bulletin, **39**, 1186 (1966).

9) T. A. Orofino, *J. Chem. Phys.*, **45**, 4310 (1966).

10) N. Kuwahara, K. Ogino, M. Konuma, N. Iida and M. Kaneko, *J. Polym. Sci., Part A*, **2**, 173 (1966).

BULLETIN OF THE CHEMICAL SOCIETY OF JAPAN VOL. 43 1883—1885 (1970)

Modified Benzyloxycarbonyl Groups for Protection of ε-Amino Group of Lysine

Kosaku NODA, Shigeyuki TERADA and Nobuo IZUMIYA

Laboratory of Biochemistry, Faculty of Science, Kyushu University, Hakozaki, Fukuoka

(Received November 18, 1969)

The benzyloxycarbonyl[1] group has been found suitable for protection of the ε-amino group of lysine in peptide synthesis by either the solution or solid phase method. Since the use of ε-Z group is compatible with that of BOC group in the solid phase method, there have been many reports regarding the use of α-BOC-ε-Z-L-lysine.[2] However, there have been suggestions that ε-Z group was partially cleaved by either N hydrogen chloride-acetic acid or 4N hydrogen chloride-dioxane used for the removal of the α-BOC group during the synthesis of oligopeptide by the solid phase method.[3] Deprotection of ε-Z group was avoided by the use of the α-N protecting group which is much more readily removed than BOC group; such sensitive α-groups so far reported are 2-(*p*-biphenyl)isopropoxycarbonyl[4] and 2-benzoyl-1-methylvinyl.[5]

Another approach to avoid partial deprotection from ε-amino group is the use of a protecting group more stable than Z. The present paper will describe the syntheses of some ε-Z-L-lysine derivatives in which phenyl is substituted with negative group and their stabilities toward treatment with hydrogen chloride as compared with ε-Z-lysine. Behavior of these protecting groups toward liquid hydrogen fluoride will also be described.

It has been observed that several ε-Z groups sub-

1) The following abbreviations are used; Z, benzyloxycarbonyl; Z(*p*-Cl), Z(*m*-Cl), Z(*p*-CN), Z(*p*-NO_2), *e. g. p*-chlorobenzyloxycarbonyl for Z(*p*-Cl); BOC, *t*-butyloxycarbonyl.

2) For example, B. Gutte and R. B. Merrifield, *J. Amer. Chem. Soc.*, **91**, 501 (1969).

3) A. Yaron and F. Schlossman, *Biochemistry*, **7**, 2673 (1968); D. A. Ontjes and C. B. Anfinsen, The 1st American Peptide Symposium, Yale Univ., New Haven, Conn., Aug., 1968.

4) P. Sieber and B. Iselin, *Helv. Chim. Acta*, **51**, 622 (1968).

5) G. L. Southard, G. S. Brooke and J. M. Pettee, *Tetrahedron Lett.*, **1969**, 3505.

Table 1. ε-*N*-Modified benzyloxycarbonyl-L-lysine

ε-*N*-Protected-L-lysine	Yield %	Mp, °C (decomp.)	$[\alpha]_D^{25}$ (*c* 2, 5N HCl)	Formula	Calcd, %			Found, %		
					C	H	N	C	H	N
Z(*p*-Cl)-Lys	81	243—245	+8.0°[a]	$C_{14}H_{19}O_4N_2Cl$	53.41	6.08	8.90	53.55	5.91	9.03
Z(*m*-Cl)-Lys	83	245—248	+10.0°	$C_{14}H_{19}O_4N_2Cl$	53.41	6.08	8.90	53.15	6.15	8.84
Z(*p*-CN)-Lys	89	240—242	+12.7°	$C_{15}H_{19}O_4N_3$	59.00	6.27	13.76	58.64	6.39	13.68
Z(*p*-NO_2)-Lys	86	233—235	+12.9°	$C_{14}H_{19}O_6N_3$	51.68	5.89	12.92	51.43	6.02	12.66

a) The solvent used was AcOH with *c* 1. Z(*p*-Cl)-Lys was hardly soluble even in hydrochloric acid.

stituted with *p*-chloro,[6] *p*-cyano,[6] and *p*-nitro,[7] are more stable toward hydrogen bromide than ε-Z group. We observed a similar tendecny regarding the stabilities toward 4N hydrochloric acid-dioxane (Table 3). The results indicate that the modified ε-Z groups can be satisfactorily used in the solid phase method if the groups are readily removed by hydrogen fluoride from a finished peptide polymer. The behavior of these groups toward hydrogen fluoride was therefore investigated. Sakakibara and Shimonishi have reported that ε-Z group is easily removed with hydrogen fluoride.[8] Sakakibara observed recently that ε-Z(*p*-Cl) group was also removed by the treatment of hydrogen fluoride.[9] We found that ε-Z groups having *p*-cyano and *p*-nitro group were highly resistant against deprotection, whereas ε-Z with *p*-chloro and *m*-chloro were removed completely within 2 to 3 hr. The ε-Z(*m*-Cl) group seemed to be slightly more resistant than ε-Z(*p*-Cl) (Table 4). Syntheses of several oligopeptides containing lysine residue by the solid phase method using α-BOC-ε-Z(*p*- or *m*-Cl)-L-lysine as a starting material are in progress in this laboratory.

Experimental

Modified Benzyloxycarbonyl Chlorides. Z(*p*-Cl)-chloride[10] and Z(*p*-NO_2)-chloride[7] were prepared as described in literature. Other chlorides were prepared as follows.

To a chilled solution of *p*-cyanobenzyl alcohol (2.66 g, 0.02 mol) or *m*-chlorobenzyl alcohol (2.85 g, 0.02 mol) in dry ether (10 m*l*) was added a solution of phosgene (10 g, 0.1 mol) in dry dioxane (10 m*l*) at −10°C. The reaction mixture was left to stand for 2 hr at −10°C and overnight at 0°C, and then evaporated *in vacuo*. The oily product, 3.92 g for Z(*p*-CN)-chloride or 4.01 g for Z(*m*-Cl)-chloride, thus obtained was used without further purification in the following reaction.

ε-*N*-Modified Benzyloxycarbonyl-L-lysines. As an example, preparation of Z(*p*-CN)-Lys is described. Others were prepared by a procedure essentially the same. To a hot solution of L-lysine hydrochloride (0.91 g, 0.005 mol) in water (15 m*l*) was added cupric carbonate (1.25 g) portionwise. The mixture was refluxed for 20 min, and the insoluble material was filtered off. To the filtrate was added sodium bicarbonate (1.2 g) at 0°C. To the solution was added Z(*p*-CN)-chloride (1.6 g, about 0.008 mol) in 3 portions over a period of 30 min under vigorous stirring. Stirring was continued for 5 hr. The alkoxycarbonylated copper complex which deposited was collected, washed successively with water, acetone and ether. After the complex was dissolved in dilute hydrochloric acid, the solution was treated with hydrogen sulfide and cupric sulfide was filtered off. The pH of the filtrate was adjusted to 6 with 6N ammonium hy-

Table 2. R_f of ε-*N*-protected-lysine on TLC[a]

ε-*N*-Protected-L-lysine	R_f [b]	
	Solvent I	Solvent II
Z-Lys	0.79	0.58
Z(*p*-Cl)-Lys	0.81	0.63
Z(*m*-Cl)-Lys	0.81	0.63
Z(*p*-CN)-Lys	0.79	0.51
Z(*p*-NO_2)-Lys	0.79	0.53
Lysine·HCl	0.25	0.03

a) Thin layer plates (20×20 cm; Merck Silica Gel G, No. 7731; thickness of Gel, approximately 0.2 mm) prepared in the usual way were used throughout these experiments. Each spot was detected by spraying 0.2% ninhydrin in acetone.

b) Solvent I, *n*-butanol-acetic acid-pyridine-water (4 : 1 : 1 : 2, v/v); solvent II, *n*-butanol-acetic acid-water (4 : 1 : 2, v/v).

Table 3. Stability of ε-*N*-modified benzyloxycarbonyl-L-lysine in 4N HCl-dioxane at 25°C[a]

ε-*N*-Protected-L-lysine	Appearance of Lys after different time intervals (hr)			
	0.5	2	12	24
Z-Lys	±	+	++	++
Z(*p*-Cl)-Lys	−	±	+	+
Z(*m*-Cl)-Lys	−	−	±	+
Z(*p*-CN)-Lys	−	−	±	±
Z(*p*-NO_2)-Lys	−	−	−	±

a) Explanation of signs: −, not cleaved; ±, cleaved about 1%; +, about 2—4%; ++, about 5—10%.

6) J. Meienhofer, "Peptides-Proceeding of the 6th European Symposium," Pergamon Press, London (1965), p. 55.

7) F. H. Carpenter and D. T. Gish, *J. Amer. Chem. Soc.*, **74**, 3818 (1952).

8) S. Sakakibara and Y. Shimonishi, This Bulletin, **38**, 1412 (1965).

9) S. Sakakibara, private communication.

10) O. L. Kisfaludy and S. Pualszky, *Acta Chim. Acad. Sci. Hung.*, **24**, 301 (1960).

Table 4. Removal of modified benzyloxycarbonyl group from ε-*N*-protected-lysine with HF and 36% HBr-acetic acid[a)]

ε-*N*-Protected-L-lysine	HF at 0°C	36% HBr-acetic acid at 25°C
	Reaction time	
Z-Lys	○ (less than 10 min)	○ (less than 0.5 hr)
Z(*p*-Cl)-Lys	○ (about 2 hr)	○ (about 1 hr)
Z(*m*-Cl)-Lys	○ (about 3 hr)	○ (about 1.5 hr)
Z(*p*-CN)-Lys	± (after 12 hr)	○ (about 4 hr)
Z(*p*-NO_2)-Lys	± (after 12 hr)	○ (about 8 hr)

a) ○, Complete deprotection; ±, deprotected about 1%.

droxide. The precipitate was collected after being left for several hours at 0°C, and washed with water and ethanol. It was recrystallized from dilute hydrochloric acid - dilute ammonium hydroxide; yield, 1.35 g (89%). Analytical data on this compound are listed in Table 1, together with those on the other derivatives.

R_f values on TLC of each ε-protected-lysine thus prepared and lysine hydrochloride are shown in Table 2.

Procedure for Treatment of ε-*N*-Protected-lysine with 4N HCl-dioxane. Fifty μmol (about 15 mg) of each of the ε-protected-lysines were dissolved in 4N HCl-dioxane (1 m*l*) at 25°C. At various time intervals, an aliquot (about 1 μ*l*) of the reaction solution was chromatographed on a plate of Silica gel G using two different solvent systems. On the same plate, aliquots (each 1 μ*l*) of lysine hydrochloride solution at various concentrations were applied as controls; thus, the amount of lysine produced from ε-protected lysine after a definite time could be estimated semiquantitatively. The results are summarized in Table 3.

Reaction of ε-*N*-Protected-lysine with Hydrogen Fluoride and 36% Hydrogen Bromide-Acetic Acid. To fifty μmol each of the ε-protected-lysines was added anhydrous HF (about 3 m*l*) at 0°C or 36% HBr - acetic acid (about 4 m*l*) at 25°C. After a certain time, the solution was evaporated *in vacuo* at 0°C (in the case of HF) or at room temperature (36% HBr), and the residue was dissolved in 10% acetic acid (1 m*l*). An aliquot (1 μ*l*) was subjected to TLC as described before, and the amount of free lysine produced by the deprotection or ε-protected-lysine remaining was estimated semiquantitatively. The results are summarized in Table 4, giving optimum reaction time for complete deprotection on each protecting group.

BULLETIN OF THE CHEMICAL SOCIETY OF JAPAN VOL. 43 1885—1889 (1970)

The Pyrolysis and Photolysis of Triphenylphosphine-carbethoxymethylene in Solution[1]

Yoshihiro NAGAO, Kensuke SHIMA and Hiroshi SAKURAI

The Institute of Scientific and Industrial Research, Osaka University, Suita, Osaka

(Received November 25, 1969)

Although there have been intensive investigations of the reaction of phosphine-ylids,[2] the pyrolysis of ylid in solution has received little attention, except for an unstable ylid, triphenylphosphine-*n*-butoxymethylene, which was studied by Wittig *et al.*[3]

We have studied the pyrolysis of a typical stable ylid, triphenylphosphine-carbethoxymethylene (I), in cyclohexene, and compared the results with those of the photolysis of I, which was reported previously.[4] In this paper, we wish to report the novel observation that, in pyrolysis, only P=C bond fission occurs, while P-phenyl bond fission occurs preferentially in photolysis.

Results and Discussion

The results of the photolysis and pyrolysis of I in cyclohexene are summarized in Table 1.

As may be seen from Table 1, I exhibited considerable thermal stability.

1) Organic Photochemical Reactions, Part XI. Part X; T. Kubota, K. Shima, S. Toki and H. Sakurai, *Chem. Commun.*, **1969**, 1462.

2) A. W. Johnson, "Ylid Chemistry," Academic Press, New York and London (1966), p. 88.

3) G. Wittig and W. Boll, *Chem. Ber.*, **95**, 2526 (1962).

4) Y. Nagao, K. Shima and H. Sakurai, *Kogyo Kagaku Zasshi*, **72**, 236 (1969).

TABLE 1. PHOTOLYSIS[a] AND PYROLYSIS[b] OF $Ph_3P{=}CHCO_2C_2H_5$ (I) IN CYCLOHEXENE
(a) in quartz tube, I; 0.87mmol, cyclohexene; 40 m*l*, high pressure mercury lamp, 40 hr.
(b) I; 1.44 mmol, cyclohexene; 15 m*l*, *ca.* 180°C, 40 hr, conversion; 34%.

products	(a) mmol×10²	(a) Yield %	(a) Quantum yield, *Φ	(b) mmol×10²	(b) Yield %
	8.7	100	0.02	—	—
$CH_3CO_2C_2H_5$	0.7	8	—	—	—
(III)	1.0	12	0.001	6.8	14
(IV)	1.6	19	0.0007	2.5	5
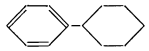	1.6	19	0.004	—	—
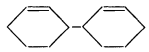 (II)	4.1	—	0.01	8.8	—
$Ph_2P(O)OH$	1.5	16	—	—	—
Ph_3P	—	—	—	0.7	2

* Quantum yields were measured by use of a low pressure mercury lamp as a light source.

TABLE 2. PYROLYSIS OF $Ph_3P{=}CHCO_2C_2H_5$ (I) IN CYCLOHEXENE
I; 1.44 mmol, cyclohexene; 15 m*l*.
(a) di-*t*-butyl peroxide; 10 mg, after 24 hr, conversion; 31%.
(b) in the presence of air, at about 180°C, after 8 hr.

products	(a) mmol×10²	(a) Yield(%)	(b) mmol×10²	(b) Yield(%)
(III)	3.5	8	28	20
(IV)	0.9	2	1.2	0.9
(II)	35	—	38	—
Ph_3P	0.7	1.7	0.2	0.1
Ph_3PO (V)	10.4	23.5	61	45

Before comparing the results of the photolysis with those of pyrolysis, it is necessary to check if the pyrolysis of I was induced by the attack of the radicals produced in this system. Therefore, a typical radical initiator, di-*t*-butyl peroxide, was added to the solution in order to verify this probability. The results are shown in Table 2.

In this case the recovered solid was found to be a mixture of unreacted I and triphenylphosphine oxide (V) from a study of its IR spectra ($\nu_{C=O}$ 1615 cm^{-1}, ν_{C-O} 1115 and 1100 cm^{-1}, $\nu_{P=O}$ 1175 cm^{-1}). The ratio of I to V was calculated by means of the intensity ratio of the signals for phenyl protons (τ=2.5) and methyl or methylene protons (τ_{CH_3}=8.92, τ_{CH_2}=6.12). Although V was produced and the yield of ethyl cyclohexaneacetate (III) increased in this reaction, it was obvious that the pyrolysis itself was not accelerated by the addition of the peroxide. V is thought to have been produced by the reaction of the *t*-butoxy radical with triphenylphosphine or with I.

Azobisisobutylonitrile was also used as an addend since it had no oxygen atom which was liable to interact with the phosphorus atom. The temperature of the bath was about 130°C, and a mixed solvent (cyclohexene 2 : benzene 1) was used to dissolve I at room temperature. In this case the decomposition caused by the attack of the radical on I was negligible.

Pyrolysis was carried out in a 100-m*l* autoclave in order to examine the effect of oxygen (Table 2b). The reaction was very fast; the conversion had reached 94% after 8 hr. In this experiment V and III were both obtained in quite good yields. It is reasonable that the yield of V increased in the presence of oxygen, but we cannot explain why the III increased also. Further studies will be necessary to explain the results of the pyrolysis of I in the presence of air.

Now let us compare the results of the pyrolysis

and photolysis of I in cyclohexene. In the case of photolysis, triphenylphosphine was not obtained at all, while diphenylphosphinic acid was obtained on the oxidation of the photolysate with hydrogen peroxide. Benzene was also formed almost quantitatively. The quantum yield of the benzene formation was 0.02. This value was equal to that for the photolysis of triphenylphosphine under the same conditions. Furthermore, the yield of benzene increased linearly with the irradiation time until the conversion reached 20%.[4] From these results, we could reject the possibility that triphenylphosphine was produced by P=C bond fission, followed by photolysis. It is most probable that P-phenyl bond breaks first in photolysis (Eq. (2a)). However, we cannot reject the probability that the electronically-excited triphenylphosphine produced in photolysis decomposes immediately (Eq. (2b)). On the other hand, in the pyrolysis no benzene and phenylcyclohexane were detected at all, while triphenylphosphine was obtained. Consequently, it is obvious that only P=C bond fission occurs, while P-phenyl bond fission does not occur at all, in the pyrolysis (Eq. (1)).

The yield of triphenylphosphine was very low, probably because of its high reactivity to the radicals.

No effect of oxygen was observed in photolysis, whereas in pyrolysis there was a remarkable effect and the decomposition was accelerated enormously.

The rate constants of this pyrolysis were obtained by titrating the unreacted ylid with HCl after the pyrolysis over the temperature range of 160—200°C.[5] The Arrhenius plot of the pyrolysis of I was linear (Fig. 1), and the activation energy of this reaction was calculated to be 28 kcal/mol.

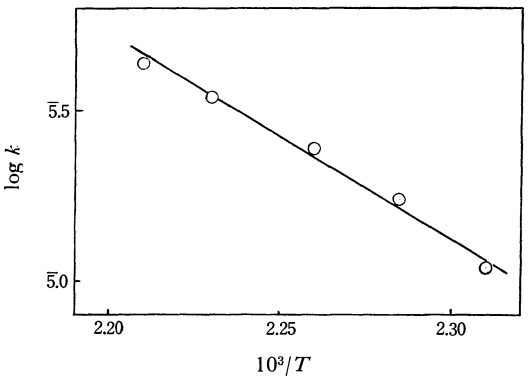

Fig. 1. Arrhenius plot of the pyrolysis.

The probable pyrolysis and photolysis mechanisms are as follows:

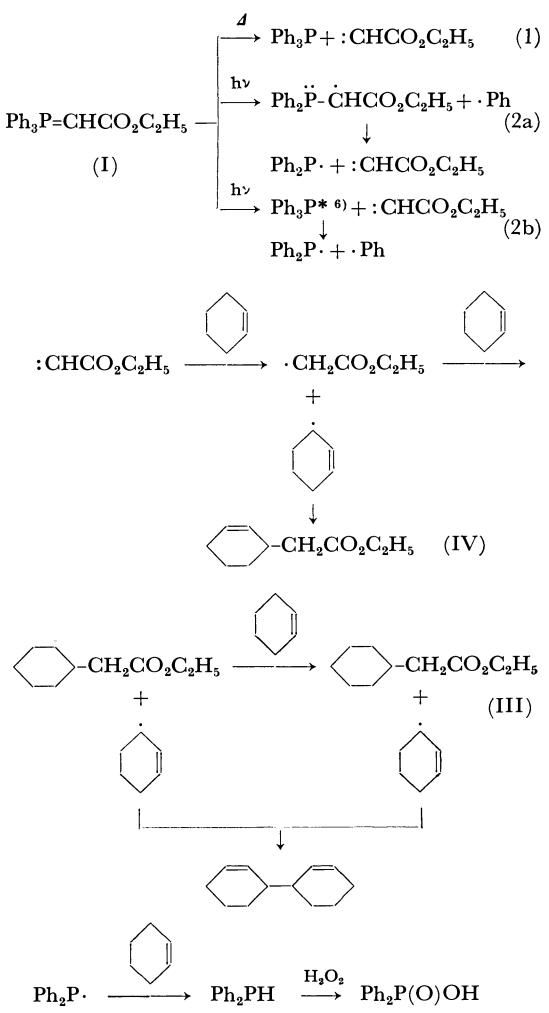

Experimental

Pyrolysis in the Pyrex Tube. A solution of I (500 mg, 1.44 mmol) in cyclohexene (15 m*l*) was degassed in a 20-m*l* Pyrex tube (10 mm I.D.) by the usual freeze-and-thaw method. This solution was then heated for 40 hr in an oil bath (at about 180°C). After cooling, the low-boiling material was distilled under reduced pressure. Benzene was not detected in this distillate. By the addition of *n*-hexane to the residue, the unreacted I was removed. The recovered I was 331 mg. 3,3′-Bicyclohexenyl (II), ethyl cyclohexaneacetate (III), and ethyl 2-cyclohexeneacetate (IV) were obtained from the *n*-hexane layer. A quantitative determination of these products were made by glc (Dinonyl phthalate), as has been described in a previous paper.[4] The triphenylphosphine was determined by glc (Thermol-3), using ethyl stealate as the internal standard.

The Isolation of $Ph_2P(O)OH$. The phosphorus-containing compound produced in the photolysis of I was isolated in the following manner.

5) The Ph_3P produced in the pyrolysis was assumed to have scarcely any effect upon the titration because of its small quantity.

6) The asterisked Ph_3P has an excess energy; hence, it decomposes as soon as it is produced.

The photolysed material was oxidized with hydrogen peroxide at pH 12—13, and then extracted with ether. A white precipitate was formed on the acidification of aqueous layer with HCl. This was extracted with ether and then recrystallized from EtOH. The IR spectrum of this material was identical with that of an authentic sample; mp 186—189°C (lit,[7] 191°C).

The Determination of the Activation Energy. After the pyrolysis at 160—200°C, the unreacted I was titrated with HCl, and the rate constants of the decomposition of I were calculated.

7) L. Horner, H. Hoffmann and H. G. Wippel, *Chem. Ber.*, **91**, 64 (1958).

BULLETIN OF THE CHEMICAL SOCIETY OF JAPAN VOL. 43 1888—1889 (1970)

The Oxidation of Thiols to Disulfides with Manganic Tris (acetylacetonate)

Tadao NAKAYA, Hideo ARABORI and Minoru IMOTO

Department of Applied Chemistry, Faculty of Engineering, Osaka City University, Sugimoto-cho, Sumiyoshi-ku, Osaka

(Received December 5, 1969)

Various methods are available for oxidizing thiols to disulfides.[1] However, only a few procedures are available for the oxidation of thiols to disulfides, in the absence of oxygen, by means of metal salts, such as lead tetraacetate,[2] ferric octanonate,[3] cupric octanonate,[3] and transition metal oxides.[4] It has recently been reported that manganic tris (acetylacetonate) (MTA) in carbon disulfide or acetonitrile acts as a coupling agent for phenols.[5]

The present note will describe a successful extension of this method to oxidizing thiols, including alkyl, benzyl, and aryl, to the corresponding disulfides. Thus, 1-pentanethiol, α-toluenethiol, benzenethiol, and 2-napthalenethiol, were readily converted into *n*-pentyl disulfide,[6] benzyl disulfide,[2b] phenyl disulfide,[2b] and 2-naphthyl disulfide,[7] respectively. All the reactions were carried out in carbon disulfide under nitrogen at room temperature. The reaction conditions employed and the results obtained are summarized in Table 1. All the yields recorded in Table 1 are based on the amount of disulfide isolated. The advantages of this convenient method are that all the reactions proceed rapidly at room temperature and that all give virtually quantitative yields of the disulfides and no other highly-oxidized products. One mole of MTA was found to oxidize about one mole of thiol. During the reaction, there was formed a precipitate which had a manganous bis (acetylacetonate) as its main component.[5] Accordingly, the following equation for the reaction is appropriate:

TABLE 1. OXIDATION OF THIOLS TO DISULFIDES WITH MTA

Reactant	Thiol/MTA[a]	Time (min)	Product	Mp or bp, °C(mmHg)		Yield[b] (%)
				Found	Reported	
1-Pentanethiol	1.05	90	*n*-Pentyl disulfide	110—113(4)	90—92(1)[6]	85
α-Toluenethiol	1.05	90	Benzyl disulfide	69—71	70—71[2b]	99
Benzenethiol	1.05	90	Phenyl disulfide	59	59—61[2b]	95
Benzenethiol	0.5	90	Phenyl disulfide			96
2-Naphthalenethiol	1.05	130	2-Naphthyl disulfide	140	138—9[7]	94

a) Molar ratio. b) Based on reacted MTA.

1) D. S. Tarbell, "Organic Sulfur Compounds," Vol. I, ed. by N. Kharasch, Pergamon Press, New York, N. Y. (1961), p. 97; A. A. Oswald and T. J. Wallace, "Organic Sulfur Compounds," Vol. II, ed. by N. Kharasch and C. Y. Meyers, Pergamon Press, New York, N. Y. (1966), p. 205.

2) a) L. Suchomelová and J. Zy'ka, *J. Electroanal. Chem.*, **5**, 57 (1963); b) L. Field and J. E. Lawson, *J. Amer. Chem. Soc.*, **80**, 838 (1958).

3) T. J. Wallace, *J. Org. Chem.*, **31**, 3071 (1966).

4) T. J. Wallace, *ibid.*, **31**, 1217 (1966).

5) M. J. S. Dewar and T. Nakaya, *J. Amer. Chem. Soc.*, **90**, 7134 (1968).

6) E. Miller, F. S. Crossley and M. L. Moose, *ibid.*, **64**, 2322 (1942).

7) V. N. Belov and M. Z. Finkel'shtein, *J. Gen. Chem. (U. S. S. R.)* **17**, 741 (1947); *Chem. Abstr.*, **42**, 1238 (1948).

Table 2. Attempted addition reactions of 1-dodecanethiol to 1-dodecene catalyzed by MTA[a)]

1-$C_{12}H_{25}SH$, mol	MTA, mol	1-$C_{12}H_{25}SH$/MTA[b)]	1-Dodecene/1-$C_{12}H_{25}SH$[b)]	Time, hr	% conversion of 1-$C_{12}H_{25}SH$	Dodecyl disulfide, mol	Dodecyl sulfide, mol
0.01	0.01	1	3.5	20	~100	5.0×10^{-3}	None
0.01	0.002	5	3.5	20	20	1.0×10^{-3}	None

a) All reactions were carried out in 50 m*l* of xylene under nitrogen at room temperature.
b) Molar ratio.

$$2RSH + 2Mn(Acac)_3 \longrightarrow RSSR + 2Mn(Acac)_2 + 2AcacH$$

As can be seen from Table 1, about one mole of MTA was consumed per mole of benzenethiol, when a one-molar excess of MTA was present. These results suggest that MTA in carbon disulfide acts as a specific oxidant for the oxidation of thiols.

For the oxidation of thiols to disulfides by ferric octanonate, Wallace[3)] proposed the following mechanism (the radical nature of the reactions was established by trapping the thiyl radical with 1-dodecene):

$$RSH + Fe(Oct)_3 \longrightarrow RS\cdot + Fe(Oct)_2 + OctH$$
$$RS\cdot \longrightarrow \tfrac{1}{2}RSSR$$

In order to obtain information regarding the nature of the oxidation of thiols to disulfides by MTA, the addition reactions of 1-dodecanethiol to 1-dodecene catalyzed by MTA were attempted in xylene according to the procedure of Wallace.[3)] The results are shown in Table 2. In contrast to the results obtained by Wallace, however, no dodecyl sulfide was detected; dodecyl disulfide was the only product. The fact that no dodecyl sulfide was formed may be explained by the following reaction scheme, involving thioxynium ion as an intermediate:[8)]

$$RSH + Mn(Acac)_3 \longrightarrow RS\cdot + Mn(Acac)_2 + AcacH$$
$$RS\cdot + Mn(Acac)_3 \xrightarrow{\text{fast}} RS^+ + Mn(Acac)_2 + Acac^-$$
$$RS^+ + RSH \longrightarrow RSSR + H^+$$

In the above reaction scheme it is assumed that MTA rapidly oxidizes the thiyl radical to the corresponding thioxynium ion because the oxidizing agent[5)] is more powerful than ferric octanonate.

8) L. S. Levitt, *Can. J. Chem.*, **31**, 915 (1953).

Experimental

Materials. The 1-pentanethiol, α-toluenethiol, benzenethiol, 2-naphthalenethiol, 1-dodecanethiol, 1-dodecene, and cetane were commercial materials and were purified by crystallization or distillation. The MTA was prepared according to the method of Charles.[9)]

General Procedure for the Oxidation of Thiols to Disulfides. The following is the general procedure by which the disulfides listed in Table 1 were prepared. Into a solution of 15.8 mmol of the required thiol in 20 m*l* of carbon disulfide, we stirred, drop by drop and under nitrogen, a solution of 15 mmol of MTA in 250 m*l* of carbon disulfide. After a while, a pale yellow crystalline solid began to separate from the solution. After the reaction mixture had been vigorously stirred at room temperature for 1 hr, the solvent was evaporated to dryness under reduced pressure. The residue was extracted twice with 100 m*l* of petroleum ether (bp 30—60°C). The insoluble material was then filtered off and washed with 30 m*l* of petroleum ether. The combined filtrate was cautiously evaporated under reduced pressure to give the crude disulfide. With the exception of *n*-pentyl disulfide, which was distilled under reduced pressure, the products were recrystallized from petroleum ether.

The elemental analyses of the products were satisfactory, and the IR and NMR spectra were consistent with the proposed structures.

The Attempted Addition Reactions of 1-Dodecanethiol to 1-Dodecene Catalyzed by MTA. The procedures were identical with those reported by Wallace.[3)] For the analyses of the reactions, a Yanagimoto Model GCG-550-FP-type gas chromatograph was used.

9) R. G. Charles "Inorganic Syntheses," Vol. VII, ed. by J. Kleinberg, McGraw-Hill Company, New York, N. Y. (1963), p. 183.

BULLETIN OF THE CHEMICAL SOCIETY OF JAPAN VOL. 43 1890—1892 (1970)

Synthesis of 2-Substituted Ethyl Hydrodisulfides

Jitsuo TSURUGI, Yasuo ABE and Shunichi KAWAMURA

Radiation Center of Osaka Prefecture, Shinke-cho, Sakai, Osaka

(Received December 8, 1969)

Alkyl hydrodisulfides synthesized so far are methyl,[1] ethyl,[1] benzyl,[1,2] benzhydryl[2] and trityl[3] hydrodisulfides, the latter three of which have been reported sufficiently stable for a few weeks. Compounds containing hydrodisulfide group (-SSH) have been postulated by biochemists as intermediates of various enzymatic reactions.[4-6] However, alanyl hydrodisulfide $HOCOCH(NH_2)CH_2SSH$, which has been called thiocysteine and proposed as an intermediate of enzymatic cleavage of cystine by Cavallini,[4] has never been isolated. Only circumstantial evidence is available to support the intermediate formation of thiocysteine[4-6] and similar polysulfidic species containing labile sulfur.[7,8] This note describes the synthesis or attempted synthesis of mono-2-substituted ethyl hydrodisulfides.

2-Hydroxyethyl hydrodisulfide (IV) was prepared as indicated in Scheme 1 by the Böhme method.[1] In Scheme 1, prior conversion of 2-mercaptoethanol (I) to 2-acetoxyethanethiol (II) was necessary, because direct reaction of I with acetyl sulfenyl chloride yielded an oily mixture, suggesting that hydroxyl group of I was also attacked by acetyl sulfenyl chloride. Compound II was then allowed to react with acetyl sulfenyl chloride to yield 2-acetoxyethyl acetyl disulfide (III). Alcoholysis of III with anhydrous methanolic or ethanolic hydrogen chloride produced IV almost quantitatively as viscous oil along with methyl or ethyl acetate. Alcoholysis of both R'SS-$COCH_3$ and CH_3CO-OR'' bonds of III apparently took place simultaneously. Compound IV seems unstable even at room temperature. Slight and continuous evolution of hydrogen sulfide was observed during alcoholysis, isolation and storing.

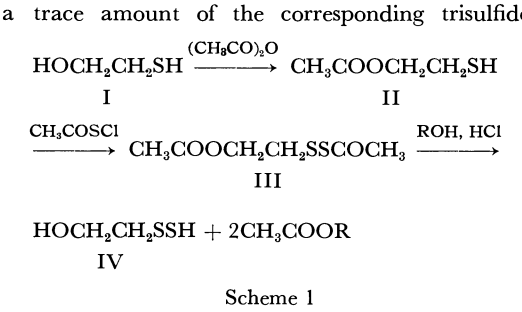

Scheme 1

Although analysis was carried out immediately after isolation, analytical values did not completely agree with calculated ones. However, NMR spectra showed the corresponding protons (-SSH, -OH and ethylenic ones) and no other signals. These results suggest that IV was contaminated with a trace amount of the corresponding trisulfide.

Contrary to our expectation that the introduction of hydroxyl group would make the hydrodisulfide water-soluble, IV was found to be insoluble in water and to decompose slowly on contact with water as evidenced by the evolution of hydrogen sulfide. More stable aralkyl hydrodisulfides also were reported to decompose on contact with water.[9]

Preparation of 2-carboxyethyl hydrodisulfide (VIII) was attempted next, as indicated in Scheme 2. Unlike Scheme 1, sulfenyl chloride reacted with 2-mercaptopropionic acid (V) exclusively on the sulfur side. Esterification took place during the alcoholysis of 2-carboxyethyl acetyl disulfide (VI). Thus 2-carboalkoxyethyl hydrodisulfides (VIIa, VIIb) were separated as oily substances in good yields. Neither hydrolysis of VII to the corresponding acid (VIII) with hydrochloric acid

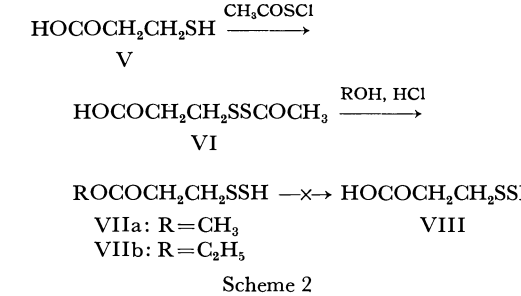

Scheme 2

1) H. Böhme and G. Zinner, *Ann.*, **585**, 142 (1954).
2) J. Tsurugi and T. Nakabayashi, *J. Org. Chem.*, **24**, 807 (1959).
3) T. Nakabayashi, J. Tsurugi and T. Yabuta, *ibid.*, **29**, 1236 (1964).
4) D. Cavallini, C. De Marco, B. Mondovi and B. G. Mori, *Enzymologia*, **22**, 161 (1960).
5) M. Flavin, *J. Biol. Chem.*, **237**, 768 (1962).
6) J. Loiselet and F. Chatagner, *Bull. Soc. Chim. Biol.*, **48**, 595 (1966).
7) O. Gawron and G. Odstrchel, *J. Amer. Chem. Soc.*, **89**, 3263 (1967).
8) J. L. Wood and N. Catsimpoolas, *J. Biol. Chem.*, **238**, 2887 (1963); N. Catsimpoolas and J. L. Wood, *ibid.*, **239** 4132 (1964); **241**, 1790 (1966).
9) S. Kawamura, Y. Abe and J. Tsurugi, *J. Org. Chem.*, **34**, 3633 (1969).

nor transesterification of VII to VIII with formic acid was successful, because the susceptibility of hydrodisulfide group to hydrolysis led to unidentified products. Instability, slight disagreement of analytical data, and NMR spectral evidence, all of which are similar to those of IV, indicate that VIIa may be also contaminated with a trace amount of the corresponding trisulfide. Compound VIIb, on the contrary, shows good coincidence of analytical data. The behavior of VII toward water was similar to that of IV.

Spectroscopic data of hydrodisulfides IV and VII are shown in Table 1 along with those of the starting thiols I and V. Proton of hydrodisulfide group of IV and VII is exchangeable with that of water, because their peaks in NMR were diminished without change in the remaining parts of the spectra by shaking with deuterated water. Although the hydrodisulfides are unstable in the presence of water as mentioned above, the decomposition of IV and VII did not disturb the NMR spectral determination. The singlet peak of each hydrodisulfide group is found in a much lower field than the triplet center of the corresponding thiol, presumably because of the anisotropic effect of additional sulfur atom. IR spectra also show that SH stretching frequency of each hydrodisulfide group is slightly lower than that of the corresponding thiol. This fact suggests that the lowering of force constant between S and H is caused by the effect of neighboring S–S bond.

Table 1. Spectroscopic data

Compound	NMR (δ, ppm)	IR (cm^{-1})
$HOCH_2CH_2$**SH**(IV)	3.09 (s)	2,500 (m)
$HOCH_2CH_2$**SH**(I)	1.45 (t)	2,560 (w)
$CH_3OCOCH_2CH_2$**SSH**(VIIa)	3.00 (s)	2,510 (m)
$C_2H_5OCOCH_2CH_2$**SSH**(VIIb)	3.06 (s)	2,510 (m)
$HOCOCH_2CH_2$**SH**(V)	1.59 (*t*)	2,600 (w)

Synthesis of 2-aminoethyl acetyl disulfide and 2-acetamidoethyl acetyl disulfide (IX) by the Böhme method was not successful. Synthesis of IX was realized, however, by the Field[10] method as shown below. By ethanolysis of IX an oily substance and ethyl acetate were obtained. The oily substance continued to evolve hydrogen sulfide during and after the evaporation of the solvent, and after one night decomposed to unidentified yellow solids, which were insoluble in most organic solvents. Although direct evidence for the formation of 2-acetamidoethyl hydrodisulfide could not be obtained, indications are the formation of ethyl acetate on ethanolysis, and a positive result in the lead acetate test characteristic for hydrodisulfides.[11] We previously reported that amines can decompose aralkyl hydrodisulfide (benzyl, benzhydryl and trityl hydrodisulfides) at room temperature.[12] The instability of this oily substance may be ascribed to the introduction of an amino group into hydrodisulfide molecule. Judging from the instability of this compound and the failure of synthesis of 2-aminoethyl hydrodisulfide, it may be concluded that the isolation of alanyl hydrodisulfide, which is considered to be an intermediate of cystine decomposition, would be difficult, even if it is formed during the enzymatic reaction.

$$CH_3CONHCH_2CH_2SSO_2CH_2CH_2NHCOCH_3 + CH_3COSH \longrightarrow \underset{\text{IX}}{CH_3CONHCH_2CH_2SSCOCH_3} + CH_3CONHCH_2CH_2SO_2H$$

Experimental

Commercial 2-mercaptoethanol and 2-mercaptopropionic acid was distilled under reduced pressure before use. Other reagents and solvents were commercial products. NMR spectra were taken on a JNM 3H-60 spectrometer with tetramethylsilane as an internal standard and IR spectra were obtained on a JASCO IR-S spectrometer.

2-Acetoxyethyl Acetyl Disulfide (III). 2-Acetoxyethanethiol (II) was prepared from 2-mercaptoethanol by the method of Miles and Owen,[13] bp 57°C/16 mmHg (lit, 62—64°C/16 mmHg). To a solution of II (15.0 g, 0.125 mol) in anhydrous ether, freshly distilled acetyl sulfenyl chloride[14] (15.2 g, 0.137 mol) in absolute ether was added with stirring at 0—5°C under a nitrogen atmosphere. Gaseous hydrogen chloride was evolved gradually. After being kept standing overnight the reaction mixture was separated off, and volatiles were removed *in vacuo*. Highly viscous oil of III was obtained in near 100% yield and proved to be pure enough for the following synthesis. Distillation did not change the properties of the product. The IR spectrum (neat) showed a strong C=O band at 1740 cm^{-1}. The NMR spectrum (10% in CCl_4) was consistent with the structure of III having two kinds of acetyl group, $OCOCH_3$, δ 2.03 and $SCOCH_3$, δ 2.43. Both IR and NMR spectra indicated no peak corresponding to sulfhydryl group.

Found: C, 36.96; H, 5.50; S, 33.35%. Calcd for $C_6H_{10}O_3S_2$: C, 37.09; H, 5.19; S, 33.01%.

2-Hydroxyethyl Hydrodisulfide (IV). To a solution of III (1 g, 5.15 mmol) in absolute methanol was added a few m*l* (0.7—2) of 5N methanolic hydrogen chloride, and the solution was kept standing for *ca.* 3 hr at room temperature. Complete removal of volatiles

10) L. Field, T. C. Owen, R. R. Crenshaw and A. W. Bryan, *J. Amer. Chem. Soc.*, **83**, 4414 (1961); L. Field and J. D. Buckman, *J. Org. Chem.*, **32**, 3467 (1967).

11) T. Nakabayashi and J. Tsurugi, *ibid.*, **28**, 813 (1963).

12) J. Tsurugi, Y. Abe, T. Nakabayashi, S. Kawamura, T. Kitao and M. Niwa, accepted by *J. Org. Chem.*

13) L. W. C. Miles and L. N. Owen, *J. Chem. Soc.*, **1952**, 821.

14) H. Böhme and M. Clement, *Ann.*, **576**, 65 (1962).

(hydrogen chloride, methanol and methyl acetate) by a rotary evaporator in a vacuum gave viscous oil of IV quantitatively. The IR spectrum (neat) exhibited a medium band at 2500 cm^{-1} characteristic for sulfhydryl groups of hydrodisulfides (*cf.* Table 1). NMR spectrum (10% in $CDCl_3$) showed a characteristic signal for singlet proton of –SSH at δ 3.09 which was exchangeable with deuteron in D_2O, as well as hydroxylic δ 3.4—4.2 (*cf.* OH of I, δ 4.12—4.60) and ethylenic protons. Qualitative test by lead acetate gave a black precipitate which resulted from the hydrodisulfide group.[11]

Found: C, 22.43; H, 5.56; S, 56.62%. Calcd for $C_2H_6OS_2$: C, 21.80; H, 5.49; S, 58.19%.

2-Carboxyethyl Acetyl Disulfide (VI). In the same way as for the preparation of III, VI was obtained quantitatively as white crystals from freshly distilled 2-mercaptopropionic acid (11.3 g, 0.106 mol) and acetyl sulfenyl chloride (26.9 g, 0.267 mol). The crystals were recrystallized from carbon tetrachloride, mp 69—70°C. The IR spectrum (KBr) showed a broad band at 1690 cm^{-1} ($SCOCH_3$). The NMR spectrum (10% in $CDCl_3$) indicated signals at δ 2.49 ($SCOCH_3$), and δ 11.70 (COOH).

Found: C, 33.20; H, 4.71; S, 35.72%. Calcd for $C_5H_8O_3S_2$: C, 33.32; H, 4.47; S, 35.58%.

2-Carboalkoxyethyl Hydrodisulfide (VII). VI (1 g, 5.55 mmol) was suspended in anhydrous methanol or ethanol (4 m*l*) with magnetic stirring. To this was added 5N methanolic or ethanolic hydrogen chloride (3 m*l*). Disulfide VI was gradually dissolved in alcohol as alcoholysis proceeded. After 3 hr, volatiles were removed by using a rotary evaporator (*in vacuo*) at room temperature. 2-Carbomethoxyethyl (VIIa) or 2-carboethoxyethyl hydrodisulfide (VIIb) was obtained as an oily substance. IR spectra (neat) of both VIIa and VIIb showed bands at 2510 cm^{-1} corresponding to hydrodisulfide group (*cf.* Table 1). NMR signals (10% in $CDCl_3$) of SSH proton were at δ 3.00 (VIIa) and δ 3.06 (VIIb) (*cf.* Table 1), and other reasonable signals were found. Addition of lead acetate solution to VII gave a black precipitate.[11]

Found: C, 31.75; H, 5.30; S, 39.49%. Calcd for $C_4H_8O_2S_2$ (VIIa): C, 31.56; H, 5.30; S, 42.13%.

Found: C, 36.26; H, 6.02; S, 38.35%. Calcd for $C_5H_{10}O_2S_2$ (VIIb): C, 36.12; H, 6.06; S, 38.57%.

Reaction of 2-Acetamidoethyl Acetyl Disulfide in Alcoholic Hydrogen Chloride. 2-Acetamidoethyl acetyl disulfide[10] was allowed to react with alcoholic hydrogen chloride under the conditions similar to those in the case of VII. After volatiles were completely evaporated, an oil remained. After a few minutes, the oily substance decomposed with evolution of hydrogen sulfide and solidified. The solid was washed with acetone and dried *in vacuo*, mp 143—146°C (unidentified). IR spectrum (KBr) showed that $SCOCH_3$ group (1734 cm^{-1}) was removed by the above treatment. In NMR (DMSO-d_6), neither the signal corresponding to $SCOCH_3$ nor SSH was found. The oily material, immediately after its formation, produced black precipitates by treatment with lead acetate solution.[11]

BULLETIN OF THE CHEMICAL SOCIETY OF JAPAN VOL. 43 1892—1894 (1970)

Hydration of Potassium Hyaluronate

Yasuko SUZUKI and Hisashi UEDAIRA

Research Institute for Polymers and Textiles, 4 Sawatari, Kanagawa-ku, Yokohama

(Received December 17, 1969)

Hyaluronic acid is one of the mucopolysaccarides, whose structure consists of a repeating disaccaride unit, D-glucronic acid and 2-acetamide-2-deoxy-D-glucose. It occurs in various animal tissues and fluids such as (bovine) vitreous humour, (human) umbilical cord and synovial fluid. One important function is to bind water in interstitial spaces of tissue and have a definite resistance to compression.[1,2] Jacobson and Laurent[3] and Laurent[4] carried out studies of streaming dielectric property and X-ray diffraction on aqueous hyaluronic acid solution, but no positive information on the interaction between hyaluronic acid and water molecules was obtained.

We present here the ultrasonic velocity data and partial specific volume for the aqueous potassium hyaluronate solutions. The adiabatic compressibility of the solution is calculated and the hydration number of hyaluronate ion is estimated.

Experimental

Potassium hyaluronate used was obtained from bovine vitreous humour (Tokyo Kasei G. R.). It was stirred in water under a stream of nitrogen at 60°C for 2 hr, filtered by Milipore filter (pore size $1.2\pm0.3\ \mu$), lyophilized and then dissolved in deionized water.

Ultrasonic velocity of solution was measured by an ultrasonic interferometer, at 5 MHz in frequency. Density was determined by picnometer (10 cc) at (25±

1) J. H. Fessler, *Biochem. J.*, **76**, 124 (1960).

2) J. S. Brimacombe and J. M. Webber, "Mucopolysaccharides Chemical Structure, Distribution, Isolation," Elsevier Publ. Co., New York (1964), Chapter 3.

3) B. Jacobson and T. C. Laurent, *J. Colloid Sci.*, **9**, 36 (1954).

4) T. C. Laurent, *Ark. Kemi*, **11**, 503 (1957).

0.01) and (30±0.01)°C. Adiabatic compressibility was calculated from the data of ultrasonic velocity and density of the solutions. Concentrations of the solutions were determined by gravimetric method and by measurement of the refractive increment using a Zeiss interferometer. The molecular weight of potassium hyaluronate was determined by a Shimazu light scattering instrument at 23°C, where the same sample solution as above was subjected to ultracentrifuging at 2.4×10^4 g and 10°C for one hour and filtered with a Corning ultrafine glass filter for optical clearance.

Results and Discussion

The weight average molecular weight of potassium hyaluronate, M_w, is obtained as 2.71×10^5 from the Zimm plot of light scattering data. The partial specific volume of potassium hyaluronate at infinite dilution, $\bar{v}_{20}$, was obtained from solution density. The values of $\bar{v}_{20}$ at 25 and 30°C are given in the table.

Table 1. The amount of hydration of potassium hyaluronate

t (°C)	M$\times10^{-5}$	$\bar{v}_{20}$ (cc)	$\bar{\kappa}_{20}\times10^{12}$ (cm²/dyn)	n_{h_1} (mol/base mol)	n_{h_2} (mol/base mol)
25	2.71	0.51	−35.0	9.22 (6.7)*	18.4 (15.9)*
30		0.55	−66.5	19.4 (16.2)*	30.8 (27.6)*

* hydration number of hyaluronate ion.

The relation between adiabatic compressibility κ, ultrasonic velocity c and density of solution ρ is given by

$$\kappa = 1/\rho c^2 \tag{1}$$

The amount of hydration is obtained from the equations

$$\omega = (n_h v_1) = \frac{\bar{\kappa}_{20} - \kappa_2}{\kappa_h - \kappa_1}\bar{v}_{20} \tag{2}$$

$$\bar{\kappa}_{20} = -\frac{1}{\bar{v}_{20}}\left(\frac{\partial \bar{v}_2}{\partial \rho}\right)_0 = -\frac{1}{\bar{v}_{20}}\left(-\bar{v}_{20} - \frac{1}{\kappa_1}\frac{\mathrm{d}\kappa}{\mathrm{d}x}\right) \tag{3}$$

where ω and n_h are the volume and number of water molecule bounded to one gram of solute, respectively.[5] v_1 and v_2 are the specific volumes of solvent and solute, respectively, and $\bar{v}_{20}$ the partial specific volume of solute at infinite dilution. κ_1, κ_2 and κ_h are the adiabatic compressibilities of solvent, solute and hydrated water respectively and $\bar{\kappa}_{20}$ the partial specific compressibility of solute at infinite dilution. The relations between the compressibilities and the concentrations of solutions at 25 and 30°C are given in Fig. 1.

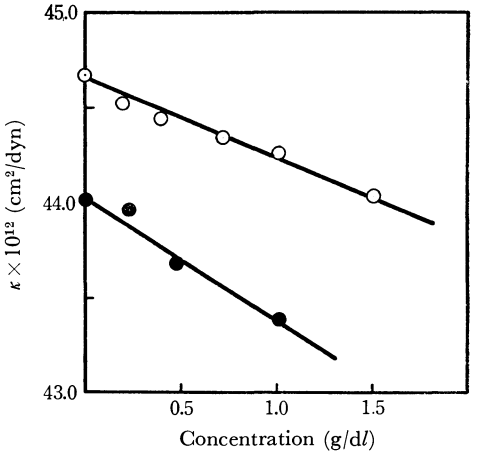

Fig. 1. The relations between adiabatic compressibilities of potassium hyaluraonate and its concentrations at 25 (open circle) and 30°C (closed circle).

In the calculation of the hydration number from Eq. (3), the following two limiting values of hydration number are obtained.

(1) When it is assumed that the solute and the water molecules very near the solute have zero compressibility (*viz.* $\kappa_h=0$ and $\kappa_2=0$), the lower limiting value of hydration number (n_{h_1}) is obtained. The values of n_{h_1} at 25 and 30°C are given in the forth column of the table.

(2) When it is assumed that the solute and bound water molecules participate in compression, the upper limiting value of hydration number (n_{h_2}) is obtained. The value of compressibility of potassium hyaluronate is not available, and so we assume its value to be the same as that of dextrin, 12×10^{-12} cm²/dyn.[6] Following Shiio, Ogawa and Yoshihashi,[6] we assume that the compressibility of hydrated water is the same as that of ice I, 1.2×10^{-11} cm²/dyn.[7] The values of n_{h_2} at 25 and 30°C are given in the fifth column of the table.

The hydration numbers of potassium ion determined from ultrasonic velocity are 2.5 and 3.2 mol/mol ion at 25 and 30°C, respectively.[8,9] It follows that the values of n_{h_1} of hyaluronate ion at 25 and 30°C are 6.7 and 16.2 mol/base mol (or 0.32 and 0.77 cc/g), respectively, and the values of n_{h_2} at 25 and 30°C are 15.9 and 27.6 mol/base mol (or 0.70 and 1.21 cc/g), respectively.

The values of n_{h_2} for glucose, sucrose, maltose and raffinose at 25°C are 0.35, 0.20, 0.22 and 0.22 cc/

5) H. Nomura and Y. Miyahara, *J. Appl. Polym. Sci.*, **8**, 1643 (1964).

6) H. Shiio, T. Ogawa and H. Yoshihashi, *J. Amer. Chem. Soc.*, **77**, 4980 (1955).

7) "International Critical Tables," Vol. 3, McGraw-Hill Book Co., New York (1928), p. 50.

8) T. Yasunaga and T. Sasaki, *Nippon Kagaku Zasshi*, **72**, 87, 89, 366 (1951).

9) *Z. Phys. Chem. Neue Folge*, **47**, 24 (1965).

g,[10] respectively. Thus, the hyaluronate ion is hydrated more strongly than sugars.

The amount of hydration of hyaluronate ion increases with increasing temperature, as in the case of polyvinyl alcohol.[11] One of the authors (H.U.) together with Uedaira[12] showed that sugars oriented the water molecules around them, and that the degree of hydration of sugars was increased by the addition of structure breaking solute. According to Samoilov's theory on salting-out,[13] the break of water structure increases the degree of hydration of the structure making solute. With increasing temperature, the water structure is destroyed by heat motion of molecule. Thus, the water molecules around hyaluronate ion are oriented more easily, and the amount of hydration increases. It is suggested that the hyaluronate ion strongly affects the hydration of ions in organism (for example, Ca^{2+}, Na^{+}, K^{+} ions).

The authors thank Assistant Professor Y. Masuda (Science University of Tokyo), Dr. T. Kamata (Government Chemical Industrial Research Institute, Tokyo) for the use of instruments, and Mrs. H. Uedaira for helpful discussions.

10) H. Shiio, *J. Amer. Chem. Soc.*, **80**, 70 (1958).

11) H. Nomura and Y. Miyahara, *Nippon Kagaku Zasshi*, **88**, 504 (1967).

12) H. Uedaira and H. Uedaira, Meeting of Colloid and Surface Chemistry (1968); *J. Phys. Chem.*, **74**, 1931 (1970).

13) O. Ya. Samoilov, "Sostoyanie i Rol' Vodny v Biologicheskikh Ob'ektakh," Nauka, Moskva (1967).

BULLETIN OF THE CHEMICAL SOCIETY OF JAPAN VOL. 43 1894—1896 (1970)

Radiation-induced Reaction of Isobutene in the Gas Phase. Effects of Pressure, Temperature and Additives on Polymerization

Yasuyuki NORO, Kenji FUEKI and Zen-ichiro KURI

Department of Synthetic Chemistry, Faculty of Engineering, Nagoya University, Chikusa-ku, Nagoya

(Received December 20, 1969)

In previous papers,[1,2] we have shown that cationic mechanism dominates in the radiation-induced polymerization of isobutene in the gas phase. The propagating rate constant and the mean lifetime of the propagating ion have also been estimated by a quantitative study of the effect of ammonia on the polymerization.[2]

We have investigated the effects of pressure, temperature and some additives to get a deeper understanding of its reaction mechanism.

Experimental

The purification of isobutene was described previously.[1] Research grade oxygen (99.9%) and nitrogen dioxide (99.0%) were dried prior to use. Sulfur hexafluoride was purified by distillation under vaccum. Methyl bromide was purified by passing through a silica gel column and by distillation under vacuum.

γ-Irradiation of samples and the analysis of products were described previously[1]. The temperature of samples was controlled using a thermostat.

1) H. Okamoto, K. Fueki and Z. Kuri, *J. Phys. Chem.*, **71**, 3222 (1967)

2) Y Noro, K. Fueki and Z. Kuri, This Bulletin, **41**, 1737 (1968).

Results and Discussion

Effect of Pressure. Figure 1 shows the effect of pressure on the polymerization rate of isobutene. We see that the polymerization rate is proportional to the square of pressure below ~800 Torr, and tends to become proportional to the pressure above ~800 Torr.

These results may be qualitatively explained in terms of the competition between fragmentation and deactivation of the excited isobutene ion, provided that a significant fraction of fragment ions do not initiate polymerization. A conventional kinetic treatment leads to the following expression for the polymerization rate:

$$R = \frac{k_p}{k_t}\left[\Phi + \Phi' \frac{k_1(\mathrm{M})}{k_2 + k_1(\mathrm{M})}\right](\mathrm{M})I_{\mathrm{abs}}, \qquad (1)$$

where Φ and Φ' are the quantities proportional to the initial yields of the ground and excited isobutene ions, k_1 and k_2 are the rate constants for deactivation and fragmentation of the excited ion, k_p and k_t are the rate constants for the propagation and termination reactions, I_{abs} is the dose rate absorbed by isobutene, and (M) is the concentration of isobutene.

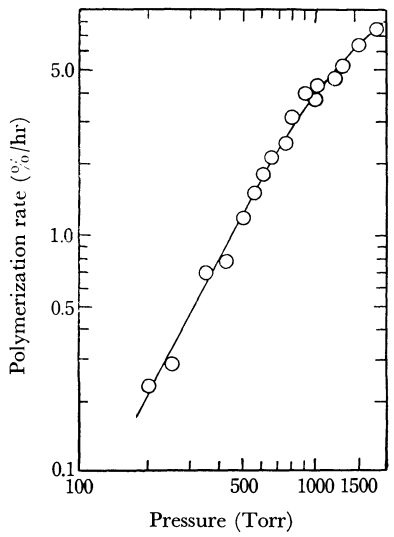

Fig. 1. Dependence of the polymerization rate on the initial pressure of isobutene.
Dose rate, 0.15 Mrad/hr; dose, 0.1—3 Mard; temperature, 20°C

If we assume that $\Phi \ll \Phi' k_1(M)/(k_2+k_1(M))$,*1 Eq. (1) is reduced to

$$R \simeq \frac{k_p}{k_t} \Phi' \frac{k_1(M)^2}{k_2 + k_1(M)} I_{abs}. \quad (2)$$

Equation (2) implies that R is proportional to $(M)^2$ at low pressures when $k_2 \gg k_1(M)$ and it is proportional to (M) at high pressures when $k_2 \ll k_1(M)$.

The molecular weight of the polymer produced, when irradiated to 0.3 Mrad at an initial pressure of isobutene of 1000 Torr, was determined to be 11000, and 5700 when irradiated to 1.2 Mrad at 500 Torr.

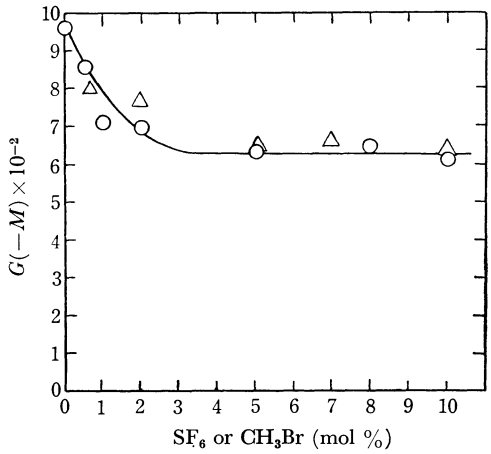

Fig. 2. Effect of sulfur hexafluoride and methyl bromide on the polymerization yield.
SF_6, ○; CH_3Br, △. Initial pressure of isobutene, 500 Torr; dose rate, 0.15 Mrad/hr; dose, 1—2 Mard; temperature, 20°C.

Effect of Temperature. The polymerization rate of isobutene irradiated to 0.3 Mrad at 0°C and at 500 Torr was 1.8 times greater than that at 20°C and at the same pressure and dose. The polymerization did not occur to an appreciable extent when irradiated to 0.3 Mrad at 50°C. At higher temperatures than 50°C, the polymerization was not observed at a dose of 1 Mrad, although a small amount of nonviscous liquid products were obtained when irradiated to 100 Mrad at 100°C. These results indicate the existence of a ceiling temperature between 50°C and 100°C.

Effect of Additives. *a) Sulfur Hexafluoride and Methyl Bromide.* Figure 2 shows the effect of SF_6 or CH_3Br on the G-value for isobutene consumption at an initial pressure of isobutene of 500 Torr at 20°C. The G-value decreases with increasing concentration of SF_6 or CH_3Br, approaching a plateau value which is about 65% of the G-value obtained for pure isobutene, at ~3 mol% of these additives.

Both SF_6 and CH_3Br are known as electron scavengers, *viz.*, they capture electrons to form negative ions:

$$SF_6 + e^- \longrightarrow SF_6^-,$$
$$CH_3Br + e^- \longrightarrow CH_3 + Br^-.$$

The retarding effect of these additives on the polymerization may be interpreted in terms of the acceleration of charge neutralization forming the negative ions. In the absence of these scavengers, the propagating ions would disappear by diffusion to the wall of the reaction vessel[2] and possibly by reacting with a trace of impurities.

If the polymerization terminates by the neutralization between the propagating cation and the negative ion in the presence of SF_6 or CH_3Br, it can be expected that the termination will be of the

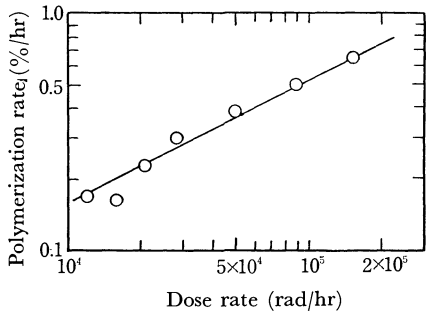

Fig. 3. Dependence of the polymerization rate on the dose rate.
Initial pressure of isobutene, 500 Torr; pressure of SF_6, 50 Torr; dose, 0.1—1 Mrad; temperature, 20°C.

*1 Abundance of the parent ion of isobutene is relatively small in its mass spectrum (E. Collinson, F. S. Dainton and H. A. Gillis, *J. Phys. Chem.*, **63**, 909 (1959)).

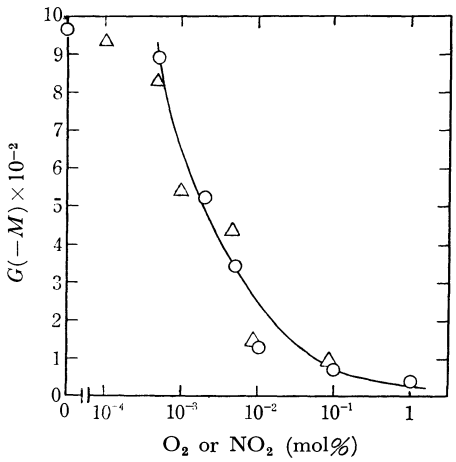

Fig. 4. Effect of oxygen and nitrogen dioxide on the polymerization yield.
O_2, ○; NO_2, △. Initial pressure of isobutene, 500 Torr; dose rate, 0.15 Mard/hr; dose, 1—5 Mrad; temperature, 20°C.

second-order with respect to the concentration of the ions. As shown in Fig. 3, it is found that the polymerization rate is proportional to the square root of dose rate, indicating a second-order termination reaction. This is in contrast with a first-order dependence of the polymerization rate on the dose rate for the case of pure isobutene in the gas phase.[1)]

b) Oxygen and Nitrogen Dioxide. Figure 4 shows the effect of O_2 or NO_2 on the G-value for isobutene consumption at an initial pressure of isobutene of 500 Torr at 20°C. Polymerization is retarded remarkably by the presence of O_2 or NO_2, and almost completely at a concentration of ~1 mol% of these additives. Such an effect of O_2 or NO_2 on the polymerization is quite different from that of SF_6 or CH_3Br, and it cannot be explained simply by electron capture by O_2 or NO_2. A similar result was obtained for N_2O.[1)] This might explain the retarding effect of oxygen-containing compounds such as O_2, NO_2 and N_2O on the polymerization of isobutene in the gas phase where these compounds*[2] capture electrons to form O^- (at least, as a fraction of negative ions), which will subsequently react with isobutene to produce water,[3)] a cation scavenger.

Conclusion

(1) The pressure effect on the polymerization of isobutene in the gas phase has been investigated over a wider range of pressure than in the previous studies. It has been interpreted in terms of the competition between fragmentation and deactivation of the excited isobutene ion.

(2) It has been found that there exists a ceiling temperature between 50°C and 100°C.

(3) The present study of the effect of electron scavengers such as SF_6 and CH_3Br has further confirmed the role of ionic processes in this polymerization. Termination of polymerization by ion neutralization has been verified by investigating the dose-rate dependence of the polymerization in the presence of electron scavengers.

(4) It has been found that the oxygen-containing compounds such as O_2, NO_2 and N_2O retard remarkably the polymerization, perhaps by producing water.

*[2] Since the ionization potentials of O_2, NO_2 and N_2O are higher than that of isobutene, the positive charge transfer from isobutene to these compounds is unlikely to occur.

3) W. J. Holtslander and G. R. Freeman, *Can. J. Chem.*, **45**, 1661 (1967).

BULLETIN OF THE CHEMICAL SOCIETY OF JAPAN VOL. 43 1897—1899 (1970)

Hydrogenolysis of a Quinonoid Oxygen of Alkoxynaphthoquinones

Teruo HAYASHI and Hiroshi KAKISAWA

Department of Chemistry, Faculty of Science, Tokyo Kyoiku University, Otsuka, Bunkyo-ku, Tokyo

(Received December 30, 1969)

During the course of our experiments on the structural determination of hydroxytanshinone[1] (I), catalytic hydrogenation of I was carried out in an acidic condition to afford two substances. One was a known orange pigment cryptotanshinone[2] (II), which was formed by hydrogenolytic removal of benzylic hydroxy group followed by autoxidation of the corresponding hydroquinone. The other was a colorless compound which was also slowly autoxidized to cryptotanshinone (II), but the structure remained undecided.

In order to determine the structure of this unusual reaction product, the hydrogenation product was isolated as a stable acetate. After prolonged hydrogenation of hydroxytanshinone (I) in the presence of palladium charcoal and acid, the reaction product was immediately acetylated to afford a monoacetate (IV). Acetate (IV) was also obtained from tanshinone-II[3] (VI) under the same conditions of reaction and time. Although quinones are usually reduced to the corresponding hydroquinones by catalytic hydrogenations and smoothly re-oxidized in the air into the original quinones, physical and chemical properties of acetate (IV) showed that, besides benzylic hydroxy group of hydroxytanshinone (I), one of the quinonoid oxygen atoms was also removed during the course of hydrogenation reaction. The position of the removed oxygen atom was first deduced from the NMR spectrum. The NMR spectrum of monoacetate (IV) is quite similar to that of cryptotanshinone (II), and shows the presence of *gem*-dimethyl group (δ 1.32, s), a methyl group (δ 1.30, d, J=6 Hz) attached to a methine group (δ 3.75, m), a methylene (δ 4.25, 4.82, dq, J=10, 9 and 6 Hz) bonded to an oxygen atom and two aromatic protons (C_9-H and C_{10}-H; δ 7.35, d, J=9 Hz and δ 7.70, brd, J=9 Hz, respectively). However, there are differences between the two spectra; whereas aromatic protons (C_9-H and C_{10}-H) of cryptotanshinone appear at δ 7.50 and δ 7.68 as sharp AB-quartet, one component (δ 7.70) of the corresponding AB-quartet of acetate (IV) is broadened by a long-range coupling[4] with epi-proton C_4-H (δ 7.12, br s). This type of long-range coupling was also found in the spectrum of a synthetic compound[5] (VII), in which the signal of C_{10}-H (δ 7.95, brd, J=9 Hz) is broadened by a long-range coupling with C_4-H (δ 6.80, brd, J=2 Hz). Benzylic protons of acetate (IV) appear at a higher field (δ 2.98, br t) than that (δ 3.24, br t) of diacetyldihydrotanshinone-II[3] (VIII), in which benzylic

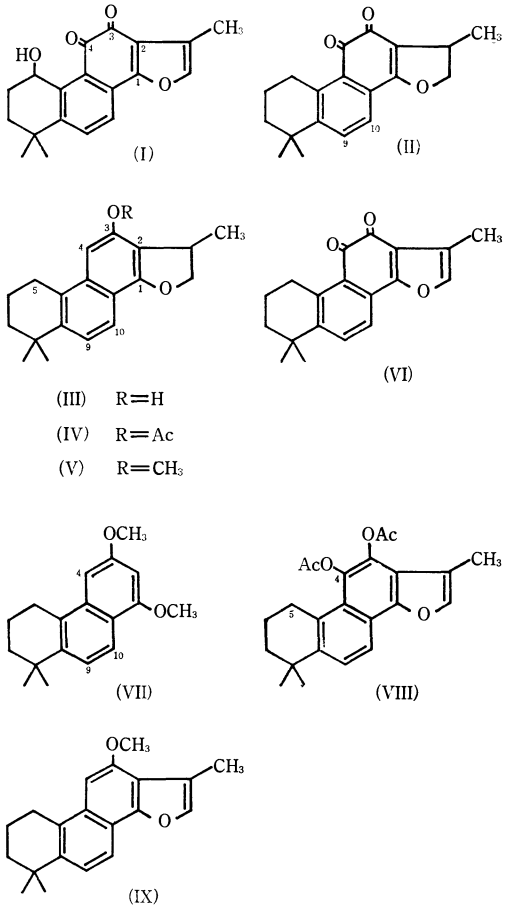

Fig. 1

1) H. Kakisawa, T. Hayashi, I. Okazaki and M. Ohashi, *Tetrahedron Lett.*, **1968**, 3231.

2) K. Takiura, *Yakugaku Zasshi* **61**, 482 (1941).

3) Y. Okumura, H. Kakisawa, M. Kato and Y. Hirata, This Bulletin, **34**, 895 (1961).

4) K. D. Bartle, D. W. Jones and R. S. Matthews, *Tetrahedron*, **25**, 2701 (1969).

5) H. Kakisawa, M. Tateishi and T. Kusumi, *Tetrahedron Lett.*, **1968**, 3783.

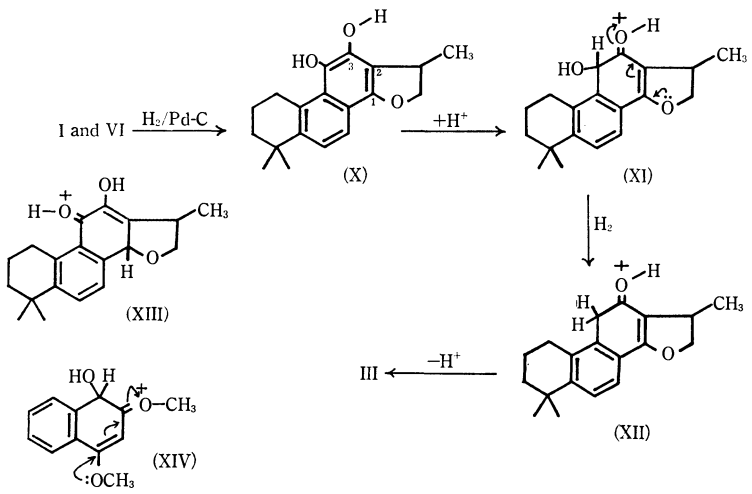

Fig. 2

protons (C_5-2H) are shifted to a low field by the deshielding effect of C_4-acetoxyl group. From these NMR properties, the position of the removed oxygen atom was assigned to C_4, and the structure of the monoacetate was deduced to be IV. For confirmation of the structure, reduction product (III) was converted into a known compound (IX). Hydrogenation product (III) was first methylated by dimethyl sulfate to afford a monomethyl ether (V). Ether (V) was dehydrogenated by refluxing with 2,3-dichloro-5,6-dicyano-1,4-benzoquinone[6] to afford a furanonaphthyl ether (IX), which was identical with the synthetic compound (IX) prepared in the total synthesis of tanshinones.[5] Thus the structure of the air sensitive compound obtained by catalytic hydrogenation in acidic condition could be assigned to III.

Catalytic hydrogenation of tanshinone-II proceeded very rapidly to afford a colorless solution of the corresponding hydroquinone within a few minutes, when the reaction was allowed to stop just to obtain a mixture of tanshinone-II (VI) and cryptotanshinone (II). On the other hand, when the hydrogenation mixture was stirred in hydrogen atomosphere for a longer time (fifteen hours or more), the sole reaction product was monohydroxy compound (III). These observations show that a hydroquinone (X) produced from tanshinone-II is an intermediate of the hydrogenolysis reaction. Protonation to a carbon atom of hydroquinone (X) forms benzyl alcohol (XI), which would readily lose a hydroxy group in hydrogenolytic condition to give (XII). Protonated ketone (XII) loses a proton to afford the monohydroxy compound (III).

The *meta*-oriented two oxygen functions (C_1–O and C_3–O) in the hydroquinone (X) have a particularly important effect on the formation of carbon-protonated species (XI), because unsubstituted 1,2-naphthoquinone showed no hydrogenolytic removal of quinonoid oxygen atom even under much severer conditions, and the product expected from another protonated intermediate (XIII) was not detected from the reaction mixture. The same effect of two oxygen atoms situated in *meta* orientation was recently found[7] in alkoxy exchange reaction of naphthyl alkyl ethers. Thus, while 1-hydroxy-2,4-dimethoxynaphthalene exchanges methoxy groups to give 1-hydroxy-2,4-diethoxynaphthalene in acidic ethanol through carbon-protonated species (XIV), 1,4-dimethoxy-naphthalene does not exchange in the same condition.

Experimental[8]

Hydrogenolysis of Tanshinone-II (VI). To a solution of 240 mg of tanshinone-II in ethanol (60 m*l*) were added 250 mg of palladium charcoal (5%) and 0.1 m*l* of concentrated hydrochloric acid. The mixture was stirred overnight at room temperature in hydrogen atmosphere. The solution was filtered and the filtrate was neutralized with saturated sodium bicarbonate solution and extracted with ether. Evaporation of the solvent afforded a white viscous oil which slowly changed into orange compound, cryptotanshinone, in the air.

Monoacetate(IV). The above reaction product (*ca.*

6) A. C. Baillie and R. H. Thomson, *J. Chem. Soc., C*, **1968**, 48.

7) J. E. Baldwin and H. H. Basson, *J. Org. Chem.*, **34**, 2788 (1969).

8) Melting points were measured by a mp apparatus, type MP-1, of Yamamoto Scientific Co. Ltd., and are uncorrected. The IR spectra were measured with a Hitachi EPI-S2. The UV spectra were measured with a Hitachi EPS-3T recording spectrometer in ethanol. The NMR spectra were measured with a Hitachi R-20 at 60 MHz in $CDCl_3$ solution using TMS as an internal reference.

100 mg) was dissolved in 1 m*l* of pyridine, acetic anhydride (2 m*l*) was slowly added, and the reaction mixture was stood overnight at room temperature. The solution was treated as usual, and the acetate was purified by repeated chromatography. λ_{max}^{EtOH} 232 (sh), 244, 293, 303, 317 and 331 mμ. $\nu_{max}^{CHCl_3}$ 1760, 1640, 1600, 1580, 1100 and 1040 cm^{-1}. *m/e* 324.175 (M^+): calcd for $C_{21}H_{24}O_3$, *m/e* 324.172.

The acetate obtained from hydroxytanshinone under the same reaction conditions is identical with this acetate.

Monomethyl Ether (V). About 100 mg of the reaction product of the hydrogenation was dissolved in 5 m*l* of acetone. To this were added 0.2 m*l* of freshly distilled dimethyl sulfate and 1 g (excess amount) of finely pulverized potassium carbonate. After refluxing the mixture under nitrogen for three hours, the same amounts of potassium carbonate and dimethyl sulfate were added, and refluxed for another three hours. The reaction mixture was filtered off while hot, and the filtrate was evaporated to dryness *in vacuo* until crystals appeared. The crude crystals were purified by column chromatography(SiO_2) and the monomethyl ether was eluted with benzene-hexane (1 : 2), and then recrystallized from ethanol to give white crystals (70 mg): mp 125—125.5°C; Found: C, 80.59; H, 8.07%. Calcd $C_{20}H_{24}O_2$: C, 81.04; H, 8.16%. λ_{max}^{EtOH} 224, 242 (sh), 248, 280, 283, 303, 317 and 332 mμ. ν_{max}^{KBr} 3090, 1635, 1603, 1520 and 1115 cm^{-1}. δ^{CHCl_3} ppm, 1.34 (s, 6H), 1.35 (d, 3H, J=6 Hz), 1.8 (m, 4H), 3.00 (brt, 2H, J=6 Hz), 3.7 (m, 1H), 3.92 (s, 3H), 4.30 (q, 1H, J=9 and 6 Hz), 4.80 (t, 1H, J=9 Hz), 6.75 (s, 1H), 7.30 (d, 1H, J=8 Hz) and 7.70 (d, 1H, J=8 Hz).

Oxidation of Monomethyl Ether (V) with 2,3-Dichloro-5,6-dicyano-1,4-benzoquinone (DDQ). To a solution of 39 mg of V in benzene (4.5 m*l*) was added 33 mg of DDQ. After the solution was refluxed under nitrogen for 75 min, separated hydroquinone was filtered off. Evaporation of the filtrate afforded white crystals (37 mg); mp 124—124.5°C (EtOH). The spectrum of UV and IR, and melting point were all identical with those of synthetic compound (IX), and the latter was not depressed in mixed melting. λ_{max}^{EtOH} 240, 248, 255.5, 275 (sh), 286 (sh), 325 and 338 mμ. ν_{max}^{KBr} 3080, 1635, 1225 and 1115 cm^{-1}. δ^{CHCl_3} ppm, 1.40 (s, 6H), 1.8 (m, 4H), 2.40 (d, 3H, J=1 Hz), 3.08 (brt, 2H, J=6 Hz) 3.98 (s, 3H), 6.80 (s, 1H), 7.35 (q, 1H, J=1 Hz), 7.45 (d, 1H, J=9 Hz) and 8.00 (d, 1H, J=9 Hz).

The authors wish to express their thanks to Dr. Nobuhide Wasada of Government Chemical Industrial Research Institute for his measurement of the mass spectrum.

BULLETIN OF THE CHEMICAL SOCIETY OF JAPAN VOL. 43 1899—1901 (1970)

Poisoning of Zeolite Catalyst with Ammonia

Hiroshige MATUMOTO, Michiaki TOKUNO, Hideo FUTAMI and Yoshiro MORITA

Department of Applied Chemistry, School of Science and Engineering, Waseda University, Nishiokubo, Shinjuku, Tokyo

(Received January 12, 1970)

In the acid-catalyzed reactions of hydrocarbons such as isomerization,[1] alkylation[2,3] and cracking,[4] the catalytic activity of zeolite increased with the amount of adsorbed water, which was controlled by thermal treatment of zeolite prior to being brought to catalysis. The activation energies of these reactions were, however, almost independent of the water content in zeolite.[1,2] The result suggests that the catalytically active surface of zeolite is regarded as homogeneous, while the existence of several different OH groups in the lattice was confirmed by IR measurements.[5] This work was carried out to confirm the homogeneity of the active surface of zeolite catalyst by means of partial poisoning with ammonia.

The reaction apparatus and its procedure were similar to those given in previous work.[6] Cumene cracking was chosen for the activity test of zeolite. The reaction was carried out at 350°C under a constant pressure of ammonia in order to measure the activity of zeolite at an equilibrium state of ammonia adsorption. The partial pressure of cumene was maintained constant (36 mmHg). Dried hydrogen was used as a carrier gas. Pretreatment of zeolite was done in a stream of hydrogen for two hours at a desired temperature and the resulting weight change was measured with a thermobalance. CaY Zeolite used in this work was prepared by the ion exchange of Linde Molecular Sieves (SK-40). The ion exchange level,

1) H. Matsumoto and Y. Morita, *Bull. Jap. Petroleum Inst.*, **11**, 40 (1969).
2) H. Matsumoto and Y. Morita, unpublished data.
3) P. B. Venuto, L. A. Hamilton and P. S. Landis, *J. Catal.*, **5**, 484 (1966).
4) P. D. Hopkins, *ibid.*, **12**, 325 (1968).
5) C. L. Angell and P. C. Schaffer, *J. Phys. Chem.*, **69**, 3463 (1965). J. B. Uytterhoven, R. Schonheydt, B. V. Lingme and W. K. Hall, *J. Catal.*, **13**, 425 (1969).
6) H. Matsumoto, K. Yasui and Y. Morita, *J. Catal.*, **12**, 84 (1968).

Table 1. Cracking activity of CaY pretreated at various temperatures

Pretreatment temperature (°C)	350	400	450	500	550
Amount of adsorbed water (mg/g)	11.4	8.9	6.7	5.2	4.1
Cracking rate[a] (g/g hr)	0.982	1.080	0.809	0.657	0.558

a) Initial rate determined by first order kinetics.

defined as the percentage of the original sodium ion replaced, was determined to be 70.

The cracking activity of CaY zeolite pretreated at various temperatures is shown in Table 1 in comparison with the amount of adsorbed water. Water content and catalytic activity of CaY decreased with the rise of pretreatment temperature. The active protonic sites of zeolite may be produced by the adsorption of water.[7] A low activity of CaY pretreated at 350°C was due presumably to poisoning by the adsorption of excessive water on the active surface.

The catalytic activity of CaY zeolite considerably decreased by the addition of ammonia to the reaction system. The relation between the cumene conversion and the on-stream period is shown in Fig. 1.

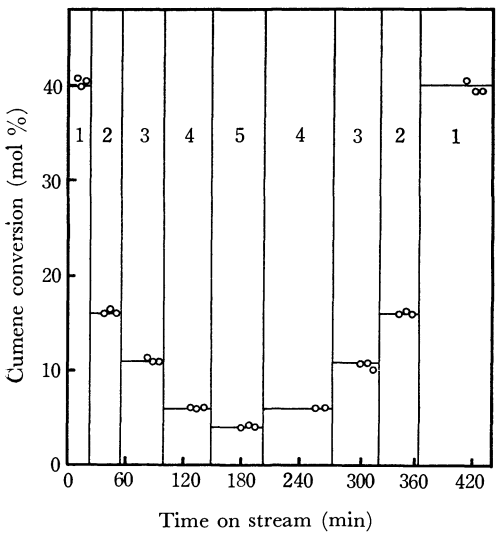

Fig. 1. Reversible poisoning of CaY with ammonia.

Pressure of ammonia; 1 0 mmHg
2 11.5
3 16.4
4 31.9
5 42.3

CaY pretreated at 450°C was brought to 350°C in a stream of hydrogen and then a continuous flow of cumene was started. During this period 40% of the conversion was observed. On the introduction of 8.23 mmHg of ammonia to the system, the conversion decreased sharply and reached the stationary value of 16% within 10 min. Cumene conversion decreased with the increase of ammonia pressure in the system. When the pressure of ammonia decreased, the conversion again increased. In this series of runs, the same conversion was obtained under the same partial pressure of ammonia. Thus, the poisoning of CaY with ammonia was completely reversible and the establishment of equilibrium was expected between the ammonia in the gas phase and that adsorbed on the active surace of zeolite.

If we postulate that the decrease in the activity of zeolite depends in first order on the amount of adsorbed ammonia, the initial rate of the reaction, r, will be expressed by the equation

$$r = r_0(1-\theta),$$

where r_0 stands for the initial rate in the absence of ammonia and θ for the fraction of the active surface occupied by ammonia. The poisoning effect of ammonia may be expressed as a function of ammonia pressure in the system (P_{NH_3}), postulating the establishment of the Langmuir assumption for the effective adsorption of ammonia on the active

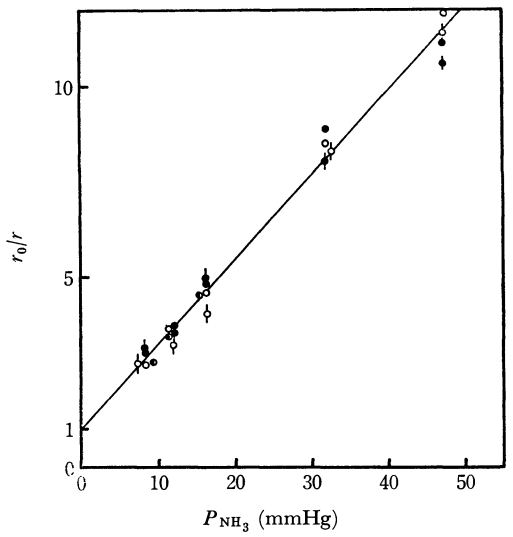

Fig. 2. Pressure dependence of ammonia poisoning of CaY pretreated at various temperatures.

CaY pretreated at
● 350°C
○ 400
○ 450
● 500
◑ 550

7) J. W. Ward, *J. Catal.*, **10**, 34 (1968); H. Hattori and T. Shiba, *ibid.*, **12**, 111 (1968).

surface of zeolite. Thus, the ratio of these initial rates, r_0/r, was evaluated by the simple relation under a constant pressure of the reactant

$$r_0/r = 1 + K \cdot P_{NH_3},$$

where K represents the constant of ammonia adsorption effective for the catalysis.

In accordance with this equation, plots of the ratio of initial rates against the pressure of ammonia should be linear. Such plots for CaY zeolite pretreated at various temperatures have been obtained in Fig. 2, where the initial rate of cumene cracking was determined by first order kinetics.[6] The data evidently satisfy the above equation. As evident from Fig. 2, the adsorption constant K was approximately independent of the pretreatment temperature (or the water content) of the zeolite, on which the catalytic activity strongly depends. This probably indicates that the catalytically active surface of CaY is nearly homogeneous.

BULLETIN OF THE CHEMICAL SOCIETY OF JAPAN VOL. 43 1901—1902 (1970)

The Dissociation of 7-Triphenylmethyl-1,3,5-cycloheptatriene in *m*-Xylene*[1]

Kunio Okamoto, Kôichi Komatsu, Tomomi Kinoshita and Haruo Shingu

Department of Hydrocarbon Chemistry, Faculty of Engineering, Kyoto University, Sakyo-ku, Kyoto

(Received January 20, 1970)

The enthalpy of the dissociation of bitropyl (bis-2,4,6-cycloheptatrien-1-yl) into the tropyl (cycloheptatrienyl) radicals has recently been evaluated to be 35 ± 1 kcal/mol using ESR spectroscopy,[1] whereas that of "hexaphenylethane," whose structure has been proved to be 1-diphenylmethylene-4-triphenylmethyl-2,5-cyclohexadiene (I),[2] into the trityl (triphenylmethyl) radicals is known to be only about 11.5 kcal/mol.[3] When these two values are available, it should be of considerable interest to know the value of the dissociation energy of 7-trityltropilidene (7-triphenylmethyl-1,3,5-cycloheptatriene), a coupling product of the trityl and the tropyl radicals.

Incidentally, we have synthesized this compound[4] by the coupling of the two unlike radicals in connection with our studies of the one-electron reduction of the tropylium ion;[5] we undertook the measurement of the degree of the dissociation by means of ESR spectroscopy in order to evaluate the enthalpy of the dissociation of this compound.

A degassed solution (0.1 M) of 7-trityltropilidene in *m*-xylene gave the ESR signals of the trityl radical at 60—100°C; the signal gradually increased in intensity and became constant after 1—5 hr at 85—90°C or after 10—20 hr at 65°C. The concentrations of the trityl radical were estimated to be 3×10^{-6}—6×10^{-5} M at 60—95°C by a comparison of the integral spectrum constructed from the first derivative spectrum, recorded under overmodulated conditions (modulation width, 5.0 G), with that of a standard diphenylpicrylhydrazyl solution. The signal intensity of the trityl radical in a sample preheated at 100°C decreased when the sample was kept at lower temperatures, thus reaching the same value as that of another sample not preheated. After each measurement, no discoloration of the solution was observed, and the TLC analysis of an aliquot gave a sole spot with the same R_f value as that of the authentic 7-trityltropilidene.[6]

*1 Presented at the 22nd Annual Meeting of the Chemical Society of Japan, Tokyo, April, 1969. Abstracts of Papers, III, p. 1712; Studies of the Dissociation of a Carbon-Carbon Bond. Part I.

1) G. Vincow, H. J. Dauben, Jr., F. R. Hunter and W. V. Volland, *J. Amer. Chem. Soc.*, **91**, 2823 (1969); we are grateful to Professor Vincow for informing us of this result before publication and for his valued correspondence.

2) a) H. Lankamp, W. Th. Nauta and C. MacLean, *Tetrahedron Lett.*, **1968**, 249; we have followed their NMR experiments and confirmed the reported structure; b) R. D. Guthrie and G. R. Weisman, *Chem. Commun.*, **1969**, 1316.

3) a) K. Ziegler and L. Ewald, *Ann.*, **473**, 163 (1929); b) E. Müller and I. Müller-Rodloff, *ibid.*, **521**, 89 (1936); c) F.S. D'yachkovskii, N.N. Bubnov and A.E. Shilov, *Doklady. Akad. Nauk S.S.S.R.*, **122**, 629 (1958).

4) 7-Trityltropilidene was first synthesized from triphenylmethylsodium and tropylium fluoroborate by M. R. Rifi and H. J. Dauben, Jr. (M. R. Rifi, Ph. D. Thesis, p. 105, the University of Washington, 1963); we are indebted to Professor K. M. Harmon of the University of Washigton for informing us of the details of Dr. Rifi's thesis.

5) K. Okamoto, K. Komatsu and H. Shingu, This Bulletin, **42**, 3249 (1969).

6) It has been found that 7-trityltropilidene gave a small amount of an oily product when heated in refluxing benzene for 4.5 days (F. R. Hunter, Ph. D. Thesis, p. 155, the University of Washington, 1966); we are grateful to Professor K. M. Harmon for informing us of the details of Dr. Hunter's thesis.

The ESR signal for the tropyl radical was not observed under the conditions here employed. This is most probably the result of the lowering of the concentration of the tropyl radical due to its dimerization to bitropyl. Since the trityl radical is also in equilibrium with the cyclohexadiene I ("hexaphenylethane"), we may assume the following equilibration scheme:

$$Ph_3C\text{-}C_7H_7 \overset{K_1}{\rightleftharpoons} Ph_3C\cdot + C_7H_7\cdot$$

K_2 ⇕ ⇕ K_3

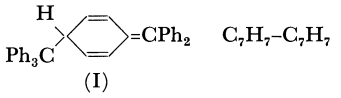

(I) $C_7H_7\text{-}C_7H_7$

If the above scheme holds under the conditions employed, the equilibrium consant, K_1, for 7-trityltropilidene can be calculated from Eq. (1):

$$K_1 = (b/a)\{-1+\sqrt{1+(16b^2/K_2K_3)+(8b/K_3)}\}(K_3/4) \quad (1)$$

where a and b are, respectively, the concentrations of 7-trityltropilidene and the trityl radical.[7] The results are summarized in Table 1, along with the thermodynamic parameters.

Thus, in the temperature range from 60 to 95°C, the values of the equilibrium constant are in the sequence: the cyclohexadiene I > $Ph_3C\text{-}C_7H_7$ > $C_7H_7\text{-}C_7H_7$, whereas the values of ΔH and of ΔS are in the sequence: $Ph_3C\text{-}C_7H_7$ > $C_7H_7\text{-}C_7H_7$ > the cyclohexadiene I. It seems to be difficult to explain the abnormally high values of ΔH and of ΔS for 7-trityltropilidene on the basis of the steric and the electronic factors which were considered in the cases of genuine hexaphenylethane[8] and bitropyl.[1] These quenstions remain to be elucidated in the future.[9]

Table 1. Equilibrium constants, enthalpy and entropy for the dissociation of 7-triphenylmethyl-1,3,5-cycloheptatriene in *m*-xylene

Temp. °C	Concn. of Ph_3C [a] M×10⁶	Equlibrium constant: $Ph_3C\text{-}C_7H_7$ $K_1\times10^{16}$ [c]	I [b] $K_2\times10^3$ [d]	$C_7H_7\text{-}C_7H_7$ $K_3\times10^{17}$ [d]
60.0	2.71	1.50	1.41	2.24
65.0	4.16	3.96	1.82	4.68
70.0	8.07	18.4	2.29	10.0
75.0	7.17	19.6	2.95	20.4
80.0	17.4	53.4	3.63	39.8
83.0	24.1	213	4.17	63.2
85.0	15.8	127	4.52	81.3
88.0	41.1	691	5.18	126
90.0	25.1	360	5.69	162
93.0	50.8	1250	6.36	235
95.0	55.0	1617	6.92	309
ΔH	(kcal/mol)	50±2	11[d]	35[d]
ΔS(60°C)(e.u.)		78.4	20.0	27.3

a) The initial concentration of 7-trityltropilidene was 0.1M.
b) I = 1-diphenylmethylene-4-triphenylmethyl-2,5-cyclohexadiene.
c) Calculated from Eq. (1) (see text).
d) The values for K's were extrapolated from data at the other temperatures: see Refs. 1 and 7.

Experimental

7-Trityltropilidene. This was synthesized by the coupling of the trityl radical with the tropyl radical in benzene-acetonitrile. To a stirred benzene solution (18 m*l*) of the cyclohexadiene I (1.13 mmol) containing zinc dust (2.94 g), an acetonitrile solution (18 m*l*) of tropylium fluoroborate (4.50 mmol) was added, drop by drop, under a nitrogen atmosphere over a 15-min period at room temperature. The reaction mixture was then filtered; the filtrate was washed with water, dried, and concentrated to give an oily solid (0.849 g), which was then chromatographed over slica gel (70 g). Bitropyl (0.185 g, 45.3%) and 7-trityltropilidene (0.459 g, 61.0% yield based on the cyclohexadiene I; 30.5% yield based on the tropylium ion) were eluted with 95 : 5 and 90 : 10 *n*-hexane - benzene respectively. 7-Trityltropilidene melts at 167—170°C (dec.) (lit, mp 156°C[4]). Found: C, 93.52; H, 6.62. Calcd for $C_{26}H_{22}$: C, 93.37; H, 6.63%. NMR spectrum: τ 2.80 (15H, singlet, aromatic), 3.25 (2H, triplet, 3- and 4-C), 3.81 (2H, multiplet, 2- and 5-C), 4.72 (2H, doublet of doublet, 1- and 6-C) and 7.06 (1H, triplet, 7-C); UV: $\lambda_{max}^{CH_3OH}$ 260 mμ (log ε=3.66) and two shoulders at 265.5 and 272 mμ (lit,[4] $\lambda_{max}^{95\%\ EtOH}$ 259 mμ ($\varepsilon=4.7\times10^3$) and 272 m$\mu$ (shoulder, $\varepsilon=3.20\times10^3$)).

ESR Measurements. The ESR spectra were taken on a Japan Electron Optics X-band spectrometer, model JES-3BS-X, equipped with a 100 kc/s field modulation unit. The evacuated sample tube to be heated was placed in a JEO Associates JES-UCT-2X quartz Dewar sleeve set in a TE_{011} JEO cavity.

7) The values of K_2 and ΔH for the dissociation of the cyclohexadiene I were taken to be, respectively, 2×10^{-4} (25°C) and 11 kcal/mol in benzene.[3b] The values of K_3 and ΔH for the dissociation of bitropyl were evaluated by means of ESR spectroscopy following the method of Vincow and his collaborators;[1] K_3 for a 2.9M solution of bitropyl in *m*-xylene, 1.2×10^{-13} (126°C); ΔH (the average value for three runs), 34.5 kcal/mol (124.5—152.0°C) (lit, ΔH for a neat sample, 35±1 kcal/mol[1]).

8) a) G. W. Wheland, "Resonance in Organic Chemistry," John Wiley & Sons, New York (1955), Section 7·6; b) S. W. Benson, *J. Chem. Educ.*, **42**, 502 (1965).

9) The sequence of ΔH $Ph_3C\text{-}C_7H_7$ > $C_7H_7\text{-}C_7H_7$ may suggest that the ΔH for the genuine $Ph_3C\text{-}CPh_3$, which has not yet been prepared,[2a] might be greater than that of $Ph_3C\text{-}C_7H_7$.

SHORT COMMUNICATIONS

The Structure of the *trans*-Dichlorobistrimethylenediaminecobalt(III) Ion, *trans*-$[CoCl_2tn_2]^+$ *1

Keiji MATSUMOTO, Shun'ichiro OOI and Hisao KUROYA

Department of Chemistry, Faculty of Science, Osaka City University, Sumiyoshi-ku, Osaka

(Received March 4, 1970)

Ethylenediamine, $H_2N-CH_2-CH_2-NH_2$ (=en), can form a stable five-membered chelate ring in combination with many transition metals; the geometry of the ring has been well established. On the other hand, trimethylenediamine, $H_2N-CH_2-CH_2-CH_2-NH_2$ (=tn), possesses one more CH_2-group than does ethylenediamine and forms a six-membered ring in chelation with several metals. The metal chelates of the trimethylenediamine are, however, less stable and less easily prepared than the corresponding ethylenediamine chelates.[1] The instability of the tn-compounds may be due to the distortion which is presumably existent in the six-membered chelate ring. In order to elucidate the conformation of the tn-chelate ring, we have attempted a crystal structure analysis of *trans*-$[Co\ Cl_2\ tn_2]Cl \cdot HCl \cdot 2H_2O$.

The crystal is green and monoclinic, with cell dimensions of $a=10.68$, $b=8.55$, $c=9.46$ Å, and $\beta=112.2°$. The space group is $P2_1/c$, and the unit cell contains two formula units ($\rho_{obsd}=1.59$ and $\rho_{calcd}=1.60\ g\cdot cm^{-3}$). The *h0l* and *hk0* intensity data were recorded on Weissenberg photographs (Ni$K\alpha$ radiation, $\lambda=1.6591$ Å). The intensities were measured visually, and no absorption corrections were applied. The positions of the heavy atoms could be obtained from Patterson projections, *P(UW)* and *P(UV)*, and those of the light atoms, from Fourier maps. The *R*-value was reduced to 0.14 by means of the usual refinements. Refinement on the basis of the three-dimensional data is now going on.

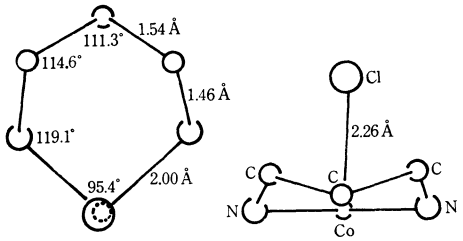

Fig. 1. The elevation and projection of *trans*-$[Co\ Cl_2\ tn_2]^+$. Asymmetric half of the cation is drawn.

The crystal structure is similar to that of *trans*-$[Co\ Cl_2\ en_2]Cl \cdot HCl \cdot 2H_2O$;[2] the crystal consists of *trans*-$[Co\ Cl_2\ tn_2]^+$, Cl^- and $[H_2O\cdots H\cdots OH_2]^+$. In Fig. 1 the structure of the complex ion is illustrated. Since the cobalt is located on a special position, the symmetry of the complex ion is $\bar{1}$.

The chelate ring takes a chair form.[3] The ring has an approximate mirror plane which is normal to the ring plane and which passes through the cobalt atom and the middle carbon atom. The bond lengths of Co–N, N–C, and C–C are in good agreement with those in *trans*-$[Co\ X_2\ en_2]^+$.[4,5] In Table 1 the average values of the two bond angles which are related by the pseudo mirror plane are compared with the corresponding values in the en-complexes. The deviation of the N–Co–N angle from 90° in the tn-complex is almost equal to that in the en-complexes. However, the values of the Co–N–C and N–C–C angles in the former are appreciably larger than 109.5°, while they are quite close to the tetrahedral angle in the latter. The lower stability in the tn-complexes may be attributable, at least in part, to these bond-angle strains. Recently a tn-ring which takes a twisted form and the N-Co-N angle of which is less than 90° was found in [Cu(*o*-haph:tn:*o*-haph)].[6]

TABLE 1

	trans-$[Co\ Cl_2\ tn_2]^+$	*trans*-$[Co\ X_2\ en_2]^+$	
		X=Cl	X=Br
∠N-Co-N	95°	86°	87°
∠Co-N-C	119	109	109
∠N-C-C	115	107	109

*1 K. Matsumoto, S. Ooi and H. Kuroya, Preprints for the 17th Annual Meeting of the Chemical Society of Japan (Tokyo, 1964), p. 491.

1) J. C. Bailar, Jr., "The Chemistry of Coordination Compounds," Reinhold Publishing Co., New York (1956).

2) A. Nakahara, Y. Saito and H. Kuroya, This Bulletin, **25**, 331 (1952).

3) T. Nomura, F. Marumo and Y. Saito, *ibid.*, **42**, 1016, (1969).

4) S. Ooi, Y. Komiyama, Y. Saito and H. Kuroya, *ibid.*, **32**, 263 (1958).

5) S. Ooi and H. Kuroya, *ibid.*, **36**, 1038 (1963).

6) K. Iida, I. Oonishi, A. Nakahara and Y. Komiyama, *ibid.*, in press.

Polymerization of *N*-Vinylcarbazole by Chlorides and Oxychlorides of Some Group V Elements. I. Polymerization by $POCl_3$, $AsCl_3$ and $SbCl_3$

Mukul Biswas and Devapriya Chakravarty

Department of Chemistry, Indian Institute of Technology, Kharagpur, India

(Received July 30, 1969)

In the course of our studies[1-3] on initiator systems for *N*-Vinylcarbazole (NVC) polymerization we have observed that $POCl_3$, $AsCl_3$ and $SbCl_3$ can effectively initiate the solution polymerization of NVC. This communication reports our preliminary observations on these systems.

Polymerization was carried out under nitrogen at 30°C with purified and dry reagents. Conversion at intervals of 2, 4, 6 and 8 up to 30 min was followed gravimetrically after purifying the polymer.[3] Molecular weights ($\bar{M}_n$) were determined cryoscopically in benzene. Polymer melting points were >350°C.

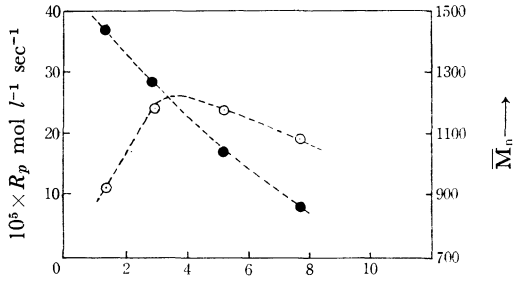

Fig. 1. Dependence of R_p on [NVC] (⊙) and of $\bar{M}_n$ on [NVC] (●); $[AsCl_3] = 16.2 \times 10^{-4}$ M.

For NVC-$AsCl_3$-benzene system, R_p was first order in $AsCl_3$ concentration. The variation of R_p and $\bar{M}_n$ with NVC concentration is shown in Fig. 1. With NVC-chloranil-nitrobenzene system, Pac and Plesch[4] found a maximum by plotting specific rate constant against NVC concentration. Dependence of the maximum on $AsCl_3$ concentration is being investigated. We feel that increased termination and transfer may be important, but any definite comment on this trend would not be justified at this stage.

The reactions were usually exothermic. R_p of NVC-$AsCl_3$ system was dependent on solvent dielectric constant (Fig. 2) and so was $\bar{M}_n$ (1269 in benzene and 3982 in nitrobenzene, for example). Additives such as water, dimethylaniline, aniline and triethylamine related the rate. These features suggest a cationic mechanism.

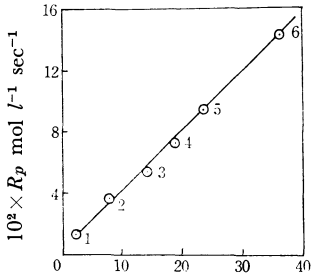

Fig. 2. Dependence of R_p on solvent dielectric constant. $[NVC] = 0.29$ M; $[AsCl_3] = 16.2 \times 10^{-4}$ M; (1) B (100%); (2) 75% B+25% NB; (3) 50% B+50% NB; (4) 37.5% B+62.5% NB; (5) 25% B+75% NB; (6) NB (100%). (B=Benzene; NB=Nitrobenzene). Values of solvent dielectric constant taken from Ref. 5.

Some experiments were performed with $POCl_3$ and $SbCl_3$. Thus $POCl_3$ (0.063—0.19 M) and NVC (0.77 M) produced (30°C; benzene; 1320 min) 94% deep yellow orange poly NVC, $\bar{M}_n$: 2704, mp >350C°. $SbCl_3$ (0.068 M) and NVC (0.29 M) produced (30°C; benzene; 765 min) 74% white poly NVC, $\bar{M}_n$: 2254, mp >350°C.

In a few cases a colour change was noted during reaction. With NVC-$Fe(NO_3)_3$, $9H_2O$ system Okamura *et al.*[6] reported a similar colour change. In our case this colour change was not a necessary condition for polymerization. In fact, colour could be produced by mixing poly NVC with $AsCl_3$ in benzene. This latter observation may be related to the possibility of charge transfer interaction between poly NVC and $AsCl_3$. Interaction between poly NVC and acceptors such as $SbCl_5$ is known.[7] Spectrophotometric investigations are in progress.

Details of all these observations will appear in due course.

1) M. Biswas and S. Ghosal, *Chem. Ind.* (London), **1966**, 1717.

2) M. Biswas and I. Kar, *Indian J. Chem.*, **5**, 119 (1967).

3) M. Biswas, M. M. Maiti and N. D. Ganguly, *Makromolecul. Chem.*, **124**, 263 (1969).

4) J. Pac and P. H. Plesch, *Polymer* (London), **8**, 237 (1967).

5) D.C. Pepper, *Trans. Faraday Soc.*, **45**, 397 (1949).

6) S. Tazuke, T.B. Tjoa and S. Okamura *J. Polym. Sci.*, A-1, **5**, 1911 (1967).

7) L. P. Ellinger, "Advances in Macromolecular Chemistry," Vol. I, ed. by W. M. Pasika, Academic Press, New York (1968), p. 180 and references cited therein.

The Molecular Structure of the Reaction Product from Sulfurdiimide and Diphenylketene

Noritake YASUOKA, Nobutami KASAI, Toru MINAMI, Yoshiki OHSHIRO, Toshio AGAWA and Masao KAKUDO

Department of Applied Chemistry, Osaka University, Yamadakami, Suita, Osaka

(Received March 7, 1970)

In a series of studies of the reaction of hetero-cumulenes with ketene, the reaction of sulfurdiimide with diphenylketene has been reported on by some of the present authors.[1] The structure of the reaction product was assumed to be 1-phenylimino-2,4,4-triphenyl-1,2-thiazetidine-3-one (I) on the basis of the IR, the mass spectra, and some chemical properties.

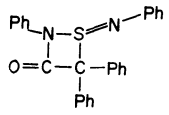

(I)

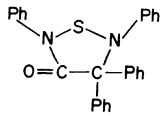

(II)

An X-ray structure investigation has, however, shown that the structure is an unexpected structure, 2,3,3,5-tetraphenyl-1,2,5-thiadiazolidine-4-one (II), instead of (I). After we completed our X-ray structure determination, Hoerhold and Eibisch have proposed a structure on the basis of some organo-chemical methods.[2] Their result agrees with ours.

The three-dimensional X-ray diffraction data were collected on a Rigaku on-line controlled single-crystal diffractometer with zirconium-filtered Mo$K\alpha$ radiation. Crystal data: $C_{26}H_{20}ON_2S$, mp=167°C, F. W.=408.5, monoclinic, $P2_1/n$, a=10.975 (5), b=15.315(6), c=12.616(6) Å, β=98.28(2)°, V=2098 Å^3, Z=4, D_c=1.29 g·cm^{-3}.

The structure was established by the heavy-atom method. The refinement was carried out by the block-diagonal least-squares procedure (R=0.089 for 1483 non-zero reflections).

The molecular is shown in the Fig. 1.

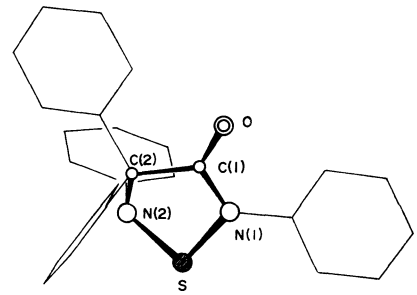

Fig. 1. The molecular structure.

Two S–N bond distances, S-N(1) and S–N(2), (Table 1) are comparable to, or somewhat shorter than, the sum of the covalent radii (1.74 Å) and are assumed to be normal single bonds. From this fact and from the N(1)–S–N(2) bond angle, the S atom seems to be bonded to nitrogen atoms using two mutually orthogonal 3p orbitals. This compound is probably the first one in which such a bonding scheme has been observed.

It is interesting to note that the C(1)–N(1) bond is significantly shorter than the C(2)–N(2) bond. The C–N bond distance in the =N–C=O group is usually shorter than the normal single bond distance: for example, the value of 1.326 Å has been reported in acetanilide.[3] The N(1) atom lies almost on the plane defined by C(1), S, and C(31). In contrast to this, the N(2) lies 0.4 Å above the plane defined by C(2), S, and C(41). These differences in the bonding states of N(1) and N(2) are interesting in connection with the reactivity of this compound.

TABLE 1.* SELECTED BOND LENGTHS AND ANGLES

S–N(1)	1.726 (0.011) Å	N(1)–S–N(2)	92.4 (0.5)°
S–N(2)	1.701 (0.009)	S–N(1)–C(1)	112.1 (0.8)
C(1)–N(1)	1.360 (0.016)	S–N(2)–C(2)	104.6 (0.6)
C(2)–N(2)	1.509 (0.014)	N (1)–C(1)–C(2)	109.7 (1.0)
C(1)–C(2)	1.564 (0.016)	N (2)–C(2)–C(1)	104.6 (0.8)
C(1)–O	1.211 (0.015)	S–N(1)–C(31)	120.9 (0.8)
C(2)–C(11)	1.523 (0.015)	C(1)–N(1)–C(31)	127.0 (1.0)
C(2)–C(21)	1.522 (0.015)	S–N(2)–C(41)	114.4 (0.7)
N(1)–C(31)	1.410 (0.015)	C(2)–N(2)–C(41)	117.6 (0.8)
N(2)–C(41)	1.473 (0.014)		

* In Table 1, C(31) and C(41) are atoms of benzene rings attached to N(1) and N(2) respectively. Similarly, C(11) and C(21) are those bonded to C(2).

1) T. Minami, O. Aoki, H. Miki, Y. Ohshiro and T. Agawa, *Tetrahedron Lett.*, **1969**, 447.

2) H. H. Hoerhold and H. Eibisch, *Tetrahedron*, **25**, 4277 (1969).

3) C. J. Brown and D. E. C. Corbridge, *Acta Crystallogr.*, **7**, 711 (1954).

Thermal *trans-cis* Isomerization of $[CrBrH_2O(NH_3)_4]Br_2$

Yoriko KAJI, Akira UEHARA, Eishin KYUNO and Ryokichi TSUCHIYA

Department of Chemistry, Faculty of Science, Kanazawa University, Kanazawa

(Received March 10, 1970)

There are only a few examples of thermal *trans-cis* isomerization of transition metal complexes in solid phase.[1] In general, the isomerization of the complexes which contain crystalline or coordinated water occurs simultaneously with dehydration or after.[2] Isomerization prior to dehydration is still unknown. One of such rare examples was investigated in the present work.

When the complex, *trans*-$[CrBrH_2O(NH_3)_4]Br_2$,[3] was heated, it turned to reddish-violet from violettish-brown, and the coordinated water was then liberated. This suggests a change from *trans* to *cis* form. The derivatogram of the *trans* complex is given in Fig. 1. It shows an endothermic peak without any mass loss in the DTA curve at 145°C.

In order to confirm the *cis-trans* isomerization, absorption spectra of the compounds obtained after heating the complex with a thermobalance at both 143 and 153°C were measured by diffusion reflectance method in solid state. They are given in Fig. 2, together with those obtained at room temperature for the starting *trans* complex and for the *cis* isomer prepared by the standard method.[3]

The *d–d* band in the long wavelength region of the starting complex is split into two peaks, indicating the validity of the *trans* form. On heating, the splitting of these peaks became gradually weaker, approaching one peak corresponding to that of the *cis* form. The results suggest that *trans-cis* isomerization occurs in thermal reaction.

The enthalpy change, ΔH, for the reaction was calculated to be 1.9 kcal·mol^{-1} by analysis of DTA, and the activation energy, $E^{\neq}$, was evaluated by the same analysis to be 87 kcal·mol^{-1}. The values are very interesting for discussing the mechanism of isomerization reaction in the solid phase.

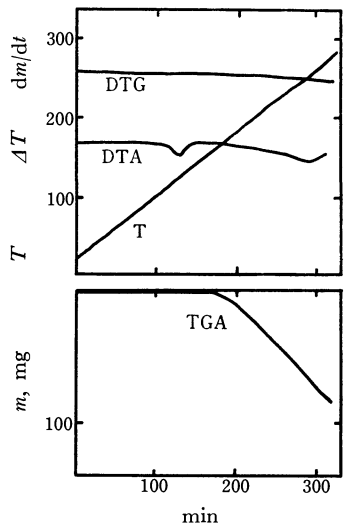

Fig. 1. Derivatogram for *trans*-$[CrBrH_2O(NH_3)_4]Br_2$.

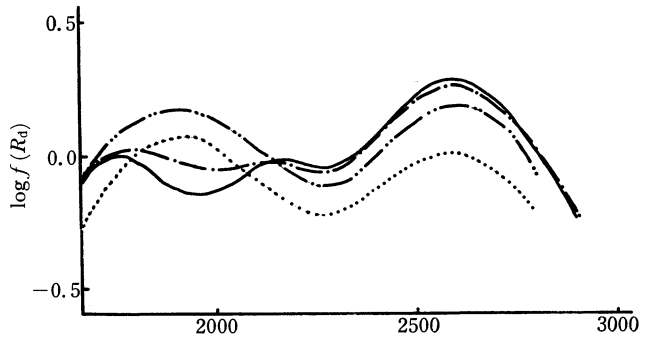

Fig. 2. Absorption spectra for *trans*-$[CrBrH_2O(NH_3)_4]Br_2$ (————), *cis*-$[CrBrH_2O(NH_3)_4]Br_2$ (·····), and the compounds obtained after heating at 143 (—·—·—) and 153°C (—··—··—).

1) H. E. LeMay, Jr., and J. C. Bailar, Jr., *J. Amer. Chem. Soc.*, **89**, 5577 (1967).

2) R. Tsuchiya, K. Murai, A. Uehara and E. Kyuno, This Bulletin, **43**, 1383 (1970).

3) D. W. Hoppenjans and J. B. Hunt, *Inorg. Chem.*, **8**, 505 (1969).

Effect of Crystal Size on the Radiolysis of Solid Succinic Acid

Tetsuo MIYAZAKI, Shigehiro OKADA, Terunobu WAKAYAMA, Kenji FUEKI and Zen-ichiro KURI

Department of Synthetic Chemistry, Faculty of Engineering, Nagoya University, Chikusa-ku, Nagoya

(Received March 14, 1970)

Recently we studied the radiolysis of hydrocarbons in the solid state and proposed that the formation of the exciton may play an important role in the radiolysis.[1,2] In the present work we have studied the radiolysis of crystalline succinic acid ($HOOCCH_2CH_2COOH$) at 77°K. The γ-irradiation of the acid was performed at 77°K in the form of a single crystal of 0.5—1.0 cm long or the powdered form. After irradiation, the sample was melted at 185°C, and then the gaseous products were analyzed as follows: the gaseous products (a mixture of CO and H_2) not condensable at the temperature of liquid nitrogen were analyzed by a gas burette connected to a Toepler pump and a cupric oxide furnace kept at 240°C, while another gaseuous product (CO_2) not condensable at the temperature of dry ice was measured by means of the gas burette alone.

The yield of $CO+H_2$ is plotted against the total dose in Fig. 1. The $G(CO+H_2)$ from the powder and the single crystal are about 0.5 and 0.1 respectively at a dose of 4.6×10^6 rad. There is no difference in the yield of CO_2 between the powder and the single crystal; in both cases it is about 1.9 G-unit. It should be noted that the $G(CO+H_2)$ from the powder is much higher than that from the single crystal. In order to examine whether the difference in $G(CO+H_2)$ can be attributed to the analytical procedure, the CO and H_2 were measured after the γ-irradiated sample had been dissolved in ethanol at room temperature without melting the sample at 185°C. The clear difference in $G(CO+H_2)$ between the powder and the single crystal was also observed in this case. In the radiolysis of succinic acid in the powdered form, the $G(CO)$ and $G(H_2)$ were about 0.4 and 0.1 respectively. Most of the CO and H_2 could be measured without melting the irradiated sample, while most of the CO_2 was not measurable until the sample had melted. The results indicate that CO and H_2 may be produced at the surface of the crystal and that $G(CO+H_2)$ may depend upon the surface area or the size of the crystal. It is conceivable that the mobile active entity formed by the γ-irradiation of the crystal migrates to its surface and produces CO and H_2.

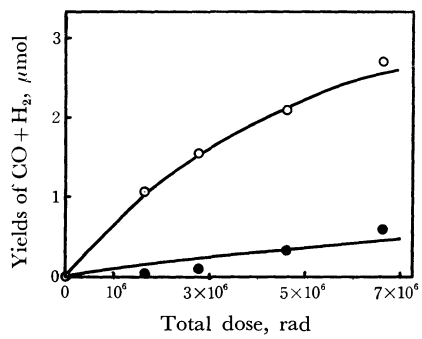

Fig. 1. Yields of $CO+H_2$ in the radiolysis of solid succinic at 77°K against the total dose.
dose rate: 3.0×10^5 rad/hr. Yields are expressed as 10^{-6} mol of products from 1 g of γ-irradiated succinic acid.
○: Yields from succinic acid in the powdered form.
●: Yields from succinic acid in the single crystal.

Since the effect of crystal size on the radiolysis has not been reported previously, it is not possible at present to discuss fully whether the mobile entity is a hole, an electron, or an exciton. It is expected, from an ESR study[3] of γ-irradiated succinic acid, that holes and electrons may be trapped in the crystal by the hydride-ion-transfer reaction and the electron-capture reaction:

$$HOOCCH_2CH_2COOH \rightsquigarrow HOOCCH_2CH_2COOH^+ + e^- \quad (1)$$

$$HOOCCH_2CH_2COOH^+ + HOOCCH_2CH_2COOH \longrightarrow HOOCCH_2CH_2COO\cdot + HOOCH_2CH_2COOH_2^+ \quad (2)$$

$$HOOCCH_2CH_2COO\cdot \longrightarrow HOOCCH_2CH_2\cdot + CO_2 \quad (3)$$

$$e^- + HOOCCH_2CH_2COOH \longrightarrow HOOCCH_2CH_2COOH^- \quad (4)$$

$$HOOCCH_2CH_2COOH^- \longrightarrow HOOCCH_2CH_3 + CO_2^- \quad (5)$$

Further studies of the effect of crystal size on the radiolysis are now in progress.

1) a) T. Wakayama, T. Miyazaki, K. Fueki and Z. Kuri, This Bulletin, **42**, 1164 (1969). b) T. Wakayama, T. Kimura, T. Miyazaki, K. Fueki and Z. Kuri, *ibid.*, **43**, 1017 (1970)

2) a) T. Miyazaki, T. Wakayama, K. Fueki and Z. Kuri, *ibid.*, **42**, 2086 (1969). b) T. Wakayama, T. Miyazaki, K. Fueki and Z. Kuri, *J. Phys. Chem.*, submitted for publication.

3) R. N. Schwartz, M. W. Hanna and B. L. Bales, *J. Chem. Phys.*, **51**, 4336 (1969).

Pure Quadrupole Resonance of Halogens in Sodium Tetrahaloaurate(III) Dihydrates and Sodium Tetrachloroiodate(III) Dihydrate[1)]

Akinobu SASANE, Takayo MATUO, Daiyu NAKAMURA and Masaji KUBO

Department of Chemistry, Nagoya University, Chikusa, Nagoya

(Received March 16, 1970)

The pure quadrupole resonance of chlorine in sodium tetrachloroaurate(III) dihydrate was observed between 77 and 400°K using a sample synthesized and identified by means of chemical analysis and X-ray powder technique. We could observe four resonance lines attributable to ^{35}Cl each showing no discontinuity in its temperature dependence. This indicates that four kinds of nonequivalent chlorine atoms exist in a crystal and that no phase transition takes place in this temperature range.

The lowest-frequency line of the quartet shows a positive temperature coefficient ($\Delta\nu/\Delta T=0.4$ and 2.5 kHz/deg at 77 and 400°K, respectively), whereas other lines have normal negative temperature coefficients in the whole range of temperature studied. Moreover, its line width is very broad and its frequency is much lower than that of other lines (25.356, 27.998, 28.867, and 29.466 MHz at 77°K).

Vaciago *et al.*[2)] have carried out X-ray analysis on this compound and found that it forms orthorhombic crystals with four formula units in a unit cell and that four chlorine atoms are crystallographically nonequivalent in a distorted square coordination in agreement with our observation of the quartet lines. In this complex ion, one chlorine atom (Cl_1) is separated from the nearest sodium ion by 4.37 Å, whereas three others are closer to sodium ions, the average distance being equal to 3.05 Å. The chlorine atom Cl_1 has four oxygen atoms at the shortest and the second shortest distances (3.36 and 3.42 Å), while other O–Cl distances are longer than 3.45 Å. The four oxygen atoms form a very flat, slightly distorted square pyramid along with the Cl_1 atom at the apex, the Au–Cl_1 axis pointing to the center of the square. Each oxygen atom has two chlorine atoms in its vicinity, *i. e.*, Cl_1 and Cl_1' belonging to different complex anions. The $\angle Cl_1$–O–Cl_1' angle (118°) is nearly equal to the valency angle of oxygen in a water molecule. Although hydrogen atoms are not located by the X-ray analysis, it is plausible that weak O–H···Cl_1 hydrogen bonds are formed in the crystal.

The positive temperature coefficient of the lowest-frequency line of the quartet can be interpreted in terms of hydrogen bond formation. To the first approximation, the quadrupole resonance frequency of a halogen is proportional to the number of unbalanced p electrons, $U_p=(N_x+N_y)/2-N_z$, where N_x, N_y, and N_z denote the number of electrons in the p_x, p_y, and p_z orbitals of the halogen atom, respectively. The origin of the coordinate system is taken at the halogen nucleus, the z axis being directed along the metal-ligand bond. When hydrogen bonds are formed, four O–H groups approximately lying on the x and y axes attract electrons from the p_x and p_z orbitals of the chlorine atom, leading to a decrease in the number of unbalanced p electrons. Accordingly, the lowest-frequency line is assigned unequivocally to Cl_1 atoms. As hydrogen bonds are weakened by thermal motion, N_x and N_y increase with increasing temperature and the resonance line shifts to a higher frequency. Because hydrogen atoms are present in the vicinity of Cl_1 atoms, the resonance line is broadened by nuclear spin-spin interaction as was observed experimentally.

We studied also the temperature dependence of the pure quadrupole resonance of ^{79}Br in sodium tetrabromoaurate(III) dihydrate ($\nu=201.70$, 217.66, 224.48, and 229.43 MHz at 77°K; $\Delta\nu/\Delta T=7$ and 18 kHz/deg at 77 and 270°K, respectively, for the lowest-frequency line) and ^{35}Cl in sodium tetrachloroiodate dihydrate[3)] ($\Delta\nu/\Delta T=0.5$ and 3.3 kHz/deg at 77 and 300°K, respectively) and found that the resonance pattern of these complexes bears a strong resemblance to that of sodium tetrachloroaurate(III) dihydrate. The crystal structures of these complexes were confirmed to be isomorphous with that of sodium tetrachloroaurate(III) dihydrate, the structural data being $a=13.29$, $b=7.28$, and $c=9.43$ Å for the former and 13.61, 7.14, and 9.24 Å for the latter.

1) Presented before the XII International Conference on Coordination Chemistry held in Sydney on August 20—27, 1969.

2) M. Bonamico, G. Dessy and A. Vaciago, *Atti Accad. Nazl. Lincei, Rend.*, **39**, 504 (1965).

3) C. D. Cornwell and R. S. Yamasaki, *J. Chem. Phys.*, **27**, 1060 (1957). Resonance frequencies observed at three different temperatures are tabulated therein.

Formation of Inclusion Compounds of β-Cyclodextrin with Hydroperoxides

Yoshihisa MATSUI, Haruki NARUSE, Kazuo MOCHIDA and Yoshio DATE

Department of Agricultural Chemistry, Shimane University, Nishikawazu-cho, Matsue

(Received March 16, 1970)

The degradation of starch by the action of *Bacillus macerans* amylase yields cyclic dextrins composed of six, seven, eight, or more α-D-glucopyranose units linked 1→4 as in amylose. They have void spaces in the molecules and enclose a number of organic compounds in it to form crystalline adducts.[1] We wish to report that various hydroperoxides are also enclosed by β-cyclodextrin (I), a cyclic dextrin with seven glucosyl residues, to form crystalline adducts.

When I (1.00 g) and *t*-butyl hydroperoxide (II) (0.50 g) were dissolved in 50 m*l* of warm water and the solution was cooled in ice water, a white precipitate was formed. On the other hand, no appreciable change occurred when D-glucose, instead of I, was dissolved in the aqueous solution of II. In the former case, the precipitate was separated from the solution by filtration, washed with cold water, dried under vacuum (2 mmHg) at room temperature, and weighed as 0.91 g. mp 215°C (decomp.). The resulting solid (III) contained 0.80 mmol/g of hydroperoxide residue, which was determined by the iodometric method.[2] The content of I in III was determined to be 0.74 mmol/g by the measurement of the optical rotation on the assumption that the specific rotation of I, determined to be +168° in water at room temperature (lit,[3] +162.5°), dose not change by the interaction with II. These results suggest that I and II form an inclusion complex with the mole-ratio of about 1 : 1.

It is interesting that II, which is fairly volatile (bp 4.5—5.0°C/2 mmHg[4]), did not evaporate even at room temperature under 2 mmHg as a result of the formation of the adduct, although at 56°C under 2 mmHg the hydroperoxide content of III decreased to 0.24 mmol/g. This indicates that II is fairly strongly bonded to I. It is considered[5] that the main forces binding the constituents of cyclodextrin complexes are hydrogen bonding, van der Waals forces, and hydrophobic interactions. In the present case, it seems that hydrogen bonding plays a major role, for hydroperoxides are known to have the strong ability of hydrogen bond. This is supported by the fact that no crystalline adduct was formed between I and *t*-butyl alcohol which has less strong ability of hydrogen bonding than II.

Hydroperoxides other than II, such as *n*-butyl, isoamyl, *t*-amyl, *s*-octyl, and cumene hydroperoxides, also formed the crystalline adducts with I. Primary and secondary hydroperoxides, as well as tertiary hydroperoxides, form the inclusion compounds of I with the mole-ratio of about 1 : 1. All the inclusion compounds studied can be dried without loss of hydroperoxides at room temperature under 2 mmHg. In the case of isoamyl, *t*-amyl, and cumene hydroperoxides vacuum drying even at 56°C caused no loss of hydroperoxides. Thus, I serves not only as a precipitant for hydroperoxides but also as a reagent making volatile hydroperoxides non-volatile by means of inclusion.

1) F. Cramer, "Einschlussverbindungen," Springer-Verlag, Heidelberg (1954).

2) E. W. Abrahamson and H. Linschitz, *Anal. Chem.*, **24**, 1355 (1952).

3) D. French, M. L. Levine, J. H. Pazur and E. Norberg, *J. Amer. Chem. Soc.*, **71**, 355 (1949).

4) N. A. Milas and D. M. Surgenor, *ibid.*, **68**, 205 (1946).

5) F. Cramer, W. Saenger and H.-Ch. Spatz, *ibid.*, **89**, 14 (1967).

Stabilization of Hydroperoxides by Means of the Formation of Inclusion Compounds with β-Cyclodextrin

Yoshihisa MATSUI, Haruki NARUSE, Kazuo MOCHIDA and Yoshio DATE

Department of Agricultural Chemistry, Shimane University, Nishikawazu-cho, Matsue

(Received March 16, 1970)

Cyclodextrins are known to stabilize a number of labile materials by means of inclusion.[1-3] We wish to report that hydroperoxides are also stabilized by the formation of inclusion compounds with β-cyclodextrin (I).

It is known[4] that *t*-butyl hydroperoxide (II) decomposes moderately at 95—100°C and explosively at 109°C. However, the crystalline adduct[5] (III) of I with II showed no change under these conditions. When the rate of the pyrolysis of II in III was measured at 160°C by means of the iodometric method, a moderate decrease of the hydroperoxide content was observed (Fig. 1). The crystalline adduct (IV) of I with *t*-amyl hydroperoxide decomposed more slowly than III at 160°C. Similarly, it was found that hydroperoxides such as *n*-butyl, isoamyl, *s*-octyl, and cumene hydroperoxides are stabilized by the formation of inclusion compound with I.

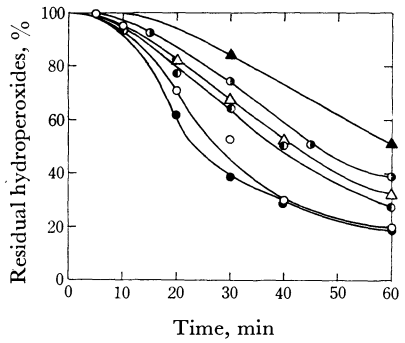

Fig. 1. Effect of I on the rate of the pyrolysis of hydroperoxides at 160°C.
△ III, ▲ IV, ○ II (0.11M) in H_2O,
◐ II (0.11M) + I (0.01M) in H_2O,
◑ II (0.11M) + I (0.02M) in H_2O,
● II (0.11M) + D-glucose (0.07M) in H_2O

The depression of pyrolysis of hydroperoxides by the interaction with I was also observed in an aqueous solution. As shown in Fig. 1, the rate of the pyrolysis of II (0.11M) in an aqueous solution was markedly decreased by the addition of 0.01M of I. The higher the concentration of I, the slower is the rate. However, the addition of D-glucose (0.07M) had no effect on the pyrolysis rate. These results clearly indicate that I stabilizes II by means of inclusion.

The stabilizing effect may be due to the formation of the strong hydrogen bonding between I and II.[5] The fact that the pyrolysis of II in an aqueous solution was depressed by the addition of I indicates that the hydrogen bond between I and II is stronger than that between I and water. It is also possible that the prevention of a chain mechanism in pyrolysis of hydroperoxides by means of inclusion may cause the stabilizing effect.[3]

1) F. Cramer, *Chem. Ber.*, **84**, 851 (1951).
2) H. Schlenk, D. M. Sand and J. A. Tillotson, *J. Amer. Chem. Soc.*, **77**, 3587 (1955).
3) J. L. Lach and T.-F. Chin, *J. Pharm. Sci.*, **53**, 924 (1964).
4) N. A. Milas and D. M. Surgenor, *J. Amer. Chem. Soc.*, **68**, 206 (1946).
5) Y. Matsui, H. Naruse, K. Mochida and Y. Date, This Bulletin, **43**, 1909 (1970).

Sulfurization of 1,3-Diphenylpropanetrione

Kōzō Inouye, Shigeru Sato and Masaki Ohta

Department of Chemistry, Faculty of Science, Tokyo Institute of Technology, Ookayama, Meguro-ku, Tokyo

(Received March 19, 1970)

During the course of synthesis of mesoionic 1,2-dithiole compounds, we attempted the sulfurization of 1,3-diphenylpropanetrione(I), expecting the formation of 1,3-dithion-2-one(II) which might be stabilized by the S–S bond formation to give mesoionic compound(V).

Treatment of a solution of I in chloroform-ethanol mixture (1 : 7) with hydrogen sulfide and hydrogen chloride afforded yellow crystalline salt (A) of mp 197—204°C (dec.) in 40% yield. The chloride is unstable and can not be purified by recrystallization. When the chloride was treated with a base such as triethylamine, pyridine, or sodium bicarbonate, chlorine-free brown crystals (B) ($C_{15}H_{10}OS_2$, mp 236—241°C, dec.) were obtained. IR (KBr): 1495 cm^{-1} (highly polarized carbonyl), 1490, 1480, 1435 cm^{-1} (aromatic 1,2-dithiolium ring).[1] UV: λ_{max}^{DMF} (log ε): 317 (3.78), 366 (3.62), 562 mμ (4.20). Mass spectrum : M^+, *m/e* 270. Compound B gave perchlorate (mp 232—233°C), picrate (mp 192—195°C) and acetylated perchlorate (mp 171—174°C) by acetyl perchlorate. Compound B was also obtained in poor yield when I was refluxed in toluene with phosphorus pentasulfide.

Recently, Schönberg[2] reported that the reaction of 1,1,3,3-tetrabromo-1,3-diphenylpropan-2-one with potassium xanthate yielded 1,3-diphenylpropane-1,3-dithion-2-one (II). The physical and chemical properties of compound B are almost the same as those of II. However, considering the reaction sequence of the formation of B from I, and its spectroscopic and chemical properties, B should be more appropriately expressed by mesoionic structure (or anhydro-3,5-diphenyl-4-hydroxy-1,2-dithiolium hydroxide (IV or V) rather than 1,3-dithion-2-one structure (II) as proposed by Schönberg.[2]

On the basis of the above observation, it may safely be concluded that the product A is 3,5-diphenyl-4-hydroxy-1,2-dithiolium chloride (III) and the deprotonated product B is mesoionic 1,2-dithiole compound (V).

$C_6H_5COCOCOC_6H_5$ I

$C_6H_5CSCOCSC_6H_5$ II

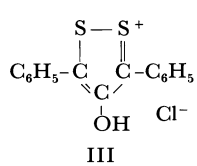

III

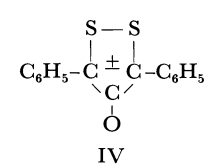

IV

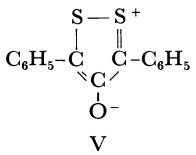

V

1) K. A. Jensen, H. R. Baccaro and O. Buchardt, *Acta Chem. Scand.*, **17**, 163 (1963).

2) A. Schönberg and E. Frese, *Tetrahedron Lett.*, **1969**, 4063.

Ethoxalylnitrene

Tadao SHINGAKI,* Masao INAGAKI,* Matsuji TAKEBAYASHI,* Rolf LEBKÜCHER** and Walter LWOWSKI**

* *Institute of Chemistry, College of General Education, Osaka University, Toyonaka, Osaka*

** *Research Center, New Mexico State University, Las Cruces, New Mexico 88001, U.S.A.*

(Received March 19, 1970)

Thermolysis of ethoxalyl azide (I) in ethanol gave quantitatively ethoxycarbonylurethane (III) *via* isocyanate (II),[1] the Curtius rearrangement product, whereas photolysis of I, with the light of a low-pressure mercury arc at −78°C, in a solution of dichloromethane with alcohols yielded *N*-alkoxyethoxalamides (IV) and ethoxalamide (V) in addition to the corresponding urethanes (III). Similarly, the photolysis of I with saturated hydrocarbons gave *N*-alkyl- or *N*-cycloalkyl ethoxalamides (VI), V and II under the same experimental condition (Table 1). The formation of IV, V and VI suggests that the reaction involves a carbonyl nitrene, ethoxalylnitrene (VII), as an intermediate in a similar manner to the cases of ethyl azidoformate[2] and pivaloyl azide.[3]

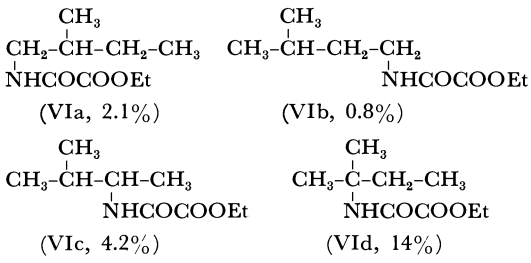

In the reaction with 2-methylbutane, the product (VI) was observed to be a mixture of four kinds of isomers (VIa—VId).

The relative reactivity of ethoxalylnitrene toward primary (1°), secondary (2°) and tertiary (3°) C–H bonds in 2-methylbutane is shown to be 1 : 6.6 (±10%) : 44 (±13%). The results indicate that the reactivity of ethoxalylnitrene is more selective than that of ethoxycarbonylnitrene[2] owing to the resonance stabilization (Table 2).

Table 2. Relative reactivities of carbonylnitrenes toward the C–H bonds in 2-methlbutane

Nitrene	1° :	2° :	3°
N·CO·COOEt	1 :	6.6(±10%) :	44(±13%)
N·COOEt	1 :	9(±10%) :	34(± 5%)
N·CO·C(CH$_3$)$_3$	1 :	8.6(±10%) :	160(±25%)

The mechanism of the insertion of ethoxalylnitrene into C–H bonds will be discussed elsewhere.

Table 1. Photolysis of ethoxalyl azide in dichloromethane

Substrate	Product (mol%)			
	OCN·COOEt (II)	RO·NH·CO·COOEt (IV)	R′·NH·CO·COOEt (VI)	H$_2$N·CO·COOEt (V)
Ethanol	45*	26	—	10
2-Propanol	45*	22	—	16
Cyclohexane	41	—	16	4
Cyclopentane	45	—	17	4
2-Methylbutane	47	—	21	9

* The yield of II shows that of urethanes derived from II.

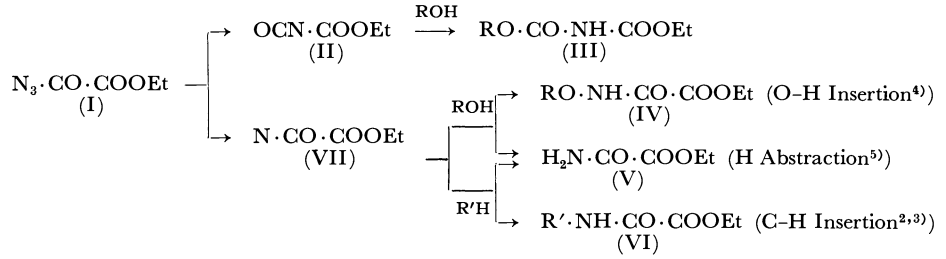

1) P. A. S. Smith, "Organic Reactions," Vol. 3, ed. by D. Adams, John Wiley & Sons, New York (1962), p. 337; "Molecular Rearrangements," Vol. 1, ed. by P. de Mayo, Interscience Publishers, New York (1963), p. 528.

2) W. Lwowski, *Angew. Chem.*, **79**, 922 (1967).

3) G. T. Tisue, S. Linke and W. Lwowski, *J. Amer. Chem. Soc.*, **89**, 6303 (1967).

4) W. Lwowski, R. A. DeMauriac, T. W. Mattingly, Jr., and E. Scheiffele, *Tetrahedron Lett.*, **1964**, 3285; R. Kreher and G. H. Bockhorn, *Angew. Chem.*, **76**, 681 (1964).

5) T. J. Prosser, A. F. Marcantonio and D. S. Breslow, *Tetrahedron Lett.*, **1964**, 2479; R. Puttner and K. Hafner, *ibid.*, **1964**, 3119.

"Reverse-oriented" Cycloaddition of Nitrone to Enamine

Yujiro NOMURA, Fumio FURUSAKI and Yoshito TAKEUCHI

Department of Chemistry, College of General Education, The University of Tokyo, Komaba, Meguro, Tokyo

(Received April 4, 1970)

In the preliminary communication[1] we showed that the reaction between benzylidenaniline *N*-oxide (diphenylnitrone) (Ia, Ar=C_6H_5) and 1-pyrrolidino-1-cyclohexene (II) gave the expected 5-pyrrolidino-isoxazolidine III.

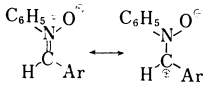

I

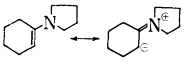

II

In the 1,3-dipolar cycloaddition between a nitrone and a monosubstituted olefin, the oxygen atom of the former generally attacks the substituted carbon atom of the olefin to give a "normal" cycloadduct, 5-substituted isoxazolidine. Thus, from 1-hexene,[2] styrene,[2] acrylonitrile,[3] or ethyl acrylate,[3] the expected normal cycloadducts are formed. If the other end of the olefinic double bond is overcrowded to a similar extent, the electronic effect will then become important; from ethyl crotonate or α,β-dimethylcrotonate, the "reverse-oriented" cycloadduct 4-ethoxycarbonylisoxazolidines are formed.[3] In such cases the reaction is under "electronic" control.

In the case of the reaction between a nitrone and an enamine, the normal cycloadduct formation is expected not only from the steric, but also from the electronic basis.

Here we report an unexpected "reverse-oriented" cycloaddition of nitrones to an enamine where no steric effect comparable to that in crotonates is involved. A dimethylformamide solution of Ib (Ar=*m*-$NO_2C_6H_4$) and 1-pyrrolidino-*cis*-3,5-dimethylcyclohexene (IV) was stirred at room temperature for 48 hr. After the removal of the solvent *in vacuo*, the residue was crystallized from ethanol to yield yellow crystals of 4-pyrrolidinoisoxazolidine Vb, mp 65—67°C, in 66% yield.

Found: C, 71.35; H, 7.60; N, 10.18%; mol wt (mass), 421. Calcd for $C_{25}H_{31}N_3O_3$: C, 71.23; H, 7.41; N, 9.97%; mol wt, 421.

The proton NMR spectrum (in $CDCl_3$) of Vb shows a sharp singlet at τ 5.60 (3-H) and a doublet at τ 6.33 (the angular 5-H, deshielded by the neighboring oxygen atom), in contrast with that of the normal cycloadduct III[1] where benzylic-H (3-H) appears at τ 5.40 as a doublet (coupled with the angular 4-H, J=*ca.* 10 Hz) and 4-H as a broad doublet centered at τ 7.35.

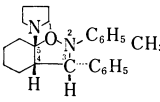

III

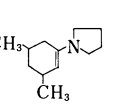

IV

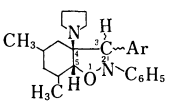

V

In a similar manner, from Ic(Ar=*p*-ClC_6H_4) and IV, 3-*p*-chlorophenyl-4-pyrrolidinoisoxazolidine Vc was obtained as colorless plates (from ethanol), mp 112—112.5°C, in 27% yield.

Found: C, 72.85; H, 7.50; N, 6.72%; mol wt (mass), 410. Calcd for $C_{25}H_{31}ClN_2O$: C, 73.01; H, 7.60; N, 6.82%; mol wt, 410.

It is well established that the electrophilic reagent attacking the β-carbon atom of cyclohexanone enamines can approach only from the direction to form the axial bond because of the large allyl strain (Johnson strain) in the enamine (or in its immonium structure).[4] Assuming that the reaction between a nitrone and an enamine is one-step concerted type,[5] and that no ring inversion is involved during the cycloaddition as we confirmed,[6] the structure of the hypothetical normal cycloadduct between I and IV would be VI. Apparently there is in VI a severe non-bonded interaction between C-aryl and one of the methyl groups. Since this interaction should be even greater in the transition state, VI is kinetically as well as thermodynamically less favorable than the reverse-oriented VII (=V) which is free from this type of interaction.

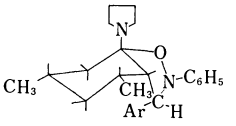

VI

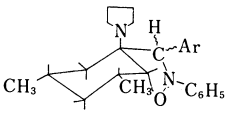

VII

This unexpected formation of reverse-oriented cycloadduct gives, in turn, a support for the stereochemistry of nitrone-enamine reaction.[6]

1) Y. Nomura, F. Furusaki and Y. Takeuchi, This Bulletin, **40**, 1740 (1967).

2) R. Huisgen, R. Grashey, H. Hauck and H. Seidl, *Chem. Ber.*, **101**, 2043, 2548 (1968).

3) R. Huisgen, H. Hauck, R. Grashey and H. Seidl, *ibid.*, **101**, 2568 (1968).

4) F. Johnson, *Chem. Rev.*, **68**, 375 (1968).

5) R. Huisgen, *J. Org. Chem.*, **33**, 2291 (1968).

6) Y. Nomura, F. Furusaki and Y. Takeuchi, unpublished studies.

Observation of Dynamic Nuclear Polarization in the Reaction of *N,N*-Dimethylaniline Oxide with Acetic Anhydride

Hiizu IWAMURA, Michiko IWAMURA,*1 Toshiaki NISHIDA*2 and Iwao MIURA*2

Department of Chemistry, Faculty of Science, The University of Tokyo, Bunkyo-ku, Tokyo

(Received March 25, 1970)

The mechanism of the reaction of *N,N*-dimethylaniline oxide (I) with acetic anhydride has been a subject of controversy.[1] Although the free radical pair mechanism seems to have been concluded by an ellegant ^{18}O-labelling experiment,[2] recent findings that 3,3-sigmatropic shift predominates in scrambling the oxygen atoms of acetyl peroxide,[3] and that even 1,3-sigmatropic rearrangement is operative in heteroatomic systems[4] prompted the present authors to reconsider these mechanistic possibilities[5] for the reaction of I to give *o*-acetoxy-*N,N*-dimethylaniline (II). A method of detecting the chemically induced dynamic nuclear polarization (CIDNP)[6] in the NMR spectrum of the reaction mixture has been employed as an operational test.

In a typical run, 32 mg of I was dissolved in a solution of 58 mg of acetic anhydride in 0.5 m*l* of benzene. The NMR trace obtained on a Varian HA 100 D spectrometer at 60 sec after mixing is reproduced in Fig. 1. In the course of the reaction which could be followed by decrease of the *N*-methyl signal at 341 Hz of I and was completed in 30 min at room temperature, a strong emission of radiation was observed at 258 Hz which decayed as shown in Fig. 2. Peaks at 196, 251 and 280 Hz increased exponentially with the progress of the reaction. It was found by comparison with the spectra in benzene of the authentic samples that the origin of the emitting line was the *N*-methyl protons of *N,N*-dimethylaniline (III) formed in 5% yield. Similarly the absorption peaks were unambiguously assigned to the methyl protons of II and *N*-methylacetanilide. Under no circumstances was observed any sign of either emission or enhanced absorption for these signals of the main reaction products. Thus the evidence is not in favor of the intermediacy of the free radical pair for the formation of II.[2] It might be argued that in the intimate radical pair in the solvent cage the singlet spin correlation between the two fragments will be kept throughout the rearrangement and there will be no chance of dynamic nuclear polarization. Mechanistically, however, the situation is indistinguishable from, and had better be described as, 1,3- and 3,3-sigmatropic rearrangements.

On the other hand, it was confirmed by the observation of CIDNP that III is indeed formed by a free radical reaction[7] and is independent of the rearrangement to give II.

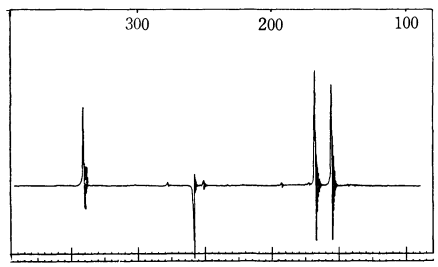

Fig. 1. The NMR spectrum of a mixture of I and acetic anhydride in benzene.

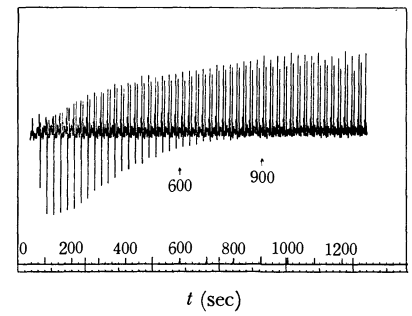

Fig. 2. Plot of signal intensities *vs.* time. The upper envelopes represent the formation of II and *N*-methylacetanilide, while the lower one demonstrates the CIDNP in III.

*1 Department of Chemistry, Faculty of Science, Toho University, Narashino-shi. J.

*2 Nippon Electric Varian, Ltd., 3-13 Azabu Iigura-machi, Minato-ku, Tokyo.

1) H. J. Shine, "Aromatic Rearrangements," Elsevier Publishing Co., New York, N. Y. (1967), p. 284.

2) S. Oae, T. Kitao and Y. Kitaoka, *J. Amer. Chem. Soc.*, **84**, 3366 (1962).

3) M. J. Goldstein and H. A. Judson, *ibid.*, in press. (1970); J. W. Taylor and J. C. Martin, *ibid.*, **89**, 6904 (1967).

4) M. J. Goldstein and H. A. Judson, *ibid.*, in press. (1970); J. C. Martin and J. H. Hargis, *ibid.*, **91**, 5399 (1969).

5) R. Huisgen, F. Bayerlein and W. Heydkarp, *Chem. Ber.*, **92**, 3223 (1959).

6) H. Fischer and J. Bargon, *Accounts Chem. Res.*, **2**, 110 (1969); J. E. Baldwin and J. E. Brown, *J. Amer. Chem. Soc.*, **91**, 3647 (1969); A. R. Lepley, *ibid.*, **91**, 748, 749, 1237 (1969); D. G. Morris, *Chem. Commun.*, **1969**, 1345; S. F. Nelsen, R. B. Metzler and M. Iwamura, *J. Amer. Chem. Soc.*, **91**, 5103 (1969).

7) V. Boekelheide and D. L. Harrington, *Chem. Ind.* (London), **1955**, 1423.

The Absolute Configuration of the Tris-*l*-propylenediaminecopper(II) Ion, $(-)_{589}$-$[Cu(l\text{-}pn)_3]^{2+}$

Tosaku OKAMOTO, Keiji MATSUMOTO and Hisao KUROYA

Department of Chemistry, Faculty of Science, Osaka City University, Sumiyoshi-ku, Osaka

(Received April, 1, 1970)

Few investigations have been made of the absolute configurations of metal complexes other than those of cobalt(III). Fortunately, we have succeeded in preparing a copper(II) complex, $(-)_{589}$-$[Cu(l\text{-}pn)_3]Br_2\cdot 2H_2O$,*1 and in determining its crystal structure. We wish here to report on its conformational features and on the absolute configuration of the complex cation.

Crystal data: monoclinic, space group $P2_1$; $a=10.71$, $b=8.93$, $c=10.88$ Å, $\beta=107.2°$; $Z=2$, $D_c=1.56$, $D_m=1.56$ g·cm^{-3}, $\mu=66.9$ cm^{-1} (for Cu$K\alpha$). The intensity data were recorded on multiple-film, equi-inclination Weissenberg photographs taken about the *a*- and *b*-axes; they were visually estimated. Absorption corrections were applied. The determination of the crystal structure was carried out by means of the three-dimensional Fourier techniques. The least-squares refinement led to the *R* value of 0.102 for 1437 reflections. In deciding the absolute configuration of the $(-)_{589}$-$[Cu(l\text{-}pn)_3]^{2+}$ ion, that of *l*-propylenediamine was cautiously referred to.

Figure 1 shows a perspective of the complex ion, viewed along the *b*-axis, the ion has an approximately three-fold axis. The *l*-propylenediamine molecules are linked to the Cu(II) atom in the "*lel*" form, every C–CH_3 bond lying in an approximately equatorial plane of the five-membered ring, as is the case with $(-)_{589}$-$[Co(l\text{-}pn)_3]^{3+}$ [1] and

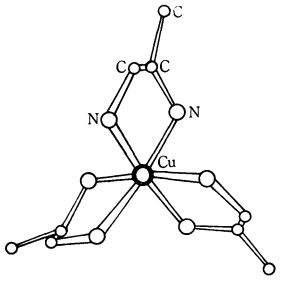

Fig. 1. A perspective of the complex ion viewed along the *b* axis.

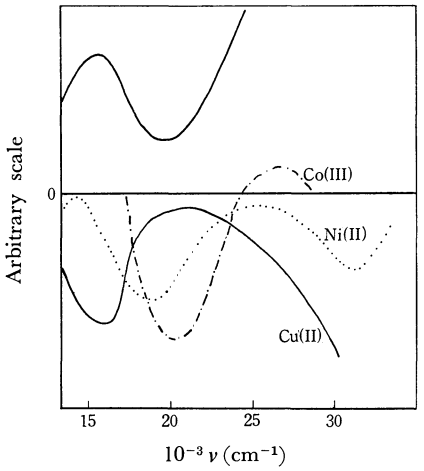

Fig. 2. The CD Spectra of tris-*l*-propylenediamine complexes and the absorption spectrum—of $(-)_{589}$-$[Cu(l\text{-}pn)_3]^{2+}$

trans-$[CoCl_2(l\text{-}pn)_2]^+$ [2]; the absolute configuration of $(-)_{589}$-$[Cu(l\text{-}pn)_3]^{2+}$ can be denoted as $\Delta(\lambda\lambda\lambda)$. The average value of the longer two of the Co–N bond lengths is 2.31 Å, and that of the other four, 2.09 Å. All the bond distances and angles within the N–C–C–N skeleton of the *l*-propylenediamine are quite normal.

Figure 2 depicts the CD curves of the tris-*l*-propylenediamine complexes of Co(III), Cu(II),*2 and Ni(II)*3 as well as the absorption spectrum of the Cu(II) complex.*2 In the first absorption-band region, a large negative CD peak can be seen for each of these three complexes; two of these have been confirmed to have the same absolute configuration. So far as this fact is concerned, it may be presumed that complexes of the same absolute configuration possess CD peaks of the same sign in the first band region, regardless of the kind of central metal atom.

*1 *l*-pn=*l*-propylenediamine.

1) H. Iwasaki and Y. Saito, This Bulletin, **39**, 92 (1966).

2) Y. Saito and H. Iwasaki, *ibid.*, **35**, 1131 (1962).

*2 The CD curve and the absorption spectrum of $(-)_{589}$-$[Cu(l\text{-}pn)_3]^{2+}$ in the bromide crystals were obtained by the present authors, but qualitatively.

*3 The CD curve of $(-)_{589}$-$[Ni(l\text{-}pn)_3]^{2+}$ was measured in a solution of its perchlorate. Crystal structure analysis of the complex is now in progress.

The Glassy Crystalline State —A Non-Equilibrium State of Plastic Crystals

Keiichiro ADACHI, Hiroshi SUGA and Syûzô SEKI

Department of Chemistry, Faculty of Science, Osaka University, Toyonaka, Osaka

(Received April 6, 1970)

In a previous paper,[1] we reported that the supercooled crystal-I (plastic crystal) of cyclohexanol showed in its heat capacity curve an anomalous jump resembling that associated with ordinary glass transition. From heat capacity data we establsihed the existence of the residual entropy for this supercooled plastic crystalline phase and also found the relaxation effect at this anomalous region. Based upon these findings we have proposed a new term "**Glassy Crystal**" for this supercooled non-equilibrium state. In the present paper we should like to report several new examples of the glassy crystal found by using differential thermal analysis method. They are 2,3-dimethylbutane, cycloheptanol, cycloheptatriene, cycloheptane, cycloheptene, cyclohexene and cyclopentanol. Among them, 2,3-dimethylbutane and cycloheptanol have been investigated in detail by measuring their heat capacities, the results of which will be reported elsewhere.

Cycloheptatriene was synthesized by photochemical reaction of benzene with diazomethane. Its purification was carried out by fractional and vacuum distillation. Cycloheptane was prepared by the catalytic hydrogenation of cycloheptatriene with use of Raney nickel. Cycloheptene was synthesized by dehydration of cycloheptanol. Cyclopentanol was obtained from the Tokyo Kasei Co. LTD. Cyclohexene was obtained from the Nakarai Chemicals LTD. Both cyclopentanol and cyclohexene were purified by means of vacuum distillation. The apparatus employed was reported previously.[2] The specimens were transferred by vacuum distillation in the sample containers. The results are shown in the figure. Measurements were performed with heating rate about 1°K min^{-1} after the plastic phases of the specimens had been supercooled down to 77°K with cooling rate of about 3°K sec^{-1}. In the cases of cycloheptatriene and cycloheptane, direct irreversible transition was observed from the supercooled plastic crystalline phase to the most stable crystalline phase just above the glass transition temperature. Cyclopentanol and cyclohexene, however, transform irreversibly and indirectly to the most stable low temperature phase by passing through the intermediate metastable crystalline states. This phenomenon may be explained by the so-called Ostwalrd's step rule. The measurements of the heat capacities of cyclohexanol, 2,3-dimethylbutane and cycloheptanol also show a similar behavior.

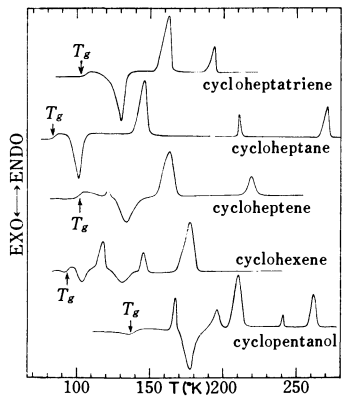

D.T.A. curves of quenched plastic crystals

TABLE

Sample	T_g (°K)	T_t (°K)	T_g/T_t
Cycloheptatriene	106	153	0.69
Cycloheptane	84	135	0.61
Cycloheptene	100	153	0.65
Cyclohexene	92	140	0.65
Cycloheptanol	135	258	0.52
Cyclohexanol	150	265	0.57
Cyclopentanol	138	201	0.69
2,3-Dimethylbutane	76	136	0.55
cis-1,2-Dimethyl-cyclohexane[3]	94	173	0.54

All the glass transition points of glassy crystals known hitherto are listed in the accompanying table where the values of the ratio of T_g to T_t (transition point from the low-temperature phase to the plastic crystalline phase) are also given. It is found that the ratio has the value 0.5—0.7 and this fact corresponds to the empirical rule known for the ordinary glass where the ratio of T_g to T_m (melting point) amounts to 0.5—0.7.

1) K. Adachi, H. Suga and S. Seki, This Bulletin, **41**, 1073 (1968).

2) H. Suga, H. Chihara and S. Seki, *Nippon Kagaku Zasshi*, **82**, 24 (1961).

3) H. M. Huffman, S. S. Todd and G. D. Oliver, *J. Amer. Chem. Soc.*, **71**, 584 (1949).

A New Synthesis of Thiophenes

Masaaki TAKAKU, Yosio HAYASI and Hitosi NOZAKI*1

Department of Industrial Chemistry, Kyoto University, Kyoto

(Received April 13, 1970)

A new route to thiophenes from 2-thiocarbonylenamines and α-bromocarbonyl compounds was reported recently.[1] In an exploration of the reactions of readily available monothio-β-diketones,[2] we eventually found an analogous way to thiophenes as outlined below. This seems to be easier and more versatile than the published methods. Physical data of products obtained (III—V) are listed in Table 1.

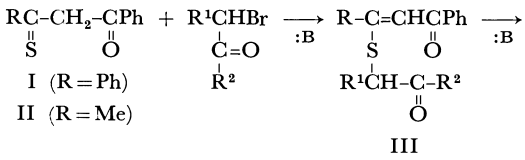

I (R=Ph)
II (R=Me)

III

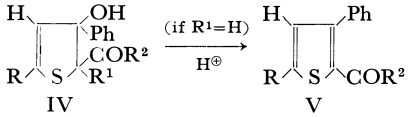

IV V

a: R=Ph, R^1=H, R^2=Ph
b: R=Ph, R^1=H, R^2=OEt
c: R=Ph, R^1=Ph, R^2=OEt
d: R=Me, R^1=H, R^2=Ph

A mixture of α-(thiobenzoyl)acetophenone (I, 5.0 mmol) and phenacyl bromide (5.0 mmol) dissolved in benzene (30 m*l*) was treated with triethylamine (15.0 mmol) at room temperature for 1 hr. Addition of water followed by extraction with benzene gave IVa in a quantitative yield. A solution of IVa (1.40 mmol) and concentrated hydrochloric acid (0.5 m*l*) in methanol (50 m*l*) was heated to reflux for 30 min and extracted with benzene to afford Va quantitatively. An S-alkylated compound IIIb (70%) was isolated in the reaction of I with ethyl bromoacetate under the same condition. In contrast, however, the use of sodium hydride (10.0 mmol) suspended in benzene (50 m*l*) in place of triethylamine yielded a cyclization product IVb (50%), whose treatment with hydrochloric acid gave Vb quantitatively.

S-alkylated products IIIc and IIId were isolated also in triethylamine-treatment of a mixture of I and ethyl α-bromophenylacetate and that of α-(thioacetyl)acetophenone (II) and phenacyl bromide in 55% and 54% yield, respectively. These are easily cyclized by more basic reagents. Treatment of IIIc (1.25 mmol) with sodium ethoxide (4.4 mmol) in ethanol (50 m*l*) at room temperature for 3 hr gave a dihydrothiophene IVc (42%), whereas that of IIId (5.0 mmol) with sodium hydroxide (10.0 mmol) in water (2.0 m*l*) and ethanol (50 m*l*) mixture yielded a thiophene Vd (60%).

The IR spectra of IIIb, IIIc and IIId showed characteristic two bands at *ca.* 1640 and 1530 cm^{-1}, which would reasonably be ascribed to the mesomeric group 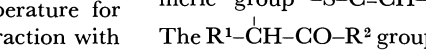 . The R^1–CH–CO–R^2 group exhibited normal absorption.

TABLE 1. MPS AND SPECTRAL PROPERTIES OF NEW COMPOUNDS[a]

Compd	Mp °C	IR[b] cm^{-1}	NMR δ ppm from TMS in $CDCl_3$
IVa	148—150	3450, 1688	5.08[c] (s, 1H), 5.40 (s, 1H), 6.15 (s, 1H), 7.2—7.8 (m, 15H)
Va	96.5—98	1634	7.1—7.8 (m)
IIIb	96—98	1738, 1635, 1532	1.17 (t, 3H), 3.26 (s, 2H), 4.02 (q, 2H), 7.11 (s, 1H), 7.3—7.6 (m, 8H), 7.9—8.2 (m, 2H)
IVb	130—132	3445, 1726	1.25 (t, 3H), 3.95[c] (s, 1H), 4.21 (q, 2H), 4.75 (s, 1H), 6.01 (s, 1H), 7.2—7.7 (m, 10H)
Vb	71—73	1708	1.26 (t, 3H), 4.25 (q, 2H), 7.2—7.8 (m, 11H)
IIIc	73—76	1733, 1634, 1530	1.09 (t, 3H), 3.95 (q, 2H), 4.65 (s, 1H), 7.03 (s, 1H), 7.2—8.1 (m, 15H)
IVc	116—118	3445, 1706	1.33 (t, 3H), 4.36[c] (broad s, 1H), 4.41 (q, 2H), 6.53 (s, 1H), 7.2—7.8 (m, 15H)
IIId	139—141	1690, 1622, 1524	2.42 (d,[d] 3H), 4.27 (s, 2H), 6.99 (q,[d] 1H), 7.3—8.1 (m, 10H)
Vd	68.5—69	1623	2.56 (d,[d] 3H), 6.92 (q,[d] 1H), 7.0—7.7 (m, 10H)

a) All gave correct analytical data. b) Taken in KBr tablets.
c) Signal disappears on treatment with D_2O. d) J=1.0 Hz.

*1 To whom all inquiries should be addressed.

1) a) E. J. Smutny, *J. Amer. Chem. Soc.*, **91**, 208 (1969); b) S. Rajappa and B. G. Advani, *Tetrahedron Lett.*, **1969**, 5067.

2) a) S. H. H. Chaston, S. E. Livingstone, T. N. Lockyer, V. A. Pickles and J. S. Shannon, *Aust. J. Chem.*, **18**, 673 (1965); b) E. Uhlemann and Ph. Thomas, *J. Prakt. Chem.*, **34**, 180 (1966).

Thermal Decomposition of Dibenziodolium Halides. Evidence for a Homolytic Pathway[1]

Takeo SATO, Shigeru SHIMADA, Kuniaki SHIMIZU and Kazuo HATA

Department of Chemistry, Faculty of Science, Tokyo Metropolitan University, Setagaya-ku, Tokyo

(Received April 16, 1970)

The thermal decomposition of dibenziodolium iodides, such as **1**/I;*1 is an efficient way of preparing 2,2′-diiodobiphenyls.[2,3] Recently, Heaney and Lees[4] reported that the thermal decomposition of dibenziodolium chloride (**1**/Cl) gave 2-chloro-2′-iodobiphenyl as the sole product. We obtained, however, conflicting results which led us to examine a series of dibenziodolium halides (**1**) in details. We here present our findings which are in accord with a radical mechanism.

Contrary to the former report by Heaney and Lees[4] the decomposition of **1**/Cl[5] at 295°C was found to produce a mixture of five halogenobiphenyls as analysed by gas chromatography using XE-60 silicone gum rubber on Chromosorb W column. They were 2-chloro-, 2,2′-dichloro-, 2-iodo-, 2-chloro-2′-iodo-, and 2,2′-diiodobiphenyls (in the order of the retention time), among which three dihalogenobiphenyls constituted major portions (Table 1). The decomposition of bromide **1**/Br occurring at 290°C again afforded five halogenobiphenyls as shown in Table 1.

Iodide **1**/I decomposed at a lower temperature of 210°C producing 98% of 2,2′-diiodobiphenyl and 2% of 2-iodobiphenyl, the ratio of which varied markedly when the reaction was performed in solvents. For example, 2-iodo- and 2,2′-diiodobiphenyls were formed in a ratio of 1 : 2 when **1**/I was heated in triethylene glycol at 240—245°C. A small amount of biphenyl was also produced. The decomposition of **1**/Cl and **1**/Br in the same solvent gave 2-iodobiphenyl even in higher yields, 77 and 60% respectively.

TABLE 1. DIHALOGENOBIPHENYLS FROM DIBENZIODOLIUM HALIDES (**1**)[a]

X	Temp. °C	Product ratio, % 2,2′-Di-X	2-X-2′-I	2,2′-Di-I	Total biphenyl yield, %
Cl	295	4	74	22	55[b]
Br	290	10	76	14	72[c]
I	210		98		84[d]

a) Reactions were carried out for 30 min in nitrogen. b, c, d) In addition, small amounts of 2-chloro-,[b] -bromo-,[c] and -iodobiphenyls[b,c,d] were detected.

Need for high temperatures and the formation of disproportionation and hydrogen transfer products suggest that these decomposition reactions are best interpreted as a radical mechanism. Increasing temperatures for decomposition as going from **1**/I to **1**/Cl seem to reflect increasing bond energies of halogen-iodine bondings. The main route of the reaction leading to 2-halogeno-2′-iodobiphenyl as well as 2-iodobiphenyl is explained in the following way.

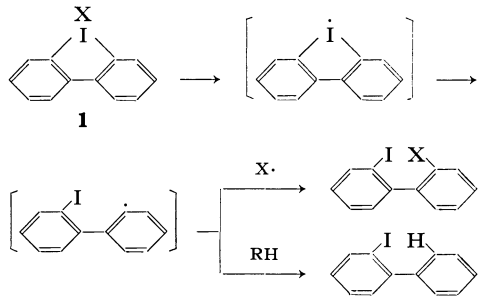

To account for the formation of dichloro-, dibromo-, and diiodobiphenyls one must postulate the cleavage of both of the carbon-iodine bonds as a minor process.[6,7] Such a cleavage was further indicated by the reaction of **1**/I in dimethyl acetylenedicarboxylate, which afforded the expected adduct, dimethyl 9,10-phenanthrenedicarboxylate, mp 127—128°C,[8] as one of the products.

1) Photo-Aryl Coupling and Related Reactions. V.

*1 Abbreviation of compound **1** where X=I.

2) D. F. Banks, *Chem. Rev.*, **66**, 243 (1966).

3) H. Irving and R. W. Reid, *J. Chem. Soc.*, **1960**, 2078; R. B. Sandin, *J. Org. Chem.*, **34**, 456 (1969) and references cited therein.

4) H. Heaney and P. Lees, *Tetrahedron* **24**, 3717 (1968).

5) J. Collette, D. Mcgreer, R. Crawford, F. Chubb, and R. B. Sandin, *J. Amer. Chem. Soc.*, **78**, 3819 (1956).

6) Existence of a biphenylyl biradical was implied by the electron impact of biphenylene [L. Friedman and D. F. Lindon, *J. Amer. Chem. Soc.*, **90**, 2324 (1968)].

7) No biphenylene formation was observed possibly due to rapid and efficient trapping of the intermediate with halogen atoms.

8) A. Jeanes and R. Adams, *J. Amer. Chem. Soc.*, **59**, 2608 (1937).

Selective *cis* Hydrogenation of *o*-Xylene and 1,2-Dimethylcyclohexene over Osmium and Iridium Catalysts

Shigeo NISHIMURA, Fuminobu MOCHIZUKI and Shigenori KOBAYAKAWA

Department of Industrial Chemistry, Tokyo University of Agriculture and Technology, Koganei-shi, Tokyo

(Received April 18, 1970)

Detailed studies by Siegel and his coworkers[1] on the stereochemistry of hydrogenation of isomeric xylenes and their tetrahydro derivatives indicated that a considerable amount of *trans* isomer was contained in the products from hydrogenation of isomeric xylenes with Adams platinum catalyst and also that desorption of the tetrahydro derivatives from the catalyst surface would be responsible for the formation of the *trans* isomer. Actually, the presence of such desorbed intermediates in the hydrogenation products has later been observed by Hartog and Zwietering[2] with nickel, rhodium and ruthenium catalysts and also by Siegel *et al.*[3] with platinum and rhodium catalysts.

The *trans* isomer was also formed in a considerable amount (18.2% at 25°C under 1 atm in acetic acid) in the platinum-catalyzed hydrogenation of 1,2-dimethylcyclohexene[4] which is expected to yield only *cis*-1,2-dimethylcyclohexane by simple *cis* addition of hydrogen.

In the study of the stereochemistry of hydrogenation of *o*-xylene and its tetrahydro derivatives with other platinum metals, it has been found that hydrogenation of *o*-xylene and 1,2-dimethylcyclohexene with osmium and iridium catalysts yield *cis*-1,2-dimethylcyclohexane with high stereospecificity. Thus, formation of the *trans* isomer was only 3.2 and 1.4% when *o*-xylene was hydrogenated over osmium and iridium catalysts in isopropyl alcohol at 25°C under one atmosphere of hydrogen.[5] The *trans* isomer was formed even in a smaller amount in the hydrogenation of 1,2-dimethylcyclohexene (1.9 and 1.3% in isopropyl alcohol and 1.4 and 1.1% in *t*-butyl alcohol, respectively with osmium and iridium metals). It is to be noted that formation of the *trans* isomer (15.0 and 17.6%) in hydrogenation of 2,3-dimethylcyclohexene with osmium and iridium catalysts as much as with the other platinum metals. Hydrogenation of *m*- and *p*-xylene with osmium and iridium catalysts also gave the *trans* isomer in a much smaller amount than with other platinum metals (9.6 and 10.3% for *m*-xylene; 18.3 and 11.1% for *p*-xylene), although the hydrogenation was less stereospecific than in the case of *o*-xylene.

The selective-formation of *cis*-1,2-dimethylcyclohexane from *o*-xylene may be explained either by selective formation of 1,2-dimethylcyclohexene as the intermediate or by only slight desorption of the intermediate 2,3-dimethylcyclohexene from the catalyst surface. The maximum amounts of 1,2- and 2,3-dimethylcyclohexene in the reaction mixture during the course of the hydrogenation over iridium were only 0.3 and 0.02%, respectively.[6] Only a slight extent of the desorption of 2,3-dimethylcyclohexene formed on the catalyst surface will explain the selective formation of *cis* isomer. The results seem to indicate that the *cis* addition of hydrogen to unsaturated hydrocarbons during a single period of residence on the catalyst surface may largely occur over osmium and iridium catalysts.[7]

The catalyst metals used in this study were prepared by the reduction of corresponding metal hydroxides (Ru, Rh, Ir) or metal oxides (Os) in water followed by a thorough washing with distilled water.

---

1) For references, see S. Siegel, *Advan. Catal.*, **16**, 123 (1966).

2) F. Hartog and P. Zwietering, *J. Catal.*, **2**, 79 (1963).

3) S. Siegel, V. Ku and W. Halpern, *ibid*, **2**, 348 (1963); S. Siegel and V. Ku, Proc. 3rd Intern. Congr. Catalysis, North-Holland Publishing Company, Amsterdam (1965), p. 1199.

4) S. Siegel and G. V. Smith, *J. Amer. Chem. Soc.*, **82**, 6082 (1960).

5) Yamamoto *et al.* reported that ruthenium gave the least amount of *trans* isomer in the vapor phase hydrogenation of *o*- and *p*-xylene with Group VIII metal catalysts other than osmium [(*Chem. Pharm Bull.* (Tokyo), **15**, 752 (1967)].

6) The maximum amounts of 1,2- and 2,3-dimethylcyclohexene in hydrogenation of *o*-xylene were 3.9 and 1.0% over ruthenium catalyst and 0.84 and 0.18% over rhodium catalyst. *Cf.* Refs. 2 and 3.

7) It was reported that only 2% of *trans*-decalin was formed in deuteration of $\Delta^{9,10}$-octalin with an iridium-carbon catalyst at 25°C under 360 to 400 psig deuterium, while hydrogenation of tetralin with the same catalyst gave 7.5% of *trans*-decalin at 25°C under 1000 psig hydrogen [A. W. Weitkamp, *Advan. Catal.*, **18**, 1 (1968)].

The Reaction of 8-Cyanoheptafulvene with Benzyne

Masaji ODA and Yoshio KITAHARA

Department of Chemistry, Faculty of Science, Tohoku University, Sendai

(Received April 25, 1970)

Heptafulvene and 8-monosubstituted heptafulvenes[1-3] undergo 8+2 cycloadditions when dimethyl acetylenedicarboxylate is used as a dienophile leading to azulene derivatives. We wish now to report a similar cycloaddition of 8-cyanoheptafulvene (I) using benzyne.

The refluxing of (I) and benzenediazonium-2-carboxylate[4] (1.2 equiv.) in methylene chloride for 70 min yielded a 1 : 1 addition product (II) in a 36% yield (based on 22% recovered I) on separation by silica-gel chromatography. Although the stereochemistry at C-3 is not yet certain, the sturcture was proved to be a 1,8-cycloaddition product, 1,2-benzo-3-cyano-3,9-dihydroazulene, from the following spectral and chemical evidence; *m/e* 205(M^+); ν_{max} (film) 3050 (w), 3020 (w), 2250 (w), 1610 (w), 750 (s) and 715 (s) cm^{-1}; λ_{max} (cyclohexane)251 (sh, log ε 3.75), 258 (3.80) and 265 nm (sh, 3.76); τ (CCl_4, TMS) 2.50—2.90 (m, 4H, aromatic), 3.38 (m, 3H, H-4~6), 3.85 (m, 1H, H-7), 4.87 (dd, J=9.5 and 4.0 Hz, 1H, H-8), 4.98 (br. s., 1H, H-3) and 6.41 (br., 1H, H-9). On dehydrogenation with *o*-chloranil (refluxing benzene, 15 min), II gave

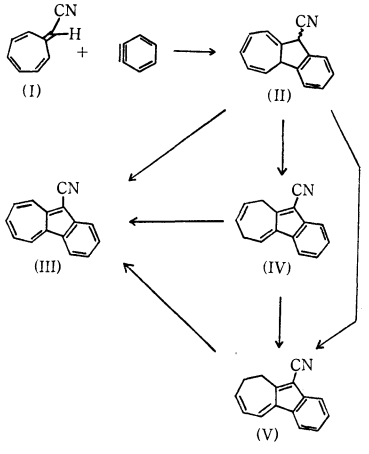

1,2-benzo-3-cyanoazulene[5] (III), (mp 153—154°C) in a 63% yield.

Compound II is liable to be isomerized to more conjugated systems by the presence of an active hydrogen at C-3. Therefore, on delayed elution from a silica-gel column, II suffered double-bond migration to give mainly 1,2-benzo-3-cyano-4,7-dihydroazulene (IV) as yellow prisms; mp 88—89°C; ν_{max} (KBr), 3040 (w), 2225 (m), 1629 (m) 1603 (w), 1557 (w), 762 (s) 733 (m) and 710 (m) cm^{-1}; λ_{max} (EtOH) 267 (log ε 4.30), 328 (3.71) and 372 nm (sh 3.45); τ (CCl_4, TMS) 2.50—3.00 (m, 5H, aromatic and H-8), 4.06 (m, 2H, H-5 and H-6), 6.51 (d-like, 4.0 Hz, 2H, H-4a and 4b) and 6.85 (t-like, 2H, H-7a and 7b). The IR and NMR spectra indicate the presence of a conjugated cyano group, an isolated double bond (from the chemical shifts and the pattern of the signals), and two kinds of doubly-allylic methylene groups. As is to be expected from the structure of IV, on treatment with triethylamine it suffered further migration of the double bond to give, quantitatively, the most conjugated isomer, 1,2-benzo-3-cyano-4,5-dihydroazulene (V), as orange needles; mp 69—70°C; ν_{max} (KBr) 3050 (w), 3010 (w), 2220 (m), 1632 (w), 1603 (w), 1577 (m), 1551 (m), 768 (s), 759 (s), 729 (s) and 710 (s) cm^{-1}; λ_{max} (EtOH) 216 (log ε 4.42), 259 (4.00), 2.66 (3.97), 295 (3.70) and 377 nm (3.95); τ (CCl_4, TMS) 2.50—3.10 (m, 5H, aromatic and H-8), 3.75 (m, 2H, H-6 and H-7), 7.10 (m, 2H, H-4a and 4b) and 7.58 (m, 2H, H-5a and 5b). In the NMR spectrum, two methylene groups, at C-4 and C-5, are assigned as above by the double resonance technique, the former being affected paramagnetically by the cyano group. Compound (V) was also rightly obtained from II with triethylamine. The dehydrogenation of IV and V also gave III; this fact further supports the above assignments.

Thus, in contrast to the results with tropone,[6] compound (I) afforded exclusively an 8+2 cycloadduct (II), and no trace of a 4+2 cycloadduct.

1) W. von E. Doering and D. W. Wiley, *Tetrahedron*, **11**, 183 (1960).

2) M. Oda and Y. Kitahara, *Chem. Commun.*, **1969**, 352.

3) M. Oda and Y. Kitahara, *Chem. Ind.* (London), **1969**, 920.

4) M. Stiles, R. G. Miller and U. Burckhardt, *J. Amer. Chem. Soc.*, **85**, 1792 (1963).

5) W. Treibs, J. Hiebsch and H. J. Neupert, *Chem. Ber.*, **92**, 606 (1959).

6) J. Ciabattoni, J. E. Crowley and A. S. Kende *J. Amer. Chem. Soc.*, **89**, 2778 (1967).

BULLETIN OF THE CHEMICAL SOCIETY OF JAPAN VOL. 43 1921—1926 (1970)

Calculation of the Chemical Shifts by the Semi-empirical SCF MO Method for All Valence-elctron Systems

Hajime KATÔ,*1 Hiroshi KATO*2 and Teijiro YONEZAWA

Department of Hydrocarbon Chemistry, Faculty of Engineering, Kyoto University, Sakyo-ku, Kyoto

(Received September 26, 1969)

The proton chemical shifts in the nuclear magnetic resonance spectra of CH_4, C_2H_6, C_2H_4, H_2CO, pyridine, and protonated pyridine were evaluated on the basis of Pople's theory (*J. Chem. Phys.*, **37**, 53 (1962)) in which the shielding tensor is expressed in terms of the magnetic susceptibility of each atom in the molecule. The wave functions were obtained using a semi-empirical SCF MO method for valence-electron systems (*Bull. Chem. Soc. Jap.*, **40**, 536, 1017 (1967)). The ^{13}C- and ^{14}N- chemical shifts in the above compounds were calculated on the basis of the "Coupled Hartree-Fock perturbation theory."

The general expression of the nuclear magnetic shielding constant for an isolated molecule was first derived by Ramsey,[1] but Ramsey's formula is not suitable for the fractional calculation of the shielding constants of large molecules. A variety of methods for the calculation of chemical shifts in molecules have been developed, such as breaking up the total shielding constants into the local contributions in some manner.[2-5] On the other hand, an attempt has been made to relate the shielding constants to other molecular properties, such as the dipole moment,[6] the electronegativities of the substituent group,[7] and the magnetic anisotropy of the bond.[8,9]

For proton shifts, an empirical correlation between the shift and the π-electron density on the atom to which it is bonded has been advocated.[10] On the other hand, more theoretical calculations have been carried out by many authors.[11] Of these, Pople[12] has proposed a formulation for the shielding constant in which a dipole approximation is used and the shielding constant is expressed in terms of the atomic contributions to the magnetic susceptibility. Although Musher[13] has given a critical discussion of a dipole approximation, it seemed that it would be of interest to calculate the shielding constant by Pople's formula. The critical discussion is based on the calculation of the Lamb term for an electron in an s or a p state using Slater atomic wave functions. In Pople's formula, the molecular orbitals are written as linear combinations of gauge-invariant atomic orbitals. It is uncertain whether or not the critical discussion is useful for the calculation based on Pople's formula. The calculation requires the knowledge of the ground-state wave function and those of the excited states. In many cases of the practical calculations, because of the lack of the knowledge of excited-state wave functions, an approximation was made.

We used the wave function obtained by a semi-empirical SCF LCAO MO method for all valence-electron system.[14] We calculated the proton chemical shifts for CH_4, C_2H_6 C_2H_4, and H_2CO without using the "mean excitation energy approximation" (ΔE approximation) used in Pople's theory. For pyridine and protonated pyridine, the calculation needs so many excitation energies that we used the ΔE approximation; some discussions of the approximation will be made.

For the investigation of ^{13}C and ^{14}N chemical shifts in the above compounds for which it is easy

*1 Present address: Department of Chemistry, Faculty of Science, Kobe University.

*2 Present address: Department of General Education, Nagoya University.

1) N. F. Ranset, *Phys. Rev.*, **78**, 679 (1950).
2) A. Saika and C. P. Slichter, *J. Chem. Phys.*, **22**, 26 (1954).
3) J. A. Pople, *ibid.*, **24**, 1111 (1956).
4) J. A. Pople, *Proc. Roy. Soc. Ser., A*, **239**, 541 (1957).
5) J. A. Pople, *ibid.*, **239**, 550 (1957).
6) A. D. Buckingham, *Can. J. Chem.*, **38**, 300 (1960).
7) B. P. Dailey and J. N. Shoolery, *J. Amer. Chem. Soc.*, **77**, 3977 (1955).
8) A. A. Bothner-By and C. J. Naar-Colin, *ibid.*, **80**, 1728 (1958).
9) A. A. Bothner-By and J. A. Pople, *Ann. Rev. Phys. Chem.*, **16**, 43 (1965).
10) G. Fraenkel. R. E. Carter, A. Mclachlan and J. H. Richards, *J. Chem. Phys.*, **35**, 731 (1961).
11) M. Karplus and H. J. Kolker, *ibid.*, **38**, 1263 (1963), **41**, 1259 (1964).
12) J. A. Pople, *J. Chem. Phys.*, **37**, 53 (1962).
13) R. M. Stevens and W. M. Lipscomb, *ibid.*, **40**, 2238 (1964).
14) T. Yonezawa, K. Yamaguchi and H. Kato, This Bulletin, **40**, 536 (1967); H. Kato, H. Konishi and T. Yonezawa, *ibid.*, **40**, 1017 (1967).

to carry out more rigorous calculation, the "Coupled Hartree-Fock perturbation thery"[15] without the ΔE approximation is applied.

Calculation

Using a dipole approximation, the mean value of the shielding tensor on the A atom has previously been given.[12]

$$\sigma^{A} = \frac{e^2}{3mc^2}\sum_{\mu}^{A} P_{\mu\mu}\langle r^{-1}\rangle_{\mu\mu} - \frac{2}{N}\langle r^{-3}\rangle_{A}\chi_{P}^{A} - \frac{1}{3N}\sum_{\alpha\beta}\sum_{B(\neq A)}\chi_{\alpha\beta}^{B}R_{B}^{-5}(R_{B}^{2}\delta_{\alpha\beta} - 3R_{B\alpha}R_{B\beta}) \quad (1)$$

$$P_{\mu\nu} = 2\sum_{i}^{occ} C_{i\mu}C_{i\nu} \quad (2)$$

$$\chi_{P}^{A} = \{(\chi_{P}^{A})_{xx} + (\chi_{P}^{A})_{yy} + (\chi_{P}^{A})_{zz}\}/3 \quad (3)$$

The first term in Eq. (1) gives the Lamb term,[16] and $\langle r^{-3}\rangle_{A}$ in the second term is the mean value of r^{-3} for the atomic orbital which contributes to paramagnetic terms on the A atom, but this term becomes zero in the calculation of the proton chemical shifts so long as the valence AO approximation is adopted. The third term, which gives the effect of currents on neighboring atoms, is divided into two terms (these two terms we shall henceforth call "the neighboring paramagnetic term" and "the neighboring diamagnetic term"). $\boldsymbol{R}_{B}$ is the radium vector to the B nucleus from the A nucleus, at which the shielding is calculated. The $R_{B\alpha}$ notation, is the $\alpha(x,y,z)$ component of the $\boldsymbol{R}_{B}$ vector, and $(\chi_{P}^{A})_{XX}$ is the diagonal x component of the paramagnetic susceptibility tensor of the A atom. In the above formula,

$$\chi_{\alpha\beta}^{B} = (\chi_{d}^{B})_{\alpha\beta} - (\chi_{P}^{B})_{\alpha\beta} \quad (4)$$

$$(\chi_{d}^{B})_{\alpha\beta} = -\frac{Ne^2}{4mc^2}\sum_{\mu}^{B} P_{\mu\mu}\langle r^2\delta_{\alpha\beta} - r_{\alpha}r_{\beta}\rangle_{\mu\mu} \quad (5)$$

$$(\chi_{P}^{B})_{\alpha\beta} = \frac{Ne^2\hbar^2}{m^2c^2}\sum_{i}^{occ}\sum_{j}^{unocc}\sum_{\mu<\nu}^{B}\sum_{A}\sum_{\lambda<\sigma}^{A} \times \frac{(C_{i\mu}C_{j\nu} - C_{i\nu}C_{j\mu})(C_{i\lambda}C_{j\sigma} - C_{i\sigma}C_{j\lambda})(l_{\alpha})_{\mu\nu}(l_{\beta})_{\lambda\sigma}}{E_{i\to j}} \quad (6)$$

where $E_{i\to j}$ is the excitation energy of the electronic transition from the ith molecular orbital to the jth molecular orbital. The other notations are the same as in Ref. 12.

Using Eqs. (1)—(6), we calculated the proton chemical shifts of CH_4, C_2H_6, C_2H_4 and H_2CO (Table 1). The coordinate axes, the x, y, and z axes, were taken on the mirror-reflection plane of these molecules. Therefore, the susceptibility tensor has nonzero values only for the diagonal elements for the sake of simplicity in calculation. (For this proof, see the appendix.) However, in the cases of pyridine and protonated pyridine (Fig. 1), according to the reason stated in the appendix, the coordinate axes chosen as has been described above do not coincide with the principal axes of the magnetic susceptibility tensor on 2C, 3C, 5C, and 6C atoms. Using the ΔE approximation, the elements of the paramagnetic susceptibility tensor in Eq. (6) are written as follows:

$$(\chi_{P}^{B})_{xx} = \frac{Ne^2\hbar^2}{m^2c^2\Delta E}\sum_{A}\sum_{i}^{occ}\sum_{j}^{unocc}(C_{iyB}C_{jzB} - C_{izB}C_{jyB}) \times (C_{iyA}C_{jzA} - C_{izA}C_{jyA}) \quad (7)$$

Table 1. Calculated and observed proton chemical shifts in CH_4, C_2H_6, C_2H_4, and H_2CO (ppm unit)

	CH_4	C_2H_6	C_2H_4	H_2CO
Calcd				
Lamb term	14.36	14.13	12.76	14.16
Neighboring diamag. term	−0.02	−0.14	−0.54	−0.28
Neighboring paramag. term	0.00	−0.23	−4.78	−4.65
Field effect due to the distortion of s-orbital	∼0	∼0	∼0	−3.82
Total	14.34	13.76	7.44	5.41
Relative to CH_4	0.00	−0.58	−6.90	−8.93
Obsd				
Relative to CH_4	0.00*	−0.75*	−5.18*	(−9)

* W. G. Schneider, H. J. Bernstein and J. A. Pople, *J. Chem. Phys.*, **28**, 601 (1958).

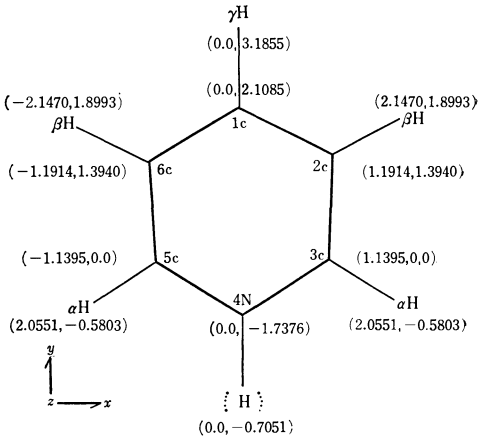

Fig. 1. Moleculer geometry for the pyridine and protonated pyridine.

15) R. A. Hegstrom and W. N. Lipscomb, This Bulletin, **46**, 1594 (1967).

16) W. Lamb, *Phys. Rev.*, **60**, 817 (1941).

$$(\chi_{\mathrm{P}}^{\mathrm{B}})_{yz} = -\frac{Ne^2\hbar^2}{m^2c^2\Delta E}\sum_{\mathrm{A}}\sum_{i}^{\mathrm{occ}}\sum_{j}^{\mathrm{unocc}}(C_{iz\mathrm{B}}C_{jx\mathrm{B}} - C_{ix\mathrm{B}}C_{jz\mathrm{B}})\times (C_{iy\mathrm{A}}C_{jz\mathrm{A}} - C_{iz\mathrm{A}}C_{jy\mathrm{A}}) \quad (8)$$

etc.

If the off-diagonal elements, $(\chi_{\mathrm{P}}^{\mathrm{B}})_{\alpha\beta}$'s are all zero, *i.e.*, if the coordinate axes are taken to be the principal axes and the summation over the A atom in the diagonal element of $(\chi_{\mathrm{P}}^{\mathrm{B}})_{\alpha\beta}$ is limited only over the B atom, the neighbouring paramagnetic constant part of Eq. (1) becomes equal to the term due to the local paramagnetic currents[5] in the shielding constant derived by the induced-current-density theory.[4]

On the basis of the relations of Eqs. (5)—(8), we have calculated the diamagnetic and paramagnetic susceptibility tensors, $\chi_{\mathrm{d}}^{\mathrm{B}}$ and $\chi_{\mathrm{P}}^{\mathrm{B}}$, on the B atom in pyridine and protonated pyridine (Tables 2, and 3, and Table 4 respectively). Using these results and Eq. (1), the proton-shielding constants of pyridine and protonated pyridine

Table 2. Components of the diamagnetic susceptibility tensor: χ_{d} in each atom in pyridine and protonated pyridine

$$\beta = \frac{Ne^2}{4mc^2}$$

B		1C	2C	3C	4N	5C	6C
Pyridine	$(\chi_{\mathrm{d}}^{\mathrm{B}})_{xx}$	-1.646β	-1.652β	-1.504β	-1.928β	-1.504β	-1.652β
	$(\chi_{\mathrm{d}}^{\mathrm{B}})_{yy}$	-1.689β	-1.651β	-1.493β	-1.713β	-1.493β	-1.651β
	$(\chi_{\mathrm{d}}^{\mathrm{B}})_{zz}$	-1.614β	-1.588β	-1.400β	-1.895β	-1.400β	-1.588β
Protonated pyridine	$(\chi_{\mathrm{d}}^{\mathrm{B}})_{xx}$	-1.583β	-1.580β	-1.535β	-1.642β	-1.535β	-1.580β
	$(\chi_{\mathrm{d}}^{\mathrm{B}})_{yy}$	-1.611β	-1.611β	-1.507β	-1.663β	-1.507β	-1.611β
	$(\chi_{\mathrm{d}}^{\mathrm{B}})_{zz}$	-1.601β	-1.528β	-1.470β	-1.540β	-1.470β	-1.528β

* The off diagonal susceptibilities: $(\chi_{\mathrm{d}}^{\mathrm{B}})_{ij}$ $(i \neq i)$ are all equal to zero.

Table 3. Components of the paramagnetic susceptibility tensor; $\chi_{\mathrm{P}}^{\mathrm{B}}$ on carbon and nitrogen atoms in protonated pyridine

$$\gamma = \frac{Ne^2\hbar^2}{4m^2c^2\Delta E}$$

B	1C	2C	3C	4N	5C	6C
$(\chi_{\mathrm{p}}^{\mathrm{B}})_{xx}$	3.268γ	5.936γ	5.315γ	4.735γ	5.315γ	5.936γ
$(\chi_{\mathrm{p}}^{\mathrm{B}})_{xy}$	0.0	0.809γ	-0.829γ	0.0	0.829γ	-0.809γ
$(\chi_{\mathrm{p}}^{\mathrm{B}})_{zx}$	0.0	0.0	0.0	0.0	0.0	0.0
$(\chi_{\mathrm{p}}^{\mathrm{B}})_{xy}$	0.0	0.841γ	-0.803γ	0.0	0.803γ	-0.841γ
$(\chi_{\mathrm{p}}^{\mathrm{B}})_{yy}$	5.657γ	4.194γ	3.480γ	6.190γ	3.480γ	4.194γ
$(\chi_{\mathrm{p}}^{\mathrm{B}})_{zy}$	0.0	0.0	0.0	0.0	0.0	0.0
$(\chi_{\mathrm{p}}^{\mathrm{B}})_{xz}$	0.0	0.0	0.0	0.0	0.0	0.0
$(\chi_{\mathrm{p}}^{\mathrm{B}})_{yz}$	0.0	0.0	0.0	0.0	0.0	0.0
$(\chi_{\mathrm{p}}^{\mathrm{B}})_{zz}$	5.579γ	5.354γ	4.685γ	4.943γ	4.685γ	5.354γ

Table 4. Components of the paramagnetic susceptibility tensor: $\chi_{\mathrm{q}}^{\mathrm{B}}$ on carbon and nitrogen atoms in pyridine

$$\gamma = \frac{Ne^2\hbar^2}{4m^2c^2\Delta E}$$

B	1C	2C	3C	4N	5C	6C
$(\chi_{\mathrm{p}}^{\mathrm{B}})_{xx}$	3.746γ	6.011γ	5.317γ	3.234γ	5.317γ	6.011γ
$(\chi_{\mathrm{p}}^{\mathrm{B}})_{yz}$	0.0	0.866γ	-0.737γ	0.0	0.737γ	-0.866γ
$(\chi_{\mathrm{p}}^{\mathrm{B}})_{zx}$	0.0	0.0	0.0	0.0	0.0	0.0
$(\chi_{\mathrm{p}}^{\mathrm{B}})_{xy}$	0.0	0.873γ	-0.893γ	0.0	0.893γ	-0.873γ
$(\chi_{\mathrm{p}}^{\mathrm{B}})_{yy}$	5.556γ	4.264γ	3.886γ	4.625γ	3.866γ	4.264γ
$(\chi_{\mathrm{q}}^{\mathrm{B}})_{zy}$	0.0	0.0	0.0	0.0	0.0	0.0
$(\chi_{\mathrm{p}}^{\mathrm{B}})_{xz}$	0.0	0.0	0.0	0.0	0.0	0.0
$(\chi_{\mathrm{p}}^{\mathrm{B}})_{yz}$	0.0	0.0	0.0	0.0	0.0	0.0
$(\chi_{\mathrm{p}}^{\mathrm{B}})_{zz}$	4.948γ	5.610γ	4.398γ	6.368γ	4.398γ	5.610γ

Table 5. Calculated proton shifts in pyridine and protonated pyridine (ppm unit)

	Pyridine			Protonated pyridine			N-H
	αH	βH	γH	αH	βH	γH	
Calcd							
Lamp term	12.812	12.210	12.724	11.430	11.430	11.554	9.729
Neighboring diamag. term	−2.19	−0.405	−0.723	−0.847	−0.234	−0.362	−1.013
Neighboring paramag. term	−3.433	−3.415	−0.574	−3.724	−3.235	−0.688	−2.575
Total	7.186	8.390	11.427	6.859	7.961	10.504	6.141
Referred to βH	−1.204	0.0	3.037	−1.102	0.0	2.543	−1.820
Obsd[a)]	−3.33	−1.87	−2.28	−3.58	−2.93	−3.50	−8.60
Referred to βH	−1.46	0.0	−0.41	−0.65	0.0	−0.57	−5.67

a) Referred to CH_2Cl_2; I. C. Smith and W. G. Schneider, *Can. J. Chem.*, **39**, 1158 (1961).

have been calculated to be as is shown in Table 5. In the ΔE approximation, ΔE was taken to be 10.0 eV.

The ^{13}C- and N^{14}-chemical shifts are calculated by the formula based on the "Coupled Hartree-Fock perturbation theory." The expressions for the diagonal component (μ is x, y, or z) of the paramagnetic and diamagnetic shielding tensors, $\sigma^{p}_{\mu\mu}$ and $\sigma^{d}_{\mu\mu}$, are given as follows:[15)]

$$\sigma^{p}_{\mu\mu} = -\alpha^2 \sum_{i}^{occ} \sum_{k}^{unocc} \times \frac{\langle\varphi_k|l_\mu|\varphi_j\rangle\langle\varphi_j|\frac{l_\mu}{r^3}|\varphi_k\rangle + \langle\varphi_j|l_\mu|\varphi_k\rangle\langle\varphi_k|\frac{l_\mu}{r^3}|\varphi_j\rangle}{\varepsilon_k - \varepsilon_j - J_{kj} + K_{kj}} \tag{9}$$

$$\sigma^{d}_{\mu\mu} = \alpha^2 \sum_{j}^{occ} \langle\varphi_j|\frac{r^2-\mu^2}{r^3}|\varphi_j\rangle \tag{10}$$

where α is the fine-structure constant and where φ_j is the jth MO. The other notations are the same as those in Ref. (23). In these ^{13}C- and ^{14}N-chemical shift calculations, only one-center terms in the matrix elements, such as $\langle\varphi_k|l_\mu|\varphi_j\rangle$, $\langle\varphi_j|l_\mu/r^3|\varphi_k\rangle$, and $\langle\varphi_j|1/r|\varphi_j\rangle$, in Eq. (9) and Eq. (10) are taken into account.

Results and Discussion

Table 1 gives the calculated and experimental proton chemical shifts, referred to CH_4 and their components, such as the Lamb term, the neighbouring diamag. term, and the paramag. term, for CH_4, C_2H_4, and H_2CO. It can be pointed out that the chemical shift of C_2H_2 comes mainly, and equally, from the Lamb term and the neighbouring paramagnetic term, while that of C_2H_4 is governed by the neighbouring paramagnetic term. In these molecules, the contribution from the field effect[6,17)] is nearly equal to zero. However, this effect arising from the electric dipole of the C–O group plays an important role, as may be seen in Table 1. For these compounds, the calculated results are in good agreement with the experimental values.

In order to investigate the practical difference between the two theories proposed by Pople in Ref. 12 and Ref. 5, further calculations were carried out for pyridine and protonated pyridine.

The calculated components of the diamagnetic susceptibility tensor, χ^{B}_{d}, and the paramagnetic susceptibility tensor, χ^{B}_{p}, on the carbon and nitrogen atoms in pyridine and protonated pyridine are shown in Tables 2, 3, and 4; $(\chi^{N}_{p})_{zz}$ shows a remarkable change from pyridine to protonated pyridine, in contrast to the conclusion of the localized-model calculations by Gil and Murrell.[18)] In the present calculation of the shielding constants, we have considered the contribution of the off-diagonal elements of the paramagnetic susceptibility tensor and found that these elements can not be ignored. This is because the exclusion of these elements leads to the dependence of the shielding constant on the choice of the coordinate.[19)] The coordinate system for pyridine and protonated pyridine in Fig. 1 does not accord with the principal axes of the magnetic susceptibility tensor on 2C, 3C, 5C, and 6V atoms. In this choice of the coordinate, the off-diagonal elements of the paramagnetic susceptibility tensor are only about 20% of the diagonal elements, but the contribution to the shielding constant through the third term in Eq. (1) is very important. For example, the contribution of the $(\chi^{C}_{p})_{yz}=0.866\gamma$ and $(\chi^{C}_{p})_{xy}=$

17) T. W. Marshall and J. A. Pople, *Mol. Phys.*, **1**, 199 (1958).

18) Y. M. S. Gil and J. N. Murrell, *Trans. Faraday Soc.*, **60**, 248 (1964).

19) H. Kato, H. Kato and T. Yonezawa, *Spect. Lett.*, **2(9)**, 267 (1969).

0.873γ (γ is a constant, see Table 4) in pyridine to the shielding constant through the neighboring paramagnetic term is -0.422 ppm, 2.985 ppm, and -0.191 ppm for αH, βH, and γH respectively. If we consider the change of the proton chemical shifts due to the field effect from the electric-charge distribution, the change of shifts due to this effect was calculated to be -0.259 ppm, -0.131 ppm, and -0.074 ppm for αH, βH, and γH, of pyridine and -0.034 ppm -0.017 ppm, -0.010 ppm, and -0.147 ppm for αH, βH, γH, and N–H of protonated pyridine respectively. In contradiction to the expreiment, the calculated shifts of γH (Table 5) in both pyridine and protonated pyridine show large shifts relative to βH. This discrepancy might be due to the difficulty involved in the MO treatment of lone-pair electrons or a non-negligible error in the dipole approximation. The relative shifts from pyridine to protonated pyridine (Table 5) are in fairly good accordance with the experimental results. In our calculation of the molecular orbitals, we have considered the interaction between the ($1s$) atomic orbital in the hydrogen atom and the (2ρ) atomic orbitals in the carbon or hygrogen atoms. Accordingly, the electric-field correction proposed by Musher,[20] which comes from the change in the local part of the Lamb contribution due to the change in the electron density, ρ^{H}, on the proton, is automatically included. Therefore, the electric-field effect due to the distortion of an spherically symmetric s state[6,17] is calculated by:

$$\sigma_{\parallel} = \frac{e^2}{3mc^2a}\left[1-\frac{439}{40}\frac{a^4E^2}{e^2}\right]$$
$$\sigma_{\perp} = \frac{e^2}{3mc^2a}\left[1-\frac{193}{15}\frac{a^4E^2}{e^2}\right] \quad (11)$$

The calculated carbon-13 chemical shifts in CH_4, C_2H_6, C_2H_4, and H_2CO which are obtained by the "Coupled Hartree Fock Method" are shown

Table 6. C^{13}-chemical shift (ppm unit) in CH_4, C_2H_6, C_2H_4, and C_2CO

	CH_4	C_2H_6	C_2H_4	H_2CO
Calcd				
paramag.	−136.8	−148.6	−251.6	−229.3
diamag.	35.5	39.9	41.3	35.3
TOTAL	−101.3	−108.7	−210.3	−194.0
Relative to CH_4	0.0	−7.4	−109.0	−92.7
Obsd				
Relative to CH_4	0.0	−8.0[a]	−126.0[b]	(−169.0)[c]

a) H. Spiesecks and W. G. Schneider, *J. Chem. Phys.*, **35**, 722 (1961).
b) Estimated from data on similar compounds by R. A. Friedel and H. L. Retcofsky, *J. Chem. Soc.*, **85**, 1300 (1963). Ref. *Mol. Phys.* **7**, 301 (1963—1964).
c) In 88% aqueous solution; P. C. Lauterbur, *J. Chem. Phys.*, **27**, 217 (1957).

Table 7. C^{13} and N^{14}-chemical shift (ppm unit) in pyridine and protonated pyridine

	Pyridine			Protonated pyridine		
C^{13}	αC	βC	γC	αC	βC	γC
Calcd						
paramag.	−263.7	−243.9	−259.1	−246.4	−210.1	−251.8
diamag.	39.9	44.4	44.8	40.9	42.7	42.8
TOTAL	−224.3	−199.5	−214.3	−205.5	−167.3	−209.0
Relative to βC	−24.8	0.0	−14.8	−38.2	0.0	−41.7
Obsd[a]	−21.72	4.59	−7.42	−13.94	−0.45	−19.84
	(−21.9)[c]	(4.2)[c]	(−7.70)[c]			
Relative to βC	−26.31	0.0	−12.01	−13.49	0.0	−19.39
	(−26.1)	(0.0)	(−11.90)			
N^{14}						
Calcd						
paramag.		−657.6			−528.8	
diamag.		86.7			75.9	
TOTAL		−588.9			−452.9	
Relative to C_5H_5N		0.0			136.0	
Obsd[b]						
Relative to C_5H_5N		0.0			123.11	

a) Relative to C_6H_6: R. J. Pugmire, Ph. D Thesis Univ. Utha, June (1966).
b) V. M. S. Gel. J. N. Murrel, *Trans. Faraday Soc.*, **60**, 248 (1964).
c) T. Tokuhiro, N. K. Wilson and G. Frankel, *J. Amer. Chem. Soc.*, **90**, 3622 (1968).

20) J. I. Musher, *J. Chem. Phys.*, **37**, 34 (1962).

Table 8. Contribution to the C_{13}-chemical shift of C_2H_4 through the paramagnetic term from each excited state

State (j — k)[b]	μ[a]	$\langle j\|L_\mu\|k\rangle$	$\langle k\|L_\mu\|j\rangle$	Contribution to C^{13} (ppm)
(4σ, $7\pi^*$)	x	−0.574	−2.772	−24.68
(6π, $8\sigma^*$)	x	0.978	4.724	−41.58
(5σ, $7\pi^*$)	y	−0.853	−4.122	−69.36
(1σ, $7\pi^*$)	y	0.015	0.072	0
(6π, $9\sigma^*$)	y	1.418	6.850	−64.96
(6π, $12\sigma^*$)	y	0.709	3.422	−6.31
(2σ, $8\sigma^*$)	z	−0.100	−0.482	−0.27
(3σ, $9\sigma^*$)	z	0.787	3.802	−16.67
(5σ, $10\sigma^*$)	z	1.079	5.214	−23.60
(4σ, $11\sigma^*$)	z	−0.364	−1.756	−2.40
(3σ, $12\sigma^*$)	z	0.393	1.899	−1.77
(1σ, $10\sigma^*$)	z	−0.019	−0.091	0

a) The molecular plane is in the xy-plane and the C-C bond is taken as the x-axis.
b) The number in the parenthesis shows the MO which is numbered from the lower to higher orbital energies.

in Table 6. The calculated values of the ^{13}C-chemical shifts, ($\delta^{13}C$), are also in fairly good agreement with the experimental values, except in the case of H_2CO. If we consider the change in the Slater exponent caused by the atomic charges in the evaluation of $\langle r^{-3}\rangle$,[21] the calculated $\delta^{13}C$ in CH_4, C_2H_6, C_2H_4, and H_2CO become −101.3 ppm, −108.2 ppm, −208.5 ppm, and −202.3 ppm respectively. The ^{13}C- and ^{14}N-chemical shifts in pyridine and protonated pyridine are shown in Table 7. The values are mainly determined by the paramagnetic term. In the $\delta^{13}C$ in pyridine, the calculated value of the paramagnetic term from the lowest (n–π^*) state is −132.8 ppm, while in protonated pyridine the corresponding contribution is −71.5 ppm. This difference corresponds to about 50% of the total difference. Table 8 shows how each excited state contributes to the paramagnetic terms in C_2H_4, as an example. The lowest excited state (5σ, $7\pi^*$) shows the largest contribution at δC^{13}. Moreover, the (6σ, $9\pi^*$) state, which needs a much larger excitation energy, shows a contribution almost comparable to that of the (5σ, $7\pi^*$) state; there are also several states which show the contribution of the same order as the (5σ, $7\pi^*$) states. In the other compounds, the same situations are found. Accordingly, it cannot be said generally that a particular state governs the chemical shift. In the present paper, we have considered only one-center terms, but it will be necessary, as a further improvement, to include two-center terms at least, as well as to refine the MO calculation. The MO calculation was carried out on a HITAC 5020E computer at the computation center of the University of Tokyo.

21) M. Karplus and J. A. Pople, *J. Chem. Phys.*, **38**, 2803 (1963).

Appendix

The susceptibility tensor, χ_M, on the M atom is a second-rank tensor:

$$\chi_M = \begin{pmatrix} \chi_{xx} & \chi_{yx} & \chi_{zx} \\ \chi_{xy} & \chi_{yy} & \chi_{zy} \\ \chi_{xz} & \chi_{yz} & \chi_{zz} \end{pmatrix}$$

If the M atom in a molecule lies on a mirror-reflection plane on the xy-plane, χ_M must satisfy the following relation:

$$\chi_M = s_h^z \chi_M {}^t s_h^z$$

where $s_h^z = \begin{pmatrix} 1 & 0 & 0 \\ 0 & 1 & 0 \\ 0 & 0 & -1 \end{pmatrix}$ *i. e.*, the matrix representation corresponding to the mirror-reflection operator. Accordingly, χ_M is as follows:

$$\chi_M = \begin{pmatrix} \chi_{xx} & \chi_{yx} & 0 \\ \chi_{xy} & \chi_{yy} & 0 \\ 0 & 0 & \chi_{zz} \end{pmatrix}$$

Further, if the M atom also lies on an other mirror reflection plane, the xz or yz plane, the susceptibility tensor should have nonzero values only for the diagonal elements.

BULLETIN OF THE CHEMICAL SOCIETY OF JAPAN VOL. 43 1927—1933 (1970)

Chemical Reaction in Silent Electric Discharge. I. The Mechanism of Ozone Formation

Hidetoshi SUGIMITSU, Ryozo ASAKURA, Satiko OKAZAKI and Momotaro SUZUKI

Science and Engineering Dept., Sophia University, Tokyo-Chiyoda

(Received October 11, 1969)

The ozone formation reactions in the silent electric discharge starting from oxygen under atmospheric pressure and varied electric conditions were investigated. The results were found to be in line with the theory based on the postulates of reactional and electrical pattern, proposed earlier by authors. The reaction regime in discharge columns where the main reactions proceed is unusual. The duration of high frequency discharge which initiates the primary reactions is extremely short compared to the apparent duration of discharge of basic primary current. Thus, in the discharge columns a non-steady reaction regime is established. A rate theory is developed for the processes in silent discharge based on a non-steady state assumption, which is acceptable in view of the experimental results. The proposed pattern of processes is useful for obtaining more detailed mechanism of the reaction involved.

Ozone formation in silent electric discharge has been a richly productive research project[1,2] for many years both from pure chemical and technical, as well as electrical viewpoints. Nevertheless, several points in the reaction mechanism, above all the dependence of the reactions on electrical processes, still remain unclarified.

The authors have tried to explain the experimental results without using a steady state assumption. It does not seem appropriate to apply this assumption to the silent discharge reaction regime of the present type, which is remarkably different from ordinary gas phase reactions.

The earlier proposed postulate is briefly summarized below.

1. The primary reaction is initiated by electrons in a high frequency electric field established by discharge due to the applied base potential of a low frequency current of 50 Hz of city source[1].

2. The rate of initiation reaction is proportional to the electric quantity, or the number of electrons, passing through the discharge space during a certain period, such as half cycle of low frequency current.

3. The discharge essentially takes place through numerous tiny columns strewn across the entire discharge space which are perpendicular to both electrode surfaces. In other words, the discharge space between the electrodes is divided into two regions,; one, the discharge columns through which displacement currents flow, and the other, the discharge free zone which is essentially free from electrons during and also after discharge.[1]

4. The number of discharge columns which are visibly observable, for instance, on photographic plates eventually serving as alternates of electrodes, is proportional to the total displacement current passing through the discharge columns under similar conditions.[1]

5. The sites of initiation reaction are then the space within the discharge columns, and further reactions will proceed either in discharge columns exclusively, or both in discharge columns and in discharge free zone according to the nature of individual chemical reactions and to the surrounding and ambient conditions.

Experimental

1. The device for the electric discharge and the flow system for the reactions were essentially similar to those described.[1] The block diagram and specifications are given in Fig. 1.

The discharge vessel or the ozonizer used was of a plate type (Fig. 2). The area of electrode, viz., the area of the copper foil pasted outside both electrodes which face each other parallel and congruently, was 37.5 cm^2, and the space gap between the electrodes was 1.25 mm for almost all runs. The pressure was maintained at 1 atm. in the ozonizer.

The reactions were highly sensitive to the chemistry and geometry of the reaction system as well as to electricity, which sometimes showed poor reproducibility of the measurements. Thus, the physical conditions, such as electrode material, thickness, nature of elec-

1) M. Suzuki, *Proc. Japan Acad.*, **26**, 21 (1950); M. Suzuki and Y. Naito, *ibid.*, **28**, 429 (1951); M. Suzuki, S. Okazaki and T. Yamamoto, *J. Amer. Chem. Soc. Advan. Chem. Ser.*, **26**, 331 (1957); K. Morinaga and M. Suzuki, This Bulletin, **34**, 157 (1961); *ibid.*, **35**, 204, 429 (1962); von A. Klemenc, H. Hintenberger and H. Höfer, *Z. Elektrochem.*, **43**, 708 (1937).

2) K. Honda and Y. Naito, *J. Phys. Soc. Jap.*, **10**, 1007 (1956); J. C. Devins, *J. Electrochem. Soc.*, **103**, 460 (1956); T. C. Manley, *Trans. Elektrochem.*, **84**, 83 (1943).

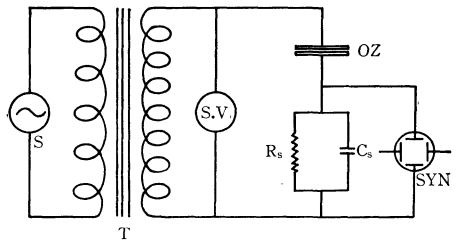

Fig. 1. Block diagram of measuring system.

S: A. C. source, 100 V, 50 Hz
T: Step-up transformer
S.V.: Static voltmeter
OZ: Ozonizer
Rs: 3 kΩ
Cs: 5300 pF
SYN: Synchroscope

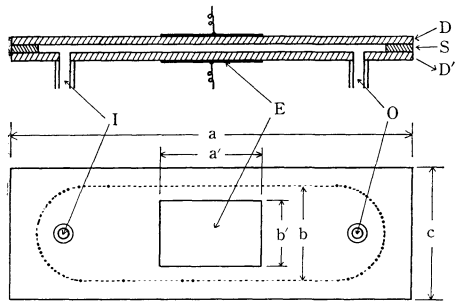

Fig. 2. Parallel plate ozonizer.

Ozonizer scales;
Whole size: a(=400 mm)×c(=100 mm).
Inside of dotted line: gas mixture streaming space, b=68 mm.
E: Cu-foil electrodes a'=75 mm, b'=50 mm.
I, O: in and outlet of gas mixture.
D=D': glass electrodes, 1.25 mm thick.
S: glass spacer, 1.25 mm thick.

trode surface, and the geometry of the experimental details or individual measurement gadgets, were kept as consistent as possible in order to eliminate cumber.

2. An optical method was employed for analysis of the produced ozone. The ozone concentration in down stream gas mixture was automatically recorded, while the absorption of 2540 Å line of ozone was continuously measured by a spectrophotometer, Hitachi EPU 2A Type, combined with a micro recorder, Hitachi QPD 33 Type. Validity of the recording scale was calibrated using the values of chemical analysis, which was found to be within 0.1% error.

3. The high frequency displacement current was sometimes unsteady and inreproducible. The electrical items involved in the measuring system were controlled with contingent precautions for each series of runs.

The high tension voltage (V) applied to the discharge system was measured by a static voltmeter (Fig. 1). The indicated values on the voltmeter gave the values of electric potential with which the condenser system (Cs and OZ in Fig. 1) should be charged. The actual field strength along the discharge path during the high frequency discharge is not yet clearly known, but some useful informations are available. The relations among various electrical quantities, such as the values of applied potential on individual condenser and the quantity of electricity were extensively discussed by Miura and Kawai.[3] This was of help in the estimation of various electric quantities from directly measured values, in spite of little knowledge of the field strength in the discharge columns.

The quantity of electricity (Q) transferred through the electrodes during a half cycle of primary base current governs the processes of chemical reactions, above all the initiation reactions originated in discharge columns.

The length of each hair[1] *i.e.* the pulse current on an oscillogram monitor of a half cycle of 50 Hz base current (Fig. 8) represents the high frequency current passing through discharge columns. From the summation of the lengths of these individual hairs the value of Q could be estimated.[1,3]

A synchroscope Iwasaki SS-5004 was used for the monitoring of discharge patterns. The indicated scale values on the gadget were taken to be valid.

Specifications of the electrical equipments were checked to ensure elimination of any possible irreproducibilities. Air or oxygen was used in the streaming gas mixture, though in the present investigation air was almost entirely used, because the theoretical treatment did not differ much for the two gas mixtures.

Results

1. Relation between the Applied Voltage and the Quantity of Electricity. The quantity of electricity carried through parallel plate electrodes is a linear function of the applied voltage on the electrodes. The slope of a straight line

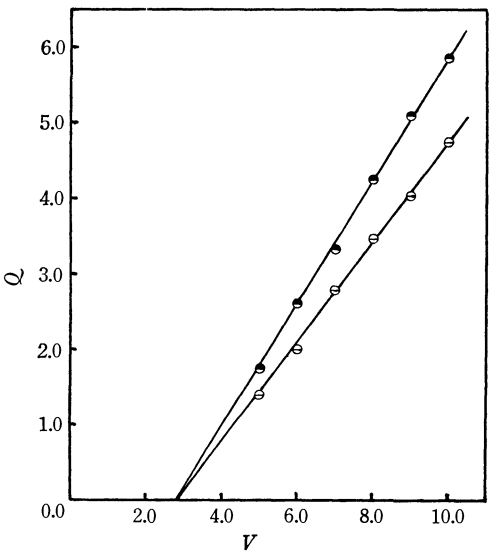

Fig. 3. Relations between quantity of electricity, $Q(10^{-7}$ coulombs) and applied voltage, V (KV).
⊖: F=2.09 cm³ sec⁻¹.
◓: F=14.26 cm³ sec⁻¹.

3) R. Miura and T. Kawai, *Kogakubu Kenkyu Hokoku (Reports on Scientific Researches), Hokkaido Univ. Eng. Dept.* No. 15, 142 (1956).

related to both quantities is governed virtually by the value of the electric constants of the discharge circuit. Such relations were obtained for a wide range of flow velocity variations. The results are shown in Fig. 3.

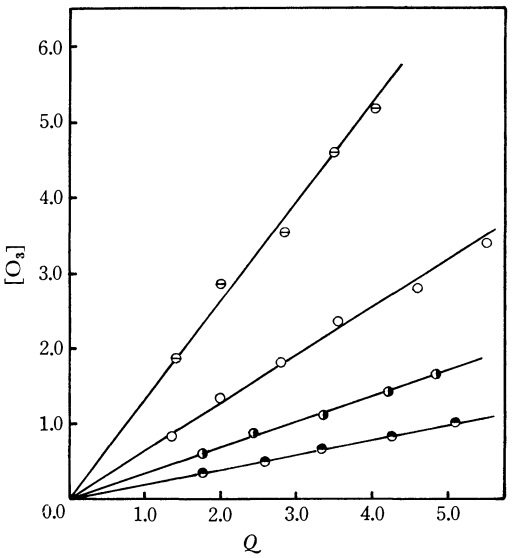

Fig. 4. Relations between quantity of electricity Q(10^{-7} coulombs) and ozone concentration [O_3] (10^{-3} g l^{-1}).
⊖: F=2.09 cm³ sec⁻¹. ○: F=3.88 cm³ sec⁻¹.
◑: F=7.44 cm³ sec⁻¹. ◓: F=14.26 cm³ sec⁻¹.

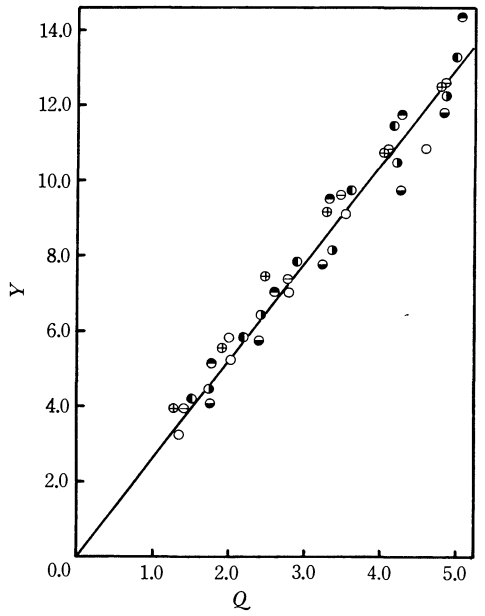

Fig. 5. Relation between quantity of electricity Q (10^{-7} coulombs) and ozone yield Y (10^{-6} g·sec^{-1}).
⊕: F=1.69 cm³ sec⁻¹. ⊖: F=2.09 cm³ sec⁻¹.
○: F=3.88 cm³ sec⁻¹. ◐: F=5.59 cm³ sec⁻¹.
◒: F=6.67 cm³ sec⁻¹. ◑: F=7.44 cm³ sec⁻¹.
◓: F=14.26 cm³ sec⁻¹.

2. Ozone Formation and Electrical Quantities. The results obtained are summarized in Table 1. In Fig. 4 the concentrations of ozone [O_3] (10^{-3} g l^{-1}) in the exit gas mixture from the discharge vessel are shown against the quantity of electricity Q (10^{-7} coulombs during a half cycle of base current) for various flow velocities F(cm³ sec^{-1}). The slopes of straight lines in sequence, each of which refers to a certain flow velocity, increase almost in proportion to the decrease of the flow velocity. The relation shows that the final ozone concentration after passing through the successive discharge columns is virtually inversely proportional to the flow velocity. The quantity $F\times$[O_3], which is in turn the ozone yield Y (10^{-6} g sec^{-1}) *vs.* Q should be expressed then as a single straight line irrespective of the flow velocities, which vary to as much as ten times (Fig. 5).

In Fig. 6 similar lines for O_3 *vs.* V are shown.

Table 1. Summarized results

F cm³ sec⁻¹	V kV	Q 10^{-7} coulombs	[O_3] 10^{-3} g l^{-1}	Y 10^{-6} g sec⁻¹
1.69	5.0	1.27	2.35	3.97
	6.0	1.92	3.33	5.63
	7.0	2.49	4.42	7.47
	8.0	3.29	5.44	9.19
	9.0	4.04	6.39	10.80
	10.0	4.79	7.41	12.52
2.09	5.0	1.40	1.88	3.93
	6.0	1.99	2.80	5.85
	7.0	2.80	3.54	7.40
	8.0	3.48	4.60	9.61
	9.0	4.04	5.17	10.81
	10.0	4.74	5.98	12.50
3.88	5.0	1.35	0.83	3.22
	6.0	2.01	1.35	5.24
	7.0	2.80	1.81	7.02
	8.0	3.54	2.35	9.12
	9.0	4.61	2.80	10.86
	10.0	5.51	3.40	13.19
5.59	5.0	1.52	0.75	4.19
	6.0	2.20	1.05	5.87
	7.0	2.92	1.40	7.83
	8.0	3.60	1.74	9.73
	9.0	4.17	2.05	11.46
	10.0	5.00	2.38	13.30
6.67	5.0	1.76	0.61	4.07
	6.0	2.41	0.86	5.74
	7.0	3.25	1.17	7.80
	8.0	4.27	1.46	9.74
	9.0	4.85	1.77	11.81
	10.0	6.13	2.09	13.94
7.44	5.0	1.75	0.60	4.46
	6.0	2.43	0.86	6.40
	7.0	3.36	1.10	8.18
	8.0	4.22	1.41	10.49
	9.0	4.85	1.65	12.28
	10.0	5.85	2.03	15.10
14.26	5.0	1.77	0.360	5.13
	6.0	2.61	0.496	7.07
	7.0	3.34	0.666	9.50
	8.0	4.27	0.823	11.74
	9.0	5.09	1.01	14.40
	10.0	5.87	1.20	17.11

The features of the lines are similar to those on Fig. 4, which is conceivable from Fig. 3.

3. Flow Velocities and Ozone Yields. The ozone concentration $[O_3]$ is inversely proportional to F as shown in Fig. 7. The diagrams are examples picked up from Table 1. The relations hold within the range given in Table 1.

Discussion

1. Electrical Pattern in Discharge Columns. In the course of ozone formation, the initiating primary step is involved in collisions between oxygen molecules and electrons. The paths of electrons are confined in discharge columns strewn across the discharge space between the two electrodes. Such columns which connect both electrodes electrically could be considered as channels solely through which electrons travel.

Neither the shape of cross sections of the channels which may be circular, nor their area which may be consistent along the channel from one electrode to the other, is known definitely, though it is almost certain that the channels are perpendicular to both electrode surfaces.

On the other hand, it is known that from the image of discharge columns on a photographic plate which served as a substitute of an electrode, the size of images of each column were found to be fairly equal.[1] The linear dimension at the bottom of columns was less than 1 mm. As the size of the columns is essentially governed by the number of electrons travelling through them, the number of electrons will be fairly consistent in each column. The current density in individual discharge columns is very likely to be constant.

The current flowing through columns is a high frequency one, or a displacement current whose frequency is dependent on the time constants of discharge circuit. Both from the oscillogram and the numerical value of actual electrical items in the measurement system, the oscillation frequency of high frequency current could be estimated to be about 10^6—10^7 Hz. Because of the high resistance of electrode material, the oscillation is highly dampened and only the first one oscillation of the high frequency current was confirmed by oscillogram patterns.[1]

When the applied high potential is gradually raised to a certain definite value, for instance V_1, a discharge or emission of electrons will take place in certain spots on one of the electrodes, which is eventually negative. A glass electrode does not usually have a perfectly flat surface, and there are numerous very small protrusions and indentations all over it. The smaller the radius of curvature r_1 of a very small protrusion, the easier the advent of a discharge from the protrusion, because the

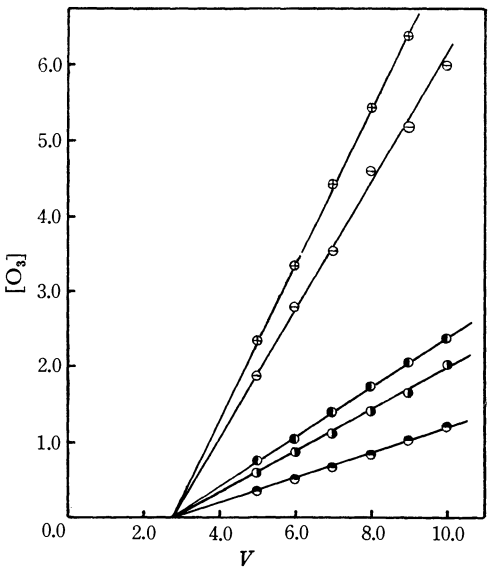

Fig. 6. Relations between ozone concentration $[O_3]$ (10^{-3} g l^{-1}) and applied voltage V (KV).
⊕: F=1.69 cm³ sec⁻¹. ⊖: F=2.09 cm³ sec⁻¹.
◐: F=5.59 cm³ sec⁻¹. ◑: F=7.44 cm³ sec⁻¹.
◓: F=14.26 cm³ sec⁻¹.

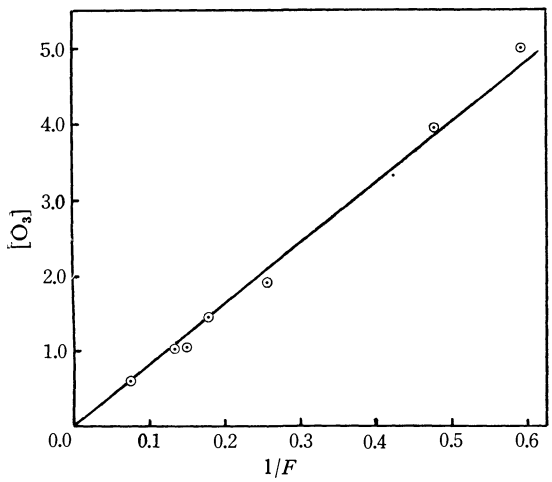

Fig. 7. Relation between ozone concentration $[O_3]$ (10^{-3} g l^{-1}) and reciprocal of flow velocity F (cm^{-3} sec).
$Q=3.0\times10^{-7}$ coulombs.

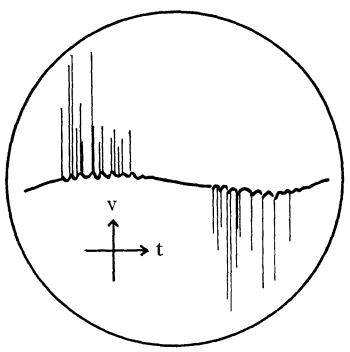

Fig. 8. Synchroscope monitoring of the pulse current (hairs) on primary current wave form.

smaller the r_1 the larger the field strength.

In Fig. 8 which shows the pulse current, the applied voltage (base line) increases from left to right, though the rise is not very distinct because of the deliberate suppression of ordinate scale. Each hair corresponds to pulse current corresponding to a certain value of applied voltage V_1. The pulse current is the sum of each individual pulse current originating from the protrusions whose radii of curvature are r_1. The pulses from left to right correspond to the protrusions for increasing r_1, corresponding to the increase of voltage which enables a discharge from the protrusions. In the other half cycle of base current analogous processes in opposite direction will take place. The high frequency discharge is actually realized only once from the same spot during course of the half cycle of basic current.

2. Reaction Mechanism in Discharge Regime. The proposed reaction sequence of ozone formation in silent discharge is as follows

$$O_2 + e \xrightarrow{k_0} O + O + e \qquad (0)$$

$$O + O_2 + M \underset{k_{-1}}{\overset{k_1}{\rightleftarrows}} O_3 + M \qquad \begin{matrix}(1)\\(-1)\end{matrix}$$

$$O_3 + e \xrightarrow{k_2} O_2 + O + e \qquad (2)$$

$$O_3 + O \xrightarrow{k_3} O_2 + O_2^* \qquad (3)$$

$$O + O + M \rightarrow O_2 + M \qquad (4)$$

$$O_2 + O_2^* \rightarrow O + O + O_2 \qquad (5)$$

where e is electron, and M could be either oxygen or nitrogen. For the sake of simplicity M is treated here exclusively to be oxygen because the effectiveness of both molecules in the reactions does not essentially show much difference.[4] Some of the values of k were estimated.

$$k_1 = 6.0\times10^7 \exp\ (+0.6/\boldsymbol{R}T)\ \ l^2\,\mathrm{mol}^{-2}\,\mathrm{sec}^{-1}$$ [4,5]

$$k_{-1} = (4.61\pm0.25)\times10^{12} \exp\ (-24.4/\boldsymbol{R}T)\ \ l\,\mathrm{mol}^{-1}\,\mathrm{sec}^{-1}$$ [5,6]

$$k_3 = (3.0\pm0.3)\times10^{10} \exp\ \{(-6.0\pm0.7)/\boldsymbol{R}T\}\ \ l\,\mathrm{mol}^{-1}\,\mathrm{sec}^{-1}$$ [6]

Reactions (3) and (4) are negligible because of the low concentration of O atoms and O_3 molecules, and reaction (5) was discarded[7] because of its eligibility only at high temperatures. Finally reaction (−1) could be put aside[4] at room temperature, which is essentially the temperature of the discharge vessel. Because of very short and intermittent advent of discharges, essentially any considerable temperature enhancement in the discharge vessel could hardly be perceptible. Thus the reactions (0), (1) and (2) are of practical interest in this reaction regime. The reaction (0) or the initiation reaction will proceed solely in discharge columns. The duration of high frequency current through columns is 10^{-6}—10^{-7} seconds. The electron drift velocity depends on E/p value in the discharge vessel, where E is the value of potential gradient (volt cm^{-1}) between the electrodes and p is the ambient pressure (mmHg), from which E/p is far less than unity.[8] In consideration of this value, the electron drift velocity could be estimated to be about 10^6—10^7 cm sec^{-1}. If the linear flow velocity of gas mixture is taken to be 10 cm sec^{-1}, and diameter of the discharge column to be 0.5 mm in average, then the resident time of gas mixture whithin a discharge column is about 5×10^{-3} sec. Now the number of columns through which streaming gas mixture passes is inversely proportional to its flow velocity. The number of electrons which shower on the gas mixture is proportional to the number of columns. Thus we conclude that the number of oxygen atoms produced by reaction (0), which in turn produced ozone molecules, should be roughly inversely proportional to the flow velocity. As the experimental results show, the ozone concentration of a certain gas mixture is really inversely proportional to the flow velocity (Fig. 7) under similar conditions.

A more detailed insight of the reaction mechanism will be discussed in the following section.

3. The Reaction Pattern based on a Non-steady State Assumption. In silent discharge both from spacial and time-resolved viewpoints three types of reaction regime could be designated: **A_1**) reactions going on in any discharge column within the time of high frequency discharge, during which the electrons reside in the column and their resident time is about 10^{-6}—10^{-7} sec; **A_2**) reactions going on in any discharge column within the interval between any two successive high frequency discharges which is 10^{-2} sec or a half cycle of base current, where any electrical phenomena are precluded; and **B**), reactions going on in the space outside discharge columns during the resident time of reaction gas mixture in the discharge vessel.

These three types of reaction regime will be discussed individually.

A_1: this is a reaction regime where electrons participate. The density of electrons will be larger on account of the smallness of the volume

4) W. M. Jones and N. Davidson, *Abstracts of Papers*, 135*th Meeting*, *Amer. Chem. Soc.*, p. 37 R. (1959).

5) S. W. Benson and A. E. Axworthy, Jr., *J. Chem. Phys.*, **26**, 1718 (1957).

6) F. Leighton, H. B. Urbach, J. A. Wojtowicz and J. A. Zaslowsky, *Abstracts of Papers*, 136*th Meeting*, *Amer Chem. Soc.*, p. 46 S. (1959); H. B. Urbach, R. J. Wunk, J. A. Wojtwicz and J. A. Zaslowsky, *ibid.*, p. 47 S. (1959).

7) R. E. Dugg, *Phys. Fluids*, **1**, 242 (1958); W. Jost, 7*th. Combus Symp.*, p. 190 (1959).

8) R. A. Nielsen and N. E. Bradbury, *Phys. Rev.*, **49**, 338 (1936), **51**, 69 (1937); R. A. Nielsen, *ibid.*, **50**, 950 (1936); R. H. Healey and J. W. Reed, "The Behaviour of Slow Electrons," Amalgamated Wireless Press Ltd., Sydney (1941), p. 94.

of columns compared to the whole discharge space, and it will tend to be smaller as the electron velocity becomes faster (up to 10^7 cm sec^{-1}).[9] The actual value of the electron concentration in the discharge columns in the present investigation is roughly estimated to be about 10^{-10}—10^{-11} mol l^{-1} during the course of high frequency discharge.

The site of reaction (0) is exclusively in the discharge columns, the produced O atoms may react according to reactions (1) and (3), but some part may flow out of the columns along with the gas stream. The electrons will play roles in reactions (0) as well as in (2). Ozone will be produced through reaction (1) and destroyed by reactions (2) and (3), and finally washed out from the columns as O atoms.

Based on a non-steady state assumption, reactions (0), (1), (2), (3) and washing out effect will be expressed in the following way, reaction (-1), (4), (5), *etc.* being discarded.

$$\frac{dx}{dt} = Ay - Bx - Fx \qquad (A_1\text{-}1)$$

$$\frac{dy}{dt} = -Ay + Bx - Fy + C, \qquad (A_1\text{-}2)$$

where $x=[O_3]$ mol l^{-1}, $y=[O]$ mol l^{-1} and $A=k_1[O_2]^2$. In this case $A=1.1\times10^4$ sec^{-1} at 300°K and at 760 mmHg.[5] Also $B=k_2[e]$, in which case [e], the electron density, is about 10^{-11} mol l^{-1}, and k_2 mol^{-1} l sec^{-1} is unknown, although from various viewpoints B is most likely less than A. In addition $C=2k_0[O_2][e]$, where k_0 is presumably 10^6—10^8 mol^{-1} l sec^{-1}, [10] although the exact value is not estimated. Finally, F is flow velocity (sec^{-1}) which is taken to be 10^{-2} sec^{-1}. F in Table 1 and Figs. 3—7 is expressed in volume velocity, whereas in this section F times concentration represents the quantity carried by flow. Although the Eq. (A_1-2) is often assumed to be zero, in the present postulate it should most likely remain finite in $\mathbf{A}_1$ regime. The above two equations could then be reduced to

$$\frac{d^2x}{dt^2} + Q\frac{dx}{dt} + Px - AC = 0, \qquad (A_1\text{-}3)$$

where $P=(A+B)F+F^2=(A+B)F$ and $Q=A+B+2F=A+B$. Eq. (A_1-3) is so simple that its general solution is obtained directly under consideration of boundary conditions. Thus we get the final result

$$Px_0 = AC[1 - \exp(-Qt_0)] \qquad (A_1\text{-}4)$$

where t_0 is the duration of high frequency oscillations, x_0 is the ozone concentration at t_0 or at the stage of reaction at the moment when the high frequency discharge is extinguished. In the course of solving the equations, a physically more suitable complementary root of the characteristic equation is selected. All the right hand side terms of (A_1-4) are independent of flow velocity, but P is proportional to it. Thus x_0 is inversely proportional to the flow velocity.

$\mathbf{A}_2$: In discharge columns after the high frequency discharge terminated, O atoms will still react according to reaction (1) and continue to flow away in the outer zone. Similarly O_3 molecules will be produced by reaction (1) and flow out in the same manner as O atoms. Electrons play no roles here.

Then the tentative equations will be

$$\frac{dx}{dt} = Ay - Px \qquad (A_2\text{-}1)$$

$$\frac{dy}{dt} = -Ay - Fy \qquad (A_2\text{-}2)$$

which can be solved easily. The solution is

$$x_1 = [x_0+y_0\{1-\exp(-At_1)\}]\exp(-Ft_1) \fallingdotseq (1-Ft_1)(x_0+y_0). \qquad (A_2\text{-}3)$$

Because of $1 \gg Ft_1$, it will further be changed into

$$x_1 \fallingdotseq x_0 + y_0, \qquad (A_2\text{-}4)$$

where t_1 is the duration which is a half period of basic current or 10^{-2} sec., and x_1 is the ozone concentration at the beginning of another overtaking high frequency discharge.

The value of y_0 or [O] at the termination of $\mathbf{A}_1$ regime can be calculated from (A_1-1) and (A_1-4), which gives

$$y_0 = (C/P)[(A+F)\exp(-Qt_0) + (B+F)] \fallingdotseq (C/P)[A\exp(-Qt_0)+B]. \qquad (A_2\text{-}5)$$

In a similar way as discussed in the foregoing section, the terms in the bracket on the right hand side of (A_2-5) are free from F, while P is proportional to F, y_0 is then inversely proportional to F. Thus the $[O_3]$ value at the termination of $\mathbf{A}_2$ is, as in $\mathbf{A}_1$, proportional to $1/F$. Furthermore, the fact that the value of x_1 in (A_2-4) is almost equivalent to (x_0+y_0) shows that, almost all O atoms react into O_3 molecules, except those washed out of the columns, which are very small, before the termination of $\mathbf{A}_2$ regime. Thus it may be concluded that the ozone formation in the zone outside of columns is very small.

B: Outside the discharge columns, O atoms and O_3 molecules are flowing, while they may react, to a very small extent, according to reaction (1). These particles may incessantly flow into and then emerge out of discharge columns, but processes in and out will obviously cancel each other, and the effect of flow could be neglected.

The required equations are then

$$\frac{dx}{dt} = Ay \qquad (B\text{-}1)$$

$$\frac{dy}{dt} = -Ay \qquad (B\text{-}2)$$

9) C. E. Normand, *Phys. Rev.*, **35**, 1217 (1936).
10) To be published.

and the solution, under the consideration of the boundary conditions is

$$x = x_a + y_a[1-\exp(-At)] \fallingdotseq x_a \quad \text{(B-3)}$$

where x is the value of $[O_3]$ at any time, so long as the gas mixture resides in the discharge zone, particularly outside discharge columns, and x_a and y_a are the $[O_3]$ and [O] at the time when the gas mixture is streaming out of a discharge column. The value of y_a is very small (*cf.* $\mathbf{A}_2$). Then x_a is equivalent to x_1 in (A_2-3) and again proportional to $1/F$. It is also conceivable from (B—3) that the extent of ozone formation in space outside discharge columns is very small, as suggested before.

Putting these three reaction regimes together, in $\mathbf{A}_1$ regime where the main part of the reaction proceeds, the ozone concentration is proportional to $1/F$; in $\mathbf{A}_2$ and **B**, where the reactional part of the substrate decreases the produced ozone concentration is again proportional to $1/F$. The experimental results show that the ozone concentration is proportional to $1/F$ for a considerable wide range of flow velocities. This agrees with the proposed theory.

In static system the ozone yield is very low. In very rapid flow where the flow velocity, or the resident time of streaming gas mixture in a column is comparable to the high frequency discharge duration, the reaction pattern should be different from those described above. The values of k_0 and k_3 of reactions (0) and (3) were left unsettled.

BULLETIN OF THE CHEMICAL SOCIETY OF JAPAN VOL. 43 1933—1939 (1970)

The Molecular Structure of Tin Tetrachloride as Determined by Gas-electron Diffraction

Hideji FUJII and Masao KIMURA

Department of Chemistry, Faculty of Science, Hokkaido University, Sapporo

(Received October 24, 1969)

The molecular structure of tin tetrachloride was determined by the sector-microphotometer method of gas-electron diffraction. By taking into account the phase-shift for the Sn-Cl pair, the following results were obtained: the tetrahedral structure with r_g(Sn–Cl)$=2.280_8\pm0.003_7$ Å, l(Sn–Cl)$=0.049_9\pm0.003_3$ Å, and l(Cl···Cl)$=0.108_6\pm0.005_0$ Å. These values, especially that of the mean amplitude, l(Sn–Cl), are different from those previously reported by other workers. This is because the effect of the phase shift was neglected in the previous investigations.

Schomaker and Glauber first pointed out the fault of the first Born approximation for the interpretation of the electron-diffraction patterns of molecules containing both heavy and light atoms;[1] subsequently, Hoerni and Ibers calculated the complex atomic-scattering factors for electrons by the partial-waves method in order to explain the observed intensities of UF_6 at 40 and 11 keV.[2,3] Since then, the angle-dependent phase factor in the scattering of electrons has been the subject of several theoretical and experimental investigations.[3] Especially, the studies carried out by Seip[4] and also Kimura *et al.*[3a] have provided extensive experimental data for solving this phase problem. The molecules treated in these experimental studies contain both very heavy and light atoms, and their diffraction patterns show distinct cut-off points in intensities at moderate scattering angles. However, the influence of the phase factor on structure analysis is not limited to such molecules. If this effect is not taken into consideration, inaccurate structure parameters might be yielded, even for molecules whose diffraction patterns have no cut-off point. The tin tetrachloride molecule is considered to be one such molecule.

There have been a few structure determinations of tin tetrachloride by electron diffraction;[5-7] the values reported by Livingston and

1) V. Schomaker and R. Glauber, *Nature*, **170**, 290 (1952).

2) J. A. Hoerni and J. A. Ibers, *Phys. Rev.*, **91**, 1182 (1953).

3) See, *e.g.*, (a) M. Kimura, V. Schomaker, D. W. Smith and B. Weinstock, *J. Chem. Phys.*, **48**, 4001 (1968); also (b) H. M. Seip, "Selected Topics in Structural Chemistry," Universitetsforlaget, Oslo (1967), pp. 26—68.

4) H. M. Seip and R. Seip, *Acta Chem. Scand.*, **20**, 2698 (1966) and the preceding papers.

5) R. Wierl, *Ann. Physik.*, **8**, 521 (1931).

6) L. O. Brockway and F. T. Wall, *J. Amer. Chem. Soc.*, **56**, 2373 (1934); L. Pauling and L. O. Brockway, *ibid.*, **57**, 2684 (1935).

7) R. L. Livingston and C. N. R. Rao, *J. Chem. Phys.*, **30**, 339 (1959).

Rao,[7] $r(\mathrm{Sn-Cl})=2.31\pm0.01_5$ Å, $r(\mathrm{Cl\cdots Cl})=3.77\pm0.03_0$ Å, $l(\mathrm{Sn-Cl})=0.08$ Å and $l(\mathrm{Cl\cdots Cl})=0.10$ Å, have often been quoted as the interatomic distances and mean amplitudes of the molecule. These values, however, have not been accurate enough to withstand recent critcal discussion of the molecular structure, for they were determined by the visual-sector method, without taking into account the phase shift for the Sn–Cl atom pair. Since, in structure analysis, the mean amplitude of the Sn–Cl stretching vibration is correlated very closely with the effect of the phase shift, the experimental mean amplitudes reported by Livingston and Rao may be larger than the true values.

It is well-known that the mean amplitudes can be calculated from the molecular geometry and the internal force field which satisfies the normal frequencies, while, conversely, unknown force constants of the internal force fields can be determined by using the observed mean amplitudes as additional information. Morino *et al.* determined, in this way, the force constants for the tetrachloride molecules, CCl_4,[8] $SiCl_4$[9] and $GeCl_4$.[8] The force constants of an internal force field can also be determined by the use of the relative intensities of the Raman lines in addition to the fundamental frequencies.[10] Chantry and Woodward applied this method to tetrahalide molecules, MX_4 (M=C, Si, Ge, and Sn; X=Br and Cl).[11] However, this method gives four sets of force constants accounting for the vibration of species, F_2, and specifies no unique set of force constants. Therefore, they selected one set from among the four by consulting the experimental mean amplitudes of vibration. Because of the inevitable ambiguities of the results for $SnCl_4$, Chantry and Woodward's choice of the force constants for $SnCl_4$ is not decisive.

Recently, Bürger and Ruoff[12] and also Kebabçioglu *et al.*[13] independently determined the force constants for the tetrachloride molecules of the group-IV_b elements by the use of the Coriolis coupling constants, which were estimated from a separation between the P and R branches of the F_2 band. The results for $SiCl_4$ and $GeCl_4$ were in reasonable agreement with each other, and also with those determined from the mean amplitudes and the relative intensities of the Raman lines. However, it seems that the values previously reported for $SnCl_4$ are inconsistent with one another. In these circumstances it is very desirable to determine the precise interatomic distances and mean amplitudes of tin tetrachloride by the sector-microphotometer method of electron diffraction. Especially, the values of the mean amplitudes are expected to be revised significantly by taking into account the phase shift for the Sn–Cl pair.

Experimental

The sample of tin tetrachloride was loaded in a sample holder by manipulating it in a dry box filled with nitrogen. The vapor pressure of the sample was about 20 Torr at 20°C.

Photographs were taken at 18°C with an r^3-sector at camera lengths of 24.430 cm and 10.930 cm; the exposure times were about 40 sec, with a beam current of about 0.15 μA. The fluctuations of the accelerating voltage (about 47.5 kV) were maintained within 0.1 per cent throughout a sequence of exposures. Carbon disulfide was employed as a reference material in determining the wavelength.[14]

The intensities of the diffraction patterns of $SnCl_4$ decreased rapidly with an increase in scattering angles, so that intensity measurements were practically impossible in a range beyond about $q=100$. This is certainly due to the effect of the phase shift in addition to the damping effect caused by molecular vibrations. This suggests that information can be obtained by using photographs taken at a long camera distance. Therefore, three plates from the long camera distance were selected for analysis; hereafter, they will be referred to as plates 1, 2, and 3 for the sake of convenience. The wavelength for each plate was determined by the use of two plates of carbon disulfide taken in the same sequence of exposures.

With a double-beam microphotometer, Model NLM-III, of the Nalumi Co., Ltd., the optical densities of the diffraction patterns were measured by the following two methods:

(1) This microphotometer was equipped with a cam converting transmission into optical density and a pen-recorder. Optical densities were read at intervals of $\Delta q=1$ on the left and right sides of the diffraction center. In this method the optical densities were determined by averaging the corresponding observed values on the two sides (the pen-recording method).

(2) By connecting an integrating digital voltmeter to the microphotometer, the values of the output voltages from the photomultiplier of the microphotometer were perforated in digits directly onto an input tape for an electronic computer. From these values, taken every one-third of a milimeter on a plate, the optical density at every integral number of q was obtained by interpolation by a second-degree polynomial which passes through the three observed points closest to each q. In this case, the diffraction center was determines so as to minimize the value of $\sum_i [D_{li}-D_{ri}]^2$, where

8) Y. Morino, Y. Nakamura and T. Iijima, *J. Chem. Phys.* **32**, 643 (1960).

9) Y. Morino and Y. Murata, This Bulletin, **38**, 104 (1965).

10) M. Wolkenstein, *C. R. Acad. Sci. U. R. S. S.*, **32**, 185 (1941); D. A. Long, *Proc. Roy. Soc.*, **A217**, 203 (1953).

11) G. W. Chantry and L. A. Woodward, *Trans. Faraday Soc.*, **56**, 1110 (1960).

12) H. Bürger and A. Ruoff, *Spectrochim. Acta*, **A24**, 1863 (1968).

13) a) C. J. Peacock, A. Müller, R. Kebabçioglu, *J. Mol. Spectry.*, **27**, 351 (1968). b) R. Kebabçioglu, A. Müller, C. J. Peacock and L. Lange, *Z. Naturforsch.*, **23A**, 703 (1968).

14) C. Kato, S. Konaka, T. Iijima and M. Kimura, This Bulletin, **42**, 2148 (1969).

the D_{li} denotes the optical density at $q=i$ on the left side of the diffraction center, and the D_{ri}, the corresponding value on the right side. Thus, by this method two sets of the observed optical densities, D_l and D_r, were obtained for each plate (the digital method). The whole process was performed by the use of an electronic computer.

The optical densities measured by the two methods differ from each other by only one per cent at most. Since the observed optical densities for all plates were below 0.7, it was assumed that the optical densities are proportional to the scattering intensities, I_T^{obs}.[15] The observed intensities ranging from $q=10$ to 70 were adopted for analysis.

Analysis and Results

The observed molecular scattering intensity, $qM(q)^{obs}$, was obtained from the I_T^{obs} and the smooth background, I_B^{obs}, according to the equation:

$$qM(q)^{obs} = q(I_T^{obs}-I_B^{obs})/I_B^{obs}. \tag{1}$$

The corresponding theoretical expression is:

$$qM(q)^{theor} = k\sum_{i,j}' A_{ij}\mu_{ij}\cos(\Delta\eta_{ij})\exp[-a_{ij}q^2] \times \sin\left[\frac{\pi}{10}q\left\{r_{aij}-\left(\frac{\pi}{10}q\right)^2\kappa\right\}\right], \tag{2}$$

$$a_{ij} = \frac{1}{2}(\pi/10)^2 l_{ij}^2, \tag{3}$$

$$A_{ij} = \frac{Z_iZ_j}{\sum_k Z_k(Z_k+1)}\cdot\frac{20}{\pi r_{aij}} \tag{4}$$

$$\mu_{ij} = \frac{\sum_k Z_k(Z_k+1)}{Z_iZ_j}\cdot\frac{|F_i||F_j|}{\sum_k\{|F_k|^2+S_k\}}, \tag{5}$$

$$|F_k| = h^2s^2|f_k|/8\pi^2me^2, \quad s=\left(\frac{\pi}{10}\right)q. \tag{6}$$

Here, all the notations follow usual usage. Starting from a trial experimental background described below, the final I_B^{obs} and $qM(q)^{obs}$ were determined according to Karle's non-negativity criterion[16] by repeating a few times the calculation of the radial distribution curve and its inverse Fourier transformation for the $r=0.00$–1.60 Å range. The trial experimental background was determined in the following way: By replacing the $q(Mq)^{obs}$ in Eq. (1) by the theoretical molecular intensity, $q(Mq)^{theor}$, the observed background can be expressed as:

$$I_B^{obs} = I_T^{obs}\frac{q}{q+kqM(q)^{theor}}.$$

From this equation a preliminary background can be calculated by using $qM(q)^{theor}$ for a reasonable molecular model and an appropriate k value.

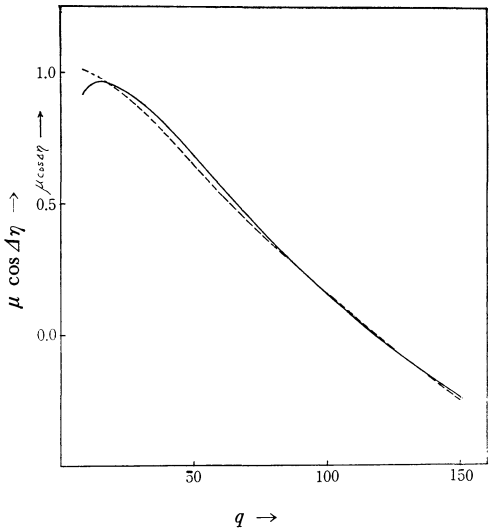

Fig. 1. $\mu_{SnCl}\cos(\Delta\eta_{SnCl})$ (the solid line) and $\chi_{SnCl}(q)$ (the broken line).

By fitting the background to a polynomial in terms of q, $\sum_{n=0}^{5} a_nq^n$, a smooth trial background, I_B^{obs}, was obtained.

Since the $\mu_{SnCl}\cos(\Delta\eta_{SnCl})$ values are far from unity, as may be seen in Fig. 1, the corrections for the non-nuclear scattering in the calculation of the radial distribution cannot be made satisfactorily by the conventional form, $1-\mu_{SnCl}\cos(\Delta\eta_{SnCl})$. Generally, the $\mu_{ij}\cos(\Delta\eta_{ij})$ values for an i and j atom pair can be approximated by the following function, $\chi_{ij}(q)$:[17]

$$\chi_{ij}(q) = \alpha_{ij} + \beta_{ij}\cos\left(\frac{\pi}{10}\Delta r_{ij}\cdot q\right) + \gamma_{ij}\exp[-\delta_{ij}q^2], \tag{7}$$

where the α_{ij}, β_{ij}, γ_{ij} and δ_{ij} are positive constant coefficients. The correction term, then, becomes:

$$\Delta qM(q) = \sum_{i,j}' A_{ij}\sin\left(\frac{\pi}{10}qr_{ij}\right)\exp[-a_{ij}q^2] \times\{\chi_{ij}(q)-\mu_{ij}\cos(\Delta\eta_{ij})\}, \tag{8}$$

and the corresponding radial distribution curve, $f(r)$, is given by:

$$f(r) = \sum_{i,j}' \frac{A_{ij}}{4}\sqrt{\frac{\pi}{a_{ij}+b}}\exp\left[-\frac{\pi^2}{400}\frac{(r-r_{ij})^2}{a_{ij}+b}\right]\alpha_{ij} + \sum_{i,j}' \frac{A_{ij}}{4}\sqrt{\frac{\pi}{a_{ij}+b}} \times\left\{\exp\left[-\frac{\pi^2}{400}\frac{(r-r_{ij}+\Delta r_{ij})^2}{a_{ij}+b}\right] + \exp\left[-\frac{\pi^2}{400}\frac{(r-r_{ij}-\Delta r_{ij})^2}{a_{ij}+b}\right]\right\}\frac{\beta_{ij}}{2} + \sum_{i,j}' \frac{A_{ij}}{4}\sqrt{\frac{\pi}{a_{ij}+b+\delta_{ij}}} \times\exp\left[-\frac{\pi^2}{400}\frac{(r-r_{ij})^2}{a_{ij}+b+\delta_{ij}}\right]\gamma_{ij}. \tag{9}$$

15) Y. Morino and T. Iijima, This Bulletin., **35**, 1661 (1962).

16) J. Karle and I. L. Karle, *J. Chem. Phys.*, **18**, 957 (1950).

17) S. Konaka, T. Ito and Y. Morino, This Bulletin, **39**, 1146 (1966).

Here, the b is an artificial damping factor, and the Δr_{ij} corresponds to an apparent splitting of the i and j interatomic distance due to the phase difference. The Δr_{ij} value was estimated from the $(\pi/10)\Delta r_{ij}\cdot q_c=\pi/2$ relation, with a theoretical first cut-off point, q_c. The anharmonicity parameter, κ, in Eq. (2) can be ignored in the calculation of the radial distribution. It readily be seen from Eq. (9) that the non-negativity criterion holds for this radial distribution curve.

In the case of $SnCl_4$ we employed the functions of $\chi_{ij}(q)$ with the following coefficients:

$\alpha_{Sn-Cl}=0$ $\alpha_{Cl-Cl}=1.20$

$\beta_{Sn-Cl}=0.625$ $\beta_{Cl-Cl}=0$

$\gamma_{Sn-Cl}=0.4$ $\gamma_{Cl-Cl}=0.3$

$\delta_{Sn-Cl}=0.00039$ $\delta_{Cl-Cl}=0.00014$

$\frac{\pi}{10}\Delta r_{Sn-Cl}=0.01333$

The broken line in Fig. 1 indicates the $\chi_{SnCl}(q)$. The final molecular intensity, $qM(q)^{obs}$, and the corresponding radial distribution, $f(r)$, are shown in Figs. 2 and 3 respectively.

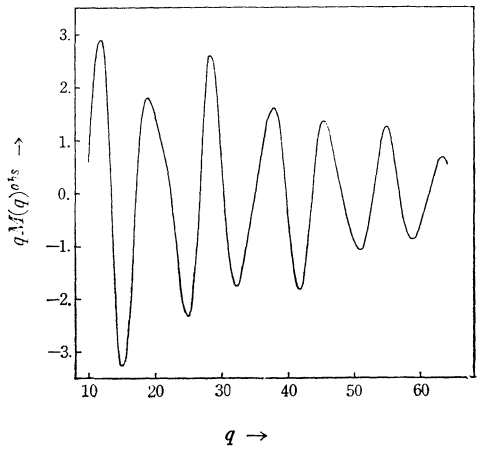

Fig. 2. The molecular intensity curve, $qM(q)^{obs}$.

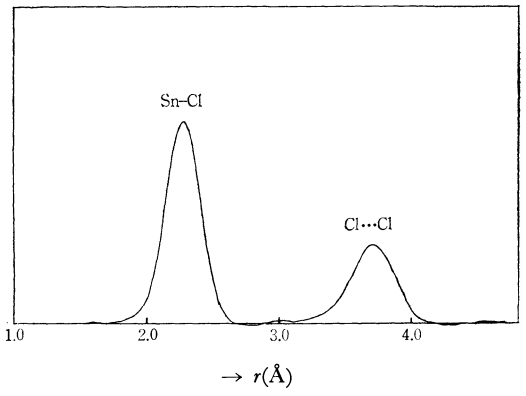

Fig. 3. The radial distribution curve, $f(r)$.

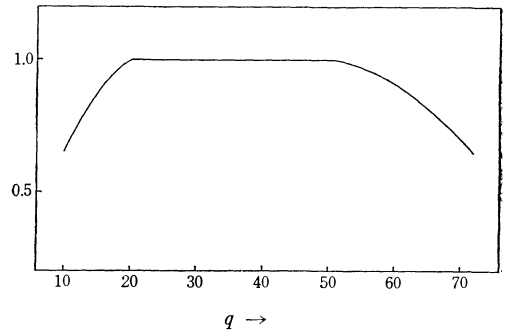

Fig. 4. The weight function employed for the least-squares fitting.

The molecular parameters were determined by the least-squares method applied to the $qM(q)^{obs}$, with the weight function shown in Fig. 4. A regular tetrahedral symmetry was assumed.

The atomic scattering factors, $|F|$, and the phase shift, $\Delta\eta$, used in the $qM(q)^{theor}$ are those calculated by Kimura *et al*,[18] the inelastic scattering factors, S, for Cl and Sn are those calculated by Tavard *et al*[19] and by Bewilogua[20] respectively.

The anharmonicity parameters, κ, fixed in the least-squares treatment were estimated to be 16×10^{-7} Å^3 for Sn–Cl and 100×10^{-7} Å^3 for Cl···Cl by following the method applied to $SiCl_4$ by Morino and Murata.[9] Errors based on the uncertainties in κ were included in the total errors, which will be described in the next section.

The measurements of the optical densities were carried out by the digital and the pen-recording methods. Table 1 shows the values of r_a observed by the digital method. The results obtained from the D_l and the D_r agree with each other within their standard deviations. The final values of r_a for each plate were determined by multiplying the averages of the two values by the scale factor. The final results obtained by the two methods for plate 1 are compared in Table 2. The two results agree with each other, but the standard deviations are about a half as much in the digital method as in the pen-recording method. This is because the smoother intensity curve was obtained by the former method than by the latter. Therefore, the results by the digital method were adopted as the final values for plates 1 and 2. Plate 3 was measured only by the pen-recording method.

18) M. Kimura, S. Konaka and M. Ogasawara, *J. Chem. Phys.*, **46**, 2559 (1967); M. Ogasawara, S. Konaka and M. Kimura, *ibid.*, **50**, 1488 (1969).

19) C. Tavard, D. Nicolas and M. Roualt, *J. Chim. Phys.*, to be published.

20) L. Bewilogua., *Physik. Z.*, **32**, 740 (1931).

TABLE 1. RESULTS OBTAINED FROM THE OPTICAL DENSITIES MEASURED BY THE DIGITAL METHOD[a)]

		from D_l[b)]	from D_r[b)]	Average
Plate 1	k	0.995 ±0.011	0.993 ±0.011	0.994 ±0.011
	r_a(Sn-Cl)	2.2795±0.0008	2.2777±0.0008	2.2786±0.0008
	l(Sn-Cl)	0.0513±0.0017	0.0519±0.0017	0.0516±0.0017
	r_a(Cl···Cl)	3.7119±0.0030	3.7125±0.0029	3.7122±0.0030
	l(Cl···Cl)	0.1117±0.0027	0.1086±0.0027	0.1102±0.0027
Plate 2	k	0.965 ±0.012	0.971 ±0.014	0.968 ±0.014
	r_a(Sn-Cl)	2.2796±0.0009	2.2797±0.0010	2.2797±0.0010
	l(Sn-Cl)	0.0494±0.0019	0.0500±0.0022	0.0497±0.0022
	r_a(Cl···Cl)	3.7165±0.0033	3.7117±0.0038	3.7141±0.0038
	l(Cl···Cl)	0.1104±0.0029	0.1104±0.0034	0.1104±0.0034

a) Distances and mean amplitudes in Å unit. The errors are the standard deviations obtained from the least-squares treatments.
b) See text.

TABLE 2. COMPARISON OF THE RESULTS FOR PLATE 1 OBTAINED SEPARATELY FROM THE OPTICAL DENSITIES BY THE PEN-RECORDING AND THE DIGITAL METHOD*

	Pen-recording	Digital
k	0.952 ±0.020	0.994 ±0.011
r_a(Sn-Cl)	2.2795±0.0015	2.2796±0.0008
l(Sn-Cl)	0.0505±0.0031	0.0516±0.0017
r_a(Cl···Cl)	3.7132±0.0052	3.7139±0.0030
l(Cl···Cl)	0.1043±0.0047	0.1102±0.0027

* Distances and mean-amplitudes in Å unit. The errors are the standard deviations obtained from the least-squares treatment. The r_a values in the third column are those in Table 1 multiplied by the scale factor.

The results of the least-squares refinements for the three plates are summarized in Table 3. The σ_1 and σ_2 values, which represent the standard deviations for the average values, were estimated according to these formulas: $\sigma_1^2=\langle\sigma\rangle^2/3$ and $\sigma_2^2=\sum V_i^2/6$. Here, $\langle\sigma\rangle$ is the average of the standard deviations for the three plates, while V_i is the residual of the value for the ith plate subtracted from the average value.[9] All the σ_1 values are larger than the corresponding values. The final random errors were, then, given by $2.5\sigma_1$, corresponding to the 99 per cent confidence intervals. Two plates of carbon disulfide were measured in order to determine the scale factor for each plate and were analyzed in the same way as were the sample plates. Therefore, various systematic errors involved in the experiment and analysis may be regarded as included in the error of the scale factor.[14] The practical procedure is to determine the scale factor for each plate by comparing the results of analysis at a presumed wavelength with the true structure of carbon disulfide. Analysis was made by assuming the two independent interatomic distances, r(C–S) and r(S···S). Then, the scale factor obtained from one plate of carbon disulfide may be given by a weighted mean of the scale factors determined from the two individual distances, while its standard deviation is given by $\sigma=[1/\sigma_{cs}^2+1/\sigma_{ss}^2]^{-1/2}$.*1 The final scale factor and its standard deviation were determined using the results for the two plates of carbon disulfide. The limit of error of the scale factor was taken as 2.5 times the standard deviation thus obtained, corresponding to 0.12 per cent in interatomic distance.

TABLE 3. SUMMARY OF RESULTS (in Å)

	Plate 1	Plate 2	Plate 3	Average	σ_1	σ_2	2.5σ
k	0.994 ±0.011	0.968 ±0.014	0.982 ±0.018	0.981	0.008	0.008	0.020
r_g(Sn-Cl)	2.2808±0.0008	2.2818±0.0010	2.2797±0.0013	2.2808	0.0006	0.0006	0.0015
l(Sn-Cl)	0.0516±0.0017	0.0497±0.0022	0.0484±0.0029	0.0499	0.0013	0.0009	0.0033
r_g(Cl···Cl)	3.7172±0.0030	3.7191±0.0038	3.7142±0.0046	3.7168	0.0022	0.0014	0.0055
l(Cl···Cl)	0.1102±0.0027	0.1104±0.0034	0.1053±0.0042	0.1086	0.0020	0.0017	0.0050
δ_g	0.0073±0.0033	0.0071±0.0041	0.0085±0.0051	0.0076	0.0024	0.0004	0.0060
method	digital	digital	pen-recording				

*1 The off-diagonal element of the error matrix, $B^{-1}{}_{cs,ss}$, is one to two hundredth as small as the diagonal elements, $B^{-1}{}_{cs,cs}$ and $B^{-1}{}_{ss,ss}$. Therefore, even if the least-squares treatment is performed under the condition that the distances, r(C–S) and r(S···S), are not independent of each other, the results do not change.

The errors associated with the ambiguity of κ were estimated from the results of the least-square fittings carried out by assuming various κ values. They were ± 0.0020 Å for r_g(Sn–Cl) and ± 0.0040 Å for r_g(Cl···Cl).

The total errors for the interatomic distances were estimated by regarding these errors independent of one another. Systematic errors for the mean amplitudes were ignored, for their magnitudes may be considered to be much smaller than the random errors. The final parameters are given in Table 4.

Table 4. Molecular parameters of tin tetrachloride at 18°C

r_g(Sn–Cl)	$2.280_8 \pm 0.003_7$ Å
r_α(Sn–Cl)	$2.274_9 \pm 0.003_7$ Å
l(Sn–Cl)	$0.049_9 \pm 0.003_3$ Å
r_g(Cl···Cl)	$3.716_8 \pm 0.008_2$ Å
r_α(Cl···Cl)	$3.712_7 \pm 0.008_2$ Å
l(Cl···Cl)	$0.108_6 \pm 0.005_0$ Å
δ_g	$0.007_6 \pm 0.006_0$

Discussion of the Results

The r_g(Sn–Cl) value, 2.281 ± 0.004 Å, determined by the present study is about 0.03 Å shorter than those reported by the previous studies[5–7] and 0.11 Å less than the sum of the covalent radii, 2.39 Å. From the results of the electron-diffraction studies of $SiCl_4$[9] and $GeCl_4$[8] the corresponding values of bond shortening are estimated to be 0.14 Å for the Si–Cl bond in $SiCl_4$ and 0.10 Å for the Ge–Cl bond in $GeCl_4$. It may be noted here that the amount of bond shortening for the Sn–Cl bond is smaller than that for the Si–Cl bond, but virtually equal to that for the Ge–Cl bond. These bond shortenings were explained by the partial ionic and the partial double-bond character of these bonds reported to Pauling.[21] From the fact that the same electronegativity value, 1.8 in Pauling's scale, is given to Si, Ge, and Sn atoms, it is reasonable to expect the same partial ionic character; consequently, the bond shortening is the same for all of the Si–Cl, Ge–Cl, and Sn–Cl bonds. Thus, the amounts of bond shortening, 0.14 Å for the Si–Cl, 0.10 Å for the Ge–Cl, and 0.11 Å for the Sn–Cl, become a measure of the extent of their double-bond character. By using the results previously reported by Pauling and Brockway[6], *i.e.*, 2.30 Å for the Sn–Cl bond length and the bond shortening of 0.07 Å, Gordy has mentioned that the quantities of double-bond character decrease in the order of the Si–Cl, Ge–Cl, and Sn–Cl bonds and that a tendency to form multiple bonds decreases with an increase in the size of the atoms.[22] It was found in the present study, however, that the amount of bond shortening for the Sn–Cl bond was similar to that for the Ge–Cl bond. It seems that, for these two bonds, the effect of the increase in atomic size from Ge to Sn is compensated for by that of the decrease in promotion energy from p to d orbitals, and that, as a result, the Ge–Cl and Sn–Cl bonds have almost the same double-bond character.

The r_g values can be converted to r_α by using the relation: $r_\alpha = r_g - [\langle \Delta x^2 \rangle + \langle \Delta y^2 \rangle]/2r_g - \delta r$, where $\langle \Delta x^2 \rangle$ and $\langle \Delta y^2 \rangle$ are the perpendicular mean amplitudes, and δr, the centrifugal stretching. Using the force constants determined from the fundamental frequencies and the Coriolis coupling constants,[13] the values of the perpendicular mean amplitudes were estimated to be 0.0054 Å for the Sn–Cl and 0.0033 Å for the Cl···Cl.*2 The stretchings, δr, were estimated by Iwasaki and Hedberg's method[23] to be 0.0005 Å for the Sn–Cl and 0.0008 Å for the Cl···Cl. The r_α values thus obtained are also listed in Table 4. The ratio of r_α(Cl···Cl) to r_α(Sn–Cl) is 1.6320 ± 0.0026, a value which is in perfect agreement with the corresponding ratio, 1.6330, for a regular tetrahedral structure.

The mean amplitude for the Sn–Cl atom pair is $0.049_9 \pm 0.003_3$ Å, which is much smaller than the value of 0.08 Å reported by Livingston and Rao.[7] Such a large discrepancy between the two results cannot have been produced simply by employing different methods of measurement, *i.e.*, the microphotometer method and the visual method. The ignorance of the phase shift in the previous study certainly led to an inaccurate mean amplitude for the Sn–Cl pair. The mean amplitudes for $SnCl_4$ were calculated by Long and Seibold[24] and also by Müller and Cyvin.[25] The former authors used the Urey-Bradley force field with the assumption that $H'=0$ and gave the values of 0.046 Å for the Sn–Cl and 0.119 Å for the Cl···Cl at 298°K, while the latter used symmetry force constants which had been calculated by the method of the "Verfahren der nächsten Lösung"[26] and gave the values of 0.046 and 0.120 Å for the respective

21) L. Pauling, "The Nature of the Chemical Bond," 3rd Ed., Cornell University Press, Ithaca, New York (1960), pp. 228, 311.

22) W. Gordy, W. W. Smith and R. F. Trambarulo, "Microwave Spectroscopy," John Wiley & Sons, Inc., London (1953), p. 318.

*2 If another set of the force constants is used, there is no significant change in the values of the perpendicular mean-amplitudes.

23) M. Iwasaki and K. Hedberg, *J. Chem. Phys.*, **36**, 2961 (1962).

24) D. A. Long and E. A. Seibold, *Trans. Faraday Soc.*, **56**, 1105 (1960).

25) A. Müller and S. J. Cyvin, *J. Mol. Spectry.*, **26**, 315 (1968).

26) A. Fadini, *Z. Naturforsch.*, **21a**, 426 (1966).

bonds at the same temperature. These calculated values are fairly close to the experimental values. The slight differences must be connected with the force constants used in the mean-amplitude calculations, and originally with the assumptions on which the force constants were given. The mean amplitudes determined in the present study will be helpful in assigning a reasonable set of force constants for tin tetrachloride. The determination and discussion of the force constants for tin tetrachloride will be described in a separate paper.

The authors wish to thank Assistant Professor T. Iijima and Dr. S. Konaka of our Laboratory for their help and discussions throughout this work. The calculations were carried out by the use of an electronic computer, FACOM 270—20. Our thanks are also due to Professor K. Ohno, Department of Chemistry, Faculty of Science, Hokkaido University, for his permission to use the computer.

BULLETIN OF THE CHEMICAL SOCIETY OF JAPAN VOL. 43 1939—1950 (1970)

A Deuteron and Proton Magnetic Resonance Study of Ammonium Oxalate Monohydrate

Takehiko CHIBA

Department of Chemistry, Nihon University, Sakurajosui, Setagaya-ku, Tokyo

(Received October 25, 1969)

The quadrupole spectra of deuteron magnetic resonance were observed on single crystals of $(ND_4)_2C_2O_4D_2O$. The quadrupole coupling tensors for stationary deuterons were determined at -110°C. eqQ/h and η are 163.7—172.8 kHz and 0.005—0.015 for the ammonium deuterons and 213.3 kHz and 0.090 for the water deuteron. The eqQ values and principal axis directions of EFG tensors are consistent with the structure deduced from the diffraction studies with the exception that the z principal axes of D in the ammonium ion deviate appreciably from the NH directions derived from neutron diffraction. From the change in the line-width with the temperature, the rate of the C_3 reorientation of ammonium ions and that of the 180° flip of water molecules were estimated at various temperatures. The ammonium-ion reorientation is found to be quite isotropic. The temperature dependence of the proton T_1 and $T_{1\rho}$ and the deuteron T_1 were measured on $(NH_4)_2C_2O_4H_2O$ and $(ND_4)_2C_2O_4D_2O$ powers. The T_1 values were then compared with the calculated values, assuming ammonium reorientation. The sharp drop of the proton $T_{1\rho}$ with the temperature above 50°C can be interpreted as being due to the 180° flip motion of water molecules through a relaxation mechanism of "slow motion." The rates of motion derived from the relaxation-time measurements are consistent with those estimated from the line-width change.

Deuteron magnetic resonance (DMR) has been successfully applied to problems of the structure and the motions of molecules in the crystals in which hydrogen atoms participate. DMR studies have often been made of O–H–bond systems, but studies of systems in which H is bonded to atoms other than O have been rather rare. The electric field gradient (EFG) at a deuteron is always nearly in the direction of the D–X bond. The DMR of an ND_4^+ ion gives, at a high temperature, a single line or a doublet of small separation due to the effect of the averaging of the EFG at each D by rapid reorientation. The doublet line may originate from the deviation from the regular tetrahedron of the ND_4^+ ion as well as from the effect due to external charge distribution. However, it is not clear what the relative importance of each contribution is. The motion of the NH_4^+ ion in ammonium salts has been studied by various techniques: IR, heat capacity, neutron diffraction, neutron inelastic scattering, proton magnetic resonance, *etc.* The mode of the NH_4^+ reorientational motion in the crystal has not been well known in most of the cases with the exception of some of the ammonium halides with a high crystal symmetry. Although reorientation about a single C_2 axis of NH_4^+ ions has been assumed in a particular case to explain the change in the second moment of the proton magnetic resonance (PMR),[1] the evidence is not fully decisive.

1) D. Pendred and R. E. Richards, *Trans. Faraday Soc.*, **51**, 468 (1955); J. B. Leane and R. E. Richards, *Spectrochim. Acta*, **10**, 154 (1957).

In DMR on single crystals, as compared to PMR, the line-width transition due to motion is often much more specific to the mode of the motion in the crystal, and if the line-width change is carefully followed it can provide more detailed information than does PMR. DMR study with single crystals, including the measurement for the stationary ND_4^+ ion, has thus far been made on ND_4Cl,[2,3] ND_4Br,[2] and $(ND_4)_2SO_4$.[4] In the cubic phase of ammonium halides, the D's are all equivalent, the bond directions are strictly fixed by the high symmetry of the crystal, and there is no preferred axes of rotational motion. Ammonium sulfate has a phase transition which complicates the DMR spectra so much that the accurate determination of quadrupole coupling for each deuteron is almost impossible. Ammonium oxalate monohydrate $(NH_4)_2C_2O_4H_2O$ provides a favorable system for a detailed study of the ND_4^+ ion—its structure and motion—because it has no phase transition in the temperature range of our interest, because each N–H bond is linked by a hydrogen bond of moderate strength, because the barrier to reorientation appears to be sufficiently high so that, for the observation of the spectra of the stationary ND_4^+ ion, one need not go down to very low temperatures, because its crystal structure is well established and is relatively simple, and because single crystals can be easily grown from the aqueous solution.

The four N–H···O hydrogen bond distances in this crystal are slightly different from each other; therefore, one might be able to detect an anisotropy in the reorientational motion. From the results of neutron diffraction study[5] the NH_4^+ ion in ammonium oxalate monohydrate can be said to assume fairly distorted tetrahedron; therefore, if one gets a quadrupole coupling tensor for each D of the four N–D bonds, one might be able to get information about the relation between the distortion of the ammonium ion and the quadrupole coupling averaged by rapid motion. These are the motivations of the present investigation.

In addition to steady-state DMR measurements of single crystals, the proton spin-lattice relaxation time in the laboratory frame, T_1, and that in the rotating frame, $T_{1\rho}$, were measured by pulse techniques on powdered samples at various temperatures. The temperature dependence of the T_1 of the deuteron in the deuterated crystal powder was also measured.

Experimental

The $(ND_4)_2C_2O_4D_2O$ was obtained by repeated exchange with D_2O of $(NH_4)_2C_2O_4$. The single crystals were grown from a saturated, heavy-water solution of deuterated ammonium oxalate by slow cooling. The single crystals used for the study were about $5\times5\times10$ mm^3. For proton resonance, a recrystallized powder sample of a reagent-grade product was used. The measurements of the steady-state DMR were made by sweeping frequency. The field was fixed at a value corresponding to the deuteron Larmor frequency of 10 MHz. The accuracy of the mounting of the crystal on the probe head was achieved by using a reflecting goniometer. In order to reduce complication in the rotation pattern as much as possible, the measurements were made with a static field (H_0) in the *ab*, *bc*, or *ac* plane. The T_1 for the proton and that for the deuteron were measured by the pulse technique at 10 MHz. The T_1 for the proton was measured at 30 MHz. The apparatus for the measurement of the steady-state type and those of the pulse type have been described previously.[6–8]

Results

According to X-ray and neutron structure analyses[9,5] the crystal is orthorhombic, belonging

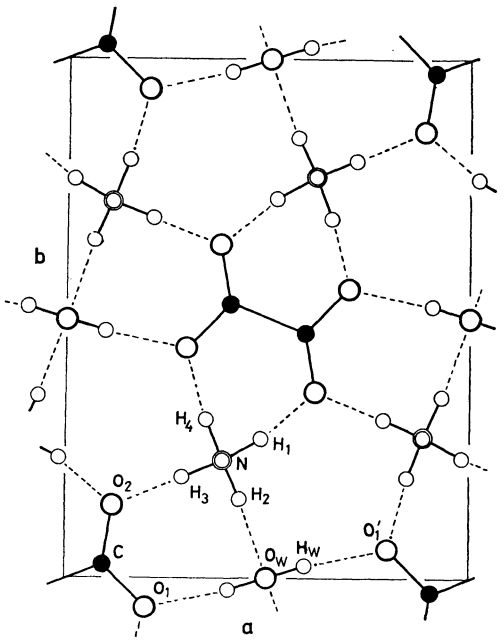

Fig 1. Crystal structure of $(NH_4)_2C_2O_4H_2O$. (001) projection.

2) V. Hovi and P. Pyykkö, *Phys. Kondens. Materie*, **5**, 1 (1966).
3) M. Linzer and R. A. Forman, *J. Chem. Phys.*, **46**, 4690 (1967).
4) D. E. O'Reilly and T. Tsang, *ibid.*, **46**, 1291 (1967).
5) V. M. Padmanabhan, S. Srikantha and S. Medhi Ali, *Acta Crystallogr.*, **18**, 567 (1965).
6) G. Soda and T. Chiba, *J. Chem. Phys.*, **50**, 439 (1969).
7) T. Chiba and Y. Kakiuchi, This Bulletin, **41**, 828 (1968).
8) T. Chiba and T. Ito, *Proceedings of the Institute of Natural Sciences, Nihon University* No. 4, Chemistry Section, (1968), pp. 15—34.
9) J. H. Robertson, *Acta Crystallogr.*, **18**, 410 (1965).

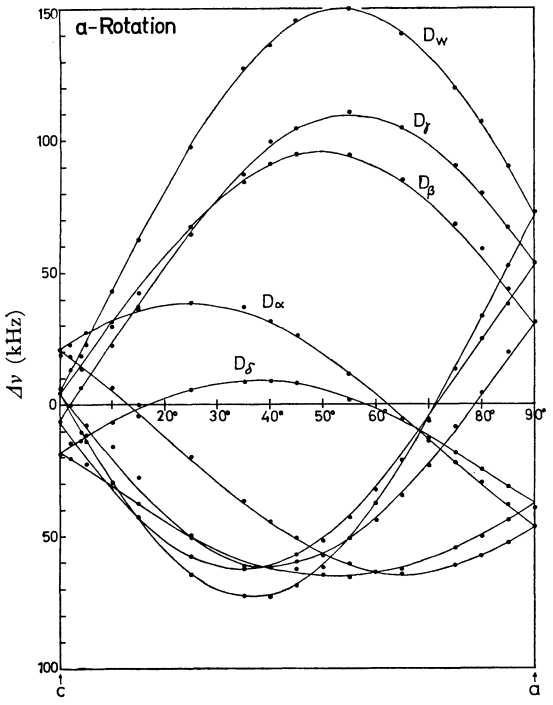

Fig. 2—1.

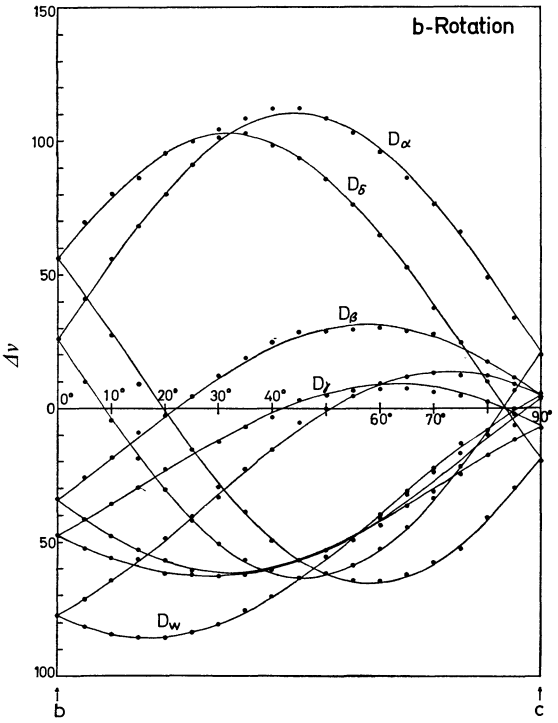

Fig. 2—2.

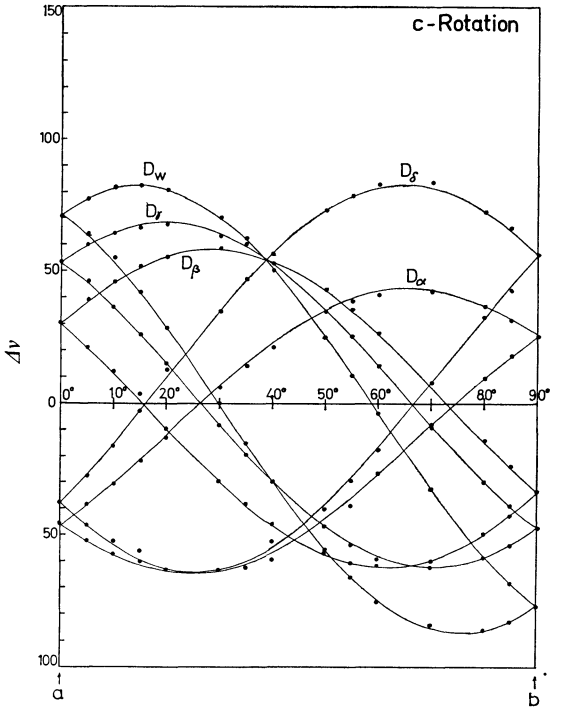

Fig. 2—3.

Fig. 2. Rotation patterns of deuteron magnetic resonance lines of $(ND_4)_2C_2O_4D_2O$ single crystal when the magnetic field is rotated about the crystalline axes *a*, *b* and *c*.

Solid lines represent calculated rotation patterns from the quadrupole coupling tensors given in Table 1.

to the $P2_12_12$ space group. A unit cell contains two formula units (Fig. 1). The ammonium ions are all crystallographically equivalent, and so are all the water molecules. Four hydrogen atoms of the ammonium ions are nonequivalent. The water oxygen atom is placed on the two-fold axis and therefore the water hydrogen atoms are equivalent. There are, thus, a total of 5 nonequivalent deuterons in the crystal of $(ND_4)_2C_2O_4D_2O$. Because a quadrupole interaction splits a deuteron resonance line into two components, from the symmetry of the crystal the maximum number of resonance-line-pairs is expected to be 10 when the static field is applied in the *ab*, *bc*, or *ac* plane, and 20 when H_0 is applied in an arbitrary direction. Spectra in accordance with the expectation are observed below -106°C. Above about -30°C a single line or a pair of lines with a small separation depending on the direction of H_0 characteristic of rapidly-reorienting ammonium ions were observed, together with the lines from the water deuterons. The water lines did not change their shape and position appreciably up to 50°C, where they started to broaden. The angular dependence of the quadrupole splitting for the stationary deuterons was measured at -110°C with H_0 in the *bc* plane (*a*-axis rotation), in the *ac* plane (*b*-axis rotation), and in the *ab* plane (*c*-axis rotation). Since the rotation patterns are symmetric about the crystalline axis direction, it is necessary only to measure the spectra for the angles between the two axes (for instance, between *b* and *c* axes in the *a*-axis rotation pattern). The rotation patterns are shown in Fig. 2.

In the first-order perturbation the frequency difference between the quadrupole-split doublet, $2\Delta\nu=\nu_+(m=1\leftrightarrow0)-\nu_-(m=0\leftrightarrow-1)$, is given by:[10]

$$2\Delta\nu = (3eQ/4\hbar)\{-q_{ZZ}+(q_{XX}-q_{YY})\cos 2\theta + 2q_{XY}\sin 2\theta\}, \quad (1)$$

where q_{ij} is the ij element of the EFG tensor in the XYZ coordinate system and where θ is the angle of rotation of H_0 about the Z-axis in the XY plane, measured from the X-axis. The estimated angular dependence of the quadrupole splitting or the "rotation pattern" was drawn with the following assumptions for the EFG. For ammonium deuterons, the EFG is axially symmetric about the direction of the N–H bond, as determined by the neutron diffraction. For water deuterons, the z principal component of EFG, q_{zz}, is along the OH bond, as determined by the neutron diffraction; the y component, q_{yy}, is perpendicular to the H_2O plane, and the asymmetry parameter $\eta=0.1$ ($|q_{zz}|\geq|q_{yy}|\geq|q_{xx}|$). Each curve of the rotation pattern is assigned to a particular deuteron with the help of this estimated pattern. The lines of the water deuterons are generally sharp and strong and can easily be discriminated from those of the ammonium deuterons, which are relatively weak, broad, and structureless. The rotation patterns of five nonequivalent deuterons are designated as D_α, D_β, D_γ, D_δ (ammonium), and D_w (water). For ammonium deuterons, due to the complexity of the rotation patterns, the assignment of each line is not as simple as for water deuterons. However, the following fact was useful for this purpose. It is seen that each rotation pattern always has one extremum about 60 kHz from the center. We expect this to occur when H_0 is perpendicular to the z axis, and $\Delta\nu$ in this case must be negative (assuming $q_{zz}>0$). Thus, in the *c* rotation pattern, the $\Delta\nu$'s of D_α and D_δ at the *b* axis are positive and those of D_β and D_γ are negative, and the sum of the four $\Delta\nu$'s is nearly zero. The sign of $\Delta\nu$ for the *a* or *b* rotation could, then, be determined referred to the above sign by comparing the $\Delta\nu$ values in the crystalline axis directions. D_α, D_β, D_γ, and D_δ are assigned to H_4, H_1, H_3, and H_2 respectively.*1 In order to determine the eqQ tensor from the rotation patterns about the *a*, *b*, and *c* axes by the method described previously,[6] we must combine the rotation patterns of the right phase, for there are two alternative rotation patterns 90° out-of-phase to each other. The four orientations for the NH_4^+ ion and the H_2O molecule will be denoted by A, B, C, and D, for which the equivalent interatomic vectors have the (xyz), $(x\bar{y}\bar{x})$, $(\bar{x}y\bar{z})$, and $(\bar{x}\bar{y}z)$ components respectively. In the *a* axis rotation, the pattern of A overlaps that of B, and the pattern of C, that of D. In the *b* rotation, the patterns of A and C, and of B and D, overlap. In the *c* rotation, the patterns of A and D, and of B and C, overlap. The rotation patterns of $\Delta\nu$ corresponding to the site-A deuterons were chosen and were combined to determine the quadrupole coupling tensor.*2 The values of eqQ, η and the direction cosines of the principal axes are given in Table 1.

The rotation patterns for the reorienting NH_4^+ deuteron were measured at room temperature. The separations are so small that it is not possible to determine the eqQ tensor. From the observed maximum separation frequency, the value of quadrupole coupling is estimated to be about 1.5 kHz.

To estimate the rate of the reorientation of the ND_4^+ ion and to get information about the mode of

10) M. H. Cohen and F. Reif, "Solid State Physics," Vol. 5, ed by F. Seitz and D. Turnbull, Academic Press Inc., New York, (1957) p. 435.

*1 The numbering of ammonium H atoms differs between Refs. 9 and 5. In this article we use Padmanabhan's (Ref. 5).

*2 All the observed points on the two sets of rotation patterns 90° out-of-phase are included in the least-square process used to determine the quadrupole coupling tensor.

Table 1. Deuteron quadrupole couplings, asymmetry parameters, and direction cosines of principal axes (x, y, z) of field gradient tensors in the coordinate system of crystalline axes (a, b, c) in $(ND_4)_2C_2O_4D_2O$, at $-110°C$

			a	b	c
Water					
$D_w(H_w)$	eqQ/h: 213.3±0.4 kHz	x	0.569 ±0.004	0.106 ±0.016	0.816 ±0.001
	η: 0.090±0.002	y	−0.229 ±0.009	0.973 ±0.002	0.033 ±0.013
		z	0.7900±0.0005	0.2051±0.0009	−0.5778±0.0007
Ammonium					
$D_\alpha(H_4)$*	eqQ/h: 170.5±0.4 kHz	x	0.34 ±0.20	−0.57 ±0.10	0.75 ±0.01
	η: 0.009±0.003	y	−0.89 ±0.08	−0.45 ±0.13	0.06 ±0.17
		z	0.3056±0.0013	−0.6831±0.0009	−0.6633±0.0010
$D_\beta(H_1)$	eqQ/h: 163.7±0.6 kHz	x	0.45 ±0.09	0.40 ±0.14	0.80 ±0.02
	η: 0.015±0.005	y	−0.55 ±0.07	0.83 ±0.07	−0.11 ±0.13
		z	−0.7054±0.0010	−0.3860±0.0016	0.5945±0.0014
$D_\gamma(H_3)$	eqQ/h: 166.1±0.5 kHz	x	−0.61 ±0.05	0.50 ±0.40	0.62 ±0.28
	η: 0.005±0.004	y	−0.10 ±0.30	−0.82 ±0.25	0.57 ±0.30
		z	0.7865±0.0008	0.2850±0.0015	0.5479±0.0012
$D_\delta(H_2)$	eqQ/h: 172.8±0.5 kHz	x	0.86 ±0.10	0.49 ±0.10	0.14 ±0.24
	η: 0.008±0.004	y	0.35 ±0.24	−0.37 ±0.14	−0.86 ±0.04
		z	−0.3738±0.0014	0.7870±0.0008	−0.4909±0.0013

* (H_4) *etc.* are H atom sites by Padmanabhan (Ref. 5).

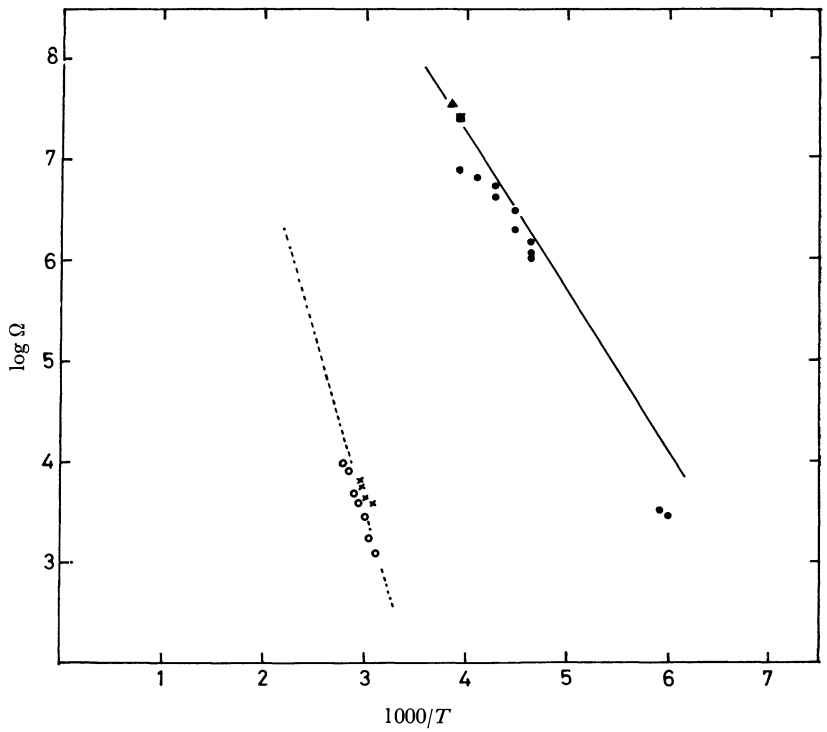

Fig. 3. Reorientation rates of water molecule and ammonium ion in $(NH_4)_2C_2O_4H_2O$. Ammonium ion (C_3) reorientation rate: ● from DMR line width change: ■ from proton T_1 minimum: ▲ from deuteron T_1 minimum. Relation of Eq. (8) is shown by a solid line. Water molecule reorientation rate: × from DMR line width change: ○ from proton $T_{1\rho}$. Dotted line corresponds to ΔE of 15.5 kcal/mol.

the motion, the line broadening of the spectra in the limits of rapid motion and of slow motion were observed. As will be mentioned in the next section, we assume only C_3 reorientations for the motion of the NH_4^+ ion in this crystal. In the case of isotropic reorientation, the average rate, Ω, of C_3 reorientation about one of the four axes is related to the average lifetime, τ, for a hydrogen atom to be in one of the four equilibrium positions by:

$$3\Omega = 1/\tau\,. \tag{2}$$

From the theory of the motional broadening of the spectral line,[11] we have, for the rapid limit spectra:

$$\Delta\nu_M = \frac{\pi}{8\Omega}\sum(\Delta\nu_i)^2\,, \tag{3}$$

and, for the slow limit spectra:

$$\Delta\nu_M = \frac{3}{2\pi}\,\Omega, \tag{4}$$

where $\Delta\nu_M$ is the line width due to the motion and where $\Delta\nu_i$ is the separation from the average frequency (here, the Larmor frequency) of the line of the stationary i-th deuteron. The broadening process is observed with H_0 in the a- and b-axisdirections. (The rapid-limit spectra, except when H_0 is in the crystalline axis directions, consist of two-line components with different degrees of broadening.) The values of $\Delta\nu_M$ at the two limiting cases were estimated by an approximate procedure from the observed line width, which includes the dipolar width.[7] These values were then used to derive the reorientation rate, Ω, of the ND_4^+ ion. The results are shown in Fig. 3. From the slope of this plot, the activation energy of reorientation, ΔE, is estimated to be 8.8 kcal/mol. The effect of the possible anisotropy of the motion will be discussed in the next section.

The lines of water deuterons start to broaden at about 50°C. The line-broadening process of water deuterons was observed, and the rate of reorientation was estimated in the same way as was done in the case of other hydrates. The reorientation rates thus derived are shown in Fig. 3.

The results of pulse measurements are shown in Fig. 4. It can be seen in this figure that the temperature dependence of the T_1 of both the proton and the deuteron is adequately explained by the reorientational motion, whose correlation frequency is expressed by the Arrhenius equation. The relevant motion is that of the NH_4^+ ion. The T_1 values will be analyzed in the next section. As is to be exprected from the theory, the log $T_{1\rho}$ *vs.* $1/T$ plot is roughly a straight line, coinciding with the log T_1 curve at the high-temperature side of the minimum and then extending further to low temperatures. The $T_{1\rho}$ could not be measured down to its minimum because of the instrumental difficulty. Above 50°C $T_{1\rho}$ starts to drop again.

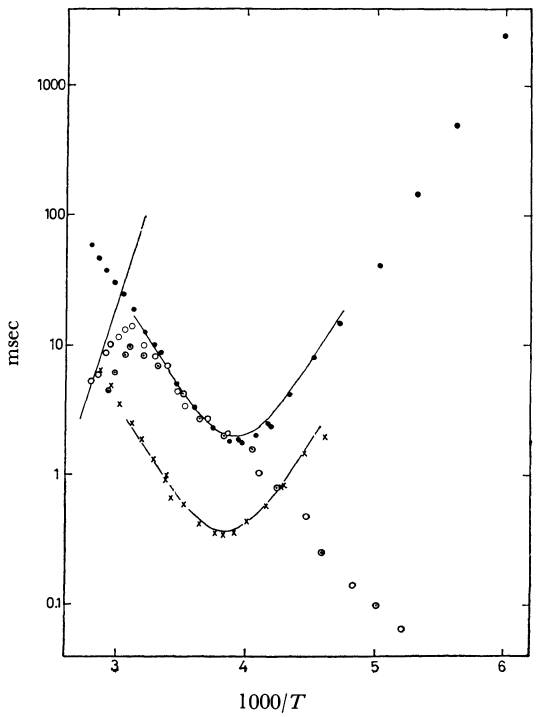

Fig. 4. Temperature dependence of the relaxation times of ammonium oxalate monohydrate powder samples.
● Proton T_1 ○ Proton $T_{1\rho}(H_1=6G)$
⊙ Proton $T_{1\rho}(H_1=4G)$ × Deuteron T_1
The straight line at the left represents $T_{1\rho}$ due to 180° flip of H_2O. Curves through T_1 minima are from Eqs. (5), (7) and (8).

This is considered to be due to the effect of the reorientation of the water molecule and will be discussed in the next section.

Discussion

In 1965, almost concurrently two independent works on the structure analysis of ammonium oxalate monohydrate were published; one was a refinement of the X-ray analysis at 30°K by Robertson,[9] and the other was a neutron diffraction study by Padmanabhan *et al.*[5] In view of the practical limits of precision of the two techniques, we will quote, in comparing the structure and EFG tensors, the heavy-atom coordinates from the X-ray study and the NH and OH bond directions from the neutron study.

Quadrupole Coupling Values. As has been discussed previously, the correlation between the O–D···O hydrogen bond length and the eqQ/h of D is fairly well represented by an empirical curve[12] or by empirical formulas.[6] The value of eqQ/h 213.3±0.4 kHz for the water deuteron is a reasonable value for a "fairly strong" hydrogen

11) P. W. Anderson, *J. Phys. Soc. Jap.*, **9**, 316 (1954).

12) T. Chiba, *J. Chem. Phys.*, **41**, 1352 (1964).

Table 2. Deuteron quadrupole coupling values, N-H bond distances and N···O hydrogen bond distances

	eqQ/h (kHz)	N-H[a] (Å)	N···O[b] (Å)
H_1	163.7	1.02	2.803
H_2	172.8	1.03	2.879
H_3	166.1	1.01	2.830
H_4	170.5	1.03	2.833

a) Ref. 5, mean standard deviations for bond lengths: 0.023 Å.
b) Ref. 9, estimated standard deviation of N···O lengths: 0.006 Å.

bond with an O-O length of 2.743 Å, and it falls on the empirical curve. This value is close to that of 209.7±2.5 kHz for D in $K_2C_2O_4D_2O$,[13] which has nearly the same hydrogen bond length, 2.744± 0.017 Å.[14] In Table 2 the eqQ values of ammonium deuterons are listed, along with the corresponding N—O hydrogen bond distances and N–H bond distances. The values of eqQ/h decrease as the N—O distance decreases and as the N–H distance increases. The correlation between eqQ and the N–D···O hydrogen bond length, similar to that in the O–D···O hydrogen bond system, is quite apparent. Table 3 lists some of the deuteron quadrupole coupling constants in the N–D bonds. It seems that it would be very interesting to know whether a curve similar to the one for the O–O system can be drawn of eqQ *vs.* the N–O distance, with eqQ/h=282 kHz as the limit of the weakest hydrogen bond. However, a few more experimental data must be added before this can be done.

Table 3. Deuteron quadrupole couplings, asymmetry parameter and N···O hydrogen bond distances in some N-H systems*

	eqQ/h (kHz)	η	N···O distance (Å)
$CO(NH_2)_2$	211[a]	0.14	3.00[b]
$(NH_4)_2SO_4$	174[c]	(0)	2.92[d]**
NH_4Cl	180.1±1.0[e,f]	0±0.01	
NH_4Br	180[e]	0	
NH_3(Solid, 75°K)	156±7[g]	0—0.3	
(Free molecule)	282±12[h]	0.05±0.06	
$(NH_4)_2C_2O_4H_2O$	168.3	0.01	2.84

* Average value is listed when more than one value are involved.
** Bifurcated or trifurcated long hydrogen bonds are not included.
a) T. Chiba, This Bulletin, **38**, 259 (1965).
b) A. Caron and J. Donohue, *Acta Crystallogr.* **17**, 544 (1964).
c) Ref. 4.
d) E. O. Schlemper and W. C. Hamilton, *J. Chem. Phys.* **44**, 4498 (1966).
e) Ref. 2.
f) Ref. 3.
g) S. W. Rabideau and P. Waldstein, *J. Chem. Phys.*, **45**, 4600 (1966).
h) P. Thaddeus, L. C. Krisher and P. Cahill, *ibid.*, **41**, 1542 (1964).

Structure of Water Molecules. The direction of the z principal axis of the water deuteron is in good agreement with the O–H bond direction obtained from the neutron diffraction, the deviation being only 3.0°. The angle between the z axes of the two water deuterons in the water molecule is 109.4°. It should be noted that the plane containing two z principal axes makes an angle of 14.6° with the crystalline a axis; this angle is in excellent agreement with 15.2°, the angle between the O_1–O_w–O_1' plane and the a axis, in contrast to a fairly large twisting of the water molecule in the hydrogen bond system (4.6° between O_1–O_1' and H_w–H_w' directions) reported in the neutron diffraction study. The principal y axis of EFG of the water deuteron is nearly perpendicular (within 2.3°) to the plane formed by the two z axes, which is in accord with the empirical relation about the y axis.[12,15]

Structure of Ammonium Ions. The directions of the z principal axes of the EFG tensors in the ND_4^+ ions are approximately in the N–H directions, as determined by the neutron diffraction, but the deviation angles, 5.2°, 2.3°, 4.6°, and 7.3° for NH_1, NH_2, NH_3, and NH_4 respectively, are somewhat larger than those usually found. The mean standard deviations in bond angles from the neutron diffraction study are estimated to be 1.9°, and the standard deviation of the z direction in this study is well below 1°. Therefore, these deviation angles exceed the limits of experimental error. The angles between the z principal axes in the ND_4^+ ion are quite close to the tetrahedral angle, as is shown in Table 4. A comparison of these with the HNH angles from the neutron diffraction study indicates a rather large distortion of the NH_4^+ tetrahedron. The small deviation angles from perfect parallelism of the z axis of the deuteron EFG with the bond direction determined from the diffraction study may be attributed to the effect of charges from the atoms which are not directly bonded to the hydrogen atom in question. In the present case of the ND_4^+ ion, however, it seems rather unrealistic that a nearly tetrahedral arrangement of the EFG tensors is due to the effect of nearby atoms on an otherwise considerably dis-

13) J. W. McGrath and G. W. Ossman, *J. Chem. Phys.*, **46**, 1824 (1967).
14) R. Chidambaram, A. Sequeira and S. K. Sikka, *ibid.*, **41**, 3616 (1964).
15) T. Chiba and G. Soda, "Magnetic Resonance and Relaxation," Proc. 14th Colloque Ampère, Ljubljana, North-Holland Publ. Co., Amsterdam (1966), p. 722.

TABLE. 4. DEVIATION FROM 109.5° OF HNH ANGLES DETERMINED BY DMR, AND BY NEUTRON DIFFRACTION STUDY (in the parentheses)

	H_1	H_2	H_3
H_2	−0.1 (−0.6)		
H_3	+0.3 (+7.6)	+0.3 (−4.4)	
H_4	+0.8 (−5.2)	−0.5 (+1.9)	−1.0 (+0.1)

torted arrangement of the z principal axes along the N-D bonds. The parallelism between the N–O directions and the z axis is to be compared with that between the N-O and N–H directions. The average angle of deviation of the N–H···O hydrogen bond from perfect linearity, assuming that the N–H bond is in the direction of the z axis, is 7.5°, while that determined by the neutron diffraction is 6.0°. Therefore, in this respect at least, the N–D bonds directed in the z axes can be almost as reasonable as the directions given by the neutron diffraction.

Let us now consider a few possible causes of these rather large discrepancies between the bond directions derived from the two methods:

a) The isotope effect as the cause of discrepancies—that is, the NH_4^+ ions in this compound are distorted, while the ND_4^+ ions are not. The changes in the bond angles seem to be too large to be ascribed to an isotope effect, however, and it is difficult to find any particular reason for such a large effect to be operative in this case.

b) The z principal direction not in the true bond direction—(1) crystalline field effect. External charges in the crystal to the EFG, the type of effect considered previously,[16,17] would cause a deviation of the z axis from the bond direction. However, it seems too artificial to say that such an effect results in the regular tetrahedral arrangement of the z directions. (2) Bent orbital effect. Assume that the bond orbitals of N are tetrahedrally directed, but the the H–N–H angle, for instance, is larger than the tetrahedral angle because of a force in intermolecular nature. In such a bent orbital or incomplete orbital-following case, the center of the overlap charge of the bond orbitals of N and H are located slightly inside the HNH triangle. A negative contribution to the EFG from this charge will have the effect of tipping the z principal axis of the total EFG at H (which is positive) in such a way that the angles between the two z directions of EFG will be closer to the tetrahedral angle than the actual HNH angle. When the HNH angle is smaller than the tetrahedral angle, the situation is reversed and again the HNH angle becomes closer to the tetrahedral angle. At least qualitatively, this seems to be a plausible explanation; it could also favorably account for the smaller net distortion of eqQ from a regularly tetrahedral arrangement in ammonium sulfate than that expected from structure analysis.[4] We have, however, no estimate of the magnitude of this effect at present. Moreover, in the case of ammonium dihydrogen phosphate (ADP), distortion from the tetrahedral symmetry determined by neutron diffraction is consistent with that estimated from the quadrupole interaction[17] despite the fact that, from the symmetry at the site of ND_4^+, a pronounced effect of deviation from the orbital following is to be expected.*3 Another experimental evidence against the above view is to be found in the deuteron-quadrupole coupling in some C–ND_3 systems where there is a rapid reorientation of the ND_3 group about the C–N bond. In triglycine sulfate, eqQ values ranging from 37.3 to 54.8 kHz have been reported from various ND_3 sites of para- and ferro-electric phases.[18,19] For CH_3ND_3Cl we obtained an eqQ value of 45 kHz from the room-temperature powder spectrum. In these cases the quadrupole coupling is given approximately by $eq_0Q(1-3\cos\theta)2$, where θ is the angle between the z axis of EFG of D at rest and the C–N bond and where q_0 is the magnitude of this EFG. Though q_0 should vary from one compound to another, the wide distribution of the observed eqQ values can be attributed to a wide distribution in θ. A definite conclusion as to the validity of the above effect must, however, be deferred until a quantitative calculation is made for this effect and until the measurements of the DMR as well as of the neutron diffraction are made on various ammonium salt crystals. Such studies seem to be of great importance because, in view of the usefulness of DMR as a means of determining the bond direction of H–(X), the limitations of this technique should be well established.

The averaging of the four quadrupole coupling tensors of the ND_4^+ ion gives $eqQ/h=-1.67$ kHz and $\eta=0.92$, values consistent with the small quadrupole coupling value of ~1.5 kHz observed at room temperature. Since the principal z directions of EFG did not agree with the bond directions by neutron diffraction, no general conclusion can be drawn concerning the relation between the averaged quadrupole coupling in the rapidly reorienting ND_4^+ ion and the distortion of the ion. However, judging from the close correlation of eqQ values with the N···O distances,

16) T. Chiba, *J. Chem. Phys.*, **36**, 1122 (1962).
17) T. Chiba, This Bulletin, **38**, 490 (1965).

*3 In the tetragonal phase of ADP, NH_4^+ forms a slightly "flat" tetrahedron (site symmetry: D_{2d}) In this structure it is not possible to form 4 equivalent orthogonal orbitals of N directed in the N–H directions from s and p orbital hybridization.

18) J. L. Bjorkstam, *Phys. Rev.*, **153**, 599 (1967).
19) R. Blinc, M. Pintar and J. Zupančič, *J. Phys. Chem. Solids*, **28**, 405 (1967).

it appears that the average eqQ is determined mainly by the local structure of the ion and that the crystalline field effect is relatively unimportant.

Motion of Ammonium Ions. For an NH_4^+ tetrahedron, reorientational motions can either by about its C_2 axes or about its C_3 axes. In ammonium halides where the crystal structure is such that a rotation about the C_2 axis is subject to a four-fold potential, 90° reorientations about the C_2 axes are considered to be the substantial ones. When the NH_4^+ ion is held by four hydrogen-bond-acceptor oxygen atoms in a nearly tetrahedral arrangement, the potential barrier to the C_3 reorientation is considered to be less than that to the C_2 reorientation, for the former requires 3 hydrogen bonds to be broken in the course of the rotation, while the latter requires 4 bonds to be broken. Therefore, we assume only C_3 reorientations in the present case.

Suppose the rate of reorientation about the N–H_1 axis, Ω_1, is different from that about the other 3 axes (N–H_2, N–H_3, and N–H_4), Ω_2. Then the probability for a given hydrogen atom in site 1 to be transferred to other sites is $3\Omega_2$, while the corresponding probability for Sites 2, 3 and 4 is $2\Omega_2+\Omega_1$. The width due to motion at the slow exchange limit (measured in angular frequency units) of a line corresponding to a particular site is just the probability of a jump from that site to others. For instance, if $\Omega_1=2\Omega_2$ the width due to the motion of the Site-1 line relative to that of the Site-2 line at the slow exchange limit will be 0.75, and if $\Omega_1=1/2\Omega_2$ it will be 1.20. The spectra near the limit of the slow exchange rate when H_0 is in the b axis direction are shown in Fig. 5. At −110°C where deuterons are practically stationary, the lines corresponding to the four sites (D_1, D_2, D_3, and D_4) are separately observed with approximately the same intensity.

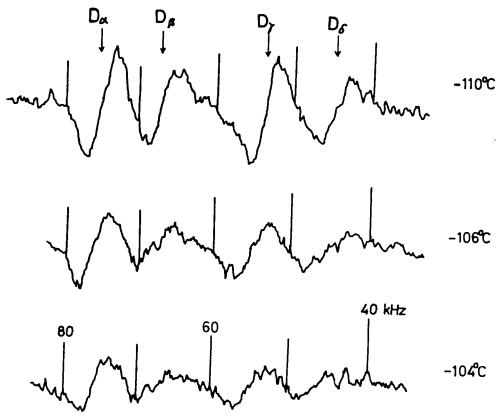

Fig. 5. Ammonium deuteron lines at the slow exchange limit recorded with H_0 in the b axis direction.

The broadened spectra at −106°C and at −104°C show no appreciable difference in the extent of broadening among the four lines. In view of the high sensitivity of the signal height as recorded as a derivative curve to the line-broadening effect, it can safely be said that the ratio of the motional line-width between any two of the four lines is well within the 0.75—1.20 range. Therefore, the reorientation of the NH_4^+ ion is considered to be quite isotropic.*4 If it is further assumed that Ω_1 and Ω_2 are governed by Arrhenius equations with the same pre-exponential factor, $\Omega_1=\Omega_0\exp(-\Delta E_1/RT)$ and $\Omega_2=\Omega_0\exp(-\Delta E_2/RT)$, $\Omega_1/\Omega_2=2$ or 0.5 gives, at −105°C, $\Delta\varepsilon=\Delta E_1-\Delta E_2=\pm 233$ cal/mol. From the rough estimate given above, it appears that the difference in the activation energy is quite small. This conclusion is unaltered when more than two different Ω values are involved. If one considers the hydrogen-bond energy to be a main factor in determining ΔE, one may conclude that the difference in hydrogen-bond energy in the four bonds is rather small, although a fairly large difference in hydrogen-bond lengths has been reported from the X-ray study. This is in contrast to the case of the H_2O flip motion, where a marked dependence of ΔE on the hydrogen-bond distance is seen.[6]

The average proton relaxation time for reorienting NH_4^+ ions (the intraionic effect only) in a powdered sample is given by O'Reilly and Tsang[4] as:

$$\frac{1}{T_1}=(1.91\times10^{10})\left(\frac{\tau_c}{1+\omega^2\tau_c^2}+\frac{4\tau_c}{1+4\omega^2\tau_c^2}\right) \quad (5)$$

where τ_c is related to the τ in Eq. (2) as:

$$\tau_c=3\tau/4\,. \quad (6)$$

with $\omega=2\pi\times10^7$ sec^{-1}, Eq. (5) gives a T_1 minimum of 2.27 msec at $\omega\tau=0.62$, or $\tau=1.31\times10^{-8}$ sec^{-1}. Since the cross-relaxation time between protons in the NH_4^+ ion and the H_2O molecule in the crystal must be much shorter than this T_1 value, the 10 protons in $(NH_4)_2C_2O_4H_2O$ are to be relaxed by this mechanism instead of the 8 protons in $2(NH_4)$. Therefore, the actual T_1 minimum will be $(10/8)\times$ 2.27 msec=2.84 msec. The observed T_1 minimum is 2.6 msec at $T=254$°K. Since the interionic contribution to relaxation is not included in Eq. (5), the agreement is quite satisfactory.

In the deuteron resonance, T_1 is determined almost entirely by the quadrupole interaction. The pulse experiment is made on the deuteron line of the reorienting ND_4^+ ion, which has a nearly zero spliting. Therefore, water deuterons which

*4 After this work had been completed we learned that, in a suitable temperature range, the $NaND_4SO_4$-$2D_2O$ crystal exhibits the DMR spectra of the ND_4^+ ion under rapid reorientation about a single C_3 axis (D. J. Genin and D. E. O'Reilly, *J. Chem. Phys.*, **50**, 2842 (1969)).

have a large splitting are not involved in the observed T_1 practically. The theoretical expression for the quadrupole relaxation in the present case is given in the Appendix. When numerical values $(eqQ/h)=168$ kHz and $\omega=6.28\times10^7$ sec^{-1} are substituted in Eq. (A9), the T_1 for a powdered sample will be given by:

$$\frac{1}{T_1}=(8.36\times10^{10})\left(\frac{\tau}{1+\omega^2\tau^2}+\frac{4\tau}{1+4\omega^2\tau^2}\right). \quad (7)$$

The T_1 minimum is attained when $\omega\tau=0.62$ or $\tau=0.98\times10^{-8}$ sec. The calculated T_1 minimum= 0.53 msec is in good agreement with the experimental value, 0.52 msec, observed at 262°K.

The values of the reorientation rate $\Omega(=1/3\tau)$ at the temperature of the T_1 minima derived above for the proton and the deuteron are found to be in satisfactory agreement with the results from the line-width transition, as may be seen in Fig. 3. The values of the activation energy, ΔE, derived from the high- and low-temperature-side slopes of the T_1 minima of log T_1 *vs.* $1/T$ curves are:

	From the high-temp. slope	From the low-temp. slope
Proton	7.07 kcal/mol	7.46 kcal/mol
Deuteron	7.27 kcal/mol	

Averaged: 7.27 kcal/mol.

With this average value of ΔE, the best fits of τ at the T_1 minimum for both the proton and the deuteron are obtained by:*5

$$\tau=10^{-14.1}\exp(7.27/RT). \quad (8)$$

log T_1 *vs.* $1/T$ curve near the T_1 minimum, calculated from Eqs. (5) and (8) for the proton and from Eqs. (7) and (8) for the deuteron, are drawn in Fig. 4. The agreement with the observed data is satisfactory.

The ΔE value of 7.27 kcal/mol obtained from the proton and deuteron relaxation times is probably more reliable than that obtained from the line-width transition. This value is higher than those for most of the ammonium salts, indicating fairly strong hydrogen bonds holding the ammonium ion.

In Fig. 3 a serious disagreement is found between the Ω derived from the line broadening at the slow exchange limit and that derived from Eq. (8) (shown by the solid line). This might seem to indicate a variation in activation energy at low temperatures. However, in the temperature dependence of T_1 in Fig. 4 no such effect is indicated. The reason for this disagreement is not clear.

Motion of Water Molecules. As has been stated before, the broadening of the water-deuteron line at about 50°C is considered to be due to the 180° flip motion about the bisector axis of the water molecule. The line broadening takes place at a considerably higher temperature than in most of the hydrates studied thus far. The water of hydration is lost before the temperature reaches the point where the motion is rapid enough to allow observation of the averaged spectrum. We estimate the value of activation energy from the reorientation rate derived from the line broadening at the slow exchange limit, assuming a pre-exponential factor of the reorientation rate to be 10^{14} sec^{-1}, a value often found for water of hydration.[6] The value of $\Delta E=15.5$ kcal/mol thus derived is the highest value obtained thus far for the 180° flip motion of water molecules. It is interesting that, in a crystal with a similar composition, $K_2C_2O_4H_2O$, a high activation energy of 14 kcal/mol has been reported.[20] In this latter compound, DMR line broadening begins just above room temperature.[13] The high activation energies in these crystals are parallel with the short hydrogen-bond distances and the small deuteron-quadrupole coupling values.

A short drop of the $T_{1\rho}$ of the proton at the high temperature in Fig. 4 can also be understood as associated with the 180° flip motion of water molecules. Since the *rf* field strength, H_1, used in the measurement of $T_{1\rho}$ is comparable to the local field, and since $T_{1\rho}$ decreases with an increase in the temperature, that is, with an increase in the assumed reorientation rate of the H_2O motion, the $T_{1\rho}$ in this range must be determined by the mechanism of "slow motion." Such cases have been dealt with by Slichter and Ailion.[21] $T_{1\rho}$ is given by the formula:

$$\frac{1}{T_{1\rho}}=\frac{2}{\tau}(1-p)\frac{H_L'^2}{H_L'^2+H_1^2}, \quad (9)$$

where $1/\tau$ is the rate of the motion and H_L' is the local field in the rotating frame and is related to the second moment, $\langle\Delta H^2\rangle$, by $H_L'^2=(1/3)\langle\Delta H^2\rangle$. The $1-p$ factor gives a measure of the effectiveness of the motion to the relaxation, and when the nuclei exchange positions between two sites, r and q, it is given by:

$$1-p=\sum_i(A_{ir}-A_{iq})^2/\{\sum_i(A_{ir}^2+A_{iq}^2)+\sum'A^2\} \quad (10)$$

where $A_{ab}=(3\cos^2\theta_{ab}-1)/r_{ab}^3$. r_{ab} is the length of the internuclear vector, $\boldsymbol{r}_{ab}$, joining a spin at Site a to that at Site b, and θ_{ab} is the angle between H_0 and $\boldsymbol{r}_{ab}$. The suffix i refers to all the stationary spins which interact with the spins, r and q, in

*5 The pre-exponential factor is dependent on the mass difference of H and D by a factor $1/\sqrt{2}$ (see Ref. 4, Appendix). In the present case, however, since unknown isotope effects of various origin may also be involved, the small correction of $1/\sqrt{2}$ is ignored.

20) J. W. McGrath and A. A. Paine, *J. Chem. Phys.*, **41**, 3551 (1964).

21) C. P. Slichter and D. Ailion, *Phys. Rev.*, **135**, A1099 (1964).

motion. The last term in the denominator represents a sum over all the spin-pairs which are motion-independent (including A_{rq}^2). To apply Eq. (9) to the present measurements, which are made on powdered samples, $1-p$ must be averaged over the direction of H_0. The denominator of Eq. (10) is just the lattice part of the second moment. The evaluation of the angular average of Eq. (10), $(1-p)_{AV}$, can be done by numerical integration, but would be quite laborious to perform. For the present discussion it may be sufficient to estimate $(1-p)_{AV}$. For this purpose it may be permitted to approximate it by taking the angular averages of the numerator and denominator separately. A second moment of about 7.5 G^2 is obtained from the powder spectrum of proton resonance at room temperature. Thus, the denominator averaged over the H_0 direction will be:

$$\langle\text{denom.}\rangle_{AV} = \langle\Delta H^2\rangle/(4/5)\cdot(3/4)^2\hbar^2 I(I+1) = 0.021\ \text{Å}^{-6}.$$

For the evaluation of the numerator, a sum is taken over all the inter-proton pairs between a given H_2O molecule and the nearest 8 NH_4^+ ions. A can be expressed in terms of the inter-proton vectors and the H_0 directions in the coordinate system of the crystalline axes. The angular average is readily made, and

$$\langle\text{num.}\rangle_{AV} \simeq 0.0022\ \text{Å}^{-6}.$$

We get $(1-p)_{AV}\sim\langle\text{num.}\rangle_{AV}/\langle\text{denom.}\rangle_{AV}=0.1$.

At $H_1=6$ G, from Eq. (9) the $T_{1\rho}$ due to the H_2O motion is given by:

$$\frac{1}{(T_{1\rho})_{H_2O}} = \frac{2}{\tau}\times 0.1\times\frac{(7.5/3)}{(7.5/3)+6^2} = \frac{1}{\tau}\times\frac{1}{77} \quad (11)$$

Near the $T_{1\rho}$ maximum, $1/T_{1\rho}$ consists of contributions from the H_2O motion and the NH_4^+ motion; that is, $(T_{1\rho})_{obs}^{-1} = (T_{1\rho})_{H_2O}^{-1} + (T_{1\rho})_{NH_4}^{-1}$. Since, in this case $\omega\tau\ll 1$ for the NH_4^+ motion, $(T_{1\rho})_{NH_4}\approx(T_1)_{NH_4}$ (see Eqs. (10) and (16) of Ref. 4). $(T_{1\rho})_{H_2O}$ is obtained from $(T_{1\rho})_{obs}$ by assuming $(T_{1\rho})_{NH_4}$ to be equal to the observed proton T_1. The values of $1/\tau(=\Omega)$ calculated from Eq. (11) at temperatures above 48°C are plotted in Fig. 3. The agreement of this result with that from the line-width change is satisfactory, considering the approximations in the analysis.*6 From the slope of $\log(T_{1\rho})_{H_2O}$ *vs.* $1/T$ curve in Fig. 4, an activation energy for the H_2O motion of about 14 kcal/mol is obtained; in view of the limited temperature range observed, this value is in good agreement with the 15.5 kcal/mol estimated in the previous section. Thus, the sharp drop of $T_{1\rho}$ at the high temperatures can be reasonably accounted for by the motion of the H_2O molecule in consistency with the line-width change of the D_2O spectra at these temperatures. It should be noted, however, that similar sharp drops of $T_{1\rho}$ are often observed in some ammonium salts at high temperatures; these drops may be considered to be due to the diffusional motion of the NH_4^+ ion or its fragments. We cannot exclude the possibility that, in the case of ammonium oxalate monohydrate, such effect is involved.

*6 Actually, in the present case H_1 (=6 G) is considerably larger than H_L'. Therefore, the application of the low-field relaxation formula of Eq. (9) may not be appropriate. However, since the difference between the high-field relaxation formula and the low-field one is small (Ref. 21, pp. 1103A—1104A), this does not have serious effect on the conclusion.

The author would like to thank Mr. Masaki Funakoshi for his great assistance in the preparation of the crystal and in the NMR measurements. Most of the measurements and the computor processing of the data were made at the Institute for Solid State Physics, the University of Tokyo. The author wishes also to thank the Institute for the use of its facilities.

Appendix

The expression for the T_1 of the deuteron is obtained from the standard treatment of the spin-lattice relaxation by a random modulation of a quadrupole interaction due to ND_4^+ reorientations. Assume an isotropic C_3 reorientation of a regularly-tetrahedral ND_4^+ ion. Let τ_c be the correlation time for this motion. The mean residence time of a spin in one site, τ, is then given by:

$$1/\tau = 3/4\tau_c \quad (A1)$$

The probability that a spin at Site 1 at $t=0$ remains in that site at $t=t$ is given by $\{1+3\exp(-t/\tau)\}/4$, and the probability that it is transferred to one of the other sites, by $\{1-\exp(-t/\tau)\}/4$. Therefore, the autocorrelation function of a given component of the EFG tensor, F, for a spin at Site 1 at $t=0$ will be:

$$F(0)F^*(t) = 1/4\{|F_1|^2(1+3x) + (F_1F_2^*+F_1F_3^*+F_1F_4^*)(1-x)\}, \quad (A2)$$

where $F_i(t)$ denotes that EFG component for a given spin at Site i at time t and $x\equiv\exp(-t/\tau)$. Since, at $t=0$, the probability of a spin in a particular site is 1/4, it follows that:

$$\langle F(0)F^*(t)\rangle_{AV} = \frac{1}{16}\{(1+3x)\textstyle\sum_i|F_i|^2+2(1-x)\sum_{i>j}|F_iF_j|\}. \quad (A3)$$

The power spectrum of F at an angular frequency, ω, $I(\omega)$, is given by:

$$I(\omega) = \int_{-\infty}^{\infty}\langle F(0)F^*(t)\rangle e^{i\omega t}dt = \left\{\frac{3}{16}\textstyle\sum_i|F_i|^2+\frac{1}{8}\sum_{i>j}|F_iF_j|\right\}j(\omega) = \left\{\sum_{i>j}\frac{1}{16}|F_i-F_j|^2\right\}j(\omega), \quad (A4)$$

with:

$$j(\omega) = 2\tau/(1+\omega^2\tau^2). \quad (A5)$$

For deuterons ($I=1$), T_1 is given by:

$$1/T_1 = P_1 + 2P_2 , \tag{A6}$$

where:

$$P_1 = (e^2Q^2/8\hbar^2)I^{(1)}(\omega) \text{ and } P_2 = (eQ^2/8\hbar^2)I^{(2)}(2\omega) . \tag{A7}$$

In $I^{(1)}(\omega)$ and $I^{(2)}(2\omega)$, the components of the EFG tensor relevant to $\Delta m=\pm 1$ and ± 2 transitions respectively are to be used for F's of Eq. (A4). Thus, for $I^{(1)}(\omega)$, $|F_i-F_j|^2$ in Eq. (A4) will be $\{(\varphi_{xz})_i-(\varphi_{xz})_j\}^2 + \{(\varphi_{yz})_i-(\varphi_{yz})_j\}^2$, and for $I^{(2)}(2\omega)$, it will be $[\{(\varphi_{xx})_i - (\varphi_{xx})_j\} - \{(\varphi_{yy})_i - (\varphi_{yy})_j\}]^2 + 4\{(\varphi_{xy})_i - (\varphi_{xy})_j\}^2$, where $(\varphi_{ab})_i$ denotes the ab element of the EFG tensor at Site i. We take, for convenience, a coordinate system of an ND_4^+ ion such that the x, y, and z axes coincide with their C_2 axes. φ's are expressed in terms of the EFG component along the D-N bond direction, q, and the direction cosines (l, m, n) of H_0 in the assumed coordinate system.

The expression of T_1 for an arbitrary direction of H_0 are computed following the procedure of O'Reilly and Tsang.[4] The symmetry consideration leads to the expression for P in Eq. (A7) of the form:

$$P = C_1 + C_2(l^4+m^4+n^4) .$$

where C_1 and C_2 are the factors to be determined. To do this it is only necessary to calculate P for two independent cases of H_0 direction, where such calculations are most conveniently made, and to solve the simultaneous equations thus obtained for C_1 and C_2. The expression for T_1 thus obtained is:

$$\frac{1}{T_1} = \frac{(eqQ)^2}{8\hbar^2}\left[(l^4+m^4+n^4)\frac{\tau}{1+\omega^2\tau^2} + \{3-(l^4+m^4+n^4)\}\frac{\tau}{1+4\omega^2\tau^2}\right] \tag{A8}$$

with a powdered sample, T_1 varies from one microcrystallite to another as $(l^4+m^4+n^4)$ takes values between 1 and 1/3, but since the orientation dependence of T_1 seen from Eq. (A8) is mild, the average T_1 measured for powdered sample may be compared with the theoretical expression, Eq. (A8), averaged over H_0 directions, as is done in the discussion of the proton T_1. Thus $\langle l^4+m^4+n^4\rangle_{AV}=3/5$ gives:

$$\frac{1}{(T_1)_{\text{powder}}} = \frac{3\pi^2}{10}\left(\frac{eqQ}{h}\right)^2\left(\frac{\tau}{1+\omega^2\tau^2}+\frac{4\tau}{1+4\omega^2\tau^2}\right) \tag{A9}$$

which is just the expression for quadrupole relaxation by the isotropic random rotation of the molecule.[22]

22) A. Abragam, "The Principles of Nuclear Magnetism," Oxford University Press (1961), p. 314.

BULLETIN OF THE CHEMICAL SOCIETY OF JAPAN VOL. 43 1950—1955 (1970)

Photochemical Reactions of Uranyl Ions with Organic Compounds. I. The Mechanism of the Uranyl Ion-Photosensitized Oxidation of Lactic Acid

Shukichi SAKURABA and Ryoka MATSUSHIMA

Faculty of Engineering, Shizuoka University, Hamamatsu

(Received November, 12, 1969)

The photochemical reaction of lactic acid with uranyl ions in an aqueous solution was studied with radiations of 4050 and 4360 Å. The quantum yields and molar ratios of the reaction products were measured under various conditions. Two competing photo-reactions appeared to take place; through them lactic acid was oxidized to form pyruvic acid at a lower pH and to form acetaldehyde, with an evolution of carbon dioxide, at a higher pH. The results obtained can be well explained by assuming that the excitation of the uranyl lactate complex is involved in the formation of acetaldehyde and that a collision between lactic acid and the excited uranyl ion, without any complex formation, is involved in the formation of pyruvic acid.

Both the intermolecular (collisional) mechanism[1,2] of the energy transfer from the excited uranyl ions to organic substrates and the intramolecular mechanism,[3-6] in which the formation of complexes between uranyl ions and substrates prior to the photolysis is involved, have been proposed for the photo-reactions of organic acids, alcohols, and aldehydes by uranyl ions in an aqueous solution. Evidence for both the mechanisms

1) R. H. Muller, *Proc. Roy. Soc., A*, **121**, 314 (1928).
2) W. C. Pierce, *J. Amer. Chem. Soc.*, **51**, 2732 (1929).
3) P. F. Büchi, *Z. Phys. Chem.*, **111**, 275 (1924).
4) W. G. Leighton and G. S. Forbes, *J. Amer. Chem. Soc.*, **52**, 3139 (1930).
5) L. J. Heidt, *J. Phys. Chem.*, **46**, 624 (1942).
6) G. E. Heckler, A. E. Taylar, C. Jenson, D. Percival, R. Jenson and P. Fung, *J. Phys. Chem.*, **67**, 1 (1963).

has been found in the photolysis of uranyl oxalate.[7,8] However, the collisional mechanism has been assumed to be less important in the photooxidations of alcohols,[9] aldehydes,[10] α-hydroxy acids,[11] and other organic acids[6] with uranyl ions.

We observed that lactic acid in an aqueous solution containing uranyl ions decomposed upon irradiation with visible light to produce acetaldehyde, carbon dioxide, pyruvic acid,*1 and uranium(IV), and that the molar ratios of the reaction products depended on the acidity of the solution, *i.e.*,

$$UO_2^{2+} + CH_3CH(OH)CO_2H + h\nu$$

$$\xrightarrow{pH \ll 1} CH_3C(=O)CO_2H + \text{U(IV) species}$$

$$\xrightarrow{pH \sim 2} CH_3C(=O)CO_2H + CH_3C(=O)H + CO_2 + \text{U(IV) species}$$

$$\xrightarrow{pH > 3.5} CH_3C(=O)H + CO_2 + \text{U(IV) species}$$

The present investigation was undertaken in order to elucidate the mechanisms by means of kinetic treatments.

Experimental

Doubly-distilled water and guaranteed reagents (Koso Chemical) were used. The solutions were de-aerated by the passage through of oxygen-free nitrogen for 40 to 60 min per 25 ml and then placed into 1-cm spectrophotometer quartz cells with pipets kept air-tight with liquid parafine; they were further de-aerated for several minutes, and then exposed to light (4050 or 4360 Å) using either an interference filter or a suitable combination of glass filters. The intensities of light absorbed by the reactants, needed for the estimation of the quantum yield, were measured by using a ferricoxalate actinometer.[13] In order to minimize the inner filter effect of the uranium(IV) formed and in order to avoid further oxidations of organic products, the measurements were carried out within 5% of the reaction extent. The light source was a 100-W high-pressure mercury lamp (Riko Co., Ltd.) or a 500-W xenon lamp (Ushio Co., Ltd.). The acidities of the solutions were adjusted with 1 N NaOH and 1 N $HClO_4$ by using a pH meter (Toa-Dempa Co., Ltd.). The pH values of the solutions were constant during the irradiation. No direct photodecomposition of lactic acid occurred in the absence of uranyl ions, and no thermal decomposition was detected in the dark in 8 hours at 70—80°C in the presence of uranyl nitrate.

The concentrations of the uranium(IV) formed were measured colorimetrically with arsenazo-III.[14] The acetaldehyde and pyruvic acid formed were identified as 2,4-dinitrophenyl hydrazones by comparing their infrared spectra, melting points, and R_f values (TLC) with those of authentic samples. To aliquots of the irradiated solutions, excess acidic solutions of 2,4-dinitrophenyl hydrazine were added; orange precipitates were then isolated and washed with water. To the precipitates, an aqueous solution of 0.5 N Na_2CO_3 and an equal volume of chloroform were added and shaken well; then the aqueous layer (containing 2,4-DNP of pyruvic acid) and the chloroform layer (containing 2,4-DNP of acetaldehyde) were separated. The absorbances of the aqueous solutions and of the chloroform solutions were measured at 380 nm and 360 nm respectively. The reproducibility of this method was checked. Carbon dioxide was identified with barium hydroxide. Spectrophotometric measurements were carried out by means of a recording spectrophotometer (Hitachi 124-Type). Fluorescence was measured by using a Hitachi fluorescence photometer.

Results

The Equilibria of the Uranyl Lactate System

Mononuclear complexes having combining ratios (lactate/uranyl) of one, two, and three to one have been reported in the uranyl lactate system in the pH range from 2 to 3.5,[15–17] while Rajan and

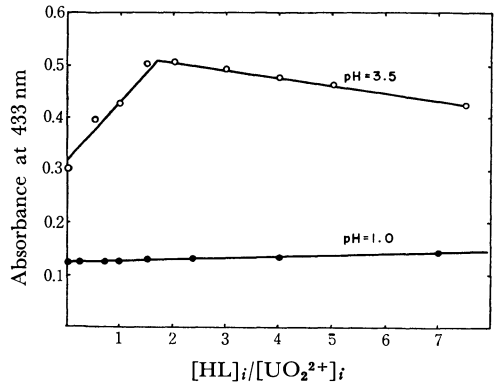

Fig. 1. Application of the molar ratio method to the uranyl-lactate system.
Initial concentration of UO_2^{2+} (as nitrate) is 0.02 M.

7) A. H. Carter and J. Weiss, *Proc. Roy. Soc., A*, **174**, 351 (1950).
8) D. H. Volman and J. R. Seed, *J. Amer. Chem. Soc.*, **86**, 5095 (1964).
9) K. Venkatarao and M. Santappa, *Indian J. Chem.*, **5**, 304 (1967).
10) K. Venkatarao and M. Santappa, *Z. Phys. Chem.*, **54**, 101 (1967).
11) S. K. Bhattacharyya and S. Guluady, *J. Indian Chem. Soc.*, **29**, 649 (1952).
*1 This product was overlooked by earlier researchers.[11,12]
12) E. Rabinowitch and R. L. Belford, "Spectroscopy and Photochemistry of Uranyl Compounds," Pergamon Press, London (1964), p. 311.
13) C. A. Parker, *Proc. Roy. Soc., A*, **220**, 104 (1953).
14) H. Onishi and Y. Toita, *Bunsekikagaku*, **14**, 1141 (1965).
15) I. Feldman and J. R. Havill, *J. Amer. Chem. Soc.*, **76**, 2114 (1954).
16) I. Feldman, J. R. Havill and W. F. Neuman, *ibid.*, **76**, 4726 (1954).
17) C. Miyake and H. W. Nurnberg, *J. Inorg. Nucl. Chem.*, **29**, 2411 (1967).

Martell[18,19] suggested the existence of polynuclear complexes as well. At the pH range of less than unity, no complexes between the uranyl and the lactate ions were found by spectrophotometric studies to exist. Examples at pH=1 and at pH=3.5 are shown in Fig. 1.

The Effect of Acidity on the Quantum Yield. The quantum yields of uranium(IV) formation at various pH's are shown in Table 1. It may be seen that the quantum yield decreases with the increase in pH, though the apparent rate of photolysis may be increased due to the remarkable increase in the absorption coefficient with the pH (Fig. 2). The acidity-dependency of the quantum yield is contrary to the view[3-6,11] that the reacting species are complexes between the uranyl ions and the substrates.

TABLE 1. EFFECT OF pH ON THE QUANTUM YIELD OF URANIUM(IV) FORMATION

pH	ϕ	pH	ϕ
1.0	0.45	3.5	0.24
1.5	0.42	4.0	0.19
2.0	0.39	4.5	0.15
2.5	0.34	5.0	0.11
3.0	0.29		

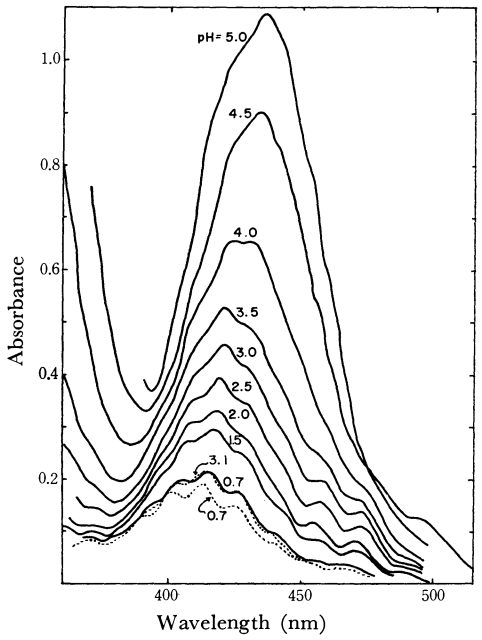

Fig. 2. Variation of the absorption spectrum of uranyl-lactic acid solution (full lines) and of a uranyl solution (dotted line) with pH.
Initial concentration of uranyl nitrate and lactic acid were 0.02 M and 0.2 M, respectively.

18) K. S. Rajan and A. E. Martell, *ibid.*, **26**, 789 (1964).
19) K. S. Rajan and A. E. Martell, *ibid.*, **26**, 1927 (1964).

The Effect of Acidity on the Molar Ratios of the Products. The molar ratios of the total organic products to the uranium(IV) are about unity, as is shown in Table 2, but the pH-dependency of the molar ratio of pyruvic to the uranium (IV) is in contrast with that of acetaldehyde (Fig. 3). The increase in acetaldehyde formation with the increase of pH is interpreted as indicating that the photoreactive species are the complexes between the uranyl and the lactate ions; this is in accord with the earlier view. However, the pH-dependency of pyruvic acid formation cannot be explained by the same theory. Further, it is noticed that the pyruvic acid formation is interfered with by the addition of a small amount of iodine, the iodide ion, the chloride ion, or oxygen (in this order), while the acetaldehyde formation is not affected. The influence of the iodide ion is shown in Fig. 4. Thus, a mechanism involving encounter collisions between the excited uranyl ion and lactic acid is proposed for the formation of pyruvic acid.

TABLE 2. THE RATIO OF THE SUM OF ACETALDEHYDE AND PYRUVIC ACID TO THE URANIUM(IV) AT VARIOUS EXTENTS OF THE PHOTOLYSIS

pH=1		pH=3.5	
Extent (%)	$(A+P)$/U(IV)	Extent (%)	$(A+P)$/U(IV)
5	0.98	6	0.94
16	0.97	16	0.97
20	1.12	26	0.99
		41	0.98
70	0.91	69	0.94

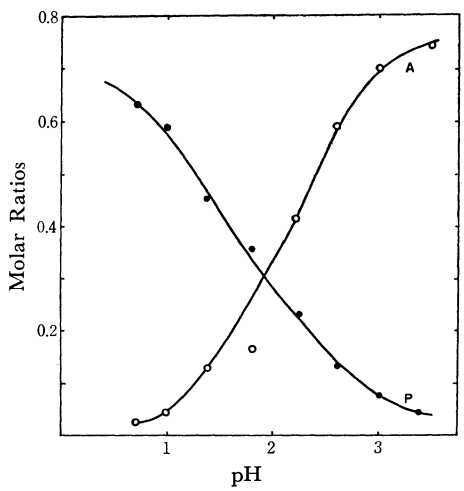

Fig. 3. Effect of pH on the molar ratios of the products. Curve A and curve P represent the molar ratios of acetaldehyde and pyruvic acid to uranium(IV), respectively.
Initial concentration of uranyl nitrate and lactic acid were 0.02 M and 0.2 M, respectively.

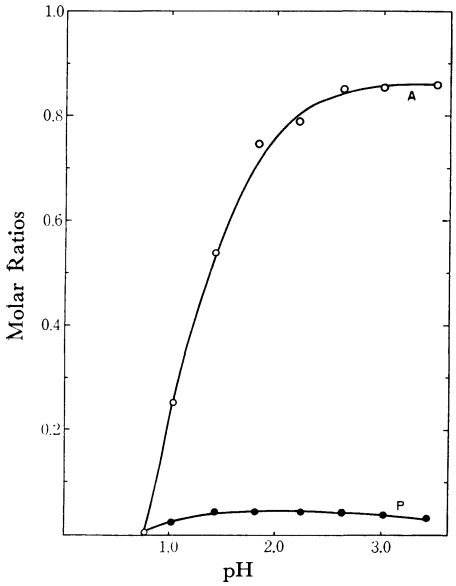

Fig. 4. Effect of iodide ions.
The concentration of potassium iodide was 0.008 M and other experimental conditions were the same as those of Fig. 3.

TABLE 3. EFFECT OF INITIAL CONCENTRATION OF LACTIC ACID ON THE QUANTUM YIELD OF URANIUM(IV) AT pH=1.0 (INITIAL CONCENTRATION OF $UO_2^{2+}=2\times10^{-2}$ M)

Initial concentration of lactic acid ($\times10^2$ M)	ϕ	Initial concentration of lactic acid ($\times10^2$ M)	ϕ
1.0	0.03	8.0	0.26
2.0	0.07	10.0	0.31
3.0	0.10	14.0	0.39
5.0	0.18	18.0	0.45

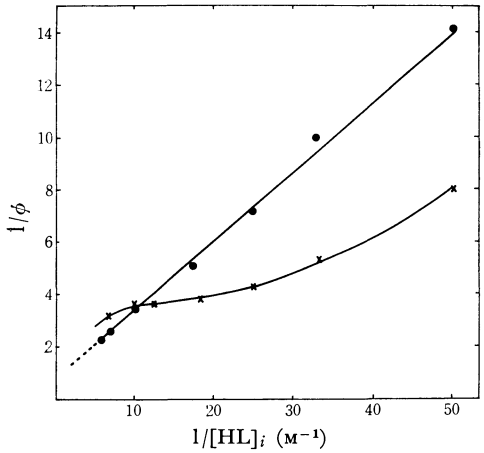

Fig. 5. Plot of reciprocal quantum yield of uranium(IV)-formation *vs.* reciprocal intial concentration of lactic acid at pH=1.0 (●) and at pH=3.5 (×).
Initial concentration of uranyl nitrate was 0.02 M.

The Effect of the Initial Concentration of Lactic Acid on the Quantum Yield. The dependency of the quantum yield on the initial concentration of lactic acid at pH=1 (not complexed) and that at pH=3.5 (complexed) are shown in Table 3 and Fig. 5 and in Fig. 6, respectively. At pH=1, a straight line of reciprocal quantum yields *versus* reciprocal initial concentrations of lactic acid was obtained, while such was not the case at pH=3.5 (Fig. 5). At pH=3.5 the quantum yield reaches a limiting value (Fig. 6).

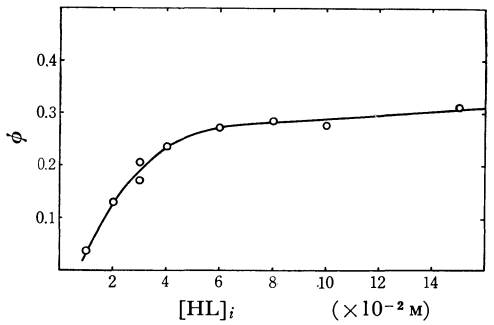

Fig. 6. Plot of the quantum yield of uranium(IV) *vs.* initial concentration of lactic acid at pH=3.5.
Initial concentration of uranyl nitrate was 0.02 M.

Discussion

The acidity-dependency of the formation of acetaldehyde is in contrast to that of pyruvic acid, as is shown in Fig. 3. Figure 1 shows that complex formation between the uranyl and lactate ions takes place in the system at pH=3.5 prior to the photolysis, while such is not the case at pH=1. Therefore, it seems reasonable to assume that the opposite dependency of the product-ratios on the acidity is attributable to the difference in the initial species of the system to be photolyzed. Further, the formation of pyruvic acid is inhibited by the trapping agents, while acetaldehyde formation is not affected (Fig. 4). This difference in the inhibitory effect suggests that the primary intermediates at pH=1 are $CH_3\dot{C}(OH)CO_2H$ and UO_2^+, while intramolecular photoredox reactions of the uranyl-substrate complexes are involved at pH=3.5. The following mechanism is, therefore, proposed for the photolysis at pH=1:

$$UO_2^{2+} + h\nu \xrightarrow{I_a} (UO_2^{2+})^*$$

$$(UO_2^{2+})^* \xrightarrow{k_1} UO_2^{2+}$$

$$(UO_2^{2+})^* + CH_3CH(OH)CO_2H \xrightarrow{k_2} CH_3\dot{C}(OH)CO_2H + UO_2^+ + H^+$$

$$CH_3\dot{C}(OH)CO_2H + UO_2^{2+} \xrightarrow{k_3} CH_3C\overset{O}{\diagdown}CO_2H + UO_2^+ + H^+$$

$$2UO_2^{+} + H^{+} \xrightarrow{k_4} UO_2^{2+} + \text{U(IV) species}^{20)}$$

I_a is the rate of light absorption in einsteins$\cdot l^{-1}\,sec^{-1}$. A similar scheme was proposed for the photolysis of uranyl oxalate by Carter and Weiss[7] and later by Volman and Seed.[8] The radical $CH_3\dot{C}(OH)CO_2H$ would be rapidly oxidized by $UO_2^{2+}(k_3)$ before the disproportionation reaction:

$$2CH_3\dot{C}(OH)CO_2H \longrightarrow CH_3C(=O)CO_2H + CH_3CH(OH)CO_2H$$

since the concentration of $CH_3\dot{C}(OH)CO_2H$ would be small compared to that of UO_2^{2+}. Assuming the steady state with respect to $(UO_2^{2+})^*$, UO_2^{+}, and $CH_3\dot{C}(OH)CO_2H$, the quantum yield of the uranium(IV) formation is given by:

$$\phi = \frac{1}{I_a}\cdot\frac{d[U(IV)]}{dt} = \frac{k_2[HL]}{k_1 + k_2[HL]},$$ HL: Lactic acid

or, $$\frac{1}{\phi} = 1 + \frac{k_1}{k_2}\cdot\frac{1}{[HL]}$$

That is, the reciprocal quantum yields *vs.* the reciprocal concentrations of lactic acid should form a straight line. This is consistent with the experimental facts (Fig. 5). In addition, the plot of the relative reciprocal intensity of uranyl fluorescence *vs.* the concentration of lactic acid obeys the Stern-Volmer equation, as in the case of isopropyl alcohol, but such is not the case at pH=3.5 (Fig. 7). It has been reported that the efficiency of intramolecular energy transfer between lanthanide ions and organic ligands is much higher than that of collisional (intermolecular) transfer between lanthanide ions and non-chelating molecules.[21-23] Figure 7 shows that the quenching constant (or the slope) of lactic acid at pH=1 nearly equals that of non-chelating isopropyl alcohol, indicating an intermolecular energy transfer from excited uranyl ions to lactic acid molecules in stronger acidic media.

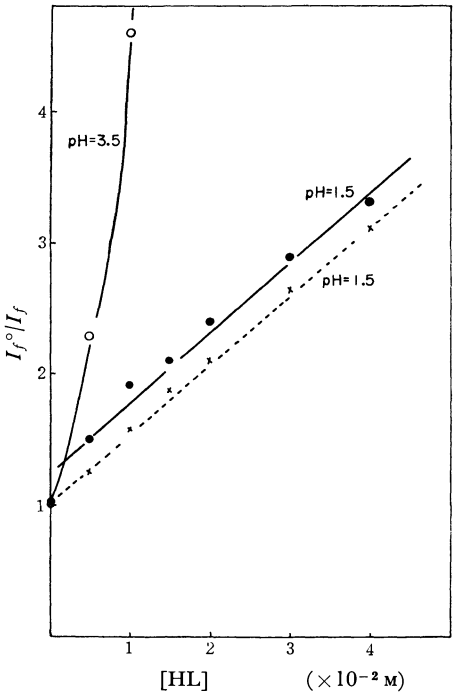

Fig. 7. Plot of I_f°/I_f *vs.* concentration of lactic acid. I_f° and I_f are the relative intensities of uranyl fluorescence at 509 nm in the absence and in the presence of lactic acid, respectively. Excitation was at 436 nm. $[UO_2(NO_3)_2]=0.02$ M. Isopropyl alcohol was included for comparison (dotted line).

The alternative explanation for the formation of pyruvic acid is a mechanism involving ester-like intermediates, as has been proposed for the thermal oxidation of α-hydroxy acid by chromic acid[24-26]:

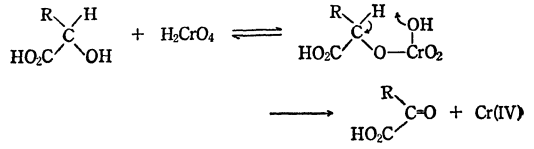

This, however, is not the case with the formation of pyruvic acid in the photolysis of lactic acid by uranyl ions, since pyruvic acid was also obtained upon the irradiation of lactic acid with cupric ions in an aqueous acidic solution, where no such ester-like intermediates are conceivable.

In the case of the photolysis at pH=3.5, the quantum yield reaches a limiting value (Fig. 6). Heckler and his co-workers[6] found a phenomenon similar to that shown in Fig. 6 for the uranyl ion-photosensitized decomposition of such organic acid as malonic, succinic and glutaric acids in solution; they concluded that the photosensitive species are complexes formed between uranyl ions and organic acid ions.

Thus, the photosensitive species for the formation of acetaldehyde are the $UO_2^{+}L$ and UO_2L_2 complexes, both formed prior to the photolysis;

$$UO_2^{2+} + HL \overset{K_1}{\rightleftharpoons} UO_2^{+}L + H^{+}$$

$$UO_2^{+}L + HL \overset{K_2}{\rightleftharpoons} UO_2L_2 + H^{+}$$

20) J. J. Katz and G. T. Seaborg, "The Chemistry of the Actinide Elements," Methuen and Co., London (1957), p. 176.

21) A. Heller and E. Wasserman, *J. Chem. Phys.*, **42**, 949 (1965).

22) R. G. Charles and E. P. Riedal, *J. Inorg. Nucl. Chem.*, **28**, 527 (1966).

23) N. Filipescu and G. W. Mashrush, *J. Phys. Chem.*, **72**, 3516 (1968).

24) G. V. Bakore and S. Narain, *J. Chem. Soc.*, **1963**, 3419.

25) T. J. Kempa and W. A. Waters, *ibid.*, **1964**, 1192.

26) G. V. Bakore and R. Shanker, *Can. J. Chem.*, **44**, 1717 (1966).

where HL and L represent $CH_3CH(OH)CO_2H$ and $CH_3CH(OH)CO_2^-$ respectively and where K_1 and K_2 are the equilibrium constants. The following mechanism may be proposed for the formation of acetaldhyde though more experimental data are needed to describe it in detail:

$$UO_2^+L + h\nu \longrightarrow (UO_2^+L)^*$$

$$(UO_2^+L)^* \longrightarrow UO_2^+L$$

$$(UO_2^+L)^* \rightleftharpoons CH_3\underset{\cdot}{C}H\begin{matrix}\diagup O \diagdown \\ \cdot\ \ \ \cdot \\ CO_2\end{matrix}UO_2^+ \longrightarrow$$

$$CH_3C\begin{matrix}\diagup O \\ \diagdown H\end{matrix} + H^+ + CO_2 + U(IV)$$

Similarly,

$$UO_2L_2 + h\nu \longrightarrow (UO_2L_2)^*$$

$$(UO_2L_2)^* \longrightarrow UO_2L_2$$

$$(UO_2L_2)^* \rightleftharpoons CH_3\underset{\cdot}{C}H\begin{matrix}\diagup O \diagdown \\ \cdot\ \ \ \cdot \\ CO_2\end{matrix}UO_2L \longrightarrow$$

$$CH_3C\begin{matrix}\diagup O \\ \diagdown H\end{matrix} + H^+ + CO_2 + U(IV) + L^-$$

Though the details of the mechanism at high pH are not clear, it may safely be concluded that the variation in the products and mechanisms with pH is to be attributed to the subject whether the formation or dissociation of the uranyl-lactate complex is predominant.

The authors wish to express their thanks to Mr. M. Koshio for a grant given to our research from the "Koshio-Hōonkai".

BULLETIN OF THE CHEMICAL SOCIETY OF JAPAN VOL. 43 1955—1962 (1970)

Relations between Intramolecular Energy Transfer Efficiencies and Triplet State Energies in Rare Earth β-diketone Chelates

Susumu SATO and Masanobu WADA

Department of Electronic Engineering, Faculty of Engineering, Tohoku University, Sendai

(Received November, 17, 1969)

The fluorescence yield of europium chelates in several solutions varies, through its maximum value, with the increase in the energy difference between the triplet state of a ligand and the emitting level of an europium ion. The time-resolved spectroscopic measurements show that the excitation energy is transferred from the triplet state to the lower and nearest resonance level of the europium ion. The intramolecular energy transfer mechanisms for europium chelates and terbium chelates are proposed, taking the resonance exchange interaction and the thermal deactivation processes from the emitting levels of rare earth ions into consideration. Steady-state rate equations are made, and the equation of the fluorescence yield is obtained. Thus, the relations between the fluorescence yield and the triplet state energy are estimated and the fluorescence properties of rare earth β-diketone chelates may be qualitatively described.

A number of europium and terbium β-diketone chelates give a narrow-band emission from the rare earth ion under near UV excitation, and some of these chelates exhibit laser action when dissolved in organic solvents.[1-3] The absorbed pump energy is transferred to a triplet state (by the intersystem crossing), and is then intramolecularly transferred to the rare earth ion.[4] Since this intramolecular energy transfer from the triplet state to the resonance level of the rare earth ion is of a spin-forbidden type, the energy is transferred by the resonant exchange interaction[5] and the role of the triplet state is very important. There have been some reports discussing the role of the triplet state, and it has been concluded that the excitation energy could not be transferred from the ligand to the rare earth ion if the triplet state of the ligand was below the resonance level of the rare earth ion.[4] However, few experimental

1) A. Lempicki and H. Samelson, *Phys. Lett.*, **4**, 133 (1963).

2) M. L. Bhaumik, P. C. Fletcher, L. J. Nugent, S. M. Lee, S. Higa and C. L. Telk, *J. Phys. Chem.*, **68**, 1490 (1964).

3) E. J. Schimitschek and R. B. Nehrich Jr., *J. Appl. Phys.*, **35**, 2786 (1964).

4) G. A. Crosby, R. E. Whan and R. M. Alire, *J. Chem. Phys.*, **34**, 743 (1961).

5) V. L. Ermolaev, V. G. Aleshin and E. A. Saenko, *Sov. Phys. Doklady (English Transl.)*, **10**, 1186 (1966).

studies have been done on the dependence of the energy transfer efficiency upon the triplet state energy. The fluorescence yield of rare earth β-diketone chelates varies widely depending on the temperatures, the solvents, the ligands, the central ions and bases, and, further, whether they are of a tris or a tetrakis form. Therefore, the dependence of the fluorescence yield upon the triplet state energy must be measured by changing only the energy level of the triplet state, maintaining the other conditions as constant as possible.

The europium β-diketone chelate derived from BTFA (benzoyltrifluoroacetone), which contains a benzene ring and a trifluoromethyl group, shows a high fluorescence yield of an europium-ion emission at room temperature. Many other β-diketone compounds similar to BTFA have been prepared in which the benzene ring was replaced by other aromatics, such as naphthalene, phenanthrene, and anthracene. The optical and fluorescent properties of europium chelates derived from substituted β-diketone compounds were measured.[6] The triplet state energy of these substituted β-diketone compounds is expected to be changed. In this paper, using europium and terbium chelates prepared from these substituted β-diketone compounds, the effects of the triplet state energy upon the energy transfer mechanism will be investigated and discussed.

Sample Preparation

The compounds discussed in the present article are listed, along with their abbreviation codes, in Table 1. In these β-diketone compounds, BTFA and TTA were obtained from Dotite reagents. All the other compounds were synthesized from the proper monoketone and ethyltrifluoroacetate by a manner reported previously.[6]

The europium, terbium, and gadolinium β-diketone chelates were synthesized by ordinary piperidine methods. The analytical data of the rare-earth-metal contents for these chelates are shown in Table 2. It can be seen that all of the

TABLE 1. β-DIKETONE COMPOUNDS

Name	Code	Formula
Benzoyltrifluoroacetone	BTFA	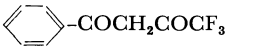
p-Chlorobenzoyltrifluoroacetone	PCBTFA	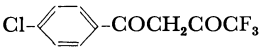
p-Bromobenzoyltrifluoroacetone	PBBTFA	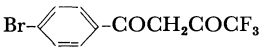
p-Phenylbenzoyltrifluoroacetone	PPBTFA	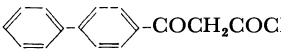
1-Naphthoyltrifluoroacetone	1NTFA	
2-Naphthoyltrifluoroacetone	2NTFA	
2-Phenanthoyltrifluoroacetone	2PTFA	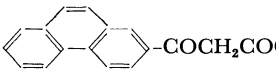
3-Phenanthoyltrifluoroacetone	3PTFA	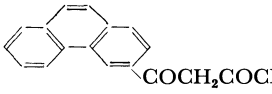
9-Anthroyltrifluoroacetone	9ATFA	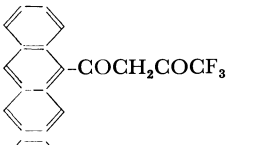
Cinnamoyltrifluoroacetone	CTFA*	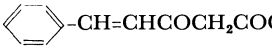
2-Thenoyltrifluoroacetone	TTA	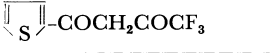

* This compound was derived from benzylideneacetone and had been named to BZDTFA previously.[6]

6) S. Sato, M. Wada and T. Seki, *Japan. J. Appl. Phys.*, **7**, 7 (1968).

Table 2. Rare earth β-diketone chelates

Ligand	Eu-chelate $\%Eu_2O_3$		Tb-chelate $\%Tb_4O_7$		Gd-chelate $\%Gd_2O_3$	
	Calcd*	Found	Calcd*	Found	Calcd*	Found
BTFA	16.2	14.5	17.1	17.2	16.4	16.2
TTA	15.9	16.4	16.8	14.6	16.1	17.6
PCBTFA	14.4	13.9	15.2	15.5	20.0**	23.2
PBBTFA	12.6	11.3	13.3	13.7	17.4**	15.3
PPBTFA	12.7	12.4	13.4	14.8	12.9	13.2
1NTFA	13.7	14.2	19.6**	18.2	19.0**	17.0
2NTFA	13.7	14.7	14.5	15.0	13.9	14.1
2PTFA	11.9	11.0	12.5	13.2	16.4**	20.9
3PTFA	11.9	11.0	16.9**	16.3	16.4**	15.4
9ATFA	11.9	11.3	12.5	12.3	12.1	12.7
CTFA	14.8	14.3	15.6	16.7	20.6**	21.6

* Calculated as the tetrakis form, (HQ) R.E. (β-diketone)$_4$ R.E.=rare earth ion, Q=pyrrolidine for europium and terbium chelates, piperidine for gadolinium chelates

** Calculated as the tris form, R.E.(β-diketone)$_3$

europium chelates and most of the terbium chelates are of the tetrakis form, (HQ)R.E.(β-diketone)$_4$ (Q=pyrrolidine, R.E.=Eu or Tb), but the gadolinium chelates are of the tetrakis form or the tris form, R.E.(β-diketone)$_3$ (R.E.=Gd), or a mixture of these two forms.

Results and Discussion

Triplet State Energy of β-Diketones. The phosphorescence spectra of gadolinium chelates were measured at 77°K in an EPA solution (5 parts diethylether, 5 parts isopentane, and 2 parts ethanol by volume). The exciting light source was a combination of a high-pressure Hg lamp and a UV-DIB bandpass filter (300—400 mμ transmission range). The phosphorescence band emission of gadolinium chelates was strong, and two or three clearly-defined bands were observed for most of the chelates investigated. The shortest-wavelength phosphorescence band was assumed to be the 0–0 transition[7], and the triplet state energy was determined. The results are summarized in Table 3. However, the phosphorescence of Gd(CTFA)$_3$ was so weak that it was very difficult to determine the triplet state energy exactly. The resonance levels of europium and terbium ions and the triplet state of each β-diketone compound listed in Table 3 are shown in Fig. 1.

Table 3. Triplet state energy of gadolinium β-diketonates

Compound	Triplet state (cm^{-1})
BTFA	21400
PCBTFA	21300
PBBTFA	21200
2PTFA	20600
PPBTFA	20400
TTA	20300
3PTFA	19800
2NTFA	19600
1NTFA	19400
CTFA	~17500
9ATFA	13600

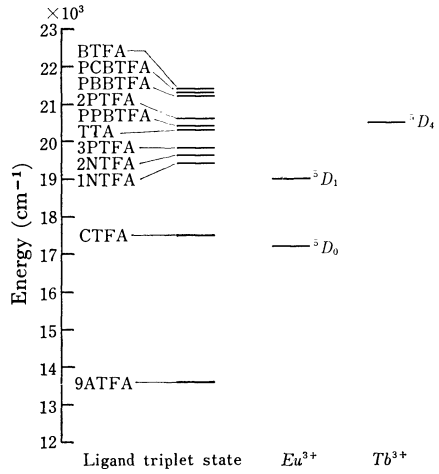

Fig. 1. Triplet states of β-diketonates and related levels of europium and terbium ions.

Europium chelates prepared from the β-diketone compounds, the triplets state of which is above the $^5D_0$ level of the Eu^{3+} ion, emit the intense fluorescence of the Eu^{3+} ion at room temperature, but $Eu(CTFA)_4^-$ fluoresces only at relatively low temperatures. $Eu(9ATFA)_4^-$ does not fluoresce even at the temperature of liquid nitrogen. On the other hand, terbium β-diketone chelates derived from the β-diketone with a triplet state higher than that of TTA emit the fluorescence of the Tb^{3+} ion at low temperatures, but no other terbium

7) W. F. Sager, N. Filipescu and F. A. Serafin, *J. Phys. Chem.*, **69**, 1092 (1965).

chelates fluoresce.

Relation between the Fluorescence Yield and the Triplet State Energy. Measurements of the fluorescence quantum yields were made at room temperature by a method similar to one reported previously.[6] The relations between the fluorescence quantum yields at room temperature and the energy difference between the ligand triplet state and $^5D_1$ level of the Eu^{3+} ion are plotted for several solutions in Fig. 2. It can be seen that the fluorescence yield varies through its maximum value as the energy difference becomes larger. In terbium chelates, the fluorescence was nearly quenched at room temperature; therefore, a relation such as that shown in Fig. 2 could not be obtained. These results will be discussed in detail later.

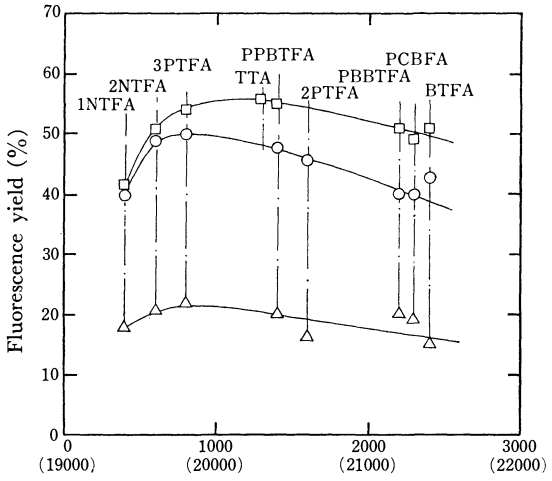

Fig. 2. Relations between fluorescence yields of europium β-diketone chelates and the energy difference between the ligand triplet state and the $^5D_1$ level of the Eu^{3+} ion.
□: acetonitrile solution
△: alcohol solution
○: dimethylformamide solution

Temperature Dependences of Fluorescence Lifetimes. The fluorescence lifetimes of the europium and terbium chelates were obtained by a stroboscopic method[6]; their values were of the order of 10^{-3}—10^{-4} sec. The normalized temperature dependences of the fluorescence lifetimes of europium and terbium β-diketone chelates are shown in Fig. 3. It can be seen that the quenching temperature moves toward the higher-temperature region as the energy difference between the triplet state of the ligand and the emitting level of the rare earth ion becomes larger. The temperature dependence of the fluorescence intensities showed thermal quenching properties quite similar to those of the temperature dependence of the fluorescence lifetimes.

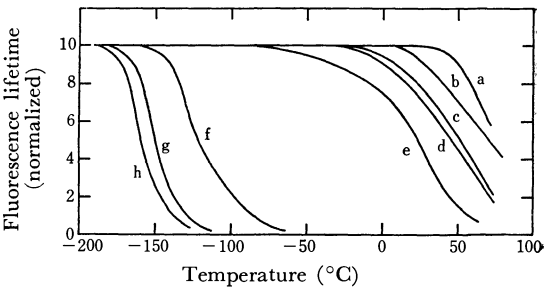

Fig. 3. Temperature dependences of fluorescence life-times. (europium chelates (a)~(e): powders, terbium chelates (f)~(h): EPA solutions)
(a): (HQ)Eu(BTFA)$_4$
(b): (HQ)Eu(PPBTFA)$_4$
(c): (HQ)Eu(TTA)$_4$
(d): (HQ)Eu(2NTFA)$_4$
(e): (HQ)Eu(1NTFA)$_4$
(f): $Tb(BTFA)_4^-$
(g): $Tb(PPBTFA)_4^-$
(h): $Tb(TTA)_4^-$
Q=pyrrolidine

Time-resolved Spectroscopy. Time-resolved spectroscopy was carried out by a stroboscopic technique similar to that described by Bhaumik *et al.*[8] The resolution time of our apparatus was about 0.3 μsec. Figures 4 (a) and (b) show the time-resolved spectra of $Eu(BTFA)_4^-$ in an acetonitrile solution at room temperature and of $Eu(CTFA)_4^-$ in an EPA solution at 77°K. For most europium chelates with the same properties as that of $Eu(BTFA)_4^-$, the emission due to the $^5D_0 \rightarrow {}^7F$ transition begins to build up as the emission due to the $^5D_1 \rightarrow {}^7F$ transition begins to decrease. On the other hand, the emission from the $^5D_1$ level of

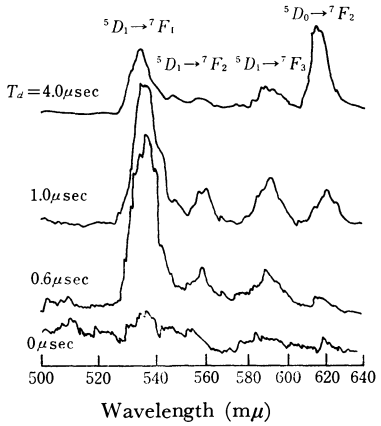

Fig. 4(a). Time-resolved spectra for (HQ)Eu(BTFA)$_4$ Q=pyrrolidine in acetonitrile solution at room temperature.
The delay time after the flash of exciting light is given by T_d.

8) M. L. Bhaumik, G. L. Clark, J. Snell, and L. Ferder, *Rev. Sci. Instr.*, **36**, 37 (1965).

*1 The same phenomenon was observed in $Eu(1NTFA)_4^-$ at room temperature; this will be discussed elsewhere.

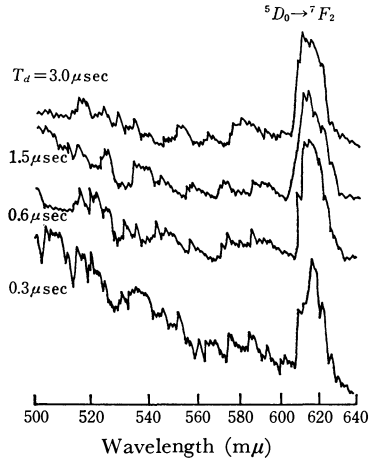

Fig. 4(b). Time-resolved spectra for (HQ)Eu-(CTFA)$_4$ (Q=pyrrolidine) in EPA solution at 77°K.
The delay time after the flash of exciting light is given by T_d.

$Eu(CTFA)_4^-$ can not be detected, and the rise time of the emission originating from the $^5D_0$ level is very short and is beyond the resolution time of the apparatus.*1 As can be seen in Fig. 1, the triplet state of CTFA exists between the $^5D_1$ level and the $^5D_0$ level of the Eu^{3+} ion, but the triplet states of all the other β-diketone compounds except 9ATFA are above the $^5D_1$ level. Therefore, in the europium chelates other than $Eu(CTFA)_4^-$, it may be concluded that the excitation energy is transferred from the ligand's triplet state to the $^5D_0$ level *via* the $^5D_1$ level of the europium ion. In $Eu(CTFA)_4^-$, it may be transferred directly from the triplet state to the $^5D_0$ level.

Intramolecular Energy Transfer Mechanism. The energy-level scheme to be used in describing the intramolecular energy transfer mechanism for europium chelates, is similar to that given by Samelson *et al.*[9]; it is shown in Fig. 5, where the wavy lines represent the energy transfer or the loss due to the radiative or nonradiative transition to the ground state, while the straight lines represent the absorption or the radiative transition due to $^5D_0 \rightarrow {}^7F_2$ or thermal-deactivation processes. In this figure, the singlet state is denoted by S, the triplet state of a ligand is denoted by T, and the $^5D_1$, $^5D_0$, $^7F_2$, and $^7F_0$ levels of the Eu^{3+} ion are shown as 4, 3, 2, and 1 respectively. The transitions associated with the other levels have not been considered. The steady-state rate equations are:

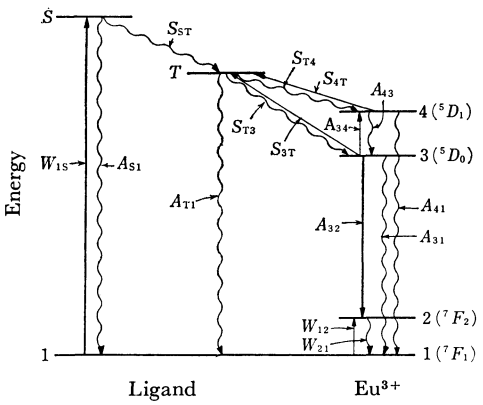

Fig. 5. Energy transfer diagram for europium chelates.

$$dN_S/dt = W_{1S}N_1-(A_{S1}+S_{ST})N_S = 0 \quad (1)$$

$$dN_T/dt = S_{ST}N_S-(A_{T1}+S_{T4}+S_{T3})N_T+S_{4T}N_4 + S_{3T}N_3 = 0 \quad (2)$$

$$dN_4/dt = S_{T4}N_T-(A_{43}+A_{41}+S_{4T})N_4+A_{34}N_3 = 0 \quad (3)$$

$$dN_3/dt = S_{T3}N_T+A_{43}N_4 -(A_{32}+A_{31}+A_{34}+A_{3T})N_3 = 0 \quad (4)$$

$$dN_2/dt = A_{32}N_3+W_{12}N_1-W_{21}N_2 = 0 \quad (5)$$

$$N_0 = N_1+N_2+N_3+N_4+N_T+N_S \quad (6)$$

where W_{1S} is the transition probability for the absorption; where A_{S1}, A_{T1}, A_{41}, and A_{31} are loss probabilities due to the transitions from the excited states to the ground state; where S_{ST}, S_{T4}, and S_{T3} are the transition probabilities for radiationless processes; where A_{32} is the radiative transition probability for the europium fluorescence, and A_{43}, the transition probability for the decay from the $^5D_1$ level to the $^5D_0$ level; where W_{12} and W_{21} are the transition probabilities for the thermal and relaxation processes between the ground state and the terminal states, and where S_{T3}, S_{T4}, and A_{34} are the probabilities for the thermal-deactivation processes and are the inverse processes of S_{T3}, S_{T4}, and A_{43} respectively. The population of the jth state is denoted by N_j, and the total concentration of molecules, by N_0. Degenerations should be considered for each level; the thermal deactivation probabilities are, then, given by:

$$S_{4T} = S_{T4}\exp(-E_{T3}/\boldsymbol{k}T) \quad (7)$$

$$S_{3T} = 3S_{T3}\exp(-E_{T3}/\boldsymbol{k}T) \quad (8)$$

$$A_{34} = 3A_{43}\exp(-E_{43}/\boldsymbol{k}T) \quad (9)$$

where E_{T4}, E_{T3}, and E_{43} are the energy differences between the corresponding respective two levels. The fluorescence yield for the $^5D_0 \rightarrow {}^7F_2$ transition is defined as follows:

$$\eta_{Eu} = A_{32}N_3/W_{1S}N_1 \quad (10)$$

Under the steady-state condition, the fluorescence yield, η_{Eu}, is obtained from Eqs. (1) to (10) as follows:

$$\eta_{Eu} = [1+(S_{T3}/S_{T4})(1+A_{41}/A_{43})+(S_{T3}/A_{43}) \times \exp(-E_{T4}/\boldsymbol{k}T)]/(1+A_{S1}/S_{ST})[(1+S_{T3}/S_{T4}$$

9) H. Samelson, A. Lempicki and C. Brecher, *J. Chem. Phys.*, **40**, 2553 (1964).

$$+ A_{T1}/S_{T4})(1+A_{41}/A_{43})(1+A_{31}/A_{32})$$
$$+ (1+A_{31}/A_{32})\{(A_{T1}+S_{T3})/A_{43}\}\exp(-E_{T4}/\boldsymbol{k}T)$$
$$+ (3S_{T3}/A_{32})\{(A_{41}/A_{43}+A_{T1}/S_{T4}+A_{T1}A_{41}/S_{T4}A_{43})$$
$$+ 3A_{T1}/A_{32}\}\exp(-E_{T3}/\boldsymbol{k}T)$$
$$+ (1+S_{T3}/S_{T4}+A_{T1}/S_{T4})(3A_{41}/A_{32})$$
$$\times \exp(-E_{43}/\boldsymbol{k}T)+(3A_{T1}S_{T3}/A_{32}A_{43})$$
$$\times \exp\{-(E_{T3}+E_{T4})/\boldsymbol{k}T\}] \quad (11)$$

Assuming that $A_{S1}/S_{ST} \ll 1$, $A_{41}/A_{43} \ll 1$, and $S_{T3}/S_{T4} \ll 1$ for the sake of simplicity, we have:

$$\eta_{Eu} = 1/[1+A_{T1}/S_{T4}+(A_{T1}/A_{43})\exp(-E_{T4}/\boldsymbol{k}T)$$
$$+ (3A_{T1}/A_{32})\exp(-E_{T3}/\boldsymbol{k}T)] \quad (12)$$

Equation (12) shows that when the temperature is low or the energy difference is large (provided that A_{T1} is constant), the exponential terms may be negligible and the fluorescence yield depends only upon S_{T4}. On the other hand, when the temperature is high or the energy difference is small, the exponential terms become large and the term of S_{T4} may be negligible.

In the case of terbium chelates, the situation is somewhat simpler; the energy transfer diagram is shown in Fig. 6.

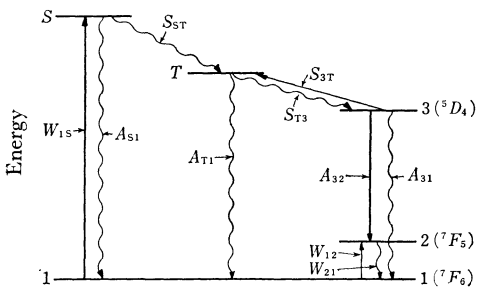

Fig. 6. Energy transfer diagram for terbium chelates.

The fluorescence yield, given by a similar way, is:

$$\eta_{Tb} = 1/[(1+A_{S1}/S_{ST})\{(1+A_{T1}/S_{T3})(1+A_{31}/A_{32})$$
$$+(A_{T1}/3A_{32})\exp(-E_{T3}/\boldsymbol{k}T)\}] \quad (13)$$

Therefore, the fluorescence yield also depends upon S_{T3} when the temperature is low or the energy difference is large, and *vice versa*.

In Eqs. (11), (12), and (13), which represent the fluorescence yields of europium and terbium chelates, the transition probability for the nonradiative energy transfer, S_{T3} or S_{T4}, is important. This transition probability was taken into consideration by Ermolaev *et al.*[5] and by Matsuda *et al.*,[10] along with the exchange-interaction theory described by Dexter.[11] The transition probability for the exchange interaction, P_{sa}, is given as follows:

$$P_{sa} = (2\pi Z^2/\hbar)\int F_s(E)\varepsilon_a(E)\mathrm{d}E \quad (14)$$

where F_s is the emission spectrum of the sensitizer (donor) and corresponds to the phosphorescence spectrum of a ligand in this case, where ε_a is the absorption spectrum of the activator (acceptor) and corresponds to the absorption spectrum for the $^7F \rightarrow {}^5D$ transition in the Eu^{3+} ion or the Tb^{3+} ion, where E is an energy (and now we use the unit of a wave number), and where Z^2 is the term of the overlap of electron clouds and cannot be determined by optical experiments. In the following discussions, the coefficient $(2\pi Z^2/\hbar)$ in Eq. (14) will be assumed to be equal and constant in all the chelates investigated.*2 Therefore, the transition probability may be proportional to the overlap between the phosphorescence spectrum and the absorption spectrum. The results obtained for the europium chelates are plotted in Fig. 7, and those for the terbium chelates are shown in

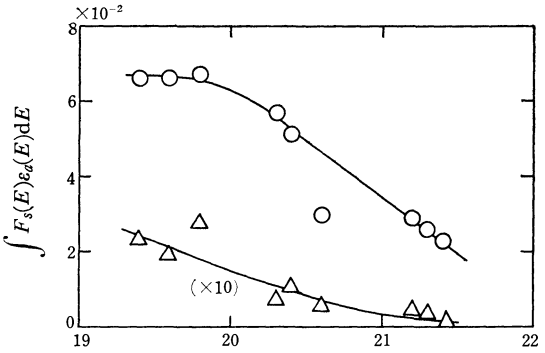

Fig. 7. Overlap for europium chelates.
○: $^7F \rightarrow {}^5D_1$ △: $^7F \rightarrow {}^5D_0$

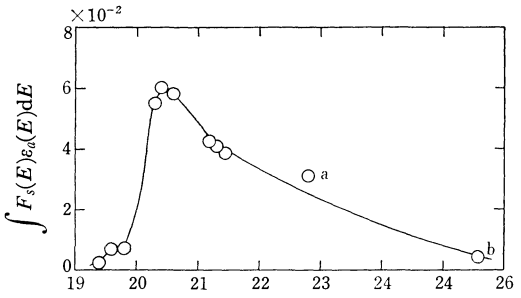

Fig. 8. Overlap for terbium chelates.
a : trifluoroacetylacetonate
b : acetylacetonate

10) Y. Matsuda, S. Makishima and S. Shionoya, This Bulletin, **42**, 356 (1969).
11) D. L. Dexter, *J. Chem. Phys.*, **21**, 836 (1953).

*2 This term may probably depend upon the mutual distance between the central ion and an oxygen atom of the ligand[10] but this distance is assumed to be not greatly changed among each β-diketone chelate in this case.

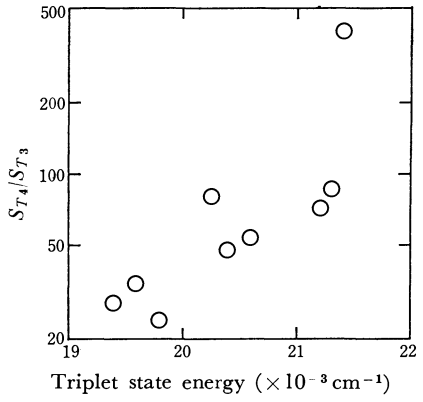

Fig. 9. The ratio of a transition probability for the $^5D_1$ level and the $^5D_0$ level of the europium ion.

Fig. 8, where the horizontal axis is the triplet state energy and where the circles show the values calculated for each β-diketone chelate. It can be seen in Fig. 7 that the overlap decreases as the triplet state energy increases. The ratio of the overlap for the $^5D_0$ and $^5D_1$ levels, that is, the ratio of the transition probability (S_{T4}/S_{T3}), is estimated from Fig. 7 and is shown in Fig. 9. As the triplet state energy increases, this ratio tends to increase exponentially, so that the excitation energy is transferred mainly from the triplet state to the $^5D_1$ level. The transition probability from the triplet state to the $^5D_0$ level is very small, but not zero. Therefore, the energy transfer to the $^5D_0$ level becomes important for the europium chelates which have the triplet state between the $^5D_1$ level and the $^5D_0$ level.

Since the energy of the $^5D_4$ level of the Tb^{3+} ion is about 20500 cm^{-1}, the value of the overlap is at its maximum for the β-diketone chelates with a triplet state energy of near 20500 cm^{-1}. This value of the overlap decreases rapidly or gradually according as the triplet state is lower or higher than the $^5D_4$ level.

The dependence of the energy transfer probabilities, S_{T4} and S_{T3}, on the energy difference must be taken into consideration, because these probabilities can reasonably be considered to depend upon the triplet state energy, as may be seen in Figs. 7 and 8. The energy transfer probability for the transition from the triplet state to the resonance level of the Eu^{3+} ion was obtained as 10^7—10^8 sec^{-1} from the quenching effects of anthracene on the fluorescence of europium chelates.[12] If the coefficient, $2\pi Z^2/\hbar$, in Eq. (14) is assumed to be 10^9, the energy transfer probability, S_{T4} (or S_{T3} from Fig. 8), can be obtained as 10^7—10^8 sec^{-1} using the values of the overlap shown in Fig. 7 or Fig. 8. This value of 10^7—10^8 sec^{-1} is coincident with the result obtained in Ref. 12 and seems reasonable. Therefore, the value of $2\pi Z^2/\hbar$ is taken as 10^9 and the energy transfer probability is obtained for each triplet state energy from the results shown in Figs. 7 and 8. Using these results, the fluorescence yield, η_{Eu}, for europium chelates is estimated from Eq. (11) and is plotted in Fig. 10,

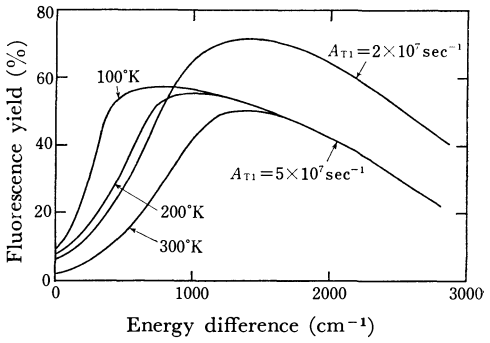

Fig. 10. Fluorescence yields *vs.* energy difference ($T-{}^5D_1$) for europium chelates.

where $A_{S1}=A_{41}=A_{31}=0$, $A_{43}=10^6$ sec^{-1}, $A_{32}=10^3$ sec^{-1}, $A_{T1}=2\times10^7$ sec^{-1} (for 300°K), and 5×10^7 sec^{-1} (for 100°K, 200°K, and 300°K) are assumed. η_{Tb} is estimated from Eq. (13) and is plotted in Fig. 11, where $A_{S1}=A_{31}=0$, $A_{32}=10^3$ sec^{-1}, $A_{T1}=2\times10^7$ sec^{-1} (for 300°K), and 5×10^7 sec^{-1} (for 100°K, 200°K, and 300°K) are assumed. In both cases, the fluorescence yield decreases because of the thermal deactivation process where the energy difference is small. Where the energy difference is large, the fluorescence yield also decreases because of the decrease in the energy transfer probability due to the diminution in the overlap between the phosphorescence spectra of the ligands and the absorption spectra of the rare earth ions. Consequently, the fluorescence yield shows a maximum for the proper energy difference between the triplet state and the resonant level of the rare earth ion; the experimental results shown in Fig. 2 are, therefore, confirmed. The temperature depen-

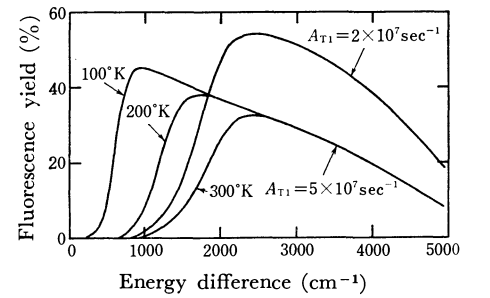

Fig. 11. Fluorescence yields *vs.* energy difference ($T-{}^5D_4$) for terbium chelates.

12) V. L. Ermolaev, E. A. Saenko, G. A. Domrachev, Yu. K. Khudenskii, and V. G. Aleshin, *Opt. Spectry.*, **22**. 466 (1967).

dences of fluorescence yields are also shown in Fig. 10 and Fig. 11, which show that the chelate compounds with small energy differences (*e.g.*, $Eu(CTFA)_4^-$, $Tb(BTFA)_4^-$, $Tb(TTA)_4^-$, and $Tb(PPBTFA)_4^-$) do not fluoresce at room temperature, but they begin to fluoresce if temperature is lowered. Since the thermal quenching for the fluorescent level decreases as the energy difference is large, the temperature dependence of fluorescence lifetimes in Fig. 3 is explained. Thus, several properties of the energy transfer mechanism for rare earth chelate compounds can be explained, but the explanation of the phenomena is qualitatively limited because so many undetermined factors in the system remain.

The authors are grateful to Dr. T. Seki and Dr. H. Watanabe for their valuable discussions.

BULLETIN OF THE CHEMICAL SOCIETY OF JAPAN VOL. 43 1962—1966 (1970)

Crystal Structure of Bis(nitrosocyclohexane)*1

Masamitsu TANIMURA,*2 Kiyotomi KOBORI,*3 Michio KASHIWAGI and Yukio KINOSHITA*3

Basic Research Laboratory, Toray Industries Inc., Tebiro, Kamakura

(Received December 1, 1969)

The crystal structure of bis(nitrosocyclohexane), $(C_6H_{11}NO)_2$, has been determined by means of three-dimensional X-ray analysis by the photographic method. The crystal belongs to the triclinic space group $P\bar{1}$, with cell parameters, $a=10.133$ A, $b=6.758$ A, $c=5.583$ A, $\alpha=121°42'$, $\beta=96°50'$, $\gamma=78°06'$. The unit cell contains one molecule. The nitrogen and oxygen atoms and the carbon atoms bound to nitroso-groups, CNO–O'N'C', are almost coplanar, and the oxygen atoms take a trans configuration around the N–N' bond. The cyclohexane ring takes a chair form and the nitrogen atom is bound to an equatorial bond. The CNO–O'N'C' plane is twisted from the cyclohexane ring by 73°.

Bis(nitrosocyclohexane), which is easily converted into cyclohexanone oxime by light, is a very important material from an industrial point of view. However, its structure has not been determined. The present investigation was carried out in order to determine a detailed structure by means of X-ray diffration.

Experimental

Single crystals of bis(nitrosocyclohexane), $(C_6H_{11}NO)_2$, were obtained by slow evaporation from methanol solution as triclinic plates tabular on (100). The cell dimensions were determined from the oscillation and Weissenberg photographs taken around the three axes using Cu$K\alpha$ radiation. The space group was determined from the measurement of piezo-electricity and from the Wilson ratio test. The results are listed in Table 1.

Intensity data were recorded on the equi-inclination Weissenberg photographs taken around b-axis up to the fifth layer and around c-axis up to the fourth layer, using the multiple film technique. The relative intensities, estimated visually with a set of standard scales, were corrected for the Lorentz-polarization factors. No absorption corrections were made. A total of 1096 independent reflections were observed.

TABLE 1. CRYSTAL DATA

Triclinic	
$a=10.133$ A	$\gamma=78°06'$
$b=6.758$	$Z=1$
$c=5.583$	$p\bar{1}$
$\alpha=121°42'$	$\mu=0.0794\,cm^{-1}$ (Cu$K\alpha$)
$\beta=96°50'$	

Structure Determination

The space group was assumed to be $P\bar{1}$. Choice of the space group was corroborated by structure determination.

An approximate structure was readily deduced from the three dimensional Patterson syntheses. The structure thus obtained was refined by Fourier

*1 Presented at the Symposium of Molecular Structure, Nagoya, October, 1965.

*2 Present address: Pioneering Research and Development Laboratories, Toray Industries Inc, Sonoyama, Otsu.

*3 Present address: Aichi Laboratory, Toray Industries Inc, Nishiku, Nagoya.

Table 2a. Atomic coordinates

Atom	$x(10^3\sigma_x)$	$y(10^3\sigma_y)$	$z(10^3\sigma_z)$	Atom	$x(10^3\sigma_x)$	$y(10^3\sigma_y)$	$z(10^3\sigma_z)$
C(1)	0.1306(4)	0.1343(5)	−0.0576(5)	H(2e)	0.0710(56)	0.5085(65)	0.2417(64)
C(2)	0.1557(5)	0.3854(5)	0.1571(6)	H(3a)	0.1793(56)	0.4580(65)	−0.1932(64)
C(3)	0.2416(6)	0.4579(6)	0.0143(7)	H(3e)	0.2524(56)	0.6503(65)	0.1859(64)
C(4)	0.3752(6)	0.2885(8)	−0.0829(7)	H(4a)	0.4218(55)	0.2877(65)	0.1004(64)
C(5)	0.3520(5)	0.0372(7)	−0.2855(7)	H(4e)	0.4279(56)	0.2931(65)	−0.2378(64)
C(6)	0.2637(4)	−0.0394(6)	−0.1519(6)	H(5a)	0.2943(56)	0.0160(65)	−0.4743(64)
N	0.0479(3)	0.0609(4)	0.0760(4)	H(5e)	0.4398(56)	−0.0661(65)	−0.3561(64)
O	0.0689(4)	0.1113(5)	0.3296(4)	H(6a)	0.3172(56)	−0.0546(65)	0.0187(64)
H(1a)	0.0860(55)	0.1213(65)	−0.2324(64)	H(6e)	0.2354(56)	−0.1914(65)	−0.3354(64)
H(2a)	0.2144(56)	0.3585(56)	0.3282(64)				

Table 2b. Anisotropic thermal parameters in the form $\exp(-(B_{11}h^2 + B_{22}k^2 + B_{33}l^2 + B_{12}hk + B_{13}hl + B_{23}kl))$

Atom	$B_{11}(10^3\sigma)$	$B_{22}(10^3\sigma)$	$B_{33}(10^3\sigma)$	$B_{12}(10^3\sigma)$	$B_{13}(10^3\sigma)$	$B_{23}(10^3\sigma)$
C(1)	0.0055 (0)	0.0228 (1)	0.0298 (2)	−0.0085 (1)	−0.0014 (1)	0.0314 (3)
C(2)	0.0129 (1)	0.0202 (2)	0.0431 (2)	−0.0090 (2)	0.0112 (2)	0.0268 (3)
C(3)	0.0179 (1)	0.0283 (2)	0.0550 (3)	−0.0236 (2)	0.0074 (2)	0.0333 (4)
C(4)	0.0108 (1)	0.0586 (3)	0.0620 (3)	−0.0332 (2)	−0.0054 (2)	0.0644 (5)
C(5)	0.0078 (1)	0.0399 (2)	0.0601 (3)	−0.0063 (2)	0.0156 (2)	0.0477 (4)
C(6)	0.0076 (0)	0.0275 (2)	0.0475 (2)	−0.0012 (1)	0.0104 (2)	0.0388 (3)
N	0.0060 (0)	0.0266 (1)	0.0243 (1)	−0.0101 (1)	−0.0041 (1)	0.0316 (2)
O	0.0137 (0)	0.0602 (2)	0.0298 (1)	−0.0385 (1)	−0.0166 (1)	0.0588 (3)
	$B(\sigma)$					
all H	3.0 (1.3)					

syntheses projected along the *b*- and *c*-axes, and later by a three dimensional isotropic least-squares method with ERBR1 program.[1] After a few cycles of this refinement, the structure was further refined by a block-diagonal anisotropic least-squares method with HBLS program.[2] Finally the difference Fourier syntheses were carried out in order to find the positions of the hydrogen atoms.

The final discrepancy factor, $R=\sum||F_o|-|F_c||/\sum|F_o|$ became 0.105 for all the observed reflections. Atomic scattering factors were taken from the International Tables for X-ray Crystallography. Final atomic parameters and their standard deviations are listed in Tables 2a and 2b. The observed and calculated structure factors are listed in Table 3.

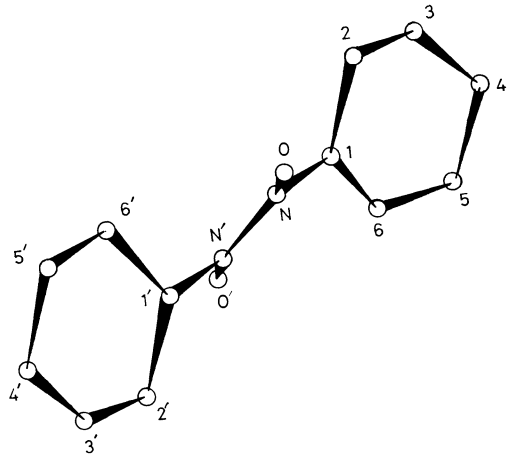

Fig. 1. Schematic diagram projected along c-axis.

Results and Discussion

The interatomic distances and bond angles are listed in Table 4. A schematic diagram of the molecule along the *c*-axis is shown in Fig. 1.

The atoms C(1), O, N, C′(1), O′ and N′ are almost coplanar, and oxygen atoms are placed *trans* with regard to the N–N′ bond. The cyclohexane ring takes a chair form, and the C(1)–N bond is equatorial.

The least-squares plane through C(1), O, N, N′, O′ and C′(1) is given by the equation.

$$0.9532X - 1.3248Y + 0.1805Z = 0 \quad (1)$$

Deviations of the atoms from this plane are apparently not significant as shown in Table 5.

The planes through C(1), C(3), C(5) and through C(2), C(4) and C(6) are given by the fol-

1) J. H. Van den Hende, "Crystallographic Structure Factor and Least-Squares Refinement Program" (1961).

2) T. Ashida, "Block-Diagonal Matrix Least-Squares Refinement Program" (1964).

lowing equations.

$$0.3534X - 0.3270Y + 0.7918Z = -0.0837 \quad (2)$$

$$0.4569X - 0.2034Y + 0.7720Z = 0.7862 \quad (3)$$

Planes (2) and (3) are almost parallel, and these planes make an average angle of 73° against plane (1).

The distances of N–N bond (1.32Å) and N–O bond (1.27 Å) suggest their double-bond characters. The N–C(1) bond (1.49 Å) has a single-bond character.

The C–C bond distances and C–C–C angles of the cyclohexane ring are normal. The bond distances and bond angles including the hydrogen atoms do not considerably deviate from the normal values as shown in Table 4. The values of other bond distances and bond angles including hydrogen are of the same order as those listed in Table 4.

All the intermolecular atomic distances observed are within the limits of experimental error, equal to or greater than the sum of the van der Waals radii of the corresponding atoms.

TABLE 3. OBSERVED AND CALCULATED STRUCTURE FACTORS

The running indices are *hl*, the value for *k* immediately precedes the group. The central column is $|F_o|$, the right hand column F_c.

	0			1 2	9.7	9.2	-5 1	1.1	0.9	2 -3	7.8	-6.9	0 -1	8.6	7.6	-4 3	2.4	-2.6	2 3	5.6	-6.1
0 1	33.4	39.7	-1 2	19.2	19.0	-5 -1	0.9	-0.8	2 4	3.3	-3.6	0 -2	1.1	0.9	-4 -3	0.9	-0.7	-2 3	1.9	1.6			
0 2	1.3	0.3	-1 -2	1.0	1.0	-5 -1	2.4	2.9	-2 4	2.9	1.2	0 -2	3.3	-2.0	4 -3	1.3	-0.6	-2 -3	0.9	-0.2			
0 3	7.0	6.7	-1 -2	6.0	-5.3	5 2	3.6	-3.2	-2 -4	1.3	-1.2	0 3	3.0	2.3	4 -4	4.3	-4.2	2 -3	1.3	0.0			
0 4	3.0	-2.9	1 3	2.0	1.6	-5 2	2.1	1.2	2 -4	7.8	7.9	0 -3	4.7	4.7	-4 5	3.9	-4.3	2 4	1.2	-1.1			
0 5	2.8	-3.2	-1 3	10.7	11.2	5 -2	6.7	6.0	-2 5	5.1	-5.0	0 4	1.4	-1.7	4 -5	2.3	-2.5	-2 4	5.5	-5.1			
1 0	33.4	29.1	-1 -3	4.3	4.3	-5 3	2.6	2.0	2 -5	1.9	1.1	0 5	1.1	0.9	-4 6	1.6	-1.5	-2 -4	1.9	1.0			
1 1	9.3	-7.9	-1 -3	5.4	5.3	-5 -3	2.9	-2.7	-2 6	2.2	-1.8	0 -5	4.5	-5.0	4 -6	0.9	0.7	2 -4	4.0	-3.8			
-1 1	2.4	4.6	1 4	3.2	-3.4	-5 4	7.3	7.5	2 -6	1.1	-0.9	1 0	4.0	-3.8	5 0	1.9	-1.9	-2 5	2.1	-2.3			
-1 2	12.3	-13.0	-1 4	1.5	-1.9	5 -4	0.7	-0.4	3 0	17.3	-18.9	-1 0	37.0	37.4	5 1	0.8	-0.4	2 -5	4.8	4.4			
1 3	5.1	4.5	-1 -4	2.3	-1.7	-5 5	4.0	4.5	-3 0	9.1	9.8	1 1	12.6	-10.8	-5 -1	0.8	-0.2	-2 6	1.3	0.9			
-1 3	3.9	5.3	1 -4	3.7	2.8	5 -5	6.1	7.0	3 1	10.5	-9.9	-1 1	3.1	-2.9	5 -1	2.1	-2.4	3 0	8.4	-8.3			
-1 4	2.2	-3.5	-1 5	4.8	-6.0	-5 6	0.9	-0.8	-3 1	7.5	7.0	-1 -1	18.1	18.0	5 2	1.2	-0.7	-3 0	3.3	3.5			
-1 5	7.9	-9.0	-1 -5	0.6	-0.8	5 -6	3.0	2.1	-3 -1	10.6	11.0	1 -1	2.6	2.5	-5 2	1.2	-1.1	3 1	4.1	3.8			
-1 6	2.2	-1.8	1 -5	2.5	-2.7	6 0	1.2	0.8	3 -1	6.1	5.7	1 2	3.5	-2.8	-5 -2	0.8	-0.6	-3 1	7.4	6.7			
2 0	23.8	22.3	-1 6	1.8	-1.7	-6 0	2.3	-2.6	3 2	1.4	-0.6	-1 2	10.9	-10.4	5 -2	9.5	10.3	-3 -1	2.7	-3.0			
2 1	4.0	2.5	1 -6	1.4	-1.3	-6 -1	2.8	-3.4	-3 2	1.6	-1.5	-1 -2	1.1	-0.2	-5 3	1.4	-1.3	3 -1	2.7	-3.0			
-2 1	13.9	13.3	2 0	12.9	12.8	-6 -1	2.3	2.9	-3 -2	8.5	8.6	1 -2	3.8	-3.6	5 -3	9.6	10.2	3 2	1.7	-1.2			
2 2	3.7	3.4	-2 0	5.0	5.4	-6 2	1.2	1.0	3 -2	10.8	10.2	1 3	6.6	-6.2	-5 4	0.9	-0.9	-3 2	2.3	1.5			
-2 2	10.2	-9.4	2 1	11.7	10.6	-6 -2	5.8	5.7	3 3	1.4	-1.4	-1 3	1.3	-0.9	5 -4	1.6	0.8	-3 -2	1.2	0.4			
-2 3	3.7	4.2	-2 1	13.3	14.2	-6 3	1.8	1.4	-3 3	3.3	2.4	-1 -3	2.6	2.0	-5 5	2.9	-3.0	3 -2	7.2	6.2			
2 4	0.8	-1.0	-2 -1	3.2	-3.4	6 -3	3.5	2.7	-3 -3	1.6	1.8	1 -3	4.3	3.4	5 -5	3.4	2.7	3 3	4.1	-4.4			
-2 4	5.6	5.7	-2 -1	17.1	18.5	-6 4	3.5	2.9	3 -3	8.7	9.4	1 4	3.4	-3.2	-5 6	2.5	-2.1	-3 3	3.8	2.9			
-2 5	3.7	-3.6	2 2	7.6	6.3	6 -4	2.3	1.4	-3 4	2.0	1.5	-1 4	4.6	-4.5	5 -6	1.7	1.2	-3 -3	0.7	0.7			
3 0	5.1	4.8	-2 2	7.7	-6.6	7 0	1.8	0.2	-3 -4	0.8	-0.9	-1 -4	2.9	-2.3	5 -7	1.5	-1.3	3 -3	8.1	-8.4			
3 1	5.4	-5.9	-2 -2	8.7	7.4	7 -1	1.3	-1.2	3 -4	13.6	17.6	1 -4	6.9	6.5	6 0	2.0	-2.3	3 4	1.1	-1.0			
-3 1	13.6	14.0	2 -2	3.3	-3.0	-7 2	2.2	2.3	-3 5	3.8	-3.3	1 5	0.8	0.7	-6 0	1.1	1.4	3 -4	1.4	1.0			
3 2	6.7	-6.5	2 3	5.1	-5.0	7 -2	3.1	-2.8	3 -5	8.0	7.5	-1 5	1.1	-0.6	6 -1	6.6	-7.2	-3 5	2.7	-3.3			
-3 2	2.7	2.2	-2 3	1.3	1.0	-7 3	5.4	5.2	-3 6	2.0	-1.7	-1 -5	3.7	-3.5	6 -2	2.2	-3.2	3 -5	8.9	8.9			
3 3	5.4	-5.5	-2 -3	5.3	5.4	7 -3	3.6	-3.6	-3 -6	1.7	-1.3	-1 6	1.6	1.5	-6 3	1.2	-0.6	3 -6	2.9	1.9			
-3 3	1.9	-1.7	2 -3	3.9	-3.4	-7 4	5.8	5.6	-4 0	1.8	-1.7	1 -6	1.8	1.4	6 -4	3.8	-3.3	-4 0	5.4	6.7			
3 4	1.4	-1.5	2 4	4.3	-4.6	7 -4	2.6	-2.2	-4 0	4.2	-3.7	2 0	14.3	-14.4	7 -1	1.0	-1.2	-4 1	9.2	9.1			
-3 4	1.8	0.8	-2 4	1.2	1.0	8 -3	1.3	-1.2	-4 1	1.0	0.9	-2 0	19.9	20.0	7 -4	3.7	-3.7	-4 -1	1.7	1.6			
-3 5	5.6	-5.2	2 -4	6.0	5.5	-8 4	1.7	1.4	4 -1	2.0	2.0	2 1	17.0	-16.6	8 -2	2.6	-2.7	4 -1	5.8	5.3			
-3 6	1.9	-1.5	-2 5	7.1	-7.6	8 -4	2.3	-2.1	4 2	1.7	-1.8	-2 1	6.5	4.8				4 2	3.1	-2.9			
4 0	3.2	-2.8	2 -5	1.6	1.0				-4 2	0.6	-0.6	-2 1	3.1	4.8	4			-4 2	3.7	3.3			
4 1	1.3	-1.4	-2 6	5.0	-4.2	2			-4 -2	0.8	0.6	-2 -1	3.7	3.0	0 0	9.1	-8.0	-4 -2	1.2	1.1			
-4 1	1.3	-1.5	2 -6	1.2	0.6	0 0	12.1	-10.7	4 -4	2.5	2.1	2 -1	12.8	12.5	0 1	6.4	-6.8	4 -2	12.9	13.1			
4 2	2.1	-1.6	3 0	17.7	-17.1	0 1	34.9	-36.9	4 3	2.8	-3.0	2 2	12.9	-11.8	0 -1	2.8	2.5	-4 3	2.1	1.9			
4 2	5.5	5.6	-3 0	2.8	1.9	0 -1	17.6	17.6	-4 3	1.3	-0.9	-2 2	0.7	-0.4	0 2	5.8	5.3	4 -3	2.9	-2.4			
4 3	1.3	-1.4	3 1	5.8	-5.2	0 2	2.7	-1.1	-4 -3	1.1	-0.7	-2 -2	0.8	-1.0	0 -2	1.3	-0.1	-4 4	1.5	1.4			
-4 3	3.1	2.5	-3 1	14.2	12.6	0 -2	1.1	-1.0	4 -3	2.0	1.5	2 -2	18.5	18.2	0 3	5.1	-5.0	4 -4	5.3	-4.7			
-4 4	5.0	4.6	-3 -1	3.9	-3.7	0 3	4.8	4.4	-4 4	1.9	0.9	2 3	9.6	-9.4	0 -3	2.9	1.9	-4 5	2.2	-2.5			
-4 5	0.9	0.4	3 -1	1.4	2.2	0 -3	5.1	4.5	4 -4	9.2	11.0	-2 3	12.1	11.1	0 4	5.7	-5.7	4 -5	4.3	4.3			
-4 6	1.4	-1.3	3 2	1.6	-1.0	0 4	4.7	-4.5	-4 5	2.4	-2.2	-2 -3	1.9	1.9	0 -4	4.6	4.4	-4 6	1.3	-1.5			
-4 7	1.8	1.8	-3 2	1.2	-0.3	0 -4	1.1	0.7	4 -5	9.0	9.8	2 -3	7.3	6.1	0 5	1.0	1.0	4 -6	1.6	1.3			
5 1	1.0	-1.3	-3 -2	2.0	1.5	0 -5	4.1	-4.7	-4 6	2.4	-2.0	2 4	1.8	-1.6	0 -5	2.3	2.7	5 0	0.8	-1.1			
-5 1	1.4	-0.8	3 -2	2.4	2.4	1 0	4.7	4.1	4 -6	0.8	0.2	-2 -4	0.7	-0.5	1 0	8.1	-7.1	-5 0	1.2	1.6			
5 2	3.7	-3.7	3 3	4.5	-4.7	-1 0	22.4	22.3	-5 0	4.5	-4.5	2 -4	6.4	5.9	-1 0	1.3	0.9	-5 1	5.7	5.9			
-5 2	3.2	3.7	-3 3	0.8	0.4	1 1	3.4	-3.0	-5 1	3.0	-2.2	-2 5	2.5	-3.1	1 1	7.1	-6.1	-5 -1	1.7	-1.9			
-5 3	1.3	1.1	3 -3	9.0	-0.0	-1 1	3.1	3.2	5 2	1.1	-0.9	-2 6	1.6	1.2	-1 1	3.4	-3.3	5 -1	1.6	-1.8			
-5 4	3.2	2.3	3 4	1.7	-1.8	-1 -1	13.9	13.2	-5 2	0.8	0.0	2 -6	0.8	-0.6	-1 -1	2.4	-1.4	-5 2	3.8	3.8			
-5 5	4.8	5.4	-3 4	5.8	5.3	1 -1	20.5	20.1	-5 -2	1.2	1.8	3 0	2.4	-1.6	1 1	17.3	16.4	-5 -2	0.8	-0.6			
-5 6	3.7	3.1	3 -4	1.8	1.8	1 2	15.3	14.3	5 -2	2.9	3.4	-3 0	11.0	11.5	1 2	5.7	-5.2	5 -2	3.7	3.3			
-5 7	2.6	2.4	-3 5	2.8	-2.7	-1 2	12.4	12.5	-5 3	0.8	0.3	3 1	4.2	4.1	-1 2	1.1	0.6	-5 3	1.3	0.9			
6 1	2.2	-2.2	3 -5	2.5	1.3	-1 -2	1.2	0.0	-5 -3	2.1	2.1	-3 1	5.1	5.2	-1 -2	4.0	-3.0	5 -3	1.2	0.3			
-6 1	1.7	1.9	-3 6	2.7	-2.1	1 -2	5.8	-5.2	-5 4	4.8	4.9	-3 -1	5.0	4.9	1 -2	6.7	5.3	5 -4	4.3	-4.0			
-6 2	7.1	7.1	-3 -6	1.0	-0.8	1 3	5.5	4.2	-5 -4	2.0	1.8	3 -1	5.0	4.2	1 3	15.8	-16.5	-5 5	4.0	-4.0			
-6 3	6.4	5.2	4 0	6.1	-6.3	-1 3	14.6	14.2	-5 5	3.0	3.4	3 2	1.6	-1.5	-1 3	3.9	-3.5	5 -5	1.4	0.8			
-6 4	1.7	1.2	-4 -0	8.3	-8.6	-1 -3	3.1	2.9	5 -5	3.9	3.4	-3 2	4.0	-3.9	-1 -3	2.5	-2.6	-5 6	3.0	-3.3			
-7 2	2.4	2.4	4 1	2.7	2.2	1 -3	5.0	4.9	-5 6	1.1	-0.9	-3 -2	2.6	2.3	1 -3	4.5	-3.9	5 -6	0.8	0.1			
-7 3	3.6	3.4	-4 1	3.7	3.5	1 4	3.3	-3.4	5 -6	0.8	-0.2	3 -2	22.3	24.2	1 4	8.1	-8.1	5 -7	1.8	-1.7			
-7 4	1.8	1.6	-4 -1	8.5	-9.5	-1 4	1.1	-1.6	5 -7	1.2	-0.6	3 3	2.7	-3.1	-1 4	5.9	-5.7	6 1	0.8	-0.6			
-8 4	2.8	-2.4	4 -1	0.4	0.5	1 -4	8.4	8.5	6 -1	4.9	-4.7	-3 3	5.5	4.2	-1 -4	3.8	-3.5	6 -1	3.0	-2.8			
			-4 2	3.4	2.8	-1 5	1.1	-0.4	6 -2	2.9	-2.6	3 -3	15.0	14.6	1 -4	3.3	3.5	6 -2	7.0	-6.2			
1			-4 -2	2.7	-2.4	-1 -5	0.7	-0.9	-6 3	1.6	-1.5	-3 4	3.7	2.7	1 5	0.7	-0.4	6 -3	8.2	-7.5			
0 1	14.2	15.4	4 -2	6.7	7.2	-1 6	1.9	1.6	6 -3	4.1	2.7	-3 -4	1.5	-1.5	-1 5	0.9	0.8	6 -4	7.7	-7.4			
0 -1	0.7	0.8	4 3	2.8	-2.8	1 -6	2.0	-1.9	-6 4	2.2	1.8	3 -4	8.9	9.8	-1 -5	1.9	-1.9	7 -4	1.2	-0.9			
0 2	6.9	5.9	-4 3	2.0	1.7	2 0	21.4	-21.3	6 -4	5.4	4.1	-3 5	3.7	-3.8	1 -5	2.9	3.4	8 -2	2.4	-2.5			
0 -2	3.7	-2.7	-4 -3	0.9	-0.1	-2 0	2.6	3.4	7 -1	1.9	-2.0	3 -5	5.7	5.6	-1 6	0.9	0.7	8 -3	1.9	-1.4			
0 3	5.9	5.4	4 -3	1.1	-0.1	2 1	19.6	-18.8	7 -2	4.6	-4.5	-3 6	1.2	-0.8	1 -6	2.1	2.0						
0 -3	4.6	3.4	-4 4	6.0	5.3	-2 1	0.7	1.3	-7 3	1.1	1.0	3 -6	0.8	-0.3	2 0	8.7	-7.9	5					
0 4	2.6	-2.0	4 -4	9.9	11.2	-2 -1	1.6	1.5	7 -3	2.9	-2.6	4 0	3.3	-3.3	-2 0	18.5	17.6	0 0	3.7	-2.8			
0 -4	3.4	-3.1	-4 5	2.6	2.4	2 -1	3.9	3.5	-7 4	2.0	1.9	-4 0	10.1	11.6	2 1	3 5	3.3	0 1	6.5	-6.2			
0 -5	2.5	-3.0	4 -5	11.5	13.4	2 2	2.5	-2.1	7 -4	2.3	-2.1	4 1	1.2	-0.3	-2 1	18.7	16.4	0 -1	9.1	9.6			
1 0	15.3	-12.8	-4 6	5.2	-4.6	-2 2	7.1	6.0	8 -2	1.6	-1.7	-4 1	8.6	8.7	-2 -1	2.7	2.3	0 2	2.9	2.2			
-1 0	34.2	34.7	4 -6	3.6	3.1	-2 -2	4.1	3.7	-8 4	2.1	2.5	-4 -1	5.0	5.7	2 -1	24.0	23.2	0 -2	1.1	-0.8			
1 1	0.7	-0.6	4 -7	1.8	1.6	2 -2	16.6	-15.7				4 -1	5.7	-6.1	2 2	1.7	1.5	0 3	7.1	-6.7			
-1 1	49.2	52.7	5 0	1.0	-0.9	2 3	5.0	-4.9	3			4 2	4.4	-4.1	-2 2	2.9	7.2	0 -3	3.1	2.6			
-1 -1	7.7	-6.8	-5 0	2.0	-1.5	-2 3	15.3	15.1	0 0	10.2	8.6	-4 2	1.2	0.4	-2 -2	0.9	-0.7	0 4	8.1	-8.4			
1 -1	8.9	-9.6	5 1	0.8	-0.8	-2 -3	2.0	2.4	0 1	13.6	-12.0	4 -2	5.5	5.9	2 -2	27.2	26.6	0 -4	8.1	8.8			

TABLE 3. (continued)

0	1	4.5	-2.1	5	-6	3.4	2.8	-4	-2	0.6	-0.7	-3	2	3.8	-3.8	-2	4	3.7	-3.9	3	2	1.3	-1.2	5	-3	2.6	-2.0
0	-5	4.4	4.2	6	0	1.9	2.0	4	-2	5.0	-4.6	3	-2	3.7	3.9	2	-4	1.7	-1.8	-3	2	2.5	-2.6	5	-4	1.0	0.8
1	0	7.5	-6.7	6	1	0.8	-0.9	4	3	2.0	2.2	3	3	1.6	1.6	2	-5	1.8	1.4	3	-2	7.9	-8.1	5	-5	2.8	-2.8
-1	0	13.0	-11.8	6	-1	1.5	-1.2	-4	3	3.4	3.3	-3	3	5.8	-6.1	3	1	3.7	-3.7	-3	3	1.7	-1.5	6	-2	2.7	-2.4
1	1	4.6	-3.1	-6	2	1.3	1.4	4	-3	2.5	2.3	-3	-3	0.7	-0.7	-3	1	1.7	-1.7	3	-3	1.0	-0.7	6	-3	3.4	-3.0
-1	1	17.0	-15.5	6	-2	5.8	-5.6	-4	4	2.1	1.7	3	-3	1.9	-1.3	-3	-1	0.8	1.3	-3	4	1.4	-1.7	6	-4	2.6	2.0
-1	-1	1.3	0.6	-6	3	1.7	1.5	4	-4	4.2	-3.7	-3	4	5.0	-4.9	-3	-1	5.5	-5.3	3	-4	2.5	-2.5				
1	-1	10.0	9.4	7	-1	2.5	-2.8	4	-5	1.0	0.9	3	-4	4.9	-4.5	3	2	5.4	-5.3	3	-5	1.2	0.7	11			
1	2	1.3	0.3	7	-2	4.4	-4.2	4	-6	3.0	2.3	-3	5	0.9	-1.0	-3	2	1.2	-0.9	4	0	0.8	0.8	0	0	1.1	-1.0
-1	-2	1.0	-0.9	8	-2	2.2	-2.1	5	0	2.6	-2.4	3	-6	1.5	1.3	-3	-2	0.8	-0.6	-4	1	1.3	-1.4	0	1	1.5	-1.5
1	-2	1.2	-0.3	8	-3	2.0	-1.2	-5	0	3.5	4.1	3	-6	1.5	1.4	3	-2	4.2	-3.9	4	-1	4.2	-4.1	0	-1	1.6	-2.4
1	3	6.1	-6.2					5	1	1.2	-1.0	4	0	6.0	-5.9	3	3	0.5	0.6	4	2	0.5	-0.1	0	2	2.0	-1.9
-1	3	1.1	-0.6	6				-5	1	1.6	-1.8	-4	0	0.7	0.5	-3	3	4.3	-3.0	-4	2	1.9	-1.7	0	-2	3.4	-3.8
-1	-3	2.8	2.5	0	0	6.2	-6.4	-5	-1	2.2	-2.8	4	1	5.3	-5.9	3	-3	1.0	0.3	4	-2	4.1	-4.2	0	-3	2.2	-2.5
1	-3	3.3	-3.0	0	1	4.6	-4.1	5	-1	9.7	-10.8	-4	1	3.3	1.4	-3	4	4.2	-4.7	-4	3	1.1	-1.1	1	0	0.9	-0.6
1	4	3.2	-3.3	0	-1	1.1	0.8	5	2	1.1	-1.0	4	-1	8.8	-8.6	3	-4	2.0	-2.0	4	-3	1.7	1.6	-1	0	0.7	-0.4
-1	4	5.4	-5.4	0	2	2.0	-2.0	5	-2	7.3	-7.5	4	2	3.2	-2.9	-3	5	1.2	-1.7	-4	4	0.9	-1.8	1	1	3.8	-3.4
-1	-4	4.1	4.0	0	-2	1.2	1.0	-5	3	1.2	1.0	-4	-2	1.0	0.1	3	-5	0.9	-0.9	4	-4	1.4	0.8	-1	1	2.1	-2.1
1	-4	5.5	5.3	0	3	6.9	-7.0	5	-3	2.1	1.0	4	-2	3.9	-3.4	4	0	2.8	2.9	4	-5	4.1	3.1	-1	-1	0.6	0.6
1	5	0.7	-0.6	0	-3	3.7	2.8	-5	4	0.9	0.9	-4	3	0.8	-0.4	4	1	0.8	-0.8	5	1	0.9	-0.8	1	-1	1.7	-2.1
1	-5	2.2	2.7	0	4	2.9	-2.7	5	-4	1.4	-1.5	4	-3	1.2	0.5	-4	-1	0.7	-0.4	5	-1	0.8	1.0	1	2	3.9	-3.9
2	0	10.4	-10.4	0	-4	3.2	3.2	-5	5	0.7	-0.6	-4	4	0.7	-0.6	4	-1	5.3	-5.8	5	-3	1.6	1.5	-1	2	2.0	-1.9
-2	0	1.0	-0.5	1	0	9.7	-9.2	5	-5	2.3	-1.7	4	-4	1.7	-2.1	4	2	1.2	-1.0	5	-4	1.1	-0.7	-1	-2	1.0	-0.9
-2	1	4.6	-4.1	1	1	2.8	-2.3	5	-6	5.1	4.6	4	-6	1.0	0.7	-4	2	0.8	-1.2	5	-5	2.3	-1.8	1	-2	3.0	-2.9
-2	-1	1.0	1.3	-1	1	6.4	-5.8	6	1	1.0	-1.5	5	0	1.9	1.9	4	-2	9.8	-10.5	6	-1	2.2	2.3	1	-3	1.5	-1.4
2	-1	1.8	-0.5	-1	-1	4.2	4.3	6	-1	1.8	-1.7	-5	0	1.7	2.0	-4	3	0.7	-0.6	6	-2	1.2	-0.9	2	0	0.8	-0.1
2	2	1.6	1.3	1	-1	2.3	2.3	-6	3	1.3	1.4	5	1	1.3	-1.6	4	-3	2.4	-2.4	6	-3	2.2	-1.9	-2	0	0.8	0.8
-2	2	4.0	3.4	1	2	3.6	-3.7	6	-3	3.1	2.4	-5	1	2.0	2.4	-4	4	2.9	-3.1	7	-2	1.8	-1.6	2	1	4.3	-4.2
-2	-2	2.9	-3.5	-1	2	2.2	-1.6	7	-1	4.1	-3.9	5	-1	1.7	1.8	4	-4	2.4	-2.4	7	-3	5.6	-5.6	-2	1	0.5	-0.3
2	-2	4.8	3.8	-1	-2	4.3	4.9	7	-2	4.4	-4.2	5	-2	2.1	-1.8	4	-6	2.9	3.2	7	-4	4.2	-3.9	-2	-1	0.9	1.0
2	3	1.3	-0.8	1	-2	13.6	13.4	7	-3	1.4	-1.0	-5	3	0.7	-0.4	5	0	1.5	1.6					-2	-1	1.6	-1.6
-2	3	3.2	2.7	1	3	3.8	-3.7	8	-4	2.3	1.2	5	-4	0.8	-1.3	-5	0	0.7	-0.7		10			2	2	2.9	-3.5
-2	-3	1.9	-1.9	-1	3	4.0	-3.5					5	-5	3.4	2.8	5	1	3.2	-3.0	0	0	5.8	-7.0	-2	2	0.5	-0.5
2	-3	3.9	3.0	-1	-3	7.1	8.2		7			6	0	3.5	-3.7	5	-1	0.8	0.2	0	1	2.9	-3.0	2	-2	1.5	-1.5
-2	4	5.3	-4.4	-1	-3	10.4	9.5	0	0	4.4	-4.3	6	-1	2.0	-1.8	-5	2	0.6	0.8	0	-1	2.6	-3.2	2	-3	2.4	2.1
2	-4	10.7	10.8	1	4	2.3	2.4	0	1	2.7	-2.3	-6	2	1.6	2.0	5	-2	4.6	-4.5	0	2	1.7	-1.9	2	-4	1.2	0.8
-2	5	1.0	-0.5	-1	4	3.7	-3.8	0	-1	8.3	8.0	6	-2	3.0	-3.1	-5	3	0.5	0.7	0	-2	1.5	1.7	3	0	5.2	-5.4
2	-5	8.5	7.7	-1	-4	4.4	4.6	0	2	3.6	-3.6	6	-4	1.2	0.8	5	-3	0.9	0.5	1	0	3.2	-3.4	3	1	0.9	0.6
-2	6	1.2	1.1	1	-4	5.8	5.2	0	-2	9.3	8.8	7	-1	1.8	1.9	5	-5	2.5	-1.9	-1	0	2.6	-3.2	3	-1	2.7	3.1
-3	0	1.0	0.7	-1	5	0.9	-0.7	0	3	8.1	-9.0	7	-3	1.8	1.3	5	-6	3.6	3.8	1	1	1.3	-0.8	3	-2	1.0	-1.0
3	1	2.6	2.2	1	-5	1.0	-1.4	0	-3	1.0	-0.6	7	-4	5.5	4.7	6	-1	1.1	1.0	-1	1	1.4	-1.2	3	-3	2.0	1.8
-3	1	3.8	2.8	2	0	7.3	-6.1	0	4	2.0	-1.9	8	-3	0.2	-1.1	6	-2	1.4	-1.3	-1	-1	1.0	0.8	3	-4	0.7	0.4
3	-1	4.5	-3.9	-2	0	0.8	-0.0	1	0	4.3	-3.9					6	-3	2.6	2.6	1	-1	2.5	-2.9	4	0	1.9	2.0
3	2	3.6	-3.7	2	1	4.2	4.2	-1	0	2.6	-2.6	8				6	-4	2.2	2.1	1	2	1.4	-1.4	4	-1	1.2	1.6
-3	2	8.0	7.7	-2	1	11.7	-11.1	1	1	2.5	2.4	0	0	3.1	2.9	7	-3	0.9	-0.8	-1	-2	3.0	2.8	4	-2	3.1	-2.7
3	-2	5.1	-4.2	-2	-1	2.3	2.2	-1	1	1.4	-2.0	0	1	2.7	2.9					1	3	0.7	0.7	4	-3	1.2	-0.8
3	3	2.8	-2.5	2	-1	9.9	-8.8	-1	-1	2.5	3.1	0	-1	6.9	7.0	9				1	-3	2.4	-2.4	4	-4	2.7	-2.2
-3	3	8.3	7.9	2	2	2.5	-2.7	1	-1	7.7	7.5	0	-2	2.2	2.2	0	0	4.5	-4.5	1	-4	1.6	-1.5	5	-1	1.5	-1.4
3	-3	5.5	-4.8	-2	2	9.3	-9.2	-1	-2	3.2	3.7	0	3	1.9	-2.0	0	1	1.2	1.0	2	0	5.5	-5.9	5	-2	1.1	-0.8
-3	4	1.1	-0.7	2	-2	1.4	0.7	-1	-2	14.4	14.8	0	-3	1.3	-1.0	0	-1	5.6	-6.1	-2	0	0.9	-1.2	5	-3	1.1	1.0
3	-4	1.9	1.5	2	-2	7.9	7.3	1	3	3.1	-3.1	0	4	0.7	0.4	0	-2	1.0	-0.1	2	1	4.6	-5.0	5	-4	1.3	1.3
-3	5	1.9	-2.1	2	3	2.8	-2.6	-1	3	6.0	-6.5	0	-4	1.6	1.3	0	3	1.0	1.1	-2	-1	0.9	1.0				
3	-5	5.4	5.2	-2	3	5.1	-4.4	-1	-3	1.6	1.1	1	0	3.2	-3.2	0	-3	2.2	2.2	2	-1	5.3	-6.0	12			
4	0	4.6	4.5	-2	-3	2.3	2.1	-1	-3	3.0	2.3	-1	0	0.8	0.6	0	4	3.4	3.7	2	2	2.6	-2.4	0	0	1.5	-1.6
4	1	3.3	2.9	2	-3	7.8	6.6	1	4	1.6	1.6	1	1	1.6	1.4	0	-4	1.4	0.6	-2	-2	1.5	1.9	0	-1	3.1	-4.6
-4	1	0.7	0.4	2	4	1.1	1.2	-1	4	3.8	-4.1	-1	1	1.2	-0.9	1	0	5.2	-5.1	2	-2	1.7	-1.4	0	-2	1.6	-2.6
-4	-1	2.0	2.3	-2	4	4.1	-3.9	-1	-4	1.8	1.7	-1	-1	3.4	3.5	-1	0	1.2	0.5	-2	3	1.1	-1.4	1	0	0.5	-0.1
4	-1	0.6	-0.5	2	-4	3.9	3.1	-1	-5	1.4	1.4	1	-1	5.6	-5.5	-1	1	2.5	2.7	2	-3	1.1	-0.9	-1	0	1.7	-2.2
-4	2	2.2	1.6	2	-5	2.3	2.6	2	0	5.6	-5.0	-1	2	1.1	-0.8	1	-1	10.3	-11.4	2	-4	0.8	-0.9	1	1	0.7	-0.5
-4	-2	2.1	1.9	2	-6	0.8	-0.5	-2	0	0.8	-0.2	-1	-2	1.2	-1.3	1	2	2.9	-2.9	3	0	2.5	-2.8	1	1	2.1	-2.3
4	-2	2.2	1.7	-3	0	3.3	3.0	2	1	2.8	2.9	1	-2	7.2	-7.0	1	-2	4.8	-4.6	3	1	4.0	-3.9	2	0	2.5	-2.5
4	3	2.4	2.1	3	1	5.5	5.6	-2	1	2.3	-2.5	1	3	0.8	0.6	1	3	0.7	-0.5	-3	1	0.6	-0.9	2	1	4.1	2.2
-4	3	3.7	3.4	-3	1	1.5	-1.7	-2	-1	2.9	3.4	-1	3	4.7	-5.4	-1	3	1.2	-1.0	-3	-1	1.1	2.1	2	-1	0.8	-1.0
4	-3	1.8	1.2	-3	-1	9.0	-8.4	2	-1	5.9	-5.6	-1	-3	0.9	-0.9	-1	-3	1.6	1.4	3	-1	3.2	-3.3	2	-2	0.7	-0.8
4	-4	3.0	-2.7	3	2	1.0	-0.8	2	2	0.8	-0.6	1	-3	5.2	-5.3	-1	4	0.8	0.7	3	2	0.8	-0.7	3	0	1.7	2.2
-4	5	1.3	-1.6	-3	2	1.4	-0.9	-2	2	3.3	-2.8	1	4	2.6	2.5	2	0	0.9	-0.5	-3	2	1.0	-1.0	3	-2	1.9	-1.8
4	-5	1.5	1.0	3	-2	3.5	3.3	-2	-2	3.4	4.5	-1	4	3.8	-4.1	2	1	1.1	1.2	3	-2	2.0	-1.8	-3	-3	2.4	-2.1
5	0	2.6	-2.4	3	3	1.5	1.3	2	-2	0.8	0.4	-1	-4	2.3	2.7	2	-1	7.2	-7.2	-3	3	1.7	-2.1	4	-1	1.5	1.6
-5	0	1.1	1.3	-3	3	2.7	3.0	-2	3	6.3	-5.9	1	-4	0.8	0.3	2	2	3.0	-2.8	3	-3	2.0	2.0	4	-3	1.4	-0.9
5	1	1.3	-1.0	-3	-3	0.9	1.0	-2	-3	1.3	1.3	1	-5	1.4	1.2	-2	2	0.8	-0.6	3	-4	3.8	3.2				
-5	1	3.1	3.5	3	-4	6.4	-6.3	2	-3	8.6	-8.8	-2	0	1.4	-1.1	-2	-2	0.8	1.4	3	-5	2.6	2.5				
-5	-1	1.1	1.2	3	-5	0.8	-0.4	2	4	2.4	-2.4	2	1	0.9	-0.5	2	-2	1.6	-0.7	4	0	2.6	2.4				
5	-1	12.9	-13.9	3	-6	0.7	0.5	-2	4	4.5	-4.8	-2	1	2.7	-2.4	-2	3	1.7	-1.8	4	1	1.3	2.4				
-5	2	4.2	4.4	4	0	7.9	-8.2	2	-4	6.4	-6.2	-2	-1	1.8	2.1	2	-3	1.2	1.3	4	-1	3.6	4.3				
5	-2	13.6	-16.1	-4	0	1.5	2.1	2	-5	1.0	1.1	2	-1	5.4	-5.2	-2	4	1.5	-1.7	-4	2	1.2	-2.2				
-5	3	3.2	3.2	4	1	2.5	-2.4	3	0	5.3	-5.2	2	2	5.0	-4.7	2	-4	2.1	-2.5	4	-2	0.8	0.9				
5	-3	6.2	-5.9	-4	1	0.9	-1.1	-3	0	2.1	1.8	-2	-2	0.8	0.7	2	-5	0.8	0.6	4	-3	1.2	1.1				
-5	4	1.0	1.1	-4	-1	1.0	1.3	3	1	3.9	-3.9	2	-2	6.7	-5.9	3	0	3.7	-3.9	4	-4	2.1	1.5				
5	-4	5.0	-4.6	4	-1	17.3	-17.6	-3	-1	0.8	0.6	-2	3	2.2	-2.0	3	1	1.4	-1.6	5	0	0.7	0.4				
-5	5	1.4	-1.2	4	2	1.6	-1.6	3	-1	5.2	-4.9	-2	-3	1.7	1.5	-3	1	2.2	-2.5	5	-1	1.5	1.6				
-5	6	0.7	-1.5	-4	2	1.2	-1.2	3	2	3.6	-3.6	-2	-3	5.2	-5.1	3	-1	11.3	-12.8	5	-2	3.2	-2.5				

TABLE 4. INTERATOMIC DISTANCES AND BOND ANGLES

N-N	1.319±0.006 A	N'-N-O	120.2±0.4°
N-O	1.272±0.006	O-N-C(1)	121.4±0.4
N-C(1)	1.488±0.006	C(1)-N-N'	118.4±0.4
C(1)-C(2)	1.532±0.007	N-C(1)-C(2)	108.8±0.4
C(2)-C(3)	1.544±0.007	N-C(1)-C(6)	108.6±0.4
C(3)-C(4)	1.523±0.007	C(1)-C(2)-C(3)	107.9±0.5
C(4)-C(5)	1.517±0.007	C(2)-C(3)-C(4)	110.6±0.5
C(5)-C(6)	1.542±0.007	C(3)-C(4)-C(5)	110.9±0.5
C(6)-C(1)	1.530±0.007	C(4)-C(5)-C(6)	111.6±0.5
C(1)-H(1a)	0.99±0.07	C(5)-C(6)-C(1)	109.3±0.5
C(2)-H(2a)	1.11±0.07	N-C(1)-H(1a)	111±4
C(2)-H(2e)	1.02±0.07	H(2a)-C(2)-H(2e)	109±6
		C(1)-C(2)-H(2a)	101±4
		C(1)-C(2)-H(2e)	115±4

Table 5. Departure from the least-squares plane (1)

O	0.002 Å
N	0.006
C (1)	0.001

Kurita *et al.*[3] determined the configuration of the C(1)–H(1a), C(1)–C(2) and C(1)–C(6) bonds around the N–C(1) bond from ESR analysis of the irradiated single crystal. The results show that the plane through C(1), N, and O makes an angle of 40° against the plane through C(2), C(1) and N. The result agrees within 5° with the value calculated from the structure of the molecule.

The authors are grateful to Dr. Y. Kurita for kindly supplying the specimen and for valuable discussions.

3) Y. Kurita, M. Kashiwagi and H. Nakata, Preprints for the Symposium of Molecular Structure, (Nagoya, 1965), p. 165.

BULLETIN OF THE CHEMICAL SOCIETY OF JAPAN VOL. 43 1966—1975 (1970)

The Crystal and Molecular Structure of Demycarosyl Leucomycin A_3 Hydrobromide

Mikio HIRAMATSU, Akio FURUSAKI, Toshiharu NODA,*1 Keizo NAYA, the late Yujiro TOMIIE and Isamu NITTA

Faculty of Science, Kwansei Gakuin University, Nishinomiya

and Tetsuo WATANABE, Teruo TAKE and Jinnosuke ABE

Research Institute, Toyo Jozo Co., Ltd., Ohito, Tagata, Shizuoka

and Satoshi OMURA and Toju HATA

Kitasato Institute, Shirokane, Sanko-cho, Shiba, Minato-ku, Tokyo

(Received December, 8, 1969)

The stereochemically-complete molecular structure of demycarosyl leucomycin A_3, $C_{30}H_{49}NO_{11}$, has been determined by means of an X-ray crystal analysis of its hydrobromide. The crystals of the hydrobromide are orthorhombic with four chemical units in a unit cell with the dimensions of $a=19.52\pm0.03$, $b=20.63\pm0.03$, and $c=9.28\pm0.03$ Å. The space group is $P2_12_12_1$. As a result of the present study, it has been found that the crystals contain about 0.6 mole of ethanol per mole of the hydrobromide as alcohol of crystallization. The intensity data were obtained from equi-inclination integrating Weissenberg photographs taken with Cu$K\alpha$ radiation around the b and c axes. The structure was elucidated by means of the minimum function, least-squares, and Fourier methods. The atomic coordinates obtained were refined by the block-diagonal least-squares method, anisotropic thermal motion being assumed for only the bromine atom. The final R factor is 14.6%. The molecular structure thus obtained corresponds exactly to that proposed in 1967 by Hata *et al.* on the chemical evidence, considering the allylic rearrangement in the hydrolysis of leucomycin A_3 with dilute hydrochloric acid. The conjugated diene system in the macro ring has the *trans-trans* configuration. The sugar component, mycaminose, forms a β-glycosidic linkage with the lactone ring.

Leucomycin A_3 is a basic macrolide antibiotic obtained from the broth-filtrate of *Streptomyces Kitasatoensis* Hata.[1] A partial structure was reported by Watanabe *et al.* for the compound,[2] which contains, as sugar components, the mycaminose and 4-*O*-isovaleryl mycarose found in many other antibiotics.[3] Later, the total structure

*1 Present address: Research Institute, Toyo Jozo Co., Ltd., Ohito, Tagata, Shizuoka.

1) T. Hata and Y. Sano *J. Antibiotics, Ser. A*, **6**, 87 (1953).

2) T. Watanabe, T. Fujii, H. Sakurai, J. Abe and K. Satake, Abstracts of papers, International Symposium on the Chemistry of Natural Products, Kyoto (1964), p. 145.

3) W. D. Celmer, *J. Amer. Chem. Soc.*, **87**, 1799 (1965).

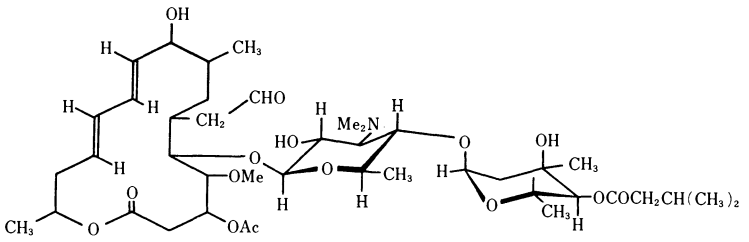

shown below was proposed by Hata *et al.* on the basis of a comparison with those of magnamycin B and spiramycin A.[4] For the purpose of confirming the proposed structure, an X-ray study of leucomycin A_3 hydrobromide has recently been undertaken by some of the present authors. However, it has been found that the bromine atom is placed at an unfavorable position in the crystal with the space group $P2_12_12_1$; thus, the analysis has been led to difficulty. Therefore, an X-ray structure determination has been tried for the hydrobromide of demycarosyl leucomycin A_3 instead of leucomycin A_3 itself. The crystal analysis of the derivative has proved successful, and the present paper will describe in detail the complete molecular structure, including the absolute configuration.

Experimental

Demycarosyl leucomycin A_3 (I) was derived from leucomycin A_3 by hydrolysis with 0.3 N hydrochloric acid and then further converted into its hydrobromide by the neutralization of an ethanol solution of I with a water-ethanol solution of hydrobromic acid. Single crystals of the hydrobromide were obtained in colorless prisms by adding ether to a methanol-ethanol solution and by then letting it stand overnight in an icebox. The crystal data determined from the present experiment are summarized in Table 1. The cell dimensions were determined from Weissenberg photographs calibrated with the standard silicon powder lines. The crystal density was measured by flotation in a mixture of carbon tetrachloride and cyclohexane.

Table 1. Crystal data

Formula	$C_{30}H_{49}NO_{11}\cdot HBr\cdot xC_2H_5OH$
Orthorhombic	
	$a=19.52\pm0.03$ Å
	$b=20.63\pm0.03$
	$c=9.28\pm0.03$
Space group	$P2_12_12_1$
U	3737 ± 23 Å
Z	4
D_m	1.258 g/cm³ (at 26°C)
D_x	1.209 g/cm³ (for $x=0.0$)
	1.258 (for $x=0.6$)
	1.291 (for $x=1.0$)

The intensities of reflections were visually measured from equi-inclination integrating Weissenberg photographs around the b and c axes taken with Ni-filtered Cu $K\alpha$ radiation. These intensities were corrected for the Lorentz-polarization factor, but not for the absorption effect, though the crystals used were not sufficiently small. The relative values of the observed structure factors of the 2450 reflections thus obtained were put on an absolute scale by Wilson's method, the estimated overall temperature factor, B, being 7.27 Å².

Structure Determination

As the first step in the structure analysis, a three-dimensional Patterson function, $P(u, v, w)$, was calculated at intervals of 1/120 for u and v and at intervals of 1/60 for w. Since all the three peaks corresponding to the Br–Br vectors were sufficiently separated from the other high peaks, though they were not always the highest in the Harker sections, it was easily found that the bromine atom might be situated at the position, (0.144, 0.098, 0.171). Five cycles of the least-squares treatment were then carried out. As a result of this treatment, it was found that the bromine position was adequate, since the temperature factor converged into a reasonable value of 6.28 Å²; the coordinates also converged into (0.144, 0.097, 0.177). At this stage, the discrepancy factor, R, was 0.48 for all the observed reflections. In order to seek for positions of light atoms, the minimum-function method was applied by using the three independent Br–Br vectors. Out of many maxima in the minimum function diagram, forty-nine were selected as the positions of light atoms on the basis of their heights; they were tested for adequacy by means of the least-squares method, with the coordinates fixed and using the atomic scattering factor of carbon for all.[5] After five cycles it was found that, out of the forty-nine positions, only eighteen were adequate. Then, the first Fourier synthesis was carried out with phases based on these eighteen positions in addition to the bromine. By applying again the above-mentioned method, it was found that thirty-one maxima in the Fourier map were adequate, five other peaks being excluded as false.

4) S. Omura, H. Ogura and T. Hata, *Tetrahedron Lett.*, **1967**, 1267.

5) M. Nishikawa, K. Kamiya, M. Tomita, Y. Okamoto, T. Kikuchi, K. Osaki, Y. Tomiie, I. Nitta and K. Goto, *J. Chem. Soc.*, *B*, **1968**, 652.

Out of these thirty-one rechosen positions, five were taken as those of oxygen atoms on the basis of their very small temperature factors. The second Fourier map thus calculated contained forty-one significant peaks, out of which seven were regarded as oxygen, one as nitrogen, and the remaining thirty-three as carbon, on the basis of both their heights and the chemical information. After three cycles of the usual least-squares refinement using the block-diagonal matrix approximation, it was further found that one of the carbon positions was inadequate and that three others were probably oxygen positions because their temperature factors were definitely small as compared with those of the carbon atoms previously established. The discrepancy factor, R, was 0.28 at this stage.

In order to look for the two atoms of I which had not yet been found, a difference synthesis was carried out. The map obtained had five peaks, with heights ranging from 1.3 to 1.7 e/Å^3. Of these peaks, two could be taken as an oxygen and a carbon atom of I on the basis of the chemical information. On the other hand, the remaining three seemed to correspond to a nonlinear triatomic molecule independent of I, judging from the calculated distances. The presence of the molecule was also supported by the consideration of the molecular packing. Thus, this was considered to be an ethanol molecule which is contained as alcohol of crystallization. However, after three cycles of the least-squares refinement, it turned out that the temperature factors of the three atoms in the alcohol molecule became abnormally large, though the R factor dropped from 0.27 to 0.24. Accordingly, excluding the parameters of the alcohol molecule for a while, six cycles of the least-squares method were repeated, assuming the anisotropic thermal motion for the bromine atom, the R factor calculated being 0.19. In the third Fourier map, computed with the parameters from the refinement, three peaks, with heights of from 1.0 to 1.7 e/Å^3, appeared again at almost the same positions as the peaks in the difference map already mentioned. Thus, it became certain that these peaks were not mere ghost peaks. The least-squares refinement including the ethanol parameters decreased the R factor to 0.177, but again made greater the thermal parameters of the alcohol molecule (20.8 Å^2 for O_E, 16.5 Å^2 for $C_E(1)$ and 20.1 Å^2 for $C_E(2)$). While so far it had been assumed that the mol ratio of ethanol to I was 1 : 1, this assumption no longer seemed to be reasonable. Accordingly, we attempted to estimate the mol ratio from a careful measurement of the crystal density and the unit-cell volume; the estimated value was about 0.6. Using, for the ethanol molecule, 0.6 times the usual values of the atomic scattering factors, three cycles of the refinement were carried out. The R factor thus reached a value of 0.152. Though four more cycles of the finement were performed in consideration of the anomalous dispersion correction of bromine for Cu $K\alpha$ radiation, the R factor did not drop ap-

TABLE 2. THE FINAL ATOMIC PARAMETERS

Atom	x/a	y/b	z/c	B	Atom	x/a	y/b	z/c	B
Br	0.6422	0.4034	0.1823	*	C (10)	0.2638	0.5294	0.2048	4.26
O (1)	0.2875	0.2592	0.2292	5.88	C (11)	0.3210	0.4874	0.1533	4.33
O (2)	0.1505	0.3150	0.1903	4.01	C (12)	0.3814	0.4877	0.2287	3.98
O (3)	0.2110	0.3651	0.0218	6.43	C (13)	0.4405	0.4455	0.1781	4.85
O (4)	0.0859	0.3262	0.4686	3.30	C (14)	0.4552	0.3840	0.2709	5.29
O (5)	−0.0045	0.4259	0.3826	2.68	C (15)	0.4035	0.3280	0.2402	4.83
O (6)	0.0245	0.3744	−0.0487	6.78	C (16)	−0.0587	0.3821	0.4025	3.01
O (7)	0.5003	0.4847	0.1998	5.96	C (17)	−0.1085	0.4125	0.5071	3.33
O (8)	0.3425	0.3427	0.3317	3.54	C (18)	−0.1748	0.3685	0.5092	2.85
O (9)	−0.0901	0.3741	0.2601	4.15	C (19)	−0.2008	0.3580	0.3616	4.27
O (10)	−0.0800	0.4121	0.6378	4.29	C (20)	−0.1431	0.3271	0.2703	3.97
O (11)	−0.2571	0.3138	0.3757	4.85	C (21)	0.1746	0.3191	0.0522	5.35
O_E	0.1432	0.1738	0.3437	9.15	C (22)	0.1530	0.2663	−0.0354	6.31
N	−0.2326	0.3973	0.5984	5.11	C (23)	0.0927	0.3335	0.6173	5.61
C (1)	0.2871	0.3071	0.3085	4.00	C (24)	0.0061	0.4754	0.0843	4.30
C (2)	0.2277	0.3295	0.3992	3.67	C (25)	−0.0101	0.4196	−0.0228	5.39
C (3)	0.1729	0.3617	0.3093	2.94	C (26)	0.1550	0.6282	0.2619	5.35
C (4)	0.1110	0.3808	0.3973	2.97	C (27)	0.4398	0.2653	0.2974	7.64
C (5)	0.0493	0.4026	0.2983	3.49	C (28)	−0.1620	0.3135	0.0996	6.75
C (6)	0.0696	0.4591	0.1897	3.48	C (29)	−0.2179	0.3943	0.7591	6.66
C (7)	0.0926	0.5196	0.2670	3.25	C (30)	−0.2563	0.4640	0.5574	6.85
C (8)	0.1391	0.5630	0.1744	3.87	$C_E(1)$	0.0916	0.1523	0.4074	10.69
C (9)	0.2040	0.5293	0.1312	3.70	$C_E(2)$	0.0430	0.1794	0.3127	8.55

* B_{11} B_{22} B_{33} B_{12} B_{23} B_{31}

0.00298 0.00547 0.06022 0.00211 −0.00066 0.00778

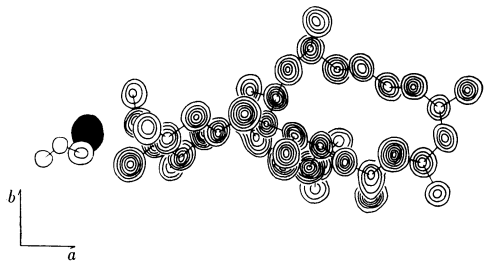

Fig. 1. A composite electron density map viewed along the *c* axis. Contours are at an interval of 2 e/Å^3, beginning at 2 e/Å^3. For the bromine atom, the region with a density above 2 e/Å^3 is blacked out.

preciably, the final value being 0.146. The final atomic parameters thus obtained are listed in Table 2, while the final electron-density distribution computed from these parameters is shown in Fig. 1. Tables of the observed and calculated structure factors are preserved by the Chemical Society of Japan.*2

The Absolute Configuration of I

When a non-centric crystal contains atoms which give rise to an observable anomalous scattering of X-rays, Friedel's law $|F(hkl)|^2=|F(\bar{h}\bar{k}\bar{l})|^2$ no longer holds.[6] Since, for the $P2_12_12_1$ space group, $|F(hkl)|^2=|F(\bar{h}\bar{k}l)|^2=|F(h\bar{k}\bar{l})|^2=|F(\bar{h}k\bar{l})|^2$ and $|F(\bar{h}\bar{k}\bar{l})|^2=|F(hk\bar{l})|^2=|F(\bar{h}kl)|^2=|F(h\bar{k}l)|^2$, pairs of (hkl) and $(\bar{h}\bar{k}\bar{l})$ reflections need not be selected for a study of the absolute configuration. In the

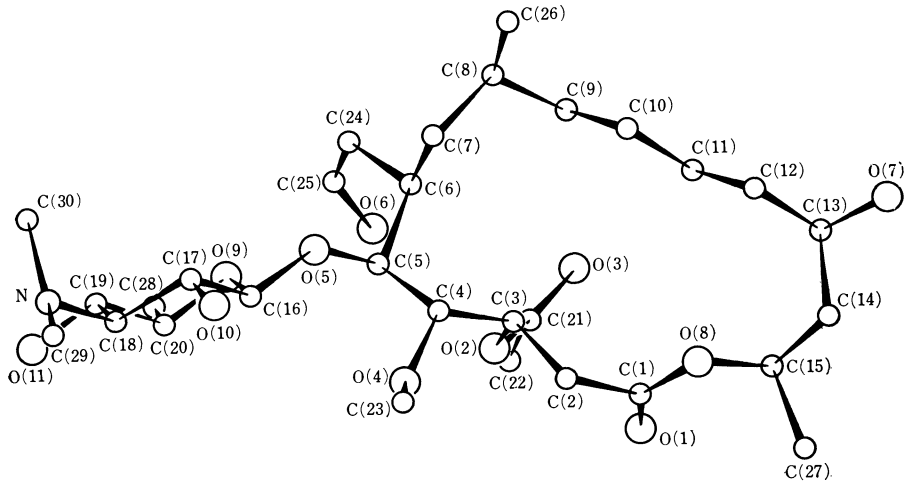

Fig. 2. The absolute configuration of the demycarosyl leucomycin A_3 molecule viewed along the normal of the mean plane of the macro ring.

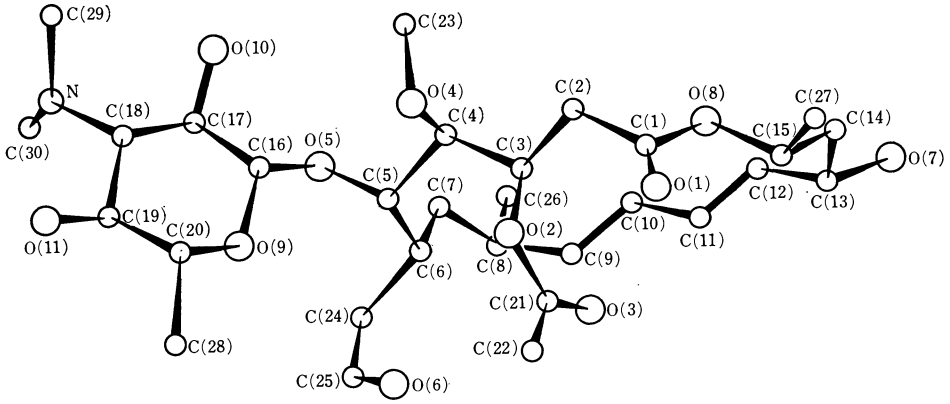

Fig. 3. The absolute configuration of the demycarosyl leucomycin A_3 molecule viewed along the *b* axis.

*2 The complete data of the F_o-F_c table are kept as Document No. 7002 at the office of the Bulletin of the Chemical Society of Japan. A copy may be secured by citing the document number and by remitting, in advance, ¥ 1,000 for photoprints. Payment may be made by check or money order payable to: Chemical Society of Japan.

6) S. Nishikawa and K. Matsukawa, *Proc. Imp. Acad. Jap.*, **4**, 96 (1928).

present study, the intensities of pairs of (hkl) and $(h\bar{k}l)$ reflections were compared with each other on the above-mentioned Weissenberg photographs around the c axis. On the other hand, the structure factors of these reflections were calculated using the atomic parameters shown in Table 2 and the imaginary part of the dispersion correction, $\Delta f''=+1.5$, for the bromine atom. The results are given in Table 3. A comparison between the observed and calculated intensities indicates that the absolute configuration of I corresponds exactly to the structure given in Table 2. The complete molecular structure thus determined is shown in Figs. 2 and 3.

Table 3. The observed and calculated intensity ratios of the reflections $(h\bar{k}l)$ to (hkl)

h	k	l	$\frac{\lvert F_c(h\bar{k}l)\rvert^2}{\lvert F_c(hkl)\rvert^2}$	$\frac{I_0(h\bar{k}l)}{I_0(hkl)}$	h	k	l	$\frac{\lvert F_c(h\bar{k}l)\rvert^2}{\lvert F_c(hkl)\rvert^2}$	$\frac{I_0(h\bar{k}l)}{I_0(hkl)}$
1	13	1	1.59	>1	1	8	3	0.91	<1
1	14	1	0.88	<1	6	1	3	1.12	>1
1	15	1	1.08	>1	6	3	3	1.16	>1
2	12	1	1.33	>1	8	1	3	1.07	>1
2	13	1	1.05	>1	9	2	3	0.95	>1*
7	1	1	1.23	>1	9	4	3	0.97	>1*
7	6	1	0.64	<1	10	1	3	1.42	>1
8	3	1	0.92	<1	10	3	3	1.01	>1
8	4	1	1.27	>1	10	9	3	0.95	<1
10	1	1	1.06	<1*	1	7	4	0.68	<1
11	1	1	0.76	<1	3	12	4	0.98	<1
11	2	1	0.97	>1*	5	2	4	1.01	>1
13	1	1	0.66	<1	5	6	4	1.11	>1
5	1	2	1.03	>1	9	4	4	1.02	<1*
5	4	2	1.00	>1*	10	2	4	1.06	>1
8	6	2	1.13	>1	11	5	4	1.00	<1*
9	1	2	0.69	<1	1	7	5	1.28	>1
10	1	2	1.02	<1*	1	13	5	1.01	>1
10	5	2	0.99	>1*	2	12	5	1.30	>1
12	1	2	0.47	<1	3	12	5	0.83	<1
13	1	2	0.81	<1	12	1	5	1.00	>1*

* The observations marked with an asterisk are not in accord with the results of the calculation.

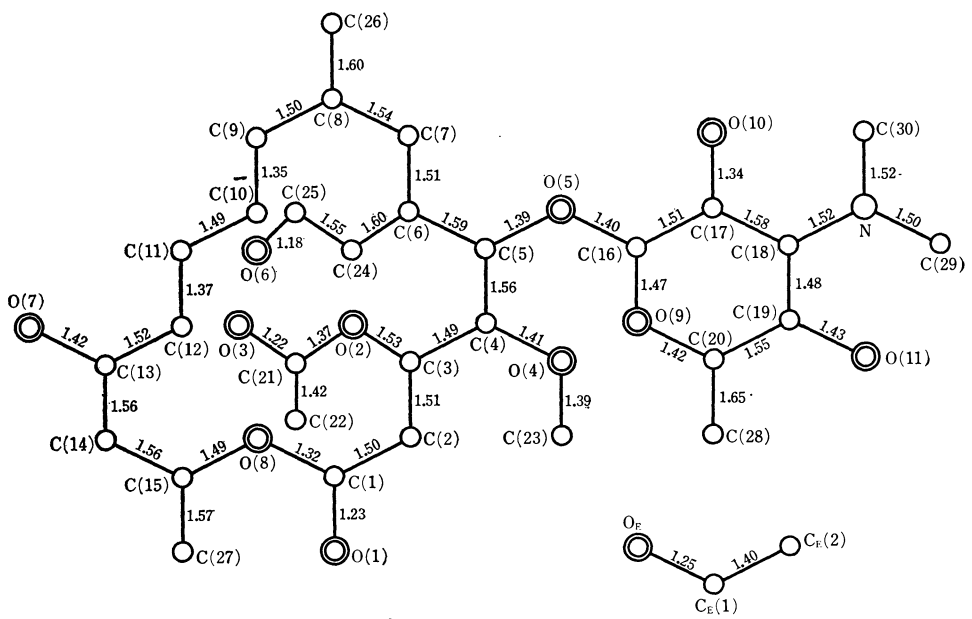

Fig. 4. The bond lengths (Å) in the demycarosyl leucomycin A_3 molecule.

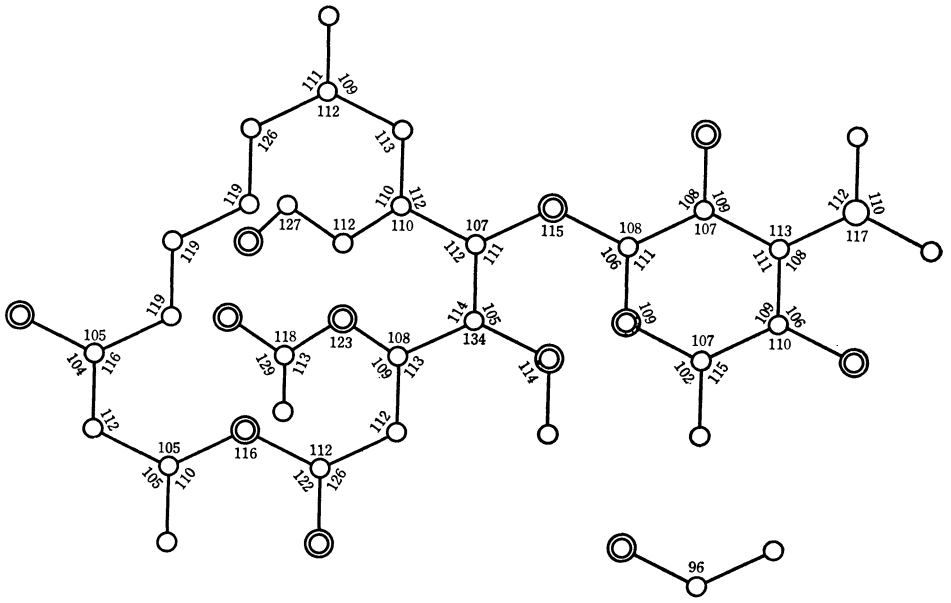

Fig. 5. The bond angles (°) in the demycarosyl leucomycin A_3 molecule.

Results and Discussion

The bond lengths and angles calculated from the final coordinates are shown in Figs. 4 and 5 respectively. The mean estimated standard deviations in the atomic distances of I are 0.025 Å for C–O, 0.028 Å for C–N, and 0.030 Å for C–C, while those of the ethanol molecule are 0.066 Å for C–O and 0.079 Å for C–C. From these lengths and angles, it is now found that demycarosyl leucomycin A_3 has the structural formula shown in Fig. 6. This is different in part from the corresponding part of the structure proposed by Hata *et al.*; that is, in the present case, the two conjugated double bonds in the macro ring are C(9)–C(10) and C(11)–C(12) and a hydroxyl oxygen, O(7), is attached to C(13), while in the latter, the diene system is C(10)=C(11)–C(12)=C(13) and O(7) is at C(9). Since, in the latter structure, the O(7)–H hydroxyl group is situated at the allylic position with respect to the C(10)=C(11) double bond, it can easily be eliminated as a hydroxide ion. If the elimination of the hydroxyl group occurs, the conjugated diene system changes easily from C(10)=C(11)–C(12)=C(13) to C(9)=C(10)–C(11)=C(12) by the successive migration of the two π-bonds, and lastly a hydroxide ion, OH^-, is connected to C(13). The new system thus formed corresponds exactly to the structure established by the present study. In fact, an organic chemical investigation has recently established that such structural changes occur in the process of the hydrolysis of leucomycin A_3 with dilute hydrochloric acid.[7] Table 4 gives the bond distances of I grouped in accordance with the chemical bond nature. In every group, the individual values deviate to some extent from the ordinary value, but the average of these is in good agreement with it.

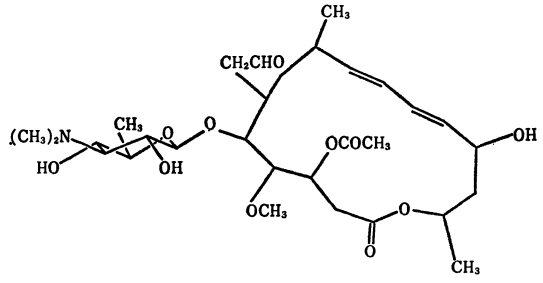

Fig. 6. The structural formula of demycarosyl leucomycin A_3 corresponding to the absolute configuration in Fig. 2.

The aglycone of demycarosyl leucomycin A_3 is composed of a sixteen-membered lactone ring with a conjugated diene system and its seven substituents, *i.e.*, a methoxyl, an acetyl, a formylmethyl, two methyl and two hydroxyl groups. The mean plane of the macro ring is represented by the equation; $0.1031x+0.3567y+0.9285z=5.850$ and is inclined by about 22° from the crystallographic c plane. The deviations of some atoms from the plane are given in Table 5. As may be seen from this table, the sixteen ring atoms deviate alternately in opposite directions except for two pairs, C(5)–C(6) and C(7)–C(8). It is of great interest to compare the conformation of the present sixteen-membered ring with that of

7) S. Omura, M. Katagiri, T. Hata, M. Hiramatsu, T. Kimura and K. Naya, *Chem. Pharm. Bull.* (Tokyo), **16**, 1402 (1968).

Table 4. The bond distances (Å) grouped in accordance with the bond nature

1. C-C distances	
(1) >C-C<	
C(2)-C(3)	1.51
C(3)-C(4)	1.49
C(4)-C(5)	1.56
C(5)-C(6)	1.59
C(6)-C(7)	1.51
C(7)-C(8)	1.54
C(13)-C(14)	1.56
C(14)-C(15)	1.56
C(16)-C(17)	1.51
C(17)-C(18)	1.58
C(18)-C(19)	1.48
C(19)-C(20)	1.55
C(6)-C(24)	1.61
C(8)-C(26)	1.60
C(15)-C(27)	1.57
C(20)-C(28)	1.65
av.	1.55±0.05
(2) >C-C(=)	
C(24)-C(25)	1.55
C(1)-C(2)	1.50
C(8)-C(9)	1.50
C(12)-C(13)	1.52
C(21)-C(22)	1.42
av.	1.50±0.04
(3) -C(=)C(=)-	
C(9)-C(10)	1.35
C(11)-C(12)	1.37
av.	1.36
(4) =C(-)C(=)	
C(10)-C(11)	1.49
2. C-O distances	
(1) >C-O	
C(3)-O(2)	1.53
C(4)-O(4)	1.41
C(23)-O(4)	1.39
C(13)-O(7)	1.42
C(15)-O(8)	1.49
C(5)-O(5)	1.39
C(16)-O(5)	1.40
C(16)-O(9)	1.47
C(17)-O(10)	1.34
C(19)-O(11)	1.43
C(20)-O(9)	1.42
av.	1.43±0.05
(2) =C(-)-O	
C(1)-O(8)	1.32
C(21)-O(2)	1.37
av.	1.35
(3) C=O	
C(1)-O(1)	1.23
C(21)-O(3)	1.22
C(25)-O(6)	1.18
av.	1.21
3. C-N distances	
(1) >C-N	
C(18)-N	1.52
C(29)-N	1.50
C(30)-N	1.52
av.	1.51

the twelve-membered ring in cyclododecane[8] and that of the thirty-four-membered ring in cyclotetratriacontane.[9] When viewed along the normal of the ring plane, the cyclododecane ring looks nearly like a square with a side of three C–C bonds, while the cyclotetratriacontane ring appears to be almost a rectangle, with one side of three bonds and the other of fourteen bonds. It is worth noticing that, in either of these cases, one side of the square or rectangle is made of three bonds. Such a partial molecular form may be the most compact and most stable one that molecules with a large ring can take. The four corners of the square or rectangle are made in such a way that two adjacent bonds take the *gauche* conformation. As may be seen from Fig. 2 and Table 6, in the present ring also, one half (from C(4) to C(13)) has a conformation very similar to that found in cyclododecane or cyclotetratriacontane, in spite of its containing

Table 5. The deviations from the mean plane of the lactone ring

Atom	Deviation	Atom	Deviation
C(1)	−0.35 Å	C(13)	−0.15 Å
C(2)	0.47	C(14)	0.23
C(3)	−0.18	C(15)	−0.56
C(4)	0.60	O(8)	0.22
C(5)	−0.22	C(24)	−1.61
C(6)	−0.70	C(26)	1.34
C(7)	0.46	C(27)	−0.45
C(8)	0.08	O(1)	−1.39
C(9)	−0.41	O(2)	−1.59
C(10)	0.34	O(4)	0.76
C(11)	−0.30	C(5)	0.57
C(12)	0.48	O(7)	0.44

8) J. D. Dunitz and H. M. M. Shearer, *Helv. Chim. Acta*, **43**, 18 (1960).

9) H. F. Kay and B. A. Newman, *Acta Crystallogr.*, **B24**, 615 (1968).

Table 6. The conformations of the sixteen bonds in the lactone ring

A-B	Angle*	Conformation**	Deviation***
C(1)-C(2)	65°	G	5°
C(2)-C(3)	177°	T	3°
C(3)-C(4)	−170°	T	10°
C(4)-C(5)	−55°	$\bar{G}$	5°
C(5)-C(6)	−61°	$\bar{G}$	1°
C(6)-C(7)	156°	T	24°
C(7)-C(8)	−61°	$\bar{G}$	1°
C(8)-C(9)	−90°	$\bar{G}$	30°
C(9)-C(10)	174°	T	6°
C(10)-C(11)	180°	T	0°
C(11)-C(12)	180°	T	0°
C(12)-C(13)	−74°	$\bar{G}$	14°
C(13)-C(14)	78°	G	18°
C(14)-C(15)	−84°	$\bar{G}$	24°
C(15)-O(8)	170°	T	10°
O(8)-C(1)	−173°	T	7°

* This is the azimuthal angle which, in the part -X-A-B-Y- of the ring, X-A and B-Y make around A-B. The positive sign denotes that the angle is measured in the right-handed way, while the negative sign denotes the measurement in the other way.

** T, G and $\bar{G}$ mean the *trans*, right-handed *gauche* and left-handed *gauche* conformations respectively.

*** This is the deviation from the perfect *trans* or *gauche* conformation.

a conjugated diene system. The diene part is incorporated into the longer side of the rectangle form because if its property of keeping six of the ring carbon atoms zig-zag in a plane. On the other hand, the conformation of the remaining half is considerably different from that of the regular part. The main difference is that the conformations of four bonds, C(1)–C(2), C(14)–C(15), C(15)–O(8), and O(8)–C(1), are, respectively, *gauche*, *gauche*, *trans*, and *trans*, while in the regular ring conformation, such as in cyclododecane or cyclotetratriacontane, they should be, respectively, *trans*, *trans*, *gauche*, and *gauche*. Such a deviating behavior of the conformations seems to be attributable mainly to the existence of the lactone group. That the C(2), C(1), O(8), C(15), and O(1) atoms lie on a plane with the C(1)–O(8) *trans* bond is due to the interaction of the π-orbitals of the C(1) and O(8) of the lactone group. The *gauche* nature of the C(1)–C(2) bond would be more favorable than the possible *trans* conformation, which makes the C(2)–C(3) bond *cis* oriented with the C(1)–O(1) bond.

The orientation of the acetyl group attached to the C(3) from the macro-ring plane is on the same side as O(1). Accordingly, some atoms of the group are near to the oxygen atom; the distances are 2.93 Å for O(2)···O(1), 3.01 Å for C(21)···O(1), and 3.27 Å for O(3)···O(1). The C(3) atom lies nearly on the mean plane of the acetyl group; its deviation from the plane is only 0.15 Å. As in the case of the lactone group, this shows that the energy of the conjugation between the C(21)–O(3) double bond and the O(2) oxygen atom is superior to the energy loss due to the close contact of 2.77 Å between C(3) and O(3). The mean plane of the acetyl makes an angle of about 82° with the macro-ring plane, and one of about 85° with the plane through C(2), C(3), and C(4). The O(2) oxygen atom has a *gauche* relation with both C(5) and O(4), and also with C(1).

The methoxyl group, O(4)–C(23), is placed on the opposite side of the ring plane from the acetyl. The plane through C(4)–O(4)–C(23) is almost perpendicular to the ring plane, the dihedral angle being about 85°. The O(4) oxygen atom has a *gauche* relation with C(2), O(2), and O(5), and a *trans* relation with C(6).

Though the formylmethyl group, O(6)–C(25)–C(24), lies on the same side of the ring as the acetyl, these two groups are not extremely close to each other; for example, the distances of O(6) from C(21), C(22), O(2), and O(3) are, respectively, 3.28, 3.36, 3.53, and 3.70 Å. Nevertheless, it must be taken into account that the two groups exert on each other some considerable attractive forces, such as electrostatic; we may thus understand the fact that the aldehydic carbonyl oxygen, O(6), is almost in a *cis* conformation with C(6) around C(24)–C(25) - in other words, the azimuthal angle for O(6) and C(6) is only 13° and, consequently, the distance between O(6) and C(6) is no more than 2.95 Å. The methylene carbon, C(24), takes a *gauche* conformation with both C(8) and O(5) around C(6)–C(7) and C(5)–C(6) respectively.

The diene system has a nearly planar *trans-trans* conformation. The mean plane of the diene part, C(9)–C(10)–C(11)–C(12), makes an angle of about 77° with the macro-ring plane. As may be seen from Table 6, one of the two double bonds, C(9)=C(10), is somewhat twisted, while the other, C(11)=C(12), is not. This twisting may be due to the incorporation into the regular part of the large ring. Since C(7)–C(8) and C(9)–C(10) make an azimuthal angle of about 90° around C(8)–C(9), though, roughly speaking, they are *gauche*, C(26) is very close to C(10), the distance being only 2.99 Å.

From Fig. 2, it can also be seen that the sugar component, mycaminose, is connected to the C(5) of the macro ring through a β-glycosidic linkage. The six-membered ring takes a regular chair form similar to that of cyclohexane, and its mean plane makes an angle of about 86° with the macro-ring plane. The five groups in the ring occupy the five possible equatorial positions, one by one. The

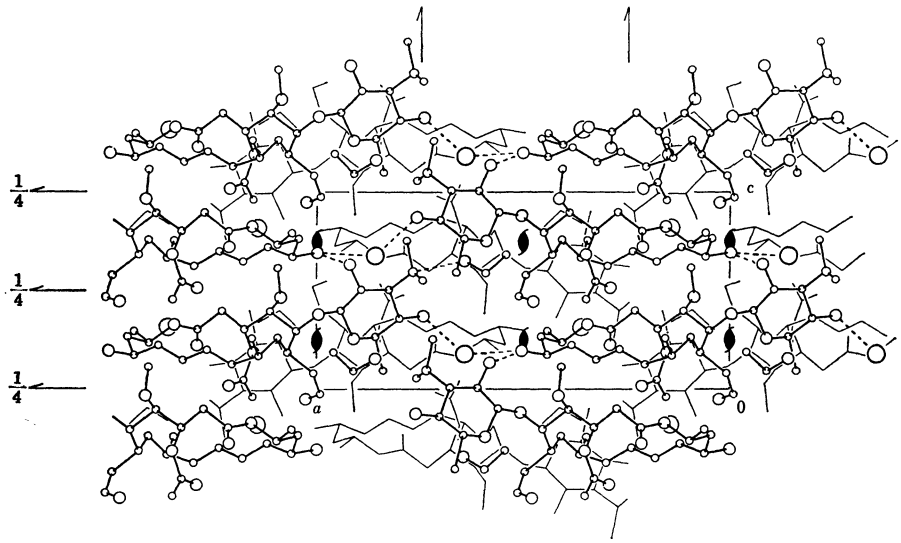

Fig. 7. The molecular arrangement viewed down along the *b* axis.

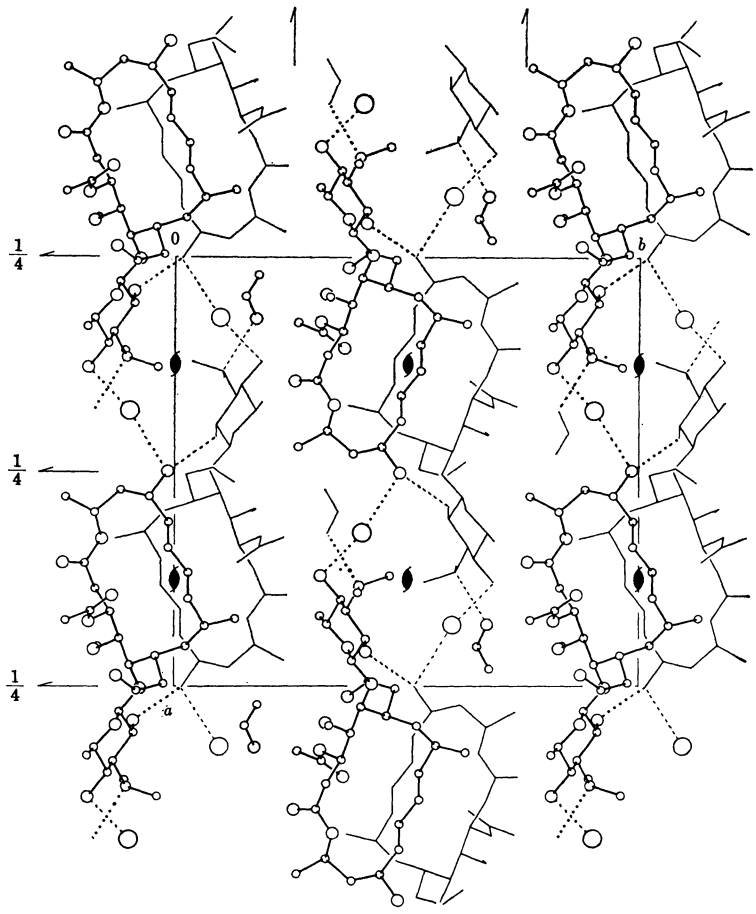

Fig. 8. The molecular arrangement viewed down along the *c* axis.

dimethylamino group takes such a conformation around N–C(18) that C(30) has a *gauche* relation with either C(17) or C(19), and C(29) also has one with C(17). As a result, the C(29) and O(10) atoms approach each other somewhat closely, the distance being 2.95 Å. As for the C(16)–O(5) bond, C(17) and O(9) are, respectively, *trans* and *gauche* with C(5).

The molecular arrangements viewed along the *b* and *c* axes are shown in Figs. 7 and 8 respectively. The macro rings of the molecules are arranged near to one another around the screw axis along the *c* axis at $x=1/4$ and $y=1/2$. The principal interatomic distances in this kind of intermolecular contact are listed in Table 7. All of these correspond to the usual van der Waals contacts except for the distance, 2.70 Å, of the O(10)-H···O(7)′ hydrogen bond. Through this hydrogen bonding, the molecules are one-dimensionally connected together around the screw axis. The molecular chains thus formed are further held together by two hydrogen bonds of the bromide ion, O(11)–H···Br^- (3.24 Å) and O(7)–H···Br^- (3.25 Å), finally making a hydrogen-bonded molecular layer parallel to the (010) plane.

Table 7. Intermolecular distances within the hydrogen-bonded molecular layer

O(3)···C(10)	3.69 Å	O(7)···C(24)	3.66 Å
O(3)···C(26)	3.56	O(7)···C(25)	3.25
O(5)···O(7)	3.48	O(8)···C(8)	3.75
O(6)···O(7)	3.76	C(2)···C(9)	3.86
O(7)···O(10)	2.70	C(4)···C(11)	3.87
O(7)···C(17)	3.50	C(12)···C(23)	3.86

Besides these strong contacts, the bromide ion is in contact with C(14), C(19), and C(30) at distances of 3.76, 3.61, and 3.71 Å respectively. The ethanol molecules are connected to the glycoside molecules only by the hydrogen bond of the N^+–H···O_E type, with a distance of 2.88 Å. The intermolecular distances from the ethanol are given in Table 8. As may be seen from this table, the hydrogen atom of the ethanol hydroxyl group does not take part in the formation of the hydrogen bonding at all. This may be one of the reasons why the ethanol molecule is easy to get out of the crystal. Between the glycoside molecules about the screw axis at $x=3/4$ and $y=1/2$, there is no intermolecular contact with a distance smaller than 4.0 Å.

Table 8. Distances from the ethanol molecule

O_E···O(1)	3.49 Å	O_E···C(30)	3.57 Å
O_E···O(2)	3.25	C_E(1)···O(2)	3.68
O_E···O(4)	3.53	C_E(1)···O(4)	3.46
O_E···O(11)	3.26	C_E(2)···O(4)	3.63
O_E···N	2.88	C_E(2)···O(11)	3.64
O_E···C(2)	3.65	C_E(2)···N	3.58
O_E···C(29)	3.20	C_E(2)···C(30)	3.83

Table 9. Intermolecular distances between the hydrogen-bonded molecular layers

O(1)···N	3.62 Å	O(11)···C(2)	3.63 Å
O(1)···C(18)	3.66	O(10)···C(27)	3.73
O(1)···C(29)	3.17	C(23)···C(27)	3.70

The relatively small interatomic distances between the molecular layers parallel to the (010) plane are listed in Table 9. These distances correspond to the ordinary van der Waals interaction, and all but one are found between the aglycone part of one molecule and the sugar part of another molecule related with the first one by the screw axis along the *a* axis.

BULLETIN OF THE CHEMICAL SOCIETY OF JAPAN VOL. 43 1976—1980 (1970)

Crystal Structure of Fukinolidol Di-Bromoacetate

Chuji KATAYAMA,*1 Akio FURUSAKI, Isamu NITTA, Mitsuo HAYASHI*2 and Keizo NAYA

Faculty of Science, Kwansei Gakuin University, Nishinomiya

(Received December 16, 1969)

Fukinolidol di-bromoacetate, $C_{19}H_{24}O_6Br_2$, is a derivative of the new sesquiterpenoids isolated from the flower stalks of wild butterburs. The crystal of this derivative is monoclinic, with two molecules in a unit cell with dimensions of $a=17.13$, $b=8.21$, $c=7.59$ Å, and $\beta=98.8°$, and with the space group $P2_1$. The structure was elucidated by the heavy-atom method, and the absolute configuration was determined by the application of the anomalous dispersion effect of bromine. The atomic parameters were refined by the least-squares method, using a block-diagonal approximation. The structure thus obtained is the same as that shown by the organic chemical investigation which was carried out parallel with the present X-ray analysis. The molecule has a novel bicyclononane structure with a *cis*-fused system of a five-membered and a six-membered ring; it also has a spiro γ-lactone ring connected to the former ring. The lactone ring is almost planar, and the other five-membered ring takes a typical envelope conformation, while the six-membered ring is of the chair form.

Three new sesquiterpenoids, named fukinolide, fukinanolide, and S-fukinolide, were isolated from the flower stalks of wild butterburs, *Petasites japonicus* Maxim (Japanese name, "Fuki").[1] By alkaline hydrolysis, these substances were then converted to fukinolidol, $C_{15}H_{22}O_4$, mp 177—178°C. In order to elucidate the molecular structure of this compound, including the absolute configuration, an X-ray analysis of its di-bromoacetate derivative was carried out in company with the organic chemical investigation.

Experimental

Fukinolidol di-bromoacetate, $C_{19}H_{24}O_6Br_2$, mp 156—158°C was prepared by the bromoacetylation of fukinolidol with monobromoacetyl bromide under reflux in benzene. This substance is easily soluble in ethyl acetate, but is nearly insoluble in ethanol and in petroleum benzine. Single crystals of a prism shape were obtained from an ethyl acetate - petroleum benzine solution by slow evaporation at room temperature, while those of a crescent shape were obtained from an ethyl acetate - ethanol solution in the same way. A preliminary experiment showed that these two types of crystals gave the same X-ray diffraction pattern. The former crystal elongates along the direction of the b axis, and the latter, along the c axis, as is shown in Fig. 1; all these crystals are monoclinic with the following cell dimensions; $a=17.13\pm0.02$, $b=8.21\pm0.01$, $c=7.59\pm0.01$Å, and $\beta=98.8\pm0.5°$. The space group was uniquely determined to be $P2_1$ from the systematic absence of the reflections. The density observed by the floatation method is 1.61g·cm^{-3}, while that calculated assuming two molecules in the unit cell is 1.607 g·cm^{-3}.

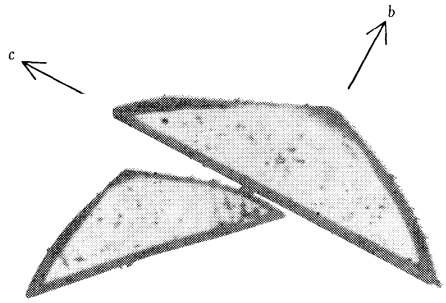

Fig. 1. The crescent shape crystals obtained from an ethyl acetate - ethanol solution.

For the purpose of collecting the intensity data, integrating Weissenberg photographs around the b and c axes were taken with nickel-filtered Cu$K\alpha$ radiation for k values from 0 to 6 and for l values from 0 to 5. The intensities were measured by visual comparison with a standard intensity scale; these values ranged between 1 and 6×10^3. The correction for Lorentz and polarization factor was made in the usual way. The relative values of the observed structure factors of 1678 reflections thus obtained were converted into an absolute scale by Wilson's method.

*1 Present address: Faculty of Science, Nagoya University, Nagoya.

*2 Present address: Research Institute, Toyo Jozo Co., Ltd., Ohito, Tagata, Shizuoka.

1) K. Naya, I. Takagi, M. Hayashi, S. Nakamura, M. Kobayashi and S. Katsumura, *Chem. & Ind.* (London), **1968**, 318.

Structure Determination

The positions of the two bromine atoms were derived from a three-dimensional Patterson function. For the elucidation of the positions of the light atoms, a Fourier synthesis by means of Sim's modified heavy-atom method[2] was carried out. The resulting map revealed that the main frame of the present molecule involves a bicyclic system of a five-membered and a six-membered ring. Besides these twenty-one light atoms, the positions of the remaining four were obtained from the second Fourier map; the R-factor was 0.32. At this stage, as a structure test, the least-squares method was performed assuming the atomic scattering factor of the carbon atom to holds for all the light atoms. After three cycles, the R-factor dropped to 0.25. Since the temperature factors of five atoms converged into values which were smaller than those of the others, these were identified as oxygen atoms. The four atoms which had been formerly regarded as an acetoxy group attached to the six-membered ring turned out to be false peaks, because their temperature factors inclined to diverge. In this way, the positions of five oxygen atoms and sixteen carbon atoms were confirmed, and the reliable positions of the acetoxy group were elucidated from another Fourier synthesis. The structure thus obtained was refined by a block-diagonal least-squares method. After three cycles of refinement using isotropic temperature factors for all the atoms, the R-factor decreased to 0.15. Three more cycles of the final refinement were carried out with anisotropic temperature factors for bromine atoms and isotropic for light atoms. Thus, the final R-factor reached a value of 0.13. The tables of the observed and calculated structure factors are kept by the Chemical Society of Japan.*3

Absolute Configuration

By applying the effect of the anomalous dispersion of bromine, the absolute configuration of the present molecule was determined. The Bijvoet inequalities for twenty pairs of $I(hkl)$ and $I(h\bar{k}\bar{l})$ were observed visually from the Weissenberg photographs around the c axis indexed on the right-handed system. On the other hand, these twenty pairs of structure factors were calculated by including the imaginary part of the anomalous dispersion correction of the scattering factor of bromine for Cu$K\alpha$ radiation ($\Delta f''=1.4$). These observed and calculated inequalities are listed in Table 1. It may be seen that the atomic coordinates correspond to the expression by the left-

Table 1. Bijvoet inequalities

h	k	l	$\lvert F_c(hkl)\rvert$	$\lvert F_c(h\bar{k}\bar{l})\rvert$	$\frac{\lvert F_c(hkl)\rvert^2}{\lvert F_c(h\bar{k}\bar{l})\rvert^2}$	$\frac{I_o(hkl)}{I_o(h\bar{k}\bar{l})}$
7	1	0	23.58	24.91	0.90	>1
13	1	0	2.12	0.79	7.24	<1
−14	1	1	15.23	16.47	0.86	>1
−8	1	1	15.86	15.02	1.11	<1
−8	2	1	16.74	19.14	0.76	>1
6	2	1	5.68	8.50	0.45	>1
7	2	1	22.25	20.67	1.16	<1
9	2	1	20.42	21.90	0.87	>1
12	4	1	6.18	7.25	0.71	>1
15	3	1	6.60	7.27	0.82	>1
17	3	1	1.10	0.44	6.37	>1
−3	2	2	13.94	11.30	1.52	<1
−12	3	2	14.18	12.95	1.20	<1
−20	1	3	5.55	5.28	1.11	<1
−9	2	3	8.35	10.35	0.65	>1
−10	1	4	13.32	11.82	1.27	<1
−5	1	4	19.81	18.16	1.19	<1
−12	2	4	14.94	16.53	0.82	>1
−5	1	5	11.82	11.23	1.11	<1
−14	1	5	8.05	8.60	0.88	>1

2) G. A. Sim, *Acta Cryst.*, **12**, 813 (1959).

*3 The complete data of the F_o–F_c table are kept as Document No. 7003 at the office of the Bulletin of the Chemical Society of Japan. A copy may be secured by citing the document number and by remitting, in advance, ¥ 500 for photoprints. Payment may be made by check or money order payable to: Chemical Society of Japan.

TABLE 2. FINAL ATOMIC PARAMETERS

Atom	x/a	y/b	z/c	B	Atom	x/a	y/b	z/c	B
Br(1)	0.2246	0.9200	0.6701	*	C(7)	0.1951	0.2794	0.1282	3.51
Br(2)	−0.0146	0.5032	0.4401	*	C(8)	0.1473	0.4243	0.0420	3.90
O(1)	0.0734	0.3792	0.0030	4.72	C(9)	0.2259	0.3282	0.3333	3.08
O(2)	0.1703	0.5527	0.0026	4.70	C(10)	0.3040	0.4065	0.3317	3.77
O(3)	0.3170	0.5285	0.6258	4.30	C(11)	0.1376	0.1495	0.1201	4.92
O(4)	0.3807	0.7438	0.5679	7.29	C(12)	0.0569	0.2319	0.0559	6.83
O(5)	0.1704	0.4431	0.3907	3.60	C(13)	0.1497	−0.0096	0.1363	7.19
O(6)	0.1647	0.3035	0.6491	4.35	C(14)	0.4171	0.0185	0.1808	6.07
C(1)	0.3589	0.4268	0.5050	3.98	C(15)	0.4134	0.3852	0.1251	4.78
C(2)	0.3834	0.2725	0.6028	6.82	C(16)	0.3320	0.6697	0.6524	4.79
C(3)	0.4275	0.1552	0.4752	4.28	C(17)	0.2889	0.7586	0.8025	6.03
C(4)	0.3707	0.1335	0.3029	4.84	C(18)	0.1417	0.4074	0.5400	3.72
C(5)	0.3443	0.2885	0.2120	3.61	C(19)	0.0835	0.5444	0.5741	4.58
C(6)	0.2755	0.2584	0.0472	3.89					

* Anisotropic temperature factors in form of $\exp(-B_{11}h^2-B_{22}k^2-B_{33}l^2-B_{12}hk-B_{23}kl-B_{31}lh)$.

Atom	B_{11}	B_{22}	B_{33}	B_{12}	B_{23}	B_{31}
Br(1)	0.00632	0.02625	0.03708	−0.00481	−0.00790	0.01023
Br(2)	0.00404	0.03287	0.04376	−0.00447	0.01348	−0.00164

TABLE 3. BOND LENGTHS AND ANGLES

Bond lengths (Å)		Bond angles (°)			
C(1) -C(2)	1.49	C(2) -C(1) -C(10)	115	C(5) -C(10)-C(9)	101
-C(10)	1.50	C(2) -C(1) -O(3)	108	C(7) -C(11)-C(12)	105
-O(3)	1.47	C(10)-C(1) -O(3)	107	C(7) -C(11)-C(13)	129
C(2) -C(3)	1.60	C(1) -C(2) -C(3)	110	C(12)-C(11)-C(13)	126
C(3) -C(4)	1.51	C(2) -C(3) -C(4)	107	C(11)-C(12)-O(1)	107
C(4) -C(5)	1.48	C(3) -C(4) -C(5)	114	C(17)-C(16)-O(3)	117
-C(14)	1.59	C(3) -C(4) -C(14)	105	C(17)-C(16)-O(4)	121
C(5) -C(6)	1.59	C(5) -C(4) -C(14)	113	O(3) -C(16)-O(4)	122
-C(10)	1.53	C(4) -C(5) -C(6)	111	C(16)-C(17)-Br(1)	104
-C(15)	1.61	C(4) -C(5) -C(10)	114	C(19)-C(18)-O(5)	107
C(6) -C(7)	1.56	C(4) -C(5) -C(15)	115	C(19)-C(18)-O(6)	124
C(7) -C(8)	1.53	C(6) -C(5) -C(10)	102	O(5) -C(18)-O(6)	128
-C(9)	1.60	C(6) -C(5) -C(15)	105	C(18)-C(19)-Br(2)	109
-C(11)	1.43	C(10)-C(5) -C(15)	109	C(8) -O(1) -C(12)	116
C(8) -O(1)	1.29	C(5) -C(6) -C(7)	105	C(1) -O(3) -C(16)	123
-O(2)	1.17	C(6) -C(7) -C(8)	111	C(9) -O(5) -C(18)	116
C(9) -C(10)	1.46	C(6) -C(7) -C(9)	102		
-O(5)	1.43	C(6) -C(7) -C(11)	121		
C(11)-C(12)	1.54	C(8) -C(7) -C(9)	107		
-C(13)	1.32	C(8) -C(7) -C(11)	104		
C(12)-O(1)	1.31	C(9) -C(7) -C(11)	111		
C(16)-C(17)	1.59	C(7) -C(8) -O(1)	108		
-O(3)	1.19	C(7) -C(8) -O(2)	129		
-O(4)	1.25	O(1) -C(8) -O(2)	123		
C(17)-Br(1)	1.90	C(7) -C(9) -C(10)	106		
C(18)-C(19)	1.53	C(7) -C(9) -O(5)	108		
-O(5)	1.30	C(10)-C(9) -O(5)	110		
-O(6)	1.21	C(1) -C(10)-C(5)	108		
C(19)-Br(2)	1.85	C(1) -C(10)-C(9)	120		

handed system. At the same time, it was established that the positive direction of the *b* axis corresponds to the direction from chord to arc of the crescent-shape crystal, as is shown in Fig. 1. The final atomic parameters, transformed into the right-handed system, are listed in Table 2. Figure 2 shows a composite diagram of the (010) sections, taken as through the atomic centers of the molecule, of the final three-dimensional electron distribution.

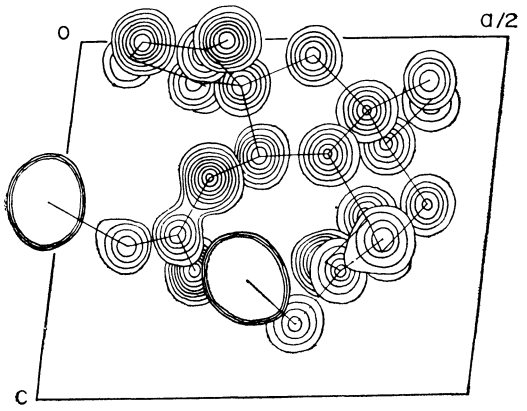

Fig. 2. The final electron distribution. Contours at 1 e.Å^{-3} beginning at 2 e.Å^{-3}.

Result and Discussion

The bond lengths and angles calculated with the final coordinates are listed in Table 3. The average estimated standard deviations of the coordinates are 0.004, 0.018, and 0.028 Å for bromine, oxygen, and carbon atoms respectively.

The molecular framework is shown in Fig. 3; the absolute configuration is taken into consideration. This is the same structure as that concluded by the organic chemical investigation. The molecule has a novel bicyclononane structure, with a

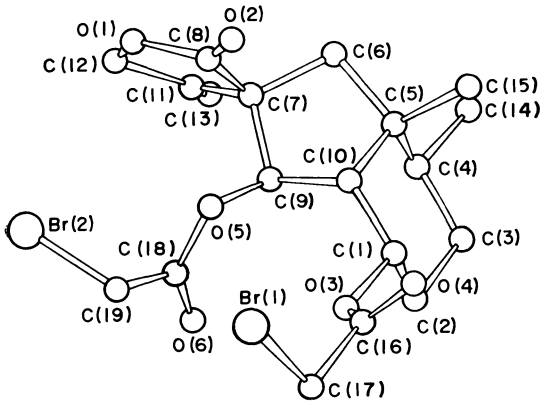

Fig. 3. The molecular framework, taking the absolute configuration into consideration.

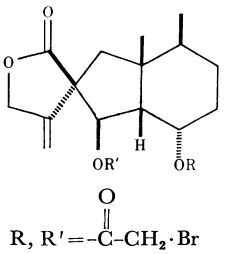

cis-fused system of a five-membered and a six-membered ring; it also has a five-membered γ-lactone ring spiro-fused with the former ring. The lactone ring is almost planar, while the other five-membered ring takes a typical envelope conformation; the C(10) atom is remarkably displaced from the mean plane through the C(5), C(6), C(7), and C(9) atoms. The six-membered ring is a chair form, and the configurations of the C(14) and C(15) atoms are β and O(3) and C(9) atoms α. The O(5), C(8), and C(15) atoms are located on the same side of the five-membered ring. Both acetoxyl groups are almost planar, including C(1) or C(9), but the bromine atoms are considerably out of these planes. The C(16)–O(4) and C(18)–O(6) bonds are orientated nearly in the same direction as the C(1)–H and C(9)–H bonds respectively.

The molecular arrangements projected along the *b* and *c* axes are shown in Figs. 4 and 5 respectively. The intermolecular distances of less than 4.0 Å are all listed in Table 4. The molecules related by a 2_1-screw axis at $x=0$ and $z=1/2$ are linked together along the *b* axis by Br–Br contacts of 3.59 Å. This contact seems to be quite strong, since twice the ordinary Van der Waals radii of bromines are 3.90 Å. Such a short contact

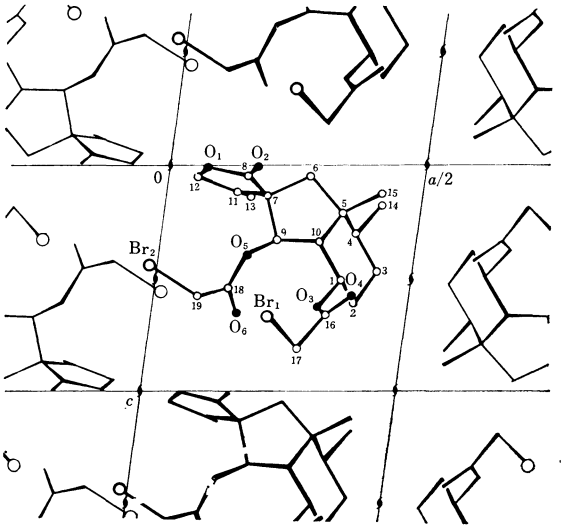

Fig. 4. The molecular arrangements along the *b* axis.

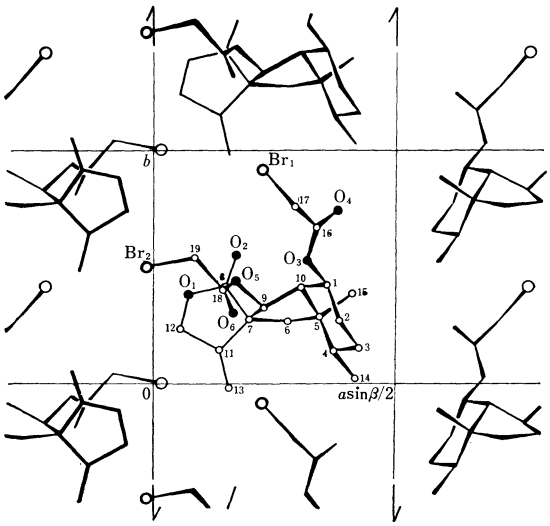

Fig. 5. The molecular arrangements along the *c* axis.

has also been found in the crystal of methyl bromide (3.57 Å).[3] The contacts along the *c* axis are concentrated between the C(8)–O(2) bond of the lactone group and the C(18)–O(6) bond of the acetyl group, related by the translation *c*. This contact seems to be caused by the dipole-dipole interaction between these polar bonds. As a whole, the contacts along the *a* axis are weak compared with those along the *b* and *c* axies.

In the early stages of the present analysis, it was not easy to elucidate the position of the acetyl group attached to the six-membered ring because of the large temperature factor of the group, especially that of the O(4) atom. In the final stages also, the temperature factor of the O(4) atom is about twice as large as those of the other oxygen atoms, and the O(3)–C(16) bond is considerably shorter than the normal bond length even if its estimated standard deviation is taken into consideration. In seeking to explain these facts, it may be considered that this acetyl group has some degree of freedom for the movement, since the group seems to be relatively free from the other part of the molecule and also from the other molecules, considering the interatomic contacts described above.

3) T. Hayafuji and Y. Tomiie, to be published.

TABLE 4. INTERMOLECULAR DISTANCES LESS THAN 4.0 Å

(i)···(ii)			(i)···(iv)		
O(6)	O(1)	3.28	O(4)	C(3)	3.55
	O(2)	3.33		C(4)	3.75
	C(6)	3.32		C(14)	3.77
	C(7)	3.55	O(2)	C(13)	3.75
	C(8)	3.14	Br(1)	O(6)	3.30
	C(11)	3.82			
	C(12)	3.78	(i)···(v)		
O(3)	O(2)	3.98	Br(1)	C(6)	3.96
	C(6)	3.98		C(13)	3.89
C(19)	O(1)	3.50	C(17)	C(14)	3.95
	O(2)	3.34			
	C(8)	3.65	(i)···(vi)		
C(18)	O(1)	3.79	Br(2)	O(6)	3.53
	O(2)	3.62		C(18)	3.96
	C(8)	3.74	Br(1)	Br(2)	3.59
C(2)	C(6)	3.98	C(19)	Br(2)	3.93
	C(15)	3.97			
C(17)	O(2)	3.14	(i)···(vii)		
			O(1)	C(12)	3.62
(i)···(iii)				C(13)	3.87
O(4)	C(3)	3.37			

Key for molecules

i: x, y, z
ii: $x, y, 1+z$
iii: $1-x, 1/2+y, 1-z$
iv: $x, 1+y, z$
v: $x, 1+y, 1+z$
vi: $-x, 1/2+y, 1-z$
vii: $-x, 1/2+y, -z$

All the numerical computations were done on the FACOM 270-20 of the Computing Center of Kwansei Gakuin University and/or the HITAC 5020E of the University of Tokyo.

BULLETIN OF THE CHEMICAL SOCIETY OF JAPAN VOL. 43 1981—1987 (1970)

Metastable Solid Solution with Nepheline-type Structure in the $CaO-Al_2O_3-SiO_2$ System

Takashi YOSHIOKA

Research Laboratory, Nihon Cement Co., Ltd., Kiyosumi, Koto-ku, Tokyo

(Received December 15, 1969)

The metastable nepheline-type solid solution in the $CaO-Al_2O_3-SiO_2$ system shows the best crystal development upon devitrification on the $CaAl_2O_4-CaAl_2Si_2O_8$ join. The crystallization occurs through the devitrification of glass at relatively low subsolidus temperatures, around 1000°C in the air. The X-ray powder diffraction patterns of the solid solution can be indexed on the basis of a hexagonal unit cell of the nepheline structure without exception. The cell parameter a of the solid solution is similar to that of nepheline, while its parameter c is smaller than that of nepheline and corresponds to that of high-temperature tridymite. When the cell parameters of the solid solution on the join are plotted against the composition, there is a break in the slope at $Ca_6Al_{12}Si_4O_{32}$, though the cell volume varies continuously. The nepheline-type solid solution on the join may be expressed as $Ca_{8-(1/2)x}\square_{(1/2)x}Al_{16-x}Si_xO_{32}$, where $\square$ means the interstitial vacant site. The relationship between the cell parameter and the composition suggests that there should be two kinds of Ca-sites in the structure of the present solid solution, and that these kinds correspond to the alkali sites of two different sizes in the nepheline structure.

Certain aluminosilicate crystals composed of a three-dimensional network of AlO_4 and SiO_4 tetrahedra are known to have crystallographic structures similar to those of some silica modifications. They have been termed "the stuffed derivatives of the silica structures".[1] A wide range of solid solutions are often formed between the stuffed derivatives and pure silica.[2-6]

Sugiura and Yoshioka[7] reported a new metastable solid solution in the $CaO-Al_2O_3-SiO_2$ system, a solid solution which was formed as a single phase over a relatively wide range of composition within a triangle having $CaAl_2O_4$, $CaAl_4O_7$, and $CaAl_2Si_2O_8$(anorthite) as the vertices; crystals of the solid solution were developed best on the $CaAl_2O_4-CaAl_2Si_2O_8$ join. Since then, it has been made clear by the present author[8] that the solid solution is structurally related to nepheline or one of the stuffed derivatives of high-temperature tridymite. The nepheline-type solid solution may be regarded as a solid solution formed between $CaAl_2O_4$,[9] one of the stuffed derivatives of the tridymite structure, and pure silica.

The present paper will deal mainly with the members formed on the $CaAl_2O_4-CaAl_2Si_2O_8$ join.

Experimental

Preparation of Glass. Homogeneous glass of the $CaO-Al_2O_3-SiO_2$ system was prepared by melting mixtures of chemicals in a platinum crucible at from 1600°C to 1700°C in an electric furnace. Pure quartz powder and guaranteed reagents of $CaCO_3$ and Al_2O_3 obtained from the Kanto Kagaku Co., Ltd., were used as the raw materials. The homogeneity of the glass was tested by the uniformity of its refractive index.

Divitrification of Glass. Crushed glass (2—8 mmϕ) was heated and devitrified under various conditions in an electric furnace equipped with SiC heating elements. The products were identified by a polarizing microscope and by the X-ray powder diffraction.

X-Ray Powder Diffraction. The cell parameter a was determined on the basis of the 52.0 reflection, using Si as the standard, and the parameter c, from the 00.4 reflection, using quartz as the standard. Diffraction

1) M. J. Buerger, *Amer. Min.*, **39**, 600 (1954).
2) R. Roy and E. F. Osborn, *J. Amer. Chem. Soc.*, **71**, 2086 (1947).
3) R. Roy, Symposium on Nucleation and Crystallization of Glasses and Melts, Amer. Ceram. Soc., Columbus, Ohio, p. 39 (1962).
4) W. Shreyer and J. F. Schairer, *Z. Kristallogr.*, **116**, 60 (1961).
5) M. D. Karkhanavala and F. A. Hummel, *J. Amer. Ceram. Soc.*, **36**, 393 (1953).
6) T. I. Prokopowicz and F. A. Hummel, *ibid.*, **39**, 266 (1956).
7) K. Sugiura and T. Yoshioka, Proc. 5th Internl. Symposium on Cement Chemistry, Tokyo, **1**, p. 370 (1968).
8) T. Yoshioka, *J. Mineral Soc. Japan*, Vol. 9, No. 6 (1970), to be published.
9) M. W. Dougill, *Nature*, **180**, 292 (1957). Also in the "Chemistry of Cements", Tailor, edited, Academic Press, London, **1**, p. 153 (1964).

conditions of the Geigerflex (Rigaku Denki Co., Ltd.) were as follows: Ni filtered Cu$K\alpha$ radiation, 40 KV-20 mA or 35KV–15 mA; slits, 1°–1°–0.1 mm; scanning speed, 0.25°(2θ)/min; chart speed, 10 mm/min; time constant, 4 sec; full scale, 200 counts/sec.

Measurement of Refractive Index. The refractive index of the phases encountered in the study was measured by the oil-immersion method with the sodium light at 20°C. The measurements were made within an accuracy of ±0.002.

Results

Mode of Formation. The subsolidus crystallization products of the glasses on the $CaAl_2O_4$–$CaAl_2Si_2O_8$ join in the CaO–Al_2O_3–SiO_2 system are given in Table 1; they are also shown in Fig. 1. As may be seen in Table 1 the single phase of the nepheline-type solid solution was obtained in the compositions between No. 4 and No. 7.

TABLE 1. SUBSOLIDUS CRYSTALLIZATION PRODUCTS OF THE GLASSES ON THE $CaAl_2O_4$–$CaAl_2Si_2O_8$ JOIN

No.	Composition of glass in weight per cent, ( ) mol ratio			Heat treatment of glass °C		Phases as determined optically and by X-ray
	CaO	Al_2O_3	SiO_2			
1	33.37 (6)	60.67 (6)	5.96 (1)	1000	5 min	Much Ks-type, little Gl.
				1000	10 min	Much Ks-type, little Ne-type, (little Gl).
				1000	30 min	Much Ks-type,little Ne-type.
				1000	2 days	Much $CaAl_2O_4$, moderate amounts Gehl and $CaAl_4O_7$.
2	32.97 (5)	59.95 (5)	7.07 (1)	950	40 min	
				1000	5 min	Much Ks-type, little Ne-type, (little Gl).
				1000	10 min	
				1000	30 min	Much Ks-type, little Ne-type.
				1000	2 days	Much $CaAl_2O_4$, moderate amounts Gehl and $CaAl_4O_7$.
				1100	12 hr	
3	32.40 (4)	58.91 (4)	8.68 (1)	950	21 hr	Much Ks-type, much Ne-type, little Gl.
				1000	5 min	Little Ks-type, little Ne-type in Gl.
				1000	20 min	Moderate amounts Ks-type, Ne-type and Gl.
				1000	13 hr	Much Ne-type, little Ks-type.
				1000	2 days	Much Ne-type, little Gehl.
				1100	12 hr	Moderate amounts Gehl, Ne-type and $CaAl_4O_7$.
				1200	3 hr	Much Gehl, moderate amounts $CaAl_4O_7$ and $CaAl_2O_4$.
4	31.49 (3)	57.26 (3)	11.25 (1)	900	19 hr	Little Ne-type in glass.
				1000	4 hr	All Ne-type.
			powdered glass	1000	14 hr	Much Ne-type, little Gehl.
				1000	2 days	
				1000	2 weeks	Much Ne-type, little Gehl, little $CaAl_4O_7$.
				1100	6 hr	
				1100	2.5 days	Much Gehl, much $CaAl_4O_7$.
				1200	6.5 hr	
5	30.80 (5)	56.00 (5)	13.20 (2)	1000	2 days	All Ne-type.
6	28.31 (3)	51.47 (3)	20.22 (2)	900	20 hr	All glass.
				950	21 hr	Much Ne-type, little Gl.
				1000	4 hr	All Ne-type
				1000	1 month	
				1100	12 hr	
		powdered Ne-type crystal		1000	12 days	Much Ne-type, litle Geh.
		powdered Ne-type crystal		1100	2.5 days	Much Ne-type, moderate amount Gehl, little An.
				1200	10 hr	Much Ne-type, moderate amount Gehl, little $CaAl_{12}O_{19}$, little An.
				1300	5 hr	Much Gehl, moderate amounts $CaAl_{12}O_{19}$ and An.
7	25.71 (1)	46.74 (1)	27.55 (1)	950	21 hr	Much Ne-type, little Gl.
				1000	2 days	All Ne-type.
				1100	2 hr	
				1100	12 hr	Much Ne-type, little An.
			powdered glass	1100	2.5 days	Much Ne-type, moderate amounts Gehl and An.
				1200	10 hr	Moderate amounts Ne-type, Gehl and An, little $CaAl_{12}O_{19}$.
				1300	5 hr	Much Gehl, much An, little $CaAl_{12}O_{19}$.

Table 1. (Continued)

No.	Composition of glass in weight per cent, ( ) mol ratio			Heat treatment of glass °C		Phases as determined optically and by X-ray
	CaO	Al_2O_3	SiO_2			
8	24.84	45.16	30.00	1000	2 days	Much Ne-type, moderate amount Un.
9	24.37 (5)	44.30 (5)	31.33 (6)	950	2 days	Little Ne-type, little Un in Gl.
				1000	2 days	Much Ne-type, much Un.
				1100	2.5 days	Much Un, little An, little Gehl.
				1200	12 hr	Much Un, moderate amounts An and Gehl.
				1300	5 hr	Much An, much Gehl, litile $CaAl_{12}O_{19}$.
10	23.42	42.58	34.00	950	2 days	Little Ne-type, little Un in Gl.
				1000	2 days	All Un.
				1100	2.5 days	Much Un, little An.
				1200	10 hr	Moderate amounts Un, An and Gehl.
				1300	5 hr	Much An, moderate amount Gehl, little $CaAl_{12}O_{19}$.
11	22.35	40.65	37.00	950	2 days	Little Ne-type, little Un, little An in Gl.
				1000	2 days	Much Un, little An, little Gl.
				1100	2.5 days	Much An, much Un.
				1200	12 hr	Much An, moderate amount Gehl, little $CaAl_{12}O_{19}$.

An anorthite, Gehl gehlenite, Gl residual glass, Ks-type kalsilite-type phase, Ne-type nepheline-type solid solution, Un unknown phase.

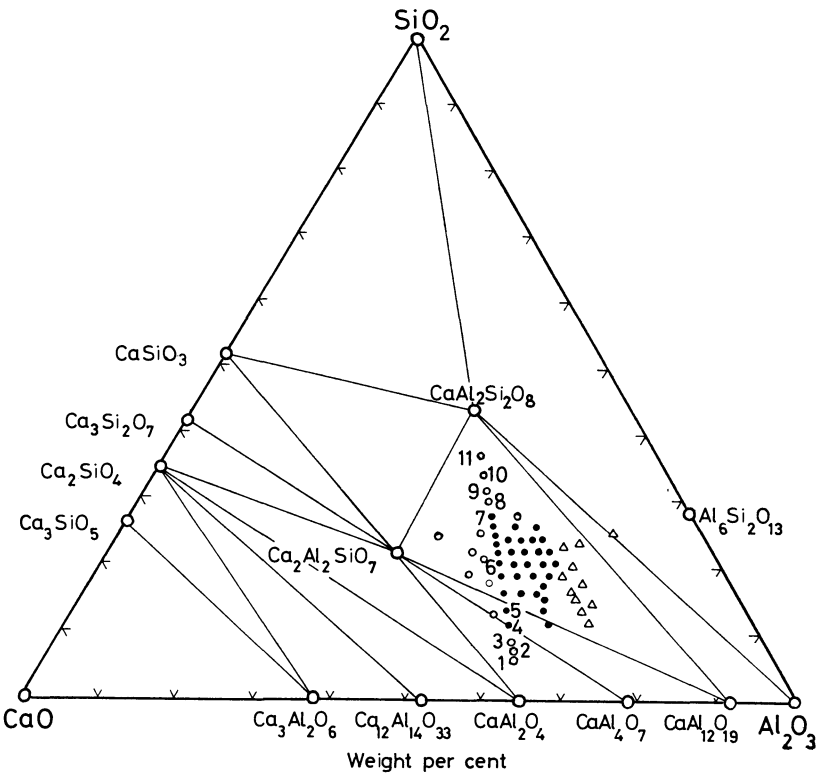

Fig. 1. Mode of formation of the nepheline-type solid solution in the CaO-Al_2O_3-SiO system.
● All nepheline-type solid solution.
○ Nepheline-type solid solution is accompanied by other crystalline phases.
△ Complete glass is not obtained, but nepheline-type solid solution is crystallized from the glassy part.
Numbers correspond to those in Table 1.

The nepheline-type solid solution appears as the first crystalline phase during the devitrification of glasses of these compositions at low subsolidus temperatures (around 1000°C).

The nepheline-type solid solution crystallized at a certain temperature decomposes when it is treated at higher subsolidus temperatures, or it decomposes when treated at the same temperature after a longer time of heating; in either case, this leads to a different assembly of crystalline products, as is shown in Table 1. This tendency was promoted when the solid solution was pulverized and reheated. In addition, the solid solution was shown by differential thermal analysis,[7] to undergo an exothermic reaction and to decompose into just the same assembly of the crystalline products described above. These results clearly suggest that the nepheline-type solid solution is of a metastable nature. The nepheline-type solid solution persists at higher temperatures or persists for much longer periods of heating at a given temperature when the solid solution increases in its SiO_2 content along the $CaAl_2O_4$–$CaAl_2Si_2O_8$ join (Table 1). A similar quality of persistence is shown by the metastable quartz-type solid solution on the SiO_2–$MgAl_2O_4$ join.[4]

X-Ray Observations. The X-ray powder patterns of the nepheline-type solid solution in the CaO–Al_2O_3–SiO_2 system are similar to those of nepheline, and all the reflections can be indexed on the basis of a hexagonal unit cell which is similar to that of nepheline. The cell parameters of the solid solution on the $CaAl_2O_4$–$CaAl_2Si_2O_8$ join are shown in Table 3. However, there are some differences between synthetic nepheline[10] and the present solid solution; they are compared in Table 2 for the sake of convenience. The cell volume of the nepheline-type solid solution on the $CaAl_2O_4$–$CaAl_2Si_2O_8$ join decreases continuously with an increase in the SiO_2 content over all the compositions. The variations in the two cell-parameters, a and c, are not thoroughly continuous against the composition; rather, they show a break in the cell parameters at the composition of No. 6 (Fig. 2).

Optical Properties. The nepheline-type solid solution on the $CaAl_2O_4$–$CaAl_2Si_2O_8$ join showed the best crystal development, while all those which were crystallized not on the join but in the lime-poor side of the CaO–Al_2O_3–SiO_2 system showed poor crystal development (Fig. 3), though they were formed as a single phase. The solid solution showed a granular or lathlike shape with an irregular outline, and those which were crystallized from the high SiO_2 compositions often showed a hexagonal skeletal development. Neither a characteristic twin nor a cleavage was ob-

10) J. V. Smith and O. F. Tuttle, *Amer. J. Sci.*, **255**, 282 (1957).

TABLE 2. INDEXED POWDER PATTERN OF THE NEPHELINE-TYPE SOLID SOLUTION

Nepheline-type solid solution No. 6 member Indexed based on hexagonal a 9.9961Å, c 8.2195Å (Da 0.0006, Dc 0.0007)			Synthetic Nepheline $Ne_{62.5}Ks_{37.5}$ J. V. Smith and O. F. Tuttle (1957)[10]		
I_{obs}	d_{obs}	Indices	I	d_{obs}	Indices
31	8.68	10.0			
36	5.00	11.0	3	5.030	11.0
2	4.31	20.0	10	4.354	20.0
—	—	—	10	4.319	11.1
22	4.11	00.2	35	4.211	00.2
—	—	—	60	3.870	20.1
9	3.71	10.2	5	3.789	10.2
28	3.280	21.0	40	3.294	21.0
11	3.175	11.2			
55	3.041	21.1	10	3.065	21.1
100	2.980	20.2	100	3.027	20.2
39	2.886	30.0	35	2.905	30.0
—	—	—	1	2.670	10.3
5	2.560	21.2	20	2.593	21.2
6	2.499	22.0	15	2.515	22.0
8	2.402	{11.3 {31.0	10	2.415	31.0
3	2.362	30.2	3	2.390	30.2
—	—	—	30	2.359	20.3
35	2.306	31.1	20	2.322	31.1
4	2.165	40.0	5	2.1773	40.0
3	2.135	22.2	1	2.1582	22.2
15	2.101	21.3	7	2.1350	21.3
26	2.074	31.2	15	2.1046	00.4
12	2.055	00.4	5	2.092	31.2
11	2.000	10.4			
3	1.986	32.0	2	1.9990	32.0
4	1.931	32.1	7	1.945	32.1
—	—	—	5	1.939	11.4
—	—	—	5	1.900	41.0
3	1.916	40.2			
18	1.856	20.4	5	1.895	20.4
11	1.841	41.1	1	1.8527	41.1
3	1.806	31.3			
10	1.788	32.2	5	1.8047	32.2
4	1.740	21.4	1	1.7200	40.3
3	1.731	50.0			
6	1.716	41.2	5	1.7051	{50.1 {30.4
2	1.674	30.4			
—	—	—	3	1.6458	{42.0 {33.1
2	1.633	33.1			
—	—	—	7	1.6276	32.3
8	1.604	42.1			
13	1.595	50.2	4	1.6094	50.2
6	1.561	{11.5 {31.4			
15	1.555	{41.3 {51.0	5	1.574	41.3
—	—	—	15	1.5705	20.5

CuKα radiation. Da, Dc standard deviation.

Table 3. Chemical compositions and physical constants of the nepheline-type solid solution on the $CaAl_2O_4$-$CaAl_2Si_2O_8$ join

No.	Chemical composition						
	Weight per cent			Atomic ratio, 0=32			
	CaO	Al_2O_3	SiO_2	Ca	Interstitial vacant site	Al	Si
3*	32.40	58.91	8.68	7.11	0.89	14.23	1.77
4	31.49	57.26	11.25	6.86	1.14	13.72	2.28
5	30.80	56.00	13.20	6.66	1.34	13.33	2.67
	29.82	54.21	15.97	6.40	1.60	12.80	3.20
	28.90	52.53	18.57	6.15	1.85	12.31	3.69
6	28.31	51.47	20.22	6.00	2.00	12.00	4.00
	27.21	49.47	23.32	5.71	2.29	11.43	4.57
	26.61	48.38	25.00	5.56	2.44	11.13	4.87
7	25.71	46.74	27.55	5.33	2.67	10.66	5.34

No.	Cell dimentions, density				Refractive index, sign		
	(Å), a	(Å), c	(Å³), V	ρ_{calcd}	ε	ω	Sign
3*	10.023	8.240	717.0	2.850	$n=1.632$		−
4	10.016	8.236	715.6	2.833	$n=1.626$		(+)
5	10.016	8.232	715.2	2.817	$n=1.622$		+
	10.009	8.224	713.5	2.801	1.617	1.614	+
	10.002	8.218	711.9	2.785			+
6	9.995	8.216	710.8	2.776	1.611	1.606	+
	9.980	8.228	709.7	2.756	1.608	1.601	+
	9.965	8.234	708.1	2.748			+
7	9.946	8.240	705.9	2.736	1.604	1.597	+

* Little gehlenite and little kalsilite-type phase coexisted.

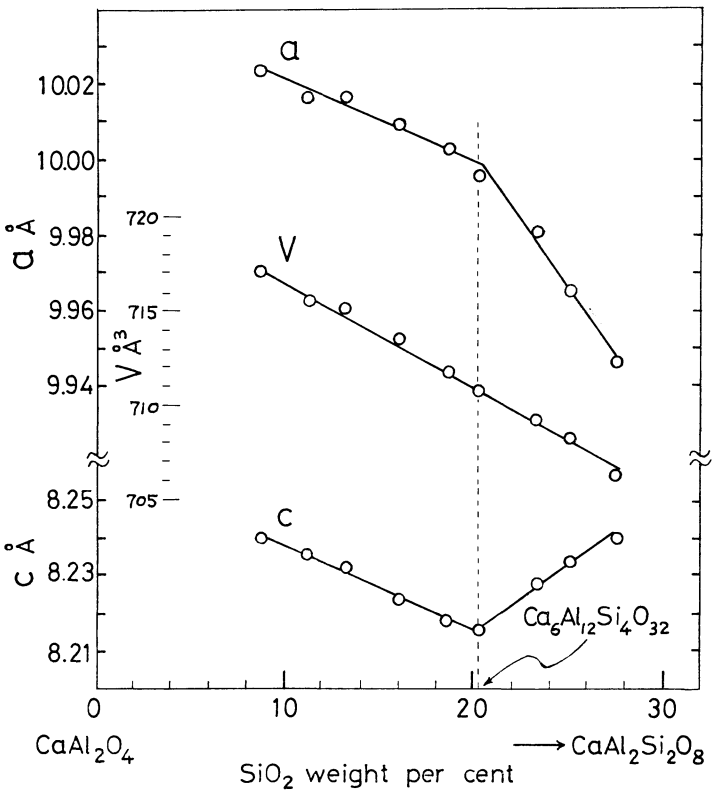

Fig. 2. Cell dimensions of nepheline-type solid solution on the $CaAl_2O_4$-$CaAl_2Si_2O_8$ join.

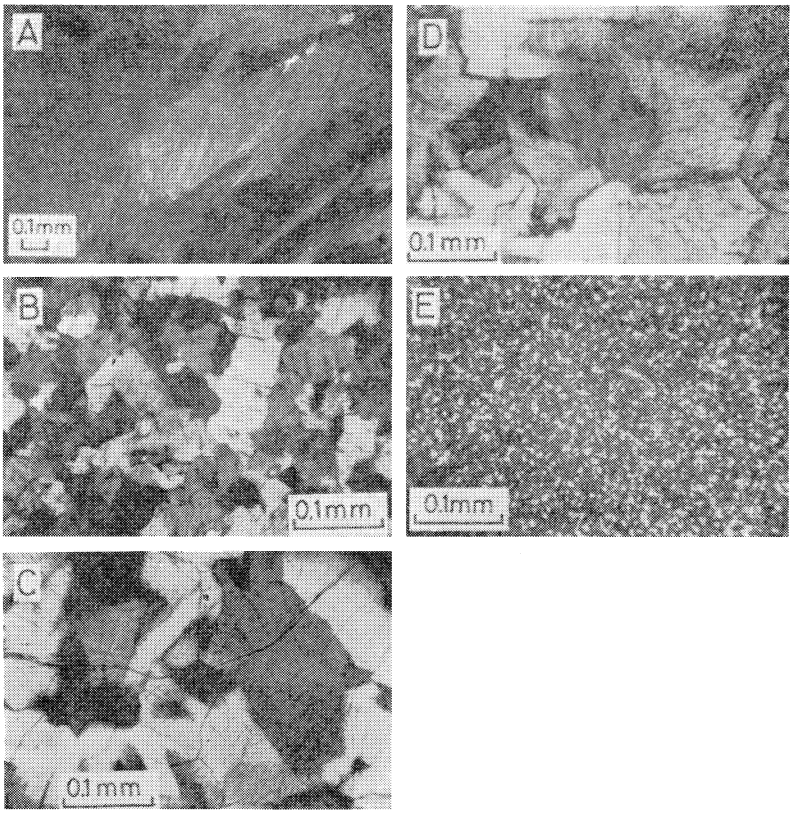

Fig. 3. Photomicrographs of the nepheline-type solid solution.

A) Crystallized from No. 3 glass, small light grains are gehlenite.
B) Member No. 6.
C) Member No. 7.
D) Crystallized from No. 8 glass showing hexagonal skeletal development.
E) Crystallized not on the $CaAl_2O_4$-$CaAl_2Si_2O_6$ join but in CaO poor side of the CaO-Al_2O_3-SiO_2 system. Single phase.

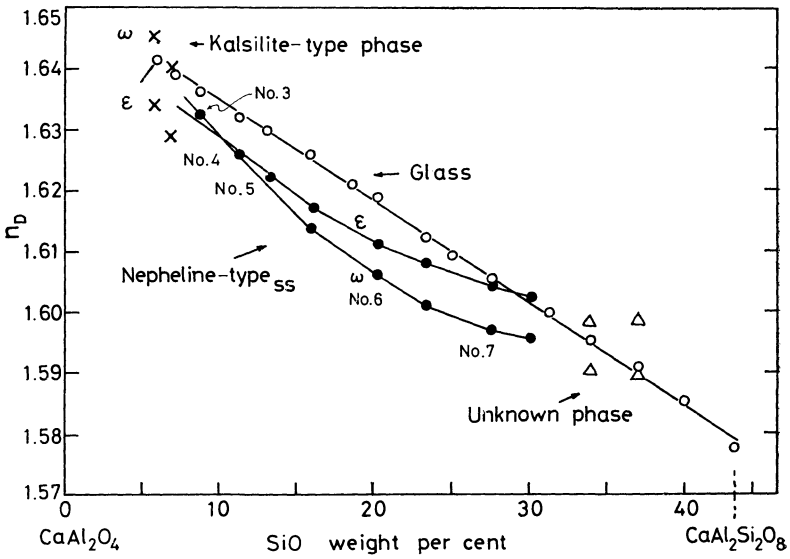

Fig. 4. Refractive index of the phases on the $CaAl_2O_4$-$CaAl_2Si_2O_8$ join. Numbers correspond to those in Table 1 and Fig. 1.

Table 4. Cell dimensions of the related crystals

		a (Å)	c (Å)
Nepheline-type solid solution	Hexagonal	9.95–10.02	8.22–8.24
Nepheline($Ne_{100-30}Ks_{0-70}$)*	Hexagonal	10.0	8.4
High temperature-tridymite*	Hexagonal	5.03	8.22

* Rock-Forming Minerals, vol. 4, (1963), London: Longmans

served.

The nepheline-type solid solution generally shows a weak birefringence. The No. 4 member shows a particularly weak birefringence, but it becomes stronger as the solid solution increases in its SiO_2 content along the join, as is illustrated in Fig. 4. The members with more SiO_2 in the composition than the No. 4 are uniaxially positive. The member crystallized from the glass, No. 3, has an appreciably stronger birefringence than does No. 4, and it is confirmed to be negative. It will be noticed, therefore, that the solid solution changes its optic sign at a certain composition between No. 3 and No. 4. as in the melilite solid solution of the gehlenite-åkermanite series. The refractive index of the phases on the join is illustrated in Fig. 4. The solid solution has a lower refractive index than that of the glass with the same composition. A similar phenomenon appears in Mg-indialite.[11]

Discussion

The cell parameter a of the nepheline-type solid solution is similar to that of nepheline, and it is twice as large as that of the ideal high-temperature tridymite. On the other hand, the parameter c is not consistent with that of nepheline but corresponds to that of the high-temperature tridymite (Table 4). The cell parameter c of the solid solution may be four times the height of a tetrahedron standing on its base, as in the ideal high-temperature tridymite.[12] The reason why, in the solid solution, the repeat distance along the a-axis is twice as large as that in tridymite is uncertain.

The nepheline-type solid solution on the $CaAl_2O_4$–$CaAl_2Si_2O_8$ join may be expressed as $Ca_{8-(1/2)x}\square_{(1/2)x}Al_{16-x}Si_xO_{32}$, where $\square$ means the interstitial vacant site, based on 32 oxygen atoms of the nepheline-unit cell. It is well known that the nepheline solid solution of $Na_{8-y}K_yAl_8Si_8O_{32}$ shows a break in the cell parameter when plotted against the composition at $y=2$ in the chemical formula.[10,13] The composition at which the break appears in the cell parameters of the present solid solution may be compared with that of the ideal nepheline as follows: the ideal composition of nepheline is known to be $Na_6K_2Al_8Si_8O_{32}$, while the present nepheline-type solid solution is represented by the formula $Ca_6\square_2Al_{12}Si_4O_{32}$, in which x is equal to 4. If there are two kinds of interstitial sites in the structure of the present solid solution, as in the nepheline structure,[14,15] six Ca^{2+} ions of the member must be situated in one kind of site, one which corresponds to the smaller Na-sites in the nepheline structure. The variation in the cell parameters in the compositions with x values smaller than 4 may be attributed to the Al–Si substitution and to the omission of Ca^{2+} ions in the larger sites, which correspond to K-sites in the nepheline structure. In the compositions with x values larger than 4, the number of the Ca^{2+} ion should be less than 6 and hence the omission of the Ca^{2+} ion will take place at the other kind of site, namely, at the smaller Na-sites in the typical nepheline structure.

The author wishes to express his thanks to Dr. K. Sugiura of the Nihon Cement Co., Ltd., for his general guidance of the study. The author is also much indebted to Professor T. Katsura, Professor H. Yamada and Professor S. Iwai of the Tokyo Institute of Technology for their critical reading of the manuscript and for their kind advice.

11) T. Iiyama, *Min. Journ.*, **1**, 372 (1956).
12) W. Eitel, *Ceram. Bull.*, **36**, 142 (1957).
13) G. Donnay, J. F. Schairer and J. D. H. Donnay, *Min. Mag.*, **32**, 93 (1959).
14) M. J. Buerger, G. E. Klein and G. Donnay, *Amer. Min.*, **39**, 805 (1954).
15) T. Hahn and M. J. Buerger, *Z. Kristallogr.*, **106**, 308 (1955).

BULLETIN OF THE CHEMICAL SOCIETY OF JAPAN VOL. 43 1988—1991 (1970)

Effect of Some Metal Oxides on the Specific Resistivities of Magnesium Oxide

Akira UEHARA, Eishin KYUNO and Ryokichi TSUCHIYA

Department of Chemistry, Faculty of Science, Kanazawa University, Kanazawa, Japan

(Received December 30, 1969)

The specific resistivities of magnesium oxide prepared by igniting magnesium hydroxide at about 1700°C were investigated in the temperature range 200—1200°C. The magnesium oxide was found to have a *p*-type character by the thermoelectric power method. Ignition at 1000°C in an oxygen stream brought about a small increase in specific resistivities, whereas ignition in a vacuum of 10^{-3} mmHg caused no appreciable change. The sample including univalent-metal oxides such as Na_2O or Li_2O showed a distinct decrease in specific resistivities and was converted from a *p*-type to an *n*-type semiconductor. Addition of tervalent-metal oxides such as γ-alumina or B_2O_3 to the magnesium oxide, however, raised the resistivities but gave no change in type.

Magnesium oxide is widely used as an excellent insulator since a long time ago.[1] Goodwin and Mailey found that the electrical conductivity increases rapidly with temperature.[2] A recent study showed that the activation energy for electrical conductivity through single crystals of magnesium oxide is 2.8±0.1 eV in 400—1800°C.[3]

Although the electrical resistivity of magnesium oxide was thought to decrease in the presence of a small amount of impurities,[4] it was found lately that some impurities raise the resistivity. It has already been reported that the addition of 0.25 mol % of TiO_2 sharply increases the electrical resistivity of magnesium oxide, while the addition of TiO_2 more than 2.5 mol % does not give any effective change in the temperature range 1200—1800°C.[5]

In this study we will discuss the electrical resistivity of magnesium oxide from the viewpoint of semiconductor. Change of the specific resistivity of magnesium oxide with temperature was measured, and classification of magnesium oxide into either *n*- or *p*-type semiconductor was decided by means of the thermoelectric power method.

On the basis of these results, considerations on the change of specific resistivities were made, and the effect of metallic oxides contained as impurities on the electrical resistivity was investigated in the temperature range 200—1200°C.

Experimental

Magnesium Oxide. Magnesium oxide was prepared by igniting magnesium hydroxide at 1700°C and by crushing it to 100—200 meshes.

Analytical results: MgO, 99.81; SiO_2, 0.06; Al_2O_3, 0.03; Fe_2O_3, 0.04; CaO, 0.06%.

Preparation of Specimen for Specific Resistivity Measurements. The resistivity measurement for the samples was carried out with the specimen as shown in Fig. 1-a. The sample powder was packed between the inner and the outer electodes. As described in Fig. 1-b, MgO powder was packed under the desired pressure by means of an oil-press. In the preliminary experiments, it was found that the effect of the packing density on the specific resistivities was not recognized within the range 2.0—3.0 g/cm³. When the density exceeded the upper limit (3.0 g/cm³), the outer electrode was broken. 2.3 g/cm³ was chosen as the optimum packing density for all the measurements. A Pt-PtRh thermocouple was spot-welded on the surface of outer electrode for temperature measurements, and leading wires for the resistivity measurements were also spot-welded as shown in Fig. 1-a.

Measurement of Specific Resistivity. Resistivity was measured by the potential drop method with a Yokogawa Teraohmmeter RM-21C. The heating rate was 5°C/min. The values of specific resistivity (R) were calculated from the equation

$$R_s = \frac{2\pi hR}{2.303 \log \frac{r_2}{r_1}} \ (\Omega\text{-cm})$$

where h is the height of MgO layer packed in specimen, R, observed resistivity, r_1, diameter of inner electrode, and r_2 is diameter of outer electrode.

Determination of *n*- or *p*-Type. The thermoelectric power method was used to decide the type of magnesium oxide (*n* or *p*) as semiconductor. Decision was made from the direction of the thermoelectric power detected by a Yokogawa Galvanometer D-2L.

1) F. Beijerinck, *Neves Jahrb. Min. B. B.*, **11**, 448 (1897).
2) H. M. Goodwin and R. D. Mailey, *Phys. Rev.*, **23**, 1 (1906).
3) T. J. Lewis and A. J. Weight, *Brit. J. Appl. Phys.*, **1**, 441 (1968).
4) G. H. Fetterley, *Electrochem. Soc.*, **83**, 191 (1943).
5) D. M. Shakhtin, E. V. Levintovich, T. L. Pivovar and G. G. Eliseeva, *Teplofiz. Vys. Temp.*, **5**, 510 (1967).

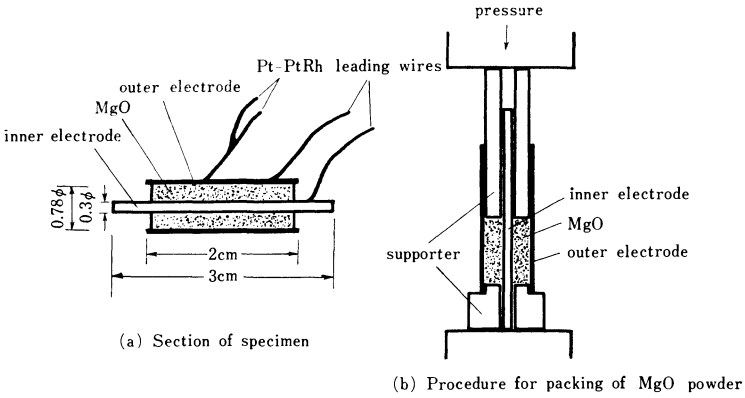

(a) Section of specimen

(b) Procedure for packing of MgO powder

Fig. 1. Specimen for the resistivity measurement.

Addition of Oxide Impurities. B_2O_3 and γ-Al_2O_3 of special grade reagents were used as tervalent-metal oxides, and Na_2CO_3 and Li_2CO_3, as univalent-metal oxides. All the compounds were added to magnesium oxide in an amount corresponding to the desired fraction, and were fully triturated in an agate mortar. The resulting mixture was ignited at 1000°C for 10 hr, and then pulverized to 100—200 meshes.

Results and Discussion

Specific Resistivity of MgO. Figure 2 shows the curves of R_s (specific resistivity) *vs.* $1/T$ (reciprocal of absolute temperature) for magnesium oxide and for the same oxide ignited in an oxygen stream for 3 hours. The resistivity of MgO itself was $\sim 10^7$ Ω-cm at 1000°K.

The specific resistivity can also be given by the equation

$$R_s = Ae^{E/kT}$$

where E is activation energy, k, Boltzmann's constant (8.63×10^{-5} eV deg^{-1}), T, absolute temperature, and A is frequency factor.

Thus, the activation energy could be estimated from the slope of R_s-$1/T$ curve as 2.68 eV. This value is close to but somewhat smaller than that of 2.8±0.1 eV estimated by Lewis and Weight with a single crystal.[3] From the study on the light absorption of magnesium oxide the intrinsic activation energy for resistivity might be 7.3 eV.[6,7] From these values the specific resistivity seems to be affected by the presence of impurities or lattice defects.

It is well known that the over-all conductivities are the sum of conductivities in donor and acceptor; *viz.*, $\sigma=\sigma_n+\sigma_p=e(N\mu_n+N\mu_p)$, where σ_n is conductivity in donor, σ_p conductivity in acceptor, e, electronic charge, N, donor concentration, P, acceptor concentration, μ_n, donor mobility, and μ_p is acceptor mobility.

The MgO prepared at high temperature was expected to be deficient in oxygen atom and to be of n-type. However, it was found to be of p-type by thermoelectric power (Sample I in Table 1). That the MgO is of p-type suggests that $N=0$ or $P>N$. Thus it can be assumed that the content of oxygen atoms in the MgO is, stoichiometrically, slightly greater than that of magnesium atoms. The magnesium oxide was ignited in a vacuum of 10^{-3} mmHg for 3 hr, but no change was found in type and resistivity. The sample ignited in an oxygen stream for 3 hr was expected to show the decrease of resistivity. However, increase was observed as shown in Fig. 2. The reason for these discrepancies is not clear, but they might be due to the change of conductivity caused by the presence of other impurities.

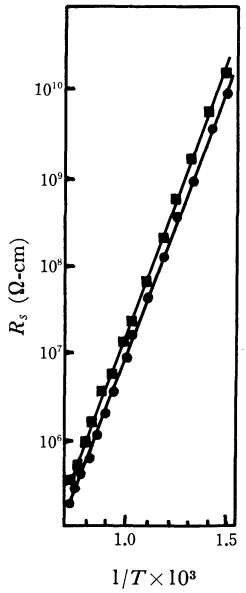

Fig. 2. R_s-$1/T$ curves for MgO (●—●) and MgO ignited in an O_2 stream (■—■).

6) P. D. Johnson, *Phys. Rev.*, **94**, 845 (1954).
7) H. Weber, *Z. Phys.*, **130**, 392 (1951).

The color of the sample ignited in an oxygen stream changed to very faint brown, while the sample ignited in a vacuum, to very faint bluish green. Though these phenomena may be ascribed to the color center related to the lattice defects, the substitution of a part of atoms and/or to the interstition of other atoms in crystal structures,[8,9] further investigations were not carried out in the present study.

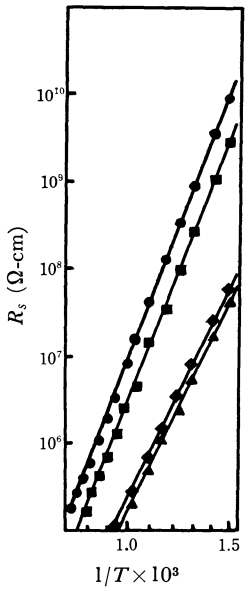

Fig. 3. R_s-$1/T$ curves for MgO (●—●), MgO+0.1%Na_2O (◆—◆), MgO+0.1%Li_2O (▲—▲), and MgO+0.1%Li_2O+10%Al_2O_3 (■—■).

TABLE 1. DETERMINATION OF *n* OR *p* TYPE

	Sample	Type
I	MgO	*p*
II	MgO ignited in an O_2 stream	*p*
III	MgO ignited in vacuum of 10^{-3} mmHg	*p*
IV	MgO+0.1%Li_2O	*n*
V	MgO+1%Li_2O	*n*
VI	MgO+1%Li_2O+10%Al_2O_3	*p*
VII	MgO+0.1%Na_2O	*n*
VIII	MgO+1%Na_2O	*n*
IX	MgO+2.5%Al_2O_3	*p*
X	MgO+5%Al_2O_3	*p*
XI	MgO+10%Al_2O_3	*p*
XII	MgO+15%Al_2O_3	*p*
XIII	MgO+2.5%B_2O_3	*p*
XIV	MgO+5%B_2O_3	*p*
XV	MgO+10%B_2O_3	*p*

8) H. G. Hecht and E. D. Taylor, *J. Phys. Chem. Solids*, **28**, 1599 (1967).

9) T. M. Searle and A. M. Glass, *ibid.*, **29**, 609 (1968).

Change in Resistivity and Transformation of Types due to Mixing Impurities. It may be expected that the addition of univalent- or tervalent-metal oxides would change the resistivity of magnesium oxide and, in some cases, transform the type into a semiconductor. Figure 3 shows the R_s-1/T curves of the samples containing univalent-metal oxides, and Table 1 shows the types of various samples. We see that the resistivity is diminished to large extent, when Na_2O or Li_2O is added to magnesium oxide, and the type is converted from *p* to *n* (samples IV, V, VII and

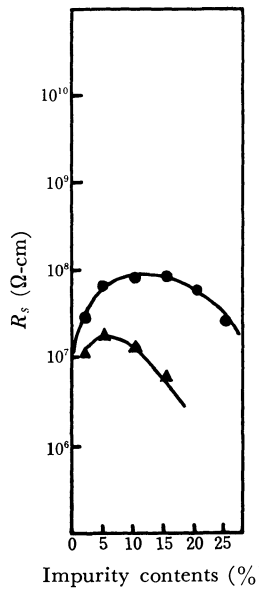

Fig. 4. R_s *vs.* impurity contents (%) curves for γ-Al_2O_3 (●—●) and B_2O_3 (▲—▲) at 1000°K.

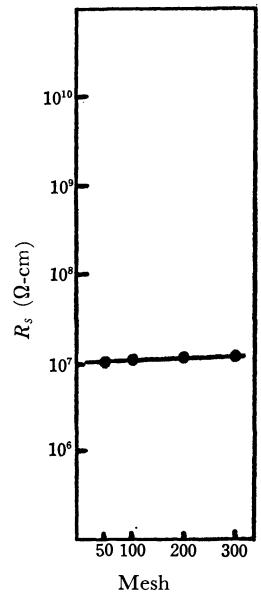

Fig. 5. R_s *vs.* grain size (mesh) curve at 1000°K.

VIII in Table 1). When γ-Al_2O_3 is added to the above samples, the resistivity is again increased (Fig. 3) and the type turned from *n* to *p* (sample VI in Table 1).

On the contrary, the addition of γ-Al_2O_3 or B_2O_3 increases the resistivity but no change is found in the type (Table 1, samples IX through XV). Figure 4 shows the curves of resistivity *vs.* the content of γ-Al_2O_3 or B_2O_3 at 1000°K. The maximum appeared at 10 % of γ-Al_2O_3 and 5 % of B_2O_3, respectively. All the samples were *p* type as shown in Table 1. Various modifications of Al_2O_3 were reported.[10-12] However, the alumina acted effectively as descrived above is γ-Al_2O_3, but not α-Al_2O_3.

10) E. Iwase, S. Nishiyama and T. Isono, This Bulletin, **29**, 147 (1956).
11) K. Funaki and Y. Shimizu, *Kogyo Kagaku Zasshi*, **56**, 53 (1953).
12) T. Sato, *ibid.*, **55**, 66 (1952).

On the activation energy for resistivity of these samples, only a small difference is found, *i.e.*, the sample containing 1 % of Li_2O showed 2.60 eV, whereas the sample containing 10 % of γ-Al_2O_3 2.72 eV.

From the principle of valency-control, it is expected that MgO containing the univalent-metal oxide should show a *p*-type character, whereas MgO with the tervalent-metal oxide, an *n*-type. The results obtained in the present work, however, can be recognized to be inconsistent with what we expected. However, the reason of this inconsistency is unknown for the present.

Grain Size and Resistivity. To observe the effect of grain size on resistivity, magnesium oxide was separated into portions 50, 100, 200 and 300 meshes with a standard sieve. Figure 5 gives the curve of the resistivity *vs.* mesh at 1000°K. The smaller the grain size, slightly larger becomes the resistivity. The resistivity hardly changes with grain size.

BULLETIN OF THE CHEMICAL SOCIETY OF JAPAN VOL. 43 1991—1998 (1970)

Radiotracer Studies on Adsorption of Surface Active Substance at Aqueous Surface. I. Accurate Measurement of Adsorption of Tritiated Sodium Dodecylsulfate

Kazuo TAJIMA, Mitsuo MURAMATSU and Tsunetaka SASAKI

Department of Chemistry, Faculty of Science, Tokyo Metropolitan University, Setagaya, Tokyo

(Received January 16, 1970)

We carried out direct measurement of adsorbed amount at the air-solution interface to confirm the validity of the Gibbs adsorption equation by using radiochemically and surface chemically pure tritiated sodium dodecylsulfate (TSDS) and a sheet scintillation counter, which was developed for the purpose of counting β-rays of tritium in air. The adsorbed amount increased with increasing SDS concentration and showed the saturation values of 3.19×10^{-10} mol/cm^2 in the concentration region from 3.2×10^{-3} to 14.4×10^{-3} mol/1000 g solution at 25°C. For the salt-free solution of ionic surfactant the Gibbs adsorption equation is confirmed to be valid for $n=2$ when activity in place of concentration is used. The equation of state for the ionic adsorbed film is further proposed. The cohesive pressure due to the attraction between hydrocarbon chains was given as a function of inverse molecular area.

The direct measurement of adsorbed amount, Γ, at the air-solution interface of ionic surfactant has been carried out by many workers to check the validity of the Gibbs adsorption equation.[1-4] Although a factor of $n=2$ in the Gibbs equation,[5] $\mathrm{d}\gamma=-\boldsymbol{R}Tn\Gamma\mathrm{d}\ln a$, is predicted theoretically, the experimental verification of the equation has

1) A. P. Brady, *J. Phys. Chem.*, **53**, 56 (1949); D. J. Salley, A. J. Weith, Jr., A. A. Argyle and J. K. Dixon, *Proc. Roy. Soc.* (London), **A203**, 42 (1950); B. A. Pethica, *Trans. Faraday Soc.*, **50**, 413 (1954); E. G. Cockbain, *ibid.*, **50**, 875 (1954); J. W. James and B. A. Pethica, "Proc. Intern. Congr. Surface Activity, 3rd," London, 2, 227 (1961).

2) J. T. Davies, *Trans. Faraday Soc.*, **48**, 1052 (1952).

3) G. Nilsson, *J. Phys. Chem.*, **61**, 1135 (1957).

4) R. Matuura, H. Kimizuka, S. Miyamoto and R. Shimozawa, This Bulletin, **31**, 532 (1958).

5) E. A. Guggenheim, "Thermodynamics," North Holland Publishing Co., Amsterdam (1949).

not been conclusive; several workers[2,3,6] indicate $n=1$ for ionic surfactant in a salt-free solution.

It is well known that the radiotracer method[7] is particularly suited for the measurement of Γ in many respects compared with the others such as "moving bubble" method[8] or microtome method.[9] However, the adsorption experiments using surfactants labelled with ^{14}C or ^{35}S involve considerable uncertainty in the measurement of Γ of ^{35}S-labelled sodium dodecylsulfate,[4] for instance, because these isotopes are not soft enough. On the other hand, owing to the extremely soft β-rays, ^{3}H renders the measurement of Γ highly accurate.[10] However, in such reports[7,11,12] which are still limited in number, the measurement of surface radioactivity is made with a 2π windowless gas-flow counter using humidified propane gas, which inevitably produces undesirable adsorption at "hydrocarbon gas-solution" interface instead of air-solution interface.

In the present paper, a radiochemically and chemically pure sample of tritiated sodium dodecylsulfate (TSDS) was synthesized and accurate determination of Γ at "air-solution" interface was made by employing a sheet scintillation counter.

Experimental

Materials. Sodium dodecyl-2,3-^{3}H,^{3}H sulfate (TSDS) was prepared by the previous method[13] with slight modifications. *n*-dodecene-2,3-ol-1 was synthesized from decanal and diethyl malonate[14] and the product was tritiated to give *n*-dodecan-2,2-^{3}H,^{3}H-ol-1 (TDOH). The unsaturated alcohol was purified by preparative gas chromatography (Yanagimoto GCG-3DH) and subsequently tritiated with tritium gas (Radiochemical Centre, Amercham, England, ca. 0.8 cc at S.T.P. 98% ^{3}H). The tritiated alcohol thus obtained was subjected to simultaneous gaschromatography (Yanagimoto GCG-5DH) for the substance and radioactivity. The results proved to be chemically and radio chemically pure for the sample obtained. It was then sulfated by the usual method[15] to give TSDS, which contained a trace amount of unreacted TDOH. The product was purified seven times by isotopic mixing with non-radioactive dodecanol in ethanol solution, followed by extraction with ether to remove dodecanol and to lower the specific activity of TDOH.[13] The specific activity of TSDS obtained was 9.16 Ci/mol. The surface-chemical purity of TSDS was confirmed by the disappearence of minimum near the critical micelle concentration (CMC) in surface tension versus concentration curve.

Thus, special care should be taken for the purity of the substance used. In fact, we had found[16] that many radioactive impurities are produced in the originally pure tirtiated stearic acid of specific activity of about 10 Ci/mol, when it is kept standing for 6.5 years in solid state. In the present experiments, therefore, the purification by Soxhlet extraction was continued until just before the adsorption experiments.

Water was distilled three times after being refluxed overnight by adding sulfuric acid and potassium permanganate. Ammonium sulfate used for the substrate solution was twice recrystallized from water and an oily substance was removed by ethereal extraction.

Apparatus. The tritium radioactivity was measured by the sheet scintillation counter,[17] modified so as to count the radioactivity at air-solution interface as shown in Fig. 1. The effective area of scintillator sheet (a) was 37.50 cm^2, and the periphery of the sheet was masked to avoid the effects of corners and edges of trough and scintillator sheet upon the scintillae. The scintillator probe was placed on the horizontally supported plate (b), which was moved vertically by the gear (c) at the rate of 2 mm per revolution. The counting was made at the applied voltage of 1250 V and with a discrimination with from 5 V to infinity.

All experiments were carried out in nitrogen gas atmosphere contained in a dark glove box. The gas controlled to 25°C by passing through a copper tube

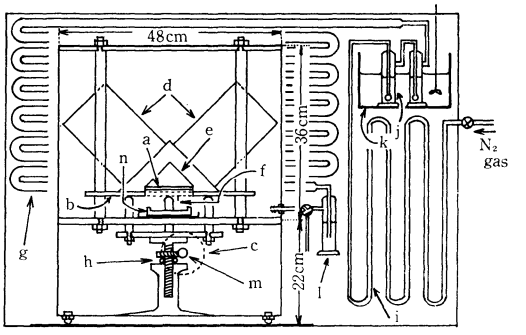

Fig. 1. Apparatus.

d: phototubes e: prism
h: ball-bearing k: water bath of 25°C
l: bubbler
For further details see text.

6) H. L. Rosano and G. Karg, *J. Phys. Chem.*, **63**, 1692 (1959); A. M. Mankowich, *J. Amer. Oil Chemists' Soc.*, **43**, 615 (1966).

7) J. K. Dixon, A. J. Weith, A. A. Argyle and D. J. Sally, *Nature*, **163**, 845 (1949); G. Aniansson and O. Lamm, *ibid.*, **165**, 357 (1950).

8) M. G. Donnan and J. T. Barker, *Proc. Roy. Soc.* (London), **A85**, 557 (1911).

9) J. W. McBain and L. A. Wood, *ibid.*, **A174**, 286 (1940).

10) G. Aniansson, *J. Phys. Chem.*, **55**, 1286 (1951).

11) M. Muramatsu, K. Tajima and T. Sasaki, This Bulletin, **41**, 1279 (1968).

12) K. Tajima, M. Muramatsu and T. Sasaki, *ibid.*, **42**, 2471 (1969).

13) M. Muramatsu and K. Tajima, *J. Labelled Compounds*, **2**, 304 (1966).

14) J. Koo, M. S. Fish, G. N. Walker and J. Blake, *Org. Syntheses*, **31**, 35 (1951).

15) E. E. Dreger, C. L. Keim, G. D. Miles, L. Shedlovsky and J. Ross, *Ind. Eng. Chem.*, **36**, 610 (1944).

16) M. Muramatsu and K. Tajima, *J. Labelled Compounds*, **3**, 343 (1967).

17) M. Muramatsu, N. Tokunaga and A. Koyano, *Nucl. Instr. Methods*, **52**, 148 (1967).

(i) and completely humidified by passing through two bubblers (j) and a long tube (g) filled with pieces of wet paper was introduced in and allowed to leak slowly out of the cell to avoid the effects of carbon dioxide and evaporation on adsorption. Humidity of the gas was measured by the weight increase of $CaCl_2$ due to passage of the gas. It was found to be $98\pm3\%$ at 25.0 ± 0.2°C.

Procedure. An aqueous solution of TSDS was introduced into a Teflon trough (n in Fig. 1), and the surface of solution was carefully swept twice by a Teflon barrier. The end of the second sweeping was taken as time zero in the surface aging of adsorption. The scintillator probe was then lowered to a fixed position about 0.8 mm above the water surface, which was assured by the electric contact of Pt-electrode (f) fixed at the scintillator probe with aqueous solution connected to another electrode. The warm gear (m) and needle point electrode in Fig. 1 enabled the distance between the probe and the aqueous surface to be adjusted to within an accuracy of 0.02 mm. The standard deviation of counting rate due to this error was less than 1%. Counting was started to measure the time dependence of radioactivity over the surface of solution.

Results

Figure 2 shows the time dependence of radioactivity at the surfaces of SDS solution varying in its concentrations. The time required for attaining the saturation value of counting rate decreased with increasing bulk concentration of solution, and the time dependence practically disappeared above CMC.

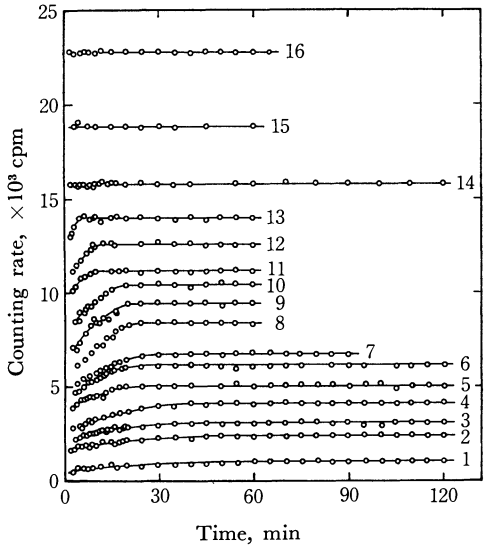

Fig. 2. Time dependence of total radioactivity on solution surface. Concentration of SDS (10^{-3} mol/1000 g solution)

1:	0.324	5:	2.02	9:	4.73	13:	8.05
2:	0.656	6:	2.47	10:	5.49	14:	9.29
3:	1.07	7:	3.04	11:	6.02	15:	11.33
4:	1.48	8:	4.09	12:	7.02	16:	14.38

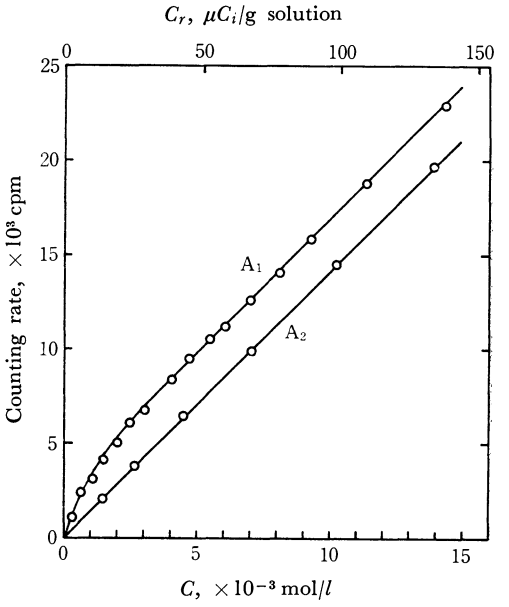

Fig. 3. A_1 plot for SDS and A_2 plot for DOH.

The counting rate of horizontal part in each curve of Fig. 2 was taken as the equilibrium value, A_1, which is plotted against SDS concentration in Fig. 3. The radioactivity due to the bulk of the solution, A_2, was determined from the radioactivity over the surfaces of the solutions of TDOH in non-radioactive DOH under the same geometrical conditions as that of A_1 determination. The A_2 values thus obtained were corrected for the difference in absorption and scattering of β-particles between water and DOH and plotted against radioactive concentration, C_r, in Fig. 3 in the same manner as in the previous report.[11] The calcu-

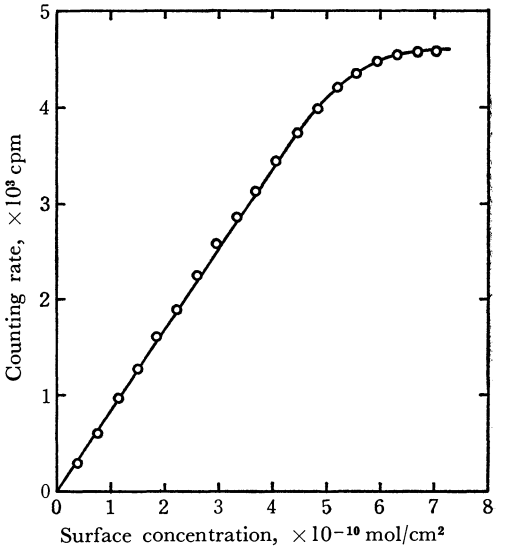

Fig. 4. Radioactivity *vs.* surface concentration for TSDS.

lation of Γ was made by

$$\Gamma = \frac{A_1 - A_2}{\kappa} \quad (1)$$

where a constant κ must be known. It was determined by counting the surface radioactivity for known amounts of TSDS film spread over the aqueous ammonium sulfate solution of 80% saturation in the Teflon trough.[18] Figure 4 shows the relationship between the surface radioactivity and the amounts of TSDS.

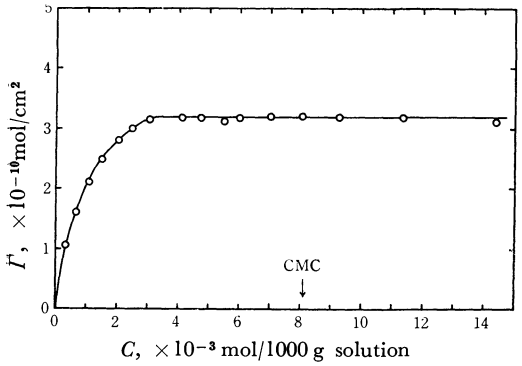

Fig. 5. Adsorption isotherm of SDS at air-solution interface (25°C).

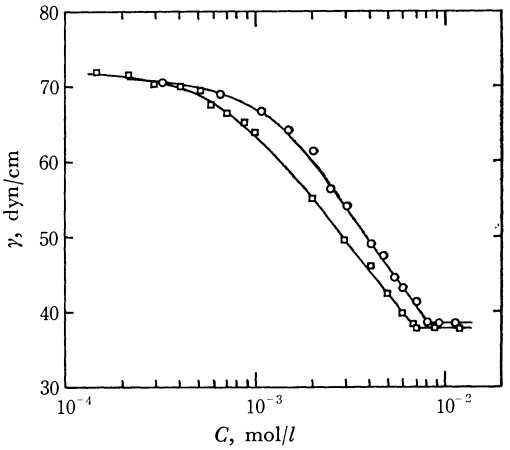

Fig. 6. Surface tension *vs.* concentration curves of SDS solution.

—○—: drop volume method
—□—: Wilhelmy plate method

The adsorption isotherm obtained is shown in Fig. 5. It can be seen that Γ markedly increases with increasing concentration of SDS and arrives at the saturated adsorption of 3.19×10^{-10} mol/cm^2 at bulk concentration of about 3.2×10^{-3} mol/1000 g solution beyond which Γ does not change

Table 1. Adsorbed amount at gas-solution interface of sodium dodecylsulfate by various methods

Method	RI species	Saturated adsorption amounts, $\times10^{-10}$ mol/cm^2	Temp. °C	Reference
RT	^{3}H	3.19	25	present paper
RT	^{3}H	5.0	25	3
RT	^{3}H	5.89	20	11
RT	^{35}S	3.7±1	28	4
RT	^{35}S	3.35		20
RT	^{35}S	7.5		21
RT	^{35}S	4.8±1		22
bubble		4.06	24—26	23
bubble		3.32	26	24
bubble		3.00	20	25
bubble		4.00	25	26
bubble		4.88	28	27
microtome		5.4	21—22	9*

* Sodium dodecylsulfonate

18) H. B. Bull, *J. Amer. Chem. Soc.*, **67**, 10 (1945).
19) M. E. L. McBain and E. Hutchinson, "Solubilization and Related Phenomena," Academic Press Inc., New York (1955).
20) J. M. Corkill, J. F. Goodman, D. R. Haisman and S. P. Harold, *Trans. Faraday Soc.*, **57**, 821 (1961).
21) R. Ruyssen and J. Maebe, *Mededeel. Koninkl. Vlaam-Acad. Wetenschap. Belg. Kl. Wetenschap.*, **15**, 5 (1953).
22) E. Hutchinson, *J. Colloid Sci.*, **4**, 599 (1949).
23) A. Wilson, M. B. Epstein and J. Ross, *ibid.*, **12**, 345 (1957).
24) J. E. Bujake and E. D. Goddard, *Trans. Faraday Soc.*, **61**, 190 (1965).
25) H. Kishimoto, *Kolloid-Z. Z. Polym.*, **192**, 66 (1963).
26) Ira Weil, *J. Phys. Chem.*, **70**, 133 (1966).
27) C. Walling, E. E. Ruff and J. L. Thornton, Jr., *ibid.*, **56**, 989 (1952).

with the concentration even beyond CMC (8.1×10^{-3} mol/1000 g solution). The area per molecule at the saturated adsorption is found to be 52.0 Å^2. The surface tension of the solution was measured by the drop volume method, the correction of Harkins and Brown being applied. The results (circles) shown in Fig. 6 show that the surfactant employed was surface-chemically pure. The Wilhelmy plate method was also adopted for the surface tension measurement for comparison.

Discussion

Evaluation of Γ. In Table 1 are shown the values obtained together with those obtained by other methods. The values are seen to fluctuate widely. Evidently the β-rays of ^{35}S are too hard for an accurate measurement of the SDS adsorption to be made, while ^3H much reduces the experimental error. However, the measurements of ^3H radioactivity with a 2π windowless gas-flow counter involve many difficulties which should be overcome. First, there is the possibility that the counting gas (humidified hydrocarbon) is adsorbed at the surface and solubilized in the bulk of surfactant solution.[19] Also, it is probable that the adsorption of the surfactant is affected by the high voltage applied and by the gas phase being hydrocarbon instead of air. These effects are unfavorable for the use of a 2π windowless gas-flow counter and the use of an end-window type is recomended.

It is seen in Table 1 that the results obtained happen to be close to some of the adsorption data obtained by the foam method. However, the latter method is not favorable because of the difference in adsorption on plane and non-plane surfaces, and also the difference in adsorption on solution surface and on two sided film where the van der Waals and coulombic interactions between the two parallel films are effective.[28] Difficulties also arise from uncertainty in the estimation of surface area, non-equilibrium state of adsorption due to the short period of passage of bubbles, and the gradual changes of bulk concentration and pH of solution during the passage of a large number of bubbles.[29] Thus, it is not surprising to find discrepancies in Γ values between the foam and the radiotracer methods, the latter being free of the difficulties mentioned above.

Surface Tension *vs.* Concentration Curve. Figure 6 shows the values of equilibrium surface tension, γ, measured by the Wilhelmy plate method[30] (squares) and by the drop volume method (circles) as a function of SDS concentration. A systematic difference seems to exist between surface tension data obtained by these methods. A similar tendency has been reported by Boucher *et al.*[31] for sodium hexyl α-sulfopelargonate. They inferred that the surface tension data obtained by these methods appear to be reliable in so far as they do not affect molecular cross-sectional areas of surfactants obtained by applying these data to the Gibbs equation. However, the results of the present measurement exhibited limiting slopes of curves being different from each other as shown in Fig. 6. This would be reasonable, when we consider marked aging phenomena observed in surface tension of detergent solution.

Gibbs Adsorption Equation. In the present system the Gibbs adsorption equation[5] is expressed by

$$-\mathrm{d}\gamma = \boldsymbol{R}T\Gamma_{Na^+}\mathrm{dln}a_{Na^+} + \boldsymbol{R}T\Gamma_{D^-}\mathrm{dln}a_{D^-} + \boldsymbol{R}T\Gamma_{H^+}\mathrm{dln}a_{H^+} + \boldsymbol{R}T\Gamma_{OH^-}\mathrm{dln}a_{OH^-} \quad (2)$$

where γ, Γ and a express the surface tension of solution, the amount of adsorption and activity, both for the solutes. The subscripts Na^+, D^-, H^+, and OH^- denote sodium, dodecylsulfate, hydrogen and hydroxyl ions, respectively. Since the SDS solution was almost neutral and pH was kept practically constant to 6.0 ± 0.2 throughout the measurements for all solution, we put for approximation $\mathrm{d}\,a_{H^+}=\mathrm{d}\,a_{OH^-}=0$. Assuming no surface hydrolysis,[32] $\Gamma_{H^+}=\Gamma_{OH^-}=0$, and electrical neutrality both in bulk and surface layer, namely $C_{Na^+}=C_{D^-}=C$, and $\Gamma_{Na^+}=\Gamma_{D^-}=\Gamma$,[33] we get from Eq. (2)

$$-\frac{\mathrm{d}\gamma}{\boldsymbol{R}T\,\mathrm{d\ln}C} = 2\Gamma\left(1+\frac{\mathrm{d\ln}f_\pm}{\mathrm{d\ln}C}\right) \quad (3)$$

where $f_\pm=(f_{Na^+}\times f_{D^-})^{1/2}$ is the mean activity coefficient of SDS. It has been reported[34] that activity coefficient of SDS solution varies according to the method of measurement such as the glass or membrane electrode methods. However, $f_\pm$ is better approximated by the Debye-Hückel second approximation. Thus, for uni-univalent

28) J. Lyklema and K. J. Mysels, *J. Amer. Chem. Soc.*, **87**, 2539 (1965).

29) F. L. Jackson and F. P. Krause, *J. Phys. Chem.*, **67**, 2355 (1963).

30) K. Nukina, Master thesis, Dept. Chem., Fac. Sci., Tokyo Metropolitan Univ., (1966).

31) E. A. Boucher, T. M. Grinchuk and A. C. Zettlemoyer, *J. Colloid Interfac. Sci.*, **23**, 600 (1967).

32) D. Eagland and F. Francks, "Proc. Intern. Congr. Surface Activity, 3rd," London, Sec. B 539 (1960).

33) R. Defay, I. Prigogine, A. Bellemans and D. H. Everett, Ed., "Surface Tension and Adsorption", Longmans, London (1966).

34) H. Huff, J. W. McBain and A. P. Brady, *J. Phys. and Colloid Chem.*, **55**, 311 (1951); C. Botre, V. L. Crescenzi and A. Mele, *J. Phys. Chem.*, **63**, 650 (1959); L. Shedlovsky, C. W. Jakob and M. B. Epstein, *ibid.*, **67**, 2075 (1963).

electrolytes, we have

$$-\ln f_{\pm} = \frac{1.18\sqrt{C}}{1+\frac{r_{\pm}}{3.08}\sqrt{C}} \tag{4}$$

where $r_{\pm}$ is the average radius of hydrated anion and cation in the solution (Å unit). According to Kielland's report[35] and in agreement with Haydon's opinion[36] that $r_{\pm}$ for alkylsulfate and quaternary ammonium ions should be slightly higher than 5 Å, we put $r_{\pm}=7$ Å in Eq. (4) for SDS ion of all concentration. Differentiating Eq. (4) we have

$$\Delta = -\frac{\mathrm{d}\ln f_{\pm}}{\mathrm{d}\ln C} = \frac{0.59\sqrt{C}}{\left(1+\frac{r_{\pm}}{3.08}\sqrt{C}\right)^2} \tag{5}$$

The values of Γ were calculated from Eq. (3) by the evaluation of $\mathrm{d}\gamma/\mathrm{d}\ln C$ from γ *vs.* C measurement and Δ from Eq. (5). The result is shown in Fig. 7 as solid and broken lines for the Wilhelmy plate and the drop volume methods, respectively. The amount of adsorption directly measured by the radiotracer method was also plotted as shown by circles in Fig. 7. The observed values are in good agreement with those calculated by Eq. (3) applying the surface tension data of the Wilhelmy plate method, compared with those of drop volume method throughout the whole range of bulk concentration. The deviation of drop volume data is marked especially at low concentration. This may be understood since the drop volume method is insufficient for giving an equilibrium surface tension at low concentration where the rate of attainment of equilibrium is slow. On the other hand, a slight discrepancy at lower concentration in the case of the Wilhelmy plate method probably comes either from the uncertainty of surface tension data or from the invalidity of Eq. (3), which has been derived by neglecting the H^+ ion terms.

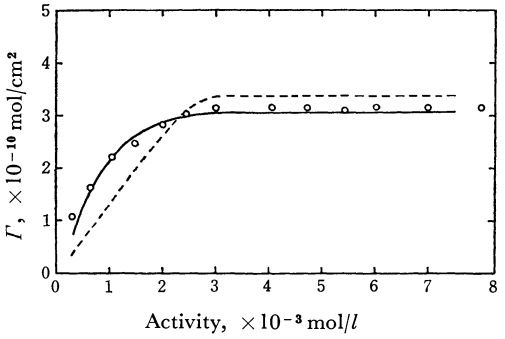

Fig. 7. Comparison of observed and calculated values of SDS adsorption using Eq. (3).

○ : observed values
··· : calculated values (drop volume method)
— : calculated values (Wilhelmy plate method)

It should be emphasized that for the salt-free solution of not so dilute ionic surfactant the Gibbs adsorption isotherm is proved to be valid for $n=2$ in the Gibbs adsorption equation, provided that activity is used in place of concentration.

Equation of State. Many investigators have reported[36,37] various types of equation of state for the monomolecular film at an air-solution interface. Davies proposed a surface equation of state,[38]

$$(\pi-\pi_s-\pi_r)(A-A_0) = \boldsymbol{k}T \tag{6}$$

for charged monolayer at air-water interface, where π is the total surface pressure, A and A_0 the area and co-area per molecule in adsorbed film, $\boldsymbol{k}$ the Boltzmann constant, T the absolute temperature, π_s the cohesive surface pressure due to the van der Waals forces of attraction between the hydrocarbon parts of the adsorbed surface-active ions as given by

$$\left.\begin{aligned} \pi_s &= -\frac{400\,m}{A^{3/2}} \\ \text{for } A>71 \text{ Å}^2\text{/molecule, and} & \\ \pi_s &= -0.67\,m \end{aligned}\right\} \tag{7}$$

for $A<71$ Å^2/molecule, with m for the effective number of CH_2 groups present in the long-chain ion. Further, π_r in Eq. (6) represents the repulsive surface pressure due to the polar head groups of adsorbed ions. Davies gave

$$\pi_r = 6.03C_i^{\frac{1}{2}} - \frac{2\boldsymbol{k}T}{A} \tag{8}$$

where C_i denotes total (uni-univalent) electrolyte concentration.

Figure 8 shows the observed equation of state for the adsorbed film of SDS, using the data of surface tension measured by the Wilhelmy plate method and the amount of adsorption by radiotracer method. In Fig. 9 plots of $1/(\pi-\pi_s-\pi_r)$ against A are shown as circles, assuming that π_s and π_r are expressed by Eqs. (7) and (8), respectively. If we draw a line with the slope of $\boldsymbol{k}T$ and through the point $A_0=33$ Å^2 given by Davies for adsorbed films of SDS, it largely deviates from the observed values (circles). This clearly shows the inapplicability of the empirical equation (7), which has been presumed from the behavior of π *vs.* A relation for the monolayer of octadecyltrimethylam-

35) J. Kielland, *J. Amer. Chem. Soc.*, **59**, 1675 (1937).
36) D. A. Haydon and F. H. Taylor, *Phil. Trans. Roy. Soc.*, **A252**, 225 (1960).
37) E. Matijevic and B. A. Pethica, *Trans. Faraday Soc.*, **54**, 1382 (1958); R. K. Schofield and E. K. Rideal, *Proc. Roy. Soc.* (London), **A109**, 57 (1925); F. M. Fowkes, *J. Phys. Chem.*, **66**, 385 (1962); E. H. Lucassen-Reynders and van den Temple, "Proc. Intern. Congr. Surface Active Substances, 4th", Brussels (1964).
38) J. T. Davies, *J. Colloid Soc.*, **11**, 377 (1956).

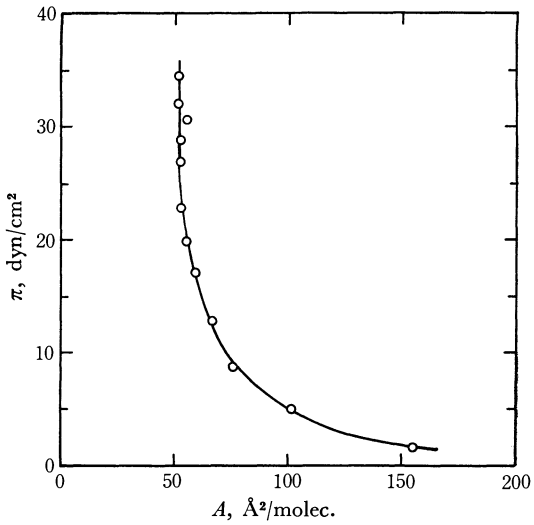

Fig. 8. Pressure *vs.* area curve of SDS at air-solution interface.

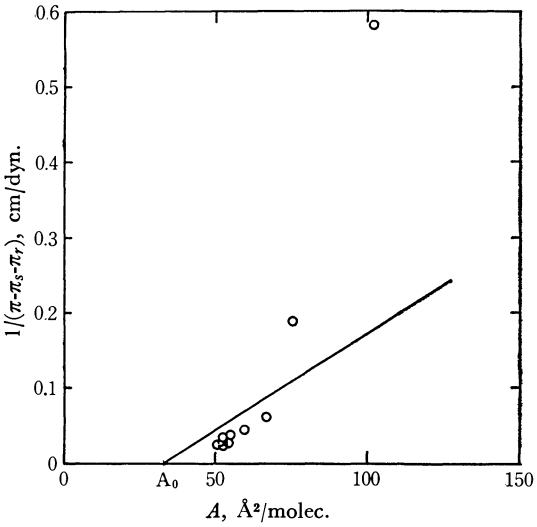

Fig. 9. Plots of $1/(\pi-\pi_s-\pi_r)$ against A for SDS.
○ : observed values
— : calculated from Davies equation

monium ions, but has not yet been confirmed actually, at least for monolayers of shorter carbon chain length. Thus, Eq. (7) turned out to be inapplicable to soluble adsorbed films, and the present authors propose the empirical equation

$$\pi_s = -\frac{K}{A} \tag{9}$$

where K is a proportionality constant, determined from the π *vs.* A curve. Substitution of Eqs. (8) and (9) into Eq. (6) yields an equation of rectangular hyperbola when $A(\pi-\pi_r)$ is plotted against A. Thus, graphical plots give

$$K = 2.43\,kT$$

$$A_0 = 38.4\ \text{Å}^2/\text{molecule}$$

and the final equation becomes

$$\left(\pi+6.03\,C_i^{\frac{1}{2}}+\frac{0.43\,kT}{A}\right)(A-A_0) = kT \tag{10}$$

Figure 10 shows the curves based on Davies' equation and Eq. (10) together with the experimental data (circles). Eq. (10) is shown to fit the actual behavior of adsorbed film better than Davies' equation. The observed π *vs.* A curve shows a more condensed film than that predicted by Davies' equation. The large deviation of Davies' equation, especially in the region of large molecular area, may be ascribed to the insufficient contribution of π given by Eq. (7) to total surface pressure. It should be emphasized that Eq. (10) holds regardless of the value of A being smaller or larger than 71 Å²/molecule, which is not the case in Eq. (7). It is shown that Eq. (10) with $K=2kT$ and $A_0=27.0$ Å²/molec. also fits the π *vs.* A curve for the monolayer of octadecyltrimethylammonium ion, while Davies' equation fairly deviates from the curve.

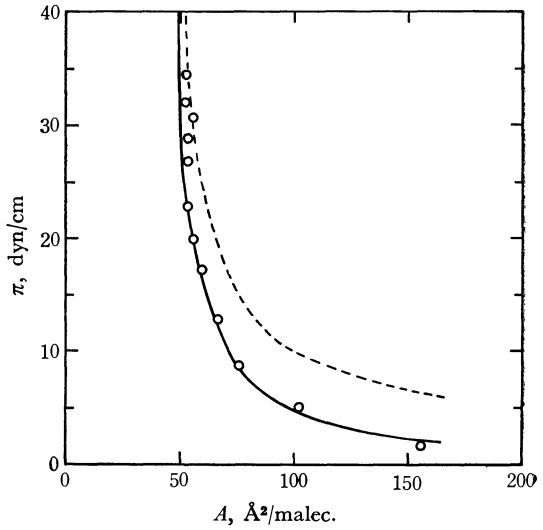

Fig. 10. π *vs.* A plot for SDS.
○ : observed values
— : Eq. (10)
··· : Davies equation

Recently, Chattoraj *et al.*[39] proposed the following equation for π_s on the basis of the two-dimentional van der Waals attraction,

$$\pi_s = \frac{\alpha_s}{A^2} \tag{11}$$

where α_s is the van der Waals constant for a surface phase. To explain the deviation of Eq. (11)

39) C. K. Chattoraj and A. K. Chatterjee, *J. Colloid Interfac. Sci.*, **21**, 159 (1966).

from their experimental data, they assumed the existence of surface micelles for the region of $A<$ 130 Å^2/molecule. In the present studies, however, Eq. (11) has been confirmed not to hold in the region of $A<150$ Å^2/molecule, suggesting the inapplicability of their equation and the uncertainty of the existence of surface micelles in adsorbed layer.

As for the value of A_0 for the charged adsorbed films, there is always disagreement among various authors. Phillips and Rideal[40] give $A_0=20$ Å^2 for the dodecylsulfate ion, and Davies[38] considers 33 Å^2 reasonable, though Cook and Tablot[41] suggest A_0 being as large as 50 Å^2. The present experiments give $A_0=38.4$ Å^2. This value is reasonable when we take account of the fact that the cross-sectional area for a hydrated sulfate ion is 28 Å^2 per molecule.[42] The difference may be ascribed to the presence of the hydrocarbon chain attached to the ion. It should be emphasized that the value A_0 obtained in the present study is based upon the equation of state which is in agreement with the direct measurement of π *vs.* A relation, while the values of other workers are based upon the equations which are not in agreement with the experimental results, at least for SDS.

40) J. N. Phillips and E. Rideal, *Proc. Roy. Soc.*, **A232**, 159 (1955).

41) M. A. Cook and E. L. Tablot, *J. Phys. Chem.*, **56**, 412 (1952).

42) R. D. Vold and M. J. Vold, Ed., "Colloid Chemistry," Reinhold Pub. Corp., N. Y. (1964), p. 100.

BULLETIN OF THE CHEMICAL SOCIETY OF JAPAN VOL. 43 1998—2002 (1970)

The Magnetic Susceptibilities and ESR of Wurster's Ions in Crystals

Jiro TANAKA, Motomichi INOUE, Masagi MIZUNO and Kazumi HORAI

Department of Chemistry and Department of Physics, Faculty of Science, Nagoya University, Chigusa-ku, Nagoya

(Received January 20, 1970)

The magnetic susceptibilities and the electron spin resonances of Wurster's blue bromide, blue iodide, and red bromide have been measured over a wide temperature range. The results show that the paramagnetism of Wurster's blue bromide above 210°K and of iodide can be explained by the linear Ising model, consistent with the crystal structure. Wurster's blue bromide showed a deviation from the linear Ising model below 210°K; the dimer model is most appropriate for the explanation of the experimental data.

The intensities of the single ESR line are consistent with the results of the static susceptivility measurements. The hyperfine structures are not observed, perhaps because of the rapid movement of the triplet exciton. The magnetic results are explained in terms of the J-values, the origin of which are discussed on the basis of the interaction between the charge-transfer states and the singlet state. The values are resonably correlated with the interaction parameter, β, as estimated from the crystal structure and the electronic spectral measurements.

The magnetic susceptibilites of Wurster's radical salts are of particular interest, as they show the effects of intermolecular spin coupling between the radicals. The electronic interaction between the radicals may be observed in several physicochemical properties; the electronic spectra have been shown to be greatly influenced by the charge-transfer effect.[1)] The singlet-triplet energy gap of the radical crystal may be produced by two mechanisms; one is a convalent-like exchange interaction between the radicals, and the other is the stabilization of the singlet ground state by the charge-transfer state. The charge-transfer interaction is more important than the exchange effect, because the electron overlap is very small between the radicals, and because the exchange interaction is second-order compared to the electron overlap.

In the present paper the result of magnetic susceptibility measurements of several Wurster's salts will be presented, together with the results of ESR measurements over a wide temperature range. The magnetic data will be discussed in terms of the exchange parameter, J. The localized spin models are most adequate for the consideration of the electronic behavior of the organic radical crystals. The observed J-values will be correlated with the calculated stabilization energies of the

*1 Present address: The Government Chemical Industrial Research Institute, Tokyo.

1) J. Tanaka and M. Mizuno, *This* Bulletin **42**, 1841 (1969).

ground state by means of the charge-transfer effects.

Experimental

The materials used in this investigation were prepared by the method of Michaelis and Granick.[2] The magnetic susceptibilities of Würster's blue iodide and bromide and Würster's red bromide have been measured by the Gouy method at temperatures between 80—300°K.

The results are shown in Fig. 1. Since the radicals are not very stable, some fluctuations are observed in the magnetic data. The accuracy of the absolute values was estimated to be about ±5%. Corrections were made for diamagnetic contributions (in 10^{-6} emu/mol) from neutral tetramethyl-*p*-phenylenediamine (−118), the bromide ion (−36), and the iodide ion (−52).[3] The value for the neutral amine was based on the observed susceptibility of *p*-phenylenediamine.[4] The susceptibility of Würster's blue iodide increases with decrease in the temperature; the maximum is reached at 140°K. The susceptibility of Würster's blue bromide gradually decreases with a lowering of the temperature and it reaches its minimum at 120°K. The susceptibility of Würster's red bromide shows only the diamagnetism at 300°K.

The ESR spectra have been observed by means of a conventional spectrometer at 9310 MHz. The intensity of the absorption lines was measured in comparison with the intensity of a small crystal of $CuSO_4 \cdot 5H_2O$ mounted in the same resonant cavity.

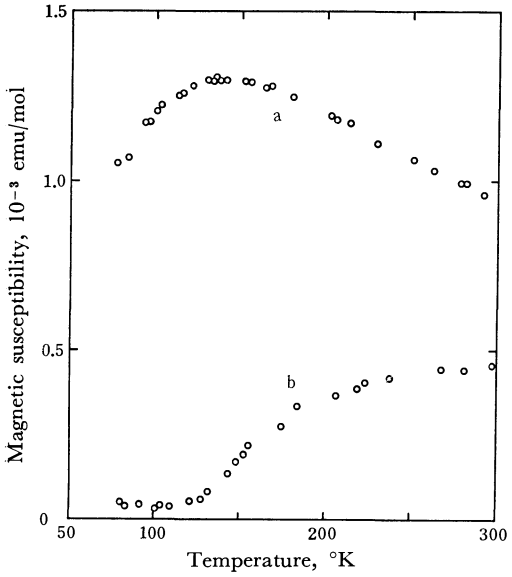

Fig. 1. Magnetic susceptibilities of Würster's Blue iodide (a) and bromide (b) at 70—300°K.

Discussion

The crystalline structure of Würster's blue iodide have been found to be a regular one-dimensional chain;[5] the structure of Würster's blue bromide has also been found to be a regular chain at room temperature.[6] The magnetic susceptibility of a regular antiferromagnetic chain will be given by the linear Ising model as

$$\chi = \frac{N_0 g^2 \mu_B^2 \exp(J/kT)}{4kT} \qquad (1)$$

where $g=2.00$ is the g-factor, μ_B is the Bohr magneton, k is the Boltzmann constant, N_0 is the Avogadro number, and J is the exchange parameter between the radical pairs.

The plot of log $(4k\chi T/N_0\mu_B^2)$ against the inverse temperature is shown in Fig. 2. The experimental values of Würster's blue iodide coincide with the line calculated by the linear Ising model, although a slight deviation from the line is found at lower temperatures. The deviation from the calculated line is monotonous; therefore, it may be ascribed to the gradual increase in the J-value, which is accompanied by a decrease in the interplanar spacing as a result of a shrinkage of the lattice dimensions. The J-values are estimated from Eq. (1) to be -59 cm^{-1} at 300°K and -83 cm^{-1} at 80°K; the average value is -71 cm^{-1} for the 80—300°K range. Since the crystal structure of Würster's blue iodide is a regular chain, the use of the linear Ising model will be most

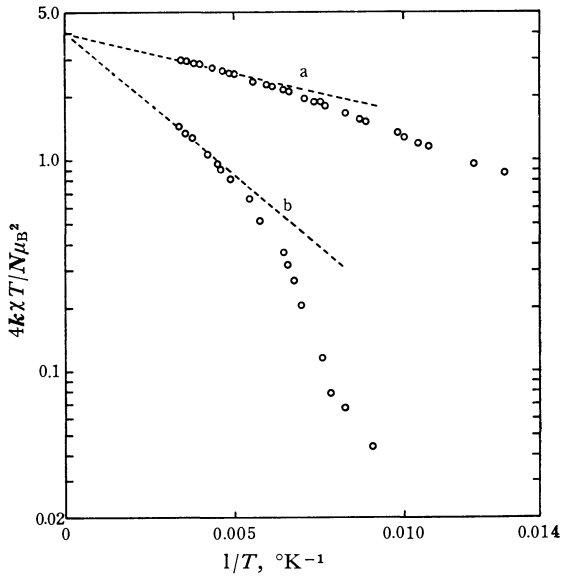

Fig. 2. The plot of magnetic data against inverse temperatures.

2) L. Michaelis and S. Granick, *J. Amer. Chem. Soc.*, **65**, 1747 (1943).

3) P. W. Selwood, "Magnetochemistry," 2nd Ed., Interscience Publishers, New York, N.Y. (1956).

4) G. Foëx, "Constantes Sélectionèes, Diamagnétisme et Paramagnétisme," Mason, Paris (1957).

5) J. L. DeBoer, A. Vos and K. Huml, *Acta Crystallgr.*, **B24**, 542 (1968).

6) Unpublished results of this laboratory.

suitable. In addition, it is most probable that the equal spacing between the radicals is maintained down to low temperatures, for no sharp change in the susceptibility with the temperature is observed. The increase in the J-values at low temperatures is also reasonable, since the interaction will be enlarged by close contact between radicals.

The results on Würster's blue bromide are in contrast to those on the iodide; a sudden change in the slope is observed at 210°K. The abnormal decrease in the susceptibility below this temperatures implies that a phase transition may take place at this temperature. Several discussions have been presented with regard to the stability of the linear interacting system;[7-9] a phase transition has actually been reported on the crystal of Würster's blue perchlorate.[9-11] Although no X-ray results have yet been found for Würster's blue bromide, a similar transition is plausible at lower temperatures. Therefore, the linear Ising model will be used above 210°K and the dimer model will be employed below this temperature. From Eq. (1) the J-value is estimated to be $-210\ \mathrm{cm}^{-1}$ in the 210—310°K range. According to the dimer model, the susceptibility is given by:

$$\chi = \frac{N_0 g^2 \mu_B{}^2}{3kT[(1 + (1/3)\exp(2|J|/kT))]} \qquad (2)$$

By the use of Eq. (2), the J-value for 120—210°K is determined to be $-350\ \mathrm{cm}^{-1}$. This value is justified in view of the value above a phase transition, since the charge-transfer interaction will be much increased by the dimer formation at low temperatures.

ESR Spectra. The intensities of the ESR spectra were measured with Würster's blue bromide and iodide for the temperature range of 80—300°K. The results are nearly in agreement with the static measurements, as is shown in Fig. 3, where the results for Würster's blue bromide is presented. The ESR spectra of these radical salts do not show any hyperfine structures; a single line is observed in both salts. The lack of the hyperfine structures may suggest that the movement of the triplet exciton is so rapid that the triplet dipolar structure is washed out.[12,13]

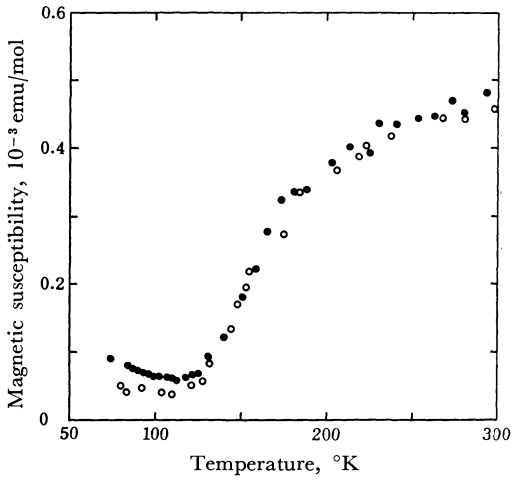

Fig. 3. The Comparison of Susceptibility Measurements by Static (○) and the ESR (●) methods.

The g-factors are those of the free spin values; the values are $g=2.0028\pm0.0005$. The measurement of the single crystal of the iodide shows no anisotropy on the g-values and the line-width. The line widths are 11 Oer (31 Mc) for iodide and 4 Oer (14 Mc) for bromide. The line-width is not changed markedly with the temperature for Würster's blue iodide. The width of Würster's blue bromide is decreased in the 120—170°K range, where the dimer is presumably formed, and it increases below 120°K because some impurities may contribute dominantly in this temperature range.

Singlet-Triplet Energy Gap. The observed J-values can theoretically be correlated with the intermolecular electronic interactions between the radicals; the values can be calculated if the molecular wave functions and the energies of the intermolecular interactions are known precisely. In a previous paper[1] we have presented the calculations for the triplet state of the dimer system.

The wave functions for the singlet ground state and the triplet state are given by;

$$\Psi_S = \frac{1}{\sqrt{2(1+S^2{}_{mm})}}[\phi_a{}^m(1)\phi_b{}^m(2) + \phi_a{}^m(2)\phi_b{}^m(1)] \times [\alpha(1)\beta(2) - \alpha(2)\beta(1)]$$

$$\Psi_T = \frac{1}{\sqrt{2(1-S^2{}_{mm})}}[\phi_a{}^m(1)\phi_b{}^m(2) - \phi_a{}^m(2)\phi_b{}^m(1)] \times \begin{cases}\alpha(1)\alpha(2)\\ \alpha(1)\beta(2) + \alpha(2)\beta(1)\\ \beta(1)\beta(2)\end{cases} \qquad (3)$$

where $\phi_a{}^m$ and $\phi_b{}^m$ denote the highest molecular orbitals which are half-occupied, where α and β are spin functions, and where S_{mm} is the overlap integral between the $\phi_a{}^m$ and $\phi_b{}^m$ orbitals.

The Hamiltonian and notations for the molec-

7) Y. Ooshika, *J. Phys. Soc. Jap.*, **12**, 1238, 1246 (1957); **14**, 747 (1959).
8) H. C. Longuet-Hitggins and L. Salem, *Proc. Roy. Soc. Ser. A*, **251**, 172 (1959).
9) D. D. Thomas, H. Keller and H. M. McConnell, *J. Chem. Phys.*, **39**, 2321 (1963).
10) K. Okumura, *J. Phys. Soc. Jap.*, **18**, 69 (1963).
11) H. Chihara, M. Nakamura and S. Seki, This Bulletin, **38**, 1776 (1965).
12) D. B. Chesnut and W. D. Phillips, *J. Chem. Phys.*, **35**, 1002 (1961).
13) Z. G. Soos and H. M. McConnell, *ibid.*, **43**, 3780 (1965).

ular integrals are the same as in the previous paper.[1] The diagonal energy for the triplet state and the separation of the singlet and the triplet state are:

$$\left.\begin{aligned} E_T &= 2\varepsilon_a - 2\langle\psi_a{}^m|1/R_b|\psi_a{}^m\rangle \\ &\quad + (\psi_a{}^m\psi_a{}^m|\psi_b{}^m\psi_b{}^m)(1+S^2{}_{mm}) \\ &\quad + \sum\frac{\delta_i\delta_j}{R_{a_i,b_j}} + 2S_{mm}\langle\psi_a{}^m|1/R_b|\psi_b{}^m\rangle \\ &\quad - 2S^2{}_{mm}\langle\psi_a{}^m|1/R_b|\psi_a{}^m\rangle \\ &\quad - (\psi_a{}^m\psi_b{}^m|\psi_a{}^m\psi_b{}^m) \\ \Delta(T-S) &= 4S_{mm}\langle\psi_a{}^m|1/R_b|\psi_b{}^m\rangle \\ &\quad - 4S^2{}_{mm}\langle\psi_a{}^m|1/R_b|\psi_a{}^m\rangle \\ &\quad + 2S^2{}_{mm}(\psi_a{}^m\psi_a{}^m|\psi_b{}^m\psi_b{}^m) \\ &\quad - 2(\psi_a{}^m\psi_b{}^m|\psi_a{}^m\psi_b{}^m) \end{aligned}\right\} \quad (4)$$

The evaluation of those integrals would require extensive calculations; however, the order of magnitudes can be estimated by an empirical relation between the overlap integrals and the assumed β values, the charge-transfer matrix elements of the previous paper. The spectral data showed that the β value between the charge-transfer and the singlet-ground configuration of Würster's blue crystals are in the vicinity of 0.1—0.2 eV, and the formula for the matrix elements showed that β should be proportional to the overlap integrals times the integrals of the $\langle\psi_a{}^m|1/R_b|\psi_a{}^m\rangle$ type. Each term in $\Delta(T-S)$ of Eq. (4) is related to the square of the overlap integrals times $\langle\psi_a{}^m|1/R_b|\psi_a{}^m\rangle$. Therefore, if we use a rough relation that:

$$\beta \simeq kS^2{}_{mm} \quad (5)$$

then Δ may be approximated by:

$$\Delta \simeq kS^2{}_{mm} \quad (6)$$

If we put $k=40$ eV (which is estimated from spectral results) then Δ can be evaluated as being smaller than a few cm^{-1} by using the overlap integrals tabulated in Table 1. This obviously shows that the exchange interaction of this type is not the true origin of the separation of the triplet and singlet energy levels.

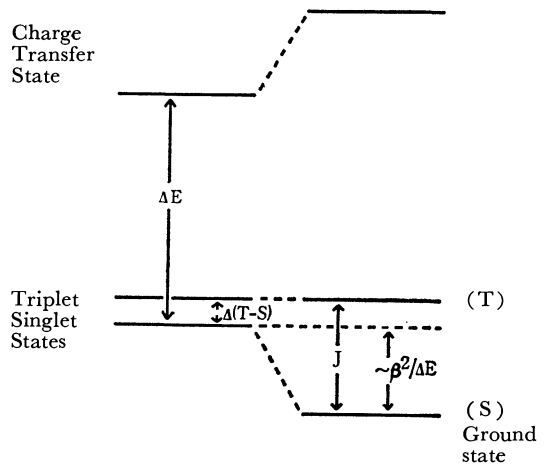

Fig. 4. Energy Levels of Singlet, Triplet and Charge Transfer States.

On the other hand, the singlet-ground state is stabilized by the charge-transfer effect, which is far more significant in the present system.[1] This resonance effect is important only for the singlet-ground state (Fig. 4); the triplet state is not stabilized at all because of the lack of the intermolecular charge-transfer effect.

The stabilization energies have been evaluated by solving Eq. (10) of the previous paper[1]; they are reproduced in Table 1. The β parameters in Table 1 were estimated by considering the spectral data, such as the energy and the intensity of the charge-transfer band.

Würster's red bromide shows only diamagnetism; this is consistent with the large stabilization energy calculated. By this mechanism it can be seen that Würster's red bromide is a diamagnetic crystal at room temperature. With other crystals,

Table 1.

		S_{mm}*	$-\beta$ (eV)	Stabilization Energy		Observed J-value
Würster's red bromide	(II)†	0.025	0.9	−0.415 (eV)	−3352 (cm^{-1})	—
	(III)		0.6	−0.187	−1500	
Würster's blue bromide	(IV)	0.0034	0.25	−0.038	−300	−210 (cm^{-1})**
	(V)		0.23	−0.0298	−238	
Würster's blue iodide	(III)	0.0025	0.11	−0.0075	−60	−70
Würster's blue perchlorate	(IX)	0.0012	0.08	−0.004	−32	−16***

* S_{mm} is the overlap integrals between the half-filled molecular orbitals.
** The value is for the 210—300°K range.
*** The value is estimated from the data of Okumura.[10]
† The numbers in parenthesis are referred to the Table 1 of Ref. 1.

the calculated energies are reasonably correlated with the observed J-values. These results show convincingly that the singlet-triplet energy gap is produced by the charge-transfer mechanism.

The magnetic interaction in such radical crystals is thus shown to be dominated by the charge-transfer mechanism. The stabilization of the ground state is approximately given by $-\beta^2/\Delta E$, where ΔE is the energy difference between the charge-transfer and the ground state and where β is the interaction energy. Since ΔE is almost constant at about 1.6—1.8 eV for all Würster's salts, the β value is very important in both spectral and magnetic studies. The motion of the triplet exciton in the crystal is governed by the transfer-matrix element between radicals and pairs; it is also connected with β-values and, hence, with the overlap integrals.

A more detailed approach to the evaluation of these intermolecular interactions would be desirable in future studies.

BULLETIN OF THE CHEMICAL SOCIETY OF JAPAN VOL. 43 2002—2007 (1970)

The Photosensitized Decomposition of Methyl Acetate at 77°K. A Kinetic Analysis of the Biphotonic Process

Shigeru MIZUTANI, Yukihiko NAKAJIMA, Kazuo SHIMOKOSHI and Shin SATO

Department of Applied Physics, Tokyo Institute of Technology, Ookayama, Meguro-ku, Tokyo

(Received January 26, 1970)

The photosensitized decomposition of methyl acetate at 77°K has been investigated using an ESR technique. Naphthalene, α-naphthol, phenanthrene, anthracene, and benzophenone were used as sensitizers. When wavelengths longer than 2700Å were used, the formation of methyl radicals was observed except in the cases of anthracene and benzophenone. For the systems containing naphthalene, phenanthrene, and α-naphthol, the rate of the formation of methyl radicals was studied in detail and was found to obey the following relation:

$$R=\alpha I^{3/2}C^{1/2}$$

Here, α is a proportional constant, I is the light intensity, and C is the solute concentration, which ranged from 5×10^{-5} to 2×10^{-3} mol l^{-1}. Possible reaction mechanisms to explain the above relation were discussed; they include the biphotonic excitation of sensitizers, the triplet-triplet annihilation for the decay of the solute triplet, and the photolysis of the radicals produced in the photosensitization.

The lowest triplet states of some aromatic compounds have very long lifetimes at 77°K.[1,2] The subsequent absorption of another photon by the triplet molecule, therefore, often occurs, even with a conventional ultraviolet light source, and produces a higher triplet state. When the ionization potential of the solute molecule is close to the energy of the higher triplet state, the charge separation takes place. Such is the case when tetramethyl-*p*-phenylenediamine (TMPD) is photolyzed in a rigid matrix.[3,4] The formation of benzyl radicals in the 2537 Å photolysis of toluene at 77°K has also been attributed to the biphotonic process.[2] The rate of the formation of this radical is reported to be proportional to $I^{3/2}$. Here, I denotes the light intensity. When an aromatic compound is dispersed in a rigid matrix solvent, the decomposition of the solvent by the biphotonic process is frequently observed.[5] Recently, one of the present authors investigated the photosensitized decomposition of methanol at 77°K using several aromatic compounds as sensitizers and concluded that the formation of CH_2OH radicals is due to the biphotonic process described above.[6]

In this paper, methyl acetate has been used as

1) D. S. McClure, *J. Chem. Phys.*, **17**, 905 (1949).
2) B. Brocklehurst, W. A. Gibbons, F. T. Lang, G. Porter and M. I. Savadatti, *Trans. Faraday Soc.*, **62**, 1793 (1966).
3) K. D. Cadogan and A. C. Albrecht, *J. Chem. Phys.*, **43**, 2550 (1965).
4) Y. Nakato, N. Yamamoto and H. Tsubomura, This Bulletin, **40**, 2480 (1967).
5) S. Siegel and K. Eisenthal, *J. Chem. Phys.*, **42**, 2494 (1965).
6) K. Shimokoshi, Y. Mori and I. Tanaka, This Bulletin, **40**, 302 (1967).

the matrix solvent, because the methyl radicals produced in the photosensitization show a clear and comparatively stable ESR spectrum. Therefore, we expected that a detailed kinetic analysis of the biphotonic process would be feasible.

Experimental

The methyl acetate (Tokyo Kasei Co.) was distilled at 57.5°C before use. The α-naphthol, phenanthrene, and benzophenone were used as supplied by the Wako Pure Chemical Co. The naphthalene and anthracene purified by the zone-melting method were kindly supplied by Professor Hayakawa of this Institute.

About 0.4 m*l* of a methyl acetate solution containing a known amount of a sensitizer was sealed in a Spectrosil quartz tube (2.5 mm in diameter) and they immersed in liquid nitrogen in an unsilvered quartz Dewar flask. The solution in the flask was irradiated with a high-pressure mercury arc (Toshiba SHL 100 UV-2) through a combination of two quartz lenzes, a glass filter, and a calibrated wire net to control the light intensity. The glass filters used were Toshiba UV-27, Corning CS-054, and Toshiba UV-33 filters; they were used to cut off the wavelengths shorter than 2700, 3000, and 3300 Å respectively.

After the irradiation, the radicals produced were examined by means of a JEP-1 X-band ESR spectrometer with a field modulation of 100 kc/sec. The concentrations of the radicals were measured by comparing the signal heights from the solutions and a Mn marker (Mn^{2+} in MgO).

In order to ascertain the kind of products formed in photolysis, prolonged irradiation was made on a rigid solution. After warming the irradiated sample up to room temperature, the gas non-condensable at −120°C was analyzed by gaschromatography.

Results

The ESR spectrum obtained with an irradiated methyl acetate solution of naphthalene is shown in Fig. 1, along with the assignment of the peaks. With other sensitizer solutions almost the same spectra were obtained, although the relative peak heights due to the different radicals were a little changed.

Table 1 summarizes the general features of the experimental results. Pure methyl acetate gave an ESR signal only when irradiated for a long period with light and through no filter. In the presence of naphthalene, it was necessary to use wavelengths shorter than 3000 Å to obtain the ESR spectrum. The strong absorption band of naphthalene has its onset at 3000 Å. When anthracene and benzophenone were used as sensitizers, no ESR signals were obtained. When a mixture of benzophenone and naphthalene was used, an ESR spectrum similar to that in Fig. 1 was obtained even by the irradiation of the light at wavelengths longer than 3300 Å. The luminescence observed from this solution was the same as that from a naphthalene solution. These results suggest an energy transfer from triplet benzophenone to naphthalene in the rigid matrix of methyl acetate. A similar observation has already been made in the matrix of methanol.[6]

Decay of Methyl Radicals in the Rigid Matrix. During the measurement of the ESR

Table 1. Radicals produced by photosensitization

Solute	Filter	Luminescence	ESR signal	τ[2]
Solvent only		violet	CH_3, CH_3O, CHO CH_2COOCH_3 or CH_3COOCH_2	
	>2700 Å			
Naphthalene	>2700 Å	yellow green	CH_3, CH_3O, CHO CH_2COOCH_3 or CH_3COOCH_2	2.5
	>3000 Å			
α-Naphthol	>2700 Å	green	CH_3, CH_3O, CHO CH_2COOCH_3 or CH_3COOCH_2	1.9
	>3000 Å	green	CH_3, CH_3O CH_2COOCH_3 or CH_3COOCH_2	
Phenanthrene	>2700 Å	yellow green	CH_3, CH_3O, CHO CH_2COOCH_3 or CH_3COOCH_2	3.3
	>3000 Å	yellow green	CH_3, CH_3O CH_2COOCH_3 or CH_3COOCH_2	
Anthracene	>2700 Å			
Benzophenone	>2700 Å			
Naphthalene + Benzophenone	>3300 Å	yellow green	CH_3, CH_3O CH_2COOCH_3 or CH_3COOCH_2	

τ: triplet lifetime (sec).

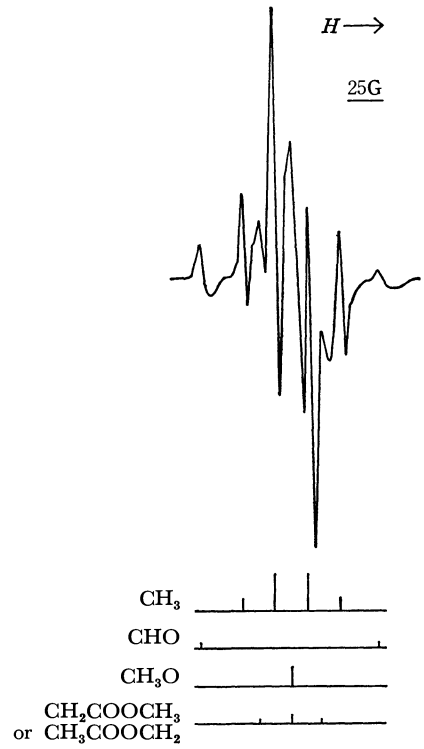

Fig. 1. ESR spectrum obtained by naphthalene photosensitized decomposition of methyl acetate (irradiated by >2700 Å at 77°K).

spectrum of the rigid matrix, the peak height due to methyl radicals gradually decreased. The rate of the decrease was dependent upon the initial peak height. The results obtained with a naphthalene solution are shown in Fig. 2. When the reciprocal of the peak height is plotted as a function of the time of measurement, a linear relationship is always obtained. This suggests that the initial decay of methyl radicals is of a second order. For the sake of simplicity, the peak heights shown in the following data are those obtained by extrapolating the linear relation to zero time, that is, the time when the irradiation was terminated.

Dependence on the Light Intensity. Using two calibrated wire nets, three light intensities were examined, one of them without a net. Figure 3 shows the irradiation-time dependence obtained with a naphthalene solution. Initially, the peak height increased linearly with the irradiation time, but on further irradiation the peak height reached a maximum and then gradually decreased. This decrease is probably due to the screening of light by decomposition products. In Fig. 4, the initial slopes obtained with three sensitizer solutions are plotted as a function of the light intensity. In every case, the rate of increase in peak height, *i.e.*, the rate of the formation of methyl radicals, was found to be proportional to $I^{1.5\pm0.1}$. Here,

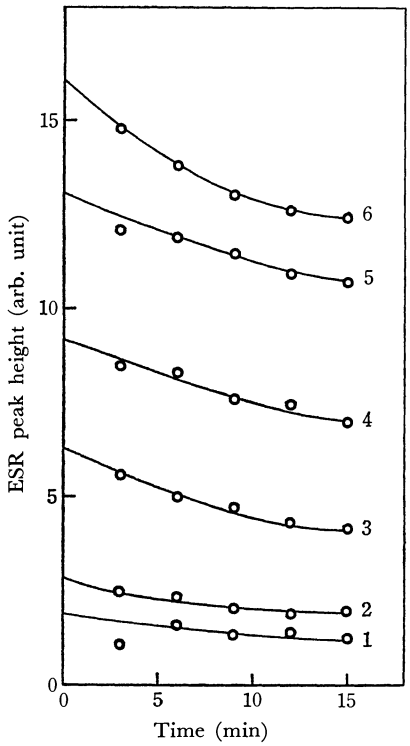

Fig. 2. Decay of methyl radicals after UV-irradiation of methyl acetate solution of naphthalene at 77°K.

1. 5×10^{-5} mol l^{-1}
2. 2×10^{-4} mol l^{-1}
3. 5×10^{-4} mol l^{-1}
4. 2×10^{-3} mol l^{-1}
5. 5×10^{-5} mol l^{-1}
6. 2×10^{-2} mol l^{-1}

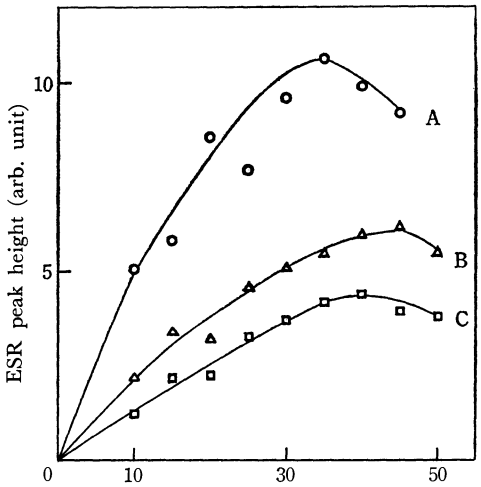

Fig. 3. ESR signal intensity of methyl radicals of naphthalene solution as a function of irradiation time.

A(○), relative light intensity= 100
B(△), relative light intensity= 60
C(□), relative light intensity= 45

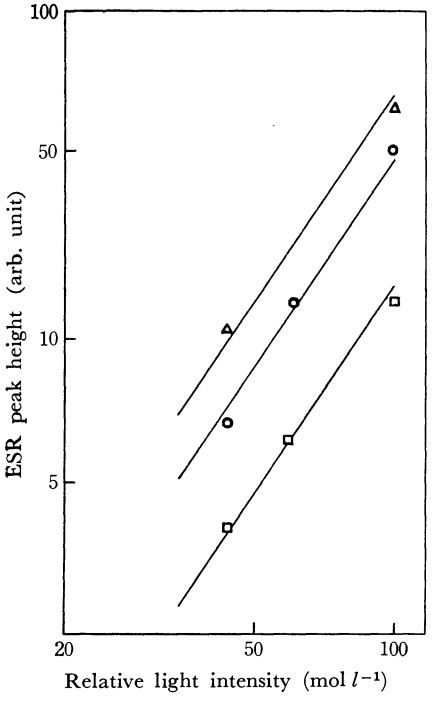

Fig. 4. ESR signal intensity of methyl radicals as a function of the light intensity. Sensitizer concentration is 2×10^{-3} mol l^{-1}. Solid curves are drawn proportionally to $I^{1.5}$.
A(○), naphthalene
B(△), α-naphthol
C(□), phenanthrene

I denotes the light intensity.

Dependence on the Concentrations of Solutes. Two series of experiments were made for each sensitizer solution. The results are shown in Fig. 5. Where the logarithm of the rate of the formation of methyl radicals is plotted as a function of the logarithm of the concentration. An approximately linear relationship was obtained over a wide range of concentrations from 5×10^{-5} to 2×10^{-3} moll^{-1} for each solution. All the slopes were nearly equal to 0.5. At concentrations higher than 10^{-2} moll^{-1}, the slope decreased with an increase in the concentration.

Reaction Products. To identify gaseous products in photolysis, a long irradiation was made on a rigid methyl-acetate solution. The products non-condensable at −120°C were analyzed by gaschromatography. The product consisted of methane and a small amount of ethane, although no quantitative measurement could be made because of their small amounts. To check whether these gases are produced during the photolysis or when the sample is warmed up for analysis, a sample kept for a long period at 77°K after irradiation, during which period most of the methyl radicals decayed, was analyzed; the amounts of methane and ethane obtained were, however, almost the same as those obtained immediately after irradiation.

Discussion

The following mechanism is usually assumed for the interpretation of the kinetics of biphotonic

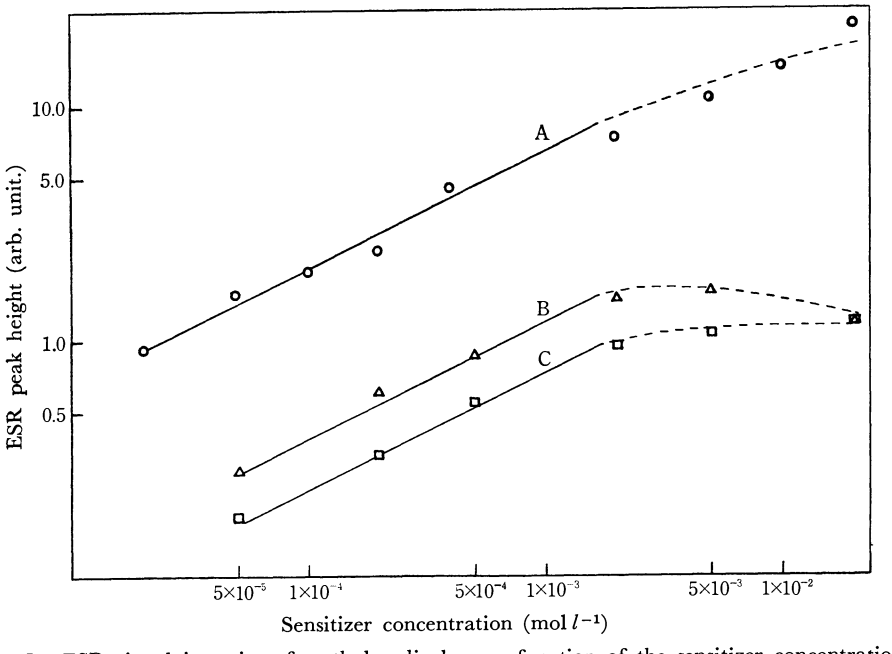

Fig. 5. ESR signal intensity of methyl radicals as a function of the sensitizer concentration.
A(○), naphthalene B(△), α-naphthol C(□), phenanthrene

processes:[2]

$S + h\nu \rightarrow S^*$ rate$=I\varepsilon_S C_S l$

$S^* \rightarrow S(+h\nu)$, $S^* \rightarrow T$ } quantum yield of $T=\phi_T$

$T \rightarrow S(+h\nu)$ rate$=(1/\tau)C_T$

$T + h\nu \rightarrow T^*$ rate$=I\varepsilon_T C_T l$

$T^* \rightarrow T$, $T^* + M \rightarrow S +$ radical } quantum yield of radical $=\phi_P$

Here, S and T represent the lowest singlet and triplet states; S^* and T^* represent the higher excited states; τ is the lifetime of the triplet state with respect to decay, $T \rightarrow S$, by phosphorescence or a radiationless process; ε_S and ε_T are the extinction coefficients; C_S and C_T are the concentrations of the ground-state and triplet molecules, and $C_S + C_T = C$ is the initial concentration. I is the light flux in the sample, and M represents the matrix solvent molecule, while l is the path of the impinging light in the matrix.

Using this mechanism, however, the experimentally-obtained relation:

$$R = \alpha I^{3/2} C^{1/2} \qquad \text{(I)}$$

cannot be easily derived. We have tried various assumptions regarding ε_S, ε_T, ϕ_T, ϕ_P and τ, but were not successful in deriving the relation (I) in the frame of the mechanism proposed above. The most stubborn difficulty was the concentration dependence.

As far as we have found in the literature, the solute concentration dependence in biphotonic processes have not been measured extensively. Brocklehurst *et al.* reported, in a study of the biphotonic photolysis of 3-methyl pentane sensitized by benzene, that the rate of the formation of radicals was not proportional to the solute concentration, but, rather increased with an increase in the concentration more slowly than the first order.[2] They tentatively attributed this to the participation of impurities.

If the triplet-triplet annihilation:

$$2T \rightarrow S^* + S \qquad \text{rate}=k_a C_T^2$$

is the most important among the decay processes of T (although this is not likely to occur in a very dilute solution such as 5×10^{-5} moll^{-1}),[7,8] the relation (I) can easily be derived as follows:

$$R = \varepsilon_T l \phi_P [\varepsilon_S l \phi_T / k_a (2-\phi_T)]^{1/2} I^{3/2} C^{1/2} \qquad \text{(II)}$$

This mechanism is very tempting, but, obviously, it needs more consideration and more extensive experiments on it before it can be adopted.

Another possible mechanism we have considered includes the participation of the produced radicals in the following manner:

$T^* + M \rightarrow S + CH_3O + CH_3CO$ (1)

$CH_3O + CH_3CO \rightarrow M$ (2)

$CH_3CO + h\nu \rightarrow CH_3^* + CO$ (3)

$CH_3^* + M \rightarrow CH_4 + CH_2COOCH_3$ or CH_3COOCH_2 (4)

$CH_3^* \rightarrow CH_3$ (5)

CH_2COOCH_3 or CH_3COOCH_2 $+ h\nu \rightarrow CH_3^* + 2CHO$ (6)

In this mechanism, a solvent molecule excited by the interaction with T^* is assumed to decompose into CH_3O and CH_3CO radicals. Moreover, the subsequent absorption of a photon by a CH_3CO radical is assumed to occur and to lead to the formation of CH_3^* and CO. Here, CH_3^* denotes an activated methyl radical; it is considered to be a precursor of methane. The absorption of a hydrogen atom by a thermal methyl radical is not probable in the matrix at the temperature of liquid nitrogen, but, as is shown in the Results section, much more methane than ethane was produced during the photolysis.

To explain the light-intensity dependence of the methyl radical formation, we did not adopt the following reactions in the above mechanism:

$T^* + M \rightarrow CH_3 + CH_3COO + S$ (7)

$CH_3COO + h\nu \rightarrow CH_3 + CO_2$ (8)

This discrimination seems to correspond to the following observations. First, as is shown in Fig. 1, the ESR spectrum we obtained has a rather large singlet at the center; this we assigned to CH_3O radicals. The formation of this radical can easily be explained by the above mechanism, but not by the mechanism consisting of the formation of methyl radicals by the reactions (7) and (8). Second, although we could not detect the formations of CO and CO_2 in photolysis because of their small amounts, the radiolysis of methyl acetate at 77°K is known to produce a large amount of CO compared with CO_2, as has been stated in a previous paper.[9] This fact seems to support the occurrence of the reaction (3) rather than the reaction (8).

Judging from the peak height of the ESR spectra of methyl radicals and the amounts of CH_4 and C_2H_6 observed, the quantum yields of these products are estimated to be very small. In other words, the reaction (2) is probably very fast in the matrix. If so, the steady-state treatment gives the following equation:

$$R = \varepsilon l I [\varepsilon_S \varepsilon_T l^2 \phi_T \phi_P \tau I^2 C / k_2 [1 + (\varepsilon_T \phi_P + \varepsilon_S \phi_T) l \tau I]]^{1/2} \qquad \text{(III)}$$

Here, ε is the extinction coefficient of the CH_3CO radical, while k_2 is the rate constant of the re-

7) T. Azumi and S. P. McGlynn, *J. Chem. Phys.*, **39**, 1186 (1963).

8) C. A. Parker, *Trans. Faraday Soc.*, **60**, 1998 (1964).

9) Y. Nakajima, S. Sato and S. Shida, This Bulletin, **42**, 2132 (1969).

action (2). Then, by assuming a tentative relation, $1 \ll (\varepsilon_T \phi_P + \varepsilon_S \phi_T) l\tau I$, we can derive an equation which has the experimentally-observed dependences of the light intensity and the solute concentration.

At higher concentrations of solutes, the rate of the formation of methyl radicals showed a tendency toward saturation. This cannot be explained by the relation (III), which has been derived on the basis of inadequate relations: the rate of light absorption by $C_S = I\varepsilon_S C_S l$ at high concentrations. If a more proper relation is used, the tendency toward saturation can easily be explained. This point has already been discussed by other investigators.[2)]

BULLETIN OF THE CHEMICAL SOCIETY OF JAPAN VOL. 43 2007—2011 (1970)

Effects of Iodine Addition on the Electrical and Optical Properties of the Semiquinoid Phenothiazine Bromide

Yoshio MATSUNAGA and Kosuke SHONO

Department of Chemistry, Faculty of Science, Hokkaido University, Sapporo

(Received January 29, 1970)

The electrical resistivity and the electronic and vibrational spectra of the semiquinoid phenothiazine bromide have been found to be drastically modified by the addition of iodine. The resistivity minimum lies around the mole ratios of 0.25 to 0.30, while the value in this composition range is from 4 to 5 ohm cm. The combined spectroscopic data indicate three different stages in the intermolecular interactions in this system; the first around a mole ratio of 0.25, the second near 0.5, and the third above 1.00. The higher the iodine content, the less conductive the adducts appear to be. Iodine addition was attempted also to the *p*-phenylenediamine bromide; however, no pronounced effect on the physical properties could be found in this system.

Earlier one of the present authors reported that the vibrational spectrum of the phenothiazine-iodine complex, which exhibits a resistivity of 20 ohm cm at room temperature, is quite different from that of the parent organic compounds, but identical with that of semiquinoid phenothiazine bromide.[1] On the basis of these observations, it was concluded that every phenothiazine molecule in the solid iodine complex bears an approximately unit-positive charge. The hypothesis that the highly-conducting iodine complexes of phenothiazine and its derivatives have essentially dative ground states seemed to receive strong support from the additional observations that the iodine adducts of semiquinoid phenothiazine chloride and bromide have resistivities of the order of 10 ohm cm. Thus far, though, no attempt has been made to determine the exact composition of such mixed halogen complexes. Now we wish to report the results of our measurements of the electrical and optical properties of the semiquinoid phenothiazine bromide-iodine system.

Experimental

Materials. Semiquinoid phenothiazine bromide was prepared by the oxidation of the parent organic compound with bromine, as has been described by Kehrmann and Diserens.[2] For example, 0.4 g of bromine, dissolved in 30 m*l* of ethyl ether, was slowly added to 1.0 g of the thiazine in 30 m*l* of the same solvent cooled with an ice-salt mixture. The greenish-black precipitate was filtered and washed with the solvent. As the bromide is not stable above 50°C, the sample was dried at room temperature over silica gel and under a vacuum.

The addition of iodine to the bromide was carried out by the careful grinding of the weighed components in the presence of a small amount of benzene. The solvent was evaporated at room temperature; then the mixture was heated to 80°C for a short time to complete the reaction and also to remove all traces of the solvent. Samples with the following mole ratios were prepared: 0.10, 0.20, 0.25, 0.30, 0.40, 0.50, 0.75. 1.00, 1.25, and 1.50.

The phenothiazine-iodine complex was precipitated by mixing 1.5 g of the thiazine in 25 m*l* of hot benzene with 3 g of iodine in 75 m*l* of the same solvent. The mole ratio of the complex is known to be 2 : 3.[1]

The *p*-phenylenediamine bromide was prepared by the oxidation of the diamine with bromine.[3] The addition of iodine to the bromide was made by the same method as has been described above.

Measurements. The electrical resistivities of the phenothiazine bromide-iodine system and the phenothiazine-iodine complex were examined on pressed pellets by a potential-probe method. The temperature de-

1) Y. Matsunaga, *Helv. Phys. Acta*, **36**, 800 (1963).
2) F. Kehrmann and L. Diserens, *Ber.*, **48**, 318 (1915).

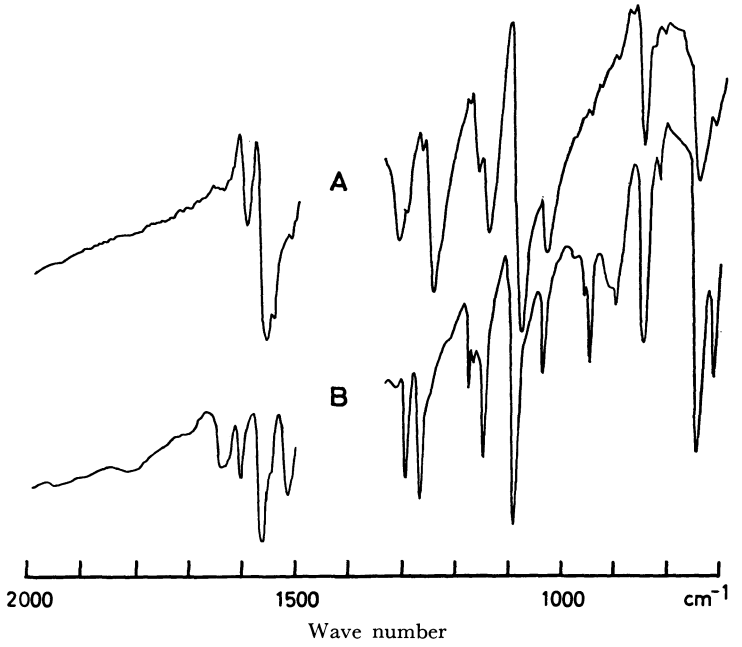

Fig. 1. Two extremes in the vibrational spectrum of semiquinoid phenothiazine bromide. The spectrum is often a superposition of these two.

pendence was measured in the range from 20 to 70°C unless otherwise stated. The resistivities observed in the *p*-phenylenediamine bromide-iodine system are in the order of 10^6 ohm cm or higher; therefore, only the values at room temperature were examined by a two-probe method employing a cell similar to that reported by LaFlamme[4] and a TOA Electronics DC microvolt ammeter, Model PM-18C.

The diffuse reflection spectra were measured with a Beckman DK-2A spectroreflectometer in the range from 4 to 30 kK. The pulverized sample was diluted with potassium bromide in concentrations of the order of 0.1 weight percent. The spectra were recorded as the difference in reflectance between the mixture and pure potassium bromide and were plotted using the Kubelka-Munk function, $f(R)=(1-R)^2/2R$, where R is the reflectance.

The vibrational spectra in the rock salt region were measured as Nujol mineral oil mulls by means of a Jasco IR-G infrared spectrophotometer. Because of the presence of an electronic absorption in this region, the reference light had to be highly attenuated in many cases in order to obtain a reasonable transmittance.

Results

Phenothiazine Bromide. We found that the vibrational spectra exhibited by the samples are often superpositions of two patterns in various ratios. The two extremes are presented in Fig. 1 as the spectra A and B. The transformation of the spectrum B to A by storage was observed on one occasion only. Although there is essentially no difference in the electronic spectrum in the region from 10 to 30 kK between the samples showing the vibrational spectra A and B, a considerable change may be noted in the region below 10 kK. As is shown in Fig. 2, the sample showing the vibrational spectrum A exhibits an electronic absorption extending into the rock salt region, but the one showing the vibrational spectrum B does not.

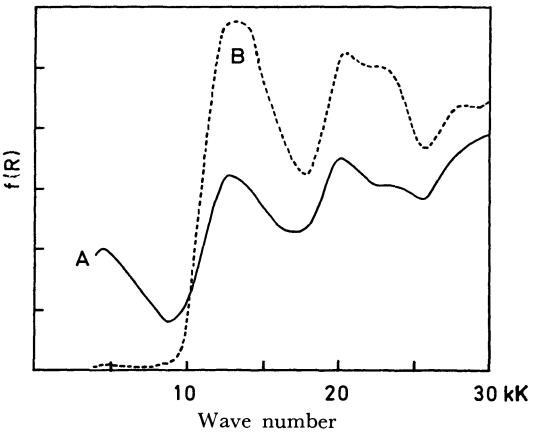

Fig. 2. Two extremes in the electronic spectrum of semiquinoid phenothiazine bromide.

The bromide samples had resistivities in the order of 10^4—10^5 ohm cm, *e.g.*, a resistivity of 1.5×10^5 ohm cm at 20°C, and an activation energy of 0.30 eV defined by $\rho=\rho_0\exp(E/kT)$ in the temperature range from 4 to 35°C was obtained by one of the

3) L. Michaelis and S. Granick, *J. Amer. Chem. Soc.*, **65**, 1747 (1943).

4) P. M. LaFlamme, *Rev. Sci. Instr.*, **35**, 1193 (1964).

preparations. Above 50°C, a rapid irreversible decrease in the resistivity was observed. The vibrational spectrum of such a heat-treated sample was found to be different from either the spectrum A or B.

Phenothiazine Bromide-iodine System. The electrical resistivity value at 20°C is plotted against the mole ratio (iodine/bromide) in Fig. 3. A deep minimum is located around mole ratios from 0.25 to 0.30, the value in this composition range being from 4 to 5 ohm cm. When the mole ratio is below these values, the vibrational spectrum of the iodine adduct consists of very broad lines as is represented by the spectrum a in Fig. 4, measured at a mole ratio of 0.25. Nevertheless, it may be noted that the whole pattern is rather close to the spectrum A of the bromide. The electronic spectrum bears also some resemblance to that of the bromide, especially the one showing the vibrational spectrum A. However, the low-energy absorption is shifted further into the rock salt region and its maximum is located below 4 kK. In addition, an extra absorption appears at about 9 kK as a shoulder. The absorption in the region above 20 kK becomes high and almost flat, as is shown in Fig. 5. The activation energies for semiconduction in the four samples in this composition range were found to be 0.10 ± 0.01 eV.

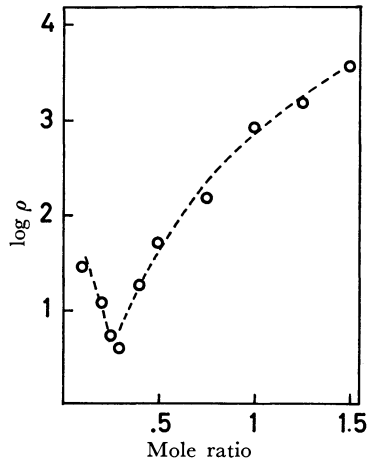

Fig. 3. Electrical resistivity plotted against the mole ratio (iodine/bromide) in the phenothiazine bromide-iodine system.

As the iodine content rises above 0.30, the resistivity increases monotonously. At a mole ratio of 0.40, a new electronic absorption is observed at 5.5 kK in addition to the one found in the low-energy region of the spectrum a in Fig. 5. By the further addition of iodine, the absorption having a maximum in the region below 4 kK is completely replaced by the one at 5.5 kK. The spectrum b in Fig. 5, recorded at a mole ratio of 0.50, represents such a stage. At this composition the resistivity at room temperature is about 50 ohm cm and the activation energy is 0.20 eV. It must be pointed out that the absorption lines in the vibrational spectrum b in Fig. 4 are a little bit sharper

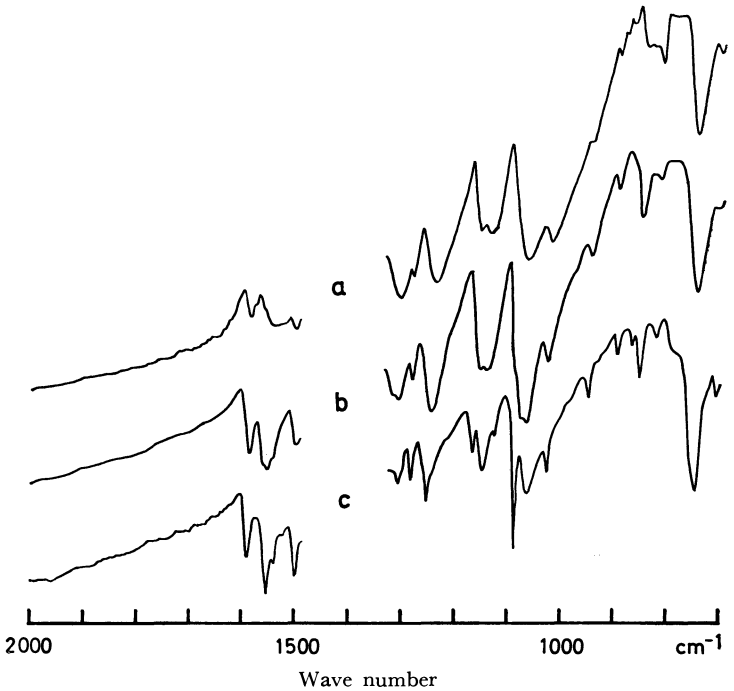

Fig. 4. Vibrational spectra in the phenothiazine bromide-iodine system; a) mole ratio 0.25, b) 0.50, c) 1.00.

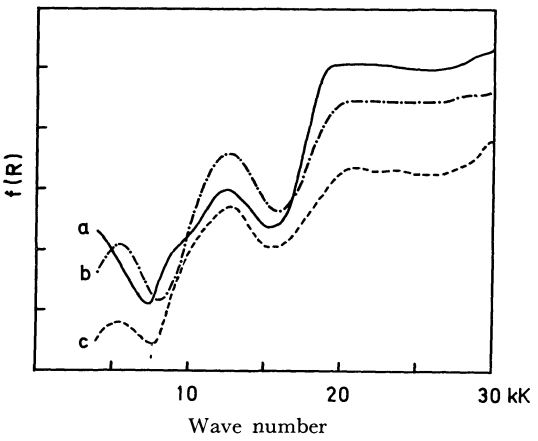

Fig. 5. Electronic spectra in the phenothiazine bromide-iodine system;
a) mole ratio 0.25, b) 0.50, c) 1.00.

than those in the spectrum a.

Then, at a mole ratio of 1.00 the intensity of the electronic absorption at 5.5 kK is markedly diminished. Moreover, the vibrational spectrum is characterized by a superposition of a pattern consisting of lines as sharp as those in the spectrum B of the bromide. The resistivity is about 8.4×10^2 ohm cm at this composition. If more iodine is added, the electronic absorption in the low-energy region disappears completely and the intensities of the sharp vibrational absorption lines belonging to the newly-appeared pattern are much enhanced. At the maximum iodine content of 1.50 the electrical resistivity is almost one thousand times as high as the minimum value.

The iodine adducts exhibiting low electrical resistivities are more stable than the semiquinoid bromide. Neither a change in the vibrational spectrum nor the vaporization of the iodine is observed by heating to 80°C. However, the coloration of polyethylene stoppers by iodine after a short storage of the samples in vials can be noticed even at room temperature if the mole ratios are higher than 0.75.

Phenothiazine-iodine Complex. An electrical resistivity of 13 ohm cm and an activation energy of 0.19 eV were obtained in the present work. These values are in good agreement with those found earlier by one of the present authors,[1] however, our resistivity is approximately two orders of magnitude lower than that reported by Gutmann and Keyzer.[5] In Fig. 6 the vibrational spectrum is compared with the spectrum of the parent organic compound. They are much better resolved than those cited in an earlier paper and are still in accordance with our previous argument.

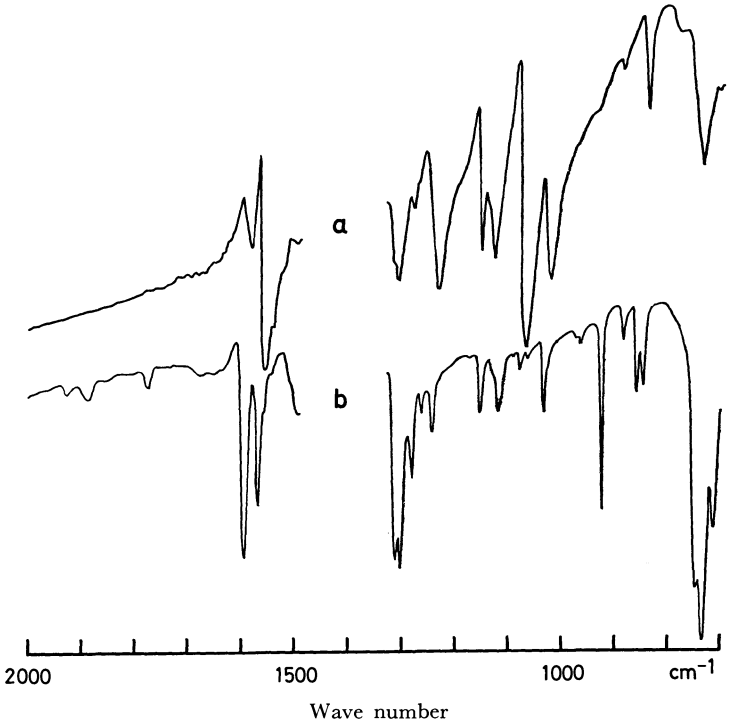

Fig. 6. Vibrational spectra of the phenothiazine-iodine complex (a) and phenothiazine itself (b).

5) F. Gutmann and H. Keyzer, *J. Chem. Phys.*, **46**, 1969 (1967).

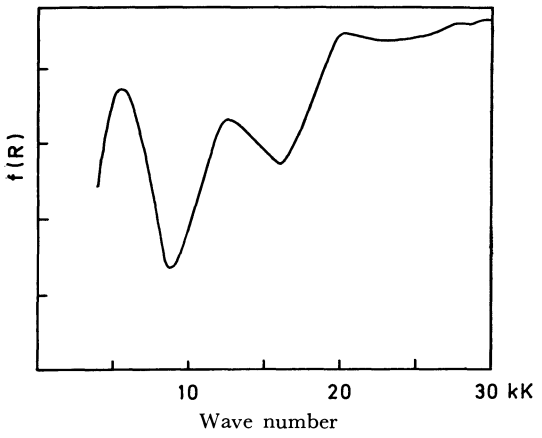

Fig. 7. Electronic spectrum of the phenothiazine-iodine complex.

It is easy to see that the spectrum of the iodine complex is quite similar to the spectrum A of the bromide, but very different from the spectrum of phenothiazine itself. The electronic spectrum was also examined. As is shown in Fig. 7, the maximum of low-energy absorption is located at 5.5 kK.

***p*-Phenylenediamine Bromide-iodine System.** The bromide has a resistivity of 5×10^7 ohm cm at room temperature. The compound becomes ten times more conductive by the addition of 0.25 to 0.75 mol of iodine. The further addition results in an increase in the resistivity again to the order of 10^7 ohm cm. Thus, this system was found to be less conductive than the iodine complex, for which Nishizaki and Kusakawa reported the minimum resistivity of 1.7×10^5 ohm cm at a mole ratio of 0.82.[6] No significant change could be observed in the electronic and vibrational spectra.

Discussion

The molecule of phenothiazine is known to have a folded configuration.[7] The large difference in the vibrational spectrum between phenothiazine and its semiquinoid bromide should be attributed to the change in the electronic and geometrical structures caused by the loss of one electron. Although the cation radical has often been assumed to be planar,[8] Pullman favored a bent form to the planar one because of its better agreement with the ESR data.[9] The barrier to the flattening the molecule is probably of about the same energy as that of a rather strong intermolecular interaction;[10] it is likely that the balance of these two forces is achieved at two different configurations, depending upon the mode of intermolecular interaction. By analogy with the electronic spectra of Würster cations,[11,12] we may assume that the cation radicals in the bromide sample showing the electronic spectrum A in Fig. 2 are in an interaction more extended than those in the sample showing the spectrum B.

In the phenothiazine bromide-iodine system the three different stages in the intermolecular interactions can be pointed out on the basis of the electrical and optical data. The first stage is represented by the adduct at mole ratios from 0.25 to 0.30. As the composition corresponds approximately to $(\text{phenothiazine})_2Br_2I$, and as the mixed halide ion, Br_2I^-, is a known species, we may suggest the formation of a complex cation radical salt, $(\text{phenothiazine})^+(\text{phenothiazine})^0Br_2I^-$, which is a cationic analogue of the TCNQ complex anion radical salts, well known for their low electrical resistivities.[13] The composition range from 0.50 to 0.75 may be considered to be the second stage, which is characterized by an electronic absorption having a maximum at 5.5 kK. This location is the same as that of the low-energy absorption appearing in the iodine complex; however, these adducts are less conductive than the complex. The shift of the low-energy absorption by the transition from the first to the second stage is parallel with an increase in the activation energy for semiconduction. It should be noted that the vibrational spectra of the iodine adducts in these two stages and also that of the iodine complex resemble the spectrum A of the semiquinoid bromide. In these adducts and the complex the intermolecular interaction is supposed to be more-than-by-pairs; otherwise, we would not observe such low electrical resistivities. These observations are in good accordance with the assumption made at the end of the last paragraph. The third stage appears in the composition range above 1.00. Not only the vibrational but also the electronic spectra are similar to the spectra B of the bromide. The high resistivities observed in this stage are consistent with such optical behavior.

The absence of a low-resistivity phase in the *p*-phenylenediamine bromide-iodine system indicates that the formation of a mixed halide complex such as the one found in the present work may be rather specific.

6) S. Nishizaki and H. Kusakawa, This Bulletin, **36**, 1681 (1963).
7) J. D. Bell, J. F. Blount, O. V. Briscoe and H. C. Freeman, *Chem. Commun.*, **1968**, 1656.
8) J. M. Lhoste and F. Tonnard, *J. Chim. Phys.*, **63**, 678 (1966).
9) J. P. Malrieu and B. Pullman, *Theoret. Chim. Acta*, **2**, 293 (1964).
10) C. J. Fritchie, Jr., *J. Chem. Soc.*, *A*, **1969**, 1328.
11) Y. Iida and Y. Matsunaga, This Bulletin, **41**, 2615 (1968).
12) A. Hakusui, Y. Matsunaga and K. Umehara, *ibid.*, **43**, 709 (1970).
13) L. R. Melby, R. J. Harder, W. R. Hertler, W. Mahler, R. E. Benson and W. E. Mochel, *J. Amer. Chem. Soc.*, **84**, 3374 (1962).

BULLETIN OF THE CHEMICAL SOCIETY OF JAPAN VOL. 43 2012—2017 (1970)

Variational Calculation of Atoms and Molecules by a Modified Hassé Method Using Hulthén Functions. I. Hydrogen and Helium Atoms

Tokio YAMABE, Shingo ISHIMARU and Kenichi FUKUI

Department of Hydrocarbon Chemistry, Kyoto University, Sakyo-ku, Kyoto

(Received February 12, 1970)

A modification of the Hassé method is presented in an attempt to describe perturbed systems. This method resolves divergence difficulties which are often encountered when the simple Kirkwood-Hassé method or Unsöld approximation is used for the coulombic perturbation problems. The procedure is illustrated for the perturbed hydrogen atom; energy values which are close to the exact ones are thus obtained. The method is also applied to the case of the ground-state helium atom; a closed-form expression of the energy is thus derived. The optimized value is −2.8983 a. u. Some other discussions are given in connection with the perturbation theory.

In the perturbation problems of atoms and molecules, the Unsöld approximation[1] is often employed to calculate the second-order perturbation energy; it is known to be equivalent to the so-called average-energy method,[2] where the operator $(H_0 - E_0)$ in the first-order perturbation equation is replaced by an average energy, ε. The approximate first-order wave function, ϕ_1, then becomes:

$$\phi_1 = -\varepsilon^{-1}(H_1 - E_1)\phi_0, \tag{1a}$$

where ϕ_0 is the unperturbed eigenfunction and where H_1 and E_1 are the perturbation and the first-order perturbation energy respectively. This wave function is also employed for the first-order wave function in the variation-perturbation method (VP method). In this case, ε^{-1} is regarded as a scale parameter; Eq. (1a) is, then, usually rewritten in the following form:

$$\phi_1 = A(H_1 - E_1)\phi_0, \tag{1b}$$

where A is a constant. In the variation method, the simple Kirkwood-Hassé form[3] is often used for the perturbative part, χ, of a trial function, $\phi = \phi_0 + \chi$:

$$\chi = AH_1\phi_0, \tag{1c}$$

which is not generally orthogonal to ϕ_0. The orthogonalized form corresponds to Eq. (1b).

It has been pointed out by several authors[2,4], however, that these approximations often lead to physically unacceptable wave-functions and, accordingly, unreasonable results for the perturbation energies. For example, consider an atomic hydrogen perturbed by the removal of a small amount (ΔZ) of the nuclear charge. In this case, $H_1 = \Delta Z/r$, where r is the distance from the nucleus to the electron. In accordance with the approximation (Eq. (1a)), ϕ_1 is singular at $r=0$; hence, the second- or the third-order perturbation energy will be infinite. Such a result can be essentially attributed to the divergency of the integrals, $\langle\phi_0|r^{-3}|\phi_0\rangle$ and $\langle\phi_0|r^{-4}|\phi_0\rangle$, involved in the energy calculations. Many other examples were given by Kirtman and Benston.[2] They applied the average-energy method to some of these examples and showed that such difficulties could be successfully avoided by making the average-energy infinite only in the neighborhood of singularity and finite elsewhere (the eae method). This method is, however, difficult to use for multidimensional problems, in particular, molecular problems.

The purpose of the present paper is to show that difficulties of divergence can be removed, easily and elegantly, not by the variation of the average energy, but by a slight modification of H_1 in Eq. (1c). In this work, we will use the variation method for energy calculations; this approximation may correspond to an extension of the simple Kirkwood-Hassé form. It will be demonstrated in the first section of this paper that the energy obtained is, besides being an upper bound, in agreement with the results of the extension of the perturbation theory to the third order. The present method is illustrated by this example and then applied to the calculation of the ground-state energy of the helium atom.

1) A. Unsöld, *Z. Phys.* **43**, 563 (1927).
2) B. Kirtman and M. L. Benston, *J. Chem. Phys.*, **46**, 472 (1967).
3) J. C. Slater and J. G. Kirkwood, *Phys. Rev.*, **37**, 686 (1931); H. R. Hassé, *Proc. Cambridge Phil. Soc.*, **27**, 66 (1931).
4) J. O. Hirschfelder, W. B. Brown and S. T. Epstein, *Advan. Quantum Chem.*, **1**, 280 (1964).

The Variation Method

Assume that a system with a Hamiltonian operator, H_0, is given, and that the function, ϕ_0, describing its state and its energy, E_0, in the state are known; then:

$$H_0\phi_0 = E_0\phi_0. \tag{2}$$

When a perturbation is applied to H_0, changing it to H_0+H_1, the energy, E, of this perturbed system, H, is optimized by the variational principle:

$$\langle H\rangle = N^2\int \phi^* H\phi \mathrm{d}\tau \geqq E, \tag{3}$$

where ϕ is an arbitrary trial function and where;

$$N = \left[\int \phi^*\phi \mathrm{d}\tau\right]^{-1/2}.$$

In Hassé's method, one may take the following type of function:

$$\phi = \phi_0(1 + v), \tag{4}$$

where v is a function to be specified later. As a consequence, Eq. (3) can be rewritten[5] in atomic units:

$$\langle H\rangle = E_0 + N^2\left\{((1 + v)^2H_1)_{00} + \frac{1}{2}\sum_i((\partial v/\partial x_i)^2)_{00}\right\}, \tag{5}$$

where $(F)_{00}$ signifies $\langle\phi_0|F|\phi_0\rangle$; that is, the matrix elements calculated with the ϕ_0 function, and where the summation extends over all the Cartesian coordinates of the problem.

Now we need a concrete form of v to calculate the energy of the perturbed system. The simplest and useful form of v is the one proportional to H_1, namely, the simple Kirkwood-Hassé form, Eq. (1c):

$$v = AH_1. \tag{6}$$

As has been pointed out in the introduction,[2,4] however, when one uses this approximation one encounters serious defects in many cases, particularly in the important case of the coulombic-type perturbation problem which we will discuss in this paper. In other words, these defects can be ascribed to the fact that the integrals in Eq. (5) diverge because of the singularities at $r=0$ (except, of course, if ϕ_0 vanishes at the nuclei). To remove the difficulties, we replaced the coulomb potential in v by the following function, $\tilde{H}_1$:

$$v = A\tilde{H}_1 = A\{\Delta Z\sum_a\sum_i(1 - e^{-\kappa_i R_{ai}})R_{ai}^{-1} + \frac{1}{2}\sum_i\sum_{(i\neq j)}(1 - e^{-\lambda_{ij}r_{ij}})r_{ij}^{-1}\}, \tag{7}$$

where:

ΔZ	:	the decrease in the nuclear charge,
a	:	the number of a nucleus,
i, j	:	the number of an electron,
κ_i, λ_{ij}	:	variational parameters,
R_{ai}, r_{ij}	:	the distances between a nucleus, a, and an electron, i, and between the i and j electrons respectively.

The function $\tilde{H}_1$ is the one known as the Hulthén function.[6] When κ and λ are positive, this function behaves like the original coulomb potential at larger distances, but it is finite as r approaches zero. In this case, the main factor underlying the correctness of Eq. (7) is that the v function is finite at $r=0$, which causes even $\langle\phi|r^{-4}|\phi\rangle$ to become finite. This is the essential point of the present method for solving this divergence problem.

The perturbed wave function that we have presented may not be considerably different from the one using the Unsöld approximation or, more generally, the Dirichlet form in the VP method. In order to investigate the relation between our method and the VP method, we will write Eq. (5) with the present $v=A\tilde{H}_1$. The perturbed wave function, ϕ, is, then obtained from Eq. (4) as:

$$\phi = \phi_0(1 + A\tilde{H}_1). \tag{8}$$

Hence, from Eq. (5):

$$\langle H\rangle = E_0 + E_1 + \frac{2A\{(H_1\tilde{H}_1)_{00} - E_1(\tilde{H}_1)_{00}\} + A^2\left\{\frac{1}{2}\sum_i((\partial\tilde{H}_1/\partial x_i)^2)_{00} + (\tilde{H}_1H_1\tilde{H}_1)_{00} - E_1(\tilde{H}_1^2)_{00}\right\}}{1 + 2A(\tilde{H}_1)_{00} + A^2(\tilde{H}_1^2)_{00}} \geqq E, \tag{9}$$

where $E_1=(H_1)_{00}$. On the other hand, following the VP theory,

$$\tilde{E}_2 = \langle\tilde{\phi}_1|H_0 - E_0|\tilde{\phi}_1\rangle + 2\langle\tilde{\phi}_1|H_1 - E_1|\phi_0\rangle \geqq E_2, \tag{10}$$

where E_2 is the second-order perturbation energy and where $\tilde{\phi}_1$ is an arbitrary function; the equality in Eq. (10) holds only when the variation function, $\tilde{\phi}_1$, is the true first-order wave function. Regarding $A\tilde{H}_1\phi_0$ as $\tilde{\phi}_1$, the approximate second and third-order energies are, respectively:

$$\tilde{E}_2 = 2A\{(H_1\tilde{H}_1)_{00} - E_1(\tilde{H}_1)_{00}\} + \frac{1}{2}A^2\sum_i((\partial\tilde{H}_1/\partial x_i)^2)_{00} \geqq E_2, \tag{11}$$

5) H. Margenau, *Rev. Mod. Phys.*, **11**, 1 (1939).

6) L. Hulthén, *Arkiv Fys.*, **28A**, 5 (1942).

$$\tilde{E}_3 = -2A\tilde{E}_2(\tilde{H}_1)_{00} + A^2\{\tilde{H}_1H_1\tilde{H}_1)_{00} - E_1(\tilde{H}_1^2)_{00}\}. \tag{12}$$[7]

Then, one obtains from Eq. (9):

$$\langle H\rangle = E_0 + E_1 + \tilde{E}_2 + \tilde{E}_3 + E_R \geqq E, \tag{13}$$

where:

$$E_R = -\frac{\{2A(\tilde{H}_1)_{00} + A^2(\tilde{H}_1^2)_{00}\}\tilde{E}_3 + A^2(\tilde{H}_1^2)_{00}\tilde{E}_2}{1 + 2A(\tilde{H}_1)_{00} + A^2(\tilde{H}_1^2)_{00}} = O(H_1^4). \tag{14}$$

The above results show that the present method is in agreement with the perturbation theory to the third order. More general investigations have been presented by Sinanoğlu.[8]

Finally, it is necessary to consider the effect of the orthogonalization. Corresponding to Eq. (1b) the orthogonalized form is given by:

$$\tilde{\psi} = \psi_0 + \tilde{\chi} \quad \text{and} \quad \tilde{\chi} = A(\tilde{H}_1 - (\tilde{H}_1)_{00})\psi_0,$$

which leads to a slight correction of the energy, $\Delta E_{\text{corr.}}$:

$$\Delta E_{\text{corr.}} = \bar{E} - \tilde{E} = \frac{-2A(H_1)_{00}\{\bar{E} - E_0 - E_1 - A(E_0\tilde{H}_1)_{00} + (H_1\tilde{H}_1)_{00})\} - A^2(\tilde{H}_1)_{00}^2(\bar{E} + E_0 + E_1)}{N^{-2} - 2A(\tilde{H}_1)_{00} - A^2(\tilde{H}_1)_{00}^2}, \tag{15}$$

where:

$$\bar{E} = \frac{\langle\psi|H|\psi\rangle}{\langle\psi|\psi\rangle}, \quad \tilde{E} = \frac{\langle\tilde{\psi}|H|\tilde{\psi}\rangle}{\langle\tilde{\psi}|\tilde{\psi}\rangle}.$$

The dependency of $\Delta E_{\text{corr.}}$ upon the arguments, κ, λ, A, and Z, is not simple. This will be given numerically in the case of the helium atom.

Applications to Hydrogen and Helium Atoms

In the first place, we would like to choose the case of a hydrogen atom merely for the purpose of illustrating our method. Consider the hydrogen atom perturbed by the removal of the ΔZ charge from the nucleus. Then, in atomic units,

$$H_0 = -\frac{1}{2}\Delta - r^{-1}, \quad H_1 = \Delta Z r^{-1}$$

$$\psi_0 = \pi^{-1/2}e^{-r}, \quad v = A(1 - e^{-\kappa r})r^{-1}. \tag{16a}$$

Hence,

$$\psi = \psi_0\{1 + A(1 - e^{-\kappa r})r^{-1}\} \tag{16b}$$

results from Eq. (4),
where, for convenience, ΔZ has been absorbed in A.

Now we are ready to obtain $\langle H\rangle$ by substituting Eqs. (16a) and (16b) into Eq. (5). In this calculation, however, there appear several well-known integrals which diverge, namely, in general forms.

$$\int_0^\infty \frac{e^{-sr}}{r}dr = -\lim_{\varepsilon\to 0} Ei(-s\varepsilon) \tag{17}$$

and:

$$\int_0^\infty \frac{e^{-tr}}{r^2}dr = \lim_{\varepsilon\to 0}\left[\frac{1}{\varepsilon} - t + tEi(-t\varepsilon)\right]. \tag{18}$$

Fortunately, however, these integrals cancel each other out in $(\tilde{H}_1H_1\tilde{H}_1)_{00}$ and $\sum_i((\partial\tilde{H}_1/\partial x_i)^2)_{00}$ respectively when our modification is used. Thus, one gets the perturbed energy in the following closed form:

$$\Delta E = \frac{2A\Delta Z(1 - 2\alpha)^2 + A^2\{4(1 - \Delta Z)\log(4\alpha^2/\beta) + \kappa^2\beta(1 - 2\alpha\Delta Z)\}}{1 + 2A(1 - 4\alpha^2) + 2A^2\kappa^2\alpha\beta}, \tag{19}$$

where:

$$\Delta E = \langle H\rangle - E_0 - E_1,$$
$$\alpha = (2 + \kappa)^{-1}, \quad \beta = (1 + \kappa)^{-1}.$$

7) H. A. Bethe and E. E. Salpeter, "Encyclopedia of Physics, Vol. 35", ed. by S. Flügge Springer-Verlag, Berlin (1957).

8) O. Sinanoğlu, *J. Chem. Phys.*, **34**, 1237 (1961).

Determining the optimum values of κ and A variationally, one obtains the minimum energy for a given ΔZ. The results listed in Table 1 are almost equal to the correct value ($\Delta E/(\Delta Z)^2=-0.5000$).

Table 1. The energy $\Delta E/(\Delta Z)^2$ for various perturbation ΔZ

ΔZ	κ	A	$\Delta E/(\Delta Z)^2$
0.0	0.000	∞	−0.5000
0.1	−0.146	25.20	−0.4999
0.2	−0.285	11.93	−0.4999
0.3	−0.415	7.39	−0.4999
0.4	−0.537	5.12	−0.4998
0.5	−0.650	3.74	−0.4997
0.6	−0.753	2.81	−0.4993
0.7	−0.843	2.13	−0.4987
0.8	−0.918	1.63	−0.4981
0.9	−0.977	1.26	−0.4982
1.0	−1.000	1.00	−0.5000

In the calculations, the value of A giving the minimum of the energy for a given κ is, of course, determined by a simple quadrature satisfying $\partial\Delta E/\partial A=0$. Figure 1 shows the relationships between the energy and κ. For large positive values of κ, where the present treatment approaches the average-energy method, the energy converges to zero, as has often been pointed out.[2] It should be noticed here that the κ giving the lowest energy is always negative in the present case. The negative κ value is not unexpected, considering that the function of Eq. (16b) is a kind of trial function. In this connection, it seems adequate to regard the present method, not as a modification of the simple Kirkwood-Hassé or Unsöld procedure, but as a method using the wave-function in which the effect of the mixing of the Os function is taken into account.[9] This can easily be understood by rewriting Eq. (16b) so that:

$$\psi = \pi^{-1/2}e^{-r} + A\pi^{-1/2}\{e^{-r} - e^{-(1+\kappa)r}\}r^{-1}. \quad (20)$$

The inclusion of the Os function into ψ seems not to be strange, considering the discussion presented by Robinson.[10] A parallelism is found between κ and ΔZ. This result is reasonable in view of Eq. (20).

Kirtman and Benston showed that, by their eae method, the difficulty of the divergency can also be avoided. They gave the exact first-order wave function for the same problem. Their way around this difficulty is to let the average energy be infinite in the neighborhood of the singularity, while the present method is to let H_1 in χ be finite; it also gives almost the exact energy, though the wave function is of a variational type.

Secondly, let us apply the present method to the ground state of the helium atom. Let the perturbed Hamiltonian, H, be split as H_0+H_1:

$$H_0 = -\frac{1}{2}(\Delta_1 + \Delta_2) - Z(r_1^{-1} + r_2^{-1})$$
$$H_1 = -\Delta Z(r_1^{-1} + r_2^{-1}) + r_{12}^{-1},$$
$$\psi_0 = \pi^{-1}Z^3e^{-Z(r_1+r_2)}, \quad (21a)$$

where: $Z + \Delta Z = 2$.

According to the present method, the perturbed wave function, ψ, is given from Eq. (4) by:

$$\psi = \psi_0(1 + A[-\Delta Z\{(1-e^{-\kappa r_1})r_1^{-1} + (1-e^{-\kappa r_2})r_2^{-1}\} + (1-e^{-\lambda r_{12}})r_{12}^{-1}]) \quad (21b)$$

for the four parameters κ, λ, A, and Z. From Eqs. (5), (21a), and (21b), one easily obtains the energy expression in a closed form (shown in the Appendix). Our result is given in Table 2, along with those calculated by other researchers. Sur-

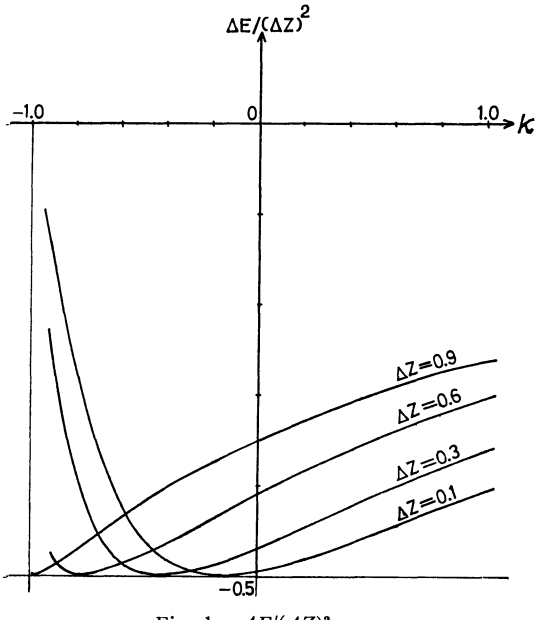

Fig. 1. $\Delta E/(\Delta Z)^2$ *vs.* κ.

Table 2. The energy of He atom (in a. u.)

Method	Energy
Experimental[a)]	−2.9033
Hartree-Fock[b)]	−2.8617
Parr and Weare[c)]	−2.8911
Snyder[d)]	−2.8979
Present result[e)]	−2.8983
Weare, Weber, and Parr[f)]	−2.9002
Pekeris[g)]	−2.9037

a) From Ref. 12. b) From Ref. 13. c) From Ref. 14. d) From Ref. 15. e) Here, $\kappa=0.891$, $\lambda=0.591$, $A=-1.1324$ and $Z=1.6108$, respectively. f) From Ref. 11. g) From Ref. 16.

9) R. McWeeny and C. A. Coulson, *Proc. Phys. Soc.* (London), *A*, **62**, 509 (1949); R. McWeeny *ibid.*, *A* **62**, 519 (1949); J. T. Zung and R. G. Parr, *J. Chem. Phys.*, **41**, 2888 (1964).

10) P. D. Robinson, *ibid.*, **45**, 1858 (1966).

prisingly, in view of the result obtained, Eq. (21b) is a very good approximation of the perturbed wave function in spite of its simple form. Orthogonalization leads no better result, *i.e.*, $\Delta E_{\text{corr.}} = -0.0006$ in the present case.

Kirtman and Benston also obtained an approximate first-order wavefunction by their eae method and computed the energies to the third order numerically. They indeed avoided the difficulties of divergency, but one will scarcely be able to find a physical meaning in the form of their wave-function. Moreover, the energy obtained is not satisfactory, namely, $E_2^{\text{eae}} = -0.135$ a.u. ($\geqq E_2$) and $E_3^{\text{eae}} = 0.01194$ a.u.*1

Recently, Weare *et al.*[11] showed that, in correlated trial wave-functions of the $\psi = \phi(r_1)\phi(r_2)(1+v(r_{12}))$ form for helium-like atoms, the Os function, when used for ϕ and/or v, gave excellent results. As one of several expected Os trial wavefunctions, they proposed $\psi = 1s_\zeta(r_1)1s_\zeta(r_2)[1+A\,Os_{\gamma\delta}(r_{12})]$, which partly resembles the present function (Eq. (21b)) in its apparent form. It should be stressed, however, that our treatment has quite a different basis than theirs, which is due to the correlated Hartree-Fock orbital approximation. In fact, our method is easily connected to the perturbation method, as has already been discussed. From Eqs. (11) and (12), we can estimate the respective energy terms from E_0 to E_R for the best variational result. As is shown in Table 3, these terms descend monotonously, disclosing the relation of the present method to the perturbational treatment. Additionally, it is worth emphasizing that the present method gives a closed form for the energy expression, whereas Weare *et al.* were unable to obtain such an expression.[11] The extension to isoelectronic atoms is trivial; further applications of this method, in particular, to the important problems of the long-range force between atoms will be presented elsewhere.

TABLE 3. THE VALUES OF RESPECTIVE ENERGY TERMS

The energy term	The value (in a.u.)
E_0	−2.59468
E_1	−0.24710
E_2	−0.06270
E_3	+0.00626
E_R	−0.00008

*1 The total energy calculated to the third order is −2.879.

Appendix

The integrals used in calculating the energy for the helium atom from Eq. (5) are as follows;

$$(H_1)_{00} = Z\left(\frac{5}{8} - 2\Delta Z\right),$$

$$(\tilde{H}_1)_{00} = Z\left[\left(\frac{5}{8} - 2\Delta Z\right) + 8\Delta Z b^2 + \frac{1}{2}df - 4df^4(\lambda+6)\right],$$

$$(\tilde{H}_1^2)_{00} = Z^2\left[\frac{2}{3} - 8\left\{\frac{1}{16}d - \frac{1}{4}df + \frac{3}{16}f + \frac{1}{4}f^2 + \frac{1}{3}f^3\right\} + \frac{1}{2}e\left\{\frac{1}{2} + \frac{1}{2}e + \frac{1}{3}e^2\right\} - 4\Delta Z\left\{\frac{3}{4} - 4b^2(1-4c^2) + df(1-16c^2) + 16d^2f^2(1-4c-4f+4g)\right\} + 2(\Delta Z)^2\{3+2a-8b-8b^2+16b^4\}\right],$$

$$(H_1\tilde{H}_1)_{00} = Z^2\left[\frac{2}{3} - 4\left\{\frac{1}{16}d - \frac{1}{4}df + \frac{3}{16}f + \frac{1}{4}f^2 + \frac{1}{3}f^3\right\} - 4\Delta Z\left\{\frac{3}{4} - 2b^2(1-4c^2) + df(1-16f^2)\right\} + 2(\Delta Z)^2\{1+2\kappa b-4b^2\}\right],$$

$$(\tilde{H}_1 H_1 \tilde{H}_1)_{00} = Z^3\left[\frac{1}{6}\lambda^2(12+15\lambda+4\lambda^2)e^2f^2 + \frac{1}{2}\log(e/4f^2) - 4\Delta Z\left\{1-d-2(1+f)f - 4(bc-cd+cf-df-cg+dg-fg) + \frac{1}{4}\lambda^2(8+9\lambda+2\lambda^2)e^2f^2 - \frac{4}{\kappa}(b-g) + 2\left(\frac{2}{\kappa^2} - \frac{1}{\kappa} + c + 2c^2\right)\log(g/2bf)\right\} + 4(\Delta Z)^2\{1-b+4c-16bc+4b^3-4f^2 + 16cfg + 2\log(2ac^2/b^3) + \kappa\lambda^2 cdf - 4\log 2b - 4\lambda^2(8-\lambda^2)d^2f^2\log 4c - 64d^2f^2\log(f/g)\} - 4(\Delta Z)^3\{3+a-8b-8b^2+16b^3 + 2\log(a/4b^2)\}\right],$$

$$\left(\sum_i\left(\frac{\partial\tilde{H}_1}{\partial x_i}\right)^2\right)_{00} = Z^4\left[\frac{1}{6}\lambda^4(3+\lambda)(4+3\lambda)e^3f^2 + 16\Delta Z\left\{\kappa^2(6+\kappa)c^2df - 16\kappa\lambda d^2f^2g + \frac{1}{2}\kappa\lambda^2(20-\lambda^2)cd^2f^2 - 2\log 2b + 2(1+\lambda^2(8-\lambda^2)d^2f^2 - (64+16\lambda^2 - 12\lambda^4+\lambda^6)d^3f^3)\log 4c\right.\right.$$

11) J. H. Weare, T. A. Weber, and R. G. Parr, *J. Chem. Phys.*, **50**, 4393 (1969).
12) G. Herzberg, *Proc. Roy. Soc.* (London), **A 248**, 309 (1958).
13) C. C. J. Roothaan, L. M. Sachs and A. W. Weiss, *Rev. Mod. Phys.*, **32**, 186 (1960).
14) R. G. Parr and J. H. Weare, *Progr. Theoret. Phys.* (Kyoto), **36**, 854 (1966).
15) L. C. Snyder, *J. Chem. Phys.*, **33**, 1711 (1960).
16) C. L. Pekeris, *Phys. Rev.*, **115**, 1216 (1959).

$$-\left(1+\frac{1}{2}\lambda-16\lambda d^2f^2+\left(64+32\lambda+16\lambda^2+8\lambda^3-12\lambda^4-6\lambda^5+\lambda^6+\frac{\lambda^7}{2}\right)d^3f^3\right)\log(f/g)\Big\}$$
$$+4(\Delta Z)^2\{\kappa^2a+4\log(4b^2/a)\}\Big],$$

where

$a=(1+\kappa)^{-1}$ $b=(2+\kappa)^{-1}$, $c=(4+\kappa)^{-1}$,
$d=(2-\lambda)^{-1}$, $e=(1+\lambda)^{-1}$, $f=(2+\lambda)^{-1}$
and $g=(2+\kappa+\lambda)^{-1}$.

The procedure of integration including $e^{-\eta r_{12}}/r_{12}{}^n$ is referred to the method presented by Page.[17]

17) C. H. Page, *Phys. Rev.*, **53**, 426 (1938).

BULLETIN OF THE CHEMICAL SOCIETY OF JAPAN VOL. 43 2017—2026 (1970)

Structure and Intramolecular Motions in Bicyclo[2.2.2]octane as Studied by Gas Electron Diffraction

Akimichi YOKOZEKI, Kozo KUCHITSU and Yonezo MORINO

Department of Chemistry, Faculty of Science, The University of Tokyo, Hongo, Tokyo

(Received February 12, 1970)

A least-squares analysis of the electron-diffraction intensities for bicyclo[2.2.2]octane in gas phase measured at 28°C has given the following structural parameters: r_g(C–C) (average) = 1.542 ±0.004Å, r_g(C–H) (average) = 1.107±0.009Å, $r_g(C_1–C_2) = 1.53_8 \pm 0.01_5$Å, $r_g(C_2–C_3) = 1.55_2 \pm 0.02_9$Å, $\angle C_1–C_2–C_3 = 109.7° \pm 0.7°$, and $\angle$H–C–H = $110._1° \pm 5._6°$, where the uncertainties represent estimated limits of error. The potential function for the twisting motion around the D_{3h} symmetry axis is found to have a broad minimum; in terms of the dihedral angle of torsion about the C_2–C_3 axis, ϕ, the potential has an rms angle of 12.0°±1.5° and a "classical turning point" of 21.5°±0.5° (7.2° and 12.8°, respectively, in terms of the dihedral angle of twist, τ). Best fit to the observed intensities has been achieved when a quartic function, $V(\phi) = k_2\phi^2 + k_4\phi^4$ with $k_2 = -4.0$ kcal/mol and $k_4 = 54.2$ kcal/mol, is assumed. The potential function probably has a hump of the order of 100 cal/mol at the D_{3h} conformation. Hence, this molecule may be regarded as having a "quasi-D_{3h} structure". The above features are consistent with those for the derivatives of this molecule in crystal phase studied by Dunitz and Ermer by X-ray diffraction, and also with semiempirical estimates based on the calculations of the intramolecular strain energy.

Bicylco[2.2.2]octane (BO) has three cyclohexane rings fused together at the carbon atoms 1 and 4 (Fig. 1). In the structure with the highest symmetry, D_{3h}, the rings are locked in a boat form, one of the unstable conformations of cyclohexane.[1] As the rings are twisted about the three-fold axis, the symmetry is lowered to D_3.

There have been controversial reports in the literature as to the symmetry of this molecule. Turner *et al.*[2] concluded from the relatively large heats of hydrogenation of bicyclo[2.2.2]octane and octadiene that BO should have a D_3 symmetry. They thought that such a twisted structure should relieve some of the torsional strain in the system, since for D_{3h} the atoms are in eclipsed positions about the C_2–C_3 axes. This structure was supported by Hendrickson,[3] who calculated the strain energy and found that it favored a structure twisted slightly around the C_3 axis. On the other hand, Gleicher and Schleyer[4] preferred a D_{3h} structure based on results from a similar calculation.

The infrared and Raman spectra of BO by MacFarlane and Ross[5] were consistent with those predicted on the assumption that the molecular symmetry was D_{3h}; the twsiting, if present, was thought to be slight. The microwave studies of 1-chloro and 1-bromo derivatives by Nethercot and Javan[6] also estimated the twist angle*1 to be essentially

1) M. Bixon and S. Lifson, *Tetrahedron*, **23**, 769 (1967).

2) R. B. Turner, W. R. Weador and R. E. Winkler, *J. Amer. Chem. Soc.*, **79**, 4116 (1957).

3) J. B. Hendrickson, *Chem. Eng. News*, **39**, 40 (1961).

4) G. J. Gleicher and P. von R. Schleyer, *J. Amer. Chem. Soc.*, **89**, 582 (1967).

5) J. J. MacFarlane and I. G. Ross, *J. Chem. Soc.*, **1960**, 4169.

6) A. H. Nethercot and A. Javan, *J. Chem. Phys.*, **21**, 363 (1953).

*1 See Analysis section for the definition of the "twist" angle and the "torsional" angle.

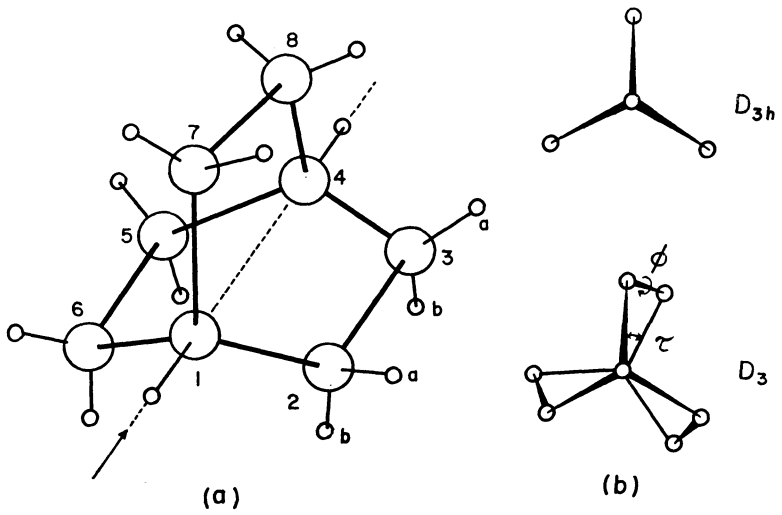

Fig. 1. a) Bicyclo[2.2.2]octane. b) Carbon skeletons as viewed from the C_1–C_4 axis.

zero (0°±4°). As for the crystal structures of BO derivatives, Cameron *et al.*[7] estimated the twist angle to be about 3°, whereas Ermer and Dunitz[8] found no significant deviation from D_{3h} symmetry in the carbon skeleton; an rms amplitude of the half-twist angle (upper limit) of 5.9°±0.2° was derived from the analysis of their anisotropic thermal ellipsoids.

From all the above studies no conclusive structure of the free BO molecule is yet known. The potential function for the twist motion may have a broad minimum near the D_{3h} conformation, where a hump may or may not exist. In this connection, a recent semiempirical calculation of Ermer and Dunitz[8,9] predicted the potential to have a small hump of only about 100 cal/mol with an rms torsional angle*1 of 13.8°. Under these circumstances, the structure of unsubstituted BO has been investigated by means of gas-phase electron diffraction with the aim of obtaining information on the twisting potential function.

Experimental

Purified sample of BO was kindly provided by Dr. Hiroshi Tanida of Shionogi Research Laboratory. Diffraction photographs were taken at 28°C on Fuji Process Hard Plates with an apparatus equipped with an r^3-sector.[10] The accelerating voltage (about 40 kV) was stabilized within 0.01% during exposure, 17—20 min for a camera length of 107.79 mm and about 7 min for 243.24 mm. The beam current was 0.31 μA, and the vacuum was kept under 5×10^{-5} Torr while the sample gas was introduced into the chamber through a nozzle of 0.2 mm diameter. The wavelength of the electron beam was calibrated to within 0.07% with reference to the r_a(C–O) bond length of carbon dioxide,[10] 1.1646 Å.

The photographs were developed at 20°C for 5 min with FD-131 developer diluted twice. Four plates for each camera length were used for density measurements. The optical densities (0.19 to 0.41) were recorded digitally at intervals of integral q values[11] (from 20 to 140 and from 8 to 65 for the short and long camera lengths, respectively); they were assumed to be proportional to the electron intensities.[12]

The intensity curve obtained above was corrected for sector imperfection and divided by a theoretical background function, which took account of elastic and inelastic atomic scattering.[13] In addition, extraneous scattering observed at large q values (15% at q=80 and 45% at 120) was subtracted so as to make the background nearly flat for all the scattering angles. This procedure seemed justified because an intensity measurement of carbon dioxide, after a similar background correction, gave experimental mean amplitudes in good agreement with their theoretical values. This procedure, however, had a significant influence on the measurement of the C_1–C_2 and C_2–C_3 bond distances, since they are so closely spaced that their mean amplitudes correlate strongly with the bond distances (see next section).*2

As illustrated in Fig. 2, the observed molecular in-

7) A. F. Cameron, G. Ferguson and D. G. Morris, *Chem. Commun.*, **1968**, 316.

8) O. Ermer and J. D. Dunitz, *ibid.*, **1968**, 567; *Helv. Chim. Acta*, **52**, 1861 (1969).

9) J. D. Dunitz and O. Ermer, *Acta Cryst.*, **A25**, S126 (1969).

10) Y. Murata, K. Kuchitsu and M. Kimura, *Japan. J. Appl. Phys.*, **9**, 591 (1970).

11) Y. Morino, K. Kuchitsu and T. Fukuyama, This Bulletin, **40**, 423 (1967).

12) Y. Morino and T. Iijima, *ibid.*, **35**, 1661 (1962); R. C. Valentine, "The Response of Photographic Emulsions to Electrons," Advances in Optical and Electron Microscopy, Vol. 1, ed. by R. Baerer and V. E. Coslett, Academic Press, New York, N. Y. (1965), p. 180.

13) T. G. Strand and R. A. Bonham, *J. Chem. Phys.*, **40**, 1686 (1964); C. Tavard, D. Nicolas and M. Rouault, *J. Chim. Phys.*, **64**, 540 (1967).

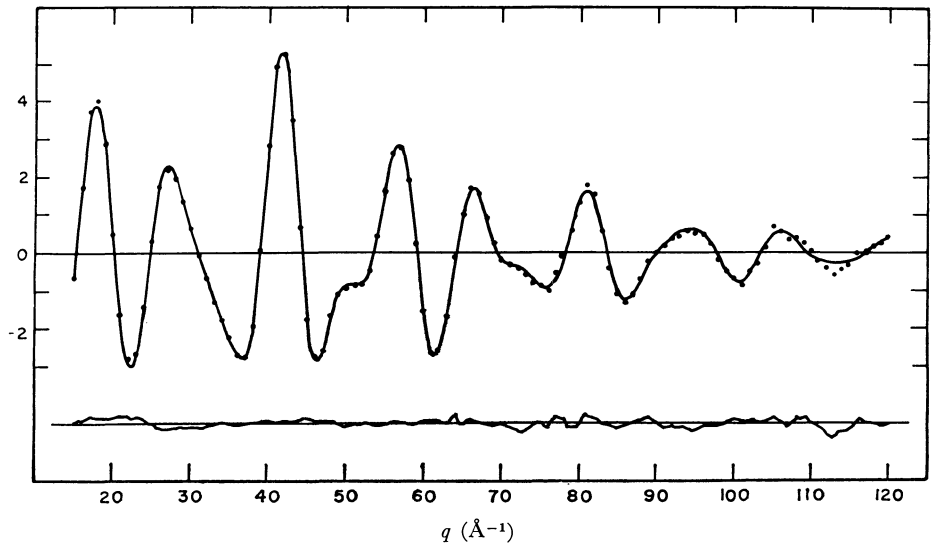

Fig. 2. Molecular intensity curves for bicyclo[2.2.2]octane.
Upper solid curve: experimental; dots: best-fit theoretical; lower curve: experimental minus theoretical.

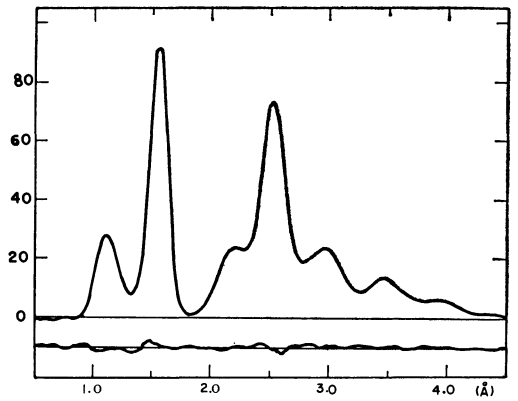

Fig. 3. Experimental radial distribution curve for bicyclo[2.2.2]octane. Lower curve: theoretical minus experimental.

tensity is in reasonable agreement with the best-fit theoretical intensity obtained from the least-squares analysis[14] described below. The corresponding radial distribution curve, calculated with an artificial damping function of the form $\exp(-0.0016s^2)$ and with a correction for nonnuclear scattering,[15] is shown in Fig. 3. Most of the computations were carried out by a HITAC-5020E computer in the Computer Centre of the University of Tokyo.

*2 Numerical experimental data of the levelled total intensity have been filed with the Chemical Society of Japan. A copy may be secured upon request to the Society.

14) Y. Morino, K. Kuchitsu and Y. Murata, *Acta Cryst.*, **18**, 549 (1965).

15) L. S. Bartell, L. O. Brockway and R. H. Schwendeman, *J. Chem. Phys.*, **23**, 1854 (1955).

Analysis

Definition of Dihedral Angles. As shown in Fig. 1, the dihedral angle between the C_1–C_2–C_4 and C_1–C_3–C_4 planes is called the "twist angle" τ about the C_3 axis, while the dihedral angle between the C_1–C_2–C_3 and C_2–C_3–C_4 planes is called the "torsional angle" ϕ about the C_2–C_3 bond. They are related by

$$\tan(\tau/2) = r_2[(r_2-2r_1\cos\alpha)^2 + 4r_1^2\sin^2\alpha\sin^2(\phi/2)]^{-1/2}\tan(\phi/2) \quad (1)$$

where the C_1–C_2 (r_1) and C_2–C_3 (r_2) distances and the C_1–C_2–C_3 angle (α) are assumed to be constant. For small ϕ, τ is equal to 0.605ϕ. In the following analysis the ϕ angle is taken instead of τ as a parameter representing the twist motion.

Choice of Independent Parameters. The number of independent parameters sufficient to describe the D_{3h} structure is seven, while for the D_3 structure, in general four additional parameters are required. In order to facilitate the analysis, the following assumptions were made:

a) The C_1–H and C_2–H bond lengths are equal. Since a weighted average, $[r_g(C_1\text{–H})\times 2/14+r_g(C_2\text{–H})\times 12/14]$, is obtained from the analysis for r_g(C–H), it is likely that r_g(C–H) represents the C_2–H bond length.

b) The angles C_1–C_2–C_3, C_2–C_3–H and H–C_2–H do not depend on the torsional angle.

c) The plane H–C_2–H is perpendicular to the C_1–C_2–C_3 plane and bisects the C_1–C_2–C_3 angle (α), and *vice versa*.

Thus for D_3 symmetry the following six independent parameters were taken: the C_1–C_2 and C_2–C_3

distances, the angles α, the equilibrium torsional angle ϕ_e, the weighted mean C–H distance, and the H–C_2–H angle.

Calculation of Mean Amplitudes. The mean amplitudes and the vibrational corrections on internuclear distances, r_a–r_α, were calculated by the method discussed in a previous paper[16] with a set of the Urey-Bradley force constants for a D_{3h} structure. The force constants, given in Table 1, were transferred mainly from those for cyclohexane.[17] The vibrational frequencies obtained from this calculation are compared in Table 2 with the observed values of Brüesch and Günthard.[18] The agreement is fair, although their assignments are still far from complete.

Table 1. Urey-Bradley force constants for bicyclo[2.2.2]octane[a] (in md/Å)

K(C-C)	2.30	F(C-C)	0.20
K(C-H)	4.10	F(C-H)	0.41
H(C-C-C)	0.32	F(H-H)	0.18
H(C-C-H)	0.225	Y[b]	0.11
H(H-C-H)	0.40		

a) Estimated from the force constants for cyclohexane.[17]
b) Defined in Eq. (3); in md·Å units.

As for the twisting mode, the symmetry coordinate is given by the equation

$$S_4(A_1'') = \frac{1}{\sqrt{3}}(\phi_{23}+\phi_{56}+\phi_{78}) \quad (2)$$

where ϕ_{ij}, the torsional coordinate about the C_i–C_j axis defined by Miyazawa and Fukushima,[19] is practically synonymous with the ϕ coordinate defined here according to the assumption (b) made above. The force constant Y for this torsional motion is defined by*3

$$V(\text{torsion}) = \frac{1}{2}Y(\phi_{23}^2+\phi_{56}^2+\phi_{78}^2) \quad (3)$$

Since the corresponding normal mode has the lowest frequency, Y has a strong influence on some of the calculated mean amplitudes. Accordingly, the mean amplitudes were calculated by the use of several different Y values. While analogous force constants for torsion about the *gauche* conformation (Y_{gauche}) have been reported for normal hydrocarbons[20] and cycloalkanes,[17] no comparable Y_{cis} constant for the *cis* conformation (possibly negative) is known. A semiempirical estimate of the potential function in terms of intramolecular strain energy (see Discussion) shows that the Y constant for this molecule (Eq. (3)) originates essentially from the positive Y_{gauche} about the C_1–C_2, C_3–C_4, ··· axes balanced by the negative Y_{cis} about the C_2–C_3, C_5–C_6, and C_7–C_8 axes. Thus the Y constant should be appreciably smaller than the Y_{gauche} given in the literature, ~0.11 md·Å, and may even be negative. For the present purpose,

Table 2. Vibrational frequencies of bicyclo[2.2.2]octane

	Calcd[a]	Obsd[b]		Calcd	Obsd		Calcd	Obsd		Calcd	Obsd
A_1'	2918	—	A_1''	2881	—	E'	2894	2918	E''	2900	—
	2889	—		1186	—		2888	2863		2883	—
	1483	1439		934	—		1480	1456		1476	—
	1282	1235		134[c]	—		1327	1348		1340	
	1028	1018	A_2''	2919	2905		1234	1266		1284	1315
	740	790		2898	2888		1164	1100		1182	1221
	537	677		1477	1453		1056	1055		1077	1131
A_2'	2892	—		1346	1340		864	866		922	955
	1173	—		864	986		735	817		523	603
	732	760		781	796		359	371		253	—

a) Calculated with the use of the force constants listed in Table 1; in cm^{-1} units.
b) Observed values[18b] in the solid or CS_2 and CCl_4 solutions.
c) The value calculated in Ref. 18a, 65 cm^{-1}, seems to be in error because of the confusion of the torsional force constant Y defined in Eq. (3) (corresponding to $3H_\tau$) with H_τ defined in Ref. 20a. See text.

16) K. Kuchitsu and S. Konaka, *J. Chem. Phys.*, **45**, 4342 (1966).
17) H. Takahashi and T. Shimanouchi, *J. Mol. Spectry.*, **13**, 43 (1964).
18) a) P. Brüesch, *Spectrochim. Acta*, **22**, 867 (1966). b) P. Brüesch and Hs. H. Günthard, *ibid.*, **22**, 877 (1966).
19) T. Miyazawa and K. Fukushima, *J. Mol. Spectry.*, **15**, 308 (1965).

*3 On the assumption (b), the force constant Y corresponds to three times the constant H_τ defined by Schachtschneider and Snyder[20] provided their definition of the torsional coordinate in regard to the *trans* conformation is translated into that in the *cis* conformation.

20) J. H. Schachtschneider and R. G. Snyder, *Spectrochim. Acta*, a) **19**, 117 (1963); b) **21**, 169 (1965).

it is sufficient to assume Y to be positive and quadratic with the above upper limit. For the Y values of 0.11, 0.08, 0.05, and 0.025 md·Å, the corresponding frequencies of the twisting motion are 134, 116, 92, and 66 cm^{-1}, respectively, whereas all the other frequencies are insensitive to Y. This indicates that this normal mode is almost completely separable from other modes. In fact, the S_4 coordinate contributes more than 95% of the potential energy distribution[21] to the lowest A_1'' mode. Calculated mean amplitudes (listed in Table 3) and vibrational corrections were used in the subsequent least-squares analyses as fixed constants so as to facilitate convergence.

Least-squares Analysis of Molecular Intensity. The experimental molecular intensity was analyzed by a standard least-squares method[14] with the sets of mean amplitudes II through V based on the above choice of the Y constant. The analysis based on Set II converged to a D_3 structure with the ϕ_e angle of 12.2°±0.7°, where the uncertainty represents standard error. For the other sets of Y, all the parameters were essentially unchanged except for ϕ_e, which decreased with the decrease in Y. For Set V, where Y=0.025, ϕ_e was essentially zero, apparently giving a D_{3h} structure. Accordingly, the shape of the potential function as derived from the above analysis depends significantly on the assumption about Y. Nevertheless, it is clear from the analysis that this molecule has a floppy structure in thermal equilibrium as regards the twisting motion. The potential function for this motion is studied in more detail in later sections.

Estimation of Uncertainties. The structural

Table 3. Calculated mean amplitudes for bicyclo[2.2.2]octane[a]

C_1–C_2	533	C–H	789	$C_7\cdots H_4$	1025
C_2–C_3	528	$C_7\cdots H_1$	1066	$C_7\cdots H_{2b}$	1055
$C_1\cdots C_4$	664	$C_1\cdots H_7$	1075	$C_1\cdots H_4$	977
$C_1\cdots C_8$	654	$C_2\cdots H_{3a}$	1077		

set[b]	I	II	III	IV	V
$C_2\cdots C_7$	729	729	732	737	742
$C_3\cdots C_7$	766	886	924	1000	1176
$C_7\cdots H_{2a}$	1557	1580	1609	1655	1740
$C_7\cdots H_{3a}$	1506	1914	2052	2318	2894
$C_1\cdots H_8$	1202	1281	1316	1384	1542
$C_7\cdots H_{3b}$	1083	1090	1092	1097	1107

a) Calculated by using the force constants given in Table 1; in 10^{-4} Å units.
b) Sets I through V correspond to the force constants for torsion defined in Eq. (3), assumed to be ∞, 0.11, 0.08, 0.05, and 0.025 md·Å, respectively. Values listed in the upper section do not depend on the choice of Y.

Table 4. Structural parameters for bicyclo[2.2.2]octane

	Exp.[a]	X.D.[b]	Calcd.[c]
C–$C_{av.}$[d]	1.542±0.004	1.541	1.543
C_1–C_2	1.53_8±0.01_5	1.540	1.542
C_2–C_3	1.55_2±0.02_9	1.543	1.544
∠C_1–C_2–C_3	109.7°±0.7°	109.9°	110.0°
$C_1\cdots C_4$	2.59_2±0.02	2.592	2.597
C–$H_{av.}$[d]	1.107±0.009	—	—
∠H–C–H	$110._1°$±$5._6°$	—	—
k[e]	0.96±0.03	—	—

a) Experimental r_g distances in Å and r_α angles determined in the present study with estimated limits of error.
b) Crystal data for bicyclo[2.2.2]octane-1,4-dicarboxylic acid observed by Ermer and Dunitz[8] by X-ray diffraction.
c) Estimates from a strain-minimization calculation by Gleicher and Schleyer.[4]
d) Weighted mean values of bond distances; see text.
e) Index of resolution.

Table 5. Error matrix[a]

	C_1–C_2	C_2–C_3	C–H	∠$C_1C_2C_3$	∠HCH	ϕ_e	k
C_1–C_2	0.0050	−0.0074	0.0016	0.0020	−0.0095	0.0044	−0.0040
C_2–C_3		0.0111	−0.0024	−0.0032	0.0143	−0.0062	0.0060
C–H			0.0035	0.0011	0.0056	0.0011	0.0028
∠$C_1C_2C_3$				0.0034	−0.0036	−0.0031	0.0025
∠HCH					0.0332	−0.0079	0.0095
ϕ_e						0.0138	−0.0013
k							0.0118

a) Error matrix for fixed mean amplitudes. Units for the distances are Å, those for the angles are rad., and the index of resolution k is dimensionless. Elements of the matrix are given by $\sigma_{ij}=\mathrm{sgn}[(B^{-1})_{ij}][|(B^{-1})_{ij}|V^*PV/(n-m)]^{1/2}$, where the notations follow Ref. 14. The diagonal element σ_{ii} represents the random standard error for the parameter i.

21) Y. Morino and K. Kuchitsu, *J. Chem. Phys.*, **20**, 1809 (1952).
22) K. Hedberg and M. Iwasaki, *Acta Cryst.*, **17**, 529 (1964).
23) K. Kuchitsu, T. Fukuyama and Y. Morino, *J. Mol. Structure*, **1**, 463 (1968).

parameters determined are listed in Table 4. The limits of error were estimated as 2.5 times the random standard errors derived from the least-squares analysis,[14] which are included in the error matrix[22] given in Table 5 as diagonal elements, plus systematic errors. Principal sources of systematic errors are as follows: a) uncertainty in the scale factor, b) sector imperfections, c) extraneous scattering, and d) the use of theoretical mean amplitudes in the analysis. The errors due to sources a) and b) are estimated to be 0.07% and 0.05% of the corresponding distances, respectively.[23] The uncertainties due to c) and d) for all the distance and angle parameters, except for the bonded C–C distances, are at most of the order of their random standard errors, since the systematic error in the estimation of extraneous scattering causes uncertainties in the mean amplitudes and the index of resolution,[14] and since all the parameters (except for the C_1–C_2 and C_2–C_3 distances) are practically uncorrelated with the mean amplitudes and the index of resolution, as confirmed by a test analysis with systematic variations of the mean amplitudes used in the analysis.

As for the C_1–C_2 and C_2–C_3 distances, their difference derived from the analysis is contingent on their estimated amplitudes. Therefore, a systematic error due to the uncertainties in the C–C bond-stretching force constants used for calculating the mean amplitudes were taken into account as well as the uncertainty in the estimation of extraneous scattering. The total systematic errors in the C–C amplitudes are thus estimated to be 0.002 Å for C_1–C_2 and 0.005 Å for C_2–C_3, resulting in the final estimates of the uncertainties in their distances given in Table 4. Thus the C_1–C_2 and C_2–C_3 distances are hardly distinguishable in the present analysis, although the most probable value of the latter distance appears to be appreciably longer than the former.*4,24,25 The weighted mean value of the r_g(C–C) distances, on the other hand, has been determined with much higher precision.

Large-amplitude Analysis. In order to further investigate the potential function $V(\phi)$ for the twisting motion as represented in terms of ϕ, the following "large-amplitude" analysis was undertaken. Since the S_4 coordinate is separable from other coordinates to a good approximation, the twisting motion can be described in terms of a single coordinate ϕ. The molecular intensity for such a nonrigid molecule may be given by a classical weighted average of the intensity in regard to the torsional angle,[26]

$$qM(q) = k\sum_{i\neq j} A_{ij}\mu_{ij}(q)\exp\left[-\frac{1}{2}(\pi l_{ij}q/10)^2\right] \int_{-\pi}^{\pi} w(\phi)\left\{\sin\left[\frac{\pi}{10}qr_{ij}(\phi)\right]\Big/r_{ij}(\phi)\right\}\mathrm{d}\phi \quad (4)$$

where k is the index of resolution, A_{ij} is a constant proportional to the atomic numbers of i and j, μ_{ij} is a known function[15] of q related to the elastic and inelastic scattering factors for i and j, and l_{ij} is the mean amplitude of the i-j pair due to the framework vibrations (*i.e.*, those apart from the twisting motion); the calculated mean amplitudes listed in Table 3 [Set I for $Y=\infty$], which were assumed to be independent of ϕ, were used for l_{ij}. The weight function w is given by Boltzmann statistics as

$$w(\phi) = \exp[-V(\phi)/\boldsymbol{k}T]\Big/\int_{-\pi}^{\pi}\exp[-V(\phi)/\boldsymbol{k}T]\mathrm{d}\phi \quad (5)$$

It is sometimes more convenient to work on the corresponding radial distribution function,[27]

$$f(r) = k\sum_{i\neq j}\frac{1}{2}A_{ij}(\pi H_{ij})^{1/2} \int_{-\pi}^{\pi}\left(w(\phi)\exp\{-H_{ij}[r-r_{ij}(\phi)]^2\}/r_{ij}(\phi)\right)\mathrm{d}\phi \quad (6)$$

where H_{ij} is defined in terms of the artificial damping coefficient b by

$$H_{ij} = (4b+2l_{ij}^2)^{-1} \quad (7)$$

In order to estimate the potential function from the present experimental data, the various functions for V, *viz.*,

(a) Square well: $V(\phi)=0$ for $\phi<\beta$ and ∞ for $\phi\geq\beta$
(b) Double parabola: $V(\phi)=a(|\phi|-b)^2$
(c) Quadratic: $V(\phi)=c\phi^2$
(d) Quadratic-quartic: $V(\phi)=k_2\phi^2+k_4\phi^4$

were applied to Eqs. (5) and (6).

A best-fit set of parameters for each potential function was searched for by a trial-and-error comparison of the observed and theoretical $qM(q)$ and $f(r)$ curves. The ranges of the experimental data most sensitive to $V(\phi)$ are q=45—60 Å^{-1} for the molecular intensity, and r=2.7—3.5 Å for the radial distribution curve. Typical examples are shown in Fig. 4.

For case (a), the limit angle β is found to be 22°± 4°. The coefficients a and b for case (b) are about 17 kcal/mol and 11°, respectively, corresponding to a potential cusp $V(0)$ of about 500 cal/mol, while for case (c) the constant c is 4.3 kcal/mol. For case (d) the set of parameters thus obtained was further refined by a least-squares analysis.

*4 Our recent electron-diffraction study of triethylenediamine (1,4-diazabicyclo[2.2.2]octane)[24] has shown that the r_g(C_2–C_3) distance is about 0.02 Å longer than that of the C–C distance in cyclohexane.[25]

24) A. Yokozeki and K. Kuchitsu, This Bulletin, to be published.

25) H. Kambara, K. Kuchitsu and Y. Morino, *ibid.*, to be published.

26) Y. Morino and E. Hirota, *J. Chem. Phys.*, **28**, 185 (1958).

27) J. Karle, *ibid.*, **15**, 202 (1947).

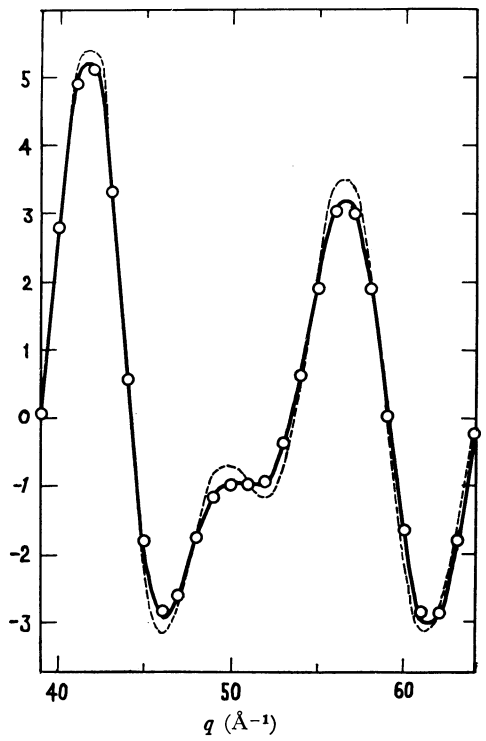

Fig. 4. (a)

The most probable set is $k_2=-4.0\pm3.3$ and $k_4=54.2\pm34.5$ (kcal/mol).

With the above adjustment of parameters, the experimental curves agree with the theoretical curves based on any one of the functions of (a) through (d) to a similar degree of consistency. As shown in Fig. 5, all the best-fit functions given above yielded a nearly equal rms angle, $\langle\phi^2\rangle^{1/2}$, of about 12° and a nearly equal "classical turning point" (the angle where the potential energy is comparable with the thermal energy at room temperature), $\phi_t\sim21°$. Since the intensity curve is sensitive to $\langle\phi^2\rangle^{1/2}$ and ϕ_t, they are the parameters readily determinable from the diffraction experiment irrespective of the type of the potential function assumed in the analysis.

On a physical basis, the function of (d) seems to be more realistic than the other functions. The most probable set of the k_2 and k_4 parameters has a potential hump of 75 ± 100 cal/mol at the D_{3h} position and a broad double minimum at about 11°; the standard error given above has been estimated by taking into account the correlation between the k_2 and k_4 parameters.[28]

Discussion

Structure. The weighted mean value of the r_g(C–C) distances, $[(2/3)r_g(C_1–C_2)+(1/3)r_g(C_2–C_3)]$

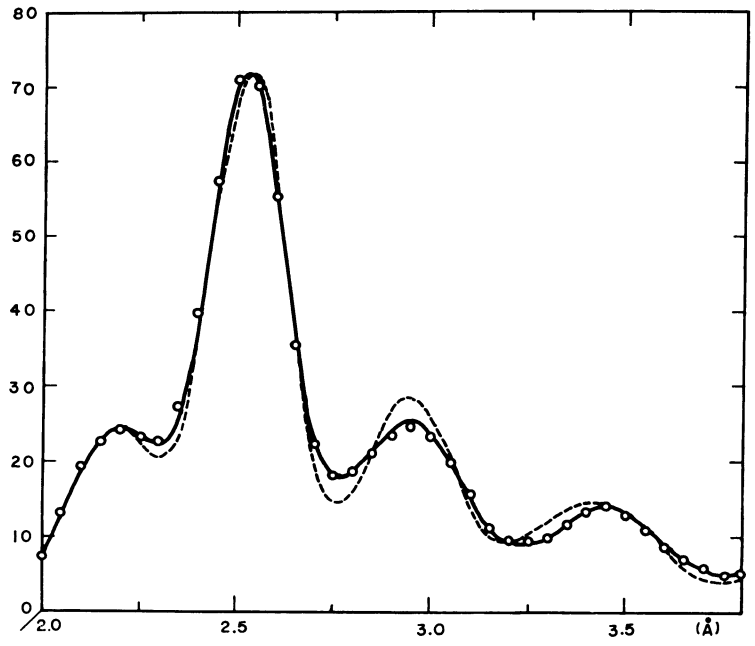

Fig. 4. (b)

Fig. 4. Dependence of the molecular intensity (a) and the radial distribution curve (b) on the potential function for twisting motion. Circles, experimental values representing their estimated uncertainties; solid curve, case (d) (quartic) potential function with the parameters given in the text; broken curve, case (c) (quadratic) potential function with $c=17$ kcal/mol corresponding to the force constant for torsion, $Y=0.08$ md·Å.

28) Y. Morino and T. Nakagawa, *J. Mol. Spectry.*, **26**, 496 (1968).

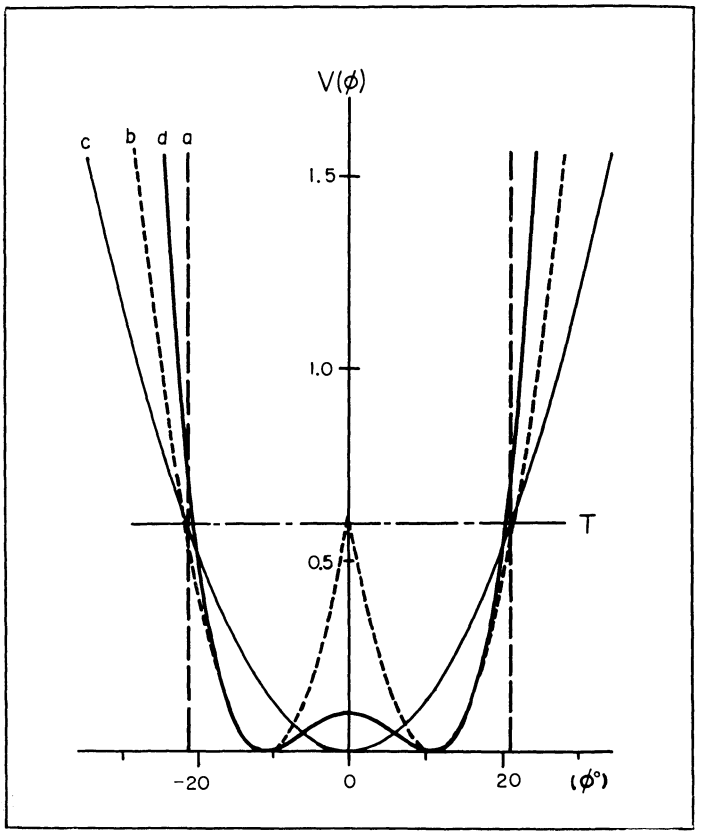

Fig. 5. Best-fit estimates of the potential functions for torsion (in kcal/mol), a—d, corresponding to the cases (a)—(d) discussed in the text. Line T denotes the thermal energy at room temperature, where the experiment was made.

$=1.542\pm0.004$ Å, is not significantly different from the r_g(C–C) distance in cyclohexane,[25] $1.540_4\pm0.001_0$ Å, indicating little overall influence of intramolecular strain on the C–C bond distances. The thermal-average C–C–C bond angle is similar to the tetrahedral angle. This structure appears to be consistent with the corresponding structures in crystalline BO derivatives determined by X-ray diffraction[8] (Table 4), although one should note that the latter parameters are based on a different definition and may also be subject to a crystal-field effect. The parameters for a free molecule estimated by a strain-minimization calculation[4] are also compatible with the present experimental values. The hydrogen parameters for the methylene group are analogous to those in cyclohexane[25] within their experimental uncertainties.

Twisting Motion. The present analysis has shown that the twisting motion has a large amplitude; the potential has a classical turning point of 21.5°±0.5° for the C–C torsional angle and an rms angle of 12.0°±1.5°, which correspond to 12.8°±0.3° and 7.2°±0.9°, respectively, in terms of the twist angle τ. The potential probably has a hump at the D_{3h} position much lower in height than the thermal energy at room temperature. Hence, the BO molecule may be said to have a "quasi-D_{3h} structure".

Semiempirical Calculation of the Potential Function It seems of interest in this connection to investigate whether the potential function derived above can be accounted for by a semiempirical model.[29] The strain energy of this molecule may be given as a function of the torsional angle by

$$E(\phi)=\frac{1}{2}H\sum_i[\alpha_i(\phi)-\alpha_0]^2+\frac{1}{2}f\sum_j(1+\cos 3\phi_j)+\sum V_{nb}(\phi) \quad (8)$$

where the bending and torsional force constants, H and f respectively, are estimated to be 98.5 kcal/mol (a bending force constant of the Urey-Bradley type for alkanes[20b,29]) and 2.93 kcal/mol (the torsional barrier for ethane[30]). The reference

29) E. J. Jacob, H. B. Thompson and L. S. Bartell, *J. Chem. Phys.*, **47**, 3736 (1967).

30) K. S. Pitzer and W. E. Donath, *J. Amer. Chem. Soc.*, **81**, 3213 (1959); S. Weiss and G. E. Leroi, *J. Chem. Phys.*, **48**, 962 (1968).

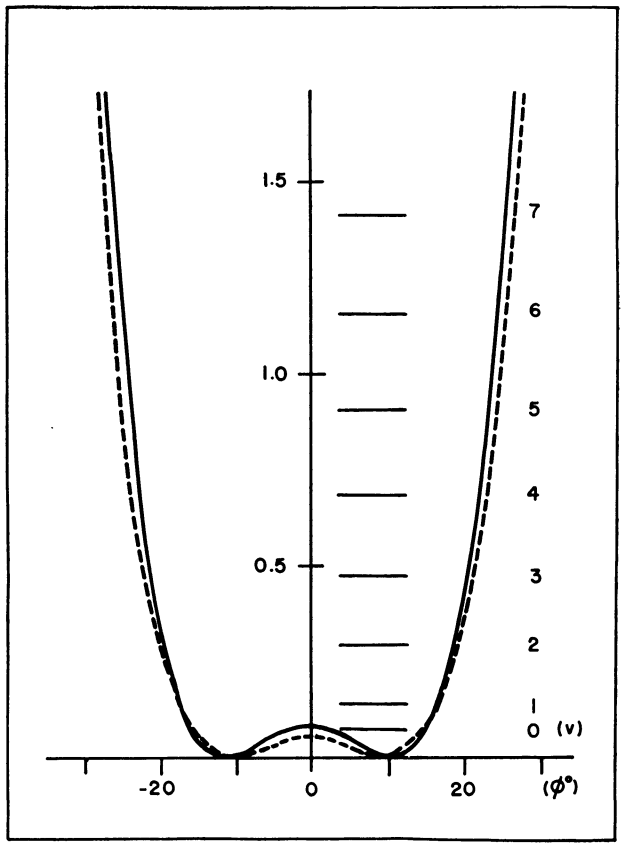

Fig. 6. Estimated potential functions for torsion (in kcal/mol).
Solid curve, best-fit function for case (d) given in the text; broken curve, a model function estimated by Eq. (8). The energy levels are estimated by the use of the d function.

for the CCC bond angle, α_0, is taken as the tetrahedral angle. In addition to the three assumptions made in the analysis section, the bond distances are assumed to be constant. The nonbonded interactions assumed for C–C, C–H, and H–H pairs (in kcal/mol) are

$$\left.\begin{aligned} V_{nb}(C\cdot\cdot C) &= 1.66\times 10^4 \exp(-3.63r) - 325/r^6 \\ V_{nb}(C\cdot\cdot H) &= 1.29\times 10^4 \exp(-4.12r) - 125/r^6 \\ V_{nb}(H\cdot\cdot H) &= 1.00\times 10^4 \exp(-4.60r) - 49.2/r^6 \end{aligned}\right\} \quad (9)$$

as taken from Hendrickson's paper.[31]

The resulting function $E(\phi)$ has a broad minimum around $\phi=10°$, as illustrated in Fig. 6, with a small hump of about 50 cal/mol at $\phi=0°$. The turning point ϕ_t is estimated to be about 23°, in good agreement with the experimental result given above. The general feature of the curve for $\phi \gtrsim 15°$ rests on the contributions from the first and third terms in Eq. 8; as the molecule is twisted from the D_{3h} conformation, the distortion of the bridgehead-carbon valence angles and the increasing interactions among the nonbonded C–C pairs contribute nearly equally to the steep rise in the potential, outweighing a slight decrease in the interactions among the nonbonded C–H and H–H pairs. For smaller torsional angles ($\phi<10°$), on the other hand, the sum of the first and third terms makes a nearly flat curve, and the potential shape is sensitive to the second term in Eq. 8. This term causes a small hump at the D_{3h} conformation, and the height and the minimum position depend on a competitive sum of six *gauche* terms (about the C_1–C_2 axis, *etc.*), which favor the D_{3h} conformation, and three *cis* terms (about the C_2–C_3 axis, *etc.*), which work in the opposite direction.

A recent calculation of this potential by Ermer and Dunitz[8,9] using a range of semiempirical functions has reached essentially the same conclusion, with a predicted minimum of about 100 cal/mol and an rms torsional angle of 13.8°.

Estimation of Energy levels. The energy levels for this twisting motion were calculated from

31) J. B. Hendrickson, *J. Amer. Chem. Soc.*, **83**, 4537 (1961).

the Hamiltonian,[32,33]

$$H = P_\phi^2/2M(\phi) + V(\phi) \quad (10)$$

where $V(\phi)$ is the quartic function estimated above, and P_ϕ is the angular momentum conjugate to ϕ. The reduced mass $M(\phi)$ was estimated with a semirigid framework,[32],*5 where, besides the assumptions (a)—(c) made in the analysis section, all the bond distances were assumed to be constant in the twisting motion. The resulting $M(\phi)$ depends only slightly on ϕ:

$$M(\phi) = 29.08 - 5.29\phi^2 + 6.54\phi^4 \text{ (amu)}$$

for ϕ (in rad.) $\lesssim 40°$. Thus the reduced mass was assumed to be constant (28.9 amu); the error due to the use of this effective mass is less than 1% of the energy levels estimated. A computer program written by Ueda and Shimanouchi[32] was used for calculating the levels listed in Table 6. Since the energy values, particularly those of lower levels, depend critically on the detailed shape of the potential, the listed values are only semiquantitative. Nevertheless, the presence of several levels under the thermal energy at room temperature is clearly demonstrated. Comparable energy values were obtained from the model potential function (8). Ermer and Dunitz[8,9] have estimated the energy differences between higher levels to be about 60 cm^{-1} by the use of their semiempirical potential functions. Though the fundamental transitions are infrared inactive, a direct measurement of the levels by some spectroscopic means, such as an analysis of combined transitions appearing in near-infrared band progressions,[34] could supply further information on this potential function.

Table 6. Estimated energy levels of the twisting motion for bicyclo[2.2.2]octane[a] (in cm^{-1} units)

v	E_v	v	E_v	v	E_v
0	24.0	3	165.8	6	403.4
1	48.4	4	237.9	7	495.0
2	103.4	5	317.5	8	591.7

a) Semiquantitative estimates based on the experimental potential function (d) given in the text.

The authors are indebted to Drs. Hiroshi Tanida and Kazuo Tori of the Shionogi Research Laboratory for their supply of the sample and for their stimulating discussions. They are also grateful to Professor J. D. Dunitz, Dr. O. Ermer and Dr. Hiizu Iwamura for their valuable comments.

*5 The method of high-frequency splitting developed by Thorson and Nakagawa[33] gave 29.14 amu for $M(0)$.

32) T. Ueda and T. Shimanouchi, *J. Chem. Phys.*, **47**, 4042 (1967).

33) W. R. Thorson and I. Nakagawa, *ibid.*, **33**, 994 (1960).

34) T. Ueda and T. Shimanouchi, *ibid.*, **47**, 5018 (1967).

BULLETIN OF THE CHEMICAL SOCIETY OF JAPAN VOL. 43 2027—2029 (1970)

A Kinetic Investigation of Oxidation of Ethyl Methyl Ketone by Manganese(III) Sulphate

K. K. BANERJI, P. NATH and G. V. BAKORE*1

Department of Chemistry, University of Jodhpur, Jodhpur, India

(Received September 10, 1969)

The oxidation of ethyl methyl ketone with manganese(III) sulphate has been studied. The main product of oxidation is acetaldehyde. The reaction is first order with respect to each manganese(III) and the ketone. The rate of oxidation is independent of acidity and is not affected by changes in solvent composition. Addition of manganese(II) also does not affect the rate. The energy of activation, the entropy of activation and free energy of activation at 35°C have values 20.5 kcal/mol, −3.50 e.u. and 21.6 kcal/mol respectively. The rate of enolisation, measured by bromination method, is less than that of oxidation under similar conditions. A mechanism involving an attack directly on the ketone by manganese(III) sulphate-complex has been suggested.

Ketones were shown to be oxidised by manganic pyrophosphate *via* their enolic form.[1] Littler,[2] however, observed that manganese(III) sulphate oxidizes cyclohexanone at a rate faster than its enolisation and suggested that oxidation of ketones does not necessarily proceed through enolisation. Oxidation of aliphatic ketones by manganese(III) has not received adequate attention and, therefore, this investigation was taken up.

Experimental

Materials. B.D.H. ethyl methyl ketone was used after fractionation. Acetic acid (B.D.H., 99.5%) was distilled over chromic acid before use. All other chemicals used were chemically pure.

Manganese(III). Sulphate was prepared by the method described by Vogel.[3] Manganese(III) solutions were standardized iodometrically.

Kinetic Measurements. Unless otherwise stated the solvent used was 20% acetic acid - 80% water (*v*/*v*). Sufficient excess of manganese(II) was added to prevent disproportionation and subsequent hydrolysis of manganese(III).

Throughout the investigation the concentration of the ketone was kept in sufficiently large excess to ensure that the rate of reduction of manganese(III) is proportional to the oxidation of the ketone itself and not to the rate of destruction of any reactive intermediate.

Reaction mixtures were prepared by mixing all reagents except the ketone, in requisite quantities and were brought to the thermostatic temperature (±0.03°C). Reaction was started by adding the ketone rapidly.

Reactions were followed by quenching aliquots, withdrawn at fixed intervals of time, in slight excess of ferrous ammonium sulphate and estimating the residual iron(II) by titrating it against standardized cerium(IV) solution using ferroin as an indicator. From this the amounts of manganese(III) left in the reaction mixture at different time intervals were calculated.

Rates of Enolisation. Enolisation rates were measured by bromination method.

The rates of bromination was followed by adding bromine to a thermostated solution of the ketone in acetic acid containing sulphuric acid. Aliquots were withdrawn at fixed intervals of time, acidity adjusted by sodium bicarbonate and bromine left unreacted was determined iodometrically.

Results

Product Analysis. Completely reduced reaction mixtures gave a blue colour with solution of morpholine and sodium nitroprusside[4] indicating that acetaldehyde is the main product of oxidation.

Rate Laws. When ketone is in excess the rate of disappearance of manganese(III) follows first order rate laws. The rate constant is independent of the initial concentration of the oxidant (Table 1). Thus the order with respect to manganese(III) is one. The order with respect to the ketone is also one (Table 2).

Under the conditions of constant ionic strength the rate of oxidation is practically independent of hydrogen ion concentration (Table 3).

Effect of Manganese(II). Addition of manganous sulphate does not affect the rate of oxidation

*1 Present address: Department of Chemistry, University of Udaipur, Udaipur, India.

1) A. Y. Drummond and W. A. Waters, *J. Chem. Soc.*, **1955**, 497.

2) J. S. Littler, *ibid.*, **1962**, 832.

3) A. I. Vogel, "A Text Book of Quantitative Inorganic Analysis," Longmans Green & Co. Ltd., London (1964), p. 327.

4) F. Fiegl, "Spot Tests in Organic Analysis," Elsevier Publishing Co., Amsterdam (1956), p. 33.

Table 1. Variation of rate with concentration of Mn(III)

[Ketone]: 4.42×10^{-2}M, [Mn(II)]: 0.20M, [H_2SO_4]: 2.0M Temperature 35°C

$[Mn(III)]\times10^3$ mol l^{-1}	2.10	3.15	4.20	6.30	8.40	10.5
$k_1\times10^3$ min^{-1}	10.6	10.8	11.0	11.0	10.8	11.0

Table 2. Variation of rate with concentration of the ketone

[Mn(III)]: 4.20×10^{-3}M, [Mn(II)]: 0.21M, [H_2SO_4]: 2.0M Temperature 35°C

$[Ketone]\times10^2$ mol l^{-1}	2.21	4.42	8.84	11.1	13.3	17.7	22.1
$k_1\times10^3$ min^{-1}	5.53	11.0	22.0	27.7	32.8	44.3	54.9
$10\cdot k_1/[Ketone]$	2.50	2.49	2.49	2.49	2.47	2.50	2.48

Table 3. Variation of rate with concentration of hydrogen ions

[Ketone]: 4.42×10^{-2}M, [Mn(III)]: 4.22×10^{-3}M, [Mn(II)]: 0.11M
[H_2SO_4+$NaHSO_4$]: 5.0M Temperature 35°C

$[H_2SO_4]$ mol l^{-1}	2.0	2.5	3.0	3.5	4.0	4.5	5.0
$k_1\times10^3$ min^{-1}	11.0	11.0	10.0	11.0	11.5	11.0	10.2

Table 4. Variation of rate with solvent composition

[Ketone]: 4.42×10^{-2}M, [Mn(III)]: 4.15×10^{-3}M, [Mn(II)]: 0.11M, [H_2SO_4]: 2.0M
Temperature 35°C

Percentage of acetic acid	20.0	30.0	40.0	50.0	60.0
$k_1\times10^3$ min^{-1}	11.0	11.5	11.0	10.8	10.8

Table 5. Effect of bisulphate ion

[Ketone]: 4.42×10^{-2}M, [Mn(III)]: 4.20×10^{-2}M, [Mn(II)]: 0.11M, [H_2SO_4]: 2.0M
Temperature 35°C

$[HSO_4^-]$ mol l^{-1}	2.0	2.5	3.0	4.0	4.5	5.0
$k_1\times10^3$ min^{-1}	11.0	11.0	10.8	10.6	10.4	10.4

Table 6. Effect of temperature

[Mn(III)]: 4.20×10^{-3}M, [Ketone]: 4.42×10^{-3}M, [Mn(II)]: 0.20M, [H_2SO_4]: 2.0M

Temperature °C	30	35	40	45
$k_1\times10^3$ min^{-1}	6.30	11.0	19.1	31.6
$k\times10^3$ l mol^{-1} sec^{-1}	2.38	4.15	7.20	11.9

of ethyl methyl ketone by manganese(III). Similar results were observed in the oxidation of cyclohexanone with manganese(III) sulphate.[5]

Similarly, change in the solvent composition caused by varying the proportion of glacial acetic acid in the solvent mixture, has no appreciable effect on the oxidation rate (Table 4).

Increase in the concentration of bisulphate ions also does not have any effect on the oxidation rate (Table 5).

Effect of Temperature. The reaction was studied at different temperatures between 30 to 45°C (Table 6). The specific rate constant, k, is defined as

$$k = \frac{k_1\ (\text{min}^{-1})}{[\text{ketone}]\times 60}$$

The plot of $\log k$ against the inverse of temperature is a straight line. The Arrhenius equation is,

5) T. J. Kemp and W. A. Waters, *J. Chem. Soc.*, **1964**, 339.

Table 7. Thermodynamic parameters

Temp. °C	$\Delta H^{\neq}$ kcal mol^{-1}	$pZ \times 10^{-12}$ l mol^{-1} sec^{-1}	$\Delta S^{\neq}$ e.u.	$\Delta F^{\neq}$ at 35°C kcal mol^{-1}
30	20.5	1.72	−3.50	21.6
35		1.69		
40		1.72		
45		1.72		
	Average	1.71		

Table 8. Rates of bromination

Temperature 35°C

Percentage acetic acid	20.0	30.0	50.0	80.0
$k_2 \times 10^4$ l mol^{-1} sec^{-1}	3.92	4.17	4.56	12.3

therefore, valid for this reaction. The thermodynamic parameters were evaluated in the usual way (Table 7).

Rates of Bromination. The bromination of ethyl methyl ketone is of first order with respect to the ketone, first order with respect to hydrogen ion but zeroth order with respect to bromine. The rate of bromination divided by concentrations of ketone and hydrogen ions gives (k_2 l mol^{-1} sec^{-1}). Table 8 records the values of k_2 at different proportions of acetic acid-water.

The rate of bromination was studied at temperatures between 30 and 40°C and thermodynamic parameters were evaluated (Table 9).

Discussion

Manganese(II) is known to affect the rate of oxidation of several compounds,[5,6] where the oxidizing species is Mn(IV) and this has been attributed to its effect on the following equilibrium:

$$Mn(IV) + Mn(II) \rightleftharpoons 2Mn(III)$$

Absence of any effect of manganese(II) on the rate of the oxidation suggests that in this case, Mn(III) is the only oxidizing species.

In sulphuric acid medium manganese(III) exists as a sulphato-complex. In stronger solutions of sulphuric acid, which are used to prepare Mn(III), sulphate ion exists as HSO_4^-. The coordination number of manganese(III) is probably six and hence the probable composition of sulphatocomplex could be $[Mn(HSO_4)_3(OH)_3]^{3-}$. Therefore, the oxidizing species is $[Mn(HSO_4)_3(OH)_3]^{3-}$.

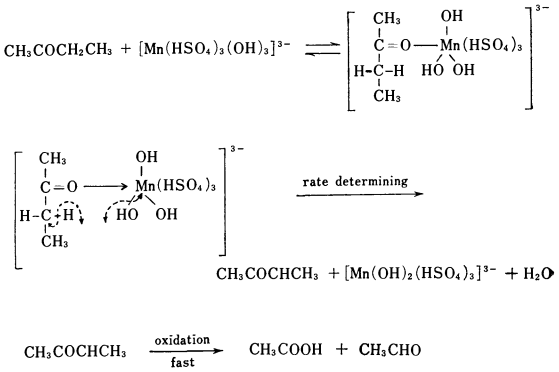

Enolisation of ethyl methyl ketone is an acid catalysed reaction, whereas the oxidation is independent of acidity. Had the enol form been involved in the oxidation, the rate expression would have included a term containing hydrogen ion concentration. Furthermore, the increase in the proportion of acetic acid in the solvent mixture decreases the dielectric constant of the medium and favours reactions involving protonation. Acid catalysed enolisation of ketone is such a reaction. No effect of the change in the solvent composition on the rate of the oxidation again suggests that enolisation is not the rate determining factor in this reaction.

The rate of enolisation of ethyl methyl ketone in 20% acetic acid solution at 35°C is 3.92×10^{-4} l mol^{-1} sec^{-1}, while the specific rate constant, k, for the oxidation under similar condition is 41.5×10^{-4} l mol^{-1} sec^{-1}. If enolisation was to precede oxidation, the rate of oxidation in the limit could be equal to the rate of enolisation, but could never exceed the rate of enolisation. This, therefore, clearly proves that oxidation of ethyl methyl ketone by manganese(III) sulphate proceeds by a direct attack on the keto- form.

The first step in the oxidation is the rapid, reversible formation of complex between the ketone and the manganese(III) sulphate complex, followed by the rate-determining step to give a radical which is then oxidized by several fast steps to acetaldehyde and acetic acid.

Table 9. Effect of temperature on the rate of bromination

Solvent: 50% acetic acid-50% water (v/v)

Temp. °C	30	35	40	$\Delta H^{\neq}$ kcal mol^{-1}	$\Delta S^{\neq}$ e.u.	$\Delta F^{\neq}$ at 30°C kcal mol^{-1}
$k_2 \times 10^4$ l mol^{-1} sec^{-1}	2.58	4.57	7.84	20.9	−6.4	22.9

6) D. R. Rosseinsky, *ibid.*, **1963**, 1181.

BULLETIN OF THE CHEMICAL SOCIETY OF JAPAN VOL. 43 2030—2038 (1970)

Oxidation of Vanadium(II) by Nitrate Ion

Kazuyoshi TANAKA

Department of Chemistry, College of Science, Rikkyo (St. Paul's) University, Nishi-Ikebukuro, Toshima-ku, Tokyo

(Received August 15, 1969)

The oxidation rates of vanadium(II) to vanadium(III) by nitrate ion were determined from the time dependence of the polarographic diffusion currents. As supporting electrolytes sodium perchlorate and sodium sulfate were used. The oxidation rates were linearly dependent on hydrogen ion concentration in strongly acidic solutions (pH<2) and independent in weakly acidic solutions (pH>2). Polarographic half-wave potentials, reversibility and diffusion currents indicated that vanadium(II) in sulfate medium formed a sulfato-complex or an ion-paired species which was oxidized faster than V^{2+} (hydrated) in perchlorate medium. The oxidation in sulfate medium proceeded mainly by a single two-electron oxidation, and further reaction between vanadium(II) and vanadium(IV) yielded a stable dimer of vanadium(III) detected by absorption experiments. The rates measured in various halide solutions, except fluoride, gave almost the same rate constants in perchlorate medium. The gaseous products from nitrate ion were identified as NO and N_2O by infrared spectrum measurements. The overall oxidation was proposed;

$$8V(II)+2NO_3^-+10H^+ \rightarrow 8V(III)+N_2O(g)+5H_2O$$

There have been a number of studies concerning the oxidation of vanadium(II) with oxidizing agents such as chlorate,[1] perchlorate,[2] oxygen and hydrogen peroxide,[3] and with higher oxidation states of metals such as vanadium(IV),[4] thallium(III),[5] chromium(III),[6] iron(III),[7] and uranium(VI).[8] The possibility of the reaction proceeding by way of a one- or a two-electron oxidation step is of interest. The vanadium is suitable for clarifying this problem because vanadium ions in aqueous solution are in various oxidation states from vanadium(II) to vanadium(V). Although the oxidation of cerium(III),[9] molybdenum(V),[10] and uranium(III)[11] by nitrate ion has been studied, no report has appeared concerning the oxidation of vanadium (II) by nitrate ion. The rates could be followed by the time dependence of polarographic diffusion current corresponding to the disappearance of vanadium(II) ion in the solution. Vanadium(II) species were polarographically investigated in various supporting electrolytes.[12,13] Many spectrophotometric measurements have been carried out in a strongly acidic solutions ($[H^+]>0.1$ M) because of the low extinction coefficient and high acidity of vanadium(II) stock solution. However, it was polarographically possible to determine the rate in weakly acidic solution of low vanadium(II) concentration.

Newton and Baker reported that the rate of reaction between vanadium(II) and vanadium(IV) changed with sulfate ion concentration, and the reaction intermediate VOV^{4+} was formed.[14] When the oxidation by nitrate ion proceeds by a single two-electron step, it is expected that the dimer of vanadium(III) may be formed and be stable in sulfate medium. This problem in particular is discussed in this paper.

Experimental

Materials. Vanadium(IV) perchlorate solutions were prepared from vanadyl sulfate solutions by adding $Ba(ClO_4)_2$ to precipitate $BaSO_4$. Vanadium(II) stock solutions were prepared by reduction of $VO(ClO_4)_2$

1) G. Gordon and P. H. Tewari, *J. Phys. Chem.*, **70**, 200 (1966).
2) W. R King, Jr., and C. S. Garner, *ibid.*, **58**, 29 (1954).
3) J. H. Swinehart, *Inorg. Chem.*, **4**, 1069 (1965).
4) T. W. Newton and F. B. Baker, *J. Phys. Chem.*, **68**, 228 (1964).
5) F. B. Baker, W. D. Brewer and T. W. Newton, *Inorg. Chem.*, **5**, 1294 (1966).
6) E. Deutsh and H. Taube, *ibid.*, **7**, 1532 (1968).
7) B. R. Baker, M. Orhanovic and N. Sutin, *J. Amer. Chem. Soc.*, **89**, 722 (1967).
8) T. W. Newton and F. B. Baker, *J. Phys. Chem.*, **69**, 176 (1965).
9) A. G. Sykes, "Advances in Inorganic Chemistry and Radiochemistry," Vol. 10, Academic Press, Inc., New York (1967), p. 233.
10) E. P. Guymon and J. T. Spence, *J. Phys. Chem.*, **70**, 1964 (1966).
11) J. Koryta, *Collect. Czech. Chem. Commun.*, **20**, 667 (1955).
12) J. J. Lingane, *J. Amer. Chem. Soc.*, **67**, 182 (1945).
13) J. J. Lingane and L. Meites, *ibid.*, **73**, 2165 (1951).
14) T. W. Newton and F. B. Baker, *Inorg. Chem.*, **3**, 569 (1964).

solutions containing perchloric acid with zinc amalgam in a pure nitrogen stream. The vanadium(IV) concentration was spectrophotometrically determined using the absorption at 720 mμ, which is mainly due to vanadium(IV). The standard vanadium(IV) solutions were prepared by dissolving vanadium metal (>99.5 %) in a dilute nitric acid. Vanadium(II) concentration was also determined as vanadium(IV) produced by air oxidation in a concentrated perchloric acid solution.

Sodium nitrate solutions were prepared from Wako reagent grade chemicals which had been dried over concentrated sulfuric acid. As supporting electrolytes used for polarographic measurements, perchloric acid (70%), sulfuric acid and their salts, sodium fluoride, chloride, bromide, and iodide were also of reagent grade. Redistilled water was used.

Measurements. The proper amount of vanadium(II) solution was added to deaerated solution containing supporting electrolytes. After the solution was vigorously stirred with nitrogen gas, d.c. and a.c. polarographic measurements were performed at 25°C to obtain the values of half-wave potential and reversibility[15] of vanadium(II). The appropriate amount of sodium nitrate was added to the solution, and mixed by passing nitrogen gas. The time dependence of the polarographic diffusion current of vanadium(II) was recorded at a constant potential (−0.1 — 0.2V *vs.* SCE) where the diffusion current appeared. In the course of these measurements, the solution was protected from air oxidation by a stream of pure nitrogen gas. In order to follow the reactions, the sensitivity of the polarograph was set at 0.10 μA/mm, and the damping capacitance at 5 μF where the current change corresponds to the derease in vanadium(II) concentration. The ionic strength was adjusted to 0.5 by adding sodium perchlorate, except for experiments in which the rates at different ionic strengths were compared.

The visible spectra of the oxidation products were obtained as follows. After vanadium(II) solution was added to a deaerated sodium nitrate solution, the solution was mixed with nitrogen gas and then taken into a capped 1 cm cell in the spectrophotometer, and the time dependence of the absorption was measured. Gas analysis was performed in the following way. After the addition of nitrate ion to vanadium(II) solution in a vacuum vessel, the gases evolved were collected in a CaF_2 gas cell with liquid nitrogen to measure their infrared spectra in the rage 1000—4000 cm^{-1}. The experiments were performed at room temperature and all pH measurements were carried out after completion of the reactions.

Instruments. A Yanagimoto d.c. and a.c. polarograph Model PA-101 was used to obtain the polarograms and the time dependence of diffusion current of vanadium(II). An H-type cell with a saturated calomel electrode was used. The reaction vessel was large enough to hold more than 100 m*l*. The dropping time of the mercury electrode was measured by a Yanagimoto polarograph timer Model SY-2. The characteristic of dropping mercury was 0.830 mg/sec at a height of mercury reservoir of 72.2 cm. All pH measurements were made by a Towadenpa pH meter Model HM-5A. Visible absorption spectra were measured by a Hitachi Model EPV-2 and infrared spectra were recorded using JASCO Model DS-301 and DS-402G infrared spectrophotometers.

15) M. Senda and I. Tachi, *J. Electrochem. Soc. Jap.*, **27**. 83 (1957).

Results and Discussion

Polarographic Behavior of Vanadium(II). Linearity between vanadium(II) concentration and its diffusion current was necessary to obtain kinetic data from the time dependence of the diffusion current. Diffusion currents were measured at various concentrations of vanadium(II) in perchlorate, and sulfate media. Typical results are shown in Fig. 1. On adding vanadium(II) to the electrolyte solution, vanadium(II) was partially oxidized by air. It was found from the value of diffusion current, however, that about 90% of the vanadium ions were in the +2 oxidation state. From Fig. 1, it is polarographically possible to follow the decrease of vanadium(II) concentration by nitrate ion and calculate the rate constant of oxidation. As shown in Fig. 1, the diffusion currents in perchlorate medium are larger than those in sulfate medium. Although the diffusion currents in perchlorate medium were independent of hydrogen ion concentration, those in sulfate medium increased with hydrogen ion concentration and decreased with sulfate ion concentration. The polarographic half-wave potentials, diffusion currents and reversibility are shown in Table 1. The half-wave potentials were almost constant below pH 2 in perchlorate medium. However, they

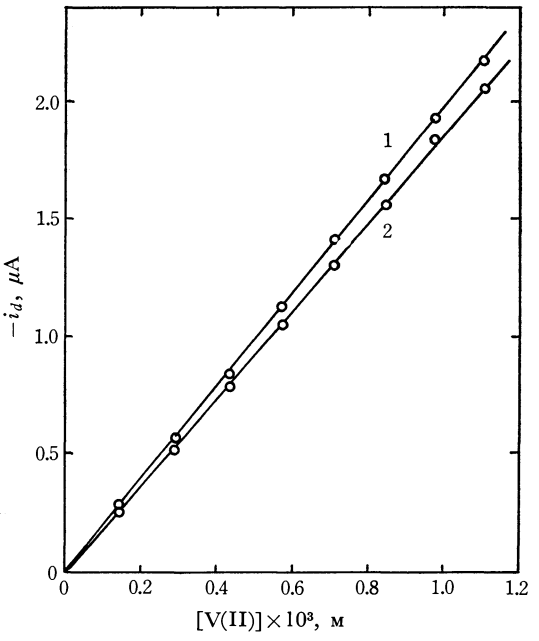

Fig. 1. Relation between vanadium(II) concentration and polarographic diffusion current at pH~4 in the solutions:
1, 0.50 M $NaClO_4$; 2, 0.25 M Na_2SO_4.

TABLE 1. HALF-WAVE POTENTIAL, DIFFUSION CURRENT, AND REVERSIBILITY OF VANADIUM(II) AT 25°C

pH	Perchlorate medium			pH	Sulfate medium		
	$-E_{1/2}$ (V *vs.* SCE)	$-i_d$ (μA)	$i_p/i_d\sqrt{\tau}$ ($\upsilon \cdot A^{-1} \cdot sec^{-1/2}$)		$-E_{1/2}$ (V *vs.* SCE)	$-i_d$ (μA)	$i_p/i_d\sqrt{\tau}$ ($\upsilon \cdot A^{-1} \cdot sec^{-1/2}$)
0.45	0.46	1.97	18.1	0.36[a]	0.50	1.93	6.4
0.69	0.46	1.96	20.3	0.58[a]	0.48	1.90	7.7
1.05	0.46	1.94	22.5	0.98[a]	0.49	1.88	11.2
2.01	0.46	1.95	23.6	1.95[b]	0.50	1.85	10.6
3.05	0.48	1.93	15.1	3.05[b]	0.51	1.82	8.8
4.01	0.50	1.96	10.5	3.94[b]	0.52	1.83	6.3
4.48	0.52	1.95	7.2	4.50[b]	0.53	1.80	4.4

a) H_2SO_4, $NaClO_4$ b) 0.05 M Na_2SO_4, $HClO_4$

shifted to more negative potential and the reversibility markedly decreased above pH 2. It was therefore concluded that vanadium(II) species was V^{2+} (hydrated) and the electro-oxidation product vanadium(III) was the same hydrated species in strongly acidic solution (pH<2). On the other hand, vanadium(III) in weakly acidic solution might form a hydrolyzed species which made the electrode reaction irreversible. In this case, the half-wave potential depends on hydrogen ion concentration. Lingane and Meites found that VO^+ in acetate buffer solution was reduced at more negative potential than VOH^{2+}.[16] However, it is more reasonable to conclude that a considerable amount of vanadium(III) ions in weakly acidic solution formed a dimer VOV^{4+}. Biermann and Wong reported that vanadium(II) species, above 2.5×10^{-3} M in perchloric acid, has a dimeric form, and below this concentration the polynucleation process seems incomplete.[17] From the diffusion currents obtained at various acidities, vanadium(II) species was, however, estimated to be mainly V^{2+}(hydrated) even in weakly acidic solution.

Although the diffusion currents in sulfate medium decreased both with sulfate ion concentration and with increasing pH values, they were linear with respect to vanadium(II) concentration. The half-wave potentials in sulfate medium were more negative than those in perchlorate medium at the same pH value. When sulfuric acid concentration decreased, the half-wave potential shifted to more positive potential and the reversibility became higher. In 0.25 M sodium sulfate, the half-wave potentials slightly shifted to more positive potential with the increase in vanadium(II) concentration, and became almost constant at the potential -0.53 V *vs.* SCE above 0.7×10^{-3} M vanadium(II). Thus, in the present work we could not obtained the results as published in which the half-wave potential is not affected by sulfate ion concentrations.[17] The second wave was observed at a more positive potential ($\sim+0.03$V *vs.* SCE) in weakly

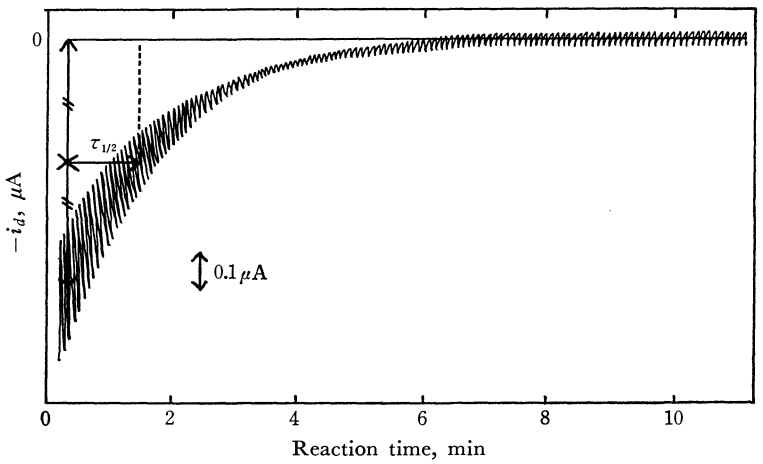

Fig. 2. Typical example of time dependence of polarographic diffusion current in 0.10 M perchloric acid at 25°C.
Initial concentration: 8.49×10^{-4} M vanadium(II), 1.84×10^{-2} M sodium nitrate

16) J. J. Lingane and L. Meites, *J. Amer. Chem. Soc.*, **70**, 2525 (1948).

17) W. J. Bierman and W-K. Wong, *Can. J. Chem.*, **41**, 2510 (1963).

acidic sulfate medium, which corresponded to the oxidation wave of vanadium(III) to vanadium-(IV). From these data, it was concluded that vanadium(II) in sulfate medium partially formed a sulfato-complex or an ion-paired species with sulfate ion and almost all vanadium(III) formed a sulfato-complex.

Zinc(II) ion was present in all of the solution used for the polarographic measurements and its concentrations were almost three times larger than those of vanadium(II). No influence of zinc ion could be observed in the polarograms of vanadium-(II).

Measurement of Rate Constant. A typical time dependence of the diffusion current obtained is shown in Fig. 2. As all reactions were carried out in excess nitrate ion, the rate constants of the oxidation reaction could be calculated from the half-life time of the reaction ($\tau_{1/2}$ shown in Fig. 2) by

$$k=0.6931/\tau_{1/2} \quad (1)$$

This relation is valid only if the rate of the oxidation is first-order with respect to vanadium(II). The logarithmic current-time plots in perchlorate, and sulfate media are shown in Fig. 3 and the rate constants calculated from Eq. (1) are listed in Table 2. From the results, the rates were indicated to be first-order with respect to vanadium(II) concentration, and the rate law is therefore given by

$$-d[V(II)]/dt = k_{obs}[V^{2+}] \quad (2)$$

where k_{obs} is equal to k in Eq. (1).

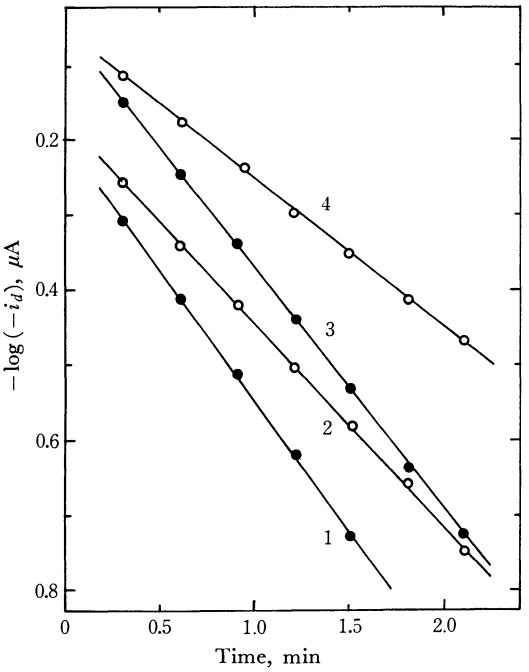

Fig. 3. Dependence of logarithmic current on time in the solutions:
1, 0.10 M H_2SO_4, pH 0.98; 2, 0.10 M $HClO_4$, pH 1.05; 3, 0.10 M Na_2SO_4, pH 4.29; 4, 0.50 M $NaClO_4$, pH 4.33. Initial concentration: *ca.* 8×10^{-4} M vanadium(II), 1.84×10^{-2} M sodium nitrate

Table 2. Dependence of k_{obs} on vanadium(II) concentration at 25°C[a]

Perchlorate medium			Sulfate medium		
pH	10^4[V(II)] M	10^3k_{obs} sec^{-1}	pH	10^4[V(II)] M	10^3k_{obs} sec^{-1}
1.05	5.12	11.2	0.98[b]	5.24	14.2
1.05	4.23	10.9	0.98	4.11	14.3
1.05	3.52	11.1	0.98	3.22	14.1
1.05	2.93	11.0	0.98	2.61	14.0
1.05	2.42	11.1	0.98	2.04	14.3
1.05	2.02	10.9	0.98	1.60	14.2
1.05	1.69	11.0	0.98	1.23	14.3
4.33	5.92	7.18	4.29[c]	5.87	12.3
4.33	4.51	7.36	4.29	4.85	12.4
4.33	3.42	7.21	4.29	3.94	12.8
4.33	2.97	7.27	4.29	2.91	12.8
4.33	2.30	7.33	4.29	2.36	12.9
4.33	1.70	7.23	4.29	1.89	12.5
4.33	1.53	7.36	4.29	1.23	12.9

a) 1.84×10^{-2} M NO^{-3} b) 0.10 M H_2SO_4
c) 0.10 M Na_2SO_4

The possibility for zinc ion to act as a catalytic impurity in this oxidation process was investigated by using electrically prepared vanadium(II). The rate constant ($k_{obs}=6.96\times10^{-3}$ sec^{-1}) at pH 1.66 was almost the same as that ($k_{obs}=6.81\times10^{-3}$ sec^{-1}) obtained using vanadium(II) prepared on zinc amalgam. Oxidation of vanadium(II) by perchlorate ion could not be detected until completion of the reaction by nitrate ion (about 30 min).

Dependence of Rate on Hydrogen Ion Concentration. The rate constants for strongly acidic solutions are plotted in Fig. 4. Sodium sulfate was added to sulfate medium in order to keep the sulfate ion concentration constant at 0.01 M assuming K_a of HSO_4^- to be 4.37×10^{-2} M.[18] Perchloric acid was used to regulate the hydrogen ion concentration of the solution. As shown in Fig. 4, the rate constants in sulfate medium were larger than those in perchlorate medium, but in both cases they were linearly proportional to the hydrogen ion concentration. The rate constants measured in weakly acidic solutions are shown in Fig. 5. In sulfate medium, 0.05 M sodium sulfate was added to the solutions and the hydrogen ion concentration was adjusted with perchloric acid. The results gave the same relationship as in strongly acidic solutions, *viz.*,

18) L. G. Sillén and A. E. Martell, "Stability Constants of Metal-ion Complexes," The Chemical Soc., London (1964), p. 232.

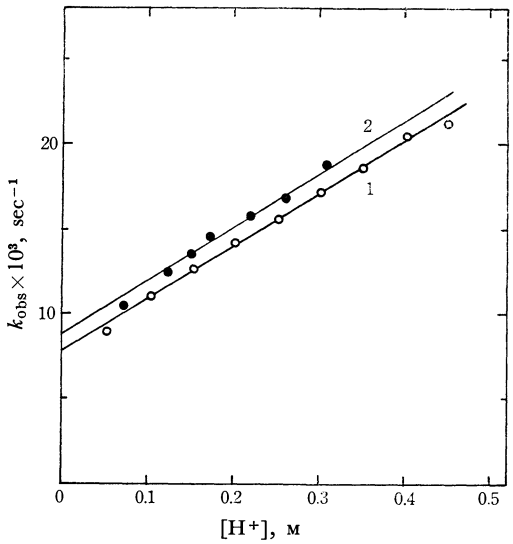

Fig. 4. Dependence of the first-order rate constant on hydrogen ion concentration at 25°C in the solution:
1, $HClO_4$; 2, $HClO_4$, 0.01 M [SO_4^{2-}].
Initial concentration: *ca.* 8×10^{-4} M vanadium-(II), 1.83×10^{-2} M sodium nitrate

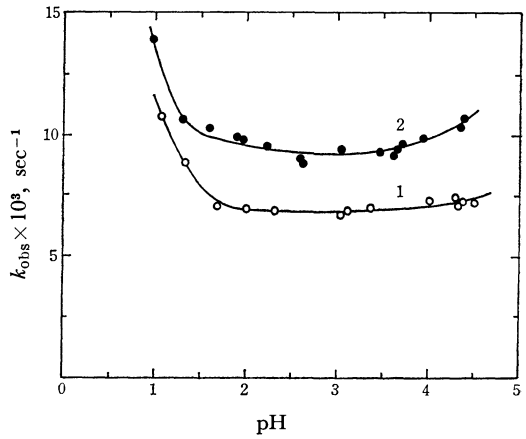

Fig. 5. Variation of the first-order rate constant by hydrogen ion concentration in the solution:
1, $HClO_4$, $NaClO_4$, 2, 0.05 M Na_2SO_4, $HClO_4$, $NaClO_4$.
Initial concentration: *ca.* 8×10^{-4} M vanadium-(II), 1.84×10^{-2} M sodium nitrate

sulfate ion increased the rate of the oxidation reaction. Although the rate constants in both media were almost independent of hydrogen ion concentration above pH 2, they slightly increased above pH 3.5, particularly in sulfate medium. The kinetic data obtained shows that the rate laws can be expressed as follows:

$$pH < 2 \qquad k_{obs} = k_1[H^+] + k_2 \qquad (3)$$

$$pH > 2 \qquad k_{obs} = \text{almost constant} \qquad (4)$$

Dependence of Rate Constants on Ionic Strength. The effects of ionic strength on the rate constant are summarized in Table 3. The results in both media indicate that the rates decreased with the increase of ionic strengths. It has been reported that the rates of the reaction between vanadium(II) and vanadium(IV) increase with ionic strength, and are in good agreement with the extended form of Debye-Hückel's equation. Since the rate of reaction between a cation and a cation system may be increased by an anion which is used for adjusting ionic strength and which decreases the effective charge of the reaction,[4,19] it can be expected that the anion suppresses the rate of reaction between anionic oxidizing agent and the cation which forms an ion-paired species. The rates obtained are interpreted by assuming that vanadium(II) formed an ion-paired species with perchlorate ion. The larger rate constants obtained in sulfate medium are thought to indicate that the reaction proceeds mainly by another oxidation path as mentioned below.

TABLE 3. EFFECT OF IONIC STRENGTH ON k_{obs} AT 25°C

Perchlorate medium (pH 4.4)		Sulfate medium (pH 4.4)[a]	
Ionic strength	10^3k_{obs}[b] sec^{-1}	Ionic strength	10^3k_{obs}[b] sec^{-1}
2.00	5.89	2.00	9.81
1.50	6.17	1.50	10.1
1.00	6.76	1.00	10.9
0.50	7.53	0.50	11.4
0.25	9.38	0.20	12.0

a) 0.10 M Na_2SO_4 b) 1.84×10^{-2} M NO_3^-

Nitrate Ion Dependence of Rate. The rates measured by varying the nitrate ion concentration in perchlorate medium are shown in Fig. 6. From

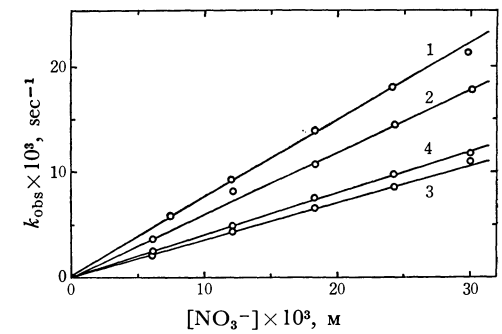

Fig. 6. Nitrate-ion-dependence of rate constant in perchlorate medium at pH 1: 0.80, 2: 1.08, 3: 3.09, 4: 4.38.
Initial concentration: *ca.* 8×10^{-4} M vanadium(II)

19) J. P. Candlin, J. Halpern and S. Nakamura, *J. Amer. Chem. Soc.*, **85**, 2517 (1963).

the results, the rates in various acid solutions were found to be first-order with respect to nitrate ion concentrations and are expressed by

$$k_{obs} = k_3[NO_3^-] \quad (5)$$

As indicated in Fig. 5, the increasing rate with pH above 3.5 in perchlorate medium is confirmed from the relation between the lines 3 and 4 in Fig. 6.

In sulfate medium, the rate increased with sulfate ion concentration and the intercepts of straight lines shown in Fig. 7 are not zero. This indicates that nitrate-ion-independent terms of the rate constants appeared. Even in sulfate medium, the rates were, however, first-order with respect to the nitrate ion concentration. The rate law is

$$k_{obs} = k_4 + k_5[NO_3^-] \quad (6)$$

When nitrate ion was not present in the solution, the diffusion current of vanadium(II) was almost constant for about 30 min, showing that no oxidation occurred by other oxidizing agents such as oxygen in the air. It was therefore concluded that the nitrate-ion-independent term was characteristic of the oxidation in the presence of sulfate ion, in which a sulfato-complex or an ion-paired species was oxidized faster than V^{2+} (hydrated).

After completion of oxidation, the polarograms indicated that the vanadium(III) concentration was about 50% of that of the initial vanadium(II). Since the polarographic wave in large excess of nitrate ion involved the catalytic wave,[20] the species of the reaction product vanadium(III) could not be determined. However, the diffusion current was not affected by vanadium(III) species.

Measurements of Visible Absorption Spectra. It was difficult to measure the rate of oxidation in a weakly acidic solution as used for the polarographic studies because of the small extinction coefficients of vanadium(II) and vanadium(III), and of the high acidity of vanadium(II) stock solution.[21] When sodium nitrate was added to the solution containing 2×10^{-2} M vanadium(II), the solution immediately exhibited a brown color, which gradually changed to green. Hydrogen ion in the vanadium(II) stock solution could be decreased somewhat by employing the experimental condition that hydrogen ion was reduced on zinc amalgam. When sodium nitrate was added to this solution, the brown color developed was so stable that absorption spectra could be measured. The spectra showed a peak at 425 mμ similar to that of the

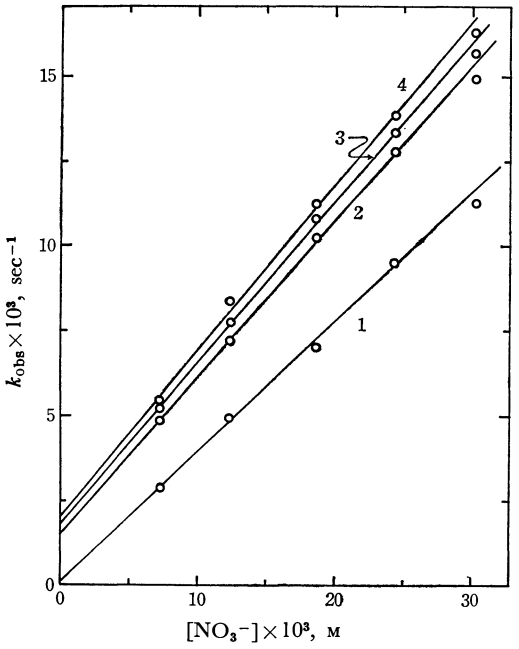

Fig. 7. Effect of sulfate ion on nitrate-ion-dependence of the first-order rate constant at pH~4.4 in the solutions:
1, 0.50 M $NaClO_4$; 2, 0.05 M Na_2SO_4; 3, 0.01 M Na_2SO_4; 4, 0.15 M Na_2SO_4.
Initial concentration: *ca.* 8×10^{-4} M vanadium(II)

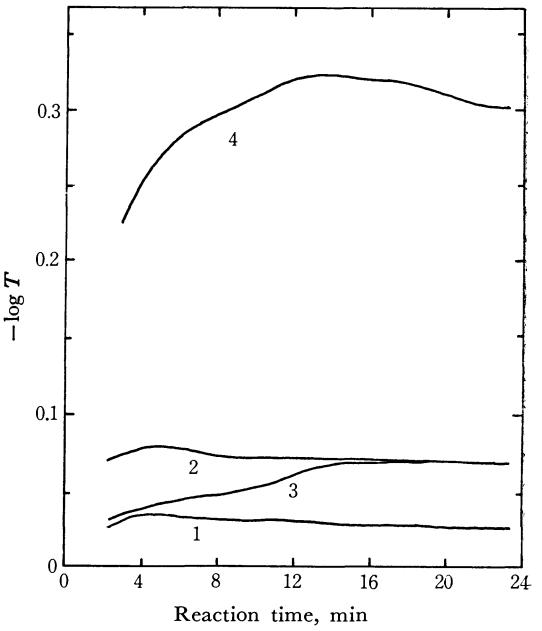

Fig. 8. Time dependence of absorbance at 425 mμ (μ=0.50):
1, 2.38×10^{-3} M vanadium(II) and 8.93×10^{-4} M sodium nitrate in 0.20 M $HClO_4$ (pH 0.80); 2, 1 in 0.20 M H_2SO_4 (pH 0.78); 3, 1.66×10^{-3} M vanadium(II) and 2.86×10^{-3} M sodium nitrate in 0.50 M $NaClO_4$ (pH 4.3); 4, 3 in 0.10 M Na_2SO_4 (pH 4.4)

20) J. W. Olver and J. W. Ross, Jr., *J. Phys. Chem.*, **66**, 1699 (1962).
21) S. C. Furman and C. S. Garner, *J. Amer. Chem. Soc.*, **72**, 1785 (1950).

intermediate VOV^{4+} of the reaction between vanadium(II) and vanadium(IV).[14] Because of a large molar extinction coefficient of this species, it was possible to follow the rate of reaction producing VOV^{4+} in almost the same composition as used for the polarographic measurements. As indicated in Fig. 8, the absorbance at 425 mμ increased both with sulfate ion concentration and with decrease in hydrogen ion. Newton and Baker found that the rate of the reaction between vanadium(II) and vanadium(IV) increased to some extent with a small amount of sulfate ion, and the reaction yielded the intermediate VOV^{4+} which decomposed to monomer in a strongly acidic solution.[14] The time dependence of absorption at 425 mμ in perchlorate medium gave the decomposition rate of the dimer VOV^{4+} to monomer. The half-life time at pH 2.59 was about 1.8 hr. The resulting solution exhibited a yellow green color which was mainly due to the absorption of vanadium(III) monomer. The result indicates that there was a reaction path between vanadium(II) and vanadium(IV) in the oxidation by nitrate ion. It was therefore considered that nitrate ion mainly acted as a one-electron oxidizing agent in strongly acidic solutions and as a two-electron one in weakly acidic solution,[22] and that vanadium(IV) produced by a single two-electron oxidation then reacted with vanadium(II) to yield the dimer. Since vanadium(III) yielded the dimer above pH 2, the dimer was not produced only by the reaction between vanadium(II) and vanadium(IV). Accordingly the oxidation in weakly acidic solutions did not always proceed by a single two-electron oxidation path.

In the present work, the rate constant of the oxidation of vanadium(III) by nitrate ion polarographically measured at pH 1.33 was smaller than 7.7×10^{-5} sec^{-1} at 1.84×10^{-2} M nitrate ion, and this rate was considerably slow compared with that of vanadium(II) by nitrate ion. When sodium nitrate was added to a strongly acidic vanadium(II) solution, the solution first developed a green color which changed to blue corresponding to the absorption of VO^{2+}. This indicates that almost all vanadium ions were once in +3 oxidation state during the course of oxidation reaction, and the polarographic measurements, therefore, followed the overall oxidation of vanadium(II) to vanadium(III).

Effects of Sulfate and Halide Ion on the Rates. The typical effects of anions on the rates of oxidation are shown in Fig. 9. The rate increased with sulfate ion and became almost constant above 0.10 M sulfate ion. The results indicate that above this sulfate ion concentration almost all of vanadium(II) formed a sulfato-complex or an ion-paired species, and the rate of oxidation of this species was not affected any more by increasing sulfate ion concentration. Newton and Baker reported that the rate of the reaction between vanadium(II) and vanadium(IV) increased by adding 4×10^{-3} M sulfate ion. This increase is probably connected with the activation process.[4] These facts lead to the conclusion that the dimer in sulfate medium may be $VOV(SO_4)^{2+}$ and was fairly stable in the solution as discussed in the absorption experiments. It is also considered from the results given in Fig. 9 that a sulfato-complex or an ion-paired species was oxidized faster than V^{2+} (hydrated).

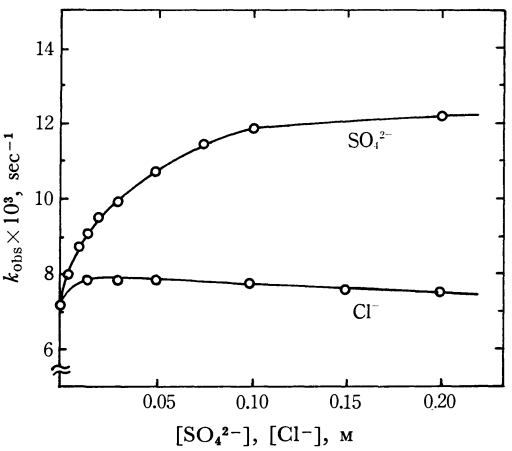

Fig. 9. Effects of sulfate and chloride ion on first-order rate constant at pH∼4.4.
Initial concentration: *ca.* 8×10^{-4} M vanadium(II), 1.84×10^{-2} M sodium nitrate

The half-wave potentials, reversibility and oxidation rates of vanadium(II) by nitrate ion are summarized in Table 4. The half-wave potential in fluoride solution indicates that vanadium(III) formed a fluoro-complex,[13] and the oxidation rate was too fast to be measured by the polarographic method. The polarographic measurements of oxidation in halide solutions, except fluoride, gave almost the same rate constants as in perchlorate medium. From these half-wave potentials, it was considered that only weak complexing took place and therefore the rates were not so much affected by halide ion concentration. However, as shown in Fig. 9, the rate increases with a small amount of chloride ion and becomes gradually suppressed above 2.5×10^{-2} M chloride ion. It has been found that the reaction between vanadium(II) and vanadium(IV) is catalyzed by chloride ion, vanadium(IV) in the presence of a large amount of chloride ion forms a chloro-complex, and the chloride ion does not increase the rate any more.[4]

The reversibility increased from fluoride to iodide solution as shown in Table 4. It was found in the oxidation of titanium(III) by chlorate ion that the smaller the rate constant, the lower the

22) M. Ardon and R. A. Plane, *ibid.*, **81**, 3197 (1957).

TABLE 4. EFFECTS OF SULFATE AND HALIDE IONS ON k_{obs} AT 25°C

Salt	Concentration M	pH	$-E_{1/2}$ V *vs.* sec	$i_p/i_d\sqrt{\tau}$ $\mu \cdot A^{-1} \cdot sec^{-1/2}$	$10^3 k_{obs}$ [a] sec^{-1}
NaF	0.20	7.20	0.67	2.0	very fast
NaCl	0.20	4.52	0.52	11.4	7.30
NaBr	0.20	4.40	0.53	28.3	7.84
NaI	0.20	4.42	0.54	42.8	7.56
Na_2SO_4	0.40	—	0.55	6.2	11.8

a) 1.84×10^{-2} M NO_3^-

reversibility.[23] However, the oxidation rates by nitrate ion increased with sulfate ion and the reversibility were lower than those in perchlorate medium. Although the rates in halide solutions, except fluoride, gave almost the same rate constants, reversibility was markedly varied. The discrepancies can be explained as follows: 1) the electrochemical oxidation product in sulfate medium may be so stable that the product makes the electrode reaction irreversible; 2) in halide solutions, the electron transfer of electrode reaction may be accelerated by halide ion specifically adsorbed on mercury.

Infrared Determination of Gaseous Products. When sodium nitrate was added to acidic vanadium(II) solutions, the solution immediately developed a brown color which gradually turned to green, yielding gaseous products. The gases produced in a vacuum line were collected in a gas cell using liquid nitrogen and determined by measuring their infrared spectra. The results are shown in Table 5. They indicate that NO and N_2O were predominant products in the ratio of 3 : 1.[25,26] However, this ratio in the polarographic measurements is considered to be more favorable to NO because of the large excess of nitrate ion. HNO_2 and NO_2 found in perchlorate medium might be produced by the oxidation of NO with oxygen in the traps, and their amounts negligibly small. The gaseous products immediately generated by the reaction between vanadium(II) and nitrite ion were also detected as NO and N_2O. The oxidizing power of nitrite ion was so strong that vanadium(IV) in acidic solution was easily oxidized to vanadium(V). Since there was such a low oxidation state of nitrogen as N_2O, it was expected that vanadium(II) would be oxidized by NO gas. NO gas easily produced by adding sodium nitrite to ferrous sulfate in sulfuric acid was bubbled through a vanadium(II) solution. The infrared spectrum of gas collected in the gas cell indicated the presence of N_2O. No N_2O was detected from the original NO gas. The solution bubbled for 3 hr developed a blue color corresponding to the absorption of vanadium(IV). The facts varified that vanadium(II) was oxidized to vanadium(IV) by NO gas, and the rate was very slow. However, all reactions investigated by the polarographic method were carried out with a considerable excess of nitrate ion to obtain feasible rates. Therefore, the amount of N_2O produced in the reaction was negligible with respect to the amount of NO. The gaseous products did not affect the time dependence of the diffusion current.

TABLE 5. INFRARED SPECTRUM MEASUREMENTS OF REACTION PRODUCTS FROM NITRATE ION

Perchlorate medium		Sulfate medium	
Observed NO str. Freq. (cm^{-1})	Compound	Observed NO str. Freq. (cm^{-1})	Compound
2223 s	N_2O	2233 s	N_2O
1873 s	NO	1871 s	NO
1678 w	HNO_2[24]	1290 s	N_2O
1620 w	NO_2		
1285 s	N_2O		

s : strong w : weak

Reaction Mechanism. The changes of diffusion currents measured in a large excess of vanadium(II) over nitrate ion showed that the amount of vanadium(II) ions oxidized by nitrate ions was approximately four times larger than that of nitrate ions consumed. In fact, the ratio of vanadium(II) to nitrate ion was 3.7 : 1 in perchlorate medium and 3.9 : 1 in sulfate medium. Therefore, overall oxidation of vanadium(II) by nitrate ion is

$$8V^{2+} + 2NO_3^- + 10H^+ \rightarrow 8V^{3+} + N_2O + 5H_2O$$

The reaction processes involved the oxidation paths of vanadium(II) by vanadium(IV), NO_2^- and NO as mentioned above. Guymon and Spence reported that NO was a major product in the oxidation of molybdenum(V) by nitrate ion and that NO^+ was assumed to be the reactive intermediate.[10] For the oxidation of vanadium(II) by nitrate ion in

23) K. Tanaka, K. Morinaga and K. Nakano, *Nippon Kagaku Zasshi*, **90**, 478 (1969).
24) T. A. Turney and G. A. Wright, *Chem. Rev.*, **59**, 497 (1959).
25) E. L. Saier and A. Pozefsky, *Anal. Chem.*, **26**, 1079 (1954).
26) G. M. Begun and W. H. Fletcher, *J. Chem. Phys.*, **28**, 414 (1958).

the present work, NO^+ was also assumed to be present as a reactive intermediate, and the following possible mechanisms in perchlorate medium were proposed.

$$V^{2+} + NO_3^- + H^+ \xrightarrow{k_I} V^{3+} + NO_2 + OH^- \quad (I)$$

$$V^{2+} + NO_3^- \xrightarrow{k_{II}} VO^{2+} + NO_2^- \quad (II)$$

$$V^{2+} + VO^{2+} \longrightarrow VOV^{4+} \quad (III)$$

$$2NO_2 \rightleftharpoons N_2O_4 \quad (IV)$$

$$N_2O_4 \rightleftharpoons NO^+ + NO_3^- \quad (V)$$

$$V^{2+} + NO^+ \longrightarrow V^{3+} + NO \quad (VI)$$

$$V^{2+} + NO_2^- + 2H^+ \longrightarrow V^{3+} + NO + H_2O \quad (VII)$$

$$2V^{2+} + 2NO + 2H^+ \longrightarrow 2V^{3+} + N_2O + H_2O \quad (VIII)$$

The oxidation rate corresponding to reaction(VII) was polarographically measured and gave a second-order rate constant of 3×10^2 M^{-1}·sec^{-1} at pH 4.70. Thus, the rate of reaction (VII) is very fast and gaseous products such as NO and N_2O were generated. Frank and Spence investigated the oxidation of molybdenum(V) by nitrite ion, and found that the rate law was dependent on nitrite ion and hydrogen ion, but independent of molybdenum (V).[27] This leads to the conclusion that nitrite ions are in the following equilibrium:

$$H^+ + NO_2^- \rightleftharpoons HNO_2 \quad (IX)$$

$$H^+ + HNO_2 \rightleftharpoons NO^+ + H_2O \quad (X)$$

The true oxidation path of reaction(VII) was therefore considered to be the same as that of reaction(VI). Reaction (I) was the predominant oxidation path in strongly acidic solutions and reaction(II) in weakly acidic solutions. The polarographic determination of the reaction between vanadium(II) and vanadium(IV) was performed, and the rate constant obtained at pH 1.66 was 0.545 M^{-1}·sec^{-1}, indicating that the rate was almost the same as that by nitrate ion.

Applying the steady-state condition to NO_2, NO_2^-, N_2O_4, NO^+, and VO^{2+}, the following rate law is obtained.

$$-d[V(II)]/dt=(2k_I[H^+] + 3k_{II})[V^{2+}][NO_3^-] \quad (7)$$

When hydrogen ion concentrations are low, that is, pH>2, Eq. (7) can be written as

$$-d[V(II)]/dt = 3k_{II}[V^{2+}][NO_3^-] \quad (8)$$

These formulas are in good agreement with the experimental rate laws, and the proposed mechanism is in line with kinetic data.

In sulfate medium, the following equilibrium between vanadium(II) and sulfate ion may exist below 0.1 M sulfate ion.

$$V^{2+} + SO_4^{2-} \rightleftharpoons VSO_4 \quad (XI)$$

where VSO_4 shows a sulfato-complex or an ion-paired species. The oxidation rate of this species is faster than that in perchlorate medium, and the following oxidation paths may be involved.

$$VSO_4 + NO_3^- + H^+ \longrightarrow VSO_4^+ + NO_2 + OH^- \quad (I')$$

$$VSO_4 + NO_3^- \longrightarrow VOSO_4 + NO_2^- \quad (II')$$

$$V^{2+} + VOSO_4 \longrightarrow VOV(SO_4)^{2+} \quad (III')$$

As mentioned in the visible absorption experiments, the stable dimer of vanadium(III) in sulfate medium might be produced by reaction (III). However, it is difficult from the present data to interpret the nitrate-ion-independent term k_4 in Eq. (6), so that further work for the oxidation in sulfate medium is necessary.

Conocchioli *et al.* investigated the oxidation of iron(II) by hypochlorate ion and suggested that iron(IV) was produced as an intermediate by a single two-electron oxidation.[28] Oxidation of vanadium(II) by thallium(III) proceeds mainly by a single two-electron step.[5] When vanadium (II) was oxidized by hydrogen peroxide and oxygen, about 30% and 60%, respectively, vanadium(III) was formed by the reaction between vanadium(II) and vanadium (IV).[3] The results obtained for the oxidation of vanadium(II) by nitrate ion might show that reactions (I) and (II) proceed by one-electron oxidation, and reactions (II) and (III) by two-electron one, the latter occurring mainly in weakly acidic solutions, particularly in sulfate medium. The two-electron oxidation would also be possible in the reaction between vanadium(II) and nitrate ion. However, when sodium nitrite was added to acidic vanadium(II) solution, the solution did not exhibit a brown color. This shows that nitrate ion acted as a one-electron oxidizing agent.

The energy of activation was determined by measuring the rate of overall reactions at five temperatures, 15, 20, 25, 30, and 38°C.[29] The results obtained are shown in Table 6.

Table 6. Activation enthalpy and entropy of overall reaction at $\mu=0.50$

Composition[a]	pH	$\Delta H^{\neq}$ Kcal	$\Delta S^{\neq}$ e.u.
0.50 M $NaClO_4$	4.45	13.3	−21.4
0.10 M Na_2SO_4	4.42	14.6	−11.9

a) 8.10×10^{-4} M V(II), 1.84×10^{-2} M NO_3^-

The author is indebted to Dr. E. Miki for the infrared spectrum measurements of gaseous products from nitrate ion.

27) J. A. Frank and J. T. Spence, *J. Phys. Chem.*, **68**, 2131 (1964).

28) T. J. Conocchioli, E. J. Hamilton, Jr., and N. Sutin, *J. Amer. Chem. Soc.*, **87**, 926 (1965).

29) K. J. Laidler, "Reaction Kinetics," Vol. **1** Pergamon Press (1963), p. 84.

BULLETIN OF THE CHEMICAL SOCIETY OF JAPAN VOL. 43 2039—2041 (1970)

The Polarography of Alkyl Hydroperoxides in an Aqueous Solution

Shigeo HAYANO and Noriko SHINOZUKA

Institute of Industrial Science, The University of Tokyo, Roppongi, Minato-ku, Tokyo

(Received November, 17, 1969)

The polarographic behavior of alkyl hydroperoxides was studied. *n*-Propyl, *n*-butyl, *n*-hexyl, and *n*-octyl hydroperoxide in an aqueous solution all show diffusion-controlled irreversible waves. The effect of the pH on the $E_{1/2}$ and $n\alpha$ values is very small. The length of the alkyl group has a marked effect on $E_{1/2}$ and $n\alpha$. The longer the chain length of the alkyl group, the larger the value of $n\alpha$ and the more positive the $E_{1/2}$. The linear free-energy relationship was found for the four alkyl hydroperoxides examined. The relation of Taft's polar substituent coefficient to $E_{1/2}$ has a negative reaction constant, which indicates a reaction promoted by high electron density in the reactive group. The electrode process seems to be the rupture of the -O–O- bond, followed by the protonation of the ions produced on the electrode.

Polarography is a versatile electrometric method that offers one of the best techniques for peroxide analysis. As most organic peroxides are polarographically reducible, their polarographic behavior has been studied for twenty years.[1-6] The electrode process may be a two-electron transfer, which leads to the rupture of the -O–O- bond, thus forming an OH group:[7]

$$ROOR + 2e + 2H \rightarrow ROH + ROH$$

The details of the above reaction have been discussed recently,[8,9] but have not yet been confirmed. The available data about the reaction of alkyl hydroperoxides provided by different authors are not sufficient for systematic discussion.

This paper will describe the polarographic behavior of the lower alkyl hydroperoxides (*n*-propyl, *n*-butyl, *n*-hexyl, and *n*-octyl hydroperoxides) synthesized in our laboratory and will discuss the electrode process in relation to the polarographic data and the organic structure. The relation of Taft's substituent coefficient to the $E_{1/2}$ values of the four compounds shows a linear line, the slope of which has a negative sign.

Experimental

All the alkyl hydroperoxides examined, *n*-propyl, *n*-butyl *n*-hexyl, and *n*-octyl hydroperoxide, were synthesized by the use of alkylmethane sulfonates.[10] The active oxygen values were determined by iodometric titration. The hydrogen peroxide and contaminated peroxides were checked by thin-layer chromatography.

Britton-Robinson's buffer solution was deaerated by N_2 bubbling for about 30 min; an alcoholic solution of a hydroperoxide was added to it with a microsyringe or a micropiette, and then N_2 was again bubbled in for a few minutes. The alcohol content was within 10 vol%.

A YEW POL-11-type polarograph (Yokogawa Denki Co.) was used for recording the d.c. polarograms. The pH of the solution was measured with a Toa Dempa PM-5A pH meter. The dropping electrode had the following characteristics: $m=2.07$ mg/sec, $t=3.58$ sec (in pure water, open circuit). No decomposition of the sample could be detected during the measurements. All the measurements were carried out at 25°C.

Results and Discussion

1) Shape of Polarographic Waves. With the four hydroperoxides examined, ill-defined waves were obtained. The wave shape indicates the irreversible nature of the step; this was confirmed by low peak height of the a.c. polarography. In both acid and alkaline solutions, the limiting currents were proportional to the hydroperoxide concentration. The half-wave potential was constant for hydroperoxide concentrations of 10^{-5}—10^{-4} M. The limiting current has a linear relation-

1) F. A. Bovey and I. M. Kolthoff, *J. Amer. Chem. Soc.*, **69**, 2143 (1947).
2) D. Swern, H. B. Knights C. O. Willits and C. Ricciuti, *Anal. Chem.*, **24**, 785 (1952).
3) H. Brüschweiler and G. J. Minkoff, *Anal. Chim. Acta*, **12**, 186 (1955).
4) D. A. Skoog and A. B. H. Lauwzecha, *Anal. Chem.*, **28**, 825, (1956).
5) R. M. Johnson and I. W. Siddigi, *J. Polarograph. Soc.*, **11**, 72 (1965).
6) H. Luck and R. Maak, *Fette, Seifen und Austrichmittel*, **68**, 305 (1966).
7) E. J. Kutta and F. W. Quackenbush, *Anal. Chem.*, **32**, 1069 (1960).
8) M. Schulz and K. H. Schwarz, *Monatsber. Deut. Akad. Wis.* (Berlin), **6**, 515 (1964).
9) E. S. Levin and A. U. Yamshchikov, *Elektrochim.*, **4**, 54 (1968).
10) H. R. Williams and H. S. Mosher, *J. Amer. Chem. Soc.*, **76**, 2984 (1954).

ship with the square root of the Hg height. The temperature coefficient of the limiting current is about 1% between 15—35°C. These results indicate that the limiting current is diffusion-controlled.

2) Dependence of Apparent $E_{1/2}$ on pH. The apparent $E_{1/2}$ values at various pH values are shown in Fig. 1. All the compounds shift with the half-wave potential more negative as the pH increases, but the effect of the pH is very small. As the number of carbon atoms increases, the half-wave potential shifts toward a more positive potential.

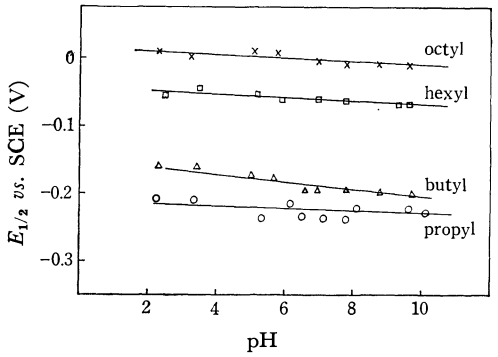

Fig. 1. Relation of $E_{1/2}$ to pH.

3) Dependence of $n\alpha$ Values on pH. As the hydroperoxides show irreversible polarographic waves, the slopes of log-plots gave $n\alpha$ values. The values of $n\alpha$ calculated at various pH are plotted in Fig. 2. Each compound seems not to change in its $n\alpha$ value with the pH of the solution. The tendency for a large alkyl group to have a large $n\alpha$ value indicates that if n=constant, a large alkyl group diminishes in polarographic irreversibility: this accords with the fact that the waves for the higher homologues are steep and well-defined.[8]

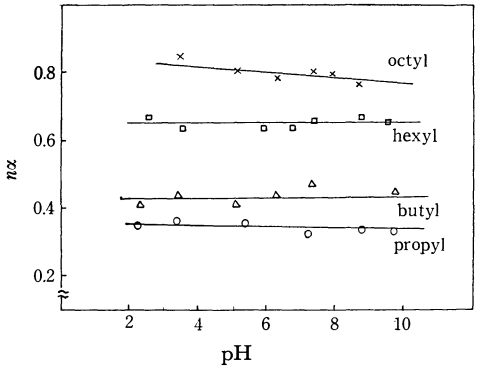

Fig. 2. Relation of $n\alpha$ to pH.

4) Effect of the Alkyl Group on $E_{1/2}$ and $n\alpha$. $E_{1/2}$ and $n\alpha$ are affected by the length of the alkyl group of the hydroperoxides. The plots of the half-wave potential and $n\alpha$ values against the chain length show a linear relation with the C_3—C_8 compounds (Figs. 3,4). The $E_{1/2}$ of C_1—C_2 hydroperoxides, quoted from Ref. (8), has a steeper slope than that of C_3—C_8.

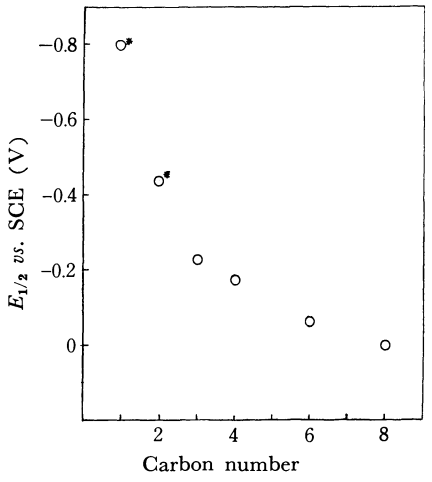

Fig. 3. Relation of $E_{1/2}$ (at pH=7) to chain length.
○*: from Ref. 8.

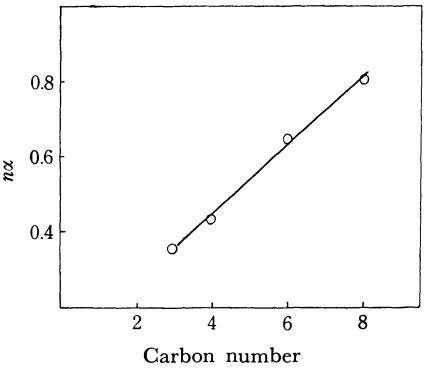

Fig. 4. Relation of $n\alpha$ to chain length.

5) The Electrode Reaction of Alkyl Hydroperoxides. The relation of the half-wave potential to Taft's polar substituent constant, σ_x*, is shown in Fig. 5. The half-wave potential of the irreversible electrode process is expressed as follows:[11]

$$E_{1/2} = E_0 + \frac{RT}{n\alpha F} \ln 0.87\, k_f^\circ \sqrt{\frac{t_1}{D}} \qquad (1)$$

$$\frac{\partial E_{1/2}}{\partial \mathrm{pH}} = -\frac{2.3RT}{\alpha F}$$

11) J. Heyrovsky and J. Kuta, "Principle of Polarography," Academic Press, New York (1966), p. 257.

where E_0 is the standard oxidation-reduction potential; R, the gas constant; T, the absolute temperature; α, the transfer coefficient; n, the number of electrons transferred in the electrode process; F, the faraday; $k_f{}^0$, the rate constant of the electrode process; t_1, the drop time, and D, the diffusion coefficient. From this equation, the linear free-energy relationship can be said to be valid when it is assumed that the value of the $dE_{1/2}/dpH$ slope and that of the transfer coefficient determined from the shape of the wave remain unchanged for all the members of the reaction series under study.[12] Therefore, strictly speaking, only with the large alkyl-group hydroperoxides which may have almost the same α values can a linear correlation be expected.

Recently Zuman has reported[13] that, in some instances, $dE_{1/2}/dpH$ and $RT/\alpha nF$ are approximately linear function of the substituent constant, $\sigma_x{}^*$. In some other cases, plots of $(E_{1/2}\cdot dE_{1/2}/dpH)$ or $(E_{1/2}\cdot RT/\alpha nF)$ against $\sigma_x{}^*$ show a better correlation than the $E_{1/2}$–$\sigma_x{}^*$ plots. On the other hand, in alkyl hydroperoxides, plots of $E_{1/2}\cdot RT/\alpha nF$ against $\sigma_x{}^*$ do not show any better correlation.

From the negative reaction constant in Fig. 5, it can be assumed that the reaction is promoted by high-electron density on the reaction group. The independence of the half-wave potential on pH suggests that the proton does not directly participate in the electrode process. The fact that in such aprotic solvent as acetonitrile and dimethylformamide the waves elongate and become ill-defined, can be interpreted in terms of the increased irreversibility in aprotic solvents. This indicates a proton contribution to the overall reaction.

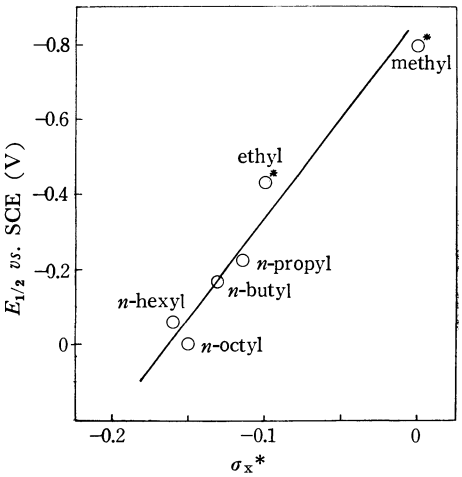

Fig. 5. Relation of $E_{1/2}$ to Taft polar substitution constant $\sigma_x{}^*$.
○*: from Ref. 8.

From the facts described above, it seems likely that the electrode process is as follows:

$$ROOH + 2e \xrightarrow{slow} RO^- + OH^-$$

$$OH^- + RO^- + 2H \xrightarrow{fast} ROH + H_2O$$

12) P. Zuman, "Substitution Effects in Organic Polarography," Plenum Press, New York (1967), p. 12.
13) *ibid.*, p. 196.

BULLETIN OF THE CHEMICAL SOCIETY OF JAPAN VOL. 43 2042—2045 (1970)

Polarographic Behaviors and Potentiostatic Determination of Kinetic Parameters for the Electrode Reaction of *trans*-1,2-Cyclohexanediaminetetraacetatochromate(III) Complexes

Nobuyuki TANAKA, Takeshi TOMITA and Akifumi YAMADA

Department of Chemistry, Faculty of Science, Tohoku University, Katahira, Sendai

(Received November 21, 1969)

The polarogographic behaviors of *trans*-1,2-cyclohexanediaminetetraacetatochromate(III) complex have been studied. The complex is reduced reversibly at the dropping mercury electrode in the solution which contains 0.4 M sodium chloride, 0.1 M acetate buffer and 2×10^{-6} M polyoxyethylene lauryl ether. The kinetic parameters of this oxidation-reduction process have been determined from the potentiostatic measurements at 25°C. The measured parameters are: the standard potential ($E_0)_{ms}=-1.198$ V *vs.* SCE, the standard rate constant $(k_s)_{ms}=2.9\times10^{-2}$ cm sec^{-1}, the transfer coefficient for cathodic process $(\alpha_c)_{ms}=0.33$ and that for anodic one $(\alpha_a)_{ms}=0.67$. The Frumkin correction for the electrical double layer has been applied to these parameters and the corrected values thus obtained are: $(E_0)_{corr}=-1.198$ V *vs.* SCE, $(k_s)_{corr}=0.93$ cm sec^{-1}, $(\alpha_c)_{corr}=0.40$ and $(\alpha_a)_{corr}=0.57$.

The theoretical treatment of the potentiostatic method for the study of fast electrode reactions and its application to the oxidation-reduction processes of Cr(II)–EDTA/Cr(III)–EDTA and Co(II)–EDTA/Co(III)–EDTA systems have been reported,[1-3] where EDTA means ethylenediaminetetraacetic acid. A ligand, *trans*-1,2-cyclohexanediaminetetraacetic acid (CyDTA), which is very similar to EDTA, also forms a stable chelate with chromium(III) ion[4] in difference of a more bulky ion.

In this report, the polarographic behaviors of Cr(III)–CyDTA have been studied and the kinetic parameters of the electrode reaction have been measured by the potentiostatic method. The Frumkin correction has been applied for the effect of electrical double layer at the electrode solution interface.

Experimental

Reagents. The stock solution of *trans*-1,2-cyclohexanediaminetetraacetatochromate(III) complex was prepared by adding the solution of hexaaquochromium(III) perchlorate (0.1 M) to the solution of disodium *trans*-1,2-cyclohexanediaminetetraacetate (0.1 M), and by heating on the water-bath for half an hour. Then, the solution was passed through a cation exchanger Dowex 50W-X8 to remove unreacted chromium ions. The concentration of the complex was determined polarographically after oxidizing chromium(III) to chromate with hydrogen peroxide.[5] All other chemicals used were of guaranteed reagent-grade.

Apparatus. Polarographic measurements were carried out with a Yokogawa Polarocorder POL-11. The potentiostat used was constructed in this laboratory and its characteristics were described previously.[3] The dropping mercury electrode used for polarographic measurements had an *m*-value of 2.02 mg sec^{-1} and a drop time t_d of 4.05 sec in 0.5 M sodium chloride solution at -0.5 V *vs.* SCE and at 63 cm mercury height. The visible absorption spectra of the solution was measured with a Hitachi EPU-2 spectrophotometer. Electrolysis at constant potential was carried out with a Yanagimoto Controlled Potential Electrolyser.

Results and Discussion

Polarographic Studies. The complex ion has two absorption maxima in the visible region at 18.3×10^3 cm^{-1} (ν_1, log $\varepsilon_1=2.05$) and 25.4×10^3 cm^{-1} (ν_2, log $\varepsilon_2=2.39$), respectively. No apparent change in visible spectra was found in the pH range from 4.2 to 7.7, and this may suggest that the predominant complex species have the ligand coordinated to the chromium(III) ion as a pentadentate or hexadentate in the same way in Cr(III)–EDTA complex.

Polarograms were obtained in a solution containing 1.0 mM Cr(III)-CyDTA, 0.4 M NaCl, 0.1 M acetate or phosphate buffer (pH 4.2 to 7.7) and 2×10^{-6} M polyoxyethylene lauryl ether (LEO) at 25°C. Examples are given in Fig. 1. As seen in Table 1, the half-wave potentials were at -1.200

1) N. Tanaka and A. Yamada, *Electrochim. Acta*, **14**, 491 (1969).

2) A. Yamada and N. Tanaka, This Bulletin, **42**, 1600 (1969).

3) A. Yamada and N. Tanaka, *Sci. Repts. Tohoku Univ. Series I*, **52**, 73 (1969).

4) A. R. Selmer-Olsen, *Anal. Chim. Acta*, **26**, 482 (1962).

5) I. M. Kolthoff and J. J. Lingane, "Polarography," Vol. 2, Interscience, New York (1952), p. 455.

Table 1. Effect of pH and surface-active substance on the polarogram of 1.0 mM Cr(III)-CyDTA in solutions containing 0.4 M NaCl and 0.1 M buffer (acetate or phosphate*) at 25°C

Surface-active substance	pH	$\bar{i}_d$ μA	$E_{1/2}$ V *vs.* SCE	Slope of log plot mV
2×10^{-6} M LEO	4.20	−3.00	−1.201	62
2×10^{-6} M LEO	4.46	−2.98	−1.202	61
2×10^{-6} M LEO	4.67	−3.00	−1.200	61
2×10^{-6} M LEO	5.02	−3.00	−1.200	61
2×10^{-6} M LEO	5.47	−2.99	−1.202	62
2×10^{-6} M LEO	*6.85	−2.97	−1.202	62
2×10^{-6} M LEO	*7.72	−2.85	−1.202	62
free		maximum wave		
1×10^{-6} M LEO	4.67	−3.00	−1.200	61
2×10^{-6} M LEO	4.67	−3.00	−1.200	61
5×10^{-6} M LEO	4.67	−2.95	−1.202	64
10×10^{-6} M LEO	4.67	−2.92	−1.204	67
5×10^{-4}% gelatin	4.67	−3.01	−1.201	61
5×10^{-3}% gelatin	4.67	−2.96	−1.202	62

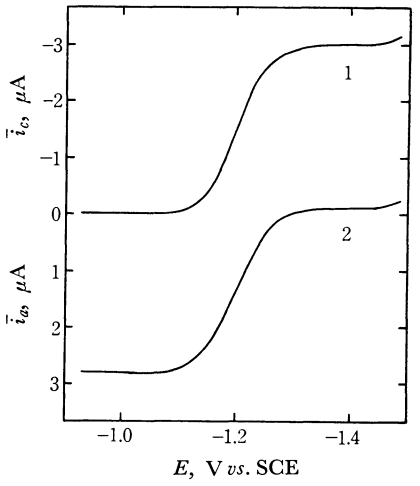

Fig. 1. Polarograms of 1.0 mM Cr-CyDTA complex in solutions of pH 4.7 containing 0.4 M NaCl, 0.1 M acetate buffer and 2×10^{-6} M LEO at 25°C: (1) Cathodic wave of Cr(III)-CyDTA; (2) anodic wave of Cr(II)-CyDTA produced by electrolytic reduction with a mercury pool electrode.

V *vs.* SCE in both cathodic and anodic processes and the limiting current, which was diffusion controlled, was of a one-electron reduction. These and the slope of log-plot indicated that the electrode processes of Cr(II, III)-CyDTA complexes are reversible. Little changes in cathodic current and $E_{1/2}$ were observed in this pH region; this may indicate that the complex species present in the solution and at the electrode surface is only one species, [Cr(III)–CyDTA]$^-$ for oxidant and [Cr(II)–CyDTA]$^{2-}$ for reductant ions.

The effect of surface-active substance on the polarographic wave was relatively small unless the concentration of the substance was too high; in the case of LEO, for example, unless its concentration exceeded about 10^{-5} M, as shown in Table 1.

Electrolysis was carried out in a deaerated solution containing 1.0 mM Cr(III)–CyDTA, 0.4 M NaCl, 0.1 M acetate buffer (pH 4.7) and 2×10^{-6} M LEO with the mercury pool electrode, the potential of which was set at −1.40 V *vs.* SCE at 25°C. A polarogram of the solution after electrolysis was given in Fig. 1, which showed a limiting diffusion current used for the determination of Cr(II)–CyDTA complex. Diffusion coefficients of Cr(III)–CyDTA and Cr(II)–CyDTA were 5.5×10^{-6} cm^2 sec^{-1} and 5.4×10^{-6} cm^2 sec^{-1}, respectively. These values are smaller than those of Cr–EDTA complexes, and seem to be reasonable because the sizes of Cr–CyDTA ions are larger than those of Cr–EDTA ions.

From these results mentioned above, the electrode process is considered as,

$$[\text{Cr(III)-CyDTA}]^- + e \rightleftarrows [\text{Cr(II)-CyDTA}]^{2-} \quad (1)$$

in which any chemical reaction, *e.g.* protonation reaction, is not involved appreciably in the range of pH 4.2 to 7.7.

Equilibrium potentials of this oxidation-reduction process were measured polarographically, using the Nernst's equation at 25°C. A straight line was obtained with a reciprocal slope of 61 mV by plotting E_e *versus* $\log\{[\text{Cr(III)–CyDTA}]/[\text{Cr(II)–CyDTA}]\}$, as shown in Fig. 2. The standard potential $(E_0)_e$ was found to be −1.199 V *vs.* SCE.

Determination of Kinetic Parameters by Means of Potentiostatic Method. When an electrode reaction is expressed as,

$$O + ne \rightleftarrows R \quad (2)$$

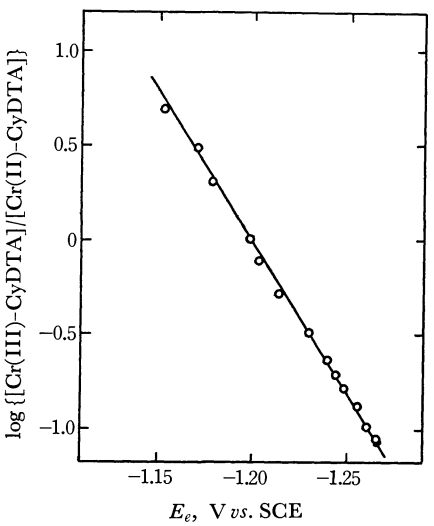

Fig. 2. Relation between equilibrium potential E_e and log{[Cr(III)-CyDTA]/[Cr(II)-CyDTA]} at 25°C. Each concentration was determined polarographically. Cr(II)-CyDTA was prepared by electrolytic reduction with a mercury pool electrode in the solution of pH 4.7 containing Cr(III)-CyDTA, 0.4 M NaCl, 0.1 M acetate buffer and 2×10^{-6} M LEO.

the relation between cathodic current i and t, time after the beginning of the electroreduction at a given potential, can be represented by the equations,[1-2]

$$\left(\frac{i}{i_d}\right)_t \Big/ \left(\frac{i}{i_d}\right)_\tau = \sqrt{\pi}\lambda_{ms}\sqrt{t}\exp(\lambda_{ms}^2 t)\operatorname{erfc}(\lambda_{ms}\sqrt{t}) \qquad \sqrt{\tau} \gg \sqrt{t} \tag{3}$$

$$(k_c)_{ms} = \lambda_{ms}\left(\frac{i}{i_d}\right)_\tau \sqrt{D_O} \tag{4}$$

$$(k_a)_{ms} = \lambda_{ms}\left\{1-\left(\frac{i}{i_d}\right)_\tau\right\}\sqrt{D_R} \tag{5}$$

where

$$\lambda_{ms} = \frac{(k_c)_{ms}}{\sqrt{D_O}} + \frac{(k_a)_{ms}}{\sqrt{D_R}} \tag{6}$$

D_O and D_R are the diffusion coefficients of oxidant and reductant, respectively. Since the ratio of $(i/i_d)_t$ to $(i/i_d)_\tau$ and time, t, are measurable, λ_{ms} can be evaluated at various potentials. The measured rate constants of the cathodic and the anodic process, $(k_c)_{ms}$ and $(k_a)_{ms}$, can be obtained with these λ_{ms} values. Kinetic parameters*1 of the electrode reaction are calculated from the relations,

$$(k_c)_{ms} = (k_s)_{ms}\exp\left[-\frac{(\alpha_c)_{ms}n\boldsymbol{F}}{\boldsymbol{RT}}(E-(E_0)_{ms})\right] \tag{7}$$

$$(k_a)_{ms} = (k_s)_{ms}\exp\left[\frac{(\alpha_a)_{ms}n\boldsymbol{F}}{\boldsymbol{RT}}(E-(E_0)_{ms})\right] \tag{8}$$

*1 The notations of parameters used here except $(k_s)_{corr}$, which corresponds practically to $(k_s)^c{}_{corr}$, are identical with those described previously.[2]

Plotting $\log(k_c)_{ms}$ against E and $\log(k_a)_{ms}$ against E (Fig. 3), the measured standard potential $(E_0)_{ms}$ can be obtained from the point of intersection of two straight lines, each slope of which gives the measured transfer coefficients $(\alpha_c)_{ms}$ and $(\alpha_a)_{ms}$ for the cathodic and the anodic process, respectively. The values of $(i/i_d)_t$ and $(i/i_d)_\tau$ which were obtained at various potentials and also those of $(k_c)_{ms}$ and $(k_a)_{ms}$ calculated therefrom are given in Table 2.

Frumkin Correction. All measured parameters involve the influence of the electrical double layer. On the assumption that neither reactant nor supporting electrolyte is specifically adsorbed, we can consider the effect of the double layer ac-

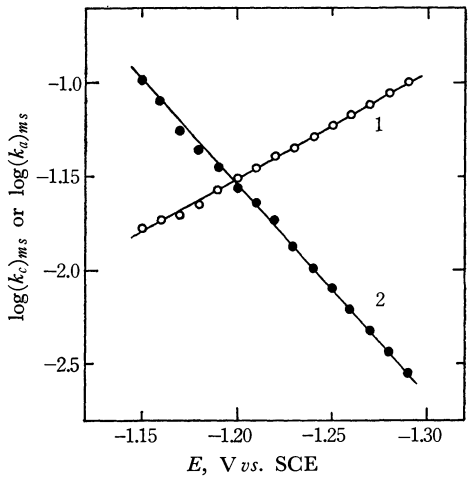

Fig. 3. Relations of (1) $\log(k_c)_{ms}$ *vs.* E and (2) $\log(k_a)_m$ & *vs.* E obtained with 1 mM Cr(III)-CyDTA in the solution of 4.7 containing 0.4 M NaCl, 0.1 M acetate buffer and 2×10^{-6} M LEO at 25°C.

TABLE 2. MEASURED KINETIC DATA OF THE ELECTRODE REACTION OF Cr(III)-CyDTA IN 0.1 M ACETATE BUFFER + 0.4 M NaCl + 2×10^{-6} M LEO (pH 4.7) 25°C

E V vs. SCE	$(i/i_d)_t$*	$(i/i_d)_\tau$**	$(k_c)_{ms}$ cm sec^{-1}	$(k_a)_{ms}$ cm sec^{-1}
−1.170	0.16_7	0.25_2	0.019_5	0.055_4
−1.180	0.21_5	0.33_1	0.022_7	0.043_8
−1.190	0.25_2	0.42_0	0.026_6	0.035_2
−1.200	0.29_7	0.51_6	0.030_3	0.027_2
−1.210	0.34_6	0.60_0	0.035_4	0.022_5
−1.220	0.39_7	0.68_6	0.040_6	0.017_7
−1.230	0.44_6	0.77_1	0.045_5	0.012_9
−1.240	0.49_6	0.83_2	0.052_0	0.010_0
−1.250	0.54_4	0.87_9	0.059_1	0.0078_0
−1.260	0.59_1	0.91_4	0.066_6	0.0060_0

* Time after beginning of electrolysis: $t=0.51_4$ msec

** Time after beginning of electrolysis: $\tau=0.11_0$ sec

cording to the Frumkin correction.

The values of ϕ_2 potential at the outer Helmholtz plane of double layer were determined by the measurements of the differential capacity and the electrocapillary curve of the supporting electrolyte solution. The ϕ_2 potentials thus obtained were shown in Fig. 4.

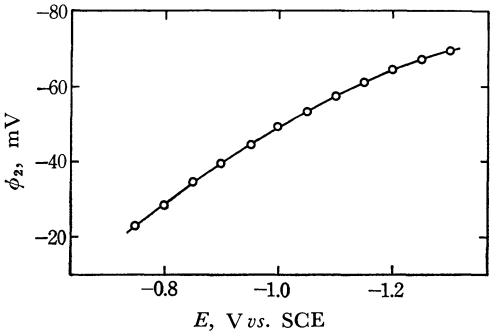

Fig. 4. Values of ϕ_2 potential at outer Helmholtz plane as a function of the electrode potential E. ϕ_2 was measured in the solution of pH 4.7 containing 0.4 M NaCl, 0.1 M acetate buffer and 2×10^{-6} M LEO at 25°C, under the assumption that no specific adsorption took place.

Arranged forms of Frumkin's equations are expressed as follows:[1]

$$(k_c)'_{ms} \equiv (k_c)_{ms}\exp\left[\frac{z_O\boldsymbol{F}}{\boldsymbol{RT}}\phi_2\right] = (k_s)_{corr}\exp\left[-\frac{(\alpha_c)_{corr}n\boldsymbol{F}}{\boldsymbol{RT}}(E-\phi_2)\right] \times\exp\left[\frac{(\alpha_c)_{corr}n\boldsymbol{F}}{\boldsymbol{RT}}(E_0)_{corr}\right] \quad (9)$$

$$(k_a)'_{ms} \equiv (k_a)_{ms}\exp\left[\frac{z_R\boldsymbol{F}}{\boldsymbol{RT}}\phi_2\right] = (k_s)_{corr}\exp\left[\frac{(\alpha_a)_{corr}n\boldsymbol{F}}{\boldsymbol{RT}}(E-\phi_2)\right] \times\exp\left[\frac{(\alpha_a)_{corr}n\boldsymbol{F}}{\boldsymbol{RT}}(E_0)_{corr}\right] \quad (10)$$

The plots of $\log(k_c)'_{ms}$ *vs.* $(E-\phi_2)$ and those of $\log(k_a)'_{ms}$ *vs.* $(E-\phi_2)$ were found to give straight lines, of which the intersection gave the corrected standard potential $(E_0)_{corr}$ and the corrected standard rate constant $(k_s)_{corr}$ and the slopes did the transfer coefficients $(\alpha_c)_{corr}$ and $(\alpha_a)_{corr}$, respectively (Fig. 5).

Kinetic parameters thus obtained are given in Table 3. The standard rate constants $(k_s)_{ms}$ and $(k_s)_{corr}$ are smaller than those of Cr–EDTA system. This may be supported by the observations that the polarographic reduction wave of Cr(III)–CyDTA complexes was more suppressed by the addition of the same amount of surface-active substances than that of Cr(III)–EDTA complexes. In this connection, it may also be interesting that on electrolysis at a constant potential, the reduced form,

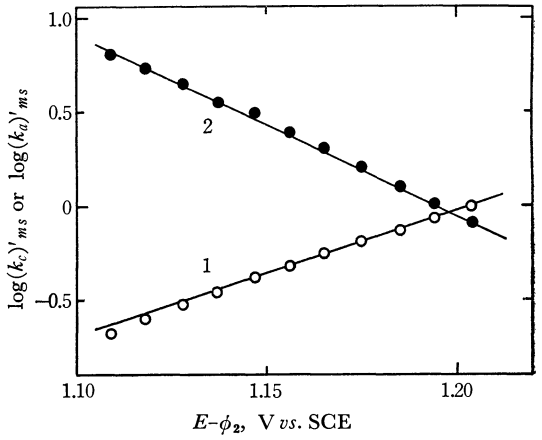

Fig. 5. (1) $\log(k_c)'_{ms}$ *vs.* $(E-\phi_2)$ and (2) $\log(k_a)'_{ms}$ *vs.* $(E-\phi_2)$ obtained with 1.0 mM Cr(III)-CyDTA in the solution of pH 4.7 containing 0.4 M NaCl, 0.1 M acetate buffer and 2×10^{-6} M LEO at 25°C. $(k_c)'_{ms}$ and $(k_a)'_{ms}$ are defined by Eqs. (9) and (10), respectively.

Table 3. Kinetic parameters of the electrode reactions of Cr(II, III)-EDTA[2] and Cr(II, III)-CyDTA systems

	Cr(II)-EDTA/ Cr(III)-EDTA	Cr(II)-CyDTA/ Cr(III)-CyDTA
$(E_0)_{ms}$, V *vs.* SCE	−1.220	−1.198
$(k_s)_{ms}$, cm sec^{-1}	0.21	0.029
$(\alpha_c)_{ms}$	0.58	0.33
$(\alpha_a)_{ms}$	0.39	0.67
$(E_0)_{corr}$, V *vs.* SCE	−1.220	−1.198
$(k_s)_{corr}$, cm sec^{-1}	17*	0.93
$(\alpha_c)_{corr}$	0.54	0.40
$(\alpha_a)_{corr}$	0.43	0.57

* This value is given for $(k_s)^c_{corr}$ in Ref. 2, which practically corresponds to $(k_s)_{corr}$ in this report.

Cr(II)–CyDTA ion, was more stable than Cr(II)–EDTA ion in the deaerated solution.

The sum of transfer coefficients, $(\alpha_c)_{ms}+(\alpha_a)_{ms}$ or $(\alpha_c)_{corr}+(\alpha_a)_{corr}$, was nearly equal to unity, and this caused $(E_0)_{ms}$ and $(E_0)_{corr}$ to be of the same value with each other.[1] Furthermore, each transfer coefficient, $(\alpha_c)_{corr}$ or $(\alpha_a)_{corr}$, seems to have a tendency to approach to 0.5 by the correction of the effect of the electrical double layer.

The polarographic half-wave potential $(E_{1/2})$, the standard potential obtained by the measurements of the equilibrium potentials, $(E_0)_e$, and those obtained by the potentiostatic method, $(E_0)_{ms}$ and $(E_0)_{corr}$, were in good agreement with each other within the experimental error.

The authors wish to thank the Ministry of Education for the financial support granted for this research.

BULLETIN OF THE CHEMICAL SOCIETY OF JAPAN VOL. 43 2046—2051 (1970)

Polarography of Halides in Dimethylformamide. III. The Chloride Ion, the Trichloromercurate Ion, and Mercuric Chloride

Yoshihisa MATSUI, Yukio KUROSAKI*1 and Yoshio DATE

Department of Agricultural Chemistry, Faculty of Agriculture, Shimane University, Nishikawazu-cho, Matsue

(Received November 27, 1969)

The polarographic behavior of the chloride ion at the dropping mercury electrode was investigated in dimethylformamide. The chloride ion gives two diffusion-controlled anodic waves. On the basis of the analysis of the waves, the first anodic wave can be ascribed to the reversible oxidation of mercury to form either the tri- or the tetrachloromercurate ion. At the more negative part of the potential in the wave, where the concentration of the chloride ion on the mercury drop is much higher than that of the mercuric ion dissolved, the higher complex species, *i.e.*, the tetrachloromercurate ion, is the main product of the electrode reaction. As the potential of the dropping electrode shifts toward less negative potentials, the concentration of the chloride ion at the electrode surface decreases more and more and the formation of the trichloromercurate ion becomes predominant. When a constant diffusion current is attained, only the trichloromercurate ion is formed and the formation of the tetrachloromercurate ion can be neglected. On the other hand, the second anodic wave can be ascribed to the reversible oxidation of mercury to mercuric chloride.

The polarographic behavior of the bromide ion, the iodide ion, and their mercuric complexes in dimethylformamide (DMF) have been reported on in previous papers.[1,2] It has been shown that each of the bromide and iodide ions gives two anodic waves; the first wave corresponds to the reversible oxidation of mercury to the trihalogenomercurate ion (HgX_3^-), and the second wave, to the reversible oxidation of mercury to mercuric halide (HgX_2).

The present investigation will deal with the mechanism of the electrode reaction of the chloride ion, the trichloromercurate ion, and mercuric chloride at the dropping mercury electrode in DMF.

Experimental

The methods of the purification of DMF and mercuric chloride and of the preparation of tetraethylammonium perchlorate and tetraethylammonium chloride were described in the previous papers.[1,2] A stock solution of tetraethylammonium trichloromercurate in DMF was prepared by adding equimolecular amounts of tetraethylammonium chloride and mercuric chloride to DMF.

The polarographic cell and the dropping mercury electrode were the same as those described previously.[1,2] D.c. polarography, controlled potential electrolysis, and conductivity measurements were carried out according to the same procedures as were used before. Likewise, all the potentials reported in the present paper refer to the aqueous saturated calomel electrode connected with the test solution by a DMF-agar salt bridge.[3]

Results and Discussion

Complex Formation between Tetraethylammonium Chloride and Mercuric Chloride in DMF. The composition of the complex ion between the chloride ion and mercuric chloride was examined in DMF by means of conductometric titration. As the previous papers showed,[1,2] information concerning the complex formation between the halide ion and the mercuric ion helps us to elucidate the mechanism of the electrode reaction of the halide ion at the dropping mercury electrode. The results are given in Fig. 1. As mercuric chloride was added to a solution of tetraethylammonium chloride in DMF, the specific conductance of the solution decreased. It attained its minimum value when the mole ratio of mercuric chloride to tetraethylammonium chloride became equal to about 0.6. This suggests that complex formation occurs in solution and that the resulting complex ion is the tetrachloromercurate ion ($HgCl_4^{2-}$). The addition of more mercuric chloride increased the specific conductance, which reached virtually a constant value when the mole ratio became equal to unity. This indicates that

*1 Present address: Matsue Technical High School, Matsue

1) Y. Matsui, R. Kawakado and Y. Date, This Bulletin, **41**, 2913 (1968).

2) Y. Matsui, Y. Kurosaki and Y. Date, *ibid.*, **43**, 1707 (1970).

3) K. Takaoka, *Rev. Polarography*, **14**, 63 (1966).

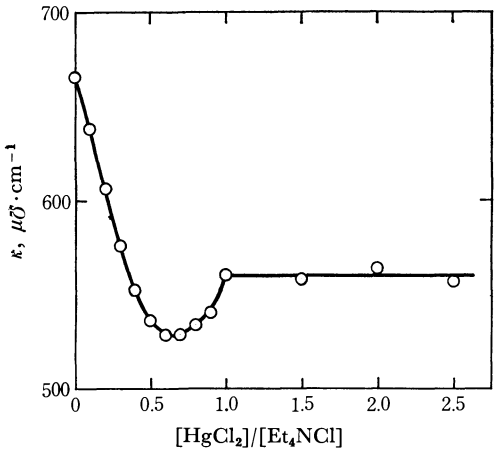

Fig. 1. Effect of $HgCl_2$ on the specific conductance of 10 mM of Et_4NCl in DMF at 25°C.

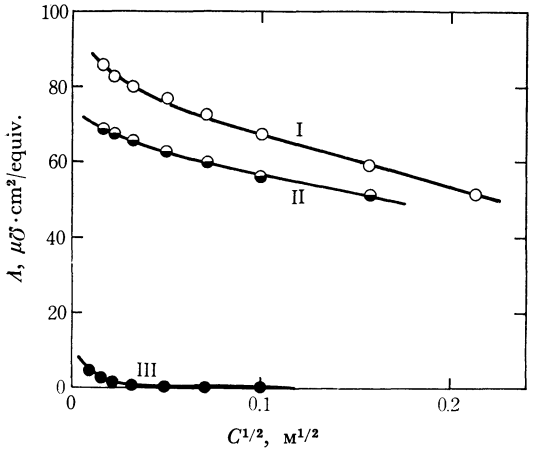

Fig. 2. Plots of equivalent conductance *vs.* square root of concentration for Et_4NCl(I), Et_4NHgCl_3 (II), and $HgCl_2$(III) in DMF at 25°C.

the formation of the trichloromercurate ion ($HgCl_3^-$) also occurs in solution. Consequently, it is necessary to consider the formation of $HgCl_4^{2-}$, as well as those of $HgCl_3^-$ and $HgCl_2$, when the mechanism of the anodic dissolution of mercury in the presence of the chloride ion is studied in DMF.

The equivalent conductances of a few connected salts are plotted as a function of the square root of the concentration in Fig. 2. The results for tetraethylammonium chloride and tetraethylammonium trichloromercurate approximately fit the Onsager equation, indicating that these salts behave as strong electrolytes in DMF. The equivalent conductance of mercuric chloride is very low, however, and its plotting does not fit the Onsager equation, which shows that the chloride is a weak electrolyte in this medium.

D.C. Palarography. Figure 3 shows the d.c. polarograms of tetraethylammonium chloride(I), mercuric chloride(III), and their equimolar mixture, *i.e.*, tetraethylammonium trichloromercurate (II) in DMF containing 0.1 M tetraethylammonium perchlorate and 0.005% polyvinyl chloride (PVC), which was added to suppress the maximum arising on the cathodic wave of tetraethylammonium trichloromercurate or on the second cathodic wave

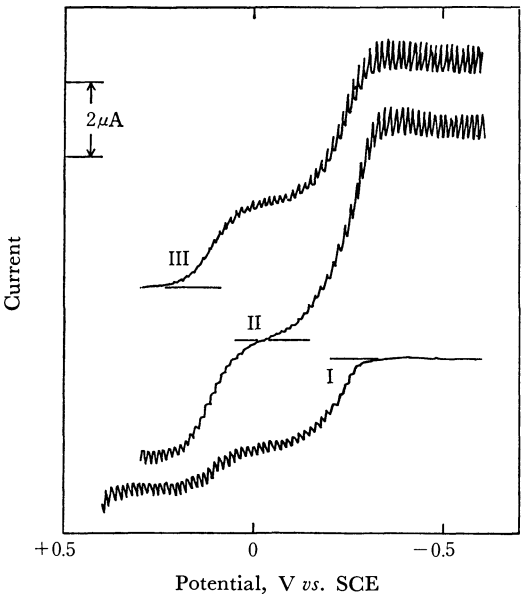

Fig. 3. Polarograms of 1.0 mM solutions of Et_4NCl (I), Et_4NHgCl_3(II), and $HgCl_2$(III) in DMF containing 0.1 M Et_4NClO_4 and 0.005% PVC at 25°C.

Table 1. Polarographic characteristics at various concentrations

Depolarizer	Concn. (mM)	$E_{1/2}$ (V *vs.* SCE) more pos.	$E_{1/2}$ (V *vs.* SCE) more neg.	I_d more pos.	I_d more neg.
Et_4NCl	0.10	+0.122	−0.136	0.59	0.94
	0.25	+0.121	−0.152	0.54	1.08
	0.50	+0.131	−0.165	0.56	1.25
	1.00	+0.131	−0.190	0.50	1.20
	2.50	+0.160	−0.213	0.51	1.24
	5.00	+0.175	−0.233	0.55	1.25
Et_4NHgCl_3	0.10	+0.110	−0.153	1.37	2.98
	0.25	+0.127	−0.179	1.51	3.15
	0.50	+0.142	−0.189	1.37	2.93
	1.00	+0.157	−0.209	1.46	2.95
	2.50	+0.173	−0.242	1.49	2.87
$HgCl_2$	0.10	+0.112	−0.164	1.14	2.38
	0.25	+0.113	−0.177	0.79	2.05
	0.50	+0.127	−0.188	0.83	2.12
	1.00	+0.140	−0.216	0.89	2.06
	2.50	+0.151	−0.234	1.10	2.06

Table 2. Relation between limiting currents of 0.50 mm of depolarizers and effective heads of the dropping mercury electrode

Depolarizer	$h_{corr.}$ (cm)	i_d, (μA) more pos.	i_d, (μA) more neg.	$i_d/(h_{corr.})^{1/2}$ more pos.	$i_d/(h_{corr.})^{1/2}$ more neg.
Et_4NCl	37.2	0.31	0.80	0.051	0.131
	43.2	0.33	0.85	0.050	0.129
	53.2	0.37	0.95	0.051	0.130
	63.2	0.38	1.01	0.048	0.127
	73.2	0.42	1.10	0.049	0.129
	82.2	0.43	1.15	0.048	0.128
Et_4NHgCl_3	37.2	0.94	2.03	0.154	0.333
	43.2	1.00	2.17	0.152	0.330
	53.2	1.12	2.40	0.154	0.330
	63.2	1.18	2.60	0.148	0.328
	73.2	1.25	2.80	0.146	0.328
	82.2	1.32	2.96	0.146	0.328
$HgCl_2$	37.2	0.53	1.30	0.087	0.213
	43.2	0.60	1.45	0.091	0.220
	53.2	0.66	1.60	0.091	0.220
	63.2	0.74	1.75	0.093	0.220
	73.2	0.79	1.88	0.092	0.220
	82.2	0.84	2.06	0.093	0.226

of mercuric chloride. The polarographic characteristics of these depolarizers at various concentrations are given in Table 1. The relation between the limiting currents and the effective heads of the dropping mercury is given in Table 2. As is shown in these tables, all the limiting currents are virtually proportional to the bulk concentrations of the corresponding depolarizers and also to the square root of the effective pressure on the mercury drop, indicating that all these waves are diffusion-controlled.

It might be considered that the mechanism of the electrolytic oxidation of mercury in the presence of the chloride ion is essentially identical with that in the presence of the bromide or iodide ion, and that it may be expressed as follows:

$$2Hg + 6Cl^- \rightleftarrows 2HgCl_3^- + 4e \quad (1)$$

$$Hg + 2HgCl_3^- \rightleftarrows 3HgCl_2 + 2e \quad (2)$$

In fact, some of the results can indeed be explained in terms of this mechanism: (1) The chloride ion gives two anodic waves, the trichloromercurate ion, two waves and anodic, cathodic, and mercuric chloride, two cathodic waves, all within the same potential region. (2) The height of the wave occurring at the more negative potential is approximately equal to twice that of the wave occurring at the more positive potential in each depolarizer.

This mechanism is also suggested by the results of the large-scale electrolysis of mercuric chloride with a controlled potential. When mercuric chloride was reduced at the potential (−0.04 V *vs.* SCE) of the plateau of the first cathodic wave, using a Hg pool cathode and a Pt plate anode, the quantity of electricity transfered per mole of the depolarizer (n) was equal to 0.77 $\boldsymbol{F}$ (calculated for Eq. (1); 0.67 $\boldsymbol{F}$); moreover, the d.c. polarogram of the catholyte agreed well with that of the trichloromercurate ion. The electroreduction of mercuric chloride at the potential (−0.62 V *vs.* SCE) of the plateau of the second cathodic wave yielded the chloride ion, the formation of which was confirmed by the d.c. polarogram of the catholyte. The value of n was equal to 2.00 $\boldsymbol{F}$ (calculated for Eqs. (1) and (2): 2.00 $\boldsymbol{F}$).

This mechanism, however, overlooks the formation of the tetrachloromercurate ion, which is clearly indicated by the conductometric titration described above. It was immediately ascertained by analyzing the d.c. polarograms of the chloride ion, that the formation of the tetrachloromercurate ion as well as that of the trichloromercurate ion must be considered. If the electrode reaction is expressed by Eqs. (1) and (2), the potential of the dropping mercury electrode is given for the first anodic wave of the chloride ion by:[1]

$$E_n = C_n + (\boldsymbol{R}T/2\boldsymbol{F}) \ln\{i/(i_d - i)^3\} \quad (3)$$

and for the second anodic wave by:

$$E_p = C_p + (\boldsymbol{R}T/2\boldsymbol{F}) \ln\{i^3/(i_d - i)^2\} \quad (4)$$

The results of the analysis of the waves are given in Fig. 4. The plot of $\log\{i^3/(i_d - i)^2\}$ against the potential for the second anodic wave gives a fairly good straight line, with a slope equal to 0.029 V (calculated for Eq. (4): 0.030 V), indicating that Eq. (2) is valid. On the other hand, the plot of $\log\{i/(i_d - i)^3\}$ against the potential for the first anodic wave became considerably curved on the less negative side. Furthermore, the slope of the

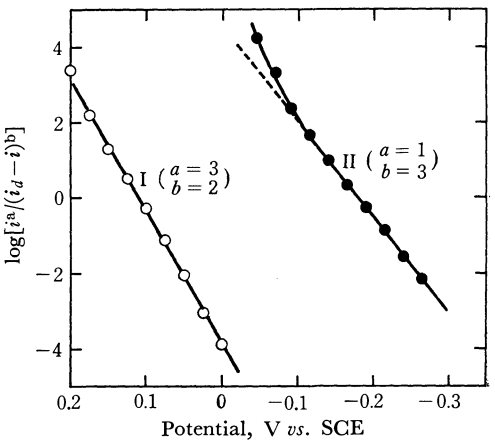

Fig. 4. Log plots for the waves of Et_4NCl.
Reciprocal slope: I, 0.029 V; II, 0.038 V

log plot (0.038 V) was somewhat greater than that expected from Eq. (3) (0.030 V).

Similar results have been reported by Given and Peover[4] in the polarographic study of lithium chloride in DMF. They assumed that the first anodic wave of the chloride ion was due to the reversible oxidation of mercury to the tetrachloromercurate ion, and they plotted log $\{i/(i_d-i)^4\}$ against the potential of the dropping mercury electrode. Their plot, however, became curved at the less negative values of the potential. They attributed the deviation of the plot to the dissociation of the tetrachloromercurate ion into the trichloromercurate ion and the chloride ion.

On the basis of these facts, we considered that the first anodic wave of the chloride ion cannot simply be ascribed to the electrochemical equilibrium expressed by Eq. (1). The tetrachloromercurate ion rather than the trichloromercurate ion is supposed to be mainly formed at the more negative part of the potential in the wave (Eqs. (5) and (6)), for here the concentration of the chloride ion on the mercury drop is much higher than that of the mercuric ion dissolved.

$$Hg \rightleftarrows Hg^{2+} + 2e \quad (5)$$

$$Hg^{2+} + 4Cl^- \rightleftarrows HgCl_4^{2-} \quad (6)$$

As the potential becomes more positive, the concentration of the mercuric ion dissolved may increase more and more and the formation of the trichloromercurate ion may become predominant (Eq. (7)):

$$Hg^{2+} + 3Cl^- \rightleftarrows HgCl_3^- \quad (7)$$

Conversely, when the trichloromercurate ion is electrolytically reduced, the tetrachloromercurate ion as well as the chloride ion may be formed at the less negative part of the potential in the cathodic wave (Eqs. (8) and (9)). Since the concentration of the trichloromercurate ion on the electrode surface may decrease with an increase in the negative potential, the formation of the tetrachloromercurate ion may be suppressed at the more negative part of the potential in the wave and the trichloromercurate ion may eventually be reduced to mercury and the chloride ion:

$$HgCl_3^- + 2e \rightleftarrows Hg + 3Cl^- \quad (8)$$

$$HgCl_3^- + Cl^- \rightleftarrows HgCl_4^{2-} \quad (9)$$

On the other hand, no data were obtained which are in conflict with the attribution of the second anodic wave of the chloride ion, as well as the anodic wave of the trichloromercurate ion and the first cathodic wave of mercuric chloride, to the electrochemical equilibrium expressed by Eq. (2).

The Equation of the More Negative Wave. If the mechanism of the anodic dissolution of mercury in the presence of Cl^- is expressed by Eqs. (5), (6), and (7), the potential at any point on the polarographic wave is given by:[5]

$$\begin{aligned} E &= C + (\boldsymbol{R}T/2\boldsymbol{F}) \ln x_0 \\ &= C' + (\boldsymbol{R}T/2\boldsymbol{F}) \ln(x_3/x_1^3) \\ &= C'' + (\boldsymbol{R}T/2\boldsymbol{F}) \ln(x_4/x_1^4) \end{aligned} \quad (10)$$

where C, C', and C'' are constant and where x_0, x_1, x_3, and x_4 are the concentrations of the simple mercuric ion, the chloride ion, the trichloromercurate ion, and the tetrachloromercurate ion respectively at the electrode surface.

Provided that a steady state is reached very quickly as the applied potential is changed, the current at any point of the wave should be equal to the sum of the rates of diffusion of the mercuric complexes formed by electrolysis. As Heyrovsky and Ilkovic[6] described, the rate of diffusion can be assumed to be directly proportional to the difference in concentration between the electrode surface and the bulk of the solution. Hence, the current should be given by:

$$i = k_3x_3 + k_4x_4 \quad (11)$$

where k_3 and k_4 are the proportionality constants of the tri- and tetrachloromercurate ions respectively, as defined by the Ilkovic equation. Likewise, the amount of the chloride ion diffusing up to the electrode surface in a unit of time should be euqal to that diffusing off from the electrode surface in the form of mercuric complexes. Hence, we obtain:

$$k_1'(*x_1 - x_1) = 3k_3x_3 + 4k_4x_4 \quad (12)$$

where k_1' is the proportionality constant of the chloride ion and where $*x_1$ is the constant concentration of the chloride ion in the bulk of the solution. The concentrations of the chloride and tetrachloromercurate ions at the electrode surface, x_1 and x_4, decrease with an increase in the anodic current of the wave, with the result that these ions are consumed for the reactions with the dissolved mercuric ion, thus forming the trichloromercurate ion. When a constant diffusion current, i_d, is attained, both x_1 and x_4 have decreased to negligibly small values. Hence, we have:

$$k_1'*x_1 = 3i_d \quad (13)$$

Eq. (13) shows that the value of k_1' is equal to three times that of the Ilkovic equation constant for the chloride ion (k_1).

By introducing Eq. (13) into Eq. (12), we obtain:

$$3i_d - k_1'x_1 = 3k_3x_3 + 4k_4x_4 \quad (14)$$

4) P. H. Given and M. E. Peover, *J. Chem. Soc.*, **1959**, 1602.

5) Since the concentrations of the species concerned are very low, we took their activity coefficients as constant for the sake of simplicity.

6) J. Heyrovsky and D. Ilkovic, *Collect. Czech. Chem. Commun.*, **7**, 198 (1935).

Since x_4 is expressed by:

$$x_4 = K_4 x_1 x_3 \tag{15}$$

where K_4 is the stepwise stability constant of the tetrachloromercurate ion, we obtain three equations for x_1, x_3, and x_4; these equations are solved as follows:

$$x_1 = (k_3/2k_1')[y - r + \{(y+r)^2 + 4ir/k_3\}^{1/2}] \tag{16}$$

$$x_3 = (1/2)[-y - r + \{(y+r)^2 + 4ir/k_3\}^{1/2}] \tag{17}$$

$$x_4 = (k_3/2k_4)[(3i_d + 2i)/k_3 + r - \{(y+r)^2 + 4ir/k_3\}^{1/2}] \tag{18}$$

where:

$$y = (3i_d - 4i)/k_3 \tag{19}$$

$$r = k_1'/k_4 K_4 \tag{20}$$

Since k_3 can be evaluated from the polarographic data, the value of y can be obtained at any point of the wave. On the other hand, the value of r is unknown; therefore, neither x_1 nor x_3 can be evaluated. However, when the plot of the potential against $\ln(x_3/x_1^3)$ calculated for an arbitrary value of r becomes linear, and when the reciprocal slope is equal to $\boldsymbol{R}T/2\boldsymbol{F}$, as is expressed by Eq. (10), the value of r must be the correct one.

Thus, as Fig. 5 shows, the linearity of the plot calculated for $r = 5 \times 10^{-4}$ M became better than that calculated for $r = \infty$ ($K_4 = 0$) and the reciprocal slope of the former (0.030 V) was in agreement with the theoretical value. In this treatment, the values of k_1' and k_3 were taken as equal to 6.63×10^{-3} and 5.28×10^{-3} A/M respectively.

The values of x_1, x_3, and x_4 calculated for $r = 5 \times 10^{-4}$ M changed with the potential of the dropping mercury electrode, as is shown in Fig. 6; the figure also clearly shows the mechanism of the electrooxidation of mercury in the presence of the chloride ion. Thus, the tetrachloromercurate ion is formed in larger quantities than the trichloromercurate ion at potentials more negative than -0.180 V *vs.* SCE. With a decrease in the negative potential, the formation of the trichloromercurate ion becomes predominant. When a constant diffusion current is attained, only the trichloromercurate ion is formed and the formation of the tetrachloromercurate ion can be neglected.

Now that the values of r and k_1' have been determined, the stepwise stability constant, K_4, of the tetrachloromercurate ion can be estimated from Eq. (20) if the value of the proportionality constant, k_4, of the tetrachloromercurate ion, as defined

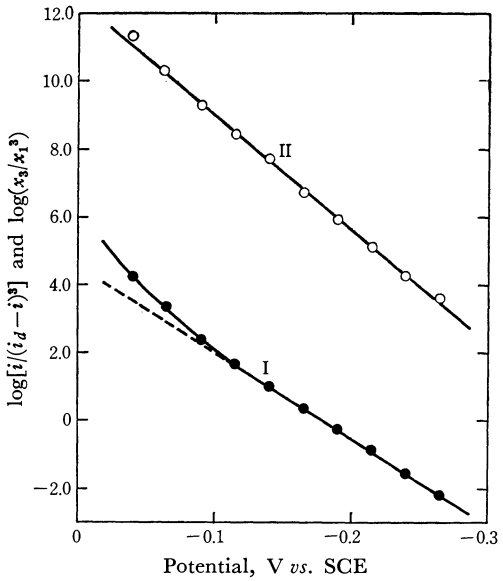

Fig. 5. Plots of $\log[i/(i_d - i)^3]$ (I) and $\log(x_3/x_1^3)$ (II) *vs.* potential for the more negative wave of Et_4NCl.

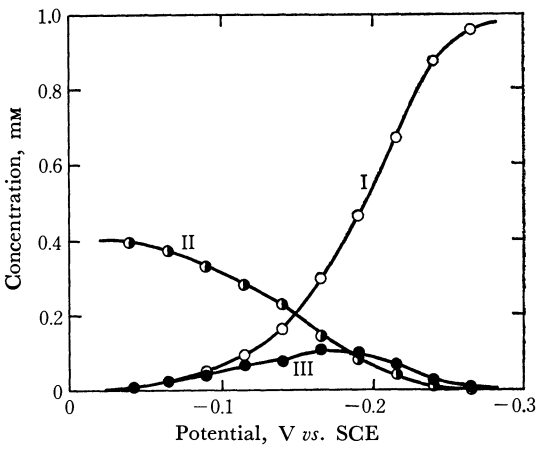

Fig. 6. Plots of the calculated concentrations of Cl^-(I), $HgCl_3^-$(II), and $HgCl_4^{2-}$(III) on the electrode surface *vs.* potential.

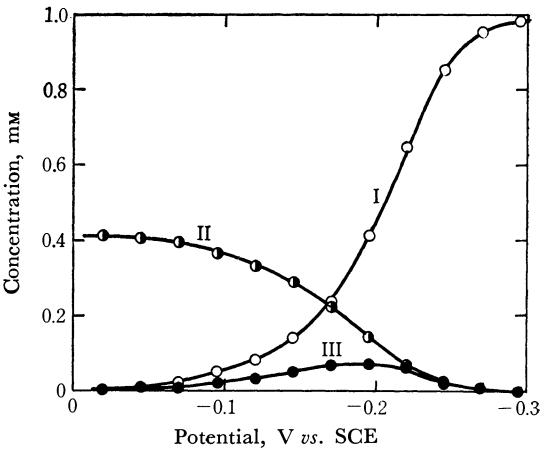

Fig. 7. Plots of the calculated concentrations of Br^-(I), $HgBr_3^-$(II), and $HgBr_4^{2-}$(III) on the electrode surface *vs.* potential.

by the Ilkovic equation, is determined. However, the value of k_4 could not be determined, because we could found no condition under which only the tetrachloromercurate ion exists as a depolarizer in the DMF solution. Assuming that k_4 is approximately equal to k_3, we can roughly estimate the value of K_4 to be 2.5×10^3 M^{-1}.

In the previous papers dealing with the polarographic behavior of the bromide ion[1] and the iodide ion,[2] the formation of the tetrahalogenomercurate ion was not considered. Indeed, it might not be necessary to consider the formation of the tetraiodomercurate ion, because the plot of log $\{i/(i_d-i)^3\}$ *vs.* the potential of the dropping mercury electrode for the first anodic wave of the iodide ion yielded a straight line of the reciprocal slope equal to 0.030 V; this is in agreement with the theoretical value obtained on the basis of the formation of the triiodomercurate ion alone. However, the reciprocal slope of such a plot for the first anodic wave of the bromide ion was equal to 0.035 V, somewhat greater than the theoretical value. Since the oxidation process was proved to be reversible, this increase in the reciprocal slope indicates that the formation of the tetrabromomercurate ion may simultaneously take place. The same method of analyzing the wave as was used for the wave of the chloride ion was applied to the first anodic wave of the bromide ion; the value of r was thus estimated to be 1×10^{-3} M ($K_4=1.3\times10^3$ M^{-1}). Figure 7 shows the change in x_1, x_3, and x_4 with the potential of the dropping mercury electrode. It is apparent that the tetrabromomercurate ion is also formed in an appreciable quantity. In the case of the wave of the iodide ion, the plot of the potential against log $(x_3/x_1{}^3)$ calculated for the r value of 1×10^{-2} M became linear and the reciprocal slope was equal to 0.0295 V, indicating that the value of K_4 for the tetraiodomercurate ion is no more than 1.3×10^2 M^{-1}.

Accordingly, it can be said that the tetrahalogenomercurate ion is always formed at the first anodic wave of any halide ion. However, the value of the K_4 of the tetraiodomercurate ion is so small that it is not necessary to consider the formation of this complex ion in the anodic dissolution of mercury in the presence of the iodide ion. On the other hand, the K_4 values of the tetrabromo- and tetrachloromercurate ions are so large that the formation of these complex ions cannot be neglected when either the bromide ion or the chloride ion is a depolarizer.

BULLETIN OF THE CHEMICAL SOCIETY OF JAPAN VOL. 43 2052—2056 (1970)

Polarography of Halides in Dimethylformamide. IV. The Stability Constants of the Halo Complexes of Mercury(II)

Yoshihisa MATSUI and Yoshio DATE

Department of Agricultural Chemistry, Faculty of Agriculture, Shimane University, Nishikawazu-cho, Matsue

(Received December 10, 1969)

The overall stability constants (β) of mercuric halide and the tri- and tetrahalogenomercurate ions in dimethylformamide containing 0.1 M tetraethylammonium perchlorate were evaluated by the polarographic method at 25°C. The values of log β obtained were: 24.16 for $HgCl_2$, 31.23 for $HgCl_3^-$, 34.57 for $HgCl_4^{2-}$, 24.17 for $HgBr_2$, 31.62 for $HgBr_3^-$, 34.73 for $HgBr_4^{2-}$, 25.93 for HgI_2, 33.34 for HgI_3^-, and 36.02 for HgI_4^{2-}.

A number of workers have evaluated the stability constants of the halo complexes of mercury(II) in an aqueous solution,[1] but only a few workers have done so in non-aqueous solutions. Ellendt and Cruse[2] have evaluated the stepwise stability constants of the tri- and tetrahalogenomercurate ions in acetonitrile by means of conductivity measurements. Given and Peover[3] and Breant and Kiet[4] have determined the overall stability constants of the tetrahalogenomercurate ion in dimethylformamide (DMF) by the polarographic method. These results show that the halo complexes of mercury(II) are generally more stable in non-aqueous solutions than in an aqueous solution.

In the previous papers of this series,[5-7] the mechanism of the electrooxidation of mercury in the presence of the halide ion was studied in DMF by means of polarography; the current-potential curve thus obtained was interpreted on the basis of the formation of complex ions of the $HgX_j^{(2-j)}$ type, where j has values from 2 to 4. In the present experiment, the overall stability constants of these complex ions were determined in DMF containing 0.1 M tetraethylammonium perchlorate by means of an analysis of the d.c. polarographic waves.

Experimental

The solvent and the supporting electrolyte used were purified as has been described previously.[6] Polarograms were obtained in a manner similar to that described before. Likewise, all the potentials reported in the present paper refer to an aqueous, saturated calomel electrode connected with a test solution by a DMF-agar salt bridge.[8]

Preparation of Solutions of Mercuric Perchlorate in DMF. According to the directions of Given and Peover,[3] mercuric perchlorate was prepared in a concentrated aqueous solution by neutralizing 60% perchloric acid with solid mercuric oxide. As a small amount of a yellow solid was precipitated, the supernatant of the mixture was pipetted out and standardized by titration against an aqueous potassium thiocyanate solution, using ferric ammonium sulfate as the indicator. Test solutions of mercuric perchlorate in DMF were then prepared from this aqueous solution. The water introduced during this procedure (*ca.* 10 mM) was not removed.

Results

The Standard Potential of Mercury in DMF. In order to evaluate the stability constants of complex ions of mercury(II) by means of polarography, it is necessary to determine the ordinary standard potential($E°$) of the mercury-mercury(II) ion half-cell,[9] which is expressed by the equation:

$$E° = E - (\boldsymbol{R}T/2\boldsymbol{F}) \ln x_0 \quad (1)$$

where x_0 is the concentration of the simple or the solvated mercury(II) ion on the dropping mercury electrode at the potential E V *vs.* SCE.[10] The value of x_0 can be obtained by:

$$x_0 = {}^*x_0 - i/k_0 \quad (2)$$

1) J. Bjerrum, G. Schwarzenbach and L. G. Sillen, "Stability Constants of Metal-Ion Complexes. Part II. Inorganic Ligands," Spec. Publ. 7, Chem. Soc., London (1958).

2) G. Ellendt and K. Cruse, *Z. Phys. Chem.*, **201**, 130 (1952).

3) P. H. Given and M. E. Peover, *J. Chem. Soc.*, **1959**, 1602.

4) M. Breant and N. V. Kiet, *C. R. Acad. Sci., Paris, Ser. C.*, **262**, 955 (1966).

5) Y. Matsui, R. Kawakado and Y. Date, This Bulletin, **41**, 2913 (1968).

6) Y. Matsui, Y. Kurosaki and Y. Date, *ibid.*, **43**, 1707 (1970).

7) Y. Matsui, Y. Kurosaki and Y. Date, *ibid.*, **43**, 2046 (1970).

8) K. Takaoka, *Rev. Polarography*, **14**, 63 (1966).

9) C. J. Nyman and G. S. Alberts, *Anal. Chem.*, **32**, 207 (1960).

where $*x_0$ is the concentration of the mercury(II) ion in the bulk of the solution; i, the cathodic current flowing at the potential E, and k_0, the Ilkovic equation constant for the mercury(II) ion. The constant k_0, which is equal to $i_d/*x_0$, can be determined by measuring the cathodic diffusion current, i_d, flowing as a result of the reduction of the mercuric perchlorate at a given concentration, $*x_0$.

Figure 1 shows a polarogram of 0.97 mM mercuric perchlorate obtained in DMF containing 0.1 M tetraethylammonium perchlorate at 25°C. An acute maximum was observed at every concentration of the mercury(II) ion studied. The height of this maximum increased with an increase in the concentration of the depolarizer. It was suppressed only a little by the addition of polyvinyl chloride, which is known to suppress the maxima given by various metal ions in DMF.[6,11] Immediately after the maximum was passed, the current suddenly decreased and reached the plateau of the wave. The height of the plateau was nearly proportional to the concentration of the depolarizer and to the square root of the effective height of the mercury head (Table 1); this indicates that the limiting current is controlled by diffusion.

From these polarographic data, k_0 was calculated to be 3.54×10^{-3} A/M. The value of E° could be determined directly from the polarographic data of the mercuric perchlorate if no maximum wave appeared. In practice, however, the value of E° was calculated from the polarographic data concerning the anodic dissolution of mercury in DMF containing 0.1 M tetraethylammonium perchlorate. The value of E at an arbitrary current of -1 μA was found to be 0.452 ± 0.004 V *vs.* SCE, while the value of E° was calculated from Eqs. (1) and (2) as 0.557 ± 0.004 V *vs.* SCE.

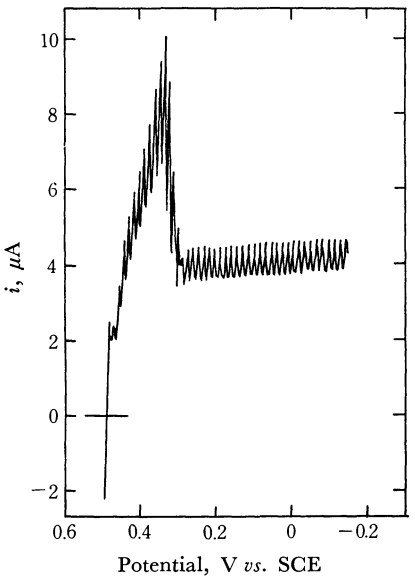

Fig. 1. Polarogram of 0.97 mM mercuric perchlorate in DMF at 25°C.

Table 1. Relation between the limiting current (i_d) of 0.97 mM mercuric perchlorate and pressure on the dropping mercury ($h_{corr.}$)

$h_{corr.}$ (cm)	i_d (μA)	$i_d/(h_{corr.})^{1/2}$
37.3	3.25	0.532
44.3	3.47	0.521
54.3	3.84	0.521
64.3	4.18	0.521
74.3	4.48	0.520

It is remarkable that the standard potential of mercury is more negative in DMF than in water ($E^\circ=0.589$ V *vs.* SCE, obtained in water at an ionic strength of 1.0 M[12]) even though the dielectric constant of DMF is lower than that of water. This indicates that the mercury(II) ion may be strongly solvated in DMF. The specific solvation of the mercury(II) ion by DMF was also suggested by the fact that the diffusion constant of the mercury(II) ion in DMF (3.92×10^{-6} cm^2 sec^{-1} at 25°C), calculated on the basis of the Ilkovic equation, was unusually small compared with that in an aqueous solution (8.2×10^{-6} cm^2 sec^{-1} at 25°C[13]). The solvated mercury(II) ion must be unstable, for it was observed that metallic mercury was separated out from the 0.1 M solution of mercuric perchlorate in DMF when it was left standing at room temperature for a few days. This may be due to the reduction of the mercury(II) ion by one-electron transfer from the solvating DMF molecules.

Evaluation of the Stability Constants of the Tri- and Tetrahalogenomercurate Ions. When the halide ion is added to a 0.1 M solution of tetraethylammonium perchlorate in DMF, two new anodic waves appear. This can be explained in terms of the formation of complexes between the halide ion and the mercury(II) ion.[5-7] The general equation, which relates the potential of the dropping mercury electrode to the current flowing when mercury is oxidized to form complex ions, is:[9]

$$E = E^\circ + (\boldsymbol{R}T/2\boldsymbol{F})\ln(i/k_c) - (\boldsymbol{R}T/2\boldsymbol{F})\ln F_0(x) \quad (3)$$

10) The concentration of the simple mercury(II) ion is, compared with that of the supporting electrolyte, so low that the activity coefficient of the former may be constant; therefore, it was assumed to be equal to one for the sake of simplicity.

11) S. Musha, T. Wasa and K. Tani, *Rev. Polarography*, **11**, 169 (1963).

12) C. J. Nyman and E. P. Parry, *Anal. Chem.*, **30**, 1255 (1958).

13) I. M. Kolthoff and C. S. Miller, *J. Amer. Chem. Soc.*, **63**, 2732 (1941).

where:

$$F_0(x) = 1 + \beta_1 x + \beta_2 x^2 + \cdots + \beta_j x^j \quad (4)$$

In this equation, x represents the concentration o the halide ion at the electrode surface; β_j, the overall stability constant of the complex $HgX_j^{(2-j)}$, and k_c, the Ilkovic equation constant for the complex ions. The value of k_c may vary with different complex ions, but the variation seems to be very slight and so the value was assumed to be constant throughout this series. The value of $F_0(x)$ can be readily obtained at every potential of the waves from Eq. (3), since the other terms in Eq. (3) are experimental quantities.

At the potential corresponding to the more negative of the polarographic waves given by the halide ion, only two halo complexes, *i.e.*, the tri- and tetrahalogenomercurate ions, are formed by the reactions:[7]

$$Hg + 4X^- \rightleftarrows HgX_4^{2-} + 2e \quad (5)$$

$$Hg + 3X^- \rightleftarrows HgX_3^- + 2e \quad (6)$$

The presence of the other complex ions can be disregarded. Thus,

$$F_0(x) = \beta_3 x^3 + \beta_4 x^4 \quad (7)$$

When K_4 denotes the stepwise stability constant of the tetrahalogenomercurate ion, we obtain:

$$F_0(x) = \beta_3 x^3(1 + K_4 x)$$

or:

$$\log F_0(x) = \log \beta_3 + 3 \log x + \log(1 + K_4 x) \quad (8)$$

In this equation, x can be expressed by the equation:[7]

$$x = (k_c/6k_x)[y - r + \{(y+r)^2 + 4ir/k_c\}^{1/2}] \quad (9)$$

where:

$$y = (3i_d - 4i)/k_c$$

$$r = 3k_x/k_c K_4$$

and where k_x is the Ilkovic equation constant for the halide ion. Since the terms on the right side of Eq. (9) are all experimental quantities except for r, which has been roughly estimated for every halide ion in a manner described in a previous paper,[7] the value of x can be evaluated at every potential of the waves.

Figure 2 is a plot of $\log F_0(x)$ *vs.* $\log x$ for the polarographic data of 1.0 mM tetraethylammonium chloride, where the value of r was taken to be 5×10^{-4} M. As is to be expected from Eq. (8), the plot becomes linear, with a slope of 3.0, in the region where the value of x is small enough for the term of $\log(1 + K_4 x)$ to be disregarded. Thus, the value of $\log \beta_3$, which is approximately equal to $\log F_0(x) - 3\log x$ if the term of $\log(1 + K_4 x)$ is negligible, was calculated to be 31.23. The value of $\log K_4$ was also determined to be 3.34 by the measurement of the deviation of the plot from linearity. The solid curve shown in Fig. 2 was calculated using these values for the stability constants obtained. It seems that the values can adequately account for the polarographic data.

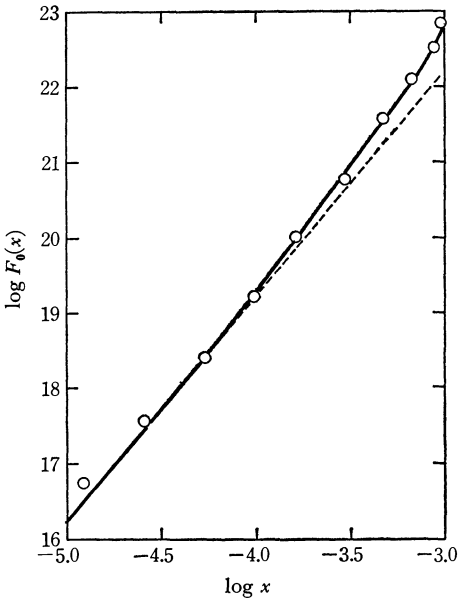

Fig. 2. Plot of $\log F_0(x)$ *vs.* $\log x$ for the more negative wave of the chloride ion.
The solid line was calculated with the stability constants in Table 2.

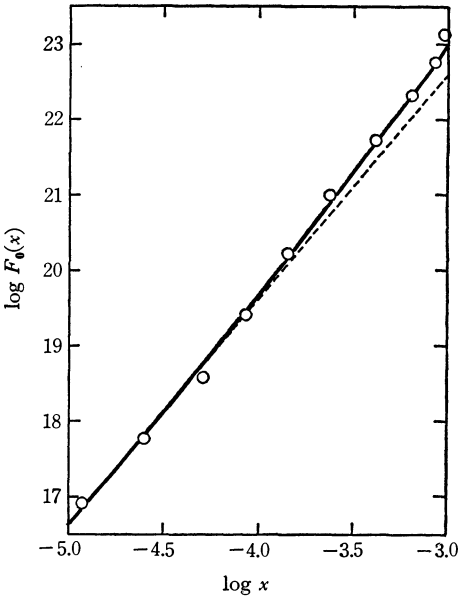

Fig. 3. Plot of $\log F_0(x)$ *vs.* $\log x$ for the more negative wave of the bromide ion.
The solid line was calculated with the stability constants in Table 2.

A similar procedure was applied to the more negative of the waves given by a 1.0-mM solution of tetraethylammonium bromide or iodide in DMF.

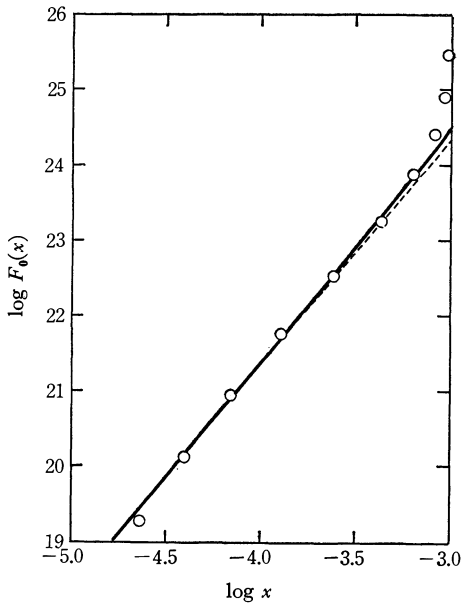

Fig. 4. Plot of log $F_0(x)$ *vs.* log x for the more negative wave of the iodide ion.
The solid line was calculated with the stability constants in Table 2.

Table 2. Stability constants of the halo complexes of mercury(II) in DMF containing 0.1 M tetraethylammonium perchlorate at 25°C

Ligand	log β_2	log K_3	log β_3	log K_4	log β_4
Cl^-	24.16	7.07	31.23	3.34	34.57
Br^-	24.17	7.45	31.62	3.11	34.73
I^-	25.93	7.41	33.34	2.68	36.02

The variation in log $F_0(x)$ with the log x value is shown in Fig. 3 for the bromide ion (r is taken as 1×10^{-3} M) and in Fig. 4 for the iodide ion (r is taken as 1×10^{-2} M). All the values of β_3, K_4, and β_4 obtained are given in Table 2. Every plot of log $F_0(x)$ *vs.* log x was found to deviate from the calculated solid curve, especially in the case of the iodide ion, in the potential range where the anodic current begins to flow. This may be due to the adsorption of the depolarizers on the electrode surface, as has previously been descrived.[6]

Evaluation of the Stability Constant of Mercuric Halide. The overall stability constant of mercuric halide can be determined more easily than those of the tri- and tetrahalogenomercurate ions. As has been described in previous papers[5-7] the more positive of the polarographic waves given by the halide ion in DMF is due to the reversible oxidation of mercury to mercuric halide. Since the concentrations of the halide ion and the tetrahalogenomercurate ion at the electrode surface become negligible at the potential corresponding to the plateau of the more negative wave, the electrode reaction at the more positive wave can be simply expressed by the equation:

$$Hg + 2HgX_3^- \rightleftarrows 3HgX_2 + 2e \qquad (10)$$

Therefore, the potential of the dropping mercury electrode at any point of this wave should be given by:

$$E = E^\circ + (\boldsymbol{R}T/2\boldsymbol{F})\ln(\beta_3^2/\beta_2^3) + (\boldsymbol{R}T/2\boldsymbol{F})\ln(x_2^3/x_3^2) \qquad (11)$$

where x_2 and x_3 are the concentrations of mercuric halide and the trihalogenomercurate ion respectively at the electrode surface. x_2 and x_3 are expressed by:

$$x_2 = 3(i-i_d)/k_c \qquad (12)$$

$$x_3 = 2(i_d'-i)/k_c \qquad (13)$$

where the current flowing at any point of the wave (i), as well as the diffusion current of the first and second anodic waves (i_d and i_d' respectively), is measured on the basis of the total anodic current. By introducing Eqs. (12) and (13) into Eq. (11) and by rearranging the resulting equation, we obtain:

$$\log\beta_2 = (1/3)\{2\boldsymbol{F}(E^\circ-E)/2.303\boldsymbol{R}T + 2\log\beta_3 + \log(27/4k_c) + \log(i-i_d)^3/(i_d'-i)^2\} \qquad (14)$$

Since the terms on the right side are either experimental quantities or known ones, the value of log β_2 can be readily calculated at any potential of the wave. As an example, the results of the calculation for the wave given by the bromide ion are given in Table 3. The mean values of log β_2 thus obtained for various halides are given in Table 2.

Table 3. Log β_2 calculated at various potentials in the more positive wave of the bromide ion

E (V *vs.* SCE)	i (μA)*	log β_2
0.056	2.31	24.19
0.081	2.34	24.13
0.106	2.37	23.99
0.131	2.54	24.19
0.156	2.72	24.21
0.181	2.87	24.19
0.206	3.02	24.21
0.231	3.10	24.22

* $i_d=2.26\,\mu$A and $i_d'=3.16\,\mu$A.

Discussion

Among the stability constants obtained in this work, only that of the tetrahalogenomercurate ion can be compared with those in earlier works, since the other constants in DMF have never been reported. Given and Peover[3] have determined the value of log β_4 to be about 30 for $HgCl_4^{2-}$ in DMF containing 1.0 M lithium perchlorate, and to be 38.79 for HgI_4^{2-} in DMF containing 0.1 M lithium perchlorate, by means of polarography at

20°C. Their procedure for determining the constants requires the measurement of the potential of the dropping mercury electrode, at an arbitrary current of $-1.0\ \mu A$, as a function of the concentration of the halide ion. In using this method, the concentration of the complexing agent in the bulk of the solution must be high enough to be effectively equal to that on the electrode surface when any slight current is flowing. Consequently, only the overall stability constant of the highest complex ion of mercury(II) can be evaluated by this procedure. Moreover, in applying this method we must pay attention to the possibility that the potential of the dropping mercury electrode at $-1\ \mu A$ can be shifted in a more negative direction by the adsorption of the depolarizer. Breant and Kiet,[4] using the same method as Given and Peover, also determined the values of log β_4 to be 32.9 for $HgCl_4^{2-}$, 35.2 for $HgBr_4^{2-}$, and 36.6 for HgI_4^{2-} in DMF containing 0.1 M perchloric acid. The values presented by them agree approximately with those in the present work, although the two sets of experimental conditions are not quite the same.

It is well known that the stabilities of the halo complexes of such metallic ions as Cu(I), Ag(I), Cd(II), and Hg(II), whose electronic configurations are representative of pseudo-inert gas ($s^2p^6d^{10}$), as opposed to those whose electronic configurations are representative of noble gas (s^2p^6), increase in an aqueous solution in the following order:

$$F^- < Cl^- < Br^- < I^-$$

This has been explained in terms of the mutual polarization of the metallic ions and ligands. The results in Table 2 show that the alteration in the stability of the complex ions with the ligands in DMF follows the same sequence as that in an aqueous solution (Table 4[1]), although the former is not so great as the latter. The difference in electronegativity between mercury and halogen ($\Delta\chi_{Hg-F}=2.1$, $\Delta\chi_{Hg-Cl}=1.1$, $\Delta\chi_{Hg-Br}=0.9$, and $\Delta\chi_{Hg-I}=0.6$[14]) indicates that all the bonds of Hg–Cl, Hg–Br, and Hg–I are rich in covalent character, and that this covalent character decreases and the ionic character increases in the following sequence:

$$Hg\text{-}I < Hg\text{-}Br < Hg\text{-}Cl < Hg\text{-}F$$

However, no such difference in bond character among them can be clearly observed in DMF. This may be due to the low dielectric constant of DMF (37.8[11]). On the other hand, the dielectric constant of water (78.54) may be high enough to distinguish the difference in bond character.

It is interesting that the values of K_4 of $HgCl_4^{2-}$, $HgBr_4^{2-}$, and HgI_4^{2-} decrease in this order. This may be related to the difference in the ionic radii of the halide ions. As has been described above, the bond between mercury and iodine is essentially covalent in character. As the value of β_3 of HgI_3^- is very large, it may be considered that each covalent Hg–I bond in HgI_3^- is readily formed without any steric hindrance from the other iodide ions. The formation of the fourth Hg–I bond, on the other hand, may be sterically hindered by the other three iodide ions already combined with the mercury(II) ion. Probably as a result, the K_4 value of HgI_4^{2-} becomes very small. As the ionic radii of I^-, Br^-, and Cl^- decrease in this order, the stepwise stability constants increase in that sequence. No such steric hindrance can be observed in an aqueous solution (Table 4), probably because, in water, the effect of the difference in bond character among Hg–Cl, Hg–Br, and Hg–I on the stability constant becomes larger than the steric effect.

TABLE 4. STABILITY CONSTANTS OF THE HALO COMPLEXES OF MERCURY(II) IN WATER CONTAINING 0.5 M SODIUM PERCHLORATE AT 25°C*

Ligand	log β_2	log K_3	log β_3	log K_4	log β_4
Cl^-	13.22	0.85	14.07	1.00	15.07
Br^-	17.33	2.41	19.74	1.26	21.00
I^-	23.82	3.78	27.60	2.23	29.83

* Ref. 1.

14) L. Pauling, "The Nature of the Chemical Bond," 3rd ed., Cornell University Press, Ithaca (1960), p. 93.

BULLETIN OF THE CHEMICAL SOCIETY OF JAPAN VOL. 43 2057—2062 (1970)

cis-Tricarbonylbistriphenylphosphinemanganese and the Related Compounds*1

Hiroaki NAKAYAMA*2

Department of Chemistry, Faculty of Science, The University of Tokyo, Hongo, Tokyo

(Received December 6, 1969)

Tricarbonyl-methylcyclopentadienylmanganese(I) (I) gives two manganese carbonyl triphenylphosphine compounds when treated with triphenylphosphine in the presence of a sodium dispersion, with tetrahydrofuran used as the solvent. One compound is a known diamagnetic $(CH_3C_5H_4)Mn(CO)_2(PPh_3)$ (II) (38% yield) formed by a ligand substitution reaction without any change in the oxidation number of the central manganese(+1). The other compound is a novel paramagnetic manganese(0) compound, *cis*-$Mn(CO)_3(PPh_3)_2$ (III) (25% yield), which may be formed by a reductive phosphination reaction. A *cis* trigonal bipyramidal configuration, as in the case reported for $Fe(CO)_3(o\text{-}(AsMe_2)_2C_6H_4)$, is proposed for III on the basis of the results of infrared spectroscopy. The compound III gives the following derivatives: $BrMn(CO)_3(PPh_3)_2$, VI, $CH_3Mn(CO)_3(PPh_3)_2$, VII, and $Mn(CO)_3(PPh_3)_2 \cdot 1/2 \cdot CHCl_3$, VIII.

Manganese carbonyl compounds are generally prepared by reductive carbonylation methods,[1,2] in which compounds of manganese in its higher oxidation state are reduced in the presence of ligand carbon monoxide in ethereal solvents. By analogy with this, triphenylphosphine (PPh_3) can also be expected to react with the metal compounds in reductive phosphination reactions in appropriate solvents. In this experiment, methylcyclopentadienyltricarbonylmanganese(I) (I), a well-known starting material for the preparation of manganese carbonyl compounds,[2] was treated reductively with a sodium dispersion in the presence of triphenylphosphine in tetrahydrofuran(THF); a novel paramagnetic manganese(0) compounds, *cis*-tricarbonyl-bistriphenylphosphinemanganese(0) (III), and a known compound, methylcyclopentadienyldicarbonyltriphenylphosphinemanganese(I) (II), were thus obtained. The latter, II, was identical with the previously-reported compound prepared by the ultraviolet radiation reaction of I and PPh_3 in cyclohexane,[3] or by heating a mixture of I and PPh_3 without any solvent at a temperature higher than 250°C.[3] With regard to the former paramagnetic compound, III, paramagnetic pentacoordinated manganese carbonyl derivatives, which do not obey the inert gas rule, have scarcely been reported. Two examples are $Mn(CO)_4PR_3$[4] and $Mn(CO)_3$(Diphos).*3,[5]

Experimental*4

Reagents. Triphenylphosphine (PPh_3) was prepared by the method in the literature[6] and then recrystallized from ethanol. All the solvents used were distilled under a nitrogen atmosphere after ordinary purification procedures. A combustion Improver 2, Ethyl Corporation, containing a small amount of organic orange dyes, was used as methylcyclopentadienyltricarbonylmanganese(I) without any further purification. A sodium dispersion, 40% in toluene (Kawaken Fine Chemicals, Co., Ltd.), was employed.

Synthesis in THF Solvent. Compound I (9.6 g; 44 mmol) was treated with PPh_3 (23.0 g; 88 mmol) and a sodium dispersion (9.3 g, 40% in toluene; Na 160 mmol) in THF (150 ml) under a nitrogen atmosphere. When the mixture was shaken, gas evolution was observed. The shaking was continued for 7 hr, after which the sodium dispersion was filtered off. Then the filtrate and the washings were evacuated under nitrogen. The dark brown tarry residue was treated with concd. hydrochloric acid and heated on a water

*1 Presented in part at the 16th Conference of Coordination Chemistry of Japan, Tokyo, December, 1966.

*2 Present address: Department of Chemistry, Faculty of Science, Hokkaido University, Sapporo, Hokkaido.

*3 (Diphos) means $Ph_2PCH_2CH_2PPh_2$.

*4 Mp uncorrected; the analytical results are shown in Table 1.

1) H. E. Podall, J. H. Dunn and H. Shapiro, *J. Amer. Chem. Soc.*, **82**, 1325 (1960); R. D. Closson, L. R. Buzbee and G. G. Ecke, *ibid.*, **80**, 6167 (1958).

2) H. E. Podall and A. P. Giraitis, *J. Org. Chem.*, **26**, 2587 (1961).

3) R. S. Nyholm, S. S. Sandhu and M. H. B. Stiddard, *J. Chem. Soc.*, **1963**, 5916.

4) W. Hieber and W. Freyer, *Chem. Ber.*, **92**, 1765 (1959).

5) A. Sacco, *Gazz. Chim. Ital.*, **93**, 698 (1963).

6) J. Dodonow and H. Medox, *Chem. Ber.*, **61**, 907 (1928).

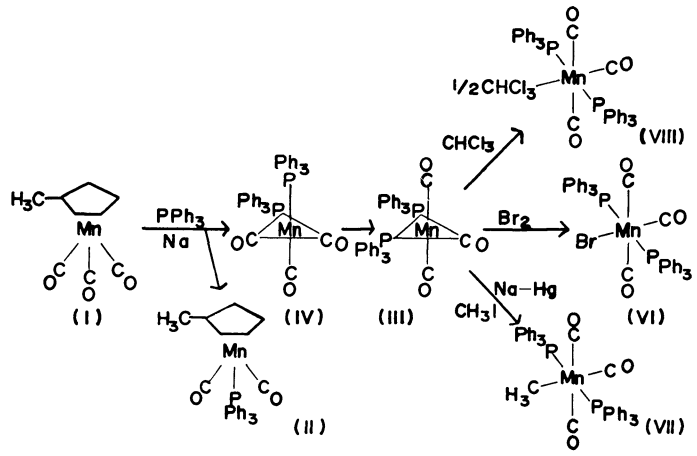

Scheme 1

bath. The residue turned into a brownish red viscous liquid; the phase of concd. hydrochloric acid was decanted away before cooling. Again concd. hydrochloric acid was added and decanted away. The residual viscous liquid was repeatedly treated with hot ethanol. Then a yellow precipitate and a brownish-red ethanol solution were obtained; they were separated by filtration. The precipitate was washed with water and then with ethanol. The crude product, tricarbonylbistriphenylphosphinemanganese, III (7.41 g, 25% yield), was recrystallized from benzene and then from acetone. The pale yellow crystals were dried *in vacuo*. A yellow chloroform adduct, $Mn(CO)_3(PPh_3)_2 \cdot 1/2\text{-}CHCl_3$, VIII, was obtained by the repeated recrystallization of III from chloroform-petroleum ether under nitrogen; it was then dried *in vacuo*. While the filtrate and the washings were combined and evaporated under reduced pressure. The crude product, methylcyclopentadienyldicarbonylmonotriphenylphosphinemanganese, II (7.75 g; 38% yield), was recrystallized from ethanol, and the resulting yellow needle crystals were measured after drying *in vacuo*. It sublimed at 100°C/10^{-4} mmHg and melted at 117°C (lit,[3] 119—20°C).

Synthesis in Dioxane Solvent. Compound I (3.35 g; 15.4 mmol) and PPh_3 (8.04 g; 30.7 mmol) were refluxed with a sodium lump (0.39 g; 17 mmol) in dioxane (55 m*l*) under a nitrogen atmosphere for 6 hr. The clear orange solution turned dark red after 30 min. After 70 min, the solution offered a clear brownish yellow color which did not change until the refluxing was stopped after 6 hr. After having been left nine days, the mixture was treated by a procedure similar to that used in the synthesis in THF. Yellow needle crystals of II were obtained in a yield of 69.4% (4.82 g), but III could not be separated in this procedure.

Synthesis in THF Solvent under Carbon Monoxide. Compound I (10.1 g; 46.1 mmol) was treated with PPh_3 (23.0 g; 88 mmol) and a sodium dispersion (16.5 g; 40% in toluene; Na 287 mmol) in THF (150 m*l*). The mixture was transferred into a 300-m*l* autoclave under a nitrogen atmosphere. The autoclave was purged twice with carbon monoxide at 60 atm and then vented to 10 atm at room temperature. It was heated to 130°C with rocking, the pressure being kept at 18 atm. When it was cooled after 6.5 hr, the barometer indicated 0 atm. The carbon monoxide was vented out, and the reaction mixture was filtered in air. The filtrate was treated by a procedure similar to that used in the synthesis under atmospheric pressure. Compound III was obtained as a yellow powder in a poor yield (44.1 mg, 0.14%); it was washed with hot ethanol, and then repeatedly with water and ethanol, and dried in air.

Reaction in THF Solvent under Atmospheric Pressure and at a Higher Temperature. Compound I (2.06 g; 9.45 mmol) and PPh_3 (5.20 g; 20 mmol) were refluxed with a sodium dispersion (1.58 g, 40% in toluene; Na 27.5 mmol) in THF (30 m*l*) under a nitrogen atmosphere for half an hour. The residual sodium was quenched with water after cooling, and phosphoric acid was added to the mixture. A suspension composed of aqueous and organic layers was thus obtained. The brown organic layer was extracted with petroleum ether; the aqueous layer was neutralized with sodium carbonate and extracted with THF. The THF extract was evacuated, and the residue was extracted with petroleum ether. The petroleum ether solution thus obtained was put together with the petroleum ether extract of the organic layer. The resulting petroleum ether solution was dried with calcium chloride and evaporated to deposit brown crystals. The crystals were dissolved with hot petroleum ether. Crystalline II was deposited instantaneously by cooling. Another brown crystal, IV, was obtained later on, although the main solute of the solution was confirmed to be II by a study of the infrared spectra.

Bromotricarbonylbistriphenylphosphinemanganese(I) (VI). Compound III (185.9 mg; 0.295 mmol) was treated with bromine (more than 29.5 mg; 0.184 mmol) in chloroform (50 m*l*). On occasional shaking, the red color turned orange, green, and at last yellow. White crystals were filtered off after 2 hr. The filtrate was evacuated to dryness. The residue was washed with diethyl ether and recrystallized from chloroform-petroleum ether. Yellowish brown crystals, VI, were thus obtained.

Methyltricarbonylbistriphenylphosphinemanganese(I) (VII). Compound III (98.5 mg; 0.149 mmol)

was treated with a sodium amalgam (prepared by dissolving 1.2 g (52 mmol) of sodium metal in 13 m*l* of mercury) in THF (35 m*l*) under a nitrogen atmosphere. The mixture was left stand with occasional shaking. The yellow color turned brown during a 4-hr period. The mercury layer was then poured off, and the THF solution was filtered. The filtrate was treated with methyl iodide (8 m*l*; 130 mmol). The color gradually turned a greyish yellow green and then a transparent, yellowish brown on leaving still. The solution was filtered and evaporated. The residue was recrystallized from benzene-petroleum ether under a nitrogen atmosphere. Yellowish brown crystals, VII, were thus obtained.

Physical Measurements. *The Molecular Weights* were determined in benzene or in methylethylketone with a Mechrolab, model 301 A, osmometer.

The Magnetic Susceptibilities were measured with Gouy balances at room temperature.*5 Cobalt(II) mercury(II) tetrathiocyanate ($\chi_g = 16.44 \pm 0.08 \times 10^{-6}$ c.g.s.e.m.u., 20°C) was used as the standard substance for III and II, while water ($\chi_g = -0.722 \times 10^{-6}$ c.g.s.e.m.u., 25°C) was used for VIII diluted with NaCl.[7]

The Infrared Spectra were recorded with Japan Optics DS-402G, Japan Optics IR-G, and Perkin Elmer model 137B Infracord recording spectrometers for the samples in the nujol mulls and KBr disks.

The ESR Spectra were recorded with a JEOL JES-118 spectrometer.

The ^1H NMR Spectra were recorded on a Varian HA-100 high-resolution spectrometer, using carbon tetrachloride as the solvent and tetramethylsilane as the internal reference.

Results and Discussion

Condition of the Synthesis. Ordinarily in the present experiment, the synthetic procedure was performed by shaking the THF solution of the reactants with a mechanical shaker at room temperature and at an atmospheric pressure of nitrogen. Two other conditions were investigated in an attempt to obtain III in a better yield and with more certainty. One of them was the reaction at so high a temperature that the sodium metal melted to react more completely with I. The THF solvent was replaced with dioxane for this purpose. Though this experiment was unsuccessful, purified II was obtained in a higher yield (69.4%) than that in the literature.[3],*6 The other reaction has at a higher temperature and at 10 atm of carbon monoxide in order to restrain the CO elimination. In this procedure, however, III was obtained in only a low yield (0.14%).

Tricarbonyl bistriphenylphosphine manganese(0) (III), $Mn(CO)_3(PPh_3)_2$. Compound III is composed of yellow, needle-like crystal readily air-oxidized in solution, although it is moderately stable against aereal oxidation in the solid state. The dilute chloroform solution of III gives no signal on an ESR spectrometer at temperature of liquid nitrogen under a nitrogen atmosphere, but it gives that of a high-spin manganese(II) compound after a short exposure to the air. Therefore, all the experiments, unless otherwise noted, were performed under a nitrogen atmosphere.

The results of the elementary analyses are listed in Table 1. The values observed on the pale yellow crystals recrystallized from benzene or from acetone do not agree well with those calculated in accordance with the formula noted above. This

Table 1

Compound	Mol wt Found (Calcd)	Elementary Analysis Found/(Calcd)% C	H	Mn[c]	Cl	μ_{eff}
II	449[a]	69.10	4.96	11.11		diamag.
$(CH_3C_5H_4)Mn(CO)_2(PPh_3)$	(452)	(69.00)	(4.87)	(12.17)		$\chi_g = -0.549 \times 10^{-6}$ c. g. s. e. m. u.
III from benzene		65.86	4.27			
III from acetone	660[b]	65.74	4.52			1.81 BM
$Mn(CO)_3(PPh_3)_2$	(663)	(70.59)	(4.52)			
$Mn(CO)_3(PPh_3)_2 \cdot (CH_3)_2CO$		(69.90)	(4.99)			
VIII		65.49	4.22		7.45	1.6 BM
$Mn(CO)_3(PPh_3)_2 \cdot 1/2\ CHCl_3$		(65.58)	(4.22)		(7.37)	
VI		62.04	4.45			
$BrMn(CO)_3(PPh_3)_2$		(62.99)	(4.04)			

a) in methylethylketone b) in benzene c) EDTA titration

*5 The author's thanks are due to Professor Yukichi Yoshino, of the College of General Education, the University of Tokyo, and to Professor Yoshio Matsunaga, of the Faculty of Science of Hokkaido University, for the use of the Gouy balances.

*6 55% by the thermal method and 36% by the UV radiation method.

7) P. E. Selwood, "Magnetochemistry," 2nd Ed., Interscience Publishers, New York, N. Y. (1956).

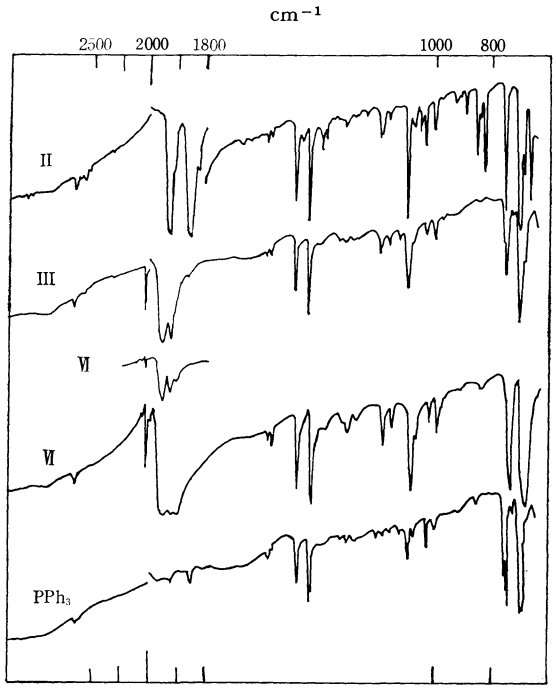

Fig. 1a. for KBr disk with DS-402 G spectrometer.

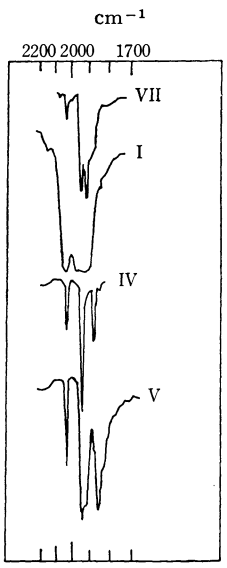

Fig. 1b. for Nujol mull with Infracord spectrometer.

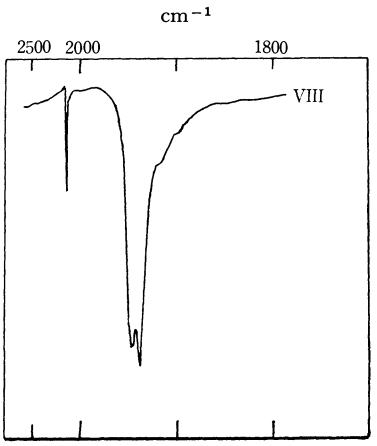

Fig. 1c. for Nujol mull with IR-G spectrometer.

Fig. 1. Infrared spectra.

cannot be attributed to the solvation of the compound (see Table 1). Though those on the yellow crystals recrystallized from chloroform-petroleum ether agree well with the solvated formula: $Mn(CO)_3(PPh_3)_2 \cdot 1/2CHCl_3$, VIII, their infrared spectra are not identical with those of the crystals recrystallized from the former two solvents (see Table 2 and Fig. 1).

The molecular weight of III in a benzene solution (Table 1) agrees very well with that calculated according to the monomeric formula, $Mn(CO)_3(PPh_3)_2$.

The infrared spectra and the wave numbers of III and VIII are shown in Fig. 1 and in Table 2. The absence of a band at about 840 cm^{-1}, characteristic of the methylcyclopentadienyl ligand, supports the idea that the $CH_3C_5H_4$ ligand of I is replaced in III. The absorption bands observed at from 760 cm^{-1} to 680 cm^{-1} can be assigned to the CH out-of-plane deformation bands of PPh_3. Three bands (one of them a doublet) in the C–O stretching region show that three CO ligands of I are not replaced. The C–O stretching pattern of pentacoordinated $M(CO)_3L_2$ was discussed by Cotton and Parish[8] and supplied by Manuel.[9] Only one infrared active band was observed for the D_{3h} symmetrical, *trans*-disubstituted trigonal bipyramidal (TBP) complexes (at 1930 cm^{-1} for rhenium[10]).

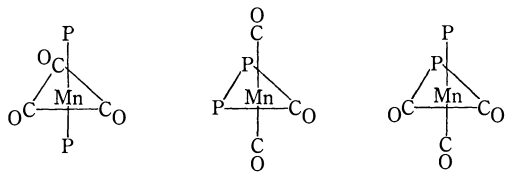

trans (D_{3h}) *cis* (C_{2v}) *cis* (C_s)

P: PPh_3

On the other hand, three bands like III were observed for most of the *cis*-$M(CO)_3L_2$, $M(CO)_3$-(Diphos),*4 and $M(CO)_3$(Diars)*7 (see Table 2). Since the (Diphos) and (Diars) ligands cannot form a monomeric *trans*-disubstituted complex, the C_{2v}

*7 (Diars) means Me_2As *o*-$C_6H_4AsMe_2$.

8) F. A. Cotton and R. V. Parish, *J. Chem. Soc.*, **1960**, 1440.

9) T. A. Manuel, *Inorg. Chem.*, **2**, 854 (1963).

10) M. Freni, D. Giusto and P. Romiti, *J. Inorg. Nucl. Chem.*, **29**, 761 (1967).

Table 2 a

Number	Compound	Sample	color	CO stretching, cm^{-1}					
VIII	$Mn(CO)_3(PPh_3)_2 \cdot 1/2\,CHCl_3$	b	yellow	2070 m	2055 sh	1948 s	1939 vs	1917 sh	1899 sh
I	$CH_3C_5H_4Mn(CO)_3$	d	pale yellow		2033 s	1940 vs,	br		
II	$CH_3C_5H_4Mn(CO)_2(PPh_3)$	a	yellow				1927 vs	1855 vs	1827 sh
III	$Mn(CO)_3(PPh_3)_2$	a *	pale yellow	2060 m	2050 m	1952 vs	1922 s	1863 sh	
IV	$Mn(CO)_3(PPh_3)_2$?	c	brown		2030 m	1950 vs		1870 m	
V	mixture	c	yellow		2030 s	1950 vs	1925 sh	1870 sh	1850 s 1830 sh
VI	$BrMn(CO)_3(PPh_3)_2$	a	yellowish brown		2040 m	1954 vs	1928 s	1908 sh	
VII	$CH_3Mn(CO)_3(PPh_3)_2$	c	yellowish brown		2035 w	1945 s	1920 vs	1880 sh	

Compound	Sample	Reference	CO stretching, cm^{-1}			
$CH_3C_5H_4Mn(CO)_2(PPh_3)$	f	3			1934	1862
trans-$Re(CO)_3(PPh_3)_2$	g	10			1930	
$Mn(CO)_3$(Diphos)	e	5	1990 s		1900 vs	
cis-$Re(CO)_3(PPh_3)_2$	e	10	2000 w		1900 s	1820 m
$Fe(CO)_3$(Diars)	e	11	2009 vs		1916 vs	1880 sh
trans-$BrMn(CO)_3(PPh_3)_2$	f	13	2046	1955	1916	
cis-$Re(CO)_3$(Diphos)	e	10		1965	1905	1855

a) KBr disk, DS-402G. b) Nujol mull, IR-G. c) Nujol mull, Infracord. d) liquid, Infracord. e) Nujol mull. f) chloroform solution. g) benzene solution. * recrystallized from benzene

Table 2 b

Compoun	Sample	C-H out of plane, cm^{-1}					
I	d		840 s				
II	a	851 s	842 m		751 s		701 s 687 s
III	a			758 s	751 s	748 s	698 s 686 s
VI	a			757 s	751 s	744 sh	693 s
PPh_3	a			758 s	752 s	746 s	701 s 694 s

or C_s symmetrical *cis*-disubstituted TBP structures were assigned to these complexes. The band pattern of III most resembles that of $Fe(CO)_3$(Diars),[11] for every band of the former is about 40 cm^{-1} higher than the corresponding band of the latter and the second bands of both compounds are more intensive than the lowest ones. Thus, the C_{2v} symmetrical TBP configuration is most likely for $Mn(CO)_3(PPh_3)_2$, much as with $Fe(CO)_3$(Diars). Now, for both $Mn(CO)_3$(Diphos) and I, two bands have been reported, but the lower intensive band might consist of two bands overlapping accidentally. $Mn(CO)_3(PPh_3)_2 \cdot 1/2CHCl_3$, VIII, shows a C–O stretching absorption band pattern similar to those of these compounds (see Fig. 1). The structure of this adduct depends on whether the chloroform molecule is only a solvent of crystallization or a definite ligand. The appearance of the highest band suggests that a linear OC–Mn–CO skeleton is preserved.*8 Therefore, two rectangular pyramidal (RP) structures, C_{2v} or C_s symmetrical, are very likely for the mother complex. The sixth coordination site of the octahedral configuration may be occupied by half-molar chloroform, though the existence of the chemical bond is uncertain. In other words, solvation may occur on the molecular plane in one of tow possible directions relative to the mother TBP complex.

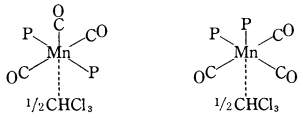

C_{2v} C_s

P: PPh_3

The magnetic susceptibilities and magnetic moments of III and VIII are listed in Table 1.*9 The value of 1.86 BM has been reported[4] for Mn-

11) H. Nigam, R. S. Nyholm and D. V. Ramana Rao, *J. Chem. Soc.*, **1959**, 1397.

*8 According to the explanation given by Angelici *et al.*[12] for the octahedral tricarbonyl complexes, the highest band can be assigned to the symmetric C–O vibration of linear OC–M–CO. C_{2v} structures (TBP and RP) and one of the RP C_s structures have this skeleton.

*9 The corrections for PPh_3 and $CHCl_3$ have been calculated to be 166 and 69 respectively on the basis of Selwood's review.[7] For three CO it was reduced from the correction given by Hieber and Freyer[3] to $-(CO)_4(PPh_3)$, 219, to 40. (All the values are in units of 10^{-6} c.g.s.e.m.u.) The formula: $\mu_{eff}=2.83\times\sqrt{\chi_M^{coor.}\times T}$ was used.

12) R. J. Angelici, F. Basolo and A. J. Poë, *J. Amer. Chem. Soc.*, **85**, 2215 (1963).

$(CO)_4(PPh_3)$, and that of 1.70 BM,[5] for $Mn(CO)_3$-(Diphos). The observed value agrees quite well with these, corresponding to one unpaired electron. This supports the idea that they are monomeric and zero valent manganese complexes, an idea which is also consistent with the observed molecular weight. In the chloroform adduct crystal VIII, the monomeric structure may be preserved for manganese because of its paramagnetism.

Two chemical reactions of III were investigated: one, its oxidation with bromine in chloroform, gave brown *trans*-$BrMn(CO)_3(PPh_3)_2$, VI, which is the usual hexa-coordinated complex. The results of CH analyses are listed in Table 1. The infrared spectra (see Table 2 and Fig. 1) are in good agreement with the results reported by Abel and Wilkinson[13] and corrected by Angelici *et al.*[14] with respect to structural assignment. The chemical shift value of the ^1H NMR spectrum (see Table 3) can be assigned to the protons of the phenyl group. The other reaction examined was the reduction of III with a sodium amalgam, followed by treatment with methyl iodide. Yellowish brown $CH_3Mn(CO)_3(PPh_3)_2$*10 VII, was thus obtained; it was identified because its infrared spectra showed a pattern similar to that of isostructural VI. Thus, the mother complex is confirmed to be *cis*-$Mn(CO)_3(PPh_3)_2$.

Methylcyclopentadienyldicarbonylmonotriphenylphosphinemanganese(I) (II), $(CH_3C_5H_4)$-$Mn(CO)_2(PPh_3)$. All the results with II are consistent with the structure reported in the literature.[3] The chemical shifts of the ^1H NMR spectra are listed in Table 3, along with the assignment of the absorptions. In the preparative reaction, sodium metal may, in the present experiment, play the same role as the ultraviolet ray in those in the literature.[3,16]

The Unidentified Yellowish Brown Crystal (IV). This was obtained by a short reaction at a higher temperature. Yellow mixture, V, noticed in the course of synthesis in dioxane consisted of II and IV judging from its infrared spectra. Three almost equi-distant intensive C–O strethcing bands are characteristic of the infrared spectra of IV (see Table 2 and Fig. 1), and their intensities are about 1 : 2 : 1. No such feature is found in I, II, or III. Shoulders on the lower side of the lower two bands are assigned to absorptions of II mixing in. In comparison with the spectra of III, the bands of IV other than the strongest center one are relatively intensive. These facts lead to two hypothetical structures for IV. One is an octahedral $Mn(CO)_3(PPh_3)_2X$, where X may be a hydrido ligand or another ligand. The other is a structural isomer of III. Neither III nor IV has a D_{3h} structure. The C_{2v} structure may be assigned to III, and the C_s structure to IV, for the weakness of the highest band in the former spectra can be attributed to the strong coupling of *trans*-2CO vibrations.*8 On the repeated recrystallization of the cruder III, the band at 1865 cm^{-1} became weak, and that at 1950 cm^{-1} intensive. This may be interpreted as resulting from the fact that the inpurity, II or IV, was taken off. However, another interpretation is possible, *i.e.*, an angular isomerization from the C_s structure to the C_{2v} one (see sheme). In the former there remains the original configuration of I for three CO, and the latter may be thermodynamically stable because of its higher symmetry. This rearrangement corresponds to the *cis-trans* isomerization of the octahedral complex for three CO ligands.[12]

TABLE 3

^1H NMR Spectra: Chemical shifts from TMS, ppm

assignments	II	VI	PPh_3
CH_3	1.42		
C_5H_4	3.39 3.54		
P-C_6H_5	6.77 6.88	7.29	7.15 7.19

The author wishes to express his hearty thanks to Professor Yukiyoshi Sasaki of the University of Tokyo for his helpful advice and encouragement throughout this work, and to Professor Shizuo Fujiwara of the University of Tokyo for his kind interest in this work.

*10 This compound was prepared by Hieber *et al.*[15] from VI by an almost identical procedure.

13) E. W. Abel and G. Wilkinson, *J. Chem. Soc.*, **1959**, 1501.

14) R. J. Angelici, F. Basolo and A. J. Poë, *Nature*, **195**, 993 (1962).

15) W. Hieber, M. Höfler and J. Muschi, *Chem. Ber.*, **98**. 311 (1965).

16) C. Barbeau, *Can. J. Chem.*, **45**, 161 (1967); W. Strohmeier and F. J. Müller, *Chem. Ber.*, **100**, 2812 (1967), and the literature cited therein.

BULLETIN OF THE CHEMICAL SOCIETY OF JAPAN VOL. 43 2063—2067 (1970)

The Separation of Gold, Platinum, and Palladium by Reversed-phase Partition Chromatography

Ikuko AKAZA, Toshiyasu KIBA and Tomoe KIBA

Department of Chemistry, Faculty of Science, Kanazawa University, Kanazawa

(Received December 6, 1969)

For the separation of gold, platinum(IV), and palladium, and for the isolation of gold from other metals, the reversed-phase partition chromatography has been used as a column process in which TBP is adsorbed on Daiflon(polytrifluorochloroethylene moulding powder) as the stationary phase and hydrochloric acid, as the mobile phase. The separation of the above three noble metals was successfully achieved by carrying out the elution with 3—4 N HCl, and the isolation of gold was attained well of itself by virture of the fact that gold is tightly retained on the column and is only released by letting concentrated HNO_3 flow through the column. The concentration and separation of gold from various solutions, such as in the presence of a large amount of iron(III) or in the presence of 19 common metals and the above three noble metals, was achieved only by allowing gold to be retained on the column and allowing ther others to flow down with a 1 N HCl eluting solution. The behavior of the three noble metals in batch extraction was also examined under the same condition as in the partition chromatography employed here; a similarity was observed between the column and the batch extraction. The principal extracted species of the noble metals might be assumed to be a hydrated and solvated ion pair, such as $H(H_2O)_nTBP_6^+ \cdot HPtCl_6^-$.

Reversed-phase partition chromatography has been used by many investigators for the separation of various metal ions. The present authors have also carried out investigations of the reversed-phase partition chromatography (not the ion-exchange) of alkali metals,[1] alkaline earth metals,[2] and hexacyanoferrate(II) and (III)[3] and established that the technique is very useful for the mutual separation of ions. In this work, reversed-phase partition chromatography was applied to the separation of gold, platinum, and palladium from each other, and to the isolation of gold from various metals. These three noble metals are the elements which come into the soluble fraction in the process of the treatment of the noble metals with aqua regia, which is still one of the best techniques available for the separation of the platinum group.[4]

With respect to the work on the reversed-phase chromatography of the noble metals, there have been descriptions by Hu *et al.*[5,6] on the chromatography using filter paper impregnated with TBP and a developing solution of hydrochloric acid. The quantitative separation of the noble metals has never been attained by means of reversed-phase partition column chromatography.

The chromatographic investigations previously performed by the present authors[1-3] have indicated that much valuable information on the chromatographic separation could be obtained from the extraction behavior of the element in question in the same system. Many articles dealing with the solvent extraction of noble metals have been cited in a review[7] and other papers; the TBP-HCl extraction system was preferred in this study as the one most suitable for a good separation of the three metals. This selection seemed to be pertinent in respect to the results of the reversed-phase partition paper chromatography by Hu[5,6], the R_f-spectra of many metals on reversed-phase thin-layer chromatography with TBP,[8] and the distribution data on the solvent extraction of the three metals in the TBP-HCl system[9] and in the counter-current extraction.[10]

1) I. Akaza, This Bulletin, **39**, 585 (1966).
2) I. Akaza, *ibid.*, **39**, 980 (1966).
3) I. Akaza, T. Kiba and M. Taba, *ibid.*, **42**, 1291 (1969).
4) I. M. Kolthoff and P. J. Elving, "Treaties on Analytical Chemistry," Part II. Vol. 8, Interscience Publishers, New York and London (1963), p. 384.
5) Chin-Te Hu and Hsiu-Chun Ssieh, *K'o Hsueh T'ung Pao*, **8**, 54 (1963).
6) Chin-Te Hu and Hsiu-Chun Shi, *Hua Hsueh Hsueh Pao*, **30**, 352 (1964).
7) F. E. Beamish, *Talanta*, **14**, 991 (1967).
8) I. S. Bark, G. Duncan and R. J. T. Graham, *Analyst*, **92**, 347 (1967).
9) T. Ishimori, K. Watanabe and E. Nakamura, This Bulletin, **33**, 636 (1960).
10) E. W. Berg and W. L. Senn, Jr., *Anal. Chim. Acta*, **19**, 12 (1958).

Experimental

Reagents and Equipments. *Daiflon M-300.* Trifluorochloroethylene polymer moulding powder was obtained from the Daikin Kogyo Co., Osaka, Japan. The material was ground with a mixing grinder and sieved; particles of 42—80 mesh were used.

TBP. *n*-tributyl phosphate of the reagent grade was washed twice with a 5% sodium carbonate solution of equal volume and then with water to remove any dibutyl- or monobutyl phosphate.

Metallic Salts Solutions. The solutions were prepared from metallic gold, palladium chloride, and chloroplatinic acid hexahydrate, all of analytical-reagent grade respectively.

Tracers. ^{195}Au, ^{113}Sn, ^{203}Hg, ^{59}Fe, ^{207}Bi, ^{110m}Ag, ^{65}Zn, ^{124}Sb were employed as tracers of the stable ions.

The other chemicals used were all of an analytical grade.

Column. The glass tube had a diamter of 0.92 cm and a length of 30 cm, and was equipped with a fritted glass disk at one end.

Measurement of Radioactivity. A scintillation counter, Kobe Kogyo Co., Model EA-14, with a NaI(Tl) crystal, and a Model SA-2 scaler were employed.

The other pieces of equipment such as a fraction collector and a spectrophotometer, were all those in ordinary use.

Organic Solvent for the Stationary Phase of the Column as Well as for the Batch Extraction. The TBP used in each experiment had been pre-equilibrated with hydrochloric acid of the same concentration as that of the acid used for the mobile phase in the column or the aqueous phase in the batch. No such diluent as benzene was added except when it was necessary to vary the TBP concentration of the organic phase.

Eluting Solution of the Column Extraction. Hydrochloric acid of various concentrations and concentrated nitric acid were used as the eluting solutions; they had been pre-equilibrated with TBP or TBP-benzene. These solutions were also used in the batch-extraction experiments as an aqueous phase.

Test Solution. Hydrochloric acid of various concentrations and of varying volumes, each portions containing 0.5 mg of a metal ion, was prepared; in this case, the concentration of hydrochloric acid was adjusted to be the same as that of the eluting solution for the column or the aqueous phase in the batch extraction.

Experimental Procedure. *The Stationary Phase of the Column.* A 5.5-g portion of Daiflon was placed in an Erlenmyer flask fitted with a stopper, and 6 m*l* of the organic solvent, prepared as above, was poured onto it. This volume of the organic solvent had been established previously to be an adsorbable amount of TBP on Daiflon.[3] The stoppered flask was shaken gently by hand until the content became homogeneous; then it was left standing over three hours. The product was then slurried with an eluting solution and packed in a column tube by gentle pressing with a glass rod every time a small portion of the slurry was added. After the column had then been washed with an eluting solution with the acidity same as the test solution, a 5 m*l* or 3 m*l* portion of the test solution was allowed to soak into the column bed at the rate of about 0.25 m*l*/min. The elution was carried out with a suitable eluting solution at the rate of 0.5 m*l*/min. The effluent was collected in suitable fractions, and the metal ion in each fraction was determined. In this study the colorimetric methods of platinum with $SnCl_2$ and of palladium with dimethylglyoxime were adopted. The gold was estimated colorimetrically with rhodamine B or radiometrically with ^{195}Au. When radioactive tracers, involving gold and other elements; were employed, all being mixed together, the nuclide separated in a fraction was identified by taking its γ-ray spectra with a 200-channel pulse-height analyzer, not only by counting the radioactivity with a scintillation counter.

Rusults and Discussion

Preliminary Experiments. *Behavior of Au, Pt, and Pd in the Batch Extraction.* The distribution behavior of the three metals was examined between the TBP adsorbed on Daiflon and an aqueous solution, not by means of liquid-liquid extraction between TBP and hydrochloric acid, in search of good conditions for separation. In this case, 4.6 g of Daiflon, adsorbing 5 m*l* of TBP, and 15 m*l* of a hydrochloric acid solution containing 0.5 mg of the metal were employed. The contents of a stoppered flask were gently shaken for a while, set aside a while, then poured them on a coarse glass filter. The aqueous solution coming through the filter was submitted to the determination of the metal ions in it. Gold shows a very high distribution in TBP on Daiflon, so this measurement method can not be applied in the case of gold. Therefore, the distribution ratio of gold was estimated only by an

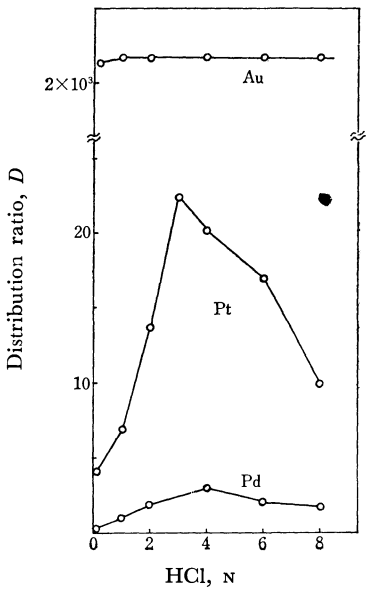

Fig. 1. The distribution curves of Au, Pt and Pd in the batch extraction.

Pt, Pd: Batch extraction with TBP-Daiflon
Au: Liq.-liq. batch extraction
TBP: 5 m*l*, Aqueous solution: 15 m*l*, Metal: 0.5 mg

ordinary liquid-liquid extraction between 5 m*l* of TBP and 15 m*l* of the aqueous solution. The results are shown in Fig. 1, from which the optimum condition for the mutual separation of the metals may be seen to be in the range of acidity between 3 to 4.

Chromatographic Behavior of Individual Ions. With 3 m*l* of a test solution containing only one of the three metals, the chromatographic behavior of the metal ion was examined by means of elution with hydrochloric acid of various concentrations. The results are shown in Fig. 2, where gold is omitted because of its absence in the effluent. Gold showed so high a distribution in TBP on the column that, even after as much as 1 *l* of the eluting solution had passed through, gold did not appear in the effluent. Thus, the separation of the three metals seemed to be attained satisfactorily by elution with 3—4 N hydrochloric acid.

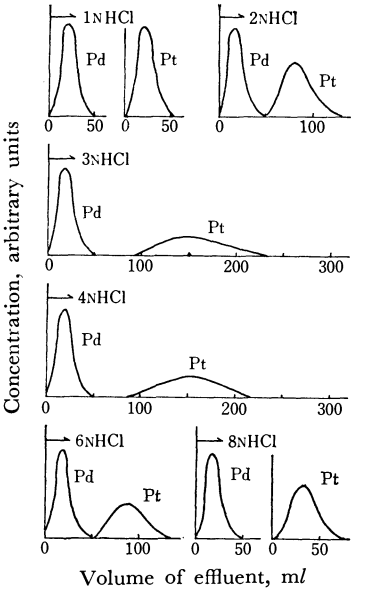

Fig. 2. The chromatographic behavior of individual ions. Gold was not eluted even after 1 *l* of eluting solution flowed.

Test solution: 3 m*l* containing metal of 0.5 mg.

Separation of Au, Pt, and Pd in the Presence of Fe(III). With the help of the results obtained for an individual ion, the separation from a test solution containing all three metals was carried out by elution with 3—4 N hydrochloric acid. Gold, which was tightly retained on the column, could be at last removed from the column by passing through concentrated nitric acid. The features of this elution scheme are shown in Fig. 3. Some interesting applications of this separation are also shown in Fig. 4, in which: (a) the quantity of each metal is in proportion to its Clarke

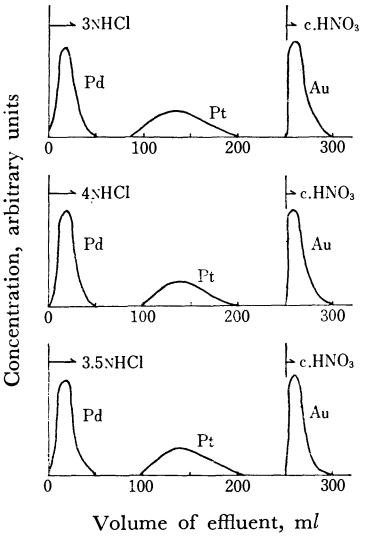

Fig. 3. The separation of Au, Pt and Pd from a mixed solution.

Test solution: 5 m*l* containing 0.5 mg of each metal.

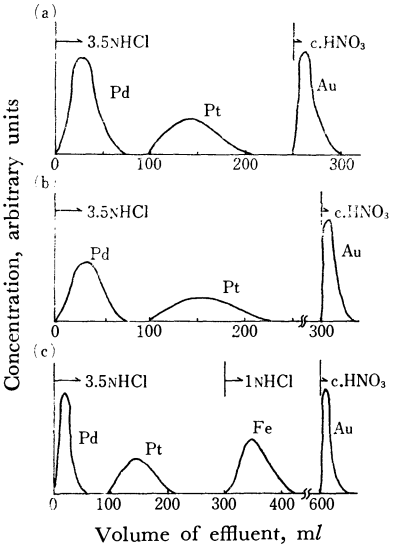

Fig. 4. The separation of Au, Pt and Pd from a mixed solution.

(a) Pd: 1 mg——Test soln.: 5 m*l*; Pt, Au: 0.5 mg
(b) Test soln.: 50 m*l*——Metal: 0.5 mg each
(c) In presence of Fe——Test soln.: 5 m*l*; metal: 0.5 mg each

number, (b) there is separation from a test solution of large a volume such as 50 m*l*, and (c) there is the separation of the three noble metals in the presence of iron(III). In the last case, iron(III) could be eluted with 1 N hydrochloric acid after the elution of Pd and Pt with 3.5 N hydrochloric acid. This seems to be very noticeable because

iron(III) is an ion which has a high distribution ratio in an ordinary TBP-HCl extraction system and is apt to exist in various samples as an impurity. All in the above experiments, gold could not be eluted by elution with hydrochloric acid, but instead was retained on the column tightly; therefore, a minute amount of gold could be successfully concentrated and separated by this column technique. As an example, 200 m*l* of a test solution containing 0.5 mg of gold and 6 g of iron(III) was adjusted to 1 N of a hydrochloric acid solution and allowed to flow through the column; followed by elution with 500 m*l* of 1 N hydrochloric acid. The iron(III) in the effluent was determined colorimetrically by the thiocyanate method, and gold(III) was detected by the tracer method with γ-counting. It was found that the gold was retained on the column completely; was concentrated and separated from a large amount of iron(III). With the elution of concentrated nitric acid, the gold could also be recovered quantitatively in the effluent. This method might be used in the chemical analysis of gold-plating materials.

Separation of Gold from Many Other Metals. To confirm the above use of this method, 50 m*l* of a test solution of 1 N hydrochloric acid was prepared, in which 0.5-mg portions of each of the following metal ions were put: Sn(IV), Hg(II), Fe(III), Zn, Bi, Ag, Co, Sb(III), Cd, Cu, Ni, Al, Mn, Pb, Ca, Sr, Ba, Mg, Pd, Pt, and Au(III). The test solution was soaked on the column, and then 950 m*l* of 1 N hydrochloric acid eluting solution was passed through. After examining all of the fractions of the effluent, it was found that only two metal ions, Au(III) and Sn(IV), were retained on the column. Then, Sn(IV) was released from the column by passing through 300 m*l* of 1 N nitric acid, and there after. Au was eluted by concentrated nitric acid. From the distribution data of the liquid-liquid extraction in the TBP-HCl system, it had been established that none of the metal ions except Sn(IV), Hg(II), Fe(III), Bi(III), Ag, Zn and Sb(III) participated in the extraction,[9] therefore, in this study the radioactive tracers of the latter seven metals and Au(III) were preferentially employed in order to detect the behavior of these metal ions. Thallium(III) is only the ion, the distribution ratio of which is so close to that of Au(III) in the TBP-2 N HCl extraction, but it was omitted in this experiment because of the lack of its γ-emitting tracer. It seems that this separation method can be used for various purposes, such as the milking of ^{195}Pt from ^{195}Au and the preparation of carrier-free ^{199}Au from irradiated platinum. The applications will be described elsewhere.

The Distribution Ratio in the Chromatographic Column and That in the Batch Extraction of the Same System. The distribution ratio in the column extraction can be calculated

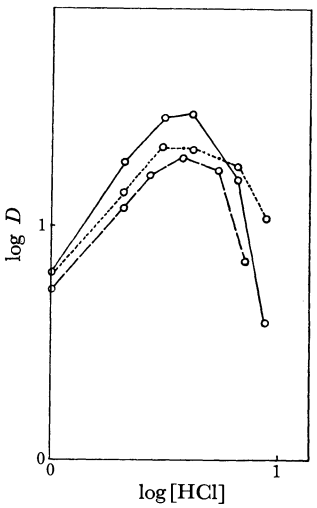

Fig. 5. Dependence of the distribution ratio of Pt on the concentration of HCl.

Solid line: Column chromatography
Dotted line: Batch extraction with TBP-Daiflon
Dashed line: liq.-liq. batch extraction

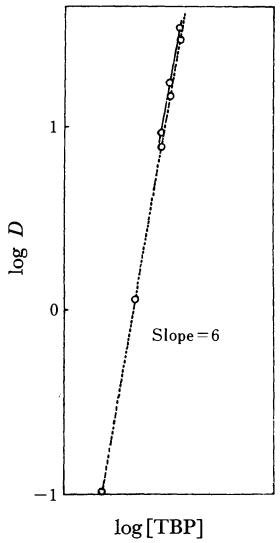

Fig. 6. Dependence of the distribution ratio of Pt upon the concentration of TBP.

Solid line: Column method
Dotted line: Batch method

by the following equation by putting the data of the elution into it: $D=(E-F)/B$, where E is the volume of the effluent before the emergence of the peak of the curve; B, the volume of the stationary phase, and F, the volume of the mobile phase. In the present column, B was 6 m*l* and F was 6.4 m*l*; 0.5 mg of platinum was loaded on and eluted with hydrochloric acid of varying concentrations. The TBP concentration of the stationary phase was also varied by diluting the organic solvent with benzene.

Thus, the dependence of the distribution ratio on the hydrochloric acid concentration of the aqueous phase, log D *vs.* log [HCl], and that on the TBP concentration of the organic phase, log D *vs.* log [TBP], were found to be as shown in Fig. 5 and Fig. 6 respectively. Along with these experiments, two other extractions were carried out by the batch system: a liquid-liquid extraction between each 5-m*l* portin of the aqueous and the organic phases, and a liquid—TBP on Daiflon extraction between 15 m*l* of the aqueous phase and 5 m*l* of the organic phase held on the adsorbent. From the distribution data thus obtained, log D *vs.* log [HCl] and log D *vs.* log [TBP] were also obtained; they are shown in Fig. 5 and Fig. 6. From the figures, it can be seen that platinum behaves similarily in all the above three extraction processes, and the chromatographic data can contribute to a knowledge of the distribution behavior of the metal ion. The lowering of the distribution ratio in the range of higher acid concentrations in Fig. 5 raises some questions to the extraction mechanism and the extracted species, but it is assumed to be caused by the competition between hydrochloric acid and the platinum ion in the extraction with TBP. Therefore, when the concentration of the chloride ion was fixed at 4 M by adding lithium chloride, the lowering of the distribution disappeared and log D *vs.* log [HCl] showed a straight line with a slope unity, as shown in Fig. 7.

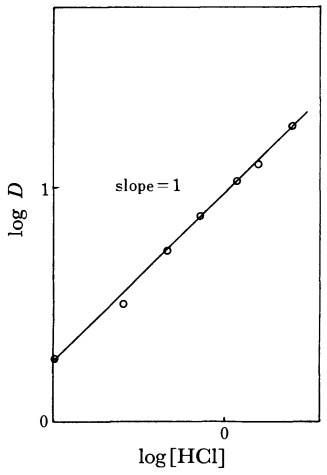

Fig. 7 Dependence of distribution ratio of Pt on the concentration of HCl.

[Cl⁻] is adjusted to 4 M with LiCl

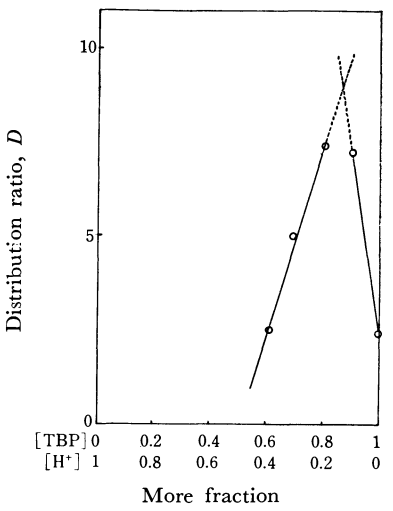

Fig. 8. Distribution of Pt under continuous variation of [TBP] and [HCl].

[Cl⁻] is kept at 4 M with LiCl
[TBP] and [HCl] are 0—3.66 M each

At last, it may be of interest to establish the extracted species of platinum in this TBP-HCl system since the species in the organic phase has not been stated anywhere. A continuous-variation method was applied to the extraction system with two variables of TBP and hydrochloric acid concentrations with a fixed concentration of 4 M lithium chloride in the aqueous phase. As is shown in Fig. 8, the maximum distribution appears at the [H] : [TBP] ratio of 1 : 6; this fact agrees well with the results shown in Figs. 5, 6, and 7. In consequence of this distribution study, though it was far from ideal, the main extracted species may be assumed to be an ion-associated one, $H(H_2O)_nTBP_6{}^+HPtCl_6{}^-$, especially in view of a previous paper concerning the extraction of metals and mineral acids,[11] and Ref. 8.

The expense of the present research was met in part by a Grant for Scientific Research from the Ministry of Education, to which the authors' thanks are due.

11) Y. Marcus, *Chem. Rev.*, **63**, 139 (1963).

BULLETIN OF THE CHEMICAL SOCIETY OF JAPAN VOL. 43 2068—2071 (1970)

Electronic Absorption Spectra of Zero-Valent* Tris-(2,2′-bipyridine) Metal Complexes

Youkoh KAIZU, Takanori YAZAKI, Yasuo TORII and Hiroshi KOBAYASHI

Department of Chemistry, Tokyo Institute of Technology, Ookayama, Meguro-ku, Tokyo

(Received December 8, 1969)

Electronic absorption spectra of zero-valent tris(2,2′-bipyridine) metal complexes of the first transition metals from titanium to cobalt have been studied. These spectra give a criterion to determine whether the central metal atom or the ligand is trapping the electrons furnished by reducing reagents upon syntheses of the complexes, if the absorption spectra of the coordinating negative ions are fairly free from the influence of the configuration interactions by the "ligand-metal" charge transfer excited states and/or by the "metal-ligand" ones. The vanadium complex is concluded as a complex of the metal atom in zero oxidation state and neutral bipyridine molecules, where the 'metal-ligand' charge transfer bands are observed. The iron- and the manganese-complexes are ionic complexes of the metal ion in a non-zero oxidation state and the negative ions of bipyridine, where the (π–π^*) absorption bands of coordinating bipyridine negative ion are observed. On the basis of their spectral character, the complexes of the other transition metals might be assigned to be a hybrid of the two typical electron traps given above.

Stabilization of complexes with a metal of lower oxidation states, $Cr(CO)_6$ for example, is well interpreted as due to the strong pi-bondings between the metal atom and the ligand molecules. The former acts as a dπ electron donor while the latter as acceptors by use of vacant anti-bonding pi-molecular orbitals of lower energy.[1] It is well known that 2,2′-bipyridine (bipy) is one of the ligands which stabilize the lower oxidation states of metals. Recently a large number of tris-bipyridine metal complexes of lower valency have been prepared by Herzog and his coworkers, and others.[2] We showed evidence of pi-bonding between the central metal atom and the ligand in the tris-bipyridine metal (II) complexes and also in the trisphenanthroline ones.[3] It might be expected that the lower the oxidation state, the more stable the pi-bonding. Although the essential role of pi-bonding in the stabilization of lower oxidation states of metals in such complexes as zero-valent bipyridine complexes should be appreciably important as was pointed out by Orgel and Jϕrgensen,[4,5] the existence of an isostructural zero-valent aluminum complexes, which is described as a complex of Al^{3+} coordinated by bipyridine negative ions, namely [Al(III)$(bipy^-)_3$], should not be overlooked, even if there exists a crucial pi-electron delocalization effect between Al^{3+} and the coordinating bipyridine negative ions.

Electron trapping seems to happen mainly in the central metal atom in the case of comparatively stable lower valency complexes of the first transition metals, *e.g.* $[Cr(I)(bipy)_3]^+$. However, the existence of coordinating negative ion, or electron trapping ligand, seems to be possible even in the first transition metal complexes depending upon the electron trapping powers of the central metal atom and the ligands.

Since bipyridine is a strong σ-donating ligand, the positive charge of the central metal ion, even in an essentially ionic complex, is almost neutralized with σ-electron charge donated by the nitrogens of the coordinating bipyridine. However, since what we discuss here is not the charge distribution of the σ-bonds in the zero-valent com-

*1 In this paper, the term "valency" stands for a net charge (electrovalency) of the complex as a whole. Therefore "zero-valent" means that no net charge is accompanied by the complex. The term "oxidation state" or "oxidation number" stands for a degree of electron detachment of the central metal or a formal charge of the central metal.

1) E. W. Abel, *Quart. Rev.* London, **17**, 133 (1963).

2) a) S. Herzog and R. Taube, *Z. Anorg. Allg. Chem.*, **306**, 160 (1960). b) S. Herzog, *ibid.*, **294**, 155 (1958). c) S. Herzog and W. Schön, *ibid.*, **297**, 323 (1958). d) F. Hein and S. Herzog, *ibid.*, **267**, 337 (1952). e) G. M. Waind and B. Martin, *J. Inorg. Nucl. Chem.*, **8**, 551 (1958).

3) I. Fujita, T. Yazaki, Y. Torii and H. Kobayashi, to be published.

4) L. E. Orgel, "An Introduction To Transition-Metal Chemistry," Second Ed., Methuen & Co., Ltd, London (1966), p. 150.

5) C. K. Jϕrgensen, "Inorganic Complexes," Academic Press, London (1963), p. 75.

plexes but the majority trapping of the extra electrons furnished by reducing reagents upon synthesis of the zero-valent complexes, the notations such as $[Al(III)(bipy^{-})_3]^0$ or $[Al(0)(bipy)_3]^0$, roughly show majority population of the molecular orbital trapping the extra electrons but not anything about the degree of σ-electroneutrality.

Analysis of ESR spectra and electronic absorption spectra give a means to determine whether the central metal atom or the ligands trap electrons. For this purpose, however, only effective magnetic moments have been measured and optical spectrum has been reported in only a few cases.[6] As far as the zero-valent complexes are concerned, only the spectrum of the iron complex[7] and the ESR of the vanadium complex[8] have been published.

In this paper, the electronic absorption spectra of the zero-valent tris-bipyridine complexes of the first transition metals from Ti to Co are presented, and the actual oxidation states of the central metals are discussed based on their absorption spectra.

Experimental

The tris-bipyridine complexes such as $[Ti(bipy)_3]$, $[V(bipy)_3]$, $[Cr(bipy)_3]$, $[Mn(bipy)_3]$, $[Fe(bipy)_3]$, and $[Co(bipy)_3]$ were prepared by the method of Herzog *et al.*[2a-2d, 9-11] The compounds were identified by elementary analysis of metal.

Tris(4,4'-dimethylbipyridine)vanadium was prepared in 50% methanol solution by the reduction of $[V(4dmbip)_3](ClO_4)_2$[3] with magnesium powder and purified by extraction with tetrahydrofuran (THF) or benzene. The compound was a blue-violet crystalline substance. Found: V, 8.31%. Calcd for $[V(4dmbip)_3]$: V, 8.44%.

Tris(5,5'-dimethylbipyridine) vanadium was prepared in 60% methanol solution by the reduction of $[V(5dmbip)_3](ClO_4)_2$[3] with magnesium powder and purified by extraction with THF. The compound was a blue-violet crystalline substance and less soluble in organic solvents than $[V(4dmbip)_3]$ and $[V(bipy)_3]$. Found: V, 8.11%. Calcd for $[V(5dmbip)_3]$: V, 8.44%.

Measurement of electronic absorption spectra. Sample solutions for spectral measurement were prepared by the method described in a previous paper.[12] Electronic absorption spectra were measured in quartz cells with light path of 0.1 cm and 1 cm, using a Shimadzu multipurpose recording spectrophotometer model MPS-50.

Results and Discussion

The electronic absorption spectra of the zero-valent tris-bipyridine complexes are given in Figs. 1—3. The general feature of their absorption spectra in the near infrared region is very diffuse and intense. Intense absorption appears in a lower wave number region than those observed for the corresponding tris-bipyridine complexes of divalent metal ions. These diffuse and intense bands might be assigned to the "metal to ligand" charge transfer bands fairly strongly red-shifted by the central metal atom M(0) with smaller ionization potential, whereas this type of charge transfer bands are usually observed in the visible region

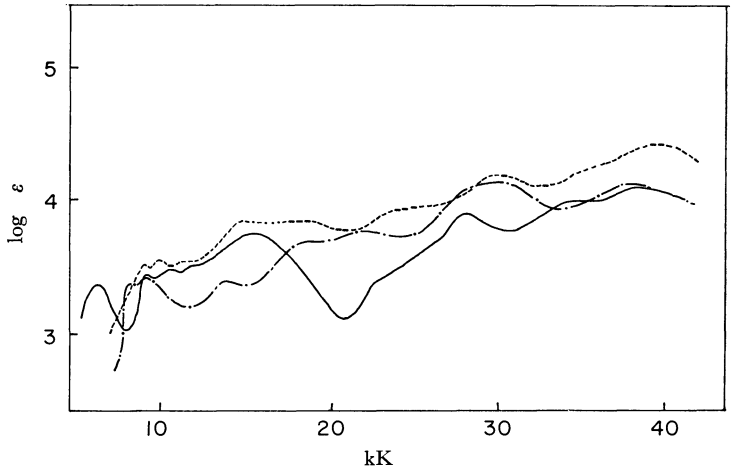

Fig. 1. Electronic absorption spectra of $[Ti(bipy)_3]$, $[Cr(bipy)_3]$ and $[Co(bipy)_3]$ in THF solution
——: Ti complex, ——: Cr complex, ----: Co complex

6) S. Herzog, E. König and H. L. Schläfer, Proc. VII Int. Conf. on Coordination Chemistry, Stockholm (1962), p. 21.
7) F. S. Hall and W. L. Reynolds, *Inorg. Chem.*, **5**, 931 (1966).
8) E. König, *Z. Naturforsch.*, **19a**, 1139 (1964).
9) S. Herzog and M. Schmidt, *Z. Chem.*, **2**, 24 (1962).
10) S. Herzog and H. Prakel, *ibid.*, **5**, 469 (1965).
11) S. Herzog, R. Klausch and J. Lantos, *ibid.*, **4**, 150 (1964).
12) Y. Torii, T. Yazaki, Y. Kaizu, S. Murasato and H. Kobayashi, This Bulletin, **42**, 2264 (1969).

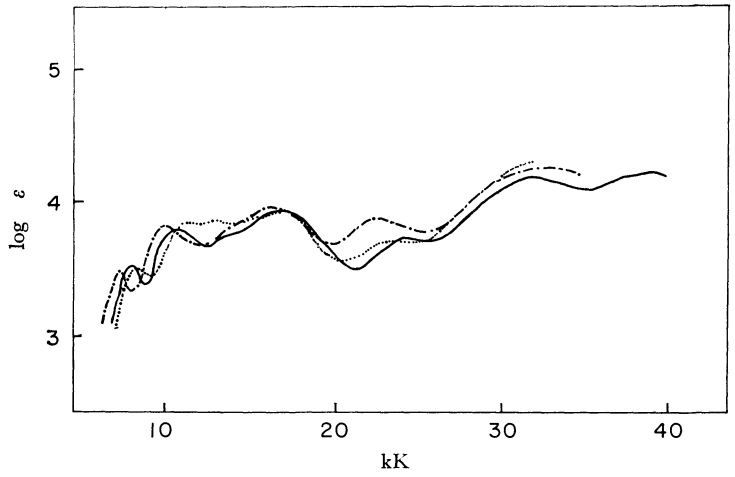

Fig. 2. Electronic absorption spectra of the V-compounds in THF solution
——: $[V(bipy)_3]$, ——: $[V(4\,dmbip)_3]$, ----: $[V(5\,dmbip)_3]$

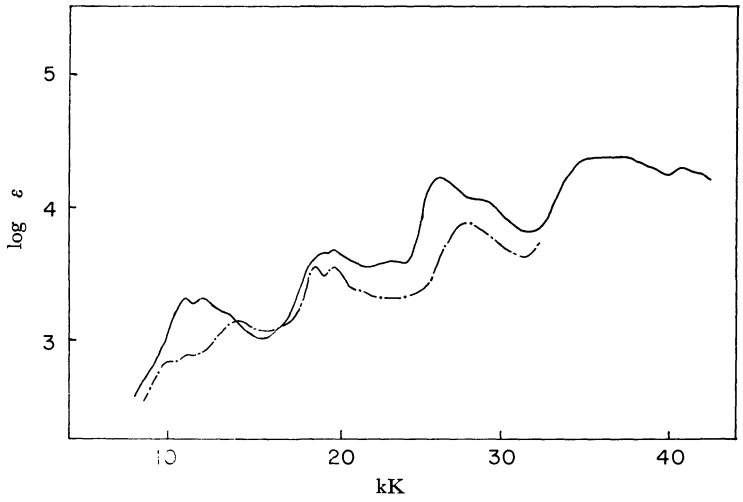

Fig. 3. Electronic Absorption spectra of $[Mn(bipy)_3]$ and $[Fe(bipy)_3]$ in THF solution. The intensity of the iron complex is in arbitrary scale ——: Mn complex, ——: Fe complex

for the corresponding tris-bipyridine complexes of such metal ions as V(II), Cr(II) and Fe(II).[3] The assignment is based on the assumption that the oxidation number of the central metals is zero, in other words the central metal atom captures electrons given by reducing reagents. On the other hand, tris(bipyridine)aluminum complex is interpreted by an approximate charge distribution such as $[Al(III)(bipy^-)_3]$,[13] since it shows an absorption spectrum very close to that observed for sodium bipyridinate and also gives ESR spectrum with a free spin g-value of 2.0037. An aluminum cation is coordinated by three bipyridine negative ions rather than an aluminum atom of zero-oxidation number is coordinated by ordinary bipyridine molecules, even if pi-electron delocalization effects between the central metal and the coordinating bipyridine are appreciable. It has also been reported for $Na[Fe(bipy)_3]$ to show similar properties.[14] In this case, the actual oxidation state of the central ion is not minus one but much more positive and the ligands are trapping a sufficient part of pi-electrons. Since these complexes are made of bipyridine negative ions coordinating to an ionic metal species, the absorption bands which appear in the near infrared region could be assigned to the (π–π^*) transitions of the coordinating bipyridine negative ion rather than the charge transfer bands mentioned above. Actually they give rise to a very similar feature to

13) Y. Torii, S. Murasato, Y. Kaizu and H. Kobayashi, to be published.

14) C. Mahon and W. L. Reynolds, *Inorg. Chem.*, **6**, 1927 (1967).

that of the bipyridine ion in alkaline salts. Among the formally zero-valent compounds of the first transition metals, $[Fe(bipy)_3]$ and $[Mn(bipy)_3]$ show a similar spectrum to that of (Na^+bipy^-) (Fig. 3). The iron complex is not so stable in solvents and decomposes so easily to Fe metal and bipyridine that $\log \varepsilon$ could not be quantitatively determined. The spectrum in the ultraviolet region could not be given because of superposing absorption bands due to the bipyridine set free in the solution (Fig. 3).

We might conclude that the Fe- and the Mn-compounds are regarded as ionic complexes of metal cation and bipyridine negative ion, $bipy^-$. The actual, but not formal, oxidation states of the central metals of these complexes could not be zero. However, molecular orbital calculations and direct experimental determinations are desirable. The Ti-, V-, Cr- and Co-compounds show another type of absorption spectra different from those for the Fe- and Mn-compounds. König interpreted his ESR spectra of the V-compound on the basis of a remarkable difference between the optical spectra observed for the V-compound and (Na^+bipy^-), assuming that trapped electrons are localized at the central metal and can not be delocalized around the ligands. Such a difference, however remarkable, does not always give a criterion when the (π–π^*) transition bands of the coordinating negative ion are drastically changed by a superposition and/or a mixing of "metal to ligand" or "ligand to metal" charge transfer bands.

In a previous paper, it was shown that small perturbations such as introduction of CH_3 group to the ligand, namely introduction of two methyl groups to the bipyridine in 4 dmbip and 5 dmbip, for example, show quite opposite spectral shifts for the "metal-ligand" charge transfer bands and the (π–π^*) transition bands of the coordinating negative ion at the lowest wave number region.[12] The charge transfer bands shift to the lower wave number in the order, 5 dmbip, bipy, 4 dmbip, while the (π–π^*) transitions of the bipyridine negative ions at the lowest wave number shift to the higher wave number in the order, 5 dmbip, bipy, 4 dmbip, which is similar to the usual (π–π^*) transitions of the bipyridines. As is shown in Fig. 2, the absorption band at the lowest wavenumber of the V-compounds shifts towards the lower wavenumber in the order, 5 dmbip, bipy, 4 dmbip. This small perturbation technique gives the criterion that the lowest wave number band of the V-compounds is due not to a (π–π^*) transition but to a "metal-ligand" charge transfer transition. This rejects the possibility of a coordinating negative ion in the case of the V-compound. We conclude that the vanadium traps electrons and is in zero oxidation state.

The Ti-compound shows a similar absorption spectrum to that of the V-compound at the near infrared and visible regions (Fig. 1). In the ultraviolet region, however, the spectra of the compounds are not identical. The absorption bands at the adjacent region of 30000 cm^{-1} are due to the (π–π^*) transition of the coordinated bipyridine. In the case of the tris-bipyridine compounds of metal(II), or metal(III), the total shift of these absorption bands ranges over several hundred wavenumbers varying with the central metal ion among the first transition metals. On the contrary, the corresponding absorption bands of the Ti-compound are observed to shift several thousand wave numbers in a comparison with the V-compound (Figs. 1 and 2): Although the (π–π^*) transition of the coordinating bipyridine changes very much in the Ti-compound, the fact that the absorption bands at the lowest wave number appear in the region lower than 10000 cm^{-1} and resemble that of the V-compound makes us conclude that the Ti-compound consists of neutral bipyridine but not negative ions. In the zero-valent complex discussed in the paper, the electron delocalization between the central metal dπ-orbitals and the ligand antibonding molecular orbitals should be appreciable even in the ground state. Since the antibonding pi-orbitals of the coordinating bipyridine is donated dπ-electron by the central metal through so-called back-donation, the (π–π^*) transitions of the coordinating bipyridine should be much modified. This type of large pi-interactions between the metal dπ-orbitals and the ligand antibonding pi-orbitals can explain not only the spectral behavior of the coordinating bipyridine but also the diamagnetism of the Ti-compound.[2a] As Fig. 1 shows, the Cr- and the Co-compounds give visible and near infrared spectra similar to those observed for the Ti-compound and the V-compound, while in the ultraviolet region, they are different from those observed for the V-compound.

Zero-valent tris-bipyridine compounds of the first transition metals can be formally classified on the basis of spectral criterion of the electronic structure: The V-compound is a complex of the metal of zero oxidation state and neutral ligands, while the Fe- and Mn-compounds are ionic complexes of the metal of non-zero oxidation state and negative ion ligands. The others seem to be in between.

BULLETIN OF THE CHEMICAL SOCIETY OF JAPAN VOL. 43 2072—2075 (1970)

The Syntheses and Properties of the Complexes of Boron with Ethylenediaminetetraacetic Acid and Its Analogs*1

Mitsuhisa NAKATANI, Yoshiaki TAKAHASHI, Akira OUCHI and Kunihiko WATANUKI

Department of Chemistry, College of General Education, The University of Tokyo, Komaba, Meguro-ku, Tokyo

(Received December 11, 1969)

Two compounds of boron with ethylenediaminetetraacetic acid, $H_6EDTA(BF_4)_2$ and $H_4EDTA\text{-}(BF_3)_2$, as well as complexes with cyclohexanediaminetetraacetic acid and nitrilotriacetic acid, have been synthesized. Their properties, including their infrared and ultraviolet spectroscopic data, have been investigated and discussed.

The syntheses and the properties of the ethylenediaminetetraacetato chelates of a large number of metals have been reported in detail.[1] The boron complexes of ethylenediaminetetraacetic acid (H_4EDTA) or other aminopolycarboxylic acids, however, have not yet been reported on. Since Gay-Lussac[2] prepared the addition compound between ammonia and boron trifluoride, $H_3N\text{-}BF_3$, about 160 years ago, a large number of complexes have been prepared by a reaction between boron trifluoride and a variety of nitrogen compounds, such as amines, imines, amides, nitriles, and nitrogen-containing hetero cyclics.[3-5] The lone-pair electrons on the nitrogen atom in these compounds readily form a coordination bond with an acceptor boron trifluoride. The carboxylic acids are less easily coordinated with boron, but some acetic acid have also been reported.[6,7] However, the coordinate compounds of boron with such aminocarboxylic acids as ethylenediaminetetraacetic acid (H_4EDTA), cyclohexanediaminetetraacetic acid (H_4CDTA), and nitrilotriacetic acid (H_3NTA) have not yet been reported on. Therefore, it seemed that it would be interesting to investigate whether or not these acids coordinate with the boron trifluoride.

Experimental

Materials and Instruments. The H_4EDTA, H_4CDTA, and H_3NTA that were used in this experiment were of all of an analytical grade. The 45% ethylether solution of boron trifluoride ethyl etherate ($BF_3\text{-}(C_2H_5)_2O$) and the acetonitrile were of an EP grade. All of them were used without further purification.

The infrared spectra were obtained by a KBr-disc or nujol-mull procedure using a Japan Spectroscopic Co. DS 403 G infrared spectrophotometer. The electronic spectra were obtained with a Hitachi EPS-2 automatic recording spectrophotometer. The pH was measured with a Toa Electronic Co. pH meter, model HM-5A.

Synthesis of the Ethylenediaminetetraacetic Acid Adduct of Boron Trifluoride, $H_4EDTA(BF_3)_2$. Two grams (0.007 mol) of H_4EDTA and 6 m*l* (0.02 mol BF_3) of a 45% ether solution of $BF_3\text{-}(C_2H_5)_2O$ were mixed with 10 m*l* of acetonitrile containing a small amount of water (about 0.3 m*l*). The mixture was warmed on a water bath for a few minutes and then dissolved. A small amount of insoluble residue was filtered off, and the filtrate was refluxed for about 2 hr. A white precipitate was thus obtained. The product was filtered off, washed well with acetonitrile and ethyl ether successively, and dried in a vacuum at room temperature. The yield was about 1.9 g (65% calculated for H_4EDTA).

Found: C, 28.08; H, 4.26; N, 6.57; B, 4.79; F, 25.83%. Calcd for $C_{10}H_{16}N_2O_8B_2F_6$: C, 28.04; H, 3.74; N, 6.54; B, 5.05; F, 26.64%.

Synthesis of Ethylenediaminetetraacetic Acidium Tetrafluoroborate, $H_6EDTA(BF_4)_2$. The acetonitrile solution of H_4EDTA and boron trifluoride ethyl etherate obtained by the former synthesis process was allowed to stand for one day at room temperature without refluxing. The white precipitate thus obtained was filtered off, washed well with acetonitrile and ethyl ether successively, and then dried in a vacuum at room tem-

*1 This paper was presented at the 19th Symposium on Coordination Chemistry, Sendai, September, 1969.

1) F. L. Garvan, in "Chelating Agents and Metal Chelates," ed. by F. P. Dwyer and D. P. Mellor, Academic Press, New York and London (1964), p. 283.

2) J. Gay-Lussac, *Mémoires de la Société d'Arcueil*, **2**, 211 (1809).

3) H. S. Booth and D. R. Martin, "Boron Trifluoride and Its Derivatives," John Wiley & Sons, New York, N. Y. (1949), p. 43.

4) N. N. Greenwood and R. L. Martin, *Quart. Rev.*, **8**, 1 (1954).

5) F. G. A. Stone, *Chem. Rev.*, **58**, 101 (1958).

6) K. J. Kunningham, *J. Chem. Soc.*, **1951**, 2305.

7) R. Beukers and A. Szent-Gyorgyi, *Rec. Trav. Chim.*, Pays-Bas **81**, 255 (1962).

perature. The yield was about 80% (calculated for H_4EDTA).

Found: C, 25.99; H, 3.87; N, 6.06; B, 3.94; F, 32.29%. Calcd for $C_{10}H_{18}N_2O_8B_2F_8$: C, 26.57; H, 3.88; N, 5.99; B, 4.62; F, 32.48%.

Synthesis of the Cyclohexanediaminetetraacetic Acid Adduct of Boron Trifluoride, $H_4CDTA(BF_3)$. About 0.5 g (0.0015 mol) of H_4CDTA, about 0.7 m*l* (0.0025 mol BF_3) of a 45% ether solution of BF_3-$(C_2H_5)_2O$, and 1 m*l* of acetonitrile were mixed and dissolved; water was not necessarily added. The solution was refluxed on a water bath for about 1 hr. After the removal of the solvent and the excess of BF_3-$(C_2H_5)_2O$ under reduced pressure, about 10 m*l* of ethyl ether was added to the brown residue. The white precipitate thus obtained was washed well with acetonitrile and ethyl ether before being dried in a vacuum at room temperature. The yield was about 0.13 g (20% calculated for H_4-CDTA).

Found: C, 39.49; H, 5.81; N, 6.21; B, 2.10; F, 14.06%. Calcd for $C_{14}H_{22}N_2O_8BF_3$: C, 40.60; H, 5.36; N, 6.76; B, 2.61; F, 13.76%.

Synthesis of Nitrilotriacetato Boron (NTA·B). The method of synthesizing $H_4EDTA(BF_3)_2$ was used. The yield was about 15% (calculated for H_3NTA).

Found: C, 34.58; H, 3.12; N, 6.99; B, 4.98%. Calcd for $C_6H_6NO_6B$: C, 36.22; H, 3.04; N, 7.04; B, 5.43%.

Results and Discussion

Typical patterns of the infrared spectra of these complexes are shown in Fig. 1, while the alkalimetric titration curve of $H_6EDTA(BF_4)_2$ in an aqueous solution is shown in Fig. 2.

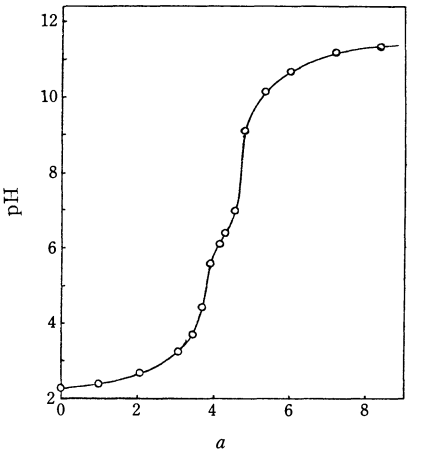

Fig. 2. Alkalimetric titration curve of $H_6EDTA(BF_4)_2$ in aqueous solution.

a = NaOH/$H_6EDTA(BF_4)_2$

Many papers have been published about the infrared spectra of ethylenediaminetetraacetato complexes as well as free acid.[8] According to these papers, the antisymmetric stretching bands of the uncoordinated and unionized carboxyl group of EDTA appears in the 1750—1700 cm^{-1} region, whereas that of the coordinated one appears in the 1650—1590 cm^{-1} region. The band of the free acid appears at 1690 cm^{-1}, and Novak and his co-workers deduced that two protonated nitrogen atoms and two $(-COOHOOC-)^-$ groups seem

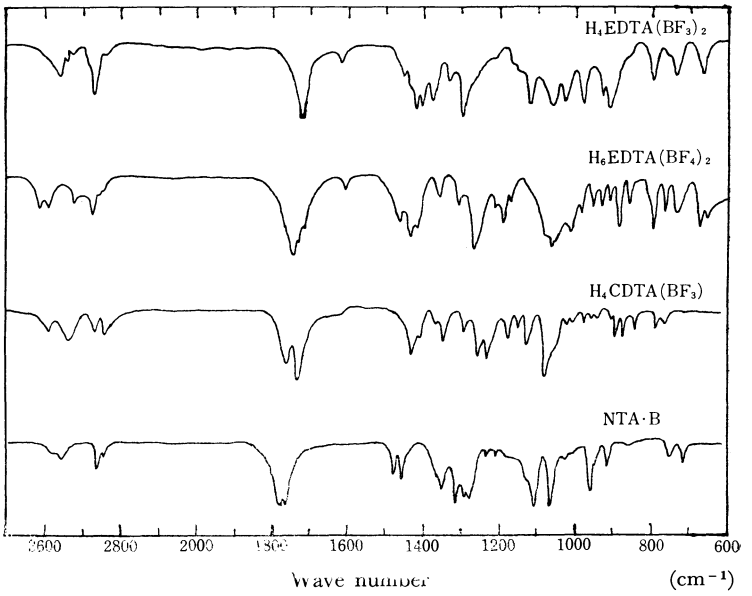

Fig. 1. Infrared spectra of the boron compounds.

8) K. Nakamoto, "Infrared Spectra of Inorganic Coordination Compounds," John Wiley & Sons, New York, N.Y. (1963), p. 205.

to exist in the free acid.[9] The fully protonated salt of ethylenediaminetetraacetic acid, $H_6EDTA \cdot Cl_2$, was also prepared by the reaction between ethylenediaminetetraacetic acid and hydrogen chloride.[10] The infrared spectra of the compound have a strong, characteristic absorption band near 1740 cm^{-1}; this can probably be assigned to the carboxyl groups attached to the protonated nitrogen atoms. There is also a broad band in the 3300—2000 cm^{-1} region; this is probably the OH stretching band of a carboxyl group.[9]

The assignments of the infrared absorption bands of $H_4EDTA(BF_3)_2$ were made with reference to the data about H_4EDTA, its metal complexes, and other B-N compounds. Therefore, the assignments are only tentative. The antisymmetric stretching band of the carboxyl group of this compound appears at 1725 cm^{-1}; this wave number is about 35 cm^{-1} higher than that of the free acid. This is probably due to the effect of coordinated boron trifluoride, which is a strong Lewis acid and which may be expected to have the same effect as a proton bonded to the nitrogen atom, as in the case of $H_6EDTA \cdot Cl_2$. Therefore, no carboxyl group of this complex seem to be coordinated with boron.

The bands near 1100 cm^{-1} are identified as B-F stretching bands following the examples given by Kreutzberger of amine adducts,[11] by Taylor of ammonia and trimethylamine adducts,[12] and by Paterson of hydrazine adducts.[13] The B-N stretching bands may be overlapping in this last case too.

A fresh aqueous solution of the complex does not give positive results in qualitative tests for the tetrafluoroborate ion using potassium chloride[3] or using nitron (1,4-diphenyl-3,5-endoanilinodihydrotriazole).[14] Therefore, the boron atoms of this compound are expected to bond with EDTA, probably with its nitrogen atoms, although no direct proof from the infrared spectra has yet been obtained.

Some peaks of the infrared spectra of $H_6EDTA(BF_4)_2$ have also been assigned by comparing them with those of $H_6EDTA \cdot Cl_2$. The strong bands at 1740—1720 cm^{-1}, the antisymmetric stretching band of the carboxyl group, and the broad band at 3200—2400 cm^{-1}, probably overlapping one of the stretching bands of N^+–H and OH, are visible. Consequently, a proton probably bonds to each nitrogen atoms of ethylenediaminetetraacetic acid, and this makes the stretching band of the carboxyl group shift to the higher-wave-number side, as in the case of $H_6EDTA \cdot Cl_2$. The other broad bands appearing in the 1100—1000 cm^{-1} region seem to be due to the B-F stretching bands of the tetrafluoroborate ion, BF_4^-, because the alkali salts show the same peak, as has been reported by Cote.[15] The broadening of this band was explained by Greenwood in term of the site symmetry and the isotope effect of the ion.[16]

The presence of the BF_4^- ion was also established by qualitative tests using potassium chloride or nitron.[3,14]

The alkalimetric titration curve of this compound, shown in Fig. 2, indicates that one mole of this compound immediately decomposes to two moles of tetrafluoroboric acid and one mole of H_4EDTA. In reality, if the solution is concentrated, a white precipitate of H_4EDTA appears. The former is a strong acid, and its hydrolysis in an aqueous solution, $BF_4^- + H_2O \rightarrow BF_3(OH)^- + HF$, is negligible during the titration, altough it may be gradually decomposed. Therefore, the inflexion point corresponds with the neutralization of two moles of HBF_4 and one mole of H_4EDTA (only to H_2EDTA^{2-}). On the other hand, boron trifluoride is rapidly hydrolysed in an aqueous solution, and the concentrations of BF_4^- and other various ionic species increase faster.[17] The acidity gradually increase during the alkalimetric titration process. In reality, in the alkalimetric titration of $H_4EDTA(BF_3)_2$ it took a long time before the equilibrium was attained after alkali was added.

Debye-Scherrer X-ray powder diffraction patterns of both $H_4EDTA(BF_3)_2$ and $H_6EDTA(BF_4)_2$ were obtained, but they were completely different from each other.

Although the attempt to recrystallize these compounds has not yet been successful, each compound seems to be nearly pure, since two products which were not only analytically but also infrared-spectroscopically characterized were reproducibly obtained in each synthesis of the compounds, even when the mole ratio of the starting materials was changed from 1 : 20 to 1 : 3.

The infrared spectra of $H_4CDTA(BF_3)$ in general resemble those of cyclohexanediaminetetraacetic acid.

The antisymmetric bands of the carboxyl group appear at 1760 and 1730 cm^{-1}, whereas the bands

9) A. Novak, M. Cotrait, J. Joussot-Dubien and J. Lascombe, *Inorg. Chem.*, **4**, 767 (1965).

10) D. C. Olson and D. W. Margerum, *J. Amer. Chem. Soc.*, **82**, 5602 (1960).

11) A. Kreutzberger and F. C. Ferris, *J. Org. Chem.*, **27**, 3496 (1962).

12) R. C. Taylor, in "Boron-Nitrogen Chemistry," ed. by K. Niedenzu, American Chemical Society, Washington (1964), p. 64.

13) W. G. Paterson and M. Onyszchuk, *Can. J. Chem.*, **39**, 986 (1961).

14) W. Lange, *Ber.*, **59**, 2107, 2432 (1926).

15) G. L. Cote and H. W. Thompson, *Proc. Roy. Soc. Ser. A*, **210**, 217 (1951).

16) D. W. A. Sharp, "Advances in Fluorine Chemistry," ed. by M. Stacey, J. C. Tatlow and A. G. Sharpe, Butterworths, London (1960), p. 68.

17) C. A. Wamser, *J. Amer. Chem. Soc.*, **73**, 409 (1951).

of the free acid appear at 1597 cm^{-1} and in the 1750—1700 cm^{-1} region (three peaks). The stretching band of B-F appears at 1100—1050 cm^{-1}. Probably the B-N band is also overlapping there.

Therefore, the structure of this complex seems to resemble $H_4EDTA(BF_3)_2$.

The infrared spectra of nitrilotriacetic acid and its metal complexes have been investigated in detail.[18,19] On the basis of all these results, the assignments of the spectra of the complex were made as follows. The antisymmetric stretching band of the carboxyl group of this compound appears at 1770 cm^{-1}, about 40 cm^{-1} higher than that of the corresponding band of the free acid (1728 cm^{-1}). This shift is probably due to the effect of the B-O and B-N bonds, which have a strong covalent character. The two strong bands at 1105 and 1070 cm^{-1} seem to be C-N and B-N stretching bands respectively. This complex is very stable towards hydrolysis because the electron shell of boron is filled with the electrons donated by the coordinated nitrogen atom. Others of the same type of compound, boroxazolidines, triethanolamine borate, for example, also show a high resistance to hydration.[20,21] Judging from these results, the ligand seems to work as a tetradentate in this complex.

Alcoholic or aqueous solution of neither $H_4EDTA(BF_3)_2$ nor $H_6EDTA(BF_4)_2$ show any peaks in the ultraviolet region, probably because of the solvolytic decomposition. However, their acetonitrile solutions show a characteristic maxima at 38200 cm^{-1} and two shoulders at about 38200 and 41000 cm^{-1}. As these compounds are only slightly soluble in a solvent, the molar extinction coefficients have not yet been determined. When the solutions were boiled for a while or allowed to stand for a few hours at room temperature, the 39400 cm^{-1} and 41000 cm^{-1}, remained. This is probably due to the solvolysis of the complex. The cyclohexanediaminetetraacetato complex shows almost the same ultraviolet spectra. The nitrilotriacetato complex is insoluble and so its spectra were not examined.

The authors are grateful to Professor Yukichi Yoshino and Dr. Toshio Takeuchi for their valuable suggestions.

18) Y. Tomita and K. Ueno, This Bulletin, **36**, 1069 (1963).

19) Y. Tomita, T. Ando and K. Ueno, *J. Phys. Chem.*, **69**, 404 (1965).

20) O. C. Musgrave and T. O. Park, *Chem. Ind.*, **1955**, 1552.

21) K. Niedenzu and J. W. Dawson, "Boron-Nitrogen Compounds," Springer-Verlag, Berlin, Heidelberg and New York (1965), p. 45.

BULLETIN OF THE CHEMICAL SOCIETY OF JAPAN VOL. 43 2076—2079 (1970)

Chemical Effects Associated with the β-Decay Process. V. Kinetic Studies of the Chemical Behavior of the ^{144}Pr Formed by the Decay of the ^{144}Ce(III)-Ethylenediaminetetraacetate and ^{144}Ce(III)-*trans*-1,2-Diaminocyclohexane-*N*,*N*′-tetraacetate

Takanobu SHIOKAWA, Hiroaki KIDO and Takashi OMORI

Department of Chemistry, Faculty of Science, Tohoku University, Katahira, Sendai

(Received December 13, 1969)

The chemical effects associated with the β^--decay of ^{144}Ce(III)-aminopolycarboxylate complexes have been further investigated. The chemical behavior of ^{144}Pr was analyzed kinetically on the basis of the isotopic exchange-reaction mechanism. The formation of the intermediate complex produced by an intramolecular electron transfer of the ^{144}Pr(IV)-aminopolycarboxylate following the β^--decay of ^{144}Ce(III) complex was also confirmed. In the ethylenediaminetetraacetate and *trans*-1,2-diaminocyclohexane-*N*,*N*′-tetraacetate systems, the values for the bond-rupture of the daughter complex ions are fairly much larger than in the diethylenetriaminepentaacetate system, suggesting that a kinetically-excited intermediate complex decomposes to a free ion to some extent.

In the β^--decay of the ^{144}Ce(III)-ethylenediaminetetraacetate(^{144}Ce(III)-EDTA) complex, the formation of an intermediate complex has been proposed on the basis of kinetic treatments.[1,2] Further investigation of the ^{144}Ce(III)-diethylenetriaminepentaacetate(^{144}Ce(III)-DTPA) complex revealed that an exhaustive bond-rupture of the daughter complex ion involves 25 per cent of the ^{144}Pr formed by the decay of the parent complex.[3]

Recently, Glentworth and Wright[4] have reported on the chemical behavior of ^{144}Pr/^{143}Pr in the aminopolycarboxylate complexes, and have proposed that a substantial fraction of the break-up of ^{144}Pr/^{143}Pr results in the multiple charging of the daughter complex as a result of the internal conversion of γ-rays and electron shake-off, as has already been pointed out in our previous papers.[2,3] However, the deactivation processes do not seem to have been established.

In order to confirm the stabilization process of ^{144}Pr on the basis of our model, the chemical behavior of ^{144}Pr was investigated in the ^{144}Ce(III)-*trans*-1,2-diaminocyclohexane-*N*,*N*′-tetraacetate (^{144}Ce(III)-DCTA) complex system. Furthermore, some additional experiments in the EDTA complex system were carried out.

Experimental

G.R.-grade EDTA and DCTA were used without further purification. The chelating agent solutions were standardized against a standard zinc(II) solution by volumetric titration, using Eriochrome Black T as an indicator. All the other chemicals and the experimental procedures employed here were substantially the same as those described previously.[2]

Results

Isotopic Exchange Reaction. Kinetic experiments on the exchange reaction,

$$^{144}Ce^{3+} + CeY^- \rightleftarrows {}^{144}CeY^- + Ce^{3+} \quad (1)$$

in the pH range from 4 to 7 at 25°C and at 5°C were carried out; here, Y^{4-} indicates the tetravalent EDTA and DCTA anions. The exchange rate between the uncomplexed cerium(III) ion and cerium(III)-aminopolycarboxylate can be expressed as follows:

For the EDTA complex system:

$$R = k_{Ce}[H^+][CeY^-] \quad (2)$$

For the DCTA complex system:

$$R = k_{Ce}[H^+][CeY^-] + k'_{Ce}[CeY^-] \quad (3)$$

The isotopic exchange rate constants, k_{Pr} and k'_{Pr}, for the analogous systems of praseodymium(III) have also been calculated using the equilibrium constant, K, for the substitution reaction[3]:

$$^{144}Ce^{3+} + PrY^- \rightleftarrows {}^{144}CeY^- + Pr^{3+} \quad (4)$$

The equilibrium constants, K, were obtained as 0.47_7 for the EDTA complex system and 0.47_2 for the DCTA complex system. The isotopic exchange rate constants for these systems are summarized in Table 1.

1) T. Shiokawa, H. Kudo and T. Omori, This Bulletin, **38**, 1340 (1965).
2) T. Shiokawa and T. Omori, *ibid.*, **38**, 1893 (1965).
3) T. Shiokawa and T. Omori, *ibid.*, **42**, 696 (1969).
4) P. Glentworth and C. L. Wright, *J. Inorg. Nucl. Chem.*, **31**, 1263 (1969).

Table 1. Isotopic exchange reaction rate constants

		Ce	Pr
EDTA			
k ($l \cdot mol^{-1} \cdot min^{-1}$)	25°C	2.1×10^5	1.0×10^5
	5°C	4.7×10^4	2.1×10^4
DCTA			
k ($l \cdot mol^{-1} \cdot min^{-1}$)	25°C	$5.7_5 \times 10^3$	2.7×10^3
	5°C	7.8×10^2	3.7×10^2
k' (min^{-1})	25°C	8.3×10^{-3}	3.9×10^{-3}
	5°C	5.5×10^{-4}	2.6×10^{-4}

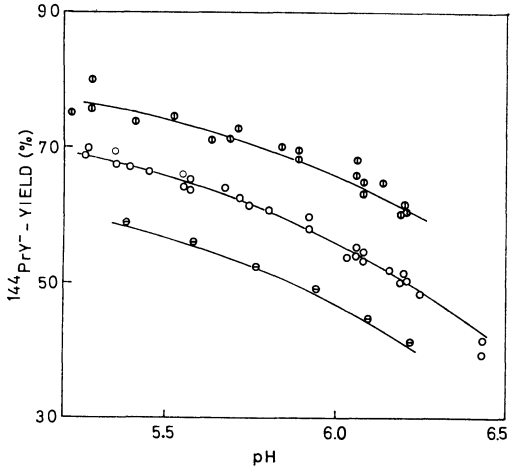

Fig. 1. Dependence of the $^{144}PrY^-$-yield on pH at 25°C in the EDTA complex system.

[Ce^{3+}] [CeY^-]
ⓘ: 1.21×10^{-4} M; 1.00×10^{-4} M
○: 0.808×10^{-4} ; 1.00×10^{-4}
⊖: 0.808×10^{-4} ; 1.50×10^{-4}
Solid curves were calculated by Eq. (11).

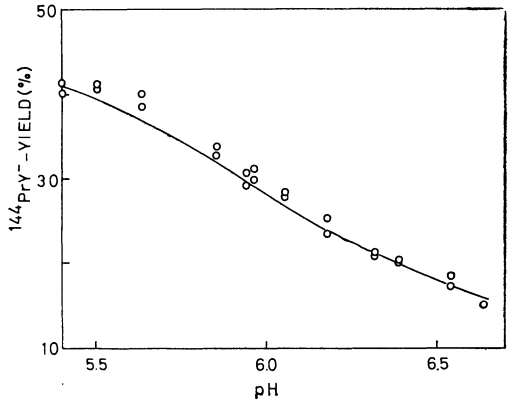

Fig. 2. Dependence of the $^{144}PrY^-$-yield on pH at 5°C in the EDTA complex system.

[Pr^{3+}]=[PrY^-]=1.14×10^{-4} M
Solid curve was calculated by Eq. (11).

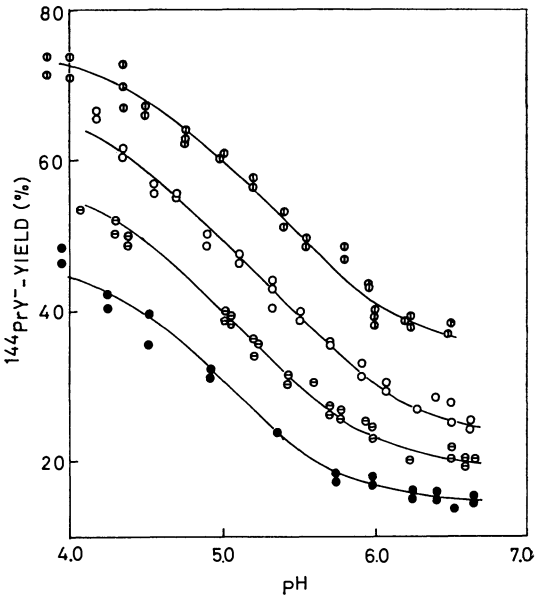

Fig. 3. Dependence of the $^{144}PrY^-$-yield on pH at 25°C in the DCTA complex system.

[Ce^{3+}] [CeY^-]
ⓘ: 1.00×10^{-4} M; 1.50×10^{-4} M
○: 1.00×10^{-4} ; 1.00×10^{-4}
⊖: 1.50×10^{-4} ; 1.00×10^{-4}
●: [Pr^{3+}]=[PrY^-]=1.00×10^{-4} M
Solid curves were calculated by Eq. (11).

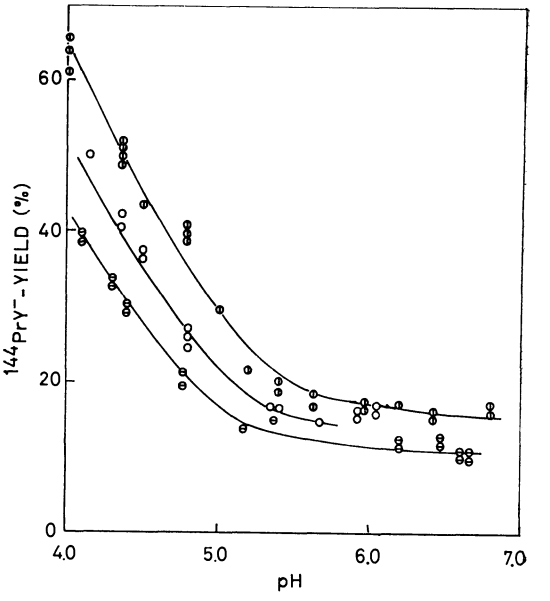

Fig. 4. Dependence of the $^{144}PrY^-$-yield on pH at 5°C in the DCTA complex system.

[Ce^{3+}] [CeY^-]
ⓘ: 1.00×10^{-4} M; 1.50×10^{-4} M
○: 1.00×10^{-4} ; 1.00×10^{-4}
⊖: 1.50×10^{-4} ; 1.00×10^{-4}
Solid curves were calculated by Eq. (11).

Chemical Behavior of ^{144}Pr. After complete equilibration with respect to ^{144}Ce in the systems represented by Eqs. (1) and (4) had been attained chemically, the yield of ^{144}Pr(III)-aminopolycarboxylate ($^{144}PrY^-$-yield) was obtained as a function of pH at 25° and 5°C. The $^{144}PrY^-$-yield is defined as the ratio of the γ-activity of the eluate to the total γ-activity. The results are shown in Figs. 1—4. In these experiments, the praseodymium ions are carrier-free when the carriers of the Ce(III) ion and Ce(III)-aminopolycarboxylate exist in aqueous solutions, and *vice versa*.

In both the systems, the $^{144}PrY^-$-yield decreases gradually with the pH, while in the DCTA complex system it seems to be constant in the higher pH regions. On the contrary, all the $^{144}PrY^-$-yield curves in the lower pH region exhibit asymptotic approaches to the equilibrium values, as is to be expected from the equilibrium constants of Reaction (4).

Discussion

The chemical behavior of the ^{144}Pr formed by the decay of ^{144}Ce(III)-DTPA was successfully explained on the basis of kinetic considerations as follows.[3] The praseodymium(IV)-DTPA complex was promptly reduced by an intramolecular electron-transfer. The trivalent ^{144}Pr, which remains complexed with a degradated DTPA radical, decomposes to a free ion by the dissociation in the substitution reaction. The uncomplexed ^{144}Pr(III) ion is also produced directly by an exhaustive decomposition of the daughter complex ion, without any formation of the intermediate. These stabilization processes of ^{144}Pr are considered to be valid also in the aminopolycarboxylate complex systems studied in this paper. Thus, the chain reactions for the stabilization of ^{144}Pr can be expressed as follows:

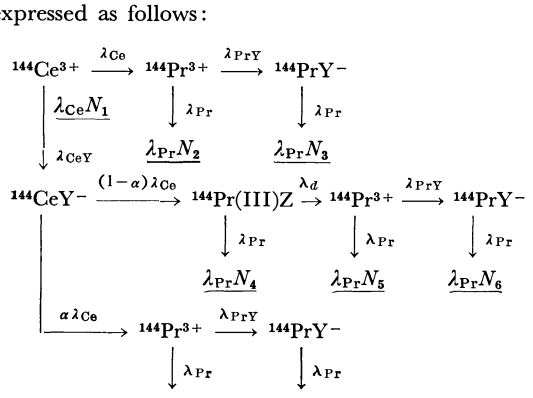

(6)

where λ_{Ce} and λ_{Pr} are the decay constants of ^{144}Ce and ^{144}Pr respectively, where λ_{CeY} and λ_{PrY} denote the respective exchange-rate constants of $^{144}Ce^{3+}$ and $^{144}Pr^{3+}$ with the aminopolycarboxylate complex, where λ_d is the decomposition rate constant of the intermediate (^{144}Pr(III)Z), and where α is the ratio of bond-rupture, which is defined as the ratio of the $^{144}Pr^{3+}$ produced directly from ^{144}Ce-(III)-aminopolycarboxylate without any formation of the intermediate possessing a finite life-time.

In Eq. (6), the fractions of $\lambda_{Pr}N_3$, $\lambda_{Pr}N_4$, $\lambda_{Pr}N_6$, and $\lambda_{Pr}N_8$ give the $^{144}PrY^-$-yield, supposing that, upon separation, the intermediate complex is not adsorbed on the ion-exchange resin. When the chemical equilibrium with respect to ^{144}Ce had been attained, and when the ^{144}Pr initially present had decayed out, the $^{144}PrY^-$-yield was obtained; therefore, the solution of Bateman's equation[5] for the respective fractions are given for the system ascribed by Eq. (1) as follows:

$$\lambda_{Pr}N_3 = \lambda_{Ce}N_1 \cdot \frac{\lambda_{PrY}}{\lambda_{Pr}+\lambda_{PrY}} \cdot \frac{[Ce^{3+}]_e}{[Ce^{3+}]_e+[CeY^-]_e} \times \frac{[^{144}PrY^-]_e}{[^{144}Pr^{3+}]_e+[^{144}PrY^-]_e} \quad (7)$$

$$\lambda_{Pr}N_4 = \lambda_{Ce}N_1 \cdot \frac{(1-\alpha)\lambda_{Pr}}{\lambda_{Pr}+\lambda_d} \cdot \frac{[CeY^-]_e}{[Ce^{3+}]_e+[CeY^-]_e} \quad (8)$$

$$\lambda_{Pr}N_6 = \lambda_{Ce}N_1 \cdot \frac{(1-\alpha)\lambda_{PrY}\lambda_d}{(\lambda_{Pr}+\lambda_{PrY})(\lambda_{Pr}+\lambda_d)} \times \frac{[CeY^-]_e}{[Ce^{3+}]_e+[CeY^-]_e} \cdot \frac{[^{144}PrY^-]_e}{[^{144}Pr^{3+}]_e+[^{144}PrY^-]_e} \quad (9)$$

$$\lambda_{Pr}N_8 = \lambda_{Ce}N_1 \cdot \frac{\alpha\lambda_{PrY}}{\lambda_{Pr}+\lambda_{PrY}} \cdot \frac{[CeY^-]_e}{[Ce^{3+}]_e+[CeY^-]_e} \times \frac{[^{144}PrY^-]_e}{[^{144}Pr^{3+}]_e+[^{144}PrY^-]_e} \quad (10)$$

where the effect of the disintegration of ^{144}Ce can be ignored. For the system expressed by Eq. (4), analogous equations are derived by exchanging the terms involving the concentrations of the metal ions. Thus, the $^{144}PrY^-$-yield is given by the sum of Eqs. (7)—(10); that is,

$$^{144}PrY^-\text{-yield}(\%) = \frac{\lambda_{Pr}(N_3+N_4+N_6+N_8)}{\lambda_{Ce}N_1} \times 100 \quad (11)$$

Since the values for λ_{Pr} and λ_{PrY} have already been established, the values for λ_d and α can be obtained by inserting the experimental values for the $^{144}PrY^-$-yields.

It was found that the ratio of the bond-rupture, α, is a constant independent of the temperature, while the λ_d depends on the temperature and is affected by the concentration of the hydrogen ion;

$$\lambda_d = k_d[H^+] \quad (12)$$

The values for the decomposition rate constant, k_d, of the intermediate, Pr(III)Z, and for the α thus obtained are summarized in Table 2, together with the data obtained in the DTPA complex system.[3] The experimental and calculated values

5) H. Bateman, *Proc. Cambridge Phil. Soc.*, **15**, 423 (1910).

Table 2. Decomposition rate constants of the intermediate complex and ratio of bond-rupture

	k_d* ($l \cdot mol^{-1} \cdot min^{-1}$)	α
EDTA (25°C)	$(2.5 \pm 1) \times 10^5$	0.7
(5°C)	$(5 \pm 2) \times 10^4$	
DCTA (25°C)	$(3 \pm 1) \times 10^4$	0.75
(5°C)	$(8 \pm 3) \times 10^3$	
DTPA (25°C)	$(5 \pm 2) \times 10^4$	0.25
(5°C)	$(2 \pm 1) \times 10^4$	

* $\lambda_d = k_d[H^+]$

for the $^{144}PrY^-$-yields are compared in Figs. 1—4.

The bond rupture of the daughter complex may be caused by the formation of a multiply-charged ^{144}Pr ion due to electron shake-off and the internal conversion of γ-rays, followed by the Auger process. In the DTPA-complex system, the ratio of the bond rupture of 0.25 corresponds to the extent of the formation of the multiply-charged ^{144}Pr ion. In the EDTA- and DCTA-complex systems, the ratios of the bond rupture of 0.70 and 0.75 respectively are much larger than that in the DTPA complex system, indicating that there is involved another process, without any formation of a stable intermediate. This process may be accounted possibly by the recoil effect. In the β^--decay of ^{144}Ce, the recoil energies imparted to free ^{144}Pr atoms range from 0 to 1.6 eV. The probability of bond rupture as a result of recoil only is very small; however, a significant fraction of the β^--decay of ^{144}Ce would leave the daughter complex in a kinetically-excited state. Thus, by taking into consideration the fact that the activation energies for the decomposition of the intermediate are estimated to be about 10 kcal/mol, it is reasonable that the kinetically-excited decomposition of the intermediate should take place, resulting in the formation of the uncomplexed $^{144}Pr(III)$ ion.

In the DTPA-complex system, the kinetically-excited decomposition of the intermediate was not observed. The differences in the chemical behavior of ^{144}Pr in the DTPA complex system from that in the EDTA and DCTA complex systems may be attributed to the difference in the molecular structures of the chelates; that is, the EDTA and DCTA are hexadentate chelating agents, while the DTPA is an octadentate.

In view of the decomposition mechanism and rate constants, the stabilization processes of ^{144}Pr proposed in the DTPA-complex system[3] are further confirmed in the EDTA- and DCTA-complex systems. In addition, a new process of the kinetically-excited decomposition of the intermediate is proposed. The stabilization processes of ^{144}Pr are shown schematically in Fig. 5.

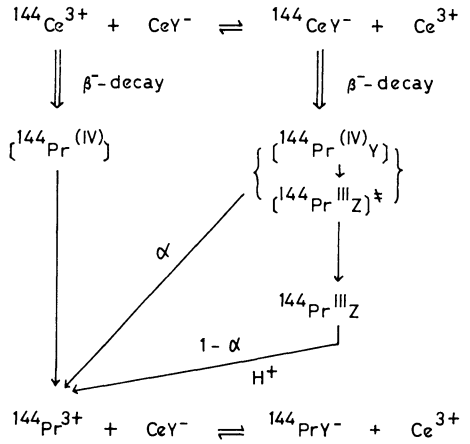

Fig. 5. Stabilization processes of ^{144}Pr produced by β^--decay of ^{144}Ce in the aminopolycarboxylate complex system.

BULLETIN OF THE CHEMICAL SOCIETY OF JAPAN VOL. 43 2080—2082 (1970)

Pyrolysis-Gas Chromatographic Analysis of Vinylchloride-Vinylacetate Copolymer

Tadaoki OKUMOTO

Engineering Department, Nagoya Rubber Co., Ltd., Haruhi-mura, Nishikasugai-gun, Aichi

and Tsugio TAKEUCHI and Shin TSUGE

Department of Synthetic Chemistry, Faculty of Engineering, Nagoya University, Chikusa-ku, Nagoya

(Received December 15, 1969)

Pyrolysis-gas chromatography was applied to rapid and precise determination of vinylchloride-vinylacetate copolymer by use of the yields of acetic acid and of benzene. The separation column was filled with packing of polymer beads (porapak Q) which are free from deterioration by hydrogen chloride evolved during the thermal degradation of copolymers. Relative yields of acetic acid, which originated from the side chains of the polymer and corresponded to vinylacetate content, and of benzene, formed mainly from successive vinylchloride units, were calculated from the relative peak area appearing on the pyrogram by making relative sensitivity correction for the flame ionization detector. By this method the composition of copolymer can be determined using 0.5—2.0 mg of sample with mean absolute deviation 0.5—0.4 wt%, with the yields of acetic acid and of benzene.

The copolymer of vinylchloride and vinylacetate (VC-VAc) shows different properties according to vinylacetate content. With the increase of vinylacetate content, solubility and adhesive affinity are imporved, and softening point is lowered. Analysis of the copolymer has mostly been carried out by means of IR, NMR and chemical determination of chlorine. A few qualitative works on the analysis of the copolymer by pyrolysis-gas chromatography (PGC), have been reported.[1-3] This is partly associated with the fact that hydrogen chloride evolved during the degradation of the polymer deteriorates the separating column, and has no sensitivity to the flame ionization detector.

Barlow *et al.*[3] reported on the analysis of the copolymer at the relatively high pyrolysis temperature of 580°C, using a hot-filament-type pyrolyzer and Katharometer detector (thermal conductivity detector). They performed the analysis with the peaks of hydrogen chloride and acetic acid on pyrogram of the copolymer with about 2% standard deviation.

In our previous works,[4,5] we characterized the microstructure of chlorine-containing polymers by PGC in which NaOH-precut column was used to adsorb hydrogen chloride evolved during the degradation of polymers.

We have worked out an analytical method for determining the composition of vinylchloride-vinylacetate copolymer with the use of PGC without NaOH-precut column.

Experimental

Materials. VC-VAc copolymers synthesized by suspension polymerization were used as samples.

The content of vinylacetate in the copolymer ranged from 0.5 to 15.7 wt% which was determined by the usual chemical analysis of chlorine.

Apparatus. A heated furnace type pyrolyzer, Hitachi KP-1, whose structure is almost the same as that used previously works[4-6] was used to decompose the polymers. It was directly attached to the inlet port of a gas chromatograph, Hitachi F6-D with flame ionization detectors.

In order to minimize the change of the pyrolysis temperature, which disturbs the reproducibility, a voltage stabilyzer was used for the pyrolyzer.

An optimum pyrolysis temperature 430°C was chosen in order to obtain characteristic, reproducible and sharp pyrograms.

A sample weighing 0.5—2.0 mg was pyrolyzed under a flow of carrier gas (N_2) at the pyrolysis temperature for 1 min. This was sufficient to achieve complete pyrolysis of the polymers.

Gas Chromatographic Conditions. Gas chromatographic analysis was carried out under the following conditions.

Column: Stainless steel tube (3 mm diam. × 0.5 m

1) Y. Mashiko, A. Echizen and A. Nakao, *Kogyo Kagaku Zasshi*, **68**, 1206 (1965).

2) R. S. Lerhle and J. C. Robb, *Nature*, **83**, 1671 (1959).

3) A. Barlow, R. S. Lehrle and J. C. Robb, *Polymer*, **2**, 27 (1961).

4) S. Tsuge, T. Okumoto and T. Takeuchi, *Makromol. Chem.*, **123**, 123 (1969).

5) S. Tsuge, T. Okumoto and T. Takeuchi, *Macromolecules*, **2**, 277 (1969).

6) S. Tsuge, T. Okumoto and T. Takeuchi, *Kogyo Kagaku Zasshi*, **71**, 1634 (1968).

7) N. Grassie, *Trans. Faraday Soc.*, **49**, 835 (1953).

length),

Packing: Polymer beads with porosity (Porapak Q; 120—150 mesh),

Temperature programing: 120—230°C, (7°C/min) isothermal after 230°C,

Carrier gas: N_2 1.0 kg/cm² inlet pressure (55 ml/min at room temperature),

Hydrogen flame: H_2 0.7 kg/cm², air 1.0 kg/cm².

Polymer beads (Porapak Q) without liquid phase and NaOH-precut column were packed in the separating column, which is not deteriorated by acidic products such as hydrogen chloride or acetic acid.

Identification of the peaks appearing on the pyrograms was carried out with the use of the retention data of various pure substances which are expected to be formed from the degradation of the polymers.

Results and Discussion

Figure 1 shows typical pyrograms of VC-VAc copolymer, PVAc (polyvinylacetate) and PVC (polyvinylchloride) at the pyrolysis temperature 430°C.

PVC yields benzene and a small amount of toluene. These degradation products are formed by dehydrochlorination reaction followed by cyclization of polymer structure.[4] On the other hand, PVAc[7] yields acetic acid and a small amount of benzene. In this case, there exist competitive thermal reactions, namely scission of the main chain followed by elimination of acetic acid and the formation of polyene structure followed by cyclization to benzene.

Although both mechanisms yield acetic acid, the former is predominant judging from the relatively small amount of benzene on pyrogram.

As might be expected from the above degradation mechanisms of PVC and PVAc, the copolymers with high content of VAc yield mainly acetic acid and a little benzene, whereas those with high content of VC yield mainly benzene.

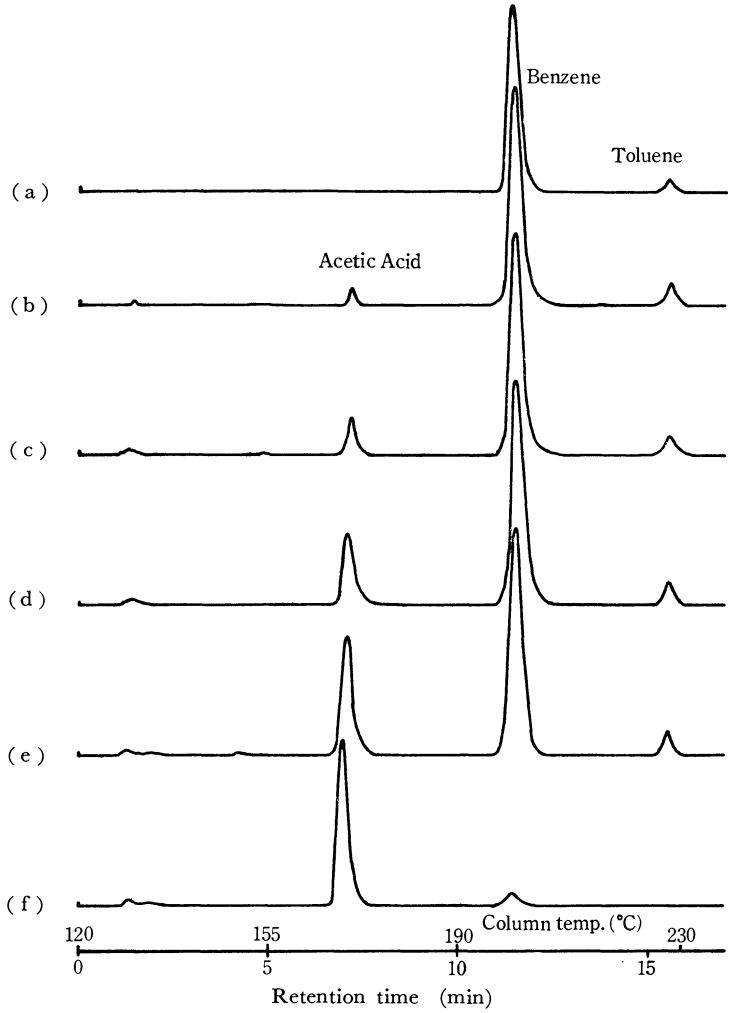

Fig. 1. Pyrogram of vinylchloride-vinylacetate copolymer at 430°C.
(a) PVC; (b)—(e) VC-VAc copolymer (VAc=2.9 (b), 5.5 (c), 11.6 (d) and 15.7 (e) wt%); (f) PVAc

For the sake of simplicity, a small amount of toluene observed with PVC and copolymers was converted into benzene in the calculation and added to the observed yield of benzene. One mole of benzene was considered to correspond to three moles of successive VC-unit, whereas one mole of acetic acid to one mole of VAc-unit.

Figure 2 shows the relation between the relative yields of acetic acid and benzene and the composition of vinylacetate (wt%). The plots (● and ▲) represent the observed values, and the solid line is obtained by the method of least squares.

The linear relations can be represented as follows:

(A) Yield of acetic acid

$$Y = 2.21\,X + 5.2 \qquad (1)$$

(B) Yield of benzene

$$Y' = 2.36\,X' - 140.1 \qquad (2)$$

where X and X' are vinylacetate and vinylchloride contents in copolymer (wt%), respectively, and $X+X'=100$. Y and Y' are the observed relative yields of acetic acid and benzene (wt%), respectively. Precision data are listed in Table 1.

With the use of Eqs. (1) and (2), the composition of vinylacetate in copolymer can be determined with mean absolute deviation 0.5 and 0.4 wt% respectively, with the yields of acetic acid and of benzene.

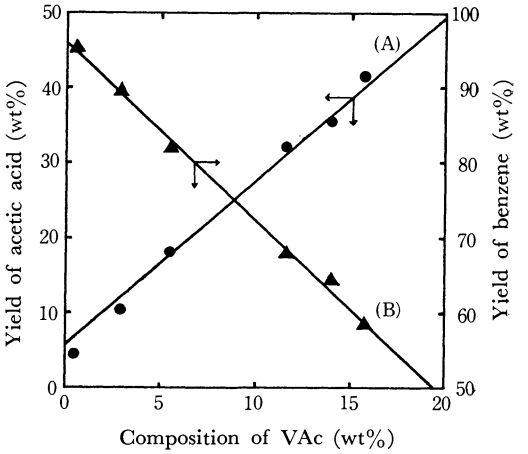

Fig. 2. Relationship between yields of acetic acid and of benzene, and composition of VAc.
(A) acetic acid; (B) benzene

Pyrolysis-gas chromatography was successfully applied to rapid and precise determination of composition of polymer evolving such acidic products as hydrogen chloride and acetic acid during its thermal decomposition without trapping the acidic substances.

Table 1. Accuracy of the determination of VC-VAc copolymer

(a) Results from the yield of acetic acid

Sample No.	Composition of* VAc (wt%) (A_1)	Yield of acetic acid (wt%)	Composition** of VAc (wt%) (B_1)	Deviation (B_1-A_1)
1	0.5	4.6	−0.3	−0.8
2	2.9	10.5	2.4	−0.5
3	5.5	18.2	5.9	0.4
4	11.6	32.1	12.1	0.5
5	14.0	35.7	13.8	−0.2
6	15.7	41.4	16.4	0.7

(b) Results from the yield of benzene

Sample No.	Composition of* VC (wt%) (A_2)	Yield of benzene (wt%)	Composition** of VC (wt%) (B_2)	Deviation (B_2-A_2)
1	99.5	95.4	99.8	0.3
2	97.1	89.5	97.3	0.2
3	94.5	81.8	94.0	−0.5
4	88.4	67.9	88.1	−0.3
5	86.0	64.3	86.6	0.6
6	84.3	58.6	84.2	−0.1

* Determined by the usual chemical method. **Calculated from Eq. (1) or (2).

BULLETIN OF THE CHEMICAL SOCIETY OF JAPAN VOL. 43 2083—2085 (1970)

On the Polarographic Limiting Current of Solubilized Dye in Nonionic Surfactant Solutions

Shigeo HAYANO and Noriko SHINOZUKA

Institute of Industrial Science, The University of Tokyo, Roppongi, Minato-ku, Tokyo

(Received December 24, 1969)

The nature of the limiting current of the reduction of solubilized dye with nonionic surfactants on a mercury-drop electrode was examined. The solution of anthraquinone derivatives solubilized in an aqueous solution of a nonionic surfactant showed a proportionality of the limiting current to the dye concentration. The linear dependence of the current on the square-root of the mercury-column height, the solpe of the log-plot, and the *i-t* curves indicated the limiting current to be diffusion-controlled. From the *i-t* curve measurements, the acceleration of the instantaneous current at the end of the mercury-drop growth was observed with the polyoxyethylene nonylphenylether and Triton X-100. This can be interpreted in relation to the reorientation of the surfactant molecules.

A previous paper treated[1] the polarographic reduction of the disperse-dyes solubilized in nonionic surfactant solutions in which the electrode process is diffusion-controlled. In that case, a linear relation of the limiting current to the dye concentration was assumed, but it could not be established.

In this paper, the nature of the limiting current of the solubilized dye will be examined in further detail in a system which shows a proportionality of the limiting current to the dye concentration.

Experimental

The 1-amino-2-methoxy-4-hydroxy anthraquinone was obtained by the recrystallization of a sample dye received through the courtesy of the Sumitomo Chemical Industry Co. from an ethanol-water mixture. Polyoxyethylene nonylphenyl ether (NP-$\overline{10}$, NP-$\overline{9}$), polyoxyethylene lauryl ether (L-$\bar{9}$), and Triton-X-100 (TX-100) were used as nonionic surfactants.

The solubilization and the polarographic procedure were the same as in the previous paper except that the solution was not irradiated with supersonic waves in this study.

The current-time curves were measured with a potentiostat (Hokuto Denko Co., Ltd.) and a XY-5121-type synchroscope (Iwasaki Tushinki Co., Ltd.) or a XY-recorder (Yokogawa Denki Co., Ltd.).

Results and Discussion

Relation of the Limiting Current to Dye Concentration. The solubilized dye in all four surfactant solutions showed a well-defined wave. $E_{1/2}$ is -0.625 V (*vs.* SCE), a value which accords with the peak potential of the ac polarogram. The dependence of the limiting current on the dye concentration is shown in Fig. 1. The linear relationship was obtained with a surfactant concentration of between 10^{-3} and 10^{-1} M. This proves that the diffusion coefficient of the surfactant micelle with the dye molecule is not affected by the surfactant concentration or the dye concentration. The value of the diffusion coefficient increases with an increase in the molecular weight of the surfactant, (NP-$\overline{10}$>L-$\bar{9}$>TX-100). The values are in accord with the volumes of these surfactant micelles, all of which have almost the same aggregation number, about 100.[2]

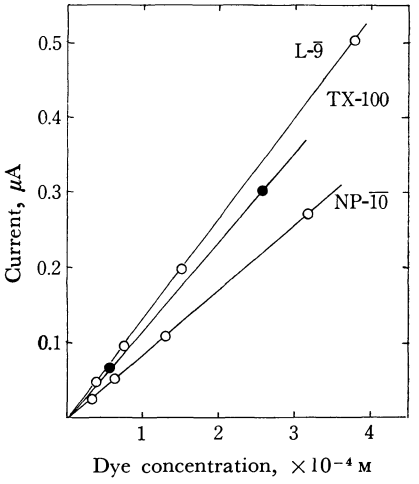

Fig. 1. Relation of limiting current to dye concentration.

1) S. Hayano and N. Shinozuka, This Bulletin, **42**, 1469 (1969).

2) P. Becher, "Nonionic Surfactants," Marcel Dekker, New York (1967), p. 495.

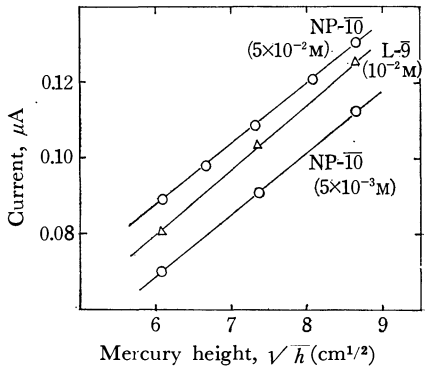

Fig. 2. Dependence of current on mercury height.

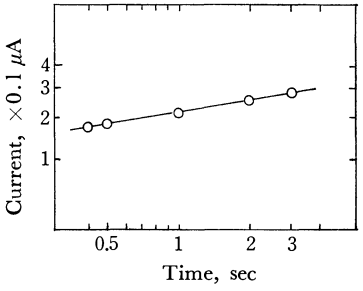

Fig. 3. log-Plots of *i-t* curve.
(L-9: 6×10^{-2} M, Dye: 2.2×10^{-4} M, at -0.7 V)

The Nature of the Limiting Current. The linear dependence of the current on the square-root of the mercury-column height indicates that the limiting current is diffusion-controlled (Fig. 2). Furthermore, the *i-t* curves of the dye at the potential of the current-plateau show the relation of $i \propto t^{1/6}$ (Fig. 3).

The log-plot of the current against the potential gives a straight line with a slope of about 30 mV/log unit, showing that the reversibility of the reduction of solubilized dye is not affected by the solubilization with surfactants.

Current-time Curves. During the measurement of the *i-t* curves, a marked current increase, an increase which gave rise to a hump on the limiting current, was observed when the mercury head was lowered or/and the surfactant concentration was decreased at potentials between -0.8 and -1.3 V (Fig. 4). The log-plots of the curve showed that the current was diffusion-controlled until there was a marked current increase. This phenomenon was not found with the L-9 surfactant in various concentrations or at various mercury-column heights. The following analysis of the curve indicates that the time of the sudden current increase corresponds to the constant surface area of a mercury drop.

The surface area of a mercury drop at time t is given as follows:[3]

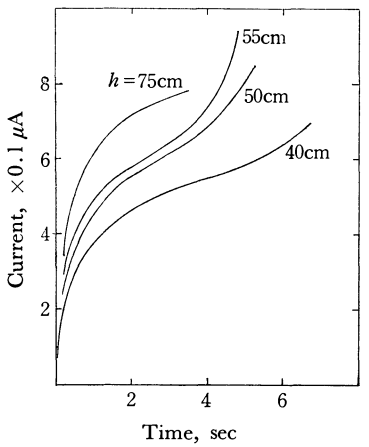

Fig. 4. Dependence of *i-t* curves on mercury height.
(NP-10: 5×10^{-2} M, Dye: 2.6×10^{-4} M at -0.8 V)

TABLE 1. DEPENDENCE OF THE TIME OF SUDDEN CURRENT INCREASE ON MERCURY COLUMN HEIGHT

Mercur height (cm)	t (sec)	$(Pt)^{2/3}$
75.5	2.2	30.2
65.5	2.5	29.9
55.5	2.9	29.5
45.5	3.5	29.3
40.5	4.1	30.1

$$a = 0.85m^{2/3}t^{2/3}$$

As the mercury flow rate, m, is proportional to the height of the mercury head, "P", and as P is easy to measure, "a" is written as,

$$a = kP^{2/3}t^{2/3} \qquad k\text{: constant}$$

From the *i-t* curves, the $(Pt)^{2/3}$ values, where t is the time at which the current increases, were calculated; they are listed in Table 1. The constant $(Pt)^{2/3}$ means that the current increases when the mercury surface attains a constant area.

It is known that surface-active cations accelerate the reduction of anions and that anionic surfactants accelerate the reduction of cations.[4] Such acceleration as in the case of a charged-type depolarizer with an ionic surfactant can be interpreted in terms of a change in the ϕ-potential due to adsorption. On the other hand, for a neutral depolarizer with a nonionic surfactant system, no acceleration has yet been reported.

Recently, Jehring has discussed the reorientation of the surfactant on mercury by means of ac polarography and has concluded that, with NP-10, a unimolecularly-dispersed surfactant is reoriented to a micelle or its hydrophilic portion extends toward

3) J. Heyrovsky, "Principles of Polarography," Acadimic Press, New York (1966), p. 40.

4) I. M. Kolthoff and Y. Okinaka, *J. Amer. Chem. Soc.*, **81**, 2296 (1959); N. Gundersen and E. Jacobsen, *J. Electroanal. Chem.*, **20**, 13 (1969).

mercury in the potential range of -0.85——-1.1 V *vs.* SCE.[5] The potential range of its appearance, the dependence on the concentration of the surfactant, and the presence of a phenyl group in the surfactant molecule were the same as in this study.

From ac polarograms it is evident that surfactant molecules are adsorbed on the electrode; therefore, the above results can be interpreted as showing that the adsorbed surfactant molecules are reoriented when the mercury-drop surface reaches a certain size. The value of the area corresponding to the reorientation varies with the applied potential, the kind of surfactant, and the surfactant concentration. For a 5×10^{-2} M solution of NP-10 at -0.8 V, the value is 2.34×10^{-2} cm^2; this is reasonable compared with the value, 2.23×10^{-2} cm^2, that corresponds to the approximate monolayer coverage of Triton -X-100.[6] The accelerated current may be related to the reorientation of the surfactant molecules.

It is interesting to note that, although the electrode reaction of the solubilized dye occurs at a potential where the surfactant is strongly adsorbed, the current is diffusion-controlled and the reversibility of the reduction is not affected.

Work is now in progress to investigate the effect of micelles on the electrode reaction of the solubilizate and the adsorption of surfactant molecules on the electrode.

5) H. Jehring and A. Weiss, *Tenside*, **6**, 251 (1969).

6) R. G. Barradas and F. M. Kimmerle, *J. Electroanal. Chem.*, **11**, 163 (1966).

BULLETIN OF THE CHEMICAL SOCIETY OF JAPAN VOL. 43 2085—2092 (1970)

Multidentate Ligand Substitution Reactions. XI. Substitution Reactions of Nickel(II) Complexes of Diethylenetriamine and Ethylenediaminemonoacetic Acid with Diethylenetriaminepentaacetic Acid and of Nickel(II) Complexes of Diethylenetriamine and Ethylenediamine with Cyclohexane-1,2-diamine-*N*,*N*,*N*′,*N*′-tetraacetic Acid

Mutsuo KODAMA, Yuki FUJII and Teiko UEDA

Department of Chemistry, Ibaraki University, Bunkyo, Mito, Ibaraki

(Received January 21, 1970)

The kinetics of substitution reactions of nickel(II) complexes of diethylenetriamine and ethylenediaminemonoacetic acid with diethylenetriaminepentaacetic acid and those of diethylenetriamine and ethylenediamine with cyclohexane-1,2-diamine-*N*,*N*,*N*′,*N*′-tetraacetic acid were studied systematically by using the polarographic technique. All the reactions studied were found to be first-order with respect to the attacking group and also first-order with respect to the nickel(II) complex of diethylenetriamine, ethylenediamine, or ethylenediaminemonoacetic acid with a 1-to-1 composition. From a comparison of the relative rate constants determined experimentally with those calculated on the basis of a postulated reaction intermediate, the reaction mechanism was described in detail. All the reactions were concluded to proceed through the mixed ligand complex reaction intermediates which are characterized as having two nitrogen (amino) groups of displaced ethylenediamine, diethylenetriamine, or ethylenediaminemonoacetate ions bonded to the nickel(II) ion. This finding is contrary to the observation obtained by Rorabacher and Margerum from their kinetic study of the exchange reaction of the ethylenediaminetetraacetate anion with nickel(II) complexes of triethylenetetramine and tetraethylenepentamine.

In previous papers,[1-3] we have studied the kinetics of nucleophilic substitution reactions involving nickel(II) and cobalt(II) complexes of ethylenediaminetetraacetic acid (EDTA) and its related substances. From a comparison of the rate constants, the reaction intermediate for these substitution reactions was characterized as having one

1) M. Kodama, This Bulletin, **40**, 2575 (1967).
2) M. Kodama, C. Sasaki and T. Noda, *ibid.*, **41**, 2033 (1968).
3) M. Kodama, C. Sasaki and K. Miyamoto, *ibid.*, **42**, 163 (1969).

nitrogen (amino) group and one acetate group of displaced aminopolycarboxylate anions bonded to the metal(II) ion (Glycinate mechanism). The nucleophilic substitution reactions involving nickel-(II)-aspartate and iminodiacetate complexes were also found to proceed through a reaction intermediate with a glycinate group bonded to the nickel(II) ion.[4] Rorabacher and Margerum studied the substitution reactions involving nickel-(II) complexes of polyamines.[5] In their kinetic studies of the displacement of triethylenetetramine and tetraethylenepentamine by the EDTA anion, they proposed a reaction intermediate in which the released polyamine forms two five-membered rings with the nickel(II) ion through three nitrogen groups. The ethylenediaminemonoacetate (EDMA) ion, in whose complexation reaction with metal ions two nitrogen groups and one acetate group can function as donor groups, was also found to be displaced from its nickel(II) complex by diethylenetriaminepentaacetic acid (DTPA) at a measurable rate. In general, the nickel(II)-nitrogen bond rupture is much slower than the nickel(II)-oxygen bond rupture.

Therefore, the nucleophilic substitution reactions involving the nickel(II)-EDMA complex can hardly be expected to proceed through a glycinate reaction mechanism. On the other hand, if the nucleophilic substitution reaction of the nickel(II)-ethylenediamine (En) complex also proceeds through a mixed ligand complex intermediate, because of steric requirements the reaction intermediate can be expected to have a structure in which a bidentate ethylenediamine occupies two of the six octahedral coordination sites of the nickel (II) ion. Thus, the substitution reaction involving an En complex would have a different reaction intermediate from those of the other polyamine complexes. In the experiments reported in this paper, we studied the kinetics of the substitution reactions of the nickel(II) complexes of diethylenetriamine (Dien) and EDMA with DTPA and of those of Dien and En with cyclohexane-1,2-diamine-*N*,*N*,*N*′,*N*′-tetraacetic acid (CyDTA) and determined the reaction mechanism and rate constants for these reactions. From comparisons of the rate constants determined experimentally and from calculations based on the relative stability of the mixed ligand complex intermediate and the electrostatic interaction between the entering group and the reactant (nickel(II) complex), the structure of the reaction intermediates in the substitution reactions involving nickel(II)-EDMA, Dien, and En complexes were determined.

Experimental

Reagents. A nickel(II) nitrate solution was prepared by dissolving a known amount of metallic nickel (99.99% pure) in dilute nitric acid (1+1) and by then removing the excess nitric acid by distillation under reduced pressure. The preparation and recrystallization of EDMA dihydrochloride have been described previously.[6] The En and Dien were purified by distillation under reduced pressure. The DTPA and CyDTA were recrystallized twice from their aqueous solutions by adding a suitable amount of pure ethanol. The other reagents were of analytical reagent grades and were used without further purification.

Apparatus and Experimental Procedures. All the d.c. polarograms and current-time curves were

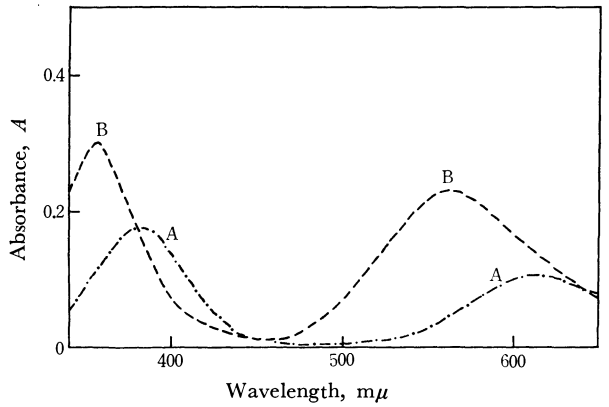

Fig. 1. Absorption curves of nickel(II) ions in the EDMA solution.
μ=0.30, 25°C
Concentration of nickel(II) ion=30.0 mM
A: Concentration of EDMA=30.0 mM, pH=6.0
B: Concentration of EDMA=80.0 mM, pH=9.0

4) M. Kodama and T. Ueda, This Bulletin, **43**, 419 (1970).
5) D. B. Borabacher and D. W. Margerum. *Inorg. Chem.*, **3**, 382 (1964).
6) Fujii, F. Kyuno and R. Tsuchiya, This Bulletin, **43**, 786 (1970).

recorded automatically by means of a Yanagimoto pen-recording polarograph, PA-102, or a Hitachi recorder, QPD-54. The characteristics of the dropping mercury electrode (DME) used in this study have been described previously.[7] For all the spectrophotometric measurements, a Hitachi EPS-3 recording spectrophotometer with a pair of 1-cm quartz cells was used. The rate of the substitution reaction was determined by measuring the change in the diffusion current of anodic waves due to the decrease in the uncomplexed DTPA or CyDTA concentration with time. In this study, all the measurements were conducted in solutions with an ionic strength of 0.30. In order to adjust the ionic strength, sodium perchlorate (the EDMA system) or potassium nitrate (the En and Dien systems) was used. In the kinetic study, measurements were made in solutions containing a large excess of complexed and uncomplexed EDMA, En, or Dien over DTPA or CyDTA in the pH range from 8.30 to 10.0 at 25°C. Therefore, all the substitution reactions could be treated as pseudo first-order reactions and no buffer reagent was required to maintain the solution's pH constant over the entire pH range covered. All the experimental procedures employed were the same as had previously been described.[7]

Results and Discussion

Spectrophotometric Determination of Formation Constants of the Nickel (II)-Ethylenediaminemonoacetate Complex. As EDMA has two amino groups and one acetate group, it can act as a tridentate ligand in the complexation with metal ions. Therefore, in order to complete the octahedral coordination sphere of a nickel(II) ion, two molecules of EDMA are required. Thus, the nickel(II) ion is expected to form complexes of 1-to-1 and 1-to-2 compositions with EDMA. In Fig. 1, typical absorption curves of the nickel-(II) ion in the EDMA solution are reproduced. In this study, we tried to determined the stability constants of the nickel(II)-EDMA complexes spectrophotometrically. If the total concentration of nickel(II) ions is kept constant throughout the experiment, the concentrations of complexed and uncomplexed nickel(II) ions in a solution containing an equimolar EDMA can be represented by the following equations:

$$[NiX^+] = \frac{A - A_{Ni}}{\varepsilon_{NiX} - \varepsilon_{Ni}} \quad (1)$$

$$[Ni^{2+}] = \frac{A_{NiX} - A}{\varepsilon_{NiX} - \varepsilon_{Ni}} \quad (2)$$

where ε's denote molar extinction coefficients, where $[Ni^{2+}]$ and $[NiX^+]$ are the concentrations of uncomplexed and complexed nickel(II) ions respectively, and where A, A_{NiX} and A_{Ni} are, respectively, the absorbance of the solutions in which complexed and uncomplexed nickel(II) ions coexist, in which all the nickel(II) ions exist in the form of NiX^+, and in which there is no EDMA. Since the concentration of uncomplexed EDMA is identical with that of the uncomplexed nickel(II) ion, the conditional formation constant of the nickel(II)-EDMA complex with a 1-to-1 composition, K'_{NiX}, is given by:

$$K'_{NiX} = \frac{K_{NiX}}{(\alpha_H)_X} = \frac{(A - A_{Ni})(\varepsilon_{NiX} - \varepsilon_{Ni})}{(A_{NiX} - A)^2} \quad (3)$$

where $(\alpha_H)_X$ is the (α_H) value of EDMA, and K_{NiX}, the formation constant of NiX^+.

Equation (3) clearly indicates that, by plotting $\log[(A-A_{Ni})(\varepsilon_{NiX}-\varepsilon_{Ni})/(A_{NiX}-A)^2]$ *vs.* $\log(\alpha_H)_X$, one can obtain a linear relation with a slope of -1.0 and that the $\log(\alpha_H)_X$ value at $\log[(A-A_{Ni})(\varepsilon_{NiX}-\varepsilon_{Ni})/(A_{NiX}-A)^2]$=zero corresponds to the $\log K_{NiX}$ value. To prepare an equimolar solution of nickel(II) ions and EDMA, we used a known amount of pure crystals of ethylenediaminemonoacetatotriaquonickel(II) chloride synthesized in our laboratory.*1 With the aid of Eq. (3), the experimental data were analyzed. The results are illustarated in Fig. 2. From the intercept of the linear relation in Fig. 2, the $\log K_{NiX}$ value was estimated to be 10.44. With an increase in the uncomplexed EDMA concentration and an increased pH value, the absorbance of the nickel (II) solution increases and the absorption curve's maxima shift to shorter wavelengths. This can be ascribed to the formation of a complex with a 1-to-2 ratio. If both the complex with a 1-to-2 ratio and that with a 1-to-1 ratio are formed, and if the uncomplexed nickel(II)-ion concentration can be disregarded as compared with the complexed nickel(II)-ion concentration, the following

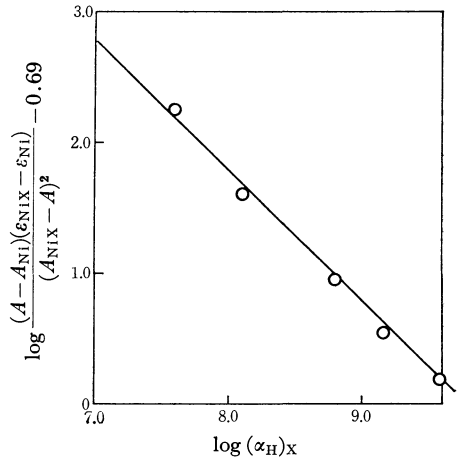

Fig. 2. The plot of $\log(A-A_{Ni})/(A_{NiX}-A)^2$ against $\log(\alpha_H)_X$.
μ=0.30, 25°C, 360 mμ
Concentration of nickel(II) ion=30.0 mM
Concentration of EDMA=30.0 mM

7) M. Kodama, *ibid.*, **42**, 2532 (1969).

*1 The preparation of ethylenediaminemonoacetatotriaquonickel(II) chloride will be described elsewhere.

relation can be derived thermodynamically for a solution containing an excess of EDMA over the nickel(II) ion:

$$\log \frac{K_2}{(\alpha_H)_X} = \log \frac{(A-A_{NiX})(\varepsilon_{NiX_2}-\varepsilon_{NiX})}{\left((A_{NiX_2}-A)\{([X]_t-2[Ni]_t)(\varepsilon_{NiX_2}-\varepsilon_{NiX})+(A_{NiX_2}-A)\}\right)} \quad (4)$$

where K_2 is defined as $[NiX_2^0]/[NiX^+]\cdot[X^-]$, where $[X]_t$ and $[Ni]_t$ denote the total concentrations of EDMA and nickel(II) ions respectively, where A_{NiX_2} means the absorbance of a solution where all the nickel(II) ions exist exclusively in the form of NiX_2^0, and where ε_{NiX_2} is the molar extinction coefficient of NiX_2. Equation (4) varified experimentally. As is illustrated in Fig. 3, the plot of the right-hand side of Eq. (4) against $\log(\alpha_H)_X$ gave a linear relation with a slope of -1.0. From this linear relation, the $\log K_2$ value was determined to be 6.34. The presence of chloride ions has no effect on the absorbance or the location of the maximum. This clearly indicates that the nickel(II) ion does not enter into the mixed ligand complex involving the chloride ion under the present experimental conditions. The numerical values determined are given in Table 1.

Kinetics Study of Substitution Reaction of Nickel(II) Complexes of Dien and EDMA with DTPA and Those of Dien and En with CyDTA. As was found in the substitution reaction of the nickel(II)-NTA complex with DTPA,[7] the linear relations passing through the point of origin could be obtained by plotting the $\log(i_0/i_t)$ against time, t, in all the substitution reactions studied in the present paper

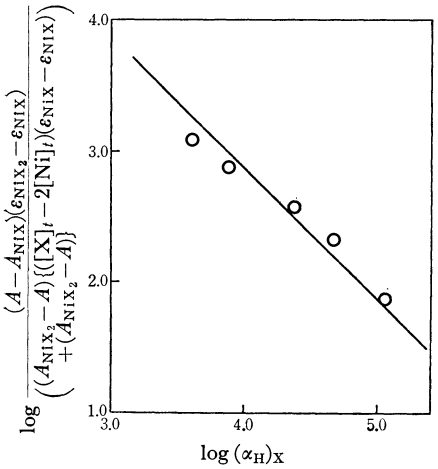

Fig. 3. The plot of $\log[(A-A_{NiX})(\varepsilon_{NiX_2}-\varepsilon_{NiX})/(A_{NiX_2}-A)\{([X]_t-2[Ni]_t)(\varepsilon_{NiX_2}-\varepsilon_{NiX})+(A_{NiX_2}-A)\}]$ against $\log(\alpha_H)_X$.
$\mu=0.30$, 25°C, 350 mμ
Concentration of nickel(II) ion=34.8 mM
Concentration of EDMA=80.0 mM

TABLE 1. NUMERICAL VALUES FOR THE NICKEL(II)-EDMA COMPLEX

i) Formation constants ($\mu=0.30$, 25°C)

$$K_{NiX} = \frac{[NiX^+]}{[Ni^{2+}][X^-]} = 2.75\times10^{10}$$

$$K_2 = \frac{[NiX_2^0]}{[NiX^+][X^-]} = 2.18\times10^6$$

ii) Molar extinction coefficients

	360 mμ	350 mμ
ε_{NI}	1.07	—
ε_{NIX}	5.98	3.31
ε_{NIX2}	—	9.80

(these results are not shown). Here, i_0 and i_t denote the wave heights of DTPA or Cy-DTA wave at time $t=0$ and $t=t$ respectively. When the other experimental conditions were kept constant, the slope of the above linear relation was not influenced by the addition of the nickel(II)-DTPA or CyDTA complex, and it was independent of the initial concentration of DTPA or CyDTA. These facts clearly indicate that the forward reaction is much faster than the backward reaction, and that the dissociation of the nickel(II) complex of Dien, EDMA, or En is not involved in any of the present substitution reactions. Therefore, the log-plot slope multiplied by 2.303 is equal to the apparent rate constant, k^+_{ap}, of the forward reaction. Furthermore, in solutions of a given pH and a given initial concentration of DTPA or CyDTA, the log-plot slope was exactly proportional to the concentration of the nickel(II)-EDMA, En, or Dien complex with a 1-to-1 ratio. The results are given in Table 2. Dien and EDMA act as tridentate

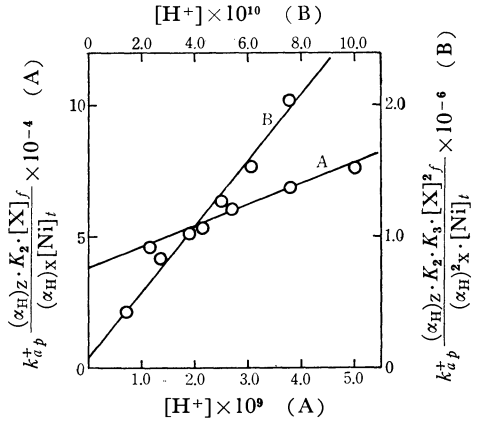

Fig. 4. The plot of $k^+_{ap}(\alpha_H)_Z K_2\cdot[X]_f/(\alpha_H)_X[Ni]_t$ or $k^+_{ap}(\alpha_H)_Z\cdot K_2\cdot K_3[X]^2_f/(\alpha_H)^2_X[Ni]_t$ against the hydrogen concentration.
$\mu=0.30$, 25°C
Initial concentration of CyDTA=0.40 mM
Concentration of nickel(II) ion=10.0 mM
A: Ni(II)-Dien system
Total concentration of Dien=30.0 mM
B: Ni(II)-En system
Total concentration of En=40.0 mM

TABLE 2. THE RELATION BETWEEN THE log-PLOT SLOPE AND THE CONCENTRATION OF NICKEL(II) COMPLEX

A) Nickel(II)-Dien - CyDTA system

Total concentration of nickel(II), $[Ni]_t$ mM	Concentration of Dien, $[X]_f$ mM	Slope S sec^{-1}	$\frac{S\times[X]_f}{[Ni]_t}$	
10.0	10.0	1.74×10^{-5}	1.74×10^{-5}	pH=8.57 μ=0.30 Initial concentration of CyDTA=0.40 mM
15.0	10.0	2.60×10^{-5}	1.72×10^{-5}	
20.0	10.0	3.50×10^{-5}	1.75×10^{-5}	
10.0	20.0	8.85×10^{-6}	1.77×10^{-5}	
10.0	30.0	5.98×10^{-6}	1.80×10^{-5}	

B) Nickel(II)-En - CyDTA system

Total concentration of nickel(II), $[Ni]_t$ mM	Concentration of En, $[X]_f$ mM	Slope S sec^{-1}	$\frac{S\times[X]^2_f}{[Ni]_t}$	
10.0	10.0	2.00×10^{-3}	2.00×10^{-5}	25°C pH=9.46 μ=0.30 Initial concentration of CyDTA=0.40 mM
16.0	10.0	3.19×10^{-3}	2.00×10^{-5}	
20.0	10.0	4.10×10^{-3}	2.05×10^{-5}	
10.0	10.0	3.32×10^{-3}	3.32×10^{-5}	pH=9.30 μ=0.30 Initial concentration of CyDTA=0.50 mM 25°C
10.0	20.0	8.00×10^{-4}	3.20×10^{-5}	
10.0	35.0	2.59×10^{-4}	3.18×10^{-5}	
10.0	50.0	1.32×10^{-4}	3.30×10^{-5}	
10.0	70.0	6.72×10^{-5}	3.29×10^{-5}	

C) Nickel(II)-Dien - DTPA system

Total concentration of nickel(II), $[Ni]_t$ mM	Concentration of Dien, $[X]_f$ mM	Slope S sec^{-1}	$\frac{S\times[X]_f}{[Ni]_t}$	
10.0	10.0	4.00×10^{-3}	4.00×10^{-3}	25°C pH=9.80 μ=0.30 Initial concentration of DTPA=0.40 mM
15.0	10.0	6.20×10^{-3}	4.13×10^{-3}	
20.0	10.0	8.00×10^{-3}	4.00×10^{-3}	
10.0	20.0	2.10×10^{-3}	4.20×10^{-3}	
10.0	30.0	1.33×10^{-3}	4.00×10^{-3}	

D Nickel(II)-EDMA - DTPA system

Total concentration of nickel(II), $[Ni]_t$ mM	Concentration of EDMA, $[X]_f$ mM	Slope S sec^{-1}	$\frac{S\times[X]_f}{[Ni]_t}$	
10.0	10.0	4.16×10^{-4}	4.16×10^{-4}	25°C μ=0.30 Initial concentration of DTPA=0.50 mM
15.0	10.0	6.22×10^{-4}	4.16×10^{-4}	
20.0	10.0	8.35×10^{-4}	4.17×10^{-4}	
10.0	15.0	2.75×10^{-4}	4.15×10^{-4}	
10.0	20.0	2.06×10^{-4}	4.13×10^{-4}	

ligands in the complex formation reaction. Therefore, the concentration of the nickel(II) complex of Dien or EDMA with a 1-to-1 ratio can be expressed by $[Ni]_t/[1+K_2[X]_f/(\alpha_H)_X]$. Here, $[X]_f$ and $(\alpha_H)_X$ denote the concentration of uncomplexed Dien or EDMA and the (α_H) value of Dien or EDMA, and K_2 is the second successive formation constant of the nickel(II)-EDMA or Dien complex. On the other hand, in the nickel(II)-En system, the concentration of the nickel(II)-En complex with a 1-to-1 ratio is given by $[Ni]_t/[1+K_2\cdot[X]_f/(\alpha_H)_X+K_2\cdot K_3\cdot[X]_f^2/(\alpha_H)_X^2]$. Here, K_2 and K_3 are the second and third successive formation constants of the nickel(II)-En complexes. As is illustrated in Figs. 4 and 5, the product of the apparent rate constant, k^+_{ap}, and $(\alpha_H)_Z(1+K_2\cdot[X]_f/(\alpha_H)_X)/[Ni]_t$(Dien and EDMA systems) or $(\alpha_H)_Z(1+K_2[X]_f/(\alpha_H)_X+K_2\cdot K_3\cdot[X]^2_f/(\alpha_H)^2_X)/[Ni]_t$ (En system) was found to be a linear function of the hydrogen ion concentration and is given by

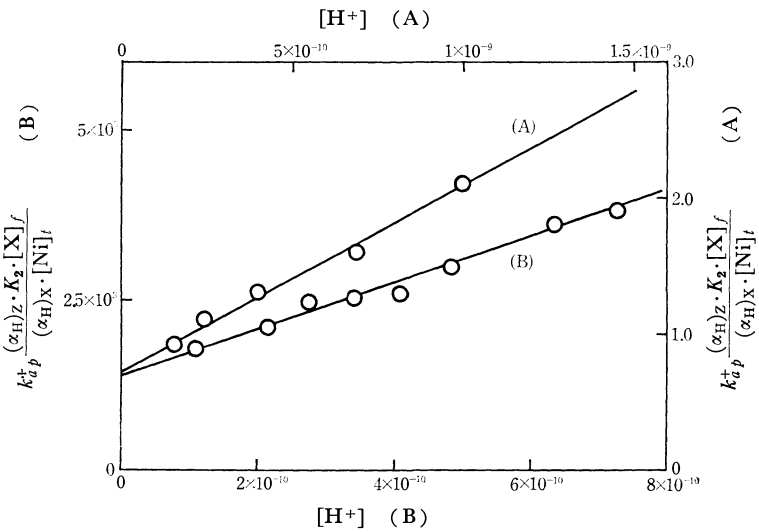

Fig. 5. The plot of $k_{ap}^{+}(\alpha_H)_Z K_2 \cdot [X]_f/(\alpha_H)_X[Ni]_t$ against the hydrogen ion concentration.
μ=0.30, 25°C
Initial concentration of DTPA=0.40 mM
Concentration of nickel(II) ion=10.0 mM
A: Ni(II)-Dien system
Total concentration of Dien=30.0 mM
B: Ni(II)-EDMA system
Total concentration of EDMA=30.0 mM

Eq. (5a) or (5b):

$$k_{ap}^{+}(\alpha_H)_Z \cdot \left(1 + \frac{K_2 \cdot [X]_f}{(\alpha_H)_X}\right) \frac{1}{[Ni]_t} = k_\alpha^{+} + k_\beta^{+}[H^+] \quad (5a)$$

$$k_{ap}^{+}(\alpha_H)_Z \cdot \left(1 + \frac{K_2 \cdot [X]_f}{(\alpha_H)_X} + \frac{K_2 \cdot K_3 \cdot [X]_f^2}{(\alpha_H)_X^2}\right) \cdot \frac{1}{[Ni]_t} = k_a^{+} + k_b^{+}[H^+] \quad (5b)$$

Here, $(\alpha_H)_Z$ in Eqs. (5a) and (5b) is the (α_H) value of DTPA or CyDTA, and $1+K_2 \cdot [X]_f/(\alpha_H)_X$ in Eq. (5a) and $1+K_2 \cdot [X]_f/(\alpha_H)_X+K_2 \cdot K_3 \cdot [X]_f^2/(\alpha_H)^2_X$ in Eq. (5b) are practically identical with $K_2 \cdot [X]_f/(\alpha_H)_X$ and $K_2 \cdot K_3 \cdot [X]_f^2/(\alpha_H)_X^2$ respectively under the present experimental conditions. From the above data, we may conclude that the mechanism of the substitution reactions of the nickel(II)-EDMA or Dien complex and that involving the nickel(II)-En complex can be expressed by (A) and (B) respectively:

(A) i) $NiX^{2-a} + Z^{m-} \overset{k_1^{+}}{\rightleftharpoons} NiZ^{2-m} + X^{a-}$

$\Big\Updownarrow$ rapid

NiX_2^{2-2a}

ii) $NiX^{2-a} + HZ^{1-m} \overset{k_2^{+}}{\rightleftharpoons} NiZ^{2-m} + HX^{1-a}$

$\Big\Updownarrow$ rapid

NiX_2^{2-2a}

where NiX_2^{2-2a} denotes 1-to-2 complex of Dien or EDMA and where Z^{m-} means a completely-deprotonated DTPA or CyDTA anion.

(B) i) $NiX^{2+} + Z^{4-} \overset{k_1^{+}}{\rightleftharpoons} NiZ^{2-} + X^{0}$

$\Big\Updownarrow$ rapid

$NiX_2^{2+} \overset{\text{rapid}}{\rightleftharpoons} NiX_3^{2+}$

ii) $NiX^{2+} + HZ^{3-} \overset{k_2^{+}}{\rightleftharpoons} NiZ^{2-} + HX^{+}$

$\Big\Updownarrow$ rapid

NiX_2^{2+}

$\Big\Updownarrow$ rapid

NiX_3^{2+}

From the above reaction mechanisms, it is very clear that k_α^{+} and k_a^{+} can be equated with k_1^{+}, and k_β^{+} and k_b^{+} with k_2^{+}/K_d. Here, K_d denotes the K_4 of CyDTA or the K_5 of DTPA. The possibility of the formation of a mixed ligand complex of nickel(II) ions involving the CyDTA anion and En can be eliminated, because the addition of En had no effect on the absorption curve of the nickel(II)-CyDTA complex. The rate constant, k_1^{+} and k_2^{+}, were determined from the linear relations shown in Figs. 4 and 5: they are listed, together with the k_2^{+} value determined for the substitution reaction of the nickel(II)-iminodiacetate (IDA) complex with DTPA, in Table 3.

8) D. W. Margerum, D. B. Rorabacher and J. F. Clarke, Jr., *Inorg. Chem.*, **2**, 667 (1963).

Table 3. Rate constants

System	k_1^+ $M^{-1}\,sec^{-1}$	k_2^+ $M^{-1}\,sec^{-1}$
Ni(II)-IDA - DTPA	3.8×10^4	6.13×10^3
Ni(II)-EDMA - DTPA	$1.3_6\times10^3$	2.58×10^2
Ni(II)-Dien - DTPA	7.2×10^5	9.80×10^4
Ni(II)-En - CyDTA	7.2×10^4	1.23×10^4
Ni(II)-Dien - CyDTA	3.8×10^4	2.97×10^1

The substitution reactions of the nickel(II)-Dien and -En complexes are much faster than their dissolication rates.[8] This clearly indicates that the presence of DTPA or CyDTA in a solution effectively aids in the removal of the Dien and En from the coordination sphere of the nickel(II) ion. To perform this function, DTPA and CyDTA may form coordination bonds with the nickel(II) ion prior to the complete dissociation of the Dien or En from the nickel(II) ion. As in the case of the reactions of Eriochrom Black T (BT) with nickel(II) and cobalt(II)-aminopolycarboxylic acids, this mechanism indicates the formation of mixed ligand intermediate complexes involving Dien or En, and DTPA or CyDTA, anion. If the substitution reaction of CyDTA with the nickel-(II)-Dien complex has a reaction intermediate quite different from that of the reaction with the nickel(II)-En complex, the rate constants of the former reaction can not reasonably be compared with those for the latter reaction. However, if the reaction with the nickel(II)-Dien complex proceeds through a reaction intermediate quite similar to that through which the reaction with the nickel(II)-En complex proceeds, the relative rate constant determined experimentally can be compared with that estimated on the basis of the proposed reaction intermediate.

In Fig. 6, the structures of some possible reaction intermediates are shown. As in the cases of the reactions of BT with the nickel(II) and cobalt(II)-EDTA and -EDTA-OH complexes,[2] the rate-

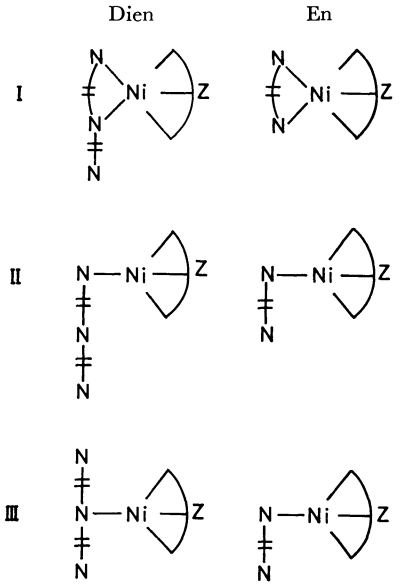

Fig. 6. Reaction intermediates for the substitutions reactions of nickel(II)-Dien and En complexes.

Table 4. Rate constant ratios

A) The reactions of CyDTA with nickel(I)-En and -Dien complexes.

System	Ratio for the elementary reaction (ii)					
	Structure I		Structure II		Structure III	
	calcd	obsd	calcd	obsd	calcd	obsd
En	7.55×10^2	4.15×10^2	1.51×10^3	4.15×10^2	3.02×10^3	4.15×10^2
Dien	1.00	1.00	1.00	1.00	1.00	1.00

B) The reactions of DTPA with nickel(II)-IDA and -EDMA complexes

System	Ratio				
	Elementary reaction (i)		Elementary reaction (ii)		
	$calcd_2$**	obsd	$calcd_1$*	$calcd_2$**	obsd
IDA	1.00	2.79×10^1	$1.34_6\times10^3$	4.27	2.38×10^1
EDMA	1.00	1.00	1.00	1.00	1.00

* Electrostatic interaction between reactants was not taken into consideration.
** Electrostatic interaction between reactants was taken into consideration.

C) The reactions of DTPA with nickel(II)-Dien and EDMA complexes

System	Ratio			
	Elementary reaction (i)		Elementary reaction (ii)	
	calcd	obsd	calcd	obsd
EDMA	1.00	1.00	1.00	1.00
Dien	6.63×10^2	5.30×10^2	1.55×10^2	3.80×10^2

constant ratios between the reaction of CyDTA with the nickel(II)-Dien complex and that with the nickel(II)-En complex were calculated on the assumption that the rates for breaking Dien and En from their mixed ligand complex intermediates are the same. In the calculation of the rate constant ratio, the stability constants of 2.34×10^{7} and 3.55×10^{10} ($\mu=0.30$) were used for the nickel(II)-En and -Dien complexes respectively, with a 1-to-1 ratio. The additional stability due to the statistical effect was also taken into account.[9] These results are listed in Table 4, together with those obtained experimentally. The calculated ratio based on structure I agrees best with the observed ratio. This finding is contrary to the observation of Rorabacher and Margerum obtained in their kinetics study of the displacement of polyamine from its nickel(II) complex by the EDTA anion.[5]

In the case of the reaction of the nickel(II)-EDMA complex, the following are considered to be possible reaction intermediates (Fig. 7). The

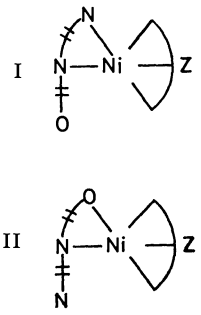

Fig. 7. Reaction intermediates for the substitution reaction of nickel-EDMA complex.

one in which only the acetate group of the displaced EDMA anion is bonded to the nickel(II) ion can be eliminated, because the nickel(II)-oxygen(acetate) bond rupture is much faster than the nickel(II)-nitrogen (amino) bond rupture[9]; hence, at least one nickel(II)-nitrogen bond rupture should be involved in the rate-determining step. Furthermore, in considering the conclusion that the reactions of the nickel(II)-aspartate and -IDA complexes with CyDTA and DTPA proceed through glycinate intermediates, the reaction intermediate having only one nitrogen group of displaced EDMA bonded to the nickel(II) ion seems unlikely. If the substitution reaction of the nickel(II)-EDMA complex with DTPA also has a glycinate mechanism, a comparison of its rate constant with that of the reaction of nickel(II)-IDA complex should be possible. The rate-constant ratio calculated on the basis of a glycinate reaction intermediate occurring between the reaction of DTPA with the nickel(II)-EDMA complex and that with the nickel(II)-IDA complex is $1 : 1.34_{6}\times 10^{3}$. In a calculation of the relative stability of the reaction intermediate, stability constants of 1.29×10^{8} and 2.75×10^{10} ($\mu=0.30$) were used for the nickel(II)-IDA and -EDMA complexes respectively, with a 1-to-1 ratio. Here, additional stabilities due to statistical and electrostatic factors were also taken into account.[9] As is clear from the data in Table 4, there is no close agreement between the calculated ratio and the observed ratio for either elementary reaction pathway, i) or ii). As was mentioned by Margerum *et al.* in their kinetic study of the formation reactions of nickel(II)-triethylenetetramine and tetraethylenepentamine complexes,[8] the electrostatic interaction between the entering group and the reactant (the nickel(II) complex) should also be taken into consideration. If the above electrostatic contribution to the rates of the reactions of nickel(II)-IDA and -EDMA complexes can be evaluated by means of Eq. (27) in Ref. (7), the rate-constant ratios for the two elementary reaction pathways, i) and ii), can be calculated to be 1 : 4.27 and 1 : 1, respectively. Even when the electrostatic interaction between the DTPA anion and the nickel(II)-IDA or -EDMA complex is taken into consideration, there is no close agreement between the calculated rate-constant ratio and the observed ratio. This disagreement clearly eliminates the possibility of a glycinate reaction mechanism (Structure II). As in the case of reactions of CyDTA with the nickel(II)-Dien and En complexes, if the reaction of DTPA with the nickel(II)-EDMA complex proceed through reaction intermediate I, the rate-constant ratios for k_1^{+} and k_2^{+} between the reaction of DTPA with the nickel(II)-Dien complex and that with the nickel(II)-EDMA complex can be estimated to be $6.63\times10^{2} : 1$ and $1.55\times10^{2} : 1$ respectively. Of course, the additional stability of the reaction intermediate due to the statistical and electrostatic effects and the contribution of electrostatic interaction between the attacking group and the nickel(II)-EDMA or -Dien complex were also taken into consideration. The agreement between the observed ratio and the calculated ratio can be regarded as satisfactory. From the results discussed in this paper, it can safely be concluded that the nucleophilic substitution reaction involving the nickel(II)-EDMA complex proceeds through a reaction intermediate in which the displaced EDMA anion is bonded to the nickel(II) ion through two nitrogen groups. This is a reasonable conclusion, because the nickel(II)-oxygen (acetate) bond cleavage is much faster than the nickel(II)-nitrogen (amino) bond cleavage.

The present authors wish to express their heartfelt thanks to the Ministry of Education for the financial support granted for this research.

9) T. J. Bydalek and D. W. Margerum, *Inorg. Chem.*, **2**, 678 (1963).

BULLETIN OF THE CHEMICAL SOCIETY OF JAPAN VOL. 43 2093—2095 (1970)

Intramolecular Electron-transfer Reactions of Ethylenediaminetetraacetatocobaltate(III) and Its Related Complexes in Solid State

Kenzo NAGASE

Department of Chemistry, College of General Education, Tohoku University, Kawauchi, Sendai

and Nobuyuki TANAKA

Department of Chemistry, Faculty of Science, Tohoku University, Katahira, Sendai

(Received January 23, 1970)

Electron transfer from a ligand to a central cobalt(III) in solid state was investigated by following the change of the valence state of coblat(III) to cobalt(II). The reaction was carried out in a vacuum as a function of sample amount, temperature and nature of a ligand and an outer-sphere cation. The electron-transfer reaction followed the first-order rate law. An outer-sphere cation had a slight effect on the reaction of the complex ion. The kinetic parameters obtained for potassium ethylenediaminetetraacetatocobaltate(III) ($E_a=38$ kcal/mol, $A=10^{14}$) differed greatly from those for potassium propylenediaminetetraacetatocobaltate(III), potassium cyclohexanediaminetetraacetatocobaltate(III) and potassium trimethylenediaminetetraacetatocobaltate(III) ($E_a\simeq 22$ kcal/mol, $A\simeq 10^6$). The kinetic behavior of the pentadentate complex, potassium hydrogen halogenoethylenediaminetetraacetatocobaltate(III), was compared with that of the hexadentate complex, potassium ethylenediaminetetraacetatocobaltate(III).

The electron-transfer reactions of cobalt(III) complexes in solid state were discussed in detail by Tanaka *et al.*[1] They proposed that the values of the activation energies increased in parallel with the increase of the ligand field.

However, it is considered that the electron-transfer reaction depends on the structure of the ligand in addition to the electronic state of the complex ion.

In the present study, a series of diaminotetraacetatocobaltate(III) complexes whose electronic spectra are almost the same but structure different were adopted, and their structural effects on the electron-transfer reaction were discussed.

Experimental

Materials. Potassium ethylenediaminetetraacetatocobaltate(III) dihydrate, K[Coedta]$2H_2O$,[2] potassium propylenediaminetetraacetatocobaltate(III) dihydrate, K[Copdta]$2H_2O$,[3] potassium cyclohexanediaminetetraacetatocobaltate(III) trihydrate, K[Cocydta]$3H_2O$,[4] potassium trimethylenediaminetetraacetatocobaltate(III) dihydrate, K[Cotrdta]$2H_2O$,[5] potassium hydrogen chloroethylenediaminetetraacetatocobaltate(III) monohydrate, K[CoCledtaH]H_2O[6], and potassium hydrogen bromoethylenediaminetetraacetatocobaltate(III) dihydrate, K[CoBredtaH]$2H_2O$,[7] were prepared according to the methods given in literature.

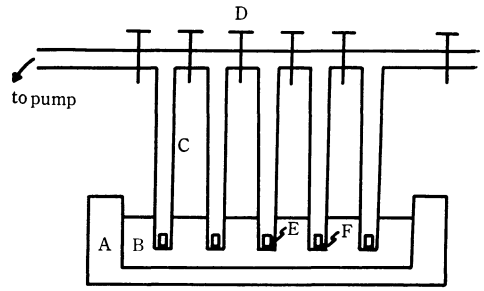

Fig. 1. Schematic diagram of apparatus: (A) bath, (B) silicone oil, (C) reaction tube, (D) cock, (E) crucible and (F) sample.

Apparatus and Procedure. Figure 1 shows the apparatus used for the thermal treatment. Samples which were smaller than 100 mesh in size weighed 2 to 4 mg in each kinetic measurement and the temperature of the sample was controlled in a range of ± 0.3°C by means of a silicone oil bath. The system was continu-

1) N. Tanaka, K. Nagase and S. Nagakura, This Bulletin, **41**, 1143 (1968).

2) H. Brintzinger, H. Thiele and U. Mueller, *Z. Anorg. Chem.*, **251**, 285 (1943).

3) F. P. Dwyer and F. L. Garvan, *J. Amer. Chem. Soc.*, **81**, 2955 (1959).

4) F. P. Dwyer and F. L. Garvan, *ibid.*, **83**, 2610 (1961).

5) N. Tanaka and H. Ogino, This Bulletin, **37**, 877 (1964).

6) M. Mori, M. Shibata, E. Kyuno and H. Nakajima, *ibid.*, **29**, 887 (1956).

7) G. Schwarzenbach, *Helv. Chim. Acta*, **32**, 839 (1949).

ously evacuated by a rotary pump during the reaction. Every one hour, the heated sample was taken out of the reaction tube and dissolved in a 25 ml deaerated solution containing 0.5 M potassium chloride. A Yanagimoto PR-2 pen-recording polarograph was used for the determination of cobalt(III) content in the solution.

Results and Discussion

The decomposition processes of diaminotetraacetatocobaltate(III) complexes were investigated by thermogravimetric analysis, gas evolution analysis and polarographic analysis. For example, the process for potassium ethylenediaminetetraacetatocobaltate(III) in a vacuum is given by the equations

$$K[Co^{III}\,edta]2\,H_2O \xrightarrow[\sim 50°C]{\text{dehydration}} K[Co^{III}\,edta] + 2\,H_2O \quad (1)$$

$$K[Co^{III}\,edta] \xrightarrow[\sim 170°C]{\text{electron transfer}} K[Co^{II}(edta')] \quad (2)$$

$$K[Co^{II}(edta')] \xrightarrow{\text{decarbonation}} \text{Products containing cobalt(II)} + CO_2 \quad (3)$$

where edta' represents the edta radical which was formed by the electron transfer from an edta to a central cobalt(III). The rate of reaction (2) was followed by the measurement of the change of the valence state of cobalt(III) to cobalt(II).

The Order of the Electron-transfer Reaction. The measurements which were carried out with various initial amounts of the sample confirmed, as shown in Fig. 2, the relation given by the equation

$$-dN/dt = kN \quad (4)$$

where N represents the number of cobalt(III) ions in the heated sample and k the rate constant. Equation (4) is modified to

$$2.303 \log x = -kt \quad (5)$$

where x is the mole fraction of cobalt(III) in the sample. A plot of $\log x$ *versus* time was made for each complex and nearly straight lines were obtained. The plots for K[Cocydta] are shown in Fig. 3 as an example.

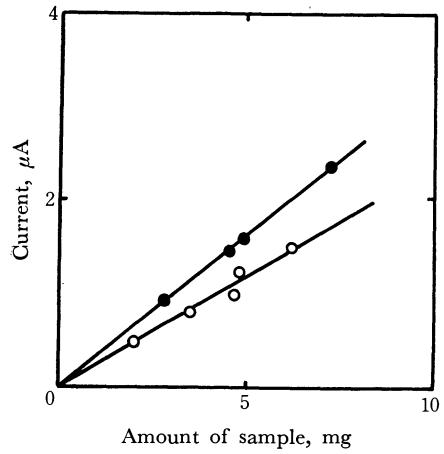

Fig. 2. Determination of cobalt(III) content for Na[Coedta] (●) before and (○) after heating at 172°C for 5 hr.

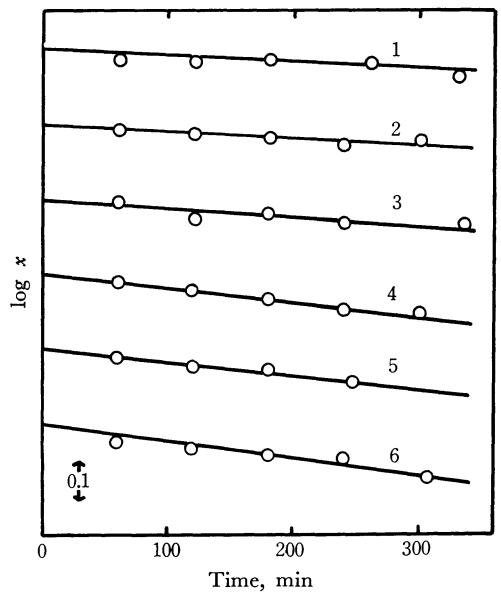

Fig. 3. Plots of log x *versus* time for K[Cocydta] at various temperatures: (1) 190, (2) 192, (3) 196, (4) 200, (5) 203 and (6) 204°C.

From these results, it is confirmed that the electron-transfer reaction follows the first-order rate law.

Effects of Outer-sphere Cations on the Electron-transfer Reaction. The kinetic parameters of ammonium, sodium and potassium salts of ethylenediaminetetraacetatocobaltate(III) are given in Table 1. The temperatures at which the rate constants are equal to 1×10^{-5} sec^{-1} are almost the same among these complexes, but the activation energies (E_a) and frequency factors (A) are slightly different. Therefore, a precise comparison of the kinetic behavior of the complex ion should be made among the complexes containing the same outer-sphere ion.

TABLE 1. EFFECTS OF OUTER-SPHERE CATION ON THE ELECTRON-TRANSFER REACTION OF EDTA COMPLEX

Complex	Temp., °C ($k = 1 \times 10^{-5}$ sec^{-1})	E_a kcal/mol	A
NH_4[Coedta]	171	43	10^{16}
Na[Coedta]	170	41	10^{15}
K[Coedta]	171	38	10^{14}

Kinetic Studies of K[Coedta], K[Copdta], K[Cocydta] and K[Cotrdta]. The first-order rate constants for potassium salts of ethylenediaminetetraacetatocobaltate(III) and its related complexes were determined from the plots of log x *versus* time. The order of the temperatures at which the rate constant is equal to 1×10^{-5} sec^{-1} is as follows:

$$\text{K[Coedta]} < \text{K[Cotrdta]} < \text{K[Cocydta]} < \text{K[Copdta]}$$

This suggests that the rate depends considerably on the nature of the ligand. The activation energies and frequency factors were obtained from the temperature dependence of the rate. The kinetic parameters obtained are given in Table 2. It is noticed that the kinetic parameters of EDTA complex are considerably higher than those of PDTA, CyDTA and TRDTA complexes, which are almost the same.

Table 2. Kinetic parameters of the electron-transfer reaction for various cobalt(III) complexes in solid state

Complex	Temp., °C ($k = 1\times10^{-5}$ sec^{-1})	E_a kcal/mol	A
K[Coedta]	171	38	10^{14}
K[Copdta]	199	22	10^{5}
K[Cocydta]	194	24	10^{6}
K[Cotrdta]	187	23	10^{6}

According to a previous paper,[1] the activation energies of the electron-transfer reaction of cobalt(III) complexes are somewhat lower than the energies of the A band of their absorption spectra and the frequency factors are smaller than the normal values for a first-order reaction, 10^{13}. From this conclusion, the values expected for EDTA, PDTA, CyDTA and TRDTA complexes are $E_a=$ 20 to 25 kcal/mol and $A=10^5$ to 10^8.

Electron transfer from a ligand to a central cobalt(III) will occur after reorganization of the structure of the cobalt complex in the formation of the transition state. Such a rearrangement in the complex containing polydentate ligand will be caused by increasing the bond distance and by varying the direction of the coordinated atom. The latter will be caused by the twist of the chelate ring as observed in racemization. From the steric relationship, the twist is easy for the EDTA complex but difficult for the other three. The difficulty of the twist for the PDTA complex results from the repulsion between methyl hydrogen atoms and methylene hydrogen atoms. The twist of the chelate ring in the CyDTA complex is impossible since the chelate ring involving two nitrogen atoms is fixed by a cyclohexane ring. In the TRDTA complex, the six-membered chelate ring is formed in contrast with the EDTA, PDTA and CyDTA complexes. The difficulty of the twist for the TRDTA complex has been reported by Ogino *et al.*[8] It is supposed that the activation energy and the frequency factor of the electron-transfer reaction are higher for the twist mechanism than for the mechanism by which the chelate ring is fixed. Therefore, the difference between kinetic parameters obtained for the EDTA complex and those for the other three may be due to whether the twist of the chelate ring is possible or not.

Kinetic Studies of Potassium Hydrogen Halogenoethylenediaminetetraacetatocobaltate(III). The kinetic parameters of the pentadentate complex, K[CoCledtaH] and K[CoBredtaH], are given in Table 3. The order of the temperatures at which the rate constant is equal to 1×10^{-5} sec^{-1} was as follows:

Table 3. Kinetic parameters of the pentadentate cobalt(III) complexes

Complex	Temp., °C ($k = 1\times10^{-5}$ sec^{-1})	E_a kcal/mol	A
K[CoCledtaH]	158	33	10^{11}
K[CoBredtaH]	144	28	10^{10}

$$\text{K[CoBredtaH]} < \text{K[CoCledtaH]} < \text{K[Coedta]}$$

This order suggests that the rate of the electron-transfer reaction was increased by substituting a halide ion for a carboxyl group. Also, the activation energies were decreased in the order

$$\text{K[Coedta]} > \text{K[CoCledtaH]} > \text{K[CoBredtaH]}.$$

These facts may be explained by the following:

i) The chelate ring of the pentadentate complex will twist more easily than that of the hexadentate complex.

ii) The energies of ligand field splitting and charge transfer from ligand to metal are lower in the order K[Coedta]>K[CoCledtaH]>K[CoBredtaH].

The authors wish to express their hearty thanks to Dr. Hiroshi Ogino for the supply of K[Cotrdta]–$2H_2O$. They also thank the Ministry of Education for the financial support granted for this research.

8) H. Ogino, M. Takahashi and N. Tanaka, presented at the 18th Symposium on Coordination Chemistry, Kyoto, Japan, October, 1968.

BULLETIN OF THE CHEMICAL SOCIETY OF JAPAN VOL. 43 2096—2102 (1970)

The Adsorption of 2,2′-Bipyridine and Its Ferrous Complex on the the Dropping Mercury Electrode

Hiromiti SAWAMOTO*1

Chemistry Institute, Faculty of Science, Kyoto University, Sakyo-ku, Kyoto

(Received January 26, 1970)

The adsorption of 2,2′-bipyridine and its ferrous complex $[Fe(bip)_3]^{2+}$ onto the electrode has been studied both by the electrocapillary method and the impedance-bridge method. Electrocapillary curves were obtained by the drop-time method. A peculiar shape was observed in the electrocapillary curve of $[Fe(bip)_3]^{2+}$, which was corrected for in the further thermodynamic treatment by taking into account the data obtained with an impedance bridge. It was found that 2,2′-bipyridine is adsorbed flat in the more positive region. At more negative potentials, the adsorption is also flat at low concentrations of 2,2′-bipyridine, but becomes perpendicular beyond 2×10^{-3} M. The $[Fe(bip)_3]^{2+}$ adsorption can be accounted for by a Langmuir isotherm. However, the isotherm for 2,2′-bipyridine adsorption varies with the potential, which can be explained in terms of the change in the adsorption structure.

The adsorption of organic compounds at the mercury electrode—solution interface has been studied for many years, mainly by the electrocapillary method and by the impedance-bridge method.[1] Attempts have been made to give a generalized interpretation of the adsorption of simple organic compounds, such as alcohols, and rather successful results have been obtained.[2] However, the adsorption of more complex organic compounds is difficult to interpret by such a generalized theory, and many complicated phenomena have been observed. For instance, certain anionic surface-active substances, such as alkyl sulfate ions, have been found to show three or four peaks in their differential capacity - potential curves.[3] In these cases, the differential capacity during a drop-life changes in a very complicated way.[4] It has also been found that the adsorption isotherms of pyridine and its derivatives vary remarkably with the electrode potential.[2,5-7]

The adsorption of organic compounds can also be studied by a.c. polarography (tensammetry), by which curves similar to the capacity - potential curves measured by the impedance-bridge method can be obtained automatically.[8] Using the a.c. polarographic method, the present author and his co-workers studied the adsorption of oxine and its derivatives and found that they showed peculiar non-faradaic peaks which were not typical of the adsorption - desorption of organic compounds.[9-13] When metal ions, such as copper and zinc, were added to the solution, the peaks disappeared by forming chelates with oxines, showing that the behavior of oxine and its derivatives differed from that of their chelates. This fact was used to detect the end point of titration of very dilute solutions of metal ions with oxines.[9-13] Scarcely a.c. polarographic (tensammetric) studies of the adsorption of chelate compounds have been reported. The present author has studied, in a previous report,[14] the a.c. polarographic behavior of chelates of 2,2′-bipyridine and 1,10-phenanthroline with metal ions, such as iron, zinc, and nickel. He found that, unlike the case of oxine chelates, these chelates

*1 Present address: Chemistry Institute, Faculty of Education, Kochi University, Asakura, Kochi.

1) "Electrosorption," ed. by E. Gileadi, Plenum Press, New York (1967).
2) A. N. Frumkin and B. B. Damaskin, "Modern Aspects of Electrochemistry," Vol. 3, ed. by J.O′ M. Bockris, Butterworths, London (1964).
3) K. Eda, *Nippon Kagaku Zasshi*, **80**, 343 (1959).
4) T. Fujinaga, K. Izutsu and H. Sawamoto, *ibid.*, **89**, 759 (1968).
5) L. Gierst and P. Herman, *Z. Anal. Chem.*, **216**, 238 (1966).
6) B. B. Damaskin, *Electrochim. Acta*, **9**, 231 (1964).
7) H. W. Nurnberg and G. Wolff, *Collect. Czech. Chem. Commun.*, **30**, 3997 (1965).
8) B. Breyer and H. H. Bauer, "Alternating Current Polarography and Tensammetry," Interscience Publishers, New York (1963).
9) B. Breyer, *Aust. J. Sci.*, **23**, 225 (1961).
10) B. Breyer, J. W. Hayes, T. Fujinaga, G. Takagi and S. Okazaki, *Bunseki Kagaku*, **14**, 1023 (1965).
11) B. Breyer, T. Fujinaga and H. Sawamoto, *ibid.*, **15**, 487 (1966).
12) T. Fujinaga, K. Izutsu and H. Sawamoto, *ibid.*, **16**, 1188 (1967).
13) T. Fujinaga, K. Izutsu, S. Okazaki and H. Sawamoto, *J. Electroanal. Chem.*, **21**, 187 (1969).
14) T. Fujinaga and H. Sawamoto, in preparation.

show typical adsorption - desorption peaks.

The present study was undertaken to investigate in more detail the above studies. The adsorption of 2,2'-bipyridine and its ferrous complex in 0.5 M KCl was measured by the impedance-bridge method and by the electrocapillary method. The a.c. polarographic method was used as an auxiliary method. The surface excess and the adsorption isotherms of these adsorbates have been obtained, and their adsorption structures have then been deduced from these results. Special attention was paid to the abnormal shape observed in the electrocapillary curves of $[Fe(bip)_3]^{2+}$ ions.

Experimental

The measurement of the differential capacity with an impedance-bridge has been described previously.[4] The bridge was balanced at the end of the life of a mercury drop. The tensammetric measurement with an a.c. polarograph has also been described previously.[13] Electrocapillary curves were usually obtained by the drop-time method. The drop time was determined by measuring the time of ten drops with a stop watch. The accuracy of the measurement of the drop time was within ± 0.01 sec, which corresponds to an interfacial tension of about ± 1 dyn/cm at the mercury/electrolyte phase boundary. The reproducibility of the dropping mercury electrode was checked before each measurement in a 0.5 M potassium chloride solution. All the chemicals were of analytical-reagent grades and were used without further purification. Drying 2,2'-bipyridine in a desiccator under reduced pressure caused no weight change. The concentration of the ferrous sulfate solution was determined gravimetrically. $[Fe(bip)_3]^{2+}$ was prepared by mixing equivalent amounts of 2,2'-bipyridine and ferrous sulfate.

Results and Discussion

Electrocapillary Curves. Among the methods for obtaining electrocapillary curves, the measurement with a Lippman electrometer is most reliable for thermodynamic treatment, but it is rather tedious, especially in the presence of organic compounds. Drop time - potential curves usually measured in polarography, on the other hand, can easily be converted to electrocapillary curves by using such relations as are shown by Eqs. (1) and (2) and can be used for further thermodynamic treatment. The relation in Eq. (1) was used by Tate, and that in Eq. (2), by Corbusier and Gierst:[15]

$$\gamma = \frac{\gamma_{ref}}{t_{ref}} t \tag{1}$$

$$\Delta\gamma = K^* \frac{\gamma_{ref}}{t_{ref}} \Delta t = 0.973 \frac{\gamma_{ref}}{t_{ref}} \Delta t \tag{2}$$

In these equations, γ and t are the interfacial tension and the drop time respectively. γ_{ref} is a known interfacial tension under the conditions chosen as a reference, and t_{ref} is the drop time obtained under the same conditions as γ_{ref}. $\Delta\gamma$ is equal to $\gamma - \gamma_{ref}$, and Δt, to $t - t_{ref}$. In the present report, the value of the interfacial tension obtained by Devanathan and Peries[16] at a potential of the electrocapillary maximum was used as γ_{ref}. K^* is a constant; a value of 0.973 was obtained experimentally by Corbusier and Gierst.[15]

The interfacial tension can also be obtained by a double integration of the differential capacity, C:

$$\iint_{Ez}^{E} C \mathrm{d}^2E = \gamma(E_z) - \gamma \tag{3}$$

where E is the electrode potential, where E_z is the potential of zero charge, and where $\gamma(E_z)$ is the known interfacial tension at E_z.

The electrocapillary curves were obtained in 0.5 M potassium chloride solutions containing various concentrations of 2,2'-bipyridine by using Eqs. (1), (2), and (3); they are compared in Fig. 1. The results obtained from Eq. (3) show slightly larger values than those obtained from Eqs. (1) and (2) in the cathodic potential region. Such differences in the presence of organic compounds have also been reported by Parsons and Zobel.[17]

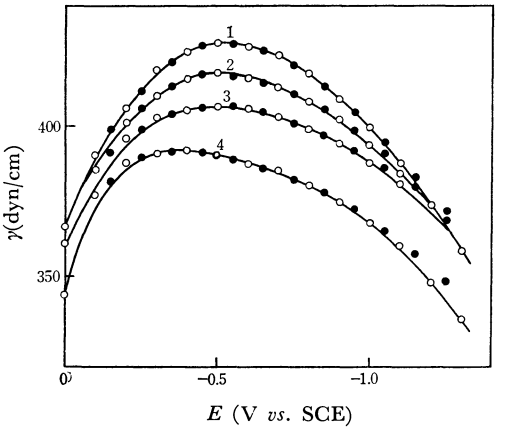

Fig. 1. Comparison of electrocapillary curves of 2,2'-bipyridine in 0.5 M KCl.
2,2'-bipyridine concentration: 1, 0; 2, 10^{-4} M; 3, 10^{-3} M; 4, 10^{-2} M.
Solid line: calculated from Eq. (1)
○: calculated from Eq. (2)
●: calculated from Eq. (3)

The results obtained from Eqs. (1) and (2) coincide well, but in the calculation from Eq. (2) the value of K^* was assumed to be 0.973, as had been obtained experimentally by Corbusier and Gierst;[15]

15) P. Corbusier and L. Gierst, *Anal. Chim. Acta*, **15**, 254 (1956).

16) M. A. V. Devanathan and P. Peries, *Trans. Faraday Soc.*, **50**, 1236 (1954).

17) R. Parsons and F. G. R. Zobel, *ibid.*, **62**, 3511 (1966).

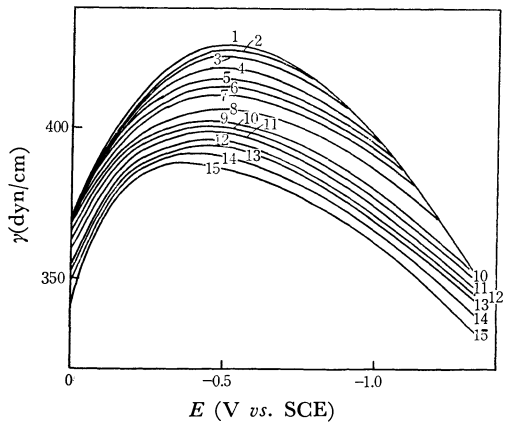

Fig. 2. Electrocapillary curves of 2,2′-bipyridine in 0.5 M KCl.
2,2′-bipyridine concentration: 1, 0; 2, 10^{-5} M; 3, 2×10^{-5} M; 4, 5×10^{-5} M; 5, 10^{-4} M; 6, 2×10^{-4} M; 7, 5×10^{-4} M; 8, 10^{-3} M; 9, 1.4×10^{-3} M; 10, 2×10^{-3} M; 11, 3×10^{-3} M; 12, 5×10^{-3} M; 13, 8×10^{-3} M; 14, 10^{-2} M; 15, 1.4×10^{-2} M

this value may not be applicable to the present dropping mercury electrode. For these reasons, the electrocapillary curves described below were obtained from Eq. (1). More detailed results on the electrocapillary curves in the presence of 2,2′-bipyridine are shown in Fig. 2.

The electrocapillary curves in the presence of $[Fe(bip)_3]^{2+}$ are shown in Fig. 3. The curves obtained in the concentration range between 5×10^{-5} M and 3×10^{-4} M show a peculiar depression in the cathodic potential range, while those obtained for $[Fe(bip)_3]^{2+}$ concentrations below 5×10^{-5} M or above 3×10^{-4} M show no such depression

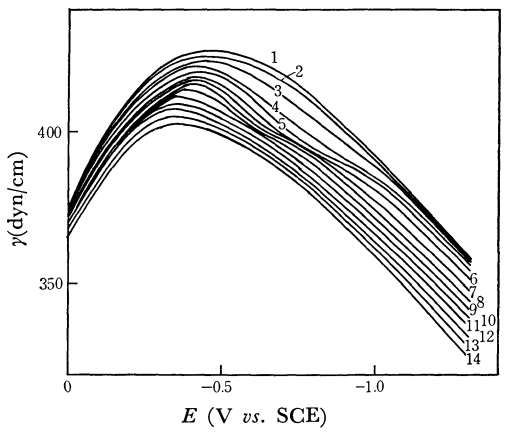

Fig. 3. Electrocapillary curves of $[Fe(bip)_3]^{2+}$ in 0.5 M KCl.
$[Fe(bip)_3]^{2+}$ concentration: 1, 0; 2, 2×10^{-5} M; 3, 3×10^{-4} M; 4, 5×10^{-5} M; 5, 7×10^{-5} M; 6, 10^{-4} M; 7, 2×10^{-4} M; 8, 3×10^{-4} M; 9, 5×10^{-4} M; 10, 7×10^{-4} M; 11, 10^{-3} M; 12, 1.4×10^{-3} M; 13, 2×10^{-3} M; 14, 3×10^{-3} M

and have normal shapes. This appearance of the depression in the electrocapillary curves is a peculiar phenomenon, because the two differentiations of the interfacial tension with respect to the potential causes a negative capacity.

It has been reported that such an abnormal depression of the electrocapillary curves was observed at a dropping mercury electrode at the potential at which the polarographic maximum appeared, but it was not observed with a Lippmann electrometer.[18] When an organic compound is reduced and gives a reductant which is strongly adsorbed onto the electrode surface, a sudden decrease in the interfacial tension is also observed at the potential at which reduction occurs.[19] In the present case, however, no faradaic current was observed in the abnormal region, as is shown in Fig. 4. As to the abnormal depression of the electrocapillary curve in the absence of electrolytic processes, only one example has been observed in anhydrous acetic acid,[20] and none in an aqueous solution.

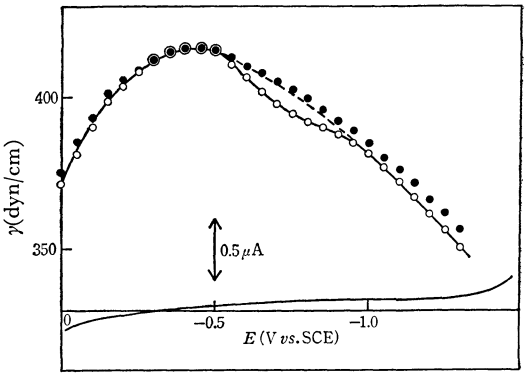

Fig. 4. Electrocapillary curve of 10^{-4} M $[Fe(bip)_3]^{2+}$ in 0.5 M KCl and its d.c. polarogram.
○: calculated from Eq. (1)
●: calculated from Eq. (3)
Dotted line shows the method of correction for the abnormal depression.

In order to test the effect of the sulfate ion introduced as $FeSO_4$ in 0.5 M potassium chloride, ferrous chloride was used instead of ferrous sulfate. As this electrocapillary curve showed the same abnormality, the effect of the sulfate ion can be disregarded.

The electrocapillary curve in the presence of both 2,2′-bipyridine and $[Fe(bip)_3]^{2+}$ also showed an abnormality at 2,2′-bipyridine concentrations above 10^{-4} M. This fact might show that the presence of both 2,2′-bipyridine and $[Fe(bip)_3]^{2+}$ is

18) J. Heyrovsky and J. Kuta, "Principles of Polarography," Academic Press, New York (1966), p. 23.
19) "Polarography," ed. by I. Tachi, Iwanami Shoten, Tokyo (1954), p. 312.
20) G. B. Bachman and M. J. Astle, *J. Amer. Chem. Soc.*, **64**, 2177 (1942).

the cause of the abnormal phenomena, and that the species obtained as a result of the dissociation of $[Fe(bip)_3]^{2+}$ might be responsible for it. However, from the calculation of the dissociation of $[Fe(bip)_3]^{2+}$ previously described,[13,21] it was found that $[Fe(bip)_3]^{2+}$ is not so dissociated as to affect the electrocapillary curves. Though the electrocapillary curve of the mixture of $[Fe(bip)_3]^{2+}$ and 2,2'-bipyridine coincides with that of $[Fe(bip)_3]^{2+}$, their C - E curves differ markedly from each other, showing that the causes of the abnormalities are not identical.

From these results, it can be concluded that the abnormality of the electrocapillary curves in the presence of $[Fe(bip)_3]^{2+}$ is not due to the presence of both $[Fe(bip)_3]^{2+}$ and 2,2'-bipyridine resulting from the dissociation of the complex in solution, though the real cause of this abnormality is still uncertain.

The electrocapillary curves calculated from Eq. (3) using the data of the impedance-bridge measurements showed no abnormality, as is shown in Fig. 4. Therefore, a correction shown by a dotted line in Fig. 4 will be made in the following discussion for the abnormality.

Adsorption Structure. The surface excess, Γ, of an adsorbed species can be obtained from the Gibbs adsorption equation:

$$\Gamma = -\left(\frac{\partial \gamma}{\partial \mu}\right)_{E,T} = -\frac{1}{2.303RT}\left(\frac{\partial \gamma}{\partial \log c}\right)_{E,T} \quad (4)$$

where μ and c are, respectively, the chemical potential and the concentration of the adsorbate in solution; R, the gas constant, and T, the absolute temperature. The value of $(\partial\gamma/\partial \log c)_{E,T}$ can be obtained by graphically differentiating the γ-$\log c$ curve as is shown in Fig. 5.

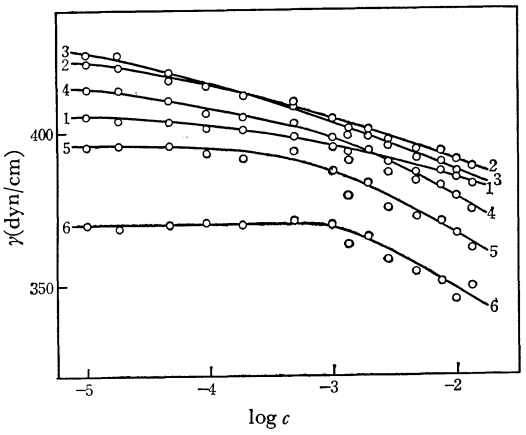

Fig. 5. Effect of 2,2'-bipyridine concentration on interfacial tension.
Potentials: 1, −0.2 V; 2, −0.4 V; 3, −0.6 V; 4, −0.8 V; 5, −1.0 V; 6, −1.2 V

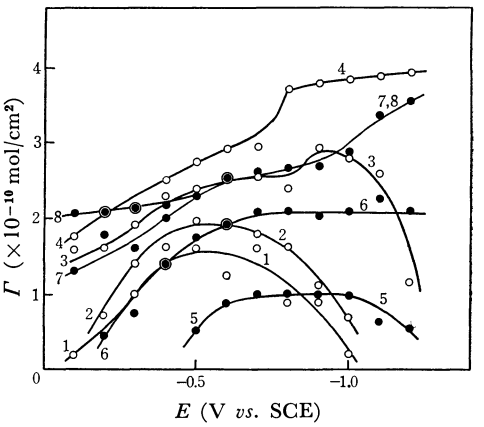

Fig. 6. Variation of surface excess with electrode potentials at different concentrations of (a) 2,2'-bipyridine and (b) $[Fe(bip)_3]^{2+}$ in 0.5 M KCl.
(a): 1, 2×10^{-5} M; 2, 10^{-4} M; 3, 10^{-3} M 4, 3×10^{-3} M
(b): 5, 2×10^{-5} M; 6, 10^{-4} M; 7, 10^{-3} M 8, 3×10^{-3} M

The variation of the surface excess with the electrode potential is shown in Fig. 6 for 2,2'-bipyridine and $[Fe(bip)_3]^{2+}$. At low concentrations of 2,2'-bipyridine, the curves are almost symmetrical, as in the case of typical neutral molecules (curves 1 and 2). The surface excess is at its maximum at the point of zero charge and decreases almost to zero at sufficiently anodic or cathodic potentials. However, as the concentration increases, asymmetrical curves are obtained whose maximum is located at a considerably negative potential (curves 3 and 4). If the 3.9×10^{-10} mol/cm² obtained from curve 4 in Fig. 6 is assumed to be the saturated surface excess for the monolayer adsorption of 2,2'-bipyridine, the area occupied by its single molecule can be calculated as 42.5 Å²/mol. The area of the electrode occupied by a molecule of α-naphthol, which is considered to be smaller than that of 2,2'-bipyridine, has been reported[22] to be 66 Å² when it is adsorbed in parallel to the electrode and 26 Å² when adsorbed perpendicularly. This shows that, at negative potentials, 2,2'-bipyridine cannot be adsorped in parallel to the electrode if a monolayer is assumed. Therefore, the adsorption of 2,2'-bipyridine at negative potentials (about −1.0 V) seems to be in multilayers or perpendicular to the electrode in a monolayer.

$[Fe(bip)_3]^{2+}$ at low concentrations is not adsorbed at sufficiently positive potentials (curves 5 and 6). At high concentrations, however, it is adsorbed in all the potential regions investigated, and the surface excess is especially large in negative regions (curves 7 and 8). This shows that [Fe-

21) L. G. Sillen and A. E. Martell, "Stability Constant of Metal-Ion Complexes," Spec. Publ., **17**, Chem. Soc., London (1964).

22) S. G. Meibuhr, *Electrochim. Acta*, **10**, 215 (1965).

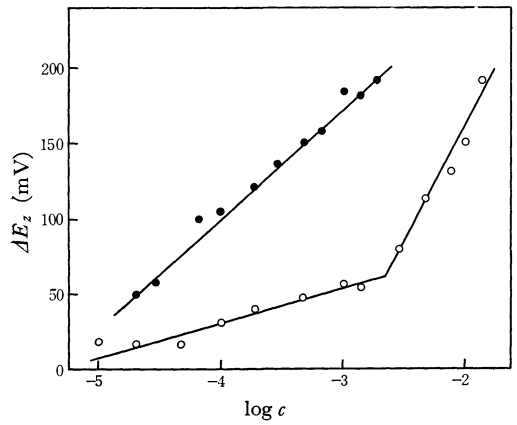

Fig. 7. Shifts of the potential of zero charge with the logarithms of adsorbate concentration in 0.5 M KCl.
○: 2,2'-bipyridine
●: $[Fe(bip)_3]^{2+}$

$(bip)_3]^{2+}$ has a character of the organic cation.

The shifts of the potential of zero charge (ΔE_z) with the logarithms of the concentrations of the adsorbates in 0.5 M KCl are shown in Fig. 7. In Fig. 7, $\Delta E_z = E_z^0 - E_z$, and E_z^0 is the potential of zero charge of the 0.5 M KCl solution, while E_z is that in a solution containing 2,2'-bipyridine or $[Fe(bip)_3]^{2+}$. The potentials of zero charge were determined from the electrocapillary curves. The change in E_z with the change in the concentration of an inorganic anion can be explained by the Esin and Markov effect,[23] which predicts that E_z will vary linearly with the logarithm of the activity of the anion. Barradas *et al.*[24] studied this effect with uncharged organic molecules and got linear relations between E_z and the logarithms of the concentrations of the organic molecules. In Fig. 7, E_z in the presence of $[Fe(bip)_3]^{2+}$ varies linearly with the logarithm of its concentration, as in the case of other inorganic ions, while the $E_z - \log c$ curve in the presence of 2,2'-bipyridine consists of two lines with different slopes. The lines cross each other at about 2×10^{-3} M, indicating a change in the structure of the adsorbed layer at this concentration.

The differential capacity - potential curves in the presence of 2,2'-bipyridine, shown in Fig. 8, do not show typical peaks, but the depression of the curves from that of the base solution indicates that 2,2'-bipyridine is adsorbed in this potential region. Above 2×10^{-3} M of 2,2'-bipyridine, a hump is observed in the adsorption region, indicating that two different adsorption structures exist on the two sides of the hump. The deep depression of the

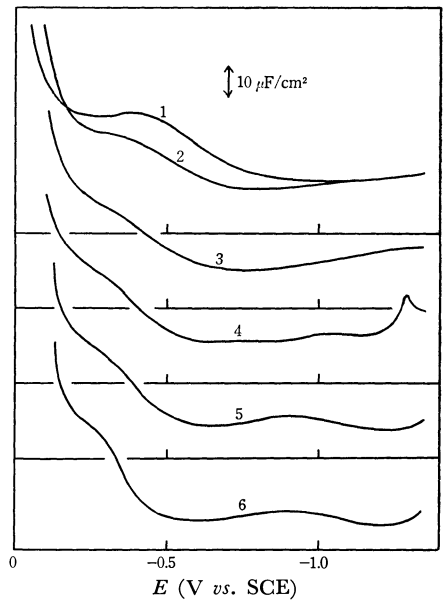

Fig. 8. Differential capacity - potential curves of 2,2'-bipyridine in 0.5 M KCl.
1, 0; 2, 5×10^{-5} M; 3, 2×10^{-4} M; 4, 2×10^{-3} M; 5, 5×10^{-3} M; 6, 10^{-2} M

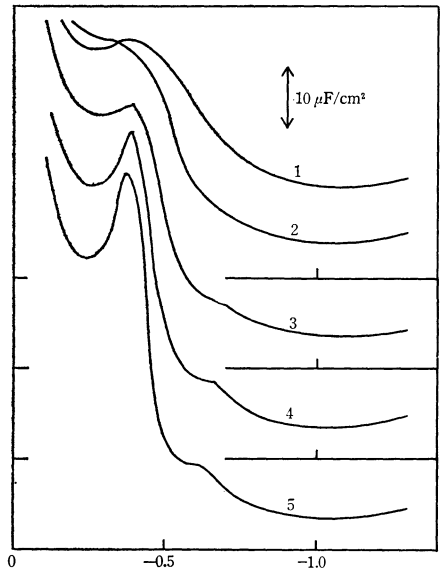

Fig. 9. Differential capacity - potential curves of $[Fe(bip)_3]^{2+}$ in 0.5 M KCl.
1, 0; 2, 5×10^{-5} M; 3, 2×10^{-4} M; 4, 5×10^{-4} M; 5, 10^{-3} M

differential capacity in the potential region more negative than the hump indicates a strong adsorption; this is in agreement with the results from the electrocapillary data shown in Fig. 6. The differential capacity - potential curves of $[Fe(bip)_3]^{2+}$

23) O. A. Esin and B. F. Markov, *Acta Physicohim. URSS*, **10**, 353 (1939).
24) R. G. Barradas, P. G. Hamilton and B. E. Conway, *J. Phys. Chem.*, **69**, 3411 (1965).

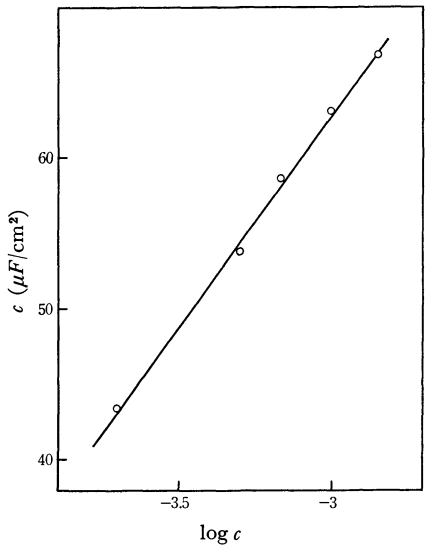

Fig. 10. Dependence of the height of capacity peak on concentration of $[Fe(bip)_3]^{2+}$.

are shown in Fig. 9. When compared with the curves in Fig. 8, distinct peaks are observed at about −0.4 V, and the capacity in the adsorption potential region is smaller in this case. As is shown in Fig. 10, the peak height varies linearly with the logarithm of the concentration. This is a characteristic trend of the adsorption - desorption peak.[2]

On the basis of the above studies, the adsorption structure can be deduced. It is preferable to assume a monolayer if there is no sure evidence for multilayers, as has been found in the case of the adsorption of certain anionic surface-active substances.[3,4] In low concentrations, 2,2'-bipyridine is adsorbed flat throughout the adsorption regions. Beyond 2×10^{-3} M, though it is still adsorbed flat in the more positive region, in the more negative region it is adsorbed perpendicularly to the electrode, probably because of the specific adsorption of nitrogen atoms onto the mercury electrode. The

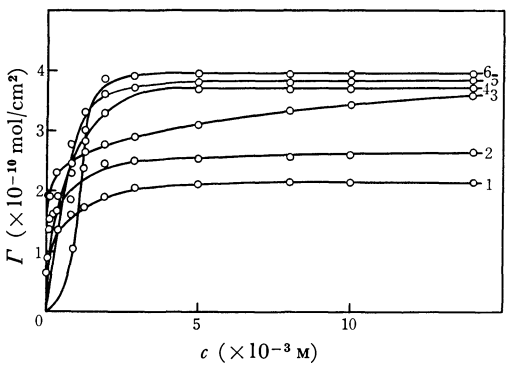

Fig. 11. Adsorption isotherms of 2,2'-bipyridine in 0.5 M KCl.
Potentials: 1, −0.2 V; 2, −0.4 V; 3, −0.8 V; 4, −0.8 V; 5, −1.0 V; 6, −1.2 V

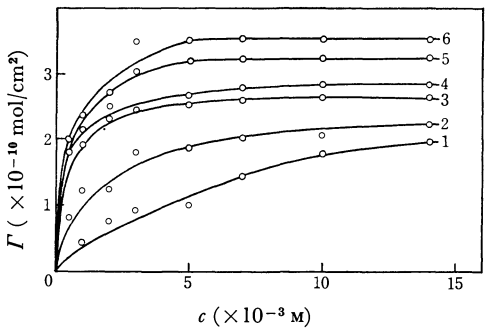

Fig. 12. Adsorption isotherms of $[Fe(bip)_3]^{2+}$ in 0.5 M KCl.
Potentials: 1, −0.2 V; 2, −0.4 V; 3, −0.6 V; 4, −0.8 V; 5, −1.0 V; 6, −1.2V

boundary of the two adsorption regions is not very distinct, so a hump is observed instead of a peak in the differential capacity - potential curves. Although the reason for the abnormal behavior of the electrocapillary curves of $[Fe(bip)_3]^{2+}$ is not yet certain, it is supposed to have only one adsorption region. As the chemical structure of $[Fe(bip)_3]^{2+}$ is almost symmetrical, the change in the orientation of the adsorbed ion cannot be considered as in the case of 2,2'-bipyridine.

Adsorption Isotherms. The surface excesses Γ of 2,2'-bipyridine and $[Fe(bip)_3]^{2+}$ at various potentials were plotted against their concentrations in the bulk of the solution. The results are shown in Figs. 11 and 12. From the figures, the isotherm for $[Fe(bip)_3]^{2+}$ is found to be of the Langmuir type, while that for 2,2'-bipyridine is not so simple and varies considerably with the electrode potential, as has been found in the case of pyridine and its derivatives.[2,5-7]

Among the many isotherms proposed up to now,[25] the Langmuir isotherm (Eq. (5)) is most commonly been used;

$$Bc = \frac{\theta}{1-\theta} \tag{5}$$

where B is the constant of the adsorption equilibrium; c, the concentration of the organic compound, $\theta=\Gamma/\Gamma_m$, the fraction of the coverage, and Γ_m, the limiting value of Γ at $c\to\infty$. Recently, however, the following Frumkin isotherm[2] has often been used:

$$Bc = \frac{\theta}{1-\theta}\exp(-2a\theta) \tag{6}$$

where a is the attraction constant, a quantity characterizing the interaction between the adsorbed particles. If a is equal to zero, Eq. (6) is converted to Eq. (5). A comparison of the experimental results with the theoretical expectations becomes much easier when Eq. (6) is modified as Eq. (7):

25) P. Delahay, "Double Layer and Electrode Kinetics," Interscience Publishers, New York (1965), p. 83.

$$\frac{c}{c_{\theta=0.5}} = \frac{\theta}{1-\theta}\exp\left[a(1-2\theta)\right] \qquad (7)$$

where $c_{\theta=0.5}$ is the concentration at which θ becomes equal to 0.5. Supposing that the Γ_m of 2,2′-bipyridine is 3.9×10^{-10} mol/cm² and that the Γ_m of $[Fe(bip)_3]^{2+}$ is 3.5×10^{-10} mol/cm², the relations of $c/c_{\theta=0.5}$ and θ were calculated; they are plotted in Figs. 13 and 14. The value of a determined from these figures is between 0 and −3 for $[Fe(bip)_3]^{2+}$, while that for 2,2′-bipyridine changes from −5 at −0.2 V to +2.5 at −1.2 V. Damaskin[26] explained the adsorption of pyridine by using the Frumkin isotherms, but he did not explain why a changed considerably with the electrode potential.

Now, from the results of the investigation of the adsorption structure of 2,2′-bipyridine, the change in a with the potential can be explained in the following way, by means of the change in the adsorption structure with the potential. In the more positive potential regions, 2,2′-bipyridine is adsorbed flat onto the electrode surface as a result of the π-electron - electrode interaction. In this case, the isotherm shown by curve 1 in Fig. 13 is obtained, and a negative attraction constant is obtained from it. In the more negative potentials, however, 2,2′-bipyridine at low concentrations is scarcely adsorbed because of the repulsion between the π-electron and the electrode. However, when the concentration is increased, it is adsorbed in a large amount perpendicularly to the electrode, resulting in an adsorption isotherm with a positive attraction constant, as in curve (8) of Fig. 13. As one adsorption structure changes in relation to another with an electrode potential, the isotherm changes between the two extreme cases with the electrode potential.

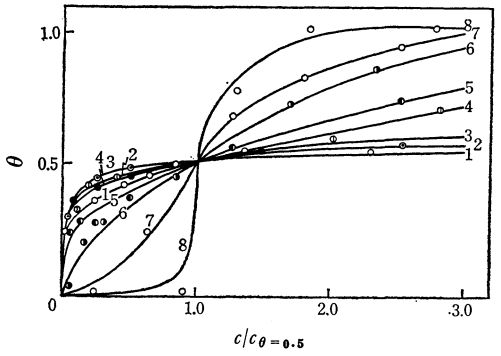

Fig. 13. Frumkin isotherms of 2,2′-bipyridine in 0.5 M KCl.
Potentials: 1, −0.2 V, $a=-5.0$; 2, −0.4 V, $a=-2.5$; 3, −0.6 V, $a=-1.0$; 4, −0.8 V, $a=-0.3$; 5, −0.9 V, $a=0.0$; 6, −1.0 V, $a=1.0$; 7, −1.1 V, $a=1.7$; 8, −1.2 V, $a=2.5$.

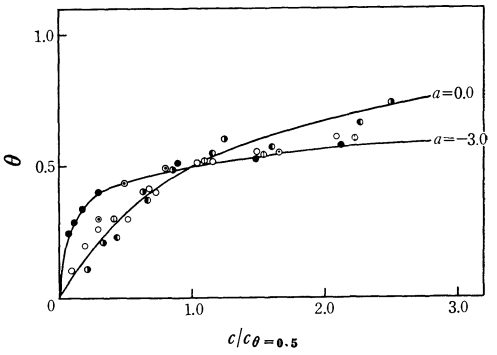

Fig. 14. Frumkin isotherms of $[Fe(bip)_3]^{2+}$ in 0.5 M KCl.
Potentials: ○: −0.2V; ●: −0.4 V; ⊙: −0.6 V; ⓘ: −1.0 V; ◐: −1.1 V; ◑: −1.2 V

The author wishes to express his deep gratitude to Professor Taitiro Fujinaga, Kyoto University, for his kind guidance and encouragement in the course of the present work, and also to Dr. Kosuke Izutsu for his helpful suggestions and discussions.

26) B. B. Damaskin, *Electrochim. Acta*, **9**, 231 (1964).

BULLETIN OF THE CHEMICAL SOCIETY OF JAPAN VOL. 43 2103—2109 (1970)

Trimethylenediamine Complexes. II. Some *cis-trans* Isomeric Pairs of Diacidobis(trimethylenediamine)cobalt(III) Complexes*[1]

Hiroshi KAWAGUCHI and Shinichi KAWAGUCHI

Department of Chemistry, Faculty of Science, Osaka City University, Sumiyoshi-ku, Osaka

(Received January 31, 1970)

Isomeric pairs of *cis*- and *trans*-dinitro-, diisothiocyanato- and cyanosulfito-bis(trimethylenediamine)cobalt(III) complexes, and *cis*-nitronitritobis(trimethylenediamine)cobalt(III) nitrite were synthesized. Their electronic and infrared spectra were compared with each other to assign their structures. The *cis*-diisothiocyanatobis(trimethylenediamine)cobalt(III) complex was resolved into optically active isomers by means of potassium antimony(III) (+)-tartrate. The circular dichroism spectra of this dissymmetric complex were measured and discussed in relation to its absolute configuration which was recently determined by X-ray analysis.

Several diacidobis(trimethylenediamine)cobalt(III) complexes were derived from *trans*-dichlorobis(trimethylenediamine)cobalt(III) chloride by the ligand substitution reactions in methanol, and all of them were assumed to have the *trans* configuration on the basis of their infrared data.[1] It is curious that there are very few reports on trimethylenediamine complexes. No example of *cis-trans* isomeric pairs of the diacidobis(trimethylenediamine)cobalt(III) complex is known. We tried to prepare these compounds and report three such pairs obtained so far.

Experimental

***cis*-Dinitrobis(trimethylenediamine) cobalt(III) Nitrite.** Five grams of *trans*-$[CoCl_2tn_2]Cl$ was dissolved in a small quantity of hot water, to which 12 g of potassium nitrite was added. The solution was heated for about 3 hr and then kept standing overnight at room temperature. Crude precipitate was recrystallized from water, washed with water and then with acetone and dried in air. Orange-yellow crystals (3.5 g) were obtained.

Found: C, 20.60; H, 5.88; N, 27.11%. Calcd for $C_6H_{20}N_7O_6Co=[Co(NO_2)_2tn_2]NO_2$: C, 20.88; H, 5.84; N, 27.40%.

The same compound was also obtained by heating an aqueous solution of *trans*-$[Co(NO_2)_2tn_2]NO_2$ for a few hours.

When excess sodium nitrite was added to an aqueous solution of $[CoCO_3tn_2]Cl$ and kept standing for 4 days at room temperature, or heated for 3 hr on a hot water bath, color of the solution turned from purple to reddish brown, and orange-yellow crystals appeared which were recrystallized from hot water. The infrared spectrum of this specimen was also identical with that of *cis*-$[Co(NO_2)_2tn_2]NO_2$ prepared by the above method.

***cis*-Nitronitritobis(trimethylenediamine)cobalt(III) Nitrite.** Five grams of *trans*-$[CoCl_2tn_2]Cl$ was dissolved in a small quantity of hot water, to which 12 g of potassium nitrite was added. The solution was heated for about 1 hr and then cooled for a few hours. Deposited crystals were washed with cold water and then with methanol and dried. Orange yellow crystals (3.1 g) were obtained.

Found: C, 20.88; H, 6.10; N, 27.46%.

***cis*-Diisothiocyanatobis(trimethylenediamine)-cobalt(III) Thiocyanate.** To a hot aqueous solution (*ca.* 70 m*l*) of *trans*-$[CoCl_2tn_2]Cl$ (5 g) was added gradually an aqueous solution (*ca.* 30 m*l*) of potassium thiocyanate (15 g). When the solution was heated for about 15 min, orange red crystals precipitated which were filtered off after cooling in ice for 2 hr, and recrystallized from hot water. Yield: 3.0 g.

Found: C, 28.41; H, 5.36; N, 25.53%. Calcd for $C_9H_{20}N_7S_3Co=[Co(NCS)_2tn_2]SCN$: C, 28.34; H, 5.29; N, 25.70%.

trans-Dinitro- and *trans*-diisothiocyanato-complexes were derived from *trans*-$[CoCl_2tn_2]Cl$ by the ligand substitution reactions in methanol as reported[1].

***cis*-Cyanosulfitobis(trimethylenediamine)cobalt(III).** This compound was prepared by following the method which Ohkawa, Hidaka and Shimura[2] had employed in synthesizing *cis*-$[CoCN(SO_3)en_2]$. To a 10 % aqueous solution of $Na_3[Co(CN)_2(SO_3)_2(NH_3)_2]\cdot 6H_2O$ (10 g), 10 g of trimethylenediamine was added. The solution was heated on a hot water bath for 5—10 hr, and then concentrated by slow evaporation to separate yellow brown crystals (1.1 g).

Found: C, 26.93; H, 6.75; N, 22.03%. Calcd for $C_7H_{20}N_5SO_3Co=[CoCN(SO_3)tn_2]$: C, 26.84; H, 6.49; N, 22.36%.

Sodium Disulfitobis(trimethylenediamine)-cobaltate(III) Trihydrate. Baldwin's method[3] of preparing the corresponding ethylenediamine complex

*1 Partly presented at the 10th International Conference on the Coordination Chemistry, Nikko, Japan, September, 1967.

1) H. Kawaguchi, N. Yano and S. Kawaguchi, This Bulletin, **42**, 136 (1969).

2) K. Ohkawa, J. Hidaka and Y. Shimura, *ibid.*, **39**, 1715 (1966).

3) M. E. Baldwin, *J. Chem. Soc.*, **1961**, 3123.

was followed. Five grams of sodium sulfite was dissolved in *ca.* 50 m*l* of hot water, to which 3 g of solid *trans*-$[CoCl_2tn_2]Cl$ was added. Orange yellow precipitate resulted, which was filtered off and recrystallized from water by adding sodium sulfite solution and ethanol.

Found: C, 16.29; H, 6.09; N, 12.86%. Calcd for $C_6H_{26}N_4S_2O_9CoNa = Na[Co(SO_3)_2tn_2]\cdot 3H_2O$: C, 16.22; H, 5.90; N, 12.61%.

Chlorosulfitobis(trimethylenediamine)cobalt(III) Monohydrate. $Na[Co(SO_3)_2tn_2]\cdot 3H_2O$ was kneaded with concentrated hydrochloric acid. Sulfur dioxide gas was evolved and the color changed to pink. The solid mass was washed with methanol, dissolved in 6 N hydrochloric acid, and recrystallized by adding methanol to this solution.

Found: C, 21.34; H, 6.72; N, 16.34%. Calcd for $C_6H_{22}N_4SO_4ClCo = [CoCl(SO_3)tn_2]\cdot H_2O$: C, 21.15; H, 6.51; N, 16.44%.

***trans* - Cyanosulfitobis(trimethylenediamine) - cobalt(III) Monohydrate.** To a 10% aqueous solution of $[CoCl(SO_3)tn_2]\cdot H_2O$ was added a concentrated solution of equimolar potassium cyanide. Yellow brown precipitate was produced but dissolved again upon prolonged stirring. To this solution five or six times the volume of ethanol was added and kept at 0°C. Yellow brown needles separated were recrystallized from water by adding ethanol. This method of preparation is analogous to that for the corresponding ethylenediamine complex.[4]

Found: C, 25.23; H, 6.79; N, 20.99%. Calcd for $C_7H_{22}N_5SO_4Co = [CoCN(SO_3)tn_2]\cdot H_2O$: C, 25.38; H, 6.69; N, 21.14%.

***cis* - Dicyanobis(trimethylenediamine)cobalt(III) Thiosulfate.** Yellow needles were obtained according to the method of Ohkawa *et al.*[5]

Found: C, 30.45; H, 6.49; N, 26.39%. Calcd for $C_{16}H_{40}N_{12}S_2O_3Co_2 = [Co(CN)_2tn_2]_2S_2O_3$: C, 30.47; H, 6.39; N, 26.66%.

***cis*-Chloroaquobis(trimethylenediamine)cobalt-(III) Chloride.** Two grams of carbonatobis(trimethylenediamine)cobalt(III) chloride monohydrate, which had been synthesized according to Werner's method,[6] was wetted with several drops of water and cooled with ice and salt. To this mass was added cold concentrated hydrochloric acid drop by drop until the evolution of carbon dioxide ceased. The purple solution was cooled with ice and salt and cold acetone was added to separate pink power. The product was filtered off, washed with cold acetone and dried over phosphorus pentaoxide *in vacuo*.

Found: C, 21.73; H, 6.82; N, 16.53; Cl, 31.60; H_2O (by the Karl Fischer method), 5.23%. Calcd for $C_6H_{22}N_4OCl_3Co = [CoCl(H_2O)tn_2]Cl_2$: C, 21.30; H, 6.69; N, 16.56; Cl, 32.09; H_2O, 5.44%.

The Optical Resolution of *cis*-$[Co(NCS)_2tn_2]SCN$. The sample was dissolved in a minimum quantity of water, to which large excess of potassium iodide was added and cooled with ice to precipitate *cis*-$[Co(NCS)_2tn_2]I$. Two grams of this iodide was mixed with 0.74 g (equimolar) of silver acetate in the presence of a small amount of water. A small quantity of cold water was added and silver iodide was filtered off. To the filtrate was added 0.74 g (half molar) of potassium antimony-(III)(+)-tartrate and the solution was kept standing overnight in an ice bath. Separated $(-)_D$-*cis*-$[Co(NCS)_2tn_2][Sb(+)\text{-tart}]$ was dissolved again in a minimum volume of water. A large excess of potassium iodide was added and the solution was cooled in an ice bath to precipitate $(-)_D$-*cis*-$[Co(NCS)_2tn_2]I$. The optical-active compound was treated with silver acetate again. After silver iodide was filtered off, excess potassium thiocyanate was added to the filtrate to precipitate $(-)_D$-*cis*-$[Co(NCS)_2tn_2]SCN$.

Spectral Measurements. Electronic absorption spectra were measured by means of a Hitachi spectrophotometer model EPS-2. Infrared absorption spectra in the region from 4000 through 650 cm^{-1} were measured with a Hitachi infrared spectrophotometer EPI-2, and those in 700—200 cm^{-1} with a Hitachi grating infrared spectrophotometer EPI-L. The optical rotatory dispersion curve was determined by means of a Yanagimoto spectropolarimeter model ORD-185 and the circular dichroism curve with a Roussel-Jouan dichrograph.

Results and Discussion

Hughes and McWhinnie[7] compared the infrared spectra of various *cis*- and *trans*-diacidobis-(ethylenediamine)cobalt(III) complexes in the lower frequency region and reported that the Co–N (en) stretching peaks in the 600—500 cm^{-1} region

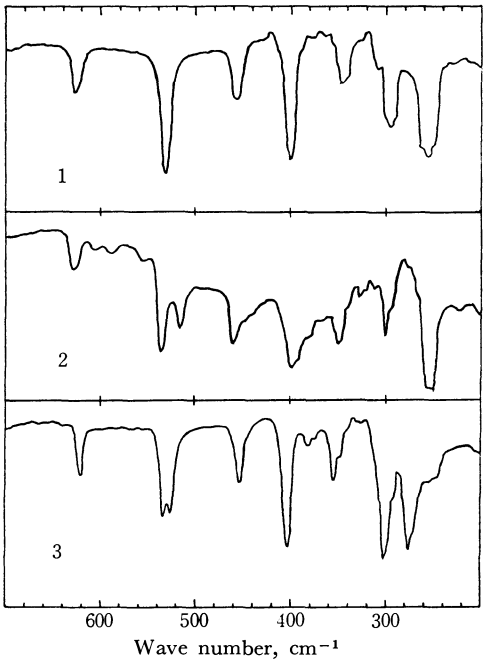

Fig. 1. Infrared spectra in the 700—200 cm^{-1} region.
(1) *trans*-$[Co(NO_2)_2tn_2]NO_2$
(2) *cis*-$[CoNO_2(ONO)tn_2]NO_2$
(3) *cis*-$[Co(NO_2)_2tn_2]NO_2$

4) S. C. Chan and M. L. Tobe, *J. Chem. Soc.*, **1963**, 966.
5) K. Ohkawa, J. Fujita and Y. Shimura, This Bulletin, **38**, 66 (1965).
6) A. Werner, *Ann.*, **386**, 264 (1912).
7) M. N. Hughes and W. R. McWhinnie, *J. Inorg. Nucl. Chem.*, **28**, 1659 (1966).

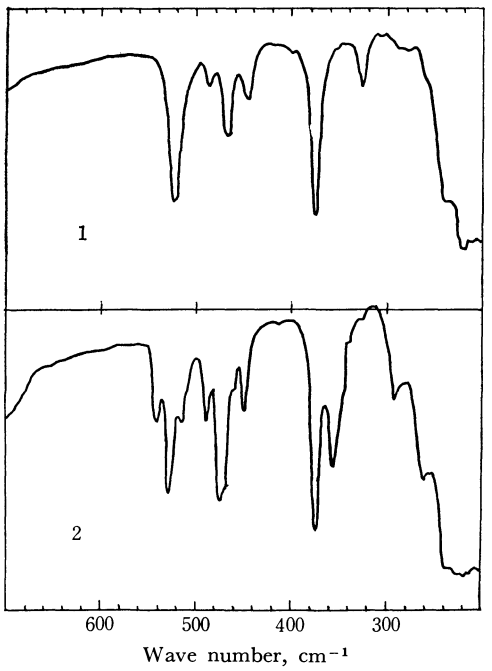

Fig. 2. Infrared spectra of $[Co(NCS)_2tn_2]SCN$ in the 700—200 cm^{-1} region.
(1) the *trans* form
(2) the *cis* form

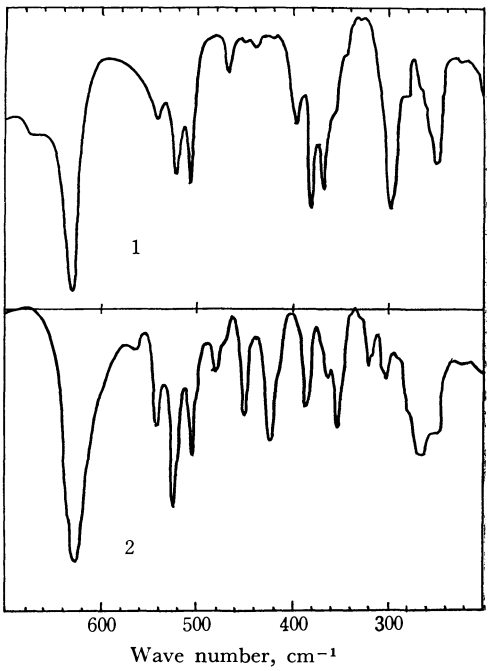

Fig. 3. Infrared spectra of $[CoCN(SO_3)tn_2]$ in the 700—200 cm^{-1} region.
(1) the *trans* form
(2) the *cis* form

were most helpful in diagnosing the geometrical configuration. In Figs. 1, 2 and 3 are presented the infrared absorption bands in the lower frequency region of the three isomeric pairs of compounds we prepared. The infrared absorption bands of these complexes are rather simple in comparison with those of diacidobis(ethylenediamine) complexes reported by Hughes and McWhinnie.[7] In the present case, too, spectra of *cis* and *trans* isomers are not identical, but the former are more complicated than the latter.

Although the reaction between *trans*-$[CoCl_2tn_2]$-Cl and excess potassium nitrite in hot methanol gave *trans*-$[Co(NO_2)_2tn_2]NO_2$, the same reaction in hot water resulted in a *cis* isomer. The *trans* form shows a single peak of Co–N(tn) stretching at 531 cm^{-1}, but the *cis* isomer two peaks at 531 and 524 cm^{-1}. In the synthetic study of this system an interesting phenomenon was observed. When a concentrated aqueous solution of excess potassium nitrite was added under stirring to an aqueous solution of *trans*-$[CoCl_2tn_2]Cl$ at room temperature or even at 0°C, yellow precipitate separated at first which was identified as potassium hexanitrocobaltate(III). However, prolonged agitation of the reaction mixture resulted in a gradual decrease of the yellow compound and increase of an orange brown precipitate which was *trans*-$[Co(NO_2)_2tn_2]NO_2$. It seems strange that two molecules of trimethylenediamine easily displaced by nitrite anions actually make a counter-attack and replace the nitrite groups. Such reactions have never been recognized in bis(ethylenediamine)cobalt(III) complexes.

It should also be noted that in reactions between hexanitrocobaltate(III) and trimethylenediamine, *trans*-$[Co(NO_2)_2tn_2]NO_2$ precipitates at room temperature, but the corresponding *cis* complex is formed at higher temperatures. If crystals of the *trans* form is redissolved in water and heated, the *cis* form is obtained. However, the reverse isomerization from *cis* to *trans* has not yet been realized.

When the heating time was relatively short, *e.g.* 1 hr, the reaction between *trans*-$[CoCl_2tn_2]Cl$ and excess potassium nitrite in water gave orange crystals. Analytical data of this compound agree with those for the dinitro complex, but its infrared spectra differ from those of *cis*- and *trans*-$[Co(NO_2)_2tn_2]NO_2$. As shown in Fig. 1 two peaks due to the Co-N(tn) stretching vibration are observed at 529 and 516 cm^{-1} suggesting the *cis* configuration of this compound. Absorption due to the wagging vibration of the nitro group[8] appears as a single peak both for *cis* and *trans* dinitro complexes. However, three peaks are observed for the new compound. A strong peak exists at 1170 cm^{-1} which is not shown by dinitro complexes and disappears on heating. The results strongly suggest that this compound is a linkage isomer, *cis*-$[CoNO_2(ONO)tn_2]NO_2$. As reported previously, *trans*-$[CoCl(ONO)tn_2]Cl$ is labile and isomerizes quickly in

methanol and so the absorption spectrum could not be observed at room temperature. The *cis*-nitronitrito compound, on the other hand, is rather inert and the isomerization to the dinitro isomer is slow even in a hot aqueous solution.

The absorption spectra of *cis*- and *trans*-[Co$(NO_2)_2tn_2]NO_2$ and *cis*-[$CoNO_2(ONO)tn_2]NO_2$ in methanol are presented in Fig. 4. It seems unlikely that the *cis*- and *trans*- dinitro complexes show practically identical spectra. The *cis-trans* isomerization equilibrium cannot possibly be attained so quickly in methanol at room temperature. The transmission spectra of solid specimen of both compounds, measured by the Nujol mull method, are also identical. The first band of the nitro-nitrito complex lies at the slightly longer wavelength side than that of the dinitro isomer (Table 1). The same trend is observed for the corresponding ethylenediamine complexes.[9]

The absorption spectra of *cis*- and *trans*-[Co$(NCS)_2tn_2]SCN$ are shown in Fig. 5. The first band of the *trans* isomer lies on the longer wavelength side than that of the *cis* isomer. This is contrary to the observation on the corresponding ethylenediamine complexes.[10] When *cis*-[Co$(NCS)_2tn_2]SCN$ was dissolved in methanol, heated for a few hours, and then concentrated by evaporation, crystals of the *trans* isomer were obtained. Reverse isomerization from *trans* to *cis* was not possible.

The infrared spectra of *cis*- and *trans*-[CoCN-

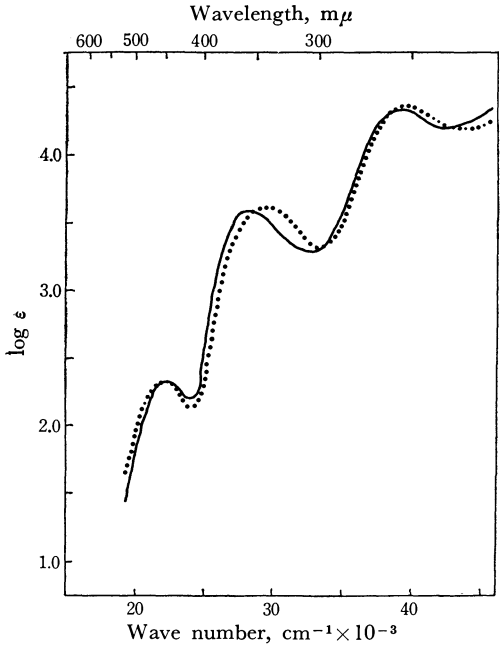

Fig. 4. Absorption spectra in methanol.
—— *trans*- and *cis*-[$Co(NO_2)_2tn_2]NO_2$
···· *cis*-[$CoNO_2(ONO)tn_2]NO_2$

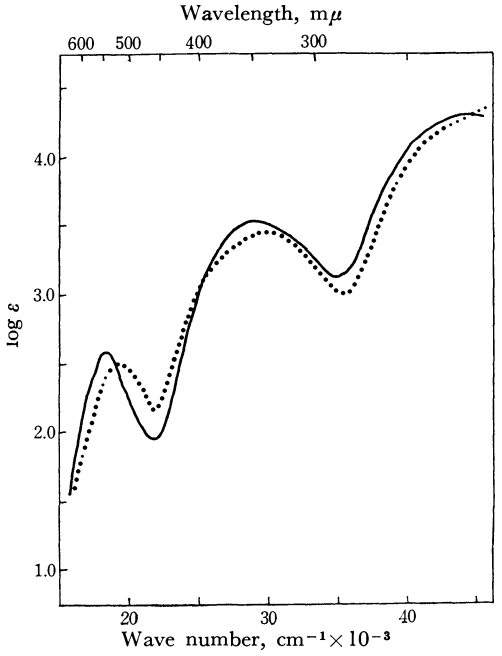

Fig. 5. Absorption spectra of [$Co(NCS)_2tn_2$] SCN in methanol.
—— the *trans* form
···· the *cis* form

TABLE 1. ABSORPTION MAXIMA OF SOME BIS(TRIMETHYLENEDIAMINE)- AND BIS(ETHYLENEDIAMINE)COBALT(III) COMPLEXES

Complex	Medium	λ_{max}, mμ(ε)		
cis-[$CoNO_2(ONO)tn_2]NO_2$	Methanol	455(214)	340(4900)	253(22000)
cis-[$Co(NO_2)_2tn_2]NO_2$	Methanol	450(220)	358(3890)	256(21200)
cis-[$Co(NO_2)_2en_2]NO_3$[10]	MeOH-H_2O	438(220)	325(5050)	240(16600)
cis-[$Co(NCS)_2tn_2]SCN$	Methanol	522(319)	340(2750)	
cis-[$Co(NCS)_2en_2]SCN$[10]	MeOH-H_2O	520(350)	335(3400)	
cis-[$CoCN(SO_3)tn_2$]	Water	433(176)	281(17000)	
cis-[$CoCN(SO_3)en_2$][2]	4% NH_3 *aq*	417(162)		
trans-[$CoCN(SO_3)tn_2$]	Water	433(148)	280(17500)	222(13400)
trans-[$CoCN(SO_3)en_2$][2]	Water	416(135)		

8) I. Nakagawa and T. Shimanouchi, *Spectrochim. Acta*, **23A**, 2099 (1967).
9) R. G. Pearson, P. M. Henry, J. G. Bergmann and F. Basolo, *J. Amer. Chem. Soc.*, **76**, 5920 (1954).
10) F. Basolo, *ibid.*, **72**, 4393 (1950).

$(SO_3)tn_2]$ in the region of 600—500 cm^{-1} are complicated and less diagnostic than those for dinitro and diisothiocyanato complexes (Fig. 3). The *cis* isomer has four peaks in this region, while the *trans* isomer three. The electronic absorption spectra of these compounds also resemble each other as shown in Fig. 6.

The absorption maxima of the new compounds reported here are summarized in Table 1 together with those of the corresponding ethylenediamine complexes. As in a previous paper,[1] the first band of each trimethylenediamine complex lies at the longer wavelength side than that of the corresponding ethylenediamine complex, indicating that the ligand field of trimethylenediamine is weaker than that of ethylenediamine.

Efforts to prepare *cis*-dichlorobis(trimethylenediamine)cobalt(III) complex have not been successful so far. Treatment of $[CoCO_3tn_2]Cl$ with concentrated hydrochloric acid at low temperatures resulted in a pink-colored compound $[CoCl(H_2O)tn_2]Cl_2$, which is unstable and changes gradually to the green dichloro complex. The infrared absorption curve of this chloroaquo complex in the potassium bromide region is complicated as shown in Fig. 7 suggesting a possible *cis* configuration. In this connection the spectrum of *cis*-$[Co(CN)_2tn_2]_2S_2O_3$ is also included in Fig. 7. Unfortunately the corresponding *trans* isomer has not been obtained so far, and the comparison of IR curves of this isomeric pair is not possible, but the splitting of the Co–N(tn) stretching band may be reconciled with the *cis* assignment by Ohkawa, *et al.*[5]

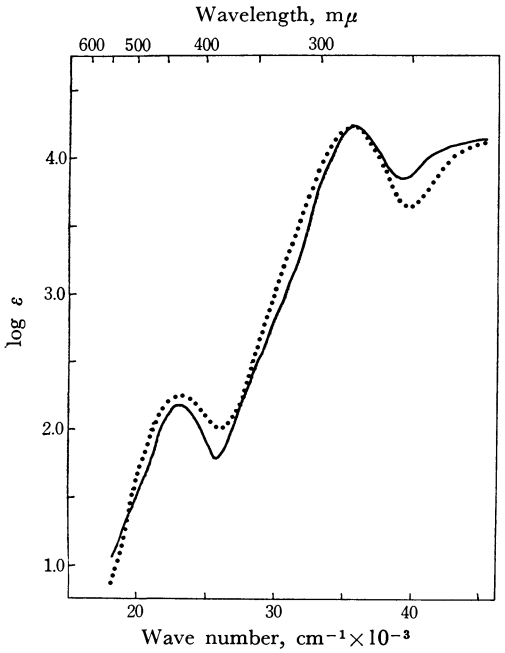

Fig. 6. Absorption spectra of $[CoCN(SO_3)tn_2]$ in water.
—— the *trans* form
···· the *cis* form

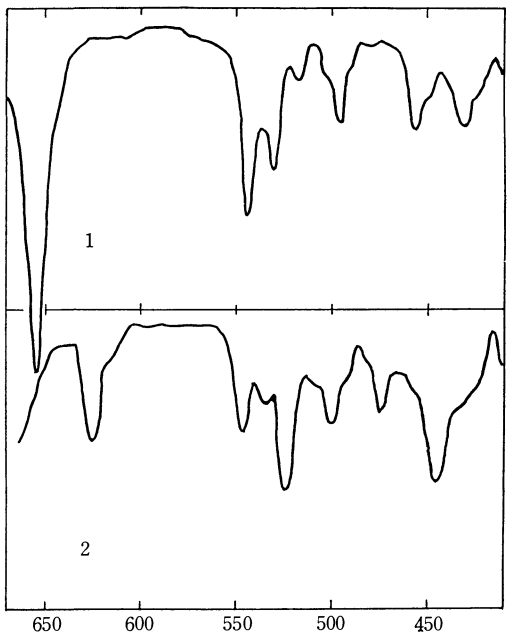

Fig. 7. Infrared spectra in the potassium bromide region.
(1) *cis*-$[Co(CN)_2tn_2]_2S_2O_3$
(2) *cis*-$[CoCl(H_2O)tn_2]Cl_2$

Hughes and McWinnie[7] compared several methods of diagnosing the geometrical configurations of diacidobis(ethylenediamine)cobalt(III) complexes, and showed that Baldwin's method[11] utilizing the CH_2 rocking peaks was the best among them. In Table 2 are summarized the CH_2 rocking peaks shown by bis(trimethylenediamine)-cobalt(III) complexes discussed in this paper. Baldwin's criterion is successful in these examples except for one case, *cis* compounds showing two

Table 2. Infrared absorption bands due to the CH_2 rocking vibration of several *cis*- and *trans*-diacidobis(trimethylenediamine) cobalt(III) complexes

Compound	cm^{-1}	
cis-$[CoNO_2(ONO)tn_2]NO_2$	895	887
cis-$[Co(NO_2)_2tn_2]NO_2$	902	894
trans-$[Co(NO_2)tn_2]NO_2$	899	
cis-$[Co(NCS)_2tn_2]SCN$	895	890
trans-$[Co(NCS)_2tn_2]SCN$	890	
cis-$[CoCN(SO_3)tn_2]$	905	890
trans-$[CoCN(SO_3)tn_2]$	900	
$[CoCO_3tn_2]Cl\cdot H_2O$	895	888
cis-$[CoCl(H_2O)tn_2]Cl_2$	888	
cis-$[Co(CN)_2tn_2]_2S_2O_3$	893	887

11) M. E. Baldwin, *J. Chem. Soc.*, **1960**, 4369.

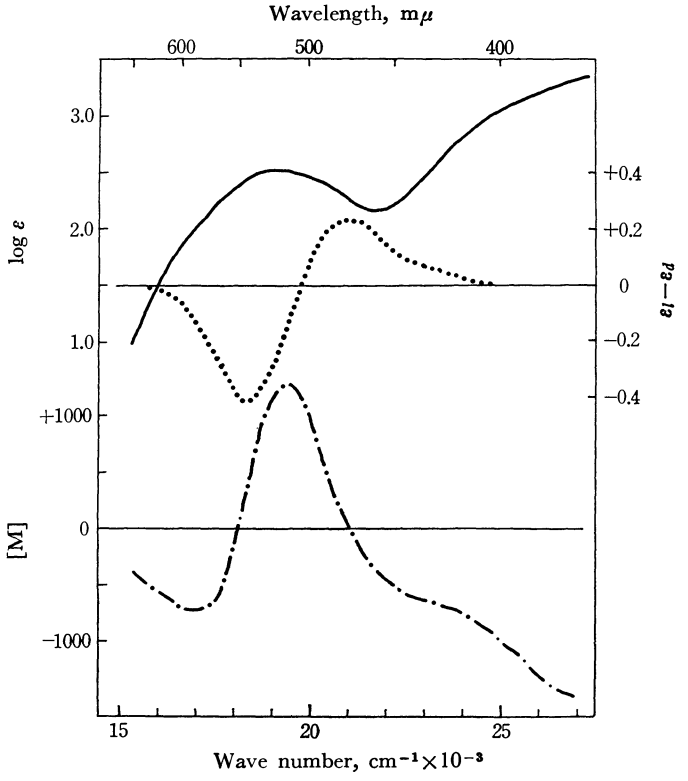

Fig. 8. Absorption(——), circular dichroism(····), and optical rotatory dispersion(·—·) curves of $(-)_D$-*cis*-$[Co(NCS)_2tn_2]SCN$ in water.

peaks while the *trans* isomers only one. The compound $[CoCl(H_2O)tn_2]Cl_2$, which was tentatively concluded to have the *cis* configuration, shows a single peak at 888 cm^{-1} violating Baldwin's empirical rule.

To establish the *cis* configuration unequivocally we tried to resolve the *cis* compounds into their optical isomers, but have succeeded only in the case of *cis*-$[Co(NCS)_2tn_2]SCN$. In Fig. 8 are shown the rotatory dispersion and circular dichroism curves of the optically active isomer. The molar rotations were calculated as follows:

$$[M]^{23}_{546} = +275°;\ [M]^{23}_{589} = -725°$$

The first example of the optically active cobalt(III) trimethylenediamine complex is $(-)_D$-$Cotn_3^{3+}$ prepared by Woldby,[12] which was shown by Saito and his coworkers[13] to have the same absolute configuration as the $(+)_D$-$Coen_3^{3+}$ ion,[14] namely Λ[15] or $P(C_2)$.[16] The crystal structure of the diastereoisomer $(-)_D$-$[Co(NCS)_2tn_2][Sb(+)$-tart]$\cdot 2H_2O$ has recently been studied and the absolute configuration of this dissymmetric complex cation was revealed to be Λ or $P(C_2)$, too.[17]

In recent years the circular dichroism spectra of a number of dissymmetric trigonal complexes have been measured and discussed in relation to their absolute configurations.[16] It was suggested[16,18] that trigonal d^3 and d^6 complexes have the same absolute configuration as $(+)_D$-$Coen_3^{3+}$ if the spin-allowed transition of lowest energy has an E_a component with a positive rotatory power. Beddoe and Mason[19] showed that the E_a component in $(-)_D$-$Cotn_3^{3+}$ has a positive rotational strength at longer wavelength, indicating that the spectroscopic criterion for the absolute configuration of trigonal metal complexes containing five-membered chelate rings may be successfully applicable to the trisdiamine complexes containing six-membered chelate rings. Consistent CD band assignments were also given by Gollogly and Hawkins to the enantiomeric $(+)_D$-$Cotn_3^{3+}$ ion.[20]

12) F. Woldby, *Record of Chemical Progress*, **24**, 197 (1963).
13) Y. Saito, T. Nomura and F. Marumo, This Bulletin, **41**, 530 (1968).
14) Y. Saito, K. Nakatsu, M. Shiro and H. Kuroya, *Acta Crystallogr.*, **8**, 729 (1955); This Bulletin, **30**, 158 (1957).
15) *IUPAC Information Bulletin*, No. 33, 68 (1968).
16) A. J. McCaffery, S. F. Mason and R. E. Ballard, *J. Chem. Soc.*, **1965**, 2883.
17) K. Matsumoto, M. Yonezawa, H. Kuroya, H. Kawaguchi and S. Kawaguchi, This Bulletin, **43**, 1269 (1970).
18) R. E. Ballard, A. J. McCaffery and S. F. Mason, *Proc. Chem. Soc.*, **1962**, 331.
19) P. G. Beddoe and S. F. Mason, *Inorg. Nucl. Chem. Lett.*, **4**, 433 (1968).
20) J. R. Gollogly and C. J. Hawkins, *Chem. Commun.*, **1968**, 689.

The relationship of absolute configuration to the optical activity of dissymmetric trigonal complexes have been extended to the *cis*-series of the bisethylenediamine complexes of cobalt(III). It was concluded that for the *cis*-complexes with the $P(C_2)$ configuration the major of the two CD bands mainly due to the E_a component of the parent trigonal complex has a positive sign and is displaced less than the minor band from the reference frequency of the $Coen_3^{3+}$ absorption.[21] The absolute configuration of $(+)_D$-$Co(CN)_2en_2^+$ was determined by Matsumoto *et al.*[22] to be Λ or P-(C_2) in accordance with this assignment by McCaffery *et al.*[23]

As shown in Fig. 8 $(-)_D$-$Co(NCS)_2tn_2^+$ gives two CD bands in the region of the long wavelength absorption band. The absolute rotational strengths of the bisdiamine complexes are usually smaller than those of the parent trisdiamine complexes owing to the reduced chelation,[24] but in the present case the CD bands of $(-)_D$-$Co(NCS)_2tn_2^+$ are more than twice as intense as those of $(-)_D$-$Cotn_3^{3+}$ (Fig. 9). If the above spectroscopic criterion concerning the absolute configurations of the bisethylenediaminecobalt(III) complexes can be extended to the bistrimethylenediamine complexes, the negative and the positive CD bands in Fig. 9 must be assigned to the A_2 and the E_a transitions in $(-)_D$-$Cotn_3^{3+}$, respectively. The positive high-energy component (E_a parentage) is displaced only by 850 cm^{-1} from the reference frequency of the $Cotn_3^{3+}$ absorption, but the negative low-energy component (A_2 parentage) is much farther displaced (1850 cm^{-1}). Thus the frequency displacement criterion holds in this case, but the relative band-area criterion fails since the negative component is larger than the positive one.

Another method of identifying the CD bands due to E_a and A_2 transition is based upon the observation that, in the presence of polarizable oxyanions such as phosphate, the areas of E_a and A_2 bands in the trigonal complexes are diminished and enhanced, respectively.[25,26] Of the various oxyanions investigated, selenite was found to be particularly convenient, producing large changes in the band area.[27] This ion-pairing effect was

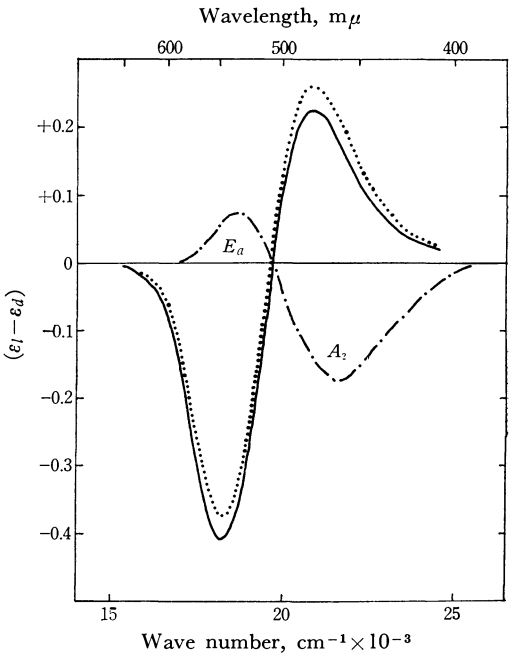

Fig. 9. Circular dichroism curves of $(-)_D$-*cis*-$[Co(NCS)_2tn_2]ClO_4$ in water(——) and in 0.05 M aqueous sodium selenite(· · · ·), and of $(-)_D$-$[Cotn_3](ClO_4)_3$ in water(— · —).

successfully applied in the case of $Cotn_3^{3+}$ ion,[19,20] but now gives inconsistent results to $(-)_D$-$Co(NCS)_2tn_2^+$. As shown in Fig. 9 the effect of selenite addition upon the CD band areas is small but obvious. The negative low-energy component is diminished and the positive high-energy component enhanced indicating that they are of E_a and A_2 trigonal parentage, respectively. Thus the CD bands assignment based on the outer-sphere coordination effect contradicts with the above assignment based on the empirical relationship between spectroscopic and configurational assignments. It is not certain at present which of them fails in the case of the bistrimethylenediamine complex, but the ion-pairing method might be less reliable. Further investigations of other dissymmetric trimethylenediamine complexes are desired.

The authors are grateful to Dr. Jinsai Hidaka of Osaka University for his help in the measurements of ORD and CD spectra and to Dr. Junnosuke Fujita of Tohoku University for his valuable discussion. Thanks are also due to Mr. Jun-ichi Gohda and Miss Takeko Inoue for organic elemental analyses and IR measurements.

21) A. J. McCaffery, S. F. Mason and B. J. Norman, *J. Chem. Soc.*, **1965**, 5094.
22) K. Matsumoto, Y. Kushi, S. Ooi and H. Kuroya, This Bulletin, **40**, 2988 (1967).
23) A. J. McCaffery, S. F. Mason and B. J. Norman, *Chem. Commun.*, **1965**, 132.
24) A. J. McCaffery and S. F. Mason, *Proc. Chem. Soc.*, **1962**, 388.
25) S. F. Mason and B. J. Norman, *ibid.*, **1964**, 339.
26) H. L. Smith and B. E. Douglas, *J. Amer. Chem. Soc.*, **86**, 3885 (1964).
27) S. F. Mason and B. J. Norman, *Chem. Commun.*, **1965**, 73.

BULLETIN OF THE CHEMICAL SOCIETY OF JAPAN VOL. 43 2110—2114 (1970)

Application of the AC Polarographic Method to the Microdetermination of the Sulfide Ion by the Methylene Blue Procedure*1

Kiyoshi HASEBE and Tomihito KAMBARA

Department of Chemistry, Faculty of Science, Hokkaido University, Sapporo

(Received February 4, 1970)

A new AC polarographic method utilizing the methylene-blue procedure was used for the determination of the sulfide ion. By means of dimethyl-*p*-phenylenediamine sulfate and iron(III) alum, the sulfide ion is converted quantitatively into methylene blue in the sulfuric-acid milieu. The methylene blue thus formed shows a prominent and reproducible AC peak, which can be suitably utilized for the indirect microdetermination of the sulfide ion. Halide ions interfere with the determination, however.

The methylene blue method is very useful for the microdetermination of sulfur. The method[1-8] consists of the photometry of the methylene blue formed by the reaction of the sulfide ion with dimethyl-*p*-phenylenediamine in the presence of the ferric ion.

The present authors tried to apply the AC polarographic method to the microdetermination of the sulfide ion by methylene-blue procedure. Although this method is found to be a little inferior to spectrophotometry as to sensitivity, the AC polarographic peaks are very prominent and reproducible and are sufficient for use in the determination of microamounts of the sulfide ion.

Experimental

Apparatus. The polarograph used was a Yanagimoto pen recording polarograph, model PA-102. The capillary characteristics at an 80-cm mercury column height were: $m=1.10_6$ mg/sec in pure water and $t=$ 4.90 sec in the polarographic solution at 0.00 V *vs.* mercury pool. The polarographic cell was thermostated to 25±0.1°C.

All the absorbance measurements were carried out by the aid of a Shimadzu photoelectric spectrophotometer, model QV-50, using 1-cm glass cells. The measurement of pH was made with a Hitachi-Horiba, model D-5, glass electrode pH meter.

Reagents. The 10^{-2} M dimethyl-*p*-phenylenediamine solutions were prepared freshly for each use by dissolving its salts (Wako Chemicals Co.), namely, hydrochloride (special grade) and its sulfate (first grade), in a 0.1 M sulfuric acid milieu. Methylene blue (for microscopy, E. Merck AG), and all the other reagents used were of analytical-reagent quality. The sodium sulfide solution was prepared afresh each day and was stored in a stoppered brown bottle protected from light. The 10^{-2} M iron(II) solution was prepared by dissolving 3.921 g of Mohr's salt in 1 *l* of 0.1 M sulfuric acid. The 10^{-2} M iron(III) solution was prepared by dissolving iron alum in 1 *l* of 0.1 M sulfuric acid.

Results

Effect of Supporting Electrolyte. As is well known methylene blue gives an adsorption prewave in DC polarography and the corresponding AC peak is remarkably prominent, suggesting a very high analytical sensitivity. The methylene-blue method, which utilizes the formation of methylene blue by the reaction of the sulfide ion with dimethyl-*p*-phenylenediamine in the presence of the ferric ion, has been carried out mainly in hydrochloric acid milieus.[1,2,4-6] The methylene-blue reaction proceeds as follows:

$$2NH_2C_6H_4N(CH_3)_2 + 6Fe^{3+} + H_2S \longrightarrow$$
$$\text{Methylene blue}^+ + 6Fe^{2+} + NH_4^+ + 4H^+$$

First of all, the effects of the various supporting electrolytes were studied. It was found that hydrochloric acid is not suitable as a supporting electrolyte for the determination of methylene blue, because the anodic peak of chloride ion partially overlaps that of methylene blue. In a 0.1 M sulfuric acid milieu and also in a solution which is 0.1 M in sulfuric acid and 0.1 M in sodium acetate, well-defined AC peak of methylene blue was ob-

*1 Part of the dissertation presented by Kiyoshi Hasebe to Hokkaido University, 1969.

1) J. K. Fogo and M. Popowsky, *Anal. Chem.*, **21**, 732 (1949).
2) S. Musha, *Nippon Kagaku Zasshi*, **71**, 572 (1950).
3) C. M. Johnson and H. Nishita, *Anal. Chem.*, **24**, 736 (1952).
4) Y. Oka and S. Matsuo, *Nippon Kagaku Zasshi*, **74**, 618 (1953).
5) H. Kitagawa and N. Shibata, *Bunseki Kagaku*, **7**, 181 (1958).
6) A. Kaya and Y. Kakita, *Nippon Kinzoku Gakkaishi*, **27**, 28 (1963).
7) Z. Marzenko and L. Chluj-Lenarczyk, *Chem. Anal.* (Warsaw), **10**, 729 (1965).
8) S. D. Yordanov and C. P. Ivanov, *C. R. Acad. Bulg. Sci.*, **21**, 451 (1968).

served.

Effect of Ferric and Ferrous Ions. For the conversion of the sulfide ion into methylene blue, the ferric ion is employed as the oxidizing agent. Hence, the effect of the excess ferric ion and the ferrous ion produced on the methylene-blue polarogram should be investigated. Figures 1 and 2 illustrate the DC and AC polarograms with the supporting electrolyte, that is, 0.1 M sulfuric acid and also in sodium acetate.

Curve (a) in Fig. 1 represents the DC polarogram of the blank solution, curve (b) was recorded after the addition of iron(III) in 5×10^{-4} M to the test solution, and curve (c) was recorded with a test solution containing the ferric ion and methylene blue in 5×10^{-5} M. When 0.1 M sulfuric acid alone is employed as the supporting electrolyte, the reduction wave of methylene blue in the DC polarogram appears *ca.* 0.3 V from the ferric ion wave, while in the AC polarography methylene blue shows a prominent peak which is not effected by the ferric ion. Therefore, the supporting electrolyte of 0.1 M sulfuric acid was employed, thereafter.

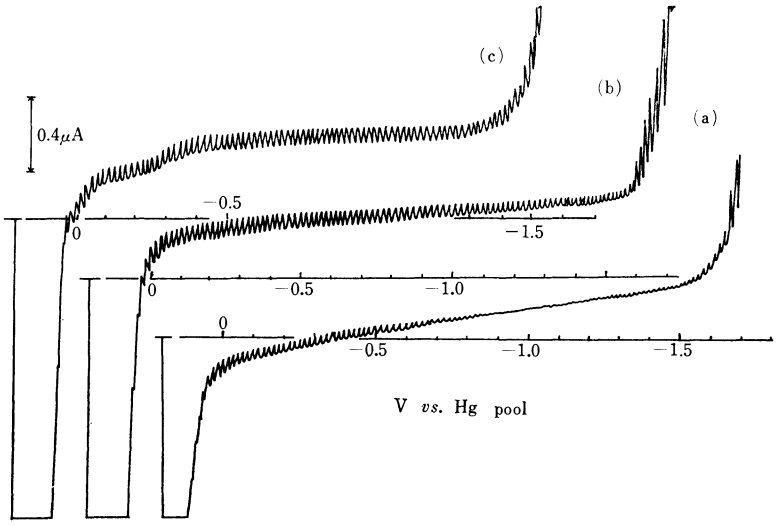

Fig. 1. Typical DC polarograms of methylene blue (Merck AG) and ferric ion.
Supporting electrolyte: (a) 0.1 M H_2SO_4+0.1 M NaOAc, (b) (a)+5×10^{-4} M Fe^{3+}, (c) (b)+5×10^{-5} M methylene blue. Parallel capacitance: 50 μF

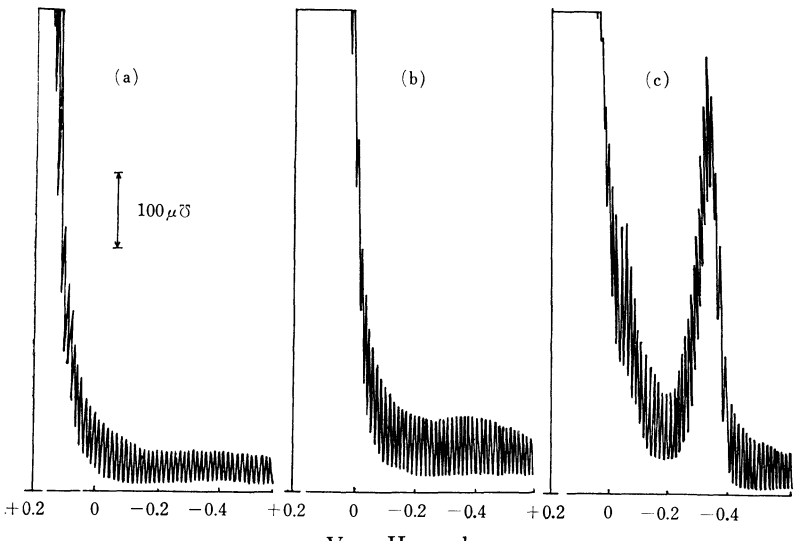

Fig. 2. The AC polarograms of methylene blue and ferric ion corresponding to Fig. 1.
Parallel capacitance: 0.05 μF.

Effect of Anions on the AC Peak of Methylene Blue. According to many authors,[2,6] the hydrochloride of dimethyl-*p*-phenylenediamine has widely been used for the color reaction forming methylene blue. When dimethyl-*p*-phenylenediamine was used, the anodic wave of the chloride ion interferes with the methylene-blue determination by the polarographic method. As the concentration of the chloride ion increases, the interference becomes especially remarkable.

Figure 3 compares polarograms of methylene blue as synthesized by dimethyl-*p*-phenylenediamine hydrochloride (a) and its sulfate (b). The prominent chloride peak appears near to the methylene blue wave. The use of sulfate is, needless to say, more advantageous than that of hydrochloride. As is well known, iodide reduces methylene blue to the leuco form, and chloride and, more strongly, the bromide ion suppress the methylene-blue peak height, as has been reported in our previous study.[9]

Effect of the Sulfuric Acid Concentration. The color development due to the formation of methylene blue from the sulfide ion and dimethyl-*p*-phenylenediamine in the presence of the ferric ion should be performed in a sulfuric acid milieu, because the chloride ion interferes with the polarographic determination of methylene blue.

The relationship between the concentration of sulfuric acid and absorbance of methylene blue, or the AC polarographic peak, was investigated. According to Rabinowitch and Epstein,[10] methylene blue exists in monomer and dimer forms in solution. On the other hand, Oka and Matsuo,[4] who discussed in detail the behavior of methylene blue in a hydrochloric acid milieu, reported the association of methylene blue with hydrochloric acid as indicated by the new absorption band at 735 mμ. Figure 4 shows the variation in the absorption spectrum of methylene blue with the sulfuric acid concentration. The new maximum in absorbance curves at 740 mμ *vs.* the reagent blank clearly shows another form of methylene blue in a sulfuric acid milieu. This maximum can be interpreted as resulting from the association of methylene blue with sulfuric acid. Thus, it is important to select a suitable acid concentration.

Figure 5 shows the relationship between the AC polarographic peak height and the sulfuric acid concentration. It can readily be seen that the optimum polarographic concentration of sulfuric acid is at 0.1—0.2 M.

Effect of the Ferric Ion Concentration and Deaeration on the AC Polarographic Peak. By applying the constant initial concentration of the sulfide ion of 4×10^{-4} M in the reaction mix-

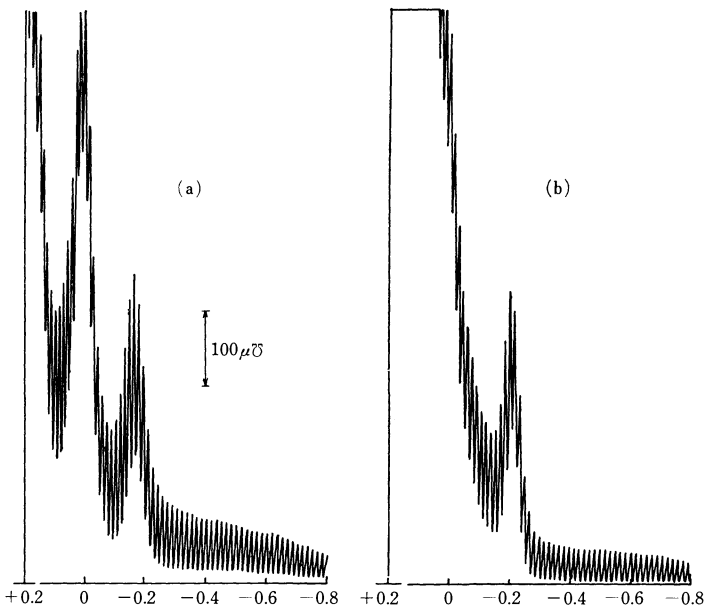

Fig. 3. The AC polarograms of methylene blue synthesized from sulfide ion by dimethyl-*p*-phenylenediamine hydrochloride (a) and its sulfate (b).
The final concentration of methylene blue: 5×10^{-5} M.
Parallel capacitance: 0.05 μF.

9) K. Hasebe and T. Kambara, Preprint of the Discussion Meeting of the Polarographic Society of Japan, Hiroshima, October, 1968; *Rev. Polarog.* (Japan), manuscript in preparation.

10) E. Rabinowitch and L. F. Epstein, *J. Amer. Chem. Soc.*, **63**, 69 (1941).

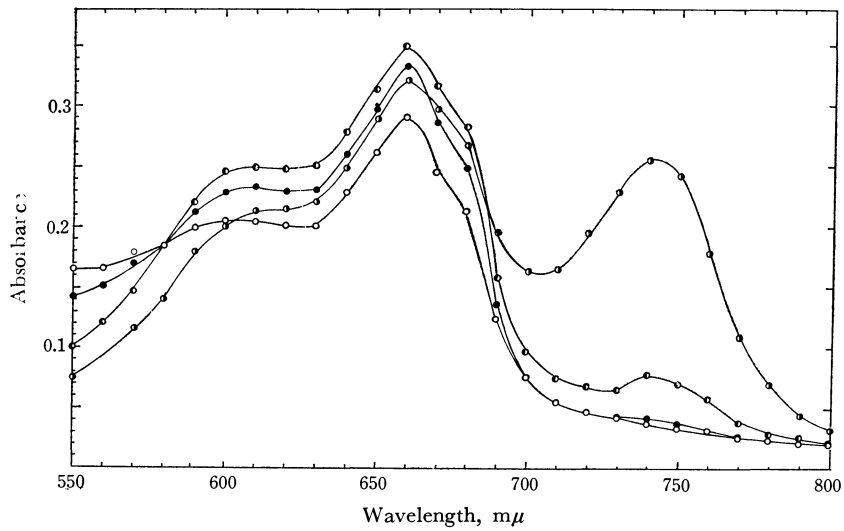

Fig. 4. Absorption spectra of synthesized methylene blue in various sulfuric acid concentrations (*vs.* reagent blank).

The concentrations of reactants in the reaction mixture is: 6×10^{-5} M S^{2-}, 5×10^{-3} M diamine, 5×10^{-4} M Fe^{3+}.

—○— 0.01 M H_2SO_4, —●— 0.05 M H_2SO_4, —◐— 0.2 M H_2SO_4, —◑— 1 M H_2SO_4.

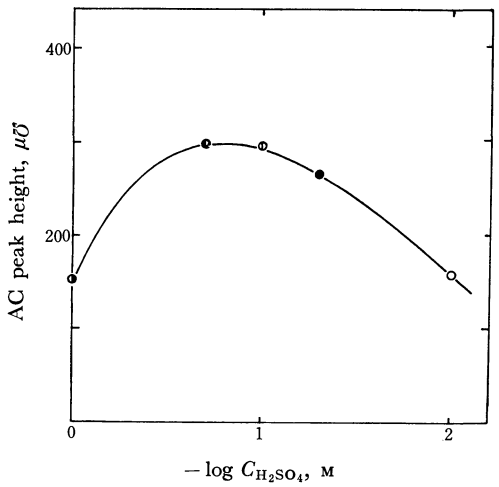

Fig. 5. Effect of the sulfuric acid concentration on the AC peak height of synthesized methylene blue corresponding to Fig. 4.

—◑— 0.1 M H_2SO_4.

Table 1. Analysis of means

Relationship between the AC peak height of methylene blue and ferric ion concn. with and without deaeration.

Ferric ion concn., M	AC peak height, μσ	
	With deaeration	Without deaeration
1×10^{-3}	132±15.6	133±15.6
5×10^{-4}	213±20.8	205±26.0
	(208, 224, 208)*	(204, 196, 216)*
1×10^{-4}	113± 5.20	111±10.4

Confidence limits 95%; * Figures in parentheses represent individual values. Parallel capacitance 0.05 μF.

The initial concentration in the reaction mixture: 4×10^{-5} M S^{2-}, 5×10^{-3} M dimethyl-*p*-phenylenediamine.

F-test shows that there is no significant difference between two variances: $F(2, 2, 0.025)=39.0>F_0=1.18$, *t*-test shows that there is no significant difference between two means: $t(4, 0.05)=2.77>t_0=1.17$.

ture, the effect of the ferric-ion concentration on the synthesis of methylene blue was studied.

Table 1 shows the relationship between the AC polarographic peak heights of methylene blue and the initial concentration of the ferric ion without deaeration. The optimum concentration of the ferric ion was found to be 5×10^{-4} M in the reaction mixture. With the ferric ion concentration of 5×10^{-4} M, the two means of obtaining the AC peak heights, with and without dissolved oxygen, were analyzed statistically. Consequently, it can be concluded that there is no significant difference between the AC peak heights obtained with and without deaeration.

Effect of the Dimethyl-*p*-phenylenediamine Concentration. The dimethyl-*p*-phenylenediamine in the electrolysis solution showed no AC peak. The optimum concentration of dimethyl-*p*-phenylenediamine was determined by employing various concentrations of the diamine from 1×10^{-4} to 8×10^{-3} M. Figure 6 shows the change in the AC polarograms of methylene blue at various

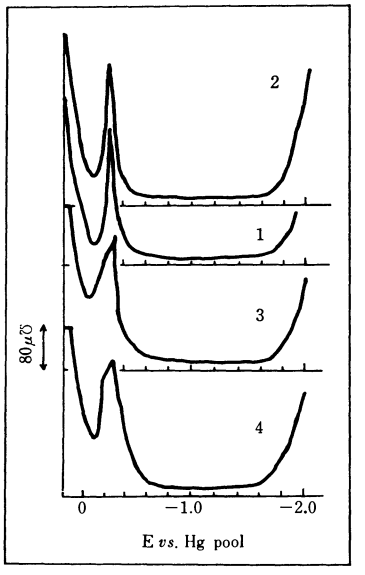

Fig. 6. Effect of dimethyl-*p*-phenylenediamine concentration on the AC polarographic peak.
Concentration in the reaction mixture is: 4×10^{-5} M S^{2-}; 5×10^{-4} M Fe^{3+}.
The diamine concentration is: (1) 5×10^{-4} M; (2) 1×10^{-3} M; (3) 5×10^{-3} M; (4) 8×10^{-3} M.

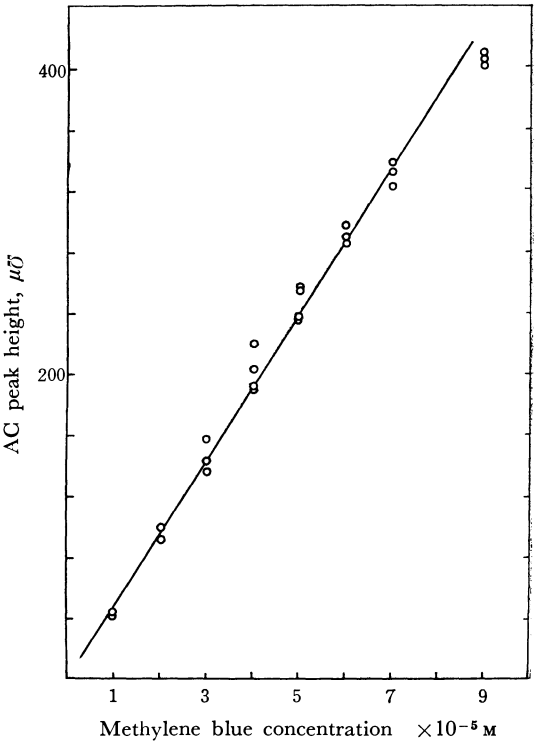

Fig. 7. Calibration curve of methylene blue.
AC peak height is plotted against the concentration of synthesized methylene blue in the electrolysis solution.

diamine concentrations.

It can be seen that 5×10^{-4} M or 1×10^{-3} M of dimethyl-*p*-phenylenediamine is most suitable for the determination of the sulfide ion. However, no peak of methylene blue appeared with 1×10^{-4} M diamine. The diamine in concentrations higher than 5×10^{-3} M interferes with the methylene blue peak, as Fig. 6 shows.

Effect of the Standing Time. At room temperature, no change in the AC polarographic peak height of methylene blue was observed over a period of 24 hr.

Established Procedure. The procedure for the sulfide determination has been established to be as follows:

To 0.5 m*l* of 2 M sulfuric acid in a 10-m*l* volumetric flask, add 0.5—1 m*l* of 10^{-2} M dimethyl-*p*-phenylenediamine in 0.1 M sulfuric acid and 0.5—0.6 m*l* of 10^{-2} M iron(III) ammonium sulfate. Add the sample solution containing the sulfide ion to the reagent mixture, shake, let stand for 15—20 min and then fill up to the mark with water. Record the AC polarogram without deaeration.

Calibration Curve. The relationship between the AC polarographic peak height of the synthesized methylene blue and the original amount of the sulfide ion was studied. The results are shown in Fig. 7.

It is possible to determine the sulfide ion, namely, methylene blue, from 1×10^{-5} M to 9×10^{-5} M in the electrolysis solution, as is shown in Fig. 7.

Discussion

It has been said that the degree of methylene-blue color development changes slightly with the sequence of reagent addition.[2,4,5] In the AC polarography, however, no significant difference could be seen by any change in reagent addition.

Breyer and Hacobian[11, 12] have reported that the sulfide ion gave a good AC polarographic peak in a supporting electrolyte of 1 M sodium hydroxide and that a linear calibration curve was obtained in the concentration range from 10^{-4} to 10^{-3} M. However, the direct determination of sulfide ion is much less sensitive than the present indirect method.

11) B. Breyer and S. Hacobian, *Aust. J. Sci. Res.*, **A4**, 610 (1951).
12) B. Breyer and H. H. Baur, "Alternating Current Polarography and Tensammetry," Interscience Publishers, New York, N. Y. (1963), p. 183.

BULLETIN OF THE CHEMICAL SOCIETY OF JAPAN VOL. 43 2115—2117 (1970)

Mössbauer Effect of ^{119}Sn in Some Organotin Compounds*1

Clive WYNTER and Louis CHANDLER

Environmental Sciences Department, Rutgers University, New Brunswick, New Jersey, U.S.A.

(Received December 1, 1969)

Mössbauer, NMR, and infrared spectroscopy have been applied to the study of a number of organometallic tin compounds containing one or more tin manganese pentacarbonyl bonds. For the $(CH_3)_{4-n}Sn[Mn(CO)_5]_n$ series ($n=0$ to 3) a linear relation between the Mössbauer isomer shift and the number of manganese pentacarbonyl ligand was consistent with the partial isomer shift theory of ^{119}Sn. A linear relation between the Mössbauer isomer shift and the methyl proton NMR chemical shift was also observed for this series. A plot of the isomer shift (δ_0) *versus* the number of p holes (h_p) for organotin manganese pentacarbonyl compounds established a relation $\delta_0 = 1.23 + 0.53\, h_p$ for sp^3 hybridized tin. From isomer shift systematics a value of ($\Delta R/R$) for ^{119}Sn was calculated to be 1.2×10^{-4}.

The preparation and properties of some mixed metal carbonyl compounds of the type $R_{4-n}Sn[Mn(CO)_5]_n$ were R=Cl, Br, C_6H_5, CH_3 and $n=0$ to 3 have been reported by Gorsich.[1] Clark and Tsai,[2] and Jetz and his co-workers[3] have studies the tin manganese bond by IR and NMR spectroscopy. Later, Graham,[4] using the Cotton-Kraihanzel (CK) approximate force constant method, separated the inductive and mesomeric effects in these types of compounds. The Mössbauer effect of a variety of these tin-transition metal bonds in organometallic compounds have been studied by Karasev[5] and his group to obtain information on the nature of the Sn–$Mn(CO)_5$ interaction, the tin-alkyl sites and the local symmetry of $Mn(CO)_5$ group in the compounds. Values of electron density at the nucleus were obtained from Ruby *et al.*[6] correlation diagram of electron density at the nucleus and the isomer shift. From this a value of ($\Delta R/R$) is obtained.

Experimental

The compounds reported in Table 1 save the monomethyl tin tris manganese pentacarbonyl, were synthesized by Gorsich's procedure.[1] A new method utilizing an inert N_2 atmosphere because of the air sensitivity of the manganese pentacarbonyl dimer was used to prepare the monomethyl tin tris manganese pentacarbonyl. An approximately 1% Na amalgam (0.5 g Na and 50 g Hg) was reacted with 2 g (5.1 mmol) $Mn_2(CO)_{10}$ dissolved in 30 m*l* of dried tetrahydrofuran. The reaction mixture was stirred for 1 hr with a magnetic stirrer and the resulting $Na^+[Mn(CO)_5]^-$ solution was decanted off from the Hg. The latter solution was mixed with 0.82 g (3.4 mmol) $MeSnCl_3$ dissolved in 4 m*l* of THF and stirred for three hours. The solid residue was filtered off and the THF solvent was removed from the mother liquor with a water aspirator. The solid residue was extracted with a 1 : 2 by volume water - THF mixture and the crude product was recovered by removing the THF from the organic layer. This yellow solid was recrystallized from *n*-hexane.

All the compounds studied gave satisfactory analytical data.

The Mössbauer spectra of these compounds at 80°K were obtained in transmission geometry with a $Ba^{119m}SnO_3$ source at room temperature. In addition proton magnetic resonance and IR spectroscopic data were taken.

TABLE 1. MÖSSBAUER PARAMETERS OF PREPARED AND RELATED TIN COMPOUNDS AT 80°K

Compounds	Isomer shift* δ_0 (mm/sec)	Quadrupole splitting ΔE (mm/sec)
$Cl_3Sn[Mn(Co)_5]$	1.63	1.62
$Br_3Sn[Mn(Co)_5]$	1.74	1.77
$\phi_3Sn[Mn(CO)_5]$	1.51	0.00
$(CH_3)_4Sn$**	1.30	0.00
$(CH_3)_3Sn[Mn(CO)_5]$	1.46	0.81
$(CH_3)_2Sn[Mn(Co)_5]_2$	1.68	0.92
$(CH_3)Sn[Mn(Co)_5]_3$	1.83	0.95

* Isomer shift relative to $BaSnO_3$ absorber
** Parameters previously reported by several works

*1 This work was supported by the U. S. Atomic Energy Commission.

1) R. D. Gorsich, *J. Amer. Chem. Soc.*, **84**, 2486 (1962).
2) H. C. Clark and J. H. Tsai, *Inorg. Chem.*, **5**, 1407 (1966).
3) W. Jetz *et al.*, *Inorg. Chem.*, **5**, 2217 (1966).
4) W. A. Graham, *ibid.*, **7**, 315 (1968).
5) A. Karasev *et al.*, *Teor. Eksp. Khim.*, **2**, 126 (1966).
6) S. L. Ruby *et al.*, *Phys. Rev.*, **159**, 239 (1967).

Table 2. Mössbauer and proton magnetic resonance parameters of $(CH_3)_{4-n}Sn[Mn(CO)_5]_n$ (n=0 to 3) compounds

Compound	Isomer shift δ_0 (mm/sec)	Quardrupole splitting ΔE (mm/sec)	Proton chemical shift (ppm)	$J(^{119}Sn-CH_3)$ cps
Me_4Sn	1.23	0.00	9.93	54.0
$Me_3Sn[Mn(CO)_5]$	1.46	0.81	9.54	48.3
$Me_2Sn[Mn(CO)_5]_2$	1.68	0.92	9.14	36.7
$MeSn[Mn(CO)_5]_3$	1.83	0.95	8.67	—

Results and Discussion

In Table 1 the Mössbauer parameters of the ^{119}Sn compounds prepared in this laboratory are reported. The quadrupole splitting in these compounds save triphenyl tin manganese pentacarbonyl are due to p holes in the "perfect" s state of sp^3 configuration arising from a disparity between the electronegativity of the R (Cl, Br, CH_3) group and the manganese pentacarbonyl radical. The question of why there is no observed quadrupole splitting in triphenyl tin manganese pentacarbonyl although there is a "p" electron defect (h_p=0.57) which is larger than in the trimethyl tin manganese pentacarbonyl (h_p=0.42) where there is a measurable quadrupole splitting is still not resolved. A reasonable guess is that the presence of the π electron clouds in the phenyl rings compensates for the field inhomogeneity at the tin nucleus and hence there is no resolvable quadrupole interaction.

Particularly interesting is the $(CH_3)_{4-n}Sn[Mn(CO)_5]_n$ series where n=0 to 3. The electrical environment around the metal atom in tetramethyl tin gives rise to the expected zero quadrupole splitting, whereas the trimethyl, the dimethyl and the monomethyl tin congeners show an almost constant quadrupole splitting of approximately

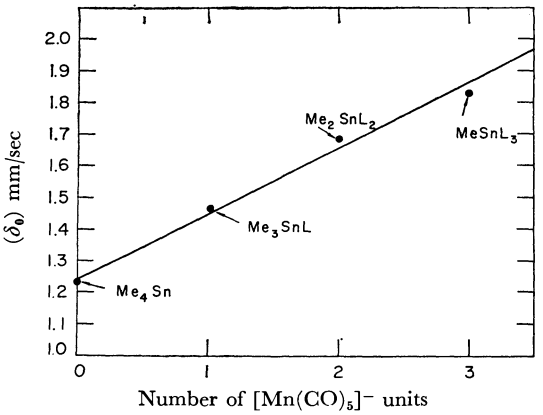

Fig. 1. A plot of the isomer shift *versus* the number of substituted $[Mn(CO)_5]$ ligand for the $(CH_3)_{4-n}Sn[Mn(CO)_5]_n$ series. (n=0 to 3)

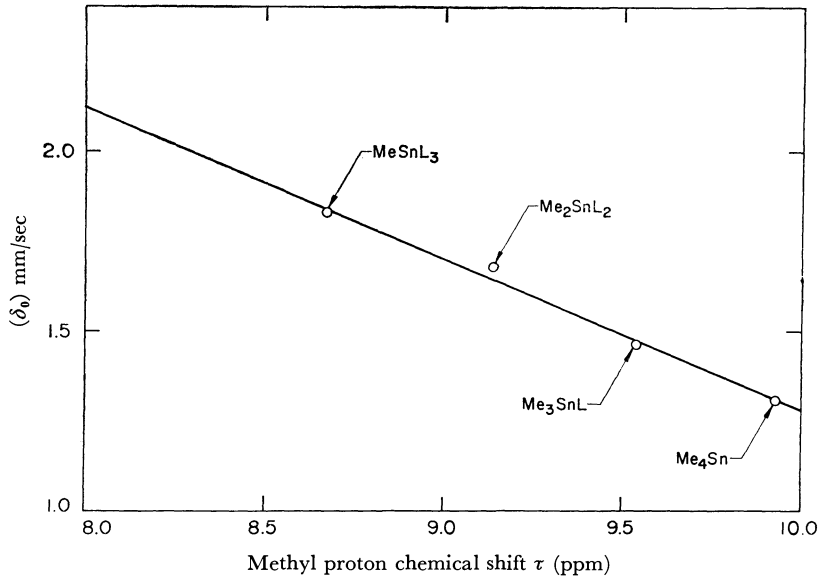

Fig. 2. Graph of the Mössbauer isomer shift *versus* the methyl proton NMR shift for the $(CH_3)_{4-n}Sn[Mn(CO)_5]_n$.

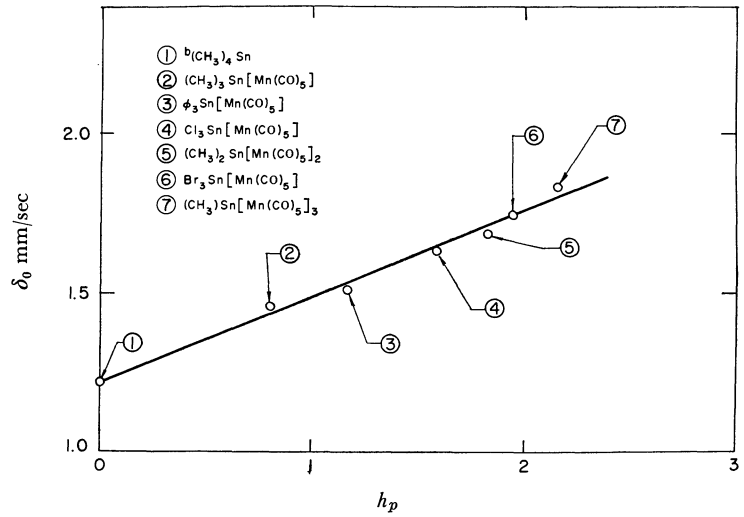

Fig. 3. A plot of the ismer shift δ_0 *versus* the number of p holes h_p for tin manganese pentacarbonyl compounds.

1 mm/sec. This lack of variance is explained by the disparity yet closeness of the group electronegativety of the $[Mn(CO)_5]$ ligand of 2.01 compared to the methyl group of 2.54.

Figure 1 shows a linear plot of the isomer shift δ_0 *versus* the number of $[Mn(CO)_5]$ ligands in the series $(CH_3)_{4-n}Sn[Mn(CO)_5]_n$, where $n=0$ to 3. This in fact lends proof to the partial isomer shift theory of tin and leads to the simple equation.

$$\delta_0(\text{relative to } BaSnO_3) = 1.23 + 0.19n \qquad (1)$$

Another interesting feature of this series is seen in Fig. 2. It establishes a linear relation between the Mössbauer isomer shift (δ_0) and the proton NMR shift τ (ppm). Holmes and Kaesz[7] have correlated the coupling constant $A_{^{119}Sn^H}$ with %5*s* character. This correlation does not work for this series and may be due to hydrogen bonding of the methyl protons in juxtaposition with oxygen of the manganese pentacarbonyl moiety. Evidence for change in local C_{4v} symmetry of the bulky manganese pentacarbonyl ligand in the monomethyl tin tris manganese pentacarbonyl derivative was furnished by the drastic change in the relative intensity of the $[2A_I+E]$ bands. It is possible that smaller changes of this sort in the other member of this series may not be detected by infrared techniques.

Spijkerman[8] has calibrated the %5*s* character and the Mössbauer chemical shift. From the measured isomer shift, %5*s* character of all compounds in this work was estimated, and electronic configurations and number of p holes h_p assuming a constant sp^3 hybridization calculated. These are shown in Table 3. Figure 3 shows a plot of the isomer shift δ_0 *versus* the number of p holes h_p leads to a linear relationship $\delta_0=1.23+0.53\ h_p$ for sp^3 hybridized tin.

Table 3. Derived parameters from the isomer shifts of ^{119}Sn compounds

Compounds	Electronic configuration	Number of p holes h_p	% 5*s* character
$Cl_3Sn[Mn(CO)_5]$	$5s^{0.745}5p^{2.22}$	0.78	34
$Br_3Sn[Mn(CO)_5]$	$5s^{0.685}5p^{2.04}$	0.96	37
$\phi_3Sn[Mn(CO)_5]$	$5s^{0.815}5p^{2.43}$	0.57	31
$(CH_3)_4Sn$	$5s^1\ 5p^3$	0.00	25
$(CH_3)_3Sn[Mn(CO)_5]$	$5s^{0.865}5p^{2.58}$	0.42	29
$(CH_3)_2Sn[Mn(CO)_5]_2$	$5s^{0.705}5p^{2.10}$	0.90	36
$(CH_3)Sn[Mn(CO)_5]_3$	$5s^{0.645}5p^{1.92}$	1.08	39

Ruby *et al.*[6] has correlated the electron density $\psi^2(0)/a_0^3$ at the nucleus and the isomer shift for ^{119}Sn. From this data values of $\psi^2(0)/a_0^3$ were obtained and a value of $\Delta R/R=1.2\times10^{-4}$ calculated. This agrees with the value obtained by their group and some previously reported values.

Further work is in progress to clear up any ambiguities in the phenyl tin manganese pentacarbonyl series.

7) R. Holmes, and H. D. Kaesz, *J. Amer. Chem. Soc.*, **83**, 3903 (1961).

8) J. Spijkerman, "Advances in Chemistry Series," No. 68, "The Mössbauer Effect and Its Application in Chemistry," 1967, p. 105.

BULLETIN OF THE CHEMICAL SOCIETY OF JAPAN VOL. 43 2118—2123 (1970)

Reactive Species in the Explosion of Silver Acetylide. II. Reaction with Olefins

Ko Taki

The Institute of Physical and Chemical Research, Yamato-machi, Saitama

(Received June 12, 1969)

The reaction of the reactive species in the explosion of silver acetylide with olefins was investigated. The main produst is acetylene. On the basis of the results of experiments on the effects of the pressure and the distance from the explosion position, the C_3 and C_4 products in the reaction with ethylene may be considered to be produced from a common precursor. The C_4 products consist mainly of vinylacetylene and diacetylene. The formation processes of the products may consist of the decomposition of the adducts of the C_2 species. The reaction with C_4 olefins gives benzene, cyclopentadiene, and other products.

In the previous paper[1] the reaction of the reactive species in the explosion of silver acetylide with saturated hydrocarbons has been reported. From the distribution[1] of the products and from the variation[1] in the ratio of C_2H_4 to C_2H_2 in various phases, it was assumed[1] that the diatomic carbon (C_2) was one of the reactive species in the explosion.

In this paper the reaction of the reactive species in the explosion of silver acetylide with olefins and their reaction processes were investigated. This reaction will be compared with the reaction of a carbon atom produced by the nuclear recoil reaction[2,3] and with the reaction of a carbon vapor produced by the carbon arc[4,5] in this paper.

Experimental

The experimental procedure and the explosion technique were essentially the same as those reported in the previous paper. The olefins (Takachiho Co., Ltd.) were used without further purification. The analyses were performed by gas chromatography using silica gel, squalane, and polyethylene glycol columns. The quantitative analyses were carried out by the internal standard system, using neopentane and chlorobenzene as standards.

Results and Discussion

In the reaction with olefins, the main product is acetylene, as has previously been described in connection with the reaction with saturated hydrocarbons.[1] This is similar to the reaction of the free carbon atom in the recoil reaction.[2] Therefore, the formation of C_3 compounds in the gas-phase reaction with the C_2 substrate may suggest that one of the reactive species is monatomic carbon. However, the yield of C_3 compounds is not high as compared with that of C_4 compounds,*1 as is shown in Table 1. Moreover, with the change in substrate from ethane to acetylene, the yields of C_3 compounds decrease, but those of C_4 compounds increase.

Table 1. C_3 and C_4 product yields in the reaction with ethane, ethylene and acetylene in the gas phase

Ag_2C_2 0.10 g
Substrate $2.3-2.5\times10^{-4}$ mol
Product $\times10^{-6}$ mol

Substrate	Product		Ratio	
	C_3	C_4	C_3/C_4	C_4H_2/C_4H_4
Ethane	2.2	1.1	2.0	1.0
Ethylene	0.51	1.9	0.3	1.3
Acetylene	0.05	3.6	0.013	7.0

These results are quite different from those with the recoil reaction[6] and the reaction of carbon vapor. In the recoil reaction,[2] as is shown in Table 2, C_3 compounds are produced in quite a large yield, and in the reaction of carbon vapor C_1 insertion intermediate and spiropentane deri-

1) K. Taki, This Bulletin, **42**, 2906 (1969).
2) M. Marshall, C. MacKay and R. Wolfgang, *J. Amer. Chem. Soc.*, **86**, 4741 (1964).
3) H. J. Ache and A. P. Wolf, *ibid.*, **88**, 888 (1966).
4) P. S. Skell and R. R. Engel, *ibid.*, **88**, 4883 (1966).
5) J. L. Sprung, S. Winstein and W. F. Libby, *ibid.*, **87**, 1812 (1965).

*1 The reaction products were catalytically hydrogenated, and the propane and butane produced were determined by gas chromatography.

6) C. MacKay and R. Wolfgang, *J. Am. Chem. Soc.*, **83**, 2399 (1961).

Table 2. In the recoil reaction, C_3 and C_4 product yield% in the reaction with ethane and ethylene[2,3]

Substrate	Product C_3%	Product C_4%	Ratio C_3/C_4
Ethane	12.5	—	—
Ethylene	27.1	10.8	2.5
Ethylene liq. −130°C	21.7	9.9	2.2
Ethylene solid −196°C	22.1	15.8	1.2

vatives[7,8] are produced in the reactions with saturated hydrocarbon and olefins respectively.

On the basis of the above results, it may be suggested that the reactitive species include not only monatomic carbon but also other carbon oligomers. By the reaction with ethylene, C_4 compounds were obtained, but higher hydrocarbons were not obtained; therefore, C_2 may be the most probable reactive species, as was suggested in the previous paper.[1] C_3 and C_4 compounds are given in the reaction of C_1 or C_2 with ethane, ethylene, and acetylene as follows:

$$\left.\begin{matrix}C_1\\C_2\end{matrix}\right\} + C_2\ \text{Substrate} \rightarrow \begin{cases}[C_2\ \text{Substrate}\ C_1]^* \rightarrow C_3\ \text{Compounds}\\ [C_2\ \text{Substrate}\ C_2]^* \rightarrow C_4\ \text{Compounds}\end{cases}$$

Reaction with Ethylene under Various Conditions. In order to examine the reaction process, a further experiment was carried out with an ethylene substrate. In the solid phase, as is shown in Table 3, and in the gas-phase reaction the main products are acetylene and C_3 and C_4 compounds. The yields of acetylene and of the C_3 and C_4 compounds increase with the ethylene pressure but the C_3/C_4 and C_4/C_2H_2 ratios are almost constant, as is shown in Figs. 1 and 2. The C_3/C_4 ratio does not depend on the distance from the explosion position,*2 as is shown in Fig. 3. Moderation of the reactive species by helium gas gave the same results. These experimental results suggest that the acetylene and C_3 and C_4 compounds may be produced from a common precursor.

Table 3. Product yields in the solid phase reaction with ethylene

Ag_2C_2 0.10 g

Ethylene 2.2—2.5×10^{-4} mol

Product	Yield×10^{-6} mol
Methane	2.5—2.7
Ethane	0.14—0.24
Acetylene	41.6—65.6
Propylene	0.43
C_3 Products	0.51
Butadiene	0.12
Ethylacetylene	0.03
Vinylacetylene	0.63
Diacetylene	0.83
C_4 Products	1.72
C_3/C_4	0.30
C_4H_2/C_4H_4	1.3

The Formation Process of C_4 Compounds. C_4 compounds consist of vinylacetylene and diacetylene,*3 and the sum of their yields increases with the ethylene pressure, as has been mentioned before. However, the ratio of diacetylene to vinylacetylene decreases with the ethylene pressure, as is shown in Fig. 4. Helium gas moderation also brought about a decrease in the C_4H_2/C_4H_4 ratio. From these facts, it may be considered that the formation processes of C_4 compounds depend on the deactivation condition of the adduct ($C_2H_4C_2$), which may be an energy-rich C_2-insertion intermediate(C_4H_4). The adduct easily gives vinylacetylene upon deactivation at a high pressure, but the adduct decomposes easily to diacetylene at a low pressure according to these reactions:

$$C_2H_4 + C_2 \rightarrow$$

$$[C_2H_4C_2]^* \begin{cases} \longrightarrow \text{acetylene}\\ \xrightarrow{\text{high pressure}} \text{vinylacetylene}\\ \xrightarrow{\text{low pressure}} \text{diacetylene}\end{cases}$$

This mechanism is also supported by the fact that the ratio of diacetylene to vinylacetylene decreases with the increase in the distance from the explosion position in the solid-phase reaction, as is shown in Fig. 5.

Harris and Skell[10] reported recently that the C_4 species (tetra atomic carbon) in carbon vapor is the precursor of the C_4 products in the reaction

*2 The explosion technique as a function of the distance from silver acetylide was also described in the previous paper.[1]

*3 The C_4 compounds were identified as vinylacetylene and diacetylene on the basis of the evidence that the catalytic hydrogenation gave *n*-butane gas chromatographically and that the retention times of these compounds on three different columns, polyethylene glycol 1000, squalane, and apiezone L columns, were the same as those of authentic vinylacetylene and authentic diacetylene. The authentic vinylacetylene was kindly given by Dr. S. Horiie (Denki Kagaku Co.), the authentic diacetylene was prepared following Ref. 9, and the catalyst, PtO_2, was kindly provided by Dr. K. Taya (Rikagaku Kenkyu Sho).

7) P. S. Skell and R. R. Engel, *ibid.*, **88**, 3749 (1966).
8) P. S. Skell and R. R. Engel, *ibid.*, **89**, 2912 (1967).
9) R. J. Tedschi and A. E. Brown, *J. Org. Chem.*, **29**, 2051 (1964).
10) R. F. Harris and P. S. Skell, *J. Amer. Chem. Soc.*, **90**, 4172 (1968).

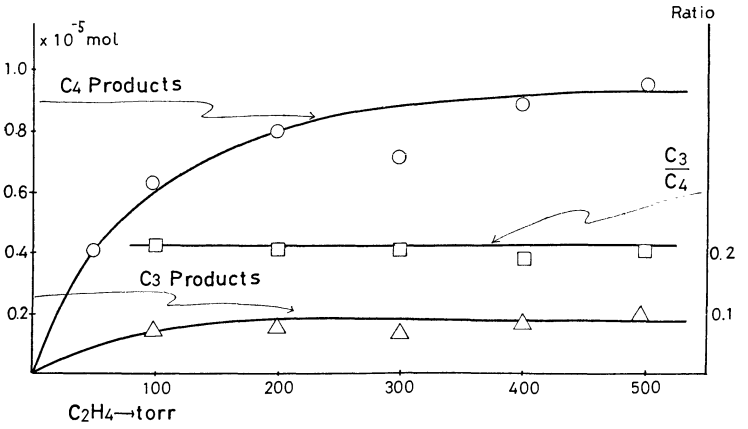

Fig. 1. C_3 and C_4 product yields as a function of ethylene pressure.

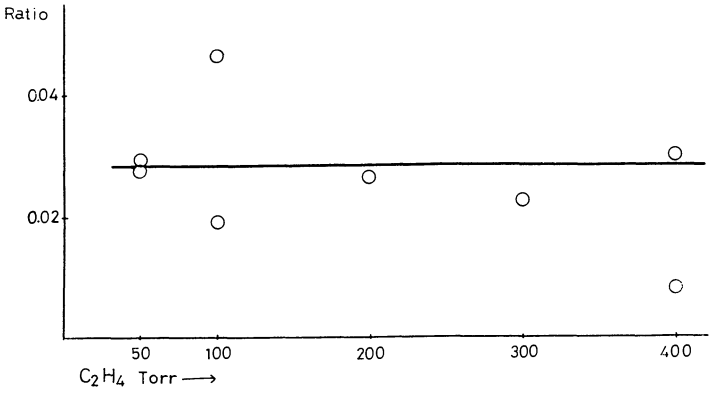

Fig. 2. C_4/C_2H_2 ratio as a function of ethylene pressure in the gas phase reaction.

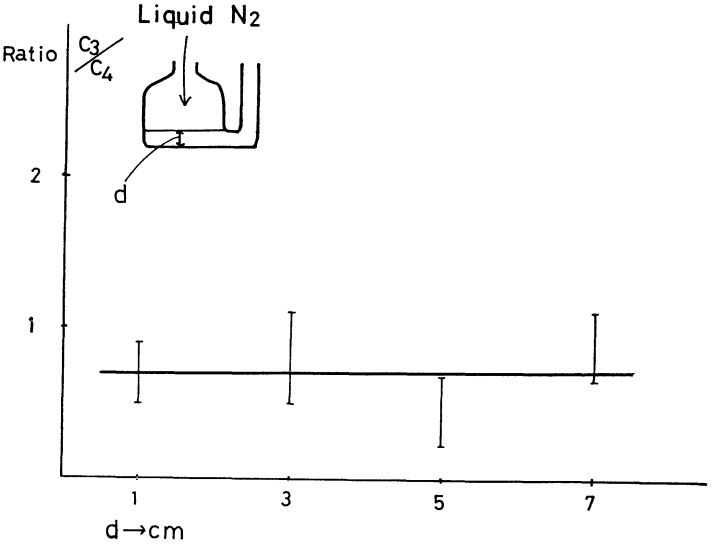

Fig. 3. C_3/C_4 ratio as a function of distance from explosion position in solid phase reaction.
Ag_2C_2 0.3 g Ethylene $2.2—2.4\times10^{-5}$ mol

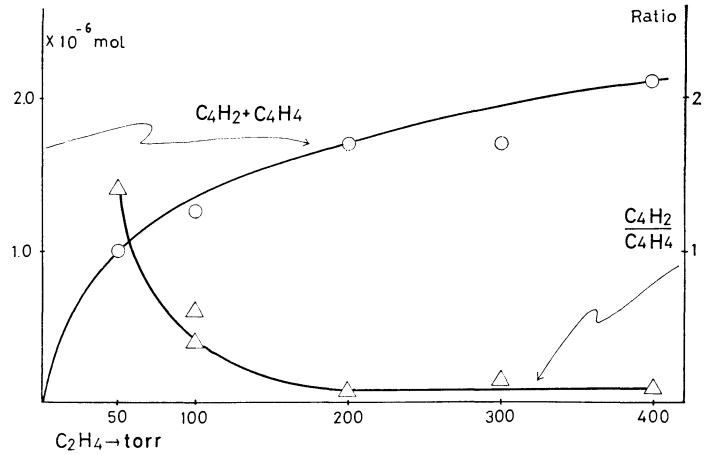

Fig. 4. C_4 product yield and C_4H_2/C_4H_4 ratio as a function of ethylene pressure.
Ag_2C_2 0.10 g

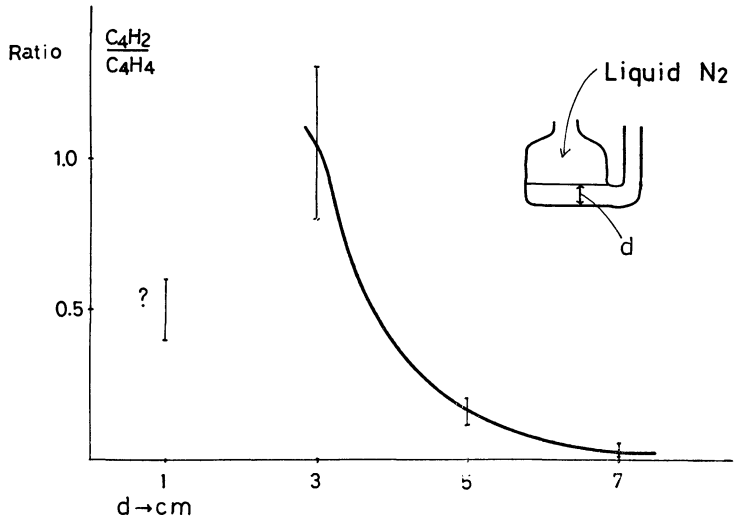

Fig. 5. C_4H_2/C_4H_4 as a function of distance from explosion position in solid phase reaction.
Ag_2C_2 0.3 g Ethylene $2.2—2.4\times10^{-5}$ mol

of various hydrocarbons. The C_4 compounds have been ethylacetylene, methylallene, 1,3-butadiene, and vinylacetylene, but diacetylene has been found only in trace quantities. In the present reaction, because of the high yield of diacetylene, C_4 compounds seem unlikely to be yielded from the reaction of the C_4 species (tetra-atomic carbon).

Reaction with C_3 and C_4 Olefins. The yields of acetylene, ethylene, cyclopentadiene, diacetylene, vinylacetylene, and benzene in reactions with various C_3 and C_4 olefins are listed in Tables 4, 5, and 6. From the fact that the reactions with isobutene and with isobutane give benzene (the yield is not high), benzene may be formed in the process of the decomposition of adducts. However, the benzene yield depends on the structure of the substrate, for the reactions with 1,3-butadiene and with 1-butene give high yields*4 of benzene. From the above facts, benzene may

*4 The yields of benzene from *cis*-butene and *trans*-butene are almost the same. In this case, the structure of the substrates does not seem to have any effect on the formation of benzene. The reason for this is not clear, but the formation of benzene might be caused by the addition of the C_2 species to the terminal double bond in the molecule and the resulting adduct may undergo cyclization; therefore, the formation might be interpreted in terms of the position of the double bond in the molecule.

Table 4. Vinylacetylene, diacetylene, cyclopentadiene and benzene yields in the solid phase reaction with C_4 olefins

Ag_2C_2 0.30 g Substrate 4.7—5.0×10^{-4} mol Product ×10^{-6} mol

Substrate	Product			
	Vinylacetylene	Diacetylene	Cyclopentadiene	Benzene
1,3-Butadiene	9.1—12.0	9.0	1.6—2.1	4.0—4.4
trans-Butene	5.6—6.2	4.5—6.5	1.9	1.5—1.8
cis-Butene	6.8—8.2	6.1—8.6	1.9—2.6	1.3—1.7
Isobutylene	2.4—3.0	4.4—5.6	0.9—1.2	2.1—2.9
1-Butene	4.3—4.6	4.3—5.1	3.0—4.0	2.4—3.1
Isobutane	3.0—3.3	4.1—4.3	1.1—1.5	0.6—0.8
n-Butane	3.2—3.7	1.4—1.5	0.2	0.1

Table 5. Product yields in the solid phase reaction with C_3 and C_4 olefines

Ag_2C_2 0.10 g Substrate 2.2—2.5×10^{-4} mol Product ×10^{-5} mol

Substrate	Product				
	Methane	Ethane	Ethylene	Acetylene	Propylene
cis-Butene	1.6	0.06	0.9	3.0	0.3
trans-Butene	1.7	0.1	0.8—1.2	1.7	0.84—6.7 ?
1-Butene	2.6	0.4	2.1	3.1	1.0
Isobutylene	2.3	0.2	0.6	1.7	0.4
n-Butane	3.0	0.5	5.6	1.1	1.0
Isobutane	4.4	0.6	2.1	1.1	2.3
Propane	4.2	0.5	5.5	2.2	0.4
Propylene	3.9	0.05	2.1	4.2	—

Table 6. Ethylacetylene, vinylacetylene, diacetylene, cyclopentadiene and benzene yields in the solid phase reaction with C_3 olefins

Ag_2C_2 0.30 g Substrate 4.5—5.0×10^{-4} mol Product ×10^{-6} mol

Substrate	Product				
	Ethylacetylene	Vinylacetylene	Diacetylene	Cyclopentadiene	Benzene
Propane	0.2	2.1—3.3	2.6—2.8	0.2	0.07
Propylene	0	2.3—2.6	5.2—5.3	0.4	0.3
Allene	0	1.1—1.2	9.0—9.4	0.09	0.08
Methylacetylene	1.1—1.3	0.9	7.7—8.1	0	0.02—0.08

be considered to be formed not only by the decomposition of adducts, but also by the cycloaddition to substrates. In the reaction with C_3 olefins, it is not clear whether diacetylene and vinylacetylene are formed by the reaction of C_1 or of C_2 species. The diacetylene yield is higher in allene and methylacetylene than in propane. On the other hand, the vinylacetylene yield is higher in propane than in allene. This fact indicates that the yields of diacetylene and vinylacetylene are affected by the structure of the substrate. The cyclopentadiene yield is also affected by the structure of the substrate, as is shown in Table 6.

The benzene formation in the reaction with C_3 olefins, and the cyclopentadiene formation in the reaction with C_4 olefins may be considered to be the reactions of the C_3 and C_1 species respectively, but the details are still not clear.

In the reaction of carbon vapor from the carbon arc[11] with ethylene, acetylene is not a main product, while in the reaction of carbon atoms from a recoil reaction[2] acetylene is a main product. Although the reaction of carbon vapor from the carbon arc deals with the reaction of carbon atoms complexed[11] by surface material rather than with the reaction of free carbon atoms, the facts that the acetylene yield diminishes sharply[12] as the carbon atoms from the recoil reaction are thermalized by a moderator and as the adducts are efficiently de-excited confirms that there is indeed no discrepancy in the two reactions. Moreover, the

11) P. S. Skell and R. R. Engle, *J. Amer. Chem. Soc.*, **87**, 1135 (1965).

12) J. E. Nicholas, C. MacKay and R. Wolfgang, *ibid.*, **87**, 3008 (1965).

yield of C_3 products is higher than that of C_4 products. On the other hand, in the present work the main products in the reaction with ethylene are acetylene and C_4 products. The C_3 products are too small in quantity as compared with the C_4 products. The difference in the results may be considered to be caused by the difference in the reactive species in the carbon vapor.

In conclusion, C_2 may be considered to be one of the reactive species in the explosion of silver acetylide. The primary step is the addition of reactive species to the substrate; the resulting adduct undergoes a secondary process to give the final products. However, the steps of the formation of benzene depend on the structure of the substrate.

The author wishes to thank Professor Shunsuke Murahashi (Osaka University) for his useful suggestions and encouragement, Miss K. Motegi for her efforts in the analysis of the reaction products, and Dr. M. Imamura and Dr. M. Matsui for their helpful discussions and suggestions.

BULLETIN OF THE CHEMICAL SOCIETY OF JAPAN VOL. 43 2123—2129 (1970)

The Synthesis and Polymerization of Vinyl- and Isopropenyl-*s*-triazines

Yasuo YUKI,*1 Toshio KAKURAI and Tatsuya NOGUCHI

Faculty of Engineering, Tokyo Institute of Technology, Ookayama, Meguro-ku, Tokyo

(Received September 4, 1969)

Some new vinyl monomers with an amino-*s*-triazinyl group were synthesized. 2,4-Amino- and substituted amino-6-vinyl-*s*-triazines were synthesized by the reaction of the substituted biguanides with acrylyl chloride, while 2-amino-4-substituted amino-6-isopropenyl-*s*-triazines were prepared from the substituted biguanides with methyl methacrylate. It has been found that vinyl-*s*-triazines thermally polymerized immediately after melting and gave insoluble polymers. Polymers with amino-*s*-triazinyl groups in the side chain were obtained by the radical polymerization of some vinyl- and isopropenyl-*s*-triazines. The copolymerization of these monomers with styrene has been investigated in dimethyl sulfoxide using α,α'-azobisisobutyronitrile as an initiator. The monomer reactivity ratios were determined, and the Q and e values for these vinyl-*s*-triazines were calculated. Some discussions are presented.

A vinyl monomer with an amino-*s*-triazine ring is interesting as a reactive monomer. Overberger and Shapiro[1,2] have reported on the synthesis and polymerization of 2,4-diamino-6-vinyl-*s*-triazine and 2-amino-4-anilino-6-vinyl-*s*-triazine from the reaction of biguanide and phenylbiguanide respectively with acrylyl chloride. Thurston[3] has reported on the reaction of biguanide with methyl methacrylate to give 2,4-diamino-6-isopropenyl-*s*-triazine. We have repeated these synthesis and, in addition, synthesized various vinyl- and isopropenyl-*s*-triazines.

The polymerizations of 2,4-diamino-6-vinyl-*s*-triazine and 2-amino-4-*o*-toluidino-6-vinyl-*s*-triazine have previously been reported.[4,5] Continuing the studies of vinyl-*s*-triazines, the homopolymerization and copolymerization of several vinyl- and isopropenyl-*s*-triazines have now been investigated. In particular, the copolymerization with styrene was studied. The copolymerization of 2,4-diamino-6-vinyl-*s*-triazine hydrochloride with styrene will also be reported here.

Experimental

Materials. The aliphatic biguanides were prepared by the method of Kono and Odo.[6] The aromatic biguanides were prepared by the method of Cohn[7] from the reaction of dicyanodiamide with aromatic amines hydrochlorides in hot water. The styrene was purified by the usual method and was distilled again before use. The initiator, α,α'-azobisisobutyronitrile (AIBN), was a commercial material. The

*1 Present address: Department of Fibers and Polymers, Nagoya Institute of Technology, Gokiso, Showa-ku, Nagoya.

1) C. G. Overberger and F. W. Michelotti, *J. Amer. Chem. Soc.*, **80**, 988 (1958).

2) C. G. Overberger and S. L. Shapiro, *ibid.*, **76**, 1061 (1954).

3) J. T. Thurston, U. S. 2461943 (1946); *Chem. Abstr.*, **43**, 3854 (1949).

4) Y. Yuki, N. Hiramatsu, T. Kakurai and T. Noguchi, *Kobunshi Kagaku*, **26**, 134 (1969).

5) Y. Yuki, T. Kakurai and T. Noguchi, *ibid.*, **26**, 141 (1969).

6) K. Kono and K. Odo, *Yukigosei Kagaku Kyokai-shi*, **20**, 649 (1962).

7) G. Cohn, *J. Prakt. Chem.*, **84**, 394 (1911).

dimethyl sulfoxide (DMSO) was fractionally distilled under reduced pressure in the presence of nitrogen. All the other reagents were commercially available and were used after purification if necessary.

2-Amino-4-anilino-6-methyl-s-triazine. Phenylbiguanide (1.77 g, 0.01 mol) was dissolved in 4 m*l* of methanol, and then 3.7 g (0.05 mol) of methyl acetate were added. After the reaction mixture had then been allowed to stand for five days at room temperature, the methanol and excess methyl acetate were removed. The residue was washed with water to give 1.2 g (60%) of a product which melted at 173—175°C.

The other 2,4-disubstituted-6-methyl-*s*-triazines were prepared in a similar manner.

2-Amino-4-anilino-6-isopropenyl-s-triazine. To a solution of 17.7 g (0.1 mol) of phenylbiguanide in 50 m*l* of methanol, we added 15.0 g (0.15 mol) of methyl methacrylate. After the reaction mixture had been allowed to stand for six days at room temperature, the methanol was removed and water was added to give 7.1 g (34%) of a white product. The product was recrystallized from a methanol-water mixture, mp 174—175.5°C.

The other 2,4-disubstituted-6-isopropenyl-*s*-triazines were prepared in a similar manner.

2-Amino-4-anilino-6-vinyl-s-triazine. 2-Amino-4-anilino-6-vinyl-*s*-triazine and the other 2,4-disubstituted-6-vinyl-*s*-triazines were prepared in a manner similar to that previously described.[5]

Procedure. All the polymerization experiments were carried out in a DMSO solution by AIBN at 60°C in a glass tube sealed under a vacuum. Methanol was used as a precipitant. The composition of the copolymer was calculated from the carbon and nitrogen contents.

Results and Discussion

Preparation of Monomers. The synthesis of 2,4-amino- or substituted amino-6-substituted-*s*-triazines was effected by the reaction of substituted biguanides with carboxylic acid derivatives (acid esters or acid chlorides).[8]

Methyl-*s*-triazines were synthesized for the model compounds of vinyl-*s*-triazines according to the directions of Overberger and Shapiro.[9] The results are shown in Table 1.

Isopropenyl-*s*-triazines were given by the reaction of substituted biguanides with methyl methacrylate in methanol,

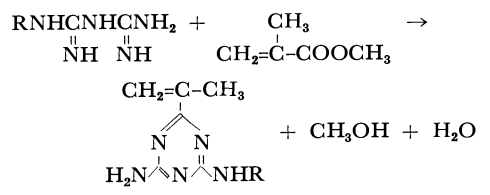

The results are shown in Table 2.

Vinyl-*s*-triazines were prepared from the reaction of the substituted biguanides with acrylyl chloride in acetone at a low temperature, as has previously been reported in the case of 2-amino-4-*o*-toluidino-6-vinyl-*s*-triazine.[5] The results are shown in Table 3.

The UV absorption data of *s*-triazines determined in ethanol are given in Table 4. When 2- and 4-substituents are amino or alkyl amino groups, the vinyl- and isopropenyl-*s*-triazines show a bathochromic shift compared with methyl-*s*-triazines. This is probably due to the conjugation of the double bond with the triazine nucleus. On the other hand, when the 4-substituents are aryl amino groups, the vinyl- and isopropenyl-*s*-triazines show a hypsochromic shift. Overberger and Shapiro[11] found this same effect on 2-amino-4-anilino-6-vinyl-*s*-triazine. These results indicate little conjugation of 4-aryl amino groups.

The thermal behavior of vinyl- and isopropenyl-*s*-triazines was studied by the techniques of differential thermal analysis (DTA) and thermogravimetric analysis (TGA). 2,4-Diamino-6-vinyl-*s*-triazine was reported to be decomposed without melting at 300—310°C[1] Figure 1 shows the DTA and TGA curves of 2,4-diamino-6-vinyl-*s*-triazine. It was found that 2,4-diamino-6-vinyl-*s*-triazine was gradually sublimed above 170°C and was thermally polymerized at about 260°C without melting. This thermally-polymerized product was insoluble, but it swelled in formic acid. Its IR spectrum was identical with that of the polymer obtained by the solution polymerization using AIBN in DMSO.[4] All the other vinyl-*s*-triazines,

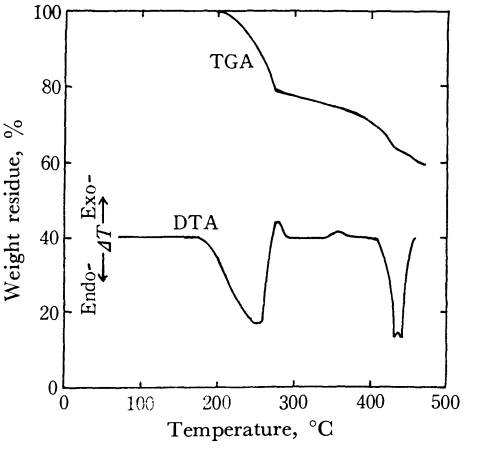

Fig. 1. Thermal analysis of 2,4-diamino-6-vinyl-*s*-triazine in air.
TGA (5°C/min), DTA (20°C/min)

8) E. M. Smolin and L. Rapoport, "*s*-Triazines and Derivatives" Interscience Publishers, New York (1959), p. 226.

9) C. G. Overberger and S. L. Shapiro, *J. Amer, Chem. Soc.*, **76**, 93 (1954).

10) S. L. Shapiro, E. S. Isaacs, V. A. Parrino and L. Freedman, *J. Org. Chem.*, **26**, 68 (1961).

11) C. G. Overberger and S. L. Shapiro, *J. Amer. Chem. Soc.*, **76**, 1855 (1954).

Table 1. 6-Methyl-*s*-triazine derivatives

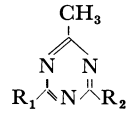

R_1, R_2	Yield (%)	Mp[a] (lit.) (°C)	Found (Calcd.) C (%)	H (%)	N (%)
R_1=NH_2					
R_2=NHC_6H_5	60	173—175 (176—177[6])			
$NHC_6H_4CH_3$(*p*)	67	204—205 (211—213[10])			
$NHC_6H_4OCH_3$(*p*)	65	213—214 (213—214[10])			
NHC_6H_4Cl(*p*)	27	195.5—196 (194—196[10])			
$NHC_6H_4NHCOCH_3$(*p*)	29	268—269	55.88 (55.81)	5.21 (5.43)	32.49 (32.56)
$NHC_6H_4COOC_2H_5$(*p*)	30	246—247	57.27 (57.14)	5.27 (5.49)	25.89 (25.64)
$NHC_6H_4CH_2CN$(*p*)	50	220—221	60.16 (60.01)	5.29 (5.00)	34.99 (34.96)
$NHC_6H_4NO_2$(*m*)	42	222—223	49.16 (48.76)	3.96 (4.09)	33.86 (34.13)
NHC_6H_4CN(*m*)	36	228—229	58.73 (58.40)	4.28 (4.46)	37.27 (37.15)
$N(CH_3)C_6H_4$	47	156—157	61.43 (61.68)	5.98 (6.07)	32.29 (32.71)
$N(C_6H_5)_2$	69	188.5—189.5	69.59 (69.31)	5.29 (5.42)	25.23 (25.27)
R_1=R_2=NHC_6H_5	35	233.5—235	68.75 (69.30)	5.39 (5.45)	25.31 (25.25)

a) Recrystallized from methanol-water or methyl cellosolve-water mixture.

Table 2. 2-Amino-4-substituted-6-isopropenyl-*s*-triazines

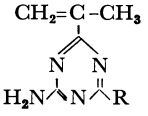

R	Yield (%)	Mp[a] (°C)	Found (Calcd.) C (%)	H (%)	N (%)
NH_2	10	247—248[b]	48.31 (47.67)	5.93 (6.00)	45.93 (46.33)
$N(CH_3)_2$	19	191—192	53.89 (53.61)	7.37 (7.31)	38.85 (39.08)
NHC_6H_5	34	174—175.5	62.81 (63.42)	5.83 (5.77)	30.43 (30.81)
$NHC_6H_4CH_3$(*p*)	14	166.5—168	63.77 (64.70)	5.89 (6.27)	28.43 (29.03)
$NHC_6H_4NHCOCH_3$(*p*)	36	144.5—145	55.09 (55.26)	5.75 (5.30)	27.62 (27.62)
$NHC_6H_5CH_3$(*o*)	5	186.5—187.5			28.69 (29.03)
$N(CH_3)C_6H_5$	16	170.5—171	65.05 (64.70)	6.33 (6.27)	29.09 (29.03)
$N(C_6H_5)_2$	54	117—119	71.79 (71.27)	5.80 (5.65)	23.32 (23.09)

a) Recrystallized from methanol-water mixture.
b) Lit,[3] 246—247°C.

Table 3. 6-Vinyl-*s*-triazine derivatives

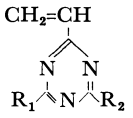

R_1, R_2	Yield (%)	Mp[a] (°C)	Found (Calcd.) C (%)	H (%)	N (%)
$R_1=NH_2$					
$R_2=NHCH_3$	31	152—153	47.78 (47.67)	5.96 (6.00)	46.57 (46.33)
$N(CH_3)_2$	26	191—192	50.33 (50.89)	6.83 (6.71)	42.80 (42.39)
	poor	170—171	58.52 (58.52)	7.28 (7.37)	34.20 (34.12)
NHC_6H_5	15	174—175.5[b]	61.72 (61.96)	5.07 (5.20)	32.73 (32.84)
$NHC_6H_4CH_3(p)$	29	180—181	63.79 (63.42)	6.17 (5.77)	30.04 (30.81)
$NHC_6H_4OCH_3(p)$	25	190.5—191.5	58.56 (59.26)	5.65 (5.39)	27.49 (28.79)
$NHC_6H_4CN(p)$	10	181—183	60.81 (60.50)	4.37 (4.23)	35.40 (35.27)
$N(CH_3)C_6H_5$	26	141.5—143	63.75 (63.42)	5.84 (5.77)	30.41 (30.81)
$R_1=R_2=NHC_6H_5$	12	166—167	71.02 (70.57)	4.81 (5.23)	24.16 (24.20)

a) Recrystallized from methanol-water mixture.
b) Lit,[2] 180—181°C.

Table 4. Ultraviolet absorption spectra of *s*-triazine

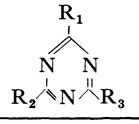

R_2, R_3	R_1 λ_{max}[a] (mμ) ($\varepsilon\times10^{-3}$) $CH=CH_2$	$C(CH_3)=CH_2$	CH_3
$R_2=NH_2$,			
$R_3=NH_2$	281 (3.2)	276 (3.8)	256 (4.0)[b]
$NHCH_3$	290 (3.5)		
$N(CH_3)_2$	296 (3.5)	292 (4.2)	264 (5.0)
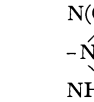	299 (3.9)		
NHC_6H_5	257 (19.4)[c]	256 (28.8)	270 (22.8)[d]
$NHC_6H_4CH_3(p)$	259 (25.7)	258 (33.7)	270 (21.0)
$NHC_6H_4OCH_3(p)$	262 (22.3)		273 (20.0)
$NHC_6H_4CN(p)$	297 (28.4)		
$NHC_6H_4NHCOCH_3(p)$		276 (32.7)	287 (28.3)
$NHC_6H_4CH_3(o)$	shoulder	shoulder	shoulder
$N(CH_3)C_6H_5$	shoulder	shoulder	shoulder
$N(C_6H_5)_2$		shoulder	255 (17.8)
$R_2=R_3=NHC_6H_5$	267 (41.1)		271 (42.8)

a) Measured in ethanol.
b—d) Ref. 11. b) 252—256 (3.2) in water, c) 255 (22.5) in methanol, d) 271 (20.38) in methanol.

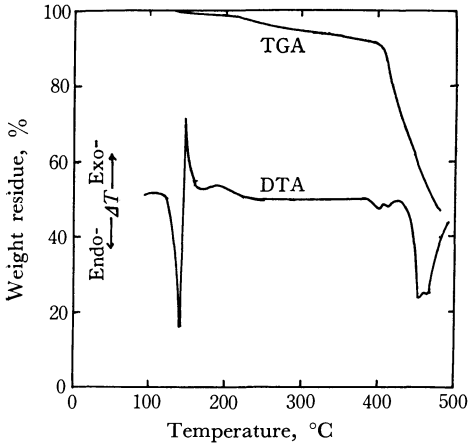

Fig. 2. Thermal analysis of 2-amino-4-*N*-methylanilino-6-vinyl-*s*-triazine in air.
TGA (5°C/min), DTA (20°C/min)

which gave a sharp melting point, were found, by a study of DTA and TGA curves, to polymerize immediately after melting. The curves of 2-amino-4-*N*-methylanilino-6-vinyl-*s*-triazine are shown in Fig. 2 as a typical example. After the exotherm, no double-bond absorption was observed in the IR spectra of the heated samples. This polymer was also insoluble. On the other hand, no thermal polymerization of isopropenyl-*s*-triazines was observed, even after its melting.

Polymerization. The results of the homopolymerization of some vinyl- and isopropenyl-*s*-triazines by AIBN in DMSO are presented in Tables 5 and 6 respectively. Poly-2-amino-4-methylamino-6-vinyl-*s*-triazine and poly-2,4-diamino-6-isopropenyl-*s*-triazine were insoluble in common organic solvents, but they were soluble in formic acid, acetic acid, and mineral acid. The polymerization of 2-amino-4-dimethylamino-6-vinyl-*s*-triazine proceeded homogeneously, but the polymer isolated was insoluble in DMSO. The polymers containing aryl amino groups were soluble in DMSO, DMF, DMA, and dioxane.

Table 5. Polymerization of vinyl-*s*-triazines

Monomer 2-amino-4-substituted-6-vinyl-*s*-triazine	Conversion (%)	η_{sp}/C[b] in DMSO	η_{sp}/C[b] in formic acid
4-Methylamino	38	insoluble	1.34
4-Dimethylamino	75	insoluble	0.58
4-Anilino	56	0.23	0.59
4-*p*-Toluidino	51	0.30	
4-*p*-Anisidino	20[a]	0.12	0.17
4-*N*-Methylanilino	86	0.10	0.21

Polymerization conditions; [M]=0.20 mol/*l*, [AIBN]=1.35×10^{-3} mol/*l*, at 60°C, 5 hr.
a) 3 hr. b) C=0.3 g/d*l*, at 30°C.

Table 6. Polymerization of isopropenyl-*s*-triazines

Monomer 2-amino-4-substituted-6-isopropenyl-*s*-triazine	Conversion[a] (%)	η_{sp}/C[b] in DMSO	η_{sp}/C[b] in formic acid
4-Amino	31	insoluble	12.2
4-Anilino	43	0.82	4.2
4-*N*-Methylanilino	62	0.67	3.4

a) Polymerization conditions: [M]=0.40 mol/*l*, [AIBN]=1.35×10^{-3} mol/*l*, at 60°C, 5 hr.
b) C=0.2 g/d*l*, at 30°C.

Copolymerization. The copolymerization of vinyl- and isopropenyl-*s*-triazines with styrene were carried out at 60°C in DMSO. The polymerization conditions were as follows; $[M_1]+[M_2]=0.20$ mol/*l* and [AIBN]=1.35×10^{-3} mol/*l*. The polymerization proceeded homogeneously. The rates of copolymerization decreased as the styrene contents in the monomer mixtures increased. The relationship between the composition of the monomer feeds and that of the copolymers is summarized in Tables 7 and 8. The copolymerization of 2,4-dianilino-6-vinyl-*s*-triazine with styrene gave a colloidal solution when the reaction mixture was poured in methanol, and the copolymer was not isolated quantitatively.

The η_{sp}/C values of several copolymers were measured in DMSO and in formic acid. The η_{sp}/C values of the copolymers in formic acid increased as the *s*-triazine content in copolymers increased.

The copolymers of 2,4-diamino-6-vinyl-*s*-triazine hydrochloride with styrene were not precipitated in methanol, but they were isolated by the addition of aqueous ammonia. The results are shown in Table 7. On the basis of these data, the

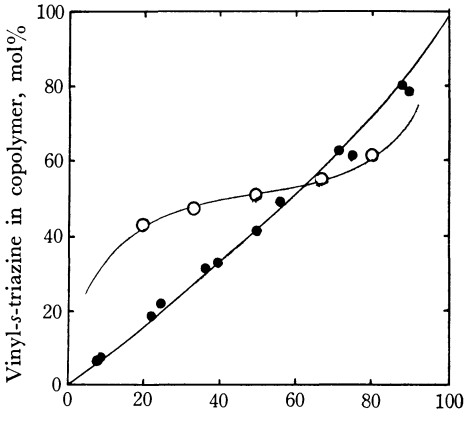

Fig. 3. Monomer-copolymer composition curves for styrene with 2,4-diamino-6-vinyl-*s*-triazine hydrochloride (○) and free base (●).[4] — calcd.

TABLE 7. COPOLYMERIZATION OF VINYL-*s*-TRIAZINES (M_2) WITH STYRENE (M_1)

M_2 in monomer (mol%)	Reaction time (hr)	Yield (%)	M_2 in polymer (mol%)	η_{sp}/C[a] in DMSO	η_{sp}/C[a] in formic acid
M_2: 2-Amino-4-*N*-methylanilino-6-vinyl-*s*-triazine					
79.54	3	17.3	74.09	0.45	2.02
66.03	3.66	11.2	63.23	0.56	2.47
49.29	3.66	16.8	51.12	0.48	2.32
32.70	4.5	14.6	38.09	0.44	1.39
19.55	6	13.4	27.11	0.37	0.79
M_2: 2-Amino-4-*p*-toluidino-6-vinyl-*s*-triazine					
79.54	3	12.0	63.80	0.52	1.55
66.03	3.17	11.2	53.57	0.52	1.61
49.29	3.5	9.3	40.66	0.54	1.61
32.70	4	1.8	30.27	—	—
19.55	5.5	8.8	20.60	0.40	0.33
M_2: 2-Amino-4-*p*-anisidino-6-vinyl-*s*-triazine					
79.83	3	10.5	64.05	0.40	1.33
66.43	3.25	10.8	53.09	0.40	1.27
49.73	4	2.5	41.67	—	—
33.10	4.5	8.5	29.56	0.34	0.86
19.83	6	9.3	20.72	0.27	0.30
M_2: 2-Amino-4-*p*-cyanoanilino-6-vinyl-*s*-triazine					
72.99	3	11.2	58.26	0.52	1.16
59.04	4	12.2	50.41	0.51	1.27
44.77	5.33	13.1	41.38	0.52	1.15
30.19	6.5	9.5	30.90	—	0.80
11.90	8	9.2	15.04	0.21	0.13
M_2: 2-Amino-4-dimethylamino-6-vinyl-*s*-triazine					
79.72	3	20.1	77.20	b)	2.46
66.28	3.33	14.4	66.26	b)	2.37
49.57	4	14.7	54.57	0.38	—
32.95	4.75	10.6	37.74	0.29	—
19.73	6	7.7	22.59	0.24	0.49
M_2: 2,4-Diamino-6-vinyl-*s*-triazine hydrochloride					
79.89	3	5.6	61.69	0.45	—
66.52	5.5	19.5	55.89	0.37	2.14
49.83	5.5	23.4	51.65	0.53	2.42
33.18	6.5	31.5	47.89	0.31	2.47
19.89	7	36.2	42.28	0.41	2.88

a) Measured $C=0.2$ g/dl at 30°C.
b) Insoluble.

monomer-copolymer composition curves are drawn in Fig. 3; they are shown in comparison with the free base previously reported on.[4]

The monomer reactivity ratios were determined by the method of Fineman and Ross.*2 The values obtained are given in Tables 9 and 10. Assuming $Q=1.0$ and $e=-0.8$ for styrene, the Q-e values for vinyl- and isopropenyl-*s*-triazines were calculated. These are summed up in Table 9 for vinyl-*s*-triazines and in Table 10 for isopropenyl-*s*-triazines.

In general, the *s*-triazinyl group acts as an electron-withdrawing group because of the electron-attracting character of nitrogen atoms. This is why 2,4-dimethyl-6-vinyl-*s*-triazine has a positive e value.[12] However, the negative e values obtained for 2,4-amino and alkylamino derivatives may be due to the presence of two strong electron-donating groups attached to the triazine ring. The

*2 In the case of copolymerization of 2,4-diamino-6-vinyl-*s*-triazine hydrochloride with styrene, the integral method of Mayo and Lewis was used.

12) A. T. Coscia, R. L. Kugel and J. Pellon, *J. Polymer Sci.*, **55**, 303 (1961).

TABLE 8. COPOLYMERIZATION OF VINYL-*s*-TRIAZINES OR ISOPROPENYL-*s*-TRIAZINES (M_2) WITH STYRENE (M_1)

M_2 in monomer (mol %)	Reaction time (hr)	Yield (%)	M_2 in polymer (mol %)
M_2: 2-Amino-4-anilino-6-vinyl-*s*-triazine			
75.0	3.25	12.0	58.1
62.5	3.33	10.2	49.9
50.0	3	6.7	44.6
50.0	4	9.8	42.7
37.5	5	9.5	37.5
25.0	3.25	5.1	27.6
M_2: 2,4-Dianilino-6-vinyl-*s*-triazine			
75.6	3.5	—	64.7
63.1	4.5	—	56.9
50.6	3	—	48.9
50.6	5	—	43.5
38.1	5.5	—	49.4
25.5	6	—	30.9
M_2: 2,4-Diamino-6-isopropenyl-*s*-triazine			
74.27	3	8.3	72.60
65.81	3.66	10.0	68.25
49.04	5.66	10.6	53.54
32.48	6.33	6.8	39.25
19.39	7	7.3	24.35
M_2: 2-Amino-4-dimethylamino-6-isopropenyl-*s*-triazine			
71.92	4	13.3	78.04
58.73	4	12.4	67.31
39.04	4.5	8.9	57.64
25.46	5	7.2	42.08
M_2: 2-Amino-4-anilino-6-isopropenyl-*s*-triazine			
74.95	3	12.5	77.38
66.61	3	10.3	68.37
49.94	3.17	7.7	55.77
33.28	3.66	6.6	44.38
19.96	4.25	6.3	30.68
M_2: 2-Amino-4-*N*-methylanilino-6-isopropenyl-*s*-triazine			
74.38	3	25.6	83.05
61.73	3	19.1	72.88
42.06	3.17	13.6	58.49
24.39	4	10.7	43.20
10.79	5	8.3	25.85

TABLE 9. THE COPOLYMERIZATION PARAMETERS OF VINYL-*s*-TRIAZINES (M_2)

6-Vinyl-*s*-triazine	r_1	r_2	Q	e
2,4-Diamino-[4]	1.30	0.65	0.55	−0.38
2-Amino-4-dimethylamino-	0.70	0.81	0.78	−0.05
2-Amino-4-*o*-toluidino-[5]	0.45	0.93	1.05	0.13
2-Amino-4-*N*-methylanilino-	0.50	0.58	0.82	0.31
2-Amino-4-*p*-toluidino-	0.80	0.30	0.48	0.40
2-Amino-4-*p*-anisidino-	0.78	0.29	0.48	0.42
2,4-Dianilino-	0.53	0.40	0.70	0.45
2-Amino-4-*p*-cyanoanilino-	0.64	0.31	0.57	0.47
2-Amino-4-anilino-	0.60	0.24	0.55	0.59
2,4-Dimethyl-[12]	0.12	0.92	2.54	0.68*
2,4-Diamino-, hydrochloride	0.09	0.14	2.08	1.29

* Coscia reported $Q=2.1$ and $e=0.92$.

TABLE 10. THE COPOLYMERIZATION PARAMETERS OF ISOPROPENYL-*s*-TRIAZINES (M_2)

6-Isopropenyl-*s*-triazine	r_1	r_2	Q	e
2,4-Diamino-	0.66	0.97	0.89	−0.13
2-Amino-4-*N*-methylanilino-	0.29	1.39	1.80	0.01
2-Amino-4-dimethylamino-	0.32	1.17	1.45	0.16
2-Amino-4-anilino-	0.39	0.78	1.07	0.29

slight effect of the *p*-substituents of substituted anilino groups on the e values and the positive e values of these monomers show a weak conjugation of anilino groups with a double bond through the triazine nucleus; these results coincide with those of the UV spectra.

The positive e value of 2,4-diamino-6-vinyl-*s*-triazine hydrochloride shows that the *s*-triazinyl cation is a strong electron-withdrawing group. It is very interesting to be able to change the Q-e values easily by using the salt of the monomer.

The authors wish to thank Mr. T. Saito of the Tokyo Institute of Technology for his elementary analysis.

BULLTEIN OF THE CHEMICAL SOCIETY OF JAPAN VOL. 43 2130—2134 (1970)

Polyamides and Polyureas Containing *s*-Triazine Rings

Yasuo YUKI,*1 Shoji SAKURAI, Toshio KAKURAI and Tatsuya NOGUCHI

Faculty of Engineering, Tokyo Institute of Technology, Ookayama, Meguro-ku, Tokyo

(Received September 4, 1969)

Several new aromatic diamines containing *s*-triazine rings were prepared by the reaction of the related dinitro-compounds prepared from biguanide derivatives and carboxylic acid chlorides. Polyamides and polyureas containing amino-*s*-triazine were synthesized by the polycondensation of these diamines with dicarboxylic acid chlorides and diisocyanates respectively. Their preparations and physical properties are described.

Among many studies for preparing thermally-stable organic polymers, the syntheses of polyamides containing heterocyclic rings from dicarboxylic acid chlorides and diamines with heterocyclic rings have been reported recently.[1)]

$$NH_2R(Het)R'NH_2 + ClCOR''COCl \longrightarrow$$
$$-(-NHR(Het)R'NHCOR''CO-)- + 2HCl$$

where Het is a heterocyclic ring.

This paper will describe the preparation of several new aromatic diamines, polyamides, and polyureas containing *s*-triazine rings.

Diamines of two types were prepared, that is, 2-amino-4-aminoanilino-6-aminophenyl-*s*-triazine and 2-amino-4-amino- or anilino-6-(3,5-diaminophenyl)-*s*-triazine. The former gave the polymers containing *s*-triazine in a main chain, while the latter gave the polymers containing it in a side chain.

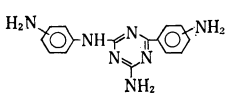

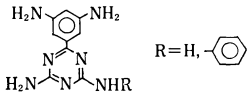

An amino group on *s*-triazine has a character like that of an amino group in the amide group because of the electron-attraction of the *s*-triazine ring, and it does not react with carboxylic acid chloride at low temperatures.[2)] In this study, an amino group on *s*-triazine was found not to be subject to a reaction with carboxylic acid chloride or isocyanate.

Results and Discussion

Preparation of Diamines. It is well known that 2-amino-4-substituted amino-6-substituted-*s*-triazines can be prepared by the reaction of substituted biguanides with carboxylic acid chlorides. The dinitro-compounds containing *s*-triazine rings were thus synthesized. 2-Amino-4-nitroanilino-6-nitrophenyl-*s*-triazine was prepared in a good yield by the reaction of nitrophenylbiguanide with nitrobenzoyl chloride. The reaction can be written as follows;

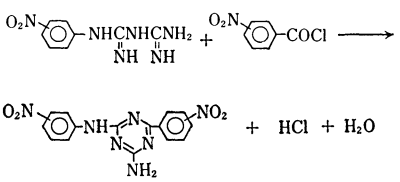

2-Amino-4-amino- or anilino-6-(3,5-dinitrophenyl)-*s*-triazine was prepared from biguanide or phenylbiguanide and 3,5-dinitrobenzoyl chloride.

These dinitro-compounds were then reduced to give diamines with tin and hydrochloric acid in ethanol. Some physical and analytical data of the reduced products are shown in Table 1. The yields were almost quantitative except in the case of 2,4-diamino-6-(3,5-diaminophenyl)-*s*-triazine (17%). Thurston[3)] has reported the synthesis of 2-amino-4-*p*-aminoanilino-6-*p*-aminophenyl-*s*-triazine dihydrochlorides.

A comparison of the UV spectra of these diamines and of 2-amino-4-anilino-6-phenyl-*s*-triazine (λ_{max} =260 mμ, ε=43.4×10^3 in ethanol[4)]) indicated the bathochromic effect of the *p*-aminophenyl group attached directly to the triazine ring.

Preparation of Polyamides. The low-temperature-solution polycondensation using organic

*1 Present address: Department of Fibers and Polymers, Nagoya Institute of Technology, Gokiso, Showa-ku, Nagoya.

1) a) J. Preston and W. B. Black, *J. Polym. Sci., Part C*, **19**, 17 (1967). b) Y. Iwakura, K. Uno, Y. Imai and M. Fukui, *Makromol. Chem.*, **77**, 41 (1964).

2) E. M. Smolin and L. Rapoport, "*s*-Triazines and Derivatives," Interscience Publishers, New York (1959), p. 333.

3) J. T. Thurston, U. S. 2447440 (1948); *Chem. Abstr.*, **42**, 9196c (1948).

4) Y. Yuki, T. Kakurai and T. Noguchi, *Yuki Gosei Kagaku Kyokai Shi*, **26**, 1119 (1968).

Table 1. Diamines containing *s*-triazine rings

Diamine	No.	Mp (°C)	Found (Calcd.) C(%)	H(%)	N(%)	UV spectra[c] λ_{max} (mμ) ($\varepsilon\times10^{-3}$)
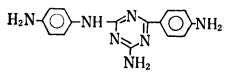	I	231—231.5	61.50 (61.42)	5.12 (5.15)	32.89 (33.43)	316(39.7)
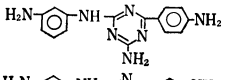	II	211.5—212	61.29 (61.42)	4.98 (5.15)	32.75 (33.43)	320(39.7)
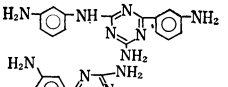	III	158.5—159	60.90 (61.42)	4.89 (5.15)	32.98 (33.43)	237 (53.9) 256[s](35.4) 306 (10.7)
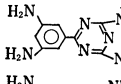	IV	258—259.5	47.36 (47.78)	5.33 (5.35)	42.54 (43.34)[a]	254[s](16.4) 284 (8.2)
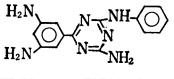	V	126—127	58.45 (58.05)	5.12 (5.20)	31.57 (31.59)[b]	256 (30.1) 294 (15.2)

a) Calcd. for $C_9H_{11}N_7\cdot\frac{1}{2}H_2O$
b) Calcd. for $C_{15}H_{15}N_7\cdot H_2O$
c) Measured in methyl cellosolve

Table 2. Polyamindes containing *s*-triazine rings

Polymer	R	No.	η_{sp}/C[a]	Elementaly analysis[b] C(%)	H(%)	N(%)
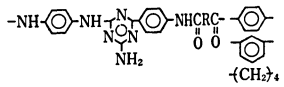		1	0.41	60.31	3.77	21.79
		2	0.38	59.93	3.76	20.81
	$-(CH_2)_4-$	3	0.29	58.11	5.43	21.82
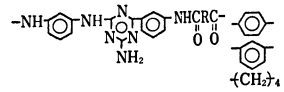		4	0.17	60.52	3.54	21.22
		5	0.26	60.13	3.59	20.67
	$-(CH_2)_4-$	6	0.17	58.62	5.51	21.69
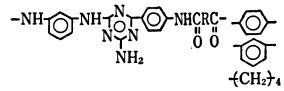		7	0.18	60.56	4.24	21.96
		8	0.52	61.50	4.17	21.18
	$-(CH_2)_4-$	9	0.22	59.23	5.36	23.79
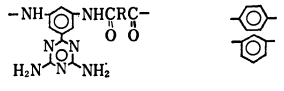		10	0.14	48.37	4.84	21.90
		11	0.33	49.73	4.78	23.81
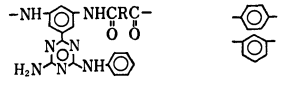		12	0.12	58.91	4.60	20.86
		13	0.19	58.58	4.38	20.27

a) Measured in DMSO at 30°C, $C=0.3$ g/dl.
b) Calcd for $C_{23}H_{17}N_7O_2\cdot2H_2O$: C, 60.12; H, 4.61; N, 21.34; about No. 1, 2, 4, 5, 7, and 8
for $C_{21}H_{21}N_7O_2\cdot2H_2O$: C, 57.40; H, 5.69; N, 22.32; about No. 3, 6, and 9
for $C_{17}H_{13}N_7O_2\cdot3H_2O$: C, 50.83; H, 3.99; N, 24.44; about No. 10 and 11
for $C_{23}H_{17}N_7O_2\cdot3H_2O$: C, 57.86; H, 4.82; N, 20.55; about No. 12 and 13

polar solvents is well known to be effective in preparing high-molecular-weight polyamides from aromatic diamines and dicarboxylic acid chlorides. This procedure was used here. The diamines used are described in Table 1; the carboxylic acid chlorides used were terephthaloyl chloride, isophthaloyl chloride, and adipoyl chloride.

The results of the preparation of polyamides by the solution polycondensation using dimethylacetamide (DMA) as a solvent are shown in Table 2. The polyamides were obtained almost quantitatively and were all a white powder except the No. 1 (yellow) and 2 (yellow) polymers. Poly-*m*-phenylene isophthalamide was prepared for the purpose of comparison.

Properties of Polyamides. Figure 1 shows the IR spectra of several polyamides. The spectra of the model compound, 2-amino-4-anilino-6-*p*-benzamidophenyl-*s*-triazine, and 2-amino-4-*p*-aminoanilino-6-*p*-aminophenyl-*s*-triazine are also shown. The bands at 815, 1390, and 1500—1600 cm^{-1} are characteristic of the amino-*s*-triazine ring. In polyamides and the model compound, the bands of amide I and amide II are masked by

Table 3. Solubilities of polyamides

Solvent	Polymer												
	1	2	3	4	5	6	7	8	9	10	11	12	13
DMF	++[a)]	++	++	++	++	++	++	++	++	+	+	++	++
DMA	++	++	++	++	++	++	++	++	++	++	++	++	++
DMSO	++	++	++	++	++	++	++	++	++	++	++	++	++
Methyl cellosolve	+	++	++	++	++	++	+	++	+	−	−	+	+
Formic acid	+	+	+	+	+	++	+	+	++	++	++	++	++
Acetic acid	−	+	+	+	−	+		+		−	−	+	+
Sulfuric acid	++	++	++	++	++	++	++	++	++	++	++	++	++

a) ++; soluble. +; partially soluble or swelling. −; insoluble.

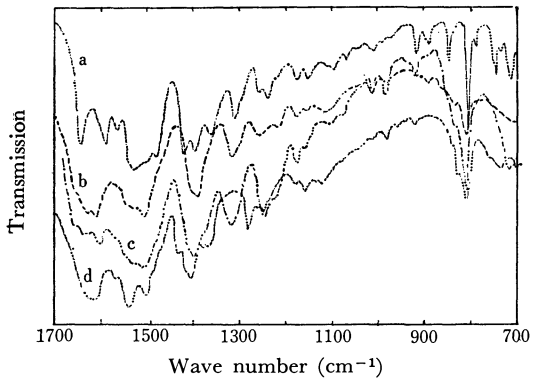

Fig. 1. IR spectra (KBr).

a : the model compound (2-amino-4-anilino-6-*p*-benzamidophenyl-*s*-triazine)
b : polyamide No. 1, c : polyamide No. 2,
d : 2-amino-4-*p*-aminoanilino-6-*p*-aminophenyl-*s*-triazine

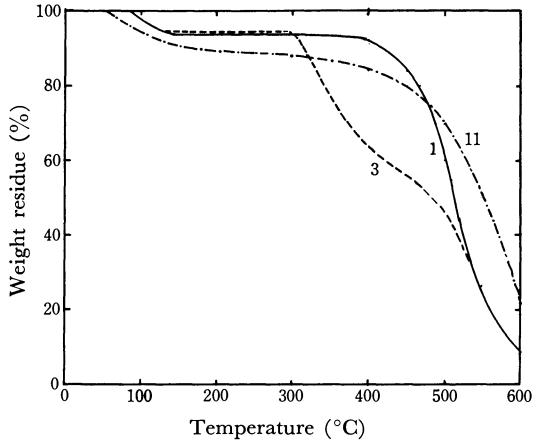

Fig. 2. TGA of some polyamide.

ΔT=5°C/min, in air, No. of polymer are shown in Table 2.

the broad bands of amino-*s*-triazine, but the band of amide III at 1320 cm^{-1} is present.

The solubilities of the polyamides are shown in Table 3. These polyamides were soluble in DMF, DMSO, DMA, and sulfuric acid, but were insoluble in the usual organic solvents. These results show that these polymers are linear and that the amino group on *s*-triazine is free.

The thermal stabilities of these polyamides were determined by thermogravimetric analysis (TGA) and by differential thermal analysis (DTA). The TGA curves of some typical polymers are shown in Fig. 2. The TGA curves of the Nos. 2, 4, 5, 7, and 8 polymers are like of No. 1, those of Nos. 6 and 9 were like that of No. 3, and those of Nos. 10, 12, and 13 were like that of No. 11. The aromatic polyamides containing *s*-triazines in the main chain showed a good thermal stability and began to decompose above 450°C. On the other hand, those containing *s*-triazines in the side chain gradually decomposed above 300°C, like poly-*m*-phenylene isophthalamide. The data of the thermal analysis of polyamides are summed up in Table 4.

Table 4. Thermal properties of polyamides

Polymer No.	DTA (°C) Tg.	DTA (°C) Mp	Decomp.[a)]	TGA (°C) 5% weight loss
1	325	410	470	445
2	315	425	455	440
3	215	320	330	320
4	300	430	460	—
5	280	435	465	480
6	215	325	420	365
7	265	438	475	430
8	295	—	465	435
9	200	340	385	360
10	325	—	420[b)]	380
11	350	—	400[b)]	410
12	240	450	500	420
13	280	445	475	440

a) A top of exothermic peak
b) Arising point of exothermic peak

Preparation of Polyureas. The polyureas were prepared by the polyaddition of diamines containing *s*-triazine with diisocyanates in DMA. The results are shown in Table 5. The polymers

Table 5. Polyureas containing *s*-triazines

Polymer	R	No.	Condition (°C/hr)	η_{sp}/C[a]	Found (calcd) C(%)	H(%)	N(%)
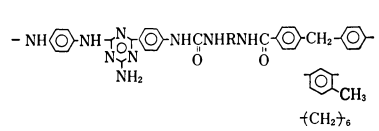		14	0/5	0.17	63.50 (62.18)	5.22 (5.01)	21.15 (21.76)[b]
		15	0/7	0.14	57.79 (57.26)	5.80 (4.97)	23.74 (25.05)[c]
		16	0/7	0.31	56.91 (55.53)	6.45 (6.24)	25.62 (25.05)[d]
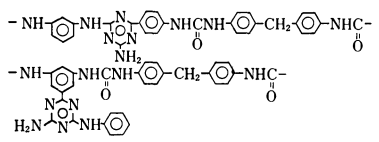		17	15/8	0.16	62.28 (62.18)	5.20 (5.01)	21.50 (21.76)[b]
		18	15/8	0.16	58.41 (58.53)	5.71 (5.40)	19.57 (20.47)[e]

a) Measured in DMSO at 30°C, C=0.3 g/d*l*.
b) Calcd for $C_{30}H_{25}N_9O_2\cdot 2H_2O$
c) Calcd for $C_{24}H_{21}N_9O_2\cdot 2H_2O$
d) Calcd for $C_{23}H_{27}N_9O_2\cdot 2H_2O$
e) Calcd for $C_{30}H_{25}N_9O_2\cdot 4H_2O$

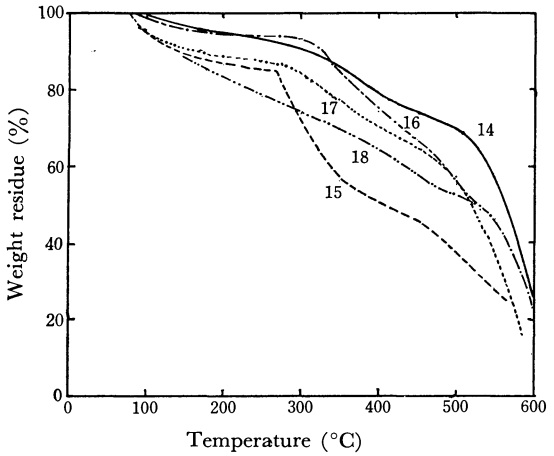

Fig. 3. TGA of polyureas.
ΔT=5°C/min, in air, No. of polymer are shown in Table 5.

showed low viscosity values except in the case No. 16.

The solubility of these polyureas was like that of the above polyamide, and they were soluble in DMSO, DMA, DMF, formic acid, acetic acid, and mineral acid.

The TGA curves of these polyureas are shown in Fig. 3. The thermal stability of polyureas was inferior to that of polyamides.

Experimental

Materials. The arylbiguanides were prepared by the reaction of dicyanodiamide with related arylamine hydrochlorides following the method of Cohn.[5] The biguanide was prepared by the method of Odo.[6] All the other reagents were commercially available and were used after purification if necessary.

2-Amino-4-p-nitroanilino-6-p-nitrophenyl-s-triazine. A suspension of 33 g (0.15 mol) of *p*-nitrophenylbiguanide in 300 m*l* of acetone was treated with 25 g (0.135 mol) of *p*-nitrobenzoyl chloride, and then 7.5 g (0.135 mol) of potassium hydroxide in water were added. Stirring and cooling at 0—5°C were continued during the reaction. After the acetone had then been removed, the yellow precipitate was separated and washed with hot water. The product was given almost quantitatively; 47.5 g, mp 300°C. (Found: N, 27.95%; Calcd.: N, 27.75%)

The other dinitro-compounds were prepared in a similar manner.

2-Amino-4-p-aminoanilino-6-p-aminophenyl-s-triazine. By stirring and refluxing, to a suspension of 11.5 g (0.033 mol) of the above dinitro-compound and 17.5 g (0.15 mol) tin in 100 m*l* of ethanol we added, drop by drop over 1-hr period, 100 m*l* of 12 N hydrochloric acid. The reaction mixture became clear and then formed a precipitate. When the precipitate was separated, dissolved in water, and treated with strong alkali, a white precipitate was also given. The product was separated; 9.0 g (93%), mp 231—231.5°C

The reduction of the other dinitro-compounds was carried out in a similar manner.

Preparation of Polyamides. In a 100-m*l*, three-necked flask equipped with a stirrer and a nitrogen inlet, we placed 7 m*l* of DMA, 0.300 g of 2-amino-4-*p*-aminoanilino-6-*p*-aminophenyl-*s*-triazine, and 0.15 g of lithium chloride; then 0.216 g of terephthaloyl chloride was gradually added at 25°C. After 8 hr, the reaction mixture was poured into methanol. The polymer was isolated, washed with water, dipped in a dilute alkali solution, repeatedly washed again with water and methanol, and dried. The polymer obtained amounted to 0.429 g.

5) G. Cohn, *J. Prakt. Chem.*, **84**, 394 (1911).

6) K. Kono and K. Odo, *Yuki Gosei Kagaku Kyokai Shi*, **20**, 649 (1962).

The other polyamides and polyureas were treated in a similar manner.

Preparation of the Model Compound. 2-Amino-4-anilino-6-*p*-nitrophenyl-*s*-triazine was prepared by the reaction of phenylbiguanide with *p*-nitrobenzoyl chloride; yellow powder, mp 206.5—208°C.

Found: C, 58.25; H, 4.13; N, 27.43%. Calcd for $C_{15}H_{12}N_6O_2$: C, 58.04; H, 3.89; N, 27.27%.

2-Amino-4-anilino-6-*p*-aminophenyl-*s*-triazine was given by the reaction of the nitro-compound with tin and hydrochloric acid in ethanol; mp 200.5—201.5°C.

The model compound, 2-amino-4-anilino-6-*p*-benzamidophenyl-*s*-triazine, was prepared by the reaction of the above amine with benzoyl chloride by a method of preparation similar to that used for the polyamides; mp 222—222.5°C, 69%. The results of elementary analysis agreed with the value calculated for semi-hydrate.

Found: C, 67.63; H, 4.70; N, 21.19%. Calcd for $C_{22}H_{18}N_6O \cdot \frac{1}{2}H_2O$: C, 67.51; H, 4.89; N, 21.47%.

The authors wish to thank Mr. T. Saito of Tokyo Institute of Technology for his elementary analysis.

BULLETIN OF THE CHEMICAL SOCIETY OF JAPAN VOL. 43 2134—2137 (1970)

Synthesis of 1,3-Thiazine Derivatives from 2-Iminocyclopentanedithiocarboxylic Acid[1)]

Motomu MURAOKA*[1], Masataka YOKOYAMA*[2], Kiyoko YAMAMOTO*[3], and Tatsuo TAKESHIMA*[2]

Department of Chemistry, Faculty of Science, Josai Uuiversity, Sakado, Saitama, and The Institute of Physical and Chemical Research, Yamatomachi, Saitama

(Received October 11, 1969)

Several new 3-substituted and 3,3-disubstituted-1,3,4,5,6,7-hexahydro-1-thioxocyclopenta[*d*]-[1,3]thiazines were obtained by the reactions of 2-iminocyclopentanedithiocarboxylic acid with some aldehydes and ketones. Some intermediate compounds in these reactions such as 2-amino-2-[2-(piperonylidenamino)-1-cyclopenten-1-yl]thiocarbonylthiocyclopentanedithiocarboxylic acid, 2-amino-2-[2-(vanillylidenamino)-1-cyclopenten-1-yl]thiocarbonylthiocyclopentanedithiocarboxylic acid, and 2-amino-2-[2-(4-methoxybenzylidenamino)-1-cyclopenten-1-yl]thiocarbonylthiocyclopentanedithiocarboxylic acid could be isolated.

Several new 1,3-thiazine derivatives were synthesized by the reactions of 2-iminocyclopentanedithiocarboxylic acid (I) with carbonyl compounds. Compound I was isolated as the intermediate during the course of synthesis of 1,3,4,5,6,7-hexahydro-1-thioxocyclopenta[*d*][1,3]thiazine-3-spirocyclopentane. The coupling reactions of I with ketones were partly reported.[2)]

The reactions in question were effected by acid or base, and 3-substituted and 3,3-disubstituted-1,3,4,5,6,7-hexahydro-1-thioxocyclopenta[*d*][1,3]-thiazines (III) were produced. Aliphatic and alicyclic ketones, in the presence of morpholine,[2)] easily reacted with I to give respective thiazine derivatives. However, aldehydes and acetophenone under the same conditions did not afford the expected products.

On treatment with sulfuric acid in place of morpholine, we have found that aldehydes such as piperonal, vanillin, anisaldehyde, acetaldehyde, salicylaldehyde, benzaldehyde, *o*-methoxy or *p*-hydroxybenzaldehyde and *p*-tolualdehyde as well as ketones such as acetophenone, methyl ethyl ketone and acetone reacted with I to afford the corresponding thiazine derivatives III. This paper deals with the results.

Evidence for the structures of IIIa—j was provided by comparison of their IR, UV and NMR spectra with those of known 1,2,5,6,7,8-hexahydro-4-thioxo-4*H*-3,1-benzo[*d*]thiazine-2-spirocyclohexane, 2-ethyl-2,4,5-trimethyl-2,3-dihydro-6-thioxo-6*H*-1,3-thiazine, and 3,3-dimethyl-1,3,4,5,6,7-hexahydro-1-thioxocyclopenta[*d*][1,3]thiazine.[2-4)] The doublet near δ 6.15 (J=4—6 Hz) was assigned to a C-3 proton, and thus structures

1) a) A part of this paper was read at the 22nd Annual Meeting of the Chemical Society of Japan, Tokyo, April 1969.

*1 Present address: Department of Chemistry, Faculty of Science, Josai University.

*2 Present address: Department of Chemistry, Faculty of Science, Chiba University.

*3 Present address: The Institute of Physical and Chemical Research.

2) T. Takeshima, M. Yokoyama, T. Imamoto, M. Akano and H. Asaba, *J. Org. Chem.*, **34**, 730 (1969).

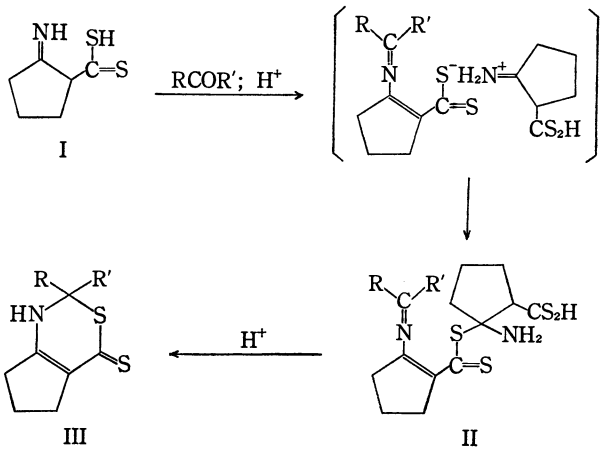

IIIa, R=H, R'=3,4(-OCH_2O-)C_6H_3
IIa, R=H, R'=3,4(-OCH_2O-)C_6H_3
IIIb, R=H, R'=3-CH_3O-4-HO-C_6H_3
IIb, R=H, R'=3-CH_3O-4-HO-C_6H_3
IIIc, R=H, R'=*p*-CH_3O-C_6H_4
IIc, R=H, R'=*p*-CH_3O-C_6H_4
IIId, R=H, R'=CH_3
IIIe, R=CH_3, R'=C_6H_5
IIIf, R=H, R'=*o*-HO-C_6H_4
IIIg, R=H, R'=C_6H_5
IIIh, R=H, R'=*o*-CH_3O-C_6H_4
IIIi, R=H, R'=*p*-HO-C_6H_4
IIIj, R=H, R'=*p*-CH_3-C_6H_4
IIIk, R=CH_3, R'=C_2H_5
IIIl, R=R'=CH_3

III were proposed as the corresponding thiazine structures.

It was shown that the reaction of methyl ethyl ketone with I was abortive.[2] However, the present experiment revealed that 3-ethyl-3-methyl-1,3,4,5,6,7 - hexahydro-1-thioxocyclopenta[*d*][1, 3]-thiazine IIIk, had a molecule of water of crystallization which was lost on heating at 138°C under reduced pressure and thus was of a different physical nature. Likewise, the thiazine derivatives IIIa and IIIj which were obtained by the reactions of I with piperonal and *p*-tolualdehyde, respectively, also had a molecule of water of crystallization which was lost on heating at 110°C under reduced pressure.

Under the acidic conditions, piperonal, vanillin and anisaldehyde gave respective intermediate compounds IIa, IIb and IIc at low temperature which changed to IIIa—b on treatment with sulfuric acid. Compound IIc was resistant to conversion into IIIc.

Structures IIa, IIb and IIc were assigned by spectral data (see Experimental).

Experimental

2-Amino-2-[2-(piperonylidenamino)-1 - cyclopenten-1-yl]thiocarbonylthiocyclopentanedithiocarboxylic acid (IIa). A solution of I (4.1 g), piperonal (4 g) and sulfuric acid (96%, 1 g) in 150 m*l* of methanol was allowed to stand for 5 min at room temperature. The yellow material was collected, washed with methanol and recrystallized from methanol-*N*,*N*-dimethylformamide. Yellow long plates (IIa): yield 4.6 g, 70%; mp 211—214°C with dec. (slow heating), 215—220°C with dec. (rapid heating); UV λ_{max}^{MeOH} 311, 397 mμ (log ε=4.04, 4.32); IR (KBr) 3380 (m, NH_2), 3296 (s, NH_2), 1609 (s, δ NH_2), 1600 (vs, C=N), 1500 (s, ring), 1486 (s, ring), 1475 cm^{-1} (m, ring); NMR (CF_3COOH) δ 9.00 (br, 1H, S<u>H</u>), 7.08 (m, 4H, $C_6\underline{H}_3$ and C<u>H</u>=N), 6.30 (s, 2H, $OC\underline{H}_2O$), 3.03 (m, 9H, C-1, 3,5,3',5' $\underline{H}_2$), 2.20(m, 4H, C-4,4'$\underline{H}_2$); NMR (CD_3SOCD_3) δ 10.80 (br, *ca.* 2H, N<u>H</u>$_2$), 9.00 (br, *ca.* 1H, S<u>H</u>); Found: C, 53.56; H, 5.09; N, 6.18; S, 28.36%. Calcd for $C_{20}H_{22}N_2S_4O_2$: C, 53.30; H, 4.92; N, 6.22; S, 28.45%.

NMR absorptions of NH_2 and SH in CD_3SOCD_3 disappeared by addition of deuterium oxide.

Conversion of IIa into IIIa. A mixture of IIa (1 g), sulfuric acid (96%, 400 mg) and 50 m*l* of methanol was refluxed for *ca.* 1 hr until a clear solution was obtained. After cooling, a yellowish orange material was collected and recrystallized from *N*,*N*-dimethylformamide-water as yellowish orange long plates: mp 177—178°C, undepressed on admixture with an authentic specimen; yield 500 mg, 77%. IR and UV spectra of both specimens also were identical.

2-Amino-2- [2-(vanillylidenamino)-1-cyclopenten-1-yl]thiocarbonylthiocyclopentanedithiocarboxylic acid (IIb). To an ice-cold solution of I (4.7 g) and vanillin (5 g) in methanol (130 m*l*), sulfuric acid (96%, 2 g) was added and the solution was kept at 0°C for 5 min. The resulting yellow material was recrystallized from acetone-water. Yellow long plates (IIb): yield 5.2 g, 77%; mp 190—192°C with dec. (slow heat-

3) T. Takeshima, T. Hayashi, M. Muraoka and T. Matsuoka, *ibid.*, **32**, 980 (1967).

4) T. Takeshima, T. Imamoto, M. Yokoyama, K. Yamamoto and M. Akano, *ibid.*, **33**, 2877 (1968).

ing), 199—201°C with dec. (rapid heating); UV λ_{max}^{MeOH} 308, 397 mμ (log ε=4.13, 4.30); IR ($CHCl_3$) 3320 (m, NH_2), 3260 (m, NH_2), 1614 (s, δ NH_2), 1603 (vs, C=N), 1510 (m, ring), 1500 (m, ring), 1472 cm^{-1} (m, ring); NMR (CF_3COOH) δ 8.97 (br, 1H, SH), 7.30 (m, 4H, C_6H_3 and CH=N), 6.12 (s, 1H, OH), 4.04 (s, 3H, OCH_3), 3.08 (m, 9H, C-1,3,5,3′,5′ H_2), 2.23 (m, 4H, C-4,4′ H_2); NMR (CD_3SOCD_3) δ 10.86 (br, *ca.* 2H, NH_2), 8.97 (br, *ca.* 1H, SH); Found: C, 53.13; H, 5.49; N, 6.16; S, 28.53%. Calcd for $C_{20}H_{24}N_2S_4O_2$: C, 53.07; H, 5.35; N, 6.19; S, 28.32%.

Conversion of IIb into IIIb. A mixture of IIb (1 g), sulfuric acid (96%, 0.5 g), *N,N*-dimethylformamide (25 m*l*) and methanol (50 m*l*) was refluxed for 15 min and allowed to stand at room temperature for 2 hr and then was added water. The resulting material was recrystallized from *N,N*-dimethylformamide-water as orange prisms: yield 400 mg, 62%; mp 229—238°C with dec., undepressed by addition of an authentic specimen. UV and IR spectra of both specimens also were identical.

2 - Amino - 2 - [2-(4-methoxybenzylidenamino)-1-cyclopenten-1-yl]thiocarbonylthiocyclopentanedithiocarboxylic acid (IIc). To an ice-cold solution of I (2.5 g) and anisaldehyde (2.5 g) in methanol (100 m*l*), sulfuric acid (96%, 1 g) was added and kept at 0°C for 10 min. The reaction mixture was worked up as above. Yellow long plates (IIc): yield 3 g, 88%; mp 209—214°C with dec. (slow heating), 213—223°C with dec. (rapid heating); UV λ_{max}^{MeOH} 275, 392 mμ (log ε=4.15, 4.27); IR (KBr) 3389 (m, NH_2), 3294 (s, NH_2), 1607 (vs. C=N), 1510 (s, ring), 1450 cm^{-1} (s, ring); NMR (CF_3COOH) δ 9.50 (br, 1H, SH), 7.18 (m, 5H, C_6H_4 and CH=N), 4.03 (s, 3H, OCH_3), 3.07 (m, 9H, C-1,3,5,3′,5′ H_2), 2.27 (m, 4H, C-4,4′ H_2); NMR (CD_3SOCD_3) δ 10.81 (br, *ca.* 2H, NH_2), 8.97 (br, *ca.* 1H, SH); Found: C, 54.96; H, 5.70; N, 6.53; S, 29.14%. Calcd for $C_{20}H_{24}N_2S_4O$: C, 55.02; H, 5.54; N, 6.42; S, 29.36%.

3 - (3,4 - Methylenedioxyphenyl) - 1,3,4,5,6,7-hexahydro-1-thioxocyclopenta[*d*][1,3]thiazine(IIIa). A solution of I (2 g), piperonal (2 g) and sulfuric acid (96%, 1 g) in methanol (100 m*l*) was refluxed for 35 min. The resulting material was collected and recrystallized from *N,N*-dimethylformamide-water and dried at 110°C under reduced pressure for 1 day to give yellowish orange plates (IIIa): yield 3.6 g, 92%; mp 178—179°C; UV λ_{max}^{EtOH} 341, 408 mμ (log ε=4.00, 4.61); IR ($CHCl_3$) 3406 (s, NH), 1541 (s, conjd C=C), 1520 (s, ring), 1506 (vs, ring), 1446 cm^{-1} (s, ring); NMR (CF_3COOH) δ 9.42 (br, 1H, NH), 7.02 (m, 3H, C_6H_3), 6.14 (d, 1H, *J*=4 Hz, C-3 H), 6.07 (s, 2H, OCH_2O), 3.05 (m, 4H, C-5,7 H_2). 2.37 (m, 2H, C-6 H_2); Found: C, 57.86; H, 4.46; N, 4.79; S. 22.08%. Calcd for $C_{14}H_{13}NS_2O_2$: C, 57.71; H, 4.50; N, 4.81; S, 21.99%.

3-(3-Methoxy-4-hydroxyphenyl)-1,3,4,5,6,7-hexahydro-1-thioxocyclopenta[*d*][1,3]thiazine (IIIb). A solution of I (2.5 g), vanillin (2.5 g) and sulfuric acid (96%, 1 g) in methanol (60 m*l*) was refluxed for 1 hr. The resulting material was worked up as above. Light lustrous orange prisms (IIIb): yield 4.1 g, 89%; mp 229—239°C with dec. (slow heating), 237—250°C with dec. (rapid heating); UV λ_{max}^{EtOH} 340, 408 mμ (log ε=3.93, 4.32); IR ($CHCl_3$) 3365 (s, NH), 1560 (s, conjd C=C), 1505 (vs. ring), 1444 cm^{-1} (m, ring); NMR (CF_3COOH) δ 9.50 (br, 1H, NH), 7.12 (m, 3H, C_6H_3), 6.15 (d, *J*=4 Hz, C-3 H), 3.97 (s, 3H, OCH_3), 3.00 (m, 4H, C-5,7 H_2), 2.36 (m, 2H, C-6 H_2); NMR (CD_3SOCD_3) δ 9.60 (s, 1H, OH), 9.37 (br, 1H, NH); Found: C, 57.31; H, 5.09; N, 4.80; S, 21.60%. Calcd for $C_{14}H_{15}NS_2O_2$: C, 57.32; H, 5.16; N, 4.78; S, 21.85 %.

3 - (4 - Methoxyphenyl) - 1,3,4,5,6,7 - hexahydro-1-thioxocyclopenta[*d*][1,3]thiazine (IIIc). To a hot solution of I (2.5 g) and anisaldehyde (2.5 g) in methanol (100 m*l*), was added sulfuric acid (96%, 1 g) and refluxed for 30 min. The resulting mixture was worked up as above. Red long prisms (IIIc): yield 3.5 g, 81%; mp 179—180°C; UV λ_{max}^{EtOH} 341, 408 mμ (log ε=3.70, 4.08): IR ($CHCl_3$) 3410 (s, NH), 1545 (s, conjd C=C), 1515 cm^{-1} (vs. ring): NMR (CF_3COOH) δ 9.39 (br, 1H, NH), 7.34 (q, 4H, C_6H_4), 6.17 (d, 1H, *J*=4 Hz, C-3 H), 4.08 (s, 3H, OCH_3), 3.03 (m, 4H, C-5,7 H_2), 2.38 (m, 2H, C-6 H_2); Found: C, 60.66; H, 5.34; N, 5.15; S, 23.13%. Calcd for $C_{14}H_{15}NS_2O$: C, 60.62; H, 5.45; N, 5.05; S, 23.11%.

3 - Methyl - 1,3,4,5,6,7 - hexahydro -1- thioxocyclopenta[*d*][1,3]thiazine (IIId). A solution of I (5 g), acetaldehyde (5 g) and sulfuric acid (96%, 2 g) in methanol (150 m*l*) was allowed to stand at room temperature for 64 hr. The resulting reaction mixture was concentrated under reduced pressure and then water was added. The purple material which separated from the solution was recrystallized from methanol-water. Light orange plates (IIId): yield 4.5 g, 78%; mp 128—129°C; UV λ_{max}^{EtOH} 337, 405 mμ (log ε=3.72, 4.26); IR ($CHCl_3$), 3405 (s, NH), 1550 (vs, conjd C=C), 1515 cm^{-1} (vs. ring); NMR (CF_3COOH) δ 9.40 (br, 1H, NH), 5.17 (m, 1H, C-3 H), 2.92 (m, 4H, C-5,7 H_2), 2.25 (m, 2H, C-6 H_2), 1.85 (d, 3H, CH_3); Found: C, 51.83; H, 5.83; N, 7.62; S, 34.87%. Calcd for $C_8H_{11}NS_2$: C, 51.85; H, 5.99; N, 7.55; S, 34.61%.

3-Methyl-3-phenyl-1,3,4,5,6,7-hexahydro-1-thioxocyclopenta[*d*][1,3]thiazine (IIIe). A mixture of I (5 g), acetophenone (5 g), sulfuric acid (96%, 2 g) and methanol (150 m*l*) was refluxed for 3 hr and the reaction mixture was worked up as above. Light orange plates (IIIe): yield 1.6 g, 19.5%; mp 183—184°C (remelted at 195—197°C); UV λ_{max}^{EtOH} 340, 407 mμ (log ε=3.70, 4.30); IR ($CHCl_3$) 3400 (m, NH), 1550 (vs. conjd C=C), 1522 cm^{-1} (s, ring); NMR (CF_3COOH) δ 9.66 (br, 1H, NH), 7.51 (s, 5H, C_6H_5), 3.03 (m, 4H, C-5,7 H_2), 2.31 (m, 2H, C-6 H_2), 2.28 (s, 3H, CH_3); Found: C, 64.41; H, 5.77; N, 5.40; S, 24.73%. Calcd for $C_{14}H_{15}NS_2$: C, 64.32; H, 5.79; N, 5.36; S, 24.53%.

3 - (2 - Hydroxyphenyl) - 1,3,4,5,6,7 - hexahydro - 1-thioxocyclopenta[*d*][1,3]thiazine (IIIf). A solution of I (2 g), salicylaldehyde (2 g) and sulfuric acid (96%, 1 g) in methanol (70 m*l*) was refluxed for 10 min and then allowed to stand at room temperature for 1 hr. The reaction mixture was concentrated under reduced pressure, then water was added. The resulting red material was recrystallized from methanol-water. Red long plates (IIIf): yield 2.2 g, 67%; mp 201—215°C with dec. (slow heating), 211—227°C with dec. (rapid heating); UV λ_{max}^{EtOH} 341, 408 mμ (log ε=3.87, 4.20); IR ($CHCl_3$) 3260 (s, OH), 3160 (s, br, NH), 1560 (s, conjd C=C), 1495 cm^{-1} (vs. ring); NMR (CF_3COOH) δ 9.43 (s, br, 2H, OH and NH), 7.28 (m, 4H, C_6H_4), 6.58 (d, 1H, *J*=5 Hz, C-3 H), 3.02 (m, 4H, C-5,7 H_2), 2.35 (m, 2H, C-6 H_2); Found: C, 59.46; H, 4.92;

N, 5.25; S, 23.95%. Calcd for $C_{13}H_{13}NS_2O$: C, 59.28, H, 4.98; N, 5.32; S, 24.34%.

3-Phenyl-1,3,4,5,6,7-hexahydro-1- thioxocyclopenta[*d*][1,3]thiazine (IIIg). A solution of I (5 g), benzaldehyde (5 g) and sulfuric acid (96%, 2 g) in methanol (150 m*l*) was refluxed for 2 hr. The resulting material was recrystallized from methanol. Red prisms (IIIg): yield 5.1 g, 66%; mp 199—200°C; UV λ_{max}^{EtOH} 340, 408 mμ (log ε=3.86, 4.28); IR ($CHCl_3$) 3400 (s, NH), 1546 (vs. conjd C=C), 1515 cm^{-1} (s, ring); NMR (CF_3COOH) δ 9.45 (br, 1H, N<u>H</u>), 7.49 (m, 5H, $C_6\underline{H}_5$), 6.13 (d, 1H, J=4 Hz, C-3 <u>H</u>), 2.97 (m, 4H, C-5,7 $\underline{H}_2$), 2.31 (m, 2H, C-6 $\underline{H}_2$); Found: C, 63.06; H, 5.11; N, 5.70; S, 25.79%. Calcd for $C_{13}H_{13}NS_2$: C, 63.12; H, 5.30; N, 5.66; S, 25.92%.

3 - (2 - Methoxypehnyl) - 1,3,4,5,6,7 - hexahydro-1-thioxocyclopenta[*d*][1,3]thiazine (IIIh). A mixture of I (5 g), *o*-methoxybenzaldehyde (5 g), sulfuric acid (96%, 2 g) and methanol (150 m*l*) was refluxed for 30 min and worked up as above. Light thick plates (IIIh): yield 5.3 g, 61%; mp 201°C; UV λ_{max}^{EtOH} 341, 408 mμ (log ε=3.88, 4.29); IR ($CHCl_3$) 3410 (s, NH), 1547 (vs. conjd C=C), 1510 cm^{-1} (s, ring); NMR (CF_3COOH) δ 9.35 (br, 1H, N<u>H</u>), 7.28 (m, 4H, $C_6\underline{H}_4$), 6.56 (d, 1H, J=6 Hz, C-3 <u>H</u>), 3.97 (s, 3H, $OC\underline{H}_3$), 3.00 (m, 4H, C-5,7 $\underline{H}_2$), 2.36 (m, 2H, C-6 $\underline{H}_2$); Found: C, 60.73; H, 5.57; N, 5.10; S, 23.10%. Calcd for $C_{14}H_{15}NS_2O$: C, 60.62; H, 5.45; N, 5.05; S, 23.11%

3 - (4 - Hydroxyphenyl) - 1,3,4,5,6,7 - hexahydro-1-thioxocyclopenta[*d*][1,3]thiazine (IIIi). A mixture of I (5 g), *p*-hydroxybenzaldehyde (5 g), sulfuric acid (96%, 2 g) and methanol (150 m*l*) was allowed to stand at room temperature for 30 min and worked up as above. Orange prisms (IIIi): yield 6.4 g, 77%; mp, 197—213°C with dec. (slow heating), 211—220°C with dec. (rapid heating); UV λ_{max}^{EtOH} 340, 408 mμ (log ε=3.88, 4.28); IR ($CHCl_3$) 3268 (s, OH), 3100 (m, br, NH), 1566 (s, conjd C=C), 1512 cm^{-1} (vs. ring); NMR (CF_3COOH) δ 9.49 (br, 1H, N<u>H</u>), 7.27 (q, 4H, $C_6\underline{H}_4$), 6.18 (d, 1H, J=4 Hz, C-3 <u>H</u>), 3.00 (m, 4H, C-5,7 $\underline{H}_2$), 2.31 (m, 2H, C-6 $\underline{H}_2$); Found: C, 59.28; H, 4.83; N, 5.33; S, 24.37%. Calcd for $C_{13}H_{13}NS_2O$: C, 59.28; H, 4.98; N, 5.32; S, 24.34%.

3 - (p-Tolyl) - 1,3,4,5,6,7-hexahydro-1-thioxocyclopenta[*d*][1,3]thiazine(IIIj). A mixture of I (3 g), *p*-tolualdehyde (3 g), sulfuric acid (96%, 1 g) and methanol (100 m*l*) was refluxed for 30 min and then water was added. The solution was allowed to stand at room temperature for 12 hr. The resulting crystalline material was recrystallized from methanol and dried at 110°C under reduced pressure. Light orange prisms (IIIj): yield 2.3 g, 44%; mp 176—177°C; UV λ_{max}^{EtOH} 340, 408 mμ (log ε=3.91, 4.34); IR ($CHCl_3$) 3420 (s, NH), 1545 (s, conjd C=C), 1515 cm^{-1} (vs. ring); NMR (CF_3COOH) δ 9.50 (br, 1H, N<u>H</u>), 7.40 (s, 4H, $C_6\underline{H}_4$), 6.17 (d, 1H, J=3 Hz, C-3 <u>H</u>), 3.08 (m, 4H, C-5,7 $\underline{H}_2$), 2.42 (s, 3H, $C\underline{H}_3$), 2.38 (m, 2H, C-6 $\underline{H}_2$); Found: C, 64.58; H, 6.05; N, 5.36; S, 24.23%. Calcd. for $C_4H_{15}NS_2$: C, 64.32; H, 5.79; N, 5.36; S, 24.53%.

3-Ethyl-3-methyl-1,3,4,5,6,7-hexahydro-1-thioxocyclopenta[*d*][1,3]thiazine(IIIk). A mixture of I (5 g), methyl ethyl ketone (22 g), morpholine (15 g) and ethanol (100 m*l*) was refluxed for 10 hr. The white precipitates which separated from the solution were filtrated, the filtrate was concentrated under reduced pressure and then water was added. The resulting yellow material was recrystallized from ethanol-water and dried at 138°C under reduced pressure for 1 day. Yellow plates (IIIk): yield 4.4 g, 67%; mp 173—174°C; UV λ_{max}^{EtOH} 336, 406 mμ (log ε=3.68, 4.25); IR (KBr) 3180 (s, NH), 1565 (m, conjd C=C), 1520 cm^{-1} (vs. ring); NMR (CD_3COCD_3) δ 9.40 (br, 1H, N<u>H</u>), 3.00 (m, 4H, C-5,7 $\underline{H}_2$), 2.25 (m, 4H, C-6 $\underline{H}_2$ and $C\underline{H}_2CH_3$), 1.85 (s, 3H, $C\underline{H}_3$). 1.15 (t, 3<u>H</u>, $CH_2C\underline{H}_3$); Found: C, 56.53; H, 7.00; N, 6.54; S, 29.99%. Calcd for $C_{10}H_{15}NS_2$: C, 56.32; H, 7.09; N, 6.57; S, 30.01%.

Compound IIIk was also obtained by refluxing a mixture of I (5 g), methyl ethyl ketone (5 g), sulfuric acid (96%, 2 g) and methanol (100 m*l*) for 1 hr; the yield was 57%.

3,3 - Dimethyl - 1,3,4,5,6,7 - hexahydro - 1 - thioxocyclopenta[*d*][1,3]thiazine (IIIl). A mixture of I (2.5 g), acetone (3 g), sulfuric acid (96%, 1 g) and methanol (100 m*l*) was refluxed for 1.5 hr and then worked up as above: yield 51%, mp 172—173°C, undepressed on admixture with an authentic specimen. IR and UV absorption spectra of IIIl were also identical with those of authentic specimen.[2)]

The authors are grateful to Dr. Hiroshi Midorikawa for his support of this work. They also wish to thank Dr. Toshio Hayashi, Miss Makiko Akano and Mr. Ichigaku Nagayama for their advice and assistance.

BULLETIN OF THE CHEMICAL SOCIETY OF JAPAN VOL. 43 2138—2142 (1970)

Geometric Configurations of α-Cyano-β-methyl-β-alkylglycidic Esters

Minoru IGARASHI,*, ** Makiko AKANO,** Akira FUJIMOTO**, *1
and Hiroshi MIDORIKAWA**

* *Department of Chemistry, Faculty of Science, Ibaraki University, Mito, Ibaraki*
** *The Institute of Physical and Chemical Research, Yamato-machi, Saitama*

(Received October 15, 1969)

α-Cyanoglycidic ester derivatives have been prepared from alkylidenecyanoacetic esters with hydrogen peroxide. The NMR technique has been applied to the study of the geometric configurations of the stereoisomeric mixture of the glycidic esters. It has been found that the β-methyl protons *cis* to the ester group respond at a higher field than do the *trans* protons.

Our search for practical methods of determining the geometric configurations of α-cyano-β-alkoxy-β-alkylacrilic esters[1] and alkylidenecyanoacetic esters[2] led to a study of nuclear magnetic resonance spectroscopy. During these studies it became apparent that the NMR non-equivalence of signals arising from geometrically-related groups of β-methylglycidic-ester derivatives which possess an oxirane ring replaced by four different groups could also serve such a purpose. Recently, Valente and Woffhagen[3] have introduced the use of this technique in the determination of the geometric configuration of β-phenylglycidic esters. We wish now to report on the chemical shifts for a number of α-cyano and α-carbamoyl-β-methyl-β-alkylglycidic esters which were gathered in order to delineate the scope of the NMR method for determining the geometric configuration.

Various conditions for epoxidation are described in the literature. The epoxidation of an alkene-bearing carbonyl substituent by a usual reagent, such as peroxy benzoic or peroxyacetic acid, is generally very slow.[4] The treatment of α,β-unsaturated nitrile with hydrogen peroxide under alkaline conditions results in the formation of epoxyamide rather than epoxynitrile.[5] We have found that the direct epoxidation of alkylidenecyanoacetic esters with hydrogen peroxide without a catalyst is satisfactory in giving the corresponding epoxynitriles. By refluxing a solution of the alkylidenecyanoacetic ester in aqueous alcohol with a small excess of 30% hydrogen peroxide for varying lengths of time, good yields of eight 2-cyano-3-methylglycidic ester derivatives (compounds I-VIII) have been obtained. That all of these compounds except 2-cyano-2,3-epoxybutanoic esters are mixtures of *cis-trans* isomers is confirmed by their NMR spectra. Table 1 shows the most important features of the NMR spectra of compounds I—VIII. The synthetic steps are shown in Chart 1.

TABLE 1. NMR SPECTRA (β-METHYL AND ESTER GROUPS) OF EPOXY ESTERS I—XVII (PPM DOWNFIELD FROM TMS).

Compound	β-CH_3		$COOCH_3$
I	1.65		4.37 ($COOC\underline{H}_2CH_3$)
			1.36 ($COOCH_2C\underline{H}_3$)
II*	1.47	1.69	3.94
IIIa	1.44	1.66	3.94
IIIb	1.41	1.65	4.37 ($COOC\underline{H}_2CH_3$)
			1.38 ($COOCH_2C\underline{H}_3$)
IV	1.42	1.66	3.94
V*	1.30	1.55	3.94
VI	1.32	1.56	3.95
VII	1.40	1.65	3.95
VIII	1.50	1.75	3.94
IX	1.45		4.33 ($COOC\underline{H}_2CH_3$)
			1.33 ($COOCH_2C\underline{H}_3$)
X*	1.42	1.46	3.86
XI	1.40	1.45	3.89
XII	1.37	1.42	3.85
XIII*	1.27	1.32	3.85
XIV	1.25	1.30	3.87
XV	1.39	1.44	3.88
XVI*	1.32		3.89
XVII	1.46	1.52	3.88

* Ref. 12.

*1 Present address: Department of Applied Science, Tokyo Electrical Engineering College, Tokyo.

1) T. Hayashi, I. Hori, H. Baba and H. Midorikawa, *J. Org. Chem.*, **30**, 695 (1965).
2) T. Hayashi, M. Igarashi, S. Hayashi and H. Midorikawa, This Bulletin, **38**, 2063 (1965).
3) V. R. Valente and J. L. Wolfhagen, *J. Org. Chem.*, **31**, 2509 (1966).
4) D. Swern, *J. Amer. Chem. Soc.*, **69**, 1692 (1947).
5) G. B. Payne and P. H. Williams, *J. Org. Chem.*, **26**, 651 (1961).

$R(CH_3)C=C(CN)COOR' \longrightarrow$
$R(CH_3)C(\diagdown O \diagup)C(CN)COOR' \longrightarrow$
$R(CH_3)C(\diagdown O \diagup)C(CONH_2)COOR'$

	R	R'
I	H	C_2H_5
II	CH_3	CH_3
IIIa	C_2H_5	CH_3
IIIb	C_2H_5	C_2H_5
IV	*n*-C_3H_7	CH_3
V	*i*-C_3H_7	CH_3
VI	*s*-C_4H_9	CH_3
VII	*i*-C_4H_9	CH_3
VIII	CH_2-*t*-C_4H_9	CH_3
IX	H	C_2H_5
X	CH_3	CH_3
XI	C_2H_5	CH_3
XII	*n*-C_3H_7	CH_3
XIII	*i*-C_3H_7	CH_3
XIV	*s*-C_4H_9	CH_3
XV	*i*-C_4H_9	CH_3
XVI	*t*-C_4H_9	CH_3
XVII	CH_2-*t*-C_4H_9	CH_3

Chart 1

The resonance positions of the methyl protons of the methoxycarbonyl group were always located in the 3.94±0.01 ppm range, while those of the methylene and methyl protons of the ethoxycarbonyl group always appeared in the 4.36±0.01 ppm and 1.37±0.01 ppm ranges respectively. The replacement of the methoxycarbonyl group by the ethoxycarbonyl group has practically no effect on the chemical shifts of the β-methyl group in the corresponding ester. Similar results have been observed in alkylidenecyanoacetic esters by some of the present authors.[2]

In the α-cyano-β,β-dimethylglycidic ester (II), the signals due to two β-methyl groups were at 1.69 and 1.47 ppm. This result indicated that the magnitude of such a chemical-shift difference was sufficient to be of practical value in the quantitative determination of geometrical isomers. In the epoxy ester, III—VIII, made by the epoxidation of alkylidenecyanoacetic esters (*cis-trans* mixture[6]), the spectra show two signals of an unequal intensity, separated by about 0.22—0.25 ppm, for the β-methyl protons. These results indicate that they contain both geometric isomers. After the products had been repeatedly distilled, their NMR showed the same pattern. It was desirable that the spectra be correlated with structures on the bases of the known configuration of the *cis* and *trans* epoxides.[7] However, no stereoisomers of a known configuration of β-alkylglycidic esters were available. Attempts to separate stereoisomers of these esters by gas and thin-layer chromatographies were unsuccessful.

In the preceding paper,[2] it was shown that the relative stabilities of the stereoisomeres of alkylidenecyanoacetic esters can be determined by means of the simple steric interaction between the β-alkyl substituent and the alkoxycarbonyl group. A similar effect may be expected for the epoxy esters. In the compounds III—VIII, models show that the *cis* configurations are to be favored over the *trans*. On the basis of this consideration, the more intense of the two signals of the β-methyl group can be assigned to the *cis* isomer, and the less intense, to the *trans*.

It is known that the ethylidenecyanoacetic ester produced by the condensation of acetaldehyde with the cyanoacetic ester is only the *trans* isomer from the NMR spectrum.[8] We have attempted to convert the *trans* isomer into the *cis* isomer. However, so far our attempts have been unsuccessful. The *trans* ethylidenecyanoacetic ester was converted into the 2-cyano-2,3-epoxybutanoic ester (I) by refluxing it with excess hydrogen peroxide or by treating it with a calculated amount of hydrogen peroxide at room temperature under alkaline conditions. The NMR spectra of the products show only one β-methyl doublet (1.65 ppm) (Fig. 1). This resonance position corresponds to that of the methyl protons at a lower field in other epoxy esters. In the case of compound I, it seems reasonable to say that the methyl group prefers a *trans* orientation, for there is a substantial difference in the steric requirements of the methyl and hydrogen groups. Thus, the result supports the structural assignment that the *trans* β-methyl group responds at a lower field than does the *cis* β-methyl group.

The methyl 1-methylpropylidenecyanoacetate used in the other experiments was prepared by the condensation of methyl ethyl ketone with cyanoacetic acid,[8] followed by esterification with diazomethane. From the NMR spectrum of the product, it has been concluded that the ester is the *cis* isomer and not a mixture of the two geometric isomers. The *cis* ester underwent 30% isomerization to the *trans* ester when refluxed in an aqueous methanol solution for six hours (NMR analysis of the product mixture). After ten hours refluxing, 47% isomerization had taken place. A longer refluxing gave no change in the *trans-cis* ratio. A more rapid isomerization of *cis* to *trans* takes place in the reaction mixture containing 0.1 N alkali. Therefore, owing to experimental difficulties arising

6) Following the notation given in Ref. 2.

7) The isomeric forms of a series of the esters are denoted as (i) *cis* (in which the β-methyl and alkoxycarbonyl groups are both on the same side of the C(—O)C bond) and (ii) *trans* (in which these groups are on opposite sides).

8) M. J. Hamelin, *C. R. Acad. Sc. Paris*, Ser. C **263**, 553 (1966).

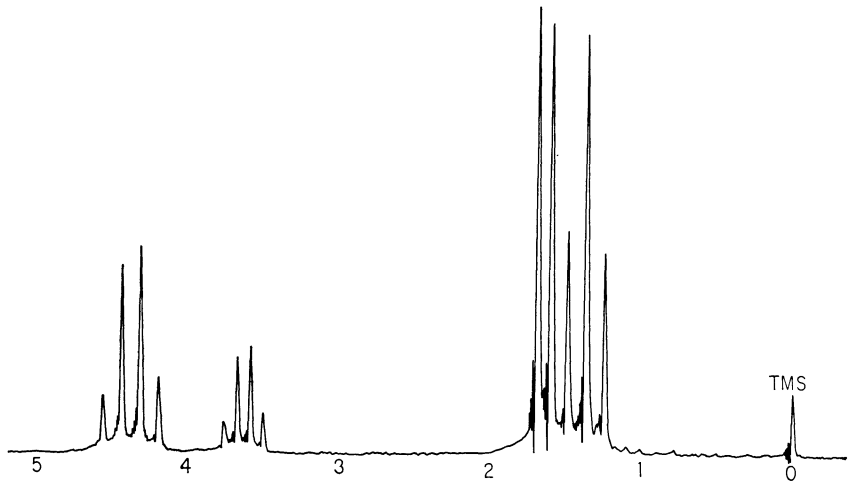

Fig. 1. The NMR spectrum of ethyl 2-cyano-2,3-epoxybutyrate.

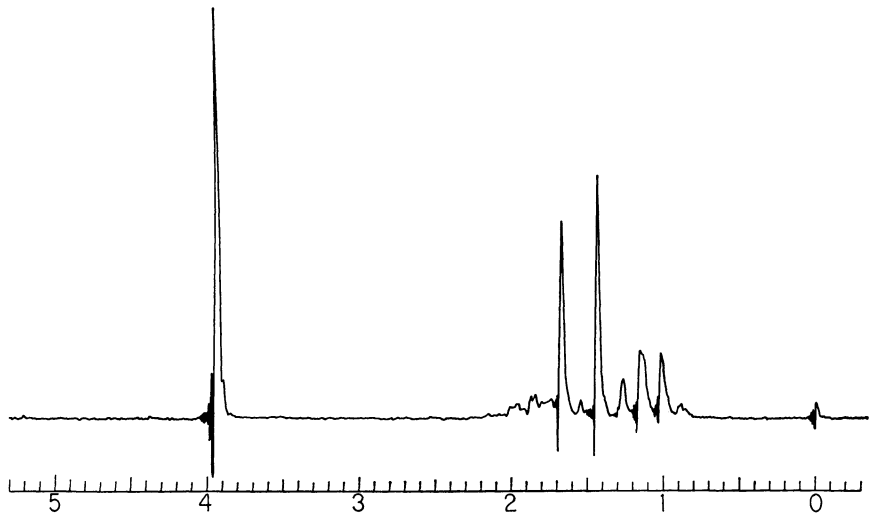

Fig. 2. The NMR spectrum of methyl 2-cyano-3-methyl-2,3-epoxyvalerate.

from the fast isomerization of the starting material, we could not obtain the pure *cis* epoxy ester.

As a typical example, the present authors analyzed the spectrum of methyl 2-cyano-3-methyl-2,3-epoxyvalerate (IIIa) (Fig. 2). The β-methyl signal appears as a doublet of an unequal intensity, with the more intense signal at the higher field (1.66 and 1.44 ppm). The intensity ratio from the analysis of the β-methylene multiplet was less certain. The γ-methyl protons appear as a doublet of an unequal intensity, with the more intense signal at the lower field (1.15 and 1.01 ppm). On the basis of the evidence just given, the more intense signal of the β-methyl protons can be assigned to that of the *cis* isomer, and the weaker signal, to that of the *trans*.

Table 2 shows the isomeric compositions of six epoxy esters and their starting unsaturated esters, which were estimated from the integration of the area under the appropriate NMR signals. The composition is little affected by the reaction conditions except in the case of VIII. Methyl 2-cyano-2,3-epoxy-3,5,5-trimethylcaproate (VIII) (*trans* percentage 60) was prepared from methyl 2-cyano-3,5,5-trimethylhexanoate (*trans* percentage 47) by heating it (70—80°C) with 30% hydrogen peroxide, while VIII (*trans* percentage 38) was obtained from the same starting ester in the presence of sodium bicarbonate at room temperature. It has already been pointed out that the *trans* isomer of this unsaturated ester is much increased by heating it to 71°C (*trans* percentage 61).[2] Accordingly, the results (Table 2) show that the *cis-trans* ratios of the products are almost the same as those of the starting materials.

On the other hand, it is known that the epoxidation of alkylidenecyanoacetic esters under alkaline conditions results in the formation of epoxy-

Table 2. *cis-trans* Composition ratios of the epoxy nitriles and their starting unsaturated esters

Compound	Method*	Composition per cent		Composition per cent of the starting material**	
		trans	*cis*	*trans*	*cis*
I	A, B	100	0	100	0
II	A, B	50	50	50	50
IIIa	A, B	43	57	47	53
V	A, B	40	60	38	62
VII	A	39	61	35	65
VIII	A	60	40	47	53
	B	38	62	47	53

* Capital letters refer to epoxidation methods designated by these letters in the Experimental Section.

** Following the method given in Ref. 2.

amides rather than epoxynitriles.[9] In the present study, the epoxynitrile was converted into epoxyamide by hydration with hydrogen peroxide in the presence of alkali. These compounds also possess an oxirane ring substituted by four different groups. Therefore, it would be interesting to use the above technique in the determination of the geometric configurations of these compounds. The NMR data are listed in Table 1.

The NMR absorptions of the β-methyl protons of the two isomers (*cis* and *trans*) were well separated, but the ratios could not be accurately determined (except for the case of XVII) from the relative areas of the two signals because of their overlap with the signals of the other alkyl groups. Therefore, when the difference in the steric requirements of the methyl and alkyl groups is relatively small, it is hard to assign signals to the two isomers by the above method.

By the epoxidation of *trans* ethyl ethylidenecyanoacetate or the hydration of *trans* ethyl 2-cyano-2,3-epoxybutyrate, ethyl 2-carbamoyl-2,3-epoxybutyrate (IX) was obtained. That this compound is a pure stereoisomer is confirmed by its NMR spectrum. The spectrum showed β-methyl protons at 1.45 ppm. This resonance position corresponds to those of signals of the lower fields of other epoxyamides (X—XII, XV) in which *cis* isomers coexist with *trans* isomers. In methyl 2-carbamoyl-2,3-epoxy-3,4,4-trimethylvalerate (XVI), prepared from the corresponding unsaturated nitrile (*trans* : *cis*=2 : 98). the only signal due to the β-methyl protons is at 1.32 ppm. In methyl 2-carbamoyl-2,3-epoxy-3,5,5-trimethylcaproate (XVII), prepared from methyl 2-cyano-2,3-epoxy-3,5,5-trimethylcaproate (VIII) (*trans* : *cis*=40 : 60), the signals due to the β-methyl protons are at 1.52 and 1.46 ppm, with the signal at the higher field much the more intense. Since there is a substantial difference between the steric requirements of methyl and hydrogen, *tert*-butyl and methyl, and neopentyl and methyl groups, it appears that the methyl group in IX, the *tert*-butyl group in XVI, and the neopentyl group in XVII prefer a *trans* orientation. By fractional crystallization, methyl 2-carbamoyl-3,4-dimethyl-2,3-epoxyvalerate (XIII) (*cis-trans* mixture) gave one isomer which was confirmed by the NMR spectrum (β-methyl protons: at 1.27 ppm). With the above data in hand, a tentative assignment of the configuration may be made. In the nine epoxyamides discussed here, the signals due to the β-methyl protons are at a higher field when they are *cis* to the ester group, and at a lower field when they are *trans*.

In the preceding papers the authors determined the geometric configurations of $R_1R_2C=C(CN)-COOR_3$ on the basis of the assumption[2] that the response for the β-methyl protons is at a higher field in the *trans* than in the *cis* configuration with respect to the ester group. The β-methyl group is more deshielded in the *cis* than in the *trans* arrangements. This trend is not followed in the case of the epoxy esters discussed here. The β-methyl protons *cis* to the ester group respond at a higher field than do the *trans* β-methyl protons because the former is more shielded. These observations can be explained consistently by considering the magnetic anisotropy of the carbonyl group. It is well established that protons located in or near the carbonyl plane experience additional deshielding, while additional shielding is observed for protons out of the plane.

Experimental

NMR Spectra. All the NMR spectra were taken with a JNM-C-60 high-resolution NMR spectrometer working at 60 MHz at a temperature of 19—20°C. The samples were examined in a chloroform solution, using tetramethylsilane as the internal reference. The chemical shifts are given as ppm downfield from tetramethylsilane.

Alkylidenecyanoacetic Esters. The ethyl ethylidenecyanoacetate was prepared according to the method of Popp and Catala.[10] The other unsaturated esters were prepared according to the method of Cope.[11] The methyl 1-methylpropylidenecyanoacetate (*cis*) was prepared by the condensation of methyl ethyl ketone with cyanoacetic acid, followed by esterification with diazomethane according to the method of Hamelin.[8]

Epoxidation of Alkylidenecyanoacetic Esters. A. A mixture of the alkylidenecyanoacetic ester (0.1 mol), 30% hydrogen peroxide (0.2 mol), and alcohol (30 ml) was refluxed for 7 hr on a water bath. To the

9) G. B. Payne, *J. Org. Chem.*, **26**, 663 (1961); M. Igarashi and H. Midorikawa, *ibid.*, **28**, 3088 (1963).

10) F. D. Popp and A. Catala, *ibid.*, **26**, 2738 (1961).

11) A. C. Cope, C. M. Hofmann, C. Wyckoff and E. Hardenbergh, *J. Amer. Chem. Soc.*, **63**, 3452 (1941).

TABLE 3. NEW EPOXY COMPOUNDS

Compound	Bp, °C/mmHg (Mp °C)	Formula	Calcd			Found		
			C, %	H, %	N, %	C, %	H, %	N, %
I	86—88/5	$C_7H_9O_3N$	54.19	5.85	9.03	54.33	5.86	9.14
IIIa	94—96/6	$C_8H_{11}O_3N$	56.79	6.55	8.28	56.80	6.57	8.54
IIIb	101—103/6	$C_9H_{13}O_3N$	59.00	7.15	7.65	58.98	7.12	7.98
IV	103—106/8	$C_9H_{13}O_3N$	59·00	7.15	7.65	59.19	7.06	7.97
VI	102—104/6	$C_{10}H_{15}O_3N$	60.89	7.67	7.10	60.53	7.57	7.33
VII	108—111/7	$C_{10}H_{15}O_3N$	60.89	7.67	7.10	60.41	7.60	7.41
VIII	110—112/13	$C_{11}H_{17}O_3N$	62.54	8.11	6.63	62.60	7.70	6.83
IX	(136—138)	$C_7H_{11}O_4N$	48.55	6.40	8.09	48.50	6.30	8.14
XI	(96—98)	$C_8H_{13}O_4N$	51.33	7.00	7.48	51.54	6.56	7.65
XII	(82—84)	$C_9H_{15}O_4N$	53.72	7.51	6.96	53.91	7.92	6.67
XIV	(95—98)	$C_{10}H_{17}O_4N$	55.80	7.96	6.51	55.49	7.76	6.24
XV	(77—79)	$C_{10}H_{17}O_4N$	55.80	7.96	6.51	55.58	7.69	6.40
XVII	(108—109)	$C_{11}H_{19}O_4N$	57.62	8.35	6.11	57.06	8.54	6.24

mixture water (100 m*l*) was added, and then it was extracted with chloroform. After the removal of the solvent, the residual oil was distilled to give epoxy nitrile.

B. To a flask equipped with a thermometer, a dropping funnel, and a stirrer, the alkylidenecyanoacetic ester (0.1 mol), sodium bicarbonate (0.05 mol), and alcohol (30 m*l*) were added. Into this 30% hydrogen peroxide (0.2 mol) was stirred, drop by drop, at room temperature. After stirring for 3 hr, the mixture was allowed to stand overnight. To the solution thus obtained we added water (100 m*l*), and then it was extracted with chloroform. After the removal of the solvent, the residual oil was distilled in a vaccum to give epoxy nitrile. The properties of the products are shown in Table 3.

Reaction of Epoxy Nitriles I—VIII with Hydrogen Peroxide. To the products (I-VIII) obtained above (0.01 mol) in alcohol (5 m*l*), we added 30% hydrogen peroxide (0.05 mol) and sodium tungstate dihydrate (0.005 mol). The mixture was then kept for 3 hr at 70—80°C on a water bath. After the removal of the solvent, the residue was extracted by the use of chloroform, and then the solvent was evaporated. The oily residue was shaken with petroleum ether to give colorless crystals (epoxy amides IX—XV, XVII).

Epoxy amide XVI was prepared from methyl 2-cyano-3,4,4-trimethylpentenoate[2] according to the method of the present authors.[12]

These epoxy amides were used for the measurement of the NMR spectra without further purification because the *cis-trans* ratios were affected by recrystallization. The samples were recrystallized from chloroform-petroleum ether prior to analyses.

Methyl 2-Carbamoyl-3,4-dimethyl-2,3-epoxyvalerate (XIII-*cis*). Compound XIII (*cis-trans* mixture) was prepared according to the general procedure. The repeated recrystallization of the product from chloroform-petroleum ether gave colorless needles; mp 135—136°C (NMR: β-methyl, 1.27 ppm).

Found: C, 53.99; H, 7.14; N, 6.95%. Calcd for $C_9H_{15}O_4N$: C, 53.72; H, 7.51; N, 6.96%.

The authors wish to express their hearty thanks to Professors Taro Hayashi and Tatsuo Takeshima for their kind advice and encouragement, and to Dr. Toshio Hayashi for his valuable discussions. Thanks are also due to Dr. Haruo Homma and his staff for their microanalyses.

12) M. Igarashi and H. Midorikawa, *J. Org. Chem.*, **32**, 3399 (1967).

BULLETIN OF THE CHEMICAL SOCIETY OF JAPAN VOL. 43 2143—2152 (1970)

Stereochemistry and Mechanism of Catalytic Hydrogenation and Hydrogenolysis. III.*1 Catalytic Hydrogenolysis of Benzyl-type Alcohols and Their Derivatives*2

Sekio MITSUI, Shin IMAIZUMI and Yasuyoshi ESASHI*3

Department of Applied Science, Faculty of Engineering, Tohoku University, Aramaki, Aoba, Sendai-shi

(Received October 25, 1969)

In order to obtain evidence for the mechanism we proposed of the catalytic hydrogenolysis of benzyl-type alcohols and their methyl ethers, optically active 2-phenyl-2-butanol (Ia), 2-phenyl-2-methoxybutane (IIa), ethyl atrolactate (Ib), and ethyl 2-phenyl-2-methoxypropionate (IIb) were hydrogenolyzed over Raney nickel and Pd(H) catalysts under hydrogen or helium atmosphere in an ethanol solution. In all cases, the hydrogenolysis proceeded stereoselectively with retention of configuration over Raney nickel catalyst but with inversion of configuration over palladium catalyst. A reverse stereoselectivity was observed when the benzyl alcohols (Ia and 2-phenyl-1,2-dihydroxypropane (Ic)) and methyl ethers (IIa) and (IIb) were hydrogenolyzed in the presence or absence of various additives over nickel catalysts. It was also found that the hydrogenolysis of benzyl alcohols always proceeds with retention of configuration over nickel catalyst containing sodium hydroxide. Various binary mixtures of Ia, IIa, Ib and IIb were hydrogenolyzed competitively over Raney nickel and Pd(H) catalysts. The order of relative rates was found to be Ia$\gtrsim$Ib$>$IIa$\gtrsim$IIb over Raney nickel, and IIa$\gtrsim$Ia$\gg$IIb$\gtrsim$Ib over Pd(H) catalyst. The results support our mechanism. The catalytic hydrogenolysis is a competitive reaction of two courses (S_Ni type and S_N2 type reactions), and the stereoselectivity reflects the difference of the free energy levels of the transition states to form π-benzylic complexes. The free energy levels of the corresponding transition states depend on stereoelectronic factor, affinity of substituents for catalyst metal, catalyst hindrance and electronic effects of substituents. The acetates (IVa) and (IVb) of Ia and IIa were hydrogenolyzed with inversion of configuration over nickel and palladium catalysts, whereas the stereoselectivity of the hydrogenolysis of the benzoate (V) of IIa depended on the kind of catalyst. The results are also explained on the basis of our mechanism.

We have shown[1] that the catalytic hydrogenolysis of optically active benzyl alcohols and their methyl ethers proceeds stereoselectivity under moderate conditions in an ethanol solution and the stereochemical results are correlated with the nature of the catalyst; the hydrogenolysis proceeds with retention over Raney nickel, cobalt, and copper catalysts but with inversion over palladium and platinum catalysts. From these results, we suggested that the hydrogenolysis proceeds through sterically different chemisorbed states of substrates which depend on the kind of catalyst metal.[1,2]

*1 Part II: S. Mitsui and S. Imaizumi, This Bulletin, **36**, 855 (1963).

*2 Part LIII in the series Studies on Hydrogenolysis: Part LII: S. Mitsui, Y. Kudo and M. Kobayashi, *Tetrahedron*, **25**, 1921 (1969). Presented in part at the 22nd Symposium of Catalysis of the Chemical Society of Japan, Osaka, April, 1968.

*3 Present address: Dainippon-Inki Chemical Industries Ltd., Urawa-shi, Saitama.

1) a) S. Mitsui, K. Iijima and T. Masuko, *Nippon Kagaku Zasshi*, **84**, 833 (1963); S. Mitsui and K. Iijima *ibid.*, **85**, 682 (1964). b) S. Imaizumi, *ibid.*, **77**, 1511 (1956); **81**, 627 (1960); S. Mitsui and S. Imaizumi, *ibid.*, **86**, 132 (1965). c) S. Mitsui, S. Imaizumi, I. Takamura and M. Takamura, *ibid.*, **84**, 838 (1963). d) K. Konno and S. Mitsui, *ibid.*, **85**, 497 (1964); Y. Senda and S. Mitsui, *ibid.*, **86**, 229 (1965); S. Mitsui, Y. Senda and K. Konno, *Chem. & Ind.*, **1963**, 1354; S. Mitsui and Y. Kudo, *ibid.*, **1965**, 381; S. Mitsui, Y. Kudo and M. Kobayashi, *Tetrahedron*, **25**, 1921 (1969). e) S. Mitsui and Y. Nagahisa, *Chem. & Ind.* (London), **1965**, 1975.

2) S. Mitsui and S. Imaizumi, *Nippon Kagaku Zasshi*, **77**, 1516 (1956); This Bulletin, **34**, 774 (1961).

Khan, McQuillin and Jardine[3] proposed a mechanism different from ours in which the reaction proceeds *via* the same intermediate(A) over any

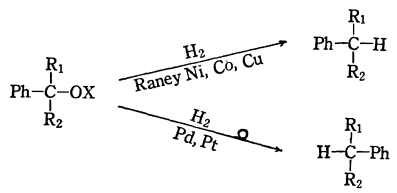

X=H or CH_3

catalyst metal, followed by hydrogen transfer with retention or inversion of configuration depending on the chemical nature of catalyst metal. They considered that nickel-carbon bond is displaced by hydrogen with retention(1), but palladium-carbon bond is displaced by hydrogen in a type of nucleophilic substitution with inversion (2), since the hydrogen supply could be critical by the faster hydrogenolysis over palladium than over nickel and because of the polarization of palladium-carbon bond. Garbisch, Jr., *et al.* offered a mechanism of the hydrogenolysis. However, no detailed process of the formation of inversed product was given.[4]

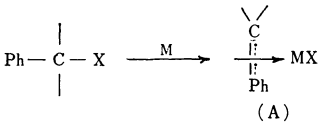

(A)

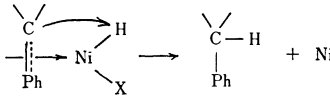

(1)

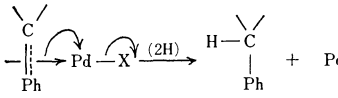

(2)

The purpose of the present study is to make a more detailed examination of the hydrogenolysis of optically active benzyl alcohols and their methyl ethers over nickel and palladium catalysts under various conditions, and to improve the mechanism from the results of this study.

Results

Catalysts. W-4 Raney nickel, "reduced nickel," 5% palladium on charcoal, Raney palladium, and "palladium hydride[5]" were used as catalysts.

The reduced nickel catalyst was prepared by reduction of finely powdered nickel oxide with hydrogen stream at about 300°C. It seems likely that no alkaline substances are contained in the catalyst, since the nickel oxide for the starting material was prepared by thermal decomposition of nickel nitrate.

The palladium hydride catalyst was prepared as follows: An aqueous solution of palladium chloride (5 per cent) was reduced with hydrogen. The metal formed was washed with water until free from chloride ion. The palladium was oxidized for one hour at 400—500°C in atmosphere and then the resulting oxide was reduced by hydrogen in an ethanol suspension. Oxidation and reduction were repeated several times until the volume of consumed hydrogen became nearly constant. The oxide consumed a greater amount of hydrogen than necessary for reduction to metal. It may be assumed that about 80 per cent of palladium was converted into palladium hydride, if all of the occluded hydrogen was consumed to form hydride. The symbols Pd(H) and $Pd(H_{0.4})$ will be used to denote the above catalyst and palladium respectively which occludes 40 per cent of the calculated amount of hydrogen corresponding to PdH.

Hydrogenolysis of Benzyl Alcohols and Their Methyl Ethers. The ethanol solution of optically active 2-phenyl-2-butanol (Ia), 1-phenyl-2-methoxybutane (IIa), ethyl atrolactate (Ib), and ethyl 2-phenyl-2-methoxypropionate (IIb) was hydrogenolyzed to 2-phenylbutane (IIIa) and ethyl 2-phenylpropionate (IIIb), respectively, over Raney nickel, Pd(H) and $Pd(H_{0.4})$ under various conditions. The results are summarized in Tables 1 and 2. In all cases, the hydrogenolysis proceeded stereoselectively with retention of configuration over Raney nickel catalyst but with inversion of configuration over palladium catalyst, the results being the same as those reported on hydrogenolysis using other palladium catalyst under ordinary reaction conditions. It is to be noted that the stereoselective inversion occurred in the hydrogenolysis over Pd(H) and $Pd(H_{0.4})$ but the retention was observed over Raney nickel not only under hydrogen atmosphere but also under helium atmosphere.

In the case of Raney nickel catalyst, the stereoselectivity of hydrogenolysis of benzyl alcohols (Ia) and (Ib) remained unaltered by the addition of

3) A. M. Khan, F. J. McQuillin and I. Jardine, *Tetrahedron Lett.*, **1966**, 2649; *J. Chem. Soc., C*, **1967**, 136.

4) E. W. Garbisch, Jr., L. Schreader and J. J. Frankel, *J. Amer. Chem. Soc.*, **89**, 4233 (1967).

5) R. J. Rennard, Jr., and R. J. Kokes, *J. Phys. Chem.*, **70**, 2543 (1966).

Table 1. Catalytic hydrogenolysis of 2-phenyl-2-butanol (Ia) and its methyl ether (IIa) under various conditions[a)]

Compd.	Catalyst (g)	Reaction conditions			Product (IIIa)[b)]		Configuration of IIIa	
		Atmosphere	Press. (atm)	Temp. (°C)	$[\alpha]_D$	Optical purity (%)	Retention	: Inversion
(+)-Ia[c)]	Raney Ni, 5	H_2	1	10	+18.4°	65.5	95.5	4.5
(+)-Ia	Raney Ni, 5	He	1	10	+18.5°	65.9	96	4
(+)-Ia	Raney Ni, 5	H_2	75	10	+16.9°	60.2	92	8
(+)-Ia	Raney Ni, 5	H_2	100	120[d)]	−2.2°[e)]	61.9	93	7
(+)-Ia	Pd(H), 3	H_2	1	10	−17.9°	63.7	5.5	94.5
(+)-Ia	Pd(H), 3	He	1	10	−17.3°	61.6	7	93
(+)-Ia	Pd($H_{0.4}$), 3	He	1	10	−17.3°	61.6	7	93
(+)-Ia	Pd(H), 3	H_2	75	10	−16.5°	58.8	9	91
(−)-IIa[f)]	Raney Ni, 5	H_2	1	20	−16.5°	58.8	94	6
(−)-IIa	Pd(H), 3	H_2	1	20	+17.1°	60.9	4.5	95.5
(−)-IIa	Pd(H), 3	He	1	20	+17.0°	60.5	5	95
(−)-IIa	Pd($H_{0.4}$), 3	He	1	20	+17.3°	61.6	4	96

a) Solvent; ethanol 20 m*l*, reaction time; 10 hr. Under these conditions, Ia and IIa were completely hydrogenolyzed to 2-phenylbutane(IIIa).
b) Solvent; benzene, $c=9.1$. The specific rotation of optically pure S(+)-IIIa is $[\alpha]_D$ +28.1° (benzene).[1a)]
c) 0.6 g, $[\alpha]_D^{19}$ +13.2° (neat), optical purity; R(+)-72%.
d) Reaction time; one hr. In this case, the product was 2-cyclohexylbutane (IIIa′).
e) This value is the specific rotation of IIIa′. The specific rotation of optically pure S(−)-IIIa′ is $[\alpha]_D$ −3.56° (benzene), as shown in experimental section.
f) 0.6 g, $[\alpha]_D^{19}$ −28.6° (neat), optical purity; S(−)-67%.

Table 2. Catalytic hydrogenolysis of ethyl atrolactate(Ib) and its methyl ether (IIb) under various conditions[a)]

Compd.	Catalyst (g)	Reaction conditions				Conv.[c)]	Product (IIIb)[b)]		Configuration of IIIb	
		Atmosphere	Press. (atm)	Temp. (°C)	Time (hr)		$[\alpha]_D$	Optical purity (%)	Retention	: Inversion
(−)-Ib[d)]	Raney Ni, 5	H_2	1	20	48	95	+62.5°	86.6	99	1
(−)-Ib	Raney Ni, 5	He	1	20	48	98	+62.4°	86.4	99	1
(−)-Ib	Raney Ni, 5	H_2	110	20	48	99	+60.2°	83.4	97	3
(−)-Ib	Raney Ni, 5	H_2	2	100	0.5	100	+58.0°	80.3	95.5	4.5
(−)-Ib	Pd(H), 6	H_2	1	20	48	90	−61.0°	84.5	2.5	97.5
(−)-Ib	Pd(H), 6	He	1	20	48	95	−60.7°	84.1	2.5	97.5
(−)-Ib	Pd($H_{0.4}$), 6	He	1	20	48	91	−57.2°	79.3	5	95
(−)-Ib	Pd(H), 6	H_2	110	20	48	97	−58.1°	80.6	4.5	95.5
(−)-Ib	Pd(H), 6	H_2	1	70	1	93	−59.0°	81.7	4	96
(−)-IIb[e)]	Raney Ni, 5	H_2	1	10	50	90	−57.6°	79.8	93.5	6.5
(−)-IIb	Raney Ni, 5	He	1	10	50	89	−60.5°	83.8	96	4
(−)-IIb	Pd(H), 3	H_2	1	10	50	93	+63.0°	87.2	2.5	97.5
(−)-IIb	Pd(H), 3	He	1	10	50	92	+61.8°	85.6	3	97
(−)-IIb	Pd($H_{0.4}$), 3	He	1	10	50	90	+63.5°	88.0	2	98

a) Solvent: ethanol 20 m*l*.
b) Solvent: ethanol, $c=9.1$. The specific rotation of the optically pure S(+)-IIIb is $[\alpha]_D$ +72.2° (ethanol).[1b)]
c) The product contained a small amount of the cyclohexyl derivatives of IIIb and Ib or IIb.
d) 1.0 g, $[\alpha]_D^{11}$ −24.27° (neat), optical purity, R(−)-88.6%.
e) 0.5 g, $[\alpha]_D^{17}$ −49.50° (neat), optical purity, S(−)-91.5%.

sodium hydroxide. On the other hand, Tables 3 and 4 clearly reveal a decrease in the proportion of the retention of configuration in the cases of methyl ethers (IIa) and (IIb) when the amount of sodium hydroxide added increased. A similar trend in the stereoselectivity was also obtained when alkali halide were added instead of sodium hydroxide.

Table 3. Catalytic hydrogenolysis of 2-phenyl-2-butanol (Ia) and its methyl ether (IIa) over nickel catalyst[a)]

Compd.	Catalyst (g)	Additive (mg)	Reaction conditions: Press. (atm)	Temp. (°C)	Time (hr)	Conv. (%)	Product (IIIa)[b)]: $[\alpha]_D$	Optical purity (%)	Configuration of IIIa: Retention	Inversion
(+)-Ia[c)]	Raney Ni, 5	——	1	10	10	100	+18.4°	65.5	95.5	4.5
(+)-Ia	Raney Ni, 5	NaOH, 400	1	70	20	17	+18.1°	64.7	95	5
(+)-IIa[d)]	Raney Ni, 5	——	1	60	120	100	+20.6°	73.3	94	6
(+)-IIa	Raney Ni, 5	NaOH, 80	1	60	120	86	+6.8°	24.2	64.5	35.5
(+)-IIa	Raney Ni, 5	NaOH, 400	1	60	120	42	−10.1°	35.9	28.5	71.5
(−)-IIa[f)]	Raney Ni, 5	——	1	60	120	100	−14.3°	50.9	88	12
(−)-IIa	Raney Ni, 5	NaOH, 80	1	60	120	75	−4.0°	14.2	60.5	39.5
(−)-IIa	Raney Ni, 5	NaOH, 400	1	60	120	47	+8.7°	31.0	27	73
(+)-Ia[c)]	Ni[e)], 2	——	100	120	5	100	−14.4°	51.3	14.5	85.5
(+)-Ia	Ni, 2	——	100	140	5	100	−11.0°	39.2	22.5	77.5
(+)-Ia	Ni, 2	NaOH, 1	100	160	10	100[g)]	+19.4°	69.1	98	2
(+)-IIa[d)]	Ni, 2	——	100	120	5	100	−7.7°	27.4	33.5	66.5

Notations b, c and f) refer to the footnotes of Table 1. a) Solvent; ethanol 20 ml.
d) 0.6 g, $[\alpha]_D^{19}$ +35.2° (neat), optical purity; R(+)-83%. e) "Reduced nickel" catalyst.
g) 2-Cyclohexylbutane(12%), IIIa(38%) and 2-cyclohexyl-2-butanol(50%) were produced.

Table 4. Catalytic hydrogenolysis of ethyl atrolactate (Ib) and its methyl ether (IIb) and 2-phenyl-1,2-dihydroxypropane (Ic) over nickel catalyst[a)]

Compd.	Catalyst (g)	Additive (mg)	Reaction conditions: Press. (atm)	Temp. (°C)	Time (hr)	Conv.[c)]	Product (IIIb)[b)]: $[\alpha]_D$	Optical purity(%)	Configuration of IIIb: Retention	Inversion
(+)-Ib[d)]	Raney Ni, 5	——	1	20	50	98	−65.0°	90.0	99	1
(+)-Ib	Raney Ni, 5	NaOH, 40	1	70	50	30	−65.1°	90.2	99	1
(+)-Ib	Raney Ni, 5	KBr, 119	1	20	150	65	−63.2°	87.6	97.5	2.5
(−)-IIb[e)]	Raney Ni, 5	——	1	20	50	95	−59.4°	82.3	95	5
(−)-IIb	Raney Ni, 5	NaOH, 40	1	20	50	94	+20.1°	27.8	35	65
(−)-IIb	Raney Ni, 5	NaOH, 80	1	20	50	77	+30.1°	41.7	27	73
(−)-IIb	Raney Ni, 5	NaCl, 58	1	20	50	70	−53.9°	74.7	91	9
(−)-IIb	Raney Ni, 5	NaBr, 103	1	20	150	72	−36.7°	50.8	78	22
(−)-IIb	Raney Ni, 5	KCl, 75	1	20	150	69	−35.9°	47.9	77	23
(−)-IIb	Raney Ni, 5	KBr, 119	1	20	150	61	+10.6°	14.7	42	58
(+)-Ib[d)]	Ni[f)], 2	——	100	110	70	58	−47.0°	65.1	85.5	14.5
(+)-Ib	Ni, 2	——	100	140	40	64	−48.6°	67.3	86.5	13.5
(+)-Ib	Ni, 2	KBr, 6	100	170	95	30	−24.0°	33.2	68	32
(+)-Ic[g)]	Raney Ni, 5	——	1	20	10	100[h)]	+15.0°[i)]	83.3	99.5	0.5
(+)-Ic	Ni[f)], 2	——	100	130	30	100[h)]	−13.2°[i)]	73.4	6.5	93.5

Notations a-c) refer to the footnotes of Table 2.
d) 1.0 g, $[\alpha]_D^{20}$ +25.16° (neat), optical purity; S(+)-91.9%.
e) 1.0 g, $[\alpha]_D^{17}$ −49.50° (neat), optical purity; S(−)-91.5%.
f) "Reduced nickel" catalyst.
g) 0.5 g, $[\alpha]_D^{16}$ +5.1° (*c*, 1.96, ethanol), optical purity; S(+)-84%.
h) 2-Phenyl-1-propanol(Ic).
i) Solvent: benzene, *c*=9.1. The specific rotation of the optically pure R(+)-Ic is $[\alpha]_D$ +18.0° (benzene).[1b)]

In order to see why the benzyl alcohols were hydrogenolyzed with retension of configuration over Raney nickel catalyst in any reaction conditions, "reduced nickel" was used as nickel catalyst which contains no alkaline substance. Hydrogenolysis proceeded only at elevated temperature, and stereoselectivity depended on the structure of benzyl alcohols as shown in Tables 3 and 4. Hydrogenolysis proceeded with predominantly retention of configuration in the case of Ib, but with predominantly inversion of configuration in the cases of Ia, IIa and 2-phenyl-1,2-dihydroxypropane (Ic). Ia was hydrogenolyzed with retention of configuration under the conditions where a trace amount of sodium hydroxide is present (Table 3).

These results suggest that the stereoselectivity of hydrogenolysis of benzyl alcohols and their methyl ethers over nickel catalyst is correlated with the structure of substrates, the kind of nickel catalyst and additives, and that an alkaline substance which is contained inevitably over Raney nickel catalyst acts as an effective factor in the stereospecific hydrogenolysis of benzyl alcohols with retention of configuration.

Competitive Hydrogenolysis of the Benzyl Alcohols(Ia) and (Ib) and Their Methyl Ethers (IIa) and (IIb). The order of relative rates of hydrogenolysis of the substrates was found to be Ia$\gtrsim$Ib$>$IIa$\gtrsim$IIb over Raney nickel catalyst, and IIa$\gtrsim$Ia$\gg$IIb$\gtrsim$Ib over Pd(H) catalyst at room temperature and atmospheric pressure in an ethanol solution. Various binary mixtures of Ia, Ib, IIa and IIb were hydrogenolyzed competitively over both catalysts under the same condition as in individual hydrogenolysis. The results are summarized in Table 5. The competitive rates in hydrogenolysis of the binary mixture of Ia and Ib were similar over Raney nickel catalyst, whereas Ia was more rapidly hydrogenolyzed than Ib over Pd(H) catalyst. In the case of the binary mixture of Ib and IIb, Ib reacted more readily than IIb over Raney nickel catalyst, while a reverse relation was observed over Pd(H) catalyst. The same competitive rates were observed in the binary mixtures of IIa and IIb, and Ia and II a,respectively.

Table 5. Competitive hydrogenolysis of various binary mixtures of benzyl alcohols(Ia and Ib) and their methyl ethers(IIa and IIb) under atmospheric pressure and room temperature

Compounds[a]	Catalyst[b]	Competitive rate of hydrogenolysis[c]	
Ia+Ib	Raney Ni	Ia=1.4	Ib=1.2
Ia+Ib	Pd(H)	Ia=50	Ib=0.1
IIa+IIb	Raney Ni	IIa=0.2	IIb=0.1
IIa+IIb	Pd(H)	IIa=53	IIb=0.1
Ia+IIa	Raney Ni	Ia=2.0	IIa=0.2
Ia+IIa	Pd(H)	Ia=33	IIa=36
Ib+IIb	Raney Ni	Ib=1.5	IIb=0.1
Ib+IIb	Pd(H)	Ib=0.2	IIb=0.5

a) The concentration of each substrate was approximately 0.2 molar ethanol solution (10 *ml*).
b) Raney Ni; 1 g (wet). Pd(H); 1 g.
c) Initial rate (at 20°C); $\times 10^{-4}$ mol/hr.

Hydrogenolysis of Benzyl Acetates and Benzoates. The ethanol solution of optically active 2-phenyl-2-acetoxybutane (IVa), ethyl 2-phenyl-2-acetoxypropionate (IVb), and ethyl 2-phenyl-2-benzoyloxypropionate (V) was hydrogenolysed to IIIa and IIIb, respectively, over Raney nickel, reduced nickel, 5% palladium on charcoal, Pd(H), and Raney palladium catalysts under various conditions. The results are summarized in Table 4. The hydrogenolysis of the acetates (IVa) and (IVb) proceeded with inversion of configuration under all reaction conditions. Hydrogenolysis of the benzoate (V) proceeded predominantly with retention of the configuration over Pd(H) catalyst, while the reverse stereoselectivity was observed over palladium on charcoal, Raney palladium and Raney nickel catalysts.

Ia: R=C_2H_5, X=H
Ib: R=$COOC_2H_5$, X=H
Ic: R=CH_2OH, X=H
IIa: R=C_2H_5, X=CH_3
IIb: R=$COOC_2H_5$, X=CH_3
IVa: R=C_2H_5, X=$COCH_3$
IVb: R=$COOC_2H_5$, X=$COCH_3$
V: R=$COOC_2H_5$, X=COPh

IIIa: R=C_2H_5
IIIb: R=$COOC_2H_5$
IIIc: R=CH_2OH

Discussion

Mechanism of the Hydrogenolysis of Benzyl-type Alcohols and Their Methyl Ethers. Khan *et al.* considered that the hydrogenolysis of benzyl alcohols and their methyl ethers over palladium catalyst proceeds with the inversion of configuration, since the hydrogen supply could be critical by rapid hydrogenolysis, *i.e.*, the intermediate (A) reacts with hydrogen from the opposite side of the catalyst surface by a deficiency of adsorbed hydrogen.[3] This prompted us to investigate the hydrogenolysis under various reaction conditions, especially over Pd(H) under helium atmosphere.

The results summarized in Tables 1 and 2 show that the stereoselectivity is independent of the kind of atmosphere. Thus, the hydrogenolysis over Pd(H) and Pd($H_{0.4}$) proceeded with the stereo-

Table 6. Catalytic hydrogenolysis of 2-phenyl-2-acetoxybutane (IVa), ethyl 2-phenyl-2-acetoxypropionate (IVb) and 2-phenyl-2-benzoyloxypropionate (V) over nickel and palladium catalysts[a)]

Compd.	Catalyst	Reaction condition			Conv. (%)	Product (III)[b)]		Configuration of III	
		Press. (atm)	Temp. (°C)	Time (hr)		$[\alpha]_D$	Optical purity (%)	Retention	Inversion
(+)-IVa[c)]	Raney Ni, 5	1	20	48	60	−16.9°	60.1	8	92
(+)-IVa	Raney Ni, 5[d)]	1	20	1	100	−18.9°	67.3	3	97
(+)-IVa	Ni[e)], 2	100	50	10	60	−19.4°	69.1	2	98
(+)-IVa	5%Pd-C, 0.5	1	20	4	100	−16.9°	60.1	8	92
(+)-IVa	Pd(H), 3	1	20	0.1	100	−16.9°	60.1	8	92
(+)-IVa	Pd(H), 3	1[f)]	20	0.5	100	−18.2°	64.9	5	95
(−)-IVb[g)]	Raney Ni, 10	1	20	72	50	+43.2°	59.8	16.5	83.5
(−)-IVb[h)]	Raney Ni, 10[d)]	1	20	6	100	+54.4°	75.3	9	91
(−)-IVb	Ni[e)], 2	100	140	15	98	+59.4°	82.3	5	95
(−)-IVb	5%Pd-C, 0.5	1	20	24	100	+58.1°	80.5	6	94
(−)-IVb	Pd(H), 3	1	20	15	100	+59.4°	82.3	5	95
(−)-IVb	$Pd(H_{0.4})$, 3	1[f)]	20	15	100	+60.7°	84.1	4	96
(+)-V[g)]	Raney Ni, 10	1	20	48	80	+23.9°	33.1	31.5	68.5
(+)-V[i)]	Raney Ni, 10[d)]	1	20	4	100	+45.3°	62.5	15	85
(+)-V[j)]	Raney Pd, 0.5	1	20	30	80	+49.7°	68.8	12.5	87.5
(+)-V	5%Pd-C, 5	1	20	10	90	+15.3°	21.2	38.5	61.5
(+)-V	Pd(H), 6	1	20	30	90	−24.2°	33.5	67	33
(+)-V	Pd(H), 3	1	20	50	60	−15.4°	21.3	61.5	38.5
(+)-V	Pd(H), 3	1	70	8	95	−35.0°	48.5	76.5	23.5

a) Substrate; 0.005 mol, solvent; ethanol 20 ml.
b) The optically pure rotations of IIIa and IIIb refer to foot note b) of Tables 1 and 2, respectively.
c) α_D^{20} +1.12 (neat, $l=1$), optical purity; R(+)-72%.
d) Sodium hydroxide (0.005 mol) was added.
e) "Reduced nickel" catalyst.
f) Atmosphere: helium.
g) Ref. 12. Optical purity; 89.1%.
h) $[\alpha]_D^{20}$ −31.7° (*c* 9.1, ethanol), optical purity; S(−)-91.9%.
i) Ref. 1c. Optical purity; 89.1%.
j) $[\alpha]_D^{20}$ +34.6° (*c* 9.1, ethanol), optical purity; S(+)-91.9%.

specific inversion of configuration not only under hydrogen atmosphere but also under helium atmosphere, in which no hydrogen is detected by means of vapor phase chromatographic analysis in the gas phase during the reaction. These results suggest that the hydrogen which takes part in the hydrogenolysis attackes an adsorbed substrate from the side of catalyst surface. Thus, the results are not in line with the consideration of Khan *et al.*,[3)] but support our mechanism.[1,2)]

It seems that the hydrogenolysis proceeds through π-adsorption of the phenyl group, followed by the formation of a π-benzylic complex with the catalyst. This complex formation will be similar to that of a π-allylic complex with transition-metal catalysts. In the transition state, thus, there is a change toward sp^2-hybridization at the benzylic carbon with the carbon-oxygen bond becoming labile. The leaving group is finally eliminated by combination with surface hydrogen π-benzylic complex being formed.[6)]

From the results, the mechanism of hydrogenolysis of benzyl-type alcohols (I) and their methyl ethers (II) may be described as follows: The substrate (B) is adsorbed over the catalyst surface. An electron attacks nucleophilically the adsorbed substrates (C) and (D) from the surface of the catalyst, and then π-benzylic intermediates (G) and (H) are produced through transition states (E) and (F), respectively. The resulting intermediates (G) and (H) decompose to the adsorbed products

6) J. J. Rooney, F. G. Gault and C. Kemball, *Proc. Chem. Soc.*, **1960**, 407; F. G. Gault, J. J. Rooney and C. Kemball, *J. Catal.*, **1**, 255 (1962); J. J. Rooney, *ibid.*, **2**, 53 (1963); J. J. Rooney and G. Webb, *ibid.*, **3**, 488 (1964); J. J. Rooney, *Chem. Brit.*, **2**, 242 (1966).

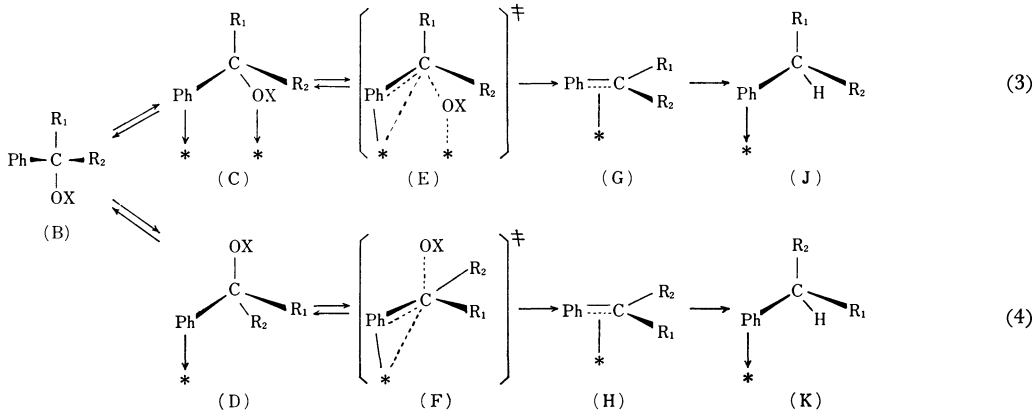

(J) and (K) by hydrogen from the surface of the catalyst with retention of configuration.

The intermediates (G) and (H) are identical in the half-hydrogenated state in the catalytic hydrogenation of styrene derivatives.[7] It has been reported that the intermediate readily decomposes to the adsorbed product by hydrogen from the catalyst surface with the retention of configuration not only over nickel catalyst but also over palladium catalyst.[7] Therefore, it seems that the stereoselectivity of hydrogenolysis is not determined by the step of the decomposition of the intermediates (G) and (H) with hydrogen.

The fact that the hydrogenolysis of I and II over palladium catalyst proceeds with the stereoselective inversion of configuration under all reaction conditions (Tables 1 and 2), suggests that the stereoselectivity is not determined by the step of the adsorption of the substrate in the mechanism. It is unlikely that both Ia and Ib are adsorbed only in one form (D) over palladium catalyst.

Therefore, the stereoselectivity over palladium catalysts may be determined by the difference in the free-energy levels of the transition states (E) and (F) to form π-benzylic complexes in the two courses (Reactions (3) and (4)), since the above results suggest that the activation energies for the cleavage of carbon-oxygen bond (C→G, and D→H) is larger than that for the adsorption of the substrate (B→C, and B→D) and that for the decomposition of carbon-metal bond of the π-benzylic complex to the adsorbed products (G→J, and H→K).

The mechanism is supported by the results of hydrogenolysis of the benzyl alcohol derivatives such as *cis*- and *trans*-1-phenylcyclohexane-1,2-diol, their monoacetates and diacetates, containing an eliminable substituents in β-position.[8]

The results of the palladium catalyzed hydrogenolysis of I and II suggest that the free energy of transition state (F) is lower than that of (E). This may be due to the fact that reaction (4) in which an electron attacks nucleophilically the asymmetric carbon from the opposite side of the leaving hydroxyl or methoxyl groups, *i.e.*, from the catalyst surface, (S_N2 type reaction on catalyst) has an advantage of fulfilling the stereoelectrical requirement in contrast with reaction (2) in which the leaving group is displaced in the same side (S_Ni type reaction on catalyst) in the same way as in homogeneous nucleophilic substitution reaction on carbon.

In the case of Raney nickel catalyst, the hydrogenolysis of I and II proceeds with the retention of configuration. Thus, the fact that the course of reaction (3) is preferable to that of reaction (4) may be due to the strong affinity of the leaving group for Raney nickel catalyst. It is well known that nickel has a strong affinity for oxygen.[9] Accordingly, Raney nickel may adsorb the groups containing oxygen more than palladium. Thus the free enrgy level of the transition state(E) may be lower than that of (F), since the strong chemisorption of the sterically small leaving groups, such as hydroxyl or methoxyl, decreases not only free energy level of adsorption state(C) but also the activation energy from (C) to intermediate(G).

The Effect of Additives over Nickel Catalysts. It was reported that the stereoselectivity of hydrogenolysis of the phenyl ether[10] of Ib and epoxides[1e,11] depended on the presence or ab-

7) G. V. Smith and J. A. Roth, *J. Amer. Chem. Soc.*, **88**, 3879 (1966); S. Mitsui, Y. Nagahisa, K. Tomomura and S. Shionoya, *Shokubai*, **10**, Preprint of 23rd Symposium on Catalysis, 74p (1968).

8) S. Mitsui, M. Fujimoto, Y. Nagahisa and T. Sukegawa, *Chem. & Ind.*, **1969**, 241; *Kogyo Kagaku Zasshi*, **73**, 97 (1970).

9) For example, K. Tanaka and K. Tamaru, *J. Catal.*, **2**, 366 (1963).

10) S. Mitsui and S. Imaizumi, This Bulletin, **36**, 855 (1963); *Kogyo Kagaku Zasshi*, **68**, 816 (1965).

sence of an additive over catalyst. However, the effect of an additive for I and II has not been studied. The mechanism presented here suggests that the reverse stereoselectivity may also be observed over nickel catalyst if the hydrogenolysis of I and II carried out under the reaction conditions which weaken the adsorption of substrate over the catalyst. In fact, the reverse stereoselectivity was observed under several reaction conditions as seen in Tables 3 and 4. Thus, the inversed product is produced predominantly by the addition of sodium hydroxide or alkali halides over Raney nickel catalyst in the hydrogenolysis of methyl ethers (IIa) and (IIb). The results may be expalined by assuming that the additives act as a catalyst poison which weakens the adsorption of substrate over the catalyst. Then the course of reaction (4) will become more advantageous to that of reaction (3) over the poisoned nickel catalyst, since hydrogenolysis may be retarded by the additives, especially in (3) which needs a strong adsorption of the leaving group.

On the other hand, the stereoselectivity of hydrogenolysis of benzyl alcohols over Raney nickel catalyst is not affected by the additives. The divergent result can be ascribed to the effect of alkaline substance contained inevitably in Raney nickel catalyst, because the inversed product is formed predominantly in the hydrogenolysis of Ia over reduced nickel catalyst but the retained product is produced in the presence of sodium hydroxide over the same catalyst (Table 3). Benzyl alcohols differ from their methyl ethers in having free hydroxyl group, and in forming their alkoxide anions with alkali over the catalyst. Therefore, the reaction of course (4) is disfavored by the decrease of the electronegativity of the leaving group, *i.e.*, by the resonance effect of the anion, resulting in the selective hydrogenolysis through course (3).

As seen in Table 3, methyl ether (IIa) was hydrogenolyzed with the inversion of configuration over the reduced nickel catalyst in contrast to the case over Raney nickel catalyst. However, it is clear that the activity of the reduced nickel catalyst is lower than that of Raney nickel catalyst because the former acts as a hydrogenolysis catalyst only at an elevated temperature. It is likely from these results that the reduced nickel behaves like the catalyst poisoned with substances other than alkali. Thus, it is assumed that the hydrogenolysis of Ia proceeds predominantly with the inversion of configuration over the reduced nickel catalyst similar to the case of IIa. It is evident that alkali acts as an effective factor for the stereoselectivity of the hydrogenolysis of benzyl alcohols because Ia is hydrogenolyzed with retention of configuration in the presence of sodium hydroxide over the reduced nickel catalyst. The result may be explained from the formation of the alkoxide anions of the benzyl alcohols with alkali over the catalyst as described before. A similar effect of sodium hydroxide has been observed in the hydrogenolysis of 2-methyl-2-phenylazilidine over palladium catalyst.[12]

In the case of ethyl atrolactate (Ib), hydrogenolysis proceeded predominantly with the retention of configuration over the reduced nickel catalyst, but the stereoselectivity was low compared with the case of Raney nickel catalyst, and decreased by the addition of potassium bromide (Table 4). Thus, it is clear that the tendency of variation of stereoselectivity is similar to that observed in the case of Ia, but the degree of variation is slight. It appears to depend on the structure of benzyl alcohols. The structure of Ib differs from that of Ia only in having the ethoxycarbonyl group instead of the ethyl group. It is clear that the bulkiness and electronegativity of the ethoxycarbonyl group are greater than those of the ethyl group, and that if the reaction proceeds *via* course (4), the ethoxycarbonyl group of Ib must be placed to the side of the catalyst surface, whereas the ethoxycarbonyl group in the reaction *via* course (3) may or may not be placed thus. The results suggest that the effect of the catalyst hindrance of the ethoxycarbonyl is larger than the electronic effect in its adsorbed state for the hydrogenolysis of Ib.

This consideration is in line with the results of the competitive hydrogenolysis of various binary mixtures of the substrates (Ia, Ib, IIa and IIb), *i.e.*, as shown in Table 5, Ia and IIa are more rapidly hydrogenolyzed than Ib and IIb, respectively, over Pd(H) catalyst, in which the hydrogenolysis proceeds with the inversion of the configuration, whereas similar rates were observed in the case of Raney nickel catalyst, in which the hydrogenolysis proceeds with the retention of the configuration.

The consideration is supported by the fact that the hydrogenolysis of 2-phenyl-1,2-dihydroxypropane (Ic) which had sterically smaller methylol group than ethoxycarbonyl group of Ib proceeds with the inversion of the configuration over reduced nickel catalyst (Table 4), similarly as in Ia.

The results led us to the conclusion that the stereoselectivity of the catalytic hydrogenolysis of benzyl alcohols and their methyl ethers depends on the difference in the free energy levels of the transition states (E) and (F). The free energy levels of E and F depend on such factors as stereoelectronic factor, affinity of substituents for catalyst metal, catalyst hindrance, and electronic effects

11) S. Mitsui and S. Imaizumi, *Nippon Kagaku Zasshi*, **86**, 219 (1965).

12) S. Mitsui and Y. Sugi, *Tetrahedron Lett.*, **1969**, 1291; This Bulletin, **43**, 1489 (1970).

of substituents.

Hydrogenolysis of Benzyl Acetates and Benzoates. Let us consider the stereochemistry of the hydrogenolysis of other derivatives of benzyl alcohols.

The hydrogenolysis of the acetates (IVa) and (IVb) proceeded with the inversion of configuration under all reaction conditions (Table 6), the results being the same as those reported in the hydrogenolysis of IVb[13] and of other benzyl acetates.[3,4,14] The stereoselectivity of hydrogenolysis of benzoate (V) depended on the kind of catalyst.

The results of benzoate(V) cannot be explained by the consideration of Khan *et al.*[3] that hydrogenolysis of the benzyl derivatives, such as acetate and benzoate, having a strongly electronegative leaving group proceeds with the inversion of configuration *via* course (2). These results may be also explained on the basis of our mechanism of the hydrogenolysis of I and II.

The fact that the acetates are hydrogenolyzed with the stereospecific inversion of configuration over both nickel and palladium catalyst suggests clearly that stereoselectivity is not determined by the difference of the step to form the adsorption states (C and D), since the acetoxyl and ethoxycarbonyl groups may be adsorbed with greater facility over the catalyst than the alkyl group. Thus, stereoselectivity may be correlated with the difference in the free energy levels of the transition states (E) and (F) to form the π-benzyl intermediates (G) and (H), in analogy with the cases of hydrogenolysis of I and II.

It is considered that S_N2 type reaction on catalyst in the hydrogenolysis of benzyl acetates proceeds with greater facility than that of benzyl alcohols and their methyl ethers, because the acetoxyl group of the acetates has a strong electron attractive nature. It seems likely therefore, that the hydrogenolysis of benzyl acetates proceeds generally with the inversion of configuration *via* course (4) under all reaction conditions.

The stereoselectivity of hydrogenolysis of benzoate (V) depended on the reaction conditions (Table 6). Thus, the hydrogenolysis proceeded predominantly with the retention of configuration over Pd(H) catalyst, but the reverse stereoselectivity was observed over palladium on charcoal, Raney palladium and Raney nickel catalysts.

These results suggest that the difference of the activation energy between the two courses (3) and (4) for V is smaller than that for the acetate(IVb). Although the benzoyloxyl group of V unquestionably possesses a stronger affinity with the catalyst and a larger catalyst hindrance than those of the acetoxyl group of IVb, the effect of the former may be larger for the hydrogenolysis of V, compared with the case of IVb, because both the carbonyl and the phenyl of the benzoyloxyl group are π-adsorbed. These effects are similar to those of the phenyl group of the phenyl ether of Ib.[10] Thus, the strong chemisorption of the benzoyloxyl group is expected to facilitate course (3) in line with the hydrogenolysis of I and II over Raney nickel catalyst. Consequently, differing from the case of acetates (IV) the stereoselectivity of hydrogenolysis of V may depend on the reaction conditions.

When a catalyst which has many suitable pores such as Raney catalyst is used, hydrogenolysis with an inversion of configuration over two phases of the catalyst surface cannot be ruled out, in analogy with the hydrogenolysis of phenyl ether[10] of Ib, since the benzoyloxyl group has a planar structure containing π-electrons, and asymmetric carbon-oxygen bond of the substrate is able to rotate freely. It is assumed that the reaction *via* this adsorption state has a smaller activation energy than that *via* the other adsorption states. Needless to say, this reaction course is included in course (4).

When the benzoyloxyl and phenyl groups of the benzoate(V) are adsorbed strongly over the catalyst, partial participation of the radical cleavage reaction on catalyst is made possible, giving a racemic product.[2,13] These factors may further complicate the stereoselectivity of hydrogenolysis of V.

Recently a similar variable stereoselectivity has been also found in the Raney nickel catalyzed desulfuration of benzylsulfone derivatives by Grimm and Bonner.[15] It is assumed that desulfuration, in analogy with the hydrogenolysis of the benzoate, may be also complicated by the participation of many reaction courses which depend on the structure of substrate and reaction conditions.

Experimental

Materials. All compounds used in this study have been previously reported; R(+)-2-phenyl-2-butanol (Ia),[1a] $[\alpha]_D^{19}+13.2°$ (neat), 72% optical purity; S(−)-2-phenyl-2-methoxybutane(IIa)[1a], $[\alpha]_D^{19}-28.6°$ (neat), 67% optical purity; R(+)-2-phenyl-2-acetoxybutane (IVa),[16] $\alpha_D^{20}+1.12°$ (neat, $l=1$), 72% optical purity; ethyl R(−)-atrolactate(Ib),[1b] $[\alpha]_D^{11}-24.27°$ (neat), 88.6% optical purity; ethyl S(−)-2-phenyl-2-methoxypropionate (IIb),[1b] $[\alpha]_D^{17}-49.50°$ (neat), 91.5% optical purity; ethyl S(−)-2-phenyl-2-acetoxypropionate (IVb),[13] $[\alpha]_D^{20}-31.7°$ (c 9.1, ethanol), 91.9% optical purity; ethyl S(+)-2-phenyl-2-benzoyloxypropionate

13) S. Imaizumi, *Nippon Kagaku Zasshi*, **81**, 631 (1965).

14) F. G. Bordwell and E. W. Garbisch, Jr., *J. Org. Chem.*, **28**, 1765 (1963).

15) R. A. Grimm and W. A. Bonner, *ibid.*, **32**, 3470 (1967).

16) D. J. Cram, *J. Amer. Chem. Soc.*, **74**, 2149 (1952).

(V),[13] $[\alpha]_D^{20}+34.6°$ (*c* 9.1, ethanol), 91.9% optical purity; S(+)-2-phenyl-1,2-dihydroxypropane(Ic),[1b] $[\alpha]_D^{16}+5.1°$ (*c* 1.96, ethanol), 84% optical purity.

Hydrogenolysis. Hydrogenolysis was carried out in 20 m*l* of ethanol containing a known amount of substrate, catalyst and additive. The catalyst was filtered. In the cases of Ia, IIa and IVa, 200 m*l* of water was added to the filtrate, and then extracted with ether. The ether layer was washed with a saturated sodium bicarbonate solution and was dried over anhydrous calcium chloride, and the solvent was removed. 2-Phenylbutane (IIIa) was then separated from the residual oil by distillation (bp 60°C/15 mmHg) or by vapor phase chromatography (2 m of column packed with a polyethylene glycol-4000 on 30—60 mesh firebrick). In the cases of Ib and IIb, the solvent was distilled, and ethyl 2-phenylpropionate (IIIb) was then separated from the residual oil by vapor phase chromatography. In the cases of IVb and V, the solvent was distilled. The residual oil was taken up in ether and extracted with a saturated sodium bicarbonate solution. The alkaline insoluble material was dried over anhydrous sodium sulfate, and the solvent removed. IIIb was then separated from the residual oil by vapor phase chromatography. In the case of Ic, the solvent was distilled. The residual oil was distilled at reduced pressure to give 2-phenyl-1-propanol (IIIc), bp 120°C/21 mmHg.

The stereochemical results are shown in Tables 1, 2, 3, 4, and 6.

Competitive Hydrogenolysis. Hydrogenolysis was carried out with each of the individual substrates and their various binary mixtures under atmospheric pressure and at room temperature (20°C). For the hydrogenolysis of the individual substrates, 10 m*l* of ethanol and 0.004 mol of the substrate were used. Hydrogenolysis of the binary mixtures of the substrates was carried out with an ethanol solution (10 m*l*) of the two substrates concerned. The concentration of each substrate was approximately 0.2 molar. Catalyst weights were 1 g of Raney nickel (wet) and 1 g of Pd (H) for each run. Small amounts of samples were extracted through a silicone rubber stopper with a hypodermic syringe at suitable intervals and analyzed by glcp procedures (45 m Golay column coated with polyethylene glycol-4000). The results are shown in Table 5.

2-Cyclohexylbutane (IIIa'). R(−)-2-Phenylbutane ($[\alpha]_D^{21}-15.4°$ (benzene), optical purity 54.8%) was hydrogenated over platinum catalyst in ethanol under hydrogen at an ordinary temperature and pressure until the hydrogen was no longer adsorbed. The catalyst was filtered and rinsed with ether. Water and ether were added to the filtrate, and ether layer was dried over anhydrous calcium chloride, and then the solvent was removed. The residual oil distilled at reduced pressure gave R(+)-2-cyclohexylbutane (IIIa'), bp 60°C/ 15 mmHg, $[\alpha]_D^{25}+1.95°$ (benzene). The specific rotation of the optically pure IIIa' is calculated to be $[\alpha]_D$ 3.56° (benzene).

The authors wish to thank the Takeda Science Foundation for their grant-in-aid.

BULLETIN OF THE CHEMICAL SOCIETY OF JAPAN VOL. 43 2153—2158 (1970)

Sulfilimine. II. IR, UV and NMR Spectroscopic Studies

Kenji TSUJIHARA, Naomichi FURUKAWA and Shigeru OAE

Department of Applied Chemistry, Faculty of Engineering, Osaka City University, Sumiyoshi-ku, Osaka

(Received October 30, 1969)

The physical properties of several *N*-*p*-tolylsulfonylsulfilimines were studied by means of infrared, ultraviolet and NMR spectroscopic determinations. Four characteristic infrared absorption bands due to both sulfonyl and sulfilimino groups are observed and those due to both N–S(IV) and N–S(VI) stretching vibrations appear at nearly the same positions and overlap with each other. The ultraviolet spectra suggest that the sulfilimino group is not an electron donor but an electron acceptor group when conjugated with a phenyl ring and could be used to measure the pK_a value of methyl-*p*-methoxyphenyl derivative. The NMR chemical shift of methyl protons attached to the S atom of *S*-methyl-*S*-*p*-tolyl derivative appears at 2.81 ppm, whereas the shifts of the corresponding sulfoxide and the sulfone groups appear at 2.69 and 3.04 ppm, respectively. From these results, it seems that the N–S(IV) bond of *N*-*p*-tolylsulfonylsulfilimine is of semipolar character while the charges on the S(IV) atom and the N atom are delocalized substantially with strong $d\pi$ conjugation into S(IV)–N–S(VI) bondings.

Sulfilimines have been known as sulfur-nitrogen ylides or ylenes. The *N*-acyl derivatives are especially well known compounds and their IR,[1] UV,[2] and X-ray data[3] have been accumulated in recent years.

The configuration of *N*-sulfonylsulfilimine is not established, though the S–N bond has been postulated from IR spectroscopic study[1] to have a double bond character. We have examined IR, UV and NMR spectra of various *N*-sulfonylsulfilimines. This paper will describe the new data and their relation to a preferable structure for *N*-sulfonylsulfilimine.

Results and Discussion

IR Spectra of *N*-*p*-Tolylsulfonylsulfilimines. The IR spectra of several *N*-*p*-tolylsulfonylsulfilimines are taken in KBr disks and shown in Table 1. All the sulfilimines have four strong characteristic IR absorption bands at around 930—980, 1070—1090, 1130—1140 and 1260—1280 cm^{-1} respectively (Fig. 1). The latter two bands, 1130—1140 and 1260—1280 cm^{-1} are well assigned to those of both symmetrical and asymmetrical stretching vibrations due to SO_2 group. The first band, 930—980 cm^{-1} has been assigned to the stretching vibration due to N–S(IV) group by Kucsman *et al.*,[1] though there are controversies in the assignment of the absorption of S–N stretching vibration.[4-6] The second band, 1070—1090 cm^{-1}, which appears in all arylsulfonamides was revealed by Tanaka *et al.* to be not of the S–N stretching absorption band from a study of the IR spectra of various sulfonamides, sulfonic acids, sulfones and other related compounds.[5]

N-*p*-Tolylsulfonylsulfilimine may be formulated by either the ylide structure, the ylene structure or by the resonance hybrid of both.

Ylide type Ylene type

Kucsman *et al.* favor the ylene structure on the basis of IR spectroscopic observations.[1] They argue that the $\bar{\nu}$ SO_2*[1] band in sulfilimine appears at a wave number considerably higher than that in sulfonate ($\bar{\nu}$ SO_3=1120 cm^{-1}) although it might

1) A. Kucsman, I. Kapovits and F. Ruff, *Acta Chim. Acad. Sci. Hung.*, **40**, 75 (1964); A. Kucsman, I. Kapovits and F. Ruff, *Tetrahedron*, **22**, 1575 (1966).

2) A. Kucsman, F. Ruff and I. Kapovits, *Acta Chim. Acad. Sci. Hung.*, **50**, 325 (1966).

3) A. Kalman, *Acta Crystallogr.*, **22**, 501 (1967).

4) J. N. Baxter, J. Cymerman-Craig and J. B. Willis, *J. Chem. Soc.*, **1955**, 669; W. Augus, A. H. Leckie and J. I. Williams, *Trans. Faraday Soc.*, **34**, 793 (1938). The bands between 1070 and 1100 cm^{-1} were assigned to the S–N stretching vibration from a study of the Raman spectra of a veriety of sulfur-nitrogen compounds.

5) D. H. Hadzi, *J. Chem. Soc.*, **1959**, 847; Y. Tanaka and Y. Tanaka, *Chem. Pharm. Bull.*, (Tokyo) **13**, 399, 858 (1965). The bands in the region near 900 cm^{-1} were assigned to the S–N stretching vibration.

6) H. J. Hofmann and K. R. Andress, *Naturwissenschaften*, **41**, 94 (1954); L. P. Bicelli, *Ann. Chim.*, **47**, 1380 (1957). It was suggested that the S–N frequency is at around 500 cm^{-1}.

*1 $\bar{\nu}$ SO_2=1/2 (ν_s SO_2+ν_{as} SO_2).

Table 1. IR spectrum of *N*-*p*-tolylsulfonylsulfilimine $R_1-\underset{\underset{NSO_2-C_6H_4-CH_3}{|}}{S}-R_2$

R_1	R_2	Mp (°C)	$\nu_{(S-N)}$	$\nu_{s(SO_2)}$	$\nu_{as(SO_2)}$	
CH_3	CH_3	157—157.5	943	1129	1265	1088
$(CH_3)_2CH$	$(CH_3)_2CH$	117—118	961	1128	1260	1082
$CH_3(CH_2)_3$	$CH_3(CH_2)_3$	59—60	965	1132	1270	1083
	$-(CH_2)_4-$	145—146	965	1132	1264	1079
	$-(CH_2)_5-$	148—149	966	1123	1257	1081
CH_3	C_6H_5	129—130	930	1139	1280	1083
CH_3	*p*-$CH_3C_6H_4$	125—126	950	1133	1270	1088
CH_3	*p*-$CH_3OC_6H_4$	144.5—145	959	1139	1281	1085
CH_3	*p*-$NH_2C_6H_4$	206—207	933	1130	1250	1083
CH_3	*p*-ClC_6H_4	112—113	957	1130	1270	1080
CH_3	*p*-$NO_2C_6H_4$	162—163	958	1133	1275	1082
CH_3CH_2	C_6H_5	97—98	971	1135	1274	1082
$(CH_3)_2CH$	C_6H_5	115—116	936	1138	1275	1085
$(CH_3)_3C$	C_6H_5	101	955	1139	1277	1088
$C_6H_5CH_2$	C_6H_5	146—147	970	1136	1275	1087
$C_6H_5CH_2$	$C_6H_5CH_2$	190—191	983	1134	1275	1086
$C_6H_5(CH_2)_2$	C_6H_5	137—138	950	1132	1270	1086
C_6H_5	C_6H_5	111—112	950	1135	1280	1082
C_6H_5	*p*-$CH_3C_6H_4$	96—98	969	1133	1273	1082
C_6H_5	*p*-ClC_6H_4	89.5—90.5	969	1130	1273	1080
C_6H_5	*p*-$NO_2C_6H_4$	148—149	955	1135	1281	1084
p-$CH_3OC_6H_4$	*p*-$CH_3OC_6H_4$	130—132	956	1131	1277	1073
	p-$CH_3C_6H_4SO_2NH_2$		906	1155	1330	1096
	[*p*-$CH_3C_6H_4SO_2NCl]^{\ominus}Na^{\oplus}$		929	1130	1246	1083

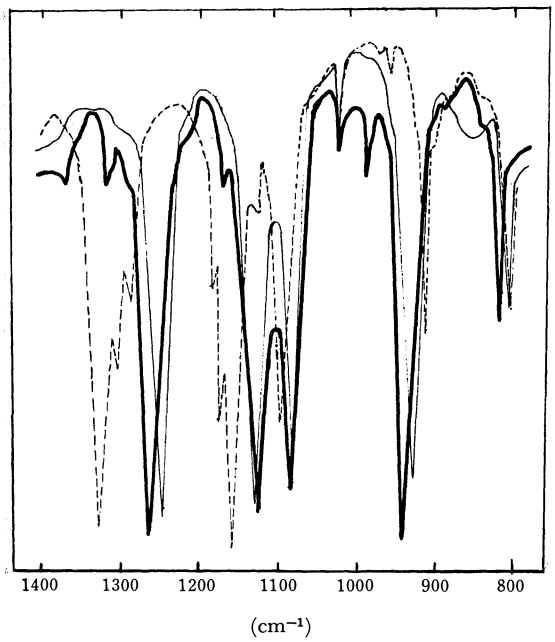

Fig. 1. IR spectra.
——— *p*-$CH_3C_6H_4SO_2N^{\ominus}-S^{\oplus}(CH_3)_2$
—— [*p*-$CH_3C_6H_4SO_2NCl]^{\ominus}Na^{\oplus}$
------ *p*-$CH_3C_6H_4SO_2NH_2$

be predicted that both SO_2 bands in the system $-SO_2-N^{\ominus}-$ and $-SO_2-O^{\ominus}$ would appear in the same region. A shift of 40—50 cm^{-1} toward a lower wave number of $\bar{\nu}$ SO_2 band in sulfilimine than that in sulfonamide or sulfone is also too small to be ascribed to the ylide structure.

However, a comparison of the two systems may not be appropriate and the shift of 40—50 cm^{-1} toward the lower wave number of SO_2 band is too large to be caused only by the electronic effect of sulfilimino group. We examined the IR spectra of sodium *N*-chloro-*p*-tolylsulfonylsulfonamide (chloramine T) which is considered to have the system $-SO_2-N^{\ominus}-$. IR spectra of *p*-tolylsulfonamide, chloramine T and *S,S*-dimethyl-*N*-*p*-tolylsulfonylsulfilimine are shown in Fig. 1. Chloramine T has four characteristic intense bands at 1255 ($\nu_{as}SO_2$), 1130 (ν_sSO_2), 1083 and 929 cm^{-1}. The whole spectrum does not resemble that of the sulfonamide but is very similar to that of sulfilimine except for the band at 929 cm^{-1} which is less intense than that of *S,S*-dimethyl-*N*-*p*-tolylsulfonylsulfilimine at 943 cm^{-1}.

The characteristic IR absorption bands of several sulfilimines, chloramine T and other related compounds are listed in Table 2. The values of $\bar{\nu}$ SO_2 of sulfilimines (1190—1210 cm^{-1}) are similar to the value of chloramine T anion (1193 cm^{-1}) but different from that of sulfonamide (1243 cm^{-1}) and

Table 2. IR spectra of sulfilimine $\begin{matrix} R_1 \\ \diagdown \\ S \\ \diagup \\ R_2 \end{matrix} \rightarrow$ NTs and related compounds

R_1	R_2	$\nu_{(S-N)}$	$\nu_{s(SO_2)}$	$\nu_{as(SO_2)}$	—	$\bar{\nu}_{(SO_2)}$
CH_3	CH_3	943	1129	1265	1088	1197
CH_3	C_6H_5	930	1139	1280	1083	1210
CH_3	p-$CH_3C_6H_4$	950	1133	1270	1088	1201
CH_3	p-$NH_2C_6H_4$	933	1130	1250	1083	1190
C_6H_5	C_6H_5	950	1135	1280	1082	1208
p-Tl-SO_2-NH_2		906	1155	1330	1096	1243
[p-Tl-SO_2-NCl]$^{\ominus}$Na$^{\oplus}$		929	1130	1255	1086	1193
Alkyl-aryl-sulfone[8]		—	1160—1150	1334—1325	—	1238—1247
p-Tl-$\overset{\uparrow O}{\underset{\|}{S}}$-$CH_3$ (I) $\underset{NSO_2\text{-Tl-}p}{\|}$		—	1150	1312	—	1231

sulfones (1238—1247 cm^{-1}). The value of $\bar{\nu}$ SO_2 of sulfoximine (I) produced by the oxidation of sulfilimine is close to that of sulfonamide but not to that of sulfilimine or chloramine T. This fact seems to be supported by the S=N double bond character of sulfoximine.[7]

The results suggest that sulfilimine and chloramine T anion have similar electronic environments around the SO_2 group, and *N*-*p*-tolylsulfonyl sulfilimine would be represented better by the ylide structure than by the ylene structure.

Recently, an X-ray crystallographic study of *S*,*S*-dimethyl-*N*-methylsulfonylsulfilimine has revealed that the bond length of N–S(IV) and N–S(VI) are 1.63 and 1.58 Å respectively,[3] which are normal values for N–S distance of sulfonamide such as *N*-phenylmethanesulfonamide[9] or sulfamide.[10] The result undoubtedly supports the consideration that the S–N bond is of semipolar nature.

$$(CH_3)_2S \qquad SO_2CH_3$$
$$1.63\ \text{Å} \diagdown \quad \diagup 1.58\ \text{Å}$$
$$N$$

The stretching vibrations of the N–S(IV) and the N–S(VI) bonds can be calculated simply by the following equation[11] using the values 1.63 and 1.58 Å, and the values 878 and 971 cm^{-1} are obtained.

$$\nu = \frac{1}{2\pi c}\left(\frac{f}{M_n \cdot M_s/M_n + M_s}\right)^{1/2}, \quad f = \frac{1.86 \times 10^5}{(r-0.88)^3}$$

where

ν: the stretching frequency (cm^{-1})
c: the velocity of light (cm/sec)
f: the force constant of bond (dyn/cm)
r: the bond length (Å)
M_n and M_s: the mass of N atom and S atom respectively (g)

N-*p*-Tolylsulfonylsulfilimine has only one very intense band around 930—980 cm^{-1} whose intensity is stronger than those of the SO_2 bands and the S–N stretching vibration of chloramine T (see Fig. 1). Thus, both bands due to both N–S(IV) and N–S(VI) stretching are considered to apper at the same or nearly the same position and would overlap each other.

UV Spectra of *N*-*p*-Tolylsulfonylsulfilimines. UV spectra of several *N*-*p*-tolylsulfonylsulfilimines are shown in Table 3. All the sulfilimines except those having *p*-amino or *p*-methoxyphenyl group give UV spectra having the maximum absorption bands (λ_{max}) at around 228 mμ with intensities (log ε_{max}) between 4.06 and 4.35.

There is practically no shift of λ_{max} when R_1 and R_2 change from dialkyl to alkylpheny or diphenyl. This suggests that the maximum absorption bands at around 228 mμ are the ^1L_a bands due to the phenyl ring of *p*-tolylsulfonyl group connected to sulfilimine group, since λ_{max} and log ε_{max} between *S*,*S*-dialkyl-*N*-*p*-tolylsulfonylsulfilimine and *p*-tolylsulfonamide having the ^1L_a band at 225 mμ are very similar.

If the S(IV)–N bond of *N*-*p*-tolylsulfonylsulfilimine has a normal double bond character, the resonance interaction between the S=N bond and the adjacent phenyl ring shown below, would lead the λ_{max} to a red-shift.

7) S–N bond of sulfoximine is considered to be of double bond character from the following evidence. i) S–N bond length obtained from X-ray analysis is appropriate for S=N double bond distance. 1.56 Å for methionine sulfoximine; B. W. Christensen and A. Kjaer, *Chem. Commun.*, **1969**, 169. 1.53 Å for methyl-*p*-nitrophenyl sulfoximine; A. Shimada, K. Hirotsu and K. Iwama, unpublished work. ii) The substituent effect of pK_a of arylmethylsulfoximine does not obey σ^+ value but σ value; S. Oae, K. Tsujihara and N. Furukawa, *Chem. Ind.* (London), **1968**, 1569.

8) L. J. Bellamy, "Advances in Infrared Group Frequencies," Methuen Co. Ltd. Londn (1968), p. 220.

9) H. P. Klug, *Acta Crystallogr.*, **24**, 792 (1968).

10) K. N. Trueblood and S. W. Mayer, *ibid.*, **9**, 628 (1956).

11) R. M. Badger, *J. Chem. Phys.*, **2**, 128 (1934).

TABLE 3. UV SPECTRA OF *N*-*p*-TOSYLSULFILIMINE

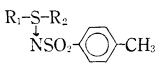

R_1	R_2	λ_{max}	log ε_{max}	Solvent
CH_3	CH_3	227	4.10	CH_3OH
$(CH_3)_2CH$	$(CH_3)_2CH$	230	4.13	CH_3OH
$CH_3(CH_2)_3$	$CH_3(CH_2)_3$	230	4.06	CH_3OH
	$-(CH_2)_4-$	228	4.07	CH_3OH
	$-(CH_2)_5-$	228	4.07	CH_3OH
CH_3	C_6H_5	226	4.26	CH_3OH
CH_3	*p*-$CH_3C_6H_4$	230	4.32	CH_3OH
CH_3	*p*-$CH_3OC_6H_4$	239	4.30	CH_3OH
		234	4.19	75%-H_2SO_4
		267	4.02	
CH_3	*p*-$NH_2C_6H_4$	222	4.17	CH_3OH
		275	4.27	
		228	4.24	75%-H_2SO_4
CH_3	*p*-$NO_2C_6H_4$	230	4.21	CH_3OH
		255*	(3.96)	
CH_3CH_2	C_6H_5	226	4.27	CH_3OH
$(CH_3)_2CH$	C_6H_5	228	4.28	CH_3OH
$(CH_3)_3C$	C_6H_5	227	4.28	CH_3OH
$C_6H_5CH_2$	C_6H_5	229	4.38	CH_3OH
$C_6H_5CH_2$	$C_6H_5CH_2$	227	4.35	CH_3OH
$C_6H_5(CH_2)_2$	C_6H_5	226	4.30	CH_3OH
C_6H_5	C_6H_5	229	4.39	CH_3OH
C_6H_5	*p*-$CH_3C_6H_4$	230	4.37	CH_3OH
C_6H_5	*p*-ClC_6H_4	232	4.46	CH_3OH
C_6H_5	*p*-$NO_2C_6H_4$	227	4.37	CH_3OH
		257*	(4.12)	CH_3OH
p-$CH_3OC_6H_4$	*p*-$CH_3OC_6H_4$	242	4.37	CH_3OH
p-$CH_3C_6H_4SO_2NH_2$		225	4.07	CH_3OH

* shoulder

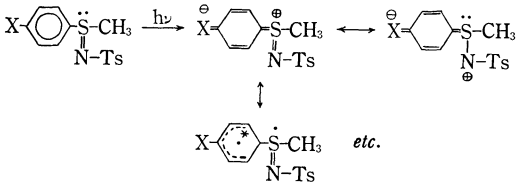

(Ts: *p*-$CH_3C_6H_4SO_2$-)

Fig. 2

Lack of such a red-shift suggests that the S(IV)–N bond in sulfilimine cannot be of the usual double bond character. This resonance interaction between the lone pair electrons on the S atom with phenyl ring is well known in sulfides.[12]

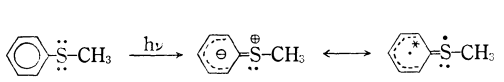

Even in the case of sulfoxides having both a lone electron pair and a somewhat positive charge on the S atom, this resonance interaction is observed.[12] In this case, however, the resonance interaction is not as large as in the case of sulfide, since the positive

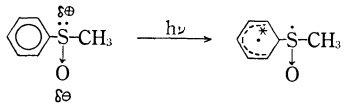

charge on the sulfoxide sulfur atom increases the energy required to excite an electron on the lone pair.

As the positive charge on the S atom becomes larger, this resonance interaction of the lone electron pair with phenyl ring would become difficult, and when the S atom bears a discrete positive charge such as in sulfonium salts, this type of resonance interaction is no longer observed.[12]

In this case, resonance involving the donation of electrons from an occupied orbital in phenyl ring into a vacant $d\pi$ orbital of the S atom would be observed. This type of interaction is known to occur in sulfones attached to a phenyl ring and occasionally in sulfoxides having a pheny ring substituted with an electron-releasing group such as amino or methoxyl group.[12]

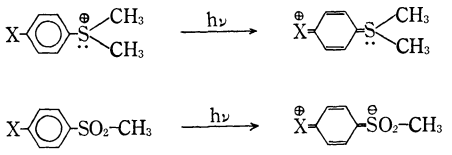

In the case of *N*-*p*-tolylsulfonylsulfilimine the lone electron pair would be bound somewhat tightly on the S atom and not readily excited to the energy level of *d* orbitals, because the λ_{max} and log ε_{max} of *p*-nitrophenyl or *p*-ammoniumphenyl-methylsulfilimine (σ_p of *p*-NO_2 and *p*-$NH_3\oplus$ are 0.778 and 0.60 respectively) scarcely alter when solvent changes from methanol or dilute sulfuric acid to 75% sulfuric acid in which sulfilimine is protonated with sulfuric acid and bears a discrete positive change on the S atom (see Table 4).

This observation indicates that the S atom of *N*-*p*-tolylsulfonylsulfilimine would bear a considerable positive charge which makes the lone electron pair tightly bound on the S atom.

UV spectra of *S*-aryl-*S*-methyl-*N*-*p*-tolylsulfonylsulfilimine in various solvents are shown in Table 4.

The maximum band of *S*-methyl-*S*-*p*-methoxyphenylsulfilimine (σ_p^+ of *p*-CH_3O is -0.778) at 239 mμ is shifted to 232 mμ with a shoulder at 242 mμ when solvent changes from methanol to water.

12) C. C. Price and S. Oae, "Sulfur Bonding," Ronald Press, New York (1962); H. H. Jaffé and M. Orchin, "Theory and Application of Ultraviolet Spectroscopy," J. Wiley and Sons, Inc., New York, (1962), p. 474.

TABLE 4. UV SPECTRA OF ARYLMETHYLSULFILIMINES

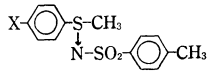

X	Solvent	λ_{max}	log ε_{max}	σ_p (σ_p^+)
H	CH_3OH	226	4.26	0
	H_2O	226	4.26	
	75%-H_2SO_4	230	4.27	
CH_3	CH_3OH	230	4.32	−0.170(−0.311)
Cl	CH_3OH	231	4.37	0.227(0.114)
NO_2	CH_3OH	230	4.21	0.778(0.790)
		255 (shoulder)	(3.96)	
	75%-H_2SO_4	235	4.23	
		254 (shoulder)	(4.07)	
OCH_3	CH_3OH	239	4.30	−0.268(−0.778)
	H_2O	232	4.25	
		242 (shoulder)		
	75%-H_2SO_4	234	4.19	
		267	4.02	
NH_2	CH_3OH	222	4.17	−0.66 (−1.3)
		275	4.27	
NH_3^+	2%-H_2SO_4	226	4.21	+0.60
	75%-H_2SO_4	228	4.24	

The increase of the concentration of sulfuric acid gives a bathochromic shift to the shoulder at 242 mμ while in 75% sulfuric acid the sulfilimine gives two isolated bands at 234 and 267 mμ. This observation obviously indicates that there is some resonance interaction between *p*-methoxyphenyl ring and the somewhat positively charged S atom, while the resonanse interaction becomes stronger when the sulfilimine group is protonated with sulfuric acid and bears a discrete positive change on the S atom as shown in Fig. 3.

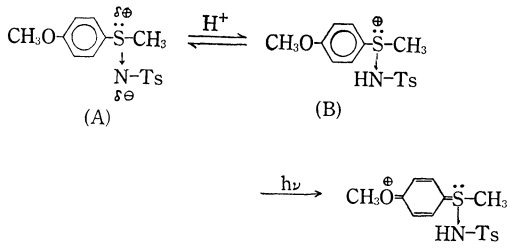

(A) (B)

(Ts: *p*-$CH_3C_6H_4SO_2$–)

Fig. 3

This type of resonance interaction can be more clearly observed in the case of *S*-*p*-aminophenyl-*S*-methylsulfilimine (σ_p^+ of *p*-NH_2 is −1.3): namely, in methanol solution in addition to 222 mμ band due to *p*-tolylsulfonyl group 275 mμ band appears and completely disappears when solvent is changed to 2% sulfuric acid in which amino group is completely protonated.

This clearly indicates that *p*-aminophenyl ring interacts with the S atom bearing somewhat positive charge as shown below.

The fact that the resonance interaction involving the donation of electrons from an occupied orbital of the phenyl ring into a vacant $d\pi$ orbital of the S

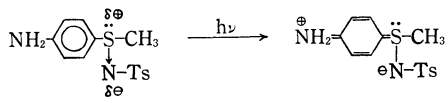

(Ts: *p*-$CH_3C_6H_4SO_2$–)

atom occurs obviously in the case of sulfilimines having an electron releasing substituent such as amino or methoxyl group, indicates that the S atom of sulfilimine possesses an appreciable positive charge.

The resonance interaction which involves the donation of electrons from the lone electron pair of the S atom into an unoccupied orbital of the benzene ring would not occur, since the UV spectra of *p*-ammoniumphenyl- and *p*-nitrophenylmethylsulfilimine are not altered when sulfilimine group protonated and bears a discrete positive charge on the S atom.

This suggests that the S(IV)–N bond is not a discrete double bond, and there is at least some positive charge on the S atom to bind the lone pair electrons tightly on the atom. From these results the S(IV)–N bond in *N*-*p*-tolylsulfonylsulfilimine is considered to be a semipolar rather than a double bond. The negative charge on the N atom is considered to be delocalized over the SO_2 and the sulfilimine groups. *p*-Methoxyphenylmethylsulfilimine gave two isolated bands at 234 and 267 mμ in aqueous sulfuric

acid. The latter band has been considered to be due to the resonance interaction between *p*-methoxyphenyl ring and the S atom having a discrete positive charge as shown in Fig. 3.

It is of interest that this observation can be used to determine the basicity of N atom of the sulfilimine group. The basicity of sulfilimine is shown in the following equation.

$$pK_a = H_0 + \log \frac{C_{B^+}}{C_A}$$

where

H_0: the acidity function

C_A and C_{B^+}: the concentrations of sulfilimine and protonated sulfilimine respectively.

When the decrease of 242 mμ band or the increase of 267 mμ band is measured, the pK_a value can be obtained from the H_0 when the sulfilimino group is half protonated. The value of pK_a of *S,S-p*-methoxyphenylmethyl-*N*-*p*-tolylsulfonylsulfilimine thus obtained is -1.78 and this value is considerably larger than that of *p*-tolylsulfonamide ($pK_a = -3.30$).[13] This fact indicates that the electron density on the N atom is increased in the form of a coordination of the lone electron pair of the S atom to the N atom.

NMR Chemical Shifts of *N*-*p*-Tolylsulfonylsulfilimines. The chemical shifts of sulfilimines are measured from TMS internal standard as a reference peak in $CDCl_3$.

N-*p*-Tolylsulfonylsulfilimine has an asymmetric center which may give the chemical shift difference between the protons of an adjacent methyl or methylene group, and the AB-type NMR spectrum due to magnetically non-equivalent protons is expected to be observed.

Actually benzyl protons of *S*-benzyl-*S*-phenyl-*N*-*p*-tolylsulfonylsulfilimine appear as double doublet ($J_{AB} = 13$ Hz). The chemical shifts of methyl protons attached to the S(IV) atom of *S*-methyl-*S*-*p*-tolylsulfilimine, sulfoxide and sulfone are 2.81, 2.69, 3.04 ppm respectively. This indicates that the sulfilimino group is somewhat more electron-withdrawing than the sulfoxide group but less than the sulfone group, while a substantial positive charge is centered on the S(IV) atom of *N*-*p*-tolylsulfonylsulfilimine.

From these IR, UV, NMR spectroscopic studies together with X-ray crystallographic data, *N*-*p*-tolylsulfonylsulfilimine is considered to be represented better by the ylide structure in which the charges on the S atom and the N atom are considerably delocalized with strong $d\pi$ conjugation into S(IV)–N–S(VI) bondings. Therefore the S–N bond of sulfilimino group is considered to be essentially semipolar.

13) H. Lemaire and H. J. Lucas, *J. Amer. Chem. Soc.*, **73**, 5198 (1951).

Experimental

Preparation of Sulfilimines. All the *N*-*p*-tolylsulfonylsulfilimines were prepared from the reaction of corresponding sulfides and chloramine T by the same procedure described previously.[14] The melting points of sulfilimines are listed in Table 1.

Measurement of the Basicity of *S*-Methyl-*S*-*p*-methoxyphenyl-*N*-*p*-tolylsulfonylsulfilimine. UV spectra of *S*-methyl-*S*-*p*-methoxyphenyl-*N*-*p*-tolylsulfonylsulfilimine were taken in sulfuric acid of several concentrations (from 0% to 75%). Increase of the concentration of sulfuric acid gave a bathochromic shift for the shoulder at 242 mμ. In 75% sulfuric acid the sulfilimine gave two isolated bands at 234 and 267 mμ, but above 75% the pattern of the spectrum no longer altered. The height of the spectrum at the suitable wavelength, for instance 266 mμ was used for calculation of the concentration in the equation

$$pK_a = H_0 + n \log \frac{C_{B^\oplus}}{C_A} = H_0 + n \log \frac{h - h_0}{h_{75} - h}$$

where

H_0: acidity function

n: constant (1.0 for Hammet base)

h, h_0 and h_{75}; height of spectrum at 266 mμ

h; at an arbitrary concentration of sulfuric acid

h_0; at 0% sulfuric acid (no protonation)

h_{75}; at 75% sulfuric acid (completely protonated)

The pK_a value was obtained from the H_0 when the sulfilimine group is half protonated ($\log(h-h_0/h_{75}-h)=0$), see Fig. 4.

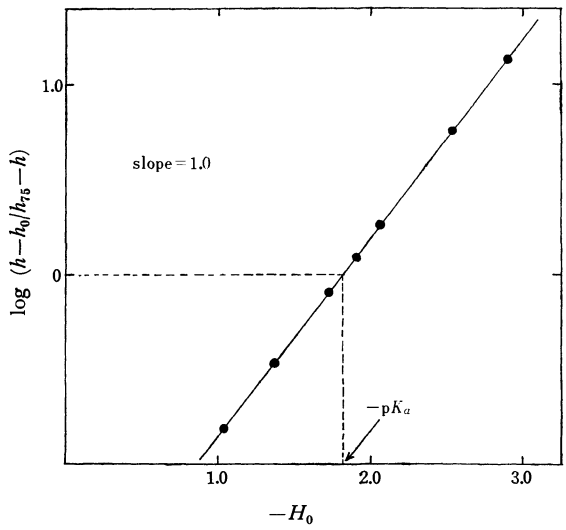

Fig. 4. Relations of $-H_0$ and log $(h-h_0/h_{75}-h)$.

14) K. Tsujihara, N. Furukawa, K. Oae and S. Oae, This Bulletin, **42**, 2631 (1969).

BULLETIN OF THE CHEMICAL SOCIETY OF JAPAN VOL. 43 2159—2161 (1970)

The Preparation of α-Amino-α-benzylmercaptopropionic Acid Derivatives

Akira KANEDA and Rokuro SUDO

Laboratory of Organic Chemistry, Tokyo Institute of Technology, Meguro-ku, Tokyo

(Received November 11, 1969)

The preparation of *N*-acyl derivatives of α-amino-α-benzylmercaptopropionic acid was investigated. It is described that pyruvic acid was treated with amides to afford *N*-acyl-α-amino-α-hydroxypropionic acids, which were then substituted into *N*-acyl-α-amino-α-benzylmercaptopropionic acids. In another experiment, Steglich's method was improved in order to afford three *N*-acyl derivatives of α-amino-α-benzylmercaptopropionic acid in a better yield.

α-Amino-α-mercaptocarboxylic acid has not been isolated in a pure form, and only two methods for the preparation of its derivatives have been reported by Steglich[1] and by Shemiyakin.[2] This paper will report a simple method for the preparation of α-amino-α-benzylmercaptopropionic acid derivatives from pyruvic acid and also an improvement of Steglich's method to give a better yield.

It has been described[3] that pyruvic acid (**1**) was heated with acetamide to give α-acetamidoacrylic acid (**2**) and α,α-diacetamidopropionic acid (**3**), which were produced through the intermediate, a complex of α-acetamido-α-hydroxypropionic acid acetamide.

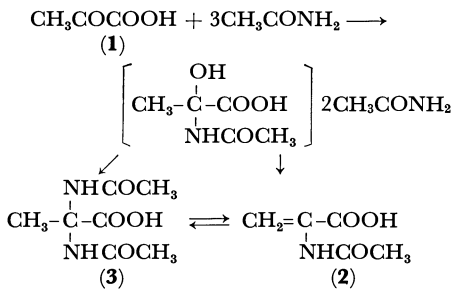

On the other hand, Shieve[4] reported that adding formamide to pyruvic acid (**1**) yielded α-formamido-α-hydroxypropionic acid (**4**), which was then isolated in a pure form.

When the acid **4** was refluxed with benzyl mercaptan in a benzene solution by means of the use of a water separator for 3 hr, 1 mol of water was separated and α-formamido-α-benzylmercaptopropionic acid (**5**) was obtained in a good yield.

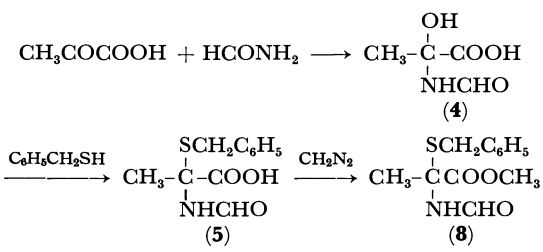

The structure of Compound **5** was characterized by elementary analysis and by a study of its IR and NMR spectrum. This reaction process was supported by the fact that carbinolamine (**6**) was replaced by mercaptan to give aminomethyl thioether (**7**).[5]

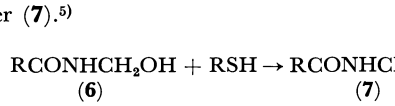

After the α-formamido-α-benzylmercaptopropionic acid (**5**) had been neutralized with a sodium bicarbonate solution, it was converted to its methyl ester with diazomethane.

On the other hand, pyruvic acid (**1**) did not react with urethane at room temperature, unlike the case of formamide. However, when pyruvic acid was refluxed with urethane in a benzene solution, it gave α-ethoxycarbonylaminoacrylic acid (**9**). Thus, pyruvic acid, urethane, and benzyl mercaptan were heated together under 60°C for 3 hr; α-ethoxycarbonylamino-α-benzylmercaptopropionic acid (**10**) was thus obtained.

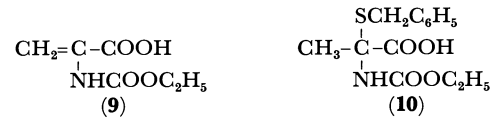

1) W. Steglich, H. Tanner and R. Hurnaus, *Chem. Ber.*, **100**, 1824 (1967).

2) M. M. Shemyakin, E. S. Chaman and L. I. Denisova, *Doklady Akad. Nauk SSSR*, **106**, 675 (1965); *Chem. Abstr.*, **50**, 13809 (1956).

3) J. P. Greestein and M. Winits, "Chemistry of Amino Acids," Vol. 1, John Wiley & Sons, Inc., New York (1961), p. 846.

4) W. Shieve, *J. Amer. Chem. Soc.*, **68**, 118 (1946).

5) H. E. Zaugg, "Organic Reactions," Vol. 14, (1965), p. 113.

Similarly, acetamide and chloroacetamide did not give α-amino-α-mercaptocarboxylic derivative, but α-acetamidoacrylic acid and α,α-diacetamidopropionic acid derivatives were formed.

Moreover, another method was investigated. Steglich[1] has described how the mercaptolysis of 2-dichloromethylene-4-methy-3-oxazolin-5-one (**11**) with ethyl mercaptan in an acetic acid solution containing hydrogen bromide gave α-dichloroacetamido-α-ethylmercaptopropionic acid and its ethyl thioester at the same time.

In our study, however, when **11** was treated with benzyl mercaptan in a solvent such as methylene-dichloride or tetrahydrofuran (THF) under neutral conditions and at room temperature, it gave only 2-dichloromethylene-4-methyl-4-benzylmercapto-2-oxazolin-5-one (**13**) and no further addition of mercaptan was observed. In an acetic acid solution however, Compound **13** reacted with another molecule of mercaptan to give α-dichloroacetamido-α-benzylmercaptopropionic acid benzyl thioester (**14**). Compound **13** was hydrolyzed, in an acetic acid solution, into α-dichloroacetamido-α-benzylmercaptopropionic acid (**12**), which was also obtained directly in low yields by the reaction of **11** with benzyl mercaptan in an acetic acid solution containing a small amount of water. Similarly, 2-benzylidene-4-methyl-3-oxazolin-5-one (**15**) also reacted with benzyl mercaptan in a THF solution; subsequent hydrolysis gave α-phenylacetamido-α-benzylacetamido-α-benzylmercaptopropionic acid (**16**), and in the case of 2-isopropylidene-4-methyl-3-oxazolin-5-one (**17**) it did not react with benzyl mercaptan in an acetic acid or THF solution, but in an acetic acid solution containing hydrogen bromide, α-isobutyrylamido-α-benzylmercaptopropionic acid (**18**) was obtained.

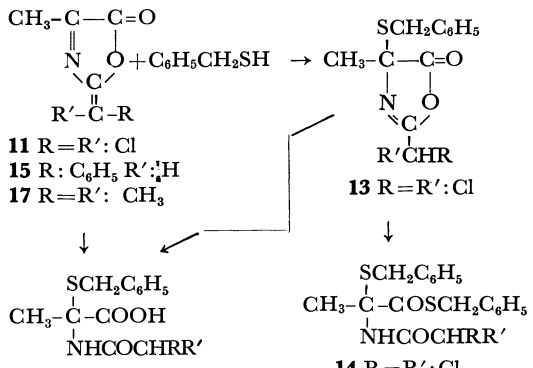

Experimental

α-Formamido-α-hydroxypropionic Acid (4). This was prepared by the method of Shieve;[4] mp 53°C, yield 98%.

α-Formamido-α-benzylmercaptopropionic Acid (5). A benzene solution (50 m*l*) of **4** (6.6 g, 1/20 mol) was heated with benzyl mercaptan (6.2 g, 1/20 mol) under refluxing for 3 hr. After cooling, the solvent was removed and the residue was treated with a sodium bicarbonate solution. The water layer was washed with ether and acidified with dilute hydrochloric acid under cooling. An oily substance was thus separated and crystallized. Recrystallization from ethanol gave white needles with a mp of 148—149°C; yield 18 g (75%). IR bands (KBr), 3290 cm^{-1} (NH), 1685, 1705 cm^{-1} (COOH), 720 cm^{-1} (C_6H_5). NMR spectrum (DMSO, TMS as internal reference), τ 8.26 (3H, singlet) for CH_3, τ 6.12 (2H, doublet) for S-$CH_2C_6H_5$, τ 2.61 (5H, singlet) for C_6H_5, τ 1.90 (1H, singlet) for NH. This compound was hydrolyzed to pyruvic acid and benzyl mercaptan under refluxing for 1 hr in water. In an attempted debenzylation and deacylation, it was unsuccessful in isolating α-mercapto-α-amino acid itself in a pure form.

Methyl α-Formamido-α-benzylmercaptopropionate (8). To a solution of 2.39 g (1/100 mol) of **5** in ether, was added, drop by drop, a solution of diazomethane in ether until nitrogen-gas ceased to be evolved. The mixture was stirred at room temperature for 0.5 hr, and the excess diazomethane was treated with a small quantity of acetic acid. The mixture was then concentrated under reduced pressure. The residue was washed with a saturated sodium bicarbonate solution, extracted with ethyl acetate, and dried over anhydrous sodium sulfate. The evaporation of the organic layer afforded 2.40 g (95%) of a methyl ester of **5**. Recrystallization from dibutyl ether gave colorless crystals; mp 57—58°C. IR (KBr) 3290 cm^{-1} (NH), 1730 cm^{-1} ($COOCH_3$), 1665 cm^{-1} (CONHR), 700, 720 cm^{-1} (C_6H_5).

Found: C, 57.05; H, 6.25; N, 5.74%. Calcd for $C_{12}H_{15}NO_3S$: C, 56.91; H, 5.97; N, 5.53%.

α-Ethoxycarbonylamino-α-benzylmercaptopropionic Acid (10). Pyruvic acid (4.4 g, 1/20 mol) and ethyl carbamate (4.4 g, 1/20 mol) were dissolved in 50 m*l* of benzene. The solution was heated at 40°C for 1 hr, and then benzyl mercaptan (6.2 g, 1/20 mol) was added to this solution. The mixture was heated for 2 hr at 60°C. After the removal of the benzene, the residue was treated with a sodium bicarbonate solution. The water layer was washed with ether and then acidified with dilute hydrochloric acid under cooling. An oily substance which separated gradually crystallized on cooling. Recrystallization from ethylene dichloride-cyclohexane gave colorless prisms with a mp of 90—91°C; yield 8.2 g (58%). IR bands (KBr), 3300 cm^{-1} (NH), 1939 cm^{-1} ($COOC_2H_5$), 1660 cm^{-1} (COOH), 715 cm^{-1} (C_6H_5). NMR spectrum ($CDCl_3$, TMS as internal reference), τ 8.78 (3H, triplet) for CH_2CH_3, τ 8.06 (3H, singlet) for CH_3, τ 6.10 (2H, singlet) for S-CH_2-C_6H_5, τ 5.88 (2H, quartet) for CH_2CH_3, τ 2.15 (5H, singlet) for C_6H_5, τ 2.15 (1H, singlet) for COOH.

2-Dichloromethylene-4-methyl-3-oxazolin-5-one (11). This was prepared by the method of Steglich;[1] mp 77°C, yield 78%.

2-Benzylidene-4-methyl-3-oxazolin-5-one (15). This was prepared by the method of Filler;[6] mp 110—

6) R. Filler and E. J. Piasek, *J. Org. Chem.*, **28**, 221 (1963).

115°C, yield 85%.

2-Isopropylidene-4-methyl-3-oxazolin-5-one (17). This was prepared by the method of Bergmann;[7] bp 56°C/1.5 mmHg, yield 62%.

2-Dichloromethylene-4-methyl-4-benzylmercapto-2-oxazolin-5-one (13). In 50 m*l* of ethylene dichloride **11** (9.0 g, 1/20 mol) was dissolved, and to this solution was added benzyl mercaptan (12.4 g, 1.0 mol). The resulting solution was kept at room temperature for 24 hr. After the evaporation of the solvent, the residual benzyl mercaptan was removed by distillation under reduced pressure. The residue was chromatographed on an alumina column in benzene to afford a syrup. This syrup could not be distilled and crystallized; yield, 11.0 g (62%). IR bands (liquid film), 1805 (C=O) and 1650 cm^{-1} (C=N). NMR bands ($CDCl_3$, TMS was used as the internal reference), τ 7.84 (3H, singlet) for CH_3, τ 6.18 (2H, singlet) for $C_6H_5CH_2$, τ 4.01 (1H, singlet) for $CHCl_2$, and τ 2.72 (5H, singlet) for $C_6H_5CH_2$.

Found: C, 47.66; H, 3.74; N, 4.36%. Calcd for $C_{12}H_{11}O_2SNCl_2$: C, 47.37; H, 3.62; N, 4.61%.

α-Dichloroacetamido-α-benzylmercaptopropionic Acid-*S*-Benzylester (14). To a solution of **13** (6.1 g, 1/50 mol) in 50 ml of acetic acid was added 2.5 g (1/50 mol) of benzyl mercaptan. The resulting mixture was kept at room temperature for 48 hr. After the evaporation of the solvent, the residue was chromatographed on an alumina column in benzene to afford a crude product, which was recrystallized from isopropyl alcohol to give colorless prisms; mp 94—95°C, yield 4.2 g (50%). IR bands (KBr), 1690 cm^{-1} ($COSCH_2C_6H_5$), 1680 and 1560 cm^{-1} (CONH).

Found: C, 53.48; H, 4.54; N, 3.42%. Calcd for $C_{19}H_{19}O_2NS_2Cl_2$: C, 53.25; H, 4.44; N, 3.27%.

α-Dichloroacetamido-α-benzylmercaptopropionic Acid (12). a) In 50 m*l* of acetic acid containing a small amount of water was dissolved 6.1 g (1/50 mol) of **13**. The resulting mixture was kept at room temperature for 48 hr. After the evaporation of the solvent, the oily residue was dissolved in a sodium bicarbonate solution and washed with ether. The aqueous solution was acidified with dilute hydrochloric acid under cooling. An oily substance which separated crystallized standing. The crystals were recrystallized from acetic acid to give colorless prisms; mp 166—167°C, yield 4.2 g (65%). IR bands (KBr), 3300 cm^{-1} (NH), 1713 cm^{-1} (COOH), 1685 and 1542 cm^{-1} (CONH).

b) To a solution of **11** (9.0 g, 1/20 mol) in 50 m*l* of acetic acid was added 6.2 g (1/20 mol) of benzyl mercaptan and a small amount of water. The resulting mixture was kept at room temperature for 2 days and they treated by a procedure similar to a) above to yield compound **12**.

α-Phenylacetamido-α-benzylmercaptopropionic Acid (16). To a solution of **15** (9.5 g 1/20 mol) in 50 m*l* of THF was added 6.2 g (1/20 mol) of benzyl mercaptan. The resulting mixture was kept at room temperature for 24 hr. After the removal of the solvent, the residue was dissolved in a mixture of 30 m*l* of acetic acid and 10 m*l* of water, and the resulting mixture was heated for 5 hr. After the removal of the acetic acid, the residue was neutralized with a sodium bicarbonate solution. This solution was acidified with dilute hydrochloric acid to give crystals. Recrystallization from ethyl acetate gave colorless crystals; mp 157—158°C, yield 11 g (66.7%). IR bands (KBr), 3300 cm^{-1} (NH), 1710 cm^{-1} (COOH), 1628 and 1516 cm^{-1} (NHCO).

α-Isobutyrylamido-α-benzylmercaptopropionic Acid (18). In an acetic acid solution containing 20% hydrogen bromide **17** was treated by a procedure similar to **16**. The recrystallization of a crude product from ethylene dichloride gave colorless prisms; mp 114—115°C, yield 40%. IR bands (KBr), 3330 cm^{-1} (NH), 1730 cm^{-1} (COOH) and 1615 cm^{-1} (NHCO).

Table 1. Elementary analysis of α-amino-α-benzylmercaptopropionic acid derivatives

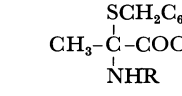

Compound number	R	Anal. % Calcd C	Calcd H	Calcd N	Found C	Found H	Found N
5	CHO	55.23	5.48	5.86	55.00	5.00	5.57
10	$COOC_2H_5$	55.12	6.05	4.95	54.91	6.02	4.87
12	$COCHCl_2$	44.75	4.04	4.35	44.99	3.97	4.38
16	$COCH_2C_6H_5$	65.64	5.82	4.25	65.71	5.71	4.23
18	$COCH(CH_3)_2$	59.77	6.81	4.98	59.86	6.55	5.09

7) M. Bergmann and S. Stern, *Ann.*, **448**, 20 (1926).

BULLETIN OF THE CHEMICAL SOCIETY OF JAPAN VOL. 43 2162—2167 (1970)

Photoreaction of Acetoacetate

Masaru TADA, Tadayoshi KOKUBO and Tadashi SATO

School of Science and Engineering, Waseda University, Shinjuku, Tokyo

(Received November 14, 1969)

Methyl acetoacetate was irradiated in the presence of cyclohexene to afford methyl 3-cyclohexyl-3-hydroxybutyrate (VIII), methyl 3-cyclohexenyl-3-hydroxybutyrate (IX), two oxetanes (Xa and Xb), and cyclohexene dimers. In contrast to acetylacetone, acetoacetate behaves as a saturated ketone rather than as an α,β-unsaturated ester on photoreaction. We concluded that the n-π^* excitation of the enol-form of β-dicarbonyl compound is responsible for photo-cycloaddition, and no effective n–π^* excitation is accesisble on irradiaron of the enol-form of acetoacetate, since the enol form of acetoacetate has its n–π^* and π–π^* absorptions in the same region.

Ultraviolet irradiation of saturated ketone in the presence of olefin gives oxetanes. β-Diketone and olefin, on the other hand, give cyclobutanes under the same condition.

Bradshaw[1] reported the formation of oxetane I, unsaturated alcohol II, and olefin dimer III on irradiation of acetone in the presence of cyclohexene. De Mayo and Takeshita[2] reported that irradiation of acetylacetone in the presence of cyclohexene afforded cyclobutane derivative IV, which was transformed to diketone V by heat. This feature of 1,3-diketone can be accounted for by the excitation of the enol-form of acetylacetone, which is the predominant species under the reaction condition. β-Ketoester is also well known to enolize to a reasonably high extent in non-polar solvents.[3] If the enol-form of β-ketoester is responsible for the photo-cycloaddition, we may expect the formation of hydroxyester VI.

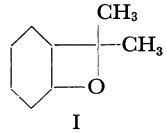

I

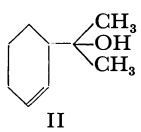

II

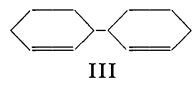

III

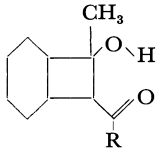

R

IV: R=CH_3
VI: R=OCH_3

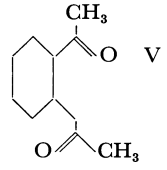

V

Our purpose in this work was to pursue the behaviour of acetoacetic ester, as saturated ketone or unsaturated ester, on irradiation in the presence of olefin.

Results and Discussion

Irradiation of methyl acetoacetate and cyclohexene with a high pressure mercury lamp gave products which were separated into C_{12}-hydrocarbons and addition products between methyl acetoacetate and cyclohexene. The structures of C_{12}-hydrocarbons were assigned to be the two isomers of tricyclododecanes (VIIa and VIIb) and bicyclohexenyl (III) respectively. The structures of VIIa and VIIb were deduced mainly from the mass spectra which showed peaks at $m/e=164$ (molecular peak), 82, and 67 for both isomers. The last two peaks are characteristic of cyclohexene[4] which is formed by the ring opening of the tricyclododecanes. Hydrocarbon III was identified with bicyclohexenyl which was unambiguously synthesized. The fraction of the adducts between acetoacetate and cyclohexene consists mostly of four components; saturated hydroxy ester VIII, unsaturated hydroxy ester IX, and two isomers of oxetanes Xa and Xb in the ratio of *ca.* 1.0 : 1.5: 2.4 : 2.2.

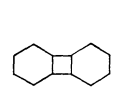

VII

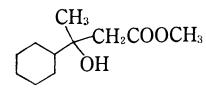

VIII

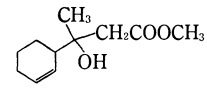

IX

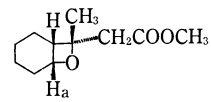

Xa

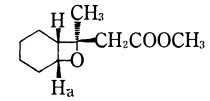

Xb

Compound VIII was identified with methyl 3-cyclohexyl-3-hydroxybutyrate which was synthesized

1) J. S. Bradshaw, *J. Org. Chem.*, **31**, 237 (1966).

2) P. de Mayo and H. Takeshita, *Can. J. Chem.*, **41**, 440 (1963).

3) A. E. Gillam and E. S. Stern, "An Introduction to Electronic Absorption Spectroscopy in Organic Chemistry," Edward Arnold Ltd., London (1958), p. 259.

4) H. Budzikiewicz, C. Djerassi and D. H. Williams, "Mass Spectrometry of Organic Compounds," Holden-Day, Inc., San Francisco (1967), p. 67.

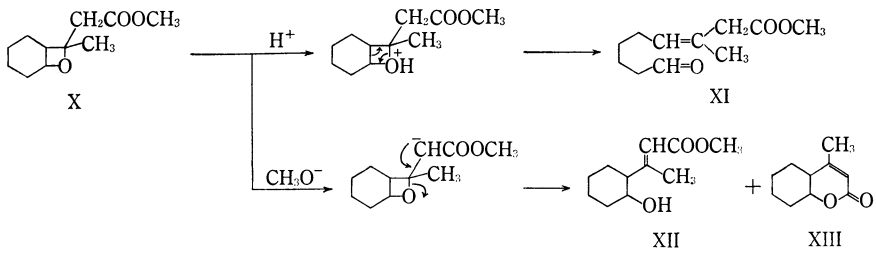

Fig. 1. Chemical behaviour of the oxetanes toward acid and base.

by the Reformatsky reaction between acetylcyclohexane and methyl bromoacetate. The structure of adduct IX was deduced to be methyl 3-(2-cyclohexenyl)-3-hydroxybutyrate from IR and NMR spectra, and was confirmed by the formation of adduct VIII by hydrogenation.

The oxetane-structures of adducts Xa and Xb were indicated by characteristic NMR signals[1] at 4.65 ppm due to the hydrogens attached to $C_6(H_a)$, and was further confirmed by the chemical behaviour toward acid and base. Acid treatment of the mixture of Xa and Xb gives two isomers of aldehyde XIa and XIb (IR: 2720, 1725 cm^{-1}, NMR: 9.62 ppm) besides a small amount of methyl acetoacetate and cyclohexene (Fig. 1). The cleavage of oxetane by acid is well known.[5] Base treatment of Xa and Xb, on the other hand, produces the hydroxyester XII (3470, and 1725 cm^{-1}) and δ-lactone XIII (1710 cm^{-1}).

NMR signals of oxetane at 4.65 ppm due to H_a are a sextet with a half-band width of 14 Hz for Xa (Fig. 2) and a quintet with a half-band width of 17 Hz for Xb, respectively. Spin decoupling between C_5-methylene (H_c and H_d) and H_a of Xa gives a doublet for H_a with a coupling constant 7 Hz (J_{ab}). Oxetane Xb gives essentially the same result except for the coupling constant between H_a and H_b being 8 Hz.

These values of J_{ab} suggest that H_a and H_b are *cis* and the oxetane rings are *cis*-fused to cyclohexane ring. This feature is further supported by the half-band width of H_a-signal and the coupling constant between H_a and C_5-methylene: $J_{ac}=J_{ad}=2.5$ Hz for Xa, and $J_{ac}=J_{ad}=4.0$ Hz for Xb. If the ring junction were *trans*, both H_a and H_b would have to occupy *quasi*-axial conformation with respect to the cyclohexane ring. In this case H_a and one of the hydrogen of C_5-methylene (H_c or H_d) must be in the relation of *trans quasi*-diaxial regardless of the conformation of the cyclohexane ring, and the larger half-band width would be observed.[6] Thus the two oxetanes must be configurational isomers at C_8. The chemical shifts of methyls (1.50 ppm for Xa and 1.33 ppm for Xb)[1] and methylene bearing carbomethoxy groups (2.60 ppm for Xa and 2.72 ppm for Xb) are in good accordance with the struc-

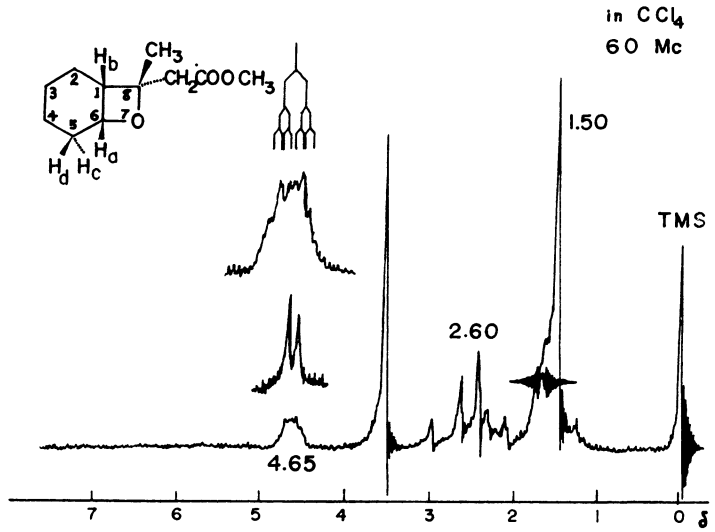

Fig. 2. NMR spectrum of oxetane Xa.

5) G. Büchi, C. G. Inman and E. S. Lipinsky, *J. Amer. Chem. Soc.*, **76**, 4327 (1954).

6) N. S. Bhacca and D. H. Williams, "Applications of NMR Spectroscopy in Organic Chemistry: Illustrations from the Steroid Field," Holden-Day, Inc., San Francisco (1964), p. 51.

tures Xa and Xb. The anisotropic effect of C_1–C_2 bond would shift to a higher field the signals of the group which is *cis* to the C_1–C_2 bond. None of the *trans* isomers other than these *cis*-oxetanes was detected at least from VPC analysis.

Types of products III, IX, Xa and Xb correspond to the irradiation products between acetone and cyclohexene reported by Bradshaw.[1] Thus the keto-form of acetoacetate must be responsible for the present photoreaction. We may expect the formation of adduct VI in the same fasion with acetylacetone, if the enol-form of acetoacetate is responsible in photoreaction. No such adduct, however, could be detected and the enol-form must be inert to the photo-cycloaddition under these irradiation.

During the course of confirming the inertness of the enol-form, the following results were obtained.

1) Irradiation of acetoacetate and cyclohexene in *n*-hexane, instead of benzene, gave the same results as in the case of the irradiation of the mixture in benzene, except for the lack of tricyclododecane (VII) in the product-mixture. Tricyclododecane was formed by the sensitization effect of benzene.

2) Irradiation with a low pressure mercury lamp (emitting strong line at 2537 Å) resulted in the production of the adducts in poor yield.

3) The enol-form of ethyl acetoacetate was fixed by making its ether (*β*-ethoxycrotonate), and acetate (*β*-acetoxycrotonate). Irradiation of these derivatives in the presence of cyclohexene did not give the expected adducts XIV and XV.

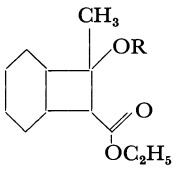

XIV: R=C_2H_5

XV: R=$COCH_3$

In view of these facts, it can be concluded that the enol-form of acetoacetate does not undergo cycloaddition at least by π–π^* excitation (246 mμ). Though n–π^* excitation of the enol-form might cause the cycloaddition, the effective n–π^* excited state is inaccessible in these systems.

Although acetylacetone (*ca.* 96% enol in *n*-hexane)[3] has a single absorption band at 272 mμ (Fig. 3), its enol ether discriminates the n–π^* band (308 mμ; ε=70) from the π–π^* band (248 mμ; ε=15900). Though we can not observe a distinct absorption maximum, the enol-form of acetylacetone must have n–π^* band in the same region as in the n–π^* band of its enol ether (308 mμ). This n–π^* excitation is believed to be responsible for the cycloaddition giving adduct IV though without rigorous evidence.[2] On the other hand, acetoacetate and its enol ether have π–π^* absorption at 246 mμ (due to enol-form, 51% in *n*-hexane)[3] and 230 mμ respectively, in *n*-hexane, and the n–π^*

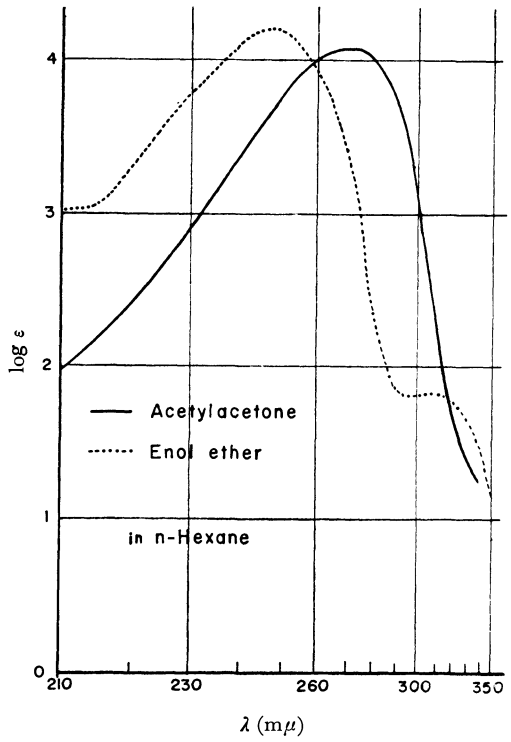

Fig. 3. UV spectra of acetylacetone and its enol ether.

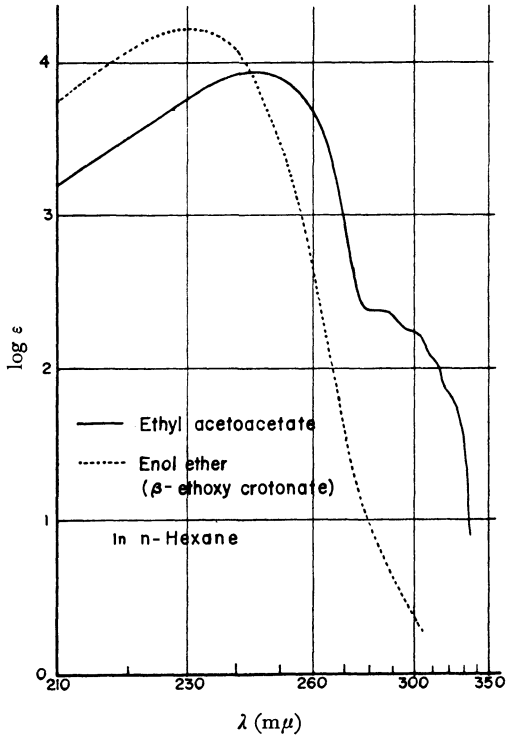

Fig. 4. UV spectra of ethyl acetoacetate and its enol ether.

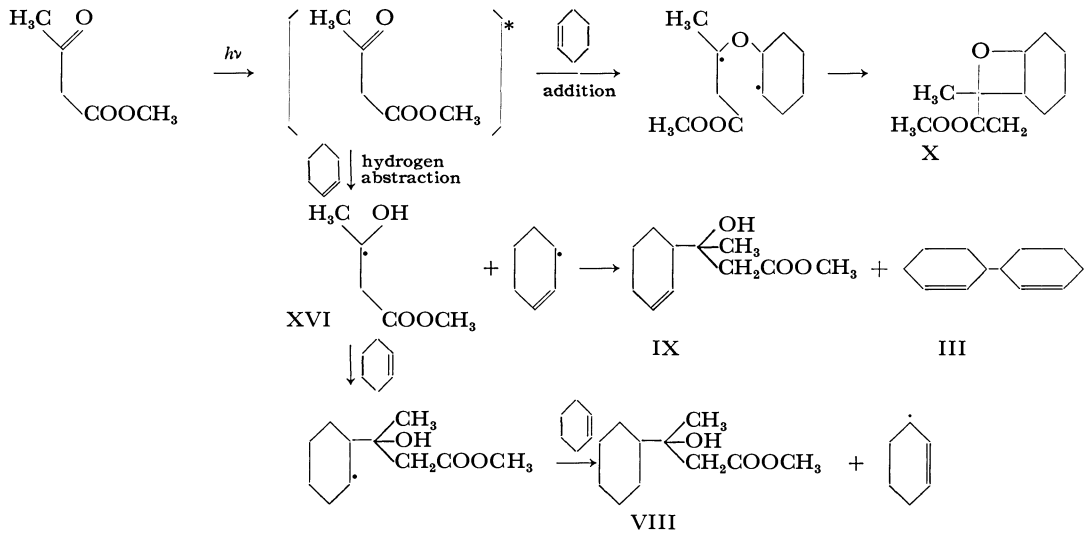

Fig. 5. Reaction scheme.

band of the enol-form can not be observed in both cases. An α,β-unsaturated ester usually has an n–π^* absorption around 240 mμ which is buried under the strong π–π^* absorption.[7] Attachment of hydroxy at β-position of α,β-unsaturated ester shifts the π–π^* absorption to longer wave length (*ca.* 40 mμ), while it possibly affects the n–π^* absorption a little.[8] The n–π^* absorption of the enol-form of acetoacetate, therefore, might be located in the same region as in its π–π^* absorption and the effective excited state (n–π^*) for the photo-cycloaddition can not be achieved.

UV spectrum of acetoacetate in n-hexane shows an absorption at 246 mμ (ε=8100) due to the π–π^* excitation of the enol-form and the shoulder at 285 mμ (ε=68) due to the n–π^* excitation of the keto-form. The latter excitation takes part in the formation of oxetane and the hydrogen abstraction from cyclohexene.

On the basis of the above discussion, the reaction of acetoacetate with cyclohexene can be rationalized as a process involving the n–π^* excitation of the keto-form of acetoacetate and can be represented by the scheme in Fig. 5. Formation of the saturated alcohol VIII can be envisaged by the initial coupling of the radical intermediate XVI and cyclohexene. The mechanism involving the coupling of cyclohexyl radical and the radical XVI can be eliminated by the fact that no bicyclohexyl can be detected in the reaction products.

Bicyclohexenyl (III) must originate from the coupling of two cyclohexenyl radicals formed by hydrogen abstraction. Formation of tricyclododecane (VII) is attributable to the sensitization by benzene used as solvent. This sensitization can be shown by the fact that cyclohexene itself gave VII on irradiation in benzene and the irradiation of acetoacetate and cyclohexene in n-hexane, instead of benezne, gave no tricyclododecane.

7) W. D. Closssen, S. P. Brady and P. J. Orenski, *J. Org. Chem.*, **30**, 2371 (1965).

8) N. J. Turro, "Molecular Photochemistry," W. A. Benjamin, Inc., New York (1965), p. 139.

Experimental

Irradiation of Methyl Acetoacetate and Cyclohexene. Methyl acetoacetate (29.0 g) and cyclohexene (82.0 g) in 350 m*l* of benzene were internally irradiated with a 450 W high pressure mercury lamp (USHIO UM-452) through a quartz immersion well in the conventional manner. Most of acetoacetate disappeared after irradiation for 14 hr and the solvent was removed under reduced pressure.

Separation and Structure of Photo-products. The crude products were distilled into two fractions, A: bp 40—50°C/1.5 mmHg, 2.4 g, and B: bp 80—90°C/1.5 mmHg, 21.8 g. Fraction A showed mainly three peaks at 7.0 (VIIa), 8.5 (VIIb), and 14.5 min (III) in the ratio of 1 : 3 : 1 on VPC analysis (2.2 m×6 mm, 10% PEG-20M on Chromosorb-W, 140°C). These products were separated and purified by preparative VPC. VIIa and VIIb were deduced to be tricyclo[6.4.0.$0^{2,7}$]dodecane. Product III was identified with the authentic sample of bicyclohexenyl.

VIIa. Mass: strong peaks at m/e=164 (M^+, $C_{12}H_{20}$), 82, 81, and 67 (base peak). IR (neat): 2850, 1445, 1340, 950 and 910 cm^{-1}. NMR (CCl_4): no olefinic hydrogen.

VIIb. Found: C, 87.62; H, 12.23%. Calcd for $C_{12}H_{20}$: C, 87.73; H, 12.27%. Mass: strong peaks at m/e=164 (M^+, $C_{12}H_{20}$), 82 (base peak), 81, and 67. IR (neat): 2850, 1449, 1320, 917, and 873 cm^{-1}. NMR (CCl_4): no olefinic hydrogen.

III. Found: C, 88.52; H, 11.17%. Calcd for $C_{12}H_{18}$: C, 88.82; H, 11.18%. IR (neat): 3010, 1650, 1435, 730, and 650 cm^{-1}. NMR (CCl_4): 5.6 ppm (4H, -CH=CH-).

Fraction B contains the adducts between acetoacetate and cyclohexene and shows four peaks at 13.4 (VIII),

14.3 (IX), 16.3 (Xa), and 20.0 min (Xb) in the ratio of 1.0 : 1.5 : 2.4 : 2.2 on VPC analysis (2.5 m×6 mm, 10% PEG-20M on Chromosorb-W, 180°C). These adducts were separated by preparative VPC.

VIII. Found: C, 66.17; H, 9.90%. Calcd for $C_{11}H_{20}O_3$: C, 65.97; H, 10.07%. IR (neat): 3560, 1717, 1200, 1005, and 893 cm^{-1}. NMR (CCl_4):*1 3.63 ($-OCH_3$), 3.2 (-OH), 2.35 (q, J_{ab}=15 Hz, $-CH_2-COO-$), 1.10 ($-CH_3$), 0.8—2.0 ppm (11H).

IX. Found: C, 66.92; H, 9.43%. Calcd for $C_{11}H_{18}O_3$: C, 66.64; H, 9.15%. IR (neat): 3550, 3020, 1720, 1205, 1005, 893, and 725 cm^{-1}. NMR (CCl_4): 5.67 (diffused d, J=5 Hz, -CH=CH-), 3.63 ($-OCH_3$), 3.3 (-OH), 2.38 (q, J_{ab}=15 Hz, $-CH_2-COO-$), 1.2—2.3 (7H), 1.16 and 1.09 ppm ($-CH_3$, 1.5H for each of the two peaks, both singlet due to the diastereomeric nature of IX).

Xa. Found: C, 66.35; H, 8.89%. Calcd for $C_{11}H_{18}O_3$: C, 66.64; H, 9.15%. IR (neat): 1740, 1195, 1095, 995, 953, 925, and 883 cm^{-1}. NMR (CCl_4): 4.65 (sextet, >CH-O-), 3.60 ($-OCH_3$), 2.60 (q, J_{ab}=16 Hz, $-CH_2-COO-$), 2.4 (multiplet, >CH-), 1.50 ($-CH_3$), 1.2—1.9 ppm (8H).

Xb. Found: C, 66.32; H, 9.16%. Calcd for $C_{11}H_{18}O_3$: C, 66.64; H, 9.15%. Mass: m/e=198 (M^+, $C_{11}H_{18}O_3$). IR (neat): 1740, 1195, 1092, 1008, 940, and 885 cm^{-1}. NMR (CCl_4): 4.65 (quintet, >CH-O-), 3.60 ($-OCH_3$), 2.72 (q, J_{ab}=15 Hz, $-CH_2-COO-$), 2.6 (multiplet, >CH-), 1.33 ($-CH_3$), and 1.2—1.9 ppm (8H).

Irradiation of Methyl Acetoacetate and Cyclohexene in *n*-Hexane. Methyl acetoacetate (3.94 g) and cyclohexene (14.0 g) in 100 m*l* of purified *n*-hexane were internally irradiated with a 100 W high pressure mercury lamp (Rikosha, UVL-700) through a quartz jacket. After irradiation for 40 hr, most of the starting acetoacetate disappeared and VPC analysis showed that the composition of the adducts was the same as that from the irradiation using benzene as solvent.

Irradiation of Enol-ether of Methyl Acetoacetate. A mixture of ethyl β-ethoxycrotonate[9] (1.0 g), cyclohexene (3.0 g) and 10 m*l* of *n*-hexane was placed in a quartz tube and was externally irradiated with a 450 W high pressure mercury lamp. VPC analysis showed that essentially no change had occured in the starting mixture.

Irradiation by a Low Pressure Lamp. Methyl acetoacetate (3.94 g) and cyclohexene (14.0 g) in 100 m*l* of *n*-hexane were internally irradiated with a 30 W low pressure mercury lamp (Rikosha UVL-300). After irradiation for 6.5 hr, VPC analysis showed that less than two per cent of the starting ester had been converted to the photo-products.

Synthesis of Bicyclohexenyl (III). Bicyclohexenyl was synthesized by an allyl coupling of 3-bromocyclohexene *via* its Grignard reagent. The reaction was carried out in the conventional manner to prepare the Grignard reagent. A mixture of 3-bromocyclohexene (6.50 g), magnesium tunings (1.07 g) and catalytic amount of iodine in dry ether (50 m*l*) was stirred overnight at room temperature under nitrogen. Work up in the usual manner and alumina chromatography gave bicyclohexenyl (1.0 g), which was identical with the product III on IR and VPC analysis.

Found: C, 88.69; H, 11.28%. Calcd for $C_{12}H_{18}$: C, 88.82; H, 11.18%.

Methyl 3-Cyclohexyl-3-hydroxybutyrate (VIII). Acetylcyclohexane (2.58 g) and freshly distilled methyl bromoacetate (3.06 g) were dissolved in 20 m*l* of dry benzene - toluene (1 : 1). To the solution was added activated zinc powder (1.31 g) and trace amount of iodine, and the reaction mixture was refluxed for 3 hr. To the reaction mixture was added dilute sulfuric acid after cooling and the organic layer was separated. The aqueous layer was further extracted with benzene, and the combined extract was washed with aqueous sodium bicarbonate and water. Evaporation of the solvent and distillation of the products after drying over magnesium sulfate gave methyl 3-cyclohexyl-3-hydroxybutyrate; bp 98—99°C/2.5 mmHg, 1.05 g (25% yield). This product was identical with the adduct VIII on IR, NMR, and VPC analysis.

Hydrogenation of the Adduct (IX). The 1 : 1 mixture of the adducts VIII and IX (400 mg) in 5 m*l* of ethanol was hydrogenated over 10% palladium - charcoal (40 mg) in the usual manner. The product consists only of the adduct VIII on IR, NMR, and VPC analysis.

Base Treatment of Oxetanes (X). The mixture of the photo-adducts (4.30 g) was dissolved in 140 m*l* of 1% sodium methoxide - methanol and was stirred overnight at room temperature. After neutralization of the reaction mixture by bubbling carbon dioxide, the solvent was evaporated and the products were dissolved in ether. Distillation under reduced pressure separated the intact adducts (VIII and IX) (fraction A; bp 95—97°C/2.0 mmHg, 1.40 g) and the degradation products (XII and XIII) from oxetanes (fraction B; bp 110—120°C/2.0 mmHg, 1.20 g). No oxetane was detected in the product-mixture. Fraction A accompanied a small amount of the α,β-unsaturated esters which were formed from the adducts VIII and IX. Fraction B consisted of hydroxy-α,β-unsaturated esters (XII) and δ-lactone XIII, which were formed by the ring opening of the oxetanes, in the ratio of 1 : 1. XII and XIII were separated and purified by preparative VPC (2.2 m ×6 mm, 10% PEG-20 M on Chromosorb-W, 200°C).

XII. Found: C, 66.25; H, 8.77%. Calcd for $C_{11}H_{18}O_3$: C, 66.64; H, 9.15%. Mass: m/e=198 (M^+, $C_{11}H_{18}O_3$). IR (neat): 3470, 1725, 1642, 980, and 865 cm^{-1}. NMR (CCl_4): 5.65 (q, J=1.0 Hz, =CH-), 4.06 (diffused, >CH-O-), 3.66 ($-OCH_3$), 2.17 (d, J=1.0 Hz, $-CH_3$), and 1.2—2.4 ppm (10H).

XIII. Mass: m/e=166 (M^+, $C_{10}H_{14}O_2$). IR (neat): 1710, 1640, 990, and 856 cm^{-1}. NMR (CCl_4): 5.60 (q, J=1.5 Hz, =CH-), 4.40 (multiplet, >CH-O-), 1.95 (d, J=1.5 Hz, $-CH_3$), and 2.3—1.0 ppm (9H).

Acid Treatment of Oxetanes (X). A mixture of the photo-adducts (2.40 g) in 50 m*l* of methylene chloride was treated with *p*-toluenesulfonic acid (50 mg), and the mixture was stirred overnight at room temperature. The solvent was removed after neutralization of the solution with aqueous sodium bicarbonate and drying over magnesium sulfate. VPC analysis showed that the alcohol (VIII and IX) persisted on acid treatment and the oxetanes (X) were converted into aldehydes (XIa and XIb) in *ca.* 70% yield and to the hydroxy-α,β-unsaturated esters (XII), which were also formed by base treatment, in *ca.* 30% yield. The aldehydes

*1 The following abbreviations were used to show signal patterns. s: singlet, d: doublet, t: triplet, q: quartet.

9) E. E. Smissman and A. N. Voldeng, *J. Org. Chem.*, **29**, 3161 (1964).

were separated by distillation under reduced pressure (bp 90—100°C/2.0 mmHg) from the products-mixture and were purified by preparative VPC (2.2 m × 6 mm, 10% PEG-20M on Chromosorb-W, 200°C).

XIa. Found: C, 66.65; H, 9.28%. Calcd for $C_{11}H_{18}O_3$: C, 66.64; H, 9.15%. IR (CCl_4): 2720, 1740, 1725, 1205, 1170, and 1015 cm^{-1}. NMR (CCl_4): 9.62 (t, J=2.0 Hz, -CHO), 5.32 (t, J=7.0 Hz, =CH-), 3.58 ($-OCH_3$), 2.90 (s, $-CH_2-COO-$), 2.36 (t, J=7.0 Hz, $-CH_2\diagdown C=O$), 1.98 (t, J=7.0 Hz, $-CH_2\diagdown C=$), 1.75 ($-CH_3$), and 1.2—1.7 ppm (4H).

XIb. Found: C, 66.28; H, 9.05. Calcd for $C_{11}H_{18}O_3$: C, 66.64; H, 9.15%. IR (CCl_4): 2720, 1740, 1725, 1260, 1160, and 1015 cm^{-1}. NMR (CCl_4): 9.62 (t, J=2.0 Hz, -CHO), 5.16 (t, J=7.0 Hz, =CH-), 3.58 ($-OCH_3$), 2.86 (s, $-CH_2-COO-$), 2.36 (t, J=7.0 Hz, $-CH_2\diagdown C=O$), 2.00 (t, J=7.0 Hz, $-CH_2\diagdown C=$), 1.66 ($-CH_3$), and 1.2—1.7 ppm (4H).

Aldehydes XIa and XIb were also formed during the VPC analysis when Chromosorb-P, instead of Chromosorb-W, was used as support for liquid phase (10% PEG-20M on Chromosorb-P, 160°C).

The authors are indebted to Kawakami Memorial Foundation for financial support.

BULLETIN OF THE CHEMICAL SOCIETY OF JAPAN VOL. 43 2167—2173 (1970)

Reactions of Some Olefins with *N*-Chlorourea in the Presence of Acetonitrile

Yasuo WADA

Koei Chemical Co., 645, *Hanaten, Jyoto-ku, Osaka*

and Ryohei ODA

Department of Synthetic Chemistry, Faculty of Engineering, Kyoto University, Kyoto

(Received November 24, 1969)

A new three-component reaction of *N*-chlorourea, olefins and acetonitrile is reported. Styrene gives *N*-(1-ureidoethylidene)-2-choro-1-phenylethylamine, *N*-(2-chloro-1-phenylethyl)acetamide and 4-phenyl-2-oxazolidone. Addition proceeds in a Markovnikov manner as shown by structural evidence. Cyclohexene gives *N*-(1-ureiodoethylidene)-2-chlorocyclohexylamine and *N*-(2-chlorocyclohexyl)acetamide. The stereochemistry of the reaction has been shown to be *trans* as demonstrated by chemical and physical evidence. Mechanisms for the reaction are proposed.

The chemistry of *N*-chlorourea given in literature is restricted predominantly to aqueous or alcoholic systems. In these cases *N*-chlorourea acts simply as a mild chlorinating or oxidizing agent. The present paper describes a new type of three-component reactions of *N*-chlorourea for the synthesis of *N*-(1-ureidoalkylidene)-2-chloroalkylamines and *N*-(2-chloroalkyl)amides. The synthesis involves interaction of *N*-chlorourea and olefin in the presence of a nitrile to give *N*-(1-ureidoalkylidene)-2-chloroalkylamine and imidochloride that can be hydrolyzed to an *N*-(2-chloroalkyl)amide.

In 1948, Ritter and co-workers discovered the reaction of nitriles with olefins in strongly acidic media to form *N*-substituted amides.[1,2]

The reaction can be explained to proceed *via* carbonium ion which is formed by addition of proton to olefins. Cairns and co-workers have discovered that halonium ion which is formed by addition of positive halogen to olefins can react with nitriles to form *N*-substituted amide.[3]

We have found the reaction of *N*-chlorourea with olefins in the presence of nitrile. The reaction has been shown to proceed in two steps.

The first step gives *N*-(1-ureidoalkylidene)-2-chloroalkylamine, chloroimide chloride and chlorinated hydrocarbon arising from the original olefin, and the second step gives an *N*-(2-chloroalkyl)-amide by the hydrolysis of chloroimide chloride.

The interaction of *N*-chlorourea and olefin in the presence of nitrile is postulated to proceed as follows:

$$NH_2CONHCl \longrightarrow Cl^+ + NH_2CONH^- \quad (1)$$

$$RCH=CH_2 + Cl^+ \longrightarrow RC^+HCH_2Cl \quad (2)$$

$$RC^+HCH_2Cl \xrightarrow{R'CN} RCHCH_2Cl \quad (3)$$

$$\qquad\qquad\qquad\qquad\qquad\qquad\quad \underset{+}{N}{=}CR' \quad [I]$$

1) J. J. Ritter and P. P. Minieri, *J. Amer. Chem. Soc.*, **70**, 4045 (1948).

2) J. J. Ritter and J. Kalish, *ibid.*, **70**, 4048 (1948).

3) T. L. Cairns, P. J. Graham, P. L. Barrick and R. S. Schreiber, *J. Org. Chem.*, **17**, 751 (1952).

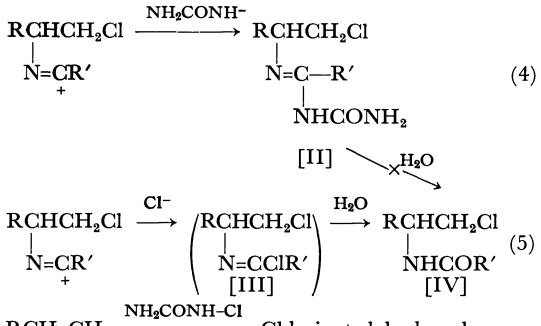

(4)

(5)

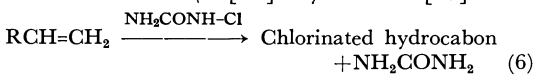

(6)

The chlorine attached to nitrogen has a positive halogen character and attacks olefin as an acidic substance Cl^+ to form a carbonium ion RC^+HCH_2Cl which may combine with nitrile. The carbonium ion [I] can be stabilized by reaction (4) with a negative ion NH_2CONH^- to produce *N*-(1-ureidoalkylidene)-2-chloroalkylamine [II]. [II] was isolated and analyzed but could not be hydrolyzed to *N*-(2-chloroalkyl)amide [IV]. Therefore, [IV] is not a hydrolyzed product of [II]. It is supposed that the carbonium ion [I] can also be stabilized by reaction (5) with a negative ion Cl^- derived from hydrogen chloride which is present in reaction medium as an impurity to produce chloroimide chloride [III]. [III] could not be isolated. But as reported by Cairns,[3] *N*-(2-chloroalkyl)amide is probably a hydrolyzed product of [III]. Reactions (4) and (5) are competing reactions and the products [II] and [IV] are expected. This interaction is a special case of the so-called Ritter reaction.[1,2]

We have studied the interaction of *N*-chlorourea with styrene and cyclohexene in the presence of acetonitrile.

Styrene reacted with *N*-chlorourea and acetonitrile at 10°C within 2.5 hr to give *N*-(1-ureidoethylidene)-2-chloro-1-phenylethylamine [V] and *N*-(2-chloro-1-phenylethyl)acetamide [VI] after treating the reaction product with water. The reaction mixture was evaporated *in vacuo*, the residue was treated with water, and the aqueous solution was extracted with benzene. From the organic layer *N*-(2-chloro-1-phenylethyl)acetamide [VI] was obtained by vacuum distillation. Neutralization of the aqueous layer with sodium hydroxide resulted in immediate precipitation of *N*-(1-ureidoethylidene)-2-chloro-1-phenylethylamine [V]. It was separated by filtration, washed with water and analyzed correctly. On evaporation of the aqueous filtrate, extraction of the residue with ethyl alcohol and distillation of the extract *in vacuo*, 4-phenyl-2-oxazolidone [VII] was obtained in poor yield. It is well known that isocyanates are formed on heating urea derivatives. Hassner and coworkers[4] have shown that 4-phenyl-2-oxazolidone can be obtained by heating β-iodoalkane isocyanate with alcohol. Katchalsky and co-workers[5] have also shown that β-halocarbamate may be converted to 2-oxazolidone by pyrolysis at 120—200°C. A reaction scheme consistent with the obtained product is as follows:

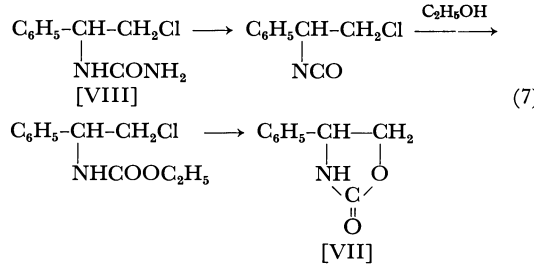

(7)

This suggests that the carbonium ion $R\overset{+}{C}HCH_2Cl$ was stabilized by NH_2CONH^- to produce *N*-(2-chloro-1-phenylethyl)urea [VIII].

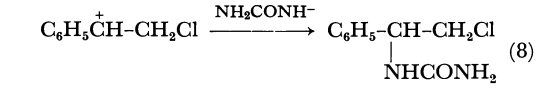

(8)

4-Phenyl-2-oxazolidone [VII] was characterized by identity of its melting point (137—137.5°C) and infrared spectrum with that of the known authentic compound prepared from styrene and iodine isocyanate followed by reaction with ethyl alcohol.[4] For 5-phenyl-2-oxazolidone the reported melting point is 88.8—90.2°C.[6]

The direction of addition is such that Cl^+ ion combines with the less substituted carbon. The composition and the structure of *N*-(1-ureidoethylidene)-2-chloro-1-phenylethylamine [V] were established by elemental analysis and infrared spectra. The spectrum shows essentially the patterns of urea, C–Cl, monosubstituted benzene and C=N bond. The structure of [V] was also established by its conversion, on treatment with aqueous sodium hydroxide solution, to 1-aminocarbonyl-2-methyl-4-phenyl-2-imidazoline [IX] and further to 2-methyl-4-phenylimidazoline [X] and 1,2-diaminoethylbenzene [XI].

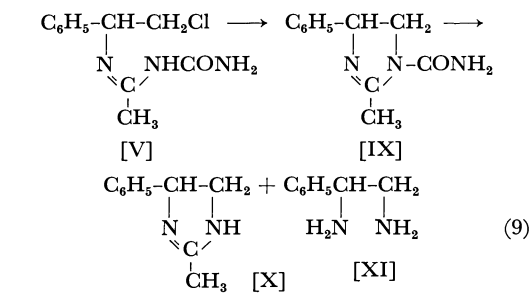

(9)

4) A. Hassner, M. E. Lobber and C. Heathcock, *J. Org. Chem.*, **32**, 540 (1967).

5) E. Katchalsky and D. B. Ishai, *ibid.*, **15**, 1067 (1950).

6) M. S. Newman and A. Kutner, *J. Amer. Chem. Soc.*, **73**, 4199 (1951).

[V] was found to be highly unstable to base hydrolysis or heat, and converted to [IX] at room temperature and more rapidly at elevated temperature. For example, when [V] was allowed to stand for one month at room temperature, complete isomerization to [IX] hydrochloride occurred. A more satisfactory procedure for the preparation of [IX] was to treat [V] with sodium hydroxide solution at elevated temperature for several minutes. A new compound [V], which was isolated and purified only by washing with cold water, had a melting point of 97—99°C and its elemental analysis corresponded to the empirical formula $C_{11}H_{14}N_3ClO$. When it was recrystallized from boiling water, however, a different substance having a melting point of 119—119.5°C was obtained. Elemental analysis of this compound corresponds to a value for [V] plus a mol of water, and infrared absorption bands at 3480 and 1130 cm^{-1} indicate the presence of C–OH.

N-(2-chloro-1-phenylethyl)acetamide [VI] was confirmed by coincidence of its melting point with that of the known compound.[7] The NMR spectrum of [VI] indicates a doublet at τ 6.18 (2H, CH_2Cl), a multiplet at 5.5 (1H, CHN) owing to additional splitting by NH, a single peak at 2.68 (5H, aromatic protons), a typically broad peak at 4.7 (the proton on nitrogen) and a triplet at 7.95 (3H, CH_3). The structure of [VI] was also established by its conversion to the known 2-hydroxyl-1-phenylethylamine [XII], picrate of [XII] and hydrochloride of [XII]. An isomeric *N*-(2-chloro-2-phenylethyl)acetamide should yield 2-phenyl-2-hydroxyethylamine.

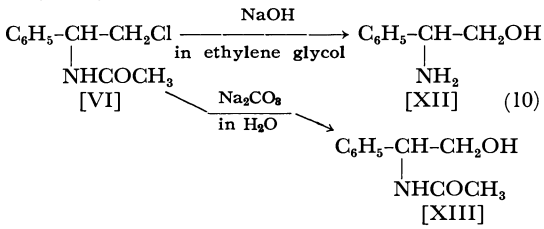

(10)

[VI] was also treated with sodium carbonate in water to give *N*-(2-hydroxy-1-phenylethyl)acetamide [XIII] having a melting point 123—124°C.[8] Lusskin and Ritter[7] reported the preparation of 2-methyl-4-phenyl-2-oxazoline having a melting point 120°C on treating chloroacetamide with potassium hydroxide at 60—65°C for 90 sec in ethyl alcohol. But the product obtained by the same reaction was a liquid having a boiling point of 96—96.5°C/5mmHg. Its infrared spectrum and elemental analysis correspond to those of 2-methyl-4-phenyl-2-oxazoline [XIV]. The hydrochloride of [XIV] had mp 145—146°C.

Cyclohexene reacted with *N*-chlorourea in the presence of acetonitrile to give *N*-(1-ureidoethylidene)-*trans*-2-chlorocyclohexylamine [XV] and *N*-(*trans*-2-chlorocyclohexyl)acetamide [XVI].

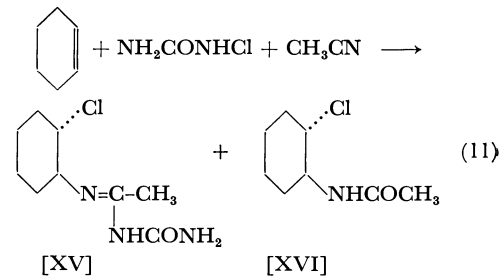

(11)

[XV] precipitated from the reaction mixture as a white solid. The filtrate was evaporated *in vacuo* to yield a very viscous semi-solid. This substance could not be recrystallized nor distilled. When it was treated with boiling water, [XVI] was obtained as white crystalline material. Reaction of cyclohexene with *N*-chlorourea and acetonitrile could yield *cis*- or *trans*-isomer. The stereochemistry of the reaction was shown to be *trans*, consistent with the ring opening of the intermediate halonium ion.[9] Thus, the product was identified as [XV] and [XVI]. The composition and structure of [XV] were established by elemental analysis and infrared spectra. The spectrum shows essentially the patterns of urea, C=N and *trans* C–Cl. The structure of [XV] was also established by its conversion to known *trans*-2-chlorocyclohexylamine [XVII] and further to *N*-(*trans*-2-chlorocyclohexyl)-acetamide [XVI].

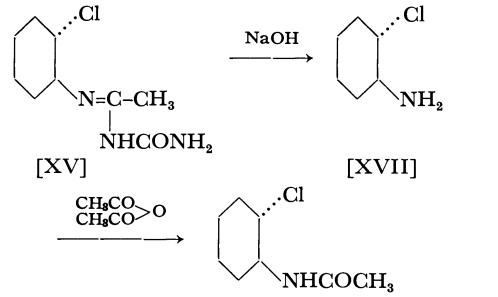

(12)

2-Chlorocyclohexylamine may exist in two diastereoisomeric forms. The infrared spectrum of [XVII], with a stretching vibration of C–Cl at 728 cm^{-1}, was identical with that reported by Yoshida[10] for *trans*. On standing at room temperature for several days, it partly decomposed to form a solid material. This confirms the previous observation for this compound.[11] The acetylated

7) R. M. Lusskin with J. J. Ritter, *ibid.*, **72**, 5577 (1950).

8) The melting point of [XIII] was reported as 114—116°C by R. M. Lusskin and J. J. Ritter.[7]

9) A. Hassner, L. A. Levy and R. Gault, *Tetrahedron Lett.*, **1966**, 3119 (1966).

10) Z. Yoshida and K. Nakagawa, *ibid.*, **1965**, 3753.

11) O. E. Paris and P. E. Fanta, *J. Amer. Chem. Soc.*, **74**, 3007 (1952).

product of [XVII] was characterized by identity of its melting point with that of [XVI]. 1,2-Diaminocyclohexane [XVIII] was also obtained on treating [XV] with sodium hydroxide in poor yield. A reaction scheme consistent with the obtained product is as follows:

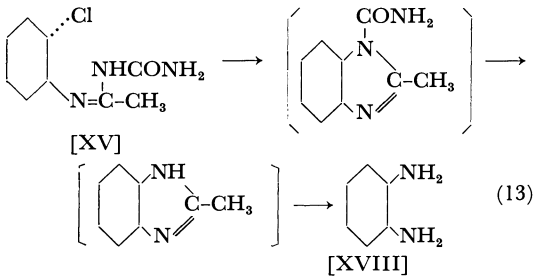

(13)

[XV] may react with sodium hydroxide to give [XVIII] *via* intermediates, imidazoline derivatives. [XVIII] reacted so readily with carbon dioxide that it was immediately converted to the picrate and subjected to analysis. [XV] was hydrogenated on treatment with sodium borohydride in ether to give *N*-(1-ureidoethyl)cyclohexylamine [XIX].

N-(*trans*-2-chlorocyclohexyl)acetamide [XVI] was confirmed by coincidence of its melting point (127.5°C) with that of the reported compound.[3] The infrared spectrum of [XVI] indicates a peak at 730 cm^{-1} based on stretching vibration of *trans* C–Cl.[10] The NMR spectrum of [XVI], in $CDCl_3$, had bands at τ 4.0 (the proton on nitrogen), 6.2 (doublet, 1H, CHCl), 7.07 (singlet, 1H, CHN), 8.0 (singlet, 3H, CH_3) and 7.7—8.87 (multiplet, cyclohexyl protons). [XVI] was hydrolyzed on treatment with aqueous hydrochloric acid solution to give *cis*-2-hydroxycyclohexylamine[3] [XX]. [XVI] was also hydrolyzed with sodium carbonate in aqueous solution or aqueous ammonium hydroxide solution to give *N*-(*cis*-2-hydroxycyclohexyl)-acetamide[12] [XXI], which was further hydrolyzed to give [XX]. [XX] was acetylated by acetic anhydride to give [XXI].[13]

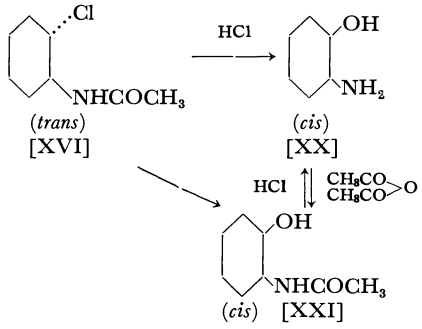

12) W. S. Johnson and E. N. Schubert, *J. Amer. Chem. Soc.*, **72**, 2187 (1950).

13) M. Mousseron and R. Jacquier, *Bull. Soc. Chim. Fr.*, **1950**, 238.

[XX], on standing at room temperature for several days, darkened and finally turned to a tarry matter. The structure of [XX] was confirmed by coincidence of the melting point of its hydrochloride (184—185°C) with that of the reported compound.[13] The infrared spectrum of [XX] had an absorption at 945 cm^{-1} based on *cis* C–O bond.[14] The NMR spectrum of [XX], in $CDCl_3$, had bands at τ 6.3 (singlet, 1H, CHO), 7.2 (singlet, 1H, CHN), 7.35 (the proton on nitrogen), 8.45 (1H, OH) and 8.55 (cyclohexyl protons). The spectrum was identical with that reported by Pavia and co-workers[15] for *cis*. Further proof of [XX] was demonstrated by its conversion to [XXI] having a melting point 145—146°C.[16] The melting point of *trans*-isomer was reported as 126—127°C.[16]

Experimental

All reagents were redistilled before use. Acetonitrile was predried over potassium hydroxide and distilled over calcium hydride. All the melting points are uncorrected. IR spectra were measured in KBr pellets or in liquid state using a Hitachi Model EPI-G3 IR spectrometer. NMR spectra were obtained using dilute solutions in CCl_4 or $CDCl_3$. Tetramethylsilane was used as an internal standard and chemical shifts are expressed in "tau" scale.

Reaction of *N*-Chlorourea with Styrene in the Presence of Acetonitrile. Simultaneous formation of *N*-(1-ureidoethylidene)-2-chloro-1-phenylethylamine[V], *N*-(2-chloro-1-phenylethyl)acetamide [VI] and 4-phenyl-2-oxazolidone [VII]. The compounds can be prepared from *N*-chlorourea or, more simply, from urea and chlorine forming *N*-chlorourea directly in the reaction solution.

A suspension of 0.6 mol (36 g) of pulverized urea in 450 m*l* of acetonitrile was cooled to 0°C and chlorinated while being stirred rapidly. Gas introduction was discontinued as soon as 0.3 mol (21.3 g) of chlorine had been absorbed. The resulting clear, colorless solution was stirred for an additional 30 min. The solution was purged with and kept under nitrogen atmosphere. A solution of 0.3 mol (31.2 g) of styrene in 100 m*l* of acetonitrile was then added dropwise over a period of 1 hr while maintaining the temperature at 10°C by external cooling. After the addition was complete, the reaction mixture was stirred for about 2 hr at 10°C until an HI test failed to produce iodine. The reaction mixture was allowed to separate into two phases. From the viscous lower phase was recovered urea after neutralizing with sodium hydroxide. The upper acetonitrile phase was then placed in a vacuum distillation flask to remove acetonitrile. The resulting viscous, pale yellow liquid was then poured into 300 m*l* of water, stirred vigorously for 20 min, and then shaken with benzene. The upper organic phase was separated and dried over

14) S. Winstein and N. J. Holness, *J. Amer. Chem. Soc.*, **77**, 5562 (1955).

15) A. Pavia, F. Winternitz and R. Wylde, *Bull. Soc. Chim. Fr.*, **1966** (8), 2506.

16) G. E. McCasland, R. K. Clark, Jr., and H. E. Carter, *J. Amer. Chem. Soc.*, **71**, 637 (1949).

anhydrous $MgSO_4$. After removing benzene and chlorinated styrene, the residue was distilled *in vacuo* to yield 14 g (23.6%) of *N*-(2-chloro-1-phenylethyl)acetamide, bp 121—127°C/1.2 mmHg, as a colorless liquid. The distillate solidified upon standing. Recrystallization from benzene gave colorless leaflets melting at 98—99.5°C (lit, mp 100°C,[7] 103—104°C[3]).

Found: C, 60.31; H, 6.28; Cl, 17.58; N, 6.94%. Calcd for $C_{10}H_{12}ClNO$: C, 60.76; H, 6.11; Cl, 17.93; N, 7.08%.

IR: 3310 (NH), 1650 (C=O), 1530 (amide II), 770, 695 (mono subst. benzene) and 725 cm^{-1} (C–Cl); NMR: τ 2.68 (phenyl, singlet), 4.7 (NH, broad peak), 5.5 (CHN, multiplet), 6.18 (CH_2Cl, doublet) and 7.95 (CH_3, triplet).

The lower aqueous phase was made alkaline (pH≒8.5) with NaOH and the resulting white precipitate was separated by filtration, washed with a large amount of cold water and dried *in vacuo* to yield 22 g (30.6%) of *N*-(1-ureidoethylidene)-2-chloro-1-phenylethylamine having a melting point 97—99°C (dec.). Insoluble in cold water, ethyl alcohol and benzene, soluble in hot water and hot ethyl alcohol. If allowed to stand for one month at room temperature, it became liquid and then resolidified.

Found: C, 54.44; H, 5.88; Cl, 15.12; N, 17.19%. Calcd for $C_{11}H_{14}ClN_3O$: C, 55.11; H, 5.88; Cl, 14.79; N, 17.52%.

IR: 3400, 3240, 3120 (NH), 1730 (C=O), 1625 (C=N), 1520 (amide II), 765, 700 (mono subst. benzene) and 710 cm^{-1} (C–Cl).

The filtrate was concentrated *in vacuo*, the residue extracted with ethyl alcohol and the extract distilled *in vacuo* to yield 1.5 g of 4-phenyl-2-oxazolidone, bp 150—160°C/1.5 mmHg. An analytical sample, mp 137—137.5°C (lit,[4] mp 138—139.5°C), was obtained by recrystallization from water. The compound gave a mp 137—137.5°C in admixture with authentic sample (mp 137.5—138°C, prepared according to the method of Hassner, Lobber and Heathcock[4]).

Found: C, 66.17; H, 5.62; N, 8.70%. Calcd for $C_9H_9NO_2$: C, 66.24; H, 5.55; N, 8.58%.

IR: 3270 (NH), 1750, 1720 (C=O), 1230, 1040 (ester) and 760, 700 cm^{-1} (mono subst. benzene).

Reaction of *N*-Chlorourea with Cyclohexene in the Presence of Acetonitrile. Simultaneous formation of *N*-(1-ureidoethylidene)-*trans*-2-chlorocyclohexylamine [XV] and *N*-(*trans*-2-chlorocyclohexyl)acetamide [XVI]. A solution of 0.3 mol of *N*-chlorourea in acetonitrile was prepared as described above. Cyclohexene (0.3 mol, 24.6 g) in acetonitrile (70 m*l*) and the *N*-chlorourea solution were reacted in a similar manner. The resulting precipitate was separated by filtration, washed with cold water, ethyl alcohol and ethyl ether. Recrystallization from hot water produced 22.5 g of white precipitate melting at 174.5—175°C (dec.), soluble in hot water, insoluble in benzene and ethyl alcohol. This product was dissolved in 60 m*l* of hot water, and the solution was made alkaline with KOH (pH≒10). After cooling the solution, the resulting precipitate was separated by filtration, washed with water and dried *in vacuo* to yield 18.5 g (28.3%) of *N*-(1-ureidoethylidene)-*trans*-2-chlorocyclohexylamine. An analytical sample, mp 113.5—114.5°C, was obtained by recrystallization from ethyl alcohol, soluble in ethyl alcohol, benzene and hot water, insoluble in ethyl ether and cold water.

Found: C, 49.28; H, 7.27; Cl, 16.70; N, 19.18%. Calcd for $C_9H_{16}ClN_3O$: C, 49.65; H, 7.40; Cl, 16.28; N, 19.30%.

IR: 3430, 3250, 3100 (NH), 1700 (C=O), 1660 (C=N), 1560 (amide II) and 730 cm^{-1} (*trans* C–Cl).

The picrate of [XV] was prepared and had mp 193°C after recrystallization from ethyl alcohol.

Found: C, 40.30; H, 4.27; Cl, 8.17; N, 18.79%. Calcd for $C_{15}H_{19}ClN_6O_8$: C, 40.32; H, 4.28; Cl, 7.93; N, 18.80%.

The filtrate from the above product was allowed to separate into two phases. From the viscous lower phase was recovered urea after neutralizing with NaOH. The upper acetonitrile phase was placed in a vacuum distillation flask to remove acetonitrile, cyclohexene and chlorinated cyclohexene. The residue was poured into 500 m*l* of water, stirred vigorously for 30 min at 90°C. The solution was then cooled to room temperature, and the resulting white needles were separated by filtration, dried *in vacuo* to give 20 g (38%) of crude *N*-(*trans*-2-chlorocyclohexyl)acetamide [XVI]. After recrystallization from benzene twice, pure [XVI] having a melting point of 127.5°C (bp 110—116°C/0.8 mmHg) was obtained. The reported melting point for this compound is 129—130°C;[3] for *cis*-isomer the melting point is 98°C.[13]

Found: C, 54.81; H, 8.02; Cl, 20.11; N, 8.03%. Calcd for $C_8H_{14}ClNO$: C, 54.70; H, 8.03; Cl. 20.18; N, 7.97%.

IR: 3200 (NH), 1630 (C=O), 1560 (amide II), and 730 cm^{-1} (*trans* C–Cl); NMR: τ 4.0 (NH, broad peak), 6.2 (CHCl, doublet), 7.07 (CHN, singlet), 7.7—8.8 (cyclohexyl protons, multiplet) and 8.0 (CH_3, singlet).

2-Hydroxy-1-phenylethylamine [XII]. Twenty grams of *N*-(2-chloro-1-phenylethyl)acetamide was refluxed with a solution consisting of 19 g of aqueous 45% NaOH solution and 48 m*l* of ethyleneglycol on an oil bath for 5 hr. After cooling the solution, the precipitate was filtered, the filtrate was acidified with HCl and then evaporated to dryness. Cold aqueous 50% NaOH solution was added to the residue and the resulting oil was extracted with ether. The ethereal extracts were dried over anhydrous $MgSO_4$, ether was removed *in vacuo* and the residue distilled *in vacuo*. 2-Hydroxy-1-phenylethylamine (9 g, 65%), bp 102—108°C/1.5 mmHg (lit,[17] bp 104—106°C/1 mmHg) was obtained, which solidified to a white solid, mp 51—52°C (lit,[17] mp 48—49.5°C).

Found: C, 69.78; H, 8.11; N, 10.20%. Calcd for $C_8H_{11}NO$: C, 70.04; H, 8.08; N, 10.21%.

IR: 3400 (OH), 3300, 1610 (NH), 1055 (C–O) and 765, 705 cm^{-1} (mono subst. benzene).

The picrate of [XII] had mp 204—204.5°C after recrystallization from ethyl alcohol. The reported melting point for this compound is 205—206°C;[18] for 2-hydroxy-2-phenylethylamine-picrate the melting point is 158°C.[19]

Found: C, 46.17; H, 4.03; N, 15.12%. Calcd for $C_{14}H_{14}N_4O_8$: C, 45.90; H, 3.85; N, 15.29%.

The hydrochloride, prepared by addition of dry HCl

17) M. S. Newman and W. M. Edwards, *ibid.*, **76**, 1840 (1954).

18) Wm. E. McEwen, W. E. Conrad and C. A. Vanderwerf, *ibid.*, **74**, 1168 (1952).

19) M. S. Kharasch and H. M. Priestley, *ibid.*, **61**, 3425 (1939).

gas to an alcoholic solution of the free base and recrystallization from ethyl alcohol, melted at 131—132°C, resolidified and subsequently remelted at 145°C. The results confirm those reported for this compound[3] (melts at 132—135°C, resolidifies and remelts at 147—149°C). The reported melting point for 2-hydroxy-2-phenylethylamine hydrochloride is 213°C.[20]

N-(2-Hydroxy-1-phenylethyl)acetamide [XIII]. Five grams of N-(2-chloro-1-phenylethyl)acetamide and a solution of 3.5 g of Na_2CO_3 in 75 ml of water were allowed to stand for 12 hr at room temperature and then refluxed for 1 hr. The solution was extracted with ethyl acetate. After removal of ethylacetate, the residue was recrystallized from benzene-ethyl alcohol to yield 3 g (66%) of white crystals, having a new mp 123—124°C (lit,[7] mp 114—116°C).

Found: C, 66.81; H, 7.38; N, 7.79%. Calcd for $C_{10}H_{13}NO_2$: C, 67.01; H, 7.31; N, 7.81%.

IR: 3350 (OH), 3140 (NH), 1650 (C=O), 1560 (amide II), 1055(C-O) and 760, 700 cm^{-1} (mono subst. benzene).

2-Methyl-4-phenyl-2-oxazoline [XIV]. N-(2-chloro-1-phenylethyl)-acetamide (0.1 mol, 19.7 g) was mixed 90 sec at 60—65°C with 0.1 mol (5.6 g) of KOH in 200 ml of ethyl alcohol. One gram of $NaHCO_3$ was added and the solution was filtered. After removal of ethyl alcohol, the residue was distilled *in vacuo* to yield 7 g (44%) of the product, bp 96—96.5°C/5 mmHg (lit,[7] mp 120°C).

Found: C, 73.94; H, 6.85; N, 8.62%. Calcd for $C_{10}H_{11}NO$: C, 74.50; H, 6.87; N, 8.68%.

IR: 1670 (C=N), 1230, 990 (C-O) and 760, 700 cm^{-1} (mono subst. benzene).

The hydrochloride, prepared by addition of dry HCl gas to an alcoholic solution of [XIV], had mp 145—146°C (lit,[3] 160.5—161°C).

IR: 2720—2400, 1980 ($C=N^+H$), 1745 ($C=N^+$), 1240, 1060, 1050(C-O) and 765, 700cm^{-1} (mono subst. benzene).

N-(1-Ureido-1-hydroxyethyl)-2-chloro-1-phenylethylamine. N-(1-Ureidoethylidene)-2-chloro-1-phenyl ethylamine was recrystallized from water. A white precipitate melting at 119—119.5°C was obtained.

Found: C, 51.28; H, 6.43; Cl, 13.80; N, 16.40%. Calcd for $C_{11}H_{16}ClN_3O_2$: C, 51.26; H, 6.25; Cl, 13.75; N, 16.30%.

IR: 3480 (OH), 3400, 3230, 3130 (NH), 1725 (C=O), 1520 (amide II), 1130 (C-O), 770, 700 (mono subst. benzene) and 720 cm^{-1} (C-Cl).

1-Aminocarbonyl-2-methyl-4-phenyl-2-imidazoline [IX]. Twenty grams of N-(1-ureidoethylidene)-2-chloro-1-phenylethylamine were mixed for 30 min at 50°C with 200 ml of aqueous 40% NaOH solution. The precipitate was separated by filtration, washed with cold water and dried *in vacuo* to yield 9 g (53%) of [IX] melting at 76—76.3°C.

IR: 3200 (NH), 1680 (C=O), 1640 (C=N), 1620 (amide II) and 755, 695 cm^{-1} (mono subst. benzene).

The picrate of [IX] had mp 139—140°C after recrystallization from ethyl alcohol.

Found: C, 47.17; H, 3.68; N, 19.39%. Calcd for $C_{17}H_{16}N_6O_8$: C, 47.22; H, 3.73; N, 19.43%.

2-Methyl-4-phenyl-2-imidazoline [X] and 1,2-Diaminoethylbenzene [XI]. Twenty-five grams of 1-aminocarbonyl-2-methyl-4-phenyl-2-imidazoline were refluxed with 90 ml of aqueous 40% NaOH solution for 2.5 hr and the resulting mixture was extracted with chloroform. The extracts were dried over anhydrous $MgSO_4$, concentrated *in vacuo* and the residue was distilled *in vacuo* to yield the following two fractions:

Cut-1, bp 95—117°C/1.5mmHg, 7 g

Cut-2, bp 135—136°C/1.5mmHg, 3 g (lit,[21] bp 121—122°C/0.2mmHg)

Cut-1 was redistilled *in vacuo* to yield pure 1,2-diaminoethylbenzene, bp 85—88°C/1.0 mmHg (lit,[22] bp 243—246°C/760 mmHg).

Found: C, 70.17; H, 8.95; N, 20.39%. Calcd for $C_8H_{12}N_2$: C, 70.55; H, 8.88; N, 20.56%.

IR: 3300, 3100, 1605, 880 (NH) and 750, 700 cm^{-1} (mono subst. benzene).

The picrate of [XI] had mp 165.5—166.5°C after recrystallization from ethyl alcohol (lit,[22] mp 160°C).

Found: C, 45.94; H, 4.09; N, 18.93%. Calcd for $C_{14}H_{15}N_5O_7$: C, 46.03; H, 4.13; N, 19.17%.

Cut-2. solidified upon standing and had mp 78.5—79°C.

Found: C, 75.08; H, 7.68; N, 17.16%. Calcd for $C_{10}H_{12}N_2$ [X]: C, 74.96; H, 7.54; N, 17.48%.

IR: 3200, 3120 (NH), 1620 (C=N, NH) and 755, 700 cm^{-1} (mono subst. benzene).

The picrate of [X] had mp 131.5—132.5°C after recrystallization from ethyl alcohol.

Found: C, 49.13; H, 3.78; N, 17.65%. Calcd for $C_{16}H_{15}N_5O_7$: C, 49.36; H, 3.88; N, 17.98%.

***cis*-2-Hydroxycyclohexylamine [XX].** Ten grams of N-(*trans*-2-chlorocyclohexyl)acetamide were refluxed with 100 ml of aqueous 20% HCl solution for 2 hr. The mixture was made alkaline with NaOH and subjected to steam distillation. The distillate was acidified with HCl and evaporated to dryness. Cold aqueous 50% NaOH solution was added to the residue. The resulting oil was extracted with ether. The etheral extracts were dried over anhydrous $MgSO_4$, concentrated *in vacuo* and the residue was distilled *in vacuo* to yield 4 g (61%) of *cis*-2-hydroxycyclohexylamine, bp 98—99°C/12 mmHg, which solidified upon standing. An analytical sample, mp 76.5—78°C, was obtained by recrystallization from ether. The product darkened on prolonged standing in air. The reported melting point for this compound is 107—108°C,[13] 72—73°C,[16] 71—72°C[12]; for *trans*-isomer the melting point is 66—67°C.[13]

Found: C, 62.25; H, 11.74; N, 12.10%. Calcd for $C_6H_{13}NO$: C, 62.57; H, 11.37; N, 12.16%.

IR: 3400 (OH), 3300, 3100, 1615 (NH), 990, 965 and 945 cm^{-1} (*cis* C-O); NMR: τ 6.3 (CHO, singlet), 7.2 CHN, singlet), 7.35 (NH_2, singlet), 8.45 (OH, singlet) and 8.55 (cyclohexyl protons).

The hydrochloride, prepared by addition of dry HCl gas to an alcoholic solution of the free base, melted at 183—184°C after recrystallization from ethyl alcohol. The reported melting point for this compound is 184—185°C[13]; for *trans* isomer the melting point is 175°C.[13]

N-(*cis*-2-Hydroxycyclohexyl)acetamide [XXI] from N-(*trans*-2-Chlorocyclohexyl)acetamide [XVI]. Five grams of N-(*trans*-2-chlorocyclohexyl)-acetamide and a solution of 3.5 g of Na_2CO_3 in 75 ml of water were allowed to stand for 12 hr at room tempera-

20) J. Read and I. G. M. Campbell, *J. Chem. Soc.*, **1930**, 2682.

21) H. Isler, U.S. 2505247, Apr. 25, 1950.

22) Beilsteins Handbuch der Organischen Chemie **13**, 177.

ture and then refluxed for 1 hr. The solution was extracted with ethyl acetate. After removal of the solvent the residue was recrystallized from benzene-ethyl alcohol to yield 2.5 g (55%) of *N*-(*cis*-2-hydroxycyclohexyl)-acetamide as a colorless plate, mp 145—146°C. The reported melting point for this compound is 146—147°C;[13,16] for *trans* isomer the melting point is 126—127°C.[16] The same result was obtained by treating [XVI] with aqueous 20% NH_4OH solution.

***cis*-2-Hydroxycyclohexylamine Hydrochloride from *N*-(*cis*-2-Hydroxycyclohexyl)acetamide.** Ten grams of *N*-(2-hydroxycyclohexyl)acetamide were refluxed with 60 m*l* of aqueous 20% HCl solution for 2 hr, and distilled *in vacuo* to dryness. The residue was recrystallized from ethyl alcohol to yield 6 g (62%) of colorless crystals, mp 183—185°C.

***N*-(*cis*-2-Hydroxycyclohexyl)acetamide [XXI] from *cis*-2-Hydroxycyclohexylamine [XX].** A solution of five grams of *cis*-2-hydroxycyclohexylamine in 20 m*l* of ethyl alcohol was added dropwise to 50 m*l* of acetic anhydride. The white precipitate was separated by filtration, recrystallized from ethyl acetate to yield 5.5 g (80%) of colorless plates, mp 145.5—146°C. The compound gave a mp 145—146°C in admixture with the sample in the preceding example prepared from *N*-(*trans*-2-chlorocyclohexyl)acetamide [XVI].

Found: C, 60.97; H, 9.78; N, 8.91%. Calcd for $C_8H_{15}NO_2$: C, 61.11; H, 9.61; N, 8.90%.

IR: 3350 (OH), 3100 (NH), 1650 (C=O), 1545 (amide II) and 985 cm^{-1} (*cis* C–O).

***N*-(1-Ureidoethyl)cyclohexylamine [XIX].** Five grams of $NaBH_4$ were added to 6.5 g of *N*-(1-ureidoethylidene)-*trans*-2-chlorocyclohexylamine [XV] solution in 150 m*l* of methyl alcohol over a period of 1 hr at 15°C. After the addition was complete, the reaction mixture was stirred for 1 hr at 15°C, then 1 hr at 40—50°C. The solution was treated with 5 m*l* of acetone, concentrated *in vacuo* to dryness and the residue extracted with ether. After drying with anhydrous $MgSO_4$, the ether was removed *in vacuo* and the resulting precipitate was separated by filtration. Recrystallization from ether gave white precipitate melting at 162—162.5°C.

Found: C, 58.31; H, 9.81; N, 22.56%. Calcd for $C_9H_{19}N_3O$: C, 58.34; H, 10.33; N, 22.68%.

IR: 3350, 3200 (NH), 1660 (C=O), 1605 (NH) and 1540 cm^{-1} (amide II).

***trans*-2-Chlorocyclohexylamine [XVII] and 1,2-Diaminocyclohexane [XVIII].** Twenty-eight grams of *N*-(1-ureidoethylidene)-2-chlorocyclohexylamine was refluxed with a solution consisting of 21 g of NaOH in 26 m*l* of water and 70 m*l* of ethylene glycol on a oil bath for 3 hr. The solution was acidified with HCl, filtered and the filtrate was evaporated to dryness *in vacuo*. Cold aqueous 50% NaOH solution was added to the residue and the resulting oil was extracted with ether. The ethereal extracts were dried over anhydrous $MgSO_4$, concentrated *in vacuo* and the residue was distilled *in vacuo* to yield the following two fractions:

Cut-1 [XVII] bp 62/9—63.5°C/8 mmHg, 4.5 g (26%) (lit,[11] bp 69°C/12 mmHg)

Cut-2 [XVIII] bp 115—121°C/3.5 mmHg, 1.0 g (7%) (lit,[23] 36—38°C/0.05 mmHg)

Cut-1 was a colorless oil when it was freshly distilled. But on standing at room temperature for several days, it decomposed to give a deposit of crystals. The result is in line with that reported for this compound.[11] IR: 3370, 3270, 1605 (NH) and 728 cm^{-1} (C–Cl).

The hydrochloride, prepared by addition of dry HCl gas to an alcoholic solution of the freshly distilled free base, melted at 208—210°C after recrystallization from ethyl alcohol. The reported melting point is 205—207°C,[24] 213—214°C;[3] the *cis*-isomer is reported to melt at 185—186°C.[16]

On being treated with acetic anhydride, the freshly distilled free base [XVII] was converted to the *N*-(*trans*-2-chlorocyclohexyl)acetamide. Recrystallization from ethyl acetate gave white needles melting at 128.5—129°C. There was no depression of melting point on admixture with the sample in the preceding example prepared from cyclohexene, *N*-chlorourea and acetonitrile.

Cut-2, obtained as a colorless oil, absorbed carbon dioxide rapidly on exposure to atmosphere as indicated by the immediate formation of solid on the surface. It was dissolved in ethyl alcohol and the solution was added to a picric acid solution in ethyl alcohol. A yellow solid precipitated immediately, the precipitate was washed with ethyl alcohol and analyzed. It became dark by heating at 220—260°C.

Found: C, 37.60; H, 3.70; N, 19.62%. Calcd for $C_6H_{14}N_2 \cdot 2C_6H_3N_3O_7$: C, 37.77; H, 3.52; N, 19.57%.

23) G. Swift and D. Swern, *J. Org. Chem.*, **32**, 511 (1967).

24) F. Winternitz, M. Mousseron and R. Dennilauler, *Bull. Soc. Chim. Fr.*, **1956**, 382. *Chem. Abstr.*, **50**, 14573 (1956).

BULLETIN OF THE CHEMICAL SOCIETY OF JAPAN VOL. 43 2174—2176 (1970)

The Characterization of Malloprenol and Its Ester with Linolenic Acid Isolated from the Leaves of *Mallotus japonicus*

Toshiharu NODA, Teruo TAKE, Tetsuo WATANABE and Jinnosuke ABE

Research Institute, Toyo Jozo Co., Ltd., Ohito, Tagata, Shizuoka

(Received December 3, 1969)

An isoprenoid alcohol (I) and the ester with linolenic acid (II) isolated from *Mallotus japonicus* of *Euphorbiaceae* were investigated. The trivial name "mallophenol" was proposed to describe the prenol (I). Nuclear magnetic resonence studies showed that the prenol contained one *trans* and six *cis* internal isoprene residues, and a *cis* 'OH-terminal' isoprene residue.

Mallotus japonicus is a deciduous tree of the *Euphorbiaceae* which has long been used in Japan as a gastrointestinal drug. In the studies of this plant, the presence of bergenin,[1] rutin,[2] and some fatty acids,[3] but not linolenic acid, has been reported.

From the nonpolar fractions of the methanol extracts of leaves which has been collected in Ohito and Nagaoka-cho, Shizuoka Prefecture, in September and October, 1968, malloprenol (I) and the ester with linolenic acid (II) were isolated. The nonpolar fractions of the extracts were then chromatographed on silica gel to give malloprenol and the ester with linolenic acid, which was less polar than the malloprenol (I). The malloprenol (I) is a colorless oil, $n_D^{23.5}$ 1.5038. The molecular formula, $C_{45}H_{74}O$ (mol wt, 631.0), was deduced from the analytical data and from the molecular weight*1 of (I) (the obsd mol wt, 652) and its derivatives. The IR spectra showed absorptions at 3325, 1005, and 1665 cm^{-1}, thus confirming the presence of a primary hydroxyl group and isolated double bonds. In the UV spectrum, there was no absorption longer than 210 mμ. The malloprenol (I) gave the acetate (III), with acetic anhydride-pyridine, $C_{47}H_{76}O_2$ (mol wt, 673.28, obsd mol wt, 669, 667), or (IV) with *p*-bromobenzoylchloride-pyridine, $C_{52}H_{77}O_2Br$ (mol wt, 814.05; obsd mol wt, 854). In the IR spectra there was no hydroxyl band, but there did appear a strong absorption of the carbonyl group at 1740 cm^{-1} in (III) and at 1730 cm^{-1} in (IV). The primary hydroxyl group in (I) was easily oxidized with the chromium trioxide-pyridine complex to give the aldehyde (V), $C_{45}H_{72}O$ (mol wt, 629.02; obsd mol wt 645). In the IR spectrum, there were absorptions of the formyl group (2740 and 1670 cm^{-1}) and the conjugated double bond (1620 cm^{-1}). The formyl proton appeared at 9.90 ppm (1H, d, J=8Hz) in the NMR spectrum. The strong absorption at 231 mμ in the UV spectrum confirmed that Compound I was a primary allylic alcohol. Compound V gave the 2,4-dinitrophenylhydrazone as a reddish oil, $C_{51}H_{76}O_4N_4$ (mol wt, 809.15; obsd mol wt, 833). From the ozonization of the malloprenol (I), followed by the reductive decomposition of the ozonide, levulinaldehyde and acetone were isolated as their 2,4-dinitrophenylhydrazones. From the above results, it appeared that malloprenol was an isoprenoid alcohol.

The NMR spectrum of (I) resembles those of solanesol[4] (all *trans*) and castaprenol-11, -12 and -15.[5] There are two peaks at 1.60 and 1.68 ppm with a shoulder at 1.73 ppm in Compound I. The relative areas under the two peaks are about six and twenty-four protons (including the shoulder at 1.73 ppm) respectively. The peak at 1.60 ppm can be assigned to two methyl groups of one internal and one ω-terminal *trans* isoprene residues. The eight methyl group at 1.68 ppm show the seven methyl groups of the six internal and one ω-*cis* isoprene residues and one methyl group of the *cis* 'OH-terminal' isoprene residue (as shoulder at 1.73 ppm.[5]) The olefinic protons give a broad peak at 5.13 ppm (8H) and a triplet at 5.42 ppm (1H, J=7Hz), corresponding to the proton on the β-carbon to the hydroxyl-group coupling with the α-methylene protons to the hydroxyl group, which appear at 4.11 ppm (2H, J=7Hz) in the malloprenol (I).

From the above observations, the prenol can be said to contain a *cis* 'OH-terminal' isoprene residue

1) K. Shibata and M. Shimogori, *Nippon Kagaku Zasshi*, **70**, 36 (1949).

2) T. Kashimoto and K. Noda, *ibid.*, **79**, 873 (1958).

3) K. Honma, Japan. 207849 (1954).

*1 The molecular weights were measured by the osmotic method on a Hitachi Perkin-Elmer Molecular-weight Apparatus 115 in a benzene solution.

4) R. L. Rowland, P. H. Latimer and J. A. Giles, *J. Amer. Chem. Soc.*, **78**, 4680 (1956).

5) A. R. Wellburn, J. Slevenson, F. W. Hemming and R. A. Morton, *Biochem. J.*, **102**, 313 (1967).

(shoulder at 1.73 ppm), one internal *trans* isoprene residue (1.60 ppm), and, of necessity, methyl groups both *cis* and *trans* to the olefinic proton in the *ω*-isoprene residue (*cis*: 1.68 ppm; *trans*: 1.60 ppm). Six of the other isoprene rdsidues are internal *cis* (1.68 ppm). In Compounds III and IV, the metyl groups of the *cis* 'OH-terminal' isoprene residue appeared at 1.75 and 1.77 ppm respectively. The allylic methylene protons appeared as two peaks, at 2.02—2.05 and 2.07—2.08 ppm, in Compounds (I—IV).

$$\begin{array}{l} \qquad\quad CH_3 \\ \qquad\quad | \\ H\text{-}(CH_2\text{-}C\text{=}CH\text{-}CH_2)_9\text{-}OR \end{array}$$

I: R=H

II: R=$CH_3(CH_2\text{-}CH\text{=}CH)_3\text{-}CH_2(CH_2)_6\cdot CO$-

The ester (II), $n_D^{19.5}$ 1.5057, showed strong absorptions at 1740 and 1170 cm^{-1}, but no hydroxyl band in its IR spectrum. The alkaline hydrolysis of the ester gave the components, an alcohol, and an acid. The NMR and IR spectra of the alcohol were the same as those of the malloprenol (I) in all respects. The acid afforded the methyl ester (VI) with diazomethane. The ester (VI) (M^+/e 292) was identified as methyl linolenate (mol wt, 292.44) by a study of its GLC, IR, and NMR spectra.

Experimental

The IR spectra were recorded on a Hitachi Grating Infrared Spectrometer EPI G-2; the UV spectra, on a Hitachi Recording Spectrophotometer EPS-3, and the NMR spectra, on a Hitachi Nuclear Magnetic Resonance Spectrometer R-20. The chemical shifts were measured on the δ scale relative to TMS as the internal standard (δ=0).

Extraction and Isolation of Malloprenol I and the Ester with Linolenic Acid (II). Dried leaves (5.1 kg) were extracted with methanol (75 *l*) at room temperature for two weeks. The methanol extract was then concentrated to 5 *l*, and water (5 *l*) was added. The solution was subsequently extracted with light petroleum ether. The evaporation of the solvent left a tarry residue (205 g), which was then chromatographed on silica gel. Ligroin/benzene (6:1) eluted fractions which gave dark brown spots (R_f 0.7) with a concentrated sulfuric acid spray on chromatoplates developed with ligroin/benzene (4:1). The fractions were combined and evaporated, and the residue was repeatedly chromatographed to give a colorless oil, (II) (1.7 g), which showed a single spot on TLC, $n_D^{17.5}$ 1.5057; Found: C, 84.85; H, 11.51%. Calcd for $C_{63}H_{102}O_2$: C, 84.88; H, 11.53%. IR: 3020, 1665, 840 (C=C), 1740, 1170 cm^{-1} ($OCOCH_3$). $\delta_{ppm}^{CDCl_3}$ 0.98 (3H, t, J=7.5 Hz, $C\underline{H}_3CH_2$-), 1.33 [10H, (-$C\underline{H}_2$)$_5$-CH_2COO-], 1.60(6H, $C\underline{H}_3\rangle C\text{=}C\langle H$), 1.67 (24H, $C\underline{H}_3\rangle C\text{=}C\rangle H$), 2.03—2.08(32H, -$C\underline{H}_2$-C=CH), 2.08(4H, $C\underline{H}_2$-CH=CH), 4.55(2H, d, J=7.5 Hz, C=CH-$C\underline{H}_2$-OH), 5.13(8H, C=C$\underline{H}$-CH_2).

Benzene subsequently eluted fractions which gave dark brown spots (R_f 0.4) with a concentrated sulfuric acid spary on chromatoplates developed with benzene. After the evaporation of the solvent, the residue was rechromatographed several times to give a colorless oil, (I) (30 g), which showed a single spot on reversed-phase partition TLC on paraffin-impregnated kieselgel (impregnated with 5%, v/v, liquid paraffin in petroleum ether) with acetone - water (23 : 2, v/v) saturated with paraffin as the mobile phase,[6] $n_D^{23.5}$ 1.5038. Found: C, 85.70; H, 11.72%; mol wt, 652. Calcd for $C_{45}H_{74}O$; C, 85.64; H, 11.82%; mol wt, 631.04. IR: 3325, 1090 (OH), 3025, 1665, 840 (C=C), 2970, 2925, 2850, 1450, 1375 cm^{-1} (-CH_2-, -CH_3). $\delta_{ppm}^{CDCl_3}$: 1.31 (1H, -$CH_2O\underline{H}$), 1.60 (6H, $C\underline{H}_3\rangle C\text{=}C\langle H$), 1.68 (24H, $C\underline{H}_3\rangle C\text{=}C\rangle H$), 2.02 and 2.07 (32H, -$C\underline{H}_2$-CH=C), 4.06 (2H, d, J= 7 Hz, C=CH-$C\underline{H}_2$-OH), 5.13 (8H, C=C$\underline{H}$-CH_2-), 5.42 (1H, t, J=7 Hz, C=C$\underline{H}$-CH_2-OH).

Monoacetate (III). The malloprenol (I) (590 mg) in 0.5 m*l* of pyridine was treated with 0.5 m*l* of acetic anhydride and then allowed to stand overnight. To the reaction mixture 15 m*l* of water were then added, and the oily product was extracted with benzene to give 522 mg of the crude acetate. Using silica-gel chromatography and elution with petroleum ether/benzene (1 : 1), 485 mg of III was obtained; $n_D^{22.5}$ 1.5047. Found: C, 83.52; H, 11.32%; mol wt, 669, 667. Calcd for $C_{47}H_{76}O_2$: C, 83.86; H, 11.38%; mol wt, 673.08. IR: 3025, 1660, 835 (C=C), 1740, 1230 cm^{-1} ($OCOCH_3$).

***p*-Bromobenzoate (IV).** The malloprenol (I) (500 mg) in 1.5 m*l* of pyridine was treated with 510 mg of *p*-bromobenzoyl chloride and then allowed to stand overnight at room temperature. To the reaction mixture, 20 m*l* of benzene were then added, after which the precipitate was filtered off and the filtrate was washed with a $NaHCO_3$ solution, 0.5N HCl, and water. After the removal of the solvent, the residue (581 mg) was chromatographed on silica gel (20 g) to give 508 mg of (IV); $n_D^{22.5}$ 1.5267. Found: C, 77.20; H, 9.73; Br, 9.70%; mol wt, 854. Calcd for $C_{52}H_{77}O_2Br$: C, 76.72; H, 9.73; Br, 9.82%; mol wt, 814.05. IR: 3030, 1665, 850 (C=C), 1730, 1590, 1270, 760 cm^{-1} (benzyl).

The Aldehyde V and Its 2,4-dinitrophenylhydrazone. To a CrO_3-pyridine complex (CrO_3 1 g, pyridine 10 m*l*) we added 1.5 g of I in 6 m*l* of pyridine with cooling at 0°; the mixture was then allowed to stand for an hour at room temperature. The reaction mixture was filtered, and the dark brown solid remaining was washed with pyridine. The combined pyridine solution was diluted with water and extracted with benzene. After drying (Na_2SO_4), the solvent was removed and the residue was chromatographed on silica gel (35 g) to give 975 mg of V; $n_D^{22.5}$ 1.5126. Found; C, 85.77; H, 11.46%; mol wt, 645. Calcd for $C_{45}H_{72}O$: C, 85.92; H, 11.54%; mol wt, 629.02. IR: 2740, 1670, 1620 cm^{-1} (C=C-CHO). λ_{max} 231 mμ (ε=1.38×10^4 in cyclohexane). $\delta_{ppm}^{CDCl_3}$ 5.86 (1H, d, J=8 Hz, C=C$\underline{H}$-CHO), 9.90 (1H, d, J=8 Hz, C=CH-C$\underline{H}$O). To 156 mg of (V), 2,4-dinitrophenylhydrazine in an EtOH solution was added; after dilution with water, a reddish oily product was extracted with benzene. After the removal of the solvent, the residue (195 mg) was chromatographed on silica gel to give 166 mg of the 2,4-dinitrophenylhydrazone.

Found: C, 75.64; H, 9.51; N, 6.57%; mol wt, 833. Calcd for $C_{51}H_{76}O_4N_4$: C, 75.70; H, 9.47; N, 6.92%; mol wt, 809.15.

6) K. J. Sone, A R. Wellburn, F. W. Hemming and J. F. Pennock, *ibid.*, **102**, 325 (1967).

Ozonolysis of the Malloprenol (I). A solution of 1.554 g of the malloprenol (I) in 150 m*l* of ethyl acetate was ozonized at −70°C until the solution became blue. The solvent was then removed *in vacuo* to give the ozonide as a pale yellow oil. To the ozonide 200 m*l* of water and 15 g of zinc dust were added and then decomposed by heating them at 95°C for 8 hr. To this reaction mixture, nitrogen gas was blown and the volatile component was collected as its 2,4-dinitrophenylhydrazone (64 mg; mp 117—119°C).

Found: C, 45.23; H, 3.99; N, 23.33%; Calcd for $C_9H_{10}N_4O_4$: C, 45.38; H, 4.23; N, 23.52%. No depression of mp was noted with an authentic sample of acetone 2,4-dinitrophenylhydrazone. After the filtration of the zinc dust, 500 m*l* of 2N HCl saturated with 2,4-dinitrophenylhydrazine was added to the filtrate. The precipitate was collected and crystallized from dimethylformamide to give 559 mg of fine needles; mp 245—246°C. Found: C, 44.25; H, 3.28; N, 24.17%. Calcd for $C_{17}H_{16}O_8N_8$: C, 44.35; H, 3.50; N, 24.34%. No depression of mp was noted with an authentic sample of levulinaldehyde 2,4-dinitrophenylhydrazone.

Alkaline Hydrolysis of II.] To the solution of II (600 mg) in 20 m*l* of benzene we added 20 m*l* of alcoholic 1N KOH, after which the mixture was refluxed for 4 hr. The organic solvents were then evaporated, leaving a residue which was dissolved in 30 m*l* of water and extracted with light petroleum ether to give a colorless oil (498 mg). The oil was identical with (I) in all respects. The aqueous solution was acidified with 1N HCl and extracted with ether to give 114 mg of a colorless oil which was esterified with diazomethane to give 105 mg of (VI); M^+/e 292. IR: 3025, 1650, 725 (C=C), 1745, 1175 cm^{-1} ($COOCH_3$). $\delta_{ppm}^{CDCl_3}$ 0.97 (3H, t, J=6.8 Hz, CH_3CH_2), 1.27—1.33 [10H, $-(CH_2)_5-CH_2COOCH_3$], 2.81 (4H, $CH_2-CH=CH$), 3.67 (3H, s, $COOCH_3$), 5.3—5.5 [6H, $(CH_2-CH=CH)_3$].

The authors wish to express their thanks to Mr. Hajime Takeuchi and Mr. Katsutoshi Ota of this Institute for their elemental analysis and for the measurements of the molecular weight.

BULLETIN OF THE CHEMICAL SOCIETY OF JAPAN VOL. 43 2176—2181 (1970)

A Study of Acyl Migration in Gallacetophenones

Kazu KUROSAWA

Department of Chemistry, Faculty of Science, Kumamoto University, Kurokami-machi, Kumamoto

(Received December 13, 1969)

3,4-Diacetoxy-2-hydroxyacetophenone, 3,4-dibenzoyloxy-2-hydroxyacetophenone and 3,4-bis(*p*-nitrobenzoyloxy)-2-hydroxyacetophenone gave corresponding 2,3-diacyl-4-methoxyacetophenones on treatment either with diazomethane or with dimethyl sulfate in the presence of potassium carbonate in acetone. Structure determination of the methylation product and also the methylation reaction of 3,4-dimethanesulfonyloxy-2-hydroxyacetophenone and 3,4-bis(*p*-toluenesulfonyloxy)-2-hydroxyacetophenone are reported.

In the course of synthetic studies of isoflavans, Gallacetophenone diacetate, mp 106—107°C,[1] was prepared as a synthetic intermediate material.[1] The structure of the diacetate was first elucidated by Perkin and Storey[1] as 2,4-diacetate on the basis of alkaline degradation of the gallacetophenone mono methyl ether, mp 132—133°C, derived from the diacetate. This ether, they claimed, afforded 2-methylpyrogallol (**6**), indicating the position of the hydroxyl group at 3. The identification, however, had been made by comparison of the melting point of the "2-methylpyrogallol diacetate" (60—63°C) only, whereas an authentic 2-methylpyrogallol diacetate has a mp 51—54°C and 1-methylpyrogallol diacetate has a mp 91—93°C.[3]

The IR spectrum of the diacetate showed a carbonyl absorption at 1648 cm^{-1}, which is slightly higher than those of other *o*-hydroxyacetophenones such as 3-acetoxy-2-hydroxy-4-methoxyacetophenone (**2b**) and 2,3-dihydroxy-4-methoxyacetophenone (**9**). Nevertheless, it is obviously a hydrogen bonded carbonyl when compared with the carbonyl absorptions of 2,3-diacetoxy-4-methoxyacetophenone (**3a**), 3-hydroxy-2,4-dimethoxyacetophenone (**10**) and 3-acetoxy-2,4-dimethoxyacetophenone (**4b**), in which *o*-hydroxyl group is absent (see Table 1). On the other hand, the NMR spectrum of the diacetate exhibited a proton signal at a lower field (δ 12.10)

1) A. G. Perkin and R. C. Storey, *J. Chem. Soc.*, **1928**, 229.

2) Beilstein's Handbuch der Organischen Chemie, Vol. 6, p. 1083 (1923).

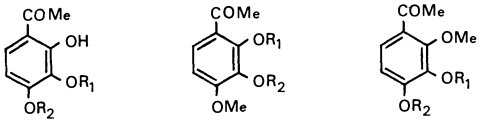

1 $R_1=R_2=H$ 3a, d-h 4b, c, g, h

2a-e, g-j

a, $R_1=R_2=Ac$

b, $R_1=Ac$, $R_2=Me$

c, $R_1=R_2=CH_2C_6H_5$

d, $R_1=R_2=COC_6H_5$

e, $R_1=R_2=COC_6H_4NO_2(p)$

f, $R_1=Me$, $R_2=COC_6H_4NO_2(p)$

g, $R_1=R_2=SO_2Me$

h, $R_1=R_2=SO_2C_6H_4Me(p)$

i, $R_1=COC_6H_4NO_2(p)$, $R_2=Me$

5, $R_1=Me$, $R_2=H$

6, $R_1=H$, $R_2=Me$

7, $R_1=Me$, $R_2=R_3=H$

8, $R_1=R_3=H$, $R_2=Me$

9, $R_1=R_2=H$, $R_3=Me$

10, $R_1=R_3=Me$, $R_2=H$

Fig. 1

which disappeared on deutration. The chemical shift is also characteristic to a hydrogen bonded *o*-hydroxyl proton as observed on *o*-hydroxyacetophenones, **9** and **2b**, while a *m*-hydroxyl proton in the compounds, **9** and **10**, appeared at a higher field (see Table 2). From this spectroscopic evidence, it is quite clear that the structure of the diacetate is neither 2,4-diacetate nor 2,3-diacetate, but undoubtedly 3,4-diacetate (**2a**) (see Fig. 1).

Diacetate (**2a**) gave a diacetyl mono methylgallacetophenone, mp 150—151°C,[1] on treatment with diazomethane, structure of which had been shown as 2,4-diacetoxy-3-methoxyacetophenone. However, this structure is also incorrect and should be revised as 2,3-diacetoxy-4-methoxyacetophenone (**3a**) by the following evidence. Diacetyl mono methylgallacetophenone was hydrolyzed to give gallacetophenone mono methyl ether, mp 132—133°C,[1] which was considered to be "2,4-dihydroxy-3-methoxyacetophenone." However, this ether was, in fact, 2,3-dihydroxy-4-methoxyacetophenone (**9**), being identical with an authentic sample, mp 132—133°C,[4] and differs from 2,4-dihydroxy-3-methoxyacetpohenone (**8**), mp 75—76°C,[5] and 3,4-dihydroxy-2-methoxyacetophenone (**7**), mp 84—85°C. It follows therefore that the two acetyl groups can be located at the position-2 and -3 in **3a**. This was further confirmed by acetylation of **9**, which gave an identical acetate, mp 150—151°C, with **3a**. The reaction could be explained in terms of a double acetyl migration during methylation. Acyl migration is fairly frequently observed in alicyclic and polyaromatic system[1,6] and extensively reviewed by Akahori[7] recently.

Various gallacetophenone 3,4-diesters (**2d**, **2e**, **2g**, **2h**) (Fig. 1) were prepared by partial esterification of Gallacetophenone (**1**) with acid anhydride or with acid chloride in pyridine (see Table 3). The position of the hydroxyl group is confirmed as ortho to the carbonyl by the presence of a hydrogen bonded carbonyl in the IR spectra and the presence of the proton signal at a lower field in the NMR spectra (see Tables 1 and 2).

Methylation of 3,4-dibenzoyloxy-2-hydroxyacetophenone (**2d**), mp 108—109°C, and 3,4-bis(*p*-nitrobenzoyloxy)-2-hydroxyacetophenone (**2e**), mp 208—209°C, gave mono methyl ethers (**3d**), mp 186—187°C,[8] and **3e**, mp 181—182°C, which were

Table 1. The carbonyl absorption bands of Gallacetophenones in IR spectra (cm^{-1})

Galloacetophenone	-COMe		-OCOR
	Free	Hydrogen bonded	
1		1628[a]	
2a		1648[b]	1779
2b		1644[b]	1768
2c		1628[a]	
2d		1640[a]	1735
2e		1638[a]	1757
2g		1643[a]	
2h		1650[a]	
2i		1640[b]	1750
3a	1681[b]		1776
3d	1673[a]		1751
3e	1674[a]		1759
3f	1692[a]		1754
3g	1700[a]		
3h	1695[a]		
4b	1673[b]		1770
4c	1668[a]		
4g	1673[a]		
4h	1679[a]		
7	1670[b]		
8		1630[b]	
9		1643[b]	
10	1672[b]		

IR spectra were determined in KBr disk (a) and in chloroform (b).

3) W. Baker, L. V. Montgomery and H. A. Smith, *J. Chem. Soc.*, **1932**, 1282.

4) W. Baker, F. H. T. Jukes and C. A. Subrahmanyan, *ibid.*, **1934**, 1683.

5) R. N. Kanna and T. S. Seshadri, *Indian J. Chem.*, **1**(9), 385 (1963); *Chem. Abstr.*, **60**, 1724h (1964).

6) A. G. Perkin and C. W. H. Story, *J. Chem. Soc.*, **1929**, 1399.

7) Y. Akahori, *Kagaku no Ryoiki*, **19**, 270 (1965).

8) Ishwar-Dass, N. Narasimhachari and T. R. Seshadri, *Proc. Indian Acad. Si.*, **37A**, 599 (1953); *Chem. Abstr.*, **48**, 7604d (1954).

TABLE 2. NMR SPECTRAL DATA FOR GALLACETOPHENONES (δ value in ppm) IN $CDCl_3$

Gallacetophenone	OH (s.)		H_6 (d.)[a]	H_5 (d.)[a]	Phenyl or *p*-substituted phenyl	OMe (s.)	COMe (s.)	Other signal	
	o-	*m*- and *p*-						δ	Assignment
2a	12.10		7.67	6.80			2.62	2.32 (s., 3H) 2.34 (s., 3H)	-OCOMe
2b	11.56		7.65	6.54		3.90	2.53	2.33 (s., 3H)	-OCOMe
2c	12.68		*ca.* 7.6	6.43	7.31 (m., 10H)		2.45	5.08 (m., 4H)	$-CH_2-$
2d	12.68		7.73	6.95	7.2—8.2(m., 10H)		2.62		
2e	12.67		7.69	6.80	6.88 (d., 2H) 6.59 (d., 2H) 7.98 (d., 2H) 8.09 (d., 2H)		2.59		
2g	12.91		7.73	7.05			2.64	3.33 (s., 3H) 3.44 (s., 3H)	$-OSO_2Me$
2h	12.65		7.69	7.06	7.25 (d., 2H) 7.35 (d., 2H) 7.60 (d., 2H) 7.81 (d., 2H)		2.60	2.46 (s., 3H) 2.40 (s., 3H)	Aromatic Me
3a			7.78	6.90		3.97	2.63	2.28 (s., 3H) 2.32 (s., 3H)	-OCOMe
4b			7.70	6.78		3.87(6H)	2.58	2.35 (s., 3H)	-OCOMe
7		5.90(2H)	7.29	6.75		3.88	2.59		
9	11.77	4.57(1H)	7.33	6.53		3.97	2.57		
10		5.87(1H)	7.38	6.74		3.75 3.97	2.62		

a) $J_{5,6}$=9.0 Hz.

TABLE 3. ESTERIFICATION OF GALLACETOPHENONES

Gallacetophenone	Reaction conditions: Reagent	Molar ratio of gallacetophenone: acylating reagent	Time (hr)	Temp. (°C)	Product	Yield (%)	Mp (°C)	Lit, mp (°C)
1	Ac_2O, AcOH, pyr.	1 : **3**	12	R.T.[a]	**2a**	59	106—107	106—107[1]
1	AcCl, pyr.	1 : 3	2	0	**2a**	29	106—107	
1	C_6H_5COCl, pyr.	1 : 3	3	100	**2d**	21	108—109	
1	*p*-$NO_2C_6H_4COCl$, pyr.	1 : 2.4	20	100	**2e**[b]	42	208—209	
1	$MeSO_2Cl$, pyr.	1 : 2.1	5	100	**2g**	23	142—143	
1	*p*-$MeC_6H_4SO_2Cl$, pyr.	1 : 3.5	19	50	**2h**	25	151—152	152—153[1]
7	$MeSO_2Cl$, pyr.	1 : 4.1	24	R.T.	**4g**	81	116—117	
7	*p*-$MeC_6H_4SO_2Cl$, pyr.	1 : 3.5	23	R.T.	**4h**	86	118—119	
9	AcCl, pyr.	1 : 1.3	2	0	**2b**	52	122—123	123.4—125.0[9]
9	*p*-$NO_2C_6H_4COCl$, pyr.	1 : 1.6	3	R.T.	**2i**[b]	20	193—194	
9	Ac_2O, pyr.	1 : 19	18	R.T.	**3a**	79	150—151	
9	C_6H_5COCl, pyr.	1 : 4.3	3.5	100	**3d**	60	186—187	185—186[8]
9	*p*-$NO_2C_6H_4COCl$, pyr.	1 : 4.8	20	120	**3e**[b]	42	181—182	
9	$MeSO_2Cl$, pyr.	1 : 11	48	100	**3g**	18	169—170	
9	*p*-$MeC_6H_4SO_2Cl$, pyr.	1 : 2.9	3	120	**3h**	34	154—155	

a) R.T. means room temperature.
b) Recrystallized from ethanol-chloroform.

Table 4. Methylation of Gallacetophenones

Gallaceto-phenone	Reagent	Reaction conditions: Molar ratio of gallaceto-phenone: methylating reagent	Time (hr)	Temp. (°C)	Product	Yield (%)	Mp (°C)	Lit, mp (°C)
2a	Me_2SO_4, K_2CO_3, Me_2CO	1 : 1.8	3.5	reflux	**3a**	59	150—151	
2a	CH_2N_2	excess	12	0	**3a**	59	150—151	150—155[1]
2d	Me_2SO_4, K_2CO_3, Me_2CO	1 : 4.5	7	reflux	**3d**	52	186—187	
2b	CH_2N_2	excess	12	0	**3d**	47	186—187	
2e	Me_2SO_4, K_2CO_3, Me_2CO	1 : 9.9	7	reflux	**3e**	6.5	181—182	
					3f	29	151—152	
2b	Me_2SO_4, K_2CO_3, Me_2CO	1 : 1.6	6	reflux	**4b**	93	112—113	110—111[10]
2i	Me_2SO_4, K_2CO_3, Me_2CO	1 : 11.5	3	reflux	**3f**	71	151—152	
2g	Me_2SO_4, K_2CO_3, Me_2CO	1 : 6.9	3	reflux	**4g**	87	116—117	
2h	Me_2SO_4, K_2CO_3, Me_2CO	1 : 9.5	14	reflux	**4h**	86	118—119	
2h	CH_2N_2	excess	12	0	**4h**	86	118—119	111—113[11]

Table 5. Analytical data for Gallacetophenones

Gallaceto-phenone	Formula	Found (%) C	Found (%) H	Found (%) N	Calcd (%) C	Calcd (%) H	Calcd (%) N
2d	$C_{22}H_{16}O_6$	69.96	4.25	—	70.21	4.29	—
2e	$C_{22}H_{14}O_{10}N_2$	56.49	3.00	5.99	56.66	3.03	6.01
2g	$C_{10}H_{12}O_8S_2$	36.91	3.73	—	37.03	3.70	—
2h	$C_{22}H_{20}O_8S_2$	55.42	4.31	—	55.46	4.23	—
2i	$C_{16}H_{13}O_7N$	57.72	3.97	4.06	58.01	3.96	4.23
3c	$C_{23}H_{22}O_4$	76.30	6.20	—	76.22	6.12	—
3d	$C_{23}H_{18}O_6$	a) 70.66	4.76	—	70.76	4.65	—
		b) 70.58	4.74	—			
3e	$C_{23}H_{16}O_{10}N_2$	a) 57.22	3.28	5.80	57.50	3.36	5.83
		b) 57.12	3.26	5.75			
3f	$C_{17}H_{15}O_7N$	a) 59.01	4.45	4.00	59.13	4.38	4.06
		b) 59.16	4.43	3.92			
3g	$C_{11}H_{14}O_8S_2$	38.99	4.17	—	39.04	4.17	—
3h	$C_{23}H_{22}O_8S_2$	56.14	4.56	—	56.31	4.52	—
4g	$C_{11}H_{14}O_8S_2$	a) 38.86	4.19	—	39.04	4.17	—
		b) 38.96	4.19	—			
4h	$C_{23}H_{22}O_8S_2$	a) 56.43	4.54	—	56.31	4.52	—
		b) 56.24	4.54	—			
7	$C_9H_{10}O_4$	59.14	5.59	—	59.33	5.53	—

a) Obtained by methylation.
b) Obtained by the esterification of corresponding monomethyl gallacetophenone.

found to be identical with those obtained by benzoylation of **9**. This indicates that the same type of benzoyl migration did occur in the reaction. In the case of **2e**, another product, mp 151—152°C, was isolated and found to be 2,4-dimethoxy-3-(*p*-nitrobenzoyloxy)acetophenone (**3f**), structure of which was confirmed by the independent synthesis of **3f** from **9**. 3-Acetoxy-2-hydroxy-4-methoxyacetophenone (**2b**), mp 122—123°C,[9] gave 3-acetoxy-2,4-dimethoxyacetophenone (**4b**), mp 112—113°C,[10] which was hydrolyzed to 3-hydroxy-2,4-dimethoxyacetophenone (**10**), mp 79—80°C,[11] indicating that the acetyl group could not migrate unless another acetyl group was present at the position-4. 3,4-Dimethanesulfonyloxy-2-hydroxyacetophenone (**2g**), mp 142—143°C, and 3,4-bis(*p*-

9) W. J. Horton and M. G. Scott, *J. Org. Chem.*, **20**, 1221 (1961).

10) W. Bradley and R. Robinson, *J. Chem. Soc.*, **1928**, 1565.

11) Beilstein's Handbuch der Organischen Chemie, **8**, II, 440 (1948).

toluenesulfonyloxy)-2-hydroxyacetophenone (**2h**), mp 151—152°C,[1] yielded 3,4-dimethanesulfonyloxy-2-methoxyacetophenone (**4g**), mp 116—117°C, and 3,4-bis(*p*-toluenesulfonyloxy)-2-methoxyacetophenone (**4h**), mp 118—119°C,[1] respectively. These sulfonates were found to be identical with those prepared from 3,4-dihydroxy-2-methoxyacetophenone (**7**), mp 84—85°C. These experiments showed that the sulfonate group did not migrate in the reaction. The results are summarized in Tables 3 and 4.

It is interesting to note that acyl migration did occur not in the sulfonates but in the carboxylic esters in the methylation. It is presumably due to the fact that O–CO bond is readily cleaved by the participation of the hydroxyl group at the neighboring position, whereas O–SO_2 bond cannot be cleaved under the condition used. Although an intermolecular reaction mechanism could not be ruled out,[12] the methylation reaction seems to proceed *via* cyclic intermediates (II and IV in Fig. 2). Anion (I) can be in equilibrium with anion (III) and anion (V) *via* the cyclic intermediates in the cases R are acetyl, benzoyl and *p*-nitrobenzoyl, and V is then methylated preferentially, as it is sterically less hindered. On the other hand, when methanesulfonyl and *p*-toluenesulfonyl groups are involved, the neighboring hydroxyl group cannot attack them and I is directly methylated. Methylation with diazomethane can also be accounted for by the same mechanism: the first step of the reaction is the capture of the proton on the hydroxyl group with diazomethane molecule, providing the anion (I), and then I is rearranged to anion (V) which is methylated.

The fact that the mono *p*-nitrobenzoate (**3f**) was obtained in the methylation of **2e** is queer. It seems that the bis-*p*-nitrobenzoate (**3e**) could be hydrolyzed with moisture and then methylated with excess dimethylsulfate present. Further investigation on this point is necessary.

Methylation of 3,4-bis(*p*-methoxybenzoyloxy)-2-hydroxyacetophenone was examined under similar conditions. However, the product has not been isolated in crystalline form as yet.

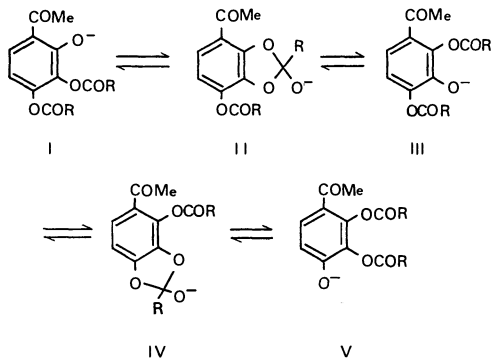

Fig. 2

Experimental

Measurements. IR spectra were recorded with JASCO Model DS 403G, a grating infrared spectrometer. Melting points were determined with Yanagimoto melting point apparatus. NMR spectra were obtained on a Varian A60 NMR spectrometer and JEOL JNM C 60H spectrometer using TMS as an internal standard.

Esterification of Gallacetophenones. a) Gallacetophenone (1 mmol) was treated with a mixture of acid anhydride (from 3 to 11 mmol) and pyridine (from 1 to 3 m*l*) at temperatures, room temperature — 120°C, for 3—24 hr. The reaction mixture was poured into ice water and the precipitates were collected. The crude ester was recrystallized from ethanol. b) Gallacetophenone (1 mmol) was dissolved in pyridine (from 1 to 3 m*l*) and treated with acid chloride (from 2 to 4.1 mmol) at temperatures 0—120°C for a period of time shown in Table 3. Working up in a similar manner to the above, a pure ester was obtained.

Methylation of Gallacetophenone. a) Gallacetophenone (1 mmol) was treated with a mixture of dimethyl sulfate (from 1.6 to 11.5 mmol) and potassium carbonate in acetone (30 to 40 m*l*). The reaction mixture was heated under reflux for a period of time shown in Table 4. After acetone was distilled off, the residue was triturated with water and the solid was collected. It was recrystallized from ethanol.

b) Gallacetophenone (1 mmol) was treated with distilled diazomethane at 0°C for 12 hr. After removal of the excess diazomethane and ether, the resulting solid was recrystallized from ethanol (see Table 4).

Preparation of Gallacetophenone (1), Gallacetophenone Monomethyl Ethers (7), (8) and (9), and 2,4-Dimethyl Ether (10). *Gallacetophenone (1).* The modified Nencki reaction of pyrogallol with boron trifluoride-acetic acid complex gave colourless needles (90%), mp 173°C.

2,3-Dihydroxy-4-methoxyacetophenone (9). 1-Methylpyrogallol[3] (4.0 g) was heated with boron trifluoride-acetic acid complex (12 m*l*) on a steam bath for an hour. The reaction mixture was poured into hot 2N hydrochloric acid (200 m*l*) and allowed to crystallize. This yielded colourless needles (4.0 g, 77%), mp 132—133°C (after sublimation) (lit,[4] mp 132—133°C).

2,4-Dihydroxy-3-methoxyacetophenone (8). 2-Methylpyrogallol[13] (839 mg) was heated with boron trifluoride-acetic acid complex (3 m*l*) on a steam bath for 30 min. The reaction mixture was poured into ice water and the precipitates were collected. Recrystallization of the crude material from water gave colourless leaves (928 mg, 85%), mp 75—76°C (lit,[5] mp 75°C).

3,4-Dibenzyloxy-2-hydroxyacetophenone (2c). A mixture of Gallacetophenone (**1**) (2 g), benzyl chloride (3.0 g), sodium iodide (4.0 g), and sodium bicarbonate (17 g) in acetone (71 m*l*) containing ethanol (6 m*l*), was heated under reflux for 19 hr. After removal of the acetone and the ethanol under reduced pressure, the residue was

12) T. H. Thompson and R. S. Wright, *J. Org. Chem.*, **26**, 4686 (1961).

13) Beilstein's Handbuch der Organischen Chemie, **6**, 1081 (1923).

triturated with water and then extracted with chloroform. The chloroform evaporated and the resulting liquid was allowed to crystallize in benzene. Recrystallization from ethanol gave colourless needles (2.01 g, 48%), mp 114—115°C (lit,[5] mp 113—114°C).

*3,4-Dibenzyloxy-2-methoxyacetophenone (**4c**).* 3,4-Dibenzyloxy-2-hydroxyacetophenone (**2c**) (4.9 g) was heated with a mixture of dimethyl sulfate (5.0 g) and potassium carbonate (6.0 g) in methyl ethyl ketone (100 m*l*) under reflux for 24 hr. After removal of the methyl ethyl ketone under reduced pressure, the residue extracted with chloroform. The chloroform was removed and the residue was crystallized from ethanol to give colourless plates (4.5 g, 88%), mp 62—63°C.

*3,4-Dihydroxy-2-methoxyacetophenone (**7**).* 3,4-Dibenzyloxy-2-methoxyacetophenone (**4c**) (1.14 g) was debenzylated with 15% hydrogen chloride-ethanol (20 m*l*), heating on a steam bath for an hour. Excess hydrogen chloride-ethanol was removed under reduced pressure and the resulting coloured liquid was separated on a silica column (Wakogel, C100, 100 g) with chloroform as an eluant. From a slow running fraction the required 3,4-dihydroxy-2-methoxyacetophenone (**7**) was crystallized on concentration, which was recrystallized from chloroform to give colourless needles (128 mg, 22%), mp 84—85°C.

*3-Hydroxy-2,4-dimethoxyacetophenone (**10**).* 3-Acetoxy-2,4-dimethoxyacetophenone (**4b**) (200 mg) was hydrolyzed with 2N hydrochloric acid (6 m*l*) in methanol (6 m*l*) under reflux for an hour. After removal of excess acid and methanol, the resulting solid was recrystallized from a mixture of benzene and light petroleum (30/70) to give micro crystals (130 mg, 78%), mp 79—80°C (lit,[11] mp 79—80°C).

The author wishes to thank Professor S. Sasaki, of Miyagi University of Education, JEOL Co., Ltd., and Dr. Y. Nakadaira, of Tohoku University for measuring the NMR spectra.

BULLETIN OF THE CHEMICAL SOCIETY OF JAPAN VOL. 43 2181—2186 (1970)

The Reactions of 1-Tropylazulenes with Phosphorus Pentachloride

Takashi TODA and Akira YAMANOUCHI[1)]

Department of Chemistry, Faculty of Science, Tohoku University, Katahira-cho, Sendai

(Received December 18, 1969)

The reactions of three 1-tropylazulenes——ethyl 2-acetamido-3-(cycloheptatrien-7-yl)azulen-1-carboxylate (I), 2-chloro-1-(cycloheptatrien-7-yl)azulene (II) and ethyl 3-(cycloheptatrien-7-yl)-azulen-1-carboxylate (III)——with phosphorus pentachloride were investigated. The reactions of I and II gave ethyl 2-acetamidoazulen-1-carboxylate and 1,2,3-trichloroazulene respectively. On the other hand, III afforded ethyl 3-chloroazulen-1-carboxylate (IV) and (3-ethoxycarbonylazulen-1-yl)tropylium perchlorate (V). The thermal isomerization of III formed *ca.* 2:3 mixtures of ethyl 3-(cycloheptatrien-3-yl)azulen-1-carboxylate (IV) and ethyl 3-(cycloheptatrien-1-yl)azulen-1-carboxylate (VII), but not ethyl 3-(cycloheptatrien-2-yl)azulen-1-carboxylate. The treatment of the above mixtures with phosphorus pentachloride raised the yield of V; however, IV was also obtained. The sodium borohydride reduction of V gave *ca.* 2:3 mixtures of VI and VII.

Syntheses of 1-tropylazulenes have been reported by Hafner and his coworkers,[2)] by Anderson and Replogle,[3)] and by the present authors.[4)] Although attempts to synthesise azulenyltropylium ions by means of the hydride abstraction of tropylazulenes have been carried out,[2,3)] there are no reports in the literature that azulenyltropylium ions have been successfully isolated in a pure state. Azulenyltropylium ions are of interest because of their possible canonical formulae, *e.g.*, the azulenyltropylium-ion type (A) and the condensed fulvalene-tropylium-ion type (B), as is shown in Fig. 1. The contribution of which canonical formula is more important is the first question. Secondly, if those types of ions are synthesized, they should be useful potential key intermediates for synthesizing non-benzenoid polycondensed aromatics, corresponding to benzanthracene, pentacene, *etc.*, in benzenoid polycondensed aromatics. Also, it is interesting to compare their properties with those of 1-azulenylfulvenes (C),[5)]

1) Present address; Kureha Chemical Co., Nakoso Works, Iwaki-shi, Fukushima-ken.

2) K. Hafner, A. Stephan and C. Bernhard, *Ann.*, **650**, 42 (1961).

3) A. G. Anderson and L. L. Replogle, *J. Org. Chem.*, **28**, 262 (1963).

4) T. Nozoe, T. Toda, T. Asao and A. Yamanouchi, This Bulletin, **41**, 2935 (1968).

5) K. Hafner and C. Bernhard, *Ann.*, **625**, 108 (1959); T. Toda, P. W. Yang and T. Mukai, *Sci. Repts. Tohoku Univ. I*, **50**, 208 (1967).

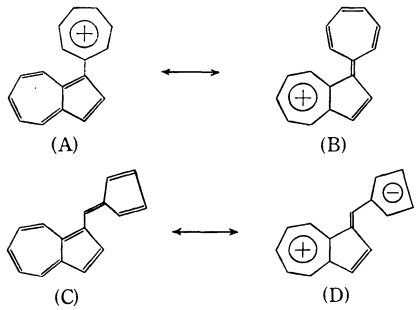

Fig. 1

which possess a (D)-type canonical formula.

In order to study the influence of substituents on azulene nuclei for hydride abstraction reactions and the stability of the formed azulenyltropylium ions, hydride abstraction reactions of three different kinds of tropylazulenes[4]——ethyl 2-acetamido-3-(cycloheptatrien-7-yl)azulen-1-carboxylate (I), 2-chloro-1-(cycloheptatrin-7-yl)azulene (II), and ethyl 3-(cycloheptatrin-7-yl)azulen-1-carboxylate (III)——were investigated. Bromination-dehydrobromination,[6] triphenylmethyl ions,[7] and phosphorus pentachloride[8] have been previously used for hydride abstraction reactions of tropylidenes. In this report, phosphorus pentachloride will be employed.

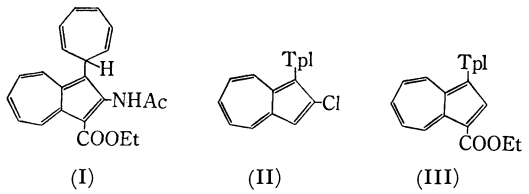

Fig. 2

The reaction of I with phosphorus pentachloride in anhydrous carbon tetrachloride afforded ethyl 2-acetamidoazulen-1-carboxylate[9] besides some intractable resinous substances. However, an attempt to isolate the removed tropylium ion as perchlorate was unsuccessful. Also, when II was treated as above, 1,2,3-trichloroazulene[9] was obtained in a 35% yield, but no other clear resultants could be identified.

The action of phosphorus pentachloride on III gave two substances, (IV) and (V). The elemental analysis ($C_{13}H_{11}O_2Cl$) and the IR spectrum (1655

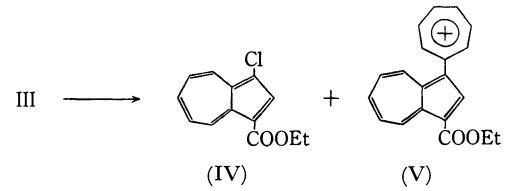

Fig. 3

cm^{-1}) of IV indicated that its structure is ethyl 3-chloroazulen-1-carboxylate. The hydrolysis and subsequent decarboxylation of IV gave 1-chloroazulene.[10] V was isolated as perchlorate salt from the water layer. The results of the elemental analysis of V are consistent with the molecular formula of ($C_{20}H_{17}O_6Cl$), and a new strong absorption band at 763 cm^{-1}, with a weakening of the 748 cm^{-1} band of III (which possesses the characteristic, very strong bands at 780, 748, and 708 cm^{-1}), is observed in the IR spectrum of V.[11] V also shows a broad strong band at 1080 cm^{-1}; presumably, this band is due to the Cl–O vibrations of the perchlorate anion.[12] Therefore, hydride abstraction must have occurred and the structure of V is (3-ethoxycarbonylazulen-1-yl)tropylium perchlorate. V is stable in air at room temperature and can be recrystallized from alcohol, but it burns explosively when heated.

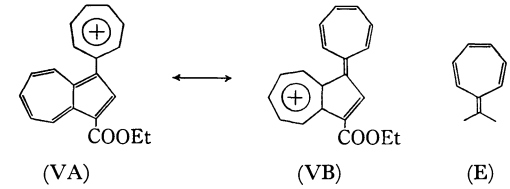

Fig. 4

As has been mentioned above, V possesses VA- and VB-type canonical formulae. If VB is the important canonical formula, the UV and a visible spectra of V should show spectra analogous to those of heptafulvenes (E). However, the spectra of V, although lacking the fine structure in the visible region, are similar to those of III, but not to those of heptafulvenes,[13] as is shown in Fig. 4. Thus,

6) W. von E. Doering and L. H. Knox, *J. Amer. Chem. Soc.*, **76**, 3203 (1954).

7) H. J. Dauben, F. A. Gadecki, K. M. Harmon and D. L. Pearson, *ibid.*, **79**, 4557 (1957).

8) D. N. Kursanov and M. E. Vol'pin, *Doklady Akad. Nauk S. S. S. R.*, **113**, 339 (1957); *Chem. Abstr.*, **51**, 1457 (1957).

9) Unpublished results obtained in the authors' laboratory.

10) A. G. Anderson, J. A. Nelson and J. J. Tazuma, *J. Amer. Chem. Soc.*, **75**, 4980 (1953).

11) All the tropylazulenes (more than thirty) which were synthesized in the authors' laboratory show characteristic, very strong bands in this region of their IR spectra.

12) P. A. Giguère and R. Savoie, *Can. J. Chem.*, **40**, 495 (1962).

13) a) W. von E. Doering and D. W. Wiley, *Tetrahedron*, **11**, 183 (1960). b) T. Nozoe, T. Mukai, K. Osaka and N. Shishido, This Bulletin, **34**, 1384 (1961). c) Y. Kitahara, K. Doi and T. Kato, *ibid.*, **37**, 1747 (1964).

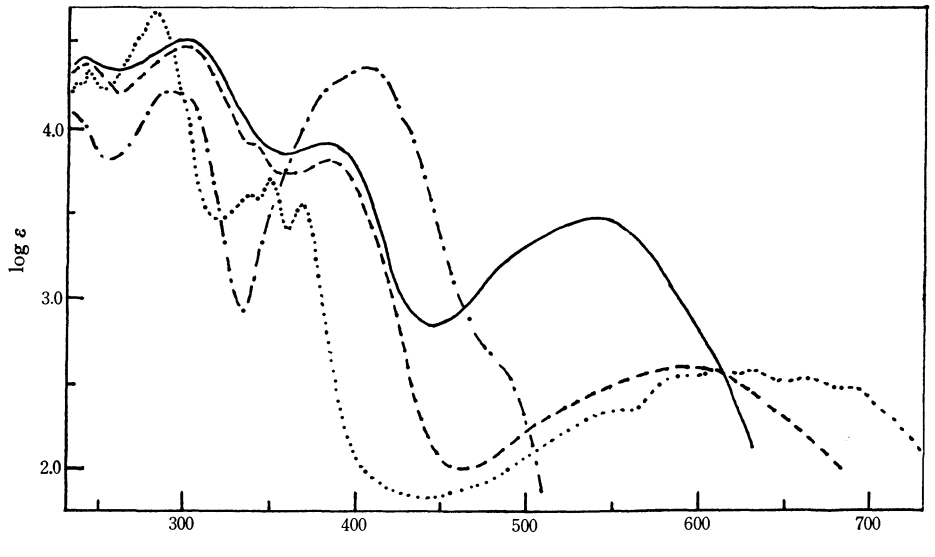

Fig. 5

-------- III —— V ---- VI

-·-·-· 8,8-Dicyano-2,3-dimethoxyheptafulvene[13c]

the contribution of the VB-type canonical formula is not important. Also, from the stereochemical point of view, this is rather reasonable, for if V takes a VB-type structure, the interference between the C_4-hydrogen of the azulene nucleus and the C_2-hydrogen of the tropylium moiety is fairly large.

The above reaction sometimes afforded a neutral substance (mp 181°C) which showed, in its IR spectrum, a strong absorption band at 1640 cm^{-1} beside the ester carbonyl band. This is presumably ethyl 3-(troponyl)azulen-1-carboxylate, which is formed from V by the attack of water and the following disproportionation reaction.[14] However, we did not obtain this in a quantity sufficient to investigate it further.

The reaction of III with chlorine was carried out for the purpose of obtaining V by chlorination-dehydrochlorination reaction. The results were the formation of IV and the recorvery of the starting substance, plus some resinous substances. Therefore, only the exchange reaction of the chlorine cation with the tropyl group occurred. Analogous types of reactions were observed when several 1-tropylazulenes were treated with cationoid reagents.[4]

The formation of 1,2,3-trichloroazulene from II and that of IV from III with phosphorus pentachloride can also be explained as exchange reactions of the chlorine cation with the tropyl groups of the above compounds, for phosphorus pentachloride is said to exist as a PCl_4^+-PCl_6^- complex[15] and it seems possible that the PCl_4^+ moiety dissociates to Cl^+ and PCl_3. The tetrachlorophosphonium cation or the formed chlorine cation then attacks the C_1- and C_3-positions of the azulene nucleus to form 1,2,3-trichloroazulene and IV respectively.[16]

Although 1-azulenyltropylium ion was obtained in the pure state, the yield of the ion was unsatisfactory because of the formation of IV as a by-product. The formation of IV can be explained as follows; if a tropyl group is attached to azulene by its C_7-position (allylic carbon), the exchange reaction takes place more readily than the hydride abstraction reaction. Therefore, if a tropyl group is attached to azulene by a carbon atom (vinyl carbon) other than C_7, the cleavage of the vinyl-carbon bond should not so easy. For this purpose, the thermal isomerization reactions of III was studied, as were the hydride abstraction reactions of the obtained isomers of III.

The thermal isomerization reactions of several different types of tropylidenes have been investigated by ter Borg *et al.*,[17] by the present au-

14) T. Ikemi, T. Nozoe and H. Sugiyama, *Chem. Ind.*, (London), **1960**, 932; A. P. ter Borg, R. van Helden, A. F. Bickel, W. Renold and A. S. Dreiding, *Helv. Chim. Acta*, **43**, 457 (1960).

15) D. Clark, H. M. Powell and A. F. Wells, *J. Chem. Soc.*, **1942** 642; E. S. Gould, "Inorganic Reactions and Structure," 2nd Ed., Holt, Rinehart and Winston, New York (1962), p. 259.

16) It is also possible that phosphorus pentachloride dissociates in small amounts to chlorine and phosphorus trichloride, and that this chlorine behaves as a cation; T. Chitani, "Inorganic Chemistry," New Ed., Sangyo Tosho KK, Tokyo (1963), p. 737.

17) A. P. ter Borg, H.K. Kloosterziel and N. van Meus, *Rec. Trav. Chim. Pays-Bas*, **82**, 717 (1963); A. P. ter Borg and H. K.Kloosterziel, *ibid.*, **82**, 741 (1963).

thors,[18] and by Murry and Kaplan;[19] the results have shown that a 1,5-hydrogen shift occurs in all cases. III was heated under a nitrogen atmosphere, and the reactions were followed by NMR spectroscopy. The methyne hydrogen of the tropyl group of III appears as a triplet (J=5.5 Hz) at 3.20 ppm in its NMR spectrum. When III was heated at 150°C, the triplet disappeared gradually and a new triplet (J=7.0 Hz) appeared at 2.38 ppm. After the disappearance of the triplet at 3.20 ppm, another new peak (doublet, J=7.5 Hz) appeared, at 2.80 ppm while the triplet at 2.38 ppm reached a maximum intensity and then decreased in intensity. The ratio of the intensities of the triplet at 2.38 ppm and the doublet at 2.80 ppm reached equilibrium (about 2:3) after *ca.* 20 hr, and no change was observed. The above peaks could be assigned to the methylene hydrogens of the tropyl groups of ethyl 3-(cycloheptatrien-3-yl)azulen-1-carboxylate (VI) and ethyl 3-(cycloheptatrien-1-yl)azulen-1-carboxylate (VII) respectively. The assignement can also be explained reasonably as follows. VI is formed from III by a 1,5-thermal hydrogen shift of the tropyl group, and then VII is formed from VI by the same procedure. The coupling constants and patterns of the above compounds are also reasonable in view of the assigned structures. Prolonged heating or heating at elevated temperature caused the formation of resinous substances, but no formation of (cycloheptatrien-2-yl)-azulene (VIII)-type isomers could be observed. Some examples of the obtained results are listed in the table.

Although the IR spectrum of III shows characteristic absorption bands at 708, 748, and 780

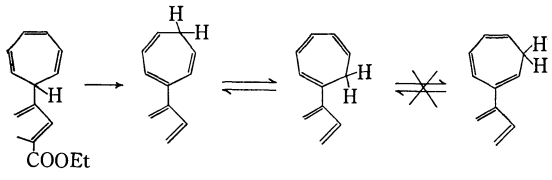

(III) (VI) (VII) (VIII)

Fig. 6

Table 1

Conditions	130°/ 1 hr	130°/ 2 hr	150°/ 3 hr	170°/ 10 hr	190°/ 18 hr
III	60%	30%	2%		
VI	40%	70%	90%	40%	56%
VII			5%	55%	
Polymers				5%	40%

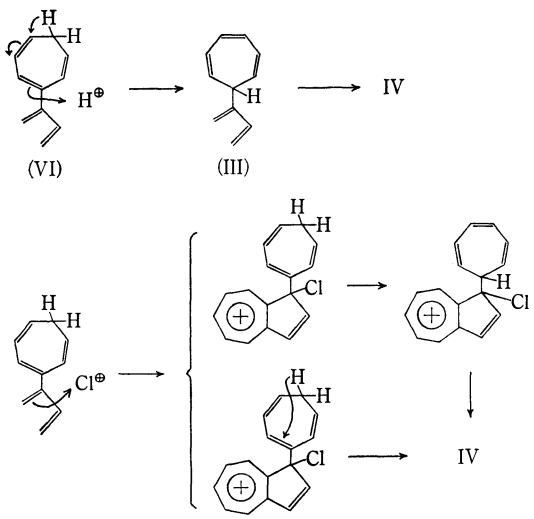

Fig. 7

cm^{-1}, the band at 708 cm^{-1} becomes very weak as the isomerization proceeds and a new, strong band appears at 730 cm^{-1}.

When the mixtures of VI and VII were treated with phosphorus pentachloride under the same conditions as in the case of III, the yield of V was raised to 50—55%. However, IV was surprisingly obtained in a 20—25% yield. These are very interesting results. The explanation was first thought to be as follows: the protons which are formed as the reaction proceeds react with VI and VII to form III, as is shown in Fig. 6, and then the exchange reaction of the tropyl group of the formed III takes place, thus giving IV. However, the treatment of the mixtures of VI and VII with hydrogen chloride under the present reaction conditions did not provide any evidence of the formation of III or ethyl azulen-1-carboxylate. The second possible mechanism of this reaction is that the attack of the chlorine cation takes place at the C_3-position of the azulene nucleus, and then the isomerization and elimination of the tropyl group occurs, either step by step or simultaneously, to give IV. Further investigation of the reaction mechanism is in progress.

The metal - hydride reductions of tropylium ions have been reported to give mixtures of several different kinds of tropylidenes by Vol'pin *et al.*,[20] and by Conrow.[21] Also, Anderson and Replogle[3] reported the formation of 1-chloro-3-(cycloheptatrien-7-yl)azulene by the reduction of the 1-(3-chloroazulen-1-yl)tropylium ion with sodium borohydride. However, they did not isolate the chloroazulenetropylium ion which was used for reduction, and the reduction product was identified only by means of its UV and visible spectra.

18) T. Nozoe and K. Takahashi, This Bulletin, **38**, 665 (1965). T. Mukai, H. Kubota and T. Toda, *Tetrahedron Lett.*, **1967**, 3581.

19) R. W. Murry and H. L. Kaplan, *J. Amer. Chem. Soc.*, **88**, 3527 (1966).

20) Z. N. Parness, M. E. Vol'pin and D. N. Krusanov, *Tetrahedron Lett.*, **1960**, 20.

The sodium borohydride reduction of V gave only 2 : 3 mixtures of VI and VII, as shown by an investigation of the IR and NMR spectra of the reduction products, but the formation of III was not observed. According to Conrow,[21] the hydride reduction of the methyltropylium ion gave mixtures of 1-methyl-, 2-methyl-, and 3-methyl-tropylidenes in more than a 95% yield and the yield of 7-methyltropylidene was about 2%. The formation of a large amount of a 7-tropyl-type compound does not seem reasonable either from the point of view of the thermodynamical stability of the resultants and the steric requirements of the reaction.

The results of the reduction of V, together with the consideration of the spectroscopic properties of V mentioned above, support the idea that the structure of V is (3-ethoxycarbonylazulen-1-yl)-tropylium perchlorate.

Experimental[22]

Hydride Abstraction Reaction of I. Into a suspension of 0.60 g of phosphorus pentachloride in 20 m*l* of anhydrous carbon tetrachloride, a solution of 0.50 g of I in 5 m*l* of anhydrous carbon tetrachloride was stirred, and then stirring was continued for 6 hr. The reaction mixture was poured into 30 m*l* of cold water, and the water layer was extracted with benzene. After separation, the combined organic layers were dried over sodium sulfate, separated from the drying reagent, and concentrated *in vacuo*; the residue was dissolved in benzene and submitted to chromatography. The first eluate gave 89 mg of dark red prisms (mp 141—142°C, which did not show any mixed-melting-point depression with ethyl 2-acetamidoazulen-1-carboxylate[9]); the second eluate gave 9 mg of violet crystalline substances (mp 111—112°C), and the third gave 23 mg of violet, crystalline substances (mp 146—182°C), the rest was composed of 156 mg of resinous, oily substances. The second crystalline substances show a positive Beilstein test: however, further purification of the second and the third eluates failed to provide pure substances.

The addition of 60% perchloric acid to the water layer did not give any crystalline substances.

Hydride Abstraction Reaction of II. A solution of II in 5 m*l* of anhydrous carbon tetrachloride and 1.0 g of phosphorus pentachloride in 20 m*l* of carbon tetrachloride was treated as above. Cyclohexane eluates of the chromatography gave 173 mg of dark blue, crystalline substances (mp 120—124°C). Recrystallization from ethyl acetate raised its melting point to 137°C; yield, 140 mg. A mixed-melting-point determination of this and 1,2,3-trichloroazulene[9] failed to show any depression.

Found: C, 51.70; H, 2.20%. Calcd for $C_{10}H_5Cl_3$: C, 51.88; H, 2.18%.

The water layer did not give any crystalline substances after the addition of 60% perchloric acid.

Hydride Abstraction Reaction of III. Into a suspension of 1.13 g of phosphorus pentachloride in 25 m*l* of anhydrous carbon tetrachloride, a solution of 0.78 g of III in 5 m*l* of carbon tetrachloride was stirred, and then the stirring was continued for 1.5 hrs. After the reaction, the reaction mixture was treated as above. The organic layer gave blue black needles (mp 62°C), after chromatography and recrystallization from cyclohexane; yield, 133 mg.

Found: C, 66.27; H, 4.30%. Calcd for $C_{13}H_{11}O_2Cl$: C, 66.30; H, 4.75%.

The addition of 60% perchloric acid to the water layer formed dark brown precipitates. The precipitates were then separated by filtration and dried in a desiccator to give 0.40 g of a dark brown powder (mp 180—182°C (dec.)). Recrystallization from alcohol raised its melting point to 205°C (dec.), and this crystalline substance vigorously burned when heated in air.

Found: C, 61.71; H, 4.30%. Calcd for $C_{20}H_{17}O_6Cl$: C, 61.79; H, 4.41%.

λ_{max}^{MeOH}, mμ (log ε); 238 (4.43), 305 (4.54), 382 (3.94), and 536 (3.49).

Hydride Abstraction Reaction of the Mixtures of VI and VII. From 0.50 g of the mixtures of VI and VII, 0.34 g of V was obtained when the reaction was carried out as above. From the organic layer, 85 mg of IV were obtained; the rest was composed of resinous, oily substances which did not give any pure substances upon further purification. The average yields of IV and V from the mixture were 20—25% and 50—55% respectively, and no remarkable change was observed when the ratio of VI and VII in the starting mixtures was changed.

Sometimes a few mg of dark blue, crystalline substances (mp 181°C) were obtained from the organic layer; these substances showed a strong absorption band at 1640 cm^{-1} (KBr pellet) besides the ester carbonyl band at 1675 cm^{-1}.

Hydrolysis and Decarboxylation of IV, 1-Chloroazolene. A solution of 50 mg of IV and 38 mg of potassium hydroxide in 3 m*l* of alcohol and 1 m*l* of water was heated under reflux for 4 hr, and then 5 m*l* of cold water were added. The pH of the solution was adjusted to *ca.* 3.0 with 6N hydrochloric acid to give 32 mg of dark violet precipitates (mp 225°C (dec.)) after having been dried *in vacuo*. The precipitates were heated in a sublimation apparatus for decarboxylation at 190°C (3 mmHg), and the blue oil thus formed was chromatographed on alumina. The cyclohexane eluate gave 21 mg of a blue oil, and its IR spectrum was superimposable upon that of 1-chloroazulene prepared by the authentic method.[10] The treatment of the oil with trinitrobenzene gave dark brown needles (mp 132—133°C) from benzene (reported, mp *ca.* 105°C).[10]

Found: C,51.26; H, 2.58; N, 10.66%. Calcd for $C_{16}H_{10}O_6N_3Cl$: C, 51.14; H, 2.68; N, 11.19%.

Reaction of III with Chlorine. To a solution of 116 mg of III in 10 m*l* of anhydrous carbon tetrachloride, 30 mg of chlorine in 0.25 m*l* of anhydrous carbon tetrachloride were added, then the mixture was allowed to stand overnight. After the solvent has then been removed, 142 mg of an oily substance were obtained; the oil was submitted to chromatography. The benzene eluate gave 88 mg of a dark blue oil, and the ethyl acetate eluate gave 24 mg of a black tar. Rechromatography of the first eluate by petroleum ether-cyclohexane (4 : 1) gave 35 mg of dark blue, crystalline substances (mp 61°C) from cyclohexane as the first eluate, and, as the second eluate, 25 mg of

21) K. Conrow, *J. Amer. Chem. Soc.*, **83**, 2343 (1961).
22) All melting points are uncorrected.

a violet oil. The former was identical with ethyl 3-chloroazulene-1-carboxylate (IV), and the latter was the recovered starting materials, as determined by a comparison of their IR spectra with those of the respective authentic samples.

Thermal Isomerization of III. III (0.51 g) was heated under a nitrogen stream at 130°C for 2 hr without any solvent; after heating, the resultant substance was chromatographed on alumina. The benzene eluate gave 0.51 g of dark blue-violet oil. The results of the elemental analysis of the resultant are as follows:

Found: C, 82.56; H, 6.38%. Calcd for $C_{20}H_{18}O_2$: C, 82.73; H, 6.25%.

The ratio of the isomers was determined by measuring the areas of the methine and methylene hydrogens of mixtures of the isomers. The NMR spectra were measured with *ca.* 10% solutions of each resultant in carbon tetrachloride, with TMS as the internal standard, using a Varian A-60-type spectrometer. Some examples of the obtained results are listed in the table.

About 2 : 3 mixtures of VI and VII were obtained when the isomerization was carried out at 150°C for *ca.* 20 hr. However, when heating was continued for more than 15 hr at 190°C, VI and VII amounted to *ca.* 56%, with the rest being a polymer which could be separated from VI and VII by means of alumina chromatography.

Sodium Borohydride Reduction of V. Into a solution of 0.20 g of V in 5 m*l* of acetonitrile, a solution of 40 mg of sodium borohydride in 2 m*l* of acetonitrile was stirred in small portions. The color of the solution changed from a dark reddish violet to brown; then 40 more mg of borohydride were added, thus causing the color of the solution to change from brown to a greenish violet. The solution was then allowed to stand at room temperature for 30 min with stirring, and water was added. The water layer was extracted with petroleum ether; the combined organic layers were then washed with water and dried over sodium sulfate, and the drying reagent was separated by filtration. The petroleum ether was removed to give 155 mg of a greenish-brown oil; the obtained oil was chromatographed on alumina. A light petroleum - benzene (9 : 1) eluate afforded 109 mg of a greenish-violet oil the IR and NMR spectra of which were identical with those of the 2 : 3 mixtures of VI and VII.

The authors wish to express their gratitude to Professor Tetsuo Nozoe for his kind encouragement and interest, to Miss Ayako Iwanaga, Miss Mutsuko Suzuki, and Mrs. Ei Arai for their elemental analyses, and to Miss Yoriko Terui and Mr. Iwao Miura for their measurement of the spectra.

BULLETIN OF THE CHEMICAL SOCIETY OF JAPAN VOL. 43 2186—2191 (1970)

The Catalytic Dehydrogenation, Dehydroxylation and Dehydroxymethylation of Benzyl Alcohol. I. The Scope and the Kinetic Study

Masayoshi ISHIGE,*1 Koji SAKAI, Masatoshi KAWAI and Kazuo HATA

Department of Chemistry, Faculty of Science, Tokyo Metropolitan University, Setagaya-ku, Tokyo

(Received December 23, 1969)

Benzyl alcohol was dehydrogenated to benzaldehyde when it was heated in the presence of various metal catalysts. It was found that the dehydrogenation was accompanied by a reductive dehydroxylation and dehydroxymethylation which led to the production of toluene and benzene respectively. The compositions of the products, which mainly consisted of benzaldehyde, toluene, and benzene, were greatly affected by the chemical nature of the catalysts used. The results of the reactions in a sealed tube or in an authoclave suggested that a pseudo-equilibrium between benzyl alcohol and benzaldehyde was attained during the reaction in a closed system. The formation of CO_2, CH_4, and other hydrocarbons as gaseous products was also observed. From these results, the catalytic dehydrogenation, dehydroxylation, and dehydroxymethylation were assumed to proceed competitively *via* a certain metal benzyl complex which is formed as an adsorbed transition complex upon the catalyst metal.

It has previously been reported[1] that a novel redox reaction was observed between benzyl alcohol and some kinds of unsaturated organic compounds, such as styrene and mesityl oxide, in the presence of nickel catalysts. In these reactions, benzyl alcohol was mainly converted into benzaldehyde by dehydrogenation (Eq. (1)), but reductive dehydroxylation (Eq. (2)) and dehydroxymethylation

*1 Present address: Chemical Laboratory, Ochanomizu University, Otsuka, Bunkyo-ku, Tokyo.

1) K. Sakai, T. Ito and K. Watanabe, This Bulletin, **39**, 2230 (1966).

(Eq. (3)) were also found to take place to some extent.

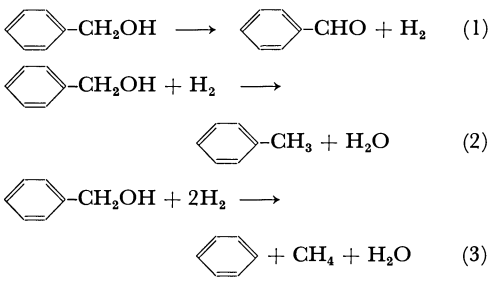

The behavior of benzyl alcohol in these reactions was considered to be much more complicated; for example, in addition to the formation of CH_4, the generation of CO_2 and of some other gaseous hydrocarbons was observed. Furthermore, the composition of the products from the alcohol was characteristically affected by the nature of the catalysts used. Nishimura[2] has also shown that the reactivity and selectivity in the hydrogenation of benzyl alcohol are dependent upon the species of the catalysts used. Thus, the study of the dehydrogenation, dehydroxylation and dehydroxymethylation of benzyl alcohol may provide an insight into the nature of the reactivity and selectivity in catalysis. For a further investigation of the relation between the catalytic reaction and the nature of the catalysts, the reactions of benzyl alcohol have been studied in the presence of various kinds of solid catalysts, including metals and metal oxides.

Results and Discussion

Benzyl alcohol afforded benzaldehyde, toluene, and benzene when heated at 140—180°C with various metal catalysts. In addition, the generation of CO_2, CH_4, and some other hydrocarbons was observed, accompanied by the formation of benzene by dehydroxymethylation.

Some experiments were carried out by refluxing under ordinary pressure; in these experiments, when the refluxing was continued for a long time, a change in the quality of the catalyst was necessarily brought

Table 1. The reactions of benzyl alcohol under ordinary pressure
benzyl alcohol 6 m*l*; catalyst 1.0 g; refluxed at 160°C for 24 hr

Catalyst	Alcohol reacted (%)	Composition of products[a] (mol %)			Selectivity $\times 10^2$		k_{alc}[b] (hr^{-1}) $\times 10^3$
		PhH	$PhCH_3$	PhCHO	PhH/PhCHO	$PhCH_3$/PhCHO	
ppt-Ni	99	1.2	38.8	60.0	2.0	64.8	96.0
$Cu_2Cr_2O_5$	51.8	—	7.7	92.3	—	8.3	30.4
S-Ni	25.0	9.6	11.2	79.2	12.0	14.3	12.0
$Ni_2Cr_2O_5$	17.4	—	2.3	97.7	—	2.4	7.8
ppt-Cu	9.1	—	26.4	73.6	—	35.9	3.9
NiO	7.2	—	4.2	95.8	—	4.4	3.1

a) The gaseous products, such as CO_2 and CH_4, are ignored.
b) The first order rate constants of the diminution of benzyl alcohol.

Table 2. The reaction of benzyl alcohol in a closed vessel

Reaction vessel	Catalyst	Alcohol reacted (%)	Composition of products[a] (mol %)			Selectivity $\times 10^2$		k_{alc}[b] (hr^{-1}) $\times 10^4$
			PhH	$PhCH_3$	PhCHO	PhH/PhCHO	$PhCH_3$/PhCHO	
Autoclave	ppt-Ni	40.5	1.5	52.8	45.7	3.3	115	216
	R-Ni (W-7)	44.7	19.4	42.6	38.0	51.0	112	246
	U-Ni-A	30.3	3.0	39.3	57.7	5.2	68.1	149
Sealed tube	S-Ni	21.2	28.8	46.7	24.5	117	190	98.8
	$Cu_2Cr_2O_5$	4.7	—	trace	<100	—	—	19.2
	$ZnCr_2O_4$	1.8	—	trace	<100	—	—	7.7
	Al_2O_3	1.4	—	trace	<100	—	—	5.8

Reaction in an autoclave: benzyl alcohol 24 m*l*, catalyst 4 g, heated at 155°C for 24 hr
Reaction in a sealed tube: benzyl alcohol 2 m*l*, catalyst 0.333 g, heated at 157°C for 24 hr
a) The quantity of gaseous products is ignored.
b) The first order rate constant of the diminution of benzyl alcohol.

2) S. Nishimura and M. Hama, *ibid.*, **39**, 2467 (1966); S. Nishimura, *ibid.*, **32**, 103 (1959); **32**, 1158 (1959).

about by the reaction with the benzaldehyde and/or benzoic acid which was formed during the reaction. The other experiments were practiced in a sealed tube or in an autoclave in order to avoid the volatilization and oxidation of the products. After the reaction was over, the reaction mixture was analyzed by gas chromatography. The results of representative experiments are summarized in Tables 1 and 2. The catalysts used were precipitated nickel (ppt-Ni), precipitated copper (ppt-Cu), Raney nickel (R-Ni), Urushibara nickel A (U-Ni-A), stabilized nickel (S-Ni), copper chromium oxide ($Cu_2Cr_2O_5$), nickel chromium oxide ($Ni_2Cr_2O_5$), zinc chromium oxide ($ZnCr_2O_4$), aluminum oxide (Al_2O_3), and nickel oxide (NiO).

The activities of these catalysts are represented in terms of the corresponding first-order rate constants of the catalytic reaction of the alcohol (k_{alc}), which were approximately calculated from the amount of unreacted alcohol. From these results, it was found that the activity of ppt-Ni is much better in dehydrogenation rather than those of the other catalysts, and that the compositions of the reaction products vary remarkably depending upon the species of the catalysts; for example, the mol percentage of toluene in the products was not very different between the different nickel catalysts used, whereas the formation of benzene was markedly influenced by the kind of catalyst, the relative yield being suppressed in the following order: S-Ni> R-Ni>U-Ni-A>ppt-Ni. It is noteworthy that benzene was not produced in the presence of metal oxide catalysts, such as $Cu_2Cr_2O_5$, $ZnCr_2O_4$, and Al_2O_3. From the viewpoint of the formation of benzene during the reaction, the catalysts used can be roughly classified into three categories: (a) the catalysts, such as S-Ni and R-Ni (W-7), which afford a large quantity of benzene. They are mainly composed of nickel crystals or crystallites; (b) the catalysts, such as ppt-Ni and U-Ni-A, which give a small quantity of benzene. Ppt-Ni, which is the precursor of U-Ni-A, is supposed to have the surface structure of an alloy-like crystal composed of nickel and zinc,[3] and (c) ppt-Cu or oxide-type catalysts which exhibit no activity giving benzene. Considering these facts, it can be assumed that the nickel crystals are generally effective in the formation of benzene.

With a veiw to getting further information on the process of the reactions of benzyl alcohol, the change in the composition of the reaction mixture was followed by gas-chromatographic analysis at successive intervals. The results of the reaction, in which benzyl alcohol was refluxed under orindary pressure in the presence of S–Ni (S 10), are shown in Fig. 1; those of the same reaction practiced in a sealed tube are illustrated in Fig. 2. Figures 1 and 2 indicate that the alcohol always reacts in the

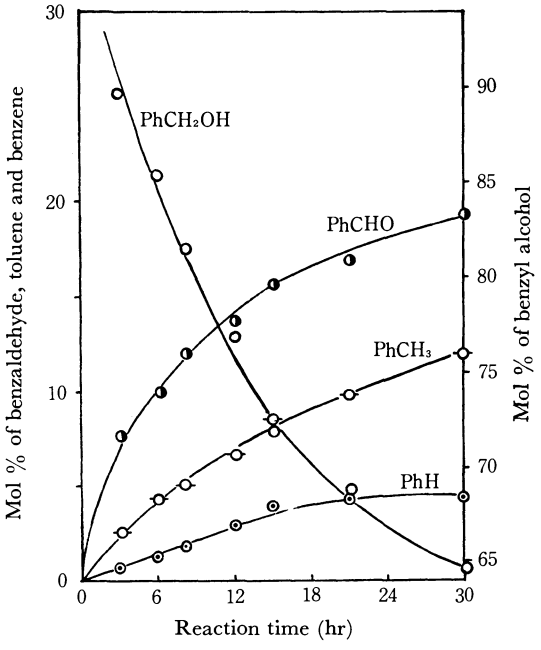

Fig. 1. The change of the composition of the reaction mixture.
substrate: benzyl alcohol, catalyst: stabilized nickel (S 10), conditions: refluxing under the ordinary pressure

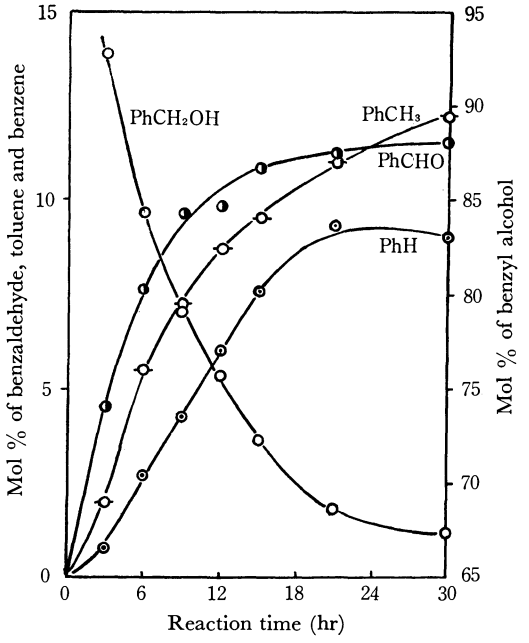

Fig. 2. The change of the composition of the reaction mixture.
substrate: benzyl alcohol, catalyst: stabilized nickel (S 10), conditions: heated at 157°C in a sealed tube

3) S. Taira, "Catalytic Engineering," Vol. 10, ed. by Catalysis Society of Japan, Chijin Shokan & Co., Tokyo (1967), pp. 498—499.

first order. In the reaction in a sealed tube, benzaldehyde and benzene increased successively in the early stages, but the rate of their formation was found to decline after the elapse of 12 hr, while toluene went on increasing.

In the redox reaction shown in Eq. (4), the rate constant of the oxidation of the alcohol (k_1) was supposed to be smaller than that of the reverse reaction (k_{-1}), because the oxidation potential of benzaldehyde is comparatively high.[4]

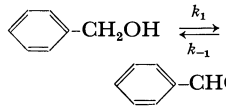

$$\text{-CHO} + H_2 \quad (k_1 < k_{-1}) \qquad (4)$$

Thus, in the state of equilibrium between benzyl alcohol and benzaldehyde, the alcohol may be predominant. Therefore, in the closed reaction system, the reduction of benzaldehyde, which corresponds to the reverse reaction in Eq. (4), may proceed concurrently with the dehydrogenation of benzyl alcohol until the pseudo-equilibrium shown in Eq. (4) is attained in the reaction system. The consumption of hydrogen produced by the dehydrogenation of benzyl alcohol will lead to the disadvantageous reductive dehydroxylation and dehydroxymethylation of the alcohol according to Eqs. (2) and (3). Of these competitive reactions, the latter was found to be more strongly suppressed (Fig. 2). This is conceivable not only because the C–C bond is more difficult to hydrogenolyze than the C–O bond, but also because the dehydroxymethylation (Eq. (3)) requires twice as much hydrogen as does dehydroxylation (Eq. (2)).

One piece of evidence leading to this conclusion comes from the results of the reactions carried out with various amounts of a nickel catalyst (S-Ni) in sealed tubes; the influence of the change in the amount of catalyst in the reactions is summarized in Table 3 and Fig. 3. As is shown in Fig. 3, a linear proportionality was observed between the amount of the catalyst and the logarithm of the rate constant. The linear relation equation can be approximately represented as follows:

$$\log k_{alc} = 6.20 \times 10^{-2} \cdot W - 2.20 \qquad (5)$$

where W is the weight of the catalyst (in gram).

The composition of each product in the reaction mixture of the above reactions is given in Fig. 4. It can be found from Figs. 3 and 4 that the rate constant of the overall reaction of benzyl alcohol and the yields of toluene and benzene increased with an increase in the amount of the catalyst. However, the yield of benzaldehyde decreased in spite of the increase in the rate of the overall reaction of benzyl alcohol. Therefore, it may be

Table 3. The reactions of benzyl alcohol in the presence of varied amount of stabilized nickel catalyst in a sealed tube

benzyl alcohol 1.0 m*l*; heated at 160° for 24 hr

Weight of catalyst (g)	k_{alc} (hr^{-1}) $\times 10^2$	log k_{alc}
0.100	0.977	−2.010
0.167	1.19	−1.922
0.250	1.95	−1.710
0.333	2.40	−1.620
0.500	5.36	−1.271

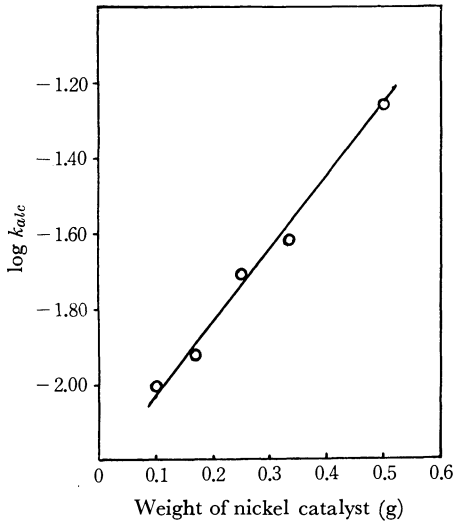

Fig. 3. Relation between k_{alc} and weight of nickel catalyst by the reactions in sealed tubes.

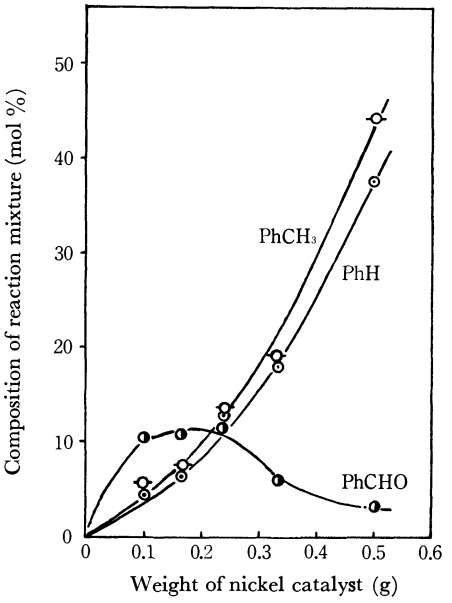

Fig. 4. The composition of products by the reactions of benzyl alcohol in the presence of varied amount of stabilized nickel catalyst in sealed tubes.

4) The values of E_0 and $-\Delta F$ for benzaldehyde are 197 mV and 9.1 kcal (25°C); H. Adkins, R. M. Elofson, A. G. Rossow and C. C. Robinson, *J. Amer. Chem. Soc.*, **71**, 3622 (1949).

Table 4. The reactions of benzyl alcohol in the presence of varied amount of stabilized nickel catalyst under ordinary pressure

benzyl alcohol 30 ml; refluxed at 150°C for 6 hr

Weight of catalyst (g)	k_{alc} (hr^{-1}) $\times 10^2$
3.0	0.766
5.0	1.11
7.5	1.66
10	2.20
15	3.33

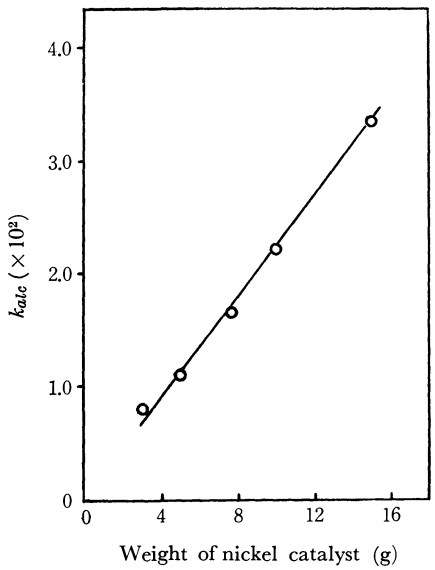

Fig. 5. Relation between k_{alc} and weight of nickel catalyst by the reactions under ordinary pressure.

assumed that the faster the dehydragenation reaction proceeds due to an increase in the amount of the catalyst, the more readily the pseudo-equilibrium shown in Eq. (4) will be attained, resulting in the promotion of the formation of benzene and toluene.

Other experiments to observe the effect of the amount of the catalyst were carried out by refluxing benzyl alcohol under ordinary pressure. The results are shown in Table 4 and Fig. 5. A linear relationship was similarly observed between the rate constant of the overall reaction of benzyl alcohol and the amount of the catalyst. The relation can be represented as in the following equation:

$$k_{alc} = 2.21 \times 10^{-3} \cdot W \qquad (6)$$

In contrast to the results in a closed reaction system, the decrease in the formation of benzaldehyde with the increase in the catalyst amount (see Fig. 4) was observed in an open reaction system under ordinary pressure. Thus, it was found that hydrogen plays an important role in determining the compositions of the products. In the closed reaction system, the high pressure of hydrogen, which is brought about by the dehydrogenation, necessarily leads to a decrease in the final yield of benzaldehyde. On the other hand, it may be advantageous to promote the formation of toluene and benzene by the reductive dehydroxylation and dehydroxymethylation. This consideration is fairly consistent with the results of another experiment in which the variation in the composition of the products under various hydrogen pressures was observed (Fig. 6). Consequently, it was concluded that the selectivity of this reaction is dependent not only upon the nature of the catalyst used, but also upon the pressure of hydrogen in the reaction system.

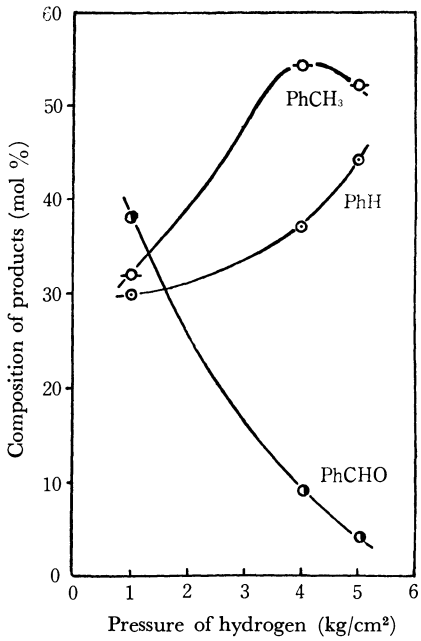

Fig. 6. The composition of products by the catalytic reactions of benzyl alcohol under varied pressure of hydrogen.
benzyl alcohol 24 ml; catalyst: stabilized nickel 4 g

It was established that benzaldehyde cannot be an intermediate in the formation of toluene or benzene, because the benzaldehyde itself was completely recovered unchanged when it was heated in the presence of a nickel catalyst in a sealed tube for more than 24 hr. The formation of methane in the dehydroxymethylation of primary alcohol has already been reported.[5] In the present study the generation of a small quantity of another gaseuous hydrocarbon besides methane was observed by gas-

5) V. N. Ipatieff, G. Czajkowski and H. Pines, *ibid.*, **73**, 4098 (1951); H. Pines, H. G. Rodenberg and V. N. Ipatieff, *ibid.*, **76**, 771 (1954); H. Pines, M. Shamaiengar and W. S. Postle, *ibid.*, **77**, 5099 (1955).

chromatographic analysis; it was assumed to be either ethane or propane on the basis of its retention time. The formaldehyde, which might be expected in dehydroxymethylation, could not be detected by any test with 2,4-dinitrophenylhydrazine, Fehling's solution, and Schiff's reagent.

It is noticeable that the generation of carbon dioxide was observed as another by-product of the dehydroxymethylation. Carbon dioxide was detected by gas-chromatographic analysis and by the formation of a $BaCO_3$ precipitate when a gaseous product was introduced into a saturated aqueous solution of $Ba(OH)_2$.

The mode of the adsorption of benzyl alcohol on the catalyst and the mechanism of the catalytic reaction are not entirely clear, but it is considered that the general scheme of the reaction may well be represented as follows, assuming the intervention of an adsorbed transition state on the catalyst:

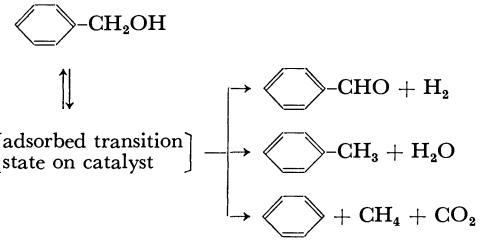

McQuillin *et al.*[6] have proposed a mechanism of the hydrogenolysis of benzylic compounds in which the reaction was presumed to proceed through a metal benzyl complex. If the formation of a π-benzyl complex intermediate in hydrogenolysis is established, it is conceivable that a similar complex, at least one of nickel, is involved in the dehydroxymethylation and dehydroxylation of benzyl alcohol in the presence of a catalyst. This consideration seems to be fairly consistent with the complicated reaction course of benzyl alcohol. Since nickel metal plays an important role in the cleavage of α-carbon from the benzene ring by dehydroxymethylation reaction, a strong interaction of nickel with the phenyl group may be expected in the adsorbed transition complex. Considering the simultaneous formation of CO_2 and CH_4 in the dehydroxymethylation, and the high yield of cyclohexylmethanol in the hydrogenation,[2,7] of benzyl alcohol, it was supposed that the formation of a π-benzyl intermediate involves the removal of either a hydrogen atom or a hydroxyl group from α-carbon, thus giving a metal benzyl complex, I or II :

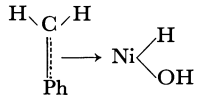

(I)

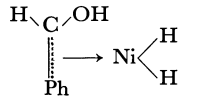

(II)

The preference for the alternative removal of either the hydrogen or hydroxyl group is probably dependent upon the chemical nature of the catalyst metal and on the reaction conditions. From the fact that scarcely no formation of benzene was observed when precipitated copper or oxide-type catalysts were used, it is reasonable to consider that the reaction in the presence of these catalysts might take place through another reaction path, without any formation of the metal complex.

Experimental

Benzyl Alcohol. Commercial benzyl alcohol of an extra pure degree was refined by distillation. The fraction boiling at 100—101°C/20 mmHg was collected. The sample was proved to be pure by gas chromatography.

The Reaction under Ordinary Pressure. In a 50-m*l* three-necked flask fitted with a Dimroth condenser and a thermometer was placed 6 m*l* of benzyl alcohol (6.25 g). The flask was then heated to 160°C, and 1.0 g of a catalyst was added through a side-neck when the contents reached a constant temperature.

Small portions of the reaction mixture were periodically taken out with a pipet and analyzed by gas chromatography: column, 1 m of 30% Silicone grease DC on Celite 480 (30—40 meshes) and 2 m*l* of 20% Apiezon grease on Chromosorb W (60—80 meshes); column temp., 150—163°C; flow rate, 40—60 m*l*/min; carrier gas, H_2.

The Reaction in a Sealed Tube. Benzyl alcohol (2.00 m*l*) and a catalyst (0.333 g) were heated at 157°C for 24 hr in a sealed tube. After the reaction was over, the tube was cooled by ice; then the reaction mixture was analyzed by gas chromatography immediately after the tube was opened. For the kinetic study in a closed reaction system, several sealed tubes with the same contents were prepared. The tubes were succesively taken out from the heating bath at adequate intervals and the reaction mixture was analyzed as has been mentioned above.

The Reaction in an Autoclave. Benzyl alcohol (24 m*l*) and a catalyst (4 g) were placed in a 200-m*l* autoclave. After the air in the autoclave had been completely displaced by hydrogen gas, the mixture was heated at 155°C for 24 hr under 1.0 kg/cm^2 pressure of hydrogen without stirring. After the reaction was over, portions of the gaseous product were introduced into various kinds of reagents in order to detect the formation of CO_2 and formaldehyde. The liquid products were analyzed by gas chromatography. Some of the gaseous products were also detected by gas chromatography.

The authors wish to express their hearty thanks to Dr. Ken-ichi Watanabe for his helpful encouragement.

6) I. Jardine and F. J. McQuillin, *J. Chem. Soc., C*, **1966**, 458; D. A. Denton, F. J. McQuillin and P. L. Simpson, *ibid.*, **1964**, 5535; A. M. Khan, F. J. McQuillin and I. Jardine, *ibid., C*, **1967**, 136; *Tetrahedron Lett.*, **1966**, 2649.

7) H. Adkins and L. W. Covert, *J. Phys. Chem.*, **35**, 1684 (1931); R. Mozingo, C. Spencer and K. Folkers, *J. Amer. Chem. Soc.*, **66**, 1859 (1944); K. Taketomo, Y. Nishimura, T. Hiraki, S. Akitomo and K. Kawamoto, Preprints for the 20th Annual Meeting of the Chemical Society of Japan, Tokyo (April, 1967), Vol. III, p. 278.

BULLETIN OF THE CHEMICAL SOCIETY OF JAPAN VOL. 43 2192—2194 (1970)

The Hydroformylation of Nitroalkenes with Rhodium Carbonyl

Masahiko TAKESADA and Hachiro WAKAMATSU

Central Research Laboratories, AJINOMOTO CO., INC., Kawasaki

(Received January 7, 1970)

The hydroformylation of butenes in nitrobenzene or nitroethane gives C_5-aldehydes in an excellent yield in the presence of tetrarhodium dodecarbonyl, but in only a poor yield in the presence of dicobalt octacarbonyl. Under hydroformylation conditions, nitrobenzene is hydrogenated to aniline above 150°C with rhodium carbonyl and at 125°C with cobalt carbonyl. The hydroformylation of nitroalkenes with rhodium carbonyl is described. 4-Nitrostyrene gives isomeric (4-nitrophenyl)-propionaldehydes in a 96% yield. 3-Nitropropene-1 gives C_4-nitroaldehydes, mostly 2-methyl-3-nitropropionaldehyde, in a 96% yield. However, no reaction of nitroethylene occurred below 140°C.

It has been already established that nitrobenzene is hydrogenated to give aniline under hydroformylation conditions at an elevated temperature and in the presence of cobalt carbonyl.[1,2] However, no study has been reported on the hydroformylation of nitroalkenes. In this paper, the hydroformylation of butenes in a solvent of nitro compounds will be described, together with the hydrogenation of nitrobenzene under hydroformylation conditions in the presence of cobalt and rhodium carbonyl. The hydroformylations of nitroethylene, 3-nitropropene-1, and 4-nitrostyrene will also be described.

Results and Discussion

Hydroformylation of Butenes. The results of the hydroformylation of butenes in a solvent of various nitro compounds are shown in Table 1. In the reaction of butene-1 with a mixture of carbon monoxide and hydrogen in nitrobenzene in the presence of dicobalt octacarbonyl, the absorption of the gas started at 120°C and more than 2 moles of the gas were consumed per mole of butene-1. However, the yield of C_5-aldehydes was only 37% and the ratio of 2-methylbutyraldehyde to *n*-valeraldehyde was 1.0 to 1.40. The yield and the isomeric ratio of the products in this system are different from those of the hydroformylation of butene-1 in benzene, where the yield of the aldehydes and the isomeric ratio were reported to be 89% and 0.23 respectively.[3] The poor yield of the aldehydes in nitrobenzene is probably due to further reactions of the aldehydes with the aniline formed from nitrobenzene under hydroformylation conditions.

TABLE 1. HYDROFORMYLATION OF BUTENES

Reaction conditions[a]					Product	
Olefin	Catalyst	Solvent	Temp. °C	Time min	Yield of aldehydes %	Ratio of isomers[c] B/N
Butene-1	Co	Nitrobenzene	120	170	37	1.40
	Rh	Nitrobenzene	60	41	95	1.19
	Rh	Nitroethane	60	42	94	1.24
	Rh	Benzene	60	33	94	1.26
trans-Butene-2	Rh[b]	Nitrobenzene	60	100	93	100
	Rh[3]	Benzene	60	120	91.4	∞

a) Other reaction conditions:
Butenes: 100 mmol, solvent: 45 ml, pressure: 200 kg/cm², $[Rh(CO)_3]_4$: 50 mg or $[Co(CO)_4]_2$: 145 mg.
b) $[Rh(CO)_3]_4$: 80 mg.
c) B: 2-methyl-butyraldehyde. N: *n*-valeraldehyde.

1) I. Wender, H. Greenfield, S. Meltin and M. Orchin, *J. Amer. Chem. Soc.*, **74**, 4079 (1952).
2) S. Murahashi, S. Horiie and T. Joh, *Nippon Kagaku Zasshi*, **79**, 68 (1958).
3) H. Wakamatsu, *ibid.*, **85**, 227(1964).

In the presence of tetrarhodium dodecacarbonyl in place of dicobalt octacarbonyl, the hydroformylation of butenes gave C_5-aldehydes in an excellent yield even in nitrobenzene or nitroethane, and the amount of gas consumed was almost the theoretical value for hydroformylation. On the hydroformylation of butene-1 or *trans*-butene-2 with rhodium carbonyl under milder conditions, there are no significant differences in the yield and isomeric distribution of the aldehydes between the benzene and the nitrobenzene used as solvents.

Hydrogenation of Nitrobenzene. In order to elucidate the catalytic activity of cobalt and rhodium carbonyl for the hydrogenation of nitro compounds to amino derivatives under hydroformylation conditions, the hydrogenation of nitrobenzene was studied. The results are shown in Table 2.

Table 2. Hydrogenation of nitrobenzene

Catalyst	Reaction conditions: Solvent	Temp. °C	Time min	Yield of aniline %
Co[a)]	Benzene	125	30	100
Rh[a)]	Benzene	180	140	94
Rh[b)]	—	150—154	105	96

Other reaction conditions:
a) Nitrobenzene (80 mmol)+benzene: 40 m*l*, pressure: 250 kg/cm² ($CO+H_2$), $[Rh(CO)_3]_4$: 73 mg or $[Co(CO)_4]_2$: 465 mg.
b) Nitrobenzene: 30 m*l*, pressure: 182 kg/cm² ($CO+H_2$), $[Rh(CO)_3]_4$: 80 mg.

Nitrobenzene is hydrogenated to aniline under hydroformylation conditions at 125°C with cobalt carbonyl as shown in Table 2. Rhodium carbonyl also catalyzed the hydrogenation of nitrobenzene above 150°C without a solvent or at 180°C in benzene, but at lower temperatures no reaction took place. A higher temperature is required for the hydrogenation of nitro groups with rhodium carbonyl than with cobalt carbonyl.

Hydroformylation of Nitroalkenes with Rhodium Carbonyl. In view of the above results, it may be expected that the hydroformylation of nitroalkenes to nitroaldehydes proceeds without hydrogenating the nitro group below 150°C with rhodium carbonyl. The hydroformylation of nitroalkenes was carried out with tetrarhodium dodecacarbonyl as a catalyst.

The hydroformylation of 4-nitrostyrene in benzene gave (4-nitrophenyl)-propionaldehydes in a 96% yield. By means of PMR study, the (4-nitrophenyl)-propionaldehydes thus produced were found to be a mixture of two isomers, [1] and [2]. The ratio of [1] to [2] was determined to be 7.3. This ratio is somewhat smaller than those of the 2-phenyl-propionaldehyde to the 3-phenyl-propionaldehyde produced by the hydroformylation of

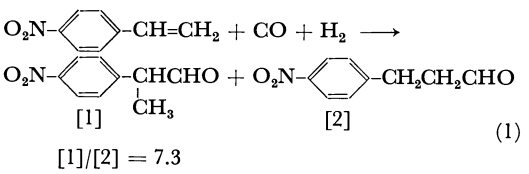

[1]/[2] = 7.3 (1)

styrene, of which ratios are 11.9 at 60°C and 13.8 at 70°C.[4] Thus, the nitro substitution on styrene is observed to induce a change in the isomeric distribution of the products, probably because of the electron-withdrawing effect of the substituent.[5]

The hydroformylation of 3-nitropropene-1 proceeded smoothly at 60°C and gave C_4-nitroaldehydes in a 96% yield. Although the formation of three isomeric aldehydes was anticipated, it was found by

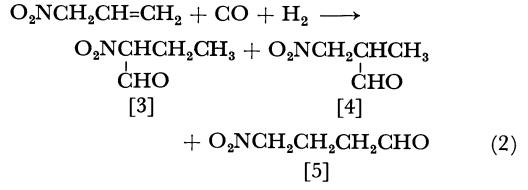

(2)

PMR that 2-methyl-3-nitropropionaldehyde, [4], was the predominant product and that the amounts of the other isomers were very small. On the hydroformylation of propene with rhodium carbonyl at 40°C, the ratio of the isobutyraldehyde to the *n*-butyraldehyde produced is 1.0 to 1.25.[3] There is a great difference in the isomeric distribution of the reaction products between 3-nitropropene-1 and propene. It is clear that a nitro-group on the olefin has a great effect on the isomeric distribution. This effect may be explained in terms of the interaction of the nitro group with rhodium in the intermediate step of the reaction, although further work on the intermediate is required to clarify this interesting observation.

Similarly, when nitroethylene was treated with a mixture of carbon monoxide and hydrogen, no absorption of the gas was observed below 140°C. When this is compared with the reaction of 3-nitropropene-1, it seems reasonable to consider that the inactiveness of nitroethylene to hydroformylation is to be ascribed to the possible deviation of the nature of the carbon-carbon double bond in nitroethylene, which may originate from the conjugation with a nitro group.

Experimental

All the melting points were uncorrected. The PMR spectra were obtained at room temperature on a Varian A-60 spectrometer, using tetramethylsilane as an internal standard. The IR spectra were recorded on a Perkin Elmer 21 spectrometer. Gas-liquid chromatographic

4) M. Takesada and H. Wakamatsu, to be published.
5) M. Kainosho, M. Takesada and H. Wakamatsu, the 20th Annual Meeting of the Chemical Society of Japan, Tokyo, April, 1967.

analyses were carried out with a Shimadzu GC-2B apparatus.

Materials. The nitrobenzene and nitroethane were obtained commercially and were rectified before use. The nitroethylene[6] and 4-nitrostyrene[7] were prepared in the manner as described in the literature. The 3-nitropropene-1 was synthesized according to the method of Askennasy[8] and was purified by fractional distillation using diphenyl ether as a diluent.

Quantitative Analyses of Aldehydes. The amount of aldehydes produced was determined by the method described previously.[3]

Hydroformylation of Butenes. The reaction and the determination of the ratio of the isomeric aldehydes were carried out in the manner described previously.[3]

Hydrogenation of Nitrobenzene. The hydrogenation was carried out similarly to the hydroformylation of butenes. The quantitative analyses of aniline were carried out by gas-liquid chromatography.

Hydroformylation of 4-Nitrostyrene. A solution (50 m*l*) of 4.7 g of 4-nitrostyrene in benzene, 88 mg of tetrarhodium dodecacarbonyl, and a small amount of hydroquinone were put into an 100 m*l*-autoclave. The mixture was then shaken for 30 min at 60—70°C under the pressure (203 kg/cm²) of an equimolar mixture of carbon monoxide and hydrogen. A part of the reaction mixture (36.6 m*l*) was concentrated to give a crystalline residue. By the fractional distillation of the residue, 3.3 g of [1] was obtained; bp 142.5—144°C/1 mmHg, mp 42—43°C recrystallized from ether (lit,[9] mp 43°C).

Found: C, 59.96; H, 5.19; N, 7.61%. Calcd for $C_9H_9NO_3$: C, 60.32; H, 5.06; N, 7.82%.

IR: 2822, 2722 (CHO), 1724 (C=O), 1519, 1352 (NO_2) cm^{-1}.

PMR (in CCl_4): 8.50 τ (doublet) for CH_3, 6.19 τ (broad quartet) for CH, 2.20 τ (multiplet) for the aromatic protons, 0.20 τ (doublet) for CHO.

The PMR spectra of the reaction mixture were obtained and the ratio of the isomeric aldehydes was calculated according to Eq. 3:

$$[1]/[2] = 4A/C = 4B/3C \quad (3)$$

A : relative intensity of the CH proton in [1], 7.02 τ.
B : relative intensity of the CH_3 protons in [1], 8.92 τ.
C : relative intensity of the CH_2 protons in [2], 7.4—8.2 τ (multiplet).

Hydroformylation of 3-Nitropropene-1. A solution (25 m*l*) of 4.4 g of 3-nitropropene-1 in benzene, 50 mg of tetrarhodium dodecacarbonyl, and a small amount of hydroquinone were put into a 50 m*l*-autoclave and then the mixture was shaken for 20 min at 60°C under the pressure (200 kg/cm²) of an equimolar mixture of carbon monoxide and hydrogen. A part of the reaction mixture (17 m*l*) was concentrated, and the residue was fractionally distilled to give 2.8 g of [4]; bp 74—75.5°C/1 mmHg, $n_D^{21.5}$ 1.4428.

Found: C, 41.19; H, 6.26; N, 12.04%. Calcd for $C_4H_7NO_3$: C, 41.02; H, 6.03; N, 11.96%.

IR: 2846, 2746 (CHO), 1723 (C=O), 1555, 1384 (NO_2) cm^{-1}.

PMR (in benzene): 9.27 τ (doublet) for CH_3, 7.42 τ (multiplet) for CH, 5.92 τ (multiplet) for CH_2, 0.78 τ (singlet) for CHO.

2,4-Dinitrophenylhydrazone: yellow needles, mp 138—139°C recrystallized from ethanol.

Found: C, 40.44; H, 4.46; N, 23.77%. Calcd for $C_{10}H_{11}N_5O_6$: C, 40.40; H, 3.73; N, 23.57%.

The PMR spectrum of the reaction mixture was virtually identical with that of [4].

The encouragement and support of Dr. Toichi Yoshida are gratefully acknowledged. The authors wish also to thank Dr. Asao Nakamura for his helpful discussion of the PMR studies, and Mrs. Keiko Terao and Mr. Nobuyoshi Kitamura for their technical assistance.

6) G. D. Buckly, *J. Chem. Soc.*, **1947**, 1471.
7) R. H. Wiley and R. Smith, "Organic Syntheses," Coll. Vol. IV, p. 731 (1963).
8) P. Askennasy and V. Meyer, *Ber.*, **25**, 1701 (1892).
9) F. Nerdel and H. Winter, *J. Prakt. Chem.*, **12**, 110 (1960).

BULLETIN OF THE CHEMICAL SOCIETY OF JAPAN VOL. 43 2195—2198 (1970)

The Stereoselectivity of the Methylcarbenoid of Zinc in the Reaction with Styrene, Indene, and Naphthalene

Jun NISHIMURA, Junji FURUKAWA and Nariyoshi KAWABATA*1

Department of Synthetic Chemistry, Kyoto University, Kyoto

(Received January 7, 1970)

The stereoselectivity of the methylcarbenoid generated from diethylzinc and ethylidene iodide was investigated in the reactions with styrene, indene, and naphthalene. 1-Methyl-2-phenylcyclopropanes (*cis*/*trans*=4.1) were obtained from styrene in a 13% yield. Indene gave exclusively the *endo*-isomer of 6-methyl-2,3-benzobicyclo[3.1.0]hex-2-ene in a 28% yield. From naphthalene, three isomers of 5,8-dimethyl-2,3-benzotricyclo[5.1.0.$0^{4,6}$]oct-2-ene were obtained favorably to the *syn*-form, as in the cases with styrene and indene, but two isomers of 7-methyl-2,3-benzobicyclo[4.1.0]-hepta-2,4-diene were formed favorably to the *anti*-form. This *anti*-selectivity was explained by the step-by-step addition mechanism which had previously been proposed for the ring-expansion reaction of alkylbenzene by the methylcarbenoid.

The stereoselectivity of unsymmetrically-substituted carbenes and carbenoids in the reaction with olefins is an interesting problem. Alkyl-,[1] phenyl-,[2] halo-,[3] phenylthio-,[4] and phenylselenocarbenes[5] and their carbenoids generally exhibit *syn*-selectivity.*2 On the other hand, alkoxy-,[6] phenoxy-,[7] carboalkoxy-,[8] and trimethylsilylcarbenes[9] and their carbenoids show *anti*-selectivity. The present authors have previously reported that the methylcarbenoid of zinc generated from diethylzinc and ethylidene iodide generally exhibits *syn*-selectivity.[1e] In general, a delicate balance of steric and electrostatic interactions among the substituents of olefins and of carbenoids in a three-centered transition state determines the stereoselectivity of the cycloaddition.[2c,d,3a,c,e]

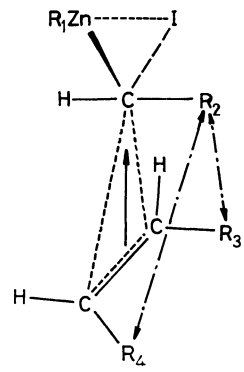

*1 Present address: Department of Chemistry, Kyoto Institute of Technology, Matsugasaki, Kyoto.

1) a) H. M. Frey, *J. Chem. Soc.*, **1962**, 2293; b) T. J. Katz and P. J. Garratt, *J. Amer. Chem. Soc.*, **86**, 4876 (1964); c) H. E. Simmons, E. P. Blanchard and R. D. Smith, *ibid.*, **86**, 1347 (1964); d) G. Wittig and M. Jautelat, *Ann.*, **702**, 24 (1967); e) J. Nishimura, N. Kawabata and J. Furukawa, *Tetrahedron*, **25**, 2647 (1969).

2) a) G. L. Closs and L. E. Closs, *Tetrahedron Lett.*, **1960**, 26; b) U. Schöllkopf and M. Eisert, *Ann.*, **664**, 76 (1963); c) G. L. Closs and R. A. Moss, *J. Amer. Chem. Soc.*, **86**, 4042 (1964); d) R. A. Moss, *J. Org. Chem.*, **30**, 3261 (1965); e) J. Furukawa, N. Kawabata and J. Nishimura, *Tetrahedron Lett.*, **1968**, 3495; f) S. H. Goh, L. E. Closs and G. L. Closs, *J. Org. Chem.*, **34**, 25 (1969);g) J. Furukawa, N. Kawabata and T. Fujita, *Tetrahedron*, **26**, 243 (1970).

3) a) G. L. Closs and J. J. Coyle, *J. Amer. Chem. Soc.*, **87**, 4270 (1965); b) D. Seyferth, H. D. Simmons, Jr., and G. Singh, *J. Organometal. Chem.*, **3**, 337 (1965); c) R. A. Moss and R. Gestle, *Tetrahedron*, **23**, 2549 (1967). d) M. Schlosser and G. Heinz, *Angew. Chem.*, **80**, 849 (1968); e) C. W. Jefford and W. Wojnarowski, *Tetrahedron Lett.*, **1968**, 193.

4) a) U. Schöllkopf and G. J. Lehmann, *ibid.*, **1962**, 165; b) U. Schöllkopf, G. J. Lehmann, J. Paust and H.-D. Härtl, *Chem. Ber.*, **97**, 1527 (1964).

5) U. Schöllkopf and H. Küppers, *Tetrahedron Lett.*, **1963**, 105.

*2 The terms *syn*- and *anti*-selectivity are used in the sense defined by Moss.[2d]

6) a) U. Schöllkopf and A. Lerch, *Angew. Chem.*, **73**, 27 (1961); b) U. Schöllkopf, A. Lerch and W. Pitteroff, *Tetrahedron Lett.*, **1962**, 241; c) U. Schöllkopf and J. Paust, *Angew. Chem.*, **75**, 670 (1963); d) U. Schöllkopf and W. Pitteroff, *Chem. Ber.*, **97**, 636 (1964); e) U. Schöllkopf, J. Paust, A. Al-Azrak and H. Schumacher, *ibid.*, **99**, 3391 (1966).

7) U. Schöllkopf, A. Lerch and J. Paust, *ibid.*, **96**, 2266 (1963).

8) a) R. R. Sauers, S. B. Schlosberg and P. E. Pfeffer, *J. Org. Chem.*, **33**, 2175 (1968); b) W. R. Moser, *J. Amer. Chem. Soc.*, **91**, 1135, 1141 (1969).

9) D. Seyferth, A. W. Dow, H. Menzel and T. C. Flood, *J. Amer. Chem. Soc.*, **90**, 1080 (1968).

TABLE 1. RESULTS[a)]

Aromatic compound	Product	Yield[b)] (%)	Isomer ratio	Bp (°C/mmHg)	n_D^{25}	Anal. Calcd (Found) C; H
Styrene	*cis*- and *trans*-1-Methyl-2-phenylcyclopropane[c)]	13	4.1 : 1	64/16	1.5200	90.85 (90.86); 9.15 (9.24)
Indene	*endo*-6-Methyl-2,3-benzobicyclo[3.1.0]-hex-2-ene	28	——	62/3	1.5465	91.61 (92.30); 8.39 (8.47)
Naphthalene	*endo*- and *exo*-7-Methyl-2,3-benzobicyclo[4.1.0]hepta-2,4-diene	14	1 : 3.5	99—100/10	1.5876	92.26 (92.52); 7.74 (7.85)
	exo, exo-, *exo, endo*- and *endo, endo*-5,8-Dimethyl-2,3-benzotricyclo[5.1.0.$0^{4,6}$]-oct-2-ene	7	1 : 9.6 : 3.9	110—112/11	1.5554	91.25 (91.51); 8.75 (8.73)

a) Reaction condition: Aromatic compound (0.20 mol), Et_2Zn (0.25 mol) and CH_3CHI_2 (0.40 mol) in *n*-
b) Based on the aromatic compound.
c) Simmons and Smith (*J. Amer. Chem. Soc.*, **81**, 4256 (1959)) reported bp 78—79°C/20 mmHg and n_D^{25}

A highly polarizable group attached to olefin is expected to increase the *syn*-selectivity of the cycloaddition. In order to examine this effect, the reactions of the methylcarbenoid with styrene, indene and naphthalene were investigated. The results are summarized in Table 1.

The reaction of styrene with twice as much of the methylcarbenoid in *n*-heptane at 80°C for 10 hours yielded a 4.1 : 1 mixture of *cis*- and *trans*-1-methyl-2-phenylcyclopropane. The *syn*-selectivity of the methylcarbenoid is higher in this reaction than in that with cyclohexene.*3

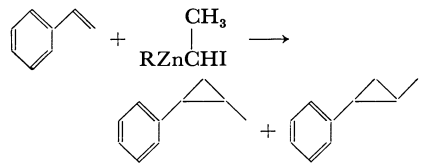

(1)

1 **2**

The structures were determined from the PMR spectra on the basis of the facts that the *cis*-methyl protons are more shielded than the *trans*-methyl protons by the anisotropy of the benzene ring[2b)] and that the absorption of the aromatic protons of the *trans*-isomer*4 becomes broader than that of the *cis*-isomer due to the shielding of an *ortho*-proton by the cyclopropane ring in a preferred conformation of the *trans*-isomer.[10)] The difference in the chemical shift between *cis*- and *trans*-methyl protons is observed to be 0.40 Hz. The aromatic proton resonances of the *cis*-isomer form a narrow band with a half-width of 1.8 Hz centered at τ 2.89. The *trans*-isomer exhibits broad highly split aromatic proton resonances extending from τ 2.7 to 3.3.

The reaction of the methylcarbenoid with indene yielded exclusively the *endo*-isomer of 6-methyl-2,3-benzobicyclo[3.1.0]hex-2-ene (**3**)

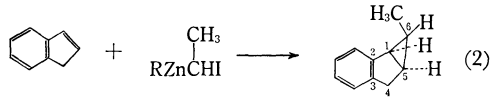

(2)

3

The PMR absorption due to the methyl protons appeared as a doublet (J=6.0 Hz) at τ 9.43. This chemical shift is higher than those of methyl groups in 1-methyl-2-phenylcyclopropanes, which appear at τ 8.8—9.2. The result can be explained by the fixing of the methyl group in the shielding region of the anisotropy by the benzene ring. The absorption due to H_1 appeared at τ 7.60 as a triplet (J=7.0 Hz). This result indicates that H_1 couples with two equivalent protons, *i.e.*, H_5 and H_6 are placed in the *cis* position with respect to H_1. These PMR findings show that the product is the *endo*-isomer.

The reactions of the methylcarbenoid with styrene and indene gave methylcyclopropanes more favorably to the *syn*-form than that with cyclohexene.*3 This result may be attributable to the large electrostatic interaction between the highly-polarizable phenyl group of olefin and the methyl group of the carbenoid. The highly *syn*-selective formation of 6-methyl-2,3-benzobicyclo[3.1.0]hex-2-ene from indene may be explained by a steric effect. The

*3 The reaction of cyclohexene with methylcarbenoid gave a 1.5 : 1 mixture of *endo*- and *exo*-7-methylnorcarane.[1e)]

*4 The structural assignment of the *trans*-isomer was also made by comparing its IR spectrum with that of the authentic sample, which was prepared in a *ca.* 50% yield by the reaction of *trans*-1-phenylpropene with diethylzinc and methylene iodide.[11)]

10) a) G.L. Closs and H.B. Klinger, *J. Amer. Chem. Soc.*, **87**, 3265 (1965); b) F. R. Jensen and D. B. Patterson, *Tetrahedron Lett.*, **1966**, 3837.

11) J. Furukawa, N. Kawabata and J. Nishimura, *Tetrahedron*, **24**, 53 (1968).

	IR ν_{max} (cm^{-1})	M^+ m/e
(*cis*)	1604 (m), 1393 (w), 1028 (m), 694 (s)	132
(*trans*)	1606 (m), 1380 (w), 1027 (m), 742 (s), 694 (s)	
	1608 (w), 1393 (w), 1021 (m), 755 (s), 717 (s)	144
	1490 (m), 1456 (m), 1383 (w), 1038 (m), 771 (s)	156
	1493 (s), 1455 (s), 1383 (m), 1022 (m), 751 (vs)	184

heptane (100 ml) at 80°C for 10 hr.

1.5204 for *cis*, *trans*-mixture.

steric interaction between the phenyl group of indene and the methyl group of carbenoid would be less than in the case of the reaction with styrene, and a strong electrostatic interaction between the phenyl group of indene and the methyl group of carbenoid

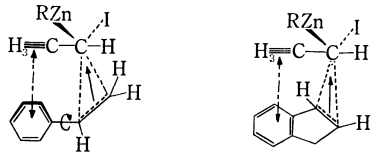

can be expected at a sufficiently close range.

A high *syn*-selectivity of the methylcarbenoid in the reaction with naphthalene, as with indene, would be expected if the reactions proceeded in a concerted mechanism similar to that proposed for the Simmons-Smith reaction.[12] 7-Methyl-2,3-benzobicyclo[4.1.0]hepta-2,4-diene and 5,8-dimethyl-2,3-benzotricyclo[5.1.0.$0^{4,6}$]oct-2-ene were obtained by reaction (3).

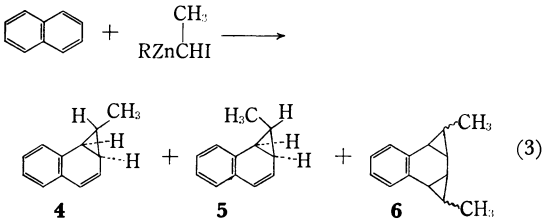

(3)

4 **5** **6**

Three kinds of 5,8-dimethyl-2,3-benzotricyclo-[5.1.0.$0^{4,6}$]oct-2-ene (**6**) were isolated, and their structures were determined to be *exo,exo-*, *exo,endo-*, and *endo,endo*-dimethyl isomers by comparing the PMR absorption of methyl groups.*5 The ratio of these isomers is given in Table 1. The ratio of the *syn*-methyl group to the *anti*-methyl group in these di-adducts (**6**) was calculated from the isomer ratios to be 1.9. This result indicates the *syn*-selective addition of methylcarbenoid to the mono-adducts (**4** and **5**). On the other hand, the mono-adducts (**4** and **5**) were not separated by glpc, although the two kinds of methyl groups were observed in the PMR spectrum (Fig. 1).*6

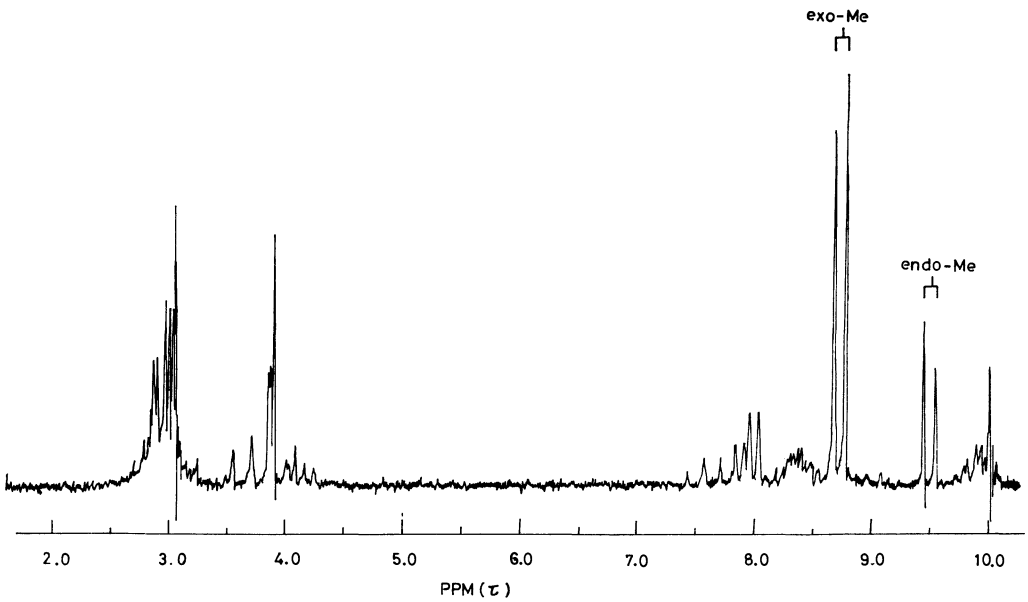

Fig. 1. The PMR spectrum of 7-methyl-2,3-benzobicyclo[4.1.0]hepta-2,4-diene (**4** and **5**).

12) a) H. E. Simmons and R. D. Smith, *J. Amer. Chem. Soc.*, **81**, 4256 (1959); b) G. Wittig and F. Wingler, *Chem. Ber.*, **97**, 2146 (1964).

*5 See Experimental Section.

*6 The spectrum is similar to that of 2,3-benzonorcaradiene-2,4-carboxylic acid reported by Huisgen *et al.* (*Chem. Ber.*, **94**, 2332 (1961)).

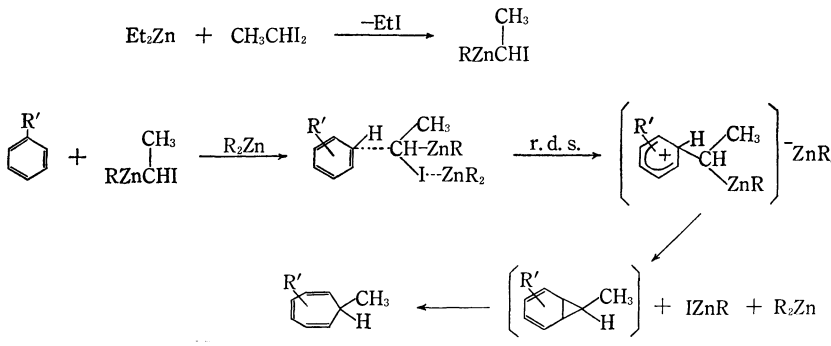

Scheme 1

One doublet peak (J=6.0 Hz), at τ 9.50, was assigned to an *endo*-methyl group, and the other one (J=6.0 Hz), at τ 8.73, to an *exo*-methyl group, by comparison with the chemical shift of the methyl group in compound (**3**). The *exo*-/*endo*-isomer ratio thus determined was 3.5, which suggests the *anti*-selective addition of methylcarbenoid to naphthalene, contrary to the above expectation.*7 This difference in the selectivity of reaction (3) from reactions (1) and (2) suggests that the mechanism of reaction (3) is different from the concerted one which was proposed for the Simmons-Smith reaction.[12] Previously, the present authors have reported that the essential features of the cycloaddition of zinc carbenoid prepared from *gem*-diiodoalkane and diethylzinc to olefin are similar to that of the Simmons-Smith reaction.[11] On the other hand, the present authors have also reported the step-by-step mechanism (Scheme 1) for the ring expansion of alkylbenzenes by methylcarbenoid.[13]

Reaction (3) may proceed by a mechanism similar to that shown in Scheme 1. The *anti*-selectivity in reaction (3) may be due to free rotation around the C_α—C_c bond in a σ-complex (**7**), which may enhance the formation of the thermodynamically more stable *exo*-isomer.*8

In a previous paper, the σ-complex formation step was concluded to determine the rate of the ring expansion.[13] The formation of *endo*- and *exo*-7-methyl-2,3-benzobicyclo[4.1.0]hepta-2,4-diene

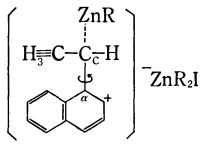

7

in reaction (3) may support the idea of the presence of a transient norcaradiene in the ring expansion reaction.

Experimental

The analyses were performed at the Elemental Analysis Center of Kyoto University. The infrared and mass spectra were recorded on a Hitachi EPI-G spectrophotometer and a Hitachi mass spectrometer, Model RMS-4, respectively. The PMR spectra were taken on a Varian Model A-60, in carbon tetrachloride, using tetramethylsilane as the internal standard. The vapor-phase chromatograms were obtained on a Shimadzu GC-2C gas chromatograph. All the boiling points were uncorrected.

Materials and Procedure. The styrene and the indene were purified by distillation before use. Reagent-grade naphthalene was used without further purification. *n*-Heptane was purified by distillation over sodium metal. The other reagents and procedure are the same as have been described in previous papers.[1e,11]

The reactions with styrene and indene gave higher-boiling materials other than listed in Table 1 in a *ca.* 10% yield. The PMR spectra of the material showed the characteristic absorption for cycloheptatrienes at τ 3—5.

5,8-Dimethyl-2,3-benzotricyclo[5.1.0.0^{4,6}]oct-2-ene (6). The fraction (bp 110—112°C/11 mmHg) of the reaction mixture with naphthalene showed three peaks on glpc analysis conducted under these conditions: 2.25 m of Apiezon-L grease and 3.75 m of Silicone DC 550, 200°C. The ratio was 1 : 9.6 : 3.9, in the order of the retention times. These three isomers were isolated by glpc. The PMR spectra of these isomers showed two kinds of methyl groups. The peaks at τ 9.0—9.1 were assigned to the *endo*-methyl group, and those at τ 8.8—8.9 to the *exo*-one, on the basis of the effect by the anisotropy of the benzene ring. These three isomers were determined to be *exo*,*exo*-, *exo*,*endo*-, and *endo*,*endo*-isomers. The configurations of the tricyclo-ring were not confirmed.

*7 The *anti*-selective formation of the mono-adducts can be concluded even if only the *endo*-isomer (**4**) further reacts with methylcarbenoid to give three kinds of di-adducts, because the ratio of di-adducts to mono-adducts was 1 : 2 (Table 1).

13) J. Nishimura, J. Furukawa and N. Kawabata, The 22nd Annual Meeting of Chemical Society of Japan, Tokyo, 1969.

*8 It is known that *exo*-phenylnorcarane is thermodynamically more stable than the *endo*-isomer.[10b,14]

14) G. L. Closs and J. J. Coyle, *J. Org. Chem.*, **31**, 2759 (1966).

BULLETIN OF THE CHEMICAL SOCIETY OF JAPAN VOL. 43 2199—2204 (1970)

Studies of Peptide Antibiotics. XX. Synthesis of Tyrocidine B[1]

Kenji KUROMIZU and Nobuo IZUMIYA

Laboratory of Biochemistry, Faculty of Science, Kyushu University, Hakozaki, Fukuoka

(Received January 9, 1970)

A cyclic decapeptide, *cyclo*-(L-Trp-D-Phe-L-Asn-L-Gln-L-Tyr-L-Val-L-Orn-L-Leu-D-Phe-L-Pro-) (XVIII), having the amino acid sequence of natural tyrocidine B has been synthesized. *p*-Methoxybenzyloxycarbonyl-Trp-D-Phe-OH was transformed into an acyldipeptide hydroxysuccinimide ester by reagents of hydroxysuccinimide-dicyclohexylcarbodiimide, and the acyldipeptide ester obtained was coupled with a neutral octapeptide. An acyldecapeptide acid thus obtained was subjected to the cyclization reaction. The antibacterial activity of the synthetic product (XVIII) toward Gram positive microorganisms is found to be nearly the same as that of synthetic tyrocidine A, indicating that the L-phenylalanine residue in tyrocidine A can be replaced by L-tryptophan without causing decrease in activity.

In 1940 Hotchkiss and Dubos discovered a basic polypeptide antibiotics named tyrocidine from autolyzed cultures of *Bacillus brevis*.[2] By means of countercurrent distribution,[3] Battersby and Craig showed that the crystalline tyrocidine hydrochloride contained at least three major components, tyrocidine A (TA), B (TB) and C. In 1955 King and Craig isolated a crystalline hydrochloride of TB and determined its amino acid composition.[4] The same authors determined its structure shown as TB in Fig. 1[5] by analyses on partial hydrolyzate with hydrochloric acid.[6]

The synthesis of a linear heptapeptide, Z-Val-Orn(δ-Ts)-Leu-Phe-Pro-Trp-Phe-OMe, related to TB has been described by Zahn and Brandenburg,[7] but the total synthesis of TB has never been accomplished. There are no reports on the quantitative feature of antibacterial activity nor data of measurements such as specific rotation and melting point on the natural TB.

→L-Val-L-Orn-L-Leu-D-Phe-L-Pro—
—L-Tyr-L-Gln-L-Asn-D-Phe-L-X←

Fig. 1. Structures of tyrocidine A (TA) and B (TB).
X represents an amino acid residue such as Phe (TA) and Trp (TB or XVIII).

We reported the syntheses of TA,[8] tyrocidine C,[9] and E,[10] and have been attempting to synthesize other components of the tyrocidine family. This paper will describe the synthesis of the cyclic decapeptide hydrochloride (XVIII·HCl) having the amino acid sequence of TB, and the chemical and biological properties of the synthetic product.

Figure 2 indicates the scheme for the synthesis of the cyclic decapeptide (XVIII). The synthesis of a tripeptide derivative, Z(OMe)-Asn-Gln-Tyr-$NHNH_2$ (VII), was achieved by stepwise elongation from the carboxyl toward the amino end as shown in Fig. 2. The condensation of the azide derived from the tripeptide derivative (VII) with a neutral pentapeptide (XI) gave an acyloctapeptide acid (XII) in 87% yield. Action of trifluoroacetic acid on XII afforded amorphous trifluoroacetate of a neutral octapeptide (XIII) in an almost quantitative yield.

The synthesis of an acyldecapeptide acid (XIV) was achieved as follows. *p*-Methoxybenzyloxycar-

1) This work was presented at the 7th Symposium on Peptide Chemistry at the University of Tokyo, Tokyo, 21 November 1969, and communicated briefly; K. Kuromizu and N. Izumiya, *Experientia*, in press.

2) R. D. Hotchkiss and R. J. Dubos, *J. Biol. Chem.*, **132**, 791 (1940).

3) A. R. Battersby and L. C. Craig, *J. Amer. Chem. Soc.*, **74**, 4019 (1952).

4) T. P. King and L. C. Craig, *ibid.*, **77**, 6624 (1955).

5) Abbreviations; Z. benzyloxycarbonyl; Z(OMe), *p*-methoxybenzyloxycarbonyl; ONp, *p*-nitrophenyl ester; HOSu, *N*-hydroxysuccinimide; DCC, dicyclohexylcarbodiimide; TsOH, *p*-toluenesulfonic acid; CMC, carboxymethylcellulose; DMF, dimethylformamide; DMSO, dimethyl sulfoxide. Amino acid symbols except D-Phe denote the L configuration.

6) T. P. King and L. C. Craig, *J. Amer. Chem. Soc.*, **77**, 6627 (1955).

7) H. Zahn and D. Brandenburg, *Ann.*, **692**, 220 (1966).

8) M. Ohno and N. Izumiya, *J. Amer. Chem. Soc.*, **88**, 376 (1966); M. Ohno, T. Kato, S. Makisumi and N. Izumiya, This Bulletin, **39**, 1738 (1666).

9) K. Kuromizu and N. Izumiya, presented at the 7th Symposium on Peptide Chemistry at the University of Tokyo, 21 November 1969.

10) N. Mitsuyasu and N. Izumiya, *Experientia*, **26**, 476 (1970); N. Mitsuyasu, S. Matsuura, M. Waki, M. Ohno, S. Makisumi and N. Izumiya, This Bulletin, **43**, 1829 (1970).

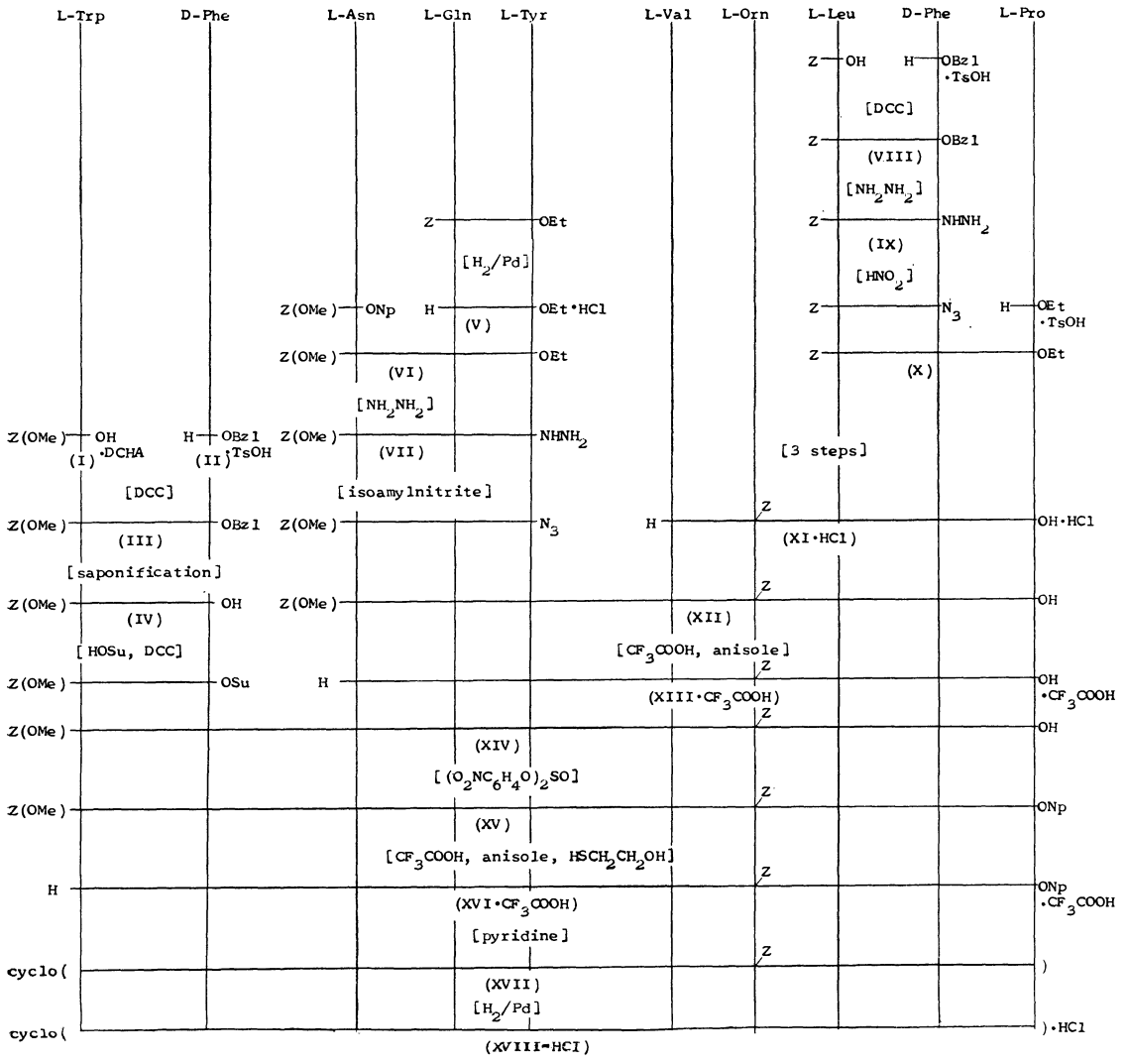

Fig. 2. Synthesis of a cyclic decapeptide hydrochloride (XVIII·HCl).

bonyldipeptide acid (IV) (1.2 equiv.) was treated with HOSu (1.4 equiv.) and DCC (1.1 equiv.). The acyldipeptide active ester, Z(OMe)-Trp-D-Phe-OSu, thus obtained was coupled with the neutral octapeptide (XIII) (1 equiv.) in the presence of triethylamine (1 equiv.) to afford the acyldecapeptide acid (XIV) in 70% yield. It was assumed that no racemization occurred on the D-Phe residue of H-Trp-D-Phe-Asn- sequence in XIV. Weygand *et al.* indicated that no racemization on a C-terminal amino acid residue in an acylpeptide acid was observed when the acylpeptide acid was treated with HOSu and DCC and subsequently the acylpeptide hydroxysuccinimide ester was coupled with an amine component.[11] Several investigators recognized also that the procedure with reagents of HOSu-DCC safely avoided racemization.[12,13] Furthermore, it was observed that the use of HOSu-DCC under the same conditions for preparation of acyldecapeptide acid (XIV) caused no racemization by an assay method using an amino acid analyzer.[13]

The protected cyclic decapeptide (XVII) was prepared as follows. Acyldecapeptide acid (XIV) was transformed to an acyldecapeptide *p*-nitrophenyl ester (XV), and its *p*-methoxybenzyloxycarbonyl group was removed by the action of trifluoroacetic acid. The cyclization reaction of the

11) F. Weygand, D. Hoffmann and E. Wünsch, *Z. Naturforsch.*, *B*, **21**, 426 (1966).

12) J. E. Zimmerman and G. W. Anderson, *J. Amer. Chem. Soc.*, **89**, 7151 (1967); G. S. Omenn and C. B. Anfinsen, *ibid.*, **90**, 657 (1968); R. Geiger, G. Jäger, W. König and A. Volk, *Z. Naturforsch.*, *B*, **24**, 999 (1969).

13) N. Izumiya and M. Muraoka, *J. Amer. Chem. Soc.*, **91**, 2391 (1969).

Table I. Inhibitory activity of the compounds on microorganisms
Minimum inhibitory concentration, $\mu g/ml$

	Staphylococcus aureus	*Bacillus subtilis*	*Escherichia coli*	*Proteus vulgaris*	*Salmonella paratyphi*	*Pseudomonas aeruginosa*	*Shigella sonnea*	*Candida albicans*
XVIII	>100	3.13	100	>100	>100	>100	>100	>100
TA	>100	3.13	100	>100	>100	>100	>100	12.5
GS	1.56	0.78	25	>100	50	50	12.5	3.13

decapeptide ester (XVI) gave a benzyloxycarbonyl-substituted cyclic decapeptide (XVII); its yield was 43% from XIV. The molecular weight determination demonstrated that the molecular size of XVII corresponded to that of cyclic decapeptide.

The hydrogenation of XVII in the presence of an equivalent amount of hydrogen chloride in methanol afforded the crystalline cyclic decapeptide hydrochloride (XVIII·HCl) in 78% yield. The homogeneity of XVIII was confirmed by elemental analysis, chromatography using several different methods (Figs. 5 and 6) and amino acid analysis. The antibacterial activities of XVIII toward several microorganisms are listed in Table 1. It was found that the degree of the activities of XVIII toward the Gram positive microorganisms was nearly the same as that of TA, indicating that the L-Phe residue in a TA molecule can be replaced with the L-Trp without seriously influencing the activity.

Experimental

Melting points were uncorrected. The optical rotations were determined with a Yanagimoto Photometric Polarimeter, OR-20 type. Thin layer chromatography was performed on Merck silica gel G with the following solvent systems: R_f^1, *n*-butanol - acetic acid - pyridine - water 4 : 1 :1 : 2 v/v; R_f^2, chloroform - methanol 5 : 1 v/v. Paper chromatography was performed on Toyo Roshi No. 52 with the following solvent systems: R_f^{I}, *n*-butanol - acetic acid - pyridine - water 4 : 1 : 1 : 2 v/v; R_f^{II}, *n*-butanol - formic acid - water 15 : 3 : 2 v/v. Spots of materials possessing free amino groups on a thin layer plate were detected by spraying ninhydrin, and those of the amino group-blocked materials, by spraying 47% hydrobromic acid and then ninhydrin. Prior to analysis, the compounds were dried over phosphorus pentoxide at 60°C and 2 mmHg to a constant weight unless otherwise described.

Z(OMe)-Trp-OH·DCHA (I). To a chilled solution of L-tryptophan (10.2 g, 50 mmol) and 2N sodium hydroxide (25 m*l*) were added *p*-methoxybenzyloxycarbonyl chloride in ether[14] (15 m*l*, 60 mmol) and 2N sodium hydroxide (30 m*l*) portionwise at −5°C. After 2 hr, the reaction mixture was extracted with ether and acidified with 0.5M citric acid solution at 0°C. The oily material formed was extracted with ethyl acetate. The organic layer was washed with water, dried over sodium sulfate and evaporated *in vacuo*. The residual oil was dissolved in ether (200 m*l*) and dicyclohexylamine (9.98 ml, 50 mmol) was added. The resulting crystals were collected by filtration, and recrystallized from ethanol - ethyl acetate - ether; yield, 19.6 g (71%); mp 151—152°C; $[\alpha]_D^{20}$ +11.5° (*c* 1, methanol); R_f^2 0.54.

Found: C, 69.55; H, 7.83; N, 7.59%. Calcd for $C_{20}H_{20}O_5N_2 \cdot C_{12}H_{23}N$: C, 69.91; H, 7.88; N, 7.64%.

H-D-Phe-OBzl·TsOH (II). A mixture of D-phenylalanine (16.5 g), *p*-toluenesulfonic acid monohydrate (20.9 g), benzyl alcohol (50 m*l*) and benzene (100 m*l*) was heated following the general procedure by Izumiya and Makisumi.[15] Yield, 36.8 g (86%); mp 166—167°C; $[\alpha]_D^{20}$ +7.5° (*c* 2, DMF) (Found: C, 64.53; H, 5.80; N, 3.26%). Reported values for the L-isomer; mp 165°C[16] and 170.5—171.5°C;[17] $[\alpha]_D$ +7.2° (DMF)[16,18] and −7.2° (methanol).[17]

Z(OMe)-Trp-D-Phe-OBzl (III). To a solution of I (2.75 g, 5 mmol) and II (2.14 g, 5 mmol) in chloroform (20 m*l*) was added DCC (1.04 g, 5 mmol) at 0°C. After being stirred for 3 hr at 0°C, the reaction mixture was left to stand overnight at room temperature. The mixture was then evaporated *in vacuo*, and ethyl acetate was added to the residue. The filtrate from dicyclohexylurea was washed successively with 10% citric acid, 4% sodium bicarbonate solution and water, and then dried over sodium sulfate. The filtrate was evaporated *in vacuo* and the residue was crystallized by the addition of ether. It was recrystallized from ethyl acetate - ether - petroleum ether; yield, 2.49 g (82%); mp 137—139°C; $[\alpha]_D^{20}$ +3.6° (*c* 0.5, methanol); R_f^1 0.92, R_f^2 0.80.

Found: C, 71.47; H, 5.96; N, 6.85%. Calcd for $C_{36}H_{35}O_6N_3$: C, 71.38; H, 5.83; N, 6.93%.

Z(OMe)-Trp-D-Phe-OH (IV). To a solution of III (1.66 g, 2.75 mmol) in methanol (5 m*l*) and dioxane (8 m*l*) was added N sodium hydroxide (5.5 m*l*). The solution was allowed to stand for 2 hr at room temperature. After the addition of water (8 m*l*), the solution was acidified with 0.5M citric acid under cooling, and concentrated *in vacuo* to remove organic solvent at 10—15°C. After the addition of water (80 m*l*), the mixture was stored in a refrigerator for several hours and the crystals were collected by filtration. The product was recrystallized from methanol - ether - petroleum ether; yield, 1.14 g (80%); mp 84—86°C; $[\alpha]_D^{20}$ −25.0° (*c* 0.24, methanol); R_f^2 0.46.

14) S. Sakakibara, I. Honda, M. Naruse and M. Kanaoka, *Experientia*, **25**, 576 (1969).

15) N. Izumiya and S. Makisumi, *Nippon Kagaku Zasshi*, **78**, 1768 (1957).

16) N. Izumiya and S. Makisumi, *ibid.*, **78**, 662 (1957).

17) L. Zervas, M. Winitz and J. P. Greenstein, *J. Org. Chem.*, **22**, 1515 (1957).

18) We wish to correct the value of the L-isomer as $[\alpha]_D^{13}$ −7.2° (*c* 2, DMF).

Found: C, 65.10; H, 5.75; N, 7.63%. Calcd for $C_{29}H_{29}O_6N_3 \cdot H_2O$: C, 65.27; H, 5.85; N, 7.87%.

H-Gln-Tyr-OEt·HCl (V). A solution of Z-Gln-Tyr-OEt[8] (6.89 g, 14.5 mmol) dissolved in DMF (60 ml) containing N ethanolic hydrogen chloride (16 ml) was hydrogenated in the presence of palladium black. The filtrate from the catalyst was evaporated *in vacuo*, and the residual crystals were collected by filtration with the aid of ether. It was recrystallized from *n*-butanol - ether - petroleum ether; yield, 5.15 g (94%); mp 157—158°C; $[\alpha]_D^{20}$ +22.4° (*c* 1, methanol); R_f^1 0.67.

Found: C, 51.42; H, 6.47; N, 11.01%. Calcd for $C_{16}H_{23}O_5N_3 \cdot HCl$: C, 51.40; H, 6.47; N, 11.24%.

Z(OMe)-Asn-Gln-Tyr-OEt (VI). To a solution of V (4.51 g, 11.3 mmol) dissolved in DMF (20 ml) and triethylamine (1.58 ml) was added Z(OMe)-Asn-ONp[19] (4.17 g, 10 mmol) in DMF (10 ml). After the solution had been stood overnight at room temperature, it was concentrated *in vacuo* and diluted with water (300 ml). The crystalline product deposited was collected by filtration and washed successively with 10% citric acid, 3% sodium bicarbonate solution and water. It was recrystallized from DMF-ether; yield, 3.90 g (63%); mp 213—214°C (decomp.); $[\alpha]_D^{20}$ −5.5° (*c* 1, DMF); R_f^1 0.84.

Found: C, 55.49; H, 6.11; N, 11.02%. Calcd for $C_{29}H_{37}O_{10}N_5 \cdot \frac{1}{2}H_2O$: C, 55.75; H, 6.13; N, 11.21%.

Z(OMe)-Asn-Gln-Tyr-NHNH$_2$ (VII). A solution of VI (3.55 g, 5.8 mmol) and hydrazine hydrate (5.58 ml, 115 mmol) in DMF (30 ml) was allowed to stand at room temperature for 2 days. The solution was then concentrated *in vacuo* in order to remove excess hydrazine, after which water (300 ml) was added to the residual solution; the resulting product was collected by filtration. It was recrystallized from DMF - ether - petroleum ether; yield, 3.3 g (95%); mp 243°C (decomp.); $[\alpha]_D^{20}$ −11.0° (*c* 1, DMSO); R_f^1 0.68.

Found: C, 53.19; H, 6.00; N, 16.50%. Calcd for $C_{27}H_{35}O_9N_7 \cdot 1/2H_2O$: C, 53.10; H, 5.94; N, 16.06%.

Z-Leu-D-Phe-OBzl (VIII). Z-L-Leu-OH·DCHA (8.95 g, 20 mmol) and II (8.55 g, 20 mmol) in chloroform (80 ml) were treated with DCC (4.14 g, 20 mmol) as described for the preparation of III. The product was recrystallized from ethanol - ether; yield, 8.22 g (79%); mp 131°C; R_f^1 0.98, R_f^2 0.78; $[\alpha]_D^{20}$ −2.0° (*c* 0.5, methanol).

Found: C, 71.72; H, 6.95; N, 5.54%. Calcd for $C_{30}H_{34}O_5N_2$: C, 7.69; H, 6.82; N, 5.57%.

Z-Leu-D-Phe-NHNH$_2$ (IX). A solution of VIII (8.25 g, 1.57 mmol) and hydrazine hydrate (15 ml) in DMF (90 ml) was treated as described for the preparation of VII. The product was recrystallized from DMF - ether - petroleum ether; yield, 6.00 g (90%); mp 162—163°C; R_f^2 0.57; $[\alpha]_D^{20}$ +3.4° (*c* 1, DMF) (Found: C, 64.72; H, 7.18; N, 13.29%). Erlanger *et al.* prepared IX from Z-Leu-D-Phe-OMe and hydrazine; mp 166°C.[20]

Z-Leu-D-Phe-Pro-OEt (X). To a solution of IX (5.34 g, 12 mmol) dissolved in a mixture of DMF (5 ml) - acetic acid (50 ml) - N hydrochloric acid (13.2 ml) were added 2N sodium nitrite (6.6 ml) and N hydrochloric acid (13.2 ml) at −5°C. After it had stood for 5 min, cold water (900 ml) was added to the solution. The azide precipitated was collected by filtration and washed with cold 3% sodium bicarbonate solution and water. After it had been dried in a vacuum desiccator, the azide was added to a chilled solution of H-Pro-OEt·TsOH (3.94 g, 12.5 mmol) dissolved in a mixture of triethylamine (1.7 ml, 12.5 mmol) and DMF (50 ml). After it had been stirred for 2 days at 0°C, the solution was evaporated *in vacuo* and the residue was dissolved in ethyl acetate (80 ml). The solution was washed with 2% hydrochloric acid, 3% sodium bicarbonate solution and water, dried over sodium sulfate, and evaporated to dryness; yield of oil, 4.93 g (76%); R_f^2 0.81. This compound was used for the preparation of H-Val-Orn(δ-Z)-Leu-D-Phe-Pro-OH·HCl (XI·HCl) as described in literature.[21]

Z(OMe)-Asn-Gln-Tyr-Val-Orn(δ-Z)-Leu-D-Phe-Pro-OH (XII). To a solution of VII (0.722 g, 1.2 mmol) in a mixture of DMF (5 ml) and DMSO (10 ml) were added N ethanolic hydrogen chloride (2.4 ml) and isoamyl nitrite[22] (0.162 ml, 1.2 mmol) at −5°C. After 5 min, triethylamine (0.336 ml, 2.4 mmol) was added to this solution. To the solution containing the azide was added a mixture of XI·HCl (0.978 g, 1.25 mmol) and triethylamine (0.344 ml, 2.5 mmol) in DMF (8 ml). The reaction mixture was stirred for 3 days at 0°C and evaporated *in vacuo* to a small volume (about 10 ml). After the addition of N ethanolic hydrogen chloride (1.2 ml) and water (150 ml), the percipitate was collected and recrystallized from DMF - ether - petroleum ether; yield, 1.35 g (87%); mp 226—227°C; R_f^1 0.85; $[\alpha]_D^{25}$ −22.2° (*c* 1, DMF).

Found: C, 59.03; H, 6.88; N, 11.67%. Calcd for $C_{65}H_{85}O_{17}N_{11} \cdot 2H_2O$: C, 58.77; H, 6.75; N, 11.60%.

The homogeneity of this product was established further by paper chromatography and paper electrophoresis after hydrogenolysis; R_f^I 0.78 and R_f 0.99× GS.[23]

H-Asn-Gln-Tyr-Val-Orn(δ-Z)-Leu-D-Phe-Pro-OH·CF$_3$-COOH (XIII·CF$_3$COOH). To a mixture of XII (1.55 g, 1.2 mmol) and anisole (1 ml) was added trifluoroacetic acid (8 ml) at −5°C. When swirled, the reaction mixture changed to a clear solution within some 10 min. After 25 min, the solution was evaporated *in vacuo* at 0°C and the oily residue was triturated with ether. The solid formed was collected by filtration and washed with ether; yield, 1.45 g (97%). The homogeneity of this product was confirmed by paper chromatography in which only one spot was detected; R_f^I 0.85. The material was used in the next reaction without further purification.

Z(OMe)-Trp-D-Phe-Asn-Gln-Tyr-Val-Orn(δ-Z)-Leu-D-Phe-Pro-OH (XIV). To a chilled solution of IV (0.805 g, 1.56 mmol) in ethyl acetate (10 ml) were added HOSu (0.207 g, 1.8 mmol) and DCC (0.297 g, 1.44 mmol) at 0°C. After the mixture had been stirred for 3 hr at 0°C, dicyclohexylurea precipitated was

19) E. Schröder and E. Klieger, *Ann.*, **673**, 208 (1964).

20) B. F. Erlanger, H. Sachs and E. Brand, *J. Amer. Chem. Soc.*, **76**, 1806 (1954).

21) M. Waki and N. Izumiya, *ibid.*, **89**, 1278 (1967); This Bulletin, **40**, 1687 (1967).

22) J. Honzl and J. Rudinger, *Collect. Czech. Chem. Commun.*, **26**, 2333 (1961).

23) Paper electrophoresis was carried out for 2.5 hr under the following conditions: solvent, formic acid - acetic acid - methanol - water (1 : 3 : 6 : 10 v/v, pH 1.8); voltage gradient, 20 V/cm.

filtered off and washed with cold ethyl acetate. The filtrate was evaporated to dryness *in vacuo* at 0°C and the residue was dissolved in cold DMF (5 m*l*). To the solution was added a mixture of XIII·CF_3COOH (1.45 g, 1.27 mmol) in DMF (10 m*l*) and triethylamine (0.356 m*l*) at 0°C. After the stirring of the reaction mixture had been continued for 5 hr at 0°C and for additional 2 hr at room temperature, the mixture was concentrated *in vacuo* to a small volume and the residue was treated with 0.5M citric acid (30 m*l*). The product was collected by filtration and recrystallized from DMF-ethyl acetate - ether; yield, 1.35 g (70%); mp 215—216°C (decomp.); $[\alpha]_D^{20}$ +33.1° (*c* 1, DMF); R_f^1 0.79.

Found: C, 61.26; H, 6.42; N, 11.85%. Calcd for $C_{85}H_{104}O_{19}N_{14}\cdot 2H_2O$: C, 61.42; H, 6.55; N, 11.80%.

The homogeneity of this material was further established by paper chromatography and paper electrophoresis after hydrogenolysis, in which only one spot was detected; R_f^I 0.69 and R_f 1.1×GS.[23]

Detection of Possible Racemization in the Coupling by HOSu-DCC Reagents. The conditions (reaction times, temperatures, mole ratios of reagents, and others) for the coupling reaction were the same as described above. Z-Gly-L-Ala-OH (1.2 equiv.) in DMF was transformed to the corresponding hydroxysuccinimide ester with HOSu (1.4 equiv.) and DCC (1.1 equiv.). To the hydroxysuccinimide ester was added H-L-Leu-OBzl (1 equiv.) in DMF. After evaporation, the residue was dissolved in ethyl acetate. The solution was washed with 2% hydrochloric acid and 4% sodium bicarbonate solution, and dried over sodium sulfate. The filtrate was subjected to hydrogenolysis and a part of the hydrogenated material was analyzed by the amino acid analyzer as described previously,[13] the extent of racemization was calculated as less than 0.1%.

Z(OMe)-Trp-D-Phe-Asn-Gln-Tyr-Val-Orn(δ-Z)-Leu-D-Phe-Pro-ONp (XV). To a solution of XIV (1.05 g, 0.65 mmol) dissolved in DMF (5 m*l*) and pyridine (5 m*l*) was added di-*p*-nitrophenyl sulfite (2.10 g, 6.5 mmol). The faintly yellow solution was allowed to stand for 18 hr at room temperature and then evaporated *in vacuo*. The oily residue was triturated several times with a mixture of ether and petroleum ether (1 : 1 v/v). The solid was collected by filtration and washed with a mixture of ether and petroleum ether until the yellow color could not be discerned upon the addition of N sodium hydroxide to the filtrate. The *p*-nitrophenyl ester content of this product (yield, 1.123 g) was estimated to be 105% measuring the optical density at 412 mμ with the solvent of DMF and N sodium hydroxide (1 : 1 v/v).[24] The product was used for the next reaction without further purification.

H-Trp-D-Phe-Asn-Gln-Tyr-Val-Orn(δ-Z)-Leu-D-Phe-Pro-ONp·CF_3COOH (XVI·CF_3COOH). To a mixture of XV (1.12 g), anisole (1.2 m*l*) and 2-mercaptoethanol (0.12 m*l*) was added trifluoroacetic acid (12 m*l*) at −5°C. When swirled, the suspension turned to a clear solution within 10 min. The solution was evaporated *in vacuo* at 0°C and the oily residue was triturated with ether. The solid was collected by filtration and washed with ether (yield, 1.092 g). This was used as such in the next step.

***cyclo*-(Trp-D-Phe-Asn-Gln-Tyr-Val-Orn(δ-Z)-Leu-D-Phe-Pro-) (XVII).** XVI·CF_3COOH (1.092 g) was dissolved in a mixture of DMF (15 m*l*) and acetic acid (0.5 m*l*). The solution was stirred drop by drop into pyridine (200 m*l*) kept at 55—60°C over 5 hr, stirring being continued for additional 3 hr at the same temperature. After the solvent had been removed, the residue was dissolved in 100 m*l* of a mixture of methanol - dioxane - water (1 : 2 : 1 v/v). This solution was passed successively through columns (1.5×12 cm) of Amberlite IRC-50 (H^+ form) and Amberlite IR45 (OH^- form). The columns were washed with the same solvent. The filtrate and washings were combined (total 300 m*l*) and then evaporated to dryness *in vacuo*. The residual product was collected by filtration with the aid of water and recrystallized from DMF-ether; yield, 0.715 g (43% from XIV); mp 198—200°C; $[\alpha]_D^{20}$ −86.9° (*c* 0.5, methanol); R_f^1 0.98, R_f^2 0.62; amino acid ratio in acid hydrolysate, Phe 1.99, Asp 0.98, Glu 1.02, Tyr 0.91, Val 0.97, Orn 1.00, Leu 1.00, Pro 0.99.[25]

Found: C, 61.79; H, 6.58; N, 13.05%; mol wt 1450.[26] Calcd for $C_{76}H_{94}O_{15}N_{14}\cdot 2H_2O$: C, 61.68; H, 6.68; N, 13.25%; mol wt, 1479.

***cyclo*-(Trp-D-Phe-Asn-Gln-Tyr-Val-Orn-Leu-D-Phe-Pro-) Hydrochloride (XVIII·HCl).** A solution of XVII (144 mg, 0.1 mmol) dissolved 0.02N methanolic hydrogen chloride (6 m*l*) was subjected to hydrogenolysis in the presence of palladium black. After 3.5 hr, the filtrate from the catalyst was evaporated to dryness *in vacuo* and ether (4 m*l*) was added to yield crystals (yield, 120 mg). Recrystallization from methanol - ether - petroleum ether gave 111 mg (78%) as the desiccator-dried product (XVIII·HCl·$5H_2O$); mp 236—237° (decomp.); $[\alpha]_D^{20}$ −93.0° (*c* 0.5, methanol).

Found: C, 56.71; H, 6.82; N, 13.62%. Calcd for $C_{68}H_{88}O_{13}N_{14}\cdot HCl\cdot 5H_2O$: C, 56.87; H, 6.95; N, 13.66%.

This desiccator-dried sample lost 6.4% of its weight after being dried for 4 hr at 110°C, 2 mmHg. Calcd for $5H_2O$: 6.3%.

Determination of Homogeneity of XVIII. The homogeneity of the compound XVIII·HCl·$5H_2O$ was ascertained further as follows. Data for TA or gramicidin S dihydrochloride (GS·2HCl) as the reference peptides are also indicated. *(a) TLC.* One spot with the com-

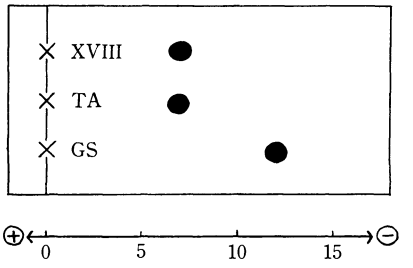

Fig. 3. Paper electrophoreses of XVIII·HCl, TA·HCl and GS·2HCl.

24) R. Schwyzer and P. Sieber, *Helv. Chim. Acta*, **40**, 624 (1957).

25) We are indebted to Mr. K. Noda in this laboratory for the amino acid analysis.

26) The molecular weight was determined on a Hitachi Osmometer, type 115, using methanol as a solvent.

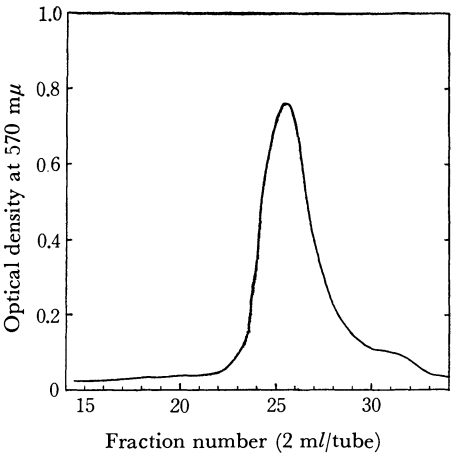

Fig. 4. CMC column chromatography of XVIII·HCl.

pound was detected; R_f^1 0.78 and R_f^2 0.02. That of TA·HCl; R_f^1 0.78 and R_f^2 0.02. *(b) Paper Chromatography.* R_f^{I} 0.98 and R_f^{II} 0.87 for the compound, R_f^{I} 0.98 and R_f^{II} 0.85 for TA·HCl. *(c) Paper Electrophoresis.*[23] The patterns of three compounds are shown in Fig. 3. The mobility of XVIII was found to be nearly the same as that of TA. *(d) CMC Column Chromatography.* A sample (0.5 mg) was dissolved in 0.4 m*l* of 0.2M pyridinium acetate buffer containing methanol (75% v/v, pH 5.0) and the solution was applied to a column (0.9×100 cm) with CMC. The mixture was developed with the same solvent and 2 m*l* fractions were collected at a flow rate of 12 m*l* per hr. The components were determined by the Yemm-Cocking method[27] after alkaline hydrolysis described previously.[8] From the chromatogram shown in Fig. 4, it was confirmed that XVIII was homogeneous. *(e) Amino Acid Analysis.* Amino acid ratios[25] in acid hydrolysate were as follows; Phe 1.86, Asp 1.01, Glu 1.02, Tyr 1.07, Val 0.97, Orn 1.00, Leu 0.97, Pro 0.96 and NH_3 2.20. Molar ratios of Trp and Tyr were determined in conformity with the extinction at 280 mμ and 294.4 mμ in ultraviolet spectrum of XVIII using a solvent of 0.1N soium hydroxide - ethanol (1 : 1 v/v) as in literature;[28] Trp 1.04, Tyr 1.05.

Microbiological Assays. The microorganisms employed are listed in Table 1. The minimum amount of the compounds necessary for the complete inhibition of growth was determined by a dilution method. TA and GS were examined as reference compounds. Table 1 indicates that the degree of the activities of synthetic XVIII toward the Gram positive microorganisms (*Staph. aureus* and *B. subtilis*) was nearly the same as that of TA except a microorganism, *Candida albicans*.

The authors wish to express their thanks to Meiji Seika Co., Ltd. for microbiological assays. The authors also express their thanks to Dr. M. Ohno, Dr. M. Waki and Mr. N. Mitsuyasu of Kyshu University for their helpful discussions and Miss T. Mizukami for her valuable assistance.

27) E. W. Yemm and E. C. Cocking, *Analyst*, **80**, 209 (1955).

28) T. W. Goodwin and R. A. Morton, *Biochem. J.*, **40**, 628 (1946).

BULLETIN OF THE CHEMICAL SOCIETY OF JAPAN VOL. 43 2204—2208 (1970)

On the Study of Various Reductions of 2-Benzoylcyclopentene-1-carboxylic Acid

Katsuo OHKATA and Terukiyo HANAFUSA

Chemistry Department, Faculty of Science, Hiroshima University, Higashisenda-cho, Hiroshima

(Received January 13, 1970)

It was found that the Clemmensen reduction of 2-benzoylcyclopentene-1-carboxylic acid (**2a**) did not give rise to 2-benzylcyclopentene-1-carboxylic acid (**1**), but to a mixture of *cis*- and *trans*-2-benzylcyclopentane-1-carboxylic acid (**6a** and **7a**) contrary to the description in literature. Unsaturated acid (**1**) was obtained as a major product by the Wolff-Kishner-Huang-Minlon reduction of **2a** accompanied with 1-carboxy-6-phenylbicyclo[3.1.0]hexane (**8**). The reduction of **2a** with zinc dust in acetic acid and the reduction of the methyl ester (**2b**) by way of its thioketal were also investigated.

Organic chemists have long been interested in selective reduction of conjugated unsaturated carbonyl compounds. A large number of such selective procedures have been published.[1] Since the preparation of 2-benzylcyclopentene-1-carboxylic acid (**1**) was necessary during the course of the other investigations, various reduction procedures of 2-

1) a) E. L. Martin, "Organic Reactions," Vol. I, ed. by R. Adams, John Wiley & Sons, Inc., New York (1942), p. 155; b) G. R. Pettit and E. E. van Tamelen, *ibid.*, Vol. XII (1962), p. 356; c) D. Todd, *ibid.*, Vol. IV (1948), p. 378.

benzoylcyclopentene-1-carboxylic acid derivatives (**2a** and **2b**) were carried out. It may be interesting to study the reduction of this compound because a double bond is placed between a carbonyl group and a carboxyl group. The results will be described in this paper.

Results and Discussion

In 1950 Sengupta and Saha reported the synthesis of the unsaturated keto-acid (**2a**) by the Friedel-Crafts condensation of cyclopentene-1,2-dicarboxylic acid anhydride (**3**) with benzene.[2] They also reported that the Clemmensen reduction of **2a** gave an oil, bp 170—173°C/4 mmHg, which was assigned as the unsaturated acid (**1**). The assignment was based on further reaction sequence including dehydrogenation step into 2,3-trimethylenenaphthalene (**4**).

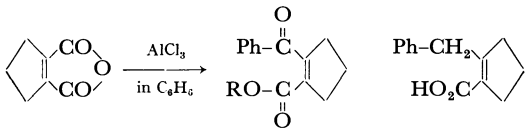

(**3**) (**2a**) R: H (**2b**) CH_3 (**1**)

We repeated the synthesis of unsaturated keto-acid (**2a**) according to Saha's method. The IR and NMR spectra of the product support the above postulated formula. Its reduction with $NaBH_4$ gave a hydroxy-acid (**5**), mp 118—119°C, in high yield. It showed a sharp singlet characteristic for benzylic α-hydrogen at $\tau=3.83$ along with other signals in its NMR spectrum. The results confirmed the presence of a tetrasubstituted double bond adjacent to the benzylic hydroxyl group.

(**4**) (**5**)

The Clemmensen reduction of **2a**[1a] was carried out with zinc amalgam in concentrated hydrochloric acid and toluene for 30 hr. IR and NMR spectra of the product oil, bp 153—154°C/2 mmHg, suggested that the product was not an α,β-unsaturated acid as reported by Sengupta and Saha but a mixture of saturated acids. Thus, the product was transformed to methyl esters with diazomethane. Vapor phase chromatography of the esters revealed that they consisted of two components, the ratio being about 1 : 2. The predominant component was purified by preparative VPC, followed by elemental analysis.

It was shown that the analytical result was consistent not with the calculated value for the unsaturated ester, $C_{13}H_{16}O_2$, but for the saturated ester, $C_{13}H_{18}O_2$. From these data it may be evident that both a carbonyl group and a double bond in the unsaturated keto-acid (**2a**) were reduced in the Clemmensen reduction to give a mixture of *cis*- and *trans*-2-benzylcyclopentane carboxylic acids, **6a** and **7a** respectively.

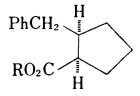

(**6a**) R: H (**6b**) CH_3

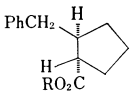

(**7a**) R: H (**7b**) CH_3

Another selective reduction for α,β-unsaturated ketone is desulfurization of its thioketal with excess of Raney-Ni.[1b] Methyl ester (**2b**) of the unsaturated keto-acid was converted into the ethylene thioketal, followed by treatment with large excess of Raney-Ni. Without further purification the oil was subjected to careful VPC analysis. It was then found that the ester was also a mixture of two components identical with the products obtained by the Clemmensen reduction. In this case, however, the ratio of two geometric isomers was reversed, *viz.*, 2 : 1.

The Wolff-Kishner-Huang-Minlon reduction is also a useful procedure for selective reduction of a carbonyl group in an unsaturated ketone.[1c] A number of such examples have been reported.[3] Keto-acid (**2a**) was treated with hydrazine hydrate in concentrated alkaline solution mixed with triethylene glycol, followed by heating the reaction mixture to 220°C for 5 hr. The product thus obtained was a mixture of solids and an oil. The former was readily purified by recrystallization from a mixture of ether and light petroleum as colorless crystals, mp 121—122°C. By its IR spectrum it was suggested that the compound was an α,β-unsaturated acid. In its NMR spectrum, it showed a sharp singlet at $\tau=2.78$ due to five aromatic protons and a characteristic singlet at $\tau=7.53$ for two benzylic protons adjacent to a tetrasubstituted double bond, along with other signals. From these data and elemental analysis the crystalline product was identified as 2-benzyl-1-cyclopentene-1-carboxylic acid (**1**).

This unsaturated acid (**1**) was then hydrogenated in glacial acetic acid using the Adams catalyst to give a saturated acid. Its methyl ester was subjected to VPC analysis proving that the ester thus obtained consisted of mainly one isomer contaminated with a small quantity of the other. Since catalytic hydrogenation should preferentially give rise to *cis* isomer, the main product in this hydro-

2) S. C. Sengupta and N. N. Saha, *Current Sci.* (India), **19**, 381 (1950); S. C. S. Gupta and N. N. Saha, *J. Indian Chem. Soc.*, **29**, 331 (1952).

3) A. Furst, R. C. Berlo and S. Hooton, *Chem. Rev.*, **65**, 51 (1965).

genation experiment could be characterized as *cis*-2-benzylcyclopentane-1-carboxylic acid (**6a**). From a comparison of the chromatogram of this methyl ester with that obtained by the above two other types of reductions, it may be evident that *trans* isomer (**7a**) predominated in the Clemmensen reduction product and that *cis* isomer (**6b**) predominated in desulfurization of thioketal.

The latter oil produced by the Wolff-Kishner-Huang-Minlon reduction was converted into its methyl ester with diazomethane and was purified by preparative VPC. From both the elemental analysis and spectra data of this methyl ester it was suggested that the compound could be characterized as 1-carboxy-6-phenylbicyclo[3.1.0]hexane (**8**). It may be noted in its NMR spectrum that a doublet at $\tau=7.10$ with $J=9$ cps for one proton was assigned to benzylic cyclopropane ring proton and that a multiplet centered at $\tau=9.85$ for one proton to the other cyclopropane ring proton attached to the bridge head.

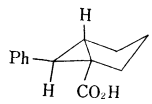

(**8**)

In analogy to the other examples[4] it seems that the intermediate hydrazone (**9**) might partially rearrange to pyrazoline derivatives (**10** and **11**), in which nitrogen molecule would be eliminated by heating the reaction mixture at higher temperature to form cyclopropane ring. Further experiments to establish the structure of **8** have not been performed.

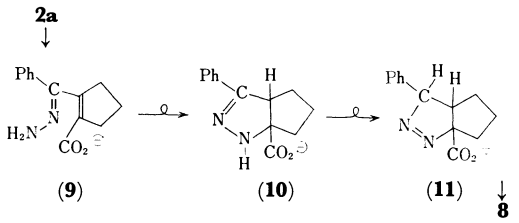

The unsaturated dione in which a double bond is inserted between two carbonyl groups has usually been reduced with zinc dust in glacial acetic acid to give a saturated dione[5] A similar result was observed in the reduction procedure of an unsaturated keto-acid in which a double bond is placed between a carbonyl group and a carboxyl group.[6] Unsaturated keto-acid (**2a**) was treated with zinc dust in glacial acetic acid under reflux for 2 hr. The reaction product, mp 80—82°C, was characterized as 2-benzoylcyclopentane-1-carboxylic acid (**12**) by spectral results and elemental analysis. Since this compound was recovered unchanged from its reaction with aqueous sodium hydroxide solution under reflux, stereochemically, the above product is assumed to be a thermodynamically more stable *trans* isomer.

All the results in the various reductions of substrates (**2a** and **2b**) are summarized in the following chart.

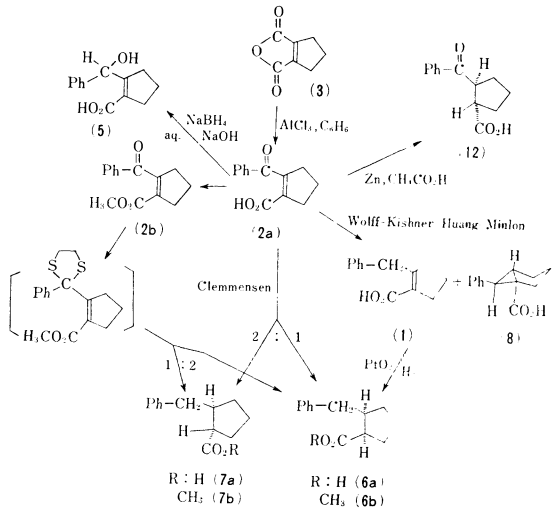

Experimental

2-Benzoylcyclopentene-1-carboxylic Acid (2a). A 200 m*l* three-necked round-bottomed flask was fitted with a mechanical stirrer, a 50 m*l* dropping funnel, a thermometer and a reflux condenser protected from the moisture in the air by means of a calcium chloride tube and also connected with a gas trap for disposing of evolved hydrogen chloride. In the flask was placed 28 g of anhydrous aluminum chloride and 40 m*l* of dry benzene. Ten and a half g of 1-cyclopentene-1,2-dicarboxylic acid anhydride (**3**)[2] was added dropwise into the flask immersed in an ice-water bath at such a rate that addition was complete in about a half hour. The reaction mixture was stirred at 0—5°C for 3 hr, at room temperature for 10 hr and then at 40—50°C for 2 hr. Cooling the resulting reaction mixture to room temperature, the mixture was poured slowly into a mixture of 100 g of ice and 50 m*l* of 6N hydrochloric acid with stirring. The light brown precipitate was separated, collected on a Buchner funnel and washed with two portions each of 10 m*l* of benzene and of 20 m*l* of water. After drying the precipitate was dissolved in a 100 m*l* of 10% sodium carbonate solution at 50°C. The solution was filtered and the filtrate was acidified with 6N hydrochloric acid. The precipitate thus formed was filtered and then washed with two portions of 20 m*l* of warm water. The final product was recrystallized from a mixed solvent of methanol and benzene. Fourteen grams of 2-benzoylcyclopentene-1-carboxylic acid (**2a**),

4) N. Kishner and A. Zavadovsky, *J. Russ. Phys. Chem. Soc.*, **43**, 1132 (1911); Y. R. Naves, *Helv. Chim. Acta*, **25**, 744 (1942); D. Davidson and J. Feldman, *J. Amer. Chem. Soc.*, **66**, 488 (1944).

5) L. F. Fieser and M. Fieser, "Reagents in Organic Synthesis," John Wiley & Sons, Inc., New York (1967), p. 1276.

6) E. Kyburz, M. V. Mijovic, W. Voser, H. Heusser, O. Jeger and L. Ruzicka, *Helv. Chim. Acta*, **35**, 2073 (1952).

mp 184—185°C (lit,[2] 181—182°C), was obtained in 85% yield. IR (Nujol), 1680, 1660, 1650 and 720 cm^{-1}; NMR ($CDCl_3$), τ, 7.6—7.8 (m, 2H, $-CH_2-$), 7.21 (t, J=7 Hz, 4H, $-CH_2-C=C$), 2.0—2.6 (m, 5H, C_6H_5), 1.56 (s, 1H, CO_2H).

The Reduction of 2a with Sodium Borohydride. Into 20 m*l* of 5% aqueous sodium hydroxide solution which contained 5 g of **2a** was added 1.9 g of $NaBH_4$ dissolved in 20 m*l* of water, then the mixture was heated at 65°C for 30 min. Twenty m*l* of aqueous sodium hydroxide solution was added and the reaction solution was heated under reflux for 1 hr. After cooling the solution was acidified with dilute hydrochloric acid to pH 3. Crude 2-(α-hydroxybenzyl)-cyclopentene-1-carboxylic acid (**5**), mp 116—119°C, was obtained in 89% yield (4.5 g). Its recrystallization from benzene gave pure sample, mp 118—119°C. IR (Nujol), 3270, 1660, 730 and 690 cm^{-1}; NMR ($CDCl_3$), τ 7.9—8.5 (m, 2H, $-CH_2-$), 7.0—7.7 (d. t, J=7 Hz, 4H, $-CH_2-C=C$), 4.83 (s, 1H, CH–O–), 2.3—2.7 (m, 7H, C_6H_5, OH, CO_2H).

Found: C, 71.54; H, 6.47%. Calcd for $C_{13}H_{14}O_3$: C, 71.59; H, 6.66%.

Clemmensen Reduction of 2a. Amalgamated zinc was prepared by shaking a mixture consisting of 32.6 g of mossy zinc, 3.2 g of mercuric chloride, 50 m*l* of water and 1.5 m*l* of concentrated hydrochloric acid for 3 min. On decanting the mixture, the following reagents were added in turn into the flask: 10 m*l* of water, 50 m*l* of concentrated hydrochloric acid, 15 m*l* of toluene and 10.8 g of **2a**. The reaction mixture was boiled with vigorous stirring for 30 hr. Three 10 m*l* portions of concentrated hydrochloric acid were added at approximately 6 hr intervals during the reaction. After cooling, the aqueous layer was diluted with 200 m*l* of water and extracted with three 20 m*l* portions of ether. The organic layer was washed with water and dried over anhydrous sodium sulfate. The solvent was removed, then 7.6 g of oily product was obtained by distillation, bp 153—156°C/12 mmHg, in 75% yield. IR (neat), 1690, 750 and 710 cm^{-1}; NMR (CCl_4), τ 7.8—8.9 (m, 6H, $-CH_2-$), 7.0—7.8 (m, 4H, $-CH_2Ph$, –CH–), 2.90 (s, 5H, C_6H_5), −1.65 (s, 1H, CO_2H). Its methyl ester was prepared with diazomethane. It was found by VPC analysis that the ester consisted of two components: retention time, 9.2 and 10.0 min; column, SE 30, 1 m, oven temp, 155°C, carrier gas flow rate, N_2, 40 m*l*/min, area ratio, 2 : 1 respectively. The major product was purified by preparative VPC.

Found: C, 77.08; H, 8.23%. Calcd for $C_{14}H_{18}O_2$: C, 77.03; H, 8.31%.

Reduction of 2b by Way of Its Thioketal. 212 mg of crude methyl 2-benzoylcyclopentane-1-carboxylate (**2b**) prepared from **2a** and diazomethane, and, 310 mg of ethanedithiol were dissolved in 10 m*l* of chloroform, then dry hydrogen chloride was passed into the solution under cooling with ice water over a period of 9 hr. The resulting solution was washed with water, 5% aqueous sodium carbonate solution and water again. Organic layer was dried over anhydrous sodium sulfate. Removing the solvent under reduced pressure, 180 mg of thioketal was obtained. The substance was heated with 3 g of Raney-Ni in 4 m*l* absolute ethanol under reflux for 30 hr. After the reaction mixture was filtered and the solvent was removed under reduced pressure, 91 mg of the crude product was obtained. It was confirmed from VPC analysis that the product was a mixture of two components identical with the Clemmensen reduction product, but their ratio was reversed, namely 1 : 2. In the preparation of the above thioketal, anhydrous zinc chloride could be used instead of dry hydrogen chloride.

Wolff-Kishner-Huang-Minlon Reduction of 2a. A 100 m*l* three-necked round-bottomed flask was fitted with a thermometer and a take-off condenser equipped with a stopcock which might be opened to permit distillation. In the flask were placed 60 m*l* of triethylene glycol and 7.0 g of potassium hydroxide. The mixture was carefully heated with swirling under nitrogen in an oil bath until potassium hydroxide was dissolved. Then 10.8 g of powdered acid (**1a**) was dissolved into the solution under nitrogen atmosphere at 100°C. Further 7.6 m*l* of 80% hydrazine hydrate was added at 80°C and the mixture was heated at 100—120°C for 1 hr. After distilled water was removed from the take-off condenser, the flask was rapidly heated until reflux began. Boiling was continued for 5 hr. The reaction mixture was poured into 50 m*l* of water after cooling, then filtered off. The filtrate was washed with two portions of 20 m*l* of ligroin and acidified with 6N hydrochloric acid. The acidified mixture was extracted with three 30 m*l* of ligroin. The combined organic layer was washed with two portions of 20 m*l* of water and dried over anhydrous sodium sulfate. After most of the solvent was removed under reduced pressure, 5 m*l* of light petroleum was added to the residue. After it had been stood in a refrigerator, solids were precipitated. Collected colorless solids weighed 5.1 g and melted between 90 and 95°C. It was recrystallized repeatedly from the mixed solvent of ether and light petroleum to give a pure sample, mp 121—122°C, which was assigned as 2-benzylcyclopentene-1-carboxylic acid (**1**) from its spectral and analytical results. IR (Nujol), 1670, 740 and 700 cm^{-1}; NMR (CCl_4), τ 7.7—8.6 (m, 6H, $-CH_2-$), 7.53 (s, 2H, $-CH_2Ph$), 2.78 (s, 5H, C_6H_5), 0.05 (s, 1H, CO_2H).

Found: C, 77.36; H, 7.12%. Calcd for $C_{13}H_{14}O_2$: C, 77.20; H, 6.98%.

The crude oily product was treated with diazomethane to give a mixture of methyl esters, which was found by VPC analysis to consist of two components. The methyl ester other than the ester of **1** was purified by preparative VPC. IR (neat), 1720, 1270, 760 and 700 cm^{-1}; NMR (CCl_4), τ 9.58—10.15 (m, 1H, bridge head H), 7.55—9.00 (m, 6H, $-CH_2-$), 7.10 (d, J=8 Hz, 1H, CH–Ph), 6.38 (s, 3H, CH_3), 2.83 (s, 5H, C_6H_5).

Found: C, 77.64; H, 7.57%. Calcd for $C_{14}H_{16}O_2$: C, 77.75; H, 7.46%.

Catalytic Hydrogenation of 1. A mixture of 103 mg of 2-benzylcyclopentene-1-carboxylic acid (**1**) dissolved in 10 m*l* of glacial acetic acid and 26 mg of Adams catalyst was shaken under hydrogen atmosphere at 20°C. Eighteen m*l* of hydrogen was absorbed. After the catalyst was filtered, the solvent was removed under reduced pressure. The residue was treated with diazomethane in ether to give its methyl ester. The identity of this ester with that of minor product in the Clemmesen reduction was confirmed by VPC analysis described below.

Vapor Phase Chromatography of the Above Four Methyl Esters. The compounds, **6b**, **7b** and methylesters of **1** and **8**, were clearly separated by

VPC, using a 2 m column packed with Carbowax 20 M coated on Celite 545 in an oven heated at 225°C with a flow rate of carrier gas 40 ml/min. Under these conditions the retention times of **6b**, **7b**, **1**-Me and **8**-Me were 7.2, 6.5, 7.8 and 8.2 min respectively.

Reduction of 2a with Zinc Dust and Glacial Acetic Acid. Into a solution of 400 mg of 2-benzoylcyclopentene-1-carboxylic acid (**2a**) dissolved in 20 ml of glacial acetic acid was added 1.6 g of zinc dust. The mixture was heated under reflux with stirring for 2 hr. After cooling the miture was filtered and zinc dust washed with small portions of acetic acid. The solvent was removed under reduced pressure. 276 mg of crude product, mp 68—73°C, was obtained. The product was recrystallized from cyclohexane to give a pure sample, mp 80—83°C. IR (Nujol), 1690, 1675 and 719 cm^{-1}; NMR ($CDCl_3$), τ, 7.55—8.52 (m, 6H, $-CH_2-$), 6.20—6.75 (m, 1H, -CH-), 5.65—6.18 (m, 1H, -CH-), 1.92—2.70 (m, 5H, C_6H_5), 0.08 (s, 1H, CO_2H).

Found: C, 71.34; H, 6.54%. Calcd for $C_{13}H_{14}O_2$: C, 71.54; H, 6.47%.

Into a solution of 1 g of sodium hydroxide in 5 ml of water was dissolved 133 mg of the above crude product. The mixture was heated under reflux for 4 hr, then acidified with dilute hydrochloric acid and extracted with ether. Evaporation of the solvent gave 110 mg of recovered acid mp 67—70°C. Both the IR and NMR spectra of the recovered acid were essentially consistent with that of the pure sample (**12**).

The authors wish to express their hearty thanks to the late Professor S. Winstein, UCLA, for his encouragement throughout this work, and to Professor Kenji Fukui for his measurement of NMR spectra and to Mrs. Shinobu Imai for her earnest assistance.

BULLETIN OF THE CHEMICAL SOCIETY OF JAPAN VOL. 43 2208—2213 (1970)

Reaction of Olefin-Palladium(II) Chloride Complexes with Amides*1

Hidefumi HIRAI and Hiroaki SAWAI

Department of Industrial Chemistry, Faculty of Engineering, The University of Tokyo, Bunkyo-ku, Tokyo

(Received January 16, 1970)

Ethylene-palladium(II) chloride complex reacts with pyrrolidone and ε-caprolactam to produce *N*-vinylpyrrolidone and *N*-vinyl-ε-caprolactam, respectively. The yield of *N*-vinylpyrrolidone increases with increasing reaction temperature up to 120°C and decreases above 120°C owing to conversion of *N*-vinylpyrrolidone to an oily polymer through thermal polymerization. By addition of quinone, the yield increases remarkably at 25°C and 90°C. Pyrrolidone - palladium(II) chloride complex, which is too stable to react with ethylene at 25°C, reacts at 120°C to give *N*-vinylpyrrolidone. Open chain amides such as *N*-ethylacetamide, acetanilide and acetamide also react with ethylene - palladium(II) chloride complex, though the corresponding *N*-vinylamides cannot be obtained. The reaction of a styrene - palladium(II) chloride complex with pyrrolidone was also investigated.

Olefin-palladium(II) chloride complexes react with various nucleophilic reagents to form carbonyl compounds or substituted olefins.[1] Little is known about the reaction with nitrogen compounds such as amines or amides. Amine or amide forms a very stable complex with palladium(II) chloride, which would prevent or complicate the reaction. Stern and Spector reported very briefly the reaction of acetamide with propylene in the presence of palladium(II) chloride and that with ethylene-palladium(II) chloride complex.[2] Destruction of the resulting stable complexes by hydrogenation yielded *N*-isopropylacetamide and *N*-ethylacetamide, respectively.

Shortly after we had shown the formation of *N*-vinylpyrrolidone by the reaction of ethylene-palladium(II) chloride complex with pyrrolidone,[3] the process for production of ethylenylated lactams

*1 The major part of this paper was presented at the 21st Annual Meeting of the Chemical Society of Japan, Osaka, April, 1968.

1) C. W. Bird, "Transitional Metal Intermediates in Organic Synthesis," Logos Press, London (1966), p. 88—112; A. Guilo, "Advances in Organometallic Chemistry," Vol 5, ed. by F. G. A. Stone and R. West, Academic Press, New York (1967), p. 321; E. W. Stern, "Catalysis Review," Vol. 1, ed. by H. Heinemann, Marcel Dekker, Inc., New York (1968), p. 74.

2) E. W. Stern and M. L. Spector, *Proc. Chem. Soc.*, **1961**, 370.

3) H. Hirai, H. Sawai and S. Makishima, Presented at the 20th Annual Meeting of the Chemical Society of Japan, Tokyo, April, 1967.

from olefins and lactams in the presence of palladium(II) chloride and cupric ion was patented.[4] This patent covered cyclic lactams such as pyrrolidone, ε-caprolactam and 2-ketopiperidone as a nucleophilic reagent, but little information on the reaction was given.

The present paper deals with the formation of *N*-vinylamides under various reaction conditions in detail to propose a reaction mechanism. The reaction of styrene-palladium(II) chloride complex with pyrrolidone is also described.

Results and Discussion

Reaction of Ethylene-Palladium(II) Chloride Complex with Pyrrolidone. Ethylene-palladium-(II) chloride complex reacted with pyrrolidone at 25°C for 2.5 hr under 10 atm of ethylene pressure to give *N*-vinylpyrrolidone (**1**) in 42 mol% yield based on palladium(II), accompanying the reduction of palladium(II) ion to the metal, as shown in Table 1. Simultaneously, a ligand substitution of the ethylene-palladium(II) chloride complex occurred to form pyrrolidone-palladium(II) chloride complex and *N*-vinylpyrrolidone-palladium(II)chloride complex. These reactions are schematically shown by the following equations.

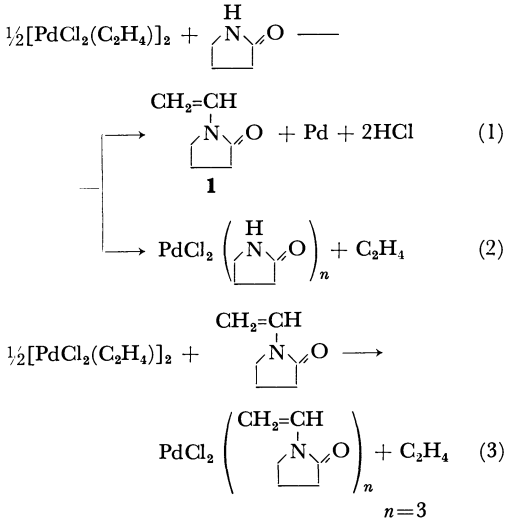

Addition of pyridine makes **1** free from the coordination state in the reaction mixture by ligand substitution, which was confirmed by the change of color of the reaction mixture. The total yield of **1** could be determined by glpc after the addition of pyridine. As shown in Table 1, the yield of **1** increased from 24 to 42 mol% by addition of pyridine to the reaction mixture at 25°C. This means that 43% of **1** formed by reaction (1) was coordinated to palladium(II) chloride.

4) J. E. Mckeon and P. S. Stracher, U. S. 3318906; *Chem. Abstr.*, **68**, 39466k (1968).

Table 1. Effect of temperature on the reaction of ethylene-palladium(II) chloride complex with pyrrolidone[a]

Temp. °C	Yield (mol%)[b] *N*-Vinylpyrrolidone free	*N*-Vinylpyrrolidone free+coordinated	Pd (metal)	Polymer[c] mg	Complex[d] mg
25	24	42	41	0	660(670)
60	32	51	49	0	570(590)
90	37	66	68	0	444(400)
120	65	72	77	100	240(260)
150	57	61	84	315	140(180)
180	13	13	88	500	50(150)

a) Reaction conditions: initial pressure of ethylene, 10 atm; time, 2.5 hr; [Pyrrolidone]/[Pd(II)]=4.
b) Based on palladium(II).
c) Crude substance.
d) Calculated amounts of the sum of pyrrolidone- and *N*-vinylpyrrolidone-palladium(II) chloride complexes are shown in parentheses.

Table 1 shows the effect of reaction temperature on the yields of reaction products. The yield of **1** increased with temperature and was nearly equal to that of palladium metal up to 90°C. Above 120°C, the yield of **1** decreased, while that of palladium metal increased and an oily resin of light greenish brown color resulted. The IR spectrum of this resin was identical with that of poly-*N*-vinylpyrrolidone. Elevation of temperature above 120°C promoted not only the extent of reaction (1) but also the polymerization of **1** by heat. The sum of the amount of pyrrolidone-palladium(II) chloride complex and that of *N*-vinylpyrrolidone-palladium(II) chloride complex in the reaction, decreased with the rise of temperature and was in fairly good agreement with the amount of these complexes calculated from unreduced palladium(II) ion.

The effects of the addition of quinone and diphenylpicrylhydrazyl on the yield of the products are shown in Table 2. Quinone is expected to regenerate palladium(II) ion in this system, forming a redox system and inhibiting thermal polymerization of **1**. Diphenylpicrylhydrazyl is known to be an inhibitor for the polymerization. Addition of quinone increased the yield of **1** remarkably at 25°C or 90°C, but depressed the formation of palladium metal less than 38 mol%. The yield of **1** became more than 100 mol% based on the initial amount of palladium(II). It is evident that quinone acted as an oxidant for the resulting palladium(0) at these temperatures. Above 150°C, however, the yield of **1** decreased remarkably, accompanying a definite increment of the yield of palladium metal, *e.g.*, about 50 mol%. The greater the amount of quinone added, the less the yield of

TABLE 2. EFFECT OF QUINONE ON THE REACTION OF ETHYLENE PALLADIUM(II) CHLORIDE COMPLEX WITH PYRROLIDONE[a]

Temp. °C	[Quinone]/[Pd(II)] molar ratio	Yield (mol%)[b] *N*-Vinylpyrrolidone free	*N*-Vinylpyrrolidone free+coordinated	Pd (metal)	Polymer
25	2	94	173	28	—
25	4	93	174	37	—
90	2	114		38	—
90	4	114	204	38	—
150	2	15	16	87	+
150	4	4	4	93	+
160	2[c]	17	17	85	+

a) Reaction conditions: initial pressure of ethylene, 10 atm; time, 2.5 hr; [Pyrrolidone]/[Pd(II)]=4.
b) Based on palladium(II).
c) Diphenylpicrylhydrazyl was used instead of quinone.

1. It can be concluded that quinone cannot inhibit the thermal polymerization of **1**. The added diphenylpicrylhydrazyl behaved in the reaction at 160°C just as quinone, as shown in Table 2.

Ethylene-palladium(II) chloride complex reacted also with sodium pyrrolidone at 25°C for 2.5 hr under 10 atm of ethylene pressure. *N*-Vinylpyrrolidone was obtained in 6 mol% yield, accompanying the formation of pyrrolidone, which was detected by glpc in the reaction mixture. This reaction can be expressed by the following equation.

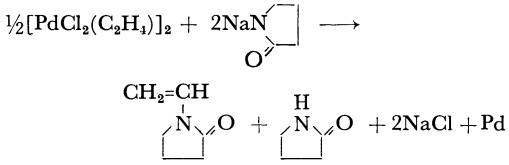

The depression of the yield is attributable to the lower solubility of sodium pyrrolidone in tetrahydrofuran.

Reaction of Tris(pyrrolidone)palladium(II) Chloride Complex with Ethylene. Tris(pyrrolidone)palladium(II) chloride complex was too stable to react with ethylene at 25°C. This complex, however, was found to react with ethylene in a good yield at 120°C as shown in Table 3.

TABLE 3. REACTION OF TRIS(PYRROLIDONE)PALLADIUM(II) CHLORIDE COMPLEX WITH ETHYLENE[a]

Temp. °C	Yield (mol%)[b] *N*-Vinylpyrrolidone free	*N*-Vinylpyrrolidone free+coordinated	Pd (metal)	Polymer
25	0	0	0	—
120	62	70	69	—

a) Reaction conditions: initial pressure of ethylene, 20 atm; time, 2.5 hr.
b) Based on palladium(II).

Reaction of Styrene-Palladium(II) Chloride Complex with Pyrrolidone. Styrene-palladium(II) chloride complex reacted with pyrrolidone at 120°C for 2.5 hr, accompanied by precipitation of palladium metal in 38 mol%. Reaction products isolated by column chromatography were *trans*-β-styrilpyrrolidone, 1,4-diphenylbutadiene and acetophenone in 20, 5 and 5 mol% yield based on palladium(II), respectively. Acetophenone can be considered to be derived from α-styrilpyrrolidone by hydrolysis in the silica gel column of chromatography. The sterical unstability of α-styrylpyrrolidone would give rise to a low yield and a high susceptibility for hydrolysis. The possibility that acetophenone is formed by the reaction of styrene-palladium(II) chloride complex with water is excluded for the following reasons. No phenylacetaldehyde was formed in the present reaction, although the styrene complex is reported to react with water to yield phenylacetaldehyde and acetophenone in a molar ratio of about 1 : 2.[5] The reaction system was prevented from water contamination, and acetophenone was formed in a yield less than 1.5 mol% in a blank test.

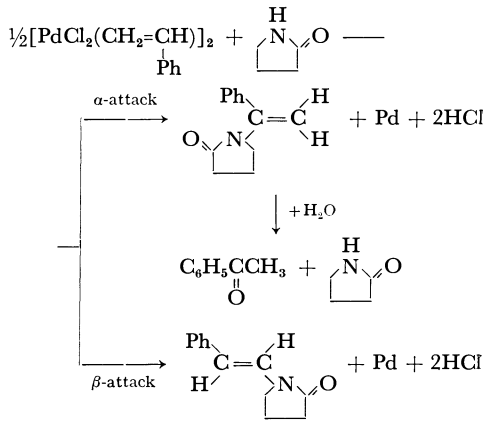

1,4-Diphenylbutadiene has been reported to be obtained from styrene in the presence of palladium(II) ion and acetate anion.[6] Pyrrolidone probably becomes pyrrolidonium anion which can play the same role of acetate anion for the formation of 1,4-diphenylbutadiene

Reaction of Ethylene-Palladium(II) Chloride Complex with Other Amides. ε-Caprolactam, *N*-ethylacetamide, acetanilide and acetamide were allowed to react with ethylene-palladium(II) chloride complex. Table 4 shows the results of glpc

5) H. Okada and H. Hashimoto, *Kogyo Kagaku Zasshi*, **69**, 2137 (1966).
6) Y. Fujiwara, I. Moritani, M. Matsuda and S. Teranishi, *Tetrahedron Lett.*, **1968**, 3863.

TABLE 4. REACTION OF ETHYLENE-PALLADIUM(II) CHLORIDE COMPLEX WITH AMIDES[a]

Amide	Temp. °C	Yield (mol%)[b]			
		N-Vinylamide		Pd (metal)	Polymer
		free	free+coordinated		
ε-Caprolactam	25	8	20	21	—
	120	10	10	80	+
N-Ethylacetamide	25	0	0	6	—
	120	0.5	0.5	74	+
Acetanilide	28	0	0	20	—
	110	0	0	56	+
Acetamide	25		19[c]	38	

a) Reaction conditions: initial pressure of ethylene, 10 atm; time, 2.5 hr; [Amide]/[Pd(II)]=4.
b) Based on palladium(II).
c) After hydrogenation, *N*-ethylacetamide was analyzed.

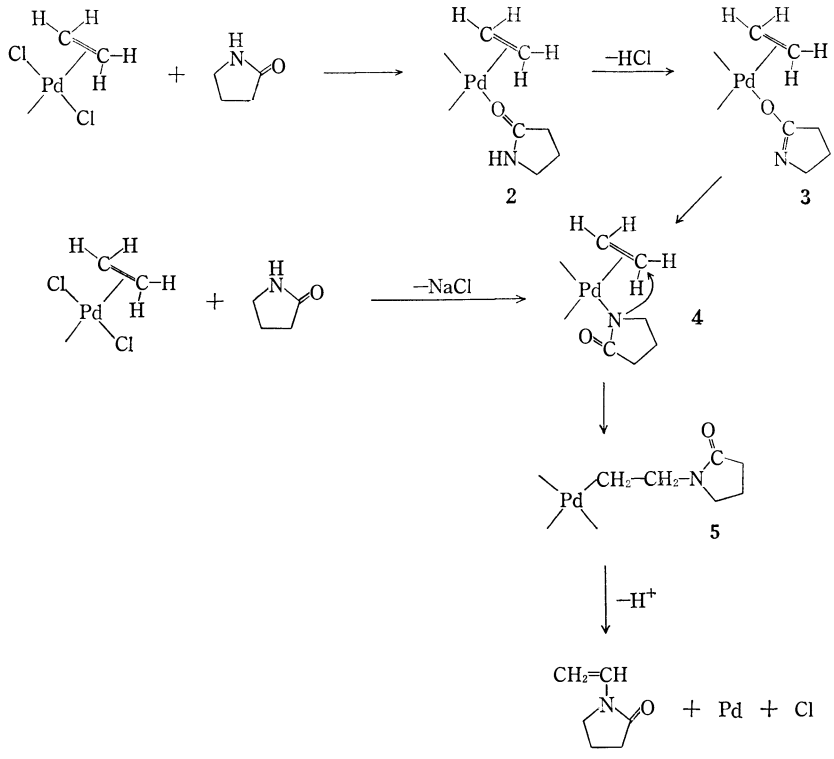

Scheme 1

analysis of the reaction products. *N*-Vinyl-ε-caprolactam was obtained in 20 mol% yield at 25°C, and the yield decreased at 120°C accompanying the formation of a large amount of polymer. *N*-Vinyl-ε-caprolactam seems to polymerize thermally more easily than *N*-vinylpyrrolidone. Cyclic amides gave *N*-vinylamides in fairly good yields, while open chain secondary amides such as *N*-ethylacetamide and acetanilide could not produce the corresponding *N*-vinylamides at room temperature. The formation of palladium metal was small in these cases. At a higher reaction temperature, the corresponding oily poly-*N*-vinylamide was obtained. In the case of open chain amides, *N*-vinylamide seems to undergo hydrolysis or polymerization easily. *N*-Vinylacetanilide is reported to undergo hydrolysis very easily in the presence of acid.[7]

In the case of acetamide, the product was analyzed by glpc after hydrogenation to *N*-ethylacetamide, because no gas chromatogram of *N*-vinylacetamide could be obtained by addition of pyridine and the

7) S. Murahashi, S. Nozakura, A. Umehara and F. Nagoshi, *Kobunshi Kagaku*, **22**, 451 (1965).

authentic sample could not be prepared with the thermal decomposition of ethylidenediacetamide.[8] In the reaction mixture, only acetamide was detected by glpc. The product probably decomposed in the column of glpc. Two types of reaction products can be considered; $CH_3CH{=}NCOCH_3$ and $CH_2{=}CHNHCOCH_3$. However, further characterization was unsuccessful.

Reaction Scheme. A scheme for ethylene-palladium(II) chloride complex with pyrrolidone is proposed (Scheme 1.)

At first pyrrolidone reacts with the ethylene complex to form ethylene-pyrrolidone-palladium(II) complex (**2**). In this complex, pyrrolidone is considered to coordinate to palladium(II) ion with the carbonyl group, because the coordination of the carbonyl group of pyrrolidone in tris(pyrrolidone)palladium(II) chloride complex has been confirmed by the shift of the IR stretching band: $\Delta\, \nu_{CO}=45\ cm^{-1}$. The proton of coordinated pyrrolidone is withdrawn to form complex (**3**) which tautomerize to complex (**4**) on account of the stronger affinity of amide nitrogen anion for palladium(II) than that of alkoxy type anion. Coordinated ethylene is then inserted into the resulting Pd–N bond to give complex (**5**) which decomposes to yield **1**. Sodium pyrrolidone reacts with ethylene complex to form complex (**4**) by the exchange reaction of chloride ion with pyrrolidonium anion. Sodium pyrrolidone cannot coordinate to palladium(II) ion by the steric and the ionic effect of sodium ion. The fact that pyrrolidone-palladium(II) chloride complex could not react with ethylene at 25°C, but could at 120°C means that the elevation of temperature makes the stable pyrrolidone complex so labile as to enable ethylene to coordinate palladium(II) ion. The high temperature also activates the withdrawal of hydrogen of coordinated pyrrolidone and promotes the extent of the reaction.

The proposed scheme is essentially the same as that for the reaction of ethylene-palladium(II) chloride complex with *n*-butylamine.[9] Usually, amine or amide in a free state cannot dissociate its *N*-proton easily, while its proton in the coordination state can be withdrawn by palladium(II) ion to its strong affinity for hydrogen to result in the reaction with ethylene[9] or carbon monoxide.[10]

Experimental

Materials. Bis(benzonitrile)dichloro palladium(II) and styrene - palladium(II) chloride complex were prepared according to Kharasch.[11] *N*-Ethylacetamide was prepared from ethylamine and acetic anhydride. ε-Caprolactam, acetanilide and acetamide were of reagent grade and dried under reduced pressure. Sodium pyrrolidone was prepared from pyrrolidone and sodium hydroxide by heating on a sand bath. Tris(pyrrolidone)-palladium(II) chloride complex was prepared from bis-(benzonitrile)dichloro palladium(II) with pyrrolidone in tetrahydrofuran in a quantitative yield, and recrystallized from methanol. Tetrahydrofuran used as a solvent was dried over lithium aluminum hydride and distilled before use.

Reaction of Ethylene-Palladium(II) Chloride Complex with Pyrrolidone. Bis(benzonitrile)dichloro-palladium(II) (0.96 g, 0.0025 mol) and dry tetrahydrofuran (20 m*l*) were charged in a magnetically stirred 100 m*l*-autoclave in a slow stream of nitrogen. In the autoclave, a glass tube was used as a reactive vessel and the stirrer was made of Teflon to prevent palladium-(II) ion from reacting with steel. Ethylene-palladium-(II) chloride complex was prepared under 10 atm of ethylene pressure for half an hour with stirring. The autoclave was then opened for addition of pyrrolidone (1 m*l*, 0.01 mol) and the reaction was carried out under 10 atm of initial ethylene pressure at 25—150°C for 2.5 hr. A similar procedure was applied for the reaction with quinone or diphenylpicrylhydrazyl.

Reaction of Ethylene-Palladium(II) Chloride Complex with Sodium Pyrrolidone. Bis(benzonitrile)dichloro palladium(II) (0.96 g, 0.0025 mol), sodium pyrrolidone (1.3 g, 0.0125 mol) and dry tetrahydrofuran were placed in the autoclave. The reaction was carried out under 10 atm of ethylene pressure at 25°C for 2.5 hr.

Reaction of Tris(pyrrolidone)palladium(II) Chloride Complex with Ethylene. Tris(pyrrolidone)-palladium(II) chloride complex (1.08 g, 0.0025 mol) and dry tetrahydrofuran were charged in the autoclave. The reaction was carried out under 20 atm of initial ethylene pressure at 25 or 120°C for 2.5 hr.

Products Analysis. *N*-Vinylpyrrolidone was analyzed by glpc (a 2 m Carbowax 20 M on Diasolid A column at 160°C and a nitrogen flow rate of 55 m*l*/min) and IR. The yield data were obtained by glpc with benzonitrile as an internal standard. Glpc analysis was carried out both before and after addition of pyridine to the reaction mixture to make the product free from coordination. Other reaction products were examined as follows. The reaction mixture was filtered through a glass filter and the residue was washed with tetrahydrofuran (Filtrate I), then with methanol (Filtrate II) and finally with dimethylformamide (Filtrate III). The resulting precipitate was palladium metal and was weighed after drying. Filtrate I was concentrated under reduced pressure to a few mililiter in order to crystallize a small amount of reddish brown complex. After removal of the crystals, a large amount of ether was added to the solution to separate an oily residue which was dried under reduced pressure and weighed. The IR spectrum of this substance was essentially the same as that of poly-*N*-vinylpyrrolidone obtained commercially.

Concentration of Filtrate II gave reddish brown

8) D. Ben-Ishai and R. Giger, *Tetrahedron Lett.*, **1965**, 4523.

9) H. Hirai, H. Sawai and S. Makishima, This Bulletin, **43**, 1143 (1970).

10) E. W. Stern and M. L. Spector, *J. Org. Chem.*, **31**, 596 (1966); J. Tsuji and N. Iwamoto, *Chem. Commun.*, **1966**, 380.

11) M. S. Kharasch, R. C. Seyler and F. R. Mayo, *J. Amer. Chem. Soc.*, **60**, 882 (1938).

crystals, which were confirmed to be a mixture of pyrrolidone-palladium(II) chloride complex and *N*-vinylpyrrolidone-palladium(II) chloride complex by IR spectrum; (3200(ν_{NH}), 2930, 2850, 1670(ν_{CO}), 1640(ν_{CO} or $\nu_{C=C}$), 1625 (ν_{CO} or $\nu_{C=C}$), 1290).

In the presence of quinone, a dark reddish brown precipitate was obtained from Filtrate III after concentration. This precipitate seems to be quinone-palladium(II) complex, but further characterization was unsuccessful.

Reaction of Styrene-Palladium(II) Chloride Complex with Pyrrolidone. Styrene-palladium(II) chloride complex (3.172 g, 0.0113 mol), styrene (2 m*l*), pyrrolidone (4.5 ml, 0.0045 mol) and dry tetrahydrofuran were charged in the autoclave. Reaction was carried out at 120°C for 2.5 hr. After the reaction, 2 m*l* of pyridine was added to the reaction mixture to make the product free from the coordination state. Then the reaction mixture was filtered through a glass filter, and the precipitate was washed with tetrahydrofuran. The filtrate was concentrated by evaporation and chromatographed on silica gel.

From the first fraction white crystals were obtained by using cyclohexane as an eluent. Recrystallization from *n*-hexane gave pure 1,4-diphenylbutadiene; mp 152—153°C (lit,[6] 149.5°C).

From the second fraction colorless liquid was obtained, which was confirmed to be acetophenone by IR and glpc.

Finally white crystals were obtained by using benzene as an eluent. Recrystallization from cyclohexane-ether gave purified *trans*-β-styrylpyrrolidone; mp 128°C (lit,[12] 129°C).

Reaction of Ethylene-Palladium(II) Chloride Complex with ε-Caprolactam, *N*-Ethylacetamide and Acetanilide. The procedure was similar to that used for the reaction of ethylene complex with pyrrolidone. Analysis of the products was carried out by glpc; A 2 m Carbowax 20 M on Diasolid A column, and a nitrogen flow rate of 60 m*l*/min, at 170°C for ε-caprolactam and acetanilide, at 122°C for *N*-ethylacetamide. The yield data were obtained by glpc with benzonitrile as an internal standard. The products were identified by comparison of gas chormatograms and IR spectra with those of authentic sample prepared according to Reppe.[13]

Reaction of Ethylene-Palladium(II) Chloride Complex with Acetamide. The reaction method was similar to that for the case of pyrrolidone. The product was analyzed by glpc; A 2 m Carbowax 20 M on Diasolid A column at 122°C and a nitrogen flow rate of 60 m*l*/min. The reaction product could not be detected by glpc, but *N*-ethylacetamide was obtained after hydrogenation of the reaction mixture catalyzed by palladium metal under 80 atm of hydrogen, as described by Stern.[2] The yield data were obtained by glpc with benzonitrile as an internal standard. The preparation of *N*-vinylacetamide as an authentic sample, reported by Ben-Ishai and Giger,[8] was unsuccessful.

12) W. Ziegenbein and W. Franks, *Chem. Ber.*, **90**, 2291 (1957).

13) W. Reppe and Mitarbeiter, *Ann.*, **601**, 81 (1956).

BULLETIN OF THE CHEMICAL SOCIETY OF JAPAN VOL. 43 2213—2217 (1970)

Reactions of Haloferrocenes. III. The Reaction of Haloferrocenes with Copper(I) Benzenethiolate, Thiocyanate, Acetate, and Benzoate

Masaru SATO, Izumi MOTOYAMA and Kazuo HATA

Department of Chemistry, Faculty of Science, Tokyo Metropolitan University, Setagaya-ku, Tokyo

(Received January 21, 1970)

Iodoferrocene reacted with copper(I) benzenethiolate in boiling pyridine to give ferrocenyl phenyl sulfide in a quantitative yield. The reaction of iodoferrocene with copper(I) thiocyanate gave diferrocenyl disulfide. The behavior of copper(I) acetate and benzoate toward haloferrocene was found to be different from those of the other copper(I) salts: the reactions in boiling pyridine gave the corresponding ferrocenyl ester, together with a small quantity of ferrocene, while the reaction in boiling toluene produced biferrocenyl as the main product. The reaction mechanism of the ferrocenyl ester and biferrocenyl formations was discussed.

It has been shown that haloferrocene has a high reactivity in the reaction with copper(I) salts in pyridine, and that chloro-, bromo-, and cyanoferrocene were obtained in good yields from the reaction of iodoferrocene with, respectively, copper(I) chloride, bromide, and cyanide in boiling pyridine.[1] Bromoferrocene was 10^3 times more reactive than bromobenzene in the reaction with copper-

1) M. Sato, T. Ito, I. Motoyama, K. Watanabe and K. Hata, This Bulletin, **42**, 1976 (1969). Part I in this series.

(I) chloride - pyridine complex in bromobenzene.[2] According to Bunnett and Zahler,[3] the reaction of this kind is classified as a nucleophilic substitution reaction participated by transition metal through an uncertain mechanism. It is surprising that haloferrocene has a high reactivity even in the nucleophilic reaction, whereas ferrocene itself shows a much higher reactivity than benzene in an electrophilic reaction such as the Friedel-Crafts acylation. In order to elucidate the nature of this reaction, the reactions of haloferrocene with copper(I) benzenethiolate, thiocyanate, acetate, and benzoate were investigated.

Results and Discussion

The treatment of iodoferrocene (**1**) with copper(I) benzenethiolate in boiling pyridine for two hours gave ferrocenyl phenyl sulfide (**2**) in a quantitative yield. Similar results have been observed in the reaction of aryl halide with copper(I) benzenethiolate.[4] No particular high reactivity of iodoferrocene over other aryl halides was observed in this reaction, although it has been found[1] that haloferrocenes generally have a higher reactivity toward copper(I) salts than do the corresponding halobenzenes. This has been supposed to be due to the special high reactivity of benzenethiolate toward both halides. Thus, this reaction is considered to be as useful as the copper-catalyzed reaction between iodoferrocene and sodium benzenethiolate[5] for the preparation of ferrocenyl phenyl sulfide.

The reaction of iodoferrocene (**1**) with copper(I) thiocyanate in boiling pyridine for two hours gave diferrocenyl disulfide (**4**) in a 48% yield instead of the expected product, ferrocenyl thiocynate (**3**), with a 42% recovery of iodoferrocene.

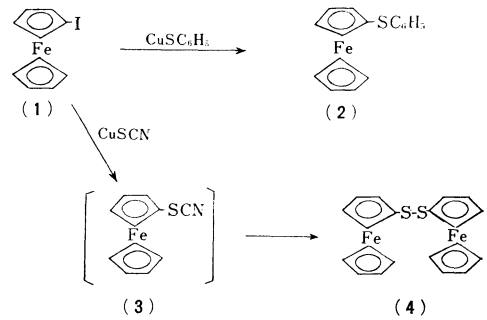

It is known that aryl halides are converted to the diaryl disulfides by the action of copper(I) thiocyanate under severe conditions[6] and that aryl thiocyanates are reduced to the corresponding disulfides with copper(I) salt.[7] The formation of diferrocenyl disulfide (**4**) is probably due to the rapid reduction of the intermediary ferrocenyl thiocyanate (**3**) to the disulfide (**4**) by an excess of copper(I) salt. The reactivity of iodoferrocene toward thiocyanate seems to be usually high, since 1-bromonaphthalene hardly reacts with copper(I) thiocyanate under similar conditions.[8] This process can be used for the preparation of diferrocenyl disulfide which was previously prepared by the oxidation of ferrocenethiol.[9]

TABLE 1. THE REACTION OF HALOFERROCENE WITH COPPER(I) ACETATE AND BENZOATE
Haloferrocene: 0.005 mol; copper(I) salts: 0.01 mol; solvent: 15 ml; reaction temp.: 120°C±5°C; reaction time: 0.5 hr

Exp. No.	Haloferrocene	Copper(I) salt	Solvent	Starting material recovered (%)	Product (%)		
					Ester	Biferrocenyl	Ferrocene
1[a]	FcI	CuOAc	Pyridine	None	62.3	4.3	20.0
2[b]	FcI	CuOBz	Pyridine	35.5	54.9	Trace	1.8
3[a]	FcBr	CuOAc	Pyridine	None	62.3	None	20.7
4	FcCl	CuOAc	Pyridine	76.8	9.6	None	11.7
5	FcI	CuOAc	Toluene	None	7.4	74.4	12.8
6[b]	FcI	CuOBz	Toluene	None	24.2	67.0	Trace
7	FcBr	CuOAc	Toluene	15.2	15.6	68.0	2.1

a) 20 ml of solvent was used.
b) A minor quantity of chloroferrocene was found in the reaction product. This halogen-exchange must be caused by hydrochloric acid during the treatment, but the reason of the exchange is not clear.

2) M. Sato, I. Motoyama and K. Hata, This Bulletin, **43**, 1860 (1970).
3) J. F. Bunnett and R. E. Zahler, *Chem. Rev.*, **49**, 273 (1951).
4) R. Adams, W. Reifschneider and M. D. Nair, *Coastica Chem. Acta*, **1957**, 29.
5) M. D. Rausch, *J. Org. Chem.*, **26**, 3579 (1961).
6) K. W. Rosenmund and H. Harms, *Ber.*, **53**, 2226 (1920).
7) R. G. R. Bacon, S. C. Rennison and O. J. Stewart, *Proc. Chem. Soc.*, **1964**, 409.
8) R. G. R. Bacon and H. A. O. Hill, *J. Chem. Soc.*, **1964**, 1097.
9) G. R. Knox and P. L. Pauson, *ibid.*, **1958**, 692.

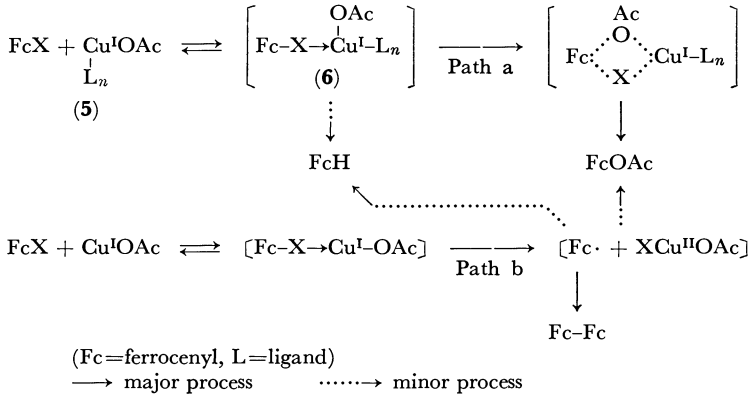

Scheme 1

The behavior of copper(I) acetate and benzoate toward haloferrocene was found to be different from that of the other salts, as is summarized in Table 1. When iodoferrocene was treated with copper(I) acetate in boiling pyridine for 0.5 hr, ferrocenyl acetate was obtained in a moderate yield, together with a small quantity of ferrocene and biferrocenyl. The formation of these by-products was not observed in the reaction described above or in the previous paper.[1] The reaction of bromo- or chloroferrocene with copper(I) acetate did not afford biferrocenyl, but it did give ferrocene in addition to ferrocenyl acetate. The reactivities of haloferrocenes toward the copper(I) acetate were in the order: FcI> FcBr>FcCl. When copper(I) benzoate, instead of copper(I) acetate, was refluxed for 0.5 hr with iodoferrocene in pyridine, ferrocenyl benzoate was similarly obtained in a moderate yield, along with traces of ferrocene and biferrocenyl. Since a considerable amount of iodoferrocene was recovered in this reaction, the reactivity of copper(I) benzoate toward iodoferrocene seems to be considerably smaller than that of copper(I) acetate.

As has been mentioned above, the reaction of haloferrocene with copper(I) acetate and benzoate in pyridine gave ferrocenyl acetate and benzoate respectively. Those results are very different from those of the halobenzene series. It has been reported that reactions of aryl halides with copper(I) acetate in pyridine generally give dehalogenation products as a sole product.[10,11] For example, naphthalene was obtained in a 60% yield by the treatment of 1-bromonaphthalene with copper(I) acetate in boiling pyridine.[10] When *o*-iodonitrobenzene, which is as reactive as iodoferrocene in the Ullmann coupling reaction,[12] was treated with copper(I) acetate in boiling pyridine, 2,2′-dinitrobiphenyl was obtained in an 84% yield, but no detectable amount of *o*-nitrophenyl acetate was produced.

The reaction of haloferrocenes with copper(I) acetate and benzoate also gave rise to the formation of ferrocene and biferrocenyl, but the formation of the latter was only observed in the reaction of iodoferrocene. The fact may be explained as follows: active copper, which was produced by the decomposition or disproportionation of copper(I) acetate, causes the coupling of iodoferrocene, just as in the reaction of iodoferrocene with active copper powder[13] prepared from copper(II) sulfate and zinc dust to give biferrocenyl. However, we cannot exclude the possibility of the process involving the reduction of iodoferrocene with copper(I) salts, followed by the coupling reaction to be described below.

The route of the reaction of haloferrocene with copper(I) acetate or benzoate in pyridine may be similar to that with the other copper(I) salts.[2] The coordination of the halogen atom of haloferrocene to the copper(I) salt-pyridine complex (**5**) may give a metastable intermediate (**6**), through which a ligand-exchange reaction leads to ferrocenyl acetate or benzoate as is shown in Path a of Scheme 1.

The fact that the dehalogenation product, *i.e.*, ferrocene, was not detected in the reaction of haloferrocene with copper(I) salts other than acetate or benzoate indicates that the existence of an acetate or benzoate ligand on the copper(I) complex (**5**) is essential for the formation of the dehalogenation product. It is considered that the dehalogenation may proceed through an intramolecular hydride shift within the intermediate complex (**6**) similar to that which was proposed by Bacon and Hill[11] in the benzene series. This consideration is supported by the fact that a larger amount of ferrocene is formed in the reaction with copper(I) acetate than with benzoate; it is possible that the hydride shift takes place more easily in the former than in the latter.

In order to examine the function of pyridine in

10) W. G. H. Edwards and R. G. Stewart, *Chem. Ind.* (London), **1952**, 472.

11) R. G. R. Bacon and H. A. O. Hill, *J. Chem. Soc.*, **1964**, 1112.

12) M. D. Rausch, *J. Org. Chem.*, **26**, 1802 (1961).

13) R. Q. Brewster and R. Groening, "Organic Syntheses," Coll. Vol. 2, p. 445 (1943).

these reactions, haloferrocenes were treated with copper(I) acetate or benzoate in boiling toluene (Table 1, Nos. 5, 6, and 7). In every case, the main product was biferrocenyl, while ferrocene and ferrocenyl ester were produced as minor by-products. The remarkable difference in the product ratio observed between the reactions in pyridine and those in toluene suggests that the coordinating ability of the solvent may be significant in these reactions. It has been established that the coordination of pyridine to copper(I) salt affords a copper(I) salt-pyridine complex (**5**). The reaction of haloferrocene with copper(I) acetate or benzoate was considered to proceed through this complex to afford the ferrocenyl ester as a main product. On the other hand, as the coordination of toluene must proceed through another process. During the reaction in toluene, a color change in the reaction mixture from orange to green was observed as the reaction proceeded. This is probably due to the formation of some copper(II) species. As no such color change was observed by refluxing copper(I) benzoate alone in toluene, the coexistence of haloferrocene seems to be necessary for the formation of the copper(II) species. On the basis of the results presented above, Path b in Scheme 1 was assumed to be a possible process: haloferrocene is reduced by some participation of copper(I) acetate or benzoate (for instance, the unstable complex-formation shown in Scheme 1) to give a ferrocenyl radical, which may interact with the excess of the salt to form ferrocenylcopper species. The ferrocenyl radicals thus formed couple with each other to give biferrocenyl, on the one hand, and abstract an acetoxy group from copper(II) acetate to give ferrocenyl acetate, on the other hand.

A similar process has been proposed for the reduction of benzyl chloride with copper(I) ion[14] or chrom(II) ion.[15] It is not apparent, however, whether or not the formation of the ferrocenyl ester is exclusively due to the process involving the ferrocenyl radical. Perhaps the ligand-exchange process through complex-formation discussed above will simultaneously contribute to the formation of the ester.[16]

Considering the results of the reactions of haloferrocenes with various copper(I) salt-pyridine complexes described in the present paper, together with those described in the previous paper,[1] it was found that the affinity of various ligands to ferrocene nucleus was in the following order: $SC_6H_5 > Cl > Br > CN > OAc > OBz > SCN$. It was also reconfirmed that haloferrocenes have a higher reactivity toward various copper(I) salt-pyridine complexes than do halobenzenes.

14) K. Wada and S. Hashimoto, This Bulletin, **41**, 3001 (1968).

15) J. K. Kochi and D. D. Davis, *J. Amer. Chem. Soc.*, **86**, 5264 (1964).

16) T. Cohen and A. H. Lewin, *ibid.*, **88**, 4521 (1966).

Experimental

Materials. Iodoferrocene was prepared from chloromercuriferrocene by a modification of a previously-reported procedure.[1] Bromoferrocene and chloroferrocene were prepared by the procedure described in a previous paper.[1] Copper(I) benzenethiolate,[4] thiocyanate,[17] acetate,[18] and benzoate[16] were prepared according to the literatures. Pyridine was distilled just before use after desiccation over potassium hydroxide.

Ferrocenyl Phenyl Sulfide. Iodoferrocene (1.56 g, 0.005 mol) and copper(I) benzenethiolate (1.73 g, 0.01 mol) were refluxed for 2 hr in 15 m*l* of pyridine. After the reaction had been completed, 80 m*l* of benzene was poured into the hot reaction mixture. The precipitate thus formed was filtered and washed with benzene. The combined benzene solution was repeatedly washed with water until the aqueous layer became neutral; then the solution was dried over anhydrous magnesium sulfate. After benzene had been evaporated off, the residue was chromatographed on alumina with hexane - benzene (1 : 1) to give 1.6 g of yellow crystals, which were then recrystallized from hexane - benzene, mp 110.0—110.5°C (lit, 111.5—112°C). Finally, 1.38 g (93.9% yield) of ferrocenyl phenyl sulfide were obtained.

The Reaction of Iodoferrocene with Copper(I) Thiocyanate in Pyridine. A mixture of 1.56 g (0.005 mol) of iodoferrocene, 1.22 g (0.01 mol) of copper(I) thiocyanate, and 15 m*l* of pyridine was refluxed for 2 hr under an atmosphere of nitrogen. Then, 80 m*l* of ether was added and the reaction mixture was filtered. The filtrate was washed with water, then with 2N hydrochloric acid to remove pyridine, and again with water. After the removal of the solvent, the residue was chromatographed on alumina. Iodoferrocene (0.65 g, 41.7%) was recovered, and diferrocenyl disulfide (0.52 g, 47.9%) was obtained as yellow crystals, which were subsequently recrystallized from hexane - benzene, mp 190—191°C (lit, 192°C,[9] 192—193°C[5]).

A General Procedure for the Reactions of Haloferrocenes with Copper(I) Acetate or Benzoate in Pyridine. Haloferrocene (0.005 mol) was refluxed, together with copper(I) acetate or benzoate (0.01 mol), in 15 m*l* of pyridine under an atmosphere of nitrogen. After 30 min, 80 m*l* of ether was added to the cooled reaction mixture, and then the mixture was filtered. The filtrate thus obtained was washed successively with water, 2N hydrochloric acid, and again with water, and then dried over anhydrous magnesium sulfate. After the removal of the solvent under reduced pressure, the residue was separated into individual compounds by chromatography.

Procedure for Exp. 1 in Table 1. The reaction product was chromatographed on silica gel with hexane - benzene (2 : 1). The product obtained from the first fraction was again chromatographed on alumina with the same solvent to give 0.24 g of yellow crystals and 0.04 g (4.3% yield) of biferrocenyl. The gas-chromatographic analysis of the former was carried out under the conditions described in a previous paper,[2] and the yellow crystalline substance was found to be a mixture

17) R. L. Demmerle, W. A. Taebel and W. F. Anderson, *Ind. Eng. Chem.*, **42**, 2 (1950).

18) M. Calvin and W. K. Wilmarth, *J. Amer. Chem. Soc.*, **78**, 1301 (1956).

of ferrocene (0.19 g, 20.0% yield) and chloroferrocene (0.05 g, 4.5% yield). The second fraction of chromatography gave ferrocenyl acetate (0.76 g, 62.3% yield), which was subsequently recrystallized from hexane, mp 66—67.5°C (lit,[19] 64.5—66.5°C).

The Reaction of Iodoferrocene with Copper(I) Benzoate in Toluene. (Table 1, Exp. 6). Iodoferrocene (1.56 g, 0.005 mol) was refluxed with copper(I) benzoate (1.85 g, 0.01 mol) in 20 m*l* of toluene under an atmosphere of nitrogen. After 30 min, the cooled reaction mixture was extracted with benzene by using a Soxhlet extractor. The concentration of the extract under reduced pressure, followed by filtration, gave orange crystals (0.56 g), which were identified as biferrocenyl on the basis of their melting point (238—240°C, lit,[12] 240—241°C) and their IR spectrum. The residue obtained from the filtrate on evaporation was chromatographed on silica gel with hexane-benzene (2:1). The first fraction was again chromatographed on alumina with the same solvent to give a trace of ferrocene and 0.06 g of biferrocenyl. The second fraction afforded 0.37 g (24.2% yield) of ferrocenyl benzoate. The total yield of biferrocenyl amounted to 0.62 g (67.0%).

The Reaction of *o*-Iodonitrobenzene with Copper(I) Acetate in Pyridine. The residue obtained from the reaction of *o*-iodonitrobenzene with copper(I) acetate under the conditions described above in the general procedure was chromatographed on silica gel with hexane-benzene (2:1) to give 0.12 g of a yellow liquid as a first fraction and 0.51 g (83.6%) of 2,2′-dinitrobiphenyl as a second fraction. The yellow liquid obtained from the first fraction was supposed to be a mixture of nitrobenzene and *o*-iodonitrobenzene, though attempts at identification failed because of the difficulty of separation.

19) A. N. Nesmeyanov, V. A. Sazonova and V. N. Drozd, *Chem. Ber.*, **93**, 2717 (1960).

BULLETIN OF THE CHEMICAL SOCIETY OF JAPAN VOL. 43 2217—2222 (1970)

Studies on Fluorene Derivatives. XXVI.[1] Radical Reactions in the Copyrolysis of Thermally-reactive Tribiphenylenepropanes

Kazuo Suzuki, Masahiro Minabe, Shozo Kubota* and Taro Isobe*

Department of Industrial Chemistry, Faculty of Technology, Utsunomiya University, Ishii-cho, Utsunomiya
* *Chemical Research Institute of Non-aqueous Solutions, Tohoku University, Katahira-cho, Sendai*

(Received January 30, 1970)

The pyrolyses of thermally-reactive tribiphenylenepropanes (mp 293°C (dec) or 257°C (dec)) in the presence of thermally-reactive 2,7,2′,7′,2″,7″-hexabromotribiphenylenepropane (mp 318—320°C (dec)) were investigated. Hydrocarbons, 2′,7′,2″,7″-tetrabromotribiphenylenepropane, 2,7-dibromo-9,9′-bifluorenyl, and -bifluorenylidene were obtained as pyrolysates from the respective thermal reactions, probably from intermolecular radical disproportionation reactions. In addition, 2,7,2′,7′-tetrabromo-9,9′-bifluorenyl, -bifluorenylidene, 2,7-dibromo-fluorene, and -fluorenone from hexabromotribiphenylenepropane, and 9,9′-bifluorenyl, -bifluorenylidene, fluorene, and fluorenone from tribiphenylenepropanes were formed by intramolecular reactions attributed to radical formation in the pyrolysis of each substrate. The pyrolyses of both tribiphenylenepropanes, 9,9′-bifluorenyl and 2,7,2′,7′,2″,7″-hexabromotribiphenylenepropane, were observed in a differential scanning calorimeter. The thermogram of tribiphenylenepropane (mp 257°C) is similar to that of 9,9′-bifluorenyl; the first endothermic peak corresponds to the melting point, and the second, broad one seems to be due to the slow formation of 9,9′-bifluorenylidene from 9,9′-bifluorenyl by means of a dehydrogenation process. In the thermogram of tribiphenylenepropane (mp 293°C), the first endothermic peak is the melting point, while the second, small one is probably caused by the overlapping of exothermic and endothermic peaks due to radical reactions during the formation and pyrolysis of tribiphenylenepropane (257°C). The thermal homolyses of solid tribiphenylenepropane isomers or those in a silicon oil solution were examined by ESR, which confirmed the radical formation in the pyrolyses.

Tribiphenylenepropanes were obtained by the Michael reaction[2] of 9,9′-bifluorenylidene (**3**) and

1) XXV of this series: K. Suzuki, M. Minabe, M. Fujimoto and N. Nohara, This Bulletin, **42**, 1609 (1969).

2) a) K. Suzuki, *Nippon Kagaku Zasshi*, **70**, 189 (1949). b) L. A. Pinck and G. E. Hilbert, *J. Amer. Chem. Soc.*, **68**, 2014 (1946).

fluorene (**13**), by the condensation of **13** with sodium amide, and by other reactions.[3] One of the isomers (mp 257°C (dec)), (**2**), is converted to the other (mp 293°C (dec)), (**1**), by the action of *N*-bromosuccinimide or Triton B.[4] We have found that the reverse process occurs during pyrolysis.

Compound **1** gave two isomers, **2** and **3**, and 9,9′-bifluorenyl (**4**) by pyrolysis, while **2** gave **3** and **4**.[2a] Additionally, 2,7,2′,7′,2″,7″-hexabromotribiphenylenepropane (**5**) yielded 2,7,2′,7′-tetrabromo-9,9′-bifluorenyl (**6**), -bifluorenylidene (**7**), and 2,7-dibromofluorenone (**12**) by pyrolysis.[5] Previously, homolytic fission was proposed as the mechanism for the formation of **2**, **3**, **4**, **6**, and **7**.[6]

The current investigation deals with the confirmation of the reaction products formed by intermolecular radical reactions during the thermolyses of tribiphenylenepropanes in the presence of **5**.

In a preliminary experiment,[2a] **13** and fluorenone (**14**) could not be isolated. A re-investigation of the pyrolysis of tribiphenylenepropane isomers showed that **1** gave **2**, **3**, **4**, **13**, and **14**, while **2** gave **3**,**4**, **13**, and **14**, as confirmed by gas-chromatographic analysis. The data are listed in Table 1.

Moreover, for the purpose of studying the thermal behavior, a differential scanning calorimeter (DSC) was employed which showed exothermic or endothermic peaks depending on the combination of physical and chemical changes proceeding at the reaction temperature. The formation of free radicals was confirmed by ESR.

Compounds **4**, **1**, **2**, and **5** are thermally-active species, each possessing two active methine groups. Under the pyrolytic conditions, the six carbon-bromine bonds in **5** are more stable than the 9-9′-9″ carbon-carbon covalent bonds in tribiphenylenepropanes.

Accordingly, the pyrolysates, **2**, 2′,7′,2″,7″-tetrabromotribiphenylenepropane (**8**), **6**, **7**, 2,7-dibromo-9,9′-bifluorenyl (**9**), -bifluorenylidene (**10**), **3**, 2,7-dibromofluorene (**11**), **12**, **13**, and **14** were observed by the copyrolysis of **1** and **5** at 320—330°C. Also, by the same process, **8**, **6**, **7**, **9**, **10**, **3**, **4**, **11**, **12**, **13**, **14**, and 2% of recovered **2** were obtained by the copyrolysis of **2** and **5** at 330—340°C.

In view of these results, it appears that all compounds participate in the fission of 9-9′-9″ carbon-carbon bonds in tribiphenylenepropanes. Moreover, the formation of the three structures, **8**, **9**, and **10**, can be explained in terms of intermolecular free radical reactions based on the thermal homolyses between the two different bromo- and nonbromo-tribiphenylenepropanes precursors. Schemes I and II summarize the pyrolytic pathways suggested for

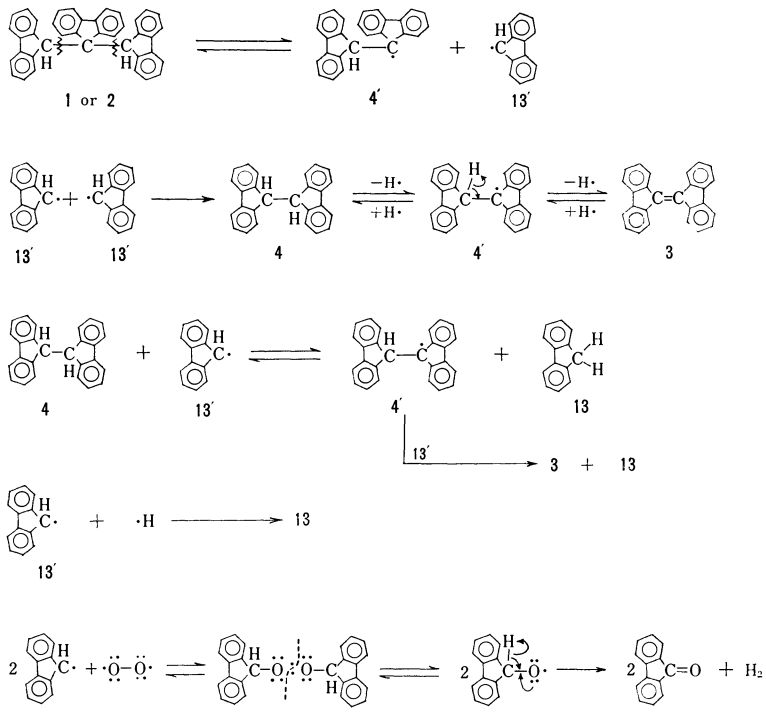

Scheme I. Pyrolyses of tribiphenylenepropanes.

3) a) K. Suzuki, *Nippon Kagaku Zasshi*, **72**, 825 (1951). b) K. Suzuki, *ibid.*, **72**, 827 (1951); **75**, 711 (1954); K. Suzuki and S. Kajigaeshi, This Bulletin, **35**, 408 (1962); K. Suzuki and M. Fujimoto, *ibid.*, **37**, 1833 (1964); K. Suzuki, M. Minabe, M. Fujimoto and N. Nohara, *ibid.*, **42**, 1609 (1969).

4) K. Suzuki and M. Minabe, unpublished.

5) K. Suzuki, *Nippon Kagaku Zasshi*, **75**, 795 (1954).

6) K. Suzuki, *Technol. Repts. Tohoku Univ.*, **19**, 63 (1955).

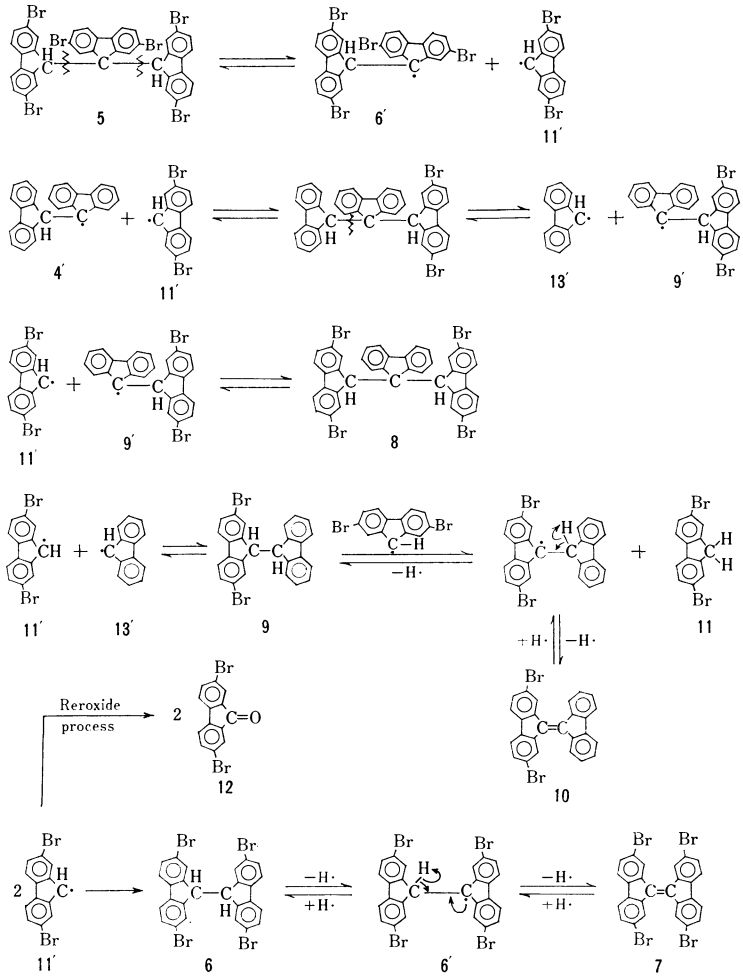

Scheme II. Pyrolyses of tribiphenylenepropanes in the presence of 2,7,2′,7′,2″,7″-hexabromotribiphenylenepropane (**5**).
(Compounds **6**, **7**, **8**, **9**, **10**, **11** and **12** were isolated.)

the formation of these compounds.

The 9-fluorenyl (**13′**) and 9-fluorenyl-9′-fluorenylidene (**4′**) radicals were presumably formed in the initial homolytic fission of **1** or **2**. A coupling reaction of **13′** could occur in the melt to give **4**, while the unsaturated hydrocarbon, **3**, may have been formed by dehydrogenation during the pyrolytic process.[2a] The formation of **13** can be explained by hydrogen abstraction from **4′** or **4** by **13′** during the formation of **3** and/or by reaction of **13′** with a hydrogen radical.

Tribiphenylenepropane (mp 257°C), (**2**), may be formed by a re-combination of the **4′** and **13′** radicals in a different steric configuration from that of the compound with a mp of 293°C (**1**). The coupling product of **4′** could not isolated; if this were formed, it might lead to the formation of **3** and **13′** by pyrolysis.

In addition, **14** was probably formed from **13′**, in the presence of trace amounts of air, *via* a peroxide mechanism by simple scission on the oxygen-oxygen bond to radicals analogous to that which would occur in peroxide, as is indicated in Scheme I.

Accordingly, the formation of compounds **6**, **7**, and **11** seems reasonable in these instances by combinations of free radical species; this is analogous with the reaction of tribiphenylenepropane, as is illustrated in Scheme II. Likewise, the formation of **12** may be similar to the case of **14**.

Our interpretation is that compound **8** is presumably formed by a combination of dissociation and coupling during the thermal reaction. The free radicals, **4′** and 2,7-dibromo-9-fluorenyl (**11′**), produce by coupling the intermediate, 2′,7′-dibromotribiphenylenepropane,[7] which may then

7) 2′,7′-Dibromotribiphenylenepropane led to 2′,7′,2″,7″-tetrabromotribiphenylenepropane (**8**) and other correlated compounds by pyrolytic reactions (see Ref. 3a).

dissociate into **13′** and 2,7-dibromo-9-fluorenyl-9′-fluorenylidene (**9′**) radicals. Thus, **8** is formed by the reaction of **11′** and **9′** radicals. In addition, **9** may have been formed by a radical reaction of **11′** and **13′**; further, **10** could conceivably result from **9** by a process analogous to that in the case of **3**.

The pyrolysates, **13**, **14**, **4**, and **3**, from **1** or **2**, in order of their retention times, were confirmed by gas-chromatographic analysis. Differential scanning calorimetry was employed to study the thermal behavior of the reactive **1**, **2**, **4**, and **5** on the basis of the pyrolyses described above. These results are illustrated in Fig. 1.

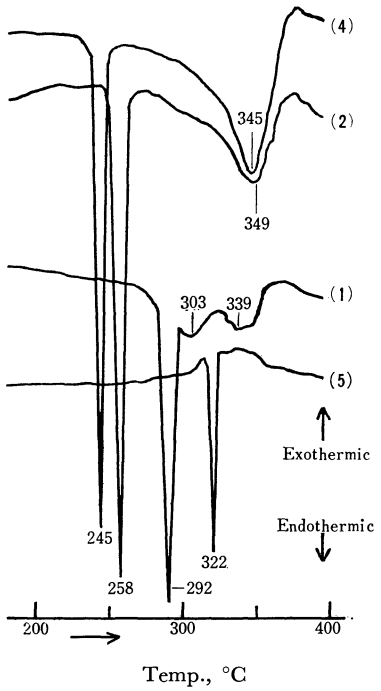

Fig. 1. Differential scanning calorimeter thermograms of **1**, **2**, **4** and **5**.

In the (4) thermogram, **4** (mp 246°C), one of the pyrolysates from **1** or **2**, can be seen to melt at the first endothermic peak (245°C), while the second, broad peak (345°C, dark red) is probably the major constituent due to the slow formation of **3** (red needles) from **4** by dehydrogenation. Moreover, the pyrolysis of **4** is known to form **3**.[2a] In this connection, the application of the DTA method to the pyrolysis of **4** has previously been reported by Lewis and Edstrom,[8] but the curves were not clear.

The two major endothermic peaks for the (2) thermogram are similar to those of **4**; the first peak corresponds to the melting point (red) at about 258°C, but a relatively slow pyrolysis[9] at the melting point was observed, unlike the case with **1**.

8) I. C. Lewis and T. Edstrom, *J. Org. Chem.*, **28**, 2050 (1963).

9) See Table 1, Run 3, for example.

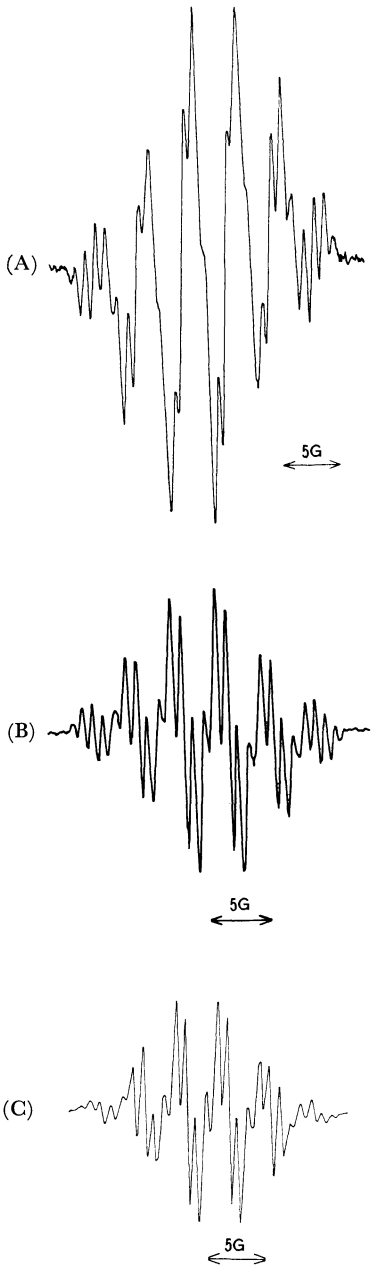

Fig. 2. Experimental spectra generated from the tribiphenylenepropane (**1**).
(A): 280°C
(B): 286°C in silicon oil solution
(C): Simulated pattern of **4′** or **13′**; 5H (1, 3, 6, 8 and 9)=3.67 gauss; 4H (2, 4, 5 and 7)=0.82 gauss; line width=0.65 gauss

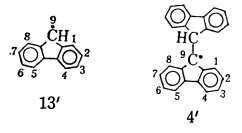

Subsequently, the slope curves suggest that the melting depression can be attributed to the progressive formation of compounds **3**, **4**, **13**, and **14** with an elevation of the temperature after the melting peaks. In addition, the broader endothermic peak (349°C) suggests that the **4**→**3** transformation is taking place.

In the thermogram of **1**, the slope curves at 200—280°C as the thermolyses increase with an elevation in the temperature. Indeed, the pyrolysis was accompanied by a readily observable red color change in addition to the temperature rise. Thus, the melting peak (292°C) is relatively small compared with that of **2**, although equal weights of the **1** and **2** isomers were used. The results of ESR show that the pyrolyses of tribiphenylenepropane isomers begin at about 200°C. The first, small peak (303°C) after the melting point suggests the formation of **2** from **1** with a consequent pyrolysis of **2** (mp 257°C), as has been described above. Accordingly, the peaks overlap as a result of compensation by exothermic and endothermic peaks. The endothermic peak (339°C) might correspond to the formation of **3** from **4**.

Although the sample weight of **5** used was roughly equal to those of **1** or **2**, the melting peak (322°C) of **5** is comparatively small; **5**, therefore, corresponds to double the molecular weight.

The solid compounds, **1**, **2**, and **4**, were degassed and their ESR spectra were measured in the range from about 200°C to near their melting points. The signals obtained from each sample were very similar. A typical pattern of **1** is shown in Fig. 2. The signal measured in a silicon oil solution is in sharp contrast to that observed in a solid sample. The same results were observed in a squalane solution instead of in the silicon oil.

As is shown by the simulation calculations, these spectra can be explained in terms of the hyperfine interaction with five equivalent protons with a large splitting constant and four equivalent protons with a small splitting constant. These splitting constants may be attributed to the two radicals, **4′** and/or **13′** (see Fig. 2). Previously Dalton and Liebman[10] observed the fluorenyl radical, **13′**, generated from 9-diazofluorene in decalin at 170°C. The ESR spectra observed in the present work are, however, in poor agreement with those observed by Dalton *et al.* Therefore, the radical is conceivably **4′** rather than **13′**.

Experimental

All the melting points are uncorrected.

The gc data were obtained with a JGC-810FP apparatus (Japan Electron Optics Lab. Co., Ltd.), using a column containing 10% Silicone SE-30 on Chromosorb W-AW. During analysis, the column temperature was programmed at 304°C, while the detector and injector temperatures were maintained at 340°C and 400°C respectively. Samples **1** and **2** were used as 2% chloroform solutions.

The infrared spectra were recorded as KBr pellets using a JASCO model IR-G spectrophotometer (Japan Spectroscopic Co., Ltd.).

Differential scanning calorimeter. The instrument used in this investigation was of the Desktop type, 8001-CS (Rigaku Denki Co., Ltd.), was equipped with α-aluminum oxide as a standard sample, and had a sensitivity of ±4 mcal/sec. The experiments were run at atmospheric pressure in air at a heating rate of 10°C per minute. Samples **4** (13.3 mg), **1** (18.1 mg), **2** (18.1 mg), and **5** (18.2 mg) were pyrolyzed in sealed aluminum pans (o.d., 5.0 mm; height, 2.0 mm; thickness, 5/100 mm) with aluminum covers (5/100 mm) which were packed with a sample clipper.

The ESR spectrometer used was an X-band JES-3BSX-type apparatus (Japan Electron Optics Lab. Co., Ltd.) with a 100-KHz-field modulation and a variable-temperature insert dewar.

Pyrolysis of Tribiphenylenepropane (1). Finely-powdered **1** (4.94 g or 0.01 mol) was placed in a 300-m*l* Erlenmeyer flask attached to an air condenser. The flask was then heated in a salt-bath to 305—308°C with shaking for 5 min. After 3—4 min, the reactant was a red melt.

After the content of the flask had resolidified, it was ground to a fine powder; this powder was then extracted with 50 m*l* of boiling cyclohexane. The residual portion (mp 245—270°C) was recrystallized from benzene to give 3.52 g (71%) of **2** (mp 257°C (dec)). Upon the evaporation of the benzene mother liquor to a small volume, 0.53 g (11%) of **1** (mp 292—293°C (dec)) was recovered.

The dilution of the last benzene mother liquor with ethanol afforded a yellow precipitate, which was recrystallized from benzene to give 0.14 g (3%) of **4** (mp 243—244°C). The residue from the evaporation of the benzene-ethanol mother solution to dryness was recrystallized from ethanol to give 0.06 g of **3** (mp 185—186°C).

The concentration of the cyclohexane extract to a small volume afforded 0.35 g of **3** (mp 184—185°C). Then the cyclohexane mother solution was evaporated to dryness and the residue was sublimed *in vacuo* at a bath temperature of 140°C, yielding 0.02 g (0.4%) of **13** (mp 110—112°C) and 0.02 g (0.4%) of **14** (mp 77—79°C), which were separated by column chromatography in benzene on alumina. The unsublimable material was recrystallized from benzene to give 0.13 g (total 0.54 g, 11%) of **3** (mp 183—185°C).

Pyrolyses of Tribiphenylenepropane (1) in the Presence of 2,7,2′,7′,2″,7″-Hexabromotribiphenylenepropane (5). Finely-powdered **1** (3.00 g; 0.006 mol) and 2.90 g (0.003 mol) of **5** were placed in a 300-m*l* Erlenmeyer flask attached to an upright air condenser. When the mixture was heated at 320—330°C for 5 min, it yielded a red pyrolysate after a few minutes.

The powdered product was extracted with 80 m*l* of boiling cyclohexane. The fractional recrystallization of the residue part from 130 m*l* of refluxing benzene yielded 0.06 g of **7** (mp 423—424°C (dec)), 0.05 g of **6** (mp 318—319°C), 0.06 g of **8** (mp 313—314°C (dec)), 0.04 g

10) D. R. Dalton and S. A. Liebman, *J. Amer. Chem. Soc.*, **91**, 1194 (1969).

Table 1. Reaction products in pyrolyses of tribiphenylenepropanes under different conditions

Run	Substrates		Reaction conditions °C×min	Products, g (%)					Recvd. g (%)
	Compds.	g (mol)		**2**	**4**	**3**	**13**	**14**	
1	**1**	4.94 (0.01)	295—300×3.5	0.94 (18)	0.04 (1)	0.11 (2)	0.01 (0.2)	0.12 (2)	3.58 (73)
2	**1**	4.94 (0.01)	305—308×5	3.52 (71)	0.14 (3)	0.54 (11)	0.02 (0.4)	0.02 (0.4)	0.53 (11)
3	**2**	4.94 (0.01)	265—267×5		0.02 (0.4)	0.02 (0.4)	trace	0.01 (0.2)	4.55 (92)
4	**2**	4.94 (0.01)	280—285×10		0.07 (1)	0.09 (2)	0.0014	0.04 (0.7)	4.45 (90)
5	**2**	4.94 (0.01)	260—290×20		2.33 (47)	0.61 (12)	0.20 (4)	0.28 (5)	1.11 (23)
6	**4**	6.6 (0.02)	Rm. temp.→390 (for 40) 390×5			0.66 (10)	1.90 (29)	0.38 (5)	0.80 (12)

of **9** (mp 265—266°C), and 0.10 g of recovered **5** (mp 318—320°C (dec)). These substances were deposited in the order of their decreasing solubilities by the removal of the benzene.

The cyclohexane extract was concentrated to a small volume. The following orange-red crystalline crops were filtered off: 0.19 g (total 0.25 g) of **8** (mp 313—314°C (dec)), 0.51 g (total 0.55 g) of **9** (mp 267—268°C), 0.08 g of **2** (mp 255—257°C (dec)), (no halogen), 0.24 g of **10** (mp 243—244°C), 1.57 g of **3** (mp 182—185°C), 0.17 g of **12** (mp 201—202°C), and a recovered 0.04 g (total 0.14 g) of **5** (mp 315—317°C (dec)). Fractional recrystallization from ethyl acetate was also employed.

The last cyclohexane mother solution was chromatographed on an alumina column. The eluant was evaporated to dryness, and the residue was fractionaly sublimed to 160°C under reduced pressure; 0.03 g of **13** (mp 108—110°C) and 0.01 g of **11** (mp 158—161°C) were thus separated. Fractions of 0.36 g of **14** (mp 79—80°C), (no halogen) and 0.05 g (total 0.22 g) of **12** (mp 195—197°C) were isolated from the yellow-absorbed band on the alumina column by established methods.

Pyrolyses of Tribiphenylenepropane (2) in the Presence of 2,7,2′,7′,2″,7″-Hexabromotribiphenyleneпropane (5). A mixture of 3.00 g (0.006 mol) of **2** and **5** (2.90 g, 0.003 mol) was pyrolyzed at 330—340°C for 3 min in an atmosphere of nitrogen. The reaction products were then worked up in a manner similar to those employed in the **1** and **5** reactions. Thus 0.13 g of **7** (mp 428°C (dec)), 0.18 g of **8** (mp 312—314°C (dec)), 0.35 g of **6** (mp 316—317°C), 1.28 g of **9** (mp 268—270°C), 0.33 g of **4** (mp 240—241°C), 0.04 g of **10** (mp 238—240°C), 0.03 g of **13** (mp 111°C), 0.33 g of **14** (mp 79—80°C), 0.04 g of **11** (mp 161—163°C), 0.05 g of **12** (mp 199—201°C), and 0.11 g of **3** (mp 180—182°C) were isolated. In addition, 0.08 g of **5** and 0.64 g of **2** were recovered.

All the pyrolysates were known compounds which were identified by a comparison of their melting points, mixed melting points, and infrared absorption spectra with those of authentic samples.

The authors wish to express their gratitude to Drs. John and Elizabeth Weisburger of the National Institutes of Health, U. S. A., for supplying editorial assistance. Thanks are also due to Mr. Koichi Kubo for measurements of the electron spin resonance, Mr. Fumio Funatani of the Japan Electron Optics Lab. Co., Ltd., for his gas chromatographic analyses, and to Mr. Kimio Satoh of the Rigaku Denki Co., Ltd., for his measurements with the differential scanning calorimeter.

This work was supported in part by a grant-in-aid from the Ministry of Education, for which the authors wish to express their appreciation.

BULLETIN OF THE CHEMICAL SOCIETY OF JAPAN VOL. 43 2223—2229 (1970)

Chemical Constituents of *Alnus firma* (BETULACEAE). I. Phenyl Propane Derivatives Isolated from *Alnus firma*

Yoshinori ASAKAWA

Department of Chemistry, Faculty of Science, Hiroshima University, Higashisenda-machi, Hiroshima

(Received February 2, 1970)

Viscous substances extracted from young shoots of *Alnus firma* were investigated, and two new hydroxyketones, named yashabushiketol (I) and dihydroyashabushiketol (II), *trans*-stilbene (III), β-phenylethyl cinnamate (IV), pinostrobin (V), alpinetin (VI), cinnamic acid (VII), paraffin hydrocarbons (*n*-, anteiso and iso) and triglycerides were identified on the basis of the chemical and spectral data. The biosynthetic pathways of the above aromatic compounds were discussed.

Alnus firma (the Japanese name is Yashabushi), which grown on poor and waste land, is a deciduous plant and a member of the birch-tree family (BETULACEAE). It is known that this plant can be used as an erosion-control plant and that its young shoots (Catkin) and leaves secrete viscous substances, late in February in Japan. No reports on the chemical constituents of *Alnus* genera have yet been presented, though. In the course of the investigation of the benzene extract of the viscous material on the young shoots, two new hydroxyketones, which possess a phenyl propane skeleton, were isolated, together with five related aromatic compounds. The present communication will be concerned with the structure elucidation and the biosynthetic pathways of these seven aromatic compounds, and with the detection of paraffin hydrocarbons and triglycerides.

Results and Discussion

The extraction of the young shoots with benzene gave a dark green, viscous material. After the removal of the acidic and phenolic constituents, the neutral portion was fractionated into three parts by silica-gel chromatography using *n*-hexane, benzene, and ethyl acetate as the eluting agents.

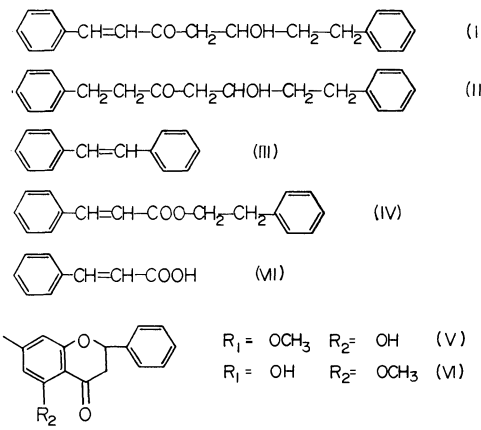

Yashabushiketol (I). 1,7-Diphenyl-5-hydroxy-1-hepten-3-one. Compound (I) was isolated as colorless needles by ethyl acetate extraction from the fractions. This compound (mp 59.5—60.5°C (from *n*-hexane), $[\alpha]_D^{20}$ +29.0°, R_f=0.14 on TLC) gives positive coloration with 2,4-DNP and with alkali-alkyl xanthate. The molecular formula of compound (I) was established as $C_{19}H_{20}O_2$ from a high-resolution mass spectrum. The UV spectrum shows λ_{max}^{EtOH} 217 mμ (log ε, 4.38), 227 (3.90) and 289 (4.18), suggesting the presence of cinnamoyl chromophore (Ar–CH=CH–CO).[1] The IR spectrum shows absorption bands at 1703 cm^{-1} (α,β-unsaturated carbonyl group), 3090, 3050, 1607, 1490, 1447, 752, and 702 cm^{-1} (monosubstituted benzene-ring), 3400 and 1100 cm^{-1} (secondary hydroxyl group), 1410 cm^{-1} (active methylene), and 3025, 1678 and 980 cm^{-1} (*trans* double bond). The NMR spectrum of I contains the following signals: a typical AB-type doublet at 7.61 and 6.71 ppm (J_{AB}=16 Hz, 1H, each) assignable to *trans* ethylenic protons of the cinnamoyl group, two overlapped singlets, at 7.27 and 7.25 ppm, accounted for by two monosubstituted benzene-ring protons (10H), a quintet at 4.07 ppm (J=7 Hz, 1H of –CH–) attributable to the presence of the $-CH_2-CHOH-CH_2-$ grouping, a complex multiplet located between 2.70 and 2.90 ppm (2H, of $-CH_2-$) assignable to the presence of the $-CO-CH_2-CHOH-$ grouping,[2,3] a triplet at 2.60 ppm (J=7 Hz, 2H of Ar–$C\underline{H}_2-$) due to the $Ar-CH_2-CH_2-$ group, a quartet at 1.89 ppm (J=7 Hz, 2H of –CH–$C\underline{H}_2-CH_2-$) due to the $-CHOH-CH_2-CH_2-$ group, and a broad singlet at 3.20 ppm (1H), which disappeared on

1) A. I. Scott, "Interpretation of the Ultraviolet Spectra of Natural Products," Pergamon Press, Oxford (1964), p. 115.

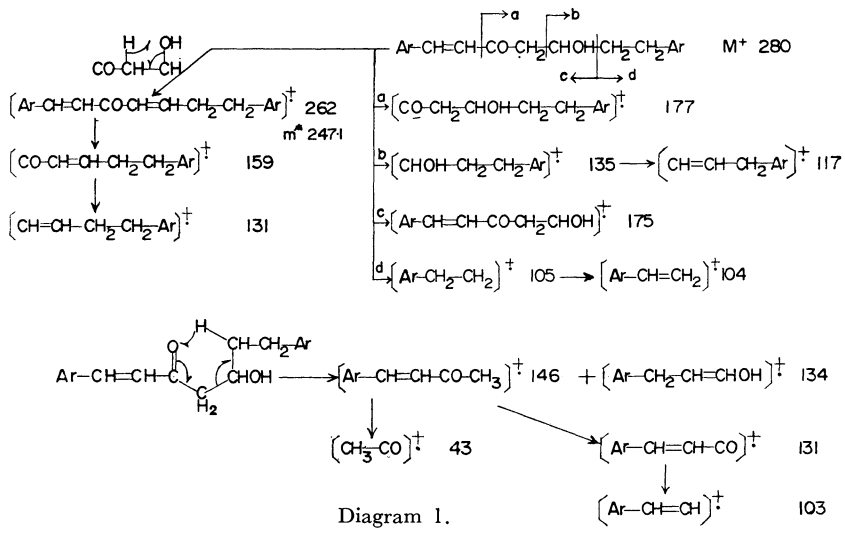

Diagram 1.

equilibration with D_2O, assignable to a hydroxy group. When I in pyridine was treated with acetic anhydride, a yellow, viscous monoacetate was obtained (IR: 1735, 1239 and 1028 cm^{-1}). That a hydroxyl group of I was secondary was proved by the fact that 4.07 ppm (quin. $J=7$ Hz, 1H) was shifted to 5.40 ppm (quin. $J=7$ Hz, 1H) after the acetylation of I.[4] Ketol (I) contains one double bond, as it absorbed one mole equivalent of hydrogen on catalytic hydrogenation over an Adams' catalyst in acetic acid and produced a dihydroderivative, $C_{19}H_{22}O_2$ (M^+ 282), mp 36.0—37.0°C, $R_f=0.25$. The IR spectrum of the dihydroderivative does not exhibit absorption bands at 3025, 1678, 1574, and 980 cm^{-1}, nor could the two doublet signals of the NMR spectrum at 7.61 and 6.71 ppm be seen. From the above chemical and spectral evidence, the following partial structures may be suggested. The ketol (I) contains the molecular

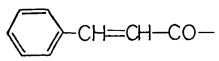

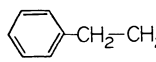

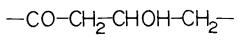

ion at *m/e* 280 ($C_{19}H_{20}O_2$ from the high-resolution mass measurements), the base peak at *m/e* 91 corresponding to a tropyrium ion, and a prominent ion corresponding to M−18 (*m/e* 262), all of which evidence indicates I to be an alcohol. The presence of characteristic ions, *m/e* 39, 51, 65, and 77 indicates I to be a monosubstituted benzene derivative. Other strong ions (*m/e* 177, 175, 159, 146, 134, 117, 105, 104, 103 and 43) in the mass spectrum may be explained as is represented in Diagram 1. The presence of the fragment ions at *m/e* 146, 134, 131, and 103 is understandable, since I, possessing a γ-hydrogen atom for a carbonyl group, undergoes β-cleavage with hydrogen transfer and the product (280→146+134) of β-cleavage is degradated by the loss of a methyl radical (146→131) and of carbon monoxide (131→103) successively. In the mass spectrum of the hydrogenated product of I, the strength of the fragment ions at *m/e* 131 decreased and the fragment of *m/e* 262 disappeared, while *m/e* 133 $(Ar\text{-}CH_2\text{-}CH_2\text{-}CO)^+$ and *m/e* 264 (M—18) newly appeared. On the basis of the above-mentioned chemical and spectral data, the structure of I was determined to be 1,7-diphenyl-5-hydroxy-1-hepten-3-one (I). We proposed the name "yashabushiketol" for this compound in a preliminary report.[5]

Dihydroyashabushiketol (II). 1,7-Diphenyl-5-hydroxy-3-heptanone. The high-resolution mass measurement of the II isolated from the ethyl acetate fraction clearly established its molecular formula as $C_{19}H_{22}O_2$. This compound, (II) (M^+ 282, mp 36.0—37.0°C (colorless needles from *n*-hexane), $R_f=0.25$), gives positive coloration with 2,4-DNP and with alkali-alkyl xanthate, and negative coloration with ferric chloride, ferric hydroxamate, and Tollens' reagent. Compound (II) is shown by its spectral properties to possess a simple ketone group

2) R. M. Silverstein and G. C. Bassler, "Spectrometric Identification of Organic Compounds," John Wiley & Sons, Inc., New York (1967), p. 129.

3) G. Rücker, *Chem. Ber.*, **102**, 2707 (1969).

4) W. Herz, K. Ueda and S. Inayama, *Tetrahedron*, **19**, 483 (1963).

5) Y. Asakawa, F. Genjida, S. Hayashi and T. Matsuura, *Tetrahedron Lett.*, **1969**, 3235.

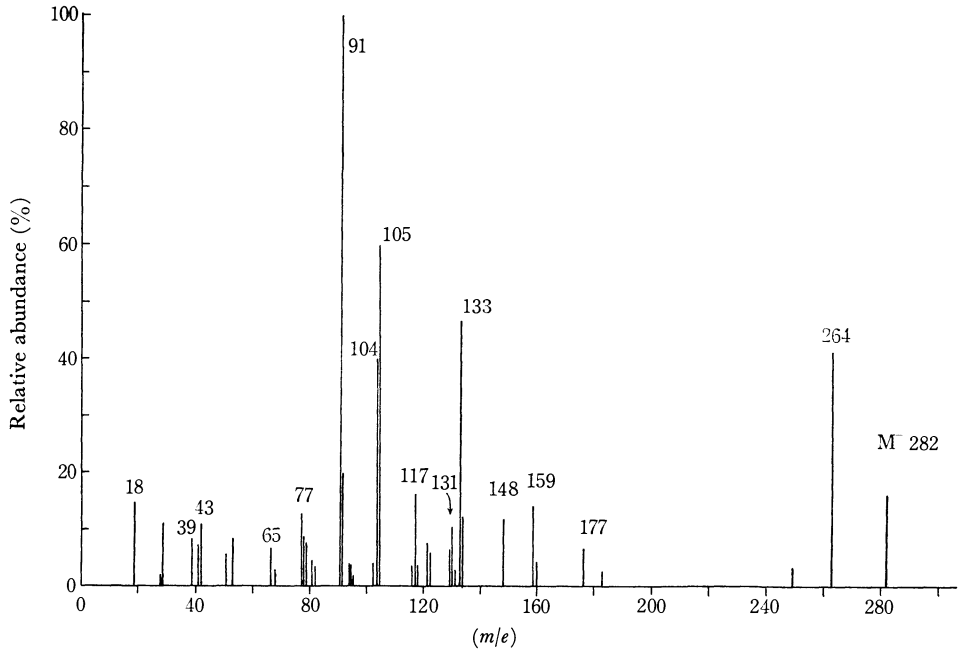

Fig. 1. Mass spectrum of dihydroyashabushiketol (1,7-diphenyl-5-hydroxy-3-heptanone).

(λ_{max}^{EtOH} 285 mμ (log ε, 2.08), ν_{max}^{liq} 1706 cm^{-1}), a mono-substituted benzene-ring (ν_{max}^{liq} 3060, 3020, 1600, 1490, 1450, 745 and 698 cm^{-1}), a non-conjugated benzene-ring (λ_{max}^{EtOH} 248 mμ (log ε, 2.50), 254 (2.53), 261 (2.54) and 268 (2.44)), active methylene (1409 cm^{-1}), and a secondary hydroxyl group (3440 and 1100 cm^{-1}). The NMR spectrum of II in $CDCl_3$ indicates signals at 7.22 ppm (s, 10H, two mono-substituted benzene-ring protons), 4.07 ppm (quin. J=7 Hz, 1H, -CH_2-C<u>H</u>OH-CH_2-), 3.10 ppm (s, 1H, O<u>H</u>), complex signals located between 2.70 and 2.90 ppm (4H, -C<u>H</u>$_2$-CO-C<u>H</u>$_2$-CHOH-), 2.55 ppm (two triplets partially overlapped, J=7 Hz, 4H, two Ar-C<u>H</u>$_2$-CH_2-) and complex multiplets located between 1.55 and 1.85 ppm (2H, -CHOH-C<u>H</u>$_2$-CH_2-). The mass spectrum (Fig. 1) of II is closely analogous to that of yashabushiketol (I). It shows the parent ion at *m/e* 282, and the base peak at *m/e* 91 corresponding to that of a tropyrium ion. An important difference between the fragmentations of these two ketols, (I) and (II), is that II possesses the molecular ion at *m/e* 282 and fragment ions at *m/e* 264 (M−18), *m/e* 148 (Ar-CH_2-CH_2-CO-CH_3)$^+$, and *m/e* 133 (Ar-CH_2-CH_2-CO)$^+$, whereas I has the molecular ion at *m/e* 280 and fragment ions at *m/e* 262 (M−18), *m/e* 146 (Ar-CH=CH-CO-CH_3)$^+$, and *m/e* 131 (Ar-CH=CH-CO)$^+$. As II has only two larger fragments and the molecular ion more than I, judging from a comparison between the mass spectra of two compounds, it seems that ketol (II) is the dihydroderivative of I. Other strong fragment ions also appear at *m/e* 177 (Ar-CH_2-CH_2-CO-CH_2-CH=OH)$^+$, *m/e* 159 (Ar-CH_2-CH_2-CO-CH=CH)$^+$ or (Ar-CH_2-CH_2-CH=CH-CO)$^+$, *m/e* 131 ($C_{10}H_{11}^+$, (Ar-CH_2-CH_2-CH=CH)$^+$ from high-resolution mass measurement), *m/e* 117 (CH=CH-CH_2-Ar)$^+$, and *m/e* 43 (CH_3-CO)$^+$. The peaks at *m/e* 39, 51, 65 and 77 constitute additional evidence for the benzene ring. These results have shown the structure of this ketol to be 1,7-diphenyl-5-hydroxy-3-heptanone (II). Furthermore, this structure was confirmed by the fact that the TLC R_f value, the mp, and the IR spectrum of II were all completely identical with those of the hydrogenated product of yashabushiketol (I). We proposed the name "dihydroyashabushiketol" for this compound in a previous communication to this bulletin.[6]

***trans*-Stilbene (III).** Colorless leaflet crystals, M$^+$ 180, mp 120.0—121.0°C, R_f=0.75, were isolated from the *n*-hexane extract. The melting point, R_f value, UV, IR, and NMR spectra of this isolated compound (III) were the same as the authentic *trans*-stilbene. There has been no report concerning the natural occurrence of *trans*-stilbene, except that Kacheler (1869) suggested the existence of stilbene on the basis of its melting point in Perubalsam oil.[7]

β-Phenylethyl Cinnamate (IV). Colorless needles (M$^+$ 252, mp 56.0—57.0°C, R_f=0.50, positive coloration with ferric hydroxamate) were isolated in a pure state (one peak, NGS 10%, 212°C) from the benzene-eluted fraction of the extract. The alkaline hydrolysis of the isolated crystals (IV) gave cinnamic acid and β-phenylethyl alcohol. The

6) Y. Asakawa, This Bulletin, **43**, 575 (1969).

7) E. Gildmeister, "Die Ätherischen Öle," Academie-Verlag, Berlin (1960), p. 413.

UV, IR and NMR spectra, the mp, the R_f value and the GLC Rt of this compound (IV) were all completely identical with those of the authentic β-phenylethyl cinnamate. It was clarified that the essential constituent with a pleasant smell in the yound shoot of *A. firma* is β-phenylethyl cinnamate, and that this compound gives rise to the viscosity of the young shoots. The only report regarding the finding of β-phenylethyl cinnamate from *Populus balsamifera* has been made by Goris and Canal.[8]

Pinostrobin (5-Hydroxy-7-methoxy-flavanone) (V). Compound (V) was isolated from the benzene-eluted fraction as colorless leaflet crystals (M^+ 270, mp 99.0—100.0°C, R_f=0.48, positive coloration with ferric chloride and with magnesium-hydrochloric acid). The mass spectrum of V is closely analogous to that of 5,7-dihydroxy flavanone.[9] When V in pyridine was treated with acetic anhydride, it gave a mono-acetate. On methylation with dimethyl sulfate, V gave pinostrobin methyl ether. The UV, IR, and NMR spectral data and the mp of the isolated original compound agreed well with those of the pinostrobin which was isolated from *Kaempferria pandurata* (ZINGIBERACEAE).[10] It is well known that pinostrobin is widely distributed in Pinaceae.[11-14]

Alipinetin (5-Methoxy-7-hydroxy-flavanone) (VI). The extensive chromatography of the phenolic portion afforded a flavanone as white needles (M^+ 270, mp 224.5—225.5°C, R_f=0.65 (benzene-methanol-acetic acid 5 : 1 : 1 vol%), negative coloration with ferric chloride and with magnesium-hydrochloric acid). The NMR spectrum of VI in trifluoroacetic acid indicates signals quite similar to those of pinostrobin. The effect upon the mass spectrum of VI is also closely analogous to that of pinostrobin and 5,7-dimethoxyflavanone. When VI was methylated, it gave pinostrobin methyl ether as fine needles. The UV and IR spectra and the mp of the isolated flavanone (VI) showed good agreement with those of alpinetin.[10]

Mongkolsuk and Dean[10] found that pinostrobin and alpinetin both occurred in *Kaempferria pandurata* (ZINGIBERACEAE) and considered that flavanoids possessing a 5-methoxy group are unusual in plants. There is no record of the coexistence of pinostrobin and alpinetin in Dicotyledoneae.

Cinnamic Acid (VII). A large quantity of colorless needles (mp 134.0—134.5°C) was isolated from the acidic portion of the extract regenerated from the sodium bicarbonate solution. The acidic compound (VII) was converted to methyl cinnamate with diazomethane. The IR and NMR spectra and the mp of the isolated acid (VII) were all completely identical with those of the authentic cinnamic acid.

In addition to the above compounds, paraffin hydrocarbons (*n*-paraffins: *n*-C_{21}—*n*-C_{33}, main component, *n*-C_{27}; anteiso: C_{22}, C_{24} and C_{26}; iso: C_{21}, C_{23} and C_{25}) and triglycerides (acid portions: saturated fatty acids, C_{16}, C_{18}, C_{20}, C_{21}, C_{22}, C_{23} and C_{24}) were tentatively identified by a comparison of the retention time with those of authentic specimens of *n*-paraffins (SE-30 2.5%, 180—300°C and 200°C) and of fatty acid methyl esters (DEGS 10%, 187°C), and by the linear relationship between the logarithm of the retention time and the number of the carbon atom of the paraffins and the fatty acid methyl esters respectively.

Biosynthetic Pathways of the Aromatic Compounds Isolated from *A. firma*. Many natural phenyl-propane derivatives have been found in organisms, and it is now recognized that the fundamental skeleton of phenyl-propane derivatives arises from phenylalanine and its congeners derived from shikimic acid and prephenic acid (these are the key compounds in this series). Birch[15] and Underhill[16] suggested that the skeletons of flavanoids and stilbenes arise from a cinnamic acid unit and three acetate units, and they assumed that, in the biosynthesis of pinosylvin (VIII), one molecule of cinnamic acid condenses with three molecules of acetic acid to give the intermediate (IX), which is then cyclized to pinosylvin carboxylic acid (X) and finally decarboxylated to give pinosylvin (VIII), as is shown in Diagram 2. This hypothesis possesses the further merit that it explains the isolation of two stilbene carboxylic acids (hydrangenic acid (XI) and phyllodulcic acid (XII)) and the coexistence of flavanoids (*e.g.*, pinocembrin (XIII) and its methyl ethers) and stilbenes (*e.g.*, pinosylvin (VIII) and its methyl ethers) in the heartwood of many pines[11] and in the buds of some species of Eucalyptus,[17] and from some of these sources cinnamic acid has been isolated. This hypothesis has been confirmed by the investigation of the biosynthesis of pinosylvin and hydrangenic acid using radioactive acetate and glucose.[18,19] Thus, it

8) A. Goris and H. Canal, *Bull. Soc. Chim. Fr.*, **1936**, 1982.
9) H. Audier, *ibid.*, **1966**, 2892.
10) S. Mongkolsuk and F. M. Dean, *J. Chem. Soc.*, **1964**, 4654.
11) V. B. Mahesh and J. R. Seshadri, *Chem. Abstr.*, **49**, 11273 (1955).
12) H. Erdtman, *ibid.*, **40**, 1309 (1946).
13) M. Sogo and K. Hata, *ibid.*, **48**, 12922 (1954).
14) G. Lindstedt and Misiorny, *Acta Chem. Scand.*, **5**, 121 (1951).
15) A. J. Birch and F. W. Donovan, *Aust. J. Chem.*, **6**, 260 (1953); A. J. Birch, *Fortschr. Chem. Org. Naturst.*, **14**, 189 (1957).
16) E. W. Underhill, J. E. Watkin and A. C. Neish, *Can. J. Biochem. Phys.*, **35**, 219, 229 (1957).
17) W. Hills and M. Hasegawa, *Biochem. J.*, **83**, 503 (1962).
18) G. Billek and H. Kindl, *Monatsh. Chem.*, **92**, 493 (1961).
19) R. K. Ibrahim and G. H. N. Towers, *Can. J. Biochem. Phys.*, **38**, 627 (1960); **40**, 449 (1962).

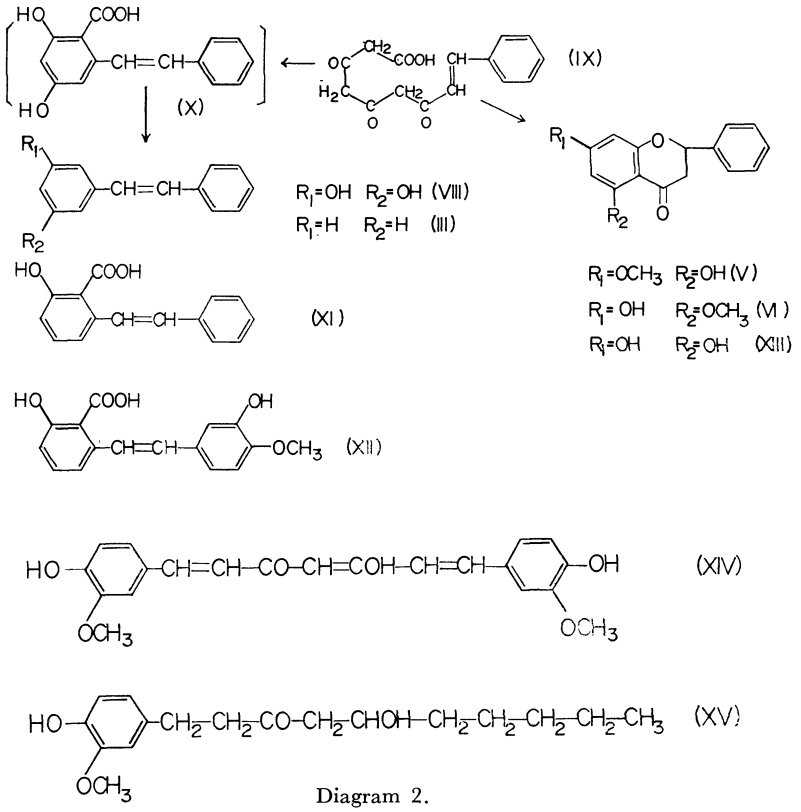

Diagram 2.

can be deduced that the *trans*-stilbene (III), *β*-phenylethyl cinnamate (IV), pinostrobin (V), and alpinetin (VI) isolated from *A. firma* result from a combination of acetic acid and shikimic acid pathways. It is noteworthy that free cinnamic acid is isolated together with pinostrobin, alpinetin, and *trans*-stilbene in this work.

There are many other natural products which also result from the condensation of cinnamic acid and acetic acid units. Thus, yashabushiketol (I) and dihydroyashabushiketol (II) are formed by the candensation of two molecules of cinnamic acid and a molecule of acetic acid. Ketol (I) and ketol (II) possess the same skeleton as the curcumin (XIV) isolated from *Curcuma longa* (ZINGIBERACEAE)[20] and are partially similar to the structure of gingeron (XV) found in *Zingiber officinalis* (ZINGIBERACEAE).[21] Recently, pinostrobin and alpinetin have been isolated from *Kaempferria pandurata* (ZINGIBERACEAE).[10] It is very interesting, from the viewpoint of biosynthesis, that the constituents isolated from *A. firma* (BETULACEAE) are closely analogous to those of ZINGIBERACEAE.

Details regarding the constituents of the cone of *A. firma* and *Alnus multinervis* (Himeyashabushi in Japan) will be reported in a later publication.

20) J. Milobedzka, S. Kostanecki and V. Lampe, *Ber.*, **43**, 2163 (1910); K. R. Srinivasan, *J. Pharm. and Pharmacol.*, **5**, 448 (1953).

21) H. Nomura, *Tohoku Riho*, **7**, 69 (1918).

Experimental

All the melting points described are uncorrected. The IR spectra were recorded on a Perkin-Elmer model 621 grating Infrared Spectrophotometer in liquid film, in chloroform, in Nujol paste, or as KBr tablets. The NMR spectra were measured on a Varian Asssociates A-60 or Hitachi Perkin-Elmer model R-20 Spectrometer, operating at 60 MHz, and were examined in a 5—10% solution of deuterochloroform, using tetramethylsilane as the internal standard, unless otherwise indicated. The following abbreviations are used for the representation of the NMR data: s=singlet, d=doublet, t=triplet, q=quartet, bs=broad singlet, quin.=quintet, and m=multiplet. The UV spectra were measured on a Shimadzu Recording Spectrophotometer, SV 50 A type, in a 95% ethanol solution. The mass spectra were recorded on a JEOL JMS-01SG Mass Spectrometer under the following conditions: ion accel. volt, 7 kV; ionizing energy, 75 eV; ionizing current, 200 μA; vacuum, 1×10^{-7} Torr; sample temp., 110°C; chamber temp., 250°C; direct sample-introduction system with a vacuum lock. The high-resolution mass spectra were measured on a JEOL JMS-01SP high-resolution mass spectrometer under the following conditions: ionizing energy, 75 eV; direct inlet system; sample temp., 120°C; reference substance, perfluorokerocene. The gas chromatograms were measured on a Hitachi Perkin-Elmer F6-D type Gas chromatograph equipped with a flame-ionization detector. Stainless-steel columns (2 m×2 mm)

coated with SE-30 2.5%, PEG 6000 10%, NGS 10% and DEGS 10% on Diasolid L (60—80 mesh) were used. Thin-layer chromatography was carried out with Silica gel G (Merck) under the following conditions: solvent system, benzene - ethyl acetate 19 : 1 vol% unless otherwise stated; chromogenic agent, iodine vapor or mixed acid (conc. H_2SO_4: conc. HNO_3 19 : 1 vol%); developing distance, 15 cm.

Extraction and Isolation Procedure. Ninety-four kg of young shoots of *A. firma* grown in Hiroshima were collected in February and were extracted with redistilled benzene for three weeks. The evaporation of the solvent gave 5 kg of a dark-green-colored slurry. The extract (18.5 g), after the acidic and phenolic constituents has been removed by treatment with 5% sodium bicarbonate and 5% sodium hydroxide solutions, was fractionated into three portions by silica-gel chromatography using *n*-hexane, benzene, and ethyl acetate as eluting agents successively. The extract (4 g) by *n*-hexane was further chromatographed over silica gel using *n*-hexane. Likewise, the extract (7 g) by benzene and the extract (4 g) by ethyl acetate were each further chromatographed using the same solvent as before. The acidic portion (4 g) regenerated from the sodium bicarbonate solution by 5% hydrochloric acid was purified through a silica-gel column using ethyl acetate. The phenolic portion (14 g) regenerated from the sodium hydroxide solution by 5% hydrochloric acid was also chromatographed on silica gel using chloroform - acetone (19 : 1).

Yashabushiketol (I) (1,7-Diphenyl-5-hydroxy-1-hepten-3-one). From the ethyl acetate fraction, a ketol was isolated as colorless needles (150 mg); mp 59.5—60.5°C (from *n*-hexane), $[\alpha]_D^{20}$ +29.0° (*c*, 1.05 in $CHCl_3$), R_f=0.14 (benzene - ethyl acetate 19 : 1 vol%) and R_f=0.52 (the same solvent 3 : 2). This compound was identified as 1,7-diphenyl-5-hydroxy-1-hepten-3-one from the chemical and spectral evidence as has been mentioned in the "Results and Discussion" section.

Catalytic Hydrogenation of Yashabushiketol (I). Yashabushiketol (37 mg) was added to a prereduced PtO_2 catalyst (20 mg) in glacial acetic acid (1.5 m*l*). The solution was then stirred at room temperature, whereupon it absorbed one mole equivalent of hydrogen in 2 hr. The catalyst was removed by filtration, and the filtrate was evaporated *in vacuo* to take off the solvent. The resulting oily yellow substance was chromatographed on a silica-gel column using ethyl acetate to give white needles (25 mg); mp 36.0—37.0°C (after crystallization from *n*-hexane), R_f=0.25 (benzene - ethyl acetate 19 : 1). Its IR and NMR spectra agreed with those of dihydroyashabushiketol, to be discussed below.

Acetylation of Yashabushiketol (I). A solution of 20 mg of yashabushiketol in 2 m*l* of anhydrous pyridine was treated with acetic anhydride and then allowed to stand overnight. The mixture was then decomposed with ice water, and the solvent was removed *in vacuo*. The product was chromatographed on a silica-gel column using ethyl acetate to give a yellow oil (12 mg). R_f=0.5; IR spectrum; ν_{max}^{liq} 3080, 3060, 3027, 2930, 1930, 1860, 1790, 1735, 1659, 1625, 1569, 1495, 1455, 1373, 1331, 1239, 1028, 969, 748 and 749 cm^{-1}, NMR spectrum; $\delta_{ppm}^{CDCl_3}$ 5.40 (quin. J=7 Hz, 1H, $-CH_2-\underline{C}HOAc-CH_2-$), 2.04 (s, 3H, $C\underline{H}_3CO-$).

Dihydroyashabushiketol (II) (1,7-Diphenyl-5-hydroxy-3-heptanone). The repeated chromatography of the substance from ethyl acetate fractions gave colorless needles (80 mg) (mp 36.0—37.0°C (after crystallization from *n*-hexane), R_f=0.25) which were identified as 1,7-diphenyl-5-hydroxy-3-heptanone on the basis of the results of chemical and spectrometric treatment. Found: C, 83.80; H, 7.68%. Calcd for $C_{19}H_{22}O_2$: C, 83.69; H, 7.80%.

***trans*-Stilbene (III).** The crude *trans*-stilbene obtained from the *n*-hexane extract was recrystallized from ether to yield colorless leaflet crystals (20 mg); mp 120.0—121.0°C (lit,[7] 120.7°C), R_f=0.75, IR spectrum; ν_{max}^{EtOH} 3016, 1590, 1491, 1451, 755 and 690 cm^{-1} (monosubstituted benzene-ring), 959 (*trans* double bond); UV spectrum: λ_{max}^{EtOH} 228.5 mμ (log ε, 4.22), 236 (4.03), 295 (4.46), 307 (4.42) and 320 (4.23), NMR spectrum: $\delta_{ppm}^{CDCl_3}$ 7.41 (symm. m, 10H, two monosubstituted benzene-ring protons) and 7.18 (s, 2H, *trans* ethylenic protons), mass spectrum; M^+ 180 (base peak), *m/e* 179, 178, 165 (M−15, m^*=151.2), 152, 91, 89, 77, 63, 51 and 39. These data agreed with those of the authentic *trans*-stilbene. The mp was not depressed on admixture with an authentic sample.

β-Phenylethyl Cinnamate (IV). From the substance of the benzene extract, a colorless, viscous oil was obtained. This oil was then chromatographed on silica gel, using benzene, to give white crystals; repeated crystallization from *n*-hexane yielded colorless needles (1.067 g). Mp 56.5—57.0°C, R_f=0.50, UV spectrum; λ_{max}^{EtOH} 216.5 (log ε, 4.29), 223 (4.13), and 277 (4.34), IR spectrum; ν_{max}^{Nujol} 3060, 3010, 1575, 1500, 1470, 760, 695 (monosubstituted benzene-ring), 1710, 1285, 1170 (α,β-unsaturated ester), 1640, 980 (*trans* double bond), 1330, 1315, 1210, 1070, 900, 865, 750, 730 and 680 cm^{-1}, NMR spectrum; $\delta_{ppm}^{CDCl_3}$ 7.43 (bs, 5H monosubstitued benzene-ring protons), 7.30 (s, 5H, monosubstituted benzene-ring protons), 7.71 (d, J=16.2 Hz, 1H, Ar–C$\underline{H}$=CH–), 6.41 (d, J=16.2 Hz, 1H, –CH=C$\underline{H}$–CO–), 4.45 (t, J=7 Hz, 2H, O–C$\underline{H}_2$–CH_2–Ar), and 3.03 (t, J=7 Hz, 2H, $-CH_2-C\underline{H}_2$–Ar), mass spectrum; M^+ 252, *m/e* 104 (base peak, Ar–CH=CH_2)$^+$, 148, 147, 131 (Ar–CH=CH–CO)$^+$, 105 (Ar–CH_2–CH_2)$^+$, 103 (Ar–CH=CH)$^+$, 91 (C_7H_7)$^+$, 77, 65, 51 and 39, GLC Rt: 36.2 min. (NGS 10%, 212°C). All these data were completely identical with those of authentic β-phenylethyl cinnamate.

Alkaline Hydrolysis of β-Phenylethyl Cinnamate (IV). A solution of β-phenylethyl cinnamate (80 mg) in methanol was hydrolyzed with an alcoholic potassium hydroxide (about 1N). Colorless oil (10 mg) was obtained from the ether extract of the reaction mixture. The IR and GLC Rt were identical with those of authentic β-phenylethyl alcohol. White crystals (30 mg) were obtained by acidifing the potassium salt of the saponified substance with dilute hydrochloric acid. The IR and NMR spectra and the mp (134.0—135.0°C) showed the crystalline substance to be cinnamic acid.

Pinostrobin (5-Hydroxy-7-methoxyflavanone) (V). From the substance of the benzene extract, pale yellow crystals (100 mg) were obtained. Crystallization from *n*-hexane afforded colorless plates; mp 99.0—100.0°C (pinostrobin, 100°C,[10] 112—113°C[11] and 90—91°C[12]), R_f=0.48. The compound showed positive coloration with ferric chloride and with magnesium - hydrochloric acid. UV spectrum; λ_{max}^{EtOH} 215 mμ (log ε, 4.38), 228.5 (4.20), 290 (4.22) and 330 (3.50), IR spectrum: ν_{max}^{KBr} 3032, 2964, 2916, 2834, 1633, 1570, 1464, 1444, 1381, 1353, 1342, 1295, 1256, 1208, 1199,

1155, 1090, 1060, 992, 941, 890, 834, 794, 765 and 745 cm^{-1}, NMR spectrum: $\delta_{ppm}^{CDCl_3}$ 12.06 (s, 1H), 7.47 (s, 5H), 6.11 (s, 2H), 5.44 (q, J_{AX}=11 Hz, J_{BX}=5 Hz, 1H), 3.81(s, 3H), 2.99 (d, J_{AX}=11 Hz, 1H) and 2.91 (d, J_{BX}=5 Hz, 1H), mass spectrum; M^+ 270 (base peak), *m/e* 269, 193, 167, 166, 159, 138, 123, 114, 110, 104, 103, 95, 91, 78, 77, 69, 51 and 39.

Pinostrobin Monoacetate. Pale yellow crystals (15 mg), mp 142.0—144.0°C, were prepared by treating a solution of 29 mg of pinostrobin in 1 m*l* of anhydrous pyridine with 3 m*l* of acetic anhydride. R_f=0.55, IR spectrum; ν_{max}^{Nujol} 1740, 1255, 1050 (acetate band), 1655, 1600, 1550, 1430, 1325, 1310, 1260, 1240, 1190, 1145, 1020, 890, 865, 835, 760 and 695 cm^{-1}.

Methylation of Pinostrobin (V). A mixture of pinostrobin (30 mg), dimethyl sulfate (5 m*l*), pottasium carbonate (150 mg), and dry acetone (10 m*l*) was refluxed on a water bath for 48 hr to give pinostrobin methyl ether as white needles. Mp 142.0—143.0°C (pinostrobin methyl ether, 144°C[10]), R_f=0.58, IR spectrum; $\nu_{max}^{CHCl_3}$ 3025, 2955, 2950, 1979, 1895, 1670, 1600, 1570, 1460, 1430, 1370, 1340, 1320, 1270, 1209, 1180, 1110, 1070, 1040, 1030, 965, 940, 890, 860, 820, 800, 700 and 660 cm^{-1}.

Alpinetin (5-Methoxy-7-hydroxyflavanone) (VI). The phenolic portion (14 g) of the extract regenerated from the sodium hydroxide solution by hydrochloric acid was fractionated through a silica-gel column with chloroform-acetone (19 : 1 vol%); a small quantity of white crystals was thus obtained. Recrystallization from methanol gave white needles (30 mg) which showed the following properties: mp 224.5—225.0°C (alpinetin, 220°C[10] 223°C[22]), R_f=0.65 (benzene - methanol - acetic acid 5 : 1 : 1). Ferric chloride and magnesium - hydrochloric acid tests were negative. UV spectrum; λ_{max}^{EtOH} 231 (log ε, 4.08), 237 (3.98), 285 (4.21) and 310 (3.75), $\lambda_{max}^{EtOH+NaOAc}$ 230 mμ (log ε, 4.06), 237 (3.87), 252.5 (3.57), 287 (4.04) and 323 (4.15), IR spectrum; ν_{max}^{KBr} 3520, 3300, 3030, 2935, 1633, 1611, 1575, 1479, 1458, 1435, 1358, 1302, 1276, 1249, 1206, 1176, 1101, 1068, 1056, 980, 833 and 766 cm^{-1}, NMR spectrum; $\delta_{ppm}^{CF_3COOH}$ 7.51 (s, 5H), 6.47 (s, 2H), 5.71 (q, J_{AX}=11Hz, J_{BX}=6 Hz, 1H), 4.30 (s, 3H), 3.49 (d, J_{AX}=11 Hz, 1H) and 3.40 (d, J_{BX}=6 Hz, 1H), mass spectrum; M^+ 270, *m/e* 166 (base peak), 193, 167, 138, 123, 114, 104, 103, 95, 78, 77, 69, 51, 39, 18 and 17.

Methylation of Alpinetin (VI). By the same method as in methylation of pinostrobin, pinostrobin methyl ether was obtained as white crystals (14 mg). Mp 144.0—145.0°C (lit,[10] 144°C), R_f=0.58. Its IR spectrum agreed with that of pinostrobin methyl ether.

Cinnamic Acid (VII). The acidic portion (4 g) of the extract regenerated from the sodium bicarbonate solution by dilute hydrochloric acid was purified through silica-gel chromatography to give white needles (1.5 g); mp 134.0—134.5°C (from ether). The IR and NMR spectra were completely identical with those of an authentic specimen.

Paraffin Hydrocarbon. The fractions eluted with *n*-hexane yielded paraffin hydrocarbons (0.8 g). Mp 51.0—54.0°C, R_f=0.78, IR spectrum; $\nu_{max}^{CHCl_3}$ 2990, 2950, 1475, 1385, 1190, 1160, 740 and 735 cm^{-1}. *n*-Paraffins (C_{21}—C_{33}), anteiso paraffins (C_{22}, C_{24} and C_{26}) and iso paraffins (C_{21}, C_{23} and C_{25}) were tentatively identified by a comparison with the retention times of the authentic *n*-paraffins.

Triglyceride. A white crystalline mass (1.76 g) was obtained from the *n*-hexane extract. When it was recrystallized from chloroform, white crystals were obtained. Mp 76.0—77.0°C, R_f=0.6, IR spectrum; ν_{max}^{KBr} 2960, 2930, 2850, 1740, 1465, 1420, 1378, 1210, 1190, 1180, 920, 725 and 718 cm^{-1}, NMR spectrum; $\delta_{max}^{CDCl_3}$ 4.08 (m), 2.25 (m), 1.28 (s) and 0.90 (m). The alkaline hydrolysis (5% NaOH-methanol) of this mass (1.0 g) gave fatty acid mixtures (saturated, C_{16}, C_{18}, H_{20}, C_{21}, C_{22}, C_{23}, C_{24} and C_{25}) which were confirmed as methyl esters by gas chromatography (DEGS 10%, 187°C).

The author wish to express his hearty gratitude to Professor Tamon Matsuura, Professor Shuichi Hayashi and Assistant Professor Takayuki Suga of Hiroshima University for their guidance and encouragement. The author is also indebted to Mr. Fumihide Genjida for his help in this investigation. Grateful acknowledgement is also made to Professor Shô Itô of Tohoku University and Dr. Hiroshi Ishii of Shionogi Research Laboratory, Shionogi & Co., Ltd. for the measurement of NMR spectra. The author also thanks for Japan Electron Optics Co., Ltd., for high-resolution mass spectral determination.

22) Y. Kimura, *Yakugaku Zasshi*, **60**, 151 (1940).

BULLETIN OF THE CHEMICAL SOCIETY OF JAPAN VOL. 43 2230—2233 (1970)

The Resolution and Rotations of *trans*-2-Aminocyclohexanecarboxylic Acids and Derivatives

Hiroyuki NOHIRA, Kenji EHARA and Akira MIYASHITA

Department of Applied Chemistry, Faculty of Science and Engineering, Saitama University, Urawa, Japan

(Received February 4, 1970)

Optically active *trans*-2-aminocyclohexanecarboxylic acids [(+)-**1** and (−)-**1**] have been prepared by a preferential crystallization of racemic *N*-benzoyl *trans*-2-aminocyclohexanecarboxylic acid [(±)-**2**]. Active **2** have been used for preparation of such active *trans*-1,2-disubstituted cyclohexanes as (+)-, and (−)-ethyl *trans*-2-aminocyclohexanecarboxylate [(+)-**3** and (−)-**3**], (+)-, and (−)-*trans*-2-aminocyclohexanemethanol [(+)-**4** and (−)-**4**], (+)-*trans*-2-bromomethylcyclohexylamine hydrobromide [(+)-**5**], and (+)- *trans*-2-methylcyclohexylamine [(+)-**6**]. Amine-nitrous acid reaction of these cyclohexylamines to give the corresponding hydroxy compounds (**7**, **8**, **9**) has also been examined. It was confirmed that the signs of optical rotations of these hydroxy compounds are the same as those of the starting amines. It has been shown that observed molecular rotations of these active 1,2-disubstituted cyclohexanes are in agreement, in sign and order of magnitude, with those calculated following Brewster's procedures presented in 1959 and in 1967.

In 1959, Brewster[1] presented a useful model for the calculation of optical rotations which has been applied to various types of optically active organic compounds.[2] Recently a more theoretical treatment has been proposed by the same author.[3] In this treatment the calculation is relatively simple in the case of 1,2-disubstituted cyclohexane systems. In this connection, Pascual[4] has reported that the observed rotation of optically active 2-hydroxycyclohexanecarboxylic acids was in good agreement with that calculated by Brewster's earlier procedure.

We also became interested in correlations between observed and calculated rotations for 2-aminocyclohexanecarboxylic acids (**1**) and their derivatives, especially rotations calculated by the procedure proposed recently. Although the racemic isomers of *cis*- and *trans*-2-aminocyclohexanecarboxylic acid are known,[5,6] there has been no investigation of their resolution.

In the present investigation, resolution of *trans*-2-aminocyclohexanecarboxylic acid [(±)-**1**] has been first realized by fractional crystallization of diastereoisomeric salts of *N*-benzoyl *trans*-2-aminocyclohexanecarboxylic acid [(±)-**2**] and an active amine, such as quinine or ephedrine. Preferential crystallization initiated by inoculation has now been found to be more convenient. When a saturated solution of (±)-**2** is carefully inoculated with a pure crystal of one of the enantiomers obtained by fractional crystallization of the diastereoisomeric salts, the crystal grows and an appreciable amount of pure crystals are separated from the racemic solution. The resulting filtrate is then saturated with addition of the racemate, and inoculation with the antipode gives another good crop of active crystals. The process can be repeated, and the optically active acids [(+)-**2** and (−)-**2**] have been prepared in large quantities.

Various optically active 1,2-disubstituted cyclohexanes have been prepared from active **2**. For example, hydrolysis of active **2** with concentrated hydrochloric acid, and then esterification with ethanol gave the active esters [(+)-**3** and (−)-**3**]. The active free amino acids [(+)-**1** and (−)-**1**] have been prepared by hydrolysis of active **3**.

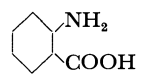

1

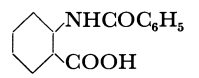

2

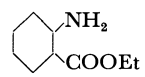

3

Active *trans*-2-aminocyclohexanemethanols [(+)-**4** and (−)-**4**], *trans*-2-bromomethylcyclohexylamine [(+)-**5**], and *trans*-2-methylcyclohexylamine [(+)-**6**] have been prepared by the following reaction sequence.

1) J. H. Brewster, *J. Amer. Chem. Soc.*, **81**, 5475, 5483, 5493 (1959).

2) E. L. Eliel, "Stereochemistry of Carbon Compounds," MaGraw-Hill Book Co., Inc., New York, N. Y. (1962), p. 401.

3) J. H. Brewster, "Helix Models of Optical Activity" in "Topics in Stereochemistry," Vol. II, ed. by N. L. Allinger and E. L. Eliel, Interscience Publishers, Inc., New York, N. Y. (1967), pp. 1—72.

4) J. Pascual, *An. Real. Soc. Espan. Fis. Quim. Ser. B*, **63**, 727 (1967).

5) S. Hünig and H. Kahanek, *Chem. Ber.*, **86**, 518 (1953).

6) E. J. Moriconi and P. H. Mazzocchi, *J. Org. Chem.*, **31**, 1372 (1966).

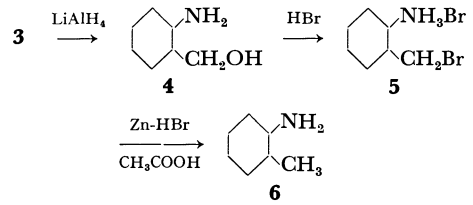

Treatment of these amines with nitrous acid gave the corresponding hydroxy derivatives:

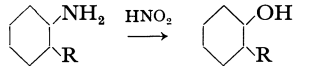

7, R=COOH
8, R=COOEt
9, R=CH_2OH

The stereochemistry of the amine-nitrous acid reaction in cyclohexane systems has been investigated extensively. It has been shown that equatorial amines react with nitrous acid to give mainly equatorial alcohols without any alteration of configuration.[7]

In the present investigation, it was also confirmed that the signs of observed optical rotations of the hydroxy compounds obtained by the amine-nitrous acid reaction are the same as those of the starting amines. The absolute configutarion of (−)-**7** has been determined by Faixat *et al.*,[8] and the result is consistent with Brewster's model. In view of this, we might conclude that (+)-**1** and (−)-**1** have absolute configurations of 1(S), 2(S) and 1(R), 2(R), respectively.

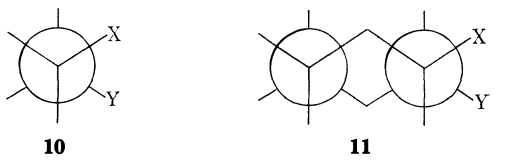

10 **11**

Fig. 1. Dextrorotatory conformations of 1,2-disubstituted ethane and cyclohexane.

Calculation of molecular rotations $[M]_D$ of these 1,2-*trans*-disubstituted cyclohexanes was performed using Brewster's theory. According to his theory, a right-handed helical chain as X–C–C–Y in Fig. 1 makes a dextrorotatory contribution to $[M]_D$. From a summation of these conformational units, a skewed conformation of 1,2-disubstituted ethane (**10**) and 1,2-diequatorially substituted cyclohexane (**11**) give the same $[M]_D$ value. In the present calculation, it has been assumed that these 1,2-*trans*-disubstituted cyclohexanes exist in the diequatorial conformation as shown in **11**.

Table 1 shows the calculated $[M]_D$ of several 1,2-*trans*-disubstituted cyclohexanes along with observed $[M]_D$. The procedures A and B are so-called semi-

Table 1. Mp, bp and molecular rotations of *trans*-1,2-disubstited cyclohexanes

Compd.	Substituents X	Substituents Y	Mp or bp/mmHg, °C racemate	Mp or bp/mmHg, °C enantiomers	Molecular rotations, $[M]_D$, deg observed value (solvent)	calculated value A	calculated value B	calculated value C
1	COOH	NH_2	274[a]	264	95 (H_2O)	69	71	82
2	COOH	$NHCOC_6H_5$	227[a]	258	110 (EtOH)	—	—	—
3	COOEt	NH_2	103—104/11[a]	109—110/13	85 (ether)	70	71	—
4	CH_2OH	NH_2	83—85/1[a]	106—108/6	28 (EtOH)	59	52	—
5	CH_2Br	NH_3Br	—	207—208	98 (EtOH)	108	—	—
6	CH_3	NH_2	150/760[c]	142—144/758	35 (ether)	59	52	55
7	COOH	OH	111[d]	107—109	70 (EtOH)	52	31	75[e]
				110—111[f]	77 ($CHCl_3$)			
8	COOEt	OH	130—132/25[d]	130—132/23	64 (ether)	53	31	—
9	CH_2OH	OH	111—113/3	119—120/4	27 (ether)	42	23	—
			122—124/2[g]	128—130/2.3[h]	28 (EtOH)[h]			

A: Calcd form the theoretical equation, $[M]_D = 251 d_1 d_2 d_3/(d_1+d_2+d_3)^2(\sum \Delta R_D) f(n)$, using $f(n) = 1.33$, in Ref. 3, p. 29.
B: Calcd from the semi-empirical equation, $[M]_D = 160(R_a^{1/2}-R_H^{1/2})(R_{a'}^{1/2}-R_H^{1/2})$, in Ref. 2, p. 404.
C: Calcd from the semi-empirical equation, $[M]_D = k(X-H)(Y-H)$, using empirical values of conformational rotatory powers in Ref. 2, p. 404.
a) Refs. 5 and 9. b) Ref. 6. c) Ref. 10. d) J. Pascual, J. Sistare and A. Regas, *J. Chem. Soc.*, **1949**, 1943. e) Ref. 4. f) M. A. Ferrer, P. Gomis and J. Pascual, *An. Real Soc. Espan. Fis. Quim., Ser. B*, **63**, 499 (1967). g) L. J. Dolby, C. N. Lieske, D. R. Rosencrantz and M. J. Schwarz, *J. Amer. Chem. Soc.*, **85**, 47 (1963). h) L. J. Dolby, F. A. Meneghini and T. Koizumi, *J. Org. Chem.*, **33**, 3060 (1968).

7) a) J. A. Mills, *J. Chem. Soc.*, **1953**, 260; b) W. Hückel, *Ann.*, **533**, 10 (1938); c) W. Hückel and K. D. Thomas, *ibid.*, **645**, 177 (1961) and Ref. 2, pp. 226—227.

8) J. E. Faixat, M. A. Febrer and J. Pascual, *An. Real Soc. Espan. Fis. Quim., Ser. B*, **57**, 705 (1961).

empirical.[1,2] Procedure C is a more exact theoretical treatment based on physical laws which govern the interaction between a helical conductor and electro-magnetic waves.[3]

It is worth noting that in this experiment our observed results of $[M]_D$ are in rough agreement with the results obtained by following Brewster's treatment, in which such a drastic model is assumed for molecular asymmetry as to consider a skewed chain of four atoms as a helical conductor.

Experimental

(±)-*N*-Benzoyl-*trans*-2-aminocyclohexanecarboxylic Acid [(±)-2]. (±)-*trans*-2-Aminocyclohexanecarboxylic acid [(±)-**1**] was prepared from anthranilic acid by the action of metallic sodium in isoamyl alcohol.[5,9] (±)-**2** was prepared by the reaction of (±)-**1** and benzoyl chloride in the usual way.

(−)-*N*-Benzoyl-*trans*-2-aminocyclohexanecarboxylic Acid [(−)-2]. To a mixture of 3.71 g (0.015 mol) of (±)-**2** and 5.18 g (0.016 mol) of quinine was added 130 m*l* of 70% methanol (methanol 70 and water 30 in volume). The mixture was briefly heated on a steam bath to dissolve all solid, then allowed to stand at room temperature. After 10 hr, the resulting fluffy needles were collected by filtration to give 6.0—6.5 g of salt, mp 125—130°C. Two or three recrystallizations of this material using 13—15 m*l* of 70% methanol per gram of salt gave 1.2—1.8 g of material whose properties did not change upon further recrystallization, mp 143—145°C, $[\alpha]_D^{20}$ −111.6° (*c* 2.5, ethanol).

With 3N hydrochloric acid the salt was converted into crude (−)-**2**, which was purified by recrystallization from 70% methanol to give 0.22—0.37 g (12—20%) of (−)-**2**, mp 257—258°C (in a capillary tube), subliming at near 240°C on an open plate, $[\alpha]_D^{20}$ −44.5° (*c* 0.67, ethanol).

Found: C, 68.26; H, 7.11; N, 5.71%. Calcd for $C_{14}H_{17}NO_3$: C, 67.99; H, 6.93; N, 5.66%.

l-Ephedrine salt of (−)-**2** melts at 186—188°C, $[\alpha]_D^{18}$ −39.7 (*c* 2.5, ethanol).

(+)-*N*-Benzoyl-*trans*-2-aminocyclohexanecarboxylic Acid [(+)-2]. To a mixture of 3.71 g (0.015 mol) of (±)-**2** and 2.75 g (0.015 mol) of *l*-ephedrine monohydrate was added 20 m*l* of 70% methanol. The mixture was heated on a steam bath to dissolve all solid. The solvent was then evaporated to dryness. The residue was recrystallized from 10 m*l* of 30% methanol to give 4.0—4.3 g of salt, melting at 160—175°C. Two or three recrystallizations of this material using 1.0—1.5 m*l* of 30% methanol per gram of salt gave 0.9—1.3 g of a material melting at above 190°C. With 3N hydrochloric acid the salt was converted into crude (+)-**2**, which was purified by recrystallization with 70% methanol, yielding 0.20—0.30 g (11—16%) of (+)-**2**, mp 257—258°C (in a capillary tube), subliming at near 240°C on an open plate, $[\alpha]_D^{20}$ +44.5° (*c* 0.67, ethanol).

Found: C, 68.13; H, 7.08; N, 5.75%. Calcd for $C_{14}H_{17}NO_3$: C, 67.99; H, 6.93; N, 5.66%.

The pure salt of *l*-ephedrine and (+)-**2** melts at 195—197°C, $[\alpha]_D^{18}$ +10.0° (*c* 2.5, ethanol). Quine salt of (+)-**2** melts at 122—123°C, $[\alpha]_D^{16}$ −72.3° (*c* 2.5, ethanol).

Resolution of (±)-2 by the Preferential Crystallization. A mixture of 10 g of (±)-**2** and 800 m*l* of 70% methanol was heated on a steam bath to dissolve all crystals, then cooled to a temperature of 50—60°C, and it was inoculated with 0.1 g of pure crystals of (−)-**2**. After standing at room temperature for about 10 hr, the inoculated solution was decanted and residual crystals were washed with 70% methanol to yield 0.5—0.8 g (10—14%) of (−)-**2**, mp 255—257°C, $[\alpha]_D^{18}$ −41±2° (*c* 0.67, ethanol).

The decanted solution was heated again with addition of 0.5—0.7 g of (±)-**2**, then inoculated with pure crystals of (+)-**2**, antipode of the seeds used in the preceding crystallization, to yield 1.1—1.6 g (20—30%) of (+)-**2**, mp 254—257°C, $[\alpha]_D^{18}$ +41±2° (*c* 0.67, ethanol).

The process was repeated in this way. Crystals separated by each inoculation were then put together and recrystallized from 95% ethanol to yield a pure sample of each enantiomer of **2**.

(+)-Ethyl-*trans*-2-aminocyclohexanecarboxylate [(+)-3]. A mixture of 24.7 g (0.1 mol) of (+)-**2** and 750 m*l* of concentrated hydrochloric acid was heated under reflux until crystals of (+)-**2** had completely dissolved (for 56—72 hr). The mixture was then cooled, and the resulting benzoic acid was removed by filtration. The filtrate was evaporated to dryness under reduced pressure. The residue was esterified by means of absolute ethanol and dry hydrogen chloride, and worked up in a known manner[9] to yield 14.9 g (87%) of (+)-**3**, bp 109—110°C/13 mmHg, $[\alpha]_D^{18}$ +49.7° (*c* 4, ether).

Similarly, (−)-**3** was prepared from (−)-**2** in 75—90% yield, bp 109—110°C/13 mmHg, 113—114°C/16 Hmmg, $[\alpha]_D^{17}$ −49.8° (*c* 4.5, ether).

Found: N, 8.05%. Calcd for $C_9H_{17}NO_2$: N, 8.18%.

N-Benzoyl derivative of (−)-**3** had a mp 146°C and $[\alpha]_D^{17}$ −38.5° (*c* 2, ethanol).

Found: N, 5.17%. Calcd for $C_{16}H_{21}NO_3$: N, 5.09%.

(+)-*trans*-2-Aminocyclohexanecarboxylic Acid [(+)-1]. A sample of (+)-**3** (1.0 g) was refluxed with 10 times its quantity of water (10 m*l*) for 10 hr. The solvent was then evaporated to dryness under reduced pressure. The residue was recrystallized from 70% ethanol, and dried over phosphorous pentoxide to yield a pure sample of (+)-**1** (0.5 g), mp 264°C, $[\alpha]_D^{17}$ +66.5° (*c* 2, water).

Found: N, 9.54%. Calcd for $C_7H_{13}NO_2$: N, 9.78%.

Similarily, (−)-**1** was prepared from (−)-**3**, mp 264°C, $[\alpha]_D^{16}$ −65.5° (*c* 2, water).

Found: N, 9.63%.

(+)-, (−)-, and (±)-*trans*-2-aminocyclohexanemethanol [(+)-**4**, (−)-**4**, and (±)-**4**] were prepared in 75—80% yield from (+)-**3**, (−)-**3**, and (±)-**3**, respectively, by the action of lithium aluminium hydride in ether[6] or tetrahydrofuran. (+)-**4**, bp 106—108°C/6 mmHg, mp 36—37°C, $[\alpha]_D^{28}$ +21.2° (*c* 5, ethanol). (−)-**4**, bp 98—102°C/3.5 mmHg, mp 37—38°C, $[\alpha]_D^{26}$ −21.6° (*c* 5, ethanol). (±)-**4**, bp 125—127°C/15 mmHg, mp 65—67°C (lit,[6] bp 83—85°C/1 mmHg).

N-Benzoyl derivative of (+)-**4** had a mp 151°C and $[\alpha]_D^{21}$ +41.2° (*c* 3.4, ethanol).

Found: N, 6.13%. Calcd for $C_{14}H_{19}NO_2$: N, 6.00%.

N-Benzoyl derivative of (±)-**4** had a mp 145°C.

Found: N, 5.95%.

(+)-*trans*-2-Bromomethylcyclohexylamine Hy-

9) A. Einhorn and A. Meyerberg, *Chem. Ber.*, **27**, 2467 (1894).

drobromide [(+)-5]. A mixture of 2.58 g (0.02 mol) of (+)-**4** and 10 m*l* of 47% hydrobromic acid was heated on an oil-bath at 160—170°C for 1 hr with bubbling dry hydrogen bromide gas. The temperature was finally raised to 200°C. The resulting material was purified by dissolving with ethanol and then precipitating with ether, giving 5.2 g (95%) of (+)-**5**, mp 207—208°, $[\alpha]_D^{20}$ +36.0° (*c* 3, ethanol).

Found: N, 5.33%. Calcd for $C_7H_{15}NBr_2$: N, 5.13%.

(+)-*trans*-2-Methylcyclohexylamine [(+)-6]. To a mixture of 4.1 g (0.015 mol) of (+)-**5**, 15 m*l* of acetic acid, and 15 m*l* of fuming hydrobromic acid was added slowly 2.5 g (0.038 atom) of zinc dust with stirring. The mixture was then heated under reflux for 2 hr. After removal of solvent under reduced pressure, the residue was dissolved in 10 m*l* of water. The resulting solution was treated with 12 g of sodium hydroxide and 20 m*l* of water, and extracted with three 4 m*l* portions of ether. The ethereal extract was dried (KOH), concentrated, and distilled giving 1.1 g (65%) of (+)-**6**, bp 142—144°C/758 mmHg, $[\alpha]_D^{19}$ +30.8° (*c* 10, ether).

Hydrobromide of (+)-**6** had a mp 299—301°C and $[\alpha]_D^{23}$ +23.0° (*c* 3, ethanol).

Found: N, 7.16%. Calcd for $C_7H_{16}NBr$: N, 7.22%.

N-Benzoyl derivative of (+)-**6** had a mp 164°C (lit,[10] (racemate) mp 146°C], and $[\alpha]_D^{20}$ +48.0° (*c* 5, ethanol).

Found: N, 6.22%. Calcd for $C_{14}H_{19}NO$: N, 6.45%.

(−)-*trans*-2-Hydroxycyclohexanecarboxylic acid [(−)-**7**], (−)-ethyl *trans*-2-hydroxycyclohexanecarboxylate [(−)-**8**], and (−)-*trans*-2-hydroxymethylcyclohexanol [(−)-**9**] were prepared from corresponding amines, that is, (−)-**1**, (−)-**3**, and (−)-**4**, respectively, according to a conventional method[7,8,11] in 50—60% yields. Their physical properties are listed in Table 1.

The authors are grateful to Professor J. H. Brewster and Dr. J. Tsunetsugu for their helpful suggestions and critical readings of the manuscript.

10) A. Skita, *Ber.*, **56**, 1014 (1923).

11) M. Mousseron, J. Jullien and F. Winternitz, *Compt. Rend.*, **226**, 1909 (1948).

BULLETIN OF THE CHEMICAL SOCIETY OF JAPAN VOL. 43 2233—2236 (1970)

Synthesis of Some New Fungicides

V. N. CHOUBEY and H. SINGH

Department of Chemistry, Banaras Hindu University, Varanasi-5, India

(Received November 25, 1969)

A number of 2-arylimino-3-aryl-4-thiazolidones and their 1,1-dioxides and 5-phenylazo derivatives have been prepared. The structure of these thiazolidones was confirmed by studying their hydrolysis products. Some of these thiazolidones were screened for their fungicidal activity against *Aspergillus niger* by agar-growth method and found to be more appropriately fungistatic and not fungicidal.

Several 4-thiazolidones and their derivatives, especially 1,1-dioxides, have been found therapeutically active as local anaesthetics,[1-3] amoebacides[4] and anticonvulsants.[5] Rout *et al.*[6-8] synthesized 2-arylimino-4-thiazolidones and their 5-substituted derivatives, and reported them to be active fungicides. Bhargava and coworkers[9-11] have demonstrated that 2-arylimino-3-aryl-4-thiazolidones with the same or different aryl groups, and 3-aryl-2,4-thiazolidiones possess considerable fungicidal activity. The acetoxymercuri derivatives of the latter were found to be the most active. Recently it has been reported that the hydrochlorides of 2-arylimino-5-methyl-4-thiazolidones[12] step the germination of spores of the fungus, *Culvularia lunata* at the concentration of 1 : 500.

1) A. R. Surrey, *J. Amer. Chem. Soc.*, **71**, 3105 (1949).
2) P. N. Bhargava and P. R. Singh, *J. Sci. Ind. Res.*, **20C**, 209 (1961).
3) P. N. Bhargava and M. R. Chaurasia, *Indian J. Pharm.*, **30**, 125 (1968).
4) A. R. Surrey and R. A. Cutler, *J. Amer. Chem. Soc.*, **76**, 578 (1954).
5) H. D. Troutman and L. M. Long, *ibid.*, **70**, 3436 (1948).
6) B. Das and M. K. Rout, *J. Indian Chem. Soc.*, **32**, 442 (1955).
7) M. K. Rout and G. N. Mahapatra, *J. Amer. Chem. Soc.*, **77**, 2427 (1955).
8) H. K. Pujari and M. K. Rout, *J. Sci. Ind. Res.*, **14B**, 448 (1955).
9) P. N. Bhargava and I. D. Saxena, *Vijnana Parishad Anusandhan Patrika* (India), **2**, 89 (1959).
10) P. N. Bhargava and Miss K. Bhargava and R. C. Kapoor, *J. Indian Chem. Soc.*, **38**, 23 (1961).
11) K. S. L. Srivastava, *Current Sci.* (India), **37**, 315 (1968).
12) P. N. Bhargava and G. C. Singh, *J. Indian Chem. Soc.*, **45**, 32 (1968).

In view of the significant biological applicability of the 4-thiazolidones and their 1,1-dioxides, it was thought worthwhile to synthesize 2-arylimino-3-aryl-5-substituted-4-thiazolidones (I) and 3-aryl-2-(substituted 2′-benzothiazolyl)imino-4-thiazolidones (III) as fungicides by the methods described earlier.[13-16]

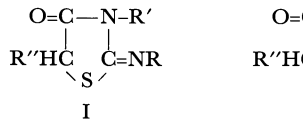

I

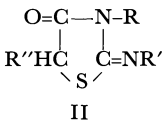

II

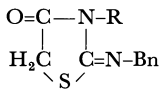

III

where R=aryl; R′=aryl; R″=H or CH_3
Bn=substituted 2-benzothiazolyl

In this communication asymmetrical *N*-aryl-*N*′-aryl thiocarbamides, needed as starting material, were prepared by interaction of aromatic primary amines and various aryl isothiocyanates in dry benzene. These thiocarbamides on condensation with monochloroacetic (α-chloropropionic) acid in absolute ethanol in the presence of sufficient anhydrous sodium acetate (which removes HCl *in situ*) yielded the corresponding 2-arylimino-3-aryl-5-substituted-4-thiazolidones. In this case formation of two possible isomeric 4-thiazolidones (I and/or II) may be assumed from the two possible tautomeric forms of thiocarbamides undergoing reaction with monochloroacetic (or α-chloropropionic) acid. The structure of the 2-arylimino-3-aryl-5-substituted-4-thiazolidones, the position of aryl groups, has been confirmed by studying their degradation products[10,13,17] and characteristic derivatives. Likewise, synthesis of 3-aryl-2-(substituted 2′-benzothiazolyl)imino-4-thiazolidones and their structures have been confirmed. The corresponding 1,1-dioxides of some of these thiazolidones were prepared by oxidizing them with $KMnO_4$ in glacial acetic acid, and 5-phenylazo derivatives

TABLE 1. 2-ARYLIMINO-3-ARYL-5-SUBSTITUTED-4-THIAZOLIDONES AND THEIR FUNGICIDAL ACTIVITY

S. No.	Aryl group R	Aryl group R′	Substituent R″	Mp °C	Molecular formula	Nitrogen, % Found	Nitrogen, % Calcd	Percentage-inhibition* at concentrations 1:1000	Percentage-inhibition* at concentrations 1:5000
1	*o*-$OCH_3\cdot C_6H_4$	*o*-$Cl\cdot C_6H_4$	H	149	$C_{16}H_{13}ClN_2O_2S$	8.19	8.42	60	19.25
2	*o*-$OCH_3\cdot C_6H_4$	*m*-$Cl\cdot C_6H_4$	H	143	$C_{16}H_{13}ClN_2O_2S$	8.50	8.42	68	34.65
3	*p*-$Cl\cdot C_6H_4$	*o*-$OCH_3\cdot C_6H_4$	H	135	$C_{16}H_{13}ClN_2O_2S$	8.30	8.42	80	53.90
4	*o*-$OCH_3\cdot C_6H_4$	*p*-$Br\cdot C_6H_4$	H	123	$C_{16}H_{13}BrN_2O_2S$	7.31	7.43	72	50.05
5	*o*-$OCH_3\cdot C_6H_4$	*p*-$I\cdot C_6H_4$	H	190	$C_{16}H_{13}IN_2O_2S$	6.45	6.60	—	—
6	*m*-$OCH_3\cdot C_6H_4$	*o*-$OCH_3\cdot C_6H_4$	H	171	$C_{17}H_{16}N_2O_3S$	8.63	8.54	72	46.20
7	*o*-$OC_2H_5\cdot C_6H_4$	*o*-$OCH_3\cdot C_6H_4$	H	131	$C_{18}H_{18}N_2O_3S$	8.27	8.19	60	30.80
8	*p*-$OC_2H_5\cdot C_6H_4$	*o*-$OCH_3\cdot C_6H_4$	H	122	$C_{18}H_{18}N_2O_3S$	8.35	8.19	—	—
9	*o*-$OCH_3\cdot C_6H_4$	β-Nathphyl	H	125	$C_{20}H_{16}N_2O_2S$	8.14	8.05	68	46.20
10	*o*-$CH_3\cdot C_6H_4$	Ph	CH_3	146	$C_{17}H_{16}N_2OS$	9.13	9.46	—	—
11	*p*-$CH_3\cdot C_6H_4$	Ph	CH_3	165	$C_{17}H_{16}N_2OS$	9.27	9.46	80	57.75
12	*o*-$Cl\cdot C_6H_4$	Ph	CH_3	161	$C_{16}H_{13}ClN_2OS$	8.47	8.84	—	—
13	*p*-$Cl\cdot C_6H_4$	Ph	CH_3	283	$C_{16}H_{13}ClN_2OS$	8.66	8.84	76	42.35
14	*p*-$OCH_3\cdot C_6H_4$	Ph	CH_3	183	$C_{17}H_{16}N_2O_2S$	8.72	8.97	64	34.65
15	*p*-$OC_2H_5\cdot C_6H_4$	Ph	CH_3	131	$C_{18}H_{18}N_2O_2S$	8.38	8.59	68	30.80
16	*p*-$Cl\cdot C_6H_4$	*p*-$CH_3\cdot C_6H_4$	CH_3	130	$C_{17}H_{15}ClN_2OS$	8.27	8.49	—	—
17	*p*-$Br\cdot C_6H_4$	*p*-$CH_3\cdot C_6H_4$	CH_3	159	$C_{17}H_{15}BrN_2OS$	7.31	7.46	80	57.75
18	*p*-$OCH_3\cdot C_6H_4$	*p*-$CH_3\cdot C_6H_4$	CH_3	184	$C_{18}H_{18}N_2O_2S$	8.32	8.59	68	46.20
19	*p*-$OC_2H_5\cdot C_6H_4$	*p*-$CH_3\cdot C_6H_4$	CH_3	161	$C_{19}H_{20}N_2O_2S$	8.07	8.23	76	50.05

Diameters of the fungus colonies of control plates in mm., at concentrations 1 : 1000 and 1 : 5000, are 25 and 26 respectively.

* Percentage inhibition$=(d_c-d_t)/d_c\times 100$ where d_c, the diameter of the fungus colony in mm in the control plates after 90 hr; d_t the diameter of the fungus colony in mm in the treated plates after 90 hr.

13) K. S. Markley and E. E. Reid, *J. Amer. Chem. Soc.*, **52**, 2137 (1930).
14) P. N. Bhargava, R. P. Rao and M. S. Sastry, *J. Indian Chem. Soc.*, **33**, 596 (1956).
15) P. N. Bhargava and G. C. Goswami, *ibid.*, **32**, 763 (1955).
16) P. N. Bhargava and A. J. Pantulu and R. P. Rao, *ibid.*, **34**, 475 (1957).
17) P. N. Bhargava and P. Ram, *ibid.*, **38**, 127 (1961).

Table 2. 3-Aryl-2-(substituted 2′-benzothiazolyl) imino-4-thiazolidones

S. No.	Substituent	Yield %	Mp °C	Molecular formula	Nitrogen, %		Sulphur, %	
					Found	Calcd	Found	Calcd
				Aryl=*p*-Cl·C_6H_4				
1	4′-Methyl	84	246	$C_{17}H_{12}ClN_3OS_2$	11.10	11.24	17.28	17.14
2	5′-Methyl	90	249	$C_{17}H_{12}ClN_3OS_2$	11.39	11.24	17.33	17.14
3	6′-Methyl	95	286	$C_{17}H_{12}ClN_3OS_2$	11.06	11.24	17.29	17.14
4	4′-Chloro	75	218	$C_{16}H_9Cl_2N_3OS_2$	10.54	10.66	16.20	16.25
5	5′-Chloro	78	245	$C_{16}H_9Cl_2N_3OS_2$	10.83	10.66	16.03	16.25
6	6′-Chloro	86	255	$C_{16}H_9Cl_2N_3OS_2$	10.75	10.66	16.38	16.25
7	4′-Methoxy	70	234	$C_{17}H_{12}ClN_3O_2S_2$	10.63	10.78	16.38	16.44
8	6′-Methoxy	82	252	$C_{17}H_{12}ClN_3O_2S_2$	10.58	10.78	16.50	16.44
9	6′-Ethoxy	89	244	$C_{18}H_{14}ClN_3O_2S_2$	10.27	10.41	16.01	15.86
				Aryl=*o*-CH_3·C_6H_4				
10	4′-Methyl	44	157	$C_{18}H_{15}N_3OS_2$	11.72	11.90	17.92	18.13
11	5′-Methyl	41	137	$C_{18}H_{15}N_3OS_2$	11.68	11.90	18.04	18.13
12	6′-Methyl	56	171	$C_{18}H_{15}N_3OS_2$	11.78	11.90	17.83	18.13
13	4′-Chloro	35	143	$C_{17}H_{12}ClN_3OS_2$	11.15	11.24	16.73	17.14
14	5′-Chloro	37	135	$C_{17}H_{12}ClN_3OS_2$	11.07	11.24	16.97	17.14
15	4′-Methoxy	48	165	$C_{18}H_{15}N_3O_2S_2$	10.84	11.39	17.15	17.35
16	6′-Methoxy	57	138	$C_{18}H_{15}N_3O_2S_2$	10.91	11.39	17.21	17.35
17	6′-Ethoxy	53	109	$C_{19}H_{17}N_3O_2S_2$	10.71	10.96	16.47	16.71

by coupling with benzenediazonium chloride in which coupling occurs at the active methylene group.

Experimental

Asymmetrical *N*-Aryl-*N*′-aryl Thiocarbamides. A mixture of arylamine (0.1 mol) and aryl isothiocyanate (0.1 mol) in dry benzene (25 m*l*) was refluxed on a water-bath for 1—2 hr during which a solid mass was obtained. Unreacted amine and isothiocyanate were removed by washing the crude product with dil. HCl and ether respectively. It was crystallized from 95% ethanol.

2-*o*-Methoxyphenylimino-3-*α*-naphthyl-4-thiazolidone. *N*-*o*-Methoxyphenyl-*N*′-α-naphthylthiocarbamide (15.4 g), monochloroacetic acid (5 g) and anhydrous sodium acetate (8 g) in absolute ethanol (60 m*l*) were refluxed on a water-bath for 7—10 hr with occasional shaking. After distilling ethanol, the gummy product was washed with hot water which solidified on being kept overnight in contact with ice-cold water. It was crystallized from ethanol, yield 72%, mp 172°C.

Found: N, 7.92; S, 9.23%. Calcd for $C_{20}H_{16}N_2O_2S$: N, 8.05; S, 9.19%.

Similarly, other 2-arylimino-3-aryl-4-thiazolidones were synthesized. Their yields, melting points and analytical data are recorded in Table 1.

2-Arylimino-3-aryl-5-methyl-4-thiazolidones. These were prepared in a similar manner as described above, using requisite amount of α-chloropropionic acid instead of monochloroacetic acid. These were crystallized from ethanol and are reported in Table 1.

***N*-Aryl-*N*′-substituted 2-Benzothiazolylthiocarbamides.** 2-Amino-(substituted)benzothiazole (0.1 mol) and arylisothiocyanate (0.1 mol) in dry benzene (110 m*l*) were heated under reflux condenser on a water-bath for 4—20 hr. The rest of the procedure for its isolation and purification was the same as above. These thiocarbamides were crystallized from glacial acetic acid.

3-*p*-Chlorophenyl-2-(2′-benzothiazolyl)imino-4-thiazolidone. A mixture of *N*-*p*-chlorophenyl-*N*′-2-benzothiazolylthiocarbamide (3 g), monochloroacetic acid (1 g) and anhydrous sodium acetate (2 g) in absolute ethanol (60 m*l*) was refluxed on a water-bath for 8—10 hr. Excess ethanol was removed by distillation and the crude product was washed with hot water to remove unchanged reactants. It was crystallized from ethanol-acetone mixture (1 : 1), yield 80%, mp 254°C.

Found: N, 11.93; S, 17.89%. Calcd for $C_{16}H_{10}ClN_3OS_2$: N, 11.68; S, 17.80%.

Following the same procedure, various 3-*p*-chlorophenyl (or *o*-tolyl)-2-(substituted 2′-benzothiazolyl)imino-4-thiazolidones were synthesized (Table 2).

2-(*o*-Methoxyphenyl)imino-3-*m*-chlorophenyl-4-thiazolidone-1,1-dioxide. 2-*o*-Methoxyphenylimino-3-*m*-chlorophenyl-4-thiazolidone (1 g) dissolved in glacial acetic acid (20 m*l*) was treated slowly with $KMnO_4$ (1 g) solution prepared in water (45 m*l*) at 0°C. The resulting mixture was allowed to stand for some time and then sodium bisulphite solution was added to discharge the colour of potassium permanganate. The residue was washed with ice-cold water, dried and crystallized from ethanol, yield 69%, mp 148°C.

Found: N, 7.53; S, 8.94%. Calcd for $C_{16}H_{13}ClN_2O_4S$: N, 7.68; S, 8.78%.

5-Phenylazo-2-*o*-ethoxyphenylimino-3-*o*-methoxyphenyl-4-thiazolidone. To a solution of benzenediazonium chloride (prepared from 2 m*l* of aniline), cooled in a freezing mixture at 0°C, a solution of the thiazolidone (2 g) in glacial acetic acid (40 m*l*) was added in small portions with continuous stirring. The resulting reaction mixture was kept for about an hour

at 0—3°C. The precipitate formed was filtered, washed with ice-cold water and, crystallized, yield 73%, mp 77°C. Found: N, 12.44; S, 7.01%. Calcd for $C_{24}H_{22}N_4O_3S$: N, 12.56; S, 7.17%.

Fungicidal Screening. Compounds 1, 2, 3, 4, 6, 7, 9, 11, 13, 14, 15, 17, 18 and 19 (Table 1) were screened for fungicidal activity against *Aspergillus niger* by agar-growth method, incubated for 90 hr at 25°C, at concn. 1 : 1000 and 1 : 5000. It is evident from the fungicidal screening results of tested compounds that these are more appropriately fungistatic and not fungicidal.

The authors wish to express their sincere thanks to Dr. P. N. Bhargava for supervision, Professor G. B. Singh, Head, Dept. of Chemistry for providing facilities, and C.S.I.R., New Delhi, India and U.G.C., India, for awarding financial assistance to them.

BULLETIN OF THE CHEMICAL SOCIETY OF JAPAN VOL. 43 2236—2240 (1970)

Studies of Ester-Containing Surfactants. Preparation and Properties of Sodium Sulfoalkyl Alkanoates

Takeshi HIKOTA

Department of Chemistry, Faculty of Science, Science University of Tokyo, Kagurazaka, Shinjuku-ku, Tokyo

(Received Junuary 20, 1970)

A series of sodium sulfoalkyl alkanoates, $RCOO(CH_2)_jSO_3Na$, were prepared by means of sodium isethionate, propane sultone, and butane sultone with normal primary fatty acid composed of 10, 11, and 12 carbon atoms respectively. The effects of the position of the ester group on the Krafft point, the critical micelle concentration (CMC), the surface tention, and the other surface and colloidal properties of these surfactants were investigated. For a given number of carbon atoms, moving the ester group from the ionic head to a more central position in the hydrocarbon chain increased the CMC value and the calcium ion stalbility, and decreased the emulsion stability and the stability to hydrolysis. However, the wetting time was not strongly influenced by the position of the ester group in these compounds. The Krafft point of these surfactants decreased as the ester group was moved to a more central position.

Many investigations have been published regarding the effect of the molecular structure on the surface and colloidal properties. For example, Stirton and his co-workers[1-4] studied the surface-active properties (the Krafft point, the critical micelle concentration, the surface tension, the detergency, the wetting time, the calcium-ion stability, *etc.*) of the sodium α-sulfo fatty ester series and observed that a good wetting agent was usually not a good detergent. Livingstone and Drogin[5] measured the CMC, the surface tension, and the detergency of alkyl thioalkyl and alkoxy alkyl sulfates. Finger and co-workers[6] measured the effect of the structure of the alkyl group in sulfate-type surfactants on the surface tension and the detergency. Previously, I have investigated the effect of the position of the ester group of alkyl sulfo acetate[7] and alkyl β-sulfo propionate[8] on the CMC, the Krafft point, and other bulk properties.

In this experiment, I prepared sodium 2-sulfoethyl alkanoates, $RCOO(CH_2)_2SO_3Na$, 3-sulfopropyl alkanoates, $RCOO(CH_2)_3SO_3Na$, and 4-sulfobutyl alkanoates, $RCOO(CH_2)_4SO_3Na$, and compared their surface-active properties in order to discuss in detail the relation between the position of the ester group and the surface activities.

1) A. J. Stirton, R. G. Bistline, Jr., J. K. Weil and W. C. Ault, *J. Am. Oil Chemists' Soc.*, **39**, 55 (1962).
2) A. J. Stirton, R. G. Bistline, Jr., J. K. Weil, W. C. Ault and E. W. Maurer, *ibid.*, **39**, 128 (1962).
3) W. C. Ault, T. J. Micich, A. J. Stirton and R. G. Bistline, Jr., *ibid.*, **42**, 233 (1965).
4) A. J. Stirton, R. G. Bistline, E. A. Barr and M. V. Numez-Ponzoa, *ibid.*, **42**, 1078 (1965).
5) J. R. Livingstone, Jr., and R. Drogin, *ibid.*, **42**, 720 (1965).
6) B. M. Finger, G. A. Gillies, G. M. Hartwig, E. E. Ryder, Jr., and W. M. Sawyer, *ibid.*, **44**, 525 (1967).
7) T. Hikota and K. Meguro, *ibid.*, **46**, 579 (1969).
8) T. Hikota and K. Meguro, *ibid.*, **47**, 158 (1970).

Experimental

Materials. The capric and lauric acids were kindly provided by the Nippon Oil & Fat Co. The purity of each fatty acid was confirmed to be above 99% by gas chromatography. Normal undecylic acid was prepared according to the following procedure. Decyl alcohol (more than 98% pure) was chlorinated with thionyl chloride; the decyl chloride was then reacted with sodium cyanide in dimethyl sulfoxide.[9] The hydrolysis of the 1-cyanodecane by refluxing it with an excess of 35% of hydrochloric acid gave an undecylic acid. After the removal of the solvent, the residue was purified by distillation; bp 182—185°C/31 mmHg. The sodium isethionate was of a reagent grade. Propane sultone manufactured by the Shell Chemical Co. was further purified by distillation; bp 130°C/3 mmHg. The butane sultone was prepared in the following way. Acetyl chloride was gradually added to tetrahydrofuran according to the method of Cloke and Pilgrim.[10] The reaction mixture was then washed with water, and the oily layer was separated. After the esterification, the solution of δ-chlorobutyl acetate was refluxed and stirred with an aqueous solution of sodium sulfite; then most of the water was removed under reduced pressure. The residue was stirred and refluxed with the excess methanol, and hydrogen chloride was passed into the solution. The reaction mixture was cooled and filtered. The distillation of the filtrate gave a transparent, colorless, and viscous liquid; bp 146°C/17 mmHg.

Preparation of Sodium 2-Sulfoethyl Caprate. A mixture of one mole of capric acid and 1.5 mol of thionyl chloride was heated and stirred at 30°C for one hour, and then at 90°C for one hour. The reaction product, capryl chloride, was distilled under reduced pressure. After the addition of 0.35 mol of sodium isethionate to 0.4 mol of the capryl chloride, the mixture was heated a 90°C for two hours. The crude product thus obtained was recrystallized three times from methanol. Then it was extracted for 100 hr with petroleum ether in order to remove all traces of the unchanged fatty acid. The pure sodium 2-sulfoethyl caprate was obtained as a white flaky powder.

Found: C, 47.45; 4H, 7.44%. Calcd for $C_9H_{19}COO(CH_2)_2SO_3Na$: C, 47.67; H, 7.67%.

Preparation of Sodium 2-Sulfoethyl Laurate. A procedure similar to that used with sodium 2-sulfoethyl caprate was used in the preparation of sodium 2-sulfoethyl laurate from lauric acid and sodium isethionate. The salt was a white, flaky powder.

Found: C, 51.01; H, 8.15%. Calcd for $C_{11}H_{23}COO(CH_2)_2SO_3Na$: C, 50.89; H, 8.24%.

Preparation of Sodium 3-Sulfopropyl Caprate. Sodium 3-sulfopropyl alkanoates was prepared as has been described by Hirai *et al.*[11] A mixture of 0.3 mol of sodium caprate (the sodium alkanoates used in this experiment had been prepared by neutralizing fatty acid with sodium methylate in the toluene), 0.3 mol of propane sultone, and 300 m*l* of toluene was refluxed for 10 hr under stirring. The reaction mixture was then cooled and diluted with 500 m*l* of acetone. The precipitated salt was filtered and recrystallized three times from methanol. Then it was extracted for 100 hr with petroleum ether in order to remove all traces of the unchanged fatty acid. The salt was a white powder.

Found: C, 48.75; H, 7.27%. Calcd for $C_9H_{19}COO(CH_2)_3SO_3Na$: C, 49.35; H, 7.65%.

Preparation of Sodium 3-Sulfopropyl Undecylate and Laurate. The esterification of undecylic and lauric acids with propane sultone was performed in a manner similar to that used with sodium 3-sulfopropyl caprate.

Found: C, 50.90; H, 8.43%. Calcd for $C_{10}H_{21}COO(CH_2)_3SO_3Na$: C, 50.89; H, 8.24%. Found: C, 51.19; H, 8.04%. Calcd for $C_{11}H_{23}COO(CH_2)_3SO_3Na$: C, 51.19; H, 8.49%.

Preparation of Sodium 4-Sulfobutyl Caprate. Sodium 4-sulfobutyl caprate was prepared by the same procedure and with the quantities as in the preparation of the sodium 3-sulfopropyl caprate, but with the propane sultone replaced by butane sultone. The product was recrystallized three times from methanol; then it was extracted for 100 hr with petroleum ether to yield a white, flaky powder.

Found: C, 50.66; H, 8.24%. Calcd for $C_9H_{19}COO(CH_2)_4SO_3Na$: C, 50.89; H, 8.24%.

Preparation of Sodium 4-Sulfobutyl Laurate. The esterification of lauric acid with butane sultone was performed in a similar manner.

Found: C, 53.45; H, 8.89%. Calcd for $C_{11}H_{23}COO(CH_2)_4SO_3Na$: C, 53.61; H, 8.72%.

Measurements. *Krafft Point.* The Krafft point was measured by the electro conductivity method,[12] which corresponds to the estimation of the Krafft point by measuring the change in solubility with the temperature. A rapid increase in solubility at the Krafft point accompanied the rapid increase in electrical conductivity. Thus, the measurement of the change in the conductivity of the surfactant solution with the temperature in a surfactant sufficent to give a solid phase made it possible to estimate the Krafft point. The conductivity measurements were made using a Leeds and Northrup Co., No. 4197, conductivity cell and a 4866 conductivity-resistivity indicator.

Critical Micelle Concentration. The critical micelle concentration (CMC) of the aqueous solution was determined by the conductivity method at 40°C. The conductivity of the water used was about 1×10^{-6} reciprocal ohm.

Surface Tension. The surface tension of the surfactants was measured by the Wilhelmy-plate (Shimadzu Instr. Co.) method at 30°C.

Emulsion Stability. The emulsion was prepared from 10 m*l* of a 20 mmol aqueous solution of the surfactant and 5 m*l* of toluene at 40°C. The emulsifying property was determined by the time (in minutes) it took for an aqueous volume separating from the emulsion layer to reach 9 m*l*, counting from the moment of the cessation of its shaking.

Wetting Property. The wetting property was measured by using a felt 20 mm in diameter and 1 mm thick at 40°C.[13] A solution of 75 m*l* of the 20 mmol surfactant

9) R. A. Smiley and C. Arnold, *J. Org. Chem.*, **25**, 257 (1960).

10) J. B. Cloke and F. J. Pilgrim, *J. Amer. Chem. Soc.*, **61**, 2667 (1939).

11) H. Hirai, Y. Ishikawa, K. Suga and S. Watanabe, *J. Japan Oil Chemists' Soc. Yukagaku*, **15**, 469 (1966).

12) T. Ino, *Nippon Kagaku Zasshi*, **80**, 456 (1959).

13) E. E. Dreger, G. I. Kelm, G. D. Miles, L. Shedlovsky and J. Ross, *Ind. Eng. Chem.*, **36**, 610 (1944).

TABLE 1. THE KRAFFT POINT TEMPERATURE AND CMC OF SURFACTANT

Derivatives	Abbreviation	Krafft point °C	CMC mol/l	
			Conductivity 40°C	Surface tension 30°C
$C_9H_{19}COO(CH_2)_2SO_3Na$	9C-2	nearly 0	0.0248	0.025
$C_{11}H_{23}COO(CH_2)_2SO_3Na$	11C-2	14.5	0.0064	0.0062
$C_9H_{19}COO(CH_2)_3SO_3Na$	9C-3	below 0	0.0192	0.0019
$C_{10}H_{21}COO(CH_2)_3SO_3Na$	10C-3	4.6	0.009	0.009
$C_{11}H_{23}COO(CH_2)_3SO_3Na$	11C-3	9.0	0.0047	0.0043
$C_9H_{19}COO(CH_2)_4SO_3Na$	9C-4	below 0	0.0126	0.013
$C_{11}H_{23}COO(CH_2)_4SO_3Na$	11C-4	below 0	0.0033	0.0025

to be tested was placed in a 150 m*l* beaker, and then the felt disk was put into the solution in such a position that the disk could run parallel to the surface of the solution. The wetting time was shown by the seconds from the moment the disk was put into the solution until the moment it stated going down.

Stability to Hydrolisys. A mixture of 10 m*l* of the 10 mmol surfactant and 10 m*l* of 2N sulfuric acid was placed in a thermostat at 40°C. The time it takes for a sample solution to be clouded as the result of hydrolysis shows the stability of the surfactant to hydrolysis.

Calcium Stability. The calcium-ion stability of a 10 mmol aqueous solution was measured by the modifide Hart method[14] using 0.1N calcium chloride.

Results and Discussion

The Krafft points of the sulfoalkyl alkanoates given in Table 1 are lower than that of surfactant with the same number of methylene groups in an alkyl chain, just as with sodium alkyl sulfate and alkyl sulfonate. This behavior suggests that the ester group introduced into the alkyl chain decreases the hydrophobic property of the hydrocarbon chain. For one series of 3-propane ester salts, 9C-3, 10C-3, and 11C-3, the Krafft point increased with the number of carbon atoms in the fatty acid chain. However, for two series with the same number of carbon atoms in the fatty acid portion, that is, 11C-2, 11C-3, and 11C-4, and 9C-2, 9C-3, and 9C-4, the Krafft point decreased with the increase in the number of methylene groups inserted between the ester group and the ionic head. For a series with the same number of carbon atoms in the surfactants, 9C-4, 10C-3, and 11C-2, the Krafft point decreased in the order of the decrease in the melting point of the corresponding fatty ester, as the ester group in the compounds was moved to a more central position. For instance, butyl caprate has a melting point of −20°C, compared with that of −10°C for the ethyl laurate of the same carbon atoms.

The CMC values of the surfactants, determined as the break points in the equivalent conductance against the concentration curves, are given in Table 1. Furthermore, the logarithm of the CMC has been plotted against the total number of methylene groups for each of the sulfoalkyl alkanoate series. For comparision, the CMC value of sodium alkyl sulfonate[15] is also presented. Figure 1, which gives examples of the plots, shows that the slopes of all of the curves (W, X, Y and Z) are parallel, following the $\log CMC = A - B \cdot N$ relationship. By measuring the horizontal distance between the curves (dotted line), one can compare the effects of the alkyl chain and of the position of the ester group on the CMC. The value of the horizontal distance was found to be 0.22 methylene groups for $\overline{WX}$ (the horizontal distance between

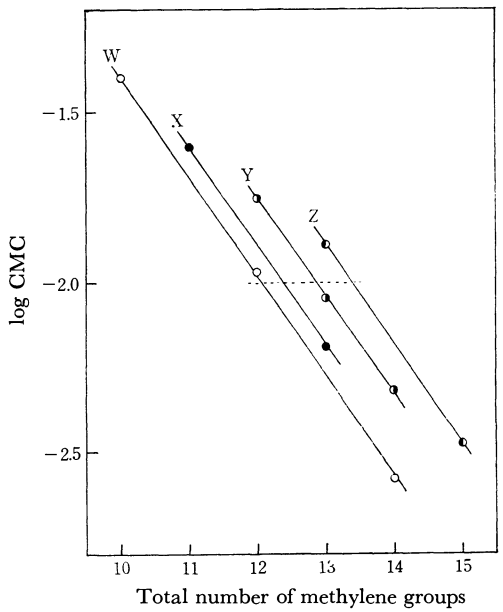

Fig. 1. Relation between log CMC and total number of mthylene groups in the chain.
RSO_3Na (○), $RCOO(CH_2)_2SO_3Na$ (●), $RCOO(CH_2)_3SO_3Na$ (◑), $RCOO(CH_2)_4SO_3Na$ (◐)

14) B. G. Wilkes and J. N. Wickert, *Ind. Eng. Chem.*, **29**, 1234 (1937).

15) K. Shinoda, T. Nakagawa, B. Tamamushi and T. Isemura, "Colloidal Surfactants," Academic Press, N. Y. (1963), p. 43.

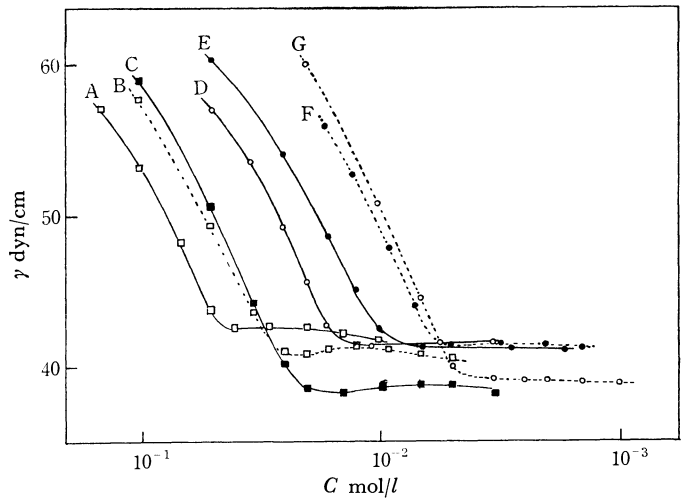

Fig. 2. Surface tension *vs.* concentration curves 11C-4 (A), 11C-3 (B), 11C-2 (C), 10C-3 (D), 9C-4 (E), 9C-3 (F) and 9C-2 (G).

the curve W and the curve X), 0.72 methylene groups for $\overline{WY}$, and 1.22 methylene groups for $\overline{WZ}$. This means that the isethionate, propane sultone, and butane sultone derivatives decrease the hydrophobic property of the hydrocarbon chain by 0.22, 0.72, and 1.22 units of the methylene group respectively with regard to the CMC value. Hence, the CMC of these surfactants increases regularly as the ester group is moved to a more central position in the chain.

The surface tension *vs.* the log concentration curve of the surfactants is shown in Fig. 2. The curve was inflected at the point which corresponds to the CMC. The CMC value estimated by means of the surface tension was in good agreement with that determined by means of the electro conductivity method, as is shown in Tables 1 and 2. The surface tension of the isethionate derivative above the CMC was about 39 dyn/cm, a little lower than that of the corresponding propane sultone and butane sultone derivatives. However, the surface tensions of these surfactants below the CMC are lower in this order: ethyl ester<propyl ester<butyl ester at the same concentration.

Table 2. Properties and stability of surfactant

Derivatives	Surface tension γ at CMC dyn/cm	Emulsion stability sec	Wetting time sec	Stability to hydrolysis min & sec
9C-2	39.10	12	3.3	43 : 51
11C-2	38.80	297	3.7	20 : 53
9C-3	41.24	146	3.8	39 : 45
10C-3	41.20	245	3.6	25 : 27
11C-3	40.40	378	4.0	18 : 39
9C-4	41.10	188	4.0	30 : 06
11C-4	42.30	442	3.5	16 : 26

The emulsion stability of the surfactants is shown in Table 2. As may be seen in the table, the emulsion stability increased with the number of the methylene group of the alkyl chain in the surfactant. For a series with the same number of methylene groups, 9C-4, 10C-3, and 11C-2, the emulsion stability increased as the ester group, was moved toward the center of the chain.

Table 3. Calcium stability and temperature

Derivative	Converted into $CaCO_3$ Temperature °C					
	10	20	30	40	50	60
9C-2	>4500	>4500	>4500	>4500	>4500	>4500
11C-2	insoluble	insoluble	260	500	1930	2380
9C-3	900	>4500	>4500	>4500	>4500	>4500
10C-3	100	700	3800	>4500	>4500	>4500
11C-3	insoluble	insoluble	100	150	700	2210
9C-4	670	>4500	>4500	>4500	>4500	>4500
11C-4	insoluble	insoluble	580	1090	2930	>4500

The wetting properties of the surfactants are shown in Table 2. These surfactants were very effective wetting agents in a distilled water solution.

The relation between the stability to hydrolysis and the chain length in the surfactant is shown in Table 2. The stability to hydrolysis decreased with the increase in the number of carbon atoms in the surfactant. The data indicates, therefore, that at the same number of the methylene group in the surfactant the relative order of stability to hydrolysis is: ethyl ester>propyl ester>butyl ester. That indicates that the sulfo group protects the ester linkage through steric hindrance.

The calcium-ion stability of the surfactants (in relation to the temperature) is shown in Table 3. It is apparent that the stability increases markedly with an increase in the temperature, but decreases with an increase in the number of methylene group in the alkyl chain length under conditions of a constant temperature. For a given number of the methylene group, moving the ester group from the terminal to a more central position in the alkyl chain increases the calcium stability. This means that the hydrophilic property of the surfactant increases with the movement of the ester group toward the the center of the chain.

The author wishes to thank Professor Kenjiro Meguro for his helpful advice, and Mr. Minori Nakamura and Miss Yōko Ohgaki for their assistance in the experiments.

NOTES

BULLETIN OF THE CHEMICAL SOCIETY OF JAPAN VOL. 43 2241—2244 (1970)

The Polymerization of Dimethallylidenepentaerythritol and Dicrotylidenepentaerythritol*1

Tatsuro OUCHI, Shozo TATSUNO, Toshiharu NAKAYAMA and Masayoshi OIWA

Department of Applied Chemistry, Faculty of Engineering, Kansai University, Senriyama, Suita-shi, Osaka

(Received September 11, 1969)

In a previous paper, the polymerization of diallylidenepentaerythritol (DAPE) has been kinetically investigated by means of degradative, effective chain transfers by the allylidene groups, and by means of cyclization by the two double bonds.[1]

This paper will deal with the polymerization of dimethallylidenepentaerythritol (DMAPE) and dicrotylidenepentaerythritol (DCPE), and with the influence of α,α'- or β,β'-methyl groups on the chain transfer and the cyclization.

Experimental

Materials. DMAPE was prepared from methacrolein and pentaerythritol by the procedure of Komori and his co-workers,[2] using phosphoric acid - phosphorus pentoxide as the catalyst; mp 115—116°C (lit,[2] 115—116°C).

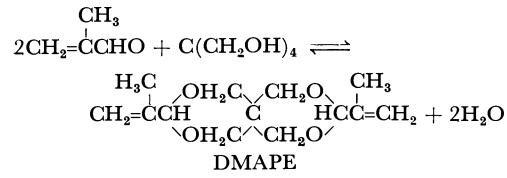

DMAPE

DCPE was prepared from crotonaldehyde and pentaerythritol by the method of Weihe and Schweitzer[3] and was purified by recrystallization from methanol-water; mp 57.5—58.0°C (lit,[3] 58°C).

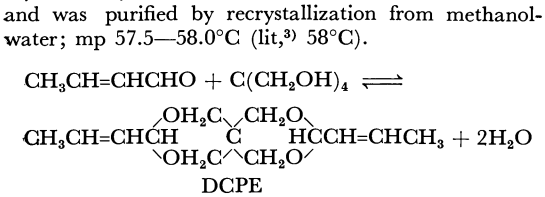

DCPE

Polymerization Procedure. DMAPE and DCPE were polymerized in benzene at 80°C with benzoyl peroxide as a radical initiator. The monomer, solvent, and initiator were charged in an ampoule; after having been degassed by the freeze-thaw method, the ampoule was sealed under a vacuum. The sealed tubes were then set in a thermostated water bath; later they were taken out into a large amount of petroleum ether and the polymers were separated by using the centrifuged, after which they were dried *in vacuo*. The conversion of the polymer was less than 10%.

Measurements of the Residual Unsaturation and the Degree of Polymerization. The residual unsaturation was calculated from the bromine value (BV) according to the usual bromite-bromate method.[4]

The molecular weight of the polymer was determined by means of a vapor-pressure osmometer (Hewlett Packard Model-302) at 37°C, using benzene as the solvent.

Results and Discussion

The conditions and the results of polymerization are summarized in Tables 1 and 2. The values of residual unsaturation and degree of polymerization shown in Tables 1 and 2 are estimated by extrapolating to zero for conversion.

If the monomer concentration is kept constant, the plots of the rate of polymerization against the initiator concentration are found to be as shown in Fig. 1 by using the values listed in Tables 1 and 2. It is found that the rate of polymerization is proportional to the first power of the initiator concentration. If the relation of $([I]/R_p - a)^{-1}$ *vs.* [M] is plotted by means of the trial-and-error method, the straight-line relationship is obtained when the values are 3.0×10^3 sec (DMAPE) and 2.0×10^4 sec (DCPE) respectively (Figs. 2 and 3). Therefore, b and c values are calculated from those slopes and intercepts as follows:

*1 Studies of the Polymerization of Diallylidenepentaerythritol. III.

1) T. Ouchi and M. Oiwa, *Kogyo Kagaku Zasshi*, **72**, 746 (1969).

2) T. Agawa, T. Ishikawa, N. Tamiya and S. Komori, *Shikizai*, **37**, 338 (1964).

3) A. Weihe and O. Schweitzer (to Deutsche Gold und Silber Scheideanstalt); U. S. 2739121 (1956).

4) I.P. Losev and O.Y. Fedotoba, "Praktikum po Khimii Vysokopolimernykh Soedinenii," Gosudarstvennoe Nauchno-Tekhnicheskoe Izdatelstvo Khimicheskoi Literatury, Moskova.

DMAPE $b = 2.53 \times 10^5$ sec, $c = 0.243$ mol/l

DCPE $b = 2.00 \times 10^7$ sec, $c = 0.044$ mol/l

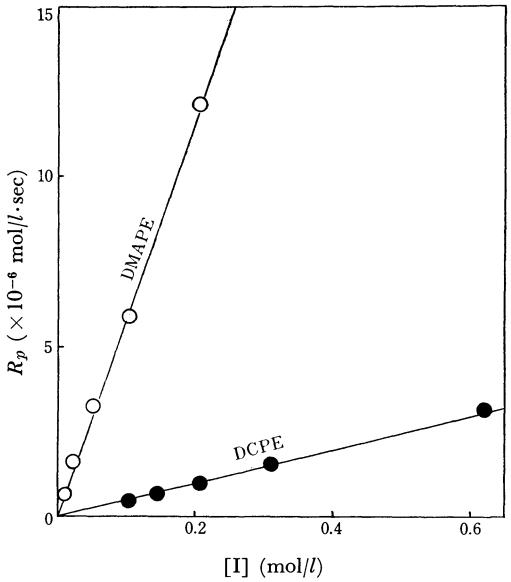

Fig. 1. Plots of rate of polymerization against the initiator concentration.

The degradative chain transfer occurred more readily on DCPE than on DMAPE. The low rate of polymerization on DCPE is due to the steric hindrance of β,β'-methyl groups.

If the monomer concentration is kept constant, the residual unsaturation does not depend on the initiator concentration. If the initiator concentration is kept constant, the residual unsaturation de-

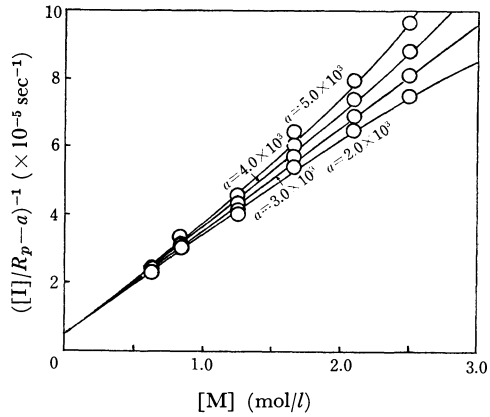

Fig. 2. Plots of $([I]/R_p-a)^{-1}$ *vs.* [M] obtained on the polymerization of DMAPE.

Table 1. The polymerization of DMAPE (80°C)

[BPO] ($\times 10^{-1}$ mol/l)	[DMAPE] (mol/l)	R_p ($\times 10^{-6}$ mol/l·sec)	BV	$2R_{us}$	Molecular weight $\bar{M}_n$	Degree of polymerization $\bar{P}_n$
2.064	2.081	12.15	62.71	0.943	1807	7.52
1.032	2.081	5.89	62.80	0.944	1812	7.54
0.516	2.081	3.23	62.83	0.945	1822	7.58
0.206	2.081	1.62	62.77	0.944	1817	7.56
0.103	2.081	0.64	62.91	0.946	1806	7.52
1.032	2.497	6.71	63.05	0.948	1896	7.89
1.032	1.664	5.02	62.19	0.935	1805	7.51
1.032	1.248	3.81	60.85	0.915	1694	7.05
1.032	0.832	2.92	58.66	0.882	1629	6.78
1.032	0.624	2.22	56.23	0.845	1416	5.89

Table 2. The polymerization of DCPE (80°C)

[BPO] ($\times 10^{-1}$ mol/l)	[DCPE] (mol/l)	R_p ($\times 10^{-6}$ mol/l·sec)	BV	$2R_{us}$	Molecular weight $\bar{M}_n$	Degree of polymerization $\bar{P}_n$
6.193	2.081	3.120	65.73	0.988	840	3.50
3.096	2.081	1.584	65.67	0.987	839	3.49
2.064	2.081	0.971	65.71	0.988	845	3.52
1.445	2.081	0.680	65.65	0.987	853	3.55
1.032	2.081	0.491	65.75	0.989	841	3.50
2.064	4.162	1.696	66.24	0.996	973	4.05
2.064	3.121	1.301	65.98	0.992	901	3.75
2.064	1.561	0.693	65.51	0.985	819	3.41
2.064	1.040	0.507	65.25	0.981	805	3.35

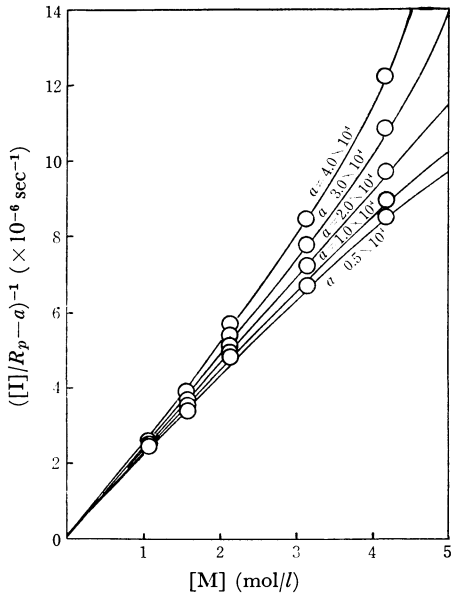

Fig. 3. Plots of $([I]/R_p-a)^{-1}$ *vs.* [M] obtained on the polymerization of DCPE.

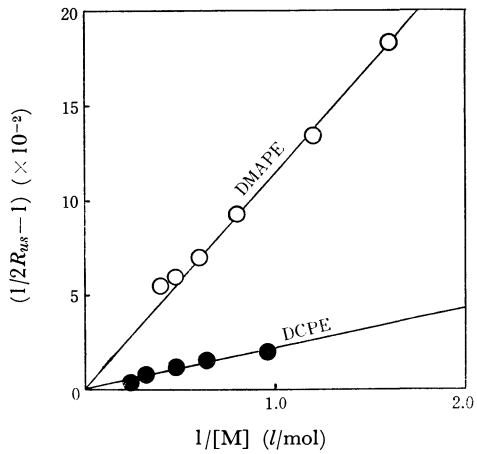

Fig. 4. Plots of $(1/2R_{us}-1)$ *vs.* 1/[M].

creases with the decrease in the monomer concentration; accordingly, there is a tendency to cyclize easily. The plots of $(1/2R_{us}-1)$ against 1/[M] are, then, shown in Fig. 4. Straight lines through the point of origin are obtained. Using their slopes, the c values of DMAPE and DCPE are computed as 0.226 mol/l and 0.044 mol/l respectively. These values agree very closely with those obtained from the trial-and-error method. Here the c value of DCPE is very small because the cyclization was sterically hindered by β,β'-methyl groups.

The degree of polymerization does not depend on the initiator concentration, but increases with the increase in the monomer concentration. It is natural that the degree of polymerization of DCPE is small, because β,β'-methyl groups influence the

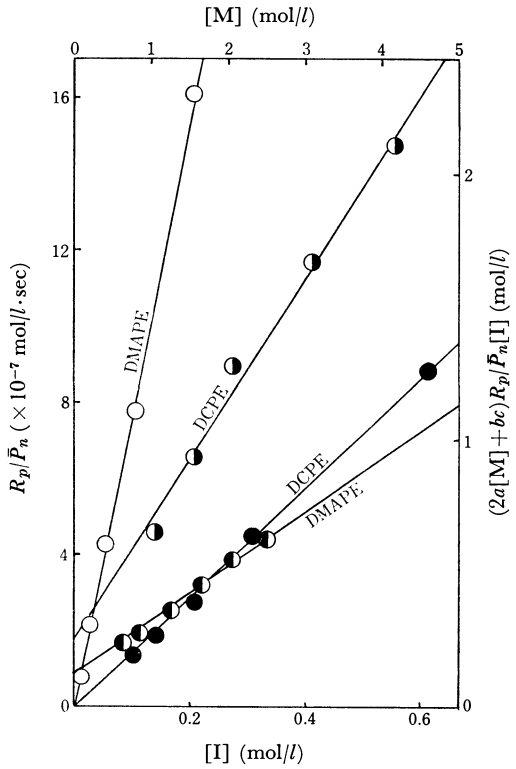

Fig. 5. Plots of $R_p/\bar{P}_n$ *vs.* [I] and $(2a[M]+bc)R_p/\bar{P}_n[I]$ *vs.* [M].

propagation and termination. The plots of $R_p/\bar{P}_n$ against [I] and of $(2a[M]+bc)R_p/\bar{P}_n[I]$ against [M] are shown in Fig. 5. Straight lines are obtained; therefore, this experimental fact seems to agree with the previous equation.[1)]

Conclusion

The polymerization of DMAPE and DCPE, which are α,α'- and β,β'-substituted derivatives of DAPE, in the initial stage were explained kinetically according to the equations suggested in a previous paper.[1)] The parameters of copolymerization for three monomers are summarized in Table 3.

Table 3. The parameters of copolymerization

Monomer	a ($\times 10^3$ sec)	b ($\times 10^4$ sec)	$\frac{k_c}{2(k_p+k_{tr}+k_{tr}^*)[M]}$
DMAPE	3.0	2.53×10	0.118
DCPE	20.0	2.00×10^3	0.022
DAPE	2.0	5.66	0.276

From the above results, it was found that $k_c/2(k_p+k_{tr}+k_{tr}^*)[M]$ were in the order of DAPE$>$DMAPE$>$DCPE, and that the cyclization was sterically hindered by methyl groups.

The a and b values varied in the following sequence:

$$\text{DAPE} < \text{DMAPE} < \text{DCPE}$$

It seemed that the degradative chain transfer occurred more readily on the methallylidene and crotylidene groups that on the allylidene group. It may be considered that allylidene groups can be resonanced easily to stabilize with methyl groups, and to hypercojugate.

BULLETIN OF THE CHEMICAL SOCIETY OF JAPAN VOL. 43 2244—2245 (1970)

Photoelectrical Response of Hydrochloric Salt of Photospiran

Takao NAKAYAMA, Isamu SHIMIZU, Hiroshi KOKADO and Eiichi INOUE

Imaging Science and Engineering Laboratory, Tokyo Institute of Technology, Ookayama, Meguru-ku, Tokyo

(Received November 20, 1969)

Photospirans (1,3,3-trimethylspiro[indoline-2,2′-benzopyran] and its derivatives) are transformed from a colorless form (A) to a colored form (C) by adding acid (Brönsted or Lewis acid) in organic solvents. (C) is converted to a colorless form by irradiation with either visible or UV light, and is gradually restored after irradiation is stopped.

The term "reverse photochromism" is given to photoreversible color changes.

During the course of our studies on the reverse photochromism of spiran-acid systems, an electrical response was observed when the colored species (C) in organic solvents was irradiated.

To measure the electrical current of the solution, a cell with two Al plate electrodes (10×10 mm^2) 10 mm apart was set up. The measurement was carried out under constant voltage 2 V (d.c.) by a micro-micro Ammeter (TR-84B). A high pressure mercury lamp fitted with a glass UV cut filter was used as the irradiation source.

A typical electrical current curve of the butanol solution of hydrochloric salt of spiran (1) is shown in Fig. 1.

The electronic current of the solution increased

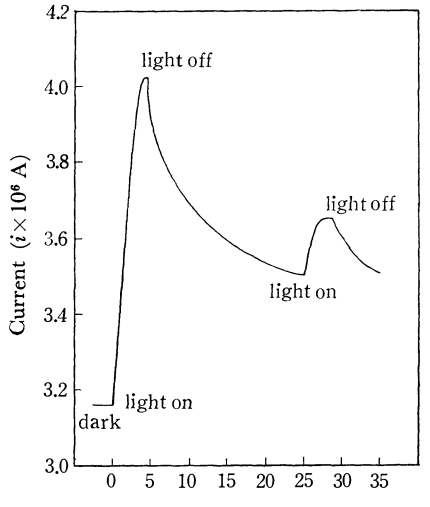

Fig. 1. Electrical current curve of the hydrochloric salt of spiran (1) in butanol.
concentration 1.7×10^{-4} mol/l
light intensity 2.1×10^{-3} W/cm^2

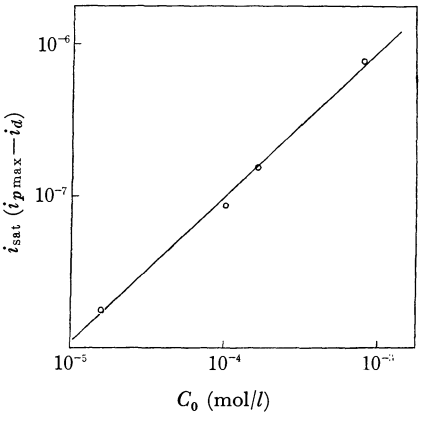

Fig. 2. Dependence of the maximum value of photocurrent on the initial concentration (C_0) of the salt.

$$[\mathrm{SPH}]^+\mathrm{Cl}^- \underset{\text{thermal}}{\overset{h\nu}{\rightleftharpoons}} \mathrm{SP} + \mathrm{H}^+ + \mathrm{Cl}^- \qquad (1)$$

(C) colored (A) colorless

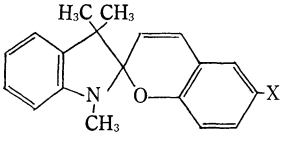

SP

X: NO_2 (1), COOH (2)

1) I. Shimizu, H. Kokado and E. Inoue, This Bulletin, **42**, 1726 (1969).

by irradiation with light, and decreased when irradiation was stopped. The value of the saturated photo-current (i_{sat}) was proportional to the initial concentration of the salt of spiran (1) as shown in Fig. 2. The dark current of the solution also increased with concentration. Though the current decreased gradually after irradiation was stopped, it did not return to the initial value. The photocurrent of the solution is assumed to be due to the generation of electrical carriers by irradiation with light undergoing photoconversion from the colored species (C) to the colorless one (A) as shown in Eq. (1). The photo-dissociated carriers seem to be partially stabilized in solvent, and neither the color nor current of the solution returns to the initial value after irradiation is stopped.

The photoelectrical phenomena mentioned above were also observed in the solution of spiran (2).

BULLETIN OF THE CHEMICAL SOCIETY OF JAPAN VOL. 43 2245—2248 (1970)

Elimination Reactions on Solid Acid Catalysts. I. A Comparison between Silica-alumina and Alumina Catalysts in the Dehydration of Ethanol by Means of the Poisoning Method

Isao MOCHIDA, Yasuhide Anju, Akio KATO and Tetsuro SEIYAMA

Department of Applied Chemistry, Faculty of Engineering, Kyushu University, Fukuoka

(Received December 15, 1969)

Silica-alumina, alumina, and alumina-boria are solid acid catalysts useful in various acid-catalyzed reactions.[1] The correlations between the acidity and the catalytic activity have been established in some reactions;[2] however, no general conclusion has yet been obtained among all the acid-catalyzed reactions.

One of the present authors has reported previously that alumina showed a characteristic behavior in contrast with silica-alumina in the reaction with methylene chloride[3] and in dehydrochlorination reactions from chloroethanes,[4] although it had a very small activity in dealkylation reactions which were explained by the protonic acidity.[5,6]

Echigoya[7] discussed the differences between these two catalysts in some reactions and explained them in terms of the acid strength and the origins of their acid sites.

The dehydration of ethanol is one of the reactions which show a distinct difference between these two catalysts, and it has been investigated for many years.[7-9] Two kinds of mechanisms have been proposed; one is the carbonium-ion mechanism,[10] and the other, the alcohoxide mechanism.[11] Pines and Pillai[12] and Jain and Pillai[13] have shown the olefin and ether formations on alumina *via* a concerted mechanism by the poisoning method, using acidic and basic inhibitors.

In the present research, the reaction mechanism was investigated by the poisoning method, using pyridine and *n*-butylamine as the basic substances and acetic acid as an acidic substance in order to clarify the differences between silica-alumina and alumina in the dehydration of ethanol. Recently,

1) a) H. H. Voge, "Catalysis," Vol. 6, ed. by P. H. Emmett, Reinhold Pub. Co., New York, N. Y. (1958), p. 407; b) S. G. Hindin and S. W. Weller, *J. Phys. Chem.*, **60**, 1506 (1956); c) Y. Izumi and T. Shiba, This Bulletin, **37**, 1797 (1964).

2) a) M. W. Tamele, *Discuss. Faraday Soc.*, **8**, 277 (1950); b) V. C. F. Holm, C. C. Bailey and A. Clark, *J. Phys. Chem.*, **63**, 129 (1959); c) K. Tanabe and T. Takeshita, "Acid-Base Catalysts," Sangyo Tosho (1965), p. 129.

3) I. Mochida, J. Take, Y. Saito and Y. Yoneda, This Bulletin, **41**, 65 (1968).

4) I. Mochida, J. Take, Y. Saito and Y. Yoneda, *J. Org. Chem.*, **32**, 3894 (1967).

5) M. E. Johnson and J. S. Melic, *J. Phys. Chem.*, **65**, 1146 (1961).

6) I. Mochida and Y. Yoneda, *J. Catal.*, **7**, 386 (1967).

7) E. Echigoya, *Nippon Kagaku Zasshi*, **79**, 426, 430 (1958).

8) M. E. Winfield, "Catalysis," Vol. 7, ed by P. H. Emmett, Reinhold Pub. Co., New York, N. Y. (1960), p. 93.

9) H. Pines and J. Manassen, *Advan. Catal.*, **16**, 49 (1966).

10) W. S. Bery and K. A. Krieger, *J. Amer. Chem. Soc.*, **71**, 3637 (1949).

11) K. V. Topchieva, K. Yun Pin and I. V. Shirnova, *Advan. Catal.*, **9**, 799 (1957).

12) H. Pines and C. N. Pillai, *J. Amer. Chem. Soc.*, **82**, 2401 (1960).

13) J. R. Jain and C. N. Pillai, *J. Catal.*, **9**, 322 (1967).

Trambouze *et al.*[11] reported common concerted mechanisms for both alumina and silica-alumina by a similar poisoning method using tetracyanoethylene (TCNE) as the acidic substance. Very recently, Parera and Figoli[15] studied the differences between these two catalysts in the dehydration and methylation of methanol, and concluded that the active sites on silica-alumina were protonic-acid sites, whereas those on alumina were Lewis-acid sites.

Experimental

Reagents. Ethanol of a G. R. grade (Hayashi Junyaku Co.) and *n*-butylamine, pyridine, and acetic acid of an E. P. grade (Wako Junyaku Co.) were used without further purification. Isopropylbenzene was used after the removal of peroxide by an adsorption column of silica and alumina gels.[16]

Table 1. Catalysts

Abbreviation	Name	Surface area (m^2/g)	Composition	Remark
A	alumina	190		(a)
A-Na	alumina-NaOH	240	0.33 meq Na/g	(b)
AB	alumina-boria	390	10% B_2O_3	(c)
AB-Na	alumina-boria-NaOH	290	0.33 meq Na/g	(d)
SA	silica-alumina	550	13% Al_2O_3	(e)
SA-Na	silica-alumina-NaOH	500	0.42 meq Na/g	(f)

a) By precipitation of $Al(NO_3)_3$ with NH_4OH.
b) By impregnation of A with aq. NaOH.
c) By coprecipitation of $Al(NO_3)_3$ and H_3BO_3 with NH_4OH.
d) By impregnation of AB with aq. NaOH.
e) Nippon Cat, a cracking catalyst of the Shokubai Kasei Co.
f) By impregnation of SA with aq. NaOH.

Catalysts. The catalysts are listed in Table 1, together with some of their properties. They were all calcined at 550° for 8 hr in the atmosphere.

Apparatus and Procedures. An ordinary pulse technique with a hydrogen carrier gas was adopted for both reactions.[17] A 1-hr pretreatment of the catalyst was carried out in a hydrogen gas flow at 450°C. For dehydration, PEG-1500 (Gas Chro Kogyo Co.) was used in the analytical column (2 m, 70°C), and the reaction temperature was 350±2°C. The gas-chromatographic peaks of the products were broad on sodium-poisoned catalysts.[18] In this case, the products were once trapped by liquid nitrogen between the reactor and analytical column, and then they were simultaneously reevaporated for gas-chromatographic analysis. For deisopropylation, the analytical column contained 3 m of TCP (Gas Chro Kogyo Co.) and the reaction temperature was 440±2°C. The conversion was proportional to the reciprocal space velocity under a low conversion, so apparent rate constant, k, was obtained from the slope. To observe the effect of a base or acid addition, poisoning reagents were injected before the reaction. As basic inhibitors did not react with ethanol, a catalyst could then be used. In the case of acetic-acid poisoning, however, ethylacetate was formed on some catalysts, so the poisoning effect was measured over the catalysts poisoned for each observation.

Results

The Catalytic Activities of Silica-alumina, Alumina, and Their Related Catalysts in Dehydration and Deisopropylation Reactions. The catalytic activities for the dehydration of ethanol and for deisopropylation from isopropylbenzene are summarized in Table 2. The six catalysts studied may be classified into two groups: SA, SA-Na, and AB belong to one group, and A, A-Na, and AB-Na to the other group. The catalyst of

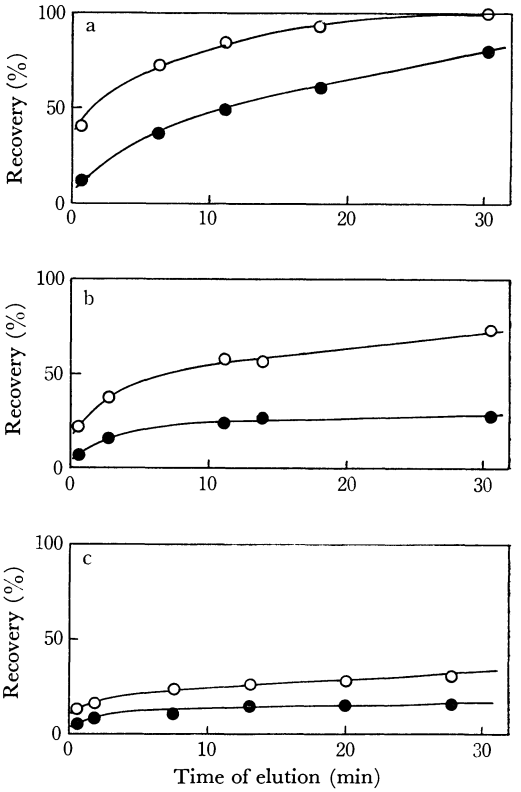

Fig. 1. Poisoning by *n*-butylamine for dehydration of ethanol at 350°C.
a, alumina; b, alumina-boria; c, silica-alumina
●, ethylene formation; ○, ether formation

14) F. F. Roca, L. De Mourgues and Y. Trambouze, *J. Catal.*, **14**, 107 (1969).
15) J. M. Parera and N. S. Figoli, *ibid.*, **14**, 303 (1969).
16) C. J. Prater and D. M. Nace, *Advan. Catal.*, **8**, 293 (1956).
17) R. J. Kokes, H. Tobin and P. H. Emmett, *J. Amer. Chem. Soc.*, **77**, 5860 (1955).
18) Y. Murakami, *Shokubai*, **5**, 192 (1963).

Table 2. Rates of dehydration of ethanol and deisopropylation of isopropylbenzene on various catalysts

Catalyst	A	AB	SA	A-Na	AB-Na	SA-Na
Rate (ml/min·g) ($\times 10^3$)[a]						
of ethanol disappearance	4.2	3.0	4.5	1.2	1.0	0.89
of ethylene formation	2.1	1.9	3.0	0.60	0.54	0.53
of ether formation[b]	2.1	1.1	1.5	0.60	0.48	0.36
Ratio of formation rate[c]	1.0	1.7	2.0	1.0	1.1	1.5
Rate (ml/min·m^2)	22	7.7	8.2	5.0	3.5	1.3
Rate (ml/min·m^2·Al-atom)	22	8.5	69	—	—	—
Rate of deisopropylation from isopropylbenzene (ml/min·g)[d]	1.3×10^{-1}	6.6×10^{2}	2.4×10^{3}	*	2.6	9.6×10

a) Reaction temperature: 350°C, flow rate: 90 ml/min.
b) Ethanol base.
c) Ratio of ethylene/ether in ethanol base.
d) Reaction temperature: 440°C, flow rate: 90 ml/min.
* Too small to be measured.

the former group had a considerable activity for deisopropylation and its ethylene/ether ratio was larger than unity, whereas the catalyst of the latter group had a very small activity for deisopropylation and its ethylene/ether ratio was about unity. Sodium ions poisoned the catalysts of both groups in both reactions. It is interesting that AB-Na behaved much like A.

Poisoning by Nitrogen Bases. The addition of a nitrogen base to a catalyst before the reaction retarded the dehydration reaction to an extent according to the kind of catalyst and base. The activity recovered gradually as the elution by hydrogen proceeded. These phenomena may be explained by the adsorption and desorption of the nitrogen base on acidic sites. The cases with *n*-butylamine and pyridine are shown in Figs. 1 and 2 respectively. With more basic *n*-butylamine, the dehydration was retarded more and the recovery of the catalytic activity was slower. The catalyst with a considerable activity for deisopropylation, the first group, was poisoned more severely, but A-Na or AB-Na suffered no effect. Generally speaking, the nitrogen base poisoned the ethylene formation more than the ether formation. This selective poisoning was most distinct with pyridine as an organic base and AB as a catalyst, when only the ethylene formation was retarded. Moreover, more poisoning of the sodium ion against ethylene formations on silica-alumina and alumina has been reported.[7,19]

Poisoning by Acetic Acid. The effect of an acid addition on dehydration was studied for SA, AB, and A from a viewpoint similar to that reported by Pines and Pillai[12] and by Jain and Pillai.[13] The results are shown in Fig. 3. Acetic acid also poisoned the ethylene formation more. Speaking of catalysts, they were poisoned in this order: A> AB>SA, which was just the reverse of that in the nitrogen-base poisoning. In the cases of SA and AB, the ester was found in the first pulse, but it disappeared in the second and following pulses, when the poisoning for ether formation also disappeared. On A, the ester was not found at all,

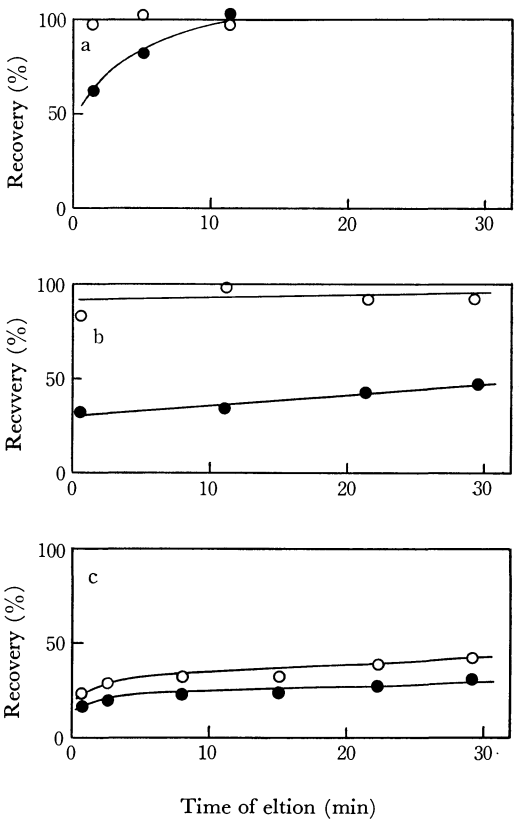

Fig. 2. Posioning by pyridine for dehydration of ethanol at 350°C.
a, alumina; b, alumina-boria; c, silica-alumina
●, ethylene formation; ○, ether formation

19) J. Take and Y. Yoneda, *ibid.*, **7**, 317 (1965).

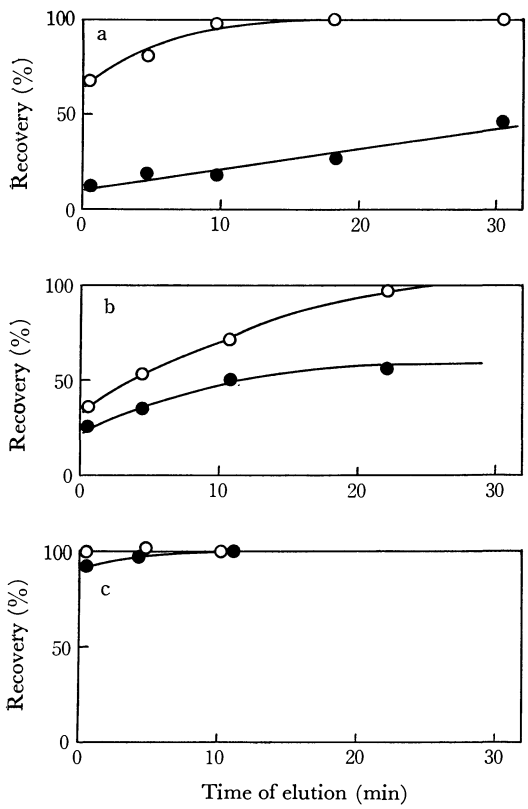

Fig. 3. Posioning by acetic acid for dehydration of ethanol at 350°C.
a, alumina; b, alumina-boria; c, silica-alumina
●, ethylene formation; ○, ether formation

although acetic acid might be adsorbed. All sodium-poisoned catalysts except SA-Na were poisoned more severely than their original catalysts.

Discussion

As has been described in the results section, the catalysts studied were classified into two groups. As for the silica-alumina group, on which a considerable deisopropylation occurred, the dehydration may take place on the strong acid sites, as is to be expected from the fact that deisopropylation proceeded on such sites.[5-7] The decrease in activity which occurred upon the addition of a sodium ion or organic bases supports the above mechanism. The active sites may not include the basic site, which is different from the sites on the alumina group, because acetic acid had little effect on dehydration, although the phenomena became complex about AB, where parts unperturbed by the presence of boria were left. Recently, Trambouze *et al.*[14] has reported that the active sites for dehydration on silica-alumina contained basic points as well as acidic points; however, the present authors observed that TCNE poisoned the deisopropylation as well. Therefore, it is possible that the adsorption of bulky TCNE on a weak basic site retarded the reaction on an acid site. The same situation may occur in dehydration. The results on alumina suggest that the ethylene formation proceeds through a concerted mechanism on an acidic site and a basic site[9,12] including an ethoxide intermediate.[20,21] The adsorption of acetic acid on basic sites may be verified by the fact that acetic acid poisoned A-Na more severely than A. Echigoya[7] defined the Lewis acid for alumina and the Brönsted acid for silica-alumina and proposed hydrated Lewis acids as active sites on alumina for dehydration. However, the aluminum ion, which can accept ethanol in an ethoxide, is more probable as the active site, although the former part of Echigoya's definition may be true. Parera and Figoli[15] reached a similar conclusion in the reaction of methanol. These differences in the mechanism and the active site might bring about the distinct difference in the dehydrations on silica-alumina and alumina.

The esterification of ethanol with acetic acid on silica-alumina was much faster than on alumina, although the esterification may proceed on weaker acid sites than dehydration. Here an interesting difference was observed between two catalysts. The results of our investigation of this reaction in connection with dehydration will be published later.

20) H. Arai, J. Take, Y. Saito and Y. Yoneda, *J. Catal.*, **9**, 146 (1967).
21) H. Arai, Y. Saito and Y. Yoneda, This Bulletin, **40**, 731 (1967).

BULLETIN OF THE CHEMICAL SOCIETY OF JAPAN VOL. 43 2249—2250 (1970)

Infrared Spectroscopic Studies on Vaska Complex using Heavy Oxygen

Kiyotomi TAKAO, Yuzo FUJIWARA, Toshinobu IMANAKA, Masao YAMAMOTO,* Kozo HIROTA* and Shiichiro TERANISHI

Department of Chemical Engineering, Faculty of Engineering Science, Osaka University, Toyonaka, Osaka
* *Department of Chemistry, Faculty of Science, Osaka University, Toyonaka, Osaka*

(Received December 30, 1969)

Recently several transition metal complexes coordinated with molecular oxygen have been described.[1-5] With respect to iridium metal in particular, the reaction of the species having the general formula $[Ir(p\text{-}p)_2]Cl$ and $IrXCO(PPh_3)_2$ (p-p: $Ph_2PCH_2CH_2PPh_2$, X: halide) with molecular oxygen has been studied in detail.[6,7] The structures of these iridium complexes have been made clear by X-ray analysis.[8,9]

In Vaska iridium oxygen complex, $(IrClCO(PPh_3)_2O_2)$, the strong IR absorption spectrum at 856 cm^{-1} is ascribed to the peroxy-vibration,[1] but no definite assignment has been made. Hirota and his coworkers[10] studied the spectra of the peroxy-complexes, $Ni(Bu^tNC)_2O_2$ and $Pd(Bu^tNC)_2O_2$ and observed three bounds due to ^{16}O–^{16}O, ^{16}O–^{18}O and ^{18}O–^{18}O.[10]

In order to investigate the nature of chemical bonds of the iridium complexes, we have studied the IR and FIR (far infrared) spectra of Vaska oxygen complex containing heavy oxygen molecule.

The iridium oxygen complex containing heavy oxygen was prepared by the reaction of $IrClCO(PPh_3)_2$ complex and heavy oxygen (25.5% as $^{18}O_2$) at 170 mmHg for 45 hr. The IR spectrum of the complex in Nujol mulls is shown in Fig. 1. The IR band at 856 cm^{-1} splites into three strong absorption bands at 856, 832 and 808 cm^{-1}. Since the iridium oxygen complex contains three molecular species such as ^{16}O–^{16}O, ^{16}O–^{18}O and ^{18}O–^{18}O, the calculation on the assumption of free diatomic molecules gives wave numbers to be 856, 832 and 807 cm^{-1}. A good agreement between the observed wave numbers and those calculated shows that the band at 856 cm^{-1} which has been reported by Vaska[1] is clearly assignable to the stretching vibration of the O–O bond.

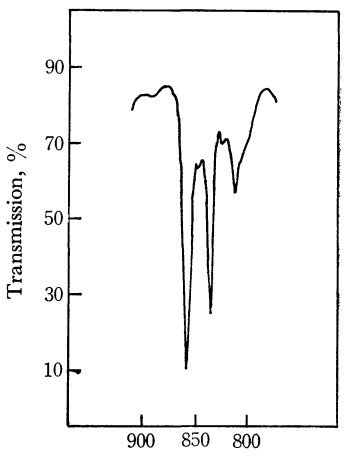

Fig. 1. Infrared spectrum of the iridium oxygen complex.

By measuring the relative intensity of the three bands at 856, 832 and 808 cm^{-1}, these bands are ascribed to such molecular species as ^{16}O–^{16}O, ^{16}O–^{18}O and ^{18}O–^{18}O, respectively. The shoulders at 843 cm^{-1} and 820 cm^{-1} are assignable to the stretching vibration of ^{16}O–^{17}O and ^{17}O–^{18}O, respectively, in comparison with the calculated.

The FIR spectra of Vaska complexes were reported already by Bennett *et al.*,[11] but those of Vaska oxygen complexes are not known and were measured accordingly.

The FIR spectrum of this oxygen adduct shown in Fig. 2 indicates that the very strong band assignable to the stretching vibration of Ir–Cl bond[11] shifts from 318 to 314 cm^{-1} and that a band at 184

1) L. Vaska, *Science*, **140**, 809 (1963).
2) G. Wilke, H. Schott and P. Heimbach, *Angew. Chem.*, **79**, 62 (1967).
3) S. Takahashi, K. Sonogashira and N. Hagihara, *Nippon Kagaku Zasshi*, **87**, 610 (1966).
4) S. Otsuka, A. Nakamura and Y. Tatsuno, *Chem. Commun.*, **1967**, 836.
5) J. T. Mague and G. Wilkinson, *J. Chem. Soc., A*, **1966**, 1736.
6) L. Vaska and D. L. Caton, *J. Amer. Chem. Soc.*, **88**, 5324 (1966).
7) P. B. Chock and J. Halpern, *ibid.*, **88**, 3511 (1966).
8) S. J. LaPlaca and J. A. Ibers, *ibid.*, **87**, 2581 (1965).
9) J. A. McGinnety, R. J. Doedens and J. A. Ibers, *Inorg. Chem.*, **6**, 2243 (1965).
10) K. Hirota, M. Yamamoto, S. Otsuka, A. Nakamura and Y. Tatsuno, *Chem. Commun.*, **1968**, 533.
11) M. A. Bennett, R. J. H. Clark and D. L. Melner, *Inorg. Chem.*, **6**, 1647 (1967).

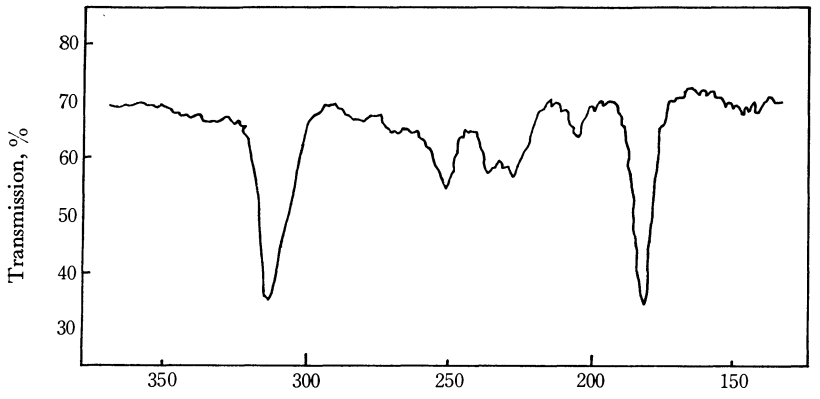

Fig. 2. Far infrared spectrum of the iridium oxygen complex.

cm^{-1} shifts to 182 cm^{-1} when heavy oxygen was used.

The stretching band of Ir–O bond which is expected in the region of 450—600 cm^{-1} can not be detected due to overlapping of the strong bands of triphenylphosphine ligand.

In addition, we have found that the oxygen complexes can easily cause the oxidation reaction of olefins under mild condition.[12]

12) K. Takao, Y. Fujiwara, T. Imanaka and S. Teranishi, This Bulletin, **43**, 1153 (1970).

BULLETIN OF THE CHEMICAL SOCIETY OF JAPAN VOL. 43 2250—2251 (1970)

Synthesis and Reactions of Sulfonium Diacylmethylide Having Active Hydrogen

Masaki TAKAKU and Hitosi NOZAKI

Department of Industrial Chemistry, Kyoto University, Sakyo-ku, Kyoto

(Received January 8, 1970)

Sulfonium diacylmethylides are easily prepared by acylating sulfonium monoacylmethylides[1] or by condensation of sulfoxides and 1,3-diketones.[2] Nevertheless few of their reactions are known with respect to the remarkable stability and inertness of these ylides.[3] We wish to report the reaction of sulfonium diacylmethylides having active hydrogens with a strong base.

Ylides Ia and Ib were prepared from the corresponding sulfonium phenacylides and phenylacetic anhydride in 71 and 72% yields, respectively, in the usual way. To a stirred solution of Ia in dimethyl sulfoxide (DMSO) under nitrogen was added equimolar sodium hydride in one portion. The reaction mixture was stirred for further 3 hr to produce a deep red solution. To this solution of IIa was added dropwise methyl iodide to give a new ylide IIIa (mp 132—133°C) in a 64% yield. Under the same conditions as above, Ib also yielded a red solution of IIb, which was treated with methyl iodide to give IIIb (mp 149—151°C) in a 70% yield. The

Fig. 1. NMR spectrum of dimethylsulfonium benzoyl(α-phenylpropionyl)methylide (IIIa).

1) H. Nozaki, M. Takaku and K. Kondo, *Tetrahedron*, **22**, 2145 (1966).

2) H. Nozaki, Z. Morita and K. Kondo, *Tetrahedron Lett.*, **1966**, 2913.

3) a) H. Nozaki, K. Nakamura and M. Takaku, *Tetrahedron*, **25**, 3675 (1969); b) M. Takaku, Y. Hayasi and H. Nozaki, *Tetrahedron Lett.*, **1969**, 2053.

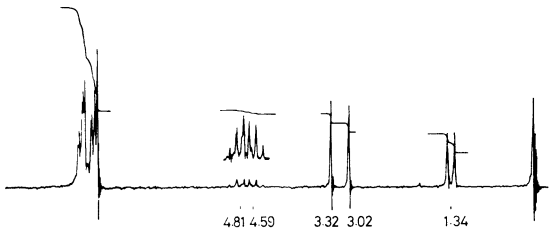

Fig. 2. NMR spectrum of methylphenylsulfonium benzoyl(α-phenylpropionyl)methylide (IIIb).

structures of IIIa and IIIb were determined on the basis of C, H analysis and spectral data. NMR spectrum of IIIa is given in Fig. 1, in which S-methyl signals were observed as two distinct singlets with chemical shift difference of 0.24 ppm. This shows that the S-methyl groups are diastereotopic to each other due to the pyramidal structure of sulfur atom and the presence of asymmetric carbon of α-phenethyl group. NMR spectrum of IIIb is given in Fig. 2. S-Methyl signals were observed as two singlets with chemical shift difference of 0.30 ppm as in IIIa. Methine protons appeared as two quartets (chemical shift difference: 0.22 ppm). The data indicate that IIIb is a *ca.* 1 : 1 mixture of two diastereomers due to two assymetric atoms (sulfur and α-phenethyl carbon), although it has a melting point 149—151°C and proved homogeneous on TLC. These diastereomers, however, have not been separated into components.

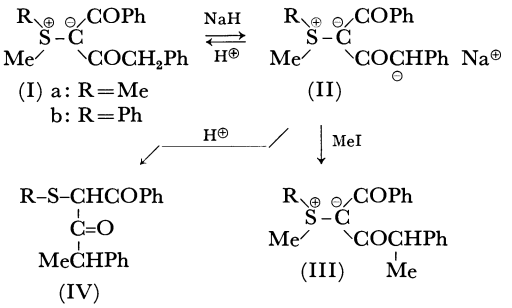

Treatment of a solution of IIa with acetic acid gave the starting ylide Ia in a 67% yield. In sharp contrast, however, treatment of IIb with acetic acid gave a rearranged product IVb (64%). The same rearrangement was also observed in DMF solvent. Simple treatment of Ib with acetic acid failed to induce the rearrangement.

Experimental

Preparation of Dimethylsulfonium Benzoyl(phenylacety)methylide (Ia). A solution of dimethylsulfonium phenacylide (3.6 g, 0.02 mol) and phenylacetic anhydride (5.1 g, 0.02 mol) in THF (100 m*l*) was stirred for 10 hr at room temperature. The reaction mixture was concentrated *in vacuo* and treated with chloroform. The chloroform solution was washed with aq. $NaHCO_3$, dried ($MgSO_4$) and concentrated. The residual solid was recrystallized from benzene to afford Ia (4.2 g, 70.5%), mp 108—110°C, IR (Nujol): 1591, 1565 and 1145 cm^{-1}, NMR: δ ($CDCl_3$) 2.86 (6H, s), 4.01 (2H, s), 7.2—7.5 (10H, m). (Found: C, 72.9; H, 6.1%. Calcd for $C_{18}H_{18}O_2S$: C, 72.5; H, 6.1%.)

Preparation of Methylphenylsulfonium Benzoyl(phenylacetyl)methylide (Ib). Treatment of methylphenylsulfonium phenacylide (4.8 g, 0.02 mol) with phenylacetic anhydride (5.1 g, 0.02 mol) in THF (100 m*l*) gave Ib (5.2 g, 72%), mp 130—132°C (from benzene), IR (KBr): 1596, 1570, 1350, 1118, 960, 735 and 710 cm^{-1}, NMR: δ ($CDCl_3$) 3.30 (3H, s), 4.09 (2H, s), 7.3—7.7 (15H, m). (Found: C, 76.8; H, 5.3%. Calcd for $C_{23}H_{20}O_2S$: C, 76.7; H, 5.6%.)

Reaction of Ia with Sodium Hydride Followed by Addition of Methyl Iodide. To a solution of Ia (3.0 g, 0.01 mol) in DMSO (50 m*l*) under nitrogen was added sodium hydride (1.0 g, 50% dispersion in mineral oil, 0.01 mol) in one portion at room temp. The reaction mixture was stirred for 3 hr to afford a red solution of IIa. To this solution of IIa was added dropwise a solution of methyl iodide (5.6 g, 0.04 mol) in DMSO (10 m*l*). After being stirred for an additional 1 hr, the reaction mixture was diluted with water and extracted with chloroform. The chloroform solution was dried ($MgSO_4$) and evaporated to afford a solid, which was recrystallized from benzene to yield IIIa (2.0 g, 64%), mp 132—133°C, IR (Nujol): 1590, 1580, 1565—1550 (broad), 1195, 1178, 1140, 1021 and 985 cm^{-1}. (Found: C, 72.8; H, 6.4%. Calcd for $C_{19}H_{20}O_2S$: C, 73.0; H, 6.5%.)

Reaction of Ib with Sodium Hydride Followed by Addition of Methyl Iodide. According to the same procedure as Ia, Ib (3.6 g, 0.01 mol) was treated with sodium hydride (1.0 g, 50% dispersion in mineral oil, 0.01 mol) followed by addition of methyl iodide (5.6 g, 0.04 mol) and gave IIIb (2.6 g, 70%), mp 149—151°C (from benzene-hexane), IR (KBr): 1580, 1570, 1295 and 1225 cm^{-1}. (Found: C, 76.6; H, 6.3%. Calcd for $C_{24}H_{22}O_2S$: C, 77.0; H, 5.9%.)

Treatment of IIa with Acetic Acid. To a solution of IIa (0.01 mol) in DMSO (50 m*l*) was added dropwise acetic acid (0.9 g, 0.015 mol) in DMSO (10 m*l*). The reaction mixture was diluted with aq. $NaHCO_3$ and extracted with chloroform. The chloroform solution was concentrated to afford Ia (2.0 g, 67%).

Treatment of IIb with Acetic Acid. A solution of IIb (0.01 mol) in DMSO (50 m*l*) was treated with acetic acid (0.9 g, 0.015 mol), diluted with water and extracted with chloroform. The chloroform solution was concentrated and ether was added to the residual oil to give a solid, which was recrystallized from ethanol to afford IVb (2.3 g, 64%), mp 90—93°C, IR (KBr): 1605, 1582, 1540 (broad), 1480 and 1380 cm^{-1}, NMR: δ ($CDCl_3$) 1.47 (3H, d, J=7.2 Hz), 4.11 (1H, s), 4.78 (1H, q, J=7.2 Hz), 7.0—7.8 (15H, m). (Found: C, 76.4; H, 5.5%. Calcd for $C_{23}H_{20}O_2S$: C, 76.7; H, 5.6%.)

BULLETIN OF THE CHEMICAL SOCIETY OF JAPAN VOL. 43 2252—2254 (1970)

The Estimation of Primary Radical Termination from Rate Data in Free Radical Polymerization

O. F. OLAJ

Institute for Physical Chemistry, University of Vienna, Austria

(Received January 20, 1970)

Recently an article has been published by Ito and Matsuda[1] in which a simple treatment of primary radical termination in free radical polymerization was proposed. Starting from the kinetic scheme for primary radical termination as it had been developed by Bamford and Jenkins,[2] however, omitting an eventual recombination of primary radicals outside the solvent cage, *viz.*,

$R_0=2(1-h)R_d$	rate of formation of primary radicals ($R_d=k_d[\mathrm{I}]$ = rate of initiator decomposition)
$R_i=k_i[\mathrm{R}][\mathrm{M}]$	rate of initiation (polymer radical formation)
$R_p=k_p[\mathrm{P}][\mathrm{M}]$	rate of chain propagation
$R_t=k_t[\mathrm{P}]^2$	rate of mutual termination between polymer radicals
$R_{ti}=k_{ti}[\mathrm{R}][\mathrm{P}]$	rate of termination of polymer radicals by primary radicals

[I], [M], [R], and [P] denoting the concentrations of initiator, monomer, primary radicals, and polymer radicals, respectively, $(1-h)$ being the fraction of primary radicals escaping the solvent cage, Ito and Matsuda simplified the cubic equation,

$$R_p^3 + (k_ik_p/k_{ti})[\mathrm{M}]^2R_p^2 + R_0(k_p^2/k_t)[\mathrm{M}]^2R_p - (k_ik_p/k_{ti})(k_p^2/k_t)R_0[\mathrm{M}]^4=0 \quad (1)$$

which is obtained after the usual stationary state treatment for primary and polymer radicals, by introducing several approximations finally arriving at an equation of the form

$$R_p/[\mathrm{M}][\mathrm{I}]^{0.5} = A - A^2B([\mathrm{I}]^{0.5}/[\mathrm{M}]) \quad (2)$$

where

$$A = k_p\{2(1-h)k_d/k_t\}^{0.5} \text{ and } B = k_{ti}/k_ik_p$$

which should allow an evaluation of the ratio $k_{ti}/k_ik_p(\equiv B)$ characteristic for the termination of the growing polymer radicals by the specific primary radicals by plotting $R_p/[\mathrm{M}][\mathrm{I}]^{0.5}$ *vs.* $[\mathrm{I}]^{0.5}/[\mathrm{M}]$ and dividing the (absolute value of the) slope by the squared intercept.

However, as had apparently escaped the notice of Ito and Matsuda, in 1965 an article had already appeared[3] in which the cubic equation (1) had been simplified on similar lines to yield another linear relationship

$$R_p/[\mathrm{M}][\mathrm{I}]^{0.5} = A - AB(R_p/[\mathrm{M}]^2) \quad (3)$$

A and B being defined identically as before. In this case which also does not require the knowledge of either k_p^2/k_t or $2(1-h)k_d$, the characteristic ratio $k_{ti}/k_ik_p(\equiv B)$ is easily calculated by dividing the absolute slope by the intercept after a plot of $R_p/[\mathrm{M}][\mathrm{I}]^{0.5}$ *vs.* $R_p/[\mathrm{M}]^2$ has been made. This method has been successfully applied to the polymerization of styrene initiated by 2,2′-azobisisobutyronitrile (AIBN) using results of Henrici-Olivé and Olivé[4] and Olaj[3] and later on also to the polymerization of styrene initiated by 1,1′-azobis-1-phenylethane and 1,1′-azobis-1-cyanocyclohexane[5] and the superiority of estimating k_{ti}/k_ik_p from rate measurements over all other methods existing at that time thoroughly discussed.[3] Although the rate of polymerization had been varied over a wide range, perfectly linear plots have been obtained within experimental accuracy.[3,5] This is in marked contrast to two of the three examples given by Ito and Matsuda[1] where strong deviations from linearity occur when experimental data are plotted according to their equation (Eq. (2)). The reason for this is that Eq. (3), which in the meantime also has been acknowledged and accepted by other workers,[6] is a clearly better approximation to the

TABLE 1

$10^5\cdot R_p$ mol/l·sec	$10^4\cdot R_0^{0.5}$ (mol/l·sec)$^{1/2}$	$10^2(R_p/[\mathrm{M}]R_0^{0.5})$ (l/mol·sec)$^{1/2}$			
		Eq. (1)	Eq. (2)	Eq. (3)	Eq. (4)
1	0.594	1.980_3	1.980_0	1.980_2	1.980_3
5	3.090	1.903	1.896	1.901	1.902
10	6.496	1.811	1.782	1.803	1.808
15	10.245	1.723	1.656	1.706	1.716
20	14.375	1.637	1.517	1.611	1.626
25	18.928	1.554	1.364	1.517	1.540
30	23.952	1.474	1.195	1.426	1.457

1) K. Ito and T. Matsuda, This Bulletin, **42**, 1758 (1969).

2) C. H. Bamford, A. D. Jenkins, and R. Johnston, *Trans. Faraday Soc.*, **55**, 1451 (1959).

3) O. F. Olaj, *Ber. Bunsenges. Phys. Chem.*, **69**, 238 (1959).

4) G. Henrici-Olivé and S. Olivé, *Makromol. Chem.*, **37**, 71 (1960).

5) O.F. Olaj, *ibid.*, **114**, 1 (1968).

6) M. Munzer, *Angew. Makromol. Chem.*, **11**, 1 (1970).

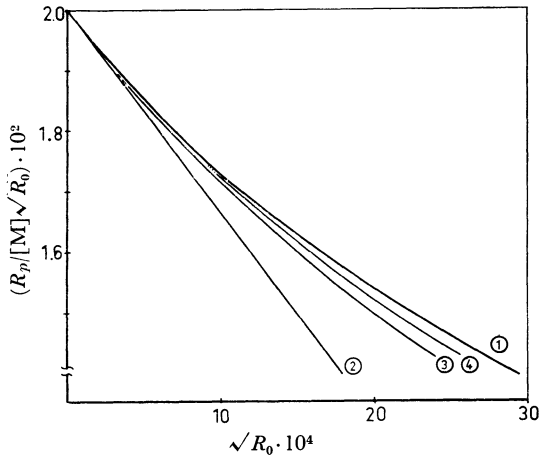

Fig. 1. $R_p/[M]R_0^{0.5}$ ($mol^{-1/2}\ l^{1/2}\ sec^{-1/2}$) calculated from given $R_0^{0.5}$ ($mol^{1/2}\ l^{-1/2}\ sec^{-1/2}$) values according to the (exact) Eq. (1) (curve 1, plot 1), Eq. (2) (curve 2), Eq. (3) (curve 3), and Eq. (4) (curve 4), plotted *vs.* $R_0^{0.5}$.
$k_ik_p/k_{ti}=1.4\times10^{-4}\ l\ mol^{-1}\cdot sec^{-1}$
$k_p^2/k_t=4.10^{-4}\ l\ mol^{-1}\cdot sec^{-1}$, $[M]=8.5\ mol\ l^{-1}$

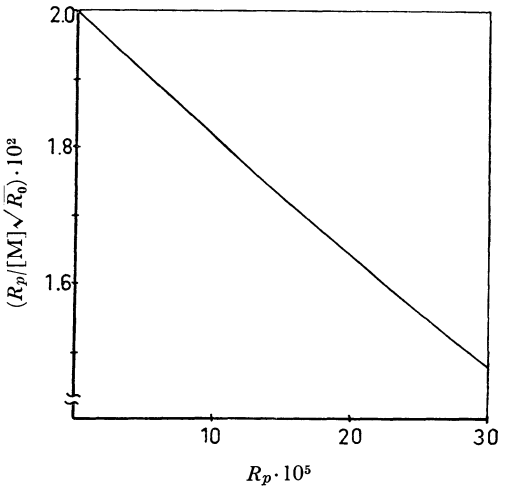

Fig. 2. $R_p/[M]R_0^{0.5}$ ($mol^{-1/2}\ l^{1/2}\ sec^{-1/2}$) calculated according to Eq. (1) and plotted *vs.* R_p ($mol\cdot l^{-1}\ sec^{-1}$) (plot 2).
(k_ik_t/k_{ti}, k_p^2/k_t, and [M] as in Fig. 1)

exact Eq. (1) than the Ito-Matsuda equation, Eq. (2). This will be shown in the following discussion.

In order to avoid ambiguity from experimental uncertainties let us assume a theoretical system with $k_p^2/k_t=4.10^{-4}\ l\ mol^{-1}\cdot sec^{-1}$, $k_ik_p/k_{ti}=1.4\times10^{-5} l\cdot mol^{-1}\cdot sec^{-1}$, and $[M]=8.5\ mol\ l^{-1}$ (for convenience a constant monomer concentration independent of the initiator concentration is used) which approximately corresponds to the system styrene - AIBN at 50°C. Let us further take a set of $R_p/[M]R_0^{0.5}-R_0^{0.5}$ pairs from the exact Eq. (1). On the other hand we use the same $R_0^{0.5}$ values and calculate the approximate $R_p/[M]R_0^{0.5}$ values according to Eqs. (2) and (3) (Table 1, columns 4 and 5). It can be easily seen from Fig. 1 that the latter (curve 3) deviate by far less from the exact values (curve 1) than Ito and Matsuda's values (curve 2). At a rate of initiation where $R_p/[M]R_0^{0.5}$ is reduced by 10% compared to its value at zero rate of initiation the deviation from the true values is *ca.* 0.45% for Olaj's equation while it amounts to *ca.* 1.65% for Eq. (2), at a 25% reduction of $R_p/[M]R_0^{0.5}$ the deviations are 3.2 and 18%, respectively.

The superiority of Eq. (3) over Eq. (2) can be demonstrated even more clearly in another way. Let us again take the true values from Table 1 and plot them according to the Eqs. (2) *vs.* $R_0^{0.5}$ (Fig. 1, curve 1) and (3) *vs.* R_p (Fig. 2). It appears from first sight that the latter plot (plot 2) is nearly linear, while Ito and Matsuda's plot (plot 1) shows a considerable curvature. Due to the small variation of $R_p/[M]R_0^{0.5}$ with R_p or $R_0^{0.5}$, respectively, the slope as the critical quantity will be comparatively sensitive to experimental error, and a least square treatment of the experimental data is often necessary. Such a treatment, however, will lead to erroneous results even from the theoretical point of view if the (theoretical) linearity of the plot is not warranted to a satisfying degree. On the other hand this difficulty is only partially circumvented if in the awareness of the limited theoretical linearity of the plot data only from low polymerization or initiation rates are used as the slope and therefore the value for k_{ti}/k_ik_p obtained in this way will be subject to considerable error due to the inevitable scatter of the experimental results. The difference between plot 1 and plot 2 becomes evident when the least square treatment is applied to the first six points in Table 1 to obtain the best slope and intercept: while plot 1 (Ito and Matsuda) gives a value of 5.04×10^4 (mol sec l^{-1}) for k_{ti}/k_ik_p which deviates by nearly 30% from the theoretical value (7.143×10^4) the value obtained from plot 2 (Olaj) is correct within 10% (6.44×10^4) which in most cases is less than the experimental uncertainty.

Mathematically the superiority of Eq. (3) over Eq. (2) can be explained as follows: When $R_p/A[M][I]^{0.5}(\equiv y)$ is expanded into a series of powers of $R_p\cdot B/[M]^2(\equiv x)$ the exact Eq. (1) will be written as

$$y = 1 - x + \frac{1}{2}x^2 - \frac{1}{2}x^3\cdots \qquad (1a)$$

Ito and Matsuda's Eq. (2) will take the form

$$y = 1 - x - x^2 - \frac{1}{2}x^3\cdots \qquad (2a)$$

while Eq. (3) will give the simple expression

$$y = 1 - x$$

Whereas the second term is represented correctly by both equations, the deviation from Eq. (1a) in the quadratic term is by far less in Eq. (3a) ($-\frac{1}{2}x^2$) than in Eq. (2a) ($-\frac{3}{2}x^2$). Furthermore Eq. (3a)

profits from a partial compensation of the deviations in the quadratic and the cubic term.

Following these considerations even further improvements in deriving a linear relationship as an approximation for Eq. (1) are possible,*1 *e. g.* adding $1/4x^2$ to the right hand side of Eq. (3a) and extracting the square root yields

$$y^{1/2} = 1 - \frac{1}{2}x$$

or as a full expression

$$(R_p/[\mathrm{M}][\mathrm{I}]^{0.5})^{0.5} = A^{0.5} - \frac{1}{2}A^{0.5}B(R_p/[\mathrm{M}]^2) \quad (4)$$

Therefore a plot of $(R_p/[\mathrm{M}][\mathrm{I}]^{0.5})^{0.5}$ *vs.* $R_p[\mathrm{M}]^2$ will give a nearly optimal linear representation of the experimental data provided they obey the kinetic scheme outlined above. From this plot B ($\equiv k_{ti}/k_i k_p$) will be available from a division of double the absolute value of the slope by the intercept, again the knowledge of k_p^2/k_t and $2(1-h)k_d$ being not necessary. $R_p/[\mathrm{M}][\mathrm{I}]^{0.5}$ values calculated according to Eq. (4) using the same kinetic parameters as before are summarized for comparison to the true values in the last column of Table 1 and plotted *vs.* $R_0^{0.5}$ (Fig. 1, curve 4). It can be seen that the deviations are reduced to 0.22 and 1.5% at a rate corresponding to an approximately 10 and 25% reduction of $R_p[\mathrm{M}][\mathrm{I}]^{0.5}$ compared to its value extrapolated to zero polymerization rate, respectively. From these examples it will appear that the fit to the theoretical curve is improved by one order of magnitude compared to the equation derived by Ito and Matsuda.[1] Using the same six $R_p-[\mathrm{I}]^{0.5}$ pairs as before the least square treatment yields a $k_{ti}/k_i k_p$ value which differs from the theoretical one by only 4.2%. This is better by a factor of 7 compared to the result obtained by application of Eq. (2) (plot 1).

After all, there will be no need to analyze primary radical termination using the method proposed by Ito and Matsuda[1] as there exist more accurate procedures which are at least as easily performed.

*1 A comprehensive survey on these improvements will be given in a separate paper.[7]

7) O. F. Olaj, to be published in *Angew. Makromol. Chem.*

BULLETIN OF THE CHEMICAL SOCIETY OF JAPAN VOL. 43 2254—2256 (1970)

Pyrolysis of the Grignard Reaction Products of Benzenesulfonyl Azide*1

Suketaka Ito, Takashi Hirabayashi and Kiyoaki Matsumoto

Department of Industrial Chemistry, Faculty of Engineering, Shinshu University, Wakasato, Nagano

(Received January 20, 1970)

Several reports have appeared concerning the reactions of arenesulfonyl azides with carbanionic or organometallic reagents.[1-7] In a previous paper,[8] we ourselves reported the preparation of phenyl azide by the pyrolysis of the triazene salt obtained from benzenesulfonyl azide and phenylmagnesium bromide.[9]

This note will describe the formation of azides, diazo-compounds, and olefins by the reaction of benzenesulfonyl azide and aliphatic Grignard reagents, or by the pyrolysis of the triazene salts resulting from the reactions.

Results and Discussion

When benzylmagnesium chloride in ether was added to the ethereal solution of benzenesulfonyl azide at −20—−10°C, a triazene salt (white pre-

*1 Presented at the 22nd Annual Meeting of the Chemical Society of Japan, Tokyo, April, 1969.

1) T. Curtius and W. Klavehn, *J. Prakt. Chem.*, **112**, 65 (1926); *Chem. Abstr.*, **20**, 1408 (1926).

2) W. von E. Doering and C. H. DePuy, *J. Amer. Chem. Soc.*, **75**, 5955 (1953).

3) M. Regitz, *Ann.*, **676**, 101 (1964); M. Regitz and G. Heck, *Chem. Ber.*, **97**, 1482 (1964); M. Regitz, *ibid.*, **98**, 1210 (1965).

4) F. Klages and K. Bott, *Chem. Ber.*, **97**, 735 (1964).

5) J. M. Tedder and B. Webster, *J. Chem. Soc.*, **1960**, 4417.

6) J. H. Boyer, C. H. Mack, N. Goebel and L. R. Morgan, Jr., *J. Org. Chem.*, **23**, 1051 (1958).

7) E. Robson, J. M. Tedder and B. Webster, *J. Chem. Soc.*, **1963**, 1863.

8) S. Ito, This Bulletin, **39**, 635 (1966).

9) After the previous paper (Ref. 8) had been published, the authors found a report which communicated that phenyl azide resulted by alkaline decomposition of the triazene salt obtained from phenylmagnesium bromide and tosyl azide: The private communication of P. A. Smith and L. Bruner to J. H. Boyer and F. C. Canter; See: J. H. Boyer and F. C. Canter, *Chem. Rev.*, **54**, 17 (1954).

Table 1. The azides, the diazoalkanes, and the olefins obtained by the reaction of Grignard reagents with benzenesulfonyl azide

Grignard reagent	Azide (Yield, %)	Diazoalkane (Yield, %)	Olefin (Yield, %)
Benzylmagnesium chloride	Benzyl Azide (7.9)	Phenyldiazomethane (0.5)	——
Benzylmagnesium chloride*	Benzyl Azide (9.1)	Phenyldiazomethane (14.1)	——
Allylmagnesium chloride	Allyl Azide (13.1)	Vinyldiazomethane (—)**	——
Methylmagnesium iodide	Methyl Azide (—)	Diazomethane (1.5)	——
n-Hexylmagnesium bromide	*n*-Hexyl Azide (trace)	Diazo-*n*-hexane (trace)	1- plus 2-Hexene (11.2)
Cyclohexylmagnesium chloride	Cyclohexyl Azide (1.6)	Diazocyclohexane (0.9)	Cyclohexene (22.3)
t-Butylmagnesium chloride	*t*-Butyl Azide (2.7)	——	Isobutylene (3.1)

* Reaction in THF.

** Red-color development in the reaction of allylmagnesium chloride showed also the formation of vinyldiazomethane, though it could not be confirmed.

cipitates) and phenyldiazomethane (0.5%) were obtained in the ether solution. Benzyl azide (7.9%) was obtained in a cold trap by the vacuum pyrolysis of the triazene salt; the additional formation of a trace of *o*-tolyl azide was confirmed by gas-liquid chromatography.

When tetrahydrofuran (THF) was used as the solvent of sulfonyl azide in the reaction of benzylmagnesium chloride, no precipitates were formed and the yield of phenyldiazomethane was considerably increased (14.1%). In this case, white precipitates could be obtained after the removal of the greater part of the THF, followed by the addition of ether. Benzenesulfinic acid and benzenesulfonamide were isolated from the residue of the pyrolysis of the precipitates.

The major product of the pyrolysis of the triazene salt from cyclohexylmagnesium chloride was cyclohexene.

Upon the addition of *t*-butylmagnesium chloride to the ethereal solution of sulfonyl azide, *t*-butyl azide and isobutylene were generated in the solution almost immediately; the azide and the olefin could not be obtained by the pyrolysis of the solid part of the reaction mixture.

The reaction of vinylmagnesium bromide in THF with sulfonyl azide was also attempted, but it did not give any vinyl azide.[10]

The Grignard reagents, the azides, the diazoalkanes, and the olefins obtained are summarized in Table 1. The low yields of these products are probably due to their high volatility or law stability, and also to the complexity of the reaction.

The reaction of aliphatic Grignard reagents with benzenesulfonyl azide can be illustrated as follows:

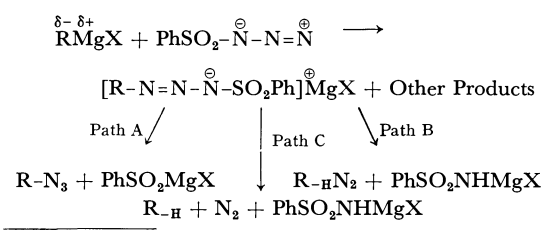

10) Nitrogen evolved and a certain polymer formed.

When the alkyl group of RMgX has no hydrogen atom in the α- and β-positions which can be eliminated, the reaction may proceed through Path A, which involves the α-elimination of the salt of sulfinic acid. On the other hand, when the alkyl group has such a hydrogen atom in the α-position, the reaction can proceed through both Paths A and B, the latter of which involves the elimination of the salt of sulfonamide.

In the reaction of benzylmagnesium chloride under the conditions of pyrolysis, no diazoalkane was obtained from the salt of triazene. However, when the triazene salt was not well dried, pyrolysis gave the benzyl azide, accompanied by a small amount of phenyldiazomethane. Furthermore, as has already been mentioned, the use of THF as the solvent in the Grignard reaction considerably increased the yield of phenyldiazomethane in the solution. Therefore, diazoalkane does not result directly from the triazene salt (I), but may be generated from a carbanion-type intermediate (II), which is itself derived from I in solution through proton transfer:

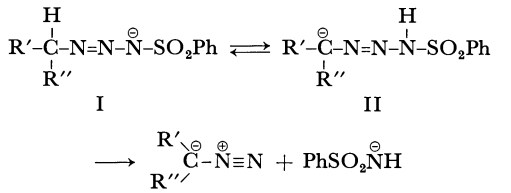

If the alkyl group has a structure in which the negative charge of the α-carbon is delocalizable by resonance, or if the R′ and/or R″ are electron-attractive groups, I can probably isomerize to II with ease, in which case the yield of the diazoalkane may increase.

The alkyl groups of cyclohexyl- and *n*-hexylmagnesium halide have eliminatable hydrogen atoms in the α- and β-positions respectively, so, in these cases, the reaction can proceed through Path A, B, or C. From the facts that 2-hexene and isobutylene were obtained, and that olefins are the major products in these types of reactions, the olefins must have been yielded through carbonium-ion

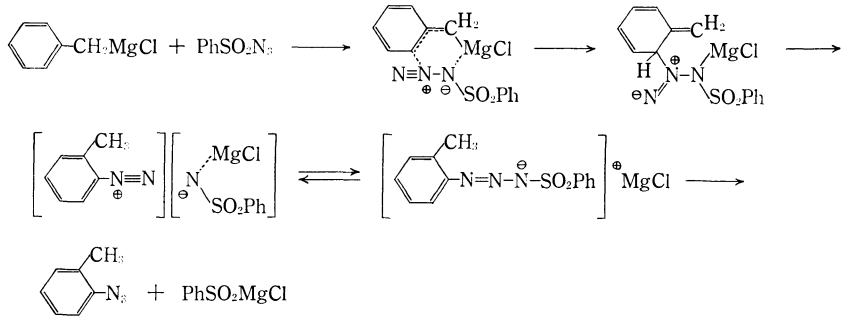

intermediates directly derived from the triazene salts.

The formation of *o*-tolyl azide can be explained by a mechanism similar to the cyclic six-membered transition state which was postulated in the reaction of benzylmagnesium chloride with formaldehyde to give 2-methylbenzyl alcohol.[11]

Experimental

Only the reaction of benzylmagnesium chloride will be described. The melting points are uncorrected. The yields of the final products are shown in percentages based on the benzenesulfonyl azide used.

The Reaction of Benzylmagnesium Chloride with Benzenesulfonyl Azide (BSA) in Diethyl Ether. Into a stirred solution of 9.2 g (0.05 mol) of BSA in 80 m*l* of dry ether, was added a solution of benzylmagnesium chloride (prepared from 7.6 g (0.06 mol) of benzyl chloride) in 70 m*l* of ether at −20—−10°C over a period of 45 min; whereupon white precipitates separated simultaneously, and the reaction mixture turned slightly red. The mixture was then separated by filtration into a reddish ether solution and a white solid (A), which was then washed with ether and dried in a vacuum desiccator. The yield of A was 16.5 g.

Upon the addition of a few drops of acetic acid, the red color of the combined filtrate and washings disappeared with an evolution of nitrogen. The ether solution, after being washed with a 5% sodium carbonate solution and then with water, and after being dried over anhydrous sodium sulfate, was concentrated to give 1.4 g of an oily residue.

By means of gas-liquid chromatography (GLC), benzyl acetate (0.5%) was found in the oily residue, which mainly consisted of unaltered BSA and benzyl chloride.

In a 200-m*l* round-bottomed flask, 16.5 g of the powdered solid (A) was placed; the flask was then connected to a series of traps and a vacuum system. The flask was heated to 40°C (oil bath temp.) (0.1 mmHg) to effect sufficient drying, and then to 120—130°C (oil bath temp.) (0.1—3.0 mmHg) in an oil bath for an hour. A colorless liquid (B) (1.57 g) was condensed at −70°C (trap temp.); from this liquid benzyl azide and *o*-tolyl azide were confirmed by means of GLC (7.9% and 0.1% respectively). The reaction of acetylenedicarboxylic acid with the colorless liquid (B) gave white granules with a mp of 183.0—184.0°C (lit,[12] 183°C for 1-benzyl-1,2,3-triazole-4,5-dicarboxylic acid). No depression of the melting point was observed on admixture with an authentic specimen of 1-benzyl-1,2,3-triazole-4,5-dicarboxylic acid.

The residue of the pyrolysis was treated with hydrochloric acid to give 3.5 g of benzenesulfinic acid, from which phenyl benzyl sulfone was then derived; mp 147.0—148.0°C (lit,[13] mp 148°C). No depression of the melting point was observed on admixture with an authentic sample.

The Reaction of Benzylmagnesium Chloride with BSA in THF. The Grignard reagent prepared from 7.6 g of benzyl chloride was allowed to react with 9.2 g of BSA in 80 m*l* of THF in the same manner as the reaction in ether. No precipitates were formed, and a homogeneous red solution was obtained.

After the greater part of the solvent had been removed from the reaction mixture *in vacuo* at 10°C, there were separated white precipitates upon the addition of each 60-m*l* portion of petroleum ether and diethyl ether. After being separated from the reaction mixture, the solid part (17.5 g) was pyrolyzed to give benzyl azide (9.1%) and *o*-tolyl azide (0.1%). From the ethereal-solution part of the reaction mixture, the amount of phenyldiazomethane (14.1%) was determined.

Benzenesulfinic acid (0.82 g, 11.6%) and benzenesulfonamide (3.1 g, 39.2%), mp 150.0—151.0°C (lit,[14] mp 153°C) were obtained from the residue of the pyrolysis of the solid part.

No depression of the melting point of the benzenesulfonamide thus obtained was observed on admixture with an authentic sample.

11) J. R. Johnson, *J. Amer. Chem. Soc.*, **55**, 3029 (1933).

12) R. H. Wiley, K. F. Hussung and J. Moffat, *J. Org. Chem.*, **21**, 190 (1956).

13) E. Knoevenagel, *Ber.*, **21**, 1349 (1888); "Beilsteins Handbuch der Organischen Chemie," Hw., Bd. VI (1923), p. 455.

14) R. L. Shriner, R. C. Fuson and D. Y. Curtin, "The Systematic Identification of Organic Compounds," Asian Edition, Maruzen Co., Tokyo (1957), p. 327.

BULLETIN OF THE CHEMICAL SOCIETY OF JAPAN VOL. 43 2257—2258 (1970)

Studies of Hydrazine Derivatives. I. A Convenient Method of Preparing Chloroacetylhydrazones*1

Suketaka Ito and Toshiaki Narusawa*2

Department of Industrial Chemistry, Faculty of Engineering, Shinshu University, Wakasato, Nagano

(Received January 27, 1970)

Although chloroacetylhydrazones are expected to be useful for synthetic purposes, only those of benzaldehyde[1,2] and of *m*-nitro- and *o*-hydroxy-benzaldehyde[1] have been reported in the literature.

Talik and Plazek[1] prepared benzaldehyde chloroacetylhydrazone by the chloroacetylation of benzaldehyde hydrazone with chloroacetyl chloride; it was also obtained by Buyle[2] from benzaldehyde and chloroacetohydrazide hydrochloride, which had been prepared from hydrazine and *p*-nitrophenyl

Table 1. Yields and melting points of chloroctylhydrazones

Original carbonyl compound	Yield (%)	Solvent for recrystallization	Melting point (°C)[a]	Crystal form
Benzaldehyde	84	Methanol	165.5—166.5 (dec.)[b]	colorless fine needles
Acetophenone	81	Methanol	137.5—138.5	colorless long needles
Benzophenone	83	Methanol	105.5—106.5	colorless prisms
Furfural	77	Methanol	151.0—152.0 (dec.)	almost colorless columns
d-Camphor	60	Methanol	189.0—190.0	colorless needles
Cyclohexanone	69	Methanol	114.0—115.0	cololress plates
Cyclopentanone	62	Methanol	123.5—124.5	colorless prisms
Pinacolone	67	Methanol	94.5— 95.5	colorless needles
Ethyl methyl ketone	72	*n*-Hexane	76.0— 77.0	colorless prisms
Acetone	53	Benzene	96.0— 97.0	colorless prisms
Acetaldehyde	73	Benzene	109.0—110.0	colorless fine plates

a) All melting points were determined in capillary, and are uncorrected.
b) Reported mp: 164°C,[1] 166°C.[2]

Table 2. Analytical data of chloroacetylhydrazones

Original carbonyl compound	Molecular weight[a,c]	Elemental analysis[b,c]		
		C%	H%	N%
Benzaldehyde	197 (197)	55.15 (54.97)	4.67 (4.61)	14.31 (14.25)
Acetophenone	218 (211)	57.07 (57.02)	5.32 (5.26)	13.39 (13.30)
Benzophenone	283 (273)	65.77 (66.06)	4.81 (4.80)	10.18 (10.27)
Furfural	174 (187)	44.99 (45.06)	3.76 (3.78)	14.88 (15.01)
d-Camphor	241 (243)	60.53 (59.38)	8.06 (7.89)	11.67 (11.54)
Cyclohexanone	224 (189)	50.84 (50.93)	7.01 (6.95)	14.78 (14.85)
Cyclopentanone	178 (175)	48.43 (48.15)	6.43 (6.35)	16.05 (16.04)
Pinacolone	203 (191)	50.70 (50.39)	8.06 (7.93)	15.09 (14.69)
Ethyl methyl ketone	157 (163)	43.94 (44.32)	6.92 (6.82)	17.03 (17.23)
Acetone	165 (149)	40.62 (40.42)	6.19 (6.11)	19.01 (18.55)
Acetaldehyde	151 (135)	35.59 (35.70)	5.22 (5.24)	20.64 (20.82)

a) A Takara Twin-type Ebulliometer Model L4 was used for the molecular weight measurement.
b) A Perkin-Elmer Elemental Analyzer Model 240 was employed for the micro-analysis.
c) Figures in parentheses are calcd values.

*1 Partly presented at the Tokai Branch Meeting of the Chemical Society of Japan, Nagoya, October 17, 1968.

*2 Present address: Fujitsu, Laboratories, Ltd., Shimo-odanaka, Kawasaki.

1) Z. Talik and E. Płażek, *Roczniki Chem.*, **33**, 379 (1959); *Chem. Abstr.*, **53**, 21660e (1959).

2) R. Buyle, *Helv. Chim. Acta*, **47**, 2449 (1964).

chloroacetate. Kupcik and others[3] reported a method for the preparation of chloroacetohydrazide and its hydrochloride from hydrazine hydrate and methyl chloroacetate.

The method of Talik and Płażek[1] is not general, but is limited in its application to carbonyl compounds that can easily give hydrazones. Buyle's method,[2] though universally applicable, is complicated and expensive. The present authors attempted to prepare chloroacetohydrazide and its hydrochloride by the method of Kupcik and others,[3] but a considerable evolution of nitrogen was observed at the reported reaction temperature (25°C) and the expected hydrazide could not be obtained even at a low reaction temperature (−25°C).

An alternative method for the preparation of chloroacetylhydrazones was devised. It consists of the previous preparation of a chloroacetohydrazide solution by the reaction of ethyl or methyl chloroacetate with 80—90% hydrazine hydrate in methanol at −30——40°C and the addition of an equimolar amount of aldehyde or ketone to the solution, without any isolation of the chloroacetohydrazide. By this simple and convenient procedure, several chloroacetylhydrazones were obtained with a higher purity and in satisfactory yields (see Tables 1 and 2).

The IR spectra of these chloroacetylhydrazones show absorptions at 3260—3350 (γ_{NH}) and 1690—1700 cm^{-1} (γ_{CO}).

Each of the NMR spectra (1—2% in CCl_4 or $CDCl_3$) shows a singlet assigned to the methylene protons of the $ClCH_2CO$- group at about 5.5 ppm (τ value) and a proton signals of the –NH– group (broad singlet) at 0—1.5 ppm (τ value).

Chloroacetylhydrazones of acetophenone and benzophenone were also synthesized by Talik and Płażek's method[1] and confirmed to be identical with those prepared by the present method.

The study of the syn-anti isomerism and tautomerism of the chloroacetylhydrazones by means of NMR analysis is now in progress.

Experimental

General Procedure. Into a stirred solution of 0.5 mol of ethyl or methyl chloroacetate (61 or 54 g) in 75 ml[4] of methanol, was added 0.5 mol (30 g) of 85% hydrazine hydrate over a period of 20—30 min at −30——40°C. After the addition was completed, the temperature of the reaction mixture was allowed to rise slowly to 0—10°C while the mixture was being stirred for an additional hour.

To this solution, was then added 0.5 mol of a carbonyl compound[5] with external cooling at such a rate that the temperature of the reaction mixture did not rise over 10°C.[6] Crystalline precipitates appeared almost immediately or after a while, so it was necessary to continue the cooling. After the reaction was over, the precipitates were collected by filtration. Washing with methanol,[7] followed by drying under a vacuum, gave fairly-pure chloroacetylhydrazone.

Further purification of the product was achieved by recrystallization from an appropriate solvent.

3) F. Kupcik, M. Liska and M. Konupcik, *Czech.*, 101955 (1961); *Chem. Abstr.*, **60**, 1606a (1964).

4) As the chloroacetylhydrazones of aliphatic carbonyl compounds are fairly soluble in methanol, it was necessary to change the quantity of the solvent as follows:

Carbonyl compound	Quantity of methanol (m*l*)
Benzaldehyde, acetophenone, and furfural	125
Benzophenone and cyclohexanone	75
Cyclopentanone, *d*-camphor, and acetaldehyde	50
Pinacolone, ethyl methyl ketone, and acetone	35

5) When it was solid, it was dissolved in a small quantity of methanol.

6) In the reaction of benzaldehyde or furfural, it was necessary to cool the reaction mixture below −30°C.

7) For aliphatic carbonyl compounds, the procedure was modified as follows. After the addition of the carbonyl compound, the reaction mixture was kept at −20——30°C for 2—3 hr, and then filtered. The resulting solid were washed with a small amount of cold methanol diluted with water (−20——30°C, 50%).

BULLETIN OF THE CHEMICAL SOCIETY OF JAPAN VOL. 43 2259—2261 (1970)

Solution Equilibria between the Nickel(II) Ion and the Ethylenediaminetetrepropionate Ion and the Substitution Kinetics of the Nickel(II)-Ethylenediaminetetrapropionate Complex with Cyclohexane-1,2-*N*,*N*,*N*′,*N*′,-tetraacetic Acid (CyDTA)

Mutsuo KODAMA

Department of Chemistry, Ibaraki University, Bunkyo, Mito, Ibaraki

(Received January 21, 1970)

In the polarographic determination of solution equilibria between ethylenediaminetetrapropionic acid (EDTP) and the cadmium(II) ion,[1] we have previously mentioned that the cadmium(II) ion can form 1 : 1 as well as 1 : 2 complexes with EDTP. The nickel(II) ion in the EDTP solution gives an absorption curve with two maxima at around 375 and 600 mμ. With an increase in both the pH value and the EDTP concentration, the absorbance increases remarkably and the absorption maxima shift to shorter wavelengths. These facts can be interpreted as resulting from the formation of the 1 : 2 nickel(II)-EDTP complex. Furthermore, the nickel(II) ion in solutions containing an excess amount of EDTP has been found to react with CyDTA at a measurable rate. In this paper, the author will attempt to estimate the second successive formation constant of the nickel(II)-EDTP complex by determining the change in the absorbance with an increase in the pH, and to analyze polarographically the kinetics of the nucleophilic substitution reaction between the nickel(II)-EDTP complex and CyDTA. He hopes to show that, by analyzing the formation of the 1 : 2 nickel(II)-EDTP complex, we can understand the kinetic behavior of the nickel(II)-EDTP complex in a substitution reaction.

Experimental

Reagents. The preparation of a standard nickel(II) nitrate solution had been described in a previous paper.[2] The EDTP and CyDTA were recrystallized twice from their aqueous solutions by adding an appropriate amount of pure ethanol. The other chemicals were of analytical reagent grades and were used without further purification.[2,3]

Apparatus and Experimental Procedures. All the apparatus (the penrecording spectrophotometer and polarograph, and the dropping-mercury electrode(DME) and the experimental procedures used in this study have been described previously.[2,3] The rate of the substitution reaction was determined by measuring changgs over a period of time in the diffusion current due to the presence of uncomplexed CyDTA. In this study, all the measurements were carried out in solutions with an ionic strength of 0.30 ($NaClO_4$) at 25°C. Kinetic measurements were conducted in solutions containing excess amounts of complexed and uncomplexed EDTP over CyDTA in the pH range from 8.50 to 9.50. Therefore, no buffer reagent is needed to keep the pH constant, and the substitution reaction can be treated as a pseudo first-order reaction.

Results and Discussion

Spectrophotometric Determination of Solution Equilibria between the Nickel(II) Ion and the Ethylenediaminetetrapropionate Anion. From observing the magnitude of both the stability constant of a 1 : 1 nickel(II)-EDTP complex and the pK values of EDTP,[4] it can safely be concluded that the complexation reaction of the nickel(II) ion in 10 mM EDTP solutions with pH's higher than 5.0 proceeds completely. As has been reported previously,[5] the nickel(II) ion in the EDTP solution gives an absorption curve with two maxima, at 375 and 600 mμ. By increasing the solution's pH value and the concentration of the uncomplexed EDTP, the absorbance in the visible region was increased remarkably and both the maxima shifted to shorter wavelengths. This fact may be interpreted as resulting from the formation of the 1 : 2 nickel(II)-EDTP complex. As has been discussed in a previous paper,[6] if the nickel(II) ion forms 1 : 1 as well as 1 : 2 complexes with EDTP, the following relation can be applied to the present system:

$$\log \frac{K_2}{(\alpha_H)_X} = \log \frac{A - A_{NiX}}{A_{NiX_2} - A} \times \frac{1}{\left([X]_t - 2\cdot[Ni]_t + \dfrac{A_{NiX} - A}{\varepsilon_{NiX} - \varepsilon_{NiX_2}}\right)} \quad (1)$$

1) M. Kodama and Y. Tominaga, This Bulletin, **42**, 2267 (1969).

2) M. Kodama, *ibid.*, **42**, 2532 (1969).

3) M. Kodama and H. Ebine, *ibid.*, **40**, 1857 (1967).

4) L. G. Sillen and A. E. Martell, "Stability Constants of Metal-Ion Complexes," 2nd Ed., The Chemical Society, London (1964), p. 696.

5) M. Kodama and K. Miyamoto, This Bulletin, **42**, 1596 (1969).

6) M. Kodama, Y. Fujii and T. Ueda, *ibid.*, **43**, 2085 (1970).

where:

K_2 = the second successive formation constant of the nickel(II)-EDTP complex

$$(\alpha_H)_X = 1 + \frac{[H^+]}{K_4} + \frac{[H^+]^2}{K_4 \cdot K_3} + \frac{[H^+]^3}{K_4 \cdot K_3 \cdot K_2} + \frac{[H^+]^4}{K_4 \cdot K_3 \cdot K_2 \cdot K_1},$$

K's = dissociation constants of EDTP,

$[X]_t$ = the total concentration of EDTP,

$[Ni]_t$ = the total concentration of the nickel(II) ion,

A_{NiX_2} = the absorbance for the solution where all the nickel(II) ions exist in the form of NiX_2^{6-},

A_{NiX} = the absorbance for the solution where all the nickel(II) ions exist in the form of NiX^{2-},

A = the absorbance of each of the solutions ($= \varepsilon_{NiX}[NiX^{2-}] + \varepsilon_{NiX_2}[NiX_2^{6-}]$),

ε's = the molar extinction coefficients.

The molar extinction coefficient for the 1 : 2 complex, ε_{NiX_2}, is much larger than that for the 1 : 1 complex, ε_{NiX}. This fact clearly shows that the EDTP anions in the 1 : 2 complex are coordinated to the nickel(II) ion through nitrogen. Equation (1) suggests that the plot of the right-hand side against log $(\alpha_H)_X$ will give a straight line with a slope of -1.0 and that the log $(\alpha_H)_X$ value at log $[(A-A_{NiX})/[(A_{NiX_2}-A)([X]_t-2[Ni]_t+(A_{NiX}-A)/(\varepsilon_{NiX_2}-\varepsilon_{NiX}))]]$ = zero can be equated with the log K_2 value. By means of this equation, the experimental data were analyzed successfully. The results are given in Fig. 1. From the intercept of the straight line, the log K_2 value was estimated to be 3.5_2.

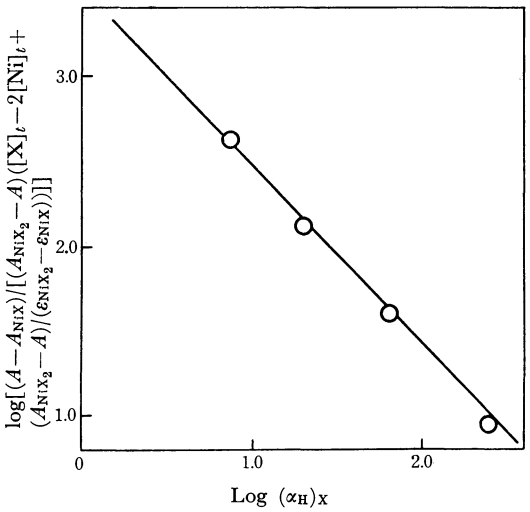

Fig. 1. The plot of $\log[(A-A_{NiX})/[(A_{NiX_2}-A)([X]_t-2[Ni]_t+(A_{NiX_2}-A)/(\varepsilon_{NiX_2}-\varepsilon_{NiX}))]]$ against log $(\alpha_H)_X$.
Total concentration of EDTP=40.0 mM
Concentration of nickel(II) ion=18.56 mM
25°C, μ=0.30

The Kinetic Study of the Substitution Reaction of the Nickel(II)-EDTP Complex with CyDTA. The CyDTA anion can displace the EDTP anion from its nickel(II) complex at a measurable rate. The present substitution reaction showed just the same kinetic behavior as that observed in the reaction of the nickel(II)-nitrilotriacetate complex with diethylenetriaminepentaacetic acid (DTPA).[2] The plot of log (i_0/i_t) against the time, t, invariably gave a straight line passing through the point of origin. Here, i_0 and i_t denote the wave heights of CyDTA at time $t=0$ and $t=t$ respectively. The slope of the above log-plot was independent of the initial concentration of CyDTA and was not influenced by the addition of the nickel(II)-CyDTA complex (the results are not shown). These facts clearly indicate that: (i) The rate of the backward reaction is negligibly small as compared with that of the forward reaction; (ii) the log-plot slope multiplied by 2.303 is equal to the apparent rate constant for the forward reaction, k_{ap}^+,[2] and (iii) the present reaction does not involve the dissociation of the nickel(II)-EDTP complex. In the solutions with constant pH's, the log-plot slope was exactly proportional to the concentration of the 1 : 1 complex, $[Ni]_t/(1+K_2\cdot[X]_f/(\alpha_H)_X)$ (Table 1). This means that the nickel(II) ion forms 1 : 1 as well as 1 : 2 complexes with an EDTP, and that the reaction proceeds exclusively through the 1 : 1 complex. Furthermore, provided that the other experimental conditions are kept constant, the product of the log-plot slope and $2.303\times(\alpha_H)_Z$

Table 1. The relation between the log-plot slope and the concentration of nickel(II)-DETP complex with a 1-to-1 composition
25°C, μ=0.30, pH=9.00
Initial cocentration of CyDTA=0.50 mM

Ni(II) ion concentration mM	EDTP concentration mM	Concentration of 1-to-1 ratio Ni(II)-EDTP complex, C_{NiX} mM	Log-plot slope, S sec^{-1}	S/C_{NiX}
5.00	35.0	1.87×10^{-1}	1.91×10^{-4}	1.02×10^{-3}
8.00	25.0	7.00×10^{-1}	7.00×10^{-4}	1.00×10^{-3}
10.00	40.0	4.38×10^{-1}	4.67×10^{-4}	1.07×10^{-3}
14.00	35.0	1.35	1.40×10^{-3}	1.04×10^{-3}

$(1+K_2\cdot[X]_f/(\alpha_H)_X)/[Ni]_t$ is a linear function of the hydrogen-ion concentration and can be given by:

$$\frac{k_{ap}^{+}\cdot(\alpha_H)_Z(1+K_2\cdot[X]_f/(\alpha_H)_X)}{[Ni]_t} = k_\alpha^{+} + k_\beta^{+}\cdot[H^+] \quad (2)$$

were $(\alpha_H)_Z$ is the (α_H) value of CyDTA. Therefore, the present reaction can be concluded to proceed through the following two simultaneous reaction pathways:

$$\text{i)}\quad NiX^{2-} + Z^{4-} \overset{k_1^+}{\rightleftharpoons} NiZ^{2-} + X^{4-}$$
$$\updownarrow \text{rapid}$$
$$NiX_2^{6-}$$

$$\text{ii)}\quad NiX^{2-} + HZ^{3-} \overset{k_2^+}{\rightleftharpoons} NiZ^{2-} + HX^{3-}$$
$$\updownarrow \text{rapid}$$
$$NiX_2^{6-}$$

where NiX_2^{6-} means the 1 : 2 nickel(II)-EDTP complex, and Z^{4-}, the completelydeprotonated CyDTA anion. Here, k_1^+ can be equated with k_α^+ and k_2^+, with the product of k_β^+ and the fourth dissociation constant of CyDTA, k_4. As was discussed with reference to the reaction of the nickel(II)-nitrilotriacetate complex with DTPA,[2] the k_1^+ and k_2^+ values in the above reaction mechanism can be determined from the intercept and the slope respectively of the straight line in Fig. 2. The k_1^+ and k_2^+ values obtained are listed in Table 2, together with the K_2 value determined spectrophotometrically. In the kinetic study of the substitution reactions of the nickel(II)-aspartate complex with CyDTA and DTPA,[7] we have previously mentioned that the six-membered ring in the nickel(II)-aspartate complex is much more substitutionlabile than the five-membered ring. Generally, the nickel(II)-oxygen bond rupture is much faster than the nickel(II)-nitrogen bond rupture. Therefore, in the substitution reaction of the nickel(II)-EDTP complex, a reaction intermediate (activated complex) having a propionate group bonded to the nickel(II) ion seems unlikely. If the present reaction proceeds through a reaction intermediate similar to that of the reaction of the nickel(II)-ethylenediamine complex with CyDTA,[6] a comparison of the rate constants for the two elementary reactions, i) and ii), with those of the reaction of the nickel(II)-ethylenediamine complex is possible. On the basis of the reaction intermediate having two nitrogen groups of EDTP or of ethylenediamine bonded to the nickel(II) ion, the k_1^+ and k_2^+ ratios between the reactions of EDTP and ethylenediamine complexes can be estimated to be $1/53._6$. When the additional stability of the reaction intermediate due to the electrostatic attraction between the nickel(II) ion and the propionate group is taken into consideration, the rate constant ratios should be larger than $1/53._6$. The observed ratios for the two elementary reactions, i) and ii), were $1/3.3\times10^2$ and $1/1.1\times10^4$ respectively. This disagreement may imply that the reaction of the nickel(II)-EDTP complex proceeds through a reaction intermediate quite different from that of the nickel(II)-ethylenediamine complex or that, although both reactions have the same reaction intermediate, the electrostatic repulsion between the nickel(II)-EDTP complex anion and the CyDTA anion makes the reaction more sluggish.

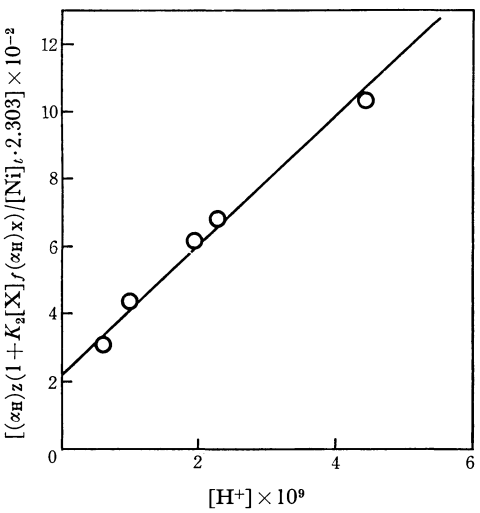

Fig. 2. The plot of k_{ap}^{+} $(\alpha_H)_Z(1+K_2[X]_f/(\alpha_H)_X)/2.303[Ni]_t$ against the hydrogen ion concentration.
Total concentration of EDTP=25.0 mM
Concentration of nickel(II) ion=8.00 mM
Initial concentration of CyDTA=0.50 mM
25°C, μ=0.30

Table 2. Formation constant and rate constans
25°C, μ=0.30

i) Second successive formation constant of the nickel(II)-EDTP compelx, K_2
$K_2 = 3.31\times10^3$

ii) Rate constants ($M^{-1}\cdot sec^{-1}$)
Reaction pathway i): $k_1^+ = 2.2\times10^2$
Reaction pathway ii): $k_2^+ = 9.45\times10^{-1}$

The author gratefully acknowledges the help of Miss Teiko Ueda during the experiments and the financial support of Ministry of Education.

7) M. Kodama and T. Ueda, This Bulletin, **43**, 419 (1970).

BULLETIN OF THE CHEMICAL SOCIETY OF JAPAN VOL. 43 2262—2263 (1970)

^{14}N Nuclear Quadrupole Resonances of 2,2′- and 4,4′-Dipyridyls

Hisao NEGITA, Masataka HAYASHI, Tadashi HIRAKAWA and Hiromu KUWATA*1

Department of Chemistry, Faculty of Science, Hiroshima University, Hiroshima

(Received February 4, 1970)

^{14}N nuclear quadrupole resonances have been observed in a number of nitrogen heterocyclic compounds, such as diazines[1] and s-triazine,[2] since Guibé found the resonance of pyridine[3] in 1960. The electronic structures of these compounds have been studied by Lucken[4] recently.

In this connection, it seemed that it would be interesting to study the ^{14}N nuclear quadrupole resonances of 2,2′- and 4,4′-dipyridyls, which are considered to be as fundamentally important as pyridine, diazines and s-triazine. When 2,2′-dipyridyl is used as a chelate reagent, it attaches a cation, itself keeping the *cis*-form, whereas it is known to exist as the *trans*-form in the crystal.[5]

Experimental

Two kinds of dipyridyls obtained from commercial sources were purified by recrystallization in organic solvents; about 10-g portions of the samples were used in the experiment. 2,2′-Dipyridyl was examined in the powder state, while 4,4′-dipyridyl was examined after having once been melted.

A frequency-modulated spectrometer of the Pound-Watkins type was used to detect the resonance signals, because large asymmetry parameters were expected in both dipyridyls.[6] For the frequency modulation, the bidirectional square wave of 140 Hz was fed to an SD-111 diode, which was connected in parallel to the tank circuit of the main oscillator.

Results and Discussion

The resonance frequencies, ν, the quadrupole coupling constants, e^2Qq, and the asymmetry parameters, η, are given in Table 1.

Since ^{14}N has a nuclear spin of unity, one can usually observe a pair of resonance frequencies, ν_{I} and ν_{II}, due to a species of nitrogen atoms as follows:

$$\nu_{\mathrm{I}} = e^2Qq\,(3-\eta)/4$$
$$\nu_{\mathrm{II}} = e^2Qq\,(3+\eta)/4 \qquad (1)$$

The numbers of the resonance lines of 2,2′- and 4,4′-dipyridyls are two and six respectively. Since the six lines of the latter compound are grouped into two sets of three lines each, as is shown in Fig. 1, it seems that there are three kinds of nonequivalent nitrogen atoms, each slightly different from the others. This situation, however, gives rise to the problem on the pairing of the six lines. It can be seen from Fig. 1 that the three lines on the higher-frequency side have different intensities, while those on the lower-frequency side are so weak as to be undistinguishable. Accordingly, it is difficult to

TABLE 1. ^{14}N NUCLEAR QUADRUPOLE RESONANCE PARAMETERS OF DIPYRIDYLS AND PYRIDINE

Compounds	Resonance frequencies		Coupling constants	Asymmetry parameters	Occupation numbers	
	ν_{I} (kHz)	ν_{II} (kHz)	e^2Qq (kHz)	η (%)	a (π)	b (σ)
2,2′-Dipyridyl	3074.0±0.1	3902.5±0.1	4152.8	35.5	1.27 (1.20)*	1.38
4,4′-Dipyridyl	3001.8±0.2	3889.0±0.3				
	2996.4±0.2	3875.0±0.2	4574.2	38.1	1.27 (1.23)	1.40
	2987.4±0.2	3835.2±0.2				
Pyridine[5]	four lines	four lines				
	(2956—3001)	(3856—3919)	4584.0	39.7	1.28 (1.20)	1.40

* The values in the parentheses were calculated by the method of LCAO MO, using parameters such as $\alpha_{\mathrm{N}} = \alpha + 0.6\beta$, $\alpha_{\mathrm{adj}} = \alpha + 0.1\beta$ and $\beta_{\mathrm{C-N}} = \beta_{\mathrm{C-C}}$.

*1 Present address: Department of Applied Chemistry, Faculty of Engineering, Hiroshima University, Hiroshima.

1) E. Schempp and P. J. Bray, *J. Chem. Phys.*, **46**, 1186 (1967).
2) L. Guibé and E. A. C. Lucken, *Mol. Phys.*, **10**, 273 (1966).
3) L. Guibé, *Compt. Rend.*, **250**, 3014 (1960).
4) E. A. C. Lucken, "Nuclear Quadrupole Coupling Constants," Academic Press, London and New York (1969), p. 235.
5) F. WM. Cagle, *Acta Crystallogr.*, **1**, 158 (1948).
6) H. Negita, *J. Chem. Phys.*, **44**, 1734 (1966).

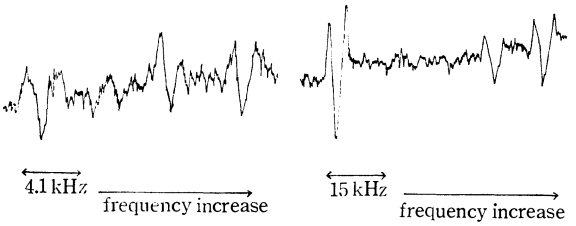

Fig. 1. ^{14}N nuclear quadrupole resonance absorption lines in 4,4′-dipyridyl.

determine which two are to be paired. The coupling constant and the asymmetry parameter of 4,4′-dipyridyl in Table 1 were derived from the two averaged values, $\nu_I(av)$ and $\nu_{II}(av)$, of three resonance frequencies grouped in the same sets.

The nitrogen atoms in dipyridyls are assumed to be in the sp^2-hybridized state and to have the maximum field gradient, q_Z, approximately in the direction of the bisector of the $\angle$CNC angle. The asymmetry parameter, η, is defined as $\eta=(q_x-q_y)/q_Z$ under the condition that $|q_y|>|q_x|$. In view of the ^{14}N nuclear quadrupole resonances of pyridine, hexamethylenetetramine, and γ-picoline,[7] it is preferable to choose the X- and Y-axes shown in Fig. 2.

From the bonding orbitals and the occupation numbers of these electrons, a, b_1, and b_2, at the nitrogen atom, the following expressions[4] are obtained:

$$U_p = [a+(b_1+b_2)/2]/2+[2-(b_1+b_2)/2]\cot^2\gamma - 2$$
$$\eta = -3[a-(b_1+b_2)/2]/(2U_p) \qquad (2)$$

7) E. A. C. Lucken, *Trans. Faraday Soc.*, **57**, 731 (1969).

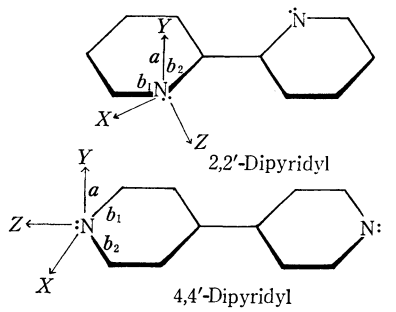

Fig. 2. Cartesian-coordinate systems at the nitrogen atoms of dipyridyls. a is the occupation number of π-orbital at the nitrogen atom, whereas b_1 and b_2 are those of σ-orbitals.

where $U_p=-e^2Qq_z/e^2Qq_p$. In Eq. (2) it is assumed that $2\gamma=\angle$CNC$=120°$ and that $e^2Qq_p=10$ MHz.

In 4,4′-dipyridyl, it is evident that $b_1=b_2=b$. Therefore, the values of a and b are calculated from e^2Qq and η. On the other hand, $b_1\neq b_2$ in 2,2′-dipyridyl; hence a, b_1, and b_2 cannot be calculated from Eq. (2). Therefore, the value of b in 2,2′-dipyridyl is obtained by averaging b_1 and b_2. As is shown in Table 1, the π- and σ- charge excesses in both dipyridyls are about 0.27 and 0.40 respectively, nearly equal to those of pyridine.

Simple LCAO MO calculations were carried out in order to compare the results with one another and also with those of NQR. The occupation numbers of the electrons calculated at the nitrogen atoms are almost all the same, as is to be expected from the experimental values, although calculated values are generally lower than experimental values. This discrepancy can be improved if a slightly smaller value than 10 MHz is adopted for e^2Qq_p.

BULLETIN OF THE CHEMICAL SOCIETY OF JAPAN VOL. 43 2264—2265 (1970)

Electrical Properties of the Platinum Anode in a Sodium Chloride Solution

Chiou-Chen Lu, Kazuo Fueki and Takashi Mukaibo

Department of Industrial Chemistry, Faculty of Engineering, The University of Tokyo, Hongo, Bunkyo-ku, Tokyo

(Received February 4, 1970)

In a previous paper[1] the present authors have shown that the anodic overpotential of chlorine evolution at the passivated platinum electrode is about 0.7 V higher than that of the activated electrode at the same current density. The purpose of the present investigation is to determine the electrical resistance, the double-layer capacitance, and the faradaic impedance of the platinum electrode in both active and passive states in a sodium chloride solution, in order to contribute to the elucidation of the passive state.

Experimental and Results

Electrolytic Cell. A platinum wire, 1 mm in diameter, was sealed in a glass tube and then cross-sectioned by grinding with emery paper. The smooth end of the platinum wire was used as the test electrode. The area of the test electrode was 0.008 cm^2. The reference electrode was a platinized platinum ring placed around the test electrode and worked as a reversible chlorine electrode. The counter electrode was a platinum plate of 8 cm^2. During the run, the solution was saturated with chlorine (1 atm).

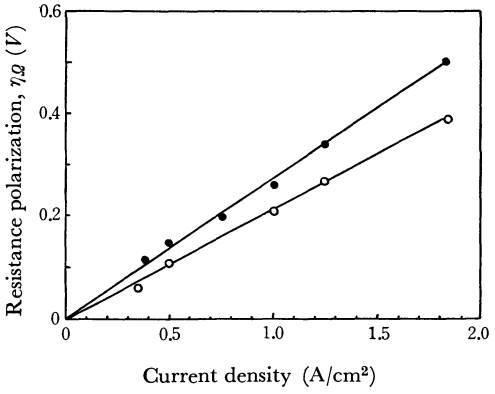

Fig. 1. Resistance polarization *vs.* current density in 5 M NaCl soln. pH 1, 40°C.
(○) activated and (●) passivated electrode

1) C. C. Lu, S. Asakura, K. Fueki and T. Mukaibo, *Denkikagaku*, **38**, 213 (1970).

TABLE 1. R_Ω, R_{soln} AND $R_{surface}$ ($\Omega \cdot cm^2$)

Temp. (°C)	R p	R a	R_{soln}	R p	R a
25	0.41	0.34	0.20	0.21	0.14
40	0.27	0.22	0.15	0.12	0.07
60	0.26	0.19	0.13	0.13	0.06
80	0.23	0.18	0.11	0.12	0.07

p : passivated electrode
a : activated electrode

The activation and passivation of the test electrode were carried out by polarizing it at −0.1 V (SCE) and 2.0 V (SCE) respectively.

Electrical Resistance. The galvanostatic transient method (current-interruptor method) was used for the measurements of the resistance and capacitance. A pulsed current was applied to the cell by means of an electrical switch. The rise time of the pulse was about 1 μs, and the potential decay from 2 to 6 μs after switching off was measured with a cathode-ray oscilloscope, the input impedance of which was 10^6 ohms. The steady-state potential before switching off was measured by means of a pen-recorder, the impedance of which was 10^6 ohms. The resistance polarization ($\eta_\Omega = \eta_{soln} + \eta_{surface}$) was determined by extrapolating the decay curves to $t=0$. An example of the plot of the resistance polarization *vs.* the current density

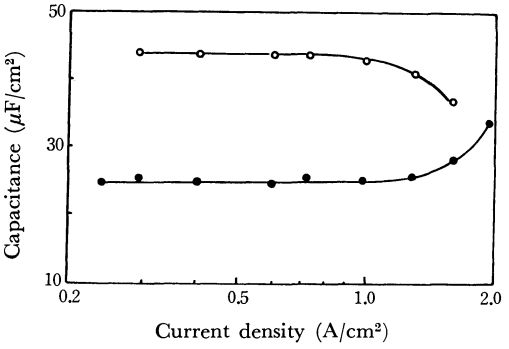

Fig. 2. Double layer capacitance of activated (○) and passivated (●) platinum electrode.
(NaCl 5M, pH 1, 25°C)

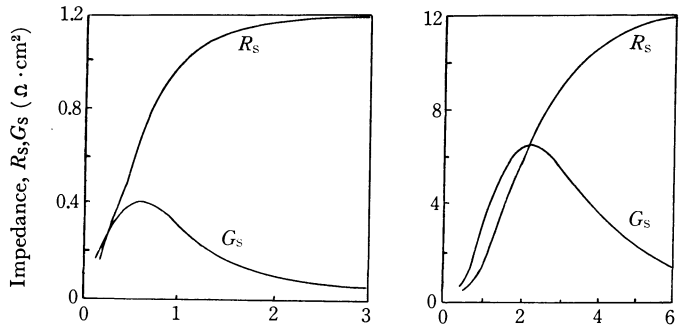

(a). Activated electrode (b). Passivated electrode

Fig. 3 (a), (b). Impedance of Pt electrode plotted against (frequency)$^{-1/2}$ in 5M solution, pH 1, 30°C.

is shown in Fig. 1. From the slope of the curves, the total resistance, R_Ω, was calculated.

For the determination of the $R_{surface}$, the test electrode was replaced by a platinized electrode of the same geometry and the R_{soln} was measured by means of an ac bridge. A preliminary experiment showed that the polarization and the resistance of the platinized platinum electrodes is negligibly small. From the values of R_Ω and R_{soln}, $R_{surface}$ was determined. The results are summarized in Table 1.

Double-layer Capacitance. The double-layer capacitance was estimated from the decay of the electrode potential by using the equation,

$$C = -I\mathrm{d}t/\mathrm{d}E$$

where I is the current density crossing the double layer during the decay period. In order to obtain the capacitance at $t=0$, the current density before switching off was taken as the value of I, $(\mathrm{d}t/\mathrm{d}E)_{t=0}$ was determined by extrapolating the values of $\mathrm{d}t/\mathrm{d}E$ at 2, 3, 4, 5, and 6 μs to $t=0$. The results are shown in Fig. 2. As may be seen from Fig. 2, the capacitance of the passivated electrode is about half that of the activated one.

Faradaic Impedance. The faradaic impedance was determined from Lissajous's figure on a cathode-ray oscilloscope. The input voltage was sine wave. Its amplitude was 3.5 mV, and its frequency was changed from 20 Hz to 30 kHz.

In Fig. 3, the ohmic component (R_s) and the capacitive component ($G_s = 1/\omega C_s$) of the electrode impedance (Z_f) are plotted against the frequency. From the shape of the curves, a surface reaction such as the recombination of chlorine atoms on the electrode is considered to be the rate-determining step.[2] The impedance of the passivated electrode was about ten times larger than that of the activated one.

2) M. Breiter, Transactions of the Symposium on Electrode Process," ed. by Yeager, John Wiley & Sons, New York (1961), p. 307.

BULLETIN OF THE CHEMICAL SOCIETY OF JAPAN VOL. 43 2266—2268 (1970)

Simultaneous Formation of Perylene Cation and Anion by Flash Excitation of Perylene in Solutions

Kiyoshi KAWAI, Naoto YAMAMOTO and Hiroshi TSUBOMURA

Department of Chemistry, Faculty of Engineering Science, Osaka University, Toyonaka, Osaka

(Received February 12, 1970)

Formation of transient cations and anions from the electron donor-acceptor interactions in the excited states was confirmed by using the flash technique in polar solutions for the first time by Leonhardt and Weller[1] and recently by Koizumi and Yamashita[2] and by us.[3]

In this note, we report a simultaneous formation of positive and negative ions of perylene revealed by the flash technique.

An acetonitrile solution of perylene (8×10^{-5}M) was used as a sample solution. It was carefully de-aerated by the usual freeze-pump-thaw method, and placed in a quartz cylindrical cell, 1.5 cm in diameter and 20 cm in length. The instrument used for the flash illumination has been described elsewhere.[4] The electric energy of a flash was about 430 J. The profile of the flash is shown in Fig. 2. A concentrated aqueous solution of sodium nitrate was used as a filter solution, which absorbed the light in the region shorter than 340 mμ, so that the perylene was excited only in the region of its ^1L_a band.

Flash illumination of the sample through the filter solution gave a transient absorption spectrum consisting of two overlapping bands at 576 mμ and 538 mμ and two others near 490 mμ and 480 mμ

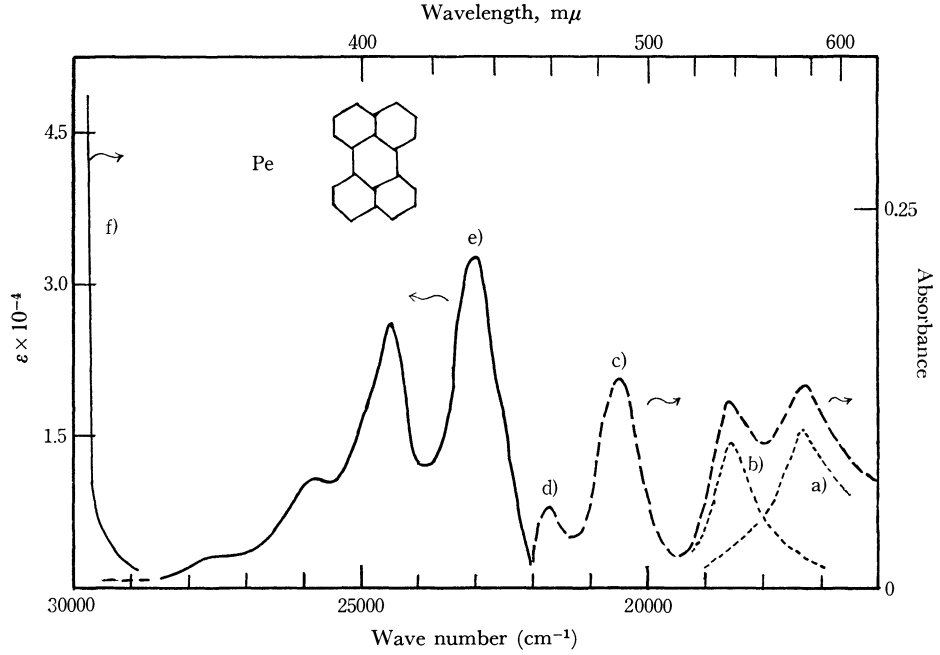

Fig. 1. Transient absorption spectrum caused by the flash illumination of perylene (8×10^{-5}M) in an acetonitrile solution. It was measured 10 μsec after illumination. Bands a) and b) correspond to perylene negative and positive ion respectively. Bands c) and d) indicate the T–T′ absorption of perylene. Spectrum e) indicates absorption of perylene in the ground state. Spectrum f) is that of the filter solution.

1) H. Leonhardt and A. Weller, *Ber. Bunsenges. Phys. Chem.*, **67**, 791 (1963).

2) M. Koizumi and H. Yamashita, *Z. Phys. Chem. N. F.*, **57**, 103 (1968).

3) K. Kawai, N. Yamamoto and H. Tsubomura, This Bulletin, **42**, 369 (1969).

4) N. Yamamoto, Y. Nakato and H. Tsubomura, *ibid.*, **39**, 2603 (1966).

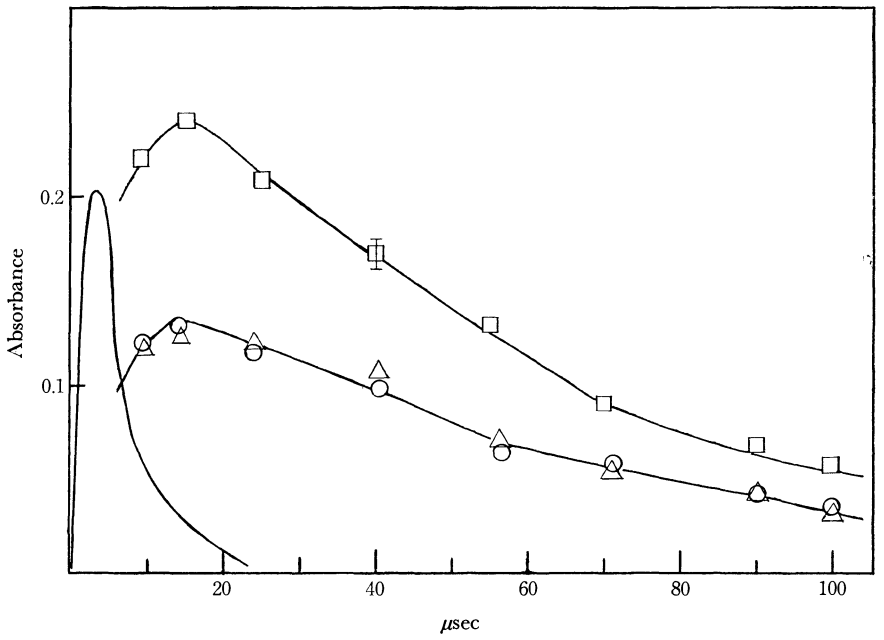

Fig. 2. The formation and decay curves of transient absorption spectra caused by flash illumination of acetonitrile solution of perylene.
-□-□- perylene in the triplet state.
-○-○- perylene anion
-△-△- perylene cation
——— flash profile.

(Fig. 1). Only two bands at 480 and 490 mμ appeared in the case where nonpolar solvents such as benzene or methylcyclohexane were used. When the acetonitrile solution of perylene was saturated with oxygen, the flash illumination of the solution resulted in the appearance of only the 538 mμ absorption band. From these results, it is highly probable that the 480—490 mμ bands are T−T′ absorption bands and the 576 mμ band is due to a negative ion.

The 576 mμ band may be ascribed to perylene mononegative ion, because it nearly agrees in position and shape with the spectrum of the perylene anion (λ_{max}: 581 mμ) formed by the action of sodium metal in a tetrahydrofuran solution.[5] The 538 mμ band is also attributed to the perylene cation, because it approximately agrees with the absorption peak at 543 mμ of perylene oxidized by antimony pentachloride in nitrobenzene.[6] The 490—480 mμ bands can be identified with the triplet-triplet absorption of perylene which Porter and Windsor found on flash illumination of perylene in solution.[7] The initial concentrations of perylene anion and cation formed at a flash energy of about 430 J was estimated to be about 2×10^{-7} M from the absorbances obtained and the molecular extinction coefficients, 4.3×10^{4} for the anion and 4.9×10^{4} for the cation.[5,6]

The absorbances of the transient species were followed in detail as the function of time. Some of the results obtained are given in Fig. 2. It was found that the ion concentrations increased during the flash illumination which continued for about 15 μsec. The decay of the ions nearly followed the second-order kinetics ($k=7\times10^{10}$ M^{-1} sec^{-1}). This result suggests that the decay of the ions is mainly due to recombination of the cations and anions and is a diffusion-controlled process.

Three mechanisms may be set up as possible routes for the simultaneous formation of perylene cation and anion:

1) *Auto-ionization* from perylene excimer.

$$^1Pe^* + Pe \longrightarrow (Pe \cdots Pe)^* \rightsquigarrow Pe^+_{solv.} + Pe^-_{solv.}$$

2) T-T annihilation.

$$^3Pe + {}^3Pe \rightsquigarrow Pe^+_{solv.} + Pe^-_{solv.}$$

3) Two-step (bi-photonic) excitation.

$$Pe + h\nu_1 \longrightarrow {}^1Pe^* \rightsquigarrow {}^3Pe$$

$$^3Pe + h\nu_2 \longrightarrow {}^3Pe' \rightsquigarrow Pe^+_{solv.} + e_{solv.}$$

$$e_{solv.} + Pe \longrightarrow Pe^-_{solv.}$$

5) P. Balk, G. T. Hoijtink and J. W. H. Schreurs, *Rec. Trav. Chim. Pays-Bas*, **76**, 813 (1957).
6) J. Hoijtink and W. P. Weijland, *ibid.*, **76**, 836 (1957).
7) G. Porter and W. H. Windsor, *Proc. Roy. Soc., Ser A*, **245**, 238 (1958).

The life time of perylene in the lowest singlet excited state (^{1}Pe) is 5×10^{-9} sec and, from this short life and low concentration of perylene in our experiment, it is unlikely that collisions of ^{1}Pe* and ground state perylene (Pe) occur to any appreciable degree. Therefore, mechanism (1) may be discarded. Also, the probability of formation of higher excited singlet state of perylene by the S—S′ absorption is very small.

The second mechanism, T–T annihilation, was assumed by Kawada and Jarnagin[8] for the explanation of photo-current of anthracene and phenanthrene in solutions. In such a process, ions need collisions of two triplet molecules. As the concentration of triplet perylene in our experimental condition is in the order of 10^{-6}M, the T–T annihilation process must be rather slow and the maximum of the ion concentration should appear at a time considerably later than that of the triplet molecules as seen in the case of Kawada and Jarnagin's work. Our experimental result shows that the concentrations of the ions increase almost in the same way as the triplet perylene and reach their maxima already at about 15 μsec after the start of the flash. Therefore, the second mechanism is also unlikely.

The third mechanism is consistent with the experimentally obtained rate of production of the ions. The ionization potential of perylene has been determined to be 7.15 eV[9] in the gas phase. Although the phosphorescence spectrum of perylene has not been observed, the lowest triplet state of perylene is estimated to be *ca.* 1.6 eV from MO calculations. As the filter solution used in the present experiment allows entrance of light having energy up to 3.6 eV, perylene can be excited to a level as high as *ca.* 5.2 eV by the T–T′ transition. This value seems to be a little too low for ionization of perylene even in a solution, based on our experience in the photo-ionization of aromatics in condensed environments.[10] In spite of this, mechanism (3) seems to be the most probable at the moment, as there is no other strong alternative. Stevens and Walker[11] have studied the photo-ionization of perylene in the rigid glass and conclude that the ionization potential of perylene is *ca.* 5.0 eV in liquid paraffine at 77°K. Photo-electron emission may then occur from the higher triplet states.

Once an electron is emitted from a highly excited perylene molecule, the electron can be captured by another perylene molecule leading to the formation of perylene anion.[10]

8) A. Kawada and R. C. Jarnagin, *J. Chem. Phys.*, **44**, 1919 (1966).

9) G. Briegleb and J. Czekalla, *Z. Electrochem.*, **63**, 6 (1959).

10) N. Yamamoto, Y. Nakato and H. Tsubomura, This Bulletin, **40**, 451 (1967).

11) B. Stevens and M. S. Walker, *Chem. Commun.*, **1965**, 8.

SHORT COMMUNICATIONS

The Photoinduced Rotational Isomerization of Benzil in a Mixture of Water and Ethanol

Hiroyasu INOUE and Toshiaki KUWAHARA*1

Department of Applied Chemistry, Faculty of Technology, Kanagawa University, Yokohama

(Received April 7, 1970)

The benzil molecule has been considered to take a nonplanar configuration in which the central carbonyl-carbonyl bond is strongly twisted.[1] Therefore, the two benzoyl parts are almost not in conjugation with each other and, consequently, benzil shows an electronic spectrum very similar to that of benzaldehyde.

Now, we wish to report on the photoinduced spectral changes of benzil in several liquid solutions. In a cyclohexane solution and in an ethanol solution the absorption spectra indicated only decompositions upon ultraviolet irradiation by means of a low-pressure mercury lamp. In a mixture of water and ethanol, however, benzil was found to show characteristic spectral changes with the irradiation. Obviously, water molecules play an essential role in this photoinduced change. As is shown in Fig. 1, the intensity of the 262 mμ band of the nonplanar species gradually decreases with the irradiation time, and at the same time an absorption band appears at 314 mμ. In this case, the isosbestic points were observed for the first several seconds of irradiation, but further irradiation shifted the absorption curves and caused them to deviate from the isosbestic points. The shift is probably due to the beginning of decomposition.

Moreover, in the initial stage of irradiation the photoproduced species absorbing at 314 mμ can be reversed to the original nonplanar benzil by heating at 83°C for 50 min in a dark room, as is indicated by curve IV in Fig. 1.

From the experimental results obtained above, the photoproduced species can be inferred to be a configurational isomer which possesses a nearly planar configuration, for the product shows a relatively longer wavelength band than that of the nonplanar species. As to the role of the water molecule, the hydrogen-bonding formation between two carbonyl groups and a water molecule can be considered plausible. The hydrogen-bonding energies may contribute to the stabilization of the nearly planar isomer of the benzil molecule, which is illustrated in Fig. 2. A detailed investigation is now in progress.

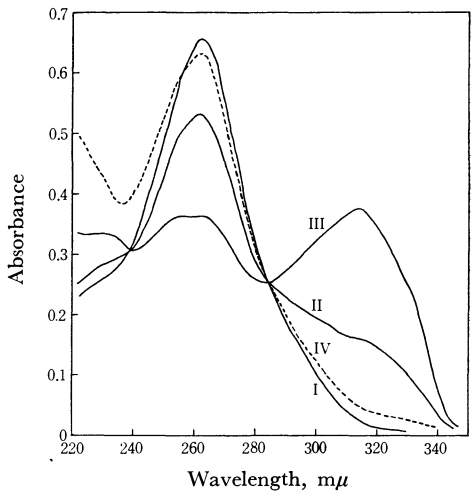

Fig. 1. The spectral changes of benzil in the mixture of water and ethanol (1:1).
I: 0 sec irradiation
II: 3 sec irradiation
III: 8 sec irradiation
IV: heat 83°C, 50 min after irradiation.

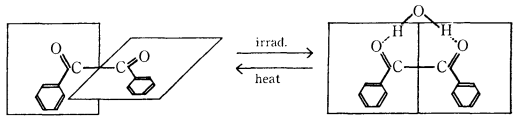

Fig. 2. Nonplanar and planar hydrogen-bonded isomers of benzil.

*1 Present address: Nippa Hososhizai Co., Ltd., Matsudo, Chiba.

1) N. J. Leonard, R. T. Rapala, H. L. Herzog and E. R. Blout, *J. Amer. Chem. Soc.*, **71**, 2997 (1949).

Ultraviolet Study for the Adsorption of Acetylacetone on D-Tartaric Acid Preadsorbed Nickel Film

Toshio NINOMIYA, Kosaku KISHI and Shigero Ikeda

Department of Chemistry, Faculty of Science, Osaka University, Toyonaka, Osaka

(Received April 2, 1970)

The ultraviolet spectra of β-diketones adsorbed on evaporated metals have been studied in order to clarify the chemical bonding of the chemisorbed species and the electronic properties of the metal surfaces.[1] The exposure of the metal films to acetylacetone vapor gives absorption peaks which can be assigned to the π–π^* transition of adsorbed acetylacetonate.

α-Amino and α-hydroxy acids function as chelating agents to metal ions. These acids are used as modifying reagents for hydrogenation catalysts, which then catalyze the asymmetric hydrogenation reaction of β-diketones.[2] The ultraviolet spectra of adsorbed β-diketones on the acid preadsorbed metal will, then, give important information shedding light on the mechanism of the modifications of catalysis and, in general, the corrosion mechanism of metal surfaces.

In the present communication, the adsorption of acetylacetone on evaporated nickel film pretreated with D-tartaric acid is studied.

The experimental apparatus shown in a previous paper[3] was improved for use here. The evaporation and other procedures have been described in the previous paper. After the nickel had been evaporated onto the quartz windows in a vacuum, a D-tartaric acid solution previously degassed was gently introduced into a quartz cell through a break-off seal broken by a glass-coated magnet. After treating the metal film with the acid solution for 30 min at 0°C, the solution was poured out from the quartz cell and the solvent water was completely removed by vacuum-distillation. Then acetylacetone was introduced, and the ultraviolet spectra of the adsorbed species were recorded on a Hitachi EPS-2 spectrophotometer.

The D-tartaric acid solutions had concentrations of 2% and were adjusted to various pH's, such as 2.0, 5.0, and 9.0, by a 1N NaOH aqueous solution.

The results are shown in Fig. 1.

In the treatment of the metal at pH 2.0, a weak, broad band was observed around 280 mμ after a 30 min adsorption of the acetylacetone. After 18 hr, the band maximum shifted to a longer wavelength.

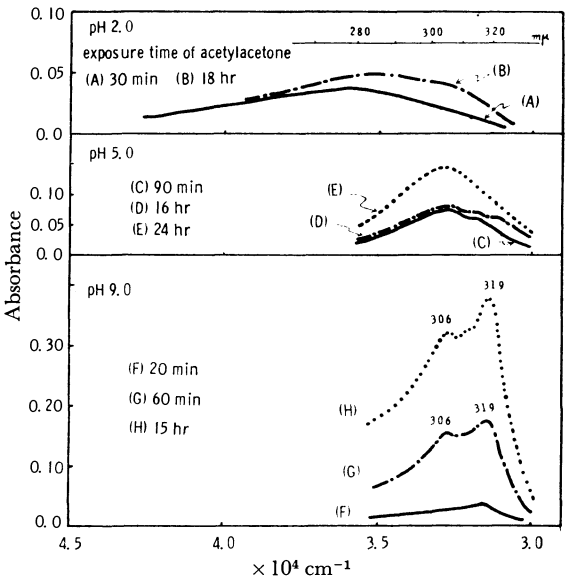

Fig. 1. Ultraviolet spectra of acetylacetone adsorbed on nickel film with preadsorbed D-tartaric acid at pH 2.0, 5.0 and 9.0.

In the case at pH 5.0, absorption peaks were obtained at 306, 316, and 322 mμ after 16 hr, and only one peak, at from 303 to 306 mμ, after 24 hr.

Figure 1 also shows the spectra obtained after the adsorption of acetylacetone on the metal film treated with the pH 9.0 solution. An absorption band was observed at 318 mμ after 20 min. After 15 hr, three intensive bands (about ten times that after 20 min) were obtained at 306, 313, and 319 mμ.

The adsorption of acetylacetone on nickel film without preadsorbed D-tartaric acid gives a band at 303 mμ which can be assigned to the π–π^* transition of adsorbed acetylacetonate.[1] In the cases with the preadsorbed acid, the absorption spectra of the adsorbed species are considerably different from that with no preadsorption procedure; furthermore, the spectra depend very significantly on the pH condition of the acid solution. By the way, the IR spectrum of D-tartaric acid adsorbed on the nickel film has been obtained, and the UV spectrum of adsorbed acetylacetonate on the nickel film treated with NaOH is different from the above spectra.

The elucidation of the relation between the spectral variation and the modification mechanism of the catalyst is now in progress.

1) K. Kishi and S. Ikeda, *J. Phys. Chem.*, **73**, 15 (1969).

2) Y. Izumi, M. Imaida, T. Harada, T. Tanabe, S. Yajima and T. Ninomiya, This Bulletin, **42**, 241 (1969).

3) K. Kishi and S. Ikeda, *J. Phys. Chem.*, **71**, 4384 (1967).

α-Chlorination of Sulfoxides by Chlorine

Gen-ichi TSUCHIHASHI and Shinobu IRIUCHIJIMA

Sagami Chemical Research Center, Ohnuma, Sagamihara, Kanagawa

(Received April 27, 1970)

Although α-halogenation of carbonyl compound is the well-established reaction in synthetic chemistry, a similar halogenation of sulfoxides was believed to be difficult until very recently.[1,2] It is now known that α-chlorination of sulfoxides can be achieved by using specific reagents such as *p*-toluenesulfonyl chloride,[1] nitrosyl chloride,[2] iodobenzene dichloride,[3] and *t*-butyl hypochlorite.[4] No research has been reported, however, on the halogenation of sulfoxides by molecular halogen. In this communication, we would like to report that sulfoxides can be easily α-chlorinated by chlorine and the reaction proceeds fairly stereo- and regioselectively.

When sulfoxides were treated with chlorine, difficulty was encountered by the evolution of hydrogen chloride which causes Pummerer-type rearrangement of sulfoxides. This was overcome by the addition of an excess amount of pyridine. Chlorine gas (5.3 mmol) was bubbled with stirring into the methylene dichloride solution (30 m*l*) of 2-phenylethyl phenyl sulfoxide (**1**) (5.3 mmol) and dry pyridine (10.6 mmol) for one hour at 0°C. The usual work-up gave 1-chloro-2-phenylethyl phenyl sulfoxide (**2**)[5] in 92% yield, which proved to be homogeneous by NMR and TLC. **2**: mp 60°C; MS, M^+ 264; NMR, τ 7.55 (1H, q), 6.45 (1H, q), 5.44 (1H, q), 2.81 (5H, s), and 2.3—2.6 (5H, m).

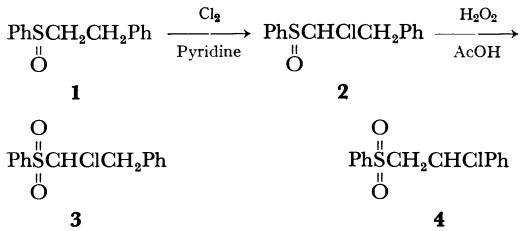

The structure of **2** was confirmed by converting **2** to the corresponding sulfone (**3**, mp 67—67.5°C). 2-Chloro-2-phenylethyl phenyl sulfone (**4**, mp 88.5—89.5°C) was synthesized according to the method in literature,[6] and from the inspection of their spectral data, **3** was proved to be the positional isomer of **4**.

It is striking that the position alpha to sulfinyl is much more susceptible to chlorination than the benzyl position, and only one diastereomer was obtained although the reaction could produce two diastereomers of **2**.

A similar reaction of tetrahydrothiophene-1-oxide (**5**) afforded 2-chlorotetrahydrothiophene-1-oxide (**6**) in 65% yield: mp 42—43°C; MS, M^+ 138; NMR, τ 7.1—8.1 (5H, m), 6.65—6.95 (1H, m), and 4.85 (1H, q). The product consists of two diastereomers in a ratio of 8 : 2, and a study of the NMR solvent-induced shift of H_a proton[7] revealed that the major isomer is *cis*-**6**.

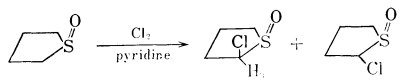

5 *cis*-**6** *trans*-**6**

In this case, the hydrogen atom *cis* to oxygen of sulfinyl group appears to be substituted preferentially.

Similarly, the reaction of methyl *p*-tolyl sulfoxide, ethyl phenyl sulfoxide, and dimethyl sulfoxide gave chloromethyl *p*-tolyl sulfoxide (mp 61.5—62°C), 1-chloroethyl phenyl sulfoxide (bp 83—84°C/1mmHg), and chloromethyl methyl sulfoxide (bp 63—68°C/0.2 mmHg, lit,[2] bp 65°/0.05 mmHg) in 70, 85, and 75% yields, respectively. Thus, this method of chlorination will provide a general route for synthesizing α-chlorosulfoxides.

The following scheme seems plausible for this reaction.

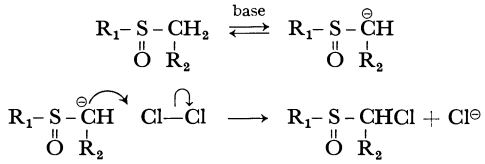

Sulfuryl chloride with pyridine can also be used as an α-chlorinating agent for sulfoxides, nearly equal to chlorine. Detailed studies on the mechanism of these chlorinations are in progress.

1) M. Hojo and Z. Yoshida, *J. Amer. Chem. Soc.*, **90**, 4496 (1968).

2) R. N. Loeppky and D. C. K. Chang, *Tetrahedron Lett.*, **1968**, 5415.

3) M. Cinquini, S. Colonna and F. Montanari, *Chem. Commun.*, **1969**, 607.

4) S. Iriuchijima and G. Tsuchihashi, *Tetrahedron Lett.*, **1969**, 5259.

5) Satisfactory data of elemental analysis were obtained for all the new compounds reported here.

6) M. Assher, D. Vofsi and A. Katchalsky, Belg. 654544 (1965); *Chem. Abstr.*, **65**, 5404e (1966).

7) E. T. Strom, B. S. Snowden, Jr, and P. A. Toldan, *Chem. Commun.*, **1969**, 50.

Reaction of Cobaltocene with Organic Compounds under an Oxygen Atmosphere: A new Route to π-Cyclopentadienyl-(1-*exo*-organylcyclopentadiene)cobalt

Hidetaka KOJIMA, Shigetoshi TAKAHASHI, Hiroshi YAMAZAKI*1 and Nobue HAGIHARA

The Institute of Scientific and Industrial Research, Osaka University, Yamada-Kami, Suita, Osaka

(Received April 30, 1970)

A number of π-cyclopentadienyl(1-*exo*-organylcyclopentadiene)cobalt complexes have been prepared by the reaction of organic halides with cobaltocene,[1] or organic alkali metals with cobalticenium perchlorate.[2]

We wish to report here a new reaction of cobaltocene with organic compounds having an active hydrogen atom under an oxygen atmosphere, which gives π-cyclopentadienyl(1-*exo*-organylcyclopentadiene)cobalt complexes in a high yield.

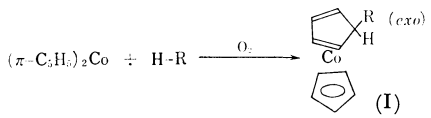

(I)

Oxygen was bubbled continuously through a dark red solution of cobaltocene in chloroform. After one hour, chloroform was removed from the resulting solution under reduced pressure to give orange red crystals of π-cyclopentadienyl(1-*exo*-trichloromethylcyclopentadiene)cobalt (Ia). The IR and NMR spectra and the melting point were identical with those of the authentic sample which was prepared by the reaction of cobaltocene with carbon tetrachloride.[3] Almost quantitative yield of Ia is a characteristic point of our method. In the case of the reaction of cobaltocene with carbon tetrachloride, the yield can not exceed 50% stoichiometrically, because half of the cobaltocene is consumed for the formation of cobalticenium chloride.

In the same way, cobaltocene reacted very smoothly with acetonitrile, propionitrile, phenylacetylene and acetone to form new complexes, $(\pi\text{-}C_5H_5)Co(C_5H_5\text{-}CH_2CN)$, $(\pi\text{-}C_5H_5)Co(C_5H_5\text{-}CH(CN)CH_3)$, $(\pi\text{-}C_5H_5)Co(C_5H_5\text{-}C{\equiv}CC_6H_5)$ and a new binuclear complex, $(\pi\text{-}C_5H_5)Co(C_5H_5\text{-}CH_2\text{-}COCH_2\text{-}C_5H_5)Co(\pi\text{-}C_5H_5)$. These complexes are summarized in Table 1.

Weiher *et al.*[4] reported smooth absorption of one mole of oxygen by four moles of cobaltocene at 0°C. They were unsuccessful in isolating and characterizing the oxygenated product. We observed that an orange solid was precipitated by the treatment of a solution of cobaltocene in ether with oxygen at −50°C. When chloroform was added to the orange solid suspended in ether under a nitrogen atmosphere, the solid was dissolved, the color of the solution turned to red, and the complex $(\pi\text{-}C_5H_5)Co(C_5H_5\text{-}CCl_3)$ was isolated in a 95% yield. This suggests that the oxygenated cobaltocene is an intermediate in the new reaction of cobaltocene. More detailed studies on the reaction mechanism are in progress.

TABLE 1. CYCLOPENTADIENYL(1-*exo*-ORGANYLCYCLOPENTADIENE)COBALT COMPLEXES*

Complex		H–R	Yield (%**)	Mp (°C)	Color
Ia	R=$-CCl_3$	$CHCl_3$	97	80—81	orange red
Ib	R=$-CH_2CN$	CH_3CN	87	58	red
Ic	R=$-CH(CN)CH_3$	CH_3CH_2CN	51	84—85	red
Id	R=$-C{\equiv}CC_6H_5$	$HC{\equiv}CC_6H_5$	56	130 (decomp.)	orange red
II***	R=$-CH_2COCH_2-$	CH_3COCH_3	70	100 (decomp.)	orange

* Satisfactory data of elemental analysis were obtained for all the new complexes.
** Based on cobaltocene. *** Binuclear complex.

*1 Present address: The Institute of Physical and Chemical Research, Yamatomachi, Saitama.

1) G. E. Herberich, E. Bauer and J. Schwartzer, *J. Organometal. Chem.*, **17**, 445 (1969), and references cited therein.

2) E. O. Fischer, W. Fellmann and G. E. Herberich, *Chem. Ber.*, **95**, 2254 (1962).

3) M. L. H. Green, L. Pratt and G. Wilkinson, *J. Chem. Soc.*, **1959**, 3753.

4) J. F. Weiher, S. Katz and A. F. Voigt, *Inorg. Chem.*, **1**, 504 (1962).

C-Band Gas-Phase EPR Spectra of the Rotational Excited $J=3$ Level of SO in the $^1\Delta$ State

Hiromichi UEHARA and Yonezo MORINO

Sagami Chemical Research Center, Sagamihara-shi, Kanagawa

(Received May 6, 1970)

We report the gas-phase C-band electron paramagnetic resonance spectra of the rotational excited $J=3$ level of the electronically excited state $^1\Delta$ of SO. The EPR spectrum of SO in the $^1\Delta$ state was first observed by Carrington *et al.*[1] for the rotational ground state ($J=2$) by using X-band microwave frequencies (*ca.* 9 GHz). By lowering the microwave frequency from X- to C-band region we have succeeded in observing the spectrum in the next higher rotational level.

A Stark modulated cylindrical TE_{011} mode detection cavity resonated at about 4.46 GHz was used with the axis of the cylinder parallel to the dc magnetic field. The C-band spectrometer used was reported elsewhere.[2] Micowave discharged oxygen gas was introduced into the resonance cavity through a gas-inlet at a pressure of 0.3 Torr and carbonyl sulfide was introduced through another inlet at a pressure of 0.1 Torr and mixed the dischagre product immediately outside the detection cavity. A strong spectrum of SO ($^1\Delta$, $J=2$) was observed in a field of 4.7 kG at a signal-to-noise ratio of about 100. Five lines of the rotational excited $J=3$ state were observed in a field of 9.1 to 10 kG, as shown in Fig. 1. Although the spectrum of the $J=3$ level consists of a sextet according to the selection rule of $\Delta M=1$, the transition to be expected at the highest field was not observed because of the restriction of the magnetic field available to us (maximum field of 10000 G).

A preliminary calculation was made with the method presented by Carrington *et al.*[1] By using the matrix elements of $(J, \Lambda, M|\mathcal{H}|J, \Lambda\, M)$ and $(J, \Lambda, M|\mathcal{H}|J+1, \Lambda, M)$ of the Hamiltonian

$$\mathcal{H} = B_0(\boldsymbol{J}-\boldsymbol{L})^2 + g_l\beta\boldsymbol{L}\cdot\boldsymbol{H}, \qquad (1)$$

we set up a 4×4 matrix and diagonalized it. The molecular constants used were $B_0=0.709$ cm^{-1} [1] and $g_l=1.00000$. The main feature of the observed five transitions were well reproduced, although a fairly large discrepancy between the calculated and the observed was noted in the absolute (about 5 gauss) and relative (a few gauss) field positions of the resonance transitions. It is expected that the electronic g factor, l-uncoupling constants, and the rotational constant may be determined accurately by analyzing the spectra of the rotational excited state $J=3$, combined with those of the ground $J=2$ state.

Carrington *et al.*[1] presented the following three features for the identification of the lines for $^1\Delta$ SO: first, the spectrum consists of four lines of similar intensity, secondly, the center of the quartet pattern indicates a molecular g value very close to the expected value 2/3, and thirdly, analysis of the splitting between the lines leads to a value of the rotational constant B_0 which is very close to that known for the $^3\sum^-$ ground state. Similarly, the present observation of the spectral lines in the $J=3$ level close to the predicted positions with the relative intensities close to the expected ratios, 3 : 5 : 6 : 6 : 5, confirms the assignment of the spectra to the $^1\Delta$ of SO.

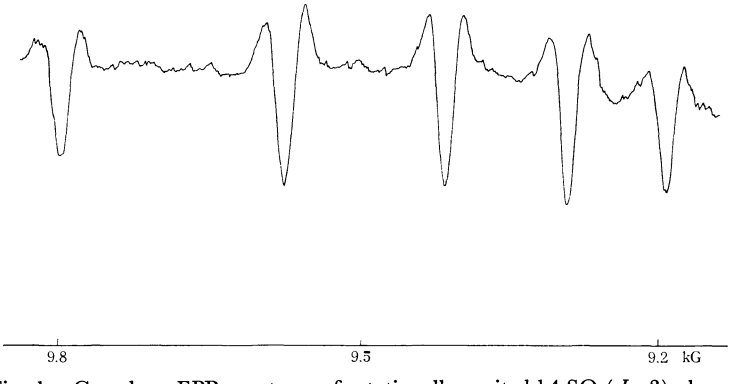

Fig. 1. Gas-phase EPR spectrum of rotationally excited $^1\Delta$ SO ($J=3$) observed with a microwave frequency of 4.46 GHz.

1) A. Carrington, D. H. Levy and T. A. Miller, *Proc. Roy. Soc.*, **A293**, 108 (1966).

2) H. Uehara and Y. Morino, *J. Mol. Spectrosc.*, to be published.

The Hydrogenation and Isomerization of Unsaturated Hydrocarbons over ZnO

Shuichi NAITO, Yuzo SAKURAI, Hazime SHIMIZU, Takaharu ONISHI and Kenzi TAMARU

Department of Chemistry, The University of Tokyo, Hongo, Tokyo

(Received May 6, 1970)

The catalytic reaction between unsaturated hydrocarbons and deuterium has been studied over several metal oxides, such as Cr_2O_3,[1] TiO_2[2] and ZnO,[3] and the main initial product in each case has been reported to be alkane-d_2. In this report, the reaction mechanism of propylene, butene, and 1,3-butadiene with deuterium was studied over ZnO. The adsorption during the course of the reaction was measured in order to study the working state of the surface. The mass and the microwave spectroscopic techniques were used to determine the deuterium content and distribution in the reactants and products.

The deuteration of propylene over ZnO proceeded readily at room temperature, and the catalytic exchange reaction between hydrogen atoms of propylene and deuterium took place simultaneously. The rate of the exchange reaction was considerably faster than that of the deuterium addition. The microwave spectroscopic measurements of propylene-d_1 demonstrated that, in the initial stage of the exchange reaction, propylene 3-d_1 predominated. As the reaction proceeded, three kinds of monodeuterio-propylene, 3-d_1, *cis*-1-d_1, and *trans*-1-d_1, were formed. However, propylene 2-d_1 was not observed during the reaction; this corresponds to the fact that the sixth hydrogen in propylene was not exchanged. These results suggest that the chemisorbed state of propylene is the π-allyl species.

The addition of deuterium to 1-butene over ZnO yielded only dideuterio-butane, and no exchange occurred in the hydrogen atoms of 1-butene in the initial stage of the reaction. During the course of the addition reaction, the isomerization of 1-butene proceeded simultaneously; this also occurred in the absence of deuterium, and the rate of isomerization was not affected by either the presence or absence of hydrogen in the ambient gas. The deuteration and isomerization of 1-butene seemingly proceed independently.

The deuteration of 1,3-butadiene over ZnO occurred easily at room temperature, and 1-butene was mainly produced (above 90%) until the 1,3-butadiene of the gas phase had been consumed; then butane started to be produced from 1-butene, accompanied by the isomerization described above. Only the dideuterio-1-butene was produced during the reaction; it was H_2DC–CHD–CH=CH_2 according to the microwave spectroscopy. On the other hand, hydrogen atoms of 1,3-butadiene did not exchange with deuterium molecules in the gas phase. When a mixed gas of 1,3-butadiene: H_2 : D_2=1 : 1 : 1 was introduced over ZnO, the main products were normal 1-butene and dideuterio-1-butene, while the amount of monodeuterio-1-butene was very small and was in proportion to the amount of HD in the gas phase.

The orders of the deuteration reaction of propylene, butene and 1,3-butadiene were all unity as to the partial pressure of deuterium and zero for the unsaturated hydrocarbons. The amounts of hydrocarbons and hydrogen chemisorbed during the hydrogenation were almost constant. In the case of 1-butene, the amounts of chemisorbed 1-butene and hydrogen were nearly half of their saturated amounts. The saturation value of the hydrogen chemisorption during the reaction between hydrogen and unsaturated hydrocarbons was in the following decreasing order: propylene, butene and butadiene, and the rates of the H_2–D_2 exchange reaction during the hydrogenation were retarded in the same order.

It can be seen from these experimental results that deuterium (or HD, H_2) participates in the addition process in a molecular form. To explain the experimental results, two alternative mechanisms may be considered. One of them is that dissociated deuterium atoms act in pairs on the surface, as if they were in a molecular form. In this case, the pair sites may be the zinc and oxygen ions on the surface, and the half-hydrogenated intermediate may be formed irreversibly. Secondly, the more probable mechanism is that deuteration proceeds by means of interaction between the chemisorbed hydrocarbons and the deuterium molecules in the ambient gas. The fact that the rate of deuteration is determined by the partial pressure of deuterium rather that by the amount of chemisorbed deuterium during the reaction favors the latter mechanism.

1) R. L. Burwell, Jr., A. B. Littlewood, M. Cardew, G. Pass and C. T. H. Stoddart, *J. Amer. Chem. Soc.*, **82**, 6272 (1960).

2) I. J. Lake and C. Kemball, *Trans Faraday Soc.*, **63**, 2535 (1967).

3) W. C. Conner, R. A. Innes and R. J. Kokes, *J. Amer. Chem. Soc.*, **90**, 6858 (1968); W. C. Conner and R. J. Kokes, *J. Phys. Chem.*, **73**, 2436 (1969).

The Reduction of 1,2-Dihalo-3,4-bis(diphenylmethylene)cyclobutenes by Lithium Aluminum Hydride

Fumio Toda, Kunihiro Kumada and Katsuhiko Akagi

Department of Industrial Chemistry, Faculty of Engineering, Ehime University, Matsuyama

(Received April 22, 1970)

Even though its calculated delocalization energy (1.21β) is comparable to that of cyclobutenedione (1.24β),[1,2] it has been established[3,4] on the basis of ultraviolet spectral data that dimethylenecyclobutene is better viewed as a cross conjugated diene rather than as a conjugated triene. Since this is probably because of the *endo*-double bond's causing ring strain, an anomalous reaction of the bond can be expected.

In the course of our studies of the title compounds (I),[5] we have found that the *endo*-double bond of I is easily reduced by lithium aluminum hydride (LAH) to afford 1,2-bis(diphenylmethylene)cyclobutane (IV).[6,7] Since no LAH reduction of carbon-carbon double bond has yet been reported, except where the double bond is conjugated with an electronegative group such as carbonyl, nitro, or cyano, the present results would seem to show an anomalous reactivity of the *endo*-double bond of I.

A mixture of Ia[5] and three equivalents of LAH in ether-tetrahydrofuran (3 : 2 ratio) was heated under reflux in a nitrogen atmosphere for 2 hr. After cooling, the reaction mixture was decomposed with water and hydrochloric acid, and then extracted with ether. The ether layer was washed with water and dried over sodium sulfate. Fractional recrystallization from the acetone of the crude product obtained by the evaporation of the solvent afforded IV and 3,4-bis(diphenylmethylene)butanedial (IX) in 33 and 8% yields respectively. The spectral data of IV (mp 180°C); $\lambda_{max}^{CHCl_3}$ 260 (23500), 357 nm (ε, 20900); NMR ($CDCl_3$) 2.89 (s, Ph, 10H), 3.30 (s, Ph, 10H), 7.16 τ (s, CH_2, 4H), and of IX (mp 208.5°C); $\lambda_{max}^{CHCl_3}$ 300 (16100), 335 sh, nm (ε, 11600); IR ($CHCl_3$) 2870 and 2750 (CHO), 1670 and

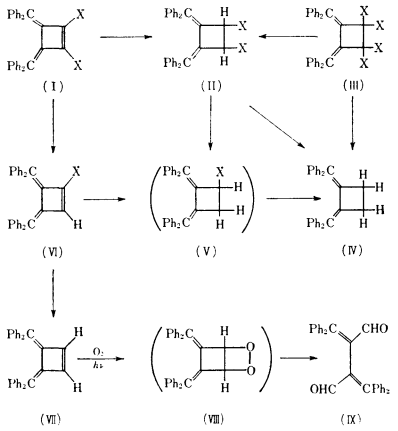

a: X=Br; b:X=Cl

1655 (CO), 1580 and 1555 cm^{-1} (C=C); NMR ($CDCl_3$) 0.45 (s, CHO, 2H), 2.90 τ (m, Ph, 20H), were identical with those of the corresponding authentic samples prepared according to the previously-reported method.[7]

Table 1. Yields (%) of the reduction products

Product	Reactant						
	Ia	Ib	VIa	VII	IIa	IIIa	IIIb
IV	33	41	30	—	78	71	67
IX	8	9	15	100	—	—	—

The yields of the reduction products, obtained by the same treatment as that employed for Ia, of 3,4-bis(diphenylmethylene)cyclobutenes (Ib,[5] VI[7] and VII[7]) and 3,4-bis(diphenylmethylene)-cyclobutanes (II[7] and III[8]) are summarized in Table 1.

The reduction of the cyclobutanes to afford IV may proceed by means of substitution processes. On the other hand, the reduction of the cyclobutenes into the two products can well be interpreted by two competing paths. One of them is the addition of hydride ion, followed by substitution, to afford IV finally. The other one is substitution to afford VII, which is photooxidized to IX, probably *via* VIII, during the course of isolation.

1) J. D. Roberts, A. Streitwieser, Jr., and C. M. Regan, *J. Amer. Chem. Soc.*, **74**, 4579 (1952).
2) S. L. Manatt and J. D. Roberts, *J. Org. Chem.*, **24**, 1336 (1959).
3) A. T. Blomquist and P. M. Maitlis, *Proc. Chem. Soc.*, **1961**, 332.
4) A. T. Blomquist and J. A. Verdol, *J. Amer. Chem. Soc.*, **77**, 1806 (1955).
5) F. Toda, H. Ishihara and K. Akagi, *Tetrahedron Lett.*, **1969**, 2531.
6) K. B. Alberman and F. B. Kipping, *J. Chem. Soc.*, **1951**, 779.
7) F. Toda, M. Higashi and K. Akagi, *Chem. Commun.*, **1969**, 1219.
8) A. Roedig and H. Niedenbruck, *Chem. Ber.*, **90**, 673 (1957).

Asymmetric Hydrogenation of C=O Double Bond with Modified Raney Nickel. XV. Asymmetric Hydrogenation of Metal Chelate Compound

Tadashi TANABE, Toshio NINOMIYA and Yoshiharu IZUMI

Division of Organic Chemistry, Institute for Protein Research, Osaka University, Kita-ku, Osaka

(Received April 22, 1970)

The asymmetric hydrogenation catalysts prepared from Raney nickel catalysts by modifications with aqueous solutions of optically-active compounds have been studied in terms of the relationships between the modifying reagent and the substrate in this series.[1,2] In the asymmetric hydrogenation of carbonyl compounds, it was found that the asymmetric yield of the product was much affected by the structure of the substrate and that the best substrate for the catalyst modified with an optically-active 2-hydroxy or 2-amino acid was a β-ketocarbonyl compound, such as a β-ketoester or a β-diketone.[1]

At an early stage of the hydrogenation of acetylacetone using the unmodified catalyst or a catalyst modified with D-tartaric acid, nickel acetylacetonate was detected in the reaction mixture, but nickel acetylacetonate was not detected at the end of hydrogenation. Moreover, it has been reported how the spectrum of acetylacetone chelating with nickel metal was observed by the exposure of the evaporated nickel film in the acetylacetone vapor.[3,4]

In view of the above-mentioned facts, the chelations of β-ketocarbonyl compounds onto the nickel surface of the catalyst might contribute to their excellent asymmetric yields of the products. Moreover, it is very important in the elucidation of the asymmetric hydrogenation mechanism of carbonyl compounds to examine the asymmetric hydrogenation of the nickel chelates of β-ketocarbonyl compounds with nickel.

In this respect, the asymmetric hydrogenation of the nickel complexes of β-ketocarbonyl compounds as the substrate, nickel methyl acetoacetate and nickel acetoacetonate,[5] were tested.

The modified Raney nickel catalysts were prepared and the optical rotation of the product was measured in ways which have been reported in a previous paper.[2] D-Tartaric acid and L-glutamic acid were used as the modifying reagents; the results are shown in Table 1.

From the results in Table 1, the asymmetric hydrogenations of the nickel chelate compounds of β-carbonyl compound are found to occur in fairly lower asymmetric yields compared with those in the asymmetric hydrogenation of methyl acetoacetate or of acetylacetone itself. These lower asymmetric yields might be caused by the change in asymmetric centers caused by the nickel metal deposited on the catalyst surface in the hydrogenation of the chelate compounds or by the difference in the structures of the β-carbonyl compound adsorbed on the catalyst surface and on the nickel chelate compound, which is a trimer in crystal and in a benzene solution. This study will be discussed in detail in this Bulletin in the near future.

Table 1. Optical rotation of product

No.	Substrate*1 (g)	Amount of R-Ni (as alloy) (g)	Modifying reagent (mod. temp. and pH)	Product	Optical rotation $[\alpha]_D^{20}$
1	$Ni(MAA)_2 \cdot 2H_2O$*2 (3.0)	3	2%-D-Tartaric acid (0°C, 5.0)	Methyl 3-hydroxybutyrate	−0.04
2	$Ni(MAA)_2 \cdot 2H_2O$ (3.0)	3	2%-D-Glutamic acid (0°C, 5.0)	Methyl 3-hydroxybutyrate	+0.15
3	$Ni(AA)_2 \cdot H_2O$*3 (5.0)	3	2%-D-Tartaric acid (0°C, 5.0)	2,4-Pentanediol	−2.88
4	$Ni(AA)_2 \cdot H_2O$ (5.0)	3	2%-L-Glutamic acid (0°C, 5.1)	2,4-Pentanediol	−0.16
5	Acetylacetone (10.0)	1	2%-L-Glutamic acid (0°C, 5.0)	2,4-Pentanediol	−1.88

*1 50 ml of benzene was used as the solvent. *2 MAA: methyl acetoacetate. *3 AA: acetylacetone.

1) Y. Izumi, M. Imaida, T. Harada, T. Tanabe, S. Yajima and T. Ninomiya, This Bulletin, **42**, 241 (1969).

2) Y. Izumi, S. Tatsumi and M. Imaida, *ibid.*, **42**, 2373 (1969).

3) K. Kishi, S. Ikeda and K. Hirota, *J. Phys. Chem.*, **71**, 4383 (1967).

4) K. Kishi and S. Ikeda, *ibid.*, **73**, 15 (1969).

5) L. March, "Inorganic Syntheses," Vol. II, McGraw-Hill Book Co., New York (1939), p. 14.

A Novel Synthesis for DL-Aspartic Acid and DL-Glutamic Acid*1

Shonosuke ZEN and Eisuke KAJI

Kitasato University, College of Pharmaceutical Sciences, Shirokane, Minato-ku, Tokyo

(Received April 27, 1970)

Our current interest in the synthesis of various amino acids[1] from α-nitroesters has led us to attempt to find an every method of synthesizing DL-aspartic acid and DL-glutamic acid.*2

The synthesis of α-nitrodicarboxylates by the *carbon-alkylation reaction* of methyl nitroacetate with the halo-ester of carboxylic acid consists of the following steps:

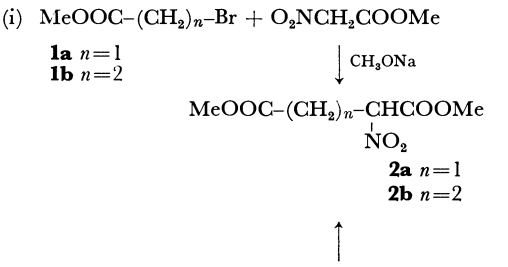

In the first method (i) sodium methylate is added to methyl nitroacetate and **1a** (or **1b**) to yield **2a** (or **2b**); the second method (ii) yields the same *C*-alkylated derivatives (**2a** and **2b**) by the reaction of sodium salt of methyl nitroacetate with **1a** (or **1b**).

Dimethyl nitrosuccinate[2] (**2a**): following Step i, an equimolecular reaction takes place between methyl nitroacetate and methyl bromoacetate (**1a**) in a dipolar aprotic solvent (such as dimethylacetamide or dimethylformamide) in the presence of sodium methylate (such as the 1N methanol solution) when it is stirred overnight at room temperature. The reaction product was extracted with benzene (from the water layer which resulted from adding water and benzene to the reaction mixture). The benzene was first distilled out; when the **2a** was further distilled under reduced pressure, its yield was 66%; bp. 70—72°C/0.05 mmHg, n_D^{20} 1.4452, IR (liquid film): 1745 (ester CO), 1565 and 1380 (C-NO_2) cm^{-1}, λ_{max}^{MeOH} 275 mμ (ε 290). Diethylammonium salt of **2a** recrystallized from ethanol - ether, melted at 103—104°C. Following Step ii, **2a** was synthesized in a 23% yield, and also the trimethyl ester of β-nitrotricarballic acid (**3a**) was obtained as colorless prismatic crystals in a 29% yield by recrystallization from an ether-isopropylether mixture; mp 88.5—89.5°C, IR (KBr): 1730 (ester CO), 1560 and 1370 (C-NO_2) cm^{-1}, λ_{max}^{MeOH} 283 mμ (ε 36).

The catalytic hydrogenation*3 of **2a** with Raney Nickel T-1[3] under 40 p.s.i.g. gave the corresponding ester of aspartic acid in a 90% yield. By the hydrolysis of the product with 6N hydrochloric acid, DL-aspartic acid was obtained in a 94% yield as HCl salt.

Dimethyl α-nitroglutarate[4] (**2b**): in a similar way, **2b** was given in an 88.5% yield by the reaction of the sodium salt of methyl nitroacetate with **1b**.

DL-Glutamic acid was then synthesized in a total yield of 83.2% from **2b** by hydrogenation and subsequent hydrolysis following the above-mentioned procedure.

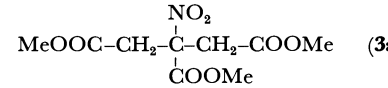

(**3a**)

Investigations into the uses of this *C*-alkylation reaction using other halogeno-compounds with the nitro ester and into the mechanism of this reaction are now in progress.

*1 Part IV in the series, "The Synthetic Reactions of Aliphatic Nitro Compounds,"

1) S. Zen, Y. Takeda, A. Yasuda and S. Umezawa, This Bulletin, **40**, 431 (1967); S. Zen, A. Yasuda, H. Hashimoto and Y. Takeda, *Nippon Kagaku Zasshi*, **90**, 110 (1969).

*2 Presented at the 23rd Annual Meeting of the Chemical Society of Japan, Tokyo, April, 1970; Preprint, Vol. III (1970), p. 1671.

2) Diethyl nitrosuccinate prepared from diethyl α-bromosuccinate and nitrite by R. Gelin and S. Gelin, (*C. R. Acad. Sci., Paris*, **256**, 3705 (1963)).

*3 Hydrogenation apparatus, Paar Instruments.

3) X. A. Dominguez, I. C. Lopez and R. Franco, *J. Org., Chem.*, **26**, 1625 (1961).

4) V. M. Belikov and Yu. N. Belokon, *Izv. Akad. Nauk, SSSR, Ser. Khim.*, **1964**(6), 1134; *Chem. Abstr.*, **61**, 7094 (1964).

Synthesis of a Heptacosapeptide Corresponding to the Human Corticotropin 1-27 Sequence

Hideo OTSUKA, Kunio WATANABE and Ken INOUYE

Biochemistry Division, Shionogi Research Laboratory, Shionogi & Co., Ltd., Fukushima-ku, Osaka

(Received May 2, 1970)

In previous communications we described the syntheses and biological properties of corticotropin (ACTH)-octadecapeptides including [β-Ala[1]]-ACTH(1-18)-NH_2.[1-3] We wish now to report the synthesis of a peptide corresponding to the amino acid sequence 1-27 of human ACTH, *viz.*, H-Ser-Tyr-Ser-Met-Glu-His-Phe-Arg-Trp-Gly-Lys-Pro-Val-Gly-Lys-Lys-Arg-Arg-Pro-Val-Lys-Val-Tyr-Pro-Asp-Ala-Gly-OH, h-ACTH (1-27)-OH (I).[4]

Z-Val-Lys(Boc)-Val-Tyr-Pro-Asp(OBu^t)-Ala-Gly-OBu^t (II) ($[\alpha]_D^{25}$ $-69.2°$ (*c* 1, methanol). Found: C, 60.30; H, 7.84; N, 10.28. Calcd for $C_{60}H_{91}N_9O_{16}$: C, 60.34; H, 7.68; N, 10.55%) was synthesized stepwise starting from the Gly-OBu^t at *C*-terminal, in which Z-Ala, Z-Asp(OBu^t) and Z-Pro were incorporated with DCC and Z-Tyr(Z), Z-Vals and Z-Lys(Boc) by the *p*-nitrophenyl ester method in combination with the hydrogenolytic removal of the N^{α}-protecting group. Z-Arg(NO_2)-Arg(NO_2)-Pro-OMe (mp 115—120°C decomp, $[\alpha]_D^{27}$ -37.1 (*c* 1, AcOH), $-30.5°$ (*c* 1, DMF)) was treated with HBr/AcOH for removal of the Z-group, followed by acylation with Z-Lys(Boc)-OCOOEt to yield a tetrapeptide ester which was readily saponified to Z-Lys(Boc)-Arg(NO_2)-Arg(NO_2)-Pro-OH (III) ($[\alpha]_D^{23}$ $-36.7°$ (*c* 1, methanol)). Compound III and an octapeptide ester, derived from II by catalytic hydrogenolysis, were coupled by the *N*-hydroxysuccinimide-mediated DCC method[5] to give Z-Lys(Boc)-Arg(NO_2)-Arg(NO_2)-Pro-Val-Lys(Boc)-Val-Tyr-Pro-Asp(OBu^t)-Ala-Gly-OBu^t (IV) ($[\alpha]_D^{23}$ $-78.5°$ (*c* 1, methanol). Found: C, 54.14; H, 7.53; N, 15.88. Calcd for $C_{88}H_{140}N_{22}O_{26}\cdot H_2O$: C, 54.48; H, 7.38; N, 15.88%). Compound IV was submitted to hydrogenolysis and the product was coupled with Z-Lys(Boc)-Pro-Val-Gly-Lys(Boc)-N_3[6] to give a heptadecapeptide, Z-Lys(Boc)-Pro-Val-Gly-Lys(Boc)-Lys(Boc)-Arg-Arg-Pro-Val-Lys(Boc)-Val-Tyr-Pro-Asp(OBu^t)-Ala-Gly-OBu^t, which was converted into the N^{α}-free peptide (V) ($[\alpha]_D^{23}$ $-74.2°$ (*c* 0.7, 50% AcOH)) by catalytic hydrogenolysis.

A decapeptide Z-Ser-Tyr-Ser-Met-Glu(OBzl)-His-Phe-Arg-Trp-Gly-OH (mp 205—210°C decomp, $[\alpha]_D^{22}$ $-13.0°$ (*c* 1, DMF)), which was synthesized from Z-Ser-Tyr-Ser-N_3[7] and H-Met-Glu(OBzl)-His-Phe-Arg-Trp-Gly-OH,[8] was esterified with *N*-hydroxysuccinimide by the DCC method[9] and the resulting active ester was allowed to react with V to afford a protected heptacosapeptide, which was treated with hydrogen fluoride[10] to liberate the free peptide (I). The crude product was purified by chromatography on a carboxymethyl cellulose column; $[\alpha]_D^{23}$ $-89.9°$ (*c* 0.5, 0.1N AcOH), $\lambda_{max}^{0.1N\ NaOH}$ $=282$ mμ ($E_{1cm}^{1\%}=25.3$), 288 mμ ($E_{1cm}^{1\%}=26.7$). Amino acid ratios in acid hydrolysate: Asp 1.07, Ser 1.72, Glu 1.02, Pro 3.17, Gly 3.15, Ala 1.03, Val 3.00, Met 0.98, Tyr 2.06, Phe 1.03, Lys 4.11, His 0.91, Arg 2.95. The Tyr/Trp ratio in intact I was 1.8 as determined spectrophotometrically. Peptide I was found to possess an adrenal-stimulating activity of 263 units/mg (3rd USP standard as standard) in the in vivo steroidogenesis.[11]

1) H. Otsuka, K. Inouye, F. Shinozaki and M. Kanayama, *J. Biochem.* (Tokyo), **58**, 512 (1965).

2) H. Otsuka, M. Shin, Y. Kinomura and K. Inouye, This Bulletin, **43**, 196 (1970).

3) K. Inouye, A. Tanaka and H. Otsuka, *ibid.*, **43**, 1163 (1970).

4) All amino acid residues are of the L-configuration. The abbreviated designation of amino acids, peptides and their derivatives accords with the proposal of the IUPAC-IUB Commission of Biochemical Nomenclature, which appeared in *Biochemistry*, **5**, 2485 (1966); *ibid.*, **6**, 362 (1967). Other abbreviations used in this paper are: Et=ethyl, Ac=acetyl, DMF=dimethylformamide, and DCC=*N*,*N*'-dicyclohexylcarbodiimide.

5) E. Wünsch and F. Drees, *Chem. Ber.*, **99**, 110 (1966).

6) H. Otsuka, K. Inouye, M. Kanayama and F. Shinozaki, This Bulletin, **39**, 882 (1966).

7) K. Hofmann, A. Jöhl, A. E. Furlenmeyer and H. Kappeler, *J. Amer. Chem. Soc.*, **79**, 1636 (1957); St. Guttmann and R. A. Boissonnas, *Helv. Chim. Acta*, **41**, 1852 (1958).

8) K. Inouye, K. Watanabe, K. Namba and H. Otsuka, in preparation.

9) G. W. Anderson, J. E. Zimmerman and F. M. Callahan, *J. Amer. Chem. Soc.*, **86**, 1839 (1964).

10) S. Sakakibara and Y. Shimonishi, This Bulletin, **38**, 1412 (1965).

11) The assay was performed by Dr. Akira Tanaka of this Laboratory according to Lipscomb and Nelson (H. S. Lipscomb and D. H. Nelson, *Endocrinology*, **71**, 13 (1962)) with a minor modification.

Hot-atom Chemistry of Tris-(acetylacetonato)-cobalt(III) in Benzene Solutions and Frozen Benzene Solutions

Takeshi TOMINAGA and Kitao FUJIWARA

Department of Chemistry, Faculty of Science, The University of Tokyo, Hongo, Tokyo

(Received May 7, 1970)

We have initiated a systematic work to irradiate the organic solutions and frozen organic solutions of metal complexes with slow neutrons in order to elucidate the mechanism of hot-atom reactions in the systems. In the present paper we report our preliminary data on the ^{60}Co recoil reactions in benzene solutions and frozen benzene solutions of tris-(acetylacetonato)-cobalt(III) and the scavenger effect of ferric chloride added to the systems for the purpose of removing free acetylacetone.

Solid $Co(acac)_3$, 0.2M $Co(acac)_3$ benzene solutions and frozen 0.2 M $Co(acac)_3$ benzene solutions were irradiated with slow neutrons for 5 min in a TRIGA Mark II reactor (thermal neutron flux: 5×10^{11} n/cm^2·sec.). The solutions were irradiated at room temperature, the solid samples and the frozen solutions at dry-ice temperature. Various amounts of $FeCl_3\cdot6H_2O$ dissolved in small amounts of ethanol, or various amounts of anhydrous $FeCl_3$, were added to the benzene solutions and frozen benzene solutions (before freezing) before irradiation. An aliquot of the irradiated benzene solution (or frozen solution) was diluted to 5 m*l* with benzene and extracted with three 5-m*l* portions of 3% EDTA aqueous solution containing 0.8% sodium potassium tartrate and 10 mg of $CoSO_4\cdot7H_2O$ as carrier. Another aliquot of the irradiated benzene solution was stored overnight at room temperature and extracted the following day. All the ^{60}Co-labeled species exchangeable with Co^{2+} are extracted into the aqueous phase whereas $^{60}Co(acac)_3$ remains in the organic phase (as retention). The broken curves in Fig. 1 correspond to retentions obtained with the stored aliquots while the solid curves represent retentions in the aliquots extracted immediately. The irradiated solid samples (30—50 mg) were dissolved in 5 m*l* of benzene, ethanol, chloroform, or acetic acid, all with or without ferric chloride additive, and analyzed by means of solvent extraction or ion exchange.

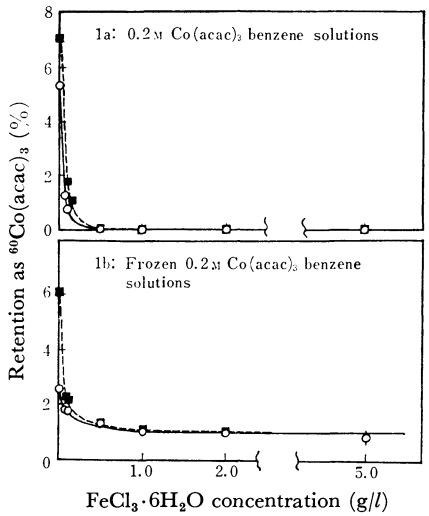

Fig. 1a-1b. Retention *vs.* ferric chloride concentration in irradiated $Co(acac)_3$ benzene solutions.

From the results we may draw the following conclusions:

1) As shown in Fig. 1a, the retention in $Co(acac)_3$ benzene solutions sharply decreases to 0% with the increase in the $FeCl_3\cdot6H_2O$ concentration. Although thermal reactions (recombination reactions) in the solutions during and after irradiation contribute appreciably to the apparent retention, their contribution can be eliminated effectively by the addition of $FeCl_3\cdot6H_2O$,*1 and the initial retention due to hot reactions alone can be estimated.

2) As seen in Fig. 1b, the retention in frozen 0.2M $Co(acac)_3$ benzene solutions decreases rapidly to a constant value (~1%) with increasing $FeCl_3\cdot6H_2O$*1 concentration. Since the most solute molecules (complex) should be precipitated as microcrystals in the frozen solutions at this concentration, it seems reasonable that the above retention value is fairly close to that observed with solid samples.

3) Retentions in solid samples fall within the range 1.3—1.5%, irrespective of solvents used, if they contain ferric chloride. Higher retentions 2.0—2.2% are obtained in the absence of ferric salts. The retention remains unchanged even after standing the solutions of the irradiated solid samples for several days if they contain ferric salts, whereas the retention increases appreciably after standing in solutions without ferric salts.

4) The effect of the ferric salt addition on the retention may be explained by assuming that ferric salts which can be easily complexed with acetylacetone work as good scavengers for free acetylacetone in solutions, and thus minimize the recombination of recoil species with acetylacetone through thermal reactions.

*1 Addition of anhydrous $FeCl_3$ is nearly as effective as $FeCl_3\cdot6H_2O$.

The Heat Capacity and the Phase Transition of the $[(C_6H_5)_3PCH_3]^+$ $(TCNQ)_2^-$ Crystal

Akio KOSAKI, Yôichi IIDA,* Michio SORAI, Hiroshi SUGA and Syûzô SEKI

Department of Chemistry, Faculty of Science, Osaka University, Toyonaka, Osaka
**Department of Chemistry, Faculty of Science, Hokkaido University, Sapporo*

(Received May 11, 1970)

The measurements of the temperature dependence of the magnetic susceptibility as well as the intensity of ESR spectra[1] of $[(C_6H_5)_3PCH_3]^+$ $(TCNQ)_2^-$ crystals have already revealed that there is some anomaly in their curves at around 40°C. The magnetic behavior has been explained in terms of a siglet - triplet transition based on the correlation between the electronic spins of each molecule, and the anomaly has been referred to a discontinuous change in the correlation energy at this temperature. The pressure dependence of the anomalous point has also been investigated by McConnell *et al.*[2] No consistent interpretation for the mechanism of this anomaly has, however, yet been given. The purpose of the present investigation is to measure the heat capacities of this radical salt precisely in order to clarify the mechanism of this anomaly.

This radical[3] was prepared by means of $(C_6H_5)_3P$ CH_3I and TCNQ (tetracyanoquinondimethan). The phosphonium salt and TCNQ were dissolved separately into acetonitrile and then mixed at about 70°C. This mixture was allowed to stand for about one day to produce black prism crystals as precipitates.

The heat capacities were measured with an adiabatic calorimeter[4] in the temperature region from 11 to 350°K.

As is shown in the following figure, the heat-capacity curve exhibited a phase transition at

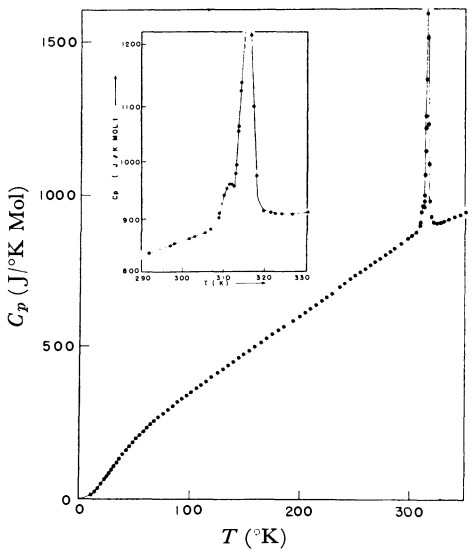

Fig. 1. Heat Capacity of $[(C_6H_5)_3PCH_3]^+$ $(TCNQ)_2^-$.

315.7°K. The enthalpy and the entropy of transition were found to be 2030.0 J mol^{-1} and 7.1989 J°K^{-1} mol^{-1} respectively. This amount of entropy cannot be explained solely by the freedom of electronic spins, as would be expected from the magnetic measurements. It may be added here that this transition is accompanied by a small hump, as is shown on an enlarged scale in the figure. In order to clarify the origin of this small anomaly as well as the mechanism of the phase transition, we are hereafter going to measure the dilution effect on the heat capacity of this compound of the formation of a series of solid solutions: $[(C_6H_5)_3PCH_3]_{1-x}^+$-$[(C_6H_5)_3As\,CH_3]_x^+(TCNQ)_2^-$, as the pure $[(C_6H_5)_3$-$As\,CH_3]^+$ $(TCNQ)_2^-$ compound has no transition point. The detailed data on these compounds will be reported in due course.

1) R. G. Kepler, *J. Chem. Phys.*, **39**, 3528 (1963); Y. Iida, M. Kinoshita, M. Sano and H. Akamatu, This Bulletin, **37**, 428 (1964); Y. Iida, M. Kinoshita, A. Kawamori and K. Suzuki, *ibid.*, **37**, 764 (1964).

2) A. W. Merkel, R. C. Hughes, L. J. Berliner and H. M. McConnell, *J. Chem. Phys.*, **43**, 953 (1965).

3) L. R. Melby, R. J. Harder, W. R. Hertler, W. Mahler, R. E. Benson and W. E. Mochel, *J. Amer. Chem. Soc.*, **84**, 3374 (1962).

4) T. Matsuo, H. Suga and S. Seki, to be published.

The Formation of 6,8-Dihydroxypurine by the Oxidation of 7-Aminooxazolo[5,4-*d*]pyrimidine with Hydrogen Peroxide-Acetic Acid[1]

Yozo Ohtsuka and Kikuo Sugimoto

Sagami Chemical Research Center, Ohnuma, Sagamihara, Kanagawa

(Received May 14, 1970)

The direct oxidation of adenine with peracetic acid has been known to afford the 1-oxide,[2,3] while hypoxanthine is not convertible to the *N*-oxide by this method.[3,4] 7-Aminooxazolo[5,4-*d*]pyrimidine (I) can be considered as a compound having a structure intermediate between adenine and hypoxanthine; accordingly, its behavior when treated with a peracid is of interest. As an analogous compound, 7-aminothiazolo[5,4-*d*]pyrimidine has been reported to be oxidized to the *N*-oxide of the adenine type.[5]

We have found that the oxidation of 7-aminooxazolo[5,4-*d*]pyrimidine (I) with hydrogen peroxide and acetic acid afforded an unexpected product, 6,8-dihydroxypurine (III). Thus, one gram of I[6] was treated with 3.7 m*l* of a 30% aqueous solution of hydrogen peroxide and 10 m*l* of acetic acid at room temperature. After 2.5 days, light yellow precipitates (0.5 g, 48%) of a single compound were obtained. Recrystallization from water yielded colorless crystals, mp >340°C, which were identical with authentic 6,8-dihydroxypurine.[7]

As has been described in a previous paper,[8] 7-aminooxazolopyrimidines are easily converted into hypoxanthine. However, there is no possibility of the formation of III *via* hypoxanthine since hypoxanthine is inert under the conditions used here. Moreover, the oxidation of the pyrimidine moiety of I would not lead to such a product. Thus, the initial step of the oxidation probably occurs at the 1-*N* position of I,[9] giving 7-aminooxazolopyrimidine 1-oxide (II) as an intermediate. The conversion of II into III can be explained by analogy with the well-known rearrangement of aldonitrons into isomeric amides under acidic conditions:[10,11]

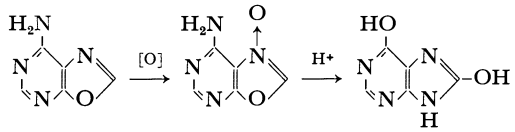

I II III

The difference in behavior towards oxidation between 7-aminooxazolo[5,4-*d*]pyrimidine and adenine or 7-aminothiazolo[5,4-*d*]pyrimidine may be attributed to the difference in the charge density on the ring-nitrogen atom, which is attacked preferentially by the electrophilic centre of the peracid. The present results may indicate that the electron-deficient character of the pyrimidine ring and the electron-excess character of the oxazole ring seem to be partly retained in the oxazolopyrimidine molecule,[12] while a more extensive donation of electrons from the five-membered ring to the pyrimidine ring takes place in purines[13] and even in thiazolopyrimidines. These factors account for the preferential oxidation on the oxazole ring in the oxazolopyrimidine.

1) Study on Oxazolopyrimidines. III.

2) M. A. Stevens, D. I. Magrath, H. W. Smith and G. H. Brown, *J. Amer. Chem. Soc.*, **80**, 2755 (1958).

3) M. A. Stevens and G. B. Brown, *ibid.*, **80**, 2759 (1958).

4) H. Kawashima, T. Meguro and I. Kumashiro, This Bulletin, **39**, 633 (1966).

5) G. B. Brown, G. Levin, S. Murphy, A. Sele, H.C. Reilley, G. S. Tarnowski, F. A. Schmid, M. N. Teller and C. C. Stock, *J. Med. Chem.*, **8**, 190 (1965).

6) Y. Ohtsuka, This Bulletin, **43**, 187 (1970).

7) R. K. Robins, *J. Amer. Chem. Soc.*, **80**, 6671 (1958).

8) Y. Ohtsuka, This Bulletin, **43**, 954 (1970).

9) Although the oxidation of azole compounds generally affords ring-opening products, the oxidation of 4-methylthiazole with hydrogen peroxide in acetic acid is known to yield the *N*-oxide [E. Ochiai and E. Hayashi, *Yakugaku Zasshi*, **67**, 34 (1947)].

10) W. Rundel, "Methoden der Organischen Chemie," ed. by E. Müller, Vol. 10/4, Georg Thieme Verlag, Stuttgart (1968), p. 428.

11) For example, pyridine *N*-oxide has been reported to afford 2-hydroxypyridine when treated with acetic anhydride [M. Katada, *Yakugaku Zasshi*, **67**, 51 (1947)]. An analogous rearrangement of pteridine derivatives [W. Hutzenlaub, G. B. Berlin and W. Pfleiderer, *Angew. Chem.*, **81**, 624 (1969)] or quinoxaline derivatives [Y. Ahmad, M S Habib, A Mohammady, B. Bakhtiari and S. A. Shamsi, *J. Org. Chem.*, **33**, 201 (1968)] seem to involve an acylation process, but we have no evidence for the involvement of acylation in the present reaction.

12) This was also suggested by the study of the spectroscopic properties of substituted 7-aminooxazolopyrimidines (see Ref. 6).

13) R. M. Acheson, "An Introduction to the Chemistry of Heterocyclic Compounds," John Wiley and Sons, New York (1967), p. 355.

Solvent and Temperature Effects on the Electronic Spectra of Mixed Nickel(II) Chelates with *N,N,N',N'*-Tetramethylethylenediamine and Acetylacetone

Yutaka FUKUDA and Kozo SONE

Department of Chemistry, Faculty of Science, Ochanomizu University, Otsuka, Bunkyoku, Tokyo

(Received May 8, 1970)

When equimolar quantities of $Ni(ClO_4)_2 \cdot 6H_2O$, *N, N, N', N'*-tetramethylethylenediamine(TMEN), acetylacetone(acaH) and sodium carbonate are mixed in ethanol, and the resulting mixture is concentrated under reduced pressure, blue crystals of the composition Ni TMEN aca $(ClO_4) \cdot 2H_2O$ separate out. This compound is stable in open air but is easily dehydrated in a P_2O_5 dessicator, and a red anhydrous compound is obtained which slowly reverts to the blue dihydrate in moist air.[1] The blue compound has a magnetic moment (μ_B) of 3.04 B.M. at 14°C, while the red one is only slightly paramagnetic ($\mu_B \sim 0.6$ B.M.).[2]

These values, and the spectral data shown below, indicate that they should be formulated as the mixed chelates, [Ni TMEN aca $(H_2O)_2$] (ClO_4) (octahedral) and [Ni TMEN aca] (ClO_4) (square-planar).

Both of these chelates are decomposed by water, but they are soluble in many organic solvents. Fig. 1 shows their spectra in some alcohols and acetone. It can be seen that in methanol both of the chelates exist as the blue octahedral species, [Ni TMEN aca $(X)_2$]$^+$ (X=H_2O or solvent); the spectra of these solutions (Curves A) are also very similar to the solid reflection spectrum of the blue chelate. On the other hand, the spectra in the other solvents show that they exist in part as blue species and in part as a red square-planar species, very probably [Ni TMEN aca]$^+$. The amount of this red species increases in the order MeOH$\ll$ EtOH$<$*n*-PrOH$<$Acetone$\ll$$CHCl_3$ or $C_2H_4Cl_2$, *i.e.* the order of decreasing coordination ability of the solvents. Corresponding to this spectral change, the color of the solution becomes gradually reddish from methanol to acetone, and the solutions in chloroform or 1,2-dichloroethane are quite red. In these two solvents, the red species clearly predominate (ν_{max}=20.5 kK; log ε=2.1—2.2).

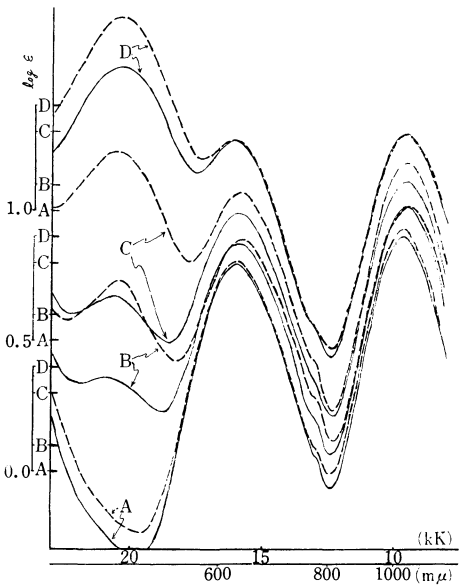

Fig. 1. Absorption spectra of the blue and red chelates at room temperature (18°C). Curves A,B,C and D refer respectively to the solutions in MeOH, EtOH, *n*-PrOH and acetone (0.8×10^{-1}—1.2×10^{-1}M); each curve is drawn in the same scale but displaced vertically (*cf.* the scale for log ε). The solid-line curves are those for the blue chelate, and the dotted-line curves for the red.

All the alcoholic and acetone solutions are thermochromic and become more reddish on heating. Spectral studies on the thermochromism show that the intensity of the band at 20.5 kK increases remarkably with the rise of temperature, showing that the equilibria [Ni TMEN aca $(X)_2$]$^+$ (octahedral)$\rightleftarrows$[Ni TMEN aca]$^+$ (square-planar)$+2X$ are shifted to the right hand side even by slight heating. It is interesting, however, to note that this type of reversible thermochromism is observed only in solvents of medium coordination ability (alcohols and acetone); the red solutions in poorly coordinating solvents($CHCl_3$ and $C_2H_4Cl_2$) as well as the blue ones in strongly coordinating solvents (DMSO and DMF) are not thermochromic, *i.e.* their colors do not changes by heating.

1) Elementary analyses of these compounds are as follows. Found for the blue compound: C, 32.40; H, 6.89; N, 6.88%. Calcd for [Ni TMEN aca $(H_2O)_2$](ClO_4): C, 32.26; H, 6.66; N, 6.84%. Found for the red compound: C, 34.65; H, 6.42; N, 7.42%. Calcd for [Ni TMEN aca](ClO_4): C, 35.37; H, 6.22; N, 7.50%.

2) The moments obtained with different samples of the red compound do not agree well with each other, and they all tend to increase slowly with time. It is therefore possible that this compound is in fact diamagnetic, and the observed moment is due to a small amount of the blue dihydrate which is readily formed in the sample. Work is now going on to confirm this view.

BULLETIN OF THE CHEMICAL SOCIETY OF JAPAN VOL. 43 2283—2290 (1970)

Chemical Species Produced from Some Diazaazulene Derivatives in Aqueous Solutions of Various Acidities

Yoshie TANIZAKI and Hiroshi HIRATSUKA

Department of Chemitsry, Faculty of Science, Tokyo Institute of Technology, Meguro-ku, Tokyo

and Toshihiko HOSHI

Department of Chemistry, College of Science and Engineering, Aoyama Gakuin University, Megurisawa, Setagaya-ku, Tokyo

(Received June 4, 1969)

Making use of the isosbestic points which appear in equilibrium between two chemical species, the chemical structures of various species produced from the diazaazulene derivatives have been investigated in aqueous solutions over a wide pH range. For 1-hydro-1,3-diazaazulene-2-one (abbreviation, HDA-1), for instance, four different species exist as stable species in the respective regions; (a) the pH region higher than 12, (b) around the neutral state, (c) the pH value of *ca.* 1.5, and (d) the strong acid state. In the (a) region, H^+ is taken off from the amino nitrogen of HDA-1 and the species becomes HDA-1^-; in (b) the species takes the HDA-1 structure, as its name indicates; in (c) it takes the H^+-HDA-1 structure protonated at the aza nitrogen, and in (d) it takes the H^+-HDA-1-H^+ structure, in which the position of the second protonation could not be clarified. In the case of 2-ethoxy-1,3-diazaazulene (EDA-2), the species corresponding to the second protonation (H^+-EDA-2-H^+) is hydrolyzed by acid catalysis and becomes H^+-HDA-1-H^+. In order to interpret the spectra of azaazulene compounds and the spectral change due to protonation, calculations by the LCAO–ASMO–SCF–CI method have been made for 1,3-diazaazulene and EDA-2. The characters of the first and the second transitions of the compounds have been satisfactorily explained by the diagrams of the AO coefficients of the LCAO-MO's representative of the transitions.

In the past two decades, a number of azaazulene compounds have been synthesized as tropolone derivatives. However, only a few physico-chemical studies have been reported, such as one on the dipole moment by Kurita and Kubo[1], and one on the electronic spectra by Nozoe and Murata.[2] As for the theoretical treatment, there seems to have been nothing except the study by Kon[3] using the simple molecular orbital method.

Nozoe *et al.*[4] have considered the product of the reaction of tropolone-methylether and guanidine hydrochloride to be a mixture of 2–amino-1, 3-diazaazulene and 1-hydro-2-imino-1,3-diazaazulene, which are tautomer with each other. Similarly, it is considered that a tautomerism exists between 2-hydroxy-1,3-diazaazulene (to be henceforth abbreviated as HDA-2) and 1-hydro-1,3-diazaazulene-2-one (HDA-1) as follows;

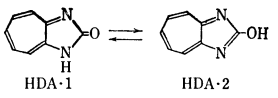

HDA·1 HDA·2 (1)

where the mole ratio of HDA-1 and HDA-2 in the methanolic solution is considered to be about 7:3.[5,6] If such an equilibrium as Eq. (1) exists, some spectral change may be expected to occur for the system when the temperature is changed. In order to determine the temperature dependence of the spectra, we measured the absorption spectra in ethanolic and aqueous solutions over the range from 25°C to 55°C. An appreciable change in spectra appeared, but the magnitude and the behavior of the spectral change were almost the same as those in the case of azulene in an ethanolic solution, in which no tautomerism like that of Eq. (1) is involved. For this reason, it is very doubtful that the above-mentioned system contains two chemical species as Eq. (1) indicates.

1) Y. Kurita and M. Kubo, *J. Amer. Chem. Soc.*, **79**, 5460 (1957).

2) T. Nozoe and T. Murata, *Proc. Japan Acad.*, **30**, 482 (1954).

3) H. Kon, *Sci. Repts. Tohoku Univ. I*, **38**, 67 (1954).

4) T. Nozoe, T. Mukai, K. Takase, I. Murata and K. Matsumoto, *Proc. Japan Acad.*, **29**, 452 (1953).

5) T. Nozoe, T. Mukai and I. Murata, *J. Amer. Chem. Soc.*, **76**, 3352 (1954).

6) I. Murata, *Sci. Rep. Res. Inst., Tohoku Univ., Ser. A*, **12**, 271 (1963).

A tautomerism is also considered to exist between anthrone and anthranole; the ratio is said to be dependent on the amount of the alkaline substance (triethylamine) added to the system.[7] If this is true, the equilibrium between HDA-1 and HDA-2 of Eq. (1) should also be shifted by the variation in the nature of the solvent, for example, by the variation in the pH of the solution. In fact, the aqueous solutions of HDA-1 show a considerable change in spectra, while retaining definite isosbestic points, upon pH variation.

In the present investigation, the chemical structures of species produced from the azaazulene derivatives in the various pH regions will be clarified.

Azulene is well known as an isomer of naphthalene; it has been investigated in detail both theoretically[8] and experimentally.[9] Concerning the diazaazulene derivatives, however, there has been only one theoretical treatment, one by Kon[3] carried out by the Hückel method. Therefore, the electronic spectra of 1,3-diazaazulene and 2-ethoxy-1,3-diazaazulene will be calculated, and the results will be discussed with reference to those for azulene, which has previously been computed using the same approximation.[10]

Experimental

The 2-ethoxy-1,3-diazaazulene and 1-hydro-1,3-diazaazulene-2-one were provided by the Sankyo Company, Ltd. The 1-ethyl-1,3-diazaazulene-2-one was synthesized following Reference 11. The melting points were determined to be 101—102°C (lit, 101°C),[11] 243°C (245°C),[4] and 138°C (140°C)[12] respectively.

The concentrations of the samples used were of the order of 10^{-4} mol/*l*. The pH value of the solution was controlled by hydrochloric acid and sodium hydroxide, and was measured by means of a Toa Denpa pH meter, HM 5A. A strong acid or a strong alkaline solution of the sample was prepared by using concentrated sulfuric acid or sodium hydroxide respectively. The conditions of the solutions used are illustrated in the figures.

The measurement of the absorption spectra was carried out by a Shimadzu MPS-50A Recording Spectrophotometer over 220—400 mμ.

Results

Figure 1 shows the absorption spectra of 1-hydro-1,3-diazaazulene-2-one (abbreviation, HDA-1) in alkaline solutions with various pH values. The isosbestic points indicate the presence of two kinds of species in equilibrium. No further spectral change appeared upon an increase in the alkaline strength to more than pH=12.4 (by 0.5N of NaOH).

Figure 2 shows the absorption spectra of HDA-1 in the week acid region of pH=5.9—1.5. In this case, isosbestic points also appear, indicating an

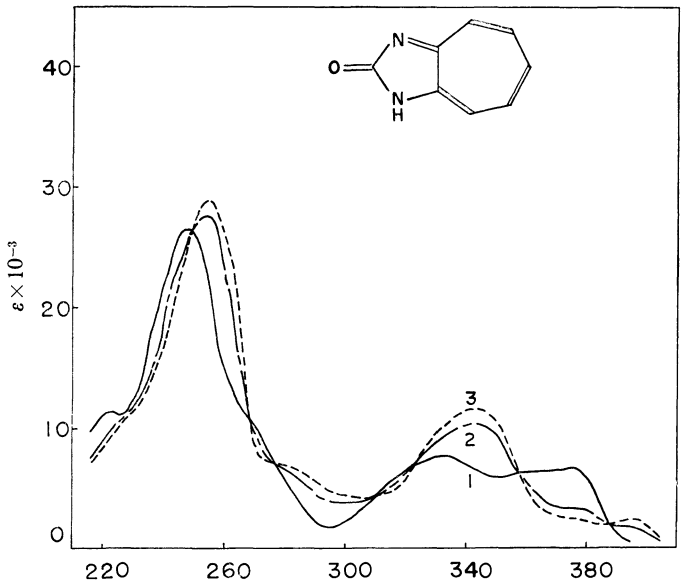

Fig. 1. Absorption spectra of (HDA-1) in aqueous alkaline solutions.
1. pH=6.10, 2. pH=10.0, 3. pH=12.40

7) H. Baba and T. Takemura, This Bulletin, **37**, 1241 (1964).

8) R. Parizer, *J. Chem. Phys.*, **25**, 1112 (1956); E. Heilbronner, "Non-Benzenoid Aromatic Compounds," D. Ginsburg, ed., Interscience, N. Y. (1960), p. 171.

9) J. W. Sidman and D. S. McClure, *J. Chem. Phys.*, **24**, 757 (1956); G. R. Hunt and I. G. Ross, *J. Mol. Spectry.*, **3**, 604 (1959); **9**, 50 (1962).

10) Y. Tanizaki, T. Kobayashi and T. Hoshi, to be published.

11) G. Sunagawa and M. Watatani, *Chem. Pharm. Bull.* (Tokyo), **16**, 1308 (1968).

12) H. Nakao, N. Soma, Y. Sato and G. Sunagawa, *ibid.*, **13**, 473 (1965).

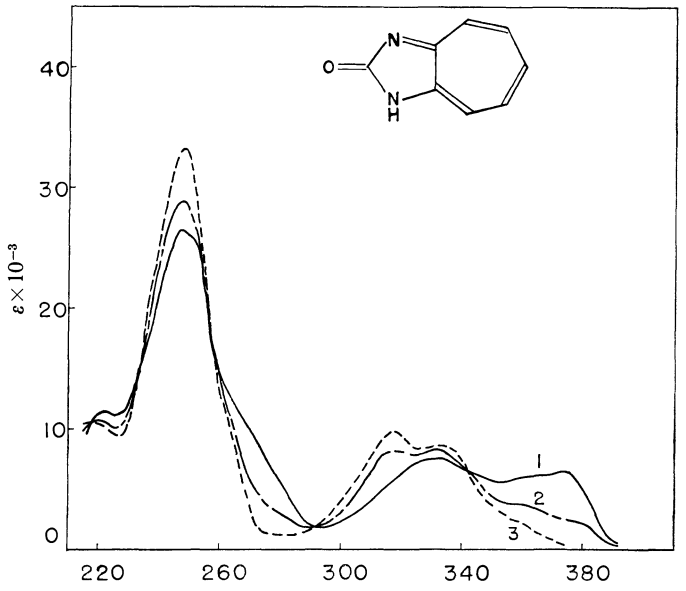

Fig. 2. Absorption spectra of (HDA-1) in aqueous acid solutions.
1. pH=5.90, 2. pH=3.90, 3. pH=1.50

equilibrium between two kinds of species. The spectrum for pH=5.9 of Fig. 2 coincides with that for pH=6.10 of Fig. 1, whereas the positions of the isosbestic points and the band shape of Fig. 2 (the acid solution) are different from those of Fig. 1 (the alkaline solution). This indicates, therefore, that the kinds of chemical species in the alkaline and the acid solution are different from each other.

With an increase in the acidity below pH=1.5, the spectral change appears again——that is, by increasing the concentration of sulfuric acid by at least from 9N to 27N, for instance, the spectrum is made to change with another set of isosbestic points. In this case, each absorption band for pH=1.50 of Fig. 2 behaves as follows. The 318 mμ band decreases in intensity, the 333 mμ band increases in intensity and shows a slight blue shift, and the 248 mμ band is only intensified, without any shift. According to the results for HDA-1, it is evident that four different kinds of species exist respectively as a stable one in four pH regions, including the strong acid and alkaline states (i.e., the extended

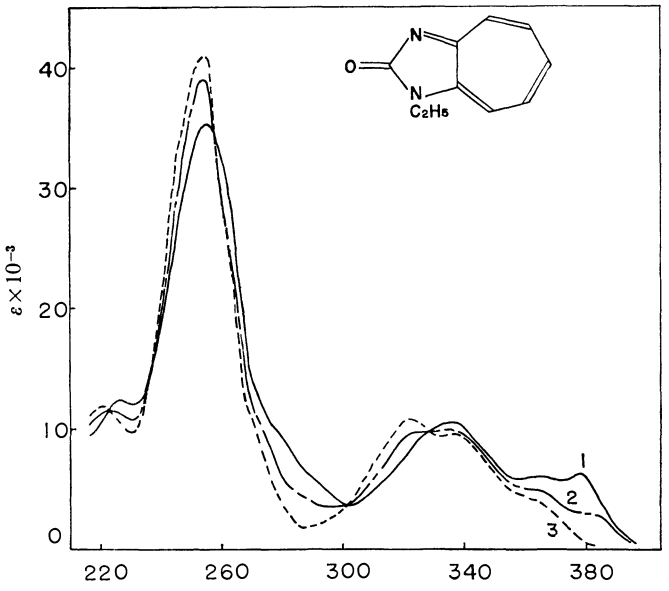

Fig. 3. Absorption spectra of (EDA-1) in aqueous acid solutions.
1. pH=5.85, 2. pH=4.01, 3. pH =1.85

pH region more than 12, the neutral state, at about the pH value of 1.5, and the strong acid state).

Figure 3 illustrates the absorption spectra of 1-ethyl-1,3-diazaazulene-2-one (abbreviated to EDA-1) in aqueous solutions from neutral to weak acid with various pH values. In addition, the spectrum of EDA-1 in an alkaline solution with a pH lower than 12.4 did not differ from that for pH=5.85 shown in Fig. 3. The behavior of the spectral change and the interval of acidity for the spectral change of EDA-1 correspond well with those in the case of HDA-1, though the absorption bands of the former are slightly longer in wavelength as a whole and are stronger in intensity than the corresponding bands of the latter. The correlation of the spectra of HDA-1 and EDA-1 in a strong acid solution is similar to that in a weak acid solution.

Consequently, in the case of EDA-1, there are a total of three kinds of species, each in one of three regions: neutral to alkaline, about pH=1.9, and strong acid.

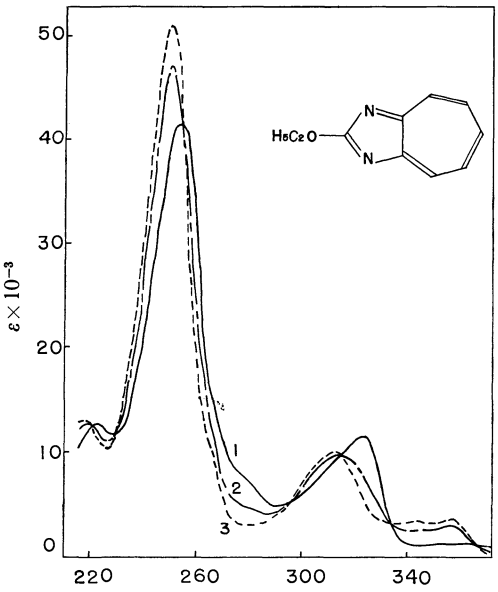

Fig. 4. Absorption spectra of (EDA-2) in aqueous acid solutions.
1. pH=5.62, 2. pH=3.30, 3. pH=1.88

Figure 4 represents the absorption spectra of 2-ethoxy-1,3-diazaazulene (abbreviation EDA-2) under conditions similar to those in Fig. 3. This sample did not show any appreciable change in spectra over the range from neutral to pH=11.9. In the strong acid solution, however, the sample showed a spectral change with the time dependence when the amount of added sulfuric acid was small, but the change was instantaneously completed when the amount was large. The resultant spectrum in either case coincided with that of HDA-1 in the strong acid solution. This suggests that EDA-2, which is stable in weak acid, is decomposed by strong acid and then becomes a species identical with that of HDA-1 in strong acid.

Accordingly, EDA-2 can exist as two independent species; one in the range from neutral to alkaline, and the other in the weak acid solution at about pH=1.90.

Calculation

The calculations were carried out by the semi-empirical method of LCAO-ASMO-SCF,[13] making use of the approximations by Pariser-Parr[14] and Nishimoto-Mataga [15] and the configuration interaction (CI). The geometry and the numbering of the atoms for 2-ethoxy-1,3-diazaazulene are shown in Fig. 5, in which the lengths of all C-C and C-N bonds are taken as 1.40Å. and in which that of C-O is taken as 1.41Å. The respective coordinates are listed in Table 1. For 1,3-diazaazulene, the same coordinates as above are taken, excluding the oxygen atom.

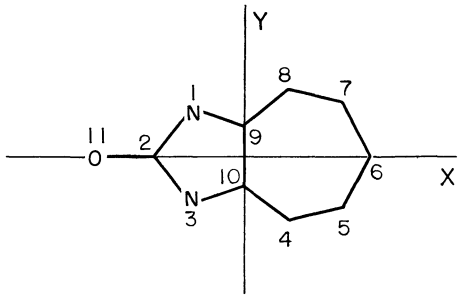

Fig. 5. Geometrical and numbering system for the 2-ethoxy-1,3-diazaazulene molecule.

For the Hückel MO calculation, the Coulomb integrals (α) and the resonance integrals (β) are used as follows:

$$\alpha_O = \alpha_C + 0.6\beta \qquad \beta_{CO} = 0.7\beta$$
$$\alpha_N = \alpha_C + 0.6\beta \qquad \beta_{CN} = 1.0\beta$$
$$\alpha_{C'} = \alpha_C + 0.1\beta$$

where α_C is the Coulomb integral of the carbon atom, where β is the resonance integral between the adjacent carbon atoms, where the subscript O or N indicates oxygen or nitrogen respectively, and where C′ indicates the carbon atom adjacent to oxygen or nitrogen.

The one-center integrals are evaluated by the Pariser-Parr's equation. The parameters employed here are summarized in Table 2. The SCF calculations were repeated ten times, and a satisfactory convergence was obtained for the respective AO

13) C. C. J. Roothaan, *Rev. Mod. Phys.*, **23**, 61 (1951).
14) R. Pariser and R. G. Parr, *J. Chem. Phys.*, **21**, 466, 767 (1953).
15) K. Nishimoto and N. Mataga, *Z. Phys. Chem. N. F.*, **13**, 140 (1957).

Table 1. Coordinate for 2-ethoxy-1,3-diazaazulene

Number of atom	X-coordinate	Y-coordinate
1	−1.33	1.13
2	−2.15	0.00
3	−1.33	−1.13
4	1.09	−1.57
5	2.46	−1.26
6	3.07	0.00
7	2.46	1.26
8	1.09	1.57
9	0.00	0.70
10	0.00	−0.70
11	−3.56	0.00

Table 2. Parameter values used

	C	O	N
Ionization potential (eV)	11.42	33.0	27.525
Electron affinity (eV)	0.58	11.48	13.435

	C–C	O–O	N–N
Core resonance integral (eV)	−2.236		
Const. in N.-M. eq.[a] (Å)	1.328	0.699	1.002

	C–O	C–N	O–N
Core resonance integral (eV)	−2.12	−2.576	
Const. in N.-M. eq.[a] (Å)	0.889	1.115	0.808

a) Nishimoto-Mataga's equation

coefficients. In the CI calculations, taking into account the SCF orbital energies, we considered the upper three occupied orbitals and the lower four unoccupied ones, and all the one-electron excitations were taken into account.

Table 3 represents the results for 1,3-diazaazulene and 2-ethoxy-1,3-diazaazulene. In the same table the results for azulene[10] are added for comparison. According to Table 3, it can be seen that both azulene and 1,3-diazaazulene have five electronic transitions in the region below 50000 cm^{-1} (above 200 mμ), and that every transition of 1,3-diazaazu-

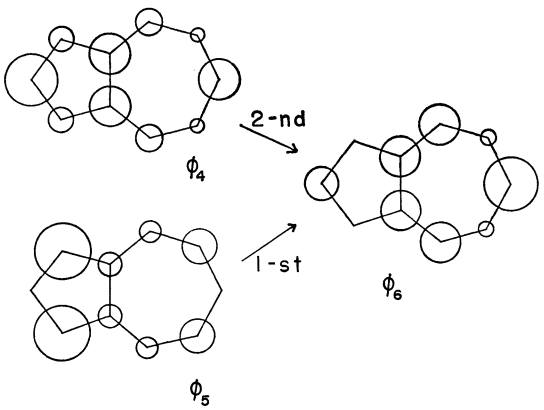

Fig. 6. Change in charge density associated with the transitions of $\Phi_5 \rightarrow \Phi_6$ and $\Phi_4 \rightarrow \Phi_6$ which are representative of the first and second transitions of 1,3-diazaazulene, respectively. Notice that the charge at 1 and 3 of Φ_5 and Φ_4 becomes zero in Φ_6.

Table 3. Calculated results for 1,3-diazaazulene and 2-ethoxy-1,3-diazaazulene

	Transition energy	Oscillator strength	Direction[a]	Assignment
azulene[b]	14798 cm^{-1}	0.026	90°	
	26667	0.007	0	
	34381	0.116	90	
	36644	1.787	0	
	45268	0.928	90	
	49328	0.026	0	
1,3-diazaazulene	21524	0.026	90	
	30445	0.062	0	
	35327	0.140	90	
	39966	1.743	0	
	45959	0.778	90	
	51336	0.247	0	
2-ethoxy-1,3-diazaazulene	22338	0.014	90	380 mμ band
	28338	0.215	0	330
	33917	0.210	90	290
	39649	1.802	0	260
	45603	0.654	90	230
	51130	0.181	0	

a) Angle of transition moment against X-axis
b) Taken from Ref. 10.

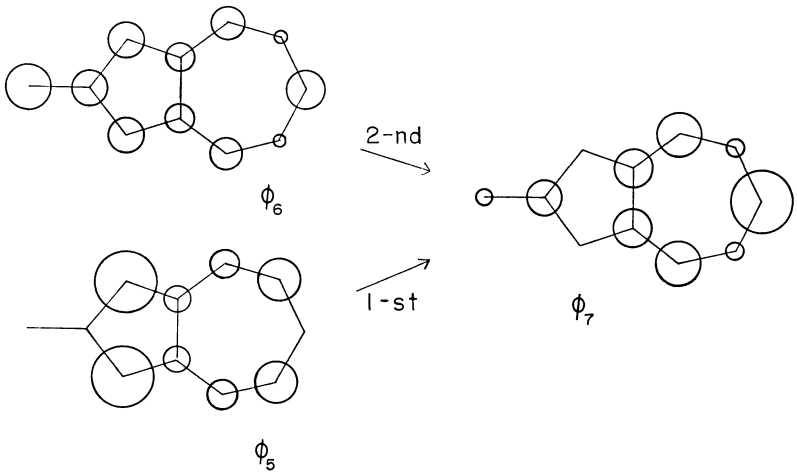

Fig. 7. $\Phi_5 \rightarrow \Phi_7$ and $\Phi_6 \rightarrow \Phi_7$ are representative of the first and second transitions of 2-ethoxy-1,3-diazaazulene (See, Fig. 6).

lene has larger wave numbers than that of azulene. This fact may be interpreted as follows. The magnitudes of the respective AO coefficients of the LCAO-MO's which are representative of the first and the second transitions, *i.e.*, $\Phi_5 \rightarrow \Phi_6$ and $\Phi_4 \rightarrow \Phi_6$ respectively, are shown diagrammatically in Fig. 6, where Φ_i represents the LCAO-MO and in which the subscript is the number in the order of increasing energy. According to Fig. 6, the change in the charge density at the positions 1 and 3 associated with the transitions $\Phi_5 \rightarrow \Phi_6$ is very large: that is to say, the large densities at 1 and 3 in Φ_5 and Φ_4 become exceedingly small in Φ_6, which is a representative MO of the excited states. Also, in the case of azulene, the corresponding transitions have the same character as above. However, the ionization potentials or the electron affinities at the positions 1 and 3 of azulene are small relative to those of 1,3-diazaazulene, because of the difference between carbon and nitrogen. Therefore, such a transition as $\Phi_5 \rightarrow \Phi_6$ or $\Phi_4 \rightarrow \Phi_6$ of 1,3-diazaazulene would need higher energies and appear at larger wave numbers than those of azulene. The same situations occur in connection with the other transitions.

2-Ethoxy-1,3-diazaazulene also possesses five electronic transitions in the range lower than 50000 cm^{-1} (above 200 mμ). The effect of the $-OC_2H_5$ substituent at the position 2 causes the first and the fifth transitions of 2-ethoxy-1,3-diazaazulene to shift to shorter wavelengths, and the rest to longer wavelengths relative to 1,3-diazaazulene. Moreover, the oscillator strengths of the second, the third, and the fourth transitions are increased, and the others are decreased, by the effect of $-OC_2H_5$. As above, the $-OC_2H_5$ substituent can cause some changes in the transition energies and oscillator strengths, but it cannot change the transition directions.

From a comparison of Figs. 6 and 7, it can be seen that the $-OC_2H_5$ group does not perturb the first and the second transitions. Especially, the character of the $\Phi_5 \rightarrow \Phi_7$ of 2-ethoxy-1,3-diazaazulene is almost the same as those representative of the first transitions of azulene and 1,3-diazaazulene.

Discussion

1. Chemical Structure. The three positions of protonation for HDA-1 or EDA-1 are considered to be aza nitrogen, amino nitrogen, and oxygen. Incidentally, a similar situation holds in the cases of the protonation of 1,6-dihydro-1-methyl-4-oxypyrimidine (expression (a), below) and 1,4-dihydro-1-methyl-4-oxypyrimidine (expression (b)).

(a) (b)

Brown *et al.*[16] have considered that a protonation occurs at the aza nitrogen atom, because the spectra of the protonated species of (a) and (b) are similar to each other.

The mechanism of the protonation to HDA-1 and EDA-1 may be different from the cases of (a) and (b). In the present case, however, let us assume that the order of the ability as the proton acceptor of the functional groups of HDA-1 and EDA-1 is similar to those of (a) and (b); that is to say, let us assume that the first protonation occurs at the aza nitrogen rather than at amino nitrogen or oxygen.

16) D. J. Brown, E. Hoerger and S. F. Mason, *J. Chem. Soc.*, **1953**, 331.

As has been shown in the "Experimental" section, all the absorption patterns over the range of 200 mμ to 300 mμ are similar to one another; no characteristic difference among them appears until above 300 mμ. For that reason, let us examine the absorption bands which appear above 300 mμ in comparing the spectra.

Murata[6] has considered that the system expressed by Eq. (1) contains HDA-1 as the main component, for the absorption pattern of the system is similar to that of EDA-1. It is natural that the electronic spectra associated with the π–π^* transitions of HDA-1 and EDA-1 are similar to each other, since they are isolectronic with respect to the π electron system. If some differences appear between the absorption patterns, it can be attributed to the difference in the substituents, –H and $-C_2H_5$. In fact, his consideration can be said to be reasonable, for the absorption spectra of HDA-1 (curve 1, Fig. 1) and EDA-1 (curve 1, Fig. 3) correspond to each other well.

We can now summarize our several results as follows. The temperature dependence of the spectrum of HDA-1 is as small as that of azulene, for which a tautomerism cannot be considered. HDA-1 and also EDA-1 can exist as independent species. HDA-1 in the neutral solution is not considered to be protonated, since no spectral change is observed in the range from neutral to pH=12. Taking these facts into account, it can safely be said that the hydrogen atom H of HDA-1 must be linked with the nitrogen atom at the position 1 of the diazaazulene skeleton in the same manner as C_2H_5 of EDA-1. If HDA-1 exists as a single species of another type (HDA-2 in Eq. (1)), then the spectrum should be correspondent to that of EDA-2. No such correspondencies, however, recognized between the curve 1 of Fig. 1 and the curve 1 of Fig. 4.

If an equilibrium such as Eq. (1) is supposed, the HDA-2 species may be found in the acid or the alkaline solutions. Let us compare the absorption spectra of HDA-1 and EDA-1 in the acid solution and that of EDA-2 in the neutral solution. In the case of EDA-1, the proton addition upon an increase in the acidity is expected to take place at the aza nitrogen atom and to produce H^+-EDA-1, as has been mentioned at the beginning of this section. The spectrum of HDA-1 in the acid state (curve 3, Fig. 2) closely resembles that of H^+-EDA-1 (curve 3, Fig. 3) rather than that of EDA-2 in the neutral state (curve 1, Fig. 4). This indicates that HDA-1 is not isomerized to HDA-2, as in Eq. (1), but is protonated and becomes H^+-HDA-1, as in the case of H^+-EDA-1.

Next, let us discuss the chemical species in the alkaline solution. As has been pointed out, EDA-1 and EDA-2 exist as a single species in the range from the neutral to the alkaline state, while HDA-1 in the alkaline state takes a spectral species different from that in the neutral state. The spectra of the chemical species may be compared as follows. The spectrum of the species of HDA-1 in the alkaline solution (curve 3, Fig. 1) does not resemble either the curve 1 of Fig. 4 in the neutral solution of EDA-2 or the curve 1 of Fig. 3, which is identical with that of EDA-1 in the alkaline solution. It is especially remarkably different from the former. This indicates that the species of HDA-1 in the alkaline state does not take the structure corresponding to EDA-2; that is, no isomerism such as Eq. (1) takes place. Moreover, the spectrum of HDA-1 in the alkaline state is not similar to that of EDA-1. Taking into consideration the possibility that a dissociation in the reverse process of the protonation occurs because of the variation from neutral to alkaline, it is reasonable that H is taken off as a proton from the amino nitrogen of HDA-1 during the variation, in some way such as $HDA\text{-}1+OH^-\rightarrow HDA\text{-}1^-+H_2O$.

When HDA-1 is protonated and becomes H^+-HDA-1, the proton will go to aza nitrogen. This theory is strongly supported by the following facts. As has been pointed out in the "Experimental" section, in the process of the first protonation of EDA-2 a proton must go to either of two aza nitrogens, and H^+-EDA-2 is produced. If the second protonation occurred, the place to be attacked by a proton would be another aza nitrogen. In order to confirm this expectation, we carefully determined the second change in spectra upon the addition of sulfuric acid. The spectrum of the doubly-protonated species (H^+-EDA-2-H^+) gradually varied and became a spectrum coincident with that of H^+-HDA-1 in the weak acid solution. Upon the further addition of concentrated sulfuric acid, the spectrum of H^+-EDA-2-H^+ completely coincided with that of H^+-HDA-1-H^+ in the strong acid solution. The above results for the second protonation of H^+-EDA-2 include two important facts — that the resultant species loses the ethyl group and that it possesses amino nitrogen. In this case, the fact that the ethyl group is separated from H^+-EDA-2 in a strong acid state can be explained by the usual mechanism of hydrolysis by acid catalysis:

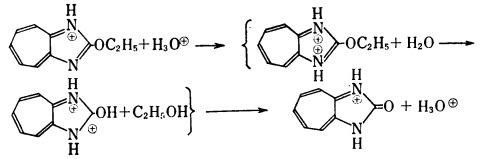

(2)

The mechanism shows that the product possesses amino nitrogen and is H^+-HDA-1 itself. Since the product shows an absorption pattern identical with that of H^+-HDA-1-H^+, the hydronium ion in the last expression of Eq. (2) may be attached as a proton to H^+-HDA-1 somewhere, but the exact position is not evident at the present stage. The

mechanism also establishes that, in the first protonation-process for HDA-1, a proton must make an attack on the aza nitrogen atom at the position 3.

Conclusively, as for HDA-1 the chemical species which can exist over the whole region from strong acid to alkaline may be summarized as follows:

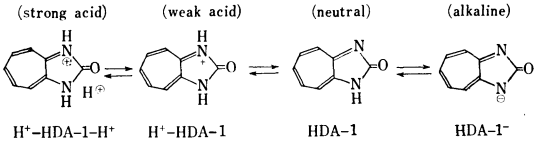

Also, the respective species considered with respect to EDA-1 and EDA-2 are;

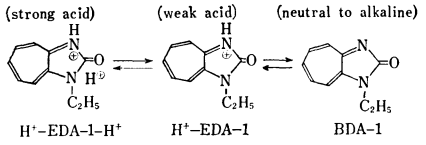

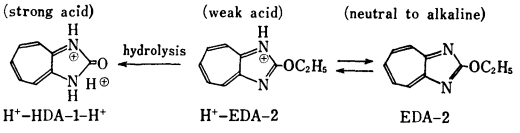

2. Interpretation of the Spectra. The absorption spectrum of EDA-2 is shown in Fig. 8, as are, for the sake of comparison, the computed results. The correlation between the observed and the computed absorption bands with respect to number, location and intensity are satisfactory. The theoretical assignments of the bands are listed in Table 3. The transition energies of azulene and 1,3-diazaazulene in Table 3 have been computed taking larger values of the ionization energy and the electron affinity at the positions 1 and 3 for the latter than for the former. The resultant transition energies of 1,3-diazaazulene are always larger (at shorter wavelengths) than the corresponding ones of azulene.

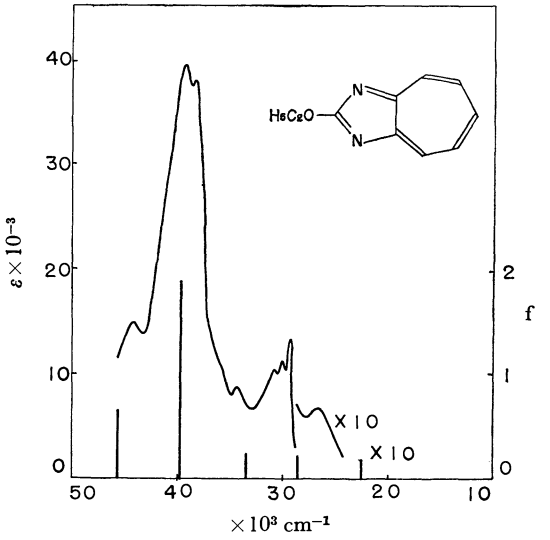

Fig. 8. Comparison of the calculated and observed (in cyclohexane) absorption bands of 2-ethoxy-1,3-diazaazulene, EDA-2.

In the case of protonation, the color bands of azobenzenes (*e.g.*, methyl-orange), for example, can remarkably shift to longer wavelengths.[17] On the contrary, in the present case, the protonation makes the π–π^* band shift to a shorter wavelength. When EDA-2 is protonated at the aza nitrogen atom and becomes H⁺-EDA-2 the apparent increase in the ionization potential and the electron affinity of the nitrogen atom results. Therefore, if we take the larger ionization potential and electron affinity at either the 1 or 3 position for H⁺-EDA-2, the resultant transition energies will become larger than those for EDA-2. Thus, the absorption bands of H⁺-EDA-2 are at shorter wavelengths than the corresponding ones of EDA-2.

The absorption bands of H⁺-HDA-1 and H⁺-EDA-1 are located at shorter wavelengths, or at least not at longer ones, than the corresponding bands of HDA-1 and EDA-1 respectively. This can be explained in the same way as above. It should be noted here that an extra band peak appears at about 330 mμ, as illustrated in Fig. 2; at the present stage, however, we cannot assign that absorption. According to the dichroism analysis,[18] however, both of the 330 mμ peaks must belong to the second electronic transition, and so they are attributed to the fine structure. The first band of H⁺-HDA-1 corresponding to the 370 mμ band of HDA-1 is the weak shoulder at about 360 mμ (curve 3, Fig. 2).

The authors are greatly indebted to Dr. H. Negoro, Dr. G. Sunagawa, Dr. N. Soma and Dr. H. Nakao of the Sankyo Company, Ltd., for providing the samples and for their helpful advice on the synthesis of the compounds. The authors are also deeply indebted to Miss K. Taniyama and Miss M. Watanabe of the Computer Center of Aoyama Gakuin University for their considerable assistance with the computer programs. This work was supported in part by a Scientific Research Grant of the Ministry of Education, to which the authors' thanks are due.

17) Y. Tanizaki, T. Kobayashi and T. Hoshi, This Bulletin, **39**, 558 (1966).

18) Y. Tanizaki, H. Hiratsuka and T. Hoshi, to be published.

BULLETIN OF THE CHEMICAL SOCIETY OF JAPAN VOL. 43 2291—2296 (1970)

Studies of the Aggregation of Dyes. The Scope of Application of the Maximum-slope Method

Mitsuhiko HIDA and Teruko SANUKI

Department of Synthetic Chemistry, Faculty of Engineering, The University of Tokyo, Hongo, Tokyo

(Received September 18, 1969)

The maximum-slope method, previously suggested by one of the authors has proved to be more advantageously applied to the determination of the aggregation constant (K_n) and the degree of aggregation (n) in a dye solution than is Zanker's method. Changes in the spectra of the aqueous or ethanolic solutions of Rhodamine 6G, 3,6-diaminoacridine and thionine were studied as their concentration increased by means of both the maximum-slope method and Zanker's method. The aggregation characteristics obtained by these two methods were then compared with each other and discussed.

Recently the aggregation of molecules in solutions has been drawing much attention from men in various fields because it has a wide application.

Spectroscopic measurement has been employed in determining the aggregation constant and the degree of aggregation because of its accuracy and its simplicity.

It is, however, rather difficult to make a reliable estimation of the aggregation parameters, even for a simple equilibrium system between a monomer and a polymer of one definite degree of aggregation, by means of the graphic analysis of the spectroscopic data. The reason for this is that there are more unknown parameters than the number of given equations.

A way to overcome this difficulty has already been developed. Zanker derived the following equation (Eq. (1))[1]:

$$\log C_0(\varepsilon_1-\varepsilon) = n\log C_0(\varepsilon-\varepsilon_n/n) + \log K_n n(\varepsilon_1-\varepsilon_n/n)^{1-n} \quad (1)$$

were ε is the apparent absorptivity at a difinite wave length, where ε_1 and ε_n are the absorptivities of the monomer and the aggregate respectively, at the same wavelength, and where C_0 is the total concentration. He assumed suitable values for ε_1 and ε_n/n, and plotted $\log C_0(\varepsilon_1-\varepsilon)$ against $\log C_0(\varepsilon-\varepsilon_n/n)$. The degree of aggregation, n, was given by the slope of this plotted straight line, and the equilibrium constant (K_n) was calculated from the intercept.

This method has been recognized as the simplest and most convenient, bus it cannot be advantageously applied to the cases where the value of either ε_1 or ε_n/n has not been determined accurately.

Another graphic method has been developed by one of the present authors (M.H.). The method, which is called "the maximum-slope method"[2], estimates the ε_1 value by extrapolating the ε-$\log C_0$ curve to an infinite dilution, while the maximum slope (m_0) is determined by the tangent of the curve. The values of n, ε_n/n, and K_n are selected in such a way that they give the best agreement with the experimental curve.

In this paper, the maximum-slope method will be compared with Zanker's method and the advantages and applicability of the former will be discussed.

Results and Discussion

1. Analysis of the Computed Aggregation System. By taking suitable values for ε_1, ε_n/n, and $\log K_n$, the apparent absorptivities were computed over a range of concentrations between 10^{-6} and 10^{-3} mol/l, and the ε-$\log C_0$ curve was analyzed graphically by both the maximum-slope method and Zanker's method. A single equilibrium system between the monomer and the dimer was postulated for the sake of simplicity. The apparent absorptivities (ε) of this system were calculated by means of following equation:

$$\varepsilon = \varepsilon_2/2 + \frac{(\varepsilon_1-\varepsilon_2/2)}{4K_2}\left(-1+\sqrt{1+8K_2C_0}\right) \quad (2)$$

Assuming ε_1 and $\varepsilon_2/2$ to be 1×10^5 and 0.0 respectively, the apparent absorptivities were computed for $\log K_2=2,3,4$ and 5. Curve (1) in Fig. 1 suggests that the dimerization of $\log K_2=5$ commences even in a very dilute range (below 10^{-5} mol/l); consequently, ε_1 cannot be accurately determined. If

1) V. Zanker, *Z. Phys. Chem.*, **200**, 250 (1952).

2) a) M. Hida, A. Yabe, H. Murayama and M. Hayashi, This Bulletin, **41**, 1776 (1968). b) Equations (4) and (6) in previous paper (Ref. 2a) should be read $f=K_nC_1^nC^{-1}$ and $\alpha=(nK_n)^{1/(n-1)}(\varepsilon_1-\bar{\varepsilon}_n)^{-1}$, respectively.

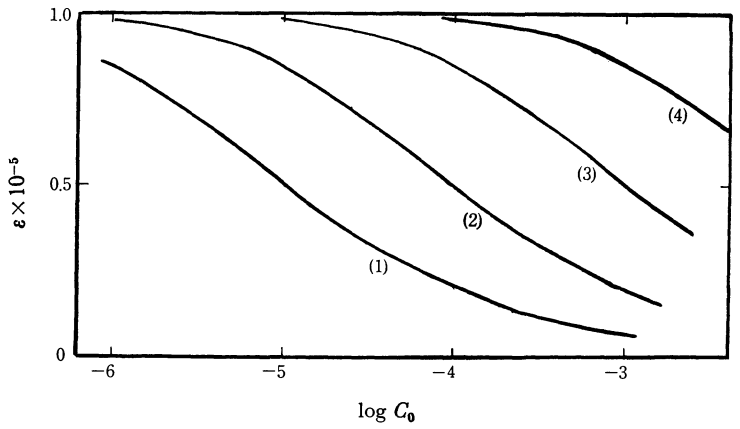

Fig. 1. Computed absorptivity *vs.* log C_0.
(1); log K_2=5.0, (2); log K_2=4.0, (3); log K_2=3.0, (4); log K_2=2.0

ε_1 is estimated by extrapolation at 0.95×10^5, $\varepsilon_2/2$ and logK_2 will be found to be -0.06×10^5 and 4.81 respectively by the use of the maximum slope method. These smaller values may be caused by the underestimation of the value of ε_1. If the errors made in estimating ε_1 and in drawing the maximum slope (m_0) are designated as $\delta\varepsilon_1$ and δm_0, the errors in the values of ε_n/n and logK_n obtained by the maximum-slope method are given by Eqs. (3) and (4):

$$\delta(\varepsilon_n/n) = \delta\varepsilon_1 - (\varepsilon_1-\varepsilon_n/n)_t(\delta m_0/m_0) \quad (3)$$

$$\delta(\log K_n) = (n-1)\delta\varepsilon_1/m_0 + n\log(\overline{1-r}/r\sqrt{n}) + (n-1)\log(1+\delta m_0/m_0) \quad (4)$$

where $r=(m/m_0)/(1+\sqrt{n})$ and where the subscript t denotes the true value.

By substituting the numerical values listed below for $\delta\varepsilon_1$, δm_0, r, and m_0 in Eqs. (3) and (4), $\delta(\varepsilon_2/2)$ and $\delta(\log K_2)$ are obtained as -0.06×10^5 and -0.114 respectively.

TABLE 1. COMPARISON OF THE TRUE AND OBTAINED VALUES OF THE AGGREGATION PARAMETERS

No.	True values		
	$\varepsilon_1\times10^{-5}$	$\bar{\varepsilon}_2\times10^{-5}$	log K_2
1	1.0	0.0	5.0
2	1.0	0.0	4.0
3	1.0	0.0	3.0
4	1.0	0.0	2.0

$$\delta\varepsilon_1 = -0.05\times10^5,$$
$$\delta m_0/m_0 = -0.01,$$
$$r = (1-0.01)/(1+\sqrt{2}) = 0.411,$$
$$m_0 = 0.396\times10^5$$

Therefore, the values of $\varepsilon_2/2$ and logK_2 obtained by the maximum-slope method would be -0.06×10^5 and 4.886 (*cf.* Table 1).

The maximum-slope method can derive correct values of $\varepsilon_2/2$ and logK_2 for the dimerization of logK_2=4 and 3, because the values of ε_1 and the maximum slope can be determined accurately. On the other hand, Curve (4) (logK_2=2) in Fig. 1 shows that the amount of the aggregate is not sufficient to determine the accurate maximum slope. If the slope at log$C_0=-3.5$, which is eight-tenths of the maximum value, is taken as the maximum slope, we obtain:

$$\delta m_0/m_0 = -0.20.$$

Consequently, $r=(1-0.20)/(1+\sqrt{2})=0.331$. The absorptivity of the monomer (ε_1) can be determined precisely by means of curve (4); that is:

$$\delta\varepsilon_1=0.$$

By substituting the numerical values for these quantities in Eqs. (3) and (4), the deviations of the values of $\varepsilon_2/2$ and logK_2 were found to be 0.2×10^5 and 0.213 respectively. Therefore, the values of $\varepsilon_2/2$ and logK_2 obtained by the maximum-slope method are 0.2×10^5 and 2.21 respectively. These

No.	Values obtained by: The maximum slope method				Zanker's method			
	$\varepsilon_1\times10^{-5}$	$\bar{\varepsilon}_2\times10^{-5}$	log K_2	n	$\varepsilon_1\times10^{-5}$	$\bar{\varepsilon}_2\times10^{-5}$	log K_2	n
1	0.95	−0.06	4.81	2	0.95	0	4.92	2
2	1.0	0.0	4.00	2	analysis is impossible			
3	1.0	0.0	3.00	2				
4	1.0	0.20	2.18	2				

Table 2. Aggregation parameters of rhodamine 6G in aqueous solution

Method	Without KCl				With KCl			
	n	$\varepsilon_1\times10^{-4}$	$\varepsilon_2\times10^{-4}$	$\log K_2$	n	$\varepsilon_1\times10^{-4}$	$\varepsilon_2\times10^{-4}$	$\log K_2$
Max. slope	2	8.50	1.50	3.41	2	8.55	0.67	3.57
Zanker	2	8.50	0.39	3.35	2	8.55	0.0	3.51

values agree well with the values shown in Table 1. Table 1 may suggest that the maximum-slope method can more reasonably be applied, if the maximum slope and either ε_1 or $\varepsilon_2/2$ are determined, than Zanker's method, which is confined within narrower limits of $\log K_2$, because the values of both ε_1 and $\varepsilon_2/2$ should be determined.

2. Aggregation of Rhodamine 6G in an Aqueous Solution. The changes in the spectrum of the solution with the dye concentration were analyzed by both methods. The results are compared in Table 2.

Baranova and Levshin reported that Rhodamine 6G aggregates in the dimerization stage at concentrations below 2×10^{-3} mol/l, but higher aggregates are formed at higher concentrations.[3] The plotting of ε against $\log C_0$ (Fig. 2) also shows that this dye appears to exist in an equilibrium between the monomer and the dimer in the concentration range below $10^{-3.5}$ mol/l, but, since there was some discrepancy between the measured value and the calculated curve ($n=2$) in the concentration range above about $10^{-3.5}$ mol/l, Rhodamine 6G is likely to exist in equilibria between the monomer and higher aggregates ($n\geq3$) in a higher concentration range.

Table 2 also shows no influence of the added potassium chloride (0.2 mol/l) on the aggregation, while Glowacki and his co-workers observed some effect of added salts (>0.24 mol/l) on the aggregation and interpreted the effect on the basis of the structural change in the aqueous solution and the salt effect. Therefore, it seems that the formation of the ion pair does play little part in the aggregation of Rhodamine 6G in a solution which has no added salt.

Figure 3 shows the spectra of the monomer and dimer, computed from those of Rhodamine 6G at different concentrations by means of the least-squares method. The spectrum of the monomer has two absorption bands in the visible region; their maximum wavelengths are 525 and about 490 mμ, while the absorption band of the dimer is at 490 mμ. This hypsochromic shift may be interpreted in terms of the weak coupling theory suggested by DeVoe.[4]

According to the weak coupling theory, the dimer absorptivity of the band M at the wave number σ is expressed by Eq. (5):

$$\varepsilon_M(\sigma) = 2\varepsilon_M^0(\sigma)[1-2(F_{MM}(\sigma)\alpha_M(\sigma)+F_{MN}(\sigma)\alpha_N(\sigma))] \quad (5)$$

where $\varepsilon_M(\sigma)$ and $\varepsilon_M^0(\sigma)$ denote the monomer and dimer absorptivities respectively, where α_M is the partial group polarizability of the band M of the

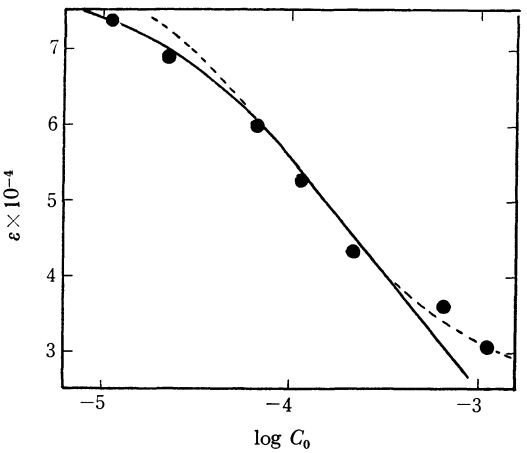

Fig. 2. Apparent absorptivity *vs.* log C_0 of rhodamine 6G in aqueous solution.
● observed
— calculated ($n=2$)
--- calculated ($n=3$)

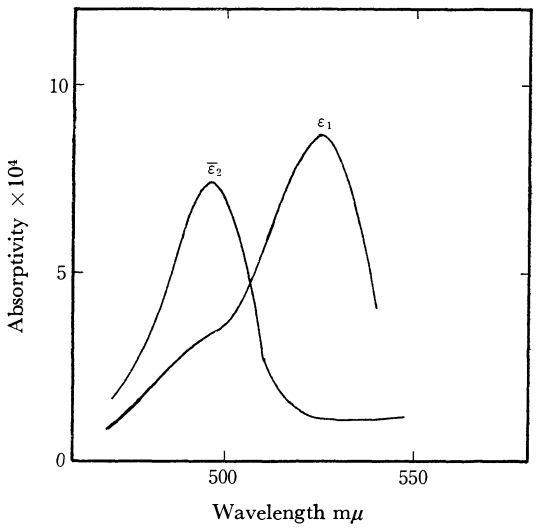

Fig. 3. Calculated absorption spectra of monomer and dimer of Rhodamine 6G in aqueous solution.

3) E. G. Baranova and V. L. Levshin, *Optika i Spektroskopia*, **10**, 182 (1961).

4) H. DeVoe, *J. Chem. Phys.*, **37**, 1534 (1962).

monomer, and where F_{MN} is a group interaction factor between the monomer bands M and N. The value of F_{MN} in (erg D^{-2}) can be calculated by means of Eq. (6):

$$F_{MN} = (10^{-36}/2)\sum_i \sum_{j \neq i} (R_{ij})^{-3} \times [\mathbf{e}_{iM}\mathbf{e}_{jN} - 3(\mathbf{e}_{iM}\cdot\mathbf{e}_{ij})(\mathbf{e}_{jN}\cdot\mathbf{e}_{ij})] \times (\mathbf{e}_{iM}\cdot\mathbf{e}_{jN}) \quad (6)$$

where R_{ij} is the distance (cm) between the molecules i and j, where $\mathbf{e}_{iM}$ and $\mathbf{e}_{jN}$ are the unit vectors of the transition moments, and where $\mathbf{e}_{ij}$ is a unit vector along the line connecting the molecules.

The partial group polarizability of the band M (α_M) is given by:

$$\alpha_M(\sigma) = 0.923 \times 10^{14} \int \frac{\varepsilon_M^0(S)}{S^2 - \sigma^2} dS$$

The value of $\alpha_M(\sigma)$ is positive for wave numbers shorter than σ_0, where a nearly maximum absorption is obtained,[5] and negative for wave numbers larger than σ_0.

If the transition moments of the two monomer bands (A and B) are perpendicular to each other, and if the molecular plane is perpendicular to a common axis,[6] the dimer spectrum may be predicted to be as follows: (1) When neighbouring moments, μ_{1A} and μ_{2A} (μ_{1B} and μ_{2B}), are parallel to each other in the dimer,

$$F_{AA} > 0,\ F_{BB} > 0, \text{ and } F_{AB} = 0;$$

namely, there is self-interaction between the monomer bands, A and B, but no mutual interaction between them.[7] In this case, both monomer bands (A and B) can be predicted to shift hypsochromically and hyperchromically. (2) On the other hand, when the monomer bands, A and B, interact with each other without self-interaction, that is, when $F_{AB} > 0$ and $F_{AA} = F_{BB} = 0$ (this is possible if the neighbouring moments, μ_{1A} and μ_{2A} (μ_{1B} and μ_{2B}), are perpendicular to each other,[8]) the absorptivity of the band with the longer λ_{max} may decrease, while that with the shorter λ_{max} may increase.

Thus, the dimer spectra observed may be understood in terms of the weak coupling mechanism, in which monomer bands interact with one another

TABLE 3. AGGREGATION PARAMETERS OF 3,6-DIAMINOACRIDINE IN AQUEOUS AND ETHANOLIC SOLUTIONS

Solvent	n	$\varepsilon_1 \times 10^{-4}$	$\bar{\varepsilon}n \times 10^{-4}$	$\log K_2$	Δ*	Method
H_2O	2	4.20	2.15	2.95	0.0139	Max. Slope
	3	4.11	2.88	7.04	0.0086	Min. Dev.
	2	4.17	2.60	3.37	—	Zanker
EtOH	2	5.20	0.0	3.52	—	Max. Slope
	2	5.20	0.0	3.74	—	Zanker

* $\Delta = \frac{1}{N}\sum|\varepsilon_{obs} - \varepsilon_{calc}|/\varepsilon_{obs}$

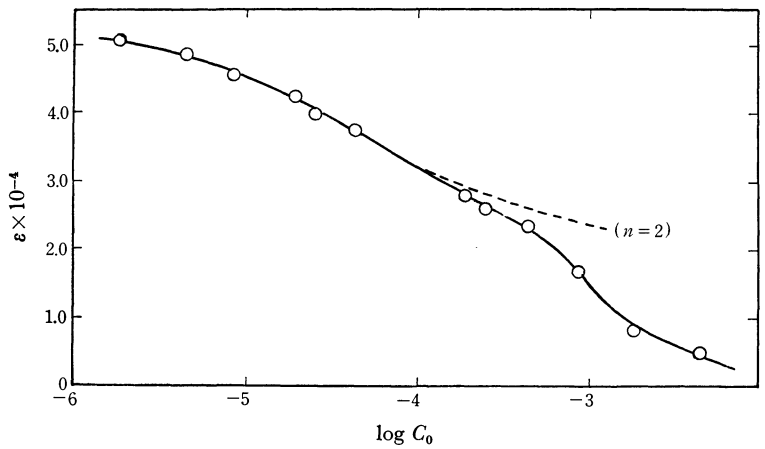

Fig. 4. Apparent absorptivity *vs.* log C_0 of 3,6-diaminoacridine in ethanolic solution.

5) The partial group polarizability is not always zero at the wave number of maximum absorption. When the monomer absorptivity ($\varepsilon_M{}^0(\sigma)$) is symmetrical about the wave number of maximum absorption, the wave number, where α_M is zero, is very near to that of the maximum absorption.

6) The spectra of dimer with another geometry will be discussed elsewhere.

7) Self-interaction means vibronic interaction of monomer band with the other wave number regions of the same band.

8) Therefore, μ_{1A} and μ_{2B} (μ_{1B} and μ_{2A}) are parallel to one another.

with or without self-interaction. However, much more work has to be done in this connection.

3. 3,6-Diaminoacridine in Aqueous and Ethanolic Solutions. Since the change in the spectrum of an aqueous solution of 3,6-diaminoacridine with the increase in the concentration was not very large, reliable results could not be obtained. Assuming that $\varepsilon_n/n=0$, Mataga determined the degree of aggregation and $\log K_n$ as 2 and 3.43 respectively by means of Zanker's method.[9]

The maximum-slope method suggested that the monomer-dimer system agrees better with the experimental data than any other system, as is shown in Table 3. If the aggregation parameters are corrected by the minimum deviation method and have a minimized mean relative deviation,[10] the monomer-trimer system seems to agree better with the experimental data. However, the two mean relative deviations (Δ) calculated by taking $n=2$ and 3 are sufficiently smaller than the experimental error (about 2%). Thus, we were not able to conclude which model was preferable.

Figure 4 shows that 3,6-diaminoacridine aggregates in two steps in an ethanolic solution. In the concentration range below 10^{-4} mol/l, 3,6-diaminoacridine seems to exist in a monomer-dimer equilibrium system, but higher aggregations proceed above 10^{-4} mol/l as:

$$nD_2 \rightleftarrows D_{2n}.$$

A specific value of n was not determined in the experiment because of a lack of sufficient reliable experimental data.

The aggregation parameters obtained by different methods are compared in Table 3.

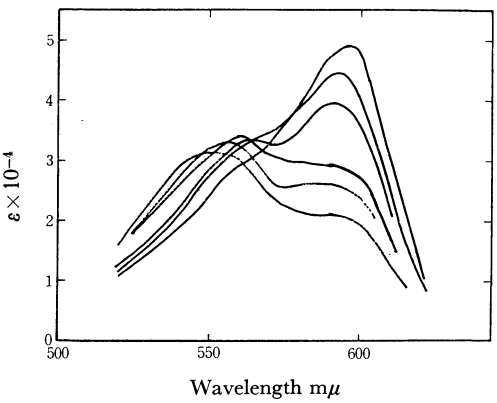

Fig. 5. Spectral change of thionine with increase of concentration.

4. Thionine (T^+Cl^-) in Aqueous Solution. Since no isosbestic point is observed, as is shown in Fig. 5, it seems that there are more than three species of thionine in its aqueous solution. The following species may be considered:

(i) several aggregates with different degrees of aggregation: $(T^+)_n$,
(ii) acid-base reaction products: TH^{2+} or TOH,
(iii) their aggregate(s), and
(iv) the ion pair and its aggregate(s): TCl and $(TCl)_n$.

In order to examine whether or not acid-base reaction products take part in the aggregation of thionine, it is necessary to determine the pK_a and pK_b values of thionine. The apparent absorptivity (ε) of the system of the protonation reaction (Eq. (7)) is given by Eq. (8):

$$T^+ + nH^+ \rightleftarrows (TH_n)^{(n+1)+} \quad (7)$$

$$\varepsilon = (\varepsilon_T[T^+]+\varepsilon_{TH_n}[TH_n])/([T^+]+[TH_n]) \quad (8)$$

By combining Eq. (8) with the law of mass action (Eq. (9)), Eq. (10) is obtained:

$$K = [TH_n]/[T^+][H^+]^n \quad (9)$$

$$\log(\varepsilon-\varepsilon_{TH_n})-\log(\varepsilon_T-\varepsilon) = n\mathrm{pH} + pK_b \quad (10)$$

If the values of both ε_T and ε_{THn} are determined, the slope and the intercept of the straight line made by plotting $\log(\varepsilon-\varepsilon_{THn})/(\varepsilon_T-\varepsilon)$ against the pH give the degree of protonation and the pK_b of thionine.[11] On the other hand, when either ε_{THn} or ε_T cannot be determined, the values of n and pK_b are obtained by a procedure similar to the maximum-slope method, because the maximum slope (m_0) of the tangent of the ε-pH curve is given by Eq. (11):

$$m_0 = \left(\frac{d\varepsilon}{d\mathrm{pH}}\right)_{max} = \frac{n}{4}(\varepsilon_T-\varepsilon_{TH_n}) \quad (11)$$

The n and pK_a values of the hydroxylation reaction can be similarly determined by analyzing the chages in the spectrum of the alkaline solution. The pK_a and pK_b values of thionine, as determined by the method described above, are shown in Table 4.

Table 4. The vlaues of pK_a and pK_b of thionine

Wavelength (mμ)	$\varepsilon_T\times10^{-4}$	$\varepsilon_{TH_n}\times10^{-4}$	n	pK_b
597	4.90	1.56	1	0.72
670	0.0	4.00	1	0.86
		mean	1	0.79
Wavelength (mμ)	$\varepsilon_{T^+}\times10^{-4}$	$\varepsilon_{TOH}\times10^{-4}$	n	pK_a
597	4.90	1.00	1	8.8

9) N. Mataga, This Bulletin, **30**, 375 (1957).

10) Adjustment of the parameters by trial and error method is repeated until the minimum value of deviation is attained and the final values of the aggregation parameters are regarded as the best ones (Ref. 2). But it can be shown that the final values obtained somewhat depend on definition of deviation. This subject will be discussed further elsewhere.

11) In very high acid concentration H_0-function should be used in site of pH.

TABLE 5. AGGREGATION PARAMETERS OF THIONININE IN AQUEOUS SOLUTION

n	$\varepsilon_1 \times 10^{-4}$	$\bar{\varepsilon}_2 \times 10^{-4}$	$\bar{\varepsilon}_3 \times 10^{-4}$	$\log K_2$	$\log K_3$	Δ	Method
2	5.25	0.0	—	2.90	—	0.0237	max. slope
3	5.25	—	1.39	—	6.52	0.0511	max. slope
2+3	5.03	2.38	0.93	2.90	6.52	0.0049	min. dev.

These results indicate that the amounts of TOH and TH^{2+} are negligibly small in the pH range between 1 and 8. Hence, the existence of acid-base reaction products and thir aggregates can be disregarded.

In addition, the ion pair and its aggregate(s), TCl and $(TCl)_n$, can also be neglected because no change was observed in the spectrum upon the addition of potassium chloride in the concentration range between 2×10^{-3} and 2 mol/l. Therefore, the absence of an isosbestic point in the change in the thionine spectrum implies that several aggregates are equilibrated; the aggregation system may, then, be in a multistage equilibrium. Although the maximum-slope method cannot be advantageously employed for the analysis of the system which includes several species with different degrees of aggregation, the change in absorptivity at 597 mμ (wavelength where the maximum absorption of the monomer is observed) was analyzed by this method, assuming that the aggregation system could be approximated by a single equilibrium system. The results (shown in Table 5) indicate that thionine may aggregate in the dimer and the trimer in an aqueous solution.

In order to minimize the mean relative deviation, the molar absorptivities of the monomer and the aggregates and the formation constants of the aggregates were adjusted by the minimum deviation method. These corrected values are also given in Table 5. Thus, thionine seems to aggregate in the monomer-dimer-trimer system. The wavelengths of the maximum absorptions of the spectra of the monomer, the dimer, and the trimer, obtained by means of least-squares calculations, are shown in Table 6. A hypsochromic shift in the spectrum of thionine was observed just as in the case of Rhodamine 6G.

TABLE 6. COMPARISON OF THE WAVELENGTHS OF MAXIMUM ABSORPTION OF THE MONOMER, DIMER AND TRIMER OF THIONINE*

	λ_{max} (mμ)/$\varepsilon_{max} \times 10^{-4}$	
Monomer	595/5.1,	~560/2.9**
Dimer	~590/3.8,**	557/6.6
Trimer	550/3.5	

* By taking $\log K_2 = 2.90$ and $\log K_3 = 6.52$, the spectra were computed by means of the least-squares method.

** shoulder.

Experimental

The prepared dye solutions were left at 25°C until no further spectral changes were observed. This took about 12 hr in the cases of Rhodamine 6G and 3,6-diaminoacridine, but 24 hr for the thionine solution.

Commercial Rhodamine 6G was purified by repeated recrystallizations from water and was then dried at 110°C in a vacuum. Pure 3,6-diaminoacridine was obtained by treating purified proflavine sulfate with aqueous ammonia. The purification of proflavine sulfate was carried out by repeated recrystallizations from an aqueous alcoholic solution. Commercial thionine was also purified by repeated recrystallizations from an aqueous ethanolic solution. The purities of the dyes were confirmed by means of paper chromatography, elementary analysis, and a study of their absorption spectra.

BULLETIN OF THE CHEMICAL SOCIETY OF JAPAN VOL. 43 2297—2306 (1970)

Thermal Decomposition of Lead Carbonate Tablets Prepared by Compressing Fine Particles

Ryozo KOMODA, Yasuhide NISHI and Matsutaro KANO

Faculty of Engineering, Ehime University, Matsuyama, Ehime

and Tatsuya IMOTO

Faculty of Engineering, Osaka City University, Osaka

(Received September 25, 1969)

The thermal decomposition of lead carbonate tablets was kinetically studied in a nitrogen gas stream at temperatures of 240, 320, and 360°C. The tablets used in this work were prepared by compressing lead carbonate particles in a steel mold under pressures of 2—15 ton/cm^2. The decomposition reaction for the tablet was represented in two ways. Rate expressions were developed from the unreacted-core shrinking model applied to the individual particles (for the first of the two decomposition processes) and to the whole tablet (for the second). The effect of the pressure applied in preparing the tablet on the decomposition rate was attributed to the deviation in the pressure profile for carbon dioxide in a tablet (for the first process) or to the variation in the effective diffusivity and bulk density of the tablet (for the second).

Publications have appeared on the non-isothermal decomposition of lead carbonate, reporting the existence of such intermediate phases as $PbO \cdot 2PbCO_3$, $PbO \cdot PbCO_3$, and $2PbO \cdot PbCO_3$ in a carbon dioxide atmosphere at 1 atm.[1-3] In 1964 Crisafe and White[4] examined the thermal decomposition of lead carbonate by equilibrium methods and found the presence of $3PbO \cdot 4PbCO_3$, which is stable under very high P-T conditions. It was recently shown, from isothermal decomposition studies[5,6] in a nitrogen-gas flow or under reduced pressure, that a mass of lead carbonate particles decomposed to form two intermediate phases, $PbO \cdot PbCO_3$ at high partial pressures of carbon dioxide and $2PbO \cdot PbCO_3$ at low partial pressures. One of the basic lead carbonates, $PbO \cdot 2PbCO_3$, is formed only in the decomposition of lead carbonate hydroxide, $2PbCO_3 \cdot Pb(OH)_2$.[7]

Few studies had been published on the rate of the decomposition of lead carbonates; therefore, kinetic studies of the thermal decomposition of these samples were previously made by the present authors,[5-7] showing that the unreacted-core shrinking model provided a good explanation for the decomposition of the samples. The thermal decomposition of a packed mass of lead carbonate particles in a small glass tube[8] was also investigated in a nitrogen-gas stream and was found to be:

$$2PbCO_3(s) \longrightarrow PbO \cdot PbCO_3(s) + CO_2(g) \quad (1)$$

$$PbO \cdot PbCO_3(s) \longrightarrow 2PbO(s, \text{litharge}) + CO_2(g) \quad (2)$$

We will refer to these processes, for convenience, as the first and second processes respectively. It was shown previously that the over-all rate of the decomposition of each process was influenced by the dissociation pressure of the reactant(s)-product(s)-product(g) system, and that it was also influenced to some extent by the carbon dioxide pressure at the gas-solid interface.[8]

In the present study, lead carbonate tablets prepared by compacting lead carbonate particles under different pressures were decomposed isothermally, and a kinetic study of the decomposition of these tablets was made in order to evaluate the effect of the compacting pressure.

Experimental

The disk-shaped tablets used in this work (11.3 mm in diameter, *ca.* 2 mm thick, and *ca.* 1 g in weight) were prepared by compressing lead carbonate particles

1) E. A. Peretti, *J. Amer. Ceram. Soc.*, **40**, 171 (1957).
2) S. St. J. Warne and P. Bayliss, *Amer. Mineralogist*, **47**, 1011 (1962).
3) G. Pannetier, S. Fénistein and G. Djega-Mariadassou, *Bull. Soc. Chim. France*, **1964**, 701 (1964).
4) D. A. Grisafe and W. B. White, *Amer. Mineralogist*, **49**, 1184 (1964).
5) R. Komoda, Y. Nishi and M. Kano, *Nippon Kagaku Zasshi*, **88**, 1038 (1967).
6) R. Komoda, Y. Nishi and M. Kano, *ibid.*, **89**, 478 (1968).
7) R. Komoda, Y. Nishi and M. Kano, *ibid.*, **90**, 30 (1969).
8) R. Komoda, Y. Nishi and M. Kano, *Kogyo Kagaku Zasshi*, **71**, 475 (1968).

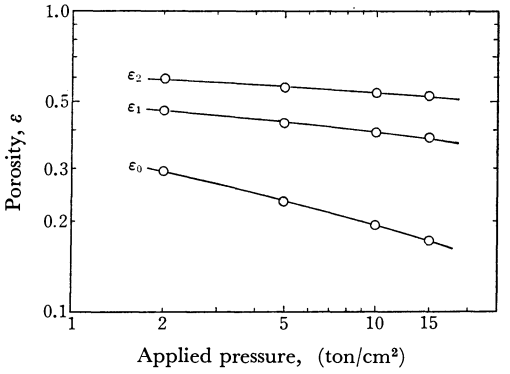

Fig. 1. Correlation between the applied pressure and porosity.

uniformly in a steel mold which consisted of a cylindrical die with two punches, lower and upper. The lead carbonate particles used (3—4 μ in diameter, as determined under an electron microscope) were prepared from cold aqueous solutions of lead acetate and ammonium carbonate, and were then compressed under pressures of 2—15 ton/cm^2 for 5 min by a hydraulic press. The lead carbonate tablets thus prepared were porous and had different porosity values as Fig. 1 shows. The porosity of the tablet was calculated from its bulk density and the theoretical net density of the sample. Some of the porosities of the tablets before decomposition, ε_0, were smaller than 0.2595, the minimum value of the theoretical porosities corresponding to that of the closest packing of equal-sized rigid spheres. This may be attributed to the fact that not all the lead carbonate particles in these tablets were exactly spherical or the same size. No change in the X-ray diffraction pattern was observed between two different lead carbonate samples, compressed and uncompressed. This fact suggests the absence of any appreciable effect of the applied pressure on the crystal structure.

The thermogravimetric apparatus used was an ordinary one consisting of a helical quartz spring and a 38-mm-i.d. $\times$ *ca.* 1-m-long quartz tube whose lower half was enclosed in an electrically-heated furnace. Preheated nitrogen-gas flows of 0.03—0.80 *l*/min were led, at 1 atm, into the vertical quartz tube at the bottom in order to sweep off the product gas or the carbon dioxide gas evolved during the decomposition runs. The tablet was supported on a stainless-steel wire sample-holder and was so suspended in the apparatus that the base of the tablet was parallel to the axis of the vertical tube. The extension of the spring was measured with a cathetometer during the decomposition reaction. The sample was also weighed exactly both before and after the run. The temperature of the sweeping gas was assumed to be close to the sample temperature and was measured with a chromel-alumel thermocouple. The decomposition runs were carried out at the constant temperatures of 240°C (for the first process) and 320 and 360°C (for the second process).

An X-ray diffractometer was also used to identify the decomposition products and to ascertain whether or not a decomposition reaction occurred.

Results and Discussion

Preliminary runs showed that the thermal decomposition of lead carbonate tablets proceeded according to Eqs. (1) and (2); this finding was in agreement with the results of the decomposition studies of the powdered mass packed tightly into a glass tube.[8] In this paper the two processes represented by Eqs. (1) and (2) are designated as the first process and the second process respectively.

For the thermal decomposition of the powdered mass, two simple, idealized models can be considered. One of them is chosen for the case where all the particles in the powdered mass decompose at all times. The other is applicable when only some particles in the outer shell of the powdered mass decompose at first, and then the decomposition zone (in which some particles are decomposing) moves inwards, leaving a completely decomposed solid behind.

In slicing and examining the inside of the partly-decomposed tablets, as will be described below, the thermal decomposition of lead carbonate (the first process) was found to occur at every individual particle within the tablet. Thus, the thermal decomposition study of the first process was made by selecting the former model, or by simultaneously applying the unreacted-core shrinking model to the individual particles within the tablet. However, the second process was found to occur at the particles localized in the outer shell of the tablet. The kinetic study of this process was made by employing the latter model.

A number of decomposition studies of solid materials have been made assuming a profile of a uniform temperature throughout the powdered mass.[8-12] This assumption is acceptable when a small amount of the sample is used and when its rate of decomposition is small, as in the present case. The theoretical expression for the effective thermal conductivity within a powdered mass[13] indicates that the effective thermal conductivity decreases with an increase in the porosity. Consequently, the rate of the heat transfer may be more rapid with the tablet compressed at the pressure of 15 ton/cm^2 than with that compressed at 2 ton/cm^2. On the other hand, experimental runs showed that the over-all rate of decomposition for the former tablet was much slower than that for the latter.

9) T. R. Ingraham and P. Marier, *Can. J. Chem. Eng.*, **41**, 170 (1963).
10) N. A. Warner and T. R. Ingraham, *ibid.*, **40**, 263 (1962).
11) A. W. Coats and N. F. H. Bright, *Can. J. Chem.*, **44**, 1191 (1966).
12) M. Hasatani and S. Sugiyama, *Kagaku Kōgaku*, **30**, 734 (1966).
13) D. Kunii and J. M. Smith, *AIChE J.*, **6**, 71 (1960).

These facts suggest that the step of heat transfer played no appreciable role in determining the rate of the decomposition reaction in our experiment. In addition, the following facts suggest the important role of the carbon dioxide pressure: during the thermal decomposition of the lead carbonate mass in a glass tube, as has been reported previously,[8] no decomposition reaction of the second process occurred at the lateral face of the cylindrical pellet, this face being surrounded by glass through which the product gas (carbon dioxide) could not be removed but through which heat could be transported. Moreover, no decomposition reaction occurred at elevated pressures of carbon dioxide. For these reasons, the temperatures within a tablet were presumed to be uniform throughout the tablet during the decomposition reaction and not practically affect the over-all rate of the decomposition. The temperature profile in each particle was also presumed to be uniform, since the expression for heat-transfer control did not fit the experimental data satisfactorily. In view of the above considerations, only the pressure profile for carbon dioxide was considered in the treatment to be described below.

Nitrogen flow rates in the range studied were found to influence the rate of the decomposition. It is obvious that the partial pressure, P_i, of carbon dioxide at the tablet surface decreases as the rate of nitrogen-gas flow increases. Therefore, the effect of carbon dioxide pressure on the decomposition rate was evaluated in this paper on the basis of the partial pressure, P_i, which was determined by means of equations to be described below.

The rate of the decomposition reaction of the lead carbonate tablet was very small; therefore, in the present work we can assume that the sample temperature is almost equal to that of the gas stream.[14]

No significant reduction in the size of the tablet during decomposition was observed, while L was constant throughout the decomposition run.

The First Process. The thermal decomposition of some solid materials occurs at an interface advancing from the outside of the particle toward the interior. The unreacted-core shrinking model proposed earlier by Yagi and Kunii[15] provides a good representation of this phenomenon. When the over-all rate of the thermal decomposition is virtually independent of the mass-transfer rates of gases through the porous solid layer, as well as across the gas-film surrounding the particle, but is controlled solely by the inherent chemical reactivity of the solid reactant, the following equation for the single particle can be developed from the model:

$$1-(1-F)^{1/3}=kt \tag{3}$$

where k is a constant which is a function of the temperature, the particle size, the specific properties of the reactant, and so on. This expression is also applicable to the powdered mass in applying the model simultaneously to all the individual particles in the powdered mass, whose constituents are practically equal in size and in the same conditions. When the decomposition of each particle in the mass is controlled by the surface phenomenon and only the partial pressure of carbon dioxide outside the particles changes, an expression of the type of Eq. (3) is still useful for the decomposition of the particles.

If the pressure profile for carbon dioxide is uniform throughout the tablet, all the individual particles in the tablet should be under essentially the same conditions. Therefore, the relationship between the conversion of the whole tablet and the decomposition time for the first process should be:

$$1-(1-F_1)^{1/3}=k_1t_1 \tag{4}$$

where the constant, k_1, comprises a decomposition rate constant which is proportional to the difference between the equilibrium partial pressure of carbon dioxide and the partial pressure of carbon dioxide within the tablet; k_1 can then be expressed as follows:

$$k_1=k_1'P_{e1}(1-P/P_{e1}) \tag{5}$$

These two expressions, (4) and (5), are useful for the decomposition study of the lead carbonate tablet with a uniform internal-pressure profile.[8]

When the pressure profile for carbon dioxide within the tablet is not uniform, consider the pressure, P, of carbon dioxide within an arbitrary volume element in the tablet ($\Delta r\cdot r\Delta\theta\cdot\Delta l$ in cylindrical coordinates) and take an average value throughout the whole tablet; then:

$$k_1=k_1'P_{e1}\frac{1}{2R^2\pi L}\int_0^R\int_0^{2\pi}\int_{-L}^{L}(1-P/P_{e1})r\,dr\,d\theta\,dl \tag{6}$$

This expression is simple and is useful for an engineer in developing approximate rate expressions without undue complexities; nevertheless, it is not strictly accurate from the mathematical standpoint.

A partly-decomposed tablet was sliced off and examined by exposing the cross-sectional surface to X-rays. In the tablet compressed at the pressure of 2 ton/cm^2, little difference was detected between the heights of the corresponding peaks of the two X-ray diffraction patterns[4,5] for the particles located in the center and near the surface, each X-ray diffraction pattern showing the existence of only two phases, $PbCO_3$ and $PbO\cdot PbCO_3$. On the contrary, a great difference between the corresponding peak heights was observed in the tablet compacted at the pressure of 15 ton/cm^2. Further experiments were made by roasting the central part of the partly-decomposed tablet and by deter-

14) N. J. Themelis and W. H. Gauvin, *Can. J. Chem. Eng.*, **41**, 1 (1963).

15) S. Yagi and D. Kunii, *Kogyo Kagaku Zasshi*, **56**, 131 (1953); "Proc. 5th Int. Symp. on Combustion," Reinhold, New York (1955), p. 231.

TABLE 1. FRACTIONAL DECOMPOSITIONS FOR THE WHOLE TABLET AND FOR ITS CENTRAL PART

Applied pressure, (ton/cm²)	2	2	5	10	15
Weight of the whole tablet undecomposed, U_u (g)	1057.4	949.4	1075.9	1071.2	1042.2
Weight of the whole tablet decomposed partly, U_p (g)[a]	1016.5	909.0	1033.4	1032.1	1002.9
Time for decomposition, t_1 (min)	16	17	20	21	25
Fractional decomposition for the whole tablet, F_1 (dimensionless)[b]	0.470	0.517	0.480	0.443	0.458
Weight of the sample: the central part of the partly decomposed tablet, U_p' (g)	143.4	123.7	127.9	82.8	134.2
Weight of the sample at the completion of decomposition, U_c (g)[c]	124.6	107.8	110.9	71.3	115.5
Fractional decomposition for the central part of the partly decomposed tablet, F_1' (dimensionless)[d]	0.470	0.504	0.445	0.364	0.358
Ratio of F_1' to F_1 at about $F_1=0.5$, F_1'/F_1 (dimensionless)	1.000	0.975	0.928	0.821	0.781

a) The decomposition runs were carried out at the temperature of 240°C in the nitrogen-gas flow of 0.40 *l*/min.

b) $F_1 = 2\times\left(\frac{U_u-U_p}{44.01}\right)\Big/\left(\frac{U_u}{267.2}\right)$

c) The samples were decomposed at 400°C in the nitrogen-gas stream for 70 min.

d) $F_1' = 2\times\left\{1-\left(\frac{U_p'-U_c}{44.01}\right)\Big/\left(\frac{U_c}{223.2}\right)\right\}$

mining its fractional decomposition. The results obtained from these experiments (see Table 1) as well as the observation of the X-ray diffraction patterns showed that the difference between the degrees of decomposition of particles at the two locations became greater with an increase in the compacting pressure (*viz.*, with a decrease in the porosity of the tablet). This fact suggests that the carbon dioxide pressure profile within a tablet becomes less uniform with a decrease in the porosity of the tablet.

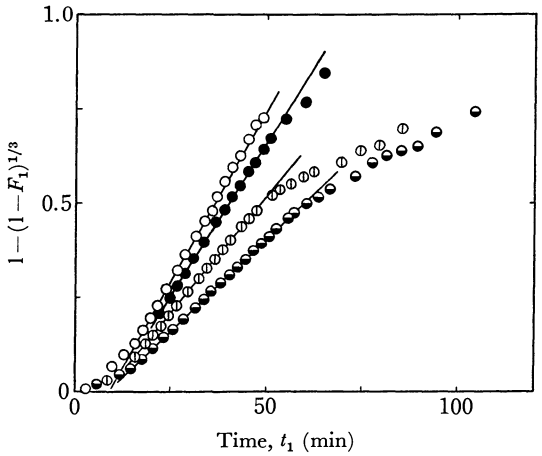

Fig. 2. Plots of $1-(1-F_1)^{1/3}$ *vs.* decomposition time for the first process at 240°C.
○: P=2 ton/cm², $G\times10^4$=2.09 g/(cm²)(sec)
●: P=2 ton/cm², $G\times10^4$=0.74 g/(cm²)(sec)
ⓘ: P=15 ton/cm², $G\times10^4$=4.01 g/(cm²)(sec)
◒: P=15 ton/cm², $G\times10^4$=2.51 g/(cm²)(sec)

Figure 2 shows some typical results obtained from the two series of experiments for the tablets prepared under two different compacting pressures. Similar plots, illustrated in Fig. 2, were obtained in the other runs, and in all cases, good, straight lines were obtained. It is evident from the linearity of the relationship in Fig. 2 that the approximate expression of Eq. (4) is applicable to the major period of the decomposition run. The slight deviations of the experimental plots from the linearity in the beginning of the decomposition reaction may be attributed to the formation and the growth of the nuclei of $PbO\cdot PbCO_3$; this initial period is usually termed an induction period. Deviations of the plots were also observed at the end of the decomposition of the tablets compressed at higher pressures, partially because of a lack of mathematical accuracy in deriving Eqs. (4) and (6). However, for the sake of simplicity, the approximate expressions of Eqs. (4) and (6) were used successfully in this work by being applied only to the experimental data in the major period.

It is now necessary to determine the partial pressure, P_i, of carbon dioxide at the external surface of the tablet. The values of P_i under the different experimental conditions were determined by calculating the following equations concerning a dimensionless factor of j_d:[16]

$$j_d = \alpha\left(\frac{\sqrt{a_p}\cdot G}{\mu}\right)^{-\beta} \qquad (7)$$

in which:

16) K. H. Yang and O. A. Hougen, *Chem. Eng. Prog.*, **46**, 146 (1950).

$$N_{Re} = \sqrt{a_p}\cdot G/\mu > 620;\ \alpha=1.25,\ \beta=0.41$$

$$N_{Re} < 620;\ \alpha=2.44,\ \beta=0.51$$

$$j_d = \left(\frac{k_f\cdot M_m\cdot P_f}{G}\right)\left(\frac{\mu}{\rho_N\cdot D}\right)^{2/3} \quad (8)$$

The rate of mass transfer in a boundary film, N', which is presumed to be equal to the apparent rate of the thermal decomposition, can be expressed as:

$$N' = k_f\cdot a_m(P_i - P_g) = r_a \quad (9)$$

Equations (7), (8), and (9) are combined to give an appropriate expression for the partial pressure:

$$P_i - P_g = \frac{1}{\alpha}\left(\frac{r_a\cdot\sqrt{a_p}\cdot M_m\cdot P_f}{\mu\cdot a_m}\right)\left(\frac{\mu}{\rho_N\cdot D}\right)^{2/3}\left(\frac{\sqrt{a_p}\cdot G}{\mu}\right)^{\beta-1} \quad (10)$$

The specific values of M_m, G, μ, and ρ_N in this equation are represented by those of nitrogen-gas at the temperature of 240°C, since the partial pressure of carbon dioxide in the bulk-gas phase was so low as to be negligible compared with that of nitrogen. The partial pressure of carbon dioxide in the main stream, P_g, was successfully regarded as zero. Let the film pressure factor, P_f, be equal to 1 atm because of the small value of P_i compared with the partial pressure of nitrogen at the solid-gas interface. The binary molecular diffusivity of interest was predicted by means of the appropriate method.[17] In this procedure, an empirical value of D, estimated at 0.6050 cm²/sec at 600°K by Walker and Westenberg,[18] was also used for the prediction. The overall rate, r_a, was empirically determined at the major period corresponding to F_1 of 0.4—0.7. The value of P_i in each run was then obtained by the substitution of the appropriate properties and empirically-determined variables into Eq. (10).

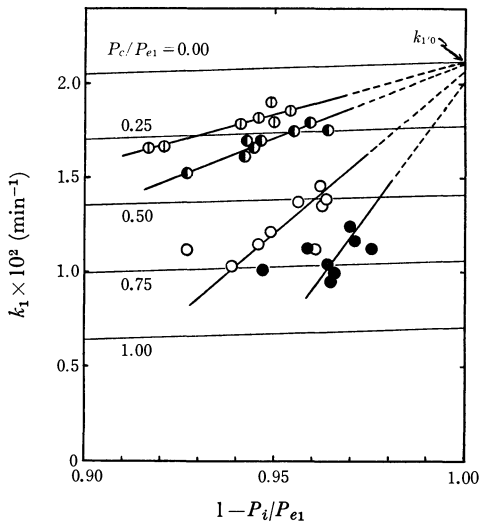

Fig. 3. Correlation between k_1 and $(1-P_i/P_{e1})$ for the first process at 240°C.
◯: P=2 ton/cm²: ◐: P=5 ton/cm²
○: P=10 ton/cm²: ●: P=15 ton/cm²

Figure 3 shows the relationship between k_1, the slope of each line illustrated in Fig. 2, and $(1-P_i/P_{e1})$, the dimensionless pressure term at the solid-gas interface as evaluated from the empirically-determined value of P_i. In estimating the $(1-P_i/P_{e1})$ quantity, the dissociation pressure of lead carbonate was determined from the experimental data by Peretti.[1] Good, straight lines were obtained in the two series of decomposition runs carried out with the tablets compacted at the pressures of 2 and 5 ton/cm². However, the empirical plots obtained from the tablets compacted at the pressures of 10 and 15 ton/cm² were scattered to some extent. This may be attributed to the large deviations of the tablet porosities. Figure 3 also shows that the rate of the decomposition, which was represented by k_1, apparently increased with the $(1-P_i/P_{e1})$ term, the function of the partial pressure at the solid-gas interface. Furthermore, it is shown that the pressure term $(1-P_i/P_{e1})$ apparently had a more significant effect on the rate of the decomposition when the compacting pressure was high (*viz.*, the porosity of the tablet was small).

It is obvious that the mean value of $(1-P/P_{e1})$, averaged through the whole tablet, necessarily exerts an influence upon the overall rate of decomposition. Since it comprises the decomposition rate constant, the k_1 constant should be affected by the averaged term of $(1-P/P_{e1})$, as is to be expected from Eq. (6). Therefore, the empirical value of k_1 gives useful information about the pressure profile within a tablet.

The dimensionless-pressure profile for carbon di-

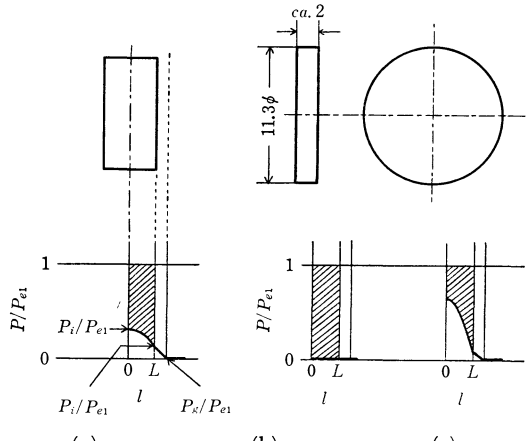

Fig. 4. Sketch of the tablet and pressure profiles for carbon dioxide.

17) E. N. Fuller, P. D. Schettler and J. C. Giddings, *Ind. Eng. Chem.*, **58**(5), 19 (1966).
18) R. E. Walker and A. A. Westenberg, *J. Chem. Phys.*, **29**, 1139 (1958).

oxide in the l-direction (the axial direction of the tablet) for the first process may be shown analogously as Profile (a) in Fig. 4, since the local pressure of carbon dioxide may be higher at the center than at the surface. It can reasonably be considered that, in estimating the rate of the decomposition of the lead carbonate tablet, the transfer of carbon dioxide in the l-direction is more important than in the r-direction (the radial direction of the tablet) because of the very small length-to-diameter ratio (L/R) of the tablet used in this work. These considerations and the symmetrical pressure distribution in the θ coordinate lead to the conclusion that Eq. (6) can be rewritten as a function of only one coordinate direction. Hence:

$$k_1 = \frac{k_1' \cdot P_{e1}}{2L}\int_{-L}^{L}(1-P/P_{e1})\mathrm{d}l \qquad (11)$$

In Fig. 3 the straight line for the tablets compacted at the pressure of 2 ton/cm^2 is extrapolated to the point $(1-P_i/P_{e1})=1$; thereby, $k_{1,0}$ is estimated at 2.12×10^{-2} min^{-1}. This constant, $k_{1,0}$, is assumed to be identical with the k_1 at $P=0$ in Eq. (11), which corresponds to that of the carbon dioxide-pressure profile (b) in Fig. 4. This assumption is reasonable because there was little difference, as has already been mentioned, between the local pressures of carbon dioxide with the tablet compressed at the pressure of 2 ton/cm^2 and because the partial pressure of carbon dioxide at the center of this tablet is, thereby, negligibly low when the partial pressure at the surface approaches zero. The integration of Eq. (11) at $P=0$ and the application of this assumption give the following equation:

$$k_{1,0} = k_1' \cdot P_{e1} \qquad (12)$$

The ratio of k_1 to $k_{1,0}$ can then be expressed as follows:

$$\frac{k_1}{k_{1,0}} = \frac{1}{L}\int_{0}^{L}(1-P/P_{e1})\mathrm{d}l \qquad (13)$$

in which the integral from zero to L with respect to l is satisfactorily used because of the symmetrical pressure profile. The integral term in Eq. (13) gives the shaded area illustrated in Profile (a) in Fig. 4 as a typical example, while the denominator, L, which is given by the integration from zero to L of the $(1-P/P_{e1})=1$ quantity, shows the area of the rectangle indicated as Profile (b) in Fig. 4. Therefore, the expression of Eq. (13) indicates that the ratio of k_1 to $k_{1,0}$ is equal to the ratio of one area to the other, each area corresponding to the overall pressure-driving force to decomposition.

It was impossible to determine the real pressure profile within a tablet because of the experimental difficulties. However, it is obvious that the partial pressure, P, of carbon dioxide at an arbitrary situation, l, varies with l; this is expressed as a continuous function of l $(-L\leqq l\leqq L)$. On introducing a dimensionless coordinate, $z=l/L$, the pressure profile within a tablet is given as $P(z)$. Noting that $P(z)=P(-z)$, the expression for $P(z)$ at $0\leqq|z|\leqq1$ can be represented by a "power series" of the type:

$$P(z) = a_0 + a_2z^2 + a_4z^4 + \cdots + a_{2n}z^{2n} + \cdots \qquad (14)$$

where:

$$\frac{a_{2n}}{a_{2n+2}z^2} > \frac{P_c}{P_c-P_i} > 1$$

for all n's greater than or equal to m.

The absolute value of the nth term in this infinite series approaches zero as $n\to\infty$. The terms with a large n value are, then, negligibly small and the approximate expression for $P(z)$ can be written with the first several terms in Eq. (14). Many of the terms should be employed for the very close approximation to $P(z)$, especially when $|z|$ approaches unity, while the value of $P(z)$ at $z=1$ is determined from the experimental data. However, in the absence of full information about the profile, the approximate expression for $P(z)$ was assumed to be given by the first two terms on the right-hand side of Eq. (14); in addition, the integral term in Eq. (13) was also assumed to give the following area in place of the real area corresponding to the overall pressure-driving force: the area being surrounded by a curved line (defined by Eq. (15)) and three straight lines ($z=l/L=0$, $z=1$, and $P/P_{e1}=1$). On the basis of these assumptions, the pressure profile in a tablet can be outlined without deviating too greatly from reality.

From the above considerations, the approximate expression presumed for the pressure profile at $0\leqq|z|\leqq1$ is:

$$P(z) = a_0 + a_2z^2 \qquad (15)$$

The boundary conditions employed are:

$$\left.\frac{\mathrm{d}P}{\mathrm{d}z}\right|_{z=0} = 0$$

$$P(0) = P_c$$

$$P(1) = P(-1) = P_i$$

The solution to Eq. (15) with these conditions is:

$$P(z) = P_c + (P_i-P_c)z^2 \qquad (16)$$

so that Eq. (13) becomes:

$$\frac{k_1}{k_{1,0}} = \frac{(1-P_i/P_{e1}) + 2(1-P_c/P_{e1})}{3} \qquad (17)$$

Since the value of $(1-P_i/P_{e1})$ in each run had already been calculated from Eq. (10), the value of $(1-P_c/P_{e1})$ in each run could be determined from the approximate expression of Eq. (17). The results for the dimensionless pressure, P_c/P_{e1}, as well as the experimental values of $k_1/k_{1,0}$ at $(1-P_i/P_{e1})=0.97$, are illustrated in Fig. 5 against the porosity, ε_1.

It is shown in Fig. 5 that the partial pressure of carbon dioxide at the center of the tablet rises with a decrease in the porosity, as was suggested earlier by the diffractmetrical and the thermogravimetrical analyses, in spite of these being the same pressure at the solid-gas interface (*viz.*, $P_i/P_{e1}=0.03$).

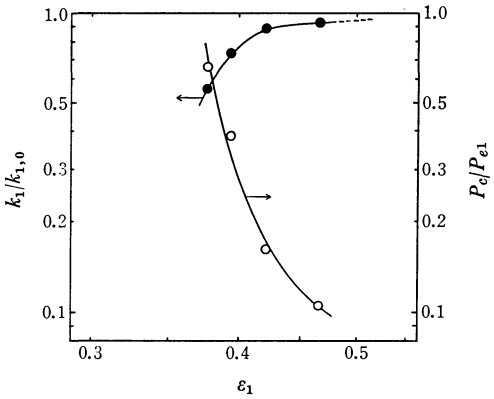

Fig. 5. Effect of porosity ε_1 on dimensionless ratios, $k_1/k_{1,0}$ (●) and P_c/P_{e1} (○).

Equation (17) with a given parameter of P_c/P_{e1} is, then, plotted in Fig. 3. The series of lines thus obtained shows how high the P_c/P_{e1} ratio was in each run. It is apparent from Fig. 3 that the carbon dioxide pressure at the center becomes higher, on the whole, with an increase in the compacting pressure; therefore, the pressure profile for carbon dioxide during the decomposition reaction is less uniform for the tablets of a lesser porosity.

The empirical plots of k_1 against $(1-P_i/P_{e1})$ for the tablets compacted at the pressure of 15 ton/cm^2 (*cf.* Fig. 3) show that the averaged value of P_c/P_{e1} can be estimated to be approximately 0.7. This fact shows that the carbon dioxide-pressure profile of this tablet might be represented analogously as Profile (c) in Fig. 4. No attempt has been made to demonstrate this simplified pressure profile, whereas these considerations are supported by the fact that the plots of $1-(1-F_1)^{1/3}$ against t_1, which give a straight line in the case of a uniform pressure profile, deviated to some extent with the tablets compacted at higher pressures. It was also considered that the simple expressions of Eqs. (4) and (11) were useful for the first process of the thermal decomposition of only the lead carbonate tablets with a greater porosity. However, these expressions proved applicable also to tablets compressed at the pressure of 15 ton/cm^2.

The Second Process. The thermal decomposition study of a mass of basic lead carbonate ($PbO \cdot PbCO_3$) particles[5] showed that the decomposition reaction of the materials occurred only at low partial pressures of carbon dioxide, and the rate of the decomposition for every single particle was found, at small nitrogen-flow rates, to be controlled by the step of the mass transfer of carbon dioxide through the atmosphere within the mass of particles. It was, then, reasonably considered that the decomposition rate of a tightly-compacted mass of the basic lead carbonate particles was controlled by the diffusional step through the powdered mass. Visual observation and the X-ray diffraction data showed that the decomposition product, PbO (litharge), formed a shell of a reddish brown color sharply separated from the grey-colored reactant, $PbO \cdot PbCO_3$, inside the shell, and that the decomposition front advanced from the outside of the lump, or of the whole tablet, to the interior. Hence, the diffusional step through the product layer (the porosity of which is given as ε_2) proves to have a significant connection with the rate of the decomposition. When the decomposition of one particle is subject to the gas-film-diffusion controlling step, the specific rate of the decomposition of this particle is constant at any given time during the decomposition run, irrespective of the size of the undecomposed-core in the particle. It can, then, be concluded that all the rates of decomposition for the particles of any conversion under the same conditions are equal during the decomposition. Therefore, the thermal decomposition of the whole tablet was reasonably considered, from a macroscopic point of view, to occur at the interface between decomposed and undecomposed materials. It is also reasonable to suppose that the decomposition interface moved inward only in the direction normal to the base of the tablet since the decomposition front, curved slightly like a lens, was taken to be almost parallel to the base of a tablet because of its small height-to-diameter ratio. Therefore, only the l component of the mass transport will be considered in this paper.

The moler flux with respect to a stationary coordinate, N_p in g-mol/(cm^2)(sec), of carbon dioxide diffusing through the porous layer of the decomposition product is expressed by the following expression, which is called Fick's first law of diffusion:

$$N_p = y_p(N_p + N_N) - c\bar{D}_e(\mathrm{d}y_p/\mathrm{d}l) \qquad (18)$$

There may be a net motion of carbon dioxide away from the decomposition interface during the decomposition run, and nitrogen-gas is stationary in a pseudo-steady-state condition; these things were assumed successfully by previous workers[19-21] and were also applicable to the present study. The molar flux of nitrogen was, thereby, taken to be zero. Then, by substituting $N_N=0$ in Eq. (18) and solving for N_p, we obtain:

$$N_p = -\frac{c\bar{D}_e}{1-y_p}\cdot\frac{\mathrm{d}y_p}{\mathrm{d}l} \qquad (19)$$

With the pseudo-steady-state approximation valid for the solid-gas system, the rate of the decomposition at any instant is, in the present case, given by the rate of diffusion of the product gas away from the decomposition interface through the product layer; therefore:

19) O. Levenspiel, "Chemical Reaction Engineering," John Wiley, New York (1962), p. 346.
20) K. B. Bischoff, *Chem. Eng. Sci.*, **18**, 711 (1963).
21) C. Y. Wen, *Ind. Eng. Chem.*, **60**(**9**), 34 (1968).

$$-\frac{dW_r}{dt}=\frac{dW_p}{dt}=2SN_p=\text{constant} \quad (20)$$

The amount of the reactant present in a tablet is expressed as the product of the molar bulk density and the volume of the undecomposed mass. The disappearance of a small amount of the solid reactant is accompanied by the decrease in its volume; thus:

$$-dW_r=dW_p=-2S\rho_a dl \quad (21)$$

Noting that the decomposition interface was taken to advance only in the l-direction, the fractional conversion for the second process can be written as follows:

$$F_2=\frac{L-l}{L} \quad (22)$$

By substituting Eqs. (19) and (21) into Eq. (20), solving with the pseudo steady-state approximation, and using the appropriate expression for F_2 we obtain the conversion-time expression for the second process of the decomposition of the tablet, or:

$$(F_2)^2=k_2t_2 \quad (23)$$

where:

$$k_2=\frac{2\bar{D}_eP_{e2}P_t}{RT\rho_aL^2(P_N)_{ln}}(1-P_i/P_{e2}) \quad (24)$$

The $(P_N)_{ln}$ term in this expression is the logarithmic mean of the partial pressures of nitrogen-gas at the solid-gas interface and at the decomposition interface, defined by the following equation:

$$(P_N)_{ln}=\frac{P_{N,t}-P_{N,l}}{\ln(P_{N,i}/P_{N,l})}=\frac{(1-P_t)-(1-P_{e2})}{\ln\dfrac{1-P_i}{1-P_{e2}}} \quad (25)$$

in which the subscripts i and l refer to the solid-gas interface and the decomposition interface respectively.

Some typical correlations between $(F_2)^2$ and t_2 for the decomposition of a lead carbonate tablet are shown in Fig. 6. These plots, as well as the similar plots from the other runs, indicate that the experimental data gave a linear relationship in almost all regions of the decomposition run, showing that Eq. (23) is valid under the present experimental conditions and can be used for the second process of the decomposition of a lead carbonate tablet. Each slope of the straight lines in Fig. 6 gives the experimental value of k_2.

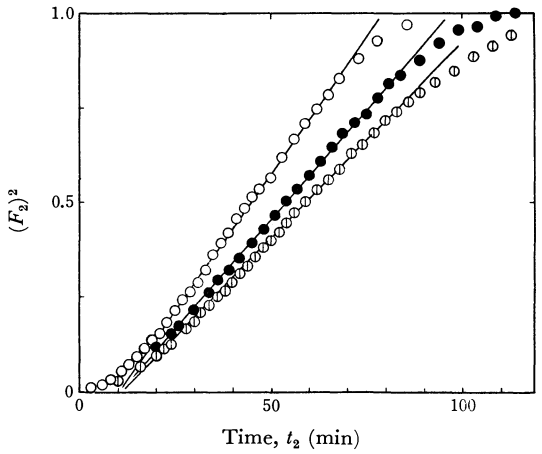

Fig. 6. Plots of $(F_2)^2$ *vs.* decomposition time for the second process at 320°C.
applied pressure P=5 ton/cm²;
○: $G\times10^4$=7.71 g/(cm²)(sec)
●: $G\times10^4$=2.67 g/(cm²)(sec)
ⓘ: G=10^4=2.01 g/(cm²)(sec)

It is now necessary to examine the effect of the compacting pressure on the decomposition rate. All the variables in Eq. (24), except for $\bar{D}_e$ and ρ_a, are naturally independent of the compacting pressure. Some variables, such as L, $(P_N)_{ln}$, and P_i, are expected to have different values varying in every run, while the rest of the variables give constant values in a series of runs carried out with tablets of the same compacting pressure. All the numerical values of $(P_N)_{ln}$ were, however, found to be almost equal in every run with the tablets of the same

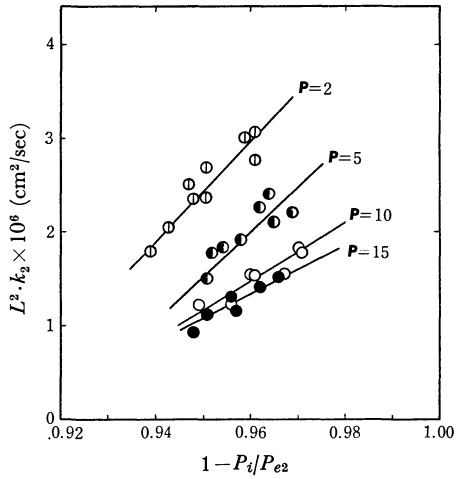

Fig. 7. Correlation between $L^2\cdot k_2$ and $(1-P_i/P_{e2})$ for the second process at 320°C.

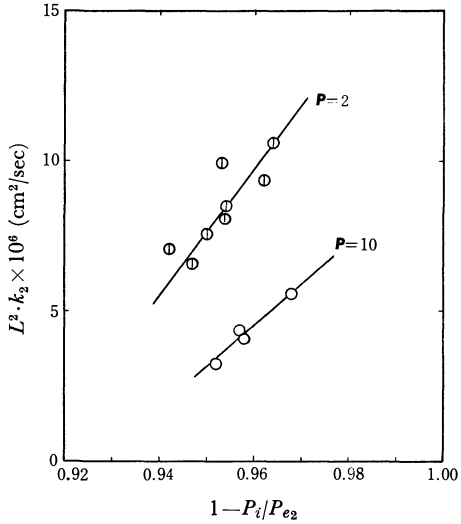

Fig. 8. Correlation between $L^2\cdot k_2$ and $(1-P_i/P_{e2})$ for the second process at 360°C.

compacting pressure (an error to within 0.2%). Consequently, a constant value of $(P_N)_{ln}$ was used for each series of runs. The plots of $L^2 \cdot k_2$ against $(1-P_i/P_{e2})$ are, then, illustrated in Fig. 7, where each experimental value of P_i was obtained from the calculation of Eq. (10). Figure 8 also shows the experimental correlation between the $L^2 \cdot k_2$ and $(1-P_i/P_{e2})$ values obtained from the other two series of experimental runs done at 360°C. Each value of the slopes in Figs. 7 and 8 was incorporated into Eq. (24); the subsequent substitution of appropriate values in the equation gave the numerical values of the mean effective diffusivity, which were subject to the influence of the compacting pressure used in the preparation of the tablet. These values of $\bar{D}_e$ are plotted against ε_2 in Fig. 9. It is apparent from Fig. 9 that the decrease in ε_2 (attributed to the increase in applied pressure) corresponds to the decrease in $\bar{D}_e$.

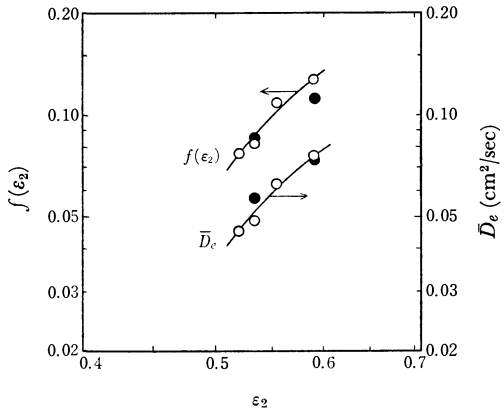

Fig. 9. Effect of Porosity ε_2 on $\bar{D}_e$ and $f(\varepsilon_2)$ at 320°C (○) and 360°C (●).

It can reasonably be concluded, on the basis of the previous considerations, that the effect of the applied pressure on the decomposition rate is reduced to that on the term $\bar{D}_e/\rho_a$ in Eq. (24). The values of $\bar{D}_e/\rho_a$ calculated from the slopes in Figs. 7 and 8 were not identical; this indicates that $\bar{D}_e$ and ρ_a were affected to different degrees by the applied pressure. Many investigations have been made of the correlation between the applied pressure and the bulk density or porosity of the powdered mass compacted. These investigations are summarized comprehensively in several papers.[22,23]

An expression between the applied pressure and the porosity, ε_0, applicable to the present work was as follows:

$$-\frac{d\varepsilon_0}{dP} = C(1-\varepsilon_0)P^{-0.9} \quad (26)$$

This expression is Nutting's Equation as modified by Kawakita and Tsutsumi.[22] The exponent, -0.9, was derived from the text.[24] Equation (26) can be easily integrated, or:

$$\ln(1-\varepsilon_0) = C_1 \cdot P^{0.1} + C_2 \quad (27)$$

The relationship between P and ρ_a can be analogously derived from Eq. (26) by noting that:

$$\varepsilon_0 = 1 - \rho_a/\rho_r \quad (28)$$

thus:

$$\ln \rho_a = C_3 \cdot P^{0.1} + C_4 \quad (29)$$

The good fits of Eqs. (27) and (29) are illustrated in Fig. 10.

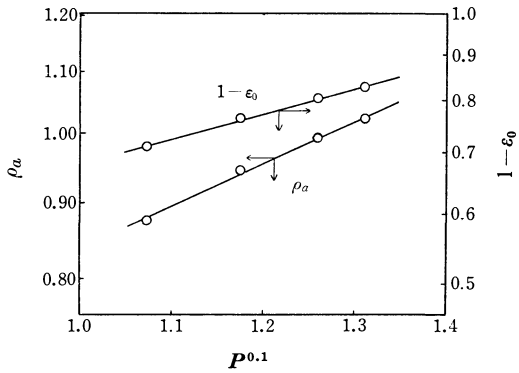

Fig. 10. Plots of log ρ_a and log $(1-\varepsilon_0)$ against $P^{0.1}$.

The mean effective diffusivity, $\bar{D}_e$, on the other hand, is a function of several variables, such as ε_2, the molecular diffusivity, the Knudsen diffusivity, and the surface diffusivity, among which ε_2 is influenced by the applied pressure, as is shown in Fig. 1. A useful study of the surface diffusion in a porous solid was made by Sakashita, Arai, and Kobayashi,[25] who concluded that the amount of carbon dioxide transported by the surface diffusion increases as the pressure of carbon dioxide rises. They also reported that, for the diffusion of carbon dioxide through a sintered mass of glass beads (ε= 0.40), the ratio of the surface diffusivity to the total effective diffusivity could be estimated to be 0.11 for CO_2–H_2 system at 1 atm. It may be analogously considered in the present case that the surface diffusion through a porous layer is almost negligible in comparison with the molecular diffusion because of the very low pressures of carbon dioxide. The empirically-determined value of $\bar{D}_e$ in the present work might include some errors due to some assumptions and errors included in Eqs. (10) or (20). For this reason and because of a lack of information about the Knudsen and surface diffusions, no explicit expression for $\bar{D}_e$ could be proposed. However, the large porosity (ε_2) values of the samples suggest that the diffusion of carbon dioxide through the product layer is predominantly

22) K. Kawakita and Y. Tsutsumi, This Bulletin, **39**, 1364 (1966).

23) R. W. Heckel, *Trans. AIME Met.*, **221**, 1001 (1961).

24) B. S. Neumann, "Flow Properties of Disperse Systems," North-Holland Publ. Co., Amsterdam (1953), p. 397.

25) K. Sakashita, F. Arai and H. Kobayashi, *Kagaku Kogaku*, **31**, 921 (1967).

influenced by the molecular-diffusional step within a macropore produced after the decomposition reaction. The plots of $f(\varepsilon_2)$ against ε_2 are shown in Fig. 9, where $f(\varepsilon_2)$, a function of ε_2, was determined from the conventional expression for the effective diffusivity, or:

$$\bar{D}_e = f(\varepsilon_2) \cdot D \qquad (30)$$

The numerical values of $f(\varepsilon_2)$ are in good agreement with the data on some other porous materials of the same porosity.[25,26]

Further information about $f(\varepsilon_2)$ or $\bar{D}_e$ should be derived from another appropriate experiment for $\bar{D}_e$. However, the approximate value of $\bar{D}_e$, varying with ε_2, was proved in the present work to be useful as a criterion by which the influence of the compacting pressure on the decomposition rate could be investigated.

Conclusions

Experiments on the rate of the thermal decomposition of a lead carbonate tablet have shown that it is possible to make kinetic studies taking into account the partial pressure distribution of carbon dioxide only in the axial direction of the tablet. It has been shown that the rate of the decomposition of the whole tablet for the first process is represented by two approximate equations, (4) and (11), which were derived from the unreacted-core shrinking model applied to the individual particles in a tablet. Consequently, the effect of the applied pressure on the decomposition rate was evaluated from the integral term in Eq. (11). The partial pressure of carbon dioxide at any location within a tablet, but outside the fine particles, was influenced by the pressure used in compressing lead carbonate particles into a tablet.

It has also been shown that the overall rate of the decomposition of the tablet for the second process is controlled by diffusion of carbon dioxide through the product layer. The rate of the decomposition for the second process was, then, expressed by two appropriate equations, (23) and (24), which were developed for the whole tablet without regard to the individual particles. The effective diffusivity and the bulk density of the tablet in Eq. (24) were affected by the applied pressure.

Notation

a, a_2, a_4, $\cdots$, a_{2n}, $\cdots$=coefficient in Eq. (14), atm
a_m=interfacial surface area per unit mass of the tablet undecomposed, cm^2/g
a_p=exterior surface area of the tablet, cm^2
c=total molar concentration in a gaseuous phase, g-mol/cm^3
C, C_1, C_2, C_3, C_4=constants in Eqs. (26), (27), and (29)
D=binary molecular diffusivity for the system CO_2–N_2, cm^2/sec
$\bar{D}_e$=mean effective binary diffusivity of carbon dioxide averaged throughout the product layer, cm^2/sec
F_1, F_2=fractional decomposition, or conversion, for the first and the second process respectively, dimensionless
G=mass velocity of the bulk flow, g/(cm^2)(sec)
j_d=dimensionless factor of mass transfer, see Eqs. (7) and (8)
k=constant in Eq. (3), min^{-1}
k_1, k_2=constants in Eqs. (4) and (23), min^{-1}
$k_{1,0}$=empirical constant of k_1 at P_i=0, min^{-1}
k_1'=proportional constant defined by Eq. (5), min^{-1} atm^{-1}
k_f=gas-film mass transfer coefficient, g-mol/(sec)(cm^2)(atm)
l=axial distance in cylindrical coordinates, cm
L=half of the thickness of a tablet, cm
m=positive integer
M_m=mean molecular weight of the gas stream, g/g-mol
n=positive integer, see Eq. (14)
N=molar flux with respect to a stationary coordinate, g-mol/(cm^2)(sec)
N'=rate of mass transfer in a boundary film, g-mol/(sec)(g)
P=partial pressure of carbon dioxide, atm, see Eq. (5) or (6)
P_e=dissociation pressure of the solid-solid-gas system, atm
P_f=film pressure factor, defined as the logarithmic mean of the partial pressures of the nondiffusing component at the solid-gas interface and in the main stream, atm
P_g, P_i=partial pressures of carbon dioxide in the main stream and at the solid-gas interface, respectively, atm
P_t=total pressure of the system, atm
$(P_N)_{ln}$=logarithmic mean of the partial pressures, atm, see Eq. (25)
$\boldsymbol{P}$=compacting pressure used in the preparation of a tablet, ton/cm^2
r=radial distance in cylindrical coordinates, cm
r_a=over-all rate of the thermal decomposition per unit mass of the tablet undecomposed, g-mol/(sec)(g)
R=radius of a tablet, cm
$\boldsymbol{R}$=gas law constant, =82.06 (cm^3)(atm)/(g-mol)(°K)
S=macroscopic area of the base of a tablet, cm
t_1, t_2=time required for the decomposition for the first and the second process, respectively, min
T=temperature of the system, °K
W_r, W_p=amount of the reactant present in a tablet and that of the product gas, respectively, g-mol
y_p=mole fraction of carbon dioxide in a gaseous phase, dimensionless
z=dimensionless coordinate, $z=l/L$
ε_0=initial porosity of a tablet, dimensionless
ε_1, ε_2=porosities of the tablet at the completion of the first and the second process, dimensionless
θ=angle in cylindrical coordinates, radians
μ=viscosity of the bulk gas phase, g/(cm)(sec)
ρ_a=molar bulk density of the tablet, g-mol/cm^3
ρ_N=density of the bulk gas phase, g/cm^3
ρ_r=theoretical net density of the reactant, g-mol/cm^3

26) J. Hoogschagen, *Ind. Eng. Chem.*, **47**, 906 (1955).

BULLETIN OF THE CHEMICAL SOCIETY OF JAPAN VOL. 43 2307—2312 (1970)

Dielectric Relaxation and Molecular Structure. I. Dielectric Relaxation in Substituted Anilines

K. K. SRIVASTAVA and J. K. VIJ*1

Department of Physics, Panjab University, Chandigarh, India

(Received December 10, 1969)

Measurements of static dielectric constant at 1 Mc, refractive index (for sodium D-line) and complex dielectric constant at 9.44 GHz (X-band) have been made to determine the relaxation times and dipole moments of *N,N'*-dimethylaniline (A), *N,N'*-diethylaniline (B), *o*-chloroaniline (C), *m*-chloroaniline (D) and *p*-chloroaniline (E) in dilute solutions of non-polar solvents. Substances A, B, C and D have been studied in *n*-heptane, benzene decalin and Nujol. The measurements for A and B have also been extended to cyclohexane, whereas E has only been studied in benzene. The values of relaxation time, calculated by Higasi's equations in terms of a_0, a', a'' and a_∞, and those of α, calculated from Cole-Cole's equation in terms of the same parameters, showed an evidence for the existence of more than one relaxation mechanism. This has been interpreted in terms of the intramolecular rotations of the amino (or the substituted amino) group occurring simultaneously with the overall molecular orientation.

A study of dipole moment and dielectric relaxation time has provided an evidence for the existence of internal or intramolecular rotations in several organic molecules.[1-3] The present work extends this study to several substituted anilines. Garg and Smyth[4] have studied liquid aniline and *N,N'*-dimethylaniline. They have analyzed their data with the help of Roberti and Smyth's[5] equation in terms of τ_1 and τ_2 which are 22.0 ps (1 ps$=10^{-12}$ sec) and 0.9 ps for aniline and 28.0 ps and 1.5 ps for dimethylaniline. The values of τ_1 and τ_2 refer to the molecular and intramolecular rotations, respectively. Smyth[6] has postulated that unusually small values of τ_2, obtained for aniline, and a small change in the value of τ_2 from aniline to dimethylaniline, can only be explained by an inversion mechanism for an amino or substituted amino group. In order to confirm his viewpoint, a systematic study of some substituted anilines has been undertaken in various solvents of different viscosity. Chitoku and Higasi[7] have recently studied a few substituted anilines in dilute solutions of benzene and dioxane. They have reported relaxation times in the main dispersion region and have predicted another dispersion region in the mm wave range.

Experimental

Purification of Materials. *Benzene* was purified by the process already described.[8]

n-Heptane (E. Merck quality) was fractionally distilled and the middle fraction was collected. It was then dried over sodium and subsequently distilled (bp 98.0°C).

Cyclohexane (L.R., B.D.H.) was treated like *n*-heptane and the final sample was collected for use (bp 80.0°C).

Decalin (Reidel, Pure grade) was used without purification.

Nujol (B. P. Grade, meant for medicinal purposes) was passed through oil-free sodium wire and was subsequently subjected to vacuum for several hours.

p-Chloroaniline (Fluka A. G., A. R. grade) was used without purification. The following chemicals were imported from Dr. Theodor Schuchardt, West Germany.

N,N'-Dimethylaniline. Analytical reagent, free from monomethylaniline.

N,N'-Diethylaniline. Pure grade.

o-Chloroaniline. Analytical reagent.

m-Chloroaniline. Analytical reagent.

Since the measured values of their physical constants tallied well with literature values, further purification was not deemed necessary.

Table 1 gives a comparative statement of the measured and literature values of physical constants which indicates

*1 Present address: Department of Physics, Punjabi University, Patiala, India.

1) I.d' Or and J. Henrion, *Physik. Z.*, **38**, 426 (1937); E. Fischer and F. C. Frank, *ibid.*, **40**, 345 (1939).

2) K. Higasi and C. P. Smyth, *J. Amer. Chem. Soc.*, **82**, 4759 (1960).

3) W. E. Vaughan and C. P. Smyth, *J. Phys. Chem.*, **65**, 98 (1961).

4) S. K. Garg and C. P. Smyth, unpublished work. (This work has been quoted in the Chemical Society Publication, "Molecular Relaxation Processes) No. 20, (1966), p. 8.

5) K. Bergmann, D. M. Roberti and C. P. Smyth, *J. Phys. Chem.*, **64**, 665 (1960).

6) C. P. Smyth, "Molecular Relaxation Processes," Chemical Society Publication, No. 20 (1966), p. 8.

7) K. Chitoku and K. Higasi, This Bulletin, **39**, 2160 (1966).

8) J. K. Vij and K. K. Srivastava, *Indian J. Pure Appl. Phys.*, **7**, 391 (1969).

Table 1. Measured and literature values of density, viscosity, refractive index (Na-D line) for all the solvents and liquid solutes

Substance	Measured values			Literature values		
	25°C d (g/cc)	25°C η (cp)	25°C n_D	25°C d (g/cc)	25°C η (cp)	25°C n_D
Benzene	0.87369	0.600	1.4979	0.87368[a]	0.599[a]	1.4980[a]
n-Heptane	0.68015	0.408	1.3851	0.67963[a]	0.388[a]	1.3852[a]
Cyclohexane	0.77375	0.878	1.4237	0.77389[a]	0.886[b]	1.4236[a]
Decalin	0.87366	2.208	1.4701	—	—	—
Nujol	0.87698	1.476	1.4800	—	—	—
Dimethylaniline	0.95343	1.378	1.5560	0.95198[a]	1.159[a]/30°C	1.5562[a]/24.6°C
Diethylaniline	0.93008	1.938	1.5392	0.9348[a]/20°C	3.251[a]/11°C	1.54105[a]/22.3°C
o-Chloroaniline	—	—	1.5832/30°C	1.21253[c]/20°C	—	1.5895[c]/20°C
m-Chloroaniline	—	—	1.5895/30°C	1.2225[b]15°C	—	1.5930[c]/20°C

a) J. Timmermans, "Physico-Chemical Constants of Pure Organic Compounds," Elsevier Press, New York (1950).
b) *Ibid*, Vol. 2, 1965.
c) J. R. A. Pollack and R. Stevens,"Dictionary of Organic Chemistry," Vol. 2, The Chancer Press Ltd., Bongay, Suffolk, Great Britain (1965), p. 595.

the extent of their purity. The melting point of *p*-chloroaniline (70°C) agreed well with the literature value (70—71°C).

Apparatus and Theory of Measurements. Dielectric constants and losses have been measured at two frequencies (1 Mc and 9.44 GHz). The measurements at 1 Mc are based on the principle of heterodyne beat method using a dielectrometer.[9] The accuracy in dielectric constant measurements is estimated to be ±0.05%. Refractive index measurements were made by means of an Abbey Refractometer (Hilger) having an accuracy upto the fourth decimal place. Viscosities were measured by means of a Ubbelohde[10] viscometer (accuracy ±0.5%). The final value was computed by applying kinetic energy corrections. Density was measured with an Oswald pycnometer (bulb capacity≈23 cc) having an accuracy of $\pm 5\times10^{-5}$ in 1. The temperature of the thermostatic bath was kept constant by means of a Thermomix within ±0.03°C.

Figure 1 shows the block diagram of the 9.44 GHz apparatus imported from Microwave Instruments, England. The measurement technique is based on the standing wave method, developed by Heston, Franklin and Smyth.[11]

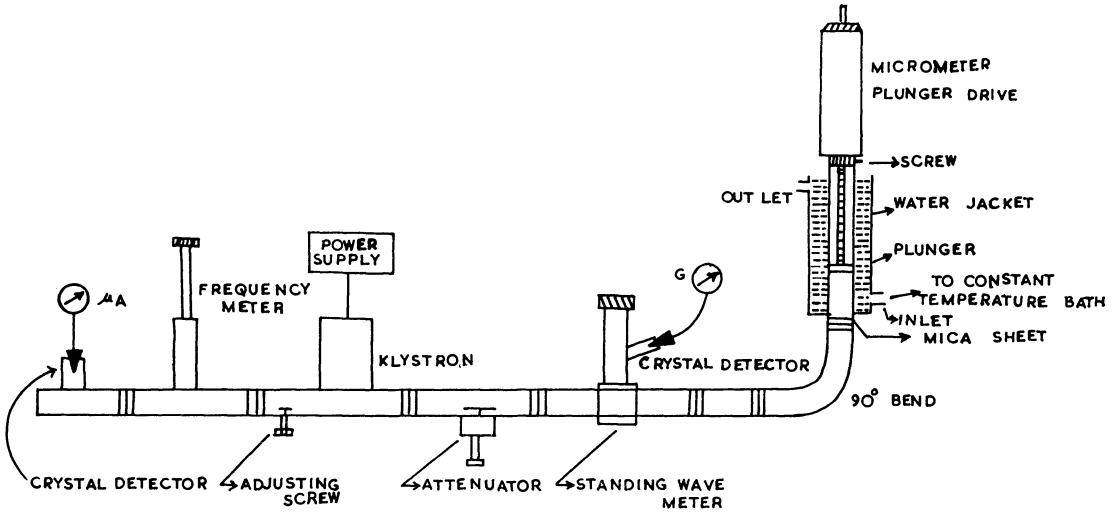

Set-up in X-band

Fig. 1

9) J. K. Vij and K. K. Srivastava, *ibid.*, **7**, 394 (1969).
10) L. Ubbelohde, *Ind. Eng. Chem., Anal. Ed.*, **9**, 85 (1937).
11) W. M. Heston, Jr., A. D. Franklin, E. J. Hennelly and C. P. Smyth, *J. Amer. Chem. Soc.*, **72**, 3443 (1950).

With the standing wave detector (SWD) at any fixed position the plunger is turned away from the mica window in the upward direction. The output of the SWD (probe position fixed) is noted at successive minima positions. The distance between the successive minima is equal to $\lambda_2/2$. The positions of at least five minima were noted and their mean value is taken as $\lambda_2/2$. In the majority of the cases, various distances between successive minima do not differ by a factor greater than the least count of the micrometer (0.001 cm). For low-loss materials the dielectric constant is given by

$$\varepsilon' \approx (\lambda_0/\lambda_c)^2 + (\lambda_0/\lambda_2)^2 \quad (1)$$

where λ_c is the cut-off wavelength, λ_0 is the free space wavelength and λ_2 is the wavelength in the dielectric filled guide of the cell.

The dielectric loss is determined by bringing the plunger down to the mica window so that the liquid length is zero. The plunger is then kept at different positions in steps of $\lambda_2/2$ and the standing wave pattern is recorded. The width at "twice minimum power points" is determined in each case and the values of the inverse voltage standing wave ratio ρ are calculated. These values of ρ are then plotted against 'n', *i. e.* the number of half wavelengths from the mica window, and the slope $(d\rho_{measured}/dn)$ is determined for each solution. The dielectric loss factor is approximated by

$$\varepsilon'' \approx (2/\pi)(\lambda_0/\lambda_2)^2(\lambda_g/\lambda_2)(d\rho_{measured}/dn)$$

where λ_g is the empty guide wavelength. The overall estimated accuracy of measurements is 0.5 to 1% for ε' and 2 to 4% for ε''.

For dilute solutions in non-polar solvents, ε, ε', ε'' and ε_∞ can be expressed as linear functions of concentration[12-14] in the following manner:

$$\left.\begin{aligned} \varepsilon &= \varepsilon_1 + a_0 w_2 \\ \varepsilon' &= \varepsilon_1' + a' w_2 \\ \varepsilon'' &= a'' w_2 \\ \varepsilon_\infty &= \varepsilon_{1\infty} + a_\infty w_2 \end{aligned}\right| \quad (3)$$

Subscript 1 refers to the pure solvent, 2 to the solute and subscript ∞ refers to the values at infinite frequency, w_2 may be taken as the weight fraction of the solute. The values of the so called slopes, *i. e.*, a_0, a', a'' and a_∞ for all the systems are given in Table 2. Most of the solutes were studied upto 0.10 weight fraction and the variable parameters were found to vary linearly with concentration. Higasi[14] showed that the Cole-Cole[15] equation can be represented in terms of the slopes a_0, a', a'' and a_∞ which would take the form

$$a' - ja'' = a_\infty + \frac{a_0 - a_\infty}{(1+j\omega\tau)^{1-\alpha}} \quad (4)$$

τ in this equation is the most probable relaxation time and α is the distribution parameter. For a system with a single relaxation time, α is zero and Eq. (4)

Table 2. Values of a_0 (slope of ε *vs.* concn. curve), a' (slope of ε' *vs.* concn. curve), a'' (slopn of ε'' *vs.* concn. curve) and a_D (slope of n_D^2 *vs.* concn. curve)

Solvent	a_0	a'	a''	a_D
		N,N'-Dimethylaniline		
n-Heptane	1.98	1.51	0.80	0.352
Benzene	2.54_5	1.76	0.98	0.160
Cyclohexane	2.17	1.29	0.64	0.276
Decalin	2.18	1.28	0.58	0.212
Nujol	2.10	0.78	0.23	0.170
		N,N'-Diethylaniline		
n-Heptane	2.00	1.14	0.92	0.325
Benzene	2.46	0.88	0.81	0.104
Cyclohexane	2.22	0.70	0.56	0.276
Decalin	2.51	0.67	0.42	0.189
Nujol	2.47	0.48	0.19	0.132
		o-Chloroaniline		
n-Heptane	2.18	2.14	0.35	0.320
Benzene	3.14	2.80	0.88	0.106
Decalin	3.00	2.22	0.74	0.187
Nujol	2.67	1.75	0.66	0.215
		m-Chloroaniline		
n-Heptance	4.27	3.54	1.08	0.324
Benzene	6.25	4.44	2.33	0.220
Decalin	5.60	3.05	1.54	0.230
Nujol	5.22	2.34	0.93	0.159
		p-Chloroaniline		
Benzene	7.96	4.90	2.49	0.256

becomes Debye's equation in terms of a', a'', *etc.*, *i. e.*

$$a' - ja'' = a_\infty + \frac{a_0 - a_\infty}{1 + j\omega\tau}$$

This equation leads to the following four relations.

$$\frac{a' - a_\infty}{a_0 - a_\infty} = \frac{1}{1 + \omega^2\tau^2} \quad (5)$$

$$\frac{a''}{a_0 - a_\infty} = \frac{\omega\tau}{1 + \omega^2\tau^2} \quad (6)$$

$$a' = a_\infty + \frac{1}{\tau}(a''/\omega) \quad (7)$$

and

$$a' = a_0 - \tau(\omega a'') \quad (8)$$

If the Debye equation for a single relaxation time is valid for the system under consideration and if the measurements are conducted with sufficient accuracy, determination of the correct value of the relaxation time could be made by means of any of the equations mentioned above. Higasi and Kiyohara,[16] in their investigation of Smyth's experimental data, compared the τ values obtained by this method and those by the

12) A. D. Franklin, W. M. Heston, Jr., E. J. Hennelly and C. P. Smyth, *ibid.*, **72**, 3447 (1950).
13) W. F. Hasel, M. D. Magee, S. W. Tucker and S. Walker, *Tetrahedron*, **20**, 2137 (1964).
14) K. Higasi, This Bulletin, **39**, 2157 (1966).
15) K. S. Cole and R. H. Cole, *J. Chem. Phys.*, **9**, 341 (1941).
16) K. Higasi and O. Kiyohara, *Oyo-Denki Kenkyusho Iho*, **18**, 24 (1966).

Table 3. Values of relaxation time, a_∞, a_D, dipole moment and distribution parameter

Solvent	τ(ps)	a_∞	a_D	$(a_\infty - a_D)$	μ(D)	α
			N,N'-Dimethylaniline			
n-Heptane	9.1	0.02	0.35	−0.32	1.61	$\leqslant 0$
Benzene	13.4	0.57	0.16	0.41	1.59	0.11
Cyclohexane	23.2	0.83	0.28	0.55	1.60	0.24
Decalin	26.1	0.91	0.21	0.70	1.49	0.32
Nujol	96.7	0.74	0.17	0.57	1.46	0.66
			N,N'-Diethylaniline			
n-Heptane	15.8	0.06	0.32	−0.26	1.82	$\leqslant 0$
Benzene	32.9	0.47	0.19	0.28	1.76	0.15
Cyclohexane	45.7	0.49	0.28	0.21	1.80	0.18
Decalin	73.8	0.57	0.19	0.38	1.80	0.44
Nujol	176.6	0.46	0.13	0.33	1.79	0.62
			o-Chloroaniline			
n-Heptane	2.4	−1.32	0.32	−1.64	1.80	0
Benzene	6.5	0.52	0.11	0.41	1.88	0.03
Decalin	17.7	1.51	0.19	1.32	1.86	0.30
Nujol	23.4	1.28	0.22	1.06	1.71	0.33
			m-Chloroaniline			
n-Heptane	11.3	1.95	0.32	1.63	2.67	0.16
Benzene	13.0	1.42	0.22	1.20	2.67	0.10
Decalin	27.8	2.12	0.23	1.89	2.60	0.34
Nujol	51.9	2.04	0.16	1.88	2.49	0.53
			p-Chloroaniline			
Benzene	20.6	2.88	0.26	2.62	3.02	0.25

usual method of Cole-Cole[15] for three different cases. The important conclusion drawn was the dependence of relaxation time upon the choice of a_∞.

In case the system has a distribution of relaxation times, values of τ and α can be calculated from the measurement of a' and a'' at a single frequency[14,17] by using the equations.

$$\tau = \frac{1}{\omega}\left(\frac{A^2 + B^2}{C^2}\right)^{1/2(1-\alpha)} \tag{9}$$

and

$$1 - \alpha = \left(\frac{2}{\pi}\right)\tan^{-1}\frac{A}{B} \tag{10}$$

where

$$\left.\begin{aligned} A &= a''\,(a_0 - a_\infty) \\ B &= (a_0 - a')(a' - a_\infty) - a''^2 \\ C &= (a' - a_\infty)^2 + a''^2 \end{aligned}\right| \tag{11}$$

Though this method has not been used by many workers yet the authors feel that it can provide more information, particularly for non-rigid molecules, in the absence of data at various frequencies. This method can, at least, determine the degree of distribution of various relaxation processes.

Method Adopted for the Calculation of Relaxation Time. If a system possesses a single relaxation time, then the values of τ calculated by using either of the four equations ((5) to (8)), should be the same within experimental errors, because all these relations are basically derived from a single equation. In the absence of an exact knowledge of a_∞, values of τ should preferably be calculated by using Eq. (8). Knowing τ for such a system, the value of a_∞ can subsequently be computed by the use of Eq. (7). This value of a_∞ should be slightly higher than the corresponding a_D value of the system, because a_∞ term involves some contribution from atomic polarization as well.

Even if the system possesses two relaxation times sufficiently far apart, values of τ can be calculated by using Eq. (8) and consequently the values of a_∞ can be estimated. Then the difference $(a_\infty - a_D)$ would give us an idea about the dispersion range to which the τ value belongs. With this picture in mind, the values of τ have been calculated for all the molecules in different solvents and these values are presented in Table 3 which also contains a_∞ values. The experimentally determined values of a_D have also been inserted in this table with a view to estimate the magnitude of $(a_\infty - a_D)$.

Discussion

A perusal of Table 3 reveals that there is a regular increase in the relaxation times of all the molecules as the solvent viscosity increases. Another noteworthy feature is the unusually high values of $(a_\infty - a_D)$ which should be negligibly small if the

17) G. L. Clark, *J. Chem. Phys.*, **25**, 125 (1956).

system has a single relaxation time. The large difference suggests that apart from relaxation in the main dispersion region, another relaxation mechanism seems to occur in the mm range which is due to the relaxation of the amino (or the substituted amino) group. One would therefore conclude that the relaxation process in anilines involves the molecular rotation as well as the intramolecular rotational mechanism. Also, it is interesting to note that the a_∞ values for all the anilines (except *m*-chloroaniline) are either less than the a_D values or negative in *n*-heptane. The values of relaxation time are also found to be relatively less in this solvent. This indicates that in *n*-heptane (having the lowest viscosity coefficient), there is a little disparity between the values of relaxation time for both processes which jointly contribute to the observed loss by competing with each other. The intramolecular process may possibly dominate.

We conclude that these relaxation times correspond to the ones in the main dispersion region.

Grubb and Smyth[18] have studied pure dimethylaniline and predicted, with reservation, two relaxation mechanisms with slightly hindered rotations of $N(CH_3)_2$ group. One of us (K.K.S.) also made a dielectric relaxation study[19] of liquid *N,N'*-dimethylaniline and *N,N'*-diethylaniline using two microwave frequencies (9.72 GHz) and 31.82 GHz), and analyzed the data with the help of "Cole-Cole plots" by taking ε_∞ as the square of refractive index. The findings show that the most probable relaxation time (τ) in both cases is frequency-dependent. The values obtained for the molecular relaxation time at 9.72 GHz are 38.2 ps for dimethylaniline and 290.3 ps for diethylaniline, whereas for 31.82 GHz, these values are 84.7 ps and 167.1 ps respectively. Furthermore, K.K.S. also found high values of distribution parameter (α), *i.e.*, 0.59 for dimethylaniline and 0.52 for diethylaniline. All these reported values correspond to the measurements at 30°C.

These observations and an examination of ($a_\infty - a_D$) values (given in Table 3) provide evidence of two relaxation mechanisms in anilines. One involves the rotation of the molecule as a whole and the other involves intramolecular or the group rotation. This suggests that the dipole in anilines is inclined at a particular angle to the C–N bond, thus making the molecule nonplaner. This possibly leads to the conclusion that the conjugation energy is insufficient to make the molecule planer. The conclusion supports the one already drawn by Tiganik[20] from the dipole moment studies. The amino group together with the benzene ring perhaps retains its pyramidal shape similar to that of an ammonia molecule even when one of its hydrogen atoms has been replaced.

Distribution Parameter (α) and Dipole Moment. In the absence of experimental data for a wide range of frequencies, the Cole-Cole[16] equation has been used in the form of relations (10—11) for the calculations of the distribution parameter (α) with the assumption that $a_\infty \approx a_D$. This will at least provide us with qualitative information about the existence of more than one relaxation mechanism. The values of relaxation time have purposely not been calculated by this method as it will give values in agreement with the values given in Table 3 only for the cases having $\alpha \approx 0$.

These values of distribution parameter are listed in Table 3 which also contains the dipole moments calculated by using the modified Higasi's equation.[8]

Study of Relaxation Time, Distribution Parameter and Dipole Moment Values. *a) N,N'-Dimethylaniline and N,N'-Diethylaniline.* Table 3 shows that for both these substances, relaxation time values increase with the increasing viscosity of the medium. Their reported[7] values in benzene are 14.5 ps and 33.2 ps at 20°C, whereas the authors found them to be 13.4 ps and 32.9 ps at 25°C. Obviously, the agreement between the two is good. Again the value of τ for dimethylaniline in benzne, determined by Kramer,[21] is 13.7 ps again in good agreement with the present value.

The reported[7] values of distribution parameter for dimethylaniline and diethylaniline in benzene, obtained by "Cole-Cole Plots", are 0.06 and 0.0 respectively as against 0.11 and 0.15 obtained by the authors. Certainly, the disparity is due to a different method adopted for calculations. The present method provides, at least qualitatively, a direct evidence of the existence of more than one relaxation mechanism, because the α values show a systematic increase with the increase in viscosity of the medium and are, in general, unusually high. Such large values cannot merely be due to the distribution of activation energies. It certainly indicates that there is more than one relaxation mechanism and that the disparity between the values of relaxation time increases with viscosity. However in *n*-heptane, α values for both these substances are slightly less than zero which perhaps indicates the predominance of intramolecular relaxation process in this solvent. These predictions are in agreement with those already drawn from the negative values of ($a_\infty - a_D$).

Small variations in the dipole moment values for different solvents are possibly due to the solvent effect.

b) o-, m-, and p-Chloroanilines. Liquid *o-* and *m*-chloroanilines have also been studied by Bhattacharyya[22] at a wavelength of 3.18 cm. His

18) E. L. Grubb and C. P. Smyth, *J. Amer. Chem. Soc.*, **83**, 4879 (1961).
19) K. K. Srivastava, *J. Phys. Chem.*, **74**, 152 (1970).
20) L. Tiganik, *Z. Physik. Chem.*, **1413**, 135 (1931).
21) H. Kramer, *Z. Naturforsch.*, **15a**, 66, 974 (1960).
22) T. J. Bhattacharyya, *Indian J. Phys.*, **36**, 533 (1962).

values of relaxation time, calculated by Debye's equation, are 12.28 ps and 12.49 ps respectively. From the existence of a loss-maxima at 30°C in both cases, he inferred that the amino group is free to rotate and the presence of a chlorine group does not hinder its rotations in any way. It was thought therefore, that the study of the relaxation time in various solvents would give more information about the nature of intramolecular process.

Table 3 again shows a regular increase in relaxation time of these anilines with the increasing viscosity of the solvent. Of course, the variation is not as large as should be expected from Debye's equation[23,24] for a rotating sphere in a continuous fluid of viscosity η. On examining α values, one finds a systematic increase as was the case for dimethyl and diethyl anilines. The increase in values with the increasing viscosity of the medium is interpreted in terms of the disparity in the two relaxation mechanisms involved in the relaxation process. The almost regular rise in α further implies that the molecular relaxation time regularly increases with viscosity, whereas the intramolecular mechanism does not seem to increase very much with the viscosity of the medium. However, one does not expect such behaviour if the amino group (or the substituted one) rotates around the (C–N) bond, because it has some effective volume and this volume goes on increasing with the substitution of the radicals: CH_3 and C_2H_5, *etc.* Amino (or the substituted amino) group possibly relaxes with an inversion mechanism similar to the ammonia molecule, as postulated by Smyth.[6] However, a detailed and systematic study of the substances with a corresponding analysis of the data in terms of τ_1 and τ_2 is required before confirming this possibility. This is not possible with the measurements at two frequencies.

The values of relaxation time for *o*-, *m*- and *p*-isomers measured in benzene at 30°C are 6.5 ps, 13.0 ps and 20.6 ps respectively. These values increase with the shift of chlorine group from *o*- to *m*-, and finally to *p*-position with respect to the amino group. A regular variation in τ values may either be due to the change in the molecular volume or due to a change in the effective length of the dipole involved in the orientation process. The molecular volume (M/d) in all the three cases is approximately the same, *i.e.*, 106 cc. It, therefore, seems that the effective change in length of the dipole is actually responsible for the observed rise in relaxation times of these substituted anilines. Another interesting feature is that the values of α for these anilines in a particular solvent, in general, increase from *o*- to *m*- to *p*-isomers. This indicates, as is expected, that the hindrance for intramolecular rotation of NH_2 group is greater in *o*-chloroaniline, less in *m*-chloroaniline and still less in *p*-chloroaniline.

The authors are grateful to Professor H. S. Hans, Head, Department of Physics, and Professor V. B. Bhanot for their interest in the work and for providing the facilities.

23) P. Debye, "Polar Molecules," Chemical Catalogue, New York (1929); *Trans. Faraday Soc.*, **30**, 679 (1934).
24) W. Kauzmann, *Rev. Mod. Phys.*, **14**, 12 (1942).

BULLETIN OF THE CHEMICAL SOCIETY OF JAPAN VOL. 43 2313—2316 (1970)

Dielectric Relaxation and Molecular Structure. II Dielectric Relaxation in Dibutyl Ether, Diphenyl Ether and Benzophenone in Various Nonpolar Solvents

J. T. VIJ*1 and K. K. SRIVASTAVA

Department of Physics, Panjab University, Chandigarh-14, India

(Received December 10, 1969)

Measurements of dielectric constant and loss have been made at 1 Mc and 9.44 GHz for dibutyl ether and benzophenone in various solvents, *e.g.*, *n*-heptane, benzene, cyclohexane, carbon tetrachloride, decalin and Nujol. Whereas, diphenyl ether has only been studied in benzene and cyclohexane. The values of relaxation time and distribution parameter have been determined by using Cole-Cole's equation in terms of the so-called slopes, a_0, a', a'' and a_∞. The relaxation time values show a regular increase with the increase in viscosity of the medium both for dibutyl ether and benzophenone. The observations seem to suggest that dibutyl ether relaxes both by molecular and intramolecular mechanisms. The dipole moments in various solvents have also been calculated.

Several workers[1-6] have reported their findings about relaxation times for diphenyl ether and benzophenone and much has been said particularly about the anomalous behavior of the former.[7-10] However, no such data on relaxation study seems to be available for dibutyl ether. A study of this molecule may provide some information about the relaxation mechanism of aliphatic ethers in contrast to aromatic ones.

Experimental

Dibutyl ether, diphenyl ether and benzophenone (all of pure grade specifications) were imported from Dr. Theodor Schuchardt, West Germany, and were used without purification. The values of density, viscosity and refractive index for dibutyl and diphenyl ethers tallied[11] with their literature values. Melting point of benzophenone (48.0°C) agreed well with its literature value (48.1°C). All the solvents were purified by the processes described in our previous communication[12] which gives the measured values of their physical constants along with their literature values.

The dielectric constant, loss (at 1 Mc and 9.44 GHz) and refractive index measurements were made as per method already discussed.[12] All the measurements were made at 25°C. The accuracy in dielectric constant (at 1 Mc) is ±0.5%, in ε' and ε'' (at 9.44 GHz) 0.5 to 1% and 2 to 4%, respectively. The values of ε, ε', ε'' and n_D^2 were found to be linearly dependent upon weight fraction (w_2) for all the systems. The values of "the so-called slopes" a_0, a', a'' and a_D were determined and are presented in Table 1.

Method of Calculations. It has been shown by Higasi[13] that Cole-Cole[14] equation can be represented in terms of a_0, a', a'' and a_∞ which would take the form

$$a' - ja'' = a_\infty + \frac{a_0 - a_\infty}{1 + (j\omega\tau)^{1-\alpha}} \tag{1}$$

where τ is the most probable relaxation time and α is the distribution parameter. τ and α can be calculated from the measurements of a' and a'' at a single frequency[13,15] and their values are obtained from Eq. (1) in the manner given below:

$$\tau = \frac{1}{\omega}\left(\frac{A^2 + B^2}{C^2}\right)^{1/2(1-\alpha)} \tag{2}$$

and

$$1 - \alpha = \frac{2}{\pi}\tan^{-1}\frac{A}{B} \tag{3}$$

*1 Present address: Department of Physics, Punjab University, Patiala, India.

1) J. Schneider, *J. Chem. Phys.*, **32**, 665 (1960).
2) F. Hufnagel, *Z. Naturforsch.*, **15a**, 723 (1960).
3) F. Hufnagel, G. Klages and P. Knoblock, *ibid.*, **17a**, 96 (1962).
4) W. E. Vaughan and C. P. Smyth, *J. Phys. Chem.*, **65**, 98 (1961).
5) W. E. Vaughan, W. S. Lovell and C. P. Smyth, *J. Chem. Phys.*, **36**, 535 (1962).
6) K. Chitoku and K. Higasi, This Bulletin, **36**, 1064 (1963).
7) D. M. Roberti, O. F. Kalman and C. P. Smyth, *J. Amer. Chem. Soc.*, **82**, 3523 (1960).
8) K. Higasi and C. P. Smyth, *ibid.*, **82**, 4759 (1960).
9) F. K. Fong, *J. Chem. Phys.*, **40**, 132 (1964).
10) K. Higasi, "Dipole, Molecule and Chemistry," Monograph series of the Research Institute of Applied Electricity, No. 13 (1965).
11) K. K. Srivastava, *J. Phys. Chem.*, **74**, 152 (1970).
12) K. K. Srivastava and J. K. Vij, This Bulletin, **43**, 2307 (1970).
13) K. Higasi, This Bulletin, **39**, 2157 (1966).
14) K. S. Cole and R. H. Cole, *J. Chem. Phys.*, **9**, 341 (1941).
15) G. L. Clark, *ibid.*, **25**, 125 (1956).

Table I. Values of a_0 (slope of ε *vs.* concn. curve), a' (slope of ε' *vs.* concn. curve), a''(slope of ε'' *vs.* concn. curve) and a_D (slope of n_D^2 *vs.* concn. curve)

	Medium	a_0	a'	a''	a_D
		Diphenyl ether			
1	Benzene	1.13_3	1.09	0.18	0.218
2	Cyclohexane	1.11	1.04	0.20	0.310
		Dibutyl ether			
1	*n*-Heptane	—	0.70_6	0.32	+0.02
2	Benzene	0.80	0.52	0.34	−0.357
3	Cyclohexane	1.02	0.68	0.40	−0.103
4	Carbon tetrachloride	1.75	1.07_5	0.90	−0.300
5	Decalin	1.16	0.64	0.47	−0.254
6	Nujol	0.96	0.42	0.36	−0.350
		Benzophenone			
1	*n*-Heptane	4.60	2.58	2.06	0.415
2	Benzene	5.90	2.47	2.42	0.281
3	Cyclohexane	4.78	2.10	2.54	0.374
4	Decalin	5.68	1.35	2.12	0.328
5	Nujol	5.62	0.78	0.85	0.270

where

$$A = a''(a_0 - a_\infty)$$
$$B = (a_0 - a')(a' - a_\infty) - a''^2$$
$$C = (a' - a_\infty)^2 + a''^2$$

The values of a_∞ are assumed to be approximately equal to a_D. This will not introduce much error in view of the inaccuracies involved in the measurements of a_0, a' and a''. Though this method has not been used by many workers, yet the authors feel that it would give reasonably accurate values of relaxation time for rigid molecules and the average values for molecular and intramolecular rotations in non-rigid molecules, depending upon their relative contributions to the overall relaxation process. The values of τ and α thus calculated are given in Table 2 along with the values of the dipole moment calculated by the method described earlier.[16]

Table 2. Values of relaxation time, distribution parameter and dipole moment for diphenyl ether, benzophenone and dibutyl ether

Solvent	τ(p.sec)	α	μ(D)
	Diphenyl ether		
Benzene	3.4	0.02	1.19
Cyclohexane	4.4	0.04	1.17
	Benzephenone		
n-Heptane	16.8	0.01	3.22
Benzene	20.1	~0	3.09
Cyclohexane	20.5	~0	3.04
Decalin	34.6	~0	3.05
Nujol	135.0	0.23	3.02
	Dibutyl ether		
Benzene	6.5	0.20	1.13
Cyclohexane	9.3	0.14	1.27
Carbon tetrachloride	11.4	0.04	0.98
Decalin	11.2	0.22	1.31
Nujol	14.2	0.40	1.25

Discussion

a) Diphenyl Ether. Values of relaxation time for diphenyl ether are 3.4 ps and 4.4 ps in benzene and cyclohexane respectively. The former compares favourably well with the literature values of 4.1[1] ps at 25°C and 4.0[3] ps at 20°C. The relaxation time for liquid diphenyl ether is 5.0 ps/30°C,[11] again in fair agreement with the value 5.1 ps/30°C as reported by Calderwood and Smyth.[17] Values of distribution parameter in both the solvents are nearly equal to zero which indicates one type of relaxation mechanism to be predominant.

The reason for a lesser value of τ for diphenyl ether as compared to a similar molecule (benzophenone) has been attributed to the internal rotations of the phenyl groups.[8] The possible mechanism responsible for giving lesser value of relaxation time is the mesomeric shift of charge due to changes in the interaction between the π-electrons in the phenyl rings and the unshared pairs on the oxygen as a function of ring twisting with respect to the C–O–C plane. However, Nelson and Smyth,[18] in a study of molecules similar in structure to diphenyl ether, seem to support Fong's[9] hypothesis that "double or coupled internal rotations, resembling a rowing motion with one oar feathered are

16) J. K. Vij and K. K. Srivastava, *Indian J. Pure Appl. Phys.*, **7**, 391 (1969).
17) J. H. Calderwood and C. P. Smyth, *J. Amer. Chem. Soc.*, **78**, 1295 (1956).
18) R. D. Nelson, Jr., and C. P. Smyth, *J. Phys. Chem.*, **69**, 1006 (1965).

Table 3. Relaxation times of benzophenone

Solvent	Present work		Literature	
	η(c.p.)	τ(ps)	η(c.p.)	τ(ps)
n-Heptane	0.408	16.8	—	—
Benzene	0.600	20.1	—	20.4/23°C[a)] 20.4/25°C[b)] 22/19°C[c)]
Cyclohexane	0.878	20.5	—	τ_1=27/20°C[d)] τ_2=3.5/20°C[d)]
Decalin	2.208	34.6	—	—
Nujol	147.6	135.0	137.8 197.0	238.0/25°C[b)] 295.0/19°C[e)]

a) E. Fisher, *Z. Naturforsch.*, **4a**, 707 (1949).
b) Ref. 6.
c) D.H. Whiffen and H.W. Thompson, *Trans. Faraday Soc.*, **42a**, 114 (1946).
d) Ref. 22.
e) Ref. 21.

responsible for the rapid relaxation mechanism". In the latter hypothesis, a fixed volume is always swept in rotation and it becomes difficult, on the basis of Debye's[19] concept of a rotating sphere in the viscous fluid characterized by its ordinary viscosity, to explain why the ratio of the rotating volume of diphenyl ether to benzophenone becomes only 2% in Nujol in comparison to 22% in benzene.[20] Indeed, some sort of internal rotation is definitely responsible for the rapid relaxation mechanism.

b) Benzophenone. Relaxation times for benzophenone along with the literature values (if available) are given in Table 3.

The value of 20.1 ps in benzene agrees fairly well with that of 20.4 ps/25°C determined by Chitoku and Higasi[6] from their study at low frequencies. However, a great disagreement appears in the case of Nujol. We found the τ value to be 135.0 ps as against 238.0 ps/25°C reported by Chitoku and Higasi.[6] and 295.0 ps/19°C reported by Jackson and Powels.[21] The reason for the large difference between the present and the literature values is perhaps due to the wide difference in frequencies at which the measurements have been carried out. Chitoku and Higasi determined the value from a study at low frequencies (~few Mc.) in which internal rotations may not have been taken into account.[6] The present value corresponds to the microwave frequency which accounts for both rotations, *i.e.*, molecular as well as intramolecular. The lesser value therefore indicates that the contributing factor of the rapid relaxation mechanism becomes predominant to the observed complex dielectric constant in the microwave range, which is obviously expected. This is further indicated by a comparatively higher value of distribution parameter (0.23) obtained in this solvent. Moreover, the existence of both processes is clearly established from the study of liquid benzophenone by Vaughan and Smyth[4,5] and from a recent study by Farmer and Walker[22] in cyclohexane. The values of τ_1 and τ_2 determined by the latter workers are also inserted in Table 3. It is interesting to note that the values of 3.0 ps[4,5] for liquid benzophenone and 3.5 ps for benzophenone in cyclohexane are nearly the same irrespective of the differences in the values of viscosity coefficients of the two media. The viscosity coefficent for liquid benzophenone is

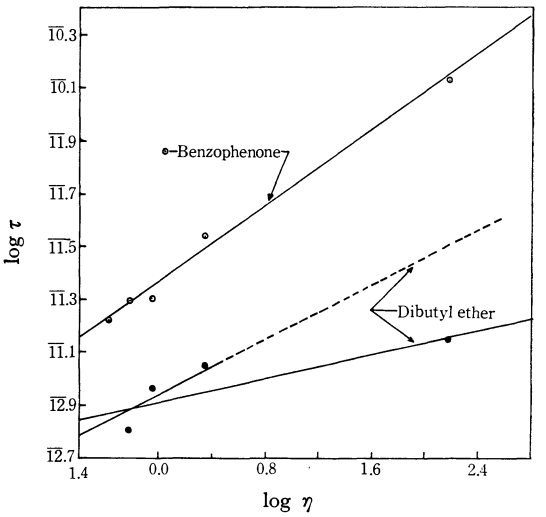

Fig. 1. Dependence of log τ upon log η.

19) P. Debye, *Trans. Faraday Soc.*, **30**, 679 (1934).
20) Ref. 10, p. 22.
21) W. Jackson and J. G. Powels, *Trans. Faraday Soc.*, **42a**, 101 (1946).
22) D. Farmer and S. Walker, *Tetrahedron*, **22**, 111 (1966).

4.19 c.p. whereas that of cyclohexane is 0.88 c.p. This suggests that the nature of rapid relaxation mechanism in this molecule is essentially the same as that of diphenyl ether. However, its contribution to the overall rotation is only about 6% in comparison to 74% for the diphenyl ether.[4,5]

The plot of log τ *vs.* log η gives a fairly reasonable linear curve and the value of x compares well with the value 0.46.[6] This confirms the viewpoint that semi-empirical equation[6] ($\tau=A\eta^x$) may replace Debye's formula[19] for a rigid sphere in a viscous fluid in which the coefficient of internal friction was taken to be the macroscopic measurable viscosity η. A systematic study of the coefficients A and X may provide a better insight into (i) the relaxation mechanism and (ii) internal rotations *vs.* overall rotations.

c) Dibutyl Ether. The relaxation time in benzene has been found to be 6.5 ps, whereas, for liquid dibutyl ether, the value (molecular relaxation time) is 5.0 ps/30°C as found by Srivastava.[11] Viscosity of dibutyl ether at 30°C is 0.58 c.p. which is almost the same as that of benzene (0.569 c.p.) A small difference between relaxation times hardly indicates any observable difference involved between the two systems.

Values of τ for this molecule, in solvents of low viscosity, show a usual trend. Ratio of relaxation times in carbon tetrachloride and cyclohexane is 1.23 as against their viscosity ratio of 1.03. This trend, possibly, is due to sticky nature[23,24] of carbon tetrachloride. Relaxation time in Nujol (having the largest viscosity coefficient) does not seem to be in accordance with its viscosity, if the molecules were considered to be of rigid structure. High value of α (0.40) in Nujol is interesting. Also a plot of log τ *vs.* log η hardly shows any trend towards linearity (see Fig. 1). This suggests intramolecular relaxation mechanism in dibutyl ether. The presence of internal rotation in the alkyl chains can also decrease the dependence of the relaxation time on the viscosity.

Considering the molecular volumes of dibutyl ether and benzophenone, one finds that these have similar values of 170.9 and 170.0 cc, but the relaxation times of these molecules in benzene are 6.5 ps and 20.1 ps respectively. This is possibly due to the reason that aliphatic groups (in comparison to phenyl groups) sweep lesser area of the solvent molecules while relaxing. This is further clear when we compare the relaxation time of this molecule with that of dipropyl ketone which has a similar molecular structure and nearly the same molecular volume (140 cc). The latter has the value of τ 5.4 ps in benzene at room temperature which compares well with that of dibutyl ether.[25]

The authors are grateful to Professor H. S. Hans, Head, Department of Physics and Professor V. B. Bhanot for their interest in the work and for providing the facilities.

23) K. Higasi, "Dielectric Relaxation and Molecular Structure," Monograph Series of the Research Institute of Applied Electricity, No. 9 (1961), p. 4.

24) K. Chitoku and K. Higasi, This Bulletin, **39**, 2160 (1966).

25) A. Vyas and H. N. Srivastava, *J. Sci. and Ind. Res.*, 399 (1959).

BULLETIN OF THE CHEMICAL SOCIETY OF JAPAN VOL. 43 2317—2321 (1970)

A New Crystal with Kalsilite-type Structure on the $CaAl_2O_4$-SiO_2 Join

Takashi YOSHIOKA

Nihon Cement Co., Ltd. Research Laboratory, Kiyosumi, Koto-ku, Tokyo

(Received December 19, 1969)

A new crystal phase with a kalsilite-type structure has been found in devitrified glass with compositions close to $CaAl_2O_4$ on the $CaAl_2O_4$-SiO_2 join. The crystal can be synthesized as a nearly pure phase by heating the glass for 5 to 20 min at 1000°C. After prolonged heating, the crystal easily decomposes into an assemblage of the stable compounds, $CaAl_2O_4$, $CaAl_4O_7$, and $Ca_2Al_2SiO_7$(gehlenite). Most of the X-ray powder diffraction lines of the kalsilite-type phase can be indexed on the basis of a hexagonal unit cell with $a=5.0$ Å and $c=8.1$ Å. In addition to these reflections, some weak ones which cannot be indexed on the basis of this unit cell are also present. The kalsilite-type phase reacts with water, resulting in heat liberation and hardening.

In the course of an experimental investigation of a nepheline-type solid solution,[1] two kinds of new crystals were found along the $CaAl_2O_4$-SiO_2 join. One was a kalsilite-type phase formed in compositions closer to $CaAl_2O_4$ than the nepheline-type solid solution, while the other was formed closer to $CaAl_2Si_2O_8$(anorthite). The latter has not yet been investigated in detail. These phases are crystallized from glass at relatively low subsolidus temperatures around 1000°C in the air and gradually disappear at the same temperatures.

In the present report, the mode of formation and some of the physical properties of the kalsilite-type phase will be described.

TABLE 1. SUBSOLIDUS CRYSTALLIZATION PRODUCTS OF GLASSES ON THE $CaAl_2O_4$-SiO_2 JOIN

No.	Composition of glass in weight per cent ( ) mol ratio			Heat treatment of glass °C		Phases as determined optically and by X-ray
	CaO	Al_2O_3	SiO_2			
	35.48 (1)	64.52 (1)	0 (0)			$CaAl_2O_4$
1	33.37	60.67	5.96	1000	5 min	Much Ks-type, little Gl.
	(6)	(6)	(1)	1000	10 min	Much Ks-type, little Ne-type, (little Gl).
				1000	30 min	Much Ks-type, little Ne-type
				1000	2 days	Much $CaAl_2O_4$, moderate amounts Gehl and $CaAl_4O_7$.
2	32.97	59.95	7.07	950	40 min	Much Ks-type, little Ne-type, (little Gl).
	(5)	(5)	(1)	1000	5 min	
				1000	10 min	
				1000	30 min	Much Ks-type, little Ne-type.
				1000	2 days	Much $CaAl_2O_4$, moderate amounts Gehl and $CaAl_4O_7$.
				1100	12 hr	
3	32.40	58.91	8.68	950	21 hr	Mcuh Ks-type, much Ne-type, little Gl.
	(4)	(4)	(1)	1000	5 min	Little Ks-type, little Ne-type in glass.
				1000	20 min	Moderate amounts Ks-type, Ne-type and Gl.
				1000	13 hr	Much Ne-type, little Ks-type.
				1000	2 days	Much Ne-type, little Gehl.
				1100	12 hr	Moderate amounts Gehl, Ne-type and $CaAl_4O_7$.
				1200	3 hr	Much Gehl, moderate amounts $CaAl_4O_7$ and $CaAl_2O_4$.

Gehl; gehlenite, Gl; residual glass, Ks-type; kalsilite-type phase, Ne-type; nepheline-type solid solution.

1) T. Yoshioka, This Bulletin, **43**, 1981 (1970).

Experimental

Homogeneous glass with compositions close to $CaAl_2O_4$ on the $CaAl_2O_4$-SiO_2 join was prepared by melting mixtures of chemicals above 1700°C in an electric furnace. Crushed glass was heated and devitrified under various conditions. The products were identified by means of a polarizing microscope and X-ray powder diffraction. The powder patterns of the kalsilite-type phase were indexed.

The rate of the heat liberation of the kalsilite-type phase in a hydration reaction was observed with a conduction calorimeter,[2] CM-502 type, of the Oyo Denki Kenkyusho Co., Ltd. Two kinds of kalsilite-type phases were synthesized by heating glass No. 1 and glass No. 2 (Table 1) for 20 min at 1000°C. They were then pulverized, and grains 4 to 16 microns in

Table 2. Indexed powder patterns of the kalsilite-type phase

Crystallized from No. 1 glass. Indexed based on Hexagonal, a 5.0268 Å, c 8.1223 Å. (Da .0003, Dc .0007)			Crystallized from No. 2 glass. Indexed based on Hexagonal, a 5.0204 Å, c 8.1673 Å (Da .0004, Dc .0009)			Kalsilite, $Ks_{100}Ne_0$. J. V. Smith and O. F. Tuttle[3]		
I_{obs}	d_{obs}	$hk.l$	I_{obs}	d_{obs}	$hk.l$	I	d_{obs}	Indices
* 3b	4.676	—						
17	4.059	00.2	23	4.085	00.2	12	4.3512	00.2
6b	3.841	10.1	55	3.840	10.1	45	3.9733	10.1
100	2.969	10.2	100	2.977	10.2	100	3.1184	10.2
* 8b	2.850	—	* 7	2.847	—			
		tri 41.0			tri 41.0			
		tetr 32.2			— —			
		ord 21.0			ord 21.0			
60	2.513	11.0	61	2.509	11.0	50	2.5789	11.0
			* 6	2.487	—			
					tri 50.1			
					tetr 53.0, 70.0			
			* 8	2.477	—			
					tetr 51.2			
36	2.401	11.1	6	2.400	11.1	15	2.4724	11.1
* 5	2.307	—						
		tetr 71.0						
6	2.299	10.3	18	2.307	10.3	10	2.4319	10.3
* 4b	2.199	—	* 4	2.205	—			
		tri 22.3			tri 22.3			
		ord 20.3			ord 20.3			
6	2.177	20.0	5	2.173	20.0	3	2.236	20.0
5	2.137	11.2	4	2.138	11.2	10	2.2183	11.2
			4	2.100	20.1	17	2.1753	00.4
8b	2.030	00.4	8	2.042	00.4	5	2.164	20.1
20	1.919	20.2	23	1.919	20.2	5	1.9868	20.2
						3	1.9546	10.4
4b	1.842	11.3	3	1.846	11.3	4	1.9270	11.3
			9	1.699	20.3	3	1.7703	20.3
			3	1.584	11.4	4	1.6621	11.4
						4	1.6580	21.1
16	1.525	21.2	13	1.529	10.5	6	1.6220	10.5
14	1.522	10.5	24	1.525	21.2	9	1.5742	21.2
* 5	1.458	—				3	1.5588	20.4
		tri 71.3						
		ord 32.3						
16	1.451	30.0	23	1.449	30.0	10	1.4895	30.0
			19	1.407	21.3	3	1.4598	21.3
			3	1.369	11.5			

tri a×3, tetr a×4, ord a×$\sqrt{3}$. Cu$K\alpha$ radiation. Da, Dc, standard deviation.

2) U. Danielson, Chemistry of Cement, Proc. 4th Internl. Symp., Washington, **1**, 519 (1960).

diameter were used for the hydration examination. Ten milliliters of water were added to 10g of the specimen. The measurement of the rate of heat liberation was performed at 20°C.

Results

Mode of Formation. The kalsilite-type phase was produced when the glass was heated for a short time at approximately 1000°C (Table 1). The crystallized products of glass No. 1 and glass No. 2 after 10 mins' heating at 1000°C were composed mostly of this phase, plus a trace of the nepheline-type solid solution or residual glass. After prolonged heating, this phase easily decomposed into an assemblage of compounds, $CaAl_2O_4$, $CaAl_4O_7$, and $Ca_2Al_2SiO_7$, as shown in the table. The crystallized product of glass No. 3, obtained by 20 mins' heating at 1000°C, was composed of both the kalsilite-type phase and the nepheline-type solid solution with residual glass. Further heating at 1000°C resulted in the formation of the nepheline-type solid solution with a concomitant disappearance of the kalsilite-type phase.

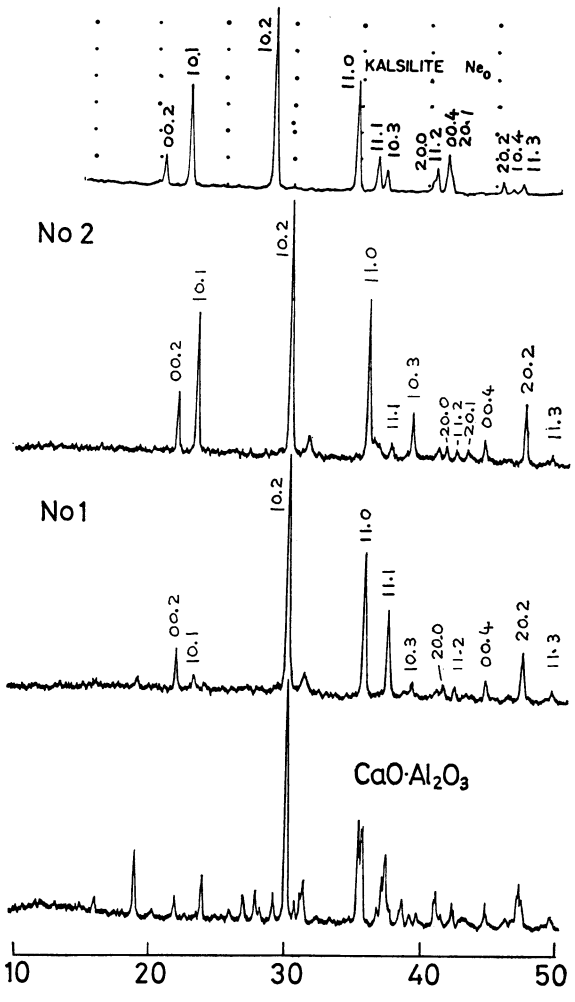

Fig. 1. X-ray powder patterns of the kalsilite-type phase.
Numbers correspond to those in Table 1. The pattern of kalsilite according to J. V. Smith and O. F. Tuttle is reproduced from Fig. 1 in p. 284 of Amer. Journ. Sci., Vol. 255 (1957). Indices are added for convenience by the present writer.

X-Ray Diffraction Pattern. In Fig. 1 powder diffraction patterns of the kalsilite-type phase obtained as a nearly pure phase (no trace of the nepheline-type solid solution was observed in the powder patterns) from glass No. 1 and glass No. 2 by 10 mins' heating at 980°C are shown, along with those of synthetic kalsilite[3] and $CaAl_2O_4$. Indexed powder data are also given in Table 2.

A close resemblance is observed between the kalsilite-type phase from glass No. 2 and the synthetic kalsilite. The diffraction pattern of the phase from glass No. 1 differs from that of the kalsilite. However, it resembles $CaAl_2O_4$ as a whole (Fig. 1). Almost all the diffraction lines of the kalsilite-type phases can be indexed on the basis of a hexagonal unit cell with $a=5.0$ Å and $c=8.1$ Å (ordinary kalsilite $KAlSiO_4$ has a hexagonal unit cell with $a=5.2$ Å and $c=8.7$ Å[3]). In addition to these reflections, some weak ones are also present, although these also are believed to be due to this phase. However, these lines cannot be indexed on the basis of the ordinary kalsilite unit cell;

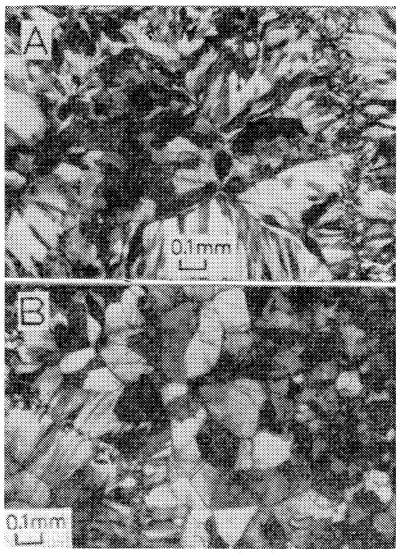

Fig. 2. Photomicrographs of the kalsilite-type phase crystallized from glass No. 2. Crossed nicols.
A) Feather-like form.
B) Granular form. Class was prepared by oxygen-acetylene flames.

3) J. V. Smith and O. F. Tuttle, *Amer. J. Sci.*, **255**, 282 (1957).

some of them can, however, be indexed by making the a parameter three or four times larger than that of the ordinary kalsilite, like that of tri-kalsilite[4] or tetra-kalsilite.[3] Also, some of them can be accounted for by the unit cell in which the a parameter is made $\sqrt{3}$ times larger than that of the ordinary cell, as in the case of ordered kalsilite.[5] However, none of these three unit cells can explain the weak reflections completely. One diffraction line remained unindexed in the pattern of the kalsilite-type phase from glass No. 1. It appears at the angle, about 19°(2θ) Cu$K\alpha$, which coincides with one of the reflections of $CaAl_2O_4$.

Optical Properties. After having been heated at 1000°C for 5 to 30 min, the glass appeared to be translucent; however, under a microscope it was observed as almost fully crystallized with a polycrystalline feature. Most of the crystals of the kalsilite-type phase appeared in a featherlike form, but they varied in their crystal habit according to the way the original glass had been prepared. They appeared in granular form when they were crystallized form the glass prepared by an oxygen-acetylene flame (Fig. 2). No difference was observed between the two forms in chemical composition, X-ray powder pattern, or refractive index. The kalsilite-type phase are uniaxially negative. The refractive indices of the one crystallized from No. 2 glass are ω 1.640 and ε 1.629, and those of the one crystallized from No. 1 glass are ω 1.646 and ε 1.636.

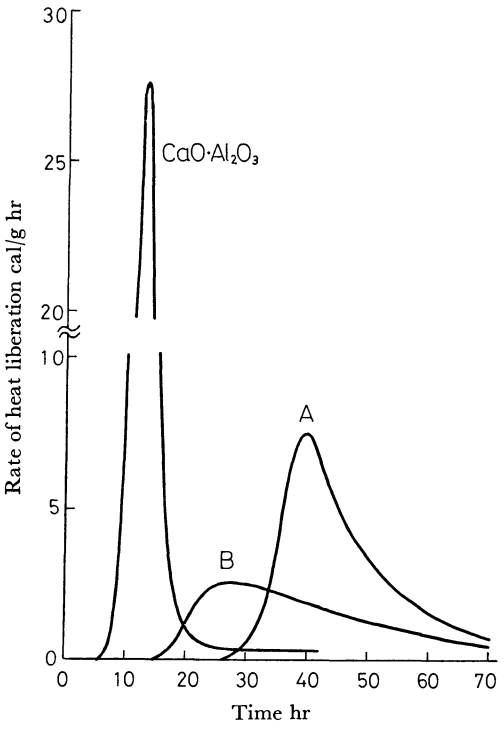

Fig. 3. Rate of heat liberation of the kalsilite-type phase.
A kalsilite-type phase cristallized from glass No. 1.
B kalsilite-type phase cristallized from glass No. 2.

Hydraulic Properties. Since the kalsilite-type phase appears in the compositions close to $CaAl_2O_4$ and has structural similarity to $CaAl_2O_4$, this phase was expected to have a hydraulic property. Generally, the cement-clinker compounds show features characteristic of heat liberation when they react with water. In the present study, therefore, the rates of the heat libetraion of the specimens of the kalsilite-type phase were examined, and they were compared with that of $CaAl_2O_4$, the grain size of which was 10—16 microns in diameter, as is illustrated in Fig. 3. Two kinds of kalsilite-type phases reacted with water, resulting in heat liberation and hardening. The rate of the heat liberation of these specimens was much smaller than that of $CaAl_2O_4$. The hydration products of the phases three days after the addition of water were composed mostly of $CaAl_2O_4 \cdot 10H_2O$, plus a small amount of $Ca_2Al_2O_5 \cdot 8H_2O$. Also, a small amount of the kalsilite-type phase remained unreacted in the No. 1 product, and much, in the No. 2 product.

Consideration

In the previous report[1] the nepheline-type solid solution on the $CaAl_2O_4$–$CaAl_2Si_2O_8$ join was expressed as:
$Ca_{8-(1/2)x}\square_{(1/2)x}Al_{16-x}Si_xO_{32}$. It takes an x value of about from 2 to 5.3. When x became less than 2, the kalsilite-type phase appeared. Kalsilite is the stable form of $KAlSiO_4$ below 850°C,[6] and its structure is based on that of the ideal, high-temperature tridymite. The kalsilite-type phases of this study can be expressed ss follows:
$Ca_{1.82}\square_{0.18}(Al_{3.64}Si_{0.36})O_8$ for the compound crystallized from glass No. 2, and $Ca_{1.85}\square_{0.15}(Al_{3.69}Si_{0.31})O_8$ for the compound crystallized from glass No. 1.

It is interesting to note that some of the weak reflections of the phases can be indexed on the basis of a unit cell similar to those of trikalsilite or tetra-kalsilite; these latter phases are regarded as metastable phases and appear only in compositions near the boundary between the stability ranges for nepheline and for kalsilite.[4,6] That the X-ray powder pattern of the No. 1 phase resembles, in general, that of $CaAl_2O_4$ more closely than that of kalsilite suggests that it is in a transitional stage

4) Th. G. Sahama and J. V. Smith, *Amer. Mineral.*, **42**, 286 (1957).
5) J. V. Smith and Th. G. Sahama, *ibid.*, **42**, 287 (1957).
6) O. F. Tuttle and J. V. Smith, *Amer. J. Sci.*, **256** 571 (1958).

to the monoclinic $CaAl_2O_4$ structure.

Rankin and Merwin[7] and Carstens[8] have reported the existence of uniaxial $CaAl_2O_4$. Recently Nurse *et al.*[9] described, in their study of the CaO–Al_2O_3 system, that the uniaxial $CaAl_2O_4$ was a spherulitic quench-growth of a melt of the composition close to $CaAl_2O_4$. It can be expected that the uniaxial $CaAl_2O_4$ in high aluminous cements will correspond to the kalsilite-type phase because high aluminous cements have compositions close to $CaAl_2O_4$ and usually contain a certain percentage of SiO_2; in addition, they are usually produced by melting.

The author wishes to express his sincere thanks to Dr. K. Sugiura at Nihon Cement Co., and Professor T. Katsura and Professor T. Mori at Tokyo Institute of Technology, for critical reading of the manuscript. Thanks are also due to Mr. H. Morikawa at the Institute and to Mr. S. Ueda at the Company, who kindly aided him in the experiments.

7) G. A. Rankin and H. E. Merwin, *J. Amer. Chem. Soc.*, **38**, 568 (1916).
8) C. W. Carstens, *Z. Kristallogr.*, **63**, 473 (1926).
9) R. W. Nurse, J. H. Welch and A. J. Majumdar, *Trans. Brit. Ceram. Soc.*, **64**, 409 (1965).

BULLETIN OF THE CHEMICAL SOCIETY OF JAPAN VOL. 43 2321—2325 (1970)

Magnetic Circular Dichroism of $[Fe(CN)_6]^{3-}$

Hiroshi KOBAYASHI, Masayuki SHIMIZU and Youkoh KAIZU

Department of Chemistry, Tokyo Institute of Technology, Ookayama, Meguro-ku, Tokyo

(Received December 25, 1969)

Magnetic circular dichroism (MCD) of $[Fe(CN)_6]^{3-}$ was measured in aqueous solution and in a polyvinylalcohol film. The use of the polyvinylalcohol (PVA) film made it possible to measure the MCD and the absorption spectrum of an electrolyte such as $K_3[Fe(CN)_6]$ at dry ice - methanol and liquid nitrogen temperatures, since the film was still optically transparent at lower temperatures. From a comparison between the observations at 300°K, 195°K and 77°K, the magnitude of an angular momentum due to the orbital motion of a hole in the ground state $^2T_{2g}$ (t_{2g}^5) was calculated to be 0.04—0.07 Bohr magneton (β). The observed reduction of the angular momentum was interpreted to be due to partial quenching of the orbital motion by the Jahn-Teller distortion, and also to the delocalization effect between the iron $d\pi$ orbital and the antibonding π molecular orbitals of the coordinating CN^- ions. The B term in $[Fe(CN)_6]^{3-}$, which had been ignored, was predicted to be non-zero and was estimated as -2.4×10^{-3} β/cm^{-1} at the band I and 0.97×10^{-3} β/cm^{-1} at the band II.

The majority of magnetic circular dichroism (MCD) measurements have been carried out with liquid solutions. However the use of the technique at low temperature makes it possible to get much more information about the electronic structure of an open-shell species such as inorganic complexes, free radicals, solvated electrons, or organic negative or positive ions. We present in this paper an MCD measurement of $[Fe(CN)_6]^{3-}$ ion which was carried out at dry ice - methanol and liquid nitrogen temperatures with a film of polyvinylalcohol (PVA) dispersing $[Fe(CN)_6]^{3-}$.

$[Fe(CN)_6]^{3-}$ has an iron(III) ion with a low spin d^5 system. A hole exists in a π molecular orbital which is delocalized over the iron $d\pi$ orbital and the antibonding orbitals of the coordinating CN^- ions. The angular momentum produced by an orbital motion of the hole in the ground state plays an important role in the temperature dependent magnetic circular dichroism. According to Buckingham and Stephens, and Schatz *et al.*,[1,2] the magnitude of molar circular dichroism observed at a transition $a\rightarrow j$ is given by

$$[\theta(a\rightarrow j)]_M = -\frac{24N}{\hbar c}\{f_1A + f_2(B+C/kT)\} \quad (1)$$

where the term C/kT is only a temperature-dependent term,

$$A = \frac{3}{d_a}\sum[\langle j|\hat{\mu}_z|j\rangle - \langle a|\hat{\mu}_z|a\rangle]\cdot \boldsymbol{I}_m[\langle a|\hat{m}_x|j\rangle\langle j|\hat{m}_y|a\rangle] \quad (2)$$

1) A. D. Buckingham and P. J. Stephens, *Ann. Rev. Phys. Chem.*, **17**, 399 (1966).

2) P. N. Schatz, A. J. McCaffery, W. Suëtaka, G. N. Henning, A. B. Ritchie and P. J. Stephens, *J. Chem. Phys.*, **45**, 722 (1966).

$$B = \frac{3}{d_a}\sum \boldsymbol{I}_m\left\{\sum_{k\neq a}\frac{\langle k|\hat{\mu}_z|a\rangle}{W_k - W_a}[\langle a|\hat{m}_x|j\rangle\langle j|\hat{m}_y|k\rangle - \langle a|\hat{m}_y|j\rangle\langle j|\hat{m}_x|k\rangle] + \sum_{k\neq j}\frac{\langle j|\hat{\mu}_z|k\rangle}{W_k - W_j}[\langle a|\hat{m}_x|j\rangle\langle k|\hat{m}_y|a\rangle - \langle a|\hat{m}_y|j\rangle\langle k|\hat{m}_x|a\rangle]\right\} \quad (3)$$

$$C = \frac{3}{d_a}\sum\langle a|\hat{\mu}_z|a\rangle \boldsymbol{I}_m[\langle a|\hat{m}_x|j\rangle\langle j|\hat{m}_y|a\rangle] \quad (4)$$

d_a is the degeneracy of the state a, and $\hat{m}$ and $\hat{\mu}$ are the electric and magnetic dipole operators, respectively. The summations are over all transitions degenerate with $a \rightarrow j$, and the state a and j are diagonal in $\hat{\mu}_z$. W_a is the energy of the state a. A correction for condensed medium effects has been avoided by expressing $[\theta(a\rightarrow j)]_M$ in terms of ratios of A, B, or C to D, the dipole strength ($D \equiv 3\sum|\langle a|\hat{m}_x|j\rangle|^2/d_a$) obtained from the observed absorption intensity.

Recently McCaffery, *et al.*[3] observed a temperature-dependent MCD of $[IrCl_6]^{2-}$ doped in a crystalline $(CH_3NH_3)_2SnCl_6$. The temperature-dependence was assumed to arise primarily from the term $C/\boldsymbol{k}T$. The term $C/\boldsymbol{k}T$ is ascribed to the orientation effect of a temperature-independent magnetic moment of the ground state in a magnetic field. However, another possibility is a temperature-dependent magnetic moment,[4] which arises from a population of the higher sublevels ($J=3/2$) other than the lowest sublevels ($J=1/2$) of the ground state $^2T_{2g}$. Since the spin-orbit coupling in $[IrCl_6]^{2-}$ is so strong that a sufficient gap exists between the sublevels $J=1/2$ and $J=3/2$, the higher sublevels are not populated.[4d] In the case of $[Fe(CN)_6]^{3-}$, however has been observed a temperature-dependent orbital contribution to the magnetic susceptibility due to a population of the higher sublevels.[4c] In this paper, a temperature-dependent MCD of $[Fe(CN)_6]^{3-}$ in a PVA matrix will be presented.

Experimental

The aqueous solution of polyvinylalcohol was added with an aqueous solution of $K_3[Fe(CN)_6]$ and the mixture was allowed to evaporate to dryness on a glass plate. When it was dried, it gave a yellow transparent film.*1 The concentrations and their mixing ratio of the solutions were adjusted to give a film with an optical density of 1.0—2.0.

Our measurement techniques of magnetic circular dichroism will be described elsewhere.[5] All measurements were carried out by a JASCO model ORD/UV-5 instrument with a drastically modified optical path for an electromagnet which produced a magnetic field up to 12000 gauss. When the current in the magnet is reversed, the signal coming out is also reversed. The deviation between two curves thus obtained (Figs. 1—3) gives an effective signal corresponding to that observed in a magnetic field of twofold strength.

The instrument was also furnished with a special Dewar system for the low temperature measurement.

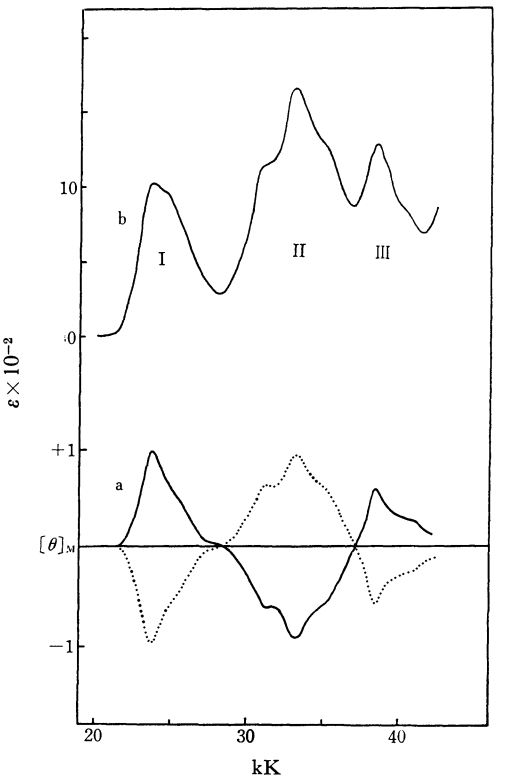

Fig. 1. (a) Molar ellipticity per unit magnetic field of $[Fe(CN)_6]^{3-}$ in aqueous solution at room temperature (300°K).
(b) Molar extinction coefficient of $[Fe(CN)_6]^{3-}$ in aqueous solution at room temperature (300°K).

3) A. J. McCaffery, P. N. Schatz and T. E. Lester, *J. Chem. Phys.*, **50**, 379 (1969).

4) a) M. Kotani, *J. Phys. Soc. Jap.*, **4**, 293 (1949); *Progr. Theor. Phys., Suppl.*, **14**, 1 (1960). b) B.N. Figgis, J. Lewis, R. S. Nyholm and R. D. Peacock, *Discuss. Faraday Soc.*, **26**, 103 (1952); B. N. Figgis, "Introduction to Ligand Fields," Interscience Publishers, New York (1966), Chap. 10. c) $[Fe(CN)_6]^{3-}$: J.B. Howard, *J. Chem. Phys.*, **3**, 813 (1935); B. Bleaney and M. C. M. O'Brien, *Proc. Phys. Soc.*, **B69**, 1205 (1956); F. R. McKim and W. P. Wolf, *ibid.*, **B69**, 1231 (1956). d) $[IrCl_6]^{4-}$: V. Norman and J. C. Morrow, *J. Chem. Phys.*, **31**, 455 (1959); A. H. Cooke, R. Lazenby, F. R. McKim, J. Owen and W. P. Wolf, *Proc. Roy. Soc.*, **A250**, 97 (1959).

*1 The authors are indebted to Dr. T. Hoshi, Department of Chemistry, Aoyama Gakuin University, who kindly showed them how to prepare a PVA film for optical measurement.

5) H. Kobayashi, M. Shimizu and I. Fujita, This Bulletin, **43**, 2335 (1970).

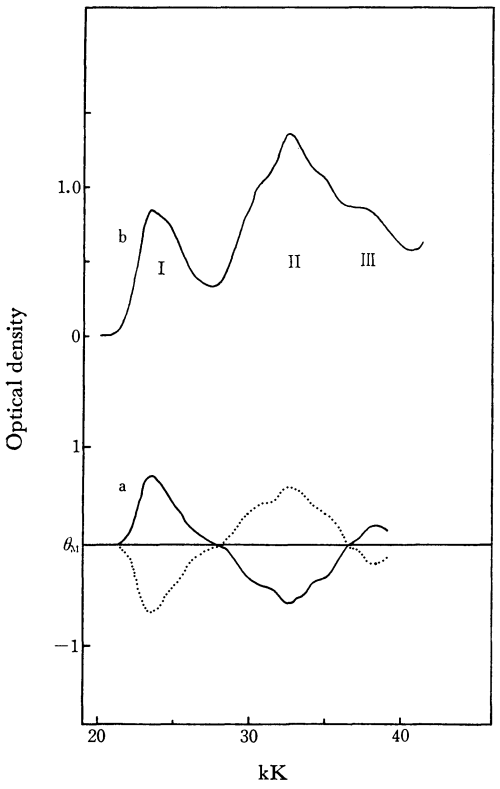

Fig. 2. (a) Ellipticity per unit magnetic field of $[Fe(CN)_6]^{3-}$ in PVA at room temperature (300°K).
(b) Absorption spectrum of $[Fe(CN)_6]^{3-}$ in PVA at room temperature (300°K).

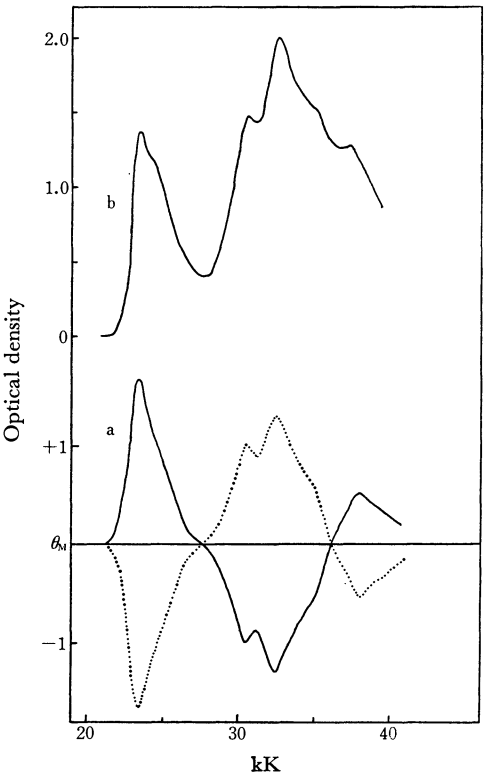

Fig. 3. (a) Ellipticity per unit magnetic field of $[Fe(CN)_6]^{3-}$ in PVA at liquid nitrogen temperature (77°K).
(b) Absorption spectrum of $[Fe(CN)_6]^{3-}$ in PVA at liquid nitrogen temperature (77°K).

Results and Discussion

The magnetic circular dichroism (MCD) and the absorption spectrum of $[Fe(CN)_6]^{3-}$ were measured with an aqueous solution and a polyvinylalcohol (PVA) matrix at room temperature. They are shown in Figs. 1 and 2. There seems to be only a little solvent effect. The magnitude of MCD was given in molar ellipticity per unit external magnetic field $[\theta]_M$. Since the concentration of $[Fe(CN)_6]^{3-}$ in PVA was unknown, the MCD was given in experimentally observed ellipticity per unit external magnetic field θ_M. The film was actually 0.25 mm thick and had an optical density corresponding to that observed for 0.82×10^{-3} mol/l aqueous solution of $[Fe(CN)_6]^{3-}$ in a 1 cm path. If it is necessary, $[\theta]_M=\theta_M/C\cdot l$, where C is the concentration, l is the path length and the product $C\cdot l$, is given by optical density measurement as 0.82×10^{-3} mol l^{-1} cm.

The observed $[\theta]_M$ of $[Fe(CN)_6]^{3-}$ arises predominantly from the term $(B+C/\boldsymbol{k}T)$, since the MCD spectrum shows its maximum at the position of an absorption maximum. If the A term plays an important role, however, the observed MCD should give a sigmoid dispersion curve at the position of the absorption maximum. The function f_1 in (1) is approximately given by a function such as

$$\{\pi^{1/2}\tilde{\nu}(\tilde{\nu}_{ja}-\tilde{\nu})\exp[-(\tilde{\nu}-\tilde{\nu}_{ja})^2/\Delta^2_{ja}]\}/\boldsymbol{h}\Delta^3_{ja}$$

which shows a sigmoid dispersion curve at the position of the absorption maximum ($\tilde{\nu}_{ja}$) and the area obtained by integration of $f_1/\tilde{\nu}$ over whole range of an absorption band should be zero. The function f_2 is approximately given by a function such as Gaussian

$$\{\pi^{1/2}\tilde{\nu}\exp[-(\tilde{\nu}-\tilde{\nu}_{ja})^2/\Delta^2_{ja}]\}/2\Delta_{ja}$$

which shows a maximum at the position of the absorption maximum ($\tilde{\nu}_{ja}$) and the area obtained by integration of $f_2/\tilde{\nu}$ over whole range of an absorption band should be $\pi/2$. The A term makes no contribution to the integrated MCD and

$$\int\frac{[\theta(a\rightarrow j)]_M}{\tilde{\nu}}d\tilde{\nu}=-\frac{24\boldsymbol{N}}{\hbar c}\frac{\pi}{2}(B+C/\boldsymbol{k}T). \quad (5)$$

We avoided troublesome correction for condensed medium effect by expressing our results in terms of a ratio of $\int[\theta]_M/\tilde{\nu}d\tilde{\nu}$ to the dipole strength D. Assuming the best fit Gaussian $\varepsilon(\tilde{\nu})$ to the molar

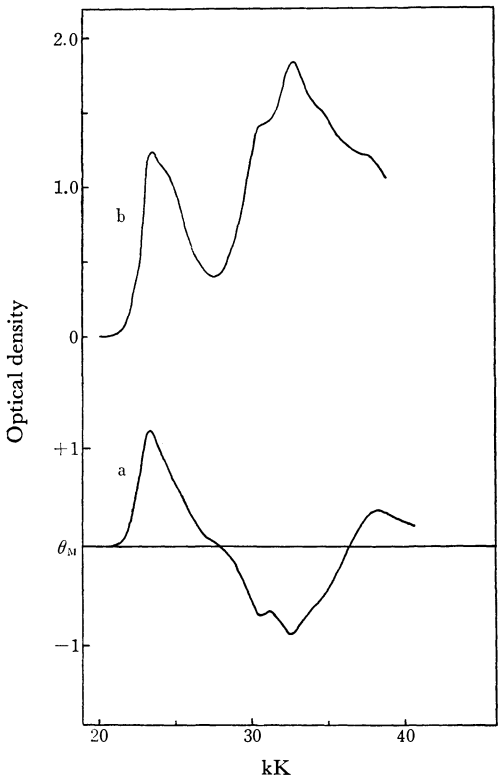

Fig. 4. (a) Ellipticity per unit magnetic field of $[Fe(CN)_6]^{3-}$ in PVA at dry ice-methanol temperature (195°K).
(b) Absorption spectrum of $[Fe(CN)_6]^{3-}$ in PVA at dry ice-methanol temperature (195°K).

absorption curve, the dipole strength D was evaluated from the area obtained by the integration of $\varepsilon(\bar{\nu})/\bar{\nu}$ over whole range of an absorption band. The value of $\int[\theta]_M/\bar{\nu}d\bar{\nu}$ was also obtained by the integration of a Gaussian which best reproduced the observed magnetic molar ellipticity curve. B and $C/\boldsymbol{k}T$ were given in units of square Debye·Bohr magneton per cm^{-1}. Our observation at room temperature and the value of C obtained by an assumption that the B term is negligibly small, are given in Fig. 1 and Table 1, respectively, and are in good agreement with the data published by Schatz, *et al.*[2] Measurements of MCD at various temperatures are expected to give a criterion to the validity of the assumption.

TABLE 1. PARAMETER VALUES FOR $[Fe(CN)_6]^{3-}$ IN AQUEOUS SOLUTION AT ROOM TEMPERATURE (300°K)

	$C(D^2\cdot\beta)$	$D(D^2)$	$C/D(\beta)$
Band I	−0.824	1.34	−0.615
Band II	0.961	3.03	0.317
Band III	−0.153	1.35	−0.113

D: Debye unit; β: Bohr magneton.

Three bands of moderate intensity (ε_{max} ~1000—2000) at 24000, 33000 and 38500 cm^{-1} have been observed.[6] These bands have been assigned to the allowed "ligand to metal" charge transfer transitions. Of these, two are $^2T_{2g}\rightarrow{}^2T_{1u}$ and one is $^2T_{2g}\rightarrow{}^2T_{2u}$. After some different assignments had been given,[7,8] the first band was assigned to $^2T_{2g}\rightarrow{}^2T_{1u}$ transition and the second to $^2T_{2g}\rightarrow{}^2T_{2u}$ transition based on magneto-optical rotatory dispersion (MORD) measurements[9] which had been carried out by Shashoua[10] and Briat.[11] Since C/D is a measure of the angular momentum of an orbital motion in the ground state, the magnitude of $|C/D|$ should not be changed from one band to another and the sign of C/D should be opposite that for the transitions to T_{1u} and T_{2u} states. Actually the MCD observed at the second band shows an opposite sign to the MCD observed at the first band and at the third band. From existing MCD data[2] including a semiquantitative measurement by Foss and McCarville[12] and also MORD data, it follows that the first band and the third band corresponding to $^2T_{1u}$ excited states show a negative C, and the second band corresponds to $^2T_{2u}$ excited state and shows a positive C.

The PVA film was optically transparent even at liquid nitrogen temperature (77°K). An optically transparent PVA film dispersing $[Fe(CN)_6]^{3-}$ was measured for MCD at various temperatures. The results are shown in Figs. 2—4. The PVA film technique made it possible to observe the MCD and the absorption spectrum of an electrolyte such as $K_3[Fe(CN)_6]$ at dry ice-methanol temperature and at liquid nitrogen temperature. When the measurements of the MCD and the absorption were carried out with exactly the same sample, the ratio of the observed value of the integrated MCD to the observed value of the integrated absorption is independent of the actual concentration of $[Fe(CN)_6]^{3-}$ in the film and gives the value of $(B+C/\boldsymbol{k}T)/D$.

TABLE 2. PARAMETER VALUES FOR $[Fe(CN)_6]^{3-}$ IN PVA FILM

	$(B+C/\boldsymbol{k}T)/D\times10^3(\beta/cm^{-1})$		
	300°K	195°K	77°K
Band I	−2.72	−3.02	−3.73
Band II	1.19	1.29	1.80

6) For example, C. K. Jørgensen, *Acta Chem. Scand.*, **10**, 518 (1956).
7) C. S. Naiman, *J. Chem. Phys.*, **35**, 323 (1961); *ibid.*, **39**, 1900 (1963).
8) G. Basu and R. L. Belford, *ibid.*, **37**, 1933 (1962).
9) P. J. Stephens, *Inorg. Chem.*, **4**, 1690 (1965).
10) V. E. Shashoua, *J. Amer. Chem. Soc.*, **86**, 2109 (1964).
11) B. Briat, *Compt. Rend.*, **259**, 2408 (1964).
12) J. G. Foss and M. E. McCarville, *J. Amer. Chem. Soc.*, **87**, 228 (1965).

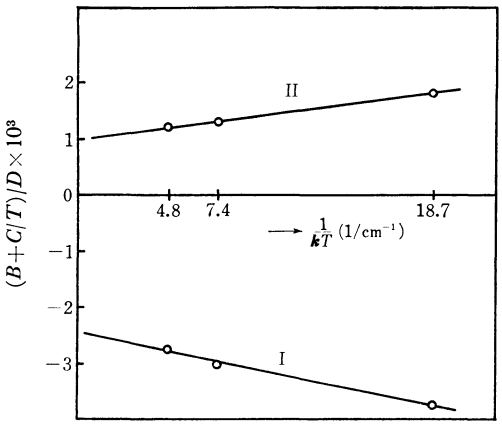

Fig. 5. Temperature dependence of $(B+C/kT)/D$.

Table 2 shows our observed values of $(B+C/kT)/D$.

As shown in Fig. 5, a plot of the observed values of $(B+C/kT)/D$ *versus* $1/kT$ gave a straight line. It gave non-zero B/D from its intercept and fairly small C/D from its slope. The value of B/D was found to be -2.44×10^{-3} β/cm^{-1} for the first band, while the value was obtained to be 0.97×10^{-3} β/cm^{-1} for the second band. The ignored angular momentum induced by magnetic field is not zero. A difference of the magnitudes of B/D between the two bands seems to be appreciable. The value of C/D was -0.070 β for the first band and $+0.044$ β for the second band. These values of C/D in the absolute value are fairly smaller than 0.5 β theoretically expected for an orbital motion of a hole at the central iron.[2] Delocalization of the hole over whole complex will reduce the absolute value of C/D. However, another important mechanism expected to reduce the value is a quenching of the orbital motion by trapping the hole in the lowest component of t_{2g} molecular orbitals split by a dynamical or static Jahn-Teller distortion of the open shell $d\pi^5$ system. As far as the MCD measurements are concerned, a population of the higher sublevels ($J=3/2$) in $[Fe(CN)_6]^{3-}$ does not seem to change the values of B and C since the plot shown in Fig. 5 gives a nice straight line. However, a theoretical approach to the problem is required. Theoretical interpretations including molecular orbital calculation will be given elsewhere.

BULLETIN OF THE CHEMICAL SOCIETY OF JAPAN VOL. 43 2326—2331 (1970)

ζ-Potentials of Natural and Synthetic Fibers in SDS Solutions and the Viscosity of SDS Solutions above the Critical Micelle Concentration*1,*2

Yoshio IWADARE and Toshiro SUZAWA

Department of Applied Chemistry, Faculty of Engineering, Hiroshima University, Senda-machi, Hiroshima

(Received December 31, 1969)

In order to investigate the adsorption behavior of an anionic surfactant on fibers, the ζ-potentials of natural and synthetic fibers in aqueous solutions of sodium dodecyl sulfate (SDS), mainly above the critical micelle concentration (CMC), were measured. Further, the change in the structure of the SDS micelle in aqueous solutions was studied by means of the viscosity method. At first the reduced viscosity for the SDS micelle, η_{spm}/c_m (c_m: the micellar concentration), increased rapidly with the c_m as long as the c_m was small; thereafter, after a break, it approximated the saturated values as a whole. The results calculated from the experimental data using Jones and Dole's equation showed two distinct breaks. The first break corresponded to the 1st CMC, and the second, nearly to the break in the η_{spm}/c_m *vs.* c_m curve. In addition, the intrinsic viscosity for the SDS micelle, $[\eta]_M$, and the effective specific volume, V, were obtained. From these results, it can be assumed that the structure of the SDS micelle is variable at the break in the η_{spm}/c_m *vs.* c_m curve. The ζ-potentials of fibers in aqueous SDS solutions changed rapidly with an increase in the concentration of SDS, but they remained approximately constant in the vicinity of the CMC. At much higher concentrations above the CMC (in the vicinity of the SDS concentration of 2×10^{-2} mol/l), the ζ values again gradually changed; thereafter, after a break, they became nearly constant again. The change in the ζ-potentials corresponds approximately to the break in the η_{spm}/c_m *vs.* c_m curve. Therefore, it may be suggested that it is connected with the change in the structure of the SDS micelle.

The adsorption of an anionic surface active agent on the fiber-solution interfaces is considered to be an important factor in problems of detergency. It is generally known that the washing power of a surfactant increases up to a certain concentration of surfactant; beyond this point, however, the further addition of the surfactant has little effect.[1-3]

On the other hand, in the case of the adsorption of a surfactant on solid materials, the appearance of maxima in adsorption isotherms has been observed by many authors.[4-11] It seems that the maxima in adsorption isotherms correspond to the critical washing concentration (CWC) in detergency. However, several investigators[12-17] did not clearly observe such maxima in isotherms.

Previous papers[18] have described the relationship

*1 This paper is Part VIII in a series on "Surface Adsorption Properties and ζ-Potentials of Fibrous Materials in Surface Active Agent Solutions"; Part VII: T. Suzawa and M. Yuzawa, *Yukagaku*, **15**, 20 (1966).

*2 Presented at the 21st Symposium of Colloid and Interface Chemistry, Kyoto, Nov. 2, 1968; at the 22nd Annual Meeting of the Chemical Society of Japan, Tokyo, April 7, 1969, and at the Meeting of Oil Chemistry of the Japan Oil Chemists' Society, Osaka, Nov. 6, 1969.

1) W. C. Preston, *J. Phys. & Colloid Chem.*, **52**, 84 (1948).
2) E. K. Goette, *J. Colloid Sci.*, **4**, 459 (1949).
3) T. Tachibana, A. Yabe and M. Tsubomura, *ibid.*, **15**, 278 (1960).
4) M. L. Corrin, E. L. Lind, A. Roginsky and W. D. Harkins, *ibid.*, **4**, 485 (1949).
5) A. L. Meader and B. A. Fries, *Ind. Eng. Chem.*, **44**, 1636 (1952).
6) R.D. Vold and A.K. Phansalkar, *Rec. Trav. Chim. Pays-Bas*, **74**, 41 (1955).
7) A. Fava and H. Eyring, *J. Phys. Chem.*, **60**, 890 (1956).
8) R. D. Vold and N. H. Sivaramakrishnan, *ibid.*, **62**, 984 (1958).
9) H. C. Evans, *J. Colloid Sci.*, **13**, 537 (1958).
10) H. J. White, Y. Gotshal, L. Robenfeld and F. H. Sexsmith, *ibid.*, **14**, 598 (1959).
11) F. Z. Saleeb and J. A. Kitchener, *J. Chem. Soc.*, **1965**, 911.
12) A. S. Weatherburn and C. H. Bayley, *Textile Res. J.*, **22**, 797 (1952).
13) M. Hayashi and Y. Nakazawa, *Radioisotopes*, **8**, 149 (1959).
14) M. Hayashi, This Bulletin, **33**, 1184 (1960).
15) C. Sakai and S. Komori, *Yukagaku*, **14**, 66 (1965).
16) J. A. Kitchener, *J. Phot. Sci.*, **13**, 152 (1965).
17) B. E. Gordon, G. A. Gillies, W. T. Shebs, G. M. Hartwig and G. R. Edwards, *J. Amer. Oil Chem. Soc.*, **43**, 232 (1966).
18) a) T. Suzawa, *Kogyo Kagaku Zasshi*, **66**, 1002 (1963). b) T. Suzawa and M. Yuzawa, *Yukagaku*, **15**, 20 (1966).

between the ζ-potentials of synthetic fibers in aqueous solutions of a surfactant and the surface-adsorption properties of its agent on the fibers below the critical micelle concentration (CMC). It was suggested that the adsorption of an anionic surfactant on fibers in an aqueous neutral solution takes place mainly by means of van der Waals' force. Further, the amount of anionic surfactant adosorbed per unit of the area of the fiber surface increased with an increase in the concentration of its agent; the increase was the greater, the smaller the degree of swelling of the fiber and the more hydrophobic the fiber. These facts indicate that the interaction between the hydrocarbon chain of an anionic surfactant and the hydrophobic part of a fiber is important for the adsorption of its agent on the fiber.

At present, in order to contribute to the study of the adsorption behavior of an anionic surfactant on the fibers in the vicinity of the CMC and above of its agent, the ζ-potentials of natural and synthetic fibers in aqueous solutions of sodium dodecyl sulfate (SDS) were measured. On the other hand, the viscosity of an aqueous SDS solution was determined in order to investigate the relationship between the structure of the micelle and the concentration of the surfactant. In this paper, the relationship between the ζ-potentials of fibers in aqueous solutions of SDS and the change in the structure of the SDS micelle will be primarily reported on.

Experimental

Apparatus and Procedures. *ζ-Potential.* The ζ-potential was measured by the method of the streaming potential described in a previous paper.[19] The streaming potential was measured by using a Transistorized Dynamic-Condenser Electrometer, Model UFE 26301 H

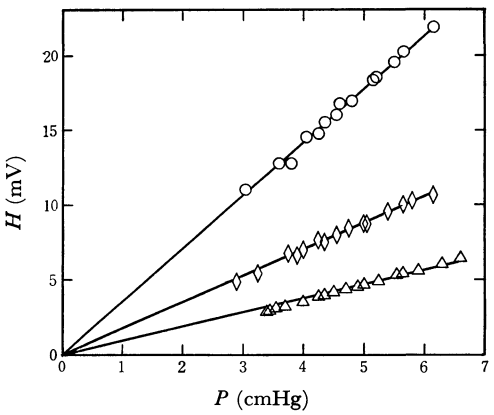

Fig. 1. Relation of streaming potential (H) to pressure (P) for Nylon 6 fiber.
SDS concentration (mol/l):
(○) 4×10^{-3}; (◇) 10×10^{-3}; (△) 26×10^{-3}

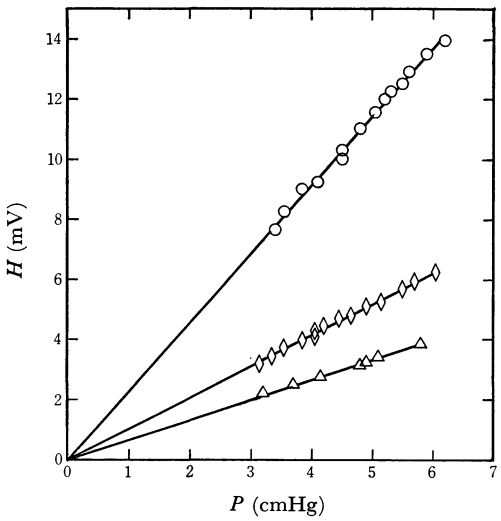

Fig. 2. Relation of streaming potential (H) to pressure (P) for Cashimilon fiber.
SDS concentration (mol/l):
(○) 4×10^{-3}; (◇) 10×10^{-3}; (△) 26×10^{-3}

(Tokyo Shibaura Electric Co., Ltd.). The relation between the streaming potential, H (mV), and the pressure, P (cmHg), is shown in Figs. 1 and 2, the figures corresponding, respectively, to Nylon 6 and Cashimilon fibers. On the basis of these results, the streaming potential can be said to be accurately proportional to the pressure (*i. e.*, to the velocity of streaming) between mercury pressures of 3 and 6 cm above the CMC as well as below it.

Actually, the streaming potential measurements were always carried out at a mercury pressure of 5 cm and at a temperature of 25 ± 0.02°C. The solutions examined all contained 10^{-4} mol/l of sodium chloride.

Critical Micelle Concentration (CMC). The critical micelle concentration was determined by measuring the surface tension, the conductance, and the viscosity of aqueous solutions of the surfactant in the presence of 10^{-4} mol/l sodium chloride and at 25 ± 0.02°C.

Surface Tension: A drop method was used for measuring the surface tension of solutions. The surface-tension values were corrected by the method of Harkins and Brown.[20]

Conductance: The conductance values were obtained by means of a Yanagimoto Conductivity Outfit, Model MY-7 (Yanagimoto MFG. Co., Ltd.).

Viscosity: The viscosities of the solutions were measured with an Ostwald viscometer prepared by reference to the British Standard,[21] so the surface tension correction was small.[22] The capillary of this viscometer was 12.5 cm long, and its average radius was 0.028 cm. Reynolds number was about 30. The kinetic correction amounted to less than 1 part in 1000 over the whole concentration range studied.[22]

19) T. Suzawa, T. Saito and H. Shinohara, This Bulletin, **40**, 1596 (1967).

20) W. D. Harkins and F. E. Brown, *J. Amer. Chem. Soc.*, **38**, 288 (1916); *ibid.*, **41**, 499 (1919).

21) A. E. Alexander and P. Johnson, "Colloid Science," Appendix IV (1949).

22) Y. Iwadare and T. Suzawa, *Nippon Kagaku Zasshi*, **90**, 1106 (1969).

The viscometer was cleaned immediately before each filling with a warm sulfuric acid-dichromate solution, rinsed numerous times in order to remove all traces of the acid, and dried with air. The flow time for water was 663.9 sec. From three to five flow-time measurements were made on each solution.

Materials. *Fibers.* Polyamide Nylon 6 (manufactured by the Toray Co., Ltd.; draw ratio, 1; denier, unknown; 30 filaments), polyvinylalcohol Vinylon (Kurashiki Rayon Co., Ltd.; 1.4 denier; monofilament; degree of formylation, 0.34), polyacrylonitrile Cashimilon (Asahi Chemical Industry Co., Ltd.; 52 counts; monofilament) and polypropylene Pylen (Toray Co., Ltd.; 100 denier; 24 filaments) were first extracted with ethanol for about 24 hr at room temperature; then they were extracted with deionized water and finally dried in air. Cotton fiber (Kanegafuchi Spinning Co., Ltd.; 30 counts; yarn) was extracted with deionized water, with ethanol, and with an ethanol-benzene mixed solvent (volume ratio 1: 1) for 24 hr at room temperature; finally it was extracted with deionized water.

Glass capillaries were used instead of glass fiber. Hario glass tubes (JIS K-250) sold by the Shibata Chemical Apparatus Mfg. Co., Ltd., were used for the capillaries. These capillaries were 23 mm long, and their average inner and outer diameters were 0.2 and 0.4 mm respectively. They were cleaned with a warm sulfuric acid - dichromate solution and rinsed numerous times with conductivity water in order to remove all traces of acid by means of suction with a aspirator.

Surface Active Agent. The sodium dodecyl sulfate (SDS) was provided by the Nippon Oils & Fats Co., Ltd. The surface tension *vs.* the log concentration curve showed no minimum. The CMC values obtained are given in Table 1.

Table 1. The CMC values of SDS in aqueous solution (NaCl: 10^{-4} mol/*l*, 25°C)

Method	CMC (mol/*l*) $\times 10^3$
Surface tension	7.1
Conductivity	7.6
Viscosimetry	7.0

Results and Discussion

Viscosity of SDS Solution and Change in the Structure of SDS Micelles. *Viscosity of Aqueous SDS Solution.* The results of the viscosity measurement for an aqueous SDS solution in the presence of 10^{-4} mol/*l* sodium chloride are shown in Fig. 3. The SDS solution was studied over the concentration range $(4—255) \times 10^{-3}$ mol/*l*.

The variation in the relative viscosity, η_r, with the SDS concentration, c_s (mol/*l*), is shown by curve I. The gentle upward curvature of the curve seems to be a result of mutual interference between the colloidal particles in motion during flow.[23]

The relation between the reduced viscosity, η_{sp}/c_s, and c_s, as is shown by curve II, reaches a minimum at the SDS concentration of 7×10^{-3} mol/*l*. This minimum point is believed to correspond to the CMC, $c_{c(1)}$, it agrees well with the CMC value obtained by surface-tension measurements (*cf.* Table 1).

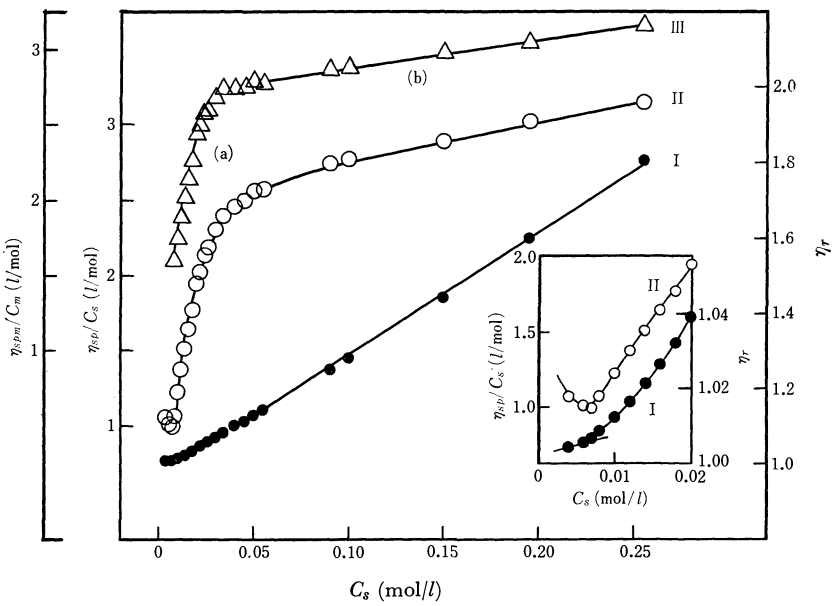

Fig. 3. Viscosity of aqueous SDS solution.
curve I: η_r *vs.* c_s; curve II: η_{sp}/c_s *vs.* c_s; curve III: η_{spm}/c_m *vs.* c_m

23) R. J. Vetter, *J. Phys. & Colloid Chem.*, **51**, 262 (1947).

Sata and Tyuzyo[24] presumed that above the 1st CMC, the concentration of a surfactant monomer in a solution which is in equilibrium with the micelle is almost constant and remains unchanged. Accordingly, the following operations were performed:

$$c_m = c_s - c_{c(1)}$$

$$\eta_{spm}/c_m = \{(\eta_r/\eta_{rc(1)}) - 1\}/(c_s - c_{c(1)}) \quad (1)$$

where;

η_{spm}/c_m: reduced viscosity for the micelle.
$\eta_{rc(1)}$: relative viscosity at the 1st CMC, $c_{c(1)}$.

Therefore, the recuced viscosity for SDS micelles, η_{spm}/c_m, is shown by curve III.

From this figure, it can be seen that the η_{spm}/c_m increases linearly with the c_m as long as the c_m is small; thereafter, after a break observed in the concentration range $(20—25)\times 10^{-3}$ mol/l, it approximates the saturated value as a whole. The second, sharper break did not appear in the concentration range studied.

Intrinsic Viscosity and Hydration of SDS Micelles. Shinoda[25] has suggested that the shape and the size of micelle depend on the concentration, the temperature, the molecular structure of the respective surface active agent, the kind of intermolecular force, and the kinds of additives. Grindley and Bury[23,26] have indicated that the micelle size increases to a maximum over a short transition concentration range. At present, while the evidence that amphipathic molecules associate to form aggregates of micelles is overwhelming, the size and shape of these micelles are still disputed.[27]

Mukerjee[28] has estimated the hydrations of micelles of SDS and dodecyl and tetradecyl trimethyl ammonium chlorides from the viscosity data in the following manner. That is, the hydration, h, in weight percentage is obtained, assuming that the micelles are spherical, from an extension of Einstein's equation:

$$[\eta]_M = 2.5(\bar{V}_s' + h) \quad (2)$$

where $[\eta]_M$ is the corrected intrinsic viscosity for the charged micelle, and where $\bar{V}_s'$ is the partial specific volume of the micelle. Consequently, it was concluded that the formation of ice-like hydration sheaths on hydrocarbon surfaces and the thickening of the shear layer on highly-charged surfaces because of the viscoelectric effect are probably unimportant.

Table 2. Intrinsic viscosities and hydration of SDS micelles

	$[\eta]_M$ (ml/g)	Hydration in weight per cent		Hydrodynamic volume	Hydration in volume per cent
		Author	Mukerjee[28]		
Portion (a)	3.3	43	39±4	1.32	24
Portion (b)	7.5	211		3.00	67

On the basis of Eq. (2), the hydration of SDS micelles obtained from the curve III are shown in Table 2. Further, in the table the hydrodynamic volumes[23] and hydrations in volume percentage, calculated from hydrodynamic volumes, are also shown. The electroviscous effect, included as part of the intrinsic viscosity, was corrected for by using the data of Parker and Wasik.[29] The partial specific volume of SDS micelles, $\bar{V}_s'$, is 0.889 ml/g.[30]

At all events, on the basis of Table 2 it seems likely that the degree of hydration and, hence, the size of SDS micelles increase to some extent with an increase in the concentration on the portion (a). As the solution becomes more concentrated, the counter-ion concentration steadily increases, with a resulting decrease in the degree of ionization of the micelles; the stability is thereby enhanced.[31] The reduced viscosity for SDS micelles, η_{spm}/c_m, linearly increases little by little with an increase in the concentration on the portion (b). This fact suggests that the micellar properties remain constant over a relatively wide range of concentration, indicating that the dimensions and the form of the micelles remain constant.[32,33]

Effective Specific Volume of SDS. Use was made of Guth and Simha's equation,[32,34,35] which is a form of Einstein's equation extended for application to more concentrated solutions:

$$\eta_r = 1 + 2.5\phi + 14.1\phi^2 \quad (3)$$

where ϕ is the volume fraction occupied by the spherical particles. The effective specific volume of 1 g of a surfactant including hydrated water, V, is expressed as follows[32,35]:

$$V = \phi/c \quad (4)$$

where c is the concentration of the solution in g/ml.

24) N. Sata and K. Tyuzyo, This Bulletin, **26**, 177 (1953).
25) K. Shinoda, T. Nakagawa, B. Tamamushi and I. Isemura, "Colloidal Surfactants," Academic Press Inc., New York (1963), p. 25.
26) J. Grindley and C. R. Bury, *J. Chem. Soc.*, **1929**, 679.
27) L. I. Osipow, "Surface Chemistry," Reinhold Publishing Corporation, New York (1963), p. 174.
28) P. Mukerjee, *J. Colloid Sci.*, **19**, 722 (1964).
29) R. A. Parker and S. P. Wasik, *J. Phys. Chem.*, **62**, 967 (1958).
30) P. Mukerjee, *ibid.*, **66**, 1733 (1962).
31) K. A. Wright and H. V. Tartar, *J. Amer. Chem. Soc.*, **61**, 544 (1939).
32) D. C. Robins and I. L. Thomas, *J. Colloid Interfac. Sci.*, **26**, 415 (1968).
33) T. Ito and H. Mizutani, *Yakugaku*, **17**, 246 (1968).
34) E. Guth and R. Simha, *Kolloid-Z.*, **74**, 266 (1936).
35) K. Shinoda, T. Nakagawa, B. Tamamushi and T. Isemura, "Colloidal Surfactants," Academic Press Inc., New York (1963), p. 115.

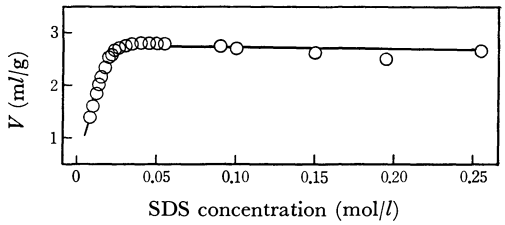

Fig. 4. Effective specific volume (V) with SDS concentration.

The values of V thus calculated are shown in Fig. 4. The effective specific volume of the dispersed colloidal particles of SDS increases with the concentration as long as the SDS concentration is small; thereafter, after a break, it remains approximately constant in the range of high concentration. This break roughly corresponds to that of curve III in Fig. 3. The constancy of the effective specific volumes is also indicative of a spherical micelle.[32,35] Therefore, the shape and size of these micelles must remain constant in the range of concentration beyond the break, but they are not constant in the smaller range.

The Change in the Structure of SDS Micelle Observed from Jones and Dole's Equation. The relative viscosity of an electrolyte solution with a molar concentration, m, is given by Jones and Dole's equation[28,36,37]:

$$\eta_r = 1 + A\sqrt{m} + Bm \qquad (5)$$

where A and B are constants. It is believed that the B coefficient for a particle in water is a positive quantity indicating a structure-forming tendency. On the other hand, if the electrolyte particle tended to destroy the structure of water and produce disorder, then the B coefficient would be a negative quantity.[37]

It is suggested that the formation of micelles is attended by a change in the structure of the solvent, that is, by an interaction between micelles and solvent.[23] If the change in the structure of the micelle were attended by a change in the structure of water, the B coefficient would be variable.

The results calculated from the experimental data are shown in Fig. 5. From this figure, it can be seen that there are two distinct breaks, at points a and b. The point a nearly corresponds to the 1st CMC, and the point b, roughly to the break of curve III in Fig. 3 and to that of the V *vs.* concentration curve in Fig. 4.

Nakagaki and Ninomiya[38] have shown the viscosity data that the 2nd CMC of SDS is 0.02

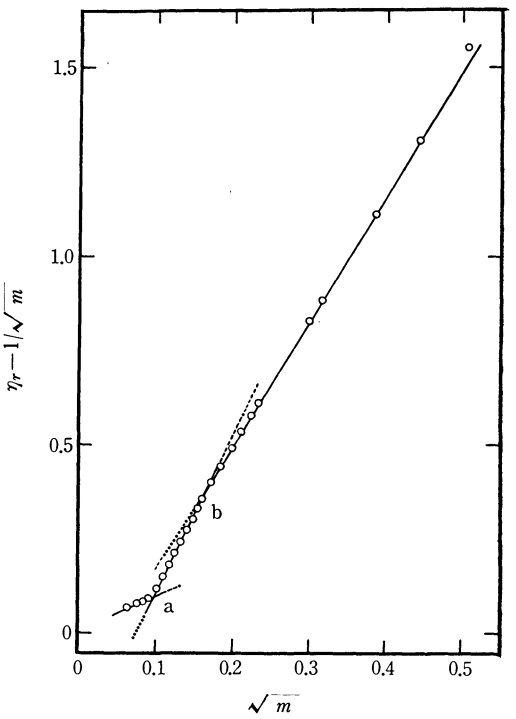

Fig. 5. Behaviour in viscosity of aqueous SDS solution observed by Jones and Dole's equation.

mol/l (40°C). This concentration nearly corresponds to that of the point b in the curve. On the basis of these results, it can be assumed that the structure of the SDS micelle is variable at the point b in Fig. 5.

ζ-Potential of Fibers in Aqueous SDS Solutions. *ζ-Potential below the CMC.* The ζ-potential was measured over the SDS concentration range $(0—30)\times10^{-3}$ mol/l in the presence of 10^{-4} mol/l sodium chloride, and every hour on the hour. The results obtained are shown in Fig. 6. These are the equilibrium values which were approximated after four hours of immersion.

The ζ-potential for the Nylon 6 fiber is negative and rapidly increases with an increase in the SDS concentration. This fact suggests that, in spite of the negative charge of Nylon 6 in an aqueous solution, the amount of SDS adsorbed on the surface of the fiber rapidly increases with an increase in the agent concentration. It can also be suggested that the Nylon 6 fiber combines mainly with SDS by means of van der Waals' force, as has been described in a previous paper.[18b]

The ζ *vs.* SDS concentration curve for the Pylen fiber resembles that for Nylon 6 very closely in its behavior, but the negative ζ values for the former are larger than those for the latter over the concentration range studied. This fact suggests that surface-surfactant adsorption for the Pylen fiber is appreciably larger than that for the Nylon 6 fiber.[18b]

36) G. Jones and M. Dole, *J. Amer. Chem. Soc.*, **51**, 2950 (1929).
37) M. Abu-Hamdiyyah, *J. Phys. Chem.*, **69**, 2720 (1965).
38) M. Nakagaki and Y. Ninomiya, This Bulletin, **37**, 817 (1964).

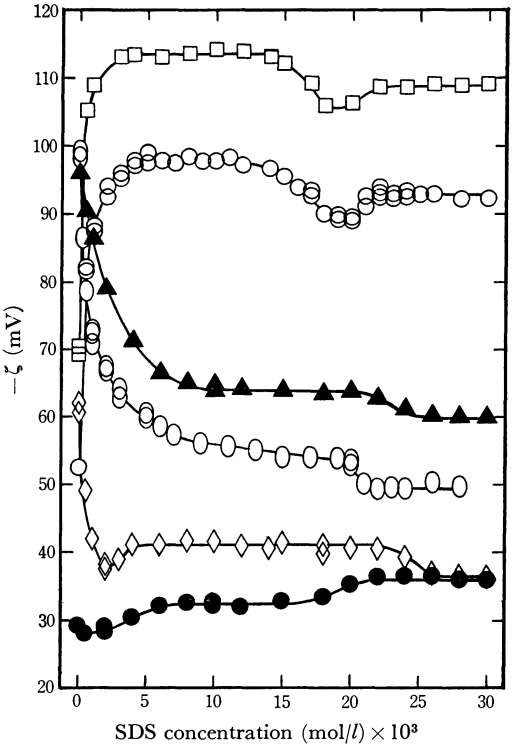

Fig. 6. ζ-potentials for fibers with SDS concentration.
(□) Pylen; (○) Nylon 6; (▲) Cashimilon; (0) glass; (◇) Vinylon; (●) cotton

On the other hand, the ζ-potentials for the glass and Cashimilon rapidly decrease with an increase in the SDS concentration. It can be suggested that the decrease in ζ values with an increase in the concentration may be due to a decrease in the thickness of the double layer, because the total ionic strength in solutions increases with an increase in the concentration. Furthermore, it may be due to a small adsorption of SDS on the surfaces of these samples, because of the large electrostatic repulsion between the surfaces of fibers and SDS anions.

A similar behavior for the ζ *vs.* SDS concen tration curve of Vinylon is also observed, except that this curve passes through a minimum at the 2×10^{-3} mol/*l* concentration. It is not at all clear why the ζ-potential of Vinylon shows its minimum at this concentration.

The negative ζ-potential for cotton increases from about 29 mV at the SDS concentration of zero to about 32 mV at the CMC. This change in the ζ-potential is small; therefore, it can be presumed that the surface-surfactant adsorption for cotton is small, in spite of the small electrostatic repulsion between the surfaces of the fiber and the SDS anions.

ζ-Potential in the Vicinity of the CMC. The ζ-potentials of all the fibers investigated remain nearly constant in the vicinity of the CMC. This constancy is also kept to some distance above the CMC. On the basis of these results, it can be presumed that the surface adsorption of SDS on fibers remains nearly constant in this concentration range.

Relationship between the Change in ζ-Potentials of Fibers and That in the Structure of the SDS Micelle. As the solution becomes more concentrated, the ζ-potentials for fibers change again; thereafter, after a minimum or a break, they again remain constant. It is rather interesting that the ranges of SDS concentration in which the apparent changes of the ζ-potentials of fibers are observed correspond approximately to the concentration for the break in curve III in Fig. 3, to that for the break in the curve in Fig. 4, and to that for the point b in Fig. 5.

From these facts, it can be presumed that, if the structure of the micelle changed at the concentration for the break in the η_{spm}/c_m *vs.* c_m curve, as has been mentioned above, there would be a change in the structure of the diffuse double layer and that, consequently, the ζ-potentials of the fibers would change.

In more concentrated solutions, the degree of ionization of the micelle must be more decreased and the stability thereby enhanced.[31] As is shown by the viscosity data (*cf.* Table 2 and Figs. 3—5), the micellar properties remain constant over a relatively wide range of concentrations, indicating that the size and the shape of micelle remain approximately constant.[32,33] Consequently, the structure of the double layer should again be kept stable. It is, therefore, understandable that the ζ-potentials for fibers are again kept constant in much higher concentration ranges, that is, in $(22—30)\times10^{-3}$ mol/*l* for Pylen, Nylon 6, and cotton, in $(25—30)\times10^{-3}$ mol/*l* for Cashimilon and Vinylon, and in $(21—28)\times10^{-3}$ mol/*l* for glass.

The authors wish to thank the Toray Co., Ltd., the Kurashiki Rayon Co., Ltd., the Asahi Chemical Industry Co., Ltd., and the Kanegafuchi Spinning Co., Ltd., for providing the fibers, and the Nippon Oils & Fats Co., Ltd., for the surfactant (SDS).

BULLETIN OF THE CHEMICAL SOCIETY OF JAPAN VOL. 43 2332—2335 (1970)

Studies of Photochemical Reactions Using Organic Photosensitizers. I. Benzene-Photosensitized Decomposition of Nitrous Oxide

Shigeru YAMASHITA, Kin-ichi ADACHI and Teruo HAYAKAWA

Department of Chemistry, Faculty of Liberal Arts and Sciences, University of Osaka Prefecture, Mozu-umemachi, Sakai, Osaka

(Received January 12, 1970)

Benzene-photosensitized decomposition of nitrous oxide has been studied in a mercury-free reaction system. 2537 Å line of low-pressure mercury lamp was absorbed by benzene and the excitation energy of benzene was transferred to nitrous oxide by triplet-triplet energy transfer mechanism. Only N–O bond rupture of nitrous oxide has been observed, which is reasonable from energetic view point. The decomposition yield of the excited triplet state of nitrous oxide was estimated to be 15% and the triplet state seems to be less than 84 kcal/mol above the ground state.

In recent years a large number of works on photochemical reactions using organic photosensitizers have been reported. Most of the work, however, has been carried out on the reactions of organic compounds in liquid phase. Since the pioneer work of Dubois and Noyes[1] only a few studies have been reported about gas phase photochemical reactions involving chemical bond splitting caused by organic photosensitizers,[2,3] although a number of gas phase photochemical reactions have been studied by mercury-photosensitization and a review of these studies has been presented.[4]

It is easy to choose organic sensitizers of various triplet state energies. However, only a few sensitizers such as Hg and Cd are available as inorganic photosensitizers. Hammond *et al.* studied the energy dependecne of *cis-trans* isomerization reactions of olefins using various organic photosensitizers.[5]

In the present work, the photochemical decomposition of nitrous oxide was studied using benzene vapor as a sensitizer. Benzene is one of the most well-studied photosensitizer in photochemical reactions,[1,6,7] and the lowest triplet energy level is known to be 84 kcal/mol.[8]

Bond energies of nitrous oxide have been studied by electron impact method[9,10] and the linear structure of nitrous oxide has been given by infrared spectroscopy.[11]

Although nitrous oxide is a simple triatomic molecule, the cross section of nitrous oxide in quenching of the excited mercury atom (Hg 6^3P_1) is relatively high compared with other simple molecules.[4] Nitrous oxide was used as a quencher competing with ketene in the mercury-photosensitized reaction for the determination of the quenching cross section of ketene.[12]

From the study of thermal decomposition of nitrous oxide, N–O bond splitting seems to occur through a triplet state about 60 kcal/mol[13,14] above the ground state.

Since the absorption band of nitrous oxide lies in vacuum-ultraviolet region,[15,16] photosensitized decomposition of nitrous oxide would be observed by some organic sensitizers as well as by excited mercury atoms[17,18] if the excited triplet state of the organic sensitizers is higher than 60 kcal/mol.

1) J. T. Dubois and W. A. Noyes, Jr., *J. Chem. Phys.*, **19**, 1512 (1951).
2) E. K. Lee, *J. Phys. Chem.*, **71**, 2804 (1967).
3) R. E. Rebbert and P. Ausloos, *J. Amer. Chem. Soc.*, **86**, 4803 (1964).
4) R. J. Cvetanović, "Progress in Reaction Kinetics," Vol. 2, ed. by G. Porter, Pergamon Press, New York (1964), p. 41.
5) G. S. Hammond, N. J. Turre and P. A. Leermakers, *J. Phys. Chem.*, **66**, 1144 (1962).
6) T. Terao, S. Hirokami, S. Sato and R. J. Cvetanović, *Can. J. Chem.*, **44**, 2173 (1966).
7) H. Ishikawa and W. A. Noyes, Jr., *J. Amer. Chem., Soc.*, **84**, 1502 (1962); *J. Chem. Phys.*, **37**, 583 (1962).
8) G. N. Lewis and M. Kasha, *J. Amer. Chem. Soc.*, **66**, 2100 (1944).
9) G. J. Schulz, *J. Chem. Phys.*, **34**, 1778 (1961).
10) R. K. Kurran and R. E. Fox, *ibid.*, **34**, 1590 (1961).
11) G. M. Begun and W. H. Fletchcer, *ibid.*, **35**, 547 (1961).
12) H. E. Avery and R. J. Cvetanović, *ibid.*, **48**, 380 (1968).
13) A. E. Stearn and H. Eyring, *ibid.*, **3**, 778 (1935).
14) H. S. Johnston, *ibid.*, **19**, 663 (1951).
15) M. Zelikoff, *ibid.*, **21**, 1647 (1953).
16) J. P. Doering and B. H. Mahan, *ibid.*, **34**, 1617 (1961).
17) R. J. Cvetanović, *J. Chem. Phys.*, **23**, 1203 (1955).
18) M. Z. Hoffman and R. B. Bernstein, *ibid.*, **33**, 526 (1960).

Experimental

For the study of benzene-photosensitized reaction, 2537 Å line of Toshiba FI-3S type low-pressure mercury lamp was used. The contribution from 1849 Å line was removed by Toshiba UVD-25 filter. In order to exclude the contribution from mercury-photosensitized decomposition of nitrous oxide, the reaction was carried out in a newly constructed, completely mercury-free reaction system and the pressure of the reaction system was measured by all-glass Bourdon pressure gauge. The reactor is a cylindrical quartz tube, 4 cm in diameter and 10 cm in length, and connected to the analyzing system. The reaction products were fractionated by cold traps and analyzed by Hitachi gas chromatograph Model K-53 and Hitachi RMU-5 mass spectrometer.

The sample of nitrous oxide used in the present work was 99.9% purity standard gas obtained from Takachiho Trading Co. The light intensity of the incident light into the reactor was measured by a ferrioxalate chemical actinometer.[19]

Results and Discussion

The decomposition of nitrous oxide was observed in the experiments of benzene-photosensitization of nitrous oxide. The reaction products which were not condensable in liquid nitrogen trap mainly consisted of nitrogen and carbon monoxide. The minor components in the noncondensable products were methane, hydrogen and sometimes a trace of oxygen.

Because of the difficulties in the identification of non-volatile species in the reaction products, material balance of the reaction was not measured.

Table 1 shows the N_2 and CO production under various benzene pressures for the same initial pressure of N_2O. The increase of N_2 formation with increase of the benzene pressure in the reaction system is seen in Fig. 1. This means that the amount of N_2 production corresponds to the number of photons absorbed by the sensitizer benzene.

Table 1. Benzene-photosensitized decomposition of nitrous oxide

Nitrous oxide pressure: 40.0 mmHg
Irradiation: 2537 Å, 60 min

C_6H_6 pressure (mmHg)	Product		N_2/CO	Quantum yield for N_2 formation
	N_2 (cc)	CO (cc)		
0	0.11×10^{-1}	—	—	—
5.2	0.44×10^{-1}	0.10×10^{-1}	4.4	2.60×10^{-2}
11.0	0.52×10^{-1}	0.10×10^{-1}	5.2	1.76×10^{-2}
13.0	0.62×10^{-1}	0.10×10^{-1}	6.2	1.75×10^{-2}
17.0	0.75×10^{-1}	0.15×10^{-1}	5.0	1.79×10^{-2}
22.5	0.94×10^{-1}	0.18×10^{-1}	5.2	1.90×10^{-2}
34.0	1.20×10^{-1}	0.36×10^{-1}	3.3	1.99×10^{-2}
35.0	1.12×10^{-1}	0.32×10^{-1}	3.7	1.84×10^{-2}
38.5	1.50×10^{-1}	0.45×10^{-1}	3.3	2.81×10^{-2}

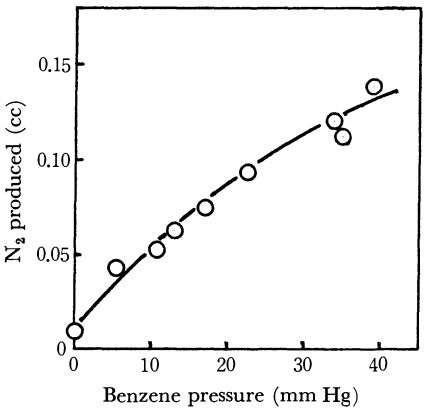

Fig. 1. The effect of benzene pressure on the amount of nitrogen formation.

Table 2 shows the N_2 and CO production with various N_2O initial pressure for the same benzene pressure. Here the apparent quantum yield presented in the table is the ratio of the mole number N_2 produced from N_2O to the number of photons absorbed by benzene.

The dissociation energies of N–N bond of nitrous oxide is 115 kcal/mol and N–O bond is 40 kcal/mol respectively,[9,10,20] and the excited triplet state energy of benzene is 84 kcal/mol.[8] It is quite reasonable, therefore, to expect that only N–O bond is split in the benzene-photosensitized decomposition of nitrous oxide. Nitric oxide was not produced and N_2 was the only nitrogen-containing product found in the reaction mixture after irradiation, which result is in agreement with the prediction of decomposition products of nitrous oxide.

While N_2 was produced by the decomposition of nitrous oxide in the present work, O_2 was not observed in almost any of the runs. Cvetanović observed that molecular oxygen was not formed when hydrocarbon was present in the reaction system of mercury-photosensitized decomposition of nitrous oxide.[17] It seems reasonable to suppose that oxygen atom, which was produced by N–O bond splitting in the benzene-photosensitized reaction of nitrous oxide, reacts rapidly with benzene before O_2 is formed by the recombination of oxygen atoms.[21] Carbon monoxide seems to be formed by the reaction of the oxygen atom from N_2O with benzene sensitizer. As seen in Tables 1 and 2, the ratio N_2/CO is larger than the stoichiometric value

19) C. A. Parker, *Proc. Roy. Soc.*, **A235**, 518 (1956).

20) V. I. Vedeneyev, L. V. Gurvich, V. N. Kondratyev, V. A. Medvedev and Ye. L. Frankevich, "Bond Energies, Ionization Potentials and Electron Affinities (English edition)," St. Martin's Press, New York (1966).

21) G. Boocock and R. J. Cvetanović, *Can. J. Chem.*, **39**, 2436 (1961).

1/1. This means that some of the oxygen atoms from N_2O molecules must have been missed in the analysis of the reaction products because of some non-volatile oxygen-containing products formed by the reaction of the oxygen atoms with benzene.[21]

The reaction scheme of the benzene-photosensitized decomposition of nitrous oxide may be presented as follows:

$$C_6H_6 + h\nu\ (2537\ \text{Å}) \longrightarrow C_6H_6^* \quad (1)$$

$$C_6H_6^* \longrightarrow C_6H_6 + h\nu' \quad (2)$$

$$C_6H_6^* \longrightarrow C_6H_6^{**} \quad (3)$$

$$C_6H_6^* + C_6H_6 \longrightarrow 2C_6H_6 \quad (4)$$

$$C_6H_6^{**} \longrightarrow C_6H_6 \quad (5)$$

$$C_6H_6^{**} + C_6H_6 \longrightarrow 2C_6H_6 \quad (6)$$

$$C_6H_6^{**} + N_2O \longrightarrow N_2O^{**} + C_6H_6 \quad (7)$$

$$N_2O^{**} \longrightarrow N_2 + O(^3P) \quad (8a)$$

$$N_2O^{**} \longrightarrow N_2O \quad (8b)$$

* and ** denote the excited state of molecule in singlet and triplet state, respectively. It is assumed that the reaction between the excited benzene and the reactant nitrous oxide can be neglected as in the case of previous workers.[1,2,6,7] The decomposition yield of nitrous oxide in the triplet state N_2O^{**} produced by the energy-transfer process (7) is expressed by $[k_{8a}/(k_{8a}+k_{8b})](N_2O^{**})$. When $k_{8a}/(k_{8a}+k_{8b})$ is replaced by n_t, the rate of N_2 formation is expressed as follows:

$$\begin{aligned} d(N_2)/dt &= n_t \cdot d(N_2O^{**})/dt \\ &= n_t k_7 (C_6H_6^{**})(N_2O) \\ &= \frac{n_t k_7 k_3 I(C_6H_6)(N_2O)}{(k_5+k_6(C_6H_6)+k_7(N_2O))(k_2+k_3+k_4(C_6H_6))} \end{aligned}$$

where, $I(C_6H_6)$ is the number of photons absorbed by benzene per unit time and k is the appropriate individual rate constant. Since the apparent quantum yield for N_2 formation Φ_t is expressed by $d(N_2)/dt \,/\, I(C_6H_6)$, we obtain

$$\begin{aligned} \frac{1}{\Phi_t} &= \frac{1}{[d(N_2)/dt]/I(C_6H_6)} \\ &= \frac{1}{n_t}\left(1+\frac{k_2+k_4(C_6H_6)}{k_3}\right)\left(1+\frac{k_5+k_6(C_6H_6)}{k_7(N_2O)}\right) \end{aligned}$$

According to the results of the previous workers,

$$k_2/k_3 = 1/4^{7,22,23)}$$

$$k_2 + k_3 = 1.7\times10^6/\text{sec}^{24)}$$

and

$$k_4 = 4.6\times10^{-13}\ \text{cm}^3/\text{molecule sec}^{7)}$$

Table 2. Benzene-photosensitized decomposition of nitrous oxide

Benzene pressure: 35.0 mmHg

Irradiation: 2537 Å, 60 min

N_2O Pressure (mmHg)	Product N_2 (cc)	Product CO (cc)	N_2/CO	Quantum yield for N_2 formation
14.0	0.22×10^{-1}	—		0.36×10^{-2}
22.0	0.40×10^{-1}	0.08×10^{-1}	4.3	0.65×10^{-2}
25.0	0.64×10^{-1}	0.13×10^{-1}	4.9	1.05×10^{-2}
29.0	0.81×10^{-1}	0.21×10^{-1}	3.9	1.33×10^{-2}
35.0	0.91×10^{-1}	0.18×10^{-1}	5.0	1.47×10^{-2}
44.0	1.12×10^{-1}	0.32×10^{-1}	3.5	1.84×10^{-2}
53.0	1.47×10^{-1}	0.38×10^{-1}	3.9	2.41×10^{-2}
55.0	1.20×10^{-1}	0.36×10^{-1}	3.3	1.99×10^{-2}
65.0	1.57×10^{-1}	0.43×10^{-1}	4.3	2.57×10^{-2}

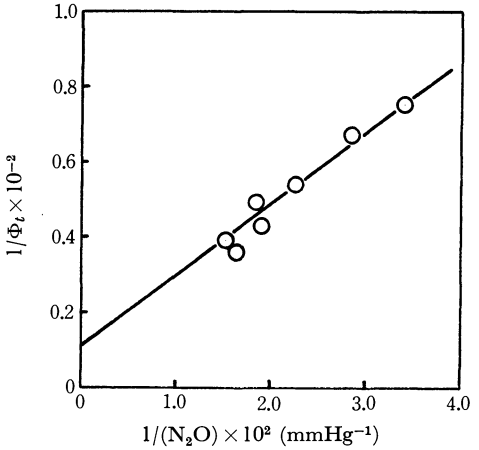

Fig. 2. Linear relation between $1/(N_2O)$ and reciprocal of apparent quantum yield for N_2 formation.

In the present work sensitizer benzene pressure was kept constant at 35.0 mmHg in every run listed in Table 2, thus

$$\frac{1}{\Phi_t} = \frac{c}{n_t}\left(1+\frac{k_5+k_6(C_6H_6)}{k_7(N_2O)}\right)$$

where the constant c denotes $\left(1+\frac{k_2+k_4(C_6H_6)}{k_3}\right)$ which was calculated using the numerical values of k_2, k_3, k_4 and (C_6H_6) mentioned above. The above equation shows the linear relation between $1/\Phi_t$ and $1/(N_2O)$. This is shown in Fig. 2 obtained from the experimental results in Table 2. From the intercept in Fig. 2, we obtain

$$c/n_t = 1.1\times10^1$$

Since the constant c is calculated to be 1.67, $n_t = k_{8a}/(k_{8a}+k_{8b})$ is evaluated to be

$$n_t = 0.15$$

We might propose that the decomposition yield of N_2O^{**} is 15%, since the material balance was not

22) R. B. Cundall, F. J. Fletcher and D. G. Milne, *Trans. Faraday Soc.*, **60**, 1146 (1964).

23) W. A. Noyes, Jr., and I. Unger, "Advances in Photochemistry," Vol. 4, ed. by W. A. Noyes, Jr., G. S. Hammond and J. N. Pitts, Jr., Interscience Publishers, New York (1966), p. 50.

24) J. W. Donovan and A. B. F. Duncan, *J. Chem. Phys.*, **35**, 1389 (1961).

obtained from the analysis of the reaction products as mentioned before.

Since the excited singlet state of nitrous oxide lies in a vacuum-ultraviolet region shorter than 2537 Å, which is the wavelength of the light source for exciting benzene sensitizer in the present work, the energy transfer process (7) seems to be exclusive for exciting nitrous oxide under the present experimental conditions.

It has been pointed out that, in mercury-photosensitized reactions of the reactant molecule species having large quenching cross sections to excited mercury atoms, triplet-triplet energy transfer process is preferable to the direct attack mechanism.[25] Nitrous oxide has a large quenching cross section compared with other simple inorganic compounds and saturated hydrocarbons.[4,26] Considering the similarity of benzene-photosensitization with mercury-photosensitization, energy transfer process (7) for N_2O excitation is more plausible than the direct attack of excited benzene molecule on the nitrous oxide molecule.

Since N–O bond splitting has been observed by the benzene-photosensitized reaction of nitrous oxide in the present work, the excited triplet state of nitrous oxide in process (7) should be located less than 84 kcal/mol above the ground state, which is consistent with the results obtained in the thermal decomposition studies of nitrous oxide by previous workers[13,14] and also with those of the biacetyl-photosensitized reaction of nitrous oxide in which N_2 formation was observed by the present authors.[27] For more elaborate discussions about the triplet excited state of nitrous oxide assumed in the present work, however, reliable experimental evidence such as emission studies would be necessary.

25) A. Jones and F. P. Lossing, *Can. J. Chem.*, **45**, 1685 (1967).

26) B. deB. Darwent and M. K. Phibbs, *J. Chem. Phys.*, **22**, 110 (1954).

27) S. Yamashita and T. Hayakawa, "Photochemical Study by Organic Photosensitizers," to be published in "Proceedings of International Conference in Mass Spectroscopy (1969)."

BULLETIN OF THE CHEMICAL SOCIETY OF JAPAN VOL. 43 2335—2341 (1970)

Magnetic Circular Dichroism of Iron Tetraphenylporphins

Hiroshi KOBAYASHI, Masayuki SHIMIZU and Ichiro FUJITA

Department of Chemistry, Tokyo Institute of Technology Ookayama, Meguro-ku, Tokyo

(Received January 12, 1970)

The magnetic circular dichroism of iron tetraphenylporphins was measured. Since the ground state of the open-shell iron porphin is degenerate and several charge-transfer excited states exist near the ^1Q and ^1B states, the A term as well as the B and C terms are very important for describing the MCD of the iron porphin, whereas the MCD at the ^1Q and ^1B bands, which arise from the pure degenerate (π,π^*) excitations in D_{4h} porphin assumed for zinc tetraphenylporphin, is ascribed to the A term. The MCD of carboxyhemoglobin, oxyhemoglobin and also deoxyhemologin was observed and compared with that of the synthesized iron porphins.

Iron porphyrin plays an essential rôle in the biological processes of hemoprotein. Current interest leans to the studies of biological processes by means of physical measurement and theoretical calculations based on molecular physics. Magnetic optical rotatory dispersion (MORD) and magnetic circular dichroism (MCD) measurements are physical techniques recently developed to obtain information on the electronic behavior in a molecule.[1] MORD measurements of myoglobin,[2] hemoglobin[3] and cytochromes,[4] which are hemoproteins

1) A. D. Buckingham and P. J. Stephens, *Ann. Rev. Phys. Chem.*, **17**, 399 (1966).

2) M. V. Volkenstein, J. A. Sharonov and A. K. Shemelin, *Nature*, **209**, 710 (1966).

3) V. E. Shashoua, "Hemes and Hemoproteins," ed. by B. Chance, R. W. Estabrook and T. Yonetani, Academic Press, New York (1966), p. 93.

4) V. E. Shashoua, *Nature*, **203**, 972 (1964); *Arch. Biochem. Biophys.*, **111**, 550 (1965); V. E. Shashoua and R. W. Estabrook, "Hemes and Hemoproteins," ed. by B. Chance, R. W. Estabrook and T. Yonetani, Academic Press, New York (1966), p. 427; M. Morrison and J. Duffield, *ibid.*, p. 431.

containing Fe(II)- or Fe(III)porphyrins, have been carried. Schooley *et al.* also reported the MCD measurements of some biologically important molecules including oxyhemoglobin, cytochrome-*c* and chlorophylls.[5]

In a magnetic field parallel to the incident light beam, the complex refractive indices of a substance for left- and right- handed circularly polarized lights, $\hat{n}_l$ and $\hat{n}_r$, respectively, are generally different because of the Zeeman splitting of the levels of orbital angular motion. The complex refractive index is given by $\hat{n}=n-ik$, where n is refractive index and k is absorption coefficient. Magnetic optical rotation arises from a magnetically induced deviation of the refractive indices for left- and right-handed circularly polarized lights, (n_l-n_r). In the region of optical absorption, a deviation in the absorption coefficients for left- and right- handed circularly polarized lights, (k_l-k_r) is observed in a magnetic field. Magnetic circular dichroism is ascribed to the difference between k_l and k_r induced by a magnetic field.

A theoretical study of the MORD observed in the region of the (π, π^*) transitions of porphyrins and phthalocyanines, first measured by Shashoua,[6] has been carried out by Stephens *et al.*[7] Since the electronic excitations corresponding to the absorption bands of iron porphyrin, however, should be interpreted in terms of a configuration-interaction admixture of the charge transfer excitations and the (π, π^*) transitions, a treatment such as employed by Stephens *et al.* can not be applied to the analysis of the MORD and the MCD of the iron porphyrins. The measurements of the MCD of the iron porphyrins have been required for further theoretical analysis of the electronic structure. In this paper, we should like to present the result of the MCD measurements of the iron tetraphenylporphins recently synthesized in this laboratory.[8]

Experimental

Materials. The free base of tetraphenylporphin (abbreviated to TPP) and Zn(II) tetraphenylporphin (TPPZn) were prepared and purified by the method given in the literature.[9] Iron tetraphenylporphins have been synthesized in this laboratory. The synthesis will be given elsewhere.[8] Samples of TPPFe(III)Cl, TPPFe(III)OCH_3, TPPFe(II)2Py, TPPFe(II)·2THF and TPPFe(II) identified by elemental analysis were used without further purification. In the formula, Py denotes the coordinating pyridine and THF the coordinating tetrahydrofuran.

Horse hemoglobin also was prepared and purified by the method in the literature.[10] Deoxyhemoglobin was prepared by adding a small amount of sodium dithionite to the buffer solution (pH 6) of freshly prepared hemoglobin. Carboxyhemoglobin was prepared by bubbling carbon monoxide into the solution of hemoglobin until the intensity of the characteristic absorption of the carboxyhemoglobin attained the highest value. The observed absorption spectra of the deoxyhemoglobin and the carboxyhemoglobin were in good agreement with those given in the literature.[10]

Preparation of the Solutions for Measurement. As solvents, tetrahydrofuran (THF) was used for TPP and TPPZn(II), benzene for TPPFe(III)Cl and TPPFe(III)OCH_3, and buffer solution (pH 6) for hemoglobins. Since ferrous tetraphenylporphins are readily autoxidized in the presence of oxygen and/or moisture in the air, the solution was prepared under inert atmosphere in a vacuum system using the solvents previously dried, distilled and degassed. The solution was transferred into a branch joined to an optical cell and the branch was then sealed off. As solvents, pyridine free from oxygen and moisture was used for TPPFe(II)·2Py, tetrahydrofuran for TPPFe(II)·2THF and benzene for TPPFe(II).

The concentration of the porphyrin in the solutions was adjusted to 10^{-4} mol/*l* for the measurement in the visible region and to 10^{-5} mol/*l* for the measurement in the near ultraviolet region.

Measurements. In a preliminary stage of this work, a permanent magnet with an 8 mm axial hole and a 13 mm pole gap was placed in the sample compartment of a JASCO automatic recording spectropolarimeter model ORD/UV-5. The external magnetic field was 3600 gauss. After a preliminary study, the light path of the spectropolarimeter was drastically modified and an electromagnet with a 15 mm pole gap was placed in the sample compartment of the spectropolarimeter. The electromagnet gave a magnetic field up to 12000 gauss. For the present work, the external magnetic field was set as 10000 gauss. When the current in the electromagnet was reversed, the reading of the out-put was completely reversed in sign over the whole range of wavenumber. A deviation between two symmetrical curves obtained for the reversed currents in the magnet, as shown in Fig. 6, gave an effective signal corresponding to one that could be obtained in a magnetic field of 20000 gauss. This technique was used for determination of the magnetic circular dichroism (MCD). The MCD of a solution was actually measured in optical density units by a deviation from the base line obtained by the first running with a pure solvent. The magnitude of MCD was given in molar ellipticity per unit external

5) D. A. Schooley, E. Bunnenberg and C. Djerassi, *Proc. Natl. Acad. Sci.*, **53**, 579 (1965).

6) V. E. Shashoua, *J. Amer. Chem. Soc.*, **86**, 2109 (1964); **87**, 4044 (1965).

7) P. J. Stephens, W. Suëtaka and P. N. Schatz, *J. Chem. Phys.*, **44**, 4592 (1966).

8) H. Kobayashi and Y. Yanagawa, This Bulletin, to be published.

9) A. D. Adler, F. R. Longs, J. D. Finarelli, J. Goldmacher, J. Assour and L. Korsakoff, *J. Org. Chem.*, **32**, 476 (1967); P. Rothermund and A. R. Menotti, *J. Amer. Chem. Soc.*, **63**, 267 (1941); **70**, 1808 (1948); G. D. Dorough, J. R. Miller and F. M. Huennekens, *J. Amer. Chem. Soc.*, **73**, 267 (1951).

10) D. L. Drabkin, "Haematin Enzymes," ed. by J. E. Falk, R. Lemberg and R. K. Morton, Pergamon Press, Oxford (1961), p. 142.

magnetic field $[\theta]_M$.[7,11] The molar ellipticity is given by the molar circular dichroism $(\varepsilon_l - \varepsilon_r)_M$ measured in a cell with 1 cm light path in a magnetic field of 10000 gauss as follows.

$$[\theta]_M = 3300\,(\varepsilon_l - \varepsilon_r)_M/10000$$

In the case of hemoglobin, even in the non-magnetic condition, it shows a circular dichroism which is ascribed to its helical structures in the counterpart of the iron porphyrin. The MCD of hemoglobin was derived from the difference between the circular dichroisms observed in the magnetic and non-magnetic conditions assuming an additivity between CD and MCD.

Results and Discussion

The structure of the coordination spheres in TPPFe(II)·2Py and TPPFe(II)·2THF is a distorted octahedron, while that of TPPFe(III)OCH_3 and TPPFe(III)Cl is a square pyramid, where the central iron might be slightly out of the porphin plane.[12,13] The structure of the coordination sphere in deoxyhemoglobin is a square pyramid[14] and that of carboxyhemoglobin is a distorted octahedron. The structure of TPPFe(II), TPP-Zn(II) and also TPP is almost planar, as shown in Fig. 1. This particular porphin has much less tendency to aggregate in solution because of the four phenyl groups perpendicular to the porphin plane.[12,15,16,] Table 1 summarizes the spin states of the iron complexes of TPP and the hemoglobins. The magnetic susceptibility measurements of the iron tetraphenylporphins have been carried out at room temperature by the Gouy method. Ferrous tetraphenylporphins were unstable in the air, so the MCD, absorption spectra and the magnetic moments were measured *in vacuo* without exposing the sample to the air.

Table 1.

	μ_{eff} (Bohr magneton)	S
TPP Fe(III) Cl	5.88	5/2
TPP Fe(III) OCH_3	1.84	1/2
TPP Fe(II)·2Py	0	0
TPP Fe(II)·2THF	2.75	1
TPP Fe(II)	4.75	2

	S
Carboxyhemoglobin	0
Oxyhemoglobin	0
Deoxyhemoglobin	2

The MCD and absorption spectra are shown in Figs. 2—6. Though TPPFe(II)·2THF and TPP-Fe(II) were of considerable interest from the electronic structure point of view, the observed MCD both in the visible and near ultraviolet regions was so low that no reliable value could be obtained in a magnetic field up to 10000 gauss. However, the magnitude of the MCD of TPPFe(II)·2Py was fairly large.

The magnitude of magnetic molar circular dichroism observed at a transition $a \rightarrow j$ is given[1,7,11] by

$$[\theta]_M = -\frac{24N}{\hbar c}\{f_1 A + f_2(B + C/rT)\} \quad (1)$$

where

$$A = \frac{3}{d_a}\sum[\langle j|\hat{\mu}_z|j\rangle - \langle a|\hat{\mu}_z|a\rangle]\cdot Im[\langle a|\hat{m}_x|j\rangle\langle j|\hat{m}_y|a\rangle] \quad (2)$$

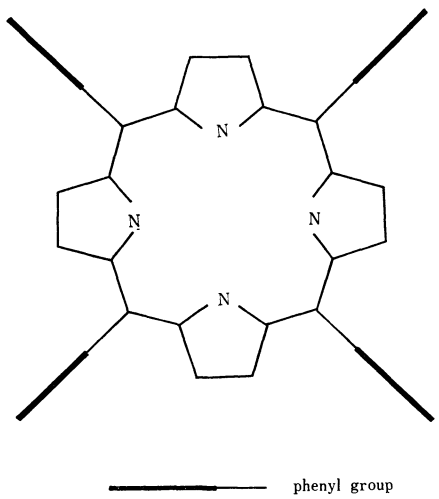

Fig. 1. Tetraphenylporphin.

11) P. N. Schatz, A. J. McCaffery, W. Suëtaka, G. N. Henning, A. B. Ritchie and P. J. Stephens, *J. Chem. Phys.*, **45**, 722 (1966); P. J. Stephens, P. N. Schatz A. B. Ritchie and A. J. McCaffery, *J. Chem. Phys.*, **48**, 132 (1968); A. J. McCaffery, P. J. Stephens and P. N. Schatz, *Inorg. Chem.*, **6**, 1614 (1967); P. N. Schatz, P. J. Stephens, G. N. Henning and A. J. McCaffery, *Inorg. Chem.*, **7**, 1246 (1968); G. N. Henning, A. J. McCaffery, P. N. Schatz and P. J. Stephens, *J. Chem. Phys.*, **48**, 5656 (1968); A. J. McCaffery, P. N. Schatz and P. J. Stephens, *J. Amer. Chem. Soc.*, **90**, 5730(1968); P. J. Stephens, A. J. McCaffery and P. N. Schatz, *Inorg. Chem.*, **7**, 1923 (1968); A. J. McCaffery, P. N. Schatz and T. E. Lester, *J. Chem. Phys.*, **50**, 379 (1969).

12) E. B. Fleischer, C. K. Miller and L. E. Webb, *J. Amer. Chem. Soc.*, **86**, 2342 (1964).

13) J. L. Hoard, M. J. Hamor, T. A. Hamor and W. S. Caughey, *ibid.*, **87**, 2312 (1965); D. F. Koenig, *Acta Cryst.*, **18**, 663 (1965); J. L. Hoard, "Hemes and Hemoproteins," ed. by B. Chance, R. W. Estabrook and T. Yonetani, Academic Press, New York (1966), p. 9.

14) M. F. Perutz, *Scientific American*, **211**, 5 (1964).

J. C. Kendrew, *Science*, **139**, 1259 (1963).

15) J. L. Hoard, M. J. Hamor and T. A. Hamor, *J. Amer. Chem. Soc.*, **85**, 2334 (1963).

16) S. Silvers and A. Tulinsky, *ibid.*, **86**, 927 (1964).

17) C. Weiss, H. Kobayashi and M. Gouterman, *J. Mol. Spectrosc.*, **16**, 415 (1965).

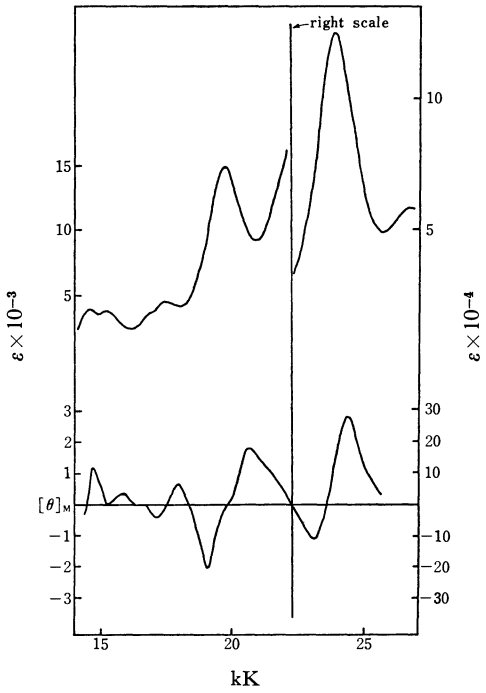

Fig. 2. MCD and absorption spectra of TPPFe(III)-Cl in benzene.

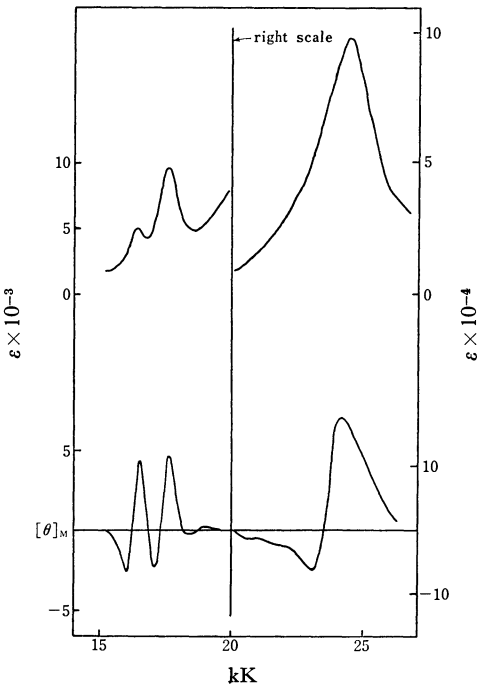

Fig. 3. MCD and absorption spectra of TPPFe(III)-OCH_3 in benzene.

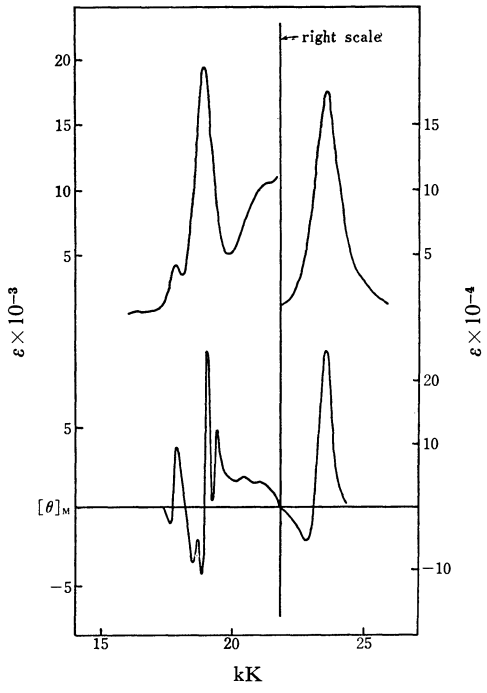

Fig. 4. MCD and absorption spectra of TPPFe(II)·2Py in pyridine.

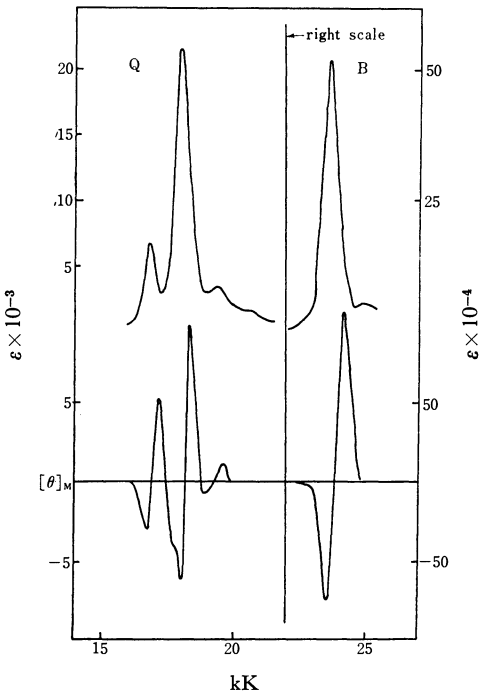

Fig. 5. MCD and absorption spectra of TPPZn in THF.

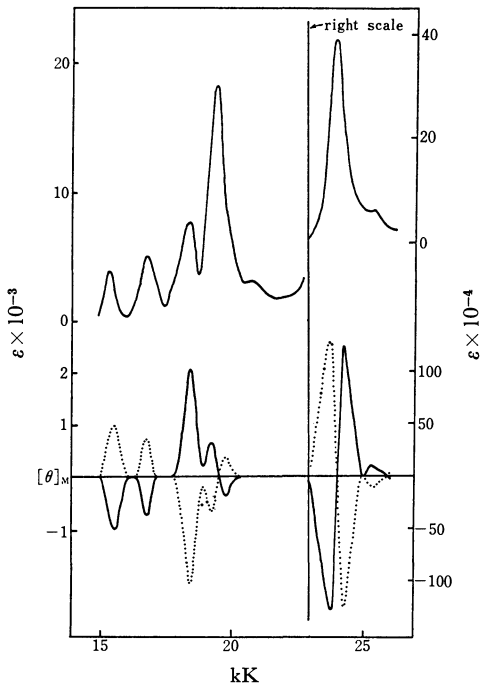

Fig. 6. MCD and absorption spectra of the metal free base of tetraphenylporphin in THF.
MCD spectra are given for a normal magnetic field (———) and a reversed magnetic field (·····). The sense of the normal magnetic field was set to that of the light beam propagation.

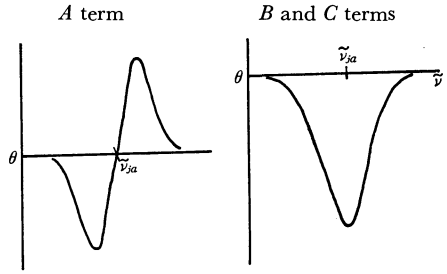

Fig. 7. The band shapes of MCD and absorption spectra.

$$B=-\frac{3}{d_a}\sum I_m\left\{\sum_{k\neq a}\frac{\langle k|\hat{\mu}_z|a\rangle}{W_k-W_a}\left[\langle a|\hat{m}_x|j\rangle\langle j|\hat{m}_y|k\rangle-\langle a|\hat{m}_y|j\rangle\langle j|\hat{m}_x|k\rangle\right]+\sum_{k\neq j}\frac{\langle j|\hat{\mu}_z|k\rangle}{W_k-W_j}\left[\langle a|\hat{m}_x|j\rangle\langle k|\hat{m}_y|a\rangle-\langle a|\hat{m}_y|j\rangle\langle k|\hat{m}_x|a\rangle\right]\right\} \quad (3)$$

$$C=-\frac{3}{d_a}\sum\langle a|\hat{\mu}_z|a\rangle I_m[\langle a|\hat{m}_x|j\rangle\langle j|\hat{m}_y|a\rangle] \quad (4)$$

W_a, W_k and W_j are the energy of the respective states, d_a is the degeneracy of the state a, and $\hat{m}$ and $\hat{\mu}$ are the electric and magnetic dipole operators, respectively.

f_1 is a function which shows a dispersion at the absorption maximum, while f_2 is a function which shows a maximum or a minimum at the absorption maximum. If term A is predominant, $[\theta]_M$ shows an anomalous dispersion at the absorption maximum, while if term B or C is predominant, $[\theta]_M$ shows an extreme value as shown in Fig. 7. Term A depends upon the absorption intensity and also the difference of angular momenta between the ground state and the excited state involved in the absorption. If the ground state is not degenerate, term A depends on the angular momentum only of the excited state. Term C depends upon the angular momentum of the ground state. Term B is ascribed to the angular momenta induced by the external magnetic field. As seen in Fig. 5 the MCD spectrum of TPPZn(II) is predominantly described by term A. As has been shown by the molecular orbital calculations,[17] the lowest (π,π^*) excited state (^1Q state) of porphin is of E_u symmetry and has an angular momentum of ± 9 in the sense of a circular box model, while the second one (^1B state) which gives rise to the Soret band, is also of E_u symmetry and has an angular momentum of ± 1. While in the case of the metal free base, the degenerate excited states of D_{4h} porphin assumed for the metalloporphins such as TPPZn(II) are split by the localization of the central two protons to the nitrogen atoms at opposite positions.[16,18] The splitting of the lowest degenerate transition in the visible region is fairly large, while that of the second one in the near-ultraviolet is usually too small to be observed. Therefore, as seen in Fig. 6 the MCD spectrum in the visible region of the metal free base should show a contribution of term B, mainly arises from the magnetically induced mixing between the split components of the degenerate excited states. The MCD observed in the near-ultraviolet region can be ascribed to term A. The ground state of TPPZn(II) and also of the metal free base can be described by a closed shell configuration, term C being vanished.

In the case of ferric porphin, the absorption spectra in the visible- and near-ultraviolet region can not be described in terms of (π,π^*) transitions, because of appreciable configuration mixings due to the charge-transfer excited states of exactly the same symmetry, E_u. The charge-transfer excited state arises from the charge-transfer from one of the top filled π molecular orbitals of porphin to one of the vacant degenerate $d\pi$ orbitals. There seem to be several excited states in the visible- and near-ultraviolet region other than the ^1Q and ^1B states which are ascribed to the (π,π^*) excitations. Thus the contribution of term B due to the magnetically induced mixings between the closely existing states is expected for the MCD of these complexes. Furthermore TPPFe(III)OCH_3 is expected to have an

18) J. Weigl, *J. Mol. Spectrosc.*, **1**, 133 (1957); B. G. Anex and R. S. Umans, *J. Amer. Chem. Soc.*, **86**, 5026 (1964).

angular momentum due to the orbital motion of a hole in the $d\pi$ orbitals in the ground state, while TPPFe(III)Cl lacks such an angular momentum. Although further experimental work under various temperatures is required to see how it depends on each of terms B and C, the MCD observed for the high-spin TPPFe(III)Cl and the low-spin TPP-Fe(III)OCH_3, as shown in Figs. 2 and 3, can be ascribed to a contribution of the terms B, C as well as A.

In the case of diamagnetic ferrous porphin, TPP-Fe(II)·2Py, the absorption spectrum in the visible- and near-ultraviolet region was very close to that of TPPZn(II). However, the MCD were quite different. A predominant contribution of term B to the MCD was observed at the Soret band and also at the 21000 cm^{-1} band. The latter can be assigned to a charge-transfer transition of a $d\pi$ electron of the iron to a vacant pyridine molecular orbital, since the piperidine adduct of TPPFe(II) does not show the 21000 cm^{-1} band.[8] Similarly near the Soret band there exist charge-transfer excited states which produce a hole in the closed $d\pi$ orbitals. These charge-transfer excited states are mixed to the Soret band by the external magnetic field. In oxyhemoglobin and carboxyhemoglobin, the iron porphyrin exists in a diamagnetic state. Their MCD and absorption spectra are given in Figs. 8 and 9. The absorption intensity of the iron porphyrin in these proteins was slightly weaker than that of TPPFe(II)·2Py, while the MCD of the iron

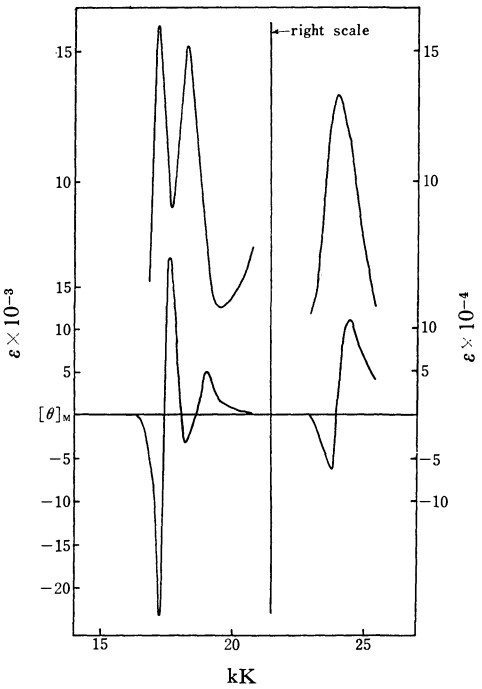

Fig. 9. MCD and absorption spectra of oxy-hemoglobin.

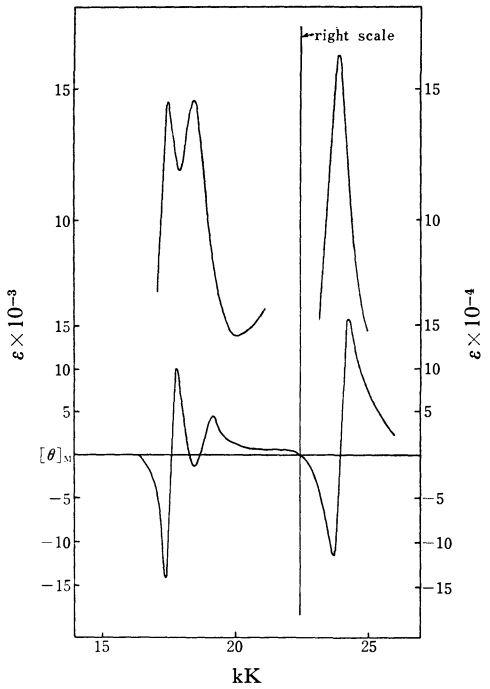

Fig. 8. MCD and absorption spectra of carboxy-hemoglobin.

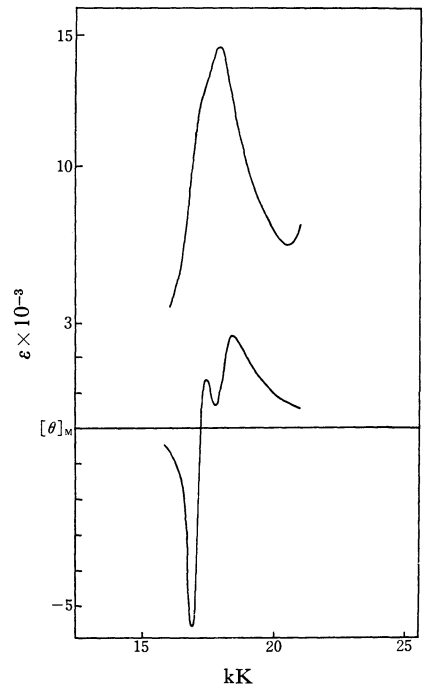

Fig. 10. MCD and absorption spectra of deoxy-hemoglobin.

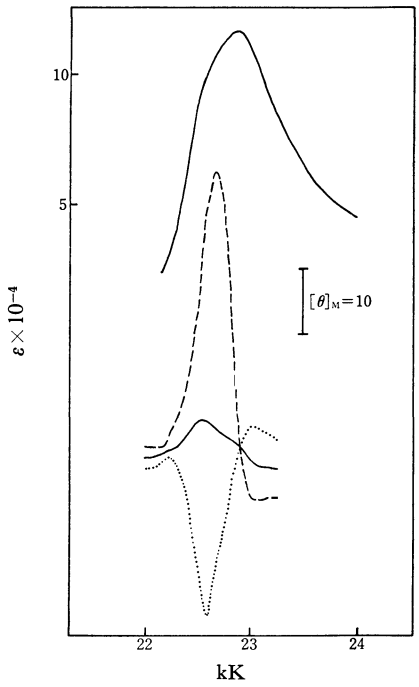

Fig. 11. A non-linear relationship between the MCD and the CD in deoxyhemoglobin.
———: Natural CD.
- - - -: MCD observed in a normal magnetic field (The sense of the magnetic field is that of the light beam propagation).
·····: MCD observed in a reversed magnetic field.

porphyrin in these proteins was much stronger. In these naturally occurring proteins, there exists a circular dichroism due to the helical structure of the counterpart of the iron porphyrin. Assuming an additivity between MCD and CD, the difference between observed CD values for the magnetic and non-magnetic conditions was assigned to the MCD of these proteins. The iron(II) porphyrin in these proteins seems to be quite free from the contribution of term *B* to the MCD at the Soret band. This indicates the charge-transfer excited states, which show an angular momentum due to a hole produced in the closed $d\pi$ shell, are fairly higher than that of TPPFe(II)·2Py.

The MCD and absorption spectra of deoxyhemoglobin are shown in Figs. 10 and 11. When the current in the electromagnet was reversed, the deviation between the circular dichroisms in the near-ultraviolet region for the magnetic and non-magnetic conditions was not symmetrically reversed in this particular case (Fig. 11). There might be a non-linear interaction between MCD and CD. The MCD of deoxyhemoglobin remarkably shows a contribution of terms *B* and *C*.

The authors wish to thank Dr. T. Samejima, Aoyama Gakuin University for kindly permitting them to use his instrument at a preliminary stage of this work. One of the authors (H.K.) is grateful to Professor S. Nagakura, The University of Tokyo for his interest in the work. Grateful acknowledgment is also made to Dr. M. Shigehisa of Japan Spectroscopic Co. Ltd. for helpful technical advice. This research was supported by a grant from the Ministry of Education.

BULLETIN OF THE CHEMICAL SOCIETY OF JAPAN VOL. 43 2342—2346 (1970)

Mössbauer Spectra of Iron Tetraphenylporphins

Hiroshi KOBAYASHI,* Yutaka MAEDA** and Yasuo YANAGAWA*

* *Department of Chemistry, Tokyo Institute of Technology Ookayama, Meguro-ku, Tokyo*
** *Research Reactor Institute, Kyoto University, Kumatori-cho, Osaka*

(Received January 23, 1970)

Mössbauer spectra were measured for a series of the central iron in Fe(II)- and Fe(III) complexes of tetraphenylporphin. The electronic structure of the central iron in the complex was modified by the axial ligand field. The Mössbauer spectra assigned the most probable electronic configurations to various iron states in the iron porphins.

Mössbauer spectroscopy provides valuable information on the electronic structure of iron complexes, complementary to those from the measurements of magnetic susceptibility and from paramagnetic resonance spectroscopy. Recently this technique has been applied to the study of some biologically important substances containing iron atom. Mössbauer effect has been observed with heme proteins such as hemoglobin, myoglobin, cytochromes, catalase, peroxidase and others.[1,2] However, a systematic investigation of the Mössbauer spectra has never been carried out with synthetic iron porphyrin complexes other than those obtained from the naturally occurring heme proteins.[3] Some studies have been performed on the adducts of nitrogeneous ligands and synthetic iron porphyrins.[4,5] Another study on the iron phthalocyanines has also been published.[6] Recently a series of the Fe(II)- and Fe(III) complexes of tetraphenylporphin (TPP) have been synthesized in our laboratory.[7] We present Mössbauer spectra observed for a series of the central iron in the tetraphenylporphin complexes.

Experimental

The Mössbauer spectra were obtained with a scanned velocity spectrometer operating in the time mode. The instrument consisting of an electromagnetic velocity transducer, a gamma-ray counting system and a Dewar has been described.[2] The radiation source was ^{57}Co diffused into metallic Pd. The absorber could be maintained at room temperature, dry ice acetone temperature (195°K) or liquid nitrogen temperature (77°K).

Since our radiation source was strong enough, it was not necessary to enrich ^{57}Fe for the measurements of Mössbauer spectra of our synthetic iron porphins. The measurements were carried out with the powder samples of TPPFe(III)Cl ($S=5/2$), TPPFe(III)OCH_3 ($S=1/2$), TPPFe(II) ($S=2$), TPPFe(II)·2THF ($S=1$) and TPPFe(II)·2Py ($S=0$), where THF denotes tetrahydrofuran and Py, pyridine. All samples had been synthesized in our laboratory and identified by elementary analysis. Their spin states determined by magnetic susceptibility measurements are given above in the brackets. The Fe(III) complexes were fairly stable even in the atmospheric circumstance, while the Fe(II) complexes were very sensitive to oxygen and moisture in the air. In a dried nitrogen atmosphere, the Fe(II) porphin was homogeneously packed and sealed in a planar capsule made of polyacrylic resin.

The velocity scale was calibrated absolutely from an independent Mössbauer run using a thin metallic iron absorber and the center of symmetry of the spectrum was taken as zero velocity. The velocity was determined to an accuracy of ± 0.06 mm/sec for the Fe(III) complexes, and ± 0.04 mm/sec for the Fe(II) complexes.

1) a) U. Gonser, R. W. Grant and J. Kregzde, *Science*, **143**, 680 (1964). b) W. Karger, *Ber. Bunsenges. Physik. Chem.*, **68**, 793 (1964). c) J. E. Maling and M. Weissbluth, "Electronic Aspects of Biochemistry," ed. by B. Pullman, Academic Press, New York (1964), p. 93. d) U. Gonser and R. W. Grant, *Biophys. J.*, **5**, 823 (1965). e) G. Lang and W. Marshall, *Biochem. J.*, **95**, 3 (1965); *J. Mol. Biol.*, **18**, 385 (1966); *Proc. Phys. Soc.*, **87**, 3 (1966). f) W. S. Caughey, W. Y. Fujimoto, A. J. Bearden and T. H. Moss, *Biochem.*, **5**, 1255 (1966). g) G. Lang, *J. Appl. Phys.*, **38**, 915 (1967). h) Y. Maeda, T. Higashimura and Y. Morita, *Biochem. Biophys. Res. Commun.*, **29**, 362 (1967); Y. Maeda and Y. Morita, *ibid.*, **29**, 680 (1967). i) J. H. Moss, A. J. Bearden, R. G. Bartsch and M. A. Cusanovich, *Biochem.*, **7**, 1583 (1968). j) R. Cooke and P. Debrunner, *J. Chem. Phys.*, **48**, 4532 (1968). k) T. H. Moss, A. Ehrenberg and A. J. Bearden, *Biochem.*, **8**, 4159 (1969).

2) Y. Maeda, *J. Phys. Soc. Jap.*, **24**, 151 (1968).

3) a) L. M. Epstein, *J. Chem. Phys.*, **36**, 2731 (1962). b) R. G. Shulman and G. K. Wertheim, *Rev. Mod. Phys.*, **36**, 459 (1964). c) U. Gonser, *J. Phys. Chem.*, **66**, 564 (1962). d) P. P. Craig and N. Sutin, *Rev. Mod. Phys.*, **36**, 437 (1964). e) A. J. Bearden, T. H. Moss, W. S. Caughey and C. A. Beaudreau, *Proc. Natl. Acad. Sci. U.S.*, **53**, 1246 (1965).

4) L. E. Epstein, D. K. Straub and C. Maricondi, *Inorg. Chem.*, **6**, 1720 (1967).

5) A. Hudson and H. J. Whitfield, *ibid.*, **6**, 1120 (1967).

6) B. W. Dale, R. J. P. Williams, P. R. Edwards and C. E. Johnson, *J. Chem. Phys.*, **49**, 3445 (1968).

7) H. Kobayashi and Y. Yanagawa, This Bulletin, to be published.

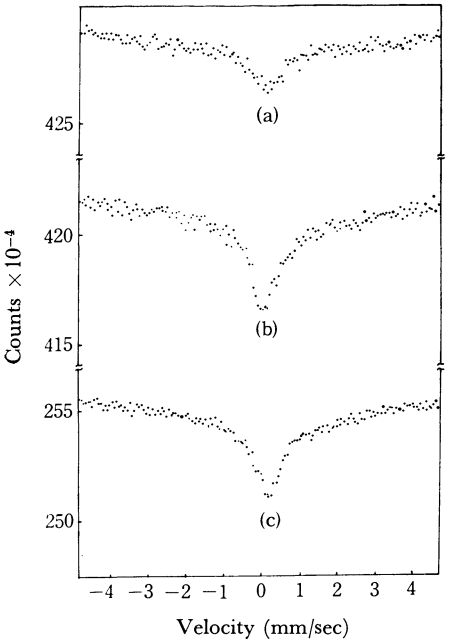

Fig. 1. Mössbauer spectrum of tetraphenylporphin iron(III) chloride.
(a) room temperature (b) 195°K and (c) 77°K

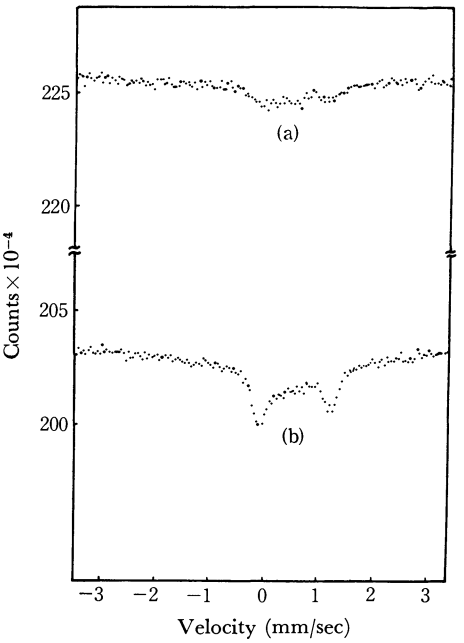

Fig. 3. Mössbauer spectrum of tetraphenylporphin iron(II).
(a) room temperature and (b) 77°K

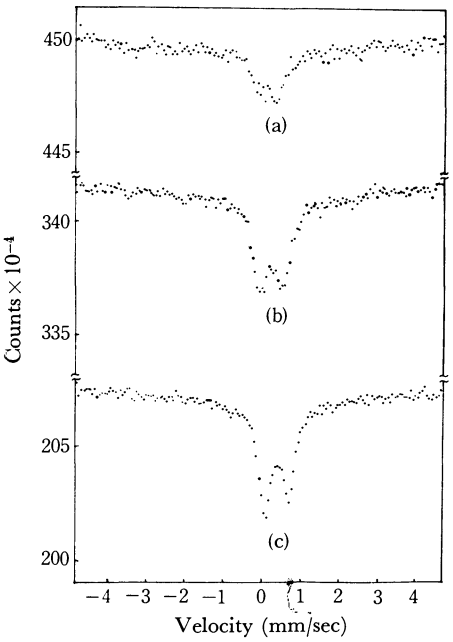

Fig. 2. Mössbauer spectrum of tetraphenylporphin iron(III) methoxide.
(a) room temperature (b) 195°K and (c) 77°K

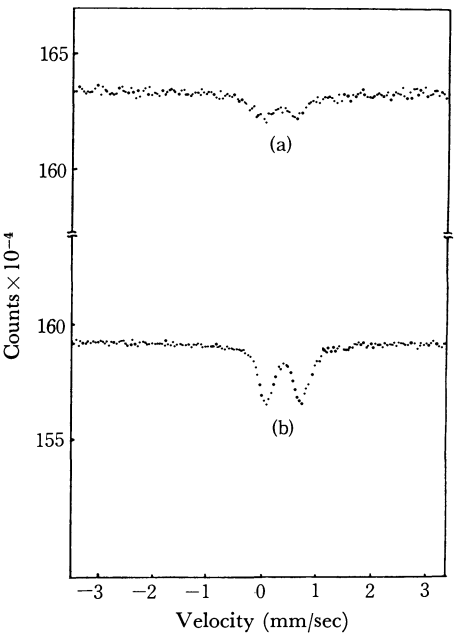

Fig. 4. Mössbauer spectrum of bis-tetrahydrofuran tetraphenylporphin iron(II).
(a) room temperature and (b) 77°K

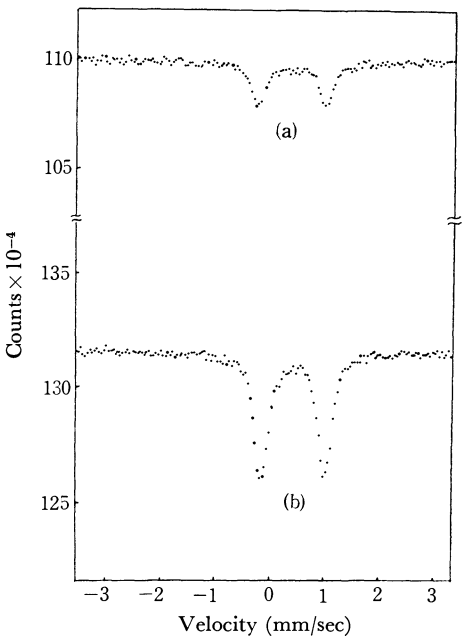

Fig. 5. Mössbauer spectrum of bis-pyridine tetraphenylporphin iron (II).
(a) room temperature and (b) 77°K.

TABLE 1. EXPERIMENTAL ISOMER SHIFT AND QUADRUPOLE SPLITTING

Material	Temperature (°K)	Quadrupole splitting (mm/sec)	Isomer shift (mm/sec)
TPPFe(III)Cl	300	0	0.08
(S=5/2)	195	0	0.00
	77	0	0.14
TPPFe(III)OCH_3	300	0.44	0.14
(S=1/2)	195	0.54	0.25
	77	0.62	0.40
TPPFe(II)	300	—	—
(S=2)	77	1.32	0.52
TPPFe(II)·2THF	300	0.57	0.26
(S=1)	77	0.64	0.33
TPPFe(II)·2Py	300	1.22	0.36
(S=0)	77	1.15	0.41

Results and Discussion

The observed spectra are shown in Figs. 1—5. The isomer shift, δ, and the quadrupole splitting, ΔE_Q, obtained from the spectra are summarized in Table 1.

(1) Isomer Shift. The isomer shift arises from the electrostatic shift of nuclear levels by an interaction between the charge distribution at the nucleus of definite dimension and the electronic charge distribution surrounding the nucleus.[8,9] The isomer shift is decreased when the s electron density at the nucleus is increased or the s orbitals are contracted, which depends upon the number of non-bonding d electrons and the charge distributions of σ-and π coordination bonds.

For ionic complexes, ferrous ion $(3d)^6$ usually shows a larger shift than ferric ion $(3d)^5$. For covalent complexes, strong σ donation by the ligands gives rise to two competitive effects to the isomer shift. The σ donation enhances the charge density in $4s$ orbital and also in $3d$ orbitals and $4p$ orbitals. An increase in the charge density in $4s$ orbital decreases the isomer shift, whereas an increase in the charge densities in $3d$ and $4p$ orbitals gives rise to an expansion of inner s orbitals and therefore an increase in the isomer shift. Another factor to be considered is an effect due to the π electron delocalization between $d\pi$ orbitals and the π molecular orbitals of the ligand.

TPPFe(III)Cl (S=5/2) shows the lowest isomer shift. In the ferric porphins, the central iron behaves like a σ and π acceptor. Since the low spin iron in TPPFe(III)OCH_3 (S=1/2) is a much stronger electron acceptor than the iron in TPPFe(III)Cl, the increase of isomer shift observed for TPPFe(III)OCH_3 can be explained by a predominant contribution from the expansion of the inner s orbitals due to an enhancement of shielding by the donated electrons. For an adduct of TPPFe(III)Cl and imidazole, of which an effective moment of S=1/2 has been observed, the value of isomer shift is still very close to that of the high spin iron in TPPFe(III)Cl.[4] Similar phenomena have been observed for the Fe(III) hemoglobins in the low spin state and in the highest spin state.[1e] In these cases, both the two competitive effects seem to be of equivalent importance.

In the case of ferrous porphin, the central iron behaves like a σ acceptor but a π donor. The iron with intermediate spin shows the lowest isomer shift. The iron has relatively higher π donating power. If there exists a significant migration of $d\pi$ electron to the ligands, a decrease in the isomer is expected. However, the iron is coordinated by relatively weak axial ligands with no electron acceptable π molecular orbital. Some migration of the $d\pi$ electron into the porphin ring is possible. The low value of isomer shift may arise from a higher population in $4s$ orbital due to the σ donations by the axial ligands and by the porphin. The iron in the highest spin state (S=2) shows the highest value of isomer shift. The iron has no axial ligand. Since it is less σ-acceptable and less π-donating, its high value of

8) See for example, A. Abragam, "L'Effet Mössbauer," Gordon and Breach Science Publishers, New York (1964).

9) G. K. Wertheim, "Mössbauer Effect," Academic Press, New York (1964).

isomer shift may readily be expected.

The diamagnetic iron(II) porphin shows an intermediate value of isomer shift. The iron is a strong σ acceptor and π-donor. Although the strong σ donation by the axial ligands and the porphin should appreciably affect the isomer shift, the migration of $d\pi$ electron seems to take an important part in this particular case. The isomer shift, however, shows almost the same values for an adduct of TPPFe(II) and pyridine and that of piperidine.[4] Pyridine has electron acceptable π molecular orbitals, whereas piperidine lacks such orbitals. Therefore the $d\pi$ electron migration to the axial ligands does not seem to be of crucial importance for the isomer shift.

(2) Quadrupole Splitting. The second nonzero term of the electrostatic interaction of a nucleus with its surrounding electrons is the electric quadrupole interaction. For the nucleus ^{57}Fe, the nuclear spins of the ground state and the excited state are 1/2 and 3/2, respectively, and the Mössbauer spectrum shows two resonance peaks. The separation between these peaks, ΔE_Q, is given by

$$\Delta E_Q = (e^2Q/2)q(1 + \tfrac{1}{3}\eta^2)^{1/2} = (e^2Q/2)X \qquad (1)$$

where Q is the quadrupole moment of the nucleus; $eq=V_{zz}$, $\eta=(V_{xx}-V_{yy})/V_{zz}$ and V_{xx}, V_{yy} and V_{zz} are the principal components of an electric-field gradient due to the electronic distribution.[8,9] For metalloporphyrin, as has been done by Weissbluth and Maling,[10] q and $(q\eta)$ are given by

$$\begin{aligned} q &= (1-R)_d q_d + (1-R)_p q_p + (1-\gamma_\infty)q_l, \\ (q\eta) &= (1-R)_d(q\eta)_d + (1-R)_p(q\eta)_p + (1-\gamma_\infty)(q\eta)_l, \end{aligned} \qquad (2)$$

in which q_d and q_p are contributions to q from the electrons occupying $3d$ and $4p$ orbitals, respectively; $(q\eta)_p$ and $(q\eta)_p$ have analogous definitions; q_l and $(q\eta)_l$ are contributions from the ligands and $(1-R)$ and $(1-\gamma_\infty)$ are Sternheimer factors.

Weissbluth and Maling have estimated the contributions to q and $(q\eta)$ from $3d$ and $4p$ orbitals and also from the ligand orbitals based on the molecular orbital calculations by Zerner, Gouterman and Kobayashi.[11] According to their estimation, the quadurpole splitting in hemoglobins predominantly arises from a charge distribution of the electrons occupying $3d$ orbitals. Therefore q and $(q\eta)$ are approximately given in terms of the contributions from the electrons occupying the molecular orbitals with equal symmetry of $3d$ orbitals.

$$\begin{aligned} q &= \sum\langle V_{zz}/e\rangle = \langle 1/r^3\rangle\sum_i A_i f_i \\ (q\eta) &= \sum\langle (V_{xx}-V_{yy})/e\rangle = \langle 1/r^3\rangle\sum_i B_i f_i \\ A_i &= -\langle 3\cos^2\theta - 1\rangle_i \\ B_i &= -\langle 3\sin^2\theta\cos 2\varphi\rangle_i \end{aligned} \qquad (3)$$

where f_i is orbital occupation number; A_i and B_i are readily calculated from the angular part of d orbital[12] and $\langle 1/r^3\rangle$ is also calculated from the radial part of d orbital, however, it can be regarded as a parameter for the intercomparison. As has been shown for the spin-orbit coupling constant in the complexes, the value of the integral $\langle 1/r^3\rangle$ should be adjusted for the molecular orbital formation.[13]

For the ferrous low spin state $(xy)^2(yz)^2(zx)^2$ and the ferric high spin state $(xy)(yz)(zx)(z^2)(x^2-y^2)$, the electronic charge distributions are approximately of spherical symmetry and therefore there are no electric field gradients. However, other electronic configurations should show electric field gradients. The values of X in (1) which actually determine the magnitude of quadrupole splittings

Table 2. The calculation of d electron contribution to ΔE_Q

			Fe(III)d^5			Fe(II)d^6				
			TPPFeCl	TPPFeOCH$_3$		TPPFe	TPPFe·2THF		TPPFe·2Py	
			$S=5/2$	$S=1/2$		$S=2$	$S=1$		$S=0$	
Isomer shift at 77°K			0.14	0.40		0.52	0.33		0.41	
Quadrupole splitting at 77°K			0	0.62		1.32	0.64		1.15	
	A	B								
x^2-y^2	4/7	0	1	0	0	1	0	0	0	0
z^2	−4/7	0	1	0	0	1	1	1	0	0
yz	−2/7	6/7	1	3/2	1	1	3/2	1	2	1
zx	−2/7	−6/7	1	3/2	2	1	3/2	2	2	1
xy	4/7	0	1	2	2	2	2	2	2	2
$\sum_i f_i A_i$			0	2/7	2/7	4/7	−2/7	−2/7	0	4/7
$\sum_i f_i B_i$			0	0	−6/7	0	0	−6/7	0	0
$X=[(\sum_i f_i A_i)^2+1/3(\sum_i f_i B_i)^2]^{1/2}$			0	2/7	4/7	4/7	2/7	4/7	0	4/7

10) M. Weissbluth and J. E. Maling, *J. Chem. Phys.*, **47**, 4166 (1967).

11) M. Zerner, M. Gouterman and H. Kobayashi, *Theoret. Chim. Acta*, **6**, 363 (1966).

12) M. Weissbluth, "Structure and Bonding," Vol. 2, Springer-Verlag, Berlin (1967), p. 1.

13) A. A. Misetich and R. E. Watson, *Phys. Rev.*, **143**, 335 (1966).

are obtained for the most probable configurations in the iron porphyrins with various spin states. The results are summarized in Table 2. For the ferric low spin state and also the ferrous intermediate spin state, two alternative configurations are possible. If an anisotropy is introduced in the porphin plane by a Jahn-Teller distortion of bi-axial ligand fields, the anisotropic contribution of B term is expected. However, as Table 2 shows, the ratios between the observed quadrupole splittings and the values of X obtained from the isotropic contributions (underlined in Table 2) are fairly constant except for the diamagnetic ferrous porphin.

In TPPFe(II)·2THF, the iron is in the intermediate spin state. As was shown by electronic absorption spectroscopy,[7] the observed intermediate spin value is not ascribed to a mixture of the state $S=2$ and the state $S=0$ but a single state $S=1$. Mössbauer spectrum also shows a spectrum characteristic of the intermediate spin iron(II) complex, which is quite different from a spectrum expected for a mixture of the high spin porphin $S=2$ and the diamagnetic one $S=0$.

The diamagnetic ferrous complex, TPPFe(II)·2Py shows a relatively higher quadrupole splitting despite its closed shell structure. Similar values have been found for carboxyhemoglobin, oxyhemoglobin[1e] and nitrogeneous base adducts of iron-porphyrins and[3e,4,5] phthalocyanine, all of which are diamagnetic. The delocalization of $d\pi$ electron to the porphin ring and also to the axial ligands produces some vacancy in the $d\pi$ orbital of the central iron. If a hole is produced in each of the degenerate yz and zx orbitals or a hole is produced in either split yz or zx orbital, the value of X (underlined in Table 2) can explain the observed quadrupole splitting. There might be anisotropy due to the coplanarity of the axial two pyridines. If this is the case, the production of an effective hole in the $d\pi$ orbital is sufficient.

A linear relationship was found between the quadrupole splitting and the isomer shift in these particular iron porphins except for the low spin ferric and also diamagnetic ferrous porphin (Fig. 6). Because of higher $d\pi$ electron affinity of the former, some of π electron charge of porphin ring can migrate into the iron and annihilates the hole existing in yz and/or zx orbital, while in the diamagnetic ferrous one, the charge migration of $d\pi$ electron over whole complex becomes significant and produces some vacancy in the $d\pi$ orbital.

(3) Temperature Dependence. The existence

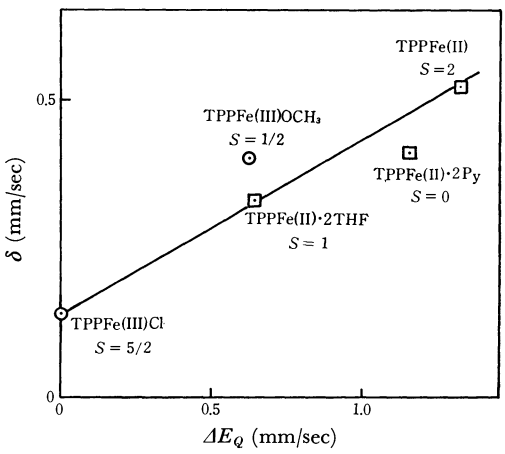

Fig. 6. The isomer shifts plotted *vs.* the quadrupole splittings.
The values were obtained at 77°K.

of low-lying excited states is theoretically and experimentally identified. Temperature dependence of Mössbauer spectrum arises from a population of higher sublevels. Remarkable temperature dependence of the spectrum had been observed for the high spin ferric porphins,[1,3] while relatively small temperature dependence was observed for the isomer shift of TPPFe(III)Cl. Asymmetric spectrum observed for TPPFe(III)OCH_3 showed a temperature dependence, which was however, less remarkable than that observed for other iron porphins of naturally occurring source. In the case of TPPFe(II), no remarkable quadrupole splitting was observed at room temperature, the splitting being observed at 77°K. Between two intense bands, there seems to exist some bands which might be assigned to the lower sublevels, although a possible contamination of the impurity formed by partial oxidation can not be eliminated.

Generally speaking, an increase in the isomer shift seems to be parallel to an increase in the quadrupole splitting observed at low temperature. An increase in the isomer shift of TPPFe(II)·2Py is observed at low temperature, while the quadrupole splitting is decreased. Similar phenomena have been observed for the diamagnetic hemoglobins[1e] and bis(pyridine)phthalocyanine iron(II).[5]

One of the authors (H.K.) wishes to express his thanks to Professor M. Kotani for encouragements and helpful discussions.

BULLETIN OF THE CHEMICAL SOCIETY OF JAPAN VOL. 43 2347—2354 (1970)

The Crystal Structure of Bis-(2-hydroxyacetophenone)-trimethylenediiminocopper(II)

Kiyoto IIDA, Isao OONISHI, Akitsugu NAKAHARA*1 and Yoshimichi KOMIYAMA*2

Department of Applied Chemistry, Faculty of Engineering, Yamanashi University, Kofu, Yamanashi

(Received January 21, 1970)

The crystal structure of bis-(2-hydroxyacetophenone)trimethylenediiminocopper(II), [Cu-(hapt)], has been determined on the basis of the X-ray diffraction data. The crystals are monoclinic. The cell dimensions are: $a=17.746$, $b=9.467$, $c=10.646$ Å, and $\beta=114.06°$. The space group is *Cc*, with four formula units in the unit cell. The structure has been refined from three-dimensional data by the least-squares method with anisotropic temperature factors to an *R*-value of 0.093. The copper atom is four-covalent, with the two planar 2-hydroxyacetophenone groups oriented so as to give a flattened tetrahedral co-ordination geometry. The six-membered copper-trimethylenediamine ring takes a "twisted boat" configuration. The Cu–O bonds are 1.88 and 1.89 Å in length, while the Cu–N bonds are 1.94 and 1.97 Å. The angle between the mean planes of the 2-hydroxyacetophenone moieties is 46.2°.

An extensive study has recently been made of the copper(II) complexes with tetradentate Schiff bases derived from several aldehydes or ketones and diamines by Nakahara and his collaborators.[1] These complexes possess three chelate rings, and their structures can be represented as follows:

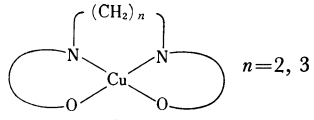

(I)

An investigation of the relative stabilities of the complexes has revealed that those complexes which have a five-membered central chelate ring ($n=2$) are generally more stable than those with a six-membered central chelate ring ($n=3$). It seemed that it would be of interest to clarify this point by determining the structure of a complex with a six-membered central chelate ring. For this purpose crystals of bis-(2-hydroxyacetophenone)trimethylenediiminocopper(II) were chosen. The complex has a 6-6-6*3 fused chelate ring structure, (II). The molecular structures of the complexes with a 6-5-6 (*N,N'*-disalicylidene-ethylenediaminecopper) and a 6-7-6 (*N,N'*-(2,2'-biphenyl)bis(salicylaldiminato)copper(II)) fused chelate ring structure have already been determined by Waters and his collaborators.[2,3] The former has a pyramidal-square coordination, while the latter has a distorted flattened-tetrahedral coordination, around the copper atom.

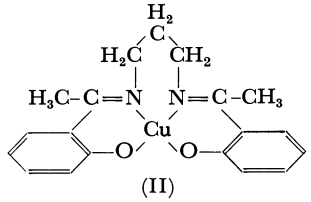

(II)

[Cu(hapt)]

The crystal and molecular structure of the complex, [Cu(hapt)], will be reported in this paper.

Experimental

The crystals of [Cu(hapt)] were prepared according to the method described by Tsumaki *et al.*[4] They are dark green in color and very stable in the air. The unit-cell dimensions were determined from higher-order reflections recorded on Weissenberg photographs (Cu$K\alpha$, $\lambda=1.5418$ Å). The possible space group was found to be $C2/c$ or Cc from the following systematic absences: hkl when $h+k$ is odd and $h0l$ when l is odd. Cc was shown to be consistent with the structure.

The specimens with dimensions of $0.05\times0.20\times0.80$ mm were used for the collection of the intensity data around the *c*-axis. Equi-inclination Weissenberg photographs were taken around the *c*-axis up to the eighth

*1 Institute of Chemistry, College of General Education, Osaka University, Toyonaka, Osaka.

*2 Deceased on Aug. 1, 1968.

*3 The abbreviation "6-6-6" indicates the fused-chelate ring structure containing six-, six-, and six-membered rings, in a clockwise direction.

1) Y. Nakao, N. Nonagase and A. Nakahara, This Bulletin, **42**, 452 (1969).

2) D. Hall and T. N. Waters, *J. Chem. Soc.*, **1960**, 2644.

3) T. P. Cheeseman, D. Hall and T. N. Waters, *ibid.*, **1966**, 1396.

4) P. Pfeiffer, E. Breith, E. Lübbe and T. Tsumaki, *Ann.*, **503**, 84 (1933).

layer, while the zero layer photograph was taken around the b-axis with Cu$K\alpha$ radiation. A multiple film technique was used. Of the 1454 independent reflections within the effective copper sphere ($\sin\theta \leqq 0.98$), 1220 non-zero reflections were observed. The intensities were estimated visually with a standard film strip. The usual Lorentz, polarization, and spot-shape corrections were applied, but the absorption correction was neglected. The crystal data are shown in Table 1.

TABLE 1. CRYSTALLOGRAPHIC DATA

Monoclinic
$a=17.746\pm0.006$Å
b$=9.467\pm0.002$Å
$c=10.646\pm0.004$Å
$\beta=114.06\pm0.02°$
$Dm=1.500$ g/cm^3
$Dx=1.511$ g/cm^3
$Z=4$
Space group C_S^4-Cc
Linear absorption coefficient for Cu$K\alpha$, $\mu=19.0$ cm^{-1}

Structure Analysis

The positions of the copper atom and the four-coordinating atoms around the copper atom could be easily deduced from the three-dimensional Patterson maps. The structure factors were calculated from the parameter values of these atoms. The discrepancy factor, R (defined as $\sum||F_o|-|F_c||/\sum|F_o|$), was 0.32. Preliminary Fourier projections of the electron density upon (010) and (001) were then synthesized, using phases determined by the parameters of these five atoms. The approximate orientation of two 2-hydroxyacetophenone moieties could be deduced from these projections, but the trimethylenediamine ring could not be fixed. The atomic parameters of the trimethylenediamine ring were, therefore, assigned by constructing a scale model of the molecule. Considerable improvement was achieved in the agreement between the observed and calculated structure factors. The structure thus obtained was refined by the three-dimensional difference synthesis to $R=0.20$, and later by a block-diagonal least-squares method using a HBLS-4 program written by T. Ashida. After six cycles of this refinement, anisotropic temperature factors were introduced. The weighting scheme for the least-squares procedure was:

$$w=0.2, \quad \text{if } F_o \leqq F_{\min} \ (4.0)$$
$$w=1.0, \quad \text{if } F_{\min} < F_o < F_{\max} \ (25.0)$$
$$w=F_{\max}/F_o, \quad \text{if } F_o \geqq F_{\max}.$$

The effect of secondary extinction was corrected for five reflections which showed a marked extinction effect ($F_o > 45$). The final R-value became

TABLE 2(a). FINAL ATOMIC COORDINATES AND THEIR E.S.D.'S ($\times10^4$)

Atom	x/a	y/b	z/c
Cu	− 3(5)	392(2)	12(10)
O(1)	− 635(7)	−1001(13)	397(14)
O(2)	643(6)	−1002(9)	− 357(11)
N(1)	− 231(6)	1803(13)	1115(15)
N(2)	234(8)	1812(11)	−1128(13)
C(1)	−1230(10)	− 757(16)	777(16)
C(2)	−1792(12)	−1895(23)	549(22)
C(3)	−2416(13)	−1770(18)	1041(19)
C(4)	−2496(12)	− 555(19)	1742(22)
C(5)	−1941(10)	545(14)	1949(18)
C(6)	−1299(9)	518(16)	1460(16)
C(7)	− 770(8)	1772(15)	1710(15)
C(8)	− 873(13)	2981(17)	2532(20)
C(9)	321(7)	3043(13)	1327(18)
C(10)	4(23)	3943(14)	6(44)
C(11)	− 312(15)	3040(19)	−1305(18)
C(12)	769(10)	1745(14)	−1652(18)
C(13)	831(14)	2951(17)	−2608(23)
C(14)	1309(9)	512(14)	−1478(18)
C(15)	1940(11)	601(23)	−1970(23)
C(16)	2490(11)	− 473(21)	−1724(20)
C(17)	2441(8)	−1705(21)	−1053(23)
C(18)	1824(9)	−1844(13)	− 579(16)
C(19)	1233(8)	− 723(13)	− 794(16)

TABLE 2(b). THE TEMPERATURE FACTORS ($\times10^4$) (The expression of the temperature factor is $\exp[-(B_{11}h^2+B_{22}k^2+B_{33}l^2+B_{12}hk+B_{13}hl+B_{23}kl)]$)

Atom	B_{11}	B_{22}	B_{33}	B_{12}	B_{13}	B_{23}
Cu	37	85	88	7	68	6
O(1)	44	109	119	− 2	105	15
O(2)	36	39	72	12	73	37
N(1)	14	92	125	28	35	105
N(2)	48	53	49	65	85	106
C(1)	44	91	32	− 5	50	−4
C(2)	41	116	121	−58	42	67
C(3)	67	97	60	−55	98	−10
C(4)	46	122	110	−73	68	−36
C(5)	39	71	73	− 1	84	−13
C(6)	34	109	29	−19	52	19
C(7)	22	91	43	−42	42	−28
C(8)	60	83	95	−33	105	−67
C(9)	15	46	131	4	45	19
C(10)	37	77	74	−25	42	66
C(11)	92	127	20	133	104	79
C(12)	39	53	84	−52	34	21
C(13)	75	80	141	−58	160	−38
C(14)	28	54	104	−29	51	−21
C(15)	39	173	144	−39	92	−138
C(16)	38	168	103	−49	102	−81
C(17)	10	162	177	19	17	−82
C(18)	34	56	52	− 3	59	38
C(19)	28	63	56	− 4	43	−27

TABLE 3. OBSERVED AND CALCULATED STRUCTURE FACTORS

Columns are h, F_o, F_c

H	FO	FC	H	FO	FC	H	FO	FC	H	FO	FC	H	FO	FC	H	FO	FC	H	FO	FC	H	FO	FC
K,L= 0 0			-12	13	13	-6	106	94	3	117	149	-20	46	48	-6	72	72	15	37	41	8	23	26	7	27	26
2	478	478	-10	95	100	-4	60	54	5	66	49	-18	58	60	-4	84	107	K,L= 4 4			10	36	34	K,L= 10 5		
4	404	431	-8	48	50	-2	113	115	7	48	65	-16	30	35	-2	72	79	-20	28	28	K,L= 5 5			-16	26	34
6	100	107	-6	105	124	0	179	181	9	79	91	-14	100	93	0	96	95	-18	27	28	-19	47	50	-8	16	28
8	206	223	-4	46	51	2	206	212	11	59	64	-12	12	19	2	94	98	-16	18	27	-17	55	57	-6	40	45
10	126	118	-2	97	117	4	96	94	K,L= 4 2			-10	47	44	4	96	98	-12	44	46	-15	29	26	-4	39	43
12	178	155	0	179	170	6	82	67	-18	32	31	-8	164	169	6	32	40	-10	86	95	-13	61	61	-2	33	43
14	75	60	2	174	209	8	25	32	-14	34	30	-6	92	79	8	56	65	-8	133	123	-11	127	129	K,L= 11 5		
16	162	144	4	61	82	10	55	44	-12	33	40	-4	114	135	10	41	42	-6	117	106	-9	151	158	-7	26	41
K,L= 1 0			6	239	226	12	26	25	-10	70	75	-2	36	59	12	35	44	-4	124	125	-7	177	174	-5	24	36
1	617	688	8	124	135	14	54	52	-8	96	115	0	149	134	K,L= 9 3			-2	98	109	-5	185	201	-3	5	14
3	22	33	10	134	129	K,L= 9 1			-6	195	200	2	151	119	-15	32	39	0	57	67	-3	318	308	K,L= 0 6		
5	184	200	12	54	53	-13	51	47	-4	180	182	4	252	226	-13	27	29	4	63	55	-1	269	244	-22	17	28
7	160	154	14	55	50	-11	26	28	-2	105	106	6	65	66	-11	54	51	6	35	42	1	134	125	-20	60	71
9	170	155	K,L= 3 1			-9	23	23	0	25	30	8	154	163	-9	36	38	8	56	56	3	48	39	-18	47	56
11	98	93	-19	44	37	-7	32	31	2	8	8	10	48	45	-7	51	50	10	39	36	5	121	105	-16	135	150
13	77	67	-17	32	35	-5	66	59	4	13	22	12	61	54	-5	65	68	12	45	38	7	128	96	-14	250	247
15	138	126	-15	55	51	-3	26	27	6	77	80	14	14	15	-3	52	53	14	23	23	9	67	63	-12	184	181
17	84	74	-13	114	105	-1	94	66	8	80	77	K,L= 3 3			-1	52	58	K,L= 5 4			11	17	27	-10	260	269
K,L= 2 0			-11	89	85	1	91	72	10	64	64	-21	29	36	1	164	164	-19	47	49	13	42	36	-8	186	181
0	113	184	-9	191	182	5	14	20	12	37	42	-19	59	61	3	82	96	-17	29	37	15	15	27	-6	42	48
4	122	119	-7	135	121	7	54	48	K,L= 5 2			-17	55	49	5	37	44	-15	33	33	K,L= 4 5			-2	118	119
6	210	207	-5	371	399	9	76	60	-15	44	38	-15	21	23	7	11	18	-13	68	71	-20	39	44	0	208	191
8	254	259	-3	135	152	11	61	45	-13	52	47	-13	46	46	11	14	23	-9	56	49	-18	60	61	2	274	216
10	104	121	-1	48	53	13	16	19	-11	81	73	-11	137	149	K,L= 10 3			-7	107	109	-16	40	40	4	145	147
12	43	46	1	41	43	K,L= 10 1			-9	59	48	-9	134	154	-12	27	33	-5	186	171	-12	63	66	6	138	133
14	118	105	3	31	46	-12	17	25	-7	15	22	-7	207	231	-10	44	45	-3	205	179	-10	250	261	8	53	56
16	123	111	5	139	155	-8	54	44	-5	53	49	-5	213	239	-8	34	32	3	59	58	-8	117	120	10	54	59
18	70	53	7	272	268	-6	59	50	-3	43	41	-3	370	344	-6	47	51	5	32	34	-6	157	154	14	26	34
20	38	43	9	111	129	-4	62	58	1	95	108	-1	138	146	-4	47	48	7	107	108	-4	49	58	K,L= 1 6		
K,L= 3 0			11	142	156	-2	20	17	3	43	38	1	95	75	-2	22	26	9	50	46	-2	165	153	-21	21	26
1	166	149	13	31	40	0	55	51	5	196	191	3	192	174	0	61	67	11	22	24	0	93	107	-19	39	41
3	161	151	15	25	31	8	31	36	7	139	135	5	184	160	2	57	72	13	14	22	2	152	142	-17	59	58
5	80	108	17	16	26	10	21	27	9	88	90	7	136	123	K,L= 6 1			K,L= 6 4			4	83	83	-15	141	160
7	224	213	K,L= 4 1			K,L= 11 1			11	77	76	9	76	82	-9	19	22	-18	32	30	6	200	209	-13	193	179
9	180	167	-20	45	51	-9	28	31	13	64	60	11	56	58	-7	30	42	-12	72	79	8	68	66	-11	219	215
11	72	60	-18	21	22	-7	66	63	K,L= 6 2			13	62	69	-5	36	39	-6	14	17	10	49	41	-9	245	259
13	30	31	-16	82	60	-5	17	26	-14	87	90	K,L= 4 3			-3	21	27	-4	40	30	12	20	21	-7	53	67
15	82	67	-14	85	61	-3	25	28	-10	59	46	-20	40	38	-1	18	21	0	81	79	14	43	50	-5	88	115
19	54	49	-12	97	87	-1	23	25	-8	31	25	-18	30	31	1	19	24	2	84	82	K,L= 5 5			-3	129	147
K,L= 4 0			-10	174	150	1	15	24	-4	47	36	-16	75	76	K,L= 0 4			4	130	134	-19	44	46	-1	124	127
0	10	17	-8	207	191	3	15	23	-2	74	62	-14	58	62	-22	45	54	6	43	34	-17	47	45	1	197	184
2	12	33	-6	292	290	5	16	20	0	50	35	-12	236	230	-20	64	63	8	37	33	-15	77	76	3	122	115
4	61	79	-4	329	354	K,L= 0 2			2	73	89	-10	160	166	-18	98	102	K,L= 7 4			-13	24	19	5	109	98
6	103	128	-2	69	30	-20	38	42	4	58	56	-8	174	165	-16	144	137	-5	66	78	-11	155	157	7	70	65
8	101	106	0	105	144	-18	28	24	6	99	105	-6	120	143	-14	208	210	-1	21	17	-9	171	186	11	23	30
10	91	77	2	38	53	-16	94	87	K,L= 7 2			-4	395	390	-12	249	244	3	79	71	-7	148	141	13	28	32
12	34	30	6	152	164	-14	183	145	-15	26	26	-2	278	274	-10	278	278	5	21	27	-5	114	118	K,L= 2 6		
14	23	17	8	40	45	-12	157	132	-13	43	37	0	118	130	-8	136	81	K,L= 8 4			-3	165	152	-20	53	49
K,L= 5 0			10	64	65	-10	120	115	-5	31	31	2	34	45	-6	154	167	-16	29	37	-1	173	162	-18	14	19
1	12	3	12	57	58	-8	258	251	1	134	130	4	56	47	-4	40	62	-14	17	21	1	141	147	-16	73	80
3	69	65	16	22	27	-6	411	393	3	69	59	6	41	42	0	70	63	-12	22	21	3	86	77	-14	58	55
5	197	190	18	13	21	-4	353	368	5	32	33	8	59	58	2	301	291	-10	20	27	5	158	165	-12	172	163
7	113	114	K,L= 5 1			2	816	798	9	34	39	10	25	32	4	176	156	-8	30	44	7	97	103	-10	145	145
9	79	75	-19	46	39	4	236	273	11	33	38	12	65	78	6	175	152	-6	18	29	9	43	39	-8	209	225
11	86	82	-17	60	46	6	250	290	K,L= 8 2			14	25	33	8	53	55	-4	18	22	11	18	18	-6	107	95
13	65	51	-15	99	80	8	138	142	-8	75	58	K,L= 5 3			10	138	144	0	51	54	13	21	26	-4	219	202
15	12	16	-13	105	91	10	108	121	-6	85	82	-19	46	48	12	98	94	10	40	45	K,L= 6 5			-2	101	104
K,L= 6 0			-11	77	64	12	81	85	-4	60	58	-17	35	38	14	65	69	K,L= 9 4			-18	51	58	0	226	228
0	29	34	-9	123	125	14	34	52	-2	71	56	-15	49	58	K,L= 1 6			-15	13	17	-16	82	86	2	69	72
2	21	26	-7	91	102	16	20	33	2	91	86	-13	92	110	-21	42	43	-13	16	19	-14	90	97	4	159	149
4	109	104	-5	286	267	18	76	108	4	12	12	-11	179	194	-19	28	34	-11	41	41	-12	121	117	6	99	102
6	42	28	-3	121	143	K,L= 1 2			6	51	47	-9	87	105	-17	96	98	-9	23	24	-10	166	160	8	53	59
12	59	52	-1	105	113	-21	19	23	8	28	29	-7	144	146	-15	92	97	-7	42	41	-8	97	87	10	34	36
16	28	32	1	146	175	-19	59	48	10	30	29	-5	142	134	-13	157	159	-5	81	87	-6	132	121	12	36	40
K,L= 7 0			3	69	78	-15	120	127	K,L= 9 2			-3	316	307	-11	209	181	-3	71	70	-4	125	115	14	11	17
1	48	39	5	99	105	-13	115	128	-11	15	20	-1	184	168	-9	82	85	-1	43	35	-2	198	206	K,L= 3 6		
3	55	59	7	116	135	-11	111	115	-9	33	35	1	188	176	-7	72	69	3	14	20	0	158	160	-21	23	33
7	56	43	9	84	75	-9	18	29	-7	100	114	3	179	164	-5	289	283	5	20	24	2	44	44	-19	60	61
9	33	29	11	100	100	-7	225	223	-5	84	78	5	128	128	-3	118	133	7	18	25	4	71	77	-17	65	66
15	35	35	13	33	32	-5	23	26	-3	78	62	7	60	61	-1	165	214	9	28	37	6	82	80	-15	27	34
K,L= 8 0			15	37	33	-3	212	231	-1	47	43	9	67	63	1	80	104	K,L= 10 4			8	25	27	-13	26	29
0	219	240	17	53	41	-1	60	42	1	86	79	11	49	48	3	294	307	-10	25	17	10	37	40	-9	43	32
2	53	38	K,L= 6 1			1	741	756	3	57	49	13	58	66	5	175	164	-8	37	33	12	15	14	-7	192	174
4	54	42	-18	34	32	3	381	353	5	77	67	K,L= 6 3			7	73	79	-6	76	90	K,L= 7 5			-5	178	154
6	39	31	-16	47	41	5	185	188	7	61	53	-18	51	63	9	61	51	-4	71	74	-17	65	78	-3	139	149
8	66	50	-14	136	127	7	90	99	9	66	70	-16	22	32	11	92	82	-2	79	86	-15	74	78	-1	98	104
10	23	24	-12	82	71	9	181	163	11	22	32	-14	34	39	13	44	37	4	50	52	-13	83	90	1	111	100
K,L= 9 0			-10	84	76	11	85	85	K,L= 10 2			-12	116	124	15	17	18	6	27	27	-11	95	113	3	59	59
1	123	117	-8	73	60	13	82	74	-12	19	20	-10	67	58	K,L= 2 4			K,L= 11 4			-9	49	48	5	186	188
5	80	61	-6	87	94	15	31	20	-10	20	17	-8	133	128	-22	21	24	-9	34	51	-7	39	40	7	96	100
7	74	59	-4	142	147	17	73	89	-8	46	46	-6	69	73	-18	53	47	-7	40	44	-3	38	36	9	85	89
9	74	67	-2	192	207	19	13	22	-6	63	49	-4	127	116	-16	44	47	-5	48	53	-1	93	91	11	34	36
11	56	42	0	195	204	K,L= 2 2			-4	46	41	-2	135	147	-14	74	70	-3	47	51	1	52	50	13	21	22
K,L= 10 0			2	237	261	-20	27	32	-2	45	35	0	142	144	-12	211	182	3	35	53	3	24	31	K,L= 4 6		
2	12	22	4	123	135	-18	84	74	2	72	59	2	206	197	-10	137	140	K,L= 1 5			5	82	77	-20	30	37
4	35	27	6	145	156	-16	69	53	4	15	23	4	271	272	-8	182	177	-21	23	32	9	32	37	-18	31	34
6	65	57	8	122	136	-14	215	212	8	51	47	6	84	83	-6	55	60	-19	55	60	11	23	27	-16	49	54
8	77	80	10	111	125	-12	149	146	K,L= 11 2			8	98	104	-4	319	267	-17	94	101	K,L= 8 5			-8	84	89
10	36	36	12	93	70	-10	90	109	-9	42	47	10	50	49	-2	352	341	-15	38	42	-16	53	65	-6	105	97
K,L= 11 0			14	79	67	-8	172	153	-7	66	73	12	58	59	0	281	249	-11	45	45	-14	62	70	-4	119	129
3	37	31	16	64	59	-6	202	187	-5	69	73	14	30	34	2	210	235	-9	39	36	-12	83	95	-2	84	79
5	57	44	K,L= 7 1			-4	118	140	-3	76	81	K,L= 7 3			4	370	357	-7	106	83	-10	79	85	0	83	72
7	73	68	-15	26	31	-2	392	382	-1	37	38	-17	48	56	6	113	99	-5	39	36	-8	60	57	4	30	31
K,L= 12 0			-13	95	79	0	224	255	1	13	18	-15	18	25	8	50	51	-1	71	69	-6	49	52	6	53	42
0	36	33	-11	26	29	2	475	515	3	36	31	-13	82	102	10	64	56	1	63	52	-4	52	51	8	56	53
2	27	32	-9	108	102	4	96	114	K,L= 1 3			-11	48	44	12	35	34	3	100	87	-2	60	57	10	20	24
K,L= 1 1			-7	79	64	8	121	132	-21	20	28	-9	38	36	14	26	26	5	32	38	0	79	83	K,L= 5 6		
-17	82	59	-5	92	80	10	138	149	-19	42	46	-7	65	58	K,L= 3 4			7	24	16	2	81	81	-19	28	27
-15	69	53	-3	95	90	12	83	73	-17	56	54	-5	53	57	-21	37	38	9	66	60	4	88	96	-17	26	28
-13	28	21	-1	219	213	14	34	34	-15	27	42	-3	61	64	-17	71	65	11	32	35	6	40	46	-15	66	65
-11	31	17	1	223	242	16	25	29	-13	62	65	-1	83	81	-13	164	175	13	27	34	8	22	24	-13	54	51
-9	234	212	3	259	264	18	20	25	-11	43	35	1	14	21	-11	164	172	15	19	20	10	19	25	-11	79	82
-7	155	161	5	76	72	K,L= 3 2			-9	42	52	3	160	152	-9	209	212	K,L= 9 5			K,L= 9 5			-9	139	129
-5	178	150	7	93	84	-19	65	44	-7	93	91	5	75	69	-7	171	152	-18	59	60	-15	25	35	-7	92	74
-3	91	90	9	15	25	-17	75	61	-5	150	137	7	53	59	-5	169	181	-16	94	91	-13	33	35	-5	86	77
1	208	181	11	38	42	-15	111	94	-3	134	105	9	57	61	-3	103	107	-12	41	31	-11	47	52	-3	113	108
3	552	531	13	17	29	-13	209	185	-1	65	49	11	37	39	-1	374	330	-10	51	52	-9	42	41	-1	107	100
5	90	113	15	63	71	-11	107	88	1	451	395	13	19	23	1	87	90	-8	83	76	-7	42	40	1	49	46
7	116	134	K,L= 8 1			-9	205	196	7	114	109	K,L= 8 3			3	262	251	-6	126	110	-5	75	74	3	74	78
11	36	46	-16	18	20	-7	346	328	9	114	109	-16	44	50	5	114	114	-4	185	161	-3	85	88	K,L= 6 6		
15	57	54	-14	76	60	-5	386	359	11	54	56	-14	57	62	7	37	39	-2	247	214	-1	51	49	-18	24	26
K,L= 2 1			-12	56	44	-3	339	359	13	14	21	-12	80	96	9	62	57	0	116	130	1	78	76	-14	28	28
-16	63	64	-10	81	70	-1	135	192	15	28	37	-10	29	40	11	65	66	2	126	178	3	75	77	-12	29	34
-14	69	56	-8	93	81	1	18	22	K,L= 2 3			-8	58	69	13	42	42	4	66	57	5	39	45	-10	21	24

Table. 3 (Continued)

H	FO	FC	H	FO	FC	H	FO	FC	H	FO	FC	H	FO	FC	H	FO	FC	H	FO	FC	H	FO	FC
-6	24	24	-4	47	46	-19	53	52	-19	18	24	-13	100	98	K,L= 10		7	1	70	70	-3	113	120	-8	74	68
-2	56	55	-2	37	39	-17	88	89	-17	74	73	-11	106	105	-6	11	15	3	118	116	-1	110	107	-6	33	31
4	66	65	0	48	63	-15	81	83	-15	76	76	-9	104	102	-4	45	45	5	68	70	1	112	114	-4	44	49
6	28	33	K,L= 1		7	-13	51	55	-13	99	98	-7	103	95	-2	14	27	7	59	57	5	25	32	0	30	37
K,L= 7		6	-17	27	31	-11	48	54	-11	53	46	-5	53	53	K,L= 0		8	9	20	30	9	37	42	2	10	25
-17	15	25	-15	35	39	-9	169	182	-9	158	150	-3	39	37	-22	42	56	K,L= 2		8	K,L= 4		8	K,L= 7		8
-15	24	28	-13	44	42	-7	155	170	-7	87	83	-1	95	80	-20	28	28	-20	36	33	-20	15	20	-15	11	18
-13	16	21	-11	44	41	-5	120	132	-5	105	101	1	103	104	-18	35	39	-18	94	90	-18	37	41	-13	29	35
-11	61	50	-9	12	25	-3	67	77	-3	75	64	3	67	62	-16	33	36	-16	78	89	-16	38	31	-9	19	27
-9	48	46	-7	125	118	-1	117	114	-1	118	116	5	62	61	-14	136	140	-14	121	124	-14	48	40	K,L= 8		8
-1	9	12	-5	61	73	1	101	97	1	93	82	7	25	26	-12	192	204	-12	119	127	-8	37	27	-14	21	21
1	21	27	-3	111	104	3	49	46	3	64	62	K,L= 8		7	-10	221	245	-10	60	65	-6	76	69	-12	20	23
K,L= 8		6	-1	134	142	5	21	27	7	94	98	-16	25	34	-8	246	265	-8	57	58	-4	64	52	-10	29	29
-16	24	29	1	134	121	7	73	85	9	41	45	-14	69	72	-4	140	155	-6	133	137	-2	96	80	-8	60	55
-14	51	46	5	24	23	9	46	53	K,L= 6		7	-12	88	93	-2	203	185	-4	49	50	0	67	61	-6	42	35
-10	27	33	K,L= 2		7	11	14	28	-18	51	47	-10	89	82	0	106	107	-2	90	90	2	46	43	-4	48	42
-4	66	65	-22	22	29	K,L= 4		7	-16	69	70	-8	71	63	2	194	206	0	35	28	10	10	20	-2	64	64
0	10	20	-20	31	20	-18	64	59	-14	108	102	-6	48	42	4	134	140	2	69	61	K,L= 9		8	0	12	19
2	19	20	-18	44	48	-16	54	54	-12	111	114	-4	57	52	6	66	70	4	41	39	-19	42	43	2	51	54
K,L= 9		6	-16	69	61	-14	108	112	-10	134	140	-2	71	66	8	58	61	6	65	63	-17	64	53	4	24	30
-13	35	34	-14	46	43	-12	96	98	-8	202	202	0	78	74	K,L= 1		8	8	28	39	-15	62	53	K,L= 9		8
-11	15	22	-12	32	29	-10	20	32	-6	126	120	2	71	77	-21	37	33	10	35	47	-11	33	39	-11	18	22
-9	62	64	-10	65	59	-8	84	87	-4	53	47	4	57	60	-19	67	53	K,L= 3		8	-9	85	83	-9	48	42
-7	20	22	-8	184	187	-6	70	74	-2	41	42	6	41	47	-17	25	33	-21	18	23	-7	86	80	-7	58	63
-5	67	64	-6	133	138	-4	116	117	0	103	97	K,L= 9		7	-15	72	63	-19	46	41	-5	93	99	-5	51	49
-3	63	68	-4	28	32	-2	159	151	2	92	89	-13	38	40	-13	167	157	-17	51	47	-3	64	53	-3	51	54
-1	49	54	-2	47	50	0	104	104	4	28	39	-11	37	38	-11	147	151	-15	78	78	-1	31	38	-1	42	37
1	41	39	0	132	103	2	109	105	6	49	49	-9	57	58	-9	136	145	-13	69	60	3	32	40	1	34	36
K,L= 10		6	2	48	40	6	56	56	8	22	29	-7	16	18	-7	174	181	-11	93	100	7	14	29			
-10	32	34	4	34	36	8	112	118	K,L= 7		7	-5	24	29	-5	83	78	-9	33	37	9	11	19			
-8	52	52	K,L= 3		7	10	41	44	-17	20	23	-3	25	23	-3	111	109	-7	88	97	K,L= 6		8			
-6	26	27	-21	36	39	K,L= 5		7	-15	48	47	3	33	40	-1	54	43	-5	53	52	-12	51	39			

0.093 for all the observed reflections. The atomic scattering factors were taken from the "International Tables for X-ray Crystallography".[5] The final atomic parameters and their estimated standard deviations are listed in Table 2. The observed and calculated structure factors are compared in Table 3.

Discussion

A perspective drawing of the [Cu(hapt)] molecule is shown in Fig. 1. The bond lengths and angles in the molecule are listed in Table 4, together with their e.s.d.'s, they are also shown in Fig. 2.

The bis-(2-hydroxyacetophenone)trimethylenediimine group is coordinated to the copper atom as a tetradentate ligand through two phenolic oxygen atoms and two nitrogen atoms of the Schiff-base linkage. The coordination around the copper atom is a distorted tetrahedron. The Cu–O distances are 1.88 and 1.89 Å, and the Cu–N distances are 1.94 and 1.97 Å. These values agree well with those found in the related complexes.[6–8] The angle between the two planes defined by Cu, O(1), and N (1) and by Cu, O(2), and N(2) is 34.4°, being equal neither to 90°, a value expected for a regular tetrahedral environment, nor to 0° for a square-planar configuration. The distorted tetrahedral configu-

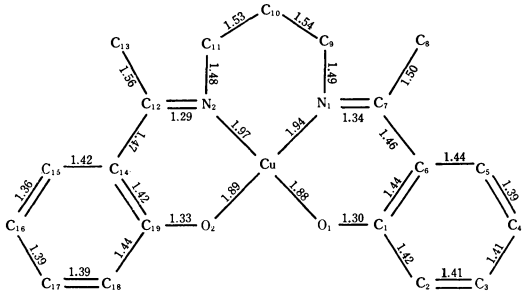

Fig. 2(a). Intramolecular bond length (in Å).

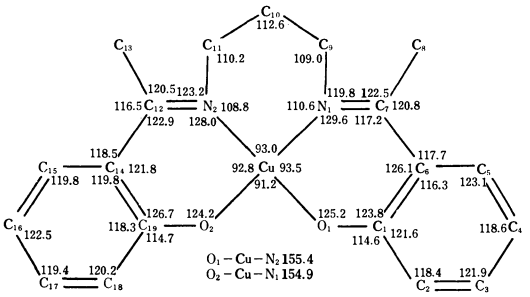

Fig. 2(b). Intramolecular bond angle (in degrees).

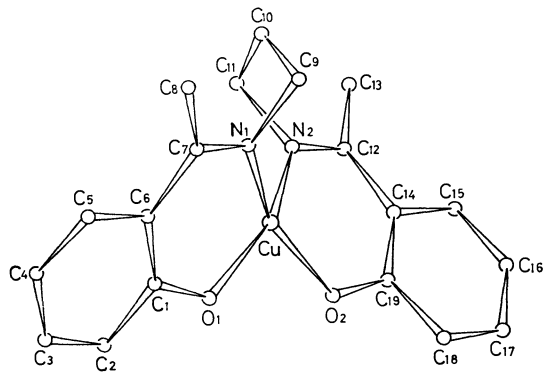

Fig. 1. Perspective drawing of the molecule.

5) "International Tables for X-Ray Crystallography," Vol. III, Kynoch Press, Birmingham (1962), p. 202.

6) E. C. Lingafelter, G. L. Simmons and B. Morosin, *Acta Cryst.*, **14**, 1222 (1961).

7) M. A. Jarski and E. C. Lingafelter, *ibid.*, **17**, 1109 (1964).

8) E. R. Boyko, *ibid.*, **21**, 614 (1966).

TABLE 4(a). INTRAMOLECUIAR BOND LENGTHS (IN Å) AND THEIR E.S.D.'S

2-haph moiety (I)		2-haph moiety (II)	
Cu - O(1)	1.88(0.02)	Cu - O(2)	1.89(0.01)
Cu - N(1)	1.94(0.02)	Cu - N(2)	1.97(0.02)
O(1)-C(1)	1.30(0.02)	O(2)-C(19)	1.33(0.02)
N(1)-C(7)	1.34(0.02)	N(2)-C(12)	1.29(0.02)
C(1)-C(2)	1.42(0.03)	C(18)-C(19)	1.44(0.02)
C(1)-C(6)	1.44(0.02)	C(14)-C(19)	1.42(0.02)
C(2)-C(3)	1.41(0.03)	C(17)-C(18)	1.39(0.03)
C(3)-C(4)	1.41(0.03)	C(16)-C(17)	1.39(0.03)
C(4)-C(5)	1.39(0.03)	C(15)-C(16)	1.36(0.03)
C(5)-C(6)	1.44(0.03)	C(14)-C(15)	1.42(0.03)
C(6)-C(7)	1.46(0.02)	C(12)-C(14)	1.47(0.03)
C(7)-C(8)	1.50(0.03)	C(12)-C(13)	1.56(0.03)
Trimethylenediamine ring			
N(1)-C(9)	1.49(0.02)		
N(2)-C(11)	1.48(0.03)		
C(9)-C(10)	1.54(0.04)		
C(10)-C(11)	1.53(0.04)		

TABLE 4(c). INTERMOLECULAR DISTANCES LESS THAN 3.6 Å

Atom 1	Atom 2	distance	e.s.d.
O(1)	N(2)	3.47	0.02
O(1)	C(12)	3.19	0.02
O(1)	C(13)	3.19	0.02
O(2)	C(13)	3.36	0.03
O(2)	C(15)	3.42	0.02
N(1)	O(2)	3.51	0.02
N(1)	C(19)	3.41	0.02
C(1)	N(2)	3.41	0.02
C(1)	C(11)	3.58	0.02
C(2)	C(11)	3.48	0.02
C(5)	O(1)	3.48	0.02
C(7)	O(2)	3.19	0.01
C(7)	C(19)	3.60	0.02
C(8)	O(1)	3.46	0.03
C(8)	O(2)	3.30	0.02
C(9)	C(18)	3.48	0.02
C(9)	C(19)	3.58	0.02

Atom 1: $(x.y,z)$
Atom 2: $(x, -y, z+1/2)$

TABLE 4(b). INTRAMOLECULAR BOND ANGLES (IN DEGREES) AND THEIR E. S. D.' S

Coordination angles			
O(1)-Cu-N(1)	93.5 (0.8)		
O(2)-Cu-N(2)	92.8 (0.7)		
O(1)-Cu-O(2)	91.2 (0.6)		
N(1)-Cu-N(2)	93.0 (0.6)		
O(1)-Cu-N(2)	155.4 (0.7)		
O(2)-Cu-N(1)	154.9 (0.7)		
2-haph moiety (I)		2-haph moiety (II)	
Cu - N(1)-C(7)	129.6 (1.1)	Cu - N(2)-C(12)	128.0 (1.2)
Cu - O(1)-C(1)	125.2 (1.2)	Cu - O(2)-C(19)	124.2 (1.0)
O(1)-C(1)-C(6)	123.8 (1.5)	O(2)-C(19)-C(14)	126.7 (1.3)
O(1)-C(1)-C(2)	114.6 (1.6)	O(2)-C(19)-C(18)	114.7 (1.2)
N(1)-C(7)-C(6)	117.2 (1.4)	N(2)-C(12)-C(14)	122.9 (1.5)
N(1)-C(7)-C(8)	122.5 (1.4)	N(2)-C(12)-C(13)	120.5 (1.5)
C(1)-C(6)-C(7)	126.1 (1.6)	C(12)-C(14)-C(19)	121.8 (1.6)
C(1)-C(2)-C(3)	118.4 (2.0)	C(17)-C(18)-C(19)	120.2 (1.4)
C(2)-C(3)-C(4)	121.9 (2.0)	C(16)-C(17)-C(18)	119.4 (1.7)
C(3)-C(4)-C(5)	118.6 (2.1)	C(15)-C(16)-C(17)	122.5 (2.1)
C(4)-C(5)-C(6)	123.1 (1.6)	C(14)-C(15)-C(16)	119.8 (2.1)
C(1)-C(6)-C(5)	116.3 (1.5)	C(15)-C(14)-C(19)	119.8 (2.1)
C(2)-C(1)-C(6)	121.6 (1.8)	C(14)-C(19)-C(18)	118.3 (1.5)
C(5)-C(6)-C(7)	117.7 (1.5)	C(12)-C(14)-C(15)	118.5 (1.6)
C(6)-C(7)-C(8)	120.8 (1.5)	C(13)-C(12)-C(14)	116.5 (1.7)
Trimethylenediamine ring			
Cu - N(1)-C(9)	110.6 (1.0)		
Cu - N(2)-C(11)	108.8 (1.3)		
N(1)-C(9)-C(10)	109.0 (1.6)		
N(2)-C(11)-C(10)	110.2 (1.8)		
C(9)-C(10)-C(11)	112.6 (1.2)		
C(7)-N(1)-C(9)	119.8 (1.3)		
C(11)-N(2)-C(12)	123.2 (1.6)		

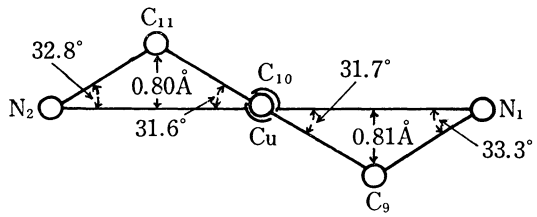

Fig. 3. Conformation of Cu(II)-trimethylenediamine ring.

rations are found in some *N*-substituted bis-salicylaldimine complexes of copper.[3,9-11] These authors claim that the substituent is sufficiently bulky to prevent the normal square-planar complex from being sterically feasible in the case of *N*-*t*-butyl[9] and *N*-isopropyl[10] complexes, and that the distortion in the *N*-ethyl[11] complex is due to packing forces in the crystal.[12] In the present compound, the two planar 2-hydroxyacetophenoneimine groups are joined by three methylene groups. Consequently, the central chelate ring is six-membered. The presence of this six-membered ring appears to give rise to the distortion of the square-planar coordination around the central copper atom. In fact, the related ethylenediamine analogue, *N*,*N*′-disalicylidene-ethylenediaminecopper,[2] exhibits a square-planar coordination. The conformation of the Cu(II)-trimethylenediamine ring is a twisted boat form, as is illustrated in Fig. 3. The six-membered chelate ring has approximately a twofold axis of rotation through the central copper atom and the central carbon atom C(10) of the ligand. The carbon atoms, C(9) and C(11), are 0.81 and 0.80 Å respectively apart from the plane defined by Cu, N(1), and N(2). It should be noted here that all the isolated metal-trimethylenediamine chelate rings

Table 5. Comparison of various fused-chelate ring structures

	a	b	c
Bond lengths and angles			
Cu–O	1.91, 2.03	1.88, 1.89	1.90, 1.90Å
Cu–N	1.94, 2.08	1.94, 1.97	1.94, 1.96Å
O–Cu–N	95°	93.5°	93.6°
O′–Cu–N′	90	92.8	93.6
O–Cu–O′	89	91.2	88.9
N–Cu–N′	82	93.0	96.1
O–Cu–N′	180	155.4	151.4
O′–Cu–N	180	154.9	154.6
Dihedral angle	0	34.4	37

Conformation of the central chelate ring

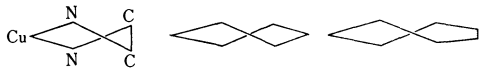

a: *N*,*N*′-disalicylidene-ethylenediaminecopper[2]
b: Present work
c: *N*,*N*′-(2, 2′-biphenyl) bis (salicylaldiminato) copper(II)[3]

Table 6. Least-squares planes

Coefficient of least-squares plane equations.

$A(x')+B(y')+C(z')+D=0$

	A	*B*	*C*	*D*
a: Coordination plane (I) [Cu, O(1), N(1)]	0.5285	0.2904	0.7977	−2.6264
b: Coordination plane (II) [Cu, O(2), N(2)]	0.5231	−0.3010	0.7974	−2.8562
c: Coordination plane (III) [Cu, N(1), N(2)]	0.7713	0.0007	0.6365	−1.4193
d: Chelate ring (I) [Cu, O(1), N(1), C(1) C(6), C(7)]	0.3761	0.3318	0.8651	−3.4027
e: Chelate ring (II) [Cu, O(2), N(2), C(12), C(14), C(19)]	0.3853	−0.3347	0.8600	−3.3655
f: Benzene ring (I) [C(1), C(2), C(3), C(4), C(5), C(6)]	0.2813	0.4024	0.8712	−3.8511
g: Benzene ring (II) [C(14), C(15), C(16), C(17), C(18), C(19)]	0.2676	−0.4099	0.8720	−3.3858
h: 2-haph moiety (I) [O(1), N(1), C(1), C(2), C(3), C(4), C(5), C(6), C(7)]	0.2825	0.3640	0.8875	−3.9227
i: 2-haph moiety (II) [O(2), N(2), C(12), C(14), C(15), C(16), C(17), C(18), C(19)]	0.2832	−0.3673	0.8859	−3.4897

$x'=ax+cz\cos\beta \qquad y'=by \qquad z'=cz\sin\beta$

9) T. P. Cheeseman, D. Hall and T. N. Waters, *J. Chem. Soc.*, **1966**, 685.
10) P. L. Orioli and L. Sacconi, *J. Amer. Chem. Soc.*, **88**, 277 (1966).
11) C. Panattoni, G. Bonbieri and R. Graziani, *Acta Cryst.*, **23**, 537 (1967).
12) D. Hall, R. H. Sumner and T. N. Waters, *J. Chem. Soc.*, **1969**, 420.

Table 7. Deviations from leas-squares planes (Å × 10^3)

	d-plane	f-plane	h-plane		e-plane	g-plane	i-plane
Cu	130	(369)	(350)	Cu	−108	(−431)	(−346)
O(1)	−146	(−125)	−98	O(2)	138	(73)	87
N(1)	− 21	(221)	134	N(2)	42	(−261)	−117
C(1)	70	−11	2	C(19)	−61	4	16
C(2)	(243)	2	61	C(18)	(−254)	1	−50
C(3)	(365)	4	53	C(17)	(−403)	1	−58
C(4)	(325)	−1	−7	C(16)	(−378)	−9	−16
C(5)	(159)	−9	−60	C(15)	(−178)	14	68
C(6)	54	15	−29	C(14)	−48	−11	53
C(7)	−75	(47)	−48	C(12)	48	(−105)	25
C(8)	(−183)	(−37)	(−187)	C(13)	(263)	(96)	(280)

( ) not included in the least-squares calculations.

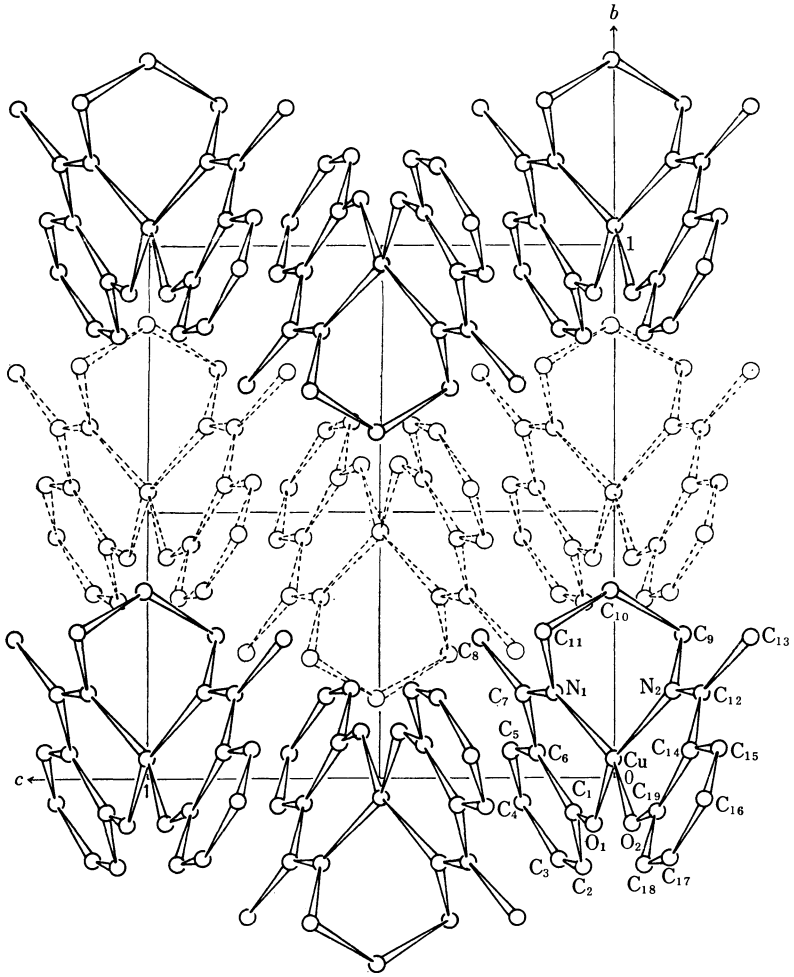

Fig. 4. Projection of the structure along the *a*-axis.

hitherto reported take a chair form.[13,14],*4 The reason for taking such a twisted boat form in the present compound may be that the arrangements of bonds around the two imino nitrogen atoms have

13) T. Nomura, F. Marumo and Y. Saito, This Bulletin, **42**, 1016 (1969).

14) E. Yasaki, I. Oonishi, H. Kawaguchi, S. Kawaguchi and Y. Komiyama, This Bulletin, **43**, 1354 (1970).

*4 The crystal structures of *trans*-$[Co(NO_2)_2(tn)_2]NO_2$ and *cis*-$[Co(NCS)_2(tn)_2]NCS$ were presented at the 22nd Annual Meeting of the Chemical Society of Japan, Tokyo, April, 1969.

to be planar.

The twofold symmetry of the fused central chelate ring is also observed in such related complexes as *N,N'*-disalicylidene-ethylenediaminecopper with a 6-5-6 fused chelate ring structure and *N,N'*-(2,2'-biphenyl)bis(salicylaldiminato)copper(II) with a 6-7-6 structure.[2,3] In Table 5, the shape and size of the central ring in the 6-*X*-6 fused chelate-ring structures are compared ($X=5$, 6, and 7). Obviously, the N–Cu–N' angle increases with the increase in X. The dihedral angles between the two coordination planes show the same tendency: 0° for $X=5$, 34.4° for $X=6$, and 37.0° for $X=7$. It seems likely that the extent of the distortion of square-planar coordination is related to the number of atoms in the central chelate ring.

Such a distorted-tetrahedral coordination around the central copper atom as is described above will certainly decrease the stability of the complex.[1]

The bond distances and angles within 2-hydroxyacetophenone moieties do not differ significantly from those reported for similar molecules.[6-8]

Equations for several least-squares planes are listed in Table 6, while the deviations from those planes are shown in Table 7. The two 2-hydroxyacetophenone moieties are approximately planar, and the deviations of the copper atom from these planes are 0.35 and 0.34 Å respectively. The angle between the two planes is 46.2°.

A projection of the structure along the a-axis is shown in Fig. 4. The molecules are alternately stacked with 2–hydroxyacetophenone groups parallel, but with Cu-C(10) directions opposite along the *c*-axis, thus forming columns. The short contacts in the columns occur between C(7) and O(2), (3.19 Å), and between C(12) and O(1), (3.19 Å). These columns of molecules are packed laterally with the usual van der waals contacts.

The numerical calculations were carried out on the HITAC 5020E at the Computer Centre of the University of Tokyo.

The authors are grateful to Professor Y. Saito for his keen interest and valuable suggestions throughout this work. Part of the cost of this work has been defrayed by a Scientific Research Grant of the Ministry of Education, to which the authors' thanks are due.

BULLETIN OF THE CHEMICAL SOCIETY OF JAPAN VOL. 43 2354—2359 (1970)

Application of the Continuous Variation Method to the Conductometric Determination of Formation Constants—Hexamminecobalt(III) Chloride - Sodium Sulfate and Tris(ethylenediamine)cobalt(III) Chloride - Sodium Sulfate Systems

Shunzo KATAYAMA and Reita TAMAMUSHI

The Institute of Physical and Chemical Research, Yamato-machi, Kita-adachi-gun, Saitama

(Received January 29, 1970)

The conductance behavior of mixtures was investigated with the following systems in aqueous solutions of various ionic strengths at 25°C; NaCl - KCl, NaCl - $NaClO_4$, NaCl - Na_2SO_4, $[CO(NH_3)_6]Cl_3$ - Na_2SO_4 and $[CO(en)_3]Cl_3$ - Na_2SO_4. Appreciable deviations of the measured conductivities from additivity were observed in the last two systems involving the cobalt(III) complexes. The deviation was attributed to the ion-pair formation of the complex cations with sulfate ions; the ion-pair formation constants at various ionic strengths were determined by means of computer analysis of the deviation without relying on the Onsager conductance equation. The thermodynamic ion-pair formation constants at 25°C were as follows: $\log K = 3.5_3$ for $[CO(NH_3)_6]^{3+} \cdot SO_4^{2-}$ and $\log K = 3.6_0$ for $[CO(en)_3]^{3+} \cdot SO_4^{2-}$. The analysis of conductance behavior of mixtures was proved to be a useful method of studying ion-pair formation particularly at relatively high ionic strengths.

The method of continuous variations is a useful technique for determining both stoichiometric compositions and equilibrium constants of complexes in solutions. The application of this method to the conductometric determination of formation constants appears to have the advantage that the measured quantities can be analysed, in principle, without relying on the quantitative validity of the Onsager conductance equation; this advantage is particularly important when the method is applied

to the systems of relatively high ionic strengths.[1] This approach, however, when applied rather loosely, often gives results which are inconsistent with those obtained by other methods, and the utility of the method has been subjected to critical discussions.[2,3] The complication involved in the application of continuous variation method to the study of the conductance behavior of mixtures lies in the fact that the deviation of the observed conductance from additivity may be caused not only by specific ionic interactions but also by the effect of the added ions on the mobility of the ions.[3,4]

This paper deals with the application of continuous variation method to the conductometric determination of ion-pair formation constants of hexamminecobalt(III) and tris(ethylenediamine)-coblt(III) ions with sulfate ions at some varying ionic strengths. The additivity rule was also examined with some mixtures of simple electrolytes, in which no specific individual effects is expected.

Experimental

Procedure and Apparatus. The electric conductivities of mixtures were measured by mixing the solutions of the same ionic strength at various volume fractions. A precision a.c. bridge (HBS-5M, Ando Electric Co., Ltd.), operated at 1000 Hz, was used for conductivity measurements; the balance of the bridge was detected by a tuned null-detector of high sensitivity. The resistance readings of the bridge were calibrated by the substitution method with a precision decade resistance box (Dekastat RS-624, Electro Scientific Industries; accuracy, $\pm 0.005\%$). The resolution of the apparatus was about one part per million, and the reproducibility of conductivity measurements was better than 0.1%. Two dipping-type cells similar to that described in previous papers[5,6] were used; the cell constants were 0.1945 and 0.7704 cm^{-1}, respectively, as determined with standard potassium chloride solutions. All measurements were carried out in a water-thermostat of 25.000 ± 0.005°C.

Hexamminecobalt(III) chloride and tris(ethylenediamine)cobalt(III) chloride were prepared according to the procedure described in literature;[7] these samples were purified by three recrystallizations from their aqueous solutions containing a few drops of acetic acid. The conventional chemical analysis and conductivity measurement showed that the samples obtained were of very high purity. Sodium sulfate of analytical reagent grade was dried at 120°C until it reached constant weight. All other chemicals were of analytical reagent grade. Each solution was carefully prepared by using the conductivity water of low specific conductance ($<2 \times 10^{-7}$ ohm^{-1} cm^{-1}) in an atmosphere of purified nitrogen gas.

Results

Mixtures of Simple Electrolytes. The conductance behavior of sodium chloride - potassium chloride and sodium chloride - sodium perchlorate mixtures showed no appreciable deviation from additivity at ionic strength, I, of 0.01 as shown in Fig. 1 (curves (1) and (2)). Sodium chloride - sodium sulfate mixtures of $I=0.01$ and 0.1, however, gave slightly smaller conductivities than those expected from additivity; the deviation reached the maximum value of about 0.5% at the volume fraction, x, of 0.5—0.6 (Fig. 1, curve (3)).

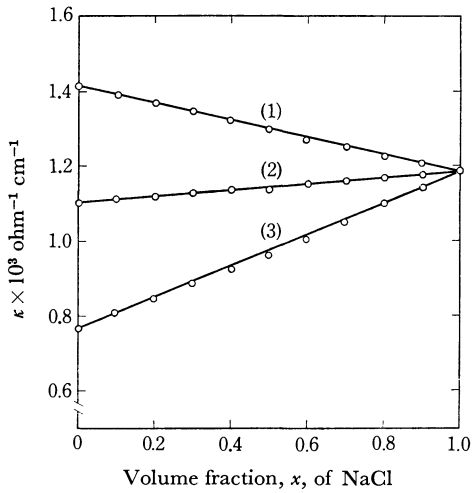

Fig. 1. Conductance behavior of mixtures (ionic strength, 0.01) of simple electrolytes measured at 1000 Hz and at 25°C.
(1) NaCl - KCl, (2) NaCl - $NaClO_4$, (3) NaCl-Na_2SO_4.
○, experimental; —, calculated by assuming additivity.

$[Co(NH_3)_6]Cl_3$ - Na_2SO_4 and $[Co(en)_3]Cl_3$ - Na_2SO_4 Mixtures. In hexamminecobalt(III) chloride-sodium sulfate and tris(ethylenediamine) cobalt(III) chloride - sodium sulfate mixtures a large departure of the measured conductance from additivity was observed at each ionic strength: the deviation, $\Delta\kappa$, between the measured and calculated conductivities is shown in Figs. 2 (a—e) as a function of the volume fraction, x, of the complex. The conductivities of the mixtures were always smaller

1) C. W. Davies, "The Structure of Electrolytic Solutions," ed. by W. J. Hamer, John Wiley and Sons, Inc., New York (1959), p. 24.
2) G. H. Nancollas, "Interactions in Electrolyte Solutions," Elsevier Publishing Co., Amsterdam (1966), pp. 30—31, and literature cited there.
3) C. W. Davies, "Ion Association," Butterworths, London (1962), pp. 27—31.
4) H. S. Harned and B. B. Owen, "The Physical Chemistry of Electrolytic Solutions," Reinhold Publishing Corp., New York (1967), pp. 200—203.
5) S. Katayama, *Rept. I. P. C. R.*, **42**, 243 (1966).
6) R. Tamamushi, T. Isono and S. Katayama, This Bulletin, **40**, 334 (1967).
7) W. C. Fernelius (ed.), "Inorganic Syntheses," II, McGraw-Hill, New York (1946), pp. 217, 221.

than those expected from additivity and showed an extreme at $x=0.5$—0.7 in each system.

Discussion

The conductivity of electrolyte mixtures is never strictly additive because of the effect of added ions on the time of relaxation;[4] in our present systems, however, this effect is shown to be negligibly small in comparison with the specific individual effects as seen from Figs. 1 and 2. Therefore, the deviation of the observed conductivities of the cobalt(III) complex - sodium sulfate mixtures from additivity may be attributed entirely to the ion-pair formation of the complex cation with sulfate ions.

Let us consider the conductance of the solution prepared by mixing xV cc of a C_1 molar solution of $M^{z_M}_{\nu_M}A^{z_A}_{\nu_A}$ and $(1-x)V$ cc of a C_2 molar solution of

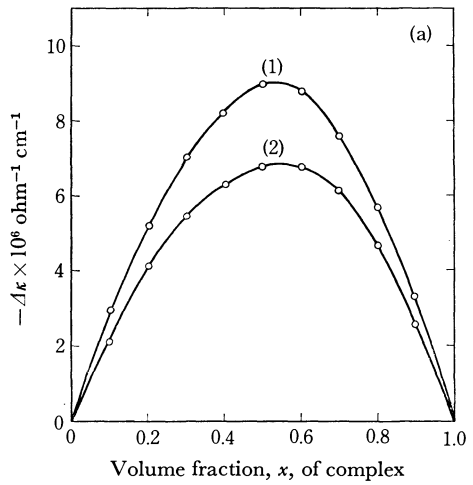

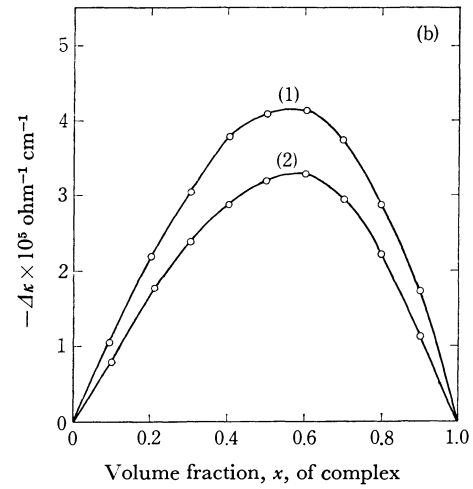

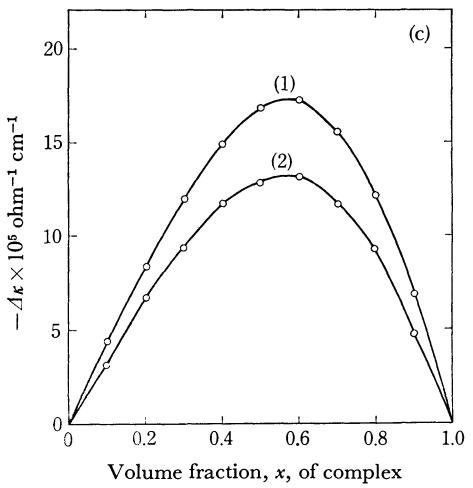

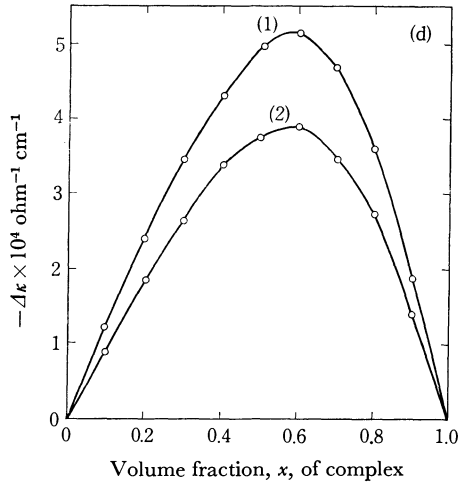

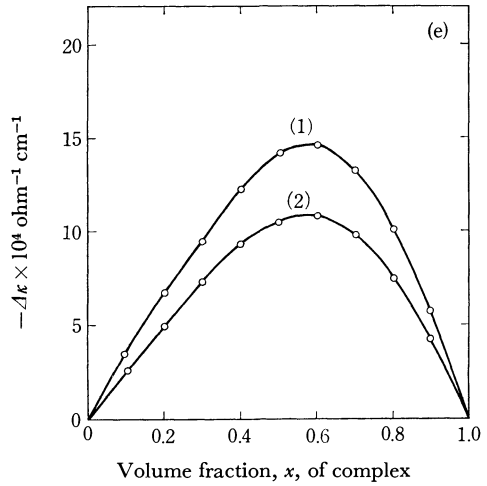

Fig. 2. Deviation of the observed conductivity from additivity, $\Delta\kappa$, as a function of the volume fraction, x, of the complex (1000 Hz, 25°C).
(1) $[Co(NH_3)_6]Cl_3$ - Na_2SO_4, (2) $[Co(en)_3]Cl_3$ - Na_2SO_4.
Ionic strength: (a) 0.001, (b) 0.003, (c) 0.01, (d) 0.03, (e) 0.1.

$N_{\nu_N}^{z_N}B_{\nu_B}^{z_B}$ to give the solution of total volume V; the concentrations, C_1 and C_2, are adjusted so that the apparent ionic strength of the mixtures is independent of x. In the following presentation of ions and ion-pairs, the ionic charge for each species will be omitted for the sake of simplicity. If the following ion-pair formations are assumed in the mixture,

$$M + B \rightleftharpoons MB,$$
$$M + A \rightleftharpoons MA,$$
$$N + B \rightleftharpoons NB,$$

the specific conductivity, κ, of the mixture is given by

$$1000\kappa = C_1 x \Lambda_m (M_{\nu_M}^{z_M} A_{\nu_A}^{z_A}) + C_2 (1-x)\Lambda_m (N_{\nu_N}^{z_N} B_{\nu_B}^{z_B}) + \alpha[MB] + \delta \quad (1)$$
$$\alpha = z_{MB}\lambda_{MB} - z_M\lambda_M - z_B\lambda_B$$

where z_i and λ_i are the ionic valence and the ionic equivalent conductance of species i, respectively, Λ_m is the molar conductance, and δ represents the contribution of ion-pairs MA and NB to the specific conductivity.

The deviation of the observed conductivity from additivity is then given by

$$\Delta\kappa' \equiv 1000\Delta\kappa = 1000\kappa - C_1 x \Lambda_m (M_{\nu_M}^{z_M} A_{\nu_A}^{z_A}) - C_2(1-x)\Lambda_m (N_{\nu_N}^{z_N} B_{\nu_B}^{z_B}) \quad (2)$$
$$= \alpha[MB] + \delta$$

Calculating [MB] by Eq. (2) and estimating the concentrations of MA and NB from their formation constants, we can determine the concentration formation constant, K_c, of MB according to the following relation.

$$K_c = \frac{[MB]}{[M][B]} = \frac{\frac{\Delta\kappa'-\delta}{\alpha}}{\left(\nu_M C_1 x - [MA] - \frac{\Delta\kappa'-\delta}{\alpha}\right)\left(\nu_B C_2(1-x) - [NB] - \frac{\Delta\kappa'-\delta}{\alpha}\right)} \quad (3)$$

In the cobalt(III) complex ($z_M=3$) - sodium sulfate mixtures, the contribution of [MA], [NB] and δ in Eq. (3) can be neglected without introducing serious errors in the determination of K_c, because the formation constants of MA and NB should be very much smaller than that of MB. Equation (3) is then simplified as

$$K_c = \frac{\frac{\Delta\kappa'}{\alpha}}{\left(\nu_M C_1 x - \frac{\Delta\kappa'}{\alpha}\right)\left(\nu_B C_2(1-x) - \frac{\Delta\kappa'}{\alpha}\right)} \quad (4)$$

Small amounts of higher order ion-pairs other than the one-to-one type may be formed between the complex cations and sulfate ions; a preliminary calculation, however, showed that the contribution of such higher order ion-pairs, if any, could be ignored in the present systems.

The determination of K_c according to Eq. (4) requires the knowledge of parameter α; the estimation of α at a given ionic strength involves some arbitrariness. In the present study, we estimated the values of α according to the following procedure: $\lambda([Co(NH_3)_6]^{3+})$ and $\lambda(SO_4^{2-})$ were obtained from the equivalent conductivities[8,9] $\Lambda([Co(NH_3)_6]Cl_3)$, $\Lambda(Na_2SO_4)$ and the corresponding transport numbers[8,10] $t([Co(NH_3)_6]^{3+})$ and $t(SO_4^{2-})$; $\lambda(Cl^-)$ from $\Lambda([Co(NH_3)_6Cl_3)$ and $t([Co(NH_3)_6]^{3+})$; $\lambda([Co(en)_3]^{3+})$ from $\Lambda([Co(en)_3]Cl_3)$ and $\lambda(Cl^-)$; and the λ-values of ion-pair MB were assumed to be equal to $\lambda(M)/3$. A slight change in the actual ionic strength is expected with varying ratio of mixing at a given nominal ionic strength; its effects, however, was ignored in the present calculation. The concentration formation constants thus determined at each nominal ionic strength are given in Tables 1 and 2.

The arbitrariness arising from the difficulty in the estimation of parameter α can be removed, when the least square method of curve fitting with the aid of a computer is applied to the analysis of the

Table 1. Logarithm of concentration formation constants, log K_c, at 25°C of ion-pair $[Co(NH_3)_6]^{3+}\cdot SO_4^{2-}$ at varying volume fractions, x, of the complex in $[Co(NH_3)_6]Cl_3$–Na_2SO_4 mixtures of various ionic strengths, I

x	I				
	0.001	0.003	0.01	0.03	0.1
0.1	3.40	3.10	2.97	2.54	1.90
0.2	3.39	3.25	2.95	2.55	1.94
0.3	3.38	3.23	2.97	2.58	1.96
0.4	3.38	3.28	3.00	2.57	2.03
0.5	3.40	3.25	3.01	2.62	2.08
0.6	3.40	3.28	3.01	2.64	2.10
0.7	3.36	3.26	3.00	2.61	2.06
0.8	3.35	3.25	3.00	2.61	2.03
0.9	3.36	3.30	2.98	2.51	2.05
Average	3.38	3.24	2.99	2.58	2.02
Computer calculation	3.18	3.26	3.03	2.75	2.23

8) G. S. Hartley and G. W. Donaldson, *Trans. Faraday Soc.*, **33**, 457 (1937).

9) Unpublished measurements of T. Shedlovsky and L. G. Longsworth, quoted by D. A. MacInnes in "Principles of Electrochemistry," Reinhold Publishing Corp., New York (1939), p. 339.

10) L. G. Longsworth, *J. Amer. Chem. Soc.*, **54**, 2741 (1932).

TABLE 2. LOGARITHM OF CONCENTRATION FORMATION CONSTANTS, $\log K_c$, AT 25°C OF ION-PAIR $[Co(en)_3]^{3+}\cdot SO_4^{2-}$ AT VARYING VOLUME FRACTIONS, x, OF THE COMPLEX IN $[Co(en)_3]Cl_3$-Na_2SO_4 MIXTURES OF VARIOUS IONIC STRENGTHS, I

x	I				
	0.001	0.003	0.01	0.03	0.1
0.1	3.30	3.14	2.71	2.22	1.84
0.2	3.35	3.20	2.89	2.45	1.84
0.3	3.36	3.15	2.86	2.47	1.92
0.4	3.33	3.19	2.92	2.52	1.96
0.5	3.32	3.18	2.90	2.52	1.99
0.6	3.34	3.22	2.92	2.56	2.00
0.7	3.36	3.22	2.89	2.51	2.00
0.8	3.35	3.19	2.91	2.51	1.96
0.9	3.32	3.23	2.81	2.40	1.96
Average	3.34	3.19	2.87	2.47	1.94
Computer calculation	3.42	3.43	2.87	2.56	2.09

following equation representing the deviation, $\Delta\kappa'$, in terms of unknown quantities K_c and α:

$$\Delta\kappa' = \frac{a+b+k_c^{-1}-\sqrt{(a+b+k_c^{-1})^2-4ab}}{2}\cdot\alpha \qquad (5)$$

TABLE 3. LOGARITHM OF THERMODYNAMIC FORMATION CONSTANTS, $\log K$, AT 25°C OF ION-PAIRS $[Co(NH_3)_6]^{3+}\cdot SO_4^{2-}$ AND $[Co(en)_3]^{3+}\cdot SO_4^{2-}$ DETERMINED BY VARIOUS METHODS

Method	$[Co(NH_3)_6^{3+}\cdot SO_4^{2-}$		$[Co(en)_3^{3+}\cdot SO_4^{2-}$	
Conductivity (present method)	3.5_3[a]	3.5_8[b]	3.6_0[a]	3.5_4[b]
Conductivity	3.56[11]		3.45[11]	
Spectrophotometry	2.89[12]	3.26[13]	3.10[13]	2.93[14]
Solubility	3.52[15]	3.60[16]		
Polarography	3.46[17]	3.21[18]	2.72[19]	
Chronopotentiometry	3.30[20]		3.22[20]	

a) determined by means of computer calculation
b) determined dy estimating parameter α

where

$$a = C_1x, \quad b = C_2(1-x)$$

By this method of computer calculation, a set of K_c and α for the best fit between the observed and calculated $\Delta\kappa'$ values can be definitely determined at each ionic strength; the K_c values obtained are given in the bottom lines of Tables 1 and 2.

These two methods of calculation resulted in the K_c-values which are in relatively good agreement. The computer method, however, is expected to give more reliable results particularly at higher ionic strengths, because the analysis can be made without assuming a quantitative expression for the

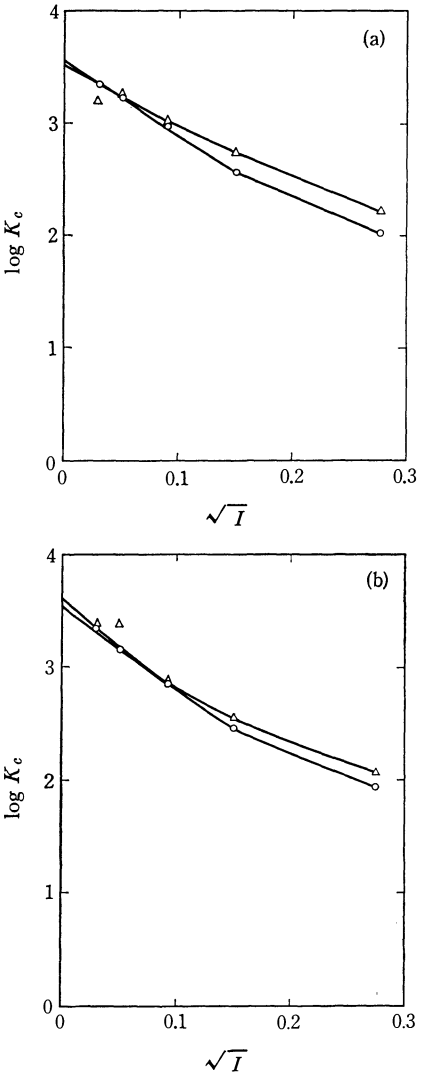

Fig. 3. Concentration formation constants of (a) ion-pair $[Co(NH_3)_6]^{3+}\cdot SO_4^{2-}$ and (b) ion-pair $[Co(en)_3]^{3+}\cdot SO_4^{2-}$ as a function of ionic strength (25°C).
—○— determined by estimating α
—△— determined by computer calculation

11) I. L. Jenkins and C. B. Monk, *J. Chem. Soc.*, **1951**, 68.
12) C. W. Davies and C. B. Monk, *J. Amer. Chem. Soc.*, **80**, 5032 (1958).
13) N. Tanaka, Y. Kobayashi and M. Kamada, This Bulletin, **40**, 2839 (1967).
14) K. Ogino and U. Saito, *ibid.*, **40**, 826 (1967).
15) C. W. Davies, *J. Chem. Soc.*, **1930**, 2421.
16) S. H. Laurie and C. B. Monk, *ibid.*, **1963**, 3343.
17) A. A. Vlček, The Proceedings of the 6th ICCC, 590 (1961).
18) N. Tanaka, K. Ogino and G. Satô, This Bulletin, **39**, 366 (1966).
19) H. A. Laitinen and M. W. Grieb, *J. Amer. Chem. Soc.*, **77**, 5201 (1955).
20) N. Tanaka and A. Yamada, *Z. Anal. Chem.*, **224**, 117 (1967).

conductance behavior of the component ions.

The thermodynamic formation constants were then determined by the extrapolation of the $\log K_c$ *vs.* $\sqrt{I}$ plots as shown in Figs. 3(a, b). The results are presented in Table 3, in which the K values determined by other methods are summarized for comparison. The good agreement of our results with those of Jenkins and Monk[11] suggests that the conductance measurement of mixtures is a useful method for determining formation constants if the method is properly applied. A great advantage of the method is expected when it is applied to the systems of relatively high concentrations where the theoretical equations of conductance behavior lose their validity.

We wish to thank Mrs. K. Takahashi for her kind collaboration in programming the computer calculation.

BULLETIN OF THE CHEMICAL SOCIETY OF JAPAN VOL. 43 2359—2363 (1970)

Photochemical Reactions of Uranyl Ions with Organic Compounds. II. The Mechanism of the Photo-Oxidation of Alcohols by Uranyl Ions

Shukichi SAKURABA and Ryoka MATSUSHIMA

Faculty of Engineering, Shizuoka University, Hamamatsu

(Received February 2, 1970)

Quantum yields were measured under various conditions for the photo-oxidation of aliphatic alcohols by uranyl ions in aqueous solutions and kinetic treatments were made. The measurements of uranyl fluorescence quenching by the alcohols showed that a complex formation between uranyl ions and alcohol molecules prior to the photolysis is not likely to be involved. The temperature effect on the quantum yield is strong evidence for a collisional energy transfer from the excited uranyl ions to the alcohol molecules. The relative rates of the photolysis of four isomeric butyl alcohols, and the isotope effect on the photo-reactivity by using alcohols labeled with deuterium, showed that the alcohol molecules are attacked on the α-hydrogen atom as a primary photochemical act.

There have been few studies of the mechanisms of the photo-reactions of uranyl ions with alcohols in aqueous solutions, and many basic problems remain unsolved. Kinetic studies have been made of the reaction mechanisms of uranyl ions with carbohydrates[1] and with alcohols,[2-4] but these experimental data are not enough to discuss the mechanism, as has been pointed out by Rabinowitch and Belford.[5] For example, a complex of an uranyl-organic substrate has been assumed to be a photosensitive cluster:

$$UO_2^{2+} + S(\text{substrate}) \rightleftharpoons UO_2S^{2+},$$

and it has been assumed to undergo an intramolecular photo-redox reaction:

$$UO_2S^{2+} + h\nu \rightarrow (UO_2S^{2+})^* \rightarrow\rightarrow U(IV) + \text{Products}.$$

However, the linear relation between the reciprocal quantum yield of the U(IV) formation, ϕ^{-1}, and the reciprocal concentration of the substrate, $[S]^{-1}$, which is inferred from the above assumed mechanism dose not support the above assumption, since the linearity can be inferred both from the mechanism assuming such a complex formation and from the alternative mechanism, in which a collisional energy transfer from the excited uranyl ions to the substrate molecules is involved.

Recently several piecies of evidence for collisional-excitation energy transfer between rare earth metal ions and α-diketones in solution have been reported.[6-8] The present investigation was undertaken

1) L. J. Heidt and K. A. Moon, *J. Amer. Chem. Soc.*, **75**, 5803 (1953).
2) L. J. Heidt, *ibid.*, **76**, 5962 (1954).
3) S. K. Bhattacharyya and S. Gulvedy, *J. Indian Chem. Soc.*, **29**, 649 (1952).
4) S. K. Bhattacharyya and S. Gulvedy, *ibid.*, **29**, 659 (1952).
5) Rabinowitch and Belford, "Spectroscopy and Photochemistry of Uranyl Compound," Pregamon Press, London (1964), p. 324.
6) A. Heller and E. Wasserman, *J. Chem. Phys.*, **42**, 949 (1965).
7) N. Filipescu and G. W. Mushrush, *J. Phys. Chem.*, **72**, 3516 (1968).
8) N. Filipescu and G. W. Mushrush, *ibid.*, **72**, 3512 (1968).

in order to elucidate in some detail the mechanism of the photo-oxidation of alcohols with uranyl ions.

Experimental

Doubly-distilled water and guaranteed reagents (Koso Chemical) were used. The solutions to be tested were de-aerated by the passage through of oxygen-free nitrogen, placed into a cylindrically-shaped, sealed pyrex cell with flat windows (5 m*l* volume), and then exposed to light of the desired wavelength by using an interference filter or by a combination of glass filters. The absorbance at every wavelength, or the rate of light absorption, I_a, of the uranyl - alcohol system was independent of the alcohol concentration. The quantum yields were measured by the usual method[9,10] by using a ferric oxalate solution. The time of exposure was so regulated that the reaction was not more than 5% completed, in order to avoid the complications which might arise from the subsequent reactions of the products or from the inner filter effect of the uranium(IV) ions. The temperature was usually 20±0.1°C. The light sources were a 500-W or 100-W high-pressure Hg lamp. The amounts of uranium(IV) formed were measured colorimetrically by the use of arsenazo III.[11] The aldehydes or ketones formed were determined by means of 2,4-dinitrophenylhydrazine. The spectrophotometric measurements and fluorescence measurements were carried out with a Hitachi 124 spectrophotometer and with a Hitachi fluorescence spectrophotometer respectively. The acidities of the solutions were regulated by using a Toa Denpa pH-meter.

Results and Discussion

Effect of Light Intensity on the Rate. Figure 1 shows that the rate of uranium(IV) formation is directly proportional to the absorbed light intensity (I_a), *i.e.*, the quantum yield is independent of I_a.

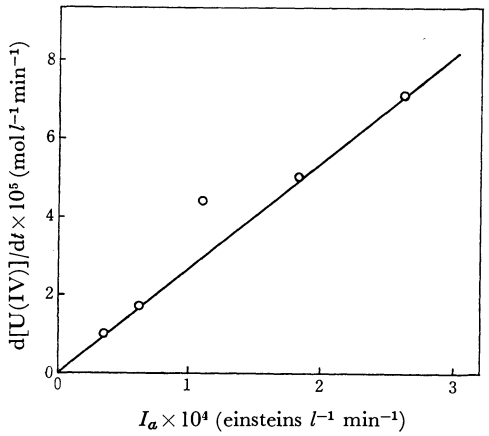

Fig. 1. Effect of light intensity on the rate.
$[UO_2^{2+}]=0.02$M, $[CH_3CH_2OH]=0.21$M
pH=1.0, λ=4047,4358 Å

Table 1. Molar ratio of the products at various of reaction
$[UO_2^{2+}(NO_3)_2]=0.02$M, $[CH_3CH_2OH]=0.2$M, pH=1.0

Reaction extent (%)	[U(IV)] ×10³M	[CH₃CHO] ×10³M	molar ratio [CH₃CHO]/[U(IV)]
2	0.4	0.5	1.2
5	1.0	1.1	1.1
10	2.0	2.0	1.0
16	3.1	3.0	1.0

Table 2. Molar ratio of the products at various pH
$[UO_2^{2+}(NO_3)_2]=0.02$M, $[CH_3CH_2OH]=0.2$M.

pH	[U(IV)] ×10³M	[CH₃CHO] ×10³M	molar ratio [CH₃CHO]/[U(IV)]
1.0	3.1	3.0	1.0
1.7	3.2	3.1	1.0
2.3	2.3	2.2	1.0
3.3	1.5	1.5	1.0
3.8	1.5	1.5	1.0
3.8	2.1	2.1	1.0

Molar Ratio of the Products at Various Extents of the Reaction and at Various pH's. Tables 1 and 2 show that the molar ratio of the products is always unity whatever the extent of the reaction and whatever the pH.

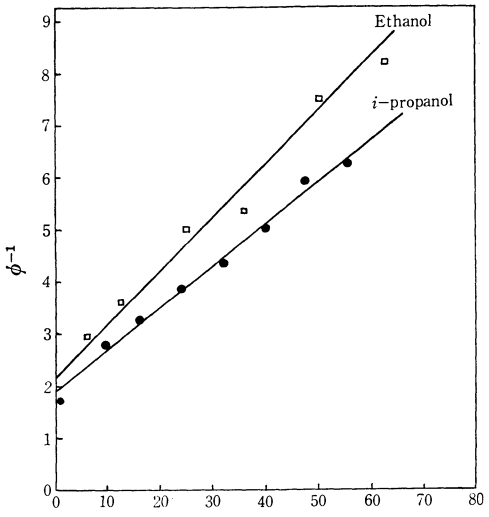

Fig. 2. Reciprocal quantum yield of formation of U(IV) as a function of reciprocal concentration of alcohol.
$[UO_2^{2+}]=0.02$M, pH=1, λ=4047, 4358 Å

9) C. A. Parker, *Proc. Roy. Soc.* (London), **A220**, 104 (1953).
10) M. Koizumi, S. Shida, S. Kato, N. Mataga and M. Imamura, "Jikken Kagaku Koza," Vol. 6, Maruzen, Tokyo (1956), pp. 282—286.
11) H. Onishi and Y. Toita, *Bunseki Kagaku*, **14**, 1141 (1965).

Effect of Alcohol Concentration on the Rate. The quantum yields of uranium(IV) formation were measured at various initial concentrations. The plot of $1/\phi$ *vs.* $1/C$ gave a straight line with an intercept $\fallingdotseq 2$, as is shown in Fig. 2. This result is similar to that obtained with the uranyl-carbohydrates system by Heidt and Moon.[1] The question as to whether a photo-activated uranyl ion reacts with a substrate molecule by encounter collisions or whether a certain complex between UO_2^{2+} and substrate is activated to produce the reaction cannot be decided on the basis of this result, since the linear relation, $1/\phi$ *vs.* $1/C$, is inferred both from the mechanism proposed by Heidt[1] assuming a complex as to be a photosensitive cluster and from the alternative mechanism assuming a collisional energy transfer.

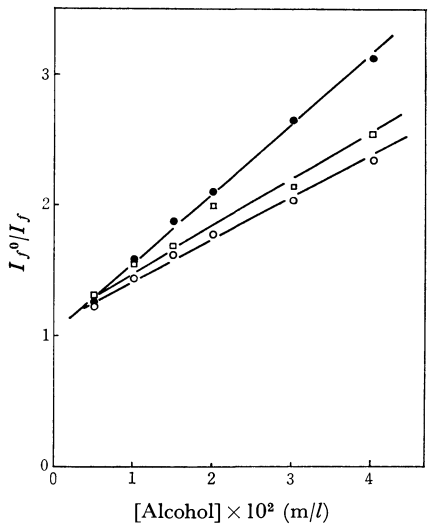

Fig. 3. Reciprocal relative fluorescence intensity of uranyl ions as a function of alcohol concentration. Excited at 4358 Å. Measured at 5090 Å. $UO_2(NO_3)_2$=0.02M.
○: Ethyl alcohol, pH=1.5, □: Ethyl alcohol, pH=3.5, ●: Isopropyl alcohol, pH=1.5, I_f^0 and I_f are the fluorescence intensities in the absence and in the presence of alcohol, respectively.

Fluorescence Intensities at Various Concentrations of Alcohol. The results shown in Fig. 3 can be expressed by the Stern-Volmer equation:

$$\frac{I_f^0}{I_f} = 1 + K_q[Q],$$

where I_f^0 and I_f are the fluoresence intensities in the absence and in the presence of a quencher respectively. K_q is the quenching constant, and [Q] is the concentration of a quencher. It can be seen that the slope, K_q, varied with the nature of the alcohol and not with the acidity of the solution.

Correlation between the Photo-Reactivity and Fluorescence Quenching. The K_q's for

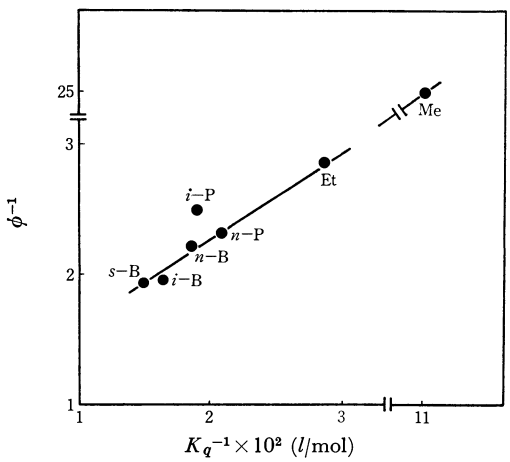

Fig. 4. Photoreactivity and fluorescence quenching constants in the system of aqueous uranyl-alcohols. ϕ_r: quantum yield of uranium(IV) formation at 3650—3606 Å, $[UO_2^{2+}]$=0.02M, [alcohol]=0.02M. pH=1.5 λ(emission)=5090 Å, λ(excitation)=4360 Å.

aliphatic alcohols were measured. Figure 4 shows the correlation between the photo-reactivity, ϕ_r, and the fluorescence quenching constant, K_q. Neither the quenching efficiency nor the photochemical reactivity of alcohols seems to be related to the stability of the uranyl-alcohol complexes assumed, on the supposition that the steric factor

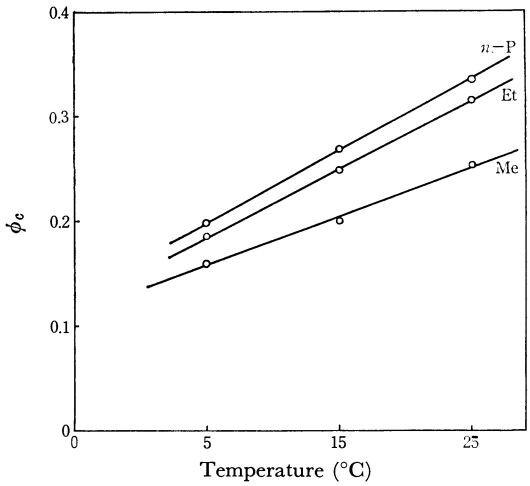

Fig. 5. Temperature effect on the rate of uranium-(IV) formation. $[UO_2^{2+}]$=0.02M. [alcohol]=0.2M. pH=1.5 λ=3650—3660 Å. The quantum yields were corrected for the self-quenching; $(UO_2^{2+})^* + UO_2^{2+} \rightarrow 2UO_2^{2+}$, on the assumption that the temperature dependence of the self-quenching is mainly due to that of the viscosity of the medium.[12]

Apparent activation energy, $\Delta E^{\ddagger}$, obtained was 8.5 kcal/mol for both ethyl alcohol and *n*-propyl alcohol.

dominates the stability of the complex; rather, it seems likely that the photo-sensitivity is related to the bond strength between the α-hydrogen atom and the carbon atom adjacent to the hydroxy group, on the assumption that the increasing order of the bond-dissociation energies in solution is approximately the same as that in the gaseous phase.

The close correlation between the quenching efficiency, K_q, and the chemical reactivity, ϕ_r, suggests that chemical quenching is predominant in the radiationless deactivation of the excited uranyl ions by alcohol molecules, while physical quenching is less important.

Temperature Effect on the Reaction Rate. The quantum yield increases with an increase in the temperature, as is shown in Fig. 5; this suggests that the reaction mechanism involves a collisional transfer from the excited uranyl ions to alcohol molecules. The values of the quantum yield in Fig. 5 were corrected for the self-quenching of uranyl ions.[12]

Relative Rates of Butyl Alcohols and the Isotope Effect on the Rate. The relative rates of *n*-butyl, isobutyl, *s*-butyl, and *t*-butyl alcohol (the last one has no α-hydrogen) were measured in order to decide which of two alternatives is the primary process. The results are listed in Table 3.

Table 3. Relative reactivity of butyl alcohols
k and k_n are relative rate constants for uranium (IV) formation with butyl alcohol isomer and with *n*-butyl alcohol, respectively.

Butyl alcohol	k/k_n
n-Butyl	1.00
Isobutyl	1.14
s-Butyl	1.05
t-Butyl	0.11

Further, the rate constants of the uranium(IV)-formation with deuteriated alcohols were compared to those with non-deuteriated alcohols in an ordinary water solution. The ratios obtained were $k_{(CH_3CH_2OH)}/k_{(CD_3CD_2OD)}=2.33$ and $k_{(CH_3CH_2OH)}/k_{(CH_3CH_2OD)}=1.02$. These results indicate that the path:

$$R_1R_2CHOH + U(VI)^* \rightarrow R_1R_2\dot{C}OH + U(V) + H^+,$$

is predominant in the primary act, while the alternative path:

$$R_1R_2CHOH + U(VI)^* \rightarrow R_1R_2CHO\cdot + U(V) + H^+,$$

is less important.

Effect of Cupric Ions. As is shown in Table 4,

Table 4. Interfering effect of cupric ions
$[CH_3CH_2OH]=0.2$M, $[UO_2(NO_3)_2]=0.02$M, $\lambda=4047$, 4358 Å
The fraction of light absorbed by cupric ions was negligible under the experimental conditions.

$[CuSO_4]$ added $\times 10^3$M	$[U(IV)]$ formed $\times 10^3$M	$[CH_3CHO]$ formed $\times 10^3$M
0.0	6.7	6.6
5.0	0.1	6.4

the formation of uranium(IV) is nearly completely interfered with by the addition of a small quantity of cupric ions, while acetaldehyde-formation is not affected.

Since cupric ions do not quench the excited uranyl ions,[13] the interfering effect must be due to the reaction between cupric ions and the intermediates, U(V); *i.e.*;

$$U(VI)^* + R_1R_2CHOH \rightarrow U(V) + R_1R_2\dot{C}OH + H^+,$$
$$U(V) + Cu(II) \rightarrow U(VI) + Cu(I),$$
$$2Cu(I) \rightarrow Cu^0 + Cu(II).$$

The selective interfering effect by cupric ions indicates that the secondary process of uranium(IV)-formation is:

$$U(V) + U(V) \rightarrow U(VI) + U(IV)$$

and not the alternative process:

$$U(V) + R_1R_2\dot{C}OH \rightarrow U(IV) + R_1R_2CO.$$

The radical intermediate, $R_1R_2\dot{C}OH$, would seem to be rapidly oxidized by the ground-state uranyl ions; *i.e.*:

$$R_1R_2\dot{C}OH + U(VI) \rightarrow R_1R_2CO + U(V) + H^+,$$

before the disproportionation reaction of the radical:

$$2R_1R_2\dot{C}OH \rightarrow R_1R_2CO + R_1R_2CHOH,$$

since the concentration of uranyl ions is much higher than that of the radical, $R_1R_2\dot{C}OH$. However, the selective inhibitory effect by maleic acid, as is shown in Table 5, indicates that the latter path (the disproportionation of the radical) is predominant.

Table 5. Effect of maleic acid
$[UO_2(NO_3)_2]=0.02$M, $[CH_3CH_2CH_2OH]=0.2$M
$\lambda=4047$, 4358 Å, Irradiation time=30 min

$[(CHCOOH)_2]$ added $\times 10^2$M	$[U(IV)]$ formed $\times 10^3$M	$[CH_3CH_2CHO]$ formed $\times 10^3$M
0.0	4.1	4.0
2.0	3.2	0.4

12) E. Rabinowitch and R. L. Belford, "Spectroscopy and Photochemistry of Uranyl Compounds," Pergamon Press, London (1964), p. 220.

13) Y. Volmar and Mathis, *Bull. Soc. Chim. Fr.*, **53**, 385 (1933).

A slight decrease in the amount of U(IV) upon the addition of maleic acid in Table 5 may be attributed to a weak masking effect of maleic acid or to a reaction between U(V) and maleic acid.

On the basis of the above data, the following mechanism may be proposed:

$$U(VI) + h\nu \xrightarrow{I_a} U(VI)^*, \text{ (absorption)} \quad (1)$$

$$U(VI)^* \xrightarrow{k_1} U(VI) + h\nu', \text{ (fluorescence emission)} \quad (2)$$

$$U(VI)^* \xrightarrow{k_2} U(VI) + \text{heat}, \text{ (radiationless deactivation)} \quad (3)$$

$$U(VI)^* + U(VI) \xrightarrow{k_3} 2U(VI), \text{ (self-quenching)} \quad (4)$$

$$U(VI) + R_1R_2CHOH \xrightarrow{k_4} U(VI) + R_1R_2CHOH, \text{ (physical quenching)} \quad (5)$$

$$U(VI)^* + R_1R_2CHOH \xrightarrow{k_5} U(V) + R_1R_2\dot{C}OH + H^+, \text{ (chemical quenching)} \quad (6)$$

$$2R_1R_2\dot{C}OH \xrightarrow{k_6} R_1R_2CO + R_1R_2CHOH, \text{ (disproportionation)} \quad (7)$$

$$2U(V) \xrightarrow{k_7, H^+} U(VI) + U(IV). \text{ (disproportionation)} \quad (8)$$

Here I_a is the rate of light absorption in einsteins$\cdot$mol$^{-1}\cdot$min^{-1}.

The steady-state assumption for U(VI),* U(V), and $R_1R_2\dot{C}OH$ leads to:

$$\phi_U = \phi_C = k_5[R_1R_2CHOH]/2\{k_1+k_2+k_3[U(VI)] + (k_4+k_5)[R_1R_2CHOH]\}, \quad (9)$$

where ϕ_U and ϕ_C are the quantum yields for the formations of U(IV) and R_1R_2CO respectively. The reciprocal expression is:

$$1/\phi_U = 1/\phi_C = 2 + 2k_4/k_5 + 2(k_1+k_2+k_3[U(VI)]/k_5[R_1R_2CHOH]. \quad (10)$$

The relative intensity of uranyl fluorescence becomes:

$$I_f^0/I_f = 1 + K_q[R_1R_2CHOH], \quad (11)$$

where:

$$K_q = (k_4+k_5)/(k_1+k_2+k_3)[U(VI)]. \quad (12)$$

The comparison of Eq. (10) with the experimental results in Fig. 2 leads to:

$$k_4/k_5 = 0 \quad (13)$$

i.e., the physical quenching is much less important than the chemical quenching. This is in agreement with the conclusion from the results shown in Fig. 4. The low probability of electronic-vibration energy transfer without a chemical reaction seems plausible.[14]

From Eqs. (10),(12) and (13), we obtain:

$$1/\phi = 2 + 2/K_q[R_1R_2CHOH]. \quad (14)$$

The plot of $1/\phi$ *vs.* $1/K_q$ should be a straight line with an intercept of 2 and a slope of $2/[R_1R_2CHOH]$. The slope in Fig. 4 is 70, roughly in agreement with the theoretical value from Eq. (14), $2/[R_1R_2CHOH]=100$. The discrepancy between Eq. (14) and the experimental results in Fig. 4 may be partly due to the inaccuracy in the value of K_q.

14) P. G. Ashmore, F. S. Dainton and T. M. Sugden, "Photochemistry and Reaction Kinetics," Cambridge University Press, London (1967), p. 133.

BULLETIN OF THE CHEMICAL SOCIETY OF JAPAN VOL. 43 2364—2366 (1970)

Spreadability of Ovalbumin Monolayers at Air-water Interface

Toshio Ishii*1 and Mitsuo Muramatsu

Department of Chemistry, Tokyo Metropolitan University, Setagaya-ku, Tokyo

(Received February 4, 1970)

The spreading processes of ovalbumin have been studied quantitatively at air-water interface with either no additive or a small amount of hydrochloric acid for controlling subphase pH. Limiting area which is obtained by extrapolating force(F)-area(A) curve to $F=0$, increases with time, t, which has elapsed after the application of protein solution at the surface of subphase. Near the isoelectric point, the spreading processes are completed instantaneously to give the equilibrated value of limiting area which is found to be 0.83 m^2/mg. The processes are much slower at both sides of the point, but the limiting area in equilibrium is found to be the same as in the case of isoelectric pH. It has also been shown that the processes are expressed in terms of two first-order reactions.

Work has been done by many investigators[1-3] on the nature of protein monolayers at air-water interfaces, in relation to the mechanism of their denaturation processes. In many cases, however, the experiments were carried out under the tacit assumption that the protein films were in the equilibrated state in which surface-chemical processes could be considered to reflect thermodynamical properties, though the assumption could hardly be verified. It is practically difficult to confirm the equilibrium state of protein monolayer at the air-water interface. In many cases, therefore, it has been assumed that the equilibrated state is attained if a monolayer gives no time effects upon the quality to be studied. This was indeed the case in determining the thermodynamical properties of monolayers of various proteins to be compared.

On the other hand, the denaturation processes are considered to take place during the course of monolayer formation by applying a protein solution to the surface of subphase water. The course is conveniently defined[4-6] to involve (1) dissolution of protein molecules into the bulk of subphase and their return to the surface by diffusion, (2) their spreading at the surface and (3) their uncoiling to form the structures of denatured protein. Thus the denaturation processes seem to be studied conveniently by elucidating the course of monolayer formation with elimination of processes (1) and (2) as much as possible. This has been achieved to some extent by the addition of a large amount of salt into subphase,[1] or of surface active, volatile solvent to spreading solution.[7] The former involves the difficulty to eliminate surface-chemical impurities from subphase,[8] while the latter gives little effects on eliminating the process (1). None of these methods always reflects the true nature of surface denaturation of protein molecules, because process (3) may be much affected by the addition of salt or solvent. Any additives should be avoided for quantitative studies on the spontaneous processes of protein denaturation. It has been pointed out[4] that the decreased contribution of processes (1) and (2) to the whole spreading course can be expected by applying dilute protein solution without additives on the top of the glass rod standing in the trough which contains water alone.[9] This has proven to be effective for decreasing the conditions of (1) and (2), making it easy to understand the surface denaturation of protein molecules in terms of unfolding processes of their polypeptide chains.[4-6] The technique has been extended in the present investigation to elucidate the kinetic processes of protein denaturation at air-water interface.

*1 Present address: Chiba Institute of Technology, Narashino, Chiba.

1) H. B. Bull, "Advances in Protein Chemistry," Vol. III, ed. by M. L. Anson, K. Bailey and J. Edsall, Academic Press Inc., New York, N. Y. (1947), p. 95.

2) E. Gorter and F. Grendel, *Proc. Kon. Akad. v. Wet.*, **29**, 1262 (1936).

3) D. F. Cheesman and H. T. Davies, "Advances in Protein Chemistry," Vol. IX, ed. by M. L. Anson, K. Bailey and J. Edsall, Academic Press Inc., New York, N. Y. (1954), p. 439.

4) M. Muramatsu and H. Sobotka, *J. Phys. Chem.*, **66**, 1918 (1962).

5) M. Muramatsu and H. Sobotka, *J. Colloid Sci.*, **18**, 625 (1963).

6) M. Muramatsu and H. Sobotka, *ibid.*, **18**, 636 (1963).

7) A. Lejtha and E. K. Rideal, *Arch. Biochem. Biophys.*, **33**, 252 (1951).

8) C. Y. C. Pak and N. L. Gershfeld, *J. Colloid Sci.*, **19**, 831 (1964).

9) H. J. Trurnit, *J. Colloid Sci.*, **15**, 1 (1960).

Experimental

A sample of ovalbumin was recrystallized seven times from aqueous ammonium sulfate and its purity was confirmed by paper electrophoresis and by microscopic observation of crystalline shape. Its aqueous solution was treated with Sephadex-G25 to remove inorganic materials and made the desired concentration (0.0859 mg/ml) which was confirmed spectrometrically. The water both for the spreading solution and for the subphase was distilled twice from alkaline permanganate in Hysil glass ware. Hydrochloric acid for controlling pH was distilled at its azeotropic point.

A glass tray, 48 cm × 15 cm in area and 0.5 cm in depth, had a well for a glass plate to be dipped for measuring surface pressure, F (dyn/cm). The plate, 2.4 cm × 3.2 cm × 0.015 cm, was cleaned by soaking it into a hot chromic acid mixture or alkali-alcohol solution prior to each measurement. The displacement of the plate was magnified by a lamp and scale system to give the surface pressure with an accuracy of 0.05 dyn/cm. The whole apparatus was thermostated at 20± 0.5°C.

The protein solution was applied onto the glass rod (0.5 cm dia. × 10 cm above the water level), which stood vertically in the subphase with pH 2.0—8.2 at such a dropping rate as to permit less than 0.1% of protein molecules to get into the subphase, the figure being based on the theoretical calculation by Trurnit.[9] Surface contamination was low enough to give $F<5$ dyn/cm when the aqueous surface was kept standing for 24 hr and then compressed to 1/20 its area.

The surface pressure was measured as a function of area, A (m²/mg), at given time, t, which had elapsed from the application of spreading solution to the surface of subphase. The limiting area, A^0, obtained by extrapolating the straight part of F-A curve was taken as a measure of the extent of the denaturation processes at given time, t.

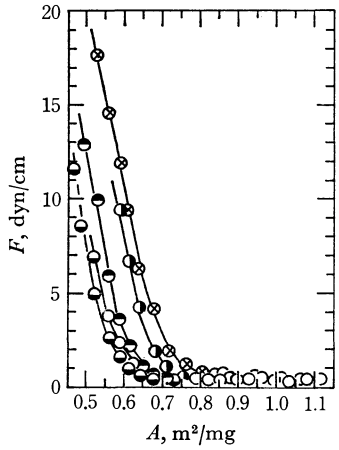

Fig. 1. Time dependence of F-A curves of ovalbumin monolayer spread on subphase of pH 5.2—6.0; —◒—, t=15 min; —○—, 1 hr; —◓—, 4 hr; —◑—, 24 hr; —⊗—, 42 hr

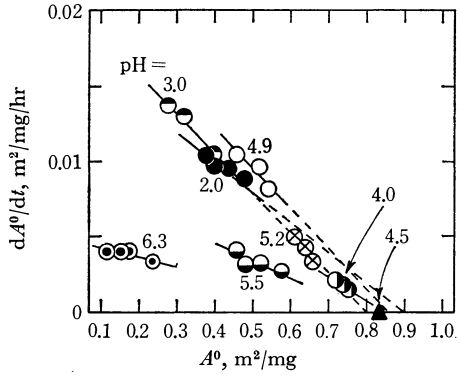

Fig. 2. The relationship of dA^0/dt and A^0 for ovalbumin nomolayers on subphases of various pH.

Results and Discussions

Figure 1 gives the F-A curves as a function of t obtained with monomolecular film of ovalbumin spread on the subphase of pH 5.2. It was inevitable to find a gradual change of pH during the elapsed time, giving the final pH of 6.0 at t=42 hr. It can be seen that the F-A curve is shifted to the right, showing an increase of limiting area with increasing time. The shift suggests an asymptotic tendency to reach the definite A^0 value at $t=\infty$. This is indeed the case of the linear relationship of log A^0 with t, suggesting the validity of the equation

$$dA^0/dt = k_2(A_\infty{}^0 - A^0), \qquad (1)$$

where $A_\infty{}^0$ is A^0 at $t=\infty$ and k_2 the constant. The relationship holds throughout the long period of t >2—3 hr.

In Fig. 2 is shown the dA^0/dt as a function of A^0 for the monolayers on subphases varying in pH values. The slope of the linear part gives the rate constant, k_2, of the first order denaturation process of ovalbumin approaching the equilibrated state, in which the monomolecular film consists of completely unfolded molecules of protein. If k_2 is plotted against pH of subphase, one finds the maximum value, as seen in Fig. 3, near the isoelectric point of protein. In both sides from the isoelectric point, k_2 decreases with increasing departure from the point. It is thus concluded that the spreading processes in the period sufficiently long after the initial spreading are expressed by

$$(A_\infty{}^0 - A^0) = (A_\infty{}^0 - A_2{}^0)\exp(-k_2 t) \qquad (2)$$

where $A_2{}^0$ is A^0 value at $t=0$.

Rigorously speaking, however, Eq. (2) does not hold in the small t region, namely, shortly after the spreading, as can be seen in Fig. 4, which gives considerable deviation of the empirical values from the calculated slope (solid lines) based on Eq. (2). If, however, we plot the deviation against t on the same figure, we have the dotted lines which show fairly linear relationships. Therefore, the whole processes could better be expressed by

$$(A_\infty{}^0 - A^0) = (A_\infty{}^0 - A_2{}^0)\exp(-k_2 t) + (A_2{}^0 - A_1{}^0)\exp(-k_1 t) \qquad (3)$$

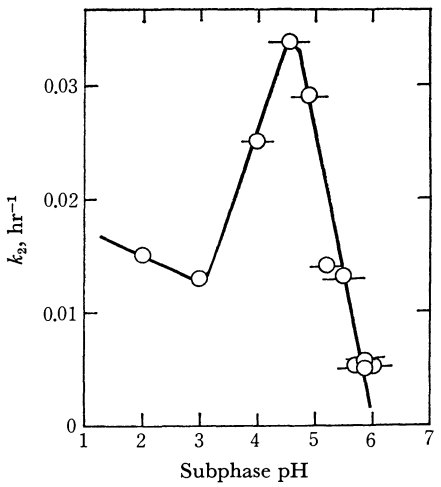

Fig. 3. k_2 as a function of subphase pH. The circles are given for the average pH from the initial and final values, which are shown as the horizontal bars.

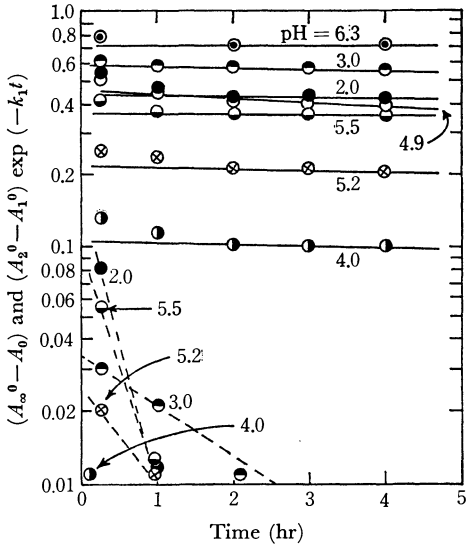

Fig. 4. Time dependences of $A_\infty^0 - A^0$ (solid lines) and $(A_2^0 - A_1^0)\exp(-k_1 t)$ (dotted).

where A_1^0 is the extrapolated value of the dotted lines to $t=0$ and k_1 the rate constant for the process shown as the dotted lines in Fig. 4. Equation (3) suggests that the spreading processes are expressed as the sum of two independent processes, one is fast and the other slow, and that, if we assume the first order reaction for one of them, the other should give the same order in its mode.

The above results suggest that the uncoiling of protein molecules at air-water interface involves the two processes; the fast process starts from A_1^0, while the slow process covers the range A_2^0 to A_∞^0. These values are plotted in Fig. 5 against the pH of subphase on which the protein is spread.

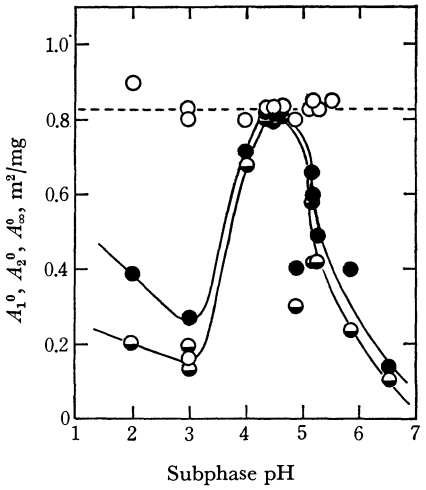

Fig. 5. A_1^0 (semiclosed), A_2^0 (closed) and A_∞^0 (open) as a function of subphase pH.

It is clear from Fig. 5 that the A^0 value (0.83 m^2/mg) is independent of pH, as mentioned previously, while A_1^0 and A_2^0 give almost the same tendency to each other, giving the maximum value near the isoelectric point, where the spreading is completed instantaneously. It should be noted that the two solid curves in the figure resemble in shape the pH dependences of limiting area reported by many investigators[1-3] who paid little attention to the time-dependent nature of protein monolayers. This means that, when subphase pH is at the isoelectric point, the spreading of protein molecules at air-water interface and the unfolding of their polypeptide chains are completed immediately after their arrival at the interface, and that, at any other pH, the protein molecules shrink to give smaller A_1^0 and A_2^0 values and then gradually uncoil to reach finally the same A_∞^0 value. This process is characterized by the slower rate of uncoiling for the more deviated pH value from the isoelectric point, as can be seen in Fig. 3.

It has been claimed by many investigators[1-3] that the limiting area of protein molecules gives the maximum value when they are spread on subphase of isoelectric pH value. It seems to be more reasonable to treat the spreading of protein at air-water interface as a reflection of kinetic processes to be characterized by the unfolding of protein molecules concerned. The subphase pH does not influence the limiting area, A_∞^0, in the equilibrium state, but affects markedly the kinetic processes with which the protein molecules uncoil to approach the equilibrated state.

In conclusion, the authors wish to express their thanks to Professor T. Sasaki for his suggestion and advice. This reseach has been supported by the Scientific Research Grant of the Ministry of Education.

BULLETIN OF THE CHEMICAL SOCIETY OF JAPAN VOL. 43 2367—2369 (1970)

The Interaction of Polymer Ions with Counterions. II. Polymethacrylates

Kunio TAMAKI and Teruo HORIUCHI

Department of Chemistry, Yokohama City University, Kanazawa-ku, Yokohama

(Received February 4, 1970)

The equivalent conductivities and the electrophoretic mobilities of sodium, tetramethyl-, tetraethyl-, and tetrabutyl- ammonium salts of polymethacrylic acid (PMA) in 0.05 M solutions of the simple salts of the corresponding cations are measured at 25°C, and the results obtained are interpreted in terms of the counterion binding. The calculated values of the apparent degree of ionization for sodium, tetramethyl-, and tetraethylammonium salts of PMA are found to be larger than those of the corresponding salts of polyacrylic acid (PAA), indicating that the methyl groups in PMA generally hinder the binding of counterions with polyions. With tetrabutylammonium salt of PMA, the apparent degree of ionization is nearly equal to that of the tetrabutylammonium salt of PAA. This fact suggests hydrophobic interaction between the methyl groups in PMA and tetrabutylammonium ions.

The role of the nonpolar side chains of polyelectrolytes in the water phase is of great interest in connection with hydrophobic interaction in grobular proteins. Polymethacrylic acid contains extra methyl groups in the main chain compared with polyacrylic acid. In the previous paper,[1] the conductivities and electrophoretic mobilities of polystyrenesulfonates, polyethylenesulfonates, and polyacrylates, measured in 0.05M solutions of the simple salt of the corresponding cations at 25°C, were discussed on the basis of the apparent degree of ionization of the polyelectrolytes. The object of the present paper is to compare the additional data on polymethacrylate with those of polyacrylates.

Experimental

Polymethacrylic acid (PMA) was prepared by the polymerization of methacrylic acid in water, in the presence of hydrogen peroxide as an initiator, according to the method described by Leyte and Mandel.[2] A commercial sample of methacrylic acid was distilled under reduced pressure before polymerization. The polymer was dissolved in methanol and fractionally precipitated by the gradual addition of ether to give different molecular weights. The fraction used in this experiment had a molecular weight of 1.11×10^6, determined from the viscosity measurement of the polymer solution in methanol using the equation proposed by Wiederhorn and Brown.[3] Sodium, tetramethylammonium (Me_4N), tetraethylammonium (Et_4N), and tetrabutylammonium (Bu_4N) salts of PMA were prepared by the neutralization of PMA with the corresponding hydroxides. The sodium hydroxide solution was preapred by diluting its saturated aqueous solution. Tetraalkylammonium hydroxides were prepared by the reaction of the respective bromide salts in aqueous solutions with silver oxide. The tetraalkylammonium bromides were purchased from the Tokyo Kasei Kogyo Co. and were recrystallized from suitable solvents: an ethanol-water mixture for Me_4NBr_4, ethanol for Et_4NBr, and ethyl acetate for Bu_4NBr. Sodium chloride was a reagent-grade sample. Water was obtained by redistillation from an alkaline permanganate solution.

The detailed procedure for measuring the equivalent conductivities and electrophoretic mobilities of polyelectrolytes in 0.05M solutions of the simple salts of the corresponding cations at 25°C was described in the previous paper.[1] As simple salts, sodium chloride was used for Na-PMA and tetraalkylammonium bromides were used for respective tetraalkylammonium salts of PMA.

The electrical conductivities were measured with a Yokogawa BVZ-13A auto-frequency bridge, using a frequency of 1000 Hz. The electrophoretic mobilities were measured with a Hitachi HTB-2 Tiselius electrophoresis apparatus, varying the electric currents from 1 to 2 mA. A polyelectrolyte solution was dialysed in a cellophane tube against a large volume of a 0.05M solution of a simple salt for 2 days. From the boundaries recorded on a photographic plate at a different time, the electrophoretic mobility was then calculated.

Results

The equivalent conductivity of polyelectrolyte in a simple salt solution, Λ_p, may be expressed;[4]

$$\Lambda_p = 10^3(K_{ps}-K_s)/N_p$$

1) K. Tamaki, M. Ozaki, M. Ogiwara and I. Takemura, *Nippon Kagaku Zasshi*, **88**, 711 (1967).

2) J. C. Leyte and M. Mandel, *J. Polymer Sci., A*, **2**, 1879 (1964).

3) N. M. Wiederhorn and A. R. Brown, *J. Polymer Sci.*, **8**, 651 (1952).

4) U. P. Strauss and S. Bluestone, *J. Amer. Chem. Soc.*, **81**, 5295 (1959).

where K_{ps} and K_s are the specific conductivities of the salt solution with and without an added polyelectrolyte, and N_p is the polyelectrolyte concentration, expressed in terms of equiv./l. Although K_s in a salt solution containing polyelectrolyte is not generally equal to that of the same concentration of a simple salt solution without an added polyelectrolyte, in this study K_s may be considered to be equal to the value of a 0.05M solution of a simple salt; this means that the 0.05M solution of a simple salt is taken to be serving as the solvent. The values of Λ_p calculated in this manner are given as a function of the polyelectrolyte concentration in Fig. 1. Λ_p shows no noticeable trend with the variation in the polyelectrolyte concentration.[4,5] Therefore, the values of Λ_p, taken as the intrinsic equivalent conductivities, are listed in Table 1, in which the values of polyacrylates under the same conditions are also included.

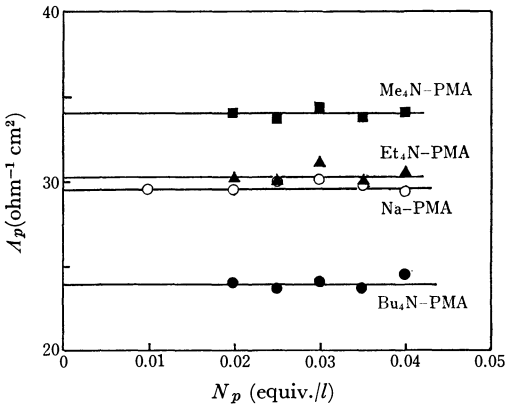

Fig. 1. Equivalent conductance in 0.05M simple salt solution as a function of the polymer concentration.

The observed electrophoretic mobility varied generally with the polyelectrolyte concentration, and it was found that the descending boudary became diffuse with the time. Thus, the mobilities of the ascending boudary as a function of the polyelectrolyte concentration are shown in Fig. 2. By extrapolation to an infinite dilution, the intrinsic mobilities of polyelectrolytes in 0.05M solutions of simple salts are obtained. The values are listed in Table 1.

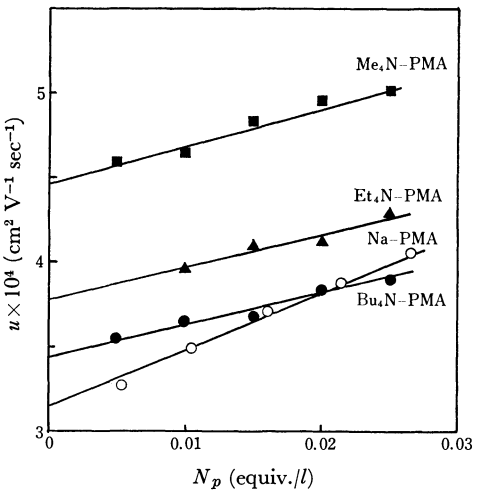

Fig. 2. Electrophoretic mobility in 0.05M simple salt solution as a function of the polymer concentration.

Discussion

As may be seen in Table 1, the electrical transport properties of the salts of PMA vary with the kinds of their counterions, indicating the difference in the strength of the interaction of this polymer with counterions. As an quantitative analysis of the data is not possible at present, the counterion-binding theory[6] is adopted as in the previous work.[1] This theory implies that part of the counterions, associated with the region of the polyion, does not contribute to the conductivity, whereas the other part of counterions remains free and behaves as in a corresponding solution of simple salt. The equivalent conductivity of polyelectrolyte can thus be written:[4]

$$\Lambda_p = i\,(\boldsymbol{F}u + l_c)$$

where i is the apparent degree of ionization, $\boldsymbol{F}$ is the faraday, and l_c is the equivalent ionic conduc-

TABLE 1

Counterion	PMA				PAA		
	$u\times10^4$ (cm^2·V^{-1}·sec^{-1})	l_c (ohm^{-1}·cm^2)	Λ_p (ohm^{-1}·cm^2)	i	$u\times10^4$ (cm^2·V^{-1}·sec^{-1})	Λ_p (ohm^{-1}·cm^2)	i
Na^+	3.15	43.1	29.4	0.40	3.27	24.4	0.33
Me_4N^+	4.45	38.2	33.9	0.42	4.84	27.3	0.32
Et_4N^+	3.77	27.3	30.2	0.47	3.89	24.4	0.38
Bu_4N^+	3.44	15.5	23.8	0.49	2.57	19.5	0.48

5) R. Varoqui and U. P. Strauss, *J. Phys. Chem.*, **72**, 2507 (1968).

6) S. A. Rice and M. Nagasawa, "Polyelectrolyte Solutions," Academic Press, London and New York (1961), p. 427.

tivity of the counterion in the solution of a simple salt. In this case, l_c can be taken as the value of the ionic conductivity of counterions in a 0.05M concentration of a simple 1-1 electrolyte.[1] Therefore, we can regard the apparent degree of ionization, i, or the apparent degree of binding, $1-i$, as a means of interpreting the strength of the interaction of the polyion with the counterion. The calculated values of i for polymethacylates are listed in Table 1; the values of polyacrylates are also shown in the table for purpose of comparison. With sodium salts, the values of i are larger in PMA than in PAA; that is, the methyl groups in PMA tend to hinder the binding of counterions with polyions. This is consistent with the finding of Crescenzi *et al.*[7] and Strauss and Leung.[8] With tetramethyl- and tetraethylammonium salts, the values of i are also about 1.2—1.3 times larger in PMA than in PAA; in fact, the binding of counterions with polycarboxylic acids is mainly determined by the size of the counterions.[1,9,10]

The value of i for Bu_4N-PMA does not increase so much as that of Et_4N-PMA, being rather equal to that of Bu_4N-PAA. From the size effect of the counterions, the values of i for Bu_4N-PMA should be much larger; however, in this case the methyl groups in PMA may play an additional part in the interaction with counterions, although the effect of the methyl groups is not so remarkable as to reverse the sequence of Et_4N and Bu_4N ions in the apparent degree of binding.

Many investigators[2,11,12] have reported the pH-induced transition of the molecular configuration of PMA in relation to the intramolecular hydrophobic or van der Waals interactions due to the methyl groups at low degrees of neutralization. However, as for the interaction of methyl groups in PMA with counterions at the full degree of neutralization, as in this study, it may be concluded that the hydrophobic effect is apparent with a strongly hydrophobic ion such as Bu_4N ion.

7) V. Crescenzi, V. DeRosa and D. Maldarella, *Ricerca Sci.*, **30**, 1680 (1960).

8) U. P. Strauss and Y. P. Leung, *J. Amer. Chem. Soc.*, **87**, 1476 (1965).

9) I. Kagawa and H. P. Gregor, *J. Polymer Sci.*, **23**, 477 (1957).

10) I. F. Miller, F. Bernstein and H. P. Gregor, *J. Chem. Phys.*, **43**, 1783 (1965).

11) A. M. Liquori, G. Barone, V. Crescenzi, F. Quadrifoglio and V. Vitagliano, *J. Macromol. Chem.*, **1**, 291 (1966).

12) E. V. Anufrieva, T. M. Birshtein, T. N. Nekrasova, O. B. Ptitsyn and T. V. Sheveleva, *J. Polymer Sci., C*, **16**, 3519 (1968).

BULLETIN OF THE CHEMICAL SOCIETY OF JAPAN VOL. 43 2370—2377 (1970)

Magnetic and Optical Properties of Ionic Electron-Donor-Acceptor Complexes

Yoichiro SATO,[*1] Minoru KINOSHITA, Mizuka SANO[*2] and Hideo AKAMATU

Department of Chemistry, Faculty of Science, The University of Tokyo, Hongo, Bunkyo-ku, Tokyo

(Received February 14, 1970)

The magnetic susceptibilities and optical absorption spectra of a number of ionic electron-donor-acceptor complexes have been studied in a solid state. The complexes of *N,N,N'N'*-tetramethyl-*p*-phenylenediamine with *o*-chloranil and *o*-bromanil were found to have a composition of 2 : 3 and their paramagnetic susceptibilities followed the Curie-Weiss law with the Weiss constant of 0 ± 5°K in the temperature range between 77°K and room temperature. It was noted that in these complexes paramagnetism is dominated by the monopositive ion radical of the amine and not by the quinone part. In contrast to this, the complexes formed by combinations of *p*-phenylenediamine and tetramethyl-*p*-phenylenediamine with *p*-chloranil and *p*-bromanil had a composition of 1 : 1 and showed paramagnetic susceptibilities which varied with temperature according to the thermal equilibrium between magnetic and non-magnetic states. The thermal equilibrium is characterized by the activation energy determined by the interaction between the monopositive and the mononegative ion radicals of the components. The absorption spectra of 1 : 1 complexes showed a charge-transfer band in the near-infrared region, while those of 2 : 3 complexes did not. The activation energy obtained magnetically is discussed in relation to the appearance of the charge-transfer absorption band. The temperature dependence of the activation energy is also discussed.

In the previous papers,[1,2] we suggested the importance of the charge-transfer interaction between ion radicals for understanding the observed magnetic susceptibilities of the crystals made of radicals. There is a correlation between the magnetic susceptibility and the appearance of a charge-transfer band in the absorption spectrum of a radical crystal. A radical crystal which shows an intense charge-transfer band is apparently diamagnetic or at most weakly paramagnetic at room temperature. The exchange coupling constant (J) for the crystal was found to be as large as 0.05 eV or more. A crystalline radical with the exchange coupling constant $J\leq0.02$ eV exhibits a fairly weak charge-transfer band. A charge-transfer band is usually undetectable for a solid with $J<10^{-3}$ eV. We have studied a similar relationship between the magnetic and optical properties for the ionic electron-donor-acceptor complexes, which may be designated as D^+A^--type complexes. In this case, the interactions between unlike molecules are of primary importance, in contrast to the systems, previously studied, of ion radical salts where interactions between like molecules are important.

We have prepared the stable solid complexes by the combination of *p*-phenylenediamines which are strong electron donors (D) with halogenated benzoquinones which are strong electron acceptors (A). In these solid complexes, an electron transfers completely from a donor molecule to an acceptor molecule, resulting in the $|D^+A^-\rangle$ ground state and $|DA\rangle$ charge-transfer excited state, when expressed in terms of a DA pair. The situation is thus reversed when compared to usual charge-transfer complexes.

Experimental

Preparation. Ionic complexes were formed between electron donors; *p*-phenylenediamine (PD), *N,N,N',N'*-tetramethyl-*p*-phenylenediamine (TMPD) and electron acceptors; chloranil (*p*-CA), *o*-chloranil (*o*-CA), bromanil (*p*-BA) and *o*-bromanil (*o*-BA), according to the method described by Kainer *et al.*[3-6] The complexes were precipitated by mixing the benzene solutions of amine

*1 Present address: National Institute for Researches in Inorganic Materials, Bunkyo-ku, Tokyo.

*2 Present address: Department of Materials Science, The University of Electro-communications, Chofu, Tokyo.

1) Y. Sato, M. Kinoshita, M. Sano and H. Akamatu, This Bulletin, **42**, 548 (1969).

2) Y. Sato, M. Kinoshita, M. Sano and H. Akamatu, *ibid.*, **42**, 3051 (1969).

3) H. Kainer, D. Bijl and A. C. Rose-Innes, *Naturwiss.*, **41**, 303 (1954).

4) H. Kainer and A. Uberle, *Chem. Ber.*, **88**, 1147 (1955).

5) H. Kainer and W. Otting, *ibid.*, **88**, 1921 (1955).

6) D. Bijl, H. Kainer and A. C. Rose-Innes, *J. Chem. Phys.*, **30**, 765 (1959).

and quinone. The composition was found to be 1 : 1 for *p*-quinone complexes. The complex formed from TMPD and *o*-BA was found to have the composition $TMPD_2 \cdot o\text{-}BA_3$. The composition of the complex formed from TMPD and *o*-CA was not determined. It was tentatively assigned, however, to be $TMPD_2 \cdot o\text{-}CA_3$, because of the close resemblance of the magnetic and optical behavior to that of $TMPD_2 \cdot o\text{-}BA_3$.

$TMPD_2 \cdot o\text{-}BA_3$ (Found: C, 28.59; H, 2.17; N, 3.19%. Calcd: C, 28.53; H, 2.07; N, 3.50%).

Measurements. The static susceptibilities of the complexes were measured as a function of temperature with a Faraday-type magnetic balance[7] in the range from 77°K to room temperature or a somewhat higher temperature according to the stability of a compound. The absorption spectra were measured in the range from 340 to 2400 mμ for a powder sample suspended in liquid paraffin.

Results

Magnetic Susceptibilities. The susceptibilities of $TMPD_2 \cdot o\text{-}CA_3$ and $TMPD_2 \cdot o\text{-}BA_3$ were found to be strongly paramagnetic at room temperature and increased with decreasing temperature, while the susceptibilities of the other complexes were diamagnetic and their temperature variations were relatively small.

For the purpose of evaluating diamagnetic contribution, the susceptibilities of the neutral component molecules were measured. The results are given in Table 1. The susceptibilities of the *o*-quinones are seen to be somewhat less diamagnetic than those of the corresponding *p*-quinones.

Table 1. Magnetic susceptibilities of the amines and the quinones

Compound	Molar susceptibility $\chi_M \times 10^6$(emu/mol)
p-Phenylenediamine	−73
N,N,N',N'-Tetramethyl-*p*-phenylenediamine	−125
Chloranil	−113
o-Chloranil	−105
Bromanil	−148
o-Bromanil	−139

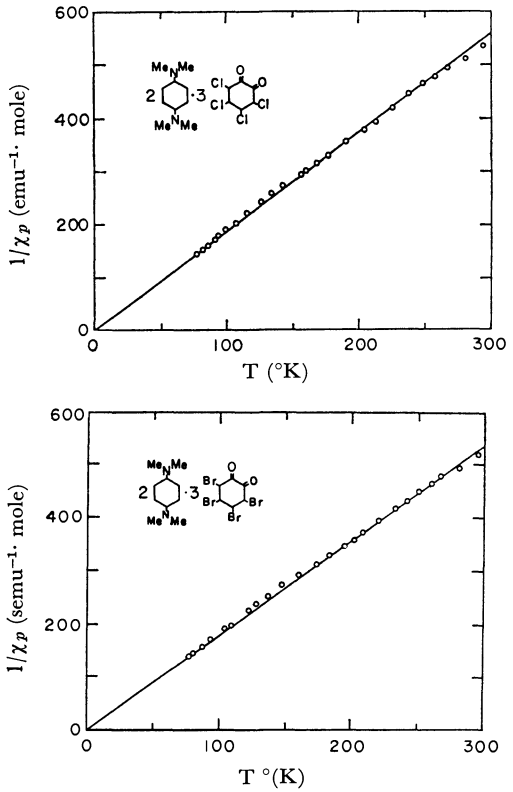

Fig. 1. Inverse paramagnetic susceptibilities of $TMPD_2 \cdot o\text{-}CA_3$ and $TMPD_2 \cdot o\text{-}BA_3$ versus temperature.

For $TMPD_2 \cdot o\text{-}CA_3$ and $TMPD_2 \cdot o\text{-}BA_3$, the sum of the susceptibilities of the neutral components was taken to be their diamagnetic susceptibility. When the inverse paramagnetic susceptibility $1/\chi_p$ was plotted against temperature, straight lines were obtained as shown in Fig. 1. The values of the Curie constant C and the Weiss constant θ were obtained from the slope of the line and its intersection on the temperature axis, respectively. The results are given in Table 2.

Table 2. Magnetic susceptibilities of the compleexes

Compound	Observed susceptibility at 296°K $\chi_M \times 10^6$ (emu/mol)	Diamagnetic susceptibility $\chi_d \times 10^6$ (emu/mol)	Paramagnetic susceptibility at 296°K $\chi_p \times 10^6$ (emu/mol)	Weiss constant θ (°K)	Curie constant C (emu °K/mol)
$TMPD_2 \cdot o\text{-}CA_3$	1297	−565	1862	0±5	0.551
$TMPD_2 \cdot o\text{-}BA_3$	1226	−694	1920	0±5	0.568
TMPD·*p*-CA	−226	−245	(19)	—	—
TMPD·*p*-BA	−230	−285	(55)	—	—
PD·*p*-CA	−180	−212	(32)	—	—
PD·*p*-BA	−231	(−259)	(28)	—	—

7) Y. Sato, M. Kinoshita, M. Sano and H. Akamatu, This Bulletin, **40**, 2539 (1967).

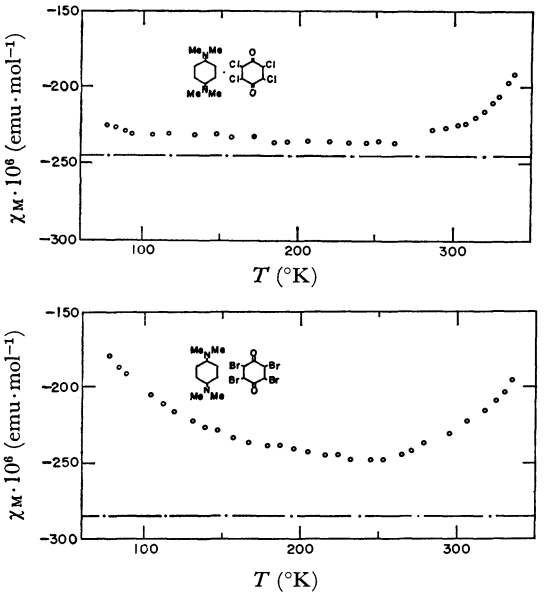

Fig. 2. Magnetic susceptibilities of TMPD·p-CA and TMPD·p-BA versus temperature.
—·—·— χ_{dia}.

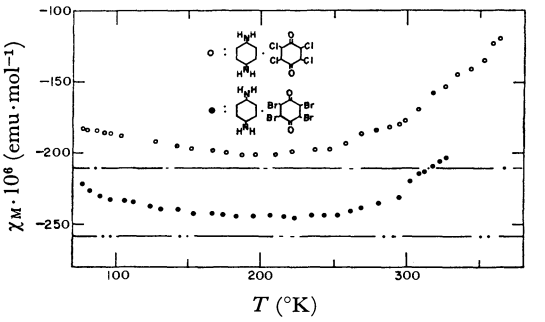

Fig. 3. Magnetic susceptibilities of PD·p-CA and PD·p-BA versus temperature.
—·—·—·—·— χ_{dia}.

The susceptibilities of TMPD·p-CA, TMPD·p-BA, PD·p-CA and PD·p-BA are plotted as a function of temperature in Figs. 2 and 3. The general feature of temperature dependence resembles each other. In a higher temperature region the susceptibility decreased with decreasing temperature, but it increased through a minimum in a lower temperature region. The diamagnetic contribution was evaluated by assuming that the susceptibility change in the lower temperature region was dominated by the paramagnetic susceptibility of an impurity which followed the Curie law.*3 The diamagnetic susceptibilities thus obtained are given in Table 3, which are in reasonable agreement with the sum of the values for neutral components. The intrinsic paramagnetic susceptibilities, after corrections for the diamagnetic and impurity parts were made, are plotted as a function of temperature in Figs. 4 and 5.

*3 The assumption seems to be plausible for the reasons mentioned in the following paragraph. It has, in fact, been supported for TMPD·p-CA by ESR experiments (Ref. 6).

Table 3. Diamagnetic parts of the complexes

Compound	χ_d(obs) $\times 10^6$ (emu/mol)	χ_d(calc) $\times 10^6$* (emu/mol)
TMPD·p-CA	−245	−238
TMPD·p-BA	−285	−274
PD·p-CA	−212	−185
PD·p-BA	(−259)	−221

* The sum of the values found for the neutral components given in Table 1.

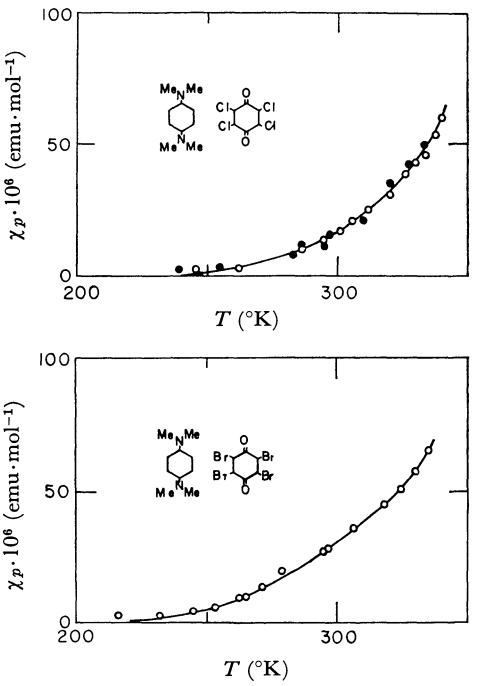

Fig. 4. Intrinsic paramagnetic susceptibilities of TMPD complexes.

The observed susceptibilities of a given complex exhibited slightly different values among the samples which had been prepared independently. The difference, however, was considered to be caused by a variation in the impurity content, since the difference in susceptibility was found to be proportional to $1/T$ within experimental errors. The intrinsic susceptibility determined after the above-mentioned corrections gave the same value for the different samples.

Electrton Spin Resonance. In order to obtain information on the origin of unpaired electrons, g-values were determined for powder samples by

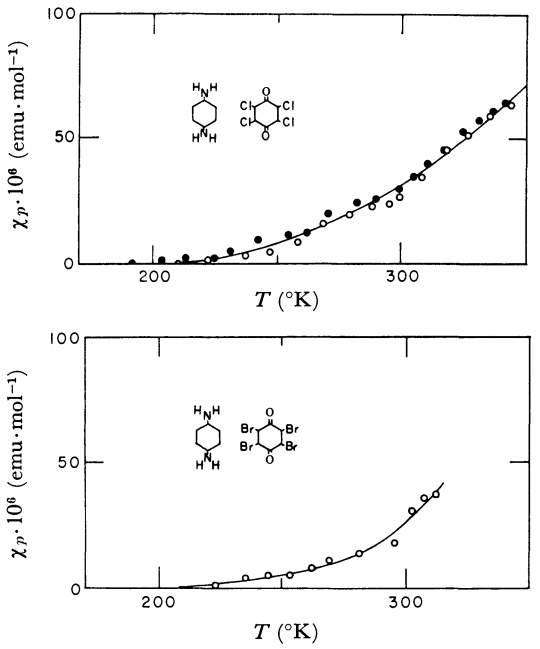

Fig. 5. Intrinsic paramagnetic susceptibilities of PD complexes.

Table 4. *g*-Factors

$TMPD_2 \cdot o\text{-}CA_3$	2.0032	$TMPD^+$	2.0032*
$TMPD_2 \cdot o\text{-}BA_3$	2.0036	PD^+	2.0030
TMPD·*p*-CA	2.0050	*p*-CA^-	2.0057**
TMPD·*p*-BA	2.0065	*p*-BA^-	2.0088**
PD·*p*-CA	2.0045 (g_{av})		
PD·*p*-BA	2.0065 (g_{av})		

* Kinoshita and Akamatu, Ref. 18.

** M.S. Blois, Jr., H.W. Brown and J.E. Maling, "Free Radicals in Biological Systems," ed. by M.S. Blois, Jr., *et al.*, Academic Press, New York and London (1961), p. 117.

ESR measurements at room temperature. The values are given in Table 4. A single exchange-narrowed absorption line was observed for the complexes; TMPD·*p*-CA, TMPD·*p*-BA, $TMPD_2 \cdot o\text{-}CA_3$ and $TMPD_2 \cdot o\text{-}BA_3$. An axially symmetric *g*-factor was observed with the *p*-phenylenediamine complexes, which is in agreement with the result obtained by Ottenberg, *et al.*[8] and Hughes and Soos.[9] The principal *g*-values were determined to be: $g_{\parallel}=2.0023$, $g_{\perp}=2.0056$ for PD·*p*-CA and $g_{\parallel}=2.0020$, $g_{\perp}=2.0087$ for PD·*p*-BA. The average value, $g_{av}=(g_{\parallel}+2g_{\perp})/3$, is given in Table 4*[4]

8) A. Ottenberg, C. J. Hoffman and J. Osiecki, *J. Chem. Phys.*, **38**, 1898 (1963); M. E. Browne, A. Ottenberg and R. L. Brandon, *ibid.*, **41**, 3265 (1964).

9) R. C. Hughes and Z. G. Soos, *J. Chem. Phys.*, **48**, 1066 (1968).

*[4] Static susceptibility data showed that the impurity paramagnetism contributed appreciably to the observed paramagnetic susceptibilities of TMPD·*p*-CA, TMPD·*p*-BA, PD·*p*-CA and PD·*p*-BA, but no separate ESR signal was observed at room temperature.

The *g*-values of the *p*-quinone complexes were found to be intermediate between the values of the components, while those of $TMPD_2 \cdot o\text{-}CA_3$ and $TMPD_2 \cdot o\text{-}BA_3$ were close to the *g*-value of Würster's blue ion ($TMPD^+$).

Absorption Spectra. The solid *p*-quinone complexes showed broad absorption bands as shown in Figs. 6 and 7. It was noted that the spectra of TMPD·*p*-CA and TMPD·*p*-BA resembled each other and also those of PD·*p*-CA and PD·*p*-BA.

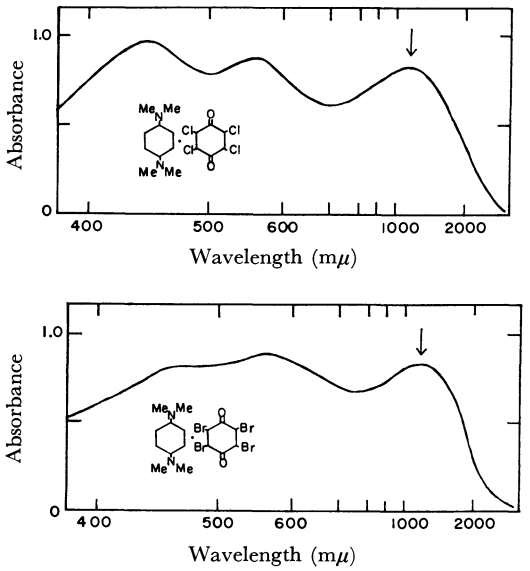

Fig. 6. Absorption spectra of solid TMPD·*p*-CA and TMPD·*p*-BA. Arrows indicate the charge-transfer bands.

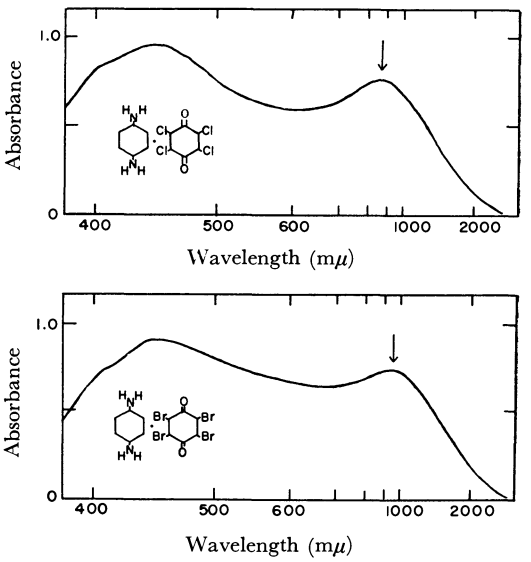

Fig. 7. Absorption spectra of solid PD·*p*-CA and PD·*p*-BA, where the charge-transfer bands are indicated by arrows.

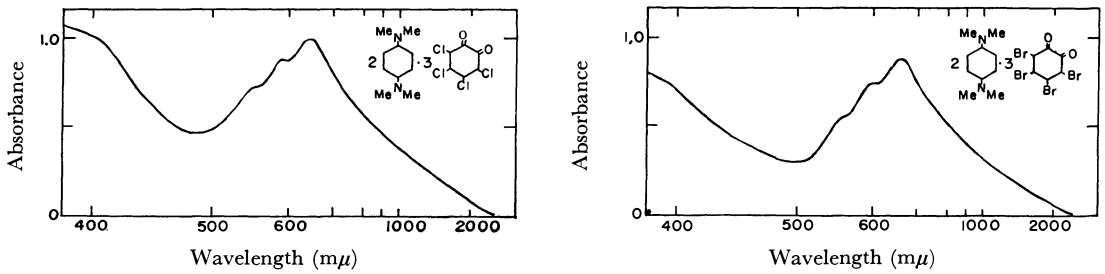

Fig. 8. Absorption spectra of solid $TMPD_2 \cdot o\text{-}CA_3$ and $TMPD_2 \cdot o\text{-}BA_3$.

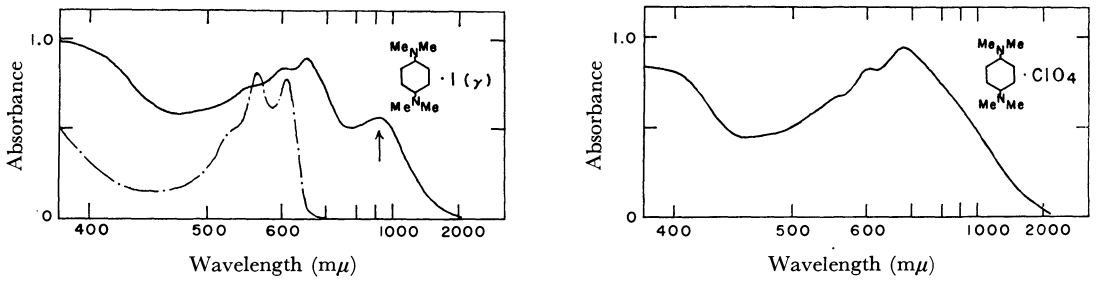

Fig. 9. Absorption spectra of TMPD·I (γ-form) and $TMPD \cdot ClO_4$.
——— Solid spectra, —·—·— $TMPD^+$ in CH_2Cl_2 solution

In contrast to the broad structureless bands of these complexes, $TMPD_2 \cdot o\text{-}CA_3$ and $TMPD_2 \cdot o\text{-}BA_3$ showed spectra in which the band around 600 mμ had a well-defined structure as seen in Fig. 8. In the observed region, the two spectra were identical as far as position and general features were concerned. For the purpose of comparison, the solid spectra of Würster's blue perchlorate ($TMPD \cdot ClO_4$) and Würster's blue iodide (TMPD·I, γ-form) are shown in Fig. 9. The spectrum of $TMPD \cdot ClO_4$ is in agreement with those observed by other investigators.[10–12] The positions of the absorption peaks are given in Table 5.

Discussion

$TMPD_2 \cdot o\text{-}TMPD_2 \cdot o\text{-}CA_3$. As evidenced by the strong paramagnetism, these complexes are considered to be fundamentally ionic, though they are expected to include a neutral quinone per formula unit. The observed value of the Curie constant indicates that there are only two free spins in a formula unit instead of four spins expected from the simple consideration that there are two monopositive $(TMPD)^+$ and two mononegative (o-CA^- or o-BA^-) ion radicals and a neutral quinone molecule per formula unit.

Table 5. Approximate positions of the absorption peaks of the solid spectra

	(mμ)
TMPD·p-CA	440, 550, 1200
TMPD·p-BA	460, 550, 1200
PD·p-CA	400, 445, 900
PD·p-BA	415, 445, 950
$TMPD_2 \cdot o\text{-}CA_3$	540, 595, 650
$TMPD_2 \cdot o\text{-}BA_3$	540, 595, 650
$TMPD \cdot ClO_4$	550, 600, 670
TMPD·I (γ-form)	550, 595, 650, 940

It is noted that the g-value of $TMPD_2 \cdot o\text{-}CA_3$ coincides with that of the monopositive ion of TMPD in $TMPD \cdot ClO_4$, and that of $TMPD_2 \cdot o\text{-}BA_3$ is close to this value. Moreover, the band structure around 600 mμ shows close resemblance with those found for $TMPD \cdot ClO_4$ and TMPD·I as compared in Figs. 8 and 9 and also in Table 5. It seems certain that the peaks are due to Würster's blue ion. Thus, it is concluded that the strong paramagnetism of these complexes is almost entirely due to $TMPD^+$ ion radicals. Since the neutrality condition requires the existence of negative ions, the question remains why the paramagnetic contribution from the quinone anion radicals is undetectable. Although no further attempts have been made to elucidate the question,*5 the following explanation is possible: 1) The cations and anions form separate column in the crystal. The cations are nearly free, while the anions are strongly coupled with each other due to the different manner of stacking in the columns. As a result, the cations contribute to paramagnetism strongly, while the

10) G. R. Anderson, *J. Chem. Phys.*, **47**, 3853 (1967).
11) Y. Iida, This Bulletin, **41**, 2615 (1968).
12) T. Sakata and S. Nagakura, *ibid.*, **42**, 1497 (1969).

*5 No detailed information on the quinone part was obtained from the absorption spectra of Fig. 8.

anions only slightly. 2) The anions exist in certain diamagnetic form, *e. g.*, as dinegative ions or as diamagnetic anions produced by chemical reaction. It is noted that the interaction between Würster's blue ions in these complexes is quite small, in fact the smallest among those observed for other Würster's blue ion radical salts.

Kainer and Überle[4] reported that the complexes formed from TMPD and *o*-quinones were 1:1 complexes. Although the absorption spectra were not explicitly shown, they described the same observations mentioned above, *i. e.*, the appearance of a band with structure in the visible region and the absence of absorption in the near-infrared region in contrast to the case of *p*-quinone complexes. Moreover, they observed strong paramagnetism which corresponded to only one spin per formula unit contrary to their expectation of two spins.[4,6] The highest radical concentration of 0.80 spins per unit of TMPD·*o*-BA in their report corresponds to 2.0 spins per unit of $TMPD_2$·o-BA_3. Therefore, their complexes also seem to have the composition 2 : 3 rather than 1 : 1.

TMPD·*p*-CA; TMPD·*p*-BA. Magnetic and optical data are in agreement with those reported by Kainer and Überle[4] and Pott and Kommandeur.[13] The absorption bands in the visible region are reasonably assigned to the intramolecular transitions of the ionized component molecules but not those of neutral components. For TMPD·*p*-CA, the bands at 550 and 440 mμ may be ascribed to $TMPD^+$ and p-CA^-, respectively, and for TMPD·*p*-BA, the bands at 550 and 460 mμ may be due to $TMPD^+$ and p-BA^-, respectively.*6 These complexes are therefore considered to consist of the amine monopositive and the quinone mononegative ions. The band at approximately 1200 mμ in each spectrum is assigned to the charge-transfer band as pointed out previously on the basis of the polarization spectrum.[14] de Boer and Vos[15] have revealed the alternant face-to-face stacking of $TMPD^+$ and p-CA^- molecules in the crystal. The interaction between D^+ and A^- is therefore thought to be important and the charge-transfer absorption should be ascribed to the transition of the type $|\cdots D^+A^-D^+A^-D^+A^-\cdots\rangle \rightarrow |\cdots D^+A^-D^0A^0D^+A^-\cdots\rangle$. The molecular stacking in TMPD·*p*-BA seems to be similar in view of the close resemblance of the magnetic and optical behavior.

The interpretation of the absorption spectra is consistent with the result from ESR measurements. The fact that the *g*-values of these complexes are close to the average *g*-values of the component ions indicates an equal contribution of the cation and anion radicals to the paramagnetism.[16] As will be discussed below, the static susceptibility data show that the spins in these complexes are coupled by rather strong antiferrromagnetic interaction of about 0.08 eV.

PD·*p*-CA; PD·*p*-BA. The absorption bands of these complexes in the visible region are also assigned to the intramolecular transitions of the amine monopositive and the quinone mononegative ions. The band in the near-infrared region in each spectrum may also be due to the charge-transfer interaction between D^+ and A^- ions.[14] The *g*-values of these complexes also indicate that the cations and anions contribute equally to paramagnetism.

Thus, the magnetic and optical properties of the complexes studied here are explained on the basis of the completely ionized component molecules in the ground state and strong antiferromagnetic interaction between D^+ and A^- ions. Moreover, it is noted that the charge-transfer bands of these complexes are strong. As a result, it is concluded that the correlation between the exchange coupling constant and the intensity of the charge-transfer band is also present in ionic donor-accepter complexes, in which the interaction between unlike molecules, D^+ and A^-, is important. This implies that the nature of the exchange interaction in D^+A^--type complexes is essentially the same as that in the previously studied D^+D^+-type or A^-A^--type complexes. It also suggests the importance of the charge-transfer stabilization of the singlet ground state in the determination of the observed values of exchange coupling constant. The same argument may also hold for the molecular complexes of diaminodurene-chloranil[17] and TMPD-tetracyano-*p*-quinodimethane.[18]

Temperature Variation of Exchange Coupling Constant

The values of exchange coupling constant (J) can be evaluated by comparison of the intrinsic paramagnetic susceptibilities with a theoretical model; the singlet-triplet model or the linear Ising model. For $TMPD_2$·o-BA_3 and $TMPD_2$·o-CA_3, the exchange coupling constants were fairly small, being estimated to be $J \leq 4\times10^{-4}$ eV from the observed Weiss constant of 0 ± 5°K. For the complexes containing *p*-quinones, the values of J were evaluated by two methods. The apparent activation energy E, expressed in the formula

$$\chi_p = (C/T)\exp(-E/kT) \qquad (1)$$

was obtained by plotting $\log(\chi_p T)$ against $1/T$. In

13) G. T. Pott and J. Kommandeur, *Mol. Phys.*, **13**, 373 (1967).

*6 The assignment of the band at 440 mμ to p-CA^- ion radical is in agreement with the argument given by Andre and Weill, *Mol. Phys.*, **15**, 97 (1968).

14) T. Amano, H. Kuroda and H. Akamatu, This Bulletin, **41**, 83 (1968).

15) J. L. de Boer and A. Vos, *Acta Cryst.*, **B24**, 720 (1968).

16) M. Kinoshita, This Bulletin, **36**, 307 (1963).

17) D. B. Chesnut and W. D. Phillips, *J. Chem. Phys.*, **35**, 1002 (1961).

18) M. Kinoshita and H. Akamatu, *Nature*, **207**, 291 (1965).

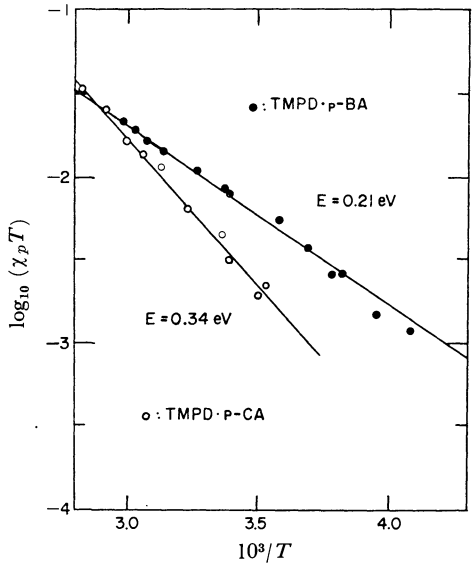

Fig. 10. Plots of log $\chi_p T$ against $1/T$ for TMPD·p-CA and TMPD·p-BA.

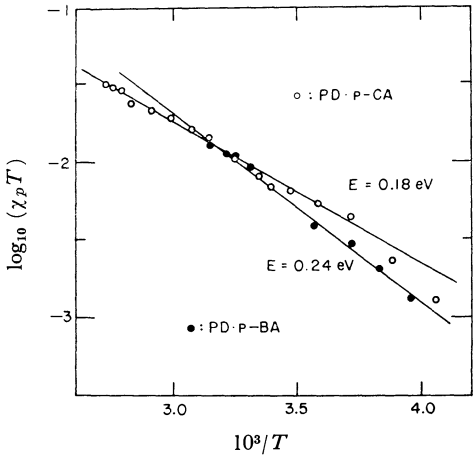

Fig. 11. Plots of log $\chi_p T$ against $1/T$ for PD·p-CA and PD·p-BA.

the case of the singlet-triplet model, E corresponds to the energy separation $\delta(=2J)$ between the singlet ground state and the thermally accessible triplet state ($E=\delta$), and in the case of the linear Ising model it corresponds to J ($E=J$). The plots of $\log(\chi_p T)$ against $1/T$ are shown in Figs. 10 and 11. Direct comparison of experimental data with theoretical curves, by finding the best fit, also gives the value of J. The singlet-triplet model with $\delta=0.15$ eV accounted for the experimental plots for TMPD·p-BA and PD·p-CA fairly well. The susceptibility rise for TMPD·p-CA and PD·p-BA, however, was so steep that neither of the models could explain the result. For a closer study, we calculated the values of J at several points of temperature by comparing the experimental susceptibilities with the theoretical ones. The results

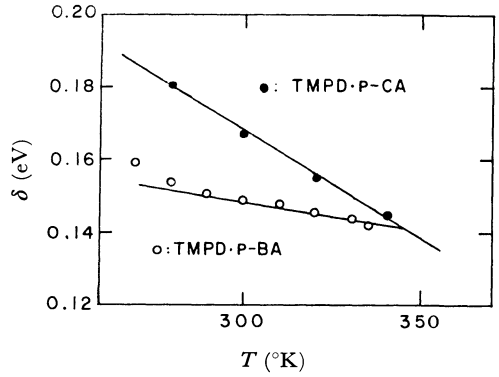

Fig. 12. Temperature variations of the singlet-triplet separation δ ($=2J$) for TMPD·p-CA and TMPD·p-BA.

Table 6. Temperature variations of exchange coupling constants

	δ_0 ($=E$) (ev)	δ(eV) at 300°K	α(ev/°K)	$\delta_0+\alpha T$ at 300°K	J(eV) at 300°K
TMPD·p-CA	0.34	0.17	-6.0×10^{-4}	0.16	0.09
TMPD·p-BA	0.21	0.15	-1.8×10^{-4}	0.16	0.08
PD·p-CA	0.18	0.15	-0.8×10^{-4}	0.16	0.08
PD·p-BA	0.24	0.15	-4.4×10^{-4}	0.11	0.08

obtained with the singlet-triplet model are shown in Figs. 12 and 13. It appears that δ is a linear function of temperature and that the temperature variation is small for TMPD·p-BA and PD·p-CA, and quite large for TMPD·p-CA and PD·p-BA. The values of δ obtained by the above procedures are given in Table 6. The largest difference between E and δ is noted for TMPD·p-CA, *i. e.*, $E=0.34$ eV and $\delta=0.17$ eV at 300°K.

If δ is a linear function of temperature, we may write

$$\delta = \delta_0 + \alpha T \qquad (2)$$

where δ_0 and α are constants. The slope of the

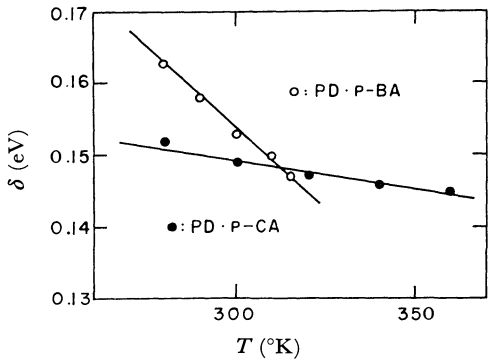

Fig. 13. Temperature variations of the singlet-triplet separation δ ($=2J$) for PD·p-CA and PD·p-BA

plot of $\log(\chi_p T)$ against $1/T$ gives δ_0 rather than δ itself. Therefore, we put $E=\delta_0$ and see if the large discrepancy between E and δ may be explained by relation (2). The values of α are obtained from the slopes of the straight lines shown in Figs. 12 and 13. The agreement between δ and $\delta_0+\alpha T$ is good as seen from Table 6, which indicates that δ decreases linearly with temperature. It would be appropriate therefore to employ the values of $J(=\delta/2)$ given in the last column of Table 6, *i. e.*, approximately 0.08 eV for all these complexes. If the linear Ising model is employed, a larger value of about 0.11 eV is obtained. It seems that the large effective change in the exchange coupling constant found for TMPD·*p*-CA and PD·*p* BA suggests the temperature variation of intermolecular interactions associated with variation in intermolecular distance. For TMPD·*p*-CA it may be related to the gradual phase transition suggested by Pott and Kommanduer.[13]

BULLETIN OF THE CHEMICAL SOCIETY OF JAPAN VOL. 43 2377—2380 (1970)

Electron Spin Resonance of Oxidized ZnO at −195°C

Morio SETAKA, Shigeaki FUJIEDA and Takao KWAN

Faculty of Pharmaceutical Sciences, The University of Tokyo, Hongo, Bunkyo-ku, Tokyo

(Received February 14, 1970)

An asymmetric ESR spectrum of ZnO at the g value of 1.96 was found to split into $g=1.957$ and 1.963 components at −195°C provided that ZnO was pretreated with oxygen. Temperature dependence of these two signals as well as the effect of doping Al^{3+} or Li^{+} on their intensities were investigated to qualify these signals. It was suggested that the $g=1.957$ signal is correlated with conduction electrons while the $g=1.963$ signal is ascribable to electrons trapped at interstitial zinc ions. The ZnO sample also gave rise to another signal at $g=2.013$ at −195°C. The signal was attributed to holes in the bulk.

As has been recognized by numerous workers, a highly outgassed ZnO sample produces a broad and asymmetric ESR spectrum around the g value of 1.96 at room temperature.[1] While this signal has been interpreted as due to electrons in the bulk, some detailed arguments were previously made concerning the origin of the electrons.[2] Recently, Codell *et al.*[3] reported that the signal splits into two components ($g=1.961$ and 1.965), when ZnO is pretreated with tertiary butyl hydroperoxide vapors and subjected to ESR mesurements at −195°C. During the course of our work,[4] we have also recognized that the $g \sim 1.96$ signal is replaced by a doublet at −195°C in accordance with the report of Codell *et al.* with respect to a ZnO sample pretreated with O_2. A similar phenomenon was reported more recently by Iyengar *et al.*[5] who pretreated ZnO with N_2O, NO or Cl_2 at 25°C.

In view of these results, it was felt necessary to further investigate the nature of the two component signals and to elucidate the relationship between the $g \sim 1.96$ signal and the two components. Since doping of ZnO with Al^{3+} or Li^{+} is expected to control the concentration of electrons or interstitial zinc in the bulk, it should be interesting to investigate ESR spectra of the doped ZnO samples and to see how the $g \sim 1.96$ signal is modified at −195°C. On the other hand, we have already noted that another signal appears at $g=2.013$ which is distinguishable from that due to adsorbed O_2^- ($g=2.002$, 2.008, 2.051)[4] when an oxidized ZnO is subjected to ESR measurement at −195°C. Undoubtedly, there still remains a question of interest on the ESR spectra of ZnO especially at low temperatures. In the present paper the results of such ESR investigations are reported using Al^{3+} or Li^{+} doped ZnO and undoped one, respectively.

1) V. J. Schneider and A. Rauber, *Z. Naturforsch.*, **16**, 712 (1961); R. J. Kokes, *J. Phys. Chem.*, **66**, 99 (1962); Y. Fujita and T. Kwan, *Shokubai*, **5**, 206 (1963); P. H. Kasai, *Phys. Rev.*, **130**, 983 (1963); M. Setaka and T. Kwan, This Bulletin, **38**, 1414 (1965); K. M. Sancier and T. Freund, *J. Catalysis*, **5**, 293 (1965).

2) M. Setaka, K. M. Sancier and T. Kwan, *J. Catalysis*, **16**, 44 (1970).

3) M. Codell, H. Gisser, J. Weisberg and R. D. Iyengar, *J. Phys. Chem.*, **72**, 2460 (1968).

4) M. Setaka, S. Fukuzawa, Y. Kirino and T. Kwan, *Chem. Pharm. Bull.* (Tokyo), **16**, 1240 (1968).

5) R. D. Iyengar, V. V. Subba Rao and A. C. Zettlemoyer, *Surface Sci.*, **13**, 251 (1969).

Experimental

ZnO of high purity (Pb: 0.003%, Fe: 0.0001%, other metal: 0.01%) supplied by Sakai Chemical Co., was used for experiments. ZnO samples doped with Al^{3+} or Li^{+} were prepared as follows. A powdered ZnO was slurried with dilute aqueous solution of $Al(NO_3)_3 \cdot 9H_2O$ (Guaranteed, Kanto Chemical Co.) and $LiNO_3$ (Guaranteed, Koso Chemical Co.) respectively and dried at 100°C. It was then calcined in air at 500°C for two hours and at 700°C for another hour. The degree of doping was so adjusted that 1.5 mol percent Li_2O or Al_2O_3 is incorporated. Li_2CO_3 was also used instead of $LiNO_3$ to investigate the effect of anion. No difference was found, however, between the two anions.

ESR measurements were made at room temperature and −195°C respectively using a JEOL-P-10 type spectrometer (X-band, 100 kcps field modulation). ZnO samples were placed in a quartz tube (4 cm long, 4 mm id), at the center of which a sealed capillary containing MgO : Mn^{2+} was inserted as a means of measuring relative ESR sensitivity. The spin concentrations of ESR signals were determined by the first moment of the derivative absorption curve, normalized with the intensity of Mn^{2+} signal which was calibrated at room temperature and −195°C with a solution of DPPH (5×10^{-5}M) in benzene substituted for the ZnO sample.

Results and Discussion

Pretreatment of vacuum outgassed ZnO with a small amount of oxygen at room temperature usually results in a decrease in the ESR spectral intensity of the $g \sim 1.96$ signal without perceptible change in its signal shape.[4] Such a spectrum observed at room temperature is illustrated in Fig. 1-a. It was found, however, that the signal is replaced by two *components* ($g = 1.963 \pm 0.001$ and 1.957 ± 0.001) as shown in Fig. 1-b when measured at −195°C. Further pretreatment of the ZnO with 30 Torr O_2 at 200°C for 30 min, followed by evacuation at room temperature, gave a spectrum of Fig. 1-c at −195°C. It is apparent from Figs. 1-b and 1-c that the spin concentrations of the $g = 1.963$ component markedly decrease with the oxygen pretreatment or oxidation of the ZnO sample, while the $g = 1.957$ signal remains nearly constant.

We shall start with a raw ZnO sample (no pretreatment) and investigate how the spin concentrations of the two signals vary with successive oxygen pretreatments of the sample. The untreated ZnO sample showed only the $g = 1.957$ signal when measured at −195°C in a vacuum (stage 1) which we have called so far the $g \sim 1.96$ signal. The ZnO sample was then outgassed at 500°C in a high vacuum for 30 min and then allowed to contact with 30 Torr O_2 at room temperature. The sample was then evacuated for residual oxygen at room temperature and subjected to ESR measurements at −195°C (stage 2). It was found that the original $g = 1.957$ signal is accompanied by the $g = 1.963$

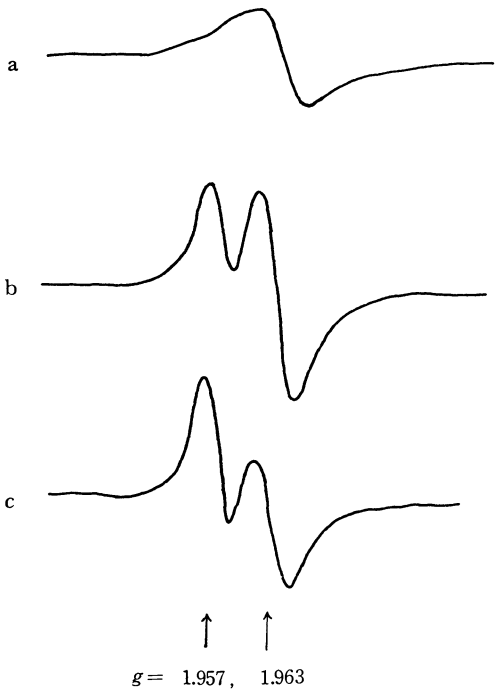

Fig. 1. ESR spectra of ZnO pretreated with oxygen measured at room temperature (a) and −195°C (b, c).

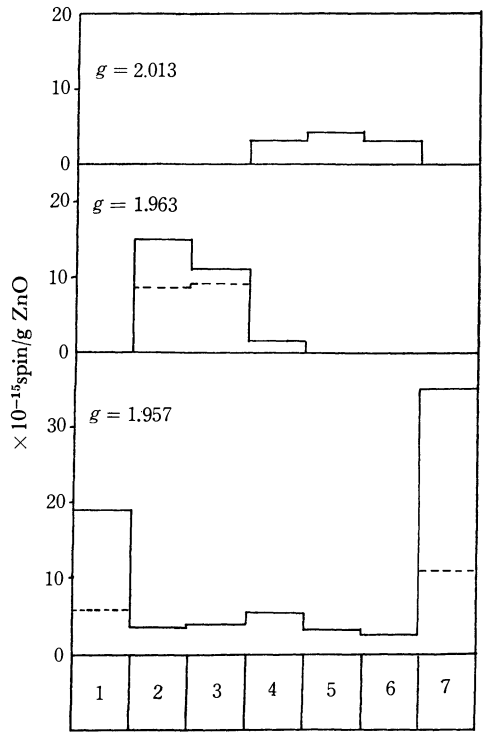

Fig. 2. Effect of successive pretreatments of ZnO on ESR signals. Dashed line indicates spin concentrations at room temperature.

signal; the $g \sim 1.96$ signal was now replaced by the $g=1.957$ and 1.963 signals as already shown in Fig. 1-b.

Changes in the spin concentrations of the two signals were further investigated by treating the ZnO sample at higher temperatures under 30 Torr oxygen (200, 350 and 500°C for stage 3, 4 and 5 respectively). It was found in this way that the $g=1.963$ signal entirely disappears by heat treatment above 350°C whereas the $g=1.957$ remains quite stable up to 500°C. The ZnO sample at stage 5 was kept at room temperature for 5 days (stage 6) where little change was observed in signal intensity. The growth or decay of the two signals with heat treatment in ambient oxygen is illustrated in Fig. 2, where annexed figures 1—6 indicate successive stages for pretreatment. It is apparent from Fig. 2 that the $g=1.957$ and 1.963 species are energetically different.

In stage 7, the ZnO sample was allowed to contact with water vapor. As a result, the 1.957 signal increased to a remarkable extent while the 1.963 signal remained unaffected. As the electric conductivity of ZnO increases on adsorbing water vapor[6] and dereases on adsorbing oxygen, the growth or decay of the 1.957 signal, as demonstrated in Fig. 2, should be correlated with the change of the concentration of conduction electrons in the bulk of ZnO.

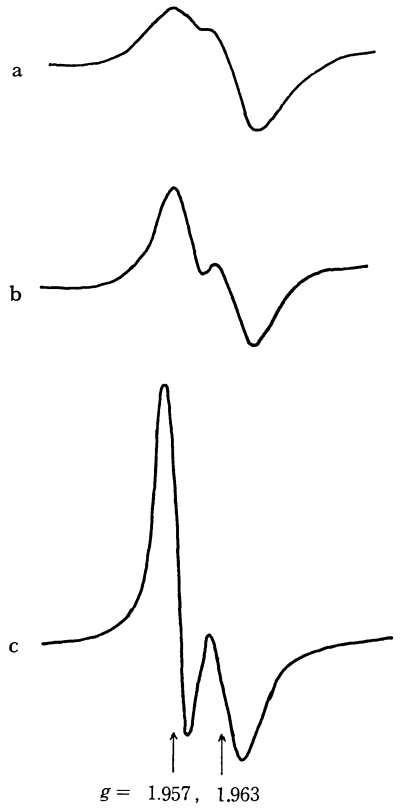

Fig. 3. ESR spectra of ZnO pretreated with oxygen measured at −100°C (a), −150°C (b) and −195°C (c).

Figure 3 indicates the temperature dependence of the $g=1.957$ and $g=1.963$ signals for the ZnO pretreated with 30 Torr O_2 at 200°C for 30 min. ESR measurements were carried out at −100°C (a), −150°C (b) and −195°C (c) respectively. According to Fig. 3, the $g=1.957$ species seems to be more temperature dependent than the $g=1.963$ species. This suggests that the $g=1.957$ species is originated from lower energy levels.

It is generally accepted[7] that Al^{3+} doped ZnO contains more electrons than an undoped one:

$$\text{ZnO crystal} + Al_2O_3 \rightleftarrows 2Al^{3+} + 2\ominus + 2ZnO + 1/2O_2$$

Conversely, Li^+ doped ZnO contains less electrons:

$$\text{ZnO crystal} + LiO_2 \rightleftarrows 2Li^+ - 2\ominus + 2ZnO - 1/2O_2$$

Attempts were made, therefore, to investigate the behavior of the $g=1.957$ signal with Al^{3+} and Li^+ doped ZnO samples respectively. The doped ZnO samples with or without oxygen pretreatment were subjected to ESR measurements at −195°C. It was found, as shown in Table 1, that the $g=1.957$ signal increases with Al^{3+} doped ZnO while it vanishes completely with Li^+ doped ZnO irrespective of pretreatment. The result is qualitatively in accord with the above equations, *viz*, the $g=1.957$ signal could be attributable to electrons whose behavior is largely in parallel with that of conduction electrons.

Table 1. Spin concentrations ($\times 10^{-15}$ spin/g) of the $g=1.957$ and 2.013 signals

Sample	Pretreatment	$g=1.957$	$g=2.013$
Al-ZnO	A	270	0
	B	120	0
Li-ZnO	A	0	7
	B	0	6

A: Sample evacuated at room temperature.
B: Sample heated at 500°C under 100 Torr of oxygen for 30 min.

Generally speaking, ZnO may contain cation and anion vacancies and many other defects which act as acceptors or donors. Electrons in the bulk of ZnO are expected to be either in the conduction band or localized in donor states, *e.g.*, interstitial Zn_i^+ ion, or trapped at oxygen ion vacancies. Oxygen ion vacancies are considered to be stable

6) H. Hasebe and A. Inoue, *Nippon Kagaku Zasshi*, **87**, 332 (1966).

7) G. Heiland, E. Mollwo and F. Stockmann, "Solid State Physics," Vol. 8, Academic Press, Inc., New York (1959), p. 191.

below the Tamman temperature of ZnO[8] (900°C) and may capture electrons produced upon Al^{3+} doping. Thus the electrons trapped at the oxygen ion vacancies could also contribute to the signal $g=1.957$. Interstitial Zn_i^+ ions are known[9] to be rather labile and may disappear completely upon heating at 550°C for a few minutes in air. It appears, therefore, that electrons responsible for $g=1.957$ may not correspond to the interstitial zinc ions. The thermal behaviour of the $g=1.963$ signal, on the other hand, seems to be consistent with that of Zn_i^+ ions; electrons responsible for the $g=1.963$ signal could be localized at these defects. However, another possibility that the $g=1.963$ signal is due to electrons trapped at the oxygen vacancies near surface[8] may not be excluded. The trapping site near the surface would be distorted to a greater extent as compared with that in the bulk, leading to a slight shift in their g values.

During the course of the above measurements the ESR spectra were accompanied with another signal at the g value of 2.013 ± 0.001. The signal does not seem to be due to contaminated impurities such as Fe^{3+} in ZnO[10] ($g=2.0056$, 2.0041) but due to intrinsic defects in ZnO. In Fig. 2, changes in the spin densities of the 2.013 signal in the successive stages were also illustrated. As shown in stage 7, the $g=2.013$ signal completely disappeared when water vapor was adsorbed on ZnO. It should be noted that the direction of change is opposite to that of the $g=1.957$ signal. This fact may suggest that the $g=2.013$ signal originates from holes in acceptor levels. The supposition is consistent with the experimental result obtained with doped ZnO samples; as shown in Table 1, Li^+ doped ZnO, that is expected to contain *holes*, definitely gave rise to the $g=2.013$ signal while it was absent with Al^{3+} doped ZnO. The $g=2.013$ signal showed no dipolar broadening at high pressures of oxygen, suggesting that it is a bulk species. It would be interesting to investigate whether or not the $g=2.013$ species are correlated with the zinc ion vacancies as suggested by Matsushita and Nakata[11] from their studies on the infrared absorption spectroscopy of a ZnO sample.

The authors gratefully acknowledge the informative discussion with Dr. Y. Fujita of this Laboratory.

8) G. Parravano, M. Boudart, *Advan. Catal.*, **7**, 53 (1955).
9) D. G. Thomas, *J. Phys. Chem. Solids*, **3**, 229 (1957).
10) A. Hausmann, *J. Phys. Soc. Japan*, **26**, 91 (1969).
11) S. Matsushita and T. Nakata, *J. Chem. Phys.*, **32**, 982 (1960).

BULLETIN OF THE CHEMICAL SOCIETY OF JAPAN VOL. 43 2381—2385 (1970)

Electrical and Optical Behaviour of Tetrathionaphthacene at High Pressures

Ichimin SHIROTANI, Kaoru KAWADA and Hiroo INOKUCHI

The Institute for Solid State Physics, The University of Tokyo, Roppongi, Minato-ku, Tokyo

(Received February 14, 1970)

The temperature dependence of the electrical resistance and the absorption spectra for tetrathionaphthacene (T.T.N.) have been studied at high pressure. It has been found that the intrinsic conduction level, which does not correspond to the observed optical transition, is located about 2 eV above the valence band. The red shift of absorption peaks with the pressure was much smaller than the contraction of the intrinsic band gap. The existence of the intrinsic conduction level is supported by the fact that the minimum of the photoemission yield arising from electron-pair production is located about 2 eV above the threshold point. The band gap of 0.4—0.62 eV previously observed seems to correspond to an acceptor level formed by chemical impurities.

Certain types of impurities and imperfections drastically affect the electrical properties of organic semiconductors. Adsorbed oxygen, as one kind of impurity, is known to modify strongly the semi- and photo-conduction of organic crystals.[1,2] For example, the semiconduction of the quaterrylene*1 film is especially sensitive to oxygen.[1] Under atmospheric circumstances, this compound is a p-type semiconductor due to an oxygen impurity level which lies 0.6 eV above the valence band. The intrinsic energy gap, observed under a high vacuum or at a high temperature, is 1.7 eV. The effect of the pressure on these energy gaps has already been studied.[3]

Tetrathionaphthacene (T.T.N.) has a low electrical resistivity, 10^4 Ωcm at room temperature. This observed value is very low when compared with others in the group of polycyclic aromatic semiconductors. Matsunaga has suggested that this anomalously low value is due to the presence of a small quantity of positive tetrathionaphthacene ions formed by oxidation with air.[4] However, no abrupt change in the electrical properties of this compound occurred when oxygen was adimitted to a sample stored in a high vacuum of 10^{-8} mmHg. Therefore, the effect of oxidation with air on the electrical resistivity may be disregard.[5] Though the activation energy and the electrical resistance of the microcrystals decrease with an increase in the pressure, these properties are not very sensitive to pres-

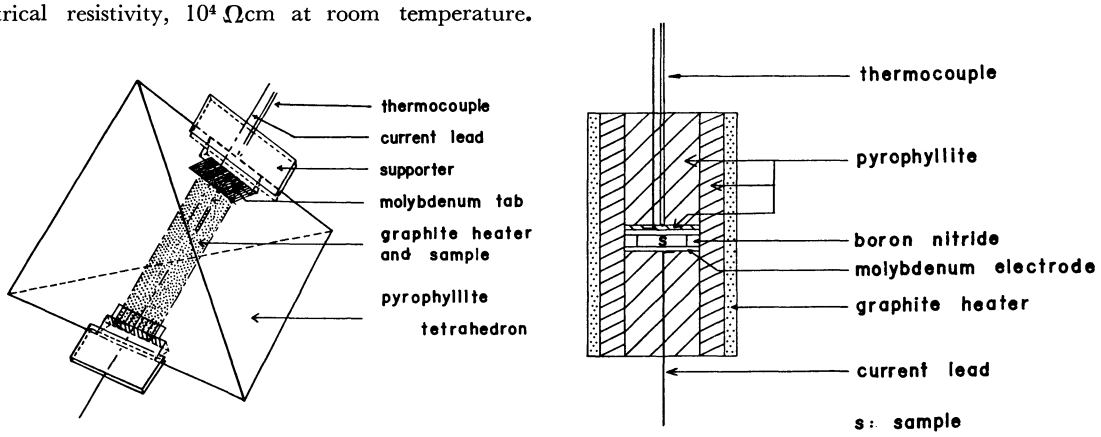

Fig. 1a, 1b. The sample assembly.

1) Y. Maruyama and H. Inokuchi, This Bulletin, **39**, 1418 (1966).

2) G. H. Heilmeier and S. E. Harrison, *Phys. Rev.*, **132**, 2010 (1963).

*1 Eleven-membered aromatic hydrocarbons, $C_{40}H_{20}$.

3) I. Shirotani, H. Inokuchi and S. Akimoto, This Bulletin, **40**, 2277 (1967).

4) Y. Matsunaga, *J. Chem. Phys.*, **42**, 2248 (1965).

5) H. Inokuchi, M. Kochi and Y. Harada, This Bulletin, **40**, 2695 (1967).

sure.[6] The anomalous electrical behaviour may arise from the chemical impurities. We have studied the temperature dependence of the electrical resistance of tetrathionaphthacene (T.T.N) at high pressures and have found the intrinsic energy gap, near 2 eV. In this report, the intrinsic conduction level of tetrathionaphthacene will be discussed.

Experimental

A tetrahedral anvil-type high-pressure apparatus similar to those described by Hall was used for this study. The present apparatus consisted of four 250-mm hydraulic rams, with 20-mm triangular tungsten carbide anvils, which were driven together simultaneously on a pyrophyllite-tetrahedron sample assembly with an edge length of 25 mm. Figures 1 (a) and 1(b) illustrate the sample assembly used for the electrical-resistance measurements. The temperature was measured with a chromel-alumel thermocouple. A tublar graphite furnace was placed nearly at the centre of gravity of the pyrophyllite-tetrahedron and was used for heating the sample. The electric power was supplied to the graphite furnace through molybdenum tabs which made contact with the faces of a pair of anvils. The sharp changes in the electrical resistances of Bi(I—II, 26 kbar),*2 Tl(II—III, 37 kbar), and Ba(I—II, 55 kbar) at their phase transitions were used to calibrate the pressure applied to the pyrophyllite-tetrahydron. The details of the high-pressure technique have already been reported.[7]

Tetrathionaphthacene ($C_{18}H_8S_4$) was provied by Matsunaga. This sulphur compound was purified by recrystallisation from trichlorobenzene and also by fractional sublimations (three times). The sample was studied as a powder which was fused into flat platelets by applied pressure.

The absorption spectra were measured by using a Shimazu SV-50A spectrophotometer. The thin tetrathionaphthacene film was grown on a glass plate by sublimation in a vacuum. The high-pressure optical cell has been described elsewhere.[3] A hydrostatic pressure up to 7 kbar was applied by means of a pressure-transmitting medium through a pressure-intensifier. The pressure was determined by a Harwood manganine resistance gauge and a Heise Bourdon tube gauge.

Results

Figure 2 shows the relation between the logaithm of the electrical resistance and the reciprocal temperature for the compressed tetrathionaphthacene at 30 kbar. For temperatures less than 340°C the impurity conduction was dominant. The temperature range of 340—400°C was the intrinsic conduction region. The sample seems to melt about 410°C. Above 430°C the electrical resistance of the compound increased slowly with an increase in the temperature; the chemical reaction must, then, occur. The behaviour of the curve was reproducible for temperatures below 400°C at high pressures.

Under 30 kbar the energy gap calculated from the temperature dependence of the conductivity over the temperature range of 300—613°K was 0.61 eV. This is assumed to be an extrinsic energy gap and is denoted as E_a. On the other hand, the energy gap from the temperature-conductivity relation, shown in Fig. 2, at 613—673°K was 1.62 eV at the same pressure. This energy gap, E_g, is considered of to be the intrinsic one. Figure 3 shows the plots of E_g and E_a as functions of the pressure. E_g decreased remarkably with an increase in the pressure. However, E_a was less affected by the pressure. If the relation between the energy gap and the applied pressure is assumed to be linear,*3 the extrapolated value of intrinsic gap at atmospheric pressure is about 2 eV. Table 1 shows the values of E_g and E_a at high pressures. From Fig. 3, we can find that the values of E_a and E_g decrease with an increase in the pressure at the rates of:

$$\left(\frac{dE_g}{dp}\right)_T \cong -15\times10^{-3} \quad \text{eV/kbar} \qquad (1)$$

and:

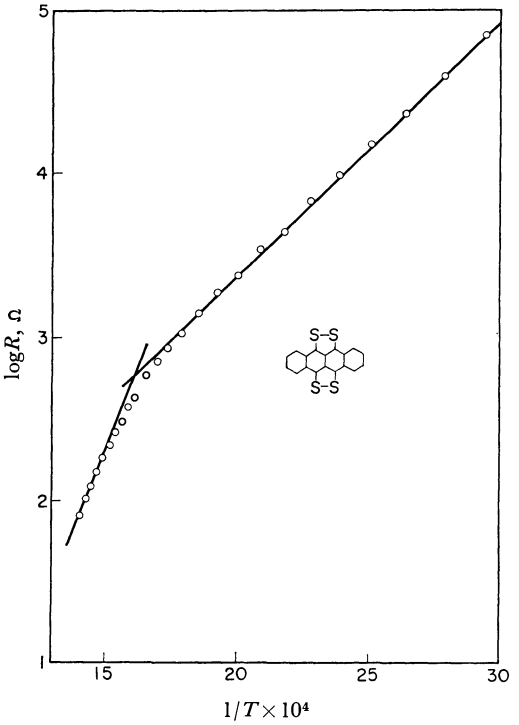

Fig. 2. The electrical resistance of tetrathionaphthacene as a function of temperature at 30 kbar.

6) I. Shirotani, H. Inokuchi and S. Minomura, *ibid.*, **39**, 386 (1966).

*2 The phase transition from Bi(I) to Bi(II) occurres at 26 kbar.

7) S. Akimoto and H. Fujisawa, *J. Geophys. Res.*, **70**, 443, 1969 (1965).

*3 For quaterrylene, E_g and E_a are proportional to the pressure, at least up to 50 kbar.

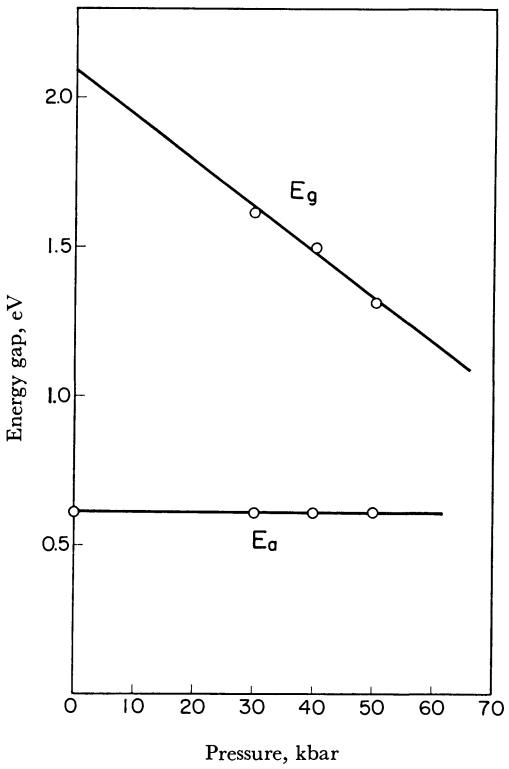

Fig. 3. The pressure dependence of the energy gaps.

$$\left(\frac{dE_a}{dp}\right)_T \cong 0 \qquad \text{eV/kbar} \qquad (2)$$

It is interesting to note that the pressure dependence of E_g is larger than that of E_a. Similar behaviour has already been found in the quaterrylene crystal.[3]

Figure 4 shows the pressure dependence of the electrical resistance at room temperature and at 360°C. The electrical resistance in the extrinsic region was insensitive to pressure, but the intrinsic resistance rapidly decreased with an increase in the pressure. These phenomena, as is shown in Fig. 3, are due to the pressure depencence of the energy gaps. Since the mobility of the charge carrier in the crystal is not so sensitive to applied pressure, the large increase in the conductivity at high pressures is mostly due to the great increment in the concentration of the charge carriers.[6]

Table 1. The pressure dependence of the thermal energy gaps of tetrathionaphthacene

Pressure (bar)	E_g (eV)	E_a (eV)
1	~2[a]	0.40—0.62[b]
30×10^3	1.62	0.61
40×10^3	1.50	0.61
50×10^3	1.32	0.61

a) extrapolated value from high pressure data.
b) Refs. 4 and 5.

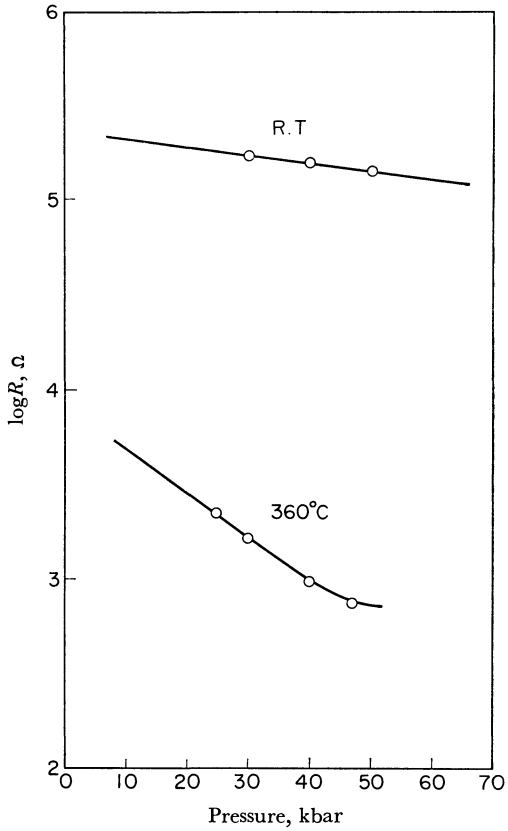

Fig. 4. The electrical resistivity of T.T.N. as a function of pressure at room temperature and at 360°C.

Figure 5 shows the electronic absorption spectra of the evaporated film and of the benzene solution of tetrathionaphthacene. The absorption band of film at 600—850 mμ may correspond to the 550—750 mμ peaks in the solution-state spectrum. Three absorption peaks of the film showed a red shift with

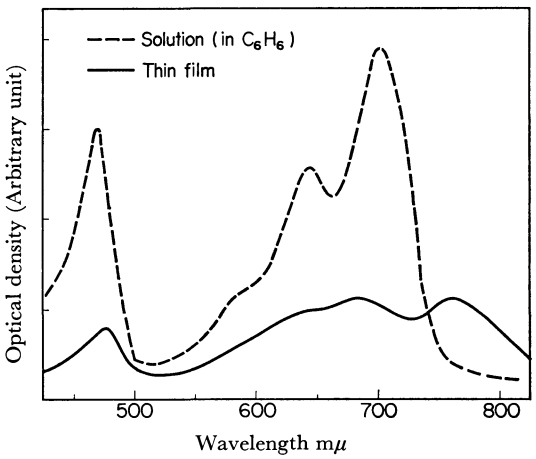

Fig. 5. The absorption spectra of T.T.N.
——— thin film ---- solution (in C_6H_6)

TABLE 2. THE RED SHIFT OF THE OPTICAL ABSORPTION PEAK FOR TETRATHIONAPHTHACENE AND NAPHTHACENE

Compound	Absorption peak mμ	Shift per unit of pressure 10^{-3} eV/kbar
Tetrathionapthacene	476	− 2.2
	680	− 2.6
	763	− 4
Naphthacene	471	− 9.4
	521	−13.4

an increase in the pressure. Table 2 illustrates the average rate of the red shift of the absorption spectra for T.T.N. and naphthacene. The values of the pressure shift for T.T.N. were much smaller than that of ordinary aromatic hydrocarbons.[8] The energy shift was approximately proportional to the applied pressure. The small red shift of T.T.N. should be noted.

Discussion

The pressure coefficient for the optical-energy gaps of such inorganic semiconductors as silicon and germanium agrees with the value determined by measuring the intrinsic resistivity as a function of the pressure.[9] In the case of the molecular crystal, similar behaviour has been observed in the absorption spectra of quaterrylene ($C_{40}H_{20}$); the rate of the red shift of the peak at 760 mμ which corresponds to the absorption peak in the solution-state spectrum, agrees approximately with that of the contraction of the thermal-energy gap. This behaviour may be useful in analyzing the mechanism of the carrier generation in quaterrylene crystal.[3]

The absorption peaks in the 575—700 mμ region observed in the benzene solution spectrum may be due to the lowest-singlet excitation of the tetrathionaphthacene molecule. The crystalline spectrum of T.T.N. corresponds to the spectrum of the free molecule, though a spectral red shift and broadening were observed. The 630, 680, and 760 mμ peaks in the film spectrum may form an exciton band arising from this lowest molecular excitation. As has been stated earlier, it was found, from the temperature dependence of the electrical resistance that the intrinsic energy gap was about 2 eV. This thermal-energy gap did not correspond with the absorption band of the T.T.N. evaporated film. As is shown in Eq. (1) and in Table 2, the red shift of the absorption peaks was very small compared with the contraction of the thermal-band gap. This suggests that the absorption band observed on evaporated film is the singlet-exciton state.

The photoconductance of anthracene crystals in the ultraviolet region (250—400 mμ) has also been investigated.[10,11] Castro and Hornig observed a peak in the photocurrent at 280 mμ which does not correspond to any known optical transition.[10] The magnitude of the 280 mμ electron photocurrent was relatively insensitive to the condition of the crystal surface. Therefore, they pointed out that the intrinsic conduction band is located in anthracene at about 4.4 eV. In the case of the tetrathionaphthacene crystal, the study of the photocurrent spectral-response curve was very difficult because of the large dark conductivity.[12] However, if the photocurrent curve can be investigated, the peak of the photoconductivity may be located near 2 eV.

The photoemission from polycyclic aromatic crystals in the vacuum ultraviolet region has also been studied.[13] Figure 6 shows the spectral distri-

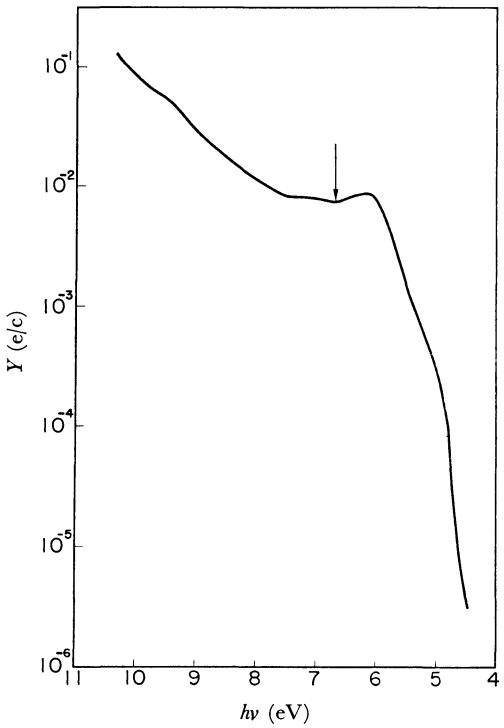

Fig. 6. Spectral distribution of the photoemission yield for T.T.N; arrow indicates the energy minimum produced from pair production scattering.

8) H. Ohigashi, I. Shirotani, H. Inokuchi and S. Minomura, *J. Chem. Phys.*, **43**, 314 (1965).

9) W. Paul and D. M. Warschauer, *J. Phys. Chem. Solids.*, **5**, 89 (1958).

10) G. Castro and J. F. Hornig, *J. Chem. Phys.*, **43**, 1459 (1965).

11) R. F. Chaiken and D. R. Kearns, *ibid.*, **45**, 3966 (1966).

12) M. Kochi, private communication.

13) Y. Harada and H. Inokuchi, This Bulletin, **39**, 1443 (1966); M. Kochi, Y. Harada and H. Inokuchi, *ibid.*, **40**, 531 (1967).

bution of the photoemission yield for T.T.N. The decrease in the yield has a minimum around 2 eV above the threshold of 4.55 eV. Kochi *et al.* have suggested[14] that this decrease in the photoemission yield arises from pair-production scattering*4 and that the threshold near 2 eV for the pair production for T.T.N. corresponds to the intrinsic-band gap. This experimental result supports the idea that the energy gap obtained from conductivity measurements under high pressure, above 2 eV, is an intrinsic one.

The inner heat of the sublimation of T.T.N. is about 36 kcal/mol. As is shown in Table 3, the sublimation energy for T.T.N. ($C_{18}S_4H_8$) and four aromatic hydrocarbons of 22 carbons is of the same order.[15] These results show that the cohesive energy of the sulphur compound is not much larger than that of aromatic hydrocarbons. The spectral red shift of the crystalline T.T.N. relative to the solution spectrum was quite small; further, the energy shift was not so sensitive to the pressure. In view of these points, the molecular interaction between T.T.N. seems to be weak. However, the electrical resistivity of this compound is quite low under atmospheric pressure. The anomalous electrical behaviour arises from the chemical impurities. Judging the photoemission data,[13] the band gap of 0.4—0.62 eV previously observed[4,5] seems to correspond to an acceptor level formed by the impurity.

Table 3. The heats of sublimation of tetrathionaphthacene and five aromatic hydrocardons

Compound	Molecular formulae	Molecular weight	ΔH kcal/mol
Benzo[*g,h,i*]perylene	$C_{22}H_{12}$	276	30.0[a]
3,4-Benztetraphene	$C_{22}H_{14}$	278	32.6[a]
1,2,5,6-Dibenzo-anthracene	$C_{22}H_{14}$	278	33.9[a]
Pentacene	$C_{22}H_{14}$	278	37.7[a]
Picene	$C_{22}H_{14}$	278	33.5[a]
Tetrathionaphthacene	$C_{18}H_8S_4$	352	36.1[b]

a) Ref. 15.
b) N. Wakayama, private communication.

The authors would like to thank Dr. M. Kochi for his useful discussions and Professor Y. Matsunaga for his gift of the chemical. Their thanks are also due to Professor S. Akimoto and Dr. M. Nishikawa for their valuable advice and kind assistance throughout this work.

14) M. Kochi, Y. Harada, T. Hirooka and H. Inokuchi, Technical Report of ISSP, Series A, No. 358 (1969).

*4 "Pair production" means the process in which the primary electron with energy E excites the second one with energy E_0 to conduction band and loses the minimum energy equal to the band gap, ΔE.

15) N. Wakayama and H. Inokuchi, This Bulletin, **40**, 2267 (1967).

BULLETIN OF THE CHEMICAL SOCIETY OF JAPAN VOL. 43 2386—2389 (1970)

Surface Properties of the System SiO_2-Al_2O_3 prepared by the Hydrolysis of Metal Alkoxides

Hiroyoshi MURAYAMA and Kenjiro MEGURO

Department of Applied Chemistry, Faculty of Science, Science University of Tokyo, Kagurazaka, Shinjuku-ku, Tokyo

(Received February 16, 1970)

The mixtures of aluminum *s*-butoxide and silicon ethoxide in different molar ratio were hydrolyzed in aqueous alcohol. The precipitates were dried, and the growth and transformation of the crystals at calcination were estimated by X-ray diffractometry. The surface properties of the oxide powder were studied by means of the heats of immersion and the adsorption of nitrogen, water vapor and ammonia. The samples calcined at 500°C have surface areas 260—600 m^2/g. Heats of immersion and surface hydrophilicity with respect to the composition, from pure silica gel to pure alumina, have a fairly good resemblance to each other, but this is not found between the heats of immersion and surface acidity.

In the preceding paper,[1] we reported surface properties of the system Al_2O_3-TiO_2 prepared by the co-hydrolysis of metal alkoxides under ion-free conditions. The study of surface properties of silica-aluminas is extremely important and interesting from a catalytic point of view.[2-5] However, few investigations have been reported on the surface properties of amorphous silica-aluminas[6-8] obtained from metal alkoxides.

In the present paper, an investigation of the surface properties of silica-aluminas produced by hydrolysis of silicon ethoxide and aluminum *s*-butoxide under ion-free conditions is reported.

Experimental

Materials. The products of hydrolysis of metal alkoxides are usually free from ionic impurities.[9-12] It is therefore advantageous to use the co-hydrolysis of aluminium *s*-butoxide and silicon ethoxide, purified by distillation, to obtain ion-free silica-aluminas. Excess aqueous ethanol was poured, with vigorous stirring, into the various mixtures of these alkoxides in *n*-butanol. Stirring was continued for 15 hr at a temperature near boiling point. The precipitate was separated by centrifuging, thoroughly washed with alcohol (by decantation) to remove undecomposed alkoxides, finely ground, and then dried at 100°C until the residual pressure of gas was less than 10^{-5} Torr. Hydrolysis of these alkoxides was confirmed by infrared analysis. The dried products were calcined for 2 hr at temperatures 100—1000°C, and the resulting samples were kept in a desiccator. The compositions of the samples determined by means of X-ray fluorescence were 0, 35.0, 64.0, 80.5, 89.6, and 100 in weight percent ratio $Al_2O_3/(Al_2O_3+SiO_2)$, respectively.

Apparatus and Procedure. The compositions of all the samples were determined by means of X-ray fluorometry with a Rigaku Denki X-ray vacuum spectrograph.[6] The analyser crystal was ethylenediamine ditartrate. The Cr-target was adjusted at 45 kV, 22 mA (for Al) and 45 kV, 12 mA (for Si). The X-ray radiation was detected by a proportional counter (90% Ar+10% CH_4) and discriminated as follows: for Al, base line 35/1000, channel width 100/100; for Si, base line 70/1000, channel width 100/100.

The differential thermal analysis curves were obtained with an automatically recording instrument, and the rate of heating was 10°C per minute. X-Ray diffraction patterns were obtained with a Geigerflex X-ray diffractometer of Rigaku Denki Co. The setting of the instrument was 35 kV, 15 mA for radiation on the target Cu$K\alpha$.

The calorimeter assembly for heats of immersion

1) H. Murayama, K. Kobayashi, M. Koishi and K. Meguro, *J. Colloid Interfac. Sci.*, **32**, 470 (1970).
2) M. W. Tamele, *Discuss. Faraday Soc.*, **8**, 270 (1950).
3) R. L. Richardson and S. W. Benson, *J. Phys. Chem.*, **61**, 405 (1957).
4) J. N. Finch and A. Clark, *ibid.*, **73**, 2234 (1969).
5) M. R. Basila, T. R. Kanter and K. H. Rhee, 145th ACS Meeting, New York, 1963, Abstr. Papers 26-I.
6) A. Léonard, S. Suzuki, J. J. Fripiat and C. De Kimpe, *J. Phys. Chem.*, **68**, 2608 (1964).
7) J. J. Fripiat, A. Léonard and J. B. Uytterhoeven, *ibid.*, **69**, 3274 (1965).
8) M. Sato, T. Kanbayashi, N. Kobayashi and Y. Shima, *J. Catal.*, **7**, 342 (1967).
9) S. J. Gregg and K. H. Wheatley, *J. Chem. Soc.*, **1955**, 3804.
10) J. F. Goodman and S. J. Gregg, *ibid.*, **1960**, 1162.
11) M. R. Harris and G. Whitaker, *J. Appl. Chem.*, **12**, 490 (1962).
12) G. C. Bye, J. G. Robinson and K. S. W. Sing, *ibid.*, **17**, 138 (1967).
13) K. Meguro, M. Koishi, M. Aizawa, N. Uchino, K. Matsumoto, H. Kimoto, Y. Kumaki and H. Sawai, *Kogyo Kagaku Zasshi*, **69**, 1724 (1964).

measurement and the experimental techniques used were the same as previously described.[13] The calorimeter was the isoperibol type equipped with a thermistor temperature sensing element. All measurements were carried out at 25±0.1°C in water with samples evacuated at 100°C for 1 hr at 10^{-5} Torr before immersion.

Adsorption isotherms were determined at −195°C, 25°C and 260°C for nitrogen, water vapor, and ammonia, respectively, by using a conventional volumetric gas adsorption apparatus. For the water vapor adsorption the apparatus was maintained at 25±0.5°C in air thermostat. Each sample for water vapor adsorption was outgassed at 100°C for 1 hr at 10^{-5} Torr to remove physically adsorbed water and cooled to 25°C prior to the adsorption studies.

Results and Discussion

(i) Bulk Properties. The typical experimental results of X-ray analysis on the samples treated at different temperatures and the differential thermal analysis curve of the 0% ($Al_2O_3/Al_2O_3+SiO_2$) sample, that is pure silica gel, are illustrated in Fig. 1. The pure alumina, 100% ($Al_2O_3/Al_2O_3+SiO_2$) sample, is the same sample used in the previous study.[1] X-ray diffraction patterns of the 100% Al_2O_3 sample heated at 500°C for 2 hr possess only very few faint lines of γ-Al_2O_3. On the other hand, all other samples calcined for 2 hr at 500, 600, 700, and 800°C are amorphous to X-ray, as can be seen from the results given in Fig. 1.

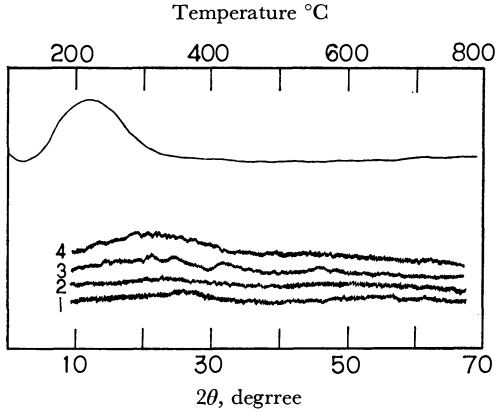

Fig. 1. X-Ray diffraction patterns at different temperatures (1: 100°C, 2: 500°C, 3: 800°C, 4: 1000°C) and differential thermal analysis curve of 0% ($Al_2O_3/Al_2O_3+SiO_2$) sample, that is pure silica gel.

Pure silica gel, 0% ($Al_2O_3/Al_2O_3+SiO_2$) sample, gives a differential thermal analysis curve which is characterized by the presence of a broad exothermic peak between 150—300°C, and a small endothermic peak at 120°C (Fig. 1). The first peak results from the loss of physically adsorbed water, and the last exothermic peak is attributed to the oxidation of chemically adsorbed butanol. The differential thermal analysis curves of other silica-alumina samples studied shows analogous features.

Changes of the surface properties of the system Al_2O_3-SiO_2 with composition were confirmed on these samples calcined at 500°C for 2 hr. Samples calcined below 500°C retain residues of butanol

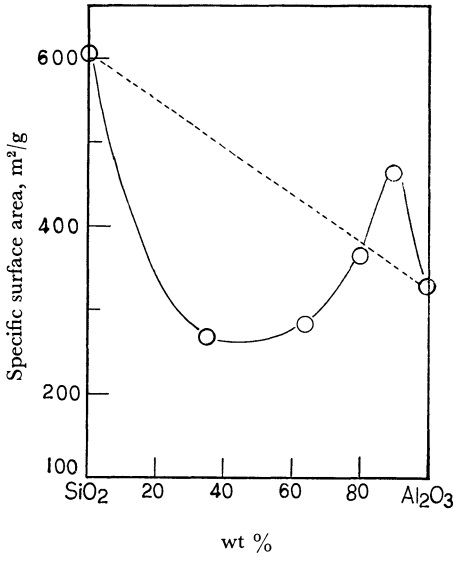

Fig. 2. Variation of specific surface areas of the system Al_2O_3-SiO_2 calcined at 500°C with composition. Dotted line is theoretical one under the assumption of additivity.

Table 1. Surface properties of the system Al_2O_3-SiO_2 prepared from alkoxides followed by heating at 500°C for 2 hr

Sample composition, % ($Al_2O_3/Al_2O_3+SiO_2$)	X-Ray analysis	S_{N_2} m²/g	S_{H_2O} m²/g	$S_{H_2O}/S_{N_2}\times 100$	ΔH_i ergs/cm²	Amounts of NH_3 adsorbed cc/m²
100	broad γ-Al_2O_3	324	140	43	423	0.0185
89.6	amorphous	464	207	45	454	0.0259
80.5	amorphous	367	236	64	498	0.0327
64.0	amorphous	279	136	49	351	0.0348
35.0	amorphous	263	89.5	34	263	0.0424
0	amorphous	600	81.3	14	119	0.0009

14) F. H. Healey, J. J. Chessick and A. V. Fraioli, *J. Phys. Chem.*, **60**, 1001 (1956).

and water, and it is only above 500°C that the structures begin to show their crystalline nature.

(ii) Specific Surface Area. Specific surface areas have been determined by standard B.E.T. procedure, using 10.8 and 16.2 Å² for the molecular cross-sectional areas of water vapor and nitrogen, respectively.[14] Specific surface areas estimated from nitrogen and water vapor adsorption are given in Table 1. The variation of the specific surface area of the system Al_2O_3-SiO_2 with composition is represented in Fig. 2, in which the surface area is plotted as a function of Al_2O_3 contents (wt%) determined by X-ray fluorometry. The dotted line in Fig. 2 shows the theoretical specific surface areas of mixtures calculated under the assumption of additivity of surface area. The surface areas observed deviate from this theoretical line. The rise of Al_2O_3 contents decreases the specific surface area to a broad minimum of about 263 m²/g obtained in the case of the 35.0% ($Al_2O_3/Al_2O_3+SiO_2$) sample, above which a slow increase in area occurs with further rise of Al_2O_3 content. The maximum in the specific surface area of silica-alumina is obtained in the case of 89.6% ($Al_2O_3/Al_2O_3+SiO_2$) sample.

Inspection of columns 3 and 4 of Table 1 reveals that the surface areas calculated from nitrogen adsorption are considerably higher than those calculated from the water vapor isotherms.

(iii) Surface Hydrophilicity and Heat of Immersion. Water vapor adsorption data were plotted as isotherms from which the monolayer capacity, V_m, was calculated by the B.E.T. method. The surface area, S_{H_2O} (m²/g), was calculated from V_m, taking the molecular area of water vapor at 25°C as 10.8 Å². The results are given in column 4 of Table 1.

Healey *et al.*[15,16] have shown that surface hydrophilicity is represented as the ratio of total surface area to hydrophilic surface area. Thus it follows that

$$\text{Surface hydrophility}(\%) = S_{H_2O}/S_{N_2} \times 100,$$

where S_{H_2O} and S_{N_2} denote the specific surface areas as based on water vapor and nitrogen adsorption, respectively. The variation of the surface hydrophilicities of the system of Al_2O_3-SiO_2 with composition is listed in Table 1 and illustrated in Fig. 3, in which the hydrophilicities are plotted as a function of Al_2O_3 contents (wt%).

The data of heats of immersion of the system SiO_2-Al_2O_3 are shown in column 6 of Table 1. The variation in heats of immersion is represented in Fig. 3, in which the heats are plotted as a function of Al_2O_3 contents (wt%).

The dotted line in Fig. 3 shows the theoretical heats calculated under the assumption of additivity. The heats observed deviate from this theoretical line, and the rise of Al_2O_3 contents increase the heats to a maximum of about 500 erg/cm² obtained in the case of the 80.5% ($Al_2O_3/Al_2O_3+SiO_2$) sample.

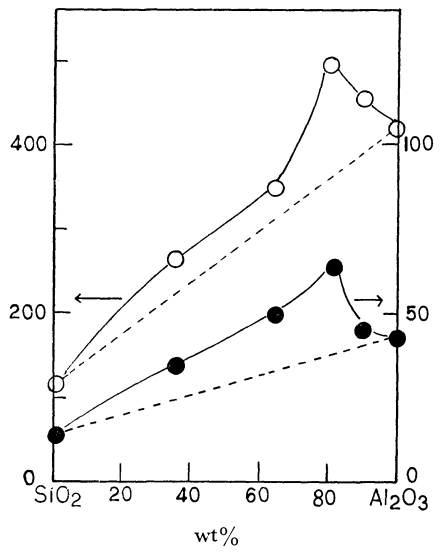

Fig. 3. Variation of surface hydrophilicities and heats of immersion of the system Al_2O_3-SiO_2 with composition.
●----Surface hydrophilicity (S_{H_2O}/S_{N_2} X 100, percent).
○----Heat of immersion (erg per square centimeter).
Dotted lines are theoretical ones under the assumption of additivity.

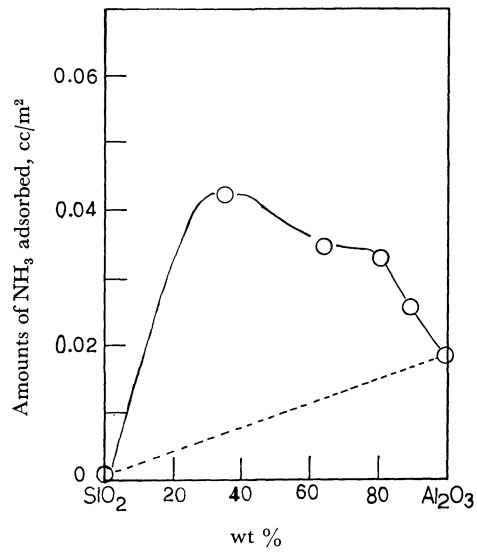

Fig. 4. Variation of amounts of ammonia adsorbed of the system Al_2O_3-SiO_2 calcined at 500°C with composition.
Dotted line is theoretical one under the assumption of additivity.

15) F. H. Healey, Y. F. Yu and J. J. Chessick, *J. Phys. Chem.*, **59**, 399 (1955).
16) A. C. Zettlemoyer, *Official Dig.*, **29**, 1238 (1957).

It is interesting to note that this tendency of the surface hydrophilicity coincides with that of heats of immersion. This strongly suggests a relationship between the magnitude of the heats of immersion and the concentration of hydroxyl sites on the surface, as pointed out by Young and Bursh,[17] and Zettlemoyer *et al.*[18]

(iv) Surface Acidity. The surface acidtiy of the system Al_2O_3-SiO_2 was determined by the chemisorption of basic gas (ammonia) at high temperature and low pressure. Ammonia adsorption isotherms at 260°C, where the highest equilibrium pressure was about 15 Torr, were determined[1] on all the samples studied after outgassing at 260°C for 1 hr at 10^{-5} Torr. The shape of the isotherms of all the samples studied is Langmuir's type. The amounts adsorbed at saturation per unit surface area calculated by the Langmuir equation are listed in Table 1 and illustrated in Fig. 4, in which the amounts of ammonia adsorbed are plotted as a function of Al_2O_3 contents. The rise of Al_2O_3 contents increases the amount of ammonia adsorbed to a maximum of about 0.04 cc/m² obtained in the case of the 35.0% ($Al_2O_3/Al_2O_3+SiO_2$) sample, above which a decrease in the amount of ammonia adsorbed occurs with further rise of Al_2O_3 contents.

From the fact[19] that silica gel does not behave as an acid-catalyst in the catalytic reaction such as propylene polymerization, it is reasonable to consider that its acidity is zero. The experiment on the ammonia adsorption at 260°C in the case of the 0% ($Al_2O_3/Al_2O_3+SiO_2$) sample gives near zero value (0.0009 cc, at S.T.P./m²) for its acidity, as indicated in Table 1.

17) G. J. Young and T. P. Bursh, *J. Colloid Sci.*, **15**, 361 (1960).

18) A. C. Zettlemoyer, R. D. Iyengar and P. Scheidt, *J. Colloid Interfac. Sci.*, **22**, 172 (1966).

19) S. E. Tung and E. Mcininch, *J. Catal.*, **3**, 229 (1964).

BULLETIN OF THE CHEMICAL SOCIETY OF JAPAN VOL. 43 2389—2394 (1970)

The Reactions of Propylene-1,3,3,3-d_4 Photosenitized by $Hg(^3P_1)$, $Cd(^3P_1)$, and Benzene-h_6 and -d_6

Shun-ichi HIROKAMI and Shin SATO

Department of Applied Physics, Tokyo Institute of Technology, Ookayama, Meguro-ku, Tokyo

(Received February 19, 1970)

A comparative study has been made of the reactions of *cis*- and *trans*-propylene-1,3,3,3-d_4 photosensitized by benzene-h_6 and -d_6 and by $Hg(^3P_1)$ at room temperature and by $Cd(^3P_1)$ at 275°C. The main reaction observed in every photosensitization was a *cis-trans* isomerization; no isomerization to propylene-2,3,3,3-d_4 was observed under the conditions employed. This is in marked contrast to the isomerization of ethylene-d_2. The ratio of *cis*- to *trans*-propylene-1,3,3,3-d_4 after prolonged irradiation was unity. The decomposition observed in the mercury photosensitization was also studied in detail; its quantum yield was less than one-tenth that of the *cis-trans* isomerization. The material balance between the decrease in the reactant and the amount of the products was well preserved, but the energy balance between the absorbed photons and the quantum yield of products was not preserved at pressures below 150 Torr. A possible mechanism is discussed.

cis- or *trans*-Dideuteroethylene, when photosensitized by benzene or $Cd(^3P_1)$, undergoes two types of reactions: (i) *cis-trans* isomerization, and (ii) hydrogen-atom scrambling, *i. e.*, the formation of 1,1-dideuteroethylene.[1-3] Since the π electronic structure of propylene is similar to that of ethylene, it seemed interesting to study whether or not propylene undergoes reactions similar to those of ethylene.

On the other hand, in the study of the reaction of 2-butene photosensitized by $Hg(^3P_1)$ we have found that the balance between the absorbed quanta and the sum of the quantum yields of products is not preserved at pressures below 150 Torr.[4] In

1) T. Terao, S. Hirokami, S. Sato and R. J. Cvetanović, *Can. J. Chem.*, **44**, 2173 (1966).

2) S. Hirokami and S. Sato, *ibid.*, **45**, 3181 (1967).

3) S. Tsunashima, S. Hirokami and S. Sato, *ibid.*, **46**, 995 (1968).

4) S. Tsunashima and S. Sato, This Bulletin, **41**, 284 (1968).

other words, a part of the energy absorbed by mercury atoms does not seem to contribute to the chemical reactions occurring in the system over a wide range of pressure. We tentatively explained this observation in terms of the formation of vibrationally-excited states of the reactant.

With these prospects in mind, a study of the reactions of partially-deuterated propylene-1,3,3,3-d_4, was made by using mercury and cadmium atoms and benzene-h_6 and -d_6 as the photosensitizers.

Experimental

trans- and *cis*-Propylene-1,3,3,3-d_4 were synthesized from methylacetylene-d_4 by a method previously described.[5] Methylacetylene-d_4 was obtained by means of a reaction between magnesium carbide and heavy water.[6] Methylacetylene was separated from other compounds by gas chromatography using a column packed with dimethylsulforane-on-celite. The mass-spectrometric analysis showed the isotopic impurities in the synthesized methylacetylene-d_4 to amount of less than 5%. Research-grade *cis*-2-butene and propylene-h_6 supplied by the Takachiho Trading Co. were used after bulb-to-bulb distillations. According to the gas-chromatographic analysis, the impurities in *cis*-2-butene amounted to less than 0.5%, and those in propylene, to less than 0.1%. Benzene-h_6 and -d_6 were both of a spectrograde; they were supplied by the Merck Co. The mass-spectrometric analysis of benzene-d_6 showed that the isotopic impurities amounted to less than 2%.

The light sources and the apparatus used were similar to those reported on in previous papers. The reaction vessels used for the mercury photosensitization had volumes of 52.3 m*l* (a), 25.4 m*l* (b), and 9.4 m*l* (c).

The isomerization products were analyzed with a Perkin-Elmer 125 double-beam grating infrared spectrometer. The absorption peak at 983 cm^{-1} was assigned to *trans*-, the peak at 785 cm^{-1}, to *cis*-propylene-1,3,3,3-d_4, and the peak at 912 cm^{-1}, to propylene-2,3,3,3-d_4.*1

In the mercury photosensitization, various products were obtained. They were analyzed as follows. After each run, the reaction products were transferred into a trap at the temperature of liquid nitrogen and non-condensables were collected in a gas buret by means of a Toepler pump. After the amount had been measured, the gas was analyzed by means of a mass-spectrometer. For the condensed part, a cold trap at −120°C was used to separate the reaction products from the reactant, propylene. The amount of propylene remaining was measured volumetrically, and the products condensed at −120°C were identified and measured with a gas chromatograph equipped with dimethylsulpholane (10 m long), dioctylphthalate columns (2 m long), and a flame-ionization detector.

The light intensity absorbed by benzene-h_6 and -d_6 was estimated by using the benzene-h_6 or -d_6-photosensitized *cis-trans* isomerization of *cis*-2-butene.[7] In the mercury photosensitization, the light intensity of the 2537 Å resonance line used for the reaction was estimated from the amount of hydrogen produced in the mercury-photosensitized decomposition of ethylene at 45 Torr, assuming the quantum yield to be 0.203.[8] The absorbed light intensity of the cadmium-resonance line at 3261 Å was estimated by using the cadmium-photosensitized *cis-trans* isomerization of *cis*-2-butene.[4]

Results

Photosensitizations by Benzene-h_6 and -d_6. By the photosensitization of benzene-h_6 or -d_6, the *cis-trans* isomerization of propylene-1,3,3,3-d_4 was observed to occur, but neither decomposition nor isomerization to propylene-2,3,3,3-d_4 was observed. Table 1 summarizes the results. After prolonged irradiation, a 1 : 1 ratio of *cis*- to *trans*-propylene-1,3,3,3-d_4 was obtained, but not even a trace of

Table 1. Isomerization of *cis*-propylene-1,3,3,3-d_4 photosensitized by benzene-h_6 and -d_6

Benzene Torr	Propylene Torr	Benzene triplet* μ mol	Products % *cis*	Products % *trans*
		Benzene-h_6		
0.22	0.40	109	49.3	50.7
0.50	0.55	11.6	86.1	13.9
0.50	0.74	13.9	87.2	12.9
0.50	0.97	21.8	85.2	14.8
0.50	1.75	43.6	82.3	17.7
0.50	5.13	11.2	85.4	14.6
0.50	6.19	11.2	87.6	12.4
0.50	8.01	11.2	88.5	11.5
3.8	6.08	12.3	85.3	14.7
3.8	8.58	16.8	84.9	15.1
3.8	14.5	39.8	79.8	20.1
		Benzene-d_6		
0.22	0.40	79.8	50.0	50.0
0.50	0.55	15.4	82.3	17.7
0.50	0.74	17.4	83.5	16.5
0.50	0.97	26.1	79.3	20.7
0.50	1.73	44.4	77.8	22.2
0.50	4.07	8.74	82.9	17.1
0.50	4.92	9.90	85.2	14.8
0.50	6.19	9.53	88.0	12.0
0.50	7.74	9.67	89.2	10.8

* Estimated by the isomerization of *cis*-2-butene. This value is related to the amount of photons absorbed by benzene as follows: [Benzene triplet]=[Photons absorbed]$\times\phi_T$. ϕ_T is the quantum yield of benzene triplet.[7,10]

5) B. S. Rabinovitch and F. S. Looney, *J. Amer. Chem. Soc.*, **75**, 2652 (1953).

6) Y. Hatano, S. Shida and S. Sato, This Bulletin, **41**, 1120 (1968).

*1 The infrared absorption spectrum of this compound was kindly supplied by the Byron Trading Co.

7) W. A. Noyes, Jr. and D. A. Harter, *J. Chem. Phys.*, **46**, 674 (1967).

8) B. DeB. Darwent, *ibid.*, **19**, 258 (1951).

propylene-2,3,3,3-d_4 was observed. The quantum yield of the formation of propylene-2,3,3,3-d_4 must be less than one-thousandth at the pressures employed, if it occurs at all.

Cadmium Photosensitization. The products obtained in the reaction of propylene-1,3,3,3-d_4 photosensitized by cadmium were *cis-trans* isomers, plus small amounts of propane and probably C_6-hydrocarbons, whose elution times on a gas chromatograph were almost equal to those of C_6 hydrocarbons. After prolonged irradiation (72 μEinstein, the pressure of the reactant being 23 Torr), equal amounts of *cis-* and *trans*-propylenes were obtained, but propylene-2,3,3,3-d_4 was again not observed.

Mercury Photosensitization. Mercury-photosentitized reactions were studied with *cis*-propylene-1,3,3,3-d_4 and propylene-h_6. Even in the mercury photosensitization, the formation of propylene-2,3,3,3-d_4 could not be observed. Table 2 summarizes the mol% of *trans-* and *cis*-propylene-d_4 observed after the mercury-photosensitized reaction.

In this photosensitization, the decomposition process cannot be ignored. Table 3 shows the pressure dependence of the quantum yields of the decomposition products observed when propylene-h_6 and *cis*-propylene-d_4 were used as the reactants. Obviously, at pressures above 20 Torr the decomposition products consist mainly of C_6-hydrocarbons. In order to check the material balance, the amount of propylene-h_6 consumed in the mercury photosensitization was measured over a wide range of pressures. The results are shown in Fig. 1, which also includes the plots of the quantum yields of the C_6-hydrocarbons and non-condensable gas formed. Obviously, the quantum yield of the consumption of propylene is about twice that of the formation of C_6-hydrocarbons.

Table 2. $Hg(^3P_1)$ photosensitized *cis-trans* isomerization of *cis*-propylene-1,3,3,3-d_4

cis-Propylene Torr	Photons absorbed μEinstein	$C_3H_2D_4$ % *trans*	*cis*	Reaction cell
48.1	97.3	50.4	49.6	c
100.9	94.2	39.9	60.1	c
103.2	64.4	30.8	69.2	c
8.9	17.4	13.4	86.6	a
10.5	4.4	2.6	97.4	a
11.0	17.4	12.4	87.6	a
12.6	4.4	2.8	97.2	a
12.7	17.4	10.8	89.2	a
13.9	17.4	11.2	88.8	a
14.1	4.4	2.4	97.6	a
15.5	4.4	2.6	97.4	a
16.4	17.4	10.2	89.8	a
17.4	4.4	2.5	97.5	a
18.1	17.4	9.1	90.9	a
25.3	18.2	13.9	86.1	b
29.3	19.6	13.9	86.1	b
33.1	19.6	12.4	87.6	b
36.3	19.8	10.9	89.1	b
45.7	39.1	19.0	81.0	b
53.4	36.3	14.5	85.5	b
68.6	43.0	17.1	82.9	b
74.0	39.6	12.6	87.4	b
98.5	21.4	15.3	84.7	c
142.8	37.4	18.0	82.0	c
178.2	43.9	17.3	82.7	c
200.8	42.8	16.8	83.2	c
229.1	46.0	16.1	83.9	c

In order to discuss the energy balance between the absorbed quanta and the quantum yields of the products, the C_6-hydrocarbons from the re-

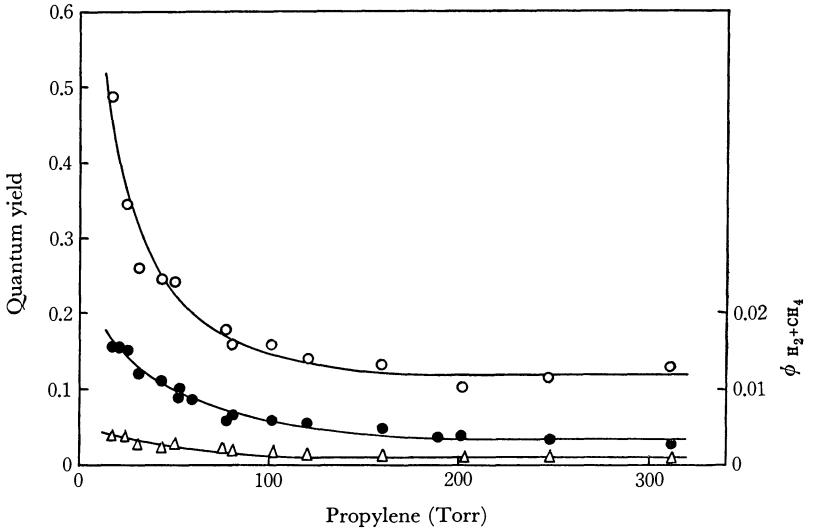

Fig. 1. Pressure dependence of the quantum yields of C_6-hydrocarbons (●), non-condensable gas (△) and propylene-h_6 consumed (○).

Table 3. Pressure dependence of quantum yields of products in the mercury photosensitization

	C_3H_6			$C_3H_2D_4$	
Reactant pressure (Torr)	21.0	53.0	80.2	19.3	82.0
Quantum Yields $\times 10^3$					
Hydrogen and Methane	7.1	4.9	3.0	—	—
Ethane and Ethylene	13.0	7.3	3.7	3.0	0.6
Propane	19.8	11.7	8.6	2.6	1.3
Acetylene	6.7	4.3	1.3	4.0	0.9
Butene-1	9.3	5.7	2.6	1.8	0.5
2,3-Dimethylbutane	26.1	16.0	10.6	5.0	2.4
4-Methylpentene-1	83.4	52.0	28.7	15.1	7.2
Hexene-1	4.8	3.2	3.2	0.7	0.5
1,5-Hexadiene	41.6	29.0	19.8	6.9	3.4
Material Balance $\phi(\Delta$ propylene$) \times 10^3$					
Calculated from					
Products	357	228	137		
Observed	380	240	160		

Table 4. Quantum yield of C_6-hydrocarbons produced in the mercury photosensitized decompostion of *cis*-propylene-d_4

Propylene Torr	Photons absorbed μEinstein	Quantum yield $\phi(C_6) \times 10^2$	Reaction cell
10.3	6.27	4.7	b
15.2	12.5	3.8	b
19.3	6.6	2.8	c
27.2	18.8	1.9	b
29.2	5.9	2.5	c
50.9	10.4	1.4	c
51.5	25.1	1.6	b
76.4	14.8	1.4	c
82.0	15.8	1.4	c
100.9	20.0	1.3	c
141.4	21.6	0.9	c
198.4	38.5	0.8	c

action of *cis*-propylene-d_4 were also measure. The results are listed in Table 4. The pressure dependence of the quantum yield is very similar to that obtained with propylene-h_6 in Fig. 1. However, the absolute value is about a quarter that obtained with propylene-h_6. This is probably due to the isotope effect in the initial process of the mercury-photosensitized reaction.

Discussion

Isomerization of Propylene-1,3,3,3-d_4. The *cis-trans* isomerization of *cis*-propylene-d_4 may be visualized as follows:

$$cis\text{-}CD_3CH{=}CDH + S^* \longrightarrow P^* + S$$
$$P^* + M \longrightarrow 1/2\ trans + 1/2\ cis + M$$

Here, S and S* represent the ground state and the excited triplet state of a photosensitizer respectively. P* is an excited state of propylene, probably the lowest triplet. M is the third body for the stabilization. In the case of *cis*-ethylene-d_2, the state corresponding to P* further isomerizes to the second excited state, which is a precursor of 1,1-dideuteroethylene, but in the present case this process is ignored because the formation of propylene-2,3,3,3-d_4 was not observed in any photosensitized reaction performed. To estimate the initial quantum yield of the isomerization, the following equation has to be applied to the data because the reverse reaction from *trans*- to *cis*-isomer is always included in a finite conversion:

$$\phi_{iso} = \frac{[C]+[T]}{2It} \ln \frac{[C]+[T]}{[C]-[T]} \qquad (I)$$

The derivation of this equation has already been shown in a previous paper.[9] Here, ϕ_{iso} is the initial quantum yield of isomerization. It is the light quanta absorbed by a photosensitizer, and the brackets show the concentrations of *cis*- and *trans*-isomers after the reaction. Thus, the relative quantum yields of isomerizations photosensitized by benzene-h_6 and -d_6 are calculated to be as is shown in Fig. 2. Although the data are scattered,

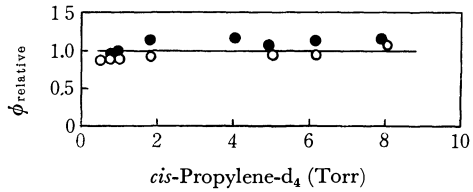

Fig. 2. Relative quantum yield of *cis-trans* isomerization of propylene-1,3,3,3-d_4 photosensitized by benzene-h_6 (○) and benzene-d_6 (●).

it may be said that the quantum yield of the *cis-trans* isomerization of *cis*-propylene-d_4 is independent of the pressure of the reactant above a few Torr. This trend has previously been observed in the isomerization of 2-butenes.[10]

As has been stated in the previous section, the formation of propylene-2,3,3,3-d_4 was not observed in any photosensitization, while this type of isomerization is important in the reaction of ethylene-d_2. The reason for this discrepancy is not clear, but a speculation may be offered. If the hydrogen-atom scrambling observed in the reaction of ethylene occurs through the formation of a structurally-symmetric intermediate such as

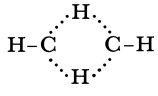

,

9) S. Tsunashima and S. Sato, This Bulletin, **42**, 329 (1969).

10) M. Tanaka, K. Kato and S. Sato, *ibid.*, **39**, 1423 (1966).

then the substitution of a methyl radical for a hydrogen atom may disturb the formation of this type of intermediate. This structure for the hydrogen-atom scrambling state was suggested by Whalley years ago,[11] but it obviously needs more deliberate theoretical consideration.

Decomposition of Propylene. An appreciable decomposition of propylene was observed only in the mercury photosensitization. The reaction mechanism has already been discussed by many investigators.[12–15] When propylene-1,3,3,3-d_4 is the reactant, the mechanism may be described as follows:

$$CD_3CH{=}CDH^* \longrightarrow D + \dot{C}D_2CH{=}CDH \quad (1)$$

$$\searrow \dot{C}D_3 + \dot{C}H{=}CDH \quad (2)$$

$$CD_3CH{=}CDH^* + M \longrightarrow 1/2\ trans + 1/2\ cis \quad (3)$$

Here, $CD_3CH{=}CDH^*$ is the excited state of the propylene produced by the mercury photosensitization. This is probably the lowest triplet state. Reference to Tables 2 and 3 makes it obvious that the process (3) is the most important at pressures higher than 10 Torr and that the process (1) is preferable the process (2), since many more C_3 and C_6 hydrocarbons than C_1, C_2 and C_4 hydrocarbons are produced. In order to estimate the quantum yields of the decomposition processes, the material balance between the consumed reactant and the observed products has to be checked. This calculation has been made regarding carbon atoms. The results are included in Table 3. Obviously, the material balance obtained is not too bad in any of the runs examined.

The formation of C_6 hydrocarbons may be described as follows (here, propylene-h_6 is used as the reactant to avoid complexity):

$$C_3H_6^* \longrightarrow H + C_3H_5 \quad (1)$$

$$H + C_3H_6 \longrightarrow C_3H_7\ (\text{mainly } CH_3\dot{C}HCH_3) \quad (4)$$

$$2C_3H_7 \longrightarrow \text{2,3-dimethyl butane} \quad (5)$$

$$\searrow C_3H_8 + C_3H_6 \quad (6)$$

$$C_3H_7 + C_3H_5 \longrightarrow \text{4-methyl pentene-1} \quad (7)$$

$$\searrow 2C_3H_6 \quad (8)$$

$$2C_3H_5 \longrightarrow \text{1,5-hexadiene} \quad (9)$$

A small amount of 1-hexene may be formed in the reaction between C_3H_5 and $CH_3CH_2CH_2$. The formation of this radical is in competition with that of the isopropyl radical in the reaction (4). The formation of 1-butene may result from the reaction of C_3H_5 with the CH_3 produced in the reaction (2). If the mechanism is correct so far, the quantum yield of the reaction (1) may be calculated by the following relations:

$$\phi_{C\text{-}H} = (C_3H_5) = \phi(C_6H_{12}) + 2\phi(C_6H_{10}) + \phi(C_4H_8) \quad (II)$$

$$\phi_{C\text{-}H} = (C_3H_7) = \phi(C_6H_{12}) + 2\phi(C_6H_{14}) + 2\phi(C_3H_8) \quad (III)$$

Here, the contribution of the reaction (8) is ignored. The quantum yield of this reaction may be comparable to that of the reaction (7). The values calculated by the relations (II) and (III), therefore, are meaningful only in their order. The calculated values are summarized in Table 5, which obviously shows a strong isotope effect on the rupture of the C–H bond. The estimation of the quantum yield of the reaction (2) may be similar but the calculation was not carried out because a large experimental error was expected.

Table 5. Estimation of the quantum yield of carbon-hydrogen bond rupture

Reactant pressure (Torr)	Propylene-h_6			Propylene-d_4	
	21.0	53.0	80.2	19.3	82.0
$\phi_{C\text{-}H}$ or $\phi_{C\text{-}D}$ (II)*	0.18	0.12	0.07	0.03	0.015
(III)*	0.18	0.11	0.07	0.03	0.015

* Calculated by Eqs. (II) and (III).

Energy Balance in the Mercury Photosensitization. It was found in the mercury-photosensitized decomposition of propylene-h_6 that the amount of the reactant consumed was almost consistent with that of the products observed, and that a large part of the products were C_6-hydrocarbons. In the case of *cis*-propylene-1,3,3,3-d_4, we could not measure the amount of the reactant consumed because the amount of the reactant itself was small

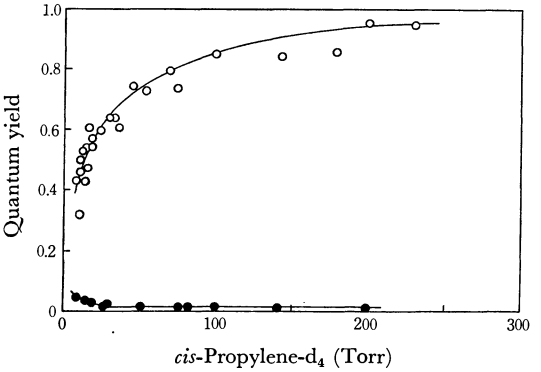

Fig. 3. Pressure dependence of the quantum yields of isomerization (○, $2\phi_{iso}$) and C_6-hydrocarbons (●, ϕ_{C_6}).

11) E. Whalley, *Can. J. Chem.*, **35**, 565 (1957).
12) H. E. Gunning and E. W. R. Steacie, *J. Chem. Phys.*, **14**, 57 (1946).
13) F. P. Lossing, D. G. H. Marden and J. B. Farmer, *Can. J. Chem.*, **34**, 701 (1956).
14) M. Avrahami and P. Kebarle, *J. Phys. Chem.*, **67**, 354 (1963).
15) C. A. Heller and A. S. Gordon, *J. Chem. Phys.*, **42**, 1262 (1965).

and we had to avoid a high conversion in order to estimate the quantum yield of isomerization. However, judging from the results obtained with propylene-h_6, the C_6-hydrocarbons obtained with *cis*-propylene-d_4 may form the main part of the decomposition products. Figure 3 shows the quantum yields of the *cis-trans* isomerization and of the formation of C_6-hydrocarbons in the reaction of *cis*-propylene-1,3,3,3-d_4 photosensitized by mercury. The quantum yield of the *cis-trans* isomerization was calculated by applying Eq. (I) to the data in Table 2. If all the photons absorbed by mercury atoms contribute to the reaction of the *cis-trans* isomerization or decomposition, the sum of the two quantum yields in Fig. 3 should be nearly equal to unity at any reactant pressure. Obviously, the sum deviates from unity with a decrease in the pressure of the reactant and approaches 0.5 at the pressure of 10 Torr. This trend has already been observed in the reaction of 2-butene photosensitized by mercury, where the quantum yield of decomposition was estimated from the formation of hydrogen.[4]

To explain this observation, we tentatively propose a mechanism including the formation of a vibrationally-excited state of olefins. The mechanism may be described as follows:

$$\mathrm{Hg^*} + \textit{cis}\text{-P} \longrightarrow \mathrm{HgP^*} \quad (10)$$

$$\mathrm{HgP^*} \longrightarrow \mathrm{Hg} + \mathrm{P^*} \quad (11)$$

$$\mathrm{HgP^*} \longrightarrow \mathrm{Hg} + \mathrm{P'} \quad (12)$$

$$\mathrm{HgP^*} \longrightarrow \mathrm{Hg} + \text{Decomposition} \quad (13)$$

$$\mathrm{HgP^*} + \mathrm{P} \xrightarrow{(\mathrm{HgP_2^*})} \mathrm{Hg} + \mathrm{P^*} + \mathrm{P} \quad (14)$$

Here, P* is the triplet state which is subject to the *cis-trans* isomerization and P′ is the vibrationally-excited state which does not isomerize. If the quantum yield of the process (12) is represented by ϕ_X, its value may be approximated by the following relation:

$$\phi_X = 1 - (2\phi_{iso} + \phi_{C_4})$$

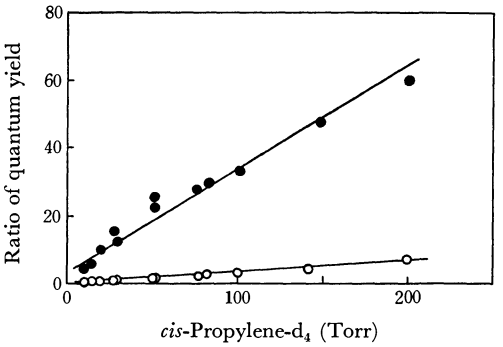

Fig. 4. Pressure dependences of the ratios, ϕ_{iso}/ϕ_X (○) and ϕ_{iso}/ϕ_{C_6} (●).

Figure 4 shows the pressure dependences of the ratios among these three quantum yields. Although the plots are scattered, it may be concluded that ϕ_{iso}/ϕ_X and ϕ_{iso}/ϕ_{C_6} are linearly dependent on the pressure. If so, and if the mechanism proposed above is correct, the contribution of the process (11) to the *cis-trans* isomerization should be small compared with that of the the process(14), because the linear relations for ϕ_{iso}/ϕ_X and ϕ_{iso}/ϕ_{C_6} have small intercepts at zero pressure. In other words, the main quenching process should occur through the formation of an unstable intermediate, HgP_2^*, in the reaction of propylene photosensitized by mercury at pressures higher than 10 Torr. Obviously, further experiments and different approaches are needed to confirm this speculation.

The authors are grateful to Dr. S. Maeda for the infrared analyses.

BULLETIN OF THE CHEMICAL SOCIETY OF JAPAN VOL. 43 2395—2397 (1970)

The Crystal and Molecular Structure of Bis(acetylacetonato)manganese(II) Dihydrate

Shigeki ONUMA and Shuzo SHIBATA

Department of Chemistry, Shizuoka University, Shizuoka

(Received February 21, 1970)

The crystal and molecular structure of bis(acetylacetonato)manganese(II) dihydrate, $Mn(C_5H_7O_2)_2 \cdot 2H_2O$, has been determined from three-dimentional X-ray diffraction data. The compound has a center of symmetry. The octahedral arrangement of the ligand atoms about the central manganese atom is distorted; the Mn–O(1) and Mn–O(2) distances are 2.129 and 2.150 Å, respectively, the Mn–O(H_2O) distance is 2.267 Å. The metal atom lies 0.561 Å out of the least-squares plane of the chelate ring. The chelate is isostructural with the cobalt, nickel, and magnesium analogues.

The molecular structures of the acetylacetonato complexes of some bivalent first transition metals were studied by gaseous electron-diffraction method by one of us (S. S.).[1] The complexes take the coordination number four in a gaseous state, but usually six in a solid state because of polymerization of the chelate or addition of solvent molecules. The purpose of the present study is to find the difference between the molecular structures in the two phases.

The crystal structure of $Mn(C_5H_7O_2)_2 \cdot 2H_2O$ has been reported recently by Montgomery and Lingafelter.[2] However, we were not aware of this when we started this work. Montgomery and Lingafelter determined the structure using 588 independent reflections recorded on Weissenberg photographs which were taken with Fe$K\alpha$ radiation and intensities of which were measured with the aid of a photometer. Comparison of their results with ours showed a good agreement between the two independent determinations.

Experimental

The crystals of bis(acetylacetonato)manganese(II) dihydrate were prepared by standard procedure.[3] The unit cell dimensions and the space group were determined from Weissenberg and rotation photographs using Cu$K\alpha$ radiation ($\lambda=1.5418$ Å). It is monoclinic with two molecules in a unit cell of the dimensions, $a=11.17$, $b=5.42$, $c=11.32$ Å and $\beta=106.2°$, and the space group is $P2_1/c$ (No. 14) which is required from the systematic absence for $0k0$ when k is odd and for $h0l$ when l is odd. The calculated density is 1.46 g cm^{-3}. A needle-shaped crystal selected carefully was used for intensity measurements. Three-dimensional intensity data were recorded on equi-inclination Weissenberg photographs taken with Cu$K\alpha$ radiation by means of the multiple film technique at room temperature. The intensities of 1202 independent reflections from $h0l$ to $h4l$ were measured visually by the use of a scale consisting of spots obtained from a selected reflection with different exposure times. All intensities were used in a least-squares calculation. Corrections for Lorentz and polarization factors were made in the usual way, while those for absorption and extinction were neglected.

Structure Determination

Since the compound $Mn(C_5H_7O_2)_2 \cdot 2H_2O$ has a center of symmetry, the manganese atom was placed at the origin of the unit cell. The two-dimensional coordinates of the five carbon and three oxygen atoms were obtained approximately from the sharpened ($B=4.0$ Å^2) Patterson projection, $P(u,w)$. Successive Fourier syntheses refined the positional parameters of the light atoms on the same plane and gave the orientation of the molecular framework. At this stage, calculated structure factors gave a discrepancy factor, $R_1=\sum||F_o|-|F_c||/\sum|F_o|$, of 0.218 for $h0l$ reflection, assuming an isotropic temperature parameter of 3.0 Å^2 for all atoms.

The three-dimensional structure which was used as the input for a least-squares calculation was assumed as follows: The acetylacetone ring takes a planar form, and the bond lengths and bond angles are equal to the average values which were estimated by Lingafelter[4] from the structures of many other acetylacetonate complexes.

The positional and the isotropic thermal para-

1) S. Shibata, Proceedings of the 10th International Conference on Coordination Chemistry (1967), p. 82.

2) H. Montgomery and E. C. Lingafelter, *Acta Crystallogr.*, **B24**, 1127 (1968).

3) R. G. Charles, "Inorganic Syntheses," Vol. 6, p. 164 (1960).

4) E. C. Lingafelter, *Coordin. Chem. Rev.*, **1**, 151 (1966).

meters were refined by a least-squares procedure with block-diagonal matrix approximation. Computations were carried out by means of a HITAC 5020E computor using a program by T. Ashida.

In the refinement procedure, the function to be minimized was $\sum w(|F_o|-|F_c|)^2$ and the weights, w, were unity for $F_o \geqq 0.5$ and zero for $F_o < 0.5$. All of the observed data including zero reflections were used in the calculation. The atomic scattering factors of manganese, oxygen and carbon atoms were taken from International Tables for X-ray Crystallography.[5] Correction for anomalous scattering of manganese atom was neglected.

Five iterations of the refinement gave a discrepancy factor R_1 of 0.139 and the isotropic temperature factors were obtained for each atom. It was noticeable that the isotropic temperature factors for the two methyl carbon atoms, C(1) and C(5), and the oxygen atom of water, O(3), are considerably large.

Refinement with a consideration of anisotropic temperature factors was carried out five cycles with the use of the same program and gave a smaller discrepancy factor R_1 of 0.093 for non-zero reflections. Anisotropic temperature factors were expressed as

$$\exp\left[-(B_{11}h^2+B_{22}k^2+B_{33}l^2+B_{12}hk+B_{23}kl+B_{13}hl)\right]$$

The final atomic coordinates with their estimated standard deviations and the anisotropic temperature factors are listed in Tables 1 and 2, respectively. The observed and the calculated structure factors are tabulated in Table 3.*1

Discussion

According to preliminary results from an electron-diffraction experiment,[1] gaseous bis(acetylacetonato)manganese(II) takes planar form and the distance between manganese and oxygen atoms is 2.28 Å. However, the present study showed that the chelate in a crystal takes distorted octahedron and the average length of the corresponding bond is 2.14 Å. A comparison between them will be made when a conclusive result of electron-diffraction is obtained.

Table 1. The final atomic coordinates and their estimated standard deviations ($\times 10^4$)

	x	y	z
Mn	0	0	0
O(1)	1538 (5)	−2281 (14)	963 (6)
O(2)	1249 (6)	1553 (14)	− 915 (5)
O(3)	613 (7)	3021 (16)	1426 (6)
C(1)	3604 (9)	−3365 (23)	2028 (8)
C(2)	2702 (7)	−1775 (19)	1107 (7)
C(3)	3145 (8)	119 (21)	499 (8)
C(4)	2434 (8)	1669 (20)	− 471 (8)
C(5)	3093 (10)	3643 (25)	−1004 (9)

The average dimension of a manganese acetylacetonate ring is shown in Fig. 1. Each manganese atom is surrounded by six coordinated oxygen atoms. Four of the coordination sites are occupied by the two bidentate acetylacetone groups and two

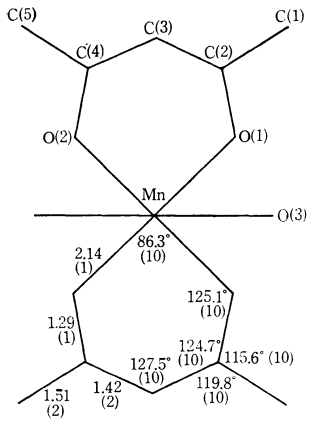

Fig. 1. The average dimensions of $Mn(C_5H_7O_2)_2 \cdot 2H_2O$.

Table 2. Anisotropic temperature factors and their estimated standard deviations ($\times 10^4$)

	B_{11}	B_{22}	B_{33}	B_{12}	B_{13}	B_{23}
Mn	31 (1)	168 (9)	36 (1)	−10 (7)	16 (2)	25 (7)
O(1)	36 (5)	145 (31)	49 (5)	−10 (19)	16 (8)	48 (20)
O(2)	42 (5)	196 (32)	37 (5)	−48 (21)	14 (8)	17 (21)
O(3)	83 (7)	248 (39)	33 (5)	−43 (26)	15 (10)	−51 (22)
C(1)	59 (9)	243 (54)	33 (7)	105 (34)	−11 (12)	53 (31)
C(2)	33 (7)	145 (47)	27 (6)	33 (26)	6 (10)	−51 (25)
C(3)	60 (8)	84 (43)	39 (7)	−26 (32)	23 (11)	− 5 (30)
C(4)	56 (8)	126 (46)	36 (7)	− 9 (29)	54 (12)	−36 (28)
C(5)	75 (10)	326 (56)	39 (7)	−132 (39)	66 (14)	1 (35)

5) "International Tables for X-ray Crystallography," Vol. III, Birmingham, Kynoch Press (1962), p. 202.

*1 The F_o–F_c table is kept as Document No. 7004 at the office of the Chemical Society of Japan. A copy may be secured by citing the document number and by remitting, in advance, ¥250 for photoprints. Payment may be made by check or money order payable to: Chemical Society of Japan.

are occupied by the water molecules. The average distance of the Mn–O($C_5H_7O_2$) is much shorter than that of Mn–O(H_2O), 2.267 Å, by 0.130 Å. However, in the crystal structure of $Zn(C_5H_7O_2)_2 \cdot H_2O$,[6] there is no considerable difference between the Zn–O($C_5H_7O_2$) distance and the Zn–O(H_2O); the average distance is 2.02 ± 0.02 Å.

The O–O separation in an acetylacetonate ring is 2.926 Å. Lingafelter[4] pointed out that the O–O distance of the acetylacetonate chelate ring decreases with the increase in an oxidation number of a metal, and the above result seems to be an additional proof to this rule.

The structure of $Mn(C_5H_7O_2)_2 \cdot 2H_2O$ is essentially the same as the structures of the corresponding cobalt,[7] nickel[8] and magnesium analogues.[9] Morosin found that in these metal acetylacetonates the metal is displaced out of the least-squares plane formed by the chelate ring OCCCO. In the present work a similar displacement was observed. The sum of the interior angles of the ring was 539.9°, although 540° must be required for planarity. Therefore the chelate ring is planar within experimental errors, and the least-squares plane has the equation $-0.2845X+0.6796Y+0.7287Z= -0.5611$ (referred to the monoclinic coordinates). The distance from the manganese atom to this ligand plane was 0.561 Å, in contrast to the corresponding distance in $Mn(C_5H_7O_2)_3$, 0.12 Å.[10] The decrement may be due to steric hindrance among the chelate frames which are considerably flexible. Deviations of the light atoms from the least-squares plane are as follows:

O(1)	0.027	O(2)	−0.019	C(1)	−0.151
C(2)	−0.039	C(3)	0.017	C(4)	0.014
C(5)	0.092	O(3)	2.655 Å		

Table 4. Intramolecular bond lengths and angles

Bond lengths (Å)

Mn	O(1)	2.150 (7)
Mn	O(2)	2.129 (8)
Mn	O(3)	2.267 (8)
C(1)	C(2)	1.504 (16)
C(4)	C(5)	1.515 (17)
C(2)	C(3)	1.401 (16)
C(3)	C(4)	1.434 (16)
O(1)	O(2)	2.926 (11)
O(1)	O(3)	3.146 (11)
O(2)	O(3)	3.035 (11)
O(1)	C(2)	1.294 (13)
O(2)	C(4)	1.280 (13)

Bond angles* (°)

O(1)	Mn	O(2)	86.3
Mn	O(1)	C(2)	125.1
Mn	O(2)	C(4)	125.1
O(1)	Mn	O(3)	90.8
O(2)	Mn	O(3)	87.3
O(1)	C(2)	C(1)	114.9
C(2)	C(3)	C(4)	127.5
C(3)	C(4)	C(5)	119.5
O(1)	C(2)	C(3)	125.1
O(2)	C(4)	C(3)	124.3
C(1)	C(2)	C(3)	120.0
O(2)	C(4)	C(5)	116.3

* Average error is 1°.

Both of the methyl groups exist significantly out of the chelate plane. The chelate ring is folded by 21° about the O(1)–O(2) axis. The intramolecular bond lengths and angles are listed in Table 4.

The intermolecular distance between O(3) (x,y,z) and O(2) $(x, 0.5-y, 0.5+z)$ and between O(2) $(-x, -y, -z)$ and O(3)$(-x, -0.5+y, 0.5-z)$ are 2.867 Å. The lengths may indicate the presence of the intermolecular hydrogen bonds between neighbouring oxygen atoms related by the twofold screw axis. Other intermolecular distances can be explained reasonably by the assumption that they are in van der Waals contact.

6) H. Montgomery and E. C. Lingafelter, *Acta Crystallogr.*, **16**, 748 (1963).
7) G. J. Bullen, *ibid.*, **12**, 703 (1959).
8) H. Montgomery and E. C. Lingafelter, *ibid.*, **17**, 1481 (1964).
9) B. Morosin, *ibid.*, **22**, 316 (1967).
10) B. Morosin and J. R. Brathovde, *ibid.*, **17**, 705 (1964).

BULLETIN OF THE CHEMICAL SOCIETY OF JAPAN VOL. 43 2398—2403 (1970)

Structural Studies of Antimony Tribromide and Its Molecular Complex with Benzene by Means of the ^{81}Br Nuclear Quadrupole Resonance

Tsutomu OKUDA, Hiromitsu TERAO, Osamu EGE and Hisao NEGITA

Department of Chemistry, Faculty of Science, Hiroshima University, Hiroshima

(Received February 25, 1970)

The structures of α-antimony tribromide and its molecular complex with benzene $2SbBr_3 \cdot C_6H_6$ were investigated by studying the Zeeman effect on the nuclear quadrupole resonance (NQR) due to ^{81}Br at room temperature. The bond angles, ∠Br–Sb–Br, of α-antimony tribromide in its solid state were found to be 94°14′±4′, 94°31′±8′, and 98°27′±7′. The polar angles specifing the directions of the Sb–Br bonds with respect to the orthorhombic crystal axes are (60°0′±9′, 62°13′±7′), (59°10′±7′, −54°35′±8′), and (57°39′±17′, 180°0′±3′). These values are consistent with those of the X-ray analysis by Cushen *et al.* within about 1°. The asymmetry parameters at the three bromine atoms were 0.068±0.002, 0.049±0.002, and 0.080±0.004. On the other hand, the bond angles, ∠Br–Sb–Br, of the $SbBr_3$ molecule in the complex $2SbBr_3 \cdot C_6H_6$ were found to be 92°24′±11′, 97°7′±14′, and 97°40′±6′. The crystal has a monoclinic symmetry, and the three Sb–Br bonds have directions making angles of 29°4′±21′, 76°26′±9′ and 63°33′±11′ relative to the *b*-axis. The asymmetry parameters at the three bromine atoms in the complex were 0.169±0.001, 0.063±0.002, and 0.094±0.002. The largest value of the asymmetry parameters seems to be the result mostly of the intermolecular bonding. From the coupling constants, the Sb–Br bond characteristics in antimony tribromide and its molecular complex, $2SbBr_3 \cdot C_6H_6$, are considered to be almost the same.

It has long been known that antimony tribromide has two distinct crystal "habits," acicular and bipyramidal. When a warm carbon disulfide solution of antimony tribromide is cooled, needle-like crystals of α-antimony tribromide are obtained, contaminated with a few crystals of the β-form. The α-form is gradually transformed into the β-form at room temperature. When the β-form is melted, it can be reversed to the α-form.

Studies of the nuclear quadrupole resonance on antimony tribromide have been made by several authors.[1-3] All of them, however, used polycrystalline samples. The X-ray analyses of the α- and β-forms were carried out by Cushen[4] and Hulme[5] respectively. The α-form is orthorhombic, with the *c*-axis as the needle axis, and it has four molecules in the unit cell. The space group is $P2_12_12_1$. The β-form is orthorhombic, with the *a*-axis as the bipyramidal axis, and it has four molecules in the unit cell. The space group is *Pbnm*. The molecule in the gaseous state has been found to have a trigonal pyramidal form by the electron diffraction method. According to the latest report by Swingle[6] it has a bond angle of 97°±2° for ∠Br–Sb–Br and a bond distance of 2.51±0.02 Å for Sb–Br.

On the other hand, it is well known that antimony tribromide forms 1 : 1 and 2 : 1 molecular complexes with aromatic compounds. Studies of the nuclear quadrupole resonances for the powder of these complexes have already been reported,[1,3] but neither a Zeeman analysis of the resonances nor X-ray analysis has been done, so far as we know. Therefore we carried out a Zeeman analysis of the single crystals of α-antimony tribromide and its molecular complex with benzene, $2SbBr_3 \cdot C_6H_6$, in order to identify the ^{81}Br resonance lines and clarify the nature of the Sb–Br bonds as well as the shape of the $SbBr_3$ molecule.

Experimental

Antimony tribromide (mp 96°C) was synthesized by the reaction of bromine and antimony powder suspended in carbon disulfide; it was then refined by distillation. A 2 : 1 molecular complex of antimony tribromide with benzene was prepared by mixing molten antimony tribromide and a small excess of benzene. It was filtered

1) V. S. Grechiskin and I. A. Kyuntsel, *Zh. Struct. Khim.*, **5**, 53 (1964).
2) S. Ogawa, *J. Phys. Soc. Jap.*, **13**, 618 (1958).
3) H. Negita, T. Okuda and M. Kashima, *J. Chem. Phys.*, **45**, 1076 (1966).
4) D. W. Cushen and R. Hulme, *J. Chem. Soc.*, **1964**, 4162.
5) D. W. Cushen and R. Hulme, *ibid.*, **1962**, 2218.
6) S. M. Swingle, *Structure Reports*, **13**, 421 (1950).

and dried in a vacuum desiccator. The melting point of the product was 93°C, whereas the literature value[1] is 92.5°C. The single crystals of these substances were obtained by a melting method. They were 15 mm in diameter and 40 mm in length. The single crystal obtained for antimony tribromide was the α-form, because a melting method was used.

An externally-quenched super-regenerative spectrometer with Lecher wires was used for the detection of the resonance absorption lines, which were displayed on an oscilloscope. The resonance frequency was measured by a frequency meter, TS-175 C/U. The single crystal was set on a goniometer equipped with a Helmholtz electro-magnet, and the magnetic field was applied on the sample from all directions in order to obtain the zero-splitting patterns. Several kinds of Zeeman fields ranging from 150 to 300 gauss were used in order to avoid misreading of the spurious signal. The crystal could be rotated about a fixed axis of the crystal, and its angle, Φ, could be measured to within 0.1°. On the other hand, the magnetic field could be rotated on a horizontal plane, and its angle, Θ, could be measured to within 1′. All of the measurements were carried out at about 20°C.

Results and Discussion

In a previous paper[3] we reported the ^{81}Br nuclear quadrupole resonance frequencies of antimony tribromide and its complexes. The ^{81}Br quadrupole resonance lines of α-antimony tribromide have been observed at 135.11, 135.32, and 140.35 MHz, with an intensity ratio of 1 : 1 : 1, at room temperature (19.5°C), as may be seen in Fig. 1 (a). In the case

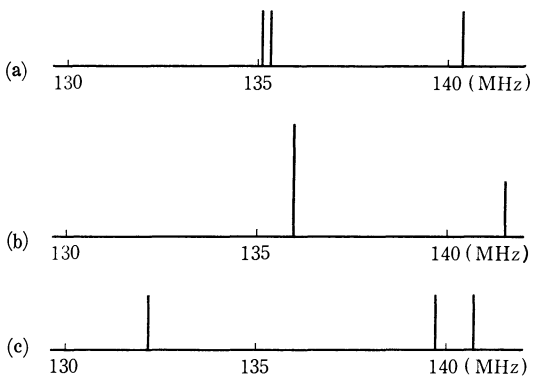

Fig. 1. Resonance spectra of antimony tribromide and its complex with benzene.
(a) α-$SbBr_3$, (b) β-$SbBr_3$, (c) $2SbBr_3 \cdot C_6H_6$

of β-antimony tribromide, the resonance lines have been observed at 135.96 and 141.49 MHz, with an an intensity ratio of 2 : 1, at room temperature (20.5°C), as may be seen in Fig. 1 (b). The resonance frequencies of α- and β-antimony tribromides are slightly different from one another. This fact reflects the delicate difference in the crystal fields surrounding the resonant nuclei in these modifications.

The quadrupole resonances of two modifications of antimony tribromide were reported by Ogawa.[2] Her synthesized antimony tribromide (1) corresponds to α-antimony tribromide, but her purchased antimony tribromide (2) is different from β-antimony tribromide. We could not obtain a sample like her second one.

As for the ^{81}Br resonance lines of $2SbBr_3 \cdot C_6H_6$, we have reported two resonance lines in a previous paper.[3] Through reexamination, however, we found a new resonance line, at about 8 MHz, below these two lines. Finally, then, three resonance lines with the same intensity have been observed; the frequencies are 132.14, 139.70, and 140.69 MHz at room temperature (21.5°C), as may be seen in Fig. 1 (c). The resonance lines in the complex are more widely spread than those of antimony tribromide, and two of them are closely spaced on the higher-frequency side. The grouping of the resonance lines is reversed from those of α- and β-antimony tribromides. We may say, however, that all resonance lines of the three samples are in nearly the same frequency regions. Thus, it can be assumed that there is no essential difference in the nature of the Sb–Br bonds, and that the shape of $SbBr_3$ molecule in its own crystal is retained in the complex.

The results of the Zeeman analyses of ^{81}Br resonance lines of α-antimony tribromide and its molecular complex with benzene $2SbBr_3 \cdot C_6H_6$ will be described below.

(a) α-Antimony Tribromide. Let us label the three resonance lines of ^{81}Br as ν_1, ν_2, and ν_3 from the lower to the higher. Then, from the number and their intensity ratio, these lines can be ascribed to three kinds of bromine atoms, Br_1, Br_2, and Br_3, in one molecule. The zero-splitting patterns of the Zeeman effect on the resonance lines are shown in Fig. 2. For the resonance lines, ν_1, ν_2, and ν_3, four, four, and two loci were obtained respectively. These loci are contributed by the Br_{1A}, Br_{1B}, Br_{1C}, and Br_{1D} atoms, the Br_{2A}, Br_{2B}, Br_{2C}, and Br_{2D} atoms, and the Br_{3A} and Br_{3B} atoms respectively. The direction of the principal z-axis of the field gradient on the bromine atom can be obtained from the zero-splitting pattern. The z-axis is usually parallel to the direction of the Sb–Br bond; the angle between any two Sb–Br bonds can thus be deduced. These angles are listed in Table 1, where the angle in parenthesis is the supplementary angle of the other. Since the gas molecule of $SbBr_3$ has been found to be a trigonal pyramid, one may expect that this molecule is nearly a trigonal pyramid in the solid state.

Taking the molecular shape and the bond angle, 97°, in the gaseous state into consideration, we find from Table 1 that each of the groups—Br_{1A}, Br_{2A}, Br_{3A}; Br_{1B}, Br_{2B}, Br_{3B}; Br_{1C}, Br_{2C}, Br_{3A}, and Br_{1D}, Br_{2D}, Br_{3B}, belongs to the same molecule. The directions of the symmetry axes of the crystal, a, b,

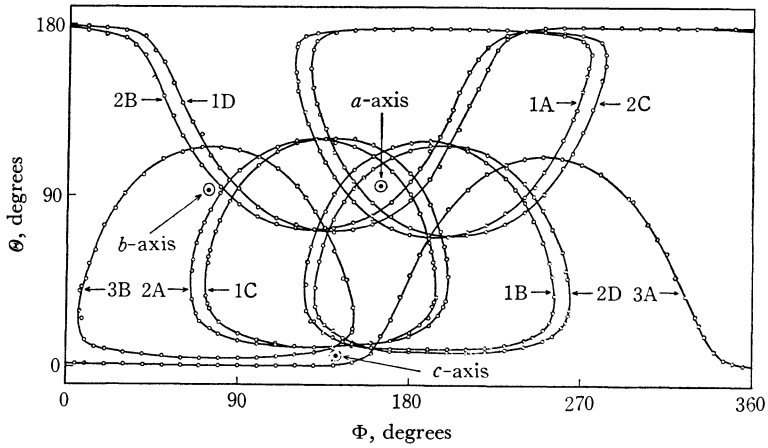

Fig. 2. Zero-splitting patterns of Zeeman lines of α-$SbBr_3$.
Θ and Φ are polar angles with respect to the orthogonal coordinate axes XYZ fixed to the sample.
1A, 1B, *etc.*, represent the zero-splitting directions of Zeeman lines at the nuclei Br_{1A}. Br_{1B}, *etc.*, respectively.

TABLE 1. THE ANGLES BETWEEN Sb–Br BONDS IN α-$SbBr_3$

∠Br–Sb–Br	Br_{1A}	Br_{1B}	Br_{1C}	Br_{1D}	Br_{2A}	Br_{2B}	Br_{2C}	Br_{2D}	Br_{3A}
Br_{1B}	119°54′ (60° 6′)*								
Br_{1C}	100° 3′ (79°57′)	47°31′ (132°29′)							
Br_{1D}	47°44′ (132°16′)	99°58′ (80° 2′)	120° 5′ (59°55′)						
Br_{2A}	**94°22′** (85°38′)	63°19′ (116°41′)	6°53′ (173° 7′)	118°49′ (61°11′)					
Br_{2B}	54° 1′ (125°59′)	**94°15′** (85°45′)	118°40′ (61°20′)	6°51′ (173° 9′)	118°19′ (61°41′)				
Br_{2C}	6°26′ (173°34′)	118°43′ (61°17′)	**94°45′** (85°15′)	53°41′ (126°19′)	88°51′ (91° 9′)	59°47′ (120°13′)			
Br_{2D}	118°45′ (61°15′)	6°23′ (173°37′)	53°25′ (126°35′)	**94°43′** (85°17′)	59°37′ (120°23′)	88°47′ (91°13′)	118°22′ (61°38′)		
Br_{3A}	**94°23′** (85°37′)	52°23′ (127°37′)	**94° 5′** (85°55′)	52°35′ (127°25′)	**98°28′** (81°32′)	45°51′ (134° 9′)	**98°46′** (81°14′)	46° 8′ (133°52′)	
Br_{3B}	52°27′ (127°33′)	**94°10′** (85°50′)	52°36′ (127°24′)	**94°17′** (85°43′)	45°52′ (134° 8′)	**98°19′** (81°41′)	46° 9′ (133°51′)	**98°14′** (81°46′)	115°18′ (64°42′)

* The value in parenthesis is supplementary angle.

and c, can easily be found from the symmetry distributions of the z-axes. These directions are shown in Fig. 2.

The values of the asymmetry parameters can be determined from the distortion of the zero-splitting loci by the following equation:[7]

$$\eta = 3(\sin^2\theta_{max} - \sin^2\theta_{min})/(\sin^2\theta_{max} + \sin^2\theta_{min}) \quad (1)$$

where θ_{max} and θ_{min} are the maximum and minimum zero-splitting angles, corresponding to $\phi = 0°$ and 90° respectively. Consequently, the quadrupole coupling constant can be calculated by substituting the value of η in the following relation:

$$\nu = (eQq_{zz}/2)(1+\eta^2/3)^{1/2} \quad (2)$$

7) C. Dean, *Phys. Rev.*, **96**, 1053 (1954).

The values of η and eQq_{zz} derived in this way are listed in Table 2.

All of the asymmetry parameters are relatively small. In the antimony trichloride, which has the same crystal structure as β-antimony tribromide and

TABLE 2. RESONANCE FREQUENCIES (ν), ASYMMETRY PARAMETERS (η) AND QUADRUPOLE COUPLING CONSTANTS (eQq_{zz}) OF ^{81}Br ATOMS IN α-$SbBr_3$ AT 19.5°C

Compound	ν,	MHz	η, %	eQq_{zz}, MHz
α-$SbBr_3$	ν_1	135.11	6.8±0.2	270.01
	ν_2	135.32	4.9±0.2	270.53
	ν_3	140.35	8.0±0.4	280.40

Table 3. The orientations (Θ', Φ') of Sb–Br bonds with respect to the crystal axes in α-$SbBr_3$

Bond	$Sb–Br_1$	$Sb–Br_2$	$Sb–Br_3$
NQR	(60°0′±9′, 62°13′±7′)	(59°10′±7′, −54°35′±8′)	(57°39′±17′, 180°0′±3′)
X-Ray	(59°28′, 62°16′)	(57°52′, −55°4′)	(58°49′, 181°18′)

which exhibits a similar pattern of NQR lines, the value of η is 15.3%[8] for the chlorine atom corresponding to the lower line, which has an intensity twice as strong as the higher. This large asymmetry parameter has been ascribed by Peterson[9] to the intermolecular bonding between the chlorine and antimony atoms.

On the basis of X-ray data, let us ascertain whether or not there are unbound Sb–Br distances which are smaller than the sum of the van der Waals radii, 4.15 Å, as preparation for discussing the effect of the intermolecular bonding in antimony tribromide. In β-antimony tribromide there are short unbound Sb–Br distances, 3.66 and 3.85 Å, for the bromine atom, which contributes to the lower NQR line. The value of 3.66 Å seems evidently to be ascribable to the intermolecular bonding, and it is thought that the bromine atom corresponding to the lower NQR line has an asymmetry parameter as large as 15.3% in antimony trichloride. On the other hand, in α-antimony tribromide there are short unbound Sb–Br distances, 3.81 and 3.84, 3.75 and 4.10, and 3.78 Å for Br_1, Br_2, and Br_3 atoms respectively. These values are, however, larger than that of 3.66 Å in β-antimony tribromide. Therefore, we consider that the intermolecular bonding in α-antimony tribromide is less considerable than in antimony trichloride and β-antimony tribromide.

Gordy[10] proposed, on the basis of an extensive study using the equation of Schomaker-Stevenson,[11] that the tendency to form a double bond by using d orbitals falls off rapidly in descending rows in the periodic table, essentially vanishing for such fifth-row elements as Sn and Sb. In the case of $SbBr_3$, the bond length, Sb–Br, calculated by means of the Shomaker-Stevenson equation is in good agreement with the experimental value calculated by means of the electron diffraction. Therefore the possibility of double-bond formation is thought to be negligibly small, so that the ionicity of the Sb–Br bond, i, may be obtained from the following equation:

$$U_p = (1-i)(1-s) \qquad (3)$$

where s is the s electron character and where U_p is the number of unbalanced p electrons. Usually s is assumed to be 0.15,[12] and U_p is evaluated from the observed quadrupole coupling constant:

$$U_p = (eQq_{zz})_{obs}/(eQq_{zz})_{atom} \qquad (4)$$

where $(eQq_{zz})_{atom}$ is 643.0 MHz.[13] From the mean value of $(eQq_{zz})_{obs}$, 273.65 MHz, one obtains the values of U_p=42.5% and i=50.0%.

The values of (Θ', Φ') specifying the direction of the Sb–Br bonds with respect to the crystal axes are listed in Table 3, together with those values obtained from X-ray analysis. In this table, the direction of $\Theta'=0°$ is chosen to be along the c-axis, and the plane of $\Theta'=0°$ is taken as the bc plane. The bond angles obtained from the Zeeman and X-ray analyses[4] are listed in Table 4, together with

Table 4. The bond angles ∠Br–Sb–Br in α-and β-$SbBr_3$

α-$SbBr_3$	$\angle Br_1$–Sb–Br_2	$\angle Br_2$–Sb–Br_3	$\angle Br_3$–Sb–Br_1
NQR	94°31′±8′	98°27′±7′	94°14′±4′
X-ray	93°38′	97°23′	95°28′
β-$SbBr_3$	$\angle Br_1$–Sb–Br_2	$\angle Br_2$–Sb–Br_3	$\angle Br_3$–Sb–Br_1
X-ray	92°48′	97°37′	97°37′

the bond angles of the β-form obtained from X-ray analysis.[5] Our values are consistent with those obtained from X-ray analysis to within about 1°. The direction of the Sb–Br_3 bond obtained from the Zeeman analysis lies on the bc plane, whereas that from X-ray analysis deviates from the bc plane by about 1°. According to the X-ray analysis, there must be four nonequivalent directions of Sb–Br_3 bonds, in each of which two directions are situated close together. However, for the Br_3 atom, which is responsible for the ν_3 line, we could observe only two loci and could not resolve either of them into two closely situated loci, even when a field of 350 gauss was used. At this stage we can not determine whether the present result and/or those obtained by the X-ray analysis are correct.

(b) The Molecular Complex $2SbBr_3 \cdot C_6H_6$. Let us label the three resonance lines of ^{81}Br as before. Again, from the number and the intensity ratio of the resonance lines, these lines can be ascribed to the three kinds of bromine atoms, Br_1,

8) T. Okuda, A. Nakao, M. Shiroyama and H. Negita, This Bulletin, **41**, 61 (1968).

9) G. E. Peterson, Thesis, Pittsburgh, 1962.

10) W. Gordy, W. V. Smith and R. F. Trambarulo, "Microwave Spectroscopy," John Wiley & Sons, Inc., New York (1953), p. 313.

11) V. Schomaker and D. P. Stevenson, *J. Amer. Chem. Soc.*, **63**, 37 (1941).

12) C. H. Townes and B. P. Dailey, *J. Chem. Phys.*, **17**, 782 (1949).

13) J. G. King and V. Jaccarino, *Phys. Rev.*, **94**, 1610 (1954).

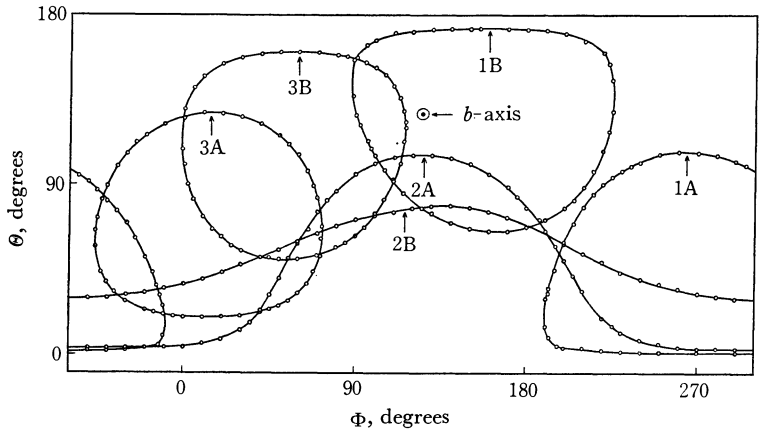

Fig. 3. Zero-splitting patterns of Zeeman lines of the complex $2SbBr_3 \cdot C_6H_6$.
Θ and Φ are polar angles with respect to the orthogonal coordinate axes XYZ fixed to the sample.
1A, 1B, *etc.*, represent the zero-splitting directions of Zeeman lines at the nuclei Br_{1A}, Br_{1B}, *etc.*, respectively.

Br_2, and Br_3, in one molecule. The zero-splitting patterns obtained for these lines are shown in Fig. 3. For each of these lines, two loci of the zero-splitting were obtained; these loci are contributed by the atoms, Br_{1A} and Br_{1B} atoms, the Br_{2A} and Br_{2B} atoms, and the Br_{3A} and Br_{3B} atoms respectively. The angles between the Sb–Br bonds (z-axes) thus obtained are listed in Table 5.

TABLE 5. THE ANGLES BETWEEN Sb–Br BONDS IN THE COMPLEX $2SbBr_3 \cdot C_6H_6$

∠Br–Sb–Br	Br_{1A}	Br_{1B}	Br_{2A}	Br_{2B}	Br_{3A}
Br_{1B}	58° 7′ (121°53′)*				
Br_{2A}	82°15′ (**97°45′**)	73°37′ (106°23′)			
Br_{2B}	105°46′ (74°14′)	**97°34′** (82°26′)	27° 9′ (152°51′)		
Br_{3A}	87°26′ (**92°34′**)	144°56′ (35° 4′)	**97°21′** (82°39′)	85° 1′ (94°59′)	
Br_{3B}	34°41′ (145°19′)	**92°13′** (87°47′)	85°13′ (94°47′)	**96°53′** (83° 7′)	52°55′ (127° 5′)

* The value in parenthesis is the supplementary angle.

Considering that the antimony tribromide molecule may retain a trigonal pyramid and take the value of the bond angle near to 97°, we find from Table 5 that each of the groups, Br_{1A}, Br_{2A}, and Br_{3A}, and Br_{1B}, Br_{2B}, and Br_{3B}, belongs to the same molecule.

Because each line has two nonequivalent z-axes (zero-splitting loci), we conclude that this complex crystal has a monoclinic symmetry.[14] However, it is impossible to distinguish between C_s, C_2, and C_{2h} on the basis of the Zeeman analysis, which always introduces the center of symmetry to the crystal. The relative orientations of the Sb–Br_1, Sb–Br_2, and Sb–Br_3 bonds with respect to the b-axis are 29°4′±21′, 76°26′±9′, and 63°33′±11′ respectively. The bond angles obtained from Table 5 are listed in Table 6. The shape of the $SbBr_3$ molecule in the complex is similar to that of β-antimony tribromide as established by X-ray analysis.

TABLE 6. THE BOND ANGLES ∠Br–Sb–Br IN THE COMPLEX $2\,SbBr_3 \cdot C_6H_6$

Bond angle	∠Br_1–Sb–Br_2	∠Br_2–Sb–Br_3	∠Br_3–Sb–Br_1
NQR	97°40′±6′	97°7′±14′	92°24′±11′

The values of the asymmetry parameter obtained from the zero-splitting loci using Eqs. (1) and the values of eQq_{zz} calculated from Eqs. (2) are listed in Table 7. The value of η at the Br_1 atom, 16.9%, is considerably larger than the remaining ones and those in α-$SbBr_3$; it is almost the same as the largest value in $SbCl_3$, which amounts to 15.3%. As we excluded the possibility of a double bond, this large value of η must be ascribed to the intermolecular bonding. Two cases of intermolecular bonding

TABLE 7. RESONANCE FREQUENCIES (ν), ASYMMETRY PARAMETERS (η) AND QUADRUPOLE COUPLING CONSTANTS (eQq_{zz}) OF ^{81}Br ATOMS IN THE COMPLEX $2\,SbBr_3 \cdot C_6H_6$ AT 21.5°C

Complex	ν,	MHz	η, %	eQq_{zz}, MHz
$2\,SbBr_3 \cdot C_6H_6$	ν_1	132.14	16.9±0.1	263.04
	ν_2	139.70	6.3±0.2	279.23
	ν_3	140.69	9.4±0.2	280.98

14) K. Shimomura, *J. Phys. Soc. Jap.*, **12**, 652 (1957).

may be thought of. One is the bonding between the Br atom and the benzene ring, this bonding being formed by charge transfer. The other is the intermolecular Sb–Br bonding among neighboring $SbBr_3$ molecules. Since the bonding by charge transfer is weak,[15] the former is not likely to be responsible for the large value of η. On the contrary, the latter case seems reasonable.

The lowest line in the complex is lower by about 3 MHz than the lowest line of antimony tribromide itself. It has been thought that the charge transfer from the benzene to the bromine atom may cause the lowering of the resonance frequency. It has been found, however, that this lowering is very small.[15,16] Thus, the relatively large frequency lowering in the complex can be considered to be caused primarily by the intermolecular Sb–Br bonding. On the other hand, the spacing of the resonance lines of this complex, as may be seen in Fig. 1 (c), resembles that of aluminum tribromide. One of the three lines is situated apart from the two closely-spaced lines on the higher-frequency side. This appearance is characteristic of the halides of the third-group elements which form the dimer.[17] The lowest line is attributed to the bridging Br atom; it is lower by about 15 MHz than those of the upper pair in aluminum tribromide.[18] The corresponding lowering in the present molecular complex is about 8 MHz.

Therefore, we consider that there exist predominantly interacting partner molecules of $SbBr_3$ in the complex crystal, and that the Br_1 atom in one molecule is bound to the Sb atom in a partner molecule to some extent. It must, however, be remembered that a slight deviation of the direction of the z-axis of the field gradient from the bond axis occurs because of moderate intermolecular covalent bonding.

At this stage, it is not evident whether the benzene ring is bound to the Br or the Sb atom in the complex. Meanwhile, Hulme and Szymański[19] have proposed, on the basis of their X-ray analysis of the complex $2SbCl_3 \cdot C_{10}H_8$ that the aromatic ring is bound to the Sb atom; they based their proposal on the distance between the Sb atom and the aromatic ring

15) H. O. Hooper, *J. Chem. Phys.*, **41**, 599 (1964).
16) D. F. R. Gilson and C. T. O'Konski, *ibid.*, **48**, 2767 (1968).
17) R. G. Barnes and S. L. Segel, *ibid.*, **25**, 180 (1956).
18) T. Okuda, H. Terao, O. Ege and H. Negita, *ibid.*, **52**, 5489 (1970).
19) R. Hulme and J. T. Szymański, *Acta Crystallogr.*, **B25**, 753 (1969).

BULLETIN OF THE CHEMICAL SOCIETY OF JAPAN VOL. 43 2404—2409 (1970)

Effect of Halogenation on Intramolecular Energy Transfer in Rare Earth Chelates

Makoto MORITA*1 and Shigeo SHIONOYA

The Institute for Solid State Physics, The University of Tokyo, Roppongi, Minato-ku, Tokyo

(Received February 27, 1970)

Using tris-dibenzoylmethanates of terbium(III) and other rare earths(III) we investigated the effect of halogenation of the central hydrogen of a 1,3-diketonate ligand on the luminescence properties of these chelates in rigid media. As a result of halogenation, all chelates display blue shift of the ligand phosphorescence, the intensity of the rare earth emission I_{RE} relative to that of the phosphorescence I_{ph} is markedly decreased in the order of H→Cl→Br, and the lifetime of the phosphorescence τ_{ph} decreases in the same order. These facts provide the evidence that the intramolecular energy transfer takes place *via* the triplet state of the ligand. In halogenated and nonhalogenated terbium chelates the ratio of the probability of energy transfer P_t estimated from the quantity $I_{RE}/I_{ph}\tau_{ph}$ to the overlap integral S between the phosphorescence spectrum and the terbium absorption spectrum is found to be roughly constant. These results lead us to the conclusion that intramolecular energy transfer is governed by the resonance mechanism due to exchange interaction.

For the intramolecular energy transfer from the ligand to the central metal ion in rare earth chelates, Crosby's proposal[1,2] has been generally accepted. This states that excitation energy is transferred from the triplet state of the ligand to the resonance level of the rare earth ion. In our previous paper,[3] we reported perturbation effects on the triplet states, such as oxygen effect and external heavy atom effect usually known in organic molecules, and gave some facts which strongly suggest Crosby's mechanism. Some other investigators[4-6] used the technique of triplet quencher to study this problem and presented some useful information.

Recently we have studied[7] this energy transfer process under the excitation of the triplet state of europium chelates by utilizing intermolecular triplet-triplet energy transfer from lanthanum chelates, and have presented evidence for Crosby's proposal. Further, we have investigated[8] the correlation between the energy transfer probability and the stretching vibration frequency of the chelate bond as obtained from infrared absorption measurements, and have concluded, according to an approximated treatment of Dexter's theory,[9] that the energy transfer process is dominated by the exchange interaction of the π electron system of the ligand triplet state with the f electron system of the central rare earth ion.

In parallel with these studies, we have continued the study of heavy atom effect on this intramolecular energy transfer with the purpose of investigating the transfer mechanism. Substitution of a halogen atom for 2-hydrogen of 1,3-β-diketonate as the ligand is expected to give an internal heavy atom effect, because this should change the probability of the transition from the triplet state to the ground singlet state and consequently influence the luminescence process of chelates. One may expect that this internal heavy atom effect is much more strongly observed than the external heavy atom effect. In the present paper, the luminescence properties of various halogenated tris-dibenzoylmethanates are reported. Exchange interaction has

*1 Present address: Department of Industrial Chemistry, College of Technology, Seikei University, Kichijoji, Musashino-shi, Tokyo.

1) G. A. Crosby, R. E. Whan and R. M. Alire, *J. Chem. Phys.*, **34**, 743 (1961).

2) G. A. Crosby and R. E. Whan, *J. Mol. Spectry.*, **8**, 315 (1962).

3) S. Shionoya, Y. Matsuda, M. Morita and S. Makishima, Proc. Internatl. Conf. Luminescence (Budapest, 1966), p. 1709 (1968).

4) M. L. Bhaumik and M. A. Elsayed, *J. Chem. Phys.*, **43**, 787 (1965).

5) V. L. Ermolaev, V. G. Aleshin and E. A. Saenko, *Dokl. Akad. Nauk SSSR*, **165**, 1048 (1965); *Sov. Phys. Dokl.*, **10**, 1186 (1966).

6) V. L. Ermolaev, E. A. Saenko, G. A. Domrachev, Yu. K. Khundenski and V. G. Aleshin, *Opt. Spectry.*, **22**, 466 (1967).

7) Y. Matsuda, S. Makishima and S. Shionoya, This Bulletin, **41**, 1513 (1968).

8) Y. Matsuda, S. Makishima and S. Shionoya, *ibid.*, **42**, 356 (1969).

9) D. L. Dexter, *J. Chem. Phys.*, **21**, 836 (1953).

been further confirmed to dominate the intramolecular energy transfer process.

Experimental

1) Samples. Tris-dibenzoylmethanates of rare earth ions were prepared by the usual procedures.[2] Halogenated chelates were obtained by the direct substitution method similar to that used by Collman *et al.*[10] for transition metal chelates. Chlorinated chelates were also prepared by the indirect method, *i. e.* by treating rare earth nitrates or acetates with 3-chloro-3-dibenzoylmethane prepared by the method reported by Kochetkov *et al.*[11] The two different methods were found to give the same chlorinated products. However, the former method was mostly employed to obtain halogenated compounds in this paper. We have synthesized various samples of $Ln[(C_6H_5CO)_2CX]_3 \cdot H_2O$ in which Ln stands for Eu, Sm, Tb, Dy, Gd and La, and X is H, Cl or Br (abbreviated hereafter as LnD, LnDCl or LnDBr). Chemical analysis of rare earth content as well as measurement of infrared absorption spectra were carried out in order to identify the obtained products.

2) Spectroscopic Measurements. Infrared absorption spectra were measured by means of the KBr disk method with a Hitachi EPI-2 infrared spectrophotometer attached with an NaCl or KBr prism (for NaCl or KBr region, respectively). Ultraviolet and visible absorption spectra were obtained at room temperature using a Cary model 14 spectrophotometer for both alcohol and chloroform solutions with chelate concentrations 5×10^{-5} mol/*l*.

Measurement of emission spectra was made at liquid nitrogen temperature by using a Kipp and Zonen prism double monochromator for ether-toluene (4 : 1) solutions with chelate concentration 5×10^{-4} mol/*l*. For the reference, powder samples of chelates were also measured. The 254 nm line obtained from the combination of a 100 W high pressure mercury lamp and an appropriate set of filters were used as the exciting source, and the response of an EMI 9558QB photomultiplier was fed to a millivolt recorder.

In the measurements of time-resolved emission spectra and emission lifetime, an Edgerton xenon flash lamp of type FX-3 attached with ultraviolet pass filters was used as the exciting light source. Chelate solutions of ether-toluene (4 : 1) with the concentration 5×10^{-3} mol/*l* were irradiated at liquid nitrogen temperature by pulse light from the flash lamp having a half-width of 2 μsec and frequency of 25 Hz. The response of an RCA 931A photomultiplier gated for 1 μsec was recorded with delay times ranging from zero to 100 μsec. Lifetime was obtained directly from the decay characteristics of the time-resolved emission spectra.

Results and Discussion

Infrared absorption spectra of halogenated rare earth chelates were found not to involve the absorption of 1200 cm^{-1} region which is due to the C–H in-plane bending mode. The carbonyl stretching bands in 1500 and 1600 cm^{-1} region are simplified in the halogenated products and the absorption band due to the M–O bond stretching does not change appreciably upon halogenation. These facts are considered to give structural evidence for the halogenation as was done for chromium

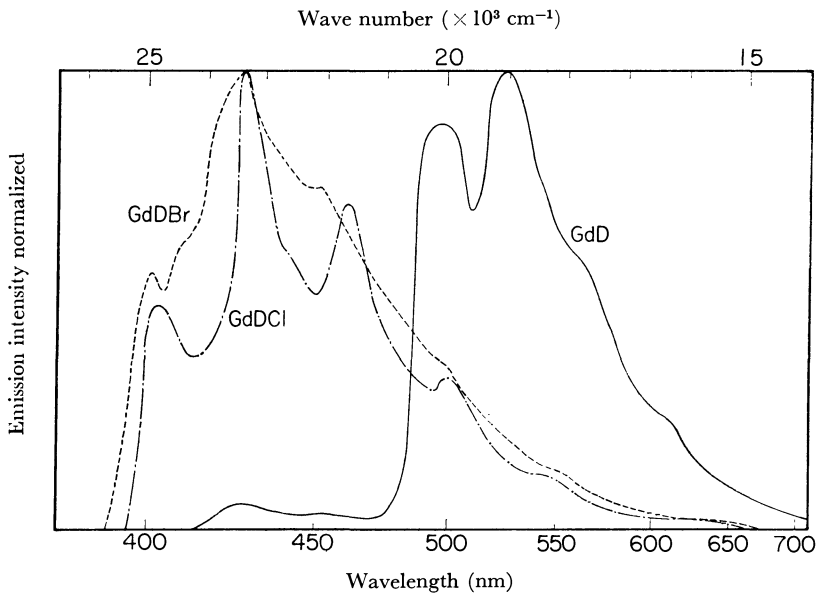

Fig. 1. Emission spectra of GdD, GdDCl and GdDBr in ether-toluene solutions (4 : 1) at 77°K under steady excitation by the 254 nm mercury line.

10) J. P. Collman, R. A. Moss, H. Maltz and C. C. Heidel, *J. Amer. Chem. Soc.*, **83**, 531 (1961).

11) N. K. Kochetkov, S. D. Sololov, N. M. Vagustova and E. E. Nifarten, *Dokl. Akad. Nauk SSSR*, **133**, 598 (1960).

chelates.[12]

The ultraviolet absorption spectra of LnD involve two broad bands at about 250 nm and 350 nm, respectively.[1] As a result of halogenation the 250 nm band strongly increases its absorbance and slightly shifts to longer wavelengths, while the 350 nm band almost disappears. We therefore used the mercury line of 254 nm as the exciting source in this study.

The emission spectra of ether-toluene solutions of GdD, GdDCl and GdDBr under steady excitation at 77°K are shown in Fig. 1. These spectra demonstrate how the ligand emission changes as a result of halogenation. If these spectra under steady excitation are compared with time-resolved emission spectra with a delay time of about 60 μsec, it turns out that in the GdD spectrum the weak band at about 430 nm is that of fluorescence while the strong band ranging from 480 to 600 nm is that of phosphorescence, and

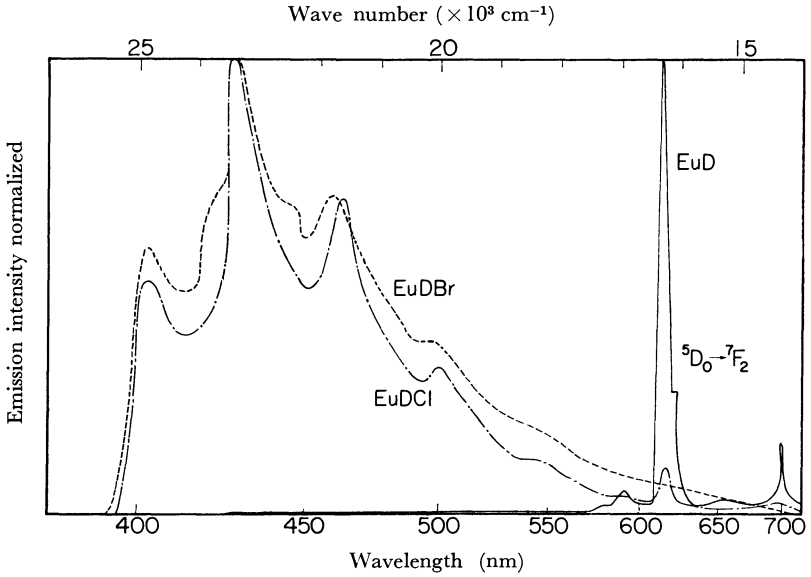

Fig. 2. Emission spectra of EuD, EuDCl and EuDBr in ether-toluene solutions (4 : 1) at 77°K under steady excitation by the 254 nm mercury line.

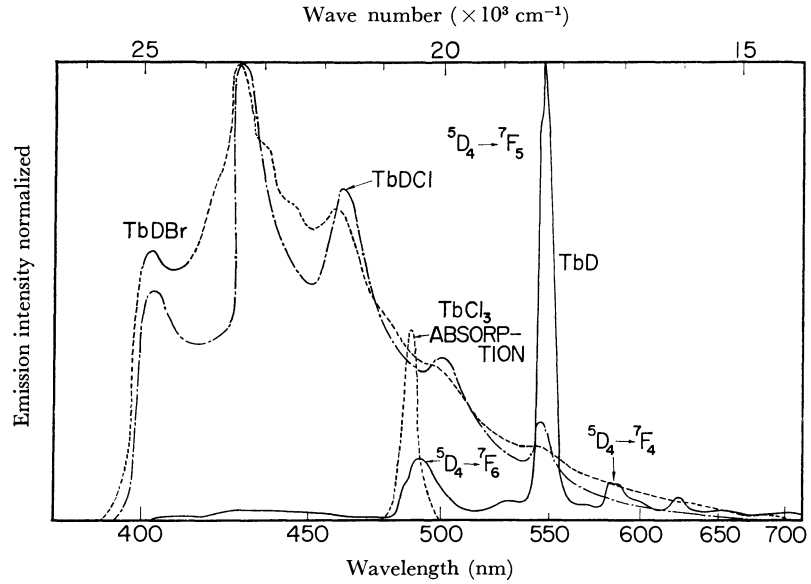

Fig. 3. Emission spectra of TbD, TbDCl and TbDBr in ether-toluene solutions (4 : 1) at 77°K under steady excitation by the 254 nm mercury line.

12) P. R. Singn and R. Sahai, *Aust. J. Chem.*, **20**, 639 (1967).

that in the case of GdDCl and GdDBr the spectra observed under steady excitation are only those of phosphorescence. It is noted that as a result of halogenation the phosphorescence spectrum is markedly blue-shifted, but the shape and peak position of the spectrum are nearly the same among the halogenated chelates.

The results of the emission spectrum measurements for a series of LaD, EuD, TbD, SmD and DyD and their halogenated derivatives are as follows. Lanthanum chelates show broad band emission of the ligand which is analogous to gadolinium chelates. Other chelates show sharp line emissions due to central rare earth ions in addition to the ligand emission. As examples, the emission spectra of europium chelates and terbium chelates are given in Figs. 2 and 3, respectively. It was found that in all cases the ligand emission spectra are quite similar to those of gadolinium chelates.

However, it should be noted, as is observed from these figures, that the intensity of the ligand emission relative to that of rare earth emission strongly increases as a result of halogenation. For example, although EuD shows hardly any ligand emission, EuDCl and EuDBr exhibit pronounced ligand phosphorescence. In the case of EuDCl the emission lines due to $^5D_0 \rightarrow {}^7F_J$ transition of Eu^{3+} ion are found only weakly at the tail of the strong ligand phosphorescence without the detectable change in the positions of the lines. In the case of EuDBr, the emission lines of Eu^{3+} ion are much more weakened. They are scarcely observed in glassy solutions as shown in this figure, although they are clearly found in a powder sample in which phosphorescence is completely quenched.

As in the case of europium chelates, terbium chelates have similar features of the halogenation effect. The variations of the emission intensity of rare earth ion as well as of the ligand are more clearly found in terbium chelates than in europium chelates. The emission spectra of samarium chelates, although not shown here, are also characterized by the halogenation effect. SmD has emissions of both ligand and rare earth ion with nearly equal intensities. However, in SmDCl and SmDBr the emission of ligand appears strongly and the emission of Sm^{3+} ion is almost quenched just as in the case of europium chelates. In the case of dysprosium chelates, the effect of halogenation is somewhat different. Namely, although DyD does not show Dy^{3+} emission, it becomes observable at around 500 nm in powder samples of DyDCl and DyDBr. This is interpreted as a result of the increase of the matching between the energies of the triplet state and the Dy^{3+} resonance levels caused by the blue shift of phosphorescence.

The decay time was obtained from time-resolved emission spectra. It was found that phosphorescence lifetime of GdD is 610 μsec while that of GdDCl and GdDBr decreases to 5.6 μsec and 4.1 μsec, respectively.

The results of the spectral measurements are summarized as follows. 1) The phosphorescence spectra of halogenated chelates are apparently blue-shifted in comparison with non-halogenated chelates, and chlorinated and brominated chelates have similar spectral features. 2) As a result of halogenation, the intensity of the ligand emission increases markedly, and instead the intensity of the rare earth emission lines decreases in the order H→Cl→Br. 3) The phosphorescence lifetime of gadolinium chelates decreases in the same order H→Cl→Br.

From these facts, one is led to the conclusion that the substitution of halogen atoms for hydrogen, *i.e.* the internal halogen effect, gives influences quite similar to the case of the external heavy atom effect.[3]

Let us next consider this substitution effect. In the case of naphthalene and its halogenated derivatives, relative decrease of the phosphorescence lifetime is H(1.0)→Cl(0.126)→Br(0.0078) against the relative increase of molecular weight of H(1.0)→Cl(1.27)→Br(1.62).[13] The internal heavy atom effect is known to depend predominantly on the weight of heavy atoms. Therefore, if we assume that for the phosphorescence lifetime of rare earth chelates the change of the same order of magnitude with halogenation as in the case of naphthalene and its derivatives is obtained, the lifetime of halogenated gadolinium chelates is estimated to fall into an order of magnitude of 10 μ to 100 μsec. The observed lifetime is comparable in magnitude with this value. However, since the peak position and shape of phosphorescence spectra change as a result of halogenation in rare earth chelates, it is inferred that the substitution effect in rare earth chelates is a pseudo-internal heavy atom effect. Hence, this substitution effect is considered to give the same conclusion as derived from the external heavy atom effect.[3] This then presents further evidence for Crosby's proposal that the intramolecular energy transfer takes place *via* the triplet states.[1,2]

Let us discuss the precise mechanism of the intramolecular energy transfer from the results obtained above. The theory of intermolecular energy transfer due to the resonance mechanism in condensed systems developed by Dexter[9] could be considered to be applicable to our present case of rare earth chelates.[5,6,8] Since intramolecular energy transfer takes place *via* the triplet state, the probability of the transfer P_t is given by the emission efficientcy of rare earth ion η divided by the lifetime of the ligand phosphorescence τ_{ph} as

$$P_t = \eta/\tau_{ph} \quad (1)$$

Here η is expressed by the intensity ratio of the rare earth emission to the ligand phosphorescence I_{RE}/I_{ph}. We have to estimate the overlapping of the

13) V. L. Ermolaev, *Opt. Spectry.*, **11**, 266 (1961).

phosphorescence spectrum of the ligand with the absorption spectrum of the rare earth ion. The overlap integral S is given by

$$S = \int I_{ph}(E)A(E)\mathrm{d}E, \qquad (2)$$

where $I_{ph}(E)$ represents the phosphorescence spectrum and $A(E)$ the absorption spectrum of rare earth ion, both being normalized to unit area.

In order to obtain the values of P_t with Eq. (1), those rare earth chelates which display appreciably both ligand phosphorescence and rare earth ion emission when halogenated must be used. Although we have examined various rare earth chelates as mentioned above, only terbium chelates were found to be appropriate for this purpose. In the case of europium and samarium chelates, the rare earth emission are almost quenched in brominated chelates in rigid media. We have further investigated the use of chelates with different ligands, but it was found that chelates with many other ligands commercially available are not so easily halogenated according to the direct substitution method. Therefore, we have to confine our discussion to terbium-(III) tris-dibenzoylmethanate and its chlorinated and brominated ones in this paper.

Let us discuss the mechanism of intramolecular energy transfer in terbium chelates. The quantities of P_t, S, η and τ_{ph} are estimated as shown in Table 1. In obtaining S, the absorption spectra of rare earth ion were substituted by those of terbium-(III) chloride in aqueous solution, because the absorption in chelate solutions is too weak to be measured. Since the ligand emission of TbD is very weak, the lifetime τ_{ph} could not be measured. Then, the relative τ_{ph} values for terbium chelates were substituted by those observed for gadolinium chelates. This substitution is allowed because only the relative value of the lifetime is important in our present analysis.

The transfer probability P_t due to exchange interaction is approximately given by[9]

$$P_t(\mathrm{exch}) = \mathrm{const.}\ S \exp(-2R/L), \qquad (3)$$

where R is, in the case of rare earth chelates, the bond distance between the metal ion and the ligand, and L is the effective Bohr radius for the excited and unexcited states of energy donor and acceptor.

On the other hand, the transfer probability P_t due to electric multipole interaction is given by

$$P_t(\mathrm{multipole}) = \mathrm{const.}\ S/R^s\tau_{ph}\tau_{RE} \qquad (4)$$

Here, s is 6, 8 or 10 corresponding to dipole-dipole, dipole-quadrupole or quadrupole-quadrupole interaction, respectively.

The magnitude of the spacial overlap of the wavefunctions of the rare earth ion and the oxygen atom of the ligand, expressed by $\exp(-2R/L)$ in Eq. (3), is nearly independent of halogenation, because the frequency of the metal-oxygen vibration as obtained by infrared absorption measurement remains nearly unchanged as a result of halogenation so that the value of R is regarded as not changing. Therfore, if the energy transfer in rare earth chelates under discussion is dominated by exchange interaction, the P_t/S values must be constant among chelates in the table. In the case of multipole interaction, since the lifetime of rare earth ion τ_{RE} is not usually affected by the kinds of ligands, the value of $P_t\tau_{ph}/S$ in Eq. (4), which is equal to η/S, must be constant. Therefore, the values of P_t/S and η/S were calculated and are shown in the table to examine which of these mechanisms is responsible.

It is noted that the values of η/S change in two orders of magnitude while those of P_t/S are in the same order. By taking account of the experimental error in estimating the shape of phsphorescence spectrum in TbD, we might be allowed to conclude that P_t/S is kept nearly constant among three compounds, although η/S changes appreciably.

Although only poor data are available for the moment, we may conclude that the intramolecular energy transfer in rare earth chelates is governed by the resonance mechanism due to exchange interaction, but not to electric multipole interaction, between the ligand triplet state and central rare earth ion. In fact, this conclusion is in agreement

TABLE 1. RELATIVE VALUES OF THE QUANTITIES CONCERNING ENERGY TRANSFER PROCESS FOR HALOGENATED TERBIUM CHELATES IN ETHER-TOLUENE SOLUTIONS AT 77°K

The meaning of the symbols is given in the text.

Compound	TbD	TbDCl	TbDBr
Overlap integral S	1.0 ±0.1	0.34 ±0.03	0.29 ±0.03
Emission efficiency η	1.00±0.03	0.0039±0.0003	0.0018±0.0002
Phosphorescence lifetime τ_{ph}	1.00±0.00	0.0092±0.0002	0.007 ±0.001
Transfer probability P_t	1.00±0.03	0.43 ±0.10	0.26 ±0.09
η/S	1.0 ±0.1	0.012 ±0.002	0.006 ±0.001
P_t/S	1.0 ±0.1	1.3 ±0.5	0.9 ±0.4

with that obtained by our previous investigation[8] in which the measurement of the infrared absorption spectra was used as the tool.

Conclusion

The substitution of chlorine and bromine atoms for the central hydrogen of the ligand has been performed in a number of dibenzoylmethanates of rare earth ions such as Eu, Tb, Sm, Dy, Gd and La. The changes of luminescence properties due to halogenation have been found to be remarkable. The intensity of the rare earth ion emission decreases in the order H→Cl→Br, while the phosphorescence spectra are blue-shifted and the intensity is strongly enhanced accompanied by the decrease of the lifetime. This is understood as being due to a pseudo-internal heavy atom effect, and provides evidence that intramolecular energy transfer takes place *via* the triplet state of the ligand. Luminescence features were examined further according to the theory of resonance energy transfer. In the case of terbium chelates, the ratio of the transfer probability to the overlap integral between the phosphorescence spectra and the rare earth absorption spectra has been found to remain nearly unchanged under halogenation. These facts lead us to the conclusion that the intramolecular energy transfer is caused by the resonance mechanism due to exchange interaction.

The authors would like to thank Dr. Y. Matsuda for his discussion. They are also indebted to Mr. S. Tamura and Miss F. Miyazawa of this Institute for the analysis of rare earth chelates.

BULLETIN OF THE CHEMICAL SOCIETY OF JAPAN VOL. 43 2409—2413 (1970)

An Electron Spin Resonance Study of 1,1′- and 2,2′-Biazulenyl Anion Radicals

Yusaku IKEGAMI and Shuichi SETO

Chemical Research Institute of Non-Aqueous Solutions, Tohoku University, Katahira-2-chome, Sendai

(Received March 2, 1970)

The electron spin resonance (ESR) spectra of the anion radicals of 1,1′- and 2,2′-biazulenyls have been examined. The ESR spectrum of the latter shows that the unpaired spin is distributed equally between both azulene rings of the molecule. Theoretical calculation of the spin densities by the McLachlan procedure gave satisfactory agreement with the experimentally estimated densities. The ESR spectrum of the anion radical of 1,1′-biazulenyl, which could only be generated by an electrolytic technique, is explained by the fact that the spin exchange between the two halves of the molecule is slow. However, the ESR spectrum of the anion radical of the 3,3′-dicarbethoxy derivative of 1,1′-isomer showed rapid spin exchange through 1,1′-bond.

Recent success in the synthesis of 1,1′- (I) and 2,2′-biazulenyls (II) by Morita and Takase[1] revealed that there is a wide difference in the physical properties of the two isomers. Difference of their absorption spectra, for example, is distinct at around 400 mμ region: the absorption maximum of I is at 382 mμ ($\varepsilon=13200$) while II has two peaks at 406 (25600) and 432 mμ (45300) in dimethoxyethane (DME). A similar tendency for the positions of the absorption maxima is noted in the spectra of 3,3′- and 2,2′-biguaiazulenyls which have been reported by Hagen, Heilbronner and Straub.[2] It is presumed that a conformational problem between two planar azulene rings of biazulenyls might be closely related to the essential features of their electronic spectra.

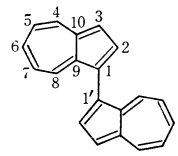

I

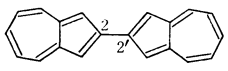

II

Several investigators[3] have studied the electron spin resonance (ESR) spectra of the anion radicals

1) T. Morita and K. Takase presented at the 20th Annual Meeting of the Chemical Society of Japan in Tokyo, 1967.

2) R. Hagen, E. Heilbronner and P. A. Straub, *Helv. Chim. Acta*, **51**, 45 (1968).

3) P. H. Rieger and G. K. Fraenkel, *J. Chem. Phys.*, **37**, 2795 (1962); **39**, 609 (1963); K. Ishizu, This Bulletin, **37**, 1093 (1964); M. Hirayama, *ibid.*, **40**, 2530 (1967).

formed by the reduction of biphenyl derivatives and have discussed the planarity of the two aromatic rings. ESR studies of azulene anion radical, a particularly interesting compound as a non-alternant hydrocarbon, have been made by some investigators,[4-6] and the π-electron densities estimated theoretically and experimentally have been discussed in detail.[4] It should be possible to obtain considerable information on the spin density contribution in the biazulenyls, as well as their molecular structures, by ESR study of their anion radicals. The ESR spectra and the calculated spin densities for the biazulenyl anion radicals are reported in this paper.

Experimental

The materials, 1,1′-biazulenyl, mp 104°C, 2,2′-biazulenyl, mp 200°C, and 3,3′-dicarbethoxy-1,1′-biazulenyl, mp 212°C, were purified by recrystallization. All solvents were degassed by at least five freezing-pumping cycles after being purified. 1,2-Dimethoxyethane (DME) and tetrahydrofuran (THF) were preserved in each flask, connected with a high vacuum apparatus as solutions of sodium anthracenide. *N,N*-Dimethylformamide (DMF) was distilled on to a molecular sieve (4A, small pellet) which had been flame dried in a vacuum. The solvents were distilled into the reaction vessels connected with the sample tube for measurement.

Reduction with alkali metal was performed by the usual method using lithium, sodium and potassium metals as reducing agents. The technique employed in the electrolytic generation of free radicals is similar to that used by Hirayama.[7] Electrolytic reduction was performed using DMF as a solvent and tetra-*n*-propylammonium perchlorate as the supporting electrolyte.

The ESR spectra were measured at room temperature with a Hitachi X-band ESR spectrometer, Model MPU-3B, using a field modulation of 100 kcps. Analysis of the spectra was confirmed by simulation for which a JEOL spectrum computer, JRA-5, was used.*1 Numerical calculation was carried out on the NEAC 2230 at the Computation Center, Tohoku University.

The absorption spectra were measured in the degassed solvent at room temperature by using a Cary Model 14 spectrophotometer.

Results and Discussion

2,2′-Biazulenyl Anion Radical. Treatment of 2,2′-biazulenyl (II) with lithium, sodium or potassium metal in degassed DME or THF caused an immediate change in color to deep blue. The

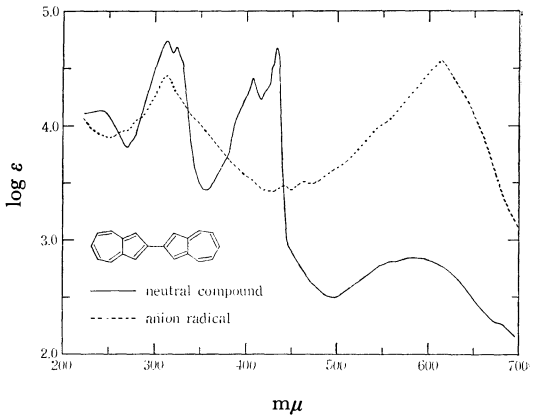

Fig. 1. Absorption spectra of 2,2′-biazulenyl (II) and its anion radical generated by the reduction of II with lithium metal in degassed DME.

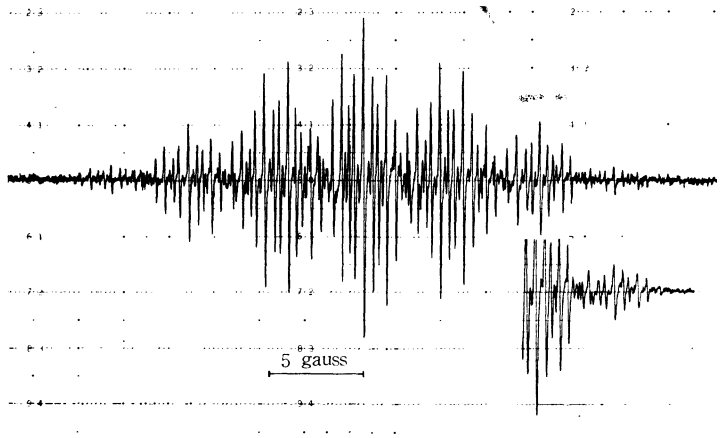

Fig. 2. ESR spectrum of 2,2′-biazulenyl anion radical generated by the reduction of II with lithium metal in DME.

4) I. Bernal, P. H. Rieger and G. K. Fraenkel, *J. Chem. Phys.*, **37**, 1489 (1962).
5) A. H. Reddoch, *ibid.*, **41**, 444 (1964).
6) A. H. Reddoch, *ibid.*, **43**, 225 (1965).
7) M. Hirayama, This Bulletin, **40**, 1822 (1967).

*1 The authors express their thanks to the computer staff of Japan Electron Optics Laboratory, Co., Ltd.

Table 1. Observed hyperfine splitting constants (a_i^H) for 2,2′-biazulenyl anion radical

Ring position (Number of H)	a_i^H, gauss						
	Metal reduction						Electrolysis in DMF
	Li-DME	Li-THF	Na-DME	Na-THF	K-DME	K-THF	
1,3,1′,3′ (4H)	0.475	0.477	0.492	0.478	0.481	0.496	0.494
4,8,4′,8′ (4H)	4.037	4.026	4.097	4.041	4.051	4.051	4.111
5,7,5′,7′ (4H)	1.200	1.227	1.239	1.219	1.233	1.239	1.248
6, 6′ (2H)	5.259	5.261	5.345	5.256	5.274	5.286	5.355
Total extent	33.4	33.4	34.0	33.5	33.6	33.7	34.1

colored solution is quite stable for a long period and shows a strong ESR signal. The absorption spectrum of the solution generated by the treatment of II with a lithium metal for a few days at room temperature is shown in Fig. 1, and compared with the spectrum of the neutral compound. Further treatment of the colored solution with the metal for a a week resulted in a loss of both the blue color and the ESR signal. This might be due to the formation of the diamagnetic dianion of II by the further reduction of the anion radical.

The ESR spectrum of the blue solution in Fig. 2 was measured at room temperature. Similar spectra were obtained by the reduction of II with sodium or potassium metal in DME or THF and by the electrolytic reduction of II in DMF using tetra-*n*-propylammonium perchlorate as the supporting electrolyte. Hyperfine structure of the spectrum was analyzed with four splitting constants (a_i^H), as expected for the symmetrical structure of II. It is thus recognized that the unpaired electron in the anion radical is distributed equally between both azulene rings. No metal coupling has been observed in all the spectra. The line widths for the spectra are between 75 and 140 milligauss. The observed splitting constants and their assignments are given in Table 1. The assignments were made reasonably by comparison with the calculated spin densities.

Calculations of unpaired spin densities (ρ_i) for the anion radical were carried out by employing both the Hückel LCAO molecular orbital theory and the approximate configuration interaction treatment proposed by McLachlan.[8] The resonance integral parameters (β_{ij}) for the 2,2′- and 9,10- (9′,10′-) bonds were varied over the following ranges:

$$0.6\beta \leqq \beta_{2,2'} \leqq 1.2\beta,$$

$$0.9\beta \leqq \beta_{9,10} = \beta_{9',10'} \leqq 1.0\beta.$$

All other bond length variations were neglected and the λ parameter in the McLachlan procedure was fixed at the value, $\lambda = 1.2\beta$, in our calculation. The $|Q_{CH}^H|$ values obtained by the relation, $a_i^H = Q_{CH}^H \cdot \rho_i$, using the observed splitting constants and the calculated spin densities, are compared with the resonance integral parameters. As easily expected from the fact that the total extent of the spectrum, 33.4—34.1 gauss, suggests the presence of negative spin densities, the McLachlan procedure showed better values than by Hückel molecular orbital calculation.

Variations of the $|Q_{CH}^H|$ values versus the parameter, $\beta_{2,2'}$, are shown in Figs. 3a and 3b for the cases in which $\beta_{9,10}$ are 0.9β and 1.0β. We see that the parameter $\beta_{2,2'}$ mostly affects the Q_{CH}^H values at the 1- and 3-(1′- and 3′-)positions. As far as the above parameters are concerned, each of the McLachlan spin densities at the positions from 4 through 8 (also

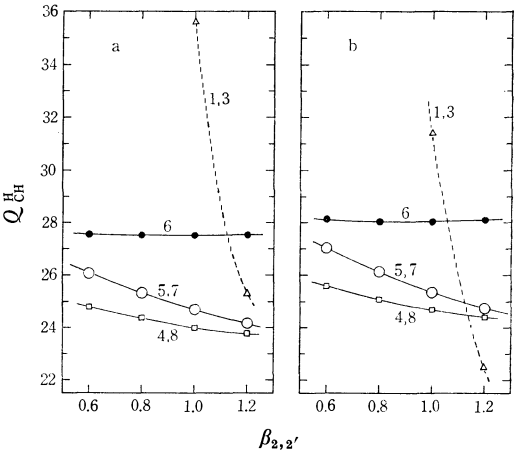

Fig. 3. Q_{CH}^H values in the relation, a_i^H(obsvd.) = $Q_{CH}^H \rho_i$ (calcd.), as a function of the resonance integral parameter for the 2,2′-bond ($\beta_{2,2'}$) of 2,2′-biazulenyl anion radical.
a: $\beta_{9,10} = 1.0\beta$, b: $\beta_{9,10} = 0.9\beta$.

4′ through 8′) in the seven membered rings differs by less than 12%. Assuming the tendency of the variation of Q_{CH}^H with bond angle in the azulene anion radical, estimated by Bernal *et al.*[4] a good agreement with the experimental splitting constants is recognized by the McLachlan method when both the parameters, $\beta_{9,10}$ and $\beta_{2,2'}$, were close to 1.0β. Using 0.9β[4] as the $\beta_{9,10}$, a good result was also obtained when $\beta_{2,2'}$ was close to 1.0β; the re-

8) A. D. McLachlan, *Mol. Phys.*, **3**, 233 (1960).

TABLE 2. CALCULATED SPIN DENSITIES (ρ_i) FOR 2,2′-BIAZULENYL ANION RADICAL

Position	$\beta_{9,10}$[a]$=0.9\beta$			$\beta_{9,10}$[a]$=1.0\beta$		
	ρ_i		$\lvert Q^H_{CH}\rvert$[b]	ρ_i		$\lvert Q^H_{CH}\rvert$[b]
	Hückel	McLachlan		Hückel	McLachlan	
1, 3,1′, 3′	0.01899	0.01553	31	0.01749	0.01366	36
2, 2′	0.04368	0.03519		0.04087	0.03139	
4, 8,4′, 8′	0.11491	0.16545	25	0.11793	0.16987	24
5, 7,5′, 7′	0.00324	−0.04853	26	0.00309	−0.04977	25
6, 6′	0.12755	0.18996	28	0.12999	0.19356	28
9,10,9′,10′	0.02724	0.00497		0.02606	0.00376	

a) The resonance integral parameters for 9,10- and 9′,10′-bonds. All other bond length variations were neglected.

b) $\lvert Q^H_{CH}\rvert$ value in the relation of $a^H_i = Q^H_{CH}\rho_i$, in which the average a^H_i observed and the McLachlan spin density were used.

sults are listed in Table 2. Thus, the π-electrons of the two halves in II conjugate freely through the central 2,2′-bond, and it is clear that the two azulene rings are co-planar in the anion radical. Bernal *et al.*[4] estimated theoretically the Q^H_{CH} value for a regular seven-membered aromatic ring to be −15.2 gauss. However, the $\lvert Q^H_{CH}\rvert$ value does not seem to be far from 23—28 gauss as seen from Table 2. Similar values are also seen for the cases of 2-methoxyazulene anion radical,[9] tropone anion radical,[10] cycloheptatrienyl radical[11] and cycloheptatrienyl dianion radical.[12]

1,1′-Biazulenyl Anion Radical. The anion radical of 1,1′-biazulenyl (I) is not so stable as that of its 2,2′-isomer. For example, the solution of I in degassed DME or 2-methyltetrahydrofuran reacted readily with an alkali metal losing its green color. However, no ESR signals were observed during the course of reaction at room temperature. Electrolysis of the green solution of I in DMF at *ca.* 2.3 V, however, resulted in a pale greenish yellow solution which exhibited a stable ESR spectrum of the anion radical. The spectrum is shown in Fig. 4. No decay of the intensity of the spectrum was observed during the course of a few hours.

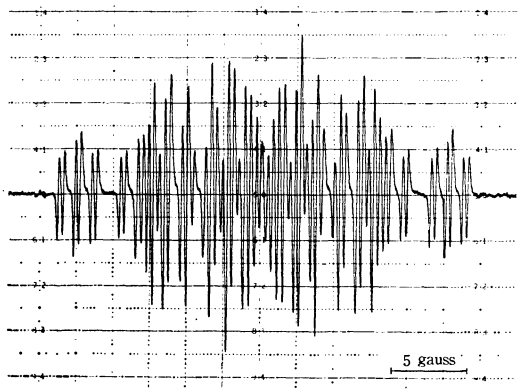

Fig. 4. ESR spectrum of 1,1′-biazulenyl anion radical generated by the electrolytic reduction in DMF.

Interesting facts seen from the spectrum are that it does not have a central strong line and that the hyperfine structure consists of five splitting constants, listed in Table 3, each of which is close to that of the azulene anion radical.[4-6] Thus, the spectrum resembles that of the azulene anion radical except that the smallest splitting is shown by doublets of relative intensities 1 : 1 as in Fig. 4. The simplest explanation of the spectrum is that spin exchange between the two halves of the molecule is slow, and the hyperfine structure originates from the seven protons on one half of the molecule. The assignment for the splitting constants is made by comparison with that for the azulene anion radical,[4] as indicated in Table 3. It might be necessary to see if the rate of intramolecular electron transfer of the anion of I can be increased by measuring its spectrum at elevated temperatures. However, measurement has not been successful because of the instability of the anion radical.

The slow spin exchange in the anion of I is analogous to the situation existing in the anion radical of

TABLE 3. OBSERVED HYPERFINE SPLITTING CONSTANTS (a^H_i) FOR 1,1′-BIAZULENYL ANION RADICAL COMPARED WITH THOSE FOR AZULENE ANION RADICAL[4]

Ring position (Number of H)		a^H_i, gauss	a^H_i for azulene anion radical
3	(1H)	0.361	0.274 (2H)
2	(1H)	4.091	3.948
4, 8	(2H)	5.903	6.219
5, 7	(2H)	1.120	1.338
6	(1H)	8.640	8.829

9) Y. Ikegami, unpublished result.

10) Y. Ikegami and S. Seto, This Bulletin, **41**, 2225 (1968).

11) A. Carrington and I. C. P. Smith, *Mol. Phys.*, **7**, 99 (1963).

12) N. L. Bauld and M. S. Brown, *J. Amer. Chem. Soc.*, **87**, 4390 (1965).

bis(*p*-nitrophenyl)ether.[13] In the anion radical of I, the localization of the unpaired electron should be attributed to the inability of the π-electrons in both azulene rings to overlap at the position of the 1,1′-bond. Moreover, the equivalence of both protons at 4- and 8-positions (and also 5- and 7-positions), shown by their splitting constants, indicates that the electronical interaction through the 1,1′-bond between the five-membered rings is small. The steric repulsion between ring protons at 2- and 8′- (2′- and 8-)positions probably makes it impossible for the two azulene rings to be co-planar. This difficulty might also be assisted by the electronical repulsion between the five-membered rings which are usually known to be negatively charged in azulene structure.[14] Such a slow spin exchange was not observed in the ESR spectrum of 1,1′-binaphthyl anion radical, prepared by the reduction of 1,1′-binaphthyl with sodium metal in DME, in which at least 135 hyperfine splitting lines with a central strong line were observed within the total extent of 22 gauss of the spectrum.[15]

The Anion Radical of 3,3′-Dicarbethoxy-1,1′-biazulenyl. In contrast to the case of I, the dicarbethoxy derivative (III) of I exhibits rapid spin exchange through 1,1′-bond.

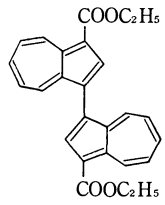

III

The anion radical of III generated by reduction with sodium metal in DME showed an ESR spectrum which is analyzed with four hyperfine splitting constants. The spectrum and the splitting constants are shown in Fig. 5 and Table 4, respectively. Each of the constants represents coupling with two equivalent protons giving triplets of relative intensities 1 : 2 : 1. A similar spectrum was obtained by the electrochemical reduction of III in DMF. The splitting constants are included in Table 4. Measurement of the spectrum at −50°C did not show any signs of slow spin exchange as in the spectrum of the anion radical of compound I.

Total extent of the spectrum (14.3 gauss) in Fig. 5 suggests that a considerable amount of spin density might be expected to be on the two carbethoxy groups in the molecule. However, an explanation of this suggestion by the calculation of the McLachlan spin densities, using some parameters related to the carbethoxy group[7,16] and resonance integral parameters for the 1,1′-bond, can not be given yet, although the two splitting constants, 2.923 and 0.640 gauss, could be easily assigned to the protons at 6- and 2- (6′- and 2′-)positions, respectively. ESR measurements of the anion radicals of other carbethoxy derivatives of azulene may provide some information on the effect of the substituents in the anion of III. However, our experiments for the cases of 1-carbethoxyazulene[17] and 1,3-dicarbethoxyazulene[18] did not show any ESR signals by standard techniques. Further attempts are being made.

Table 4. Observed hyperfine splitting constants (a_i^H) for the anion radical of 3,3′-dicarbethoxy-1,1′-biazulenyl

Reducing method	a_i^H*, gauss				Total extent
Na in DME	2.923	1.906	1.663	0.640	14.3
Electrolysis in DMF	2.882	1.845	1.691	0.737	14.3

* Each represents coupling with two equivalent protons.

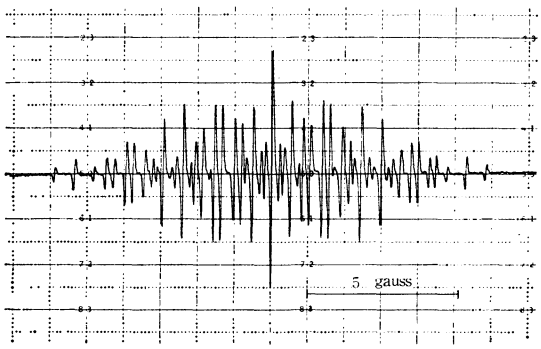

Fig. 5. ESR spectrum of the anion radical of 3,3′-dicarbethoxy-1,1′-biazulenyl (III) generated by the reduction with sodium metal in DME.

The authors wish to express their appreciation to Professor K. Takase and Mr. T. Morita for their donation of materials. We are also grateful to Professor T. Isobe, Dr. M. Hirayama and Dr. H. Yokoi for their helpful discussions.

13) J. E. Harriman and A. H. Maki, *J. Chem. Phys.*, **39**, 778 (1963).
14) A. Julg, *Compt. Rend.*, **239**, 1498 (1954); *J. Chem. Phys.*, **52**, 377 (1955); A. G. Anderson, Jr., and B. M. Steckler, *J. Amer. Chem. Soc.*, **81**, 4941 (1959).
15) Y. Ikegami, unpublished result.
16) M. Hirayama and T. Isobe, This Bulletin, **41**, 1502 (1968).
17) W. Treibs, H.-J. Neupert and J. Hiebsch, *Chem. Ber.*, **92**, 1216 (1959).
18) T. Nozoe, S. Seto, S. Matsumura and T. Asano, *Proc. Japan Acad.*, **32**, 339 (1956).

BULLETIN OF THE CHEMICAL SOCIETY OF JAPAN VOL. 43 2414—2418 (1970)

Electronic Absorption Spectra and Electronic Structures of Some Würster's Blue Salts

Tadayoshi SAKATA and Saburo NAGAKURA

The Institute for Solid State Physics, The University of Tokyo, Roppongi, Minato-ku, Tokyo

(Received March 4, 1970)

Electronic absorption spectra were measured at various temperatures for Würster's blue iodide, bromide, and chloride. The charge-transfer bands were found to be strongly dependent upon temperature. Concerning the iodide, the temperature dependency can be explained quantitatively, or at least semiquantitatively, by the aid of the linear Ising model in relation to the local ordering of the electron spins of Würster's blue cation radicals. This model gives the exchange energy of 99 ± 23 cm^{-1} for the iodide. For the bromide and the chloride, the dimer model was successfully applied to the analysis of the temperature dependence of the charge-transfer bands, giving singlet-triplet energy separations of 248 ± 30 cm^{-1} and 255 ± 30 cm^{-1} for the bromide and the chloride, respectively. The electronic structure and the intermolecular interaction were discussed for these radical salts, their electronic absorption spectra being compared with one another.

The Würster's blue radical salts are interesting research subjects because of their peculiar physicochemical properties.[1-12] For example, Würster's blue perchlorate (WBP) exhibits an unusual temperature dependency in the intensity of its electronic absorption spectrum. In previous papers[11,12] we studied this phenomenon, paying special attention to the phase transition mechanism and concluded that the dimerization mechanism of the phase transition is appropriate to solid WBP and that the disproportionation mechanism proposed by Kommandeur *et al.*[7-10] may be disregarded.

In the present paper, the temperature dependence of electronic absorption spectra was measured for the other Würster's blue salts: Würster's blue iodide (WBI), Würster's blue bromide (WBB), and Würster's blue chloride (WBC). The X-ray crystal analysis study of WBI was performed by de Boer *et al.*[13] According to their result, WBI takes a crystal structure in which the Würster's blue cations pack face-to-face to form regular columns parallel to the *b*-axis. The magnetic susceptibility of WBI was found to be well explained in the temperature range of 77—300°K by the aid of the linear Ising model.[14,15] From this it is revealed that the phase transition observed for WBP may not occur WBI in this temperature range. In view of this, we have undertaken to measure the temperature dependence of the electronic absorption spectra of WBI, WBB, and WBC and to compare the results with those for WBP.

Experimental

WBI and WBB were prepared by the method described in the literature.[16] WBC was prepared by oxidizing *N,N,N',N'*-tetramethyl-*p*-phenylenediamine in methanol with chlorine gas.

A Cary recording spectrophotometer model 14 M was used for the measurement of the electronic absorption spectra of solid samples. Solid, thin films used for the

1) K. H. Hausser, *Z. Naturforsch.*, **11a**, 20 (1956).
2) W. Duffy, Jr., *J. Chem. Phys.*, **36**, 490 (1962).
3) K. Okumura *J. Phys. Soc. Japan*, **18**, 69 (1963).
4) H. Chihara, M. Nakamura and S. Seki, This Bulletin, **38**, 1776 (1965).
5) D. D. Thomas, H. Keller and H. M. McConnell, *J. Chem. Phys.*, **39**, 2321 (1963).
6) K. Uemura, S. Nakayama, Y. Seo, K. Suzuki and Y. Ooshika, This Bulletin, **39**, 1348 (1966).
7) H. J. Monkhorst and J. Kommandeur, *J. Chem. Phys.*, **47**, 391 (1967).
8) G. T. Pott and J. Kommandeur, *ibid.*, **47**, 395 (1967).
9) H. J. Monkhorst, G. T. Pott and J. Kommandeur, *ibid.*, **47**, 401 (1967).
10) G. T. Pott, C. F. van Bruggen and J. Kommandeur, *ibid.*, **47**, 409 (1967).
11) T. Sakata and S. Nagakura, This Bulletin, **42**, 1497 (1969).
12) T. Sakata and S. Nagakura, *Mol. Phys.*, to be published.
13) J. L. de Boer, A. Vos and K. Huml, *Acta Crystallogr.*, **B24**, 542 (1968).
14) M. Inoue and J. Tanaka, presented at the Symposium on Molecular Structure, Tokyo, October, 1968.
15) M. Mizuno, T. Sakabe, M. Inoue and J. Tanaka, presented at the 20th Annual Meeting of the Chemical Society of Japan, Tokyo, April, 1967.
16) G. K. Hughes and N. S. Hush, *J. Proc. Roy. Soc. N. S. W.*, **81**, 48 (1947).

absorption measurements were prepared by coating powdered samples on quartz plates by a stainless steel spatula.[11]

Absorption measurements at low temperatures were made by using glass Dewar vessels containing liquid helium or liquid nitrogen as a refrigerant, the temperature being measured by a thermocouple of (Au–Co) and Cu.

Results and Discussion

The Temperature Dependence of the Charge-Transfer Band of WBI. According to the X-ray crystal analysis data, WBI takes the crystal structure in which WB cations are located face-to-face forming one-dimensional columns.[13] Since the overlap between the π-electron orbitals of the neighboring cations is expected to be largest in the direction parallel to the columns, the one-dimensional model is applicable to the study of the charge-transfer (abbreviated hereafter to CT) interaction in solid WBI.

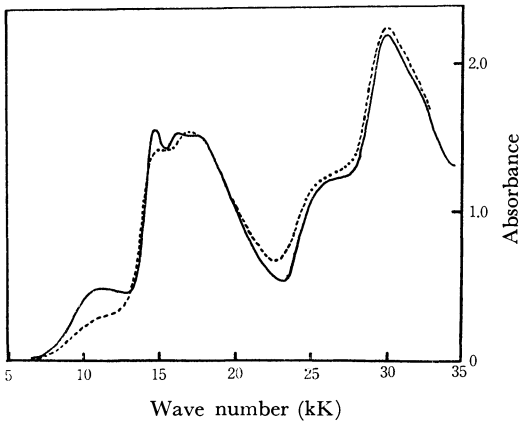

Fig. 1. The electronic absorption spectrum of the solid WBI.
---- at 260°K, ——— at 40°K

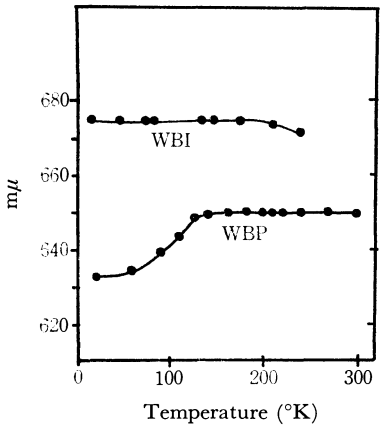

Fig. 2. Temperature dependence of the peak position of the first vibronic band for WBI and WBP.

The electronic absorption spectra of WBI measured at 260°K and at 40°K are shown in Fig. 1. First, let us consider the 600 mμ band due to the $^2B_{1u} \leftarrow {}^2B_{3g}$ transition of the WB cation. The peak position of this band is almost independent of temperature, though the vibrational structure becomes sharp with the decreasing temperature. The temperature dependence of the first vibronic band position observed for WBI is shown in Fig. 2, together with that for WBP. The peak position is almost constant for WBI in the temperature range of 40—260°K, while it varies greatly for WBP below the phase transition point. This suggests that the phase transition does not occur for WBI in this temperature range.

The 900 mμ band observed for solid WBI can safely be regarded as the CT band due to electron transfer between the half-occupied orbitals of the WB cation radicals. Its intensity greatly depends on temperature and increases with the decreasing temperature, as seen in Fig. 3. Since WBI shows no phase transition as mentioned above, it is not probable that solid WBI takes the dimer model which can be successfully applied to WBP. Therefore, we have undertaken to interpret the temperature dependency of the CT band of WBI by the aid of the one-dimensional Ising model, taking only the two neighboring WB cations in a chain.

The CT transition corresponding to the electron

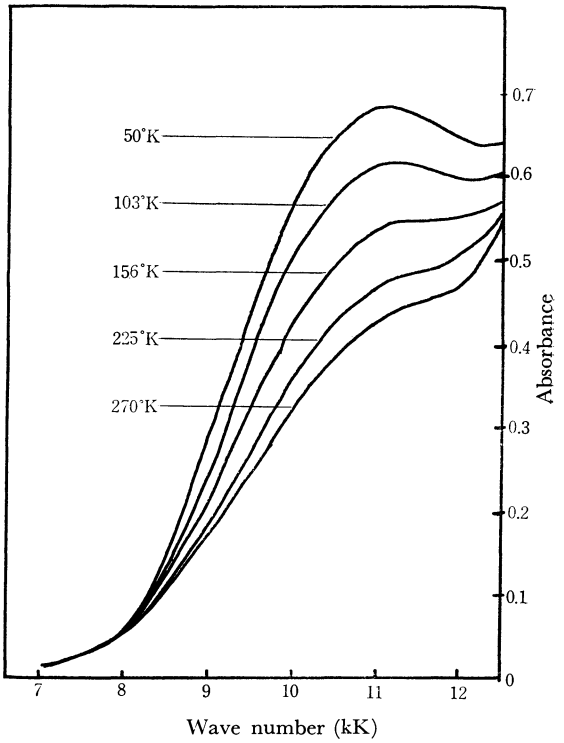

Fig. 3. The temperature dependence of the CT band of solid WBI.

transfer between the half-occupied orbitals of the two WB cation radicals is allowed, when the unpaired electron spins on these two orbitals are antiparallel with each other in the ground state ($S_1^zS_2^z=-1/4$). When they are parallel ($S_1^zS_2^z=1/4$), however, the transition is forbidden. This rule comes from the facts that the two spins must be antiparallel in the CT state from Pauli's principle and that the electron does not change its spin in the optical transition. We define the normalized intensity of the CT band, I_{CT}, in such a way as it takes 1 and 0 for the allowed and forbidden transitions, respectively; it is expressed with regard to the spin of the ground state as follows:

$$I_{CT} = -2S_1^zS_2^z + \frac{1}{2} \tag{1}$$

The above consideration can be generalized for a regular linear chain as follows:

$$I_{CT} = -2\langle S_i^zS_{i+1}^z\rangle + \frac{1}{2} \tag{2}$$

where $\langle\ \rangle$ represents the statistical average for the system. Now let us write the Ising Hamiltonian of the system by the aid of the exchange energy, J, as follows:[17]

$$\boldsymbol{H} = 2J\sum_i S_i^zS_{i+1}^z \tag{3}$$

The solution of this Hamiltonian is well known, and $\langle S_i^zS_{i+1}^z\rangle$ is given as follows:

$$\langle S_i^zS_{i+1}^z\rangle = -\frac{1}{4}\tanh\frac{J}{2kT} \tag{4}$$

Accordingly, the following equation can be obtained from Eqs. (2) and (4):

$$I_{CT} = \frac{1}{2}\left(\tanh\frac{J}{2kT} + 1\right) \tag{5}$$

Figure 4 shows the temperature dependence of the normalized intensity of the CT band.*1

We can obtain J from the temperature, T_1, at which I_{CT} equals 3/4, namely, $\tanh J/2kT_1=1/2$. From Fig. 4, T_1 may be taken to be 130 ± 30°K; J is evaluated to be 99 ± 23 cm^{-1}. The theoretical curve for $J=99$ cm^{-1} is also shown in Fig. 4 for the purpose of comparison. The discrepancy between the theoretical and observed curves becomes predominant at higher temperatures. There may be two reasons for this discrepancy: 1) the J value and the transition probability may be dependent upon the temperature through the intermolecular distance, and 2) the Ising model may be applied inadequately. At any rate, it may be said that the calculated I_{CT} values are at least semiquantitatively

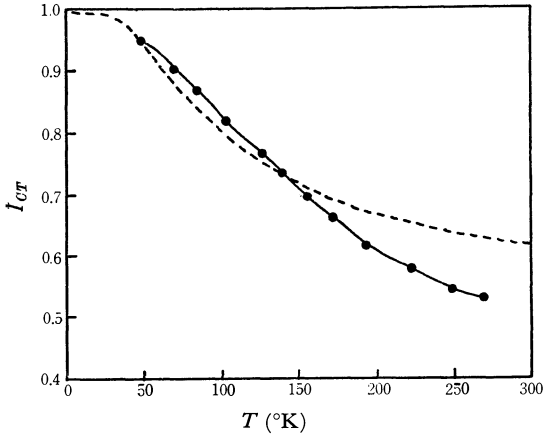

Fig. 4. The temperature dependence of the normalized intensity of the CT band.
----- theoretical curve by the linear Ising model
——— experimental curve

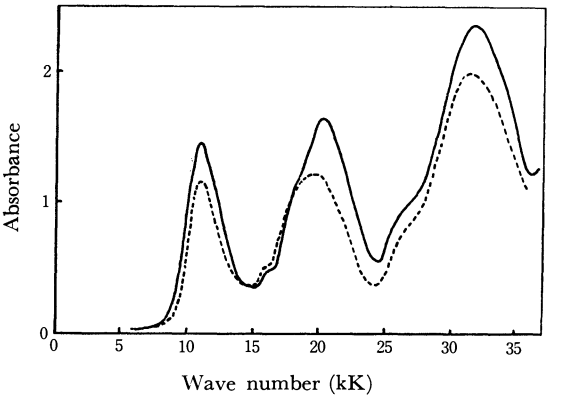

Fig. 5(a). The absorption spectra of WBC and WBB.
——— WBC ---- WBB

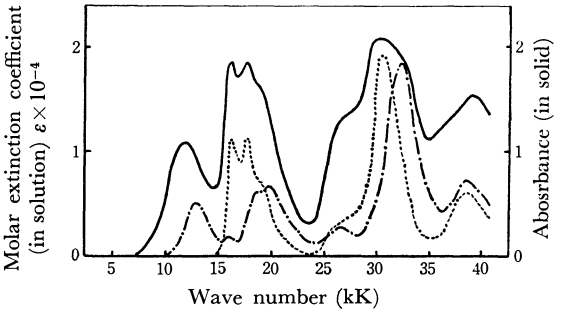

Fig. 5(b). The absorption spectra of WPB in solid and solution.
——— solid at 48°K, ---- ethanol solution at 295°K, —·— ethanol solution at 110°K

17) R. Kubo, H. Ichimura, T. Usui and N. Hashizume, "Statistical Mechanics," North-Holland Publishing Company, Amsterdam (1965), p. 348.

*1 The CT band intensity was obtained by integrating the area below the respective absorption curve over the frequency region lower than 11300 cm^{-1}. Since, in our experiment, the lowest temperature was 50°K, the intensity at 0°K was estimated approximately by extrapolation.

Table 1. The peak positions (cm^{-1}) of the absorption bands of various Würster's blue salts

		CT	lst LE	3 rd LE
Solution	WBP monomer	—	17000	30700
	WBP dimer	12900	19800	32300
Solid	WBP (high temp.)	11700	16500	30000
	WBP (low temp.)		17000	30800
	WBI (77°K)	11300	17000	30000
	WBB (77°K)	11200	19600	31600
	WBC (77°K)	11100	20500	31900

coincident with the observed values at lower temperatures. The J value obtained by this method agrees with that obtained from the magnetic susceptibility (83 cm^{-1}) measurements within the expermental error.[14] This seems to mean that our explanation on the temperature dependence of the CT band intensity is essentially correct for solid WBI.

The Absorption Spectra of Solid WBB and WBC. The absorption spectra of solid WBB and WBC were measured at ~77°K; the results are shown in Fig. 5(a). In Fig. 5(b) the absorption spectra of solid WBP and the free WB cation in solution are shown for the purpose of comparison. As is clearly seen in Fig. 5, the absorption spectra of solid WBB, WBC, and WBP are different from one another in their peak positions and in their shapes.

In Table 1, the peak positions in the absorption spectra of the solid Würster's blue salts under consideration are shown, together with those for WBP in solution. In this table, the first and third locally excited (LE) bands correspond, respectively, to the ~600 mμ and ~330 mμ ones of the WB cation radical monomer. Approximate values are taken for the peak positions of the first local excitation bands of WBP and WBI, since it is difficult to obtain their values definitely because of the vibrational structure. As is seen in Table 1, the first LE band shifts to higher frequencies in the order of WBP (high-temperature form)<WBI<WBP (low-temperature form)<WBB<WBC. The same tendency was observed for the third LE band. Furthermore, the ratio of the intensity of the CT band to that of the first or the third LE band also increases in the above order. This means that the ~600 mμ and ~330 mμ bands of the monomer are increasingly perturbed by the intermolecular interaction in the above order. That is to say, the strong interaction between the WB cation radicals is not only the source of the CT band but also has an influence on the intramolecular excitation band. In this connection, it may be noticed that the vibrational structures characteristic of the first absorption band of the WB cation radical disappear in solid WBB and WBC and that their band shapes resemble the spectra of the dimer in solution as seen in Fig. 5.

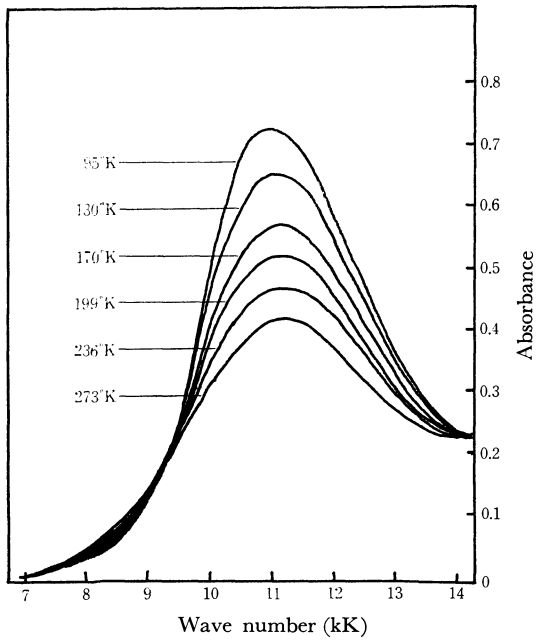

Fig. 6(a). The temperature dependence of the CT band of solid WBC.

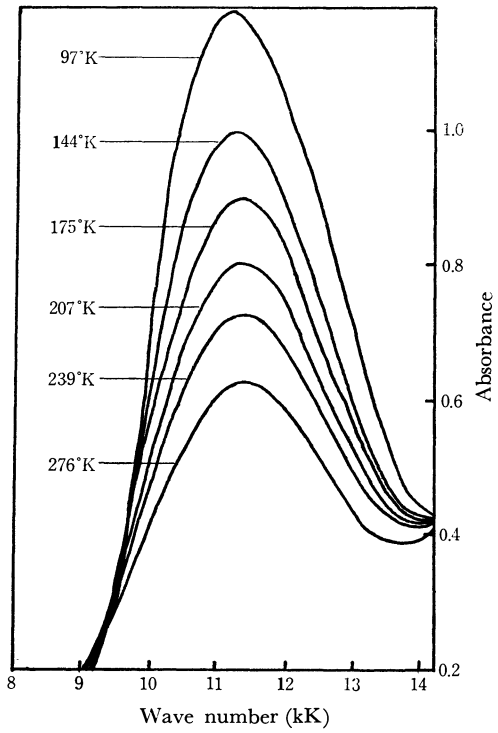

Fig. 6(b). The temperature dependence of the CT band of solid WBB.

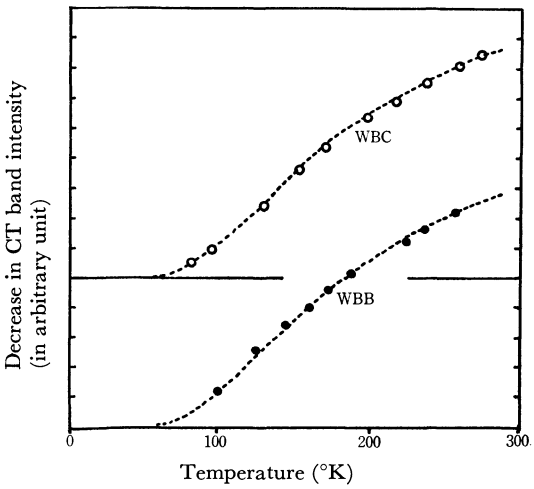

Fig. 7. Temperature dependence of the CT band intensity for WBC and WBB. The circles represent the observed values and the broken lines the theoretical ones.

The temperature dependence of the CT band was measured for WBB and WBC; we found an increase in its intensity with the decreasing temperature. Since this tendency observed for WBB and WBC is similar to that for WBP in the low-temperature phase, it may be expected that the temperature dependence of the CT band observed for the former salts can be explained by the dimer model which was successfully applied to the latter.[11] According to this model, the decrease in the CT band intensity turns out to be proportional to the population on the thermally accessible triplet exciton state caused by the exchange interaction between the two radical monomers. Actually, we applied the analytical method described in a previous paper[11] to the experimental data given in Fig. 6 and evaluated the singlet-triplet separation, J', as 248 ± 30 cm^{-1} and 255 ± 30 cm^{-1} for WBB and WBC, respectively. The theoretically expected temperature dependence of the CT band, calculated by the aid of the evaluated singlet-triplet separation, is shown in Fig. 7 for WBC and WBB. In this figure the observed values are also plotted for the purpose of comparison. We can find good agreement between the theoretical and experimental values for both WBC and WBB.

The authors should like to express their deep thanks to Dr. Akio Sakurai of this Institute for his helpful discussion.

BULLETIN OF THE CHEMICAL SOCIETY OF JAPAN VOL. 43 2418—2421 (1970)

Studies of Helical Aggregates of Molecules. II. The Sense of Twist in the Fibrous Aggregates from the Alkali Metal Soaps of Optically Active 12-Hydroxystearic Acid

Taro TACHIBANA, Shyoko KITAZAWA and Hideko TAKENO

Department of Chemistry, Ochanomizu University, Bunkyo-ku, Tokyo

(Received March 12, 1970)

Under an electron microscope, it was observed that the alkali metal soaps of 12-D(or L)-hydroxystearic acid separated out twisted fibers from various solutions. A symmetrical relationship regarding the sense of the twist was found between the soap fibers of the D-enantiomer and those of the L-enantiomer. In the case of the soap fibers of the D-enantiomer, the sense of twist was right-handed for the Li soap and left-handed for the Rb and Cs soaps. The Na- and the K- soap fibers produced both right-handed and left-handed fibers. A solvent effect with respect to the sense of twist was found for the fibers of the free acid and its Li soap. The cause of the twisting was discussed in connection with the structure and the growth process of the soap crystal.

In the preceding paper[1] we reported that optically active 12-hydroxystearic acid and its lithium soap produced twisted fibers when allowed to crystallize out from appropriate solvent and that the sense of twist is related to the optical isomerism of this hydroxy acid. Studies have since been extended to other univalent metal soaps, as has been described in part in a preliminary report.[2]

1) T. Tachibana and H. Kambara, This Bulletin, **42**, 3422 (1969).

2) T. Tachibana and H. Kambara, *J. Colloid Interfac. Sci.*, **28**, 173 (1968).

The sense of twist has been found to be associated with the cation size. This paper will describe the results obtained mainly with a series of the alkali metal soaps; the solvent effect on the sense of twist is also included.

Experimental

The purification of D-12-hydroxystearic acid from the commercial product and the preparation of L-12-hydroxystearic acid have been described previously.[1] The alkali metal soaps were prepared by neutralizing the acid with the desired metal hydroxide in anhydrous ethanol or in aqueous ethanol, by then recrystallizing several times from ethanol, and finally by drying over P_2O_5 *in vacuo*. The purity of these soaps was checked by elementary analysis, infrared absorption spectroscopy, and differential thermal analysis. The infrared spectra of these samples showed no peak at about 1700 cm^{-1} (the C=O stretching vibration for carboxylic acid) or at from 1600 to 1650 cm^{-1} (the deformation vibration for water). The absence of water was also confirmed by the use of differential thermographs. These results show that these soaps were reasonably pure and in an anhydrous form. The sample of the Rb soap was mixed with the K soap, since it was prepared by using RbOH, which had been found by fluorescent X-ray analysis to contain K in a Rb/K ratio of 80/20.

The sample of the NH_4 soap was a gift of Dr. Yoshiro Tsutsui, who prepared it by reacting the D-acid with liquid ammonia under 59 atm at 110°C for 24 hr in an autoclave.

The Ag soap was prepared by the metathesis of the Na soap in aqueous ethanol in a dark room.

The Tl(I) soap was prepared by neutralizing the D-acid in ethanol with an aqueous solution of thallous hydroxide.

The soap fibers are formed in the grease or the gel, which is made by dissolving the soap in a solvent at a high temperature and by then cooling the hot solution to room temperature. Since it was considered that the free acid may have been formed by the thermal decomposition of the soap during the preparation of the grease, the soap samples recovered from the grease were subjected to infrared analysis. It was confirmed that these samples contain no free acid.

The procedure of observing the fibers by means of an electron microscope was described in the preceding paper.[1]

Results

a) The Alkali Metal Soaps. Under the electron microscope, the grease or gel from the soaps was observed to consist of twisted fibers with a certain thickness, the thickness being dependent on the procedure used in making the grease. Figure 1 shows typical micrographs of the fibers of the alkali metal soaps.

As has been stated previously,[1] the Li soap produced twisted fibrils about 0.03 μ in width from ethanol, while helical ribbons of from 0.03 to 0.3 μ in width were produced from mineral oil and from Nujol. The Na and K soaps formed twisted fibers and ribbons from 0.02 to 0.3 μ in width, depending on the conditions used in the grease preparation. The Rb and Cs soaps produced ribbons of the form characteristic of these soaps, in addition to the fibers of a form such as was observed in the other alkali metal soaps.

The sense of twist was characteristic of the respective soaps. It is represented, together with the results for the free acid, in Table 1; it is found that

Table 1. The sense of twist in the fibers from both enantiomers of 12-hydroxystearic acid and their alkali metal soaps

Enantiomer	The sense* of twist					
		Alkali metal soap				
	Acid	Li	Na	K	Rb	Cs
D	l	r	r&l	r&l	l	l
L	r	l	r&l	r&l	r	r

* r: right-handed twist, l: left-handed twist

there is an enantiomorphic relationship between the D-enantiomer and the L-enantiomer for the alkali metal soaps as well as for the free acid. From this table, it can be seen also that the sense of twist for the soaps of the D-acid changes from right to left with an increase in the cation radius; it is right-handed for the Li soap of the D-acid, while it is left-handed for the Rb and Cs soaps of the D-acid.

The Na and K soaps, which occupy the intermediate positions, did not always give reproducible results. Usually, but not always, they were inclined to exhibit both right-handed fibers and left-handed fibers from the same sample. In detail, the same sample of the Na soap or the K soap produced either of these fibers alone on one occasion, and both right-handed and left-handed fibers at the same time on another occasion. In the latter case, the right-handed and the left-handed fibers appeared as separated groups, either group being predominant. These results led us to draw a hasty conclusion in a previous communication[3] that the sense of twist was always right-handed for the Na and K soaps.

Since the non-reproducible results were considered to be due to the slight difference in the soap samples, a further investigation was made with the samples of the Na and K soaps, which had been prepared by the reaction of the D-acid in its ethanol solution, (1) with an NaOH (or KOH) aqueous solution, (2) with an NaOH (or KOH) ethanol solution, and (3) with Na (or K)-alcoholate. The samples thus obtained showed identical infrared absorption spectra, X-ray diffraction patterns, and differential thermographs, indicating that they

3) T. Tachibana and H. Kambara, *J. Amer. Chem. Soc.*, **87**, 3015 (1965).

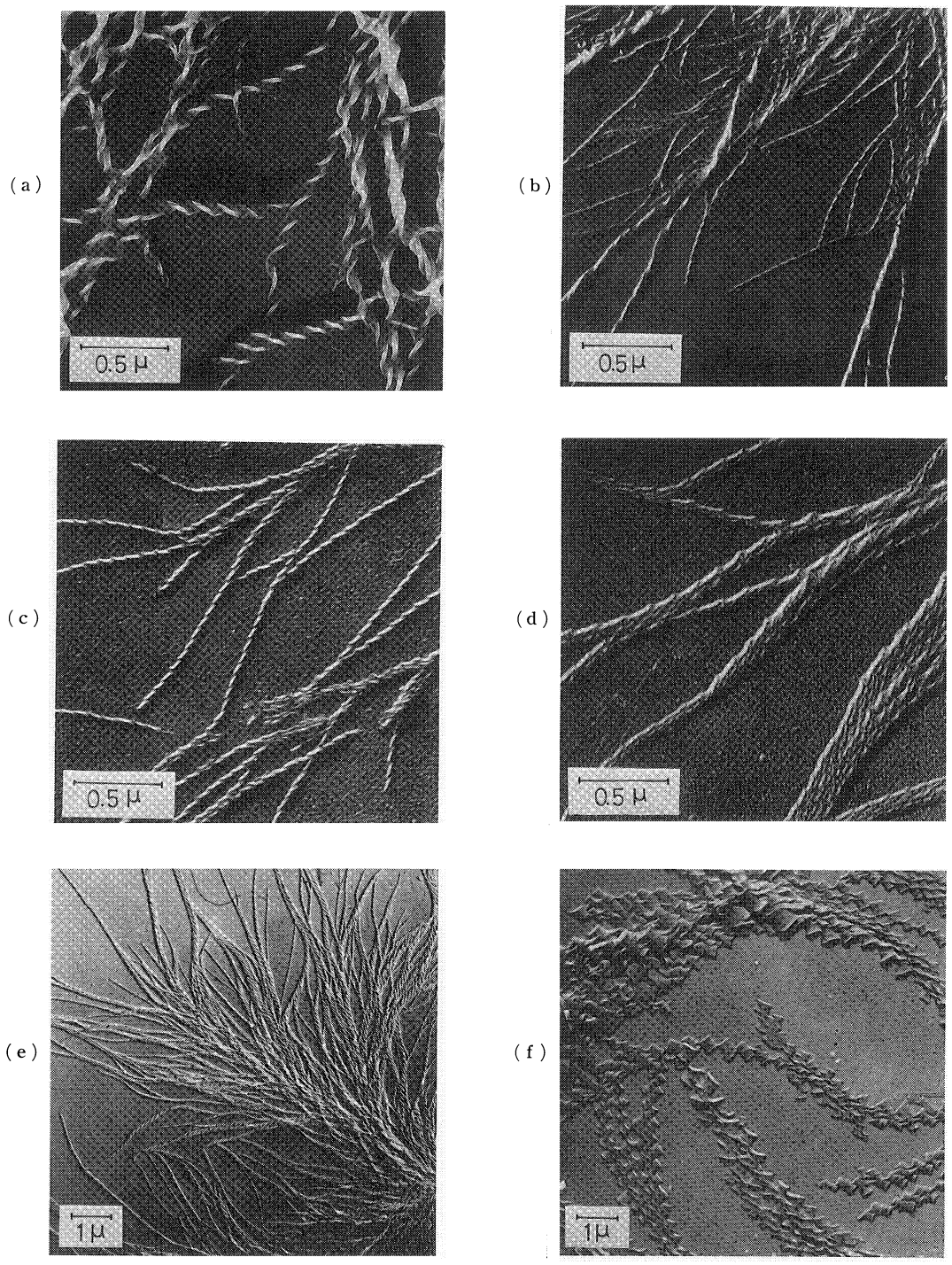

Fig. 1. The twisted fibers of the alkali metal soaps of D-12-hydroxystearic acid.
(a) Li soap from mineral oil, right-handed twist.
(b) Na soap from ethanol, right-handed & left-handed twists.
(c) K soap from hexanol, right-handed twist.
(d) K soap from nonanol, left-handed twist.
(e) Rb soap from hexanol, left-handed twist.
(f) Cs soap from hexanol, left-handed twist.

(a)

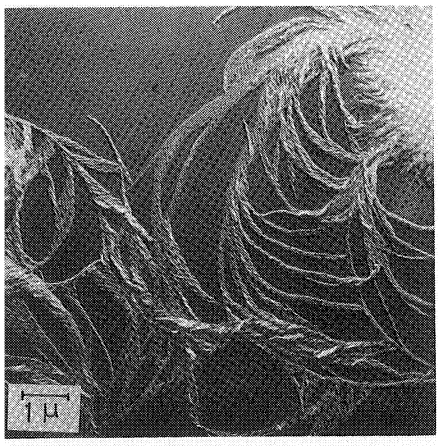

(b)

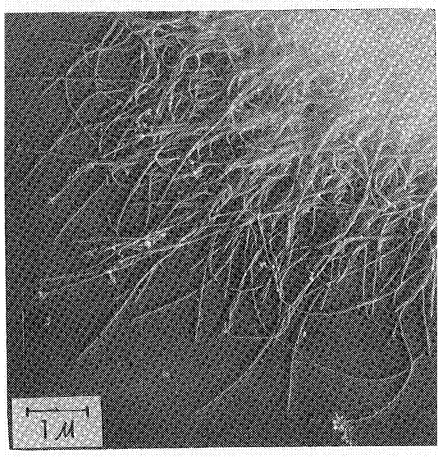

(c)

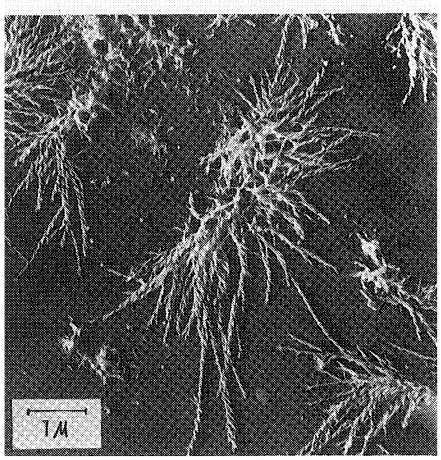

Fig. 2. The twisted fibers of the NH_4, Ag and Tl soaps of D-12-hydroxystearic acid.
(a) NH_4 soap from ethanol, left-handed twist.
(b) Ag soap from ethanol, left-handed twist.
(c) Tl soap from *n*-butanol, left-handed twist.

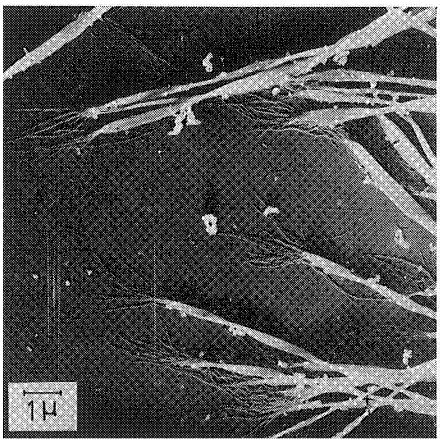

Fig. 3. The twisted fibers of D-12-hydroxystearic acid from nonanol.

belong to the same crystalline phase. Moreover, it was confirmed from these measurements that these samples are samples of the neutral soap, but not so-called acid soaps. The greases were prepared from these samples under the same conditions as far as was possible; consequently, all of the greases gave the same results. These Na-(or K-) soap samples produced both right-handed fibers and left-handed fibers from mineral oil or Nujol as well as from ethanol. Each fiber appeared as a separated group from the same sample; for the Na-soap fibers from mineral oil or Nujol, one group consisted of uniformely-thin fibrils with a right-handed twist, and another, of wide ribbons with a left-handed or right-handed twist. One may consider the possibility that the left-handed fibers consist of the free D-acid produced by the thermal decomposition of the Na soap during the preparation of the grease. However, the infrared analysis showed no free acid in the sample of the Na soap recovered from the grease. Therefore, the fact that both fibers were produced from these samples of the Na soap is to be ascribed to a property of this metal soap. Almost the same result was also obtained in the case of the K soap. Probably, the fibers twist in either the right-hand or the left-hand direction as a result of some slight difference in the conditions under which the fibers are formed. It can thus be suggested that the energy difference which determines whether the Na(or K)-soap fibers twist to the right or to the left is very slight, so that the effect of the asymmetric molecule is obscured. On the other hand, the Li-soap fibers twist stably to the right, and the Rb- and the Cs-soap fibers do so to the left. On the basis of these results, a specific effect of the alkali-metal cations can clearly be seen on the sense of twist.

b) The Other Soaps. The NH_4, Ag, and Tl(I) soaps of the D-acid were also investigated. Figure 2 shows typical micrographs of the fibers of these soaps. Since the NH_4 soap is readily decomposed with a rise in the temperature, the crystallization was done in a refrigerator after the saturated solution in ethanol had been prepared at room temperature. The precipitate thus obtained was found to contain more or less the free D-acid by infrared analysis; it was found to consist of fibers of the left-handed twist alone. These results strongly suggest that the NH_4-soap fibers exhibit a left-handed twist.

The Ag soap produced left-handed fibers from its ethanol solution.

The Tl(I) soap produced left-handed fibers from its ethanol, *n*-butanol, or *n*-octanol solution, although sometimes right-handed fibers were included. From these results, it can be roughly concluded that the fibers from the univalent metal soaps of the D-acid having a cation of a comparatively large size are inclined to twist to the left.

c) The Solvent Effect. An investigation was made into the effect of various solvents on the sense of twist in the fibers from the free D-acid and from its soaps. When the solvents used for the preparation of the grease were mineral oil, Nujol, ethanol, carbon bisulfide, nitrobenzene, and dimethyl formamide, it was found that these solvents greatly affect the form of the twisted fibers produced, but they had no influence on the sense of twist.

When a series of *n*-aliphatic alcohols were used as the solvents, a notable effect on the sense of twist was found only for the free D-acid and its Li soap, the cation sizes of which are comparatively small. The results are shown in Table 2. The free D-acid and its Li soap produced both left-handed fibers and right-handed fibers from the solution in an alcohol of from C_6 to C_{10}, while from the shorter-chain (C_2 to C_4) alcohols the D-acid fibers exhibited only a left-handed twist, and the Li-soap fibers, a right-handed twist alone. No solvent effect on the sense of twist was found for the fibers from the Na, K, Rb, and Cs soaps.

TABLE 2. THE EFFECT OF *n*-ALIPHATIC ALCOHOLS AS THE SOLVENT ON THE SENSE OF TWIST IN THE FIBERS OF D-12-HYDROXYSTEARIC ACID AND ITS ALKALI METAL SOAPS

Sample	Carbon number of *n*-aliphatic alcohols as the solvent								
	C_2	C_3	C_4	C_5	C_6	C_7	C_8	C_9	C_{10}
Free acid	l	l	l	r&l	r&l	r&l	r&l	r&l	r&l
Li soap	r	r	r	r	r&l	r&l	r&l	r&l	r&l
Na soap	r&l	r&l	r&l	r&l	r&l	r&l	r&l	r&l	r&l
K soap	r&l	r&l	r&l	r&l	r&l	r&l	r&l	r&l	r&l
Rb soap	l	l	l	l	l	l	l	l	l
Cs soap	l	l	l	l	l	l	l	l	l

r: right-handed twist, l: left-handed twist

The crystalline aggregates of the D-acid or its Li soap recovered from *n*-heptanol solution showed a melting point, an X-ray diffraction pattern, and an infrared spectrum identical to those of the samples from ethanol solution. This indicates that the observed effect is not due to the difference in the crystalline phase of the fibers produced. Probably, in any stage of the growth of the fibrous crystal the solvent molecules may act so as to obscure the asymmetrical effect of the enantiomer molecule through the solvation. Here it is interesting to note that the molecules of these alcohols approximate a fragment of 12-hydroxystearic acid molecules.

In this connection, it may be mentioned that cyclohexanol, which is a cyclic alcohol, did not exhibit this abnormal behavior, but functioned much like the normal C_2- to C_4-alcohols.

An attempt was made to investigate the effect of an optically-active solvent. The D-acid, the L-acid, and the respective soaps produced twisted fibers from solutions in optically active amyl alcohol (L-form). The results regarding the sense of twist

were quite identical with those with the solution in *n*-amyl alcohol. Accordingly, no effect of the optically-active solvent was observed.

Discussion

Twisted crystal shapes are not unique to soap fibers, but they have been observed for quartz and various whiskers. Wilman[4] explained such structures as the results of the rotational slip of crystal layers parallel to the cleavage plane. McClellan[5] explained the shape of soap fibers in terms of an equation derived by Eshelby,[6] who showed that a whisker containing an axial-screw dislocation must be uniformly twisted by an amount equal to the Burger vector of the dislocation divided by the crosssectional area of the whisker. However, the explanation that the twisting is a result of the dislocation seems doubtful in the case of the soap fibers, because it is difficult to explain why the Li soap of 12-D(or L)-hydroxystearic acid forms twisted fibers, whereas the racemic soap always forms non-twisted fibers.

All our findings described in the preceding paper and in the present paper have demonstrated that the sense of twist is determined by the chemical species and is, furthermore, dependent on the conformation of the molecule. Thus, the twisting should be explained by a mechanism which reflects the conformation of the molecule. Recently, in our laboratory, it has been found that the Na soap of a paraffin-chain fatty acid, for example, Na myristate, sometimes forms twisted fibers. In such a case, both right-handed and left-handed fibers are observed. Therefore, twisting is considered to be common for soap fibers and particularly likely in fibers with such asymmetric molecules as optically active 12-hydroxystearate.

Generally the crystal of a paraffin-chain compound is composed of alternating ionic and hydrocarbon layers. While the complete crystal structure determination has not yet been achieved for 12-hydroxystearic acid and its soaps, they may be regarded as being composed of such a layer structure, since these compounds also showed a long spacing, about 48 Å, in the X-ray powder patterns. Bird and Rooney[7] presented evidence of such a structure for Ca-soap fibers from a commercial fatty acid; they obtained that evidence by means of a high-resolution electron microscope. This structure must be responsible for the growth of the soap crystal in the form of a ribbon or a fiber.

If one of the surfaces of a thin ribbon is different from another surface in the structure, the distortion or twisting will tend to occur as a result of a surface stress which develops from the difference in the surface energy between the two surfaces. When the soap ribbon is produced from such a nonpolar solvent as Nujol, free-energy considerations require the development of the nonpolar surfaces in a manner that exposes the methyl groups to Nujol. Consequently, both surfaces of the ribbon would have the same structure, and would thus not cause any twisting. However, in the course of crystallization the two surfaces of a ribbon do not always have the same structure. In certain cases this may be caused by the adsorption of impurities on either surface. The case is the same with the ribbons deposited from any polar solvent. There could possibly also be a case in which one surface is polar, and the other, nonpolar. In these cases a surface stress would develop, leading to a twisting of the thin ribbon. Furthermore, when the molecules have an asymmetric conformation, the ribbon itself has an asymmetric structure and the surface stress acts to twist the ribbon favorably in a certain sense. Consequently, all the ribbons would twist in the same direction. In this view, twisting is considered to occur rather generally in thin ribbons. However, the surface stress decreases rapidly with an increase in the thickness, so the twisting becomes more difficult for too wide or too thick a ribbon. The analogy with a gross physical ribbon is useful in explaining the interesting electron-micrograph shown in Fig 3, which was obtained with a sample of the free D-acid from a nonanol solution. In this micrograph one can see many thin and twisted fibers split from an end of a straight and wide ribbon. Evidently twisting is likely in very thin ribbon-like fibers. However, there is a limitation in explaining the twisting phenomenon by this analogy alone. For instance, it is thereby difficult to explain why some soap fibers twist easily and others do not.

The fact that the sense of twist for the fibers of the free D(or L)-acid is opposite to that of the Li soap suggests that the sense of twist is associated with the structure of the ionic layers in crystal. The effect of the cation size was observed in a series of the alkali metal soaps. This fact suggests that the packing arrangement in the ionic layers plays an important role in determining the helical sense, but the nature of this role has yet to be determined. The solvent effect exhibited by particular alcohols is also suggestive in explaining the twisting phenomenon, since these alcohols may be involved in the formation of the soap-crystal structure and may affect the packing arrangement of molecules. Further studies are also in progress with bivalent-metal soaps, giving complicated results which will be presented in a subsequent paper.

These studies were supported by a Scientific Research Grant from the Ministry of Education.

4) H. Wilman, *Proc. Phys. Soc.* **64A**, 329 (1951).
5) A. L. McClellan, *J. Chem. Phys.*, **32**, 1271 (1960).
6) J. D. Eshelby, *J. Appl. Phys.*, **24**, 176 (1953).
7) R. J. Bird and G. Rooney, *Nature*, **190**, 337 (1961).

BULLETIN OF THE CHEMICAL SOCIETY OF JAPAN VOL. 43 2422—2429 (1970)

Studies of the Liquid-Liquid Partition Systems. VII. The Solvent Extraction of Mercury(II) Chloride, Bromide, Iodide and Thiocyanate with Some Organic Solvents

Tatsuya SEKINE and Teruhiko ISHII

Department of Chemistry, Science University of Tokyo, Kagurazaka, Shinjuku-ku, Tokyo

(Received March 13, 1970)

The liquid-liquid distribution of mercury(II) has been determined when the organic phase was benzene, hexane containing tributylphosphate(TBP), methylisobutylketone(MIBK), or nitrobenzene, and when the aqueous phase was 0.5M sodium perchlorate containing chloride, bromide, iodide, or thiocyanate ions. The stability constants for the mercury(II) complexes in the aqueous phase and the distribution constants for the extractable complexes were determined by a graphic analysis of the distribution data, which were measured as a function of the ligand concentration. It was concluded that the stability constants determined from the present results agree almost entirely with the previous values and that the only extracted species into benzene and hexane containing TBP is the non-charged complex (HgX_2, where X^- is the ligand) in all cases, whereas those extracted into MIBK or nitrobenzene include not only the non-charged but also the charged species (HgX_3^- and sometimes HgX_4^{2-}) except in the case of the chloride system. The distribution ratio in the hexane-TBP system was further determined by changing the TBP concentration in the hexane phase, and the equilibrium constants for the adduct formation between the HgX_2 species and TBP molecules were determined. Finally, some discussion was made of the relation between the distribution behavior of the mercury(II) complexes and the natures of the ligands and the solvents.

It has been known for a long time that mercury(II) halides are somewhat soluble in organic solvents, while they are rather insoluble in water. This has been explained in terms of the formation of stable coordinate complexes which dissociate only slightly into mercuric ion and halide ions in aqueous solutions.

The stability constants of these complexes have been determined repeatedly by many authors by using various different experimental methods.[1] Of these, Sillén and his co-workers[2] determined these constants very comprehensively in a 0.5M sodium perchlorate constant ionic medium; their findings are listed in Table 1. Later, Marcus[3] published a series on the solvent extraction of mercuric halides or mixed halides with benzene. He concluded that the distribution ratio of mercury(II) between benzene and aqueous halide solutions can be explained in terms of the complex formation in the aqueous phase and the extraction of the non-charged dihalide mercury(II) complex into the benzene phase.

In the present investigation, the authors have studied the solvent extraction of mercury(II) in aqueous chloride, bromide, iodide, and thiocyanate solutions with four organic solvents, benzene, hexane containing tributylphosphate (TBP), methylisobutylketone (MIBK), and nitrobenzene. These solvents were chosen in order to examine how the nature of the organic solvent influences the distribution behavior of mercury(II) complexes. We determined that benzene has no lone-pair electrons, but can form π-complexes with an acceptor, that TBP coordinatedly solvates metal ions rather strongly in non-

TABLE 1. STABILITY CONSTANTS FOR Hg(II) COMPLEXES AT 25°C

Previous work

	Cl^-	Br^-	I^-	SCN^-	
log K_1	6.74*	9.05*	12.87*	—**	—***
log K_2	6.48	8.28	10.95	—	—
log K_3	0.85	2.41	3.78	2.71	2.88
log K_4	1.00	1.26	2.23	1.98	1.99

Present work

	Cl^-	Br^-	I^-	SCN^-
log K_3	0.85	2.27	3.78	2.73
log K_4	1.00	1.60	2.23	2.02

* in 0.5M Na (X, ClO_4), from Ref. 2
** in 0.2M Na (X, NO_3), from Ref. 7
*** in 1M Na (X, ClO_4), from Ref. 8

1) L. G. Sillén and A. E. Martell, "Stability Constants," The Chemical Society Spec. Pub. **17** (1964).
2) L. G. Sillén, *Acta Chem. Scand.*, **3**, 539 (1949).
3) Y. Marcus, *ibid.*, **11**, 329, 599, 610, 811 (1957).

polar solvents such as hexane, that MIBK also can solvate the metal ion, and the solvent itself is somewhat polar, and that nitrobenzene has one of the highest dielectric constants among the water immiscible organic solvents. The aqueous phase was kept as a 0.5M sodium perchlorate constant ionic medium in order to compare the present results with the previous results obtained in the same medium.

The changes in the distribution ratio, determined as a function of the ligand concentration, has been analyzed graphically, and the equilibrium constants in these systems were determined. There is some discussion of the distribution behavior of the complexes in these systems in connection with the chemical properties of the solvent and the ligand. The role of sodium ions in the organic phase for the extraction of the anionic complexes is also discussed.

Experimental

Reagents. About 0.2 g of mercuric dichloride was irradiated with thermal neutrons in the Triga III reactor at the Nuclear Research Laboratory of St. Paul's University, Kanagawa. It was dissolved in 5 m*l* of concentrated hydrochloric acid and then to the solution there was added an excess of zinc powder; the mixture was left standing overnight in order to reduce the mercury(II) to metallic mercury, and then the supernatant solution was decanted off. To the residue there was added a small amount of sulfuric acid in order to dissolve the excess of the zinc powder, and then the metallic mercury which remained was washed with water several times and finally dissolved in nitric acid. The solution was then evaporated in order to expel the excess acid, dissolved in 0.05M nitric acid, and stored for about one month in order to make the Hg-197 isotope decay out. The solution thus prepared was used as the stock tracer solution. The sodium-24 was obtained from the Japan Atomic Research Institute as a sodium chloride solution. It was diluted with a large amount of water and used as the stock solution. All of the reagents used were reagent-grade. The sodium perchlorate was recrystallized twice from water. The MIBK or TBP was washed with 0.1M perchloric acid, water, and 0.1M sodium hydroxide, and then several times with water. The other reagents were used without further purification. The concentration of the sodium thiocyanate solutions was determined by means of argentmetry, but the other concentrations were determined by means of gravimetry.

Procedures. All of the procedures were carried out in a thermostatted room at 25°C. Stoppered glass tubes (volume, 20 m*l*) were used to equilibrate the two phases. Five-milliliter portions of an aqueous solution containing mercury(II) labelled by the Hg-203 isotope, various amounts of ligand anions, and a 5-m*l* portion of one of the organic solvents were placed in the tubes. The initial concentration of the hydrogen ions in the aqueous phase was 1×10^{-3}M, and that of the mercury(II) ions was 1×10^{-5}M. The two phases were agitated mechanically for 30 min and then centrifuged off. A two-milliliter portion was pipetted from each phase and transferred into small test tubes. The γ-radioactivity in the sample solutions was measured with a well-type (NaI) scintillation counter, and the distribituion ratio of mercury(II) was calculated as follows:

$$D = [\mathrm{Hg(II)}]_{org,total}/[\mathrm{Hg(II)}]_{total} = \frac{\gamma\text{-count-rate per m}l\text{ of the org. phase}}{\gamma\text{-count-rate per m}l\text{ of aq. phase}}$$

Statistical

The complex formation of mercury(II) with these monovalent anions, X^-, can be described as follows:

$$\mathrm{Hg^{2+}} + n\mathrm{X^-} \rightleftarrows \mathrm{HgX}_n^{2-n} \quad (1)$$

$$\beta_n = [\mathrm{HgX}_n^{2-n}]/[\mathrm{Hg^{2+}}][\mathrm{X^-}]^n \quad (2)$$

or the stepwise formation constants can be described as follows:

$$\mathrm{HgX}_{n-1}^{3-n} + \mathrm{X^-} \rightleftarrows \mathrm{Hg}_n^{2-n} \quad (3)$$

$$K_n = [\mathrm{HgX}_n^{2-n}]/[\mathrm{HgX}_{n-1}^{3-n}][\mathrm{X^-}] \quad (4)$$

The solvent extraction of the neutral mercury(II) complexes may be described as follows;

$$\mathrm{HgX_2} \rightleftarrows \mathrm{HgX_2}(org) \quad (5)$$

$$K_{D2} = [\mathrm{HgX_2}]_{org}/[\mathrm{HgX_2}] \quad (6)$$

It would be also possible to extract the ion-pairs of the mercury(II) complex anion with sodium ions as:

$$\mathrm{HgX_3^-} + \mathrm{Na^+} \rightleftarrows \mathrm{NaHgX_3}(org) \quad (7)$$

$$\mathrm{HgX_4^{2-}} + 2\mathrm{Na^+} \rightleftarrows \mathrm{Na_2HgX_4}(org) \quad (8)$$

These ion-pairs could dissociate in the organic phase as:

$$\mathrm{NaHgX_3}(org) \rightleftarrows \mathrm{Na^+}(org) + \mathrm{HgX_3^-}(org) \quad (9)$$

$$\mathrm{Na_2HgX_4}(org) \rightleftarrows \mathrm{Na^+}(org) + \mathrm{NaHgX_4^-}(org) \quad (10)$$

$$\rightleftarrows 2\mathrm{Na^+}(org) + \mathrm{HgX_4^{2-}}(org) \quad (11)$$

The third complex in the organic phase may be treated as follows. The equilibrium constant for the ion-pair extraction in Eq. (7) is:

$$K_{ex3} = \frac{[\mathrm{NaHgX_3}]_{org}}{[\mathrm{HgX_3^-}][\mathrm{Na^+}]} \quad (12)$$

The dissociation constant for Eq. (9) is:

$$K_{diss3} = \frac{[\mathrm{HgX_3^-}]_{org}[\mathrm{Na^+}]_{org}}{[\mathrm{NaHgX_3}]_{org}} \quad (13)$$

The total concentration of the third complex in the organic phase can, then, be described from Eqs. (12) and (13) as follows;

$$[\mathrm{NaHgX_3}]_{org} + [\mathrm{HgX_3^-}]_{org} = [\mathrm{HgX_3^-}](K_{ex3}[\mathrm{Na^+}] + K_{ex3}K_{diss3}[\mathrm{Na^+}]/[\mathrm{Na^+}]_{org}) \quad (14)$$

From this, the distribution of the $\mathrm{HgX_3^-}$ species in the organic phase could be said to be dependent on the sodium concentration in the aqueous and the organic phases. However, it was concluded that both the aqueous and the organic sodium concen-

trations can be regarded as practically constant under the conditions employed in the present study, thus, the terms in parentheses in Eq. (14) can be regarded as constant. The terms in parentheses will be denoted in this study by a constant, "K_{D3}", as:

$$K_{D3} = ([NaHgX_3]_{org} + [HgX_3^-]_{org})/[HgX_3^-] \quad (15)$$

The same type of arguement, but a more complicated one, could be made for the fourth complex species in the organic phase, and for the same reason a "K_{D4}" constant can be defined as:

$$K_{D4} = ([Na_2HgX_4]_{org} + [NaHgX_4^-]_{org} + [HgX_4^{2-}]_{org})/[HgX_4^{2-}] \quad (16)$$

In the ligand-concentration range where the Hg^{2+} and HgX^+ species are negligible, the distribution ratio may be generally described as:

$$D = \frac{[HgX_2]_{org}+[HgX_3^-]_{org,total}+[HgX_4^{2-}]_{org,total}}{[HgX_2]+[HgX_3^-]+[HgX_4^{2-}]} \quad (17)$$

where $[HgX_3^-]_{org,total}$ and $[HgX_4^{2-}]_{org,total}$ stand for the total organic concentrations of the third complex species (HgX_3^- and $NaHgX_3$) and of the fourth complex species (HgX_4^{2-}, $NaHgX_4^-$ and Na_2HgX_4) respectively.

When the organic sodium-ion concentration is assumed to be constant, it can be described from Eqs. (4), (6), (15), and (16) as;

$$D = \frac{K_{D2}+K_{D3}K_3[X^-]+K_{D4}K_3K_4[X^-]^2}{1+K_3[X^-]+K_3K_4[X^-]^2} \quad (18)$$

When to the non-charged mercury(II) complex in an organic solvent there is added a non-charged organophilic ligand, L, the equilibrium constants can be described as:

$$HgX_2(org) + L(org) \rightleftarrows HgX_2L(org) \quad (19)$$

$$HgX_2(org) + 2L(org) \rightleftarrows HgX_2L_2(org) \quad (20)$$

$$\beta_1^\circ = [HgX_2L]_{org}/[HgX_2]_{org}[L]_{org} \quad (21)$$

$$\beta_2^\circ = [HgX_2L_2]_{org}/[HgX_2]_{org}[L]_{org}^2 \quad (22)$$

When the organic phase contains these adduct complexes as well as the HgX_2 species, but no charged complexes, the following holds;

$$[Hg(II)]_{org,total} = [HgX_2]_{org} + [HgX_2L]_{org} + [HgX_2L_2]_{org} = [HgX_2]_{org}(1 + \beta_1^\circ[L]_{org} + \beta_2^\circ[L]_{org}^2) \quad (23)$$

When the ligand-anion concentration in the aqueous phase, $[X^-]$, is kept at "a", the following equation may be introduced from Eqs. (18) and (23);

$$D = \frac{K_{D2}(1+\beta_1^\circ[L]_{org}+\beta_2^\circ[L]_{org}^2)}{1+K_3a+K_3K_4a^2} \quad (24)$$

When the distribution ratio at the same anionic-ligand concentration, but in the absence of the adduct-forming ligand, is denoted by D_0, the following equation is obtained;

$$\log D = \log D_0 + \log (1+\beta_1^\circ[L]_{org}+\beta_2^\circ[L]_{org}^2) \quad (25)$$

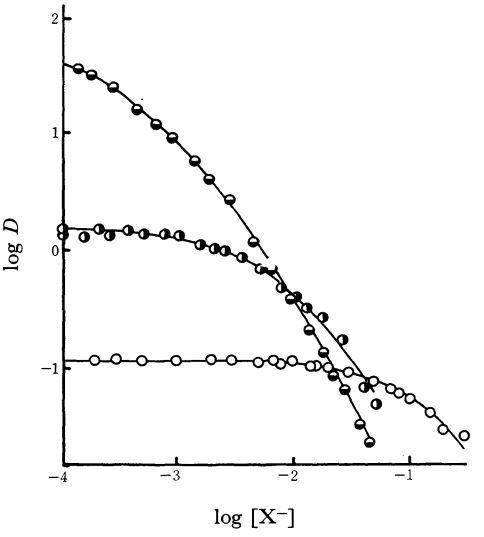

Fig. 1. Distribution of Hg(II) between benzene and 0.5M Na(X, ClO_4).
○: Cl^-, ◑: Br^-, ◒: I^-
Distribution ratio in the thiocyanate system is very low.

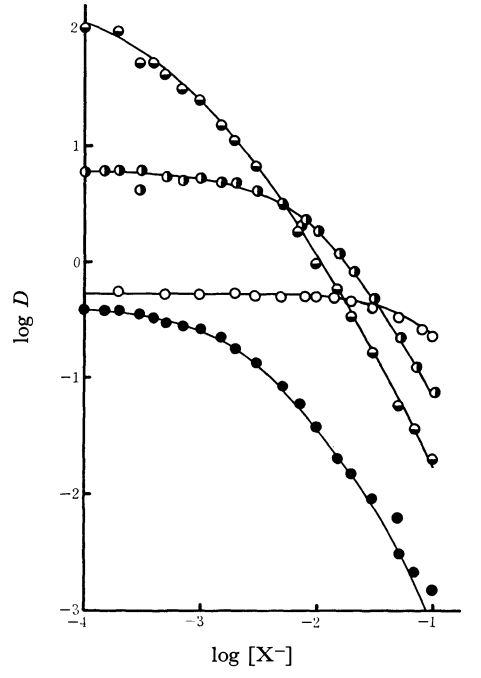

Fig. 2. Distribution of Hg(II) between hexane containing 0.1M TBP and 0.5M Na(X, ClO_4).
○: Cl^-, ◑: Br^-, ◒: I^-, ●: SCN^-

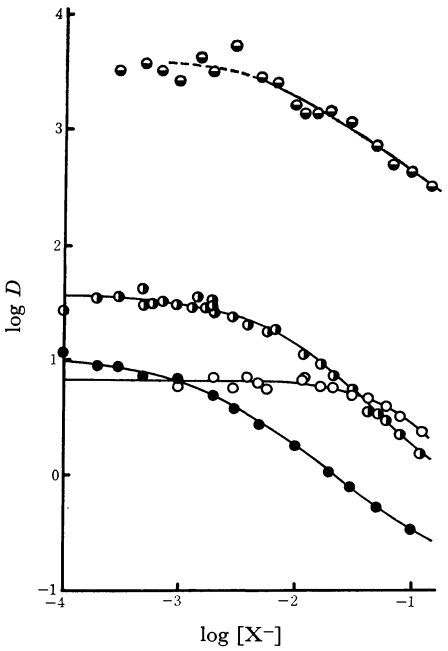

Fig. 3. Distribution of Hg(II) between MIBK and 0.5M Na(X, ClO_4).
○: Cl^-, ◑: Br^-, ◒: I^-, ●: SCN^-

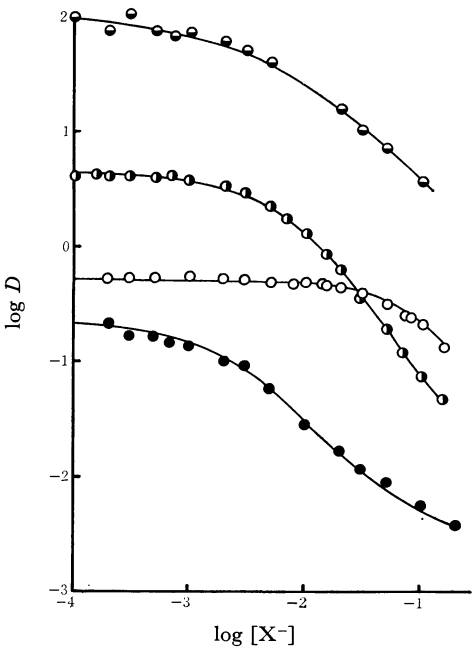

Fig. 4. Distribution of Hg(II) between nitrobenzene and 0.5M Na(X, ClO_4).
○: Cl^-, ◑: Br^-, ◒: I^-, ●: SCN^-

Results

Figures 1 to 4 give the changes in the distribution ratio as a function of the ligand concentration in the aqueous 0.5M perchlorate constant ionic medium when the organic phase was benzene, hexane containing 0.1M TBP, MIBK, and nitrobenzene, respectively.

It can be assumed that the concentration of the Hg^{2+} or HgX^+ species is very small in the ligand-concentration range studied[2]; when it is assumed that the extraction of the ion-pair species, $NaHgX_3$ and Na_2HgX_4, into benzene or into hexane containing a small amount of the extractant, TBP, is almost negligible, the follwing equation can be employed for the analysis of the data in Figs. 1 and 2;

$$D = \frac{K_{D2}}{1 + K_3[X^-] + K_3K_4[X]^{-2}} \qquad (18')$$

By using the following family of standard curves:

$$Y = -\log(1+pv+v^2),\quad X = \log v \qquad (26)$$

the equilibrium constants for the data in Figs. 1 and 2 were determiend by a curve-fitting method.[4-6] The stability constants and the distribution constants thus determined are listed in Tables 1 and 2. It was concluded that the stability constants for the HgX_3^- and HgX_4^{2-} complexes agree well with the values previously pointed by Sillén[2] within the limits of experimental error except for those for the bromide complexes. The equilibrium constants in the benzene system also agreed very well with the values reported by Marcus.[3] The stability constants for the thiocyanate complexes were also determined from Fig. 2; they are given in Table 1. They also agree with the constants in 0.2M nitrate media reported by Tanaka, Ebata, and Murayama[7] and with those in 1M perchlorate media reported by Nyman and Alberts.[8]

By introducing the constants, K_3 and K_4, determined from Figs. 1 and 2 into Eq. (18), the data in Figs. 3 and 4 were also analyzed graphically in order to obtain the distribution constants. After several attempts, it was found that the extraction constants for the charged complexes, K_{D3} and K_{D4}, should be taken into account as well as that for the non-charged complex, K_{D2}. However, the extraction curve of iodide in the MIBK system could be explained only in terms of the extraction of the charged complexes, HgI_3^- and HgI_4^{2-}, for a reason to be given below.

In order to ascertain the effect of the coexisting salt, some experiments were carried out in the absence of sodium perchlorate in the aqueous phase; that is, the aqueous phase contained only sodium halide, and the ionic concentration was not con-

4) D. Dyrssen and L. G. Sillén, *Acta Chem. Scand.* **7**, 663 (1953).
5) L. G. Sillén, *ibid.*, **10**, 186 (1956).
6) T. Sekine and M. Ono, This Bulletin, **38**, 2087 (1965).
7) N. Tanaka, K. Ebata and T. Murayama, *ibid.*, **35**, 124 (1962).
8) C. J. Nyman and G. S. Alberts, *Anal. Chem.*, **32**, 207 (1960).

TABLE 2. EXTRACTION CONSTANTS FOR Hg(II) COMPLEXES

		Benzene	Hexane	0.1M TBP-Hexane	MIBK	Nitrobenzene
Cl^-	$\log K_{D_2}$	−0.95(−0.96*)	−2.1	−0.72	0.83	−0.28
	$\log K_{D_3}$	—	—	—	—	—
Br^-	$\log K_{D_2}$	0.16(0.155*)	−1.70	0.79	1.57	0.63
	$\log K_{D_3}$	—	—	—	0.81	−0.84
I^-	$\log K_{D_2}$	1.84(1.760*)	0.39	2.28	—**	2.10
	$\log K_{D_3}$	—	—	—	3.68	1.81
	$\log K_{D_4}$	—	—	—	2.28	—
SCN^-	$\log K_{D_2}$	$<-2(-2.2^*)$	−2.4	−0.38	1.00	−0.66
	$\log K_{D_3}$	—	—	—	0.31	−1.60
	$\log K_{D_4}$	—	—	—	−0.82	−2.57

$$K_{D_2} = \frac{[HgX_2]_{org}}{[HgX_2]} \qquad K_{D_3} = \frac{[NaHgX_3]_{org} + [HgX_3^-]_{org}}{[HgX_3^-]}$$

$$K_{D_4} = \frac{[Na_2HgX_4]_{org} + [NaHgX_4^-]_{org} + [HgX_4^{2-}]_{org}}{[HgX_4^{2-}]}$$

* Taken from Ref. 3

** This value could not be determined but it was supposed that the extraction constant for the HgI_2 species with MIBK should be very large.

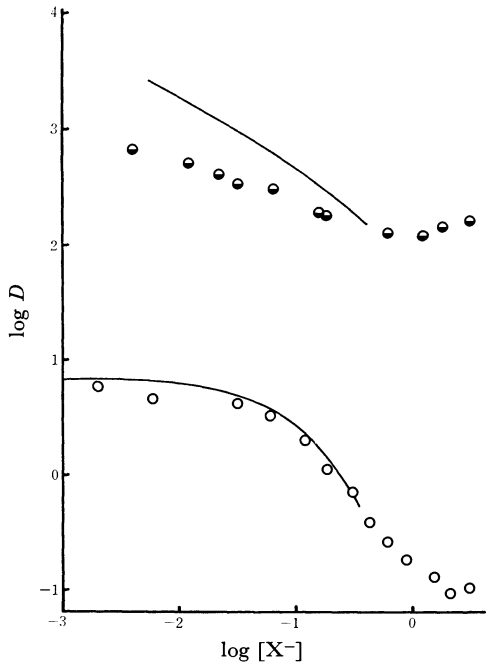

Fig. 5. Changes in the distribution of Hg(II) into MIBK when the aqueous phase containes sodium chloride(○) or sodium iodide(◒) but no sodium perchlorate (concentration of the ionic medium is not kept constant).

stant. Figure 5 gives some of the results of these experiments. In Fig. 5, the half-closed circles and the open circles show the extraction of mercury(II) with MIBK from aqueous sodium iodide and chloride solution respectively. The solid lines show the MIBK extraction curves from the 0.5M constant ionic media taken from Fig. 3. It can be seen that the extraction is not very different in the chloride system, but it is somewhat different in the iodide system.

The coextraction of sodium as ion-pairs with the anionic mercury(II) complex was also studied by using a sodium-24 radioactive tracer. An aqueous 0.1M sodium iodide solution containing no mercury-(II) was equilibrated with MIBK, and from the measurement of the γ-radioactivity of sodium-24 in the two phases, the organic sodium concentration was determined. Then, from 0.002M to 0.01M of mercury(II) nitrate, (which was not labelled) was added to this aqueous 0.1M sodium iodide solution, the aqueous phase was equilibrated with MIBK, and the organic sodium concentration was determined. In the absence of mercury, the sodium content in the organic phase was about 1×10^{-4}M; this is probably due to the extraction of sodium iodide. Upon the extraction of mercury, the organic sodium concentration increases; when the total organic mercury concentration was 0.002M, 0.003M, 0.005M, and 0.01M, the organic sodium concentration was 1.8×10^{-3}M, 3.4×10^{-3}M, 7.8×10^{-3}M, and 1.3×10^{-2}M. These results indicate that one molecule of the mercury iodide complex coextracts one or two sodium ions. As has been pointed out, the extracted mercury-iodide complexes in this iodide concentration are the HgI_3^- and HgI_4^{2-} species, and they should coextract one and two sodium ions respectively. The results of the above sodium coextraction, determined by means of radiometry, seem to be explained by this assumption regarding the complex species in the organic phase.

Figure 6 shows the dependence of the distribution ratio on the TBP concentration in hexane when the

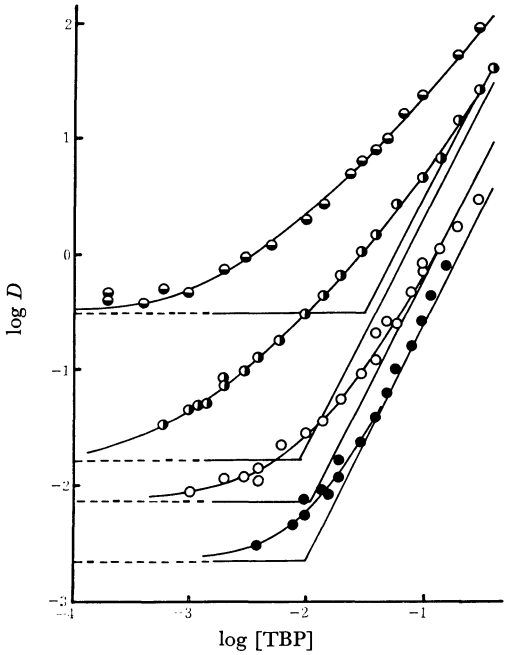

Fig. 6. The increase in the distribution of Hg(II) into hexane by the addition of TBP into the organic phase.
○: Cl^-, ◑: Br^-, ◒: I^-, ●: SCN^-.
The aqueous phase is 0.5M $NaClO_4$ containing 1×10^{-3}M of the ligand. The broken lines represent the distribution ratio of the HgX_2 in the absence of TBP in hexane.

aqueous phase contains ligands at 1×10^{-3}M. It was found that some mercury(II) is extracted from these aqueous phases even into hexane containing no TBP. The distribution ratio into pure hexane is given in Table 3 as D_0. The distribution ratio increases as the TBP concentration increases. The plot was also analyzed by the curve-fitting method by using Eq.(24). The adduct-formation constants in Eqs. (21) and (22) thus determined are given in Table 3.

The distribution constant of the HgX_2 complex between pure hexane and the aqueous phases given by Eq. (6) was calculated by using the D_0 values and the stability constants in Table 1, for at this ligand concentration (1×10^{-3}M), the aqueous phases contain not only the HgX_2 but also the HgX_3^- and HgX_4^{2-} species except in the case of the chloride system. The K_{D2} values are also given in Table 3.

Table 3. Equilibrium constants for the extraction TBP and adduct formation of HgX_2 in hexane when the aqueous phase is 0.5M $NaClO_4$ containing 1×10^{-3}M of the ligand

	$\log D_0$	$\log K_{D2}$	$\log \beta_1^\circ$	$\log \beta_2^\circ$
$HgCl_2$	−2.1	−2.1	2.24	3.88
$HgBr_2$	−1.80	−1.70	3.32	4.08
HgI_2	−0.52	0.39	2.80	3.00
$Hg(SCN)_2$	−2.7	−2.4	1.70	4.00

$$D_0=\frac{[HgX_2]_{org}}{[HgX_2]+[HgX_3^-]+[HgX_4^{2-}]}$$ (org. phase; pure hexane)

$$K_{D2}=\frac{[HgX_2]_{org}}{[HgX_2]}$$ (org. phase; pure hexane)

$$\beta_1^\circ=\frac{[HgX_2TBP]_{org}}{[HgX_2]_{org}[TBP]_{org}} \qquad \beta_2^\circ=\frac{[HgX_2 2TBP]_{org}}{[HgX_2]_{org}[TBP]_{org}^2}$$

Discussion

The results given in Figs. 1 to 6 and in Tables 1, 2 and 3 may be summarized as follows; i) In the benzene and 0.1M TBP-hexane systems, the only metal species in the organic phase is the HgX_2 species.

ii) In the MIBK and nitrobenzene systems, only the HgX_2 species is extracted from the chloride media, but anionic complexes, HgX_3^- and HgX_4^{2-} species, are also extracted as ion-pairs with sodium ions from other media.

iii) The extraction of the HgX_2 species into pure hexane grows larger in this order; $Hg(SCN)_2<HgCl_2<HgBr_2<HgI_2$. This extraction is increased by the addition of TBP. The increase can be explained in terms of the formation of TBP adduct complexes, HgX_2TBP and $HgX_2(TBP)_2$, in hexane. No systematic explanation has yet been made of the stability order of these adduct complexes of the different mercury(II) complexes.

iv) The stability constants for the HgX_3^- and HgX_4^{2-} species in the chloride and iodide systems agreed well with the data given by Sillén,[2] but those in the bromide system are slightly different. The same type of disagreement in the stability constants of the bromide complexes was also observed in the distribution work by Marcus[3] ($\log K_3$ and $\log K_4$ for the bromide complexes are 2.27 and 1.75), but the present results are closer to his values. Equilibrium constants in the benzene system agreed very well with the values reported by Marcus,[3] who also did his work in 0.5M sodium perchlorate constant ionic media.

The stability constants of the thiocyanate complexes obtained in the present study also agreed almost entirely with the previous data.[7,8]

As has been pointed out, the data in Figs. 3 and 4 were analyzed by using Eq. (18); that is, no effect of the organic sodium concentration on the distribution of the charged species was assumed. This is reasonable for the following reasons. According to the other studies, the sodium concentration in the organic phase equilibrated with 0.5M sodium perchlorate is about 5×10^{-5}M for nitrobenzene[9] and almost 1.5×10^{-3}M for MIBK (a small part of

9) T. Sekine and D. Dyrssen, *Anal. Chim. Acta*, **45**, 433 (1969).

these sodium ions could associate with perchlorate ions and form ion-pairs in MIBK).[10] The sodium concentration in the organic phases in the present systems can be described as follows:

$$[Na^+]_{org} = [ClO_4^-]_{org} + [X^-]_{org} + [HgX_3^-]_{org} + [NaHgX_4^-]_{org} + 2[HgX_4^{2-}]_{org} \quad (27)$$

In the ligand-concentration range studied, the aqueous sodium perchlorate concentration was kept pratically at 0.5M and the sums of the first and the second terms on the right side of Eq. (27) were 5×10^{-5}M and 1.5×10^{-3}M in nitrobenzene and MIBK respectively. On the other hand, as the total mercury concentration in the initial aqueous phase was 1×10^{-5}M, the maximum of the sum of the third, fourth and the fifth terms of Eq. (27) should be 2×10^{-5}M (when the HgX_4^{2-} species is dominant in the organic phase). However, as may be seen from Figs. 3 and 4 and Tables 1 and 2, this does not happen under the present experimental conditions. On the contrary, it is most probable that this sum is smaller than 1×10^{-5}M. From these points, it can be assumed that the sodium ions coextracted with the anionic mercury(II) complexes do not change the total organic sodium concentration seriously; in other words, the total sodium in the organic phase given by Eq. (27) is practically constant: 5×10^{-5}M in nitrobenzene and 1.5×10^{-3}M in MIBK.

Until now, not very much seems to have been discovered about the activity coefficient of ionic species in the organic phase in solvent extraction systems. The present results indicate that the activity coefficients of the ionic species in the organic phase can be controlled if the concentration of the metal complexes is very low. When the organic concentration of sodium perchlorate is much larger than that of the extracted metal ions in the organic phase, and when the aqueous phase is kept at a constant ionic medium by using sodium perchlorate, the concentration of the bulk sodium perchlorate in the organic phase is kept constant; in other words, this organic phase is a kind of constant ionic medium.

The distribution ratio of the complexes in these systems is probably influenced by many factors. When the interactions in the organic phase are not large as in hexane, the distribution ratio should be affected mainly by the interactions with the aqueous phase. Thus, the K_{D2} into pure hexane shown in Table 3 reflects the differences in the interactions with the aqueous phase. The order of the values of this K_{D2}, $HgCl_2 < HgBr_2 < HgI_2$, is the same as the order of the sizes of these complexes, which is in turn parallel with the difficulty of the dissolution into water with a hydrogen-bonded structure. The small distribution ratio of the thiocyanate complex could be due to another effect of the polyatomic nature of this ion.

The extraction of the dihalides into benzene becomes larger than that into hexane, but the difference is rather small with the dithiocyanate. This increase in the extraction can be explained in terms of the π-complex formation of the mercury dihalides, and the data seem to show a smaller tendency toward π-complex formation in the dithiocyanate.

The TBP adduct formation also increases the extraction, as may be seen from Fig. 6 and Table 3. Many neutral metal complexes have been known to be extracted into various solvents as TBP adducts, and the solvation number of TBP has been given to many of them on the basis of the TBP dependence of the extraction. As the neutral complex is usually extracted into an "inert diluent" only very poorly, not very much has been known about the adduct-formation constants, β°, except for the adduct metal chelate complexes which are known as "synergic complexes." Thus, although it is known to be a general tendency, for complexes of a certain metal with a series of similar ligands to be extracted better with a neutral extractant such as TBP when the size of the ligand is large, there has been little discussion as to whether this is due to the larger extraction into the diluent or whether it is due to the larger stability of the adduct complexes. The results shown in Table 3, however, indicate that the greater extraction into hexane, in other words, the larger "aquofobic" tendency, is more important in causing the larger extraction (the larger K_{D2} in Table 3) of the bis-mercury(II) complexes into hexane containing TBP.

It is remarkable that the extraction of the ion-pairs of the third complex anion and the sodium ion is larger in this order; chloride (no extraction) < thiocyanate < bromide < iodide, an order which is parallel to the order of K_{D2}. The extraction of the ion-pairs should be effected by the dissociation and the solvation in the organic phase, and when the extracted complexes dissociate more in the organic phase, the distribution ratio should be higher. As has been pointed out, no information about the dissociation of the ion-pairs in the organic phase has been obtained from the present distribution constant, not only for the neutral complex (K_{D2}), but also for the anionic complexes (K_{D3} and K_{D4}), probably indicates a larger contribution of the solvation than of the dielectric constant, because nitrobenzene has a higher dielectric constant ($\varepsilon=34.82$ at 25°C)[11] than MIBK ($\varepsilon=13.11$ at 20°C)[11]: However, the latter is obviously more favorable for the solvation than the former; this higher ability of solvation should make MIBK a better extractant of the charged complexes than nitrobenzene.

The distribution ratio of the iodide complexes in MIBK is too high to allow an accurate determina-

10) Y. Hasegawa, T. Ishii and T. Sekine, to be published.

11) A. A. Maryott and E. A. Smith, Table of Dielectric Constant of Pure Liquids NBS Circular 514 Aug. 10 1951.

tion, especially in the lower-iodide-concentration region, where an extraction of the HgI_2 species could be expected ($[I^-] < 10^{-2}$M). Thus, the data used for the analysis were taken from the region where the iodide concentration was above 5×10^{-3}M when the concentration of the HgI_2 species was calculated to be lower than 1.8% of the mercury(II) content, neglecting the extraction of this species; the K_{D2} value for the iodide complex could not be determined. The K_{D2} for this species in the MIBK system, however, is probably very large because the K_{D2} can be assumed to be larger than the very large K_{D3}, $10^{3.68}$.

Due to the change in the ionic concentrations in the experiments in Fig. 5, no statistical analysis of the data has been carried out. However, the following qualitative discussion is possible. In the chloride system, the addition of the sodium perchlorate may change the activity coefficients of the species, but we observed a not very large effect in the experimental data. In the iodide system, however, the extraction of the ion-pairs is probably influenced by the change in the sodium concentration, as can be seen from Eq. (14) or from the discussion which has been given above. Therefore, the extraction of mercury(II) can be increased by an increase in the aqueous sodium concentration (*cf.* Eqs. (21) to (24)). Figure 6 shows the rather prominent independence of the iodide extraction on the sodium iodide concentration. This may be explained as follows; the increase in the sodium iodide concentration will increase the concentration of iodide ions, which in turn changes the metal species from the HgI_3^- species to the less extractable HgI_4^{2-} species. In consequence, this should decrease the extraction. At the same time, however, the increase in the salt concentration of the sodium ions may increase the extraction, as we can see from Eq. (14). By the combination of these two inverse effects, the increase or the sodium iodide concentration has a rather small effect on the net distribution ratio.

Part of this work has been carried out at the Laboratory of Nuclear Chemistry, Institute of Physical and Chemical Research. The authors are grateful to Professor Nobufusa Saito, the head of the laboratory. They are also grateful to Dr. Tadashi Nozaki of the same laboratory for his valuable discussions and continuous interest for this work. The authors wish to express their gratitude to Messrs. Hirokazu Fukuda, Masaaki Suzuki, and Michio Ohtsuki of the present laboratory for their experimental aid. This work has been financially supported by a research grant from the Ministry of Education.

BULLETIN OF THE CHEMICAL SOCIETY OF JAPAN VOL. 43 2429—2434 (1970)

Physical Chemistry of Binary Plastic Crystals. II. Dielectric Constant of the System, Carbon Tetrachloride and *t*-Butyl Chloride

Kayako KOTAKE,*1 Nobuo NAKAMURA and Hideaki CHIHARA

Department of Chemistry, Faculty of Science, Osaka University, Toyonaka, Osaka

(Received March 19, 1970)

Careful measurements of the dielectric constant of a binary system of *t*-butyl chloride and carbon tetrachloride were made in the entire composition range and in three different phases, the liquid, the fcc solid, and the rhombohedral phases. The simple Debye theory applies to the liquid and the fcc solid, giving an effective dipole moment of *t*-butyl chloride of 2.11 ± 0.01 D whereas in the rhombohedral phase, it was 2.00 ± 0.03 D. Molecular polarization shows no discontinuity between the vapor, the liquid, and the fcc solid but there is a jump between the fcc and the rhombohedral solids. The molecular rotation in the plastic rhombohedral phase is more hindered by 450 cal/mol than in the liquid or the fcc phase. The 1 : 1 solid solution data were examined on the basis of the Onsager theory.

In the previous paper,[1] a dielectric and NMR study of *t*-butyl iodide dissolved in carbon tetrachloride in liquid and solid states was reported. It was then found that the solid solution formed a plastic crystal in which molecules not only reorient themselves but diffuse through the lattice with an

*1 Present address: Institute for Scientific and Industrial Research, Osaka University, Suita, Osaka.

1) H. Chihara, M. Otsuru and S. Seki, This Bulletin, **39**, 2145 (1966).

activation energy of 6.8 kcal/mol. The solid solution was dealt with by the theory of regular solutions. The stable solid phase I immediately below the melting point was then believed to be of the fcc structure, but as Post reported later[2] it was rhombohedral phase. The fcc phase of carbon tetrachloride and its solid solution does exist, however, as a metastable phase as our reexamination of the phase relations has shown.[3] The question now arises if there is any difference in the state of molecular motion in the two plastic phases, fcc and rhombohedral. The difference between the liquid and the solid phases, if any, is also of great interest in view of elucidating the nature of plastic crystals.

t-Butyl chloride forms two plastic solid solutions with carbon tetrachloride, having different structures, fcc and rhombohedral. The fcc phase becomes metastable where the concentration of *t*-butyl chloride is low. This binary system has been investigated by the dielectric[4] and the NMR[5] methods but the studies emphasized the similarity of the motional behavior between the liquid and the plastic phases. The present paper describes a careful dielectric measurements on the binary system in an attempt to learn about the motion of solute molecules in different matrix structures of carbon tetrachloride.

Experimental

Materials. Commercial special grade carbon tetrachloride and *t*-butyl chloride were distilled after drying over calcium chloride; carbon tetrachloride bp 76.7—76.8°C, n_D^{20} 1.45986, *t*-butyl chloride, bp 50.5—50.8°C, n_D^{20} 1.38550, literature values are as follows: *t*-butyl chloride bp 50.5,[6] 51.0°C,[7] n_D^{20} 1.38470,[8] 1.38786.[7]

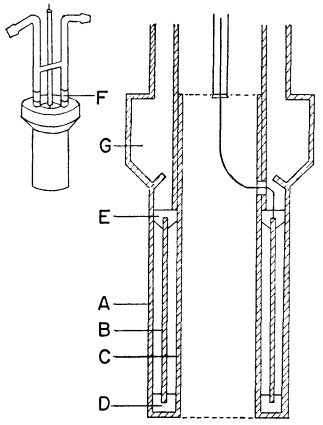

Fig. 1. The dielectric cell.

Equipments. The apparatus of the differential thermal analysis (DTA) is the same as the one reported earlier.[9]

The dielectric constant was measured by the heterodyne-beat method at the frequency of 1 MHz.

Two sample cells were used. One was the glass cell as described previously,[1] which often broke where the electrode leads were fused when the sample solution was remelted. A new cell, shown in Fig. 1 consists of three coaxial cylinders of nickel-plated copper A, B, and C that served as the electrodes: B is insulated from the cylinders A and C by the Teflon spacers D and F. To secure uniform temperature in the specimen, thermal conduction from the outside was reduced to a minimum by using thin-walled stainless steel pipes F through which the solution was charged or discharged. G is the space to allow for the thermal expansion of the specimen through the cutting of the spacer E. The new cell is sturdier than the previous one and also suffers smaller disturbances from environment. The air capacitance of either cell was about 18 pF. The cell was placed in a thick copper holder which was filled with toluene as the heat-exchange medium. The holder was cooled with Dry Ice in a Dewar vessel and the temperature of the cell, measured by a chromel-P-constantan thermocouple, was controlled manually with the heater wound around the holder.

Density was measured by a pycnometer[10] in the liquid state.

The dielectric constants and the densities of liquids were in good agreement with the literature values.[11]

Results and Discussion

1) Differential Thermal Analysis (DTA). Recent X-ray studies[2] of carbon tetrachloride showed that under certain conditions it exhibits monotropy immediately below the melting point; *i. e.*, the crystal formed upon solidification is of metastable cubic phase, which is transformed to a rhombohedral crystal on further cooling. Such phase relations were substantiated by our DTA work.[3] Figure 2 is a reproduction of the DTA result of pure carbon tetrachloride. The figure is self-explanatory but it is to be noted that the melting point of the cubic phase (peak G) is about 3.8°C lower than the melting point of the rhombohedral phase (peak E). Similar DTA curves were obtained, though the tem-

2) R. Rudman and B. Post, *Science*, **154**, 1009 (1966).

3) K. Kotake, N. Nakamura and H. Chihara, This Bulletin, **40**, 1018 (1967).

4) W. P. Conner and C. P. Smyth, *J. Amer. Chem. Soc.*, **63**, 3424 (1941).

5) J. G. Powles and H. S. Gutowsky, *J. Chem. Phys.*, **21**, 1704 (1953).

6) A. Turkewich and C. P. Smyth, *J. Amer. Chem. Soc.*, **62**, 2468 (1940).

7) J. Timmermans and Y. Dolcourt, *J. Chim. Phys.*, **31**, 85 (1934).

8) W. O. Baker and C. P. Smyth, *J. Amer. Chem. Soc.*, **61**, 2798 (1939).

9) H. Suga, H. Chihara and S. Seki, *Nippon Kagaku Zasshi*, **82**, 24 (1961).

10) M. R. Lipkin, J. A. Davison, W. T. Harvey and S. S. Kurtz, Jr., *Ind. Eng. Chem., Anal. Ed.*, **16**, 55 (1944).

11) a) R. Guillien, *J. Phys. Radium*, **1**, 29 (1940). b) A. Mansingh and D. B. McLay, *Can. J. Phys.*, **45**, 3815 (1967). c) A. Audsley and F. R. Goss, *J. Chem. Soc.*, **1941**, 864.

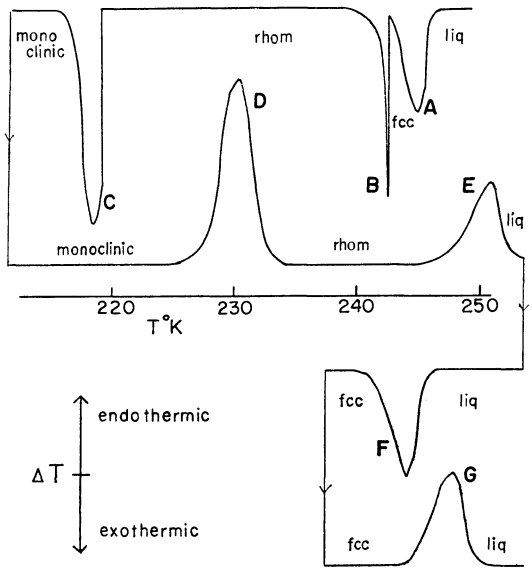

Fig. 2. DTA curves of carbon tetrachloride.

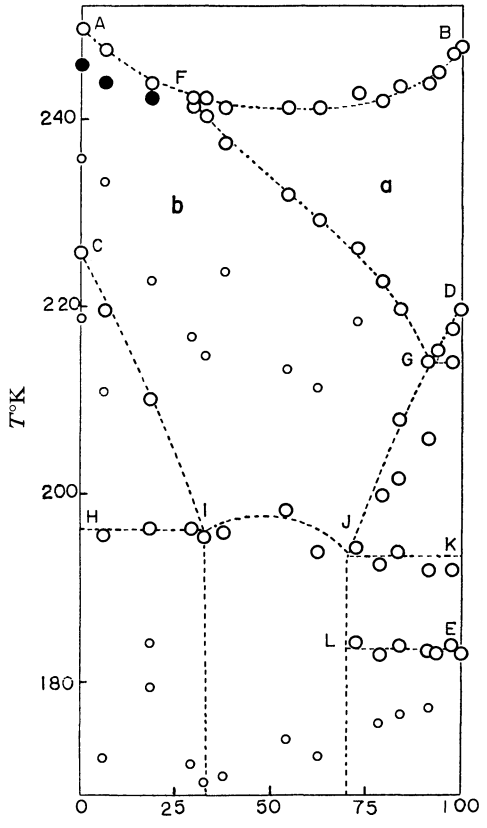

Fig. 3. The phase diagram of the system, CCl_4 - *t*-BuCl. Large and small circles represent the peaks on warming and on cooling, respectively. Closed circles represent the mp of metastable fcc phases. Dashed lines and capital letters refer to the work by Smyth *et al.*

peratures of transitions were displaced for binary mixtures of CCl_4 and *t*-BuCl where the concentration of the latter was less than 25 mol%. For more concentrated solutions, the melting and freezing points coincide and the second exotherm (B in Fig. 2) is replaced by a stable transformation corresponding to the curve FG in Fig. 3. The phase diagram determined by the DTA method (Fig. 3) confirms the dielectric result.[4]

Because the structure of the plastic phase of *t*-butyl chloride is fcc,[12] the area a of Fig. 3 must correspond to the fcc phase, the area b similarly corresponding to the rhombohedral phase.

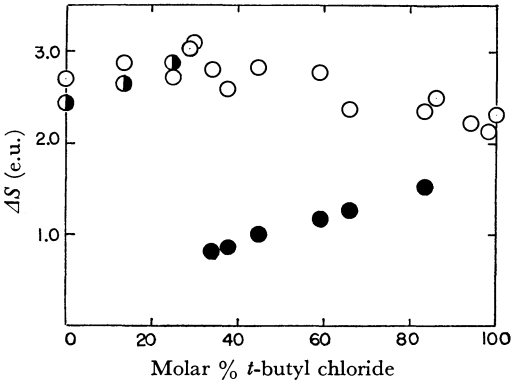

Fig. 4. Entropy of phase changes of CCl_4 - *t*-BuCl. ● rhombohedral → fcc, ◑ rhombohedral → liquid, ○ fcc → liquid.

The entropy changes of the phase transitions were estimated from the area under the peak in the DTA curves and are shown in Fig. 4. To obtain the internal consistency, the experimental conditions including the volume of the specimen in the measuring tube were fixed for all compositions. The literature values of the entropy of fusion is 2.401 cal/deg·mol[13] for carbon tetrachloride and 2.00 cal/deg·mol[14] for *t*-butyl chloride. It is interesting to note that the entropy of fusion of the fcc phase, either stable or metastable, changes almost linearly with the composition, *i. e.*, the solid solution is very close to the ideal solution. Also, the entropy change from the rhombohedral to the stable fcc phase increases linearly as the solution becomes more concentrated in *t*-butyl chloride. Extrapolation of the line back to the zero concentration gives about 0.3 cal/deg·mol to the entropy of transition from the rhombohedral to the metastable fcc phase of

12) R. S. Schwartz, B. Post and I. Fankuchen, *J. Amer. Chem. Soc.*, **73**, 4490 (1951).

13) J. F. Hicks, J. G. Hooley and C. C. Stephenson, *ibid.*, **56**, 31 (1944).

14) A. Dworkin and M. Guillamin, *J. Chim. Phys.*, **63**, 53 (1966).

15) C. P. Smyth, "Dielectric Behavior and Structure," McGraw-Hill Book Co., Inc., New York, N. Y. (1955).

pure carbon tetrachloride.

2) Dielectric Constants and Density. Uncertainty in the dielectric constant measurements was less than 0.1 pF, which arose from repeated assembly and disassembly. Samples were carefully frozen into plastic crystal phase to fill the space between the electrodes by slow cooling and annealing thereafter, and the dielectric constant values on warming and on cooling agreed well except in the region of the supercooled fcc phase, in contrast to the result of Smyth *et al.*,[4] who reported that the runs on two directions did not agree and that the dielectric constants were smaller on cooling. The values of the present work were reproducible to within 1%. The smoothed values for each temperature are listed in Tables 1—3. The values of the density are given in terms of the coefficients of the formula

$$\rho = a + bx + cx^2$$

where ρ is the density, x is mole% of *t*-butyl chloride and a, b and c are the coefficients.

Table 1. The dielectric constant and the density in liquid solutions

The density is given in terms of a, b, and c in the formula $\rho=a+bx+cx^2$.

(mole %)	Temperature (°C)				
	20.0	10.0	0.0	−11.4	−22.0
0.00	2.240	2.258	2.276	2.300	2.324
1.39	2.319	2.347	2.374	2.407	2.437
4.23	2.471	2.509	2.548	2.592	2.632
8.87	2.712	2.760	2.812	2.875	2.937
11.98	2.936	3.000	3.068	3.151	3.227
21.05	3.505	3.612	3.723	3.855	3.978
37.26	4.731	4.911	5.114	5.360	5.603
51.03	5.775	6.036	6.283	6.636	6.782
64.16	6.762	7.122	7.487	7.913	8.178
77.69	7.832	8.270	8.720	9.276	9.855
100.00	10.04	10.61	11.25	12.05	12.09
a	1.5935	1.6116	1.6316	1.6519	1.6740
$b\cdot10^2$	−8.279	−8.336	−8.448	−8.636	−8.755
$c\cdot10^6$	7.664	7.725	7.949	9.176	9.569

Table 2. The dielectric constant in the S.C. phase

x (mole %)	Temperature (°C)				
	−30.0	−35.0	−40.0	−45.0	−50.0
21.05	4.28	4.31	—	—	—
37.26	—	6.39	6.50	—	—
51.03	—	8.06	8.25	8.38	—
64.16	—	9.68	10.06	10.37	10.64
77.69	11.28	11.68	12.00	12.27	12.49
100	15.85	16.11	16.34	16.53	16.68

Table 3. The dielectric constant in the rhombohedral phase

x (mole%)	Temperature (°C)					
	−25.0	−30.0	−40.0	−50.0	−60.0	−70.0
0.00	2.40	2.41	2.43	—	—	—
1.39	—	2.51	2.52	—	—	—
4.23	—	2.71	2.72	—	—	—
8.78	—	3.04	3.07	3.09	—	—
11.98	—	3.37	3.42	3.46	—	—
21.05	—	—	4.13	4.16	—	—
37.26	—	—	6.14	6.29	6.38	—
51.03	—	—	7.54	7.72	7.87	7.99
64.16	—	—	—	9.69	9.97	10.20
77.69	—	—	—	10.82	11.03	11.23

3) Polarization at Infinite Dilution. The dielectric constant in both the cubic and the rhombohedral phases has negative temperature coefficients as is evident from Tables 2 and 3. The negative coefficient is commonly encountered in polar plastic crystals[1,15] and is generally interpreted as being due to the effect of thermal agitation opposing the orientation of molecules in the electric field. It is therefore interesting to see if the Debye theory for the liquid solution applies to the plastic solid solution. This is equivalent to seeing if the application of the Debye theory might lead to a reasonable value of the effective dipole moment of solute molecules in the solid state.

To obtain the specific polarization at infinite dilution, the Halverstadt-Kumler's method[16] was used. If linear relationships hold for the dielectric constant and the density,

$$\varepsilon_{12} = \varepsilon_1 + \alpha w_2$$

and

$$\rho_{12} = \rho_1 + \beta w_2 \qquad (1)$$

the specific polarization is given by the equation

$$p_\infty = p_1\left\{1 + \frac{3\alpha}{(\varepsilon_1-1)(\varepsilon_1+2)} - \frac{\beta}{\rho_1}\right\} \qquad (2)$$

where w_2 is the weight fraction of the solute, the suffix 1 referring to the solvent and the suffix 2 to the solute. The experimental results of Tables 1 to 3 were used to derive the values of α and β in the region of dilute solutions. In the absence of the density values of the solid solution, the ρ_1 values of pure carbon tetrachloride were taken from Ref. 17 and the β value was assumed to be equal to that in the liquid solution. This assumption would not lead to a serious error in p_∞ since a variation of 10% in the value of β changes the value of p_∞ by only 1%.*2 The values of moler polarization at

16) R. J. W. Le Fevre, "Dipole Moments," Methuen & Co. Ltd., John Wiley & Sons, Inc., London-New York (1953).

17) P. F. Higgins, R. A. B. Ivor, L. A. K. Staveley and J. J. des C. Virden, *J. Chem. Soc.*, **1964**, 5762.

*2 The use of the liquid β value in the solid solution may be justified by considering that the solid solution can be described by the regular solution theory.[18]

18) I. Prigogine and V. Mathot, *J. Chem. Phys.*, **20**, 49 (1953); V. Mathot and A. Desmyter, *ibid.*, **21**, 782 (1953).

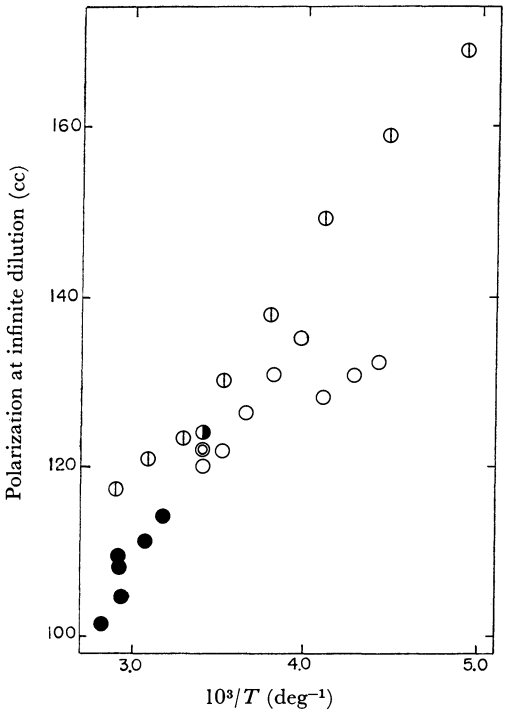

Fig. 5. Polarization at infinite dilution.
○; Present work, ●; in vapor,[20] ⓘ; in *n*-heptane,[19] ◑; in benzene,[21] ◎; in CCl_4[11c]

infinite dilution thus derived are plotted against $1/T$ in Fig. 5, which also shows the results of other investigations.[19-21] Our values for the liquid solution lie on a line extended from the values in the vapor phase, whereas there is a jump in the polarization between the liquid and solid (rhombohedral) phases and their slopes are also different.

Other conditions being equal, the difference in slope means a difference in the effective dipole moment between the liquid and the solid phases. By taking the electronic and atomic polarization to be 1.05 times the molar refraction, or 26.8 cc,[22] the magnitude of the dipole moment is estimated as 2.00 ± 0.03 D for the solid (rhombohedral) phase as compared with 2.11 ± 0.01 D for the liquid phase. The smaller effective dipole moment in the solid should be an indication of the effect of a stronger intermolecular interaction, which also accounts for the jump of the polarization at the melting point. After Debye,[23] we take

$$U = -\mu F\cos\theta' - V\cos\theta \tag{3}$$

as potential energy of a solute molecule in the solid solution, where the first term represents the part due to the external field and the second term represents the potential energy hindering the molecular rotation. The angle θ is measured from the direction of the minimum hindering potential that is determined by the structure of the solid solution. The orientation polarization is given by

$$P^{o} = \frac{4}{3}\pi N\frac{\mu^2}{3kT}\left\{1 - L^2(V/kT)\right\} \tag{4}$$

where $L(y)$ is the Langevin function. Since there is a smooth continuity in the polarization between the vapor and the liquid, we assume that $L(y)=0$ in the liquid and the jump at the melting point is entirely due to non-zero $L(y)$ in the solid solution. Inserting the numerical values into Eq. (4), we obtain $V=0.9kT=450$ cal/mol. That $L(y)$ is put to zero in the liquid should not be taken to imply that there is no potential barrier in the liquid but it should be interpreted as meaning that the apparent potential barrier vanishes after averaging over all possible values of θ' and θ because of the symmetry of the barrier,[24] its existence being expected from the structure of the liquid.[25]

4) More Concentrated Solutions. We shall consider a more concentrated solution. If we take a 51.03% solution, the cubic and rhombohedral phases may be compared on similar grounds. To make a comparison with the case of dilute solutions meaningful, we deduce a quantity which corresponds to the orientation polarization in the Debye theory by applying the Onsager formula[26] in the form

$$\frac{4\pi N\mu^2}{9kT} = \frac{1}{3}v_{12}\frac{100}{x}\left\{\frac{(\varepsilon-1)(2\varepsilon+1)}{3\varepsilon} - \frac{(2\varepsilon+1)(n_1^2-1)}{2\varepsilon+n_1^2}\frac{v_1}{v_{12}}\frac{100-x}{100} - \frac{2(\varepsilon+1)(n_2^2-1)}{2\varepsilon+n_2^2}\frac{v_2}{v_{12}}\frac{x}{100}\right\}\Big/ \left\{\frac{2\varepsilon+1}{2\varepsilon+n_2^2}\cdot\frac{n_2^2+2}{3}\right\}^2. \tag{5}$$

Here ε is the dielectric constant of the solution, n is the refractive index, and v is the molar volume. Rough estimate of the molar volume of solid solution may be made on the basis of the theory of Pople and karasz,[27] which relates the volume change to the entropy of fusion for the plastic crystals. Though

19) C. P. Smyth and R. W. Dornte, *J. Amer. Chem. Soc.*, **53**, 545 (1931).
20) R. H. Wiswall, Jr., and C. P. Smyth, *J. Chem. Phys.*, **9**, 356 (1941).
21) A. Partz, *Z. Phys. Chem.*, **B7**, 327 (1930).
22) "Kagaku Binran," ed. by the Chemical Society of Japan, Maruzen, Tokyo (1966).
23) P. Debye, *Phys. Z.*, **36**, 100 (1935).
24) H. Fröhlich, "Theory of Dielectrics," Oxford University Press, London (1958), p. 51.
25) R. W. Gruebel and G. T. Clayton, *J. Chem. Phys.*, **46**, 693 (1967); A. H. Narten, M. D. Danford and H. A. Levy, *ibid.*, **46**, 4875 (1967).
26) L. Onsager, *J. Amer. Chem. Soc.*, **58**, 1486 (1936).
27) J. A. Pople and F. E. Karasz, *J. Phys. Chem. Solids*, **18**, 28 (1961).

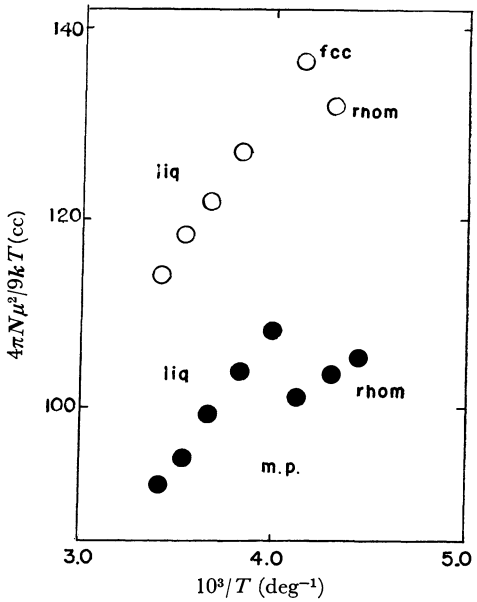

Fig. 6. Orientation polarization extrapolated to infinite dilution.
○ 51% mixture, derived by use of Eq. (5).
● dilute mixtures, derived by Halverstadt-Kumler method.

this theory was constructed for the pure substances, the extention to mixtures is possible on the assumption of perfectly random mixing in either phases. Precise application of this theory is not possible for rhombohedral phase of carbon tetrachloride, presumably due to the lower symmetry of the potential. Table 4 shows the parallelism of ΔS and $\Delta V/V_s$ among the fcc phases. V_s is estimated to be 92 cc, which is consistent with the density value, 1.349 g/cc, obtained from the equation $\rho=a+bx+cx^2$, where a is 1.760 g/cc for the fcc phase of carbon tetrachloride from the X-ray analysis[5] and b and c are mean values in liquid phase. The same value of molar volume is used for the rhombohedral phase of the mixture, though the actual value must be certainly less than it. The results

TABLE 4. THE RELATION OF THE ENTROPY CHANGES ΔS FROM DTA AND THE RELATIVE VOLUME CHANGES $\Delta V/V_s$ ON FUSION

V and V_s are molar volumes of liquid and solid phases at the melting point, respectively, and the former are obtained by extrapolation of density *vs.* temperature curves for each concentration.

	CCl_4 fcc	*t*-BuCl fcc	51% mixture fcc
ΔS	2.7	2.0	2.9
$\Delta V/V_s$	0.050	0.046	0.051*
V	91.8	103.4	96.3
V_s	87.4	98.9	92*

* estimated values

are shown in Fig. 6, compared with the value of the orientation polarization obtained in the preceding section. An inspection of the figure immediately reveals that:

1) the orientation polarization P^o derived from Onsager's equation are systematically larger than P^o at the infinite dilution, but the slopes are almost equal in the liquid phases.

2) P^o for the fcc and liquid phases lie on a straight line, whereas P^o for the rhombohedral phase falls short of the line.

These facts indicate that Onsager's treatment of dipole-dipole interaction is not adequate, mainly in the account of the short range interaction. However the defect of the theory is displayed in the liquid as well as in the solid phase in a similar fashion. The molecules are not as free in the rhombohedral phase as in the liquid or the cubic phases. The different behavior in the two solid phases is probably due to the different symmetry of the hindering potential of molecular rotation and is related to the factor $\overline{Z\cos\gamma}$ in the Kirkwood formula[28] which probably vanishes in the liquid and cubic phases.

28) J. G. Kirkwood, *J. Chem. Phys.*, **7**, 911 (1939).

BULLETIN OF THE CHEMICAL SOCIETY OF JAPAN VOL. 43 2435—2439 (1970)

Absorption Spectra of Gaseous Benzo[*g,h,i*]perylene and Coronene

Jun-ichi AIHARA*1, Koichi OHNO and Hiroo INOKUCHI

The Institute for Solid State Physics, The University of Tokyo, Roppongi, Tokyo

(Received March 30, 1970)

The gas-phase spectra of typical polycyclic aromatic hydrocarbons benzo[*g,h,i*]perylene and coronene, were measured. These data can be used as criteria for the solvent shifts and the molecular excitons.

One of the most refined analytical approaches to the molecule is to examine the gaseous behaviour of the isolated molecule. The conventional way of doing so is to make an experimental determination of the electronic transition energies. Further, the gas-phase spectra play an important role in the estimation of the energies in the crystalline phase and in solution.

For these purposes, several absorption spectra have been obtained for the vapours of various aromatic compounds.[1,2] However, in spite of many investigations, the absorption spectra have not been measured for benzo[*g,h,i*]perylene and coronene, which are typical higher polycyclic aromatic hydrocarbons. The latter is a famous example of the Shpolskii effect.[3]

We overcame the experimental difficulties resulting mainly from their lower volatility, and we succeeded in measuring their absorption spectra by the aid of a powerful electric furnace.[4]

This paper will report the optical absorption band positions of compounds, benzo[*g,h,i*]perylene and coronene, in the near-ultraviolet region, and will compare these results with the solution data.

Experimental

Benzo[*g,h,i*]perylene (Benzoperylene). The absorption spectra of benzo[*g,h,i*]perylene (Fig. 1) in the gas phase were observed as follows: Below 3.2×10^4 cm^{-1}, an Aminco 4-8401 monochromator was used. Above 3.2×10^4 cm^{-1}, a Cary recording spectrophotometer 14 was employed. The light sources were a 300-W tungsten lamp and a hydrogen discharge tube. Sodium and mercury lamps were employed to calibrate the spectral wavelengths.

The optical cell used was a Pyrex one, 30 cm in length, and also a silica cell, 2 cm long. A small quantity of benzoperylene crystals was placed in the cell, which was then evacuated to less than 10^{-5} mmHg pressure. The absorption coefficients of both compounds range from 10^2 to 10^4.[5] Therefore, the temperature must be varied widely in order to obtain the appropriate concentration of the gaseous specimen for observing their absorption spectra. In the case of coronene, the temperature ranges from 250 to 450°C.

When the absorption spectra of benzoperylene in the longer-wavelength region were observed, the Pyrex cell was maintained in a 50-KW electric furnace equipped with a temperature controller because the cell had to be kept at a fairly high temperature. To detect the spectra in the shorter-wavelength region, a small 80-W furnace for heating the cell was placed in the spectrophotometer. The spectra were taken after the specimen had been kept at the chosen temperature for at least 20 min. No condensation of the sample on the windows was detected during the measurement. The blank determination for the spectra was done by carefully cleaning and replacing the cell without changing the optical arrangement.

Benzo[*g,h,i*]perylene used was a synthetic one, prepared by Iwashima; it was purified by the chromatographic method.[6]

Coronene. For spectral measurements, a Spex spectrograph equipped with a 300-W tungsten lamp was used. The spectra were recorded photographic sheet films, Fuji Neopan SS. The spectral response on the films was determined by means of a Shimadzu microdensitometer. Iron lines were used for the wavelength calibration.

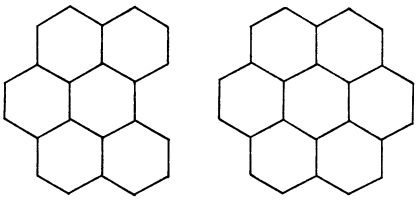

Fig. 1. Benzo[*g,h,i*]perylene and coronene.

*1 Present address: Department of Chemistry, Faculty of Science, Hokkaido University.

1) T. Kitagawa, *J. Mol. Spectry.*, **26**, 1 (1968).
2) G. C. Morris, *Australian J. Chem.*, **17**, 1288 (1964).
3) E. V. Shpolskii, *Soviet Phys. -Usp.*, **2**, 51 (1959).
4) N. Wakayama and H. Inokuchi, This Bulletin, **40**, 2267 (1967).
5) E. Clar, Polycyclic Hydrocarbons, Vols. 1 and 2, Academic Press Inc., New York (1964).
6) S. Iwashima, K. Ogino, T. Kajiwara and J. Aoki, *Nippon Kagaku Zasshi*, **89**, 1157 (1968).

The cell used for coronene was a Pyrex one used to measure the absorption spectra of benzoperylene vapour; the 50-kW furnace was also employed. The third band could not be observed because of the limitation of the optical absorption of the Pyrex cell.

Coronene (Fig. 1) used was a commercial one; it had been purified by recrystallization from xylene and by sublimination *in vacuo*.

For a complete investigation of absorption spectra of coronene, thirty hours were needed, but measurements of such a long duration scarcely affected the sample at all.*2

Results

The gaseous absorption spectra of benzoperylene are shown in Figs. 2, 3, and 4, which correspond to the region of the first, second, and third electronic transitions respectively. The spectra in an *n*-hexane solution were added for the sake of comparison. Table 1 gives the absorption bands observed in the various phases.[7]

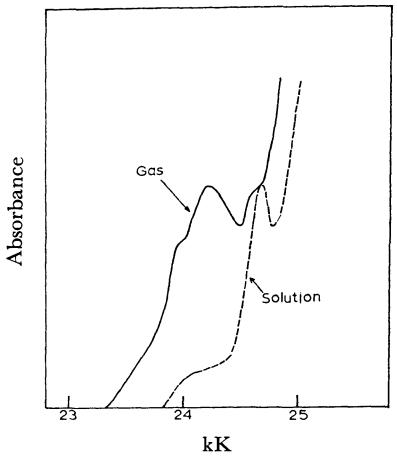

Fig. 2. Absorption spectrum of the α-band of benzo[*g*,*h*,*i*]perylene.

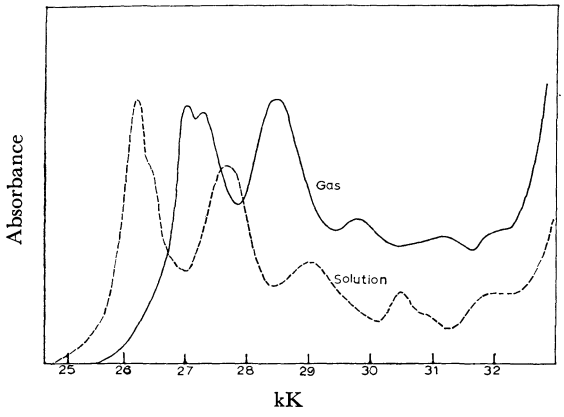

Fig. 3. Absorption spectrum of the *p*-band of benzo-[*g*,*h*,*i*]perylene.

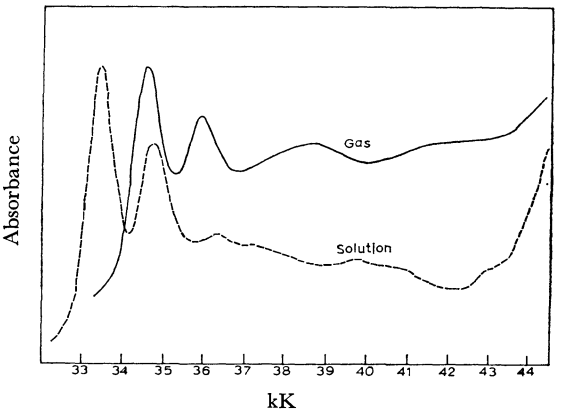

Fig. 4. Absorption spectrum of the β-band of benzo[*g*,*h*,*i*]perylene.

This compound has been subjected to scarcely experimental or theoretical treatments for the determination of its electronic transition energies, except for the case of the fluorescence spectra in the condensed phases.[8] As to benzoperylene, the best, and almost the only calculations, have been those of Hummel and Rüdenberg's, whose results are also listed in Table 1.[9]

Figures 5 and 6 show the spectra of gaseous coronene in the first two transition regions. The density on the films is plotted against the wave-numbers. Table 2 shows the bands of coronene which appeared in the various phases. The recent Pariser-Parr calculations for coronene are also listed.[10]

TABLE 1. ABSORPTION BANDS OF BENZO-[*g*,*h*,*i*]PERYLENE

Band	Gas phase (cm^{-1})	*n*-Hexane solution (cm^{-1})	Crystal[10] (cm^{-1})	Theoretical[9] (cm^{-1})
α-Band	24230	24690	21685	26847
				(f=0.008)
p-Band	27025	26075	24185	27077
	27315	~26460		(f=0.525)
	28490	27610	25560	
	29815	29015	26955	
	~31200	30415	28170	
β-Band	34565	33410		37239
	35880	34735		(f=2.084)

*2 We also tried to detect the absorption spectrum of gaseous violanthrene B. This attempt was unsuccessful because of its thermal instability. In comparison with the other polycyclic aromatics, coronene is one of the most stable hydrocarbons.

7) J. Tanaka, This Bulletin, **38**, 86 (1965).
8) B. C. Mukherjee and S. C. Ganguly, *Proc. Phys. Soc.*, **83**, 93 (1954).
9) R. L. Hummel and K. Rudenberg, *J. Phys. Chem.*, **66**, 2334 (1961).
10) J. E. Bloor and B. R. Gilson, *Theoret. Chim. Acta*, **8**, 35 (1967).

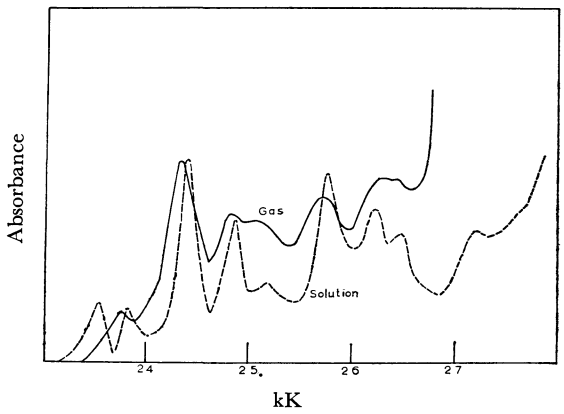

Fig. 5. Absorption spectrum of the α-band of coronene.

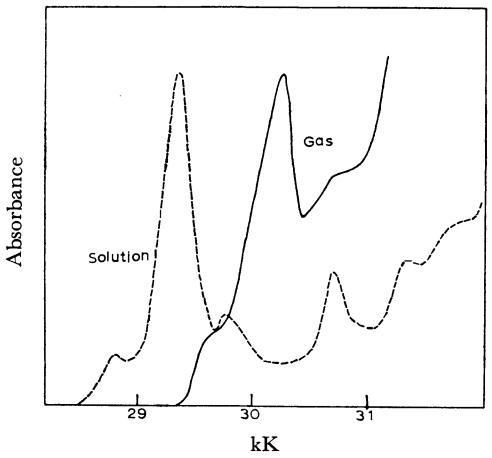

Fig. 6. Absorption spectrum of the *p*-band of coronene.

Table 2. Absorption bands of coronene

Band	Gas phase (cm^{-1})	Benzene solution (cm^{-1})	Crystal[7] (cm^{-1})	Analysis[15] (cm^{-1})	Theoretical[10] (cm^{-1})
α-Band	—	23365	21800	ν_{00}	24985 (f=0)
	23756	23810	22130	$\nu_{00}+350$	
	24366	24390	—	$\nu_{00}+350+650$	
	24832	24875	23250	$\nu_{00}+1450$	
	~25150	25220	—	$\nu_{00}+1450+350$	
	25727	25775	24140	$\nu_{00}+350+650+1350$	
	26178	26210	24620	$\nu_{00}+1450+1350$	
	~26450	26455	—	$\nu_{00}+1450+1600$	
p-Band	~29700	28780	27200		35190
	30250	29285	28350		(f=2.113)
	~30700	29760	30090		
		30720	31850		
		31300			
		31600			
β-Band		32787	32985		
			33570		
			36440		

Discussion

The first transition bands of these compounds, *i. e.*, the α-bands according to Clar's notation, have very weak oscillator strengths, *f*. (f=0.008 for benzoperylene and f=0 for coronene.[9]) Especially, the first singlet-singlet transition of coronene is forbidden by symmetry, but it is slightly allowed by vibrational perturbations, as in the case of benzene.[10]

Accordingly, it is the vibronic bands coupled with asymmetric vibrations that appeared with the stronger intensities. The 0–0 band is very weak, and it completely disappears in the gas phase. In both cases, the extinction coefficients are of the order of 10^2 in the solution.[5]

To aid the analysis of these bands, the behaviour in various solvents was taken into consideration. According to McRae's theory of the solvent effect, the molecule is affected by the interaction between the induced dipoles in the following way:[11]

$$h\Delta\nu = A\frac{n^2-1}{2n^2+1} \quad (1)$$

where $h\Delta\nu$ is the spectral shift, where A is a constant characteristic of the transition of the solute, and where n is the refractive index of the solvent. The solvent-shifts are plotted for various kinds of solvents in Figs. 7 and 8.[12] As to benzoperylene, Eq. (1)

11) E. G. McRae, *J. Phys. Chem.*, **61**, 562 (1957).
12) H. Matsushita, *Nippon Kagaku Zasshi*, **84**, 110 (1963).

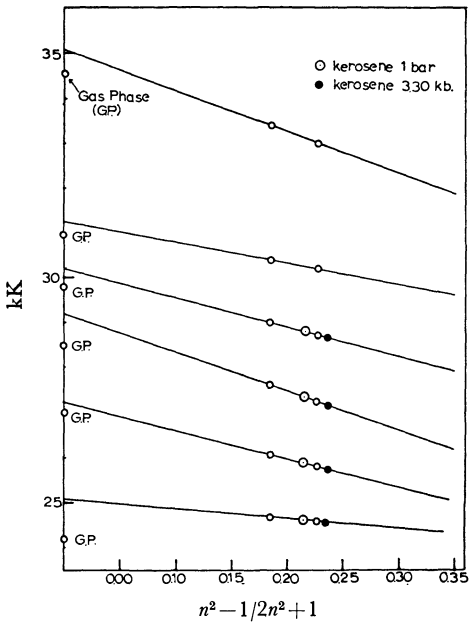

Fig. 7. Solvent effect for benzo[*g,h,i*]perylene.

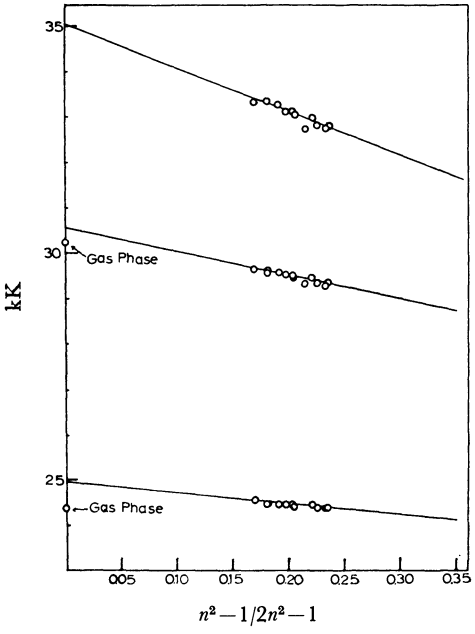

Fig. 8. Solvent effect for coronene.

is valid for the non-polar solvents, since it has a permanent dipole in the ground state.

The values extrapolated to the point of origin approximately indicate the positions of the spectra in the gaseous phase, but they generally exceed them to some extent. The discrepancies of the α-band are the greatest in both cases. The transitions with such small transition dipoles should not be expressed simply by Eq. (1), since the apparent amount becomes larger than the actual value, indicated by the abbreviation employed in the derivation of Eq. (1).[12,13]

The difference between the α-bands of benzoperylene in the gas phase and in solution is 460 cm^{-1}, while that of coronene is very little; the difference in f-values is thus reflected. This phenomenon is based on the fact that the solvent-shift is linearly correlated with the oscillator strength of the band to the second order of perturbation.[13]

However, the gaseous spectra became more diffuse than those in solution. This fact is the opposite of the general tendency, especially in the case of small molecules.

This line broadening can be explained if the following phenomenon is taken into consideration: in the first place, the thermal population can be considered in the vibrationally-excited states in the electronic ground state, which causes the hot bands in the excited states. The thermal energy kT amounts to 500 cm^{-1} when the α-band of coronene is measured. Considerable modes of fundamental vibration are obscured by this effect. This seems to have a very great effect on the line broadening. The relaxation process due to the intermolecular collisions may also be effective, thus reducing the lifetime of each vibronic band.

Coronene has many vibronic bands in the condensed phase, even at room temperature; this is rare among higher polycyclic aromatic hydrocarbons. These vibronic structures are reproduced in the gaseous spectrum. The redistribution of the oscillator strengths among the vibronic bands are not very distinguishable. The vibrational spacings are not changed. Several vibrational progressions, with fundamentals of 365, 650, 1440 cm^{-1}, *etc.*, are observed. These lines can be assigned by the aid of the studies in the rigid solution.[14,15]

From the two distinct lines, 4104 Å and 3887 Å, the location of the 0–0 band of coronene was deduced to be at 23390 cm^{-1}.

The second-transition bands of benzoperylene and coronene are called p-bands by Clar; they are theoretically-allowed transitions.[9,10] These two transitions have very similar red shifts in going from vapour to solution; the transitions amount to about 1000 cm^{-1}, corresponding to the fact that both transitions have nearly the same strong oscillator strengths (f= 2.08—2.20).

The spectrum of benzoperylene consists of four main peaks. The redistributions of the intensities were clearly observed in the passage from gas to solution. The shoulder on the band at 26075 cm^{-1} in solution grew into a distinct peak in the gas phase. The second vibronic peak augmented its intensity

13) Y. Ooshika, *J. Phys. Soc. Japan*, **9**, 591 (1954).
14) E. G. Moisya, *Opt. Spectry.*, **21**, 59 (1966).
15) N. Mentzel and H. Zimmermann, *Ber. Bunsenges. Phys. Chem.*, **67**, 582 (1963).

in comparison with the other bands. The solvent effect of this band is apparently twice as large as those of the others. The pressure effect on these bands is consistent with the behaviour mentioned above.[16]

It is likely, in view of only the intensities and the shifts of the absorption spectra, that the p-band of benzoperylene consists of two or more transitions. However, theoretical studies do not suggest that there exists another transition near the 27025 cm^{-1} band system.[9] Therefore, the most reasonable interpretation should be based on the assumption that there are two (or more) vibrational progressions, beginning at 27025 cm^{-1} and 27315 cm^{-1}. When these progressions are very similar to each other, the overlapped band shapes are probably directly dependent on the difference in the solvent effects of the two progressions. The apparent peaks even in the same transition will sometimes behave differently, as in the case of benzoperylene.

It may be remarked incidentally that the pressure shifts can be explained in terms of the change in the refractive index of the solvent due to the applied pressure. In Fig. 7, the spectral shifts induced by the pressure of 3.30 kb are also plotted, along with the linear relationship of the solvent effect expressed by Eq. (1); all the evidence points to the same n-value, 1.501. This interpretation is slightly different from the popular explanation based on the change in the density of the solvent.[17] Therefore, it must be further examined both experimentally and theoretically.

In the case of coronene's p-band, one main peak and two subsidiary shoulders were detected. No other vibrational structure was observed. The behaviour in this region seems unchanged, except for the shifts of the spectral lines.

The third-transition system of benzoperylene, which is ordinarily called the β-band, begins at 34565 cm^{-1} in the gas phase. This intense system shifts to an energy lower by as much as 1165 cm^{-1}. The β-band of coronene may be supposed, on the basis of the solvent-shifts, to be located at about 35000 cm^{-1}.

The comparison of the gaseous spectra with those in crystalline states will be made elsewhere.

It is a pleasure to acknowledge our helpful and stimulating discussion with Drs. Takashi Kajiwara, Ichimin Shirotani, and Tadayoshi Sakata of the Institute for Solid State Physics, The University of Tokyo, during the course of this work.

16) T. Kajiwara, Thesis, University of Tokyo (1969).

17) W. W. Robertson, D. E. Weigand, Jr., and F. A. Matsen, *J. Mol. Spectry.*, **1**, 1 (1957).

BULLETIN OF THE CHEMICAL SOCIETY OF JAPAN VOL. 43 2439—2441 (1969)

Direct Determination of Charge Transfer Energy

Jun-ichi AIHARA,*1 Motoyuki TSUDA*1 and Hiroo INOKUCHI

The Institute for Solid State Physics, The University of Tokyo, Roppongi, Tokyo

(Received March 30, 1970)

The absorption spectrum of the gaseous anthracene - chloranil complex was measured. The Coulomb energy contributing to the charge-transfer transition was determined to be 3.03 eV. The polarization energy for the transition was 0.17 eV in an *n*-heptane solution.

Since the charge-transfer theory was advocated by Mulliken, various theoretical and experimental investigations have been made of the charge-transfer complexes.[1,2] By means of the theory, approximate linear relations between the energy of the charge-transfer transition and the ionization potential of the donor or the electron affinity of acceptor have been derived and experimentally confirmed.[3,4]

According to McConnell *et al.*, the energy of the charge-transfer transition, W, can often be expressed simply by the following relation:[5]

$$W = I - A - C - P \qquad (1)$$

*1 Present address: Department of Chemistry, Faculty of Science, Hokkaido University.

1) R. S. Mulliken, *J. Amer. Chem. Soc.*, **74**, 811 (1952).

2) G. Briegleb, Elektronen Donator-Akzeptor Komplexe, (Springer-Verlag, Berlin, 1961).

3) R. Foster, *Nature*, **183**, 1253 (1959).

4) M. Kinoshita, This Bulletin, **35**, 1609 (1962).

5) H. McConnell, J. S. Ham and J. R. Platt, *J. Chem. Phys.*, **21**, 66 (1953).

where I is the energy required to take an electron out of the highest occupied molecular orbital of a donor and where A is the energy gained as an electron is brought to the lowest vacant molecular orbial of an acceptor. C is a Coulomb-energy term, and P is a polarization-energy term.

If the geometrical configuration of the complex is known, the Coulomb term can be calculated by the following equation:[6]

$$C = \int \phi^2(1) \frac{e^2}{r_{12}} \theta^2(2) d\tau_1 d\tau_2 \qquad (2)$$

where ϕ is the molecular orbial of a donor and θ is that of an acceptor. However, the polarization energy is rather difficult to estimate theoretically, as it depends on the properties of the solvent as well as on the geometry of the complex. Moreover, the electron affinity of the acceptor can not be obtained accurately.

Because of these ambiguities, the estimation of Eq. (1) is very difficult as long as the available data are restricted to the optical absorption in condensed phases. Fortunately, the electron affinity of chloranil has recently been determined by the magnetron method to be 2.45 eV.[7] In order to make a rigorous analysis of each term in Eq. (1), we tried to observe the gaseous absorption spectrum of the anthracene-chloranil complex. The ionization potential of anthracene was determined to be 7.38 eV by the photoionization method.[8]

Experimental

Anthracene used in this work was a synthetic and zone-refined material prepared by Iwashima.[9] Chloranil was purified by recrystallization from benzene. The *n*-heptane solution of the anthracene - chloranil complex was prepared by mixing equimolecular components to an appropriate concentration.

The optical data for the complex in the gas phase were obtained by means of an Aminco 4-8401 monochromator. Anthracene and equimolecular chloranil were placed in a Pyrex-glass cell 30 cm long; the cell was sealed off after evacuation. The vapour pressure of chloranil is very low, so the cell was heated to around 250°C in a 50-kW electric furnance.[10] The absorption spectrum of the gaseuous complex was measured rapidly with a 200-W tungsten lamp.

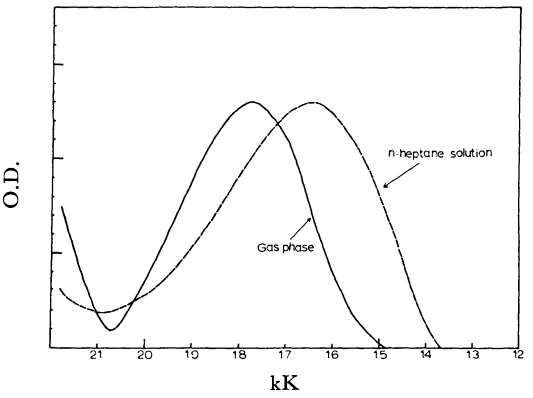

Fig. 1. Absorption spectra of the anthracene-chloranil complex.

Results and Discussion

Figure 1 shows the absorption spectrum of the anthracene - chloranil complex in the gas phase. The solution spectrum in *n*-heptane is added for the sake of comparison. Heptane was chosen as a common inert solvent in view of its solvent effect.[11]

The complex vapour gave evidence of a charge-transfer absorption maximum at 17800 cm^{-1} as compared with a value of 16400 cm^{-1} in an *n*-heptane solvent.

The shapes of the charge-transfer bands in the gaseous state and in solution are almost the same; the bands are all broad and diffuse. The asymmetry of bands is preserved in the vapour. However, the half-width, δ, in the gas phase is considerably smaller than that in solution (*e. g.*, $\delta = 3060$ cm^{-1} in gas and $\delta = 3930$ cm^{-1} in solution). The wave-number-shift from gas to solution amounts to 1400 cm^{-1} in this complex; this is considerably smaller than those in the complexes with TCNE.[11]

It has been shown that the width and diffuseness of the charge-transfer bands result from the difference in the form of the potential curves for the ground and excited states of the complex.[12] Therefore we tried to estimate the location of the 0–0 band with the aid of the fluorescence spectra, since the spectrum for the anthracene complex is deficient, but our efforts were in vain. Therefore, by analogy with the general behaviour of the mirror points of the fluorescent chloranil complexes, the 0–0 band of the anthracene - chloranil was estimated to be at 15400 ± 300 cm^{-1}, which is equivalent to 1.91 eV.[2]

As a considerable amount of the change in the molecular coordinate is caused by the augmentation of the Coulomb energy in the excited state,

6) H. Kuroda, T. Amano and H. Akamatu, *J. Amer. Chem. Soc.*, **89**, 6056 (1967).
7) A. F. Farragher and F. A. Page, *Trans. Faraday Soc.*, **62**, 3073 (1966).
8) A. Terenin and F. Vilessov, *Advan. Photochem.*, **2**, 385 (1964).
9) S. Iwashima, K. Ogino and J. Aoki, *Nippon Kagaku Zasshi*, **89**, 338 (1968).
10) K. H. Hausser and R. S. Mulliken, *J. Phys. Chem.*, **64**, 367 (1960).
11) J. Aihara, M. Tsuda and H. Inokuchi, This Bulletin, **42**, 1824 (1969).
12) J. Prochrow and A. Tramer, *J. Chem. Phys.*, **44**, 4545 (1966).

the 0–0 position generally shifts to the band edge of the charge-transfer transition. Therefore, it is understandable that the band width of the absorption spectrum is often broader than that of the fluorescence.[2]

In 1964, Chakrabarti *et al.*,[13] using the relation concerning the solvent shifts, estimated the location of the band maximum of gaseous anthracene - chloranil at 21000 cm^{-1}. This overestimated value may be due to the misapplication of the solvent effect. They also failed to explain the dipole moment in the ground state.

In a previous paper,[11] we ourselves have reported the gaseous absorption spectra of aromatic-TCNE complexes. We concluded that the charge-transfer bands obey the McRae's formula of solvent effect, so the gas phase spectra can be regarded as the origin of that effect. This implies that the charge distribution of the complex is nearly preserved in normal solvents and in the gas phase.

Presupposing that this theory is valid for the anthracene - chloranil complex, we will proceed in our discussion. In the first place, the Coulombic-attraction term contributing to the charge-transfer transition can be directly deduced from Eq. (1), as the polarization energy vanishes in the gas phase. Therefore, the Coulomb term of the anthracene - chloranil amounts to 3.03 eV. It is a quite reasonable value compared with those calculated for a series of aromatics-TCNE complexes (*e. g.*, 3.34 eV for the naphthalene-TCNE, 3.10 eV for the pyrene-TCNE, and 2.91 eV for the perylene-TCNE).[14] These calculations have been made on every configuration, using Eq. (2) with the point-charge approximation. In view of their origin, the constancy of these attraction terms among various complexes is quite natural.

Employing the calculated Coulomb energy, we shall now determine the electron affinity of TCNE again. The ionization potential of naphthalene is 8.12 eV.[15] As the transition energy of the naphthalene-TCNE complex is considered to be around 2.23 ± 0.05 eV, its electron affinity can be estimated as 2.55 eV. This value is in good agreement with the 2.60 eV assumed in the previous paper.[11]

The smaller affinity was also estimated to be 2.10 eV from the SCFMO calculations performed by Flurry's laboratory.[16] The value derived by Briegleb from the spectroscopic data, 1.80 eV, seems too small.[17]

As to the polarization energy term, we define the spectral shift in the condensed phase as the polarization energy.

Table 1. The results of the charge transfer energies (eV)

	Anthracene-chloranil	Naphthalene-TCNE
Ionization potential of donor	7.38	8.12
Electron affinity of acceptor	2.45	2.55 ± 0.05
Coulomb energy	3.03 ± 0.05	3.34
Polarization energy		
in *n*-heptane	0.17	0.29
in carbon tetrachloride	0.22	0.38

So far, the physical meaning of the polarization energy has been very obscure, since the difference between the absorption maximum and the theoretically-calculated transition energy is considered to be the energy. This term often grows to 1 eV, depending on the MO adopted.[6] According to our definition, the transition energies of the anthracene - chloranil are 0.17 eV in *n*-heptane and 0.22 eV in carbon tetrachloride. Those of the naphthalene-TCNE are 0.29 eV in *n*-heptane and 0.38 eV in carbon tetrachloride.[11] (Summarized in Table 1) Consequently, the dipole-polarization force acting on the charge-transfer transition of the naphthalene-TCNE is stronger than that of the anthracene - chloranil by a factor of 1.7. This quantity can be explained by the usual McRae's formula.[18]

In the above treatment, we neglected an ionic character of several percent which stabilizes the complex in the ground state.[19] Probably, it influences each term in Eq. (1) within an accuracy of 0.20 eV. In the case of the TCNE complex, this effect may contribute to the increase in the electron affinity of TCNE, since its ionicity is considerably stronger than that of the chloranil complex.[19]

For further investigations of the charge-transfer complex, it is desirable to determine wavefunctions such as we obtained in this experiment wihch will accurately reproduce the energy diagram.

Giacometti *et al.*, who first treated the chloranil complex theoretically, adopted a complex with *p*-phenylenediamine in their MO calculations.[20] The SCFMO approach to the molecular complex system also seems fruitful.[21]

13) S. K. Chakrabarti and S. Basu, *Trans. Faraday Soc.*, **60**, 465 (1964).
14) I. Ikemoto, private communication.
15) K. Watanabe, *J. Chem. Phys.*, **26**, 542 (1957).
16) R. L. Flurry, Jr., *J. Phys. Chem.*, **73**, 2111 (1969).
17) G. Briegleb, *Angew. Chem.*, **76**, 326 (1964).
18) E. G. McRae, *J. Phys. Chem.*, **61**, 562 (1957).
19) G. Briegleb, J. Czekalla and G. Ruess, *Z. Phys. Chem.* (Frankfurt), **30**, 333 (1961).
20) G. Giacometti, P. L. Nordio and G. Rigatti, *Nuovo Cimento*, **23**, 433 (1962).
21) T. Ohta, T. Kunii, H. Kuroda and H. Akamatu, Simposium on Molecular Structures held at Fukuoka (1969).

BULLETIN OF THE CHEMICAL SOCIETY OF JAPAN VOL. 43 2442—2444 (1970)

Ion-Solvent Interaction of Tetraalkylammonium and Some Common Ions in *N*-Methylformamide from Viscosity Data

Pushti Prakash RASTOGI

Chemistry Department, Lucknow University, Lucknow, India

(Received November 4, 1969)

Solute-solvent interaction of tetraalkylammonium iodides (R_4NI) and some common electrolytes has been studied in *N*-methylformamide (NMF) from the viscosity point of view. From the obtained results it has been concluded that common electrolytes like LiCl, KI, CsI are net structure promoters while R_4NI salts are net structure breakers in this solvent.

The interaction of the tetraalkylammonium (R_4N^+) ions with *N*-methylacetamide (NMA) molecules has already been reported from the point of view of conductance in a previous[1] communication. Another method commonly employed, for investigating ion-solvent interaction in solution, is to study the temperature dependence of the coefficient B of the viscosity equation of Jones and Dole,[2] namely,

$$\eta = \eta_0(1+A\sqrt{C}+BC)$$

or

$$(\eta/\eta_0-1)/\sqrt{C} = A + B\sqrt{C} \qquad \text{(i)}$$

This approach provides valuable information about the mode of solute-solvent interaction[3] on account of the fact that the coefficient B represents the interaction between the solvent molecules and the ions of the dissolved electrolyte. Ion-solvent interaction in aqueous solutions, from this point of view, has been studied by several workers.[4-6] According to Kaminsky[4] the coefficient B has a negative temperature coefficient for the highly hydrated ions like Li^+, Be^{2+}, Mg^{2+}, Ce^{3+}, *etc.*; on the other hand, B has a positive temperature coefficient for the less hydrated ions like Cs^+, Rb^+, I^-, NO_3^-, *etc.* These results led him to suggest that the former are net structure makers while the latter are net structure breakers in aqueous solutions. Nightingale[5] and Kay and coworkers[6] concluded that Pr_4N^+ and Bu_4N^+ ions are excellent structure promoters but Me_4N^+ ion is a net structure breaker, while the structure breaking and making effects almost balance one another for Et_4N^+ ion in aqueous solutions. In view of the current interest in the behaviour of R_4N^+ ions, on account of their "abnormal" properties in aqueous solutions and of their special structual features, one is tempted to investigate their behaviour in solvents other than water but similar to water in having high dielectric constant so that the complications arising out of ion-association may be avoided. Some interesting solvents of this type are monoalkyl-substituted amides, *e.g.*, NMF, NMA and *N*-methylpropionamide (NMP).

The present communication reports a study of the ion-solvent interaction of R_4NI salts in NMF from the viscosity data. Some common salts like LiCl, KI and CsI have also been included in the study for the sake of comparison.

Experimental

R_4NI salts were purified in the usual manner as described.[1] Merk's A. G. reagents LiCl, KI and CsI were twice recrystallized from conductivity dried in an electric oven and were kept in a vacuum desiccator until used.

NMF, obtained from M/s Distillation Products Industries, U.S.A., was left overnight on some freshly ignited quicklime and was then distilled under reduced pressure. The middle fraction of the distillate was collected and redistilled. The process of purification was continued until the specific electrical conductance of the middle fraction of the distillate was reduced to less than 10^{-6} ohm^{-1} cm^{-1}. The purified samples were collected in dark amber-coloured bottles which were kept in a dry box. A rapid variation in electrical conductance and viscosity of NMF with time was observed immediately after distillation. However, after several hours the changes were slow. Hence NMF was used after keeping it for about 24 hr.

Measurements of density and viscosity were carried out in a thermostat with maximum temperature fluctuation ± 0.01°C. Solutions were prepared on molar basis at 25°C and were corrected for the changes in volume at other temperatures.

1) R. D. Singh, P. P. Rastogi and R. Gopal, *Can. J. Chem.*, **46**, 3525 (1968).

2) G. Jones and M. Dole, *J. Amer. Chem. Soc.*, **51**, 2950 (1929).

3) R. W. Gurney, "Ionic Processes in Solution," McGraw Hill Book Co. Inc., New York (1953), pp. 159—171.

4) M. Kaminsky, *Discuss. Faraday Soc.*, **24**, 150 (1957).

5) E. R. Nightingale, Jr., *J. Phys. Chem.*, **66**, 894 (1962).

6) R. L. Kay, T. Vituccio and D. F. Evans, *ibid.*, **70**, 2336 (1966).

Table 1. Values of $\eta_{sp}/\sqrt{C}$ from viscosity data in NMF

$C\times10^2$	25°C	30°C	35°C
	Me_4NI		
0.25	0.019	0.025	0.030
0.50	0.026	0.035	0.042
1.00	0.038	0.046	0.051
1.43	0.042	0.050	0.061
2.00	0.053	0.060	0.068
	Et_4NI		
0.25	0.026	0.030	0.039
0.50	0.041	0.043	0.046
1.00	0.052	0.059	0.067
1.43	0.061	0.067	0.074
2.00	0.073	0.081	0.090
	Pr_4NI		
0.25	0.035	0.042	0.047
0.50	0.050	0.055	0.059
1.00	0.066	0.073	0.078
1.43	0.079	0.086	0.094
2.00	0.095	0.102	0.106
	Bu_4NI		
0.25	0.041	0.046	0.051
0.50	0.060	0.063	0.068
1.00	0.080	0.087	0.095
1.43	0.100	0.106	0.112
2.00	0.111	0.121	0.128
	Pen_4NI		
0.25	0.052	0.057	0.061
0.50	0.068	0.075	0.081
1.00	0.094	0.102	0.108
1.43	0.113	0.119	0.127
2.00	0.133	0.140	0.148
	Hex_4NI		
0.25	0.057	0.062	0.069
0.50	0.082	0.086	0.091
1.00	0.110	0.118	0.121
1.43	0.131	0.140	0.148
2.00	0.158	0.162	0.168
	Hep_4NI		
0.25	0.063	0.067	0.074
0.50	0.090	0.094	0.106
1.00	0.103	0.136	0.141
1.43	0.151	0.160	0.164
2.00	0.180	0.189	0.197
	LiCl		
0.25	0.035	0.030	0.025
0.50	0.046	0.042	0.037
1.00	0.065	0.060	0.054
1.43	0.072	0.067	0.060
2.00	0.083	0.078	0.074
	KI		
0.25	0.040	0.036	0.031
0.50	0.049	0.044	0.037
1.00	0.061	0.057	0.050
1.43	0.072	0.067	0.060
2.00	0.088	0.082	0.075
	CsI		
0.25	0.036	0.032	0.026
0.50	0.045	0.040	0.036
1.00	0.065	0.058	0.054
1.43	0.072	0.067	0.060
2.00	0.089	0.080	0.074

Density was determined with a dilatometer which was provided with a graduated stem on which volume could be read upto 0.005 m*l* within an error of ±0.002 m*l*. A modified Ubbelohde viscometer with a flow time of about 500 sec, for NMF at 25°C, was employed for measuring the viscosity. The readings within the maximum deviation of ±0.1 sec were recorded and taken into account while the widely varying ones were discarded. A 40% sugar solution of known viscosity was used to determine the viscosity of NMF. The density and viscosity of NMF determined at different temperatures, were found to agree very closely to those reported in literature as is clear from the following table:

Temp. °C	Density and Viscosity of NMF			
	Density in g/ml		Viscosity in poise	
	Exptl.	Literature*	Exptl.	Literature*
25	0.9990	0.9988	0.0168	0.0165
30	0.9947	—	0.0155	—
35	0.9905	—	0.0144	—

* C.M. French and K.H. Glover, *Trans. Faraday Soc.*, **51**, 1418 (1955).

The viscosity of solution was calculated with help of the usual relation, namely,

$$\eta = \frac{d}{d_0} \times \frac{t}{t_0} \times \eta_0 \qquad \text{(ii)}$$

The viscosity data were subjected to the kinetic energy corrections which were usually negligible. From the corrected data, the factors $\eta_{sp}/\sqrt{C}$ ($\eta_{sp}=\eta/\eta_0-1$) were obtained for different solutions at various temperatures. The values of $\eta_{sp}/\sqrt{C}$ are given in Table 1. The factor $\eta_{sp}/\sqrt{C}$ was plotted against $\sqrt{C}$ for different salts at different temperatures. The plots are almost linear, the slopes of which give the values of B and are summarized in Table 2, whereas the ordinate intercepts give the coefficients A (which represent the contribution from interionic forces[7]).

Table 2. Viscosity B coefficients in *N*-methylformamide

Salt	25°C	30°C	35°C
Me_4NI	0.38	0.42	0.48
Et_4NI	0.49	0.52	0.57
Pr_4NI	0.68	0.71	0.75
Bu_4NI	0.81	0.85	0.88
Pen_4NI	0.97	1.00	1.03
Hex_4NI	1.11	1.15	1.17
Hep_4NI	1.28	1.30	1.33
LiCl	0.59	0.55	0.53
KI	0.56	0.54	0.51
CsI	0.60	0.58	0.57

7) H. Falkenhagen and E. L. Vernon, *Phys. Z.*, **33**, 140 (1932).

Results and Discussion

It may be noted from Table 2 that B values increase with the increase in the radius of the ion, *i.e.*, dB/dr (r being the radius of the ion) is positive, which leads to the conclusion that R_4N^+ ions behave, more or less, like large spheres moving in a dielectric continuum as was postulated by Einstein. The value of B according to the Einstein theory[8] is given by:

$$B = 2.5(v/C) \qquad \text{(iii)}$$

where v is the total volume of the ions per ml of solution and C the molar concentration. So, for a particular solvent the value of B for different ions should be proportional to v. If the crystal radii of these ions as estimated by Robinson and Stokes[9] are used, it is found that $B \propto r^3$ as is clear from Fig. 1, in which the experimental values of B are plotted against r^3. Thus the ion-solvent interaction as shown by the dependence of B on radius of the R_4N^+ ions, shows that the larger the ion, the greater the resistance for its movement in the solvent medium and there is no other ion-solvent interaction. However, the variation of B with temperature does indicate some interaction.

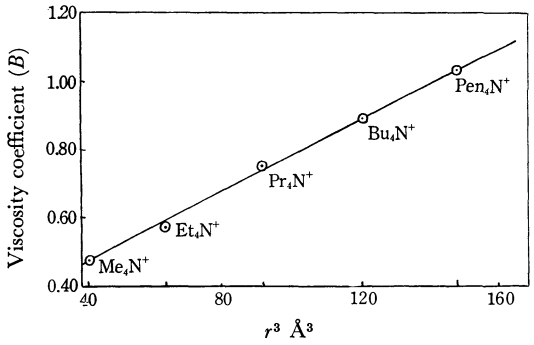

Fig. 1 *N*-Methylformamide temperature 35°C.

B values given in Table 2 indicate that dB/dt is positive for the R_4NI salts and negative for common electrolytes like LiCl, KI, CsI studied here in NMF. A positive dB/dt implies a net structure-breaking of the solvent at lower temperature in the presence of R_4NI salts so that the local viscosity around the ions does not decrease with temperature rise as rapidly as the viscosity η_0 of the pure solvent. The temperature coefficient (*i.e.*, dB/dt) is negative for common electrolytes containing cations like Li^+, K^+, Cs^+ *etc.*, because of the possible long range ordering (or secondary solvation) of the solvent molecules around them. As the temperature rises, long range ordering is disturbed by the thermal agitation and the local viscosity around the ions decreases faster than η_0 and this leads to a negative dB/dt. Although R_4NI salts appear to be structure breakers in these solvents, they do not give rise to long range ordering because of the low surface charge density, and hence dB/dt is positive. This is in contrast with their behaviour in aqueous solutions in which the temperature coefficient of B, *i.e.*, dB/dt, is negative[5,6] for the R_4N^+ (except Me_4N^+); this has been explained on the ground of the strong "hydrophobic solvation" of the R_4N^+ ions; strong hydrophobic solvation is equivalent to long range ordering of the water structure, similar to the electrostatic hydration of Li^+, Be^{2+}, Mg^{2+} and Ce^{3+} ions for which dB/dt is negative.[4-6,10] For larger common cations and for the halide ions, dB/dt is positive in aqueous solutions. In NMF, such hydrophobic ordering of the solvent by R_4NI salts does not occur, presumably because the solvents and R_4N^+ ions have methyl or similar organic groups, in both of them making the solvent and the solute similar in nature.

It appears that structure breaking effect goes on decreasing with the increase in the radius of the ion. This can be expected because the larger R_4N^+ ions have low surface change density; so the electrostatic ion-solvent interaction is not strong enough to break the hydrogen-bonded structure of the solvent.

It appears that R_4N^+ ions are net structure breakers (in the sense of breaking of hydrogen bonds) whereas the alkali metal ions are structure promoters (*i.e.*, the long range order makers) in NMF solutions.

The author thanks Dr. Ram Gopal for providing the laboratory facilities and valuable suggestions.

8) A. Einstein, *Ann. Phys.*, **19**, 289 (1906); **34**, 591 (1911).

9) R. A. Robinson and R. H. Stokes, "Electrolyte Solutions," Butterworths Publications, Ltd., London (1959), pp. 124—126.

10) D. Feakins and K. G. Lawrence, *J. Chem. Soc.*, *A*, **1966** 217.

BULLETIN OF THE CHEMICAL SOCIETY OF JAPAN VOL. 43 2445—2449 (1970)

Oxidation of Substituted Glycollic Acids by Ce(IV) in Sulphuric Acid Solutions

V. K. GROVER and Y. K. GUPTA

Department of Chemistry, University of Rajasthan, Jaipur, India

(Received December 15, 1969)

A comparison of the rate constants, dissociation constants, tendency of complex formation and catalytic activity of Mn(II) in the oxidation of substituted glycollic acids (benzilic, DL-atrolactic, 2-hydroxyisobutyric, *p*-chloromandelic, *p*-bromomandelic, mandelic and lactic acids) by Ce(IV) in sulphuric acid solutions has been made. Hydrolyzed species of Ce(IV) are reactive and the kinetics conform to the empirical rate law

$$-\frac{d[Ce(IV)]}{dt} = \frac{kK[Ce(IV)][Org.\ Acid]}{[HSO_4^-]^2([H^+]+K[Org.\ Acid])}$$

The reactivity and the chelating tendency of the acids seem to follow the substituent order, $C_6H_5 > CH_3 > H$. The catalytic activity of Mn(II) appears to follow the same order as in the oxidation of these acids by Mn(III).

Oxidation of glycollic acid by Ce(IV) has been studied by McAuley,[1] and Bakore *et al.* and rupture of C–H bond is said[2] to be rate determining. In the oxidation of substituted acids also, *i.e.*, mandelic and lactic acids, Krishna and Tewari,[3] and Bhargava *et al.*[4] assume the same mechanism, while Kemp and Waters[5] from their experiments with deuterated mandelic acid showed that the slow step preferably involves C–C bond breaking. A detailed systematic study was, therefore, considered desirable and the present paper reports and compares the rate and other data of the phenyl and methyl substituted acids.

Experimental

Reagents. Ceric sulphate (E. Merck G. R.) was used without further purification. Benzilic, mandelic, *p*-chloromandelic and *p*-bromomandelic acids were Riedel products. DL-Atrolactic and 2-hydroxyisobutyric acids were obtained from Koch-Light Co. All other chemicals were either B.D.H. Analar and E. Merck G. R. quality.

Preparation of Solutions. Ce(IV) solutions in sulphuric acid were prepared as described[6] earlier. Ceric perchlorate was prepared in the following way. Ceric ammonium hydroxide was precipitated from a solution of ceric ammonium nitrate by ammonium hydroxide. The precipitate was allowed to settle (48 hr), leached several times with water, dissolved in perchloric acid and filtered. Ce(IV) solutions were standardized against ferrous ammonium sulphate using *N*-phenyl anthralinic acid indicator. Solution of benzilic, mandelic, *p*-chloromandelic and *p*-bromomandelic acids were prepared by dissolving them in equivalent amounts of caustic soda and adjusting the pH between 6—8. 2-Hydroxyisobutyric acid was dissolved in hot water. All other acids were soluble in cold eater.

Kinetic Procedure. Reactions were carried out at 35±0.05°C in a thermostat. They were initiated by adding a temperature equilibrated solution of the organic acid to the reaction vessel containing the desired amount of ceric solution, sulphuric acid and water at 35°C. The kinetics were followed by removing a 10 m*l* aliquot portion after suitable intervals and quenching the reaction by adding it to a known excess of ferrous ammonium sulphate solution. The excess was determined against standard ceric solution using *N*-phenylanthranilic acid indicator. The maximum error in the analysis of the aliquots was ±0.02 m*l* of Ce(IV). This introduced an error of ±1 to 6% in the rate constants depending on the volume of the titrant. In most cases duplicate rate measurements were reproducible to ±5%.

Spectrophotometric Work. Optical density measurements were made on Beckmann spectrophotometer (DU-G 2400) using 1 cm cell. Measurements were carried out to obtain information about the complex formation between Ce(IV) and the organic acid. All the measurements were done in perchloric acid solutions because in sulphuric acid solutions strong sulphate complexes of Ce(IV) are formed, and any complex with the organic substrate, even if formed, would not be indicated spectrophotometrically.

Ionization Constants. Ionization constants of the organic acids were determined in water-dioxane (1:4 v/v) potentiometrically.

1) A. McAuley, *J. Chem. Soc.*, **1965**, 4054.
2) G. V. Bakore, R. Dayal and P. Nath, *Z. Physik. Chem.*, **227**, 19 (1964).
3) B. Krishna and K. C. Tewari, *J. Chem. Soc.*, **1961**, 3097.
4) K. P. Bhargava, R. Shankar and S. N. Joshi, *J. Sci. Ind. Res., India*, **218**, 573 (1963).
5) T. J. Kemp and W. A. Waters, *J. Chem. Soc.*, **1964**, 1192.

Stoichiometry. The stoichiometry was determined as described[6] earlier. In each case two moles of Ce(IV) were used up by one mole of the organic acid. The products of oxidation, benzophenone, *p*-chlorobenzaldehyde, *p*-bromobenzaldehyde, methyl ethyl ketone and acetone were estimated either as such or as hydrazones. The yields were 70—80%. The volume of carbon-dioxide was measured in case of benzilic acid and was found to be about 90% of the expected amounts. Stoichiometry for lactic and glycollic acids was not determined, but it is reported[3] to be 5.75 and 4 mol of Ce(IV) for each mole of the acid respectively.

Products. The products of oxidation of the organic acids were as follows:

Benzilic acid - benzophenone; *p*-chloromandelic acid - *p*-chlorobenzaldehyde; *p*-bromomandelic acid - *p*-bromobenzaldehyde; DL-atrolactic acid - methyl phenyl ketone; 2-hydroxyisobutyric acid - acetone. Products of oxidation of lactic and glycollic acids have already been identified. Benzophenone and *p*-bromobenzaldehyde were obtained as white insoluble solid from concentrated solution. They were recrystallised from alcohol or benzene and were identified by melting points, IR spectra and other tests. In the case of *p*-chloromandelic acid, the white crude solid product responds to the tests of *p*-chlorobenzaldehyde, but it undergoes slow air oxidation yielding the acid. It is interesting to note, however, that experiments on stoichiometry indicate no oxidation of *p*-chlorobenzaldehyde by Ce(IV). Acetone was identified in the form of hydrazone. Methyl phenyl ketone was obtained as a solid at about 0°C and was identified by the melting point and its characteristic hydrazone.

Results and Discussion

The orders with respect to the various reactants conform to either of the following two empirical rate laws:

$$-\frac{d[Ce(IV)]}{dt} = \frac{k_{11}[Ce(IV)][Org.\ Acid]}{[HSO_4^-]^2[H^+]} \quad (1)$$

and

$$-\frac{d[Ce(IV)]}{dt} = \frac{kK[Ce(IV)][Org.\ Acid]}{[HSO_4^-]^2([H^+]+K[Org.\ Acid])} \quad (2)$$

The results are shown in Table 1 and Figs. 1 and 2. Although kinetic evidence for complex formation has been obtained[6] only in the case of benzilic acid, spectrophotometric results provide evidence in all the cases and hence in general, rate law (2) appears to be applicable in all the cases. The various equilibria,[6-9] involving the cerium(IV) species and the mechanism are given below:

$$Ce^{4+} + H_2O \overset{K_{h1}}{\rightleftharpoons} CeOH^{3+} + H^+ \quad (3)$$

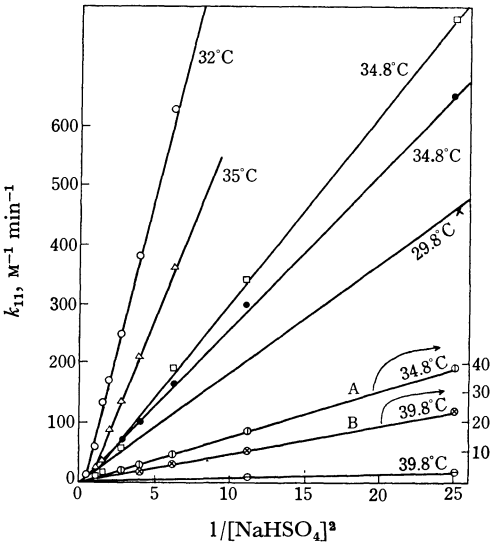

Fig. 1. Effect of bisulphate ion.
$[HClO_4]=0.5$M. ○, benzilic acid; △, atrolactic acid; ●, mandelic acid; □, *p*-chloromandelic acid; ×, *p*-bromomandelic acid; ⊕, 2-hydroxy isobutyric acid; ⊗, lactic acid; ⊖, glycollic acid. Straight lines A and B refer to the right scale.

$$CeOH^{3+} + H_2O \overset{K_{h2}}{\rightleftharpoons} Ce(OH)_2^{2+} + H^+ \quad (4)$$

$$Ce^{4+} + HSO_4^- \overset{K_5}{\rightleftharpoons} CeSO_4^{2+} + H^+ \quad (5)$$

$$CeSO_4^{2+} + HSO_4^- \overset{K_6}{\rightleftharpoons} Ce(SO_4)_2 + H^+ \quad (6)$$

$$Ce(SO_4)_2 + HSO_4^- \overset{K_7}{\rightleftharpoons} HCe(SO_4)_3^- \quad (7)$$

$$\text{Org. Acid} \overset{K_d}{\rightleftharpoons} \text{Anion} + H^+ \quad (8)$$

$$R_1\!\!\diagdown\!\!\overset{OH}{\underset{}{C}}\!\!\diagup\!\!R_2 \quad \diagdown\!\!COO^- + Ce(OH)_2^{2+} \overset{K_9}{\rightleftharpoons}$$

$$\left[R_1\!\!\diagdown\!\!\overset{H}{\underset{}{C}}\!\!\diagup\!\!R_2 \quad O\!\!\diagdown\!\!Ce(OH)_2 \quad \diagdown\!\!COO\!\!\diagup\right]^+ \quad (9)$$

(complex)

$$\text{Complex} \xrightarrow[\text{slow}]{k_{10}} R_1\!\!\diagdown\!\!\overset{H}{\underset{}{C}}\!\!\diagup\!\!R_2 \quad O + CO_2 + Ce(III) \quad (10)$$

$$R_1\!\!\diagdown\!\!\overset{H}{\underset{}{C}}\!\!\diagup\!\!R_2 \quad O + Ce(IV) \xrightarrow{\text{fast}}$$

$$R_1\!\!\diagdown\!\!C{=}O + Ce(III) + H^+ \quad (11)$$
$$R_2\!\!\diagup$$

The predominant species[8,9] of Ce(IV) is $Ce(SO_4)_2$ in bisulphate solutions employed in this work, but the reactive species as indicated by bisulphate and hydrogen ion effects, is $Ce(OH)_2^{2+}$. The rate law can be deduced only on such basis.

6) V. K. Grover and Y. K. Gupta, *J. Inorg. Nucl. Chem.*, **31**, 1403 (1969).
7) S. K. Mishra and Y. K. Gupta, *ibid.*, **29**, 1643 (1967).
8) T. J. Hardwick and E. Robertson, *Can. J. Chem.*, **29**, 828 (1951).
9) F. G. Soper, *J. Chem. Soc.*, **1935**, 802.

The above equations and equilibria lead to the rate law

$$-\frac{d[Ce(IV)]}{dt} = \frac{2k_{10}K_9K_{h1}K_{h2}K_d[Ce(IV)][Org.\ Acid]}{K_5K_6[HSO_4^-]^2([H^+]+K_9K_d[Org.\ Acid])} \quad (12)$$

which has the same form as (2). An alternative mechanism conforming to the rate law (1) is as follows.

$$Ce(OH)_2^{2+} + Anion \xrightarrow{k_{13}}$$
$$Org.\ free\ radical + CO_2 + Ce(III) + H^+ \quad (13)$$

$$Org.\ free\ radical + Ce(IV) \xrightarrow{fast}$$
$$product + Ce(III) \quad (14)$$

The complete rate law similar to (1) is:

$$-\frac{d[Ce(IV)]}{dt} = \frac{2k_{13}K_{h1}K_{h2}K_d[Ce(IV)][Org.\ Acid]}{K_5K_6[HSO_4^-]^2[H^+]} \quad (15)$$

These rate laws explain the observed order of the bisulphate ion. The rate decreases by the increase of hydrogen ion too, but a plot of k_{11} (observed second order rate constant) against $1/H^+$ does not yield a straight line as expected from (1) or (15). Thus these rate laws are not of the correct form so far as hydrogen ion dependence is concerned. On the other hand (2) or (12) conform to the observed hydrogen ion dependence (Fig. 2), but absence of kinetic evidence for complex formation does not justify their forms. Unfortunately the study with regard to hydrogen ion effect and complex formation could not be made under identical conditions. The effect of hydrogen ion was studied by varying perchloric acid concentration in a constant bisulphate medium. The reaction was fast in this medium. It could be made of measurable speed only by employing low concentrations of the reactants, particularly the organic acid, and consequently a study of complex formation could not be made.

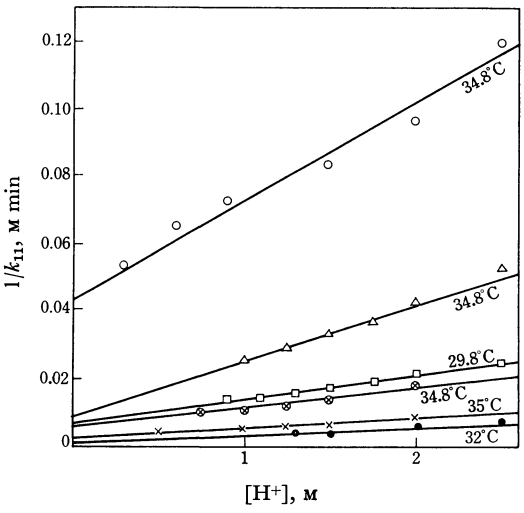

Fig. 2. Effect of hydrogen ions.
○, 2-hydroxy isobutyric acid, $[HSO_4^-]=0.4$M
△, *p*-chloromandelic acid, $[HSO_4^-]=1.0$M
□, *p*-bromomandelic acid, $[HSO_4^-]=0.5$M
⊗, mandelic acid, $[HSO_4^-]=0.5$M
×, atrolactic acid, $[HSO_4^-]=0.5$M
●, benzilic acid, $[HSO_4^-]=1.0$M

Under such a situation, in view of the general characteristics of Ce(IV) oxidation of hydroxy acids, tendency of complex formation from optical density measurements and kinetic evidence for the complex formation in the oxidation of benzilic acid,[6] we are inclined to regard (12) as the correct form of the rate expression. However, since no kinetic evidence for complex formation has been obtained in other cases, it is better to retain it in the same form but with 'A' as unspecified constant in the denominator in place of K_9K_d[Org. Acid]. The second order rate constant, k_{11} which has no reference to Eq. (11) can be defined by

$$k_{11} = \frac{2k_{10}K_9K_dK_{h1}K_{h2}}{K_5K_6[HSO_4^-]^2([H^+]+A)} \quad (16)$$

Table 1. Pseudo-first order and second order rate constants of the reaction between Ce(IV) and the organic acids in sulphuric acid solutions
$[Ce(IV)] = 5\times10^{-4}$M

$[H_2SO_4]$ M	[Org. Acid] M $\times10^3$	Pseudo-first order rate constant $k_1\times10$ min^{-1}	$k_{11}=k_1/$[Org. Acid] l/mol·min
DL-Atrolactic acid, t=35°C			
1.5	6.44	1.70	26.4
1.5	5.52	1.44	26.8
1.5	5.06	1.33	26.3
2.0	6.44	0.81	12.6
2.0	4.60	0.60	13.0
2.5	5.52	0.35	6.5
2.5	4.60	0.28	6.0
2-Hydroxyisobutyric acid, t=34.8°C			
0.5	14.0	1.10	7.8
0.5	10.0	0.80	8.0
0.5	7.0	0.56	8.0
0.75	16.0	0.58	3.62
0.75	7.0	0.25	3.57
p-Chloromandelic acid, t=34.8°C			
1.0	5.0	0.97	19.4
1.0	10.0	1.96	19.6
1.5	6.0	0.42	7.0
1.5	15.0	1.07	7.1
p-Bromomandelic acid, t=29.8°C			
1.0	6.0	0.62	10.3
1.0	12.0	0.12	10.0
1.5	4.5	0.19	4.2
1.5	10.0	0.42	4.2
Benzilic acid, t=32°C			
1.5	2.0	2.26	113
1.5	3.5	3.68	103
2.0	1.5	0.78	52
2.0	4.5	2.13	47

Table 2. Oxidations of substituted glycollic acids by Ce(IV)
10^3[Ce(IV)]=1.0 M; [H_2SO_4]=1.0 M, t=35°C

Acid	Concn. M×10^4	k_{11} l/mol·sec ×10^2	Ionization constant ×10^5	Maxima of the complex in the UV spectrum mμ	k_{Mn} l/mol·sec ×10^{-4}	E_a kcal
Benzilic	5.0	560	17.80	255	33 (2M H_2SO_4, 32°C)	18.7 (1.0M H_2SO_4)
DL- Atrolactic	5.0	113	8.320	242	14 (1.5M H_2SO_4, 34.8°C)	21.3 (1.5M H_2SO_4)
p-Chloromandelic	5.0	66.6	14.45	256	2.4 (1M H_2SO_4, 34.8°C)	19.8 (0.5M H_2SO_4)
p-Bromomandelic	5.0	64.4	12.88	255	2.0 (0.5M H_2SO_4, 29.8°C)	19.7 (0.5M H_2SO_4)
Mandelic	5.0	58.8	10.96	251	——	19.9 (1.0M H_2SO_4)
2-Hydroxyisobutyric	160	3.90	3.80	flat band 245—255	1.0 (0.5M H_2SO_4 34.8°C)	23.2 (0.5M H_2SO_4)
Lactic	160	1.60	4.40	flat band 245—255	——	27.4 (0.5M H_2SO_4)
Glycollic	400	0.11	6.17	flat band 245—255	——	25.5 (0.15M H_2SO_4)

Ce(IV) oxidation in general is without any isotopic effect as shown by Waters and coworkers in the oxidation of deuterated alcohols[10] and mandelic acid.[5] We have also carried out rate experiments with deuterated acids and the ratio k_H/k_D was in no case more than 1.1. Hence C–C fission is considered to be rate determining in the oxidation. The products of oxidation of the organic acids also support the involvement of C–C cleavage in the slow step. On the other hand Cr(VI) and V(V) oxidation is characterized by large isotopic effect suggesting C–H fission. Reactions in the presence of acrylamide further show that C–C fission occurs with the evolution of carbon dioxide. Acrylamide does not react[11] with Ce(IV), but it captures the free radical produced in step (10). This strongly suggests that carbon dioxide is produced in the slow step rather than in the fast step suggested by other workers.[2,3,12]

Mn (II) greatly catalyzes all these oxidations as is obvious from Fig. 3. These results can be expressed in the form

$$k_T = k_{11} + k_{Mn}[Mn(II)] \quad (16a)$$

where k_T and k_{11} are the rate constants in the presence and absence of Mn(II) and k_{Mn} is the specific rate constant for the catalyzed path. The catalytic activity of Mn(II) is ascribed to the rapid equilibrium[13]

$$Ce(IV) + Mn(II) \rightleftharpoons Ce(III) + Mn(III) \quad (17)$$

and the larger rate[5,14] for the oxidation of the organic acids by Mn(III). Table 1 shows the various data for all the acids. Mandelic acid is more readily oxidized than 2-hydroxyisobutyric acid[14] or lactic acid[15] by Mn(III) sulphate. Some visual observations have also indicated that the order of oxidation of different acids by Mn(III) is the same as given by the values of k_{Mn} of Table 2.

Spectrophotometric results indicate complex formation between Ce(IV) and the organic acid. Absorption curves typical of complex formation have

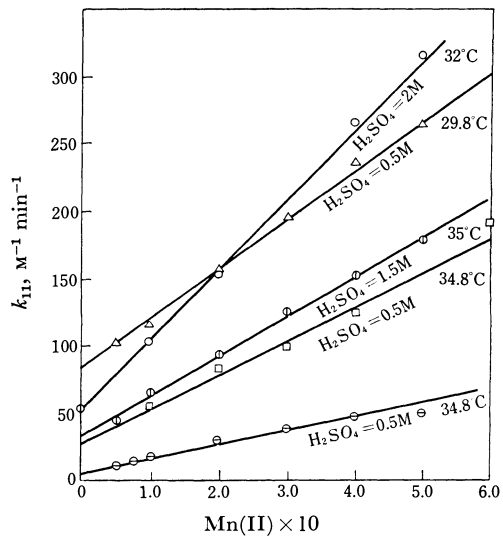

Fig. 3. Effect of Mn(II) on the oxidations of organic acids by Ce(IV).
○, benzilic acid; △, *p*-bromo mandelic acid; □, *p*-chloro mandelic acid; ⓛ, atrolactic acid; ⊖, 2-hydroxy isobutyric acid

10) J. A. Littler and W. A. Waters, *J. Chem. Soc.*, **1960**, 2767.
11) A. A. Katai, V. K. Kulshreshtha and R. H. Marchessault, *J. Poly. Sci.*, **2**, 403 (1963).
12) A. McAuley and C. H. Brubaker, Jr., *J. Chem. Soc.*, **1966**, 960.
13) M. J. Aspray, D. R. Rosseinsky and G. R. Shaw, *Chem. Ind.*, **1963**, 911.
14) T. J. Kemp and W. A. Waters, *J. Chem. Soc.*, **1964**, 339, 1610.
15) R. N. Mehrotra, *Z. Physik. Chem.*, **43**, 140 (1964).

been shown earlier[6] in the oxidation of benzilic acid. Similar curves were obtained for mandelic, *p*-chloromandelic, *p*-bromomandelic and DL-atrolactic acids. Flat bands with less absorption than that of Ce(IV) were obtained in case of 2-hydroxyisobutyric, lactic and glycollic acids. Complex formation seems to depend on two factors; the ionization constant of the organic acid and the substituted group C_6H_5 or CH_3 for H in CH_2. The ionization constants are in the sequence as expected from the $-I$ effect of C_6H_5 and $+I$ effect of CH_3 groups, it being largest for two C_6H_5 groups (benzilic acid) and lowest for two CH_3 groups (2-hydroxyisobutyric acid). The larger the ionization constant the greater is the tendency of complex formation as is obvious from Eq. (9). Another factor which seems to influence this tendency is the size of the group. A bulky group like C_6H_5 in benzilic acid facilitates complex formation. The larger value of the equilibrium constant[16] in case of *trans*-1,2-cyclohexanediol than that of *trans*-2-methoxycyclohexanol, has been explained on the basis of the steric hindrance. The same reason has been assigned to the failure for the complex formation by 2,3-butanediol as compared to ethylene glycol.[10] At first sight the formation of a complex in case of benzilic acid seems to violate the principle of steric hindrance, but closer examination would reveal that the steric hindrance of the phenyl groups brings the hydroxyl and the carboxyl groups closer facilitating the chelate formation with Ce(IV). On the other hand in case of *trans*-2-methoxy-cyclohexanol and 2,3-butanediol the substitution is in the hydroxyl group which may prevent the chelate formation. No maximum was obtained for lactic and 2-hydroxyisobutyric acids. On the other hand the corresponding absorption curves run below the curve of Ce(IV). A probable explanation for this may be the fact that the steric effect of the methyl group is less important than its inductive effect as suggested,[17] in the rare earth chelates of these organic acids. Kinetic evidence for the complex formation was obtained only in the case of benzilic acid obviously because both the factors, inductive and steric effects of the phenyl group act in the same direction.

The order of reactivity of different acids in general can be explained on the basis of free radical character developing in the activated complex at the carbon atom.[19] The formation of free radical is facilitated by the substituents of R in the order $C_6H_5 \gg CH_3 > H$.

k_{11} of Table 2 is a complex rate constant. It may be regarded as a product kK, where k and K are rate and equilibrium constants, respectively. It has not been possible to separate these two constants but it appears that the overall rate constant k_{11} follows the same order as that of the tendency of complex formation. Co(III) and V(V) oxidation of these acids also probably takes place *via* complex formation. The overall rate constants are in the same order, *i.e.*, atrolactic>mandelic>2-hydroxyisobutyric>lactic in 3.14M $[ClO_4^-]$ at 15°C in the case of Co(III)[20,21] and, mandelic>2-hydroxyisobutyric>lactic in 5M $[ClO_4^-]$ at 25°C in the case of V(V).[22]

16) H. L. Hintz and D. C. Johnson, *J. Org. Chem.*, **32**, 556 (1967).

17) Stagg and Powell, *Inorg. Chem.*, **3**, 242 (1964).

18) Choppin and Chopoorian, *J. Inorg. Nucl. Chem.*, **22**, 97 (1961).

19) W. H. Urry, F. W. Stacey, E. S. Huyser and O. O. Juveland, *J. Amer. Chem. Soc.*, **76**, 450 (1954).

20) D. G. Hoare and W. A. Waters, *J. Chem. Soc.*, **1964**, 2552, 2560.

21) A. A. Clifford and W. A. Waters, *ibid.*, **1965**, 2796.

22) J. R. Jones, W. A. Waters and J. S. Littler, *ibid.*, **1961**, 630.

BULLETIN OF THE CHEMICAL SOCIETY OF JAPAN VOL. 43 2450—2457 (1970)

Polarographic Study of Metal Complexes. X.[1] The Disulfitotetracyanocobaltate(III) Complex[2]

Nobufumi MAKI and Kouei YAMAMOTO*1

Department of Chemistry, Faculty of Engineering, Shizuoka University, Johoku, Hamamatsu

(Received December 25, 1969)

The sodium disulfitotetracyanocobaltate(III), $Na_5[Co^{III}(SO_3)_2(CN)_4]\cdot 3H_2O$, was found to be irreversibly reduced in one step to the cobalt(I) state in a 0.5M Na_2SO_3 aqueous solution at the dropping mercury electrode (DME). As for the resulting cobaltate(I) complex, neither further reduction to the metal nor oxidation was observed in the potential range of 0——2.0 V (*vs.* SCE). Above 40°C, a partial reduction to the metal was observed to take place at about −1.9 V (*vs.* SCE). The reduction was interpreted as being of the "*inert-inert*" type, as shown below:

$$trans\text{-}[Co^{III}(SO_3)_2(CN)_4]^{5-} \xrightarrow{2e} trans\text{-}[Co^{I}(SO_3)_2(CN)_4]^{7-}.$$

Here, the disulfito complex was presumed to take a *trans*-configuration rather than that of a *cis*-form on the evidence of its polarographic behavior and the absorption spectrum. That is, the tetracyano complexes with a *cis*-configuration are considered to be reduced to the metal, whereas those with a *trans*-configuration are reduced to the cobalt(I) state, and not to the metal polarographically, at the DME.

In earlier papers,[3] we reached some significant conclusions about the electrode reaction of the tetracyanocobaltate(III) complex, $K[Co^{III}(CN)_4en]\cdot H_2O$ (*cis*-form). Namely, the *cis*-$[Co(CN)_4en]^-$ ion gave rise to an apparent one-step wave of a three-electron reduction, representing a direct reduction from the cobalt(III) complex to the metal in aqueous solutions at the DME. In the presence of ethylenediamine (2M), however, the *cis*-$[Co(CN)_4en]^-$ ion was reduced to the metal *via* the cobaltate(I) complex. The hexa-coordinated cobalt(I) ion $[Co^{I}(CN)_4en]^{3-}$, was presumed to be able to exist under the conditions where aquation is prevented.

Recently, in examining the *cis*-dicyanobis(ethylenediamine)cobalt(III) complex polarographically, we ascertained the binuclear tetracyanocobaltate(II) ion,[4] $[Co^{II}(CN)_4\text{-}en\text{-}Co^{II}(CN)_4]^{4-}$, to be formed in the course of reductions by the rearrangement of cyanide ligands; the ion undergoes the step-by-step reduction of Co(II)→Co(I)→Co(0) at the DME.[5]

In connection with these results, several kinds of pentacyanocobaltate(III) complexes of the $[Co^{III}X(CN)_5]$-type have also been reported to be all reduced to the cobalt(I) state in aqueous solutions at the DME.[6-8] Neither further reduction of the pentacyanocobaltate(I) complex to the metal nor oxidation from the cobalt(I) state was observed in the potential range of 0——2.0 V (*vs.* SCE).

The present paper is concerned with the behavior of the disulfitotetracyanocobaltate(III) complex, $Na_5[Co(SO_3)_2(CN)_4]\cdot 3H_2O$, in aqueous solutions.

Experimental

Apparatus. A Yanagimoto Polarograph, Model P8-DP, was used for the measurements of the d.c. polarograms. The *iR* drop was corrected automatically with a compensator for the liquid resistances, Yanagimoto Model P8-PT. The other experimental set-up and the measurements were the same as those employed previously.[3,5] The characteristics of the capillary used were as follows: $m=1.38$ mg/sec, $t=4.50$ sec, both measured on an open circuit in a 0.5M Na_2SO_3 aqueous solution (25°C).

The absorption spectra in the visible and ultraviolet regions were determined manually with a Beckmann DU spectrophotometer.

1) Previous paper of this series: N. Maki, Y. Ishiuchi and S. Sakuraba, This Bulletin, **42**, 3166 (1969).

2) Briefly reported in part: N. Maki and R. Tsuchida, This Bulletin, **34**, 891 (1961).

*1 Present address: K. Y., Hamamatsu TV company Inc., Ichino-cho, Hamamatsu.

3) N. Maki and K. Okawa, *J. Electroanal. Chem.*, **8**, 262 (1964); This Bulletin, **37**, 1233 (1964).

4) R. Ripàn, A. Farcăs and O. Piringer, *Z. Anorg. Allgem. Chem.*, **346**, 211 (1966).

5) N. Maki, K. Yamamoto, H. Sunahara and S. Sakuraba, This Bulletin, **42**, 3159 (1969).

6) D. N. Hume and I. M. Kolthoff, *J. Amer. Chem. Soc.*, **71**, 867 (1949).

7) N. Maki, J. Fujita and R. Tsuchida, *Nature*, **183**, 458 (1959); N. Maki, *ibid.*, **185**, 682 (1960).

8) N. Maki, Proceeding 3rd International Congress of Polarography, Vol. 1, ed. by G. J. Hills, MacMillan & Co., London (1966), p. 505.

Materials. The complex, $Na_5[Co(SO_3)_2(CN)_4]\cdot 3H_2O$,*2 was prepared by the method of Rây and Chackrabarty[9] and purified according to the directions of Chen *et al.*[10] The purifications were essential for obtaining the pure aimed-at complex and were carried out five times here. The complex thus obtained has this formula: $Na_5[Co(SO_3)_2(CN)_4]\cdot 12H_2O$ (orange-yellow); it is efflorescent in an open state and the crystallization water is lost partly in the air. The anhydrous salt, which had been dried *in vacuo* at 100—110°C (in an Abderhalden apparatus) for six hours, assumed a brown color and was very hygroscopic. Hence, the trihydrate salt used for the polarographic measurements was obtained by drying it *in vacuo* at 60°C overnight. Found: Co, 11.57; C, 10.03; N, 11.30; H, 1.35%. Calcd for $Na_5[Co(SO_3)_2(CN)_4]\cdot 3H_2O$: Co, 11.98; C, 9.76; N, 11.39; H, 1.23%.

The diaquotetracyanocobaltate(III) complex, $K[Co(OH_2)_2(CN)_4]\cdot \frac{3}{4}H_2O$, was also prepared by the method of Rây and Chackrabarty[9] according to the following reaction of scheme:

$$Na_5[Co(SO_3)_2(CN)_4]\cdot 3H_2O \xrightarrow{HNO_3} [Co(SO_4)_2(CN)_4]^{5-} \xrightarrow{H_2O} [Co(OH_2)_2(CN)_4]^- \xrightarrow{AgNO_3} Ag[Co(OH_2)_2(CN)_4]\ \text{ppt.} \xrightarrow{KI} K[Co(OH_2)_2(CN)_4]\cdot \tfrac{3}{4}H_2O.$$

The diaquo complex can not be stored for more than two weeks, because it decomposes gradually even in the solid state to yield an unknown product insoluble in water. The causes of this deterioration are not clear, but probably it is due to the polymerization of the complex. Therefore, the elementary analyses and the polarographic measurements were always carried out on a freshly-prepared complex. Found: Co, 24.09; C, 19.83; N, 22.97; H, 1.62%. Calcd for $K[Co(OH_2)_2(CN)_4]$: Co, 24.75; C, 20.18; N, 23.53; H, 1.69%.

The sulfitopentacyanocobaltate(III) complex, $K_4[Co(SO_3)(CN)_5]\cdot 3H_2O$, was prepared from the $K_3[CoBr(CN)_5]$ complex by the method of Fujita and Shimura.[11] Found: Co, 12.26; C, 12.38; N, 14.77; H, 1.32%. Calcd for $K_4[Co(SO_3)(CN)_5]\cdot 3H_2O$: Co, 12.29; C, 12.52; N, 14.61; H, 1.26%. The other complexes used in this work were lots prepared in our previous experiments.[3,5]

Results and Discussion

The disulfito complex, $Na_5[Co^{III}(SO_3)_2(CN)_4]\cdot 3H_2O$, gave rise to a well-defined wave of one step at the DME in a 0.5M sodium sulfite supporting electrolyte. This wave, corresponding to a gain of two electrons, represents the reduction from the cobalt(III) to the cobalt(I) state. No further reduction to the metal was found over the potential range of 0——2.0 V (*vs.* SCE). Figure 1 shows the dependence of the current-potential curves upon the concentration of the complex in the 10^{-2}—10^{-3}M range in a 0.5M Na_2SO_3 aqueous solution. In the figure, the current-scale is individually curtailed, lest it should change with the concentration of the complex. Scarcely no changes were found in the

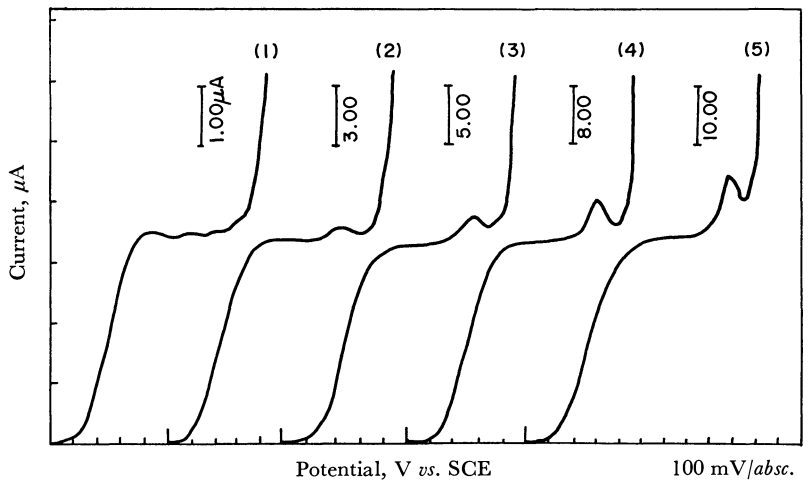

Fig. 1. The dependence of the current-potential curves upon the concentration of the complex, $Na_5[Co(SO_3)_2(CN)_4]\cdot 3H_2O$, in a 0.5M Na_2SO_3 aqueous solution (25°C). Concentration of the complex, (1) 10^{-3}; (2) $3\cdot 10^{-3}$; (3) $5\cdot 10^{-3}$; (4) $8\cdot 10^{-3}$; (5) 10^{-2}M; recorded from −1.00 V (*vs.* SCE).

*2 The sulfite ion, OSO_2^{2-}, can be bound to the cobalt either by the oxygen or by the sulfur atom; the former is named the sulfito complex, and the latter, the sulfono complex.

9) P. R. Rây and S. Ch. Chackrabarty, *Z. Anorg. Allgem. Chem.*, **211**, 173 (1933).

10) H. H. Chen, M-S. Tsao, R. W. Gaver, P. H. Tewari and W. K. Wilmarth, *Inorg. Chem.*, **5**, 1913 (1966).

11) J. Fujita, Ph. D. thesis (1959); J. Fujita and Y. Shimura, This Bulletin, **36**, 1281 (1963).

TABLE 1. THE RELATIONSHIP BETWEEN THE HEIGHT OF THE MERCURY RESERVOIR AND THE LIMITING CURRENT

$h_{corr.}$ (cm)	i_l (μA)	$i_l/\sqrt{h_{corr.}}$
92.0	18.5	1.93
82.0	17.3	1.92
72.0	16.5	1.93
62.0	15.1	1.92
52.0	13.7	1.90
42.0	12.3	1.89

Concentration of the complex: $5.0 \cdot 10^{-3}$M in a 0.5M Na_2SO_3 i_l=the limiting current at -1.50 V *vs.* SCE (25°C)

shape of the wave with the concentration. The limiting current and the concentration of the complex were ascertained to be strictly linearly related in the concentration range of 10^{-4}—10^{-2}M.

Table 1 shows that the limiting current is proportional to the root of the height of the mercury reservoir; the values $i_l/\sqrt{h_{corr.}}$ are almost constant, irrespective of the mercury pressure.

Figure 2 shows the temperature-dependence of the limiting current in the range of 0—60°C. Above 40°C, the current values were seen to deviate from the straight line of the plot; the current increases remarkedly with the temperature, indicating a kinetically-controlled feature. This seems to be due to the disruption of the cobaltate(I) complex in solution. Below 40°C, the current increases linearly with the temperature; its coefficient was 1.70%/degree at 25°C. Figure 3 shows the temperature-dependence of the current-potential curves in a 0.5M Na_2SO_3 supporting electrolyte. On the whole, scarcely no deformations of the wave with the temperature were observed, but the partial reduction to the metal could be discerned to appear at around -1.98 V (*vs.* SCE) above 50°C.

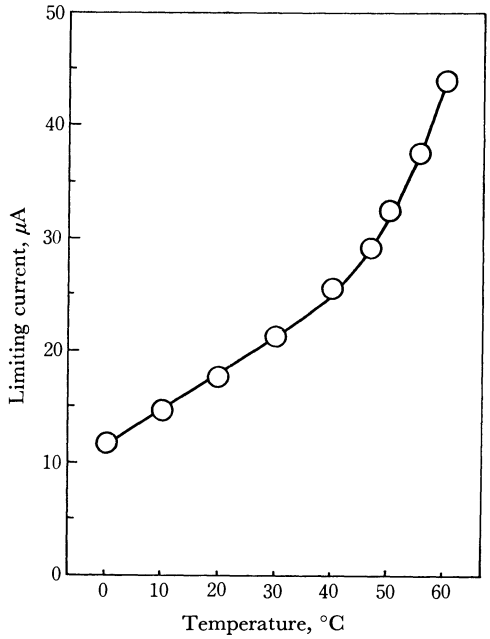

Fig. 2. The relationship between the limiting current and the temperature for the $Na_5[Co(SO_3)_2(CN)_4] \cdot 3H_2O$ complex in a 0.5M Na_2SO_3 solution (25°C).

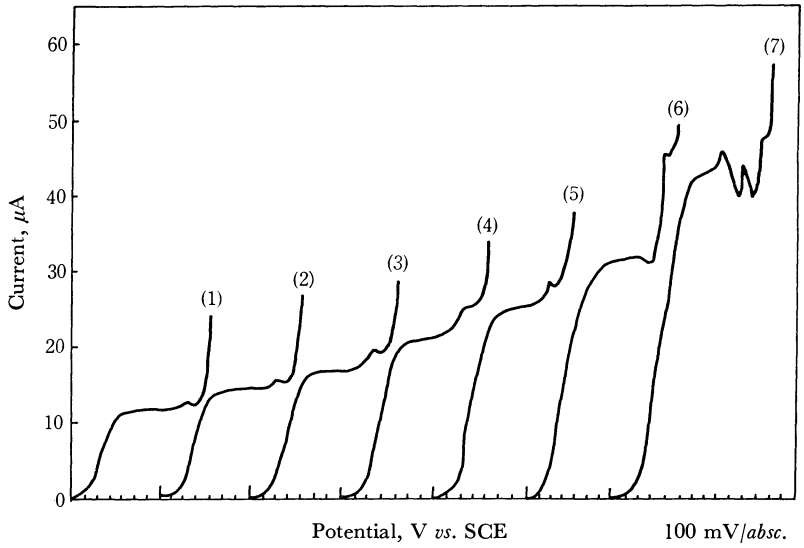

Fig. 3. The temperature-dependence of the current-potential curves for the $Na_5[Co(SO_3)_2(CN)_4] \cdot 3H_2O$ complex in a 0.5M Na_2SO_3 solution. The concentration of the comeplx, $5 \cdot 10^{-3}$M, the temperature, (1) 0; (2) 10; (3) 20; (4) 30; (5) 40; (6) 50; (7) 60°C. Recorded from -1.00 V (*vs.* SCE).

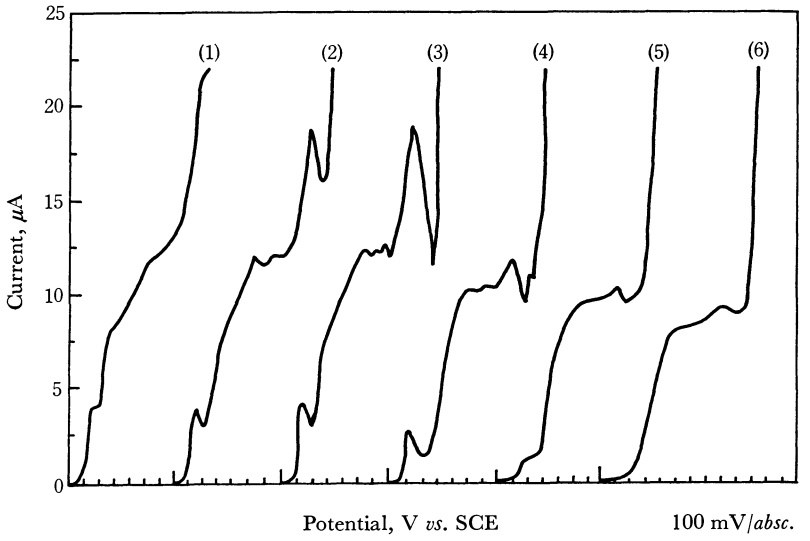

Fig. 4. The effect of sulfite ions upon the current-potential curves for the complex, $Na_5[Co(SO_3)_2(CN)_4]\cdot 3H_3O$, under a unit ionic strength ($Na_2SO_3+Na_2SO_4$). The concentration of SO_3^{2-} ions, (1) 0; (2) 0.005; (3) 0.01; (4) 0.05; (5) 0.1; (6) 0.5M. Recorded from −0.90 V (*vs.* SCE).

From these results, the limiting current may well be concluded to be diffusion-controlled below 40°C.

Figure 4 shows the effect of sulfite ions on the current-potential curves in solution under a unit ionic strength. The disulfitotetracyano complex has previously been described as not being able to exist stably in solution unless sulfite ions are present in excess. That is, the cobaltate(III) complex in solution decomposes with time to yield unknown yellow precipitates insoluble in water. Polarographic measurements were, however, practically possible on the freshly-prepared solution. The limiting current decreases with the increase in the concentration of the sulfite ions by about 15%.

Figure 5 shows oscillopolarograms of the Heyrovský-Forejt type photographed for the disulfito-, diaquo-tetracyanocobaltate(III), and sulfitopentacyanocobaltate(III) complexes in aqueous solutions. For the sulfito- and disulfito-complexes, only one incision was observed, at −1.26 or at −1.24 V (*vs.* Hg pool) respectively on the cathodic branch of the dE/dt - E curves, whereas no incision was found on the anodic branch; this is in agreement with the findings on the aquopentacyanocobaltate(I) ion by Kolthoff and Hume.[6] Moreover, in the solution not containing an excess of sulfite ions, the disulfitotetracyano complex also exhibited oscillopolarographic behavior quite similar to that in the presence of sulfite ions; neither further reduction to the metal nor oxidation from the tetracyanocobaltate(I) complex was found on the oscillopolarogram. On the other hand, for the diaquotetracyano complex, two incisions were recorded, at −0.59 and −1.39 V (*vs.* Hg pool) on the cathodic branch, while no incision was found on the anodic branch, just as above. The former two incisions correspond to the

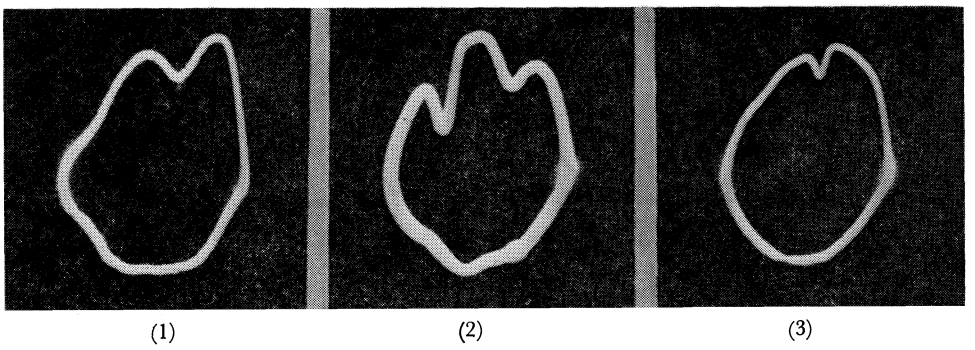

Fig. 5. The current-controlled oscillopolarograms of dE/dt-E curves measured at $5\cdot 10^{-3}$M complex ion (25°C). (1) $Na_5[Co(SO_3)_2(CN)_4]\cdot 3H_2O$ in 0.5M Na_2SO_3 aqueous solution; (2) $K[Co(OH_2)_2(CN)_4]\cdot \frac{3}{4}H_3O$ in 0.5M Na_2SO_4 aqueous solution: (3) $K_4[Co(SO_3)(CN)_5]\cdot 3H_2O$ in 0.5M Na_2SO_4 aqueous solution. Voltage unit: V *vs.* Hg pool.

double wave in the conventional polarography, as will be described later. Therefore, we may conclude that the tetracyanocobaltate(I) complexes for these disulfito and diaquo complexes as well as for the sulfitopentacyano complex do not electrochemically take any oxidation at the DME.

From these results, it seems to be most likely that the following process of electrode reaction takes place at the DME:

$$\underset{inert}{trans\text{-}[Co^{III}(SO_3)_2(CN)_4]^{5-}} \xrightarrow{2e} \underset{inert}{trans\text{-}[Co^{I}(SO_3)_2(CN)_4]^{7-}}.$$

The cobaltate(III) and cobaltate(I) complexes may be considered to take a *trans*-configuration rather than that of a *cis*-form on the following evidence.

The diaquo complex, $K[Co^{III}(OH_2)_2(CN)_4]\cdot \frac{3}{4}H_2O$, which had been prepared from the disulfito complex was found to be reduced in two steps to the cobalt(I) state, but not to the metal at the DME, in a 0.5M Na_2SO_4 aqueous solution.

$$trans\text{-}[Co^{III}(OH_2)_2(CN)_4]^{-} \xrightarrow{e} trans\text{-}[Co^{II}(OH_2)_2(CN)_4]^{2-} \xrightarrow{e} trans\text{-}[Co^{I}(OH_2)_2(CN)_4]^{3-}.$$

On the other hand, the ethylenediaminetetracyano complex, $K[Co^{III}(CN)_4en]\cdot H_2O$ (*cis*-form), was found to be reduced directly to the metal in the same supporting electrolyte of a 0.5M Na_2SO_4 aqueous solution; no cobalt(II) and cobalt(I) states were detected by means of conventional polarography in the course of reductions.[3] The cobalt(I) state was detectable only in the presence of an excess of ethylenediamine, *i.e.*, under conditions where the aquation was prevented. In other words, the resulting cobaltate(I) ion, *cis*-$[Co^{I}(CN)_4en]^{3-}$, certainly aquates rapidly, unless an excess of ethylenediamines is present in the solution, to yield the *cis*-diaquo complex ion, *cis*-$[Co^{I}(OH_2)_2(CN)_4]^{3-}$. This diaquo-cobaltate(I) complex with a *cis*-form is immediately reduced to the metal at the DME.

Figure 6 shows the current-potential curves of the disulfitotetracyano and its related mixed cyanocobaltate(III) complexes measured in an aqueous solution under the same conditions, employing the same capillary, concentration, height of mercury head and temperature. Since the limiting currents to be investigated here are all diffusion-controlled, we can ascertain the number of electrons participating in the electrode process from the ratio of the wave-heights.

The electrode process for the tetracyano complex with a *cis*-form may be speculated to be as follows:

$$cis\text{-}[Co^{III}(CN)_4en]^{-} \xrightarrow{2e} cis\text{-}[Co^{I}(CN)_4en]^{3-} \xrightarrow{aquation} cis\text{-}[Co^{I}(CN)_4(OH_2)_2]^{3-} \xrightarrow{e} Co(metal).$$

in a 0.5M Na_2SO_4 aqueous solution.

In the dimethyl sulfoxide (DMSO), however,

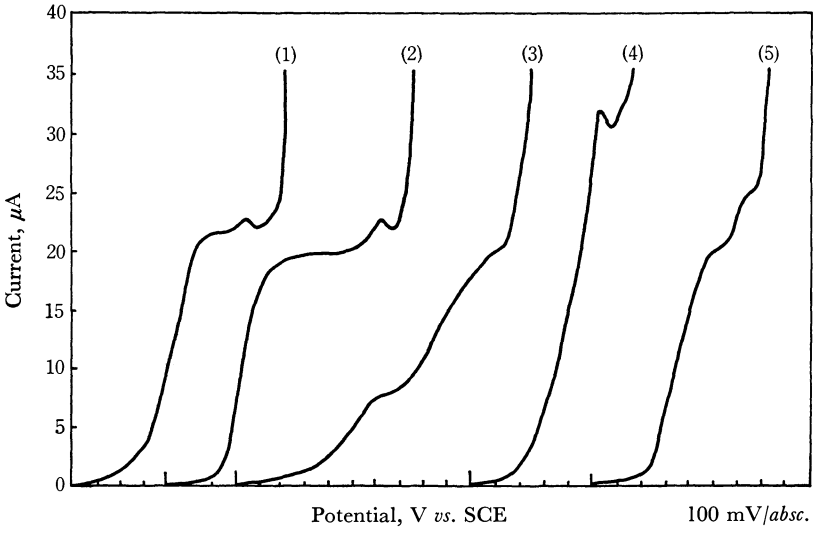

Fig. 6. The current-potential curves of the mixed cyano cobaltate(III) complexes at $5\cdot10^{-3}$ M complex ion measured under the same experimental conditions (25°C). The cobaltate(III) complexes are as follows: (1) $K_4[Co(SO_3)(CN)_5]\cdot 3H_2O$, recorded from −1.10 V; (2) $Na_5[Co(SO_3)_2(CN)_4]\cdot 3H_2O$ in 0.5M Na_2SO_3 solution, from −0.90 V; (3) $K[Co(OH_2)_2(CN)_4]\cdot \frac{3}{4}H_2O$, from −0.60 V; (4) $Na[Co(CN)_4en]\cdot 3.5H_2O$, recorded from −0.80 V; (5) $Na[Co(CN)_4en]\cdot 3.5H_2O$, in 0.5M Na_2SO_4 solution containing 1M ethylenediamine, recorded from −0.80 V (*vs.* SCE). The supporting electrolyte is an aqueous solution of 0.5M Na_2SO_4, except the cases (2) and (5).

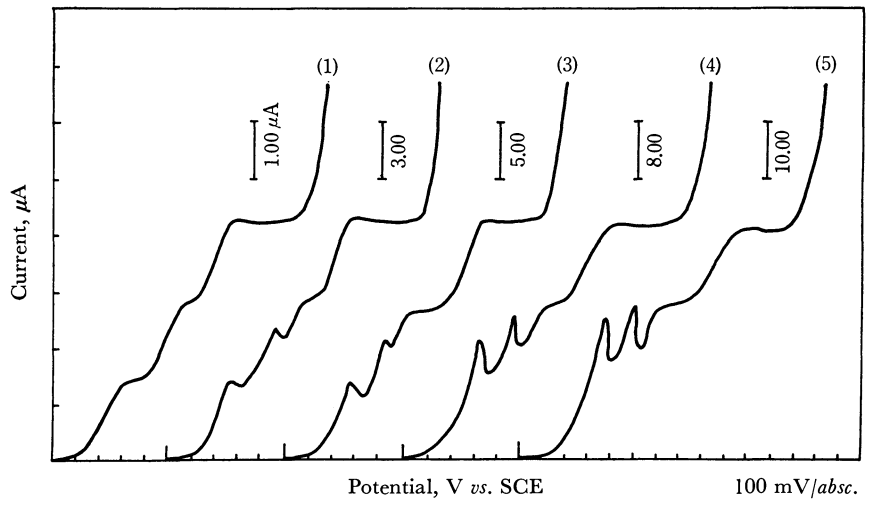

Fig. 7. The dependence of the current-potential curves upon the concentration of the complex, $Na[Co(CN)_4en]\cdot 3.5H_2O$, in the DMSO (100%) solution containing 0.1M $[(C_2H_5)_4N]ClO_4$(25°C). The concentration of the complex, (1) 10^{-3}; (2) $3\cdot10^{-3}$; (3) $5\cdot10^{-3}$; (4) $8\cdot10^{-3}$; (5) 10^{-2}M. Recorded from −1.40 V (*vs.* SCE).

the *cis*-tetracyano complex, $Na[Co^{III}(CN)_4en]\cdot 3.5H_2O$,*3 taking up three electrons, one by one, undergoes the step-by-step reduction of Co(III)→Co(II)→Co(I)→Co(*metal*) at the DME. In an aprotic non-aqueous solvent such as DMSO, it may be considered that all the cobalt complexes of the oxidized and reduced-forms are of the "*inert*" type for substitution, unlike those in aqueous solutions. Therefore, the cobaltate(III) complex may be presumed to be reduced, as it were, without any accompanying structural changes throughout the reduction; neither the aquation nor the rearrangements of ligands need be considered during reductions in DMSO. Hence, the *cis*-$[Co^{I}(CN)_4en]^{3-}$ ion of the "*inert*" type is interpreted as undergoing subsequent reduction to the metal in DMSO.

Figure 7 shows the dependence of the current-potential curves upon the concentration of the complex in the DMSO(100%) containing 0.1M $[(C_2H_5)_4N]ClO_4$. The following net processes of the electrode reaction are considered to be most reasonable:

$$\underset{inert}{cis\text{-}[Co^{III}(CN)_4en]^-} \xrightarrow{e} \underset{inert}{cis\text{-}[Co^{II}(CN)_4en]^{2-}} \xrightarrow{e}$$

$$\underset{inert}{cis\text{-}[Co^{I}(CN)_4en]^{3-}} \xrightarrow{e} Co(metal).$$

From the above-mentioned results, it would not be out of the way to assume that the tetracyanocobaltate(III) complexes with a *cis*-configuration are finally reduced to the metal *via* the cobalt(I) state, while those with a *trans*-configuration are reduced to the cobalt(I) state, but not to the metal at the DME. This difference in their polarographic behavior may be understood in terms of the configuration of four cyanides, which exerts a considerable effect on the stability of a cobalt(I) state, since the d^8-complexes of the univalent cobalt tend to get a coplanar structure with a *trans*-form rather than an octahedral configuration with a *cis*-form, a structure similar to that of nickel(II) complexes,

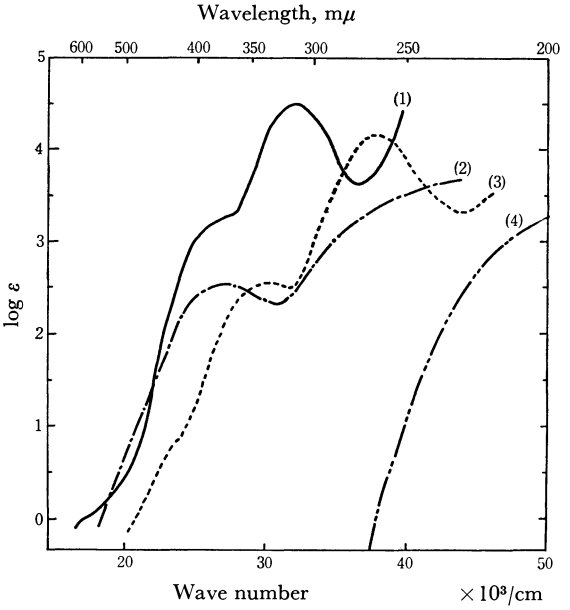

Fig. 8. The absorption spectra of the cyano cobaltate(III) complexes in water solutions (25°C). (1) ——— $Na_5[Co(SO_3)_2(CN)_4]\cdot 3H_2O$ in 0.5M Na_2SO_3; (2) -—-—- $K[Co(OH_2)_2(CN)_4]\cdot \frac{3}{4}H_2O$ in 0.1M HNO_3; (3) -------- $K_4[Co(SO_3)(CN)_5]\cdot 3H_2O$ in H_2O; (4) ——-—- Na_2SO_3 in H_2O.

*3 The sodium salt was used here, since it is more soluble in a DMSO solvent than the potassium salt.

through a dsp^2-hybridization. Taking account of the Jahn-Teller effect, it might happen that, in solution, the coordinate bonds of the fifth and the sixth sulfite ligands became longer at the cobalt(I) state than those for the cobaltate(III) complex.

Figure 8 shows the absorption spectra of the tetracyano- and pentacyano-cobaltate(III) complexes in the visible and ultraviolet regions in water. Since the disulfito- and diaquo-complexes both gradually decompose even in a crystal state, the spectrum had to be measured in the solution of a freshly-prepared complex. The spectrum revealed that the disulfito complex can not be stored in the pure state for more than two weeks. In fact, the spectrum of the disulfito complex, $Na_5[Co(SO_3)_2(CN)_4]\cdot 3H_2O$, does not necessarily coincide in detail with that reported in 1941 by Kiss *et al.*[12]

Table 2 summarizes the absorption maxima and intensities of the cyano cobaltate(III) complexes measured in water. The first d–d transition band shifts towards a shorter wavelength in the following order of ligands: OH_2, SO_3, en. According to Shimura and Tsuchida,[13] however, the spectrochemical series for both the *cis*-tetrammine- and *cis*-bis(ethylenediamine)-cobalt(III) complexes of the $[CoX_2(NH_3)_4]$- and $[CoX_2en_2]$-types is in this order of ligands: OH_2, en, SO_3. Hence, the order for the *cis*-type complexes does not agree with that for the tetracyano complexes. This disagreement seems likely to be due to the *trans*-configuration of the disulfito complex. Since the diaquotetracyano complex was prepared from the disulfito complex, and since it exhibited quite different polarographic behavior from that of the aquated species of the *cis*-ethylenediaminetetracyano

Table 2. Absorption maxima and intensities of the cyano-cobaltate(III) complexes

Compound	I-Band	II-Band
$K[Co(OH_2)_2(CN)_4]\cdot \frac{3}{4}H_2O$	27.03(2.56)	—*
$Na_5[Co(SO_3)_2(CN)_4]\cdot 3H_2O$	27.30(3.23)	31.95(4.52)
$K[Co(CN)_4en]\cdot H_2O$	28.43(2.26)	36.13(2.28)
$K_4[Co(SO_3)(CN)_5]\cdot 3H_2O$	29.87(2.59)	37.87(4.16)

* shoulder band kK (10^3 cm^{-1})

Table 3. Half-wave potentials of the waves for the tetracyano- and pentacyano-cobaltate(III) complexes (25°C)

Complex compound	$E_{1/2}$	$E_{1/2}$	Supporting electrolyte
trans-$K[Co(OH_2)_2(CN)_4]\cdot \frac{3}{4}H_2O$	−1.03 ($Co^{III}\rightarrow Co^{II}$)	−1.41 ($Co^{II}\rightarrow Co^{I}$)	0.5M Na_2SO_4 aq. soln.
trans-$Na_5[Co(SO_3)_2(CN)_4]\cdot 3H_2O$	*ca* −1.21 ($Co^{III}\rightarrow Co^{I}$)		0.5M Na_2SO_4
	−1.22 ($Co^{III}\rightarrow Co^{I}$)		0.5M Na_2SO_3
cis-$Na[Co(CN)_4en]\cdot 3.5\ H_2O$	−1.17 ($Co^{III}\rightarrow Co^{0}$)		0.5M Na_2SO_4
	−1.12 ($Co^{III}\rightarrow Co^{I}$)	−1.39 ($Co^{I}\rightarrow Co^{0}$)	0.5M Na_2SO_4+1M en
	−1.59 ($Co^{III}\rightarrow Co^{II}$)	−1.78 ($Co^{II}\rightarrow Co^{I}$) −2.09 ($Co^{I}\rightarrow Co^{0}$)	DMSO(100%) containing 0.1M $[(C_2H_5)_4N]ClO_4$
$K_4[Co(SO_3)(CN)_5]\cdot 3H_2O$	−1.55 ($Co^{III}\rightarrow Co^{I}$)		0.5M Na_2SO_4 aq. soln.

Volt *vs.* SCE

Table 4. Apparent kinetic parameters of the electrode process for the $Na_5[Co(SO_3)_2(CN)_4]\cdot 3H_2O$ complex in a 0.5M Na_2SO_3 solution

T°K	288	293	298	303	313
$E_{1/2}$ (V *vs.* NHE)	− 0.969	− 0.976	− 0.980	− 0.993	− 1.003
i_d (μA)	1.80	2.02	2.18	2.50	3.04
αn	0.55	0.56	0.53	0.57	0.61
D_{ox} ($cm^2\cdot sec^{-1}$)	$3.13\cdot 10^{-6}$	$3.96\cdot 10^{-6}$	$4.62\cdot 10^{-6}$	$6.10\cdot 10^{-6}$	$9.00\cdot 10^{-6}$
$\log k_f^a$	−12.57	−12.48	−12.28	−12.18	−12.04
k_f^a (cm/sec)	$2.67\cdot 10^{-13}$	$3.32\cdot 10^{-13}$	$5.29\cdot 10^{-13}$	$6.56\cdot 10^{-13}$	$9.12\cdot 10^{-13}$

Characteristics of capillary: m=0.54 mg·sec^{-1}, t=4.00 sec $\Delta H^{\neq}$=4.7 kcal/mol

12) P. Pascal (ed.), "Nouveau Traite de Chimie Minerale," Tome XVIII, Masson et Cie, Editeurs, Paris (1959), pp. 697—698; A. Kiss, G. Auer and E. Major, *Z. Anorg. Allgem. Chem.*, **246**, 28 (1941).

13) Y. Shimura and R. Tsuchida, This Bulletin, **29**, 311 (1956).

Table 5. Apparent kinetic parameters of the electrode process for the $K_4[Co(SO_3)(CN)_5]\cdot 3H_2O$ complex in a 0.5M Na_2SO_4 solution

T°K	283	288	293	303
$E_{1/2}$ (V *vs.* NHE)	−1.305	−1.305	−1.299	−1.286
i_d (μA)	1.64	1.78	1.94	2.01
αn	0.59	0.56	0.61	0.61
D_{ox} ($cm^2\cdot cm^{-1}$)	$2.37\cdot10^{-6}$	$2.82\cdot10^{-6}$	$3.31\cdot10^{-6}$	$3.57\cdot10^{-6}$
$\log k^a_f$	−16.78	−16.51	−16.18	−15.82
k^a_f (cm/sec)	$1.66\cdot10^{-17}$	$3.06\cdot10^{-17}$	$6.62\cdot10^{-17}$	$15.03\cdot10^{-17}$

The same capillary in Table 4 was employed. $\Delta H^{\neq}=20.8$ kcal/mol

complex, it may also be interpreted as getting a *trans*-configuration rather than a *cis*-form.

Table 3 summarizes the half-wave potentials and the corresponding electrode processes of the cyano cobaltate(III) complexes in various kinds of supporting electrolytes. Since the disulfito-, diaquotetracyano, and sulfitopentacyano complexes are quite insoluble in such organic solvent as DMSO, acetonitrile (AN), dimethylformamide (DMF), and ethanol, it was impossible for us to obtain the reduction waves of these complexes in such aprotic solvents.

Tables 4 and 5 show the apparent kinetic parameters for the irreversible electrode process of Co(III)→Co(I) in an aqueous solution, such parameter having been determined by a method described previously;[8] the terms have their usual significance. Here, the so-called "Frumkin's correction" was not taken into consideration in estimating these data. Since a plot of $\log k^a_f$ (apparent rate constant) against $1/T$ should be linear with a slope equal to $\Delta H^*/2.303\ R$, the activation energies at a constant pressure (ΔH^*) can be calculated; these values are shown below the respective tables. The ΔH^* value for the disulfito complex was found to be far smaller than that for the sulfitopentacyano complex, although it is noteworthy that these parameters have, ultimately, only a relative meaning.[14]

The authors wish to thank Professor Shukichi Sakuraba for his helpful discussions.

14) R. Tamamushi, *Rev. Polarography* (Kyoto), **10**, 1 (1962).

BULLETIN OF THE CHEMICAL SOCIETY OF JAPAN VOL. 43 2457—2462 (1969)

Studies of the Ion-pairing of Hexylate and Picrate Ions with Alkali Metal Ions by Capillary Analysis

Kazuaki SANO, Michio SAKUMA,*1 Syoji MOTOMIZU, Tadashi IWACHIDO* and Kyoji TÔEI

Department of Chemistry, Faculty of Science, Okayama University, Tsushima, Okayama
* *College of Liberal Arts, Okayama University, Tsushima, Okayama*

(Received December 30, 1969)

The hexyl (Dipicrylamine) anion, hexylate, and picrate form weak ion-pairs with alkali metal cations in an aqueous solution. The composition and the association constants of the ion-pairs are determined by capillary analysis based on the difference in the adsorbability of the anions and of the ion-pairs on a filter paper. A new constant temperature-humidity apparatus is devised, and by means of it the analysis is successfully carried out. The compositions of the cation and the anion in the ion-pairs formed are 1 : 1, in either case; the association constants of the ion-pairs for Li, Na, K, Rb, and Cs cations are about 10^2, and they tend gradually to decrease with the ionic radii.

Interactions in electrolyte solutions can largely be explained by assuming that electrolytes completely dissociate into rigid, spherically-symmetrical ions and that the resulting ions exert long-range

*1 Present address: Kohkoku Chemical Industry Co., Ltd., Nishimiya-cho, Ashikaga-shi.

electrostatic forces on the other ions through the medium of the dielectric constant, ε. The interaction increases with the decrease in the distance of charge separation; that is, a small cation and a small anion may have enough attractive force compared with the thermal energy. Bjerrum[1] calculated the critical distance to be 3.57 Å for 1 : 1 electrolytes in water at 25°C and regarded ions which can approach within the distance as a virtually new entity, an ion-pair, of a sufficient stability. The association equilibrium between free ions and ion-pairs is expressed by means of K, and the ion-pair species is treated as neutral molecules of unit activity, if the electrolyte is symmetrical. So long as only the Coulomb force is assumed between the adjacent ions, ion-pairing would be at minimum in the salts of alkali metals with large, univalent anions. However, the reverse is true in the present case, so some other forces must be considered.

Several methods have been adopted to determine the association constant, K,——for example, conductivity[2] and solubility[3] measurements, polarography,[4] and spectrometric methods.[5] In any case, it is important to find a suitable way to detect a certain difference in physical properties between free ions and an ion-pair. In the present case, the method of capillary analysis was found to be successful in ascertaining the significant difference between them.

The so-called "capillary analysis" is a kind of paper chromatography. One end of a paper strip is dipped into the solution to be tested (which is in striking contrast to the usual paper chromatography). When the system is saturated as much as possible by water vapor in order to avoid undesirable vaporization during the development, the ratio of the movements of the solute and the solvent can be related to the association constant with the aid of the following assumptions: 1) the paper is regarded as being divided into successive layers of such a thickness that the solution issuing from each layer is in equilibrium with the mean concentration of the solute in the stationary phase throughout the layer; 2) the diffusion from one plate to another is negligible, and 3) the partition coefficient of the solute between two phases is independent of its concentration.

The purpose of the present paper is to show that, contrary to our expectations judging from the Bjerrum theory, there is a considerable amount of ion-pairing between alkali metal cations and large organic anions, such as picrate or hexylate, in an aqueous solution, that the largest cation, Cs^+, forms the most stable ion-pair with such anions, and that the method of capillary analysis is useful in determining the association constant of such ion-pairs.

Theoretical

The theory of capillary analysis was first proposed by Hayama[6] based on analogy with the plate theory of liquid-partition chromatography; Hayama applied it to the complex formation between dyes and non-ionic surfactants.

Hexylate and picrate anions form precipitates with heavy alkali metal cations in an aqueous solution; hence, it may be assumed that hexylate and picrate associate with alkali metal ions to form ion-pairs even in a dilute solution and that each species has different adsorbabilities on cellulose. In such a solution, the associated ion-pairs are in equilibrium with the free ions; also, each species is equilibrate with those in the stationary phase, as is shown in Fig. 1. and Eqs. (1) to (4).

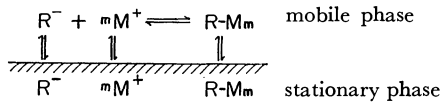

Fig. 1. Schematic representation of the behavior of hexylate and picrate, alkali metal ion and the ion-pair formed in an aqueous solution against a filter paper.

$$K = \frac{[\mathrm{R\text{-}M}_m]_a}{[\mathrm{R}^-]_a[\mathrm{M}^+]_a{}^m} \tag{1}$$

(K: Association constant)

$$K_1 = \frac{[\mathrm{R}^-]_s}{[\mathrm{R}^-]_a} \tag{2}$$

(K_1: Distribution coefficient of the reagent anion)

$$K_2 = \frac{[\mathrm{R\text{-}M}_m]_s}{[\mathrm{R\text{-}M}_m]_a} \tag{3}$$

(K_2: Distribution coefficient of the ion-pair)

$$K_3 = \frac{[\mathrm{R}^-]_s + [\mathrm{R\text{-}M}_m]_s}{[\mathrm{R}^-]_a + [\mathrm{R\text{-}M}_m]_a} \tag{4}$$

(K_3: Distribution coefficient of the total reagent)

where R^- denotes the reagent anions; M^+ and $R\text{-}M_m$, the alkali metal cations and ion-pairs; brackets, the concentration of each species, and the suffixes a and s, an aqueous and a stationary phase respectively.

From Eqs. (1), (2), (3), and (4), we obtain:

$$K_3 = \frac{K_1 + KK_2[\mathrm{M}^+]_a{}^m}{1 + K[\mathrm{M}^+]_a{}^m} \tag{5}$$

As the concentration of the reagent ions is much

1) N. Bjerrum, *K. Danske Vidensk. Selsk. (Math. fys. Medd.)* **7**, 1 (1926).
2) T. Shedlovsky, *J. Franklin Inst.*, **225**, 739 (1938).
3) H. E. Blayden and C. W. Davies, *J. Chem. Soc.*, **1930**, 949.
4) E. Gelles and G. H. Nancollas, *ibid.*, **1956**, 4847.
5) V. S. K. Nair, *Trans. Faraday Soc.*, **57**, 1988 (1961).
6) N. Hayama, *Nippon Kagaku Zasshi*, **84**, 943 (1963).

lower than that of alkali metal ions, the equilibrium concentration of alkali metal cations, $[M^+]_a$, may be approximately replaced by the total concentration, neglecting the formation of the ion-pair.

On the other hand, according to the equation of capillary analysis, the distribution coefficient, K_3, is related to R_h by the following equation:

$$\alpha K_3 = \frac{1 - \ln 2}{R_h - \ln(1+R_h)} - 1 \quad (6)$$

where α is the ratio of volumes of the stationary phase (cellulose) and the mobile phase (solution), and R_h, the ratio of the movement of the solute and the solvent.

By combining Eq. (5) with Eq. (6), we obtain Eq. (7), in which R_h is related to the concentration of free alkali metal ions.

$$\alpha K_3 = \frac{\alpha K_1 + \alpha K K_2 [M^+]_a{}^m}{1 + K[M^+]_a{}^m} = \frac{1 - \ln 2}{R_h - \ln(1+R)} - 1 \quad (7)$$

When alkali metal cations are absent in the solution to be tested, $[M^+]_a = 0$, we denote the values of R_h by $R_h{}^0$:

$$\alpha K_1 = \frac{1 - \ln 2}{R_h{}^0 - \ln(1+R_h{}^0)} - 1 \quad (8)$$

On the contrary, when these cations are present in a large excess, and when most of the reagent anions associate completely to form ion-pairs, R_h is denoted by $R_h{}^\infty$. Then we obtain:

$$\alpha K_2 = \frac{1 - \ln 2}{R_h{}^\infty - \ln(1+R_h{}^\infty)} - 1 \quad (9)$$

By substituting Eqs. (8) and (9) into Eq. (7), we obtain the following expression:

$$\frac{[R\text{-}M_m]_a}{[R^-]_a} = K[M^+]_a{}^m = \frac{\dfrac{1}{R_h{}^0 - \ln(1+R_h{}^0)} - \dfrac{1}{R_h - \ln(1+R_h)}}{\dfrac{1}{R_h - \ln(1+R_h)} - \dfrac{1}{R_h{}^\infty - \ln(1+R_h{}^\infty)}} \quad (10)$$

Equation (10) shows that the logarithmic plot of $[M^+]_a$ against the right-hand side of the equation allows us to estimate the K and m values. For the first approximation, $[M^+]_a$ was made equal to the initial concentration of the alkali metal cations; then K was determined, and the $[M^+]_a$ value calculated from the K value was used to determine a more accurate K value, after which the procedure was continued until a constant K value was obtained. Only for the values of picrate, activity correction was made simultaneously.

Experimental

Reagents. Hexyl (2,2′,4,4′,6,6′-hexanitrodiphenylamine) was prepared by treating an aqueous solution of a commercial Hexyl calcium (Mitsubishi Chemical Industries, Ltd.) with dil. hydrochloric acid, by filtering the hexyl thus formed, and by then purifying it by recrystallization from acetic acid.

The hexyl was dissolved by warming it in a lithium carbonate solution (0.006%); reagent-grade picric acid was then dissolved in water to give 2.62×10^{-4}M and 2.000×10^{-3}M solutions respectively.

Apparatus and Procedures. The ordinary procedure of capillary analysis is not siutable for the present purpose because of the unavoidable vaporization of the solvent during the development, as has previous been described. To avoid such trouble, a vessel of a constant humidity and temperature was devised (Fig. 2). A

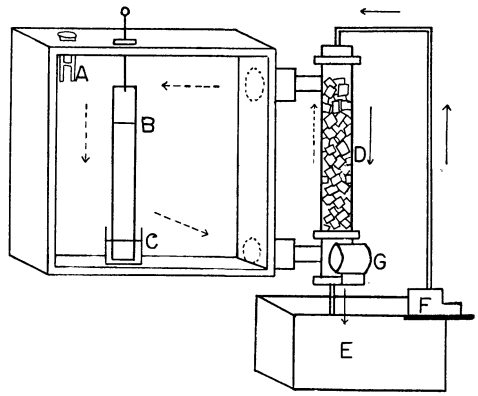

Fig. 2. Schematic representation of the apparatus. A: Assmann aspiration psychrometer, B: Filter paper (No. 50; 2×40 cm^2, Toyo Roshi Kaisha, Ltd.), C: Sample solution, D: Water vapor saturating tower, E: Water bath (25°C), F: Pump, G: Air blower

developing box was made of wood lined with a polyvinylchloride sheet and with a wet cloth on it. A gentle stream of water vapor introduced into the box from a saturation tower moistened the paper strips hung in it. The humidity was monitored by an Assmann aspiration psychrometer. A tower was filled with small pieces of polyvinylchloride pipes (2 cm in length and 1.5 cm in diameter). The water from a water bath was spreaded at the top of the tower, and the air in the box was blown upwards from the bottom through a column. Thus the humidity and the temperature in the box were kept at a constant values of 95 per cent and 25°C respectively. The room temperature was also controlled at 25°C.

Some paper strips previously moistened in another vessel for 24 hr were hung upon the hooks of the supporting rods at the upper wall of the box. Under each strip, 50 ml of 1.31×10^{-4}M hexyl or 1.00×10^{-3}M picric acid solutions containing alkali salts in various amounts (10^{-4} to 10^{-1} g-ion/l for hexyl solutions or 10^{-3} to 10^{-1} g-ion/l for picric acid solutions) were placed.

On dipping the paper strips into the test solution, it was always necessary to adjust exactly the solution level to the mark on the paper by handling the supporting rods. When the solvent fronts came near the upper ends of the strips, the front panel of the box made of double-walled transparent acrylate resin plate was removed and the detached strips were laid on a large sheet of filter paper and dried quickly by using a hot blower. Then the fronts of the solvent and of the solute

were marked. About two hours were requied for a single run.

Results and Discussion

The relationship between the R_h value and the free alkali metal ion concentration, $[M^+]_a$, is shown in Figs. 3a and 3b. The R_h^0 values are obtained by extrapolating the curves to an infinite dilution, $[M^+]_a=0$. To determine R_h^∞ values, R_h is plotted against the reciprocal of the alkali metal-ion concentration; the curves obtained are then extrapolated as in Figs. 4a and 4b.

The right-hand side of Eq. (10), evaluated in such a way, was plotted against the free alkali metal-ion concentration; these plots gave straight lines, as Figs. 5a and 5b show. The slopes of the five lines obtained are approximately unity; the $\log K$ values obtained by extrapolating these lines to $\log[M^+]_a=0$ are about 2 for hexylates, are slightly larger for picrates, and slightly increase in the order of Li, Na, K, Rb, and Cs in either case, as is shown in Table 1. The agreement between the results of the capillary analysis and the solvent

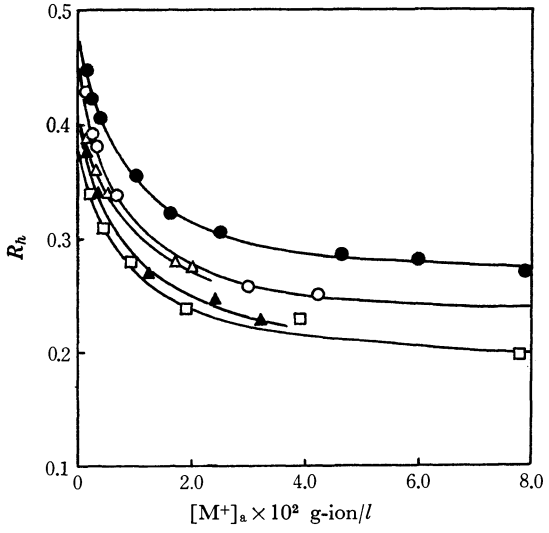

Fig. 3a. Relation between R_h and alkali metal ion concentration.
● Li, ○ Na, □ K, △ Rb, ▲ Cs-hexylate

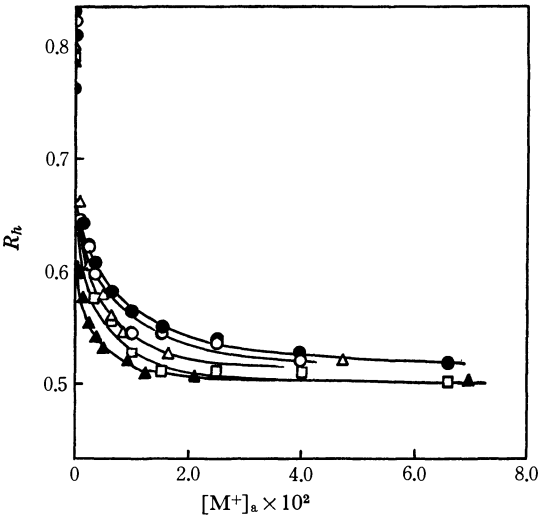

Fig. 3b. M-picrate.

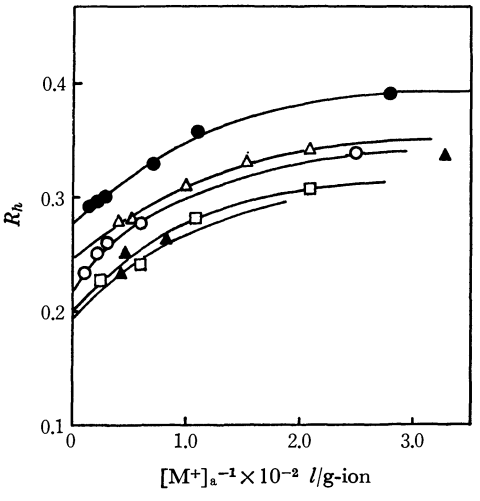

Fig. 4a. Relation between R_h and reciprocal of alkali metal ion concentration.
● Li, ○ Na, □ K, △ Rb, ▲ Cs-hexylate

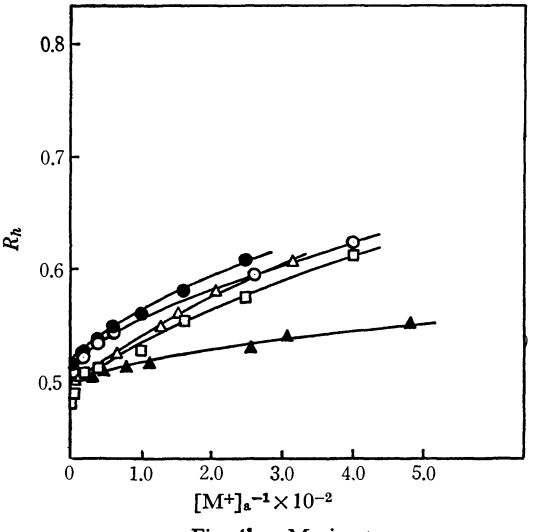

Fig. 4b. M-picrate.

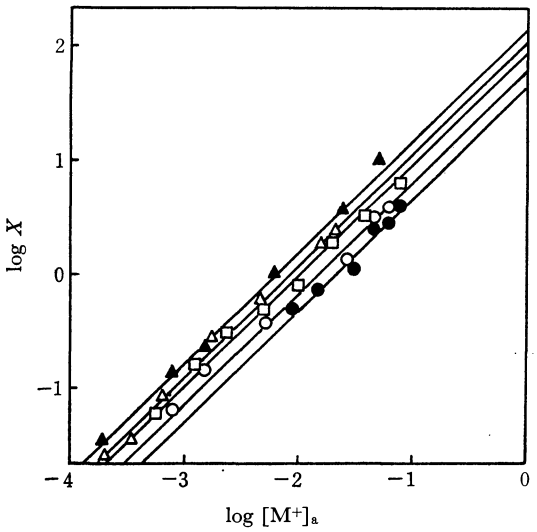

Fig. 5a. Interaction between Hexyl and alkali metals.
● Li, ○ Na, □ K, △ Rb, ▲ Cs-hexylate
$X=\frac{1/[R_h^0-\ln(1+R_h^0)]-1/[R_h-\ln(1+R_h)]}{1/[R_h-\ln(1+R_h)]-1/[R_h^\infty-\ln(1+R_h^\infty)]}$

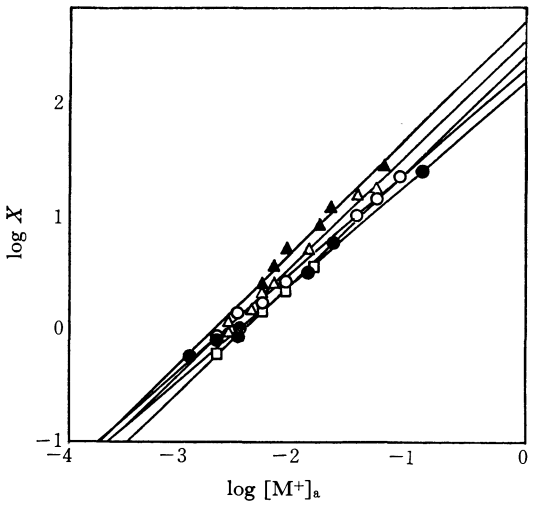

Fig. 5b. M-picrate.

extraction previously reported[7] is fairly good.

The log K value for sodium hexylate was also obtained by using a pNa-meter (Horiba Instruments, Inc., Type N-5 Sodium Ion Indicator). The concentration of free sodium ions was determined with a pair of electrodes, *i. e.*, a glass electrode especially sensitive to sodium ions and a reference electrode of the double-junction type, with a sodium chloride solution as the liquid junction to prevent the direct contact of the potassium ions in the inner solution of the electrode with the hexylate anions, and thus precipitating potassium hexylate at the junction.

The instrument was calibrated with 0.1 and 0.001M standard sodium chloride solutions. Consequently, the pNa-meter directly measures the sodium-ion concentration in terms of moles per liter instead of activity.

Table 1. Combination ratio and association constant

	Alkali metal-ion	Li^+	Na^+	K^+	Rb^+	Cs^+
Hexylates	Combination ratio	0.95	0.95	0.98	1.0	1.0
	log K	1.7	1.9	1.9	2.0	2.1
Picrates*	Combination ratio	0.88	0.90	0.98	0.98	1.0
	log K	2.2	2.3	2.4	2.5	2.7

* Correcteed by activity coefficient.

7) S. Motomizu, K. Tôei and T. Iwachido, This Bulletin, **42**, 1006 (1969).

Two sodium solutions, one with and one without hexyl, were prepared (Table 2); a certain amount of sodium hydroxide was added equally in order to avoid the hydrolysis of the hexylate anion. A few pairs of such solutions, differing only in total sodium concentration, were also prepared, the concentration of sodium hydroxide being kept unchanged.

The free sodium ion in each pair was measured, and the two were then compared with each other. The solution with hexyl is less alkaline than that without hexyl because of the neutralization of the hydroxide ion with hexyl. In order to estimate the effect of the hydroxide ion on the glass electrode, the solution without hexyl was neutralized with acetic acid just as with hexyl, and then the free sodium ion was measured. The pNa values thus obtained are in good agreement with those calculated on the assumption that the acetate ion does not form an ion-pair with the sodium ion.

From these findings, it can be concluded that, in the solutions without hexyl, the differences in pNa between the measured and the calculated values, Δ, are attributable to the large amount of hydroxide ions present, and that, in the solutions with hexyl, the sodium ion is determined correctly and the increases in pNa can be considered as a measure of the extent of ion-pairing.

The equilibrium in the solution with hexyl can be written as follows:

$$\text{Hexyl}^- + \text{Na}^+ \rightleftarrows \text{Hexyl-Na}$$

$$K=\frac{[\text{Hexyl-Na}]}{[\text{Hexyl}^-][\text{Na}^+]} \qquad (11)$$

If the total concentrations of hexyl and the sodium ion are denoted by C_R and C_{Na} respectively, we obtain:

$$C_R = [\text{Hexyl-Na}] + [\text{Hexyl}^-]$$
$$C_{Na} = [\text{Hexyl-Na}] + [\text{Na}^+] \qquad (12)$$

Table 2. Determinination of $\log K_2$ by using pNa-meter

Reagent concn., 10^2C_R(M)	Sodium concn. 10^2C_{Na}(M)		pNa			log K
	NaOH*	NaCl	measured	calcd.	Δ	
0	2.02	0	1.609	1.695	0.086	
2.0	2.02	0	1.908			1.72±0.02
0	2.02	0.10	1.584	1.674	0.090	
2.0	2.02	0.10	1.875			1.69±0.04
0	2.02	1.00	1.428	1.520	0.092	
2.0	2.02	1.00	1.686			1.66±0.05
0	2.02	10.00	0.896	0.920	0.034	
2.0	2.02	10.00	0.979			1.46±0.36
0	4.04	0	1.250	1.394	0.144	
4.0	4.04	0	1.699			1.72±0.01

* Sodium content was checked by flamephtometry.

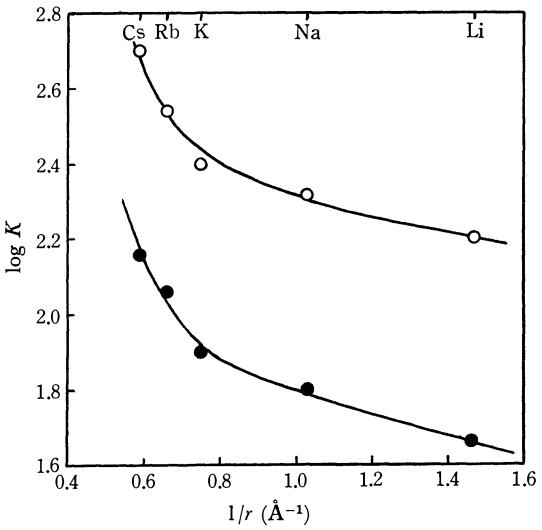

Fig. 6. log K's of alkali metal salts.
○ Picrate, ● Hexylate

By substituting Eq. (12) into Eq. (11), we obtain:

$$K = \frac{C_{Na} - [Na^+]}{(C_R - C_{Na} + [Na^+])[Na^+]} \qquad (13)$$

Thus, an association constant can be calculated from Eq. (13). The data necessary for the above calculation are given in Table 2, along with the log K values. The log K values thus obtained are very close to those obtained by capillary analysis.

Figure 6 shows the log K data for hexylates and picrates, plotted against the reciprocal of the radii of unhydrated cations. The curves thus obtained have negative slopes, unlike the common pattern of ion-pairing; that is, the cesium ion in the aqueous solution must be considered to be the smallest among the alkali metal cations as far as only the electrostatic force is concerned. In the ion-pairing of this type, it may be thought that the hydration of the cation is a predominant factor; *i. e.*, adjacent water dipoles rather than the hexylate or picrate ion are strongly affected by the field of the cation, and it is difficult for the hydration shell of the cation to be penetrated by such anions. The formation of the solvent-separated ion-pair is supported by the fact[7] that, with hexyl salts in dry nitrobenzene, lithium associates more firmly than cesium, while in nitrobenzene saturated with water the extent of ion-pairing decreases and by the fact that water is co-extracted with alkali metals into nitrobenzene.

The order among K values may be explained by the hydration, but it is difficult to explain these large values only in terms of the long-range, electrostatic force between adjacent ions; therefore, these large values lead us to suspect other forces, for example, the formation of a chemical bond, the contribution of the Van der Waals force, and the role of water-structure for the ion-pairing. It is of much interest to consider the last possibility, suggested by Diamond.[8] Considerations of these possibilities will, however, be described elsewhere; the present discussion will be confined to pointing out the similarity in ion-pairing between some oxy-acid anions and picrate or hexylate.

Some oxy-acid anions such as iodates[9] and thiosulfates[10] are known to associate with cations of the noble-gas configuration to form an ion-pair of this type; these anions have some common features with hexylate or picrate—for example, every ligand is large and has many ionic resonance forms, so that the negative charges on the ligands can be distributed over all the ligands.

The authors wish to thank Dr. Naomi Hayama for many helpful discussions and suggestions during this work.

8) R. M. Diamond, *J. Phys. Chem.*, **67**, 2513 (1963).
9) W. C. Wise and C. W. Davies, *J. Chem. Soc.*, **1938**, 273.
10) T. D. Denny and C. B. Monk, *Trans. Faraday Soc.*, **47**, 992 (1951).

BULLETIN OF THE CHEMICAL SOCIETY OF JAPAN VOL. 43 2463—2469 (1970)

Ionic Equilibria in Mixed Solvents. V. Intermediates of Polymerization of Aluminum Ion in a 0.2 Mole Fraction Dioxane-Water Mixture

Hitoshi OHTAKI

The Laboratory of Analytical Chemistry, Faculty of Science, Nagoya University, Chikusa, Nagoya

(Received January 7, 1970)

Formation of highly polymerized hydroxo-complexes of aluminum ions proceeded so slowly in a dioxane-water mixture that less polymerized intermediates were detected by means of the usual emf titration techniques. The titrations were performed at 25° in solutions of total aluminum concentrations of 0.00500, 0.0100, 0.0200, 0.0399, 0.0400 and 0.0798M in a 0.2 mol fraction (55.01 % w/w) dioxane-water mixture containing 3M $LiClO_4$ as an ionic medium. The emf data obtained can be explained in terms of the formation $Al_2(OH)_2^{4+}$ ($\log {}^*\beta_{2,2} = -6.95 \pm 0.07$) and $Al_2(OH)_3^{3+}$ ($\log {}^*\beta_{3,2} = -10.02 \pm 0.03$) assuming equilibrium conditions. It was observed that these complexes proceed further slowly to form highly polymerized complexes.

Several works have been made on the hydrolysis reaction of aluminum ion, and various conclusions have been reported on the formulae of the species formed. In dilute solutions a series of mononuclear complexes, $Al(OH)_n^{(3-n)+}$, may be formed. However, in more concentrated solutions formation of polynuclear complexes is certain. Treadwell and Zürcher[1] have found a dimerized species, $Al_2(OH)_5^+$, at room temperature. Formation of another dimer complex, $Al_2O(NO_3)_3^+$, and a highly polymerized complex, $(AlONO_3)_{\sim 8}$, has been reported by Jander and Jahr[2] by a diffusion method. Formation of a dimerized $Al_2(OH)_2^{4+}$ complex, which has recently been confirmed by some workers, was first suggested by Faucherre[3] in 1948 and he determined the formation constant of the species.[4] The same complex has been found by Jahr and Brechlin[5] at 0°C, Kenttämaa,[6] Kubota[7] and Aveston[8] at 25°C. In a crystalline state of a basic aluminum sulfate or selenate, a group of $Al_2(OH)_2(H_2O)_8^{4+}$ was found to construct a unit cell of the crystals.[9] For higher complexes several authors have described the formation of cationic trimers,[10,11] tetramers[5,6] and sometimes octamers.[12]

After X-ray analysis of another basic aluminum sulfate ($13Al_2O_3 \cdot 6SO_3 \cdot xH_2O$)[13] and the corresponding selenate ($Na[Al_{13}O_4 \cdot (OH)_{24} \cdot (H_2O)_{12}](SeO_4)_4 \cdot xH_2O$)[14] had been carried out by Johansson, Sillén[15] reexamined his results[16] in order to explain the data[16] in terms of the formation of the $Al_{13}(OH)_{34}^{5+}$ complex together with the $Al_7(OH)_{17}^{4+}$ complex. From the results obtained by ultracentrifugal methods and by emf measurements, Aveston[8] concluded that the highly polymerized cationic species has the formula $Al_{13}(OH)_{32}^{7+}$.

As has been pointed by Brosset[17] and Aveston,[8] diverse formulae of species hitherto reported may mainly be due to a slow reaction rate of the hydrolysis reaction of aluminum ions. Different conclusions may also have resulted from different accuracies of measurements by different authors. For such a complicated system of the complex formation, accuracy of measurements substantially affects the ratio of OH/Al in the complexes.

1) W. D. Treadwell and Zürcher, *Helv. Chim. Acta*, **15**, 980 (1932).
2) G. Jander and K. F. Jahr, *Kolloid-Beih.*, **43**, 296 (1936).
3) J. Faucherre, *Compt. Rend.*, **227**, 1367 (1948).
4) J. Faucherre, *Bull. Soc. Chim. France*, **1954**, 253.
5) K. F. Jahr and A. Brechlin, *Z. anorg. Chem.*, **270**, 257 (1952).
6) J. Kenttämaa, *Suomen Kem.*, **28B**, 172 (1955).
7) H. Kubota, Thesis, Univ. Wisconsin, 1956, University Microfilms 16182.
8) J. Aveston, *J. Chem. Soc.*, **1965**, 4438.
9) G. Johansson, *Acta Chem. Scand.*, **16**, 403 (1962).
10) L. K. Leptin and A. Ya. Vaidave, *Zhur. fiz. Khim.*, **27**, 217 (1953).
11) H. Tanabe, *J. Pharm. Soc. Jap.*, **74**, 866 (1954).
12) E. Matijevic, K. G. Mathai, R. H. Ottewill and M. Kerker, *J. Phys. Chem.*, **65**, 826 (1961).
13) G. Johansson, *Arkiv Kemi*, **20**, 321 (1963).
14) G. Johansson, *ibid.*, **20**, 305 (1963).
15) L. G. Sillén, "Hydrolytic Aqueous Species," Lecture, Houston, Texas, November 1962.
16) C. Brosset, G. Biedermann and L. G. Sillén, *Acta Chem. Scand.*, **8**, 1917 (1954).
17) C. Brosset, *ibid.*, **6**, 910 (1952).

Schwarzenbach and Wenger[18] also reported that the hydrolysis reaction of aluminum ion proceeds rather slowly. Yotsuyanagi and Aoyama[19] reported that it reaches equilibrium after two to three years in aqueous solutions.

Although Brosset[17] pointed out that equilibrium potentials might be obtained on standing a solution tens of hours after the addition of an alkaline solution, no intermediate could be detected during the course of the formation of highly polymerized complexes of aluminum ion in aqueous solutions. However, in the aqueous dioxane solution the rate of polymerization reactions was so slow that some intermediates could be found and the data obtained could be treated assuming equilibrium conditions.

The present study deals with the hydrolysis reactions of aluminum ion in a 0.2 mol fraction dioxane-water (55.01% w/w dioxane) mixture containing 3M $LiClO_4$ as an ionic medium.

The hydrolysis reaction of aluminum ion may be written as

$$qAl^{3+} + pH_2O = Al_q(OH)_p^{(3q-p)+} + pH^+ \quad (1)$$

In Eq. (1) solvated dioxane and water molecules are omitted,[20] and ${}^*\beta_{p,q}$ was calculated, which is defined by

$${}^*\beta_{p,q} = [Al_q(OH)_p^{(3q-p)+}][H^+]^p/[Al^{3+}]^q = [Al_q(OH)_p^{(3q-p)+}]h^p/b^q \quad (2)$$

Here the brackets denote the concentration of the relevant species.

Symbols

h	Hydrogen ion concentration at equilibrium
H	Concentration of analytical excess of hydrogen ions $=[ClO_4^-]-3B-[Li^+]$
B	Total concentration of aluminum
b	Concentration of free aluminum ions
Z	Average number of hydrogen ion set free per aluminum atom $=(h-H)/B$
p	Number of OH groups bound to hydrolyzed species
q	Number of Al atoms present in hydrolyzed species
${}^*\beta_{p,q}$	Equilibrium constant of the formation of $Al_q(OH)_p^{(3q-p)+}$
E	Emf

Experimental

Reagents. Aluminum perchlorate was prepared from aluminum chloride and perchloric acid as follows. Reagent grade aluminum chloride was recrystallized three times from aqueous solution by bubbling dry hydrogen chloride, The aluminum chloride crystals were dissolved in a small amount of water and then an excess of perchloric acid was added. Hydrochloric acid thus liberated was evaporated repeatedly under an infrared lamp. Aluminum perchlorate crystals prepared were recrystallized from water. Neither chloride nor iron(III) was detected.

The concentration of aluminum ion in the stock solution was determined as Al_2O_3 by igniting aluminum hydroxide at about 1100°C.

The concentration of free acid in the aluminum perchlorate solution was determined in a similar way to that employed in the preceding works;[21-24] that is, aliquot of a dilute solution of aluminum perchlorate, which contained a known amount of the stock solution, was titrated with a standard perchloric acid, and then, the amount of free acid present was estimated from a plot of $V_{tot}.10^{E/59.15}$ *vs.* volume of the perchloric acid added (Gran plot[25]), where V_{tot} denotes the total volume of the solution in a titration vessel.

Lithium Perchlorate was prepared as described by Biedermann and Ciavatta.[26]

Dioxane was purified by the method described elsewhere.[21]

Apparatus. *Glass Electrodes and pH Meter.* Beckman Nos. 40498 and 41263 glass electrodes were used in combination with a Beckman 101900 Research pH Meter.

The Wilhelm-type Half-cell described by Forsling, Hietanen and Sillén[27] was used for emf measurements.

All emf measurements were performed at 25.00± 0.01°C in a paraffin oil thermostat in a room thermostated at 25±1°C. Air in a titration vessel was replaced by nitrogen gas free from carbon dioxide during the titration.

Methods of Investigation. The hydrolysis reactions were studied from the measurements of the hydrogen ion concentration of a series of aluminum perchlorate solutions at 25°C using a glass electrode. During the potentiometric titration B was kept constant. The values of B studied were 0.00500, 0.0100, 0.0200, 0.0399, 0.0400 and 0.0798M. All solutions were prepared with a 0.2 mol fraction dioxane-water mixture (55.01% w/w dioxane).

Emf Measurements. The general composition of a test solution may be described as: $B\,Al^{3+}$, $H\,H^+$, $(3-3B-H)\,Li^+$, 3M ClO_4^-, where H, the analytical excess of hydrogen ion, is either positive or negative depending on the degree of hydrolysis of aluminum ion. The original composition of the test solution, S_1, has a composition, $S_1 = B\,Al(ClO_4)_3$, $H_0\,HClO_4$, $(3-3B-H_0)$ $LiClO_4$. Values of H_0, the initial concentration of acid in the solution taken in a titration vessel, were controlled to fall in the range from 0.01 to 0.03M, where the acidity

18) G. Schwarzenbach and H. Wenger, Proceedings of the 11th International Conference on Coordination Chemistry, Haifa and Jerusalem, September, 1968.

19) T. Yotsuyanagi and K. Aoyama, Annual Meetings of the Chemical Society of Japan, Osaka, April, 1968.

20) J. F. Hinton, L. S. McDowell and E. S. Amis (*Chem. Commun.*, **1966**, 776) reported solvation of dioxane in aqueous dioxane solutions of $Al(ClO_4)_3$.

21) H. Ohtaki, *Inorg. Chem.*, **6**, 808 (1967).

22) H. Ohtaki and H. Kato, *ibid.*, **6**, 1935 (1967).

23) H. Ohtaki, *ibid.*, **7**, 1205 (1968).

24) C. Bercki-Biedermann, *Arkiv. Kem.*, **9**, 175 (1956).

25) G. Gran, *Analyst*, **77**, 661 (1952).

26) G. Biedermann and L. Ciavatta, *Acta Chem. Scand.*, **15**, 1347 (1961).

27) W. Forsling, S. Hietanen and L. G. Sillén, *ibid.*, **6**, 901 (1952).

of the solution is sufficiently high to prevent any appreciable hydrolysis of aluminium ion.

Compositions of titransts were as follows: $T_1=A$ LiOH, $(3-A)$ $LiClO_4$: and $T_1'=2B$ $Al(ClO_4)_3$, X $HClO_4$, $(3-6B-X)$ $LiClO_4$. Equal volumes of T_1 and T_1' were added to S_1 in order to keep B constant during the course of titration. Concentration of the added hydroxide ion was calculated from the difference of A and X.

The concentration of hydrogen ion was measured by means of the cell

$$(-)\text{GE}\,|\,\text{solution}\,|\,\text{Ref}\,(+) \qquad (3)$$

where GE denotes a glass electrode and Ref the reference half-cell,

3.00M $LiClO_4$ in 0.2 mol fraction aqueous dioxane	2.99M $LiClO_4$ and 0.01M $AgClO_4$ in aqueous solution	AgCl-Ag

The emf of the cell (3) at 25°C may be written as

$$E = E^\circ - 59.15 \log h - 59.15 \log f_H - E_J(h,B) \qquad (4)$$

where E° is a constant and f_H represents the activity coefficient of hydrogen ion. As described in the previous works,[21-23] the standard state is defined so that f_H, as well as the activity coefficients of the other reacting species, tends toward unity as the composition of the solution approaches 3M $LiClO_4$ in 0.2 mol fraction of aqueous dioxane. During the course of titration Z varied from zero to 0.3 at the lowest B and to 0.08 at the highest. Nevertheless, we assume that the activity coefficients of the reacting species to be constant as long as B is maintained constant and the ionic medium in the solution is sufficiently high.

The liquid-junction potential at the junction, test solution | 3M $LiClO_4$ in 0.2 mol fraction of aqueous dioxane, is described as $E_J(h,B)$ in Eq. (4). At $B=0$ it was found in a cell of similar design that $E_J(h,0)=-8.3h$ mV.[21] In the present study $E_J(h,B)$ can be assumed to be equal to $E_J(h,0)$ without causing any appreciable error in the evaluation of the hydrogen ion concentration from emf measurements.

A glass electrode is calibrated against a perchloric acid through a Gran plot.[25] The value, $E^0-59.15\cdot\log f_H$, in Eq. (4) thus obtained is assumed to be kept constant throughout titration.

At a sufficiently low pH range where no appreciable hydrolysis occurred, a stable potential was established within 5 to 10 min after addition of the titrants. However, in the range where the hydrolysis occurred, reactions seemed to progress rather slowly. At lower Z ($Z\lesssim 0.1$) and relatively low pH range, stable emf's were obtained only after two to three hours. When Z increased ($Z>0.1$), the reaction seemed to be so accelerated that the stable potential was established more rapidly (within half an hour or less). Finally the solution was distinctly turbid and the potential was nearly unchanged in systems of lower B. When the solution was clear and the emf remained unchanged for at least an hour, we recorded the emf value as the final one. In fact the emf was still maintained constant within an accuracy of ±0.1 mV for at least 5 hr thereafter.

Titration in the reverse way was demonstrated as follows: A test solution was prepared by the addition of LiOH solution into an aluminum perchlorate solution until precipitates formed. The solution was left for two months in a thermostated room at 25°C with occasional shaking. The precipitates were separated by centrifugation and a portion of the supernatant was subjected to gravimetric determination of the concentration of aluminum ion in the test solution. Another portion of the supernatant was used for emf measurements, in which the solution was gradually acidified by adding a titrant, whose composition was $T_2=B$ $Al(ClO_4)_3$, X' $HClO_4$ (back titration). In the present case $B=0.02913$M and $X'=0.1032$M.

All processes of preparation of the test solution and of transfer of solutions were performed in a glove box which was filled with air free from carbon dioxide.

The maximum Z value found was 0.6 which was almost three times as large as that expected from the ordinary forward titrations. At lower Z less than 0.3, reactions between the hydrogen ions added and the hydrolyzed aluminum species present in the solution progressed very slowly and no stable potential was obtained even after more than 24 hr. However, in a strong acid solution having pH lower than 1.9, all the hydrolysis products were decomposed and a stable emf was obtained within 5—10 min.

Table 1. Survey of experimental data

B=0.00500M		B=0.0100M		B=0.0200M	
$-\log h$	Z	$-\log h$	Z	$-\log h$	Z
2.979	0.00320	3.134	0.01807	2.746	0.00100
3.092	0.00378	3.305	0.03957	2.881	0.00435
3.212	0.01292	3.381	0.05414	3.038	0.01333
3.342	0.02859	3.451	0.07036	3.172	0.02944
3.466	0.05362	3.513	0.09859	3.261	0.05087
3.567	0.08653	3.569	0.1271	3.329	0.07412
3.647	0.1238	3.609	0.1561	3.300	0.09783
3.702	0.1647	3.645	0.1846	3.432	0.1221
3.750	0.2063	3.679	0.2248	3.464	0.1458
3.784	0.2557	3.699	0.2642	3.501	0.1690
3.819	0.2912			3.520	0.1925
				3.544	0.2154
				3.571	0.2377

B=0.0399M		B=0.0400M		B=0.0798M	
$-\log h$	Z	$-\log h$	Z	$-\log h$	Z
2.649	0.00272	2.626	0.00368	2.531	0.00440
2.786	0.00594	2.739	0.00563	2.678	0.00820
2.925	0.01281	2.866	0.00929	2.833	0.01408
3.035	0.02389	2.947	0.01337	2.937	0.02342
3.102	0.03783	3.008	0.01950	3.016	0.03392
3.165	0.05208	3.087	0.02985	3.063	0.04483
3.217	0.06657	3.151	0.04585	3.101	0.05563
3.270	0.08611	3.209	0.06224		
3.300	0.1058	3.261	0.08298		
3.334	0.1251	3.303	0.1034		
3.359	0.1476	3.322	0.1281		
		3.361	0.1509		
		3.383	0.1732		
		3.407	0.2019		

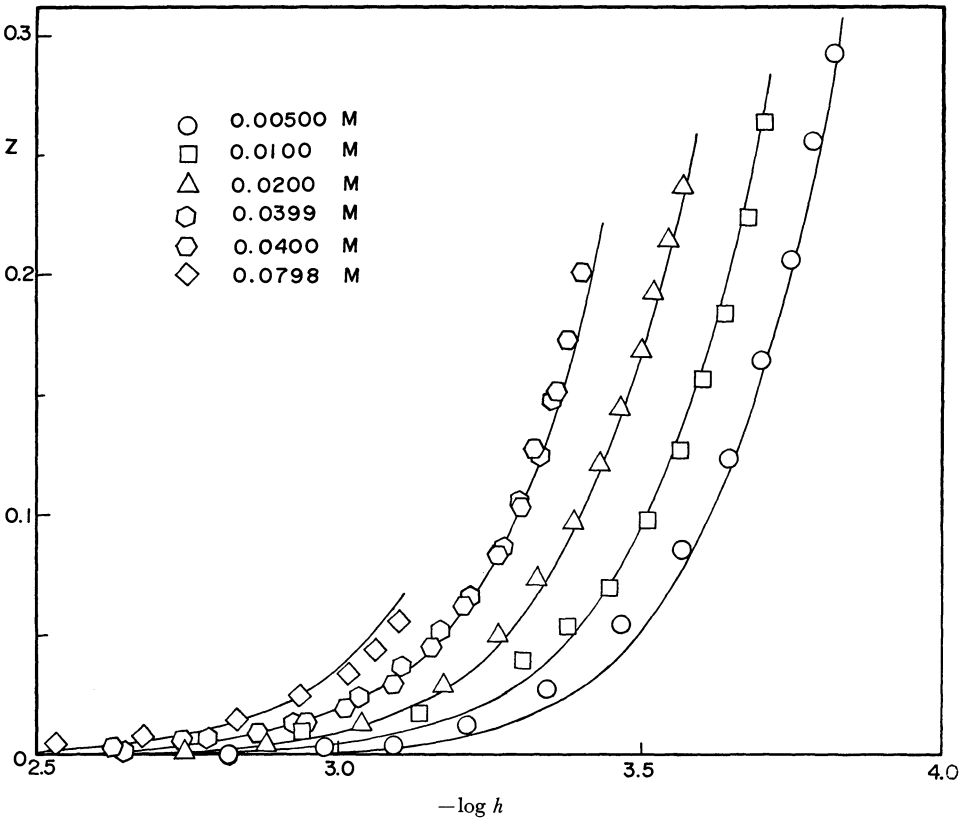

Fig. 1. Z as a function of $-\log h$. Curves were calculated with $^*\beta_{2,2}=1.16\times10^{-7}$ and $^*\beta_{3,2}=9.55\times10^{-11}$.

Results

Results obtained by means of forward titrations were treated with the assumption of the equilibrium condition. Values of $-\log h$ and Z at each series of B were calculated from the emf data obtained. They are shown in Table 1 and also represented graphically in Fig. 1.

The concentration of hydrogen ion set free by hydrolysis, BZ, is given by the general formula

$$BZ=\sum_p\sum_q p[\mathrm{Al}_q(\mathrm{OH})_p{}^{(3q-p)+}]=\sum_p\sum_q p{}^*\beta_{p,q}h^{-p}b^q \quad (5)$$

and B is given as

$$B=b+\sum_p\sum_q q[\mathrm{Al}_q(\mathrm{OH})_p{}^{(3q-p)+}]$$
$$=b+\sum_p\sum_q q{}^*\beta_{p,q}h^{-p}b^q \quad (6)$$

Plots of $\log B$ against $-\log h$ gave a set of straight lines with a slope of 2.7—3.0, which approximately corresponds to t in the formula $[\mathrm{Al}(\mathrm{Al}(\mathrm{OH})_t)_n]$ according to the core-link treatment.[28]

As a preliminary consideration, simple assumptions were made as follows: only a complex, $\mathrm{Al}_Q(\mathrm{OH})_P{}^{(3Q-P)+}$, is mainly formed and an approximation of $B\approx b$ is applied. Thus,

$$Z\approx P{}^*\beta_{P,Q}h^{-P}B^{Q-1} \quad (7)$$

or

$$\log Z\approx\log P{}^*\beta_{P,Q}B^{Q-1}-P\log h \quad (8)$$

An examination was made for the assumption of the formation of $\mathrm{Al}_{13}(\mathrm{OH})_{32}{}^{7+}$ which has been proposed by Aveston.[8] In the formula of this complex t is described as $32/12=2.667$ which is fairly close to that found in the present case. The following relations can be derived:

$$BZ=32{}^*\beta_{32,13}h^{-32}b^{13} \quad (9)$$

$$B=b+13{}^*\beta_{32,13}h^{-32}b^{13} \quad (10)$$

Then,

$$Z=32{}^*\beta_{32,13}\{B(1-0.406Z)^{13/12}\cdot h^{-32/12}\}^{12} \quad (11)$$

All points obtained in this work fell on a straight line of $\log Z$ plotted against $\log B+13/12\log(1-13/32.Z)-32/12\log h$. However, the slope of the line was not 12 but only 1. From this observation the main complex was not $\mathrm{Al}_{13}(\mathrm{OH})_{32}{}^{7+}$ but the formation of dimerized species ($q=2$) might be expected.

When we plotted $\log Z$ against $-\log h$ a set of straight lines with a slope of 2.4—2.6 was obtained, which corresponds to the value of P in Eq. (8).

28) L. G. Sillén, *Acta. Chem. Scand.*, **8**, 299 (1954).

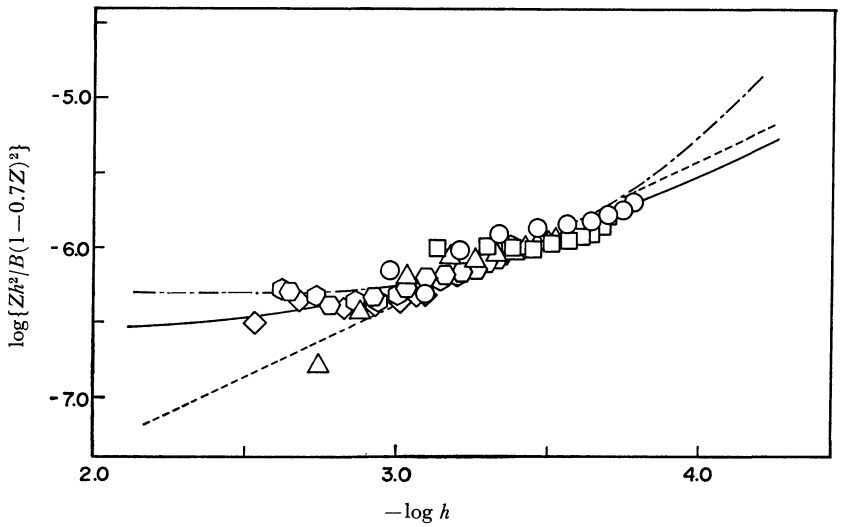

Fig. 2. log $(Zh^2/B(1-0.7Z)^2)$ as a function of $-\log h$.
————— , Assumption of the formation of both $Al_2(OH)_2^{4+}$ and $Al_2(OH)_3^{3+}$;
-·-·-·- , $Al_2(OH)_2^{4+}$ and $Al_2(OH)_4^{2+}$; ------ , $Al_2(OH)_3^{3+}$ only.
Symbols used are the same as those in Fig. 1.

Since P is given as nt in the $[Al(Al(OH)_t)_n]$ complex and t was found to be 2.7—3.0, the value of n should be unity and thus, the main species formed should contain two Al atoms.

The second step of the approximation was made for a nonstoichiometric complex such as $Al_2(OH)_{2.4}^{3.6+}$. A plot of Z against $\log B+2\log(1-0.833Z)-2.4\log h$ systematically deviated from a normalized curve, $y=x=f(\log x)$, which led to the conclusion that the average value of p ($\bar{p}$) of the complexes must be larger than 2.4. An examination with another assumption that $Al_2(OH)_3^{3+}$ is the unique complex formed led to the conclusion that $\bar{p}$ must be smaller than 3. Thus, the average value of p, *i.e.*, $\bar{p}$, must lie between 2.4 and 3.

It may be natural to assume the formation of two complexes both of which contain two aluminum atoms. An approach was tried for the formation of complexes of $Al_2(OH)_2^{4+}$ and $Al_2(OH)_3^{3+}$. The following approximation was made for calculation of b:

$$b = B(1-\alpha Z) \qquad (12)$$

For the value of α, we put $\alpha=0.7$ which is a number between 0.667 (for $\bar{p}=3$) and 0.833 ($\bar{p}=2.4$). The variation of α was insensitive to the present calculations. Inserting Eq. (12) into Eqs. (5) and (6), the following equation was readily derived:

$$BZ = 2{}^*\beta_{2,2}B^2(1-0.7Z)^2h^{-2} + 3{}^*\beta_{3,2}B^2(1-0.7Z)^2h^{-3} \qquad (13)$$

Table 2. Various sets of complexes assumed and error square sums obtained with a generalized least squares method

Complexes assumed (p,q)			U
1,1	2,2	3,2	3.019×10^{-3}
2,2	3,2		3.077×10^{-3}
2,2	3,2	4,2	5.430×10^{-3}
2,2	4,2		7.189×10^{-3}
2,2	5,2		1.391×10^{-2}
1,1	2,2	4,2	1.641×10^{-2}
2,2	6,4		5.709×10^{-2}
2,2	3,3		7.231×10^{-2}
2,2	15,6		1.125×10^{-1}
2,2	32,13		1.290×10^{-1}
2,2	17,7	34,13	8.790
17,7	34,13		15.58

Table 3. Equilibrium constants of the hydrolysis reaction of aluminum ion†

Author	log $*\beta_{1,1}$	log $*\beta_{2,2}$	log $*\beta_{3,2}$	log $*\beta_{6,15}$	log $*\beta_{7,17}$	log $*\beta_{13,32}$	log $*\beta_{13,34}$
Brosset[17]				−47			
Kentämaa[6]	−4.96	−7.55					
Kubota[7]	−5.03	−6.27					
Sillén[15]					−48.8		−97.6
Aveston[8]		−7.07				−10.45	
Present Work		−6.95	−10.02				

† Except for the present work all the measurements were performed in aqueous solutions.

or

$$\frac{Zh^2}{B(1-0.7Z)^2} = 2{}^*\beta_{2,2} + 3{}^*\beta_{3,2}h^{-1} \qquad (14)$$

Plots of log $(Zh^2/B(1-0.7Z)^2)$ against log h^{-1} were compared with a normalized curve, $y=\log(1+x)$ plotted against log x. It is seen from Fig. 2 that all the points examined fall on a single curve which overlapped with the normalized curve. From the position of the best fit of curve we evaluated that log ${}^*\beta_{2,2}=-6.92$ and log ${}^*\beta_{3,2}=-10.02$. Another assumption that complexes formed were $Al_2(OH)_2^{4+}$ and $Al_2(OH)_4^{2+}$ gave a worse agreement. Evidently the assumption of the formation of $Al_2(OH)_3^{3+}$ complex only did not explain the experimental results.

Finally the data have been treated by a generalized least-squares method with the help of an electronic computer HITAC 5020E for various sets of complexes in order to find the best set of the complexes. Calculation of Z_{calc} ($Z_{calc}=\sum_p\sum_q \beta^*\beta_{p,q}\, h^{-p}b^q/B$ for a particular set of constants ${}^*\beta_{p,q}$) with a set of ${}^*\beta_{2,2}$ and ${}^*\beta_{3,2}$ resulted in a satisfactory agreement with the experimental data.

The other sets of ${}^*\beta_{p,q}$ gave more or less worse agreement *i.e.*, larger error square sums, U ($U=\sum(Z-Z_{calc})^2$) were obtained. Highly polymerized complexes such as $Al_7(OH)_{17}^{4+}$, $Al_{13}(OH)_{32}^{7+}$ or $Al_{13}(OH)_{34}^{5+}$ were thus excluded. Formation of any monomeric complexes was not conclusive in the present work. Various sets of complexes assumed and square sums obtained are listed in Table 2. The final values of the constants obtained by the computer calculation are $\log{}^*\beta_{2,2}=-6.95\pm0.07$ and $\log{}^*\beta_{3,2}=-10.02\pm0.03$. They are listed in Table 3 together with values reported by some workers in aqueous solutions.

Discussion

Although we could not estimate the composition of complexes formed after two months of aging, the following conclusions may be drawn from the results obtained by back titration: precipitates of aluminum hydroxide once formed dissolve slowly and, as a result, the value of the maximum Z increases to nearly threefold of that expected from the ordinary forward titration at the same B, and binuclear $Al_2(OH)_2^{4+}$ and $Al_2(OH)_3^{3+}$ complexes may coagulate, releasing some protons to form higher polynuclear complexes which result in the increase of the hydrogen ion concentration at equilibrium. Thus, the hydrolysis reactions of aluminum ion may be schematically described as follows:

$$2Al^{3+} + \begin{Bmatrix} 2H_2O \\ 3H_2O \end{Bmatrix} \overset{{}^*\beta_{p,q}}{\rightleftharpoons} \begin{Bmatrix} Al_2(OH)_2^{4+} + 2H^+ \\ Al_2(OH)_3^{3+} + 3H^+ \end{Bmatrix} \xrightarrow[k]{\text{slow}} \text{High polymers}$$

The rate constant k is so small that the formation

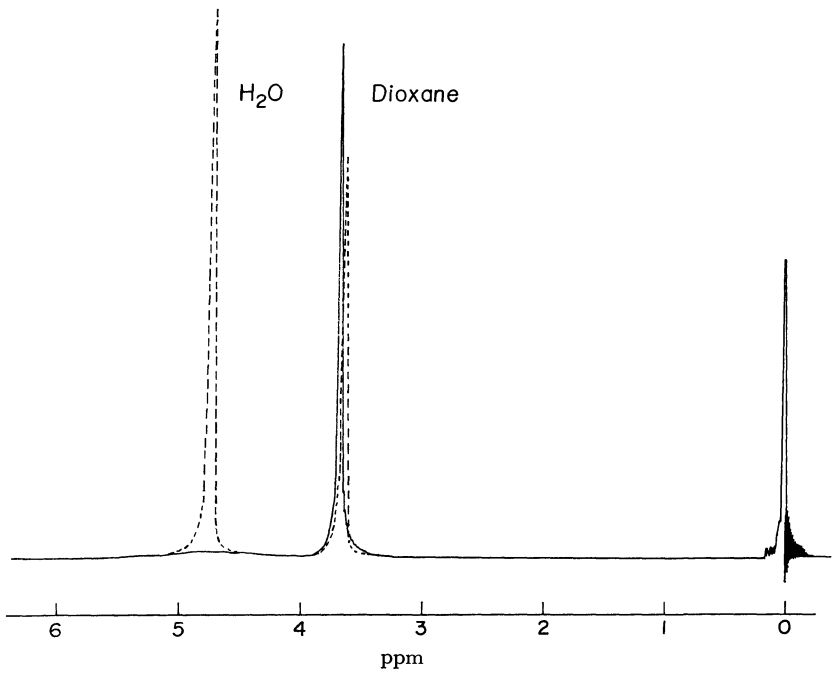

Fig. 3. Proton NMR spectra of water and dioxane in pure water (-----), pure dioxane (-----) and in 80% w/w dioxane-water mixture containing 0.35M $Al(ClO_4)_3$ (————).

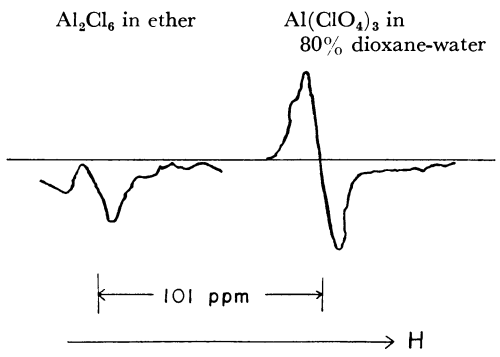

Fig. 4. NMR spectra of ^{27}Al of Al_2Cl_6 in ether and of $Al(ClO_4)_3$ in 80% w/w dioxane-water mixture.

reaction of higher polymers does not noticeably proceed during measurements. Thus, the formation constant obtained in the present work, $*\beta_{p,q}$ are for the intermediates on the way to higher polymers.

The solvent effect on the formation constants of hydrolysis reactions of aluminum ion may be seen from a comparison of $\log *\beta_{2,2}$ found in various media. In aqueous solutions at zero ionic strength the value of $\log *\beta_{2,2}$ spread from -7.55[6] to -6.27[7] at 25°C. In 1M sodium perchlorate solution $\log *\beta_{2,2}$ is evaluated to be -7.07,[8] which differs only slightly from that in 0.2 mol fraction (55.01% w/w) dioxane-water mixture.

NMR spectra of protons and aluminum ions (^{27}Al) in an acid aqueous dioxane (80% w/w dioxane) solution were measured and are shown in Fig. 3 and 4, respectively. In Fig. 3 a peak caused by protons in water becomes broad but no apparent shift in position compared with the peak in pure water (dotted line) was observed. On the other hand, a peak caused by hydrogen atoms in dioxane molecules remained almost unchanged both in shape and in position. Thus, it may be concluded that even in the aqueous dioxane solution with fairly high dioxane concentration, aluminum ions are surrounded only by water molecules.

The NMR spectra of ^{27}Al (Fig. 4) showed that a peak caused by the aluminum ion in the aqueous dioxane solution is located at about 101 ppm higher side of the magnetic field compared with that in Al_2Cl_6 in ether. We concluded that, at least in acid aqueous dioxane solution, aluminum ion has an octahedral configuration which is so in aqueous solutions. If we assume that the aluminum ions still keep the octahedral configuration even in hydrolyzed complexes, the structure of the $Al_2(OH)_2^{4+}$ complex may be similar to that depicted in Fig. 5,

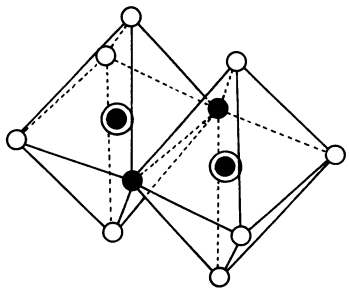

Fig. 5. A model proposed for the $Al_2(OH)_2^{4+}$ complex.

which has been determined by X-ray analysis of a basic aluminum sulfate crystal.[9] The $Al_2(OH)_3^{3+}$ complex may be formed by releasing another proton from one water molecule which occupies an apex of an octahedron of aluminum atom.

The author wishes to thank Professor M. Tanaka for his continued interest in this work. He is indebted to Prof. S. Fujiwara and Dr. H. Haraguchi of Tokyo University for their kind help in NMR measurements of ^{27}Al. The work has been financially supported by the Ministry of Education.

BULLETIN OF THE CHEMICAL SOCIETY OF JAPAN VOL. 43 2470—2474 (1970)

Metal Chelates of Some β,δ-Triketone Homologues. Copper(II) Chelates of 2,6-Diacetyl-4-methylphenol, 2,2′-Dihydroxybenzophenone, 2-Acetoacetylphenol and 2-Acetyl-1,8-dihydroxynaphthalene*1

Yoshio TAGUCHI,*2 Fumio SAGARA, Hiroshi KOBAYASHI and Keihei UENO

Department of Organic Synthesis, Faculty of Engineering, Kyushu University, Fukuoka

(Received January 30, 1970)

Copper(II) chelates of 2,6-diacetyl-4-methylphenol, 2,2′-dihydroxybenzophenone, 2-acetoacetylphenol and 2-acetyl-1,8-dihydroxynaphthalene were synthesized. The first and last ligands give only a mononuclear chelate of type CuL_2 respectively, whereas the second and third ones give a binuclear complex of type Cu_2L_2 in addition to the mononuclear complex. In the cases of the latter ligands two types of complexes are interconvertible and in a solution phase there exists an equilibrium between them. Higher temperature favors a binuclear form and lower temperature another form. Structures of the complexes are assigned with spectroscopic and thermogravimetric data.

In relation to our work on the metal chelates of 2,4,6-heptanetrione and related compounds,[1] the following four ligands have been synthesized and the properties of copper(II) chelates of the ligands have been investigated. The ligands synthesized are 2,6-diacetyl-4-methylphenol (Hdap), 2,2′-dihydroxybenzophenone (H_2dhb), 2-acetoacetylphenol (H_2aap) and 2-acetyl-1,8-dihydroxynaphthalene (H_2ahn), which are illustrated in Fig. 1. Although the compounds have been reported in literature, no systematic investigation concerning multidentate ligands was reported.

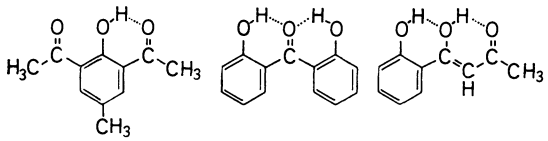

(Hdap) (H_2dhb) (H_2aap)

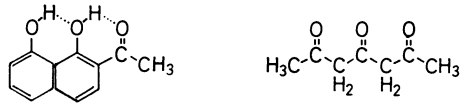

(H_2ahn) (H_2daa)

Fig. 1. Structure of the ligands.

The coordinating moiety of these ligands resembles that of 2,4,6-heptanetrione. However, features of the ligands are that the mono- or dienol tautomeric structures of the trione is fixed on certain oxygen atoms and that the free rotation of the coordinating site is partly restricted by fused aromatic rings. By analogy with 2,4,6-heptanetrione, the ligands are also expected to behave as bidentate as well as terdentate ligands. Thus, an investigation on the structures and properties of the metal chelates of the ligands may provide us with additional information for understanding 2,4,6-heptanetrione metal chelates.

In the cases of unsymmetrical ligands such as 2-acetoacetylphenol and 2-acetyl-1,8-dihydroxynaphthalene, it is also of interest to study which coordinating sites are preferred for metal chelation if they behave as bidentate ligands.

Experimental

Synthesis of the Ligands. All ligands were synthesized according to the methods given in literature, and were identified by means of their melting points, ultraviolet and infrared absorption spectra, nuclear magnetic resonance spectra and elemental analyses. Melting points and the appearence of the ligands are summarized in Table 1.

Synthesis of the Chelates. Lower temperature favors the mononuclear 1 : 2 chelate formation, while higher temperature favors the binuclear 2 : 2 chelate formation. Thus for preparation of 1 : 2 chelate, procedure A was followed. For preparation of 2 : 2 chelate, procedure B or C was followed.

Procedure A. To a methanolic solution of the ligand (2 mol), an aqueous solution of copper acetate (1 mol) was added with stirring below 15°C. Then pH of the solution was adjusted to 9 with aqueous ammonia. The resulting precipitates were recrystallized from ap-

*1 Contribution No. 202 from the Department of Organic Synthesis, Kyushu University, Fukuoka, Japan.

*2 Present address; Sanyo Kasei Industries, Ltd., 11 Hitotsubashi-Nomotomachi, Higashiyama-ku, Kyoto.

1) Fumio Sagara, Hiroshi Kobayashi and Keihei Ueno, This Bulletin, **41**, 266 (1968).

Table 1. Ligands synthesized

Ligand	Mp °C (reported mp)	Solvent for recryst.	Appearance*
Hdap	83.1—83.3 (83)[a]	Ligroin	Y-n
H_2dhb	59.2—59.8 (59—60)[b]	Ligroin	Y-p
H_2aap	88.1—88.8 (90.5—91.5)[c]	Benzene	Cl-n
H_2ahn	97.0—99.8 (101—103)[d]	Chloroform	Y-n unstable in air

a) K. W. Rosemund and W. Schunurr, *Ann. Chem.*, **460**, 85 (1928)
b) R. Richter, *J. prak. Chem.*, **28**, 285 (1883)
c) G. Wittig, *Ann. Chem.*, **446**, 173 (1926)
d) J. C. Overeen, *Rec. Trav. Chim. Pays-Bas*, **83**, 1017 (1964)
* Y: yellow, Cl: colorless, n: needles, p: plates

propriate solvents whenever possible.

Procedure B. Equimolar amounts of the ligand and the metal salt were dissolved in methanol and pH of the solution was adjusted to 9 with aqueous ammonia. The solution was then refluxed for a few hours, until the precipitate of binuclear 2 : 2 chelate came out.

Procedure C. A solution of the mononuclear 1 : 2 chelate in ethanol, chloroform, benzene or pyridine, was refluxed for a few hours, until the precipitates of 2 : 2 chelate came out. If the 1 : 2 chelate was not soluble enough in these solvents, the 1 : 2 chelate was placed in an extraction thimble of a Soxhlet extraction apparatus, and was extracted with hot benzene. The 2 : 2 chelate was precipitated in a refluxing flask.

The results on synthesis of the copper(II) chelates are summarized in Table 2.

Apparatus and Procedure. All melting points are uncorrected. Ultraviolet and visible spectra were measured with a Hitachi 124 recording spectrophotometer. Solid reflectance spectra were measured with a Hitachi EPU-2A spectrophotometer. Infrared absorption spectra and nuclear magnetic resonance spectra were recorded with a JASCO DS-301 spectrophotometer and a Varian A-60 operating at 60 MHz, respectively. Molecular weights were determined with a Mechrolab vapour pressure osmometer. Thermogravimetric analyses on the pyridine adducts were conducted with a Shimadzu automatic recording thermobalance TB-10B. A weighed amount of a chelate (20—100 mg) was placed on a weighing pan of the thermobalance and a few drops of pyridine was added to it. After the sample was left at room temperature until its weight became constant, the temperature of the furnace was raised at a rate of 5°C per minute under atmospheric pressure, and the weight change was recorded automatically up to 150°C. The results are summarized in Table 3.

Table 3. Thermogravimetric analysis of the pyridine adducts

Starting material: Composition	Starting material: Color	Temp. where elimination occurs	Final-product
$Cu(dap)_2 \cdot Py$	drak green	34— 54°C	$Cu(dap)_2$
$Cu(Haap)_2 \cdot 2Py$	green	26	$Cu(Haap)_2 \cdot Py$
		45— 62	$Cu(Haap)_2$
$Cu_2(aap)_2 \cdot 3Py$	green	34— 60	$Cu_2(aap)_2 \cdot 2Py$
		62—102	$Cu_2(aap)_2 \cdot Py$
		102—108	$Cu_2(aap)_2$
$Cu(Hdhb)_2 \cdot 2Py$	dark green	34—125	$Cu(Hdhb)_2$
$Cu_2(dhb)_2 \cdot 6Py$	dark green	25—72	$Cu_2(dhb)_2 \cdot Py$

Table 2. Copper (II) chelates

Chelates	Method of synthesis	Yield %	Molecular formula	Elemental analysis Found (Calcd.) C%	H%	M%	Appearance[a]
$Cu(dap)_2$	A	27	$C_{22}H_{22}O_6Cu$	59.06 (59.25)	4.90 (4.97)	14.35 (14.25)	YO-n (Cl)
$Cu(Hdhb)_2 \cdot 1/2\ H_2O$	A	35	$C_{26}H_{18}O_6Cu \cdot 1/2\ H_2O$	62.83 (62.58)	3.81 (3.84)	12.25 (12.74)	YB-pd
$Cu_2(dhb)_2$	B C	45 51	$C_{26}H_{16}O_6Cu_2$	57.27 (56.62)	3.11 (2.92)	21.78 (23.04)	YB-pd M.W. 512 (551)[b]
$Cu(Haap)_2$	A	63	$C_{20}H_8O_6Cu$	57.49 (57.48)	4.50 (4.34)	14.96 (15.21)	YG-n (Et)
$Cu_2(aap)_2 \cdot H_2O$	B C	62 26	$C_{20}H_{18}O_6Cu_2 \cdot H_2O$	48.01 (48.29)	3.65 (3.65)	24.98 (25.55)	G-n (Th-Lg) M.W. 442 (497)[b]
$Cu(Hahn)_2$[d]	A	38	$C_{24}H_{18}O_6Cu$	61.30 (60.69)	4.01 (4.32)	13.08 (13.38)	YB-pd M.W. 463 (466)[b]
$Cu_2(ahn)_2$[d]	B	35	$C_{24}H_{20}O_9Cu_3$[c]	45.01 (44.82)	3.33 (3.14)	29.93 (29.64)	B-pd

a) Appearance. YO: yellow orange, YB: yellow brown, YG: yellow green, G: green, B: brown, n: needles, pd: powder. Solvent for recrystallization in parentheses. Cl: chloroform, Et: ethanol, Th-Lg: tetrahydrofurane-ligroin mixture.
b) Molecular weight was determined in pyridine. The observed value is followed by the theoretical one in parentheses.
c) A possible structure is discussed in the text.
d) The reaction is carried out under nitrogen stream.

Results and Discussion

Copper(II) chelates of Hdap, H_2dhb, H_2aap and H_2ahn were prepared according to the procedure in Experimental. As in the case of 2,4,6-heptanetrione metal chelates,[2] the chelates of different ratio of metal to ligand were obtained according to the conditions of synthesis

The 1 : 2 chelates are obtained by procedure A, whereas the 2 : 2 chelates are obtained by either procedure B or C. In general, the 1 : 2 chelate is fairly soluble in various organic solvents such as ethanol, chloroform, benzene and pyridine. Thus, in most cases, they can be obtained as crystalline form by recrystallization from such solvents. On the other hand, the 2 : 2 chelates are hardly soluble in organic solvents except pyridine. The only exception is the 2 : 2 chelate of 2-acetoacetylphenol, which can be recrystallized from a mixture of tetrahydrofurane and ligroin. All chelates obtained do not show any definite melting points below 300°C.

As observed in the copper(II) chelates of 2,4,6-heptanetrione, the 1 : 2 chelate of the diprotonic ligands such as H_2dhb, H_2aap and H_2ahn can be converted into 2 : 2 chelates of the respective ligands, as described in the preparation of 2 : 2 chelates by procedure C. Reversely the 2 : 2 chelate can be converted into a 1 : 2 chelate when the solution of the 2 : 2 chelate in pyridine containing an excess of the ligand is kept at a lower temperature. Thus, the equilibrium seems to occur

$$2Cu(HL)_2 \rightleftarrows Cu_2L_2 + 2L \text{ (in pyridine)}$$

and the higher temperature favors the 2 : 2 chelate and lower temperature the 1 : 2 chelate.

Since the ligands chosen in this investigation are terdentate, there remains the possibility of their affording polymeric forms, especially in the case of the 2 : 2 chelates. The 1 : 2 chelates are, however, so soluble in various organic solvents that they are not likely to be of polymeric form. Moreover, the fairly fast rate of interconversion between the 1 : 2- and 2 : 2 chelates in pyridine suggests that the drastic rearrangement of the chelation is not likely to occur in the process of conversion in a solution phase. The results of the molecular weight determination of the 2 : 2 chelates in pyridine also support the monomeric form. Thus, there is no doubt that the 1 : 2- and 2 : 2 chelates are monomeric at least in a pyridine solution, and this may also be true in solid state. Although there is no positive reason to reject the possibility of affording the polynuclear chelates in solid state, a study with molecular models shows that the polymeric structures can be constructed only with heavy steric hinderance and strain, because free rotation of the coordinating sites is partly restricted by fused aromatic rings.

When the chelates are treated with pyridine, they easily form pyridine adducts, and the number of moles of pyridine per mole of the chelate varies from one to six depending upon the kind of ligand as summarized in Table 3. The reversible pyridine adduct formation is indicative of the vacancy of the coordinating sites of copper(II) on z axis. Two copper(II) ions in the chelate can accept at most four moles of pyridine. Thus, in the case of Cu_2-$(dhb)_2 \cdot 6Py$, two of the six moles of pyridine are not coordinated to copper ions. It is also noted that the last one mole of pyridine does not dissociate up to 150°C. The stepwise dissociation of pyridine with increasing temperature is clearly observed in the chelates of H_2aap, whereas the pyridine on the rest of the chelates dissociates gradually.

Chelate of 2,6-Diacetyl-4-methylphenol (Hdap). The chelate prepared by procedure A is found to have the formula of $Cu(dap)_2$. As this ligand has only one dissociable proton, the binuclear chelate of type Cu_2L_2 can not be obtained even under the condition of procedure B or C. $Cu(dap)_2$ is obtained as well defined green yellow needles after recrystallization from aqueous methanol, and its formula is confirmed by elemental analysis.

The infrared spectrum of the free ligand is characterized by a broad band of ν_{O-H} at 3000 cm^{-1} and a doublet band of free and hydrogen bonded carbonyl groups at 1669 and 1640 cm^{-1}, respectively. The infrared spectrum of the copper chelate, on the other hand, shows no ν_{O-H} band, but still shows $\nu_{C=O}$ bands at 1670 and 1619 cm^{-1} in addition to the new bands at 1530 and 1520 cm^{-1} which are related to the coordinated carbonyl group.

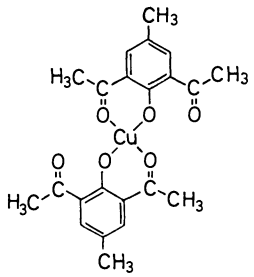

(I) Structure I

From the results, structure I is proposed for the chelate $Cu(dap)_2$. However, the question remains whether the two ligands take *cis* or *trans* arrangement as regards the central metal ion.

Chelates of 2-Acetoacetylphenol (H_2aap). The free ligand may possibly exist as three tautomeric forms A, B and C. The solid H_2aap, however, seems to exist as form B or C, since a free carbonyl band at 1730 cm^{-1} which is observed in chloroform

2) Ref. 1. More details will be published elsewhere.

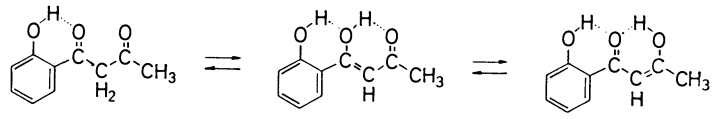

(A) (B) (C)

Scheme 1.

solution, can not be found in the spectrum of a solid sample. In the latter spectrum, absorption bands observed at 1680, 1615 and 1580 cm^{-1} can be assigned to those of the hydrogen bonded carbonyl and the conjugated olefinic groups.

The 1 : 2 chelate, which is obtained as yellow green needles by procedure A, is found to have the formula of $Cu(Haap)_2$. The infrared spectrum of the 1 : 2 chelate does not show a band due to the free carbonyl group, but shows new bands at 1570 and 1515 cm^{-1} which may be related to the coordinated carbonyl groups. From the above results, either of the following two structures, (II) and (III), can be proposed for the 1 : 2 chelate.

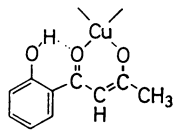

(II)

Structure II

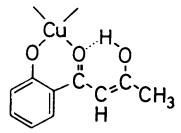

(III)

Stucture III

Of the two structures, the chelating moiety of (II) resembles that of bis(benzoylacetonato)copper-(II), and structure (III) resembles that of bis(*o*-hydroxyacetophenonato)copper(II). Comparison of the electronic spectra of $Cu(Haap)_2$ with those of the above two model compounds suggests the probable chelate structure of this compound. The results of the visible absorption spectra of the pyridine solution and the reflectance spectra of solid samples are summarized in Table 4.

Table 4. Electronic spectra of the copper (II) chelates of 2-acetoacetylphenol, benzoylacetone and *o*-hydroxyacetophenone

Ligand of Cu (II) chelate	Visible absorption spectra in pyridine λ_{max} mμ, (log ε)	Solid reflectance spectra λ_{max} mμ
2-Acetoacetylphenol	680 (1.19), 353 (4.33)	640
Benzoylacetone	664 (1.92), 368 (4.48)	645
o-Hydroxyacetophenone	628 (2.01), 566 (2.14), 362 (3.90)	595

The bands in the range 500—600 mμ can be assigned to the ligand field *d–d* transition band, and the spectrum of $Cu(Haap)_2$ is more closely similar to that of bis(benzoylacetonato)copper(II) than that of bis(*o*-hydroxyacetophenonato)copper-(II) which has two peaks in this region. Thus, it is very likely that the structure of $Cu(Haap)_2$ is that shown in II.

As to the question of the two ligands taking either *cis* or *trans* arrangement, the *trans* structure is more probable because the *cis* structure may suffer from the steric hinderance of phenolic protons.

The binuclear chelate $Cu_2(aap)_2 \cdot H_2O$ can be obtained either by procedure B or C as green needles, the yield being higher by procedure B. Molecular weight determined in pyridine solution supports the above formula. No significant difference in infrared spectra is observed between 1 : 2- and 2 : 2 chelates. Thus, it is likely that the structure of $Cu_2(aap)_2$ is that shown in IV.

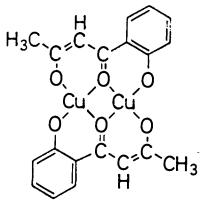

(IV)

Structure IV

Chelates of 2,2′-Dihydroxybenzophenone (H_2dhb). The 1 : 2 copper(II) chelate is obtained as a yellow brown powder by procedure A, and elemental analysis supports the formula $Cu(Hdhb)_2 \cdot 1/2H_2O$. The hydrogen bonded carbonyl band of the free ligand at 1630 cm^{-1} disappeared in the infrared spectra of the 1 : 2 chelate, and a new

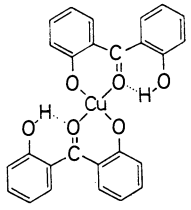

(V)

Structure V

band appearing at 1520 cm^{-1} is assigned to the coordinated carbonyl group. The results suggest structure V for the 1 : 2 chelate. The *trans* form is more probable than the *cis* form because of the steric hindrance of the phenolic protons.

The 2 : 2 copper chelate was obtained as yellow brown powder by procedure B or C, with a slightly higher yield by the latter procedure. The results of elemental analysis and molecular weight determination support the formula $Cu_2(dhb)_2$.

Infrared spectra of the 2 : 2 chelate in 1600—1500 cm^{-1} region differ from those of the 1 : 2 chelate, but structure VI is the most probable for this chelate. It has been reported that the hydrogen atoms at 6- and 6′-positions of the free ligand interfere with each other sterically.[3] Accordingly, the planer structure around copper atoms may be distorted to some extent.

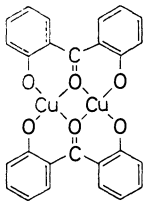

(VI)

Structure VI

Chelates of 2-Acetyl-1,8-dihydroxynaphthalene (H_2ahn). As this ligand is found to be sensitive to atmospheric oxygen, all the procedure with this ligand is carried out in a nitrogen stream.

The 1 : 2 copper(II) chelate is obtained as yellow brown powder by procedure A, and elemental analysis as well as molecular weight determination supports the formula of $Cu(Hahn)_2$. Hydrogen bonded carbonyl band of the free ligand at 1640cm^{-1} disappears in the infrared spectrum of the 1 : 2 chelate, and a new band is observed at 1520 cm^{-1} which is assigned to the coordinated carbonyl groups. These results suggest structure VII for the 1 : 2 chelate. The *trans* form is more probable than *cis* form as discussed previously.

3) J. R. Merrill, *J. Phys. Chem.*, **65**, 2023 (1961).

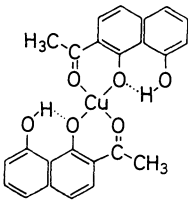

(VII)

Structure VII

An attempt to prepare a 2 : 2 chelate of 2-acetyl-1,8-dihydroxynaphthalene by procedure B, results in a chelate of 3 : 2 composition, whose empirical formula is found to be $C_{21}H_{20}O_9Cu_3$. In this procedure, when pH is adjusted to 9, a 3 : 2 chelate is obtained, whereas a 1 : 2 chelate is obtained when the reaction is carried out at pH 6—7. As the infrared spectrum does not show a sharp band at around 3600 cm^{-1}, it is not likely that the chelate contains copper hydroxide. In contrast to the chelates of 2,4,6-heptanetrione, 2-acetoacetylphenol and 2,2′-dihydroxybenzophenone where the interconversion of the 1 : 2- and 2 : 2 chelates is observed, the 3 : 2 chelate of 2-acetyl-1,8-dihydroxynaphthalene can not be converted into a 1 : 2 chelate. Furthermore, the 3 : 2 chelate is hardly soluble in pyridine, whereas 2 : 2 chelates of the other ligands are fairly soluble in pyridine. Thus, the 3 : 2 chelate may possibly be of an ionic complex or a highly polymeric form. One of the possible structures of this chelate may be something like that shown in VIII.

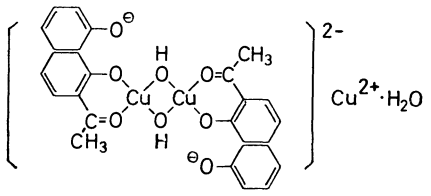

(VIII)

Structure VIII

The authors are grateful to the Ministry of Education for a grant-in-aid for scientific research.

BULLETIN OF THE CHEMICAL SOCIETY OF JAPAN VOL. 43 2475—2478 (1970)

Titanium and Zirconium in Hydrothermally-altered Rocks from the Tateyama Jigokudani Hot Springs, Toyama, Japan

Masayuki IMAHASHI

Department of Chemistry, Faculty of Science, Tokyo Metropolitan University, Setagaya, Tokyo

(Received February 3, 1970)

Hydrothermally-altered rocks and muds collected from the Tateyama Jigokudani hot springs were analysed for titanium and zirconium. In order to estimate the acidity of the thermal waters which contributed to these altered rocks, the concentration factor of the elements relative to SiO_2 was used for convenience. The titanium and zirconium contents of the alteration products are approximately equal to those of the fresh rocks. This seems to indicate that most of these elements remain in the rocks during the alteration under acidic conditions. The muds are characterized by high values of the concentration factors and the factors proved to be dependent on the acidity of the mud-suspending waters. From the relation between the concentration factors and the pH's of the waters, we could estimate the acidities of the thermal waters which attacked the altered rocks in the earlier stages.

The alteration of silicate rocks generally involves a change in their chemical composition. Under strongly acid conditions, all the chemical constituents except SiO_2 and TiO_2 are almost entirely leached out and the altered rocks are enriched in SiO_2 and H_2O.[1] Iwasaki *et al.* reported on the chemical compositions of alteration products in the Tamagawa hot springs.[2] According to their data, the TiO_2 and SiO_2 contents of these products are larger than those of the original rocks, and the concentration factors of TiO_2 relative to SiO_2 for these alteration products have values ranging from 0.77 to 1.07. The variation in the values of the factors may depend on the nature of the thermal waters which attack the rocks. Therefore, the factor may give some useful indications for use in estimating the environmental conditions of the alteration.

Zirconium can be expected to behave like titanium because of the similarity in chemical properties. Between titanium and zirconium, however, there may be some differences in leachability and in mobility in acid solutions. The differences may depend on the acidity of the thermal waters dominating during the alteration; the changes in the pH of the waters may, that is, reflect in some way the concentrations of these elements in hydrothermally-altered rocks.

There have been no detailed studies of the distribution of titanium and zirconium in altered rocks under acid conditions. The purpose of this investigation is to determine the titanium and zirconium contents of hydrothermally-altered rocks in an acid hot spring area and to estimate the acidity of the thermal waters using the concentration factor of these elements.

1) J. Ossaka, *Chinetsu*, **17**, 65 (1968).

2) I. Iwasaki, T. Katsura, T. Tarutani, T. Ozawa, M. Yoshida, B. Iwasaki, M. Hirayama and M. Kamada, "Geochemistry of the Tamagawa Hot Springs," Minami Sensei Kanreki Kinen Jigyo-kai, Tokyo (1963), p. 35.

Experimental

Samples. The alteration products were collected from the Tateyama Jigokudani hot springs, Toyama Prefecture, where there is still volcanic actions and where there are many acid hot springs. The alteration products collected were divided into two groups according to where they occurred. The first group consisted of altered rocks; most of these are silicified and contain iron sulfide and free sulfur in small amounts. In general, the center part of the altered rocks is gray or a blackish gray, and the surface is white or a grayish white. Suffixes are used to distinguish the center part from the surface; "a" indicates a sample of the center part, "b" idicates the surface. These rocks are probably the alteration products of an earlier stage.

The second group consisted of the muds which were suspended in acid thermal waters. These samples are extremely fine-grained and contain considerable amounts of free sulfur and iron sulfide. These muds are denoted in the sample number by the prefix "s". They are presently undergoing active alteration. The fresh rocks were identified as augite hypersthene andesite by microscopic examination and by X-ray diffraction.*1

Chemical Analysis. Titanium and zirconium were determined colorimetrically using disodium 1,2-dihydroxy-benzene-3,5-disulfonate (Tiron) and 2,7-bis-(azo-2)-phenylarsono-1,8-dihydroxynaphthalene-3,6-disulfonic acid (Arsenazo-III) respectively. A 0.2 g—0.4 g portion of a powdered sample (under 100 mesh) was

*1 The identification was performed by Dr. J. Ossaka, to whom the author wishes to express his thanks.

decomposed with 10 m*l* of concentrated hydrofluoric acid on a hot plate. One milliliter of concentrated perchloric acid was then added, and the mixture was evaporated to dryness. The evaporated residue was fused sodium bisulfate, and the cooled melt was dissolved in dilute hydrochloric acid. The volume of the solution was made up to 50 m*l* with water.

An 1—2 m*l* aliquot of this solution was taken out and titanium was determined according to the method described by Rygg and Wagenbauer,[3] To determine the zirconium, a 5—10 m*l* aliquot of this solution was taken out and evaporated to white fumes with 1 m*l* of concentrated perchloric acid. The solution was then transferred to a 25 m*l* volumetric flask; 13 m*l* of concentrated nitric acid, 2 m*l* of a 10% urea solution, and 2 m*l* of a 0.1% Arsenazo-III solution were added, and the mixture was diluted with water to 25 m*l*. The zirconium content was determined from the absorbance at 660 mμ.[4] Elements commonly in rocks scarcely interfered with the determination at all. The experimental errors (relative) for the titanium and zirconium determinations were within $\pm 3\%$ and $\pm 5\%$ respectively.

Results and Discussion

Contents of Titanium and Zirconium. The titanium and zirconium contents of the alteration products and of fresh rocks are shown in Table 1, along with the percentage of SiO_2 and the ignition loss. Although the SiO_2 content of the altered rocks is larger than that of the fresh rocks, the titanium and zirconium contents are not necessary so; these, rather, have a tendency to scatter. This indicates that considerable portions of all the major constituents except SiO_2 were removed, while titanium and zirconium partly remained in the rocks or were leached out according to the environmental conditions. There is, at any rate, no considerable difference in the contents between the altered and the fresh rocks, so it may be considered that these elements in the rocks are generally resistant to alteration.

In the case of the muds, the SiO_2 content is apparently smaller than that of the altered rocks because considerable portions of these samples are ignition losses largely of free sulfur and water. On the other hand, the titanium and zirconium contents of the muds are approximately equal to those of the altered rocks; this leads to the conclusion that the concentration factors of the these elements in the muds are above unity, as will be discussed below.

Concentration Factors. In order to normalize the concentrations of these elements, relative to

TABLE 1. TITANIUM AND ZIRCONIUM CONTENTS OF ALTERATION PRODUCTS

No.	SiO_2 (%)	Ign. loss (%)	Ti (%)	Zr (%)	r(Ti)*	r(Zr)*	r(Ti)/r(Zr)
1	56.82	1.42	0.42	0.017	—	—	—
2a	65.11	11.71	0.32	0.0088	0.68	0.45	1.5
2b	87.72	9.03	0.28	0.0094	0.44	0.36	1.3
4	65.78	20.09	0.35	0.0080	0.74	0.41	1.8
5	77.62	10.46	0.58	0.019	1.04	0.82	1.3
6	81.27	9.95	0.54	0.018	0.92	0.75	1.2
7a	78.84	11.52	0.44	0.022	0.78	0.94	0.83
7b	89.72	7.35	0.61	0.026	0.95	0.97	0.98
8	64.05	0.80	0.47	0.019	—	—	—
13a	85.34	7.93	0.38	0.016	0.62	0.63	0.98
13b	91.63	6.57	0.42	0.013	0.64	0.48	1.3
14a	65.16	15.11	0.50	0.019	1.07	0.98	1.1
14b	73.73	13.35	0.93	0.030	1.74	1.37	1.3
24a	66.00	14.86	0.46	0.011	0.97	0.56	1.7
24b	73.19	12.70	0.57	0.014	1.08	0.65	1.7
s-1	42.44	33.82	0.64	0.018	2.10	1.43	1.5
s-2	21.91	71.13	0.49	0.016	3.12	2.46	1.3
s-3	49.07	25.94	0.62	0.016	1.75	1.09	1.6
s-4	42.11	42.83	0.63	0.016	2.09	1.28	1.6
s-5	50.17	20.31	0.49	0.010	1.36	0.67	2.0
s-8	53.33	30.04	0.60	0.015	1.56	0.95	1.6
s-9	39.00	50.74	0.38	0.0093	1.33	0.80	1.7
s-11	39.38	50.22	0.60	0.019	1.67	1.62	1.0
s-12	49.72	36.50	0.82	0.023	2.30	1.55	1.5

* Average values of fresh rock samples, Nos. 1 and 8, were used for the calculations

3) T. Rygg and H. A. Wagenbauer, *Anal. Chem.*, **33**, 1347 (1961).

4) O. Kammori, I. Taguchi and R. Komiya, *Bunseki Kagaku*, **14**, 106 (1965).

SiO_2, for the alteration products, the concentration factor, denoted by r, is used. It is expressed by the following relation; $r(M)=(M/SiO_2)_a/(M/SiO_2)_f$, where M is the element to be considered and where the subscripts "f" and "a" stand for the fresh and the altered rocks respectively. In the case of discussion of the concentration factors, it must be assumed that the titanium and zirconium contents of the original rocks are essentially constant.

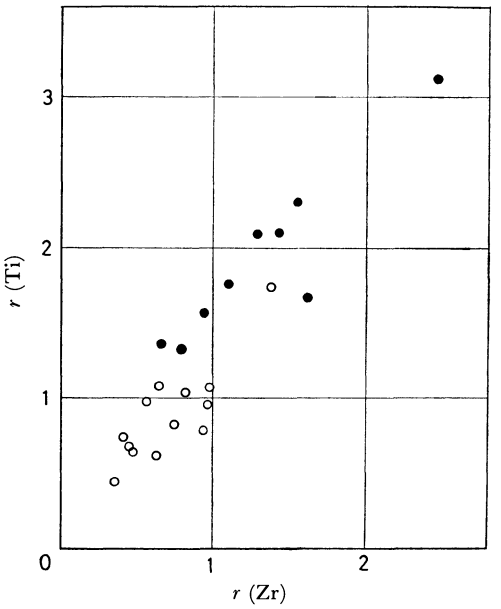

Fig. 1. Relationship between r(Ti) and r(Zr).
○: altered rock, ●: mud

The r values for titanium and zirconium and the ratio of r(Ti) to r(Zr) are shown in Table 1. Figure 1 represents the relationship between these values. These values fluctuate rather widely. However, it is certain that the values of the muds are above unity and that those of the altered rocks are below unity, with a few exceptions. As Fig. 1 shows, there is a linear relationship between these values, but the values of the muds are apparently different from those of the altered rocks. This suggests that there is no considerable difference in the rate of leaching between titanium and zirconium, but that the rates of these elements are different from those of silica. That is, the leaching rates of titanium and zirconium for the altered rocks were higher than those of silica, in contrast with the case of the muds. This may also suggest that the altered rocks were attacked by thermal waters with slightly lower pH values.

The large r values of the muds can be explained in terms of the difference in the leachabilities between these elements and silica and the occurrence of these elements in a resistant fraction in such an environment. Thus, the r values may be effectively used in estimating the conditions of the alteration.

Estimation of the Acidity of Thermal Waters. The variation in r values found for the muds and the altered rocks may be due to the environmental characteristics of the sample locality. The mobility and the leachability of a chemical element during alteration are known to be greatly affected by the acidity of the environment. Therefore, it can be assumed that the acidity is a factor governing the differences in leachability between titanium and zirconium. In Table 2, the acidity and the temperature of the mud-suspending waters are given. Because the disparity of temperature of the mud-suspending waters is not very large, as is shown in Table 2, and as the chemical compositions of the waters are nearly equal to each other, it may be possible to disregard the influences of other factors. In Fig. 2, the r(Ti)/r(Zr) ratio is plotted against the pH of the water in which the mud was suspended. The figure shows that the ratios tend to increase with an increase in the pH of the waters. Thus, these ratios prove to be affected by the pH of the mud-suspending waters; the ratios may provide some indications for use in estimating the acidity of the thermal waters dominating during the alterations.

As is shown in Table 1, the ratios of the altered rocks have values ranging from 0.83 to 1.8. From these values and from Fig. 2, it can be estimated

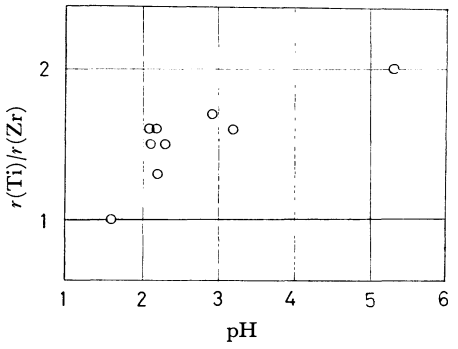

Fig. 2. Relationship between r(Ti)/r(Zr) ratio of muds and pH of the mud-suspending waters.

Table 2. Acidity and temperature of mud-suspending waters

No.	pH	T (°C)	SO_4^{2-} (g/l)	Cl^- (g/l)
s-1	2.3	51	1.22	0.00
s-2	2.2	75	1.09	0.09
s-3	2.1	71	1.49	0.00
s-4	3.2	62	0.12	0.03
s-5	5.3	29	0.16	0.23
s-8	2.2	88	0.91	0.03
s-9	2.9	77	0.15	0.26
s-11	1.6	80	1.61	0.02
s-12	2.1	83	0.92	0.02

that the pH values of the thermal waters which attack the altered rocks range from about 1 to 4, provided that none of the conditions except the acidity in the earlier stage change up to the final stage. It may be concluded that the pH values of the thermal waters are slightly lower than, or approximately equal to, those of the mud-suspending waters. This is consistent with the pH's of hot spring waters in the Tateyama Jigokudani area.[5]

In igneous rocks, most of titanium and zirconium may be incorporated in resistant minerals, such as ilmenite and zircon.[6] In a certain stage of the alteration, however, these elements gradually enter into solutions, but the titanium in an acid solution is slightly less mobile than is zirconium; the pH values of solutions which give rise to the precipitates of titanium and zirconium hydroxides are 1.4 and 2.0 respectively.[7] Moreover, titanium secondary minerals, such as rutile and anatase, are generally resistant to acid.[8] Consequently, during the alteration the Ti/Zr ratio in an alteration product may be changed and it may gradually increase in the later stage of the alteration. The higher the pH values of thermal waters, the larger will be the ratios.

It is necessary to make further leaching experiments on titanium and zirconium obtained from rocks with acid solutions and to study the occurrences of these elements in hydrothermally-altered rocks. These results will be reported in a future paper.

The author wishes to express his thanks to Prof. Masami Ichikuni for his valuable advice and for his critical reading of the manuscript.

5) K. Noguchi and T. Nishiido, *Nippon Kagaku Zasshi*, **90**, 781 (1969).

6) K. Rankama and Th. G. Sahama, "Geochemistry," The University of Chicago Press, Chicago (1950), p. 557.

7) B. A. Gavrusevich, "Fundamentals of General Geochemistry," Nedra, Moskow (1968), p. 291.

8) W. A. Deer, R. A. Howie and J. Zussman, "Rock-forming Minerals," Vol. 5, Longmans, London (1962), p. 34.

BULLETIN OF THE CHEMICAL SOCIETY OF JAPAN VOL. 43 2478—2481 (1970)

Studies of Thin-layer Chromatography of Inorganic Salts. IV. Chromatographic Behavior of Square Planar Complexes in Comparison with that of Octahedral Complexes

Tetsuo BABA[1] and Hayami YONEDA

Department of Chemistry, Wakayama University, Masagocho, Wakayama

(Received February 4, 1970)

The chromatography of copper(II) and platinum(II) complexes on silica gel was investigated in comparison with that of cobalt(III) and nickel(II) complexes. Each complex showed various R_f values from zero to unity, when it was developed with aqueous solutions of various salts. This was interpreted to be due to different degrees of anionic association with the complex. The pattern of deversity of R_f values in copper(II) and platinum(II) complexes was found to be definitely different from that in cobalt(III) and nickel(II) complexes. Thus, different association mechanisms were proposed for both cases. In copper(II) and platinum(II) complexes, association occurs through the direct coordination of the anion to the metal ion, while, in cobalt(III) and nickel(II) complexes, association takes place at the outer-sphere of the complex.

We were interested in obtaining information concerning the behaviors and dissolved states of ions in solution through chromatographic studies. In a previous study[2] it was revealed that silica gel is charged negatively in contact with water and adsorbs cations so strongly that the R_f value of the complex cation is almost zero when developed with distilled water. Such strong adsorption is palliated and the increase of the R_f value is observed, when an aqueous solution of salts such as NaCl or Na_2SO_4 is used as a developer. The sample is eluted mainly through ionic association with anions contained in

1) On leave from the Minoshima High School, Arita-shi, Wakayama.

2) T. Baba, H, Yoneda and M. Muto, This Bulletin, **41**, 1965 (1968).

the developer. In other words, such association reduces the apparent positive charge of the complex cation, which results in the decrease of the electrostatic attraction by the adsorbent and in the increase of the R_f value of the sample. Thus, we undertook to study the feature of ionic association by means of thin-layer chromatography. In the preceding paper[3] the effect of hydration of anions upon association was investigated using the crystal violet cation. In the present paper, we should like to report the characteristic features of association involving square planar complexes in compariosn with those involving octahedral complexes.

Experimental

Thin-layer Chromatography. As an adsorbent, Merck's silica gel H was used without further purification. This was spread on a glass plate with length 25 cm and thickness 0.25 mm.

The complexes used in this investigation were [Co en$_3$]Cl$_3$ [Co gly$_3$], [Cu en$_2$] (NO$_3$)$_2$, [Cu gly$_2$], [Pt en$_2$]Cl$_2$, [Ni en$_3$] (NO$_3$)$_2$ and [Ni gly$_2$ (H$_2$O)$_2$]. Each complex was dissolved in water to 1/50M, and 2.5μl of the solution was spotted at a starting point 5 cm above the lower edge of the plate.

The salts used in development were sodium salts of Cl$^-$, Br$^-$, I$^-$, NO$_2^-$, NO$_3^-$, HCOO$^-$, CH$_3$COO$^-$, SO$_3^{2-}$, SO$_4^{2-}$ and S$_2$O$_3^{2-}$, and potassium salts of OCN$^-$, SCN$^-$ and SeCN$^-$. To obtain the best separation, different salt concentrations of developers were used, *viz.*, 0.2M for cobalt(III), 0.1M for nickel(II), 0.5M for copper(II) and platinum(II) complexes.

Development was carried out at room temperature (20—23°C). For detection of the developed spot an aqueous solution of potassium sulfide was sprayed on the cobalt(III) complex, while the alcoholic solution of rubeanic acid was sprayed on the other three complexes. For visualization of the platinum complex, a special procedure was necessary. Rubeanic acid must be acidified with a small amount of hydrochloric acid, and the sprayed plate must be heated to 100°C.

UV Spectral Measurement. The absorption spectra were recorded with a Hitachi Spectrophotometer Model 124.

Results and Discussion

The R_f values of the complexes are summarized in Table 1. In order to understand the characterisrics of the chromatography of square planar complexes, it is advantageous to discuss the chromatography of typical octahedral complexes first.

The tervalent complex cation is adsorbed so strongly on silica gel, that it can be eluted only through ionic association with anions contained in the developer. Thus, various R_f values of the [Co en$_3$]$^{3+}$ complex were obtained as shown in Table 1. This seems to reflect various degrees of anionic association. A marked feature of the chromatography of the [Co en$_3$]$^{3+}$ complex is that the difference in R_f values among univalent anions is not so marked, and that there is a definite difference in R_f values between univalent and bivalent anions. This seems to be the characteristics of octahedral complexes. In fact, the R_f value pattern of the

TABLE 1. R_f VALUES OF THE OCTAHEDRAL AND THE SQUARE PLANAR COMPLEXES DEVELOPED WITH SOLUTIONS OF VARIOUS SALTS

Anion	Complex					
	[Co en$_3$]$^{3+}$	[Co gly$_3$]^0	[Nien$_3$]$^{2+}$	[Cu en$_2$]$^{2+}$	[Cu gly$_2$]^0	[Pt en$_2$]$^{2+}$
H$_2$O	0.02	0.90	0.01	0.01	0.03	0.02
Cl$^-$	0.24	0.91	0.23	0.14	0.13	0.37
Br$^-$	0.23	0.92	0.23	0.16	0.08	0.39
I$^-$	0.26	0.94	0.21	0.44	0.81	0.52
NO$_3^-$	0.19	—[a]	0.24	0.13	0.12	0.34
NO$_2^-$	0.18	—[a]	0.24	0.27	0.49	0.29
HCOO$^-$	0.11	—[a]	0.20	0.22	0.40	0.19
CH$_3$COO$^-$	0.07	—[a]	0.19	0.15	0.39	0.13
OCN$^-$	0.12	—[a]	0.13	0.63	0.95	0.27
SCN$^-$	0.32	—[a]	0.32	0.67	0.88	0.58
SeCN$^-$	0.30	—[a]	0.96	1.00	0.97	—[c]
SO$_4^{2-}$	0.57	0.90	0.62	0.33	0.30	0.36
SO$_3^{2-}$	0.70	0.93	0.50	0.95	0.90	0.78
S$_2$O$_3^{2-}$	0.79	0.96	0.53	1.00	—[b]	0.52

a) Development was not carried out, as no special difference of R_f values was expected.
b) The complex was reduced by the thiosulfate.
c) The developed spot was not identified, because red selenium appeared over the plate surface during the heating process for visualization of the spot.

3) T. Baba, K. Sakushima, and H. Yoneda, This Bulletin, **43**, 931 (1970).

$[Ni\ en_3]^{2+}$ complex is quite similar to that of the $[Co\ en_3]^{3+}$ complex as seen in Table 1.

In the neutral $[Co\ gly_3]^0$ complex, the R_f value is very large even with distilled water and is not affected much with salt solutions. This suggests that the octahedral neutral complex has little tendency towards association. A marked contrast to this can be seen in the R_f value pattern of the corresponding $[Cu\ gly_2]^0$ complex. As shown in Table 1, the $[Cu\ gly_2]^0$ complex is so strongly adsorbed on silica gel, it remains near the starting point when developed with distilled water. Such strong adsorption can not be explained by a simple electrostatic attraction between silica gel and the complex, because the complex as a whole is elecrically neutral. We must, therefore, assume that the adsorption of the complex takes place through the direct coordination of SiO_2 to the copper(II) ion. In other words, the oxygen atom of SiO_2 occupies the axial position of the square planar copper complex. Any kind of anion can make such direct coordination. Thus, a wide variety of R_f values were observed, when various salt solutions were used as a developer. This is considered to correspond to a wide variety of degree of coordination equilibrium between the complex and the anion. This makes a marked contrast to the case of the octahedral $[Co\ gly_3]^0$ complex which has no more reserved coordination seat to be occupied by the anion. It should be noted that the R_f value of the copper complex seems to depend not on the ionic charge of anions but on the kind of anion, especially on the kind of donor atoms. Thus, the R_f value is definitely larger in the case of I^- than in the cases of Br^- and Cl^-, and the large R_f values in the cases of $S_2O_3^{2-}$, SO_3^{2-}, NCS^- and $NCSe^-$ can be regarded to result from the coordination through sulfur and selenium atoms. On the other hand, the R_f value is relatively small in the case of SO_4^{2-}, which can be understood by considering that the coordination is made through the oxygen atom. A quite similar pattern of R_f value variation is observed in the $[Cu\ en_2]^{2+}$ complex too, as can be seen in Table 1. In this case the R_f value also depends not on the ionic charge of anions but on the kind of donor atoms. This is in contrast to the corresponding $[Co\ en_3]^{3+}$ complex.

The characteristics of the chromatography of the typical square planar $[Pten_2]^{2+}$ complex is quite similar to that of $[Cuen_2]^{2+}$ complex. The R_f value is definitely larger in the case of I^- than in the cases of Br^- and Cl^-, and definitely smaller in the case of SO_4^{2-} than in the cases of SO_3^{2-} and $S_2O_3^{2-}$. Therefore, in the platinum(II) complex also, association of anions is presumed to occur not in an equatorial direction but along the axial direction of the complex. In the case of $[Ni\ gly_2(H_2O)_2]^0$, though the complex has an octahedral configuration, the R_f value pattern appears to be similar to that of the square planar complex (R_f-value: 0.06 with H_2O, 0.82 with I^-, and 0.85 with SO_4^{2-}). Therefore, it is presumed that the water

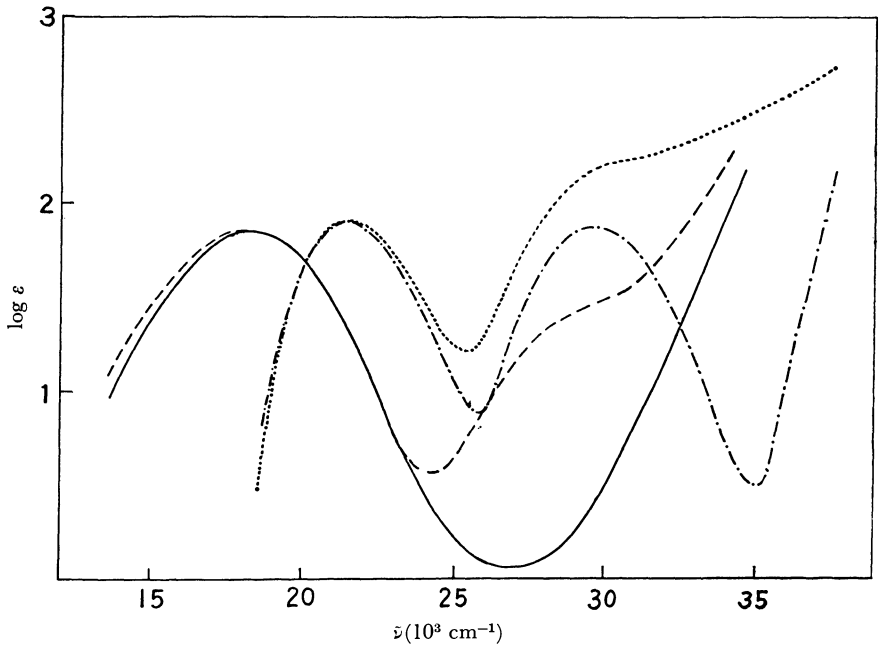

Fig. 1. Electronic spectra of $[Cu\ en_2)](ClO_4)_2$ and $[Co\ en_3](ClO_4)_3$.
———— $[Cu\ en_2]^{2+}$ in distilled water
------ $[Cu\ en_2]^{2+}$ in 1M Na_2SO_3 aqueous solution
-·-·-·- $[Co\ en_3]^{3+}$ in distilled water
····· $[Co\ en_3]^{3+}$ in 1M Na_2SO_3 aqueous solution

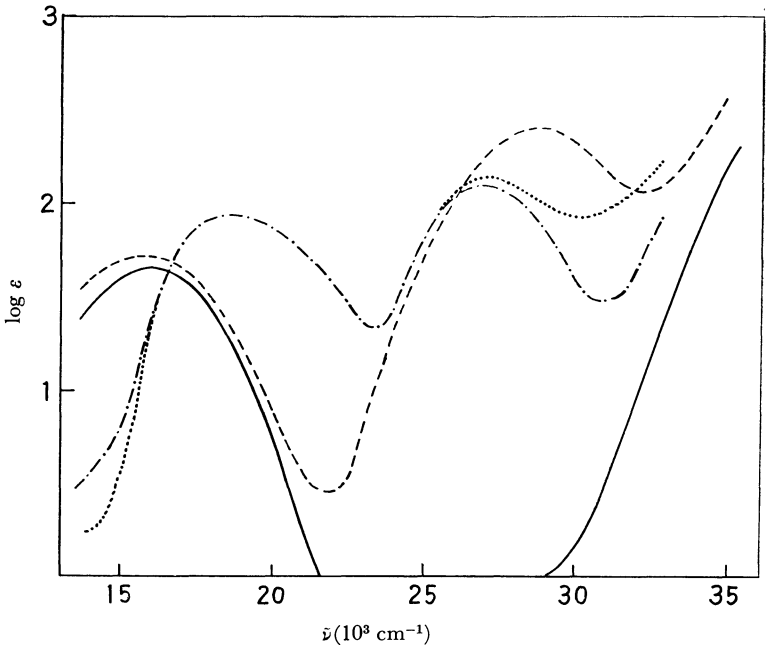

Fig. 2. Electronic spectra of $[Cu\,gly_2]^0$ and $[Co\,gly_3]^0$.
———— $[Cu\,gly_2]^0$ in distilled water
------ $[Cu\,gly_2]^0$ in 1M Na_2SO_3 aqueous solution
-·-·-·- $[Co\,gly_3]^0$ in distilled water
····· $[Co\,gly_3]^0$ in 1M Na_2SO_3 aqueous solutions

molecules at the axial positions can be replaced by the anion.

The above-mentioned ionic association can be supported from the spectral data of the complex. As can be seen in Fig. 1, the UV spectra of the $[Coen_3]^{3+}$ and $[Cuen_2]^{2+}$ complexes dissolved in 1M Na_2SO_3 solution show a new band in the near ultraviolet region, which is not observed in water. Such a band can be regarded as a charge-transfer band due to ionic association. A similar charge-transfer band was also observed in the $[Cugly_2]^0$ complex (See Fig. 2). It should be noted that the intensity of the charge-transfer band in the $[Cu\,gly_2]^0$ complex is much larger than that in the $[Cu\,en_2]^{2+}$ complex. Thus a greater interaction is presumed between SO_3^{2-} and $[Cugly_2]^0$ than between SO_3^{2-} and $[Cuen_2]^{2+}$.[4] On the contrary, the absorption spectrum of $[Cogly_3]^0$ is almost the same both in water and in 1M Na_2SO_3 solution, which suggests no marked interaction between the complex and SO_3^{2-}.

4) The association constant for $[Cu\,alanin_2]^0$ and SO_3^{2-} is 240, while that for $[Cu\,en_2]^{2+}$ and SO_3^{2-} is only 25. H. Yoneda, This Bulletin, **29**, 68 (1956); *ibid.*, **29**, 319 (1956).

BULLETIN OF THE CHEMICAL SOCIETY OF JAPAN VOL. 43 2482—2486 (1970)

Photon-Activation Analysis for Iodine by Using Cesium as the Internal-Reference Element*1

Hui-Tuh Tsai, Toyoaki Kato and Yoshinaga Oka

Department of Chemistry, Faculty of Science, Tohoku University, Katahira-cho, Sendai

(Received February 6, 1970)

The internal-reference method proposed previously has been applied to the determination of iodine by photon-activation analysis, using cesium as the internal-reference element. The present method is based on the measurement of the ^{126}I, ^{124}I and ^{123}I activities produced by the neutron-emitting reactions in iodine, and on the comparison of these activities with that of ^{130}I coming from cesium by the (γ, 2pn) reaction. A lithium-drifted germanium diode with a sensitive volume of 36 cm^3 was used as the detector. The yields of various photonuclear reactions in both elements have also been examined as a function of the bremsstrahlung maximum energies up to 65 MeV. A series of synthetic mixtures of iodine-cesium with known weight ratios has been used to check the sensitivity and the accuracy of this method. We found that we could determine amounts of iodine down to 0.2 μg under the present experimental conditions.

Recently, photon-activation analysis has been established as a useful analytical method for the determination of a number of elements in the periodic table. One of the advantages of photon-activation analysis, as compared with high-flux thermal neutron activation analysis, is that interferences due to ^{24}Na and ^{38}Cl encountered in the thermal neutron activation of various biological materials can be eliminated. Thus, Anderson *et al.*[1] and Wilkniss and Linnenbom[2] utilized the ^{19}F-(γ,n)^{18}F reaction in the determination of fluorine in biological samples and in sea water respectively. The bremsstrahlung-activation technique was also applied to the determination of iodine in biological materials,[3,4] in pharmaceuticals,[5] and in sodium chloride and sodium bromide media.[6]

On the other hand, the present authors have proposed the internal-reference method of activation analysis and have applied this method to the determination of silver in palladium[7] and to that of antimony in tin[8] by activation with thermal neutrons. By this method, the sources of errors associated with activation analysis, such as flux irregularities, can be avoided and no correction for the chemical yield is necessary. Another possible application of this method lies in photon-activation analysis. The residual activities from (γ,xn) reactions in an element to be determined can be compared with those from the (γ,p), the (γ,2pn), the (γ,α), or another charged particle emitting reactions in an internal-reference element. Recently, methods of photon-activation analyses for the determinations of arsenic and niobium have been reported; these methods use selenium and molybdenum respectively as the internal reference elements.[9,10]

The present work concerns a method for the determination of iodine by using cesium as the internal-reference element, along with bremsstrahlung from a linear electron accelerator. The present method depends on the much greater resolving power of a lithium-drifted germanium detector. A study is also included of the yields of photonuclear reactions at several different bremsstrahlung maximum energies up to 65 MeV.

*1 Study of the Activation Analysis Using the Internal-Reference Method. Part XIII. Part XII: Y. Oka, T-C. Pung and T. Saito, This Bulletin, **43**, 1083 (1970).

1) G. H. Anderson, F. M. Graber, V. P. Guinn, H. R. Lukens and D. M. Settle, Proceedins of the Symposium on Nuclear Activation Techniques in the Life Sciences, Amsterdam, IAEA (1967), p. 99.

2) P. E. Wilkniss and V. J. Linnenbom, *Limnol. Oceanog.*, **13**, 530 (1968).

3) P. F. Mulvey, Jr., J. A. Cardarelli, M. Zonkis, R. D. Cooper and B. A. Burrows, *J. Nucl. Med.*, **7**, 603 (1966).

4) R. D. Cooper, D. M. Linekin and G. L. Brownell, Proceedings of the Symposium on Nuclear Activation Techniques in the Life Sciences, Amsterbam, IAEA (1967), p. 65.

5) D. Brune, S. Mattsson and K. Liden, *Anal. Chim. Acta*, **44**, 9 (1969).

6) S. Abe, *Nippon Kagaku Zasshi*, **87**, 426 (1966).

7) Y. Oka, T. Kato, H-T. Tsai and K. Nomura, This Bulletin, **41**, 329 (1968).

8) Y. Oka, T. Kato and H-T. Tsai, *ibid.*, **41**, 2427 (1968).

9) Y. Oka, T. Kato and Y. Konami, *Bunseki Kagaku*, **18**, 971 (1969).

10) Y. Oka, T-C. Pung and T. Saito, This Bulletin, **43**, 1083 (1970).

Table 1. Separation scheme

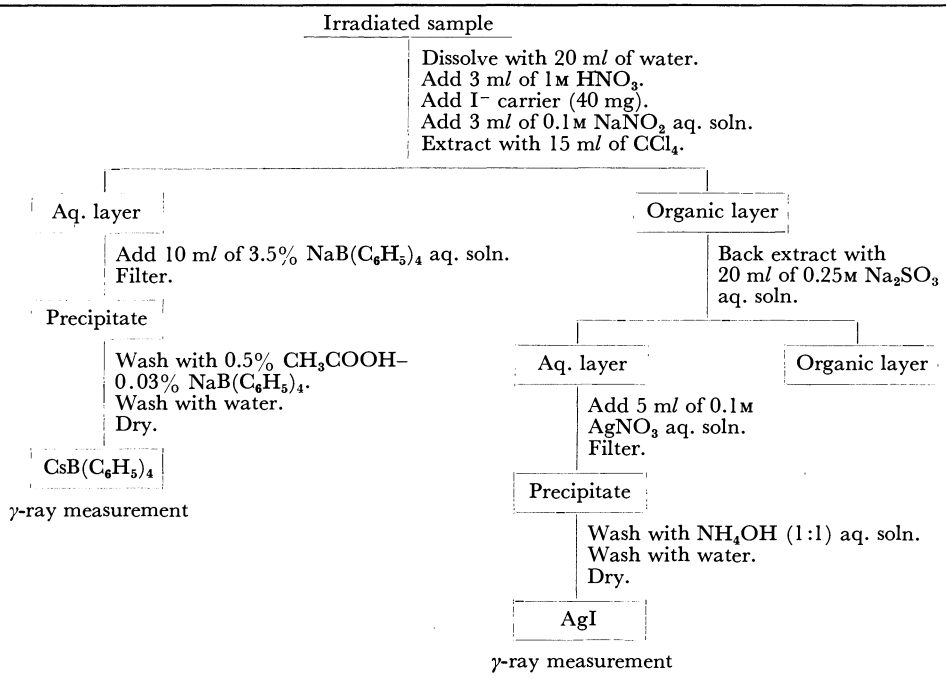

Experimental

Materials and Irradiation. Cesium chloride and potassium iodide of guaranteed reagent grades were used as the sample materials. A series of synthetic iodine-cesium mixtures with known weight ratios, ranging from 8.87×10^{-3} to 2.64×10^{-4}, were prepared by mixing these two kinds of compounds. Each sample, weighing about 500 mg, was placed in a quartz tube with an internal diameter of 6 mm, and was irradiated by bremsstrahlung with maximum energies up to 65 MeV. Irradiations were terminated after from 30 min to 2 hr. A linear electron accelerator of Tohoku University was used as the bremsstrahlung source. The electron beam was converted to bremsstrahlung photons by a platinum converter with a thickness of 3 mm. In the energy range from 40 to 65 MeV, the range used in this experiment, the average beam current was at least 100 μA, measured at the position of the converter using a current monitor. The pulse-repetition rate was 250 pps, with a pulse width of 3 μsec. During irradiation, the samples were located in a water-cooled sample holder on the bremsstrahlung-beam axis immediately behind the converter. To monitor the bremsstrahlung flux to which the samples were exposed, a thin sheet of gold was wrapped around each sample tube; this was irradiated together with the sample.

Radiochemical Separation. After irradiation, each sample was dissolved with water, and 40 mg of an iodine carrier were added; the sample was subjected to the radiochemical procedure diagrammed in Table 1.

After oxidation with sodium nitrite, the iodine was extracted with chloroform and then back-extracted with an aqueous solution of sodium sulfite. The iodide was precipitated as silver iodide, filtered, washed, and dried. After the removal of the radioiodine, cesium was precipitated as its tetraphenylborate from the aqueous layer, filtered, washed, and dried. The final precipitates were packed in thin aluminum foil for the determination of the chemical yield and for the measurement of the γ-ray spectra. The chemical yield of iodine was 70—75%.

Radioactivity Measurements. The γ-ray spectra were measured with a lithium-drifted germanium detector with a sensitive volume of 36 cm^3, coupled to a TMC 1024-channel pulse-height analyzer. A sample was measured at a fixed position, 9 mm from the active surface of the detector. The counting efficiencies of this detector had previously been determined as a function of the source distance and the γ-ray energy, by counting a series of calibrated sources of known activities. The counting system had a resolution of 4 keV for the 661.6 keV γ-line of ^{137}Cs.

Yield Determination. A photonuclear yield is defined as the rate of the production of a given radioactive nuclide per mole of the target nuclide when a standard amount of bremsstrahlung radiation with a given maximum energy has passed through the target during the irradiation period. In the present experiment, the initial decay rates of the various activities produced were determined from a decay curve analysis of the counting rate of the relevant photopeak area. The corresponding saturation rates were computed and normalized for the bremsstrahlung dose rate, which was measured in terms of the amount of ^{196}Au activity produced by the $^{197}Au(\gamma,n)^{196}Au$ reaction in gold foil irradiated together with the sample.

After correcting for chemical yields, counting efficiencies, branching ratios,[12] and the internal conversion

12) The decay schemes used were those listed in G. M. Lederer, J. M. Hollander and I. Perlman, "Table of Isotopes," Sixth Ed., John Wiley & Sons, New York (1967).

Table 2. Photonuclear reactions and nuclear characteristics of the product iodine nuclides[a)]

Parent nuclide	Reaction path	Threshold energy (MeV)	Product nuclide	Half-life of product	γ-Ray (MeV) (Branching ratio, %)
^{133}Cs	(γ,2p)	17.3	^{131}I	8.05 d	0.284(5.1), 0.364(85.6), 0.637(6.9), others
	(γ, pd) (γ, 2pn)	21.9 24.1	^{130}I	12.4 hr	0.419(35.0), 0.538(100), 0.743(87), 0.669(100), 1.15(13)
	(γ, αn), (γ, ^{3}He2n), (γ, 2dn), (γ, pd2n), (γ, 2p3n), (γ,dt),	11.2, 31.8, 35.0, 37.2, 39.5, 28.8	^{128}I[b)]	25 min	0.411(~13), 0.528, 0.743, others
	(γ, α3n), (γ, ^{3}He4n), (γ, 2d3n), (γ, pd4n), (γ, 2p5n), (γ, dt2n),	27.1, 47.7, 51.0, 53.2, 55.4, 44.7	^{126}I[b)]	13.0 d	0.386(34.2), 0.48(4.15), 0.667(29.3), 0.751(3.6), 0.870(0.85), 1.43 (3.6)
	(γ, α5n), (γ, dt4n), (γ, ^{3}He6n)	43.8, 61.4, 64.5	^{124}I[b)]	4.2 d	0.603(~61), 0.644(21), 0.722(17.9), 0.714(11), 1.298(0.385), 1.326(0.34), 1.692(13.8), others
	(γ,α6n)	51.4	^{123}I	13.3 hr	0.159(98.8), 0.430(4.56), others(weak)
^{127}I	(γ,n)	9.2	^{126}I[b)]	13.0 d	0.386(34.2), 0.48(4.15), 0.667(29.3), 0.7151(3.6), 0.870(0.85), 1.43(3.6)
	(γ,3n)	25.8	^{124}I[b)]	4.2 d	0.603(61), 0.644(21), 0.722(17.9), 0.714(11), 1.298(0.385), 1.326(0.34), 1.692(13.8), others
	(γ,4n)	33.2	^{123}I	13.3 hr	0.159(98.8), 0.430(4.56), others(weak)
	(γ,6n)	51.3	^{121}I[b)]	2.1 hr	0.212(90)
	(γ,7n)	61.3	^{120}I[b)]	1.3 hr	0.562(100)

a) The data for ^{125}I and ^{122}I are not included because the former nuclide emites only very weak γ-ray (35 keV, 100%) and the latter has a short half-life (3.5 min).
b) Positron emitter.

electrons,[13] the yields were expressed relative to that of the ^{133}Cs(γ,n)^{132}Cs processes, which was measured by means of the amount of the 0.667 MeV γ-ray (95.6%) of 6.5d-^{132}Cs.

Results and Discussion

Photonuclear Reaction. Although the yield is strongly dependent on the photon energy, and, although, hence, higher sensitivities can be expected with higher maximum electron energies, it should be noted that interferences due to the competitive nuclear reactions would also increase in such circumstances. In order to determine the most suitable conditions for the determination of iodine in iodine-cesium mixtures, therefore, the induced photonuclear reactions and their production rates were investigated by irradiating the two elements individually by bremsstrahlung with several different maximum energies, 40, 45, 60, and 65 MeV. The possible reactions leading to the production of radionuclides of the present importance in this energy region, as well as their nuclear characteristics, are summarized in Table 2. The *Q*-values of the reactions were calculated on the basis of the difference in mass between the target and the product nuclei.

The threshold energy considerations show that the excitation of a nucleus by photons with energies up to 65 MeV produces excited states of the compound nucleus which can emit up to seven nuclei, leading to the production of several activities. Iodine and cesium are both elements with a single-isotopic composition. This makes the assignment of reaction paths for the (γ,xn) processes easy. On the other

Table 3. Photopeak activities of iodine nuclides formed by ^{127}I (γ,xn) reaction with 45 MeV bremsstrahlung

Nuclide	γ-ray energy (MeV)	Photopeak activity[a)] (cpm/mg)	Limit of determination (μg)
^{126}I	0.386	5.20×10^4	0.2
	0.48	2.73×10^3	3.7
	0.751	2.47×10^3	4.0
	0.870	4.92×10^2	20
^{124}I	0.603	2.69×10^3	3.7
	0.722	3.45×10^2	29
^{123}I	0.159	1.79×10^4	0.6

a) At the end of 2 hr-irradiation with a dose rate of bremsstrahlung with which 0.60 μCi^{196}Au is produced by the (γ,n) process in 1 mg Au.

13) The tables in M. E. Rose, "Internal Conversion Coefficients," North-Holland Publ. Co., Amsterdam (1958), were used.

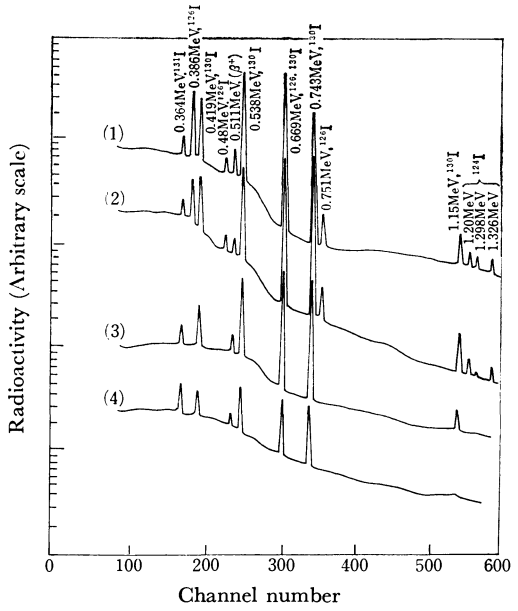

Fig. 1. γ-Ray spectra of iodine activities separated from cesium samples.
1) Irradiated with 65 MeV bremsstrahlung for 30 min; 13 hr after irradiation.
2) Irradiated with 60 MeV bremsstralung for 1 hr; 5.5 hr after irradiation.
3) Irradiated with 45 MeV bremsstrahlung for 1 hr; 9 hr after irradiation.
4) Irradiated with 40 MeV bremsstrahlung for 1 hr; 30 hr after irradiation.

hand, as Table 2 shows, all the iodine nuclides from ^{133}Cs except ^{131}I, can be formed through several different reaction paths.

When an iodine sample was irradiated by 45 MeV bremsstrahlung for a period of 2 hr, the production of ^{126}I, ^{124}I, and ^{123}I was recognized by means of their characteristic γ-rays in the γ-ray spectra. The areas under the photopeaks of the principal γ-rays from those nuclides are given in Table 3. The radioactivity strength of the 0.386 MeV γ-ray from ^{126}I produced by the (γ,n) reaction on ^{127}I was the highest over the energy range investigated; hence it provided the most sensitive method for the determination.

Figure 1 shows the γ-ray spectra of the iodine fractions separated from the cesium samples. It can be seen that ^{131}I, ^{130}I, and ^{126}I were produced at 60 MeV and at 65 MeV, but that the ^{126}I activities can not be detected in any appreciable amounts at excitation energies below 45 MeV. The data listed in Table 2 show that the only possible reaction leading to the production of ^{126}I from cesium at 45 MeV is the ^{133}Cs(γ,α3n)^{126}I reaction. The Coulomb barrier height for this reaction can be calculated as 14.5 MeV; this would restrict the emission of α-particles from an excited state of the cesium nucleus. The yields of the photonuclear reactions for the productions of those nuclides are shown in Table 4.

It should be noted that, with a maximum excitation energy of more than 60 MeV, the more deficient in neutron number the iodine nuclides are, the higher are their yields. This behavior has been emphasized in the previous photospallation work with bremsstrahlung photons up to 250 MeV.[14]

The Determination of Iodine. In the determination of iodine, irradiation were performed by

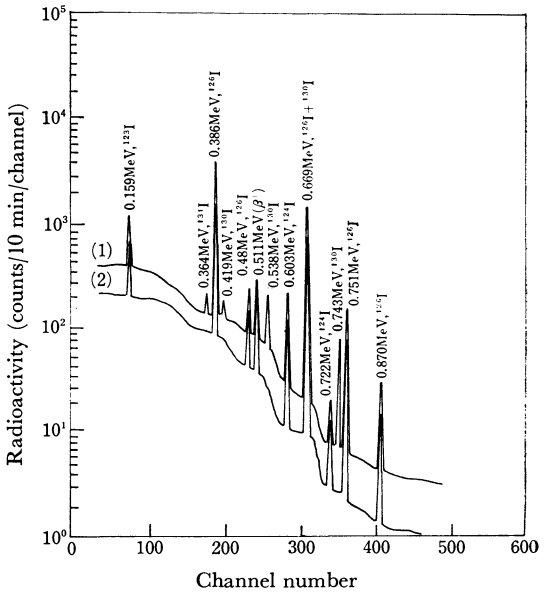

Fig. 2. γ-Ray spectra of radioiodine; (1) separated from an irradiated iodine-cesium mixture (I/Cs=2.64×10^{-4}), 7.5 hr after irradiation, and (2) of iodine sample.

Table 4. The yields of ^{133}Cs (γ, 2pxn) reactions as a function of bremsstrahlung maximum energy

Reaction	Yield relative to ^{133}Cs(γ,n))^{132}Cs			
	40 MeV	45 MeV	60 MeV	65 MeV
^{133}Cs(γ, 2p)^{131}I	7.20×10^{-7}	2.32×10^{-6}	1.27×10^{-5}	1.44×10^{-5}
^{133}Cs(γ,2pn)^{130}I	3.27×10^{-7}	1.87×10^{-6}	1.39×10^{-5}	1.61×10^{-5}
^{133}Cs(γ,2p5n)^{126}I	Not detected	Not detected	1.65×10^{-4}	2.48×10^{-4}

14) T. Kato, H-T. Tsai and Y. Oka, This Bulletin, **43**, 576 (1970).

TABLE 5. R_W *vs* R_{A_0} FOR IODINE-CESIUM MIXTURES

R_W	R_W/R_{A_0}						
	^{126}I				^{124}I		^{123}I
	0.386 MeV	0.48 MeV	0.751 MeV	0·870 MeV	0.603 MeV	0.722 MeV	0.159 MeV
8.87×10^{-3}	5.07×10^{-5}	1.00×10^{-3}	1.01×10^{-3}	5.31×10^{-3}	0.93×10^{-3}	0.74×10^{-2}	1.39×10^{-4}
3.47×10^{-3}	5.05×10^{-5}	0.94×10^{-3}	1.01×10^{-3}	5.52×10^{-3}	0.91×10^{-3}	0.73×10^{-2}	1.41×10^{-4}
1.82×10^{-3}	4.94×10^{-5}	0.95×10^{-3}	1.07×10^{-3}	5.48×10^{-3}	0.96×10^{-3}	0.79×10^{-2}	1.35×10^{-4}
5.25×10^{-4}	4.94×10^{-5}	0.94×10^{-3}	1.00×10^{-3}	5.45×10^{-3}	0.94×10^{-3}	0.71×10^{-2}	1.49×10^{-4}
2.64×10^{-4}	5.02×10^{-5}	0.94×10^{-3}	1.06×10^{-3}	5.98×10^{-3}	0.97×10^{-3}	0.76×10^{-2}	1.46×10^{-4}
Mean:	$5.0_0\times10^{-5}$	$0.9_6\times10^{-3}$	$1.0_3\times10^{-3}$	$5.5_5\times10^{-3}$	$0.9_4\times10^{-3}$	$0.7_5\times10^{-2}$	$1.4_2\times10^{-4}$
Std. dev.:	$\pm0.0_5\times10^{-5}$	$\pm0.0_2\times10^{-3}$	$\pm0.0_3\times10^{-3}$	$\pm0.2_3\times10^{-3}$	$\pm0.0_2\times10^{-3}$	$\pm0.0_3\times10^{-2}$	$\pm0.0_5\times10^{-4}$
	(±0.9%)	(±2.4%)	(±2.8%)	(±4.1%)	(±2.2%)	(±3.7%)	(±3.4%)

bremsstrahlung with a maximum energy of 45 MeV, and the photopeak activities due to ^{126}I, ^{124}I and ^{123}I were compared with the reference activity, ^{130}I, from cesium. The synthetic iodine-cesium mixtures were irradiated for a period of 2 hr. A typical γ-ray spectrum of the iodine fraction is shown in Fig. 2, together with that of the iodine sample. From the composite spectra obtained, the photopeak areas under the 0.386, 0.480, 0.751 and 0.870 MeV γ-rays from ^{126}I, the 0.603 and 0.772 MeV γ-rays from ^{124}I, and the 0.159 MeV γ-ray from ^{123}I were measured. Then the ratios of all of those activities to the photopeak area under the 0.538 MeV of ^{130}I were computed. All the activity data were corrected for decay to the end of irradiation. Table 5 shows the results, where the R_{A_0}'s represent the activity ratios and where the R_W's are the weight ratios, I/Cs. A good proportionality is given in each case between the R_{A_0}'s and the R_W's. A relative standard deviation of within ±4% was obtained in the weight-ratio range examined here. When the amount of iodine needed to give 100 cpm is defined as the limit of determination, the sensitivities of this method can be calculated to be as given in the last column of Table 3.

Under the present experimental conditions, amounts of iodine down to about 0.2 μg can be determined.

An increase in sensitivity may be expected with a higher bremsstrahlung dose rate and with a longer period of irradiation. A general applicability of this method will be found in the determination of the iodine content in samples to be analyzed when we add a proper amount of cesium as the internal-reference element.

Considerations were then given to the elements which would cause interferences in this method. The iodine nuclides can be produced by the (γ,pxn) reactions on xenon, *e. g.*, ^{129}Xe(γ,p2n)^{126}I, $-Q=$ 24.22 MeV. However, considering the abundance of xenon in samples ordinarily encountered, it may not appear to be a serious source of interference. The ^{130}Ba(γ,3pn)^{126}I ($-Q=29.36$ MeV) reaction is also a possible source of interference. However, the production rate of this reaction is low because of the small natural abundance of ^{130}Ba(0.101%) and because of the Coulomb barrier restriction inherent in this reaction. In the present case, the neutron reactions which arise from photoneutrons cause no serious problems.

In conclusion, the authors believe that the method presented here holds considerable promise for the accurate determination of iodine in samples of various origins.

BULLETIN OF THE CHEMICAL SOCIETY OF JAPAN VOL. 43 2487—2491 (1970)

A New Method of Preparing θ-Alumina and the Interpretation of Its X-Ray-powder Diffraction Pattern and Electron Diffraction Pattern

Goro YAMAGUCHI, Itaru YASUI and Wen-Chau CHIU

Department of Industrial Chemistry, Faculty of Engineering, The University of Tokyo, Hongo, Tokyo

(Received February 12, 1970)

Highly crystallized θ-alumina was obtained by a two-step treatment, by hydrothermal and thermal treatment, of γ-alumina. Its X-ray-powder diffraction pattern was interpreted based on the structure of β-gallia, and least-squares refinements were carried out. The electron diffraction pattern of θ-alumina from boehmite was also interpreted, and the directional relations between the phases were established.

The preparation of θ-alumina has been studied since θ-alumina was recognized as a transient alumina by Stumph *et al.*[1-3] As to the structure of θ-alumina, an attempt has been made to index the X-ray-powder diffraction peaks using a hexagonal cell, but the proper indices have not yet been given.[4]

On the other hand, β-gallia, the high-temperature form of gallias, was revealed to have an isostructure with θ-alumina.[5-7] The single crystal of β-gallia was prepared, and its structure analysis was carried out by X-ray diffraction.[8-10] The X-ray powder diffraction pattern of θ-alumina has, however, not been interpreted so precisely that the identification of pure θ-alumina is unperfect, this makes the studies of the alumina polymorphs unsure.

In the present study, a new method of preparation will be described, the X-ray-powder diffraction and the electron diffraction pattern will be interpreted, and a least-squares refinement of the structure will be reported.

Experimental

Preparation of θ-Alumina from γ-Alumina (The New Method). The method of preparing the γ-alumina used as the starting material of θ-alumina was as follows.[11] Alumina gel was prepared by the procedure

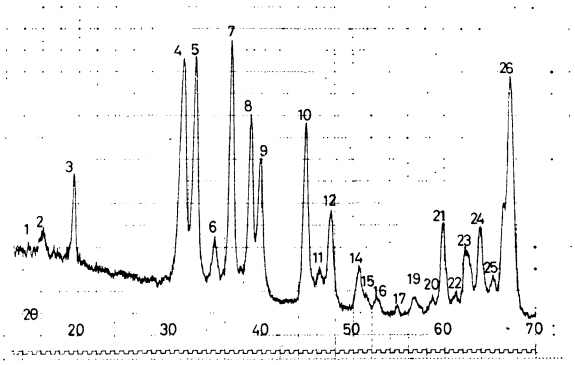

Fig. 1. X-Ray powder diffraction pattern of θ-alumina prepared by the new method.

1) H. C. Stumph, A. S. Russel, J. W. Newsome and C. M. Tucker, *Ind. Eng. Chem.*, **42**, 1393 (1950).
2) M. K. B. Day and V. J. Hill, *J. Phys. Chem.*, **57**, 946 (1953).
3) D. J. Stirland, A. G. Thomas and N. C. Moore, *Trans. Brit. Ceram. Soc.*, **57**, 69 (1958).
4) R. Tertian, *Compt. Rend*, **230**, 1677 (1950).
5) V. M. Goldschmidt, T. Barth and G. Lunde, *Mat. Naturv. Klasse*, **7**, 24 (1925).
6) L. M. Foster and H. C. Stumph, *J. Amer. Chem. Soc.*, **73**, 1590 (1951).
7) R. Roy, V. G. Hill and E. F. Osborn, *Ind. Eng. Chem.*, **45**, 819 (1953).
8) J. A. Kohn, G. Katz and J. D. Broder, *Amer. Miner.*, **42**, 398 (1957).
9) H. Saalfeld, *N. Jb. Miner. Abh.*, **95**, 1 (1960).
10) S. Geller, *J. Chem. Phys.*, **33**, 676 (1960).
11) G. Yamaguchi and W.-C. Chiu, This Bulletin, **41**, 348 (1968).

TABLE 1. PEAK NUMBER, INTENSITIES, *etc.*

Peak No.	*hkl*	*I* (obsd)	*I* (calcd)	*d* (obsd)	*d* (calcd)	sp. *HKL*	Mul.
1	200	1	1	5.7	5.7324		
2	001	9	9	5.45	5.4606		
3	20$\bar{1}$	17	15	4.535	4.5345		
4	400	80	81 (29, 48, 4)	2.837	2.8662		
	40$\bar{1}$				2.8330		
	100				2.8169		
5	20$\bar{2}$	64	67 (26, 41)	2.730	2.7327		
	002				2.7303		
6	11$\bar{1}$	14	12	2.566	2.5658		
7	111	62	60	2.444	2.4454	311	4
8	401	46	44 (33, 11)	2.315	2.3191		
	310				2.3132	222	4
9	40$\bar{2}$	37	41 (4, 5, 32)	2.257	2.2673	222	2
	202				2.2631	222	2
	31$\bar{1}$				2.2506		
10	311	45	40 (8, 32)	2.019	2.0268		
	11$\bar{2}$				2.0210	400	4
11	60$\bar{1}$	8	8	1.9544	1.9558		
12	600	30	32 (14, 12, 6)	1.9094	1.9108	400	2
	312				1.9068		
	112				1.9052		
13	20$\bar{3}$	0	0		1.8690		
14	003	14	15 (0, 0, 15)	1.7998	1.8202	331	2
	51$\bar{1}$				1.8142	331	4
	510				1.8001		
15	602	5	3 (1, 2)	1.7765	1.7788		
	402				1.7755		
16	40$\bar{3}$	4	4	1.7376	1.7376		
17	601	2	1	1.6807	1.6821		
18	51$\bar{2}$	0	0 (0, 0)		1.6527		
	312				1.6506		
19	203	5	4 (2, 2)	1.6216	1.6259		
	511				1.6212		
20	11$\bar{3}$	2	4	1.5715	1.5716		
21	313	23	23	1.5426	1.5436	511	4
22	603	5	5	1.5120	1.5115	333	2
23	113	26	29 (20, 9)	1.4883	1.4893		
	80$\bar{1}$				1.4759		
24	020	26	23 (23, 0)	1.4526	1.4530	440	2
	71$\bar{1}$				1.4570		
25	800	10	10 (1, 9, 0, 0, 0)	1.4264	1.4331		
	710				1.4268		
	51$\bar{3}$				1.4207		
	213				1.4189		
	802				1.4165		
26	602	100	100 (0, 0, 19, 2, 39, 39, 1)	1.3883	1.4142		
	220				1.4085		
	20$\bar{4}$				1.4062	440	2
	403				1.3927		
	71$\bar{2}$				1.3894	440	4
	512				1.3875	440	4
	22$\bar{1}$				1.3837		

through which an aluminum chloride of a 0.5-mol/*l* aqueous solution was neutralized with a 14% ammonia aqueous solution to pH 7.5; the gel thus precipitated was filtered out and rinsed. The gel was then aged in ethylenediamine, a 5% aqueous solution, for 3 days at 30—40°C, by which time it had crystallized into nordstrandite. This nordstrandite was then heated and dehydrated at 700°C in air for 1 hr; the η-alumina was thus obtained.

This η-alumina was treated hydrothermally at 500°C, under 150 atm, for 45 hr; quite well-crystallized θ-alumina was thus obtained. When this θ-alumina was heated again at 1000°C in air for 0.5 hr, it became highly well-crystallized θ-alumina.

Preparation of θ-Alumina from Boehmite. Well-crystallized boehmite was prepared from gibbsite by

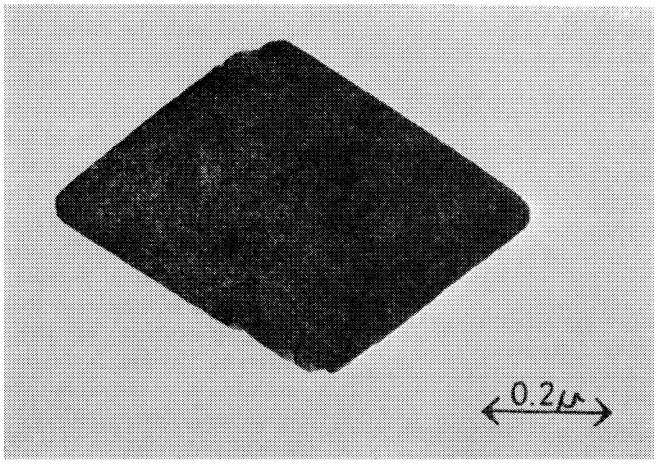

Fig. 2. Electron-micrograph of θ-alumina having the initial own shape of boehmite from well-crystallized boehmite.

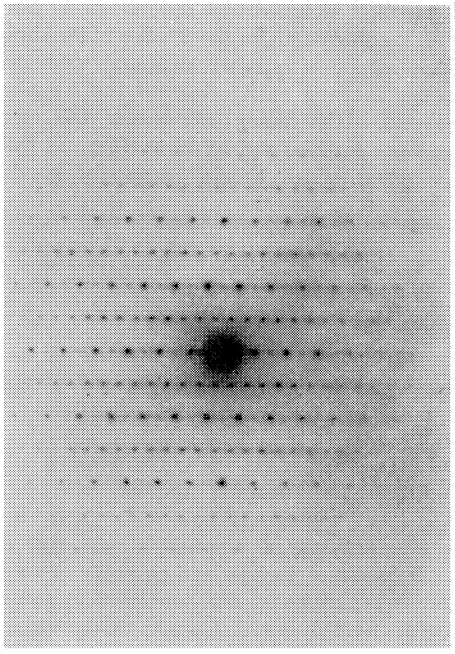

Fig. 3. Electron diffraction pattern of θ-alumina from well-crystallized boehmite.

hydrothermal treatment. This boehmite was heated at 1100°C in air for 2 hr, θ-alumina with the initial shape of boehmite was thus obtained.

X-Ray Powder Diffraction. The X-ray-powder diffraction pattern of θ-alumina from η-alumina was taken with a recording X-ray diffractometer, using Ni filtered Cu$K\alpha$ radiation, as is illustrated in Fig. 1. This pattern shows a fairly good crystallinity.

The numbers of the peaks and the relative intensities obtained from the areas of the peaks are given in the 1st and 3rd columns of Table 1 respectively.

Electron Diffraction. An electron-micrograph of θ-alumina with the shape of boehmite was taken, as is illustrated in Fig. 2. The electron-diffraction pattern of θ-alumina was also taken, as is illustrated in Fig. 3. In Fig. 2, the *a*-axis of boehmite lies in the direction of the short diagonal of the rhombus, the *b*-axis is parallel to the long diagonal, and the *c*-axis is parallel to the incident electron beam.

Results and Discussion

Analysis of the Lattice and Atomic Parameters and the Indexing of the Powder-diffraction Pattern. The programs for the calculation of the atomic and lattice parameters were written for the HITAC 5020E computer by the authors. On the basis of the structure of β-gallia,[10] the intensities were computed on the assumption that aluminum atoms occupy the positions of gallium atoms as substitutes. Moreover, the index of each peak and its overlapping state were confirmed, as is shown in Table 1.

The lattice parameters calculated by the least-squares method are given in Table 2.

Table 2. Lattice dimensions of θ-alumina

Monoclinic	$C_{2h}-C_{2/m}$
$a=$	11.813 ± 0.010Å
$b=$	2.906 ± 0.002Å
$c=$	5.625 ± 0.005Å
$\beta=$	$104.1\quad\pm0.1°$

The transformation matrix from the cubic lattice (*HKL*), that is, the lattice of spinel, to θ-alumina's monoclinic lattice (*hkl*) is given as follows:

$$\begin{pmatrix} h \\ k \\ l \end{pmatrix} = \begin{pmatrix} -1/4 & 1/4 & -3/2 \\ 1/4 & 1/4 & 0 \\ 1/2 & -1/2 & 0 \end{pmatrix} \begin{pmatrix} H \\ K \\ L \end{pmatrix}$$

The spinel indices corresponding to θ-alumina and their multiplicities are given in the 7th and 8th columns of Table 1.

TABLE 3. ATOMIC PARAMETERS AND THEIR STANDARD DEVIATIONS OF β-GALLIA

	x	z
Ga(1)	0.0904(2)	−0.2052(5)
Ga(2)	0.3414(2)	−0.3143(5)
O(1)	0.1674(19)	0.1011(41)
O(2)	0.4957(16)	0.2553(34)
O(3)	0.8279(15)	0.4365(34)

TABLE 4. ATOMIC PARAMETERS AND THEIR STANDARD DEVIATIONS OF θ-ALUMINA

	x	z
Al(1)	0.0843(19)	−0.2071(37)
Al(2)	0.3400(14)	−0.3168(33)
O(1)	0.1614(20)	0.1071(53)
O(2)	0.4980(19)	0.2602(35)
O(3)	0.8326(24)	0.4404(54)

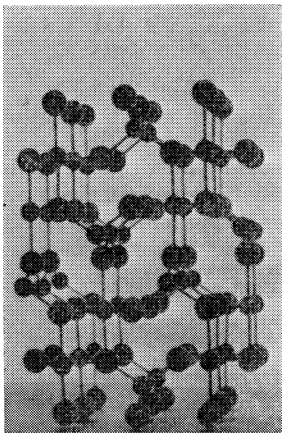

Fig. 4. Structure model of θ-alumina.
Large sphere: Oxygen
Small sphere: Aluminum

The least-squares refinement of the structure was executed with the initial value given in Table 3,[10] and the reliability factor was reduced from 0.17 to 0.08. The final coordinate, along with their estimated standard deviations, are given in Table 4, while the structure model is illustrated in Fig. 4.

This refinement reveals shifts of aluminum atoms from the ideal positions. The interatomic distances are given in Table 5. These interatomic distances show that the $Al(1)O_4$ tetrahedron is more distorted than that of β-gallia, but that the $Al(2)O_6$ octahedron is similar to that of β-gallia.

Interpretation of the Electron-diffraction Pattern. In Fig. 5, (a) is the shape of boehmite and (b) is a spinel lattice of the corresponding θ-alumina. Accordingly, in the electron-diffraction pattern of θ-alumina (Fig. 3), the horizontal direction corresponds to the c-axis of the spinel lattice of Fig. 5(b). This direction corresponds to one of the three diagonal directions of oxygen octahedrons in cubic closest packing of θ-alumina; it can thus be concluded that the horizontal direction in Fig. 2 corresponds to the a^*-axis of θ-alumina or to one of the two other diagonal axes perpendicularly crossing each other on the b-c plane of θ-alumina. Of these three cases, the electron-diffraction pattern clearly shows (Fig. 3) that the horizontal direction should correspond to the a^*-

TABLE 5. INTERATOMIC DISTANCES AND STANDARD DEVIATIONS

Atomic pair	Distance Å	σ Å
Tetrahedron		
Al(1)-O(1)	1.78	0.03
Al(1)-O(2)	1.73	0.02
Al(1)-O(3)	1.82	0.04
Octahedron		
Al(2)-O(1)	1.87	0.02
Al(2)-O(2)	1.86	0.03
Al(2)-O(3)	1.99	0.03
Al(2)-O(3)$_{II}$	1.98	0.02

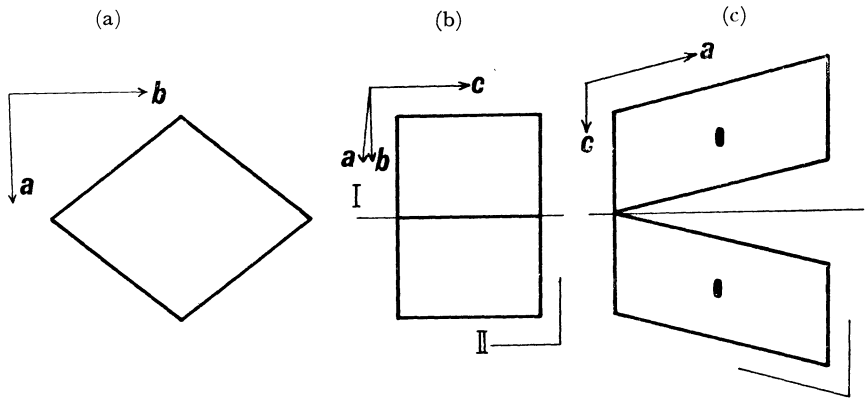

Fig. 5. Shape of θ-alumina from boehmite and lattices of spinel and θ-alumina with mirror planes.

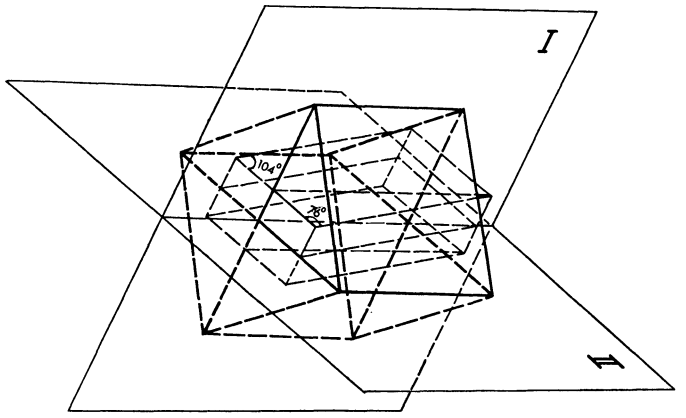

Fig. 6. Perspective drawing of the lattice of spinel with that of θ-alumina.

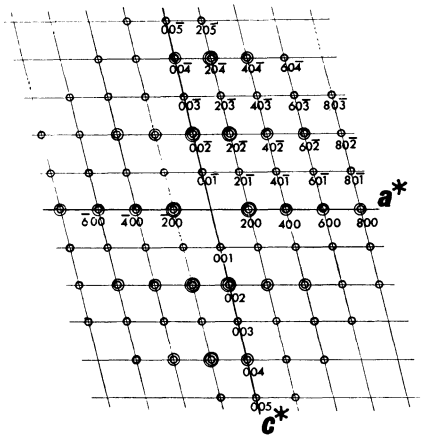

(a)

Fig. 7(a). Indices of electron diffraction pattern of θ-alumina from boehmite.

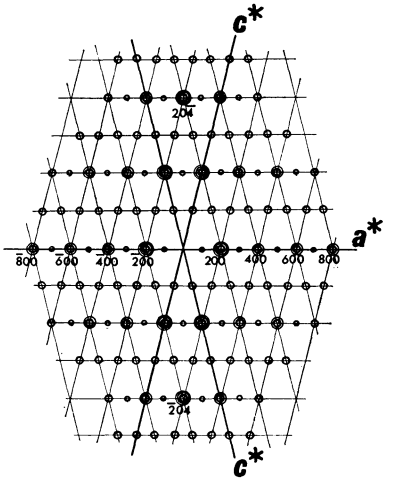

(b)

Fig. 7(b). Indices with the assumption of the twinning structure or the twinning like aggregate.

axis of θ-alumina, in view of the possible reflections of $h0l$. This relation is shown in Fig. 5(c) and Fig. 6.

In this case, θ-alumina has a twinning structure or a twinning-like aggregate structure. The twinning phenomenon can be explained as follows: there are mirror planes parallel to the (110) planes in the spinel lattice, as is shown in Fig. 6, and two mirror planes, I and II, perpendicularly crossing each other are to be considered. The other (110) plane need not be considered, because it is not a mirror planes in γ-alumina through which θ-alumina is formed from boehmite. If one of the two mirror plane, plane II, is conserved as a mirror plane in the θ-alumina ($C_{2h}C_{2/m}$) lattice, the other, plane I, can not become a mirror plane, but it can possibly become a twinning plane. On the assumption of this twinning structure, the reciprocal lattice of θ-alumina is illustrated in Fig. 7(b). This figure is in good agreement with the observed electron-diffraction pattern. Figure 7(a) represents the indices of θ-alumina without a twinning structure. The reason why the two planes do not alternate must be investigated in the future.

In the electron-diffraction pattern, weak spots are observed; they are shown in Fig. 3 and are expressed by the smallest circles in Fig. 7(b). These spots show the distortion of the crystal structure from $C_{2/m}$, but the X-ray-powder diffraction does not show any evidence for this distortion. Therefore, it can be said that the true space group is distorted from $C_{2/m}$, but that the atomic arrangement of the structure analyzed above with $C_{2/m}$ is almost true.

All the calculations were performed with a computer of the Computation Center of Tokyo University.

BULLETIN OF THE CHEMICAL SOCIETY OF JAPAN VOL. 43 2492—2494 (1970)

Complexes Coordinated by 2,2′-Bipyridine Negative Ion. I. Synthesis of Sodium 2,2′-Bipyridinetetracarbonylchromium

Youkoh KAIZU and Hiroshi KOBAYASHI

Department of Chemistry, Tokyo Institute of Technology, Ookayama, Meguro-ku, Tokyo

(Received March 10, 1970)

Bipyridinetetracarbonylchromium was reduced by sodium metal in tetrahydrofuran. The first stage product of the reduction which showed a spectrum similar to that of sodium bipyridine (Na^+bipy^-) was isolated. The complex was identified as $Na[Cr(CO)_4bipy]$ by elementary analysis. On the basis of the electronic absorption spectrum and the electron spin resonance, the complex formed in the reduction was concluded to be complex coordinated by mononegative ion of bipyridine and should be named sodium 2,2′-bipyridine(1−)-tetracarbonylchromium(0).

An electronic configuration of the rare gas is required for the central metal atom in a stable compound of a transition metal in the lower oxidation state. Sidgwick's rule states that no open-shell exists in a stable compound. This rule has been found to be satisfied in various systems including organic and organometallic species. In the higher oxidation state, however, the transition metal ions with open *d* electron shell can exist in various stable coordination complexes. Even in an essentially ionic complex charge delocalization effect is crucial in coordination binding. However, the unpaired electron existing in the complex has been detected mainly on the central metal orbitals by physical measurements such as ESR.

For the past decade, tris-bipyridine complexes in the lower oxidation states have been prepared[1] and their electronic structures have been studied.[2-4] These compounds, even if in the lower oxidation states, can exist with open shell electronic configurations.[1] Monomeric tris-bipyridine complexes of the lower oxidation states are stabilized partly by chelate effect and partly by back-donation due to a higher π acceptability of the coordinating bipyridine. Migration of $d\pi$ electron into the antibonding π molecular orbital of the coordinating bipyridine makes the central metal more positive and therefore more σ-acceptable.

Some monomeric metal carbonyls of open shell electronic configuration have recently been succesfully prepared. An open shell metal carbonyl $[V(CO)_6]$ was obtained by oxidation of a closed shell metal carbonyl, $[V(CO)_6]^-$.[5] Oxidation or reduction of closed shell metal carbonyl is expected to give an open shell structure. However, in many cases it forms a dimer with carbonyl groups bridging or with metal-metal bonds.

In this paper, we present the synthesis of a new type of metal carbonyl with coordinating negative ion of 2,2′-bipyridine.

Experimental

Materials. 2,2′-Bipyridine (bipy) and its 4,4′-dimethyl (4dmbip) and 5,5′-dimethyl (5dmbip) derivatives were synthesized by the method of Sasse and Whittle.[6] Hexacarbonylchromium $Cr(CO)_6$ was of reagent grade (Strem Chemical Incorporated, Mass. U.S.A.) and was used without further purification. All other reagents and solvents were commercially available. Tetrahydrofuran (THF) used for solvent was purified by careful distillation over cuprous acetate, and a trace of water was removed by $LiAlH_4$.

Preparation of Compounds. $Cr(CO)_4bipy$ was prepared by the method of Stiddard.[7] Dimethyl substituted bipyridine complexes also were prepared by the same method. $Cr(CO)_4$4dmbip: Hexacarbonylchromium (1.1 g) and 4dmbip (0.95 g) were refluxed in toluene (50 ml) for 2 hr under oxygen-free, dry nitrogen atmosphere. Unreacted hexacarbonylchromium sublimed from the reaction vessel into the reflux condensers in the course of reaction. After cooling, deep reddish orange crystals (0.5 g) were collected, washed with light petroleum (60 ml) and dried *in vacuo*. The yields were not so high since hexacarbonylchromium sublimed during the reaction.

1) S. Herzog and R. Taube, *Z. Anorg. Allgem. Chem.*, **306**, 160 (1960).
2) E. König, *Z. Naturforsch.*, **19a**, 1139 (1964).
3) C. Mahon and W. L. Reynolds, *Inorg. Chem.*, **6**, 1927 (1967).
4) Y. Kaizu, T. Yazaki, Y. Torii and H. Kobayashi, This Bulletin, **43**, 2068 (1970).
5) R. L. Pruett and J. E. Wyman, *Chem. Ind.* (London), **1960**, 119; F. Calderazzo, R. Cini and R. Ercoli, *ibid.*, **1960**, 500, 934.
6) W. H. F. Sasse, *J. Chem. Soc.*, **1956**, 618; W. H. F. Sasse and C. P. Whittle, *ibid.*, **1961**, 1347.
7) M. H. B. Stiddard, *ibid.*, **1962**, 4712.

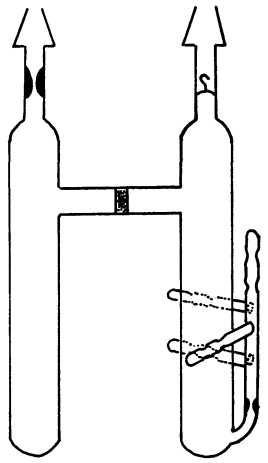

Fig. 1. Apparatus for reduction.

$Cr(CO)_4$bipy Found: Cr, 16.5%. Calcd for $Cr(CO)_4$bipy: Cr, 16.2%.

$Cr(CO)_4$4dmbip Found: Cr, 15.1%. Calcd for $Cr(CO)_4$4dmbip: Cr, 14.9%.

$Cr(CO)_4$5dmbip Found: Cr, 14.9%. Calcd for $Cr(CO)_4$5dmbip: Cr, 14.9%.

Reductions of $Cr(CO)_4L$. $Na[Cr(CO)_4L]$, where L is bipy, 4dmbip or 5dmbip, was prepared by reduction with sodium metal in the apparatus shown in Fig. 1 in a high vacuum using the method described in a previous paper.[8] $Na[Cr(CO)_4$4dmbip]: A mixture of $Cr(CO)_4$4dmbipy and a little excess amount of sodium metal in 15 m*l* of dried THF was shaken for 10 hr. After the solution was filtrated, the solvent was removed by distillation into a liquid-nitrogen cooling trap jointed to the vacuum system, the product was collected and dried *in vacuo*.

$Na[Cr(CO)_4$bipy] Found: Cr, 15.4%. Calcd for $Na[Cr(CO)_4$bipy]: Cr, 15.2%.

$Na[Cr(CO)_4$4dmbip] Found: Cr, 13.9%. Calcd for $Na[Cr(CO)_4$4dmbip]: Cr, 14.0%.

$Na[Cr(CO)_4$5dmbip] Found: Cr, 14.4%. Calcd for $Na[Cr(CO)_4$5dmbip]: Cr, 14.0%.

Electronic Absorption Spectra. Measurements of the electronic absorption spectra of air-sensitive compounds were described in a previous paper.[8] Spectra were measured using a Shimadzu automatic recording spectrophotometer Model MPS-50.

Electron Spin Resonance. ESR spectra were measured in THF solution at room temperature using a Japan Electron Optics Laboratory spectrometer Model JES-3BSX. The *g*-value was determined by the aid of the standard sample of Mn^{2+} ion.

Results and Discussion

Until quite recently no electronic absorption and electron spin resonance (ESR) studies had been carried out on complexes such as $[Al(bipy)_3]$, $[Mn(bipy)_3]$[4] or $Na[Fe(bipy)_3]$.[3] However, it has been recognized since a few years ago that the complexes, at least, $[Al(bipy)_3]$ should consist of a metal cation and bipyridine negative ions.[9] The low-valent tris-bipyridine complexes show a spectrum similar to that of bipyridine negative ion and an ESR spectrum of the free electron *g*-value (2.003).[4,10] The tris-bipyridine complexes are concluded to consist of bipyridine negative ions and a metal cation.

When zero-valent bipyridinetetracarbonylchromium was reduced by sodium metal in THF, the absorption spectrum of the solution changed stepwise and showed that there were two or more stages in the reduction. To obtain a complex coordinated by bipyridine negative ion, we tried to isolate a complex formed at the first stage of reduction.

The electronic absorption spectra of the bipyridine complexes isolated in this work are shown in Fig. 2. In such a low oxidation state, an extra electron donated by a reducing reagents in the preparation should be delocalized over the whole complex. However, partial localization of the trapped electron in some part of the complex has been reported.[4] The electronic absorption spectra, at least, of tris-bipyridine complexes have been reported to give a criterion on the major location of the trapped electron.[4] When the trapped electron is mainly localized on the coordinating bipyridine, it does not show charge transfer bands characteristic to the electron trapping by the central metal but a spectrum similar to that of the bipyridine negative ion. As shown in Fig. 2, the

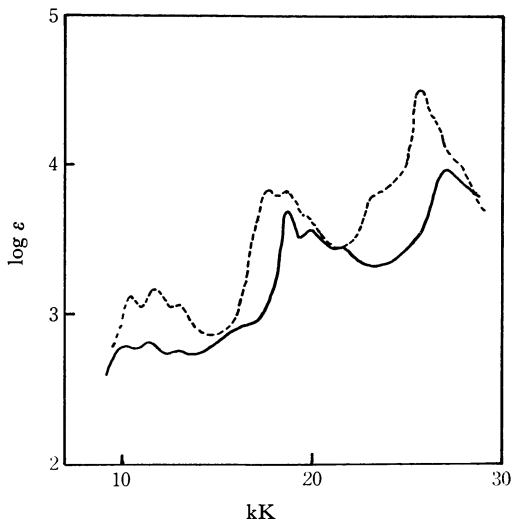

Fig. 2. Electronic absorption spectra in THF.
——: $Na[Cr(CO)_4$bipy], ----: Na bipy

8) Y. Torii, T. Yazaki, Y. Kaizu, M. Murasato and H. Kobayashi, This Bulletin, **42**, 2290 (1969).

9) L. E. Orgel "An Introduction To Transition-Metal Chemistry," Second Ed., Methuen Co. Ltd., London (1966), p. 150; C. K. Jørgensen "Inorganic Complexes" Academic Press, London (1963), p. 75.

10) Y. Torii, M. Murasato and Y. Kaizu, *Nippon Kagaku Zasshi*, **91**, 549 (1970).

complex reported here gave a spectrum similar to that of the mononegative ion of bipyridine in Na bipy. However, they did not coincide in details. The exact position of the absorption peak at about 19000 cm^{-1} of the complex was slightly shifted to the higher wavenumber. This tendency was observed for the other two complexes, $Na[Cr(CO)_4$-4dmbip] and $Na[Cr(CO)_4$5dmbip], and also in the case of zero-valent tris-bipyridine aluminum complex.[10] For such a small perturbation as introduced by two methyl groups, the absorption peak at about 19000 cm^{-1} of the bipyridine negative ion was blue-shifted in the order 5dmbip, 4dmbip and bipy.[8] When the extra electron was trapped by the central metal, the metal-ligand charge transfer bands found in the visible region showed a quite different behavior for the methyl substitutions. The absorption peaks at about 19000 cm^{-1} of $Na[Cr(CO)_4$-5dmbip], $Na[Cr(CO)_4$4dmbip] and $Na[Cr(CO)_4$-bipy] show the negative ion type of spectral shift. These findings on the electronic absorption spectra suggest that the bipyridine attached to the central chromium is not a neutral molecule but a negative ion. The ESR spectrum of $Na[Cr(CO)_4$bipy] in Fig. 3 gives a g-value close to that of a free electron

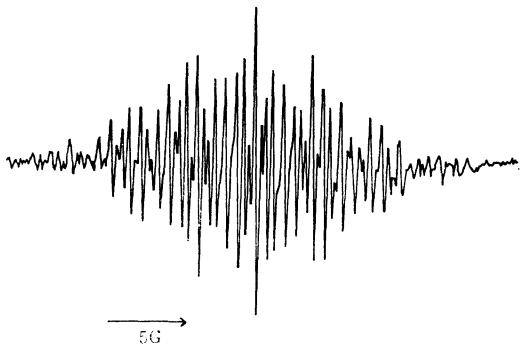

Fig. 3. The ESR spectrum of $Na[Cr(CO)_4$bipy] in THF at room temperature.

(g=2.0025) and a well-dispersed hyperfine structure. The hyperfine constants in the coordinating bipyridine negative ion were not so different from those of K bipy, even if the negative ion was strongly attached to the central chromium. In the case of K bipy, the binding between K^+ and $bipy^-$ is essentially ionic and the trapped electron in $bipy^-$ has a very poor population on K^+. As a matter of fact, the ESR spectrum of K bipy does not show the hyperfine structure due to the nuclear spin of potassium ion.[11] The ESR spectrum of Na bipy clearly shows the hyperfine structure due to the nuclear spin of sodium ion,[11] whereas in the case of $Na[Cr(CO)_4$bipy], it does not show any hyperfine structure due to either sodium or chromium. This is explained by the fact that an unpaired electron in an antibonding π orbital of bipyridine can not strongly interact with the closed shell $d\pi$ electron of the chromium and does not migrate over the outer sodium ion.

All of the complexes reported here are extremely soluble in polar organic solvents such as THF. They are very sensitive to oxygen and moisture in the air and are readily oxidized to the corresponding zero-valent complexes.

These observations and chemical analyses give sufficient evidence to conclude that the complexes synthesized in this work are the kind coordinated by bipyridine negative ion.

The sum of the numbers of the valence electrons in the central chromium and the σ electrons contributed by the ligands is the number of electrons in Kr atom. The paramagnetic character of the complex $Na[Cr(CO)_4$bipy] was identified by ESR, though, it still satisfies Sidgwick's rule as mentioned above. Since the complex is made of zero-valent chromium atom, four carbon monoxides and a bipyridine negative ion, the compound should be named sodium 2,2′-bipyridine(1−)tetracarbonyl-chromium(0).

The authors are indebted to Professor M. Nakahara, St. Paul's University for his advice concerning nomenclature.

11) E. König and H. Fischer, *Z. Naturforsch.*, **17a**, 1063 (1962); J. S. Veiga, W. L. Reynolds and J. R. Bolton, *J. Chem. Phys.*, **44**, 2214 (1966).

BULLETIN OF THE CHEMICAL SOCIETY OF JAPAN VOL. 43 2495—2500 (1970)

Alkoxysilanes. V. The Preparation of Polyalkyl(aryl) Silicates

Yoshimoto ABE, Takeo TAKEUCHI and Ichiro KIJIMA

Department of Industrial Chemistry, Faculty of Engimeering, Science University of Tokyo, Kagurazaka, Shinjuku-ku, Tokyo

(Received March 18, 1969)

Silicon-containing novel polymers, polyalkyl(aryl) silicates $(-\overset{\overset{OR}{|}}{\underset{\underset{OR}{|}}{Si}}-O-R'-O-)_n$ (R=Bu^t and $(Bu^tO)_3Si$, R'=$-(CH_2)_{2 \text{ or } 4}-$, $-C_6H_4-$ or $-C_6H_4-\overset{\overset{Me}{|}}{\underset{\underset{Me}{|}}{C}}-C_6H_4-$), were prepared by the reaction of diaminosilanes with aliphatic or aromatic diols. The products were a white powder (fused at about 300°C), a highly viscous liquid, or a glassy solid; these products were soluble in common organic solvents, but insoluble in methanol. The results of the molecular-weight determination by the vapour-pressure method indicated that some of polymers had a molecular weight of 5000 or 6000. A study of the thermal stability of the polymers by means of TGA and DTA analysis made clear that the polymers with the aryloxy group in the molecular main chain were remarkably more stable than those with the alkoxy group. The former indicated a weight loss of about 50% at 350—400°C. An investigation of the TGA curve and thermal decomposition products allowed us to discuss the probable process for the degradation of the polymers. The reaction of the diaminosilanes with 1,4-butanediol afforded distillable products rather than the expected polymers; these products were identified as being cyclic alkoxysilanes.

In order to obtain thermally-stable polymers, many experiments[1] have been carried out concerning the preparation of polymers containing metal atoms. Although it is well-known that polyalkylsiloxanes have a superior thermal stability, they are also pyrolyzed at temperatures higher than 300°C to form ring compounds of a low molecular weight. Therefore, an attempt has been made to prevent the degradation and to increase the thermal stability by replacing the side[2] and main[3] chain of the polysiloxane by other groups or metals. Recently, Dunnavant[4] has synsesized polyaryloxysilanes with aryloxy groups in the main chain and the phenyl group in the side chain; his polyaryloxysilanes have excellent thermal and mechanical properties.

Polyalkyl(aryl) silicate $(-\overset{\overset{OR}{|}}{\underset{\underset{OR}{|}}{Si}}-O-R'-O-)_n$, however, has not been prepared; in it both the main and side chain are replaced by an alkoxy or aryloxy group. Probably, the reason is that the alkoxysilanes $(RO)_nSiX_{4-n}$ (n=2 and 1) have various functional groups and their reactivities have not yet been investigated. Since we have already reported on our study of the preparation and reaction of alkoxysilanes containing functional groups,[5,6] in this experiment we tried to prepare polyalkyl(aryl) silicates and to investigate their thermal stability.

Experimental

Material. The di-*t*-butoxydiaminosilane[7] and bis(tri-*t*-butoxysiloxy)diaminosilane[6] were prepared by the reaction of the corresponding dichlorosilanes with dry ammonia gas. The ethylene glycol and 1,4-butanediol were purified by distillation after having been dehydrated over anhydrous sodium sulfate. The hydroquinone and bisphenol A were recrystallized from methanol and benzene respectively.

1) D. N. Hunter, "Inorganic Polymers," John Wiley & Sons, New York (1963); V. V. Korshak, "Progress of Polymer Chemistry," Izdatelystovo Nauka, Moskva (1965), p. 323.

2) S. M. Atlas and H. F. Mark, *Angew. Chem.*, **72**, 249 (1960).

3) C. M. Murphy, C. E. Saunder and D. C. Smith, *Ind. Eng. Chem.*, **42**, 246 (1950).

4) W. R. Dunnavant, R. A. Markle and P. B. Stickney, *J. Polym. Sci., Part A-1*, **5**, 707 (1967).

5) Y. Abe and I. Kijima, This Bulletin, **42**, 1118 (1969).

6) Y. Abe and I. Kijima, *ibid.*, **42**, 2570 (1969).

7) C. S. Miner, L. A. Bryan, R. P. Holysz and G. W. Pedlow, *Ind. Eng. Chem.*, **39**, 1368(1947).

Polymerization and Measurement of the Reaction Rate. To a solution of diols dissolved into dry ethyl ether or benzene, diaminosilanes were added. After the solvent (ether) had been removed off along with stirring and the introduction of dry nitrogen gas, the residue was polymerized under the conditions shown in Tables 1 and 2. When the benzene was used as a solvent, the mixture was refluxed under the boiling point of the solvent. When the reaction was carried out without a solvent, the mixture was heated at the temperatures shown in Tables 1 and 2. The raw product (a highly viscous liquid or a glassy solid) thus formed was dissolved into benzene, and filtered off; the filtrate was then added, drop by drop, into vigorously stirred methanol. The precipitate was separated by decantation and dried *in vacuo*. When a white precipitate was produced from the reaction mixture, it was filtered off, extracted with benzene, and dried *in vacuo*.

The polymerization rate in the reaction of the diaminosilanes with hydroquinone or bisphenol A was determined by introducing ammonia evolved under the following conditions into a sulfuric acid solution: a mixed solution was heated up to 70°C for 30 min, and then the ether was removed. When the temperature rose to 70°C during the next 30 min, the residue was further heated for 170—180°C. The results are shown in Fig. 1.

The Reaction of Di-*t*-butoxydiaminosilane with 1,4-Butanediol. A mixture of 21.8 g (0.1055 mol) of the diaminosilane, 9.5 g (0.1055 mol) of 1,4-butanediol, and 50 m*l* of benzene was refluxed with stirring. After 3.5 hrs' heating (45%, ammonia evolved), the solvent was evaporated off; the residue was then further heated for 7.5 hr at 150—160°C (80.4%, ammonia evolved). The distillation of the residue *in vacuo* gave 11.0 g of a distillate (bp 115°C/21 mmHg) and 17.3 g of a brown, highly viscous liquid. The redistillation of the distillate yielded 7.5 g of a colorless, transparent liquid. The results of elemental analysis, the measurement of the NMR spectra, and the yield are shown in Table 3.

The Reaction of Bis(tri-*t*-butoxysiloxy)diaminosilane with 1,4-Butanediol. A mixture of 11.0 g (0.0188 mol) of the diaminosilane, 1.7 g (0.0188 mol) of 1,4-butanediol, and 30 m*l* of toluene was heated while being stirred. The mixture was refluxed for 6.5 hr (93%, ammonia evolved), and the solvent was removed off. Then the residue was distilled *in vacuo* to give 8.3 g of a solid; 160—161°C/1 mmHg. The solid was recrystallized with petroleum ether with a boilling point below 45°C, giving a needle crystal. The results are shown in Table 3.

Thermal Decomposition of the Polymer

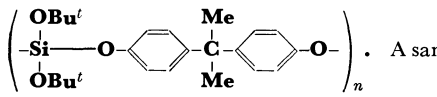

. A sample (9.1 g) was decomposed at 290—300°C *in vacuo* to form a gas, which was trapped into a vessel cooled by dry ice-acetone. The weight loss of the polymer was 2.1 g (23%). The residue (T-1), insoluble in solvents, was finely powdered, extracted with benzene, and subjected to elemental analysis (Found: C, 54.39; H, 5.08; Si, 9.48%) and IR-spectra measurements (Fig. 6). The gas, becaming a liquid under the cooling, was absorbed into a carbon tetrachloride-bromine solution. The solution was washed, dehydrated over anhydrous calcium chloride, and subjected to gas chromatography.

The T-1 (7.0 g) was further pyrolyzed at 480°C *in vacuo* to form a volatile liquid and a solid. To the mixture, carbon tetrachloride was added. Then the solid was filtered off and recrystallized with the solvent to give a crystal; mp 151—152°C (bisphenol A). The filtrate, having a phenolic odor and showing a positive color test for ferric chloride, was brominated to give a precipitate, which was then recrystallized with an aqueous alcohol, mp 91—93°C (tribromophenol). The weight loss of T-1 was 2.9 g (55%, total weight loss in relation to the initial polymer). The residue which remained was subjected to elemental analysis (Found: C, 41.60; H, 3.92; Si, 15.87%) and IR-spectra measurements (Fig. 6) after it had been treated as has been described above.

Results and Discussion

Preparation of Polyalkyl(aryl) Silicates. Polyalkyl(aryl) silicates were obtained by the following reactions:

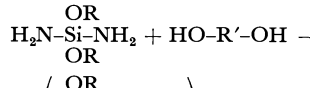

where R=Bu^t and (Bu^t O)$_3$Si, R'=-(CH$_2$)$_2$-, -(CH$_2$)$_4$-,

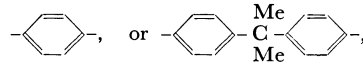

At first, the reactivity of the diols to the diaminosilanes was investigated by measuring the ammonia evolved by the reaction of the diaminosilanes with hydroquinone or bisphenol A under definite conditions. The results are shown in Fig. 1. Figure 1 indicates that the reactions are completed within about 3 hr (90%, ammonia evolved); thus, it is clear that the polymerization proceeds easily. This figure also suggests that di-*t*-butoxydiaminosilane reacts more easily with hydroquinone or bisphenol

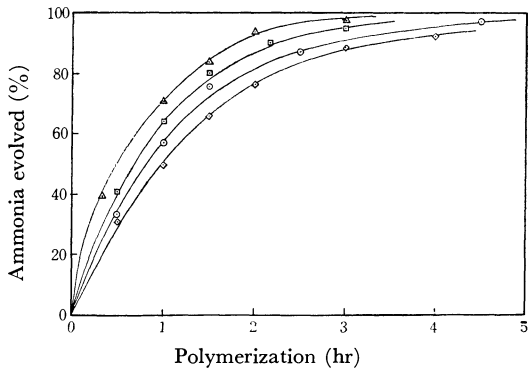

Fig. 1. The rate in the reaction of diaminosilanes with hydroquinone or bisphenol A.
△: c, ▣: d, ◉: C, ◇: D

Table 1. Reaction conditions and products in the reaction of $(Bu^tO)_2Si(NH_2)_2$ with HO-R'-OH

Exp. No.	R'	Reaction Condition			Product			
		Reaction Temp., °C	Reaction Time, hr	Solvent	Mp, °C	Anal., Found (Calcd) % C	H	Si
a-1	$-(CH_2)_2-$	70—80	2.5	Benzene	300	21.24 (51.25)	6.34 (9.46)	23.44 (11.19)
b-1	$-(CH_2)_4-$	70—80	3.5	Benzene	Liq	53.32 (54.92)	10.75 (9.99)	10.52 (10.70)
b-2	$-(CH_2)_4-$	184—208	4.5	—	Liq	54.09 (54.92)	10.80 (9.99)	— (10.70)
c-1	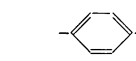	136—204	3.5	Ether	79–84	58.29 (59.54)	8.48 (7.85)	9.71 (9.96)
d-1	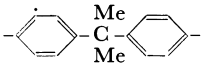	120—160	2.5	Ether	68–75	67.81 (68.96)	8.51 (8.06)	6.98 (7.01)

Molar ratio=1:1, Liq=liquid

Table 2. Reaction conditions and products in the reaction of $[(Bu^tO)_3SiO)]_2Si(NH_2)_2$ with HO-R'-OH

Exp. No.	R'	Reaction Condition			Product			
		Reaction Temp., °C	Reaction Time, hr	Solvent	Mp, °C	Anal., Found (Calcd) % C	H	Si
A-1	$-(CH_2)_2-$	81–83	6.0	Benzene	300	50.60 (50.80)	10.29 (9.50)	13.72 (13.70)
A-2	$-(CH_2)_2-$	100–199	1.5	—	300	— (50.80)	— (9.50)	13.75 (13.70)
A-3	$-(CH_2)_2-$	80–84	2.0	Benzene	160–170	50.92 (50.80)	10.59 (9.50)	13.26 (13.70)
B-1	$-(CH_2)_4-$	150–231	4.5	—	125–135	52.02 (52.30)	10.39 (9.71)	12.80 (13.10)
C-1	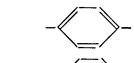	200–260	4.0	Ether	Liq	53.36 (54.35)	9.50 (8.82)	12.57 (12.71)
C-2	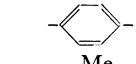	250–285	1.5	Ether	56–63	49.54 (54.35)	7.75 (8.82)	12.58 (12.71)
D-1	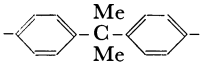	165–194	4.0	Ether	53–56	60.42 (59.96)	9.01 (8.77)	10.05 (10.78)

Molar ratio 1:1 or 1 : 2 diol (A-3)

A than with bis(tri-*t*-butoxysiloxy)diaminosilane. This results from the smaller steric hindrance of the *t*-butoxy group than that of the tri-*t*-butoxysiloxy group. Further, in comparison with bisphenol A, hydroquinone is more reactive to di-*t*-butoxydiaminosilane (or bis(tri-*t*-butoxysiloxy)diaminosilane). This may be explained by the stronger acidity of hydroquinone than that of bisphenol A.

On the basis of the above results, polymerization was attempted; it gave the polymers shown in Tables 1 and 2. The products were a white powder (A-1, 2, 3; B-1; a-1; c-1), a highly viscous liquid (b-1,2; C-1), and a glassy solid (C-2; d-1; D-1); some of them (c, C, d, and D) form fiber when fused at elevated temperatures. The a-1, A-3, and B-2 polymers are soluble in hot benzene, but A-1 and 2 are insoluble in solvents. The others are soluble in all common organic solvents, such as benzene, *n*-hexane, ether, acetone, and carbon tetrachloride, but not methanol; hence, the polymers can be purified by adding them, dissolved in benzene, into vigorously-stirred methanol. The results of elemental analysis after the purification are shown in Tables 1 and 2. The tables indicate that the values, except for in the cases of a-1 and C-2, agree with those calculated for the linear structure $(-Si(OR)_2-O-R'-O-)_n$. It seems to support the above structure that the products are soluble in organic solvents and form fiber. The IR spectra are essentially identical and show absorption peaks at 2900 (Me), 1605 and 1505 (Ph), 1390 and 1365 (Bu^t), and 1100—1000 (Si–O–Si, Si–O–C) cm^{-1}. As Fig. 2 shows, the NMR spectra of the polymer (d) exhibit the proton signals at 2.87—3.27 (Ph), 8.38 (Me), and 8.66 (Bu^t) τ. These spectroscopic data also imply that the above

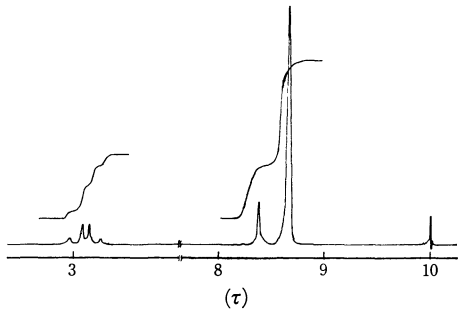

Fig. 2. NMR spectrum of polyaryloxy silicate d.

structure is reasonable. The polymer C and especially the polymer c are apt to discolor, probably due to the susceptibility of hydroquinone to oxidation. The results of the molecular-weight determination for D and d in benzene by the vapor-pressure method indicated the values of 6100 and 4800, which corresponded to the degrees of polymerization of 8 and 16 respectively. The X-ray powdery diffraction of D also showed no crystallinity. In general, it has been established that alkyl silicate are susceptible to hydrolysis and alcoholysis, but these polyalkyl(aryl) silicates have a remarkable stability.

The results of the elemental analysis for a-1 and C-2 are different from the values calculated for the structure. It is found that the deviation in the case of a-1 is due to a cross-linking of the polymer by ethylene glycol, which results from the alcohol-exchanging reaction between the *t*-butoxy and the hydroxy group of ethylene glycol, for *t*-butyl alcohol was detected in the gas chromatography of the solvent removed from the reaction mixture. Additional evidence of the cross-linking lies in the IR spectra of the product; a strong absorption peak appears at 3425 (OH) cm^{-1}, while the peaks at 1390 and 1360 cm^{-1} due to the *t*-butyl group almost disappear. Therefore, the product is a polymer partially crosslinked by ethylene glycol; however, the degree of the cross-linking seems to be low, for it is soluble in hot benzene. The deviation in c-2 may be ascribed to a partial decomposition during the course of polymerization at a high temperature (280°C).

On the other hand, distillable products rather than polymeric substances were obtained when the reaction of the diaminosilanes with 1,4-butanediol was carried out using toluene as the solvent. These products were found to be cyclic alkoxysilanes by elemental analysis, by molecular-weight determination (Table 3), and by means of examining the NMR spectra (Fig. 3). In the reaction of di-*t*-

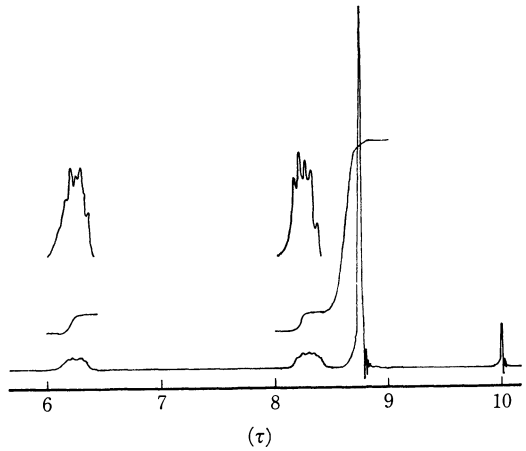

Fig. 3. NMR spectrum of cyclic alkoxysilane (R=Bu^t).

butoxydiaminosilane with the diol, a polymeric substance was formed in addition to the cyclic alkoxy silane; the ratio of the products was about 5 : 3 (by weight). On the other hand, in the reaction of bis(tri-*t*-butoxysiloxy)diaminosilane, only a distillable product was obtained.

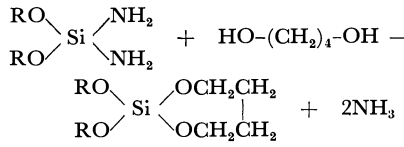

where R=Bu^t and (Bu^{t}O)$_3$Si.

The tendency toward cyclization rather than the expected polymerization seems due to the length of the methylene linkage and the steric hindrance, since no distillable product was afforded by the reaction of the diaminosilanes with ethylene glycol

TABLE 3. PRODUCTS IN THE REACTION OF DIAMINOSILANES WITH 1,4-BUTANEDIOL

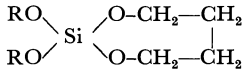

R	Yield %	Bp, °C/mmHg (Mp, °C)	Mol. wt. Found (Calcd)	Analysis Found (Calcd) % C	H	Si	NMR (τ) (Proton Ratio) Me	CH_2	$\underline{CH_2}$
Bu^t	40	n_0^{20} 106.5/1 1.4217	261 (261)	54.94 (54.93)	10.75 (9.98)	10.70 (10.52)	8.92 (4.5)	8.16–8.37 (1)	6.1 –6.35 (1)
(Bu^{t}O)$_3$ Si	70	160–161/1 (62–63)		52.57 (52.30)	10.30 (9.71)	12.95 (13.10)	8.71 (14.7)	8.15–8.36 (1)	6.02–6.22 (1)

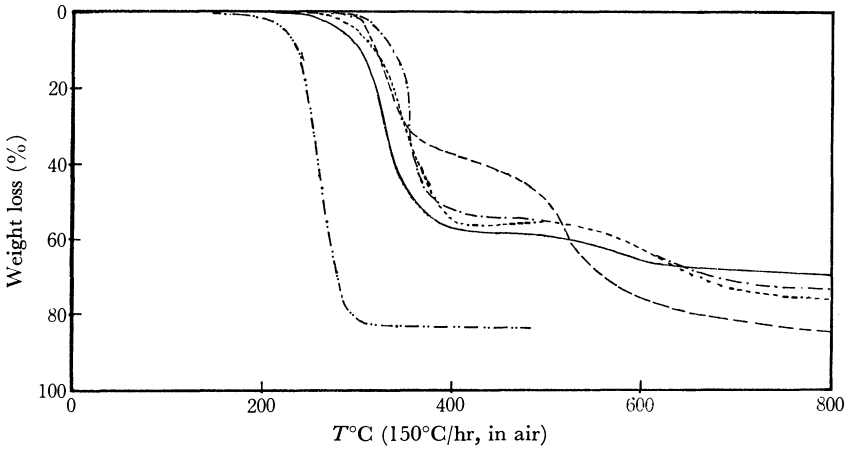

Fig. 4. TGA curve of A (—··—), C (———), D (—·—), c (·····), and d (----).

and only the cyclic alkoxysilane was formed in the case of bis(tri-*t*-butoxysiloxy)diaminosilane. These facts suggest that the seven-membered ring is more favorable to ring formation than the five-membered ring and that the steric hindrance of tri-*t*-butoxysiloxy group greatly contributes to the cyclization. Probably, the reactions proceed *via* the initial formation of the intermediate $(RO)_2Si(NH_2)(OCH_2CH_2CH_2CH_2OH)$, and at this stage it may undergo an intramolecular condensation, for the intermolecular condensation appears to be more difficult due to the steric hindrance of the RO groups. Indeed, the assumption that the intermediate is formed seems to be supported by the reports by Miner[7] and by our previous investigation.[6]

Thermal Properties of Polyalkyl(aryl) Silicates. The TGA curves of polyalkyl(aryl) silicates (Fig. 4) indicate that the weight loss of A-1 amounts to about 80% at 200—300°C, whereas those of c, C, d, and D amount to about 50—60% at 350—400°C and 70—80% at 900°C. Obviously the polymers with aromatic rings in the molecular main chain have a superior thermal stability to the A-1 with the methylene linkage. When c, C, or D is compared with d, no remarkable difference in thermal stability is observed, except that the weight loss of d is less than that of the others at 400—500°C. However, as Tables 1 and 2 show, there is a tendency for the fusing points of polymers with a butoxy group in the side chain are to be higher than those with a tri-*t*-butoxysiloxy group. This seems to be explained by considering that the flexibility of the molecule increased by the Si–O–Si linkage in the side chain of C and D results in a lowering their fusing points compared with those of c and d without the linkage.

The results of the differential thermal analysis of D and d are shown in Fig. 5. Figure 5 indicates that D and d have endo- or exothermic peaks at about 60 and 360°C. The endothermic peaks at about 60°C correspond to the fusing points, which are in good accordance with the results shown in Tables 1 and 2. The peaks at 360°C are due to decomposition, but the thermal behavior is

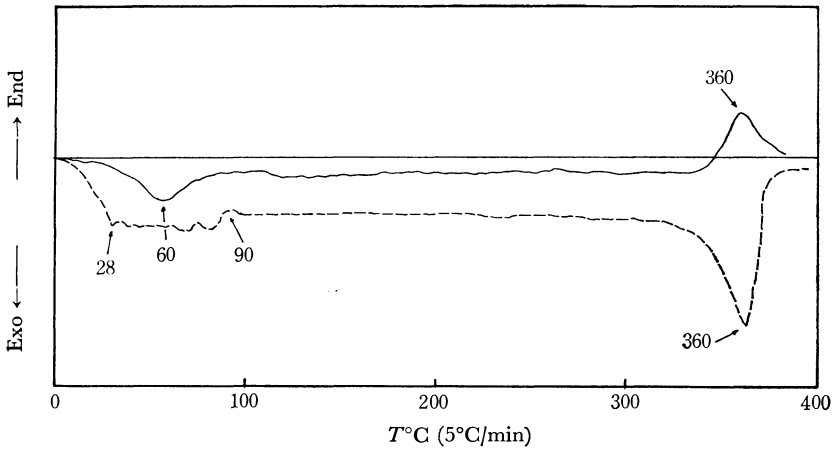

Fig. 5. DTA curve of D (----) and d (——).

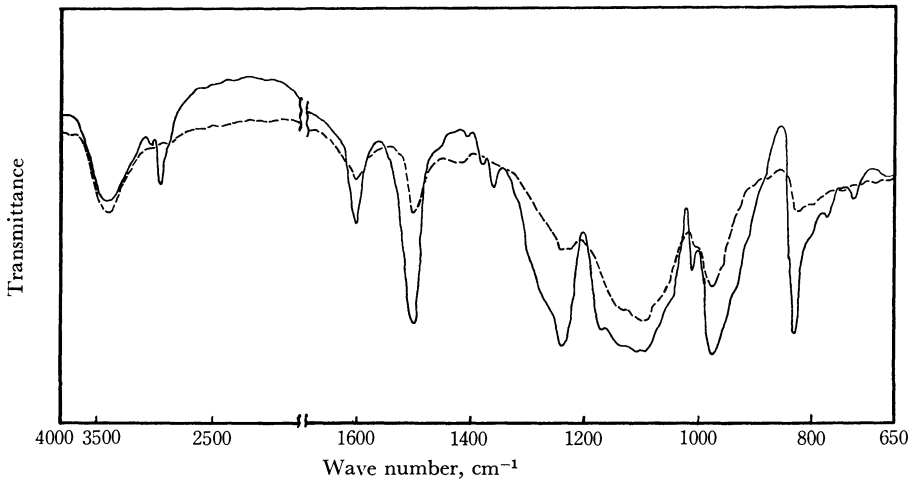

Fig. 6. IR spectra of $T-1$ (——) and $T-2$ (----).

different, as may be seen when d is compared with D. This may be thought to be caused by the different side chains, the butoxy and butoxysiloxy groups.

During the investigation of the thermal stability by means of the TGA curves, it has been observed that the decomposition of all the polymers except A proceeds through two steps, as is shown by Fig. 4. This suggests that either step is caused by the degradation of the side or main chain; hence, the identification of thermal decomposition products would allow us to discuss the process of the degradation. With this in view, the d polymer was pyrolyzed at 300 and 480°C *in vacuo*; a gas evolved, and the residue was subjected to analysis. Consequently, the following facts were made clear: 1. The gas evolved at 300°C was confirmed to be 2-methyl propene by means of gas chromatography after it had been brominated. Moreover, as is shown in Fig. 6, the IR spectra of the residue (T-1) at this temperature exhibited absorption peaks at 1500 and 820 cm^{-1} due to the phenyl group, but lack the peaks at 1380 and 1360 cm^{-1} attributed to the branching of the alkyl group; therefore, the above facts seem to support the idea that the first step is the degradation of the side chain. 2. The volatile substances obtained at 480°C were identified as phenol and bisphenol A; besides, the IR spectra of the residue (T-1) at 480°C lack the peaks ascribed to not only the branching of the alkyl group, but to the phenyl group. These facts imply that the second step is the decomposition of the main chain. On the basis of the above results, it is thought that the probable decomposition process of the polymers proceeds step by step, as is shown by the following scheme:

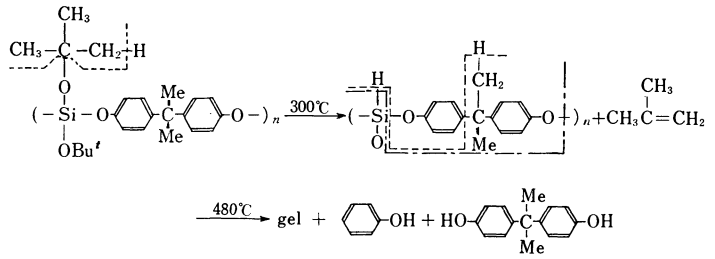

The authors wish to thank Professor Yojiro Tsuzuki for his interest and helpful advice. Acknowledgement is also due to Mr. Takao Aoki of the Laboratory of the Physical Chemistry for his measurements of the molecular-weight determination, the Laboratory of the Chemical Engineering for the permission to employ its thermovalance, Assistant Professor Keizo Ogino for his suggestions regarding the differencial thermal analysis, and Mr. Tetsuo Kanamoto for his measurements of the X-ray powder diffraction for this work and for Part II.

BULLETIN OF THE CHEMICAL SOCIETY OF JAPAN VOL. 43 2501—2506 (1970)

Synthese der Epiminozucker

Kunihiro ICHIMURA

Institut für Polymer- und Faserforschung, Yokohama, Kanagawa-ku, Sawatari, Yokohama

(Eingegangen am 20. September, 1969)

Two-step conversion of aldehydes to 2-monosubstituted aziridines has been extended to sugar derivatives. Treating *O,O'*-isopropylidene-D-glyceraldehyde with benzenesulfonyl chloride and sodium cyanide, 2-benzenesulfonyloxy-3,4-isopropylidenedioxybutyronitrile is obtained as a mixture of the diastereomers in a good yield, and is converted to the corresponding ketalaziridine, 2-(1,2-isopropylidenedioxyethyl)aziridine, by the reduction with lithium aluminum hydride. When the partially racemized isopropylideneglyceraldehyde is used, the diastereomers obtained are successfully separated by the fractional recrystallization. Each diastereomeric α-sulfonyloxynitrile is reduced by lithium aluminum hydride to afford the ketalaziridine, which is *p*-nitrobenzoylated and rearranged to the derivative of 1,3,4-trihydroxy-2-amino-butane by means of sodium iodide. Analogously, 3-*O*-benzyl-1,2-*O*-isopropylidene-α-D-glucopentodialdo-1,4-furanose was converted to two urononitriles, 3-*O*-benzyl-5-*O*-benzenesulfonyl-1,2-*O*-isopropylidene-α-D-glucofuranurononitrile and the epimeric β-L-idofuranurononitrile. The reduction of the former yielded 5,6-epimino-5,6-dideoxy-β-L-idofuranose.

Wegen ihrer reaktionsfreudigen Eigenschaften können Aziridine als Ausgangsmaterial zur Herstellung stickstoffhaltiger Verbindungen dienen. Vor kurzem wurde die stereospezifische Synthese von β-Aminoalkoholen[1] und von 1,2-Diaminen[2] mitgeteilt, indem zugängliche Verfahren zur Gewinnung der Aziridine von Olefinen aus beschrieben wurden.[3]

Wie in der voranstehenden Mitteilung erwähnt, haben wir eine zweistufige Umwandlung von Aldehyden in 2-monosubstituierte Aziridine aufgefunden, die vorteilhaft unter verhältnismäßig milderen Reaktionsbedingungen stattfinden kann.[4]

Ergebnisse

In dieser Arbeit haben wir diese Umwandlung an Zucker-Derivaten angewandt. Zuerst wird *O,O'*-Isopropylidenglycerinaldehyd gewählt. Um die unangenehme Nebenreaktion der Hydrolyse des Ketalrings oder der Aldolkondensation zu vermeiden, versetzt man zuerst ein Drittel des gebräuchlichen Natriumcyanids und anschließend Benzolsulfonylchlorid mit Aldehyd in Acetonitril und setzt dem Gemisch die wäßrige Lösung des übrigen Natriumcyanids zu. Dann entsteht α-Benzolsulfonyloxynitril vom Schmp 47—49°C (IIIa), dessen Struktur nach der Analysenwert und dem IR-Spektrum bestätigt wird.

Obwohl sich in dieser Reaktion zwei Diastereomere bilden könnten, ist es uns nicht gelungen, diese Diastereomere durch fraktionelle Kristallisation oder durch Dünnschichtchromatographie abzuteilen.

Bei dieser Umwandlung handelt es sich hauptsächlich um das Molverhältnis des Ausgangsmaterials, wie man in der Tabelle 1 sehen kann.

Im Versuch Nr. 2 entsteht vielmehr hydrolysiertes 2-Benzolsulfonyloxy-3,4-dihydroxybutyronitril (IVa), das durch die Dünnschichtchromatographie mit der bei der essigsauren Hydrolyse des Ketalnitrils (IIIa) erhaltenen Produkts vom Schmp 136—139°C identifiziert wurde. Im Gegensatz dazu färbt sich das Reaktionsgemisch nach der Umsetzung mit einer größeren Menge Natriumcyanid, und die Ausbeute des Ketalnitrils nimmt stark ab. Die besten Ergebnisse (85%-ige Ausbeute) erhält man bei der Benutzung des heterogenen Systems des Acetonitrils und der Na_2HPO_4-NaH_2PO_4-Pufferlösung von pH etwa 7.40 statt reinen Acetonitrils und bei einem Molverhältnis wie das des Ausgangsmaterials wie in Versuch Nr. 5.

Im Vergleich zum Hydrolysat (IVa) des Ketalnitrils (IIIa) mit Essigsäure entsteht bei der salzsauren Hydrolyse neben Ammoniumchlorid eine unreine Verbindung, die nach dem IR-Spektrum vermutlich γ-Lakton ist. Ferner fanden wir, daß D-Glycerinaldehyd selber bei der Einwirkung des Natriumcyanids und Benzolsulfonylchlorids in Dihydroxynitril (IVa) übergeführt wird.

Wenn man das so erhaltene Ketalnitril (IIIa)

1) C. Heathcock und A. Hassner, *Angew. Chem.*, **75**, 344 (1963).

2) G. Swift und D. Swern, *J. Org. Chem.*, **31**, 4226 (1966); **32**, 511 (1967).

3) In Ref. 4) angeführt.

4) K. Ichimura und M. Ohta, Dieses Bulletin, **43**, 1443 (1970).

TABELLE 1. SYNTHESE DES 1-BENZOLSULFONYLOXY-3,4-ISOPROPYLIDENDIOXYBUTYRONITRIL (III)

Versuch Nr.	Molverhälthis			Rohprodukt		
	D-Aldehyd	NaCN	$C_6H_5SO_2Cl$	Schmp °C	Ausbeute %	Lösgm.
1	1.05	1.10	1.00	36–42	46.5	CH_3CN
2	1.00	1.05	1.00	90–130*	41	CH_3CN
3	1.05	1.11	1.00	36–42	57	CH_3CN
4	1.12	1.12	1.00	40–50	59.5	CH_3CN
5	1.15	1.25	1.00	40–57	85	Pufferlösung**

* Hydrolysiertes Nitril.

** pH 7.40 von Na_2HPO_4- NaH_2PO_4 (s. Beschreibung der Versuche).

mit Lithiumaluminiumhydrid reagieren läßt, entsteht Ketalaziridin (Va) in 55%-iger Ausbeute. Die Abtrennung der Diastereomere durch Gaschromatographie war auch hier erfolglos.

Bei der Oxydation des D-Mannitols durch Bleitetraacetat entsteht bei längerem Erhitzen ein sehr zähes Öl, das bei etwa 200°C in teilweise racemisiertes Isopropylidenglycerinaldehyd entpolymerisiert wird.

Bei der Einwirkung von Natriumcyanid und Benzolsulfonylchlorid auf diesen Isopropylidenglycerinaldehyd erhält man zwei verschiedene Produkte. Diese beiden können durch fraktionelle Kristallisation mit 2-Propanol in fast gleicher Ausbeute abgetrennt werden. Das eine (IIIb) schmilzt bei 100—102°C und das andere (IIIc) bei 52—56°C. Beide zeigen die gleichen Analysenwerte des Ketalnitrils vom Schmp 47—49°C, und die Anwesenheit des Ketalrings und des Sulfonsäureesters in den IR-Spektren. Die IR-Spektren dieser drei Isomere im festen Zustand sind aber im wesentlichen nicht identisch. Bei der essigsauren Hydrolyse liefern ferner die Kristalle (IIIb) vom Schmp 100—102°C das Dihydroxynitril (IVb) vom Schmp 89—90°C, und die Kristalle (IIIc) vom Schmp 53.5—56°C das entsprechende isomere Dihydroxynitril (IVc) vom Schmp 156—157°C.

Beim Vergleich der IR-Spektren dieser drei Ketalnitrile (IIIa, IIIb und IIIc) in Chloroform kann man vermuten, daß die Kristalle vom Schmp 47—49°C ein Gemisch von IIIb und IIIc sind. Diese Vermutung wird durch die NMR-Spektren bestätigt. Während die eine Methylgruppe der *gem*-Dimethylgruppe im Dioxolanring in beiden Kristallen (IIIb und IIIc) die gleichen chemische Schiebung bei τ 8.69 zeigt, tritt das andere Methylsignal von IIIb bei τ 8.60, und das von IIIc bei 8.57 auf. Die Protonen der Isopropyliden-Gruppe der Kristalle vom Schmp 47—49°C absorbieren doch bei τ 8.69, 8.57 und 8.60, im Stärkeverhältniss etwa 2 : 1 : 1. Auch die anderen Signale unterstützen die Vermutung, daß IIIa das Gemisch von IIIb und IIIc ist.

Diesen Tatsachen nach schließt man, daß die vom teilweise racemisierten Isopropylidenglycerinaldehyd aus stammenden beiden Verbindungen (IIIb und IIIc) die Diastereomere sind, und daß das vom optisch aktiven Aldehyd erhaltene Produkt (IIIa) ein Gemisch der beiden Diastereomere im Verhaltniss etwa 1 : 1 ist.

Diese beiden Diastereomere (IIIb und IIIc) liefern auch bei der Reduktion mit Lithiumaluminiumhydrid die entsprechenden Aziridine (Vb und Vc), deren IR-Spektra sehr verwandt sind.

Das aus IIIb erhaltene Aziridin (Vb) wird *p*-nitrobenzoyliert und anschließend mit Natriumjodid behandelt unter Bildung des Oxazolins vom Schmp 123—124.5°C (VIIb).

Indem 1-Acyl-2-alkylaziridin mittels Natriumjodids in 4-alkylsubstituiertes Oxazolin umgelagert wird,[5] ist das erhaltene Umlagerungsprodukt ein Derivat des 1,3,4-Trihydroxy-2-aminobutans.

Das andere Diastereomer des Trihydroxyaminobutan-Derivats (VIIc) vom Schmp 107—110°C wird nach gleicher Behandlung wie Vc dargestellt.

Als nächstens konnte Epiminozucker in analoger Weise hergestellt werden. 1,2:5,6-Diisopropylidenglucofuranose wird über partielle saure Hydrolyse durch Natriumperjodat oxydiert, und das rohe Prodkt wird wie unter den oben erwähnten Bedingungen mit Benzolsulfonylchlorid und Natriumcyanid behandelt.[4] Aus dem Reaktionsgemisch kann man keine einheitliche Substanz isolieren. Die Entstehung des erwarteten α-Sulfonyloxynitrils gelingt durch die Dimerisierung des Aldehyds und/oder durch die Bildung des Addukts mit Formaldehyds nicht, worüber vor kurzem Paulsen und Todt berichtet haben.[6]

Um diese unangenehmen Phänomene zu vermeiden, wird 1,2:5,6-Isopropyliden-α-D-glucofuranose nach Benzylierung partiell hydrolysiert, um 3-*O*-Benzyl-1,2-*O*-isopropyliden-α-D-glucofuranose zu gewinnen, das durch Natriumperjodat oxydiert wird.

Wenn man auf das rohe Aldehyd (IX) Benzolsulfonylchlorid und Natriumcyanid in gewöhnlicher Weise einwirken läßt, so erhält man α-Sulfonyloxynitril-Gruppe tragendes Produkt, in dessen IR-

5) H. W. Heine, *Angew. Chem.*, **74**, 772 (1962).

6) H. Paulsen und K. Todt, *Chem. Ber.*, **101**, 3358 (1968).

Spektrum die charakteristischen Absorptionen der Sulfonsäureester auftritt.[4] Sie zeigt auch keine deutlichen Bande der Nitril-Gruppe. Im NMR-Spektrum des rohen Produkts treten bei τ 5.50 und 5.65 zwei Dublette des Protons der 5-Stellung der Furanose im Stärkeverhältniss 19 : 10 auf, was zeigt, daß die rohe Verbindung ein Gemisch der zwei erwarteten Diastereomere ist. Wenn das rohe Produkt aus Tetrachlorkohlenstoff umgelöst wird, scheiden sich farblose Nadeln vom Schmp 137—139°C in 20%-iger Ausbeute in bezug auf 3-*O*-Benzyl-1,2-isopropyliden-α-D-glucofuranose. Im NMR-Spektrum dieser Verbindung tritt das anomere Proton bei τ 5.93 als eine Dublette (J=3 Hz) und das Proton in der 5-Stellung bei τ 5.46 (J=7.15 Hz) als eine Dublette auf, was zeigt, daß diese Verbindung das Hauptprodukt ist.

Aus dem vom kristallinen Hauptprodukt (X) freigesetzten Rückstand, der dem NMR-Spektrum nach ein Gemisch von X und dessen Epimer im Verhältniss 1 : 2 ist, fraktioniert man durch nochmalige Umkristallisationen das andere Epimer vom Schmp 106—108°C als farblose Blättchen. Im NMR-Spektrum tritt das anomere Proton bei τ 5.87 als Dublette (J=3 Hz) auf, das Proton in der 5-Stellung bei τ 5.29 als Dublette (J=8.2 Hz), was die Struktur und die Einheitlichkeit der Substanz stützt. Die beiden Epimere haben einen gleichen R_f-Wert bei der Dünnschichtchromatographie mit Silikagel oder Alumina, und die Abtrennung durch Säulenchromatographie gelingt dann nicht.*1

Wenn man als Sulfonylchlorid *p*-Toluolsulfonyl- und *p*-Brombenzolsulfonylchlorid benutzt, erhält man die entsprechenden α-Sulfonyloxynitrile, deren Strukturen durch IR- und NMR-Spektren festgestellt werden. Die beiden Rohprodukte enthalten zwei Epimere im Verhältniss von etwa 2 : 1 nach den NMR-Spektren, ganz analog wie im Fall vom 5-*O*-benzolsulfonylierten Uronsäurenitril. Es ist noch nicht gelungen, die Epimere in den beiden Fällen abzutrennen, außer dem Minorprodukt des *p*-Brombenzolsulfonyloxynitrils.

Der Cram-Karabatsos-Regel nach[8] wird vermutet, daß sich die Konfiguration des Kohlenstoffs der 5-Stellung des Benzolsulfonyloxygruppe tragenden Hauptprodukts (X) in der *R*-Chiralität befindet und daß es nämlich ein Derivat des D-Glucuronsäurenitrils ist, während das andere Epimer ein L-Idouronsäurenitril-Derivat (XI) ist, was durch die unten beschriebene Methode festgestellt wurde.

Wenn man X in THF mittels Lithiumaluminiumhydrids reduziert, ist ein Epiminozucker erhältlich, der im IR-Spektrum bei 3300 cm^{-1} absorbiert. Obwohl die Benzoyl-, Phenylcarbamoyl- und *p*-Nitrobenzoyl-Derivat alle nicht kristallin erhältlich sind, erhält man Kristalle vom Schmp 188—189°C nach der Behandlung des *N*-Nitrobenzoyl-Derivat mit Natriumjodid. Die Kristalle zeigen einen Oxazolinring bei 1650 cm^{-1} im IR-Spektrum,und der erhaltene Zucker ist also vermutlich ein Derivat des 5-Amino-5-desoxy-zuckers (XIII).

Wie in der voranstehenden Arbeit mitgeteilt, werden α-Chlor- und Bromnitrile stereospezifisch über *trans*-Eliminierung zum Ringschluß gebracht, und α-Sulfonyloxynitrile sind auch offenbar in gleicher Weise stereospezifisch umgewandelt.[4] Der durch LAH-Reduktion erhaltene Epiminozucker (XII) ist daher 5,6-Epimino-5,6-didesoxy-β-L-idofuranose. Gerade wie im Fall von VII erwähnt, ist der Oxazolinzucker (XIII) deswegen ein Derivat der 5-Amino-5-desoxy-β-L-idofuranose.

Um die Konfiguration von XII mehr ins klare zu bringen, synthetisiert man XII in der folgenden Weise, die vor kurzem Saeki und Ohki mitgeteilt haben.[9a] Nach der Tosylierung der 3-*O*-Benzyl-1,2-isopropyliden-α-D-glucose und der chromato-

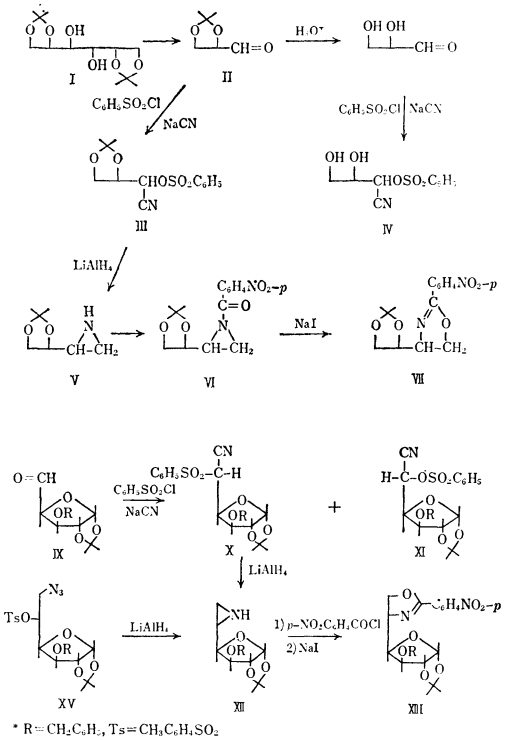

Fig. 1. Synthese der Epiminozucker.

*1 Von Saeki und Ohki wurde vor kurzem unabhängig mitgeteilt, daß das Cyanhydrin des 1,2:3,4-di-*O*-Isopropyliden-α-D-galactohexodialdo-1,5-pyranoses tosyliert und analog mit Lithiumaluminiumhydrid in Epiminozucker umgewandelt wird.[7]

7) H. Saeki und E. Ohki, *Chem. Pharm. Bull.* (Tokyo), **17**, 1974 (1969).

8) a) D. J. Cram und D. R. Wilson, *J. Amer. Chem. Soc.*, **85**, 1245 (1962). b) G. J. Karabatsos, *ebd.*, **89**, 1367.

9) a) H. Saeki und E. Ohki, *Chem. Pharm. Bull.* (Tokyo), **16**, 2471 (1968). b) *ebd.*, **16**, 2477 (1968). c) *ebd.*, **17**, 1664 (1969).

graphischen Reinigung läßt man den ditosylierten Zucker mit Natriumazid in DMF reagieren. Wenn man das so erhaltene Azid-Derivat (XV) in THF durch LAH reduziert, entsteht der rohe Epiminozucker, dessen IR- und NMR-Spektrum mit denen von XII ähnlich sind. Für die Identifizierung des Produkts mit XII wird der Aziridinzucker über die *p*-Nitrobenzoylierung in das Oxazolin mittles Natriumjodids umgewandelt, das durch Mischprobe und IR-Spektrum mit XIII praktisch identisch ist. Der oben erhaltene Epiminozucker wird nach Destillieren kristallin erhalten und mit von Saeki und Ohki dargestelltem 5,6-Epimino-5,6-didesoxy-*β*-L-idose-Derivat identifiziert.*2 Die struktuelle Feststellung deutet nämlich daraufhin, daß die Konfiguration von X mit der nach der Cram-Karabatsos-Regel geschlossenen Konfiguration im Übereinstimmung steht.

Beschreibung der Versuche

IR-Spektra wurden mit Hitachi EPI und NMR-Spektra mit Japan Elektron Optik Laboratorium JNM C-60HL alle in $CDCl_3$ aufgenommen. Die Schmelzpunkte wurden nicht korrigiert.

***O,O'*-Isopropyliden-D-glycerinaldehyd.** Zu der Lösung des 22.2 g Bleitetraacetats in 60 m*l* wasserfreiem Benzol setzt man 13.1 g 1,2: 5,6-Diisopropyliden-D-mannitol in kleinen Portionen unterhalb 20°C unter Rühren zu und rührt eine Weile. Nach dem Freisetzen und Waschen des Unlöslichen mit Benzol versetzt man die vereinte benzolische Lösung mit wasserfreiem Kaliumcarbonat und rührt das Gemisch bis zum Ende der Entwicklung des Kohlendioxyds. Nach Filtrieren des Niederschlags destilliert man die Lösung im verminderten Druck ab, und erhält 7.8 g *O,O'*-Isopropyliden-D-glycerinaldehyd vom Kp 53°C/17 mmHg. (Ber Kp 27°C/2 mmHg).[10] $[\alpha]_D = +64.9°$. Das Aldehyd wird sofort nach dem Destillieren zur Umsetzung benutzt.

2-Benzolsulfonyloxy-3,4-isopropylidendioxybutyronitril aus Isopropylidenglycerinaldehyd von $[\alpha]_D = +64.9°$. Man versetzt 7.40 g *O,O'*-Isopropyliden-D-glycerinaldehyd und 8.75 g frisch destilliertes Benzolsulfonylchlorid mit M/20 30 m*l* Pufferlösung (NaH_2PO_4-Na_2HPO_4) von pH 7.40 und 20 m*l* Acetonitril unter Eis-Kochsalzkühlung. Unter gutem Rühren setzt man die wäßr. konz. Lösung des 3.01 g Natriumcyanids zu dem Gemisch unterhalb 7°C tropfenweise zu und rührt 30 Min bei Raumtemperatur. Nach Versetzen mit Wasser wird das Reaktionsgemisch mit Äther ausgezogen und mit Wasser gewaschen. Nach Trocknen über wasserfreiem Kaliumcarbonat und Entäthern der Lösung erhält man die Kristalle, die mit Aceton-Trockeneis abgekühltem 2-Propanol gewaschen werden. Ausbeute, 11.32 g (77% d. Th.). Schmp 40—47°C. Aus dem Filtrat werden 1.18 g (8.0% d. Th.) Kristalle vom Schmp 38—47°C zurückgewonnen. Sie werden aus abgekühltem 2-Propanol umkristallisiert und schmelzen bei 47—49.5°C. Ausbeute, 8.77 g $[\alpha]_D^{25} = -13.2°$ (*c* 0.5 $CHCl_3$). IR-Spektrum (KBr): 1380, 1220, 1190, 1180, 1095, 1070, 980, 730 cm^{-1}. Gef: C, 52.38; H, 4.91; N, 5.05%. Ber für $C_{15}H_{15}NO_5S$: C, 52.52; H, 5.09; N, 4.71%.

2-Benzolsulfonyloxy-3,4-dihydroxybutyronitril (IVa). *a) mit Essigsäure.* Das oben erhaltene Ketalnitril (IIIa) wird eine Weile in 50%-iger Essigsäure bei 60—70°C erwärmt, und anschießend dampft man die Lösung unter verm. Druck bei dieser Temperatur ein und erhält den kristallinen Rückstand, der aus Isobutylalkohol umkristallisiert wird. Schmp 136—139°C. Gef: C, 46.82; H, 4.19; N, 5.63%. Ber für $C_{10}H_{11}NO_5S$: C, 46.70; H, 4.31; N, 5.45%. IR-Spektrum (KBr): 3340, 3330, 1370, 1195, 1010, 731 cm^{-1}.

b) aus D-Glycerinaldehyde. 5.2 g *O,O'*-Isopropyliden-D-glycerinaldehyd wird in 10%-iger Essigsäure gelöst, über Nacht stehen gelassen und unter verm. Druck eingedampft. Den Rückstand löst man in 20 m*l* Wasser und versetzt dazu die Acetonitril (10 m*l*)-Lösung von 5.60 g Benzolsulfonylchlorid. Unter Rühren setzt man 1.88 g Natriumcyanid in 5 m*l* Wasser in die Lösung unterhalb 30°C zu. Beim anschließenden Versetzen mit Wasser scheiden sich die Kristalle aus, die aus Isobutylalkohol umkristallisiert werden, bei 136—138°C schmelzen und 0.85 g betragen. Sie werden mit dem oben erhaltenen Dihydroxynitril (IVa) durch Mischprobe identifiziert.

2-Benzolsulfonyloxy-3,4-isopropylidendioxybutyronitril (IIIb und IIIc) aus Isopropylidenglycerinaldehyd von $[\alpha]_D = +14.9°$. Diaceton-D-mannitol (15.2 g) wird in Benzol mittels Bleitetraacetat oxydiert und wie oben aufgearbeitet. Nach Behandlung mit Kaliumcarbonat destilliert man das Lösungsmittel unter gewöhnlichem Druck ab. Wenn man den öligen zähen Rückstand unter verm. Druck destilliert, so geht nach wenigem Vorlauf 8.2 g Isopropylidenglycerinaldehyd vom Kp 70°C/30 mmHg erst beim Erhitzen des Umsetzungsprodukts bei 160—200°C über. Nach einmaligem Destillieren zeigt das Aldehyde $[\alpha]_D^{25} = +14.6°$ (*c* 2.754 Bzl). Man läßt 2.38 g Natriumcyanid auf so erhaltenes 6.50 g Isopropylidenglycerinaldehyd und 7.75 g Benzolsulfonylchlorid in M/20 Pufferlösung und Acetonitril einwirken und arbeitet auf, genau so wie in der oben beschriebenen Weise. So erhält man die Kristalle vom Schmp 51—88°C, die aus Isobutylalkohol umkristallisiert werden und 4.02 g betragen. Schmp 90—100°C. Wenn man die Mutterlauge bei der Umkristallisation mit großer Menge Petroläther versetzt und sie im Eisschrank stehen läßt, so scheiden sich 6.95 g Kristalle vom Schmp 44—50°C ab. Nach nochmaligen Umkristallisationen der beiden Kristalle aus Isobutylalkohol schmelzen die einen bei 101.5—102.5°C, die anderen bei 52—54.5°C. 2-Benzolsulfonyloxy-3,4-isopropylidendioxybutyronitril vom Schmp 101.5—102.5°C (IIIb), Gef: C, 52.67; H, 5.36; N, 4.76%. Ber für $C_{13}H_{15}NO_5S$: C, 52.52; H, 5.09; N, 4.71%. $[\alpha]_D^{27} = \pm 0.0$ (*c* 0.5 $CHCl_3$). Das Diastereomer vom Schmp 52—54.5°C (IIIc), Gef: C, 52.65; H, 5.36; N, 4.82%. Ber für $C_{13}H_{15}NO_5S$: C, 52.52; H, 5.09; N, 4.71%. $[\alpha]_D^{27} = -4.0°$ (*c* 0.5 $CHCl_3$). IIIa, IIIb und IIIc haben alle die gleichen R_f-Werte bei der Dünnschichtchromatographie mittels Silikagels.

Essigsaure Hydrolyse von IIIb und IIIc. Genau so wie im Fall von IIIa hydrolysiert man IIIb vom Schmp 100—102°C und umkristallisiert aus Isobutylalkohol/Petroläther. Schmp 89—90°C. Gef: C, 46.89; H, 4.48; N, 5.41%. Ber für $C_{10}H_{11}NO_5S$: C, 46.70; H, 4.31; N, 5.45%. IR-Spektrum (KBr); 3450, 3250,

*2 Der Autor dankt Dr. Ohki und Saeki für die Anweisung der spektroskipischen Daten.

10) E. Baer, *J. Amer. Chem. Soc.*, **67**, 338 (1945).

1370, 1190, 1180, 970 cm^{-1}.

Nach dem analogen Aufarbeiten erhält man das Hydrolysat (IVc) aus IIIc vom Schmp 50—52°C und umkristallisiert es aus Isobutylalkohol. Schmp 155—157°C. Gef: C, 46.72; H, 4.29; N, 5.77%. Ber für $C_{10}H_{11}NO_5S$: C, 46.70; H, 4.31; N, 5.45%. IR-Spektrum (KBr); 3450, 3300, 1375, 1195, 1180, 1000 cm^{-1}.

Reduktion von IIIa, IIIb und IIIc mit Lithiumaluminiumhydrid. Man löst 7.50 g Ketalnitril (IIIa) in 30 m*l* 1 : 1 Lösung von THF und Äther und tropft die Lösung in die Suspension von 1.82 g Lithiumaluminiumhydrid in 50 m*l* Äther unterhalb 0°C ein. Nach vierstündigem Rühren bei Raumtemperatur behandelt man das Reaktionsgemisch in gewöhnlicher Weise und erhält 2.00 g (55.4% d. Th.) 2-(1,2-Isopropylidendioxyäthyl)aziridin (Va) vom Kp 112°C/23 mmHg. n_D^{25} 1.4491. $[\alpha]_D^{25}=+7.51°$ (*c* 1.385 Bzl). In der Gaschromatographie mittels Carbowax 20 M-Säule beobachtet man nur eine einzige Spitze. Gef: C, 58.45; H, 9.05; N, 9.67%. Ber für $C_7H_{13}NO_2$; C, 58.72; H, 9.12; N, 9.78%. IR-Spektrum (Flüssigkeit); 3300, 3050, 1385, 1375, 1220, 1070 cm^{-1}.

IIIb liefert in analoger Weise das Aziridin (Vb) vom Kp 106—110°C/26 mmHg in 57%-iger Ausbeute. n_D^{25} 1.4450. $[\alpha]_D^{25}=+0.8°$ (*c* 0.5 Bzl). IIIc gibt das diastereomere Aziridin (Vc) vom Kp 107—109°C/28 mmHg in 60%-iger Ausbeute. n_D^{25} 1.4483, $[\alpha]_D^{25}=-4.2°$ (*c* 0.5 Bzl).

2-(*p*-Nitrophenyl)-4-(1,2-isopropylidendioxyäthyl)-2-Oxazolin (VIIb und VIIc). *VIIb vom Schmp 123—124.5°C.* Man setzt die ätherische Lösung des 1.10 g *p*-Nitrobenzoylchlorid in die Lösung des 0.80 g Ketalaziridins (Vb) und 1.13 g Triäthylamins in 30 m*l* wasserfreiem Äther unterhalb 7°C unter Rühren zu, und nach zweistündigem Rühren versetzt man das Reaktionsgemisch mit Wasser. Die ätherische Schicht wird abgetrennt, zweimal mit 2N Natronlauge und zweimal mit Wasser nachgewaschen und über wasserfreies Kaliumcarbonat getrocknet. Nach Entäthern erhält man 1.40 g (86% d. Th.) 1-(*p*-Nitrobenzoyl)-aziridin (VIb) als öligen Rückstand. Das IR-Spektrum zeigt die Amid-Bande bei 1680 cm^{-1}. Man löst den Rückstand in 60 m*l* wasserfreiem Aceton, versetzt die Lösung mit 7.0 g Natriumjodid und läßt sie 20 Std bei Raumtemperatur stehen. Bei Verdünnen mit Wasser erhält man das umgelagerte Produkt vom Schmp 115—121°C, das aus 2-Propanol umkristallisiert wird. Gelbliche Prismen vom Schmp 123—124.5°C. Gef: C, 57.29; H, 5.40; N, 9.61%. Ber für $C_{14}H_{16}N_2O_5$: C, 57.53; H, 5.52; N, 9.59%. IR-Spektrum (KBr): 1647, 1515, 1375, 1380, 1210, 1070 cm^{-1}.

VIIc vom Schmp 107—110°C. Von Ketalaziridin (Vc) ausgehend, erhält man nach der gleichen Aufarbeitung das diastereomere Oxazolin (VIIc), das aus wäßr. Äthanol umkristallisiert wird. Gelbliche Nadeln vom Schmp 107—110°C. Gef: C, 57.27; H, 5.50; N, 9.78%. Ber fur $C_{14}H_{16}N_2O_5$: C, 57.53; H, 5.52; N, 9.59%. IR-Spektrum (KBr); 1650, 1530, 1375, 1380, 1215, 1070 cm^{-1}.

3-*O*-Benzyl-5-*O*-benzolsulfonyl-1,2-isopropyliden-α-D-glucofuranuronsäurenitril (X) und 3-*O*-Benzyl-5-*O*-benzolsulfonyl-1,2-isopropyliden-β-L-idofuranuronsäurenitril (XI). 3-*O*-Benzyl-1,2:5,6-isopropyliden-α-D-glucofuranose (40 g) wird in 28 m*l* 5%-iger Schwefelsäure und 220 m*l* THF partiell hydrolysiert, und mittels Dünnschichtchromatographie geprüft. Danach wird das Gemisch mit Natriumbicarbonat neutralisiert. Man löst so erhaltene rohes 20.9 g 3-*O*-Benzyl-1,2-isopropyliden-α-D-glucofuranose in 100 m*l* Chloroform und versetzt mit 80 m*l* Wasser. 14.4 g Natriumperjodat wird anschließend in kleinen Portionen unter Eiskühlung zugesetzt, und man rührt das Gemisch 30 Min. Nach dem Filtrieren wäscht man die Chloroformschicht dreimal mit Wasser, trocknet mit Natriumsulfat, dampft sie ein und erhält Pentodialdose (IX) als Syrup. Man löst den Rückstand und 12.5 g Benzolsulfonylchlorid in 70 m*l* Acetonitril, versetzt 70 m*l* M/15 Pufferlösung von pH 7.40 (NaH_2PO_4-Na_2HPO_4) und setzt die konz. waßr. Lösung von 3.81 g Natriumcyanid tropfenweise unter Eiskühlung und gutem Rühren zu. Nach halbstündigem Rühren unter Eiskühlung versetzt man das Gemisch mit Wasser und zieht zweimal mit Äther aus. Die ätherische Lösung wird mit Wasser nachgewaschen, über Magnesiumsulfat getrocknet und eingedampft. Im NMR-Spektrum dieses Rückstands treten zwei Dublette bei τ 5.28 und 5.46 im Stärkeverhältniss 10 : 19 auf. Der Rückstand wird in 25 m*l* Tetrachlorkohlenstoff umgelöst und im Eisschrank stehen gelassen. Man nutscht 9.24 g (20% d. Th.) Kristalle vom Schmp 134—137°C ab, die mit kaltem Tetrachlorkohlenstoff gewaschen, aus Äthanol umkristallisiert werden und bei 137.5—139°C schmelzen. 3-*O*-Benzyl-5-*O*-benzolsulfonyl-1,2-isopropyliden-α-D-glucofuranuronsäurenitril (X) als farblose Nädeln. $[\alpha]_D^{25}=-29°$ (*c* 2.27 $CHCl_3$). Gef: C, 59.60; H, 5.21; N, 3.15%. Ber für $C_{22}H_{23}O_7NS$: C, 59.31; H, 5.20; N, 3.14%. IR (KBr); 1375, 1190, 1080, 990 cm^{-1}.

Man engt das von den Kristallen freigesetzte Filtrat unter verm. Druck ein, und im NMR-Spektrum des Rückstands treten zwei Dublette bei τ 5.28 und 5.46 im Stärkeverhältniss 31 : 13 auf. Die Dünnschichtchromatographie des Rückstands mittels Silikagels ergibt keine Abtrennung. Die Säulenchromatographie mittels Silikagels war auch zur Abtrennung der Diastereomere vergeblich: das Reaktionsgemisch jeder Fraktionen zeigt das gleiche NMR-Spektrum. Das kristalline Gemisch (6.27 g) wird dann mit Äthanol dreimal zur Fraktionierung umkristallisiert, und man erhält das Diastereomer (XI) vom Schmp 106—108°C als farblose Blättchen. $[\alpha]_D^{25}=-8.3°$ (*c* 2.06 $CHCl_3$). Die Kristallisation von XI ist langsamer als die von X in Äthanol. Gef: C, 59.36; H, 5.15; N, 3.04%. Ber für $C_{22}H_{23}O_7NS$: C, 59.31; H, 5.21; N, 3.14%.

5-Amino-5-desoxy-β-L-idose-Derivat (XIII). Man tropft 2.00 g X in 15 m*l* THF in die THF-Lösung von 0.34 g LAH unter Eiskühlung unterhalb 10°C ein und rührt bei Raumtemperatur 4 Std. Nach Stehenlassen über Nacht zersetzt man den Metallkomplex mit wenigem Wasser, nutscht den Niederschlag ab, dampft die Lösung unter verm. Druck ein, löst den Rückstand in Äther, wäscht die äther. Lösung mit Wasser zweimal und dampft sie nach Trocknen über Natriumhydroxyd ein. Der Rückstand zeigt die infraroten Banden bei 3300, 1385, 1375, 1210, 1165, 1070, 1020 cm^{-1}. Man löst oben erhaltenene rohen Aziridinylzucker und 2.00 g Triäthylamin in Benzol und setzt die benzolische Lösung von 1.08 g *p*-Nitrobenzoylchlorid unter Eiskühlung zu. Nach Filtrieren und Waschen mit Natriumbicarbonatlösung und Wasser dampft man die Lösung unter verm. Druck ein. Der Rückstand zeigt die Amid-Bande bei 1680 cm^{-1}. Man versetzt den Rückstand mit 5.10 g

Natriumjodid in 60 ml Aceton, läßt über Nacht stehen und verdünnt mit Wasser zur Bildung der kristallinen Substanz, die aus Äthylacetat umkristallisiert wird. 0.658 g (33% d. Th. in bezug auf X). Gelbliche Nädelchen vom Schmp 188—189°C. $[\alpha]_D^{25} = -48.3°$ (*c* 1.45 $CHCl_3$). Gef: C, 62.71; H, 5.49; N, 6.24%. Ber für $C_{23}H_{24}O_7N_2$: C, 62.72; H, 5.49; N, 6.36%. IR (KBr): 1650, 1515, 1375, 1350, 1080, 1015 cm^{-1}.

3-*O*-Benzyl-1,2-isopropyliden-5,6-*O*-ditosyl-α-D-glucofuranose (XIV). Man setzt 24 g *p*-Toluolsulfonylchlorid in Pyridin (20 ml)-Lösung der 8.46 g rohen 3-*O*-Benzyl-1,2-isopropyliden-α-D-glucofuranose und läßt das Gemisch 24 Std bei Raumtemperatur stehen. Nachdem man zur Lösung Wasser und Chloroform zusetzt und eine Weile stark rührt, trennt man die org. Schicht ab, die mit Wasser nachgewaschen, über Magnesiumsulfat abgetrocknet und eingeengt wird. Der Rückstand wird säulenchromatographisch mittels Silicagels gereinigt, und 12.7 g (64% d. Th.) ditosyliertes Produkt (XIV) wird erhalten. IR: 1370, 1190, 1180, 1095, 920 cm^{-1}. Dünnschichtchromatographisch einheitlich.

6-Azido-3-*O*-Benzyl-1,2-isopropyliden-5-*O*-*p*-toluolsulfonyl-6-desoxy-α-D-glucofuranose (XV). Man rhürt 1.51 g Natriumazid und 12.1 g oben erhaltene ditosylierte Glucofuranose (XIV) in 80 ml DMF eine Std bei Raumtemperatur und eine Std bei 120°C. Nach Stehenlassen über Nacht versetzt man die Lösung mit Xylol und nutscht den Niederschlag mit aktiver Kohle ab. Nach Einengen löst man den Rückstand in Äther und Petroläther (1 : 1), wäscht die Lösung dreimal mit Wasser, trocknet über Magnesiumsulfat ab und dampft sie ein. Man reinigt den Rückstand säulenchromatographisch mittels Silikagels. Ausbeute, 8.30 g (87% d. Th.). IR: 2100, 1375, 1190, 1180, 1095, 1080, 920 cm^{-1}.

5-Amino-5-desoxy-β-L-idose-Derivat (XIII) aus 6-Azido-3-*O*-benzyl-1,2-isopropyliden-5-*O*-*p*-toluolsulfonyl-6-desoxy-α-D-glucofuranose (XV). Man reduziert 2.34 g oben erhaltene Azidofuranose (XV) mit 0.40 g Lithiumaluminiumhydrid in THF und erhält 1.33 g öligen Rückstand, dessen infraroten Spektrum mit dem des oben dargestellten Epiminozuckers (XII) sehr verwandt ist. Wie oben beschrieben, *p*-nitrobenzoyliert man den Rückstand und versetzt das acylierte Produkt mit 5.1 g Natriumjodid in Aceton. Nach Eindampfen der Acetonlösung versetzt man das Reaktionsgemisch mit Wasser unter Bildung der Kristalle, die aus Äthylacetat umkristallisiert werden. Ausbeute, 0.608 g. Die erhaltene Nadeln vom Schmp 187—188°C sind durch Mischprobe und IR-Spektrum mit oben synthetisiertem Oxazolin (XIII) identisch.

In einem anderen Versuch erhält man kristalline 5,6-Epimino-5,6-didesoxy-3-benzyl-β-D-idofuranose (X) nach Destillieren (Kp 170—175°C/1 mmHg) und umkristallisiert aus Cyclohexan. Schmp 93—95°C (Ber Schmp 91—94°C).[9a] $[\alpha]_D^{25} = -59.3°$ (*c* 1.99 $CHCl_3$) (Ber $[\alpha]_D^{21} = -62.1°$ (*c* 1.8 $CHCl_3$)).[9a] Gef: C, 65.32; H, 7.48; N, 4.69%. Ber für $C_{16}H_{21}O_4N$; C, 65.96; H, 7.22; N, 4.81%.

BULLETIN OF THE CHEMICAL SOCIETY OF JAPAN VOL. 43 2506—2511 (1970)

Cyclic Diacylcarbene Generated from Iodonium Ylides and Diazodiketones

Yosio HAYASI, Taiiti OKADA and Mituyosi KAWANISI

Department of Industrial Chemistry, Kyoto University, Sakyo-ku, Kyoto

(Received December 12, 1969)

The preparative method of iodonium ylides, $Ph\text{–}\overset{\oplus}{I}\text{–}\overset{\ominus}{C}(COR)(COR')$, is improved by condensation of active methylene compounds, $H_2C(COR)(COR')$, with iodosobenzene in the presence of acetic anhydride. Thermal and Cu-catalyzed decomposition of iodonium ylides can be differentiated and both are explained in terms of diacylcarbene intermediate with different multiplicity. For the sake of comparison diazodimedone and related compounds are also decomposed by Cu-catalysis as well as by photochemical reaction. Carbene is also found to be a highly probable intermediate. Throughout these investigations the spin multiplicity of the carbene is discussed on the basis of product distributions. Notably in the presence of homogeneous Cu-catalyst in ethanol, diazodimedone gives an insertion product to O–H bond, 2-ethoxy-3-hydroxy-5,5-dimethyl-2-cyclohexenone (XVII), whereas the iodonium ylides do not give such a compound. The formation of XVII is explained by assuming a ketocarbene-Cu-chelate complex.

Ylides and carbenes are structurally related chemical species[1,2] and their reactions have often been interpreted in terms common to both.[3] Neilands *et al.* have carried out an extensive work on the

1) W. Kirmse, "Carbene Chemistry," Academic Press, New York, N. Y. (1964).

2) A. W. Johnson, "Ylid Chemistry," Academic Press, New York, N. Y. (1966).

3) *Inter alia* W. Ando, T. Yagihara, S. Tozune and T. Migita, *J. Amer. Chem. Soc.*, **91**, 2786, 5164 (1969).

preparation of iodonium ylides,[4] but not much is known on the chemistry of an acylcarbene produced by the cleavage of the ylide bond $-\overset{\oplus}{I}-\overset{\ominus}{C}=$. We have been engaged in the iodonium ylide chemistry[5] and found some aspects of the reaction which suggests the carbene intermediacy. In order to gain further insight on the behavior of the cyclic diacylcarbene the reaction of cyclic diazodiketones was also investigated.

Results

Preparation of Iodonium Ylides. We were able to improve the Neilands method and prepared some compounds which could not be obtained by the original method.[4] A convenient method of preparation of sulfonium ylides previously reported[6] has now been extended to the reaction of iodosobenzene and active methylene compounds. Thus phenyl- (I, 74%), *p*-tolyl- (II, 70%), mesityl-iodonium dimedone betaine (III, 40%) and phenyl-iodonium cyclohexa-1,3-dione betaine (IV, 32%) were prepared by condensing respective active methylene compounds with iodosobenzene in the presence of acetic anhydride. An attempted synthesis of II and III according to the Neilands method which involves heating of iodosobenzene and active methylene compounds in chloroform resulted only in the formation of thermally rearranged products.

We were not successful in the preparation of the open chain ylide (V) from dibenzoylmethane presumably because of the instability of the ylide toward acetic acid generated in the reaction. Condensation of malononitrile or bisbenzenesulfonylmethane with iodosobenzene was also unsuccessful. Physical properties of iodonium ylides prepared by our method were reasonable as compared with those of the corresponding sulfonium ylides.[7]

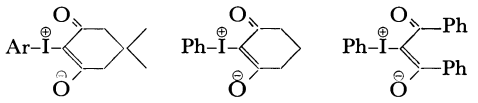

I: Ar=Ph IV V
II: Ar=4-MeC_6H_4
III: Ar=2,4,6-$Me_3C_6H_2$

Thermal and Catalytic Decomposition of Iodonium Ylides. Thermolysis of I in pyridine, water, dioxane and toluene reported by Neilands[4] in which phenyl migration from iodine to oxygen was included has been discussed in detail in the previous paper.[5b] Heating of I in absolute ethanol for 2 hr under reflux afforded dimedone (VI, 10%), dimedone ethyl ether (VII, 32%) and iodobenzene in addition to the rearranged product (VIII, 15%). Analogous results were obtained with II and III.

In the presence of cuprous chloride an exceedingly facile decomposition of I took place at room temperature and a significant difference was observed in the product distribution between the simple thermal and copper-catalyzed decompositions. The major product was 2-iododimedone (IX, 56%) and the rearranged product (VIII) was obtained in only 2% yield. Additional products were phenethole (X, 6%),*1 ethyl 4,4-dimethyl-2-ketocyclopentanecarboxylate[8] (XI, 25%) and iodobenzene.

The thermal reaction of the open chain ylide (V) has never been reported. Heating of V in absolute ethanol under reflux for 2 hr yielded dibenzoylmethane (40%) as a major product along with ethyl benzoylphenylacetate (XII, 17%), ethyl benzoate (5%) and iodobenzene. In contrast to the reaction of I, no detectable amount of the thermally rearranged product (XIII) was obtained.

In the presence of cuprous chloride the spontaneous decomposition of V in ethanol took place at room temperature and afforded XII (46%), tetrabenzoylethylene (21%),[7] ethyl benzoate (5%) and iodobenzene. No detectable amount of dibenzoylmethane was produced.

Decomposition of Diazodimedone in the Presence of Homogeneous Copper Catalyst. When pyrolyzed in refluxing xylene diazodimedone (XIV)[9] was reported to give a dimeric product (XV).[8] Stetter and Kiehs obtained a similar product by an analogous treatment of 2-diazocyclohexane-1,3-dione.[10] The decomposition of XIV in aniline gave 4,4-dimethyl-2-ketocyclopentanecarboxanilide (XVI).[11] The results can be explained by assuming ketoketene intermediate. When XIV was decomposed in the presence of copper catalyst the reaction took a somewhat different course. Thus when XIV was heated in ethanol under reflux in the presence of homogeneous copper catalyst, bis-[*N*-α-phenethylsalicylaldiminato]copper(II),[12] three

4) B. Karele and O. Neilands, *Zh. Org. Khim.*, **4**, 1818 (1968) and references cited therein.

5) a) H. Nozaki, Z. Morita, T. Yamaguti and K. Kondo, 21st Annual Meeting of Chemical Society of Japan, No. 1217, April (1968). b) M. Takaku, Y. Hayasi and H. Nozaki, *Tetrahedron*, in press.

6) H. Nozaki, D. Tunemoto, Z. Morita, K. Nakamura, K. Watanabe, M. Takaku and K. Kondo, *Tetrahedron*, **23**, 4279 (1967).

7) H. Nozaki, M. Takaku, D. Tunemoto, Y. Yamamoto and K. Kondo, *Nippon Kagaku Zasshi*, **88**, 1 (1967).

*1 The yield of X was not definite since it was very difficult to isolate X from the mixture.

8) a) H. Veschambre and D. Vocelle, *Can. J. Chem.*, **47**, 1981 (1969). b) R. N. Chakravarti, *J. Chem. Soc.*, **1947**, 1028.

9) a) J. B. Hendrikson and W. A. Wolf, *J. Org. Chem.*, **33**, 3610 (1968). b) M. Regitz, *Angew. Chem., Int. Ed.*, **6**, 733 (1967).

10) H. Stetter and K. Kiehs, *Chem. Ber.*, **98**, 1181 (1965).

11) B. Eistert, H. Elias, E. Kosch and R. Wollheim, *ibid.*, **92**, 130 (1959).

12) H. Nozaki, H. Takaya, S. Moriuti and R. Noyori, *Tetrahedron*, **24**, 3655 (1968).

products, XI (39%), XVII (25%) and XVIII (14%) were obtained.*2 The product, XVII, mp 94.5°C showed IR absorption band at 1570 cm^{-1} which is ascribed to the monosubstituted dimedone derivative.*3 NMR signals due to the *gem*-methyl and ethyl groups were observed at δ 1.10 (singlet, 6H), 1.27 (triplet, 3H) and 4.04 (quartet, 2H), respectively. Ring methylene protons showed slightly broadened singlet at 2.35 and hydroxyl proton signal appeared at 6.61 as a very broad singlet which indicates the existence of five-membered enolic hydrogen-bonded hydroxyl group.[13] Analysis also supported the assigned structure, XVII. Another crystalline product (XVIII), mp 205°C, had molecular weight of 366 (by mass spectroscopy) corresponding to $C_{20}H_{30}O_6$. Its IR spectrum showed two kinds of carbonyl absorption band at 1732 and 1709 cm^{-1}, and NMR spectrum indicates the presence of both ethoxyl (1.35 and 3.34) and *gem*-methyl (0.83 and 1.72). Ring proton signals appeared as a quartet (geminal AB type; $J=15$ Hz) at 2.45 and 3.20 slightly broadened presumably due to the W-type long-range coupling. The stereochemistry of ring junction is undetermined, but the molecular model suggests that the *trans* configuration is highly probable. Thus we tentatively assigned structure XVIII to this compound. Compound XVII was considerably unstable and turned into XVIII when kept under atmospheric oxygen at room temperature. Thus XVIII can be considered as an oxidative coupling product of XVII.

Photolysis of Diazodimedone. When XIV was photolyzed directly in ethanol, Veschambre and Vocelle[8] observed the formation of VI, dimedone derivative of acetaldehyde (XIX) and 4,5-diketo-2,2,7,7,9-pentamethyloctahydroxanthene (XX) along with XI. We have also obtained the same results in the same reaction.[14] In addition we could confirm that photolysis of XIV in 2-propanol gave acetone which was not easily condensed with dimedone under the present conditions. However, when the reaction was carried out in the presence of an excess amount of benzophenone in ethanol, XIX was detected in the photolysate. Despite every effort we could not detect the presence of XI among the reaction products. It should be noted that benzopinacol was a minor product in this photoreaction with good recovery of benzophenone.

An attempted photolysis of diazomeldrum's acid (5-diazo-2,2-dimethyl-1,3-dioxane-4,6-dione) (XXI)[15] in ethanol resulted only in the formation of meldrum's acid (XXII, 67%)[16] after evolution of 76% of nitrogen.

Discussion

In thermolysis of I, the mechanism of phenyl migration has been discussed.[5b] The formation of other substances may be best rationalized by assuming the cleavage of I-C bond in the yildes to yield a diketocarbene (XXIII) and iodobenzene. The carbene abstracts hydrogen from ethanol to give dimedone (VI) and its ethyl ether (VII). From this chemical behavior the spin multiplicity

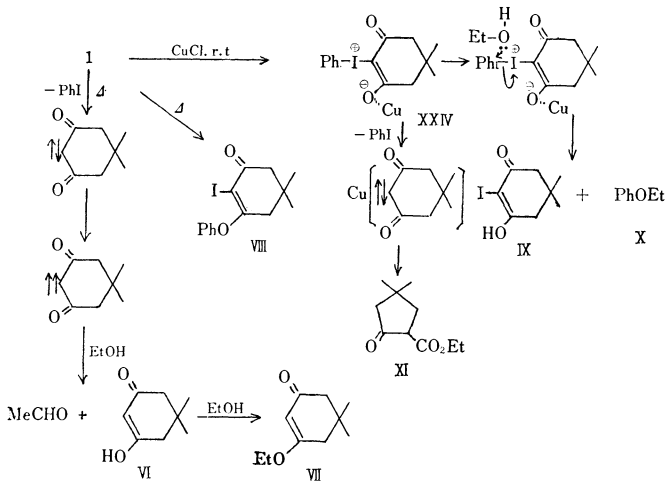

Scheme 1

*2 The reaction catalyzed by $Cu(acac)_2$ or CuCl was extremely complex and detailed analysis of the products was impossible.

*3 For example, 2-methyldimedone absorbs at 1570 cm^{-1}.

13) H. A. Szymanski and R. E. Yelin, "NMR Band Handbook," IFI/Plenum Data Corporation, New York, N. Y. (1968), p. 309.

14) M. Kawanisi, K. Kamogawa, T. Okada and H. Nozaki, 22nd Annual Meeting of Chemical Society of Japan, No. 16322, April, 1969.

15) M. Regitz and D. Stadler, *Ann.*, **687**, 214 (1965).

16) D. Davidson and S. A. Bernhard, *J. Amer. Chem. Soc.*, **70**, 3426 (1948).

of the carbene (XXIII) which is responsible for the reaction is estimated to be triplet in view of the results obtained from the sensitized photolysis of diazodimedone described below. The reason for the facile intersystem crossing from singlet to triplet state is unknown at present, but it may be partly ascribed to the external heavy atom effect[17] due to the presence of iodobenzene.

The Cu-catalyzed reaction is clearly different from the purely thermal one. The formation of phenethole (X) and 2-iododimedone (IX) can be explained by assuming the Cu-coordinated intermediate (XXIV), and subsequent nucleophilic attack of ethanol as depicted in Scheme 1, whereas the formation of the ester (XI) is the result of the Wolff-rearrangement of XXIII in ethanol. The reactive species which is responsible for the Wolff-rearrangement has been claimed to be ketocarbene[18] whose multiplicity is considered to be singlet in view of the discussion by Padwa and Layton.[19] In the present case also the diketocarbene in singlet state should be produced. The presence of Cu salt may prohibit the intersystem crossing and the Wolff-rearrangement became predominant at the expense of hydrogen abstration reaction. This was also the case with V when decomposed by the action of Cu catalyst (Scheme 2). The yield of XII surprisingly increased while no dibenzoylmethane was detected. The absence of XIII among the products of purely thermal reaction may be attributed to the intrinsic lability of V. With respect to the formation of tetrabenzoylethylene the same rationalization as described for the sulfonium ylide should be taken into account.[7]

In conclusion the cleavage of phenyl-iodine bond occurs predominantly in the Cu-catalyzed decomposition of I, while the ylide bond is always broken in the case of V. The reason for this difference should be clarified by further investigation.

The decomposition of XIV in the presence of homogeneous copper catalyst presents a striking contrast to the non-catalyzed reaction as mentioned above. In this case the Wolff-rearrangement was a minor process and the insertion reaction to the solvent alcohol O–H bond became important. The insertion product (XVII) and its oxidation product (XVIII) were produced. Takebayashi and coworkers studied in detail the catalytic decomposition of diazoacetophenone in alcohol in the presence of copper chelates under heterogeneous conditions, and they obtained the insertion products at the expense of the rearranged product.[20] The observation was explained by assuming an intermediary ketocarbene-metal chelate complex. Our results can also be accomodated to this hypothesis except for the formation of the rearranged products (Scheme 3). This may be due to the difference existing in the intermediate carbene complexes or the reaction condition.

The photolysis of diazoacetophenones has been

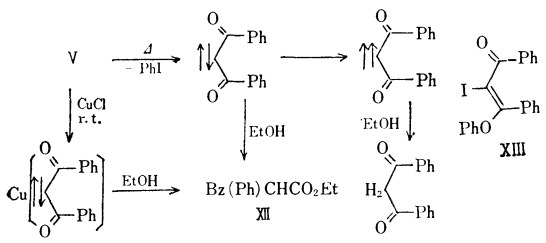

Scheme 2

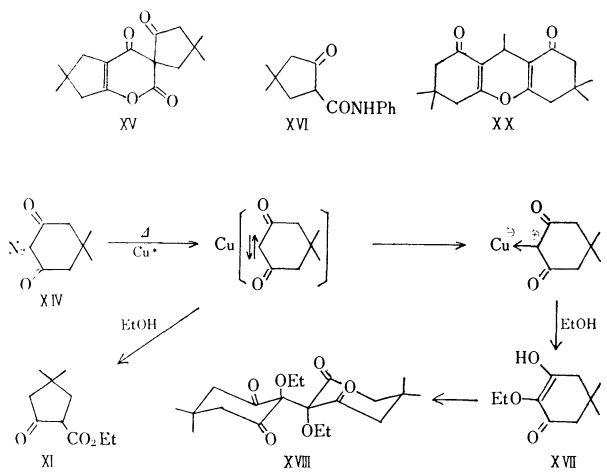

Scheme 3

17) D. S. McClure, *J. Chem. Phys.*, **17**, 905 (1949). *Cf.* U. Schoelkopf and M. Reetz, *Tetrahedron Lett.*, **1969**, 1541.

18) A. Melzer and E. F. Jenny, *ibid.*, **1968**, 4503.

19) A. Padwa and R. Layton, *ibid.*, **1965**, 2167.

20) M. Takebayashi, T. Ibata, H. Kohara and B. H. Kim, This Bulletin, **40**, 2392 (1967).

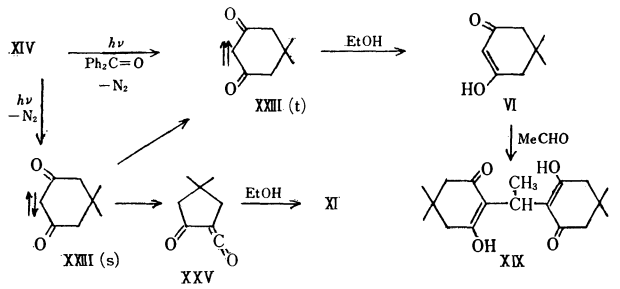

Scheme 4

investigated by several workers[19,21,22] and explained by assuming that triplet benzoylcarbene abstracts hydrogen to give acetophenones and the intersystem crossing of triplet ketocarbene to singlet species efficiently competes with the hydrogen abstraction. Although much has been done with respect to the photochemical generation of ketocarbene, little attention has been focused on the one of β-diketocarbenes.[8,23,24] Direct photolysis of XIV in ethanol gave VI, XIX, XX and XI.[8a] The sensitized photolysis of XIV in the presence of large excess of benzophenone has now clearly demonstrated that only VI was produced through XXIII in triplet state. VI then condensed with acetaldehyde generated in the reaction mixture (Scheme 4). Thus in the case of cyclic diketocarbene the intersystem crossing of triplet XXIII to singlet multiplicity is clearly ruled out, and ester (XI) must be derived from only XXIII in singlet state *via* ketoketene (XXV). It is still open to question as pointed out by Hammond[21] under the present circumstance whether the evolution of nitrogen takes place after or before the intersystem crossing of the excited diazodimedone.

Experimental

All melting points and boiling points are uncorrected. Microanalyses were performed at the Elemental Analyses Center of Kyoto University. The NMR spectra were obtained on a JEOL C-60-H spectrometer with $CDCl_3$ or CCl_4 as solvent and data are given in the order of multiplicity (s=singlet, d=doublet, t=triplet, q=quartet and m=unresolved multiplet), integration. Chemical shifts are reported in δ values relative to TMS as an internal standard. Mass spectra were obtained with a Hitachi RMU-6D mass spectrometer with a direct inlet (200°C) at 80 eV. Plates of Silicagel G were used for thin layer chromatography (TLC) and the spots were visualized with iodine vapor.

Preparation of Iodonium Ylides. A solution of PhIO (0.8 g, 3.6 mmol) and dimedone (0.5 g, 3.6 mmol) in Ac_2O (10 m*l*) was allowed to stand for 10 hr at room temp. The reaction mixture was made basic (pH *ca.* 10) with 20% NaOH aq. and then extracted with $CHCl_3$. Drying ($MgSO_4$) and concentration of the extract *in vacuo* gave an oil which solidified upon addition of ether. This solid substance was recrystallized from PhH to afford 0.9 g (74%) of I, mp 126—128°C(dec) (lit,[25] 132—133°C), IR (Nujol): 1530 cm^{-1}, λ_{max}^{EtOH}: 261 nm (log ε 4.0), NMR: δ 1.05 (s, 6H), 2.48 (s, 4H), 7.2—7.9 (m, 5H).

An analogous procedure was used for the preparation of III (40%), mp 133—135°C. Found: C, 52.60; H, 5.48. Calcd for $C_{17}H_{21}IO_2$: C, 53.14; H, 5.51%. IR (Nujol): 1560 cm^{-1}, λ_{max}^{EtOH} 266 nm (log ε 4.2), NMR: δ 1.02 (s, 6H) 2.30 (s, 3H), 2.43 (s, 4H), 2.75 (s, 6H), 6.9—7.1 (m, 2H), from iodosomesitylene and dimedone, and IV (32%), mp 109—110°C. Found: C, 46.00; H, 3.24. Calcd for $C_{12}H_{11}IO_2$: C, 45.88; H, 3.53%. IR (Nujol): 1530—1550 cm^{-1}, λ_{max}^{EtOH} 259 nm (logε 4.29), from iodosobenzene and dihydroresorcinol.

3-Mesityloxy-5,5-dimethyl-2-iodo-2-cyclohexenone. A $CHCl_3$ (20 m*l*) suspension of iodosomesitylene (1.32 g, 5 mmol) and dimedone (0.7 g, 5 mmol) was refluxed for 1 hr according to the Neilands method. Evaporation of the solvent afforded a crystalline solid, which was recrystallized from EtOH to give 1.2 g (60%) of 3-mesityloxy-5,5-dimethyl-2-iodo-2-cyclohexenone, mp 148—150°C, IR (nujol): 1660, 1583, 1130 cm^{-1}, NMR: δ 1.30 (s, 6H), 2.07 (s, 2H), 2.13 (s, 6H), 2.29 (s, 3H), 2.47 (s, 2H), 6.87 (s, 2H). Found: C, 53.01; H, 5.61. Calcd for $C_{17}H_{21}IO_2$: C, 53.14; H, 5.51%.

Thermolysis of I in EtOH. A solution of I (6 g, 17.5 mmol) in EtOH (100 m*l*) was refluxed for 10 hr under a slow stream of nitrogen. Removal of the solvent in a vacuum gave a mixture of products (4.1 g) from which a crystalline solid precipitated. Collection by filtration followed by recrystallization from EtOH afforded 0.9 g (15%) of VIII, mp 164—165°C (lit,[26] 165—166°C), IR(nujol): 1670, 1580, 1230 cm^{-1}, λ_{max}^{EtOH}: 275 nm (log ε 4.07), NMR: δ 1.05 (s, 6H), 2.30 (s, 2H), 2.50 (s, 2H), 6.9—7.5 (m, 5H). Distillation of the filtrate *in vacuo* afforded PhI and VII (0.95 g, 32%). bp 77—81°C/2 mmHg (lit,[27] 252°C), which solidified

21) D. O. Cowan, M. M. Cough, K. R. Kopecky and G. S. Hammond, *J. Org. Chem.*, **29**, 1922 (1964) and references cited therein.

22) N. R. Gohsh, C. R. Goshal and S. Shan, *Chem. Commun.*, **1969**, 151.

23) L. Horner and E. Spietschka, *Chem. Ber.*, **85**, 225 (1952).

24) F. Weygand, H. Dworschak, K. Koch and S. Konstas, *Angew. Chem.*, **73**, 409 (1961).

25) E. Gudriniece and O. Neilands, *Chem. Abstr.*, **52**, 7177e (1958).

26) O. Neilands, G. Vanago and E. Gudriniece, *ibid.*, **52**, 19988c (1958).

27) A. W. Crossley and N. Renouf, *J. Chem. Soc.*, **93**, 640 (1908).

to give white crystals on standing in a refrigerator, mp 58—59°C (lit,[27] 59.5—60°C), IR(Nujol): 1660, 1610, 1220, 1140 cm^{-1}, NMR: δ 1.10 (s, 6H,), 1.37 (t, 3H), 2.20 (s, 2H), 2.28 (s, 2H), 3.90 (q, 2H), 5.35 (s, 1H). (Found: C, 71.14; H, 9.51). The residue afforded VI (0.24 g, 10%) upon addition of ether. The evolved N_2 gas was passed into the 2,4-dinitrophenylhydrazine solution. The yellow precipitates obtained were identical with the authentic specimen of acetaldehyde 2,4-dinitrophenylhydrazone.

Copper-catalyzed Decomposition of I. Cuprous chloride (0.16 g, 1.6 mmol) was added in one portion to a solution of I (6 g, 17.5 mmol) in absolute EtOH (100 m*l*) under N_2 atm and stirred at room temp for 10 hr. Copper catalyst combined with iododimedone was removed by filtration and the filtrate was concentrated *in vacuo*. From the residual oil crystals were formed, collected by filtration and washed with PhH to yield IX (2.6 g, 56%), mp 150—152°C (lit,[28] 160—162°C), IR (Nujol): 1570 cm^{-1}. (Found: C, 36.18: H, 4.36.)

The filtrate was concentrated *in vacuo* and the residual oil (2.0 g) was subjected to chromatography (Silicagel), followed by preparative GLC giving VIII (0.1 g, 2%), phenethole (X) (0.12 g, 6%), PhI (0.3 g) and an oil XI (0.8 g, 25%). The compound XI showed IR (neat) absorptions at 3475, 1760, 1730 and 1190 cm^{-1}; NMR ($CDCl_3$) signals at δ 1.16 (s, 3H), 1.25 (s, 3H), 1.28 (t, 3H), 1.99 (d, 1H, J=14 Hz), 2.40 (s, 2H), 2.43 (d, 1H, J=14 Hz), 3.75 (broad s, 1H) and 4.23 (q, 2H), which were identical with those of authentic ethyl 4,4-dimethyl-2-oxocyclopentane-1-carboxylate.[8]

Thermolysis of V in EtOH. A solution of V (11 g, 25.8 mmol) in absolute EtOH (200 m*l*) was refluxed for 2 hr. After evaporation of the solvent, the residual oil (8.54 g) was chromatographed on a Silica gel column with PhH as an eluant to give PhI (3.2 g, 60%), dibenzoylmethane (2.3 g, 40%), ethyl benzoate (0.2 g, 5%) and XII (1.1 g, 17%), mp 89—90°C (from *i*-PrOH) (lit,[29] 90—91°C), IR (Nujol): 1750, 1685, 1260 cm^{-1}.

Copper-catalyzed Decomposition of V. Cuprous chloride (0.3 g, 3 mmol) was added to a solution of V (9 g, 21.2 mmol) in absolute EtOH (250 m*l*) under N_2 atm and stirred at room temp. for 12 hr. After filtration, the solvent was removed in a vacuum. The residual oil (6.3 g) was distilled *in vacuo* to yield an oily mixture, which was subjected to GLC analysis. Iodobenzene, ethyl benzoate (0.16 g, 5%) and XII (2.5 g, 44%) were identified by comparison of the retention times on GLC and IR spectra with those of authentic specimens. From the distillation residue, 2.0 g (21%) of tetrabenzoylethylene was obtained which melted at 183—185°C (lit,[30] 184°C) upon recrystallization from EtOH. (Found: C, 81.21; H, 4.80%. Calcd for $C_{30}H_{20}O_4$: C, 81.06; H, 4.54%.)

Thermal Decomposition of XIV in the Presence of the Homogeneous Catalyst. A solution of diazodimedone (XIV)[9] (3 g, 18 mmol) in EtOH (120 m*l*) in the presence of bis(*N*-α-phenethylsalicylaldiminate)copper(II)[12] (50 mg) was heated under reflux for 15 hr. Quantitative amount of nitrogen gas was evolved. After removal of the solvent, the resulting masses were collected by filtration and recrystallized from ethyl acetate to afford XVIII (0.47 g, 14%), mp 205—206°C IR(KBr): 1732, 1709, 1140 and 1098 cm^{-1}, NMR: δ 0.83 (s, 6H), 1.11 (s, 6H), 1.26 (t, 6H), 2.83 (q, (*gem*-AB), J=15 Hz, 8H), 3.35 (q, 4H). Found: C, 65.66; H, 8.30%. Calcd for $C_{20}H_{30}O_6$: C, 65.66; H, 8.25%. Mass spectra had parent peak at *m/e* 366. From these data XVIII was assigned to be bis-2,2'-(2-ethoxy-5,5-dimethyl-1,3-cyclohexanedione). The filtrate was concentrated and chromatographed on Silicagel column. The following compounds were isolated and identified: XI (1.29 g, 39%), bp 75—80°C/2 mmHg, 2-ethoxy-3-hydroxy-5,5-dimethyl-2-cyclohexenone (XVII), (0.83 g, 25%), mp 94.5°C (from cyclohexane), very hygroscopic, fairly unstable crystalline solid. IR (Nujol): 2600 (weak) 1570, 1250, 1120, 1035 cm^{-1}, NMR: δ 1.10 (s, 6H), 1.27 (t, 3H), 2.35 (s, 4H), 4.04 (q, 2H), 6.61 (s, 1H, enolic proton*4). Found: C, 65.19; H, 8.75%. Calcd for $C_{10}H_{16}O_3$: C, 65.32; H, 8.80%. Exposure of XVII to atmospheric oxygen resulted in the formation of XVIII almost quantitatively.

Photochemical Decomposition of Diazodimedone, a Sensitized Experiment. A solution of XIV (1.0 g, 6 mmol) in EtOH (20 m*l*) containing benzophenone (5 g, 28 mmol) was irradiated by means of 200 W high pressure mercury arc (Pyrex filter) for 12 hr. Under this condition almost all the incident light was absorbed by benzophenone.*5 After evolution of the theoretical amount of nitrogen gas the reaction mixture was concentrated *in vacuo* and the residue was chromatographed on Silicagel column. The following compounds were isolated: XIX (0.47 g, 51%), benzopinacol (0.16 g, 1.6%) and recovered benzophenone (4.28 g, 96%).

Photolysis of XIV in 2-Propanol. A solution of XIV (1 g, 6 mmol) in 2-propanol (20 m*l*) was irradiated by means of Pyrex-filtered Hg arc. The reaction mixture was subjected to distillation and the distillate was poured into a solution of 2,4-dinitrophenylhydrazine. 2,4-Dinitrophenylhydrazone of acetone precipitated. From the distillation residue VI (0.68 g, 80%) was isolated.

Photochemical Decomposition of 5-Diazo-2,2-dimethyl-1,3-dioxa-4,6-dione (Diazomeldrum's Acid). A solution of 2-diazomeldrum's acid[9] (2 g, 12 mmol) in EtOH (80 m*l*) was irradiated by means of a 200 W high pressure Hg arc (Pyrex filter) for 50 hr. Seventy per cent of theoretical amount of nitrogen gas was evolved. The reaction mixture was concentrated *in vacuo* and the residue was recrystallized from EtOH to afford meldrum's acid (1.12 g, 67%), mp 94°C (lit,[16] 94—95°C).

The authors are grateful to Professors Keiiti Sisido and Hitosi Nozaki for help and encouragement. They are also indebted to Messrs. Zyun-iti Morita, Tadasige Yamaguti and Koiti Kamogawa for valuable assistance.

28) D. Vorlaender and M. Kohlmann, *Ann.*, **322**, 254 (1902).

29) W. Wislicenus, H. Eichert and M. Marquardt, *ibid.*, **436**, 92 (1924).

30) H. von Halban and H. Geigel, *Z. Phys. Chem.*, **96**, 233 (1920).

*4 Enolic proton of hydrogen-bonded five-membered ring appears in this region. See Ref. 13.

*5 *Cf.* benzophenone; $\varepsilon_{300nm}^{EtOH}$ 700, diazodimedone: ε_{300}^{EtOH} 52.

BULLETIN OF THE CHEMICAL SOCIETY OF JAPAN VOL. 43 2512—2515 (1970)

The Codimerization of Styrene with Ethylene Catalyzed by Olefin-palladium(II) Chloride Complexes

Keiji KAWAMOTO, Toshinobu IMANAKA and Shiichiro TERANISHI

Department of Chemical Engineering, Faculty of Engineering Science, Osaka University, Machikaneyama, Toyonaka, Osaka

(Received December 12, 1969)

The codimerization of styrene with ethylene catalyzed by the olefin-palladium chloride complexes was investigated in a homogeneous system under mild conditions; di-μ-chloro-dichlorobis-(styrene)dipalladium(II), $(Pd(C_6H_5CH{=}CH_2)Cl_2)_2$, was found to be an effective catalyst. When ethylene was bubbled into a styrene solution containing the styrene-palladium complex at 50°C for 6 hr, codimers including *trans*-1-phenyl-1-butene, *cis*-1-phenyl-1-butene, and *trans*-1-phenyl-2-butene were obtained in 1278, 57 and 170% yields respectively, based on palladium(II) used. However, the absence of ethylene resulted in the formation of a 70% yield of the dimer of styrene, *trans*-1,3-diphenyl-1-butene. The order of the solvent effect on the rate of the codimerization was as follows: nitrobenzene>nitromethane>acetic acid, phenol>dioxane≫benzene≫acetonitrile. A possible mechanism for this reaction was discussed on the basis of the present results.

Many investigations have recently been reported into the cooligomerizations of conjugated dienes with mono-olefins catalyzed by transition-metal compounds.[1] Only little is known, however, about the codimerization of styrene with ethylene catalyzed by transition-metal compounds. Müller and his co-workers have reported that the cocatalyst consisting of nickel acetylacetonate, trialkylaluminum, and phosphite catalyzes the codimerization of styrene with ethylene to give cocyclic higher oligomers and a small amount of codimer.[2] Alderson and his co-workers described how rhodium chloride and ruthenium chloride also catalyze the codimerization of styrene with ethylene under a high pressure to give 2-phenyl-2-butene.[3]

As has been reported in a preliminary communication,[4] we have found that di-μ-chloro-dichlorobis-(styrene)dipalladium(II) is an effective catalyst for the codimerization of styrene with ethylene. In this paper detailed studies of the reaction catalyzed by olefin-palladium chloride complexes will be reported.

Experimental

Codimerization of Styrene with Ethylene by a Styrene-palladium Complex Catalyst. A reaction vessel was charged with 4.5 g of styrene-palladium chloride and 150 m*l* of styrene, and then ethylene was bubbled into the mixture at 50°C for 6 hr. This solution became a reddish-yellow. The color did not vary during the reaction, indicating that the complex functions as a stable catalyst, although only a slight precipitation of metallic palladium was observed in the final stage of the reaction. The resulting solution was diluted with petroleum ether after the unreacted styrene had been removed under reduced pressure at 50°C; then it was filtered in order to remove the palladium complex and palladium metal. The distillation of the filtrate gave 27.1 g of *trans*-1-phenyl-1-butene, 1.2 g of *cis*-1-phenyl-1-butene, 3.6 g of *trans*-1-phenyl-2-butene, and 0.4 g of acetophenone, all of which were identical with authentic samples.[5]

trans-1-Phenyl-1-butene: IR spectrum: *trans*-HC=CH- 960 cm^{-1}, phenyl 740 and 690 cm^{-1}. NMR spectrum: CH_3 τ 8.80 (triplet), CH_2 τ 7.70 (quintet), -HC=CH- τ 3.70 (multiplet), phenyl τ 2.38 (multiplet). Found: C, 90.92; H, 9.13%. Calcd for $C_{10}H_{12}$: C, 90.90; H, 9.12%.

cis-1-Phenyl-1-butene: NMR spectrum: CH_3 τ 8.95 (triplet), CH_2 τ 7.63 (quintet), -HC=CH- τ 3.67 and 4.40 (multiplet), phenyl τ 2.83 (multiplet).

trans-1-Phenyl-2-butene: IR spectrum: *trans*-HC=CH- 968 cm^{-1}, phenyl 745 and 695 cm^{-1}. NMR spectrum: CH_3 τ 8.31 (doublet), CH_2 τ 6.73 (doublet), -HC=CH- τ 4.50 (multiplet), phenyl τ 2.85 (multiplet).

Reaction Kinetics. The apparatus and procedure used to measure the reaction rates were similar to those employed before.[6] The reaction rates were determined

1) See, for example, C. W. Bird, "Transition Metal Intermediates in Organic Synthesis," Logos Press, London (1967), p. 50.

2) H. Müller, D. Wittenberg, H. Seibt and E. Scharf, *Angew. Chem. Intern. Ed.* **4**, 327 (1965).

3) T. Alderson, E. L. Tenner and R. V. Lindsey, Jr., *J. Amer. Chem. Soc.*, **87**, 5638 (1965).

4) K. Kawamoto, T. Imanaka and S. Teranishi, *Kogyo Kagaku Zasshi*, **72**, 1612 (1969).

5) a) A. Klages, *Ber.*, **37**, 2312 (1904). b) E. Erlenmeyer, *Ann.*, **135**, 122 (1865). c) F. R. Mayo, *J. Amer. Chem. Soc.*, **90**, 1289 (1968).

6) K. Kawamoto, T. Imanaka and S. Teranishi, *Nippon Kagaku Zasshi*, **89**, 639 (1968).

by measuring the amount of *trans*-1-phenyl-1-butene formed and that of ethylene absorbed.

Results and Discussion

Products. The codimerization reaction of styrene with ethylene catalyzed by the styrene - palladium chloride was carried out at 50°C for 6 hr, ethylene being bubbled into the styrene solution containing the catalyst.[4] The following products were obtained:

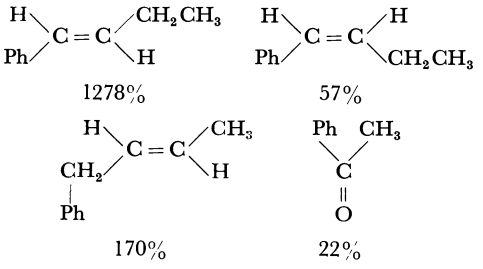

(based on palladium(II))

The total amount was more than 15 mol equivalents of the palladium complex, indicating that the styrene - palladium complex is an effective catalyst for the codimerization reaction under the mild conditions here adopted.

It is interesting that no dimers of styrene and ethylene were formed. In the absence of ethylene under the same conditions, the dimer of styrene, *trans*-1,3-diphenyl-1-butene, and acetophenone were formed in 70 and 30% yields respectively, on the basis of palladium(II). It has previously been reported[6] that the dimerization reaction of ethylene proceeded when ethylene was bubbled into a reaction mixture of dioxane and ethylene - palladium chloride. These facts indicate that the coexistence of styrene and ethylene inhibits the dimerization reactions.

The formation of acetophenone may be due to the reaction of styrene with the moisture, since a partial precipitation of metallic palladium in the course of the reaction was observed.[7]

Activity of Styrene-, Ethylene-palladium Complexes and Palladium Chloride. The codimerization reaction of styrene with ethylene was studied by using styrene- and ethylene-palladium complexes and palladium chloride. The results are shown in Fig. 1, where the amount of ethylene absorbed from the gas phase and that of the *trans*-1-phenyl-1-butene formed are plotted *vs.* the reaction time. From the gas-chromatographic analysis, it

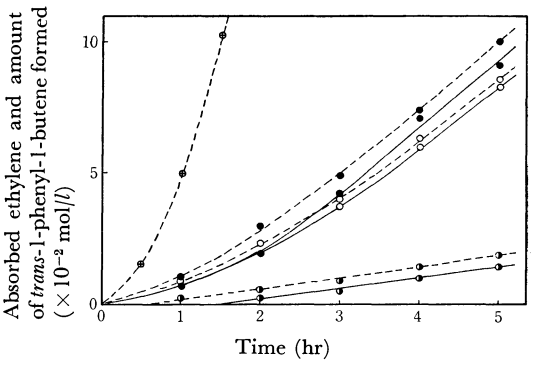

Fig. 1. The time dependences of the absorption of ethylene and the formation of *trans*-1-phenyl-1-butene.
——: amount of *trans*-1-phenyl-1-butene, ------: absorbed ethylene, ⊕: ethylene-palladium complex-dioxane system, ●: styrene-palladium complex, ○: ethylene-palladium complex, ◑: $PdCl_2$, neat(styrene at 8.72 mol/*l*), (Pd): 1.06×10^{-2} mol/*l*, concentration of ethylene: 6.36×10^{-2} mol/*l*, 50± 0.2°C.

was found that the amounts of the other codimers were proportional to that of *trans*-1-phenyl-1-butene, and that the absorbed ethylene was almost completely consumed in the codimerization. As is shown in Fig. 1, the reaction has an induction period (*ca.* 30 min) which was slightly different for various solvents.

The dimerization of ethylene, which was observed in the reaction system of dioxane and ethylene-palladium complex, is also shown in Fig. 1. It is necessary to point out that the dimerization reaction of ethylene is much faster than the codimerization reaction of styrene with ethylene. However, no dimer of ethylene has been formed in the present system.

The reactivities of palladium complexes decreased in the following order: styrene complex≳ethylene complex≫palladium chloride.

Solvent Effect. The solvent effect on the codimerization reaction of styrene with ethylene is summarized in Table 1. The dipole moments and the dielectric constants of the solvents are also shown in Table 1.

The reaction rate is subjected to restriction in both a nonpolar solvent such as benzene and a strongly polar solvent such as acetonitrile. In acetonitrile palladium complex is changed into an insoluble yellow complex. The reaction rate is particularly enhanced in a solvent containing oxygen atom. A similar effect was also observed in the dimerization reaction of ethylene.[9]

The rate decreases in the following sequence: nitrobenzene > nitromethane > acetic acid > phenol > dioxane. Table 1 shows that the sequence agrees

7) The formation of acetophenone from styrene and water by palladium salts is well known. For example, (i) J. Smidt, W. Hafner, R. Jira, J. Sedlmeiner, R. Sieber, R. Ruttinger and H. Kojer, *Angew. Chem.*, **71**, 176 (1959). (ii) J. Smidt, W. Hafner, R. Jira, R. Sieber, J. Sedlmeier and A. Sabel, *ibid.*, **74**, 93 (1962).

9) K. Kawamoto, T. Imanaka and S. Teranishi, *Nippon Kagaku Zasshi*, **91**, 39 (1970).

TABLE 1. EFFECT OF SOLVENTS

Solvent	Concentration of ethylene ($\times 10^{-2}$mol/l)	Rate of formation for *trans*-1-phenyl-1-butene ($\times 10^{-2}$ mol/l hr)	Dipole moment[8] μ	Dielectric constant[8] ε (°C)
Nitrobenzene	4.46	6.36	4.21	34. 8 (25)
Nitromethane	4.90	4.60	3.46	35. 9 (30)
Acetic acid	6.36	2.25	1.73	6.15 (20)
Phenol	3.65	1.90	1.14	9.87 (60)
Dioxane	6.37	1.25	—	2.28 (0)
Benzene	6.01	0.96	0	2.44 (0)
Acetonitrile	5.41	0.22	—	37. 5 (20)
Styrene	6.36	1.38	—	2.43 (25)

Styrene-palladium complex (Pd): 1.12×10^{-2} mol/l. Solvent+styrene (1:1 vol. ratio): 80 cc.
Reaction temperature: 50±0.2°C.

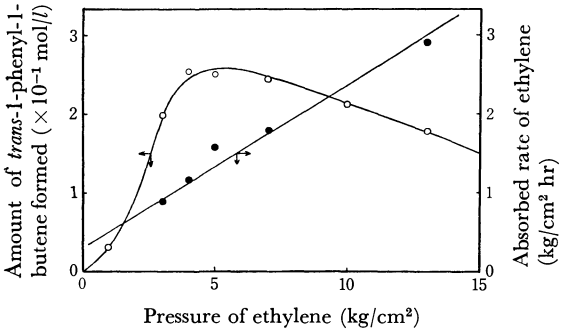

Fig. 2. The dependence of ethylene pressure on the amount of *trans*-1-phenyl-1-butene formed.
styrene - palladium complex (Pd): 2.97×10^{-2} mol/l, styrene+benzene (1 : 1 vol. ratio) : 60 cc, 100 cc glass autoclave, 50°C, 5 hr.

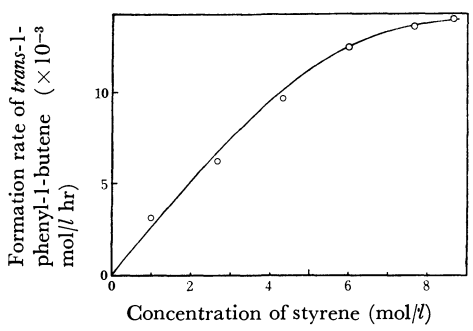

Fig. 3. The dependence of the concentration of styrene on the formation rate of *trans*-1-phenyl-1-butene.
styrene-palladium complex (Pd): 1.12×10^{-2} mol/l, concentration of ethylene: 6.01×10^{-2} mol/l, solvent: benzene, 50±0.2°C.

with the decreases in the dipole moment (μ) and dielectric constant (ε).

It should be noted here that; (i) the complex is partly reduced to metallic palladium in the early stage of the reaction in phenol, and (ii) the liquid-phase concentration of ethylene is much lower in phenol than in acetic acid. These facts indicate that the corrected rate of the codimerization in phenol is faster than that in acetic acid.

Effect of Ethylene Pressure. The codimerization was examined as the ethylene pressure increased from 1 to 15 atm. The results are shown in Fig. 2. The styrene - palladium complex was used as a catalyst. The amount of *trans*-1-phenyl-1-butene formed initially increases, reaches a maximum at an ethylene pressure of 4 atm, and then gradually decreases. At a high pressure of ethylene, the rate of the formation of butene increases with an increase in the ethylene pressure.

These results indicate that the codimerization reaction is favored at low pressures of ethylene and that the dimerization reaction of ethylene predominates above an ethylene pressure of 4 atm.

Effect of Styrene Concentration. The formation rate of *trans*-1-phenyl-1-butene was measured by diluting styrene with benzene. In benzene the codimerization and dimerization reactions did not occur. The results are shown in Fig. 3. The reaction rate increased with an increase in the styrene concentration, and the order of the reaction changed from one to zero.

Reaction Mechanism. In view of the above facts, we propose the reaction mechanism of the codimerization shown in Scheme 1.

The styrene-palladium complex (1) initially dissociates into the complex (2) in the presence of a solvent. The coordination of ethylene with the complex (2) results in the complex (3). In the complex (3) the insertion between the coordinated styrene and ethylene produces the complex (4). Finally styrene rapidly displaces the coordinated dimer in the complex (4), reforming the complex (2). In the stage of changing from the complex (4) to (2), the amount of coordinated ethylene instead of styrene can be ignored, since the liquid-

8) The Chem. Soc. Japan, "Kagaku Binran, Kisohen I," Maruzen, Tokyo (1966), pp. 1003, 1226.

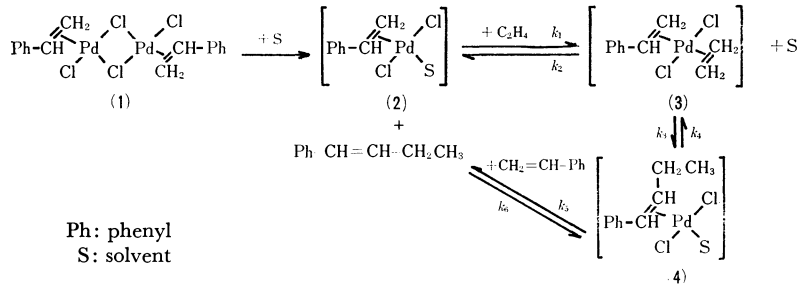

Scheme 1

phase concentration of styrene is more than 100 mol equivalents of that of ethylene at a low pressure of ethylene. However, with an increase in the pressure of ethylene, this amount can not be ignored, and another complex coordinated by ethylene and the solvent must be formed. In this case, another circulation was previously proposed for the dimerization of ethylene by the present authors.[6]

In the stage of changing from the complex (2) to (3), it is natural that the complex coordinated by two molecules of styrene is formed, since the concentration of styrene is much higher than that of ethylene. Therefore, the fact that styrene does not undergo the dimerization suggests that the insertion reaction between coordinated styrene and ethylene is much faster than that between coordinated styrenes.

When the stage of changing from the complex (3) to (4) is the rate-determining step,[6] the rate of the codimerization is given by;

$$r_c = k(\mathrm{St})(\mathrm{S})/\{(k'+k''(\mathrm{St}))(\mathrm{S})+k'''(\mathrm{St})\}$$

where $k=k_1k_3k_5/(k_2+k_3)$, $k'=k_1k_3/(k_2+k_3)+k_6(\mathrm{C})$, $k''=k_5/(\mathrm{E})$, and $k'''=k_1k_5/(k_2+k_3)$, and where (C), (E), (St), (S) represent the liquid-phase concentration of the codimer, ethylene, styrene, and the solvent respectively.

The above equation shows that the reaction order changes from one to zero with an increase in the styrene concentrations. The experimental evidence in the reaction order can, therefore, be interpreted on the basis of Scheme 1.

The fact that solvents containing oxygen atom are effective in the codimerization reaction can be reasonably understood by considering that the oxygen atom tends to have a moderate ability of coordination. The ease of the solvents in both coordination to and dissociation from the complex leads to a promotion of the reactivity of the coordination site. The same argument was previously made by the present authors for the dimerization of ethylene.[9]

BULLETIN OF THE CHEMICAL SOCIETY OF JAPAN VOL. 43 2515—2518 (1970)

The Synthesis of Poly-L-arginine*1

Junzo NOGUCHI and Yukihiko FUJIWARA

Department of Polymer Science, Faculty of Science, Hokkaido University, Sapporo

(Received December 25, 1969)

N^{ω}-Tosyl-L-arginine-N^{α}-carboxylic acid anhydride hydrochloride was obtained as a crystal by the reaction of N^{α}-carbobenzyloxy-N^{ω}-tosyl-L-arginine and thionyl chloride. After treatment with silver oxide to remove the hydrochloride, N^{ω}-tosyl-L-arginine-N^{ω}-carboxylic acid anhydride (NCA) was prepared; it was then polymerized to poly-N^{α}-tosyl-L-arginine ($M \fallingdotseq 16200$, $n \fallingdotseq 52$), which was subsequently converted into poly-L-arginine hydrochloride by treating it with hydrogen fluoride and by passing it through a column of the hydrochloride form of the IRA-400 resin.

Poly-L-arginine is an interesting model of the natural basic proteins, such as curpeine or sarmine, containing large amount of arginine.

The preparation of the *N*-carboxylic acid anhydride (NCA) of the L-arginine derivative has been studied in order to synthesize poly-L-arginine,

*1 Presented at the Autumn Meeting of the Chemical Society and the related Societies of Japan, Nagoya, Oct. 14, 1969.

but the results were almost entirely unsuccessful with regard to the chemical specificity of the guanido group, although all of native amino acids except arginine have been converted into their NCA's. However, arginine NCA was recently prepared in the case of the arginine derivative whose N^{δ}-imino group was protected as the carbobenzyloxy group, because when the arginine derivative is treated by the Leuchs method[1] or the Fuchs-Farthing method,[2] the α-carboxyl group tends to form a closed ring with the N^{δ}-imino group of arginine. Poly-L-arginine has been prepared by the following three methods: **a**) poly-ornithine, which had itself been prepared from δ-protected ornithine NCA, was guanidized with 1-guanyl-3,5-dimethyl pyrazole[3] or with methyl isothiourea[4] into polyarginine; **b**) poly-L-nitroarginine, which had been prepared by the *N*-carbothiophenyl method,[5] was reduced in formic acid with stannous chloride into poly-L-arginine,[6] and **c**) $N^{\omega},N^{\omega'}$-dicarbobenzyloxy-L-arginine NCA hydrochloride,[7] which had been prepared from $N^{\alpha},N^{\omega},N^{\omega'}$-tricarbobenzyloxy-L-arginine and thionyl chloride, was polymerized, after treatment with silver oxide in order to remove its hydrochloride, into poly-$N^{\omega},N^{\omega'}$-dicarbobenzyloxy-L-arginine, which was then decarbobenzyloxylated with hydrogen bromide in acetic acid in order to convert it into poly-L-arginine.[7]

However, the quantitative guanidation of all the ornithine residues of poly-ornithine is not easy with the method a), poly-L-arginine is hard to get in a high polymer with the method b), and $N^{\alpha},N^{\omega},N^{\omega'}$-tricarbobenzyloxy-L-arginine can not easily be prepared in a good yield in the method c) and, for the complete decarbobenzyloxylation of poly-$N^{\omega},N^{\omega'}$-dicarbobenzyloxy-L-arginine, it is necessary to employ the drastic step of heating it at 50°C for 90 min in 6N HBr - glacial acetic scid. The chemical properties of the N^{ω}-carbobenzyloxy group are so different from those of an ordinary *N*-carbobenzyloxy group that such a drastic step to removing the protecting group is not generally applicable to the synthesis of an arginine copolymer without a cleavage of the peptide bond.

In this investigation, the synthesis of N^{ω}-tosyl-L-arginine NCA was studied, because the nature of N^{α}-carbobenzyloxy-N^{ω}-tosyl-L-arginine is such that it is hard to form a N^{δ}-closed ring with the α-carboxyl group in peptide syntheses and the tosyl of guanido group can easily be removed by hydrogen fluoride. N^{ω}-Tosyl-L-arginine NCA hydrochloride was obtained for the first time as a crystal without protecting an N^{δ}- or N^{ω}-imino group of L-arginine. After the removal of hydrogen chloride from the NCA hydrochloride with silver oxide, the resulting syrupy NCA was ploymerized into poly-N^{ω}-tosyl-L-arginine which was then converted to poly-L-arginine with hydrogen fluoride.[8]

Results and Discussion

The synthetic route of poly-L-arginine is summarized in Scheme 1.

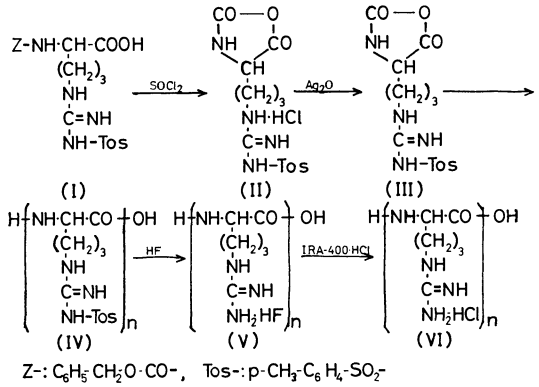

Scheme 1. The synthetic route of poly-L-arginine hydrochloride.

A syrupy N^{ω}-tosyl-L-arginine NCA (III) was obtained from II by treating the dry acetone solution with silver oxide in order to remove the hydrogen chloride and by evaporating the solvent after the acetone solution had been passed through a column of dry active charcoal. This NCA was immediately dissolved in dimethylacetamide (DMA), dioxane, hexamethyl phosphoramide (HMPA), or dimethyl sulfoxide (DMSO), and polymerized at room temperature in a sealed flask with a mercury manometer. The highest molecular weight was obtained in DMA ($M\fallingdotseq16200$, $n\fallingdotseq52$, $[\alpha]_D^{30}$ +9.9°). The polymerization in dioxane and DMSO gave a lower polymer ($M\fallingdotseq8400$, $n\fallingdotseq27$, $[\alpha]_D^{30}$ +7°). The difference in $[\alpha]_D$ between the two polymers may be due to the difference in molecular weight, for their hydrolysates, when treated with 6N hydrochloric acid at 110°C for 22 hr, gave only L-arginine without any racemization. Poly-N^{ω}-tosyl-L-arginine (IV) was treated with hydrogen

1) H. Leuchs, *Ber.*, **39**, 857 (1906).
2) A. C. Farthing and R. J. W. Reynolds, *Nature*, **165**, 647 (1950).
3) S. Ariely, M. Wilcheck and A. Patchornik, *Biopolymers*, **4**, 91 (1966).
4) E. Katchalski and P. Spitnik, *J. Amer. Chem. Soc.*, **73**, 3992 (1951).
5) T. Hayakawa, T. Mizuno and J. Noguchi, *Nippon Kagaku Zasshi*, **81**, 618 (1960).
6) T. Hayakawa, Y. Fujiwara and J. Noguchi, This Bulletin, **40**, 1205 (1967).
7) T. Hayakawa, Y. Kondo, H. Yamamoto and Y. Murakami, *ibid.*, **42**, 479 (1969).
8) S. Sakakibara, Y. Shimonishi, Y. Kishida, M. Okada and H. Sugihara, This Bulletin, **40**, 2164 (1967); S. Sakakibara, Y. Kishida, R. Nishizawa and Y. Shimonishi, *ibid.*, **41**, 438 (1968); S. Sakakibara, N. Nakamizo, Y. Kishida and S. Yoshimura, *ibid.*, **41**, 1477 (1968).

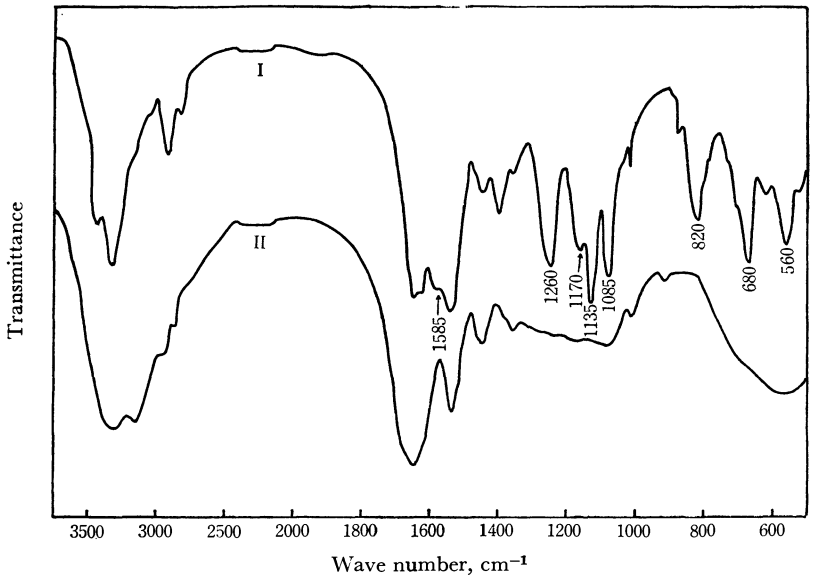

Fig. 1. Infrared absorption spectra of poly-N^{ω}-tosyl-L-arginine (I) and poly-L-arginine hydrochloride (II).

fluoride[8] at 0°C for 1 hr to remove the tosyl groups and then converted into poly-L-arginine hydrochloride by passing it through a column of the HCl type of resin (IRA-400). The infrared spectrum of poly-L-arginine (Fig. 1) shows the absence of the absorptions at 1585, 1265, 1085, 820, 680, 560, 1170, and 1135 cm^{-1} which are due to the benzene and SO_2 groups of the tosyl residue. The hydrolysate of poly-L-arginine gave only L-arginine (R_f 0.16)*2 and did not show any trace of ornithine (R_f 0.12)*2 or citruline (R_f 0.20)*2 on paper chromatography. Therefore, the complete detosylation proceeded by means of the HF method.[8]

Experimental

N^{α}-Carbobenzyloxy-N^{ω}-tosyl-L-arginine (I). N^{α}-Carbobenzyloxy-L-arginine,[9] which had been prepared from L-arginine hydrochloride and carbobenzyloxy chloride, was tosylated with tosyl chloride according to the procedure of Ramachandran and Li.[10]

N^{ω}-Tosyl-L-arginine NCA Hydrochloride (II). Five grams (10.8 mmol) of I were dissolved in 10 m*l* of thionyl chloride at room temperature for 5 hr, and then the excess thionyl chloride was evaporated *in vacuo* at room temperature. The residual syrup was crystallized with dry ether, and the crystal was centrifuged and washed with ether. It was then recrystallized from acetone and ether. Yield, 3.8 g (90%); mp 75°C (dec.); $[\alpha]_D^{23}$ −9.0° (*c* 2.6, acetone). The equivalent molecular weight, as determined by CH_3ONa titration, was 390 calcd 390).

Found: C, 43.4; H, 5.5; N, 13.8; Cl, 8.8%. Calcd for $C_{14}H_{19}O_5N_4SCl$: C, 43.1; H, 4.9; N, 14.3; Cl, 9.1%.

N^{α}-Tosyl-L-arginine NCA (III). Two grams (5.1 mmol) of II were dissolved in 20 m*l* of dry acetone, and then 2 g (8.0 mmol) of silver oxide were added. After the mixture had been stirred at room temperature until the chloride ion in the solution disappeared, it was filtered and the filtrate was passed through a column of dry active charcoal.[11] The colorless solution was evaporated *in vacuo*, and N^{ω}-tosyl-L-arginine NCA was obtained as a syrup. Yield, 1.6 g (89%). The NCA test with barium hydroxide was positive. The fresh syrup was used in the polymerization.

Poly-N^{ω}-tosyl-L-arginine (IV). a) N^{ω}-Tosyl-L-arginine NCA (III), 1.6 g (4.5 mmol), was dissolved in 4.2 m*l* of DMA and polymerized by the addition of triethylenediamine (TEDA) (0.045 mmol) as an initiator at room temperature over a 3-day period. After the mixture had been refluxed for 2 hr on a boiling water bath, it was cooled and poured into water to precipitate the polymer. The precipitate was then centrifuged and washed water. Yield, 0.7 g (50%). $[\alpha]_D^{30}$ +9.9° (*c* 2.0, DMF). The equivalent molecular weight was 16200 ($n \fallingdotseq 52$); it was measured by carboxyl-end titration with 0.02N CH_3ONa in methanol. b) 2 g (5.6 mmol) of IV were dissolved in 8 m*l* of dioxane and then polymerized with TEDA (0.028 mmol). The polymer which was separated out of the solution after it was stood for 16 hr was redissolved with the addition of DMSO (4 m*l*), and then the solution left to stand for a further 3 days. The reaction mixture was treated by the same procedure as that of a). Yield, 1.6 g (94%); $[\alpha]_D^{23}$ +7° (*c* 2.0, DMF). The equivalent molecular weight as determined by 0.02N CH_3ONa titration, was 8400 ($n \fallingdotseq 27$).

*2 Developed with an *n*-butanol-glacial acetic acid-water mixture (4 : 1 : 5).

9) L. Zervas, M. Winitz and J. P. Greenstein, *J. Org. Chem.*, **22**, 1515 (1957).

10) J. Ramachandran and C. H. Li *ibid.*, **27**, 4006 (1962).

11) J. Noguchi, N. Nishi, M. Itaya and S. Tokura, *Kogyo Kagaku Zasshi*, **69**, 745 (1966).

Found: C, 47.8; H, 6.15; N, 16.8%. Calcd for $(C_{13}H_{18}O_3S \cdot H_2O)_n$: C, 47.8: H, 6.10; N, 17.2%.

Hydrolysis of Poly-N^{ω}-tosyl-L-arginine. IV was hydrolyzed with 6N hydrochloric acid at 110°C for 22 hr; when the hydrolysate was then analyzed by paper chromatography, it showed only one spot of arginine with ninhydrin. The quantity was determined by means of a colorimetric densitometer and compared with that of standard ariginine, it corresponded to the arginine content of the polymer. The optical rotation of hydrolysate was $[\alpha]_D^{19}$ +22.3° (*c* 0.7, 6N HCl); this is in good agreement with that of a standard arginine hydrochloride and shows no racemization.

Poly-L-arginine Hydrochloride (VI). Poly-N^{ω}-tosyl-L-arginine (IV) (1.4 g), containing 1.4 m*l* of anisole was treated with liquid hydrogen fluoride at 0°C for 1 hr by the procedure of Sakakibara *et al.*[8] After evaporating the hydrogen fluoride, the poly-L-arginine hydrofluoride (V) was taken out with ether and alcohol. It was dissolved in 10 m*l* of water and dialyzed against water. The solution was then treated with a HCl form of the IRA-400 resin in order to remove the fluoride ion and then evaporated *in vacuo*. The residue was washed with alcohol and dried. Yield, 0.6 g (62%); $[\alpha]_D^{17}$ −71.8° (*c* 1.9, water).

Found: C, 39.1; H, 7.52; N, 25.9; Cl, 16.7%. Calcd for $(C_6H_{13}ON_4Cl \cdot \frac{1}{2} \cdot C_2H_5OH)_n$: C, 39.3; H, 7.49; N, 26.0; Cl, 16.5%.

Hydrolysis of Poly-L-arginine Hydrochloride. A part of the VI was hydrolyzed with 6N hydrochloric acid at 110°C for 22 hr; when the hydrolysate was then analyzed by paper chromatography, it showed only one spot of arginine. The optical rotation of the hydrolysate was $[\alpha]_D^{22}$ +22.5° (*c* 1.0, 6N HCl); this is in good agreement with standard L-arginine hydrochloride and shows no racemization of the polymer.

The authors are very mcuh indebted to Dr. S. Sakakibara for his kind help and useful advice with the hydrogen fluoride; they wish also to thank Dr. S. Tokura for his kind support. This work was also supported by the Fuji Photofilm Co., Ltd., and by the Institute of Polymer Science.

BULLETIN OF THE CHEMICAL SOCIETY OF JAPAN VOL. 43 2518—2523 (1970)

Syntheses of Organic Phosphates. II. 3-Hydroxy-2-pyridylmethyl, 6-Methyl-2-pyridylmethyl, 3-Pyridyl and 8-Quinolyl Phosphate*1

Yukito MURAKAMI, Junzo SUNAMOTO, Hiromi SADAMORI, Hiroki KONDO and Makoto TAKAGI

Department of Organic Synthesis, Faculty of Engineering, Kyushu University, Hakozaki, Fukuoka

(Received October 11, 1969)

The phosphorylation of 3-hydroxy-2-pyridylmethanol and 6-methyl-2-pyridylmethanol was carried out with pyrophosphoric acid. 3-Pyridinol and 8-quinolinol were phosphorylated in pyridine by using five- to ten-fold molar amount of phosphoryl chloride at room temperature or below. The chromatographic elution of the reaction mixtures on a column of cation-exchange resin, with water as an eluent, was found to be effective for separation and purification of the products in most cases, while 8-quinolyl phosphate was obtained directly from the concentrated reaction mixture. These phosphates, with the exception of 3-hydroxy-2-pyridylmethyl phosphate, follow acid dissociation processes similar to the case of pyridylmethyl phosphates. The effect of the 3-hydroxy group in 3-hydroxy-2-pyridymethyl phosphate on its acid dissociation processes was discussed. A symmetric pyrophosphate ester was also isolated in the course of phosphorylation of 3-pyridinol.

In an earlier paper[1] from our laboratories, synthesis and purification of 2-, 3- and 4-pyridylmethyl phosphate were reported in connection with the studies of biochemically interesting model compounds, such as vitamin B_6 phosphate. Hydrolysis of these pyridylmethyl phosphates was also investigated in the absence and presence of metal ions.[2-4] As a result, it became desirable to investigate the participation of a neighboring functional group

*1 Contribution No. 195 from the Department of Organic Synthesis, Faculty of Engineering, Kyushu University.

1) Y. Murakami, M. Takagi and H. Nishi, This Bulletin, **39**, 1197 (1966).

2) Y. Murakami and M. Takagi, *ibid.*, **40**, 2724 (1967).

3) Y. Murakami and M. Takagi, *J. Amer. Chem. Soc.*, **91**, 5130 (1969).

4) Y. Murakami and M. Takagi, This Bulletin, **42**, 3478 (1969).

in the hydrolysis of pyridylmethyl phosphate and the related compounds. The role of a hetero-aromatic nitrogen in such solvolysis reactions also needs to be clarified. In the present work, therefore, 3-hydroxy-2-pyridylmethyl phosphate (**1**), 6-methyl-2-pyridylmethyl phosphate (**2**), 3-pyridyl phosphate (**3**), and 8-quinolyl phosphate (**4**) have been synthesized. In addition, their ionization constants have been determined and discussed in terms of the structural effect.

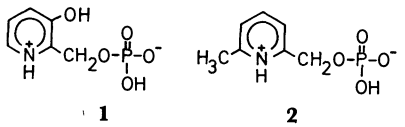

1

2

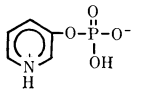

3

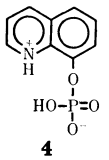

4

Syntheses and Purification. The phosphorylation of 3-hydroxy-2-pyridylmethanol and 6-methyl-2-pyridylmethanol, by using pyrophosphoric acid, was carried out according to the previous method for the syntheses of the unsubstituted pyridylmethyl phosphates.[1] Figure 1 shows the eluting behavior

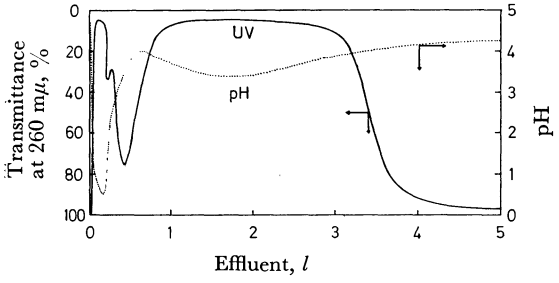

Fig. 1. Chromatographic separation of 3-hydroxy-2-pyridylmethyl phosphate from the phosphorylation mixture.
Mixture: 3.0 g of the alcohol underwent reaction with 23 g of pyrophosphoric acid
Column: Dowex 50W-X8 [H^+] (312 meq.), 3×34 cm
Eluent: mineral-free water
Elution rate: 300 ml/hr

of the phosphorylation mixture of 3-hydroxy-2-pyridylmethanol on a chromatographic column of cation-exchange resin, Dowex 50W-X8, with water as an eluent. The front effluent (about 100—150 ml) was strongly acidic (pH=1.0). The ultraviolet measurement of this effluent showed the presence of aromatic species (λ_{max}=294 mμ), and the paper chromatogram indicated the presence of some phosphate compounds. However, no organic phosphates could be isolated from this portion because of their low yield. 3-Hydroxy-2-pyridylmethyl phosphate was obtained in a comparatively good yield from the following fractions, as described in the experimental section.

Since 3-hydroxy-2-pyridylmethanol has two phosphorylation sites, it was necessary to confirm which group, the 2-hydroxymethyl or the 3-hydroxy, was predominantly phosphorylated. Nuclear magnetic resonance spectra directly provide an evidence for the phosphorylation of the former group. The singlet resonance signal of the methylene group in 3-hydroxy-2-pyridylmethanol, the original alcohol, was found to shift downfield and to become the doublet signal through coupling with ^{31}P upon phosphorylation.

6-Methyl-2-pyridylmethanol was phosphorylated nearly quantitatively by a method similar to that used for 3-hydroxy-2-pyridylmethanol. The phosphorylation mixture showed an eluting behavior similar to that case 3-hydroxy-2-pyridylmethanol.

Phosphorylation of 3-pyridinol and 8-quinolinol was carried out by using five- to ten-fold molar amount of phosphoryl chloride at room temperature or below in pyridine. The phosphorochloridate of 3-pyridinol thus produced was hydrolyzed with a sufficient amount of water. After the reaction mixture was neutralized with ammonia, the products were separated chromatographically. Figure 2 shows the eluting behavior of the phosphorylation mixture of 3-pyridinol on a column of cation-exchange resin, Dowex 50W-X8, with water as an eluent. Effluent I was found to contain the corresponding symmetric pyrophosphate ester, which was not isolated because of its low yield. 3-Pyridyl phosphate was obtained from effluent II. When the reaction mixture was treated with just enough amount of water to hydrolyze all the phosphorochloridate in the presence of pyridine, the major product was identified to be the symmetric pyrophosphate ester, P^1,P^2-di(3-pyridyl) pyrophosphate (**5**), and no detectable amount of 3-pyridyl

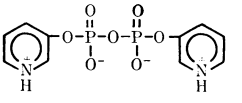

5

phosphate was found in the reaction mixture as the eluting profile in Fig. 3 indicates. Meanwhile, 8-quinolyl phosphate was obtained exclusively as precipitates from the concentrated phosphorylation mixture even though the phosphorochloridate was hydrolyzed with a just enough amount of water in the presence of pyridine.

Acid Dissociation Constants. 3-Hydroxy-2-pyridylmethyl phosphate was found to be a tetrabasic acid, while the remaining orthophos-

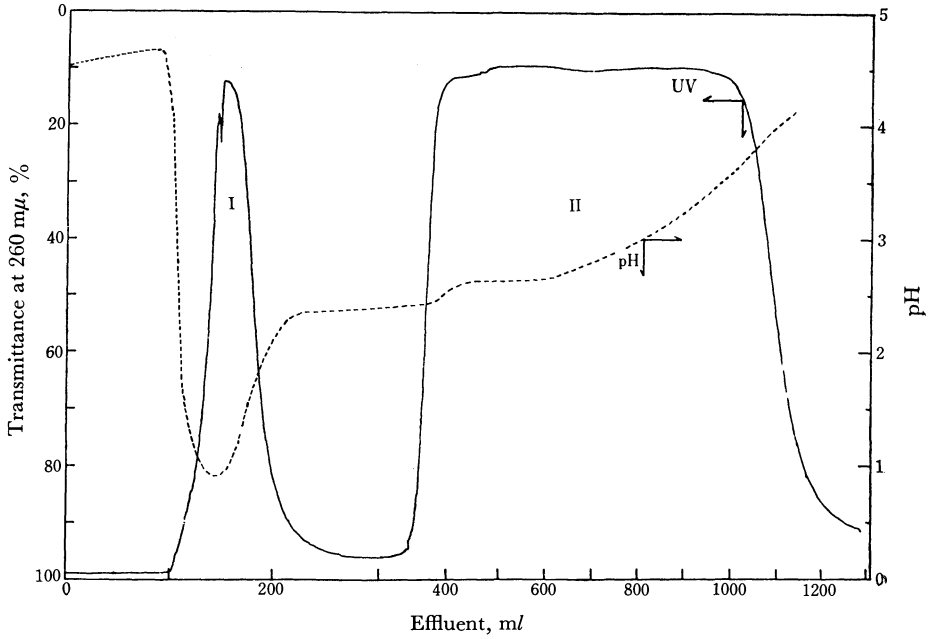

Fig. 2. Chromatographic separation of 3-pyridyl phosphate from the phosphorylation mixture.
Mixture: the phosphorylation mixture of 3-pyridinol (2.00 g) was hydrolyzed and neutralized with concd. ammonia; divided into two portions
Column: Dowex 50W-X8 [H^+] (50—100 mesh, 430 meq.), 2.8×48.5 cm
Eluent: distilled water
Elution rate: 2 ml/min for effluent I, 4 ml/min thereafter

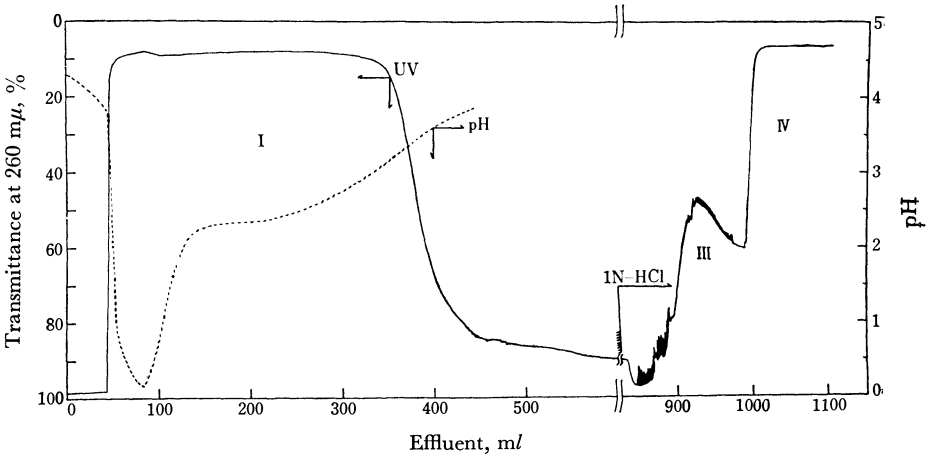

Fig. 3. Chromatographic separation of P^1,P^2-di(3-pyridyl) pyrophosphate from the phosphorylation mixture.
Mixture: the hydrolyzed phosphorylation mixture obtained from 1.4 g of 3-pyridinol
Column: Dowex 50W-X8 [H^+] (50—100 mesh, 240 meq.), 2.8×25 cm
Eluent: distilled water; 1N HCl for effluents III and IV
Elution rate: 2 ml/min
Effluent: I, the pyrophosphate ester; III, 3-pyridinol; IV, pyridine

phates were to be tribasic acids. Acid dissociation constants of these phosphates along with those of the related compounds are listed in Table 1.

Since pK_{H_2A} and pK_{HA} values for the tribasic phosphates are comparable in a qualitative sence with the corresponding values for pyridylmethyl

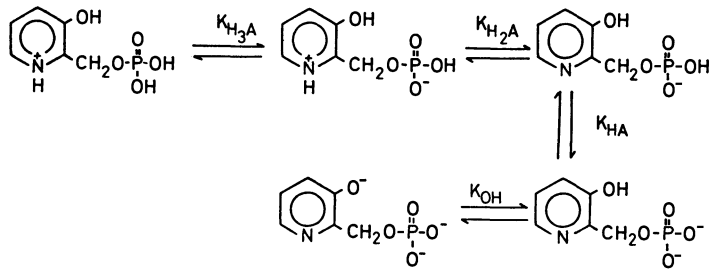

Chart 1. Acid dissociation processes for 3-hydroxy-2-pyridylmethyl phosphate.

Table 1. Acid dissociation constants

25.0±0.1°C, μ=0.10M (KNO_3)

Acid	pK_{H_2A}	pK_{HA}	pK_{OH}[a]
2-Pyridylmethyl phosphate[1]	4.42	6.29	—
3-Pyridylmethyl phosphate[1]	4.86	6.23	—
6-Methyl-2-pyridylmethyl phosphate	4.74	6.64	—
3-Hydroxy-2-pyridylmethyl phosphate	4.54	5.75	9.67
3-Pyridyl phosphate	3.86	5.64	—
8-Quinolyl phosphate	4.17	6.42	—
P^1,P^2-Di (3-pyridyl) pyrophosphate	3.58	4.51	—
3-Pyridinol	—	—	8.54
3-Hydroxy-2-pyridylmethanol	—	—	8.76

a) K_{OH} is the dissociation constant for the hydroxy proton.

phosphates, the present phosphates may undergo dissociation processes similar to those described previously.[1] Thus, K_{H_2A} is attributable to the dissociation constant of a pyridinium proton, while K_{HA} refers to that of the second phosphate proton. The most plausible proton-dissociation processes for 3-hydroxy-2-pyridylmethyl phosphate are shown in Chart 1 in the light of the acid dissociation steps for ordinary dibasic phosphates and hydroxypyridines.

3-Pyridyl phosphate demonstrated the lowest values of both pK_{H_2A} and pK_{HA} among the present six different phosphates listed in Table 1. This may be due to the phenolic character of the ester oxygen which may facilitate the electronic interaction between a pyridine ring and a phosphate group, while such an interaction would be minor in the remaining phosphates.

A comparatively low pK_{HA} value was observed for 3-hydroxy-2-pyridylmethyl phosphate. Through electron-withdrawing effect of the 3-hydroxy group and its participation in intramolecular hydrogen bonding with the phosphate group, the acidic nature of the phosphate proton seems to be greatly increased in this case. The above intramolecular hydrogen bonding is further confirmed by the fact that the dissociation of the 3-hydroxy proton is much suppressed as shown in Table 1.

The acid dissociation constants for pyrophosphoric acid have been evaluated at 20°C and the ionic strength of 0.1 in potassium chloride: pK_{H_3A} 2.22, pK_{H_2A} 6.08, pK_{HA} 8.45.[5] It is clear that the pK-values for P^1,P^2-di(3-pyridyl) pyrophosphate given in Table 1 are much higher than those of the first and the second protons of pyrophosphoric acid (pK_{H_4A} and pK_{H_3A}). Since these pK-values are comparable with those pK_{H_2A} values for other phosphate esters listed in Table 1, both K_{H_2A} and K_{HA} for the pyrophosphate ester may be attributed to the dissociation constants of pyridinium protons.

Experimental

3-Hydroxy-2-pyridylmethanol. To a mixture of sodium hydroxide (1.3 g), water (12.6 m*l*) and 3-pyridinol (3.0 g), 37% aqueous formaldehyde solution (2.5 m*l*) was added. After stirring for 3 hr at about 90°C, the mixture was neutralized with acetic acid, and evaporated to dryness. The yellow solid obtained was extracted with 200 m*l* of hot acetone. Through introduction of hydrogen chloride into the resulting extracts, the white hydrochloride was precipitated; yield 2.1 g (41%) upon recrystallization from ethanol; mp 213—216°C (dec.) (lit,[6] mp 209—211°C).

NMR (0.5M in D_2O, HOD as an internal standard): methylene, 0.31 ppm (singlet), ring protons, 3.22—3.57 ppm (multiplet).

This hydrochloride was converted to the corresponding free base with aqueous potassium hydroxide, and further purified by recrystallization from acetone followed by sublimation under reduced pressure; mp 145.4—146.5°C (lit,[6] mp 137—139°C) (Found: C, 57.62; H, 5.69; N, 11.12%).

3-Hydroxy-2-pyridylmethyl Phosphate. A mixture of 3-hydroxy-2-pyridylmethanol (3.0 g) and pyrophosphoric acid (23 g), which was freshly prepared by the brief heating of 85% orthophosphoric acid (13 g) and of phosphorus pentoxide (10 g), was placed in a 50 m*l* three-necked flask protected from moisture. This reaction mixture, after being heated at 80—85°C for

5) L. G. Sillén and A. E. Martell, "Stability Constants of Metal-Ion Complexes," Special Publication No. 17, the Chemical Society, London (1964).

6) N. Elming, *Acta Chem. Scand.*, **11**, 1496 (1957).

5 hr with sufficient stirring, was diluted with 16 ml of water and then reheated at 96°C for 30 min to hydrolyze any polyphosphates produced. After being cooled down to room temperature, an equal volume of water was added into the hydrolyzate. The resulting aqueous solution was applied to the top of a column (3×34 cm) of Dowex 50W-X8 [H^+] resin (312 meq.) and eluted with mineral-free water at 300 ml per hour. The ultraviolet absorption of the effluent was checked at 260 mμ with a ultraviolet detector, JEOL Model JLC-2B or Toyo UVICON-540, for the presence of aromatic species and the corresponding pH value was measured with a Hitachi-Horiba Model H-5 pH meter. After the front effluent (about 150 ml, pH=1.0) with absorption at 294 mμ came off, the acidity of the effluent gradually lowered, reaching pH 4.0 at a total effluent of 800 ml, in line with a decrease in the optical density. As the elution proceeded further, the effluent turned slightly acidic (pH=3.5), and the corresponding optical density at 295 mμ increased. After 3000 ml of the subsequent effluent was collected, the pH returned to 4.0 and the ultraviolet measurement did not show the presence of aromatic species. These fractions containing the phosphate ester (about 3000 ml, pH=3.5—4.0) were concentrated under reduced pressure below 30°C; white crystals precipitated; yield 2.53 g (66%) upon recrystallization from water, mp 201—203°C (dec.); neutralization equivalence 104.6 (calcd 102.5); $\lambda_{max}^{H_2O}$ (10^{-4}M) 252 mμ (ε 1270) and 288 mμ (ε 6910).

IR (KBr disc): 1250, 1175 cm^{-1} ($\nu_{P=O}$), and 1080 cm^{-1} ($\nu_{P-O-C(alk.)}$).

NMR (0.05M in D_2O, HOD as an internal standard): methylene, 0.64 ppm (doublet, J_{P-H}=7.40 Hz); ring protons, 3.33—3.62 ppm (multiplet); the accumulation (16 times) was carried out.

Found: C, 34.90; H, 4.02; N, 6.57; P*[2], 14.2%. Calcd for $C_6H_8NO_5P$: C, 35.14; H, 3.93; N, 6.83; P, 15.1%.

6-Methyl-2-pyridylmethanol. This was obtained from 2,6-lutidine *via* 2,6-lutidine *N*-oxide and 6-methyl-2-acetoxymethylpyridine in succession by a modification of the method in literature[7]; bp 86—92°C/0.2 mmHg; mp as the picrate 134.0—135.0°C (lit,[7] mp 129—132°C) (Found: C, 44.67; H, 3.38; N, 15.88%).

6-Methyl-2-pyridylmethyl Phosphate. A mixture of 44 g of phosphorus pentoxide and 56 g of 85% orthophosphoric acid were heated at 90—100°C with stirring. To the resulting viscous pyrophosphate, 5.4 g of 6-methyl-2-pyridylmethanol was added with caution at 67.5°C. Reaction temperature then immediately rose to about 110°C. After the exothermic reaction ceased, the reaction mixture was heated again up to 90—95°C and stirred for 9.5 hr. After being cooled down to room temperature, 100 ml of water was added and then reheated at 80—85°C for 1 hr in order to hydrolyze any polyphosphates produced. The hydrolyzate was subjected to the cation-exchange column chromatography by the use of Dowex 50W-X8 [H^+] resin (50—100 mesh, 425 meq.). Elution was carried out with mineral-free water at about 97 ml per hour. Eluting behavior was quite similar to that of 3-hydroxy-2-pyridylmethyl phosphate. From the later fractions of effluent (about 3840 ml), which were concentrated under reduced pressure at 40—45°C, white needle-like crystals were obtained; yield 7.5 g (92.7%) upon recrystallization from aqueous ethanol; neutralization equivalence 100.64 (calcd 101.57); $\lambda_{max}^{H_2O}$ (10^{-4}M) 269 mμ (ε 8350).

IR (KBr disc): ~3400 cm^{-1} (ν_{O-H}); 1268 cm^{-1} ($\nu_{P=O}$); 1182, 1164, 1102, and 1060 cm^{-1} ($\nu_{P-O-C(alk.)}$).

NMR (0.5M in D_2O, HOD as an internal standard): methyl, −1.87 ppm (singlet); methylene 0.44 ppm (doublet, J_{P-H}=8.29 Hz); 5H, 2.87 ppm (doublet); 3H, 2.93 ppm (doublet); 4H, 3.49 ppm (triplet, $J_{3-4} \simeq J_{4-5}$=7.80 Hz and J_{3-5}<1.0 Hz).

Found: C, 40.94; H, 5.04; N, 6.64; P, 14.6%. Calcd for $C_7H_{10}NO_4P$: C, 41.39; H, 4.96; N, 6.96; P, 15.3%.

3-Pyridyl Phosphate. A 2.00 g sample of 3-pyridinol dissolved in 25 ml of dry pyridine was added dropwise for 40 min into a mixture of 16.4 g of phosphoryl chloride and 25 ml of dry pyridine protected from moisture. The reaction flask was cooled with ice. The reaction mixture was then stirred for 3 hr at room temperature (10—15°C), followed by cooling with a freezing mixture (ice-sodium chloride). After the precipitated pyridine hydrochloride was removed immediately by filtration, pyridine and unreacted phosphoryl chloride were taken out by distillation *in vacuo* at 50°C from the filtrate. The residue was dissolved in 25 ml of acetonitrile, and then added in 80—90 ml of cold water in about 10 min with sufficient stirring. This aqueous mixture was neutralized with concd. ammonia, divided into two portions, each of which was concentrated to 10—15 ml *in vacuo* at 40°C and below. Each portion was then applied to the top of a column (2.8×48.5 cm) of Dowex 50W-X8 [H^+] resin (50—100 mesh, 430 meq.) and eluted with water at 2 ml per min until the front effluent (Fig. 2, I) came through; elution rate was doubled after then. The second part of eluted fractions (Fig. 2, II) was concentrated to about 10 ml *in vacuo* at 40°C and below; white needle-like crystals were precipitated by adding acetone; total yield 1.81 g (49%); mp 145.8—146.8°C (part. dec.); R_f 0.15—0.27 (Toyo filter paper No. 51A; developer, isopropanol : concd. ammonia : water=7 : 1 : 2 by volume); neutralization equivalence 87.4 (calcd 87.5); $\lambda_{max}^{H_2O}$ (2×10^{-4}M at pH 13) 268 mμ (ε 3340).

Found: C, 34.01; H, 3.62; N, 8.12; P, 17.5%. Calcd for $C_5H_6NO_4P$: C, 34.29; H, 3.46; N, 8.00; P, 17.7%.

***P*[1],*P*[2]-Di(3-pyridyl) Pyrophosphate.** The phosphorylation of 3-pyridinol (1.4 g) with phosphoryl chloride (11.4 g) was carried out in 80 ml of dry pyridine in a manner similar to that for 3-pyridyl phosphate. The unreacted phosphoryl chloride and pyridine were distilled off *in vacuo* from the reaction mixture without removing pyridine hydrochloride produced in the course of reaction. The mixture was stirred for 30 min at room temperature after addition of 40 ml of dry pyridine and 1 ml of water in succession, and was allowed to stand overnight. The solution was then concentrated to about 20 ml *in vacuo*, and charged to the top of a column (2.8×25 cm) of Dowex 50W-X8 [H^+] resin (50—100 mesh, 240 meq.). The elution was conducted with water at the flow rate of 2 ml per min, and with 1N hydrochloric acid subsequently as shown in Fig. 3.

*[2] A sample was decomposed by heating with concentrated nitric acid and 60% perchloric acid. The product was then analyzed for phosphorus by colorimetric method (R. J. L. Allen, *Biochem. J.*, **34**, 858 (1940)).

7) G. Kobayashi, S. Furukawa and Y. Kawada, *J. Pharm. Soc. Japan.*, **74**, 790 (1954).

The fractions of pH above 2 in the front effluent (Fig. 3, I) were collected, and concentrated *in vacuo* at 40°C and below; white precipitate (985 mg) was obtained upon addition of acetone. Repeated precipitation with water-acetone gave 100 mg of pure phosphate; mp 180—190°C (part. dec.); R_f 0.62; neutralization equivalence 165.3 (calcd 166.1)

Found: C, 35.74; H, 3.30; N, 8.84; P, 18.2%. Calcd for $C_{10}H_{10}N_2O_7P_2$: C, 36.16; H, 3.03; N, 8.43; P, 18.7%.

8-Quinolyl Phosphate. A 7.25 g sample of 8-quinolinol dissolved in 70 m*l* of dry pyridine was added dropwise in 2 hr into a mixture of 38.2 g of phosphoryl chloride and 70 m*l* of dry pyridine, while the reaction vessel was cooled with ice. Stirring was continued for another 5 hr. Pyridine hydrochloride formed was then recovered by filtration, and the filtrate was distilled *in vacuo* at 50°C to remove pyridine and the unreacted phosphoryl chloride. Into the residue, 100 m*l* of dry pyridine in one portion and subsequently 2.5 m*l* of water was added dropwise with shaking. Shaking was continued for another 30 min, and the reaction mixture was allowed to stand overnight at room temperature. The resulting yellowish brown mixture was concentrated *in vacuo* to 20—30 m*l*; filtered off to recover white precipitate (4.0 g). Repeated recrystallization from water-acetone (1 : 1) gave 1.95 g (17.5%) of needle-like crystals; mp 208—223°C (part. dec.); R_f 0.2—0.3 (developer, isopropanol : concd. ammonia : water=7 : 1 : 2), ~0.4 (developer, pyridine : concd. ammonia : water=6 : 3 : 1); neutralization equivalence 111.3 (calcd 112.6).

Found: C, 47.79; H, 3.66; N, 5.87; P, 13.0%. Calcd for $C_9H_8NO_4P$: C, 48.01; H, 3.58; N, 6.22; P, 13.8%.

The filtrate was applied to the top of column (3.0× 42.5 cm) of Dowex 50W-X8 [H^+] resin (50—100 mesh, 430 meq.) and eluted with water as described for 3-pyridyl phosphate; the eluting behavior was quite similar. Isolation of the pyrophosphate ester in its pure form from the front effluent was unsuccessful.

Acid Dissociation Constants. The acid dissociation constants of the phosphates prepared in this work were determined potentiometrically, with the use of a Hitachi-Horiba Model P pH meter with extension glass and calomel electrodes, at 25.0±0.1°C and the ionic strength of 0.10M in potassium nitrate.

BULLETIN OF THE CHEMICAL SOCIETY OF JAPAN VOL. 43 2523—2526 (1970)

Ring-opening Reactions of Cyclic Ethers. VIII.*1 Acid-catalyzed Ring-opening Reactions of Isobutylene Oxide in Alcohols

Shizen SEKIGUCHI, Kohji MATSUI and Yoshihiro YASURAOKA

Department of Synthetic Chemistry, Faculty of Engineering, Gunma University, Tenjin-cho, Kiryu, Gunma

(Received January 20, 1970)

The rates of the ring-opening reaction of isobutylene oxide have been measured in methyl, ethyl, *n*-propyl and isopropyl alcohols in the range from 10 to 40°C under conditions where the molar ratio of an alcohol to the epoxide was kept at 10 and the range of the concentration of boron trifluoride etherate was *ca.* 1.0×10^{-3} to *ca.* 4.0×10^{-3} mol/*l*. The rate equation is expressed as follows: $-d[\text{epoxide}]/dt=k_2[C_0][\text{epoxide}]$, where $[C_0]$ is the initial concentration of the catalyst and [epoxide] is the instantaneous concentration of the epoxide at time *t*. The rate constants (k_2) decreased in the order, $CH_3OH>C_2H_5OH>n\text{-}C_3H_7OH>i\text{-}C_3H_7OH$. The entropies of activation decreased in the same order, while the energies of activation were not appreciably changed. A plot of $\log k_2$ against $1/D$ (D, the dielectric constant of the mixture of each alcohol and the epoxide) was found to be linear, its slope being -61.2. The results support the fact that the reaction is bimolecular.

Although the acid-catalyzed ring-opening reactions of epoxides in various solvents, such as water, alcohol, *etc.*, have recently received intensive attention,[1,2] there have still been controversies on their mechanisms. Long *et al.* reportrd that the acid-catalyzed hydrolyses of epichlorohydrin, propylene and isobutylene oxides were unimolecular (A-1).[3] On the other hand, that of epichlorohydrin was shown by le Noble and Muffy.[4] to proceed by

*1 Part VII: S. Sekiguchi, H. Inoue, M. Hayashi and K. Matsui, *Kogyo Kagaku Zasshi*, **71**, 1943 (1968).

1) R. E. Parker and N. S. Isaacs, *Chem. Rev.*, **59**, 737 (1959).

2) S. Winstein and R. B. Henderson, "Heterocyclic Compounds," Vol. 1, ed. by R. C. Elderfield, John Wiley and Sons, Inc., New York, London (1950), p. 1.

3) F. A. Long and J. G. Pritchard, *J. Amer. Chem. Soc.*, **78**, 2667, 6008 (1956).

4) W. J. le Noble and M. Duffy, *J. Phys. Chem.*, **68**, 619 (1964).

a bimolecular process(A-2)and Koskikallio *et al.* gave the same conclusion for those of propylene oxide and isobutylene oxide.[5]

An unsymmetrical epoxide reacts with excess alcohol to give the following products:

$$\begin{matrix}R\\R\end{matrix}\!\!>\!C\!-\!CH_2 + R'OH \rightarrow \underset{\underset{OH\ OR'}{|\quad|}}{\overset{R}{\underset{R}{>}}C\!-\!CH_2} + \underset{\underset{OR'\ OH}{|\quad|}}{\overset{R}{\underset{R}{>}}C\!-\!CH_2}$$

(I) (II)

(1)

In a previous paper*1 we determined the total amounts of I and II and the ratios (II/I) for the reaction of propylene oxide or isobutylene oxide with alcohols using boron trifluoride etherate as a catalyst. From the results obtained, we inferred that in the case of isobutylene oxide an A-1 reaction might perhaps take place. In the present investigation, kinetic measurements were carried out in excess alcohols using the same catalyst in order to obtain a closer insight into the reaction mechanism.

Results and Discussion

Reaction Products. In a previous investigation*1 the acid-catalyzed ring-opening reaction of isobutylene oxide was carried out in methyl, ethyl and isopropyl alcohols under conditions where the molar ratio of an alcohol to isobutylene oxide was kept at 10 and the concentration of boron trifluoride etherate was 1.2×10^{-3} mol/*l*. The values of II/I after three hours' reaction were found to be as follows:

Alcohol	Reaction temp. (°C)	II/I
CH_3OH	20	54.5
C_2H_5OH	20	42.4
	30	76.1
i-C_3H_7OH	20	II only
	30	II only

The figures indicate that II is the main product in the reactions.

Rate Constants. The rates of the reactions were followed by measuring a decrease in the concentration of isobutylene oxide under conditions where the molar ratio of an alcohol to the epoxide was kept at 10 and the range of the concentration of boron trifluoride etherate was *ca.* 1.0×10^{-3} to *ca.* 4.0×10^{-3} mol/*l*.

The data of a decrease in the concentration of the epoxide were found to obey the standard first-order kinetic equation:

$$k_1 = \frac{1}{t}\log\frac{a}{a-x} \qquad (2)$$

where a is the initial concentration and x is the instantaneous concentration at time t of the epoxide, respectively. When k_1 was plotted against the initial concentration of the catalyst for the reaction with ethyl alcohol, a straight line was obtained as shown in Fig. 1. Similar results were obtained for other alcohols.

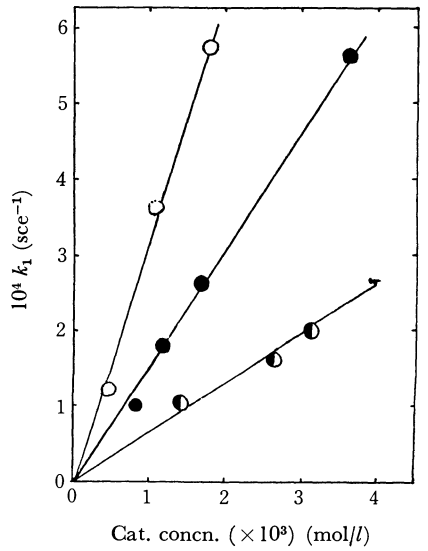

Fig. 1. Relation between rate constants and catalyst concentrations (EtOH).
○ 40°C, ● 30°C, ◐ 20°C

From the results the following equation was obtained.

$$k_1 = k_2[C_0] \qquad (3)$$

where $[C_0]$ is the initial concentration of the catalyst.

Therefore, the rate equation can be written as

$$\frac{-d[\text{epoxide}]}{dt} = k_2[C_0]\,[\text{epoxide}] \qquad (4)$$

The results of the rate measurements are tabulated in Table 1 together with the activation parameters.

It is evident from the results in Table 1 that the variations in the rates of the ring-opening reaction of isobutylene oxide are largely due to changes in the entropy of activation ($\Delta S^{\neq}$).

In their discussion of the acid-catalyzed hydration of olefins, Taft *et al.*[6,7] suggested that an A-1 reaction should be characterized by relatively more positive entropies of activation than an A-2 reaction.

5) J. Koskikallio and E. Whalley, *Trans. Faraday Soc.*, **55**, 815 (1959).

6) R. W. Taft, Jr., *J. Amer. Chem. Soc.*, **74**, 5374 (1952).

7) R. W. Taft, Jr., E. L. Purlee, P. Riesz and G. A. De Frazio, *ibid.*, **77**, 1584 (1955).

Table 1. Rate constants and activation parameters for the ring-opening reaction of isobutylene oxide in alcohols

Alcohol	10°C	k_2 $l\cdot mol^{-1}\cdot sec^{-1}$ 20°C	30°C	40°C	E kcal·mol^{-1}	$\Delta S^{\neq}$ (20°C) e.u.
CH_3OH	1.20×10^{-1}	3.25×10^{-1}	6.60×10^{-1}	—	14.4	−13.5
C_2H_5OH	—	6.71×10^{-2}	1.58×10^{-1}	3.30×10^{-1}	14.9	−15.0
n-C_3H_7OH	—	2.75×10^{-2}	6.25×10^{-2}	1.50×10^{-1}	14.8	−17.9
i-C_3H_7OH	—	1.23×10^{-2}	2.97×10^{-2}	6.00×10^{-2}	14.9	−18.7

Table 2. Values of $\Delta S^{\neq}$ for several acid-catalyzed hydrolyses in aqueous solution

Substrate	Mechanism	$\Delta S^{\neq}$ (e.u.)
Ethyl orthoformate[a]	A-1	+5.8
Sucrose[b]	A-1	+7.9
Methylal[c]	A-1	+7.3
Dimethoxymethane[d]	A-1	+6.8
Dialkoxyethane[d]	A-1	+7.0∼+13
Alkyl-1,3-dioxolane[e]	A-1	−3.8∼+7.9
Benzaldehyde diethyl acetals[f]	A-1	+7.0∼+2.0
2-(Substituted phenyl)-1,3-dioxolanes[f]	A-1	−6.9∼−9.6
Methyl orthobenzoate[g]	A-1	+8.4
Ethyl orthobenzoate[h]	A-1	−0.3
Ethyl orthoacetate[h]	A-1	+5.5 (40% dioxane)
Methoxymethyl acetate[i]	A-1	+3.7
Methoxymethyl formate[i]	A-1	+2.7
Methyl acetate[b]	A-2	−21.3
Ethyl acetate[b]	A-2	−23.0
γ-Valerolactone[j]	A-2	−24.6
γ-Butyrolactone[j]	A-2	−20.9

a) F. Bresica and V. K. Lamer, *J. Amer. Chem. Soc.*, **62**, 612 (1940).
b) E.A. Moelwyn-Hughes, "Kinetics of Reactions in Solution," Second Edition, Oxford University Press, Oxford, (1947), p. 321.
c) D. McIntyre and F. A. Long, *J. Amer. Chem. Soc.*, **76**, 3240 (1954).
d) J. Koskikallio and E. Shalley, *Trans. Faraday Soc.*, **55**, 809 (1959).
e) P.Salomaa and A.Kankaanperä, *Acta Chem. Scand.*, **15**, 871 (1961).
f) T. H. Fife and L. K. Jao, *J. Org. Chem.*, **30**, 1492 (1965).
g) J. G. Fullington and E. H. Cordes, *ibid.*, **29**, 970 (1964).
h) R.H. Dewolfe and J.L. Jensen, *J. Amer. Chem. Soc.*, **85**, 3264 (1963).
i) P. Salomaa, *Suomen Kemistilehti*, **B33**, 11 (1960).
j) F. D. Coffin and F. A. Long, *J. Amer. Chem. Soc.*, **74**, 5767 (1952).

Schaleger and Long[8] reported that the entropies of activation should be used as a criterion of mechanism for acid-catalyzed reactions in aqueous solution.

Whalley[9] further deduced that (i) if $\Delta S^{\neq}$ was less than zero then the reaction was probably A-2 and (ii) if $\Delta S^{\neq}$ was greater than zero the mechanism could be either A-1 or A-2. Stimson *et al.*[10,12] showed that the hydrolyses of *t*-butyl benzoate and *t*-butyl formate in acidified 60% acetone-water gave the $\Delta S^{\neq}$ values of +9.5 and −23.7 e.u., respectively, indicating that the former hydrolysis proceeds by an A-2 mechanism and the latter by an A-2 mechanism and that the hydrolysis of *t*-butyl 2,4,6-trimethylbenzoate in acidified 90% ethanol - water gave an $\Delta S^{\neq}$ of +8.1 by an A-1 mechanism.

Further examples that show the relation between $\Delta S^{\neq}$ and mechanism are listed in Table 2. The data in Table 2 show that the $\Delta S^{\neq}$ values fall into two groups, corresponding to the two types of mechanism. The $\Delta S^{\neq}$ values in Table 1 are closer to the value for the A-2 reactions rather than for the A-1 reactions. Therefore, we conclude that A-2 mechanism holds for the acid-catalyzed ring-opening reaction of isobutylene oxide.

Relationship between Rate Constants and Dielectric Constants of Media. The relationship between reaction rates and dielectric constants of media (D) have so far been studied by many investigators. Hiromi[12] further developed the theories of Kirkwood[13] and Laidler *et al.*[14] and concluded that the slope in a plot of logarithms of k_2 against reciprocals of dielectric constants of media was less than about −150 for A-1 reactions and greater than about −100 for A-2 ones. Hiromi's theory was applied by Parker *et al.*[15] to elucidate the mechanism of the reaction of benzylamine with 1,2-epoxyethylbenzene.

8) L. L. Schaleger and F. A. Long, "Advances in Physical Organic Chemistry," Vol. 1, ed. by V. Gold, Academic Press Inc., London (1963), p. 1.
9) E. Whalley, *Trans. Faraday Soc.*, **55**, 798 (1959).
10) V. R. Stimson, *J. Chem. Soc.*, **1955**, 4020.
11) V. R. Stimson and E. J. Watson, *ibid.*, **1954**, 2848.
12) K. Hiromi, This Bulletin, **33**, 1251 (1960).
13) J. G. Kirkwood, *J. Chem. Phys.*, **2**, 351 (1934).
14) K. J. Laidler and P. A. Landskroener, *Trans. Faraday Soc.*, **52**, 200 (1956).
15) R. E. Parker and B. W. Rockett, *J. Chem. Soc.*, **1965**, 2569.

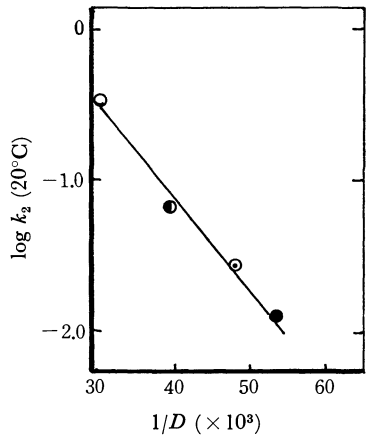

Fig. 2. Relation between rate constants and dielectric constants.
○ Methyl alcohol, ◐ Ethyl alcohol
⊙ *n*-Propyl alcohol ● Isopropyl alcohol

As shown in Fig. 2, the slope is −61.2, indicating that the reaction under investigation proceeds by a bimolecular process.

Our result is in agreement with the conclusion of Koskikallio *et al.*[5]

As shown in Table 1, the $\Delta S^{\neq}$ values for this ring-opening reaction are a little larger than those for the usual A-2 reactions and the rates increase in the increasing order of the polarity of alcohols.

As Parker *et al.*[1] proposed, we assume that the transition state for this ring-opening reaction is as follows:

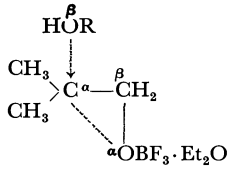

where the extent to which bond breaking (C^{α}–O^{α}) has progressed is larger than the extent to which bond forming (C^{α}–O^{β}) has progressed. As the crowding in such a transition state should be less than the one in the usual bimolecular reaction, the lower $\Delta S^{\neq}$ values would be expected.

We conclude that this ring-opening reaction may be a borderline case between A-1 and A-2 reactions, but essentially is an A-2 reaction.

Experimental

Materials. *Alcohols.* Commercial reagents were purified by the usual procedures.

Boron Trifluoride Etherate. Commercial reagent of boron trifluoride etherate was distilled under a nitrogen atmosphere before use, bp 124.0—125.0°C.

Isobutylene Oxide. Isobutylene chlorohydrin was prepared from isobutylene and hypochlorous acid according to the method of Michael *et al.*,[16] bp 63.0—65.0°C/74 mmHg (lit, 128—129°C[16]).

Found: C, 44.18; H, 8.20%. Calcd for C_6H_9OCl: C, 44.27; H, 8.31%.

The yield was 40% (based upon isobutylene).

Isobutylene oxide was prepared according to the method of Ishida,[17] bp 49.6—60.2°C (lit, bp 50°C[17]). The yield was 83% (based on isobutylene chlorohydrin). n_D^{20} 1.3732 (lit, 1.3730[17]).

Kinetic Measurements. The reaction was followed by the determination of isobutylene oxide according to the method of Swan.[18] About 1.0 g of a sample was pipetted out at different times from the reaction mixture and added to 30 m*l* of a saturated aqueous sodium sulfite solution. Sodium sulfite reacted smoothly and quantitatively with the epoxide, liberating an equivalent of sodium hydroxide.

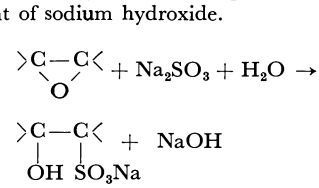

The epoxide was determined by the titration of liberated sodium hydroxide with standard hydrochloric acid. A simple kinetic data for a representative run is shown in Table 3.

Table 3. Simple kinetic data for the ring-opening reaction of isobutylene oxide in ethyl alcohol[a]

Time min	Sample pipetted g	Titer[b] HCl cc	Epoxide %	$10^2 k_1$ min^{-1}
0	—	—	13.52	—
14.63	0.9643	6.08	8.23	3.43
20.84	1.0949	5.67	7.09	3.31
26.70	1.1812	5.30	6.40	3.11
32.39	1.0100	3.45	4.47	3.40
38.58	1.0543	3.00	3.72	3.33
44.42	1.3086	3.13	3.14	3.27
50.38	1.2392	2.68	2.83	3.08
			Average:	3.37

a) Concentration of $BF_3 \cdot Et_2O$ was 3.55×10^{-3} mol/*l*.
b) Concentration of HCl was 0.1792N.

Measurement of Dielectric Constants. Dielectric constants of the mixtures of isobutylene oxide and alcohols were measured by the phase difference compensation method with a Shibayama SS-207 type apparatus (Shibayama Scientific Co.).

16) A. Michael and V. L. Leighton, *Ber.*, **39**, 2157 (1906).
17) S. Ishida, This Bulletin, **33**, 924 (1960).
18) J. D. Swan, *Anal. Chem.*, **26**, 878 (1954).

BULLETIN OF THE CHEMICAL SOCIETY OF JAPAN VOL. 43 2527—2530 (1970)

Reaction of P-N Compounds with Alkylating Reagents such as Alkyl Benzenesulfonates and Dialkyl Sulfates[1]

Jugo KOKETSU*1 and Yoshio ISHII

Department of Synthetic Chemistry, Faculty of Engineering, Nagoya University, Nagoya

(Received January 24, 1970)

The reaction of *N,N*-dialkyl-diphenylphosphinous amides (I) with alkyl benzenesulfonates (III) or dialkyl sulfates (IV) took place exothermally, giving phosphonium salts (V). When phosphonium salts (V) were heated at 100°C for 5—10 hr, asymmetric phosphine oxide (VI) and *N,N*-dialkyl-benzenesulfonamides (VII) or polymeric materials were obtained. In the case of diphenyl dialkylphosphoramidites (II), no quaternization was observed at room temperature. However, diphenyl alkylphosphonates (VIII) and *N,N*-dialkylbenzenesulfonamides (VII) or the same polymeric materials were obtained through intermediate phosphonium salts when the mixture was heated.

The reaction of P–N compounds with phenyl cyanate[2] or cyclic carbonate esters[3] have been studied. In the reaction, the P–N compound behaved as an ambident reagent. When it was treated with an onium ion, the reaction took place at the phosphorus center, as exemplified by the reaction with phenyl cyanate:

$$R_2PNR_2' + PhOCN \rightarrow [R_2P^+(NR_2)(OPh)][CN^-] \rightarrow R_2POPh + R'_2NCN \quad (1)$$

In contrast, when the reaction partners were ester-carbonyl compounds, the P–N compound reacted as the N base and the phosphorus atom would attack ester oxygen or carbonyl oxygen synchronously:

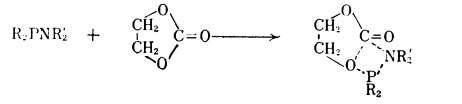

$$\longrightarrow R_2POCH_2CH_2OC(O)NR'_2 \quad (2)$$

In reaction (2), predominancy of the nucleophilic attack of the nitrogen atom to the carbonyl carbon was confirmed by the kinetic study of the reaction of P–N compounds with acetic anhydride.[4]

The reaction between *N,N*-dialkyl-diphenylphosphinous amide (I) or diphenyl dialkylphosphoramidites (II) and alkyl benzenesulfonates (III) or dialkyl sulfates (IV), which would give phosphonium salts through a reaction similar to (1) are reported in this publication.

Results

A: Reaction of *N,N*-Dimethyl-diphenylphosphinous Amide (Ia) with Alkyl Benzenesulfonates (III) or Dialkyl Sulfates (IV). When Ia was added to equimoler amounts of III or IV at room temperature, an exothermic reaction took place with the formation of stable phosphonium salts (V), as shown in the following equations.

$$Ph_2PNMe_2 + PhSO_2OR''$$

Ia; IIIa: R″=Me, IIIb: R″=Et

$$\longrightarrow [Ph_2P^+(R'')NMe_2][PhSO_2O^-] \quad (3)$$

Va: R″=Me, Vb: R″=Et

$$Ph_2PNMe_2 + SO_2(OR'')_2$$

Ia; IVa: R″=Me, IVb: R″=Et

$$\longrightarrow [Ph_2P^+(R'')NMe_2][(R''O)SO_2O^-] \quad (4)$$

Vc: R″=Me, Vd: R″=Et

These phosphonium salts (Va—Vd) are insoluble to benzene, petroleum ether, dioxane, or carbon tetrachloride, but soluble to chloroform, acetone, or water. IR (KBr disk) and NMR (in $CDCl_3$) spectral data of Vb and Vd are shown in the Table 1.

When the phosphonium salts were heated at 100°C for 5 hr in a sealed tube under an atmosphere of nitrogen, the corresponding asymmetric phosphine oxides (VI) were obtained, along with

*1 Department of Synthetic Chemistry, Faculty of Engineering, Nagoya University; Furo-cho, Chikusa-ku, Nagoya, Japan

1) Part IV. J. Koketsu, S. Kojima, S. Sakai and Y. Ishii, *Kogyo Kagaku Zasshi*, **73**, 1004 (1970).

2) J. Koketsu, S. Sakai and Y. Ishii, *ibid.*, **72**, 2503 (1969).

3) J. Koketsu, S. Sakai and Y. Ishii, *ibid.*, **73**, 201 (1970).

4) J. Koketsu, S. Sakai and Y. Ishii, *ibid.*, **73**, 205 (1970).

Table 1. IR and NMR spectra of phosphonium salts; Vb and Vd

Compounds	IR spectra ν (cm^{-1})	NMR spectra τ (TMS)
Vb	3060(w), 2980(w), 2940(w), 2910(w), 1585(w), 1480(m), 1438(m), 1352(s), 1220—1180(vs, br), 1118(s), 1165(m), 1033(m), 1019(m), 997(m), 915(w), 755(s), 730(s), 698(s), 611(s), 586(w), 562(s).	8.55—9.10(m); $PCH_2\mathbf{CH_3}$ 6.60—7.45(m); $\mathbf{PCH_2}CH_3$ 7.22(d); J=11 Hz; $PN\mathbf{Me_2}$ 2.30—2.80(m); $P\mathbf{Ph_2}$
Vd	3055(w), 2980(w), 2945(w), 2910(w), 1585(w), 1484(m), 1440(s), 1385(m), 1250—1190(vs, br), 1119(s), 1060(m), 1023(s), 996(m), 915(s), 759(s), 732(s), 698(s), 620(s), 578(s), 564(m).	8.40—9.00(m); $PCH_2\mathbf{CH_3}$ and $\mathbf{CH_3}CH_2OSO_2O$ 6.40—7.30(m); $\mathbf{PCH_2}CH_3$ 5.90(q); J=7Hz; $-\mathbf{CH_2}CH_3$ 2.30—2.80(m); $P\mathbf{Ph_2}$

N,N-dimethylbenzenesulfonamide (VIIa) in the case of two phosphonium salts Va and Vb (Eq. (5)). However, pyrolysis (100°C for 5 hr) products of Vc and Vd were phosphine oxides (VIa and VIb) and polymeric materials which showed a broad ν_{SO_2} band at 1220—1180 cm^{-1}.

$[Ph_2P^+(R'')NMe_2][PhSO_2O^-]$

Va: R″=Me
Vb: R″=Et

$\longrightarrow Ph_2P(O)R'' + PhSO_2NMe_2$ (5)

VIa: R″=Me VIIa
VIb: R″=Et

$[Ph_2P^+(R'')NMe_2][(R''O)SO_2O^-]$

Vc: R″=Me
Vd: R″=Et

$\longrightarrow Ph_2P(O)R''$ + Polymeric materials (6)

VIa: R″=Me
VIb: R″=Et

N,N-dimethylbenzenesulfonamide (VIIa) was identified by comparison of its IR and NMR spectra with those of an authentic sample.

B: Reaction of *N,N*-Diethyl-(Ib) and *N,N*-Di-*n*-propyl-diphenylphosphinous Amide (Ic) with Alkyl Benzenesulfonates (III) and Dialkyl Sulfates (IV). In the same manner as Ia, Ib and Ic reacted with III or IV, affording stable phosphonium salts. The phosphonium salts were subsequently heated to afford the corresponding phosphine oxide (VIa) and *N,N*-dialkylbenzenesulfonamides (VIIb and VIIc) or polymeric materials:

$Ph_2PNR'_2 + PhSO_2OR''$

Ib: R′=Et IIIa: R″=Me
Ic: R′=Pr^n

$\longrightarrow Ph_2P(O)R'' + PhSO_2NR_2'$ (7)

VIa: R″=Me VIIb: R′=Et
VIIc: R′=Pr^n

$Ph_2PNR'_2 + SO_2(OR'')_2 \rightarrow Ph_2P(O)R''$

Ib: R′=Et IVa: R″=Me VIa: R″=Me
+ Polymeric material (8)

C: Reaction of Diphenyl Dialkylphosphoramidites (II) with Alkyl Benzenesulfonates (III) or Dialkyl Sulfates (IV). Diphenyl dialkylphosphoramidite (II) did not react with III or IV at room temperature. However, when a mixture of equimolar amounts of II and III or IV was heated at 100°C under an atmosphere of nitrogen in a sealed tube for about 10 hr, a similar reaction took place with the formation of final deoxygenation products and counter products (probably through unstable phosphonium salts, Eqs. (9) and (10)). The results were supported by the appearance of the IR band characteristic of benzenesulfonamide at 1360 cm^{-1} ($\nu_{SO_2asym.}$) and 1160 cm^{-1} (ν_{SO_2sym}), and also by a sharp singlet at τ (in CCl_4) 7.40 for NMe_2 protons and complex ethyl protons at τ (in CCl_4) 7.9—9.2 for P(O)Et in the NMR spectra. After distillation and subsequent column chromatographic treatments of the reaction mixtures, diphenyl alkylphosphonates (VIII) and *N,N*-dialkylbenzenesulfonamides (VII) or polymeric materials were obtained:

$(PhO)_2PNR'_2 + PhSO_2OR''$

IIa: R′=Me IIIb: R″=Et
IIb: R′=Et IIIa: R″=Me

$\longrightarrow (PhO)_2P(O)R'' + PhSO_2NR'_2$ (9)

VIIIb: R″=Et VIIa: R′=Me
VIIIa: R″=Me VIIb: R′=Et

$(PhO)_2PNR_2' + SO_2(OR'')_2$

IIa: R′=Me IVb: R″=Et
IIb: R′=Et IVa: R″=Me

$\rightarrow (PhO)_2P(O)R''$ + Polymeric materials (10)

VIIIb: R″=Et
VIIIa: R″=Me

The structures of VIIIa and VIIIb were determined by IR and NMR spectra and elemental analyses, and those of VIIa and VIIb by comparison of their IR and NMR spectra with those of authentic samples.

Discussion

In the reaction with electrophilic reagents, the P–N compound exhibited an ambident property. When the reaction partners were typical soft acids such as carbonium ions and PhO^+, the P–N compound behaved as the P base. In this case, *N,N*-dialkyl-diphenylphosphinous amide (I) reacted more readily than diphenyl dialkylphosphoramidite (II). This can be ascribed to the fact that the phosphorus atom of I has higher electron density than II, because II has more electronegative oxygen atoms as substutients on the phosphorus atom. In addition, the phenyl group attached to the phosphorus atom donates an electron to the phosphorus center because of (p–d)π interaction between electrons of phenyl groups and an empty 3d orbital of the phosphorus atom.[5] On the other hand, when reaction partners were hard acids, *i.e.* ester-carbonyl compounds, the reverse reactivity order II$>$I was observed.[6] In this case the nucleophilic site of P–N compounds is considered as the nitrogen atom, and the phosphorus atom would attack ester or carbonyl oxygen synchronously as seen in Eq. (2). The different reactivity order between I and II (II$>$I) stems from the different affinity of the phosphorus atom to the oxygen atom. That is, II has more electronegative oxygen atom bonded to the phosphorus atom directly, hence, electron density on the phosphorus atom of II is reduced considerably. This electron attractive effect of oxygen gives large octet expansion ability,[7] *i.e.* an oxygen affinity to the phosphorus atom.

The structures of the phosphonium salts (V) resulting from the reaction between I and III or IV were confirmed by IR and NMR spectra (see Table 1) In the IR spectra, there were absorption bands characteristic of sulfonate ion at 1220—1180 cm^{-1} ($\nu_{SO_2asym.}$), 1120 cm^{-1} ($\nu_{SO_2sym.}$), and 610 cm^{-1} ($\nu_{SO_2-O^-}$). In the NMR spectra, NMe_2 protons showed doublet near τ (in $CDCl_3$) 7.1 (d, J=11 Hz) and PCH_2CH_3 protons showed complex multiplet signals at τ (in $CDCl_3$) 6.6—7.4 (PCH_2-CH_3) and 8.4—9.1 (PCH_2CH_3) as the result of large J_{PCCH} and J_{HCCH}[8]. The results indicate that quaternization occurred at the phosphorus center, being consistent with the results of Trippett[9] and Burg.[10] They suggested that the phosphorus atom has larger nucleophilicity than the nitrogen atom owing to (p–d)π conjugation between the phosphorus atom and the nitrogen atom. II could not be quaternized at room temperature. This phenomenon was already observed in the reaction of II with phenyl cyanate.[2] When the phosphonium salts (V) or the mixture of II with III or IV, were heated at 100°C, not only alkylation reaction of the phosphorus atom but also deoxygenation reaction from the sulfonate group took place, giving phosphine oxide (VI) or phosphonate (VIII). This reaction was assumed to proceed *via* a four centered mechanism as follows.

$$R_2PNR_2' + R'''SO_2(OR'') \rightarrow [R_2P^+(R'')NR_2'][R'''SO_2O^-] \xrightarrow{\text{heat}} \text{(cyclic intermediate)} \rightarrow R_2P(O)R'' + R'''SO_2NR_2' \quad (11)$$

The alkylation reactions of phosphorus by alkylbenzenesulfonate and dialkyl sulfate can be applied generally to P–N compounds as well as the alkylation reaction of P–N compounds by the Grignard reagent.[10]

Experimental

General Remarks. IR and NMR spectra were measured on a Nippon Bunko IR 403 G Spectrometer and a Japan Electron Minimer Spectrometer. By using benzene as solvent, thin layer chromatography (TLC) was carried out on 250μ thick WAKO Gel-5G (silica gel) layer. Column chromatography was performed in a column 50 cm long (ratio of column to diameter= 20 : 1). Into the column filled with 40 g of 100 mesh silica gel (Mallinckrodt Chemical Works) was put 1—2 g of the sample by the wet method (solvent benzene) which was then eluted by benzene.

Reagents. *N,N*-Dialkyl-diphenylphosphinous amides (I) and diphenyl dialkylphosphoramidites (II) were prepared by the same method as described previously.[2] Alkyl benzenesulfonates (III) and dialkyl sulfates (IV) were purified by distillation before use.

N,N-Dialkylbenzenesulfonamides (VII) were prepared from benzenesulfonyl chloride and the corresponding amine.

$PhSO_2NMe_2$(VIIa): bp 103—110°C/0.1 mmHg; mp 46—47°C; TLC, R_f=0.30; IR (KBr disk), 1324 (ν_{SO_2asym}), and 1158 cm^{-1} (ν_{SO_2sm}).

$PhSO_2NEt_2$(VIIb): bp 120—121°C/1.0 mmHg; n_D^{23} 1.5361; TLC, R_f=0.23; IR (KBr disk), 1332 (ν_{SO_2asym}), and 1158 cm^{-1} (ν_{SO_2sym}).

$PhSO_2NPr_2^n$(VIIc): bp 154—156°C/2.5 mmHg; n_D^{23} 1.5181; TLC, R_f=0.28; IR (KBr disk), 1338 (ν_{SO_2asym}), and 1170 cm^{-1} (ν_{SO_2sym}).

5) E. A. Yakovleva, E. N. Tsvetkov, D. I. Lobanov, A. I. Shatenstein and M. I. Kabachnik, *Tetrahedron*, **25**, 1165 (1969).

6) J. Koketsu, S. Sakai and Y. Ishii, Preprint of Autumn Meeting of the Chem. Soc. of Japan (Nagoya, 1969), p. 139.

7) F. Ramirez and A. Aguiar, Abstr. of Papers, 134th Meeting, Am. Chem. Soc., (Chicago, III, 1958), p. 42N.

8) J. B. Hendrickson, N. L. Maddox, J. J. Sims and H. D. Haesz, *Tetrahedron*, **20**, 449 (1964).

9) S. Trippett and D. M. Walker, *J. Chem. Soc.*, **1961**, 2130.

10) A. B. Burg and P. J. Slota, Jr., *J. Amer. Chem. Soc.*, **80**, 1107 (1958).

Reaction of *N,N*-Dimethyl-diphenylphosphinous Amide (Ia) with Methyl Benzenesulfonate (IIIa). An equimolar mixture of Ia and IIIa reacted exothermally, and the product became turbid and separated into two layers. Further stirring of the product for 5 hr gave a homogeneous and clear solution. This product was heated at 100°C for 5 hr in a sealed tube under a nitrogen atmosphere. When the reaction mixture was distilled, a distillate with boiling point range 104—140°C/mmHg was obtained *viz.*, two spots on TLC at R_f=0.0 and R_f=0.3. From the mixture, 1.17 g (82% yield) of diphenylmethylphosphine oxide (VIa) was separated as crystals from cyclohexane solution, and the filtrate gave 0.81 g (78% yield) of *N,N*-dimethylbenzenesulfonamide (VIIa).

VIa: bp 132—134°C/0.04 mmHg; mp 111.5—112.5°C (lit, 112.5—113°C,[11] 111°C[12]), IR (KBr disk) 1170 cm^{-1} ($\nu_{P=O}$); NMR (in $CDCl_3$) τ 7.79 (d, 3H, J=11Hz, P-CH_3), 2.20 and 1.86 (m, 10H, phenyl). Found: C, 71.99; H, 6.06; P, 14.35%. Calcd for $C_{13}H_{13}PO$: C, 72.22; H, 6.06; P, 14.33%.

VIIa was identified by a comparison of IR and NMR spectra with those of an authentic sample.

Reaction of *N,N*-Diethyl-diphenylphosphinous Amide (Ib) with Methyl Benzenesulfonate (IIIa). When the product from equimolar reaction (6.30 mmol) of Ib and IIIa was heated at 100°C for 5 hr, IVa and VIIb were obtained in 87% and 92% yield, respectively. The structure of VIIb was confirmed by comparison with the corresponding product by a standard procedure.

Reaction of *N,N*-Dimethyl-diphenylphosphinous Amide (Ia) with Ethyl Benzenesulfonate (IIIb). A mixture of 6.19 mmol of Ia and 6.25 mmol of IIIb reacted at room temperature to give the phosphonium salt (Vb) (see Table 1). The subsequent heating of Vb at 100°C for 6 hr in a sealed tube afforded 1.23 g (90% yield) of diphenylethylphosphine oxide (VIb) and 0.82 g (85% yield) of VIIa.

VIb: bp 145—147°C/0.2 mmHg; mp 120—122°C (lit, 124°C,[13] 121°C[12]); IR (KBr disk) 1178 cm^{-1} ($\nu_{P=O}$); NMR (in $CDCl_3$) τ 7.20—7.90 (m, 2H, P**C**H_2-CH_3), 8.45—9.10 (m, 3H, PCH_2**C**H_3), 2.18 and 1.86 (m, 10H, phenyl).

Reaction of *N,N*-Di-*n*-propyl-diphenylphosphinous Amide (Ic) with Methyl Benzenesulfonate (IIIa). From equimolar reaction of Ic and IIIa, 88% yield of VIa and 78% yield of VIIc were obtained.

Reaction of *N,N*-Dimethyl-diphenylphosphinous Amide (Ia) with Diethyl Sulfate (IVb). When 7.95 mmol of Ia was added to IVb (7.90 mmol), phosphonium salt (Vd) was formed exothermally (see Table 1). When Vd was heated in a sealed tube at 100°C for 7 hr, 82% yield of VIb was obtained, which was identified by comparison with the above products. The distillation residue was dark polymeric material, which showed a broad IR absorption band at 1220—1180 cm^{-1} attributable to ν_{SO_2} frequency, and was assumed to be the decomposition product of "$ROSO_2$-NR_2."

Reaction of *N,N*-Diethyl-diphenylphosphinous Amide (Ib) with Dimethyl Sulfate (IVa). In the same manner as in the above experiment, VIa was isolated in 50% yield by the reaction of equimolar mixture of Ib and IVa. The viscous distillation residue had the same IR spectrum as that obtained in the above experiment.

Reaction of Diphenyl Dimethylphosphoramidite (IIa) with Ethyl Benzenesulfonate (IIIb). When IIa was added to an equimolar amount of IIIb, heat evolution could not be observed. Even after standing for one week at room temperature, the IR and NMR spectrum of the mixture showed no change. When the mixture was heated in a sealed tube under a nitrogen atmosphere at 100°C for 10 hr, the mixture turned to yellowish brown. The reaction products showed IR and NMR spectra corresponding to the final alkylation-deoxygenation products as described (see Result). By distillation under reduced pressure, 2.70 g of the distillate with boiling point range 130—150°C/0.03 mmHg was obtained. The distillate gave two reaction products, which were separated on a chromatographic column. Thus, 73% yield of diphenyl ethylphosphonate(VIIIb) and 86% yield of *N,N*-dimethylbenzenesulfonamide (VIIa) were obtained.

VIIIb: bp 113.5—114.0°C/0.03 mmHg; n_D^{23} 1.5540; TLC, R_f=0.14; IR(KBr disk), 1265 cm^{-1} ($\nu_{P=O}$); NMR (in CCl_4), τ 7.80—9.00 (m, 5H, P**C**H_2**C**H_3), 2.85 (s, 10H, phenyl), (Found: P, 11.65% Calcd: P, 11.80%.)

Reaction of Diphenyl Diethylphosphoramidite (IIb) with Methyl Benzenesulfonate (IIIa). When an equimolar mixture of IIb and IIIa was heated at 100°C for 10 hr in a sealed tube under a nitrogen atmosphere, diphenyl methylphosphonate (VIIIa) and VIIb were isolated by distillation and subsequent column chromatography in 87% and 77% yields, respectively.

VIIIa: bp 110—112°C/0.01 mmHg; n_D^{23} 1.5480; TLC, R_f=0.17; IR (KBr), 1264 cm^{-1} ($\nu_{P=O}$); NMR (in CCl_4) τ 8.33 (d, 3H, J=18 Hz, PCH_3), 2.23 (S, 10H phenyl). Found: C, 62.69; H, 5.75; P, 12.20%. Calcd for $C_{13}H_{13}PO_3$: C, 62.91; H, 5.23; P, 12.43%.

Reaction of Diphenyl Dimethylphosphoramidite (IIa) with Diethyl Sulfate (IVb). No reaction took place between equimolar amounts (8.10 mmol) of IIa and IVb at room temperature. However when the mixture was heated at 100°C, VIIIb was isolated in 63% yield by distillation. The distillation residue was 2.0 g of dark polymeric material which showed the same IR spectrum as those of the above experiments.

Reaction of Diphenyl Diethylphosphoramidite (IIb) with Dimethyl Sulfate (IVa). By the same treatment as that mentioned above, VIIIa was obtained in 54% yield from an equimolar mixture (6.50 mmol) of IIb and IVa. In this case too, the counter product was dark polymeric material (1.80 g).

11) D. Seyferth, D. E. Welch and J. Heeren, *ibid.*, **85**, 642 (1963).

12) G. M. Kosolapoff, "Organophosphorus Compounds," John Wiley, New York (1958).

13) G. Aksnes and D. Aksnes, *Acta Chem. Scand.*, **18**, 38 (1964).

BULLETIN OF THE CHEMICAL SOCIETY OF JAPAN VOL. 43 2531—2535 (1970)

Cyclizations of Thioureas with a Hydroxy Group at the β-Position of the *N*-Substituent. I. Reaction with Cupric Acetate

Yoshio IWAKURA, Tadahiro KAYA*1 and Keisuke KURITA

Department of Synthetic Chemistry, Faculty of Engineering, The University of Tokyo, Bunkyo-ku, Tokyo

(Received January 27, 1970)

The reaction of 1-(3-phenoxy-2-hydroxypropyl)-3-phenyl-2-thiourea (thiourea I) with cupric acetate was investigated. The desulfurization reaction by the cupric ion proceeded in refluxing ethanol to yield 2-anilino-5-phenoxymethyl-2-oxazoline. At room temperature, thiourea I and cupric acetate gave a copper complex and the oxazoline. When the complex was heated in ethanol, the same oxazoline and thiourea I were obtained, along with inorganic copper compounds. On the basis of an investigation of the structure of the complex and the decomposition of the complex, the reaction mechanism involving copper-complex formation was discussed. On the other hand, the reaction of 1-(3-phenoxypropyl)-3-phenyl-2-thiourea with cupric acetate under the same conditions gave 1-(3-phenoxypropyl)-3-phenyl-3-acetylurea.

The desulfurization reaction of thiourea bearing a hydroxy group at the β-position of the *N*-substituent (hydroxythiourea) to give an oxazoline derivative was first reported by Söderbaum,[1] who used mercuric oxide to effect such a desulfurization-cyclization reaction. This method was later elaborated by Dains and his co-workers.[2,3] However, their version requires the use of a large excess of the metal oxide to complete the reaction. Adcock and his co-workers[4–6] used methyl iodide for such a desulfurization of hydroxythioureas.

In an earlier paper,[7] it was reported that 2-anilino-5-phenoxymethyl-2-oxazoline was obtained from 1-(3-phenoxy-2-hydroxypropyl)-3-phenyl-2-thiourea by treatment with *p*-toluenesulfonyl chloride. As part of a continuing investigation of the cyclization reaction of hydroxythiourea, the reaction of 1-(3-phenoxy-2-hydroxypropyl)-3-phenyl-2-thiourea with cupric acetate was attempted with the expectation that the oxazoline derivative would be formed by a homogeneous reaction.

Results and Discussion

The reaction of 1-(3-phenoxy-2-hydroxypropyl)-3-phenyl-2-thiourea (thiourea I) with an equimolar amount of cupric acetate proceeded readily in refluxing ethanol to give 2-anilino-5-phenoxymethyl-2-oxazoline in a 73% yield along with some blue-black inorganic precipitate. On the other hand, 1-(3-phenoxypropyl)-3-phenyl-2-thiourea (thiourea II), which has no hydroxy group, was found to afford 1-(3-phenoxypropyl)-3-phenyl-3-acetylurea in an 83% yield, along with a black, inorganic precipitate, under the same reaction conditions.

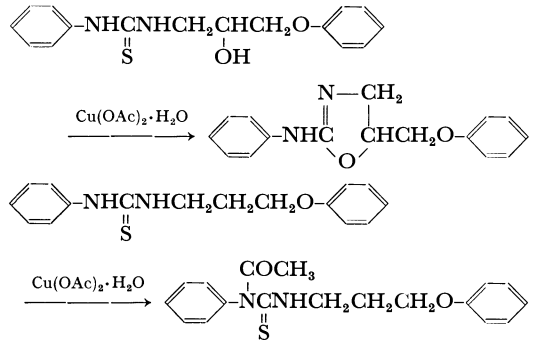

In order to obtain some clue to the reaction mechanism, the reaction of thiourea I and cupric acetate was examined at room temperature. When the solutions of thiourea I and cupric acetate in 70% aqueous dioxane were mixed at room temperature, a brown-black solution resulted and the color of the solution immediately turned yellow. From the yellow solution, yellow crystals containing copper (complex I) appeared gradually.

*1 Present address: Sankyo Chemical Industries, Ltd., 3-Chome, Ginza, Chuo-ku, Tokyo.

1) H. G. Söderbaum, *Ber.*, **28**, 1897 (1895).
2) F. B. Dains, R. Q. Brewster, J. S. Blair and W. C. Thompson, *J. Amer. Chem. Soc.*, **44**, 2637 (1922).
3) F. B. Dains, R. Q. Brewster, I. L. Malm, A. W. Miller, R. V. Maneval and J. A. Sultzaberger, *ibid.*, **47**, 1981 (1925).
4) B. Adcock, A. Lawson and D. H. Miles, *J. Chem. Soc.*, **1961**, 5120.
5) B. Adcock and A. Lawson, *ibid.*, **1965**, 474.
6) B. Adcock and A. Lawson, *ibid.*, *C*, **1966**, 65.
7) Y. Iwakura, K. Kurita and F. Hayano, *J. Polym. Sci.*, in press.

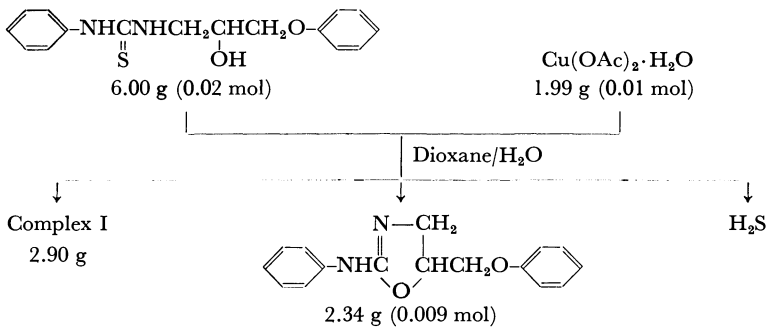

When the moler ratio of thiourea I to cupric acetate was exactly 2 : 1, only the oxazoline and acetic acid were found in the mother liquor obtained after the filtration of complex I from the reaction mixture mentioned above, while neither of the reactants remained unchanged. However, if the ratio was less than 2 : 1, the cupric acetate remained unchanged; on the contrary, if the ratio was larger than 2 : 1, thiourea I was recovered. These facts suggest that the formation of complex I and the oxazoline requires only a half mole of cupric acetate for each mole of thiourea I. Furthermore, a quantitative study of the reaction showed that two moles of thiourea I gave one mole of the oxazoline when the molar ratio of thiourea I to cupric acetate was just 2 : 1. This indicates that one of the two moles of thiourea I added was consumed in the formation of complex I. The elemental analysis of complex I indicated that it contained thiourea I and copper in a 1 : 1 ratio. These results are summarized in the following diagram, along with the quantitative relationship of the materials. Hydrogen sulfide was detected in the reaction mixture by gas chromatography.

Complex I is soluble in polar solvents, such as dimethylformamide and dimethyl sulfoxide, but insoluble in usual organic solvents, such as dioxane, toluene, benzene, methanol, and acetone. These facts suggest that the complex has a polymeric rather than a monomeric structure. From the elemental analysis, the empirical formula, $C_{16}H_{18}N_2SO_3Cu$, was obtained; this formula corresponded well with the composition, thiourea I·Cu·OH. On the basis of these facts, a dimeric olation structure was considered for complex I, since it is well known that a copper complex is apt to form a dimeric olation structure in an aqueous medium. The ESR measurement and particularly the thermoanalysis of the complex, to be described below, seemed to support the structure. Complex I showed a sharp signal in the ESR; this indicated that the copper was in the cupric rather than the cuprous state. The complex prepared from thiourea I and cuprous chloride showed no signal in the ESR.

When complex I was heated while suspended in refluxing ethanol, it gradually decomposed, giving rise to a blue-black powdery material which was insoluble in ethanol. From the ethanolic solution, the oxazoline and thiourea I were obtained in equimolar amounts. The blue-black powder was considered to be a 1 : 1 mixture of cupric sulfide and cupric hydroxide on the basis of the following facts: (1) The sulfur content of the powder was found to be 17.00%, this value was in good agreement with the calculated value, 16.67%. (2) In a thermogravimetric analysis, the powder showed a 9.00% weight loss after being kept at 350°C for 4 hr in a nitrogen atmosphere. If the cupric hydroxide in the mixture loses water to give cupric oxide, the weight loss should be 9.30%. After heating, the color of the powder was black, suggesting a change from cupric hydroxide (blue) to the oxide (black). Complex I and its decomposition in boiling ethanol may be depicted thus:

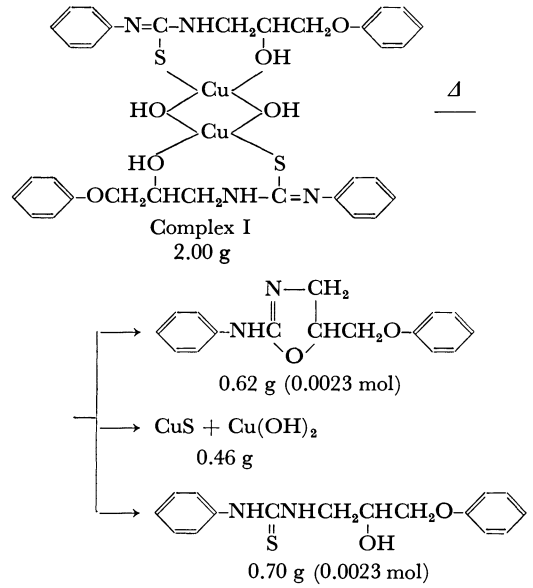

Thus, on the basis of theses data, the reaction scheme between two moles of thiourea I and one mole of cupric acetate at room temperature was presumed to be as follows. Two molecules of thiourea I were co-ordinated to a cupric ion at the initial stage; then one molecule of thiourea I was removed to produce the oxazoline and hydrogen sulfide, and simultaneously the co-ordinated water

was changed to hydroxide to form the olation structure.

If it is assumed that the reaction of thiourea I with cupric acetate in refluxing ethanol also proceeds *via* the formation of complex I, the whole reaction sequence between equimolar amounts of thiourea I and cupric acetate at an elevated temperature would be as follows. Two moles of thiourea I and one mole of cupric acetate react to give one mole of the oxazoline and a half mole of complex I. Then complex I decomposes to give a half mole of the oxazoline and a half mole of thiourea I, along with inorganic materials. The half mole of thiourea I freed from complex I again reacts with a quarter mole of cupric acetate to repeat the sequence. Therefore, the minimum amount of cupric acetate required to convert one mole of thiourea I to the oxazoline completely should be 2/3 mol.

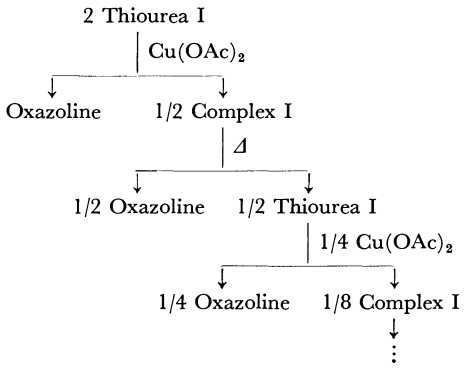

This sequence may be summarized as in the following equation.

$$2\ \text{Thiourea I} + 4/3\ \text{Cu(OAc)}_2 \longrightarrow 2\ \text{Oxazoline}$$

The experimental results showed that the reaction of one mole of thiourea I with 2/3 mol of cupric acetate in refluxing ethanol gave the oxazoline in a 67% yield, with no recovery of thiourea I or cupric acetate.

Figure 1 represents the infrared to far-infrared spectra of thiourea I, complex I, and the oxazoline.

The copper complex of thiourea II (complex II) was obtained by the procedure described for the preparation of complex I. The results of the elemental analysis of complex II agreed well with the calculated value for the 1 : 1 complex of thiourea II and copper. In contrast to complex I, complex II showed no signal in the ESR and was soluble even in a non-polar solvent such as benzene. From these facts, this complex may be considered to consist of thiourea II and copper in a cuprous state in a 1 : 1 ratio and to have no polymeric olation structure. Therefore, the mechanism of the reaction of cupric acetate with thiourea I and that with thiourea II are considered to be quite different; in the latter case, the cupric ion has been reduced to the cuprous ion during the formation of complex II. This problem is under investigation.

Figure 2 represents the infrared to far-infrared spectra of thiourea II, complex II, and the *N*-acylurea.

Experimental

1-(3-Phenoxy-2-hydroxypropyl)-3-phenyl-2-thiourea. This compound, prepared from 1-phenyl-3-amino-2-propanol and phenyl isothiocyanate, has been reported previously.[7]

3-Phenoxypropylamine. This compound was pre-

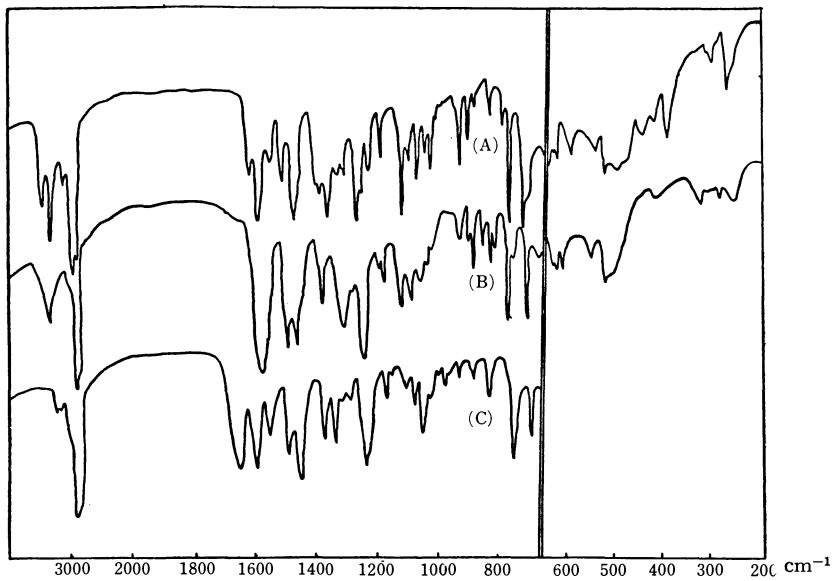

Fig. 1. Infrared to far-infrared spectra of thiourea I (A), complex I (B), and the oxazoline (C), (Nujol).

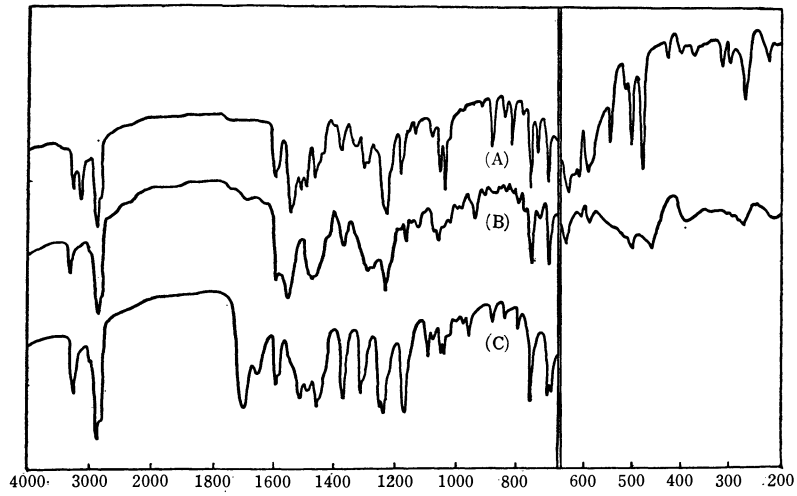

Fig. 2. Infrared to far-infrared spectra of thiourea II (A), complex II (B), and the *N*-acylurea (C), (Nujol).

pared from 3-phenoxypropyl bromide[8] and was synthesized from phenol, 1,3-dibromopropane, and potassium phthalimide according to the Gabriel synthesis. The yield was 64%, bp 138—139°C/23 mmHg.

1-(3-Phenoxypropyl)-3-phenyl-2-thiourea. Into a solution of 15.1 g (0.1 mol) of 3-phenoxypropylamine in 100 m*l* of methanol, we stirred 13.5 g (0.1 mol) of phenyl isothiocyanate, drop by drop, over a period of 30 min. The mixture was then stirred for 4 hr at room temperature; then the solvent was evaporated under reduced pressure. The residual white solid was recrystallized from toluene to give 25.4 g (89.0%) of the product; mp 89—90°C.

Found: C, 67.39; H, 6.42; N, 9.57%. Calcd for $C_{16}H_{18}N_2SO$: C, 67.10; H, 6.33; N, 9.78%.

2-Anilino-5-phenoxymethyl-2-oxazoline. 1-(3-Phenoxy-2-hydroxypropyl)-3-phenyl-2-thiourea (1 g; 0.0033 mol) was refluxed with 0.66 g (0.0033 mol) of cupric acetate monohydrate in 20 m*l* of ethanol. After 5 hr heating, the blue-black precipitate was filtered off and the filtrate was evaporated under reduced pressure. The residue was dissolved in 20 m*l* of toluene and extracted with dilute hydrochloric acid. On the basification of the aqueous extract with aqueous sodium hydroxide, 0.6 g (73%) of 2-anilino-5-phenoxymethyl-2-oxazoline was obtained; this was identical with the authentic sample prepared by the dehydration of 1-(3-phenoxy-2-hydroxypropyl)-3-phenylurea.[7]

1-(3-Phenoxypropyl)-3-phenyl-3-acetylurea. To a solution of 0.95 g (0.0033 mol) of 1-(3-phenoxypropyl)-3-phenyl-2-thiourea in 20 m*l* of ethanol, we added a solution of 0.66 g (0.0033 mol) of cupric acetate monohydrate in 30 m*l* of ethanol. After the mixture had been refluxed for 7 hr, the black precipitate which had formed was filtered off. The filtrate was evaporated under reduced pressure, and the residual solid was recrystallized from *n*-hexane to give 0.86 g (83%) of colorless needles, mp 84°C.

Found: C, 69.40; H, 6.53; N, 8.88% Calcd for $C_{18}H_{20}N_2O_3$: C, 69.21; H, 6.45; N, 8.97%

Reaction of 1-(3-Phenoxy-2-hydroxypropyl)-3-phenyl-2-thiourea with Cupric Acetate at Room Temperature. Cupric acetate monohydrate (1.99 g; 0.01 mol), dissolved in 120 m*l* of 70% aqueous dioxane, was added to a solution of 6.00 g (0.02 mol) of 1-(3-phenoxy-2-hydroxypropyl)-3-phenyl-2-thiourea in 120 m*l* of 70% aqueous dioxane. The mixture immediately became a brown-black solution, and then the solution turned yellow. When this yellow solution was allowed to stand yellow crystals began to appear. The mixture was allowed to stand at room temperature for 6 hr. The crystals were then collected by filtration and weighed 2.90 g; mp 115°C (decomposition).

Found: C, 49.71; H, 4.88; N, 7.51; Cu, 16.66%. Calcd for $C_{32}H_{36}N_4S_2O_6Cu_2$: C, 50.18; H, 5.00; N, 7.32; Cu, 16.59%.

The filtrate was evaporated under reduced pressure, and the residue was dissolved in toluene. The toluene solutions was extracted with dilute hydrochloric acid, and the aqueous extract was basified with aqueous sodium hydroxide to precipitate 2-anilino-5-phenoxymethyl-2-oxazoline in a yield of 2.34 g.

Copper Complex from Thiourea I and Cuprous Chloride. To a solution of 1.00 g (0.0033 mol) of 1-(3-phenoxy-2-hydroxypropyl)-3-phenyl-2-thiourea in 30 m*l* of 70% aqueous dioxane, we added a solution of 0.33 g (0.0033 mol) of cuprous chloride and 0.3 g of sodium chloride, which was added to dissolve the cuprous chloride, in 50 m*l* of 70% aqueous dioxane at room temperature. Aqueous sodium hydroxide was added to the reaction mixture to maintain the pH at 6.8, which was the value of the reaction mixture of the thiourea I and cupric acetate, since the complex was not formed in the low pH region. The precipitated yellow crystals weighed 0.95 g; mp 134°C (decomposition.

Reaction of 1-(3-Phenoxypropyl)-3-phenyl-2-thiourea with Cupric Acetate at Room Temperature. Cupric acetate monohydrate (0.697 g; 0.0033 mol) was dissolved in 40 m*l* of 70% aqueous dioxane, and then the solution was slowly added to a solution of 2.00 g

8) C. S. Marvel and A. L. Tanenbaum, "Organic Syntheses," Coll. Vol. I, p. 435 (1956).

(0.0067 mol) of 1-(3-phenoxypropyl)-3-phenyl-2-thiourea in 40 m*l* of 70% aqueous dioxane. The brown-black mixture changed to yellow, and yellow crystals gradually precipitated. The mixture was kept at room temperature for 6 hr. The crystals were then filtered off; they weighed 0.86 g; mp 104°C (decomposition).

Found: C, 55.31; H, 5.16; N, 8.38%. Calcd for $C_{16}H_{17}N_2SOCu$: C, 54.92; H, 5.18; N, 8.01%.

The filtrate was evaporated, and the residue was dissolved in toluene; the organic solution was washed with aqueous sodium hydroxide to remove the acetic acid, and then with water, and dried over sodium sulfate. The solvent was evaporated to give 0.80 g of 1-(3-phenoxypropyl)-3-phenyl-3-acetylurea.

Thermal Decomposition of Complex I. Complex I (2.00 g) was heated in 60 m*l* of refluxing ethanol for 7 hr heterogeneously. The yellow-orange complex decomposed, giving a blue-black powder. The blue-black powder was filtered, washed with ethanol and weighed; 0.46 g. The filtrate was evaporated under reduced pressure, and the residue was dissolved in toluene. The toluene solution was extracted with dilute hydrochloric acid. When the organic layer was evaporated, 0.70 g of thiourea I was obtained, while, from the aqueous extract, 0.62 g of 2-anilino-5-phenoxymethyl-2-oxazoline was obtained by basification.

BULLETIN OF THE CHEMICAL SOCIETY OF JAPAN VOL. 43 2535—2539 (1970)

Cyclizations of Thioureas with a Hydroxy Group at the β-Position of the *N*-Substituent. II. Oxidation with Thionyl Chloride to Benzothiazoles

Yoshio IWAKURA and Keisuke KURITA

Department of Synthetic Chemistry, Faculty of Engineering, The University of Tokyo, Hongo, Bunkyo-ku, Tokyo

(Received January 27, 1970)

The reaction of *N*-alkyl and *N'*-phenyl substituted thioureas with a hydroxyl group at the β-position of the *N*-substituent with thionyl chloride gave benzothiazole derivatives by an oxidative cyclization reaction; no other products, such as thiazolines or oxazolines, were formed. The structure was confirmed by the various spectral and chemical data.

The dehydration of *N*-acyl derivatives of β-hydroxyalkylamines with thionyl chloride has been one of the most useful methods for preparing oxazoline derivatives since Bergman and Brand[1,2] found in thionyl chloride a mild and effective cyclizing agent; in this manner, 2-phenyl-5-phenoxymethyl-2-oxazoline was obtained from 1-benzamido-3-phenoxy-2-propanol in a quantitative yield, as has been described in a previous paper.[3] Roggero and Metzger[4] investigated the cyclization reaction of 1-thiobenzamido-2-propanol by several reagents, such as thionyl chloride, *p*-toluenesulfonyl chloride, and phosphorus pentoxide, and reported that the cyclization by thionyl chloride led to a mixture of 2-phenyl-5-methyl-2-thiazoline and the corresponding oxazoline, and that the product composition varied with the reaction temperature.

In a preceding paper,[5] it was shown that the cyclization of 1-(3-phenoxy-2-hydroxypropyl)-3-phenyl-2-thiourea by various acids gave thiazoline, oxazoline, or a mixture of them, depending on the character of the acid used. The present investigation was undertaken in order to determine the cyclization products by thionyl chloride.

Results and Discussion

Reaction with Thionyl Chloride and Identification of the Products. The treatment of *N*-alkyl and *N'*-phenyl substituted thioureas with a hydroxyl group at the β-position of the *N*-substituent

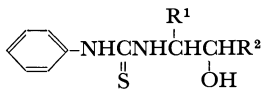

Ia: $R^1=R^2=H$
Ib: $R^1=H$, $R^2=CH_3$
Ic: $R^1=H$, $R^2=CH_2O-C_6H_5$
Id: $R^1=CH_3$, $R^2=CH_3$ (*threo*)

1) M. Bergmann and E. Brand, *Ber.*, **56**, 1280 (1923).
2) M. Bergmann, E. Brand and F. Weinmann, *Z. physiol. Chem.*, **131**, 1 (1923).
3) Y. Iwakura, S. Izawa, F. Hayano and K. Kurita, *Makromol. Chem.*, **104**, 66 (1967).
4) J. Roggero and J. Metzger, *Bull. Soc. Chim. Fr.*, **1963**, 2531
5) Y. Iwakura, K. Kurita and F. Hayano, *J. Polym. Sci., Part A-1*, in press.

(hydroxythioureas) of such types as Ia—d with a large excess of thionyl chloride at room temperature resulted in the formation of the hydrochlorides of the basic materials, which were then converted to the free bases (IIa—d) with aqueous ammonia. The elemental analyses and the infrared spectra of these compounds showed, however, that they were identical with neither the thiazolines nor the oxazolines, nor were they identical with mixtures of the two, contrary to expectation. 1-Isopropyl-3-phenyl-2-thiourea (Ie), non-hydroxythiourea, gave a similar basic compound (IIe) by the same procedure, suggesting that this reaction proceeded independently of the existence of a hydroxyl group in the thioureas.

It is well known that thioureas are oxidized with bromine or thionyl chloride in chloroform to give the salts of bis(substituted formamidine)disulfides. However, the possibility that the above-obtained reaction products of thioureas Ia—e with thionyl chloride might be the bis(substituted formamidine)-disulfides can be ruled out, though the results of the elemental analysis were close to the calculated values. The salt of bis(substituted formamidine)-disulfide is known to be unstable to water or ethanol, and one of the two sulfur atoms is extruded on treatment with absolute ethanol or a mixture of absolute ethanol and benzene to give the monosulfide salt, followed by isomerization and cyclization to the so-called Hector's or Hugershoff's base.[6-14] Moreover, it has been reported that the disulfide base is too unstable to exist as a free base, and that it decomposes instantly, with the elimination of sulfur.

On the basis of the spectral and chemical data, as will be mentioned later, it is very likely that IIa—e has a benzothiazole structure. The oxidation of aryl thioureas with bromine[15] is a very convenient method for preparing benzothiazoles; other oxidizing reagents, such as sulfuryl chloride and sulfur monochloride, have also been reported

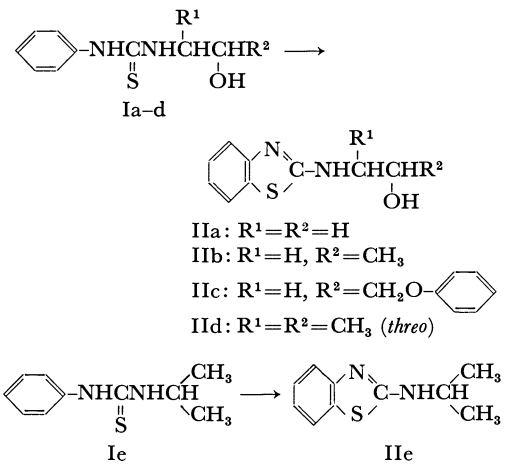

in several papers[16-18] and patents.[19-21]

The products obtained here were found to be resistive to such reducing agents as lithium aluminum hydride and zinc in acidic media. For instance, IIc was recovered quantitatively after being heated in refluxing tetrahydrofuran with a large excess of lithium aluminum hydride for 20 hr. Thermal analysis revealed that they were fairly stable to heat, that they decomposed thermally in a nitrogen atmosphere above 200°C, and that each compound showed only one DTA peak (endothermic) corresponding to its melting point. The molecular weight of IIc as determined by the Rast method (299), was very close to that of the starting thiourea, Ic (302). The mass spectra of IIa, IIb, IIc, IId, and IIe exhibited the molecular ion peak at *m/e*, 194, 208, 300, 222, and 192 respectively, as was to be expected from the benzothiazole structure. In the NMR spectra of IIc and IId, the ratio of the integration of aromatic protons to that of the aliphatic ones gave a better agreement with the benzothiazole than with the disulfide structure: 9/5 for IIc and 4/8 for IId. Figure 1 represents the NMR spectrum of IId. Beilstein's test was negative for all the compounds, IIa—e, showing that none of these was chlorinated under the conditions used.

Tables 1 and 2 summarize the properties of the benzothiazoles obtained. The melting point of IIe was practically the same as that of the reported 2-isopropylaminobenzothiazole, mp 95°C, prepared from 2-methylsulfonylbenzothiazole and isopropyl-

6) D. S. Hector, *Ber.*, **22**, 1176 (1889); *ibid.*, **25**, 799 (1892).
7) A. Hugershoff, *ibid.*, **34**, 3130 (1901).
8) F. Kurzer and P. M. Sanderson, *J. Chem. Soc.*, **1957**, 4461; *ibid.*, **1959**, 1058; *Chem. Ind.*, **1962**, 1681.
9) C. P. Joshua, V. K. Verma and K. S. Suresh, *Tetrahedron Lett.*, **1961**, 663.
10) C. P. Joshua, *Indian J. Chem.*, **1**, 391 (1963).
11) P. K. Srivastava, *ibid.*, **1**, 354 (1963); **1**, 432 (1963); **2**, 154 (1964).
12) P. K. Srivastava and Y. R. Rao, *J. Indian Chem. Soc.*, **40**, 803 (1963).
13) G. Barnikow and J. Bödeker, *Chem. Ber.*, **100**, 1394 (1967).
14) P. K. Srivastava and M. Saleem, *Tetrahedron Lett.*, **1968**, 2725.
15) J. M. Sprague and A. H. Land, "Heterocyclic Compounds," ed. by R. C. Elderfield, John Wiley, New York (1957), p. 581.
16) C. F. H. Allen and J. Van Allen, "Organic Syntheses," Coll. Vol. III, p. 76 (1955).
17) R. D. Desai and C. V. Mehta, *Indian J. Pharm.*, **13**, 205 (1951).
18) R. Sahasrabudhey and H. Krall, *J. Indian Chem. Soc.*, **21**, 17 (1944).
19) I. G. Farbenind. A.-G., Brit. 345735 (1929) (*Chem. Abstr.*, **26**, 1944 (1932)).
20) I. G. Farbenind. A.-G., German 537105 (1929) (*Chem. Abstr.*, **26**, 1000 (1932)).
21) I. G. Farbenind. A.-G., French 688867 (1930) (*Chem. Abstr.*, **25**, 968 (1931)).

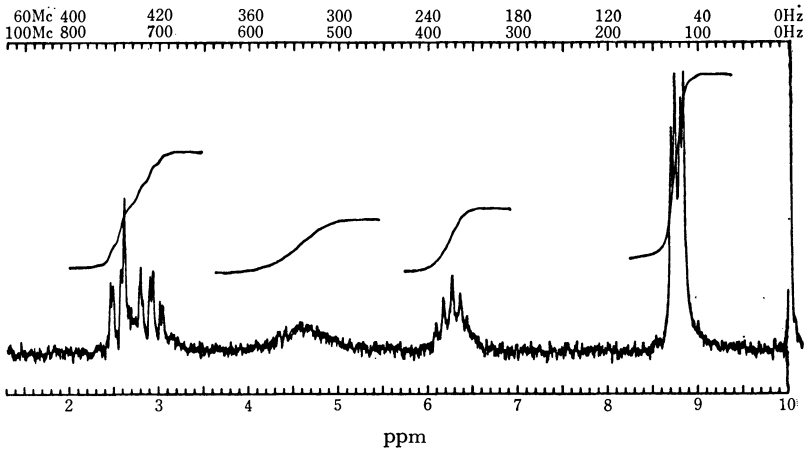

Fig. 1. NMR spectra of IId in $CDCl_3$ (60 Mc).

Table 1. Properties of the benzothiazoles (1)

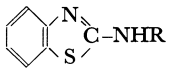

No.	Yield %	Mp °C	Calcd, %				Found, %			
			C	H	N	S	C	H	N	S
IIa	88	104—105.5	55.66	5.19	14.43	16.48	55.18	5.06	14.25	16.63
IIb	80	107—108.5	57.68	5.81	13.46	15.37	57.23	5.57	14.20	15.63
IIc	91	137—139	63.99	5.37	9.33	10.66	64.11	5.35	9.22	11.08
IId	78	109—111	59.45	6.35	12.60		59.05	6.47	12.10	
IIe	90	93— 94.5	62.48	6.29	14.58	16.65	62.09	6.15	14.44	16.56

Table 2. Properties of the benzothiazoles (2)

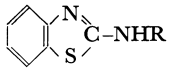

No.	Mass *m/e*	IR cm^{-1}	Picrate								
			Mp °C	Calcd, %				Found, %			
				C,	H,	N,	S,	C,	H,	N,	S,
IIa	194	1600 1570 1560	199—200								
IIb	208	1600 1580 1560	176—177.5	43.94	3.46	16.02		43.65	3.38	16.24	
IIc	300	1600 1580 1560	194—196.5	49.90	3.62	13.23	6.06	49.87	3.66	12.96	6.01
IId	222	1595 1575 1540	183.5—185	45.24	3.80	15.52	7.10	45.49	3.87	15.96	7.18
IIe	192	1615 1575 1550	211—212	45.61	3.59	16.62		45.58	3.58	16.90	

Table 3. Absorption maxima of the benzothiazoles

No.	λ_{max} mμ (log ε)	
IIa	226 (4.54)	268 (4.18)
IIb	225 (4.59)	268 (4.22)
IIc	223 (4.56)	269 (4.26)
IId	226 (4.57)	269 (4.22)
IIe	226 (4.57)	269 (4.21)

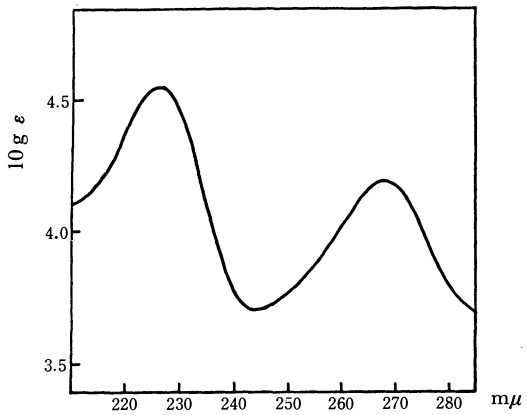

Fig. 2. UV spectra of IId in 95% ethanol.

amine.[22] The elemental analyses of IIa—e and those of the picrates show good agreement with the calculated values for benzothiazoles and their picrates, as these tables show.

The ultraviolet spectra of IIa—e in 95% ethanol were very similar to each other and showed the λ_{max} at 223—226 and 268—269 mμ. The results (Table 3) correspond very well with the reported data that 2-aminobenzothiazole has the λ_{max} at 222 (log ε=4.52) and 264 mμ (log ε=4.09),[23] or 263 mμ (log ε=4.11)[24] in ethanol in the UV. A typical example of the ultraviolet spectrum is shown in Fig. 2.

The Acetylation of IIc and the Hydrolysis of IIc Diacetylate. Acetylation of IIc was carried out by treating IIc with a mixture of pyridine and acetic anhydride to give a diacetylated compound (IIIc).

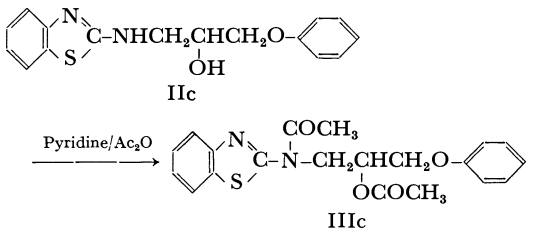

22) E. Hoggarth, *J. Chem. Soc.*, **1949**, 3311.
23) J. Okamiya, *Nippon Kagaku Zasshi*, **80**, 783 (1959).
24) J. R. Edisbury, R. F. Hunter and A. D. Scott, *J. Chem. Soc.*, **1948**, 1497.

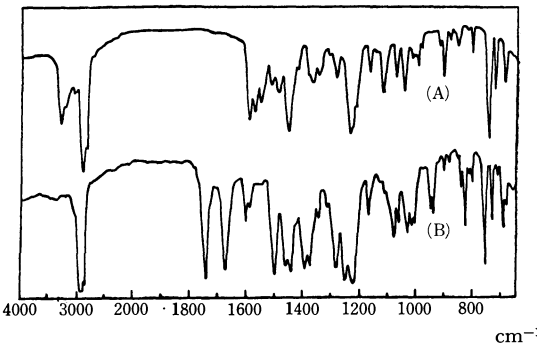

Fig. 3. Infrared spectra of IIc (A) and IIIc (B), (Nujol).

The infrared spectra of IIc and IIIc are shown in Fig. 3. The most characteristic absorption bands of IIIc are found at 1740 and 1670 cm^{-1}, assignable to the carbonyl groups of the *O*- and the *N*-acetyl group respectively. The NMR spectrum of IIIc in $CDCl_3$ showed two singlets at 8.00 τ and 7.46 τ (both 3 protons), indicating that acetylation had taken place at both OH and NH, and a peak due to the methine proton which appeared at 5.75 τ in IIc, was shifted downfield by the acetylation of hydroxyl group and appeared as a multiplet at 4.30 τ.

Diacetylated benzothiazole, IIIc, was subjected to alkaline hydrolysis to give the original benzothiazole, IIc, in a quantitative yield.

In view of the above facts, it can be concluded that the benzothiazoles were obtained quantitatively by the oxidation reaction of 1-aryl-3-alkyl-2-thioureas with thionyl chloride. Benzothiazoles are at a higher oxidation stage than disulfides, and Barnikow and Bödeker[13] have reported that the disulfides which were obtained by the oxidation of thioureas with bromine were further oxidized by bromine to give benzothiazoles. This reaction presumably proceeds also through the disulfides; then these disulfides are oxidized further by thionyl chloride to yield the benzothiazoles.

It is noteworthy that the hydroxythioureas, Ia—d, gave the benzothiazoles in preference to the thiazolines or the oxazolines, since a thioamide with a hydroxyl group at the β-position gave a mixture of a thiazoline and an oxazoline, as has already been mentioned in the introduction.

Experimental

Thioureas. The hydroxythioureas, Ia, Ib and Id, and the non-hydroxythiourea, Ie, were synthesized from the corresponding aminoalcohols or amine and phenyl isothiocyanate by the method previously used in the preparation of hydroxythiourea, Ic.[5] The results are listed in Table 4.

2-(3-Phenoxy-2-hydroxypropylamino)benzothiazole. To 20 ml of thionyl chloride we added 5 g (0.0165 mol) of 1-(3-phenoxy-2-hydroxypropyl)-3-

Table 4. Preparation of thioureas

No.	Yield %	Mp °C	
Ia	90	136—137	(lit, 138[25])
Ib	81	105—106	(lit, 108—109[26])
Ic	85	142—143.5[5]	
Id	84	97—99*	
Ie	85	99—100	(lit, 100—101[27])

* Found: C, 58.96; H, 7.09; N, 12.63%. Calcd for $C_{11}H_{16}N_2SO$: C, 58.91; H, 7.19; N, 12.49%.

phenyl-2-thiourea at 0°C. After the vigorous evolution of gas had ceased, the reaction mixture was allowed to warm to room temperature and was then stirred for an additional hour. The solution was then poured into 300 m*l* of ether and allowed to stand in a refrigerator overnight. The precipitated salt was collected by filtration, washed with ether to remove the excess thionyl chloride, and dried. The benzothiazole hydrochloride was treated with aqueous ammonia to give the free base, which weighed 4.5 g (9.1%). Recrystallization from a mixture of benzene and *n*-hexane gave white crystals; mp 137—139°C.

The other benzothiazoles were prepared by virtually the same procedure.

Acetylation of Benzothiazole, IIc. A mixture of pyridine and acetic anhydride (15 m*l* each)was added to 1.7 g (0.0057 mol) of benzothiazole, IIc. The solution was allowed to stand at room temperature for 1 day and was then concentrated under reduced pressure. The residual solid was recrystallized from cyclohexane to give 1.8 g (83%) of diacetylated benzothiazole, IIIc; mp 149—150°C.

Found: C, 62.64; H, 5.36; N, 7.16; S, 8.29%. Calcd for $C_{20}H_{20}N_2SO_4$: C, 62.49; H, 5.24; N, 7.29; S, 8.33%.

Alkaline Hydrolysis of Diacetylated Benzothiazole, IIIc. To a solution of 0.7 g (0.0018 mol) of diacetylated benzothiazole, IIIc, in 50 m*l* of acetone, we added 20 m*l* of 0.2N sodium hydroxide. The mixture was stirred at 50°C for 5 hr, and then the solvent was evaporated under reduced pressure. The residual white solid was washed well with water and dried. The benzothiazole, IIc, was thus obtained; it weighed 0.53 g (97%).

25) L. Knorr and P. Rössler, *Ber.*, **36**, 1280 (1903).
26) S. Gabriel and H. Ohle, *ibid.*, **50**, 809 (1917).
27) D. C. Iffland and F. A. Cassis, Jr., *J. Amer. Chem. Soc.*, **74**, 6284 (1952).

BULLETIN OF THE CHEMICAL SOCIETY OF JAPAN VOL. 43 2539—2543 (1970)

Bromodenitrogenation of N^2-Benzoylarginine Ethyl Ester with *N*-Bromosuccinimide

Kentaro ANZAI

The Institute of Physical and Chemical Research, Yamato-machi, Saitama

(Received February 3, 1970)

N^2-benzoylarginine ethyl ester (II) reacted with *N*-bromosuccinimide at pH's above 7 to yield, as the main product, N^2-benzoyl-N^5-cyanoornithine ethyl ester (VII), as well as N^3,N^6-bis(4-benzamido-4-ethoxycarbonylbutyl)*s*-tetrazine-3,6-diimine (VIII), *N*,*N*′-di(4-benzamido-4-ethoxycarbonylbutyl)urea (IX), and N^2-benzoylcitrulline ethyl ester (X) as minor products. On acid hydrolysis, VII afforded the following amino acids: ornithine (III), citrulline (IV), N^6-[(4-amino-4-carboxybutyl)-carbamoyl]arginine (V), and *N*,*N*′-di(4-amino-4-carboxybutyl)urea (VI). The mechanism of these reactions was also discussed.

Amino acids react with *N*-bromosuccinimide (NBS), with the evolution of carbon dioxide, to produce corresponding aldehydes.[1] According to Okuyama *et al.*,[2,3] arginine, acetyl arginine, and DNP-arginine as well as guanidine react with NBS, with the evolution of nearly equimolar amounts of nitrogen gas, at pH's above 7. Some proteins, *e. g.*, clupein, gelatin, and the crude urease extract, also suffer from NBS oxidation. On the basis of the above findings the chemical modification of a peptide antibiotic, triculamin,[4,5] which contains two arginine residues in a molecule, was attempted. However the product obtained was an intractable mixture which could hardly be separated chromatographically and this unfruitful result prompted

1) N. Konigsberg, G. Stevenson and J. M. Luck, *J. Biol. Chem.*, **235**, 1341 (1960).

2) N. Okuyama, N. Sato and M. Hirota, *Nippon Kagaku Zasshi*, **86**, 443 (1965).

3) N. Okuyama, private communication, Feb. 16, 1968.

4) S. Suzuki, K. Asahi, J. Nagatsu, Y. Kawashima and I. Suzuki, *J. Antib.*, **20A**, 126 (1967).

5) K. Anzai and S. Suzuki, *Agr. Biol. Chem.*, **33**, 1737 (1969).

us to study the reaction path of NBS oxidation on arginine.

Okuyama *et al.*[3,6] postulated an intermediate, I, from which, on further oxidation, nitrogen could evolve, leaving N^2-formyl ornithine. However, an attempt to isolate the latter compound failed, though ornithine was obtained upon the hydrolysis of the oxidation product.

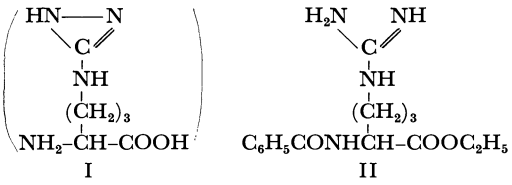

I II

N^2-Benzoylarginine ethyl ester (II) was allowed to react with an excess amount of NBS under neutral conditions at room temperature. The product was extracted with ethyl acetate, and then hydrolysed with hydrochloric acid. CM Sephadex chromatography afforded the following five amino acids (yields): ornithine (III), 52%; citrulline (IV), 29%; N^6-[(4-amino-4-carboxybutyl) carbamoyl] arginine (V), 8%; N,N'-di(4-amino-4-carboxybutyl)urea (VI), 3%; arginine, 2%.

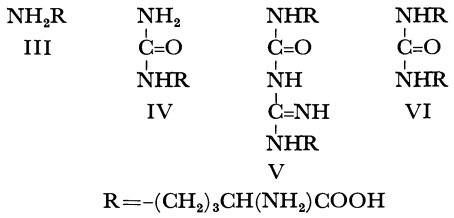

III IV V VI

R=$-(CH_2)_3CH(NH_2)COOH$

V is a strong base; it is eluted from CM Sephadex column closely after arginine, and it is obtained as an acetate. It showed a positive ferricyanide-nitropurside reaction (substituted guanidine). NMR shows the presence of two methylene and two methine groups: δ 3.24 (t, J=5 Hz, 2H), δ 3.35 (t, J=7 Hz, 2H), δ 3.71 (t, J=7 Hz, 1H), δ 3.75 (t, J=5 Hz, 1H). Though the trifluoroacetylated methyl ester of V does not give the parent peak, the

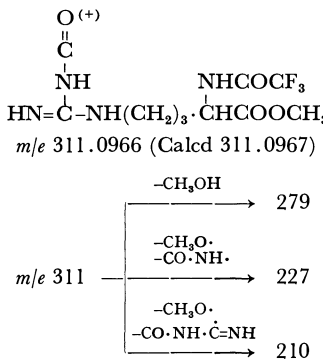

m/e 311.0966 (Calcd 311.0967)

Scheme 1

fragmentations, shown in Scheme 1, can be reasonably explained on the basis of the structure V.

The NMR of VI shows one methylene (δ 3.15, t, J=6 Hz) and one methine (δ 3.75, t, J=6 Hz) proton signals, showing that it is a symmetrically-substituted compound. The trifluoroacetylated methyl ester of VI shows a very weak parent peak at *m/e* 510. However, the intense fragmentations shown in Scheme 2 can reasonably be explained on the basis of the structure VI.

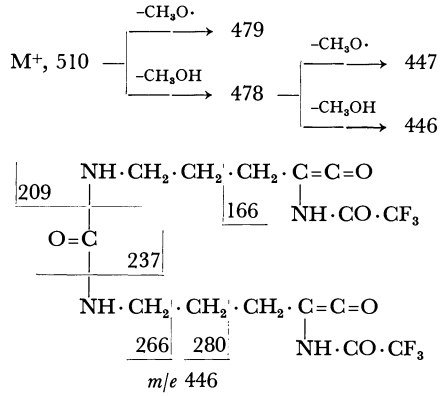

Scheme 2

We attempted to isolate the NBS oxidation product of II using silicic acid chromatography. The main product was identified as N^2-benzoyl-N^5-cyanoornithine ethyl ester VII; three minor products were also obtained.

The IR of VII shows a strong band at 2210 cm^{-1} attributable to a cyano group. Though the analytical and NMR data support the structure VII, the mass spectrum shows some ambiguity. Though the operation conditions can be chosen so as to give the expected parent peak at *m/e* 289.1418 (calcd for $C_{15}H_{19}N_3O_3$ 289.1426), unexplicable peaks at higher mass are observed on an elevation of the temperature: These can possibly be ascribed to the polymerization of the sample. VII also afforded III, IV, V, and VI on acid hydrolysis; a reasonable reaction path from VII to the three amino acids is shown in Scheme 3:

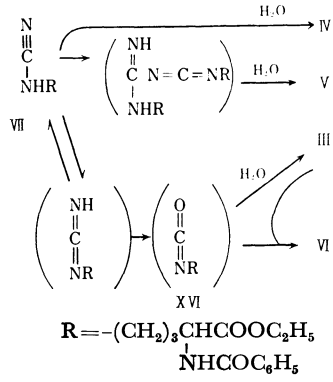

R=$-(CH_2)_3CHCOOC_2H_5$
$NHCOC_6H_5$

Scheme 3

6) K. Niijima and N. Okuyama, *Seikagaku*, **35**, 396 (1963).

The three minor products were identified as N^3,N^6-bis(4-benzamido-4-ethoxycarbonylbutyl)-*s*-tetrazine-3,6-diimine (VIII), *N,N'*-di(4-benzamido-4-ethoxycarbonylbutyl)urea (IX), and N^2-benzoyl-citrulline ethyl ester (X).

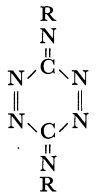

VIII

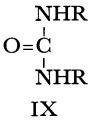

IX

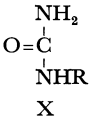

X

$R=-(CH_2)_3CHCOOC_2H_5$
$NHCOC_6H_5$

The intense UV absorption of VIII ($\lambda_{max}^{methanol}$ 222, ε 83000; 303 mμ, ε 7000), as well as the absence of IR absorption in the 1800—2900 cm^{-1} region, exclude other possible structures, XI and XII, which

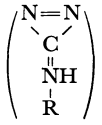

XI

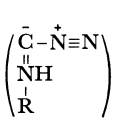

XII

$R=-(CH_2)_3CHCOOC_2H_5$
$NHCOC_6H_5$

could be expected to give the same analytical data and an NMR spectra similar to that of VIII. XI or XII was first postulated[7] as an intermediate through which N^2-benzoyl-N^5-formylornithine ethyl ester might be given, along with the evolution of nitrogen gas.

IX and X gave the corresponding amino acids, VI and IV, on acid hydrolysis; the analytical and spectral data are also consistent with the proposed structures.

After VII, VIII, IX, and X had been extracted with ethyl acetate, the aqueous layer was heated with sodium hydroxide. Subsequent CM Sephadex chromatography afforded N^2-benzoylornithine (XIII).

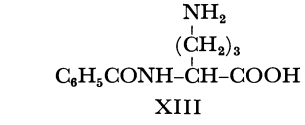

XIII

The product analysis leads to the possible reaction path outlined in Scheme 4; by postulating an intermediate, XIV, all the products mentioned above can reasonably be situated there.

The compound XV was once obtained; though its poor reproducibility made satisfactory identification difficult, the analytical data and the MS

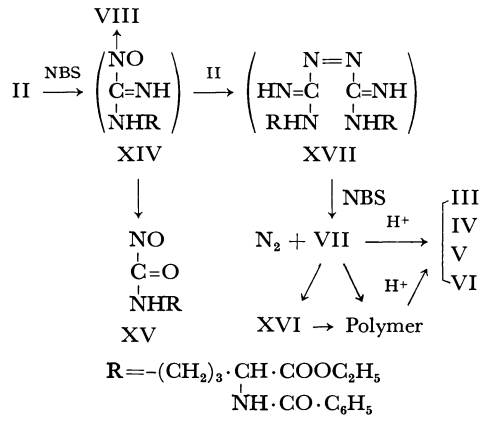

$R=-(CH_2)_3\cdot CH\cdot COOC_2H_5$
$NH\cdot CO\cdot C_6H_5$

Scheme 4

fragmentation pattern suggested it to be 2-benzamido-5-(2-nitrosoformamido)valeric acid ethyl ester (XV) (See Experimental section).

Possibly the main reaction proceeds *via* II, XIV, XVII, and VII, with the evolution of nitrogen from XVII. According to this process, 1.5 mol of NBS is needed for the oxidation of 1 mol of II. VII as well as its hydrolysed product, XVI, might have a tendency to polymerize easily under the present reaction conditions, resulting in an unexpectedly low yield of VII (20% after purification). A polymerized product, which was separated roughly by means of silicic acid chromatography, also gave four amino acids, *i. e.*, III, IV, V, and VI, on acid hydrolysis.

VII was still hydrolysed in a neutral solution, the reaction might proceed in a way similar to that shown in Scheme 3, giving IX, X, and the ethyl ester of XIII.

According to the reaction path proposed here, the two atoms of a nitrogen molecule do not originate from the same guanidine residue, as was first postulated.[7] Ammonia, liberated from VII by hydrolysis, may also be oxidized to a nitrogen molecule.

Experimental

Reaction Procedure. In 25 m*l* of a 0.1N phosphate buffer solution at pH 7, 171 mg (5×10^{-3}M) of the hydrochloride of N^2-benzoylarginine ethyl ester (II) were dissolved. A solution of 178 mg (10^{-2}M) of NBS in 25 m*l* of acetone was added dropwise with stirring and the reaction proceeded with an evolution of nitrogen gas accompanying the decrease in the pH. If the insoluble product separated, acetone was added until a homogenous solution was obtained; the pH of the solution was kept at 7—8 with sodium hydroxide throughout the reaction. The decrease in the pH ceased before the addition of NBS was completed. Five grams of ammonium sulfate were added to diminish the excess NBS.

Acid Hydrolysis of the Reaction Product Yielding Ornithine (III), Citrulline (IV), N^6-[(4-Amino-4-carboxybutyl)carbamoyl]-arginine (V), and *N,N'*-Di(4-amino-4-carboxybutyl)urea (VI). The reaction

7) In a letter to Dr. N. Okuyama the present author suggested the reaction path to be II→I→XI or XII $\xrightarrow{H_2O}$ N^2-benzoyl-N^5-formylornithine ethyl ester+N_2. This mechanism can be rejected on the basis of this paper.

mixture described in the preceding section was extracted with ethyl acetate; then, after the solvent had been evaporated, the residue, which weighed 1.15 g, was dissolved in a mixture of acetic acid and conc. HCl (1 : 1) and the solution was heated at 105°C for 14 hr. The acids were then evaporated, and the residue was dried over sodium hydroxide *in vacuo*. Water was added, and the water-insoluble part, from which 130 mg of benzoic acid was obtained after crystallization from ethanol and water, was excluded by filtration; we thus obtained a mixture of amino acids, which were separated chromatographically as will be described below.

The amino acid mixture was charged on a column (2×90 cm) of CM Sephadex and developed with a 0.4N pyridine solution buffered at pH 5.0 with acetic acid. Three fractions, all of which showed a positive ninhydrin reaction, were thus obtained. The first one (a fraction at 100—190 ml) consisted of two amino acids as the main components; they were separated further chromatographically on a cellulose column using a mixture of propanol, pyridine, acetic acid, and water (15, 10, 3, 10) as the developing solvent. The one which was eluted first was identified as citrulline (IV) by comparing it with an authentic sample; yield, 250 mg.

The latter one (yield, 20 mg) was crystallized from water and ethanol and was identified as *N,N'*-di(4-amino-4-carboxybutyl)urea (VI). It gradually decomposed above 240°C and did not show a definite mp; $[\alpha]_D$= +2.3 (20°C, *c* 1, H_2O).

Found: C, 44.62; H, 7.55; N, 20.05%. Calcd for $C_{11}H_{22}N_4O_5$: C, 45.50; H, 7.63; N, 19.30%. NMR (D_2O) δ 3.15 (t, J=6 Hz, $-NH\cdot C\underline{H}_2\cdot CH_2-$), δ 3.75 (t, J=6 Hz, $CH_2-C\underline{H}(NH_2)-COOH$): IR, ν_{max}^{KBr} 3350, 2940, 1625, 1583, 1417, 1347 cm^{-1}.

The second fraction (420—530 ml), which was eluted from the CM Sephadex column, consisted mainly of one amino acid; this amino acid was purified further chromatographically on a cellulose column and was identified as the acetate of ornithine (III) by comparing it with an authentic sample.

The third fraction (540—750 ml) consisted of two amino acids which were separated chromatographically on a cellulose column (2×90 cm; propanol, pyridine, acetic acid and water; 15, 10, 3, 10). The one which was eluted first was crystallized from water and ethanol and was identified as arginine acetate; yield, 29 mg.

The second one, which was eluted later, was identified as the acetate of N^6-[(4-amino-4-carboxybutyl)carbamoyl]arginine (V); yield, 78 mg, mp 178—183°C.

Found: C, 42.64; H, 7.03; N, 20.62%. Calcd for $C_{14}H_{28}N_6O_7$: C, 42.85; H, 7.19; N, 21.42%.

NMR (D_2O) δ 1.91 (s, $C\underline{H}_3COO^-$), δ 3.24 (t, J=5 Hz, $-NH\cdot C\underline{H}_2\cdot CH_2-$), δ 3.35 (t, J=7 Hz, $-NH\cdot C\underline{H}_2\cdot CH_2-$), δ 3.71 (t, J=7 Hz, $-CH_2\cdot C\underline{H}(NH_2)COOH$), δ 3.75 (t, J=5 Hz, $-CH_2\cdot C\underline{H}(NH_2)COOH$).

Isolation of N^2-Benzoyl-N^5-cyanoornithine Ethyl Ester (VII), N^3,N^6-Bis(4-benzamido-4-ethoxycarbonylbutyl)-*s*-tetrazine-3,6-diimne (VIII), *N,N'*-Di(4-benzamido-4-ethoxycarbonylbutyl)urea (IX), and N^2-Benzoylcitrulline Ethyl Ester (X). The ethyl acetate extract of the reaction mixture was dried *in vacuo*, and the residue was chromatographed on a silicic acid column (2×50 cm) using a mixting of ethyl acetate and benzene as the developing solvent, while the ratio of the former to the latter was gradually increased. The fractions, all of which showed single spots on TLC with a Greig-Leaback reagent, were then collected.

The main product, N^2-benzoyl-N^5-cyanoornithine ethyl ester (VII), was eluted with a mixture of benzene and ethyl acetate (2 : 3). After the solvent had been evaporated, the solidified residue was washed with benzene; yield, 290 mg; mp 85—85.5°C.

Found: C, 61.79; H, 6.59; N, 14.31%. Calcd for $C_{15}H_{19}N_3O_3$: C, 62.26; H, 6.62; N, 14.52%.

NMR ($CDCl_3$), δ 1.30 (t, J=7 Hz $-OCH_2C\underline{H}_3$), δ 1.85 (m, $-C\underline{H}_2\cdot C\underline{H}_2\cdot CH\swarrow$), δ 3.08 (m, $-NH\cdot C\underline{H}_2\cdot CH_2-$), δ 4.22 (q, J=7 Hz, $OC\underline{H}_2CH_3$), δ 4.70 (m, $-CH_2\cdot C\underline{H}\cdot NH-$), δ 5.30 (broad $N\equiv C\cdot N\underline{H}\cdot CH_2-$), δ 7.2—8.0 (complex, $-C_6\underline{H}_5$): ν_{max}^{KBr} 3300, 2930, 2210, 1735, 1640, 1535, 1490, 1215, 1030, 720, 700 cm^{-1}.

The molecular weight determination by the V.P.O. method gives much larger values (chloroform, 757; ethyl acetate, 839) than that calculated (289.33), suggesting that some molecules associate in the solvent.

After VII and two other minor products (one of which was identified as succinimide (yield, 90 mg), and the other of which was not yet been identified because of its low yield) had been eluted, the solvent for the development was changed to ethyl acetate. Two products were thus obtained.

The one which was eluted first was crystallized from ethyl acetate and ligroin and was identified as N^3,N^6-bis(4-benzamido-4-ethoxycarbonylbutyl)-*s*-tetrazine-3,6-diimine (VIII); yield, 31 mg; mp 157—158°C.

Found: C, 59.30; H, 6.10; N, 17.99%. Calcd for $C_{30}H_{36}N_8O_6$: C, 59.59; H, 6.00; N, 18.53%.

IR, ν_{max}^{KBr} 3280, 3050, 2920, 1740, 1633, 1604, 1580, 1540, 1210, 1193 cm^{-1}: $\lambda_{max}^{methanol}$ 222 (ε, 83000), 303 mμ (ε, 7000).

The other product, which was eluted later than VIII with ethyl acetate, was crystallized from ethanol and ligroin and was identified as *N,N'*-di(4-benzamido-4-ethoxycarbonylbutyl)urea (IX); yield, 32 mg; mp 196—197°C.

Found: C, 61.78; H, 7.06; N, 10.26%. Calcd for $C_{29}H_{28}N_4O_7\cdot\frac{1}{2}H_2O$: C, 61.78; H, 6.97; N, 9.94%.

M^+, 554 (weak): IR, ν_{max}^{KBr} 3360, 3260, 1740, 1648, 1605, 1570, 1540, 1490, 1470, 1340, 1260, 1035, 715 cm^{-1}: the acid hydrolysis (acetic acid-conc. HCl (1 : 1), 105°C, 16 hr) of IX gave VI, which was identified by comparison with a sample obtained as has been described in the second section.

When the developing solvent was changed to a mixture of ethyl acetate and methanol (9 : 1), a brownish-colored fraction was rapidly eluted; yield of the residue, 160 mg. No crystalline material was obtained from this dirty fraction. It exhibited a tailing aspect on TLC and may be a mixture of the polymerized products. As in the case of VII, it afforded four amino acids, *i. e.*, III, IV, V, and VI, on acid hydrolysis.

Another product was eluted with the same solvent mixture after the brownish fraction had been eluted and crystallized from ethanol and ligroin. The analytical and spectral data of the compound show that it is N^2-benzoylcitrulline ethyl ester (X), with one mole of succinimide as an adduct; yield, 90 mg; mp 196—197°C.

Found: C, 56.04; H, 6.27; N, 13.79%. Calcd for $C_{19}H_{26}N_4O_6$: C, 56.14; H, 6.45; N, 13.79%.

NMR (DMSO-d_6): δ 1.18 (t, J=7Hz, $-O\cdot CH_2\cdot C\underline{H}_3$), δ 1.7 (m, $NH\cdot C\underline{H}_2\cdot C\underline{H}_2\cdot CH\swarrow$), δ 2.4 (partially overlapped with the peak of DMSO, $2C\underline{H}_2$ of succinimide), δ 3.2 (m, $-NH\cdot C\underline{H}_2\cdot CH_2-$), δ 4.07 (q, J=7 Hz, $-OC\underline{H}_2$

CH_3), δ 4.25 (m, $-CO\cdot NH\cdot C\underline{H}\cdot CH_2-$), δ 6.75 (s, $N\underline{H}$ of succinimide), 7.2—8.0 (complex, $C_6\underline{H}_5CO$), δ 8.30 (t, J=6 Hz, $-NH_2\cdot CO\cdot N\underline{H}\cdot CH_2-$), δ 8.70 (d, J=8 Hz, $C_6H_5\cdot CO\cdot N\underline{H}\cdot CH<$), δ 10.25 (s, $N\underline{H}_2\cdot CO\cdot NH-$): $\lambda_{max}^{methanol}$ 223 mμ (ε, 14200): IR, ν_{max}^{KBr} 3400, 3290, 3060, 2920, 1757, 1688, 1667, 1638, 1550, 1520, 1385, 1250, 1218, 1183, 1160 cm^{-1}: M^+, 307 (weak), M^+-NH_3, 290.1260 (Calcd for $C_{15}H_{18}N_2O_3$, 290.1267), M^+ of succinimide, 99 (intense). On acid hydrolysis (using a mixture of acetic acid and conc. HCl (1 : 1), 105°C, 20 hr) X afforded citrulline, which was identified by comparison with an authentic sample.

The Isolation of N^2-Benzoylornithine (XIII). After the reaction mixture described in the first section had been extracted with ethyl acetate, the volume of the aqueous layer was diluted to 100 m*l* and 4 g of sodium hydroxide were added. After the solution had been heated at 100°C for 2 hr, it was passed through an IR 120 (H-cycle) column (3×50 cm). With 1N aqueous ammonia a ninhydrin-positive fraction was eluted; it was shown to be almost homogeneous on TLC. Further purication was effective with chromatography on a CM Sephadex column (2×90 cm) using a 0.4N pyridine solution buffered at pH 5.0 with acetic acid. After the solvent had been evaporated, the residue was crystallized from water and ethanol; yield, 33 mg; mp 227—228°C.

Found: C, 60.48; H, 6.44; N, 11.76%. Calcd for $C_{12}H_{16}N_2O_3$: C, 61.00; H, 6.83; N, 11.86%. NMR (D_2O) δ 1.85 (complex, $-CH_2\cdot C\underline{H}_2\cdot C\underline{H}_2\cdot CH<$), δ 3.02 (t, J=6 Hz, $-NH\cdot C\underline{H}_2\cdot CH_2-$), δ 4.38 (t, J=6 Hz, $-CH_2\cdot C\underline{H}\cdot NH\cdot CO-$) δ 7.6 (complex, $-C_6\underline{H}_5$): IR, ν_{max}^{KBr} 3350, 2900, 1652, 1633, 1590, 1532, 1495, 1465, 1410, 1370, 1345, 1307, 1299 cm^{-1}. The methyl ester of XIII, prepared by the method of McLaffaty *et al.*[8], afforded the expected parent peak at 250. The acid hydrolysis of XIII (6N HCl, 105°C, 16 hr) afforded ornithine, which was identified by comparison with an authentic sample.

2-Benzamido-5-(2-nitrosoformamido)valeric Acid Ethyl Ester (XV). The reaction mixture described in the first section was extracted with ethyl acetate, the solvent was evaporated, and the residue, after dried *in vacuo*, was dissolved in hot benzene. Usually on standing in a refrigerator only an oily substance was separated. However, in a few cases a small amount of crystals was obtained; yield 10 mg; mp 183—184°C. The effort to create conditions which would give a good reproducibility in obtaining the compound was unfruitful. The attempt to separate the same compound by means of silicic acid chromatography was also unsuccessful. Though the sample obtained was too scanty to make a full identification, the analytical and spectral data suggested it to be 2-benzamido-5-(2-nitrosoformamido)valeric acid (XV).

Found: C, 53.23; H, 5.93; N, 12.53%. Calcd for $C_{15}H_{19}N_3O_5\cdot H_2O$: C, 53.09; H, 6.24; N, 12.39%. The parent peak was not observed: M^+-HNO, 290.1258 (calcd for $C_{15}H_{18}N_2O_4$ 290.1267). Other fragmentations, the compositions of which were confirmed by high-resolution MS, are shown in Scheme 5. IR, ν_{max}^{KBr} 3440, 3340, 3200, 3120, 3000, 1733, 1687, 1640, 1615, 1580, 1537, 1443, 1345, 1222, 1203, 1028, 710 cm^{-1}.

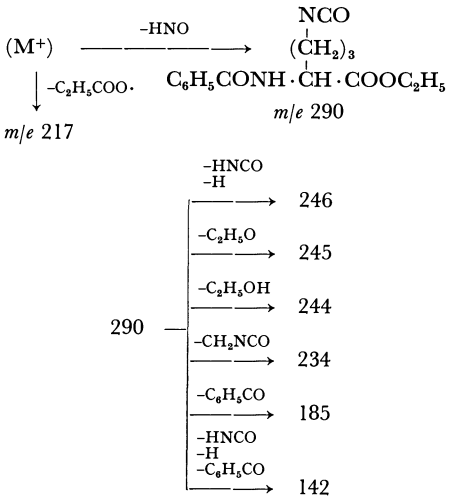

Scheme 5

The author wishes his hearty thanks to Dr. S. Suzuki, the chief of the Laboratory of Antibiotics, this institute, for his kindly giving him a chance to study on this subject and for his encouragement, and to Dr. S. Emoto, this institute, and Dr. N. Okuyama, Tokyo Metropolitan University, for their useful suggestions.

8) M. Senn, R. Venkataraghavan, and F. W. McLafferty, *J. Amer. Chem. Soc.*, **88**, 5593 (1966).

BULLETIN OF THE CHEMICAL SOCIETY OF JAPAN VOL. 43 2544—2548 (1970)

Lactone Carboxylic Acids. VII. Reaction of Lactone Pyrazolines with Acetic Anhydride. A Preparation of Lignans Skeleton by Thermal Decomposition of Pyrazoline

Sigeru Torii and Takuya Furuta

Department of Industrial Chemistry, Okayama University, Okayama

(Received February 9, 1970)

Cycloaddition of diazomethanes to aconic acids (**4** and **14**) gave 1-pyrazolines (**5**, **7** and **15**). Thermal decomposition of **7** afforded γ-phenyl-α-benzylaconic acid **8** having a lignans skeleton. By the action of phosphoric acid **5** was converted into 2-pyrazoline **12**. The chemical nature of pyrazolines (**5** and **12**) is discriminated by treatment with acetic anhydride in the presence of *p*-toluenesulfonic acid. Thus, 1-pyrazoline **5** gave the corresponding derivatives (**10**, **11** and **13**), and **12** gave **13**. The thermochemical stability of the pyrazolines (**15** and **16**) were also studied. A possible mechanism of the formation of **10** and **13** is described.

In the preceding paper of this series, the synthesis of γ-butyrolactones having lignans skeleton was reported.[1] The present paper describes an alternative route to ligans-like compounds and some new properties of pyrazoline derivatives[2] obtained by the addition of diazomethanes to aconic acid (**4** and **13**).

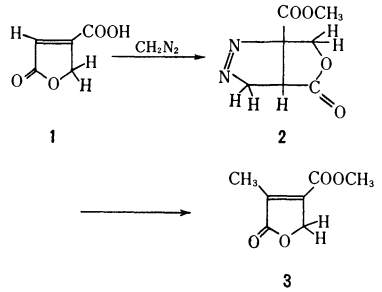

1 **2** **3**

The reaction of aconic acid **1** with diazomethane gives the corresponding pyrazoline **2** which undergoes thermal decomposition to afford **3**.[3] The applicable mode of cycloaddition of diazomethane to aconic acid has led to an extensive study on the preparation of lignans.[4] γ-Phenylaconic acid **4**, obtained in good yield by treatment of α-benzylidenesuccinic acid[5] with bromine in water followed by hot water, was characterized by the absorption spectrum: 1733 (carbonyl $\nu_{C=O}$) and 1645 cm^{-1} and by hydrolysis[6] with alkali to γ-keto acid **9**.[7]

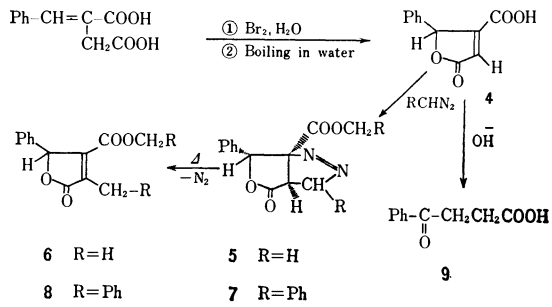

6 R=H **5** R=H **9**

8 R=Ph **7** R=Ph

Scheme I

The adduct[8] of **4** with diazomethane gave **6** in a quantitative yield, when heated at 145°C for 30 min. Similarly, phenyldiazomethane[9] in the same reaction yielded crystalline pyrazoline **7** which was subjected to thermal decomposition to give **8**. The structural assignment of **8** was carried out by the infrared and NMR spectra which revealed the pres-

1) A. Takeda and S. Torii, This Bulletin, **41**, 1468 (1968).

2) See Reviews "Cycloaddition of Diazoalkanes," A. Ohta, *Yuki Gosei Kagaku Kyokai Shi*, **26**, 115 (1968).

3) R. F. Rekker, J. P. Brombacher and W. Th. Nauta, *Rec. trav. chim. Pays-Bas*, **73**, 417 (1954).

4) W. M. Hearon and W. S. MacGregor, *Chem. Rev.*, **55**, 957 (1955); F. M. Dean, "Naturally-occurring Oxygen Ring Compounds," Butterworths, London (1963), p. 29.

5) H. J. Bestmann and H. Schulz, *Chem. Ber.*, **95**, 2921 (1962).

6) A. Takeda, K. Takahasi, S. Torii and T. Moriwake, *J. Org. Chem.*, **31**, 616 (1966).

7) L. F. Somerville and C. F. H. Allen, "Organic Syntheses," Coll. Vol. II, p. 81 (1943).

8) It is expected that considering the Stuart model of **4** the bulkiness of the phenyl group provides a back side attack of diazomethane. Selective decomposition of these kinds of adducts to the corresponding unsaturated compounds such as **6** and **8** has been reported: *e.g.*, a) J. Hamelin, *C. R. Acad. Sci., Paris, Ser.* c, **261**, 4776 (1965); b) J. Hamelin and R. Carrie, *ibid.*, **261**, 5545 (1965).

9) R. J. Mohrbacher and N. H. Cromwell, *J. Amer. Chem. Soc.*, **79**, 401 (1957).

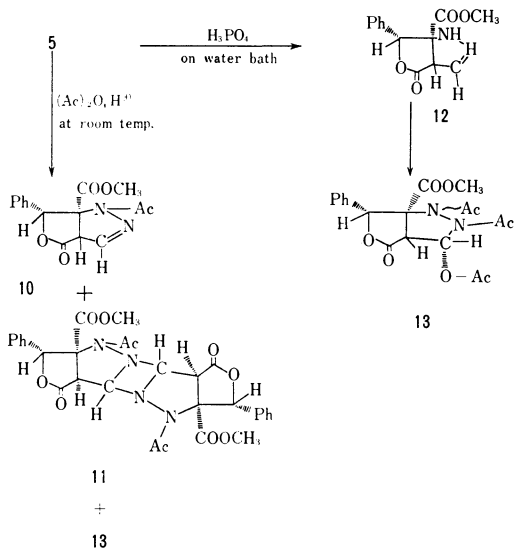

Scheme II

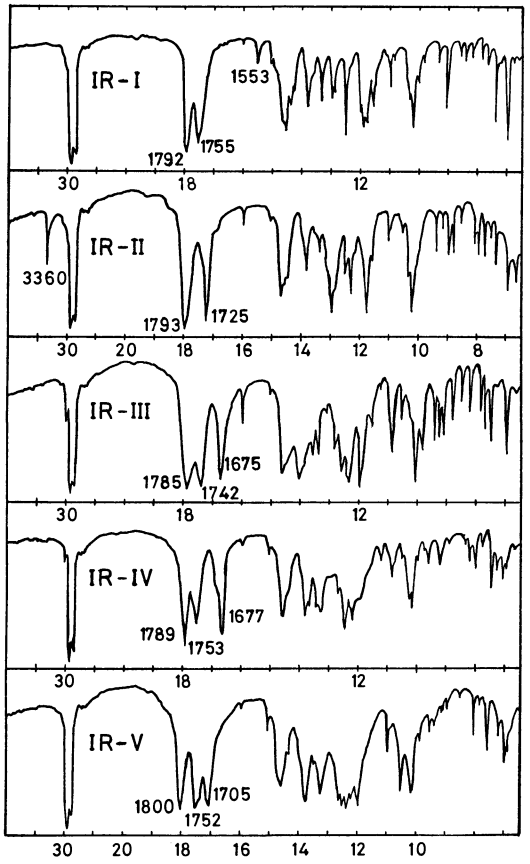

Fig. 1. IR spectra of the key compounds are as follows: IR-I, methyl γ-phenyl-α,β-(1-pyrazolino)-paraconate **5**; IR-II, methyl γ-phenyl-α,β-(2-pyrazolino)paraconate **12**; IR-III, *N*-Acetyl-2-pyrazoline **10**; IR-IV, Dimer of **10**; IR-V, the compound **13**.

ence of lactone, ester and double bond functions, 1785, 1725 and 1670 (shoulder) cm^{-1}, respectively, and also the presence of two kinds of methylene group (C=C-CH_2-Ph, τ 7.00, q, and -O-CH_2-Ph 5.03, q).

Many papers concerning cycloaddition of diazoalkanes to suitable unsaturated compounds have recently appeared.[2,10] However, concerning the isolation of the products, it was difficult to obtain the tautomers concurrently,[11] *i. e.*, 1-prazolines and 2-pyrazolines,[2] and the reactivities of these tautomers have not yet been examined. 2-Pyrazolines **12**, readily obtained by the treatment of **5** with phosphoric acid[12] at 70—80°C, can be distinguished by its infrared spectrum as shown in Fig. 1, since instead of the absorption band at 1553 cm^{-1} due

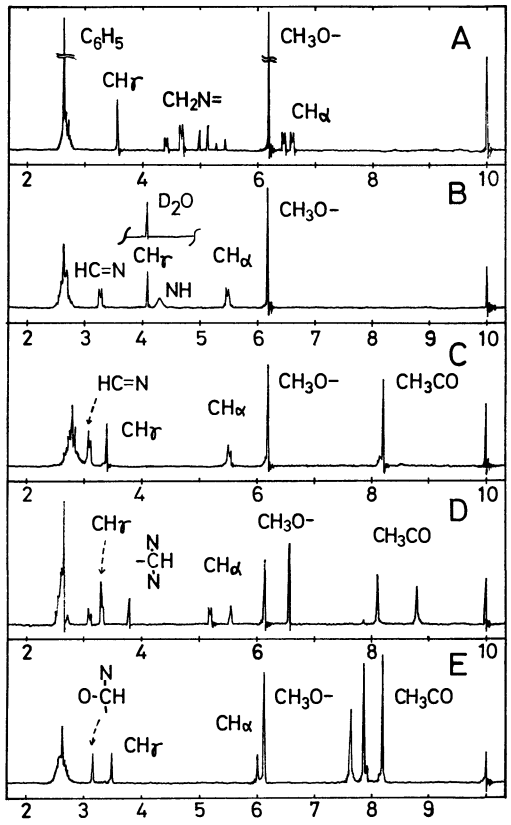

Fig. 2. NMR spectra of methyl γ-phenyl-α,β-(1-pyrazolino)paraconate (A), methyl γ-phenyl-α,β-(2-pyrazolino)paraconate (B), *N*-acetyl-2-pyrazoline **10** (C), Dimer of **10** (D), and the compound **13** (E).

10) R. Huisgen, R. Grashey and J. Sauer, "The Chemistry of Alkenes," John Wiley and Sons, Inc., New York N. Y., (1964), p. 826.

11) W. M. Jones, *J. Amer. Chem. Soc.*, **81**, 5153 (1959).

12) Acid-catalysed isomerization of 1-pyrazoline to 2-pyrazoline has been attempted: K. von Auwers and F. König, *Ann. Chem.*, **496**, 27, 252 (1932).

Table 1.

Compd.	Mp°C, (Bp °C/mmHg)	Formula	Calcd, %			Found, %		
			C	H	N	C	H	N
4	142—143.5	$C_{11}H_8O_4$	64.71	3.95	—	64.88	3.96	—
5	141.8 (decomp)	$C_{13}H_{12}N_2O_4$	60.00	4.66	10.76	60.26	4.82	10.59
6	(120/0.001)	$C_{13}H_{12}O_4$	67.23	5.21	—	66.88	5.28	—
7	143 (decomp)	$C_{25}H_{20}N_2O_4$	72.80	4.89	6.79	72.72	4.82	6.71
8	a	$C_{25}H_{20}O_4$	78.11	5.24	—	77.95	5.33	—
10	189	$C_{15}H_{14}N_2O_4$	59.60	4.67	9.27	59.90	4.92	8.98
11	218.5—220.5	$C_{30}H_{28}N_4O_{10}$	59.60	4.67	9.27	59.94	4.79	9.04
12	106	$C_{13}H_{12}N_2O_4$	60.00	4.65	10.76	59.81	4.59	10.89
13	185.5	$C_{19}H_{20}N_2O_8$	56.44	4.99	6.93	56.36	5.02	6.79
15	50.5—51.5	$C_9H_{12}N_2O_4$	50.94	5.70	—	50.63	5.72	—
16	b	$C_9H_{12}N_2O_4$	50.94	5.70	13.45	50.43	5.45	12.45
17	b	$C_9H_{12}O_4$	58.69	6.57	—	58.61	6.99	—

a) Purification was performed by column chromatography (see Experimental).
b) Separation and purification were carried out by preparative vpc.

to the diazo group[8a,13] of **5** a new band at 3360 cm^{-1} (ν_{NH}) was observed. Concerning the ester carbonyl of **12** the hydrogen bonding of the imino group may cause a shift of the absorption band from 1755 to 1725 cm^{-1}.

A mixture of 1-pyrazoline **5** and acetic anhydride in the presence of *p*-toluenesulfonic acid, on standing at room temperature for 24 hr, gave three compounds (**10**, **11**, and **13**) with a ratio of 90 : 7 : 3, respectively, whereas 2-pyrazoline **12** in the same treatment gave **13** exclusively. An attempt to prepare similar derivatives using acetic anhydride, upon standing for 2 days at room temperature, was unsuccessful.[13b,14]

The structural assignments of **10**, **11** and **13** were based on spectral and microanalytical data. The infrared spectrum of **10** shows a normal absorption band at 1742 cm^{-1} consistent with ester carbonyl owing to the loss of the hydrogen-bridge with the imino group observed on **12**. The NMR spectrum of **10** reveals that the proton at γ-position of the lactone ring is affected with the deshielding effect of acetyl carbonyl as shown in Fig. 2. Similarly, the NMR spectrum of **13** (Fig. 2) indicates that the deshielding effect of the neighbouring *N*-acetyl group is also expected to affect the hydrogen atom attached to the C_3 carbon atom and causes a pronounced shift to the lower field, while the shielding effect of the acetoxy group shifts the signal of the CH_α proton upfield. A structure of **11** for one of the minor products, mp 218—220°C, 7% of yield, consistent with the spectral and microanalytical evidences (See Table 1), is considered tentatively as a dimer of **5**. The infrared spectrum of **11** (Fig. 1) is subequal to that of **5**. The NMR spectrum of **5** shows a complex pattern, but number of the whole protons appearing in the chart of Fig. 2 coincides exactly with that of **11**.

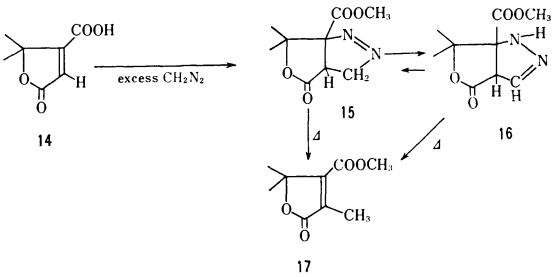

Scheme III

The thermochemical stability about the tautomers (**15** and **16**) was found to be structure dependent when examined by vpc, since most of **15** was converted into **17** smoothly, whereas about 20% of change for **16** was noted as indicated in Table 2. It seems that the conversion of **16** into **17** may proceed *via* 1-pyrazoline **15**.[15] The partial change from **15** to **16** occurred spontaneously during storage.

As illustrated in Scheme IV, a mechanistic consideration of the formation of **10** and **13** involves the assumption that **12** is first protonated and then followed by combination with anionic acetoxy group to give **19**, which leads to **13** by further *N*-acetylation. On the other hand, the formation of **10** seems to result from a direct attack of cationic acetyl group on **5** owing to the weak polarization

13) a) C. G. Overberger, J.-P. Anselme and J. R. Hall, *J. Amer. Chem. Soc.*, **85**, 2752 (1963); b) C. G. Overberger and J.-P. Anselme, *ibid.*, **86**, 658 (1964); c) C. G. Overberger, N. Weinshenker and J.-P. Anselme, *ibid.*, **87**, 4119 (1965).

14) C. G. Overberger and J.-P. Anselme, *ibid.*, **84**, 869 (1962).

15) W. M. Jones, *ibid.*, **80**, 6687 (1958).

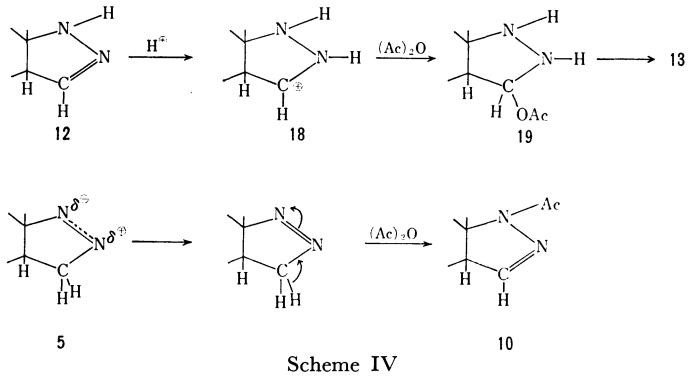

Scheme IV

of the azo bond. In the course of the reaction from **12** to **18** the dimer **11** may be obtained by addition of **12** with the cation intermediate **18**.

Table 2

Compound		Product, yield (%)		
		15	**16**	**17**
A	**15**	0	10	90
	16	0	80	20
B	**15**	40	60	0

A: Passing on vpc column, SE-30, 3 m long at 160°C;
B: Standing for 1 month at room temperature.

Experimental[16]

Preparation of γ-Phenylaconic Acid 4. To a suspension of α-benzylidenesuccinic acid[5] and 50 m*l* of water 6.3 m*l* of bromine was added with stirring for 2 hr at room temperature and then stirred for an additional 10 hr. After the precipitate was filtered the crude solid was allowed to react with boiling water. From the aqueous layer separated by decantation, after cooling to room temperature, the precipitates were collected and recrystallized from benzene giving 12.7 g (64% based on the dicarboxylic acid) of **4**, mp 142—143.5°C; IR (Nujol) 3300—2400 (COOH), 1733 (lactone C=O), 1700 (COOH, shoulder), 1645 (C=C), 1220, 990 and 690 cm^{-1}.

β-Benzoylpropionic Acid 9 from 4. A solution of **4** (1 g) in 50 m*l* of 0.1N ethanolic sodium hydroxide solution was allowed to stand for 0.5 hr. After acidification of the alkaline solution with dilute sulfuric acid, β-benzoylpropionic acid **9** was obtained in a quantitative yield. The IR spectrum of **9** was identical with that of the authentic sample;[7] IR 1710 (acid C=O), 1675 (ketone C=O) cm^{-1}.

Methyl γ-Phenyl-α,β-(1-pyrazolino)paraconate 5. To an ethereal solution of **4** (1 g) excess diazomethane solution was added. After standing for 10 min removal of the solvent gave **5** in a quantitative yield, which on crystallization from benzene-*n*-hexane melted at 141.8°C; IR (Nujol) 1792 (lactone C=O), 1755 (ester C=O), 1553 (-N=N-) cm^{-1}; UV λ_{max}^{EtOH} 324 mμ (ε_{max} 298) and 289 mμ (ε_{max} 270)[13c]; NMR ($CDCl_3$) τ 2.62 (5H s, C_6H_5), 3.58 (1H s, CH_γ), 4.64 and 5.61 (2H each q, $C-CH_aH_b-N=N$, J_{AB}=18.0, J_{AC}=8.7, J_{BC}=2.3 Hz), 6.19 (3H s, $-OCH_3$), 6.54 (1H q, $CH_c-C-N=N$).

Thermal Decomposition of 5. Pyrolytic decomposition of **5** was carried out by heating at 145—150°C for 30 min. Distillation of the residue afforded 1.6 g (*ca.* 90%) of methyl α-methyl-γ-phenylaconate **6**, bp 120°C/0.001 mmHg; IR 1766 (lactone C=O), 1725 (ester C=O), 1665 (C=C) cm^{-1}; UV λ_{max}^{EtOH} 217 mμ (ε_{max} 15000); NMR ($CDCl_3$) τ 7.77 (3H d, CH_3), 6.35 (3H s, $-OCH_3$), 4.05 (1H q, CH_γ), 2.78 (5H m, C_6H_5). A long range coupling (J=1.9—2.0 Hz) between methyl protons at α-position and a proton at γ-position was observed.

Benzyl γ-Phenyl-α,β-(3-phenyl-1-pyrazolino)paraconate 7. To an ethereal solution of **4** (1 g) excess phenyldiazomethane solution,[9] prepared from the oxidation of an ethereal solution of benzaldehydrazone with silver oxide, was added. After standing for 30 min the solid precipitated was filtered and recrystallized from benzene giving 1.7 g (88%) of **7**, mp 143°C (decomp); IR (Nujol) 1785 (lactone C=O), 1755 (ester C=O), 1553 (-N=N-) cm^{-1}; NMR ($CDCl_3$) τ 6.57 (1H d, CH_α), 4.78 (2H d, $O-CH_2-Ph$), 4.78 (1H d, CH-Ph), 3.67 (1H s, CH_γ), 2.70 (15H m, C_6H_5).

Thermal Decomposition of 7. Decomposition of **7** at 145—155°C for 30 min gave **8** in good yield. Purification of the crude product of **8** was performed on column chromatograph with Wako Gel-C200 using benzene-acetone-*n*-hexane (8 : 1 : 1.5) as an elute; IR 1785 (lactone C=O), 1725 (conjugated ester C=O), 1670 (C=C shoulder) cm^{-1}; UV λ_{max}^{EtOH} 225 mμ (ε 6600), NMR ($CDCl_3$) τ 6.97 and 7.20 (2H d, CH_AH_BPh J_{AB}=5.4 Hz), 5.10 and 5.21 (2H d, OCH_AH_BPh J_{AB}=7.8 Hz) 3.91 (1H s, CH_γ), 2.87 (15H m, C_6H_5).

Isomerization of 5. A mixture of **5** (0.5 g) and 20 m*l* of phosphoric acid was heated slowly with stirring for 10—15 min at 70—80°C. Upon cooling to room temperature, the reaction mixture was diluted with 50 m*l* of water and then the organic layer was taken up in ether. The extracts were washed with aqueous sodium chloride, next with saturated sodium bicarbonate solution and finally with sodium chloride solution, and

16) All melting and boiling points are uncorrected. Infrared spectra were determined with a Hitachi EPI-S2 and ultraviolet spectra on a Hitachi EPS-3T spectrophotometer. NMR spectra were obtained on a Japan Electron Optics Laboratory spectrometer (JNM-C-60) in deuteriochloroform with TMS as internal standard. Microanalyses were performed by Mr. E. Amano of the Department of Synthetics Chemistry in this Faculty and the results are listed in Table 1.

dried on Na_2SO_4. Removal of the solvent gave 0.4 g (80%) of 2-pyrazoline **12**, mp 106°C; IR (Nujol) 3360 (>NH), 1793 (lactone C=O), 1725 (ester C=O), 1600 (-C=N-) cm^{-1}; NMR ($CDCl_3$) τ 6.17 (3H s, $-OCH_3$), 5.52 (1H d, CH_α), 4.33 (1H broad, >NH), 4.09 (1H s, CH_γ), 3.27 (1H d, N=CH-), 2.68 (5H m, C_6H_5).

Acetylation of 1-Pyrazoline 5. A mixture of **5** (1 g) and 10 m*l* of acetic anhydride in the presence of a small amount of *p*-toluenesulfonic acid was kept for 24 hr at room temperature. After the reaction mixture was diluted with 20 m*l* of water and neutralized with solid sodium bicarbonate to pH 8, the organic layer was extracted with ether. The extracts were washed with saturated sodium chloride solution and dried on Na_2SO_4. Removal of the solvent gave 1 g of crude crystals which were allowed to dissolve in a hot solution of benzene-*n*-hexane (1 : 1), then standing for several hours, to give **10**. The filtrate, when allowed to stand for another day, gave **11**. After the filtrate was concentrated, 3 m*l* of hot benzene-*n*-hexane (2 : 3) was added. On cooling to room temperature, **13** was precipitated. Total yield of **10**, **11**, and **13** was in the ratio of 90 : 7 : 3. The ultraviolet spectrum of **11** showed two absorption bands at λ_{max}^{EtOH} 258 mμ (ε 5200) and 407 mμ (ε 240), whereas that of **10** showed an absorption at λ_{max}^{EtOH} 246 mμ (ε 7600). The infrared and NMR charts of these compounds (**10**, **11**, and **13**) are illustrated in Figs. 1 and 2. The physical constants together with microanalytical results are indicated in Table 1.

Acetylation of 12. Acetylation of **12** (0.2 g) was carried out in a similar manner as for **5**. After the usual treatment, 0.2 g of **13** was obtained.

Preparation of 15. To an ethereal solution of γ,γ-dimethylaconic acid **14**[17] excess diazomethane solution was added. After standing for 30 min, removal of the solvent gave **15** in a quantitative yield which melted at 50.5—51.5°C; IR (Nujol) 1775 (lactone C=O), 1735 (ester C=O) and 1558 (N=N) cm^{-1}; UV λ_{max}^{EtOH} 328 mμ (ε 210); NMR ($CDCl_3$) τ 4.72 and 5.24 (2H each q, C-CH_aH_b-N=N, J_{AB}=18.0, J_{AC}=8.0, J_{BC}=1.5 Hz), 6.12 (3H s, $-OCH_3$), 6.36 (1H q, CH_c-C-N=N), 8.40 and 8.09 (6H each s, gem CH_3).

Thermal Isomerization of 1-Pyrazoline 15 and 2-Pyrazoline 16 on VPC Column. When **15** was passed on 10% Diasolid-L Silicone (SE-30) coated column with a 3 m long, carrier gas H_2, 20 m*l*/min, operating at 160°C, two peaks of **17** and **16** were observed in a ratio of 9 : 1 (Rt: 5 and 17 min, respectively). Each component was isolated by VPC preparatively. On the other hand, the purified **16**, when passed on the same column in the similar condition, gave two peaks of **16** and **17** in a ratio of 4 : 1. These data are indicated in Table 2. The microanalyses of both **15** and **16** are recorded in Table 1. The spectral data are as follows: methyl γ,γ-dimethyl-α,β-(2-pyrazolino)-paraconate **16**, IR 3320 (NH), 1770 (lactone C=O), 1736 (ester C=O), 1588 (C=N-) cm^{-1}; NMR ($CDCl_3$) τ 8.57 and 8.40 (6H s, $-CH_3$), 6.16 (3H s, $-OCH_3$), 5.43 (1H d, CH_α J=2.6 Hz), 3.24 (1H, broad, CH=N), 2.5—4.0 (1H broad, NH); methyl γ,γ-dimethyl-α-methylaconate **17**, IR 1765 (lactone C=O), 1724 (conjugated ester C=O), 1661 (C=C) cm^{-1}; NMR ($CDCl_3$) τ 8.40 (6H s, $-CH_3$), 7.28 (3H s, α-CH_3), 6.07 (3H s, $-OCH_3$).

The authors wish to express their thanks to Professor Akira Takeda, Department of Synthetics Chemistry, for helpful discussions and encouragement.

17) R. Fittig and B. Frost, *Ann. Chem.*, **226**, 370 (1884).

BULLETIN OF THE CHEMICAL SOCIETY OF JAPAN VOL. 43 2549—2553 (1970)

The Condensation Reactions of Bivalent Sulfur Compounds-Copper(II) Complexes with Nucleophiles

Teruaki MUKAIYAMA, Koichi NARASAKA, Kazuo MAEKAWA and Hisao HOKONOKI

Laboratory of Organic Chemistry, Tokyo Institute of Technology, Ookayama, Meguro-ku, Tokyo

(Received February 10, 1970)

It was found that the bivalent sulfur compounds such as benzaldehyde diethylmercaptal, benzophenone diethylmercaptole, ethyl orthotrithioformate and benzyl methylsulfide, react with copper(II) salts of 1,3-dicarbonyl compounds, active methylene compounds or anisole, in the presence of cupric chloride, to give condensation or substitution products in good yields accompanied with carbon-sulfur bond cleavage. On the other hand, in the absence of cupric chloride, the bivalent sulfur compounds underwent no reaction and the starting materials were recovered. These results can be explained by assuming initial formation of active complexes from the bivalent sulfur compounds and copper(II).

The condensation reactions of bivalent sulfur compounds, such as benzaldehyde diethylmercaptal [Ia], benzophenone diethylmercaptole [Ib] and ethyl orthotrithioformate [Ic], with active methylene compounds were reported briefly in a previous paper[1]. In the present report, these reactions are explained in detail with new results.

The new condensation reaction of carbon-carbon bond formation accompanied with carbon-sulfur bond cleavage was carried out on the assumption that the bivalent sulfur compound would be activated by coordination with the so-called soft acids,[2] such as Cu(II), Ag(I) and Hg(II), forming a reactive complex. Copper(II) was chosen as the acid because it has a soft character and is known to form mercaptide easily. The coordinated compounds of bivalent sulfur compounds and copper(II) would act as an electrophile and cleavage of the carbon-sulfer bond would occur without difficulty. Based on this assumption, the condensation reactions of the bivalent sulfur compounds [I] with nucleophilic reagents, such as copper(II) salts of 1,3-dicarbonyl compounds [II], active methylene compounds and anisole, were studied in the presence of cupric chloride.

Little work has been done on a synthetic study with the used of copper(II) salts of 1,3-dicarbonyl compounds [II] since they are very stable toward electrophiles.[3] For example, it is known that alkyl halide does not react with the copper(II) salts [II]. Instead, the condensation reaction occurs when 1,3-dicarbonyl compound is used as an alkali metal salt. In this reaction, *O*-substituted compound is always accompanied with *C*-substituted compound. On the other hand, when copper(II) salt is used for alkali metal salt, it is expected that the copper(II) atom would protect the *O*-position by chelation. Therefore, *C*-substituted products would result exclusively by treating copper(II) salts with bivalent sulfur compounds [I] under a nearly neutral condition.

At first, bis(acetylacetonato)copper(II) [IIa] and ethyl orthotrithioformate [Ic] were refluxed in dioxane, but the reaction did not occur and the starting materials were recovered quantitatively. However, when a half molar amount of cupric chloride was added to the tetrahydrofuran [THF] solution of Ic and IIa, the blue precipitate of IIa disappeared and a green precipitate appeared immediately. After being stirred for 8 hr and kept standing overnight, the green precipitate disappeared and a grey substance deposited. After filtration of the substance and purification by silica gel column chromatography and distillation, the condensation product, 3-(α-ethylthioethyl-

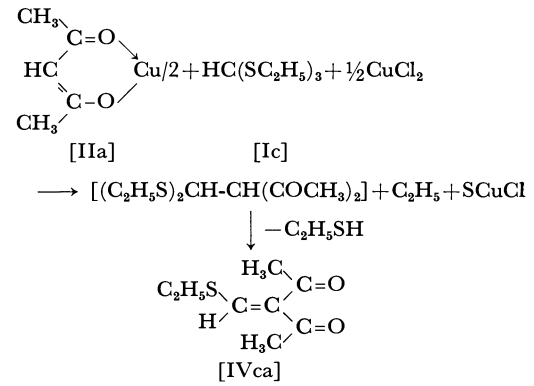

1) T. Mukaiyama, K. Narasaka and H. Hokonoki, *J. Amer. Chem. Soc.*, **91**, 4315 (1969).

2) R. G. Pearson and J. Songstad, *ibid.*, **85**, 3533 (1963); R. G. Pearson and J. Songstad, *ibid.*, **89**, 1827 (1967).

3) M. Conrad and M. Guthzert, *Ber.*, **19**, 19 (1886); H. D. Murdock and D. C. Nonhebel, *J. Amer. Chem. Soc.*, **84**, 2153 (1962).

idene)-pentane-2,4-dione [IVca] was obtained in 65% yield.

Similarly, bivalent sulfur compounds [Ia,b,c] reacted with copper(II) salts of 1,3-dicarbonyl compounds such as acetylacetone [IIa], dibenzoylmethane [IIb] or ethyl acetoacetate [IIc] in the presence of cupric chloride at room temperature and the condensation products, [III] or [IV], were obtained. The results are shown in Table 1.

TABLE 1

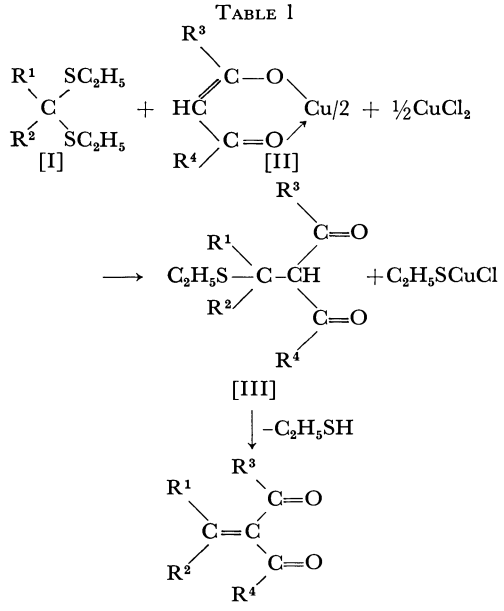

[I] R¹	[I] R²	[II] R³	[II] R⁴	Yield, % (III)	Yield, % (IV)
H	C_2H_5S	CH_3	CH_3		65
H	C_6H_5	CH_3	CH_3	92	
C_6H_5	C_6H_5	CH_3	CH_3	55	
H	C_2H_5S	C_6H_5	C_6H_5	73	
H	C_6H_5	C_6H_5	C_6H_5	82	
H	C_2H_5S	CH_3	OC_2H_5	58	
H	C_6H_5	CH_3	OC_2H_5		46

In all cases, *C*-substituted products were produced exclusively, as expected, and no detectable amount of *O*-substituted product was obtained.

In the absence of cupric chloride, the sulfur compounds [I] did not react with copper(II) salts [II] even at an elevated temperature, while, in the presence of cupric chloride the reaction proceeded smoothly under a mild condition.

This may be explained by assuming a double nuclear complex [V][4] of copper(II) salts [II] and cupric chloride. [V] readily affords chelate [VI] by coordination to a sulfur atom of bivalent sulfur compound [I]. Chelate [VI] thus formed decomposes into a condensation product [III] and ethylmercapto cupric chloride by way of an internal nucleophilic displacement as described in the following equation.

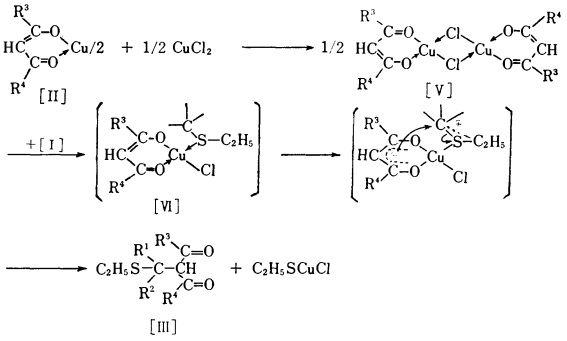

The result suggests that a complex of bivalent sulfur compounds [I] and cupric chloride would act as an electrophile and react with nucleophilic reagent [$Nu^{\ominus}$] giving a condensation product [$\geqslant$C–Nu] and ethylmercapto cupric chloride as shown below.

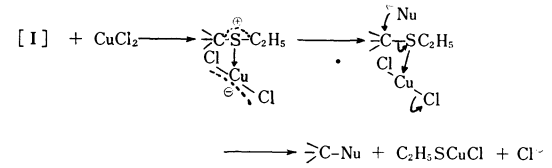

Based on this assumption, the reactions of sulfur compounds [I] and active methylene compounds in the presence of cupric chloride were investigated. Acetylacetone and benzaldehyde diethylmercaptal [Ia] were allowed to react for 12 hr at room temperature in the presence of 2 equimolar amounts of cupric chloride and an equimolar amounts of 2,6-lutidine, a hydrogen chloride catcher, in THF. After removal of the precipitate by filtration and purification by silica gel column chromatography, 3-(α-ethylthiobenzyl)pentane-2,4-dione was isolated in 79% yield as a white crystal. Similarly, 1,3-indandione, malononitrile or ethyl malonate reacted with sulfur compounds [Ia,b,c] to give condensation products, [VII] or [VIII]. The results are summarized in Table 2.

By this procedure, the condensation products can be directly prepared from 1,3-dicarbonyl compunds and sulfur compounds [I], without preparation of their copper(II) salts. It was confirmed that malononitrile and 1,3-indandione, which do not form their copper(II) salts, can react with sulfur compounds [I] in this way.

In the cases of cyclohexanone and benzaldehyde diethylmercaptal [Ia], a similar reaction did not occur and the starting materials were recovered. On the other hand, when they were refluxed in ether in the presence of 4 equimolar amounts of cupric chloride and a catalytic amount of Et_2O·

4) The double nuclear complex of IIa and cupric chloride, μ-dichloro-bis(acetylacetonato)dicopper(II), was isolated as a green precipitate by treating equimolar amounts of IIa and cupric chloride in THF under a dry nitrogen atmosphere. Elemental analysis gives $(C_5H_7O_2CuCl)_n$. It was found that the complex is readily hydrolyzed to give IIa and cupric chloride.

Table 2

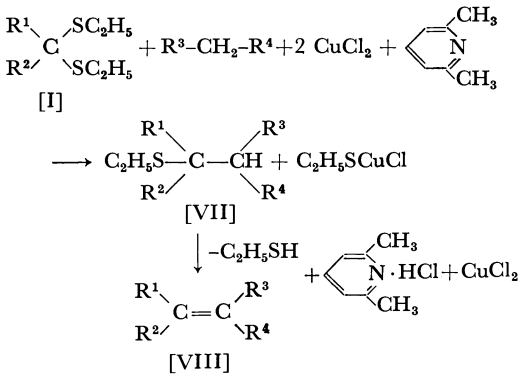

[I]		Active methylene		Yield, %	
R^1	R^2	R^3	R^4	(VII)	(VIII)
C_6H_5	H	CH_3CO	CH_3CO	79	
C_6H_5	H	CN	CN		62
C_6H_5	H	$COOC_2H_5$	$COOC_2H_5$	63	
C_6H_5	H	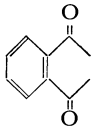			53
C_2H_5S	H	CN	CN		45
C_2H_5S	H	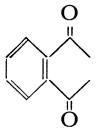			62
C_6H_5	C_6H_5	CN	CN		64

BF_3, the condensation product, 2,6-dibenzylidenecyclohexanone [IX], was obtained in 62% yield.

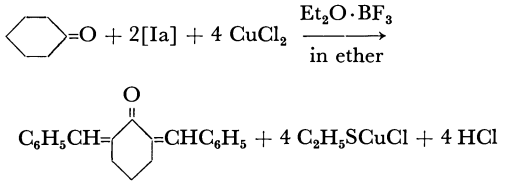

[IX]

The effects of the solvents on this type of reaction were studied by treating cyclohexanone and 2 equimolar amounts of Ia in the presence of 4 equimolar amounts of cupric chloride, in various solvents at room temperature. Among various solvents examined, ethyleneglycoldimethylether afforded the best result and the condensation product [IX] was obtained in 64% yield.

It was found that anisol also reacted with Ia,c and benzyl methylsulfide [XV] in the presence of cupric chloride to afford substituted products. When benzaldehyde diethylmercaptal [Ia] was

Table 3

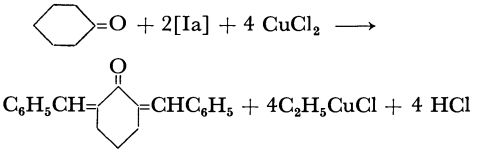

[IX]

Solvent	[IX], Yield	Solvent	[IX], Yield
$C_2H_5OC_2H_5$	17%	CCl_4	45%
	15%	$CHCl_3$	28%
$(CH_3OCH_2)_2$	64%	CH_2Cl_2	41%
$(CH_3OCH_2CH_2)_2O$	50%	$(ClCH_2)_2$	35%
C_6H_{12}	24%	$CH_3COOC_2H_5$	53%
C_6H_6	58%	DMSO, DMF	0%

treated in the presence of an equimolar amount of cupric chloride in anisole, even at room temperature, hydrogen chloride evolved vigorously and after purification by silica gel column chromatography, a monosubstituted compound, anisylphenylmethyl ethylsulfide [X] and a disubstituted product, dianisylphenylmethane [XI] were obtained in 62% and 19% yields, respectively. When the molar ratio of cupric chloride to Ia was increased to 2 or 3, the disubstituted compound [XI] only was formed in a good yield according to the following equation.

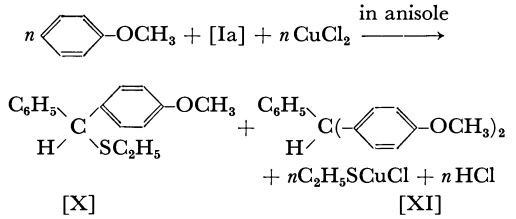

[X] [XI]

	Yield, %	
	[X]	[XI]
$n=1$	62	19
$n=2$		83
$n=3$		100

Similary, ethyl orthotrithioformate [Ic] reacted with anisole to give the following products.

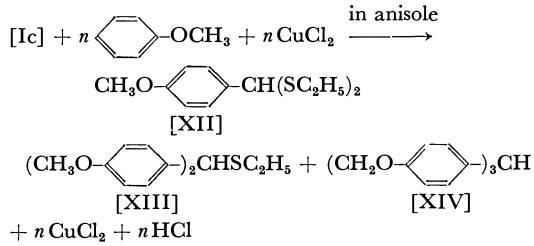

[XII] [XIII] [XIV]

	Yield, %		
	[XII]	[XIII]	[XIV]
$n=1$	5	31	
$n=2$			32
$n=3$			38

It was also confirmed that anisylphenylmethane [XVI], was obtained in 51% yield by refluxing benzyl methylsulfide [XV] in anisole in the presence of an equimolar amount of cupric chloride.

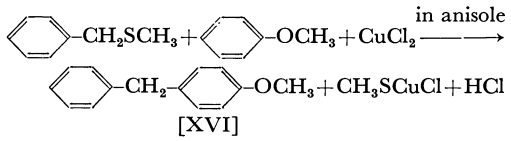

[XVI]

Experimental

Material. Commercial cupric chloride was used. It was ground and dried over phosphorus pentoxide *in vacuo* at about 130°C before use. Bivalent sulfur compounds, [Ia,b,c] and [XV] were prepared according to the procedures in literature and purified by distillation.

[Ia][5] 135—136°C/8 mmHg; [Ib][5] 146—150°C/0.07 mmHg; [Ic][6] 129—132°C/14 mmHg; [XV][7] 97—101°C/27 mmHg.

Copper salts of 1,3-dicarbonyl compounds [IIa,b,c] were prepared from cupric acetate and 1,3-dicarbonyl compounds according to general procedure.[8]

Reaction of Bis(acetylacetonato)copper(II) [IIa] with Benzaldehyde Diethylmercaptal [Ia]. Into a suspension of 0.68 g (0.005 mol) of cupric chloride and 1.31 g (0.005 mol) of IIa in dry THF (35 m*l*) was added 2.12 g (0.001 mol) of Ia in one portion. The mixture was stirred for 8 hr and kept standing overnight at room temperature. After removal of 0.69 g of grey precipitate, the filtrate was concentrated under reduced pressure. The residue was then purified by silica gel column chromatography (silica gel column chromatography was used in order to remove ethylmercapto cupric chloride completely.), and a white crystal, 3-(α-ethylthiobenzyl)-pentane-2,4-dione was obtained; 2.20 g (92%), mp 71—72°C (recrystallized from ethanol, mp 71.5—73°C). Found: C, 67.25; H, 7.33; S, 12.88%. Calcd for $C_{14}H_{18}O_2S$: C, 67.18; H, 7.25; S, 12.79%. The infrared spectrum showed a strong absorption band at 1690 cm^{-1} assigned to the C=O group. The NMR spectrum showed absorption bands at τ 8.86 (triplet) 3H, 8.68 (singlet) 3H, 7.68 (singlet) 3H, 7.22 (quartet) 2H, 5.83 (doublet) H, 5.51 (doublet) H and aromatic protons 5H.

Similarly, the condensation products [III] or [IV] were obtained by the reaction of copper(II) salts of 1,3-dicarbonyl compounds [IIa,b,c] with sulfur compounds [Ia,b,c]. Physical properties and analytical data are summarized in Table 4.

Isolation of μ-Dichloro-bis(acetylacetonato)dicopper(II) by the Reaction of Bis(acetylacetonato)-copper(II) [IIa] with Cupric Chloride. When 2.62 g (0.01 mol) of [IIa] and 1.36 g (0.01 mol) of cupric chloride were allowed to react in 200 m*l* of dry THF stirred in a dry nitrogen atmosphere, the blue precipitate of IIa disappeared immediately and a green precipitate appeared soon. The green substance was collected by filtration in a dry nitrogen atmosphere and washed with THF. It was then dried *in vacuo* and analyzed. Found: C, 32.32; H, 4.44; Cl, 17.37%. Calcd for $C_{10}H_{14}O_4Cu_2Cl_2$: C, 33.29; H, 3.91; Cl, 17.90%.

Reaction of Acetylacetone with Benzaldehyde Diethylmercaptal [Ia]. Into a suspension of 2.68 g (0.02 mol) of cupric chloride and 1.07 g (0.01 mol) of 2,6-lutidine in THF (35 m*l*), 1.00 g (0.01 mol) of acetylacetone and 2.12 g (0.01 mol) of Ia were added in one portion. The solution was then stirred for 12 hr and kept standing overnight at room temperature. After filtering off a solid (3.76 g,) the filtrate was evaporated under reduced pressure. Purification of the residue by silica gel column chromatography gave 1.96 g (79%) of 3-(α-ethylthiobenzyl)pentane-2,4-dione (mp 68—72°C), which showed an infrared spectrum identical with that of the authentic sample obtained by the above mentioned reaction.

TABLE 4

[I]		[II]		Products	Mp (Bp)	Anal Found (Calcd)		
R^1	R^2	R^3	R^4	[III]	[IV]	C	H	S
H	C_2H_5S	CH_3	CH_3		(121°C/1 mmHg)	55.76	6.81	18.80
						(55.80)	(7.03)	(18.59)
H	C_2H_5S	C_6H_5	C_6H_5	101—102°C		81.75	5.02	8.39
						(81.46)	(4.97)	(8.64)
H	C_2H_5S	CH_3	OC_2H_5		(129°C/1 mmHg)	53.62	7.21	15.86
						(53.46)	(6.98)	(15.82)
H	C_6H_5	CH_3	CH_3	71.5—73°C		67.25	7.33	12.88
						(67.18)	(7.25)	(12.59)
H	C_6H_5	C_6H_5	C_6H_5	111—113°C		76.75	5.97	8.47
						(76.98)	(5.92)	(8.55)
H	C_6H_5	CH_3	OC_2H_5	(115—115.5°C/3 mmHg)		64.57	7.46	10.78
						(64.27)	(7.19)	(11.42)
C_6H_5	C_6H_5	CH_3	CH_3	124.5—126°C		73.38	7.06	9.62
						(73.60)	(6.79)	(9.81)

5) M. L. Wolform and J. V. Karavinos, *J. Amer. Chem. Soc.*, **66**, 909 (1944).

6) G. Holber, *Ber.*, **40**, 1740 (1907).

7) J. V. Brown and P. Engelbertg, *ibid.*, **56**, 1573 (1923).

8) H. D. Murdoch and D. C. Nonhebel, *J. Chem. Soc.*, **1962**, 2153.

Table 5

(I)	Active methylene	Products [VII]	Mp (Bp) [VIII]	Anal, Found (calcd) C	H	N	S
Ia	Malononitrile		82.5—84°C	78.18	3.67	18.20	
				(77.90)	(3.92)	(18.17)	
Ia	Ethylmalonate	(137°C/0.6 mmHg)		62.09	6.89		10.21
				(61.92)	(7.15)		(10.31)
Ia	1,3-Indandione		152.—153°C	81.89	4.10		
				(82.04)	(4.30)		
Ib	Malononitrile		139.5—140.5°C	83.27	4.38	12.30	
				(83.45)	(4.38)	(12.17)	
Ic	Malononitrile		39—41°C	52.41	4.23	20.30	22.90
				(52.17)	(4.38)	(20.28)	(23.17)
Ic	1,3-Indandione		129—130.5°C	65.81	4.34		14.57
				(66.05)	(4.62)		(14.66)

Similarly, the products [VII] or [VIII] were obtained by treating acetylacetone, malononitrile, ethyl malonate and 1,3-indandione with Ia,b,c. Their physical properties and analytical data are shown in Table 5.

Reaction of Cyclohexanone with Benzaldehyde Diethylmercaptal [Ia] in the Presence of a Catalytic Amount of $Et_2O \cdot BF_3$. 4.24 g (0.02 mol) of [Ia], 0.98 g of cyclohexanone and three drops of $Et_2O \cdot BF_3$ were added to a suspension of 5.44 g (0.04 mol) of cupric chloride in 40 ml of ether. The mixture was refluxed for 2 hr with stirring and kept standing overnight at room temperature. 2,6-Dibenzylidenecyclohexanone [IX] was obtained through the same procedure as described in the above reaction. 1.72 g (62%) (recrystallized from ligroin; mp 115—117°C). Found: C, 87.64; H, 6.40%. Calcd for $C_{20}H_{18}O$: C, 87.56; H, 6.61%.

Reaction of Cyclohexanone with Benzaldehyde Diethylmercaptal [Ia] in Various Solvents. Into a suspension of 2.68 g (0.02 mol) of cupric chloride in 50 m*l* of solvent were added 0.49 g of cyclohexanone and 2.12 g (0.01 mol) of Ia. The mixture was then stirred for 7 hr and kept standing 15 hr at room temperature. The reaction mixture was purified in a similar manner as mentioned above. The yields of IX in various solvents are summarized in Table 3.

Reaction of Anisole with Benzaldehyde Diethylmercaptal [Ia]. A mixture of 6.36 g (0.03 mol) of Ia and 4.08 g (0.03 mol) of cupric chloride in dry anisole (50 m*l*) was stirred at room temperature. Hydrogen chloride was evolved vigorously. A white precipitate (1.07 g) was filtered off and the filtrate was condensed in reduced pressure. Two substances, an oily substance and a white crystal, were separated by silica gel column chromatography. The oily substance was then fractionated, giving 4.73 g (62%) of anisylphenylmethyl ethylsulfide [X]. bp 147—155°C/0.05 mmHg. Found: C, 74.11; H, 6.79; S, 12.13%. Calcd for $C_{16}H_{18}OS$: C, 74.39; H, 7.02 ;S, 12.38%. The white crystal was dianisylphenylmethane [XI]. 1.71 g (19%) (recrystallized from ethanol. mp 96—97°C). Found: C, 82.81; H, 6.35%. Calcd for $C_{21}H_{20}O_2$: C, 82.86; H, 6.62%. The NMR spectrum of both X and XI has only one absorption band assigned to OCH_3 group at τ 6.45 and 6.33, respectively. The results show that *para*-substituted products were obtained exclusively.

Reaction of Ethyl Orthotrithioformate [Ic] with Anisole in the Presence of an Equimolar Amount of Cupric Chloride. A mixture of 3.92 g (0.02 mol) of Ic and 2.72 g (0.02 mol) of cupric chloride in dry anisole (40 m*l*) was stirred for 12 hr and kept standing overnight at room temperature. Through the same procedure as described above, an oily substance was obtained and distilled *in vacuo*. Ic was recovered in 21% and 0.24 g (5%) of methoxybenzaldehyde [XII] (bp 162—164°C/0.08 mmHg) was obtained. In addition to XII, 1.78 g (31%) of dianisylmethylethylsulfide [XIII] was fractionated at 192°C/0.08 mmHg. Found: C, 71.11; H, 7.20; S, 11.10%. Calcd for $C_{17}H_{20}SO_2$: C, 70.81; H, 6.99; S, 11.17%.

Reaction of [Ic] with Anisole in the Presence of Two Equimolar Amounts of Cupric Chloride. When 5.44 g (0.04 mol) of cupric chloride was used in the above experiment, 2.13 g (32%) of trianisylmethane [XIV] was isolated. (recrystallized from ethanol. mp 56—58°C). Found: C, 78.72; H, 6.50%. Calcd for $C_{22}H_{22}O_3$: C, 79.01; H, 6.63%.

Reaction of Benzyl Methylsulfide [XV] with Anisole. When a mixture of 4.14 g (0.03 mol) of XV and 6.00 g (0.044 mol) of cupric chloride in 60 m*l* of dry anisole was refluxed for 11 hr, the color of the solution turned black and a white precipitate was deposited. The precipitate was filtered off and the filtrate was concentrated *in vacuo* and purified by silica gel column chromatography. The eluate was concentrated and distilled, giving 3.02 g (51%) of anisylphenylmethane [XVI] (bp 112—114°C/1.5 mmHg). Found: C, 85.03; H, 7.31%. Calcd for $C_{14}H_{14}O$: C, 84.81; H, 7.12%.

BULLETIN OF THE CHEMICAL SOCIETY OF JAPAN VOL. 43 2554—2558 (1970)

The Resolution of *N*-Benzyloxycarbonyl-DL-amino Acids Using Ephedrine*1

Katsue Oki, Kuniyoshi Suzuki, Seiichi Tuchida, Tomoo Saito and Hiroshi Kotake

Department of Chemistry, Faculty of Science, Kanazawa University, Kanazawa

(Received February 10, 1970)

The use of ephedrine has here been proposed to be of value in the direct resolution of racemic *N*-benzyloxycarbonylamino acids. By using a half equi-amount of natural (−)-ephedrine, *N*-benzyloxycarbonyl derivatives of β-methyl DL-aspartate, DL-leucine, DL-methionine, and *O*-benzyloxycarbonyl-DL-serine resulted, each in turn producing a salt of the respective D-isomer. On the other hand, DL-isoleucine, *erythro*-β-methyl-DL-leucine, *threo*-*N*,β-dimethyl-DL-leucine, DL-valine, and DL-phenylalanine each produced a salt of each L-isomer with the same base. It should be better to protect, if possible, the third functional groups of three functional amino acids before the resolution. Each antipode of the optically active *N*-benzyloxycarbonylamino acid obtained above was also conveniently produced, in a high optical purity, by using (+)-ephedrine alternately. However, a few limitations on the desirable method of resolution have also been observed.

Varieties of *N*-protecting groups for amino acids have recently been developed by splendid studies of peptide syntheses and have been used well. The *N*-benzyloxycarbonyl group, explored by Bergmann and Zervas in 1932[1], is, however, still one of the most favorable *N*-protecting groups for the sequential synthesis of peptides. The direct resolution of *N*-benzyloxycarbonyl derivatives of racemic amino acids would, therefore, be a much more convenient way of preparing optically active *N*-benzyloxycarbonylamino acids than the route of incorporating the protecting group onto optically active amino acids obtained *via* the appropriate resolution of temporary derivatives of racemic amino acids, *e.g.*, *N*-acetyl ones.

In this paper, the resolution of racemic *N*-benzyloxycarbonylamino acids by using (−)- and (+)-ephedrine alternately and a survey of the resolution will be described. In these experiments, a half equi-amount of ephedrine in relation to racemic *N*-benzyloxycarbonylamino acids was used principally. Although ethyl acetate could be employed as a predominant solvent in many cases, ethyl acetate-petroleum ether (2 : 3v/v) for *N*-benzyloxycarbonyl-DL-leucine and ether for *N*-benzyloxycarbonyl-DL-isoleucine and *N*-benzyloxycarbonyl-DL-phenylalanine were also effectively used in concentrations of *N*-benzyloxycarbonylamino acid and ephedrine of 0.45—4.68 and 0.25—2.58 M respectively. The selection of a suitable solvent for the aforementioned resolution is important, especially in the case of phenylalanine; usually only a racemate or a partially-resolved salt was deposited from a solution in a solvent such as ethyl acetate, benzene, or chloroform, though when ether was used the resolution was favored. The results obtained with salts with natural (−)-ephedrine are listed in Table 1. Of all the amino acids used, *N*-benzyloxycarbonyl derivatives of amino acids without a β-methyl side group—β-methyl DL-aspartate, DL-leucine, DL-methionine, and *O*-benzyloxycarbonyl-DL-serine—deposited to afford predominantly, if not exclusively, salts of the D-isomer of amino acids with natural (−)-ephedrine. Unlike the above cases, however, the same derivatives of amino acids with a β-methyl side group—DL-isoleucine, *erythro*-β-methyl-DL-leucine, *threo*-*N*, β-dimethyl-DL-leucine, and DL-valine—afforded salts bearing a reverse configuration, L, at the α-carbon atom of the amino acids. Entirely opposite results yielding each antipode were attained when (+)-ephedrine was used instead of (−)-base. Thus, it is possible to choose either antibode of ephedrine before the resolution, because it is possible, as a rule, to predict the configutarion of the amino acid to be obtained as an insoluble salt, depending on the presence of a β-methyl side group. This would be especially useful for the resolution of a new amino acid, as we have shown successfully in a preceding paper.[2] In consonance with this view, the preceding observation, made by

*1 Presented, in part, at the 22nd annual meetings of the Chemical Society of Japan, held at Tokyo, April 1969. Copies of the paper are available from T.S. or H.K. on request.

1) M. Bergmann and L. Zervas, *Ber.*, **65**, 1192 (1932).

2) H. Kotake, T. Saito and K. Ōkubo, This Bulletin, **42**, 1367 (1969).

Table 1

Salt of *N*-Benzyloxycarbonylamino Acid with (−)-Ephedrine	Molecular Formula	Analysis Calcd C	Calcd H	Calcd N	Found C	Found H	Found N	Yield (%)	Mp (°C)	$[\alpha]_D$** (deg)
β-Methyl D-aspartate	$C_{23}H_{30}O_7N_2$	61.87	6.77	6.27	61.84	6.74	6.60	71	141	−30.3
D-Leucine	$C_{24}H_{34}O_5N_2$	66.95	7.96	6.51	66.44	8.06	6.44	78	92— 94	−12.3
D-Methionine	$C_{23}H_{32}O_5N_2S$	61.59	7.19	6.25	61.40	7.29	5.96	89	129—130	−28.1
O-Benzyloxycarbonyl-D-serine	$C_{29}H_{34}O_8N_2$	64.67	6.36	5.20	64.87	6.61	5.17	95	133—134	−33.8
L-Isoleucine	$C_{24}H_{34}O_5N_2$	66.96	7.96	6.51	66.68	7.95	6.69	89	138	−17.2
erythro-β-Methyl-L-leucine*	$C_{25}H_{36}O_5N_2$	67.54	8.16	6.30	67.50	8.09	6.28	45	124—125	−17.6
threo-*N*, β-Dimethyl-L-leucine*	$C_{26}H_{38}O_5N_2$	68.09	8.35	6.11	68.26	8.24	6.27	94	160—161	−75.0
L-Valine	$C_{23}H_{32}O_5N_2$	66.32	7.74	6.73	66.27	7.83	6.43	78	145	−20.3
L-Phenylalanine	$C_{27}H_{32}O_5N_2$	69.80	6.94	6.03	69.97	7.04	6.28	85	139—140	+11.3

* Represented from our preceding paper.[2]
** All optical rotation values were measured in a solution of absolute alcohol, at 22—27°C.

Overby and Ingersoll,[3] that a salt of *N*-benzyloxycarbonyl-D-alanine with (−)-ephedrine was produced as a less soluble product when *N*-benzyloxycarbonyl-DL-alanine was allowed to react with natural ephedrine in ethyl acetate, also supports our above conclusion. An exception to the rule was, however, observed in the case of phenylalanine, which bears a β-aromatic group but no β-methyl group; thus, a salt of the L-isomer with natural (−)-ephedrine was deposited preferentially. In order to determine the effect of a β-aromatic side group on the resolution, further attempts have been made to resolve *N*-benzyloxycarbonyl-DL-tyrosine and -DL-tryptophan into their respective isomers, but these attempts have so far been unsuccessful. Even if the base was used in a half- or equi-molar amount ratio in various solvents, neither *N*-benzyloxycarbonyl-DL-aspartic acid nor *N*-benzyloxycarbonyl-DL-glutamic acid have provided favorable results. A successful resolution of DL-aspartic acid was, however, achieved by protecting β-carboxyl as its methyl ester. An additional attempt to resolve the γ-methyl DL-glutamate was unsuccessful, though. Similarly, the resolution of DL-serine was performed successfully only when its *N*,*O*-dibenzyloxycarbonyl derivative was employed. Thus, one recommendation, that the third functional groups of amino acids should be protected for the favorable resolution, can be made on the basis of our experiments involving aspartic acid and serine. Each antipode of *N*-benzyloxycarbonylamino acid with an entirely optical purity resulted, when (+)-ephedrine was used alternately, from a solution of the same solvent used in the corresponding case (Table 2), though it could also be produced in an optically active state from the mother liquor obtained after the removal of the

Table 2

Salt of *N*-Benzyloxycarbonylamino Acid with (+)-Ephedrine	Analysis Found C	Found H	Found N	Yield (%)	Mp (°C)	$[\alpha]_D$** (deg)
β-Methyl L-aspartate	62.31	6.81	6.29	53	141—142	+31.0
L-Leucine	66.43	8.01	6.47	68	91—93	+12.3
L-Methionine	61.27	7.27	6.09	82	130—131	+28.2
O-Benzyloxycarbonyl-L-serine	64.50	6.39	5.36	91	132	+33.0
D-Isoleucine	67.06	8.00	6.36	83	139	+15.7
erythro-β-Methyl-D-leucine*	67.60	8.14	6.32	50	124—125	+17.7
threo-N, β-Dimethyl-D-leucine*	67.97	8.31	6.16	89	159—160	+73.5
D-Valine	65.98	7.73	6.82	96	145	+19.1
D-Phenylalanine	69.44	7.05	6.28	85	139—140	−11.1

* Represented from our preceding paper.[2]
** All optical rotation values were measured in a solution of absolute alcohol, at 22—27°C.

3) L. R. Overby and A. W. Ingersoll, *J. Amer. Chem. Soc.*, **82**, 2067 (1960).

salts with natural ephedrine. All the salts obtained herein were treated with 2N hydrochloric acid to remove the basic moieties and to produce optically active *N*-benzyloxycarbonylamino acids. Each amino acid was then regenerated in an optically pure state by the removal of the benzyloxycarbonyl

Table 3

	N-Benzyloxycarbonyl derivative			Free amino acid regenerated
	Yield (%)	Mp (°C)	$[\alpha]_D$** (deg)	$[\alpha]_D$*** (deg)
β-Methyl D-aspartate	88	98—99	+17.8[a]	
D-Leucine	100	oil		−15.9 (lit, −15.1[11,e])
D-Methionine	95	70—71 (lit, 69—70[4])	+17.2 (lit, +18.2[7])	−26.0 (lit, −23.9[12,e])
O-Benzyloxycarbonyl-D-serine	96	83—84	−4.3, −23.5[b]	−14.0[f] (lit, −14.3[13])
L-Isoleucine	100	oil		+40.8 (lit, +40.7[11,14])
erythro-β-Methyl-L-leucine*	100	oil		+38.9[e]
threo-*N*, β-Dimethyl-L-leucine*	92	98—99	−75.9	+38.3[e]
L-Valine	96	66—67 (lit, 66—67[4] 57—61[8])	+ 0.7 (lit, +0.1[4] −4.3[8,c])	+29.5 (lit, +28.8[14])
L-Phenylanine	94	86—89 (lit, 88—89[4])	+ 8.4 (lit, +5.1,[4] +5.3[9,c])	−31.9[g] (lit, −34.8[14,g])
β-Methyl L-aspartate	90	96 (lit, 96—98[5])	−16.5[a] (lit, −17.4[5,a])	
L-Leucine	100	oil		+14.6 (lit, +14.9[14])
L-Methionine	93	69—70 (lit, 68—69[4])	−19.4 (lit, −16.6[10])	+23.4 (lit, +23.5[14])
O-Benzyloxycarbonyl-L-serine	95	83—84	+4.4, +23.6[b]	+13.9[f] (lit, +14.5[14,f])
D-Isoleucine	100	oil		−40.3 (lit, −40.7[11])
erythro-β-Methyl-D-leucine*	100	oil		−39.4[e]
threo-*N*, β-Dimethyl-D-leucine*	93	98—99	+75.3	−39.3[e]
D-Valine	93	66—67 (lit, 60—62[6])	−0.53 (lit, +5.0,[6,d] +4.2[8,c])	−28.3 (lit, −26.4[12,e])
D-Phenylalanine	91	86—87 (lit, 88—89[4])	−8.3 (lit, −4.6[4,c])	+32.4[g] (lit, +33.9[12,e])

* Represented from our preceding paper.[2]
** Measured in solution of absolute alcohol unless stated otherwise, at 22—26°C.
*** Measured in a solution of 6N hydrochloric acid unless stated otherwise, at 22—25°C.
a) Measured in pyridine. b) Measured in ether. c) Measured in glacial acetic acid. d) Measured in methanol. e) Measured in 5N hydrochloric acid. f) Measured in 1N hydrochloric acid. g) Measured in water.

4) J. P. Greenstein and M. Winitz, "Chemistry of the Amino Acids," Vol. 2 John Wiley & Sons Inc., New York (1961), pp. 892—894.
5) H. Schwarz, F. M. Bumpus and I. H. Page, *J. Amer. Chem. Soc.*, **79**, 5701 (1957).
6) R. Sargers and B. Witkop, *ibid.*, **87**, 2020 (1965).
7) N. F. Albertson and F. C. McKay, *ibid.*, **75**, 5323 (1953).
8) E. Schröder, *Ann. Chem.*, **692**, 241 (1966).
9) D. W. Clayton, J. A. Farrington, G. W. Kenner and J. M. Furner, *J. Chem. Soc.*, **1957**, 1398.
10) K. Hofmann, A. Jöhl, A. E. Furlenmeier and H. Kappeler, *J. Amer. Chem. Soc.*, **79**, 1636 (1957).
11) W. A. H. Huffman and A. W. Ingersoll, *ibid.*, **73**, 3366 (1951).
12) J. R. Parikh, J. P. Greenstein, M. Winitz and S. M. Birnbaum, *ibid.*, **80**, 953 (1958).
13) E. Fischer and W. A. Jacobs, *Ber.*, **39**, 2942 (1906).
14) S. Akabori and S. Mizushima (Eds.), "Protain Chemistry" (Tanpakushitu Kagaku) Vol. 1 Kyoritsu Shuppan K.K., Tokyo (1952), pp. 112.

group using hydrogen bromide in glacial acetic acid,[15] followed by neutralization with triethylamine, with the exception of the deprotection of *N,O*-dibenzyloxycarbonyl serine. In the latter case, the protecting groups were removed by catalytic hydrogenation, using palladium-black as a catalyst in ethyl alcohol, in order to avoid any *O*-acylation, which is likely caused by the action of hydrogen bromide in glacial acetic acid.[16] The specific rotations of resolved *N*-benzyloxycarbonylamino acids and free amino acids are listed in Table 3, and their values are compared with those reported in the literature. The specific rotation value of β-methyl *N*-benzyloxycarbonyl-D-aspartate is comparable in magnitude to that of its L-antipode. The value of *N*-benzyloxycarbonyl-L-phenylalanine, along with that of the D-isomer, is relatively higher in magnitude than those reported. A striking difference is found to exist in the optical-rotation values of benzyloxycarbonyl valine reported in the literature; there are only a few values compatible with that of benzyloxycarbonyl valine obtained in this experiment. However, the two isomers of benzyloxycarbonyl valine afforded optically pure L- and D-valine respectively by debrocking.

Experimental

All the melting points are uncorrected. The optical rotation values were measured with a Jasco DIP-SL-type polarimeter.

Starting Materials. *A) (−)- and (+)-Ephedrine Hemihydrate Used Throughout This Work.* Commercially-available (−)-ephedrine hydrochloride, with a specific rotation value of −33.8° in water, was treated with a slight excess of N sodium hydroxide, and the organic base thus liberated was immediately taken up into ethyl acetate. The organic layer was dried over anhydrous sodium sulfate, filtered, and evaporated to dryness *in vacuo* to afford a crystalline material. This was then recrystallized from petroleum ether and dried spontaneously under an atmosphere to give (−)-ephedrine hemihydrate as needles; the melting point was 39—40°C, $[\alpha]_D = -5.8°$ in water. Found: C, 68.80; H, 9.14; N, 8.09%. Calcd for $C_{10}H_{15}ON \cdot 1/2H_2O$: C, 68.93; H, 9.26; N, 8.04%. Similarly, from (+)-ephedrine hydrochloride ($[\alpha]_D = +33.1°$ in water), (+)-ephedrine hemihydrate was obtained; mp 40°C, $[\alpha]_D = +5.9°$ in water. (Found: C, 69.29; H, 9.27; N, 8.21%).

B) N-Benzyloxycarbonyl Derivatives of Racemic Amino Acids. The compounds were prepared, in excellent yields, by the generally-applicable Schotten-Baumann method. Recrystallization from appropriate solvents afforded pure products as follows [name of *N*-benzyloxycarbonyl-DL-amino acid, mp°C, (lit, mp°C).]: β-methyl DL-aspartate, 110—112°C, (112°C).[17] DL-Isoleucine, 64—66°C, (48°C[18]). *erythro*-β-Methyl-DL-leucine, 62—64°C.[2] *threo-N,β*-Dimethyl-DL-leucine, 79°C.[2] DL-Leucine, 53—54°C, (52—55°C[4]). DL-Methionine, 112°C, (112°C[4]). DL-Phenylalanine, 102°C, (103°C[4]). *O*-Benzyloxycarbonyl-DL-serine, 93°C, (94°C[4]). DL-Valine, 74—75°C, (76—78°C[4]).

General Procedure for the Resolution of *N*-Benzyloxycarbonyl-DL-amino Acids. To a solution of 0.100 mol of *N*-benzyloxycarbonyl-DL-amino acid in ethyl acetate at a suitable concentration, depending on the amino acid employed, as will be shown below individually, 0.055 mol of (−)-ephedrine hemihydrate was added; then the solution was allowed to stand at room temperature (or stored in a refrigerator in some cases) until there was an adequate amount of a precipitate (this took from several hours to several days, depending on the materials employed.). The precipitate was collected by filtration and washed with ethyl acetate. An almost pure product was recrystallized from ethyl acetate to afford a fine salt of optically active *N*-benzyloxycarbonylamino acid with (−)-ephedrine (Table 1).

The suitable solvents and concentrations for *N*-benzyloxycarbonylamino acid favored for the resolution were as follows [name of *N*-benzyloxycarbonylamino acid, solvent (ethyl acetate was used unless stated otherwise), concentration in mole (M)]: β-methyl DL-aspartate, 0.45. DL-Isoleucine, ether, 2.49. *erythro*-β-Methyl-DL-leucine, ether, 2.00. *threo-N,β*-Dimethyl-DL-leucine, 1.00. DL-Leucine, ethyl acetate - petroleum ether (2 : 3 V/V), 2.62. DL-Methionine, 2.46. DL-Phenylalanine, ether, 0.17. *O*-Benzyloxycarbonyl-DL-serine, 1.00. DL-Valine, 4.68.

The above mother liquor was washed with a small amount of N hydrochloric acid and then water. The organic layer was dried over anhydrous sodium sulfate and evaporated to dryness *in vacuo*. The residue thus obtained was redissolved in a half volume of the same solvent as was used in the initial resolution stage, and 0.055 mol of (+)-ephedrine was added. The solution was then allowed to stand. The deposition of salt was usually much faster than in the initial case. The precipitate was filtered and washed with ethyl acetate. Recrystallization from ethyl acetate gave pure antipodal salt (Table 2).

Liberation of Optically Active *N*-Benzyloxycarbonylamino Acids from Salts. A suspension of the salt of optically active *N*-benzyloxycarbonylamino acid with ephedrine in ethyl acetate was treated with a slight excess of 2N hydrochloric acid, and the organic layer was washed with a small amount of water. The solution of ethyl acetate was then dried over anhydrous sodium sulfate. After filtration, the filtrate was evaporated to dryness *in vacuo* to give an almost optically pure material. Recrystallization from an appropriate solvent was performed to afford pure materials (Table 3).

Regeneration of Free Amino Acids Bearing Entirely Optical Activities. *A)* According to the usual way, optically active *N*-benzyloxycarbonylamino acid was dissolved in threefold equi-amounts of 30% hydrogen

15) D. Ben-Ishai and A. Berger, *J. Org. Chem.*, **17**, 1564 (1952); D. Ben-Ishai, *ibid.*, **19**, 62 (1954).

16) K. Okawa, This Bulletin, **30**, 977 (1957); J. Noguchi, T. Saito, T. Hayakawa and Y. Hayashi, *Nippon Kagaku Zasshi*, **80**, 299 (1959).

17) C. H. Bamford, A. Elliot and W. E. Hanby, "Synthetic Polypeptides," Acad. Press, New York (1956), p. 46.

18) Yu. I. Khurgin and M. G. Dmitrieva, *Tetrahedron*, **21**, 2305 (1965).

bromide in glacial acetic acid. After about one hour, much anhydrous ether was added and deposition was collected by fitration. A solution of the resulting hydrobromide in ethyl alcohol was neutralized with triethylamine to deposit free amino acid. This was recrystallized from water or water–ethyl alcohol to give optically pure amino acids (Table 3).

B) In the case of serine, optically active *N,O*-dibenzyloxycarbonylserine was dissolved in ethyl alcohol and a palladium-black catalyst was added. Hydrogenolysis was carried out under slight pressure for 6 hr at room temperature with the aid of an efficient shaking machine. Then the catalyst, with the substance adhering to it, was filtered and the product was separated from the catalyst by extraction with hot water. To the aqueous solution, dioxane was added to complete the precipitation. Recrystallization from water and acetone afforded optically active serine (Table 3).

The authors wish to express their gratitude to Dr. Eishin Kyuno of this Department and to Fuji Pharmaceutical Industries Co., Ltd., for their kind donation of (+)-ephedrine.

BULLETIN OF THE CHEMICAL SOCIETY OF JAPAN VOL. 43 2558—2566 (1970)

Conformations of the Ester Group

Michinori Ōki and Hiroshi Nakanishi

Department of Chemistry, Faculty of Science, The Univercity of Tokyo, Hongo, Tokyo

(Received February 16, 1970)

In some esters of formic acid which carry bulky alkyl groups (*e .g*, *t*-butyl formate, 1,1-diethylpropyl formate, and triphenylmethyl formate), the presence of *s-cis* conformer has been confirmed by various spectroscopic techniques. The dipole-moment measurements also support the conclusion drawn from the spectroscopic data.

It has been reported that the *s-cis* conformer as well as the *s-trans* conformer is present in many carboxylic acids[1-3] and amides.[4,5] The presence of these isomers can be attributed to the partial double bond character of the C–O or C–N bond due to delocalization of the electrons. Although the ester is an analogous compound, its conformation has been reported to be *s-trans*, chiefly on the basis of the results of dipole moment measurements[6] and microwave spectroscopy.[7,8] The *s-cis* conformer has only rarely been found.[9,10]

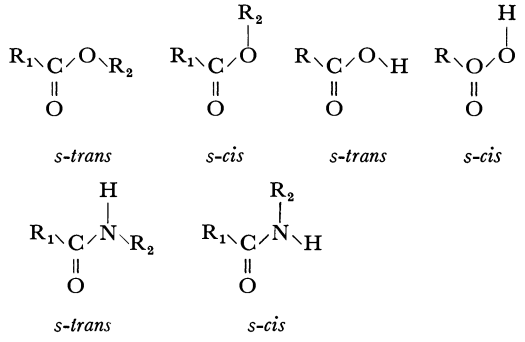

Fig. 1. Conformations of ester, carboxylic acid and amide.

However, it is well known that the C–O bond of

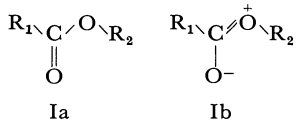

Ia Ib

1) M. Ōki and M. Hirota, *Nippon Kagaku Zasshi*, **81**, 855 (1960).

2) M. Ōki and M. Hirota, This Bulletin, **33**, 119 (1960).

3) M. Ōki and M. Hirota, *ibid.*, **34**, 374 (1961).

4) L. A. LaPlanche and M. T. Rogers, *J. Amer. Soc.*, **86**, 337 (1964).

5) H. Kessler and A. Rieker, *Ann. Chem.*, **708**, 57 (1967).

6) a) A. Euker and L. Meyer, *Z. Phys.*, **30**, 397 (1929). b) C. T. Zahn, *ibid.*, **33**, 70 (1952). c) L. Meyer, *Z. Phys. Chem. Ber.*, **8**, 27 (1930). d) J. M. Sturtevant, *J. Amer. Chem. Soc.*, **55**, 4478 (1933). e) C. T. Zahn, *Trans. Faraday. Soc.*, **30**, 804 (1934). f) R. J. B. Marsden and L. E. Sutton, *J. Chem. Soc.*, **1936**, 1383. g) M. L. Bender, *Chem. Rev.*, **60**, 53 (1960).

7) J. M. Ogorman, W. Schand, Jr., and V. Schomaker, *J. Amer. Chem. Soc.*, **72**, 4222 (1950).

8) R. F. Curl, *J. Chem. Phys.*, **30**, 1529 (1959).

9) B. Krishna, S. C. Srivastava and S. V. Mahadame, *Tetrahedron*, **23**, 4801 (1967). Krishna reported on the basis of dipole moment data that geranyl formate had the *s-cis* conformation, but there are not sufficient data to confirm the existence of the *s-cis* isomer.

10) D. N. Hall and J. Lamb, *Trans. Faraday Soc.*, **55**, 784 (1959).

the ester also has a partial double bond character due to the delocalization of electrons, as is exemplified by the resonance structures, (Ia, Ib). Therefore, *s-cis* conformers like carboxylic acid and amide may exist in some esters if either the *s-cis* conformer is stabilized or the *s-trans* is destabilized for some reason.

The purpose of this paper is to present the spectroscopic evidence, as well as the support from the dipole moment data, for the presence of *s-cis* conformers in some alkyl formates; it will also consider the effect of the bulkiness of the alkyl part of alkyl formates on the presence of the rotational isomers about the C–O bond of the esters.

Experimental

Materials. The simple esters were prepared by the standard methods. The *t*-butyl acetate was prepared from anhydrous acetic acid and *t*-butyl alcohol in the presence of zinc chloride. The *t*-butyl formate, *t*-amyl formate, 1-ethylpropyl formate, 1,1-diethylpropyl formate, phenyl formate, 2,6-dimethylphenyl formate, and geranyl formate were prepared from mixed anhydride of formic and acetic acid and the corresponding alcohol according to the Stevens method.[11] The triphenylmethyl formate was prepared from sodium formate and triphenylmethyl chloride.[12]

The γ-butyrolactone and cyclopentadecanolide were of commercial origin and were purified before the measurements.

The ε-caprolactone and cyclododecanolide were prepared from the corresponding ketone and perbenzoic acid. The physical constants of the compounds used in this study agree with those previously reported in the literature.

Apparatus. The IR spectra were measured by using a Perkin-Elmer 112G grating spectrometer, (1800—1700 cm^{-1}) (the precision of the instrument was believed to be 0.5 cm^{-1} at 1750 cm^{-1}), a JEOC-DS-402G infrared spectrophotometer (4000—400 cm^{-1}), a Hitachi EPI-G2 grating infrared spectrophotometer (1200—400 cm^{-1}), and a Hitachi EPI-L grating infrared spectrophotometer (700—200 cm^{-1}).

The UV spectra were measured on a Hitachi EPS-3 recording spectrophotometer.

The NMR spectra were measured on a JNM-C-60 spectrometer and on a JNM-4H-100 spectrometer.

The dipole moment was measured by the heterodine-beat method. (The estimated error was about 0.05D at 1.5D and about 0.02D at 2.5D).

Results and Discussion

The three chief factors governing the preference of the conformations of ester can be considered to be: the dipole-dipole interaction between C=O and O–R_2 bonds (Fig. 2a), the repulsion between lone-pair electrons of two oxygen atoms (Fig. 2b), and

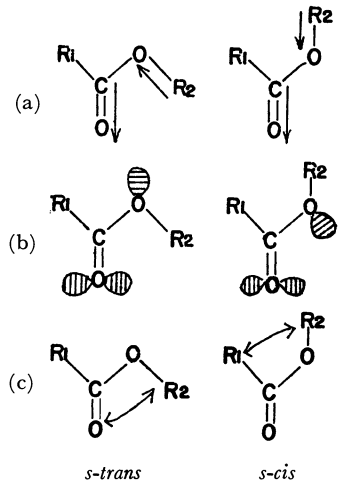

Fig. 2. The chief factors governing ester conformation.

the steric repulsion either between C=O and R_2 or between R_1 and R_2 (Fig. 2c).

The direction of the dipoles of the two bonds is roughly antiparallel in the *s-trans* conformer and roughly parallel in the *s-cis*. Therefore, the *s-trans* conformer is favored over the *s-cis* in less polar media as far as the first factor is concerned. In the second factor, the repulsion is considered to be very small in the *trans* conformer compared to that in the *s-cis*. Thus, the *s-trans* conformer is more stable than the *s-cis*. As to the third factor, when R_1 is bulky, the steric repulsion between C=O and R_2 in the *s-trans* conformer should be smaller than that between R_1 and R_2 found in the *s-cis*. Thus, the *s-trans* conformer is more stable in the ordinary esters. However, when R_1 is small, and R_2 bulky, the situation may be reversed; the *s-cis* conformer could be favored over the *s-trans* because of the increase in the interaction between R_2 and O relative to that between R_1 and R_2. These considerations lead to the conclusion that a *s-cis* conformer of the ester may exist when the ester has a small R_1 and a bulky R_2, which is possible in some formates which carry a large alkyl group.

Infrared Spectra

From the results obtained with carboxylic acids[13] and ketones,[14] it is natural to consider that the *s-cis* and *s-trans* conformations of the ester are reflected in the C=O stretching absorptions of these compounds. The results obtained with solutions in nonpolar solvents are shown in Table 1. It may be pointed out that some formates and acetates with

11) W. Stevens and A. van. Es, *Rec. Trav. Chim. Pays-Bas*, **83**, 1287 (1964).

12) S. L. Fires, *J. Amer. Chem. Soc.*, **71**, 2571 (1949)

13) M. Ōki and M. Hirota, This Bulletin, **34**, 374 (1961).

14) M. Hirota, T. Hagiwara and H. Satonaka, *ibid.*, **40**, 2439 (1967).

Table 1. Absorption maxima due to carbonyl stretching vibration of esters (in CCl_4 or CS_2)

Compound	ν_{CO} (cm^{-1})	Compound	ν_{CO} (cm^{-1})
HCO_2CH_3	1733	$CH_3CO_2CH_3$	1749
$HCO_2C_2H_5$	1729	$CH_3CO_2C_2H_5$	1741
$HCO_2CH(CH_3)_2$	1725	$CH_3CO_2CH(CH_3)_2$	1737
$HCO_2C(CH_3)_3$	1722	$CH_3CO_2C(CH_3)_3$	1736
$HCO_2C(C_2H_5)_3$	1723		
$HCO_2C_{10}H_{17}$*	1728		

* geranyl formate

rather bulky alkyl groups show absorptions at the lower frequencies. However, this can not be taken as positive evidence for the presence of rotational isomers, because the absorption band is rather symmetrical except in the cases of isopropyl acetate and *t*-butyl acetate*[1] (see the discussions of the solvent effects). The present authors presume that the shift is the mere reflection of some effects of the electrical and bonding natures.

There are some lactones which are forced to take the *s-cis* conformation. Therefore, if the C=O absorption due to the lactones of the smaller ring and that due to the large lactone ring are compared, there will be a chance of finding the difference between the two conformers. Thus, the infrared C=O absorptions of various lactones were measured; the results are given in Table 2. The extraordinarily high frequency of γ-butyrolactone is, of course, attributable to the ring strain or the angle deviation, whereas ε-caprolactone is a compound which can take the *s-cis* conformation only. Judging from the knowledge of other esters, it may be assumed that cyclopentadecanolide exists in the *s-trans* conformation only. The data in Table 2 indicate that there

Table 2. Absorption maxima due to carbonyl stretching vibration of lactones (in CCl_4)

n	Compound	ν_{CO} (cm^{-1})	
5	γ-butyrolactone	1783	
7	ε-caprolactone	1740	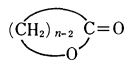
13	cyclododecanolide	1736	
16	cyclopentadecanolide	1735	

is not much difference between these two compounds. Cyclododecanolide is expected to be a composite of *s-cis* and *s-trans* conformers, since the analogous C_{12} lactam is known to be so from NMR spectroscopy.[15] However, it shows only one sharp absorption in the carbonyl region. These results, although negative, may be interpreted as indicating that the *s-cis* and *s-trans* conformations of the ester can not be distinguished by the infrared C=O absorptions as measured in carbon tetrachloride or carbon disulfide.[16] Although the investigation of the infrared spectra in the C=O stretching region may not reveal the presence of the *s-cis* and *s-trans* conformers, the skeletal deformation region may be useful to this end, because the skeletal deformation is known to be sensitive to conformational change and because it has been shown recently that the spectra of amides in the 1200—200 cm^{-1} region reflect the presence of conformers superbly.[17]

The Effect of Temperature on the Absorptions in the 1200—200 cm^{-1} Region. The infrared spectra of *t*-butyl formate (II) were thus measured in various states and at various temperatures. The results are shown in Figs. 3 and 4.

Apparently, the intensities of absorptions bands change with a change in the temperature from 20°C (liquid) to <-100°C (solid), as is shown in Fig. 3;

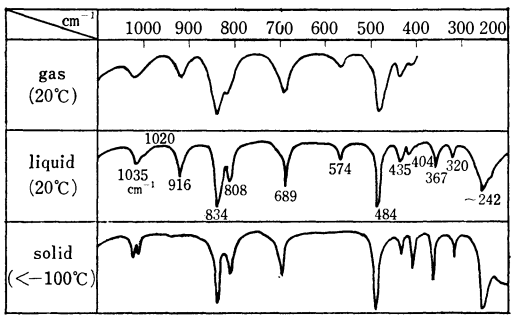

Fig. 3. IR spectra of *t*-butyl formate in three phases.

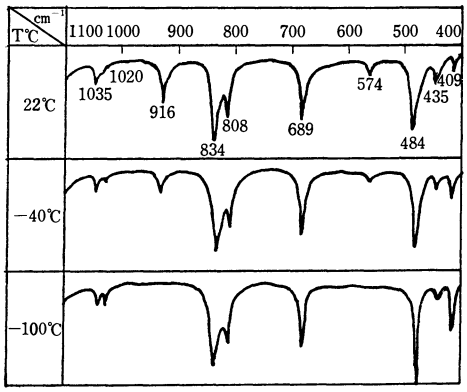

Fig. 4. Temperature change of IR spectra of *t*-butyl formate in liquid state.

*[1] In these acetates, the absorptions are unsymmetrical. Regarding this phenomena, an extensive discussion will be presented in subsequent papers.

15) R. M. Moriarty and J. M. Kliegman, *Tetrahedron Lett.*, **1966**, 891.

16) Owen and Sheppard could not find the *s-cis* conformer by means of the infrared spectra. N. L. Owen and N. Sheppard, *Proc. Chem. Soc.*, **1963**, 264.

17) Y. Koyama. the university of Tokyo, private communication.

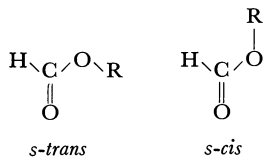

s-trans *s-cis*

II: R=*t*-Bu
III: CEt_3
IV: $R=C_{10}H_{17}$ (geranyl)

for example, the absorptions at 916 cm^{-1} and 574 cm^{-1}, which are present at 20°C, disappear in the spectrum of the solid. In the gas phase at a lower pressure, the absorptions become broader than those in the liquid phase, although all the absorptions which are present in the liquid phase also exist in the spectra of the gas.

A temperature dependence (Fig. 4) study of the spectra of liquid *t*-butyl formate has shown the interesting features of some bands; the intensities of the bands at 916, 574, and 435 cm^{-1} decrease as the temperature is lowered, whereas those at 1020, 484, 409, and 242 cm^{-1} increase at low temperatures. The temperature dependence study of the spectra of gaseous *t*-butyl formate at 20—70°C reveals the same tendency. These phenomena may be explained by asuming the presence of conformational isomers. These studies alone not establish how many conformers are present, but, from the considerations of structure, it may now be said that *t*-butyl formate has two conformers, *s-cis* and *s-trans*, and that the populations of these isomers change as the temperature varies, and that these changes are reflected in the far-infrared spectra. It is not easy to assign these bands at the present time; further sutdy will be necessary to clarify this point.[18]

A far-infrared spectral study of 1,1-diethylpropyl formate (III) and geranyl formate (IV) was also carried out, because the former compound has a bulkier alkyl group than *t*-butyl formate, while the latter has been reported, on the basis of dipole moment data, to exist as an *s-cis* conformer.[9]

The spectra of these compounds measured under various conditions (gas, liquid, solid, and temperature range 81.0°C to −100°C) show very complicated changes. However, these changes may not be directly related to the *s-cis* and *s-trans* conformers of the ester group, because there are many rotational isomers possible for the alkyl part also. *t*-Butyl formate is simple in this respect; the only rotational axis considered is C_{co}–O_{ether}; rotation about the other axes produces the same conformation because of the symmetry of the substituent. 1,1-Diethylpropyl formate, on the other hand, has two different conformations (Va, Vb), in addition to the *s-cis* and *s-trans* conformers, because of rotation about the C–C axis of the ethyl group. There is no doubt about the presence of more possible conformers in geranyl formate. Although desirable, it was even impossible to correlate these spectra with those of *t*-butyl formate, because the absorptions are seriously shifted by the mass effect.

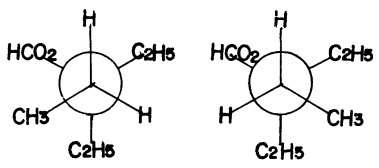

Va Vb

Solvent Effect in the 1200—400 cm^{-1} Region. The *s-cis* conformer of ester is considered to be more polar than the *s-trans*, judging from the arrangement of bond dipoles, and the dipole moments are calculated to be 3.04 and 1.53 D for the *s-cis* and *s-trans* conformers respectively. This implies that the population of the *s-cis* conformer will become greater in a polar solvent relative to the nonpolar solvent. Thus, it may be possible to assign some bands to the respective conformations.

The infrared spectra of *t*-butyl formate and 1,1-diethylpropyl formate were thus measured in carbon disulfide (2.64),*2 acetone (20.7), acetonitrile (37.5), and *N*,*N*-dimethylformamide (DMF) (37.7). The results are shown in Fig. 5.

Apparently, the intensities of all the absorptions change. The outstanding feature of the change is

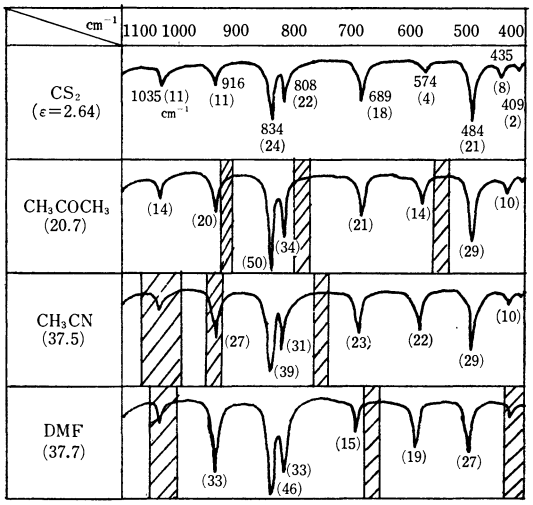

Fig. 5. Solvent effect of IR spectra of *t*-butyl formate.
The figures in parentheses are molar absorption coefficients.
The shaded range is a part of strong absorption of solvent itself.

18) In this skeletal deformation region, the assignment and calculation of each absorption of the ester were made only with methyl formate, methyl acetate, ethyl acetate, and methyl propionate. S. Ichikawa, Tokyo University, private communication.

*2 The numbers shown in parentheses are dielectric constants.

that the intensities of the absorptions at 916 and 574 cm^{-1} become larger in comparison with the band at 689 cm^{-1}, as the solvent polarity increases.*3 The results mean that the bands at 916 and 574 cm^{-1} can be assigned to some modes of vibration of the *s-cis* conformer. Since, as has been mentioned before, the intensities of these bands decrease on lowering of the temperature, it may now be said that the *s-cis* conformer of *t*-butyl formate is less stable than the *s-trans*. The solvent effect on the spectra of the 1,1-diethylpropyl formate is large, as is on *t*-butyl formate. This fact may be considered as a reflection of the presence of *s-cis* and *s-trans* isomers, since the population of the rotational isomers about the C–C axis of the ethyl groups is not affected to a great extent by the solvent polarity change; the dipole moment should not be affected too much by rotation about the bond in question.

Solvent Effect in the Region of the Carbonyl Stretching Vibration. The solvent effect on the far-infrared spectra of formates, as has been described above, naturally led the present authors to reinvestigate the carbonyl stretching region by means of the polar solvents. The results are given in Fig. 6.

It is apparent that *t*-butyl formate has at least two peaks in acetonitrile and dimethyl sulfoxide (DMSO) and that graphical seperation of these bands gives two peaks, the molecular extinction coefficients of which and the wave numbers of the absorption maxima of which, are also shown in Fig. 6. There are two possible reasons for the fact that *t*-butyl formate gives two absorption maxima in the polar solvents, whereas it gives only one peak in carbon disulfide. The first is the possibility that, although there is only one conformation, there are at least two species of solvation, the lower band representing the molecular species which are strongly solvated by the polar solvent. In this case, the exchange among these species is slow enough for resolution by infrared light. The second is the possibility that *s-cis* and *s-trans* conformers now give resolvable two bands. If the first possibility were really the case, however, other esters which exist in

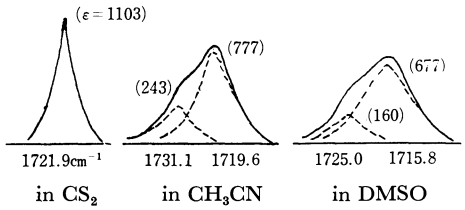

Fig. 6. Solvent effect on ν_{CO} of *t*-butyl formate.

Table 3. Solvent effect on ν_{CO} of esters

($c \approx 0.05$ mol/*l* at 20°C)

Compound \ Solvent	CS_2 (2.64)*		CH_3CN (37.5)*		DMSO (48.9)*	
HCO_2Me	1733.2 cm^{-1}	(1150)**	1727.0 cm^{-1}	(1102)**	1719.0 cm^{-1}	(1111)**
HCO_2Et	1729.0	(1146)	1721.9	(1164)	1715.2	(1430)
HCO_2CHMe_2	1725.4	(1018)	1718.9	(901)	1716.6	(637)
HCO_2CMe_3	1721.9	(1103)	1719.6 1731.1	(777) (243)	1715.8 1725.0	(677) (160)
HCO_2CMe_2Et	1724.4	(1471)	1717.6 1731.0	(911) (281)	1714 1730	(851) (104)
HCO_2CMeEt_2	1723.1	(1356)	1716.8 1728.0	(820) (305)	1712 1725	(686) (104)
HCO_2CEt_3	1722.6	(1095)	1716.7 1727.7	(867) (219)	1715.6 1726	(730) (70)
$HCO_2C_{10}H_{17}$	1728.2	(1133)	1720.1 1724.2	(746) (244)		
HCO_2CPh_3	1740.8 1746.5	(684) (262)	1736 broad	(568)		
HCO_2Ph	1775.1	(—)	1762.2	(—)		
$HCO_2C_6H_3Me_2$-2,6	1769 1771	(—)*** (—)	1757 1768	(—)*** (—)		
$CH_3CO_2C_6H_3Me_2$-2,6	1763.2	(1127)	1759.1	(724)		
$(CH_2)_{14}$ C=O, O	1734.6	(772)	1727.6	(557)		

* Numericals shown in parentheses are dielectric constants at 20°C.

** Numericals shown in parentheses are molar absorption coefficients.

*** The molar absorption coefficients of the lower absorption of this compound are stronger than that of the higher in these two solvents.

*3 The wave numbers referred to are those observed in carbon disulfide.

one conformation should also give two bands in these polar solvents. Thus, the C=O stretching absorptions of various esters were determined and the results are shown in Table 3. It can immediately be pointed out that methyl formate, ethyl formate (whose conformations has been established to be *s-trans* by microwave spectroscopy),[7] and isopropyl formate have only one sharp symmetrical absorption in carbon disulfide, acetonitrile, and DMSO. The first possibility is, thus, not very likely. Therefore, the second becomes likely, since the existence of conformers has been proved for *t*-butyl formate from the far-infrared spectra (see below).

The reason why this compound gives only one band for C=O stretching in carbon disulfide may be that the wave number difference between the two conformers is so small that it cannot be resolved by the present optical instrument. As for the assignment of the two bands, the band at the higher wave number seems to correspond to the *s-cis* isomer. The reason for this assignment is two-fold. The first comes from a consideration of the population. The temperature dependence study has established that the *s-cis* isomer is the less stable one. Therefore, the weak band will correspond to less stable isomer. It may be argued that the absorption intensities per molecule for *s-cis* and *s-trans* are not known and that the reverse may be possible. However, consideration of bond dipole leads to the conclusion that, if the absorption intensity per molecule is different, it is the *s-cis* molecule which gives rise to a stronger absorption.*4 The second reason for the assignment comes from the location of maximum absorption. From the same consideration as the intensity, it is natural to expect the *s-cis* conformer to give absorption due to C=O stretching at a higher frequency than the *s-trans*, since a higher energy will be necessary to excite the molecule when the two dipoles are arranged roughly parallel.

Table 3 shows that formate esters with bulky alkyl groups give two C=O stretching absorptions in polar solvents, whereas isopropyl formate gives only one absorption in any of the solvents investigated. These results indicate that the alkyl group in formate esters should at least be tertiary in order to make the existence of the *s-cis* conformer possible.

The aryl esters in Table 3 are worthy of special mention. Phenyl formate has only one absorption due to C=O stretching in both carbon disulfide and acetonitrile. It is expected to exist as the *s-trans* isomer. On the other hand, 2,6-dimethylphenyl formate shows two bands due to C=O stretching even in carbon disulfide. It is believed that the resolution is now possible between the *s-cis* and *s-trans* conformers in carbon disulfide. The same is true of triphenylmethyl formate. This assignment may be explained as follows: The conformation of phenyl formate (VII) must, at least, be nearly planar because of the resonance stabilization. However, the planar conformation is not possible for 2,6-dimethylphenyl formate (VIII) because of the steric effect of the methyl groups. If the models of the latter compound are written schematically, the *s-trans* and *s-cis* conformers may be represented as in Fig. 7. (VIIIa, VIIIb). In the *s-trans* conformation, those which cause the repulsion are the *p*-electron pair of oxygen and the π-electrons of the benzene ring. On the other hand, in the *s-cis* conformation, the interaction takes place between hydrogen of the formyl group and the π-electrons of the benzene ring. The latter interaction, which could even be rather attractive, is at least expected to be less repulsive because the van der Waals radius of hydrogen is far less than that of oxygen. Thus the *s-cis* conformer becomes less unstable than that

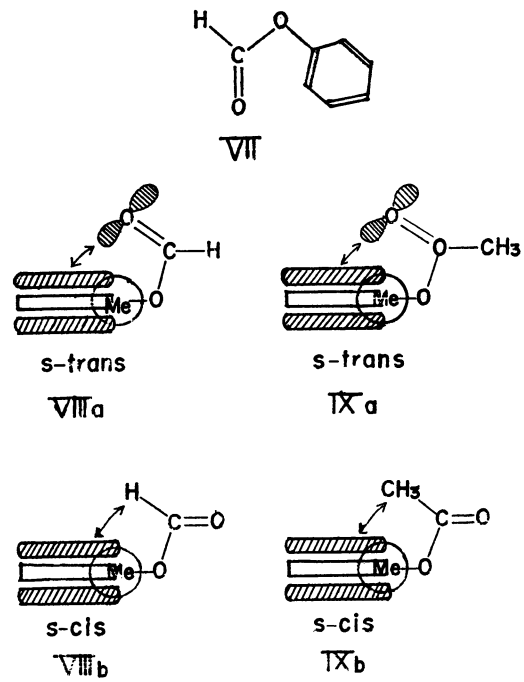

Fig. 7. Conformations of phenyl formate, 2,6-dimethylphenyl formate and 2,6-dimethylphenyl acetate.

*4 It is well known that α-halocyclohexanone derivatives give stronger absorption due to C=O stretching per molecule when halogen is equatorial. This effect can be explained by considering the direction of the bond

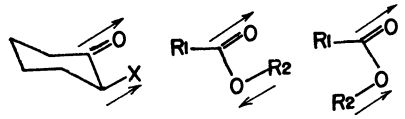

VI *s-trans* *s-cis*

dipoles; the equatorial α-halocyclohexanone (VI) has dipoles as is shown above, which makes the change in dipole moment small on stretching the C=O bond. The situation is similar with the *s-cis* isomer of esters.

of the *s-trans*, although the interaction of the lone pair electrons of the two types of oxygen is still large in the *s-cis* conformation.

In this connection, the situation of 2,6-dimethylphenyl acetate (IX) is a different case. The repulsive interaction between the benzene ring and the methyl group of the acetyl seems to become large (Fig. 7, IXa and IXb), and this compound gives only one absorption due to C=O stretching in either carbon disulfide or acetonitrile.

Dipole Moment

It is known that the dipole moments of most esters are in the range from 1.4 to 2.0 D. Using the usual bond moments, the calculated values are 1.53 D and 3.40 D for the *s-trans* and *s-cis* isomers respectively. (The dipole moment of δ-valerolactone, which can take only the *s-cis* conformation, has been determined as 4.22 D[19]). Thus, the conformations of the ordinary esters are considered to be *s-trans*.

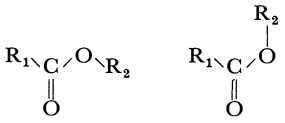

1.53 D 3.40 D

Calculated Dipole Moments.

In view of the above knowledge, it can be expected that the dipole moment data will provide another proof for the existence of the *s-cis* isomer. Krishna and his co-workers investigated along this line.[9] The results of the present work are tabulated in Table 4. Although the data are rather scattered, it may safely be said that methyl and ethyl formates and other acetates exist as *s-trans* conformers.

However, those of *t*-butyl formate, 1,1-diethylpropyl formate, and geranyl formate are a little too large to be attributed to the *s-trans* conformer only. Two reasons for the unusually high dipole moment may be considered. The first is the nonplanarity of the formate molecule ($\theta \neq 0$). Because of the steric requirement of the bulky alkyl group, the carbon atom attaching to the ether oxygen may not lie on the plane which is made by the formyloxy group. These conformations can be considered for both the *s-trans* and *s-cis* isomers. The second is the presence of both *s-trans* and *s-cis* conformers.

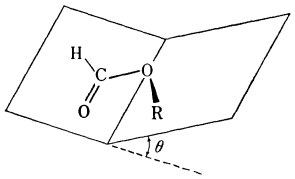

To clarify this point, the dipole moments of methyl formate, *t*-butyl formate, and 1,1-diethylpropyl formate were measured at various temperatures in benzene. The dipole moments of the compounds with bulky groups varied as the temperature changed, but that of methyl formate remained intact within the range of errors (Table 4). These results supported the idea that the second possibility is actually the case. The dipole moments of these compounds with bulky alkyl groups become large as the temperature becomes higher. This shows that the *s-cis* conformer is more unstable than the *s-trans* and agrees with the results obtained from the infrared spectra data.

Although it is now proved that the second possibility is actually the case, the first possibility cannot be ruled out. Indeed, the rather small excess of the dipole moment of *t*-butyl formate and 1,1-diethylpropyl formate over that of *s-trans* may reflect the nonplanarity of the molecule, since the nonplanar *s-cis* conformer may be expected to possess a smaller dipole moment as a result of the smaller contribution of the dipolar canonical structure. It is interesting to know in this connection that *t*-butyl acetate and ethyl acetate show larger dipole moments, in that order, than methyl acetate, whose structure has been shown by the microwave spectroscopic data to be planar.[7,8]

Table 4. Dipole moments of esters (in C_6H_6)

Compound	μ (D)	T°C	Compound	μ (D)	T°C
HCO_2CH_3	1.67	5	$HCO_2C(C_2H_5)_3$	2.23	15
	1.73	25		2.28	25
	1.73	35		2.29	35
$HCO_2C_2H_5$	1.96	25	*$HCO_2C_{10}H_{17}$[9]	2.57	25
$HCO_2C(CH_3)_3$	1.67	5	$CH_3CO_2CH_3$	1.45	25
	2.10	25	$CH_3CO_2C_2H_5$	1.88	25
	2.26	45	$CH_3CO_2C(CH_3)_3$[20,21]	1.91	25

* geranyl formate

19) R. Huisgen and H. Ott, *Tetrahedron*, **6**, 253 (1959).
20) C. P. Smyth and W. S. Walls, *J. Amer. Chem. Soc.*, **53**, 527 (1931).
21) C. P. Smyth, "Dielectric Behavior and Structure," McGraw-Hill, New York, (1955), pp. 303—309.

TABLE 5. n-π^* ABSORPTIONS OF CARBONYL OF FORMATES AND ACETATES (in n-hexane or isooctane)

Compound	λ_{max} (mμ)	ε	Compound	μ_{max} (mμ)	ε
HCO_2CH_3	215.2	71	$CH_3CO_2CH_3$	209.8	57
$HCO_2C_2H_5$	215.7	82	$CH_3CO_2C_2H_5$	210.0	58
$HCO_2{}^nC_3H_7$	215.7	79*	$CH_3CO_2{}^nC_3H_7$	209.8*	56
$HCO_2{}^iC_3H_7$	215.9	75	$CH_3CO_2{}^iC_3H_7$	211.7	64
$HCO_2{}^nC_5H_{11}$	215.5	77*	$CH_3CO_2{}^nC_5H_{11}$	210.4*	63
HCO_2CMe_3	217.8	80	$CH_3CO_2CMe_3$	216.2	53
HCO_2CMe_2Et	218.5	72			
HCO_2CMeEt_2	223	116			
HCO_2CEt_3	226	155			
$HCO_2C_{18}H_{17}$**	238	163			

* Data from W. D. Closson and P. Haug[23]
** geranyl formate

Ultraviolet Absorption Spectra.

The ultraviolet absorption spectra of esters and lactones were measured by Closson and Orenski,[22] who pointed out that the n–π^* absorption of the carbonyl oxygen appeared at a longer wavelength with the *s-cis* conformation than with the *s-trans*. Therefore, the UV spectral technique will give another clue in the reseach for the *s-cis* conformer.

The ultraviolet absorption spectra of various esters have been determined; the results are shown in Table 5. It is apparent that those which have been proved by the other techniques to exist as conformational mixtures have absorptions at wavelength longer than 216 mμ. The absorption maximum is still shifted bathochromically when the alkyl group becomes bulkier. The ultraviolet absorption may be used as supplementary evidence for the presence of the *s-cis* isomer in esters.

Nuclear Magnetic Resonance Spectra.

It is not possible to learn the population of the *s-cis* and *s-trans* conformers of the ester by means of infrared spectroscopy because of the nonidentical absorption intensity per molecule. Nor is it possible to do so by dipole moment measurements, because the absolute value for each isomer is not known. However, it is possible by means of NMR spectroscopy, provided the exchange of the isomers is sufficiently slow on the NMR time scale. Thus, it seemed that it would be interesting to measure the NMR spectra of several formates at various temperatures. Methyl, ether, isopropyl, and *t*-butyl formates show sharp singlets at 7.97, 7.87, 7.88, and 7.83 ppm respectively in carbon tetrachloride at room temperature. Although it might be hoped that the signal might be resolved into two singlets in a solvent which would give a specific solvent effect, *t*-butyl formate shows a sharp singlet at 7.68 ppm from tetramethylsilane (TMS) in benzene. Thus, it is necessary to lower the temperature in order to slow down the rate of exchange. DMF has been chosen as a solvent for this study because it has a rather low melting point (−61°C) and its proton signal may be used as a control. The concentration of this solution was *ca.* 50% to avoid freezing during the measurement at about −100°C. *t*-Butyl formate in DMF has a singlet peak at 8.04 ppm from TMS at 20°C. whereas the peak broadens at −64°C. The signals are resolved into two at −94°C, the chemical shifts beeing 8.88 and 8.03 ppm from TMS. The chemical shifts do not change at −99°C. The area under the peak at 8.88 ppm corresponds to 14% of the total signals of formyl proton. The peak at 8.88 ppm is assigned to the *s-cis* isomer, and that at 8.03 ppm, to the *s-trans* isomer, because it is established by the infrared study that the *s-cis* isomer is less stable.*[5]

The rough thermodynamic parameters for the *s-cis* and *s-trans* isomers are shown in Table 6; they

22) W. D. Closson and P. J. Orenski, *J. Org. Chem.*, **32**, 3160 (1967).
23) W. D. Closson and P. Haug, *J. Amer. Chem. Soc.*, **86**, 2384 (1964).

*[5] It may be argued that *t*-butyl formate and *N*,*N*-dimethylformamide (DMF) may form a complex and that there is an equilibrium between the complex and the monomer of the ester. In this case, the exchange between these species is slow enough to be detected on the NMR time scale at these low temperatures. In order to clarify this point, the NMR spectra of methyl formate were measured in DMF at a *ca.* 50% concentration at temperatures between 30°C and −95°C. The peak heights of formyl protons of methyl formate and DMF remained unchanged, although the chemical shift of the formyl proton of methyl formate shifted a little to a lower field (from 8.03 ppm to 8.06 ppm from TMS) as the temperature was lowered. These results support the idea that the splitting of the signal of *t*-butyl formate is due to the presence of rotational isomers and not to the presence of a complex molecule.

Table 6. The thermodynamic parameters for the *s-cis* and *s-trans* isomer equilibration of *t*-butyl formate

ΔH	-2.2 ± 0.7 kcal/mol
ΔS	-9 ± 2 e.u.

are obtained from the equilibrium constants at -94°C and -99°C. It is impossible at the present to obtain the kinetic parameters for the rotation about the $C-O_{ether}$ axis of *t*-butyl formate, for the intensities of the two peaks are not the same and, moreover, vary according to the temperature. However, judging from the large chemical shift, $\Delta\nu=0.85$ ppm (*cf*, the fact that *t*-butyl formamide has a $\Delta\nu$ value of 0.23 ppm and shows two peaks at room temperature[4]), it is apparent that the activation energy for the rotation of *t*-butyl formate is smaller than that of the corresponding amide.

Conclusion

It has been established, by various spectroscopic techniques and by dipole moment measurements, that *t*-butyl formate exists as a mixture of the *s-cis* and the *s-trans* conformers. The other formate, which has a rather bulky group, shows also the presence of two isomers. These may be attributed to the steric effect of the alkyl group, which interfers severely with carbonyl oxygen; the steric repulsion is relieved when the *s-cis* conformation is taken, because the hydrogen of the formyl group is less bulky than the carbonyl oxygen.

A rather striking example is geranyl formate. Every piece of evidence studied so far has indicated the presence of the *s-cis* isomer in this compound. Geranyl is the primary alkyl group, and we cannot expect a great steric bulkiness. A further surprising fact is that neryl formate, an isomer of geranyl formate, shows no evidence of the presence of the *s-cis* isomer. These puzzling facts must be studied further.

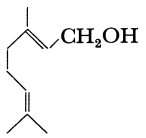

Geraniol

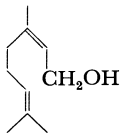

Nerol

The authors wish to express their hearty thanks to Professor T. Shimozawa of Saitama University for the measurement of the dipole moments and to Dr. Y. Kawazoe of the National Cancer Center Reseach Institute for the NMR measurements. The authors are also indebted to Mrs. S. Ichikawa and Dr. Y. Koyama for their help in measurement of the far-infrared spectra and for their helpful discussions.

BULLETIN OF THE CHEMICAL SOCIETY OF JAPAN VOL. 43 2566—2570 (1970)

The Reactions of Sulfur Ylides with Cyclic Carboxyl Compounds and Isocyanates

Teruaki MUKAIYAMA, Moriaki HIGO and Hisashi TAKEI

Laboratory of Organic Chemistry, Tokyo Institute of Technology, Ookayama, Meguro-ku, Tokyo

(Received February 19, 1970)

It was found that the reactions of dimethyloxosulfoniummethylide (II) with cyclic carboxyl compounds (I), such as lactones, carboxylic anhydrides and imides, gave the corresponding stable oxosulfonium ylides (III). In addition, the reaction of phenyl isocyanate dimer (IX) and dimethylsulfoniummethylide (X) afforded a 1 : 1 adduct (XI), which, on heating, decomposed to give a ring expansion product (XIV). Hydantoin derivatives (XVII) were also produced by treating dimethylsulfonium-α-methylacylmethylide (XVI) with two moles of isocyanates in dimethyl sulfoxide. On the other hand, when the same reactions were carried out in benzene, XVI reacted with an equimolar amount of isocyanates to give acrylamide derivatives (XVIII) in high yields by the rearrangement of the intermediate sulfoniummethylide (XX).

In the previous paper,[1] it was shown that 3-hydroxyfuran derivatives were synthesized in good yields from ketene dimer and stable sulfonium or oxosulfonium[2] ylides accompanied with ring expansion.

In the present paper, in connection with this methylene transfer reaction, the reactions of sul-

1) H. Takei, M. Higo, K. Saito and T. Mukaiyama, This Bulletin, **41**, 1738 (1968).

2) unpublished result.

fonium and oxosulfonium ylides with some cyclic carboxyl compounds (I) such as lactones, imides[3] or carboxylic anhydrides, and isocyanates[4] were studied. When I and dimethyloxosulfonium-methylide (II) were allowed to react in tetrahydrofuran (THF), stable oxosulfonium ylides (III)[5] were produced in high yields instead of the expected ring expansion compounds (IV). The reaction may proceed through an initial formation of a betaine intermediate (V), which in turn changed to III by an intramolecular proton transfer. The results are summarized in Table 1.

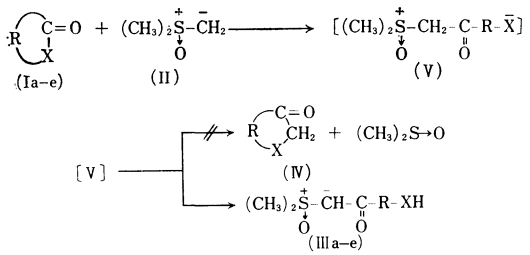

Table 1. Reactions of dimethyloxosulfonium-methylide (II) with cyclic carboxyl compounds (I)

(I)	(III) -R-X-H	Yield, %
(Ia)	$-(CH_2)_2-OH$	93
(Ib)	$-(CH_2)_3-OH$	99
(Ic)	$-(CH_2)_2-C(=O)-NHC_6H_5$	94
(Id)	$-(CH_2)_2-COOH$	69
(Ie)	$-o-C_6H_4-COOH$	55*

* IIIe was not isolated but subsequently treated with phenyl isocyanate to give *N*-phenylphthalimide (VIII) in a 55% yield.

In the case of succinic anhydride (Id), IIId was very hygroscopic and identified as its acylurea derivative (VI) by treating with phenyl isocyanate

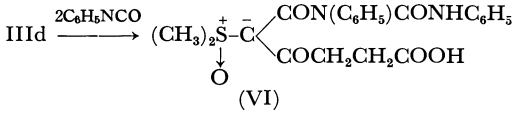

(VI)

(VII). On the other hand, when the mixture resulted from the reaction of Ie and II was treated with VII, *N*-phenylphthalimide (VIII) was produced with evolution of carbon dioxide.

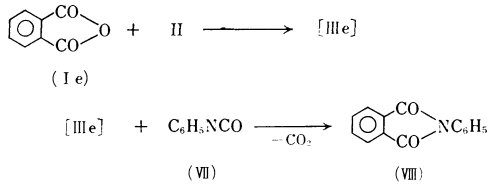

Several attempts to convert III into IV were unsuccessful (See Experimental).

The reaction of phenyl isocyanate dimer (IX) with dimethylsulfoniummethylide (X) was carried out at −15°C, and dimethylsulfonium-bis(phenylcarbamoyl)-methylide (XI), dimethylsulfonium-1,3-diphenylbarbiturylide (XII)[6] and 1,3-diphenylurea (XIII) were obtained in 15, 4 and 16% yields, respectively.

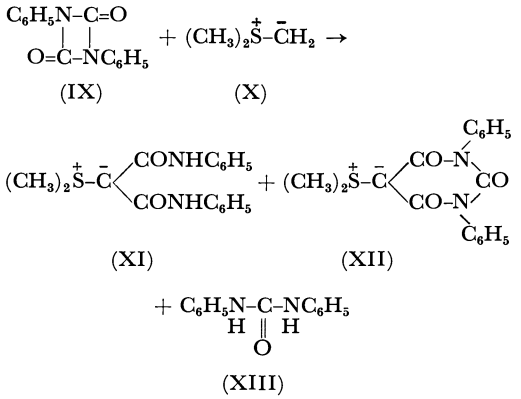

It seems reasonable to consider that the reaction proceeds *via* such two ylide intermediates as sketched below.

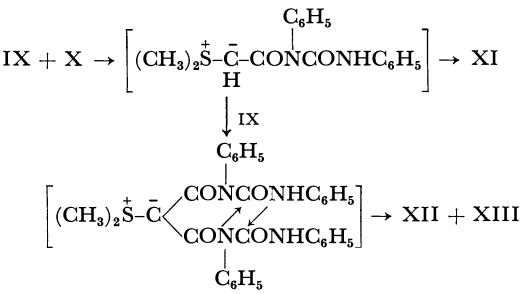

When XI was heated[7] at 160—170°C in a sealed tube, 1,3-diphenylhydantoin (XIV) was obtained with elimination of dimethyl sulfide probably

3) P. T. Izzo, *J. Org. Chem.*, **28**, 1713 (1963).
4) H. König and H. Metzger, *Chem. Ber.*, **98**, 3733 (1965).
5) J. C. Sheehan and J. H. Beeson, *J. Amer. Chem. Soc.*, **89**, 362 (1967).
6) a) R. Gompper and H. Euchner, *Chem. Ber.*, **99**, 527 (1966). b) A. Hochrainer, *Monatsh. Chem.*, **97**, 1 and 823 (1966).
7) C. Kaiser, B. M. Trost, J. Beeson and J. Neinstock, *J. Org. Chem.*, **30**, 3972 (1965).

through a betain intermediate (XV), which decomposed to give XIV by an intramolecular nucleophilic displacement.

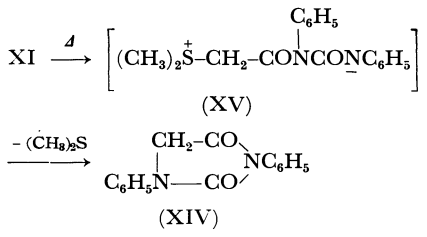

(XV)

(XIV)

The result indicates that IX was transformed into XIV accompanied with ring expansion *via* XI. In addition, it was found that the intermediate XI was easily obtained from X and two moles of VII. Thus, it will be possible to obtain hydantoin derivatives directly from two moles of isocyanates and sulfur ylides through such intermediates as XV.

Based on the above assumption, the reactions of VII with stable sulfonium ylides having no proton on the ylide carbon atom, *e. g.*, dimethylsulfonium-α-methylphenacylide (XVIa), were investigated. When XVIa was treated in dimethyl sulfoxide (DMSO) with two moles of VII at 70°C, 1,3-diphenyl-5-benzoyl-5-methylhydantoin (XVIIa)[9] was obtained with evolution of dimethyl sulfide, as expected.

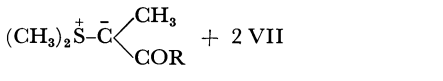

(XVI)

a, R=C_6H_5
b, R=CH_3

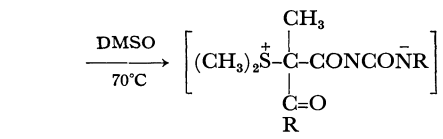

(XXIII)

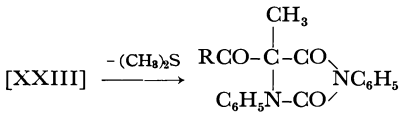

(XVII)

a, R=C_6H_5 52%
b, R=CH_3 49%

On the other hand, when the same reaction of XVIa with VII was carried out in benzene, evolution of dimethyl sulfide was not observed and α-methyl-β-methylthiomethoxy-β-phenylacrylanilide (XVIIIa) was obtained in a good yield along with the recovery of one mole of VII.

The structural assignment was made on the basis

XVIa + RNCO

R=C_6H_5 (VII)
R=C_2H_5
R=c-C_6H_{11}

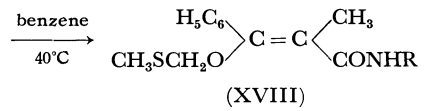

(XVIII)

a, R=C_6H_5 73%
b, R=C_2H_5 86%
c, R=c-C_6H_{11} 80%

of elemental analyses and IR, NMR and mass spectra. The configuration about the carbon-carbon double bond is still not determined, but it is suggested that phenylcarbamoyl and phenyl groups have *trans* relationship because of bulkiness of these two groups.

In a similar manner, reactions of XVIa with ethyl and cyclohexyl isocyanates gave XVIIIb and XVIIIc, respectively.

The reaction is considered to proceed through a 1,4-betaine (XIX), which changed to an ylide intermediate (XX) by a proton transfer. The XX in turn undergoes the rearrangement reported by Ruiz[9] and by Ratts and Yao[10] to give XVIII.

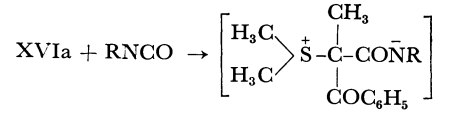

(XIX)

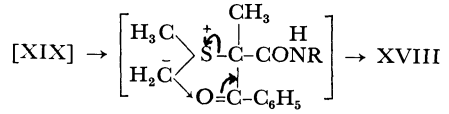

(XX)

The difference in the reaction course between the two reactions mentioned above can be explained by considering that the intermediate XIX, formed from XVI and one mole of isocyanate, reacts rapidly with another mole of isocyanate in DMSO to give a 1,6-betaine (XXIII) (path a), and that, in benzene, the formation of XX from XIX by an intramolecular proton transfer proceeds more rapidly (path b) than that of XXIII.

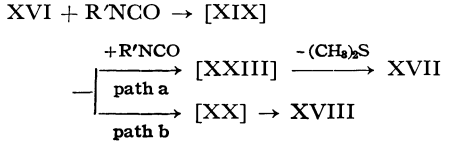

8) F. Ramirez, S. B. Bhatia and C. P. Smith, *J. Amer. Chem. Soc.*, **89**, 3030 (1967).

9) E. B. Ruiz, *Acta Salmenticensia, Ser. cienc.*, **2**, 64 (1958); *Chem. Abstr.*, **54**, 7623 (1960).

10) K. W. Ratts and A. N. Yao, *J. Org. Chem.*, **33**, 70 (1968).

It was found that XVIIIa obtained by the above reaction gave *p*-methylthiomethylanisole (XXI) in a 38% yield along with α-benzoylpropionanilide (XXII) by heating at 60°C with excess anisole in the presence of a catalytic amount of boron trifluoride etherate.

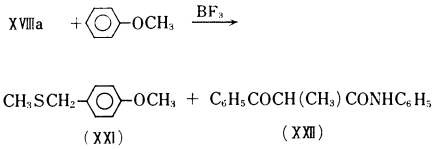

Experimental

Most of these reactions were carried out in the atmosphere of dry nitrogen. All melting and boiling points are uncorrected.

Reaction of β-Propiolactone (Ia) with Dimethyloxosulfoniummethylide (II). To a solution of II (25 mmol) in 40 m*l* of dry tetrahydrofuran (THF), a solution of Ia (1.80 g, 25 mmol) in 18 m*l* of dry THF was added over a period of 10 min with stirring at −15°C. An exothermic reaction soon took place to give a semi-crystalline mush, which, after warming at 50—60°C for 4 hr, afforded 3.80 g (in a 93% yield) of dimethyloxosulfonium-ω-hydroxypropionylmethylide (IIIa), mp 94.5—95.5°C (recrystallized from ethyl acetate). Found: C, 44.09; H, 7.70; S, 19.48%. Calcd for $C_6H_{12}O_3S$: C, 43,90; H, 7.37; S, 19.49%. IR (KBr): 3380, 1030 (OH); 1552 (C=O); 1172 cm^{-1} (S→O). NMR (DMSO-d_6): δ=2.20 (2H, t, CH_2–CO), 3.43 (6H, s, $2CH_3$), 3.62 (2H, t, CH_2–O), 4.40 (1H, s, OH), and 4.78 (1H, s, CH).

In a similar manner, dimethyloxosulfonium-ω-hydroxybutyrylmethylide (IIIb) was obtained from γ-butyrolactone (Ib) and II in a quantitative yield, mp 55—67°C (ethyl acetate). Found: C, 46.91; H, 8.28%. Calcd for $C_7H_{14}O_3S$: C, 47.18; H, 7.96%. IR (KBr): 3400, 1030 (OH); 1552 (C=O); 1172 cm^{-1} (S→O). IIIb was very hygroscopic and decomposed slowly even when stored in a desiccator over phosphorus pentoxide.

Attempts to Obtain IVa from IIIa. *1) Thermolysis of IIIa.* When 0.82 g (5.0 mmol) of IIIa was heated in a distilling flask under reduced pressure, decomposition started at 215°C and 0.27 g (70%) of dimethyl sulfoxide (DMSO) was distilled out. The resulting black tar prevented further purification.

2) Reaction of IIIa with Cupric Chloride.[11] A mixture of IIIa (1.00 g, 6.1 mmol) and anhydrous cupric chloride (0.82 g, 6.1 mmol) in 20 m*l* of dry dioxane was heated at 90°C for 1.5 hr to give dark brown resinous material which prevented further purification.

3) Reaction of IIIa with Triphenyl Phosphite.[12] When 1.64 g (10 mmol) of IIIa was heated in a distilling flask with 3.10 g (10 mmol) of triphenyl phosphite, a vigorous reaction took place at the bath temperature of 120°C. After cooling, 0.84 g (90%) of phenol was distilled from the reaction mixture. The expected IVa (lit. bp 137—138°C) was not obtained.

Reaction of *N*-Phenylsuccinimide (Ic) with II. To a solution of II (10 mmol) in 35 m*l* of dry THF, a solution of Ic (1.75 g, 10 mmol) in 30 m*l* of dry THF was added at room temperature with stirring. After stirring for 2 hr, followed by refluxing for 2 hr, the solvent was evaporated. The residue was recrystallized from benzene to give dimethyloxosulfonium-ω-phenylcarbamoylpropionylmethylide (IIIc), 2.52 g (94%), mp 131.5°C. Found: C, 58.27; H, 6.16; N, 5.17%. Calcd for $C_{13}H_{17}NO_3S$: C, 58.42; H, 6.41; N, 5.24%. IR (Nujol): 3320 (NH); 1660, 1534, 1294, 1254 (–CO–NH–); 1572 cm^{-1} (C=O).

Thermolysis of IIIc. When 0.82 g (3 mmol) of IIIc was heated in a distilling flask under reduced pressure, decomposition occurred at the bath temperature of 180°C and DMSO was distilled out, bp 75—76°C/11 mmHg, 0.23 g (quantitative yield). The resulting solid was recrystallized from ethanol to give Ic, 0.29 g (53%), mp and mmp 154°C.

Reaction of Succinic Anhydride (Id) with II. A solution of Id (1.00 g, 10 mmol) in 24 m*l* of dry THF was added to a solution of II (10 mmol) in 35 m*l* of dry THF over a period of 30 min with stirring at −15°C. The reaction started at once with evolution of heat to afford colorless precipitates. After stirring for 1.5 hr with the cooling bath removed, the precipitates were filtered and washed with dry THF. The resulting precipitates were very hygroscopic and prevented further purification. However, they were identified as dimethyloxosulfonium-ω-carboxypropionylmethylide (IIId), 1.30 g (69%), by the following manner. Thus, to a suspension of IIId in dry THF prepared from Id (10 mmol) and II (10 mmol) by the method described above, a solution of phenyl isocyanate (VII) (1.19 g, 10 mmol) in 30 m*l* of dry dioxane was added dropwise. The reaction mixture turned to a clear solution by warming at 30—60°C for 2 hr. After removal of the solvents, the resulting colorless solid was submitted to a silica gel column to afford 1,3-diphenylurea (XIII), 0.42 g (40%), and dimethyloxosulfonium-ω-carboxypropionyl-(2,4-diphenylallophanyl)-methylide (VI), 0.35 g (17%), mp 135—136°C (benzene). Found: C, 58.92; H, 5.13; N, 6.27%. Calcd for $C_{21}H_{22}N_2O_6S$: C, 58.60; H, 5.15; N, 6.51%. IR (KBr): 3320 (NH); 1700 (COOH); 1667 (C=O); 1614, 1545 cm^{-1} (C=O).

Reaction of Phthalic Anhydride (Ie) and II. When a solution of Ie (1.26 g, 8.5 mmol) in 25 m*l* of dry THF was added dropwise to a solution of I (8.5 mmol) in 32 m*l* of dry THF with stirring at −15°C, the reaction soon took place to give colorless precipitates, to which, after stirring for 2 hr with the cooling bath removed, VII (1.01 g, 8.5 mmol) in 20 m*l* of dry dioxane was added dropwise at room temperature. The mixture was stirred at 60—70°C for 3 hr and turned to a clear solution. During the time, 145 m*l* (15°C, 760 mmHg) of carbon dioxide (76%) was evolved. The solvents were evaporated and the residue was recrystallized from methanol to give *N*-phenylphthalimide (VIII), 1.05 g (55%), mp 205.5—206.5°C.

Reaction of Phenyl Isocyanate Dimer (IX) with Dimethylsulfoniummethylide (X). A solution of IX (2.14 g, 9.0 mmol) in 75 m*l* of dry THF was added to a solution of X (10 mmol) in dry DMSO with stirring at −15°C. Stirring was continued for 40 min, followed by an additional two hours' stirring with the cooling bath removed. The reaction mixture was poured into

11) J. Selbin, W. E. Bull and L. H. Holmes, Jr., *J. Inorg. Nucl. Chem.*, **16**, 219 (1961).

12) E. H. Amonoo-Neizer, S. K. Ray, R. A. Shaw and B. C. Smith, *J. Chem. Soc.*, **1965**, 4296.

200 ml of cold water, and the suspension was extracted with three 80 ml portions of ether, and then with three 100 ml portions of chloroform. The ethereal extract was dried over anhydrous sodium sulfate and the solvent was evaporated to give slight yellow crystals, to which a small amount of dichloromethane was added. The undissolved crystals were filtered, washed and recrystallized from ethanol to give XIII, 0.30 g (16%), mp 238°C (dec.). The filtrate was chromatographed over silica gel. Elution with dichloromethane gave dimethylsulfonium-bis(phenylcarbamoyl)-methylide (XI), 0.43 g (15%), mp 165°C (dec.) (benzene). IR (KBr): 3290, 1632, 1570, 1530, and 1510 cm^{-1}. NMR ($CDCl_3$): τ=6.95 (6H, s, $2CH_3$) and 2.45—3.00 (12H, m, $2C_6H_5$ and 2NH). The chloroform extract was dried over anhydrous sodium sulfate and the solvent was removed under reduced pressure. The resulting red-brown oil was chromatographed over silica gel. By elution with methylene chloride, dimethylsulfonium-1,3-diphenylbarbiturylide (XII) was obtained, 0.06 g (4%), mp 289°C (dec.) (methanol). Found: C, 63.50; H, 4.74; N, 8.49; S, 9.78%. Calcd for $C_{18}H_{16}N_2O_3S$: C, 63.52; H, 4.74; N, 8.23; S, 9.40%. IR (KBr): 3020, 1705, 1640, 1610, and 1595 cm^{-1}.

Thermolysis of XI. When XI (1.50 g) was heated in a sealed tube at 160—170°C for 2 hr, formation of dimethyl sulfide was observed by its characteristic odour. The resulting slight yellow solid was dissolved in a small amount of dichloromethane and chromatographed over silica gel to give 1,3-diphenylhydantoin (XIV), 0.15 g (13%), mp 137.0—137.5°C (ligroin). Found: C, 71.45; H, 4.99; N, 11.43%. Calcd for $C_{15}H_{12}N_2O_2$: C, 71.41; H, 4.80; N, 11.11%.

Reaction with VII and X. To a solution of X (30 mmol) in dry DMSO, a solution of VII (3.57 g, 30 mmol) in 10 ml of dry THF was added with stirring at −15°C. An exothermic reaction started at once. After stirring for 50 min with the cooling bath removed, the reaction mixture was treated in the same way as described for the reaction of IX and X to give XI (26%), XII (10%) and XIII (4%). From the water layer, kept standing after extraction with ether and chloroform, colorless precipitates were deposited, which were recrystallized from ligroin and identified as XIV, 0.17 g (5%).

In a similar way, the reaction of X with 2 mol of VII gave XI, XII and XIII in 32, 22 and 23% yields, respectively. The reaction of X with 4 mol of VII also gave XII (24%) and XIII (22%).

Reaction of Dimethylsulfonium-α-methylphenacylide (XVIa) with 2 mol of VII in DMSO. XVIa,b were newly prepared from the corresponding bromides by a method similar to that described for the preparation of dimethylsulfoniumcarbethoxymethylide.[13] To a suspension of XVIa (0.97 g, 5 mmol) in 18 ml of dry DMSO, VII (1.19 g, 10 mmol) was added portionwise. The mixture was stirred for a while, and then turned to a clear solution. When the solution was heated at 70°C, evolution of dimethyl sulfide was observed. After heating for 6 hr, the solvent was removed under reduced pressure at 50°C to give a slight yellow viscous oil, which was chromatographed over silica gel. Elution with benzene afforded XIII, 0.45 g (43%), and 1,3-diphenyl-5-benzoyl-5-methylhydantoin (XVIIa), 0.97 g (52%), mp 138.5—140°C (ligroin). Found: C, 74.84; H, 4.84; N, 7.72%. Calcd for $C_{23}H_{18}N_2O_3$: C, 74.58; H, 4.90; N, 7.56%. IR (KBr): 1775, 1716, and 1685 cm^{-1}. NMR ($CDCl_3$): τ=8.16 (3H, s, CH_3) and 2.15—2.90 (15H, m, $3C_6H_5$).

Similarly, 1,3-diphenyl-5-acetyl-5-methylhydantoin (XVIIb),[8] mp 135—137°C (ligroin), was obtained from XVIb and 2 mol of VII in a 49% yield along with XIII (24%). Found: C, 70.22; H, 4.90; N, 9.11%. Calcd for $C_{18}H_{16}N_2O_3$: C, 70.11; H, 5.23; N, 9.09%. IR (KBr): 1780 and 1720 cm^{-1}.

Reaction of XVIa with 1 mol of VII in Benzene. When 0.60 g (5.0 mmol) of VII was added portionwise to a suspension of XVIa (0.97 g, 5. 0mmol) in 20 ml of dry benzene, an exothermic reaction took place and the mixture turned into a clear solution. The solution was warmed at 40°C for 4 hr and the solvent was removed *in vacuo*. The residue was chromatographed over silica gel. Elution with benzene gave 1.13 g (73%) of α-methyl-β-methylthiomethoxy-β-phenylacrylanilide (XVIIIa), mp 118.5—119°C (ligroin). Found: C, 69.25; H, 5.85; N, 4.32; S, 10.11%. Calcd for $C_{18}H_{19}NSO_2$: C, 68.99; H, 6.11; N, 4.47; S, 10.22%. IR (KBr): 3300, 1640, 1535, 1340, and 1112 cm^{-1}. NMR ($CDCl_3$): τ=8.16 (3H, s, CH_3–C), 7.86 (3H, s, CH_3–S), 5.28 (2H, s, S–CH_2–O), 2.20—3.05 (10H, m, $2C_6H_5$), and 0.24 (1H, s, NH). Mass: *m/e* 251, 222, 146, 119, 105, and 77.

In a similar manner, *N*-ethyl- and *N*-cyclohexyl-α-methyl-β-methylthiomethoxy-β-phenylacrylamide, (XVIIIb) and (XVIIIc), were obtained by the reactions of XVIa with ethyl and cyclohexyl isocyanates, respectively. XVIIIb (in an 80% yield), mp 77—78°C (petroleum ether). Found: C, 67.50; H, 8.10; N, 4.35; S, 9.99%. Calcd for $C_{18}H_{25}NO_2S$: C, 67.69; H, 7.89; N, 4.39; S, 10.02%. XVIIIc (in an 86% yield), bp 141.0°C/0.073 mmHg. Found: C, 63.37; H, 7.13; N, 5.29; S, 11.83%. Calcd for $C_{14}H_{19}NO_2S$: C, 63.38; H, 7.22; N, 5.28; S, 12.06%.

Reaction of XVIIIa with Anisole. To a solution of XVIIIa (1.57 g, 5.0 mmol) in 25 ml of anisole, several drops of boron trifluoride etherate were added. Evolution of heat was observed and the color of the solution turned slightly yellow. After stirring for 1.5 hr at room temperature, followed by warming at 60°C for 6 hr, anisole was evaporated and dry ether was added to the residue to precipitate α-benzoylpropionanilide (XXII), 0.70 g (67%), mp 137.0—138.5°C (benzene). Found: N, 5.53%. Calcd for $C_{16}H_{15}NO_2$: N, 5.58%. From the filtrate, *p*-methylthiomethylanisole (XXI) was obtained, 0.31 g (38%), bp 80—81°C/1.6 mmHg. Found: C, 63.98; H, 7.43; S, 18.83%. Calcd for $C_9H_{12}OS$: C, 64.27; H, 7.19; S, 19.03%. NMR ($CDCl_3$): τ=8.08 (3H, s, CH_3–S), 6.43 (2H, s, $-CH_2-$), 6.28 (3H, s, CH_3–O), 3.22 and 2.85 (4H, a pair of doublets with a coupling constant of 8.5 Hz, $-C_6H_4-$).

13) G. B. Payne, *J. Org. Chem.*, **32**, 3351 (1967).

BULLETIN OF THE CHEMICAL SOCIETY OF JAPAN VOL. 43 2571—2574 (1970)

Studies on Pyrophosphates. I. A Selective Degradation of Pyrophosphates by Means of 2,6-Dichloroquinone *N*-Chloroimide

Kyu-Jang CHONG, Sheng-Shung PONG and Tsujiaki HATA

Department of Chemistry, Tokyo Institute of Technology, Ookayama, Meguro-ku, Tokyo

(Received February 19, 1970)

Reaction of P^1,P^2-dialkyl pyrophosphate with alcohols or water in the presence of 2,6-dichloroquinone *N*-chloroimide (CQC) was studied. It was found that alkyl *p*-nitrophenyl phosphates are obtained in high yields by treating P^1,P^2-di-*p*-nitrophenyl pyrophosphate with alcohols in the presence of CQC. Similarly, alkyl phosphates are selectively produced by the reaction of P^1,P^2-dialkyl pyrophosphates with water in the presence of CQC. These reactions afford a new procedure for the selective degradation of P^1,P^2-dialkyl pyrophosphates, especially nucleoside pyrophosphates.

The method of phosphorylation with the use of tetraalkyl pyrophosphates (**1**) is a versatile one[1-3] that has been applied to nucleotide synthesis.[4]

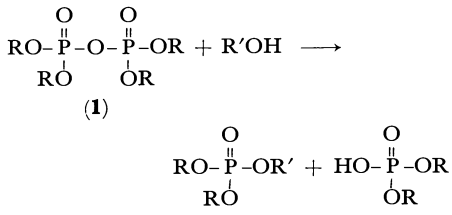

However, only a few studies[5-7] have been reported on P^1,P^2-dialkyl pyrophosphates (**3**) as applied to the phosphorylation of alcohols, since pyrophosphates (**3**) are generally unreactive compared with tetraalkyl pyrophosphates (**1**).

In the present study, phosphorylation of alcohols with P^1,P^2-dialkyl pyrophosphates (**3**) and 2,6-dichloroquinone *N*-chloroimide (CQC) was investigated.

It was found that P^1,P^2-di-*p*-nitrophenyl pyrophosphate (**3a**) was obtained in high yield by treating CQC with *p*-nitrophenyl phosphate (**2a**) in dry pyridine at room temperature for 5 hr.

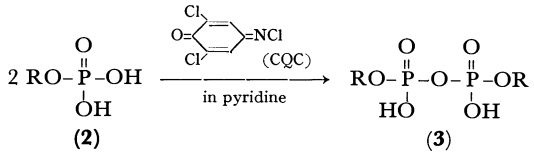

2a and **3a**, R=*p*-nitrophenyl

This result suggests that CQC participates in the activation of *p*-nitrophenyl phosphate (**2a**), which leads us to surmise that it would be used as an active condensating reagent for the preparation of diesters of phosphoric acid (**4**) from **2a** and alcohols. When a mixture of 1 equiv. of **2a** and *n*-octanol in dry pyridine was treated with 3 equiv. of CQC at room temperature for 19 hr, *n*-octyl *p*-nitrophenyl phosphate (**4f**) and **3a** were produced in 15% and 77% yields, respectively.

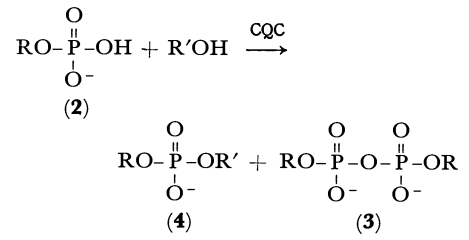

After being kept standing for several days, **3a** decreased significantly and **4f** was obtained as the main product. This indicates that **3a**, initially formed, further reacts with CQC to yield an intermediate (**5**), which in turn reacts with alcohol to give a diester of phosphoric acid (**4**) and *p*-nitrophenyl 2,6-dichloroquinoneoxime phosphate (**6**). **6** thus formed also reacts with another alcohol to yield **4** and 2,6-dichloroquinone oxime (**7**).

1) H. S. Mason and A. R. Todd, *J. Chem. Soc.*, **1951**, 2267.
2) G. O. Dudek and F. H. Westheimer, *J. Amer. Chem. Soc.*, **81**, 2641 (1959).
3) J. G. Moffatt and H. G. Khorana, *ibid.*, **79**, 3741 (1957).
4) R. W. Chambers, J. G. Moffatt and H. G. Khorana, *ibid.*, **79**, 3747 (1957).
5) F. Cramer and H. J. Baldauf, *Angew. Chem.*, **72**, 627 (1960).
6) F. Cramer and K. H. Scheit, *Chem. Ber.*, **95**, 1657 (1962).
7) M. Smith, G. I. Drummond and H. G. Khorana, *J. Amer. Chem. Soc.*, **83**, 698 (1961).

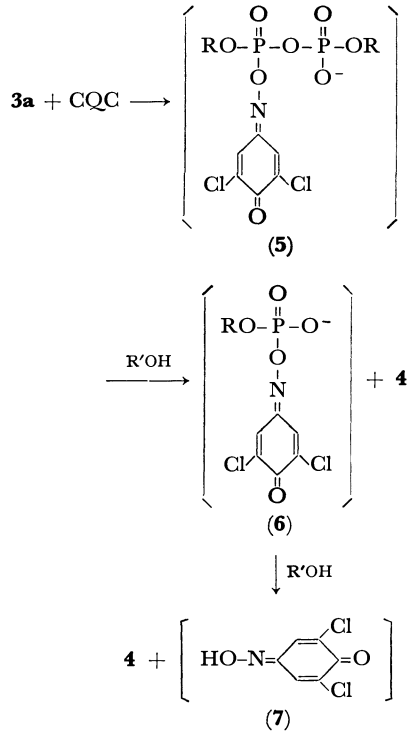

Based on the above mechanism, phosphorylation of alcohols with the use of CQC and P¹,P²-di-*p*-nitrophenyl pyrophosphate (**3a**), obtained from *p*-nitrophenyl phosphate (**2a**) and dicyclohexylcarbodiimide, was tried.

When a mixture of 3 equiv. of CQC and 1 equiv. of **3a** in methanol was heated at 100°C for 2 hr, methyl *p*-nitrophenyl phosphate (**4a**) was obtained in 91% yield, as expected.

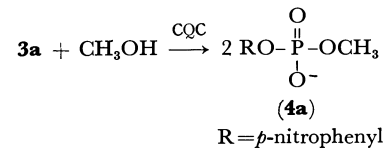

R=*p*-nitrophenyl

This shows that the pyrophosphate can be effectively used as a phosphorylating reagent when it is treated with CQC. By this method, several alkyl *p*-nitrophenyl phosphates (**4**) were obtained in high yields from the corresponding alcohols as shown in Table 1. In the cases of *n*-octanol and *n*-hexadecanol, **2a** was produced as a by-product probably by way of a direct nucleophilic attack of alkoxide anion on phosphorus atom of **3a** to give **2a** and **4**.

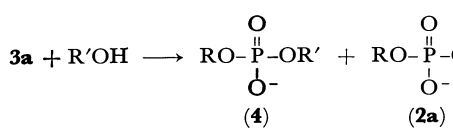

R=*p*-nitrophenyl

Table 1. Preparation of alkyl *p*-nitrophenyl phosphate (**4**)

No.	alkyl (R)	yield (%)	R_f value
4a	methyl	91	0.75
4b	ethyl	85	0.76
4c	*n*-propyl	82	0.81
4d	*n*-butyl	93	0.82
4e	*n*-pentyl	72	0.85
4f	*n*-octyl	65	0.91
4g	*n*-hexadecyl	59	0.92

Solvent system: isopropyl alcohol : conc. ammonia : water=8 : 1 : 1 (v/v)

A nucleoside pyrophosphate, P¹,P²-di-thymidine 5′-pyrophosphate (**8a**) was also degradated in methanol to methyl thymidine 5′-phosphate and thymidine 5′-phosphate by treating with CQC.

A further study to extend the reaction for a selective hydrolysis of the pyrophosphates was carried out with the assumption that 2 mol of alkyl phosphate (**2**) is exclusively produced, when **3** is treated with water in place of alcohols in the above reaction.[8]

When a mixture of 1 equiv. of **3a** and 3 equiv. of CQC in aqueous pyridine was heated at 100°C for 2 hr, **2a** was exclusively obtained in 95% yield as expected. This non-enzymatic method can be applied to the hydrolysis of nucleoside pyrophosphates such as thymidine-, uridine-, adenosine-, guanosine-, and cytidine-pyrophosphate. These results are summarized in Table 2.

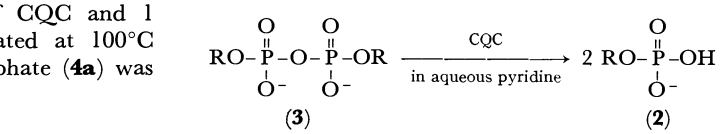

In the above reactions, six coloured substances were always detected by paper chromatography. All of the compounds contain no phosphate group and seem to be derivatives of CQC. Failure to isolate and identify the coloured substances makes the interpretation of the reaction mechanism more difficult.

Experimental

General Methods. Paper chromatography was carried out by the descending technique using Toyo Roshi No. 51 and No. 51A papers. The solvents used were isopropyl alcohol-concentrated ammonia - water (7 : 1 : 2 v/v) (Solvent A), or (8 : 1 : 1 v/v) (Solvent B) and isoamyl alcohol-5% disodium hydrogen phosphate (1 : 1 v/v) (Solvent C). The R_f values of different compounds are given in Tables 1 and 2. Except for

8) In general, on hydrolysis in aqueous alkali solution, P¹,P²-dialkyl pyrophosphate does not afford the single phosphate (**2**), but inorganic phosphate, pyrophosphoric acid and alcohol are always contaminated.

Table 2. Hydrolysis of P^1, P^2-di-nucleoside 5′-pyrophosphates (**8**)

No.	Pyrophosphate (NppN)	(μmol)	CQC (mM)	Mixed solvent (ml)	Product: Yield of phosphate (pN) (%)	Product: R_f value*	Product: pN/NppN***
8a	Di-thymidine(5′)	4.4	0.1	DMF(2) water (0.05)	80	0.10	0.89
8b	Di-uridine(5′)	5.5	0.1	DMF(2) water (0.05)	72	0.05	0.76
8c	Di-adenosine(5′)	3.5	0.1	pyridine(1.75) DMF (1.75) water (0.05)	77	0.71**	0.72
8d	Di-N^6,*O*,*O*-tribenzoyl guanosine(5′)	19.0	0.25	pyridine(8) water(0.1)	32	0.07	0.74
8e	Di-cytidine(5′)	16.0	0.1	pyridine(8) DMF (2.4) water (1.6)	41	0.08	0.75

* Development with Solvent A.
** Development with Solvent C.
*** Mobility relative to the corresponding pyrophosphate.

the use of Solvent C, phosphorus compounds were made visible on paper chromatograms after spraying the chromatograms with the Isherwood Reagent[9] and exposing them to ultraviolet lamp. The ε_{max} value at 290 mμ used for alkyl *p*-nitrophenyl phosphates (**4**) was 10000 (pH : 7). Paper electrophoresis was carried out in an apparatus in which the paper was immersed in carbon tetrachloride. The buffers used were phosphate 0.05M KH_2PO_4 (pH 6, pH 7 and pH 8).

Materials. 2,6-Dichloroquinone *N*-chloroimide was a commercial sample (Tokyo Kasei Co., Tokyo, Japan). Alcohols and pyridine were purified and dried by ordinary procedures. *N*-Benzoyl guanosine 5′-phosphate,[7] *N*-benzoyl cytidine 5′-phosphate,[7] P^1,P^2-dithymidine 5′-pyrophospate (TppT),[11,12] P^1,P^2-di-adenosine 5′-pyrophosphate (AppA)[7] and P^1,P^2-di-uridine 5′-pyrophosphate (UppU)[10] were prepared by the procedures in literature. P^1,P^2-Di-*p*-nitrophenyl pyrophosphate (**3a**), P^1,P^2-di-*N*-benzoyl guanosine pyrophosphate ($G^{Bz}ppG^{Bz}$) and P^1,P^2-di-*N*-benzoyl cytidine pyrophosphate ($C^{Bz}ppC^{Bz}$) were prepared by a modification of Khorana's method[7,11] as described below.

P^1,P^2-Di-*p*-nitrophenyl Pyrophosphate. To a solution of *p*-nitrophenyl phosphate (**2a**) (0.438 g, 0.2 mM) in dry pyridine (5 ml) was added dicyclohexylcarbodiimide (0.247 g, 1.2 mM). To the mixture, after being stirred for 2 hr at room temperature, was added 1 ml of water. Stirring was continued for 1 hr at room temperature. A white precipitate, dicyclohexylurea, was filtered and washed with water. The filtrate and the washings were combined and concentrated under reduced pressure at a temperature below 40°C.

Evaporation was then repeated twice or three times with pyridine.

The flask was kept standing in a refrigerator overnight to afford P^1,P^2-di-*p*-nitrophenyl pyrophosphate (0.550 g, 95%) as a white powder: mp 166—167°C (di-pyridinium salt).

Found: C, 45.86; H, 3.59; N, 9.90. Calcd for $C_{22}H_{20}O_{11}N_4P_2$: C, 45.67; H, 3.46; N, 9.70%; mol wt, 578.

P^1,P^2-Di-*N*-benzoyl Guanosine 5′-Pyrophosphate ($G^{Bz}ppG^{Bz}$). *N*-Benzoyl guanosine 5′-phosphate (0.056 mM)[7] was rendered anhydrous by three repeated evaporations of 4 ml of dry pyridine. A gummy *N*-benzoyl quanosine 5′-phosphate was dissolved in 10 ml of dry pyridine and dicyclohexylcarbodiimide (35 mg) was then added. The reaction mixture was heated at 100° for 20 min and allowed to stand at room temperature overnight. The precipitate was filtered and washed with pyridine. The filtrate and the washings were combined and evaporated to dryness. White powder, thus obtained, was dissolved in 15 ml of water. The aqueous solution was washed with four portions of 20 ml of petroleum ether. The aqueous layer was treated with 2 ml of pyridine and evaporated to dryness. White powder was obtained and dry pyridine was added. The precipitate was filtered and washed with pyridine. The filtrate was evaporated to dryness. P^1,P^2-Di-*N*-benzoyl guanosine 5′-pyrophosphate (0.019 mM, 38%) was obtained as syrupy substance which was chromatographically pure. The yield was estimated spectrophotometrically. $\lambda_{max}^{H_2O}$ 292 mμ (ε : 16200), $\lambda_{max}^{H_2O}$ 259 mμ, $\lambda_{max}^{H_2O}$ 278 mμ.

P^1,P^2-Di-*N*-benzoyl Cytidine 5′-Pyrophosphate (CppC). *N*-Benzoyl cytidine 5′-phosphate[7] (0.046 mM) and 4-morpholine-*N*,*N*′-dicyclohexylcarboxamidine(13.5 mg) were dissolved in 10 ml of pyridine under anhydrous conditions at 100°C. After addition of dicyclohexylcarbodiimide (25 mg, 0.12 mM), the mixture was kept at 100°C for 10 min and was allowed to stand at room temperature for 1 day. After removal of pyridine, 10 ml of water was added. The gel was filtered and washed with three portions of petroleum ether. The aqueous layer was concentrated to dryness. The gummy residue was dissolved in 0.5 ml of ethanol and treated

9) C. S. Hanes and F. A. Isherwood, *Nature*, **164**, 1107 (1949).
10) M. Smith, J. G. Moffatt and H. G. Khorana, *J. Amer. Chem. Soc.*, **80**, 6204 (1958).
11) H. G. Kohrana and J. P. Vizsolyi, *ibid.*, **81**, 4660 (1959).
12) M. W. Moon and H. G. Khorana, *ibid.*, **88**, 1798 (1966).

with 1 m*l* of concentrated ammonium hydroxide. The mixture was allowed to stand at room temperature for 3 days. A white precipitate appeared and the suspension was treated with 2 m*l* of pyridine. After removal of solvent, the residue was dissolved in 3 m*l* of water and neutralized with Dowex 50W-X8 (pyridinium form). The resin was filtered and washed thoroughly with water. The filtrate and the washings were concentrated to a small volume. Electrophoresis showed that the product contained almost pure P^1,P^2-di-cytidine 5′-pyrophosphate. The solution was passed through a column (45 cm × 2 cm dia.) of commercially available diethylaminoethyl cellulose (DEAE) (bicarbonate form), elution being carried out with a linear salt gradient, 1*l* of water and 1*l* of 0.05M triethylammonium bicarbonate in a reservoir. About 15 m*l* fractions were collected every 10 min. Fractions 47—56 contained P^1,P^2-di-cytidine 5′-pyrophosphate. The yield of this product, as estimated spectrophotometrically, was 69%. The product obtained as the triethylammonium salt was converted in to the pyridinium salt by treatment with Dowex 50W-X8 (pyridinium form) and the solution was lyophilized.

Alcoholysis of P^1,P^2-Di-*p*-nitrophenyl Pyrophosphate (3a) in the Presence of CQC. To a solution of **3a** (0.134 g, 0.2 mM) and an alcohol (2 mM) in 20 m*l* of dry pyridine was added CQC (0.132 g, 0.63 mM), and the mixture was heated at 100°C for 2 hr. The solution was concentrated to a syrup, which was washed thoroughly three times with chloroform. The chloroform was combined and evaporated to dryness. The residue was washed three times with benzene. The benzene was evaporated and the residual oil was dissolved in 30 m*l* of water and washed with two portions of 30 m*l* of ether. After removal of water under reduced pressure, chromatographically pure alkyl *p*-nitrophenyl phosphate (**4**) was obtained as shown in Table 1. Estimation of the yield of this product was carried out spectrophotometrically after elution of spot from paper chromatogram run in Solvent A.

Hydrolysis of P^1,P^2-Di-*p*-Nitrophenyl Pyrophosphate (3a) in the Presence of CQC. To a solution of **3a** (0.314 g, 0.2 mM) in aqueous pyridine was added CQC (0.132 g, 0.63 mM), and the mixture was heated at 100°C for 2 hr. *p*-Nitrophenyl phosphate (**2a**) was obtained in 93% yield which was estimated spectrophotometrically after elution of the spot from paper chromatogram run in Solvent A.

Hydrolysis of P^1,P^2-Di-nucleoside 5′-Pyrophosphate in the Presence of CQC. In Table 2 are summarized the reaction under various conditions. A typical procedure is described below.

Hydrolysis of P^1,P^2-Di-adenosine 5′-Pyrophosphate. To a solution of P^1,P^2-di-adenosine 5′-pyrophosphate in 2.5 m*l* of pyridine-dimethylformamide (1 : 1) was added water and then CQC. The mixture was heated on a boiling water bath for 2 hr. Adenosine 5′-phosphate was obtained (see Table 2) which was estimated spectrophotometrically after elution of the spot from Toyo Roshi No. 51A paper run in phosphate buffer (pH 6) by electrophoresis.

We heartily thanks Professor Teruaki Mukaiyama for his encouragement and discussion throughout the investigation. We also wish to thank Mr. Masaru Koezuka for his help with elemental analysis.

BULLETIN OF THE CHEMICAL SOCIETY OF JAPAN VOL. 43 2574—2581 (1970)

Thermal Demercuration Reactions of Organomercurials

Naoki INAMOTO and Masaaki YOSHIFUJI

Department of Chemistry, Faculty of Science, The University of Tokyo, Hongo, Bunkyo-ku, Tokyo

(Received February 23, 1970)

Thermal demercuration reactions of organomercurials (RHgX) alone or with mercuric salts (HgY_2) were performed (where R=*n*-butyl, *s*-butyl, cyclohexyl, benzyl, phenyl, and *p*-tolyl; X,Y=Cl, Br, CN, SCN, and OAc). Alkyl chlorides were obtained in good yields in the cases of alkylmercuric chlorides. The results in the reactions of cyclohexylmercuric halides with mercuric salts suggested the exchange reaction between them. Thermal demercuration reactions of arylmercurials gave the corresponding aromatic hydrocarbons as main product, and their mechanisms which involve generation of aryl radicals were discussed. General mechanisms of demercuration reaction of organomercurials alone were also discussed, and the importance of intermolecular interaction between organic group and chlorine was suggested in the cases of aliphatic organomercuric chlorides.

French, Inamoto and Wright[1] found that mercurous salts are the most effective catalyst for redistribution reaction of the bis-organomercurials. As impure bis-organomercurials redistributed more readily than pure materials, the following mechanism

1) W. E. French, N. Inamoto and G. F Wright, *Can. J. Chem.*, **42**, 2228 (1964).

was postulated for the formation of mercurous salts as a catalyst.

$$RHgR \xrightarrow[\text{peroxide}]{\text{heat or}} R\text{-}R + Hg \quad (1)$$

$$RHgX \rightarrow RX + Hg \quad (2)$$

$$2\ RHgX \rightleftarrows R_2Hg + HgX_2 \quad (3)$$

$$HgX_2 + Hg \rightarrow Hg_2X_2 \quad (4)$$

The reaction (2) has not been reported except for some vinylmercuric salt,[2] although it is well known that organomercuric salts give mercurous salts by thermal decomposition,[3] photolysis,[4-6] or the action of peroxide.[1,7]

$$2\ RHgX \rightarrow 2R\cdot + 2\cdot HgX\ (\rightarrow Hg_2X_2)$$

According to the reactions (2) and (4), the following reaction would be expected to occur.

$$RHgX + HgX_2 \rightarrow RX + Hg_2X_2 \quad (5)$$

Inamoto and Wright[8] carried out the reactions of organomercurials with mercuric salts and obtained the following preliminary results. Reaction of cyclohexylmercuric or *n*-butylmercuric chloride with a slight excess of mercuric chloride at 150—240°C gave cyclohexyl chloride (isolated in 68% yield under reduced pressure) or *n*-butyl chloride (isolated in 40% yield), respectively, and mercurous chloride was produced in nearly quantitative yield in both cases. Therefore, it was proved that the reaction (5) occurs. On the other hand, phenylmercuric or *p*-tolylmercuric chloride gave benzene or toluene (isolated in 20—30% yield by distillation), respectively, instead of the corresponding aryl chloride, under similar conditions, and the yields of mercurous chloride were not quantitative. These results indicate that the reaction of arylmercuric chlorides does not follow the reaction (5). Furthermore, the similar reaction of cyclohexylmercuric bromide with mercuric chloride gave no cyclohexyl bromide but cyclohexyl chloride.

In order to clarify these reactions, we investigated the thermal decompositions of organomercurials alone or with mercuric salts in more detail.

Results and Discussion

Alkylmercuric Chloride, Bromide, and Cyanide. The thermal reaction of *s*-butylmercuric chloride with a slight excess of mercuric chloride at about 260°C for 2 hr gave *s*-butyl chloride in 64% yield after distillation.

Table 1 shows the results on the thermal reactions of the cyclohexylmercuric halide-mercuric halide system. The ratio of cyclohexyl bromide to the chloride increased with the bromine content in the system. The formation of the chloride, moreover, is apparently considered to be more favorable than that of the bromide. This result suggests that an exchange reaction occurs between cyclohexylmercuric halide and mercuric halide. Formation of considerable amount of cyclohexyl bromide in the thermal reaction of cyclohexylmercuric bromide with an insufficient amount of mercuric chloride is presumably attributed to a self-decomposition of an excess cyclohexylmercuric bromide.

Some attention should be given on the de-

Table 1. Thermal reactions of cyclohexylmercuric chloride and cyclohexylmercuric bromide (at 230—265°C, under a pressure of 50 mmHg for 1.5 hr)

C$_6$H$_{11}$-HgX (I) X	HgY_2 (II) Y	II/I mole ratio	Composition of products (mol %) C$_6$H$_{11}$-Cl	C$_6$H$_{11}$-Br	C$_6$H$_{10}$	C$_6$H$_{12}$	Hg[a] (%)	Recovery of R (%)	C$_6$H$_{11}$-HgX recovered (%)
Cl	—	0	61		34	5	67	88	12
Cl	Br	0.25	49	7	39	5	49	97	3
Cl	Br	1.14	55	12	30	3	0	98	1
Cl	Br	3.00	45	21	34	1	0	94	—
Br	Cl	1.18	70	2	27	1	0	100	—
Br	Cl	0.27	26	35	33	7	39	91	4
Br	—	0		35	41	24	24	93	7

a) Yield from RHgX used.

2) E. Tobler and D. J. Foster, *Z. Naturforsch.*, *B*, **17**, 136 (1962).
3) M. M. Koton and F. S. Florinskii, *Zh. Obshch. Khim.*, **9**, 2196 (1939).
4) V. Weinmayr, *J. Amer. Chem. Soc.*, **81**, 3590 (1959).
5) D. H. Hey, D. A. Shingleton and G. H. Williams, *J. Chem. Soc.*, **1963**, 1958.
6) K. Yoshida and S. Tsutsumi, *Tetrahedron Lett.*, **1966**, 281.
7) J. H. Robson and G. F Wright, *Can. J. Chem.*, **38**, 1 (1960).
8) N. Inamoto and G. F Wright, unpublished work; see N. Inamoto, *Nippon Kagaku Zasshi*, **86**, 1223 (1965).

Table 2. Thermal reactions of phenylmercuric chloride and phenylmercuric cyanide (for 1.3 hr)

PhHgX	HgY_2	Temp. (°C)	Composition of products			Hg[a]	Recovery of R
X	Y		PhH	PhCl (mol %)	PhCN	(%)	(%)
Cl	—	300—340	99	1		0.4	35
Cl	Cl	300—320	91	9		0	41
Cl	Cl	260—280	97	3		0	45
Cl	Cl	200—220	~100	0.02		0	46
Cl	CN	310—320	96	1	4	29	48
CN	—	300—340	94		6	62	54
CN	CN	240—265	99.5		0.5	1	30
CN	CN	280—295[b]	99		1	11	48
CN	CN	320—350	95		5	148	26
CN	Cl	300—350	94	3	3	0	50

a) Yield from PhHgX used.
b) Reaction was carried out *in vacuo* in a sealed tube.

mercuration reaction of cyclohexylmercuric chloride or bromide alone as in the following. First, the yield of mercury metal liberated in the latter was smaller than that in the former. Secondly, the yield of cyclohexane from the latter was much larger than that in the former, partly because of the formation of cyclohexyl radicals due to the weaker bond strength of C–Hg in the bromide than that in the chloride,*1 followed by hydrogen abstraction from the surrounding organomercurials. Partial formation of cyclohexyl radicals is evident from the detection of a trace of dicyclohexyl by means of vapor phase chromatography (VPC).

Another pathway of the formation of cyclohexane is a reaction of unchanged cyclohexylmercuric bromide with hydrogen bromide generated by mercuric bromide - catalyzed dehydrobromination of cyclohexyl bromide produced during the reaction,[10] because of facile dehydrobromination of organic bromide. This pathway is considered to be reasonable, because of the formation of a considerable amount of cyclohexene.

The demercuration reaction of cyclohexylmercuric cyanide alone at 240—265°C under reduced pressure gave cyclohexane (4%), cyclohexene (66%), cyclohexyl cyanide (9%), mercury metal (84%), and hydrogen cyanide.

Mechanisms of these demercuration reactions will be discussed later.

Phenylmercuric Chloride, Cyanide, and Thiocyanate. Table 2 shows the results on the thermal reactions of phenylmercuric chloride or cyanide*2 under various conditions. In every case, the main product was benzene (25—50% yields), and the yield of chlorobenzene or/and benzonitrile was very poor, but increased at higher temperatures. The benzene formation can be explained by assuming generation of phenyl radicals, followed by hydrogen abstraction from the surrounding organomercurials. It is confirmed by the presence of diphenyl among the products.

The reaction of phenylmercuric cyanide and mercuric cyanide at 350°C gave a large amount of mercury, which might be attributed to the

Table 3. Thermal reactions of phenylmercuric thiocyanate (for 1.5 hr)

HgY_2	Temp.	Composition of products			Hg[a]	Recovery of R
Y	(°C)	PhH	PhCN (mol %)	PhSCN	(%)	(%)
—	270—300	98	2	0	21	31
SCN	220—290	96	3	1	23	33
CN	210—285	98	1	1	76	40

a) Yield from PhHgSCN used.

*1 *e. g.*, compare the following bond dissociation energy D(R–HgX);[9] D(Et–HgCl) = 60.3 ± 3 and D(Et–HgBr) = 57.6 ± 3 (kcal/mol).

9) H. A. Skinner, in F. G. A. Stone and R. West, "Advances in Organometallic Chemistry," Vol. 2, Academic Press, New York (1964), p. 49.

10) F. Swarts, *Bull. Classe Sci., Acad. Roy. Belg.*, **22**, 784 (1936).

*2 Our present results on the thermal reactions of phenylmercuric cyanide with mercuric cyanide were quite different from those reported by one of the authors (N. I.).[8]

Table 4. Thermal reactions of bis-organomercuries with mercuric salts (for 1 hr)

R_2Hg (III) R	HgX_2 (IV) X	IV/III mole ratio	Temp. (°C)	Composition of products (mol %) RH	RX	Hg (%)	Recovery of R (%)
Ph	Cl	3.30	260—290	91	9	0	66
Ph	CN	2.28	240—290	98	2	1	25
PhC≡C–	CN	2.31	250 (50 mmHg)	98	2	96	14

decomposition of mercuric cyanide at higher temperatures.[11]

Table 3 shows the results on the thermal reactions of phenylmercuric thiocyanate. The main product was also benzene, together with a considerable amount of mercury metal and mercuric sulfide. Phenyl isothiocyanate was not detected. In the demercuration reaction of phenylmercuric thiocyanate alone, no phenyl thiocyanate was obtained.

The demercuration reaction of *p*-tolylmercuric chloride alone gave toluene (47%) as a main product, together with a trace of *p*-tolyl chloride, dibenzyl, di-*p*-tolyl, phenyl-*p*-tolylmethane and mercury metal.

Bis-organomercuries. In order to test the possibility of the reaction (3), the reactions of diphenyl mercury with mercuric salts were carried out (Table 4). The thermal reaction of diphenylmercury with mercuric chloride (or cyanide) gave almost the same products as those of phenylmercuric chloride (or cyanide) with mercuric chloride (or cyanide).

The thermal reaction of bis-phenylethynylmercury with mercuric cyanide was similar to that of diphenylmercury with mercuric cyanide, but mercury liberated was almost quantitative.

Acetoxymercurials. The results of the thermal reactions of acetoxymercurials are summarized in Table 5.

n-Butylmercuric acetate gave metallic mercury in 72% yield, but only a small amount of *n*-butyl acetate (9.6%) was obtained together with a considerable amount of very volatile material, which is supposed to be butane or butene. Other products were acetic acid (24%), a considerable amount of acetic anhydride, and a trace of methyl acetate. In the presence of a slight excess of mercuric acetate, the yield of *n*-butyl acetate was rather small (5%). A considerable amount of very volatile material was also observed in this case.

Benzylmercuric acetate gave metallic mercury in 68% yield, but only a trace of benzyl acetate was formed, together with a considerable amount of dibenzyl and acetic acid and a trace of toluene, acetic anhydride and methyl acetate. In the presence of slight excess of mercuric acetate, the amount of benzyl acetate increased and the amount of dibenzyl decreased.

The demercuration reaction of phenylmercuric acetate alone or with mercuric acetate gave acetic acid, benzene (50%), and a trace of methyl acetate, together with mercury metal. Neither phenyl acetate nor toluene were detected.

In this connection, the thermal reaction of mercuric acetate alone was performed, and the products

Table 5. Thermal reactions of acetoxymercurials (for 1—1.5 hr)

RHgOAc R	HgX_2 X	Temp. (°C)	Products (%) ROAc	RH	AcOH[a]	R–R[b]	Hg[c]	Recovery of R (%)
–	OAc	210—220	—	—	63	—	90	—
n-C_4H_9	—	215—253	10	—	24[d]	—	72	—
n-C_4H_9	OAc	250—258	5	—	56	—	80	—
$PhCH_2$	—	255—260[e]	0.2	1	44[d]	31	68	64
$PhCH_2$	OAc	250—315[e]	18	2	54	8	90	36
Ph	—	180—230	0	52	72	—	66	52
Ph	OAc	180—230	0	48	64	—	26	48

a) Yield based on acetoxy group.
b) Yield based on R group.
c) Yield based on total mercury in the system.
d) Acetic anhydride was also obtained.
e) The reaction was carried out under a pressure of 40 mmHg.

11) J. P. Galvin and H. O. Pritchard, *J. Phys. Chem.*, **68**, 1035 (1964).

Table 6. Thermal reactions of organomercuric salt alone[a)]

RHgX		Temp. (°C)	Products (%)				RHgX recovered (%)
R	X		RX	R(−H)[b)]	RH	Hg	
n-C_4H_9	Br	~245	29.5	—	—	33	12
cyclo-C_6H_{11}	Cl	230—265[c)]	54	30	4	67	13
cyclo-C_6H_{11}	Br	~250[c)]	33	37.5	23	24	7
cyclo-C_6H_{11}	CN	240—265[c)]	9	66	4	84	10
C_6H_5	Cl	300—340	0.4	—	33	0.4	5
C_6H_5	CN	300—340	3.4	—	50	62	3
C_6H_5	SCN	270—300	0.5 (PhCN)	—	30.5	21	2
p-$CH_3C_6H_4$	Cl	285—310	2.4	—	47	4	1

a) Acetates were excluded.
b) Denotes the corresponding olefin.
c) The reaction was carried out under a pressure of 50 mmHg.

were metallic mercury (90%), a large amount of acetic acid and a trace of methyl acetate. Thus the thermal reactions of organomercuric acetate proved to involve the self-decomposition of mercuric acetate itself.

The formations of acetic acid and methyl acetate are reasonably explained by radical mechanism including acetoxy radicals.*3

Mechanisms of Demercuration Reactions. The results on the thermal reactions of organomercuric halides alone are very interesting: although cyclohexylmercuric chloride liberated a large amount of mercury metal and gave cyclohexyl chloride, phenylmercuric and p-tolylmercuric chlorides gave the corresponding aromatic hydrocarbons and only a trace of mercury (Table 6). Moreover, cyclohexylmercuric and n-butylmercuric bromides gave smaller amount of mercury metal than cyclohexylmercuric chloride.

These results show that the appearance of the demercuration reaction depends upon both organic and inorganic groups, and that the demercuration reactions of alkylmercuric halides are different from those of arylmercuric halides.

Three mechanisms are possible for thermal demercuration of organomercuric salt alone.

Mechanism A

$$\text{R–Hg–X} \rightarrow \text{R}\cdot + \cdot\text{HgX} \quad (6)$$

$$\text{R}\cdot + \cdot\text{HgX} \rightarrow \text{RX} + \text{Hg} \quad (7)$$

$$2\cdot\text{HgX} \rightarrow \text{Hg}_2\text{X}_2$$

Mechanism B

$$2\ \text{R–Hg–X} \rightleftarrows \begin{bmatrix} \text{R–Hg–X} \\ \vdots \quad \vdots \\ \text{R—Hg–X} \end{bmatrix} \rightleftarrows \text{R}_2\text{Hg} + \text{HgX}_2 \quad (8)$$

$$\text{R–Hg–R} \rightarrow 2\text{R}\cdot + \text{Hg} \quad (1)$$

$$\text{R}\cdot + \text{HgX}_2 \rightarrow \text{RX} + \cdot\text{HgX} \quad (9)$$

$$\text{Hg} + \text{HgX}_2 \rightarrow \text{Hg}_2\text{X}_2 \quad (4)$$

$$2\cdot\text{HgX} \rightarrow \text{Hg}_2\text{X}_2$$

Mechanism C

$$\text{R–Hg–X} \rightleftarrows [\text{–X}\cdots\text{R–Hg–X}\cdots\text{R–Hg–}]$$

$$\text{or} \begin{bmatrix} \text{R–Hg–X} \\ \vdots \quad \vdots \\ \text{X–Hg–R} \end{bmatrix} \rightarrow \text{RX} + \text{Hg} \quad (10)$$

If the mechanism A is correct, organomercuric bromides would give larger amount of mercury metal than the corresponding chlorides, from a consideration of bond energy of R–HgX and ·Hg–X. However, as the results are opposite, the mechanism A seems to be unlikely.

In the mechanism B, the position of the equilibrium (reaction (8)) generally lies by far to the left-hand side, but, if at least one of the components in the right-hand side is unstable to heat, the equilibrium would shift to the right-hand side. Since bis-organomercurials are usually less stable to heat than organomercuric salts, organic free radicals would generate from bis-organomercurials thus produced, and would react according to the reaction (9), which would compete with the reaction (4). Thus the formation of mercury metal would be considerably supressed. Therefore, the formation of large amounts of mercury metal could not be explained by the mechanism B.

Kharasch *et al.*[12] and Shoolery *et al.*[13–15] have

*3 It is considered that the acetoxy radicals may be stabilized by some interaction with mercury metal, because completely free acetoxy radical would rapidly decompose into methyl radical and carbon dioxide.

12) M. S. Kharasch and M. W. Grafflin, *J. Amer. Chem. Soc.*, **47**, 1948 (1925); M. S. Kharasch and R. Marker, *ibid.*, **48**, 3130 (1926); M. S. Kharasch and A. L. Flenner, *ibid.*, **54**, 674 (1932); M. S. Kharasch, H. Pines and J. H. Levine, *J. Org. Chem.*, **3**, 347 (1938); M. S. Kharasch and S. Swartz, *ibid.*, **3**, 405 (1938); M. S. Kharasch, R. R. Legault and W. R. Sprowls, *ibid.*, **3**, 409 (1938).

13) B. P. Dailey and J. N. Shoolery, *J. Amer. Chem. Soc.*, **77**, 3977 (1955).

14) J. R. Cavanaugh and B. P. Dailey, *J. Chem. Phys.*, **34**, 1099 (1961).

15) M. A. Davis, *J. Org. Chem.*, **32**, 1161 (1967).

established the relative electronegativities of organic and inorganic groups as follows:

$$p\text{-}CH_3C_6H_4 > C_6H_5 > CH_3 > n\text{-}C_4H_9 > C_6H_5CH_2 > cyclo\text{-}C_6H_{11};$$
$$OAc > Cl > Br > SCN > CN$$

Since aryl groups are more electronegative than cyclohexyl, the intermolecular interaction between cyclohexyl and chlorine seems to be more strong than that between aryl and chlorine. From these considerations, the demercuration reactions of alkylmercuric chlorides are considered to proceed mainly through the mechanism C. Thus, the corresponding chlorides are obtained in good yields. Partial formation of alkyl radicals is attributed to the mechanisms A (may be less probable) and B.

In the cases of alkylmercuric bromides, intermolecular interaction between alkyl group and bromine is considered to be not so strong as in the alkylmercuric chlorides because of less electronegativity of bromine. Therefore, the contribution of the mechanism C decreases and both liberation of metallic mercury and the formation of organic bromide decrease.

Arylmercuric chlorides, on the contrary, might decompose on heating to generate aryl radicals mainly through mechanism B, because an intermediate complex in the reaction (8) seems favorable over that in the mechanism C from a consideration of the electronegativities of aryl group and chlorine. Formation of the corresponding aromatic hydrocarbon is presumably attributed to hydrogen abstraction from the surrounding organomercurials by aryl radicals. Thus the reaction (9), in which aryl radical is considered to be more favorable over alkyl radical, scarcely occurs.

In organomercuric cyanides, considerable amount of mercury metal was always liberated. These facts indicate that the demercuration reaction of organomercuric cyanides proceeds mainly through the mechanism B, because mercuric cyanide produced is also unstable to heat.[11]

A large amount of cyclohexene in the case of cyclohexylmercuric cyanide is presumably formed through homolytic β-elimination of aliphatic organomercurials[16] by cyano radical, which is produced by thermal decomposition of mercuric cyanide,[11] because the formation of a considerable amount of hydrogen cyanide was observed.

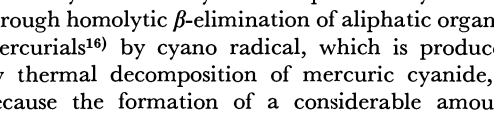

The demercuration reaction of phenylmercuric thiocyanate is considered to be very similar to that of the corresponding cyanide, excepting that no phenyl thiocyanate was obtained. This is explained by the following decomposition, because a large amount of mercuric sulfide was obtained and then liberated mercury metal decreased.

$$Hg(SCN)_2 \rightarrow HgS + \cdot CN + \cdot SCN$$
$$Hg + \cdot SCN \rightarrow HgS + \cdot CN$$

In the cases of organomercuric acetates, since mercuric acetate was almost decomposed to give metallic mercury under similar conditions, the demercuration reaction proceeds mainly through the mechanism B.

Phenylmercuric acetate gave neither phenyl acetate nor toluene. This fact shows that the mechanism C does not occur at all, because acetoxy group is more electronegative than chlorine. From the result, it is considered that the reaction (9) is also unlikely in other cases. Thus, the formation of a trace of RX is probably attributed to a small contribution of the mechanism C.

The following two mechanisms are possible for the demercuration reaction of organomercuric salt in the presence of mercuric salt.

Mechanism D

$$\begin{matrix} R\text{-}Hg\text{-}X \\ + \\ HgY_2 \end{matrix} \rightleftarrows \begin{bmatrix} R\text{—}Hg\text{-}X \\ \vdots \quad \vdots \\ Y\text{-}Hg\text{-}Y \end{bmatrix} \rightleftarrows RHgY + HgXY \quad (11)$$

$$RHgX(\text{or } RHgY) \xrightarrow[B,\ C \text{ or } E]{\text{Mechanism}}$$

Mechanism E

$$RHgX + HgY_2 \rightleftarrows [\cdots X\text{-}Hg\text{-}R\cdots Y\text{-}Hg\text{-}Y\cdots R\text{-}Hg\text{-}X\cdots] \rightarrow RY + Hg \quad (12)$$
$$Hg + HgY_2 \rightarrow Hg_2Y_2$$

In cyclohexylmercuric halide - mercuric halide systems, the ratio of cyclohexyl bromide to the chloride increased with the bromine content in the system, and the formation of the chloride was more favorable than that of the bromide (Table 1). These facts can be explained considering that the position of the equilibrium (11) lies to the side of cyclohexylmercuric chloride and that organomercuric salts thus produced decompose through the mechanism C or E depending on the amount of mercuric salts present.

Generally, it is concluded that alkylmercuric halides also decompose mainly through the mechanisms C and E in the presence of mercuric halides. In the cases of arylmercuric salts, the reactions presumably proceed through the mechanisms D and E. This conclusion is also supported from the facts that the results of the reactions of diphenylmercury with mercuric salts were very similar to those of phenylmercuric salts with mercuric salts.

In organomercuric acetate, the demercuration reaction proceeds through the mechanism B as described before. Thus, *n*-butylmercuric or benzylmercuric acetate gave the corresponding organic acetate only in a poor yield. In the case of *n*-butylmercuric acetate, the yield of *n*-butyl acetate

16) F. R. Jensen and H. E. Guard, *J. Amer. Chem. Soc.*, **90**, 3250 (1968).

decreased from 10% to 5% in the presence of mercuric acetate. This fact can be reasonably explained by a large contribution of homolytic β-elimination[16] similarly to that of cyclohexylmercuric cyanide.

On the other hand, in the case of benzylmercuric acetate, the yield of benzyl acetate increased considerably and the yield of dibenzyl decreased in the presence of mercuric acetate. Since benzyl group is much less electronegative and acetoxy group is much more electronegative, the observed results can be explained by the absence of homolytic β-elimination and by the contribution of the mechanism E in the presence of mercuric acetate.

Experimental*4

Materials. Organomercurials were prepared by usual methods: *n*-butylmercuric bromide, mp 129.5—131°C (lit,[17] 136°C); *n*-butylmercuric acetate, mp 54—55.5°C (lit,[17] 56°C); *s*-butylmercuric chloride, mp 26.5—29.5°C (lit,[18] 28°C); benzylmercuric acetate, mp 124—125°C (lit,[19] 128—128.8°C); cyclohexylmercuric bromide, mp 151—153°C (lit,[20] 153°C); cyclohexylmercuric chloride, mp 160—161.5°C (lit,[21] 163°C); cyclohexylmercuric cyanide, mp 147—148.5°C (lit,[21] 146°C); phenylmercuric acetate, mp 148.5—150°C (lit,[22] 149°C); phenylmercuric chloride, mp 249.4—249.7°C (lit,[21] 251°C); phenylmercuric cyanide, mp 203—205°C (lit,[21] 209°C); phenylmercuric thiocyanate, mp 230—231°C (decomp.) (lit,[23] 231—232.5°C (decomp.)); diphenylmercury, mp 125—127°C (lit,[24] 122—124°C); *p*-tolylmercuric chloride, mp 232.5—234.5°C (lit,[21] 233°C); bis-phenylethynylmercury, mp 123—124°C (lit,[25] 124.5—125°C).

Mercuric thiocyanate was prepared by the usual method.[26] Other inorganic mercuric salts were obtained commercially.

Authentic samples were prepared by the methods described in the literature: cyclohexyl cyanide,[27] bp 183—187°C (lit,[28] 184—185°C); dicyclohexyl, bp 110°C/15 mmHg, n_D^{19} 1.4800 (lit, bp 233°C/750 mmHg,[29] n_D^{20} 1.47954[26]); phenyl thiocyanate, bp 104—106°C/15.5 mmHg (lit,[23] 232—233°C), IR: 2150 cm^{-1} (-S-C≡N); *p*-tolyl chloride, bp 155—156.5°C, n_D^{16} 1.5231 (lit, bp 162—162.2°C,[30] $n_D^{18.20}$ 1.5199[31]); di-*p*-tolyl, mp 118—120°C (lit,[32] 121°C); phenyl-*p*-tolylmethane, bp 141°C/13 mmHg (lit,[33] 144°C/16 mmHg); phenylethynyl cyanide, bp 101°C/12 mmHg, mp 37.5—39°C (lit,[34] bp 105—106°C/13 mmHg, mp 41°C); benzyl acetate, bp 104°C/17 mmHg, n_D^{21} 1.5008 (lit,[35] bp 213°C, $n_D^{19.93}$ 1.50324).

Other samples were obtained commercially.

General Methods for Thermal Reactions. About 2 g of organomercurial or a mixture of about 2 g of organomercurial and an appropriate amount of mercuric salt, which was softly covered with glass wool to prevent from sublimation of mercurials, was placed without a solvent in a reaction tube equipped with a thermometer and a cold trap, and heated at 200—300°C for 1—2 hr under ordinary or/and reduced pressure. Volatile liquid was collected in the cold trap cooled with dry ice-ethanol, weighed, and submitted to VPC*5 or distilled. Nonvolatile material in the reaction tube was extracted with ether or petroleum ether, with ethanol, methanol or acetone, and with water, successively, and each extract after evaporation was submitted to determination of melting point and/or to thin layer chromatography for identification. Metallic mercury liberated was isolated from the residual material and weighed.

Some typical examples are described below, and the results are summarized in Tables 1—6.

s-Butylmercuric Chloride with Mercuric Chloride. A mixture of 4.917 g (16.7 mmol) of *s*-butylmercuric chloride and 6.091 g (22.4 mmol) of mercuric chloride was heated at 250—260°C under ordinary pressure for 2 hr. Generation of hydrogen chloride was observed. Volatile liquid (1.420 g) was distilled, and 0.977 g (10.6 mmol, 63.5%) of *s*-butyl chloride, bp 61—68°C, was obtained.

Cyclohexylmercuric Chloride with Mercuric Bromide. A mixture of 2.003 g (6.27 mmol) of cyclohexylmercuric chloride and 2.579 g (7.18 mmol) of mercuric bromide (mole ratio 1 : 1.14) was heated at 240—265°C under a pressure of 50 mmHg for 1.5 hr. Volatile liquid (0.683 g) was submitted to VPC, and cyclohexane (0.20 mmol), cyclohexene (1.87 mmol), cyclohexyl chloride (3.36 mmol) and cyclohexyl bromide (0.74 mmol) were determined. A trace of dicyclohexyl was also detected. From the ethanol extract of nonvolatile material 0.302 g (11.7%) of unchanged mercuric bromide was recovered. The residue consisted of 2.828 g of white insoluble material, and no metallic mercury was observed.

*4 All the melting points and boiling points described here were not corrected.

17) K. H. Slotta and K. R. Jacobi, *J. Prakt. Chem.*, **120**, 249 (1929).

18) H. B. Charman, E. D. Hughes and C. Ingold, *J. Chem. Soc.*, **1959**, 2523.

19) G. H. Coleman, L. A. Weed and C. D. Myers, *J. Amer. Chem. Soc.*, **59**, 2703 (1937).

20) G. Grüttner, *Ber.*, **47**, 1651 (1914).

21) E. Carr, I. B. Johns and R. M. Hixson, *J. Amer. Chem. Soc.*, **60**, 891 (1938).

22) J. L. Maynard, *ibid.*, **46**, 1510 (1924).

23) E. Söderbäck, *Ann. Chem.*, **419**, 267 (1919).

24) W. E. Bachmann, *J. Amer. Chem. Soc.*, **55**, 2827 (1933).

25) J. R. Johnson and W. L. McEwen, *ibid.*, **48**, 469 (1926).

26) A. A. Blanchard, J. W. Phelan and A. R. Davis, "Synthetic Inorganic Chemistry," John Wiley, New York (1936), p. 234.

27) C. H. Tilford, M. G. Van Campen and R. S. Shelton, *J. Amer. Chem. Soc.*, **69**, 2902 (1947).

28) M. Godchot, *Bull. Soc. Chim. Fr.*, **1911**, 261.

29) J. H. Gardner and P. Borgstrom, *J. Amer. Chem. Soc.*, **51**, 3375 (1929).

30) W. H. Perkin, *J. Chem. Soc.*, **1896**, 1203.

31) K. Seubert, *Ber.*, **22**, 2519 (1889).

32) L. Gattermann, *ibid.*, **23**, 1223 (1890).

33) K. V. Auwers and A. Frühling, *Ann. Chem.*, **422**, 192 (1921).

34) Ch. Moureu and I. Lazennec, *Bull. Soc. Chim. Fr.*, **1906**, 520.

35) S. T. J. Tromp, *Rec. Trav. Chim. Pays-Bas*, **41**, 278 (1922).

*5 Diisodecyl phthalate, Apiezon "L" grease, di-2-ethylhexyl sebacate and succinic polyester of diethylene glycol were used as liquid phase.

Phenylmercuric Thiocyanate with Mercuric Thiocyanate. A mixture of 2.003 g (5.96 mmol) of phenylmercuric thiocyanate and 2.013 g (6.34 mmol) of mercuric thiocyanate was heated at 220—290°C under atmospheric pressure for 1 hr and then under a pressure of 20 mmHg at 270°C for 45 min. The volatile liquid (0.327 g) was submitted to VPC, and benzene (1.92 mmol, 32.3%), benzonitrile (0.471 mmol), and phenyl thiocyanate (0.0232 mmol) were determined. No phenyl isothiocyanate was detected. From the petroleum ether extract of nonvolatile material, 6 mg (0.036 mmol) of diphenyl was obtained, and from the ethanol extract 20 mg (1%) of unchanged phenylmercuric thiocyanate was recovered. The residue consisted of a considerable amount of insoluble black material and 243 mg (1.21 mmol) of metallic mercury. The black material proved to contain mercuric sulfide by the usual analytical method.

The authors wish to express their thanks to Professor G. F Wright, The University of Toronto, Canada, for his valuable comments throughout this work.

BULLETIN OF THE CHEMICAL SOCIETY OF JAPAN VOL. 43 2581—2588 (1970)

Imidazole Catalyses in Aqueous Systems. IV. Bimolecular and Michaelis-Menten-Type Catalyses of a Phenyl Ester Hydrolysis by Some Hydrophobic Imidazole Derivatives*1

Toyoki KUNITAKE and Seiji SHINKAI

Department of Organic Synthesis, Faculty of Engineering, Kyushu University, Fukuoka

(Received February 23, 1970)

Catalytic hydrolyses of *p*-acetoxybenzoic acid by several imidazole derivatives were conducted at 15—40°C in aqueous systems using a pH-stat. Imidazole compounds containing the naphthalene ring catalyzed the hydrolysis following the Michaelis-Menten kinetics as in enzymatic reactions, while catalysis by less hydrophobic imidazoles followed the second-order kinetics. Enhancement of the overall catalytic efficiency in the Michaelis-Menten pathway was estimated to be ten times at most as compared with the bimolecular pathway. The thermodynamic and activation parameters were obtained at 15—40°C for the Michaelis-Menten pathway. The binding of catalyst and substrate was characterized by small positive enthalpy changes ($\Delta H \cong +3.5$ kcal/ mol) and large positive entropy changes ($\Delta S_u \cong +28$ eu), indicating that the complex formation was ascribable to hydrophobic interactions. The intra-complex product formation was characterized by not unreasonable $\Delta H^{\neq}$ values and extraordinarily large negative $\Delta S^{\neq}$ ($\cong -50$ eu) values. The unexpectedly small rate enhancement in the Michaelis-Menten pathway was attributed to the unfavorable $\Delta S^{\neq}$ term, which suggested that the structure of the Michaelis complex was quite different from that of the transition state of the product formation.

In a previous publication of this series, we showed that a naphthylimidazole derivative (I) catalyzed the hydrolysis of a phenyl ester by the Michaelis-Menten kinetic as in enzymatic reactions.[1]

$$\text{catalyst} + \text{substrate} \underset{K_m}{\rightleftharpoons} \text{catalyst}\cdot\text{substrate} \xrightarrow{k_{cat}} \text{catalyst} + \text{product}$$

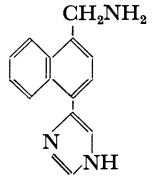

I

The substrate binding was attributed to hydrophobic interactions between catalyst and substrate. Apparently the naphthalene ring was hydrophobic enough to bind the substrate, *p*-acetoxybenzoic acid, under the hydrolytic conditions. In fact, naphthalenesulfonic acid and other water-soluble naphthalene derivatives were shown by NMR spectroscopy to associate with methanol or acetone in an aqueous system.[2] Occurrence of the substrate saturation in the hydrolysis of phenyl esters due to the hydrophobic interaction

*1 Contribution No. 203 from this department.

1) a) C. Aso, T. Kunitake and S. Shinkai, *Chem. Commun.*, **1968**, 1483. b) T. Kunitake, S. Shinkai and C. Aso, This Bulletin, **43**, 1109 (1970).

2) E. S. Hand and T. Cohen, *J. Amer. Chem. Soc.*, **87**, 133 (1965).

have been observed increasingly in polymeric[3-6] and non-polymeric[7,8] systems. Interest in these studies arises from the fact that the active site of many hydrolytic enzymes comprises hydrophobic regions and the hydrophobic interaction with substrate is intrinsic in determining the specificity and efficiency of the active site.[9]

We showed that the catalytic efficiency was quite different in the neutral and monoprotonated spcies of I, indicating that the structural difference of the catalyst affected its catalytic activity appreciably. On the other hand, remarkable rate enhancement which might be expected from formation of the Michaelis complex was not observed because of rather small k_{cat} values.

Thus it was felt necessary to study in more detail the influence of hydrophobicity on the catalytic behavior of imidazoles. In the present investigation thermodynamic and activation parameters were estimated for the catalytic process in the hydrolysis of *p*-acetoxybenzoic acid (Eq. (2)) by several imidazole derivatives (Bz-Im, Ph-Im, N-oyl-Im, and N-yl-Im), in the hope that the results would be useful for designing more efficient catalytic systems.

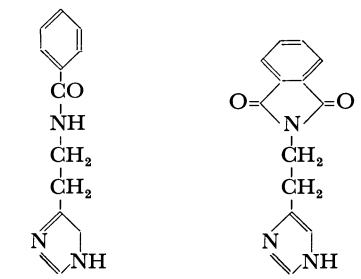

Bz-Im

Ph-Im

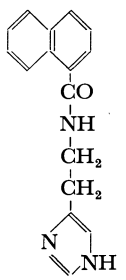

N-oyl-Im

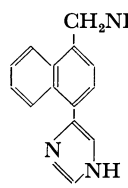

N-yl-Im

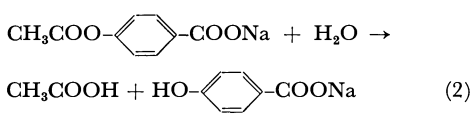

(2)

Experimental

***N*-Benzoylhistamine (Bz-Im)** was prepared by reaction of histamine and benzoyl chloride in the presence of triethylamine,[10] mp 148.5—149.5°C (lit,[10] 148°C).

***N*-[4(5)-Imidazolylethyl]-phthalimide (Ph-Im).** *o*-Phthaloyl chloride was prepared from phthalic anhydride and phosphorus pentachloride in 90% yield, bp 142—146°C/15 mmHg (lit,[11] 131—133°C/9—10 mmHg). Histamine dihydrochloride (1.8 g, 0.01 mol) was dissolved in 60 m*l* of 4 N NaOH in a three-necked flask equipped with a mechanical stirrer. *o*-Phthaloyl chloride (1.0 g, 0.005 mol) in 30 m*l* of chloroform and 3.0 m*l* of 4 N NaOH were separately added dropwise over a 15 min period of ice cooling. The solution was confirmed to be alkaline and then stirred for 1 hr. Sodium chloride was added and the chloroform layer was separated. The aqueous layer was extracted with 30 m*l* of chloroform, and the combined chloroform solution was washed with dil. aqueous alkali and with a small amount of water. Chloroform was evaporated and the residue was recrystallized from water, colorless plates, mp 221—225°C (dec.), yield 45%. IR (KBr): $\nu_{C=O}$ 1700, 1772 cm^{-1}. Found: C, 64.59; H, 4.60; N, 15.99%; Calcd for $C_{13}H_{11}O_2N_3$: C, 64.72; H, 4.60; N, 17.43%; mol wt, 241.24. The equivalent weight determined from titration of the imidazole group was 244.

***N*-α-Naphthoylhistamine (N-oyl-Im).** Histamine dihydrochloride (1.8 g, 0.01 mol) was dissolved in a mixture of methanol (150 m*l*) and water (20 m*l*), containing 7.2 g (0.072 mol) of triethylamine. To this solution was added at 0—4°C 2.1 g (0.01 mol) of *N,N'*-dicyclohexylcarbodiimide in 40 m*l* of acetonitrile and 1.7 g (0.01 mol) of naphthalene-α-carboxylic acid in 20 m*l* of methanol in succession. The reaction mixture was kept with occasional shaking at 0—4°C for three days and at room temperature for four days. The unreacted carbodiimide was converted to *N,N'*-dicyclohexylurea by addition of 5 m*l* of glacial acetic acid. Upon addition of 3 m*l* of concentrated hydrochloric acid, the mixture was concentrated to about 20 m*l*, separated from dicyclohexylurea formed, added to saturated aqueous sodium carbonate and extracted with chloroform. Evaporation of chloroform and recrystallization of the residue from water yielded colorless needles

3) a) C. Aso, T. Kunitake and F. Shimada, *J. Polym. Sci., Part B*, **6**, 467 (1968). b) T. Kunitake, F. Shimada and C. Aso, *J. Amer. Chem. Soc.*, **91**, 2716 (1969). c) T. Kunitake, F. Shimada and C. Aso, *Makromol. Chem.*, **126**, 276 (1969).

4) R. L. Letsinger and I. S. Klaus, *J. Amer. Chem. Soc.*, **87**, 3380 (1965).

5) Yu. E. Kirsh, V. A. Kabanov and V. A. Kargin, *Vysokomol. Soedin.*, **A10**, 349 (1968).

6) a) C. G. Overberger, R. Corett, J. C. Salamone and S. Yaroslavsky, *Macromolecules*, **1**, 331 (1968). b) C. G. Overberger, M. Morimoto, I. Cho and J. C. Salamone, *ibid.*, **2**, 553 (1969).

7) a) R. L. VanEtten, J. F. Sebastian, G. A. Clowes and M. L. Bender, *J. Amer. Chem. Soc.*, **89**, 3242 (1967). b) R. L. VanEtten, G. A. Clowes, J. F. Sebastian and M. L. Bender, *ibid.*, **89**, 3253 (1967).

8) R. G. Shorenstein, C. S. Pratt, C.-J. Hsu and T. E. Wagner, *ibid.*, **90**, 6199 (1968).

9) W. P. Jencks, "Catalysis in Chemistry and Enzymology," McGraw-Hill, Inc., New York (1969), Chapter 8.

10) G. Gerngross, *Z. physiol. Chem.*, **108**, 58 (1915).

11) E. Ott, "Organic Syntheses," Coll. Vol. II, p. 528 (1943).

in 67% yield, mp 112—114°C (dec.). Found: C, 72.15; H, 5.85; N, 14.45%. Calcd for $C_{16}H_{15}ON_3$: C, 72.43; H, 5.70; N, 15.84%; mol wt, 265.32. The equivalent weight determined by titration of the imidazole group was 270.5.

1-Acetamidomethyl-4-[4(5)-imidazolyl]naphthalene (N-yl-Im). 265 mg of 1-aminomethyl-4-[4(5)-imidazolyl]naphthalene[1b] (10^{-3} mol) was reacted with 79 mg (10^{-3} mol) of acetyl chloride in a mixture of 10 m*l* of triethylamine and 100 m*l* of acetonitrile in an ice bath. Upon stirring for 1 hr solvents were evaporated, and the solid residue taken up in 0.1 N hydrochloric acid was reprecipitated by addition of saturated aqueous sodium carbonate. The precipitate was recrystallized from 3 : 2 water - ethanol, mp 144—150°C (dec.), 60% yield. IR (KBr): $\nu_{C=O}$, 1640 cm^{-1} (broad). Found: C, 72.04; H, 5.99; N, 15.35%. Calcd for $C_{16}H_{15}ON_3$: C, 72.43; H, 5.70; N, 15.84%; mol wt, 265.32. The equivalent weight determined by titration of the imidazole was 272.1.

Substrate. *p*-Acetoxybenzoic acid was prepared as described before.[1b,12]

Titration and Hydrolysis Procedures. Titration and hydrolyses were carried out at several temperatures using a pH-stat connected with a recorder (TOA Electronics, Ltd., Models HS-1B and EPR-2T, respectively). The water-jacket holding the reaction vessel was maintained at given temperatures by circulating water from a constant temperature bath. The pH meter was calibrated at two pH values at the respective temperatures. Further details of the procedures have been described previously.[3b]

NMR Measurements. The imidazole derivative N-oyl-Im was saturated at room temperature in D_2O containing a trace of ethanol, and its NMR spectrum was obtained with a Varian A-60 spectrometer. Acetonitrile and contaminating water were used as internal standards. The imidazole protons at the 2 and 4(5) positions appeared at 7.56 and 6.80 ppm, respectively. Histamine dihydrochloride was dissolved in D_2O (30 mg/m*l*) and neutralized to pH 7—8. At this pH range, only the amino group is protonated. The imidazole protons at the 2 and 4(5) positions appeared at 8.11 and 7.39 ppm, respectively.

Results

Spontaneous Hydrolysis. Table 1 gives the rate of spontaneous hydrolysis of the substrate and pK_a of the resulting *p*-hydroxybenzoic acid at several temperatures. Spontaneous hydrolysis was undetectably slow at 15°C and increased with temperature. Dissociation of *p*-hydroxybenzoic acid is as follows.

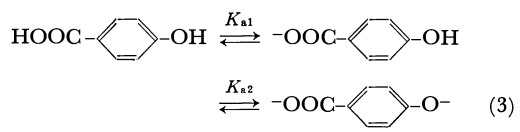

That the phenol group was partially dissociated at pH 8 was taken into consideration in calculating the rate of hydrolysis from alkali consumption.

Table 1. Spontaneous hydrolysis of substrate and pK_a of *p*-hydroxybenzoic acid

Temp. (°C)	k_{spont} (10^{-4}M^{-1}min^{-1})[a]	pK_{a1}[b]	pK_{a2}[b]
15	~0	—	—
20	0.78±0.05	4.51	9.05
30	4.23±0.02	4.44	9.17
40	14.7 ±0.4	4.34	8.94

a) pH 8.0, 1M KCl.
b) 1 M KCl. Experimental error, ±0.05.

Catalytic Hydrolysis by Bimolecular Mechanisms. The total rate of hydrolysis in the presence of the catalyst consists of the two terms—spontaneous and catalytic hydrolyses.

$$v = v_{cat} + v_{spont} \quad (4)$$

Throughout the present investigation v_{cat} represents the initial rate of catalytic hydrolysis. Spontaneous hydrolysis prior to the addition of catalyst was small and necessary corrections were made for substrate concentration. Figure 1 shows the relation between v_{cat} and substrate concentration with Bz-Im catalyst. In the temperature range from 15°C to 40°C, v_{cat} values are reasonably proportional to substrate concentration, and the catalytic hydrolysis with Bz-Im was concluded to proceed *via* the common second-order kinetics:

$$\text{catalyst} + \text{substrate} \xrightarrow{k'} \text{catalyst} + \text{product} \quad (5)$$

$$v_{cat} = k'[C][S] \quad (6)$$

where C and S denote catalyst and substrate, respectively. In Fig. 2 is given v_{cat} *vs.* [S] with Ph-Im as a catalyst. Similarly, a linear relationship was obtained. The second-order rate con-

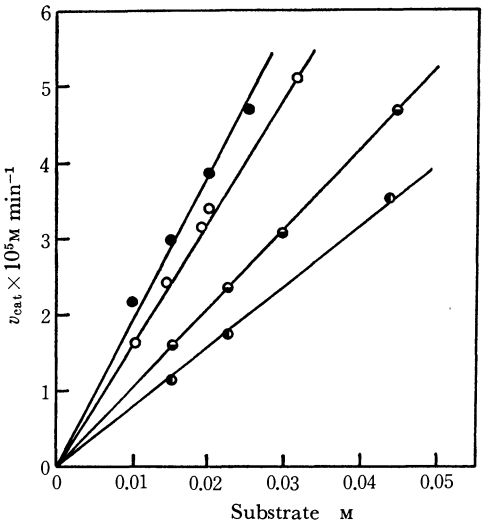

Fig. 1. Catalytic hydrolysis.
catalyst, Bz-Im 3.22×10^{-3}M; pH 8.0; 1.0M KCl.
●, 40°C; ○, 30°C; ◒, 20°C; ◐, 15°C.

12) E. R. Marshall, J. A. Kuck and R. C. Elderfield, *J. Org. Chem.*, **7**, 450 (1942).

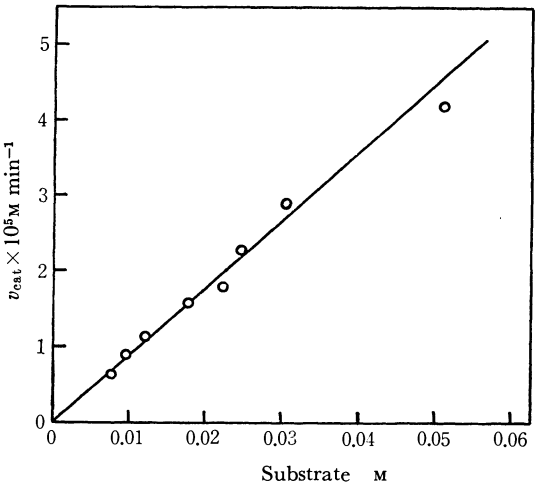

Fig. 2. Catalytic hydrolysis. catalyst, Ph-Im 2.16×10^{-3}M; pH 8.0; 1.0M KCl; 30°C.

TABLE 2. SECOND ORDER RATE CONSTANT OF CATALYTIC HYDROLYSIS

Catalyst	Temp. (°C)	pK_a[a]	k'($M^{-1}min^{-1}$)[b]
Bz-Im	15	7.35	0.24_6
Bz-Im	20	7.24	0.33_6
Bz-Im	30	7.21	0.50_7, 0.49[c]
Bz-Im	40	7.20	0.64_1
Ph-Im	30	6.75	0.40_5, 0.39[c]
Iimidazole[d]	30	7.13±0.03	0.32_5

a) 1M KCl. Experimental error: ± 0.05 unless stated otherwise.
b) pH 8.0, 1M KCl.
c) Catalyst concentration was varied instead of substrate concentration.
d) from Ref. 1b.

stants k' were obtained from these data and are given in Table 2, together with the data with imidazole catalyst. When the catalyst concentration was varied ($(1—10) \times 10^{-3}$M) at a constant substrate concentration ([C]=0.020M, 30°C, 1.0M KCl), the relationships between v_{cat} and [S] were similarly linear, with the second-order rate constant of 0.49$M^{-1}min^{-1}$ and 0.39$M^{-1}min^{-1}$ for Bz-Im and Ph-Im, respectively. Since the imidazole groups are partially protonated at pH 8.0, the effective catalyst concentrations ($[C]_{eff}$) were calculated from the corresponding pK_a values

$$[C]_{eff} = [C]_{total} \cdot \frac{K_a}{K_a + a_H} \quad (7)$$

where K_a is the acid dissociation constant of the conjugate acid and a_H is the hydrogen ion activity. Bz-Im and imidazole show similar catalytic activities, whereas Ph-Im is somewhat more efficient.

Catalytic Hydrolysis by the Michaelis-Menten Mechanism. The relationships between v_{cat} and [S] at four temperatures are given for imidazole derivative N-oyl-Im in Fig. 3. Undoubtedly, v_{cat} showed substrate saturation which was particularly clear at high temperature. A similar catalytic behavior was previously observed for a related imidazole derivative[1] and some imidazole-containing polymers.[3] These kinetic patterns, typical of the enzyme-catalyzed reaction, can be described by Eq. (1) and the corresponding catalytic rate is expressed by

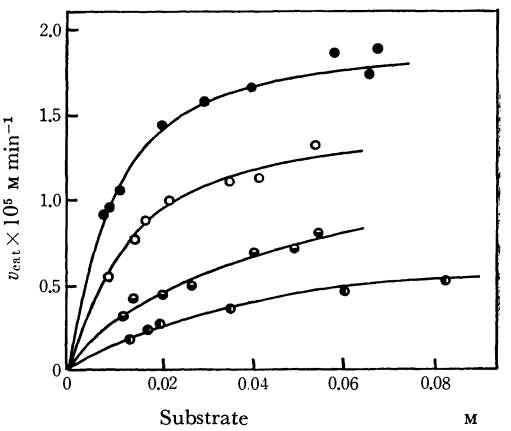

Fig. 3. Catalytic hydrolysis. catalyst, N-oyl-Im 0.82×10^{-3}M; pH 8.0; 1.0M KCl.
●, 40°C; ○, 30°C; ◒, 20°C; ◐, 15°C.

$$v_{cat} = \frac{k_{cat}[C][S]}{K_m + [S]} \quad (8)$$

Since k_{cat} values for the imidazole catalysts used are sufficiently small, the Michaelis constant K_m is considered to represent the true dissociation constant.[3b] The kinetic constants in the equation are determined from the Lineweaver-Burk plotting[13]

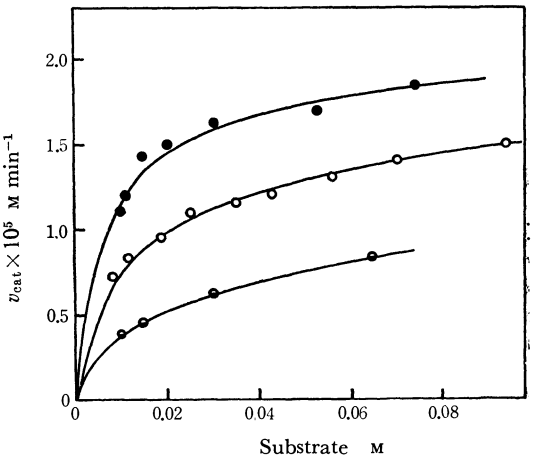

Fig. 4. Catalytic hydrolysis. catalyst, N-yl-Im 0.31×10^{-3}M; pH 8.0; 1.0M KCl.
●, 40°C; ○, 30°C; ◒, 20°C.

13) H. Lineweaver and D. Burk, *J. Amer. Chem. Soc.*, **56**, 658 (1934).

Table 3. Kinetic parameters of Michaelis-Menten-type hydrolysis

Catalyst	Temp. (°C)	pK_a[a]	K_m(mM)[b]	k_{cat}(min^{-1})[b]	k_{cat}/K_m(min^{-1}M^{-1})
N-oyl-Im	15	6.88	40.0	0.0095	0.24
N-oyl-Im	20	6.80	20.4	0.012	0.59
N-oyl-Im	30	6.75	16.4	0.021	1.3
N-oyl-Im	30	—	14.9[c]	0.017[c]	1.2
N-oyl-Im	40	6.58	13.7	0.029	2.1
N-yl-Im	20	6.06	16.7	0.033	2.0
N-yl-Im	30	6.00	13.9	0.054	3.9
N-yl-Im	40	5.86	11.1	0.071	6.4

a) 1M KCl. Experimental error, ±0.05.
b) pH 8.0, 1M KCl.
c) pH 7.0, 1M KCl.

of $1/v_{cat}$ *vs.* 1/[S]. The plots were sufficiently linear, showing the validity of the Michaelis-Menten expression of the rate data. Substrate saturation curves were similarly observed for the catalytic hydrolysis with N-yl-Im as a catalyst (Fig. 4). The corresponding Lineweaver-Burk plots were sufficiently linear. The kinetic constants for the enzyme-like catalysis are summarized in Table 3. Also included are kinetic constants obtained from hydrolysis at pH 7.0 with N-oyl-Im at 30°C.

The effect of ionic strength of the reaction medium was studied for the substrate-binding catalysts as shown in Fig. 5. v_{cat} increased with increase in ionic strength for both systems. Catalysis with N-oyl-Im was more sensitive to ionic strength as compared with N-yl-Im.

Thermodynamic and Activation Parameters of Catalytic Hydrolysis. From these kinetic data are obtained the activation parameter of the bimolecular catalysis by Bz–Im and the thermodynamic and activation parameters of the Michaelis-Menten-type catalysis by N-oyl-Im and N-yl-Im. The free energy of activation $\Delta G^{\neq}$ was calculated from k_{cat} or k' from the relationship $\Delta G^{\neq} = \boldsymbol{R}T\ln(\boldsymbol{k}T/\boldsymbol{h}k_r)$,[14] and plotted against T. Satisfactorily linear relationships were obtained as shown in

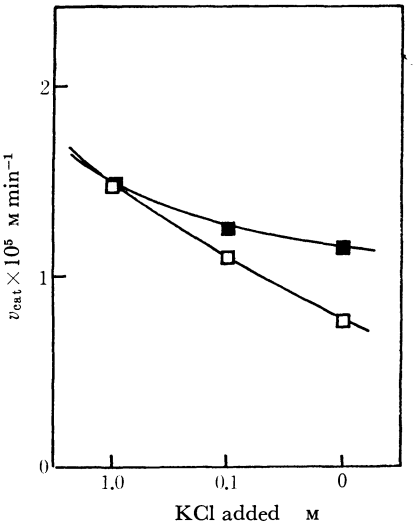

Fig. 5. Effect of ionic strength on catalytic rate. pH 8.0 : 30°C
□: catalyst, N-oyl-Im 0.82×10^{-3}M; substrate, 0.022M.
■: catalyst, N-yl-Im 0.31×10^{-3}M; substrate, 0.020M.

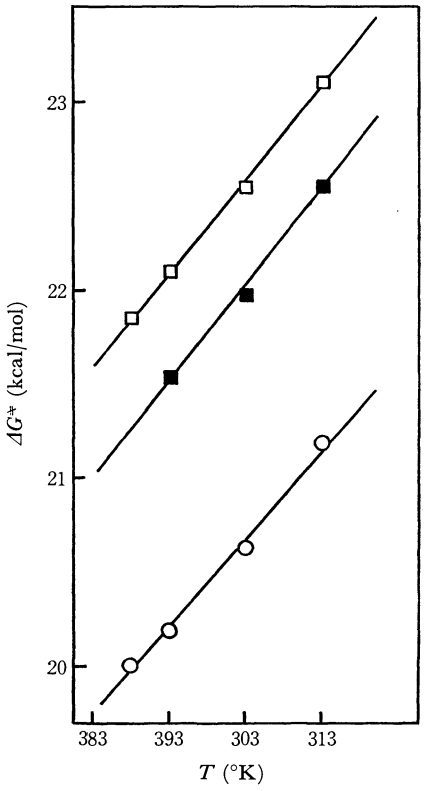

Fig. 6. Free energy of activation *vs.* absolute temperature.
catalyst: ○, Bz–Im; □, N-oyl-Im; ■, N-yl-Im.

14) A. A. Frost and R. G. Pearson "Kinetics and Mechanisms," 2nd. Ed. John Wiley & Sons, Inc., New York (1961), p. 98.

TABLE 4. THERMODYNAMIC AND ACTIVATION PARAMETERS OF CATALYTIC HYDROLYSIS

Catalyst	Substrate Binding			Bimolecular and Intra-complex Processes	
	ΔH (kcal/mol)	ΔS (eu)	ΔS_u (eu)	$\Delta H^{\neq}$ (kcal/mol)	$\Delta S^{\neq}$ (eu)
Bz-Im[a)]	—	—	—	6.43	−47.0
N-oyl-Im[b)]	3.74	20.5	28.5	7.31	−50.4
N-yl-Im[b)]	3.44	19.9	27.9	6.26	−52.0

a) Bimolecular pathway
b) Michaelis-Menten pathway

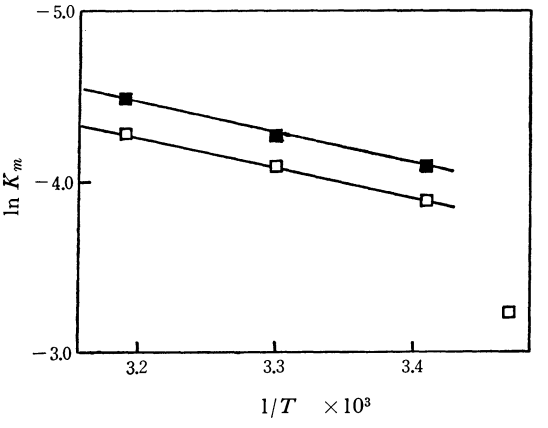

Fig. 7. Temperature dependence of the Michaelis constant. catalyst: □, N-oyl-Im; ■, N-yl-Im.

Fig. 6. $\Delta H^{\neq}$ and $\Delta S^{\neq}$ were obtained from intercept and slope, respectively, from the relationship $\Delta G^{\neq} = \Delta H^{\neq} - T\Delta S^{\neq}$, and are given in Table 4. Particularly noteworthy are exceptionally large negative entropies of activation obtained for the pseudo-intramolecular process.

The thermodynamic parameters of the dissociation process of the Michaelis complex were obtained from plots of $\ln K_m$ *vs.* $1/T$ (Fig. 7). Linear relationships are obtained for the respective catalysts except for a plot at 15°C for N-oyl-Im catalyst. The deviation may indicate that the bimolecular process is involved at this temperature. The enthalpy and entropy changes of the binding process are obtained from the relationship using the equation $\ln K_m = \Delta H/\boldsymbol{R}T - \Delta S/\boldsymbol{R}$. The thermodynamic parameters of binding are very similar for these two catalysts and characterized by small positive enthalpies and large positive entropies (see Table 4). The unitary entropy change was obtained from the relation $\Delta S_u = \Delta S + 7.98$.[15)]

Discussion

The results given above clearly demonstrate the different catalyst behavior between imidazole derivatives containing the naphthalene ring and less hydrophobic imidazole compounds. Thus, v_{cat} increased linearly with substrate concentration with the latter catalysts, whereas the Michaelis-Menten kinetics were observed for the former catalysts. The kinetic difference can be attributed to a large hydrophobicity of the naphthalene ring sufficient to bind a substrate molecule prior to the catalytic process. The benzene ring in Bz–Im or Ph–Im was not sufficiently hydrophobic to bind a substrate molecule under hydrolysis conditions and the formation of the Michaelis complex, if any, was not significant for these catalysts.

On the other hand, a bimolecular catalytic process by uncomplexed catalyst molecules might coexist in the overal Michaelis-Menten kinetics as long as the binding of catalyst and substrate occurs.[3b)] In this case the relative importance of the two processes is determined from a comparison of k_{cat}/K_m and k'. The second-order rate constants k' for three non-binding catalysts are 0.3—0.5 $min^{-1}M^{-1}$ at 30°C. Therefore, the hypothetical k' values for N-oyl-Im and N-yl-Im will certainly not be greater than 0.3—0.5 $min^{-1}M^{-1}$, considering their lower pk_a values. Since k_{cat}/K_m at 30°C is 1.3 and 3.9 for N-oyl-Im and N-yl-Im, respectively, the enzyme-like catalytic pathways are considered to be preferred to with these catalysts. At lower temperatures, however, the dissociation constant increases and the overall rate enhancement due to complexation is less pronounced. In fact, substrate saturation was not very clear for the catalytic hydrolysis at 15°C (Fig. 3). Deviation of the corresponding $\ln K_m$ plot from linearity in Fig. 7 and comparable k_{cat}/K_m and k' values (0.24 *vs.* 0.25 $min^{-1}M^{-1}$) obtained for closely related catalysts (Bz-Im and N-oyl-Im) suggest that the significance of the two catalytic processes becomes comparable at this temperature.

The tendency of non-polar groups to adhere to one another in aqueous environments has been referred to as hydrophobic bonding,[15)] and this process is usually accompanied by a large positive entropy change and a small enthalpy change. The thermodynamic parameters obtained (large positive ΔS_u and small ΔH for the binding process) clearly indicate that hydrophobic forces are responsible for substrate binding. Very close values obtained for both ΔH and ΔS_u with catalysts N-oyl-Im and N-yl-Im seemingly reflect the fact that the naphthalene

15) W. Kauzmann, *Advan. Protein Chem.*, **14**, 1 (1959).

ring is the major site of binding in these catalysts.

The pseudo-intramolecular rate constant k_{cat} was greater (about 2.5 times at 30°C) for imidazole N-yl-Im than for N-oyl-Im in spite of the lower pK_a value for the former. Since the nucleophilicity of simple imidazoles in the hydrolysis of *p*-nitrophenyl acetate was proportional to pK_a of the conjugate acid,[16] reversal in the intra-complex rate constant may be attributed to the structural difference of the Michaelis complexes. It was found that k_{cat} differed considerably between catalysts I and its protonated form (0.19 *vs.* 0.036 min^{-1}),[1b] and we anticipated a much greater difference in catalytic activity between N-oyl-Im and N-yl-Im, because k_{cat} was expected to be particularly sensitive to the spacial disposition of the imidazole group relative to the bound substrate. However, the difference in k_{cat} was rather small, although it would be greater if the difference in pK_a is to be corrected. Appearance of the imidazole proton peaks in N-oyl-Im at higher magnetic fields than the corresponding peaks in histamine by about 0.6 ppm can be ascribed to the paramagnetic shielding of the former proton by the naphthalene ring. Thus, the imidazole group in N-oyl-Im is conceivably located at a position fairly close to the plane of the naphthalene ring. The difference in pK_a between Bz-Im and N-oyl-Im also supports this supposition. Klotz and Lyndrup[17] noted that the charged state of an N-ethylimidazole residue placed in a polyvinylpyrrolidone matrix was destabilized relative to the uncharged state, because of changes in the local polymer or solvent environment, causing lowering of pK_a by about 1.15 pK units. Similarly we found that pK_a of the benzimidazole unit in polymers decreased with increasing hydrophobicity of the polymer in aqueous systems.[18] Thus the decreased pK_a of N-oyl-Im relative to that of Bz-Im can be considered to arise from destabilization of the charged state of the imidazole group due to the nearby hydrophobic naphthalene ring. The greater sensitivity to the ionic strength of the medium of the catalytic efficiency of N-oyl-Im as compared with that of N-yl-Im (Fig. 5) may be also ascribed to the conformational flexibility of N-oyl-Im molecules. Thus, a compact conformation of N-oyl-Im at $\mu=1.0$ will tend to lessen the difference in catalytic activity between N-oyl-Im and N-yl-Im, since the location of the imidazole group relative to the naphthalene ring will not be very different in these catalysts.

The overall enhancement in the catalytic efficiency due to substrate binding can be estimated from k_{cat}/K_m *vs.* k'. The rate enhancement observed in the present study was at most ten times (Table 2 *vs.* 3). A similar extent of rate enhancement was observed for related polymer catalysts, and some discussions were made concerning small k_{cat} values.[3b] These results are in a sharp contrast with much greater rate enhancement observed in imidazole-catalyzed hydrolyses of phenyl esters[8,19,20] and acylation of amines[21,22] where the hydrophobic interaction of long hydrocarbon chains significantly contributed to rate enhancement. The small rate enhancement in the present system is associated with a small k_{cat}. Bruice and Benkovic showed that intramolecular catalysis was characterized by favorable entropy terms (*ca.* 15 eu) compared with those of bimolecular catalyses.[23] The remarkable efficiency of enzyme-catalyzed reactions is commonly attributed to formation of the Michaelis complex and to the facile intra-complex reaction. However, the activation parameters shown in Table 4 indicate that the activation entropies are extremely unfavorable for the intra-complex process. The large negative $\Delta S^{\neq}$ observed betrays our expectation that the intra-complex product formation would be facilitated by the favorable entropy term. In fact $\Delta S^{\neq}$ for k_{cat} was more negative than that for k'.

The unfavorable entropy factor for k_{cat} may be explained by either or both of the following assumptions: (1) The relative disposition of catalyst and substrate in the Michaelis complex may be very different from the structure of the transition state, and extensive reorganization of the structure of the complex becomes necessary for the action of the imidazole group on the ester group to occur. In this case, k_{cat} will increase greatly if suitable combinations of catalyst and substrate are selected. Connors and coworkers[24] made extensive studies on the modification of reaction rates by complex formation in aqueous solutions. An analogous study may be necessary in order to establish the structure-reactivity relationship in the complex. Also interesting is the finding by Gitler and Ochoa-Solano that elongation of the hydrocarbon chain in substrate decreased the activation energy of the imidazole-catalyzed ester hydrolysis in micelles,[19]

16) T. C. Bruice and G. L. Schmir, *J. Amer. Chem. Soc.*, **80**, 148 (1958).

17) I. M. Klotz and M. L. Lyndrup, *Biopolymers*, **6**, 1405 (1968).

18) T. Kunitake, S. Shinkai and C. Aso, to be published.

19) a) A. Ochoa-Solano, G. Romero, and C. Gitler, *Science*, **156**, 1243 (1967); b) C. Gitler and Ochoa-Solano, *J. Amer. Chem. Soc.*, **90**, 5004 (1968).

20) J. R. Knowles and C. A. Parsons, *Nature*, **221**, 53 (1969).

21) J. R. Knowles and C. A. Parsons, *Chem. Commun.*, **1967**, 755.

22) a) I. M. Klotz and V. H. Stryker, *J. Amer. Chem. Soc.*, **90**, 2717 (1968). b) G. P. Royer and I. M. Klotz, *ibid.*, **91**, 5885 (1969).

23) T. C. Bruice and S. J. Benkovic, *ibid.*, **85**, 1 (1963).

24) a) J. A. Mollica, Jr., and K. A. Connors, *ibid.*, **89**, 308 (1967). b) P. A. Kramer and K. A. Connors, *ibid.*, **91**. 2600 (1969). c) K. A. Connors, M. H. Infeld, and B. J. Kline, *ibid.*, **91**, 3597 (1969).

since their results suggest that the disposition of substrate relative to catalyst possibly affects the activation energy.[25] (2) If it is assumed that acetylimidazoles are intermediates of the pseudo-intramolecular transformation, the transition state for the acyl transfer is considered to be rather polar. The polar transition state will not be favored on the surface of the hydrophobic naphthalene ring. Thus, the hydrophobic interaction between catalyst and substrate may have to be largely destroyed for the intra-complex reaction to occur, resulting in the large negative entropy of activation.

25) Recently this problem was discussed also by Cordes and Dunlop: E. H. Cordes and R. B. Dunlop, *Accounts Chem. Res.*, **2**, 329 (1969).

In conclusion, both of the bimolecular and Michaelis-Menten-type catalyses were observed for the imidazole-catalyzed hydrolysis of *p*-acetoxybenzoic acid in aqueous systems. Unfortunately, however, the rate acceleration expected from formation of the catalyst-substrate complex was not remarkable because of the highly unfavorable entropy of activation. We are now attempting syntheses of related catalytic systems which presumably possess different organizations of the catalytic site from those of the present one.

The authors are deeply grateful to Professor C. Aso of this department for his unfailing encouragement and advice.

BULLETIN OF THE CHEMICAL SOCIETY OF JAPAN VOL. 43 2588—2591 (1970)

Stereochemical Studies of Monoterpene Compounds. VIII.[1] The Stereochemistry of Dihydro-β-campholenolactone and 1,2-Campholide[2]

Toshifumi HIRATA, Takayuki SUGA[3] and Tamon MATSUURA

Department of Chemistry, Faculty of Science, Hiroshima University, Hiroshima

(Received February 25, 1970)

The stereochemistry of (+)-dihydro-β-campholenolactone (II) and (−)-1,2-campholide (III) was clarified to be IIa and IVc, respectively, by a combination of nuclear magnetic resonance, optical rotatory dispersion and circular dichroism measurements.

The reaction of α-campholenic acid (I) with sulfuric acid has been reported[4] to produce only dihydro-β-campholenolactone (II). However, no report has been given on that with organic acid. The stereochemistry of lactone II has been only presumed[5] by considering the reaction of pinonic acid with sulfuric acid. While the peracetic acid oxidation of camphor[5] has been reported to produce 1,2-campholide (III), its stereochemistry has not been reported yet. Our recent study of the stereochemistry and rearrangement of 2-hydroxypinocamphone necessitated our working on the reaction of α-campholenic acid (I) with anhydrous oxalic acid, and the stereochemistry of (+)-dihydro-β-campholenolactone (II) and (−)-1,2-campholide (III) produced.[6-8] The present paper deals with the stereochemistry of these lactones.

Results and Discussion

A mixture of (+)-α-campholenic acid (I) and anhydrous oxalic acid suspended in acetone was refluxed for 6 hr. The reaction gave not only

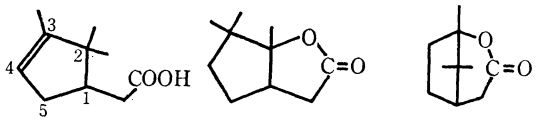

I II III

1) Paper VII of this series: T. Shishibori, T. Suga, S. Watanabe and T. Matsuura, This Bulletin, **42**, 3284 (1969).

2) Presented at the 20th Annual Meeting of the Chemical Society of Japan, Tokyo, April, 1967.

3) To whom all inquiries should be addressed.

4) R. R. Sauers, *J. Amer. Chem. Soc.*, **81**, 925 (1959).

5) M. Harispe and D. Mea, *Bull. Soc. Chim. Fr.*, **1962**, 1340.

6) T. Suga, K. Mori and T. Matsuura, *J. Org. Chem.*, **30**, 669 (1965).

7) T. Suga, T. Shishibori, T. Hirata and T. Matsuura, This Bulletin, **41**, 1180 (1968).

8) R. G. Carlson, J. K. Pierce, T. Suga, T. Hirata, T. Shishibori and T. Matsuura, *Tetrahedron Lett.*, **1968**, 5941.

(+)-dihydro-β-campholenolactone (II) but also (−)-1,2-campholide (III) in 74% and 25% yield, respectively, in contrast to the reaction with mineral acid.[4] Lactones II and III were identified by a combination of infrared and nuclear magnetic resonance spectra measurements and the conversion to 1-(2-hydroxyethyl)-2,3,3-trimethyl-2-cyclopentanol and 1-(2-hydroxyethyl)-2,2,3-trimethyl-3-cyclopentanol respectively.

The Stereochemistry of (+)-Dihydro-β-campholenolactone (II). The spatial arrangement of the lactone ring of II was decided by the solvent effect of NMR spectra with benzene and pyridine. A reference plane was imagined through the carbonyl carbon atom at right angles to the carbon-oxygen bond of the carbonyl group as an aid in predicting the benzene-induced shift of methyl groups (*cf.* Fig. 1).[9] For the *cis*-form, a large upfield

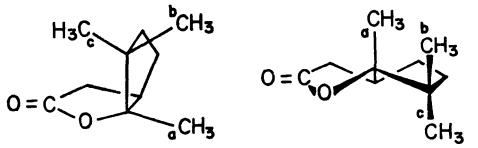

cis-form *trans*-form

Fig. 1. *cis* and *trans*-Forms of dihydro-β-campholenolactone (II).

shift by the solvent is predicted to occur equally on the a- and b-methyl signals (*cf.* Fig. 1), and a smaller upfield shift for the c-methyl group. For the a-methyl group of the *trans*-form, a large upfield shift is predicted and a small one for the b- and c-methyl groups. The a-, b- and c-methyl resonances underwent an upfield shift by 0.43, 0.39 and 0.10 ppm, respectively, by changing a solvent from deuteriochloroform to benzene.

In order to predict the pyridine-induced shift, the reference plane was drawn through the α-position to the carbonyl group[10] (*cf.* Fig. 1). For the a- and b-methyl groups of the *cis*-form, a large upfield shift is expected, and a down field shift for the c-methyl group. The a-, b- and c-methyl signals of γ-lactone II exhibited shifts by +0.17, +0.27 and −0.08 ppm, respectively. It was thus found that the spatial arrangement of the lactone ring is *cis*. The stereochemistry of γ-lactone II is therefore assigned as either IIa or its optical antipode (IIb).

The octant and the sector projection diagrams of each conformer are shown in Fig. 2. According to the lactone sector rule,[11] the sign of the Cotton effect is predictable to be positive for IIa and negative for IIb. The ORD and CD curves of (+)-γ-lactone II exhibited the positive Cotton effect as shown in Fig. 3. The stereochemistry of (+)-dihydro-β-campholenolactone (II) was consequently found to be IIa.

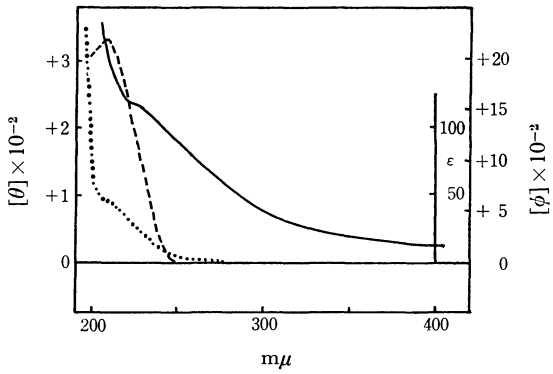

Fig. 3. Optical rotatory dispersion (the full line) and circular dichroism curves (the broken line) and ultraviolet spectrum (the dotted line) of (+)-dihydro-β-campholenolactone (II) in methanol.

The Stereochemistry of (−)-1,2-Campholide (III). Examination of the stereochemical structure of III by a molecular model[12] indicated that it was impossible for the lactone to take the *trans*-form. The stereochemistry of III is consequently

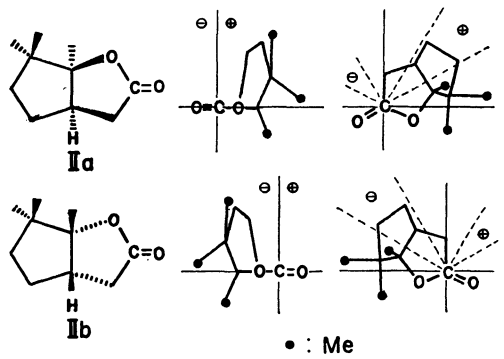

Fig. 2. Octant and sector projections of stereoisomers IIa and IIb.

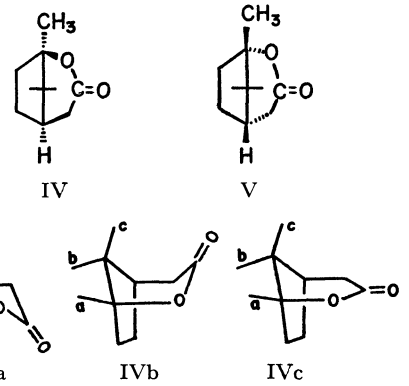

9) J. D. Connolly, *Chem. & Ind.* (London), **1965**, 2066.
10) D. H. Williams, *Tetrahedron Lett.*, **1965**, 2305.
11) J. P. Jennings, W. Klyne and P. M. Scopes, *J. Chem. Soc.*, **1965**, 7211.
12) Examined by "HGS Molecular Structure Model," Maruzen Co., Tokyo.

assigned as either IV or its optical antipode (V). Conformers IVa, IVb and IVc are considered the possible preferred conformation for IV. Three conformers are also possible for V. A large upfield shift of the NMR spectrum by the solvent effect of benzene is expected equally for the a- and c-methyl groups of conformer IVa, and a smaller one for the b-methyl signal. The a- and b-methyl signals of conformer IVb may exhibit a large upfield shift, and the c-methyl signal a very small one. Three methyl signals of conformer IVc will show larger upfield shifts in the order of the b-, a- and c-methyl groups. The a-, b- and c-methyl signals of campholide III were observed to shift upfield by 0.37, 0.31 and 0.52 ppm, respectively.

Pyridine may induce the large upfield shift on a-, b- and c-methyl signals of IVa. On the other hand, a- and b-methyl groups of IVb may be shifted to a large upfield, and the c-methyl group to a down field shift. The a- and b-methyl signals of IVc may exhibit a large upfield shift, and the c-methyl signal a small one. The experimental data were +0.29, +0.13 and +0.08 ppm for a-, b- and c-methyl groups, respectively. The preferred conformation of III was thus found to be either IVc or its optical antipode (Vc).

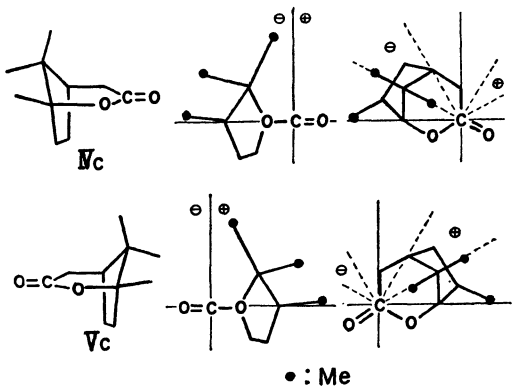

Fig. 4. Octant and sector projections of stereoisomers IVc and Vc.

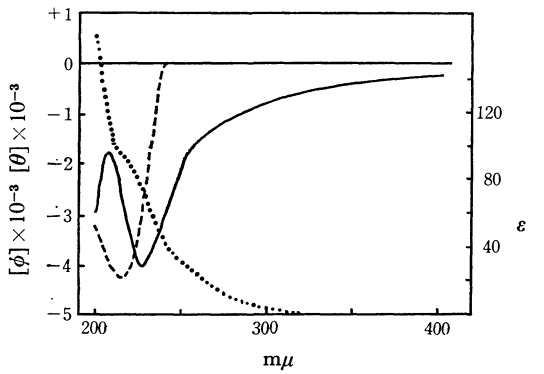

Fig. 5. Optical rotatory dispersion (the full line) and circular dichroism curves (the broken line) and ultraviolet spectrum (the dotted line) of (−)-1,2-campholide (III) in methanol.

The octant and the sector projection diagrams for IVc and Vc are shown in Fig. 4. According to the lactone sector rule,[11] a negative Cotton effect was predicted for IVc, and a positive one for Vc. The ORD and CD curves of (−)-1,2-campholide (III) showed a negative Cotton effect (Fig. 5). The stereochemical structure of III was thus concluded to be IVc.

The mechanism of the lactonization of α-campholenic acid (I) by anhydrous oxalic acid will be discussed in the near future.

Experimental

The NMR spectra were recorded with a Varian Associates A-60 spectrometer using tetramethylsilane as an internal standard. The ORD curves were obtained at 25°C with a Japan Spectroscopic Co. Ltd. automatically recording spectropolarimeter, Model ORD/UV-5, using the normally programmed slit width, and a cell 1 mm long. A monochromator and a cell compartment of the spectropolarimeter were kept in an atmosphere of dry nitrogen. The CD curves were also obtained by the same spectropolarimeter equipped with a circular dichroism attachment. Microanalyses were performed at the Microanalytical Center in the Faculty of Pharmacy of Kyoto University.

(+)-α-Campholenic Acid (I). A mixture of 25 g of (+)-10-camphorsulfonic acid, mp 192°C, $[\alpha]_D^{20}$ +37.5° (*c* 10.2, ethanol) and 25 g of potassium hydroxide was fused for 30 min in an iron crucible with stirring. After cooling, the mixture was dissolved in 200 m*l* of water. After the reaction mixture was washed with ether, then with dichloromethane, the mixture was acidified with 6N-hydrochloric acid solution and then extracted with ether. The usual treatment of the ether extract afforded 9.5 g of crude acid. The crude acid was rectified by distillation under reduced pressure to yield 6.6 g of pure (+)-α-campholenic acid (I): bp 138°C/8 mmHg (lit,[5] bp 95.5—97.5°C/0.54—0.65 mmHg), n_D^{25} 1.4675 (lit,[5] n_D^{25} 1.4695), d_4^{25} 0.9922, $[\alpha]_D^{25}$ +7.21° (*c* 10.1, ethanol).

(+)-Dihydro-β-campholenolactone (II) and (−)-1,2-Campholide (III). A mixture of 35 g of (+)-α-campholenic acid (I) and 140 g of anhydrous oxalic acid suspended in 112 m*l* of acetone was heated under reflux for 6 hr with stirring. After removal of acetone under reduced pressure, the reaction miture dissolved in water was extracted with ether to obtain 21.8 g of a reaction product. The product was subjected to column chromatography on silica gel with a mixture of ethyl acetate and *n*-hexane to separate into two kinds of lactone. The initial eluate gave 15.6 g of (+)-β-lactone II and the second eluate 5.9 g of (−)-δ-lactone III. The lactones were identified by a combination of physicochemical measurements and chemical treatment as follows.

(+)-Dihydro-β-campholenolactone (II) (15.6 g) was obtained from the initial eluate and showed following properties: mp 30—31°C (lit,[5] mp 32°C); $[\alpha]_D^{25}$ +49.9° (*c* 10.0, ethanol); $\nu_{C=O}$ 1774 cm^{-1} (lit,[4] 1786 cm^{-1}); $\lambda_{shoulder}^{MeOH}$ 210 mμ (ε 44.6); ORD (*c* 2.64, methanol),

$[\phi]_{400}$ +272, $[\phi]_{225}$ +1550, $[\phi]_{210}$ +2000; CD (*c* 2.64, methanol), $[\theta]_{250}$ 0, $[\theta]_{210}$ +328, $[\theta]_{200}$ +300.

Found: C, 71.45; H, 9.70%. Calcd for $C_{10}H_{16}O_2$: C, 71.39; H, 9.59%.

The methyl proton signals of the NMR spectra appeared at δ 0.90 (a-CH_3), 1.29 (b-CH_3) and 1.08 ppm (c-CH_3) in 10% deuteriochloroform solution and δ 0.53 (a-CH_3), 0.90 (b-CH_3) and 0.98 ppm (c-CH_3) in 10% benzene solution and δ 0.73 (a-CH_3), 1.02 (b-CH_3) and 1.16 ppm (c-CH_3) in 10% pyridine solution.

The reduction of 0.30 g of γ-lactone II with 0.3 g of lithium aluminum hydride in 50 m*l* of dry ether gave 0.24 g of 1-(2-hydroxyethyl)-2,3,3-trimethyl-2-cyclopentanol: mp and mixed mp 147—148°C (lit,[5] mp 147°C); $[\alpha]_D^{25}$ +38.9° (*c* 1.49, ethanol) (lit,[5] $[\alpha]_D^{25}$ +15±2° (*c* 2, alcohol); $\nu_{OH(free)}^{CCl_4}$ 3626 cm^{-1}, $\nu_{OH(bonded)}^{CCl_4}$ 3462 cm^{-1}.

Found: C, 69.86; H, 11.93%. Calcd for $C_{10}H_{20}O_2$: C, 69.72; H, 11.70%.

(−)-1,2-Campholide (III) (5.9 g) was obtained from the second eluate and showed the following properties: mp 162—163°C (lit,[4] 168.5—171.5°C); $[\alpha]_D^{25}$ −43.0° (*c* 3.0, ethanol) (lit,[4] $[\alpha]_D^{25}$ −37°); $\nu_{C=O}$ 1729 cm^{-1} (lit,[4] 1745 cm^{-1}); $\lambda_{shoulder}^{MeOH}$ 215 mμ (ε 95.4); ORD (*c* 1.62, methanol), $[\phi]_{400}$ −250, $[\phi]_{227}$ −4010, $[\phi]_{208}$ −1770, $[\phi]_{200}$ −2970; CD (*c* 1.62, methanol), $[\theta]_{242}$ 0, $[\theta]_{215}$ −4270, $[\theta]_{200}$ −3200.

Found: C, 71.41; H, 9.73%. Calcd for $C_{10}H_{16}O_2$: C, 71.39; H, 9.59%.

The methyl proton signals of the NMR spectra appeared at δ 1.07 (a-CH_3), 1.29 (b-CH_3) and 1.00 ppm (c-CH_3) in 5% deuteriochloroform solution and δ 0.70 (a-CH_3), 0.98 (b-CH_3) and 0.48 ppm (c-CH_3) in 5% benzene solution and δ 0.78 (a-CH_3), 1.16 (b-CH_3) and 0.91 ppm (c-CH_3) in 5% pyridine solution.

Reduction of 0.20 g of lactone III with 0.20 g of lithium aluminum hydride in 100 m*l* of dry ether afforded 0.09 g of 1-(2-hydroxyethyl)-2,2,3-trimethyl-3-cyclopentanol: mp and mixed mp 93—94°C (lit,[4] 91—93°C); $[\alpha]_D^{25}$ +72.4° (*c* 1.85, ethanol); $\nu_{OH(free)}^{CCl_4}$ 3624 cm^{-1}.

Found: C, 70.00; H, 11.76%. Calcd for $C_{10}H_{20}O_2$: C, 69.72; H, 11.70%.

The authors wish to express their thanks to Dr. Marcelle Harispe of College of Paris for a gift of 1-(2-hydroxyethyl)-2,3,3-trimethyl-2-cyclopentanol, to Dr. J. D. Connolly of the Glasgow University for a gift of 1-(2-hydroxyethyl)-2,2,3-trimethyl-3-cyclopentanol, and Dr. Shô Itô of Tohoku University for measuring the NMR spectra.

BULLETIN OF THE CHEMICAL SOCIETY OF JAPAN VOL. 43 2591—2596 (1970)

Reactions of Aziridines with Acetyl Chloride and Related Compounds

Itaru OKADA, Toshio TAKAHAMA and Rokuro SUDO

Laboratory of Organic Chemistry, Tokyo Institute of Technology, Ookayama, Meguro-ku, Tokyo

(Received March 25, 1970)

When aziridines (**1**) were treated with acetyl compounds, such as acetyl chloride, acetic acid, acetic anhydride, and thioacetic acid, the corresponding acetamide derivatives were obtained in good yields. In the case of acetyl chloride, some derivatives of *N*-(2-chloroethyl)acetamide (**5**) were found to be unstable in the face of moisture; they were easily hydrolyzed to give *N*-(2-hydroxyethyl)acetamide hydrochlorides (**3**). The NMR spectrum of *N*-(2-mercaptoethyl)-*N*-benzylacetamide (**12**) was discussed.

The reactions of aziridine with acid chlorides to give *N*-(2-chloroethyl)amide derivatives have been described.[1,2] On the other hand, at least two examples of the reactions of *N*-substituted aziridines with acid chlorides have been reported.[3,4] However, no systematic study of this type of reaction has yet been reported. In the present investigation, we studied the reactions of *N*-substituted aziridines with acetyl chloride and other acetyl compounds.

1) H. Bestian, *Ann. Chem.*, **566**, 210 (1950).
2) H. W. Heine, *J. Amer. Chem. Soc.*, **85**, 2743 (1963).
3) L. J. Dolby and H. Biere, *ibid.*, **90**, 2699 (1968).
4) K. Tanaka, *Yakugaku Zasshi*, **70**, 220 (1950).

Results and Discussion

Reaction of Aziridines with Acetyl Chloride. When *N*-benzylaziridine (**1a**) was treated with acetyl chloride in dry benzene under ice cooling, a light yellow sirup was obtained. After being kept for 7 day at room temperature, the sirup crystallized. The crude product was recrystallized from ethanol. *N*-(2-Hydroxyethyl)-*N*-benzylacetamide hydrochloride (**3a**) was thus obtained in a 66% yield. **3a** was characterized by elemental analysis and by means of its IR and NMR spectra. The IR spectrum had absorptions at 2750—2350 cm^{-1} (ν_{NH^+}), 1735 cm^{-1} ($\nu_{C=O}$), and the NMR spectrum

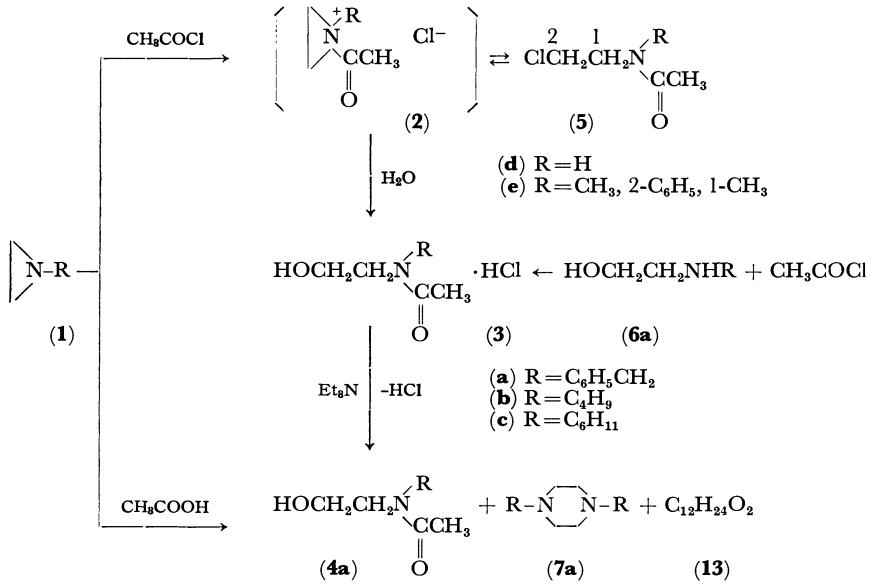

Scheme 1

exhibited a broad peak at τ 0.1 (2H) due to -OH and $-NH^+$.

Furthermore, the fact that the reaction of **3a** with triethylamine in benzene yielded triethylamine hydrochloride and *N*-(2-hydroxyethyl)-*N*-benzylacetamide (**4a**) supported the idea of the structure of **3a**, while **4a** was also prepared by the reaction of *N*-benzylaziridine (**1a**) with acetic acid. On the other hand, the product prepared from *N*-benzylaminoethanol (**6a**) with acetyl chloride was identical with **3a** in its IR spectrum, and a mixed-melting-point determination showed no depression.

A probable pathway for this reaction involves an initial electrophilic attack of the acetyl group on the basic aziridine nitrogen, followed by the ring opening of the intermediate aziridinium salt (**2a**) to give *N*-(2-chloroethyl)-*N*-benzylacetamide (**5a**). This compound was unstable in the face of moisture and was easily hydrolyzed to **3a**. This fact was explained by the change in the IR bands from 1650 cm^{-1} ($\nu_{>N-C=O}$) to 1735 cm^{-1} ($\nu_{C=O}$).

Analogous reactions of *N*-butylaziridine (**1b**) and *N*-cyclohexylaziridine (**1c**) with acetyl chloride resulted in the formation of the corresponding *N*-(2-hydroxyethyl)amide hydrochloride derivatives (**3b**, **3c**). These results are summarized in Table 1.

On the contrary, when aziridine (**1d**) or 1,2-dimethyl-3-phenylaziridine (**1e**) was treated with acetyl chloride, a stable *N*-(2-chloroethyl) amide derivative (**5d** or **5e**) was obtained in a 95% or

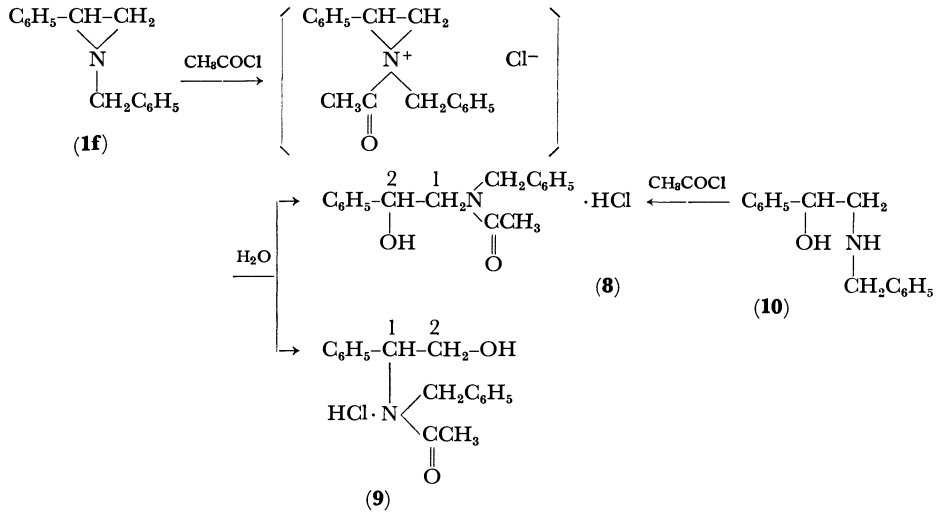

Scheme 2

Table 1. Reactions of aziridines with acetyl compounds

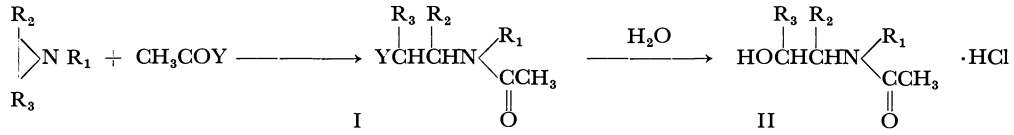

Compound	R_1	R_2	R_3	Y	Product	Mp°C or Bp°C/mmHg	Yield, %	IR(C=O) cm^{-1}
3a	$C_6H_5CH_2$	H	H	Cl	II	152–153	66	1735
4a				OH	I	174/1.5	58	1620
11				$OCOCH_3$	I	150–151/0.5	72	1650, 1740
12				SH	I	158–160/1.2	73	1640
3b	C_4H_9	H	H	Cl	II	182–183	69	1735
3c	C_6H_{11}	H	H	Cl	II	171–172	95	1745
5d	H	H	H	Cl	I	131/6	95	1655
5e	CH_3	CH_3	C_6H_5	Cl	I	122–124[a]	99	1635
8	$C_6H_5CH_2$	H	C_6H_5	Cl	II	178–181	93	1725

a) Lit, mp 124°C.[4]

Table 2. Elemental analysis

Compound	Formula	Calcd, %				Found, %			
		C	H	N	Cl(S)	C	H	N	Cl(S)
3a	$C_{11}H_{16}NO_2Cl$	57.50	6.70	6.10	15.44	57.68	6.84	6.18	15.51
4a	$C_{11}H_{15}NO_2$	68.37	7.82	7.25		68.36	7.99	7.24	
11	$C_{13}H_{17}NO_3$	66.36	7.28	5.95		65.79[a]	7.22	6.28	
12	$C_{11}H_{15}NOS$	63.14	7.23	6.69	15.29	64.18[a]	7.14	6.96	14.83
3b	$C_8H_{18}NO_2Cl$	49.10	9.21	7.16		49.17	9.04	7.38	
3c	$C_{10}H_{20}NO_2Cl$	54.20	9.04	6.32	16.05	54.46	8.92	6.56	16.52
5d	C_4H_8NOCl	39.51	6.58	11.52		39.65	6.82	11.67	
5e	$C_{12}H_{16}NOCl$	63.83	7.15	6.21	15.75	63.99	6.89	6.08	15.71
8	$C_{17}H_{20}NO_2Cl$	66.78	6.55	4.58	11.62	66.57	6.43	4.42	11.73

a) The elemental analysis did not give a good agreement with the calculated values because of a very viscous oil.

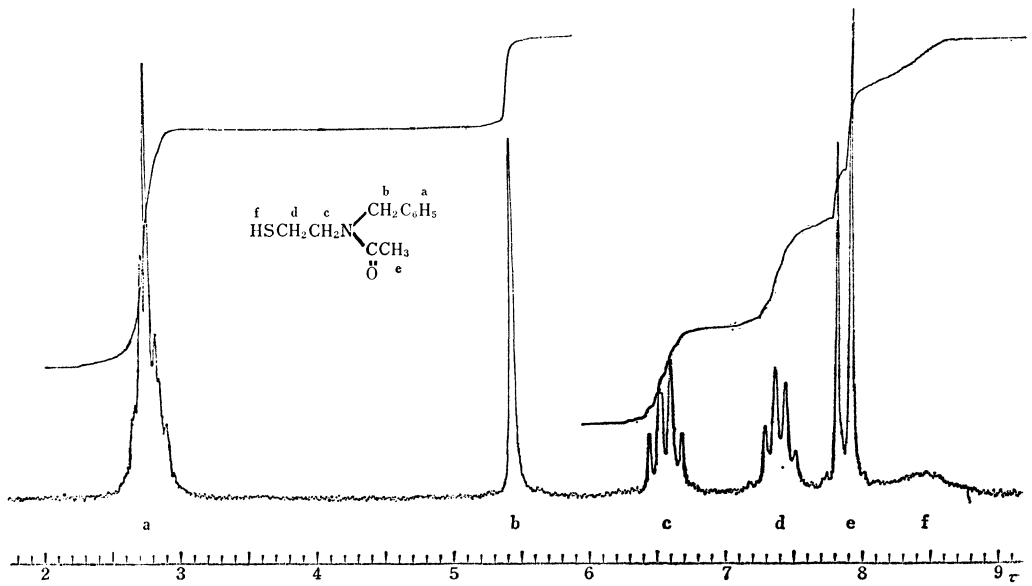

Fig. 1. NMR spectrum of *N*-(2-mercaptoethyl)-*N*-benzylacetamide (**12**) at 100 Mc in $CDCl_3$ using TMS as standard (23°C).

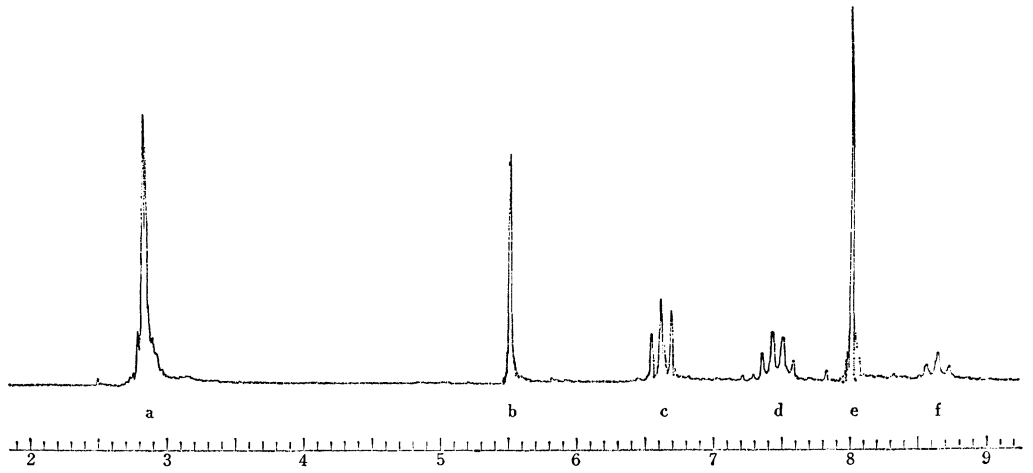

Fig. 2. NMR spectrum of **12** (100°C).

99% yield (Scheme 1).[5]

Two isomers (**8**,**9**) are possible through the ring opening of the aziridine moiety in the reaction of 1-benzyl-2-phenylaziridine (**1f**) with acetyl chloride. The product was found to be *N*-(2-phenyl-2-hydroxyethyl)-*N*-benzylacetamide hydrochloride (**8**). **8** was identified by a comparison of its IR spectrum with that of a sample prepared from 1-phenyl-2-benzylaminoethanol (**10**) with acetyl chloride; a mixed-melting-point determination supported this structure (Scheme 2).

Reaction of Aziridines with Other Acetyl Compounds. When 1-benzylaziridine (**1a**) was treated with other acetyl compounds, such as acetic acid,[6] acetic anhydride[7] or thioacetic acid,[6] the corresponding acetamide derivatives (**4a**, **11**, **12**) were obtained in good yields. When a reagent with a lower electrophilicity, such as acetamide, was used as an acetyl compound, the starting materials were recovered even after refluxing for 7 hr.

In the NMR spectra of these compounds (**4a**, **11**, **12**), acetyl protons exhibited a doublet at 23°C, and the doublet became a singlet at 100°C. This fact establishes that acetyl protons are nonequivalent due to the partial doublebond character of the >N–C-bond. As an example, the NMR spectrum of **12** is shown in Fig. 1 and Fig. 2.

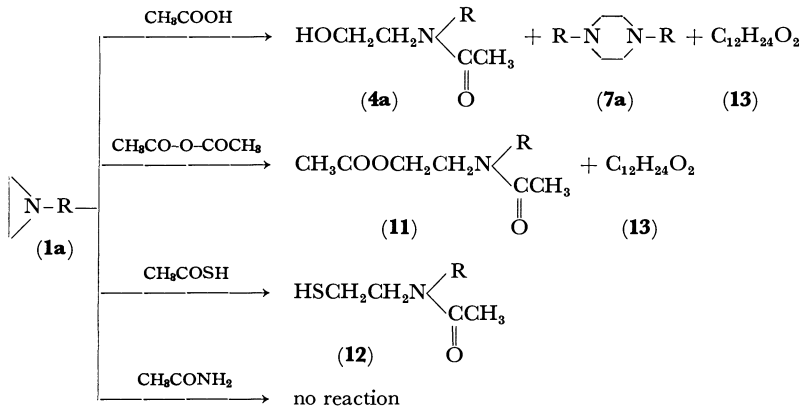

Scheme 3

5) *N*-(2-Chloroethyl)-*N*-methylacetamide was already prepared, bp 100—101°C/5 mmHg. A. F. Nikolaev, M. E. Rosenberg, N V. Daniel and G. P. Tereschenko, *Zh. Obshch. Khim.*, **33**, 391 (1963); *Chem. Abstr.*, **59**, 424d (1963).

6) P. E. Fanta, "Heterocyclic Compounds with Three- and Four-Membered Rings," Part I, ed. by A. Weissberger, Interscience Publishers, Inc., New York. N.Y. (1964), pp. 553—554.

7) P. Loewrigkeit, G. J. Del Franco and N. Georgalas, *J. Org. Chem.*, **33**, 3344 (1968); M. G. Voronkov and L. A. Fedotova, *Khim. Geterotsikl. Soedin*, 302 (1967); *Chem. Abstr.*, **67**, 116687 s (1967); Badische Anilin- & Soda-Fabrik Akt.-Ges., Brit. 784058 (1957): *Chem. Abstr.*, **52**, 5034 h (1958).

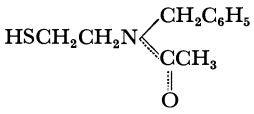

(12)

In the cases of acetic acid or acetic anhydride, an unknown substance with the composition of $C_{12}H_{24}O_2$ (**13**) was obtained as a by-product; this substance's structure is now under investigation (Scheme 3).

Experimental

Benzene was dried over sodium. All the concentrations and evaporations were carried out under reduced pressure. All the melting points and boiling points are uncorrected.

Aziridines (**1**). These compounds were prepared by the methods in the literature. *N*-Benzyl-(**1a**), bp 77.5°C/7 mmHg;[8] *N*-butyl-(**1b**), bp 102—105°C;[9] *N*-cyclohexyl-(**1c**), bp 64.5—65.5°C/25 mmHg;[8] 1,2-dimethyl-3-phenyl-(**1e**), bp 82°C/14 mmHg;[10] 1-benzyl-2-phenylaziridine (**1f**), bp 138—139°C/1 mmHg[10] and aziridine (**1d**) 56—57°C, a commercial product.

Reaction of *N*-Benzylaziridine (1a) with Acetyl Chloride. A solution of acetyl chloride (2.36 g, 0.03 mol) in benzene (10 m*l*) was stirred, drop by drop, into a solution of **1a** (3.99 g, 0.03 mol) in benzene (30 m*l*) under ice cooling. The mixture was stirred at room temperature for 1 hr, and then refluxed for 3 hr. The mixture was concentrated to give a light yellow sirup, which was identified as *N*-(2-chloroethyl)-*N*-benzylacetamide (**5a**) by means of its IR spectrum. After standing for 7 day at room temperature, the sirup crystallized to give *N*-(2-hydroxyethyl)-*N*-benzylacetamide hydrochloride (**3a**). The crude product was collected by filtration, washed with benzene, and dried (4.55 g, 66% yield). Recrystallization from ethanol gave colorless needles; mp 152—153°C. IR (KBr): 2920, 2770, 2550, 2350, 1735, 1430, 1240, 1065, 980, 745 and 700 cm^{-1}; NMR (CD_3SOCD_3): τ 7.95 (3H, singlet) due to CH_3CO, τ 6.85 (2H, triplet) due to $>NCH_2-$, τ 5.83 (2H, singlet) due to $C_6H_5-CH_2-$, τ 5.65 (2H, triplet) due to $HOCH_2-$, τ 2.25—2.7 (5H, multiplet) due to aromatic protons, and τ 0.1 (2H, broad) due to –OH and $-NH^+$.

An attempt to obtain *N*-(2-chloroethyl)-*N*-benzylacetamide hydrochloride by the treatment of the sirup with hydrogen chloride failed, while **3a** was obtained through hydrolysis.

In a similar procedure, other aziridines (**1b**, **1c**, **1e**) were treated with acetyl chloride; the results are summarized in Table 1.

Reaction of 2-Benzylaminoethanol (6a) with Acetyl Chloride. A solution of acetyl chloride (7.85 g, 0.1 mol) in benzene (20 m*l*) was stirred, drop by drop, into a solution of **6a** (15.10 g, 0.1 mol) in benzene (100 m*l*) under cooling. The mixture was stirred for 5 hr at room temperature, and then refluxed for 1 hr. After cooling, the precipitated **3a** (16.70 g, 73%) was collected by filtration. Recrystallization from ethanol afforded colorless plates, mp 151—153°C; this was shown to be the same product as that prepared by the reaction of **1a** with acetyl chloride by a mixed-melting-point determination and by a study of its IR spectrum.

Reaction of Aziridine (1d) with Acetyl Chloride. A solution of acetyl chloride (7.85 g, 0.1 mol) in chloroform (10 m*l*) was stirred, drop by drop, into a solution of **1d** (4.31 g, 0.1 mol) in chloroform (50 m*l*) under ice cooling. The mixture was stirred at room temperature for 1 hr and then concentrated to give a light yellow oil; this oil was distilled to give *N*-(2-chloroethyl)-acetamide (**5d**) (7.30 g, 60%); bp 131°C/16 mmHg.

Reaction of 1-Phenyl-2-benzylaminoethanol (10)[10] with Acetyl Chloride. A solution of acetyl chloride (4.71 g, 0.06 mol) in benzene (15 m*l*) was stirred, drop by drop, into a solution of **10** (4.54 g, 0.02 mol) in benzene (100 m*l*) under ice cooling. The mixture was refluxed for 3 hr and then concentrated to give a light yellow oil. Ethanol containing hydrochloric acid (10 m*l*) was added to the oil, after which the mixture was concentrated to give *N*-(2-phenyl-2-hydroxyethyl)-*N*-benzylacetamide hydrochloride (**8**) (6.10 g, 99%); mp 178—181°C.

Found: C, 66.67; H, 6.42; N, 4.68%. Calcd for $C_{17}H_{20}NO_2Cl$: C, 66.78; H, 6.55; N, 4.58%.

Reaction of 1-Benzylaziridine (1a) with Acetic Acid. A solution of acetic acid (2.40 g, 0.04 mol) in benzene (12 m*l*) was added, drop by drop, to a solution of **1a** (5.30 g, 0.04 mol) in benzene (40 m*l*). The mixture was refluxed for 3 hr and then concentrated to give a light yellow oil; this oil was subsequently distilled at 53—65°C/2 mmHg (redistilled, 89°C/18 mmHg) to give **13** (1.00 g). IR (NaCl): 3300, 2900, 1705, 1460, 1375 and 1035 cm^{-1}. NMR ($CDCl_3$): τ 9.1, τ 8.7, τ 8.0, τ 7.15, τ 6.5 and τ 6.05.

Found: C, 71.39; H, 13.00%, MW 190—200 (VPM). After the mixture had stood for a day, the precipitated 1,4-dibenzylpiperazine (**7a**)[11] (0.53 g, 10%) was filtered off. The filtrate was redistilled to give *N*-(2-hydroxyethyl)-*N*-benzylacetamide (**4a**) (4.47 g, 58%); bp 174°C/1.5 mmHg.

Reaction of 1-Benzylaziridine (1a) with Acetic Anhydride. A solution of acetic anhydride (3.06 g, 0.03 mol) in benzene (9 m*l*) was added, drop by drop, to a solution of **1a** (3.99 g, 0.03 mol) in benzene (30 m*l*). The mixture was refluxed for 3 hr and then concentrated to give a light yellow oil; this oil was distilled at 50—54°C/4 mmHg to give **13** (0.90 g). This product was identified as **13** by a comparison of its IR spectrum with that of the product from the reaction of **1a** with acetic acid. Distillation at 155—159°C/1 mmHg gave *N*-(2-acetoxyethyl)-*N*-benzylacetamide (**11**) (5.40 g, 72%). An analytical pure sample was obtained by redistillation; bp 150—151°C/0.5 mmHg.

Reaction of 1-Benzylaziridine (1a) with Thioacetic Acid. A solution of thioacetic acid (1.52 g, 0.02 mol) in methanol (10 m*l*) was stirred, drop by drop, into a solution of **1a** (2.66 g, 0.02 mol) in methanol (10 m*l*) under ice cooling. The mixture was refluxed for 3 hr and then concentrated to give a red viscous

8) A. T. Bottini and J. D. Poberts, *J. Amer. Chem. Soc.*, **80**, 5203 (1958).

9) R. C. Elderfield and H. A. Hageman, *J. Org. Chem.*, **14**, 605 (1949).

10) I. Okada, K. Ichimura and R. Sudo, This Bulletin, **43**, 1185 (1970).

11) I. Okada, N. Itoh and R. Sudo, *ibid.*, **42**, 547 (1969).

oil; this oil was distilled at 159—163°C/1.5 mmHg to give *N*-(2-mercaptoethyl)-*N*-benzylacetamide (**12**) (3.05, 73%). An analytical pure sample was obtained by redistillation; bp 158—160°C/1.2 mmHg.

Treatment of *N*-(Hydroxyethyl)-*N*-benzylacetamide Hydrochloride (3a) with Triethylamine. **3a** (4.60 g, 0.02 mol) and triethylamine (3.03 g, 0.03 mol) were dissolved in benzene (50 m*l*), after which the mixture was stirred. The triethylamine hydrochloride thus precipitated was filtered off. The filtrate was concentrated to give an oil which was subsequently distilled at 174—175°C/1 mmHg. Its IR spectrum was superimposed on that of **4a**.

Found: C, 67.91; H, 7.30; N, 7.12%. Calcd for $C_{11}H_{15}NO_2$: C, 68.37; H, 7.82; N, 7.25%.

BULLETIN OF THE CHEMICAL SOCIETY OF JAPAN VOL. 43 2596—2598 (1970)

Synthesis of [9]Heterophanes from 2-Cyclododecenone

Shinsaku FUJITA, Takeyuki KAWAGUTI and Hitosi NOZAKI

Department of Industrial Chemistry, Kyoto University, Yoshida, Kyoto

(Received March 26, 1970)

[9](3,5)Pyrazolophane (V) and 11-methyl[9](2,4)furanophane (IX) were prepared from 2-cyclododecenone (I) and their spectral properties were discussed. A new route to I from cyclododecanone is described.

The unusual properties of cyclophanes have received considerable attention. In particular, NMR investigations of the conformational changes have been conducted extensively.[1] Interest has also been focused on their heteroaromatic analogs (heterophanes[2,3]), as two natural products, muscopyridine[4] and metacycloprodigiosin,[5] were shown to have [10](2,6)pyridinophane and [9](2,4)pyrrolophane structure, respectively. In continuation of studies on the heterophanes,[2,6] we carried out the synthesis of [9]heterophanes from 2-cyclododecenone (I).*1

cis- and *trans*-2-cyclododecenone (I) were prepared from cyclododecene oxide.[8] An alternative route to I has been explored in this study starting from commercially available cyclododecanone. Bromination of cyclododecanone ethylene acetal (II) followed by dehydrobromination of the resulting III with potassium *t*-butoxide in dimethyl sulfoxide afforded IV, which was in turn hydrolyzed to I (*cis* : *trans*=1 : 4). The stereoisomeric mixture of I was subjected to further reactions without separating the components. The spectral data of these compounds supported their assigned structures.

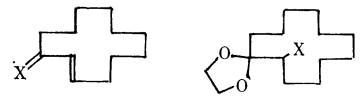

I: X=O II: X=H
IV: X=$-OCH_2CH_2O-$ III: X=Br

[9](3,5)Pyrazolophane (V) was synthesized as follows. Treatment of I with hydrazine hydrate in ethanol gave the corresponding pyrazoline (VI) which was a distillable but quite labile solid (MS, *m/e* 194 (M^+)). Freshly distilled VI was admixed with powdered sulfur and dehydrogenated at 200—220°C to afford pyrazolophane V. Compound V showed IR absorptions characteristic of the pyrazole ring (3200, 3025 and 1580 cm^{-1}). The NMR spectrum of V (Fig. 1) was consistent with the assigned structure (*vide infra*).

1,2-Addition of lithium acetylide to I gave 1-ethynyl-2-cyclododecen-1-ol (VII) whose spectral

1) F. Vögtle, *Chem. Ber.*, **102**, 3077 (1969) and references cited therein.

2) H. Nozaki, T. Koyama and T. Mori, *Tetrahedron*, **25**, 5357 (1969).

3) In agreement with Vögtle's proposal, we will call this kind of compound "heterophane" rather than "heterocyclophane." See F. Vögtle and P. Neumann, *Tetrahedron Lett.*, **1969**, 5329.

4) K. Biemann, G. Büchi and B. H. Walder, *J. Amer. Chem. Soc.*, **79**, 5558 (1957).

5) H. H. Wasserman, G. C. Rodgers and D. D. Keith, *ibid.*, **91**, 1263 (1969); H. H. Wasserman, D. D. Keith and J. Nadelson, *ibid.*, **91**, 1264 (1969).

6) H. Nozaki, S. Fujita and T. Mori, This Bulletin, **42**, 1163 (1969).

*1 When the present investigation of [9]heterophane was almost completed, Bradamante *et al.* reported a different approach to several [9]heterophanes.[7] This communication prompted us to report independent results obtained at present by using I as a starting material.

7) S. Bradamante, R. Fusco, A. Marchesini and G. Pagani, *Tetrahedron Lett.*, **1970**, 11.

8) H. Nozaki, T. Mori and R. Noyori, *Tetrahedron*, **22**, 1207 (1966).

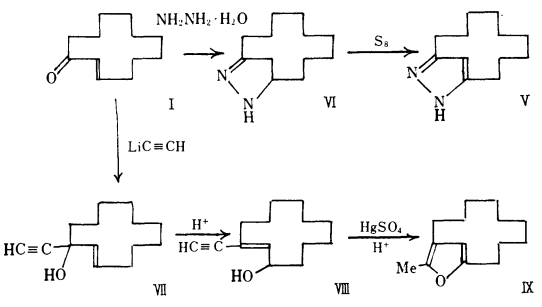

data were consistent with the assigned structure. Acid catalyzed isomerization of VII yielded 3-ethynyl-2-cyclododecen-1-ol (VIII). Subsequent treatment of VIII with mercuric sulfate under acidic condition resulted in cycloaddition of hydroxyl on ethynyl group to afford 11-methyl [9](2,4)furanophane (IX) which displayed IR absorptions due to the furan ring (3100, 1579 and 798 cm^{-1}).

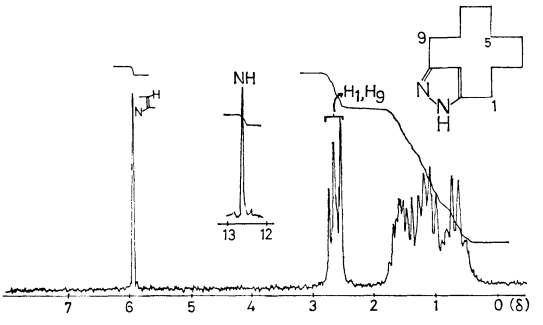

Fig. 1. The NMR spectrum of V (CCl_4, at 24°C, 60 MHz).

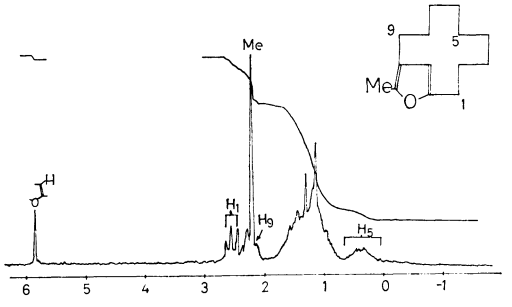

Fig. 2. The NMR spectrum of IX (CCl_4, at 60 MHz, 24°C).

The NMR spectra of the heterophanes prepared are shown in Figs. 1 and 2. Each nonamethylene chain should be flexible at room temperature, since the signal due to C_1 and C_9 protons can be approximately regarded as a triplet. Several methylene protons of chains were magnetically shielded as compared with the usual paraffinic methylene. The shielding effect may be ascribed to the diamagnetic ring current of pyrazole and furan ring. In particular, one of IX (*cf.* Fig. 2) made the signal of one methylene group separate from other peaks (δ 0.6—0.1 in CCl_4 and in CS_2). It is tentatively assigned to C_5 protons on the basis of conformational inspection by the Dreiding model. The position of the signal was dependent on temperature and shifted to a much higher field (δ 0.0——0.7, one proton) upon cooling to −72.5°C (Fig. 3). Probably, at this temperature the nonamethylene chain of IX is fixed to some extent and one of the C_5 methylene protons is forced close to the π-cloud of the furan ring. Since the UV spectrum of furanophane IX shows a considerable red shift as compared with 2,5-dimethylfuran (λ_{max} 218.5 nm), the furan ring of IX appears to suffer a distortion from coplanarity[9] similar to that of [8](2,5)furanophane.[2]

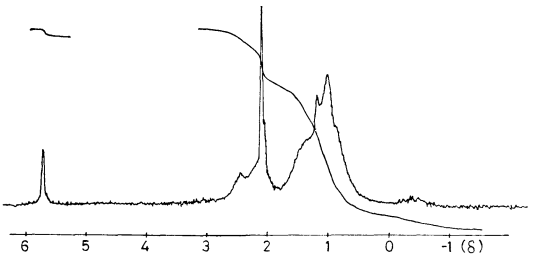

Fig. 3. The NMR spectrum of IX (CS_2, at 60 MHz, −72.5°C).

Experimental

All melting points are uncorrected. NMR data were obtained on a JEOL C-60-H spectrometer. Mass spectra were taken on a Hitachi RMS-4 spectrometer.

Cyclododecanone Ethylene Acetal (II). A solution of cyclododecanone (150 g, 0.82 mol), ethylene glycol (60 g, 0.97 mol) and *p*-toluenesulfonic acid (catalytic amount) in dry benzene (700 m*l*) was heated to reflux for 110 hr using a Dean-Stark condenser. The mixture was washed with water, dried over sodium sulfate and concentrated *in vacuo*. Distillation of the crude crystals through Vigreux column gave II (155 g, 84%) as pale yellow crystals, bp 104—105°C/0.2 mmHg, mp 68—71°C (ethyl acetate) (lit,[10] bp 125—130°C/3 mmHg, mp 70°C). IR (Nujol): 2948, 1480, 1390, 1231, 1124, 1064, 996, 957 and 875 cm^{-1}.

2-Bromocyclododecanone Ethylene Acetal (III). To a solution of II (22.6 g, 0.10 mol) in dry ether (70 m*l*) bromine (18.0 g, 0.11 mol) was added dropwise for 3 hr with vigorous stirring. The reaction mixture was neutralized with monosodium ethylene glycolate. After the ethereal layer was separated, the aqueous layer was thoroughly extracted with ether. The combined extracts were washed with water, dried over sodium sulfate and concentrated *in vacuo*. Fractional distillation of the residue yielded III (24.0 g, 79%), bp 120—124°C/0.08 mmHg, mp 72.9—73.6°C (ethyl acetate). IR

9) B. H. Smith, "Bridged Aromatic Compounds," Academic Press, New York, N. Y. (1964).

10) Haarmann and Reimer G. m. b. H., Fr. 1393647 (1965); *Chem. Abstr.*, 6886 (1965).

(Nujol): 2930, 2860, 1470, 1382, 1223, 1144, 1128, 1064, 984, 957 and 880 cm^{-1}. NMR (CCl_4): δ 4.4—4.7 (4H, m, $-OCH_2CH_2O-$) and 2.3—1.1 (21H, m).

Found: C, 55.0; H, 8.3%. Calcd for $C_{14}H_{25}O_2Br$: C, 55.1; H, 8.2%.

2-Cyclododecenone Ethylene Acetal (IV). A mixture of III (16.7 g, 55 mmol), potassium *t*-butoxide (12.3 g, 110 mmol) and dimethyl sulfoxide (70 m*l*) was mechanically stirred for 5 hr at 90°C under nitrogen atmosphere. The mixture was diluted with water and extracted with ether. The extracts were washed with water, dried (sodium sulfate) and concentrated *in vacuo*. Distillation of the residue gave IV (8.6 g, 70%), bp 150—153°C/5 mmHg. IR (neat): 3017, 2922, 1667, 1465, 1448, 1168, 1135, 1038, 983 and 946 cm^{-1}. NMR (CCl_4): δ 5.99—5.08 (2H, m, olefinic), 3.75 (4H, s, $-OCH_2CH_2O-$) and 2.5—1.2 (18H, m).

Found: C, 74.5; H, 10.6%. Calcd for $C_{14}H_{24}O_2$: C, 75.0; H, 10.8%.

2-Cyclododecenone (I). Hydrolysis of IV with dilute sulfuric acid gave a mixture of *cis*- and *trans*-2-cyclododecenone (*cis* : *trans*=1 : 4) in 74% yield, bp 127—134°C/7 mmHg (lit,[8] 95—105°C/3 mmHg).

3,5-Nonamethylene-2-pyrazoline (VI). A solution of I (1.85 g, 10.3 mmol) and hydrazine hydrate (80%, 1.37 g) in ethanol (30 m*l*) was heated to reflux for 1.5 hr. After concentration, the residue was distilled *in vacuo* to yield VI, as a white solid (1.10 g, 55%), bp 95—98°C/0.07 mmHg. The solid was so labile as to turn into a viscous yellow oil on exposure to air. The IR spectrum(neat) showed prominent peaks at 3302, 2902, 1624, 1471, 1293, 845 and 812 cm^{-1}, and MS exhibited a molecular ion peak at *m/e* 194.

[9](3,5)Pyrazolophane (V). Freshly distilled VI (1.10 g, 5.7 mmol) was admixed with powdered sulfur (0.18 g, 5.7 mmol) and heated at 200—220°C under nitrogen atmosphere for 2 hr. After the evolution of hydrogen sulfide had ceased, the crude product was subjected to separation on a silica gel column to afford crystalline V (0.77 g, 71%), mp 109—109.7°C (*n*-hexane). IR (Nujol): 3200, 3130, 3100, 3025, 2922, 2850, 1580, 1460, 1371, 1148 and 782 cm^{-1}. λ_{max} (EtOH): 207 nm (log ε 4.54). MS *m/e* (intensity): 192 (26), 177 (2), 163 (11), 149 (29), 135 (10), 124 (18), 110 (22), 109 (23) and 95 (100). The NMR is shown in Fig. 1.

Found: C, 75.1; H, 10.5%. Calcd for $C_{12}H_{20}N_2$: C, 75.0; H, 10.5%.

1-Ethynyl-2-cyclododecen-1-ol (VII). To a freshly prepared solution of lithium acetylide (from 0.13 g lithium) in liquid ammonia[11] a solution of I (2.41 g, 13 mmol) in dry ether (10 m*l*) was added dropwise in 10 min and mechanical stirring was continued for 2 hr at −35°C. The reaction mixture was treated with ammonium chloride (1.0 g) and allowed to stand overnight at room temperature. The residue was mixed with water and extracted with ether. The combined extracts were washed with water, dried over sodium sulfate, concentrated under reduced pressure and distilled to yield VII (1.41 g, 51%), bp 85—91°C/0.06 mmHg. IR (neat): 3425, 3332, 2120, 1625, 1464, 1448, 1111, 1015, and 978 cm^{-1}. NMR (CCl_4): δ 2.40 (1H, s, OH), 2.80 (1H, s, C≡CH), 5.75 (2H, m) and 2.45—0.77 (18H, m).

Found: C, 81.3; H, 10.7%. Calcd for $C_{14}H_{22}O$: C, 81.5; H, 10.8%.

3-Ethynyl-2-cyclododecen-1-ol (VIII). A solution of VII (1.27 g, 6.2 mmol) in tetrahydrofuran (15 m*l*) and 4% sulfuric acid (10 m*l*) was magnetically stirred at 100°C for 45 min under nitrogen atmosphere. After evaporation of tetrahydrofuran, the residual aqueous layer was extracted with ether, washed with water, dried over sodium sulfate and concentrated *in vacuo*. Distillation of the residue afforded VIII (1.10 g, 87%) as a highly viscous oil, bp 90—105°C/0.06 mmHg. IR (neat): 3372, 3325, 2079, 1621, 1464, 1447, 1111, 1034, 1009, 979 and 847 cm^{-1}. NMR (CCl_4): δ 5.73 (1H, d, J=9 Hz, C=CH), 3.94 (1H, s, OH), 3.26—2.88 (1H, m), 3.14 (1H, s, C≡CH) and 2.58—0.61 (18H, m).

Found: C, 81.3; H, 10.7%. Calcd for $C_{14}H_{22}O$: C, 81.5; H, 10.8%.

11-Methyl[9](2,4)furanophane (IX). A solution of VIII (0.25 g, 1.2 mmol), mercuric sulfate (92 mg) and 2% sulfuric acid (10 m*l*) in dioxane (15 m*l*) was heated to reflux at 100°C for 1.5 hr under nitrogen atmosphere. The mixture was neutralized with aqueous sodium hydrogen carbonate and extracted with ether. The ether extracts were washed with water, dried over sodium sulfate and concentrated *in vacuo*. The crude mixture was purified through a silica gel column and distilled under reduced pressure to give IX (0.045 g, 18%), bp 72—75°C/1.5 mmHg. IR (neat): 3100, 2927, 2862, 1637, 1579, 1467, 1346, 1217, 1191, 997, 929 and 798 cm^{-1}. λ_{max} (EtOH): 225 nm (log ε 2.68). MS *m/e* (intensity): 206 (49), 191 (16), 177 (11), 163 (35), 149 (34), 135 (48), 121 (60) and 108 (100).

Found: C, 81.7; H, 10.6%. Calcd for $C_{14}H_{22}O$: C, 81.5; H, 10.8%.

The NMR spectra at room temperature and at −72.5°C are shown in Figs. 2 and 3, respectively.

The authors are grateful to Professor Keiiti Sisido for his generous help and to Mr. Tamejiro Hiyama for his assistance. Financial support from Toray Science Foundation is acknowledged.

11) R. A. Raphael, "Acetylenic Compounds in Organic Syntheses," p. 193, Academic Press, New York, N. Y. (1955).

BULLETIN OF THE CHEMICAL SOCIETY OF JAPAN VOL. 43 2599—2603 (1970)

Effect of Coexisting Minerals on the Graphitization of Carbon under Pressure. IV. Accelerating Effect of Calcium Oxide

Shin-ich HIRANO, Hajime SAITO and Michio INAGAKI

Faculty of Engineering, Nagoya University, Chikusa-ku, Nagoya

(Received January 22, 1970)

Heat treatments of polyvinylchloride coke in the presence of three kinds of calcium oxide calcined at different temperatures were carried out in order to study the effect of the reactivity of calcium oxide on the acceleration of graphitization of carbon under the quasihydrostatic pressure of 3.2 kbar. A remarkable difference in the accelerating effect on graphitization was confirmed. In the presence of the most reactive calcium oxide calcined at 920°C, the graphitization of the carbon began at about 1100°C and the content of the graphitic component became 100% by heat treatment at 1500°C for 60 min. While in the presence of the least reactive calcium oxide calcined at 1470°C, the graphitic component, an even hump on the corresponding diffraction angle, could not be detected in specimens heat-treated below 1500°C. The content of graphitic component and the distribution of calcium in heat-treated specimens were measured by an electron microprobe analyzer. It was found that the part having a larger content of calcium had a larger content of the graphitic component. A possible mechanism of the accelerating effect of calcium compound on graphitization is considered to be chemical concerning the intermediate formation of carbide or metal. The formation of the graphitic component seems to proceed by the reaction:

$$CaO+C\ (amorphous) \rightarrow Ca+CO \rightarrow CaO + C\ (graphite) \quad (1)$$

below 1300°C, and above 1300°C, mainly by the reaction:

$$CaO+3C(amorphous) \rightarrow CaC_2+CO \rightarrow CaO+3C\ (graphite) \quad (2)$$

and also by reaction (1). The driving force of the formation of the graphitic component through these reactions is the difference in the free energy between amorphous carbon and graphite, *viz.*, disordered and ordered graphite.

It was reported previously[1-3] that the graphitization of carbon was accelerated by the coexistence of calcium carbonate and hydroxide during heat treatment under the pressure of 3.2 kbar. A graphitic component began to appear in the carbon specimen at about 1100°C[1,2] in contact with calcium carbonate or limestone and at about 600°C[3] in contact with calcium hydroxide. The (002) diffraction line of these carbon specimens had a composite profile, *viz.*, graphitic component existed side by side with turbostratic component. The turbostratic component had transformed directly to the graphitic component without going through intermediate state. Though this heterogeneous process of graphitization seems to be similar to that observed on the same carbon heat-treated under pressure without any coexisting mineral,[2,4] the mechanisms of accelerating effects of these two processes were considered to be different from each other. The intermediate formation of unstable carbide seems to be formed by a chemical reaction of carbon and coexisting calcium compounds as one of the possible mechanism of the accelerating effect.

In the present work, calcium oxide specimens calcined at different temperatures were used as the coexisting mineral in the heat treatment of carbon under the pressure of 3.2 kbar. The object of the experiments was to study the effect of reactivity of calcium oxide on the acceleration of graphitization.

Experimental

The carbon sample used was the same polyvinyl chloride coke (PV-7) as that used in the previous works.[1-3] Three kinds of calcium oxide were prepared by the calcination of calcium carbonate at 920, 1050 and 1470°C for 60 min and were pressed into disks of 8.0 mm in diameter and 3.5 mm in thickness. It was confirmed by X-ray diffraction method whether calcium carbonate had decomposed completely or not. The disks were covered with calcium oxide powder and kept in an evacuated desiccator. The crystallite size

1) T. Nod, M. Inagaki, S. Hirano and K. Amanuma, This Bulletin, **41**, 1245 (1968).

2) T. Noda, M. Inagaki, S. Hirano and H. Saito, *Kogyo Kagaku Zasshi*, **72**, 643 (1969).

3) T. Noda, M. Inagaki, S. Hirano and H. Saito, This Bulletin, **42**, 1738 (1969).

4) T. Noda, K. Kamiya and M. Inagaki, *ibid.*, **41**, 485 (1968).

TABLE 1

Sample	Calcination °C	Calcination min	Crystallite size, Å	Bulk density g/cm	Prosity %
CaO-9	920	60	720	2.78	18
CaO-10	1050	60	950	2.88	15
CaO-11	1470	60	1000	2.95	13

and bulk density of the three kinds of calcium oxide (designated as CaO-9, CaO-10 and CaO-15) are given in Table 1. Calcium oxide calcined at lower temperature is known to be more reactive than that calcined at higher temperature.[5-7]

The heat treatment of the carbon sample in the presence of calcium oxide was carried out at various temperatures between 900 and 1500°C for 60 min under the quasi-hydrostatic pressure of 3.2 kbar in a simple piston-cylinder type pressure vessel. The cell arrangement and the procedure for the experiments were exactly the same as reported previously.[1-3] Temperature of heat treatment was estimated from the relation between temperature and input power. Pressure was calibrated by the transition points of KNO_3 and AgI.[8]

The diffraction profile of (002) line was measured for the central part of the heat-treated carbon specimen by using Ni-filtered Cu$K\alpha$ radiation and a recording goniometer. The composite profile observed was separated graphically into two component profiles corresponding to the graphitic component GM and turbostratic component AM.*1 The c_0-spacing and crystallite size L_c were measured from the (002) profile by the same method as reported previously.[1] The content of the graphitic component GM was obtained from the ratio of the area under the profile for the component GM to the total area under the composite profile. The area ratio was corrected for the preferred orientation of crystallite in the X-ray specimen by a conventional method.[2] The heat-treated specimens were also observed under an electron microscope. The specimen for electron microscopy was dispersed in trichloroethylene by ultrasonic vibration and then supported on an evaporated carbon film.

Results and Discussion

Each carbon specimen heat-treated above 1000°C was obtained as a caked tablet. In these caked specimens, calcium oxide was always detected by X-ray diffraction method. Its amount increased with the increase in heat treatment temperature (HTT). In the specimens heat-treated above 1300°C in the presence of CaO-9 and those heat-treated above 1400°C in the presence of CaO-10, calcium carbide was detected in the part where carbon and calcium oxide contacted each other. Recrystallization of calcium oxide was not observed

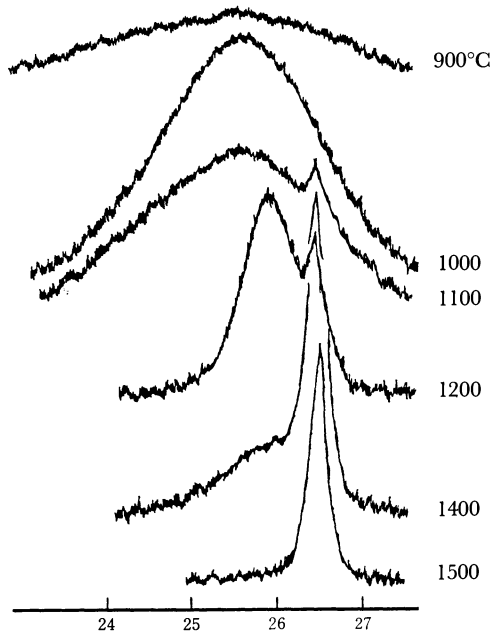

Fig. 1. Profiles of (002) diffraction line of carbon (PV-7) heat-treated under 3.2 kbar.
a) in the presence of calcium oxide calcined at 920°C for 60 min (CaO-9)

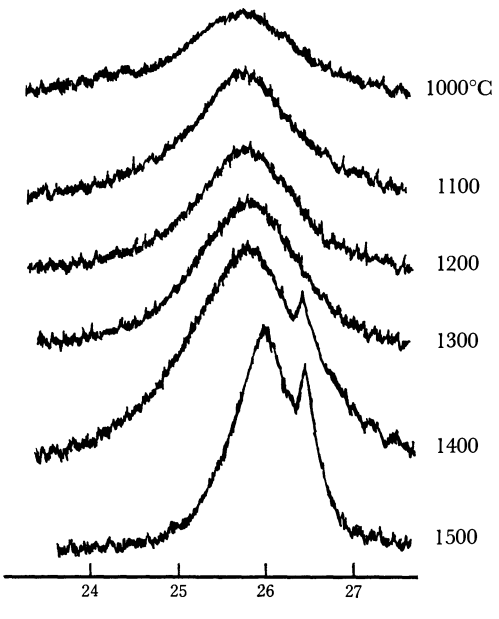

b) in the presence of calcium oxide calcined at 1050°C for 60 min (CaO-10)

5) H. C. Fischer, *J. Amer. Ceram. Soc.*, **38**, 245, 284 (1955).
6) T. Noda, *Kogyo Kagaku Zasshi*, **40**, 195, 196 (1937).
7) Y. Ono and T. Matsuoka, *Yogyo Kyokai Shi*, **59**, 284, 341 (1951).
8) M. Inagaki, S. Hirano and H. Saito, *ibid.*, **76**, 264 (1968).
*1 Suffix denotes these components were formed in the presence of a mineral.

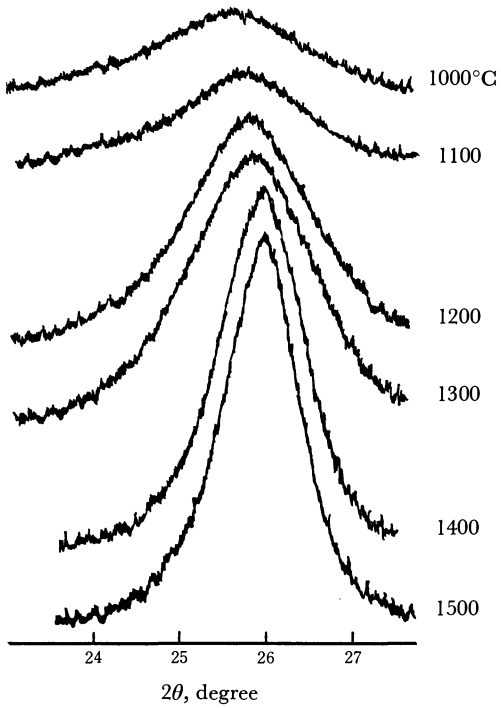

c) in the presence of calcium oxide calcined at 1470°C for 60 min (CaO-15)

in the present experiment.

Changes of the profile of (002) diffraction line with HTT are shown in Fig. 1 a), b) and c). We see that there is a remarkable difference in the accelerating effect of the three kinds of calcium oxide on graphitization of carbon. In the presence of CaO-9, the graphitization of carbon began at about 1100°C and the profile for the graphitic component developed rapidly with the increase in HTT. The graphitization of the same carbon was found to begin at about the same HTT in the presence of limestone[1] and calcium carbonate.[2] In the presnece of CaO-10, the graphitic component G_M could be detected on (002) profile of the specimen heat-treated above 1400°C. In the presence of CaO-15, however, the graphitic component, an even hump at the corresponding diffraction angle, could not be detected in specimens heat-treated below 1500°C. From profiles of (004) line, the same results were deduced.

The variation of content of the graphitic component G_M is shown in Fig. 2 as a function of HTT. In the presence of the most reactive calcium oxide CaO-9, the graphitic component G_M increased very rapidly. The content of G_M turned out almost 100% at HTT of 1500°C. In the presence of less reactive CaO-10, however, only a small amount of the graphitic component G_M was found above 1400°C, and in the presence of CaO-15 no graphitic component G_M was observed at least up to 1500°C. The changes of c_0-spacing and crystallite size L_c with HTT are given in Figs. 3 a) and b), together with the results obtained in the presence of calcium

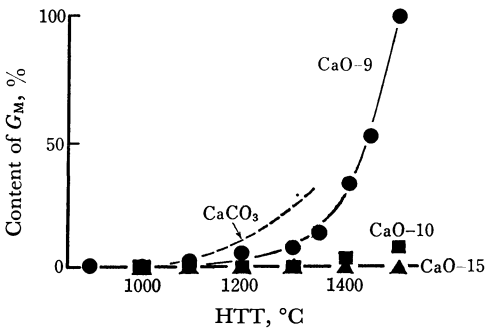

Fig. 2. The variations of content of the graphitic component G_M with HTT under 3.2 kbar for 60 min.
●: in the presence of CaO-9
■: in the presence of CaO-10
▲: in the presence of CaO-15

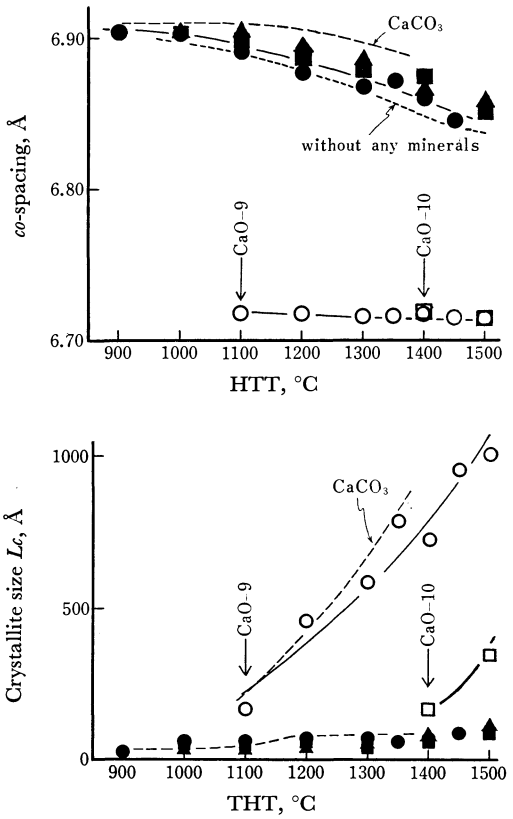

Fig. 3. Changes of c_0-spacing and crystallite size L_c of carbon (PV-7) with HTT, which was heat-treated under 3.2 kbar.

Turbostratic component A_M	Graphitic component G_M	
●	○	in the presence of CaO-9
■	□	in thejpresence of CaO-10
▲	△	in the presence of CaO-15

carbonate and without any coexisting mineral.[2] The c_0-spacing of the graphitic component G_M was almost constant at 6.72 Å as in the cases of coexistence of limestone or calcium carbonate and without any mineral.[2,3] The crystallite size L_c of G_M increased with the increase in HTT, and became larger than 1000 Å at 1500°C in the case of CaO-9. The c_0-spacing of the turbostratic component A_M decreased gradually and its crystallite size L_c increased only silghtly with the increase in HTT.

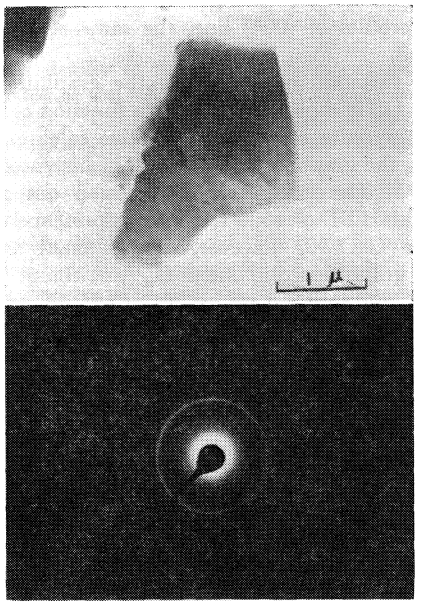

Fig. 4. Bright-field electron micrograph and selected area electron diffraction pattern of turbostratic particle under 3.2 kbar in the carbon specimen heat-treated at 1100°C for 60 min under 3.2 kbar in the presence of calcium oxide CaO-9.

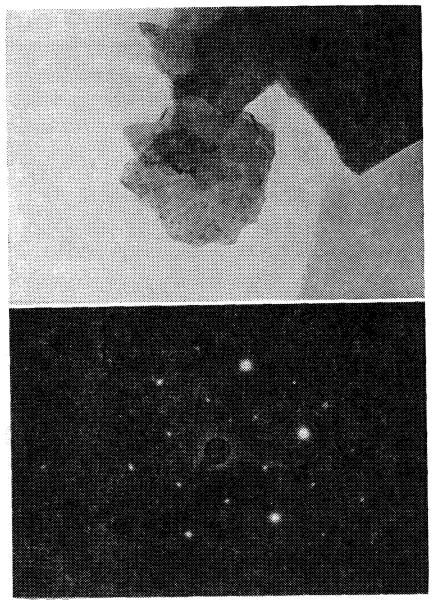

Fig. 5. Bright-field electron micrograph and selected area electron diffraction pattern of graphitic particle in the carbon specimen heat-treated at 1100°C for 60 min under 3.2 kbar in the presence of calcium oxice CaO-9.

In the specimens heat-treated above 1100°C in the presence of CaO-9 and those heat-treated above 1400°C in the presence of CaO-10, well-crystallized flaky particles having the same six-fold diffraction pattern as graphite single crystal were found under an electron microscope, besides the particles having continuous diffraction rings (Figs. 4 and 5).

The distribution of the graphitic component G_M in the caked specimens was examined by taking samples from different parts. The change of profiles and the distribution of the content of G_M in the specimen heat-treated at 1400°C in the presence of CaO-9 are shown in Fig. 6 as an example. The part closer to calcium oxide disk was found to have a larger content of G_M. The distribution of calcium element was measured by using an electron microprobe analyzer. In Fig. 7, the distribution of calcium across the thickness is shown on the specimen heat-treated at 1400°C in the presence of CaO-9. It is shown that the closer to calcium oxide disk, the larger the content of calcium.

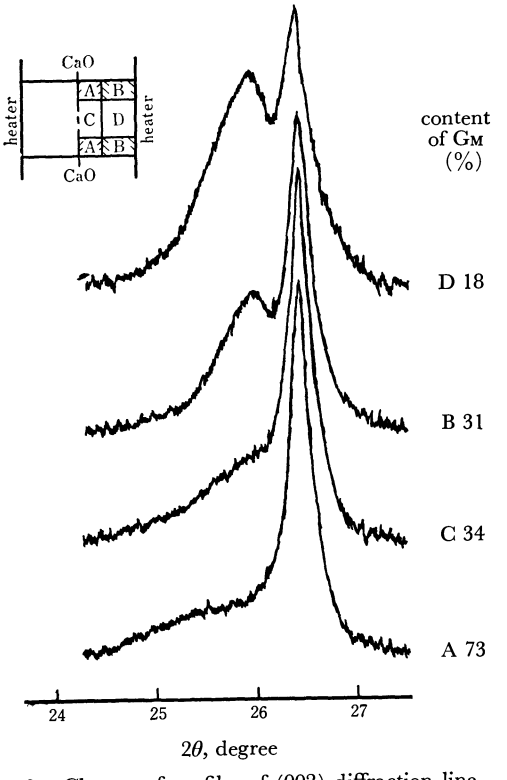

Fig. 6. Change of profiles of (002) diffraction line and distribution of content of graphitic component G_M in the specimen heat-treated at 1400°C for 60 min under 3.2 kbar in the presence of CaO-9.

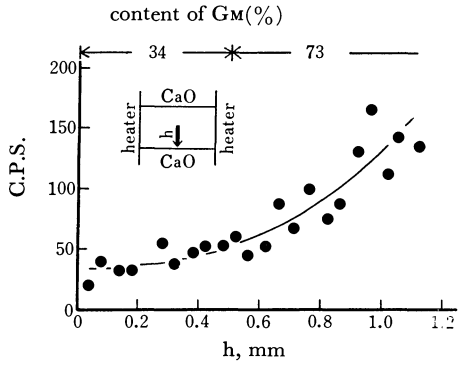

Fig. 7. Relation between distribution of calcium across the thickness and content of graphitic component G_M in the specimen heat-treated at 1400°C for 60 min under 3.2 kbar in the presence of CaO-9.

Generally, the part having the larger content of calcium has the larger content of the graphitic component G_M. The same relation between calcium content and content of G_M was observed in the specimens obtained by heat treatment in the presence of calcium carbonate under 3.2 kbar.[9]

It is suggested that the formation of the graphitic component in the presence of calcium compounds under pressure proceeds by the mechanisms explained below. The fact that calcium carbide was detected above around 1300°C, in the part where the carbon specimen contacted the calcium oxide disk, suggests that the intermediate formation and subsequent decomposition of calcium carbide may mainly lead to the formation of the graphitic component in the carbon specimen:

$$CaO+3C\ (\text{amorphous}) \rightarrow CaC_2+CO \quad (1)$$
$$CaC_2+CO \rightarrow CaO+3C\ (\text{graphite}). \quad (2)$$

Calcium oxide distributed in the carbon specimen must be the decomposition product of calcium carbide according to Eq. (2). The content of graphitic component should vary with the content of calcium oxide in the carbon specimen. This was in good accordance with experimental results.[9] On the other hand, the fact that calcium carbide was not detected below 1200°C in the specimen and the difficulty of the decomposition of calcium carbide under such condition make it impossible to explain the formation of the graphitic component at lower temperatures below 1300°C by the same mechanism as that above 1300°C. In this case, the formation of the graphitic component may proceed through the following reaction:

$$CaO+C\ (\text{amorphous}) \rightarrow Ca+CO \rightarrow CaO+C\ (\text{graphite}). \quad (3)$$

The results[11] concerning heat treatments of carbon in the presence of magnesia, alumina and silica under pressure also support this mechanism. The formation of the graphitic component by this mechanism is also possible for high temperature process. The driving force of the graphite formation through the intermediate formation of calcium carbide or calcium metal is the difference in the free energy between amorphous carbon and graphite, *viz.*, disordered and ordered graphite.[12]

The more reactive calcium oxide reacts with carbon more easily at lower temperature.[10] This was verified by the fact that carbide was detected in the carbon specimen heat-treated at 1300°C in the presence of CaO-9 and at 1400°C in the presence of CaO-10. This low reaction temperature of active oxide is closely related to the low temperture formation of the graphitic component in the presence of reactive oxide. When calcium carbonate (limestone) or calcium hydroxide was used as the coexisting mineral, nascent oxide formed during the heat treatment may have reacted with carbon to form calcium metal.

An apparent close association[1] of recrystallization and melting of coexisting calcium carbonate and hydroxide with the acceleration of graphitization is mainly due to the increased rate of reaction of the coexisting minerals with carbon at temperatures where recrystallization of minerals becomes vivid, or when the minerals melt.

The authors are indebted to Dr. T. Noda, President of Mie University, for many helpful suggestions and discussions on this work.

9) S. Hirano, H. Saito and M. Inagaki, This Bulletin, **43**, 2624 (1970).

10) T. Mukaibo and Y. Yamanaka, *Kogyo Kagaku Zasshi*, **56**, 232 (1953).

11) S. Hirano, M. Inagaki and H. Saito, unpublished.

12) E. Fitzer and B. Kegel, *Carbon*, (Oxford), **6**, 433 (1968).

BULLETIN OF THE CHEMICAL SOCIETY OF JAPAN VOL. 43 2604—2608 (1970)

The Adsorption of Polyvinyl Pyrrolidone on Silver Iodide Surfaces

Masaaki SUGIURA

7th Division, Government Chemical Industrial Research Institute, Tokyo, 85 Shinshuku, Hiratsuka-shi, Kanagawa

(Received March 7, 1970)

Adsorption isotherms for four kinds of polyvinyl pyrrolidone (PVP), having different molecular weights, on the sol particles and the powder of silver iodide at 25°C were obtained. Further, the adsorption of PVP on the sol particles was investigated by means of the electrophoresis method. All of the PVP materials give approximate adsorption isotherms of the Langmuir type, at least up to the PVP concentration of 0.4 g/*l*. At higher concentrations, the amounts of PVP adsorbed gradually increase with the increase in the PVP concentration. The effect of the molecular weight on the PVP adsorption is not observed except for the lowest-molecular-weight material, which displays a lower adsorption. The tendency for the ζ-potential of the sol particles to increase with an increase in the PVP concentration almost coincides with that of the amount of PVP adsorbed.

In previous works, the present author and co-worker have studied the adsorption of several lyophilic polymers (gelatin,[1] polyvinyl alcohol[2] and polyacrylamide[3]) on the sol particles of silver iodide as part of an investigation of the photographic emulsion of synthetic polymers. The adsorption isotherms of these polymer materials at low concentrations are roughly of the Langmuir type. However, considerable differences among the polymer materials in the limiting adsorption or in the ζ-potential for the sol particles are observed, as will be described later.

In this work, polyvinyl pyrrolidone (PVP), as a markedly water-soluble, nonionic polymer, was taken as the adsorbate to silver iodide. By measuring the amounts of PVP adsorbed on the sol particles and the powder of silver iodide and the ζ-potential of the sol particles, the adsorption behavior of PVP on the silver iodide surface could be discussed, and the values obtained were compared with those obtained for the polymers in previous works.[1-3]

Experimental

Materials. As PVP materials, PVP K-90, K-30 and K-15 obtained in the form of powder from the General Aniline & Film Co. and PVP K-60 obtained as a 45% aqueous solution from the Tokyo Kasei Kogyo Co. were used. The PVP materials were purified as follows: PVP was precipitated at room temperature (20—25°C) by the addition of freshly-distilled acetone to a concentrated solution obtained by dissolving PVP in water. The precipitate was again dissolved in small quantities of water, and then this procedure was repeated. The precipitate thus obtained was repeatedly washed with acetone and then vacuum-dried to free it from acetone and water at temperatures up to 100°C. The PVP solutions used for adsorption and electrophoretic experiments were prepared by dissolving the dry polymers in water. The concentrations of the PVP K-90 and K-60 solutions were determined by weighing the polymer films, prepared from 5-m*l* portions of the solutions cast on a stainless steel plate, after they had been vacuum-dried at 100°C for one hour. Those of the PVP K-30 and K-15 solutions were estimated from the weights of the dry polymers added to the water. The molecular weights of the PVP materials after purification were calculated from their intrinsic viscosities by the relationship;[4]

$$[\eta]=6.76\times10^{-2}M^{0.55},$$

where $[\eta]$ is the intrinsic viscosity in ml/g, and M, the viscosity-average molecular weight. The molecular weights of PVP K-90, K-60, K-30, and K-15 were 9.3×10^5, 3.0×10^5, 4.0×10^4, and 7.6×10^3 respectively.

Preparation of Silver Iodide Sol. Into the solution obtained by mixing 11 m*l* of a 0.1M potassium iodide solution and 69 m*l* of water, we vigorously stirred 10 m*l* of a 0.1M silver nitrate solution. This procedure was repeated six to ten times. All the silver iodide sols prepared in this manner were then combined and transferred into a flask with a 1-*l* capacity. After aging at room temperature for 18—24 hr, the silver iodide sol whose turbidity was in a range to be given below was used for the adsorption or electrophoretic experiments; when the sol was diluted by the addition of water to make the concentration of silver iodide 0.01 mol/*l*, the turbidity of the diluted sol was in the 0.89—1.02 cm^{-1} range. The surface area of the sol particles at a turbidity of 0.94 cm^{-1} was 1.7×10^5 cm^2/g, based on the adsorption of 1,1′-diethyl-2,2′-cyanine iodide with an assumed

1) M. Sugiura, *Kogyo Kagaku Zasshi*, **73**, 92 (1970).
2) M. Sugiura and A. Yabe, *ibid.*, in press.
3) A. Yabe and M. Sugiura, *ibid.*, **72**, 2356 (1969).
4) G. B. Levy and H. P. Frank, *J. Polym. Sci.*, **17**, 247 (1955).

molecular area of 43 Å².[5] On the basis of this particle size, assuming that the sol particles were spherical, the surface areas for other silver iodide sols were estimated from their turbidities by applying Rayleigh's law. The turbidity measurements were carried out using a Tokyo Koden nephelometer, and the dye-adsorption experiment was done by the method of Suzuki and Ishida.[6]

Preparation of Silver Iodide Powder. A silver iodide powder was prepared in the manner described by Mathai and Ottewill.[7] The surface area determined by the adsorption of the cyanine dye mentioned above was 6.7×10^3 cm²/g. This dye-adsorption experiment, considering that the dye adsorption was affected by cosolutes, was carried out by suspending the powder in a solution which had the same composition as the solvent of the sol described above. The particle size of this powder, obtained by the dye adsorption, roughly agreed with the results of observation using an electron micrograph.

Adsorption of PVP on Silver Iodide Sol Particles. 45 m*l* of the silver iodide sol were added to 5 m*l* of the PVP solution at 25±0.1°C. The mixture was maintained at this temperature for 1 hr, with occasionally shaking, and then centrifuged at room temperature for 30 min at 15000 g. The PVP concentration of the supernatant solution was determined interferometrically. For this we used a Zeiss interferometer with a 4- or 8-cm cell. The standard solutions used in constructing the calibration curves were prepared by mixing 5-m*l* portions of PVP solutions of known concentrations and a 45-m*l* portion of the supernatant solution obtained by centrifuging the silver iodide sol used for PVP adsorption.

The time dependence of the PVP adsorption was not recognized at times longer than 15 min, as is shown by the four examples in Fig. 1. The silver iodide particles dispersed in the sols were not precipitated in the presence of PVP during the adsorption process. However, since the particles were aggregated in the presence of PVP in the low concentration range, the aggregation was confirmed by the turbidity measurements.

Adsorption of PVP on Silver Iodide Powder. A 5-g portion of silver iodide powder was added to 50 m*l* of the PVP solution in a conical flask with a 100-m*l* capacity. After sealing, the contents were agitated with a magnetic stirrer for 1 hr in a thermostatted chamber at 25±1°C, and then centrifuged at room temperature for 15 min at 9000 g. The PVP concentration of the supernatant solution was determined interferometrically, as has been described above. In these measurements, since the adsorption equilibrium was almost established for 30 min, as is shown in Fig. 1, one hour was chosen as the time for the equilibration of PVP with the powder.

Electrophoretic Measurements. The electrophoretic measurements of the sol particles were carried out at 25±1°C using an ultramicroelectrophoresis apparatus described previously.[1] The sols used for these measurements were prepared as follows: a silver iodide sol having the same composition as the sol used for the adsorption experiment was diluted five-fold by a supernatant solution obtained by centrifuging the same sol, and then 45 m*l* of the diluted sol were added to 5 m*l* of the PVP solution. The ζ-potential of the sol particles was calculated using Henry's equation:[8]

$$\zeta=4\pi\eta u/Df(\kappa a), \qquad (2)$$

where η is the solvent viscosity; u, the mobility of the particle; D, the dielectric constant of the medium, and $f(\kappa a)$, the Henry factor, in which κ is the Debye-Hückel function, and a, the particle radius; the η values were obtained from the viscosity measurements of solutions with the same compositions as the solvents.

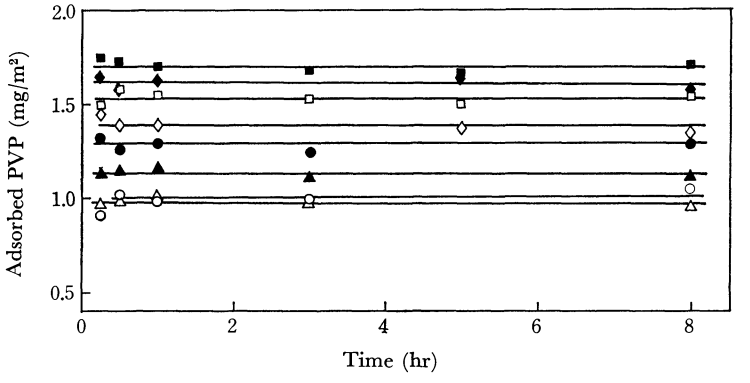

Fig. 1. Time dependence of PVP adsorption. Adsorption of PVP on silver iodide sol particles from the solutions of added concentration.
□ K-90 8.73×10^{-2} g/*l*, ■ K-90 4.37×10^{-1} g/*l*,
◇ K-15 1.73×10^{-1} g/*l*, ◆ K-15 8.64×10^{-1} g/*l*
Adsorption of PVP on silver iodide powder from the solutions of added concentration.
○ K-90 8.73×10^{-2} g/*l*, ● K-90 4.37×10^{-1} g/*l*,
△ K-15 1.73×10^{-1} g/*l*, ▲ K-15 8.64×10^{-1} g/*l*

5) R. Peacock and A. M. Kragh, *J. Photogr. Sci.*, **16**, 229 (1968).
6) S. Suzuki and T. Ishida, *J. Soc. Sci. Phot. Jap*, **25**, 30 (1962).
7) K. G. Mathai and R. H. Ottewill, *Trans. Faraday Soc.*, **62**, 750 (1966).
8) D. C. Henry, *Proc. Roy. Soc., Ser. A*, **133**, 106 (1931).

Results

Adsorption of PVP on Silver Iodide Sol Particles. The adsorption isotherms for PVP K-90, K-60, K-30, and K-15 on the sol particles are given in Fig. 2, plotted as mg PVP adsorbed per m^2 of the surface against the PVP concentration. There is no significant difference in the amounts adsorbed among PVP K-90, K-60, and K-30; PVP K-15, which has the lowest molecular weight, alone gives a lower adsorption.

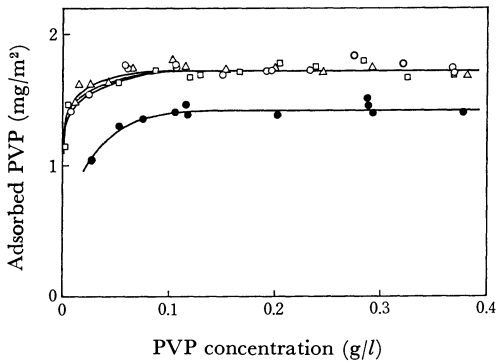

Fig. 2. Adsorption isotherms for PVP on silver iodide particles.
○ K-90, △ K-60, □ K-30, ● K-15

The turbidity-*versus*-PVP-concentration curves for silver iodide sols in the presence of PVP K-90, K-60, K-30, and K-15 are given in Fig. 3; the sols used for these measurements were prepared by adding the silver iodide sols, which gave a turbidity of 0.94 cm^{-1} in the absence of PVP, to various PVP solutions; then, after an hour, the turbidities were measured. The sol particles were aggregated in the presence of a PVP of a high molecular weight, such as PVP K-90 or K-60.

Adsorption of PVP on Silver Iodide Powder. The adsorption isotherms for PVP K-90, K-60, K-30, and K-15 on the silver iodide powder up to the PVP concentrations of 0.4 g/*l* and 4.5 g/*l* are given in Fig. 4 and Fig. 5 respectively. These isotherms in low PVP concentrations show tendencies similar to those shown in Fig. 2. At higher

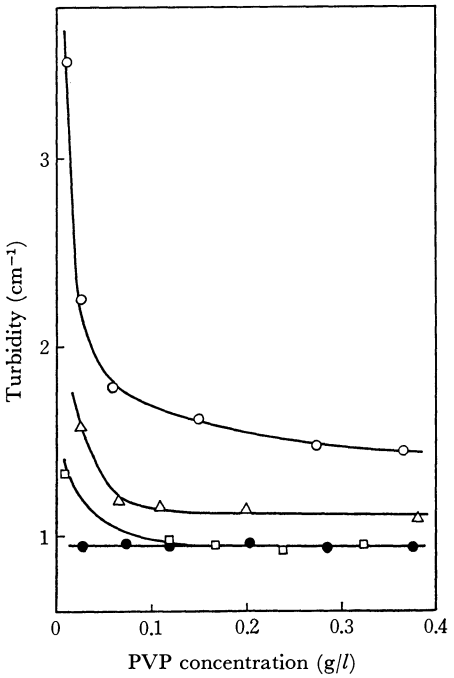

Fig. 3. Turbidity *vs.* PVP concentration curves for silver iodide sols in the presence of PVP.
○ K-90, △ K-60, □ K-30, ● K-15

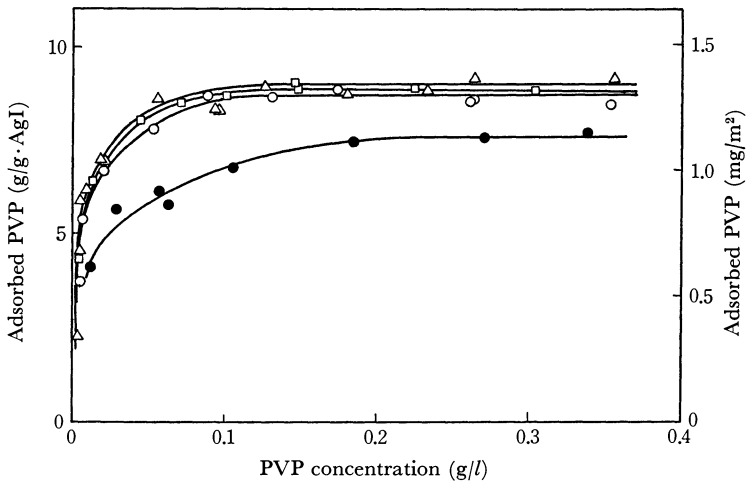

Fig. 4. Adsorption isotherms for PVP on silver iodide powder up to PVP concentration of 0.4 g/*l*.
○ K-90, △ K-60, □ K-30, ● K-15

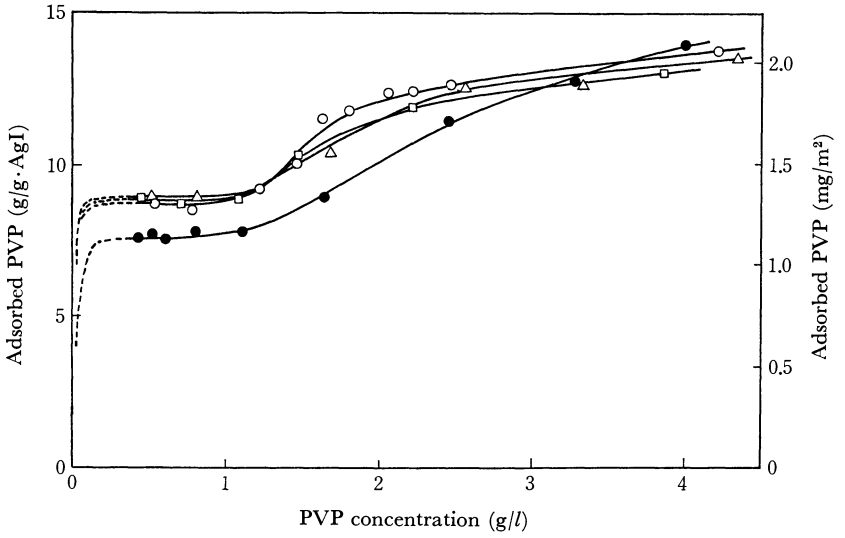

Fig. 5. Adsorption isotherms for PVP on silver iodide powder up to PVP concentration of 4.5 g/*l*.
○ K-90, △ K-60, □ K-30, ● K-15

PVP concentrations, the amounts of PVP adsorbed gradually increase with an increase in the PVP concentration.

ζ-potential of Sol Particles. The ζ-potential-*versus*-PVP-concentration curves for silver iodide sols in the presence of PVP K-90, K-60, K-30, and K-15 are given in Fig. 6; the free PVP concentrations were estimated from the relation between the added element and the equilibrium concentration of the PVP obtained from the measurements of the PVP adsorption on the sol particles, assuming that the amounts of PVP adsorbed per unit of the surface area of the particles in the diluted sols were equal to those in the concentrated sols. The ζ-potential of the sol particles in the absence of PVP was −75.6 mV. The tendency for the ζ-potentials to increase with an increase in the PVP concentration coincides with that of the amounts of PVP adsorbed.

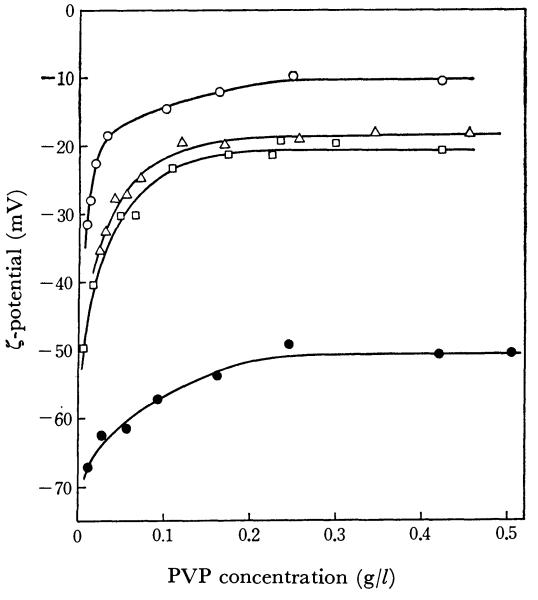

Fig. 6. ζ-Potential *vs.* PVP concentration curves for silver iodide sols in the presence of PVP.
○ K-90, △ K-60, □ K-30, ● K-15

Discussion

The adsorption isotherms and the turbidity curves for PVP in the low-concentration region are similar to those for polyvinyl alcohol and polyacrylamide, both nonionic, lyophilic polymers, obtained in previous works.[2,3] It can be considered that the plateaux of the isotherms in Fig. 2 or Fig. 4 are suitable for the monolayer saturation of PVP, since the ζ-potential curves, suggesting the coverages of the silver-iodide surfaces, approach constant values at the PVP concentrations reaching the plateaux. At higher concentrations of PVP, the increase in the isotherms, therefore, intimates that the adsorption extends to two or more molecular layers. In fact, in all cases considerable amounts of PVP were confirmed to be adsorbed at high PVP concentrations, up to about 30 g/*l*, though their exact values could not be obtained because of the difficulty of measuring the slight difference between the added element and the equilibrium concentration of PVP.

The difference in the amount of PVP adsorbed per unit of surface area between the sol particles and the powder, presented in Fig. 2 and Fig. 4, is mainly caused by a disagreement between the surface

TABLE 1. LIMITING ADSORPTION AND ζ-POTENTIAL FOR VARIOUS POLYMER MATERIALS ON SILVER IODIDE SOL PARTICLES, AND VALUES OF ν

Polymer	Molecular weight	Limiting adsorption (mg/m²)	Limiting ζ-potential (mV)	ν**
PVP	9.3×10^5(K-90)	1.7	−10	1.2
	3.0×10^5(K-60)	1.7	−18	1.0
	4.0×10^4(K-30)	1.7	−21	1.0
	7.6×10^3(K-15)	1.4	−51	1.0
Gelatin	1.1×10^5	6.0	−11	1.5
	8.8×10^4 (pH 6.0	4.8	−13	1.2
	7.3×10^4 —6.5)	4.3	−14	1.0
	6.1×10^4	4.0	−13	1.0
	8.8×10^4(pH 4.7)	6.0	0	1.0
	8.8×10^4(pH 3.6)	4.0	+12	3.0
Polyvinyl alcohol	1.2×10^5(99.4)*	1.95	− 6	1.5
	6.4×10^4(99.4)*	1.9	− 8	1.5
	2.9×10^4(99.4)*	1.9	− 9	1.45
	1.7×10^4(99.4)*	1.9	−12	1.3
	7.7×10^4(98.8)*	1.9	− 7	1.5
	7.7×10^4(96.5)*	1.95	− 6	1.5
	7.7×10^4(94.4)*	2.2	− 6	1.5
	7.7×10^4(92.3)*	2.75	− 7	1.5
	7.7×10^4(90.6)*	3.1	− 7	1.5
Poly-acrylamide	7.1×10^5	3.6	− 3	1.0
	2.2×10^5	3.4	− 6	1.0
	8.9×10^4	2.4	−13	1.0
	5.2×10^4	1.5	−16	1.0

* % hydrolysis

** The values for PVP were calculated from the isotherms in Fig. 4 and for gelatin from those obtained for ten-fold diluted sols.

area required for PVP adsorption and that derived from the cyanine dye adsorption, except for the difference in the adsorption behaviour of PVP molecules at the surfaces; the low ionic strength in the solvent tends to decrease the adsorption. In this regard, further investigation is necessary.

The values of the limiting adsorption and the ζ-potential for PVP on the sol particles at monolayer saturation are listed in Table 1 and compared with those obtained for gelatin,[1] polyvinyl alcohol[2] and polyacrylamide[3] in previous works; the sols used all contained the same quantity of silver iodide per unit of volume, and the surface areas of the sol particles, to facilitate comparison, were recalculated from the turbidities of the sols in the absence of the polymers by applying Rayleigh's law on the basis of the particle size of the sols used for PVP. These values for PVP are smaller than those for the other polymers. This indicates that the surfaces of the silver iodide particles were more loosely covered with PVP molecules. On the other hand, as has been shown in previous paper, the power of PVP to protect gold sol against an electrolyte is stronger than that of polyvinyl alcohol and only slightly inferior to that of gelatin.[9,10] Therefore, it may be considered that PVP molecules, in consequence of their orientation, form a more stable hydration shell around silver iodide particles than those of polyvinyl alcohol.

Table 1 also includes the parameters, ν, estimated from the Frisch-Simha-Eirich[11] (FSE) equation:

$$\theta/\nu(1-\theta)^\nu = KC \qquad (3)$$

where θ is the surface converge; C, the equilibrium concentration of the polymer, and K, a constant; θ is replaced by a/a_∞ where a is the amount of polymer adsorbed at the concentration, C, and where a_∞ is the limiting adsorption. The ν parameter does not represent the number of anchor segments adsorbed per polymer chain, as has been described by Frisch *et al*, but only the deviation from the Langmuir form on the polymer adsorption, as has been pointed out by Curme and Natale.[12] From the values of ν, PVP also follows roughly the Langmuir-type adsorption in the low-concentration region, and the PVP molecules appear to be adsorbed from an aqueous solution on the silver-iodide surfaces without any remarkable transfiguration.

9) M. Sugiura and E. Fujii, *Kogyo Kagaku Zasshi*, **67**, 268 (1964).

10) E. Fujii and M. Sugiura, *ibid.*, **65**, 1609 (1962).

11) H. L. Frisch, M. Y. Hellman and J. L. Lundberg, *J. Polym. Sci.*, **38**, 441 (1959).

12) H. G. Curme and C. C. Natale, *J. Phys. Chem.*, **68**, 3009 (1964).

NOTES

BULLETIN OF THE CHEMICAL SOCIETY OF JAPAN VOL. 43 2609—2612 (1970)

A Spectrophotometric Study of the Formation and Thermochromism of the Nickel(II)-Piperidine Complexes in *N*,*N*-Dimethylformamide Solutions

Akira OUCHI, Toshio TAKEUCHI and Iwao TAMINAGA

Department of Chemistry, College of General Education, The University of Tokyo, Komaba, Meguro-ku, Tokyo

(Received November 14, 1969)

The transition energy between the pair of coordination states in a nickel(II) complex is sometimes low. In such a case, the state changes only upon a slight heating, so its solution shows a characteristic thermochromism. Such kinds of thermochromism of nickel(II) complexes have already been reported by several authors. Sone and Kato have studied the thermochromism of the ethylenediamine chelate of nickel(II),[1] Cotton and others studied the thermal change of bis(acetylacetonato)-nickel(II) in solution,[2] and several authors have reported about the formation of the $[NiCl_4]^{2-}$ ion at high temperatures.[3-5] Recently we have found that the nickel(II) chloride - piperidine complex formed in the *N*,*N*-dimethylformamide (DMF) solution containing a large excess (with a mole ratio of about 10 to 30 : 1) of piperidine is remarkably thermochromic. The solution which was yellow at room temperature became violet at high temperatures, and the color change was quite reversible. These observations led us to study the complex species formed in such solutions.

Experimental

The visible absorption spectra at 25°C were obtained with a Hitachi EPS-2 type automatic recording spectrophotometer. The spectra at high temperature were obtained with an Ito Model QU-3 spectrophotometer, with heated paraffin oil being circulated around the cell chamber. The reagents used were all GR grade, the $Ni(ClO_4)_2 \cdot 6DMF$ was made by the method reported by Gutmann.[6]

The Preparation of the Sample Solution. In general, a mixed solution of nickel(II) chloride and amine in DMF was stable for about 6 hours, and practically no spectral change could be observed in it. However, a gradual spectral change then appeared as a result of the aging of the solution. Consequently, the spectral measurements at 25°C were carried out within five hours after the preparation of the sample. The concentration of the nickel ion in the sample solutions was 0.04 M. The optical path length of the cell was 5.5 mm. The absorption coefficient of the solution showed a little deviation from Beer's law even at the concentration of 0.01 M. When the concentration of the nickel salt was higher, precipitation occurred when much amine was added.

Results and Discussion

The visible absorption spectra of the DMF solutions containing piperidine and nickel(II) chloride, where the mole ratio of the former to the latter was 0 to 101, were examined. Typical results are shown in Fig. 1. Many peaks which are considerably overlapping are observed, but no exact isosbestic points can be detected.

The relation between the absorption coefficients at various wave numbers and the mole ratio of amine to nickel are shown in Fig. 2. These curves seem to have a bending point at the mole ratio of 1 : 1, and probably another at about 2 : 1.

The DMF solution of nickel(II) chloride (curve a, Fig. 1) shows one low peak at 23800 cm^{-1}, a high peak at 16100 cm^{-1} with two shoulders at 17200 cm^{-1} and 15400—14300 cm^{-1} at its sides, and a small peak at 8050 cm^{-1}. The application of the band assignments proposed by Gutmann[6] for the DMF solution of the nickel(II) perchlorate-tetramethylammonium chloride system to our data

1) K. Sone and M. Kato, *Z. Anorg. Allg. Chem.*, **301**, 277 (1959).

2) F. A. Cotton and J. P. Fackler, Jr., *J. Amer. Chem. Soc.*, **83**, 2870, 3775 (1961).

3) R. K. Scarrow and T. R. Griffiths, *Chem. Commun.*, **1967**, 425.

4) D. E. Saife and K. P. Wood, *Inorg. Chem.*, **6**, 358 (1967).

5) C. Furlani and G. Morpurgo, *Z. Phys. Chem.*, **28**. 93 (1961).

6) H. Hubacek, B. Stancic and V. Gutmann, *Monatsh. Chem.*, **94**, 1118 (1963).

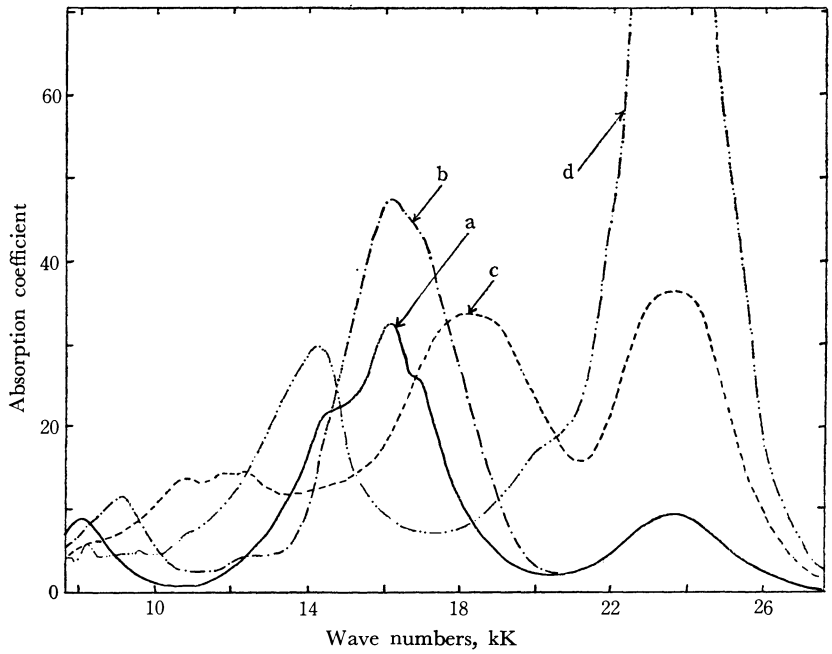

Fig. 1. Spectra of nickel(II) chloride - piperidine - DMF system. $Ni^{2+}=0.04$ M, at 25°C. Piperidine/Ni^{2+}(M/M) are a) —— 0, b) —·— 0.45, c) ---- 6.0, d) —··— 101.

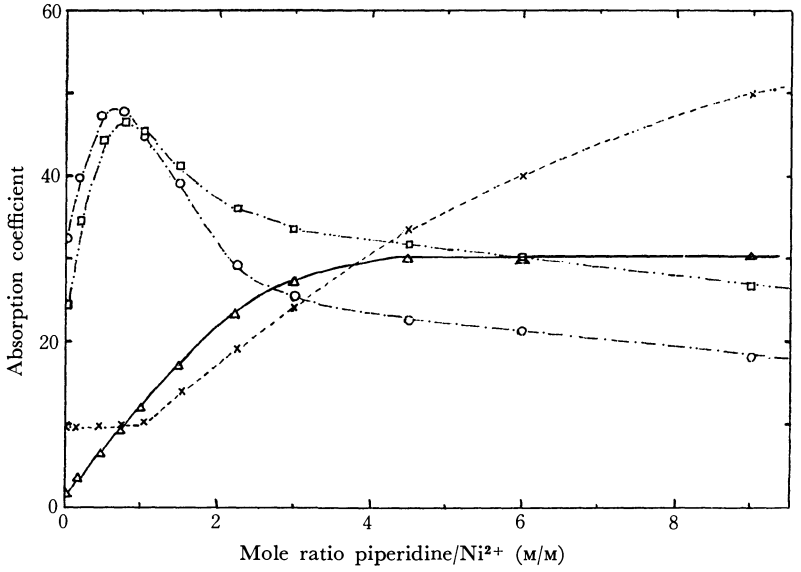

Fig. 2. The relation between the absorption coefficients at various wave numbers and the ratio of piperidine to nickel chloride in the DMF solutions. $Ni^{2+}=0.04$ M, at 25°C. a) --×-- 23800 cm^{-1}, b) —△— 19200 cm^{-1}, c) —··—□—··— 17200 cm^{-1} and d) —·—○—·— 16100 cm^{-1}

indicates that the main peak at 16100 cm^{-1} and the shoulder at 17200 cm^{-1} are the $^3T_1(F)\rightarrow{}^3T_1(P)$ absorptions of the tetrahedral $[Ni(DMF)Cl_3]^-$ and $[Ni(DMF)_3Cl]^+$, while the smaller peak at 23800 cm^{-1} is the $^3A_{2g}\rightarrow{}^3T_{1g}(P)$ absorption of such coexisting octahedral species as $[Ni(DMF)_4Cl_2]^0$ and $[Ni(DMF)_6]^{2+}$. Among these, the intensities of the peaks at about 16000—17000 cm^{-1} are far lower than the values to be expected from the $^3T_1(F)\rightarrow{}^3T_1(P)$ band of the pure tetrahedral species. This is probably due to the fact that a considerable amount of nickel is in the form of

octahedral species in the solution.[7-15]

When lithium chloride was added to the solution, the intensity of the shoulder at 15400—14300 cm^{-1} increased very rapidly and the other peaks disappeared. Consequently, it can be inferred that this peak corresponds to the $^3T_1(F) \rightarrow {}^3T_1(P)$ transition band of the tetrahedral $[NiCl_4]^{2-}$.

The results shown in Fig. 2 indicate that the dominant complex species in the solution containing a little amine have the amine : nickel composition of 1 : 1. They are probably such slightly distored tetrahedral species as $[Ni(DMF)_2(pip)Cl]^+$ and $[Ni(DMF)(pip)Cl_2]^0$. When the concentration of amine in the solution is increased, the species with the amine : nickel composition of 2 : 1 begins to appear, and in the concentrated amine solution, this diamine complex becomes predominant. Therefore the original tetrahedral species change into pentacoordinate species; probably they are such distorted square-pyramidal species as $[NiCl_2(DMF)(pip)_2]^0$ or $[NiCl(DMF)_2(pip)_2]^+$. This fact also seems to be proved by the spectral data. The spectra of the penta-coordinate bis(diethyldithiophosphate)diethylamine nickel(II) complex, for example, shows main peaks at about 6500 cm^{-1} (12), 9500 cm^{-1} (26), 12700 cm^{-1} (131), 17400 cm^{-1} (30) and 21500 cm^{-1} (250) (where the approximate ε's are shown in parentheses).[16] As is shown in Fig. 1, the spectra of the sample solutions in this study, especially those of the solutions containing a large excess of amine, show peaks at 14300, 19200 and 23800 cm^{-1} (curve d, Fig. 1.), and their general features resemble those of the penta-coordinate species.

The precipitate obtained from the concentrated DMF solution containing nickel(II) chloride and piperidine was always $NiCl_2(pip)_2 \cdot \frac{1}{2}DMF$, even if a large excess of amine was added. Moreover, the morpholine adduct of nickel sulfate was found to be $Ni(morph)_2SO_4$ (where morph means morpholine).[17] Therefore, it may be concluded that at most two molecules of amine can coordinate to one central nickel ion. The solid $NiCl_2(pip)_2 \cdot \frac{1}{2}DMF$ and the complex solutions always show their magnetic moments between 3.0 and 3.3 B.M. Therefore, the possibility of the presence of the square-planar complex species can be rejected.

It is expected that the equilibrium of the system under consideration is affected by the nature of the chloride ion, piperidine, and DMF. When the nickel perchlorate, $Ni(ClO_4)_2 \cdot 6DMF$, was used in place of nickel chloride, the intensities of

Table 1. The thermal change of the absorption spectra of nickel(II) chloride- piperidine-DMF solutions

The concentration of nickel(II) ion is 0.04 M.

The numbers in the table are apparent molar extinction coefficients (ε), and the wave numbers of the maxima of the respective peaks (kK) are given in parentheses.

Piperidine/Ni^{2+} (M/M)	I			II			III		
	25°C	50°C	75°C	25°C	50°C	75°C	25°C	50°C	75°C
0	11.6	10.4 (23.8)	12.3	23.7	34.5 (17.2 sh)	43.2	31.4	41.4 (16.1)	50.0
0.45	10.0	10.3 (23.8)	9.10	36.8	42.5 (17.2 sh)	42.8	39.0	45.5 (16.1)	49.6
2.25	18.2	14.3 (23.8)	13.2	22.3	29.0 (17.2)	35.0	19.1	27.8 (15.9 sh)	33.2
6.0	37.4	27.5 (23.8)	21.6	18.0 (18.9)	23.4 (17.9)	28.6 (17.7)			
12.0	51.1	46.9 (23.7)	39.2	14.8 (20.0)	20.5 (19.1)	34.5 (18.5)	19.5	13.4 (14.3)	10.6
30	72.7	57.8 (23.7)	45.5	12.1 (20.0)	20.5 (19.3)	28.1 (17.8)	21.1	16.5 (14.3)	14.5
101	82.4	78.7 (23.7)	49.2	10.9	14.3 (20.0 sh)	12.3	26.3	23.9 (14.1)	13.6

7) R. S. Drago, D. W. Meek, R. Longhi and M. D. Joesten, *Inorg. Chem.*, **2**, 1056 (1963).

8) S. Buffagni, L. M. Vallarino and J. V. Quagliano, *ibid.*, **3**, 671 (1964).

9) M. A. Robinson and T. J. Hurley, *ibid.*, **4**, 1716 (1965).

10) M. R. Rosenthal and R. S. Drago, *ibid.*, **4**, 840 (1965).

11) L. Sacconi, I. Bertini and F. Mani, *ibid.*, **6**, 262 (1967).

12) W. Ludwig and G. Wittmann, *Helv. Chim. Acta*, **47**, 1265 (1964).

13) D. M. Goodgame, M. Goodgame and F. A. Cotton, *J. Amer. Chem. Soc.*, **83**, 4161 (1961).

14) S. Buffagni, L. M. Vallarino and J. V. Quagliano, *Inorg. Chem.*, **3**, 480 (1964).

15) D. Foster and D. H. L. Goodgame, *ibid*, **4**, 823 (1965).

16) A. Sgamelloti, C. Furlani and F. Magrini, *J. Inorg. Nucl. Chem.*, **30**, 2655 (1968).

17) J. S. Ahuja, *Inorg. Chim. Acta*, **3**, 110 (1969).

the peaks were extensively lowered. The change in the spectra according to the variation of the amine concentration is small, and the thermochromism phenomenon was not observed. Probably it is due to the high stability of the $[Ni(DMF)_6]^{2+}$ ion.

Second, dimethylsulfoxide (DMSO) was used in place of DMF. The spectral change caused by the variation in the piperidine-nickel chloride mole ratio was examined. Although some spectral change according to the variation in the amine concentration was observed, it was not very remarkable, probably because of the high stability of the $[Ni(DMSO)_6]^{2+}$ ion which was dominant in the solution.

Third, various amines were added in place of piperidine to the DMF solution of nickel(II) chloride. When morpholine or pyrrolidine was used, the spectral change depending on the amine concentration was almost the same as when piperidine was used. On the other hand, in the case of using aniline, benzylamine or pyridine the change in the spectra depending on the amine concentration was not much. When diethylamine, di-*n*-butylamine, or isopropylamine was used, the spectral change and its dependence on the amine concentration were intermediate between these extremes. These results show that the amines which show the thermochromism are those which have a relatively high base dissociation constant, K_b, of about 10^{-3}. The K_b values of the amines which do not caused the thermochromism are much lower. The change in the spectra of nickel(II) chloride-DMF-piperidine solution with the variation in the temperature was then investigated; the results are shown in Fig. 3 and Table 1. The experimental results show that the spectra of a mixed sample at a high temperature resembles one which contains less amine, or one containing the same concentration of amine and an excess of chloride.

Therefore, the mechanism of the thermochromism of these complexes is explained the amine molecule in the complex species is replaced by a chloride ion or by a DMF molecule when the temperature is raised.

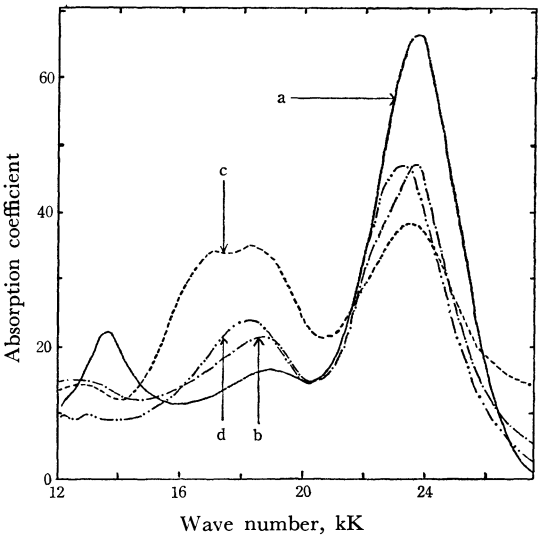

Fig. 3. The thermal change of the spectra of $NiCl_2$-piperidine-DMF system. The mole ratio of piperidine to nickel ion is 18.0, $Ni^{2+}=0.04$ M. a) —— 25°C, b) —·— 50°C, c) ---- 75°C and d) —···— 25°C, with 0.456 M LiCl.

The enthalpy change of the reaction obtained from the relation between the $1/T$ of the solution and the absorption coefficients of the main peaks of the spectra are about 3 kcal/M, far lower than those of the tetrahedral⇄octahedral or tetrahedral⇄square planar change described in the literature.[2,4]

The authors wish to thank Professors Y. Yoshino and K. Watanuki and the other colleagues of our laboratory for their helpful discussions.

BULLETIN OF THE CHEMICAL SOCIETY OF JAPAN VOL. 43 2613—2614 (1970)

The Preparation of 2-Chloroalkane-1-phosphonic Acid

Yoshiki OKAMOTO and Hiroshi SAKURAI

The Institute of Scientific and Industrial Research, Osaka University, Yamada-kami, Suita-shi, Osaka

(Received November 18, 1969)

It is well known that 2-chloroalkane-1-phosphonic acid is a phosphorylation reagent[1,2] and a useful intermediate for the preparation of 1-alkane-1-phosphonic acid.[3]

The preparation of 2-chloroalkane-1-phosphonic acid or 1-alkene-1-phosphonic acid by the reaction of phosphorus pentachloride with a terminal olefin such as styrene derivatives has been reported by many investigators,[4] but in most cases the yields were unsatisfactory because of the side reaction. The yields of the desired products by this procedure usually ranged between 40—50%.

In the present experiments, it has been found that 2-chloroalkane-1-phosphonic acid can be prepared in a high yield by adding an adequate amount of phosphorus trichloride to the reaction medium. (see Table 1)

TABLE 1. THE RESULTS OF THE REACTION OF OCTENE-1 AND PHOSPHORUS PENTACHLORIDE[a]

Exp. No.	PCl_3/PCl_5	Time (hr)	Conversion[b] (%)	Yield (%) I	Yield (%) II
1	0	24	97	49	41
2	0.2	24	58	47	7
3	1	24	56	50	1
4	1	24	42	39	0
5	9	24	30	27	0
6	1	72	99	92	2
7	2	72	97	93	0

a) The PCl_5/octene-1 ratio was 2:1; benzene was used as the solvent, and the total volume of benzene+PCl_3 was maintained at 300 m*l*. The reaction temperature was 25°C.

b) The yields of 2-chlorooctane-1-phosphonic acid (I) and 1,2-dichlorooctane (II) were based upon the amount of octene-1 employed. The conversions of octene-1 were calculated from the amounts of them recovered.

When a larger amount of phosphorus trichloride was added to the reaction mixture, the rate of the reaction became much slower and the formation of 1,2-dichlorooctane was much suppressed. When the reaction time was lengthened to 72 hr, the conversion of the olefin increased to 97% and 2-chlorooctane-1-phosphonic acid was obtained in a 93% yield.

The reaction mechanism of the formation of 2-chloroalkane-1-phosphonic acid is considered to proceed *via* Eqs. (1) and (2):[5]

$$2PCl_5 \rightleftarrows PCl_4^+ + PCl_6^- \quad (1)$$

$$PCl_4^+ + CH_2{=}CHR \rightleftarrows PCl_4CH_2\overset{+}{C}HR \xrightarrow{Cl^-} PCl_4CH_2CHClR \quad (2)$$

1,2-Dichloroalkane may be produced by the addition of chlorine to the olefin by reactions (3) and (4).

$$PCl_5 \rightleftarrows PCl_3 + Cl_2 \quad (3)$$

$$Cl_2 + CH_2{=}CHR \longrightarrow ClCH_2CHClR \quad (4)$$

The equilibrium (3) may migrate to the left upon the addition of phosphorus trichloride, and the generation of chlorine may be suppressed; this latter may consequently decrease the formation of 1,2-dichlorooctane. When a large amount of phosphorus trichloride is present, the formation of the chloride is completely restrained and the side reaction (4) can be prevented. The slower rate of the reaction (2) may be due to the small concentration of PCl_4^+, caused by the nucleophilic attack of PCl_3 on PCl_4^+, as is shown in the reaction (5):

$$PCl_4^+ + PCl_3 \longrightarrow [PCl_4 \cdot PCl_3]^+ \quad (5)$$

Experimental

Preparation of 2-Chlorooctane-1-phosphonic Acid. Typical Procedure. Twenty-two grams (0.2 mol) of octene-1, 83.3 g (0.4 mol) of phosphorus pentachloride, 54.8 g (0.4 mol) of phosphorus trichloride, and 265 m*l* of absolute benzene were added to a 500 m*l*, three-necked flask fitted with a condenser protected by a drying tube. After the mixture had then been stirred for 24 hr, it was poured into ice water and stirred for 2 more hours. The oily layer was se-

1) J. A. Maynard and J. M. Swan, *Aust. J. Chem.*, **16**, 596 (1963).

2) V. M. Clark, *Proc. Chem. Soc.*, **1964**, 129.

3) Y. Okamoto, T. Nitta and H. Sakurai, *J. Oil Chemists' Soc. Japan*, **12**, 882 (1969).

4) G. M. Kosolapoff, "Organic Reactions," Vol. VI, ed. by R. Adams, John Wiley & Son, New York (1957), p. 273.

5) A. J. Kirby and S. G. Warren, "The Organic Chemistry of Phosphorus," Elsevier Publishing Co., New York (1967), p. 262.

parated, and the aqueous layer was extracted with ether. The oily layer and the ether extract were combined and distilled. After the ether had been removed by atmospheric pressure, the remainder was distilled under reduced pressure below 100°C. The distillate was a mixture of octene-1 (9.0 g, bp 87—89°C/250 mmHg) and 1,2-dichlorooctane (0.4 g, bp 80—81°C/1 mmHg, Found: Cl, 38.14; C, 52.52; H, 8.89%. Calcd for $C_8H_{16}Cl_2$: Cl, 38.72; C, 52.46; H, 8.81%). From the residue, 22.8 g of pure 2-chlorooctane-1-phosphonic acid (mp 85—86°C. Found: P, 12.89; Cl, 14.81; C, 40.11; H, 7.53%. Calcd for $C_8H_{18}ClP$: P, 12.92; Cl, 14.79; C, 40.09; H, 7.57%) were obtained by recrystallization from petroleum ether.

BULLETIN OF THE CHEMICAL SOCIETY OF JAPAN VOL. 43 2614—2616 (1970)

The Liquidus Curve of the ZrO_2-Y_2O_3 System as Measured by a Solar Furnace

Tetsuo NOGUCHI, Masao MIZUNO and Toyoaki YAMADA

Government Industrial Research Institute, Nagoya

(Received November 19, 1969)

A subliquidus phase in the ZrO_2-Y_2O_3 system was studied by Duwez *et al.*,[1] who claimed an eutectic with 70 mol% Y_2O_3 at 2100°C and a peritectic at 2500°C, and by Otto[2] who claimed them at 2260°C and 2580°C respectively. More recently (1962) Fu-Kan *et al.*[3] have reported on a subliquidus-phase study of the system and demonstrated $Y_2Zr_2O_7$ compound at 2530±30° C. Liquidus curves in the ZrO_2-Ln_2O_3 systems[4] and the phase diagram of the ZrO_2-Y_2O_3 system[5] were also studied at the Ultra-Refractory Laboratory of Mont-Louis, France, using a heliostat-type solar furnace. The present authors have previously studied the high-temperature phases in ZrO_2–CaO[6] and ZrO_2–MgO[7] systems with a heliostat-type solar furnace; we found anomalies in the liquidus curves in the ZrO_2-rich side region. This note will be concerned with the liquidus curve measurement in the ZrO_2-Y_2O_3 system and with anomalies in the curve of the system.

Experimental

By the use of a brightness pyrometer the freezing points of a composition in the ZrO_2-Y_2O_3 system were measured by means of the specular reflection method.[8] The brightness temperature of the freezing point of the respective composition was obtained from the cooling curve. The spectral reflectivity of the specimen was also measured at 0.65 μm by the use of a shadowing plate, and the spectral emissivity was estimated from the reflectivity data. Thus, the true temperature of the freezing point was calculated. The materials used were ZrO_2 (99.8% pure, from the Yokozawa Chemicals Co.) and Y_2O_3 (99.9% pure, from the Johnson Matthey & Co., London). The carefully-mixed specimen was pressed into a $6\times6\times35$ mm bar under a pressure of 4000 kg/cm^2 and sintered at 1700°C for 3 hr with two heating and grinding cycles.

Results

The cooling-curve data are summarized in Fig. 1, while the mean values of from forty to fifty individual readings of the freezing point for each composition are indicated in Table 1. Anomalies in the liquidus curve not previously reported were found with compositions of 7.5, 15.0, and 20.0 mol% Y_2O_3.

In order to examine the stoichiometry of a composition quenched from the melt, the Y_2O_3 content of a specimen was analysed by chelate titration with an EDTA solution. The results obtained are shown in Table 2; the deviation from the stoichiometry was found to be almost negligible.

The findings on X-ray powder diffraction patterns of quenched specimens form the melt at the quenching rate of about 2000°C/sec are shown in Table 3. The Y_2O_3 solid solution was confirmed by means of diffraction lines from (332), (510), (541), and (631). The diffraction patterns of a 15 mol% Y_2O_3 composition quenched from the melt showed a broadening of peaks, though no extra reflection line was observed

1) P. Duwez, F. H. Brown, Jr., and F. Odell, *J. Electrochem. Soc.*, **98**, 356 (1951).

2) L. E. Olds and H. E. Otto, "Phase Diagram for Ceramists," ed. by E. M. Levin, C. R. Robbins and H. F. McMurdie, Amer. Ceram. Soc., Columbus, Ohio (1964).

3) Fan Fu-Kan, A. K. Kuznetsov and E. K. Keler, *Izv. Akad. Nauk SSSR, Otd. Khim. Nauk*, No. 7, 1141 (1962).

4) M. Foex and A. Rouanet, *C. R. Acad. Sci., Paris, Ser. C*, **264**, 947 (1967).

5) A. Rouanet, *ibid.*, **267**, 1581 (1968).

6) T. Noguchi, M. Mizuno and W. M. Conn, *J. Solar Energy*, **11**, 136 (1967).

7) T. Noguchi and M. Mizuno, This Bulletin, **41**, 1583 (1968).

8) T. Noguchi and T. Kozuka, *J. Solar Energy*, **10**, 125 (1966).

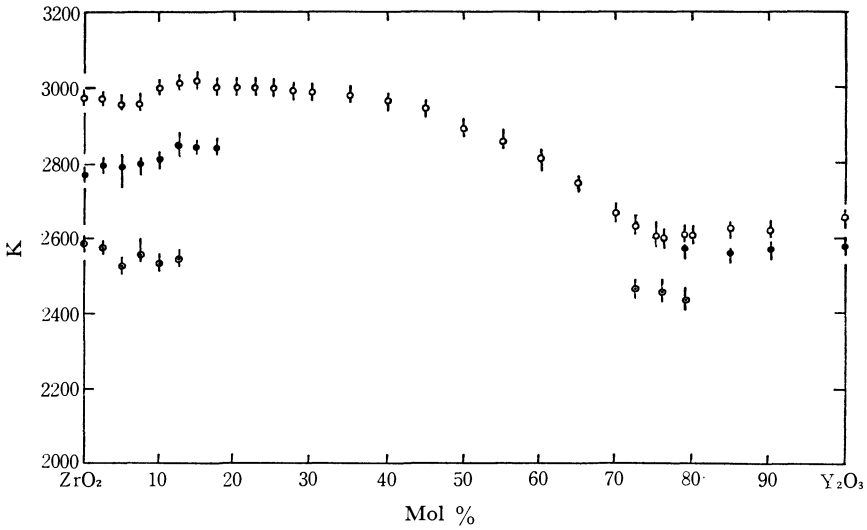

Fig. 1. Freezing point data in the ZrO_2-Y_2O_3 system.
○ Freezing point
● 2nd exothermic peak } (solid state)
⊙ 3rd exothermic peak }

Table 1. Freezing point data of ZrO_2-Y_2O_3 system

Composition ZrO_2 (mol%)	Composition Y_2O_3 (mol%)	Freezing point (±20°C)	Spectral emissivity at 0.65 μm
100		2706	0.81
97.5	2.5	2704	0.83
95	5	2690	0.88
92.5	7.5	2689	0.88
90	10	2728	0.89
87.5	12.5	2751	0.86
85	15	2746	0.89
80	20	2736	0.88
77.5	22.5	2735	0.87
75	25	2732	0.86
72.5	27.5	2720	0.88
70	30	2717	0.89
65	35	2708	0.90
60	40	2700	0.90
55	45	2675	0.89
50	50	2622	0.90
45	55	2592	0.89
40	60	2545	0.91
30	70	2449	0.89
25	75	2398	0.90
24	76	2330	0.92
20	80	2342	0.87
10	90	2351	0.87
	100	2376	0.96

through 2θ 160°. The high-temperature X-ray diffraction data for this specimen through 2θ 25°—38° up to 1350°C showed a cubic modification in both heating and cooling processes. The lattice

Table 2. Chemical analysis of quenched specimens from the melt in the ZrO_2-Y_2O_3 system

Sample	Y_2O_3 content (Theoretical) wt%	Y_2O_3 content (Determined) wt%	Y_2O_3 content (Determined) mol%	Difference mol%
Y 10	16.91	17.21	10.19	+0.19
Y 22.5	34.73	34.38	22.23	−0.27
Y 30	43.99	43.32	29.43	−0.57
Y 45	59.99	59.57	44.57	−0.43
Y 75	84.61	85.04	75.62	+0.62
Y 90	94.28	94.26	89.96	−0.04

Table 3. X-Ray diffraction data of quenched specimens from the melt in ZrO_2-Y_2O_3 system

Composition ZrO_2 (mol%)	Composition Y_2O_3 (mol%)	Phase present after quenching		
97.5	2.5	M (m)		
95	5	M (vw)	C*(m)	
92.5	7.5		C*(s)	
90	10		C*(s)	
85	15		C*(s)	
80	20		C (s)	
70	30		C (s)	
60	40		C (s)	
50	50		C (s)	
40	60		C (s)	Y (vw)
30	70		C (m)	Y (w)
25	75		C (w)	Y (m)
20	80			Y (s)
10	90			Y (s)

M: monoclinic zirconia solid solution; C: cubic zirconia solid solution; C* cubic not resolved; Y: yttria solid solution

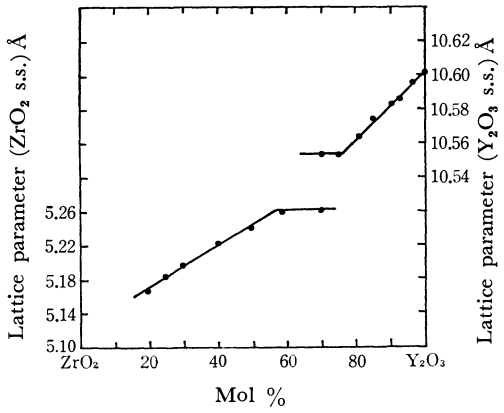

Fig. 2. Lattice parameters of cubic solid solutions.

parameters of the cubic zirconia solid solution were obtained at 2θ 1/8° from the diffraction lines with $2\theta > 90°$, and those of the yttria solid solution, with (332), (510), (541), and (631). The two-phase region containing a cubic zirconia solid solution and a yttria solid solution extended from 57—76 mol% Y_2O_3, as is shown in Fig. 2.

In a microscopic observation of the thin section of specimens quenched from the melt, the sample with a 15 mol% Y_2O_3 composition showed biaxial negative crystals with an optic angle of $2V = -80°$ unlike that of the monoclinic crystals ($-30°$), as in the cases of 7 mol% CaO and 12.5 mol% MgO compositions. The zirconia modification of this type is possibly of the rhombic form, though verification by X-ray diffraction data was not possible at present because of the difficulty in obtaining the single crystal.

These results suggest that the liquidus curve in the ZrO_2-rich side region of the ZrO_2-Y_2O_3 system is located at higher temperatures than those of ZrO_2-MgO and ZrO_2-CaO systems, as is shown in Fig. 3. An eutectic point on the yttria side was located at 76 mol% Y_2O_3 and at 2330°C. Further investigations should be focussed on the high-

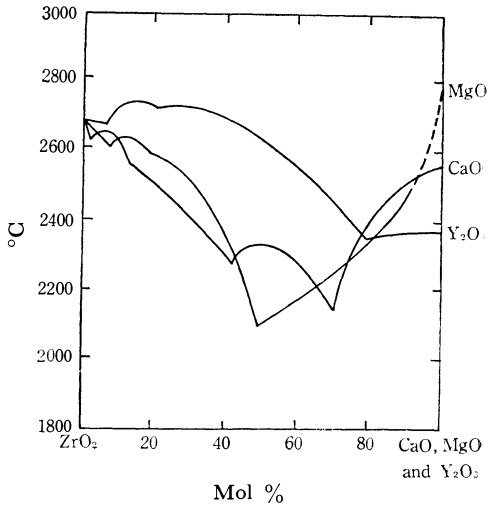

Fig. 3. Liquidus curves for binary oxide systems containing ZrO_2.

temperature phase study in the ZrO_2-rich side region in order to establish the complete phase diagram in the system.

Yttria showed its exothermic peak at about 2283°C in the solid state in the cooling curve; this might be ascribed to the cubic-hexagonal transition, as has been proposed by Rouanet.[5] However, the two phase-region of the cubic and hexagonal yttria solid solutions could not be clearly determined from the cooling-curve data.

The very narrow region for the monoclinic zirconia solid solution and the transformation of 15 mol% Y_2O_3 composition at a very high temperature might be assumed. The existence of the compound claimed by Fu-Kan *et al.* was not confirmed in this study.

The authors wish to express their appreciation to Dr. Hiroshi Hayashi for his help in the chemical analysis of the quenched specimen and in the microscopic work.

BULLETIN OF THE CHEMICAL SOCIETY OF JAPAN VOL. 43 2617—2619 (1970)

Solubility of Antimony Oxyhalides in Water

Toshiaki KISHIKAWA and Taizo YOSHIDA

Department of Industrial Chemistry, Faculty of Engineering, Kumamoto University, Kurokami-cho, Kumamoto

(Received December 8, 1969)

The hydrolytic behavior[2] of a neutron-irradiated antimony tribromide has indicated the presence of free bromine(^{82m}Br) at the end of the irradiation. Such a bromine atom must be the result of hydrolysis, of a solubility equilibrium of the hydrolyzed product, or of the Szilard-Chalmers process.[3] The present paper will deal with the hydrolytic behavior of antimony trihalides (chloride, bromide, and iodide), a study conducted by means of a radiotracer technique, X-ray diffractional identification, and X-ray spectrochemical analysis, and with the radiometric determination of the solubilities of the hydrolyzed products.

If water is added to antimony trihalides, various oxyhalides can be obtained, depending on the amount of water added and on the amount of free acid in the solution.[4] When 1 mol of antimony trihalide is treated with 8 mol of water, antimony monooxyhalide is formed (1). When 27 mol of water are used, the oxyhalide shown in Eq. (2) is formed:[4a]

$$SbX_3 + H_2O \rightarrow SbOX + 2HX \quad (1)$$

$$4SbX_3 + 5H_2O \rightarrow Sb_4O_5X_2 + 10HX \quad (2)$$

Experimental

Stoichiometric Determination of the Composition of Antimony Oxyhalides. Antimony oxybromide was chosen as a sample of the oxyhalides.

Materials. Radiobromine (^{82}Br) produced[5] from neutron-irradiated ammonium bromide, the radiochemical purity of which had been tested by measuring its gamma-spectrum and half-life, was introduced, after it has passed through a dehydrating agent ($CaCl_2$), into a cooled trap containing antimony powder suspended in carbon disulfide. After the reaction (performed at room temperature) had been completed, the excess antimony powder was filtered off, and then the solvent was evaporated. Antimony tribromide (^{82}Br) was thus obtained.

Procedure. About 36 mg of antimony tribromide (^{82}Br) were treated with 1 m*l* of water[6] in a small test tube. After thorough shaking for 3 min, the contents were centrifuged for 5 min (2000 rpm). Then the centrifugate was pipetted out and the residue was washed with water. The radioactivities of both the centrifugate plus washings and the residue were counted by using an NaI(Tl) well-crystal scintillation detector and a scaler.

X-Ray Diffraction. *Sample Preparation.* The antimony trihalides (Cl, Br, and I) were obtained commercially or were prepared by methods similar to that described above. Each of them was dissolved in carbon disulfide. Hydrolysis was done by thorough shaking from a two-phase mixture of the carbon disulfide solution and water in the same $SbBr_3/H_2O$ proportions as have been described above. After aging, the precipitate was filtered out and dried in a desiccator until use. The precipitate was finely powdered by means of a spatula.

Measurement. Powder X-ray diffraction patterns of the samples were recorded with a Tokyo Shibaura Electric, Model ADX-103, X-Ray Diffractometer. Mn-filtered Fe$K\alpha$ radiation at 35 kV and 7 mA was used. A G-M counter was used as an X-ray detector. The intensities reported are described in terms of peak heights above the background, so scaled that the most intense line is given a value of 100.

X-Ray Spectrochemical Analysis. *Sample Preparation.* An addition technique was carried out. As additives, Wako Pure Chemicals' antimony powder and ammonium halides (Br and I) were used. Each additive was homogeneously mixed in the oxyhalide by the use of a mortar and a pestle.

Measurement. The instrument used for the X-ray specter measurements was a Tokyo Shibaura Electric, Model AFX-103, Spectrometer. A Toshiba AF-50W-type tungsten target tube operated at 35 kV and 25 mA was used. A LiF plane-crystal and an NaI(Tl) crystal were used for diffracting the fluorescent spectrum and for the X-ray detection respectively. The peak measurements of the elements were corrected for the background near the peak to provide the net peak-intensity values. The position of each $K\alpha$ peak was located approximately by scanning the spectrum of the element and was then

1) Part V on Hot-Atom Chemistry of Bromine. Presented at the Joint Local Meeting of Chugoku-Shikoku and Kyushu Branches of the Chemical Society of Japan, Tokushima, November 1968.

2) T. Kishikawa, Y. Aratono and C. Shinomiya, This Bulletin, **43**, 1276 (1970).

3) L. Szilard and T. A. Chalmers, *Nature*, **134**, 462 (1934).

4) a) C. Lea and J. K. Wood, *J. Chem. Soc.*, **125**, 137 (1934). b) V. von Richiter, *Ber.*, **4**, 408 (1871). c) G. Peason, *Trans. Roy. Soc.* (London), **81**, 323 (1891). d) J. Davy, *ibid.*, **102**, 190 (1912). e) J. M. van Benmelen, P. A. Meerburg and U. H. Noodt, *Z. Anorg. Allg. Chem*, **33**, 272 (1803); J. W. Mellor, "A Comprehensive Treatise on Inorganic and Theoretical Chemistry," Vol. 9, Longmans, London (1929), Chapter 52.

5) F. Weygand, H. Grisevach, K.-D. Kirchner and M. Haselhorst, *Chem. Ber.*, **88**, 487 (1955).

6) In such proportion hot-atom data (Ref. 2) have been obtained.

more exactly located by point-set readings using mannual control.

Radiometric Determination of Solubilities. *Materials.* As a radiotracter, an ^{124}Sb isotope of a known radioactivity (*ca.* 10^5 cpm/mmol-oxyhalide) was precipitated according to the directions presented above. The radiochemical purity was also checked by the manner described above.

Procedure. A known amount of the antimony oxyhalide(^{124}Sb) was suspended in a reaction flask containing 50 m*l* of distilled water. After the suspension had been equilibriated for 20 hr (in a thermostat ± 0.2°C), an aliquot (*ca.* 2 m*l*) of the suspended solution was pipetted out and centrifuged for 5 min. A known amount of the centrifugate was then pipetted into a measuring tube and counted with an NaI(Tl) well cristal and a scaler. The comparison of the activity with that of a standard specific-activity solution indicated the solubility.

Results and Discussion

Hydrolytic Behavior of Antimony Tribromide. If the radioactivities of the residue and the centrifugate are *m* and *n* respectively, the following equation can be proposed:

$$\frac{m+n}{3}SbBr_3^* + \frac{n}{2}H_2O \rightarrow Sb_{(m+n)/3}O_{n/2}Br_m^* + nHBr^* \quad (3)$$

where an asterisk represents the ^{82}Br isotope. The *m* and *n* values thus obtained in cpm or in percentage of the total activity, are listed in Table 1.

Table 1. Radiometric determination of the hydrolytic behavior of antimony tribromide by using bromide-82 as a tracer

No.	Radioactivities of Residue (antimony oxybromide) *m*		Centrifugate (bromide ion) *n*	
	cpm	%	cpm	%
1	18361	19.7	74714	80.3
2	18963	20.4	74037	79.6
3	16040	17.4	76304	82.6
4	16160	17.7	74981	82.3
5	19430	19.4	79486	80.6
6	13932	15.7	74891	84.3
7	18044	19.6	74007	80.4
Av.		18.4±1.6		81.6±1.6

If the reaction (1) is predominant, the *m* value in percentage should be close to 33.3; if the reaction (2) is predominant, the *m* value in percentage should be close to 16.7. The average value of *m* in percentage in Table 1 is 18.4±1.6, which indicates that the composition of the obtained antimony oxybromide is $Sb_4O_5Br_2$.

Identification by X-Ray Diffraction. The X-ray diffraction patterns of the samples are shown in Fig. 1. The results of the diffraction of the oxychloride and the -bromide showed them to be $Sb_4O_5Cl_2$ and $Sb_4O_5Br_2$ respectively, according to the data of the ASTM cards.[7]

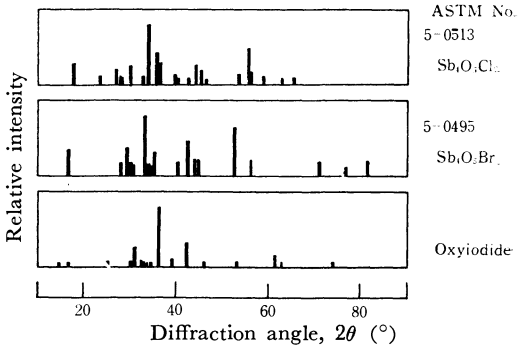

Fig. 1. X-Ray diffraction patterns of antimony oxyhalides.

X-Ray Spectrochemical Analysis. The $K\alpha$-line intensity of the relevant element was measured before and after the addition of a known amount of the element to the sample. After the determination of the intensity ratio of these two, the percentage of the element in the original sample could be calcurated from the following relationship:[8]

$$x = \frac{R \cdot w}{(1-R) \cdot W + w} \times 100(\%) \quad (4)$$

where x, R, W, and w are the percentage of the element in the original sample, the intensity ratio (intensity of the $K\alpha$ element before addition, I_x)/(intensity of the $K\alpha$ element after addition, I_s), the weight of the sample, and the weight of the standard element respectively.

The analyzed elements were Sb, Br, and I. The results of the X-ray spectrochemical analysis are listed in Table 2. The values of oxygen were calculated by subtracting the percentages of two atoms from 100%.

These results establish that the composition of the hydrolyzed product of antimony trihalides is $Sb_4O_5X_2$.

Table 2. Results of X-ray spectrochemical analysis

Element	Antimony oxibromide		Antimony oxyiodide	
	%	atoms[a]	%	atoms[a]
Sb	65.7	4	57.5	4
O	10.3	4.8	8.5	4.5
X	24.0	2.2	34.0	2.2

a) Normalized to Sb: 4.

7) ASTM Cards No. 5-0495 and 5-0513; M. Estrand, *Acta Chem. Scand.*, **1**, 178 (1947).

8) W. J. Campbell and H. F. Carl, *Anal. Chem.*, **26**, 800 (1954).

Table 3. Heat of solution

	Q, kcal/mol
$Sb_4O_5Cl_2$	21.0±0.1
$Sb_4O_5Br_2$	23.3±0.2
$Sb_4O_5I_2$	32.7±0.3

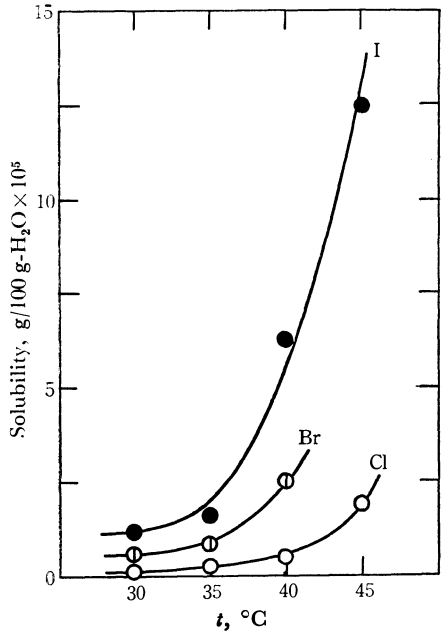

Fig. 2. Solubility curves of $Sb_4O_5X_2$ (X: Cl, Br, I). Thermostat±0.2°C

Radiometric Measurement of Solubilities. The data summarized in Table 3 and Fig. 2 indicate that the solubility increases in the following order: Cl<Br<I.

When the solubility, S, is expressed as mol/kg-solvent, the plots of log$S$ against $1/T$ gives a straight line, as is shown in Fig. 3. When a solid dissolves in a liquid, and when the state of equilibrium is reached, the van't Hoff equation holds between the equilibrium constant, K, and the absolute temperature, T:

$$\partial \ln K/\partial T = Q/RT^2 \qquad (5)$$

where Q is the heat of solution. If the heat of solution is taken as constant over the given range of temperature, the general integration of the van't Hoff equation gives, when the equilibrium constant, K, is replaced by the solubility, S:

$$\log S = -\frac{Q}{2.303R}\cdot\frac{1}{T} + \text{constant} \qquad (6)$$

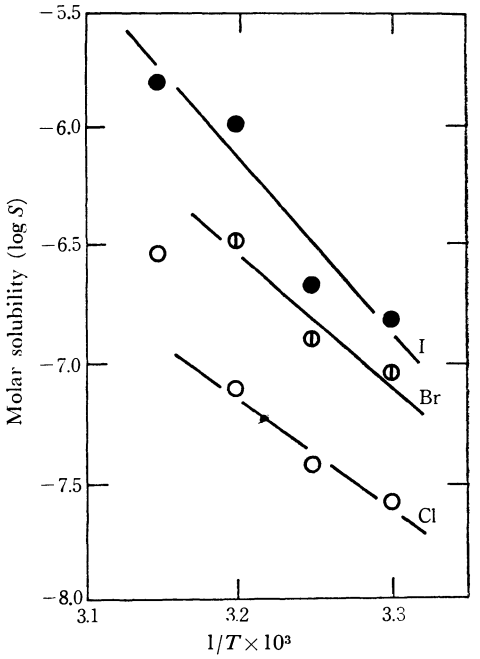

Fig. 3. Dissociation of $Sb_4O_5X_2$ (X: Cl, Br, I).

Equation (6) is shown in Fig. 3. From the slope, which is equal to $-Q/2.303R$, the heat of solution, which represents the heat of absorption when 1 mol of solution is dissolved afresh in a saturated solution, can be found in Table 3 over the given range of temperature.

The authors wish to thank Professor Chiro Shinomiya and Dr. Akira Oyoshi for their encouragement and valuable advice. Thanks are also due to Mr. Yoriyuki Ogawa of the Center for Engineering Research of this University for X-ray measurements. A part of the investigation was supported by the Joint Universities Facilities at the Tokai Establishment, the Japan Atomic Energy Research Institute, to the personnel of which thanks are also due.

BULLETIN OF THE CHEMICAL SOCIETY OF JAPAN VOL. 43 2620—2622 (1970)

The Reaction of 3,4-Dihydroxyphenylalanine with *p*-Benzoquinone under Physiological Conditions

Aizo HIKOSAKA and Ju KUMANOTANI

Engineering Research Institute, Faculty of Engineering, University of Tokyo, Bunkyo-ku, Tokyo

(Received December 23, 1969)

When 3,4-dihydroxyphenylalanine (dopa) is oxidized in the presence of tyrosinase, the oxidation is considerably enhanced by *p*-benzoquinone.[1] However, the stimulation by the quinone has not yet been elucidated.

This study was undertaken in order to examine the interaction of dopa and *p*-benzoquinone *in vitro* under physiological conditions. Two types of reactions were expected to occur; one of these was the ring amination of the quinone with dopa (Eq. (1)), and the other was the oxidation of dopa with the quinone (Eq. (2)).

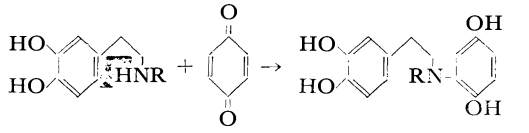

(1)

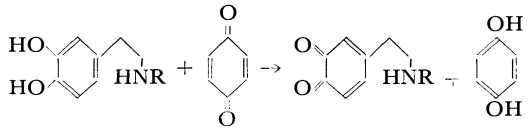

(2)

In this study, the spectrum for the enzymic oxidation of dopa[2] was compared with that of the reaction of dopa with *p*-benzoquinone. It was found that these spectra were essentially identical.

The scheme for the enzymic oxidation of dopa by tyrosinase[3] has been confirmed polarographically.[4] The oxidation products of dopa give polarographic waves. In this study, by a comparison of the observed polarogram for the enzymic oxidation of dopa with that for the reaction of dopa with *p*-benzoquinone *in vitro* under physiological conditions (*i.e.*, in a buffer solution of pH 7.0 at ordinary temperatures), it was found that the polarograms (Fig. 2) were essentially identical, except that the anodic-cathodic wave for the hydroquinone and the quinone appeared in the dopa-*p*-benzoquinone reaction.

In view of the above facts, it appears that the reaction of dopa with *p*-benzoquinone *in vitro* under physiological conditions involves mainly the redox reaction.

The other expected course of the reaction was the amination of the quinone ring by the amino group of dopa. Polarographic investigation showed, however, that the rate of the reaction was much smaller than that of the redox reaction of dopa with *p*-benzoquinone. It is likely that the contribution of amination to the overall reaction was very small.

Experimental

Materials. Dopa (mp 271—272°C decomp. Found: C, 54.73; H, 5.59; N, 6.89%. Calcd for $C_9H_{11}O_4N$: C, 54.82; H, 5.62; N, 7.10%) was obtained commercially. No polarographic reduction wave was found in a solution of dopa. *p*-Benzoquinone (mp 116°C) was purified by the sublimation of commercially available chemicals. The buffers used were prepared according to the method of Sörensen in our laboratory. A tyrosinase preparation from a mushroom was kindly supplied by Prof. Y. Ogura.

Apparatus. The visible spectra were recorded on a Hitachi Recording Spectrophotometer, Model EPS-2U. The polarographic determinations were made with a Yanagimoto Pen Recording Polarograph, PA-102.

The Determination of 2,3-Dihydroindol-5,6-quinone (Red Quinone). 1) *Visible Spectroscopy. Enzymic Oxidation of Dopa*: To 3.0 m*l* of a solution buffered at pH 6.8 and containing 0.214 mg (1.09×10^{-6} mol) of dopa per m*l*, we added about 0.1 m*l*, of a tyrosinase solution. The absorption spectra were then immediately measured. The results are depicted in Fig. 1. The absorption spectra of intermediates between dopa and the pigment did not become evident. The experiment was conducted at room temperatures.

Reaction of Dopa with p-Benzoquinone: To 2.0 m*l* of a solution buffered at pH 6.8 and containing 0.106 mg (9.8×10^{-7} mol) of dopa per m*l*, we added 1.0 m*l* of a solution buffered at pH 6.8 and containing 0.229 mg (2.1×10^{-6} mol) of *p*-benzoquinone per m*l*. The experiment was conducted at room temperatures. The absorption spectrum of the pigment obtained in this manner was the same as that found in the enzymic oxidation.

2) *Polarography*. The experimental conditions were the same as those of the spectrophotometric studies.

1) Private communication.
2) H. S. Mason, *J. Biol. Chem.*, **172**, 83 (1948).
3) H. S. Mason, "Advances in Enzymology," Vol. 16, Interscience, New York, London (1955), p. 105.
4) H. S. Raper, *Biochem. J.*, **21**, 89 (1943).
5) K. Wiesner, *Biochem. Z.*, **314**, 2214 (1943).

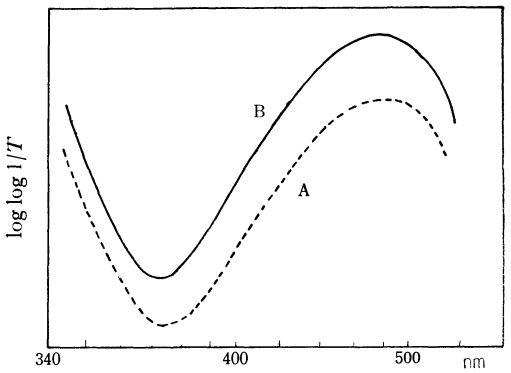

Fig. 1. Absorption spectra of oxidized dopa.
A: Enzymically catalyzed oxidation of dopa. Three m*l* of a solution containing 0.624 mg of dopa buffered at pH 6.8 and 0.1 m*l* of enzyme solution.
B: Oxidation of dopa with *p*-benzoquinone. Two m*l* of a solution containing 0.212 mg of dopa buffered at pH 6.8 and 1.0 m*l* of a solution containing 0.229 mg of *p*-benzoquinone.

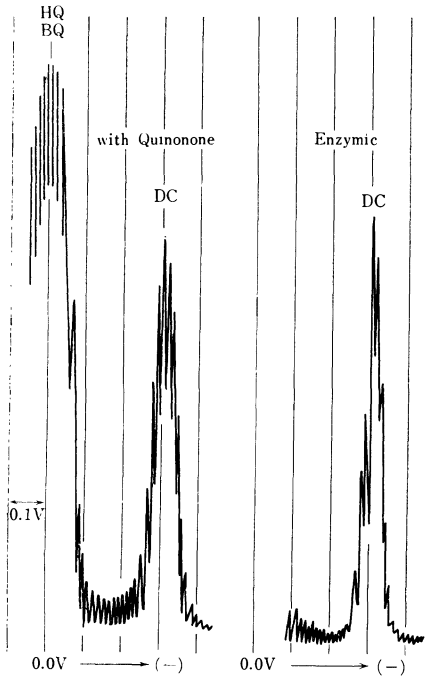

Fig. 2. Polarograms of dopachrome from tyrosinase catalyzed oxidation of dopa and from dopa-*p*-benzoquinone reaction.
DC; Dopachrome, BQ; *p*-Benzoquinone, HQ; Hydroquinone

Enzymic Oxidation of Dopa: The reaction mixtures showed a polarographic wave at −0.20 V.

Reaction of Dopa with p-Benzoquinone: The reaction mixtures showed two polarographic waves, at −0.20 and at 0.0 V. The polarograms are all essentially identical with the exception of the anodic-cathodic wave (at 0.0 V) for the hydroquinone and the quinone.

Reaction of Dopa with *p*-Benzoquinone. The buffered solution of dopa and that of the quinone were deoxygenated by passing nitrogen through, and then they were mixed in a polarographic cell in order to initiate the reaction. Nitrogen was bubbled through the reaction mixture in order to remove any oxygen and agitate the solution. The bubbling was stopped during the recording of the polarograms. Polarographic curves were registered at regular intervals, and the amounts of the unchanged quinone and its hydroquinone were determined by means of the polarograms.

To 3.0 m*l* of an oxygen-free solution buffered at pH 7.0 (phosphate buffer) and containing 0.091 mg (4.6×10^{-7} mol) of dopa per m*l*, we added 3.0 m*l* of an oxygen-free solution buffered at pH 7.0 (phosphate buffer) containing 0.15 mg (1.4×10^{-6} mol) of *p*-benzoquinone per m*l*. The rate of the reduction of the quinone was obtained at 28°C by polarography. The results are given in Fig. 3.

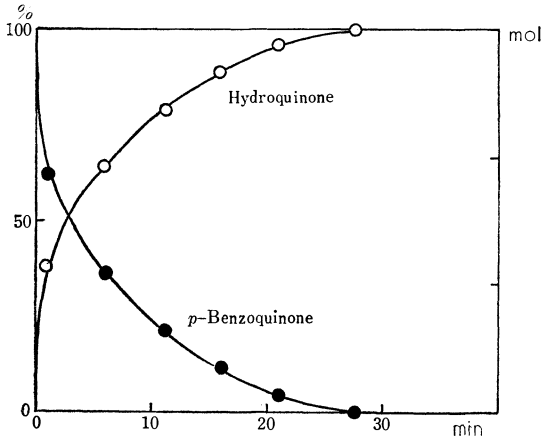

Fig. 3. Change of amount of *p*-benzoquinone and that of hydroquinone in dopa-*p*-benzoquinone reaction. The final reaction mixtures contained 4.6×10^{-7} mol of dopa and 1.4×10^{-6} mol of the quinone in a total volume 6.0 m*l* in 0.03 M phosphate buffer at pH 7.0. The experimental was run in a polarographic cell at 25°C.

The experimental results show that, at any instant, the amount of hydroquinone formed was equal to the amount of quinone that had disappeared. Three moles of the quinone were quantitatively reduced to hydroquinone by one mole of dopa. Therefore, one might conclude that the redox reaction took place. When more than three moles of the quinone were used, hydroquinone was not quantitatively formed, although the amount of excess quinone decreased.

Results

The experimental results showed that dopa was oxidized to indol-5,6-quinone by *p*-benzoquinone. The oxidation was similar to the oxidation by phenoloxidase or that by inorganic oxidants.

One molecule of dopa is capable of reducing 3 molecules of the quinone. The following scheme can be put forward to explain the reaction:

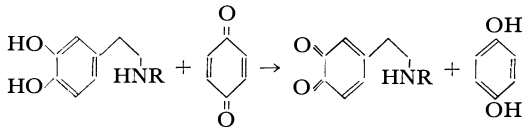

Next, the quinon undergoes an intramolecular change, with the production of 5,6-dihydroxy-2,3-dihydroindol derivatives:

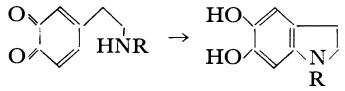

This is in turn oxidized to its quinone, which is the red pigment which appears in the first of the reaction stages:

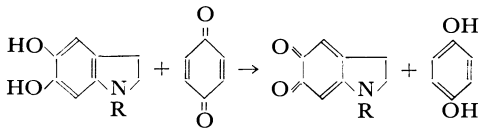

This pigment undergoes further change on standing and yields 5,6-dihydroxyindole derivatives:

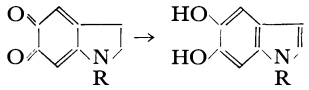

These are oxidizable in the air or by the quinone and yield indol-5,6-quinone derivatives:

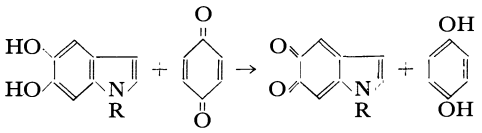

The problem of the fate of indol-5,6-quinone derivatives is not discussed in the present paper.

BULLETIN OF THE CHEMICAL SOCIETY OF JAPAN VOL. 43 2622—2623 (1970)

The Reaction Route of 2,4,6-Triphenyl-*s*-triazine to the C=N Conjugated Polymer

Eizo OIKAWA and Atsushi OHKUMA

Faculty of Engineering, Niigata University, Nagaoka, Niigata

(Received January 13, 1970)

The heating of 2,4,6-triphenyl-*s*-triazine (cyaphenin) with a metal halide afforded a black polymer. A similar polymer was obtained from the benzonitrile complex with a metal halide. In this note, the reaction route of cyaphenin to the polymer was investigated in order to determine whether or not the polymerization proceeds by the usual ring-opening, since Kabanov *et al.*[1] have reported the conversion of cyaphenin to the polymer as a ring-opening. Their meaning was, however, ambiguous.

The reaction of cyaphenin[2] with zinc chloride[3] was carried out in an about-20-m*l*, vacuum-sealed ampule by heating a mixture in the molar ratio of 2 : 3 (2 : 1 based on the benzonitrile unit) at 350—430°C in both the presence and absence of metaphosphoric acid (MPA) for from 1 to 13 hr. The black solid formed was dissolved in sulfuric acid and precipitated by pouring the solution into water. The weight difference between the initial cyaphenin and the precipitates gave the weight of the benzonitrile, which remained unchanged. The unreacted cyaphenin was recovered by sublimation. The polybenzonitrile from the zinc chloride complex was prepared by heating a mixture of benzonitrile and zinc chloride in a 2 : 1 molar ratio. The black product was extracted with hot toluene. The toluene was removed by distillation, and the residue was sublimed at about 200°C to give cyaphenin.

The relation between the polymer yields and the reaction time at different reaction temperatures in the presence of MPA is shown in Fig. 1. Similar curves were obtained in the absence of MPA. The apparent activation energy was calculated to be 14 kcal/mol in the presence of MPA and 16 kcal/mol in the absence of MPA, on the basis of the maximum slope in the yield-time curves.[4] The heating of cyaphenin without zinc chloride in either the presence or absence of MPA in an ampule at 430°C for 4 hr gave no appreciable amounts of benzo-

1) B. A. Kabanov, V. P. Zubov, V. P. Kobaleba and V. A. Kargin, *J. Polym. Sci., Part C*, **No. 4**, 1009 (1963).

2) A. H. Cook and D. G. Jones, *J. Chem. Soc.*, **1941**, 278.

3) Guaranteed grade: commercially available.

4) E. Oikawa and S. Kambara, *J. Polym. Sci., Part B*, **2**, 649 (1964).

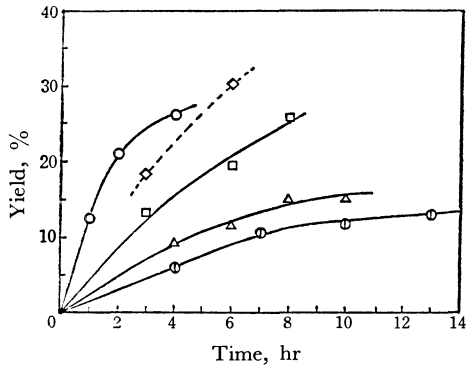

Fig. 1. Polymer yields in the presence of MPA.
○ 430°C, □ 400°C, △ 370°C, ◐ 350°C,
◇ from $2C_6H_5CN : ZnCl_2$ at 400°C

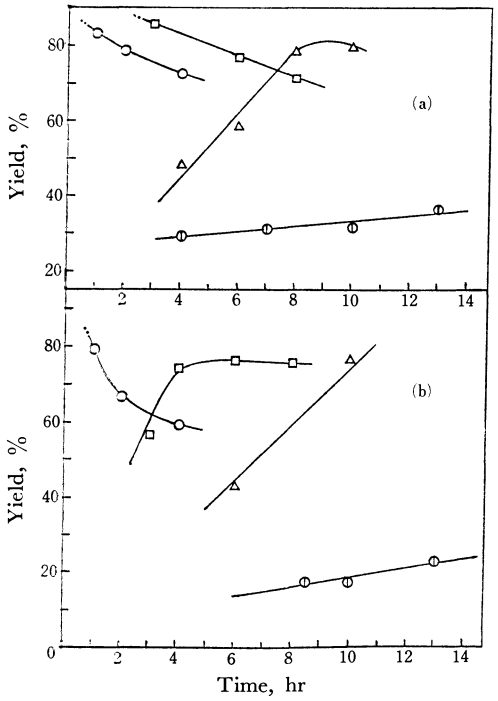

Fig. 2. Yields of unreacted benzonitrile in the presence (a) and absence (b) of MPA.
○ 430°C, □ 400°C, △ 370°C, ◐ 350°C

nitrile, although in the presence of MPA a little stronger smell of benzonitrile was perceived. In order to examine the influence of MPA on the trimerization, benzonitrile was heated with 5% MPA in an autoclave at 300°C for 24 hr. This gave only a 0.3% yield of cyaphenin. These facts indicate that MPA neither initiates the trimerization nor decomposes the trimer by itself.

Unreacted benzonitrile, as is shown in Figs. 2 (a) and (b), was formed by the decomposition of cyaphenin and was not changed to either the polymer or cyaphenin. The yields of benzonitrile decreased at higher temperatures and increased at lower temperatures with the reaction time. The decrease in the yields of the unreacted nitrile reveals that the decomposition of cyaphenin took place in the initial reaction period and in the subsequent reaction period the benzonitrile thus formed was converted to the polymer. In other words, the rate of the decomposition of cyaphenin is very rapid compared with the rate of the polymer formation at higher temperatures. On the other hand, the increase in the yields of the unreacted nitrile at lower temperatures corresponds to the accumulation of benzonitrile due to the difference between the decomposition and the polymer-formation rate of cyaphenin, since the decomposition of cyaphenin to benzonitrile proceeds at a higher rate than the conversion of benzonitrile to the polymer. Therefore, the activation energies noted above indicate those of the polymerization reaction of benzonitrile. The variations in the yields of the unreacted benzonitrile indicate that MPA acts as a promoter in the decomposition of the trimer to the monomer in the presence of zinc chloride. These results can be summarized as in the following diagram:

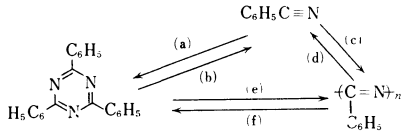

The once-produced polymer is thermally stable and remains unchanged except for a slight decomposition, accompanied by NH_3 formation.[5] The routes (d) and (f) can, therefore, be neglected compared with the other routes. The ring-opening path of cyaphenin *via* (b) to give benzonitrile is made possible by the preferential formation of benzonitrile in Figs. 2 (a) and (b). The route (c) from the benzonitrile complex with zinc chloride to the polymer is preferential to the route (a) back to cyaphenin, as is demonstrated by the higher yields of the polymer. Consequently, the route (e) should not be appreciable compared with (b) and (c). The presence of the equilibrium between (a) and (b) is demonstrated by the higher polymer yields from the complex than those from cyaphenin at 400°C, as is shown in Fig. 1, and by the simultaneous formation of cyaphenin from the complex.

5) E. Oikawa and S. Kambara, This Bulletin, **37**, 1849 (1964).

BULLETIN OF THE CHEMICAL SOCIETY OF JAPAN VOL. 43 2624—2625 (1970)

Effect of Coexisting Minerals on the Graphitization of Carbon under Pressure. V. Distribution of Calcium and Graphitic Components in Heat-Treated Carbon Specimens

Shin-ichi HIRANO, Michio INAGAKI and Hajime SAITO

Faculty of Engineering, Nagoya University, Chikusa-ku, Nagoya

(Received January 22, 1970)

The accelerating effect of coexisting calcium compounds on the graphitization of carbon under pressure has been reported.[1-4] The mechanism of the accelerating effect on the graphitization seems to consist of the formation and the successive decomposition of calcium carbide and/or the formation and the successive reaction of calcium metal and carbon monoxide.

In the present work, the distribution of calcium in carbon specimens heat-treated in the presence of calcium compounds under pressure was determined by using an electron microprobe analyser. The distribution was compared with that of the graphitic component G_M which was determined by the X-ray diffraction method.[1]

Specimens were prepared from a polyvinylchloride coke, carbonized at 680°C (PV-7) by heat treatment under 3.2 kbar for 60 min at 1090 and 1360°C in the presence of calcium carbonate, and at 1100, 1400 and 1500°C in the presence of calcium oxide precalcined at 920°C. All the five specimens were obtained as caked pieces.

Details on the apparatus and the procedure for the preparation of the caked specimens were reported previously.[2,4] The size of the caked specimens was about 7.6 mm in diameter and 2.5 mm in thickness.

The specimens were cut into halves (a) and (b) across their diameter, one half for the electron microprobe analysis and the other for the X-ray diffraction analysis.

Sample (a) was mounted in resin. The surface of the cross section was ground on an abrasive paper and finished to a very flat surface by polishing on a felt with very fine corundum powder dispersed in ethanol in order to avoid reactions between calcium compounds and water. Electron beam of 100μ width was scanned along the thickness (h-direction) and also along the radial direction (r-direction) on the polished section of the caked specimen (Fig. 1).

For X-ray diffraction analysis, sample (b) was cut down to pieces along the thickness and also

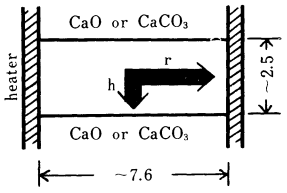

Fig. 1. Scheme of direction scanning electron beam.

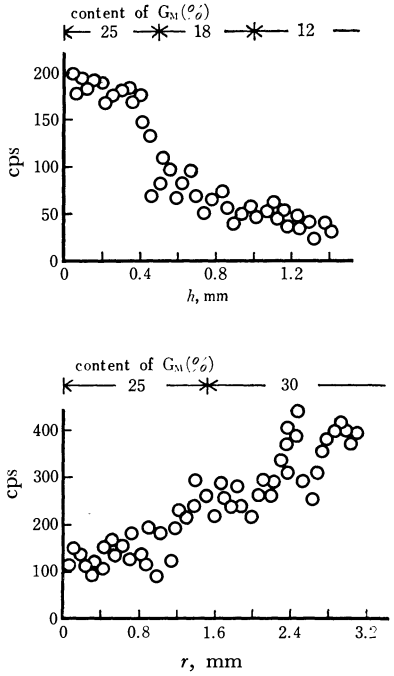

Fig. 2. Relation between distribution of calcium and content of graphitic component G_M in the specimen heat-treated at 1360°C under 3.2 kbar in the presence of calcium carbonate.

1) T. Noda, M. Inagaki, S. Hirano and K. Amanuma, This Bulletin, **41**, 1245 (1968).
2) T. Noda, M. Inagaki, S. Hirano and H. Saito, *Kogyo Kagaku Zasshi*, **72**, 643 (1969).
3) T. Noda, M. Inagaki, S. Hirano and H. Saito, This Bulletin, **42**, 1738 (1969).
4) S. Hirano, H. Saito and M. Inagaki, *ibid.*, **43**, 2599 (1970).

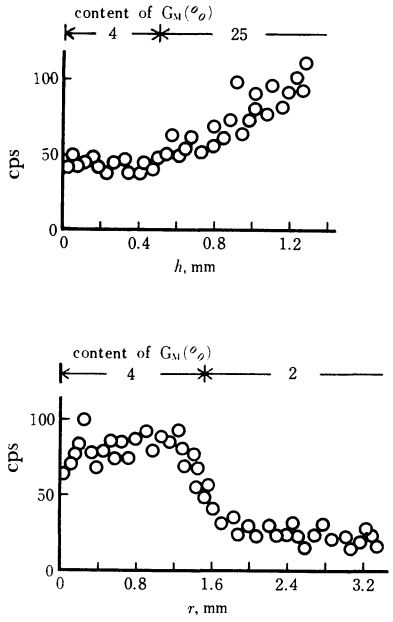

Fig. 3. Relation between distribution of calcium and content of graphitic component G_M in the specimen heat-treated at 1100°C under 3.2 kbar in the presence of calcium oxide.

along the radial direction, and the content of graphitic component G_M was measured for each piece.

Two examples of results are shown in Figs. 2 and 3. In the presence of calcium carbonate, the content of graphitic component G_M was found to be larger in the central part of the specimen than in the peripheral part which was close to carbonate layer. This distribution of graphitic component was attributed to a temperature gradient in the specimen.[2] In the presence of calcium oxide, however, the reverse distribution of graphitic component G_M was observed,[4] that is, the content of graphitic component was smaller in the central part than in the peripheral part. The reason for this difference in the distribution of graphitic component in the heat-treated carbon specimens is not clear. However, in both cases the part having a larger content of graphitic component G_M has larger calcium concentration. The same relation was observed for all the specimens.

X-ray fluorescence photographs of carbon and calcium in the central area (400 $\mu \times 400\ \mu$) of a specimen are shown in Figs. 4a and 4b. The concentration variation of calcium scanned with electron beam width of 10 μ from A to B (Fig. 4 b) across a carbon grain is shown in Fig. 4c. From the figures we see that calcium was accumulated in the boundaries of carbon grains. The concentration of calcium in the carbon grain decreased very steeply in the layer about 10 μ from the boundary and only a minute amount of calcium was detected in the inner part.

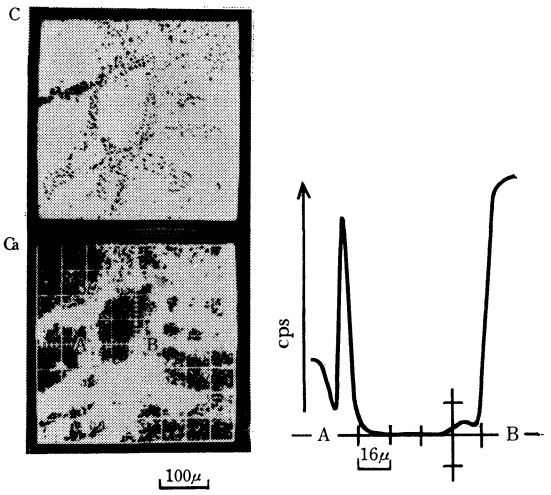

Fig. 4. a) X-ray fluorescence photograph of carbon in the central area of the specimen heat-treatd at 1360°C under 3.2 kbar in the presence of calcium carbonate.
b) X-ray fluorescence photograph of calcium in the same area as in Fig. 4a.
c) Concentration variation of calcium scanned from A to B in Fig. 4b.

The fact that the content of graphitic component G_M and the concentration of calcium were closely related to each other supports the proposed mechanism of the acceleration of graphitization in the presence of calcium compounds,[4] *viz.*, the intermediate formation of calcium carbide and/or calcium metal.

The authors wish to thank Dr. T. Noda, President of Mie University, for his helpful discussion and The Toyota Central Research Laboratory for kind arrangements for use of the Shimadzu-ARL electron microprobe analyser.

BULLETIN OF THE CHEMICAL SOCIETY OF JAPAN VOL. 43 2626—2628 (1970)

Reactions of Recoil ^{35}S Atoms with Organic Compounds. I. The Distribution of ^{35}S Atoms on Mercaptobenzothiazole

Ko Taki

The Institute of Physical and Chemical Research, Yamato-machi, Saitama

(Received January 28, 1970)

The reaction of ^{35}S atoms produced by neutron irradiation has been studied recently.[1,2] An appreciable proportion of the ^{35}S appears in oxidized forms,[3,4] especially as sulfate. Several investigations[5,6] have been reported regarding the chemical forms of ^{35}S, and extensive studies of the sulfur atom produced by the photolysis[7,8] of SCO have also been reported. However, few investigations[9] have been reported regarding the reaction of a sulfur atom produced by nuclear recoil reaction with organic compounds.

In this paper, the distribution of ^{35}S atoms in the molecules of mercaptobenzothiazole (I) and methylmercaptobenzothiazole (II) was studied; some differences in the reactions of the ^{35}S atoms formed by the $^{35}Cl(n,p)^{35}S$ and $^{34}S(n,\gamma)^{35}S$ processes were also investigated.

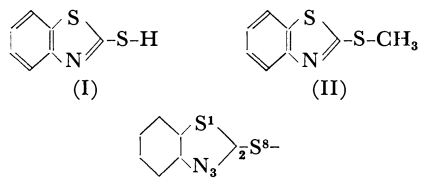

(I) (II)

Experimental

Mercaptobenzothiazole (I) and methylmercaptobenzothiazole(II) (Tokyo Kasei Co.) were irradiated with JRR-1,2 and 3 reactors of the Japan Atomic Energy Research Institute in the absence of and in the presence of trichlorobenzene as a chlorine source. The irradiations were performed in a quartz ampule (0.5×3.0 cm) containing the sample.*1

Separation and Purification of an Irradiated Sample. For the degradation of an activated compound, the starting material (I and II) was added as a carrier to the irradiated sample; the purification was performed by recrystalization, reprecipitation, and solvent extraction.

Measurement of Radioactivity. All the samples were oxidized by the Shöniger[10] method or by the method using a Pirie reagent,[11] and the sulfate thus produced was precipitated by barium chloride. The activity of the barium sulfate thus obtained was measured at an infinite thickness by an end-window-type Geiger Müller counter. The specific activity of each compound was calculated from the saturation value of the apparent activity. The measurement of the total activity was carried out by the simultaneous irradiation of $(NH_4)_2SO_4$, NH_4Cl, and the targets. At each step of degradation of the sulfur compounds, the relative activity was measured. The degradation was performed by the following processes:[12]

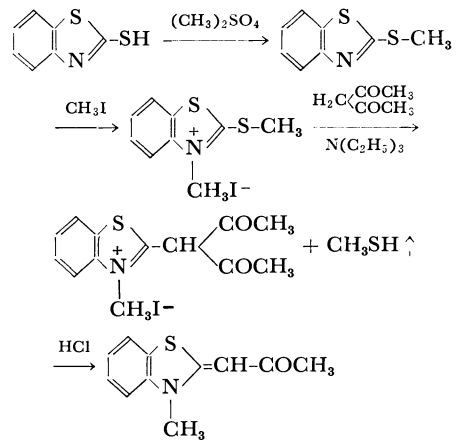

Results and Discussion

As is listed in Table 1, the reactions of the ^{35}S atoms in the presence and in the absence of ben-

*1 For the purpose of degassing, the sample was dissolved in pyridine or alcohol, and then the solvents were removed.

1) C. Chiotan, I. Zamfir and M. Szabo, *J. Inorg. Nucl. Chem.*, **26**, 1132 (1964).
2) K. Yoshihara, Ting-Chia Huang, H. Ebihara and N. Shibata, *Radiochim. Acta*, **3**, 185 (1964).
3) J. Cifka and V. Bracokova, *J. Inorg. Nucl. Chem.*, **28**, 2483 (1966).
4) K. Taki and Y. Hishiki, *J. Phys. Chem. Inst.*, **37**, 106 (1961).
5) J. H. Freeman, M. Kasrai and A. G. Maddock, *Chem. Commun.*, **1967**, 979.
6) C. Chiotan, I. Zamfir and T. Costera, *J. Inorg. Nucl. Chem.*, **30**, 2857 (1968).
7) E. M. Lown, E. L. Dedio, O. P. Strausz and H. E. Gunning, *J. Amer. Chem. Soc.*, **89**, 1056 (1967).
8) E. M. Lown, H. S. Sandhu, H. E. Gunning and O. P. Strausz, *ibid.*, **90**, 7164 (1968).
9) K. Taki, *J. Phys. Chem. Inst.*, **38**, 419 (1962).
10) W. Schöniger, *Mikrochim. Acta*, **1956**, 869.
11) N. W. Pirie, *Biochem. J.*, **26**, 2041 (1932).
12) B. Beilenson and F. M. Hamer, *J. Chem. Soc.*, **1939**, 143.

Table 1. Distribution (%) of ^{35}S produced by $^{35}Cl(n, p)^{35}S$ process in the presence and absence of benzoquinone

Benzoquinone %	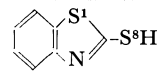 S_1-position	S_8-position
0	2.4	97.6
3.9	1.6	98.4

Mercaptobenzothiazole 0.2 g
1,2,4-Trichlorobenzene 0.1 g
Irradiation 2.5×10^{13} n/cm² sec, about 200 hr

Benzoquinone %	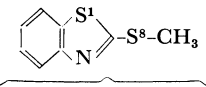 S_1-position	S_8-position
0	2.2	97.8
3.5	5.7	94.3

Methylmercaptobenzothiazole 0.4 g
1,2,4-Trichlorobenzene 0.1 g
Irradiation 2.5×10^{13} n/cm² sec, about 200 hr

zoquinone and oxygen as a radical scavenger[13] gave almost the same ^{35}S distribution. This experimental fact suggests that all the reactions may be considered to be hot reactions and not thermal reactions. The radiochemical yield of the activated parent molecule (retention value) is about 2—5% for the $^{35}Cl(n,p)^{35}S$ process and about 30% for the $^{34}S(n, \gamma)^{35}S$ process. The distribution of the ^{35}S atoms in the molecule is much greater in the S_8-position than in the S_1-position in both mercaptobenzothiazole (I) and methylmercaptobenzothiazole (II). The experimental results can not be reasonably interpreted, but it may be considered that the collisional exchange (a knock on exchange in terms of a billiard-ball model) of the sulfur atom is easier in the S_8-position than in the S_1-position in the molecule. By the collision of a hot atom, C–S–C bond rupture may occur in a moment. A large number of bond-cleaved intermediates may decompose, and some of them may combine in a short duration with slow-downed ^{35}S atoms which are located near the molecule. Therefore, the distribution of the ^{35}S atoms may be dependent on the stability of the bond-cleaved intermediate. It may be considered that the intermediate which is bond-cleaved at the S_8-position 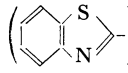 is more stable than that at the S_1-position 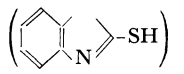 in the mercaptobenzothiazole molecule.

Table 2. Distribution (%) of ^{35}S produced by $^{34}S(n, \gamma)^{35}S$ and $^{35}Cl(n, p)^{35}S$ process

Process	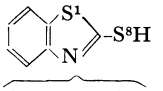 S_1-position	S_8-position	$\frac{S_8}{S_1}$	(Retention value) yield %
$^{34}S(n, \gamma)^{35}S$	12.6	87.4	6.9	27.5
$^{35}Cl(n, p)^{35}S$	5.4	94.6	17.5	4.8

Cl source: *p*-Dichlorobenzene (^{35}Cl atoms/^{34}S atoms=10)
Irradiation 3×10^{11} n/cm² sec, 240 hr
Targets were not degassed.

$^{34}S(n, \gamma)^{35}S$	6.4	93.6	14.6	
$^{35}Cl(n, p)^{35}S$	3.6	96.4	26.8	

Cl source: Trichlorobenzene (^{35}Cl atoms/^{34}S atoms=11
Irradiation 4×10^{13} n/cm² sec, 144 hr

Reaction of ^{35}S Atoms Formed by Two Nuclear Reactions. In the presence of trichlorobenzene, since the activation cross-section of ^{34}S and ^{35}Cl is almost the same (0.26 barn for ^{34}S and 0.17 barn for ^{35}Cl) and since the number of atoms of ^{35}Cl is much larger than that of ^{34}S, the $^{34}S(n, \gamma)^{35}S$ process can be disregarded. In this case the reactions are brought about by hot ^{35}S atoms produced by the $^{35}Cl(n, p)^{35}S$ process. On the other hand, in the absence of trichlorobenzene the reactions are brought about by hot ^{35}S atoms produced by the $^{34}S(n, \gamma)^{35}S$ process. The experimental results on hot ^{35}S atoms from the two formation processes are listed in Table 2. The ratio of ^{35}S atoms at the S_8-position to those at the S_1-position is smaller in the process of $^{34}S(n, \gamma)^{35}S$ than in that of the $^{35}Cl(n, p)^{35}S$ process in all the runs, as is shown in Table 2; the ^{35}S atoms formed from ^{34}S exchange with S_8-sulfur more easily than the ^{35}S atoms formed from ^{35}Cl.

The chemical reaction may occur when hot atoms have been slowed[14] sufficiently (25 eV—50 eV).

Process	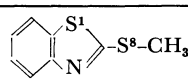 S_1-position	S_8-position	$\frac{S_8}{S_1}$	(Retention value) yield %
$^{34}S(n, \gamma)^{35}S$	12.5	87.5	7.0	
$^{35}Cl(n, p)^{35}S$	7.1	92.9	13.1	

Cl source; Trichlorobenzene (^{35}Cl atoms/^{34}S atoms=10)
Irradiation 4×10^{13} n/cm² sec, 200 hr

$^{34}S(n, \gamma)^{35}S$	17.1	82.9	4.8	29.7
$^{35}Cl(n, p)^{35}S$	10.5	89.5	8.5	2.1

Cl source: Trichlorobenzene (^{35}Cl atoms/^{34}S atoms=20)
Irradiation 1×10^{11} n/cm² sec, 288 hr

13) A. F. Trotman-Dickenson, "Free Radicals: An Introduction," Methuen & Co. Ltd., London (1959), p. 14

14) A. P. Wolf, C. S. Redvanly and R. C. Anderson, *J. Amer. Chem. Soc.*, **79**, 3717 (1957).

The reaction of sulfur atoms may not be affected by the initial recoil energy, about 17 keV for the $^{35}Cl(n, p)^{35}S$ process and about 1 keV for the $^{34}S(n, \gamma)^{35}S$ process, because the recoil energy is too high to react with an organic compound. Also, because of the simultaneous irradiation of the sample for two nuclear reactions, the effect of radiation damage may be disregarded.

It has been reported that, in the reaction of the ^{11}C formed from the $^{12}C(n, 2n)^{11}C$, $^{12}C(p, pn)^{11}C$,[15,16] and $^{12}C(\gamma, n)^{11}C$[17] processes, no essential differences are found among the processes.

The present author does not have any reasonable explanation for the experimental facts. It may, however, be presumably postulated that the distribution of ^{35}S atoms is affected by the original position of the nuclear-transformed atom in the molecule.

The author wishes to acknowledge the valuable assistance of Miss K. Motegi as well as to express his appreciation to Dr. T. Nozaki for his helpful discussions and suggestions. A part of this research was carried out with a Scientific Research Grant from the Ministry of Education, to which the author's thanks are due.

15) G. Stöcklin H. Stangl, D. R. Christman, J. B. Cumming and A. P. Wolf, *J. Phys. Chem.*, **67**, 1735 (1963).

16) G. Stöcklin and A. P. Wolf, *J. Amer. Chem. Soc.*, **85**, 229 (1963).

17) MacKay and R. Wolfgang, *ibid.*, **83**, 2399 (1961).

BULLETIN OF THE CHEMICAL SOCIETY OF JAPAN VOL. 43 2628—2630 (1970)

The Action of Boron Trifluoride Etherate on *l*-Menthol

Kimiko NAGAI

Fukuyama Women's Junior College, Fukuyama

(Received February 4, 1970)

The reaction of menthol with sulfuric acid has been reported by Wagner,[1] who detected *p*-menthane and alkane, bp 178.0—180.0°C/13 mmHg, in the reaction product. Aizawa *et al.*[2] have reported that the reaction of menthyl chloride with anhydrous aluminum chloride resulted in the formation of *p*-menthane, a dimer ($C_{20}H_{36}$), 1-*p*-menthene and 3-*p*-menthene via the menthyl cation. In this work, *l*-menthol was reacted with an equimolar amount of boron trifluoride etherate at 80°C for 45 min. A light-yellow oil separated as an upper layer; it consisted of a low-boiling part and a high-boiling part. Six components were isolated from the low-boiling part by preparative gas chromatography, and one component from the high-boiling part by column chromatography.

(a) Low-boiling Component. Component (1), 3-isobutyl-1-methylcyclopentane: The molecular formula is found to be $C_{10}H_{20}$ from the mass spectrum (parent peak M^+, *m/e* 140, Fig. 1). The IR and NMR spectra showed the bands at 1384, 1368, and 1169 cm^{-1} associated with a branched dimethyl group and the signals corresponding to three methyl groups (9H) between 0.80 and 1.00 ppm (Fig. 2). This component is a saturated mono-cyclic hydrocarbon which differs from *o*-, *m*- and *p*-menthane in its IR and NMR spectra. The main peaks of *m/e* 97, 83, 69, 55, and 41 in the mass spectrum can be well explained as those of 3-isobutyl-1-methylcyclopentane, which has not previously been reported.

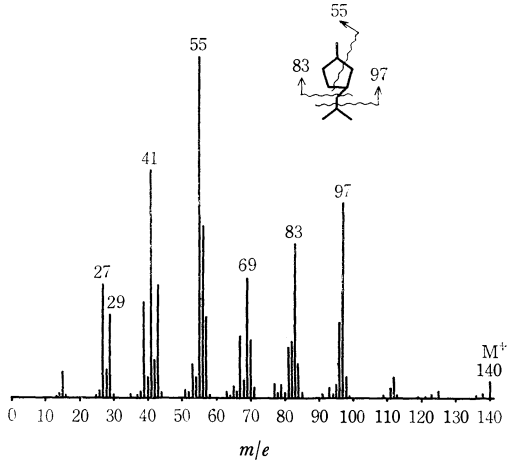

Fig. 1. Mass spectrum of 3-isobutyl-1-methylcyclopentane.

Component (2): The molecular formula is found to be $C_{10}H_{18}$ from the mass spectrum (parent peak M^+, *m/e* 138). The IR spectrum showed the bands at 1386, 1370, and 1167 cm^{-1} associated with a branched dimethyl group. The compo-

1) G. Wagner, *Ber.*, **27**, 1636 (1894).

2) F. Aizawa, M. Arai and M. Yamaguchi, *Nippon Kagaku Zasshi*, **90**, 497 (1969).

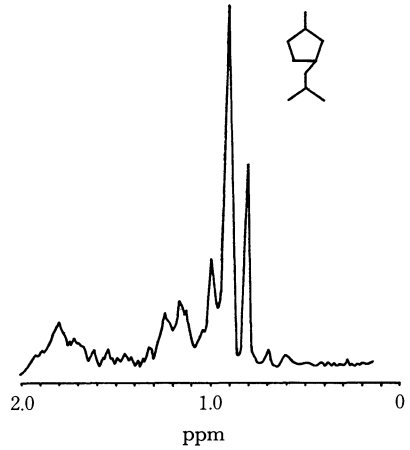

Fig. 2. NMR spectrum of 3-isobutyl-1-methylcyclopentane.

nent (2) seems to have been found to be a mixture of two compounds through careful gas chromatography using Carbowax 6000 as a stationary phase. When this component was hydrogenated in the presence of platinum oxide, it absorbed one mole of hydrogen and changed to 3-isobutyl-1-methylcyclopentane. Judging from the base peak of *m/e* 81 in the mass spectrum, this component seems to be an unsaturated five-membered ring compound having the same carbon skeleton as 3-isobutyl-1-methylcyclopentane.

Components (3), (4), (5) and (6) were identified as *trans-p*-menthane, *cis-p*-menthane, 3-*p*-menthene, and 1-*p*-menthene respectively by comparing them with authentic specimens by gas chromatography or by comparing their IR spectra and also by the preparation of nitrosochloride.

(b) High-boiling Component. A colorless and rather viscous oil was isolated from the high-boiling part by elution chromatography. The molecular formula is found to be $C_{20}H_{38}$ from the mass spectrum (parent peak M^+, *m/e* 278). Peaks at *m/e* 139 corresponding to a half of the molecular weight of this component and at *m/e* 235 ($M^+ - C_3H_7$) appeared in the mass spectrum. It was suggested that this compound was bis-menthyl.

The reaction of boron trifluoride etherate with *l*-menthol was carried out under various conditions (Experiment (1), temp. 25°C, reaction period 30 days; (2) temp. 60°C, reaction period 6.5 hr; (3) temp. 80°C, reaction period 45 min). The contents of C_{10}- and C_{20}-hydrocarbons identified in Experiment (3) were as follows: 3-isobutyl-1-methylcyclopentane 2%, 3-isobutyl-1-methylcyclopentene 1%, *trans-p*-menthane 9%, *cis-p*-menthane 2%, 3-*p*-menthene 10%, 1-*p*-menthene 2%, $C_{20}H_{38}$ 30%.

trans-p-Menthane was produced in a large quantity at room temperature (25°C), but the amount of 3-*p*-menthene increased with a rise in the reaction temperature. Also, C_{20}-hydrocarbon was

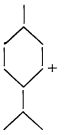

[I]

obtained in a large quantity in every experiment. It seems that 3-isobutyl-1-methylcyclopentane and 3-isobutyl-1-methylcyclopentene were formed through a ring contraction of the cation [I]. It is interesting that 3-isobutyl-1-methylcyclopentane and 3-isobutyl-1-methylcyclopentene were produced from *l*-menthol by ring contraction; these two compounds have not yet been reported.

Experimental

1. Sample. *l*-Menthol: mp 42.5—43.5°C, $[\alpha]_D^{25}$ —46.7° (in ether), phenylurethane, mp 111.0—111.5°C. The sample exhibited only one peak on gas chromatography with either Carbowax 6000 and Neopentyl glycol succinate. Neoiso-menthol which shows the same retention value at *l*-menthol, could not be detected on the basis of the IR spectrum (lack of bands, 795 and 629 cm^{-1} characteristic of the neoiso-isomer).

Boron trifluoride etherate: Commercially-available boron trifluoride ehterate (BF_3 47%) of the first grade was used.

2 Identification of the Reaction Product. Three hundred grams of *l*-menthol and 300 m*l* of boron trifluoride etherate were reacted at 80°C for 45 min; 260 g of the oil were thus obtained from the upper layer. The oil, washed with a saturated aqueous solution of sodium carbonate and water, was distilled under reduced pressure to 7 fractions. Six components were isolated from fractions (1) to (4) by preparative gas chromatography using Carbowax 6000 at 65°C.

Component (1), 3-isobutyl-1-methylcyclopentane: The component corresponding to the peak (1) on gas chromatography was a colorless oil with petroleum-like smell. The mass and NMR spectra are shown in in Figs. 1 and 2.

Component (2): This was a colorless oil with a petroleum-like smell; it corresponded to the peak (2). This oil was shown to be a mixture of two compounds by gas chromatography, but the two compounds could not be separated. When 0.5 g of the oil was hydrogenated on platinum oxide, it absorbed one molar equivalent of hydrogen and changed into 3-isobutyl-1-methylcyclopentane.

Components (3), (4), (5), and (6) were identified by the following measurements and by the preparation of derivatives. Their IR and GLC were compared with those of authentic specimens.

Component (3): *trans-p*-menthane, mol wt, 139 (Rast), Elementary analysis: $C_{10}H_{20}$, IR, GLC

Component (4): *cis-p*-menthane, IR, GLC

Component (5): 3-*p*-menthene, IR, GLC, nitrosochloride

Component (6): 1-*p*-menthene, IR, GLC, nitrosochloride

High-boiling component: The oil was isolated from the fraction (6) by passing *n*-hexane through a silica gel column. The component showed a spot of R_f 0.88

on thin-layer chromatography. Bp 145.0—145.5°C/5 mmHg, d_4^{25} 0.8829, n_D^{25} 1.4820, mol wt, 278 (mass spectrum); elementary analysis, $C_{20}H_{38}$. This component seemed, on the basis of the IR and NMR spectra, to be a saturated hydrocarbon with two separated C_6-rings and an isopropyl group.

Gas chromatography. A Shimadzu GC-2 apparatus equipped with a thermal conductivity detector was used. Carrier gas, helium; flow rate, 60 ml/min. For hydrocarbon analysis, Celite 545 (60—80 mesh) coated with Carbowax 6000 (30%) was used at 65°C.

The author wishes to express her sincere gratitude to Professor Tamon Matsuura and Professor Shuichi Hayashi, of Hiroshima University, for their kind guidance and discussions during this work.

BULLETIN OF THE CHEMICAL SOCIETY OF JAPAN VOL. 43 2630—2631 (1970)

Biogenesis of the Essential Oils in Camphor Trees. XXVI. On the Components of the Essential Oil of *Cinnamomum daphnoides* Sieb. et Zucc.*[1]

Yasuji FUJITA,* Shin-ichi FUJITA** and Hisashi YOSHIKAWA*

* *Government Industrial Research Institute, Osaka, Midorigaoka, Ikeda-shi, Osaka*

** *Faculty of Engineering, Doshisha University, Kamikyo-ku, Kyoto*

(Received February 4, 1970)

Cinnamomum daphnoides Sieb. et Zucc. (Japanese name, Marubanikkei) of Lauraceae is an endemic plant growing chiefly on the shores of the Osumi Peninsula and the Islands of Tane and Yaku in Kagoshima Prefecture, Japan.[1)]

This plant had been utilized as a linalool resource since a field survey of the senior author on Tane and Yaku Islands in 1947.[2)] Nakahara has reported that the plant obtained from Tane Island affords the essential oil in a 0.25% yield by the steam distillation of the twigs, and that the oil contains *l*-linalool (65—70%) and an unidentified high-boiling compound (15%) as the main components, besides α-pinene, *p*-cymene, cineole, and an ester.[3)]

The present investigation consists of the further study of this essential oil from the viewpoint of chemical systematics; in this paper, the authors will report on the results of their examination of the essential oil of the plant, bred from seeds collected on Tane Island in 1947.

The essential oil was obtained in a 0.15% yield by the steam distillation of fresh leaves and branchlets. The chemical composition of this oil is shown in Table 1. The characteristic of the oil is the abundant existence of *l*-linalool (69—75%) and elemicine (16—19%), the total amounting to 88.2—90.6%; the content of camphor is so small that it is not detected by the ordinary procedure.

A comparison with the essential oils of the relative species will be published later.

Experimental

Materials. Two plants in an experimental garden (Ikeda, Osaka), bred from seeds collected from a tree at Nishino-omote, Tane Island, Kagoshima Prefecture, on November 8, 1947.

Isolation of the Essential Oils. Sample I. On July 25, 1962, material gathered at the beginning of the flowering stage (21.7 kg) (the average length of a twig: 44 cm; its weight: 48 g, consisting of 69% leaves, plus a small amount of flowers, and 31% branchlets) was subjected to steam distillation. The distilled oil was extracted with ether, and then dried over anhydrous sodium sulfate. The oil (33.4 g) obtained in a 0.15% yield had the following properties: d_4^{30} 0.9208, n_D^{30} 1.4784, α_D^{10} −12.45°, A.V. 7.0, E.V. 3.1.

Sample II. On October 15, 1964, material gathered at fruiting stage (18.2 kg) (the average length of a twig: 44 cm; its weight: 42 g, consisting of 57% leaves, 42.6 % branchlets, and 0.4% fruits) was subjected to steam distillation; the oil (27.5 g) thus obtained in a 0.15% yield had the following properties: d_4^{30} 0.9077, n_D^{30} 1.4765, α_D^{10} −12.80°, A.V. 7.0, E.V. 2.4.

Gas-chromatographic Analysis. The gas chromatography was carried out by means of Shimadzu GC-1B Model equipment with a thermal conductivity detector. A 150×0.5-cm stainless steel column was packed with PEG 6000 (30%) on Celite 545 (100 mesh), and hydrogen was used as the carrier gas.

Separation and Identification of the Individual Components. The essential oil was fractionated by

---

*1 Presented at the 11th Symposium on the Chemistry of Terpenes, Essential Oils and Aromatics, Matsuyama, October, 1967.

1) Y. Fujita, *J. Jap. Bot.*, **28**, 255 (1953); *Bot. Mag. Tokyo*, **80**, 216 (1967).

2) Y. Fujita, *Koryo*, **3**, 33 (1948).

3) K. Nakahara, Abstract of the Reports of the Annual Meeting of the Chem. Soc. of Japan, **5**, 105 (1952).

Table 1. Compositions of the essential oils of *C. daphnoides*

Peak No.	Rt.* (min) A	Rt.* (min) B	Component	Sample I (%)	Sample II (%)	Remark
1	1.7		α-Pinene	0.5	0.5	
2	2.2		Camphene	0.3	0.3	
3	2.6		β-Pinene	0.3	0.3	
4	3.3		Limonene	0.4	0.3	IR
5	3.6		1,8-Cineole	1.0	1.0	IR
6	4.3		*p*-Cymene	0.2	0.2	IR
7	4.8		*n*-Hexanol	0.2	0.1	IR
8	5.6		*cis*-3-Hexen-1-ol	0.2	0.2	IR
9	6.5		unidentified alcohol	trace	0.1	
10	8.0	3.8	*trans*-Linalooloxide	0.5	0.4	IR
11	8.8	4.2	*cis*-Linalooloxide	0.5	0.3	IR
12	11.0	4.8	*l*-Linalool	**69.4**	**74.5**	IR, a
13		4.8	α-Ylangene	0.1	0.1	
14	14.0		Linalyl acetate	0.2	0.2	
15	16.5	5.9	unidentified alcohol	0.5	0.3	b
16	16.5	5.9	Camphor	trace	trace	
17		6.5	Terpinen-4-ol	0.2	0.2	
18		6.5	β-Elemene	trace	trace	
19		7.4	Caryophyllene	1.0	1.0	IR
20		8.8	α-Terpineol	0.6	0.5	IR
21		8.8	unidentified sesquiterpene hydrocarbon (S. H. C.)	trace	trace	
22		9.6	*trans*-2,6,6-Trimethyl-2-vinyl-5-hydroxy-tetrahydropyran	0.1	0.1	IR
23		9.6	Humulene	0.3	0.2	
24		10.0	*cis*-2,6,6-Trimethyl-2-vinyl-5-hydroxy-tetrahydropyran	0.1	0.1	IR
25		10.2	unidentified S. H. C.	0.3	0.2	
26		12.0	Nerol	0.3	0.1	
27		12.0	δ-Cadinene	0.4	0.2	
28		14.0	Geraniol	0.5	0.3	IR
29		14.0	unidentified S. H. C.	0.1	trace	
30		17.5	Safrole	0.3	0.2	
31		17.5	unidentified S. H. C.	trace	trace	
32		19.5	unidentified S. H. C.	trace	trace	
33		27.0	Methyleugenol	0.6	0.3	
34		45.0	Eugenol	1.7	1.5	IR
35		58.5	Elemicine	**18.8**	**15.8**	IR, c
36		63.0	Chavicol	0.2	0.2	

* A: 145°C, 60 ml/min H_2, B: 165°C, 80 ml/min H_2 on PEG 6000 column (5 mmϕ × 1.5 m).

a) d_4^{30} 0.8690, n_D^{30} 1.4571, α_D^{19} −17.50°.

b) This compound shows the bands at 3400, 1100, 885 cm^{-1}.

c) Bp 272°C/756 mmHg, d_4^{30} 1.0519, n_D^{30} 1.5228. Trimethylgallic acid (mp 169°C) was obtained by oxidation with potassium permanganate.

distillation under reduced pressure into nine fractions. Each fraction was further divided into hydrocarbons and oxygenated compounds by alumina-column chromatography.

The components were isolated by preparative gas chromatography using a PEG 6000 column (2 m × 10 mmϕ) and were identified by a comparison of the IR spectra and retention times (Rt.) with those of authentic samples. Some minor components were identified by Rt's. only using two kinds of columns (PEG 6000 and Silicone DC-550).

The results are shown in Table 1.

BULLETIN OF THE CHEMICAL SOCIETY OF JAPAN VOL. 43 2632—2633 (1970)

A Convenient Method for the Preparation of Thiolesters

Tadashi ENDO, Shinichi IKENAGA and Teruaki MUKAIYAMA

Laboratory of Organic Chemistry, Tokyo Institute of Technology, Ookayama, Meguro-ku, Tokyo

(Received February 12, 1970)

In connection with a continuing investigation on the new synthetic reactions by the use of a disulfide as an oxidant, it was reported in the preceding paper that bis(diethylthiocarbamoyl) disulfide or benzenesulfenyl chloride reacts with mercuric carboxylates to give carboxylic acid anhydrides in high yields.[1] The present paper describes a convenient method for the preparation of thiolesters from free carboxylic acids by the use of triphenylphosphine and diphenyl disulfide.

It is known that dibenzoyl or bis(dimethylthiocarbamoyl) disulfide reacts with triphenylphosphine in refluxing benzene to give the corresponding sulfide and triphenylphosphine sulfide.[2]

$$(C_6H_5)_3P + RS\text{-}SR \rightarrow (C_6H_5)_3P{=}S + RSR$$
$$(R = C_6H_5\overset{\overset{\|}{O}}{C},\ Me_2N\overset{\overset{\|}{S}}{C})$$

Schönberg reported that 2 equiv. of benzenethiol and triphenylphosphine oxide resulted in low yields by treating diphenyl disulfide with triphenylphosphine in the presence of water in boiling benzene.[3]

$$(C_6H_5)_3P + (C_6H_5S)_2 + H_2O \rightarrow 2C_6H_5SH + (C_6H_5)_3P{=}O$$

This result suggests that the use of carboxylic acids in place of water as proton donors in the above reaction would lead to the formation of thiolesters, benzenethiol, and triphenylphosphine oxide. As expected, carboxylic acids reacted readily with diphenyl disulfide and triphenylphosphine in boiling acetonitrile to give thiolesters, benzenethiol, and triphenylphosphine oxide in high yields as shown in Table 1.

$$RCO_2H + (C_6H_5S)_2 + (C_6H_5)_3P \rightarrow RC(=O)SC_6H_5 + C_6H_5SH + (C_6H_5)_3P{=}O \quad (1)$$

Except for the case of crotonic acid, analytically pure thiolesters were easily isolated by chromatography over silica gel.[4] However, in the case of crotonic acid, phenyl *dl*-3-phenylthiothiolbutyrate (I) was obtained in 77% yield. The adduct (I)[5] resulted from the addition of benzenethiol to phenyl thiolcrotonate initially formed by the reaction (Eq. (1)).

$$CH_3CH{=}CHC(=O)SC_6H_5 + C_6H_5SH \rightarrow CH_3CH(SC_6H_5)CH_2C(=O)SC_6H_5 \quad (I)$$

The reaction can be explained by considering an initial formation of the first phosphonium salt (II) from diphenyl disulfide and triphenylphosphine. The intermediate (II) is in turn changed into the second phosphonium salt (III) by nucleophilic attack of a carboxylic acid on phosphorus of II with the elimination of benzenethiol. The intermediate (III) is further converted to the third phosphonium salt (IV) by the intramolecular oxidation-reduction reaction. In this process, the phenylthio moiety attached to phosphorus in the intermediate (III) accepts two electrons from phosphorus to be reduced to the benzenethiolate anion of the intermediate (IV). The intermediate (IV) undergoes decomposition to a thiolester and triphenylphosphine oxide.

TABLE 1. REACTIONS OF CARBOXYLIC ACIDS WITH DIPHENYL DISULFIDE AND TRIPHENYLPHOSPHINE

Carboxylic acid	Time hr	Yield, %		
		Thiol-ester	C_6H_5SH	$(C_6H_5)_3P{=}O$
Acetic	3	90	75	94
Propionic	3	94	80	92
Benzoic	3	89	73	90
Succinic	5	81	73	89
Crotonic	5	77[a]		90
Chloroacetic	3	81	64	92

a) The yield of the adduct (I)

1) T. Mukaiyama, T. Endo, S. Ikenaga and K. Osonoi, *J. Org. Chem.*, **33**, 2242 (1968).

2) A. Schönberg and M. Z. Barakat, *J. Chem. Soc.*, **1949**, 892.

3) A. Schönberg, *Ber.*, **68**, 163 (1935).

4) With chloroacetic acid, phenyl chlorothiolacetate and benzenethiol were obtained in 81 and 64% yields, respectively, indicating that phenyl chlorothiolacetate is unreactive with benzenethiol.

5) A. A. Schleppnik and F. B. Ziently, *J. Org. Chem.*, **29**, 1910 (1964).

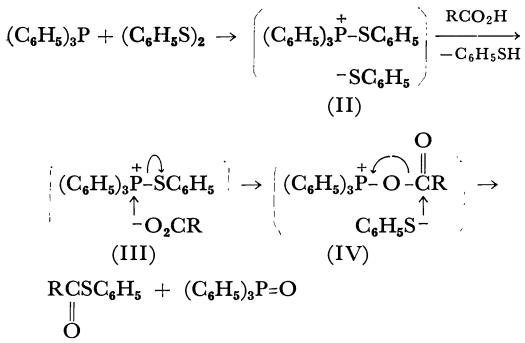

When diethyl disulfide was used as an oxidant, no reaction took place and the starting materials were recovered almost quantitatively. This result suggests that the reactivities of the disulfides in this reaction depend on the oxidizing power of the disulfides, which was found to decrease in the order of decreasing stabilities of the corresponding thiolate anions of the disulfides.[6]

Experimental

Materials. Various carboxylic acids, diphenyl disulfide, and triphenylphosphine were all commercial materials and purified by distillation or recrystallization before use. Acetonitrile was purified by the conventional procedure.

Preparation of Phenyl Thiolpropionate. Propionic acid (0.74 g, 0.01 mol), diphenyl disulfide (2.18 g, 0.01 mol), and triphenylphosphine (2.62 g, 0.01 mol) were refluxed in 30 m*l* of acetonitrile for 3 hr. After the reaction mixture was concentrated under reduced pressure, the residue was chromatographed on silica gel. Elution first with petroleum ether gave benzenethiol (0.88 g, 80%), bp 50—55°C/10 mmHg, and phenyl thiolpropionate (1.44 g, 94%), bp 112—113°C/10 mmHg. The infrared spectrum of this thiolester showed carbonyl absorption at 1710 cm^{-1}. Elution with ethyl acetate gave triphenylphosphine oxide (2.56 g, 92%), which was recrystallized from methylene chloride - petroleum ether, mp 154—156°C.

Preparation of Phenyl Thiolsuccinate. Succinic acid (0.60 g, 0.005 mol), diphenyl disulfide (2.18 g, 0.01 mol), and triphenylphosphine (2.62 g, 0.01 mol) were refluxed in 30 m*l* of acetonitrile for 5 hr. After the reaction mixture was concentrated *in vacuo*, the residual oil was chromatographed on silica gel to isolate three products. Elution first with petroleum ether gave benzenethiol (0.80 g, 73%), bp 50—53°C/10 mmHg. Elution next with methylene chloride - petroleum ether (1 : 1) gave first phenyl thiolsuccinate (1.23 g, 81%), mp 89—90°C, after recrystallization from isopropanol, then gave triphenylphosphine oxide (2.42 g, 89%).

Reaction of Crotonic Acid with Diphenyl Disulfide and Triphenylphosphine. Crotonic acid (0.86 g, 0.01 mol), diphenyl disulfide (2.18 g, 0.01 mol), and triphenylphosphine (2.62 g, 0.01 mol) were refluxed for 5 hr in 30 m*l* of acetonitrile. After removal of the solvent from the reaction mixture, the resulting oil was chromatographed on silica gel. Elution with petroleum ether gave phenyl *dl*-3-phenylthiothiolbutyrate (I) (2.31 g, 77%), bp 148—150°C/0.07 mmHg, n_D^{22} 1.6114 (lit,[5] bp 172—173°C/0.2 mmHg, n_D^{25} 1.6106). (Found: C, 66.50; H, 5.59; S, 21.94%). Elution next with methylene chloride gave triphenylphosphine oxide (2.54 g, 90%).

6) T. Mukaiyama and T. Endo, This Bulletin, **40**, 2388 (1967).

BULLETIN OF THE CHEMICAL SOCIETY OF JAPAN VOL. 43 2633—2634 (1970)

The Synthesis of 5,5′-Di-(2-methoxycarbonyl-vinyl)-2,2′-bifuryl by the Electrolysis of Methyl 3-(2-Furyl)acrylate[1]

Hajime SATONAKA, Zei SAITO and Toshio SHIMURA

Industrial Research Institute of Kanagawa Prefecture, Tomioka-machi, Kanazawa-ku, Yokohama

(Received February 23, 1970)

The present authors previously reported the synthesis of methyl 3-(2,5-dimethoxy-2,5-dihydrofuryl)acrylate (**2**) by the electrolysis of methyl 3-(2-furyl)acrylate (**1**) and the decomposition of **2**.[2-5]

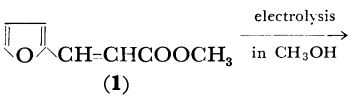

(**1**)

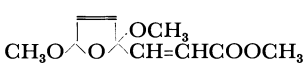

(**2**)

1) Paper 5 on "The Synthesis of Unsaturated Carboxylic Acid by the Ring-opening Reaction of Furan Compounds."

2) T. Shimura and Z. Saito, *Nippon Kagaku Zasshi*, **89**, 695 (1968).

3) T. Shimura, Z. Saito, M. Koizumi and H. Satonaka, *ibid.*, **90**, 96 (1969).

4) T. Shimura, Z. Saito and H. Satonaka, *ibid.*, **90**, 716 (1969).

5) T. Shimura, Z. Saito and H. Satonaka, *ibid.*, **90**, 1173 (1969).

This paper will describe a new compound formed by the electrolysis of methyl 3-(2-furyl)acrylate (**1**) in methyl alcohol at low temperatures (−40—−50°C). When the electrolysis was carried out by use of the Clauson-Kaas method,[6] methyl 3-(2,5-dimethoxy-2,5-dihydrofuryl)acrylate (**2**) was mainly formed, a yellow precipitate was also obtained.

The IR spectrum of the yellow product showed an unsaturated ester carbonyl band at 1721 cm^{-1}, an olefinic band at 1638 cm^{-1}, and bands of the furan ring at 1023 and 881 cm^{-1}. The UV spectrum in methyl alcohol showed a maximum peak with a molecular extinction coefficient of 46000 at 392 mμ and a shoulder band at 410 mμ.

The NMR spectrum showed signals at τ 2.59 (2H, doublet, J=15 Hz), 3.27 (2H, doublet, J=5 Hz), 3.35 (2H, doublet, J=5 Hz), 3.62 (2H, doublet, J=15 Hz), and 6.21 (6H, singlet). The signals at τ 2.59 and 3.62 with the spin-spin coupling constant of 15 Hz were assigned to the methin protons of –CH=CH– in the acrylate group. The doublets at 3.27 and 3.35 with the J of 5 Hz were assigned to the protons of the furan ring. The signal at τ 6.21 was assigned to the methyl protons of the methyl ester. The elementary analysis data agreed with the formula of $C_{16}H_{14}O_6$.

On the basis of these results, the product was determined to be a dimer of methyl 3-(2-furyl)-acrylate, 5,5′-di(2-methoxycarbonyl-vinyl)-2,2′-bifuryl (**3**).

This dimer seems to be formed at the anode. The reactions may proceed as follows:

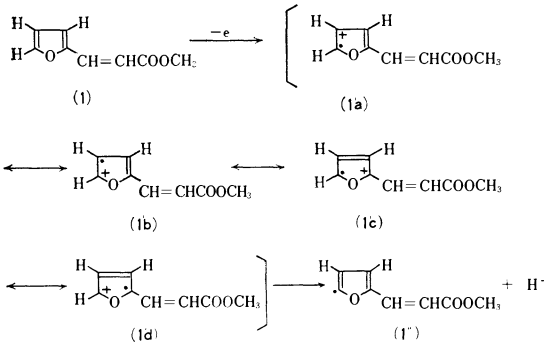

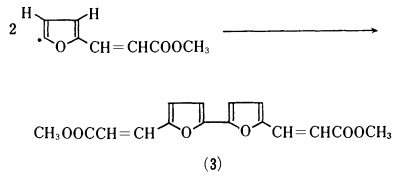

The anodic oxidation of furylacrylate (**1**) may give a radical cation which can be expressed in terms of the resonance hybrid of the four structures, **1′a**, **1′b**, **1′c**, and **1′d**, and this radical cation may then turn into a radical **1″** and a proton. At last, the coupling reaction of **1″** takes place to give **3**. The bifuryl thus formed seems to be deposited from the reaction mixture because of its small solubility.

This dimer is an interesting material which belongs to an unsaturated dibasic carboxylic acid and which contains two furan rings.

Experimental

Methyl 3-(2-Furyl)acrylate (1). This material was prepared by the condensation of furfural with methyl acetate by the method of Gilman *et al.*[7] Yellow crystals; mp 27°C.

5,5′-Di(2-methoxycarbonyl-vinyl)-2,2′-bifuryl (3). To a solution of 20 g of methyl 3-(2-furyl)acrylate in 250 m*l* of methyl alcohol, 1 m*l* of concentrated sulfuric acid was added; the mixture was then electrolyzed in a Clauson-Kaas electrolyser[6] for 6 hr with 10—12 V, 1.5 A at −40——50°C. A yellow product was obtained by the subsequent filtration of the electrolyzed solution. Recrystallization from methyl alcohol gave yellow needles with a melting point of 184°C; 2 g (10%).

Found: C, 63.40; H, 4.77%. Calcd for $C_{16}H_{14}O_6$: C, 63.57; H, 4.67%.

IR (cm^{-1}, KBr): 3130($\nu_{=C-H}$), 1721($\nu_{C=O}$), 1638 ($\nu_{C=C}$), 1023, 881(furan nucleus).

UV(λ_{max} mμ(ε), in CH_3OH): 392 (46000), 410 (39000), 228 (22000), 289 (9000).

NMR (τ, in $CDCl_3$): 6.21 (6H, s), 3.62 (2H, d, J=15 Hz), 2.59 (2H, d, J=15 Hz), 3.35 (2H, d, J=5 Hz), 3.27 (2H, d, J=5 Hz).

The authors wish to express their thanks to Dr. Minoru Hirota, Yokohama National University, for his kind suggestions and encouragement, and to Mr. Takayoshi Ozawa for his assistance in the elementary analysis.

6) N. Clauson-Kaas and F. Linborg, *Acta Chem. Scand.*, **6**, 531 (1952).

7) H. Gilman and R. E. Brown, *Iowa State College J. Sci.*, **2**, 317; *Chem. Abst.*, **22**, 4524 (1928).

BULLETIN OF THE CHEMICAL SOCIETY OF JAPAN VOL. 43 2635—2637 (1970)

Equilibria of the Isomerization of Xylene at 290°C under a Pressure of 300—6000 kg/cm²

Haruo TAKAYA,* Naoyuki TODO,* Tadasuke HOSOYA,* Toshio MINEGISHI* and Mikio YONEOKA**

* *The Government Chemical Industrial Research Institute, Tokyo, Mita, Meguro-ku, Tokyo*
** *Japan Gas-Chemical Company Inc., Niigata Laboratory, Enoki-cho, Niigata*

(Received February 23, 1970)

It is known that the isomeric forms of xylene, *i.e.*, *ortho*-xylene, *meta*-xylene and *para*-xylene, can be converted into one other by isomerization over acid catalysts under heterogeneous conditions. However, as has been reported by Taylor,[1] the *para*-xylene content in the mixture of xylene at equilibrium is 23—24% in the temperature range from 100°C to 600°C.

Recently a patent presented by Hepp[2] has reported an improved process for isomerizing xylenes; in this process the yield of the *para* isomer is about 58%, and that of the *ortho* isomer is almost twice that which can be obtained by a conventional operating process, when the reaction is conducted at 327°C and at a pressure of 5400 kg/cm². If such a process can be possible, both the economical and thermodynamical interests of the isomerization would be enhanced. However, it has been realized that the influence of the pressure on an equilibrium of a reaction is determined by the difference between the molar volumes of the product and the reactant.[3] The molar volumes of *ortho*-, *meta*- and *para*-xylene at 25°C are 121.2 ml/mol, 123.5 ml/mol, and 123.9 ml/mol respectively.[4] Hence, under a high pressure, the differences between the molar volumes of these isomers seem to be small even at a high temperature of 327°C, where the molar volumes of the xylenes are nearly equal to those at 25°C.

The present authors have previously developed high-pressure equipment for both the batch and the flow reactions and have investigated the rate of the isomerization of xylenes over acid catalysts under heterogeneous conditions.[5,6] This study was undertaken in order to examine the pressure dependency of the compositions of the mixtures of xylenes at equilibrium at 290°C and to confirm the improved process described above.

Experimental

The xylene isomerization was carried out by the contineous-flow method using the high-pressure equipment reported in the previous paper.[5] The catalyst used was powdered Nikki X633L silica-alumina. The feeds were prepared by mixing pure xylenes in the desired proportions; the compositions used are given in the column 2 of Table 1. The products were analyzed by gas chromatography in the same manner as has been described in a previous paper.[6]

Results and Discussion

The compositions of the xylene fraction in the reaction product at 290°C at pressures between 300 and 6000 kg/cm² are shown in column 3 of Table 1.

It has been proposed by Hanson that *para*-xylene and *ortho*-xylene do not directly interconvert,[7] that is, that the migrating methyl group moves around the benzene ring in steps of one ring position at a time. This can be represented schematically as;

$$ortho \rightleftharpoons meta \rightleftharpoons para$$

Hence, the results on the equilibrium composition of xylenes were treated with the following two reactions: *para*⇄*meta* and *meta*⇄*ortho*. The ratios of *para*-xylene and *ortho*-xylene to *meta*-xylene are also tabulated in column 2 (Reactant) and 3 (Product) of Table 1 and are shown in Fig. 1. The ratios of the products should approach closer to those at equilibrium than the ratios of the reactants. For example, the ratio of *p*/*m* at equilibrium under the pressure of 2000 kg/cm² can be obtained by the following procedure. The ratio of *p*/*m*

1) W. J. Taylor, D. D. Wagman, M. G. Williams, K. S. Pitzer and F. D. Rossini, *J. Res. Nat. Bur. Stand.*, **37**, 95 (1946).

2) H. J. Hepp and M. M. Johnson, U. S. 3363017.

3) S. D. Hamann, "High Pressure Physics and Chemistry," ed. by R. S. Bradley, Academic Press, London and New York (1963), p. 134.

4) J. A. Riddick and E. E. Toops, Jr., "Organic Solvents," 72nd ed., Interscience Publisher, New York (1955), pp. 74—76.

5) T. Hosoya, T. Minegishi, H. Takaya, M. Yoneoka and N. Todo, *Tokyo Kogyo Shikenjo Hokoku*, **64**, 499 (1969).

6) H. Takaya, N. Todo, T. Hosoya, T. Minegishi and M. Yoneoka, *Kogyo Kagaku Zasshi*, **73**, 1831 (1970).

7) K. L. Hanson and A. J. Engel, *A.I.C.E.J.*, **13**, 260 (1967).

Table 1. Compositions and ratios* at 290°C under various pressures

Pressure I kg/cm²	Reactant II %			Reactant II Ratio*			Product** III %			Product** III Ratio*			W/F IV h.g-cat./g
	p	*m*	*o*	*p*/*m*	*m*/*m*	*o*/*m*	*p*	*m*	*o*	*p*/*m*	*m*/*m*	*o*/*m*	
300	33.3	33.3	33.3	1.00	1.00	1.00	26.8	45.5	27.7	0.59	1.00	0.61	0.45
300	0.2	99.6	0.2	0.00	1.00	0.00	22.0	59.0	18.8	0.38	1.00	0.32	1.24
2000	18.8	55.9	25.3	0.34	1.00	0.45	19.9	54.4	25.7	0.37	1.00	0.47	0.78
2000	33.3	33.3	33.3	1.00	1.00	1.00	23.1	51.1	25.8	0.45	1.00	0.51	0.43
2000	0.3	99.4	0.3	0.00	1.00	0.00	21.8	59.0	19.2	0.37	1.00	0.33	1.13
5000	17.5	58.4	24.1	0.30	1.00	0.41	20.9	53.2	25.9	0.39	1.00	0.49	0.85
5000	52.5	14.9	32.6	3.52	1.00	2.19	29.2	47.1	23.9	0.62	1.00	0.51	0.80
5000	27.7	54.1	18.1	0.51	1.00	0.34	23.9	53.3	22.8	0.45	1.00	0.43	0.80
5000	24.1	53.6	22.3	0.45	1.00	0.42	22.0	52.2	25.7	0.42	1.00	0.49	0.80
5000	20.0	56.0	24.0	0.36	1.00	0.43	20.4	54.6	25.0	0.37	1.00	0.46	0.08
6000	18.2	56.7	25.1	0.32	1.00	0.44	20.8	52.7	26.5	0.40	1.00	0.50	0.81
6000	33.3	33.3	33.3	1.00	1.00	1.00	20.1	54.7	25.2	0.37	1.00	0.46	0.45

* Ratio of *para*-xylene or *ortho*-xylene to *meta*-xylene.
** Xylene fraction of the product.

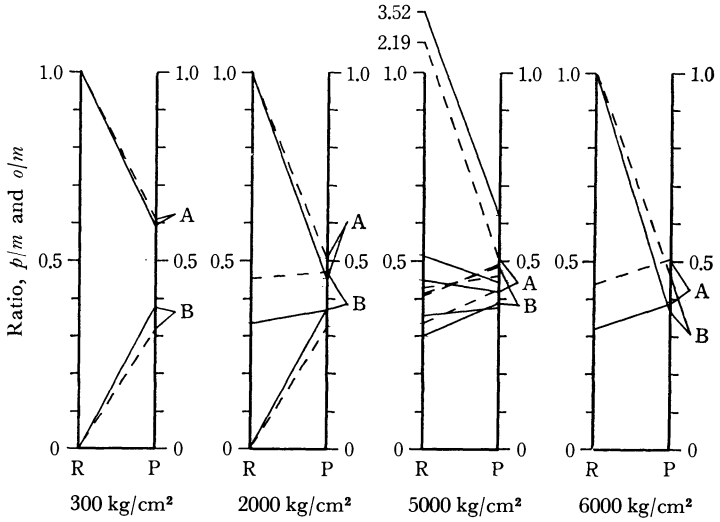

Fig. 1. Ratios, *p*/*m* and *o*/*m*, of reactants and products.
——: *p*/*m*, ----: *o*/*m*
R: Reactant P: Product
A and B are the maximum and the minimum value of the probable ratio at equilibrium respectively.

Table 2. Compositions at equilibrium

Pressure kg/cm²	Composition at B** in Fig. 1 Ratio			Composition at B** in Fig. 1 %			Composition at A* in Fig. 1 Ratio			Composition at A* in Fig. 1 %		
	p/*m*	*m*/*m*	*o*/*m*	*p*	*m*	*o*	*p*/*m*	*m*/*m*	*o*/*m*	*p*	*m*	*o*
300	0.38	1.00	0.32	22	59	19	0.59	1.00	0.61	27	46	28
2000	0.37	1.00	0.47	20	54	26	0.45	1.00	0.51	23	51	26
5000	0.39	1.00	0.49	21	53	26	0.42	1.00	0.51	22	52	26
6000	0.37	1.00	0.46	20	55	25	0.40	1.00	0.50	21	53	27

* A is the maximum value of the probable ratio at equilibrium.
** B is the minimum value of the probable ratio at equilibrium.

decreases from 1 to 0.45 upon the isomerization; thus, the ratio at equilibrium should be smaller than 0.45 (A in Fig. 1). The ratios of p/m increase from 0 to 0.37 and from 0.34 to 0.37; thus, the ratio at equilibrium should be larger than 0.37 (B in Fig. 1). Consequently, the ratio at equilibrium under 2000 kg/cm² should be 0.37(B)—0.45(A). The A and B values obtained from such a procedure, and also the corresponding compositions, are shown in Table 2 and in Fig. 2. Figure 2 clearly indicates that a mixture of xylenes at equilibrium, even under a pressure of 6000 kg/cm², consists of 20—21% *para*-xylene, 53—55% *meta*-xylene, and 25—27% *ortho*-xylene; these findings practically agree with those obtained under ordinary conditions, although the experiment in this study was carried out at 290°C, a temperature lower by 37°C than that in Hepp's work. However, it seems unlikely that the difference in the reaction temperature between the both cases greatly influences the equilibrium composition, for it is very difficult to suppose that by such a temperature difference discrete phenomena can occur.

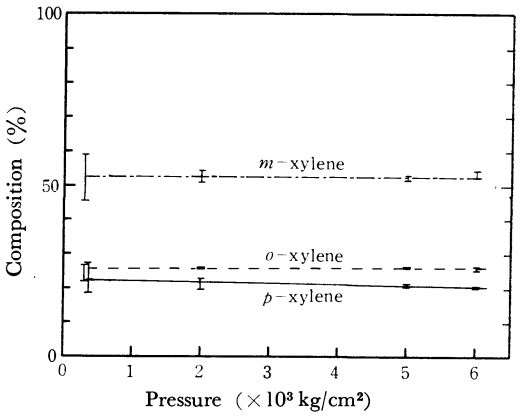

Fig. 2. Pressure dependency of the composition at equilibrium.

This conclusion is consistent with the thermodynamical consideration presented in the first paragraph.

BULLETIN OF THE CHEMICAL SOCIETY OF JAPAN VOL. 43 2637—2638 (1970)

trans-Shisool (*trans*-8-*p*-Menthen-7-ol) Isolated from the Essential Oils of *Perilla acuta* Nakai and *P. acuta* f. *viridis* Nakai*[1]

Yasuji FUJITA, Shin-ichi FUJITA and Yoshiko HAYAMA

Government Industrial Research Institute, Osaka, Midorigaoka, Ikeda-shi, Osaka

(Received March 4, 1970)

We have examined the essential oils of *Perilla acuta* (Thunb.) Nakai[1] (=*P. frutescens* Brit. var. *acuta* Kudo[2]) (Japanese name "Shiso") and *P. acuta* f. *viridis* (Makino) Nakai[1] (=*P. frutescens* var. *acuta* Kudo f. *viridis* Kudo[2]) (Japanese name "Aojiso") of the mint family, and have isolated a new monoterpene alcohol, amounting to 2.2—8.2% of the oil.

This alcohol was purified by preparative gas-liquid chromatography and was identified as *trans*-8-*p*-menthen-7-ol (I) by a comparison of its IR spectrum and of the retention time of its gas-liquid chromatography with those of the synthesized compound. The content of the *cis*-isomer (II) in the oils was very small.

We propose the name "Shisool" for these alcohols.

Ito[3] has reported the isolation of dihydroperillyl alcohol from *P. frutescens* Brit. var. *crispa* Decaisne f. *viridis* Makino (Japanese name "Chirimen-aojiso"); he showed the structure to be 8-*p*-menthen-7-ol, but did not mention anything about its configuration.

In a more recent report, Kayahara *et al.*[4] obtained these alcohols by the reduction of *l*-perillaldehyde (III) with sodium in aqueous ammonia; they proved the conformations of I and II clearly by means of NMR and IR spectra.

Many years ago, Semmler and Zaar[5] synthesized dihydroperillyl alcohol in the course of the determination of the structure of III; they showed its physical properties to be: bp 114—115°C/10 mmHg, d^{19} 0.9284, n_D 1.4819.

*1 Presented at the 13th Symposium on the Chemistry of Terpenes, Essential Oils, and Aromatics of the Chem. Soc. of Japan (Kagoshima, October, 1969).

1) T. Nakai, *Bot. Mag. Tokyo*, **42**, 474 (1928).

2) Y. Kudo, *Mem. Fac. Sci. Agri., Taihoku Imp. Univ.*, **2**, 74 (1929).

3) H. Ito, *Shōyakugaku Zasshi*, **18**, 24 (1964).

4) H. Kayahara, H. Ueda, K. Takeo and C. Tatsumi, *Agr. Biol. Chem.*, **33**, 86 (1969).

5) F. W. Semmler and B. Zaar, *Ber.*, **44**, 56 (1911).

Experimental

Isolation. The essential oils were obtained by the steam distillation of fresh materials, while the monoterpene alcohols were separated from the bp 111—115 °C/20 mmHg fraction of the oil, by the following procedures.

The perillaldehyde of this fraction (90 g) was eliminated by shaking it with a saturated sodium sulfite solution; the residual oil (8.5 g) was then heated with phthalic anhydride at 80°C in a pyridine solution for one hour, and the esterified part was extracted by means of a sodium bicarbonate solution. The sodium salt of the phthalic acid ester was saponified by potassium hydroxide, and the regenerated alcohol was distilled with steam. The oil thus obtained (1.2 g) contained 85.5% of I.

The alcohol (I) was purified by preparative gas-liquid chromatography. This alcohol is a colorless oil: bp 225°C/760 mmHg (uncorrected), d_4^{30} 0.9212, n_D^{30} 1.4796, $\alpha_D \pm 0.00°$, and shows bands at 3350(s), 3080 (w), 2930(s), 2860(s), 1640(m), 1445(s), 1375(m), 1185 (w), 1090(m), 1035(s), 965(m), 885(s), and 530(w) cm^{-1} in its IR spectrum.

Synthesized I and II. These compounds were prepared by the method of Kayahara *et al.*[4] Namely, to a stirred mixture of III (0.5 g), benzene (2.5 m*l*), and 28% aqueous ammonia (2.0 m*l*), metallic sodium (0.2 g) was gradually added with cooling by ice water. The product was extracted with ether, the ether extract was washed with a dilute hydrochloric acid solution and water successively, and dried over anhydrous sodium sulfate, and the ether was distilled off. The oil thus obtained (0.3 g) consisted of 28.0% I and 57.5% II, besides other compounds.

The specific retention times of the gas-liquid chromatography relative to perillyl alcohol (PEG 6000, 175°C) are 0.70 and 0.78 for I and II respectively.

BULLETIN OF THE CHEMICAL SOCIETY OF JAPAN VOL. 43 2638—2639 (1970)

Mutual and Acid Distribution in Methyl Isobutyl Ketone-Water System

Tatsuya SEKINE, Toshio FUKUSHIMA and Yuko HASEGAWA

Department of Chemistry, Science University of Tokyo, Kagurazaka, Shinjuku-ku, Tokyo

(Received March 4, 1970)

Many authors have reported on the mutual and acid distribution equilibria in extraction systems containing carbon-bonded oxygen-type solvents.[1] However, this kind of knowledge about the MIBK (methyl isobutyl ketone)-water system seems to be rather limited. In order to obtain further information on the system, the present authors have carried out the following measurements.

Experimental

Reagents. The MIBK was washed with 0.1 M perchloric acid, water, and 0.1 M sodium hydroxide respectively, and then several times with water. It was dried with anhydrous sodium sulfate and distilled. The distillate at 116°C was used for the experiments. All of the other reagents were of an analytical grade and were used without further purification.

Procedure. All of the procedures were carried out in a thermostatted room at 25°C. Stoppered glass tubes (volume, 20 ml) were used to equilibrate the two phases. Organic and aqueous solutions were placed in the tubes and agitated mechanically for one hour. They were then centrifuged at 1000 rpm for 3 min, with some portion being pipetted from each phase. The content of the material in these samples were determined as follows: the MIBK in an aqueous phase was determined by spectrophotometry at 273 mμ. The molar extinction coefficient of MIBK in water at this wavelength was 20, and the absorption obeyed Lambert-Beer's law, at least between 8.5×10^{-3} and 5.0×10^{-2} M. The concentration in the organic phase was calculated from the initial concentration and the aqueous concentration at the equilibrium. The water content was determined by Karl-Fischer titration. The acid concentrations in the organic and aqueous phases were determined by titration with standard barium hydroxide solutions.

Results

The distribution ratio of a material, M, is defined as;

$$D = [\mathrm{M}]_{\mathrm{org,total}}/[\mathrm{M}]_{\mathrm{total}}$$

The percentage concentration is given by the volume percentage. The density of water-saturated MIBK at 25°C is 0.793 g/ml; thus, the molar concentration is 7.8 M.

Mutual Distribution. The mutual solubility is 1.8×10^{-1} mol/l (18 g/l) for MIBK in water and 8.5×10^{-1} mol/l (15.3 g/l) for water in MIBK. The mutual distribution ratios of these materials have been calculated to be as is shown in Table 1.

Acid Distribution. The distribution ratios of five mineral acids are given in Fig. 1 as a function of the queous acid concentration. The results shown in Fig. 1 agree with the general tendency

1) Y. Marcus and A. S. Kertes, "Ion Exchange and Solvent Extraction of Metal Complexes," Wiley-Interscience, New York (1969), pp. 575, 617.

Table 1. Distribution of materials and effect of dilution with hexane

The figures show the distribution ratio of the materials ($D=[M]_{org}/[M]$).

Material	Organic phase		
	MIBK	50% MIBK*	Hexane
MIBK	4.3×10	3.3×10	1.0×10
Water	1.5×10^{-2}	3.1×10^{-3}	7×10^{-6}
$HClO_4$**	1.4×10^{-1}	5.2×10^{-4}	very low

* by the volume percent

** Values obtained when the aqueous concentration is 1.0 M.

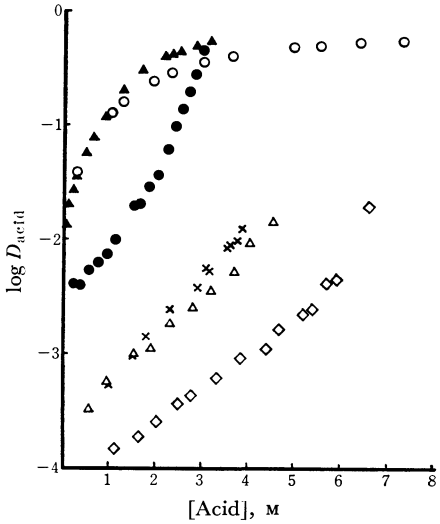

Fig. 1. Distribution of mineral acids as a function of the aqueous acid concentration. The organic phase is undiluted MIBK except the data given by ×.
▲: $HClO_4$, ○: HNO_3, ●: HI, △: HBr, ◇: HCl, ×: $HClO_4$ distributed between 50% MIBK (diluted with hexane) and water

of the distribution of mineral acids, that is, the extraction grows larger in this order; $HClO_4>HNO_3>HI>HBr>HCl$.[2)]

2) R. M. Diamond and D. G. Tuck, *Progress in Inorganic Chemistry*, **2**, 109 (1960).

It was observed that the mutual solubility of the organic and the aqueous phases increases with the increase in the acid concentration; the contact of the same volume of MIBK and the aqueous solution formed a single layer when the initial acid concentration was above 8 M (hydrochloric acid), 5 M (hydrobromic acid), or 3.5 M (perchloric acid and hydroiodic acid), but two immiscible layers were always observed in the nitric acid system, even when the initial acid concentration was 13 M.

Effect of Dilution with *n*-Hexane. The dilution of MIBK with an "inert diluent" changes the distribution of the materials. Figure 2 shows the effect of the dilution with *n*-hexane on the distribution of MIBK and water. The distribution of perchloric acid between 50% (*v*/*v*) MIBK and water is also shown in Fig. 1.

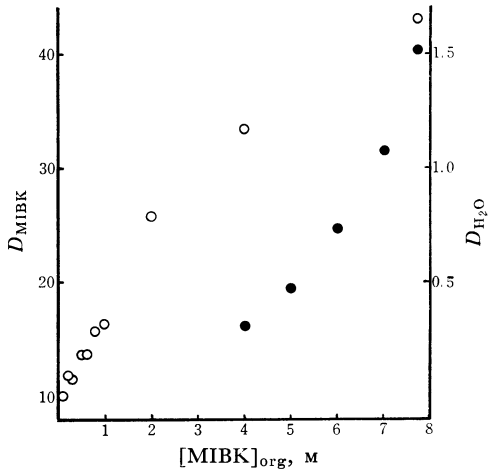

Fig. 2. Effect of the dilution with hexane on the distribution of MIBK (○) and water (●).

The effect of the dilution with *n*-hexane can be summarized as is shown in Table 1. It may be seen from Table 1 that the effect of the dilution can be quite different for different materials. MIBK has been used very often without any dilution. However, the results seem to indicate that dilution with an inert solvent could improve the efficiency of the separation of materials or that of back-extraction in MIBK-water systems.

BULLETIN OF THE CHEMICAL SOCIETY OF JAPAN VOL. 43 2640—2641 (1970)

The Crystal and Molecular Structure of *O,O',N*-Trimethylpyoluteorin, $C_{14}H_{13}O_3NCl_2$

Yoshihisa UTSUMI,*1 Akio FURUSAKI and Yujiro Tomiie*2

Faculty of Science, Kwansei Gakuin University, Nishinomiya

(Received March 26, 1970)

Pyoluteorin, $C_{11}H_7O_3NCl_2$, mp 174—175°C (dec.), is an antibiotic produced by *Pseudomonas aeruginosa* it has been found to be efficacious against cholera germs, *etc.* For this antibiotic, the following structural formula (I) has been proposed on the basis of chemical evidence:[1]

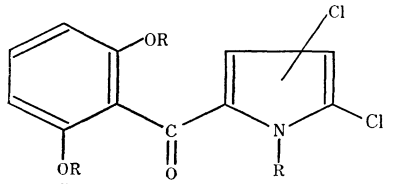

I: R=H II: R=CH_3

However, the position of one of the chlorine atoms in the pyrrole ring has remained uncertain. Using single crystals of *O,O',N*-trimethylpyoluteorin (II) kindly supplied by Dr. Masao Nishikawa, Chemical Research Laboratories, Research and Development Division, Takeda Chemical Industries, Ltd., an X-ray-crystal structural analysis of the derivative has been undertaken in order to determine the chlorine position and in order to obtain more detailed information about the stereostructure of the molecule.

O,O',N-Trimethylpyoluteorin, $C_{14}H_{13}O_3NCl_2$, crystallizes in yellow needles and gives the crystal data shown in Table 1. The reflection intensities were visually measured from equi-inclination integrating Weissenberg photographs taken with Cu$K\alpha$ radiation for 0—5 layers around the *b* axis and for 0—10 layers around the *a* axis. To these intensities, the usual Lorentz and polarization corrections were applied. Thus, the structure factors of 1363 independent reflections were obtained.

TABLE 1. CRYSTAL DATA

Monoclinic	
	$a = 14.51 \pm 0.04$ Å
	$b = 7.71 \pm 0.03$
	$c = 14.60 \pm 0.04$
	$\beta = 116.5 \pm 0.3°$
Space group	$P2_1/a$
Z	4

The positions of the two independent chlorine atoms could be easily found from a three-dimensional Patterson function. These coordinates were refined by the diagonal-matrix least-squares method. As a result of five cycles of this refinement, the *R* factor dropped only a little from the initial value, 0.50, while the temperature factor converged into a value of about 6 Å^2 for either one of the chlorine atoms. The approximate coordinates of all the light atoms were obtained from the first Fourier map, calculated with the sign based on only the chlorine atoms. The coordinates of the two chlorine and eighteen light atoms thus obtained were refined at first by the diagonal-matrix least-squares method with individual isotropic temperature factors, and then by the block-diagonal-matrix least-squares method with anisotropic temperature factors. The final *R* factor thus obtained was 0.137. The atomic parameters obtained are given in Table 2, while the molecular framework is further shown in Fig. 1.

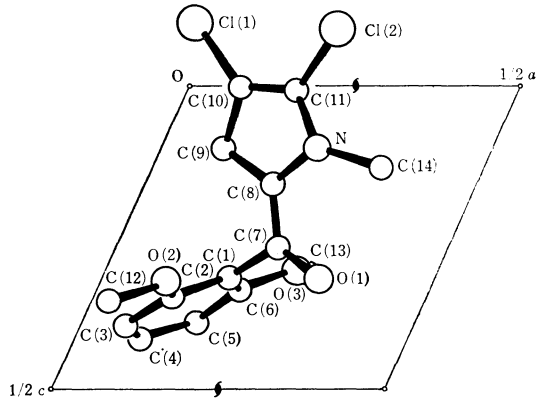

Fig. 1. The molecular framework viewed along the *b* axis.

As is shown in Fig. 2, the bond lengths and angles calculated with the final coordinates are all reasonable considering the mean standard deviations of the coordinates (0.007 Å for Cl, 0.014 Å for O, 0.016 Å for N, and 0.021 Å for C); for example, as to the benzene ring, they are 1.36—1.47 Å and 113—125° respectively. The molecular structure

*1 Present address: Fujitsu, Ltd., Marunouchi, Chiyoda-ku, Tokyo.

*2 Deceased May 31, 1967.

1) R. Takeda, *J. Amer. Chem. Soc.*, **80**, 4749 (1958).

Table 2. The atomic parameters

Atom	x/a	y/b	z/c	B_{11}	B_{22}	B_{33}	B_{12}	B_{23}	B_{31}
Cl(1)	−0.0384	0.2541	−0.1046	830	3062	495	−306	181	−99
Cl(2)	0.1800	0.4397	−0.0948	1377	2035	547	−832	245	1125
O(1)	0.3408	0.3175	0.3248	364	1084	577	−175	−4	487
O(2)	0.1129	0.3873	0.3287	460	962	909	440	102	966
O(3)	0.2998	−0.0889	0.3107	544	1004	700	288	71	888
N	0.2381	0.3604	0.1040	449	661	469	−138	142	594
C(1)	0.2052	0.1463	0.3233	299	649	397	306	266	422
C(2)	0.1345	0.2217	0.3553	306	854	440	−39	14	392
C(3)	0.0877	0.1182	0.4046	338	1512	301	−281	−12	289
C(4)	0.1184	−0.0511	0.4266	429	1776	400	−391	432	162
C(5)	0.1899	−0.1376	0.3983	226	1704	389	−520	0	206
C(6)	0.2299	−0.0240	0.3436	246	1407	383	104	−68	243
C(7)	0.2547	0.2509	0.2719	337	555	448	239	80	507
C(8)	0.1991	0.2784	0.1646	390	641	379	170	293	417
C(9)	0.0985	0.2269	0.1055	571	1128	556	−137	−49	689
C(10)	0.0764	0.2787	0.0016	547	1064	459	269	191	169
C(11)	0.1628	0.3555	0.0072	746	925	528	−355	−46	767
C(12)	0.0427	0.4738	0.3623	490	1606	1127	314	−157	1126
C(13)	0.3199	−0.2726	0.3149	720	768	879	918	541	987
C(14)	0.3481	0.4165	0.1375	595	2689	707	−1151	−298	856

The thermal parameters are given in values multiplied by 10^5.

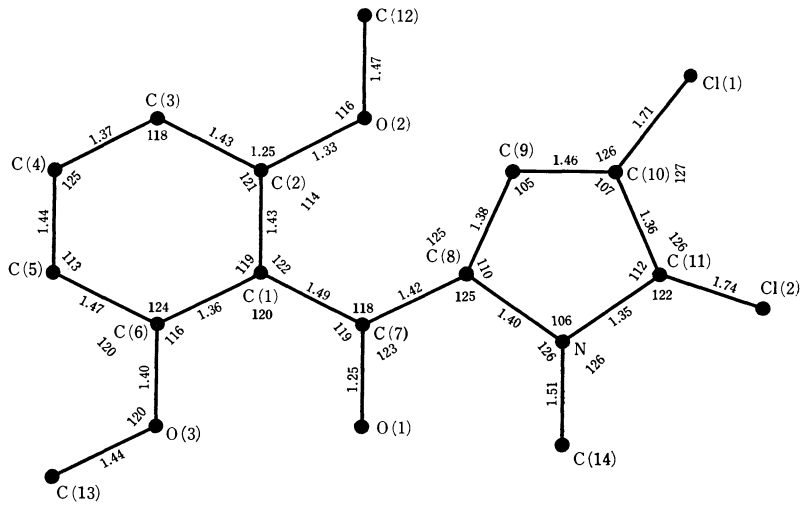

Fig. 2. The bond lengths (Å) and angles (°).

found in the present experiment corresponds exactly to Formula II, as may be seen from Fig. 1. One of the two chlorine atoms is situated at the 5′-position of the pyrrole ring, as was expected on the basis of chemical evidence, while the other is located at the 4′-position, the distance between them being about 3.41 Å. The pyrrole ring plane makes a dihedral angle of only about 7° with the carbonyl plane, while the benzene plane makes an angle of no less than 83° with it. This shows that the carbonyl group is considerably conjugated with the pyrrole ring, but is little conjugated with the benzene ring. Further, it is noteworthy that the *N*-methyl carbon atom, C(14), deviates to a considerable extent from the pyrrole ring plane, the distance being about 0.16 Å. Though one of the two methoxyl carbon atoms, C(12), lies almost on the benzene plane, the other, C(13), deviates from the plane by about 0.24 Å.

In conclusion, the authors would like to express their thanks to Professor Isamu Nitta of this university for his valuable discussions. The authors also wish to express their thanks to Dr. Masao Nishikawa, Chemical Research Laboratories, Research and Development Division, Takeda Chemical Industries, Ltd., for providing them with the sample.

BULLETIN OF THE CHEMICAL SOCIETY OF JAPAN VOL. 43 2642—2643 (1970)

X-Ray Diffraction Studies on *cis*- and *trans*-[Co $en_2(CH_3COO)_2$]ClO_4

Luigi CAMPANELLA

Institute of Analytical Chemistry, University of Rome, Italian National Researches Council, Rome, Italy

(Received February 23, 1970)

In a previous paper[1] X-ray crystallographic data of *cis*- and *trans*-[Co en_2Cl_2]ClO_4 and of *cis*- and *trans*-[Co $en_2(C_6H_{11}COO)_2$]ClO_4 were reported. Extending now the studies to another couple of *cis*- and *trans*-isomers of Co(III) complexes having formula $[Co\ en_2X_2]^+$, *cis*- and *trans*- [Co $en_2(CH_3COO)_2$]ClO_4 are examined and characterized by the X-ray powder patterns by means of a Debye-Scherrer camera of diameter 114.8 mm with monochromatized Cu$K\alpha_1$ and Fe$K\alpha_1$ radiations. The salts are prepared as described by Linhard and

TABLE 1. X-RAY POWDER PATTERNS DATA OF *cis*-[Co $en_2(CH_3COO)_2$]ClO_4

Power diagram line	d_{hkl} (Å)	I/I_0 (visual inspection)	Q ($=1/d^2$) obsd.	Q computed	hkl
1	9.466	6	0.0111	0.0112	200
2	7.969	6	0.0157	0.0157	201
3	6.705	10	0.0222	0.0222	220
4	6.305	8	0.0252	0.0252	300
5	6.087	3	0.0270	0.0269	221
6	6.000	8	0.0278	0.0280	310
7	5.801	3	0.0297	0.0297	301
8	5.534	4	0.0327	0.0325	311
9	4.972	6	0.0405	0.0405	003
10	4.727	4	0.0448	0.0448	400
11	4.580	5	0.0477	0.0476	410
12	4.279	9	0.0546	0.0545	213
13	3.991	1	0.0628	0.0628	402
14	3.779	1	0.0700	0.0700	500
15	3.651	1	0.0750	0.0748	104
16	3.598	8	0.0772	0.0773	511
17	3.506	1	0.0814	0.0812	520
18	3.464	5	0.0833	0.0832	204
19	3.211	1	0.0970	0.0972	304
20	3.110	1	0.1034	0.1036	610
21	2.927	2	0.1167	0.1165	621
22	2.841	1	0.1239	0.1237	205
23	2.700	2	0.1372	0.1372	700
24	2.333	1	0.1837	0.1837	801
25	2.315	1	0.1866	0.1865	811
26	2.293	2	0.1902	0.1900	316
27	2.064	1	0.2347	0.2348	516
28	1.990	1	0.2525	0.2525	{715 555
29	1.858	1	0.2897	0.2896	942

1) L. Campanella, This Bulletin, **41**, 2814 (1968).

TABLE 2. X-RAY POWDER PATTERNS DATA OF *trans*-[Co $en_2(CH_3COO)_2$]ClO_4

Power diagram line	d_{hkl} (Å)	I/I_0 (visual inspection)	Q ($=1/d^2$) obsd.	Q computed	hkl
1	8.421	8	0.0141	0.0141	201
2	7.619	8	0.0172	0.0172	211
3	7.189	10	0.0193	0.0192	202
4	6.675	3	0.0224	0.0223	212
5	6.141	8	0.0265	0.0265	221
6	5.540	9	0.0326	0.0327	311
7	5.136	3	0.0379	0.0378	312
8	4.694	8	0.0454	0.0456	105
9	4.290	3	0.0543	0.0544	411
10	4.209	1	0.0564	0.0564	402
11	3.966	10	0.0636	0.0637	421
12	3.692	6	0.0734	{0.0735 0.0736	315 206
13	3.381	4	0.0875	0.0874	512
14	3.283	3	0.0928	0.0928	503
15	3.030	4	0.1089	0.1088	008
16	2.993	4	0.1116	0.1116	600
17	2.905	3	0.1185	0.1184	602
18	2.834	1	0.1245	0.1243	218
19	2.748	3	0.1324	0.1324	525
20	2.679	1	0.1393	0.1393	623
21	2.570	5	0.1514	0.1512	624
22	2.524	1	0.1570	0.1572	615
23	2.478	7	0.1629	0.1629	641
24	2.405	2	0.1729	0.1728	606
25	2.350	1	0.1811	0.1815	731
26	2.300	1	0.1890	0.1891	650
27	2.120	1	0.2225	0.2223	735
28	2.106	1	0.2255	0.2255	726
29	2.060	2	0.2356	0.2362	752
30	2.009	2	0.2478	0.2480	840
31	1.973	1	0.2569	0.2566	744
32	1.927	1	0.2693	0.2695	913
33	1.907	1	0.2750	0.2752	844
34	1.790	1	0.3121	0.3117	10,01
35	1.770	1	0.3192	0.3199	10,12
36	1.753	1	0.3254	0.3253	10,09
37	1.668	1	0.3594	0.3592	857

Stirn.[2]

Ito's method[3] is successful in indexing powder patterns. The use of an IBM computer is helpful in applying this method.

The experimental data for d_{hkl}, I/I_0 and Q of the two compounds are listed in Tables 1 and 2 and compared with the Q values computed on the basis of the indexing. Studies so far perfomed lead to the following conclusions:

a) *cis*-$[Co\,en_2(CH_3COO)_2]ClO_4$: The unit cell is tetragonal with dimensions $a=b=(18.898\pm0.007)$ Å, $c=(14.908\pm0.005)$Å. The measured density is 1.48 g cm^{-3}; the cell content is 12 formula units, giving a calculated density of 1.48 g cm^{-3}.

b) *trans*-$[Co\,en_2(CH_3COO)_2]ClO_4$: The unit cell is tetragonal with dimensions $a=b=(17.953\pm0.007)$ Å, $c=(24.213\pm0.008)$Å. The measured density is 1.34 g cm^{-3}; the cell content is 16 formula units, giving a calculated density of 1.35 g cm^{-3}.

2) V. M. Linhard and G. Stirn, *Z. Anorg. Allgem. Chem.*, **268**, 105 (1952).

3) T. Ito, "X-Ray Studies on Polymorphism," Maruzen Co., Ltd., Tokyo (1950), pp. 187—228.

BULLETIN OF THE CHEMICAL SOCIETY OF JAPAN VOL. 43 2643—2645 (1970)

The Mechanism of the Oxidation of Acetaldehyde by Chromic Acid

C. GOSWAMI and K. K. BANERJI

Department of Chemistry, University of Jodhpur, Jodhpur, India

(Received March 16, 1970)

Aliphatic ketones are oxidized by chromic acid *via* their enol form.[1] There is a possibility that oxidation of aldehydes may also involve the enol intermediate. Chromic acid oxidation of aromatic aldehydes[2-4] and formaldehyde[5] has been studied in detail, but these aldehydes cannot enolize. Some preliminary studies have been carried out on the oxidation of acetaldehyde by Roček[6] and by Chat terji and Antony.[7] In the present investigation the role of enolization in the oxidation process has been studied.

Results

Product Study. Oxidation of acetaldehyde by aqueous chromic acid yielded acetic acid. The completely reduced reaction mixture gives a blue-brown colour with lanthanum nitrate and a drop of iodine solution in the presence of ammonia.[8]

Rate Laws. The rate of disappearance of Cr(VI) followed first order law, but the values of rate constants decreased with increase in the concentration of chromium(VI). The results show that the reaction is strictly of first order with respect to acid chromate ion, $HCrO_4^-$ (Table 1). The concentrations of $HCrO_4^-$ were calculated assuming a value 2.3×10^{-2} for association constant for dichromate formation ($K=[HCrO_4^-]^2/[Cr_2O_7^{2-}]$) at 25°C.[9]

The reaction is also of first order with respect to acetaldehyde (Table 2).

Under the conditions of constant ionic strength the rate is proportional to the square of hydrogen ion concentration (Table 3) and there is also a marked positive ionic salt effect.

Effect of Solvent Composition. Increase in proportion of acetic acid in the solvent mixture

TABLE 1. OXIDANT CONCENTRATION DEPENDENCE OF THE REACTION RATE

$[CH_3CHO]$: 4×10^{-2}M, $[H^+]$: 0.5M, Temp. 25°C

10^3[Ce(VI)] mol/l	$10^4[HCrO_4^-]$ mol/l	$10^2\,k_1$ min^{-1}	10^2k_1[Cr(VI)] / $[HCrO_4^-]$
1.00	9.24	6.91	7.47
2.50	21.2	6.30	7.42
4.00	31.7	6.00	7.57
5.00	38.0	5.50	7.23
10.00	64.9	4.80	7.40

1) P. A. Best, J. S. Littler and W. A. Waters, *J. Chem. Soc.*, **1962**, 822.
2) E. Lucchi, *Boll. Sci. Fac. Chim. Ind. Bologna*, **228**, 333 (1940); *Gazz. Chim. Ital.*, **71**, 729, 752 (1941).
3) K. B. Wiberg and T. Mill, *J. Amer. Chem. Soc.*, **80**, 3022 (1958).
4) G. T. E. Graham and F. H. Westheimer, *ibid.*, **80**, 3030 (1958).
5) T. J. Kemp and W. A. Waters, *Proc. Roy. Soc.*, **A274**, 480 (1963).
6) J. Roček, *Tetrahedron Lett.*, **1959**, No. 5, 1.
7) A. C. Chatterji and V. Antony, *Z. Phys. Chem.* (Leipzig), **210**, 103 (1959).
8) F. Feigl, "Spot Tests in Organic Chemistry," Elsevier (1966), p. 454.
9) F. H. Westheimer and A. Novick, *J. Chem. Phys.*, **11**, 506 (1943).

Table 2. Substrate concentration dependence of the reaction

[Cr(VI)]: 1×10^{-3}M, [H$^+$]: 0.5M, Temp. 25°C

10^2[CH_3CHO] (mol/l)	1.00	2.00	3.00	4.00	5.00
10^2k_1 (min^{-1})	1.73	3.50	5.20	6.91	8.70
k_1/[CH_3CHO]	1.73	1.75	1.73	1.73	1.76

Table 3. Acidity dependence of the reaction velocity

[CH_3CHO]: 1×10^{-2}M, [Cr(VI)]: 1×10^{-3}M
Temp. −25°C, Ionic strength (μ)=2M

[H$^+$] (mol/l)	0.25	0.50	0.75	1.00	1.25	1.50
10^2k_1 (min^{-1})	0.691	2.53	6.15	10.1	16.1	23.0
k_1/[H$^+$]^2	11.0	11.2	10.9	10.1	10.3	10.2

increases the rate of oxidation (Table 4), probably because of the lowering of dielectric constant of the medium,[10] which favours reactions involving protonation. In acetic acid chromic acid exists as acetochromic acid, $CH_3COOCrO_3H$, which is assumed to be a stronger acid and a very powerful oxidizing agent[4,11] and hence the rate increases.

Table 4. Solvent composition dependence of the reaction rate

[CH_3CHO]: 1×10^{-2}M, [Cr(VI)]: 1×10^{-3}M
[H$^+$]: 0.5M, Temp. 25°C

Precentage acetic acid	20	40	50	60	70	80
10^2 k_1 min^{-1}	1.73	2.30	3.45	5.07	10.4	18.4

Effect of Manganese(II). Addition of manganese(II) did not affect the rate of oxidation. This prevents any conclusion as to whether chromium(IV) or chromium(V) is formed in the rate-determining step. A similar effect was noted in the oxidation of cyclohexanone[1] and has been attributed to the rapid oxidation of the organic substrate by Mn(III), formed by the reaction.

$$Cr(IV) + Mn(II) \longrightarrow Cr(III) + Mn(III) \quad (1)$$

Effect of Temperature. Data on the effect of temperature on the reaction rate are summarized in Table 5. A plot of $\log k_1$ against reciprocal of temperature gave a straight line. The specific rate constant, k, is defined by

$$k = \frac{k_1\ (\text{min}^{-1})}{60\cdot[CH_3CHO][H^+]^2}$$

The activation parameters were evaluated in the usual manner.

Table 5. Effect of temperature on the reaction rate

[CH_3CHO]: 1×10^{-2}M, [Cr(VI)]: 1×10^{-3}M
[H$^+$]: 1.0M

Temp. °K	10^2 k_1 min^{-1}	$k\times10^2$ $l^3\cdot$mol$^{-3}\cdot$ sec^{-1}	$\Delta H^{\ddagger}$ kcal/mol	$\Delta S^{\ddagger}$ e.u.
293	5.53	9.21	9.03	−33.2
298	7.14	11.90	$\Delta F^{\ddagger}$	
303	9.21	15.35	298°	
308	11.7	19.50	18.9 kcal/mol	

Rates of Enolization. The rates of enolization were measured by bromination method.

The rate of bromination of acetaldehyde is of first order with respect to acetaldehyde and hydrogen ions but of zero-order for bromine. Table 6 records the rate constants of bromination (k_2) at different temperatures and activation parameters.

Table 6. Effect of temperature on the bromination rate

Temp. °K	10^4 k_2 $l\cdot$mol$^{-1}\cdot$sec^{-1}	$\Delta H^{\ddagger}$ kcal/mol	$\Delta F^{\ddagger}$ 298° kcal/mol
293	1.08	15.3	
298	1.63	$\Delta S^{\ddagger}$	22.8
303	2.50	−25.3 e.u.	
308	3.83		

Discussion

A comparison of Tables 5 and 6 shows that oxidation is much faster than enolization. Moreover, the activation energy is much lower in the chromic acid oxidation than in enolization. On these grounds we are forced to conclude that enolization cannot be an essential step in the oxidation reaction.

The results obtained here are consistent with the following rate equation, which is very similar to that previously derived for the oxidation of isopropyl alcohol.[9]

$$-d[Cr(VI)]/dt = k[CH_3CHO][HCrO_4^-][H^+]^2$$

It has been proposed that aliphatic aldehydes are oxidized *via* their hydrates.[5,6] The kinetic solvent isotope effect demonstrated by acetaldehyde[12] is of the same order as that by formaldehyde[5] and hence either the acetaldehyde hydrate or its simple derivative is the most likely intermediate. Because the aldehyde hydrates so closely resemble alcohols both is structure as well as in practically all aspects of oxidation, it is reasonable

10) M. Cohen and F. H. Westheimer, *J. Amer. Chem. Soc.*, **74**, 4387 (1952).
11) K. B. Wiberg and H. Schäfer, *ibid.*, **91**, 927 (1969).
12) K. B. Wiberg and W. H. Richardson, "Oxidation in Organic Chemistry," ed. by K. B. Wiberg, Academic Press, New York (1965), p. 175.

to expect a similarity in the mode of their oxidation as well.

Very recently Wiberg and Schäfer have established that oxidation of alcohols proceeds *via* chromate esters.[13] Analogously the oxidation of acetaldehyde can best be interpreted by assuming the reversible formation of a similar intermediate, which will then decompose in the rate-determining step. As long as the chromic acid ester is in rapid equilibrium with acetaldehyde and its hydrate, it is immaterial whether it is formed by the esterification to the hydrate or by a carbonyl addition reaction to the free aldehyde.

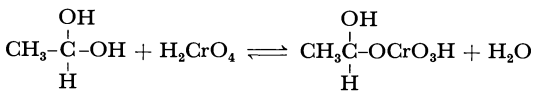

(2)

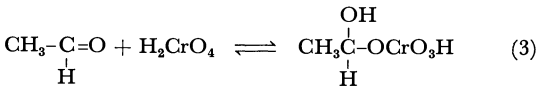

(3)

However, the second-order dependence on $[H^+]$ and magnitude of kinetic solvent isotope effect[12] ($k_{D_2O}/k_{H_2O}=6.29$), show that the rate-determining step must involve a protonated reaction complex. Thus formation of ester is followed by protonation of the chromic acid moiety of the ester.

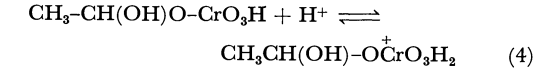

(4)

The activation parameters suggest that C–H bond is ruptured in the rate-determining step[14,15] and this reasoning is made clear by the fact that both formaldehyde[5] and acetaldehyde[16] show a primary isotope effect. It is, however, far less clear whether hydrogen leaves as a proton, an atom or an anion. Westheimer[4] prefered the abstraction of proton in cyclic process by one of the chromate oxygen atoms. Roček,[6,17] however argued in favour of a hydride transfer. There are no data which permit one to distinguish conclusively between these two mechanisms. Recently, however, it has been shown that several two-electron oxidants oxidize alcohols by a hydride transfer mechanism[18,19] and it is likely that oxidation of acetaldehyde by chromic acid involves a hydride transfer as follows.

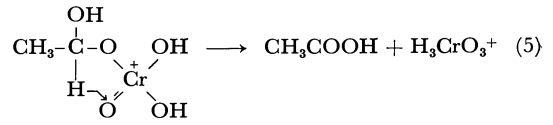

(5)

Experimental

Materials. Perchloric acid (60%, E. Merck) was used as a source of hydrogen ions; sodium perchlorate (Riedel) was used to adjust the ionic strength. Acetaldehyde (B.D.H.) was purified by the usual method. Acetic acid (99.5%, B.D.H.) was distilled over chromic acid before use. All other chemicals used were of "AR" grade.

Kinetic Measurements. The reactions were carried out at constant temperature (±0.05°C). Unless otherwise stated, the solvent was 20% acetic acid. The concentration of acetaldehyde was always kept in excess. Reactions were followed iodometrically.

13) K. B. Wiberg and H. Schäfer, *J. Amer. Chem. Soc.*, **91**, 933 (1969).
14) G. V. Bakore and S. Narain, *J. Chem. Soc.*, **1963**, 3419.
15) G. V. Bakore and S. Narain, *Z. Phys. Chem.*, **227**, 8 (1964).
16) J. W. Corniforth and G. Popjak, *Nature*, **164**, 1053 (1949).
17) J. Roček, in "The Chemistry of Carbonyl Compounds," ed. by Saul Patai, Interscience Publishers, New York (1966), pp. 461—474.
18) K. K. Banerji and P. Nath, This Bulletin, **42**, 2038 (1969).
19) R. N. Barter and J. S. Littler, *J. Chem. Soc., B*, **1967**, 205.

BULLETIN OF THE CHEMICAL SOCIETY OF JAPAN VOL. 43 2646—2647 (1970)

Studies in Haloketones. I. Synthesis and Reactions of α-Bromo-β-chlorovinyl Aryl Ketones

T. C. SHARMA, H. PATEL and M. M. BOKADIA

School of Studies in Chemistry, Vikram University, Ujjain, India

(Received May 20, 1969)

The reactivity of halogen atom in haloketones varies considerably depending upon the nature of the organic moiety and the position of the halogen atom with respect to the carbonyl group. The halogen atom of α-haloketones is activitated for S_N2 displacement reactions and is attributed with positive character. When these compounds are warmed with acidified potassium iodide solution, iodine is liberated.[1,2] Usually a vinylic halogen atom is very inert and cannot be replaced by direct substitution reactions. However, a keto group at the β-position of the vinyl moiety makes this halogen atom very susceptible to displacement reactions. For example, β-chlorovinyl aryl ketones react with ammonia[3,4] and amines[5,6] to eliminate hydrogen chloride and form corresponding amino compounds.

In the present work α-bromo-β-chlorovinyl ketones (I) have been synthesised by the following general route. These ketones are quite stable at room temperature.

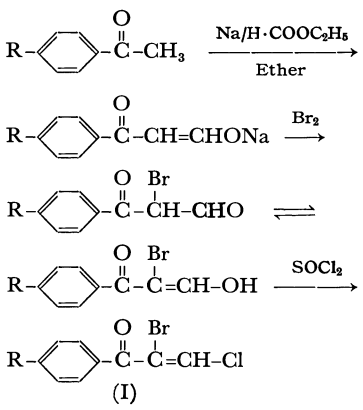

(I)

(a) R=H (b) R=CH_3 (c) R=Cl
(d) R=Br

The reactions of these compounds with ammonia and anilines have also been studied. It has been observed that it is only β-chlorine atom that undergoes substitution, whereas α-bromine atom remains intact in all the reactions.[7]

(The structures of the reaction products are as follows.)

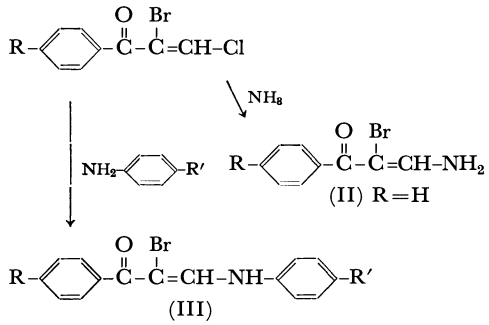

(II) R=H

(III)

(III) (a) R=R'=H (b) R=H, R'=Cl
(c) R=H, R'=Br (d) R=CH_3, R'=H
(e) R=CH_3, R'=Cl (f) R=CH_3, R'=Br

Experimental

Synthesis of α-Bromo-β-chlorovinly *p*-Chlorophenyl Ketone (Ic). A mixture of equimolecular quantities of α-bromo-β-hydroxy vinyl *p*-chlorophenyl ketone (10 g), thionyl chloride (4.5 g) and dry benzene (40 m*l*) was refluxed on a water bath for eight hours. Benzene was removed by distillation and the residue, when distilled under reduced pressure (140°C/1 mmHg), yielded yellow coloured oil (4 g). IR spectrum (liquid film of the compound) showed a carbonyl frequency at 1667 cm^{-1}.

Found: C, 38.8; H, 1.9; (Cl+Br), 53.3%. Calcd for $C_9H_5OCl_2Br$: C, 38.6; H, 1.8; (Cl+Br), 53.9%.

The same procedure was adopted for the synthesis of other ketones. Data for these products are given in Table 1.

Action of Ammonia on α-Bromo-β-chlorovinyl Phenyl Ketone (II). α-Bromo-β-chlorovinyl phenyl ketone (1 g) was treated with aqueous ammonia (10 m*l*) (in the presence of air) at room temperature. The reaction mixture was kept for three days for the completion of the reaction when a brown coloured solid separated. It was filtered, washed with water and crystallised

1) K. H. Mayer, *Ber.*, **44**, 2755 (1911); **46**, 2847 (1912).
2) M. M. Bokadia and S. S. Deshpande, *J. Indian Chem. Soc.*, **27**, 548 (1957).
3) A. Nesmeyanov, N. Kochetkov and Ya. Dombrovskii, *Izv. Akad, Nauk SSSR, Otd Khim. Nauk*, **1955**, 179.
4) N. Kochetkov, and Ya. Dombrovskii, *Zh. Obshch, Khim*, **26**, 3081 (1956).
5) N. Kochetkov, *et al. ibid.*, **27**, 1626 (1957).
6) N. Kochetkov, *Izv. Akad. Nauk SSSR, Otd. Khim. Nauk.*, **1953**, 991.
7) H. G. Garg, Y. Singh and M. M. Bokadia, *J. Indian Chem. Soc.*, **23**, 353 (1956).

TABLE 1

Compd. No.	Formula	Boiling point	Yield %	Calcd % (Cl+Br)	Found % (Cl+Br)
Ia	C_9H_6OBrCl	145°C/1 mmHg	30	47.0	47.1
Ib	$C_{10}H_8OBrCl$	144°C/1 mmHg	33	44.5	44.7
Id	C_9H_5OBrCl	150°C/1 mmHg	30	60.3	59.8

TABLE 2

Compd. No.	Solvent	Formula	Mp °C	Yield %		C %	H %	N %	Halogen %
IIIb	Alcohol	$C_{15}H_{11}OBrClN$	165	40	Calcd	53.4	3.2	4.1	34.3
					Found	53.6	3.2	4.3	34.6
IIIc	Alcohol	$C_{15}H_{11}OBr_2N$	174	38	Calcd	47.2	2.9	3.7	41.9
					Found	47.4	3.2	3.6	41.5
IIId	Alcohol	$C_{16}H_{14}OBrN$	126	41	Calcd	60.7	4.4	4.4	25.3
					Found	60.9	4.4	4.3	25.6
IIIe	Alcohol	$C_{16}H_{13}OBrClN$	156	37	Calcd	—	—	—	32.8
					Found	—	—	—	32.4
IIIf	Alcohol	$C_{16}H_{13}OBr_2N$	162	39	Calcd	—	—	—	40.5
					Found	—	—	—	40.4

from benzene to furnish light yellow needles (0.4 g, mp 136°C). The compound was characterised as α-bromo-β-aminovinyl phenyl ketone by elemental analysis and IR spectrum. Strong absorption bands in the spectrum are 3250, 1600, 1310, 1050 and 835 cm^{-1}. The lowering of keto frequency (1600 cm^{-1}) may be due to H-bonding in the molecule.

Found: C, 47.6; H, 3.6; N, 6.1; Br, 35.3%. Calcd for C_9H_8OBrN: C, 47.8; H, 3.5; N, 6.2; Br, 35.4%.

Similar treatment of the ketone with alcoholic ammonia also yielded the same product.

Action of Aniline on α-Bromo-β-chlorovinyl Phenyl Ketones (IIIa). A mixture of α-bromo-β-chlorovinyl phenyl ketone (2 g), sodium carbonate (2 g), aniline (1.6 g) and alcohol (10 m*l*) was shaken for eight hours and then refluxed for 15 min. It was cooled to room temperature and poured into cold water (150 m*l*). A yellow coloured solid separated. It was filtered, washed with water and crystallised from alcohol to provide yellow prisms (1 g, mp 127°C). The product was characterized as α-bromo-β-anilinovinyl phenyl ketone by chemical analysis and IR spectrum.

The presence of NH group is indicated by infrared absorption at 3100 cm^{-1}. A weak absorption peak at 1610 cm^{-1} and a strong broad band at 1570 cm^{-1} indicate carbonyl frequencies. This considerable shift in NH and carbonyl frequencies can be ascribed to hydrogen bonding in the molecule.

Found: C, 59.7; H, 4.2; N, 4.3; Br, 26.6%. Calcd for $C_{15}H_{12}OBrN$: C, 59.6; H, 4.0; N, 4.0; Br, 26.5%.

Data of other products of this series prepared by the same method are given in Table 2.

The authors are thankful to Professor W. V. Bhagwat for providing laboratory facilities and to the authorities of chemistry department I. I. T. Kanpur for providing analytical and spectral data.

BULLETIN OF THE CHEMICAL SOCIETY OF JAPAN VOL. 43 2648—2649 (1970)

Tautomerism of Phenols—A Theoretical Study

Z. MAJERSKI[1] and N. TRINAJSTIĆ[2]

Institute "Rudjer Bošković," Zagreb, Croatia, Yugoslavia

(Received February 27, 1970)

Keto-enol tautomerism in the polyacene series presents an interesting theroretical problem, since in the higher polyacene phenols the keto form is more stable, in contrast to the lower polyacene phenols where the enol form is more stable.[3] Although this displacement of equilibrium in the keto-enol tautomerism of phenols has been known for some time,[3] there are only a few theoretical studies, within the framework of the HMO theory, reported for these systems.[4]

Here we wish to report calculations of keto-enol tautomerism of the phenols based on Dewar's variant of the SCF π-MO method, which has been described in detail elsewhere.[5]

Theoretical Method

The location of a chemical equilibrium is determined by the variation of free energy (ΔF). Since free energy depends upon enthalpy and entropy, the equilibrium constant (K) can be expressed as a function of the variations of enthalpy (ΔH) and entropy (ΔS) of the compounds in the equilibrium:

$$-RT\ln K = \Delta F = \Delta H - T\Delta S \qquad (1)$$

The entropy variation for a given reaction occurring in a series of related compounds under the same experimental conditions remains essentially constant and thus can be neglected.[6] Making the usual assumption[6,7] that the difference in the keto and enol forms is due to changes in the heats of atomization rather than the enthalpy of reaction, the equilibrium can be expressed as follows:

$$-RT\ln K = \Delta H_a^A - \Delta H_b^B \qquad (2)$$

where ΔH_a^A and ΔH_a^B are the heats of atomization of the keto and enol form, respectively. Therefore, the position of equilibrium is determined essentially by the difference in the heats of atomization between the two tautomeric forms of phenols. The heats of stomization for the tautomeric forms in question can be calculated by Dewar's SCF π-MO (variable β)[4b] procedure.[4]

Results and Discussion

The systems studied are presented below.

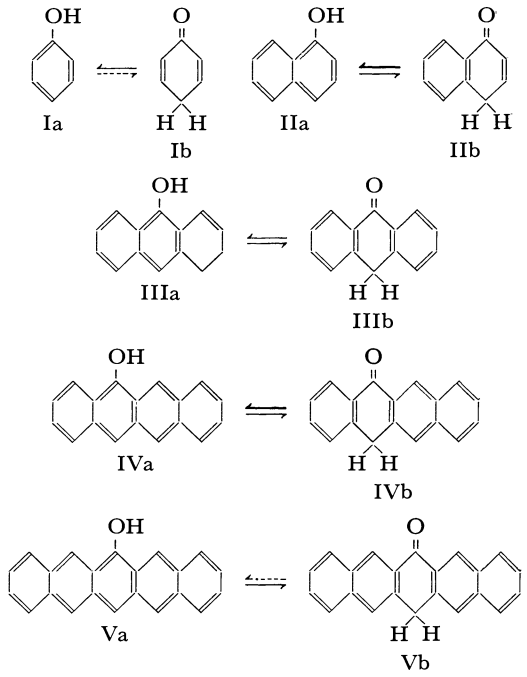

Table 1 lists the heats of atomization of tautomeric forms of phenols (A being phenol forms, B being

1) address (unitl October 1970): University of Princeton, Department of Chemistry, Princeton, New Jersey 08540, U.S.A.

2) address (unitl October 1970): University of Texas, Department of Chemistry, Austin, Texas 78712, U.S.A.

3) E. Clar, "Polycyclic Hydrocarbons," Vol. 1, Academic Press, New York (1964), p. 108.

4) a) A. Streitwieser, Jr., "Molecular Orbital Theory for Organic Chemists," Wiley, New York (1961), p. 250. b) B. Pullman and A. Pullman, Quantum Biochemistry, Interscience Publishers, New York (1963), p. 123.

5) a) A. L. H. Chung and M. J. S. Dewar, *J. Chem. Phys.*, **42**, 756 (1965). b) M. J. S. Dewar and G. J. Gleicher, *J. Amer. Chem. Soc.*, **87**, 685 (1965). c) M. J. S. Dewar and C. de Llano, *ibid.*, **91**, 789 (1969). d) M. J. S. Dewar and T. Morita, *ibid.*, **91**, 796 (1969). e) M. J. S. Dewar, "The Molecular Orbital Theory of Organic Chemistry," McGraw-Hill, New York (1969).

6) M. J. S. Dewar, *Advan. Chem. Phys.*, **8**, 65 (1965).

7) a) M. J. S. Dewar and T. Morita, *J. Amer. Chem. Soc.*, **91**, 802 (1969). b) M. J. S. Dewar and N. Trinajstić, *Tetrahedron*, **25**, 4529 (1969).

Table 1. Heats of atomization of tautomeric forms of phenols

Tautomer A	ΔH_a^A (eV)	Tautomer B	ΔH_a^B (eV)	$\Delta H_a^A - \Delta H_a^B$ (kcal/mol)
Phenol (Ia)	− 61.6675	Keto form (Ib)	− 60.6913	−22.5
α-Naphthol (IIa)	− 95.1193	Keto form (IIb)	− 94.5830	−12.4
Anthranol (IIIa)	−128.4071	Anthranone (IIIb)	−128.4679	+1.4
Hydroxytetracene (IVa)	−161.6223	Tetracenone (IVb)	−161.9402	+7.3
Hydroxypentacene (Va)	−194.8007	Pentacenone (Vb)	−195.4114	+14.5

keto forms) and the differences in the heats of atomization between these forms. The obtained results appear to be in a good agreement with present experimental evidence.

The experimental evidence can be summarized as follows; there is no indication in literature that phenol (Ia) exists to any appreciable extent in the keto form (Ib), the equilibrium being heavily located on the phenol form. However, the keto form (Ib) is apparently quite stable when substituents are attached to the ring;[8] the substituents may stabilize this form considerably. Naphthol (IIa) shows some reactions which point to existence of keto form (IIb), but here again as in the case of phenol only the substituted keto form (IIb) is stable enough to be isolated.[9] In anthracene series the keto form (IIIb) is in a slightly more stable form in the equilibrium. The equilibrium anthranol (IIIa) $\rightleftharpoons$ anthranone (IIIb) has been fairly thoroughly investigated recently by Löber[10] and Baba and Takemura[11] using spectrometric methods (absorption and fluorescence spectrometry). The equilibrium was found[11] to be solvent dependent and the enthalpy change indicated a slight displacement of the equilibrium to the keto form (IIIb) in the less polar solvents ($_{293}\Delta H$=2.6 kcal/mol in benzene; $_{293}\Delta H$= 3.3 kcal/mol in isooctane).[11] The anthranol/anthranone equilibrium can be pushed on the anthranol side by adding basic substances.[13] This has been used for the preparation of anthranol from anthranone.[12,13] However, even pure anthranol is not stable and after some time a chemical equilibrium sets up between these two tautomers.[14] Tetracenone is a stable species and well known.[15] It can be transformed into hydroxytetracene (IVa) only in an alcoholic alkali solution.[15] There is no evidence, so far, that pentacenone (Vb) can be enolized to hydroxypentacene (Va),[3,16] although the pure keto form (Vb) has been isolated and studied.[16,17]

8) *i. e.* H. E. Zimmerman and D. I. Schuster, *J. Amer. Chem. Soc.*, **84**, 4527 (1962); V. Ershov, A. A. Volod'kin and G. N. Bogdanov, *Uspekhi himii*, **32**, 1954 (1963); W. Ried and E. Torok, *Liebigs Ann. Chem.*, **687**, 232 (1965); B. Miller, *Tetrahedron Lett.*, **1964**, 3527; *ibid.*, **1965**, 1727; G. Legler and B. Quiring, *Tetrahedron*, **23**, 2683 (1967).

9) *i. e.* R. T. Arnold, J. S. Buckley, Jr., and J. Richter, *J. Amer. Chem. Soc.*, **69**, 2322; (1947); H. E. Zimmerman, R. C. Hahn, H. Morrison and M. C. Wani, *ibid.*, **87**, 1138 (1965); J. W. Huffman and T. W. Bethea, *J. Org. Chem.*, **30**, 2956 (1965); V. D. Shteingarts, G. G. Jakobson and N. N. Vorozhtsov, Jr., *Doklady Akad. Nauk SSSR*, **170**, 1348 (1966); L. H. Klemm, J. Shabatai and P. R. Taylor, *J. Org. Chem.*, **33**, 1480, 1489 (1968); P. B. D. de la Mare and H. Suzuki, *J. Chem. Soc., C*, **1968**, 648.

10) G. Löber, *Acta Chim Acad. Sci. Hung.*, **40**, 9 (1964); *Z. Wiss. Phot. Photophys. Photochem.*, **59**, 20 (1965); *Z. Phys. Chem.* (Frankfurt), **54**, 73 (1967).

11) H. Baba and T. Takemura, This Bulletin, **37**, 1241 (1964); *Tetrahedron*, **24**, 4779, 5311 (1968).

12) K. H. Mayer, *Liebigs Ann. Chem.*, **397**, 37 (1911); K. H. Mayer and A. Sander, *ibid.*, **396**, 133 (1913); *ibid.*, **420**, 113 (1920).

13) Anthranol has been obtained from anthranone also by the irradiation of the degassed ether solution by a light flash (S. Kanamaru and S. Nagakura, This Bulletin, **39**, 1355 (1966).

14) Y. Bonsho and K. Nukada, This Bulletin, **33**, 579 (1960).

15) L. F. Fieser, *J. Amer. Chem. Soc.*, **53**, 2329 (1931); E. de B. Barnett and R. A. Lowry, *Ber.*, **65B**, 1649 (1932); C. Dufraisse and H. Vayson de pradenne, Festhr. Arthur Stoll 1957, 701.

16) E. Clar, *Chem. Ber.*, **82**, 495 (1949).

17) W. H. Mills and M. Mills, *J. Chem. Soc.*, **1912**, 2194; C. Marshalk, *Bull. Soc. Chim. Fr.*, **1937**, 1381, 1547.

SHORT COMMUNICATIONS

The Photochemical Reactions of Several Mesoionic Compounds

Akiko CHINONE, Yoshiharu HUSEYA and Masaki OHTA

Department of Chemistry, Faculty of Science, Tokyo Institute of Technology, Ookayama, Meguro-ku, Tokyo

(Received March 30, 1970)

Since interest in the photochemistry of mesoionic compounds is increasing,[1-3] we wish now to report a part of the results of our studies of this subject, which are going on in our laboratory.

The irradiation of a dioxan solution of 3,4-diphenylsydnone (Ia) in a Pyrex vessel under nitrogen and with a high-pressure mercury lamp (100 W, 30 hr) gave white plates (yield, 15%; mp 119—120°C [UV λ_{max} (dioxan) 298 mμ (ε 7660); IR ν(KBr) 3050, 1595, 1493, 1455, 1439, 775, 756, 700, 693 cm^{-1}; NMR τ_{Me_4Si} ($CDCl_3$) 1.75—1.95(2H), 2.30—2.50(3H), 2.50—2.70 (5H); Mass spectra M$^+$, *m/e* 194 (11%)]) whose spectral characteristics are consistent with its formulation as 1,3-diphenyldiazirine (IIa). This reaction seems to proceed by a mechanism analogous to that of the photolysis of 3-phenylsydnone.[1] The irradiation of Ib and Ic gave seven and fourteen products respectively; those products were only detected with vpc and were not isolated.

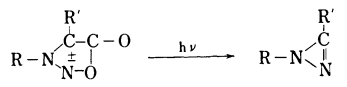

I II

Ia: R=C_6H_5 R'=C_6H_5 IIa: R=C_6H_5 R'=C_6H_5
Ib: R=C_6H_5 R'=$COCH_3$
Ic: R=$N(CH_3)_2$ R'=H

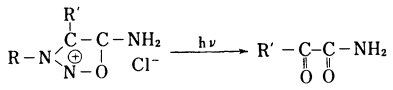

III IV

IIIa: R=C_6H_5 R'=C_6H_5 IVa: R'=C_6H_5
IIIb: R=C_6H_5 R'=CH_3 IVb: R'=CH_3

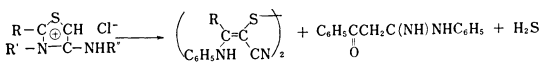

V VI VII

Va: R=R'=C_6H_5 R''=H VIa: R=C_6H_5
Vb: R=C_6H_5 R'=C_6H_5 R''=H VIb: R=CH_3
Vc: R=R'=C_6H_5 R''=$COCH_3$

Ve:

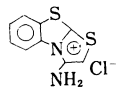

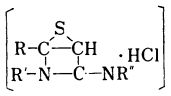

VIII

The irradiation of an aqueous solution of IIIa and IIIb for 20—40 hr gave IVa (yield, 9%; white needles with a mp of 79—81°C [UV λ_{max} (EtOH) 253 and 357 mμ (ε 10500 and 1300); IR ν(KBr) 3440, 3300(w), 3210, 1695, 1660, 1240 cm^{-1}; NMR τ_{Me_4Si} ($CDCl_3$) 1.6—1.8(2H), 2.3—2.6(3H), 2.8—3.2(1H), 3.7—4.1(1H)]) and IVb (yield, 8%; white prisms with a mp of 120—123°C [IR ν(KBr) 3400, 3280(w), 3200, 1730, 1680, 1360 cm^{-1}]) respectively.

The irradiation of an aqueous solution of Va for 6 hr gave VIa (($C_{15}H_{11}N_2S)_2$, yield, 23%; yellow needles with a mp of 230—231°C [UV λ_{max} (EtOH) 265, 325 and 385 mμ (ε 23400, 18500 and 15300); IR ν(KBr) 3300, 3250, 2180, 1580, 1545 cm^{-1}; mol wt (in DMF) 444.7]), VII (yield, 70%; white needles with a mp of 165—166°C [UV λ_{max} (EtOH) 235 and 333 mμ (ε 12000 and 24600); IR ν(KBr) 3480, 3310, 3190, 1680, 1600 cm^{-1}; Mass spectra M$^+$, *m/e* 238 (63%)]), and H_2S, which was removed in a stream of N_2 and which was characterised by reaction with lead(II) acetate. The irradiation of an aqueous solution of Vb gave VIb (yield, 12%; mp 215—216.5°C [UV λ_{max} (EtOH) 275, 295 and 355 mμ (ε 15700, 12200 and 17800); IR ν(KBr) 3220, 2180, 1560, 1540 cm^{-1}]) and H_2S. These results show that the photolyses of thiazone imine derivatives most likely proceed *via* bicyclic intermediates (VIII). However, the irradiation of Vc in an aqueous solution gave no detectable products and resulted in the recovery of the starting material, while the irradiation of Vd gave only a resinous oil. No change was observed by the irradiation of Ve in an aqueous solution.

1) C. U. Krauch, J. Kuhls and H.-J. Piek, *Tetrahedron Lett.* **1966**, 4043.
2) R. M. Moriarty, J. M. Kliegman and R. B. Desai, *Chem. Commun.*, **1967**, 1255.
3) R. M. Moriarty and R. Mukherjee, *Tetrahedron Lett.*, **1969**, 4627.

Synthesis of Succinonitrile by the Catalytic Reaction of Acrylonitrile in a Gaseous Phase

Michiaki OSHIO and Tadashi HARA

Department of Chemical Engineering, Faculty of Engineering, Doshisha University, Kamikyo-ku, Kyoto

(Received April 16, 1970)

During the course of an investigation of synthesizing adiponitrile by hydrodimerization of acrylonitrile in a gaseous phase, it has been found that succinonitrile is selectively produced from acrylonitrile by the catalytic reaction on a catalyst consisting of alkali and alkaline earth metal oxides. The conventional methods for the preparation of succinonitrile are based on, 1) the reaction between acrylonitrile and hydrogen cyanide in a liquid phase,[1] 2) the reaction between ethylene and hydrogen cyanide in a gaseous phase,[2] and 3) the irradiation of γ-rays onto acetonitrile molecule,[3] *etc.* The present work has an advantage in that succinonitrile can be prepared from acrylonitrile alone.

Acrylonitrile was made to react in a tubular flow reactor with fixed bed under the following conditions; fused silica tube 750×12 mm diam., catalyst 15 g (magnesium oxide: sodium oxide= 2 : 1 in moles, calcined at 500°C for 6 hr), reaction temp. 250—500°C, pressure 1 atm, W/F= 30—100 g-cat·hr/mol-feed, and hydrogen or nitrogen as a carrier gas. Gaseous components were trapped by ice-water, and analyzed by a gas chromatograph.

The liquid trapped weighed 90% of the acrylonitrile fed, and the succinonitrile content in the product was around 90 mol%. The results obtained are shown in Table 1 and Fig. 1. No acetylene was detected in the exhaust gas for 2 hr after initiation of the reaction, while it was confirmed in the sample prepared after 6 hr. This may be understood by taking the acetylide formation into consideration, that is, the reaction between alkali metal and acetylene. Hydrogen cyanide was more or less detected irrespective of the reaction time. It was further confirmed that acrylonitrile is not thermally decomposed if the reaction temperature is below 500°C and the catalyst is absent.

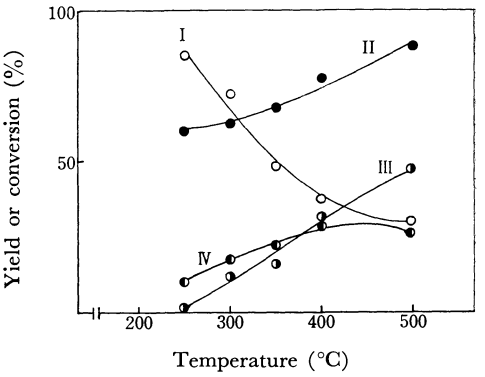

Fig. 1. Relationship between the yield or conversion and reaction temperature.
I: Succinonitrile, II: Conversion, III: Propionitrile, IV: Acetonitrile

From the results the reaction is supposed to proceed in accordance with the following in which acrylonitrile is decomposed into acetylene and hydrogen cyanide, followed by the Michael-type addition.

$$CH_2{=}CHCN \rightarrow CH{\equiv}CH + HCN \quad (1)$$

$$HCN + CH_2{=}CHCN \xrightarrow{\text{base catalyst}} NCCH_2CH_2CN \quad (2)$$

As seen in Fig.1, the yield of succinonitrile decreased with the rise of temperature while the yields of propionitrile and acetonitrile increased. In general, succinonitrile is synthesized favorably at 250°C or below.

TABLE 1.

Feed of Hydrogen (ml/min)	Feed of AN (g/hr)	Liquid trapped/hr					Untrapped products (g/hr)
		Weight (g)	AN obtained (mol)	SN obtained (mol)	AcN obtained (mol)	PN obtained (mol)	
100	0.88	0.75	0.32×10^{-2}	0.70×10^{-2}	0.04×10^{-2}	0.01×10^{-2}	0.13
150	1.16	1.08	1.45×10^{-2}	0.37×10^{-2}	0.02×10^{-2}	0.02×10^{-2}	0.08
200	1.87	1.81	2.92×10^{-2}	0.25×10^{-2}	0.04×10^{-2}	0.04×10^{-2}	0.06
300	2.43	2.38	3.90×10^{-2}	0.22×10^{-2}	0.16×10^{-2}	0.10×10^{-2}	0.05

AN: Acrylonitrile, SN: Succinonitrile, AcN: Acetonitrile, PN: Propionitrile
The reaction was carried out under the following conditions: reaction temperature 250°C, catalyst 15 g (MgO: Na_2O=2 : 1 in mol), and pressure 1 atm.

1) P. L. Heider and H. M. Walker, U. S. 2698337 (1954).
2) C. R. Harris, U. S. 2427601 (1948).
3) D. Bradley and J. Wilkinson, *J. Chem. Soc., A*, **1967** 531.

A New Dynamic Approach for Elucidating the Mechanism of Catalytic Reactions. The Mechanism of the Decomposition Reaction of Methyl Alcohol on ZnO

Akifumi UENO, Takaharu ONISHI and Kenzi TAMARU

Department of Chemistry, The University of Tokyo, Hongo, Bunkyo-ku, Tokyo

(Received May 2, 1970)

Many reports[1] have been published on the infrared spectra of the species on the catalyst surface, but most of them have dealt only with the kind or with the structure of the species when no catalytic reaction takes place. The importance of observing the amounts and the dynamic behavior of the chemisorbed species on the catalyst surface in the course of the reaction in order to elucidate the mechanism of the catalytic reaction was previously emphasized by one of the present authors.[2] Accordingly, the mechanism of the H_2-D_2 exchange reaction,[3] the decomposition of formic acid,[4] and the water-gas shift reactions[5] on zinc oxide have been elucidated by means of a new dynamic approach, measuring the infrared spectra of the surface species.

The mechanism of the decomposition reaction of methyl alcohol on ZnO was studied by means of a new dynamic treatment. When CD_3OD was introduced to ZnO at 200°C, the CD_3O(a), OD (a), and DCOO(a) chemisorbed were observed by means of infrared spectroscopy, but CD_3OD(a) was not. The behavior of these surface species as well as that of the ambient gas and the overall reaction rates were simultaneously examined under various reaction conditions, including non-stationary conditions.

D_2, CO_2 and CO were formed by the decomposition of CD_3OD on ZnO at 200°C, but when CD_3OD was trapped out of the system by a dry ice-methanol mixture or in the absence of an ambient methanol vapour, the evolution of D_2 and CO_2 stopped correspondingly, though that of CO from the surface species continued during the trapping. The amount of CD_3O(a) on the catalyst decreased, but that of DCOO(a) increased, during the trapping. The decrease in the CD_3O(a) was nearly equal to the total increase in DCOO(a) and CO(g). Most of the CD_3O(a) on the surface disappeared during the trapping at 240°C, though DCOO(a) still remained on the catalyst, whereas the evolution of CO(g) was uninfluenced and continued at a rate comparable to the overall rate. When the CD_3OD collected in the trap was released into the gas phase, the amounts of D_2 and CO_2 were increased rapidly, but that of CO continued to increase without any change. It was, consequently, concluded that the CO was produced mainly from the decomposition of DCOO(a) on ZnO, and that the D_2 and CO_2 resulted from the interaction between the CD_3OD in the ambient gas and the surface DCOO(a). The results are shown in Fig. 1.

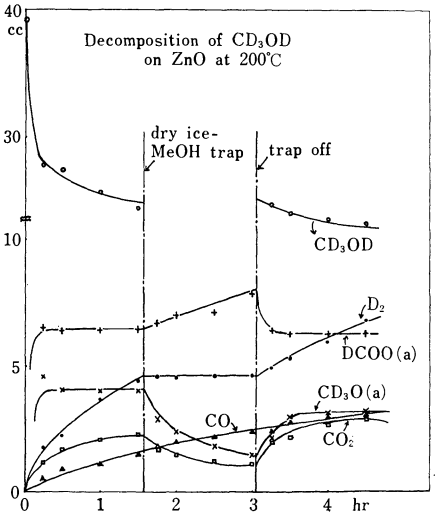

Fig. 1.

When CH_3OD was introduced onto the catalyst, the surface of which had been covered by OD(a), the hydrogen produced contained overwhelmingly more deuterium than protium. It was, accordingly, demonstrated that CH_3OD reacted not only with the surface formate, but also with the hydroxide on the surface of ZnO. It was, consequently, concluded that the mechanism of the decomposition of methyl alcohol on ZnO is shown as follows:

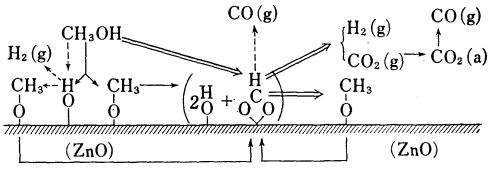

1) L. H. Little, "Infrared Spectra of Adsorbed Species," Academic Press, N. Y. (1966). Micheal L. Hair, "Infrared Spectroscopy in Surface Chemistry," Marcel Deeker, (1967).
2) K. Tamaru, *Adv. Catalysis*, **15**, 65 (1964); *Nippon Kagaku Zasshi*, **87**, 1007 (1966).
3) S. Naito, H. Shimizu, E. Hagiwara, T. Onishi and K. Tamaru, This Bulletin, **43**, 974 (1970).
4) Y. Noto, K. Fukuda, T. Onishi and K. Tamaru, *Trans. Faraday Soc.*, **63**, 3072 (1967).
5) A. Ueno, T. Onishi and K. Tamaru, *ibid.*, **66**, 756 (1970); This Bulletin, **42**, 3040 (1969).

Single, Double and Triple Insertion of Cyclohexyl Isocyanide into Methyl-Palladium Sigma Bond

Yasuhiro YAMAMOTO and Hiroshi YAMAZAKI

The Institute of Physical and Chemical Research, Yamatomachi, Saitama

(Received May 20, 1970)

Recently Otsuka *et al.* reported that the reaction of tetrakis(*tert*-butyl isocyanide)nickel with methyl iodide or benzoyl chloride undergoes multiple successive insertions of isocyanide molecules.[1] They pointed out that the insertion reaction suggested a mechanism for the polymerization of isocyanides. During our studies on the interaction of isocyanide with alkyl transition metal complexes,[2] we found that a similar successive insertion occurred in the reaction of cyclohexyl isocyanide(I) with *trans*-iodo-bis(tertiary phosphine)-methylpalladium. We wish to report on this subject.

Addition of I to *trans*-iodo-bis(methyldiphenylphosphine)methylpalladium(IIa) in benzene at 0°C gave yellow orange crystals IIIa[3] (49%, mp 134—137°C dec.). The dimeric structure was confirmed by molecular weight determination, IR and NMR spectra. Treatment of IIIa with I in the presence of methyldiphenylphosphine produced yellow complex IVa[3] (57%, mp 126—130°C dec.). The IR spectrum showed two carbon - nitrogen double bonds at 1630 and 1585 cm^{-1}. The NMR spectrum*[1] showed a singlet peak at 8.47($C-CH_3$), three broad signals at 8.72, 8.43 and 2.35 (two cyclohexyl and four phenyl groups) and a triplet signal at 8.07 τ($P-CH_3$), indicating the *trans*-configuration for IVa. The complex IVa was also obtained from the reaction of IIa with I in 1 : 2 molar ratio.

When IVa was treated with I in benzene, stepwise-inserted reaction took place, affording a trisimino complex Va[3] (67%, mp 138—141°C dec.). Va was identified to be the five-membered chelate structure coordinated to palladium through the lone pair electrons of terminal imino nitrogen atom, based on its monomeric nature, electronic configuration of palladium atom and spectroscopic studies.[4] The IR spectrum showed carbon-nitrogen double bonds at 1636 and 1598 cm^{-1}. The NMR spectrum showed a sharp singlet peak at 7.68($C-CH_3$), a doublet resonance at 7.80($P-CH_3$, $J_{P,H}=9.0$Hz) and two broad signals at 8.50 and 2.60 τ(cyclohexyl and phenyl groups), in addition to two broad signals due to α-protons of two internal cyclohexyl groups (7.30 τ) and that of a terminal one(6.50 τ). Complex Va was also obtained from the reaction of IIa with I in 1 : 3 molar ratio. A series of reactions indicates the stepwise-inserted reaction of isocyanides.

The reaction of *trans*-iodo-bis(triphenylphosphine)methylpalladium (IIb) with I in 1 : 1 molar ratio gave an air-sensitive yellow complex VIb[3] (53%, mp 98—102°C dec.). Treatment of IIb with I in 1 : 2 molar ratio produced yellow crystals IVb[3] (51%, mp 117—119°C dec.). The IR and NMR spectra were in complete agreement with the suggested structure.

No reaction of I with VIb was observed, indicating that the reaction did not proceed stepwise as IIb→VIb→IVb.

It is interesting to note that the insertion proceeds stepwise or nonstepwise depending on the nature of tertiary phosphine ligand.

Detailed studies will be reported in the near future.

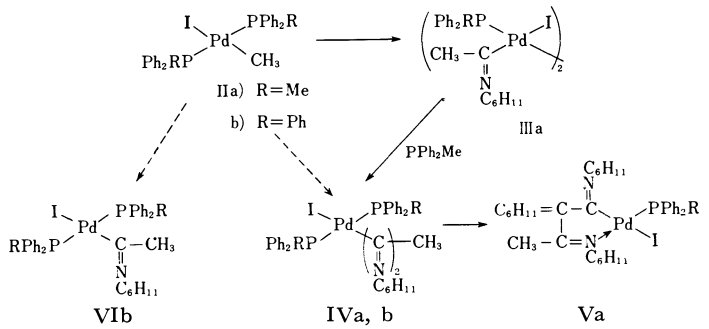

1) S. Otsuka, A. Nakamura and T. Yoshida, *J. Amer. Chem. Soc.*, **91**, 7196 (1969).

2) Y. Yamamoto, H. Yamazaki and N. Hagihara, This Bulletin, **41**, 532 (1968); *J. Organometal. Chem.* **18**, 189 (1969); Y. Yamamoto and H. Yamazaki, This Bulletin, **43**, 143 (1970).

3) All complexes gave satisfactory results in elementary analysis.

*[1] measured in $CDCl_3$ with TMS as the internal standard.

4) A similar structure has been postulated in the nickel complex; see Ref. 1.

Optical Resolution of a Heteropolymolybdate Anion

Tomoharu AMA, Jinsai HIDAKA and Yoichi SHIMURA

Department of Chemistry, Faculty of Science, Osaka University, Toyonaka, Osaka

(Received May 22, 1970)

Shimura[1] studied the electronic absorption spectrum of a dark olive green heteropolymolybdate containing cobalt(III) in a ratio of Co : Mo= 1 : 5, and concluded that the heteropoly anion contains two or more central cobalt(III) atoms with a linkage of Co^{III}–O–Co^{III}. Recently, Evans and Showell[2] determined the crystal structure of the ammonium salt of this anion and proved the dimeric structure of the anion, $[H_4Co_2Mo_{10}O_{38}]^{6-}$ with the two CoO_6 octahedra sharing two oxygens. They showed that the dicobalt(III)-decamolybdate(VI) anion has a point group symmetry D_2, and that it might be possible to resolve the complex ion into the optical antipodes.

We have succeeded in the optical resolution as follows. To a solution of $(NH_4)_6[Co_2Mo_{10}O_{34}(OH)_4]\cdot 7H_2O$ (1.0 g, 0.5 mmol, in 1000 m*l* of water) was added a solution of $(+)_{589}$-[Co en_3]-$Br_3\cdot H_2O$ (0.25 g, 0.5 mmol, in 200 m*l* of water). After the solution had been kept at 55°C for 4 hr, the less soluble dark yellowish green diastereomer deposited was collected by filtration.

Found: C, 6.20; H, 3.03; N, 7.19%. Calcd for $(+)_{589}$-[Co $en_3]_2\cdot(+)_{589}$-$[Co_2Mo_{10}O_{34}(OH)_4]\cdot 9H_2O$: C, 6.18; H, 3.00; N, 7.21%. The diastereomer was stirred with the cation-exchange resin (Dowex 50 W×8, 200—400 mesh, NH_4^+ form) in water. After the resin had been filtered off, ammonium chloride was dissolved in the green filtrate. The solution was kept in a refrigerator overnight in order to complete the crystallization of the optically active isomer. $[\alpha]_{589}^{25}=+100°$.

Found: H, 1.99; N, 4.42%. Calcd for $(+)_{589}$-$(NH_4)_6[Co_2Mo_{10}O_{34}(OH)_4]\cdot 5H_2O$: H, 2.03; N, 4.45%.

The electronic absorption and circular dichroism (CD) spectra are shown in Fig. 1. Four CD bands, (−), (+), (−) and (−) listing from the longer wavelength side, are observed in the region of d-d absorption bands of the $(+)_{589}$ isomer. The isomer shows two rather strong CD bands in the region of near ultraviolet absorption band, which may be assigned to a charge-transfer band characteristic to the bridging oxygen ligands in the linkage of $Co^{III}\langle{}^{O}_{O}\rangle Co^{III}$. Similar CD bands have also been reported for some tetranuclear Co(III) complexes containing OH-bridges.[3]

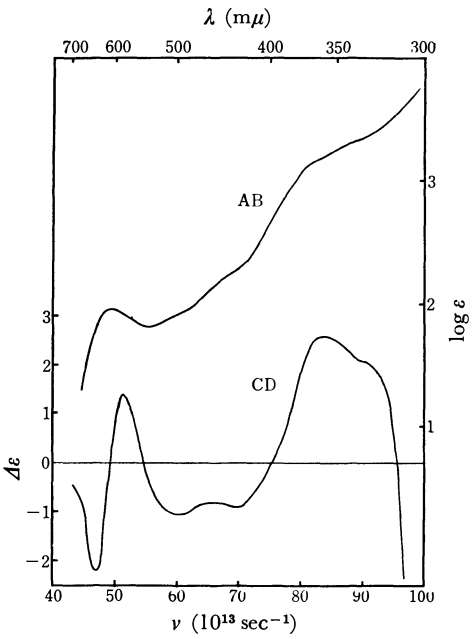

Fig. 1. Absorption AB and CD curves of $(+)_{589}$-$(NH_4)_6[Co_2Mo_{10}O_{34}(OH)_4]\cdot 5H_2O$.

This heteropolymolybdate anion appears to be the first heteropoly complex which has been optically resolved.

1) Y. Shimura, H. Ito and R. Tsuchida, *Nippon Kagaku Zasshi*, **75**, 560 (1954).

2) H. T. Evans, Jr., and J. S. Showell, *J. Amer. Chem. Soc.*, **91**, 6881 (1969).

3) S. F. Mason and J. W. Wood, *Chem. Commun.*, **1967**, 209.

Preparation of Methyl 2,3-Anhydro-4,6-*O*-benzylidene-3-deoxy-3-nitro-β-D-allopyranoside and Some C^2-Branched-Chain Derivatives of Methyl 4,6-*O*-Benzylidene-2,3-dideoxy-3-nitro-β-D-glucopyranoside

Tohru SAKAKIBARA, Satoru KUMAZAWA and Toshio NAKAGAWA

Department of Chemistry, Tokyo Institute of Technology, Ō-okayama, Meguro-ku, Tokyo

(Received May 29, 1970)

In a previous paper[1] we reported that new nucleosides (**3** and **4**) were easily formed on treatment of 3-nitroglucoside **1** with theophylline or 2,6-dichloropurine in the presence of sodium bicarbonate via a two-step mechanism, *i.e.* (i) elimination of acetic acid from 1 to yield α-nitroolefin **2** and (ii) nucleophilic addition of the purine bases to **2**. Recently Newman and Angier[2] described α-nitroepoxides, a new class of compounds, generated from α-nitroolefins with alkaline hydrogen peroxide.

We have found that on treatment with sodium hypochlorite in THF **2** also gives nitroepoxide **5** as the first member in the field of sugar chemistry. When the solvent was changed from THF to acetone, an unexpected addition of acetone, a very weak nucleophile(K_a[3] 10^{-20}), to **2** predominantly occurred[4] and a branched-chain compound **6** was obtained.

In THF (20 m*l*) **2**[5] (293 mg) was stirred with sodium hypochlorite (*ca.* 20% aq., 1.8 m*l*) for 2 hr at room temperature. It was then diluted with water (40 m*l*), condensed *in vacuo* to a half volume, extracted with chloroform, and on evaporation the remaining material was recrystallized from ethanol/water to give in 74% yield epoxide **5**, $C_{14}H_{15}NO_7$,[6] mp 184—185°C, $[\alpha]_D^{20}$ −96.2° (*c* 1, MeOH).

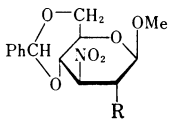

1 R=OAc
3 R=7-theophyllinyl
4 R=2,6-dichloro-9-purinyl
6 R=CH_2-C(=O)-CH_3
7 R=$CH(CN)_2$
8 R=$CH(CO_2Et)_2$
9 R= 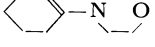

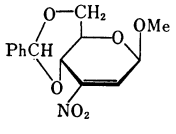

2

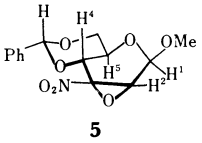

5

When stirred in acetone instead of THF overnight at room temperature, **2** gave in 91% yield adduct **6**, $C_{17}H_{21}NO_7$,[6] mp 176—177°C (from EtOH), $[\alpha]_D^{20}$ −66.9° (*c* 1, MeOH), IR(KBr) 1715 cm^{-1} (C=O), NMR($CDCl_3$) 7.89τ (3H-*s*, Ac).

Similarly, addition of malononitrile (K_a[3] 6.5×10^{-12}) and ethyl malonate (K_a[3] 5×10^{-14}) to **2** afforded the following, in an over 88% yield, respectively: *2-C-Dicyanomethyl derivative* **7**, $C_{17}H_{17}N_3O_6$,[6] mp 177—178°C (from EtOH), $[\alpha]_D^{20}$ −40.2° (*c* 1, MeOH); *2-C-(Diethoxycarbonyl)methyl derivative* **8**, $C_{21}H_{27}NO_{10}$,[6] mp 109—110°C (from EtOH), $[\alpha]_D^{20}$ −61.2°C (*c* 1, MeOH).

Under similar conditions cyclohexanone was shown to be inactive as a nucleophile, but its morpholino enamine was made to react with **2** without a catalyzer to afford adduct **9** in 76% yield, $C_{24}H_{32}N_2O_7$,[6] mp 145.5—146°C (from EtOH), $[\alpha]_D^{20}$ −135° (*c* 0.5, $CHCl_3$).

Structures of the products obtained were deduced from NMR-data: The fact that $J_{1,2}$=0(dihedral angle of H^1,H^2=100°) and $J_{4,5}$=9.5 Hz(diaxial of H^4,H^5) in **5** permits only a distorted β-*allo* structure, as shown in the figure. Large values of coupling constants (≳8 Hz) of H^1 - H^5 in **6**—**9** indicate their β-*gluco* configurations.

TABLE 1. 100 MHz NMR SPECTRA IN $CDCl_3$ (TMS as an internal standard)

Compound	Chemical shifts in τ					Coupling constants			
	H^1	H^2	H^3	H^4	$-CH\langle_O^O$	$J_{1,2}$	$J_{2,3}$	$J_{3,4}$	$J_{4,5}$
5	5.21	6.25	—	4.98	4.30	0	—	—	9.5
6	5.30	?	5.00	5.87	4.47	8	10.5	9.5	9.5
7	5.41	7.16	5.12	5.79	4.44	8	10.5	9.5	9.5
8	4.87	7.10	4.97	?	4.46	8	11.5	10	?
9	5.51	?	5.01	5.87	4.48	8	10.5	10.5	9.5

1) T. Nakagawa, T. Sakakibara and S. Kumazawa, *Tetrahedron Lett.*, **1970**, 1645.
2) H. Newman and R. B. Angier, *Chem. Commun.*, **1969**, 369.
3) Value in water at 25°C [R. G. Pearson and R. L. Dillon, *J. Amer. Chem. Soc.*, **75**, 2439 (1953)].
4) In this case sodium hypochlorite is likely to behave as a basic catalyzer. The reaction proceeds also in the presence of a trace of sodium hydroxide instead of sodium hypochlorite, to give **6** in 86% yield.
5) H. H. Baer and T. Neilson, *Can. J. Chem.*, **43**, 840 (1965).
6) All the new compounds give satisfactory results in elementary analyses.

The Reactivity of Electron Donor-acceptor Complexes. The Effect of the Complex Formation on the Reduction of Methylene Blue in the Presence of Aromatic Hydrocarbons

Yasuhiro IWASAWA, Tamotsu KONDOW, Mitsuyuki SOMA, Takaharu ONISHI and Kenzi TAMARU

Department of Chemistry, The University of Tokyo, Hongo, Bunkyo-ku, Tokyo

(Received January 27, 1970)

The hydrogen transfer from dihydro-aromatic hydrocarbons to methylene blue was chosen for study, with methylene blue being regarded as a model compound of flavin co-enzymes, and the effect of aromatic hydrocarbons added was studied.

Various aromatic hydrocarbons, such as naphthacene, perylene, anthracene, and pyrene, were purified by recrystallization and sublimation, while commercial methylene blue and dihydro-aromatic hydrocarbons, such as 9,10-dihydroanthracene, 9,10-dihydrophenanthrene, 4,5-dihydropyrene, and 5,12-dihydronaphthacene, were employed. The reaction was handled in the absence of air or oxygen at 0°C in 1,2-dichloroethane.

It was observed that the reduction of methylene blue, (Mb) (1.6×10^{-5} mol/l) by di-hydro-aromatic hydrocarbons, (ZH_2) (2.2×10^{-4} mol/l) was a Michaelis-Menten type with respect to the initial concentrations of aromatic hydrocarbons, $(Ar)_0$, in the concentration range from 5.45×10^{-7} to 5.45×10^{-4} mol/l.

The scheme and the rate of the overall reaction may be given as follows:

$$2Mb + Ar \underset{k_{-1}}{\overset{k_1}{\rightleftarrows}} (Mb_2\cdot Ar)$$

$$(Mb_2\cdot Ar) + ZH_2 \underset{k_{-2}}{\overset{k_2}{\rightleftarrows}} (Mb\cdot ZH_2) + Mb + Ar$$

$$(Mb\cdot ZH_2) \xrightarrow{k_3} MbH_2 + Z$$

for $d(Mb\cdot ZH_2)dt=0$ and $k_1,\ k_{-1}\gg k_2$,

$$-d(Mb)/dt = \frac{k_2k_3K(ZH_2)_0(Ar)_0(Mb)^2}{k_3+k_{-2}(Ar)_0(Mb)},$$

which is also equal to $k'(Mb)$, provided that $(Mb)_0\ll(ZH_2)_0$, where $(Mb_2\cdot Ar)$ and $(Mb\cdot ZH_2)$ represent the EDA complex of Mb with Ar and ZH_2 respectively, and where K is equal to k_1/k_{-1}.

Besides such kinetic investigations, new absorption bands were observed in the range between 500 and 600 mμ in the solution of Ar and Mb; for the absorption band of the EDA complex of pyrene and Mb, as a typical example, it was found at 530 mμ. The plots of $(Mb)_0/(O.D.)$ against $1/(Ar)_0^{1/2}(O.D.)^{1/2}$ gave a linear relation according to the Benesi-Hildebrand equation. It is of great interest to note that methylene blue formes EDA complexes with a molar ratio of 2 : 1 with various aromatic hydrocarbons. It was also observed that Mb forms EDA complexes with a molar ratio of 1 : 1 with ZH_2. When ZH_2 was 9,10-dihydroanthracene, the new absorption band was found at 618 mμ.

The reduction of methylene blue by various dihydro-aromatic hydrocarbons was accelerated by a factor of 50 by the formation of the EDA complexes with aromatic hydrocarbons. The rate constant, k', was determined in the initial stage of the reaction when the Z produced from ZH_2 is negligible. The k_1/k_{-1} and k_2/k_{-2} in the above scheme must have some relation with the stabilization energy of the EDA complex formation of Mb with Ar. In fact, the plots of the logarithms of both k_1/k_{-1} and k_2/k_{-2} against the reciprocal of the ionization potential of Ar, a measure of the stabilization energy of the EDA complex formation,

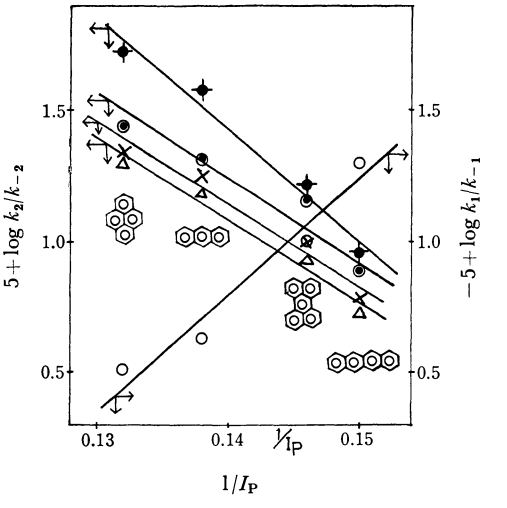

Fig. 1. The ionization potentials of aromatic hydrocarbons and the k_1/k_{-1} in the right scale and the k_2/k_{-2} in the left scale, respectively, in the concentration of aromatic hydrocarbons, 5.45×10^{-4} mol/l: for the k_2/k_{-2}, ●: 9,10-dihydroanthracene, ⊙: 9,10-dihydrophenanthrene, ×: 5,12-dihydronaphthacene, △: 4,5-dihydropyrene

gave a good linear relation, as is shown in Fig. 1. This shows that the EDA-complex formation plays a part in the redox reaction.

The Dehydration of Surface Silanol on Silica Gel

Seiichi KONDO* and Masa-aki MUROYA**

* *Osaka University of Education, Tennoji-ku, Osaka*

** *Osaka Electro-Communication University, Neyagawa, Osaka*

(Received February 23, 1970)

The thermal behavior of surface silanol groups on silica gel has been extensively studied.[1-3] Several authors have suggested various models, including the quasi-crystalline structure of the silica substrate, for the configuration and the dehydration reaction of free and hydrogen-bonded silanol groups. If the dehydration reaction occurs, the heat of reaction can be expected. In the present paper, some experimental findings derived by means of differential thermal analysis and thermogravimetric analysis are reported.

Silica gel was washed until the remaining sodium impurity became about 70 ppm of Na_2O. The presence of less than 100 ppm of the Na ion was shown to have a negligible effect on the thermal properties of silica gel.[4] The BET N_2 specific surface area of this material was 690 m^2/g.

The simultaneous measurements of DTA and TGA were carried out by means of two apparatuses, a Rigakudenki Co. Model 8001 CSL and a Shimadzu Model MTG-11. The sensitivities of the former instrument were ± 0.005°C and ± 0.02 °C using Chromel-Alumel and Pt-PtRh thermocouples respectively for DTA and ± 0.03 mg for TGA. About 30 mg of a powdered sample was heated in air in a shallow-dish-type platinum cell, using α-Al_2O_3 as the reference material, at a heating rate of 10°C and 20°C per minute.

Four endothermic DTA peaks, accompanied by four steps of weight decreases in the TGA curves and two exothermic DTA peaks, without any observable discontinuity in the TGA curves, were obtained in the range from room temperature to 1100°C, as shown in Fig. 1.

The largest DTA peaks at 150°C with the biggest weight decreases is obviously due to the desorption of adsorbed water. Three small peaks, 1, 2, and 3, at about 200, 400, and 500°C, and the corresponding small weight decreases are the facts newly found in this investigation. The pure sample which had preliminarily been heated at 570°C for six hours and then exposed to humid air with a 90% relative humidity for six hours showed

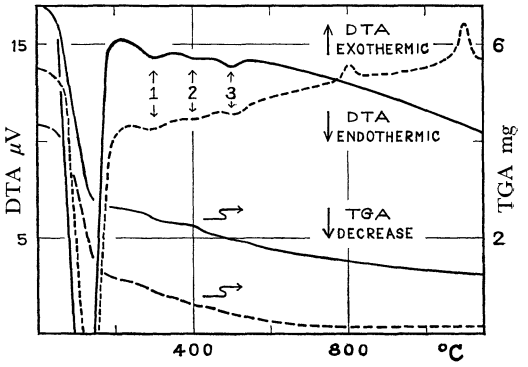

Fig. 1. DTA and TGA curves of silica gel. Full and dotted lines show pure and impure samples containing 70 and 800 p.p.m. Na_2O respectively. Sample weight was 30 mg and heating rate was 20°C/min in air.

smaller DTA and TGA changes at the same temperatures as that above. The ratio of these changes to each other was roughly equal to those obtained without preheating.

According to the preliminary test of the infrared spectroscopy in this laboratory, four absorption bands were observed in the O–H stretching vibration region, *i.e.*, at 3230, 3460, 3620, and 3750 cm^{-1}. These bands disappear, one after another, in the order from lower to higher wave numbers (except the 3750 cm^{-1} band assigned to the free silanol group) by successive heating at about the same temperatures where DTA peaks disappear. Therefore, it seems reasonable to relate the DTA peaks 1, 2, and 3 to the bands at 3230, 3460, and 3620 cm^{-1} respectively. These considerations suggest the existence of four species of silanol groups, one free and three hydrogen-bonded silanol species. According to the quasi-crystalline structure model,[2] the surface of the silica particle might have various kinds of planes, which may give rise to various types of silanol groups, similar to the crystal planes, such as (100), (110), (210) and (211), of cristobalite or similar planes of other silica crystals. The present results seem to support this theory.

No endothermic DTA peaks were found above 600°C. Two exothermic peaks, shown in Fig. 1 on samples impregnated with some metallic salts, were interpreted as the heats of crystallization to cristobalite at 800°C and to quartz or tridymite at 1000°C.[4]

1) McIntosh, "Dielectric Behavior of Physically adsorbed Gases," Marcel Dekkar, Inc. New York (1966).

2) S. Kondo and M. Muroya, This Bulletin, **42**, 1165 (1969).

3) J. B. Peri, *J. Phys. Chem.*, **70**, 2937 (1966).

4) S. Kondo and M. Muroya, presented at the 22nd annual meeting of the Chem. Soc. Japan, 1969.

The Reaction of Allene with Palladium(II) Acetate

Tadashi OKAMOTO, Yasumasa SAKAKIBARA* and Sango KUNICHIKA

Institute for Chemical Research, Kyoto University, Gokasho, Uji

* *Chemical Laboratory of Textile Fibers, Kyoto University of Industrial Arts and Textile Fibers, Kyoto*

(Received March 17, 1970)

A recent note on the reaction of allene with π-allylpalladium(II) acetylacetonate to give 2,2'-bi-π-allyl complex of palladium[1] prompts us to report another bridged π-allyl complex obtained from allene and palladium acetate.

Palladium(II) acetate and allene were stirred in benzene at room temperature overnight; subsequent separation with a silica-gel column gave a yellow crystal, di-μ-acetato-[2,2'-(1-methyleneethylene)bis-π-allyl]dipalladium (I), in about a 20% yield. The structure of I was established by chemical and spectroscopic methods. Found: C, 34.63; H, 4.10%; mol wt (benzene, 37°C), 466. Calcd for $(C_3H_4)_3Pd_2(CH_3COO)_2$: C, 34.58; H, 4.11%; mol wt, 451. The hydrogenation of I gave 2,3,5-trimethylhexane and partially-hydrogenated products, 2,3,5-trimethyl-2-hexene and 2,4,5-trimethyl-2-hexene, which were determined by a study of

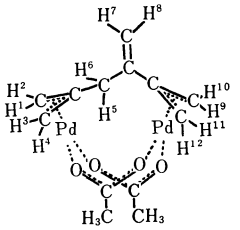

(I)

the mass and NMR spectra. The NMR spectrum of I shows singlet absorptions at 5.67 (1H, H^7), 5.21 (1H, H^8), 3.95 (2H, H^{10} and H^{12}), 3.77 (2H, H^2 and H^4), 3.26 (2H, H^5 and H^6), 2.90 (2H, H^1 and H^3), 2.80 (2H, H^9 and H^{11}), and 2.05 ppm [(6H), acetoxy protons] at 100°C in acetic acid-d_4, with TMS used as the internal reference. At −28°C in deuterochloroform, the absorptions at 3.95, 3.26, and 2.90 ppm each separated into two peaks (Fig. 1). The couplings of the AB-type by H^5 and H^6 protons at the low temperature are not clear because of the disturbance by neighboring absorptions. The IR spectrum of I shows two broad absorptions, at 1570 and 1410 cm^{-1}, which

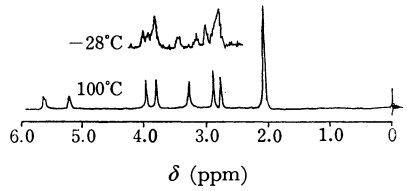

Fig. 1. NMR spectra of I.

can be assigned to the carboxylate ion. Acetate ligands were replaced, resulting in an insoluble complex, when I was treated with an aqueous sodium chloride solution.

An iron complex of a ligand with the same carbon skeleton was also obtained by Otsuka *et al.*[2] from hexacarbonyl 2,2'-bi-π-allyldiiron and allene. A similar route may be supposed for the formation of complex I, but no absorption due to 2,2'-bi-π-allylpalladium acetate was observed on the NMR spectrum of our reaction mixture.

When an aqueous sodium chloride solution was added to the reaction mixture, di-μ-chloro-bis-[2-(1-(acetoxymethyl)vinyl)-π-allyl]dipalladium (II) and di-μ-chloro-bis(2-acetoxy-π-allyl)dipalladium (III) were isolated from the solution in a total yield of 52%. The NMR spectrum of II shows singlet absorptions at 5.68 (1H, $=CH_2$), 5.46 (1H, $=CH_2$), 4.86 (2H, H^3), 4.18 (2H, H^4), 2.90 (2H, H^5) and 2.20 ppm (3H, acetoxy protons) in deuterochloroform at room temperature, with TMS used as the internal reference.

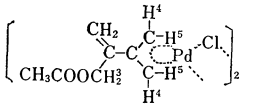

(II)

Although the mechanisms of these reactions are not yet clear, the newly-obtained complexes are the first examples of a stable complex obtained from palladium acetate.

1) R. P. Hughes and J. Powell, *J. Organometal. Chem.*, **20**, p. 17 (1969).

2) S. Otsuka, A. Nakamura and K. Tani, Symposium on Organometallic Chemistry, Osaka, Japan, September, 1969, Abstract 25.

Catalytic Diacetoxylation of *cis*- and *trans*-Dichloroethylenes by Means of Palladium(II) Chloride

Masahiro YAMAJI, Yuzo FUJIWARA, Toshinobu IMANAKA and Shiichiro TERANISHI

Faculty of Engineering Science, Osaka University, Machikaneyama, Toyonaka, Osaka

(Received May 15, 1970)

It is well known that palladium(II) chloride and sodium acetate cause the displacement reaction of vinylic halides to give vinyl acetate derivatives.[1] However, examples are limited to only monohalides such as vinyl chloride or 2-chloropropylene. In order to study whether dihalides also undergo displacement reaction or not, we have carried out the reactions of *cis*- and *trans*-dichloroethylenes. Interestingly enough we have found that in the presence of catalytic amounts of palladium(II) chloride, *cis*-dichloroethylene reacts with acetate ions to produce *trans*-diacetoxyethylene[2] in high yield with a small amount of unidentified products. Similarly *trans*-dichloroethylene afforded *trans*-diacetoxyethylene in a 137% yield based on palladium(II) chloride used.

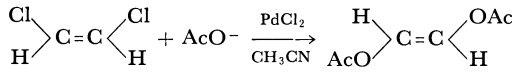

AcO: CH_3COO

This is the first example of direct diacetoxylation ethylene derivatives to give unsaturated diacetates by the nucleophilic substitution of halides with an acetate anion.

The following procedure is a representative one. A mixture of 0.09 mol of *cis*-dichloroethylene, 0.18 mol of sodium acetate, and 0.03 mol of $PdCl_2$ in 200 m*l* of acetonitrile under air was stirred at 80°C for 8 hr. The resulting mixture was filtered to remove $PdCl_2$ and Pd metal, and the filtrate was poured into water, and the organic layer was then separated. After drying over $MgSO_4$, the solvent was evaporated. The residual heavy oil crystallized on standing. The mixture was filtered and the crystals were washed with petroleum ether. From the mother liquor, a very small amount of two unidentified products was detected by glpc. The crude substance was recrystallized from ether-petroleum ether, then sublimed at 4 mmHg, to give 5.31 g (123% yield based on $PdCl_2$) of *trans*-diacetoxyethylene[3] as colorless crystals, mp 44—44.5°C, IR, 1720 (C=O), 1600 (C=C), 1188 (C-O-C) and 970 cm^{-1} (*trans*-C-H); NMR,[4] 3.29 (olefinic protons, s, 2H) and 7.80 τ (methyl protons, s, 6H).

The reaction provides an extremely convenient method for the synthesis of olefinic diacetate derivatives.

Further works on this reaction are now in progress together with mechanistic investigation, and details will be described in a full paper.

1) E. W. Stern, M. L. Spector and H. P. Lefti, *J. Catalysis*, **6**, 152 (1966); C. F. Kohll, R. Van Helden, *Rec. Trav. Chim. Pays-Bas*, **87**, 481 (1968); H. C. Volger, *ibid.*, **87**, 501 (1968); M. Tamura and A. Yasui, *Kogyo Kakagu Zasshi*, **72**, 572 (1969).

2) No *cis*-isomer was obtained, but it is presumably formed at first and then rapidly isomerized to a *trans*-isomer in the reaction.

3) M. F. Shostakovskii, N. V. Kuznetsov and Chemin Yang, *Izv. Akad. Nauk SSSR, Ser. Khim.*, **1962**, 710; *Chem. Abstr.*, **57**, 16389 (1962).

4) Taken with a Japan Electron Optics JNH-MH-100 spectrometer.

A New Synthesis of Organosilicon Azo Compounds

Hamao WATANABE, Kyoichi INOUE and Yoichiro NAGAI

Department of Applied Chemistry, Faculty of Technology, Gunma University, Tenjin-cho, Kiryu, Gunma

(Received May 16, 1970)

Although numerous methods have been proposed for synthesizing azo compounds, there are only a few reports on the formation of organometallic azo compounds with one or two silicon atoms substituted on nitrogen atoms. Mixed aryl azo organosilanes have been prepared in low yields by Krüger and Wannagat.[1] However, their method is circuitous and troublesome[2] and purity of the products was at best 90%.

We wish to report a new synthetic method for the preparation of organosilyl azo compounds in good yields by the reaction of organosilylhydrazines with radical generating agents such as di-*t*-butyl peroxide or azobisisobutyronitrile.

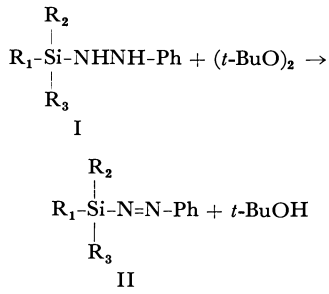

a) $R_1=Ph$, $R_2=R_3=Me$
b) $R_1=R_2=R_3=Et$

A mixture of Ia[3] (3.63 g, 15 mmol) and di-*t*-butyl peroxide (3.30 g, 22.5 mmol) was refluxed on a metal bath (210—230°C) for 3 hr under nitrogen and heated further at 180—200°C (metal bath temp.) for 1—1.5 hr, during which a mixture of low boiling materials (3.25 g; mainly *t*-butyl alcohol and the unreacted peroxide) was distilled off. Distillation of the resulting mixture gave 2.02 g (56%) of IIa, a deep blue liquid, bp 162—165°C/11 mmHg. Similarly, the reaction was effected employing Ib[4] and the peroxide to give a deep blue liquid of IIb. The analytical results are summarized in Table 1.

Compounds IIa and IIb are shown to be distillable, stable under nitrogen and considerably stable in dry air, and the solution in cyclohexane remains unchanged for a few months.

The present method is especially suitable for the preparation of such organometallic compounds sensitive to moisture or water in the reaction system. The results show that the isolation of the product from the reaction mixture is carried out with great ease due to the simplicity of the reaction system.

It is of interest to apply this method to the synthesis of other types of azo compounds. The usefulness is shown by the following example: hydrazobenzene (1.84 g, 10 mmol) was treated with the peroxide (2.02 g, 15 mmol) and worked up as described above to yield a dark-brown molten mass which was solidified on cooling. Purification of the solid by alumina column chromatography with benzene as an eluent afforded, after recrystallization from ethanol, 1.40 g, (77%) of orange-red fine crystals of azobenzene, mp 66.5—68.0°C.

TABLE 1. ANALYTICAL RESULTS OF DEEP BLUE PRODUCTS

Compound	Yield %	Elemental anaysis Found %	Calcd %	Bp °C/mmHg	NMR spectrum[a] δ, ppm	IR spectrum N=N[b]; Si-C cm^{-1}	λ_{max}[c](mμ); ε, $n\rightarrow\pi^*$
IIa	56	Si 11.85 C 70.16 H 6.94	11.68 69.95 6.71	162—165/11	7.85—7.17 (m)[d] 0.59 (s)[e]	1450 ; 1250 923	581 ; 39
IIb	59	Si 12.49 C 66.11 H 9.63	12.74 65.40 9.15	125—130/10	7.85—7.17 (m)[f] 0.99 (m)[g]	1447 ; 1240 925	592 ; 25

a) CCl_4 solution; TMS internal standard, b) see Ref. 1, c) cyclohexane solution, d) and f) phenyl protons, e) methyl protons, g) ethyl protons

1) C. Krüger and U. Wannagat, *Z. Anorg. Allg. Chem.*, **326**, 288, 296, 304 (1964).

2) Wiberg and his co-workers have prepared bis-(trimethylsilyl)diimine by another method; see *Angew. Chem.*, **80**, 661 (1968).

3) Bp 185—187°C/10 mmHg; n_D^{20} 1.5736; Analysis, Found: C, 69.12; H, 7.62%. Calcd for $C_{14}H_{18}N_2Si$: C, 69.37; H, 7.48%.

4) U. Wannagat and W. Liehr, *Z. Anorg. Allg. Chem.*, **299**, 341 (1959).

The Substitution Reaction of Ligands in Copper(II) Acetylacetonate with Pyridine on a Molecular Sieve 13X

Yoshio YAMADA, Akinori HASEGAWA and Masaji MIURA

Department of Chemistry, Faculty of Science, Hiroshima University, Higashisenda-machi, Hiroshima

(Received May 22, 1970)

It has been reported that well-resolved hyperfine structures of ESR spectra are obtained for copper(II) acetylacetonate ($Cu(acac)_2$) on silica gel.[1] The present authors found that the complex also presents a distinct ESR spectrum on a Molecular Sieve 13 X (MS). In this paper, it will be reported that the substitution of a part of the ligands in $Cu(acac)_2$ with pyridine is observed on the MS surface, but not in solutions containing pyridine.

The MS powder (Linde Lot No. 1380019) was treated in a vacuum for 5 hr at 500°C. The amount of $Cu(acac)_2$ used as the adsorbate was adjusted so as to be included in the cages of the MS in the ratio of one molecule to 20 cages. The solution of $Cu(acac)_2$ in chloroform was outgassed and introduced to the MS through a breakable seal. After the chloroform had been eliminated by means of a vacuum line, the complex adsorbed on the MS was exposed to pyridine vapor at room temperature and the ESR spectrum was measured at 77°K.

The spectral lines of perpendicular g components for the $Cu(acac)_2$ on MS were replaced upon the adsorption of pyridine by those consisting of about 11 lines, with a splitting of 16 gauss, as is shown in Fig. 1. The latter spectral lines can be explained by supposing that, in addition to the hyperfine splitting due to the copper nucleus, there exists a superhyperfine structure arising from ligand nitrogen atoms. On the other hand, none of the superhyperfine structure due to the ligand nitrogen atoms was observed in $Cu(acac)_2$ dissolved in 60% pyridine - 40% chloroform, 60% pyridine - 40% methanol, or 25% pyridine-25% water-50% methanol at 77°K.[2] Moreover, no ESR signal was obtained upon the adsorption of pyridine alone on MS. These results may imply that some of the ligands of the complex are substituted on the MS with pyridine molecules, but not in the solution containing pyridine. This conclusion is supported by the IR measurements; the absorption band at 1580 cm^{-1} of $Cu(acac)_2$ on MS, which has been assigned to the stretching of chelated carbonyl groups, disappears in $Cu(acac)_2$-pyridine on MS. The formation of $Cu(pyridine)_4^{2+}$ is not possible since the idea of a charge transfer during the substitution with pyridine is unreasonable. Consequently, the spectral lines exhibited in Fig. 1 seems to be due to the signal of a new complex in which two of four oxygen atoms originally coordinated with copper are replaced by two nitrogen atoms of pyridine. The observed spectral lines can be satisfactorily explained by the assumption that the ratio of the splitting constant of the copper nucleus to that of two ligand nitrogen atoms is 2 : 1 and that the separation of perpendicular g components can be disregarded.*1 A spectrum similar to that of $Cu(acac)_2$-pyridine on MS was observed when 4-methylpyridine was used instead of pyridine. It can be deduced from these results that such a characteristic substitution reaction is caused by the excitation of $Cu(acac)_2$ arising from the interaction of the complex with the active site on MS.

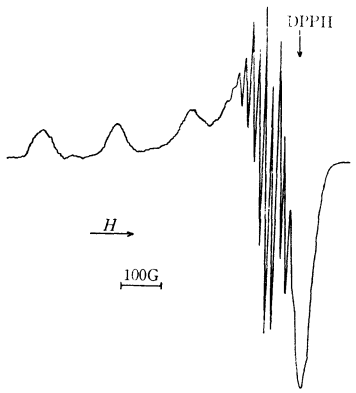

Fig. 1. ESR spectrum of $Cu(acac)_2$ on MS in the presence of pyridine at 77°K.

1) E. V. Kavalerova, V. B. Golubev and V. B. Evdokimov, *Zhur. Fiz. Khim.*, **37**, 226 (1963).

2) H. Yokoi, M. Sai and T. Isobe, This Bulletin, **43**, 1078 (1970).

*1 This was confirmed by means of a K-band ESR spectrometer.

The Mechanism of the Formation of Tropolone from the Adduct of Cyclopentadiene and Dichloroketene*[1]

Toyonobu ASAO, Takahisa MACHIGUCHI*[2] and Yoshio KITAHARA

Department of Chemistry, Faculty of Science, Tohoku University, Katahiracho, Sendai

(Received May 29, 1970)

We have previously reported[1] the novel rearrangements of the adduct of 6,6-dimethylfulvene with dichloroketene, and have proposed a mechanism for the formation of tropone derivatives from the adduct involving a norcaradienone intermediate. We have also proposed a similar mechanism for the rearrangement[2] of the adduct of cyclopentadiene with dichloroketene to tropolone. This report will present evidence to support the proposed mechanism by a tracer experiment.

The reaction of cyclopentadiene with dichloroketene-2-^{14}C, produced by the reaction of the dichloroacetyl chloride-2-^{14}C and triethylamine, in boiling *n*-hexane afforded a 1 : 1 adduct (**1**).[2,3]

The adduct (**1**) was rearranged to ^{14}C containing tropolone (**2**) under solvolytic condition (potassium acetate in acetic acid and water) according to the method of Stevens *et al.*[2]

The tropolone was submitted to catalytic hydrogenation in the presence of the Adams catalyst to give ^{14}C containing cycloheptane-1,2-diol (**3**). The diol (**3**) was degraded to trimethylenediamine (**7**) and carbon dioxide via pimelic acid (**4**), pentamethylenediamine (**5**), and glutaric acid (**6**) by repeated oxidations and Schmidt reactions, as is shown in the following scheme.

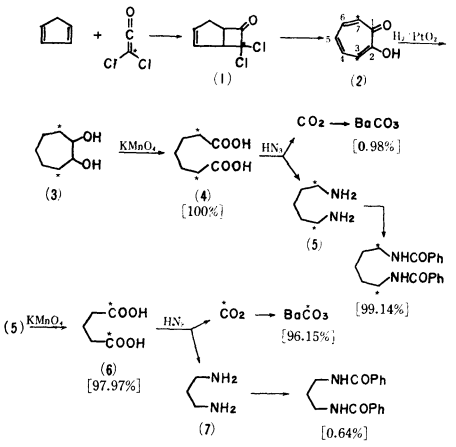

Pimelic acid (**4**) shows a radioactivity*[3] of 152,883 dpm/mM; the activities of the consecutive degradation products or their derivatives are shown in parentheses in terms of a percentage of the activity based on the activity of pimelic acid.

It is clear from the above results that all the ^{14}C are located at the 3- or 7-carbon in the tropolone (**2**); this supports the previously-proposed mechanism for the formation of tropolone by way of the attack of the nucleophile at the 7-position of the norcaradienone intermediate (**8**). The details will be reported elsewhere.

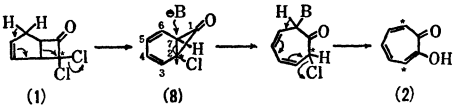

*[1] Presented at the 23rd Annual Meeting of the Chemical Society of Japan, Tokyo, April, 1970.

*[2] Present address: Department of Chemistry, Faculty of Science and Engineering, Saitama University, Urawa, Saitama.

*[3] The activities of the compounds (**4**), (**6**) and dibenzoate of (**5**) and (**7**) were measured in dioxane, and those of $BaCO_3$ were measured in toluene on TEN Liquid Scintillation Counter GSL-111.

1) T. Asao, T. Machiguchi, T. Kitamura and Y. Kitahara, *Chem. Commun.*, **1970**, 89.

2) H. C. Stevens, D. A. Reich, D. R. Brandt, K. R. Fountain and E. J. Gaughan, *J. Amer. Chem. Soc.*, **87**, 5257 (1965).

3) L. Ghosez, R. Montaigne and P. Mollet, *Tetrahedron Lett.*, **1966**, 135.

New Types of Copper(II) Complexes with Subnormal Magnetic Moments

Shoichiro YAMADA and Kuniko YAMANOUCHI

Institute of Chemistry, College of General Education, Osaka University, Toyonaka, Osaka

(Received June 12, 1970)

It is known that Schiff bases of a type represented by Formula I*[1] form copper(II) complexes of a Cu(X-SAL.$CH_2CH_2CH_2O$) type with subnormal magnetic moments, which are considered to be due

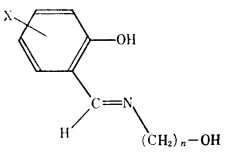

Formula I

to an interaction between two copper(II) ions within the binuclear molecule.[1,2] With Schiff bases of different series, we have recently succeeded in isolating crystals of new copper(II) complexes having subnormal magnetic moments.

A copper(II) complex shown by Formula II*[2]

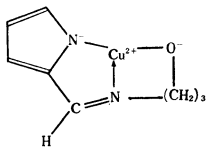

Formula II

was prepared as follows. An aqueous solution of copper(II) nitrate (0.005 mol) was added drop by drop to a solution of the Schiff base (0.01 mol) in ethanol, followed by addition of an aqueous solution of sodium carbonate (0.005 mol). After the solution was stirred at 60°C for one hour, it was allowed to cool to room temperature. A brown precipitate was collected and recrystallized from benzene or chloroform to yield brown crystals. Found: C, 44.87; H, 4.70; N, 12.43%. Calcd for Cu(Pra.$CH_2CH_2CH_2O$), $C_8H_{10}N_2OCu$: C, 44.96; H, 4.72; N, 13.11%.

By a similar method except that 2-hydroxyacetophenone was used instead of pyrrole-2-carboxyaldehyde, a copper(II) complex shown by Formula III*[3] was obtained as olive-colored crystals. This complex could also be obtained without sodium carbonate. Found: C, 52.04; H, 5.17; N, 5.53%. Calcd for Cu(Hap.$CH_2CH_2CH_2O$), $C_{11}H_{13}NO_2Cu$: C, 51.86; H, 5.14; N, 5.50%.

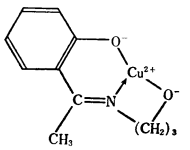

Formula III

The magnetic moments for Cu(Pra.CH_2CH_2-CH_2O) and Cu(Hap.$CH_2CH_2CH_2O$), which have been determined at room temperature to be 0.60 and 1.09 B.M., respectively, are significantly smaller than the spin-only moments expected for normal copper(II) complexes. The subnormal magnetic moments of these complexes are considered to be due to an antiferromagnetic interaction between copper(II) ions. One most probable structure may be a binuclear structure similar to that of the corresponding salicylideneiminato-complex.

It should be noted that similar methods using ethanol-amine instead of *n*-propanol-amine yielded compounds of a different type. Further study of copper(II) complexes with related ligands is now in progress.

*[1] Abbreviated as X-SAL.Y-OH.

1) S. Yamada, Y. Kuge and K. Yamanouchi, *Inorg. Chim. Acta*, **1**, 139 (1967); S. Yamada, H. Nishikawa, Y. Kuge and K. Yamanouchi, *Sci. Rep.* (College of General Education, Osaka Univ.), **16**, 11 (1967).

2) M. Kato, Y. Muto, H. B. Jonassen, K. Imai and A. Harano, This Bulletin, **41**, 1864 (1968).

*[2] Abbreviated as Cu(Pra.$CH_2CH_2CH_2O$).

*[3] Abbreviated as Cu(Hap.$CH_2CH_2CH_2O$).

Structure and Rotational Isomerism of Ethylenediamine by Gas Electron Diffraction—Evidence for a Dominant *gauche* Conformer

Akimichi YOKOZEKI and Kozo KUCHITSU

Department of Chemistry, Faculty of Science, The University of Tokyo, Hongo, Tokyo

(Received June 16, 1970)

Ethylenediamine is known as a typical chelating agent, and the structures of its complexes have been investigated extensively by X-ray crystallography.[1] However, only a little is known about the structure of free ethylenediamine. Neither the geometrical parameters nor the rotational isomerism have been studied in detail, while the spectroscopic data (IR and Raman) have been only tentatively assigned to a single (*cis*) conformer.[2] The present communication will report on the average structure of ethylenediamine and the rotational isomerism as studied by gas electron diffraction.

Anhydrous ethylenediamine (Guaranteed Reagent) was purchased from the Tokyo Chemical Industry Co., Ltd. Diffraction photographs (q= 7 to 130) were taken at various temperatures between 55°C and 118°C using 40 kV electrons with a high-temperature nozzle[3] and with camera lengths of 114 mm and 249 mm. The experimental and analytical procedures are analogous to those reported elsewhere.[4]

The average structure was determined by a least-squares analysis on the molecular intensity. The hydrogen positions were assumed to be similar to those for methylamine[5] and ethane.[6] The mean amplitudes of vibration were calculated by the use of a plausible force model.[7] The skeleton parameters and their limits of error were found to be: r_g(C–C)=1.55$_6$±0.01 Å, r_g(C–N)= 1.468±0.005 Å, and ∠C–C–N=110.2±0.8°. The C–C bond length was about 0.02 Å longer than those in ethane and other *n*-alkanes, whereas the C–N distance was similar to that in methylamine[5] within the limits of error.

The above analysis also gave the average N–C–C–N dihedral angle of 64.0±5.0°, as measured from the *cis* position. Thus, ethylenediamine is dominantly in the "*gauche*" conformation about the C–C axis at the above temperature range. This is also supported by the outstanding peak around 2.85 Å in Fig. 1 (essentially composed of the nonbonded N–N pair), where the experimental radial distribution curve with a damping factor, exp(−0.00062 q^2), is compared with the theoretical curves for different conformers. On the other hand, a small peak around 3.8 Å in the experimental curve indicates that a small fraction of the *trans* conformer may also be present.

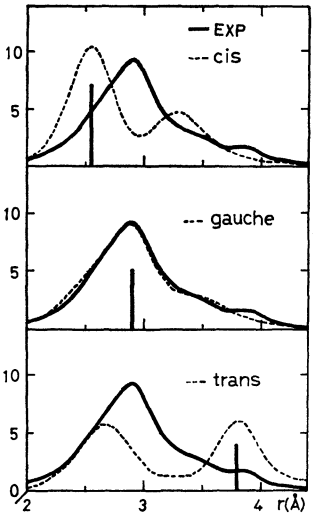

Fig. 1. Radial distribution curves. Solid line: experimental curve, from which the contribution from pairs independent of the internal rotation about the C–C and C–N axes are subtracted to accentuate the comparison. The subtracted peak, 16.4 at 2.5 Å and 1.0 at 2.8 Å, can be reproduced to within 0.2 by a theoretical curve based on the skeleton parameters given in the text with the index of resolution of 100%. The experimental error is estimated to be of the order of 0.4 in the whole region illustrated. Broken lines: corresponding theoretical curves for *cis*, *gauche* and *trans* conformers about the C–C axis with the index of resolution of 100%. Vertical line indicates the nonbonded N–N distance for each conformer.

In the above calculations, the NH_2 group was assumed to have a three-fold potential around the C–N axis with a barrier height of 1.6 kcal/mol, as in the case of ethylamine;[8] a classical average was taken to account for the effect of this motion.[4] The results presented in the preceding paragraphs are, however, found to be essentially independent of the assumptions as to the NH_2 conformation. A further analysis of the internal rotation about the C–C and C–N axes and the geometrical parameters is now being made.

1) For example, M. Iwata, K. Nakatzu and Y. Saito, *Acta Crystallogr.*, **B25**, 2562 (1969).

2) A. Sabatini and S. Califano, *Spectrochim. Acta*, **16**, 677 (1960).

3) A. Yokozeki and K. Kuchitsu, to be published.

4) A. Yokozeki and K. Kuchitsu, This Bulletin, **43**, 2017 (1970).

5) D. Lide., Jr., *J. Chem. Phys.*, **27**, 343 (1957); H. K. Higginbotham and L. S. Bartell, *ibid.*, **42**, 1131 (1965).

6) L. S. Bartell and H. K. Higginbotham, *ibid.*, **42**, 851 (1965).

7) I. Suzuki, This Bulletin, **35**, 1456 (1962).

8) M. Tsuboi, A. Y. Hirakawa and K. Tamagake, *Nippon Kagaku Zasshi*, **89**, 821 (1968).

BULLETIN OF THE CHEMICAL SOCIETY OF JAPAN VOL. 43 2665—2670 (1970)

The Behavior of Indium(III) Complexes in Several Liquid-Liquid Distribution System. I. A Solvent Extraction Study of Indium(III) Complexes in Aqueous Perchlorate Media Containing Several Anionic Ligands

Yuko HASEGAWA

Department of Chemistry, Science University of Tokyo, Kagurazaka, Shinjuku-ku, Tokyo

(Received April 2, 1969)

The stabilities of the indium(III) complexes in 4 M sodium perchlorate solutions with eight univalent anionic ligands have been studied at 25°C by using a TTA-chelate extraction method and a TBP adduct extraction method. The following conclusions have been reached. The stabilities of the indium(III) halide complexes are larger in this order; $Cl^- > Br^- > I^-$; on the other hand, those of indium(III) complexes with the halate anions increase in the order: $ClO_3^- < BrO_3^- < IO_3^-$. The former forms more stable complexes than the latter. Thiocyanate ions form the most stable indium(III) complexes (the first to the fifth complexes), while nitrate ions form the least stable one (only the first complex). The values obtained by the TTA method are almost identical with those obtained by the TBP method. It was also concluded that although the TTA method could be applied to all the systems studied, it is more suitable for the examination of the lower complexes; the TBP method, on the other hand, could be used only for the systems in which an extractable third complex is formed, but it could give more accurate constants for the higher complexes. Thus, only a combination of these two methods can give all the equilibria in a system where many complexes are formed.

Many kinds of indium(III) complexes in aqueous solutions have been reported. Among these, the halide complexes seem to have been most extensively studied and are known to be rather stable.[1)]

The present author grew interested in the differences in stability among the indium(III) complexes with halide ions and among those with the other univalent ions. In order to determine stabilities of these different complexes, measurements over a wide ligand-concentration range were necessary; thus an ionic medium, 4 M Na(ClO_4), has been employed throughout the study for this purpose. Two different solvent extraction methods, a TTA (thenoyltrifluoroacetone) chelate extraction method and a TBP (tributylphosphate) adduct extraction method, were used for the determination of the stability constants. Indium(III) in aqueous solutions containing different concentrations of the ligand was extracted by using these extracting agents, and the stability constants were determined by a graphic treatment. Some discussion was made regarding the stabilities of these complexes and regarding the solvent extraction method as a technique for the determination of the stability constants.

1) L. G. Sillén and A. E. Martell, "Stability Constants", Spec. Pub. No. 17, The Chemical Society, London (1964).

Statistical

The complex formation of indium(III) in aqueous solutions containing a univalent ligand, L^-, may be described as follows:

$$In^{3+} + nL^- \rightleftarrows InL_n^{3-n} \quad (1)$$

$$\beta_n = [InL_n^{3-n}]/[In^{3+}][L^-]^n \quad (2)$$

or:

$$K_n = [InL_n^{3-n}]/[InL_{n-1}^{4-n}][L^-] \quad (2')$$

The total indium(III) concentration in the aqueous phase may be described as:

$$[In(III)]_{total} = [In^{3+}] + [InL^{2+}] + \cdots + [InL_n^{3-n}] \quad (3)$$

The distribution ratio of indium(III) in a solvent extraction system is defined as follows (it can be measured radiometrically):

$$D = [In(III)]_{org,\ total}/[In(III)]_{total} = \frac{\gamma\text{-count-rate per m}l \text{ of the org. phase}}{\gamma\text{-count-rate per m}l \text{ of the aq. phase}}$$

(i) Extraction with an Organophilic Chelating Acid. The tripositive indium ion could be extracted with an organophilic chelating acid HA, in an immiscible organic solvent as follows:

$$In^{3+} + 3HA(org) \rightleftarrows InA_3(org) + 3H^+ \quad (4)$$

$$Kex_0 = [InA_3]_{org}[H^+]^3/[In^{3+}][HA]^3_{org} \quad (5)$$

When the aqueous phase contains only uncomplexed indium ions, the net distribution ratio may be described as follows:

$$D_0 = [InA_3]_{org}/[In^{3+}] \quad (6)$$

where the subscript "0" denotes no complex formation in the aqueous phase. The extraction constant can, then, be described as:

$$Kex_0 = D_0[H^+]^3[HA]_{org}^{-3} \quad (7)$$

When the indium ion undergoes complex formation with a uninegative ligand, L^-, and when only the InA_3 species is extractable, the net distribution ratio may be described as:

$$D = \frac{[InA_3]_{org}}{[In^{3+}] + [InL^{2+}] + \cdots + [InL_n^{3-n}]} = \frac{[InA_3]_{org}}{[In^{3+}](1 + \sum \beta_n[L^-]^n)} \quad (8)$$

From Eqs. (7) and (8), we obtain:

$$D[H^+]^3[HA]_{org}^{-3}/Kex_0 = (1 + \sum \beta_n[L^-]^n)^{-1} \quad (9)$$

(ii) Extraction as Adduct Neutral Complexes. The uncharged complex species in an aqueous phase, InL_3, could be extracted as an adduct with an organophilic neutral extractant, E, in the organic phase:

$$InL_3(org) + eE(org) \rightleftarrows InL_3E_e(org) \quad (10)$$

$$\beta_e^{\circ} = \frac{[InL_3E_e]_{org}}{[InL_3]_{org}[E]^e_{org}} \quad (11)$$

The net distribution ratio of indium(III) in such systems can be described as:

$$D = \frac{[InL_3]_{org} + [InL_3E]_{org} + [InL_3E_2]_{org} + \cdots + [InL_3E_e]_{org}}{[In^{3+}] + [InL^{2+}] + \cdots + [InL_n^{3-n}]} = \frac{[InL_3]_{org}(1 + \sum \beta_e^{\circ}[E]^e_{org})}{[In^{3+}](1 + \sum \beta_n[L^-]^n)} \quad (12)$$

When the concentration of the extractant is kept at a constant value, c_1, we can define the following partition coefficient for this complex:

$$K_{DM} = \frac{[InL_3]_{org}(1 + \sum \beta_e^{\circ}c_1^e,_{org})}{[InL_3]} \quad (\text{at } [E]_{org} = c_1) \quad (13)$$

From Eqs. (2), (12), and (13), the following equation is obtained:

$$D = \frac{K_{DM}\beta_3[L^-]^3}{1 + \sum \beta_n[L^-]^n} \quad (\text{at } [E]_{org} = c_1) \quad (14)$$

On the other hand, when the ligand concentration, $[L^-]$, is kept at a constant value, c_2, the distribution ratio is dependent on the $[E]_{org}$, and from Eq. (12) the following is obtained:

$$D = D_0(1 + \sum \beta_e^{\circ}[E]^e_{org}) \quad (15)$$

where D_0 stands for the $[InL_3]_{org}/[In^{3+}](1 + \sum \beta_n c_2^n)$ term, that is, the distribution ratio when the $[E]_{org}$ is zero.

If the "eth" adduct, InL_3E_e, is dominant in the organic phase, Eq. (15) can be described as:

$$\log D = \log D_0\beta_e^{\circ} + e \log [E]_{org} \quad (16)$$

Therefore, the plot $\log D$ *vs.* $\log[E]_{org}$ should be a straight line with the slope of $+e$, and from the value of $+e$, we can determine the number of the extractant molecules in the organic complex species.

Experimental

Reagents. The indium-114 m tracer was obtained from the Radiochemical Center, Amersham, England, as a hydrochloric acid solution. This was diluted with a large amount of 0.1 M perchloric acid and used as the stock tracer solution. All of the reagents used were of a reagent grade. The TTA was obtained from Dojindo & Co. The TBP was obtained from the Tokyo Kasei Co. and was washed with 0.1 M perchloric acid, water, and 0.1 M sodium hydroxide, and then several times with water. The chloroform was washed three times with water; The sodium perchlorate was recrystallized twice from water. The other reagents were used without further purification.

Procedures. All of the procedures were carried out in a thermostatted room at 25±0.5°C. Stoppered glass tubes (volume 20 m*l*) were used to equilibrate the organic and aqueous phases. The tracer and various amounts of ligand solutions and the sodium perchlorate solution were placed in the tubes, and then the organic solution was added. The hydrogen-ion concentration was adjusted by the addition of perchloric acid. A small amount (0.01 M at initial) of sodium acetate was added as a buffer for the iodate (pK_a, *ca.* 0.7) and thiocyanate (pK_a, *ca.* 0.8) systems in order to prevent the association of the ligand with the portion. The initial volume of each phase was 5.0 m*l*. The aqueous phase was kept at a constant ionic medium, 4 M $Na(ClO_4)$. The two phases in the tubes were agitated mechanically for one hour and then centrifuged. A two-milliliter portion was pipetted from each phase and transferred into a small test tube. The γ-radioactivity of these sample solutions was measured with a well-type(NaI) scintillation counter. A small portion was also pipetted from the aqueous phase and transferred into a small glass vessel, and the hydrogen-ion concentration was measured potentiometrically by using a standard solution containing 0.0100 M perchloric acid and 3.99 M sodium perchlorate as a standard of $-\log [H^+]$ 2.00.

Results

TTA-Extraction. Figure 1 shows the $-\log[H^+]$ dependence of the indium(III) extraction into the chloroform phase containing 0.02 M TTA from a 4 M sodium perchlorate medium containing no ligand. It may be seen from the figure that the slope of the plot is +3. The extraction constant, K_{ex_0} in Eq. (7), was obtained as $\log K_{ex_0} = -3.62$. Figures 2 to 5 give the $\log D[H^+]^3 \cdot [HA]_{org}^{-3}/K_{ex_0}$ *vs.* $\log[L^-]$ plot. The $-\log[H^+]$ for these experiments was kept at 2.0, but it was kept around 3 for the experiments with iodate and thiocyanate ions. The stability constants of the

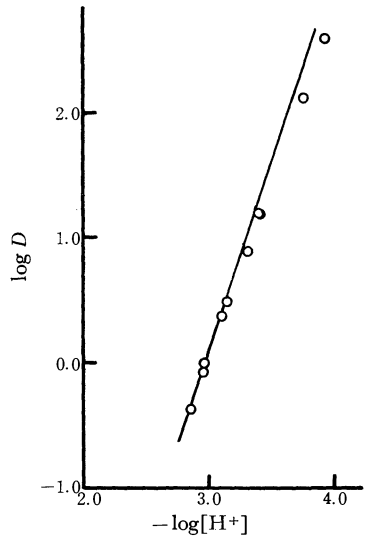

Fig. 1. Extraction of In(III) from aqueous phase containing no complexing ligands.
Organic phase: $CHCl_3$ containing 0.02 M TTA
Aqueous phase: 4 M $NaClO_4$
The straight line gives $\log D = -3 \log [H^+] - 8.72$

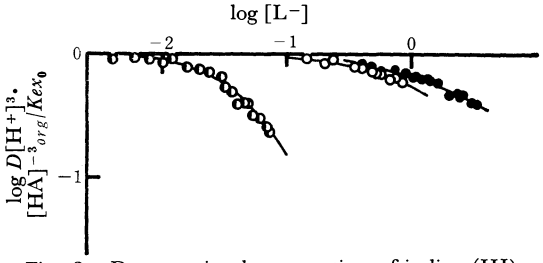

Fig. 2. Decrease in the extraction of indium(III) as a function of the ligand concentration.
● 0.2 M TTA-$CHCl_3$, 4 M $Na(ClO_3, ClO_4)$
○ 0.2 M TTA-$CHCl_3$, 4 M $Na(BrO_3, ClO_4)$
◐ 0.02 M TTA-$CHCl_3$, 4 M $Na(IO_3, ClO_4)$
The solid curves were calculated using the stability constants in Table 1.

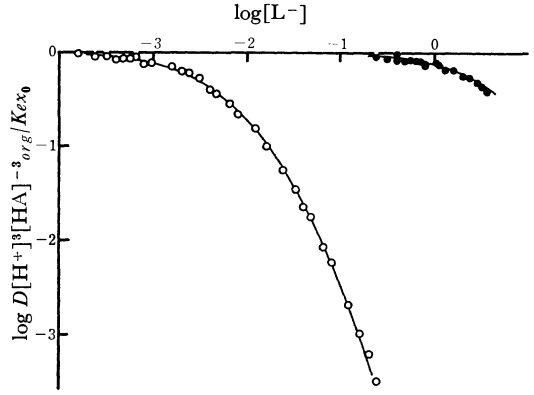

Fig. 3. Decrease in the extraction of indium(III) as a function of the ligand concentration.
● 0.2 M TTA-$CHCl_3$, 4 M $Na(NO_3, ClO_4)$
○ 0.02 M TTA-$CHCl_3$, 4 M $Na(SCN, ClO_4)$
The solid curves were calculated using the stability constants in Table 1.

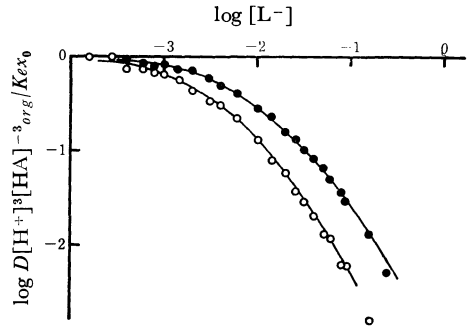

Fig. 4. Decrease in the extraction of indium(III) as a function of the ligand concentration
● 0.2 M TTA-$CHCl_3$, 4 M $Na(Br, ClO_4)$
○ 0.2 M TTA-$CHCl_3$, 4 M $Na(Cl, ClO_4)$
The solid curves were calculated using the stability constants in Table 1.

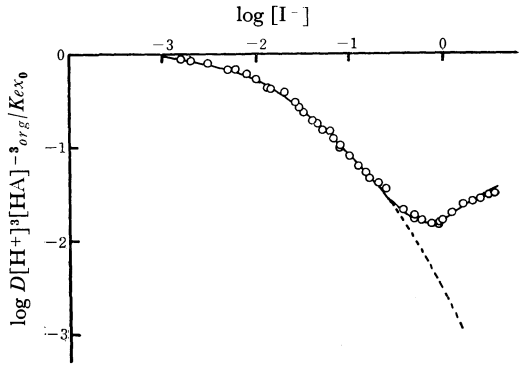

Fig. 5. Decrease in the extraction of indium(III) as a function of the iodide ion concentration (0.2 M TTA-$CHCl_3$, 4 M $Na(I, ClO_4)$).
The solid curve was drawn as:

$$y = \log(1+5[I^-]^3) - \log(1+93[I^-] + 190[I^-]^2 + 78[I^-]^3)$$

(The extraction of the InI_3 complex is taken into account for the calculation, *cf.* Eqs. (13) and (14)). The dotted curve was drawn as

$$y = -\log(1+93[I^-]+190[I^-]^2+78[I^-]^3)$$

(A statistical curve assuming no InI_3 extraction, *cf.* Eq. (8))

complexes of indium(III) with these ligands were determined by a curve-fitting method.[2,3] They are summarized in Table 1-a.

As may be seen from Fig. 5, the slope for the plot obtained in the iodide system decreases in a manner to be expected from Eq. (9) in the lower ligand concentration region; however, the slope increases as the ligand concentration increases, and finally it becomes positive after a pronounced

2) F. Rossotti and H. Rossotti, "The Determination of Stability Constants," McGraw-Hill, New York (1961).

3) T. Sekine, M. Sakairi and Y. Hasegawa, This Bulltin, **39,** 2141 (1966).

Table 1. Equilibrium constants for In(III) complexes

a) Stablity constants determined by TTA chelate extraction method

Ligand	$\log\beta_1$	$\log\beta_2$	$\log\beta_3$	Ligand	$\log\beta_1$	$\log\beta_2$	$\log\beta_3$
Cl^-	2.61	4.18	—	NO_3^-	−0.43	—	—
Br^-	2.36	3.16	—	ClO_3^-	−0.37	—	—
I^-	1.97	(2.28)*	(1.89)*	BrO_3^-	−0.12	—	—
SCN^-	2.44	4.11	5.10	IO_3^-	1.02	2.64	—

* These stability constant for the iodide complexes were calculated by Eq. (14) in which $K_{DM}=[InI_3]_{org}/[InI_3]=10^{-1.2}$ (0.2 M TTA-$CHCl_3$) had been introduced, but the values in Table 1-b are recommended instead of these constants.

b) Distribution constants and stability constants by TBP-adduct extraction method.

Ligand	$[TBP]_{hexane}$	$\log K_{DM}$	$\log\beta_1$	$\log\beta_2$	$\log\beta_3$	$\log\beta_4$	$\log\beta_5$
Br^-	0.1 M	0.11	~1.9*	3.32	3.24	2.18	—
I^-	0.01 M	1.63	~2.0*	2.18	2.20	—	—
SCN^-	0.01 M	0.70	~2.4*	4.11	5.10	4.57	5.45

* The values for the β_1 have not been determined accurately by this method.

minimum of D at about 0.7 M. From the statistical analysis of the data, it was concluded that the decrease in the distribution ratio in the lower iodide concentration region is caused by the iodide complex formation, but in the higher region the tris-iodide complex is assumed to be extracted into the chloroform phase. This may be the reason why the extraction curve deviates from that to be expected from Eq. (9).

The distribution ratio in this system may be described as:

$$D=\frac{[InA_3]_{org}+[InI_3]_{org}}{[In^{3+}]+[InI^{2+}]+[InI_2^+]+[InI_3]} \quad (13)$$

and from Eqs. (8) and (10), Eq. (13) can be described as:

$$D=\frac{K\varepsilon x_0[HA]^3_{org}\times[H^+]^{-3}+K_{DM}\beta_3[I^-]^3}{1+\beta_1[I^-]+\beta_2[I^-]^2+\beta_3[I^-]^3} \quad (14)$$

At first, the values β_1 and β_2 were determined, by the curve-fitting of the plot in the lower iodide concentration region in Fig. 5, to be $\log\beta_1=1.97$ and $\log\beta_2=2.28$. However, after several trials the data in Fig. 5 were concluded to be too errorneous to determine the β_3 and K_{DM} in Eq. (14). The equilibrium constants, β_2, β_3, and K_{DM}, only tentatively determined from the data in Fig. 5, are given in Table 1-a.

TBP Extraction. It was found that some of the tris-indium(III) complexes in the aqueous phase were extracted with TBP in hexane. Figure 6 shows the extraction of indium(III) from solutions containing 3 M sodium perchlorate and 1 M sodium bromide, iodide, or thiocyanate as a function of the TBP concentration in hexane. In Fig. 6 we can see that the slope of the log D *vs.* log $[TBP]_{org}$ plot ("e" in Eq. (16)) is +2 for the bromide and iodide systems, but +3 for the thiocyanate system. The dominant species in the organic phase may, then, be regarded as InL_3-

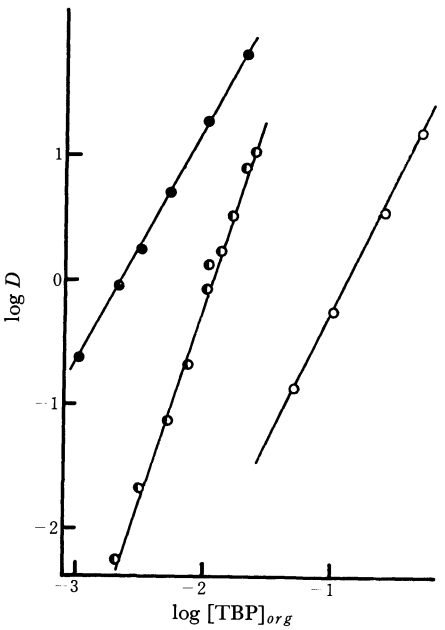

Fig. 6. TBP dependence of the distribution ratio.
Organic phase: hexane containing TBP.
Aqueous phase:
○ 1 M NaBr+3 M $NaClO_4$
● 1 M NaI+3 M $NaClO_4$
◐ 1 M NaSCN+3 M $NaClO_4$
The straight lines for the bromide and iodide plots show a slope of +2 and that for the thiocyanate plot shows a slope of +3.

$(TBP)_2$ for the former two systems and $InL_3(TBP)_3$ for the latter system. Figure 7 shows the log D *vs.* log $[L^-]$ plot when the ligand anion, L^-, is a bromide ion ($[TBP]_{org}=0.1$ M), an iodide ion ($[TBP]_{org}=0.01$ M), and a thiocyanate ion ($[TBP]_{org}=0.01$ M). The plot in Fig. 7 was explained in terms of the extraction of the neutral complex

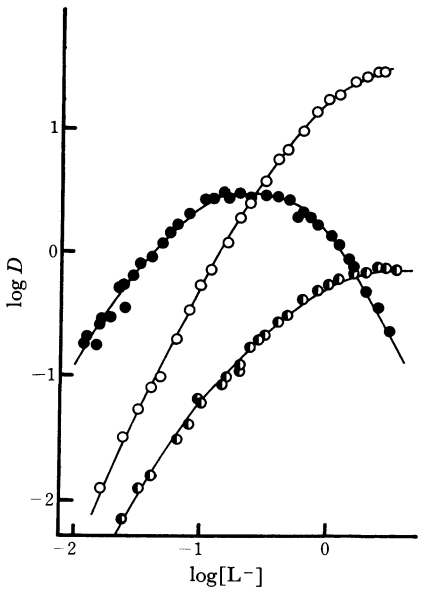

Fig. 7. TBP extraction of InL_3 complexes as a function of ligand concentrations.
○ 0.01 M TBP-hexane, 4 M Na(I, ClO_4)
◐ 0.1 M TBP-hexane, 4 M Na(Br, ClO_4)
● 0.01 M TBP-hexane, 4 M Na(SCN, ClO_4)
The solid curves were calculated using the stability constants in Table 1.

into the organic phase. The partition coefficient, K_{DM}, in Eq. (13) and the stability constants, β_n, were determined graphically by Eq. (14) as follows. In all cases, the slope of the log D *vs.* log [L^-] plot is smaller than +3 over the entire ligand concentration range studied; that is, even at the lowest concentration some of the indium ions are already complexed, and it is not possible to determine the β_1 accurately. For this reason, the values for β_1 determined by the TTA extraction method were introduced into Eq. (14); the rest of the stability constants and the partition coefficient, K_{DM}, were determined by a graphical method based on a successive approximation. The constants finally determined are listed in Table 1-b.

The extraction of indium(III) from 4 M Na(Cl, ClO_4) into hexane containing 0.1 M TBP was very poor over the entire chloride concentration range. When the TBP concentration was elevated, for example, to 1 M, a measurable extraction, one which was dependent on the chloride concentration, was observed. However, it was not possible to determine the stability constants of the chloride complexes from the analysis of these data by using Eq. (14), because those complexes which were extracted were assumed to be indium species containing perchlorate ions or both perchlorate and chloride ions.

Discussion

The Stabilities of the Complexes. It has previously reported[1] that indium(III) forms stable complexes with halide ions. The present results also indicate this. The stabilities of the halide complexes increase in the decreasing order of the ionic radii. Table 2 summarizes some of the earlier data on indium(III) complexes. The present values of log β_1 of chloride and bromide complexes seem to agree with the earlier data, but literature values of the stability constants of higher complexes are quite different from the present results. The literature constants for iodide complexes, especially, are not consistent.

It is remarkable that most of the earlier reports indicate the formation of such higher thiocyanate complexes as $In(SCN)_3$ and $In(SCN)_4^-$. The present results also indicate larger stabilities of the thiocyanate complexes.

The stabilities of indium(III) complexes with the halate and halide ions increase with the increase in the basicity of the ligands, as is usually to be expected. The nitrate ion, which has a

Table 2. Summary of the representative earlier work on the indium(III) halide and thiocyanate complexes

Ligand	log β_1	log β_2	log β_3	log β_4	Medium	Ref.
Cl^-	2.26	2.50	3.55	—	4 M Na(NO_3)	4
	2.15	3.59	—	—	2 M Na(ClO_4)	5
Br^-	1.36	1.52	—	—	4 M Na(NO_3)	4
	2.08	3.36	3.96	4.81	4 M Na(ClO_4)	6
I^-	1.00	2.26	—	—	2 M Na(ClO_4)	7
SCN^-	2.58	3.60	4.63	—	2 M Na(ClO_4)	7
	2.08	3.20	4.24	4.23*	2 M Na(ClO_4)	8

* log β_5=4.81, log β_6=4.84 are also reported.

4) Ya D. Fridman, R. I. Sorochan and N. V. Dolgashova, *Zhur. Neorg. Khim.*, **7**, 2127 (1962).
5) N. Sundén, *Svensk Kem. Tidskr.*, **66**, 20 (1954).
6) E. A. Burns and D. N. Hume, *J. Amer. Chem. Soc.*, **79**, 2704 (1957).
7) N. Sundén, *Svensk Kem. Tidskr.*, **66**, 50 (1954).
8) J. Selbin and L. H. Holmes, Jr., *J. Inorg. Nucl. Chem.*, **24**, 1111 (1962).

planar structure, forms the least stable indium complex among those studied; this may be explained in terms of the decrease in the polarity under steric conditions.

The Solvent Extractions for the Determination of the Stability Constants. As the distribution ratios in this study were always determined radiometrically, it was supposed that the distribution ratios would be accurate enough when they were between 10^{-2} and 10^{2}; thus, only the data in this range were used for the calculation and the discussion. The TTA extraction method may be applied to almost all complex formation systems, because it can determine the concentrations of the uncomplexed metal ion, which should decrease even upon the formation of a very weak complex. This method, however, is not appropriate for higher complexes with larger stability constants because, in such cases, the uncomplexed metal concentration is very low and, consequently, the distribution ratio is too low for an accurate determination ($D<10^{-2}$). Statistically, it would be possible to determine the distribution even under those conditions if the concentration of the chelating extractant is increased or if the hydration ion concentration is decreased ($[HA]_{org}/[H^+]$ is increased).

However, it is not always practically possible to carry out the above method practically because the aqueous chelate is very often formed in the higher $[HA]_{org}/[H^+]$ range, thus causing a systematic error in the stability constants.[4] Therefore, we should always confirm the constancy of K_{ex_0} value, $D_0[H^+]^3[HA]_{org}^{-3}$, in the absence of the ligand throughout the $[HA]_{org}/[H^+]$ region to be studied.

As may be seen from Fig. 1, the slope of the $\log D$ *vs.* $-\log [H^+]$ plot is $+3$ when the $\log D$ is smaller than $+1$. Thus, from Eq. (9) an accurate determination of the stability constants by the TTA method is possible when $10^3<(1+\sum\beta_n\cdot[L^-]^n)$. This fact and the results in Figs. 3 and 4 show that the TTA method can be applied only when the ligand concentration is lower than about 0.2 M.

When only the TTA method was used, no formation constants of the higher complexes could be determined, as may be seen in Table 1-a.

On the other hand, as may be seen from Fig. 7, the TBP method can cover the higher ligand-concentration region, where the TTA method can not be applied.

Statistically, it would be also possible to determine the complexes in the lower ligand-concentration range by the TBP method. Under such conditions, the distribution ratio should be very low if the TBP concentration is kept constant, as may be seen from Fig. 7. However, as may be seen in Fig. 6, the extraction of the TBP adduct increases when the TBP concentration is increased, and the distribution ratio becomes higher; consequently, a measurable distribution ratio should be obtained even in the ligand concentration range by the use of a high TBP concentration. However, when the TBP concentration is higher, the extraction of mixed complexes, such as $InX_n(ClO_4)_{3-n}$ or of such ion-pairs as $Na^+InX_4^-$ might be effected.

In the present paper, the ligand-concentration ranges studied have been too wide to allow for an accurate determination by using only one of these two methods. Only the combination of the two methods has made it possible to determine reasonable sets of stability constants for many such complexes. The agreement of the results obtained by these two different methods, shown in Tables 1-a and 1-b, is good.

The author is very grateful to Professor Tatsuya Sekine, of the Science University of Tokyo, for this invaluable discussions and helpful suggestions. She is also grateful to Mr. Akira Kaneko for his experimental aid.

BULLETIN OF THE CHEMICAL SOCIETY OF JAPAN VOL. 43 2671—2676 (1970)

Studies on Associated Solutions. II. Heat of Mixing of Methanol with Aliphatic Amines

Koichiro NAKANISHI, Hidekazu TOUHARA and Nobuatsu WATANABE

Department of Industrial Chemistry, Kyoto University, Sakyo-ku, Kyoto

(Received November 19, 1969)

The heat of mixing has been measured at 25.00°C and 45.00°C for binary mixtures of methanol with *n*-butylamine, diethylamine and triethylamine. A twin-type conduction calorimeter was used. All the systems exhibit large negative enthalpies of mixing, which become slightly less negative as the temperature increases. From the present results and vapor-liquid equilibrium data, the excess free energy and entropy of mixing at 25.00°C have been calculated for each system. The sign and magnitude of the excess functions were as follows: $H^M < TS^E < G^E < 0$ for methanol with *n*-butylamine and diethylamine, $G^E > 0$, $TS^E < H^M < 0$ for methanol with triethylamine. These facts were interpreted in terms of steric effects and specific solvation in the hydrogen bonding between hydroxyl group and amino bases.

Since Barker's theory based on a lattice model appeared,[1] theories of associated solutions have been developed by Prigogine and Defay,[2] Kehiaian and Sonkowaska-Kehiaian[3], and Renon and Prausnitz.[4] The theories interpreted with considerable success the behavior of excess functions of some types of associated solutions, such as those composed by an associated liquid (*e.g.*, aliphatic alcohol) and a nonpolar liquid (*e.g.*, hydrocarbon, CCl_4). Although there remains much ambiguity as to the species, role and behavior of the associated complex, we can visualize these solutions as being useful as a basis for more elaborate theoretical treatment.

However, for the solutions in which both components are associated, we have at present no satisfactory theory nor important experimental information. If the modes of association in both components are similar to each other, we may expect nearly ideal behavior for their mixtures. Mixtures of two aliphatic alcohols are such examples.[5] On the other hand, the mixtures with components each having a different mode of association exhibit peculiar anomalies in their thermodynamic properties. Aqueous solutions of alcohol are typical examples of those systems which show much complexity in their structural and thermodynamic properties.[6] We can expect many other combinations of associated liquids to show similar anomalies hitherto not yet fully understood.

Apart from general interest in associated solutions, we have paid attention in particular to the thermodynamic properties of aliphatic amine+alcohol solutions. It was found that a positive deviation from the ideal solution occurs with a methanol+triethylamine (Et_3N) solution, while binary solutions of methanol with *n*-butylamine (*n*-$BuNH_2$) and diethylamine(Et_2NH) have negative excess free energies.[7] On the other hand, the infrared spectra[8] indicate that the N–OH interactions in these solutions are always stronger than those for H–OH. Thus the question arises as to why G^E is positive, in other words, which of H^M and TS^E is responsible for the unexpected behavior of tertiary amine. For an answer, it is necessary to measure the heat of mixing and combine the results with G^E data in order to obtain the excess entropy value.

In this paper, we will report the data for the heat of mixing in binary mixtures of methanol with above mentioned three aliphatic amines. Based on these data and the values in literature, we will discuss the relationship between the thermodynamic properties and steric effects in hydrogen bond.

1) J. A. Barker, *J. Chem. Phys.*, **20**, 1526 (1952).
2) I. Prigogine and R. Defay, "Chemical Thermodynamics," Longmans Green, London (1954).
3) H. Kehiaian and K. Sonkowaska-Kehiaian, The series paper in *Bull. Acad. Polon. Sci., Ser. Sci. Chem.*, (1964).
4) H. Renon and J. M. Prausnitz, *Chem. Eng. Sci.*, **22**, 299 (1967).
5) W. D. Hill and M. van Winkle, *Ind. Eng. Chem.*, **44**, 205 (1952).
6) F. Franks and D. J. G. Ives, *Quart. Rev.* (London), **20**, 1 (1966).
7) a) J. L. Copp and T. J. V. Findlay, *Trans. Faraday Soc.*, **56**, 13 (1960). b) K. Nakanishi, H. Shirai and T. Minamiyama, *J. Chem. Eng. Data*, **12**, 591 (1967).
8) K. Nakanishi, S. Ichinose and H. Shirai, *Ind. Eng. Chem. Fundam.*, **7**, 381 (1968).

Experimental

Materials. All the samples were purified from the purest products commercially available according to the methods described in literature.[9] They were distilled twice before use under nitrogen with a 30 plate fractionating column. The purified samples showed no trace of impurity peaks on a gas chromatogram. Mercury was shaken with samples and then distilled.

Apparatus and Procedures. A twin-type conduction calorimeter based on the principle developed first by Tian and Calvet was used.[10] The apparatus, originally produced as model CM-502 by Oyodenki Kenkyusho Co., Japan, was modified for the purpose of detecting a very small amount of heat change. The calorimeter is surrounded by adiabatic materials and fixed in a submarine vessel. The submarine vessel is installed in a water thermostat, the temperature of which is kept within ±0.005°C. The temperature change due to the mixing is detected by the difference in thermal electromotive force of the thermoelement between the mixing vessel and the reference one. The electric potential is amplified by a dc-ac amplifier, the output signal of which is fed to an automatic pen recorder. With the present amplifying system we could detect the change $\pm 1 \times 10^{-6}$ V. The maximum sensitivity is about 1.5×10^{-4}°C under the present conditions. The experimental procedure was similar to that described previously.[11]

Calibration of Apparatus. In order to check the accuracy of the calorimeter, the heats of mixing were measured for the benzene + carbon tetrachloride system at 25.00°C. The results are given in Fig. 1, together with those obtained by Larkin and McGlashan,[12] and fitted by the method of least squares to an equation of the type

$$H^M = x_1x_2[A + B(x_1 - x_2) + C(x_1 - x_2)^2 + D(x_1 - x_2)^3] \quad (1)$$

where H^M is the enthalpy of mixing, x is the mole fraction and A, B, C and D are constants. The values of the constants are given in Table 1. The standard and maximum deviations of the experimental points from Eq. (1) are 0.58 and −1.1 cal/mol, respectively. Table 1 and Fig. 1 indicate that there is a reasonable agreement between our results and those of Larkin and McGlashan within 3 percent for x_1=0.1—0.9.

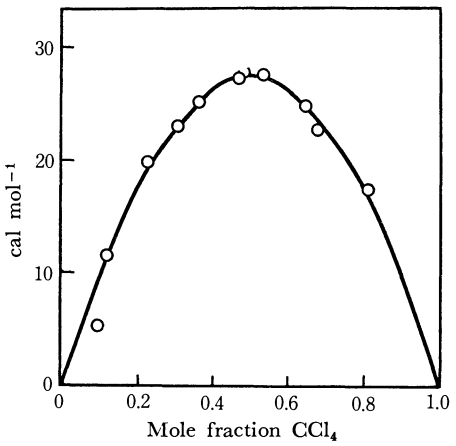

Fig. 1. Heat of mixing at 25.00°C: CCl_4 + Benzene.
—— Larkin and McGlashan
○ This Work

TABLE 1. VALUES OF CONSTANTS IN EQ. (1) FOR CARBON TETRACHLORIDE (1)+BENZENE (2) AT 25.00°C

Constants (cal/mol)	A	B	C	D
Larkin and McGlashan*	110.09	−5.58	10.27	3.35
This Work	109.79	−17.66	3.35	41.74

* Ref. 12.

Results and Discussion

Heat of Mixing. The data for the heats of mixing of binary solutions of methanol with n-$BuNH_2$, Et_2NH, and Et_3N at 25.00°C and 45.00°C are given in Tables 2 to 4 and are plotted in Fig. 2. The values of constants in Eq. (1) are given in Table 5, together with their estimated uncertainties δ, where x_1 refers to the mole fraction of methanol.

The results obtained in the present study together with a brief qualitative interpretation may be summarized as follows. 1) All the systems exhibit large negative enthalpy of mixing with the sequence of triethylamine, n-butylamine and diethylamine. The curves of H^M *vs.* x_1 (the mole

TABLE 2. HEAT OF MIXING FOR METHANOL (1) +n-BUTYLAMINE (2)

25.00°C		45.00°C	
x_1	$-H^M$ cal/mol	x_1	$-H^M$ cal/mol
0.199	453.9	0.102	229.0
0.207	483.5	0.263	618.2
0.244	569.4	0.382	769.8
0.284	605.6	0.521	884.5
0.358	773.9	0.618	843.1
0.391	801.1	0.706	768.4
0.445	857.1	0.722	742.3
0.469	878.0	0.874	425.8
0.508	886.7	0.901	311.5
0.804	602.6	0.918	280.1
0.900	305.4		

9) A. Weissberger and E. S. Porskauer, "Organic Solvents," Interscience Publishers Inc., New York (1955).

10) E. Calvet and H. Prat, "Recent Progress in Microcalorimetry," Pergamon Press, London (1963).

11) S. Murakami and R. Fujishiro, This Bulletin, **40**, 1784 (1967).

12) J. A. Larkin and M. L. McGlashan, *J. Chem. Soc.*, **1961**, 3425.

fraction of methanol) are slightly asymmetric, each having a minimum at about $x_1=0.6$. This is consistent with the postulate that H^M results from the contributions of two effects,[13] a positive one, due to the breaking of hydrogen bonds between alcohol molecules, and large asymmetrical negative one, due to the formation of hydrogen bonds between free alcohol and amine molecules. The latter is approximately symmetrical with respect to mole fraction.

Table 3. Heat of mixing for methanol (1) + diethylamine (2)

25.00°C		45.00°C	
x_1	$-H^M$ cal/mol	x_1	$-H^M$ cal/mol
0.239	655.5	0.302	762.3
0.269	701.1	0.341	858.1
0.285	803.3	0.445	1002.1
0.362	906.3	0.624	995.3
0.401	1011.1	0.701	880.2
0.515	1091.5	0.853	523.9
0.556	1096.5	0.908	350.0
0.598	1094.5		
0.605	1091.0		
0.667	1090.6		
0.706	1029.0		
0.740	900.7		
0.846	566.2		
0.932	256.3		

Table 4. Heat of mixing for methanol (1) + triethylamine (2)

25.00°C		45.00°C	
x_1	$-H^M$ cal/mol	x_1	$-H^M$ cal/mol
0.201	219.4	0.327	300.7
0.235	238.0	0.398	344.1
0.349	312.3	0.551	455.0
0.409	386.6	0.601	460.9
0.450	424.5	0.685	453.8
0.509	455.9	0.906	240.6
0.532	487.6	0.935	223.8
0.698	440.1		
0.867	303.9		
0.903	231.2		

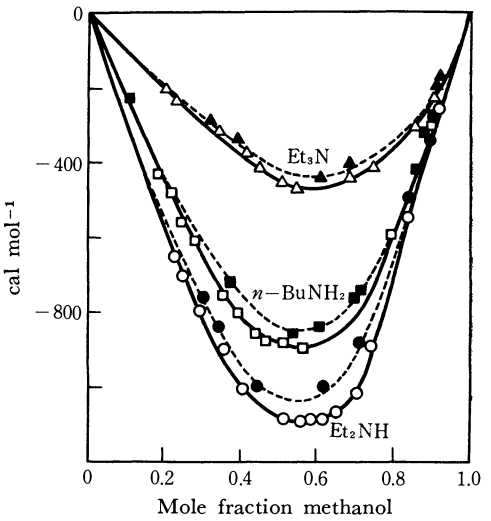

Fig. 2. Heat of mixing: MeOH + n-$BuNH_2$, Et_2NH, Et_3N.
—— 25°C, ---- 45°C

2) There is a slight tendency for H^M to become less negative as the temperature increases, that is, the excess heat capacity C_P^E is small and positive. The order of magnitude for C_P^E is less than 3 cal/deg. mole. This fact is in contrast to the system of alcohols[14] or aliphatic amines[15] with nonpolar liquids for which the temperature dependence of H^M is fairly large. This suggests that the hydrogen bonding OH–N is somewhat stronger than the OH–H hydrogen bonding in alcohols or NH–N in amines and that moderately stable complexes between alcohol and amine are formed. In fact,

Table 5. Values of constants in eq (1) for methanol (1)+aliphatic amine (2) and estimated uncertainties

Amine	Temp. (°C)	Constants (cal/mol)				δ
		A	B	C	D	
n-Butylamine	25.00	−3617.1	−1095.6	+852.9	+997.5	2.1
	45.00	−3537·9	−588.9	+677.7	−219.5	2.2
Diethylamine	25.00	−4457.1	+47.4	+2606.3	−2383.1	3.1
	45.00	−4163.2	−553.1	+1568.0	−1124.3	0.8
Triethylamine	25.00	−1776.4	−1020.4	−274.4	+230.8	2.4
	45.00	−1676.5	−678.3	+1120.4	+2900.6	4.1

13) J. S. Rowlinson, in "Hydrogen Bonding," paper for symposium, Ljubljana, Pergamon Press, London (1957), p. 423.
14) J. E. A. Ottersted and R. W. Missen, *Trans. Faraday Soc.*, **58**, 879 (1962).
15) H. Wolff and R. Wirtz, *Ber. Bunsenges. Phys. Chem.*, **72**, 101 (1968).

Lambert and Zeegers-Huyskens[16] have shown calorimetrically that there is a considerably large association energy for some aliphatic alcohols with aliphatic amines.

Other Excess Functions. The excess free energy of mixing has been calculated from isobaric vapor-liquid equilibrium data[8] by means of equations

$$\mu_1^E = RT \ln (y_1P/x_1P_1) + (P_1 - P)(V_1 - B_{11}) + 2P\delta B_{12}y_2^2 \quad (2)$$

$$\mu_2^E = RT \ln (y_2P/x_2P_2) + (P_2 - P)(V_2 - B_{22}) + 2P\delta B_{12}y_1^2 \quad (3)$$

$$G^E = x_1\mu_1^E + x_2\mu_2^E \quad (4)$$

In the present case, the correction factors due to the vapor phase imperfection can be neglected.[8] The G^E values at 25.00°C can be evaluated from these data, since the heat of mixing has been measured as a function of temperature. For this purpose, the Gibbs-Helmholtz equation was used in the form

$$(G^E/T)_{T_2} - (G^E/T)_{T_1} = -\int_{T_1}^{T_2} H^M dT/T^2 \quad (6)$$

The excess entropies of mixing at 25.00°C have been calculated from the analytically smoothed values of H^M and G^E.*1

The results for each system are shown in Figs. 3—5. We see that the sign and magnitude of excess functions are as follows: $H^M < TS^E < G^E < 0$ for methanol with *n*-butylamine and diethylamine, $G^E > 0$, $TS^E < H^M < 0$ for methanol with triethylamine. For all the systems, both H^M and S^E exhibit large negative deviations, while the absolute value of G^E is relatively small owing to the counterbalance of two contributions, H^M and TS^E.

On the other hand, a large volume contraction has been observed in methanol solution with aliphatic amines. The absolute values of excess volumes of mixing were in the increasing order of *n*-$BuNH_2$, Et_3N and Et_2NH.[17] This sequence is not same as that for H^M.

Steric and Solvation Effects on H^M. The above results reveal that the thermodynamic properties of MeOH+Et_3N solution are somewhat anomalous, that is, G^E becomes positive because the absolute value of TS^E is larger than that of

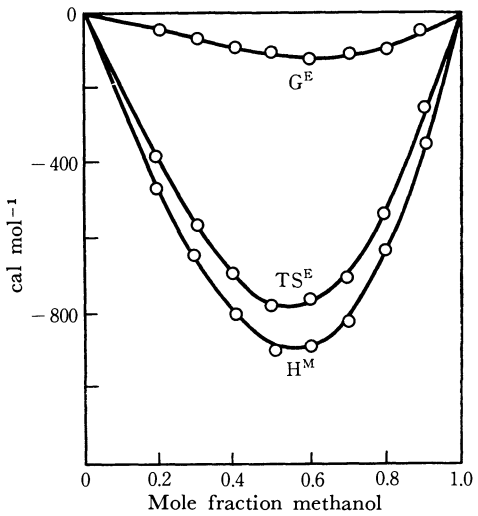

Fig. 3. Excess thermodynamic functions at 25.00°C: MeOH + *n*-$BuNH_2$.

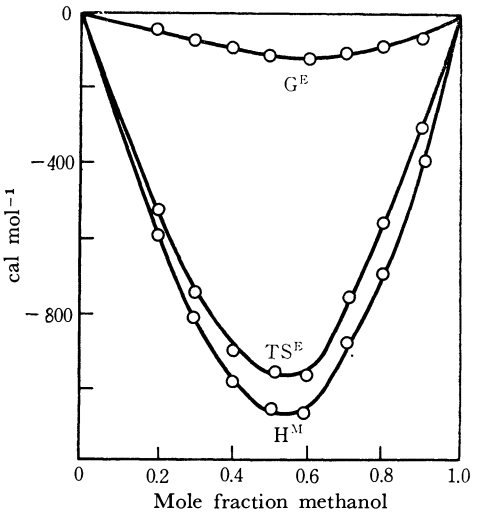

Fig. 4. Excess thermodynamic functions at 25.00°C: MeOH + Et_2NH.

H^M. In the following discussions, we will compare this with other evidences for the purpose of examining the effects of geometric characteristics on physical and chemical properties.

The specific interaction between alcohol and amine, which makes the values of H^M negative, is due to a strong hydrogen bond between hydroxyl and amino groups. This interaction can be considered as the reaction between alcohol as a Lewis acid and amine as a Lewis base. An absolute Lewis base strength of aliphatic amines may be measured by the ionization potential, I, and the acidic dissociation constant, p*Ka*. Kaufman and Koski[18] estimated the ionization potential of alipha-

16) L. Lambert and T. Zeegers-Huyskens, *J. Chim. Phys.*, **60**, 435 (1963).

*1 Strictly speaking, evaluation of S^E at 25.00°C should be made with the G^E values obtained at the same temperature. With lack of such data, we have used those at varying temperatures. However, for the present purpose of comparing the sign and the relative magnitude of excess functions, this may be justified since the excess heat capacity of the present system is very small as evident from Tables 2—4.

17) K. Nakanishi and H. Shirai, This Bulletin, **43**, 1643 (1970).

18) J. J. Kaufman and W. S. Koski, *J. Amer. Chem. Soc.*, **82**, 3262 (1960).

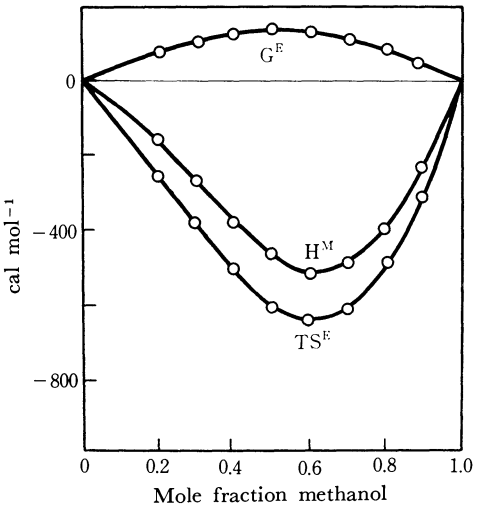

Fig. 5. Excess thermodynamic functions at 25.00°C: MeOH + Et_3N.

tic amines and defined the order as follows: $NH_3 < RNH_2 < R_2NH < R_3N$. The order is coincident with that for p*Ka* of aliphatic amines predicted by induced effect.

On the other hand, in hydrogen bonding solvents such as water or dioxane, the base strength or reactivity of amine with H^+ does not vary in the same manner.[19] We see that the order for this reactivity is in accordance with that for H^M obtained in the present work:

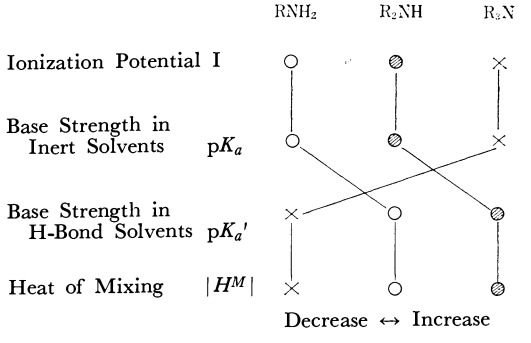

The phenomena, *viz.*, inversions of the sequence, have been ascribed to the steric strains and/or specific solvation effects.[20-22]

Brown *et al.*[23-25] have proposed that there should be two kinds of steric effect in determining the dissociation constant of amine. They defined them as B-strain and F-strain. The term, B-strain,[23] refers to the interference which is localized at the back of the molecule, and the term, F-strain,[24-25] refers to the repulsions due to the bulky alkyl groups in an ion pair. In the present case, rather bulky ethyl groups attached to the small nitrogen atom in Et_3N molecule tend to repel each other. This sets up the B-strain which reduces the stability of the hydrogen bonded complex, but co-ordination of an acidic proton of alcohol with the nitrogen atom of Et_3N does not cause an appreciable F-strain. Thus a certain amount of B-strain may be responsible for the relative decrease of alcohol-tertiary amine interaction, and the negative contribution to H^M will become smaller.

Another important factor which might influence H^M is the specific solvation. The amino hydrogen is considered to be a weak acidic proton, and co-ordinates to oxygen atom of alcohol. The interaction due to solvation is not as large compared with hydrogen bonding between hydroxyl group and amino bases, but it would affect the stability of hydrogen bonded complexes to some extent. Since tertiary amine has no acidic proton, its proton accepting ability is exceedingly small in comparison with that of primary or secondary amine. Thus, the two effects might be responsible for the smaller H^M of alcohol with tertiary amine system, though it is impossible to determine the dominant factor. Since no inversion in the order between R_2NH and RNH_2 is observed, steric and other effects for these two kinds of amine may be negligible.

The negative contribution discussed above is even larger than positive contributions due to the break-up of self-association of both components. In the present case, the contribution due to the break-up of alcohol structure is common to all the systems. A possible positive contribution due to the break-up of amine association should be proportional to the amino hydrogen contact number.[26] Since this contribution is negligible for Et_3N, the H^M value with Et_3N is expected to become more negative. The fact that this is not the case furnishes another support to the above interpretation.

There have been many works on the steric effects of hydrogen bonding in sterically hindered alcohols and phenols.[27-30] The low equilibrium constants of self-association have often been as-

19) R. G. Peason and D. C. Vogelsong, *J. Amer. Chem. Soc.*, **80**, 1038 (1958).
20) D. H. Everett and W. F. K. Wynne-Jones, *Proc. Roy. Soc.* (London), **A177**, 499 (1941).
21) R. G. Peason, *J. Amer. Chem. Soc.*, **70**, 204 (1948).
22) A. F. Trotman-Dickenson, *J. Chem. Soc.*, **1949**, 1293.
23) H. C. Brown, H. Bartholomay, Jr, and M. D. Taylor, *J. Amer. Chem. Soc.*, **66**, 435 (1944).
24) H. C. Brown, *J. Chem. Soc.*, **1956**, 1248.
25) H. C. Brown, *J. Amer. Chem. Soc.*, **67**, 1452 (1945).
26) K. Sonkowska-Kehiaian, K. Orzel and H. Kehiaian, *Bull Acad. Polon. Sci., Ser. Sci. Chem.*, **14**, 711 (1966).
27) B. G. Somers and H. S. Gutowsky, *J. Amer. Chem. Soc.*, **67**, 303 (1945).
28) I. Yamaguchi, This Bulletin, **34**, 451 (1961).
29) S. Singh and C. N. R. Rao, *J. Phys. Chem.*, **71**, 1074 (1967).
30) S. Singh and C. N. R. Rao, *J. Amer. Chem. Soc.*, **88**, 2142 (1966).

cribed exclusively to entropy factors. In the present case where the alkyl groups attached to nitrogen atom are not too bulky, an enthalpy factor seems to be responsible for anomalous behavior of excess functions.

The authors thank Mr. Isao Matsumoto for his assistance in some of the experiments.

BULLETIN OF THE CHEMICAL SOCIETY OF JAPAN VOL. 43 2676—2679 (1970)

The Dipole Moments of α,ω-Alkanediols

Yoshio Toshiyasu,*1 Ko Kimura*2 and Ryoichi Fujishiro*2

Science Education Institute of Osaka Prefecture, Sumiyoshi-ku, Osaka

(Received January 24, 1970)

The electric dipole moments of α,ω-alkanediols such as HO-$(CH_2)_n$-OH (n being varied from 2 to 5) were measured both in dioxane and in a mixed solvent of dioxane with carbon tetrachloride at 25°C. The observed dipole moments increase with the increasing n until $n=4$, and then decrease for $n=5$, while the calculated dipole moments based on the vector addition of group moments on the assumption of the random coil model for alkane chains increase monotonously as n increases from 2 to 5. It is concluded that for both propanediol and butanediol the conformations forming the intramolecular hydrogen-bond which have the larger dipole moments contribute appreciably to the observed dipole moments. The dipole moment of pentanediol is close to the calculated one for the random coil model, whereas that of ethylene glycol suggests the existence of the intramolecular hydrogen-bond. Population analysis of the hydrogen-bonded species in solutions is also given.

The electric dipole moments of molecules with multiple degrees of freedom of internal rotation were already discussed.[1] Recently, the anomalous dipole moments of 1,4-dichlorobutane or 1,4-dibromobutane were reported by Thompson and Hanson,[2] and led to the conclusion that the steric hindrance between two halogen atoms attached at the end positions of the aliphatic chain excludes some of the conformations which have larger dipole moments. The dipole moments of these compounds are, therefore, anomalously small.

When the two halogen atoms in 1,4-dihalogenobutane are replaced by hydroxy groups, the intramolecular hydrogen-bond may be formed. Study of the intramolecular hydrogen-bonding in solutions is carried out extensively by help of the infrared absorption spectra, but α,ω-alkanediols dissolve scarcely in solvents commonly used in the infrared absorption study. Nevertheless, the formation of the intramolecular hydrogen-bond for some of α,ω-alkanediols in solutions is inferred from the infrared absorption[3] or from NMR spectra[4] by making suitable device. It is interesting and valuable to investigate the intramolecular hydrogen-bond in mixed solvents from the view point of dipole moments.

In this paper, the electric dipole moments of α,ω-alkanediols such as HO-$(CH_2)_n$-OH (n being varied from 2 to 5) are measured and discussed in connection with the intramolecular hydrogen-bonding.

Experimental

All the alkanediols used in this work were purified by the fractional distillation through a 100 cm column packed with stainless-steel helices, dried over molecular sieves and distilled in vacuum. Dioxane used as a solvent was refluxed over fresh sodium for a few days and distilled through the same column as that just mentioned. A mixed solvent of dioxane with carbon tetrachloride was also used, when necessary. Carbon tetrachloride was purified by shaking it with alcoholic sodium hydroxide, dried, and then distilled through

*1 This paper is based on a thesis submitted by Y. Toshiyasu to the Graduate School of Osaka City University, in partial fulfillment of the requirements for the degree of Master of Science.

*2 Permanent address: Department of Chemistry, Faculty of Science, Osaka City University, Sumiyoshi-ku, Osaka.

1) C. P. Smyth, "Dielectric Behavior and Structure, McGraw Hill, New York, N. Y. (1955), p. 368; J. W. Smith, "Electric Dipole Moments" Butterworths Scientific Publications, London (1955), p. 292.

2) H. B. Thompson and S. L. Hanson, *J. Phys. Chem.*, **65,** 1005 (1961).

3) L. P. Kuhn, *J. Amer. Chem. Soc.*, **74,** 2492 (1952).

4) K. Fukui, T. Yonezawa, H. Saito and S. Matsuoka, This Bulletin, **38,** 1431 (1965).

the same column.[5]

Measurements of the dielectric constants, ε's and the specific volumes, ρ's were carried out by the same apparatus and method as in the previous work.[6] All the data were obtained at 25±0.02°C. In the present investigation, the weight fractions, w's of solutes range over from zero to about 0.02.

Results

The observed values of ε's and of ρ's are fairly well expressed by the linear equations of w's. The molecular polarizations, p's were obtained from these experimental data according to Halverstadt-Kumler's method.[7] The molecular refractions, R_D's for the sodium D line were calculated on the assumption of the additivity of bond refractions, and distortion polarizations were assumed to be equal to $1.05\times R_D$. The polarization values and the observed dipole moments, μ's are tabulated in Table 1, together with the linear equations of ε's and ρ's to w's. Data for ethyl alcohol are also given in Table 1.

Table 1. Dipole moment data

	Dioxane	A mixed solvent*
$n=2$	$\varepsilon=2.2079+10.61w$	$\varepsilon=2.2470+14.48w$
	$\rho=0.9729-0.08w$	$\rho=0.7123+0.20w$
	$p=124.5$ cc	$p=123.0$ cc
	$R_D=14.4$ cc	$R_D=14.4$ cc
	$\mu=2.31$ D	$\mu=2.30$ D
$n=3$	$\varepsilon=2.2090+10.53w$	$\varepsilon=2.2480+15.60w$
	$\rho=0.9726-0.03w$	$\rho=0.7126+0.29w$
	$p=152.6$	$p=163.0$
	$R_D=19.1$	$R_D=19.1$
	$\mu=2.55$	$\mu=2.65$
$n=4$	$\varepsilon=2.2061+9.10w$	$\varepsilon=2.2470+13.68w$
	$\rho=0.9726+0.01w$	$\rho=0.7127+0.29w$
	$p=160.7$	$p=172.6$
	$R_D=23.7$	$R_D=23.7$
	$\mu=2.58$	$\mu=2.69$
$n=5$	$\varepsilon=2.2083+7.46w$	$\varepsilon=2.2476+10.48w$
	$\rho=0.9725+0.04w$	$\rho=0.7117+0.31w$
	$p=158.4$	$p=160.3$
	$R_D=28.3$	$R_D=28.3$
	$\mu=2.51$	$\mu=2.53$
C_2H_5OH**	$\varepsilon=2.2095+9.40w$	$\varepsilon=2.2725+6.83w$
	$\rho=0.9726+0.04w$	$\rho=1.14619+0.19w$
	$p=77.8$	$p=77.7$
	$R_D=12.9$	$R_D=12.9$
	$\mu=1.77$	$\mu=1.77$

* A mixed solvent is composed of one volume of dioxane and two volumes of carbon tetrachloride.

** Measurements were carried out not in the mixed solvent but in both dioxane (the left column) and benzene (the right column).

Discussion

The mean square dipole moment, $\overline{\mu^2}$ of α,ω-disubstituted alkanes can be written on the assumption of the vector addition as

$$\overline{\mu^2}=\mu_1^2+\mu_n^2+2\overline{(\vec{\mu}_1\cdot\vec{\mu}_n)} \quad (1)$$

where $\vec{\mu}_1$ and $\vec{\mu}_n$ mean moment vecotrs of polar groups located at the both ends, and μ_1 and μ_n scalar quantities of $\vec{\mu}_1$ and of $\vec{\mu}_2$, respectively. The third term of Eq. (1) in the right hand side may be easily calculated by the use of transformation matrix.[8] The coordinate system is chosen as

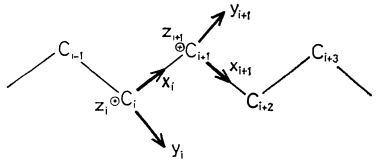

Fig. 1. The coordinate system.
⊕ Upwards from the plane
⊙ Downwards from the plane

follows, which is depicted in Fig. 1: the x_i axis of the origin C_i is taken in the direction of C_i-C_{i+1} bond of a chain, the z_i axis in the direction of the vector product of C_i-C_{i+1} and C_{i-1}-C_i, and the y_i axis in the direction to constitute the right-handed coordinate system. The coordinate system of the origin C_{i+1} is chosen in the same way as already mentioned. The transformation from the coordinate system$(x_{i+1}, y_{i+1}, z_{i+1})$ to (x_i, y_i, z_i) is carried out by help of the following transformation matrix:

$$T_{i,i+1}=\begin{pmatrix}\cos\chi & \sin\chi & 0\\ \sin\chi\cos\varphi_i & -\cos\chi\cos\varphi_i & -\sin\varphi_i\\ -\sin\chi\sin\varphi_i & \cos\chi\sin\varphi_i & -\cos\varphi_i\end{pmatrix} \quad (2)$$

where the valence angles$(\pi-\chi)$ are assumed to be tetrahedral, and φ_i is an angle of the internal rotation measured from the *trans*-form about C_i-C_{i+1} bond. The successive operation of this transformation on the third term of Eq. (1) gives

$$\overline{\mu^2}=\mu_1^2+\mu_n^2+2\overrightarrow{\mu_1(T_{1,2}\cdots\cdots T_{n-1,n})\mu_n}. \quad (3)$$

If all the internal rotations are free, the mean square dipole moment of α,ω-alkanediol becomes independent on φ_i's, and is given by[1]

5) A. Weissberger *et al.*, "Organic Solvents," Interscience Publishers, New York, N. Y. (1955).

6) K. Kimura and R. Fujishiro, This Bulletin, **39,** 608 (1966).

7) I. F. Halverstadt and W. D. Kumler, *J. Amer. Chem. Soc.*, **64,** 2988 (1942).

8) S. Oka, *Proc. Phys. Math. Soc. Japan*, **24,** 657 (1942); J. Marchal and H. Benoit, *J. Chim. Phys.*, **52,** 818 (1955); M. V. Volkenstein, "Configurational Statistics of Polymer Chains," Interscience Publishers, New York, N. Y. (1963).

$$\overline{\mu^2} = 2\mu_1^2(1-\cos^2\theta\cos^n\chi) \quad (4)$$

where μ_1 is the magnitude of the moment vector $\vec{\mu}_1$ for a HO-C group and is assigned to be 1.77D[1),9)] and θ is an angle between the moment vector $\vec{\mu}_1$ and the position vector, $\overrightarrow{C\text{-}O}$ bond and is equal to 62°. Dipole moments calculated by the use of Eq. (4) are summarized in Table 2, together with those obtained from Eq. (3) by assigning appropriate angles to φ_i's, which are determined by the intramolecular hydrogen-bonded conformations. Tables 1 and 2 show that the observed dipole moments increase with the increasing n until n=4, and then decrease for n=5, whereas the calculated moments on the assumption of the random coil model increase monotonously, as is expected from Eq. (4), when n increases from 2 to 5. This phenomenon is observed remarkably in the mixed solvent of dioxane with carbon tetrachloride, as is shown in Table 1. Agreement between the observed value and the calculated average one is good only for n=5 irrespective of solvents used in this research. If it is assumed that the vector addition of group moments is valid even for the hydrogen-bonded system, a pentanediol molecule forms no intramolecular hydrogen-bond at all in solutions. This result is supported by the infrared absorption spectra,[3)] and also by NMR spectra.[4)] On the contrary, the observed dipole moments for 1,3-propanediol and for 1,4-butanediol are larger than the calculated average moments. Difference between the calculated average moment and the calculated moment for the intramolecular hydrogen-bonded conformation amounts to about 1D for the former and to about 0.5D for the latter. Small but not negligible increase of the observed dipole moments over the calculated average moments is due to the appreciable contribution of the intramolecular hydrogen-bonded conformations to the observed dipole moments. The same kind of research as mentioned above was carried out recently by Toshiyasu and Fujishiro[10)] both for 1,3-dimethoxypropane or 1,4-dimethoxybutane and for monomethyl ether of 1,3-propanediol or 1,4-butanediol, although the former corresponds to the case of α, ω-dihalogenoalkane reported by Thompson *et al.*,[2)] and the latter to the present research. Hence, it is possible to infer the existence of the intramolecular hydrogen-bond in solutions from measurements of dipole moments together with the calculations of dipole moments based on the vector addition of group moments both for the random coil model and for the intramolecular hydrogen-bonded conformations. The intramolecular hydrogen-bond for ethylene glycol in solutions was confirmed by the infrared absorption spectra, but any information can not be obtained from dipole moment data, as is seen from Table 2.

Table 2. Calculated dipole moments

	The average moment μ_r (the random coil model)	The moment for the intramolecular hydrogen-bond conformations* μ_h	
$n=2$	2.47D	TGG' (TG'G)	2.51D
$n=3$	2.48	TGG'G (TG'GG')	3.54
$n=4$	2.49	TGG'GG' (TG'GG'G)	3.06
		GGG'GG' (G'G'GG'G)	
$n=5$	2.50		

* T and G represent *trans*- and *gauche*-form, respectively.

Population analysis of rotational isomers in solutions is performed by the help of the theory of chemical equilibrium. According to the statistical thermodynamic treatment of associated solutions by Saroléa-Mathot,[11)] the partition function Ω is given by

$$\Omega = \phi_a^{N_a}\phi_d^{N_d}\phi_c^{N_c}\frac{(x-z-u+N_d+N_c)!}{x!y!z!u!v!(N_d-y-2\cdot z-v)!N_c!} \times \exp[-1/kT\{x_1f_1+x_2f_2+x_3f_3 + (y+2\cdot z+v)\Delta E_{\mathrm{I}} + (u+v)\Delta E_{\mathrm{II}}\}] \quad (5)$$

where ϕ_a, ϕ_d, and ϕ_c represent the internal partition functions of alkanediols, dioxane and carbon tetrachloride, respectively, and N_a, N_d, and N_c are the number of molecules corresponding to each suffix. The total number of molecules for alkanediols, N_a is divided into five molecular species, that is,

$$N_a = x + y + z + u + v$$

where x is the number of molecules with the free hydroxy groups without any hydrogen-bond, y the number of molecules with one free hydroxy group and the other hydrogen-bonded with dioxane, z the number of molecules with both hydrogen-bonded with dioxane, u the number of molecules with one free hydroxy group and the other forming the intramolecular hydrogen-bond, and v the number of molecules with one hydrogen-bonded with dioxane and the other forming the intramolecular hydrogen-bond. Interaction parameters f_1, f_2, and f_3 are defined as follows:

9) In order to confirm the value assigned by Smyth, the dipole moment measurement for ethyl alcohol was carried out in the same condition as that for α, ω-alkanediols. The observed value is fairly close to that given by Smyth, as is shown in Table 1.

10) Y. Toshiyasu and R. Fujishiro, to be published.

11) L. Saroléa-Mathot, *Trans. Faraday Soc.*, **49**, 8 (1953).

$$\left.\begin{aligned} f_1 &= f_{cd} - 1/2(f_{cc}+f_{dd}) \\ f_2 &= f_{ad} - 1/2(f_{dd}+f_{aa}) \\ f_3 &= f_{ac} - 1/2(f_{cc}+f_{aa}) \end{aligned}\right\} \quad (6)$$

where f_{ij} is the interaction energy due to dispersion force between two contact molecules i and j. The quantities x_1, x_2, and x_3 represent the number of contact pairs corresponding to each suffix. ΔE_{I} and ΔE_{II} are energies of the intermolecular hydrogen-bond and of the intramolecular hydrogen-bond, respectively. Equality of the chemical potentials of all species in the equilibrium state gives equilibrium concentrations of all species as functions of ΔE_{I}, ΔE_{II}, and $C=N_d/(N_d+N_c)$. On the assumption ($N_a \ll N_d$ or N_c) in dilute solutions, one obtains

$$\left.\begin{aligned} x &= N_d/[1+\exp(-\Delta E_{\mathrm{II}}/\boldsymbol{k}T) + C\cdot\exp(-\Delta E_{\mathrm{I}}/\boldsymbol{k}T) \\ &\quad \times \{1+\exp(-\Delta E_{\mathrm{II}}/\boldsymbol{k}T)\}+C^2\cdot\exp(-2\cdot\Delta E_{\mathrm{I}}/\boldsymbol{k}T)] \\ y &= N_d/[1+\exp(-\Delta E_{\mathrm{II}}/\boldsymbol{k}T) + 1/c\cdot\exp(\Delta E_{\mathrm{I}}/\boldsymbol{k}T) \\ &\quad \times \{1+\exp(-\Delta E_{\mathrm{II}}/\boldsymbol{k}T)\} + c\cdot\exp(-\Delta E_{\mathrm{I}}/\boldsymbol{k}T)] \\ z &= N_d/[1+1/c\cdot\exp(\Delta E_{\mathrm{I}}/\boldsymbol{k}T)\{1+\exp(-\Delta E_{\mathrm{II}}/\boldsymbol{k}T)\} \\ &\quad + 1/c^2\cdot\exp(2\cdot\Delta E_{\mathrm{II}}/\boldsymbol{k}T)\{1+\exp(-\Delta E_{\mathrm{II}}/\boldsymbol{k}T)\}] \\ u &= N_d/[1+\exp(\Delta E_{\mathrm{II}}/\boldsymbol{k}T)+c\cdot\exp(-\Delta E_{\mathrm{I}}/\boldsymbol{k}T) \\ &\quad \times \{1+\exp(\Delta E_{\mathrm{II}}/\boldsymbol{k}T)\} \\ &\quad + c^2\cdot\exp\{(\Delta E_{\mathrm{II}}-2\cdot\Delta E_{\mathrm{I}})/\boldsymbol{k}T\}] \\ v &= N_d/[1+\exp(\Delta E_{\mathrm{II}}/\boldsymbol{k}T) + 1/c\cdot\exp(\Delta E_{\mathrm{I}}/\boldsymbol{k}T) \\ &\quad \times \{1+\exp(\Delta E_{\mathrm{II}}/\boldsymbol{k}T)\} \\ &\quad + c\cdot\exp\{(\Delta E_{\mathrm{II}}-\Delta E_{\mathrm{I}})/\boldsymbol{k}T\}] \end{aligned}\right\} \quad (7)$$

Then, the observed dipole moments are approximately given by

$$\mu^2_{\mathrm{obs}} = (x+y+z)\mu_r^2 + (u+v)\mu_h^2 \quad (8)$$

where μ_r and μ_h represent the average dipole moment for the random coil model and that for the intramolecular hydrogen-bonded conformation, respectively, which are given in Table 2. When ΔE_{I} is assigned to be -4 kcal/mol,[12] a value of ΔE_{II} for $n=3$ and that for $n=4$ are -2.2 kcal/mol and -2.9 kcal/mol, respectively, each of which is close to already reported value[13], *i.e.*, -2.1 kcal/mol for $n=3$ and -2.7 kcal/mol for $n=4$. Population analysis in solutions was performed by using these energy values. Table 3 gives the equilibrium concentrations of all species present in solutions. This table is suggestive in giving information about what kind of molecular species is predominant in a solvent: for $n=3$, the species v is scarcely present in pure dioxane, but for $n=4$, it amounts to about 13% even in pure dioxane, and the amount of species v becomes significant in a mixed solvent(1 volume dioxane to 2 volumes carbon tetrachloride) both for $n=3$ and for $n=4$.

Table 3. Mole fractions of species present in solutions

		x	y	z	u	v
$n=3$	Dioxane	0	0.001	0.953	0	0.046
	A mixed solvent	0	0.003	0.880	0	0.117
$n=4$	Dioxane	0	0.001	0.865	0	0.134
	A mixed solvent	0	0.002	0.696	0.001	0.301

In conclusion, dipole moment study makes it possible in some cases of α,ω-alkanediols to confirm the existence of the intramolecular hydrogen-bonded species and to do population analysis of all species in solutions.

12) G. C. Pimentel and A. L. McClellan, "Hydrogen Bonding," W. H. Freeman and Company, Reinhold Publishing Corp., New York N. Y. (1960).

13) L. P. Kuhn and R. A. Wires, *J. Amer. Chem. Soc.*, **86**, 2161 (1964).

BULLETIN OF THE CHEMICAL SOCIETY OF JAPAN VOL. 43 2680—2689 (1970)

Kinetic Studies of Adsorbed Films of Tritium-labelled Sodium Stearate at the Air/Water Interface

Tsutomu SEIMIYA

Department of Chemistry, Faculty of Science, Tokyo Metropolitan University, Setagaya, Tokyo

(Received January 30, 1970)

The adsorption of tritium-labelled sodium stearate at the air/water interface was directly measured radiometrically using an ultra-thin-windowed Geiger-Müller tube for varying soap concentrations, pH values, and temperatures. The changes in the amount of adsorption and in the surface tension were simultaneously traced with the lapse of time. The pressure-area curve was then obtained by the successive plotting of the surface pressure against the area at the same aging; the curve at equilibrium was also obtained. Thus, the pressure-area relationship of the adsorbed monolayer was automatically measured during the course of adsorption approaching equilibrium. A close resemblance was observed between the monolayer of stearic acid on neutral water and the adsorbed films on the stearate solution of pH values from 8.85 to 9.30 at 30°C. The amount of adsorption measured for an alkaline solution often exceeds the value to be expected from the saturation value for a completely-ionized stearate monolayer. The pressure-area characteristics suggested a transition from the condensed state of the adsorbed film at a higher surface concentration to an expanded state at a lower concentration. It was also confirmed, by measuring the amount of adsorption in the atmospheres of both nitrogen and air containing carbon dioxide, that the atmospheric carbon dioxide acts to increase the adsorption of stearic acid on the aqueous surface. The diffusion coefficient of the adsorbing solute, calculated from the initial rate of adsorption, showed a smaller value than that obtained by conductometric measurements.

A number of investigations have been presented by many workers into the properties of adsorbed monolayers at both air/water and oil/water interfaces. Efforts have also been made to obtain the pressure-area relationship for the adsorbed monolayers of soluble, surface-active substances. In some of these studies, a monolayer was spread on an aqueous surface,[1,2] and from the observed surface pressure changes against the time, the surface pressure extrapolated to time zero was plotted against the area per molecule, assuming that no molecule was lost by desorption or evaporation.

In other studies the pressure-area relationships were obtained by spreading the film substances on aqueous substrates that contained excess salt, thus preventing the desorption of film molecules by decreasing the solubility of the film substance.[3-8] These methods may be convenient and easy to practise for the study of the soluble monolayer, but at the same time they involve several disadvantages. The major disadvantages exist in using a sufficiently concentrated solution of inorganic salt and/or a solution of a restricted pH as a substrate, especially for a monolayer of an ionizable nature. Another question is an uncertainty arising as to the amount of film substances remaining on the surface. For the theoretical treatment of the adsorbed film, it is also necessary to have exact knowledge regarding the dissolved state of the solute, which may suffer from hydrolysis or association.

In the present report, pressure-area studies were made for the soluble, adsorbed films of tritium-labelled sodium stearate, the amounts being determined directly by the radiotracer method. The pressure-area characteristics at the air/water interface have been investigated under various conditions of the substrate pH, solute concentration, and temperature. The results have then been discussed from both kinetic and equilibrium aspects.

Experimental

The Effect of Evaporation on the Surface Concentration. One of the major troubles encountered

1) H. L. Rosano and G. Karg, *J. Phys. Chem.*, **63**, 1692 (1959).
2) L. Ter Minassian-Saraga, *J. Colloid Sci.*, **11**, 398 (1956).
3) J. A. Spink, *ibid.*, **18**, 512 (1963).
4) E. D. Goddard, *ibid.*, **18**, 585 (1963).
5) E. D. Goddard, *ibid.*, **21**, 320 (1966).
6) E. D. Goddard, 4 th Int. Congr. Surface Activity (Brussel) B/II. 6.
7) E. D. Goddard, *J. Colloid Sci.*, **24**, 297 (1967).
8) J. T. Davies, *Trans. Faraday Soc.*, **48**, 1052 (1952).

in the study of the properties of the air/water interface is the evaporation of a solute or solvent from the solution surfaces. This evaporation affects the surface properties of liquid in a complicated manner by lowering surface temperature[9] and changing the surface concentration.[10] The first change subsequently changes other surface properties, such as the surface tension, and disturbs the system by promoting the convection current. The change in the concentration of a solute near the surface of the solution depends on a dynamic equilibrium between the rate of evaporation and the convection current occurring near the surface of the liquid. Preliminary radiotracer experiments have proven that only 60 seconds' exposure of the surface of an aqueous solution containing a 1.97×10^{-3} mol/l surface inactive sodium sulfate to an atmosphere of 40% relative humidity at 20°C without any air current produced the accumulation of a solute which is shown in Table 1. The accumulation was detected by the increase in the surface count rate of beta-rays from ^{35}S, with which Na_2SO_4 was labelled. The changed count rate was soon restored to its original value by suppressing the evaporation. Simple calculation shows that the amount of surface-concentration increase is about 50% of the amount of the maximum adsorption of such commonly-used surfactants as sodium dodecyl sulfate. Thus, it can be demonstrated that even a slight evaporation produces a serious error in the measurement of the properties concerning the liquid surface. Great care to prevent evaporation was taken in the present study by placing the trough containing the solution for study in a compact enclosure saturated with water vapor, as will be described later.

Table 1. Effect of evaporation of water on surface concentration of aqueous Na_2SO_4 solution

	Surface	Surface count rate (cpm)	Mean
1	Measured after 240 secs' stirring without evaporation	6460 6530 6530 6415 6510 6600	6518±81 ±1.24%
2	After 60 secs' exposure to open air	6760 6590 6600 6710 6740 6690 6860	6707±82 ±1.22%
3	After suppressing the evaporation of the above surface 2	6550 6510 6550 6460	6519±81 ±1.24%

$Na_2{}^{35}SO_4$: 1.97×10^{-3} mol/l
Specific activity: 1.09×10^{-12} mol/cpm. cm²
Room temperature: 20°C
Humidity of the atmosphere: 40% R.H.

Measurement of Tritium Radioactivity from an Aqueous Surface. The extremely soft beta-radiation is best suited for surface analyses, as has been mentioned above; unfortunately, however, the softness itself renders the detection of tritium very difficult.

Here, a windowless gas-flow 2π counter is generally used because of its high counting efficiency[11], as in the study of the adsorption of tritium-labelled sodium dodecyl sulfate[12] on an aqueous surface. In this case, however, the aqueous surface was inevitably exposed to hydrocarbon counting gas and to a high electrical field applied for the measurement of radioactivity.[13] To avoid such disturbances, we attempted to measure the tritium beta-radiation using an end-windowed Geiger-Müller counter tube equipped with a thin polycarbonate window. A thin film of polycarbonate was prepared by the following procedure,[14] The polycarbonate was dissolved in an equi-volume mixture of dioxane and ethylene dichloride up to 0.4 % and was then spread on a clean glass plate with an optically-flat surface, using a glass applicator composed of two glass rods tightly bound together with steel wire which determined the thickness of the liquid film. After slowly evaporating the solvent, the deposited film was removed and transferred on the water surface by immersing the plate in water. The thin film, floating on the aqueous surface was scooped up with a steel ring, treated with an aqueous polyvinyl alcohol solution in order to fill up the pinholes inevitably formed in the film, and dried at 100°C. After the vacuum deposition of gold on one side of the film, the film was fixed to an attachment grid with a 75% opening. The thin film thus prepared and attached to the end-windowed Geiger-Müller tube (type FC-16, Japan Radiation and Medical Electronics, Inc.) proved successful for the measurement of the soft beta-radiation of tritium from aqueous surfaces, a measurement which had hitherto been impossible with the ordinary Geiger-Muller tube with a thick window. The optimal thickness of the polycarbonate film used was 15—20 $\mu g/cm^2$. The overall counting efficiency attained for tritium was 9% of that obtained by using a windowless gas-flow 2π counter when polyvinyl alcohol-treated polycarbonate windows of 17.5 $\mu g/cm^2$ were used at a distance of 1 mm from an infinitely thin tritium sample in air. Further, th film proved to suffer no perceptible change in counting efficiency over several months. The details of the method of preparation and the properties of the film may be found in a former report.[14]

The Trough and Surface Balance. The surface tension of the aqueous sodium stearate solution was measured by a self-recording Wilhelmy-type surface balance[15]; the surface radioactivity was simultaneously measured. The apparatus is shown in Fig. 1. A Teflon trough ($120\times61\times5.6$ mm) was put in a jacket

9) N. L. Jarvis, *J. Colloid Sci.*, **17**, 501, 512 (1962).
10) T. Seimiya and T. Sasaki, *J. Colloid Interfac. Sci.*, **21**, 229 (1966).
11) G. W. Eulitz, *Rev. Sci. Instrum.*, **34**, 1010 (1963).
12) G. Nilsson, *J. Phys. Chem.*, **61**, 1135 (1957).
13) G. Nilsson and G. Aniansson, *Nucleonics*, **13**, 38 (1955).
14) T. Seimiya, K. Sekine and T. Sasaki, *J. Sci. Instrum.*, **42**, 906 (1965).
15) K. Ohbu, T. Seimiya and T. Sasaki, 18th Colloid Symposium (Shimane University 1965).

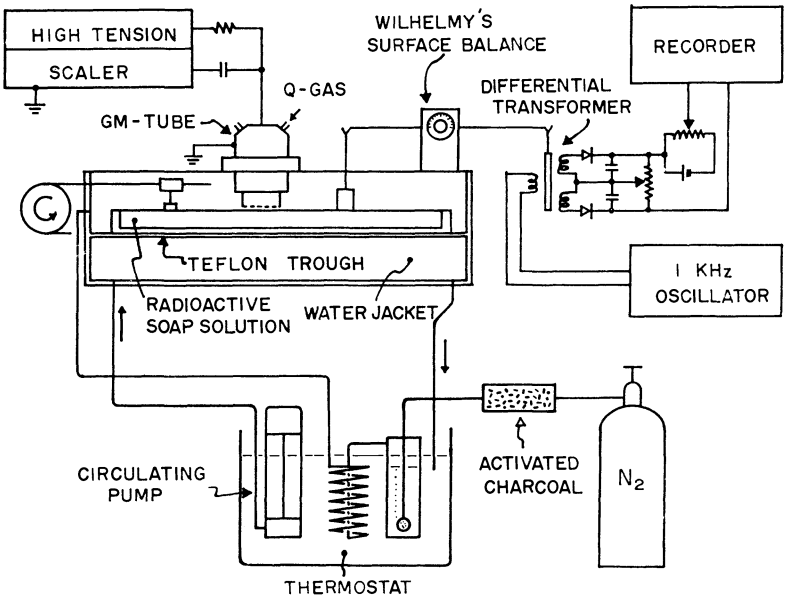

Fig. 1. Apparatus for simultaneous measurements of amount of adsorption and surface tension.

box, and the temperature of the solution in the trough was kept constant by the circulation of thermostatted water through the jacket surrounding the trough. The evaporation of water from the aqueous surface was prevented by slowly introducing nitrogen gas saturated with water vapor into the space above the trough. The radioactivity and surface-tension measurements were started just after the sweeping of the surface by a Teflon barrier which could be operated outside the lagged box. The Wilhelmy surface balance was equipped with a differential transformer (type DS-36-LM, Shinkoh Electric Works, Tokyo) which converted the minute displacement of the hanging plate to a proportional electrical output.[15] The primary input for the differeytial transformer was supplied by a 1-kHz oscillator. The output was then rectified and recorded by means of a Hitachi QPD 33 recorder after an appropriate application of bias voltage in order to put the desired part of the surface-tension change into the range of the recorder scale. Thus, the surface tension change could be recorded within an accuracy of ± 0.09 dyne/cm.

Materials. The tritium-labelled sodium stearate used was prepared[16] by dissolving tritium-labelled stearic acid[17] (specific activity, 7 Ci/mol) in absolute alcohol freshly distilled over sodium hydroxide; an amount of sodium hydroxide slightly less than that required for the neutralization of the acid was added as an alcoholic solution. The soap solution thus prepared was evaporated to dryness in vacuo, and the residue was washed with benzene to remove excess stearic acid by using a Soxhlet extractor. The water used in this experiment was obtained by first refluxing distilled water in an alkaline permanganate solution for 24 hours, and by then distilling it three times from a Hysil flask. The carbon-dioxide contamination from the air was removed by boiling the water for about ten minutes and then cooling it in a nitrogen atmosphere. The supernatant solution of saturated aqueous sodium hydroxide, after being centrifuged, was used to control the pH of the stearate solution.

Procedures. The conversion factor used for calculating the amount of adsorption from the observed counting rate was obtained by measuring the counting rate of a known amount of a radioactive stearic acid monolayer spread on the water surface. For this purpose, tritium-labelled sodium stearate was spread on distilled water from a 2.40×10^{-4} mol/l benzene solution by means of a microsyringe. At a low surface concentration, the heterogeneity of the monolayer and its time dependence were usually observed.[16] However, when left standing at 20°C for at least several hours, the film became homogeneous and the time dependence practically disappeared as far as the surface radioactivity was concerned. As the surface concentration increased, the surface film became more homogeneous and the time effects disappeared. The counting rate versus surface concentration curve was obtained from radioactivity measurements made at various surface concentrations by means of the compression and expansion of the monolayer. A linear relationship was confirmed within the limits of counting errors. For the measurement of the adsorption of sodium stearate at the air/water interface, a radioactive sodium stearate solution with a $1.0—5.0\times10^{-5}$ mol/l concentration was put in the Teflon trough used in the monolayer measurement, and the counting of the surface radioactivity was started immediately after the sweeping of the surface by the barrier. The bulk-count rate should be subtracted from the total count rate observed to give the surface radioactivity due to the adsorption of stearate at the air/water interface. In this experiment, the bulk-count rate was comparable to the background, so it was negligibly small compared with the total count rate. This

16) K. Sekine, T. Seimiya and T. Sasaki, This Bulletin, **43**, 629 (1970).

17) M. Muramatsu and T. Sasaki, *Radioisotope*, **10**, 100 (1961).

can reasonably be expected from the extremely low concentration of the solution used and the small range of beta-rays, about 1 micron in water. It is also confirmed by the fact that, for some solutions, the surface count rate at the initial stage of adsorption is comparable to that of the background. Therefore, the bulk-count rate can safely be neglected within the limits of counting error in the present experiment. The pH of these solutions was kept constant (within +0.1) throughout the experiment by keeping the trough in a humidified nitrogen atmosphere and by avoiding the dissolution of carbon dioxide from the air. The measurements were carried out at both 40°C and 30°C for the solutions with pH values from 8 to 11, and at concentrations from 1 to 5×10^{-5} mol/*l*.

Results and Discussion

Effect of Propane Gas. As for the measurement of tritium radioactivity using windowless gas-flow 2π counter mentioned above,[13] the aqueous surface must be exposed to the propane gas, and an appreciable change in the adsorption of the surface-active agent can subsequently be expected to occur. In this connection, the surface tension was measured for the aqueous sodium dodecyl sulfate solution in atmospheres of both nitrogen and propane gas. The results are shown in Fig. 2. In this figure, a remarkable drop in surface tension was observed upon the introduction

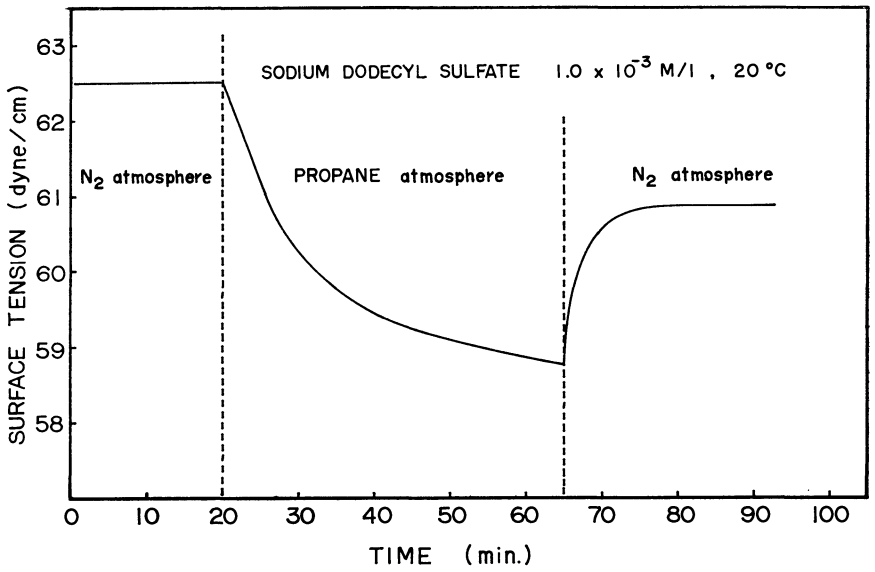

Fig. 2. Effect of propane gas on surface tension of aqueous sodium dodecylsulfate solution.

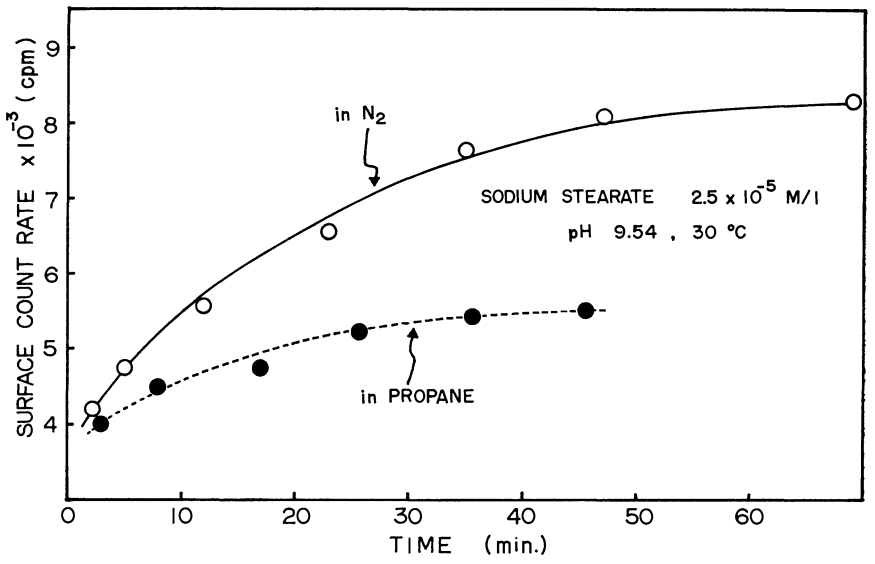

Fig. 3. Effect of propane gas on adsorption of sodium stearate at aqueous surface.

of propane gas to the aqueous surface of the sodium dodecylsulfate solution. The original value was only partially recovered by flushing the propane out with nitrogen. The effect of propane gas on the adsorption was further examined for the aqueous sodium stearate solution, as is shown in Fig. 3. An appreciable difference in the amount of the adsorption of stearate can be seen between the propane/water and nitrogen/water interfaces. The adsorption of stearate is lower for the propane/water interface than the nitrogen/water one, presumably because of the formation of a mixed film of stearate and propane at the aqueous surface, as was to be expected from the surface tension lowering shown in Fig. 2. The dissolution of propane into the aqueous stearate may also be expected to affect the stearate adsorption, although no tacit proof was found in this experiment. These experiments clearly show the considerable influence of atmospheric propane gas upon the adsorption of soap at the air/water interface.

Kinetic Aspects of Adsorpsion. Typical examples of the simultaneous measurement of the surface tension and the amount of adsorption at 30 and 49°C are presented in Fig. 4. The surface tension decreases and the amount of adsorption increases with the lapse of time. An amount of adsorption of about 8.5×10^{-10} mol/cm^2, nearly equal to that corresponding to the closely-packed monolayer of stearic acid, can be seen for the adsorption curve at 30°C. The surface tension curve in its early stage of aging, within 10 min, exhibits a gradual change which indicates the expanded nature of the adsorbed film at this stage. This tendency is more pronounced for the solution with a lower temperature (Fig. 4), pH (Fig. 5), and soap concentration (the third factor is not shown in the figure); the initial plateau appears in the surface tension, though a considerable increase in the amount of adsorption with time occurred during this stage. From the observed adsorption rate at an early period of aging, the diffusion coefficient of the solute can be calculated according to the equation of Ward and Tordai,[18] assuming the rate-determining process of adsorption to be the diffusion of the solute from the bulk to the sublayer of the surface, and assuming that the electrostatic potential barrier does not affect the diffusion practically in this early period of adsorption. The diffusion coefficient was calculated by the following equation;

$$\left(\frac{d\Gamma}{dt}\right)^2\cdot\frac{\pi t}{C_0^2}=D$$

where Γ denotes the amount of adsorption at time t, C_0 the bulk concentration of solute, and D, the diffusion coefficient. The observed D values for various C_0 and pH values at various temperatures are listed in Table 2, along with the values obtained by various other workers.[19-22] Although no comparison can be made between these data in a strict sense, it can at least be noted that the

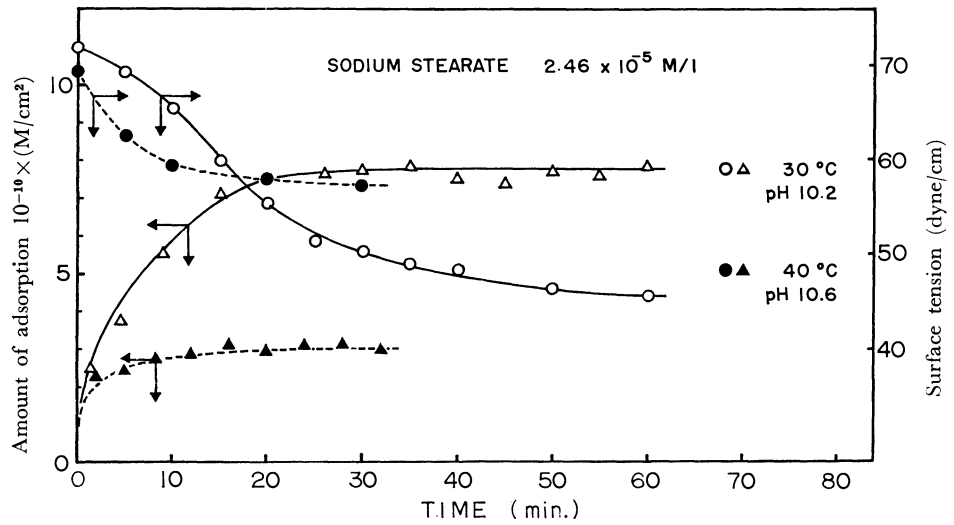

Fig. 4. Simultaneously measured amount of adsorption and surface tension for aqueous sodium stearate.

18) A. F. H. Ward and L. Tordai, *J. Chem. Phys.*, **14**, 453 (1946).
19) R. Matsuura, H. Kimizuka, S. Miyamoto, R. Shimozawa and K. Yatsunami, This Bulletin, **32**, 404 (1959).
20) D. J. Salley, A. J. Weith, Jr., A. A. Argyle and J. K. Dixon, *Proc. Roy. Soc.*, **A203**, 42 (1950).
21) S. N. Flengas and E. Rideal, *Trans. Faraday Soc.*, **55**, 339 (1959).
22) C. C. Addison and S. K. Hutchinson, *J. Chem. Soc.*, **1949**, 3387.

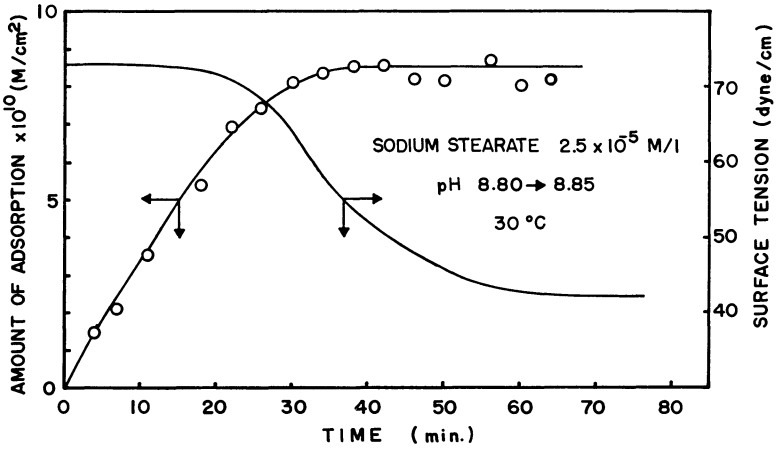

Fig. 5. Simultaneously measured amount of adsorption and surface tension for aqueous sodium stearate.

Table 2. Diffusion coefficient of surface active substances in aqueous solution

Surface active substance	C_0 (mol/l)	Temp., °C	pH	D_{obs} (cm²/sec)	D_{cal} (cm²/sec)
Sodium stearate	1.00×10^{-5}	40	11.0	1.88×10^{-6}	
	2.00		10.6	1.64×10^{-6}	
	3.00		10.7	1.40×10^{-6}	
	4.00		10.5	8.49×10^{-7}	
	5.00		10.7	1.51×10^{-7}	
	2.46×10^{-5}	30	10.2	9.35×10^{-7}	
Sodium hexadecylsulfate[19,20]		28		6.32×10^{-7}	4.01×10^{-6}
Sodium stearate[21]	3.26×10^{-5}	25	10.0	1.29×10^{-6}	
n-Octanol[22]	3.26×10^{-5}	20		5.94×10^{-6}	6.0×10^{-6}

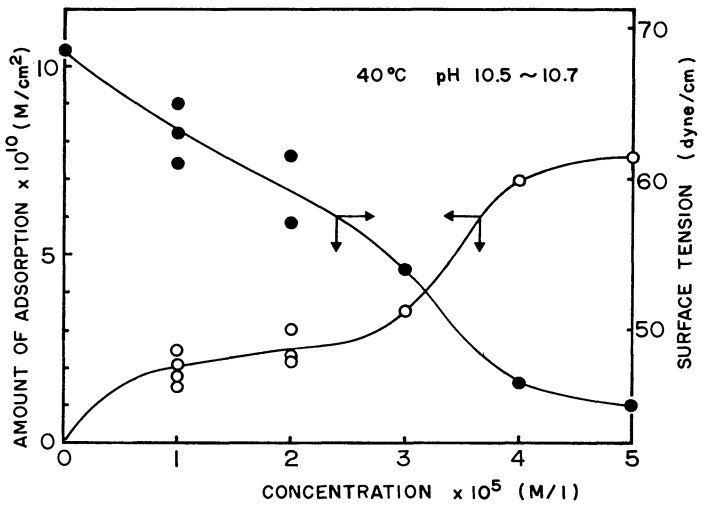

Fig. 6. Equilibrium values of surface tension and amount of adsorption for various concentrations of sodium stearate.

results of the present experiment are comparatively direct and accurate as far as the diffusion to the surface is concerned. There is also a tendency for the D value for a stearate to decrease with an increase in the solute concentration C_0. This presumably due to the effect of the electrostatic barrier assuming some importance.

Concentration Dependence of the Adsorpsion and Surface Tension. From these time-dependent curves of the surface tension and adsorption for various concentrations of stearate at a constant temperature and pH, equilibrium values were obtained; they are plotted against the concentration in Fig. 6. The adsorption isotherm appears step-by-step, on the whole, and shows two plateaus. The amount of adsorption in the lower concentration region is about one-third of that in the higher concentration region. The former corresponds closely to the state of saturation of the ionized monolayer,[23] while the latter corresponds to that of stearic acid. Such a step-by-step adsorption may presumably be interpreted as the superposition of two isotherms for species differing in the area of surface occupation, such as a stearate ion and a stearic acid molecule, the latter being the hydrolysis product of a stearate in the solution. The stearate ion, requiring a larger area, is predominant in the low concentration region, while the stearic acid molecule, with a smaller molecular area, appears in the higher concentration region at constant pH. Although the amount of stearic acid adsorbed is not in agreement with that expected from the bulk hydrolysis calculated by using the ordinary pK of the stearate, the discrepancy may be explained by the difference in pK between the bulk and the surface, or by the adsorption of some surface active associates between stearate and the stearic acid molecule.[4] These explanations are further supported by the pressure-area characteristics of the film, which will be described below.

Pressure-area Curve. From the time-dependence curves of the amount of adsorption, $\Gamma(t)$, and the surface tension, $\sigma(t)$, shown in Figs. 4 and 5, a Γ-σ or F-A plot can be constructed by eliminating the parameter, t, where $F=\sigma_0-\sigma$ denotes the surface pressure, σ_0 being the surface tension of water, and $A=1/\Gamma$ the area occupied by a stearate ion or a stearic acid molecule in the monolayer. In Fig. 7 such plots are constructed for varying concentrations of stearate solutions. The plots for F and A values in equilibrium appear at the end of the series of plots for each solution concentration. F-A curve thus obtained for the non-equilibrium state runs closely to that in the equilibrium state. Namely, Γ and σ change with the time in such a manner as F-A plot moves along the equilibrium F-A curve, and the successive steps of the kinetic state closely resemble that of equilibrium. In this respect, we cannot distinguish between the compression of an insoluble monolayer by a barrier in the usual monolayer technique and the compression of the soluble film due to the increase in the amount of adsorption. Thus, an automatic scanning of the pressure-area curve is made for the soluble monolabers by the simultaneous measurement of the surface tension and the amount of adsorption. The slower compression is more desirable for the surface-pressure measurements from the viewpoint of the homogeneity of the monolayer.[16] Here, the time re-

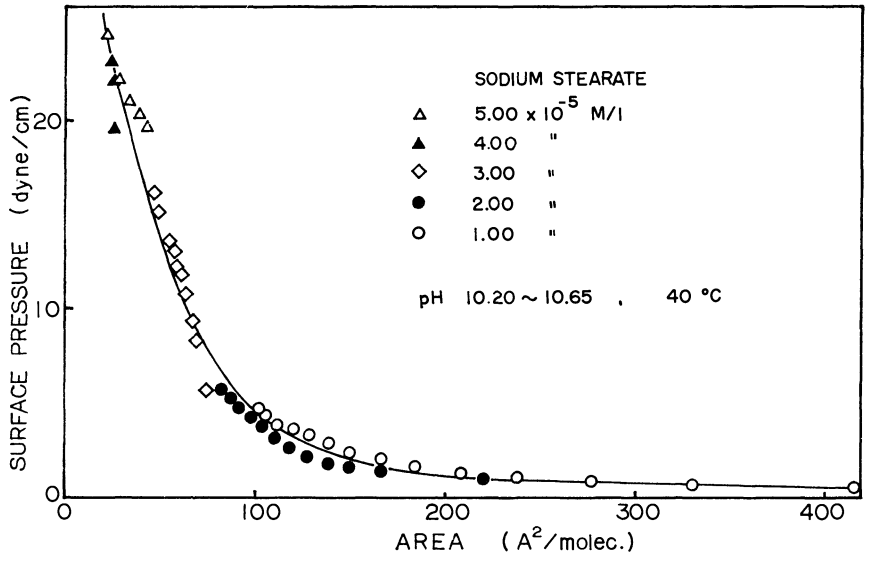

Fig. 7. Pressure-area relationship for adsorbed stearate films.

23) E. H. Lucassen-Reynders, *J. Phys. Chem.*, **70**, 1777 (1966).

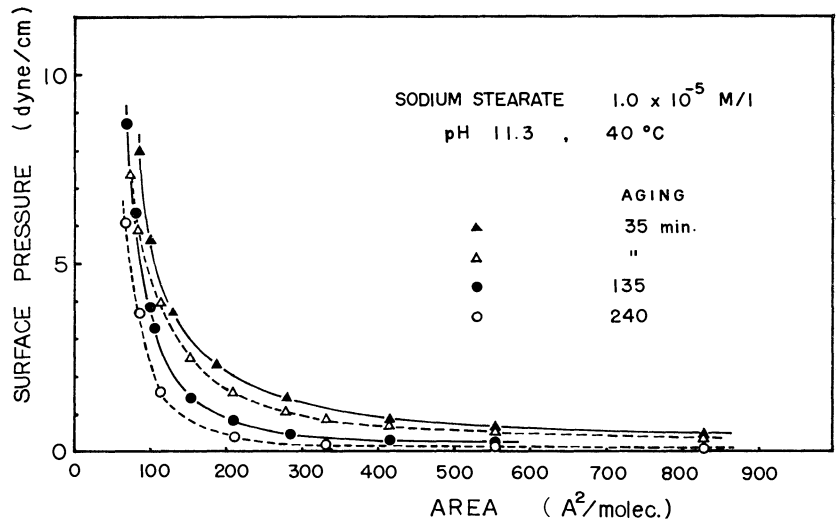

Fig. 8. Effect of bulk aging of stearate solution on pressure-area characteristics.

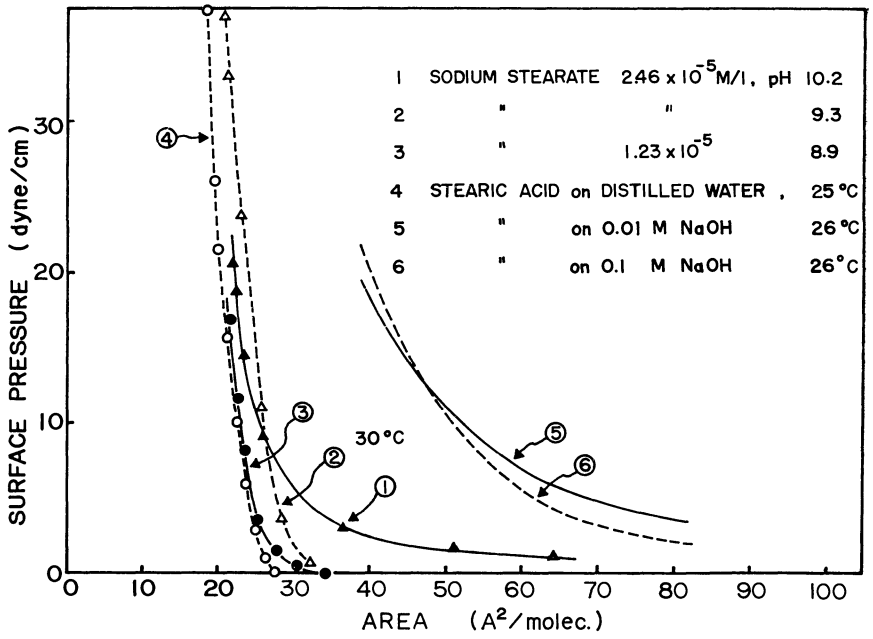

Fig. 9. Effect of pH on pressure-area relationship of adsorbed stearate films at 30°C.

quired for the establishment of the adsorption equilibrium is about 60 min, while in the usual monolayer technique about 10 min or so is required for complete compression.

The method of preparing a stearate solution markedly affects the pressure-area characteristics of the adsorbed monolayer (Fig. 8). The amount of adsorption increases, but the surface pressure decreases, with the increase in the age of the solution from 35 to 240 min before use. The effect of the pH of the stearate solution on the pressure-area relation is shown in Fig. 9, together with, for the sake of comparison, the curves for stearic acid on alkaline and neutral substrates at 30°C.[7] There is a close resemblance between the monolayer of stearic acid on neutral water and the adsorbed films on the stearate solution at pH values from 8.85 to 9.30. The difference in pH from 10 to 12 dose not produce any appreciable difference in the pressure-area relation, as is shown in Fig. 10.

The adsorption of stearic acid as a result of surface hydrolysis[24] is also expected to occur in these films. In the case of a stearate film adsorbed at

[24] M. A. Cook and E. L. Talbot, *ibid.*, **56**, 412 (1952).

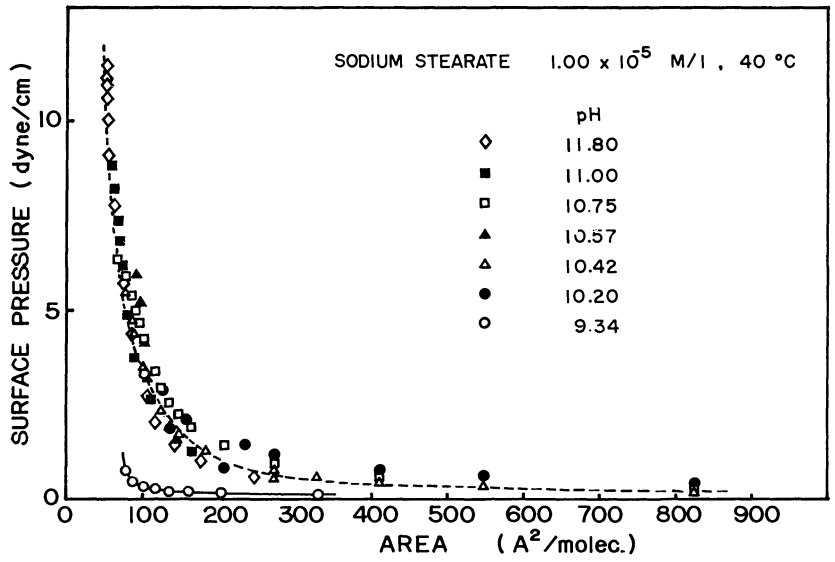

Fig. 10. Effect of pH on pressure-area relationship of adsorbed stearate films at 40°C.

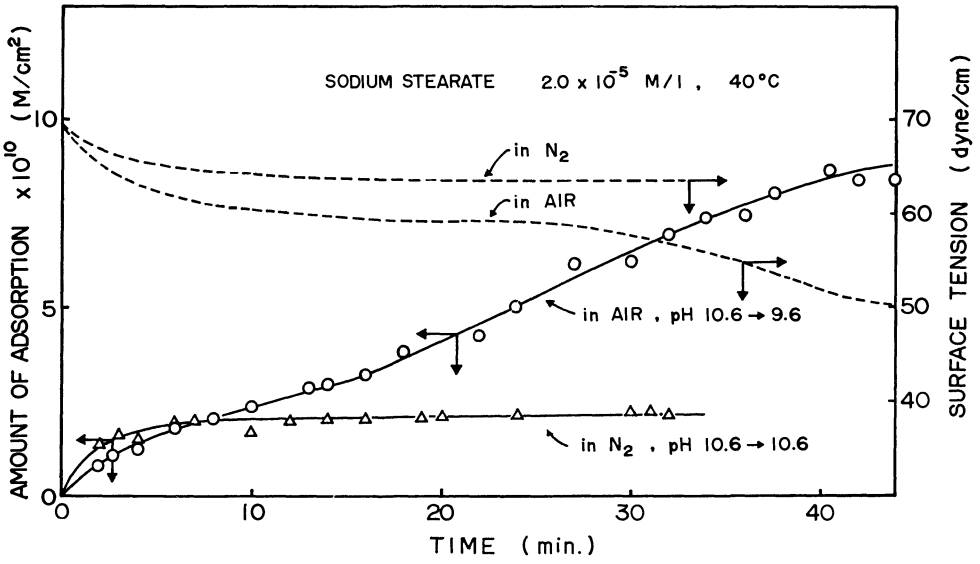

Fig. 11. Effect of atmospheric carbon dioxide on stearate adsorption.

pH 10.2, a transition from a condensed state at a higher surface concentration to an expanded state at a lower concentration can be observed. This behavior is in accord with the explanation of the step-by-step increase in Γ shown in Fig. 6, although the details are somewhat different because of the difference in temperature. The surface properties of soap are greatly affected by the presence of carbon dioxide either in solution or in atmosphere, as has been predicted by various workers.[3,5,25] In this experiment, extreme care was taken to avoid the contamination of either the surface or the bulk of the solutions by using carbonate free sodium hydroxide and sodium stearate, and by performing the experiments in a nitrogen atmosphere. In Fig. 11, the effects of carbon dioxide on the surface tension of stearate solution and on the amount of adsorption are shown by comparing the measurements in atmospheres of air (containing carbon dioxide) with those in carbon dioxide-free nitrogen. The exposure of an aqueous surface to air containing carbon dioxide increases the amount of adsorption and decreases the surface tension compared with the corresponding values obtained in nitrogen. From the observed change in the pH of the bulk solution, it is evident

25) J. Lucassen, *ibid.*, **70**, 1824 (1966).

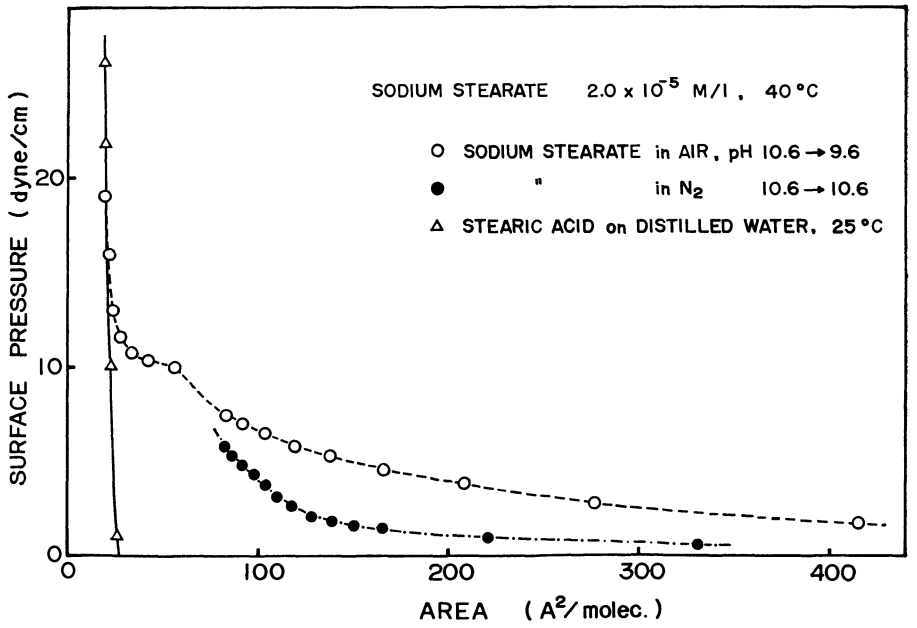

Fig. 12. Effect of atmospheric carbon dioxide on stearate adsorption.

that a considerable amount of carbon dioxide was absorbed by the solution from the air. This carbon dioxide distinctly lowers the pH of the surface layer of the solution and accelerates the hydrolysis to form free stearic acid or other surface-active associates[4,21,26] of a solute containing stearic acid, associates which preferentially adsorb at the surface and which often produce an abnormally large amount of adsorption. This tendency is also apparent in the pressure-area characteristic as shown in Fig. 12, which takes a form different from that obtained in an nitrogen atmosphere because of the dissolution of carbon dioxide into the solution. However, the curve coincides with that for stearic acid at a high surface pressure.

Author expresses his hearty thanks to Professors T. Sasaki and M. Muramatsu of Tokyo Metropolitan University for their kind discussions and suggestions. The cost of this research has been frayed by a Scientific Research Grant of the Ministry of Education given to Professor Sasaki.

26) J. Marsden and J. H. Schulman, *Trans. Faraday Soc.*, **34**, 748 (1938).

BULLETIN OF THE CHEMICAL SOCIETY OF JAPAN VOL. 43 2690—2702 (1970)

Photoemission from Organic Crystal in Vacuum Ultraviolet Region. IV

Masakatsu KOCHI,*1 Yoshiya HARADA, Tomohiko HIROOKA and Hiroo INOKUCHI

The Institute for Solid State Physics, The University of Tokyo, Roppongi, Tokyo

(Received February 7, 1970)

The quantum yield and the energy distribution of photoelectrons were measured for organic crystals in the vacuum ultraviolet region. A model was presented for the photoemission from organic crystals with a narrow valence band, and a semiempirical power law was derived for the yield near the threshold. The ionization potentials found from the spectral distribution of the quantum yield using this model were as follows: anthracene—5.68 eV, naphthacene—5.43, pentacene—5.04, perylene—5.33, indanthrone—5.17, and tetrathionaphthacene—4.42. The effect of electrons which escape after one inelastic scattering was observed. It was shown how the contribution of once-scattered electrons can be separated in the energy distribution. The threshold for "pair production" was estimated to be nearly equal to the band gap for perylene and a little higher than the band gap for quaterrylene. The fine structures observed both in the yield spectra and in the energy distribution can be accounted for by assuming the existence of additional valence bands.

Photoemission from solids is considered to be a three-step process: first, electrons are optically excited into high energy states; second, the excited electrons move to the surface of solids, with or without inelastic scattering, and third, they escape over the surface barrier into a vacuum. We define the first process as an optical excitation process, and the latter two as transport processes. In order to study these processes in solids, measurements of the spectral distribution of the photoelectric yield and the energy distribution of photoemitted electrons at individual photon energies can be used. As a result, the analysis of photoemission from solids gives us information on the electronic states and the transport phenomena in the solids. Recently, ultraviolet photoemission has received increasing attention as an experimental method of probing the electronic structure in solid.[1-4]

Although the external photoelectric emission from organic cystals has been measured by several workers,[5-10] there have been no systematic studies about the total process mentioned above.

In this paper, the photoemission both at photon energy near the threshold and well above the threshold is investigated. The well-known fact that an intermolecular interaction in organic crystal is very weak as compared with that in metal or inorganic semiconductor is taken into account by considering the intramolecular vibrations. With regard to the transport process, inelastic scattering between electrons and the tunneling effect over the surface barrier is emphasized. By these means, general results are obtained which allow a considerably detailed interpretation of the photoemissive characters of the organic crystals.

Method of Analysis

1.1 A Model for the Photoemission from Organic Crystals. In the study of photoelectric phenomena in solids, the photoemission from metals has been investigated most extensively, and the work functions of metals have been obtained by using a method developed by Fowler.[11]

The photoemission from inorganic semiconductors is treated on the assumption of "density of state" considerations. Precise studies[12] of weak

*1 Present address: The Institute of Space and Aeronautical Science, The University of Tokyo, Komaba, Tokyo.

1) C. N. Berglund and W. E. Spicer, *Phys. Rev.*, **136**, A 1030 (1964).
2) A. J. Blodgett, Jr., and W. E. Spicer, *ibid.*, **146**, 390 (1966).
3) T. M. Donovan and W. E. Spicer, *Phys. Rev. Lett.*, **21**, 1572 (1968).
4) D. E. Eastman, *Phys. Rev.*, **40**, 1387 (1969).
5) L. E. Lyons and G. C. Morris, *J. Chem. Soc.*, **1960**, 5192.
6) A. Terenin and F. Vilessov, *Doklady Akad. Nauk, SSSR*, **134**, 71 (1960).
7) R. C. Nelson, *J. Opt. Soc. Amer.*, **51**, 1186 (1961).
8) D. R. Kearns and M. Calvin, *J. Chem. Phys.*, **34**, 2026 (1961).
9) Y. Harada and H. Inokuchi, This Bulletin **39**, 1443 (1966).
10) M. Kochi, Y. Harada and H. Inokuchi, *ibid.*, **40**, 531 (1967).
11) R. H. Fowler, *Phys. Rev.*, **38**, 45 (1931).
12) G. W. Gobelli and F. G. Allen, *ibid.*, **127**, 141 (1962).

photoelectric emission from silicon metal near the threshold on atomically-clean surfaces reveal direct and indirect thresholds. The plot of the quantum yield against the photon energy is linear when photoelectrons are generated by optical direct transition in the bulk. An indirect transition results in the cube-root of the quantum yield becoming proportional to the photon energy. These results are in agreement with Kane's theory.[13] Kane's power laws near the threshold mainly depend on the shape of the upper edge of the valence band. Therefore, his formula can not be applied to organic crystals with narrow valence bands.

Therefore, we wish now to propose a simple model for interpreting the general results of the photoemission from organic crystals. This model uses the following assumptions:

(a) the crystal is composed of vibrating molecules, and

(b) the wavefunction of an electron part may be described by Bloch representation inside the crystal, which joins smoothly through the surface barrier to a free electron state of equal energy.

Molecular vibrations in aromatic molecules typically have energies of approximately 0.4 eV (corresponding to C–H stretching), while the bandwidths for excess holes in molecular crystals of the naphthalene · anthracene type are very narrow—0.2 eV at the largest, and possibly smaller than that by an order of magnitude or more.[14] Thus, the effect of molecular vibrations is to split each hole band into many well-separated bands, all separated by the energy of a vibrational quantum. On the other hand, an excess electron band may not be separated by a vibrational quantum, because the ionized state with a wide electronic band is considered in the study of photoemission. Figure 1 illustrates a simplified case where there is only one vibrational frequency. A parabolic band is assumed for the conduction band. The energy difference, Δ, between the vacuum level and the bottom of the band will act as a surface barrier for slow photoelectrons. The valence bands are considered to be almost flat against the change in the k vector. The energy states which should exist below the conduction band for organic crystals are omitted in Fig. 1 for the sake of simplicity.

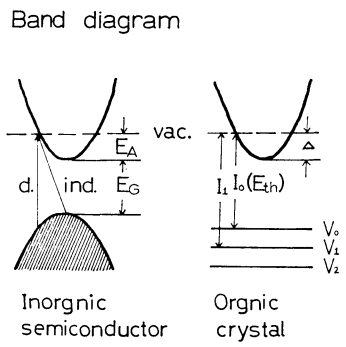

Fig. 1. Band diagram in photoemission from organic crystals including the vibronic bands. associated with hole bands.
The pure hold band is labeled V_0. Vibrationally excited bands are lebeled V_1, V_2, and so on.
(Band diagram for inorganic semiconductors is illustrated for reference; d. and ind. correspond to direct and indirect threshold, respectively.)

Assuming that no vibrational states are excited in the initial ground state, the electronic transition which puts a hole into V_0 requires only electronic excitation. The photon energy required for this pure electronic transition corresponds to the photoelectric threshold energy, E_{th}. It is denoted as I_0 in Fig. 1. Since the electronic transition which puts a hole into V_1 requires simultaneous electronic and vibrational excitation, it requires more energy than the excitation in V_0. For this reason, the vibrationally-excited hole bands are drawn downwards with increasing energy, as in Fig. 1.

1.2. The Form of the Spectral Distribution of the Quantum Yield near the Threshold. The quantum yield, $Y(h\nu)$, is designated by $Y(h\nu)$=number of electrons emitted/number of incident quanta. We assume that all the incident quanta are absorbed.*2 Then, using the first-order time-dependent perturbation theory, the quantum yield can be written as:

$$Y(h\nu) = \sum_i \int_0^\infty \int_{B.Z.} \delta(E_f - E_i - h\nu)|H_{if}|^2 \times \rho(E_f)D(E_f, x)I\mathrm{e}^{-\alpha x}\mathrm{d}x\mathrm{d}E_f \Big/ \int_0^\infty I\alpha \mathrm{e}^{-\alpha x}\mathrm{d}x$$

and

$$\alpha = \sum_i \int_{B.Z.} \delta(E_f - E_i - h\nu)|H_{if}|^2 \rho(E_f)\mathrm{d}E_f, \quad (1)$$

if all the photons of energy, $h\nu$, are absorbed in exciting electrons in the crystal. Here, I is the intensity of incident light; the absorption coefficient, $\alpha(h\nu)$, corresponds to the total absorption of the crystal at the photon energy, $h\nu$; H_{if} is the matrix element of the momentum; $\rho(E_f)$ is the state density, and $D(E_f,x)$ is the escape probability of an electron excited to a certain energy, E_f, at a certain distance, x, from the crystal surface. In Eq. (1) the state density of initial states is elimi-

13) E. O. Kane, *ibid.*, **127**, 131 (1962).

14) O. H. LeBlanc, *J. Chem. Phys.*, **40**, 2223 (1964); J. L. Katz, S. A. Rice, S. I. Choi, and J. Jortner, *ibid.*, **39**, 1683 (1963); R. Silbey, J. Jortner, S.A. Rice and M. Vala, *ibid.*, **42**, 733 (1965).

*2 This assumption was valid for the crystals several microns thick in the vacuum ultraviolet region. However, it may be necessary to take into account the optical reflectivity at the crystal surface for a more precise study.

nated because of the narrow band, the photoemissive crystal is assumed to be semiinfinite, and the integral with respect to E_f extends over the Brillouin zone (B.Z.).

The $D(E_f,x)$ term generally involves both the scattering probability and the surface transmission probability, $T(E_f)$. Near the threshold, $D(E_f,x)$ may be represented only by $T(E_f)$, because the scattering probability varies slowly near the threshold. The subsequent integration with respect to x gives the result:

$$Y(h\nu) = \frac{1}{\alpha(h\nu)} \sum_i \int_{\text{B.Z.}} \delta(E_f - E_i - h\nu) |H_{if}|^2 \times \rho(E_f) T(E_f) \mathrm{d}E_f. \quad (1')$$

With the adiabatic approximation, H_{if} is expressed as follows;

$$H_{if} = M_{if}(R_0) \cdot \langle n|0\rangle. \quad (2)$$

where $M_{if}(R_0)$ is the matrix element of the electronic part at the equilibrium atomic distance, R_0, and where $<n|0>$ is the "overlap integral" concerned with the vibrational part. By substituting Eq. (2) into Eq. (1'), we obtain:

$$Y(h\nu) = \frac{1}{\alpha(h\nu)} \sum_i \int_{\text{B.Z.}} \delta(E_f - E_i - h\nu) |\langle n|0\rangle|^2 \times |M_{if}|^2 T(E_f) \rho(E_f) \mathrm{d}E_f. \quad (3)$$

In Eq. (3) we assume that $\alpha(h\nu)$, M_{if}, and $\rho(E_f)$ are slowly varying in the vicinity of the threshold, because, in the absorption spectra, no drastic change is found near the photon energy corresponding to the threshold energy of photoemission.[5] Hence, Eq. (3) may take the following form near the threshold:

$$Y(h\nu) \propto \sum_i \int_{\text{B.Z.}} \delta(E_f - E_i - h\nu) |\langle n|0\rangle|^2 T(E_f) \mathrm{d}E_f. \quad (4)$$

The delta function in Eq. (4) gives the energy conservation relation:

$$E_f - E_i - h\nu = E + I_n - h\nu = 0 \quad (5)$$

In Eq. (5) the energy zero is taken to be a vacuum, E is the kinetic energy of a free electron, and I_n is the threshold energy corresponding to the n'th vibrational level:

$$I_n = I_0 + n\hbar\omega \quad (6)$$

I_0 corresponds to the ionization potential, I_c, of the crystal, and $\hbar\omega$ is the vibrational energy quanta, where the diversity of vibrational quanta due to many kinds of vibrational modes is neglected for the sake of simplicity. The critical escape condition:

$$\mathrm{E} \geq 0, \quad (7)$$

can be expected from the transmission probability, $T(E)$. From Eqs. (4), (5), (6), and (7), the following relation is obtained:

$$Y(h\nu) \propto \sum_n [|\langle n|0\rangle|^2 \cdot T(E)] \quad 0 \leq E = h\nu - I_0 - n\hbar\omega \leq h\nu - I_0. \quad (8)$$

Since it is difficult to calculate both factors, $T(E)$ and $|<n|0>|^2$, especially for polyatomic molecular crystals, we determine their forms empirically as follows.

The Form of $T(E)$. The surface transmission probability, $T(E)$, is difficult to determine exactly, for it depends on the shape of the surface barrier. However, it is evident that $T(E)$ must be zero for $E=0$ and that it must increase at higher values of E. In a first approximation we set:

$$T(E) \begin{cases} = 0 & \text{for } E < 0 \\ \propto E^l \left(\frac{1}{2} \leq l \leq 1\right) & \text{for } E \geq 0 \end{cases} \quad (9)$$

Note that it is for slow electrons that the shape of the surface potential barrier becomes important and that $T(E)$ usually becomes nearly constant for a large value of E. $T(E)$ is one of the main factors determining the energy distribution of slow electrons and the form of the quantum yield near the threshold.

The Form of $|<n|0>|^2$. Condon's "overlap integral," $<n|0>$, in Eq. (8) was considered in connection with diatomic molecules by Mannenback.[15] In general, if the change of equilibrium interatomic distances through the excitation process is large, a $<0|0>$ factor often becomes small and the overlap integral in the $<n|0>$ progressions will increase slowly with the increase in n. The energy distribution due to the $|<n|0>|^2$ factor is observed as a broadened band in the energy-loss curve, because there are many kinds of vibrational modes in polyatomic molecules, each having different vibrational quanta. It will be found in the energy-loss curves that the number of slower electrons increases almost linearly with the increase in the energy-loss, that is to say, with the increase in the vibrational quantum number, n, commencing at the electron energy corresponding to the $0\leftarrow0$ vibrational transition, and reaching the first maximum. Therefore, as a first approximation we replace the $|<n|0>|^2$ factor by a linear equation of n, setting $|<0|0>|^2 \simeq 0$.

Replacing $T(E)$ and $|<n|0>|^2$ in Eq. (8) by $E^l (1/2 \leq l \leq 1)$ and n respectively, and integrating over n in place of the summation in Eq. (8), we obtain the following relation:

$$Y \propto (h\nu - E_{th})^m, \left(\frac{5}{2} \leq m \leq 3\right) \quad (10)$$

This semi-empirical power law for the yield near the threshold will be compared with the experimental results in Section 4.1.

1.3. The Effect of Pair-production Scattering on the Energy Distribution. "Pair-production scattering" means the process by which the primary electron, with the energy of E', excites the second one, with the energy of E_0, to the

15) C. Mannenback, *Physica*, **17**, 1001 (1951); *ibid.*, **20**, 497 (1954).

conduction band and loses the minimum energy equal to the band gap energy, $\Delta\varepsilon$. In most organic crystals, the energy loss per collision is several eV for this process.

On the other hand, electron-phonon scattering involves a small energy loss per collision. Assuming that the phonon energy corresponds to the Debye temperature (for instance, it has been reported to be about 0.01 eV in naphthalene and anthracene.[16]), the average energy loss per collision at 300°K in organic crystals can be estimated to be about 0.003 eV. Note that it takes several hundred phonon-scattering events to produce as large an energy loss as one pair production event. Therefore, we consider pair-production scattering to be the main factor in the energy distribution of secondary electrons.

In their study of the energy distribution of photoelectrons from Cs_3Sb, Apker *et al.*[17] found evidence for the production of hole-electron pairs by energetic electrons. Spicer[18] determined the thresholds and the mean free path for pair production in semiconductors. Recently, pair-production scattering was investigated in detail by Spicer *et al.* for Cu and Ag[1] and by Kane for Si.[19]

In this work, we will consider only the escape probability of once scattered electrons in a way similar to that used for metal by Spicer *et al.*

Using a one-dimensional model, the total rate of the escape of electrons with energies between E and $E+dE$ after one scattering is*3:

$$N_s(E)dE \simeq AT(E)dE\int_{E+\varepsilon_{th}}^{h\nu-E_{th}} W(E')p(E,E')dE' \quad (11)$$

where $W(E')$ is the optical transition probability, where $p(E,E')$ is the probability that a primary electron with the energy of E' will be inelastically scattered to an energy between E and $E+dE$, where $T(E)$ is the surface transmission probability, where A is the function depending on the absorption coefficient and the scattering length, and where ε_{th} is the threshold energy for pair production.

Since we do not have enough information about the wavefunctions, particularly for excited states, the matrix element of electron-electron scattering is assumed to be constant. Under this approximation, and using the Fermi function at $T=0$, the following equation for $p(E,E')$ is obtained.[20]:

$$pdE = \frac{\rho(E)\left[\int \rho(E_0)\rho(E_0+E'-E)dE_0\right]dE}{\iint \rho(E)\rho(E_0)\rho(E_0+E'-E)dE_0dE} \quad (12)$$

Here, the scattering process by which an electron in the $(E,\vec{k'})$ state is scattered to the $(E,\vec{k})$ state and excites an electron in the $(E_0,\vec{k_0})$ state to the $(E_1,\ \vec{k_1})$ state is considered.

To ascertain the characteristic effects of a once-scatterd electron on the energy distribution, we assume a simple model. Assuming that $\rho(E)$, $\rho(E_0)$, and $\rho(E_0+E'-E)$ are constant, Eq. (12) reduces to:

$$pdE = dE\Big/\int_{-\Delta}^{E'-\varepsilon_{th}} dE = dE/(E'-\varepsilon_{th}+\Delta). \quad (13)$$

the lower limit of the integral means that we can neglect the interband transition for primary electrons. By substituting Eq. (13) into Eq. (11) and by assuming $AW(E')=W_0$ (const.) in Eq. (11), the following equation is derived:

$$N_s(E)dE \simeq W_0dET(E)\ln\frac{h\nu-E_{th}-\varepsilon_{th}+\Delta}{E+\Delta} \quad (14)$$

In Fig. 2 the energy distribution of secondary electrons, $N_s(E)$, is shown for several photon ener-

16) D. W. J. Cruickshank, *Rev. Mod. Phys.*, **30**, 163 (1958); M. L. Canut and J. L. Amaros, *J. Phys. Chem. Solids*, **21**, 146 (1961).

17) L. Apker, E. A. Taft and J. Dickey, *J. Opt. Soc. Amer.*, **43**, 78 (1953).

18) W. E. Spicer, *J. Phys. Chem. Solids*, **22**, 365 (1961).

19) E. O. Kane, *Phys. Rev.*, **159**, 624 (1967).

*3 Consider an electron excited to the energy of E' at a certain distance, x from the surface; the probability of this electron escaping with an energy between E and $E+dE$ after one scattering is the product of three probabilities: (1) the probability, p_1, that the primary electron will scatter after moving a certain distance, r, in the solids: (2) the probability, $p(E,E')$, that this electron will be scattered to an energy between E and $E+dE$, and (3) the probability, p_3, that it will escape without further scattering. Using a one-dimensional model, p_1 and p_3 are given as:

$$p_1 = \frac{1}{2}e^{-c'r}(c'dr),\ p_3 = \frac{1}{2}T(E)e^{-c(x\pm r)},$$

where c' is the reciprocal scattering length for an electron with the energy of E' and where, generally, $c'>c$. The distance of the electron from the surface is $x-r$ $(0\leq r\leq x)$ and $x+r(0\leq r\leq\infty)$. The factor, 1/2, reflects the fact that the electron can go either towards the surface or away from it.

In an optical absorption process, the rate per unit of length at which electrons are excited to energies between E' and $E'+dE'$, in a slab with a width of dx located at a certain distance, x, from the surface, has the form:

$$G(E',x) = W(E')dE'e^{-\alpha x}dx.$$

By integrating the product of p_1, $p(E,E')$, p_3 and $G(E',x)$ over r and x under the assumption that the photoemissive crystal is semi-infinite, we obtain the following equation:

$$N_s(E',E)dEdE' = \left(\frac{2c'}{c'+c}-\frac{\alpha+c}{\alpha+c'}\right) \times \frac{c'}{4(c'-c)(\alpha+c)}T(E)W(E')p(E,E')dEdE'.$$

By setting $A = \left(\frac{2c'}{c'+c}-\frac{\alpha+c}{\alpha+c'}\right) \times \frac{c'}{4(c'-c)(\alpha+c)}$ in the above equation, we obtain Eq. (11).

20) Ref. 1, p. A1035; Peierls, Quantum theory of solids (Oxford, 1955) p. 131.

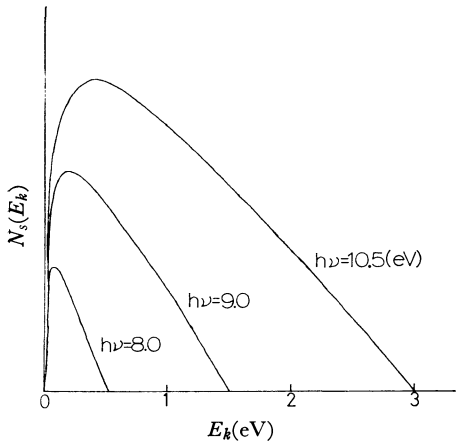

Fig. 2. Theoretical energy distribution of once-scattered electrons.

gies, setting $T(E) \propto E^{1/2}$, $E_{th}=5.5$ eV, $\varepsilon_{th}=2.0$ eV, and $\Delta \simeq 0$ in Eq. (14).

The most important feature of Fig. 2 is that pair-production scattering gives a low energy peak in the energy distribution of photoemitted electrons. The position of the peak remains almost constant in energy above the vacuum level and the height of the peak increases, as the photon energy increases. These results are in qualitative agreement with the results obtained for metal by Spicer:[1] Spicer used a three-dimensional model and introduced the "threshold function" in place of $T(E)$. Though the choice of Δ(defined in Fig. 1) has a slight influence on the curvature and the position of the peak, its behaviour described above does not change.

Experimental

The details of the purification of samples and the arrangement of the specimens in the photoemission measurement have been reported previously.[9,10],*4

2.1. Sample. Figure 3 shows the materials—anthracene, naphthacene, pentacene, perylene, quaterrylene, tetrathionaphthacene, and indanthrone—used in the present work. All the purified samples except anthracene were deposited on a copper disk, 10 mm in diameter, by means of a sublimation method *in vacuo* (10^{-6} Torr), the thickness of the film being a few microns. The single crystal of zone-refined anthracene[21] was attached to the copper disk by silver paste, its thickness being about 100 μ.

2.2. Experimental Technique. The photoemission was measured with a 0.5-metre Seya-Namioka-type vacuum ultraviolet monochromator. A concave grating coated by MgF_2, with 1200 grooves /mm, has a reciprocal linear dispersion at the exit slit of 16 Å/mm. A lithium fluoride window, which was attached with an O-ring to the exit slit, transmitted to a photon energy of about 11.5 eV. As a light source, a Hinteregger-type hydrogen discharge lamp was used. A collector was a glass sphere about 13 cm in diameter; on the inside it was coated with a conducting layer of colloidal graphite, Aguadag. An organic compound deposited onto a copper disk was fixed at the centre of the collector. Light was focussed on the sample in a spot with dimensions of about 6 mm×6 mm.

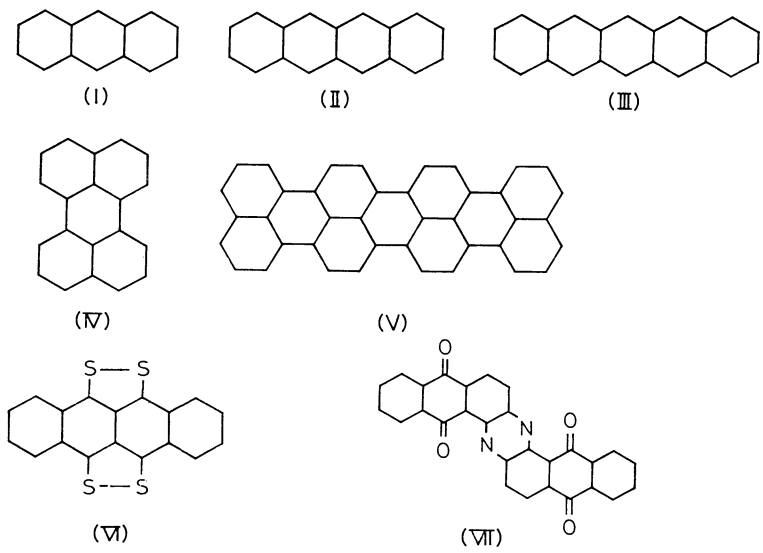

Fig. 3. Structural formula of materials.
(I) anthracene, (II) naphthacene, (III) pentacene, (IV) perylene, (V) quaterrylene, (VI) tetrathionaphthacene, and (VII) indanthrone.

*4 The method of purifying quaterrylene was reported by Y. Maruyama, H. Inokuchi and Y. Harada, This Bulletin, **36**, 1193 (1963).

21) S. Iwashima, K. Ogino and J. Aoki, *Nippon Kagaku Zasshi*, **89**, 338 (1968).

The photoemission current was amplified and observed by a Cary 31 vibrating-reed electrometer. Its spectral response was measured at intervals of 20 Å under an applied potential of 10 V, high enough to collect all the photoemitted electrons.[22]

One-mm slits were used in these experiments. The 16 Å/mm reciprocal dispersion at the exit slit gives, then, a photon-energy spread of 0.05 eV at 6.20 eV (2000 Å) and one of 0.13 eV at 10.33 eV (1200 Å).

The quantum yield, Y, was found from the ratio between the number of the photoemitted electrons and that of the incident photons. The absolute measurement of the incident photons was made by means of an Epply circular thermopile. The relative value of the light intensity was obtained by measuring the fluorescence intensity from a coronene film[23] evaporated onto a glass plate with a RCA 5819 photomultiplier tube.

The energy distribution curves (EDC) were obtained by differentiating graphically the current-voltage characteristics, which had been measured by the spherical retarding-potential method and recorded with a Yokogawa X-Y recorder, PRO-12. The estimated uncertainty in the location of structures in EDC was ±0.2 eV.

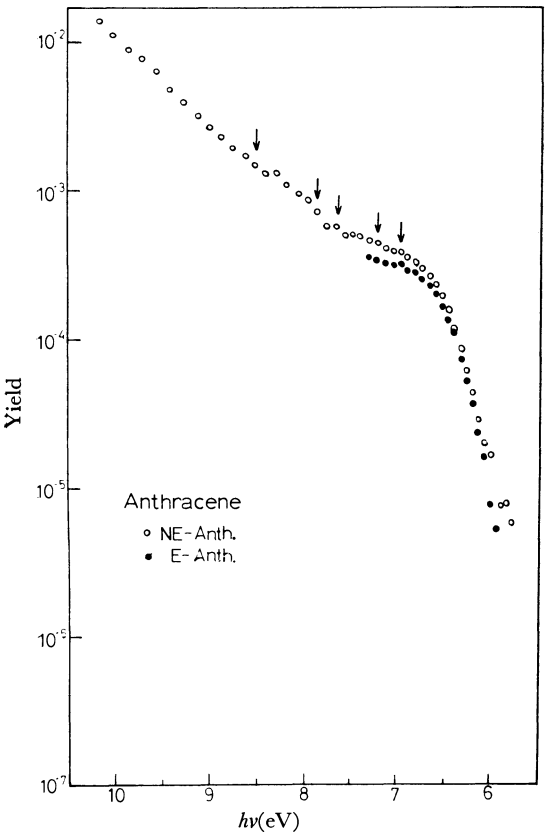

Fig. 4. Spectral distribution of the quantum yield for anthracene.

Results

3.1. Quantum Yield. Figure 4 shows the spectral distributions of the quantum yield for anthracene single crystal on the *a-b* plane under illumination. This single crystal was measured under a pressure of 10^{-3} Torr, because it evaporated easily in a high vacuum. One distribution was observed as soon as the photo-cell had been evacuated to a pressure of 10^{-3} Torr (this will be referred to as not-evaporated-anthracene, NE-Anth.). The other distribution was observed after more than five hours evacuation*5 (this will be referred to as evaporated-anthracene, *E*-Anth.). The most conspicuous difference between the two cases was that a tail appeared for NE-Anth. in the photon-energy region lower than 5.9 eV. This seems to indicate that NE-Anth. has two kinds of ionization potential, the larger value corresponding to that of anthracene itself, and the smaller one, to that of the impurity formed on the surface layer of the anthracene crystal. We will again discuss this problem in Section 4.4. The other features of the spectra were not so different in the two cases, though the magnitude of the yield for NE-Anth.

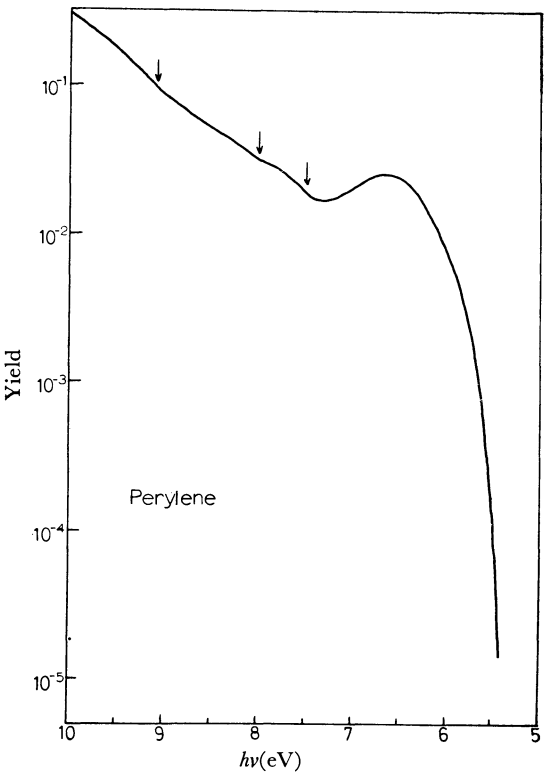

Fig. 5. Spectral distribution of the quantum yield for perylene.

22) T. Hirooka, M, Kochi, H. Inokuchi, Y.Harada and J. Aihara, This Bulletin **42**, 1481 (1969).

23) H. Inokuchi, Y. Harada and T. Kondow, *J. Opt. Soc. Amer.*, **54**, 842 (1964).

*5 There was hardly any influence of evacuation when the photo-cell was evacuated for more than two hours.

was slightly higher than that for *E*-Anth.

Figure 5 shows the spectral response of the quantum yield for perylene. As can be seen in Fig. 5, a decrease in the yield was observed at photon energies between 6.8 and 7.3 eV. In Section 4.2, using the data of the energy distribution, it will be found that this decrease can be interpreted as the effect of pair-production scattering.

As may be seen from Figs. 4 and 5, the quantum yield of organic crystals rose with a considerable sharpness at the threshold and increased quickly with an increase in the photon energy. In the higher-energy region, the value of the yield increased gradually, reaching the order of 10^{-2}—10^{-1} electrons/photon at a photon energy of about 10 eV. Further, some inflection points were observed in the region more than 1 eV above the threshold.

3.2. Energy-distribution Curve and Energy-loss Curve. Figures 6, 7, and 8 show the energy distribution curves (EDC) for anthracene,*[6] perylene, and quaterrylene respectively, normalized

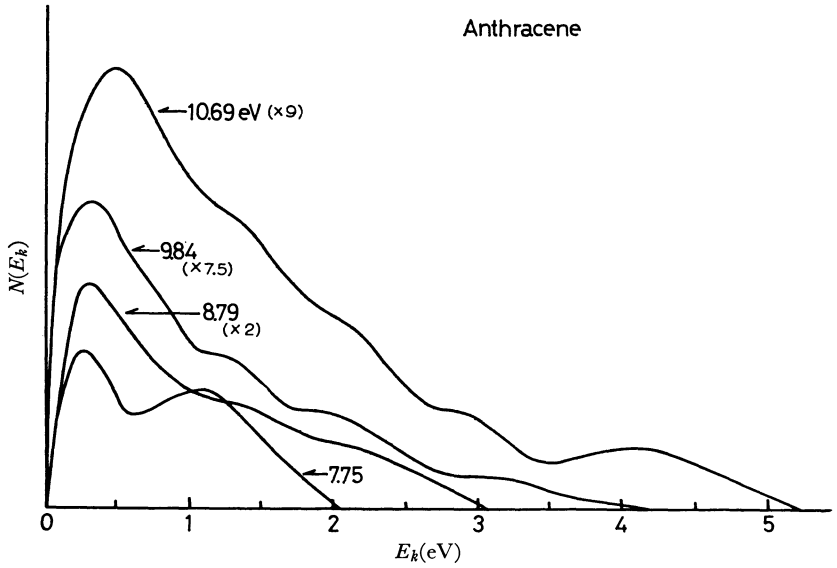

Fig. 6. Energy distribution curve for anthracene.

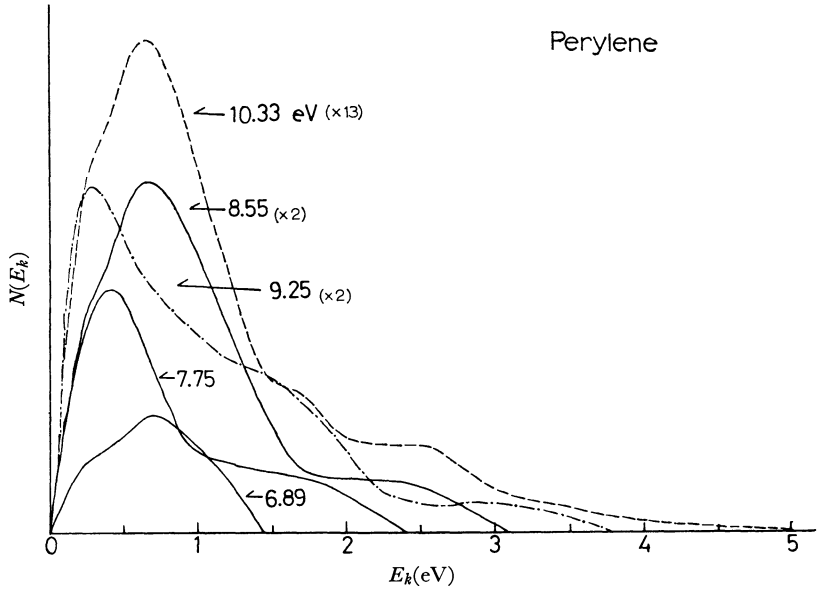

Fig. 7. Energy distribution curve for perylene.

*[6] A very slight increase in the current was observed above the saturation point in the current-voltage characteristics of the anthracene single crystal. Therefore, in the EDC for anthracene the tails due to an unsaturated current were cut off at the saturation voltage.

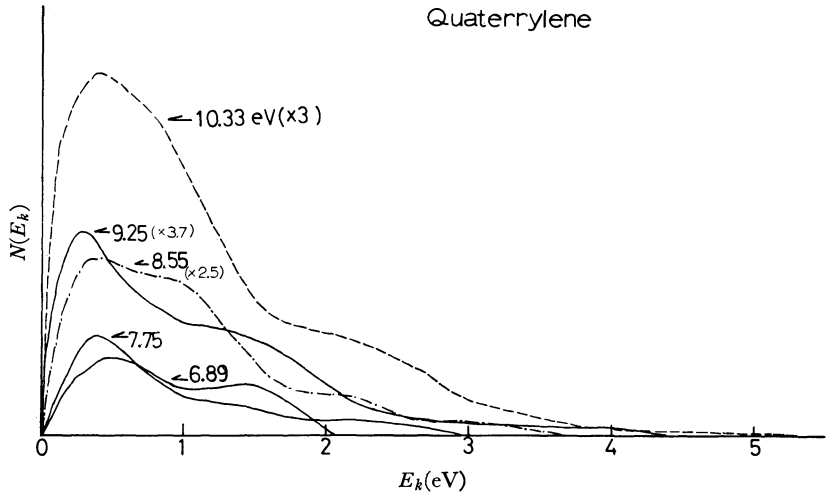

Fig. 8. Energy distribution curve for quaterrylene.

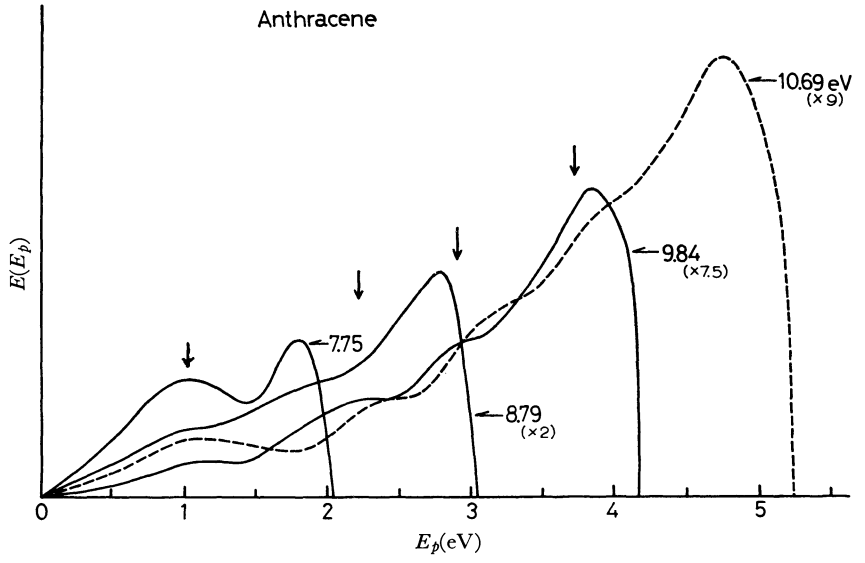

Fig. 9. Energy-loss curve for anthracene.

to the yield. On the ordinate axis, the relative numbers of the emitted electrons, $N(E)$, are plotted; on the abscissa axis, the electron energies, E_k, are stated relative to the vacuum level.

In Figs. 9, 10, and 11 the energy-loss curves (ELC) are shown; in them the difference, E_p, ($E_p = E_m - E_k$, E_m is the maximum kinetic energy) has been chosen on the abscissa axis instead of the electron kinetic energy, E_k. In this representation the $E_p=0$ point corresponds to electrons with a limiting maximum kinetic energy at any photon energy. The numerical values, increasing to the right, represent a deficiency in kinetic-energy losses.

As can be seen from EDC (Figs. 6, 7, and 8), two groups of photoelectrons were observed. The one formed by slow electrons was almost stationary in the same kinetic energy range (0.3—0.5 eV), independent of the increase in photon energy, while the height of their peaks increased as the photon energy increased. The group of fast electrons was regularly shifted to kinetic energies higher by the same amount as the photon energy increased.

The behaviour of the fast electrons can be described more pertinently in ELC. For the anthracene single crystal (see Fig. 9), at the photon energy of 7.75 eV ELC had a maximum at $E_p \simeq$ 1.0 eV. When the photon energy was increased to 8.79 eV, a shoulder appeared at $E_p \simeq 2.0$ eV. Subsequent shoulders appeared at $E_p \simeq 2.9$ and 3.7 eV at higher photon energies. The positions of the maxima and shoulders were independent

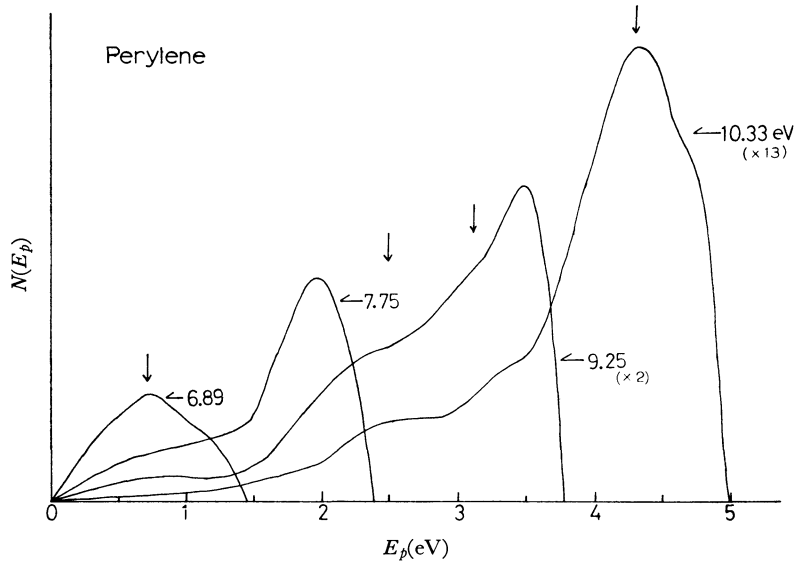

Fig. 10. Energy-loss curve for perylene.

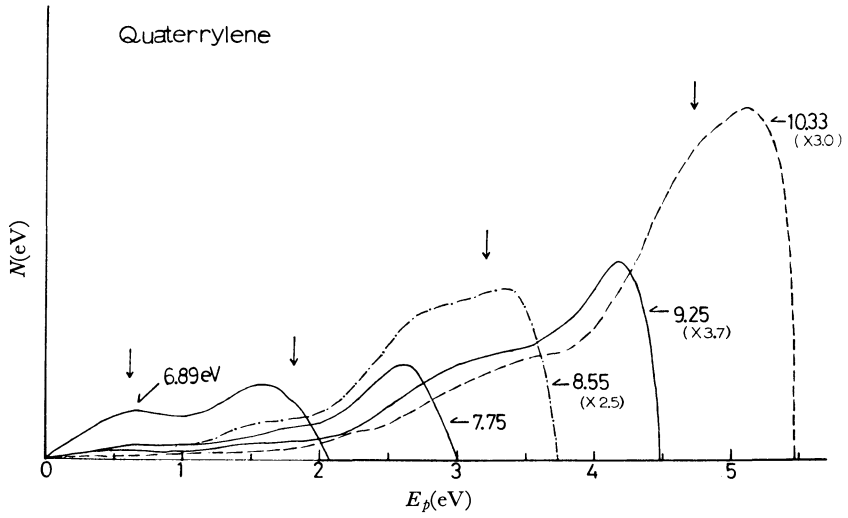

Fig. 11. Energy-loss curve for quaterrylene.

of the photon energy. The ELC of other compounds were qualitatively similar to that of anthracene.

For photon energies at which inelastic scatterings were not so frequent, broad energy-loss distributions due to vibrational excitation were clearly observed, with the maxima between $E_p=0.6$ eV and 1.0 eV (see Figs. 9, 10, and 11). Those distributions increased almost linearly with the increase in the energy-loss, commencing at $E_p=0$.

Discussion

4.1. Application of the Model to Organic Crystals. The quantum yield near the photoelectric threshold for all compounds was plotted on various power-law assumptions in order to establish the spectral characteristics. A typical example of such data is shown in Fig. 12, where the yield for the anthracene single crystal is plotted to the 1,1/2, and 1/3 power versus $h\nu$. These results, and those for other samples, indicate that the cubic power most closely represents the data and that the yield in this region obeys the relations:

$$Y \propto (h\nu - E_{th}^*)^3 \qquad (15)$$

where E_{th}^* is defined as the extraporated threshold value of the cube-root plots, such as are shown in the insets of Fig. 13. This empirical cube-law is in good agreement with the power-law predicted by Eq. (10), which may be considered to show that the form of the yield near the thresh-

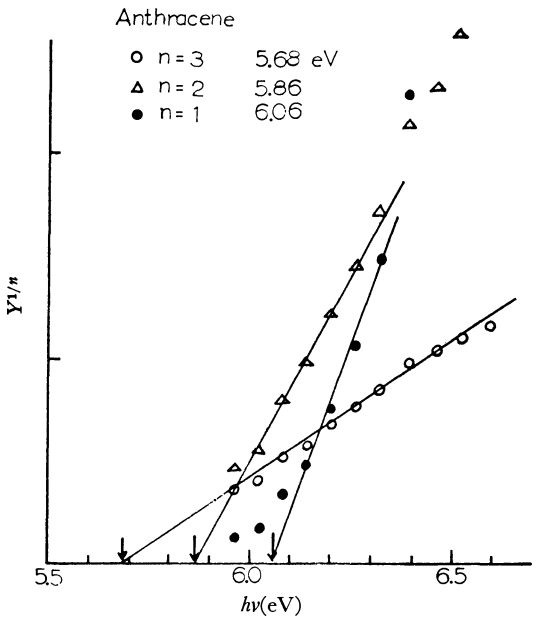

Fig. 12. Power-law fit for the photoelectric yield near the threshold for anthracene.

old for organic crystals can be effectively determined by the vibrational transition probability $|<n|0>|^2$ and the surface transmission probability $T(E)$. The importance of the $|<n|0>|^2$ factor in the photoemission of organic crystals and its linearity for n were implied by Williams and Dresner.[24]

The semi-empirical cube-power law expressed by Eq. (10) has certain limits for its validity, limits which come from the form of $T(E)$ assumed by Eq. (9). However, it is theoretically known that the $T(E) \propto E^{1/2}$ relation corresponds to the case of a rectangular potential wall.[25] Apker *et al.* used the $T(E) \propto E$ form in their analysis of the energy and spectral distribution of semiconductors.[26] Regarding the (b) assumption of our model, localized states are generally expected to exist in the continuum in molecular crystals. Although its influence was not observed in the present work, it is an important subject deserving future attention.

Figure 13 shows a cube-root-plot for each compound. In Table 1 the threshold values, E_{th}* and E_{th}, are listed and compared with those obtained by other workers. E_{th} was determined by extrapolation to a quantum yield of 10^{-7} electrons per incident photon. As can be seen from Table 1, the E_{th}* values show reasonable agreement with the E_{th} values and those of other workers.

In addition, the cube-law had been applied to determine the photoelectric threshold energy of charge-transfer complexes.[22] For those complexes the quantum yield near the threshold dropped so slowly that the threshold energy could not be determined by the extrapolation method.

4.2. Pair-production Scattering. As can be seen from EDC for perylene (Fig. 7), a remarkable low-energy peak appeared at $h\nu=7.75$ eV. Since an electron with the energy of E, less than ε_{th}, cannot escape after pair-production scattering, a low-energy peak due to pair production begins to appear in EDC at the photon energy of $h\nu \geq E_{th}+\varepsilon_{th}$. Note that perylene has a threshold energy of $E_{th} \simeq 5.40$ eV and a bandgap energy of $\Delta\varepsilon=1.95$—2.2 eV.[27] At photon energies of more than 7.75 eV, the low-energy peak was almost stationary at $E_k \simeq 0.5$ eV and grew rapidly in relative height with the increase in photon energy. Further, it was found that relatively few electrons escaped into a vacuum with kinetic energies larger than about 2 eV (see Fig. 7). These phenomena are expected from theoretical considerations for pair production (see Fig. 2). Now, we can attribute the behaviour of the low-energy peak and the scarcity of electrons with higher kinetic energies to pair-production scattering.

On the other hand, the decrease in the quantum yield is expected to occur in the $h\nu \leq E_{th}+\varepsilon_{th}$ region of the photon energy if the inelastic scattering takes place efficiently. The pair-production process is a kind of multiple process, and a decrease in quantum yield due to this process was observed in the photoemission of alkali halides.[28] For perylene, the decrease in the yield was observed in the $h\nu=6.8$—7.3 eV region (see Fig. 5). Therefore, we estimate that the threshold for the pair production of perylene is nearly equal to its band-gap energy.

For quaterrylene there are few electrons with energies larger than about 2 eV (see Fig. 8). Further, a decrease in the yield for quaterrylene had been observed between 2.2 and 2.7 eV above the photoelectric threshold by Harada.[29] The band-gap energy of quaterrylene has been reported to be 1.7 eV or more.[30] Therefore, the threshold for pair production is estimated to be a little more than its band gap.

24) R. Williams and J. Dresner, *J. Chem. Phys.*, **46**, 2133 (1967).
25) L. D. Landau and E. M. Lifshitz, "Quantum Mechanics, Nonrelativistic Theory," Pergamon Press, New York (1965), p. 77.
26) L. Apker, E. Taft and J. Dickey, *Phys. Rev.*, **74**, 1462 (1948).
27) M. Sano and H. Akamatu, This Bulletin, **34**, 1569 (1961); D. C. Northrop and O. Simpson, *Proc. Roy. Soc.*, **A234**, 124 (1956).
28) P. H. Metzger, *J. Phys. Chem. Solids*, **26**, 1879 (1965).
29) Y. Harada, The thesis for the degree of doctor (Tokyo University).
30) Y. Maruyama and H. Inokuchi, This Bulletin, **39**, 1418 (1966).

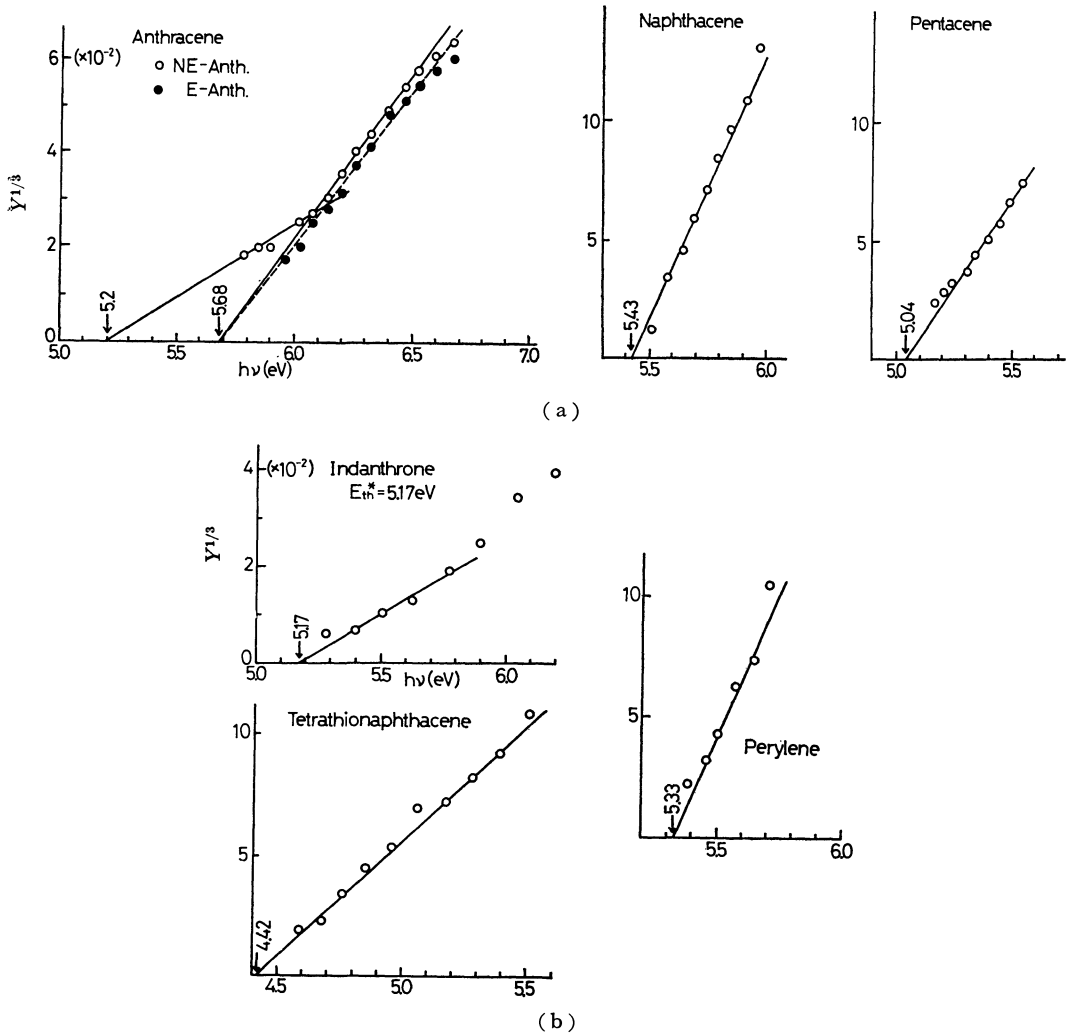

Fig. 13. Cube power-law fit for the photoelectric yield near the threshold.

Table 1. Photoelectric threshold and ionization potential for the organic crystals (in eV)

Compound	E_{th}	E^*_{th} $(=I_c)$	Other Work	I_G
Anthracene	5.65	5.68 (5.2)	5.65[a], 5.0—5.6[b]	7.38[b]
Naphthacene	5.40	5.43	5.24[c], 5.25[b], 5.31[d]	6.88[b]
Pentacene	5.06	5.04	5.06[c], 5.1[b]	
Perylene	5.40	5.33	5.40[d]	7.22[f], 7.06[g]
Indanthrone	5.10	5.17		
Tetrathionaphthacene	4.55	4.42	4.56[c], 4.45—4.54[e],*	

a) Ref. 5, b) Ref. 31, c) Ref. 9, d) Ref. 37, e) Ref. 34, f) Ref. 38, g) Ref. 39.
* This value was obtained using the observed values for work function and band gap energy (see H. Inokuchi, M. Kochi, Y. Harada, This Bulletin, **40**, 2695 (1967)).

37) M. Batley and L. E. Lyons, *Mol. Cryst.*, **3**, 357 (1968).
38) J. Briegleb, "Electronen-Donator-Acceptor-Komplexes," Springer-Verlag, Berlin (1961).
39) M.Kinoshita, This Bulletin, **35**, 1609 (1962).

For the anthracene single crystal, the threshold for pair production could not be estimated because the scarcity of energetic electrons in EDC and the decrease of the yield were not remarkable. It may be due to the inelastic scattering on the crystal surface.

4.3. Energy Structures of Organic Crystals. In ELC for anthracene (Fig. 9) the position of the first maximum was located at $E_p \simeq 1.0$ eV; the second shoulder, at $E_p \simeq 2.2$ eV; the third, at 2.9 eV, and the fourth at 3.7 eV, independent of the photon energy, meaning losses of 1.2, 1.9, and 2.7 eV respectively relative to the position of the first maximum. These results are in good agreement with that of Vilessov and Terenin.[31]

We reported[10] previously that the structures of this kind observed in ELC should be ascribed to those of valence bands. The structures which do not shift in ELC and which do shift in EDC linearly with the photon energy can be explained in terms of the so-called nondirect transition.[1,2] Schechtman and Spicer[32] found that these structures were observed very clearly for phthalocyanines under a high vacuum of 10^{-9} Torr.

At energies near the threshold for transitions from deeper bands, the yield may be expected to rise as a result of the larger density of possible initial states. In Figs. 4 and 5 the inflection points are illustrated by arrows. For anthracene they were situated at 6.93, 7.18, 7.61, 7.83, and 8.48 eV, thus meaning energies higher by 1.28, 1.53, 1.96, 2.18, and 2.83 eV respectively relative to the threshold energy, $E_{th} \simeq 5.65$ eV.

In Table 2, the discrete energy losses and the inflection points are given relative to the position of the first maximum and to the threshold value, respectively.*[7] In the table of anthracene, the two sets of values marked by(*) may show the lifting-up of the accidental degeneracies of the π-orbital energy, which are annexed to the LCAO method.[33] As may be seen from Table 2, the sequence of the descrete energy losses is well reproduced in the sequence of the inflection points in the yield, taking into consideration the resolution of ELC. This means that the discrete energy losses in ELC and the occurrence of inflection points in the yield spectra can be accounted for by assuming the existence of additional valence bands. It should also be noted that the fairly broad width of the first peak in ELC is due to the vibrational structure of the valence band. In order to ensure our observed valence band structure, a reliable method for the calculation for organic molecules is under consideration.

Table 2. Energy structure of the valence band (in eV)

Anthracene

Y		ΔY	E_p	ΔE_p
5.65		0	1.0	0
6.93 7.18	(*)	1.28 1.53	2.2	1.2
7.61 7.83	(*)	1.96 2.18	2.9	1.9
8.48		2.83	3.7	2.7

Perylene

Y	ΔY	E_p	ΔE_p
5.40	0	0.7	0
7.53	2.13	2.5	1.8
8.00	2.60	3.1	2.4
9.05	3.65	4.3	3.6

Quaterrylene

Y*	ΔY	E_p	ΔE_p
4.76	0	0.6	0
—	—	1.8	1.2
7.6	2.8	3.2	2.6
8.5	3.7	4.7	4.1

* Ref. 29.

4.4. Photoelectric Threshold Energy of Organic Crystals. The energy required to extract an electron from an organic crystal to a point in a vacuum outside its surface, *i.e.*, the photoelctric threshold energy, was obtained by measuring the quantum yield. The threshold energy, E_{th}*, corresponds to the ionization potential, I_C, of the crystal.

Table 1 summarizes the data for the threshold energies for the different organic crystal compounds studied in the present work. The table also includes data obtained by other workers and those for molecular ionization potentials, I_G. The values for I_C were obtained by extrapolation to $Y=0$ using the power-law of $Y \propto (h\nu - E_{th}^*)^3$. Regarding the column of "Other Work", Terenin and Vilessov[31] obtained their values from the measurement of the maximum kinetic energy. Kotani and Akamatu[34] determined the work function of organic crystals using a contact potential-difference method.

The table shows that the I_C values of the organic crystals under consideration are below I_G by 1—

31) A. Terenin and F. Vilessov, "Advances in Photochemistry," Vol. 2, Interscience Publ., New York (1964), p. 385.

32) B. H. Schechtman and W. E. Spicer, *Chem. Phys. Lett.*, **2**, 207 (1968).

*7 When ELC are measured with sufficient accuracy in the future, the rising points in ELC should be compared with the inflection points in the yield spectra.

33) C. A. Coulson, *J. Phys. Soc.*, **60**, 257 (1948).

34) M. Kotani and H. Akamatu, private communication.

2 eV. As has been suggested by Lyons,[35] this difference may be due to the polarization energy of the crystal by a positive centre.

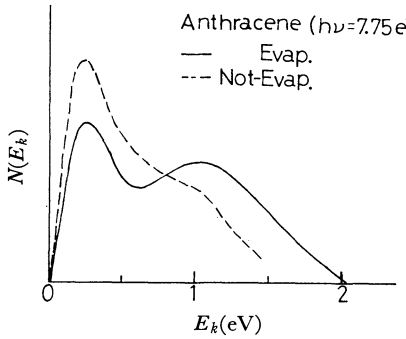

Fig. 14. Effect of oxygen on EDC for anthracene single crystal.

35) L. E. Lyons, *J. Chem. Soc.*, **1957**, 5001; L. E. Lyons and J. C. Mackie, *Proc. Chem. Soc.*, **1962**, 71.

For the I_C of the anthracene single crystal, we obtained two values for NE–Anth. One was 5.68 eV, which agreed with the I_C of E–Anth.; the other was about 5.2 eV. As Pope and Burgos[36] pointed out, the lower value for I_C seems to be caused by the oxygen-anthracene pair formed on the surface of the anthracene crystal. Figure 14 shows the energy distribution curves at $h\nu$= 7.75 eV for both E–Anth. and NE–Anth. It can be seen from the figure that the number of slow electrons for NE–Anth. is larger than that for E–Anth.; this may be attributed to an inelastic collision on the crystal surface between photoelectrons and the oxygen-anthracene pair.

The authors gratefully acknowledge their valuable discussions with Professor Yutaka Toyozawa, The University of Tokyo.

36) M. Pope and J. Burgos, *Mol. Cryst.*, **1**, 395 (1966).

BULLETIN OF THE CHEMICAL SOCIETY OF JAPAN VOL. 43 2702—2705 (1970)

Ionic Dissociation. II. An Extended Hückel Treatment of the Dissociation of Pseudo Acids

Hiroko YAMABE, Hiroshi KATO*1 and Teijiro YONEZAWA

Department of Hydrocarbon Chemistry, Faculty of Engineering, Kyoto University, Sakyo-ku, Kyoto

(Received February 14, 1970)

The electronic structures of several pseudo acids are studied, in connection with their reactivity and stability, by the Extended Hückel method. The linear relationship between the observed pK_a value and the change in the calculated electronic energy, ΔE, in the course of the dissociation of the pseudo acids is also observed. The order of the stability of the carbanion, referred to its parent acid, as estimated from our calculations, is; $CH_2NO_2^- > CH_2COCH_3^- > CH_2CN^-$. Di- or tri- substituted carbanions should be more stable. This order is parallel with that of the electron-attracting abilities of the groups adjacent to the methylene group. The highest-occupied MO of the carbanion is remarkably unstable, resembling a lone-pair level, and the atomic orbital population of that MO is large at the P_z AO of the carbon. This reflects the high reactivities of the carbanion as a reaction intermediate; the electrophilic addition probably takes place at the carbon atom.

Carbanions are known as important intermediates in many organic and biological reactions,[1] especially in various condensations such as those of the aldol-type. The more easily the carbanion is generated, and the more stabilized it is, the more enhancement of the reaction may be expected. Therefore, it would be significant to ascertain what kinds of carbanions satisfy these conditions.

Studies of the carbanions have been carried out by many authors. Especially, there are many reports by Cram *et al.*[2] paying particular attention to their sterochemistry. However, as far as we know, there have been few discussions of the stabilities and the reactivities of the carbanions,

*1 Present address; Department of General Education, Nagoya University, Chikusa-ku, Nagoya.

1) L. L. Ingraham, "Biochemical Mechanics", John Wiley & Sons, Inc., New York (1962), Part Two, Codensation. M. J. S. Dewar, "The Electronic Theory of Organic Chemistry", The Clarendon Press in the University of Oxford (1949), Chapter VII.

2) D. J. Cram, A. Langemann, J. Allinger and K. R. Kopecky, *J. Amer. Chem. Soc.*, **81**, 5740 (1959) and subsequent several papers.

on the basis of the calculated electronic structures. Nagakura *et al.*[3] studied the dissociation of pseudo acids from the spectroscopic point of view and discussed their π electronic structures. However, they did not refer to the stability and reactivity of the carbanions.

In this paper, as one of a series of studies of the ionic dissociation,[4] we will report some findings on the electronic structures, including the π and σ electronic systems, of some pseudo acids which dissociate in water as in Eq. (1) and which give carbanions.

$$HA \rightleftarrows A^- + H^+ \qquad (1)^{*2}$$

Also the relationship between pK_a[5] and the change in the calculated electronic energy, ΔE, in the course of dissociation (Eq. (1)) will be presented.

Calculations

The electronic energy and the electronic structure of the molecule and its anion were calculated by using the Extended Hückel method proposed by Hoffmann,[6] in which all the valence atomic orbitals (AO) are taken into account. For the coulomb integrals, H_{rr}, the following valence-state ionization potentials (eV) for the hydrogen, carbon, oxygen, and nitrogen have been used:

H_{rr}(H1S) = −13.6 H_{rr}(C2S) = −21.43
H_{rr}(C2P) = −11.42 H_{rr}(O2S) = −35.30
H_{rr}(O2P) = −15.45 H_{rr}(N2S) = −27.50
H_{rr}(N2P) = −14.49

The resonance integrals, H_{rs}, have been calculated by means of $H_{rs}=(1/2)KS_{rs}(H_{rr}+H_{ss})$, where $K=1.75$[6] and where S_{rs} is the overlap integral between the rth and sth AO's. The electronic energy change, ΔE, in the dissociation process is estimated by means of the difference of the calculated total electronic energy as follows:

$$\Delta E = E(\text{final}) - E(\text{initial}) \qquad (2)$$

The bond lengths employed are given in Table 1. The bond angles are assumed to be as follows: ∠ONO in CH_3NO_2: 127°; for a sp^2 carbon, 120°, and for a sp^3 carbon, 109.5°. The Z axis is chosen in the direction of the π orbital. The calculation of the final state as an anion is made in the configuration of the sp^2 hybridization of the methylene carbon (abbreviated hereafter as the sp^2 configuration). For the anions of CH_3NO_2 and CH_4, two anionic forms, the sp^3 and sp^2 configurations, are calculated. As it is revealed that the sp^2 configuration is more stable for these molecules, the sp^2 configuration is adopted as the final anionic form of the other molecules.

Table 1. Interatomic distances (Å)

C-H	1.09
N-O (in CH_3NO_2)	1.21
C-N (in CH_3NO_2)	1.46
C-N (in CH_3CN)	1.16
C-C (in CH_3CN)	1.46
C-C (in CH_3COCH_3)	1.54
C-O (in CH_3COCH_3)	1.22

For $CH_2(NO_2)_2$, the cofiguration (1) is adopted; in our calculations it is slightly stable than the other configuration (2).

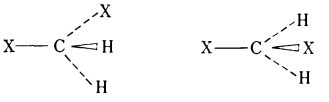

(1) (2)

In both (1) and (2), X denotes the NO_2 substituent and the central carbon has an sp^3 hybridization.*3 One of the reasons for this seems to be a rather large π-conjugation in the X–C bond of the configuration (1). For CH_3COCH_3, the following configuration is assumed, in which the central carbon has an sp^2 hybridization:

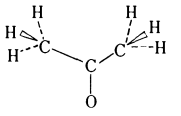

Results and Discussion

As many authors have pointed out, the charge distribution calculated by this method is unrealistic. Therefore, the absolute values of the electron densities and the energy levels have little meaning. However, the trend of their variation in a series of molecules may be discussed meaningfully. The calculated results are given in Table 2, together with the observed values of pK_a. The values of pK_a are plotted against ΔE (eV) for various pseudo acids as in Fig. 1. A linear

3) S. Nagakura, *Mol. Phys.*, **1960**, 152; F. Hashimoto, J. Tanaka and S. Nagakura, *J. Mol. Spectry.*, **10**, 401 (1963).

4) T. Yonezawa, G. Del Re and B. Pullman, This Bulletin, **37**, 985 (1964). T. Yonezawa, H. Yamabe and H. Kato, "Ionic Dissociation I. A Hückel Molecular-Orbital Treatment of the Dissociation of Carboxylic Acids and Some Bases," (to be published in this Bulletin).

*2 The presence of the H_2O molecule and its effect on the dissociation process is not taken into account in the present work.

5) P. G. Pearson and A. L. Dillon, *J. Amer. Chem Soc.*, **75**, 2439 (1953).

6) R. Hoffmann, *J. Chem. Phys.*, **39**, 1397 (1963).

*3 The configurations (1) and (2) are apparently different, because the substituent $N\langle^{O}_{O}$ is not spherical.

TABLE 2. CALCULATED ΔE AND OBSERVED pK_a VALUES

Compounds	Obsd.[5] pK_a	Calcd. ΔE (eV)
CH_4	40	6.783
CH_3NO_2	11	5.006
$CH_2(NO_2)_2$	4	4.576
$CH(NO_2)_3$	0	4.468
CH_3CN	25	5.876
$CH_2(CN)_2$	12	5.368
$CH(CN)_3$	0	5.011
CH_3COCH_3	20	5.791

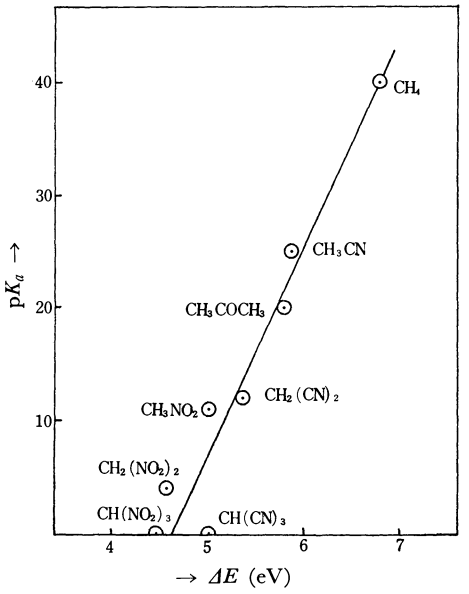

Fig. 1. The dissociation constant pK_a *vs* ΔE.

relationship between the pK_a's and the ΔE's is observed. That is the pseudo acid is ionized more easily as the ΔE is smaller. Therefore, the order of the stability of the carbanion referred to its parent acid, as estimated from our calculations, should be:

$$CH_2NO_2^- > CH_2COCH_3^- > CH_2CN^-$$

and di- or tri- substituted carbanion should be more stable still. On the other hand, the common order of the electron-attracting abilities of the groups adjacent to the methylene group is $NO_2 > CO > CN$. This order is also confirmed by the population analysis in our calculation to be $NO_2 > COCH_3 > CN$. Therefore, it can be said that the greater the ability of the substituent to bear a negative charge generated in the carbanion, the more stable is the carbanion to the parent acid and the smaller is the pK_a value of the parent acid.

Next we would like to give a detailed discussion of the electronic structure and energy levels of CH_3NO_2, picked as an example from the obtained results. In Fig. 2, atomic populations are given for the parent acid, CH_3NO_2 (I), and the anionic form, $CH_2NO_2^-$, in the sp^3 (II)*4 and sp^2 (III) configurations. The coordinate axes and the numbering of the three H atoms are also shown. The C atoms of CH_3NO_2 (I) and $CH_2NO_2^-$(II) have an sp^3 hybridization, and that of $CH_2NO_2^-$ (III) has an sp^2 hybridization. The NO_2 group is in the x–y plane, and $CH_2NO_2^-$(III) is planar. It may be seen that an electron released by the dissociation of the proton delocalizes on a whole molecule. The total electronic energy and the π atomic orbital population of the P_z AO in the highest occupied (HO) orbitals are shown in Table 3. In Table 3 and Fig. 2 it may be observed that, in spite of the delocalization of an electron released on a whole molecule, the π atomic orbital population of the p_z AO of the carbon atom C(Z) in the highest occupied orbital of the anion, which is a frontier orbital for the electrophilic attack,[7] becomes much larger than that of the parent acid. This means that the electrophilic addition must take place at the carbon atom; this is in agreement with the experimental suggestion.

Furthermore, the energy levels adjacent to the HO level and the lowest unoccupied (LU) level are illustrated in Fig. 3. The qualitative correlation between the energy levels of CH_3NO_2 (I) and its anion is studied. The third highest occupied MO (denoted by C–H in Fig. 3) of CH_3NO_2 (I) is considerably localized at the C–H_3 bond*5 to be dissociated*3). This C–H level corresponds to the HO level of the anion. (See the dotted line in Fig. 3.) These levels of the anions are remarkably unstable and seem to resemble a lone-pair level in which almost one electron localizes at the P_z AO of the carbon (See Table 3). This reflects the high reactivities of a carbanion as a reaction intermediate. The features of the elctronic structure and the energy levels of CH_3NO_2 and $CH_2NO_2^-$, which have been described above, are also seen in the cases of CH_4 and CH_3^- in the sp^3 and sp^2 configurations.

It is said that such carbanions as $CH_2NO_2^-$ and CH_2CN^- planar and π electron systems must develop a whole molecule. When the configuration of a carbanion, $CH_2NO_2^-$, is changed from an sp^3 to an sp^2, the following variations in

*4 In our calculations, the anionic form induced by the dissociation of the H_3 of CH_3NO_2 (I) becomes more stable than that induced by the dissociation of the H_1. The stable form is shown in Fig. 2 as CH_3NO_2 (II).

*5 The MO coefficients of the s, p_x, p_y and p_z AO's of the atoms C and H_3 in this level are as follows: C(s:−0.001, p_x:0.028, p_y: 0.000, p_z:−0.565), H_3 (s: −0.437)

7) K. Fukui, T. Yonezawa, C. Nagata and H. Shingu, *J. Chem. Phys.*, **22**, 1433 (1954).

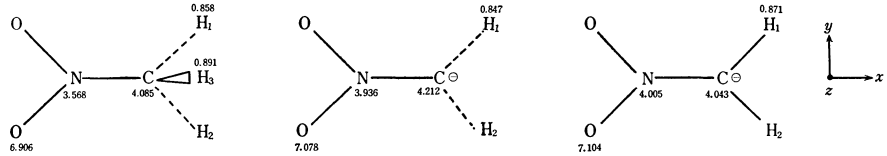

CH_3NO_2 (I) $CH_2NO_2^-$ (II) $CH_2NO_2^-$ (III) (in plane)

Fig. 2. Atomic populations of CH_3NO_2(I) and its anions are shown. The coordinate axis and the numbering of the three H atoms are also shown. The C atoms of CH_3NO_2(I) and $CH_2NO_2^-$(II) have an sp^3 hybridization, and that of $CH_2NO_2^-$(III) has an sp^2 hybridization. The NO_2 group is in the x-y plane and $CH_2NO_2^-$(III) is planar.

Table 3. Total electronic energy and the atomic orbital population of the P_z AO and that in the highest occupied MO

Compounds		CH_3NO_2(I)	$CH_2NO_2^-$(II)*	$CH_2NO_2^-$(III)*
Total electronic energy (eV)		−493.71	−487.92	−488.70
Atomic orbital population of the P_z AO in the H.O.**	C(z)	0.004	0.970	0.966
	N(z)	0.000	0.369	0.446
	O(z)	0.000	0.264	0.294
Atomic orbital pop. of the P_z AO	C(z)	1.059	1.068	1.009
	N(z)	0.815	1.198	1.274
	O(z)	1.661	1.832	1.858

* $CH_2NO_2^-$(II), $CH_2NO_2^-$(III) denote the sp^3 and the sp^2 configuration, respectively.
** Highest occupied level

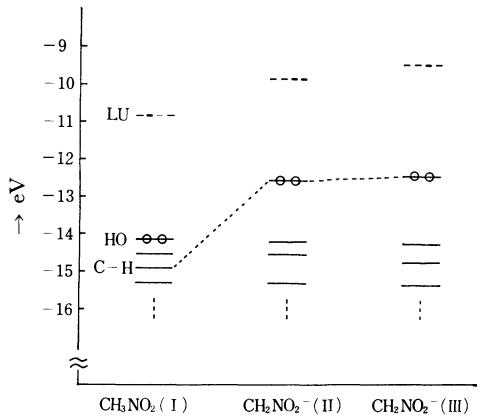

Fig. 3. Energy levels adjacents to the highest occupied level(HO) and the lowest unoccupied level(LU). C-H denotes the level, of which MO is considerably localized at the C-H bond to be dissociated. The dotted line shows the correspondence between the C-H level and HO of the anions.

the energy and the population are observed in our calculations:

1. An electron released is much delocalized over a whole molecule. That is the π conjugation strongly prevails.

2. The total electronic energy becomes lower in an sp^2 than in an sp^3. That is a carbanion treated here becomes more stable in the sp^2 configuration.

3. The highest occupied level becomes higher. That is, a carbanion becomes more reactive.

These results indicate that the configuration of the carbanion will be changed from the sp^3 to the sp^2 by the dissociation of the proton.

As for the electronic transition of the carbanion Nagakura *et al.*[3] observed that the ultraviolet absorption spectrum of the carbanion has a strong band at wavelengths longer than in the parent pseudo acid; they ascribed this to the intramolecular charge transfer band of the anion. In the present calculations, too, the π–π^* transition energy of the anion is certainly smaller than that of the neutral molecule. However, we can not discuss the electronic transition in more detail, for the approximation of our calculation is very rough.

The calculation was carried out on a HITAC 5020 computer at the computation center of the University of Tokyo.

BULLETIN OF THE CHEMICAL SOCIETY OF JAPAN VOL. 43 2706—2713 (1970)

Group Interactions in Polyelectrolytes. III. The Electrostatic Effect of Neighboring Groups on the Ionization of Polyelectrolytes

Hiroshi KAWABE and Masaya YANAGITA

The Institute of Physical and Chemical Research, Yamato-machi, Saitama

(Received February 17, 1970)

The two parameters in the modified Henderson-Hasselbach equation, $pH=pK_a-n'\log[(1-\alpha)/\alpha]$, where pK_a and n' are empirical constants and where α is a degree of the ionization of a polymeric acid, were evaluated on the assumption that the ionization of polyelectrolytes is electrostatically affected in the main by a few neighboring ionized groups and that the overall ionization is composed of only a few elementary ionization. The titration curves of various polyelectrolytes in the absence of salt could be classified into two types: $\Delta pK' \geqq 2$ and $\Delta pK' < 2$, where $\Delta pK'$ is the difference between the succeeding ionization constants. The maleic acid-styrene copolymer and polyvinyl amine belong to the former type, while polyacrylic acid and pectinic acid belong to the latter. In the former, a plot of pH against $\log[(1-\alpha)/\alpha]$ nearly falls on a line in only a limited range and n' is substantially equal to the number of elementary ionizations. In the latter, both pK_a and n' are related to the distance between the groups. The titration curve of polyacrylic acid, drawn by means of the above equation with the parameters calculated on the basis of the kinetic data of the alkaline hydrolysis of polymethyl acrylate, was in good agreement with the observed titration curve. The titration data of other polyelectrolytes also fall nearly on their calculated titration curves.

The potentiometric titration curves of polymeric acids (or polymeric bases) do not obey the Henderson equation for monomeric acids (or bases), and their apparent dissociation constant, K_{app}, decreases with an increase in the degree of ionization in the case of polymeric acids and increases in the cases of polymeric bases depending on the electrostatic effect of the ionized groups fixed on the macromolecule. Although it is difficult to eliminate the electrical effect entirely by adding neutral salt, Katchalsky *et al.*[1] showed that the titration data of some polyelectrolytes could be expressed by a single dissociation constant of their monomeric unit when the correction for an electric field was properly made.

On the other hand, Marcus[2] presented a theory of the potentiometric titrations of polymeric acids taking into account only electrical interaction between neighboring groups; he suggested that the polymeric acids under the conditions given in his theory would behave much like dibasic acid. Katchalsky *et al.*[3] found that the electrostatic interaction between neighboring ionized groups of polyvinylamine could not be eliminated by the addition of salt in a very high concentration or even by making a correction for electrostatic field, and showed that its behavior in the titration with hydrobromic acid in the presence of sodium chloride was also similar to that of diamine. It was also reported that the titration curve of the maleic acid-styrene copolymer resembled that of dibasic acid.[4,5]

The titration curves of polymeric acids in the absence of salt are difficult to analyze theoretically because of the intense electrostatic effect of neighboring ionized groups, and the Henderson-Hasselbach-Katchalsky equation[6] is the only empirical relation to describe their titration data. In the present study, the empirical constants in the equation have been evaluated by assuming that the ionization of polyelectrolytes is electrically affected mainly by a few neighboring charged groups; the titration curves of several polymeric acids and bases have been interpreted on this basis.

Experimental

Commercial anhydrous ethylenediamine of a reagent grade was distilled before use; it was proved to be pure by its refractive index. Crystalline 1,3-propanediamine dihydrochloride was dissolved in water, and the solution was passed through a column of Dowex-2 X-8 in the hydroxide form to remove the hydrogen chlo-

1) A. Katchalsky, N. Shavit and H.Eisenberg, *J. Polymer Sci.*, **13**, 69 (1954).

2) R. A. Marcus, *J. Phys. Chem.*, **58**, 621 (1954).

3) A. Katchalsky, J. Mazur, P. Spitnik, *J. Polymer Sci.*, **23**, 513 (1957).

4) E. R. Garret and R. L. Guile, *J. Amer. Chem. Soc.*, **73**, 4533 (1951).

5) J. D. Ferry, D. C. Udy, F. C. Wu, G. E. Heckler and D. B. Fordyce, *J. Colloid Sci.*, **6**, 429 (1951).

ride. Aqueous solutions of the amines (0.01 M) were titrated with 0.1 N hydrochloric acid at 25°C, and the pH of the solution was measured with a Beckman Model G pH meter.

Evaluation of the Parameters in the Henderson-Hasselbach-Katchalsky Equation

Katchalsky and spitnik[6] found that the potentiometric titration curves of some polymeric acids could be described by the generalized Henderson-Hasselbach relation:

$$\mathrm{pH} = \mathrm{p}K_a - n' \log \frac{1-\alpha}{\alpha} \tag{1}$$

where $\mathrm{p}K_a$ and n' are empirical constants and where α is a degree of ionization of an acid. For a monobasic acid, n' is unity.

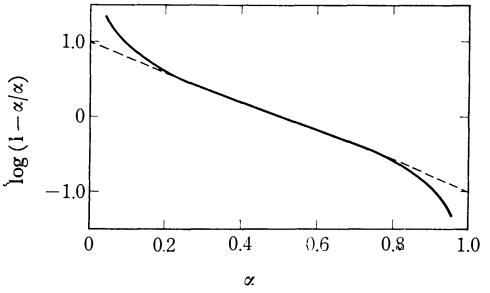

Fig. 1. Plot of $\log[(1-\alpha)/\alpha]$ against α.

As is shown in Fig. 1, $\log[(1-\alpha)/\alpha]$ is approximately proportiona to α over a wide range of α, 0.2—0.8:*1

$$\log \frac{1-\alpha}{\alpha} = 1 - 2\alpha \tag{2}$$

The introduction of Eq. (2) into Eq. (1) gives:

$$\mathrm{pH} = (\mathrm{p}K_a - n') + 2n'\alpha \tag{3}$$

Hence, n' may be estimated from the slope of a titration curve in its middle range at $(\Delta\mathrm{pH}/\Delta\alpha)/2$. Equation (3) also indicates that the main part of the titration curve of any monobasic acid ($n'=1$) is within 2 pH, and also suggests that in the titration curve of a dibasic acid or a mixture of two monobasic acids, two ionizable groups can be distinguished only when $\mathrm{p}K_2 - \mathrm{p}K_1 \gtrsim 2$.

In the titration of a polybasic acid with σ ionizable groups, the degree of ionization with respect to the nth ionized group, *i.e.*, the degree of the nth elementary ionization, α_n', is given by:

$$\mathrm{pH} = \mathrm{p}K_n' - \log \frac{1-\alpha_n'}{\alpha_n'} \tag{4}$$

or:

$$\alpha_n' = 1/[1+10^{(\mathrm{p}K_n'-\mathrm{pH})}] \tag{5}$$

where $\mathrm{p}K_n'$ is the negative logalithms of the nth elementary ionization constant.. If $\Delta\mathrm{p}K' \equiv \mathrm{p}K'_{n+1} - \mathrm{p}K'_n \geq 2$, α'_n can be estimated over a wide range of α'_n by the following relation:

$$\alpha_n' = \sigma\alpha - (n-1) \qquad \Delta\mathrm{p}K' \geq 2 \tag{6}$$

Since the α'_n of a polybasic acid is calculated by Eq. (5) when $\mathrm{p}K_n'$ is known, the over-all degree of ionization of an acid with σ groups is given by:

$$\alpha = (\sum_{n=1}^{\sigma} \alpha_n')/\sigma \tag{7}$$

The titration curves of several imaginary polybasic acids with various $\Delta\mathrm{p}K'$ values have been drawn in this manner. The titration curves calculated by arbitrarily taking $\mathrm{p}K'_1$ as unity in the case $\sigma=4$ are shown in Fig. 2, in which the circles indicate the points where $\alpha'_n=0.5$ and in which the four vertical lines correspond to $\alpha=1/8$, 3/8, 5/8, and 7/8. In the figure, the calculated plots of pH against $\log[(1-\alpha)/\alpha]$ are also shown. It may be seen that the plots can be represented by a line over a wide range. Upon the examination of the case when $\sigma=2$, the plot was also found to be substantially linear over a wide range of α provided that $\Delta\mathrm{p}K'<2$. The values of n' thus determined are listed in Table 1. It was also found that the value of n' is closely equal to

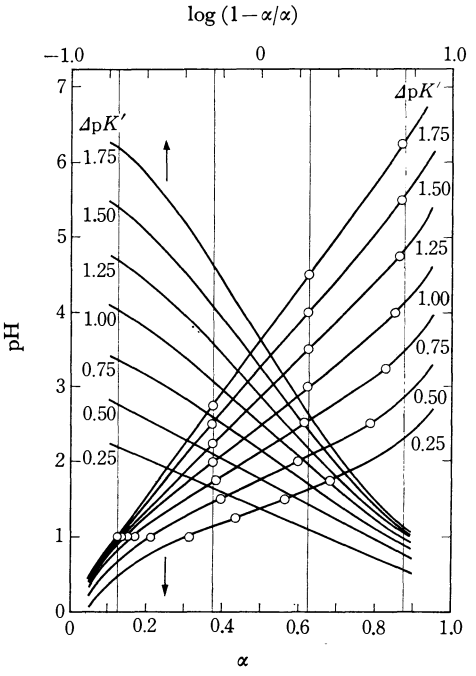

Fig. 2. Calculated titration curves of tetrabasic acids. ($\mathrm{p}K_1'=1$)

6) A. Katchalsky and P. Spitnik, *J. Polymer Sci.*, **2**, 432 (1947).

*1 Since the left term of Eq. (2) can be expanded as follows:

$$\log[(1-\alpha)/\alpha] = 2[(1-2\alpha) + (1-2\alpha)^3/3 + (1-2\alpha)^5/5 + \cdots]/2.303$$

this term is near to $(1-2\alpha)$.

TABLE 1. VALUES OF n' FOR SOME IMAGINARY POLYBASIC ACIDS

σ	$\Delta pK'$						
	0.25	0.50	0.75	1.00	1.25	1.50	1.75
2	1.02	1.12	1.16	1.28	1.45	1.66	1.87
4	1.09	1.32	1.69	2.10	2.58	3.06	3.58

the number of elementary ionization, σ, when $\Delta pK' \approx 2$. In the case when $\Delta pK' > 2$, it was found that the plots fall on σ parallel lines with the same slope, $n' = \sigma$, and that the distance between the lines is equal to $(\Delta pK' - 2)$ pH. Hence, when $\Delta pK' \geq 2$, n' is an integer which represents the total number of elementary ionizations. However, some difficulties are encountered when a plot of pH against $\log [(1-\alpha)/\alpha]$, based on the experimental titration data, is expressed by a single line with n' closely equal to an integer, since, for instance, $n' \approx 2$ will be realized not only when $\sigma = 2$ and $\Delta pK' = 2$, but also when $\sigma = 4$ and $\Delta pK' < 2$. The criterion is that if the titration curve is divided into two equal parts at the middle ionization point, the data of each part will fit Eq. (4) in the former case, but not in the latter case.

On the basis of the above-mentioned nature of the titration curve, the parameters in Eq. (1) will be evaluated in the following two cases: $\Delta pK' \geq 2$ and $\Delta pK' < 2$.

1) **$\Delta pK' \geq 2$.** On the basis of Eqs. (2) and (6), the following approximate relatoin is given for the case when $\Delta pK' \geq 2$:

$$\log \frac{1-\alpha_n'}{\alpha_n'} = \sigma \log \frac{1-\alpha}{\alpha} - (\sigma + 1 - 2n) \tag{8}$$

The introduction of the relation to Eq. (4) gives:

$$pH = [pK_n' + (\sigma + 1 - 2n)] - \sigma \log \frac{1-\alpha}{\alpha} \tag{9}$$

By comparing Eq. (9) with Eq. (1), we obtain:

$$\left.\begin{aligned} pK_a &= pK_n' + (\sigma + 1 - 2n) \\ n' &= \sigma \end{aligned}\right\} \tag{10}$$

Hence, the difference in pK_a between succeeding ionization steps, ΔpK_a, is:

$$\Delta pK_a = \Delta pK' - 2 \tag{11}$$

If $\Delta pK' = 2$, pK_a takes a single value. Therfore, the plot of pH against $\log [(1-\alpha)/\alpha]$ may be represented by a line with a slope of $n' = \sigma$. If $\Delta pK' > 2$, the plot may be represented by σ parallel lines separated by a distance of $(\Delta pK' - 2)$. It can thus be concluded that when $\Delta pK' \geq 2$ the constant n' does not correlate with the magnitude of the electrostatic effect, but is equal to the number of elementary ionizations. In this case, each ionization step is characterized substantially by a single ionizable group, and the electrostatic free energy of the nth elementary ionization, $(\Delta F^i{}_{el})_n$, is given by:

$$(\Delta F^i{}_{el})_n = 2.303 \boldsymbol{R}T [pK_n' + \log \frac{\sigma - n + 1}{n} - pK_0] \tag{12}$$

where pK_0 is the intrinsic ionization constant.

2) **$\Delta pK' < 2$.** When $\Delta pK' < 2$, each elementary ionization is no longer distinguishable in the titration curve, because the ionization of one kind of group is accompanied by that of certain number of other groups. When the ionizations of several kinds of groups overlap, the electrostatic free energy of ionization at a given α, $(\Delta F^i{}_{el})_\alpha$, may be given by:[*2]

$$\begin{aligned} (\Delta F^i{}_{el})_\alpha &= \sum_{n=1}^{\alpha} f_n (\Delta F^i{}_{el})_n \\ &= 2.303 \boldsymbol{R}T [\sum_{n=1}^{\sigma} f_n \left(pK_n' + \log \frac{\sigma - n + 1}{n} \right) \\ &\quad - pK_0 \sum_{n=1}^{\sigma} f_n] \end{aligned} \tag{13}$$

where f_n is the mole fraction of the nth ionizable group at a given α. Since a differential amount of the nth elementary ionization is given, from Eq. (4), by $d\alpha'_n / dpH = \alpha'_n (1 - \alpha'_n)$, f_n is defined as follows:

$$\left.\begin{aligned} f_n &= \alpha_n' (1 - \alpha_n') / \sum_{n=1}^{\sigma} \alpha_n' (1 - \alpha_n') \\ \sum_{n=1}^{\sigma} f_n &= 1 \end{aligned}\right\} \tag{14}$$

The second term of Eq. (13) is equal to pK_0 by the definition. The first term of Eq. (13) was computed for the imaginary acids given in Table 1 and then compared with the $pH + \log [(1-\alpha)/\alpha]$ term. In Fig. 3, the numerical difference between the two terms is plotted against α for various

*2 Since pK_n' is given by Eq. (4), the first term of Eq. (13) is transformed as follows:

$$\begin{aligned} &\sum_{n=1}^{\sigma} f_n \left(pH + \log \frac{(1-\alpha_n')(\sigma - n + 1)}{\alpha_n' \times n} \right) \\ &= \sum_{n=1}^{\sigma} f_n \left(pH + \log \frac{N_n (\sigma - n + 1)}{N_n' \times n} \right) \\ &= \log \prod_{n=1}^{\sigma} \frac{(m_n) f_n}{(m_n') f_n \times m_{H^+}} = -\log K_\alpha \end{aligned}$$

where N_n and N'_n are the numbers of the elements which concern the nth elementary ionization and which contain $(\sigma - n + 1)$ unionized groups and n ionized groups respectively, where m_n and m'_n are the molarities of unionized and ionized groups of the respective elements, and where K_α is the ionization constant defined in the equation. Hence,

$$(\Delta F^i{}_{el})_\alpha = 2.303 \boldsymbol{R}T (pK_\alpha - pK_0)$$

By comparing this equation with Eq. (16), pK_α can be estimated by:

$$pK_\alpha = pH + \log \frac{1-\alpha}{\alpha}$$

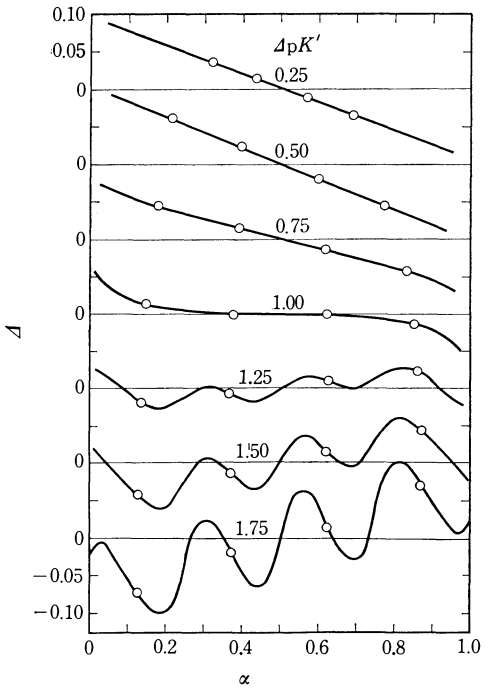

Fig. 3. Calculated difference $\Delta=\sum_{n=1}^{4}\left(pK_n'+\log\frac{5-n}{n}\right)-\left(pH+\log\frac{1-\alpha}{\alpha}\right)$ as a function of α.

$\Delta pK'$ values when $\sigma=4$. In the figure, the circles indicate the points where $\alpha'_n=0.5$. For the case when $\Delta pK'=2$, the difference amounts to about 0.2. Accordingly, the two terms may be equal within an error of ±0.1 when $\Delta pK'<2$; therefore:

$$\sum_{n=1}^{\sigma}f_n\left(pK_n'+\log\frac{\sigma-n+1}{n}\right)=pH+\log\frac{1-\alpha}{\alpha} \quad (15)$$

Hence, in the case when $2>\Delta pK'$, Eq. (13) may be transformed into the familiar equation:

$$pH=pK_0-\log\frac{1-\alpha}{\alpha}+\frac{(\Delta F^i{}_{el})_\alpha}{2.303\boldsymbol{R}T} \quad (16)$$

This equation was derived by Katchalsky and Gillis[7] for polymeric acid and transcribed, in the neighborhood of the half-ionization point, in the form of Eq. (1).[1,7]

The first term of Eq. (13) was also numerically compared with the term, $pK'+\log[(\sigma-n+1)/n]$, in Eq. (12) for the imaginary acids given in Figs. 2 and 3 ($\sigma=4$); the two terms were found to have almost the same value (within ±0.05) at $\alpha'_n=0.5$ when $n=2$ and 3. Hence, $(\Delta F^i{}_{el})_\alpha$ can be replaced by $(\Delta F^i{}_{el})_n$ at the points:

$$(\Delta F^i{}_{el})_\alpha=(\Delta F^i{}_{el})_n \qquad \alpha_n'=0.5\ (n=2 \text{ and } 3) \quad (17)$$

The fact that the titration curves of polyelectrolytes are independent of the chain length suggests that the electrical interaction between ionized groups which are situated close together compared with the over-all distance of the polyion contributes significantly to the electrostatic free energy of ionization.[8] Such an interaction was actually observed in the alkaline hydrolysis of polymethyl acrylate; the reaction in a 29% aqueous acetone solution proceeded in four distinct steps, and the rate constant of each step remained substantially unchanged.[9] This can be understood by assuming that the hydrolysis of an ester group is affected mainly by the electrical charges of the first and second neighboring groups. If the same assumption holds in the ionization of polyacrylic acid,*3 the ionization of the acid may be considered to be composed of four elementary ionizations ($\sigma=4$) and the electrostatic free energy of the nth ionization may be given by:

$$(\Delta F^i{}_{el})_n=(\boldsymbol{Ne}^2/D)\sum_i(z_i/\bar{r}_i) \quad (18)$$

where D is the effective dielectric constant, where z_i is the number of the electrical charge in the ith group apart from the ionizing group ($z_i=0,1$ or 2, and $i=1$ and 2), and where $\bar{r}_i$ is the average distance between the ionizing group and the ith group.

From Eqs. (12) and (18), it follows that:

$$pK_0=pK_n'+\log\frac{\sigma-n+1}{n}-\frac{\boldsymbol{Ne}^2}{2.303\boldsymbol{R}TD}\sum_i\frac{z_i}{\bar{r}_i} \quad (19)$$

Since $\sum_i(z_i/\bar{r}_i)$ is considered to be $2/\bar{r}_2$, $2/\bar{r}_1$, and $2(1/\bar{r}_1+1/\bar{r}_2)$ when $n=2$, 3, and 4 respectively, when $\sigma=4$, as has been illustrated in a previous paper,[9] this term can be represented by:

$$\sum_i(z_i/\bar{r}_i)=[2/k-1)\{(n-1)-2\}^2+(n-1)]/\bar{r}_1 \quad n\neq1 \quad (20)$$

where $k=\bar{r}_2/\bar{r}_1$.

Although Eq. (6) has been found to be correct for the case when $\Delta pK'\geqq2$, the relation still

7) A. Katchalsky and J. Gillis, *Rec. Trav. Chim. Pays-Bas*, **68**, 879 (1949).

8) H. Morawetz. "Macromolecules in solution," Interscience Publishers, New York (1965), p. 354; P. Doty and G. Ehrlich, *Ann. Rev. Phys. Chem.*, **3**, 81 (1952); See also Ref. 1.

9) H. Kawabe and M. Yanagita, This Bulletin, **42**, 3109, (1969).

*3 The reason why the four-step ionization does not appear in the titration curve of polyacrylic acid is that the $\Delta pK'$ is proportional to the increase in $(\Delta F^i{}_{el})_n$, whereas the rate constant of the alkaline hydrolysis of polymethyl acrylate, K_n, is an exponential function of $(\Delta F^{\neq}_{el})_n$, the electrostatic free energy of activation. The succeeding step of ionization is distinguishable if $\Delta pK'>2$, which corresponds to $\Delta(\Delta F^i{}_{el})_n>2.8$ kcal. On the other hand, the succeeding steps of the chemical reaction are distinguishable if the ratio of the succeeding rate constants is more than 2, which corresponds to $\Delta(\Delta F^{\neq}_{el})_n>0.5$ kcal.

holds at $\alpha' = 0.5$, at least when n=2 and 3 in the case when $\sigma=4$, even if $\Delta pK' < 2$.
Hence:

$$\alpha = (2n-1)/8 \qquad \alpha_n' = 0.5 \ (n=2 \text{ and } 3) \qquad (21)$$

It may be seen in Fig. 2 that the values of α at $\alpha'_n=0.5$ are almost equal to those given by Eq. (21) when $n=2$ and 3 (within an error of ± 0.05). It follows from Eqs. (2) and (21) that:

$$(n-1) = \frac{3}{2} - 2\log\frac{1-\alpha}{\alpha} \qquad (22)$$

The combination of Eqs. (16), (17), (18), (20), and (22) yields the relation:

$$\mathrm{pH} = \mathrm{p}K_0 + \frac{\Phi}{\bar{r}_1}\left[\frac{3}{2}+\frac{1}{4}\left(\frac{2}{k}-1\right)\right] - \left\{1+\frac{\Phi}{\bar{r}_1}\left[2-(6-8\alpha)\left(\frac{2}{k}-1\right)\right]\right\}\log\frac{1-\alpha}{\alpha} \qquad (23)$$

where $\Phi = Ne^2/2.303RTD$. This equation is derived under the conditions given by Eqs. (17) and (21). It has been shown that these conditions are well satisfied at the points where $\alpha'_n=0.5$ ($n=2$ and 3), whereas the equations yield larger errors if $n=1$ and 4. Additionally, Eqs. (2) and (15), which are also used in the derivation of Eq. (23), give a better approximation for the former points than the latter. Hence, the pH values at $\alpha'_n=0.5$ for $n=2$ and 3 are given, in good approximation, by Eq. (23). The values of α at the two points are estimated, according to Eq. (21), to be 3/8 and 5/8 respectively, and the corresponding pH values are given by Eq. (23). Provided that both the points are on a line represented by Eq. (1), $\mathrm{p}K_a$ and n' are given by:

$$\mathrm{p}K_a = \mathrm{p}K_0 + \frac{\Phi}{\bar{r}_1}\left[\frac{3}{2}+\left(\frac{1}{4}+\log\frac{5}{3}\right)\left(\frac{2}{k}-1\right)\right] = \mathrm{p}K_0 + \frac{Ne^2}{2.303RTD\bar{r}_1}\left(1.03+\frac{0.94}{k}\right) \qquad (24)$$

$$n' = 1 + \frac{\Phi}{\bar{r}_1}\left[2-2\left(\frac{2}{k}-1\right)\right] = 1 + \frac{4Ne^2}{2.303RTD\bar{r}_i}\left(1-\frac{1}{k}\right) \qquad (25)$$

From Eqs. (24) and (25) a parameter which is only a function of k is obtained:

$$\frac{\mathrm{p}K_a - \mathrm{p}K_0}{n'-1} = \frac{1}{4}\left(\frac{1.03k+0.94}{k-1}\right) \qquad (26)$$

Since k is the relative distance concerning the first and second neighboring groups, the left term of Eq. (26) will be more or less sensitive to the stereoisomerism of polyelectrolytes.

Discussion

1) **$\Delta pK' \geq 2$.** The plots of pH against log $[(1-\alpha)/\alpha]$ derived from some potentiometric titration data are shown in Fig. 4, where the solid lines are calculated on the basis of Eqs. (1) and (10) as below. Garret and Guile[4] and Ferry et al.[5] found that the titration curve of the maleic acid-styrene copolymer (MA–ST) was composed of two parts, which could be expressed by Eq. (1) with $n'=1$ and 2. If the second-half part ($n'=2$), which is plotted in Fig. 4 on the basis of Ferry's data,[4] is further divided into two parts, each of them can be represented by a line with a slope of unity. Hence, the corresponding dissociation constants can be determined on the basis of Eq. (4): $\mathrm{p}K'_2=9.4$ and $\mathrm{p}K'_3=11.4$. ($\mathrm{p}K'_1=4.4$ is given by Ferry for the first-half ionization). Upon substitution $\Delta \mathrm{p}K' = \mathrm{p}K'_3 - \mathrm{p}K'_2 = 2.0$ in Eq. (11), we obtain $\Delta \mathrm{p}K_a = 0$. Hence, the constants of Eq. (1) for the second-half ionization are given by Eq. (10). Since $\sigma=2$ in this case, the calculated values are $n'=2$ and $\mathrm{p}K_a=10.4$; these are close to the values observed by Ferry: $n'=2.2$ and $\mathrm{p}K_a=10.35$.

The behavior of MA–ST in the second-half ionization will be illustrated by the ionzation of 1,3-propanediamine (PDA), whose acidic dissociation constants are $\mathrm{p}K'_1=8.6$ and $\mathrm{p}K'_2=10.6$. The constants for PDA are calculated to be $n'=2$ and $\mathrm{p}K_a=9.6$. The line in Fig. 4, which is calculated by substituting these value in the parameters of Eq. (1), fits the titration data.

When $\Delta pK' > 2$, the plot of pH *vs.* log $[(1-\alpha)/\alpha]$ will be represented by σ parallel lines separated

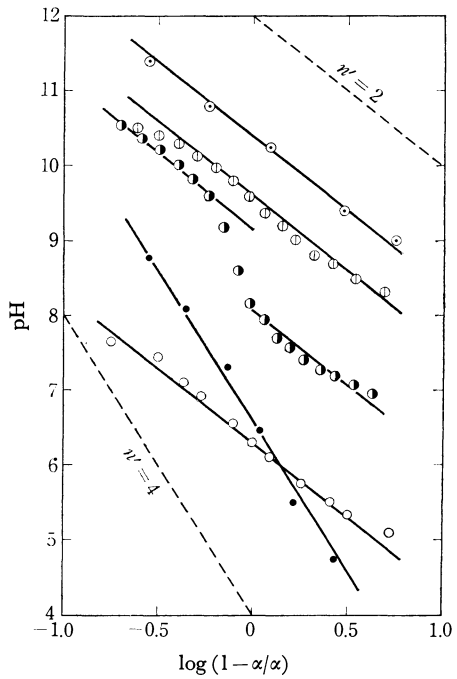

Fig. 4. Plot of pH *vs.* log $[(1-\alpha)/\alpha]$ from the potentiometric titration data in water.
⊙ MA-ST[5] (second-half ionization)
◑ PDA ◑ EDA ● PVAM[3]
○ PVAM[3] (in 2 N NaCl, second-half ionization)
— calculated on the basis of Eqs. (1) and (10)

by a distance of ($\Delta pK'-2$), as was pointed out in the previous section. This situation will be illustrated by the ionization of ethylenediamine; $pK'_1=7.1$, $pK'_2=10.0$, and $\Delta pK'=3.0$. Actually, the titration data shown in Fig. 4 nearly all fall on two parallel lines with a slope of $n'=2$ and separated by a distance of 1.0 ($\Delta pK_a=3.0-2=1.0$).

It is interesting to note that polyvinylamine (PVAM) behaves similarly to MA-ST when it is titrated in the presence of salt. It is shown on the basis of the data in the 2N sodium chloride solution[3] that the titration curve can be divided into two parts. The plot of pH *vs.* $\log[(1-\alpha)/\alpha]$ for the first-half ionization is represented by a line of $n'=1$, and the corresponding acidic dissociation constant is $pK'_3=9.6$. The plot for the second-half ionization shown in Fig. 4 has a slope of $n'=2$, and the data of this part can be expressed by Eq. (4) if they are further divided into two parts. Thus, the acidic dissociation constants in the second part can also be determined; they are $pK'_2=7.3$ and $pK'_1=5.3$. Here, it is seen again that $\Delta pK'=pK'_2-pK'_1=2.0$ and $\Delta pK_a=0$; hence, the parameters of Eq. (1) are given by Eq. (10). The line in Fig. 4 drawn with the calculated values, $n'=2$ and $pK_a=6.3$, can well represent the plot for the second ionization.

On the other hand, polyvinyl amine behaves differently in the absence of salt. The data[3] can be expressed by Eq. (1), with $n'=4$ and $pK_a=6.6$ in the middle range of the titration curve, as is shown in Fig. 4. If the titration curve is divided into four even parts and if Eq. (4) is applied to the data of each part, the corresponding four acidic dissociation constants can be determined: $pK'_1=4.1$, $pK'_2=5.6$, $pK'_3=7.6$, and $pK'_4=9.3$. The linearity of the plot in the middle ionization range shown in Fig. 4 can be explained by $\Delta pK'=pK'_3-pK'_2=2$. Since $\sigma=4$ in this case, the parameters are determined on the basis of Eq. (10) to be $n'=4$ and $pK_a=6.6$.

Since the ionization of all the acids and bases shown in Fig. 4 satisfies the condition $\Delta pK'\geq 2$, their titration curves can be determined by the use of their pK'_n values on the basis of Eqs. (5) and (7). The observed values fall excellently on the calculated titration curves of MA–ST and PVAM, as is shown in Fig. 5, where β is the degree of the ionization of PVAM ($\beta=1-\alpha$).

2) **$\Delta pK'<2$.** polyacrylic acid was titrated with sodium hydroxide in the absence of salt;[9] the data are shown in Fig. 6, where the solid lines are calculated as below. The titration data are expressed by Eq. (1) with the parameters of $pK_a=6.9$ and $n'=2.4$; these values are in accordance with those given by Gregor and Frederic.[10]

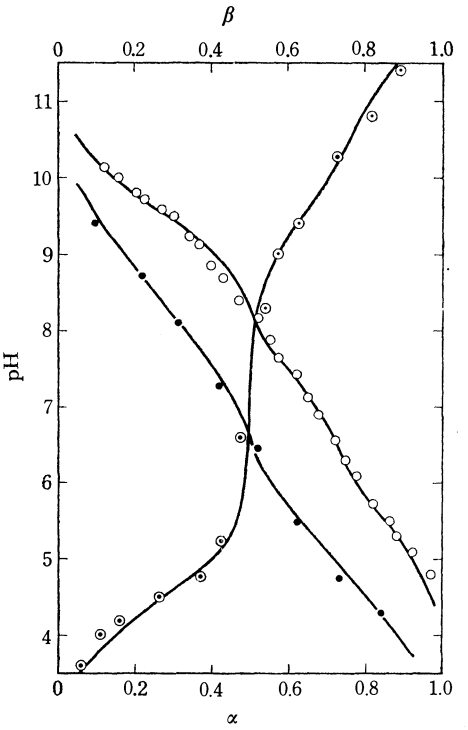

Fig. 5. Titration curves of the polyelectrolytes.
⊙ MA-ST[5] ● PVAM[3]
○ PVAM[3] (in 2N NaCl)
— calculated on the basis of Eqs. (5) and (7)

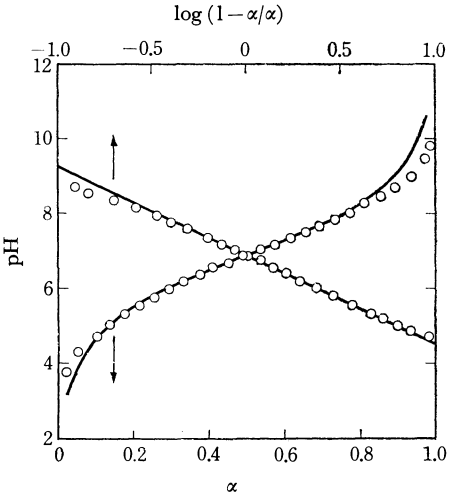

Fig. 6. Titration curve of polyacrylic acid.[9]
— calculated on the basis of Eq. (1) with $pK_a=6.89$ and $n'=2.35$.

The data do not fit Eq. (4) when they are divided into two equal parts. In the previous section, Eq. (23) was derived on the assumption that the ionization of polyacrylic acid is composed of four elementary ionizations, by analogy with the kinetic behavior in the alkaline hydrolysis of polymethyl acrylate. The distance between the groups

10) H. P. Gregor and M. Frederic, *J. Polymer Sci.*, **32**, 451 (1957).

TABLE 2. INTRINSIC IONIZATION CONSTANT OF POLYACRYLIC ACID

n	$\alpha(\alpha_n'=0.5)$	pH	$\sum z_i/\bar{r}_i$	pK_0	
2	3/8	6.40	$2/\bar{r}_2$	5.38	5.36
3	5/8	7.39	$2/\bar{r}_1$	5.34	

determined on the basis of the kinetic data are $\bar{r}_1=3.25$ and $\bar{r}_2=5.07$ Å.[9] The parameters in Eq. (23) are $k=1.56$ and $\Phi=3.04$ ($T=298$ and $D=80$). The intrinsic ionization constant, pK_0, can be determined on the basis of Eq. (19), in which pK'_n is given by pH at $\alpha'_n=0.5$. An approximate value of α corresponding to $\alpha'_n=0.5$ is given by Eq. (21); a better approximation is obtained when $n=2$ and 3 than when $n=1$ and 4, as has been discussed in the previous section. The calculated values of pK_0 are shown in Table 2; the average value is 5.36. This value is slightly higher than the dissociation constant of isobutylic acid, 4.86, but it is comparable with the value determined from the pH value of an aqueous solution of polyacrylic acid on the basis of the approximate relation, $pK_0=2pH-\log$ [COOH], where [COOH] represents the concentration of polyacrylic acid expressed by monomole/l. The value estimated from the present experimental data is 5.4 ([COOH]=0.019 and pH=3.57); the value of 5.2 is obtained from Gregor's data.[10] The empirical constants in Eq. (1) are calculated on the basis of Eqs. (24) and (25): $n'=2.35$ and $pK=6.89$. These values are in good agreement with the observed values of the parameter. The titration curve determined on the basis of the equation, $pH=6.89-2.35\log[(1-\alpha)/\alpha]$, fits the titration data in the middle range of the curve, as is shown in Fig. 6.

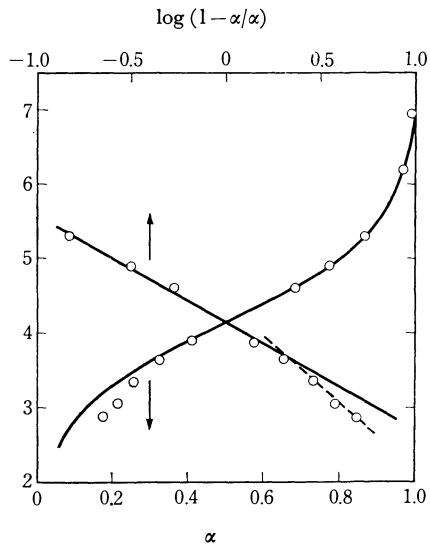

Fig. 7. Titration curve of pectinic acid.[11]
— calculated on the basis of Eq. (1) with $pK_a=4.15$ and $n'=1.44$.

Equation (23) is also applicable to the ionization of pectinic acid. The titration data of the acid[11] is shown in Fig. 7, in which the solid lines are drawn by means of Eq. (1) with the values of the parameter calculated as below. The plot of pH *vs.* $\log[(1-\alpha)/\alpha]$ is linear in the $\alpha>0.3$ range, and the empirical parameters determined from the titration data are $n'=1.5$ and $pK_a=4.1_5$. It may be presumed that pectinic acid has an elongated structure similar to cellulose when the ionization proceeds, for an intense repulsing force emerges among the charges formed on the macromolecule. It can thus be assumed that $r_2=10.3$ Å on the basis of the fiber period of cellulose.[12]*4 On the assumption of the elongated pectinic acid structure, $\bar{r}_1$ is estimated to be 7.5 Å on the basis of the length and angle of the bond. By assuming $\sigma=4$ for the ionization of pectinic acid, the pK_0 value is calculated on the basis of Eq. (19); the obtained values are shown in Table 3. The

TABLE 3. INTRINSIC IONIZATION CONSTANT OF PECTINIC ACID

n	$\alpha(\alpha_n'=0.5)$	pH	$\sum z_i/\bar{r}_i$	pK_0	
2	3/8	3.80	$2/\bar{r}_2$	3.45	3.45
3	5/8	4.45	$2/\bar{r}_1$	3.47	

mean value, $pK_0=3.45$, is in good agreement with the $pK=3.42$ of D-garacturonic acid,[12] the monomeric homologue of pectinic acid. The parameters of Eq. (1) can now be calculated on the basis of Eqs. (24) ayd (25) to be $n'=1.44$ and $pK_a=4.1_5$; those values are in accordance with the observed values. All the titration data except for the extent $\alpha<0.3$ fall excellently on the titration curve drawn by means of $pH=4.15-1.44\log[(1-\alpha)/\alpha]$, which is shown in Fig. 7. The structural transformation of pectinic acid presumably occurs in this range on account of an increase in the repulsion force among the fixed charges.

It has been pointed out in the previous section that the left term of Eq. (26) may correlate with the steric arrangement of the groups; this seems

11) R. Speicer, C. H. Hills and C. R. Eddy, *J. Phys. Colloid Chem.*, **49**, 328 (1945).

12) K. J. Palmer, M. B. Hartzog, *J. Amer. Chem. Soc.*, **67**, 1865 (1945). See also Katchalsky's paper.[13]

13) A. Katchalsky and J. Feitelson, *J. Polymer Sci.* **13**, 385 (1945).

*4 By treating the kinetic data of the alkaline hydrolysis of pectin at 4°C in an aqueous solution[13] according to the procedure described in a previous paper,[9] the rate constans of $k_3=6.6$ and $k_4=1.7$ l/mol min are obtained; from them we obtain $\bar{r}_2=11$ Å.

really to be the case with polyacrylic acid and pectinic acid. The average distance from an ionizing group to the ith group, $\bar{r}_i$, is defined as follows:[9]

$$1/\bar{r}_i = \sum_j (X_{i,j}/r_{i,j})$$

where j is related to the steric configuration, where r is the distance between two groups, and where X is the mole fraction ($\sum_j X_{i,j}=1$). If the planar zig-zag structure is assumed in the vicinity of an ionizing group of polyacrylic acid, the value of $(pK_a-pK_0)/(n'-1)$ for an atactic isomer, whose structure is completely random, is estimated to be 1.0. The value obtained from the titration data is 1.1, close to the calculated one. If it is assumed that pectinic acid has an elongated structure like cellulose and that carboxylic acid groups are situated alternatively on the opposite sides of the plane consisting of piranose rings, $(pK_a-pK_0)/(n'-1)$ will be 1.5; this is close to the value obtained from the titration data, 1.4.

BULLETIN OF THE CHEMICAL SOCIETY OF JAPAN VOL. 43 2713—2718 (1970)

A Theoretical Consideration of the Electron-scavenging Process in Liquid Hydrocarbons

Hideo YAMAZAKI and Kyoji SHINSAKA

Laboratory of Physical Chemistry, Tokyo Institute of Technology, Meguro-ku, Tokyo

(Received February 27, 1970)

The electron-scavenging process by a scavenger and the random recombination between ions and electrons in a spur in the radiolysis of nonpolar hydrocarbons have been investigated theoretically on the basis of the extended type of Smoluchowski equation. To obtain the approximate solutions, a model of the distribution of charged species in which a positive ion core is surrounded by electrons is assumed; several approximations are also made during the calculation. The reaction rate of the electron scavenging is expressed by the overlapping integral between the concentration of the electrons and that of the scavenger. The rate of the recombination reaction is approximately expressed as the total flux of the electrons flowing into the core of parent ions. The G value of electron scavenging shows a Langmuir-type dependence on the concentration of the electron scavenger. The values of the slope of the sigmoidal curve at the mid point and of the corresponding scavenger concentration almost agree with the experimental value.

In recent years a considerable number of experiments have been made on the ionic process in the radiation chemistry of liquid hydrocarbons; the quantitative interpretations of the experiments have become more important in ascertaining the various rates in the primary process. The theoretical treatments proposed hitherto for the reactions of the primary ionic process can be classified into the following four groups. The first method, utilized by Freeman[1,2] and by Sato *et al.*,[3,4] deals with the geminate recombination of ions, assuming an initial distribution of ion pairs. They evaluated the G value of free-electron formation as a function of the concentration of scavengers. The method seems to be successful in explaining the experimental results in nonpolar solvents. The second method, used by Monchick,[5] Mozumder,[6] and Hummel,[7] is based on the Smoluchowski equation of the distribution function of ion pairs in a static electric field. The third method, used by Schuler *et al.*,[8] investigates the reactions of ionic species by the scavenger technique and derives a simple formula from the nonhomogeneous kinetics of the recombination and scavenging processes. The last method, used by Schiller,[9,10] attempts to discuss the expansion and contraction of a spur or a track

1) G. R. Freeman, *J. Chem. Phys.*, **46**, 2822 (1967).
2) G. R. Freeman and J. M. Fayadh, *ibid.*, **43**, 86 (1965).
3) S. Sato, T. Terao, M. Kono and S. Shida, This Bulletin, **40**, 1818 (1967).
4) S. Sato, *ibid.*, **41**, 304 (1968).
5) L. Monchick, *J. Chem. Phys.*, **24**, 381 (1956).
6) A.Mozumder, *ibid.*, **48**, 1659 (1968).
7) A. Hummel, *ibid.*, **48**, 3268 (1968).
8) J. M. Warman, K. -D. Asmus and R. H. Schuler, *Advan. Chem. Ser.*, **82**, 25 (1968).
9) R. Schiller, *J. Chem. Phys.*, **43**, 2760 (1965).
10) R. Schiller, *ibid.*, **47**, 2278 (1967).

using a thermodynamic consideration with Debye's linear response between electric field and electric displacement, and to compare the theoretical values. These theories have been tested by the following experiments: (1) scavenger method,[3,8] (2) decay of the solvated electrons in pulse radiolysis,[11] (3) luminescence intensity due to the recombination after pulse radiolysis.[12,13]

Even in the detailed calculations of the first and second methods, the random recombinations between ions and electrons in a spur or a track have been ignored. This corresponds to the assumption of a simplified spur involving an electron and an ion. However, this effect of random recombination in a spur is important, especially for a spur or a track with a high ionization density. This paper will present a theory using a distribution function of ionic species and considering random recombination in a spur or a track, as in the diffusion theory of radicals.[14] Since the effect of dielectric relaxation in nonpolar solvents can be ignored, it is necessary only to consider the movements of ionic species under a static electric field.

Theory

A) Basic Equation and Its Approximation. The basic equation of distribution functions for positive and negative species may be represented in the following form of the extended Smoluchowski equations:

$$\frac{\partial C^-}{\partial t} = u \text{ grad } C^- \cdot \text{grad}\phi + uC^- \nabla^2\phi + D_- \nabla^2 C^- - k_S^- S^- C^- - k_C C^+ C^- \quad (1)$$

$$\frac{\partial C^+}{\partial t} = -u \text{ grad } C^+ \cdot \text{grad}\phi - uC^+ \nabla^2\phi + D_+ \nabla^2 C^+ - k_S^+ S^+ C^+ - k_C C^+ C^- \quad (2)$$

where the plus and minus signs of the superscripts and the subscripts denote the quantities for positive ions and electrons; C is the distribution function, D is the diffusion constant, u is the mobility, ϕ is the static electric potential, S is the concentration of the scavenger, and k_S and k_C are the rate constants. ϕ and C are connected by the Poisson equation (3):

$$\nabla^2\phi = 4\pi e(C^+ - C^-) \quad (3)$$

where e is the electron charge.

The G value of the recombination reaction can be expressed as the overlapping of the concentrations of the species, as shown in Eqs. (4), (5) and (6), if the original equations can be solved:

$$S_\beta^\pm = k_S^\pm S^\pm \iint C^\pm \mathrm{d}v\mathrm{d}t \quad (4)$$

$$S_n = k_C \iint C^+ C^- \mathrm{d}v\mathrm{d}t \quad (5)$$

$$(G_\pm/G_\pm^0) = 1/\left\{1 + (k_S^\pm S^\pm \iint C^\pm \mathrm{d}v\mathrm{d}t/k_C \times \iint C^+ C^- \mathrm{d}v\mathrm{d}t)\right\} = 1/(1+S_\beta/S_n) \quad (6)$$

where $G_\pm^0$ is the G value of total ionization and where $G_\pm$ is the G value of the recombination reaction of positive ions and electrons.

The last terms in Eqs. (1) and (2) are important, especially for the track with a high ionic density. However, in a track or in a spur ions and electrons seem to be separated from each other as a central ion core surrounded by the electron cloud, so that the overlap of these species can be neglected in the initial distribution. The term of overlapping can be approximated as the total flux of electrons flowing into the central ion core, where the overlap of the distribution of the ions and electrons is quite appreciable in the course of reaction. However, due to the non-linearity of the equations it is generally difficult to solve these equations. Therefore, appropriate approximations are required to obtain the distribution of electrons. Equations (1), (2), and (3) may be expressed as a function of r and t in the cylindrical or spherical coordinate by ignoring the last term of the second-order reaction:

$$\frac{\partial C^-}{\partial t} = u\left(\frac{\partial \phi}{\partial r}\right)\frac{\partial C^-}{\partial r} + C^- u(1/r^n)\frac{\partial}{\partial r}\left(r^n \frac{\partial \phi}{\partial r}\right) + D_-(1/r^n)\frac{\partial}{\partial r}\left(r^n \frac{\partial C^-}{\partial r}\right) - k_S^- S^- C^- \quad (7)$$

$$\frac{\partial C^+}{\partial t} = -u\left(\frac{\partial \phi}{\partial r}\right)\frac{\partial C^+}{\partial r} - C^+ u(1/r^n)\frac{\partial}{\partial r}\left(r^n \frac{\partial \varphi}{\partial r}\right) + D_+(1/r^n)\frac{\partial}{\partial r}\left(r^n \frac{\partial C^-}{\partial r}\right) - k_S^- S^- C^- \quad (8)$$

($n=1$, cylindrical coordinate; $n=2$, spherical coordinate)

The potential function in the equation is given by Eq. (9) for the spherical coordinate:

$$\phi(r,t) = e(N^+)r,t(-N^-(r,t))/\varepsilon r \quad (9)$$

where ε is the dielectric constant and where

$$N^\pm(r,t) = \int_0^r C^\pm(r,t)\mathrm{d}v \quad (10)$$

One of the simplest models of the distribution of species is that the positive ion cluster is surrounded by the electrons ejected from the central ion cluster. If the ions are confined within the radius, r, the force from the central ion cluster is expressed by Eq. (11). In this approximation the motion of the electrons is much faster than that of ions, so that the spacial distribution of electrons is given by Eq. (12), which is reduced to the usual form of the Smoluchowski equation when $N^+(t)=1$ and $k_S^- S_S^- = 0$

11) J. P. Keene, E. J. Land and A. J. Swallow, *J. Amer. Chem. Soc.*, **87**, 5284 (1965).
12) P. K. Ludwig and M. Burton, *Advan. Chem. Ser.*, **82**, 542 (1968).
13) P. K. Ludwig, *J. Chem. Phys.*, **50**, 1787 (1969).
14) A. H. Samuel and J. L. Magee, *ibid.*, **21**, 1080 (1953).

$$\nabla^2\psi = 0 \quad r>R_0,$$

$$\mathrm{grad}\psi\cdot\mathrm{grad}\ C^- = \left(\frac{\partial C^-}{\partial r}\right)\left(\frac{N^+(t)e}{\varepsilon r^2}\right) \tag{11}$$

$$\frac{\partial C^-}{\partial t} = \left\{\frac{uN^+(t)e}{\varepsilon r^2}\right\}\frac{\partial C^-}{\partial r} + \frac{D_-}{r^2}\frac{\partial}{\partial r}\left(r^2\frac{\partial C^-}{\partial r}\right) - k_S^-S^-C^- \tag{12}$$

where R_0 means the radius of the central ion core. In the following discussion, the plus and minus signs of the superscripts and the subscripts are omitted for the sake of simplicity, because only the distribution of electrons is going to be discussed. The total amount of the recombination reaction can be approximated by the total flux of the electrons flowing into the core of the parent ions in place of Eq. (5). The flux consists of the terms of the diffusion and the electric potential:

$$S_n = u\int\int_{R_0}\left(C\,\mathrm{grad}\psi + \frac{D}{u}\mathrm{grad}C\right)\mathrm{d}s\mathrm{d}t \tag{13}$$

When G_- and G_-^0 are expressed by G_e and G_e^0 respectively, Eq. (6) gives Eq. (14). The two terms in Eq. (13) are going to equilibrate at the r_c distance.

$$(G_e/G_e^0) = 1/(1+S_\beta/S_n) \tag{14}$$

$$[u\ C\ \mathrm{grad}\psi + D\ \mathrm{grad}C]_{r_c} = 0 \tag{15}$$

The electrons separated by a longer distance than r_c become free electrons. In the case of a pair consisting of an ion and an electron, the scavenging probability is expressed by the function of r/r_c, and r_c is a constant. However, in the ion-cluster system it varies with the time. The next step is the actual calculation of the concentration distribution. Several models may be proposed for evaluating the distribution function.

B) Model I. The first model is derived by ignoring the diffusion term and by using $\bar{N}$, the mean number of ions for $N^+(t)$ in Eq. (11):

$$\frac{\partial C}{\partial t} = \frac{\alpha}{r^2}\frac{\partial C}{\partial r} - \beta C \tag{16}*1$$

where $\alpha=\bar{N}eu/\varepsilon$ and $\beta=k_sS$. When $C(r,t)$ is factorized by $T(t)\cdot R(r)$, the factorized functions are given by the following equations:

$$T(t) = c\ \exp\{(-\beta + m\alpha)t\},\quad R(r) = c\ \exp(mr^3/3) \tag{17}$$

where c and m are constants. The solution is obtained by the superposition of these solutions. One of the boundary condition is $C(\infty,\infty)=0$, so m should be negative.

By substituting n for $|m|$, the solution is given by Eq. (18):

$$C(r,t) = \sum_n c_n\ \exp\{-(\beta+n\alpha)t\}\cdot\exp(-nr^3/3) \tag{18}$$

where c_n are constants determined by the initial distribution. The distribution of electrons can be approximated by considering only one term in the summation of Eq. (18). The probability of the initial distribution, $\phi(r,0)=(1/N^-)C(r,0)\cdot$

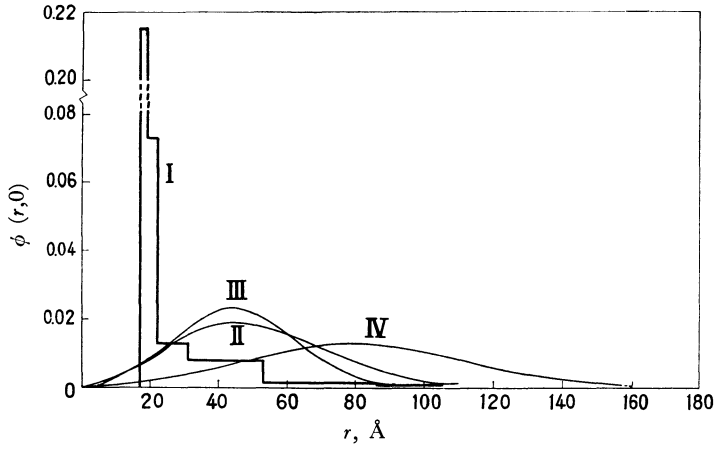

Fig. 1. The initial distribution of the separation distance between the positive-ion core and the surrounding negative electron cloud along with those estimated by Freeman and by Sato for ion pairs.

ϕ $(r, 0)$: the probability of initial distribution of the separation distance between the ion pairs in the cases of I and II and between the potitive-ion core and the surrounding negative electron cloud in the cases of III and IV; I: by Freeman, see Ref. 1 and Ref. 4; II: by Sato, see Ref. 4; III: this work, assuming that the distance, r_{max}, at a maximum initial distribution coincides with the distance where curve II reaches its maximum ($r_{max}\cong 45$ Å); IV: this work, assuming that $r_{max}=80$ Å.

*1 The general solution of Eq. (16) can be expressed by:

$$C(r,t) = \exp(-\beta t)\cdot f(t+r^3/3\alpha) \tag{18'}$$

where f is an arbitrary function.

$4\pi r^2$, obtained by means of Eq. (18) is shown in Fig. 1, along with the results of Freeman and of Sato. The value of r_{max} was chosen as 80 Å in the tentative calculations in view of the previous values,*2 but the curve corresponding to 45 Å is also shown in Fig. 1. The overlap between the electron and scavenger distribution may be evaluated as follows:

$$S_\beta = k_S S \int_{R_0}^{\infty} C(r,t)\ 4\pi r^2 \mathrm{d}r\mathrm{d}t = \frac{4\pi C k_S S\ \exp(-nR_0^3/3)}{n(\beta+n\alpha)} \tag{19}$$

In the vicinity of the ion cluster, the total current of electrons can be approximated by the electric potential term. The flux of electrons flowing into the central ion cluster is, then, obtained by means of Eq. (20):

$$S_n = \frac{4\pi \bar{N} e u C}{\varepsilon(\beta+n\alpha)} \exp(-nR_0^3/3) \tag{20}$$

The ratio of the G values, G_e/G_e^0, of the electron formation is given by Eq. (21). The G_e/G_e^0 is expressed as a sigmoidal curve of the first order of the concentration of the electron scavenger:

$$(G_e/G_e^0) = 1/(1+k_S S\varepsilon/\bar{N}eun) \tag{21}$$*3

C) Model II. In the second model the diffusion term is ignored. However, the change in the number of ions in the central cluster is considered to be a function of the time. The basic equation is, then, given by Eq. (22):

$$\frac{\partial C}{\partial t} = \frac{N(t)eu}{\varepsilon r^2}\frac{\partial C}{\partial r} - k_S S C \tag{22}$$

As in the previous model, the use of factorization, $C(r,t)=T(t)\cdot R(r)$, yields the following equation:

$$\frac{1}{\alpha(t)T(t)}\frac{\partial T(t)}{\partial t} + \frac{\beta}{\alpha(t)} = m \qquad \frac{1}{r^2 R(r)}\frac{\partial R(r)}{\partial r} = m \tag{23}$$

where $\alpha(t)$ and β are given by $\alpha(t)=N(t)eu/\varepsilon$ and $\beta=k_S S$. By the integration of these equations, $T(t)$ and $R(r)$ are obtained:

$$T(t) = c\ \exp(-\beta t)\cdot\exp\left\{m\int^t \alpha(t)\mathrm{d}t\right\} \tag{24}$$

$$R(r) = c\ \exp(mr^3/3)$$

Therefore, the general solution of Eq. (22) is given by the superposition of the product of $T(t)$ and $R(r)$ and by the substitution of n for $|m|$, since m should be negative.

$$C(r,t) = \sum_n c_n\ \exp(-\beta t) \times \exp\left\{-n\int^t \alpha(t)\mathrm{d}t\right\}\exp(-nr^3/3) \tag{25}$$

The overlapping, S_β, and the flux, S_n, can be evaluated as in the case of the first model.

$$S_\beta = 4\pi k_S S \sum_n c_n \int_0^{\infty} \exp\left\{-\beta t - n\int^t \alpha(t)\mathrm{d}t\right\} \times \frac{1}{n}\exp(-nR_0^3/3)\mathrm{d}t \tag{26}$$

$$S_n = 4\pi \sum_n c_n \int_0^{\infty} \alpha(t) \times \exp\left\{-\beta t - n\int^t \alpha(t)\mathrm{d}t\right\}\exp(-nR_0^3/3)\mathrm{d}t \tag{27}$$

Therefore, the S_β/S_n ratio is given by Eq. (28):

$$S_\beta/S_n = k_S S\varepsilon/eu\langle N(t)\cdot n\rangle \tag{28}$$

where $N(t)\cdot n$ is given by Eq. (29):

$$\langle N(t)\cdot n\rangle = \frac{\int \sum_n N(t)\cdot n\cdot\frac{c_n}{n}\exp\left\{-\beta t - n\int^t \alpha(t)\mathrm{d}t\right\}\exp(-nR_0^3/3)\mathrm{d}t}{\int \sum_n \frac{c_n}{n}\exp\left\{-\beta t - n\int^t \alpha(t)\mathrm{d}t\right\}\exp(-nR_0^3/3)\mathrm{d}t} \tag{29}$$

The final expression of the G value as a function of the scavenger concentration is given by Eq. (30):

$$(G_e/G_e^0) = 1/\{1+k_S S\varepsilon/eu\langle N(t)\cdot n\rangle\} \tag{30}$$

where the brackets express the average of the quantities. The average value can be written by the one-term approximation:

$$\langle N(t)\cdot n\rangle = \frac{n\int_0^{\infty} N(t)\exp\left\{-n\int_0^t \alpha(t)\mathrm{d}t - \beta t\right\}\mathrm{d}t}{\int_0^{\infty}\exp\left\{-n\int^t \alpha(t)\mathrm{d}t - \beta t\right\}\mathrm{d}t} \tag{31}$$

If $\alpha(t)$ is assumed to be a decreasing function expressed by a second-order reaction, $\alpha(t)=1/(1/\alpha(0)+bt)$, Eq. (31) is reduced to Eq. (32):

$$\langle N(t)\cdot n\rangle = \frac{n\varepsilon}{eu}\frac{\int_0^{\infty}(1/\alpha(0)+bt)^{-n/b-1}\exp(-\beta t)\mathrm{d}t}{\int_0^{\infty}(1/\alpha(0)+bt)^{-n/b}\exp(-\beta t)\mathrm{d}t} \tag{32}$$

where $\alpha(0)$ and b denote the initial value of $\alpha(t)$ at $t=0$ and a positive constant respectively. Therefore, after the integration of Eq. (32), and assuming $n/b\approx 1$ and $\alpha(0)/\alpha\approx 2$, (G_e/G_e^0) can be expressed as in Eq. (33):

$$(G_e/G_e^0) = 1/\{1+k_S S\varepsilon/1.4eu\bar{N}n\} \tag{33}$$

D) Model III. In the third model the effect of diffusion is taken into account, so that the

---

*2 For example, Sato,[4] r_{max} ($\cong$45 Å); Ludwig,[13] r_{max} (=80 Å, 112 Å).

*3 By using the general solution (18″),

$$C(r,t) = \exp(-\beta t)\int_0^{\infty} F(n)\exp\{-n(\alpha t + r^3/3)\}\mathrm{d}n \tag{18''}$$

where $F(n)$ is an arbitrary function of n, the G value is evaluated as a function of the scavenger concentration.

$$(G_e/G_e^0) = 1/\left\{1+(\beta\int_0^{\infty} F(n)e^{-nR_0^3/3}\frac{1}{n(\beta+n\alpha)}\mathrm{d}n \Big/ \alpha\int_0^{\infty} F(n)e^{-nR_0^3/3}\frac{1}{(\beta+n\alpha)}\mathrm{d}n\right\} \tag{21'}$$

basic equation of the distribution is as given by Eq. (34):

$$\frac{\partial C}{\partial t}=\left(\frac{u\bar{N}e}{\varepsilon r^2}\right)\frac{\partial C}{\partial r}+\frac{D}{r^2}\frac{\partial}{\partial r}\left(r^2\frac{\partial C}{\partial r}\right)-k_S SC \quad (34)$$

The following two equations are obtained by factorizing $C(r,t)$:

$$\frac{1}{T(t)}\frac{\mathrm{d}T(t)}{\mathrm{d}t}+\beta=-n\alpha$$

$$\frac{\mathrm{d}^2R(r)}{\mathrm{d}r^2}+\left(\frac{2}{r}+\frac{\alpha}{Dr^2}\right)\frac{\mathrm{d}R(r)}{\mathrm{d}r}+\frac{n\alpha}{D}R(r)=0 \quad (35)$$

By multiplying the appropriate coefficient M_n, the solution is expressed by an integral form:

$$C(r,t)=\sum_n M_n\cdot R_n(r)\cdot T_n(t) \quad (36)$$

S_β and S_n are then evaluated from $C(r,t)$ by:

$$S_\beta=k_S S\sum_n M_n\int R_n(r)\mathrm{d}v\cdot\int T_n(t)\mathrm{d}t \quad (37)$$

$$S_n=\frac{u\bar{N}e}{\varepsilon R_0^2}\sum_n M_n\int R_n(R_0)\mathrm{d}s\int T_n(t)\mathrm{d}t \quad (38)$$

(G_e/G_e^0) can be expressed by a formula of the Langmuir type:

$$(G_e/G_e^0)=1/\left[1+\left(\frac{k_S S\varepsilon R_0^2}{u\bar{N}e}\right)\frac{\sum_n M_n\left\{\int R_n(r)\mathrm{d}v\right\}\left\{\int T_n(t)\mathrm{d}t\right\}}{\sum_n M_n\left\{\int R_n(R_0)\mathrm{d}s\right\}\left\{\int T_n(t)\mathrm{d}t\right\}}\right] \quad (39)$$

Since S is involved in the integrals of $R_n(r)$ and $T_n(t)$, the actual result is generally quite a complicated function of S. However, a simplified approximation of the integrals gives a Langmuir formula of the first order of S:

$$(G_e/G_e^0)=\left\{1+\frac{k_S S\varepsilon}{ue\bar{N}}\cdot K\cdot\frac{1}{n}\right\} \quad (40)$$

and:

$$K=\frac{1+\{\Gamma(7/3)3^{4/3}-(1/7)\Gamma(10/3)3^{7/3}\}(D/\alpha n^{1/3})\exp(nR_0^3/3)}{[1+DnR_0^4/\alpha-Dn^2R_0^7/7\alpha]}$$

where n is a constant.

E) Results and Discussion. The result of the scavenger reaction is usually expressed by a plot of G_e/G_e^0 against the logarithm of the scavenger concentration, which shows a sigmoidal which is characterized by the concentration of the midpoint of the curve and the value of the slope at that point.

As the first step in comparing theory and experiment, let us examine the slope of the sigmoidal curve. In this theory the slope at the middle of the sigmoidal curve is given by Eq. (41):

$$\left(\frac{\mathrm{d}(G_e/G_e^0)}{\mathrm{d}\log[S]}\right)_{1/2}=-\frac{1}{4\log\mathrm{e}}[S]_{1/2}\left(\frac{\mathrm{d}(S_\beta/S_n)}{\mathrm{d}[S]}\right)_{1/2} \quad (41)$$

where the 1/2 suffix indicates the values corresponding to $G_e/G_e^0=1/2$.

Table 1. Comparison of theory and experiment of the slope at $G_e/G_e^0=1/2$

Theoretical	Experimental
First model: $-\frac{1}{4\log\mathrm{e}}=-0.58$[a]	-0.50[e]
	-0.47[f]
Second model: $-\frac{1}{4\log\mathrm{e}}=-0.58$[b]	-0.49[g]
	-0.57[h]
Third model: $-\frac{1}{4\log\mathrm{e}}=-0.58$[c]	-0.40[i]

(a), (b) and (c) are calculated according to Eqs. (21), (33) and (40), respectively.
(d) All the experimental values in Table 1 are obtained by assuming that $G_e^0=3.0$.
(e) Obtained from the curve of cyclohexane-N_2O system in Ref. 4.
(f) Obtained from the curve of cyclohexane-C_2H_5OD system in Ref. 4.
(g) Obtained from the curve of cyclohexane-N_2O system in Ref. 1.
(h) Obtained from the curve of cyclohexane-D_2S system in Ref. 1.
(i) Obtained from the curve of cyclohexane-CH_3Cl system in Ref. 8.

Table 2. Comparison of theory and experiment of the scavenger concentration at $G_e/G_e^0=1/2$

Theoretical (mol/l)	Experimental (mol/l)
First model: $\frac{u\bar{N}en^{(a)}}{k_S\varepsilon}=0.17$—$0.017$	0.020[e]
	0.131[f]
Second model: $\frac{1.4\,u\bar{N}en^{(b)}}{k_S\varepsilon}=0.24$—$0.024$	0.019[g]
	0.131[h]
Third model: $\frac{u\bar{N}en^{(c)}}{k_S\varepsilon K}=0.17$—$0.017$	0.056[i]

* The superscripts in this table, (a)—(i), are the same with those in Table 1.

** In the calculation the following values are used: ε; the dielectric constant, 2, u; the mobility of electron for unit force, $6.0\times10^{-1\sim-2}$ esu cm sec^{-1} dyn^{-1} ($=2\times10^{-3\sim-4}$ cm^2 v^{-1} sec^{-1}), r_{max}; the radius where the distribution probability, $\frac{4\pi}{N^-}r^2C(r,t)\mathrm{d}r$ becomes maximum, 80 Å, $\bar{N}$; the average number of positive ions in cluster, 3, k_S; the reaction constant of electron with scavenger, 10^{10} M^{-1} sec^{-1}, e; the electron charge, 4.8×10^{-10} esu.

*** The following points are also taken into consideration. n can be replaced by $2/r_{max}^3$. D is the diffusion constant of electron calculated from the relation, $D=ukT/e$ where k is Boltzmann's constant, 1.38×10^{-16} erg·deg^{-1} and T is the absolute temperature taken as 300°K in this calculation and the evaluated value of D is $5.1\times10^{-5\sim-6}$ cm^2 sec^{-1}. K is the correction factor for diffusion process and the evaluated value of K is 1.

The values evaluated from the various models are shown in Table 1 along with the experimental values.

As the second measure, the value of the concentration at the mid-point of the sigmoidal curve is shown in Table 2. As is shown in Table 1 and Table 2, the theoretical values agree almost entirely with the experimental values. An even more plausible result can be obtained by changing N, *e.g.*, from four to zero, and by combining solutions with various values of N. The theory can be extended for the analysis of the effect of LET and the dependence of the density of the reactant on the electron-scavenging process.

The authors wish to thank Professor S. Shida and Dr. S. Sato of the Tokyo Institute of Technology and Dr. K. Fueki of Nagoya University for reading the preliminary manuscript of this paper and for many helpful discussions.

BULLETIN OF THE CHEMICAL SOCIETY OF JAPAN VOL. 43 2718—2723 (1970)

Sound Velocity in Aqueous Non-Electrolyte Solutions in Relation to Water Structure

Otohiko NOMOTO*,** and Harumi ENDO*

* *Department of Applied Physics, Defense Academy, Yokosuka*
** *Kobayasi Institute of Physical Research, Kokubunzi, Tokyo*

(Received March 4, 1970)

An acoustic interferometer is employed to obtain the variation of sound velocity with concentration and temperature in hexamethylenetetramine (HMT), urea, thiourea, acetamide and *N*,*N*-dimethylformamide (DMF) and their aqueous solutions. The plot of velocity of aqueous solutions of these organic substances against temperature gives parabolic curves similar to one for pure water. In these curves, the maximum height of sound velocity is higher than that for pure water and the temperature at maximum point is lower than for water. The curves of sound velocity *vs.* concentration at various temperatures show values of maximum velocity at intermediate concentrations. The maximum value decreases with increasing temperature and finally disappears in some cases. Results show that the velocity dependency on temperature and concentration are qualitatively determined by the relative concentration of non-associated water to cluster. The sound velocity of acetamide and DMF is 1404.4 m/sec (65°C) and 1478.8 m/sec (20°C), respectively, and shows negative temperature coefficients of −2.68 m/sec/deg and −3.90 m/sec/deg, respectively.

All pure liquids, except water[1] and heavy water,[2] are found to have negative temperature coefficients of sound velocity V. Randall[1] found that water has a large positive coefficient of sound velocity at room temperature. The temperature coefficient (dV/dT) decreases to zero at 74°C and then becomes negative as for ordinary liquids. The origin of such an anomalous behaviour is sought in the structure of water.

According to the two-state model, liquid water consists of two species; a non-associated, close-packing-state water, and a bulky, associated state or cluster. According to the molecular view of the acoustic compression of water, compression of the former state is attributed to the compression of the free space among non-associated water molecules, while the compressibility of the latter part mainly results from the breaking of the hydrogen bonds and accordingly the partial destruction of the associated bulky structure. The structural sound absorption in pure water is explained along these lines by Hall.[3] The amount of the cluster part of water decreases with increasing temperature, resulting in a decrease of the structural part of the compressibility, while an increase in molecular distance with temperature rise accompanies an increase in ordinary compressibility. These opposing effects make the compressibility curve a minimum at an intermediate temperature, or the maximum of the sound velocity at a slightly different temperature.

Sound velocity in aqueous solutions is a function of both temperature T and concentration c, *i.e.*,

1) R. Randall, *Bur. Standards J. Res.*, **8**, 79 (1932).
2) M. Pancholy, *J. Acous. Soc. Amer.*, **25**, 1003 (1953).
3) L. Hall, *Phys. Rev.*, **73**, 775 (1948).

$V=V(T, c)$. Temperature dependence of sound velocity $V=V(T)$ at constant concentration and concentration dependence of sound velocity $V=V(c)$ at constant temperature are the two main aspects. An aqueous solution of any substance, either organic[4,5] or inorganic,[4,5] shows parabolic $V(T)$-curves similar to that of water. When the substance is dissolved in water, a part of the clusters in solution is decreased and the peak temperature T_m (temperature for velocity maximum V_m) is lowered, the peak velocity V_m becoming greater than that of pure water. The concentration dependence of sound velocity $V(c)$ in aqueous solutions, however, has hitherto been studied only in some primary alcohols, amines, amides, ketones, carboxylic acids and heterocyclic compounds.

In the present study, sound velocity in aqueous solutions of HMT, urea, thiourea, acetamide, and DMF is measured and the dependence on concentration and temperature is studied with the purpose of elucidating the molecular mechanism of the sound propagation in aqueous solutions.

Experimental

Materials. HMT, urea (mp 133.6°C), thiourea (mp 181.3°C) and acetamide (mp 83.1°C) were purified by recrystallization from absolute alcohol, from reagent grade products. The melting point of HMT was not measurable because of sublimation. DMF (bp 152.8—153.6°C) was purified from reagent grade product by drying with anhydride sodium sulfate and distillation.

Apparatus. A crystal-controlled ultrasonic interferometer with frequency of 5 MHz was used to measure the sound velocity. One hundred standing waves were counted. Solutions in the measuring cell were immersed in an oil bath. The temperature was kept constant within ±0.1°C.

Results and Discussions

The sound velocity in solutions of HMT, urea, thiourea, acetamide and DMF is plotted against temperature in Figs. 1—5. It should be noted that for dilute solutions the $V(T)$-curves change in a systematic manner with concentration keeping the parabolic form nearly the same as that for water. We see that the peak velocity V_m becomes higher than that of pure water with increasing concentration, and at the same time the temperature corresponding to peak velocity (T_m) becomes lower than that for pure water. In concentrated solutions, a small amount of remaining

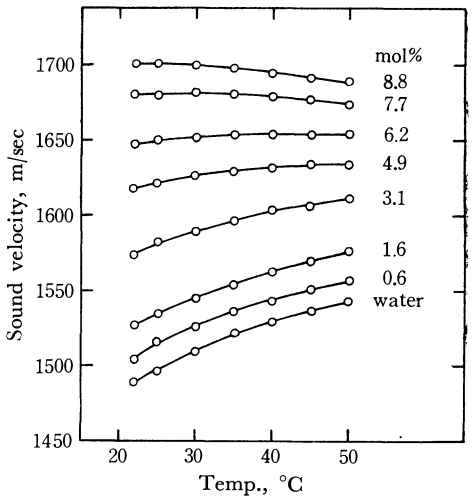

Fig. 1. Sound velocity *vs.* temperature of aqueous HMT solutions at various concentrations.

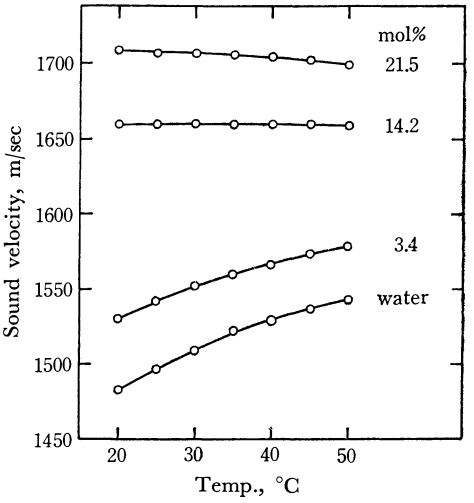

Fig. 2. Sound velocity *vs.* temperature of aqueous urea solutions at various concentrations.

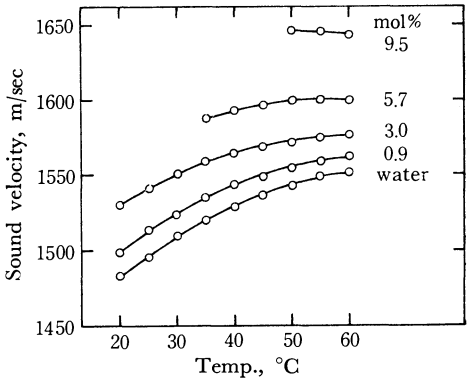

Fig. 3. Sound velocity *vs.* temperature of aqueous thiourea solutions at various concentrations.

4) J. Saneyoshi, K. Kikuchi and O. Nomoto, "Tyo-onpa Gizitu Binran," *Nikkan Kogyo Sinbunsya, Tokyo* (1966), pp. 1254—1267.

5) W. Schaaffs, Landolt-Börnstein, Zahlenwerte und Funktionen. Gruppe II, Band 5, "Molekularakustik," Springer-Verlag, Berlin, Heidelberg, New York (1967), pp. 89—125.

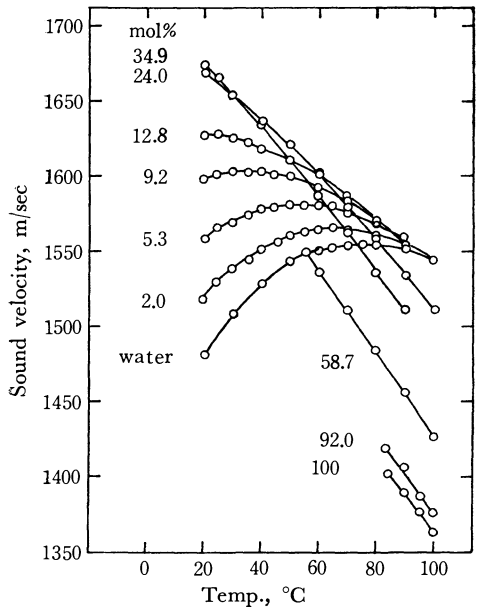

Fig. 4. Sound velocity *vs.* temperature of aqueous acetamide solutions at various concentrations.

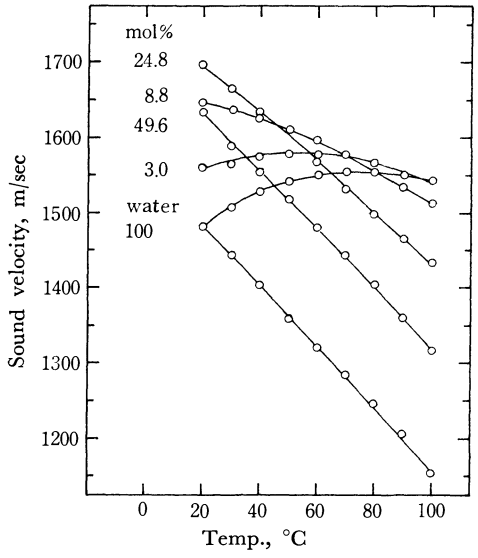

Fig. 5. Sound velocity *vs.* temperature of aqueous DMF solutions at various concentrations.

water makes the sound velocity considerably higher than that of pure solute (acetamide or DMF), the $V(T)$-curves becoming linear as in pure liquids (Figs. 4 and 5).

It is to be expected that a small amount of water in high-concentration solutions is almost in non-associated state, so that structural compressibility is absent. This makes the sound velocity in "non-associated water" much higher than in ordinary water, accompanying the great rise in velocity in highly concentrated solutions.

By extrapolating the sound velocity for pure water from that in the high-concentration region we obtain $V_2=2140$ m/sec and 2160 m/sec respectively, from acetamide solutions and DMF-solutions at 20°C, if the thermodynamic Kudriavtsev equation[6] for the sound velocity in ideal mixtures

$$V^2 = \mu\frac{M_1}{\bar{M}}V_1^2 + (1-\mu)\frac{M_2}{\bar{M}}V_2^2$$

is used. Here V_1, M_1 and μ mean sound velocity, molecular weight, and molar fraction of the first component, respectively, and V_2,M_2 and $(1-\mu)$ are the corresponding quantities for the second component. $\bar{M}=\mu M_1+(1-\mu)M_2$ is the average molecular weight. This value of V_2 is appreciably higher than the usual sound velocity for pure water (1483 m/sec at 20°C) and represents the sound velocity of virtual non-associated water.

The sound velocity V_1 in pure acetamide and DMF is found to be 1404.4 m/sec (85°C) and 1478.8 m/sec (20°C), respectively. The temperature coefficients of sound velocity in these substances are found to be -2.68 m/sec/deg and -3.90 m/sec/deg, respectively. Reported values for DMF (20°C) are $V_1=1497$ m/sec, $dV_1/dT=-4.0$ m/sec/deg[7] and $V_1=1478$ m/sec, $dV_1/dT=-3.62$ m/sec.[8]

Parshad[9] found that when alcohol is added to water, the peak temperature (74°C in pure water) becomes lower with increasing concentration. Willard[10] studied the relation between velocity and concentration in the same system and found that the shapes of curves are parabolic as for water. He assumed that for $V(T)$-curves in aqueous solutions over a wide temperature range parabolas shifted in a systematic manner with concentration are obtained. Even when we cannot find an actual velocity peak, we can determine the height and temperature of the hypothetical peak outside the measured range, by assuming that the shape of the $V(T)$ curve for solution remains the same with that of pure water, and by shifting the latter curve along the both coordinate-axes T and V till the both curves do overlap. (The hypothetical velocity peak sometimes comes below melting point.)

We assumed that the shift of the peak temperature is determined by the increment of non-associated water molecules exclusively add that this increment depends on the total surface area of solute molecules in water, considering that larger the surface area, the larger the number of single water

6) B. B. Kudriavtsev, *Soviet Physics-Acoustics*, **2**, 36 (1956).

7) I. Larionov, A. Dmitrieva and V. Goryatchoko, *Primenenie Ultraakustiki*, **2**, 75 (1958).

8) W. Schaaffs, Landolt-Börnstein, "Molekular-akustik," Springer Verlag, Berlin, Heidelberg, New York (1967), p. 18.

9) R. Parshad, *Indian J. Phys.*, **15**, 323 (1941).

10) W. Willard, *J. Acous. Soc. Amer.*, **19**, 234 (1947).

molecules which might be oriented in the neighbourhood of the solute resulting in the breaking of clusters. Assuming the solute molecules to be hard spheres with surface area $S_0=k_0(M/\rho N)^{2/3}$, the total surface area of the solute in 100 g aqueous solution of p wt% becomes

$$S_t = k\frac{p}{(\rho^2 M)^{1/3}},$$

where k_0 and k are constants, and N, ρ, and M are the Avogadro number, density and the molecular weight of the solute, respectively. In Fig. 6, the peak temperatures in solutions are plotted against $p/(\rho^2\mathrm{M})^{1/3}$, a quantity proportional to the total surface area S_t. As can be seen, a simple linear relation exists between the peak temperature and surface area up to about 30 wt%. This shows, at least qualitatively, the validity of our assumption that the shift of the peak temperature is determined by the relative concentration of non-associated water molecules.

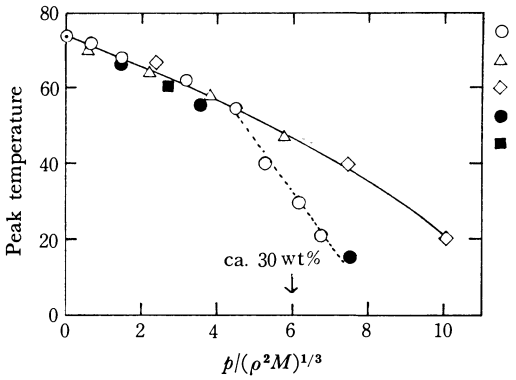

Fig. 6. Peak Temperature *vs.* $p/(\rho^2 M)^{1/3}$.
○ HMT, △ thiourea, ◇ urea, ● acetamide, ■ DMF

In Figs. 7—11 the sound velocity is plotted against molar fraction for aqueous solutions of HMT, urea, thiourea, acetamide and DMF over the whole range of concentration (up to the solubility limit in the case of HMT, urea and thiourea), and at temperatures 20—100°C. In case of sufficient solubility, these $V(c)$-curves exhibit maximum each at a fixed concentration, the maximum value gradually decreasing and shifting towards lower concentration with increasing temperature.

As seen in Figs. 10 and 11, the $V(c)$-curve at 100°C has no longer a maximum but exhibits a nearly linear relation. The aqueous solution hitherto investigated, which exhibit maximum in the $V(c)$-curve are those of primary alcohols, amines, amides, ketones, carboxylic acids and heterocyclic compounds. These compounds are known to be water-soluble non-electrolytes with radicals OH, NH_2, NH, CO, COOH and C_5H_5N, *etc.*, with tendency to form a hydrogen-bonded

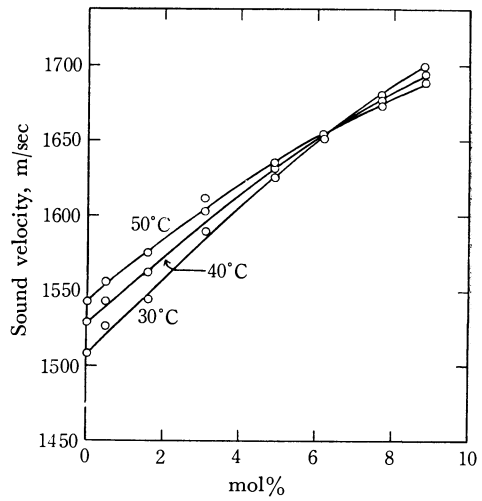

Fig. 7. Sound velocity *vs.* concentration of aqueous HMT solutions at various temperatures.

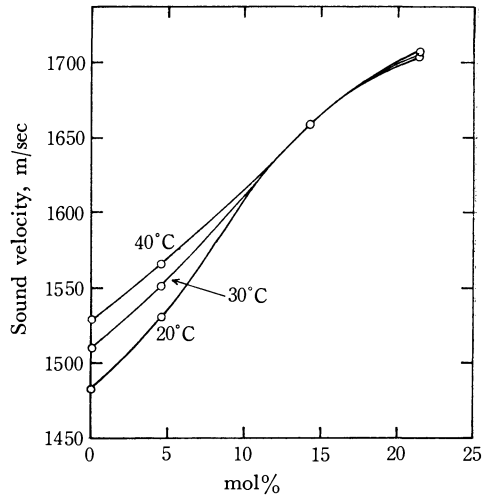

Fig. 8. Sound velocity *vs.* concentration of aqueous urea solutions at various temperatures.

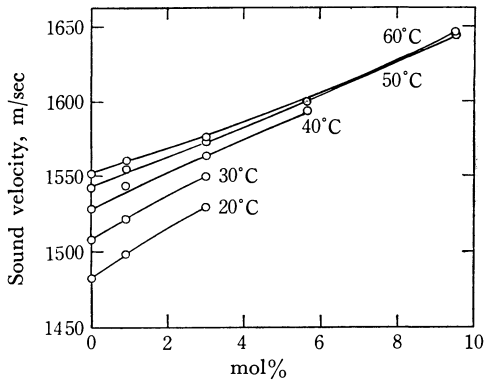

Fig. 9. Sound velocity *vs.* concentration of aqueous thiourea solutions at various temperatures.

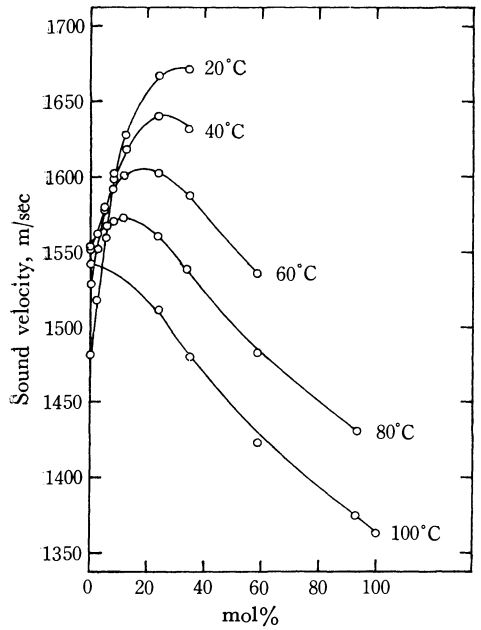

Fig. 10. Sound velocity *vs.* concentration of aqueous acetamide solutions at various temperatures.

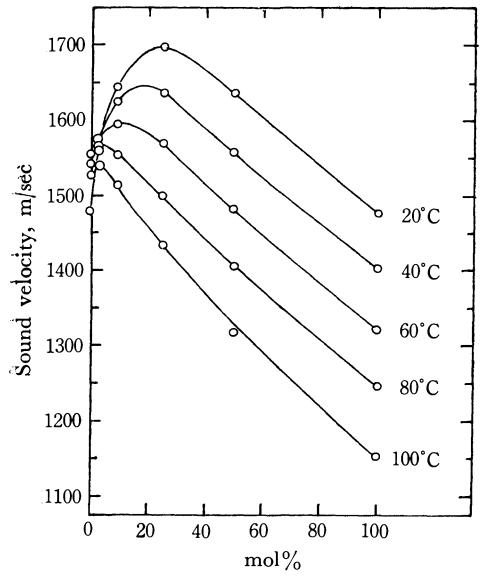

Fig. 11. Sound velocity *vs.* concentration of aqueous DMF solutions at various temperatures.

structure with water. By addition of these substances to water, it is to be expected that the available number of single water molecules decreases, so that the clusters of associated water molecules may dissolve to some extent until a new equilibrium is established.

Figure 12 gives the viscosity curves in the system water-DMF at various temperatures. The viscosity curves of aqueous solutions, especially primary alcohols[11,12] and carboxylic acids,[12,13] when plotted as functions of concentration at various temperatures, also show the maximum each at a fixed concentration, the maximum becoming lower and slightly shifting towards higher concentration with increasing temperature. It should be noticed that the direction of the shift of the viscosity peak is opposite that of the velocity peak. Recent data by Kikuchi and Oikawa[14] show no shift of viscosity peak with temperature. At any rate, the shift of viscosity peak is smaller than that of the sound velocity-peak.

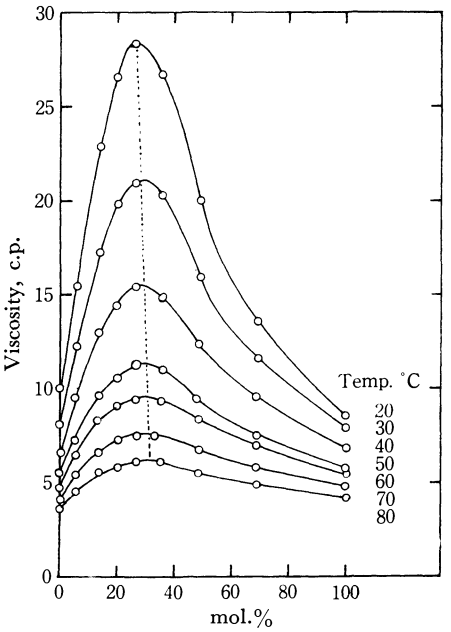

Fig. 12. Viscocity vs. concentration of aqueous DMF solutions at various temperatures. The dotted line shows the position of maximum viscocity (Larionov *et al.*[7]).

The maximum viscosity dependent on concentration is attributed to the molecular complex formation[12,15] among non-associated water molecules and the solute molecules. The viscosity maximum mighy shift towards higher concentration with temperature rise because of the increase in coordination number in the neighbourhood of the solute due to the increased fraction of the single water molecules, favouring complex formation at higher concentrations.

11) C. Bingham and F. Jackson, *Bull. Nat. Bur. Standards*, **14**, 59 (1917).
12) T. Ishikawa, "Kongoeki Nendo no Riron," Maruzen, Tokyo (1968).
13) J. Traube, *Ber.*, **19**, 871 (1886).
14) M. Kikuchi and E. Oikawa, *Nippon Kagaku Zasshi*, **88**, 19 (1967).
15) E. Hatschek, "The Viscosity of Liquids," Bell, London (1928), Chap. IX.

The solute-water-complex itself, however, does not influence sound velocity so much, because the complex is presumably of the same density and compressibility as the constituent parts before complex formation(solutes plus single-water molecules), approximately. The existence ratio of the single water molecules and clusters, however, changes with complex formation, and this gives rise on a shift towards lower concentration of the velocity peak with temperature rise.

We conclude that the maximum velocity observed for some aqueous solutions at a certain concentration at constant temperature does not correspond to the decrease in comressibility resulting from solute-water association, but is attributed to the balance between the relative magnitudes of the structural compressibility of the water-clusters and the ordinary compressibility of non-associated water molecules and solutes. Parshad[16] and Yasunaga *et al.*[17] attained analogous conclusions by adding small amounts of salt to ethanol-water system at constant temperature.

16) R. Parshad, *J. Acous. Soc. Amer.*, **21**, 175 (1949).
17) T. Yasunaga, N. Tatumoto and M. Miura, This Bulletin, **37**, 867 (1963).

BULLETIN OF THE CHEMICAL SOCIETY OF JAPAN VOL. 43 2723—2726 (1970)

The Effect of Adsorbed Amines on the ESR of Copper Oxide

Hisashi UEDA and Naoyuki TODO

Government Chemical Industrial Research Institute, Tokyo, 2-19-19 Mita Meguro-ku, Tokyo

(Received March 6, 1970)

The effect of several additives on the ESR of copper oxide was studied. Among the additives studied, amines and NH_3 had peculiar effects on the ESR spectra. From the spectrum formed by NH_3, it is concluded that the $(Cu–NH_3)^{2+}$ complex cation is formed on the surface of a CuO particle. The formation of this complex cation obeyed a pseudo-first-order rate and can be interpreted in terms of the surface reaction between the exposed Cu^{2+} and NH_3. Among the amines studied, only primary amines gave ESR spectra which provide evidence for the existence of $(Cu\text{-amine})^{2+}$ complex cations. The foregoing fact and the results obtained on the three isomers of chloroaniline indicate that a strong *s*-character of the lone-pair orbital is needed if an amine molecule is to occupy a surface defect of the O^{2-}, by which the Cu^{2+} is exposed on the surface, thus forming a complex cation. By these facts, the *d*-orbital of Cu^{2+}, which can overlap with the nitrogen lone pair of the amine molecule, is concluded to be d_z^2. The three principal values of the *g*-tensor for the $(Cu–NH_3)^{2+}$ complex cation depend greatly on the temperature, indicating that this cation has some rotational and vibrational motions below 130°C, at which point Cu^{2+} and NH_3 dissociate.

The electron spin resonances of copper complex have been studied in both the liquid and solid states.[1] The paramagnetic species, which exist only on the surfaces of particles of copper compounds, have been studied little, however. The paramagnetic species formed on the surface of CuO particles by various solid additives have been observed by one of the present authors.[2] In that work, it was found that the effect of the aromatic amines on the surface of the oxides studied is different from those of the other types of aromatic compounds. In the present report, the effect of NH_3 and a few aromatic amines on the ESR of cupric oxide is studied in order to discuss the nature of the paramagnetic species thus formed.

1) H. R. Gersman and J. D. Swalen, *J. Chem. Phys.*, **36**, 3221 (1962); A. H. Maki and B. R. McGarvey, *ibid.*, **29**, 31 (1958).

2) H. Ueda, This Bulletin, **43**, 319 (1970).

Experimental

The cupric oxide used was prepared by the oxidation of cupric carbonate. The adsorption of an amine on CuO particles was carried out by adding a solution of it (0.2 mM amine in 2.0 m*l* of purified benzene per 1.000 g of CuO) to copper oxide powder. After the evaporation of the solvent, the CuO-amine mixture was placed in an ESR sample tube and evacuated to 10^{-4} mmHg or to the vapor pressure of the additive. NH_3 and five other additives, used for comparison, were added in the gas phase at the pressure of 405 mmHg (N_2O), 653 mmHg (H_2), 294 mmHg (NH_3), 107 mmHg (tetrahydrofuran), 63 mmHg (benzene), and 89 mmHg (1,2-dichloroethane), all at 28.0°C.

Results

In Table 1 the relative intensities and the δH_{msl} values obtained from the ESR spectra of CuO with several additives are shown. It may be seen

that only NH_3 affects the spectrum considerably and that only it yields the narrow ESR absorption in addition to the broad absorption which it yields in common with the other additives. This paper will descuss only the narrow component of the ESR spectra obtained from NH_3 and aromatic amines. In Fig. 1, a-d, the narrow components of the ESR spectra obtained from a CuO–NH_3 sample at various measurement temperatures are shown. The thermal change in the shape of the spectra is reversible in the temperature region below 140°C. When the sample is heated to as much as 300°C, the paramagnetic species (giving rise to the a–d spectra) receive some irreversible thermal damage; the resulting spectrum, measured at 20°C, is shown as e. If a CuO–NH_3 sample which is heated to 135°C (showing the *d* spectrum) is quickly cooled to 103°C, and if the spectra are repeatedly recorded, the intensity of the absorption spectrum, to be identified as I_t, begins to increase with the rate, as is shown in Fig. 2. As is shown in the figure, $\log(I_\infty - I_t)$ changes linearly with respect to time, t, indicating that the formation is a first- (or a pseudo-first-) order reaction. The spectrum (Fig. 1a) indicates three principal values of the g-factor, as has been observed with several cupric-ammonium complex salts.[3,4] The magnitude of the three principal

TABLE 1. ESR OF CUPRIC OXIDE WITH VARIOUS ADDITIVES

Additive	Relative intensity*	δH_{msl} (gauss)
None	3.38×10^5	700±40
H_2	4.50×10^5	950±40
NH_3, broad comp.	3.08×10^5	800±40
NH_3, narrow comp.	3.60×10^3	see text
C_6H_6	2.11×10^5	730±40
1,2-Dichloroethane	3.42×10^5	800±40
N_2O	2.27×10^5	800±40
Tetrahydrofuran	2.70×10^5	800±40

* Integrated value. The average g-factor is 2.21.

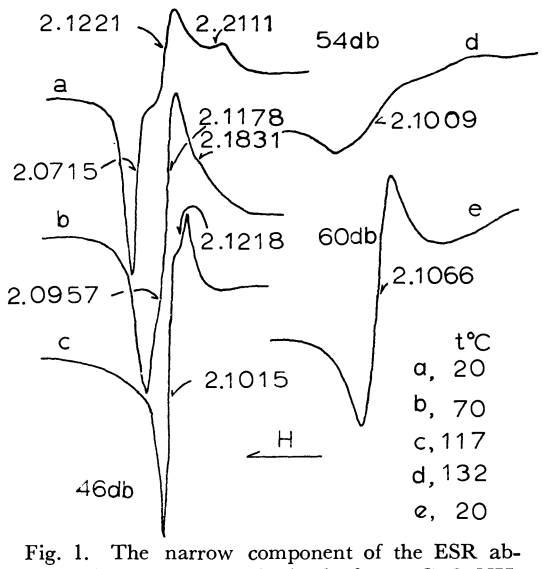

Fig. 1. The narrow component of the ESR absorption spectrum obtained from CuO–NH_3 sample. The g-factor is indicated with an arrow pointing the position on the curve. The temperature at which measurements were made are shown in the right bottom corner. The curve e is after thermal treatment at 300°C. The amount of current amplfication is shown in db.

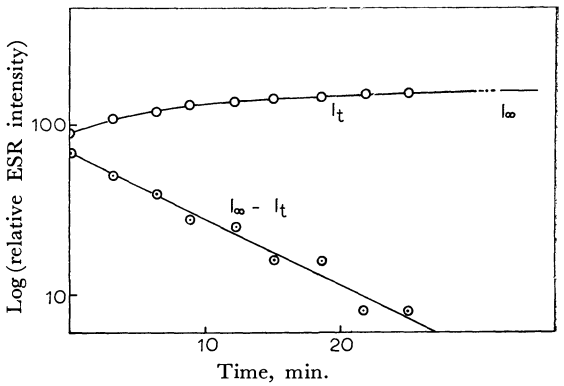

Fig. 2. The growing rate of the intensity of the narrow component of the ESR signal from a sample of CuO–NH_3 at 103°C. I_∞ is for time infinity and I_t is for time=t.

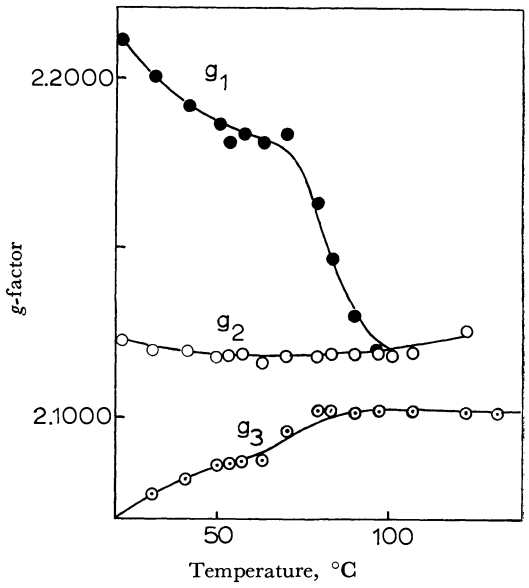

Fig. 3. The dependence of the three principal values of the g-tensor obtained by a (CuO–NH_3) sample upon the temperature of measurement.

3) T. Okamura and M. Date, *Phys. Rev.*, **94**, 314 (1954).

4) E. H. Carlson and R. D. Spence, *J. Chem. Phys.*, **24**, 471 (1956).

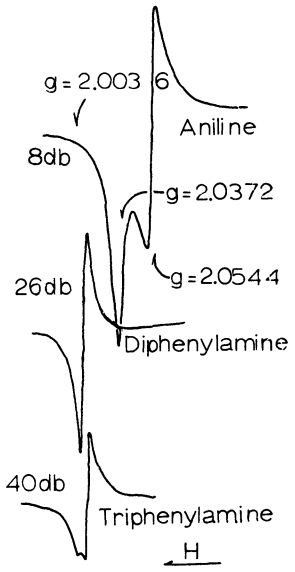

Fig. 4. The central components of the ESR spectra obtained with CuO and aromatic amines. The amount of current amplification is indicated in db. Measurements were made at 20°C.

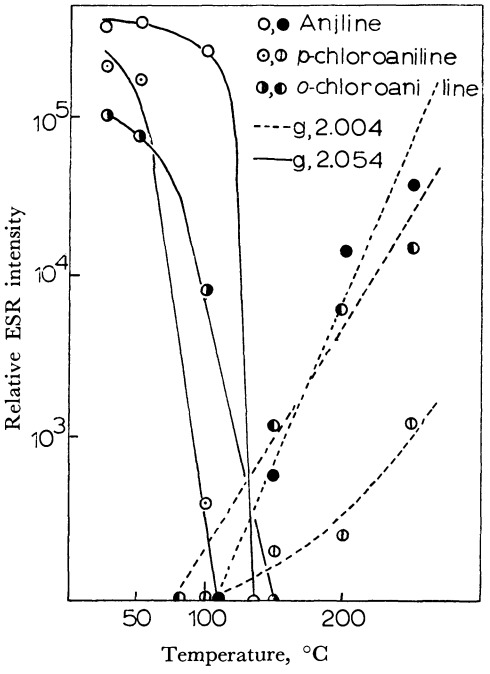

Fig. 5. The dependence of the relative intensities of the narrow ESR components of the (CuO-aromatic amine) specimens on the temperature of the thermal treatment, which is on the abscissa. Measurements were made at 20°C.

values of the g-tensor depend on the temperature of measurement, as is shown in Fig. 3. According to previous studies,[4] it seems reasonable to assign the g_1 to the $g_{\parallel}$, and the g_2 and g_3, to the $g_{\perp}$. When aromatic amines are used as additives, the ESR spectra shown in Fig. 4 are observed. Only primary amines, aniline, *o*- and *p*-chloroanilines but not *m*-chloroaniline, give spectra which are identical. In Fig. 5 the temperature dependence of the ESR intensities obtained by aniline and isomeric chloroanilines are shown.

Discussion

The ratio between the area covered by the narrow component of the spectrum obtained in the CuO–NH_3 sample at 29°C and the broad component of the same spectrum is approximately 0.0117, as may be seen in Table 1. If the surface Cu^{2+} is all converted to $(Cu–NH_3)^{2+}$-type complex ions, and if all the other Cu^{2+} (the second and the inner layers under the surface of a CuO particle) are not affected, the above-mentioned ratio can be shown to be a function of the dimensions of the particles. If the formation of $(Cu–NH_3)^{2+}$ is limited to some particular Cu^{2+} points on the surface, or if some of the Cu^{2+} are completely covered by O^{2-} ions, the ratio (the surface Cu^{2+} to combine with NH_3)/(the total surface and bulk Cu^{2+}) becomes smaller than expected. The observed ratio of the two spectral components is not unreasonable for considering the formation of $(Cu–NH_3)^{2+}$ exclusively at some or all of the surface Cu^{2+} points.

The reaction rate, $Cu^{2+}+NH_3 \rightarrow (Cu–NH_3)^{2+}$, also indicates that this is a surface process. The reaction rate is proportional to the product of the concentrations, $[Cu^{2+}][NH_3]$. If the reaction occurs under the surface, the $[NH_3]$ will be controlled by the velocity of the penetration of NH_3 into and through the CuO particles and will not depend much on the time, for the pressure of NH_3 is constant. $[Cu^{2+}]$ will also be constant, and the reaction rate will be zeroth order. However, if the reaction on the surface is assumed, $[NH_3]$ or p_{NH_3} is constant because of its excess amount, and $[Cu^{2+}]=[Cu^{2+}]_{total}-[(Cu–NH_3)^{2+}]$, where $[Cu^{2+}]_{total}$ signifies the amount of Cu^{2+} on the surface prior to the introduction of NH_3. The rate of the formation of $(Cu–NH_3)^{2+}$ is equal to the rate of the decay of the surface Cu^{2+}, therefore, it proceeds with a pseudo-first-order rate. Therefore, the surface reaction model agrees well with the observed rate.

The results in the previous paper indicated that, in the case of alumina, the chemisorption occured between the *p*-orbitals of the oxygen anions and the π-orbital of the aromatic additive, both having the same symmetry. In contrast with it, the chemisorption in the case of CuO was considered to occur between the 3d orbital of Cu^{2+} and the additive. Acturally, in some cases the unpaired electron was found on both Cu^{2+} and the nitrogen of the additive molecule.[2] If all the surface *d*-orbitals of Cu^{2+} are occupied or covered by O^{2-}

ligands, there will be no way for a NH_3 to occupy or overlap with one of them. Therefore, it can be concluded that the $(Cu\text{–}NH_3)^{2+}$ complex is formed when a NH_3 molecule fills the defect of a O^{2-} ligand on the surface. As NH_3 is a neutral molecule and so has no net negative charge on it, this chemisorption will partly consist of the formation of a covalent bond between the Cu^{2+} and NH_3, and partly of a polarization of the lone-pair orbital of the NH_3 toward the Cu^{2+}. In the case of aromatic amines, only primary amines gave ESR spectra with $g=2.03$—2.06. In the case of secondary and tertiary amines, the lone pair of the nitrogen will possess a considerably more *p*-character than that of aniline. Therefore, the stronger *s*-character of the lone pair bond is the better for a foreign ligand to occupy the O^{2-} defect on the surface. Since the H–N–H angle in NH_3 is 107.3°[5,6] and deviates somewhat from the pure sp^3 angle of 109°28′, the lone pair of NH_3 has a small *p*-character.

Though the *g*-factors observed in the CuO-aniline sample are closer to those of DPPH than those of the CuO–NH_3 sample, it is certain that the unpaired electron is on both Cu^{2+} and aniline; in other words, the $(Cu\text{-aniline})^{2+}$ complex is formed. The temperature dependence of the intensity of the line with $g=2.054$ is also similar to that of the $(Cu\text{–}NH_3)^{2+}$ complex (Fig. 5), and they both disappear above 130°C. In the cases of *o*- and *p*-chloroanilines, the double-bond character of C–Cl induces some negative electron density on the carbon atom to which the NH_2 group is attached. Probably because of the electrostatic repulsion, the configuration in which the nitrogen lone pair is out of the C_6H_4-plane is avoided and the *s*-character of the lone pair is strong. In the case of *m*-chloroaniline, the negative electron densities are distributed on the carbon atoms next to the $\rangle C\text{–}NH_2$ group; probably for this reason the nitrogen lone pair possesses some *p*-character of overlapping with the molecular π-bond.

As the O^{2-} ions are in the tetrahedral directions with respect to Cu^{2+},[7] the defect of one of the four O^{2-} ligands surrounding one Cu^{2+} ion leads to a electrostatic field of the C_{3v} symmetry. In the T_d symmetry, the unpaired electron occupies one of the ^2E_g orbitals, *i.e.*, $x^2\text{–}y^2$ and z^2. If the symmetry goes down to C_{3v}, it is uncertain which orbital accommodates the unpaired electron. The experimental evidence that the foreign or amine ligand orbital has a strong *s*-character suggests that the corresponding Cu^{2+} orbital has an A_1 symmetry or z^2. As the electronic state of a Cu^{2+} is considered to consist of a hole in a completely-filled 3d-shell, the energy eigenvalue of the z^2 orbital without an O^{2-} in the *z*-direction will be higher than that with an O^{2-}. Thus, it is possible that the energy level of the orbital with A_1 symmetry eventually becomes higher than those of the other orbitals with E symmetry when the crystal field symmetry goes down to C_{3v}. Therefore, for this reason too, it is likely that the unpaired electron occupies the z^2 orbital. The molecular orbitals formed may be written as $k\cdot z^2+l\cdot\phi_{\sigma N}$ where k and l are coefficients to be determined by the relative weights of the spin densities in each orbital.

The relatively smaller *g*-factor of $(Cu\text{-aniline})^{2+}$ absorption is due to the greater polarizability of the H–C_6H_4–NH_2 bonds toward Cu^{2+} than that of H–NH_2 bonds toward Cu^{2+}; as a result, the l for aniline is larger than that for NH_3. As the unpaired electron is in an antibonding molecular orbital with coefficients (k and $-l$), the larger l value for $(Cu\text{-aniline})^{2+}$ makes the complex less stable and the *g*-factor closer to that of DPPH.

The temperature dependence of the *g*-factor in Fig. 3 indicates that the three components of the *g*-factor at relatively low temperatures are reduced to two components at higher temperatures. This is due to the rotational and vibrational motion of the Cu^{2+}–NH_3 (partially covalent) bond. The anisotropy in the *g*-tensor is averaged out by thermal motions at elevated temperatures. Somewhere above 140°C, but below 300°C, the surface Cu^{2+} species decompose or react irreversibly with NH_3 and yield some paramagnetic species which give the ESR spectrum shown in Fig. 1e.

The active site of a solid catalyst may be described in two ways. One is in terms of the geometrical positions at which they are located on the surface of a particle, while the other is a description in molecular- or atomic-orbital language. The geometrical problems can be studied by means of an electron microscope and other optical techniques. The bulk symmetry of the orbitals and the crystal field in the solid state can be studied by X-ray and other methods. The symmetry of the atomic- or molecular-orbitals or crystal field on the surface, however, has not been investigated much. From such a point of view, the method employed in the present work would seem to have some significance even when the catalytic importance of CuO is considered to be rather meager.

5) G. Herzberg, "Infrared and Raman Spectra of Polyatomic Molecules," van Nostrand Co., New York, N. Y. (1945).

6) M. T. Weiss and M. W. P. Strandberg, *Phys. Rev.*, **83**, 567 (1951).

7) R. Kiriyama, "Kozomukikagaku," Vol. 1, Kyoritu Publ. Co., Tokyo (1958), p. 110.

BULLETIN OF THE CHEMICAL SOCIETY OF JAPAN VOL. 43 2727—2731 (1970)

The Electronic Nature of Paramagnetic Oxygen Species Combined with Metal Ions at Surface and in Solution

Morio SETAKA and Takao KWAN

Faculty of Pharmaceutical Sciences, The University of Tokyo, Bunkyo-ku, Tokyo

(Received March 6, 1970)

ESR spectra of adsorbed oxygen species were investigated on cadmium, cerium and uranium oxides supported on alumina. The principal g values, g_x, g_y and g_z of the oxygen species were computed and compared with those on the other metal oxides. It was pointed out that the principal g values observed on cerium and uranium oxides are interpretable by a peroxy-like model rather than an O_2^- radical. ESR spectra due to radicals formed on mixing solutions of VO^{2+} or UO_2^{2+} (containing Ti^{3+}) with H_2O_2 were also investigated by a rapid-mixing flow technique. The g value of the radicals was very close to the isotropic one of the peroxy-like species adsorbed on the corresponding metal oxide. The electronic nature of the interaction of oxygen species with metal ions at surface and with those in solution was comparatively discussed.

ESR spectra of adsorbed oxygen species on various metal oxides[1-11] have been reported by many workers. These spectra were asymmetric and characterized generally with three different principal g values near 2.0, which varied from one metal oxide to the other. The observed shifts in the principal g values have been discussed in terms of an adsorbed O_2^- model; effect of the electric charge of the constituent metal ion of the oxides on the O_2^- radical was taken into consideration.[3,6] According to Kasai[12] who had studied ESR spectra of γ-irradiated zeolites in the presence of oxygen, the principal g values of the O_2^- radical were strongly dependent on the electric charge associated with the zeolite cation (Na^+ or Ba^{2+}).

The shift of the principal g values has been recognized also by us[8] with respect to the O_2^- radical adsorbed on ZnO, TiO_2 and ZrO_2. It was felt worthwhile, therefore, to extend this sort of study to metal oxides having different electric charges of the constituent metal ion. Thus, in the present paper, special interest will be placed on the ESR of oxygen species adsorbed on metal oxides of higher valencies *e.g.* CeO_2 and UO_3.

Literature shows that a mixture of metal ion and H_2O_2 produces an ESR signal near the g value of 2.0. We have already reported[13] that a mixture of $VOSO_4$ and H_2O_2 yields an ESR signal near $g=2.0$ characterized with eight hyperfine lines due to vanadium nucleus ($I=7/2$) and that the signal is attributable to a *complex* hydroperoxy radical. The observed resemblance in the g values between the complex peroxy-like species in solutions[13] and the oxygen species adsorbed on the surface of V_2O_5[9] is worthy of note. Since the nature of the hydroperoxy or peroxy-like species often observable in solutions of metal ion and H_2O_2 is still unknown, it would be pertinent to investigate ESR spectra of such solutions with particular interest in the valencies of metal ions and to compare the g value of generated radicals with that of adsorbed oxygen species on the corresponding metal oxide. Thus in the present work, solutions containing metal ions such as Ti^{3+}, VO^{2+} and UO_2^{2+} mixed with H_2O_2 were also subjected to ESR studies by using a rapid-mixing flow technique.

1) R. Kokes, Proceeding of the Third International Congress on Catalysis. North-Holland Publishing Company, Amsterdam (1964), p. 484.
2) Y. Fujita and T. Kwan, *Shokubai*, **5**, 206 (1963).
3) J. H. Lunsford and J. P. Jayne, *J. Chem. Phys.*, **44**, 1487 (1966).
4) R. D. Iyenger, M. Codell, J. S. Karra and J. Turkevich, *J. Amer. Chem. Soc.*, **88**, 5055 (1966).
5) Y. Fujita and J. Turkevich, *Discuss. Faraday Soc.*, **41**, 407 (1966).
6) I. D. Mikheikin, A. I. Maschenko and V. B. Kasanskii, *Kin. i Kat.*, **8**, 1363 (1967).
7) J. H. C. Van Hooff and J. F. Van Helden, *J. Catalysis*, **8**, 199 (1967); J. H. C. Van Hooff, *ibid.*, **11**, 277 (1968).
8) M. Setaka, S. Fukuzawa, Y. Kirino and T. Kwan, *Chem. Pharm. Bull. Tokyo*, **16**, 1240 (1968); M. Setaka and T. Kwan, This Bulletin, **38**, 1414 (1965); M. Setaka and T. Kwan, *Shokubai*, **7**, 335 (1965).
9) V. A. Shvets, M. E. Sarichev and V. B. Kasanskii, *J. Catalysis*, **11**, 378 (1968).
10) K. Tarama, S. Yoshida, S. Ishida and Y. Doi, This Bulletin, **42**, 1161 (1969).
11) K. M. Sancier, *J. Catalysis*, **5**, 314 (1966).
12) P. H. Kasai, *J. Chem. Phys.*, **43**, 3322 (1965).
13) M. Setaka, Y. Kirino, T. Ozawa and T. Kwan, *J. Catalysis*, **15**, 209 (1969).

Experimental

Preliminary investigations indicated that the metal oxide such as CeO_2 or UO_3 gives only a weak ESR signal due to adsorbed oxygen species. Moreover the oxides became rather metallic, when outgassed at or above 500°C, leading to a decrease in the sensitivity of the cavity. Therefore, in the present work, we used Al_2O_3 as the support, and the supported Ce or U oxide sample (denoted as the Ce or U sample) was studied after appropriate pretreatment. The valency state of the cerium or uranium ion in the sample should therefore be regarded as indefinite. CdO was also investigated as an example of metal oxide having a lower valency.

A sample of Al_2O_3 powder (standardized, E. Merck AG) was impregnated with an aqueous solution of cadmium nitrate (guaranteed, Koso Chemical Co.), ceric ammonium nitrate (guaranteed, Wako Pure Chemical Co.) and uranyl nitrate (standardized, E. Merck AG), respectively. The samples were then dried at 100°C and calcined in a stream of oxygen (760 Torr) for four hours at 500°C except for the Cd sample which was pretreated below 400°C. The amount of added salts was so controlled that the metal ions were 5 wt% of the Al_2O_3. The calcined samples were white (Cd sample), pale yellow (Ce sample) and reddish brown (U sample).

A given amount of each sample was placed in individual quartz tubes (4 mm dia.). The Cd sample was evacuated for thirty minutes at 400°C and heated in a hydrogen atmosphere (50 Torr) for one hour at 300°C and then evacuated for another hour at the same temperature. When the sample was treated with hydrogen at temperatures higher than 300°C, cadmium sublimed and condensed in a metallic state on the wall of the sample tube. The Ce and U samples were evacuated for thirty minutes at 500°C and treated with 50 Torr of hydrogen for one hour and evacuated for another hour at the same temperature. The color was greyish white for the Cd sample and greyish brown for the Ce and U samples.

A capillary tube containing MgO powder dispersed thermally with Mn^{2+} ion was inserted into the center of the sample as a means of measuring relative ESR sensitivity. The g values were calculated on the basis of the g value ($g=2.0036$) of DPPH. Signal simulation of the sample was made with a computer (Hitachi, HITAC 5020) to confirm the obtained g-values. ESR measurements were carried out at room temperature with a JEOL P-10 spectrometer (X band, 100 kcps field modulation).

A rapid-mixing flow technique coupled with ESR was utilized to detect peroxy-like species formed on mixing solutions of Ti^{3+}, VO^{2+} or UO_2^{2+} with H_2O_2. The experimental procedures were nearly the same as those reported earlier.[13]

Results

1. Supported Oxides. So far we have observed ESR spectra of adsorbed oxygen species on a number of metal oxides with or without support.[8] For TiO_2 and SnO_2 supported on Al_2O_3, ESR spectra due to adsorbed oxygen species were essentially the same as those reported for the unsupported oxides.[7,8] On the metal oxide such as MoO_3, it was difficult to distinguish the signal of adsorbed oxygen species from that due to molybdenium ion. Thus we confined ourselves to investigating the Cd, Ce and U samples, which exhibited distinct ESR signals due to adsorbed oxygen species as will be shown later.

No ESR signal was detectable at least in the magnetic field investigated ($g=1.8$—2.2) with the Cd and U samples outgassed in a high vacuum at room temperature. Neither heat treatment in a high vacuum nor hydrogen pretreatment resulted in ESR signals. However, when 50 Torr of oxygen was introduced to the pretreated Cd and U samples at room temperature, followed by slight outgassing, ESR signals as shown in Figs. 1 and 2 were obtained. For the Ce sample, a very small signal consisting of six resonance lines was detected.

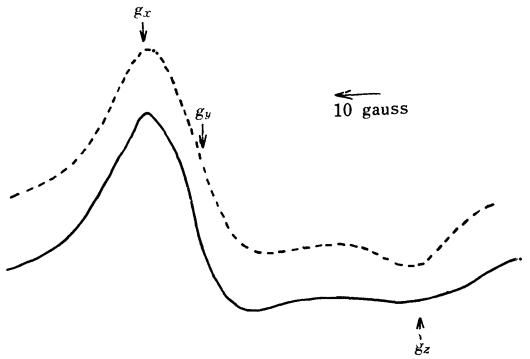

Fig. 1. ESR(X-band) spectrum of adsorbed oxygen species on a pretreated CdO-Al_2O_3 sample. Dotted curve: simulated

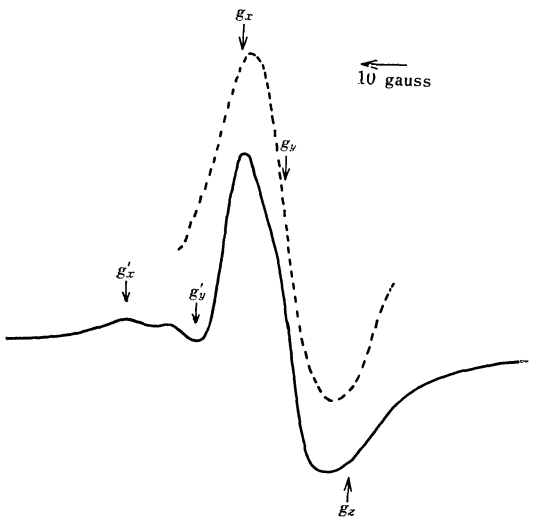

Fig. 2. ESR spectrum of adsorbed oxygen species on a pretreated UO_3-Al_2O_3 sample.
Dotted curve: simulated
g_x, g_y and g_z: g values for the major signal
g_x' and g_y': g values for the minor signal

for both untreated and pretreated samples. It was attributed to manganese impurities. The Ce sample showed, after a similar oxygen pretreatment, a large signal which overlapped the signal of manganese impurities. The manganese signal was so small compared with the major signal due to adsorbed oxygen species (1/300) that it could be neglected as shown in Fig. 3. The Al_2O_3 support itself gave no ESR signal even after pretreatment.

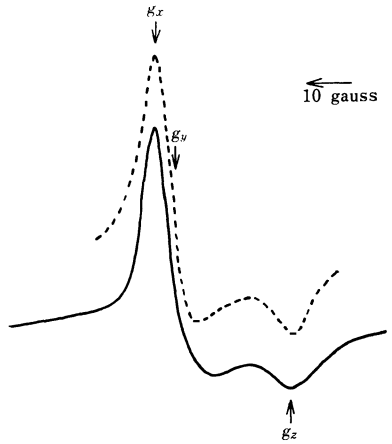

Fig. 3. ESR spectrum of adsorbed oxygen species on a pretreated $CdO-Al_2O_3$ sample.
Dotted curve: simulated

The ESR signals shown in Figs. 1, 2 and 3 were completely broadened by exposure to air. They were restored, however, by slight outgassing at room temperature. This phenomenon suggests that the signals are due to the surface paramagnetic species. When 50 Torr of NO was introduced onto the samples showing these signals, they disappeared in an irreversible manner. A chemical reaction probably had occurred between the paramagnetic species and NO. Although cerium and uranium ions of some lower valencies are indeed paramagnetic and hence may exhibit ESR signals, the observed g values are apparently different from those of the reported spectra.[14] Consequently, the ESR signals of Figs. 1, 2 and 3 should be regarded as due to adsorbed oxygen species.

In the case of the U sample, the major signal (g_x, g_y, g_z) appeared to overlap the minor one (g_x', g_y'). The two signals behaved quite similarly with respect to exposure to air or NO. It seems likely that there are two kinds of adsorped oxygen species on the surface.

It was rather difficult to obtain accurate ESR parameters directly from the maximum or the inflection point of the first derivative curve. The situation became more serious especially when the half width (ΔH) between the maximum slope of the derivative of the absorption line was large. Thus, signal simulation was carried out with a computer on the basis of the theoretical equation of the line shape given by Kneübuhl[15] for a polycrystalline sample having three principal g values.

The computed curves (dotted lines) are compared with the experimental curves (solid lines) in Figs. 1, 2 and 3. Agreement of both curves was rather poor with the U sample where two signals overlapped. The ESR spectrum of the O_2^- radical on ZrO_2[8] is reproduced in Fig. 4 where the signal simulation was similarly carried out and the g values were computed.

In Table 1, the principal g values reported for adsorbed oxygen species on various metal oxides

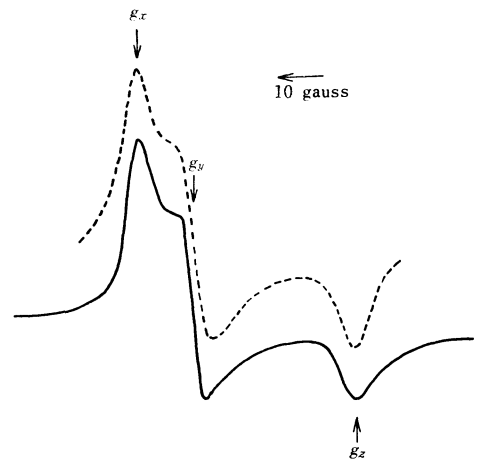

Fig. 4. ESR spectrum of adsorbed oxygen species on a pretreated ZrO_2 sample.

TABLE 1. THE PRINCIPAL g VALUES FOR PARAMAGNETIC OXYGEN SPECIES ADSORBED ON VARIOUS METAL OXIDES

Metal oxide	g_z	g_y	g_x	K[a]	Ref.
UV irrad. MgO	2.077	2.0073	2.0011	27	3
ZnO	2.051	2.0082	2.0020	41	3
TiO	2.024	2.009	2.003	92	6
SnO_2	2.028	2.009	2.002	78	7
$V_2O_5-SiO_2$	2.025	2.011	2.005	88	9
Vycor glass	2.030	2.014	2.002	72	5
ZrO_2	2.032	2.010	2.002	67	8
$CdO-Al_2O_3$	2.039	2.009	2.002	55	
$CeO_2-Al_2O_3$	2.030	2.014	2.011		
$UO_3-Al_2O_3$	2.035	2.025	2.018		
	—	2.012	2.003[b]		

a) $K \equiv 2/(g_z - g_e)$.
b) g Values for the minor signal of adsorbed oxygen radical.

14) W. Low, "Paramagnetic Resonance in Solid, Solid State Physics Supl." Academic Press, **2**, pp. 128, 140 (1960).

15) F. K. Kneübuhl, *J. Chem. Phys.*, **33**, 1074 (1960).

were listed in addition to those on the Cd, Ce and U samples determined in the present work.

2. Solutions. The rapid-mixing flow technique was applied to $UO_2(NO_3)_2$–H_2O_2 similarly as in the case of $VOSO_4$-H_2O_2 system.[13] Since UO_2^{2+} does not act as electron donor, a very small amount of Ti^{3+} we added to the mixing solution in advance. In other words, we expected that UO_2^{2+} would capture peroxy-like species produced by Ti^{3+}–H_2O_2. As a result, the Ti^{3+}–UO_2^{2+}–H_2O_2 system yielded a signal of the g value of 2.023 entirely different from that due to Ti^{3+}–H_2O_2. It is suggested that the $g=2.023$ signal is atrributed to a peroxy-like species combined with UO_2^{2+}.

ESR spectra of a mixture of Fe^{2+}–H_2O_2 or Ti^{3+}–H_2O_2 with organic additives have been the subject of many investigations. Nevertheless, the signal near $g=2.9$ observable for Ti^{3+}–H_2O_2 has not been well identified[16-18] while the nature of organic radicals produced was extensively worked out for both systems. We were able to show an ESR signal near $g=2.0$ for a $VOSO_4$-H_2O_2 system in sulfuric iacid by utilizing a rapid-mixing flow technique.[13] The g value of the signal was found to be 2.0016, and the signal was characterized with eight hyperfine resonance lines due to vanadium nucleus ($I=7/2$). On the basis of these findings, we have proposed that the signal is due to a HO_2 radical complexed with VO^{3+}. Ti^{3+} or Ce^{4+} is reported to give an ESR signal having g values of 2.01195, 2.1335 or 2.016[19] when mixed with H_2O_2 while no such signal is reported for Fe^{2+}–H_2O_2.[20] In the second column of Table 2, the reported g values of the signal observed for various metal ion-H_2O_2 systems are listed together with that of the Ti^{3+}–UO_2^{2+}–H_2O_2 system. In Table 2 are shown the isotropic g values for the oxygen radical adsorbed on the corresponding metal oxides for comparions. It is rather surprising to see that the g values of the peroxy-like species produced from a mixture of metal ions and H_2O_2 is nearly the same as that of the radical adsorbed on the corresponding metal oxide.

Discussion

It can be seen from Table 1 that g_z is, in general, larger than the g value of a free spin ($g_e=2.0023$), while g_x remains nearly constant around g_e. The principal g values of the O_2^- ion trapped in the lattice of alkali halide have been formulated by Kanzig and Cohen.[21] This approach was applied

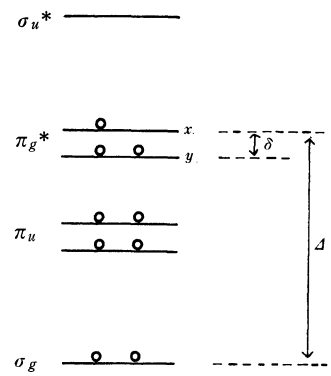

Fig. 5. Electronic energy levels of O_2^- after Kasai (Ref. 12).

here to the study of the adsorbed O_2^- radical. The ground-state electronic configurat on of O_2^- is $(\sigma_g\,2P)^2(\pi_u\,2P)^4(\pi_g^*\,2P)^3$. When O_2^- is adsorbed and exposed to the asymmetric surface field of the metal oxide, the originally degenerated π_g^* orbitals are expected to split into two orbitals, π_g^* $(2P_x)$ and π_g^* $(2P_y)$, as shown schematically in Fig. 5. The three principal g values are then given by

$$g_x = \frac{g_e\delta}{(\delta^2+\lambda^2)^{1/2}} + \frac{\lambda}{\Delta}\left[\frac{\delta+\lambda}{(\delta^2+\lambda^2)^{1/2}} - 1\right]$$
$$\simeq g_e - \frac{\lambda^2}{\delta^2} + \frac{\lambda^2}{\Delta\delta} \qquad (1)$$

TABLE 2. THE ISOTROPIC g VALUES FOR PARAMAGNETIC OXYGEN SPECIES COMBINED TO METAL IONS AT SURFACE AND IN SOLUTION

Metal ion-H_2O_2	g_{iso}	Metal oxide-O_2	g_{iso}	Ref.
Ti^{3+}-H_2O_2	2.01195 2.01335	TiO_2-O_2	2.011 (O^-) 2.012 (O_2^-)	15, 16, 17
VO^{2+}-H_2O_2	2.0116	V_2O_5-O_2	2.0137	13
Ce^{4+}-H_2O_2	2.016	CeO_2-O_2	2.018	18
UO_2^{2+}-H_2O_2 containing Ti^{3+}	2.023	UO_3-O_2	2.026	

16) Y. S. Chiang, J. Craddock, D. Mickewich and J. Turkevich, *J. Phys. Chem.*, **70**. 3509 (1966).
17) H. Fisher, *Ber. Bunsenges. Phys. Chem.*, **71**, 689 (1967).
18) R. E. Florin, F. Sicilio and L. A. Wall, *J. Phys. Chem.*, **72**, 3154 (1968).
19) E. Saito and B. H. J. Bielski, *J. Amer. Chem. Soc.*, **83**, 4467 (1961).
20) T. Shiga, *J. Phys. Chem.*, **69**, 3805 (1965).
21) W. Kanzig and M. H. Cohen, *Phys. Rev. Lett.*, **3**, 509 (1959).

$$g_y = \frac{g_e\delta}{(\delta^2+\lambda^2)^{1/2}} - \frac{\lambda}{\Delta}\left[\frac{\delta-\lambda}{(\delta^2+\lambda^2)^{1/2}} + 1\right]$$
$$\simeq g_e + \frac{2\lambda}{\Delta} - \frac{\lambda^2}{\delta^2} - \frac{\lambda^2}{\Delta\delta} \quad (2)$$

$$g_z = g_e + \frac{2\lambda}{(\delta^2+\lambda^2)^{1/2}} \simeq g_e + \frac{2\lambda}{\delta} \quad (3)$$

where, z is chosen along the internuclear axis of O_2^-, δ and Δ are the energy separations shown in Fig. 5. λ is the spin-orbit coupling constant for O_2^-. Approximate equations are useful when $\Delta > \delta \gg \lambda$.

As shown from the approximate equations, the principal g value, which deviates farthest from g_e, should be assigned to g_z, while g_x should be closest to and slightly below g_e. The obtained data except for the Ce and U samples are well explained by such an O_2^- radical model. The effect of a trapping site, which gives rise to the energy separation (δ) of the two π_g^* orbitals, is well reflected in the deviations in g_z values. The value, $K=2/(g_z-g_e)\simeq\delta/\lambda$ was calculated as a possible measure of the interaction of O_2^- with a cation. The results are shown also in Table 1 together with some results of K given by the other workers.[3,6] The K value is expected to increase when the interaction energy between the O_2^- radical and the trapping site increases.

The sequence of this effect, according to Table 1, is given by

$TiO_2 > V_2O_5/SiO_2 > SnO_2 >$ Vycor glass $>$
$ZrO_2 > CdO > ZnO > MgO$

It should be recognized, however, in view of the uncertainty in the g values and also in the approximation used in the theory that the sequence is only qualitative. Nevertheless, it may be inferred from the above sequence that the O_2^- radical is bound more strongly on oxides with cations of higher valencies.

The important role of metal cations for the adsorption of oxygen has already been pointed out by Schvets *et al.*[9] as well as by Kasai.[12] In this connection, mention should be made of the fact that the g_x values (2.011, 2.018) obtained for the Ce and U samples are considerably larger than that of a free spin. The fact suggests that the positive electric charge of Ce and U ions is large enough to interact with the O_2^- radical so that the O_2^- radical model is no longer applicable to these oxides. Probably, a peroxy-like model would be adequate.

Let us review the ESR spectra of hydroperoxy radical trapped in organic or inorganic matrices, since the principal g values of the spectra are known to be similar to those of the O_2^- radical adsorbed on the metal oxides. For example, $g_1=2.0495$, $g_2=2.0081$, $g_3=2.0018$ and $g_1=2.0353$, $g_2=2.0086$, $g_3=2.0042$ have been reported for HO_2 radicals generated in a γ-irradiated single crystal of H_2O_2–$CO(NH_2)_2$ and in a γ-irradiated H_2O_2-water matrix at 77°K, respectively.[22,23] Such O_2^--like spectra could be anticipated, if the unpaired electron, in the π * orbital, is affected by the field of the proton,[24] and moreover if the unpaired electron is located on the unprotonated oxygen.

The ESR of the organic peroxy radicals has been summarized by Bersohn and Thomas.[25] Accordingly, the g values differs slightly but significantly from one organic peroxy radical to another. For example, the principal g values ($g_1=2.0267$, $g_2=2.0193$, $g_3=2.102$) have been reported by Lontz[26] to an organic peroxy radical, $CF_3CF(\text{-}OO\cdot)CONH_2$, generated on a γ-irradiated single crystal of $CF_3CF_2CONH_2$. It is interesting to note that the observed g values are not much different from those of the oxygen species adsorbed on the supported Ce and U samples.

It can be seen from Table 2 that any metal ion that gives rise to an ESR signal of the complexed radical in a mixed solution with H_2O_2 also produce an ESR signal due to adsorbed oxygen on its oxide surface and that the g shifts are parallel at surfaces and in solutions. The phenomena led us to presume that the electronic nature of paramagnetic oxygen species combined with metal ion at surface is similar to that in solution.

22) T. Ichikawa, M. Iwasaki and K. Kuwata, *J. Chem. Phys.*, **44**, 2979 (1966).
23) S. J. Wyard, R. C. Smith and F. J. Adrian, *ibid.*, **49**, 2780 (1968).
24) P. W. Atkins and M. C. R. Symons, "The structure of Inorganic Radicals," Elsevier Publ. Comp. (1967), p. 156; F. J. Adrian, *J. Chem. Phys.*, **46**, 1543 (1967).
25) M. Bersohn and J. R. Thomas, *J. Amer. Chem. Soc.*, **86**, 59 (1964); K. U. Ingold and J. R. Morton, *ibid.*, **86**, 3400 (1964).
26) R. Lontz, *Bull. Amer. Phys. Soc.*, **8**, 328 (1963).

BULLETIN OF THE CHEMICAL SOCIETY OF JAPAN VOL. 43 2732—2739 (1970)

Studies on Triplet Energy Transfer by Means of an Emission-Absorption Flash Technique. I. Reversible Energy Transfer between Xanthene Dyes and Anthracenes

Koichi KIKUCHI, Hiroshi KOKUBUN and Masao KOIZUMI

Department of Chemistry, Faculty of Science, Tohoku University, Katahira-cho, Sendai

(Received March 24, 1970)

Choosing eosin and erythrosin as donor and anthracene and 9-methylanthracene as acceptor, we have kinetically investigated the triplet energy transfer process by flash technique involving emission measurement. In these systems the differences of T-levels of donor and acceptor are of the order of kT at most, and it was anticipated that a reversible energy transfer would occur. It has been established that it actually occurs in eosin-anthracene and erythrosin-anthracene, and very likely occurs in erythrosin-9-methylanthracene. Furthermore, it has been found that in the first two systems the energy transfer rate for the process, donor→acceptor is about half that for the process, acceptor→donor. This means that the rate in the present systems is determined by some other factor than the triplet level. Discussions have been given on the model for energy transfer.

According to Parker *et al.*,[1] triplet energy transfer between some dyes and aromatic hydrocarbons gives rise to various types of delayed fluorescence. Their observations, however, were qualitative in nature. By a flash apparatus modified so as to measure the emission as well as absorption,[2] the present authors made a quantitative study on the reversible energy transfer between eosin and anthracene.[3] We could demonstrate that an equilibrium, $D^T+A \rightleftarrows D+A^T$ practically holds between donor and acceptor.

The result of our studies will contribute to our knowledge concerning the efficiency of the triplet energy transfer. It is often assumed that when the transfer is highly exothermic its rate is diffusion-controlled.[4,5] But when the triplet levels of donor and acceptor are close to each other the rate becomes slower; Bäckström and Sandros proposed that in endothermic transfer the rate is governed by an exponential factor $\exp(-\Delta E)$, where ΔE is an endothermic energy.[5] Recent work has raised some criticism on the condition for diffusion controlled energy transfer.[6] It has been suggested that the energy transfer in less viscous solvents competes with the diffusion apart of donor and acceptor, which makes the energy transfer rate appreciably slower than the diffusion rate.[7] Such a suggestion has been made chiefly on the basis of the viscosity dependence of the bimolecular rate constant between quencher and triplet molecule. It may be expected that clearer understanding will be obtained by comparing the forward and backward energy transfer rates of a reversible system, for which the encounter rate is practically the same for forward and backward processes. Furthermore, such studies will enable us to examine experimentally whether and how the transfer efficiency is influenced by other factors than the triplet levels of donor and acceptor.

The object of the present paper is to describe the details on the reversible energy transfer be-

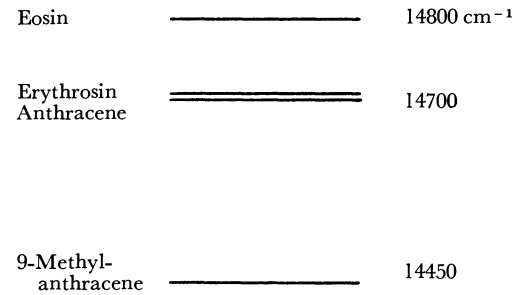

Fig. 1. Triplet energy levels.

1) C. A. Parker, C. G. Hatchard and T. A. Joyce, *Nature*, **205**, 1285 (1965).

2) K. Kikuchi, H. Kokubun and M. Koizumi, *Photochem. Photobiol.*, **7**, 499 (1968); This Bulletin, **41**, 1545 (1968).

3) K. Kikuchi, H. Kokubun and M. Koizumi, *Z. Physik. Chem. N. F.*, **62**, 75 (1968).

4) A. D. Osborne and G. Porter, *Proc. Roy. Soc.* (London), **A284**, 9 (1965). W. G. Herkstroeter and G. S. Hammond, *J. Amer. Chem. Soc.*, **88**, 4769 (1966).

5) H. L. J. Bäckström and K. Sandros, *Acta Chem. Scand.*, **16**, 958 (1962).

6) S. Nordin and R. L. Strong, *Chem. Phys. Lett.*, **2**, 429 (1968).

7) P. J. Wagner and I. Kochevar, *J. Amer. Chem. Soc.*, **90**, 2232 (1968).

tween eosin and anthracene which has already been communicated briefly,[3] and to extend a similar study to the systems, erythrosin-anthracene eosin-9-methylanthracene and erythrosin-9-methylanthracene, all in ethanol.

The triplet levels of these substances are very close to each other[8] as shown in Fig. 1; in particular, the levels of erythrosin and anthracene are almost the same.

Experimental

Materials. 9-Methylanthracene of K & K Lab., Inc. was subjected to zone-melting and recrystallized from ethanol. G. R. grade ethanol of Wakojunyaku was used without further purification. Other substances were purified by standard methods.

Apparatus and Procedures. Essentially the same as has been described.[2]

Results

The elementary processes related with the energy transfer are those involved in the scheme

$$\begin{array}{ccccc} {}^3D + A & \underset{k_4}{\overset{k_2}{\rightleftharpoons}} & {}^3A + D & & \\ \downarrow k_1 \quad +A \quad k_3 \downarrow & & \downarrow k_6 \quad +D \quad k_5 \downarrow & & \\ D \qquad D + A & & A \qquad A + D & & \end{array}$$

in which D is a xanthene dye and A, anthracene. The differential equations to be solved are

$$-\frac{d[^3D]}{dt} = \{k_1+(k_2+k_3)[A]\}[^3D] - k_4[D][^3A] \quad (1)$$

$$-\frac{d[^3A]}{dt} = \{k_6+(k_4+k_5)[D]\}[^3A] - k_2[A][^3D] \quad (2)$$

When the dyes as donor are excited exclusively by means of a suitable filter, the initial condition is put as

$$[^3D] = [^3D]_0 \qquad [^3A] = 0$$

In the early stage of the decay, the above equations are written as follows with a good approximation, since most donor molecules are in the triplet state and the concentration of triplet acceptor is small.

$$-\frac{d[^3D]}{dt} = \{k_1 + (k_2 + k_3)[A]\}[^3D] \quad (3)$$

$$\frac{d[^3A]}{dt} = k_2[A][^3D]$$

Thus the rate constant of ^{3}D-decay is given by $k_1+(k_2+k_3)$ [A]. In order to keep such a situation for a long time, the concentrations of donor and acceptor should be made as low as possible. Of course the later stage under such a condition is not observable on account of very low concentrations of ^{3}D.

In order to study the later stage, higher concentrations of donor and acceptor must be used. In the later stage where the concentrations of donor and acceptor are approximately constant, the solution of (1) and (2) are expressed as the sum of two exponential terms in which the exponents of the two terms are given correctly as follows.

$$\beta_2^1 = \frac{1}{2}\{k_1 + (k_2 + k_3)[A] + k_6 + (k_4 + k_5)[D]\} \pm \frac{1}{2}[\{k_1 + (k_2 + k_3)[A] - k_6 - (k_4 + k_5)[D]\}^2 + 4k_2k_4[A][D]]^{1/2} \quad (4)$$

But one terms with an exponent β_1 can safely be neglected and the exponent β_2 ($=\beta$) for the remaining term is approximated as

$$\beta = \frac{k_2[A]\{k_6 + k_5[D]\} + k_4[D]\{k_1 + k_3[A]\}}{k_2[A] + k_4[D]} \quad (5)$$

if

$$k_2[A] > k_3[A] + k_1 \qquad k_4[D] > k_5[D] + k_6 \quad (6)$$

Furthermore the relation

$$[^3A]/[^3D] \simeq k_2[A]/k_4[D] \quad (7)$$

holds which shows the existence of equilibrium, $^3D+A \rightleftarrows D+{}^3A$. Although an attempt to give exact criterion for the above two extremes was not made, the two extremes could be distinguished by the linear relations in the log[^{3}D] *vs.* *t* plot and with quite different slopes.

It will be seen that relations (5) and (7) really hold in the case of eosin-anthracene and erythrosin-anthracene, and approximately in erythrosin-9-methylanthracene but not in eosin-9-methylanthracene.

Eosin-anthracene. The dependence of the decay curves of eosin at low concentrations (1.0×10^{-6}, 5×10^{-7} M) upon the concentration of anthracene was studied. The observed first order rate constants are plotted against the anthracene

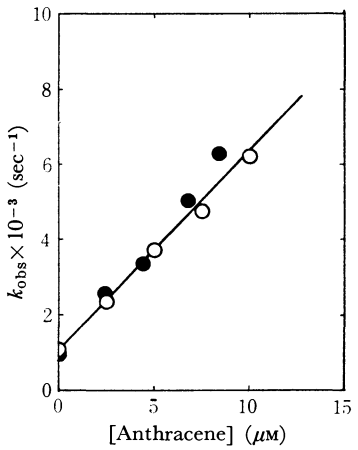

Fig. 2. Effect of anthracene concentration on the first-order rate constant of triplet eosin.
○ [Eosin]$=1\times10^{-6}$ M ● [Eosin]$=5\times10^{-7}$ M

8) K. Gollnick, "Advances in Photochemistry," Vol. VI, ed. by W. A. Noyes, Jr., G. S. Hammond and J. N. Pitts, Jr., Wiley (Interscience), New York (1968), p. 40.

concentration in Fig. 2. From the plot one obtains

$$k_2 + k_3 = (5.1 \pm 0.5) \times 10^8\ \text{M}^{-1}\,\text{sec}^{-1} \quad (8)$$

In a similar way the dependence of the decay constant of triplet anthracene on [eosin] was studied. The result is shown in Fig. 3. As is expected, the slopes in the initial stage are linear but decrease remarkably in the later stage. The dependence of the observed first order rate constant on [eosin] is given in Fig. 4. From the slope we get

$$k_4 + k_5 = (1.2 \pm 0.2) \times 10^9\ \text{M}^{-1}\,\text{sec}^{-1}$$

Figure 5 gives the decay curves of triplet eosin*1 for 10^{-5} M eosin at various concentrations of anthracene. It is seen that the slopes are almost independent of the anthracene concentrations.

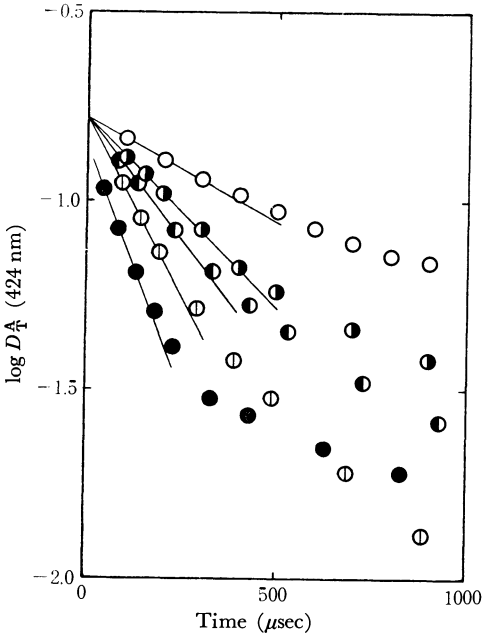

Fig. 3. Effect of eosin concentration on the decay curve of triplet anthracene.
[Anthracene] = 2×10^{-6} M
[Eosin]: ○ 0 M ◑ 5×10^{-7} M ◐ 1.2×10^{-6} M ⓘ 2.7×10^{-7} M ● 5.8×10^{-6} M

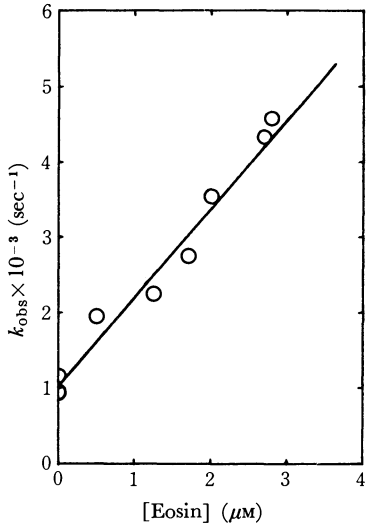

Fig. 4. Effect of eosin concentration on the first-order rate constant of triplet anthracene.
[Anthracene] = 2×10^{-6} M.

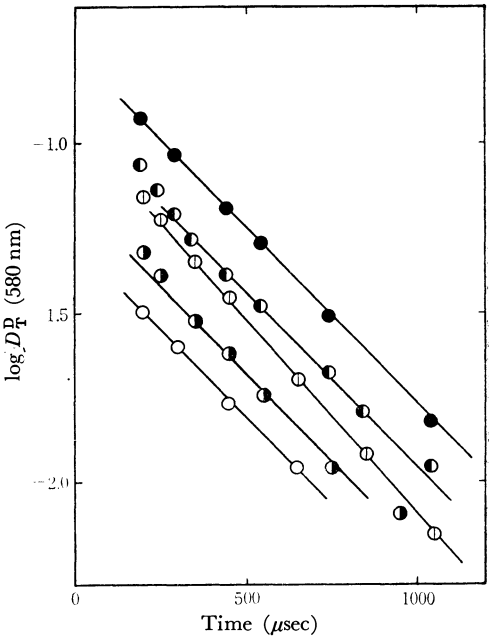

Fig. 5. Effect of anthracene concentration on the decay curve of triplet eosin.
[Eosin] = 1×10^{-5} M
[Anthracene]: ● 0 M ◐ 5×10^{-6} M ⓘ 1×10^{-5} M ◑ 2×10^{-5} M ○ 4×10^{-5} M

The decay of triplet anthracene in this case can be studied either by its triplet-triplet absorption or by the intensity of the delayed fluorescence. The latter is related to the former by the relation, $I_{DF}^A = \alpha\phi_F p k_{TT}^A [D_T^A/\varepsilon]^2$ (I_{DF}^A, intensity of the anthracene delayed fluorescence; α, experimental parameter; ϕ_F, fluorescence quantum yield; p, efficiency for the formation of singlet excited state. Other constants are the usual ones). In the present case, the latter method is more suitable because the anthracene T-T absorption is superposed by the absorption of eosin semiquinone[9] which is produced by a reaction between triplet eosin and alcohol. The relations between coexisting triplet eosin and triplet anthracene are

*1 Decay curves are shown by the log D_T^D *vs.* t plots, where D is the optical density and, suffixes D, T mean donor and triplet.

9) A. Kira and S. Kato, *Sci. Rep. of Tohoku Univ., Ser.* 1, **48**, 142 (1965).

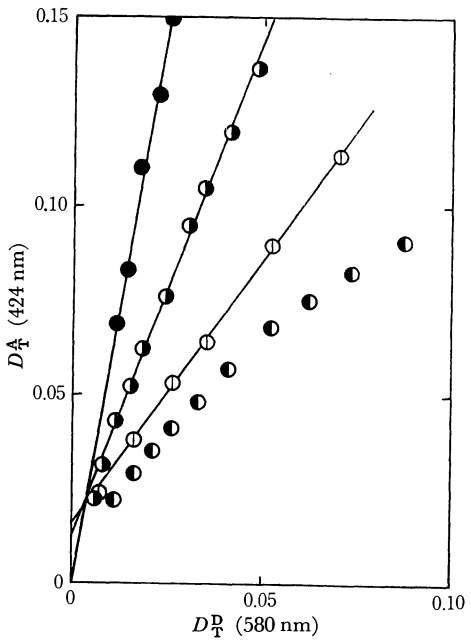

Fig. 6a. Relationship between triplet-triplet absorption of eosin and of anthracene.
[Eosin] = 1×10^{-5} M
[Anthracene]: ◐ 5×10^{-6} M ◑ 2×10^{-5} M ○ 1×10^{-5} M ● 4×10^{-5} M

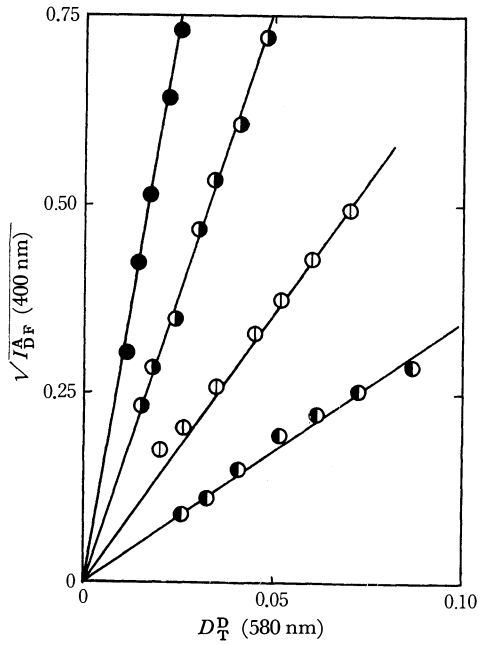

Fig. 6b. Relationship between triplet-triplet absorption of eosin and delayed fluorescence of anthracene.
[Eosin] = 1×10^{-5} M
[Anthracene]: ◐ 5×10^{-6} M ◑ 2×10^{-5} M ◌ 1×10^{-5} M ● 4×10^{-5} M

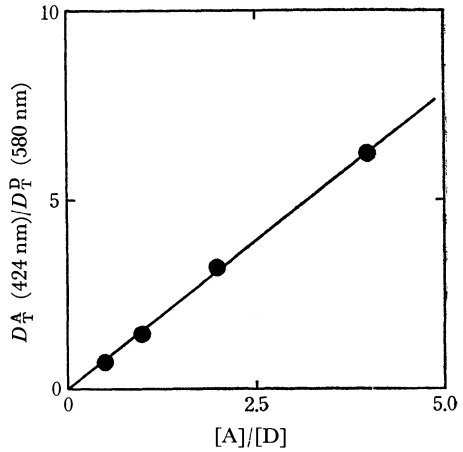

Fig. 7. Proof of the existence of equilibrium.
$^3D + A \rightleftarrows D + {}^3A$, [D] = 1×10^{-5} M

given in Figs. 6a, b and 7. It is clearly seen that a linear relation holds more satisfactorily between $\sqrt{I_{DF}^A}$ and D_T^D than between D_T^A and D_T^D. This, as stated above, is due to the superposition of the absorption from eosin semiquinone over the triplet anthracene absorption. Such situations are frequently encountered in the study of the behavior of the triplet state. Mixed T-T annihilation is another point to be noted. Although a mixed T-T annihilation $^3D+{}^3A\rightarrow A^*+D$ does not occur in the present system, another type, $^3D+{}^3A\rightarrow D^*+A$ does occur; this however does not prohibit the usage of delayed fluorescence intensity of anthracene as a measure of its triplet concentration. If the former were to occur, I_{DF}^A would not simply represent the concentration of triplet anthracene. The linear relation between D_T^A/D_T^D and [A]/[D] shown in Fig. 7 is nothing but the one expected from the existence of equilibrium, $^3D+A\rightleftarrows D+{}^3A$. Using the values of molecular extinction coefficient of ^3D and ^3A, the value of k_2/k_4 is evaluated to be 0.40*2±0.05.

The above result, however, is not enough to verify the existence of the equilibrium in question; it must be shown that the relation $k_2[A], k_4[D] \gg k_1+k_3[A], k_6+k_5[D]$ really holds. The values of k_3 and k_5 can be estimated as follows. Putting

$$k_2[A]/(k_2[A] + k_4[D]) = f \qquad (9)$$

one can transform eq. (5) as follows.

$$\beta = f(k_6 + k_5[D]) + (1 - f)(k_1 + k_3[A]) \qquad (10)$$

Hence

$$\beta - k_1 = f\{k_6 - k_1 + (k_5 + k_4k_3/k_2)[D]\} \qquad (11)$$

It was experimentally found that β is practically equal to k_1, independent of [A]. One can use this result to estimate the values of k_3 and k_5 as follows. The right side of eq. (11) should be less

*2 The value reported in Ref. 2 should be corrected.

than $0.1 \times k_1$, if one assumes the experimental error for the decay constant as *ca.* 10%. Thus

$$-2 \times 10^2 < f\{(k_6 - k_1) + (k_5 + k_3k_4/k_2)[\mathrm{D}]\} < 2 \times 10^2 \qquad (12)$$

Inserting the value of $k_2/k_4=0.40$ and the values of [A] and [D] into Eq. (9), f is found to change from zero to 0.54 and further from Eq. (12) one obtains the following relation.

$$1.2 \times 10^8 < k_5 + 2.5\,k_3 < 1.9 \times 10^8$$

From this, we get

$$k_5 < 1.9 \times 10^8 \qquad k_3 < 7.6 \times 10^7$$

In the case that $k_3=k_5$, we have $3.5 \times 10^7 < k_3 = k_5 < 5.5 \times 10^7$ Thus the values of k_3 and k_5 are estimated to be at most less than 10% of k_2 and k_4 respectively. The values of (k_2+k_3) and (k_4+k_5) then give $k_2/k_4 \approx 0.4$ which agrees satisfactorily with the one already described.

Erythrosin-anthracene. This system is particularly interesting because the triplet levels of donor and acceptor are almost the same. Similar experiments as in eosin-anthracene system were performed. Figure 8 shows the dependence of the decay constant of triplet erythrosin, k_{obs} upon [anthracene] at [erythrosin] $= 1.0 \times 10^{-6}$ M. From the slope we get,

$$k_2 + k_3 = (7.3 \pm 1.0) \times 10^8\ \mathrm{M^{-1}\,sec^{-1}}$$

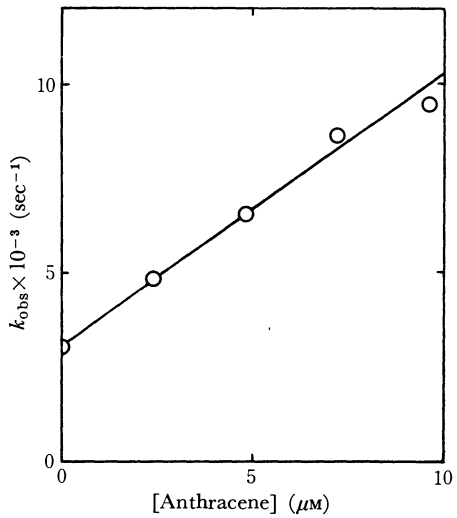

Fig. 8. Effect of anthracene concentration on the first-order rate constant of triplet erythrosin.
[Erythrosin] $= 1 \times 10^{-6}$ M

From the dependence of ^{3}A decay on [erythrosin] at low anthracene and erythrosin concentrations, we obtain $k_4+k_5=(1.7+0.2) \times 10^9\ \mathrm{M^{-1}\,sec^{-1}}$. Putting $k_2/k_4=0.45$ (see below) and $|\beta - k_1| = 0.1\,k_1$ we obtain the following relation by similar reasoning as performed for eosin

$$-5 \times 10^2 < 0.6\{-4.7 \times 10^3 + (k_5 + 5.5k_3)10^{-5}\} < 5 \times 10^2$$

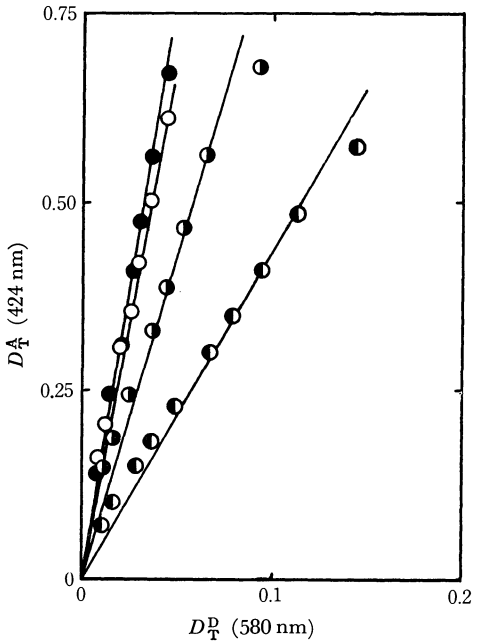

Fig. 9a. Relationship between triplet-triplet absorption of erythrosin and of anthracene.
[Erythrosin] $= 1 \times 10^{-5}$ M
[Anthracene]: ◐ 3×10^{-6} M ○ 9×10^{-6} M ◑ 6×10^{-6} M ● 1.2×10^{-5}

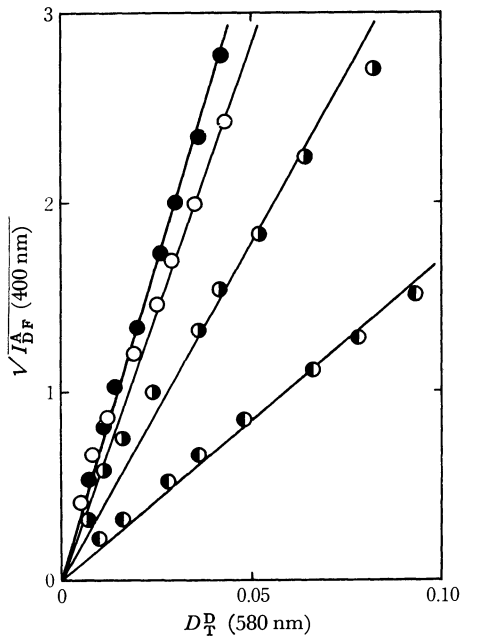

Fig. 9b. Relationship between triplet-triplet absorption of erythrosin and delayed flurescence of anthracene.
[Erythrosin] $= 1 \times 10^{-5}$ M
[Anthracene]: ◐ 3×10^{-6} M ○ 9×10^{-6} M ◑ 6×10^{-6} M ● 1.2×10^{-5} M

The results obtained are summarized as follows.

$$k_5 < 5.3 \times 10^8 \qquad k_3 < 2.5 \times 10^8$$

In the case $k_5 = k_3$, we have

$$1.2 \times 10^8 < k_5 = k_3 < 1.8 \times 10^8$$

In the system the values of k_3 and k_4 are 30% of the values of k_2 and k_4, respectively at most.

At 1.0×10^{-5} M of erythrosin, the $\log D_T^D$ *vs.* t plots in the later stage give almost the same slope from [anthracene]=0 to 12.0×10^{-5} M. The relation between the coexisting ^3D and ^3A in the later stage are given in Figs. 9 and 10.

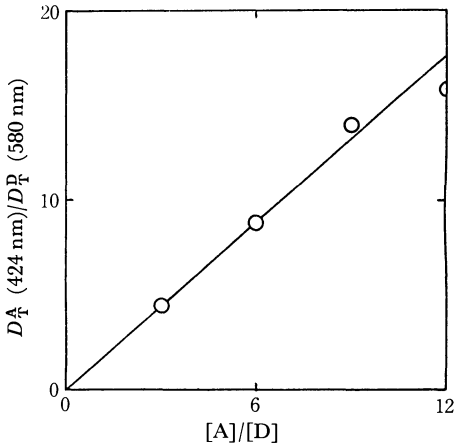

Fig. 10. Proof of the existence of equilibrium.
$^3D + A \rightleftarrows D + {}^3A$, [D]=$2.6 \times 10^{-5}$ M

It is seen that quite a similar relation to that in the case of eosin (Figs. 6 and 7) holds. It is to be noted that a good linear relation in Fig. 9a suggests that there is scarcely any absorption of intermediate such as semiquinone in the region of T-T absorption of anthracene. The value of k_2/k_3 was evaluated to be 0.45+0.05.

Erythrosin-9-methylanthracene. It is expected that the quasi-equilibrium $^3D+A \rightleftarrows D+{}^3A$ is more difficult to hold in this case than in the former two cases, because the difference of triplet levels of donor and acceptor is more than twice as large as that of eosin and anthracene and the decay constant of triplet erythrosin is also about two times larger than that of eosin. Figure 11 gives the plot of decay constant of triplet erythrosin, k_{obs} against [9-methylanthracene] at low [erythrosin]. From the slope, we get

$$k_2 + k_3 = 2.2 \pm 0.4 \times 10^9 \text{M}^{-1}\,\text{sec}^{-1} \qquad (12)$$

From a similar experiment for the triplet 9-methylanthracene, we have

$$k_4 + k_5 = (3.3 \pm 0.3) \times 10^8 \text{M}^{-1}\,\text{sec}^{-1} \qquad (13)$$

At higher concentrations of erythrosin (2.6×10^{-5} M), the plots of $\log D_T^D$ *vs.* t at various acceptor concentrations, give about the same slopes as in the previous two cases. Figure 12 gives the relation between the triplet absorbance of erythrosin

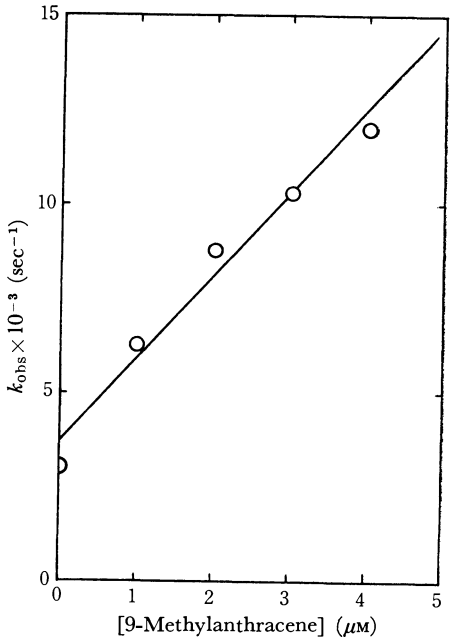

Fig. 11. Effect of 9-methylanthracene concentration on the first-order rate constant of triplet erythrosin.
[Erythrosin]=1×10^{-6} M

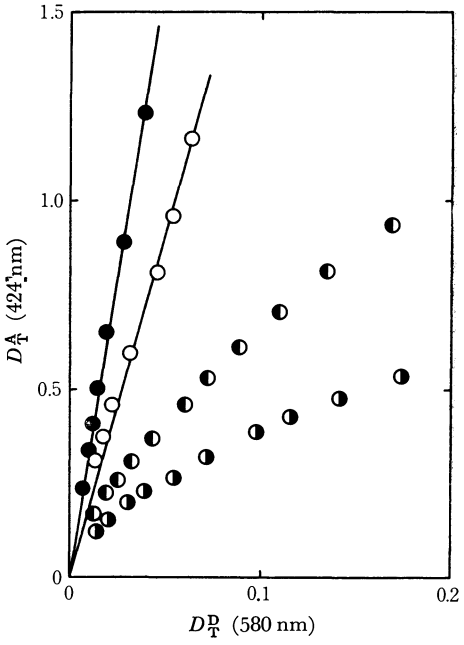

Fig. 12. Relationship between triplet-triplet absorption of erythrosin and of 9-methylanthracene.
[Erythrosin]=2.6×10^{-5} M
[9-Methylanthracene]: ◑ 4.7×10^{-6} M
◐ 9.5×10^{-6} M
○ 1.9×10^{-5} M
● 3.8×10^{-5} M

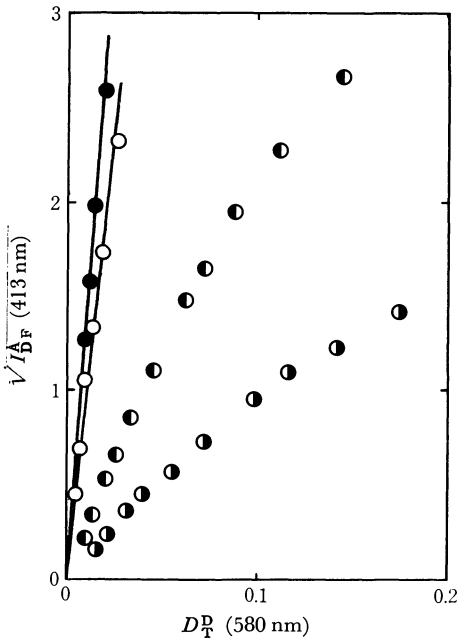

Fig. 13. Relationship between triplet-triplet absorption of erythrosin and delayed fluorescence of 9-methylanthracene.
[Erythrosin] $=2.6\times10^{-5}$ M
[9-Methylanthracene]: ◑ 4.7×10^{-6} M
◐ 9.5×10^{-6} M
○ 1.9×10^{-5} M
● 3.8×10^{-5} M

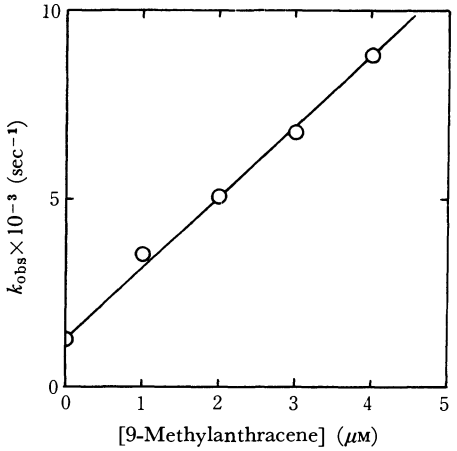

Fig. 14. Effect of 9-methylanthracene concentration on the first-order rate constant of triplet eosin.
[Eosin] $=2\times10^{-6}$ M

and 9-methylanthracene and Fig. 13, the relation between the delayed fluorescence of 9-methylanthracene and triplet erythrosin. It is seen that the linear relation holds approximately in both cases, suggesting the existence of quasi-equilibrium. However, the upper limits estimated for k_3 and k_5 are, respectively, 2.1×10^9 and 3.3×10^8 which are comparable with the values of (k_2+k_3) and (k_4+k_5). Hence it is somewhat doubtful that the approximate equilibrium in question really holds.

Eosin-9-methylanthracene. Since the difference in triplet levels of donor and acceptor is still larger than that for erythrosin-9-methylanthracene, it is expected that the quasi-equilibrium does not hold in this case. In fact, the existence of triplet eosin could not be observed at high concentration of donor and acceptor. From the plot of decay constant of triplet eosin, k_{obs} against [9-methylanthracene] at low [eosin] (2.0×10^{-6}), we obtain $k_2+k_3=(1.9+0.2)\times10^9$ M^{-1} sec^{-1} and from a similar experiment for the decay of 9-methylanthracene $k_4+k_5=(2.1+0.4)\times10^8$ M^{-1} sec^{-1}.

All the rate constants evaluated in the present paper are summarized in Table 1.

Discussion

In the present work it has been fully established that a quasi-equilibrium, $^3D+A\rightleftarrows D+{}^3A$ holds in eosin-anthracene and erythrosin-anthracene. It is well known that Bäckström and Sandros[5] found the reversible energy transfer between donor and acceptor with triplet levels close together. But they did not observe the establishment of a relation $[^3A]/[^3D]=\text{const}\cdot[A]/[D]$, as shown in the present paper. Besides, the present study demonstrates definitely that the rate constant for $^3D+A\rightarrow D+{}^3A$ (k_2) is smaller than that for the reverse transfer (k_4). Thus in erythrosin-anthracene where $\Delta E\sim0$, and in eosin-anthracene

Table 1. Rate constants for elementary reactions involved in energy transfer

	Eosin Anthracene	Erythrosin Anthracene	Erythrosin 9-Methylanthracene	Eosin 9-Methylanthracene
k_1 (sec^{-1})	$(2.4\pm0.3)\times10^3$	$(5.5\pm0.5)\times10^3$	$(5.5\pm0.5)\times10^3$	$(2.4\pm0.3)\times10^3$
k_2+k_3 (M^{-1} sec^{-1})	$(5.1\pm0.5)\times10^8$	$(7.3\pm1.0)\times10^8$	$(2.2\pm0.4)\times10^9$	$(1.9\pm0.2)\times10^9$
k_4+k_5 (M^{-1} sec^{-1})	$(1.2\pm0.2)\times10^9$	$(1.7\pm0.2)\times10^9$	$(3.3\pm0.3)\times10^8$	$(2.1\pm0.4)\times10^8$
k_6 (sec^{-1})	$(7.6\pm1.0)\times10^2$	$(7.6\pm1.0)\times10^2$	$(2.5\times0.5)\times10^2$	$(2.5\pm0.5)\times10^2$
k_3 (M^{-1} sec^{-1})	$<7.6\times10^7$	$<2.5\times10^8$	$<2.1\times10^9$	—
k_5 (M^{-1} sec^{-1})	$<1.9\times10^8$	$<5.3\times10^8$	$<3.3\times10^8$	—
k_2/k_4	0.40 ± 0.05	0.45 ± 0.05	6.4 ± 0.7	—
$(k_2+k_3)/(k_4+k_5)$	0.43 ± 0.10	0.43 ± 0.10	6.7 ± 1.0	—

where donor triplet level is 100 cm^{-1} higher than that of acceptor, the k_2-values are about twice as small as the k_4-values. This implies that for the system where $\Delta E \lesssim kT$, ΔE is not the only important factor for determining the transfer efficiency.

For interpreting the present results, it is helpful to refer to the results and the interpretations of other workers on the related phenomena. For the system in which the reversible energy transfer occurs, Sandros[5] proposed that the encounter complex is formed with a diffusion controlled rate and that the probability for the forward and backward energy transfer is determined only by the energy difference between ^{3}D and ^{3}A. Thus they inferred that the rate constant for endothermic transfer is essentially determined by a factor $e^{-\Delta E/RT}$ where $\Delta E = E(^3\mathrm{D}) - E(^3\mathrm{A})$. The same assertion was made also by Stevens and Walker.[10] Wagner,[7] on the other hand, studied the system in which energy transfer is irreversible and obtained results which lead to the conclusion that the transfer efficiency can be much smaller than the diffusion-controlled one, on account of the competition between the transfer process and the diffusion apart of ^{3}D and A. Richtol and Belorit[11] and also Borkman and Kearns[12] studied the irreversible energy transfer and found that the ^{3}D+A→D+A process occurs to some extent. Both groups proposed the following scheme where (^{3}D···A) is an encounter complex.

$$\begin{array}{ccccccc} {}^3\mathrm{D} + \mathrm{A} & \rightleftarrows & (^3\mathrm{D}\cdots\mathrm{A}) & \rightarrow & \mathrm{D} & + & {}^3\mathrm{A} \\ & & \downarrow & & & & \\ & & \mathrm{D} + \mathrm{A} & & & & \end{array}$$

Their conclusion is similar to Wagner's in that the overall rate constants for energy transfer and energy dissipation are small on account of the backward reaction (^{3}D···A)→^{3}D+A.

In view of all the previous results, it is quite reasonable to assume the following scheme for the present system.

$$\begin{array}{ccccc} {}^3\mathrm{D} + \mathrm{A} & \underset{k'_{\mathrm{ID}}}{\overset{k'_{\mathrm{DI}}}{\rightleftarrows}} & {}^3(\mathrm{D}\cdots\mathrm{A}) & \underset{k'_{\mathrm{AI}}}{\overset{k'_{\mathrm{IA}}}{\rightleftarrows}} & \mathrm{D} + {}^3\mathrm{A} \\ & & \downarrow k'_d & & \\ & & \mathrm{D} + \mathrm{A} & & \end{array}$$

In this scheme, ^{3}(D···A) is an intermediate (I) with perhaps a specific configuration by way of which the forward and backward energy transfer (^{3}D+A→D+^{3}A and D+^{3}A→^{3}D+A) and also the energy dissipation process (^{3}D+A→D+A, ^{3}A+D→A+D) can occur.*3

As to the interchange between I and the encounter complex, two typical models are to be discriminated. The first is a model in which the intermediate is very easy to reach from the encounter state, (^{3}D···A) and (D···^{3}A). In this case the forward and backward energy transfer is repeated and a certain equilibrium state is realized during the encounter state. If one assumes that the encounter rate k_e controlled by diffusion is the same for forward and backward reactions, k_2 and k_4 can be written as

$$k_2 = k_e k_{\mathrm{IA}}/(k_{\mathrm{IA}} + k_{\mathrm{ID}} + k_d)$$
$$k_4 = k_e k_{\mathrm{ID}}/(k_{\mathrm{IA}} + k_{\mathrm{ID}} + k_d)$$

where k_{IA} and k_{ID} is the rate constant for processes I→(D···^{3}A) and I→(^{3}D···A), respectively. Then the equilibrium constant $K=k_2/k_4$ is reduced to $k_{\mathrm{IA}}/k_{\mathrm{ID}}$ and this reflects the equilibrium state in the encounter complex. It should be added that this model requires $k_3 \approx k_5$.

The second is a model in which the intermediate is difficult to reach from the encounter state and only a small fraction α_f and α_r, respectively of (^{3}D···A) and of (D···^{3}A) goes to the ^{3}(A···D) state. In this case, k_2 and k_4 are written, respectively as follows.

$$k_2 = k_e \alpha_f k_{\mathrm{IA}}/(k_{\mathrm{IA}} + k_{\mathrm{ID}} + k_d)$$
$$k_4 = k_e \alpha_r k_{\mathrm{ID}}/(k_{\mathrm{IA}} + k_{\mathrm{ID}} + k_d)$$

Thus the equilibrium constant $K=k_2/k_4$ depends not only on $k_{\mathrm{IA}}/k_{\mathrm{ID}}$ but also on α_f/α_r. k_3/k_5 is then expected to be equal to α_f/α_r. If this model fits the truth, the result $k_2/k_4 < 1$ suggests that the intermediate has a configuration closely resembling that of an encounter compex (D···^{3}A) because the value of k_2/k_4 depends most likely on α_f/α_r much more than $k_{\mathrm{IA}}/k_{\mathrm{ID}}$.

Of the two models described above, the first appears to interpret the present results better than the second. Thus according to the first model, the sum of (k_2+k_3) and (k_4+k_5) should be the diffusion rate constants, and the experimental values are really very near them.

Apart from the argument as to which model is more suitable, it should be noted that the equilibrium state in the present system, contrary to Sandros' system,[5] is not determined only by an energy factor. As a possible factor, an overlap integral $\int^{\infty} f_{\mathrm{D}}(\nu)\varepsilon(\nu)\,d\nu$ involved in Dexter's theory[13] is conceivable. Since the longest absorption band of donor is located in the longer wavelength region than that of acceptor, this factor is expected to be favorable to k_{ID} than k_{IA}, resulting in a larger k_4 than k_2 according to the first model.

One of the authors (H.K.) wishes to thank Matsunaga Science Foundation for financial support.

10) B. Stevens and M. S. Walker, *Proc. Chem. Soc.*, **1964**, 26, 109.

11) H. H. Richtol and A. Belorit, *J. Chem. Phys.*, **45**, 35 (1966).

12) R. H. Borkman and D. R. Kearns, *J. Amer. Chem. Soc.*, **88**, 3467 (1966).

*3 It is possible that the forward and backward reaction occurs via a different intermediate state. Even in this case the conclusions for $K=k_2/k_4$ described below will be essentially the same.

13) D. L. Dexter, *J. Chem. Phys.*, **21**, 836 (1953).

BULLETIN OF THE CHEMICAL SOCIETY OF JAPAN VOL. 43 2740—2745 (1970)

Mercury-Photosensitized Reaction of Acetylene

Shoji SHIDA and Masao TSUKADA

Laboratory of Physical Chemistry, Tokyo Institute of Technology, Ookayama, Meguro-ku, Tokyo

(Received April 8, 1970)

The mercury-photosensitized reaction of acetylene has been studied with equimolar mixtures of C_2H_2 and C_2D_2 under various conditions of pressure, temperature, and additives. It is shown that the distribution of isotopically substituted benzenes can be explained by a modified excited state mechanism equally as well as, or more favourably than by the free radical mechanism. The results on deuterium-acetylene mixtures photosensitized by $Hg(^3P_1)$, however, suggest that benzene is also formed by the reaction of hydrogen atoms and acetylene molecules. The rates of benzene formation and of the polymer formation increased gradually with pressure in low pressure region to attain a maximum and then decreased. Argon very strongly inhibited the benzene formation and, to a less extent, the polymer formation. The primary process is explained by assuming the formation of a transient complex of a triplet mercury atom and an acetylene molecule.

Since the early work of Bates and Taylor,[1] photopolymerization of acetylene has been the subject of a number of studies. In spite of the simplicity of the over-all reaction, which produces mainly benzene and an involatile solid polymer, cuprene, no final agreement on the mechanism of the reaction has yet been attained, although the free radical mechanism appears to be predominant at the present stage. For the formation of benzene, an excited molecule mechanism was suggested for the mercury-photosensitized reaction,[2] though LeRoy and Steacie[3] proposed a free radical mechanism to explain the formation of polymer and volatile products from the fact that nitric oxide inhibited the polymerization. Mains, Niki and Wijnen[4] found that isotopic benzenes including an odd number of H or D atoms were produced in significant yields in mercury-photosensitization of C_2H_2-C_2D_2 mixtures, suggesting a free radical mechanism again. However, the observed distribution of isotopic benzenes can not necessarily support the free radical mechanism, which can also be explained by a modified excited molecule mechanism.[5]

Experimental

Acetylene (purity, 99.6%) supplied by Takachiho Trading Co. was passed through a silica gel column and further through a trap immersed in a carbon dioxide-acetone mixture followed by bulb-to-bulb distillation, and the middle third was used. No impurity was detected by gas chromatography or by mass spectrometry. Acetylene-d_2 was prepared by passing D_2O through high-purity carbide, purified with a dimethyl sulfolane column and degassed by bulb-to-bulb distillation. Less than 1.3% C_2HD was found as an impurity. Nitric oxide and argon (Takachiho Trading Co., purity, 98.5 and 99.999% respectively) were used without further purification.

The light source was a low-pressure mercury resonance lamp. Between the lamp and the quartz reaction vessel, a UV-25 filter (Toshiba Denki Co.) which eliminated a light shorter than 2300 Å was placed. The reactant was circulated through a closed loop system having a mercury vapor saturator and a glass pump circulator. Total pressure change was measured with a mercury manometer and a travelling microscope.

Benzene formed as a product was analyzed by gas chromatography under reduced pressure. The column used was packed with dioctyl phthalate at 80°C. The distribution of isotopically substituted benzenes was analyzed by means of a mass spectrometer using ionizing electrons of 10 eV which produce almost only the parent ions of benzenes.

Results and Discussion

Reaction Products. The products formed from C_2H_2 were hydrogen, diacetylene, vinylacetylene, benzene, cyclooctatetraene, polymer, and C_2HD in the case of C_2H_2-C_2D_2 mixtures. No attempt was made to measure quantitatively other products except for benzene, C_2HD, and polymer, since it was confirmed that they were formed only in very small amounts. These products are in general accord with those found by

1) J. R. Bates and H. S. Taylor, *J. Amer. Chem. Soc.*, **49**, 2438 (1927).
2) S. Shida, Z. Kuri and T. Furuoya, *J. Chem. Phys.*, **28**, 131 (1958).
3) D. J. LeRoy and E. W. R. Steacie, *ibid.*, **12**, 117 (1944).
4) G. J. Mains, H. Niki and M. H. J. Wijnen, *J. Phys. Chem.*, **67**, 11 (1963).
5) S. Shida, M. Tsukada and T. Oka, *J. Chem. Phys.*, **45**, 3483 (1966).

Table 1. Distribution of isotopic benzenes formed in the mercury-photosensitized reaction of C_2H_2-C_2D_2 mixtures

Acetylene initial press. mmHg	9.4	14.2	24.0	36.0	49.0	118.0
C_6H_6	8.3%	8.4%	9.2%	9.0%	9.8%	10.0%
C_6H_5D	8.4	7.1	6.8	7.0	6.5	6.4
$C_6H_4D_2$	26.2	26.4	25.9	27.0	27.4	28.9
$C_6H_3D_3$	17.7	14.3	13.9	13.7	12.5	12.0
$C_6H_2D_4$	23.8	27.1	26.4	27.1	28.1	28.2
C_6HD_5	9.7	7.3	7.4	7.1	6.1	5.7
C_6D_6	7.6	9.5	10.2	9.1	9.6	8.8

earlier workers.[2,3,6]

Isotopic Studies. The mercury-photosensitized reaction of an approximately equimolar mixture of C_2H_2 and C_2D_2 resulted in the mixture of isotopically substituted benzenes shown in Table 1. The yields of C_6H_5D, $C_6H_3D_3$, and C_6HD_5 are too large to be accounted for by statistical inclusion of C_2HD, because the concentration of C_2HD formed is nearly less by a few per cent of the initial acetylene.[7] It can be seen that the yields of C_6H_6, $C_6H_4D_2$, $C_6H_2D_4$, and C_6D_6 are relatively larger than those of C_6H_5D, $C_6H_3D_3$, and C_6HD_5, and that the distribution of isotopic benzenes is almost constant at higher pressures.

As suggested by LeRoy,[8] this isotopic distribution may be explained by a free radical mechanism initiated by hydrogen atoms such as

$$\left.\begin{aligned} &C_2H_2 + H \rightarrow C_2H_3 \\ &C_2H_3 + C_2H_2 \rightarrow C_4H_5 \\ &C_4H_5 + C_2H_2 \rightarrow C_6H_7 \\ &C_6H_7 \rightarrow C_6H_6 + H \end{aligned}\right\} \quad (I)$$

The distribution of various benzenes predicted on the basis of the free radical mechanism (I) would be, in decreasing order of H atom content, 9.4%, 6.25%, 28.2%, 12.5%, 28.2%, 6.25%, 9.4%. The calculation is performed on the assumption that the quenching cross sections for the formation of H or D atoms from C_2H_2 and C_2D_2 are equal and that the probability of eliminating a D or H atom from a terminal =CHD group on cyclization is 0.5. The calculated percentages are nearly in agreement with the distributions except for those in the low pressure region.

As shown in Table 1, the observed distribution depends on the acetylene pressure in the low pressure region and the yields of benzenes containing an odd number of D atoms tend to increase as the acetylene pressure decreases.[9] The distribution of isotopic benzenes expected to be formed in the radical mechanism should be independent of the acetylene pressure. Thus, the free radical mechanism could not explain the change of the isotopic distribution at low pressures. The close agreement between the distribution observed in the higher pressure region and the calculated one can not necessarily support such a radical mechanism.

The observed distribution can be as well accounted for by a modified excited molecule mechanism as by the radical mechanism.[5] This mechanism which involves redissociation of a hot acetylene dimer molecule is shown as follows:

$$\left.\begin{aligned} &C_2H_2^* + C_2H_2 \rightarrow \begin{matrix} CH{=}CH^* \\ | \quad | \\ CH{=}CH \end{matrix} \\ &\begin{matrix} CH{=}CH^* \\ | \quad | \\ CH{=}CH \end{matrix} \rightleftarrows \begin{matrix} CH{-}CH^* \\ \| \quad \| \\ CH{-}CH \end{matrix} \\ &\begin{matrix} CH{-}CH^* \\ \| \quad \| \\ CH{-}CH \end{matrix} \rightarrow C_2H_2^{**} + C_2H_2 \\ &C_2H_2^{**} \xrightarrow[+C_2H_2]{} C_4H_4^{**} \xrightarrow[+C_2H_2]{} C_6H_6 \end{aligned}\right\} \quad (II)$$

where * denotes highly (electronically or vibronically) excited states and ** lower excited states. In this mechanism, $C_2H_2^*$ and $C_2D_2^*$ will be in the ratio 1 : 1 and no C_2HD^* exists, but $C_2H_2^{**}$, C_2HD^{**}, and $C_2D_2^{**}$ are produced in the ratio 3 : 2 : 3 in an equimolar C_2H_2-C_2D_2 mixture. Consequently, the benzene formed *via* the path including excited acetylene would again consist of the distribution, 9.4%, 6.25%, 28.2%, 12.5%,

6) J. K. Cashion and D. J. LeRoy, *Can. J. Chem.*, **32**, 906 (1954).

7) Recently, Fujisaki *et al.* studied the radiolysis of C_2H_2-C_6D_6 mixtures and found that benzene formed was only C_6H_6. N. Fujisaki and S. Shida, unpublished. From this, it can be confirmed that the isotopic exchange between acetylene and benzene formed does not occur in the mercury-photosensitized reaction of C_2H_2-C_2D_2 mixtures.

8) D. J. LeRoy, *J. Chem. Phys.*, **45**, 3482 (1966).

9) In the direct-photolysis of acetylene at 1849 Å, the distribution of isotopic benzenes and the change of it at lower pressures was just the same as in mercury-photosensitization. S. Shida and M. Tsukada, unpublished. In the radiolysis, the distribution was the same as in mercury-photosensitization at higher pressures and was constant in the higher pressure region than 20 mm. S. Shida and T. Oka, unpublished.

28.2%, 6.25%, 9.4%. However, the distribution would be independent of acetylene initial pressure also in this case.

In the reaction mechanism (II), it may be assumed that C_4H_4** is unstable and decomposes into two acetylene molecules or further reacts with an acetylene molecule. If this is the case, C_4H_4** might dissociate into no two ground state acetylene molecules but give C_2H_2** molecule as follows:

$$C_4H_4^{**} \rightarrow C_2H_2^{**} + C_2H_2 \qquad \text{(III)}$$

If the mechanism including reaction (III) is assumed as

$$\left.\begin{aligned} &C_2H_2^{*} + C_2H_2 \rightarrow C_4H_4^{*} \\ &C_4H_4^{*} \rightarrow C_2H_2^{**} + C_2H_2 \\ &C_2H_2^{**} + C_2H_2 \rightarrow C_4H_4^{**} \\ &C_4H_4^{**} \rightarrow C_2H_2^{**} + C_2H_2 \\ &\qquad\qquad \longrightarrow C_6H_6 \end{aligned}\right\} \qquad \text{(IV)}$$

the distribution of isotopic benzenes formed in C_2H_2-C_2D_2 mixture would be 8.6%, 7.8%, 25.8%, 15.6%, 25.8%, 7.8%, 8.6%.

If the reaction conforms to mechanism (II) at higher pressures and if the cyclobutadiene** molecules partially dissociate to give acetylene** molecules before coming into collision with acetylene at lower pressures, this mechanism would explain the result that the yields of isotopic benzenes containing an odd number of H or D atoms tend to increase at lower pressures. It seems that the modified excited state mechanism would be more favourable that the radical mechanism in this respect.

A fact which has been considered as a direct support for the radical mechanism is the benzene formation in the reaction of acetylene with hydrogen atom.[4,6] However, the formation of benzene in the Cd($^3P_1$)-photosensitized reaction of acetylene studied by Tsunashima and Sato[10] seems to strongly suggest that benzene is also formed by some excited molecule mechanism, because the dissociation energy of the C–H bond of acetylene molecule (114 kcal)[11] is larger than the energy of triplet cadmium (87.7 kcal) even when the heat of formation of cadmium hydride (15.5 kcal) is taken into account.

A single determination of isotopic cyclooctatetraene (COT) formed in the mercury-photosensitized reaction of C_2H_2-C_2D_2 mixture was also made (Table 2). If COT is formed from the reaction of free radicals as

$$H \xrightarrow[+4C_2H_2]{} C_8H_9$$

$$C_8H_9 \rightarrow C_8H_8 + H,$$

10) S. Tsunashima and S. Sato, This Bulletin, **41**, 2281 (1968).

11) B. E. Knox and H. B. Palmer, *Chem. Rev.*, **61**, 247 (1961).

TABLE 2. DISTRIBUTION OF ISOTOPIC CYCLOOCTATETRAENES FORMED IN THE MERCURY-PHOTOSENSITIZED REACTION OF C_2H_2-C_2D_2 MIXTURES[a]

C_8H_8	6.3%
C_8H_7D	2.1
$C_8H_6D_2$	23.1
$C_8H_5D_3$	4.6
$C_8H_4D_4$	32.6
$C_8H_3D_5$	3.5
$C_8H_2D_6$	21.3
C_8HD_7	1.1
C_8D_8	5.4

a) Acetylene initial pressure 574 mm

the isotopic distribution predicted will be 4.7%, 3.1%, 18.8%, 9.4%, 28.1%, 9.4%, 18.8%, 3.1%, 4.7%. But if COT is assumed to be formed from the reaction of C_6H_6*, the precursor of benzene, with C_2H_2, just the same distribution as above is predicted. Consequently, it is impossible to determine from the isotopic distribution of COT whether the free radical or the excited state mechanism is more favourable.

Effect of Acetylene Pressure. Figures 1 and 2, respectively, show the pressure depend-

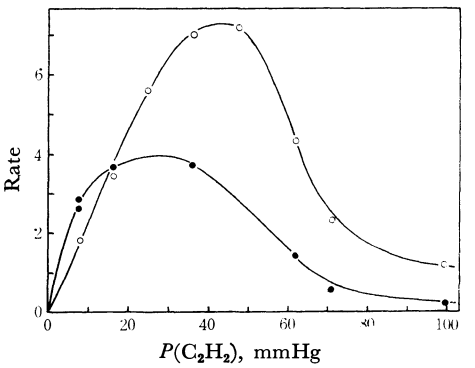

Fig. 1. Rates of formation of benzene and C_2HD.
—○— C_6H_6 ($\times 10^{-8}$ mol/min)
—●— C_2HD ($\times 10^{-7}$ mol/min)

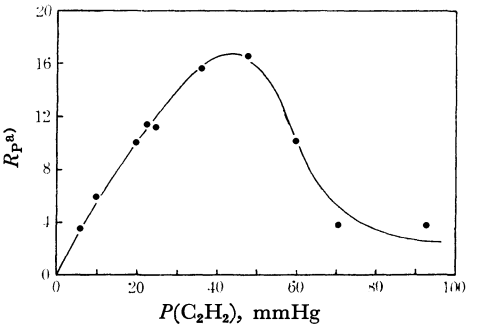

Fig. 2. Rate of polymer formation (acetylene consumed for cuprene).
a) $\times 10^{-7}$ mol/min

ence of the rate of benzene formation and of the rate of polymer formation. The shapes of both the curves are very similar. The rates increase gradually with pressure in the low pressure region to attain a maximum and then decrease. This fact has not been noted by previous investigators.[2,3] Although mercury vapor may be consumed by some reaction with actylene,[3,12] the decrease of the rates in the higher pressure region can not be ascribed to the deficiency of mercury vapor, because a mercury saturator is used in the present experiment. A similar pressure dependence has also been found in the cadmium-photosensitized reaction[10] and also in the radiolysis[13,14] of acetylene.

Effect of Argon. Figure 3 shows the effect of the addition of argon on the rates. Argon very strongly inhibits benzene formation and, to a less extent, polymer formation. It is considered that mechanisms of both benzene and polymer formation include a certain excited intermediate in some stage of reaction, because argon acts only as the deactivator under the experimental conditions. It should be noted here that argon does not quench the excited mercury atom, because the quenching cross section of argon for $Hg(^3P_1)$ is almost zero while that of acetylene is much larger.

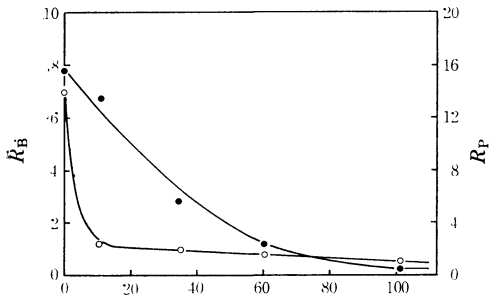

Fig. 3. Effect of argon on the rates of polymer formation and benzene formation.
—○— C_6H_6 ($\times 10^{-8}$ mol/min)
—●— Polymer Formation ($\times 10^{-7}$ mol/min)
Acetylene initial pressure 36.0 mmHg

Primary Process. If an initially excited acetylene decomposes to give an H atom and a C_2H as

$$\left.\begin{aligned} C_2H_2 + Hg^* &\rightarrow C_2H_2^* + Hg \\ C_2H_2^* &\rightarrow C_2H + H \end{aligned}\right\} \quad (V)$$

the formation of diacetylene C_4H_2 is to be expected. However, no significant amount of diacetylene was formed. It might be considered that C_2H radicals add to acetylene rather than recombine to give C_4H_2. But in the direct-photolysis of acetylene at 1849Å, diacetylene was formed as one of the major products as shown in Table 3. In the direct-photolysis, the initial absorption of light by acetylene leads to dissociation along with the formation of excited molecule, and C_4H_2 may be formed by the recombination of C_2H radicals.[15] Thus, the simple mechanism (V) is inadequate for the explanation of the initial stage of mercury-photosensitized reaction.

Table 3. Products in the direct-photolysis of acetylene at 1849 Å

C_2H_2 init. press. mmHg	C_6H_6[a]	C_4H_2[a]
11.0	1.8	6.3
36.0	3.5	4.5
64.5	3.7	4.1
92.0	4.8	3.8

a) $\times 10^{-8}$ mol/min

Sherwood and Gunning[16] showed that a stable mercury compound, probably a mercury carbide, is formed in the reaction and that enriched isotopic composition of ^{202}Hg was obtained in the solid reaction products under ^{202}Hg monoisotopic photosensitization. Furthermore, they studied the mercury-photosensitized decomposition of acetylene in the presence of nitric oxide using a fast-flow apparatus.[17] From the results they proposed the primary process

$$\left.\begin{aligned} Hg^* + C_2H_2 &\rightarrow HgH + C_2H \\ &\rightarrow HgC_2H + H \\ &\rightarrow Hg + C_2H_2^* \end{aligned}\right\} \quad (VI)$$

where $C_2H_2^*$ is not chemically reactive and only collisionally deactivated.

However, the deactivation effect of argon and the formation of only a small amount of diacetylene are probably not explained by a mechanism initially including the process (VI).

We suggest that the following primary sequence is in agreement with the observed data

$$\left.\begin{aligned} Hg^* + C_2H_2 &\rightarrow (HgC_2H_2)^* \\ (HgC_2H_2)^* &\rightarrow Hg + C_2H_2^* \\ &\rightarrow HgC_2H + H \\ (HgC_2H_2)^* + M &\rightarrow Hg + C_2H_2 + M \end{aligned}\right\} \quad (VII)$$

where $C_2H_2^*$ does not decompose to give an H atom any more.

12) H. W. Melville, *Trans. Faraday Soc.*, **32**, 258 (1935).
13) F. H. Field, *J. Phys. Chem.*, **68**, 1039 (1964).
14) J. H. Futrell and L. W. Sieck, *ibid.*, **69**, 892 (1965).
15) M. Zelikoff and L. M. Aschenbrand, *J. Chem. Phys.*, **24**, 1034 (1956).
16) A. G. Sherwood and H. E. Gunning, *Can. J. Chem.*, **38**, 466 (1960).
17) A. G. Sherwood and H. E. Gunning, *J. Phys. Chem.*, **69**, 1732 (1965).

TABLE 4. EFFECT OF NITRIC OXIDE, ARGON, AND TEMPERATURE ON THE DISTRIBUTION OF ISOTOPIC BENZENES[a)]

	Additives		Temp., °C		
	1.3% NO	61.2 mmHg	150	270	262[b)]
C_6H_6	7.9%	9.9%	7.7%	6.9%	5.6%
C_6H_5D	6.5	6.8	6.4	7.5	9.2
$C_6H_4D_2$	24.6	28.1	26.1	24.3	20.7
$C_6H_3D_3$	16.8	12.3	14.0	15.8	19.6
$C_6H_2D_4$	28.9	27.8	28.6	26.9	23.5
C_6HD_5	6.6	5.6	6.8	8.4	12.9
C_6D_6	8.8	9.5	10.4	10.2	8.7

a) Acetylene initial pressure 36.0 mmHg
b) Ref. 4

The primary process of photosensitization in which the photosensitizer interacts chemically or forms chemically reactive intermediates by bonding or complexing with the non-absorbing molecules can not always be distinguished from simple physical transfer of energy in collisions. However, it was suggested that a water molecule, for example, reacts with an excited mercury atom to give an excited complex, $(HgH_2O)^*$, which results in decomposition through a second collision with a third body.[18] In the cadmium($^3P_1$)-photosensitization, Tsushima and Sato[10] suggested the formation of the transient complex of a triplet cadmium atom and an acetylene molecule, $(CdC_2H_2)^*$.

As shown in Fig. 3, it seems that the deactivation effect of argon differs for polymer formation and benzene formation. From mechanism (VII), if excited species (some of $C_2H_2^*$, $C_2H_2^{**}$, $C_4H_4^*$, or $C_4H_4^{**}$) is deactivated in addition to the deactivation of $(HgC_2H_2)^*$, the rate of benzene formation will be much affected.

Using the method of the mercury-photosensitized decomposition of acetylene at very low pressure in the presence of excess amounts of helium, Kebarle[19] suggested that the primary decomposition of acetylene is very small which is about 7% of decomposition of ethylene having a similar quenching cross section. The deactivation of $(HgC_2H_2)^*$ based on analogous arguments as used above can interpret the fact.

Influence of Nitric Oxide. Effect of nitric oxide on the rates of pressure decrease and benzene formation is shown in Fig. 4. Nitric oxide largely suppresses the benzene formation. Nitric oxide usually behaves as a radical scavenger. But, at the same time, nitric oxide which is a paramagnetic molecule may quench the excited triplet species like oxygen.[20]

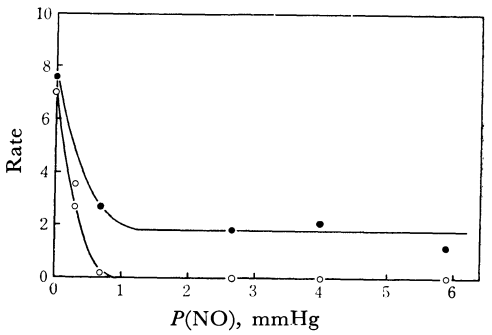

Fig. 4. Effect of nitric oxide on the rates of pressure decrease and of benzene formation.
—○— C_6H_6 ($\times 10^{-8}$ mol/min)
—●— Press. Decrease ($\times 10^{-2}$ mm/min)

Effect on Distribution of Isotopic Benzenes. Table 4 shows the effects of nitric oxide, argon, and temperature on the distribution of isotopic benzenes. Addition of nitric oxide or argon does not affect distribution so much, at least under the experimental conditions. It may be seen that the isotopic benzenes having an odd number of H or D atoms appreciably increase with the rise of temperature. On the basis of the modified excited state molecule mechanism shown above, the change of distribution can be understood on the assumption that the rate of decomposition of cyclobutadiene increases with the rise of temperature.

Effect of Hydrogen Atom. It is known that the hydrogen atom induces the polymerization of acetylene.[4,6,10] Table 5 shows the effect of addition of excess amount of D_2. Benzene formed from the reaction of C_2H_2-D_2 mixture photosensitized by Hg($^3P_1$) consists of a mixture of C_6H_6,

TABLE 5. ISOTOPIC BENZENES FORMED IN THE MERCURY-PHOTOSENSITIZED REACTION OF C_2H_2-D_2 MIXTURE

C_2H_2 (mmHg)	12	12
D_2 (mmHg)	300	494
C_6H_5D/C_6H_6	0.58	0.58

18) H. E. Gunning and O. P. Strausz, "Advances in Photochemistry," Vol. 1, ed. by W. A. Noyes, G. S. Hammond and J. N. Pitts, Interscience Publishers, New York (1963).
19) P. Kebarle, *J. Chem. Phys.*, **39**, 2218 (1963).
20) For example, G. Porter and M. R. Wright, *Discuss. Faraday Soc.*, **27**, 18 (1959).

C_6H_5D and $C_6H_4D_2$. This suggests that a part of the benzene is actually formed by the reaction of hydrogen atoms.

Conclusion

The formation of benzene in the mercury-photosensitization of acetylene could be explained by a modified excited state mechanism equally as well as, or more favourably than, by the free radical mechanism on the basis of the distribution of isotopic benzenes. The effects of additives and of acetylene initial pressure suggest that the primary process is constituted including a transient complex of a triplet mercury atom and an acetylene molecule.

BULLETIN OF THE CHEMICAL SOCIETY OF JAPAN VOL. 43 2745—2749 (1970)

Radiation Chemical Studies with Cyclotron Beams. II. The Radiolysis of an Aqueous Ferrous Ammonium Sulfate Solution with Carbon- and Nitrogen-Ion Radiations[1)]

Masashi IMAMURA, Masao MATSUI and Takashi KARASAWA

The Institute of Physical and Chemical Research, Yamato-machi, Saitama

(Received April 13, 1970)

The yield of ferric ions in the radiolysis of an aqueous ferrous ammonium sulfate solution has been determined in the very high LET (linear energy transfer) range. The radiations used were ions of carbon-12 and nitrogen-14, which were accelerated by means of the IPCR cyclotron and which had energies (E_s) of 31—77 MeV for C-ions and of 17—78 MeV for N-ions; the LET ranges for water were 24—46 eV/Å and 26—85 eV/Å respectively. From the plot of $G(Fe^{3+})E_s$ *vs.* E_s, the value for $G(Fe^{3+})$ at an infinite LET was found to be in the vicinity of 2.9. It has also been shown that there is a substantial difference in the instantaneous yield (G_i) between the two ion radiations of the same LET; this may be ascribed to the differences in the track structures of the heavy-ion radiations.

In most of the experimental work on the LET (linear energy transfer) effect in radiolysis, protons, deuterons, or helium ions have usually been used as radiation sources with a high LET.[1-8)] The maximum LET available in water, however, is approximately 7 eV/Å for protons and 25 eV/Å for helium ions. It is expected that a much higher LET can be obtained from fission fragments of ^{235}U (several hundred eV/Å), but they are attended with some inevitable experimental difficulties.

Schuler[9)] has used ^{12}C-ions accelerated with a HILAC and has made measurements of the yields for aqueous ferrous ammonium sulfate solutions; the energy of the C-ions was in the range of 54—102 MeV. Other heavy ions, such as ^{14}N- and ^{20}Ne-ions, have been used by Burns and his colleague for the radiolysis of liquid cyclohexane and benzene.[10)]

We have initiated radiolysis studies using heavy-ion radiations made available by the IPCR 160 cm cyclotron, which can accelerate several heavy ions at variable energies. While the previous paper[1)] of this series has reported the radiolysis of aqueous ferrous ammonium sulfate solutions with protons and helium ions, the present paper

1) Part I of this series: M. Matsui, H. Seki, T. Karasawa and M. Imamura, *J. Nucl. Sci. Tech.*, **7**, 97 (1970).

2) a) R. H. Schuler and A. O. Allen, *J. Amer. Chem. Soc.*, **77**, 507 (1955). b) R. H. Schuler and A. O. Allen, *ibid.*, **79**, 1565 (1957).

3) a) R. H. Schuler and N. F. Barr, *ibid.*, **78**, 5756 (1956). b) N. F. Barr and R. H. Schuler, *J. Phys. Chem.*, **63**, 808 (1959).

4) H. A. Schwarz, J. M. Caffrey, Jr., and G. Scholes, *J. Amer. Chem. Soc.*, **81**, 1801 (1959).

5) A. Appleby and H. A. Schwarz, *J. Phys. Chem.*, **73**, 1937 (1969).

6) A. R. Anderson and E. J. Hart, *Radiat. Res.*, **14**, 689 (1961).

7) G. L. Kochanny, Jr., A. Timnick, C. J. Hochanadel and C. D. Goodman, *ibid.*, **19**, 462 (1963).

8) For organic compounds, see, W. G. Burns and R. Barker, "Progress in Reaction Kinetics," Vol. 3, ed. by G. Porter, Pergamon Press, Oxford (1965), p. 303.

9) R. H. Schuler, *J. Phys. Chem.*, **71**, 3712 (1967).

10) a) W. G. Burns, W. R. Marsh and C. R. V. Reed, *Nature*, **218**, 867 (1968). b) W. G. Burns and C. R. V. Reed, *Chem. Commun.*, **1968**, 1468.

will concern the results with C- and N-ions, which had energies of 31—77 and 17—78 MeV respectively; a single result with 58 MeV ^{16}O-ions is also included.

By extrapolating the present results at very high LET's, one could obtain the value for $G(Fe^{3+})$ at an infinite LET and, therefore, the limiting yield of water decomposition, G_{-H_2O}. It has also been shown that there is a substantial difference in the instantaneous yield among C-, N-, and O-ions. This may be explained by the differences in the track structures of these heavy-ion radiations.

Experimental

The irradiation arrangement and experimental procedure were similar in outline to those described previously.[1] The ions accelerated in the cyclotron had a charge of +4.[11] The accelerated ions were withdrawn through a beam duct (10 m long) to a target. In the vicinity of the exit window of the duct, the ion beams were passed through a thin gold foil (2μ) and a small fraction of them were elastically scattered by it. The number of ions passing through the foil was thus monitored by counting the number of the scattered ions by a solid-state detector. Meanwhile, the beam currents of ions passing through the foil were determined with a Faraday cup. The number of ions collected in a Faraday cup was then calculated from the total charge, Q, and the average charge, $\langle z\rangle_f$, of ions collected in a Faraday cup after passing through the gold foil; the average charges of ions were obtained in a manner described below. As the number counted by the solid-state detector should be proportional to the number of ions collected in the Faraday cup, one can readily obtain the total number of ions deposited in the solution by assuming no loss of ions between the scattering foil and the solution. The ratio of the number of the scattered ions to that of the collected ions was determined before and after each run; the data were in agreement, within an error of 3%, for each run.

The incident energies of ions were obtained within an error of $\pm 2\%$ by $E_c(\mathrm{MeV}) = 0.107Af^2$, where A is the mass number of the ion and, f(MHz) the radio frequency of the cyclotron being operating. As the ion beams were passed through the scattering foil (2μ Au), the exit window (10μ Al), the air layer (10 mm), and the cell window (10μ mica), the incident energy, E_c, was reduced to E_s when the ions entered the solution. The initial energies of ions entering the solution, E_s, were estimated by the use of the range-energy relations given by Northcliffe.[12]

The principal difference between protons (or helium ions) and heavy ions is that the former can be regarded as charge-invariant over most of the energy region, while the latter can not. With an increase in the atomic number of the ion, there is an expansion of the velocity region in which charge variation is of importance. Northcliffe[13] summarized experimental equilibrium charge distribution data for several heavy ions. It seems that the data can be represented reasonably well by a single universal curve for each value of $z-z'$ (z: atomic number; z': net charge). In the present experiment, the total thickness of absorbers was sufficient to allow the heavy ions to be charge-equilibrated before entering the solution. We have calculated the average charge of ions entering the solution, $\langle z\rangle_s$, by taking weighted means of each fraction of ions having a charge, z', in a charge-equilibrated monoenergetic beam. Table 1 lists the values of z' and $\langle z\rangle_s$ for each ion used in this experiment.

A ferrous ammonium sulfate solution (10^{-2} M $Fe(NH_4)_2(SO_4)_2$, 10^{-3} M NaCl, 0.8 N H_2SO_4) in triply-

Table 1. Average charges, initial LET's and overall yields for heavy ions

Ion	E_c*1	E_s*2	Fraction of ions having charge z' of					$\langle z\rangle_s$	Initial LET (eV/Å)	$G(Fe^{3+})$
			+4	+5	+6	+7	+8			
^{12}C	54.1	31.0	2	23	75	—	—	5.7_3	45.5	3.8_3
^{12}C	73.5	57.0	0	8	92	—	—	5.9_2	30.0	4.1_1
^{12}C	74.2	58.0	0	8	92	—	—	5.9_2	29.6	4.2_0
^{12}C	91.5	77.0	0	4	96	—	—	5.9_6	23.7	4.9_1
^{14}N	51.8	17.0*3	3	29	49	19	—	5.8_4	84.7	3.3_9
^{14}N	52.7	17.0	3	29	49	19	—	5.8_4	84.7	3.4_3
^{14}N	66.8	35.5	0	6	36	58	—	6.5_2	59.8	3.7_7
^{14}N	82.2	61.5	0	1	17	82	—	6.8_1	42.3	4.1_2
^{14}N	96.6	78.5	0	0	12	88	—	6.8_8	35.5	4.4_6
^{16}O	91.7	58.0	0	0	4	33	63	7.5_9	59.2	4.3_2

*1 The energy of ions accelerated in the cyclotron.
*2 The energy of ions entering the solution.
*3 A Ni (3 μ) scattering foil was used.

11) Y. Miyazawa, T. Tonuma, I. Kohno, S. Nakajima, T. Inoue, A. Shimamura, K. Yoshida and T. Karasawa, *Japan J. Appl. Phys.*, **9**, 532 (1970).
12) L. C. Northcliffe, "Studies in Penetration of Charged Particles in Matter," Publication 1133, National Academy of Sciences-National Research Council, Washington, D. C. (1964), p. 173.
13) L. C. Northcliffe, *Ann. Rev. Nucl. Sci.*, **13**, (1963).

distilled water was used under aerated conditions. The irradiation cells were the same as those used previously;[1] the aperture of the cell (10 mm in diameter) was glazed with mica (10 μ thick), the range of which was estimated to be 2.7 mg/cm^2. The solution was stirred during irradiation by means of a magnetic stirrer at a speed of 36 rps.

The oxidation yields of ferrous ions (the number of Fe^{3+} ions oxidized by 100 eV of energy deposited in the solution) were calculated by the equation:[1]

$$G(Fe^{3+}) = 0.96\times10^{7}\times\frac{DV}{\varepsilon d}\times\frac{\langle z\rangle_f}{E_sQ}$$

where: D: the optical density at 304 nm,
ε: the molar extinction coefficient of Fe^{3+} at 304 nm in $M^{-1}\,cm^{-1}$,
d: the optical path-length for D-measurement in cm,
V: the volume of the irradiated solution in ml,
E_s: the initial energy of ions entering the solution in Mev,
Q: the total charge collected in a Faraday cup in nanocoulomb, and
$\langle z\rangle_f$: the average charge of ions collected in a Faraday cup.

The initial LET values for ions with an energy of E_s and a net charge of z' were calculated by the reduced Bethe equations:

$$-\frac{dE}{dx} = \frac{22.2z'^2}{E_s}\log(2.75E_s) \quad \text{for } C^{+z'}\text{-ions}$$

$$-\frac{dE}{dx} = \frac{25.9z'^2}{E_s}\log(2.36E_s) \quad \text{for } N^{+z'}\text{-ions}$$

where the mean excitation potential (I) is assumed to be 66 eV for water and where $-dE/dx$ is expressed in eV/Å when E_s is in MeV. The effective values of $-dE/dx$ for ions with an average charge of $\langle z\rangle_s$ were obtained by taking the weighted means of the value for each z'-value; they are summarized in Table 1.[14]

Results and Discussion

The oxidation yield of ferrous ions was found to be linearly dependent on the dose. Some typical examples are given in Fig. 1; Figure 1 also shows that the yield is independent of the beam current in the range of 0.1—3 nA;[15] above 5 nA the yield decreases.

The radiation chemical yields ($G(Fe^{3+})$) were calculated from the slopes of these linear yield-dose plots and are summarized in Table 1. Figure 2 shows the dependence of the observed $G(Fe^{3+})$ value on the initial LET's of ions. The yields obtained by Schuler[9] with C-ions, also plotted in Fig. 2, indicate good agreement with the present C-ion data. It does not seem, however, that the data for the three ions are superimposable: the heavier the ion, the greater the yield. A similar discrepancy has also been observed between protons or deuterons and helium ions.[16] Furthermore, it seems that the yields at higher LET's can be extrapolated to a value lower than 3.6, which was assumed by Schuler and Allen[2b] to be a limiting yield at an infinite LET.

The $G(Fe^{3+})$-values have hitherto been determined by using accelerated protons, deuterons, and helium ions (LET as high as ~5 eV/Å) and

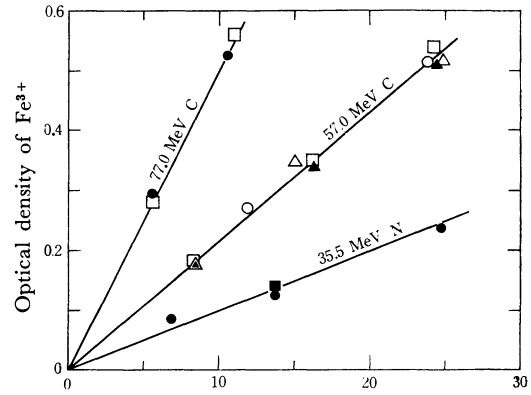

Fig. 1. Plots of Fe^{3+}-yield *vs.* number of ions scattered by a gold foil at various beam currents. The number of scattered ions is proportional to the total number of ions deposited in the solution. The optical densities (d= 10 mm) were determined at 304 nm.
○, 0.1 nA; ●, 0.2 nA; □, 0.5 nA; ■, 0.7 nA; △, 1.5 nA; ▲, 3.0 nA

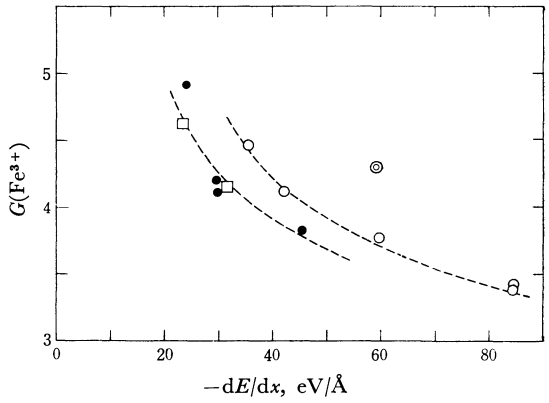

Fig. 2. A plot of the observed $G(Fe^{3+})$ *vs.* reciprocal LET. The initial LET values were calculated by the equations described in the text.
●, C-ions; ○, N-ions; □, C-ions by Schuler (Ref. 9); ◎, O-ions

14) Table 1 also contains a single result with O-ions; the experimental procedure was quite similar to that for C- or N-ions. The initial LET for O-ions is given by $(-dE/dx)=(29.6\,z'^2/E_s)\log(2.06\,E_s)$.

15) The beam currents determined by the use of a Faraday cup.

16) A. O. Allen, "The Radiation Chemistry of Water and Aqueous Solutions," Van Nostrand, Princeton, N. J. (1961), p. 54.

the recoil particles from (n,α) reactions of Li and B (~25 eV/Å).[17] These results indicate that the $G(Fe^{3+})$ decreases as the LET of the radiation is increased. No experimental value of $G(Fe^{3+})$ at the LET's higher than the above value has been reported except for those by Schuler with C-ions (LET's as high as ~30 eV/Å) shown in Fig. 2.[9] The present results indicate that the $G(Fe^{3+})$ still decreases at LET's above 30 eV/Å.

The integrated yield of ferric ions produced by an ion with E_s is given by:

$$G(Fe^{3+}) \times E_s = \int_0^{E_s} G_i dE \qquad (E_s \text{ in } 100\,eV)$$

where G_i represents an instantaneous yield at a a given energy. In Fig. 3 the values of $G(Fe^{3+}) \times E_s$ for C-, N-, and O-ions are plotted as a function of E_s; the data of Schuler with C-ions[9] are also included. It seems that, in unexpected contrast to Fig. 2, all the data fit a universal curve, as is shown in Fig. 3. The instantaneous yields, G_i, for given values of E_s are readily obtained from the slopes at the corressponding points on this curve, *i.e.*,

$$G_i(Fe^{3+}) = \frac{d[G(Fe^{3+})E_s]}{dE_s}$$

The values of $G_i(Fe^{3+})$ thus obtained are plotted as a function of the reciprocal LET in Fig. 4 for C-, N-, and O-ions. The dotted line in Fig. 3 represests the tangent at an infinite LET, which gives $G_i(Fe^{3+}) = 2.9$.

As may be seen in Fig. 3, the data for C- and N-ions and probably for O-ions apparently fit a single universal curve within the limits of experimental error. This is presumably adventitious; the curves may not coincide with each other at higher E_s's. Figure 4 clearly indicates the existence of substantial differences in $G_i(Fe^{3+})$ among these ions at the same LET. These differences may be explained by assuming the different contribution of high-energy secondary electrons; the heavier ion ejects the more energetic secondary electrons. The net yield is, therefore, a combination of the yields for the "core" of the track and for the emergent secondary electrons. The higher yields of heavier ions can thus be understood by assuming the effective expansion of the heavy-ion tracks; such a model has been proposed by Mozumder *et al.*[18] A similar effect observed with deuterons and helium ions has been discussed in terms of the kinetics of secondary electron production.[19] Further experimental study on this effect due to the quality of heavy ions is in progress by using C-, N-, and O-ion radiations.

The oxidation yield of ferrous ions in an aerated aqueous solution is given by the equations:

$$G(Fe^{3+}) = G_{OH} + 3G_H + 2G_{H_2O_2}$$
$$= G_{-H_2O} + 3G_H = 2G_{H_2} + 4G_H$$

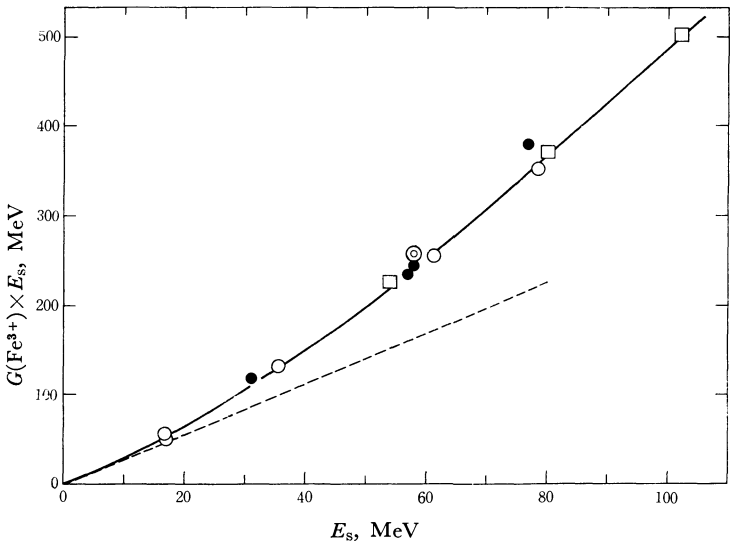

Fig. 3. A plot of the integrated yield of ferric ions *vs.* energy of the heavy ions entering the solution. The dotted line represents the limiting yield of $G(Fe^{3+}) = 2.9$ at an infinite LET.
●, C-ions; ○, N-ions; □, C-ions by Schuler (Ref. 9) ◎, O-ions

17) W. R. McDonell and E. J. Hart (*J. Amer. Chem. Soc.*, **76**, 2121 (1954)) have obtained $G(Fe^{3+}) = 5.2$ and 4.2 for $^6Li(n, \alpha)^3H$ and $^{10}B(n,\alpha)^7Li$ recoils and R. H. Schuler and N. F. Barr (Ref. 3a) 5.69 and 4.22, respectively.

18) a) A. Mozumder, A. Chatterjee and J. L. Magee, *Advan. Chem. Ser.*, **81**, 27 (1968). b) A. Mozumder, *Advan. Radiat. Chem.*, **1**, 1 (1969).

19) R. E. Faw and H. J. Donnert, *Nucl. Instr. Methods*, **58**, 307 (1968).

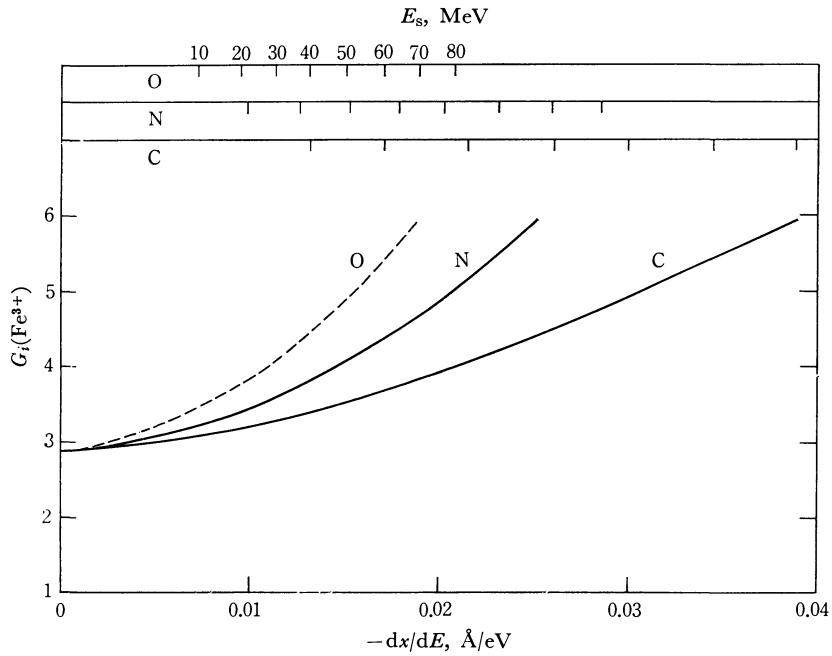

Fig. 4. Dependence on reciprocal LET of the instantaneous yields for C- and N-ions obtained from Fig. 3. Probable dependence for O-ions is also shown.

At an infinite LET, the free radical yields will vanish;[6,20] $G(Fe^{3+})$ will, therefore, approach G_{-H_2O} or $2G_{H_2}$. Schuler and Allen[2b] have assumed the limiting $G(Fe^{3+})=3.6$ from the values for G_{-H_2O} $(=3.6)$ or $2G_{H_2}(=3.4)$ in the radiolysis of an aqueous solution with $^{10}B(n,\alpha)^7Li$ recoil particles. As has been mentioned above, the present results gave the value of 2.9 for the limiting $G(Fe^{3+})$ at an infinite LET, which would mean $G_{-H_2O}\simeq 2.9$ according to the above argument.[21]

According to Allen,[22] the G_{-H_2O} for the 0.8 N H_2SO_4 solution decreases with an increase in the LET to about 3.6 at about 5 eV/Å; then it becomes constant in the higher LET range. In a neutral solution the G_{-H_2O} increases with an increase in LET above 5 eV/Å. However, Anderson and Hart,[6] who investigated the LET dependence of the initial yields from water using a formic acid solution saturated with oxygen, found that the value for G_{-H_2O} decreases with an increase in LET down to 2.4—2.6 for helium ions of about 10 MeV (LET ~5 eV/Å), and then increases slightly.

The present results indicate that the G_{-H_2O} in the 0.8 N H_2SO_4 solution seems substantially lower than the 3.6 estimated by Schuler and Allen.[2b] Although some discussions have been made concerning the value of G_{-H_2O} at very high LET's[21-24] and concerning the difference in that value between acid and neutral solutions,[6] more data should be accumulated in the higher LET region, and the variation in the value of G_{-H_2O} at LET's above 5 eV/Å is still open to question.

The authors wish to express their gratitude to the members of the cyclotron operation group, and also to Hiroshi Seki and Takahisa Imai for their experimental assistance.

20) A. Kuppermann, "Radiation Research 1966," ed. by G. Silini, North-Holland Publ. Co., Amsterdam (1967), p. 212.

21) In the high-LET tracks, some reactions between molecular products and free radicals may be taken into consideration. The most noteworthy reaction of them may be: $H_2O_2+OH\rightarrow H_2O+HO_2$ (*cf.* Ref. 16, p. 51). The formation of HO_2 in the α-ray tracks has been reported by Donaldson and Miller (*Trans. Faraday Soc.*, **52**, 652 (1956) and Appleby and Schwarz (Ref. 5). However, the rate constant of this reaction is not high (4.5×10^7 M^{-1} ses^{-1}, Schwarz, *J. Phys. Chem.*, **66**, 255 (1962)) and the yield has not been established. If this reaction is assumed to occur at all, the $G(Fe^{3+})$ is given, by assuming the material balance suggested by Allen (Ref. 16, p. 51(, by $G(Fe^{3+}(=G_{-H_2O}+G_{HO_2}$ at an infinite LET, yielding the value of G_{-H_2O} lower than 2.9.

22) A. O. Allen, Ref. 16, p. 58.

23) C. J. Hochanadel, "Comparative Effects of Radiation," ed. by M. Burton, J. S. Kirby-Smith and J. L. Magee, John Wiley & Sons, New York (1960), p. 151.

24) M. Anbar, "Fundamental Processes in Radiation Chemistry," ed. by P. Ausloos, Interscience, New York (1968), p. 651.

BULLETIN OF THE CHEMICAL SOCIETY OF JAPAN VOL. 43 2750—2758 (1970)

Fluorescence Quenching Reactions due to the Intermolecular Electron Transfer Process in Solution

Tadashi OKADA, Hiroo OOHARI and Noboru MATAGA*[1]

Department of Chemistry, Faculty of Engineering Science, Osaka University, Toyonaka

(Received April 13, 1970)

Mechanisms of the intermolecular electron transfer process in the electronically excited states of solute molecules have been studied in relation to the fluorescence quenching reactions in solution, employing pyrene as a fluorescer and some aromatic amine and cyano compounds as quenchers. The quenchers showed various strengths of the quenching actions which were classified and discussed on the basis of a new theoretical model of electron transfer process in excited state. Tetracyanoethylene showed a quite strong quenching action which was interpreted in terms of a long range electron transfer from excited pyrene to tetracyanoethylene. The relation between the exciplex formation, the electron transfer reaction due to the short range interaction and that due to the long range interaction have been discussed.

The mechanism of fluorescence quenching in solution has been studied for a long time.[1] Although there are diverse mechanisms of the luminescence quenching reactions, the intermolecular electron transfer or charge transfer processes in the excited state seem to be one of the most important mechanisms for fluorescence quenching reactions.[2] The mechanism may be connected with the fact that the electron affinity of a molecule is larger and its ionization potential is smaller in the electronically excited state than in the ground state and, the electron donor-acceptor interaction can arise in the excited state even though there is no interaction in the ground state. Recent studies[2] on exciplex (or heteroexcimer) luminescence are making important contributions to this fluorescence quenching mechanism.

The results of observations concerning exciplex fluorescence have indicated that the exciplex formed in a polar solvent by the encounter collision between the fluorescer (F*) and the quencher (L) molecule gradually shifts to the solvated ion-pair or to the dissociated ion-radicals during the lifetime of the excited state as follows:

$$F^* + L \underset{k_2}{\overset{k_1}{\rightleftarrows}} \text{exciplex} \xrightarrow{k_3} F_S^{\pm}\cdots L_S^{\mp} \rightarrow F_S^{\pm} + L_S^{\mp} \quad (1)$$

Although Eq. (1) seems to be important for fluorescence quenching due to the electron transfer, it might not be correct to say that the electron transfer in the fluorescence quenching reaction occurs always *via* the formation of a "complex" where the interaction between the electron donor and the acceptor is considerable. In principle, it may be possible for the electron transfer to occur by very weak interaction in a quite loose encounter complex, so weak that the states of the system before and after the electron transfer can be regarded as independent stationary states between which the quantum mechanical transition occurs.[3] Accordingly, it is necessary and important to examine various quenchers of different strengths in detail for the elucidation of the electron transfer processes.

In the following, we show the results of our measurements on the quenching of pyrene fluorescence by various quenchers in various solvents.

Experimental

Materials. Pyrene was chromatographed on activated alumina and silica gel, and extensively

*1 To whom correspondence should be addressed.

1) Th. Förster, "Fluoreszenz Organisher Verbindungen," Vandenhoeck Ruprecht, Göttingen (1951).

2) H. Leonhardt and A. Weller, *Ber. Bunsenges. Phys. Chem.*, **67**, 791 (1963); N. Mataga, K. Ezumi and K. Takahashi, *Z. Phys. Chem. N.F.*, **44**, 250 (1965); N. Mataga, T. Okada and K. Ezumi, *Proc. International Conf. on Luminescence*, Budapest, 431 (1966); *Mol. Phys.*, **10**, 201, 203 (1966); T. Miwa and M. Koizumi, This Bulletin, **39**, 2603 (1966); N. Mataga, T. Okada and and N. Yamamoto, *ibid.*, **39**, 2562(1966); N. Mataga, T. Okada and H. Oohari, *ibid.*, **39**, 2563 (1966); N. Mataga and K. Ezumi, *ibid.*, **40**, 1355(1967); K. Kaneta and M. Koizumi, *ibid.*, **40**, 2254(1967); H. Knibbe, D. Rehm and A. Weller, *Z. Phys. Chem. N. F.*, **56**, 95, 99(1967); N. Mataga, T. Okada and N. Yamamoto, *Chem. Phys. Lett.*, **1**, 119 (1967); H. Beens, H.Knibbe and A. Weller, *J. Chem. Phys.*, **47**, 1183(1967); H. Knibbe, K. Rolleg, F. P. Schafer and A. Weller, *ibid.*, **47**, 1184 (1967); H. Knibbe, D. Rehm and A. Weller, *Ber. Bunsergs. Phys. Chem.*, **72**, 257 (1968); W. R. Ware and H. P. Richter, *J. Chem. Phys.*, **48**, 1595 (1968); T. Okada, H. Matsui, H. Oohari, H. Matsumoto and N. Mataga, *ibid.*, **49**, 4717 (1968).

3) N. Mataga and O. Tanimoto, *Theoret. Chim. Acta*, **15**, 111 (1969).

zone-refined. *N,N*-Dimethylaniline (DMA) was refluxed with acetic anhydride, washed with water, dried over potassium hydroxide, and distilled in a vacuum several times. G. R. grade tetracyanoethylene (TCNE) was recrystallized from monochlorobenzene and sublimated several times in a vacuum. 1,2,4,5-tetracyanobenzene (TCNB) was synthesized and purified in this laboratory.[4] Isomeric dicyanobenzenes (DCNB) were recrystallized from ethanol and sublimated in a vacuum. *n*-hexane was passed through a column of activated silica gel and distilled. Pyridine was refluxed with 28% aqueous solution of sodium hydroxide, dried over sodium hydroxide and potassium hydroxide and after refluxing with potassium hydroxide distilled carefully. Ethanol was treated with sulfuric acid and silver nitrate, dried over aluminium amalgam and activated silica gel, distilled carefully. Acetonitrile was refluxed repeatedly over phosphorus pentoxide, distilled into potassium carbonate and distilled from it. Spectrograde *N,N*-dimethylformamide (DMF) was used without further purification.

All solutions for the measurement were carefully deaerated by freeze-pump-thaw cycles.

Apparatus and Measurements. Fluorescence spectra were measured with an Aminco-Bowman spectrophotofluorometer which was calibrated to obtain the correct fluorescence quantum spectrum. Absorption spectra were measured by a Cary 15 spectrophotometer.

In order to measure the fluorescence decay times, the specimens were excited by a pulse which was made monochromatic through a monochromator (335 mμ). The fluorescence pulses were received by a photomultiplier of 1P28 type. Responses from the photomultiplier were guided to a synchroscope(Tektronix 585A) and the decay curve was photographed, or they were led to a sampling oscilloscope(Tektronix 661) and the decay curves were recorded on a X-Y recorder.

The exciting pulsed lights were produced by discharging a specially designed capacitor (of a few hundreds pF and charged up to 2000—4000 V) through a gap of about 0.5 mm between small platinum electrodes in air. The half width of the pulsed light was about 15 ns.

The measurement of the temperature effect on the fluorescence was conducted by using a metal dewar with quartz windows (for the temperature range below −50°C) or by using a quartz dewar which contains purified ethanol as a refrigerant (for measurements above −50°C). In the case of the former, the temperature of a solution in a quartz cuvette placed in the dewar was controlled by a constant flow of cold nitrogen gas. The flow of the gas was controlled by heating liquid nitrogen, and the temperature of the solution was measured by a thermocouple. In the case of the latter, the temperature of the solution in the cuvette was controlled by dropping appropriate amounts of liquid nitrogen into the refrigerant.

The measurements of the absorption spectra of transiently produced ion radicals were made by means of an ordinary flash photolysis apparatus. Both the first and the second flash lights have a half-value width of 3 μsec. The spectra were photographed by using a Shimazu GE 100 type spectrograph.

Experimental Results and Discussion

In such polar solvents as ethanol, DMF and acetonitrile, the fluorescence of pyrene is quenched by DMA completely. As an example, the quenching curves in acetonitrile and DMF are shown in Fig. 1, where the simple Stern-Volmer equation (2) is well satisfied with respect to the fluorescence quantum yield as well as the fluorescence decay time.

$$\eta'_F/\eta_F = \tau'_F/\tau_F = 1/(1 + \gamma k_1 \tau_F[L]) \qquad (2)$$

where $\gamma = k_3/(k_2+k_3)$ according to Eq. (1).

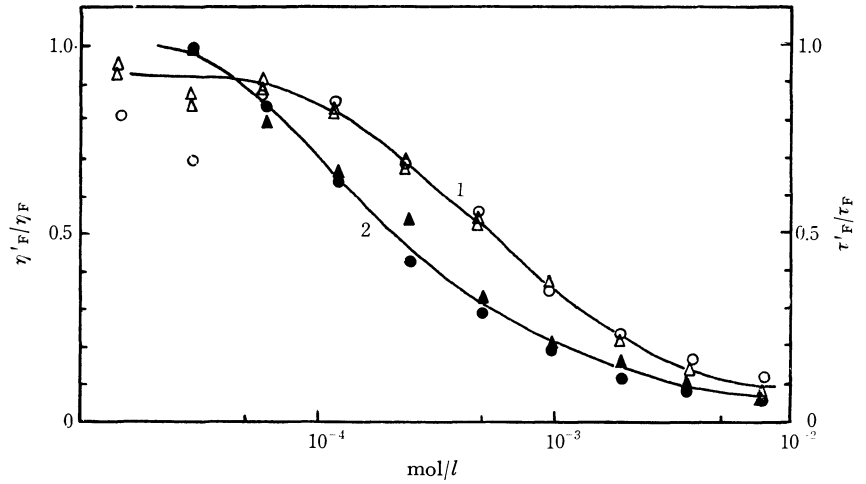

Fig. 1. η'_F/η_F or τ'_F/τ_F *vs.* [L] relations for pyrene - DMA system in acetonitrile (1) and DMF (2) at 300°K.
●, ○: η'_F/η_F ▲, △: τ'_F/τ_F [Pyrene]: 1×10^{-5} mol/l

4) N. Mataga and Y. Murata, *J. Amer. Chem. Soc.*, **91**, 3144 (1969).

The quenching rate constants γk_1 at 300°K for the pyrene-DMA system were 1.3×10^{10} l/mol·sec in acetonitrile, 5.7×10^{9} l/mol·sec in DMF and 6.9×10^{9} l/mol·sec in ethanol, respectively. Similar results have been obtained also in the case of the quenching of pyrene fluorescence by TCNB and isomeric dicyanobenzenes in polar solvents. In the case of pyrene - TCNB system in acetonitrile, the quenching curve can be reporduced accurately by Eq. (2) and the γk_1 value at 300°K has been evaluated to be 1.6×10^{10} l/mol·sec.

When isomeric dicyanobenzenes are used as quenchers, the quenching curves are not exactly reproducible by Eq. (2), but η'_F/η_F value is a little smaller than τ'_F/τ_F value at the same [L] value, although $\tau'_F/\tau_F=(1+\gamma k_1\tau_F[L])^{-1}$.

It is well-known that a more detailed consideration based on the diffusion-controlled encounter process of Eq. (3), leads to Eqs. (4) and (5).[5]

$$F^* + L \underset{k_2}{\overset{k_1}{\rightleftarrows}} F^* \cdots L \xrightarrow{k_3} \text{intermediate} \longrightarrow \quad (3)$$

$$\eta'_F/\eta_F = \delta/(1 + \gamma k_1\tau_F[L]) \quad (4)$$

$$\delta = \exp\left[-4\pi(\gamma R_0)^2\{D\tau_F(\eta'_F/\eta_F)\}^{1/2}N'[L]\right] < 1$$

$$\tau'_F/\tau_F = 1/(1 + \gamma k_1\tau_F[L]) \quad (5)$$

where, $D=D_{F^*}+D_L$, the sum of the diffusion coefficients of F* and L, N' is the Avogadro number per 1 ml and γR_0 is the effective encounter distance. When the electron transfer interaction in the encounter complex is a sufficiently short range one, Eq. (4) is reduced to the simplest case of Eq. (1) because $\delta\simeq1$.

From the results, the mechanism of Eq. (1) seems to be correct at least for the pyrene-TCNB systems.

If the mechanism of Eq. (1) is correct and the ion radicals are formed, we should be able to observe the absorption spectra of transiently produced ion radicals by means of the flash photolysis method. Actually, we have observed such spectra for pyrene - DMA system in acetonitrile as well as in ethanol (Figs. 2 and 3).

In Fig. 2, we see clearly the absorption peaks due to pyrene anion radical at 20.3×10^3, 22.0×10^3 and 26.0×10^3 cm^{-1}. The peak at *ca.* 24×10^3 cm^{-1} may be ascribed to the T-T absorption, while shoulders around this peak can neither be ascribed to the absorption of radicals nor the T-T absorption. The small shoulder at *ca.* 21.3×10^3 cm^{-1} might be assigned to the absorption band of DMA cation radical.

In the case of Fig. 3, we can observe more clearly the absorption bands of both ion radicals. The spectrum in Fig. 3c where no added DMA is present is due to the T-T absorption. In the presence of DMA((a), (b)), the absorption bands at 22.0×10^3 and 20.3×10^3 cm^{-1} due to pyrene anion radical as well as those at 22.2×10^3 and 21.3×10^3 cm^{-1} which can be ascribable to DMA cation radical have been observed. From comparison of Fig. 3b and Fig. 3a, we see that in ethanol, pyrene anion is rather unstable and decays more

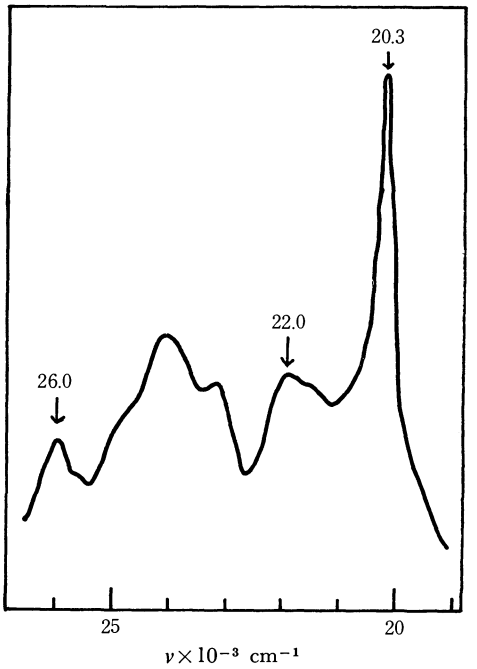

Fig. 2. Transient absorption spectra of pyrene - DMA system in acetonitrile.

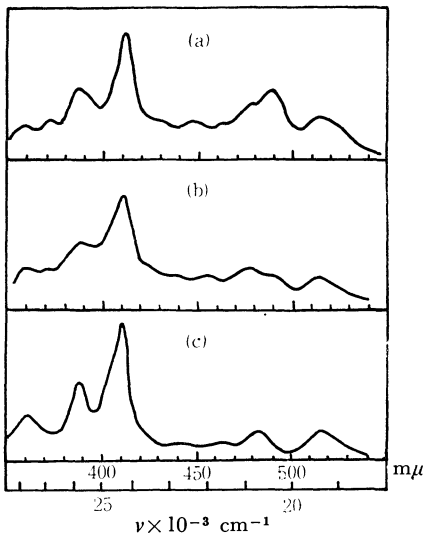

Fig. 3. Transient absorption spectra in ethanol.
(a), (b): pyrene - DMA system, the intervals between the peaks of the main flash and second one were 3 μsec(a) and 50 μsec(b)
(c): T−T absorption bands of pyrene, the interval between the two peaks was 3 μsec
[Pyrene]: 1×10^{-5} mol/l, [DMA]: 1×10^{-2} mol/l

5) A. Weller, *Z. Phys. Chem. N. F.*, **13**, 335 (1957); *ibid.*, **15**, 438 (1958); *ibid.*, **18**, 163 (1958).

rapidly compared with DMA cation. Contrary to this, the spectrum DMA cation can hardly be observed in the case of acetonitrile solution. Presumably, the ion radicals will decay partly due to the reaction with solvent molecules or unknown impurities in the solvent in addition to the bimolecular recombination reaction between anion and cation radicals (electron transfer from anion to cation). At any rate, the ion radical formation according to the mechanism of Eq. (1) has been confirmed experimentally.

The fluorescence of pyrene is quenched completely even in a non-polar solvent by the strong quencher, TCNE. The quenching curve in *n*-hexane is shown in Fig. 4. This quenching curve of pyrene - TCNE - *n*-hexane system can be well reproduced by Eq. (2); $\gamma k_1 = 2.5 \times 10^{10}$ *l*/mol·sec at 300°K. However, the formation of ion radicals cannot be observed by means of flash photolysis studies on this system. Presumably, the ion radicals are extremely unstable in this non-polar solvent. Therefore, the encounter collision may lead to the formation of charge transfer type complex which is non-fluorescent.

$$F^* + L \xrightarrow{k_1} \text{Complex} \longrightarrow \text{Product} \qquad (6)$$

Because there is a large energy difference between the state (F^*+L) and the complex, the back reaction from the complex to the (F^*+L) state can be neglected. The energy difference is estimated to be *ca.* 13×10^3 cm^{-1} from the CT absorption band of pyrene-TCNE CT complex and the excitation energy of pyrene.

The fluorescence of pyrene is strongly quenched by TCNE in acetonitrile solution. In contradistinction to the case of *n*-hexane solution, there is a quite large difference between the quenching curve for the fluorescence quantum yield and that for the decay time as shown in Fig. 5. Namely, $\eta'_F/\eta_F < \tau_F'/\tau_F$ for the same [L] value in general. The quenching curves in acetonitrile can be reproduced by Eqs. (4) and (5). In this polar solvent, the electron transfer from excited pyrene to TCNE may occur and ion radicals may be produced. We have confirmed by flash photolysis the transient production of TCNE anion radical in addition to the formation of pyrene cation radical with absorption band at 22.2×10^3 cm^{-1}.

We obtain from Eqs. (4) and (5),

$$\ln \delta = \ln [(\eta'_F/\eta_F)(\tau_F/\tau'_F)] = -4\pi(\gamma R_0)^2(D\tau_F)^{1/2}N'(\eta'_F/\eta_F)^{1/2}[L] \qquad (7)$$

From the plot of $\ln[(\eta'_F/\eta_F)(\tau_F/\tau'_F)]$ against $(\eta_F'/\eta_F)^{1/2}[L]$, we can obtain the value of $4\pi(\gamma R_0)^2(D\tau_F)^{1/2}N'(=v)$. As we can evaluate γk_1 from the quenching curve of (τ'_F/τ_F) and $\gamma k_1 = 4\pi\gamma R_0 DN'$, the γR_0 value can be given by

$$\gamma R_0 = [v^2/4\pi\gamma k_1 \tau_F N']^{1/3} \qquad (8)$$

Thus, it is possible to evaluate (γR_0) experimentally without knowing the value of the diffusion coefficient which, in general, does not seem to be known accurately. The γR_0 value obtained in this way was 47±8Å irrespective of the temperature at which the measurement was made. This γR_0 value is so large that one cannot regard $R_0 \geqq \gamma R_0$ as physically meaningful for the actual encounter distance in the loose complex F*···L.

It might be argued that the pyrene - TCNE CT complex is formed in the ground state, which causes the large difference between η'_F/η_F and τ'_F/τ_F values. However, this possibility can be rejected

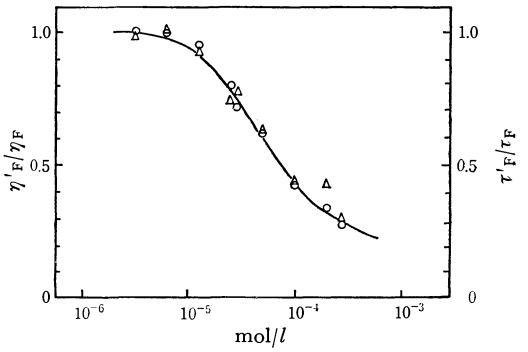

Fig. 4. Fluorescence quenching curve for pyrene - TCNE system in *n*-hexane at 300°K.
[Pyrene]: 1×10^{-5} mol/*l*, ○: η'_F/η_F, △: τ'_F/τ_F

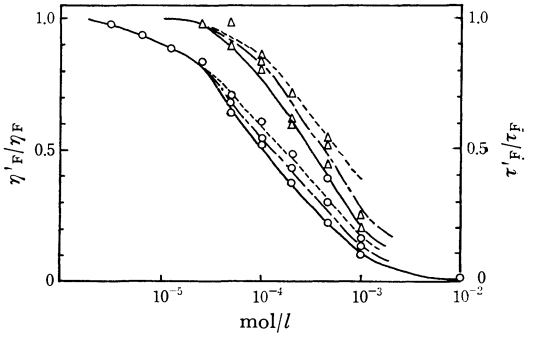

Fig. 5. Fluorescence quenching curve for pyrene - TCNE system in acetonitrile at various temperatures.
——: at 25°C, ———: at 0°C, ----: at −40°C
○: η'_F/η_F, △: τ'_F/τ_F [Pyrene]: 1×10^{-5} mol/*l*

because of the fact that the absorption spectrum does not show any change in the range of TCNE concentration used here, and because of the more important fact that the extent of the quenching with respect to both of the quantum yield and the decay time is greater at higher temperatures.

One should note that Eq. (4) and, accordingly, (7) and (8) contains rather drastic approximations. One should not regard R_0 as the actual intermolecular distance in the encounter complex, in general. These approximate equations may not be

valid for this quite strong quenching action of TCNE in acetonitrile. Nevertheless, the quite strong quenching and the anomalously large R_0 value seem to indicate a long range interaction between the fluorescer and the quencher.

The diffusion equation for the encounter and electron transfer process may be written as

$$-\frac{\partial\Phi(R,t)}{\partial t} = -D\nabla^2\Phi(R,t) + \frac{1}{\tau_F}\Phi(R,t) + \sum_i W(|R-R_i|)\Phi(R,t) \qquad (9)$$

where $\Phi(R,t)$ is the distribution function for F^* and $W(|R-R_i|)$ is the electron transfer probability.

In the case of the long range electron transfer caused by the very weak interaction, $W(|R-R_i|)$ represents the electronic transition probability which depends on the intermolecular distance $|R-R_i|$ between the fluorescer and the quencher. If W is hard core type, *i.e.*,

$$\begin{aligned} W &= 0 \quad \text{at } |R-Ri| > \gamma R_0 \\ W &= 1 \quad \text{at } |R-R_i| \leqq \gamma R_0 \end{aligned} \qquad (10)$$

then the bimolecular reaction rate constant should be proportional to the diffusion coefficient D. However, if W has a long range part, the bimolecular rate constant should be proportional to D^m, where $m<1$. Such a long range effect was actually observed in the case of the singlet excitation transfer from pyrene to perylene in fluid solution,[6] where W has been proved to be proportional to inverse sixth power of $|R-R_i|$.[7] Namely, it has been confirmed that the bimolecular rate constant for the quenching of pyrene fluorescence caused by the excitation transfer is proportional to D when the D value is relatively large, while it is proportional to $D^{3/4}$ at relatively small values of D in accordance with the theoretical consideration.[8]

From the viewpoint of the above consideration, we have examined the dependence of γk_1 value (which can be determined accurately by the measurement of the decay times) on the diffusion coefficient for the pyrene - TCNE - acetonitrile system.

The temperature dependences of $1/\tau_F$ and $1/\tau'_F$ values are shown in Fig. 6. These curves were obtained by repeating the measurement of the decay time many times at each temperature and averaging them. The accuracy of the measurement was not so good for curve (4) compared to the others, because of a little smaller number of measure-

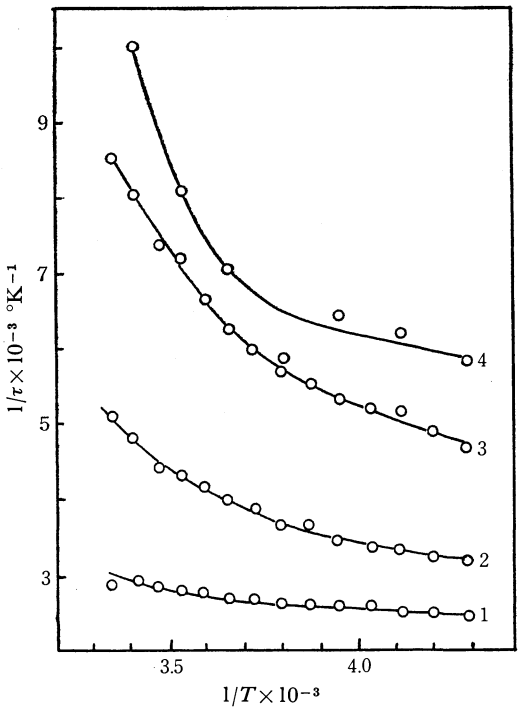

Fig. 6. $1/\tau_F$ or $1/\tau'_F$ *vs.* $1/T$ relations for pyrene - TCNE system in acetonitrile.
[TCNE]: (1) 0, (2) 2×10^{-4}, (3) 4×10^{-4}, (4) 9×10^{-4} mol/*l*, [Pyrene]: 1×10^{-5} mol/*l*

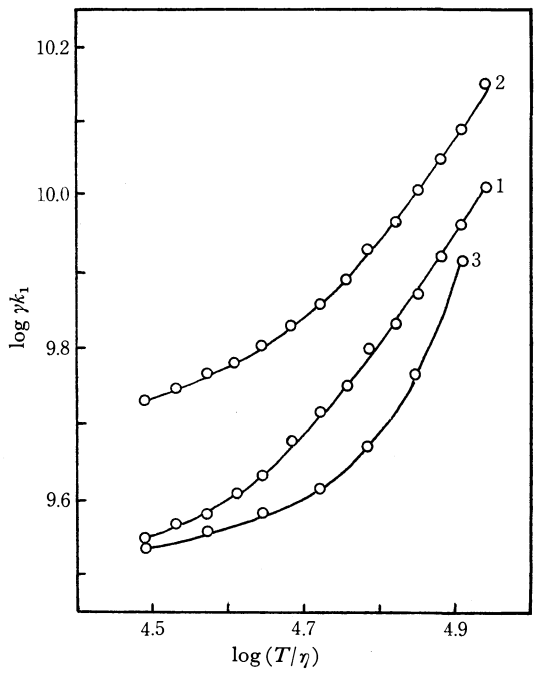

Fig. 7. log γk_1 *vs.* log (T/η) relations for pyrene - TCNE system in acetonitrile.
[TCNE]: (1) 2×10^{-4}, (2) 4×10^{-4}, (3) 9×10^{-4} mol/*l*, [Pyrene]: 1×10^{-5} mol/*l*

6) M. Tomura, E. Ishiguro and N. Mataga, *J. Phys. Soc. Japan*, **22**, 1117 (1967); *ibid.*, **25**, 1439 (1968).
7) N. Mataga, H. Obashi and T. Okada, *Chem. Phys. Lett.*, **1**, 133 (1967); *J. Phys. Chem.*, **73**, 370 (1969).
8) M. Yokota and O. Tanimoto, *J. Phys. Japan*, **22**, 779 (1967).

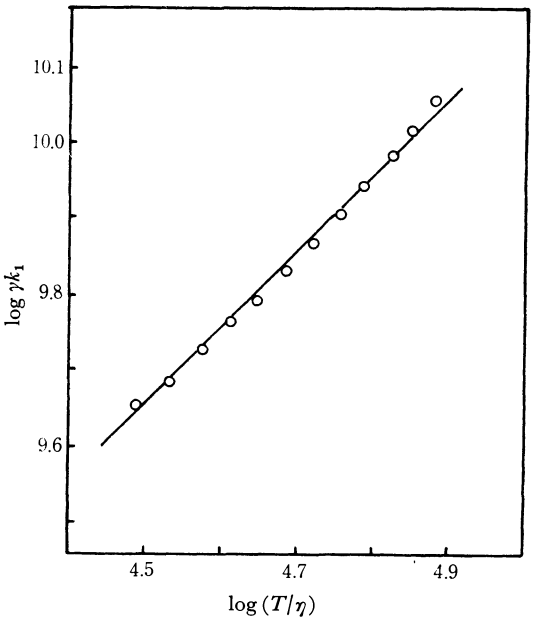

Fig. 8. log γk_1 *vs.* log (T/η) relation for pyrene - DMA system in acetonitrile.
[Pyrene]: 1×10^{-5} mol/*l*, [DMA]: 4×10^{-4} mol/*l*

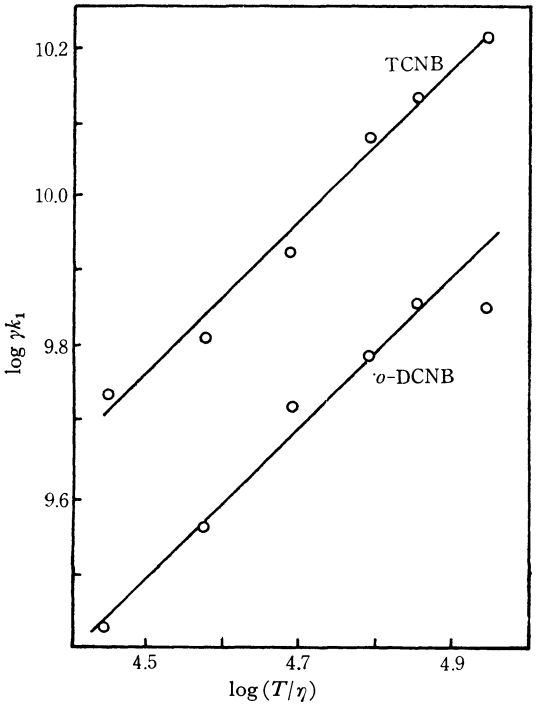

Fig. 9. log γk_1 *vs.* log (T/η) relations for pyrene - TCNB and pyrene - *o*-DCNB systems in acetonitrile.

ments. From these values of decay times, the γk_1 values have been obtained by means of the equation $\gamma k_1=(\tau_F/\tau_F'-1)/\tau_F[L]$.

In Fig. 7, log γk_1 values are plotted against log

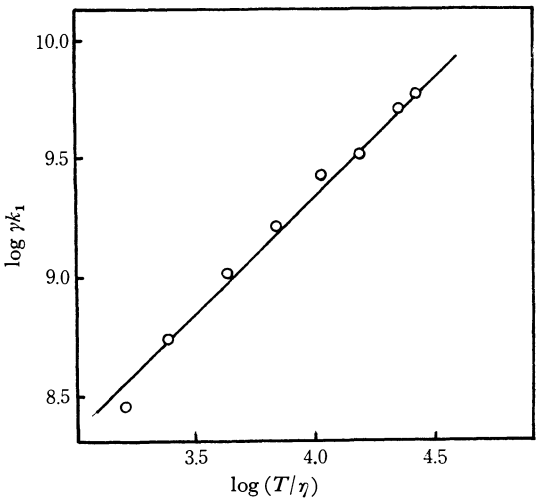

Fig. 10. Log γk_1 *vs.* log (T/η) relation for pyrene - *p*-DCNB system in ethanol.
[*p*-DCNB]: 1×10^{-3} mol/*l*, [Pyrene]: 1×10^{-5} mol/*l*

(T/η), where T is the absolute temperature and η is the viscosity of the solution. Although the absolute value of γk_1 for each [L] value is not very accurate, the shapes of the curves in Figs. 6 and 7 are certainly reliable. Of course, the correction for the change of the concentration of the quencher due to the change of the temperature of the solution has been taken into concideration. As (T/η) is proportional to the diffusion coefficient, this plot will provide the desired information as described above.

We see clearly from Fig. 7, that $m\simeq1$ in the range of relatively large (T/η) values, while $m<1$ at relatively small (T/η) values. Moreover, the long range effect appears to be more predominant in the case of higher concentrations of TCNE. Thus, the long range electron transfer process due to the very weak interaction seems to play an important role and the hard sphere model provides only a poor approximation for the pyrene - TCNE system in acetonitrile.

As the fluorescence quenching reaction of pyrene-DMA system in acetonitrile can be reproduced satisfactorily by Eq. (2) the long range effect may not be important in this system. Thus, one may expect a straight line with $m=1$ when log γk_1 is plotted against log (T/η). The relation is actually satisfied (Fig. 8).

Since quite an analogous result to the case of pyrene - DMA system has been observed for the quenching curve of pyrene-TCNB system in acetonitrile, we can expect that $m\simeq1$ also for this system. When *p*-DCNB and *o*-DCNB were used as quenchers for pyrene fluorescence in acetonitrile solution, there is a little tendency that $\eta'_F/\eta_F\lesssim\tau_F'/\tau_F$. By means of Eqs. (7) and (8), the γR_0 values have been evaluated to be 29Å for *p*-DCNB and 24Å

for *o*-DCNB in acetonitrile. These γR_0 values are much smaller than in the case of the fluorescence quenching due to TCNE. Therefore, it is possible that a similar result to the case of pyrene-TCNB system (*i.e.* $m \simeq 1$) can be obtained also for the pyrene - *o*-DCNB system, because the difference between the value of η'_F/η_F and that of τ'_F/τ_F is rather small.

As indicated in Fig. 9, log γk_1 is linear with log (T/η) and $m \simeq 1$ for both systems. In contrast to this, although log γk_1 is approximately linear with log (T/η), m is a little smaller than unity in the case of pyrene - *p*-DCNB system in acetonitrile. We have further examined pyrene - *p*-DCNB system in ethanol and also, in pyridine solution. Although η'_F/η_F is a little smaller than τ'_F/τ_F in ethanol solution, γk_1 is proportional to (T/η) and $m \simeq 1$ as shown in Fig. 10. In the case of pyridine solution, the quenching curve and the change of the fluorescence spectrum are shown in Figs. 11 and 12, respectively. The quenching curve can be well reproduced by the simple Stern-Volmer equation (2). However, as shown in Fig. 12, one can observe the fluorescence of pyrene - *p*-DCNB exciplex. Since the yield of this exciplex fluorescence is quite small, it is probable that the ion-pair formation process (k_3) as indicated in Eq. (1), is competing with the fluorescence transition, the probability of which may be rather small because of the very polar structure of the exciplex. In a more polar solvent such as ethanol, process k_3 is certainly much more dominant than the exciplex fluorescence transitions so that the exciplex fluorescence cannot be observed in ethanol solution.

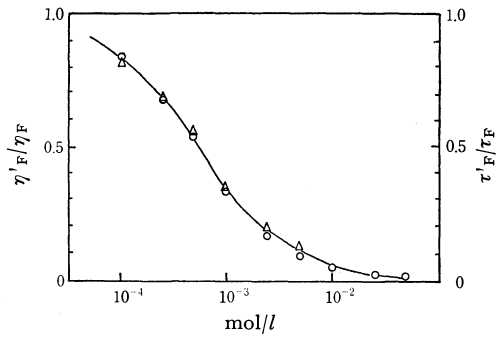

Fig. 11. η'_F/η_F or τ'_F/τ_F *vs.* [L] relation for pyrene - *p*-DCNB system in pyridine at 25°C.
○: η'_F/η_F, △: τ'_F/τ_F

We can summarize the results as follows. In non-polar and less polar solvents, the exciplex formation occurs between the fluorescer and the quencher molecules. The exciplex is either fluorescent or non-fluorescent. Furthermore, in a slightly polar solvent, there arises a solvated ion-pair via the exciplex. In the more polar solvents, there occurs an electron transfer from the fluorescer to the quencher and *vice versa* due to the short

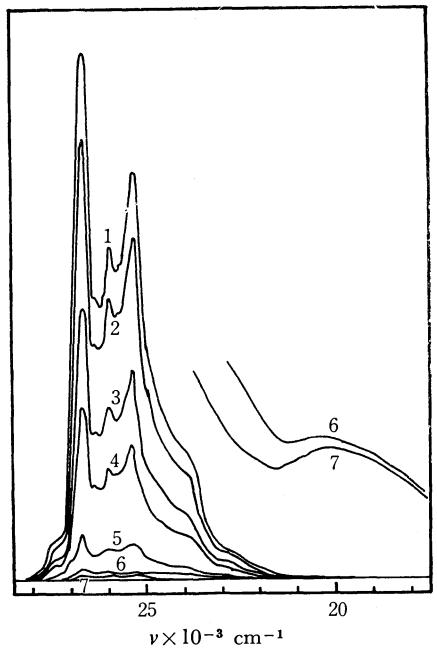

Fig. 12. Fluorescence spectra of pyrene - *p*-DCNB in pyridine at 25°C.
[*p*-DCNB]: (1) 0, (2) 1×10^{-4}, (3) 5×10^{-4}, (4) 1×10^{-3}, (5) 5×10^{-3}, (6) 2.5×10^{-2}, (7) 5×10 mol/l
[Pyrene]: 1×10^{-5} mol/l

range interaction or the long range very weak interaction depending on the strength of the quencher. The long range electron transfer process due to the very weak interaction may be a non-adiabatic quantum mechanical transition as will be described below.

Let us denote the energies of the various states in Eq. (1) as follows: $U_1 = U(F^* + L)$, $U_2 = U$ (exciplex), $U_3 = U(F_S^{\pm} \cdots L_S^{\mp})$ and $U_4 = U(F_S^{\pm} + L_S^{\mp})$ When $U_2^\circ > U_3^\circ$ or U_4°, the solvated complex will immediately shift to the solvated ion-pair or dissociate into the solvated ion radicals, where U_i°'s represent the values for the equilibrium state with respect to the solute-solvent interactions. If the interaction between the fluorescer and the quencher is not very weak, the reaction will proceed on the adiabatic potential energy surface and the probability W may be of a hard core type.

When the interaction between the partners in the exciplex is weak, its wavefunction may be written as

$$\Psi \sim c_1(s)\Phi_i^\circ(F^* \cdots L) + c_2(s)\Phi_f^\circ(F^+ \cdots L^-)$$
$$\text{or} \qquad (11)$$
$$\Psi \sim c_1(s)\Phi_i^\circ(F^* \cdots L) + c_2(s)\Phi_f^\circ(F^- \cdots L^+)$$

where s symbolizes the nuclear configurations including the surrounding solvent molecules. When the electronic interaction between F* and L in the loose encounter complex F*···L is very weak

in a sufficiently polar solvent, the isoenergetic electronic transition will occur from the state Φ_i° to Φ_f°. The electron transfer by this process may be given schematically by configuration coordinate diagrams as shown in Fig. 13. In this figure, the long range electron transfer is represented by the quantum mechanical tunnelling through the potential barrier as indicated by the horizontal wavy line. In the case of curve (a) for U_3, the barrier may be too high for the tunnelling to occur while it may be possible in the case of curve (b).

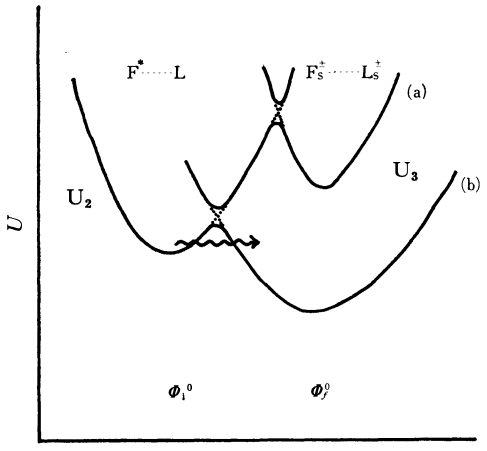

Fig. 13. Schematic diagrams of the electron transfer process by very weak interaction.

The energy of the curve U_3 depends upon the magnitudes of ionization potential of the donor and the electron affinity of the acceptor on the one hand and upon the solvation energies of the ion radicals on the other hand. Among the cyano compounds used in the present work, the electron affinity of TCNE is the largest. Moreover, the solvation energy of its anion in polar solvent may be the largest because its molecular radius is the smallest among others. Therefore, U_3 may be the lowest in the case of pyrene - TCNE - acetonitrile system.

The tunnelling efficiency depends also upon the magnitude of the matrix element of the perturbation Hamiltonian between Φ_i° and Φ_f°. As the spatial dimension of TCNE is the smallest among the quenchers employed, the overlap between the electron donating orbital of excited pyrene and the accepting orbital of TCNE may be large compared to those of the other systems, which results in a relatively large value of the perturbation matrix element.

We have discussed the long range electron transfer in analogy to the long range singlet-singlet excitation transfer. Let us examine the matrix elements responsible for the excitation transfer as well as the electron transfer transition. We assume both F and L are closed shell molecules and denote their MO's as ψ_m^F's and ψ_m^L's respectively, where the m-th MO's are the highest occupied ones in the ground state. The Hamiltonian $\mathscr{H}$ can be separated into the core part $\mathscr{H}_c=\sum f_c(i)$ and the electron interaction part $G=\sum g(ij)$. Then, the matrix elements for the following excitation transfer processes

$$F^*(^1L_a) + L \rightarrow F + L^*(^1L_a)$$
$$F^*(^1L_b) + L \rightarrow F + L^*(^1L_a)$$

can be written as

$$\langle\Phi_i^\circ(^1L_a)|\mathscr{H}|\Phi_f^\circ(^1L_a)\rangle = 2(\langle\psi_m^L\psi_{m+1}^F|g|\psi_{m+1}^L\psi_m^F\rangle - \langle\psi_m^L\psi_{m+1}^F|g|\psi_m^F\psi_{m+1}^L\rangle) \quad (12a)$$

$$\langle\Phi_i^\circ(^1L_b)|\mathscr{H}|\Phi_f^\circ(^1L_a)\rangle = \sqrt{2}(\langle\psi_m^L\psi_{m+2}^F|g|\psi_{m+1}^L\psi_m^F\rangle - \langle\psi_m^L\psi_{m+2}^F|g|\psi_m^F\psi_{m+1}^L\rangle - \langle\psi_m^L\psi_{m+1}^F|g|\psi_{m+1}^L\psi_{m-1}^F\rangle + \langle\psi_m^L\psi_{m+1}^F|g|\psi_{m-1}^F\psi_{m+1}^L\rangle) \quad (12b)$$

In contrast to this, the matrix elements for the electron transfer transitions

$$F^*(^1L_a)\cdots L \rightarrow F^+\cdots L^-$$
$$F^*(^1L_b)\cdots L \rightarrow F^+\cdots L^-$$

are given by[3]

$$\langle\Phi_i^\circ(^1L_a)|\mathscr{H}|\Phi_f^\circ(F^+\cdots L^-)\rangle = \langle\psi_{m+1}^F|f_c|\psi_{m+1}^L\rangle + \sum_{\lambda_k\neq\psi_{m+1}^F}\{\langle\psi_{m+1}^F\lambda_k|g|\psi_{m+1}^L\lambda_k\rangle - \langle\psi_{m+1}^F\lambda_k|g|\lambda_k\psi_{m+1}^L\rangle\} + \langle\psi_m^F\psi_{m+1}^F|g|\psi_{m+1}^L\psi_m^F\rangle \quad (13a)$$

$$\langle\Phi_i^\circ(^1L_a)|\mathscr{H}|\Phi_f^\circ(F^+\cdots L^-)\rangle = \frac{1}{\sqrt{2}}[\langle\psi_{m+1}^F|f_c|\psi_{m+1}^L\rangle + \sum_{\lambda_k\neq\psi_{m+2}^F}\{\langle\psi_{m+2}^F\lambda_k|g|\psi_{m+1}^L\lambda_k\rangle - \langle\psi_{m+2}^F\lambda_k|g|\lambda_k\psi_{m+1}^L\rangle\} + \langle\psi_{m+1}^F\psi_m^F|g|\psi_{m+1}^L\psi_{m-1}^F\rangle + \langle\psi_m^F\psi_{m+2}^F|g|\psi_{m+1}^L\psi_m^F\rangle - 2\langle\psi_{m+1}^F\psi_m^F|g|\psi_{m-1}^F\psi_{m+1}^L\rangle] \quad (13b)$$

For the excitation transfer, only the electron interaction integral plays an important role while both the core part and the electron interaction part may be important for the electron transfer. It is well-known that the Coulomb integral in $\langle\Phi_i^\circ|\mathscr{H}|\Phi_f^\circ\rangle$ plays the dominant role for the excitation transfer. Since the matrix elements in the r.h.s. of Eqs. (13a,b) are roughly proportional to the intermolecular overlap of MO's, the transition matrix elements for the electron transfer will be smaller than the Coulomb integrals (which do not depend on the intermolecular overlap) in Eq. (12), at a sufficiently large intermolecular distance. However, the matrix elements in Eq. (13) have a much longer range interaction than the corresponding matrix element for the triplet-triplet excitation transfer, where the electron exchange integral which is roughly proportional to the square of the intermolecular overlap plays the dominant role.

Although only the electronic part of the interaction is shown in Eqs. (12) and (13), Φ^0's are

also function of the nuclear coordinates of solute as well as the surrounding solvent molecules. As U's are adiabatic potential energies, the tunnelling may be caused essentially by the vibronic interactions between transferring electron and the nuclear motions. Presumably, the interaction process between the polarization motion (mainly orientational) of the solvent molecules and the transferring electron is the dominant mechanism for tunnelling. This sort of interaction may be large in a polar solvent such as acetonitrile, which is in accord with the observed results.

The intermolecular electron transfer by very weak interaction in the excited state, as demonstrated here, will be found out for other systems. Studies along this line are in progress.

BULLETIN OF THE CHEMICAL SOCIETY OF JAPAN VOL. 43 2758—2761 (1970)

Methane Formation in the Radiolysis of Neopentane and Isooctane

Shuichi IIDA, Rei YUGETA and Shin SATO

Department of Applied Physics, Tokyo Institute of Technology, Ookayama, Meguro-ku, Tokyo

(Received April 21, 1970)

The formation of methane and hydrogen in the γ-radiolysis of neopentane and isooctane has been studied in the presence of an electron scavenger (N_2O) and/or a radical scavenger (styrene). The *G*-value of nitrogen from neopentane solutions of nitrous oxide was found to be about twice the sum of the decrease in the *G*-values of methane and hydrogen. From isooctane solutions, $G(N_2)$ was more than three times the sum of the decrease in $G(H_2)$ and $G(CH_4)$. This can be interpreted on the assumption that a significant part of the neutralization of isooctane ions with electrons induces the fragmentation into C_4-hydrocarbons. It was also found that a part of the methane formed (0.9 *G* in neopentane and 0.2 *G* in isooctane) was not produced by the reactions of ions or methyl radicals, but by a "molecular" process, probably the decomposition of the highly-excited states.

Because of its large *G*-value, the formation of hydrogen in the radiolysis of liquid hydrocarbons has been studied by many investigators in an attempt to clarify the primary process of the radiation-induced reactions.[1,2] In the case of branched hydrocarbons, it is well known that methane formation is important and that the *G*-value of methane increases with the increase in the number of the branched chain.[3] Several papers have reported on the effect of electron scavengers on the *G*-value of the formation of methane.[4,5] However, the mechanism of the formation of methane has not been discussed systematically in connection with the primary process.

Neopentane and isooctane are typical branched hydrocarbons, and their radiolyses have been studied by several groups.[6-9] Recently, Tanno and his collaborators investigated the fragmentation process of the radical ions produced in the radiolysis of branched hydrocarbons, including neopentane and isooctane.[10,11] In this paper, we will report on the effect of electron and radical scavengers on the *G*-values of methane and hydrogen, and will discuss the mechanism of the formation of these products.

Experimental

The neopentane (Matheson Co., pure grade) was used as supplied. The isooctane (Tokyo Kasei Co., spectro grade) was used after passing it through a 1-m silica gel column. Gaschromatographic analysis showed that both hydrocarbons contained impurities of less than 0.01%. The nitrous oxide and sulfur hexafluoride (Matheson Co., pure grade) were used after bulb-to-bulb distillations. The styrene monomer (Tokyo Kasei Co., pure grade) was distilled *in vacuo* before use.

1) J. P. Manion and M. Burton, *J. Phys. Chem.*, **56**, 560 (1952).
2) J. M. Warman, K. -D. Asmus and R. H. Schuler, Advances in Chemistry Series, **82**, 25 (1968).
3) H. Yamazaki and S. Shida, *Isotopes and Radiation* (Tokyo) **2**, 119 (1959).
4) K. Shinsaka and S. Shida, This Bulletin, **40**, 2796 (1967).
5) R. A. Holroyd, Advances in Chemistry Series, **82**, 488 (1968).
6) W. H. Taylor, S. Mori and M. Burton, *J. Amer. Chem. Soc.*, **82**, 5817 (1960).
7) R. A. Holroyd, *J. Phys. Chem.*, **65**, 1352 (1961).
8) J. A. Knight, R. L. McDaniel, R. C. Palmer and F. Sicilio, *ibid.*, **65**, 2109 (1961).
9) T. Kudo and S. Shida, *ibid.*, **67**, 2871 (1963).
10) K. Tanno, T. Miyazaki, K. Shinsaka and S. Shida, *ibid.*, **71**, 4290 (1967).
11) K. Tanno, S. Shida and T. Miyazaki, *ibid.*, **72**, 3496 (1968).

Irradiation samples were prepared by repeated freeze-and-thaw cycles. The samples (2 or 10 m*l*), sealed in glass tubes, were irradiated by ^{60}Co-γ rays at a dose rate of 1.25×10^{6} R/hr. All the additives were assumed to be completely soluble, because the gas-phase volume above the irradiation liquid was less than a half of the liquid volume.

Non-condensable gas at 77°K was collected by a Toepler pump, and its amount measured by means of a gas buret. A cuprous oxide furnace at 240°C was used to combust hydrogen into water, which is condensable in a liquid nitrogen trap. The remainder (methane and nitrogen) was analyzed by gas-chromatography. The column used contained activated charcoal (2 m).

Results and Discussion

Neopentane. As is shown in Fig. 1, the *G*-value of nitrogen increased with an increase in the concentration of nitrous oxide and did not attain a limiting value even at 0.8 mol/*l*, the highest concentration examined. This is a typical trend observed in the charge scavenging. The *G*-values of methane and hydrogen decreased with an increase in the concentration of nitrous oxide and seemed to level off at 2.6 and 0.8 respectively.

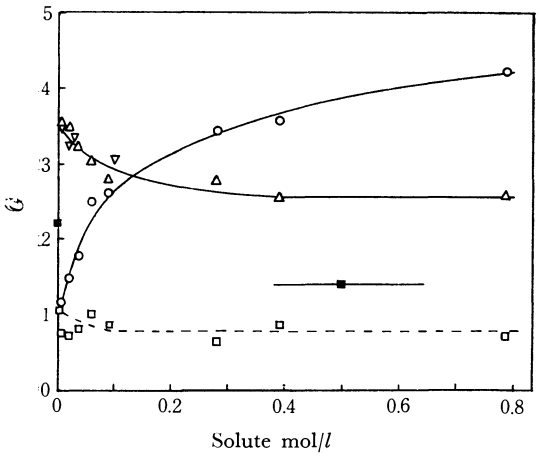

Fig. 1. *G*-Values of nitrgen (○), methane (△) and hydrogen (□) from neopentane solutions of nitrous oxide and the *G*-value of methane (▽) from SF_6 solutions. The irradiation dose is 2.0×10^{20} eV/m*l* except for (■) which is $G(H_2)$ obtained with the irradiation dose of 1.7×10^{18} eV/m*l*.

Table 1. Dose dependence of $G(H_2)$ from a neopentane solution

Additive	Irradiation dose 10^{18} eV/m*l*	$G(H_2)$
None	1.1	2.2
	1.7	2.2
	78	1.2
	115	1.1
0.4 mol/*l* N_2O	1.7	1.4

However, these values may be somewhat underestimated because the irradiation dose used for the data in Fig. 1 is not low enough to disregard the build-up of radical scavengers such as isobutene during the radiolysis.[7] The data shown in Table 1 were obtained with much lower irradiation doses. Obviously, the *G*-value of hydrogen is very much dependent upon the dose, as has already been reported by Holroyd.[7] The dose dependence of $G(CH_4)$ was, however, found to be small. This is consistent with the observation of Holroyd. Therefore, the decreases in the *G*-values of methane and hydrogen in the presence of 0.4-mol/*l* N_2O may be estimated to be 0.9 (=3.5−2.6) and 0.8 (=2.2−1.4) respectively. The sum of these values (0.9+0.8) is nearly equal to a half of the *G*-value of nitrogen (3.6/2) from a 0.4-mol/*l* N_2O solution.

The effect of sulfur hexafluoride was also examined. The results are plotted in Fig. 1. The effects of the two electron scavengers on the *G*-value of methane are almost the same. This observation is compatible with the conclusion that the electron scavenging process in the radiolysis of cyclohexane is diffusion-controlled.[12]

Table 2. The effect of styrene monomer on the *G*-values of products from neopfntane solutions of nitrous oxide

N_2O mol/*l*	Styrene mol/*l*	$G(H_2)$	$G(CH_4)$	$G(N_2)$
0	0.43	0.63	1.04	0
0.52	0.26	0.66	1.24	3.97
0.53	0.43	0.64	0.91	3.98
0	0.086	0.85	1.50	0

Use was made of the styrene monomer as a radical scavenger. As is shown in Table 2, the *G*-values of methane and hydrogen decreased rapidly with an increase in the concentration of styrene and leveled off at 0.9 and 0.6 respectively, while the *G*-value of nitrogen was not affected by the presence of styrene. These results suggest that the main precursor of methane is the methyl radical, whose *G*-value is estimated to be 2.6 (=3.5−0.9). Holroyd and Klein experimented with the radiolysis of neopnetane in the presence of iodine and found the *G*-value of methyl iodide to be 2.3.[13] The decrease in $G(H_2)$ from 2.2 to 0.6 due to the presence of styrene may be explained similarly. The difference, $\Delta G=1.6$, probably corresponds to the *G*-value of the thermal hydrogen atoms produced.

According to Tanno *et al.*,[10] primarily-produced

12) S. Sato, T. Terao, M. Kono and S. Shida, This Bulletin, **40**, 1818 (1967).

13) R. A. Holroyd and G. W. Klein, *J. Amer. Chem. Soc.*, **87**, 4983 (1965).

parent ions in the radiolysis of liquid neopentane can be classified into two types. One consists of highly-excited ions which decompose instantaneously into a methyl radical and a *t*-butyl ion, even in the liquid phase; the other consists of stable neopentane ions which are subject to charge neutralization. They estimated the *G*-value of the former process to be 1.0.

On the basis of the results presented above, we have tentatively constructed the following reaction mechanism for the formation of methane and hydrogen:

$$(CH_3)_3CCH_3 \rightsquigarrow (CH_3)_3C^+ + CH_3 + e^- \quad (1)\ G\sim 1.0$$

$$\rightsquigarrow (CH_3)_3CCH_3^+ + e^- \quad (2)\ \sim 2.2$$

$$\rightsquigarrow CH_4 + (CH_3)_2C{=}CH_2 \quad (3)\ \sim 0.9$$

$$\rightsquigarrow H_2 + \text{residue} \quad (4)\ \sim 0.6$$

$$(CH_3)_3CCH_3^+ + e^- \rightarrow (CH_3)_3C + CH_3 \quad (5)\ \sim 1.6$$

$$\rightarrow (CH_3)_3CCH_2 + H \quad (6)\ \sim 0.6$$

$$(CH_3)_3C^+ + e^- \rightarrow H + (CH_3)_2C{=}CH_2 \quad (7)\ \sim 1.0$$

$$CH_3 + (CH_3)_3CCH_3 \rightarrow CH_4 + (CH_3)_3CCH_2 \quad (8)$$

$$H + (CH_3)_3CCH_3 \rightarrow H_2 + (CH_3)_3CCH_2 \quad (9)$$

Here, the numbers shown after each reaction are the estimated *G*-values. When nitrous oxide is present in the system, nitrogen becomes an important product. As has been assumed in the radiolysis of the N_2O - cyclohexane solution, if $G(N_2)$ is twice the *G*-value of electrons scavenged by N_2O,[12] the $G(N_2)$ from the N_2O - neopentane solution should be equal to twice the sum of the decreases in $G(CH_4)$ and $G(H_2)$ for according to the above mechanism, each electron should produce a methyl radical or a hydrogen atom when they are neutralized. In fact, this relationship was observed, as has already been stated.

The reactions (3) and (4) are very tentative at present. In their studies of the radiolysis of olefins, Hatano and his collaborators discovered that hot-hydrogen-atom reactions play an important role in the formation of hydrogen and suggested that reactive species are formed from the superexcited state of the olefin.[14] In the radiolysis of neopentane, therefore, the corresponding reactive species might be hot methyl radicals and hot hydrogen atoms, which in turn give rise to the reactions (3) and (4).

Isooctane. Exactly the same experiments as those of neopentane were done with isooctane. The results are shown in Figs. 2 and 3 and in Table 3.

The isooctane molecule has two C–C bonds, whose splitting does not lead to the formation of a methyl radical. This is an essential difference from neopentane when considering the formation of methane. According to Tanno *et al.*,[10] highly-excited isooctane ions decompose into C_4-fragments, but the *G*-value is reported to be only 0.36. On the other hand, the *G*-values of isobutane and isobutene from isooctane have been reported to be about 3.0.[8] One of the possible origins is the following neutralization reaction:

$$iso\text{-}C_8H_{18}^+ + e^- \rightarrow t\text{-}C_4H_9 + iso\text{-}C_4H_9 \quad (10)$$

If so, the *G*-value of the electrons consumed for this reaction is estimated to be 1.1 (=3.0/2−0.36).

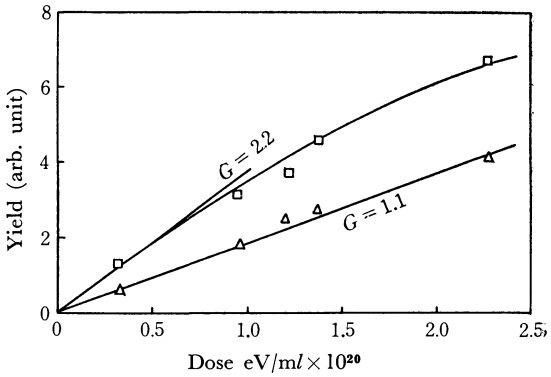

Fig. 2. Irradiation does dependence of *G*-values of hydrogen (□) and methane (△) from isooctane.

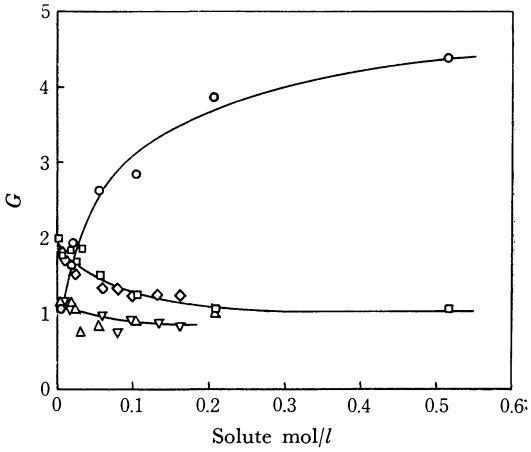

Fig. 3. *G*-Value of nitrogen (○), hydrogen (□) and methane (△) from isooctane solutions of nitrous oxide and *G*-values of hydrogen (◇) and methane (▽) from SF_6 solutions. The irradiation dose is 1.5×10^{20} eV/ml.

14) Y. Hatano, S. Shida and S. Sato, This Bulletin, **41**, 1120 (1968).

TABLE 3. THE EFFECT OF STYRENE MONOMER ON THE G-VALUES OF GASEOUS PRODUCTS FROM ISOOCTANE SOLUTIONS OF NITROUS OXIDE

N_2O mol/l	Styrene	$G(H_2)$	$G(CH_4)$	$G(N_2)$
0	0.43	0.83	0.38	0
0.52	0.43	0.70	0.23	4.6

As is shown in Fig. 3, the decrease in $G(H_2+CH_4)$ due to the presence of electron scavengers is about 1.2 and the corresponding G-value of nitrogen is more than 4.0. If $G(N_2)$ is equal to twice the G-value of the electrons scavenged by nitrous oxide, the following reaction mechanism may be constructed:

$$iso\text{-}C_8H_{18} \rightsquigarrow C_4H_9^+ + C_4H_9 + e^- \quad (11) \quad \sim 0.4$$
$$\rightsquigarrow C_8H_{18}^+ + e^- \quad (12) \quad \sim 3.1$$
$$\rightsquigarrow H_2 + \text{residue} \quad (13) \quad \sim 0.7$$
$$\rightsquigarrow CH_4 + \text{residue} \quad (14) \quad \sim 0.2$$
$$C_8H_{18} + e^- \rightarrow 2C_4H_9 \quad (10) \quad \sim 1.1$$
$$\rightarrow CH_3 + C_7H_{15} \quad (15) \quad \sim 0.9$$
$$\rightarrow H + C_8H_{17} \quad (16)$$
$$C_4H_9^+ + e^- \rightarrow H + C_4H_8 \quad (17) \quad \sim 1.5$$

Here, the G-value of the electrons was assumed to be 3.5 in order to make the G-values of the products self-consistent. The reactions (13) and (14) are tentative as the reactions (3) and (4) in the radiolysis of neopentane.

BULLETIN OF THE CHEMICAL SOCIETY OF JAPAN VOL. 43 2761—2766 (1970)

Mechanism of Redox Surface Reaction between Wüstite and CO_2 or CO

Seiichi KURIHARA, Kazuo FUEKI, Takashi MUKAIBO and Yasuo WADA

Department of Industrial Chemistry, Faculty of Engineering, The University of Tokyo, Hongo, Bunkyo-ku, Tokyo

(Received April 25, 1970)

The redox reaction between thin wüstite foil and CO_2 or CO was studied by means of a microbalance in a temperature range 900—1075°C. It was found that the reaction at the gas-wüstite interface is rate-controlling and that the reaction rate is expressed as

$$V_{ox} = k_O P_{CO_2} a_O^{-m/3} \quad \text{and} \quad V_{red} = k_O' P_{CO} a_O^{n/3},$$

where a_O is the oxygen activity of wüstite, and m and n are 2.1—2.2 and 0.8—1.2, respectively. On the basis of the theory by Kobayashi and Wagner, the most predominant mechanism is concluded to be

$$CO_2 + 2\ominus \rightleftarrows CO + O^{2-}$$

Actigation energies for k_O and k_O' were 35+3 and 32+3 kcal/mol, respectively.

In the redox reaction at the gas-solid interface, chemical species in the solid phase take part in the reaction as well as gaseous reactants. Therefore, in order to elucidate the reaction mechanism, it is necessary to determine the reaction rate as a function not only of the partial pressure of reactant gases but also of the activity of chemical species in the solid phase. Kobayashi and Wagner[1] constructed electrochemical cells, such as Ag|AgI|Ag_2S|Pt and Cu|CuI|Cu_2S|Pt, and measured the rate of reduction of the sulfides by hydrogen under the controlled metal activity by using the coulometric titration technique. They also proposed a new theory whereby the experimental results can be explained. Thereafter, new experimental techniques such as the isotopic exchange method[2,3] and the chemical relaxation method[4] have been developed in addition to the coulometric titration technique.

Grabke[2] has studied the exchange reaction between $^{14}CO_2$ and ^{12}CO on the wüstite surface at 800—985°C and found that the exchange rate is a function not only of the partial pressures of CO_2 and CO but also of the oxygen activity of wüstite. He has also discussed the reaction mechanism on the basis of the Kobayashi-Wagner theory.

In order to investigate the mechanism of the reaction at the gas-solid interface, we have devised

1) H. Kobayashi and C. Wagner, *J. Chem. Phys.*, **26**, 1609 (1957).

2) H. J. Grabke, *Ber. Bunsenges, Physik. Chem.*, **60**, 48, (1965).

3) K. Fueki, H. Inaba and T. Mukaibo, This Bulletin, **43**, 23 (1970).

4) S. Stotz, *Ber. Bunsenges, Physik. Chem.*, **70**, 37 (1966).

a new technique which uses a microbalance and studied the redox reaction between wüstite and CO_2 or CO. The purpose of the present paper is to report the result of the study.

Experimental

a) Principle of Microgravimetric Technique. Wüstite is a metal-deficit type nonstoichiometric compound and often expressed by the chemical formula $Fe_{1-\delta}O$. The equilibrium relation between δ and $a_O(\equiv P_{CO_2}/P_{CO})$ has been determined precisely by Darken and Gurry[5] and by other investigators.[6] According to the result of their thermodynamic investigations, the homogeneous nonstoichiometric range of wüstite is fairly wide, for instance, δ ranges from 0.05—0.15 at 1000°C. Thus, the change in δ within the stable region of wüstite can be followed gravimetrically.

According to a study of iron oxidation in CO_2–CO gas mixtures,[7] the oxidation is controlled by the gas-oxide interface reaction in the initial period of oxidation where the oxide scale is thin. Therefore in the case of oxidation and reduction of wüstite, the overall reaction is expected to be controlled by the reaction on the wüstite surface, if the wüstite specimen is sufficiently thin. In such a case, the surface reaction rate can be obtained by measuring the weight change of wüstite as a function of time. When the reaction is controlled by the surface reaction, δ is constant throughout the specimen. Thus, the value of δ of wüstite at every moment can be determined by following the weight change during the run. Since there is a close relationship between δ and a , we can determine the surface reaction rate as a function of a_O.

b) Apparatus. Figure 1 shows a schematic diagram of the apparatus. The reaction tube (A) was a mullite tube, 3.6 cm in inner diameter and 72 cm long, to which upper and lower glass tubes were connected by glass joints. The upper glass tube (B) was connected to a stainless steel inner tube (C). The outer tube (D) which was also made of stainless steel, can be raised or lowered together with the balance chamber (E) above it. In order to secure a vacuum seal, an O-ring (F) was inserted between the outer stainless steel tube and the inner one. Gas was passed upward through the reaction tube. The furnace (G) was wound with Kantal wire. The temperature gradient was less than 0.2 deg/cm over the region where the specimen (H) subjected to reaction. Temperature was controlled by means of an electronic controller within +1.5°C and measured by a calibrated Pt-Pt.Rh thermocouple (I). The weight change of wüstite specimen was followed continuously by means of Cahn RG electrobalance (J).

c) Purification of Gases. CO_2 was passed successively through a $Mg(ClO_4)_2$ column and an activated copper column to remove water vapor and oxygen. CO was passed through $Mg(ClO_4)_2$ to remove water vapor and then through an activated copper column to convert O_2 into CO_2, which was absorbed in a soda lime column.

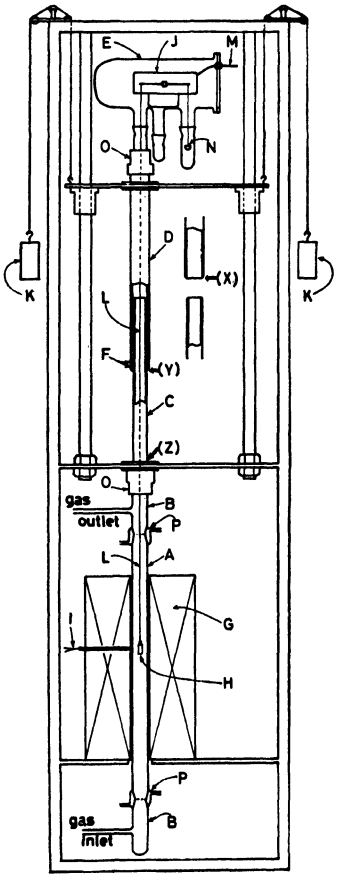

Fig. 1. Schematic diagram of the apparatus.
A: reaction tube (Mullite), B: glass tube, C: stainless steel inner tube, D: stainless steel outer tube, E: balance chamber, F: O-ring, G: furnace, H: specimen, I: thermocouple J: Cahn's RG electrobalance, K: weight, L: silica fibre, M: electric cable, N: counter weight, O: glass/stainless tube junction, P: water jacket to cool the glass/Mullite junction region.

d) Preparation of Wüstite Specimen. Wüstite specimens were prepared as follows. A rectangular coupon, approximately 1.2 cm long by 0.8 cm wide was taken from a sheet of electrolytic iron 0.14 mm thick. Results of spectroscopic analysis is shown in Table 1. A hole, 1 mm in diameter was drilled near one end of the coupon and the coupon was washed with soap and water, rinsed in alcohol, dried in a desiccator and weighed. A Pt hock was then attached through the hole. After the outer tube (D) was raised to position X so as to be detached from the inner one, the coupon was suspended from the balance with a silica fibre. The outer tube was then lowered to position Y and the reaction apparatus was evacuated. After evacuation CO_2 was admitted to the system and let to flow at a flow rate of 20 cc/min. The outer tube was then lowered to position Z in order to oxidize the iron specimen at 1050°C. When the weight reached the

5) L. S. Darken and R. W. Gurry, *J. Amer. Chem. Soc.*, **67**, 1398 (1945).

6) I. Bransky and A. Z. Hed, *J. Amer. Ceram. Soc.*, **51** (4), 231 (1968).

7) F. S. Pettit and J. B. Wagner, Jr., *Acta Met.*, **12**, 35 (1964).

Table 1. Spectroscopic analysis of electrolytic iron

Impurity	Content (ppm)	Impurity	Content (ppm)
Ni	150	Cr	10
CO	130	Si	10
Zn	110	Al	5
Mo	50	Mg	5
Cu	30	V	1
Mn	20	Pb	nil
Ca	16	B	nil

value corresponding to the nearly stoichiometric ratio of iron to oxygen, the oxidized specimen was raised from the hot zone by raising the outer tube to position Y and the furnace temperature was changed to the desired reaction temperature. Then the reaction apparatus was evacuated and a CO_2–CO mixture whose CO_2/CO ratio was 2/3 was introduced to the system. The oxidized specimen was lowered to the furnace and equilibrated with the gas mixture at the reaction temperature. When the weight became constant, the metal deficit, δ, was calculated from the weight change the specimen before and after oxidation. Data of the present work agreed well with Darken's. The thickness of wüstite specimen was about 0.3 mm and the average grain size was about 100 μ.

e) Measurement of Surface Reaction Rate. After the reaction apparatus was evacuated, CO_2 gas desired partial pressure was introduced to the system to oxidize the wüstite. Since the length of time needed for the introduction of gas was less than 15 sec, weight change during the introduction was negligibly small. Thus, the value of log a of wüstite at the beginning of oxidation was thought to be equal to log 2/3. When the weight of the specimen reached the value corresponding to log a =0.6, CO_2 was removed from the system to stop the oxidation, and CO of desired partial pressure was introduced to initiate the reduction. In this way, the same wüstite specimen was used repeatedly for the kinetic measurement of oxidation in CO_2 and reduction in CO at desired partial pressures in a range of log a_O=−0.18—0.6. The wüstite specimen was kept in the furnace during the kinetic measurement to prevent the wüstite specimen from decomposing by quenching, since the wüstite phase is unstable below 570°C. After repetition of oxidation and reduction, a gas mixture of P_{CO}/P_{CO}=2/3 was introduced into the reaction apparatus to equilibrate the wüstite specimen with the gas mixture. A comparison of the equilibrium weight at the end of the run with that at the beginning showed the difference between the two weights to be less than 10% of the total weight change of the oxidation or reduction of wüstite.

The measurement was carried out in a temperature range 950—1075°C and at pressures of 70—300 mmHg.

Results

Typical oxidation curves of wüstite in CO_2 and reduction curves in CO are shown in Figs. 2 and 3. respectively. In these figures the scale of δ is also given. The wüstite specimen employed in this

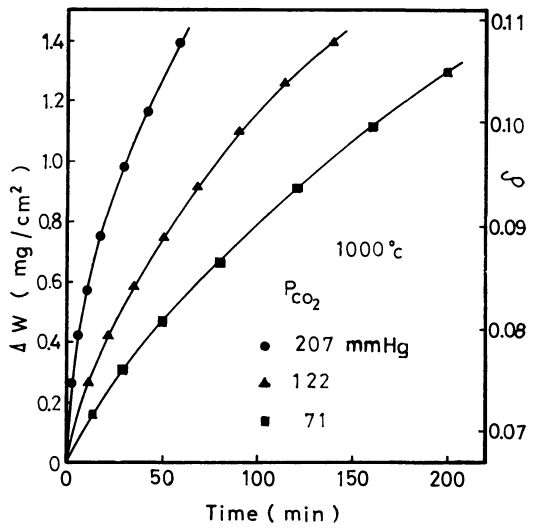

Fig. 2. Oxidation curves of wüstite by CO_2.

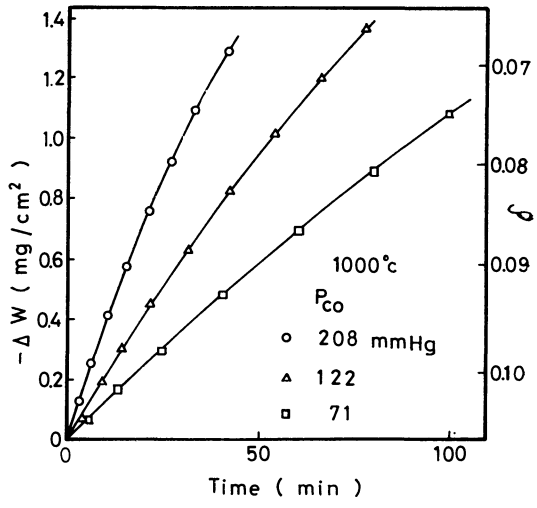

Fig. 3. Reduction curves of wüstite by CO.

experiment was so thin that the overall reaction is supposed to be controlled by the surface reaction. It is thought that the gradient of δ is not formed in the specimen, and the surface reaction rate, V, at a specified value of δ is determined from the slope of tangent drawn to the curve at the δ value. Since there is a relationship between the oxygen activity in wüstite (a_0) and δ, the relationship between V and a_0 is determined.

Figure 4 shows the plots of log V *vs.* log a_O. In the case of reduction, the plots of log V *vs.* log a_0 show a good linearity. In the case of oxidation, an abnormally high rate was observed in the initial period of oxidation, especially at high pressures of CO_2. However, even in such cases the reduction performed immediately after the oxidation showed no abnormality. At low CO_2 pressures,

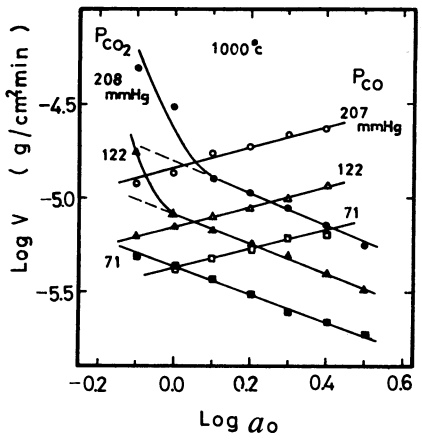

Fig. 4. Relationship between V and a_O.

the plots of log V *vs.* log a_0 give a good linearity. The cause of abnormally high rate of oxidation has not been elucidated yet.

Figures 5 and 6 show the dependence of V on partial pressures of CO_2 and CO at constant a_0, respectively. V linearly depends on gas pressures. This clearly shows that the overall reaction is controlled by the reaction at the surface.

Accordingly, the rate of oxidation, V_{red}, and the rate of reduction, V_{red}, are expressed in terms of P_{CO_2}, P_{CO} and a_O as follows:

$$V_{ox} = k_O P_{CO_2} a_O^{-m/3} \quad (1)$$

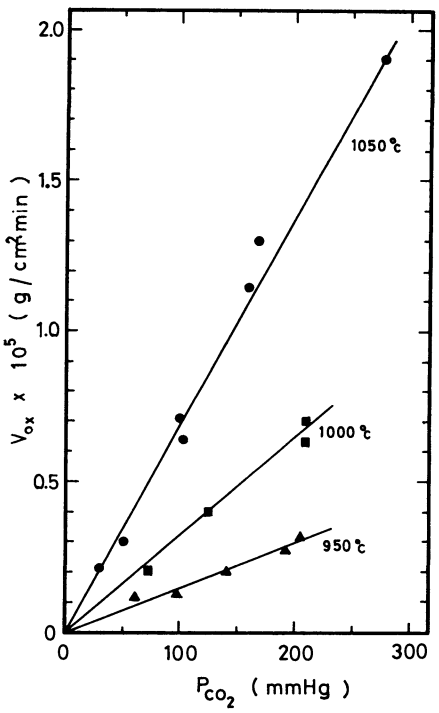

Fig. 5. Dependence of oxidation rate, V_{ox}, on partial pressure of CO_2, P_{CO_2} at $a_O=25$.

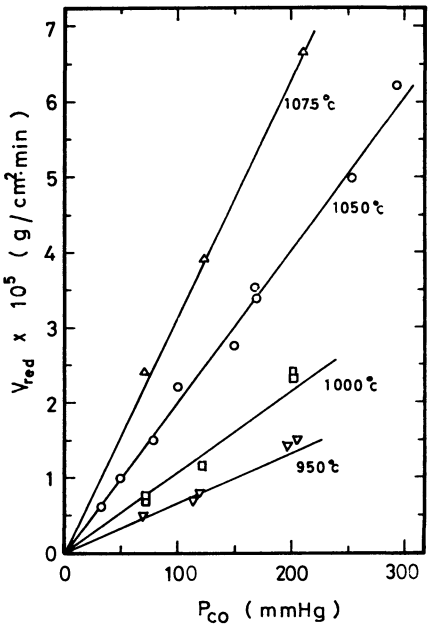

Fig. 6. Dependence of reduction rate, V_{red}, on partial pressure of CO, P_{CO} at $a_O=25$.

$$V_{red} = k_O' P_{CO} a_O^{n/3} \quad (2)$$

The values of m and n at various temperatures are listed in Table 2. It is noteworthy that m is approximately 2 and n is approximately 1. Rate constants k_O and k_O' defined in Eqs. (1) and (2) were obtained by extrapolating the linear relationship in Figs. 5 and 6 to the gas pressure of 1 atm. and substituting 2.5 for a_O. The Arrhenius plots of k_O and k_O' obtained in this way are shown in Fig. 7. From the definition of $a_O \equiv P_{CO_2}/P_{CO}$ and the equilibrium condition, $V_{ox}=V_{red}$, k_O and k_O' should be equal to each other. However, as seen in Fig. 7, a discrepancy of about 25% exists between k_O and k_O'. In the case of oxidation, experimental results showed a rather large deviation at high pressures of CO_2. Therefore, the value of k_O is thought to be less accurate than the value of k_O'. Activation energy for k_O and k_O' are 35.0+3 kcal/mol and 33.0±3 kcal/mol, respectively. Grabke[2] found 33.5±2 kcal/mol as the activation energy of of dissociative adsorption of CO_2 on wüstite in the kinetic study of isotopic exchange between $^{14}CO_2$ and ^{12}CO at temperatures from 800°C to 983°C.

TABLE 2. VALUES OF m AND n

Temp. (°C)	m	n
950	2.1	1.2
975	2.1	1.1
1000	2.2	1.3
1025	2.1	0.9
1050	2.2	1.2
1075	—	0.8

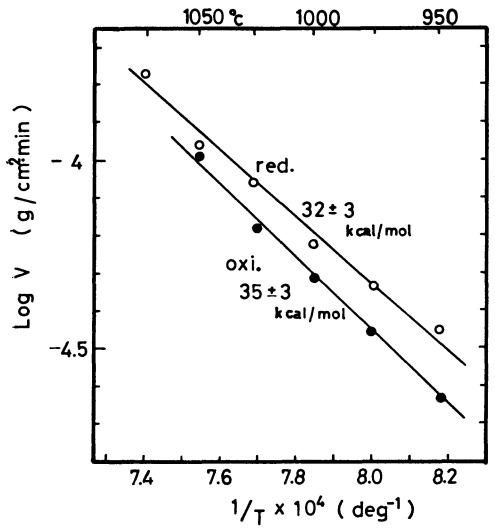

Fig. 7. Arrhenius plots of k_O and k'_O.

The present activation energy is nearly the same as Grabke's.

Discussion

The reaction mechanism can be discussed on the basis of the Kobayashi-Wagner theory as follows. The reaction between CO_2 and CO on the wüstite surface proceeds by the parallel reactions

$$CO_2 \rightleftarrows CO + O \quad (3.A)$$

$$CO_2 + \ominus \rightleftarrows CO + O^- \quad (3.B)$$

$$CO_2 + 2\ominus \rightleftarrows CO + O^{2-} \quad (8.C)$$

where O, O^-, and O^{2-} represent adsorbed oxygen atoms, monovalent oxygen ions and divalent oxygen ions, respectively, and $\ominus$ electrons in wüstite.

Assuming that the adsorbed oxygen atoms and oxygen ions are in equilibrium with those in bulk of wüstite and that the adsorption of CO_2 and CO is weak, we can write the rate equations as

$$V_A = k_1 P_{CO_2} - k_1' P_{CO} a_O \quad (4.A)$$

$$V_B = k_2 P_{CO_2} a_\ominus - k_2' P_{CO} a_{O^-} \quad (4.B)$$

$$V_C = k_3 P_{CO_2} a_\ominus^2 - k_3' P_{CO} a_{O^{2-}} \quad (4.G)$$

where a_O, a_{O^-}, $a_{O^{2-}}$ and $a_\ominus$ denote the activities of respective species.

Assuming the equilibrium among positive holes ($\oplus$), cation vacancies ($Fe_{\square}''$) and oxygen atoms in wüstite, we obtain

$$O \rightleftarrows FeO + Fe_{\square}'' + 2\oplus$$

$$\frac{a_{Fe_{\square}''} a_\ominus^2}{a_O} = k_1 \quad (5)$$

Because of the low concentration of $Fe_{\square}''$ and $\oplus$, we have

$$x_{Fe_{\square}''} \approx a_{Fe} \quad (6)$$

$$x_\oplus \approx a_\oplus \quad (7)$$

where x denotes the concentration.

From the charge neutrality condition

$$2x_{Fe_{\square}''} = x_\oplus \quad (8)$$

it follows that

$$a_\oplus = K_2 a^{1/3} \quad (9)$$

Other equilibrium conditions and mass action laws are

$$\ominus + \oplus \rightleftarrows \text{Null}$$

$$a_\ominus \cdot a_\oplus = K_3 \quad (10)$$

$$O^- \rightleftarrows O + \ominus$$

$$a_O \cdot a_\ominus = K_4 a_{O^-} \quad (11)$$

$$O^{2-} \rightleftarrows O + 2\ominus$$

$$a_O \cdot a_{\ominus^2} = = K_5 a_{O^{2-}} \quad (12)$$

Combination of Eqs. (9), (10), (11) and (12) yields

$$a_\ominus = K_6 a_O^{-1/3}$$

$$a_{O^-} = K_7 a_O^{2/3} \quad (14)$$

$$a_{O^{2-}} = K_8 a_O^{1/3} \quad (15)$$

Inserting these equations into Eqs. (4.A)—(4.C), we obtain

$$V_A = k_1 P_{CO_2} - k_1' P_{CO} \quad (16.A)$$

$$V_B = k_2 K_6 P_{CO_2} a_O^{-1/3} - k_2' K_7 P_{CO} a_O^{2/3} \quad (16.B)$$

$$V_C = k_3 K_6^2 P_{CO_2} a^{-2/3} - k_3' K_8 P_{CO} a_O^{1/3} \quad (16.C)$$

The generalized rate equation is

$$V = k_O P_{CO_2} a_O^{-m/3} - k_O' P_{CO} a_O^{3/n} \quad (17)$$

where m and n are integers characteristic of reaction mechanism as listed in Table 3. The first term

Table 3. Predominant reaction mechanism and values of m and n

Mechanism	m	n
(A) $CO_2(ads) \rightleftarrows CO(ads) + O(ads)$	0	3
(B) $CO_2(ads) + \ominus \rightleftarrows CO(ads) + O^-(ads)$	1	2
(C) $CO_2(ads) + 2\ominus \rightleftarrows CO(ads) + O^{2-}(ads)$	2	1

on the right side represents the oxidation rate of wüstite by CO_2 and the second term represents the reduction rate of wüstite by CO, namely,

$$V_{ox} = k_O P_{CO_2} a^{-m/3} \quad (18)$$

$$V_{red} = k_O' P_{CO} a_O^{n/3} \quad (19)$$

In the present work, values of m and n were determined experimentally, so we can conclude the predominant mechanism of the three. From a comparison of Tables 2 and 3 it is concluded that the most predominant mechanism of the surface reaction is

$$CO_2 + 2\ominus \rightleftarrows CO + O^{2-}$$

Summary

(1) Oxidation of wüstite by CO_2 and reduction by CO in a homogeneous range of wüstite were

studied kinetically by the microgravimetric method. The reactions were found to be countrolled by gas-oxide interface reaction.

(2) The surface reaction rate was determined as a function of gas pressure and oxygen activity in wüstite, a_O, in a temperature range 950—1075°C at pressures of 70—300 mmHg.

(3) The oxidation rate in CO_2 and reduction rate in CO were expressed respectively as

$$V_{ox} = k_O P_{CO_2} a^{-m/3} \qquad (m = 2.1—2.2)$$

$$V_{red} = k_O' P_{CO} a_O^{n/3} \qquad (n = 0.8—1.2)$$

(4) Activation energies for rate constants k_O and k_O' were 35±3 kcal/mol and 32±3 kcal/mol respectively and coincided with those obtained by Grabke.

(5) From Wagner's theory the predominant mechanism was determined as the two electron transfer mechanism:

$$CO_2 + 2\ominus \rightleftarrows CO + O^{2-}$$

Support by Takeda Science Foundation is gratefully acknowledged.

BULLETIN OF THE CHEMICAL SOCIETY OF JAPAN VOL. 43 2766—2771 (1970)

Ionic Processes in the Radiolysis of Nitrous Oxide. The Effect of Electron Scavenger and Rare Gas Sensitization

Satoshi TAKAO and Shoji SHIDA

Laboratory of Physical Chemistry, Tokyo Institute of Technology, Meguro-ku, Tokyo

(Received April 28, 1970)

The effect of electron scavenger (SF_6) on the radiolysis products of N_2O was examined. The sensitization of N_2O by various rare gases was also measured. In the presence of an electron scavenger we got 3.0 for the value of $-\Delta G(-N_2O)$ in good agreement with the value of $G(e^-)$ for N_2O. In the experiments of Xe or Kr containing small amounts of N_2O, the $G(-N_2O)$ values were nearly equal to the respective $G(e^-)$ values for the rare gases, and the addition of SF_6 to the Xe-N_2O system almost completely inhibited nitrogen formation. The results show that one electron decomposes just one molecule of N_2O. This fact can not be accounted for by the hitherto assumed mechanism, and a new mechanism involving N_2O^- is proposed for ionic processes in the radiolysis of N_2O. In the N_2O-rare gas mixtures of various compositions, the sensitized yields of N_2O decomposition per 100 eV energy absorbed by rare gases were divided into two groups, *e.g.*, the yields from He, Ne mixtures were about twice as large as those from Ar, Kr and Xe mixtures. This result is discussed in terms of charge transfer and the Penning ionization.

Nitrous oxide has been currently used as an effective electron scavenger in the study of liquid[1] and gaseous[2] hydrocarbon radiolysis. In these systems, the nitrogen yields which are considerably in excess of the estimated yields of electrons have been found, and many discussions are raised on the mechanism of the radiolytic formation of nitrogen from nitrous oxide in hydrocarbons.[3]

The study of the radiolysis of nitrous oxide in the gas phase has long received considerable attention in relation to the gas dosimeter, and a number of determinations of the radiolysis products have been reported,[4] but nothing definite has yet been established about the reaction mechanism.

The present study was undertaken in order to obtain a better insight of the mechanism for ionic processes in the radiolysis of N_2O by using SF_6 as an electron scavenger and various rare gases, especially Xe, as electron supplier.

Experimental

Nitrous oxide from a cylinder supplied by the Takachiho-Shoji Co. was freed from nitrogen and oxygen by careful degassing.

The gases SF_6 and CO_2 were used after the usual degassing. The rare gases were of high purity and used as obtained, the stated purities being 99.99%, 99.99%, 99.999%, 99.9% and 99.9% for He, Ne, Ar,

1) S. Sato, R. Yugeta, K. Shinsaka and T. Terao, This Bulletin, **39**, 156 (1966); N. H. Sagert and A. S. Blair, *Can. J. Chem.*, **45**, 1351 (1967).

2) for example, N. H. Sagert, R. W. Robinson and A. S. Blair, *Can. J. Chem.*, **46**, 3511 (1968).

3) for example, J. M. Warman, *J. Phys. Chem.*, **71**, 4066 (1967).

4) for example, J. A. Hearne and R. W. Hummel, *Radiat. Res.*, **15**, 254 (1961); G. R. A. Johnson, *J. Inorg. Nucl. Chem.*, **24**, 461 (1962); F. T. Jones and T. J. Sworski, *J. Phys. Chem.*, **70**, 1546 (1966).

Kr and Xe, respectively.

Irradiations were done in a cylindrical vessel of about 50 cc with ^{60}Co γ-rays at 25°C at a dose rate of 3.0×10^{19} eV/g/hr and the highest dose used was 7.2×10^{20} eV/g.

The initial products of radiolysis of nitrous oxide are N_2, O_2 and NO, but NO and O_2 were known to react to form NO_2 in a cold trap[5] and so the products, N_2 and O_2, after the cold trap reaction were measured by gas chromatography (a 5 m column of Molecular Sieve-5 A at room temperature). The initial amounts of NO formed were calculated stoichiometrically from the measured amounts of N_2 and O_2 and the initial amount of nitrous oxide.

The total energy absorbed in pure N_2O or mixtures was measured by the Fricke dosimeter making appropriate corrections for electron density. In the calculation of the total energy absorbed in these systems and the energy partition in mixtures, especially in the rare gas sensitization experiments, it would be better to use the relative stopping powers and the so-called effective atomic numbers suggested by Klots.[6] The results brought about slightly larger G-values (about 15% for all G_{sens}-values described below), but this does not change our conclusion. We advance discussions using the G-values obtained by the usual electron density corrections.

Results

The initial products, N_2, O_2 and NO from pure nitrous oxide of 50 to 400 mmHg pressures at room temperature have been determined. The observed G-values at 200 mmHg were $G(N_2)=10.1$, $G(O_2)=3.8$ and $G(NO)=5.1$ which were almost independent of pressure within experimental error. From these values we get 12.6 for the value of $G(-N_2O)$ in good agreement with those of Sworski[4] and other earlier investigators.

Although nitrous oxide is known to be an effective electron scavenger, SF_6 is much more effective in the gas phase,[7] and we could estimate the role of electrons in the radiolysis of N_2O by the addition of SF_6 to N_2O. The effect of adding SF_6 to N_2O of a constant pressure of 200 mmHg is shown in Fig. 1. The addition of very small amounts of SF_6 rapidly reduced the yields of N_2, O_2 and NO, which then remained constant on further addition of SF_6. The observed decreases were $-\Delta G(N_2)=2.1$, $-\Delta G(O_2)=0.6$ and $-\Delta G(NO)=1.8$, and thus the value of $-\Delta G(-N_2O)$ is calculated to be 3.0.

In Fig. 2 are shown the results with CO_2[8] which

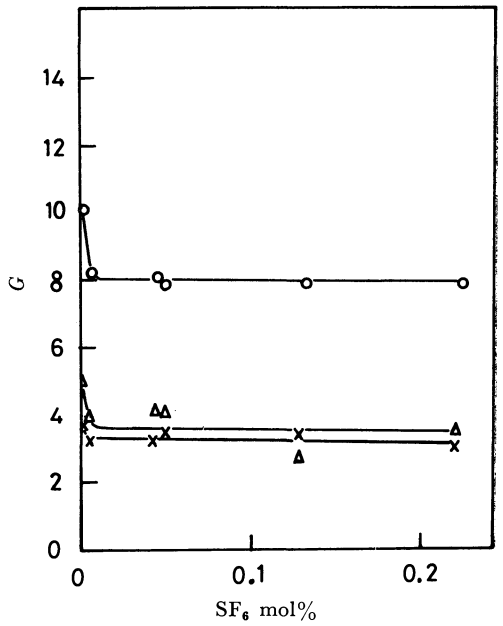

Fig. 1. The effect of adding SF_6 to N_2O on the yields of the products: ○, N_2; ×, O_2; △, NO.

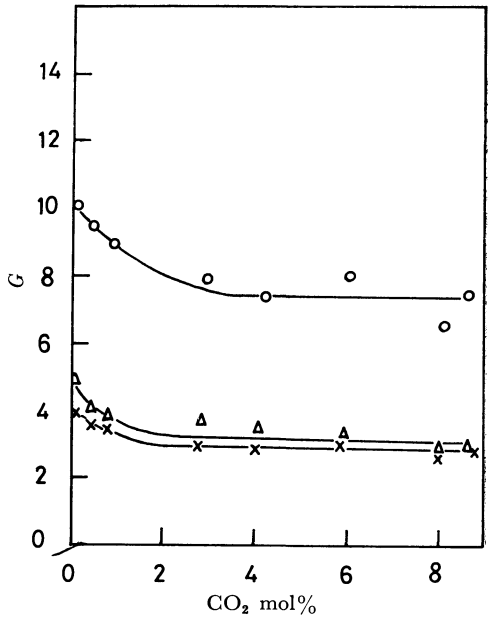

Fig. 2. The effect of adding CO_2 to N_2O: ○, N_2; ×, O_2; △, NO.

are similar to the above except for much slower levelling off of the G-values.

Figures 3 and 4 show, respectively, the results of the addition of N_2O to Xe and Kr of a constant pressure of 600 mmHg. All these values are corrected for the products formed by the direct radiolysis of N_2O.

Next, the effect of adding SF_6 to Xe including 5 mol% of N_2O was examined. Addition of

5) P. Burtt and J. F. Kircher, *Radiat. Res.*, **9**, 1 (1958).
6) C. E. Klots, *J. Chem. Phys.*, **46**, 3468 (1967).
7) G. R. A. Johnson and J. M. Warman, *Trans. Faraday Soc.*, **61**, 1709 (1965).
8) There are few reports in which CO_2 is used as an electron scavenger in the gas phase and no evidence in the electron attachment experiments that CO_2 is an electron scavenger (L. C. Christophorou and J. A. D. Stockdale, *J. Chem. Phys.*, **48**, 1956 (1968)). The results in Fig. 2 show nearly the same G-values as those in Fig. 1. In the present system, CO_2 may act as an electron scavenger.

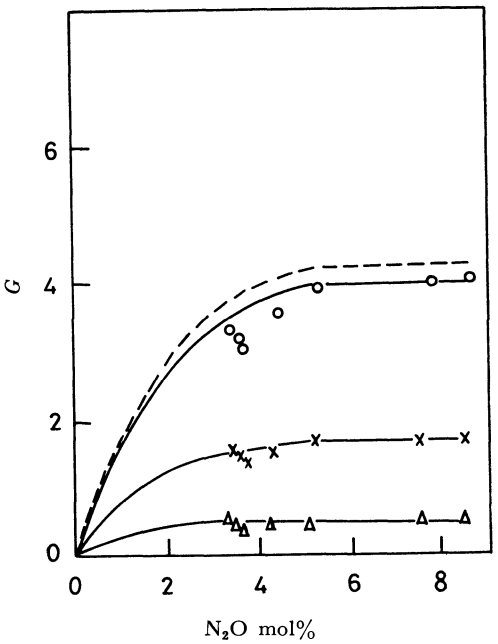

Fig. 3. The effect of adding N_2O to Xe: ○, N_2; ×, O_2; △, NO; ----, yields for $-N_2O$. In this figure and Fig. 4, corrections were made for the products arising from the direct radiolysis of N_2O.

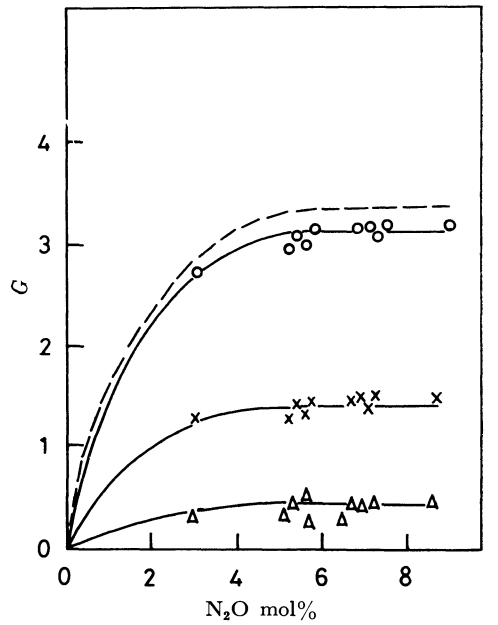

Fig. 4. The effect of adding N_2O to Kr: ○, N_2; ×, O_2; △, NO; ----, yields for $-N_2O$.

SF_6 of only 0.1% with respect to Xe completely inhibits nitrogen formation, indicating the electrons to be the primary precursor of products (Fig. 5).

We further studied the radiolysis of N_2O with

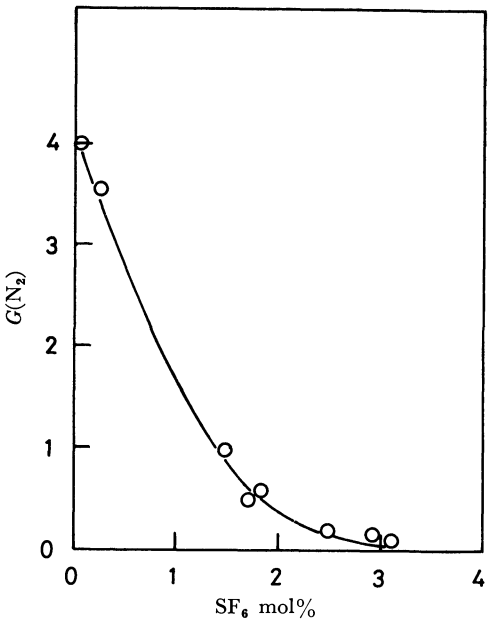

Fig. 5. The effect of adding SF_6 to Xe including 5 mol.% of N_2O. In this figure, SF_6 mol% shows the value with respect to N_2O.

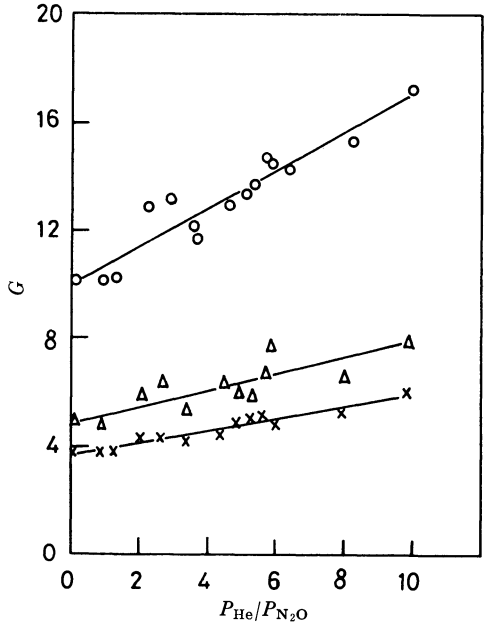

Fig. 6. Sensitization by He: ○, N_2; ×, O_2; △, NO. $P_{N_2O}=50$ mmHg.

various rare gases including those of higher ionization energies and metastable excitation energies. In Figs. 6—10, the results are shown with various ratios of rare gas to N_2O; the G-values are expressed as the number of molecules of products formed per 100 eV absorbed directly by N_2O. The amounts of N_2, O_2 and NO all increased linearly in the system of He and Ne, while in the

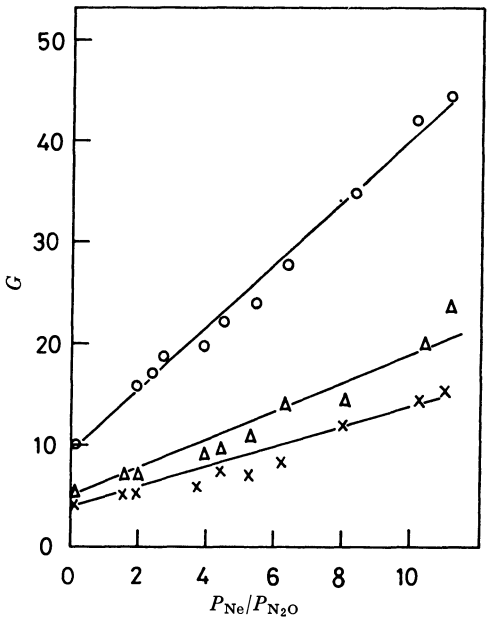

Fig. 7. Sensitization by Ne: ○, N_2; ×, O_2; △, NO. P_{N_2O} = 50 mmHg.

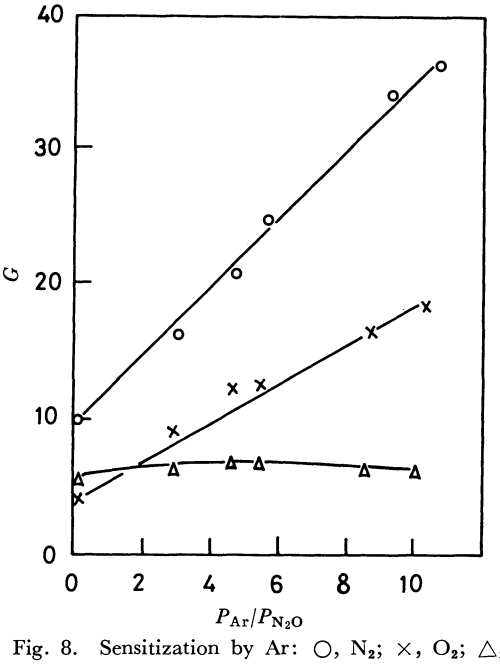

Fig. 8. Sensitization by Ar: ○, N_2; ×, O_2; △, NO. P_{N_2O} = 50 mmHg.

system of Ar, Kr and Xe, N_2 and O_2 increased linearly but the amounts of NO did not increase at all.

In order to investigate the effects of rare gas sensitization more quantitatively, we calculate the value represented as G_{sens}, that is, the increase in the G-value of a product by sensitization based on the energy absorbed by the rare gas as defined by the equation

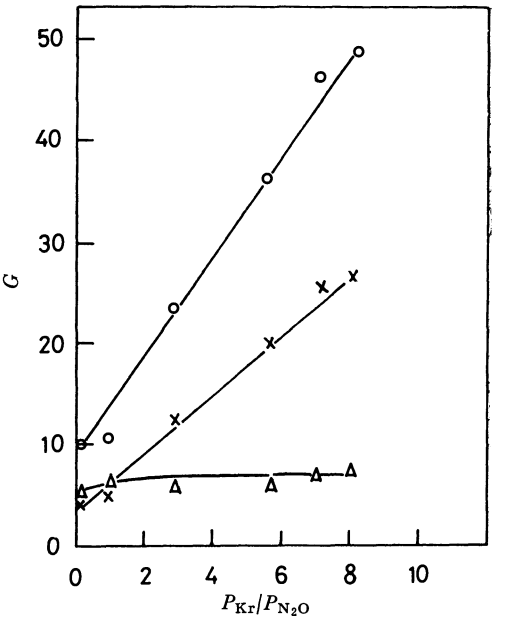

Fig. 9. Sensitization by Kr: ○, N_2; ×, O_2; △, NO. P_{N_2O} = 50 mmHg.

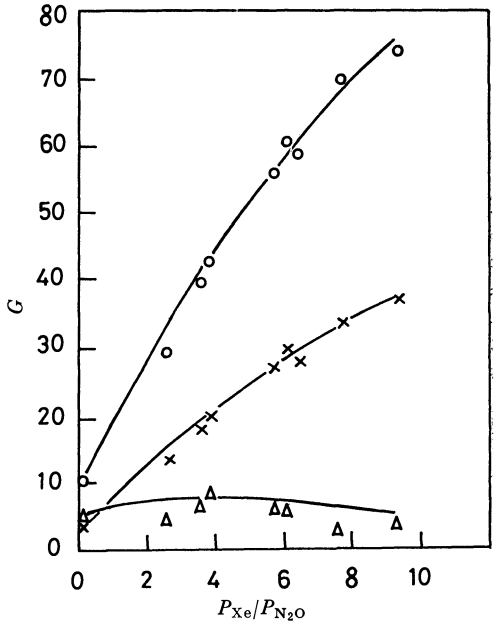

Fig. 10. Sensitization by Xe: ○, N_2; ×, O_2; △, NO. P_{N_2O} = 50 mmHg.

$$G_{sens} = (G_N R_N - G^\circ_N R_N)/R_r$$

where G°_N and G_N represent the values of the particular product based on the energy absorbed by N_2O in the N_2O pure system and in the sensitization experiment, respectively, and R_N and R_r the energy absorbed by N_2O and rare gas, respectively. The values obtained from the above equation are shown in Table 1.[9]

TABLE 1. G_{sens} VALUES FOR VARIOUS RARE GASES (The W-values and $G(e^-)$ values are also presented.)

G_{sens}	He	Ne	Ar	Kr	Xe
N_2	7.3	6.3	3.0	2.9	3.8
O_2	2.8	2.4	1.5	1.6	1.8
NO	3.0	3.2	0.0	0.5	0.5
$-N_2O$	8.8	7.9	3.0	3.2	4.1
W(eV)	42	37	26	24	22
$G(e^-)$	2.5	2.8	3.9	4.1	4.4

Discussion

From the experiments shown in Fig. 1, we get 3.0 for the value of $-\Delta G(-N_2O)$. This is in good agreement with the value of $G(e^-)=3.0$ calculated from $W(N_2O)=33$ eV.[10] If we assume that all electrons are scavenged by SF_6 and that the resulting SF_6^- does not contribute in any way to the decomposition of N_2O, it seems that one electron produced by the ionization of N_2O decomposes just one molecule of N_2O. If this is correct, the addition of small amounts of N_2O to Xe may result in the decomposition of N_2O close to the value of $G(e^-)$ expected from the W-value of Xe. This is the case for Xe and approximately for Kr (Figs. 3 and 4).

It is noted here that Xe has lower ionization energy than N_2O, while Kr has a higher one. However, experimental results showed that there was no appreciable difference between the Xe and the Kr systems and the product distributions were nearly the same in both cases. Thus in spite of the higher ionization potential of Kr, the charge transfer from Kr^+ to N_2O does not seem to occur effectively.

In the Xe-N_2O system as well as in other rare gas-N_2O systems, there is the possibility of excitation energy transfer from rare gas to N_2O besides that from the ionic processes:

$$Xe^* + N_2O \rightarrow N_2O^* + Xe$$

$$N_2O^* \rightarrow N_2 \text{ or other products}$$

Many photolysis data of nitrous oxide (λ: 1470, 1830 or 1849 A)[11-13] show that the ratio of NO to O_2 is greater than unity, but in the present Xe-N_2O system the ratio of NO to O_2 is less than 0.3. In the Xe-N_2O-SF_6 system, the formation of nitrogen was almost completely inhibited by SF_6, and we consider that there is no appreciable contribution from the excitation transfer processes.

Quite recently after the present work had been completed, Sears[14] reported the effect of addition of a small amount of SF_6 on the radiolysis of N_2O. His results and conclusion are not inconsistent with ours. Hummel[15] also reported experiments to determine the effect of small amounts of SF_6 on $G(N_2)$ at temperatures from 30 to 200°C. His results, however, were different from ours. We thought this discrepancy might lie mainly in the experimental conditions (he used a very large vessel of 1.9 l). Therefore we also examined the same system by using a larger vessel of about 400 cc, but the results obtained did not differ much from our earlier results obtained with a small vessel.

Thus we conclude that one electron decomposes one molecule of N_2O and yields one or less molecule of N_2 (0.7 and 0.9 molecules in pure N_2O and in Xe, respectively).

The results obtained here for ionic processes can not be accounted for by the hitherto assumed mechanism:[16]

$$e^- + N_2O \rightarrow N_2 + O^-$$

$$O^- + N_2O \rightarrow N_2 + O_2^- \text{ and } NO + NO^-$$

According to this mechanism, more than one molecule of N_2 should be produced per electron, instead of the observed values of 0.7 and 0.9.

In order to explain the observed facts, we assumed a long-lived N_2O^- molecule resulting from the electron capture by N_2O, and proposed the following mechanism for the ionic processes in the radiolysis of pure N_2O.[17]

$$e^- + N_2O \rightarrow N_2O^-$$

$$N_2O^- + N_2O^+ \rightarrow N_2 + O + N_2O \text{ and } N + NO + N_2O.$$

Consideration of the possible reaction schemes and reaction rate constants[18] led us to the assumption that the resulting O and N atoms react to form O_2 and NO through NO_2. Of course, the presence of other positive ions (NO^+, N^+, *etc.*) other than N_2O^+ could be considered as possible participants. There is the possibility that the difference of positive ions changes the decomposition mode and product formation. However, from the mass spectra of N_2O[19] it can be seen that only 36% of the parent ions decomposes. A number of studies have been reported of the mass spectra of N_2O, but ion-molecule reactions

9) Ausloos *et al.* (R. Gordon and P. Ausloos, *J. Res. Natl. Bur. Std.*, **69A**, 79 (1965)) studied the rare gas sensitization of $^{15}N^{14}NO$ by Kr and Xe and reported rather qualitative ion pair yields for nitrogen. Their results were consistent with ours qualitatively but not quantitatively. Their ion pair yields are approximate calculated values.

10) G. G. Meisels, *J. Chem. Phys.*, **41**, 51 (1964).

11) J. P. Doering and B.H. Mahan, *ibid.*, **36**, 1682 (1962).

12) N. R. Greiner, *ibid.*, **47**, 4373 (1967).

13) J. Y. Yang and F. M. Servedio, *ibid.*, **47**, 4817 (1967).

14) J. T. Sears, *J. Phys. Chem.*, **73**, 1143 (1969).

15) R. W. Hummel, *Chem. Commun.*, **1969**, 995.

16) for example, J. M. Warman, *Nature*, **213**, 381 (1967).

17) S. Takao, S. Shida, Y. Hatano and H. Yamazaki, This Bulletin, **41**, 2221 (1968).

18) G. B. Kistiakowsky and G. G. Volpi, *J. Chem. Phys.*, **27**, 1141 (1957).

19) R. C. Taylor, R. A. Brown, W. B. Young and C. E. Headington, *Anal. Chem.*, **20**, 396 (1948).

between positive fragment ions from N_2O^+ and N_2O molecules and their rate constants are not known in detail.[20] Charge transfer reaction is a likely one among many possible reactions. We assume then that some of these ions transfer their positive charge to N_2O to produce N_2O^+, eventually resulting in the neutralization of N_2O^+ with N_2O^-.

Recently, Warman and Fessenden[21] and Phelps and Voshall[22] reported the experimental facts showing that the electron capture of N_2O proceeds by a three-body process and suggested that N_2O^- ion is initially formed. Their results are consistent with our ionic processes in the radiolysis of N_2O.

In Table 1, we can classify the rare gases into two groups, *viz.*, He, Ne group and Ar, Kr, Xe group. The He, Ne group has much higher $G_{sens}(-N_2O)$ values than the Ar, Kr, Xe group. In the case of He and Ne the product distributions were nearly the same as in the direct radiolysis of N_2O, but in the case of Ar, Kr and Xe the yields of oxygen amount to about one-half of the nitrogen yields, NO being a minor product.

As mentioned before, the energy transfer from excited rare gas atom (X*) or ion (X^+) to N_2O molecule and the resulting decomposition of N_2O is possible in the rare gas sensitization such as

$$X^* \text{ or } X^+ + N_2O \rightarrow N_2 \text{ or other products.}$$

In the experiments with Ar, Kr and Xe, however, the $G_{sens}(-N_2O)$ values are nearly equal to the values of $G(e^-)$, and we believe that the energy transfer (charge or excitation) from Ar or Kr to N_2O does not occur in spite of the higher ionization potentials of Ar and Kr.

In the experiments with He and Ne, we observed nearly the same product distributions as in the direct radiolysis of N_2O and large $G_{sens}(-N_2O)$ values. We think that N_2O^+ ion produced by charge transfer in these systems could have considerable energy in excess of the ionization energy and that this might cause NO formation and large $G_{sens}(-N_2O)$ values in the rare gas sensitization by He and Ne. Of course, there is no saying that the difference in the object of neutralization of N_2O^- plays some part in the overall decomposition mechanism. In the case of He and Ne, the neutralization occurs between N_2O^+ resulting from charge transfer from He^+ or Ne^+ and N_2O^-, while in the case of Ar, Kr and Xe, the neutralization occurs between Ar^+, Kr^+ or Xe^+ and N_2O^-.

In the case of He and Ne, we must further take into account the formation of products from excitation energy transfer processes besides those from electron capture by N_2O and charge transfer to N_2O. We mentioned above that the results shown in Table 1 can be classified into two groups. From the discontinuity lying between Ne and Ar with respect to the product distributions and $G_{sens}(-N_2O)$ values, we remarked that the ionization potential of N_2O lies between the metastable energies of Ne and Ar. These conditions are shown in Table 2. It seems true that the product formation initiated from the Penning ionization of N_2O by metastable He or Ne atoms takes considerable part in the sensitization experiments with He and Ne, though we can not say to what extent.

Table 2. Ionization potentials and metastable excitation energies of rare gases[a]

	I.P. (eV)	E_m^* (eV)
He	24.6	19.8
Ne	21.7	16.1
Ar	15.9	11.6
Kr	14.5	9.9
Xe	12.1	8.8
N_2O	12.9	—

a) G. R. A. Johnson and G. Scholes, "The Chemistry of Ionization and Excitation," Taylor and Francis Ltd., London (1967), p. 145.

The total processes in the rare gas sensitization are described as follows.

$$X \rightsquigarrow X^+ + e^- \quad (1)$$

$$\rightsquigarrow X_m^* \quad (2)$$

$$X^+ + N_2O \rightarrow N_2O^+ + X \quad (3)$$

$$X_m^* + N_2O \rightarrow N_2O^+ + X + e^- \quad (4)$$

$$e^- + N_2O \rightarrow N_2O^- \quad (5)$$

$$N_2O^- + N_2O^+ \rightarrow N_2 \text{ and other products} \quad (6)$$

$$N_2O^- + X^+ \rightarrow N_2 \text{ and other products} \quad (7)$$

where X_m^* represents the metastable rare gas atom. Reactions (3), (4) and (6) do not occur in the case of Ar, Kr and Xe. Reaction (7) does not occur in the case of He and Ne. For overall radiolytic decomposition of N_2O in rare gases, the contribution from the neutral excited molecule decomposition by excitation transfer must be added except for the case of Ar, Kr and Xe. In the latter case, neither the excitation transfer from rare gas to N_2O nor the charge transfer takes place.

The authors wish to thank Dr. Y. Hatano and Dr. H. Yamazaki for many valuable suggestions throughout the course of this work. The authors gratefully acknowledge discussions with Professor G. R. Freeman, University of Alberta.

20) G. R. A. Derwish, A. Galli, A. Giardini-Guidoni and G. G. Volpi, *J. Chem. Phys.*, **40**, 3450 (1964).
21) J. M. Warman and R. W. Fessenden, *ibid.*, **49**, 4718 (1968).
22) A. V. Phelps and R. E. Voshall, *ibid.*, **49**, 3246 (1968).

BULLETIN OF THE CHEMICAL SOCIETY OF JAPAN VOL. 43 2772—2776 (1970)

The Electronic Spectra of the Anion Radical Salts Derived from Halogen-substituted *p*-Benzoquinones*[1]

Yôichi IIDA

Department of Chemistry, Faculty of Science, Hokkaido University, Sapporo

(Received April 30, 1970)

The anion-radical salts derived from *p*-chloranil, 2,5-dibromo-3,6-dichloro-1,4-benzoquinone, and *p*-bromanil were prepared. The absorption spectra in an acetone solution and the diffuse reflection spectra of the solid salts were examined. These solid salts were then classified into three groups, namely, those showing the spectrum of the anion-radical monomer, those showing a strong charge-transfer band characteristic of the solid salts, and, finally, those showing not only the spectrum of the anion-radical monomer but also an intermolecular charge-transfer band. The mode of intermolecular interaction in these anion-radical salts was discussed according to this classification. Their magnetic behaviour was also speculated upon on the basis of the charge-transfer interaction.

Solid ion-radical salts are particularly interesting because, in crystals of such ion-radical salts, the ion-radical molecules form, in themselves, a plane-to-plane stacking into columns so as to make a large overlap between their half-filled molecular orbitals.[1] Since, in this case, any individual radical molecule interacts through charge transfer most strongly with one or two other radicals, the electronic spectrum of the solid salt is expected to be different from the monomer spectrum in solution and to show an intermolecular charge-transfer band. In this respect, it was interesting to examine the solid-state spectra, particularly of Würster cation-radical salts and of 7,7,8,8-tetracyanoquinodimethane (TCNQ) anion-radical salts.[2-4]

The present paper will describe the solid-state spectra, as well as the absorption spectra in solution, of some stable anion-radical (*i.e.*, semiquinone ion) salts derived from halogen-substituted *p*-benzoquinones (see Fig. 1). The purpose of this paper is to report the results of our electronic-spectrum measurements and to show that a charge-transfer interaction similar to those in Würster cation-radical salts and in TCNQ anion-radical salts takes place in these anion-radical salts. It is also interesting to discuss their magnetic properties on the basis of the charge-transfer interaction.

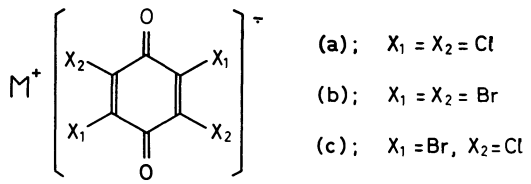

Fig. 1. The anion-radical salts of (a) *p*-chloranil, (b) *p*-bromanil, and (c) 2,5-dibromo-3,6-dichloro-1,4-benzoquinone. M^+ represents a diamagnetic counter cation.

Experimental

Materials. The *p*-chloranil and *p*-bromanil were commercially available. The 2,5-dibromo-3,6-dichloro-1,4-benzoquinone (*p*-QBr_2Cl_2) was synthesized by the bromination of 2,5-dichloro-1,4-benzoquinone. These compounds were purified by recrystallization from benzene or acetic acid.

The following six anion-radical salts were prepared according to the method of Torrey and Hunter[5]: Na^+ *p*-Chloranil$^-$, K^+ *p*-Chloranil$^-$, Na^+ *p*-$QBr_2Cl_2^-$, K^+ *p*-$QBr_2Cl_2^-$, Na^+ *p*-Bromanil$^-$, and K^+ *p*-Bromanil$^-$. In this method, the anion-radical salts were made by the one-electron reduction of the corresponding quinones with alkali metal iodides in a cold acetone solution.

Measurements. The absorption spectra in an acetone solution were measured at room temperature, using a Beckman DK-2A spectrophotometer at concentrations of the order of 10^{-4} mol/*l*.

The diffuse reflection spectra of the solid salts were

*1 This work was presented at the 22nd Annual Meeting of the Chemical Society of Japan, Tokyo, April, 1969, and at the Symposium on Molecular Structure, Fukuoka, October, 1969.

1) G. R. Anderson and C. J. Fritchie, Jr., Second National Meeting, Society for Applied Spectroscopy, San Diego, October, 14, Paper 111 (1963); C. J. Fritchie, Jr., *Acta Crystallogr.*, **20**, 892 (1966); C. J. Fritchie, Jr., and P. Arthur, Jr., *ibid.*, **21**, 139 (1966); P. Goldstein, K. Seff and K. N. Trueblood, *ibid.*, **B24**, 778 (1968); J. Tanaka and N. Sakabe, *ibid.*, **B24**, 1345 (1968).

2) Y. Iida and Y. Matsunaga, This Bulletin, **41**, 2615 (1968).

3) Y. Iida, *ibid.*, **42**, 71 (1969).

4) Y. Iida, *ibid.*, **42**, 637 (1969).

5) H. A. Torrey and W. H. Hunter, *J. Amer. Chem. Soc.*, **34**, 702 (1912).

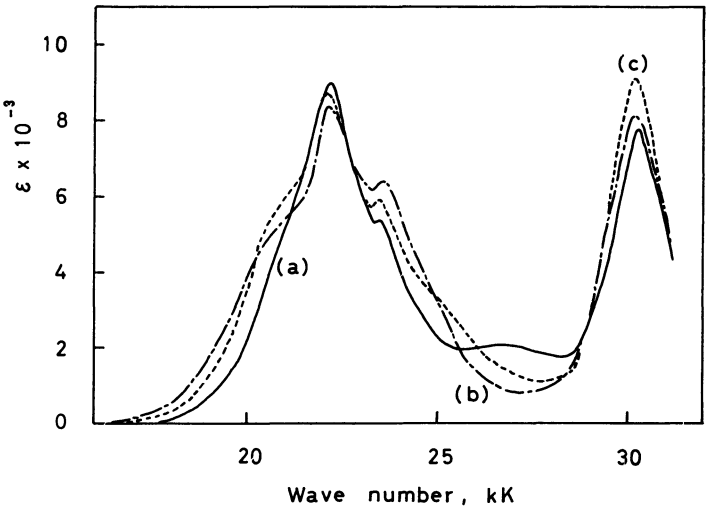

Fig. 2. The absorption spectra of (a) K^+ *p*-Chloranil$^-$, (b) K^+ *p*-Bromanil$^-$ and (c) K^+ *p*-$QBr_2Cl_2^-$, in acetone solution.

recorded on a Beckman DK-2A spectroreflectometer in the range from 4.0 to 30.8 kK at room temperature. In order to avoid cation exchange between the salt and the diluent, the sodium salts were ground with sodium chloride, and the potassium salts, with potassium bromide. The solid-state spectra were then obtained by plotting the diffuse reflection spectra using the Kubelka-Munk equation, $f(R)=(1-R)^2/2R$, in which R is the reflectance. The experimental details were the same as those in previous papers.[2-4]

The Absorption Spectra in Solution

Some of the absorption spectra of these anion-radical salts in an acetone solution are given in Fig. 2. The spectra are not changed when the counter cation of the salt is replaced. Since the concentrations are so dilute, the salts seem to be completely dissociated. The obtained spectra are those of the anion-radical monomer, because the counter cations of the salts are simple alkali metal cations.

The *p*-Chloranil Anion Radical (Fig. 2, Curve a). The absorption spectrum of this anion was found to be very similar to that of the *p*-benzoquinone anion-radical reported by Harada and Inokuchi.[6] The spectrum of the *p*-chloranil anion-radical consists of bands at 22.2 kK, 26.7 kK, and 30.3 kK, while that of the *p*-benzoquinone anion-radical has bands at 22.7 kK, 27.0 kK, and 31.3 kK. We can see that the introduction of the chlorine substituents into the *p*-benzoquinone anion-radical causes slight shifts in their corresponding bands. Therefore, it may be assumed that the π-conjugated system for the *p*-chloranil anion-radical may be approximated by that for the *p*-benzoquinone anion-radical. According to Harada's calculations,[7] the ground configuration of the *p*-benzoquinone anion-radical belongs to the $^2B_{3g}$ representation. He assigned the bands at 22.7 kK, 27.0 kK, and 31.3 kK to the transitions of $^2B_{3g}\rightarrow{}^2B_{1u}$, $^2B_{3g}\rightarrow{}^2A_u$, and $^2B_{3g}\rightarrow{}^2B_{1u}$ respectively. Therefore, the same assignments seem to be applicable to the bands at 22.2 kK, 26.7 kK, and 30.3 kK for the *p*-chloranil anion-radical.

On the other hand, Shirotani *et al.* have found the monomer-dimer equilibrium for the *p*-chloranil anion-radicals in an ethanolic solution at low temperatures.[8] At this time, the charge-transfer band of the dimer*2 appears around 14.9 kK; this value is smaller than that of 17.1 kK for the dimer of the *p*-benzoquinone anion-radical reported by Kimura *et al.*[9]

The *p*-Bromanil Anion Radical (Fig. 2, Curve b). Because both were similar to those for the *p*-chloranil anion-radical, the bands at both 22.2 kK and 30.2 kK for the *p*-bromanil anion-

6) Y. Harada and H. Inokuchi, *Mol. Phys.*, **8**, 265 (1964).

7) Y. Harada, *ibid.*, **8**, 273 (1964).

8) I. Shirotani, N. Sakai and S. Minomura, This Bulletin, to be published.

*2 According to the Hausser and Murrell's theory, the ion-radicals in a dimer may lie in parallel planes, one above the other, and the spin-exchange interaction leads to a singlet ground state and an excited triplet state. Therefore, we must take into consideration the fact that intermolecular charge-transfer may make a significant contribution to stabilizing the ground singlet state of the dimer. The low-energy charge-transfer absorption characteristic of the dimer arises from a transition from the thus-stabilized ground state to an excited singlet state expressed by an antisymmetric combination of the wave-functions for charge-transfer structures, $R\text{-}R^{2-}$. See K. H. Hausser and J. N. Murrell, *J. Chem. Phys.*, **27**, 500 (1957).

9) K. Kimura, H. Yamada and H. Tsubomura, *J. Chem. Phys.*, **48**, 440 (1968).

radical were assigned to the transitions of $^2B_{3g} \rightarrow {}^2B_{1u}$. However, it was noted that, unlike the *p*-chloranil anion-radical, the transition due to $^2B_{3g} \rightarrow {}^2A_u$ was not detected, while a shoulder appeared around 20.5 kK.

The *p*-QBr_2Cl_2 Anion Radical (Fig. 2, Curve c). The point group for this molecule belongs to the C_{2h} symmetry, which is degraded from the D_{2h} symmetry for the above two molecules. Therefore the bands at both 22.1 kK and 30.2 kK must belong to the $^2B_g \rightarrow {}^2A_u$ transitions. Except for this difference, the electronic structures of the *p*-QBr_2Cl_2 and *p*-bromanil anion-radicals seem to be much alike.

The Solid-State Spectra

K^+ *p*-Chloranil$^-$ (Fig. 3, Curve a). The solid-state spectrum of this salt shows a low-energy band at 11.8 kK, a strong high-energy band at 23.3 kK, and a shoulder around 30 kK. Except for the appearance of the low-energy band, the bands seem to be similar to those for the *p*-chloranil anion-radical monomer in an acetone solution. Therefore, the high-energy band at 23.3 kK and the shoulder around 30 kK can be assigned to the $^2B_{3g} \rightarrow {}^2B_{1u}$ transitions at 22.2 kK and at 30.3 kK respectively for the monomer. Unfortunately, in the present investigation, the band due to the $^2B_{3g} \rightarrow {}^2A_u$ transition for the monomer spectrum was not observed for the solid-state spectrum. Although the value of the low-energy band, 11.8 kK, of the solid-state spectrum is a little bit lower than that of 14.9 kK of the charge-transfer band of the *p*-chloranil anion-radical dimer in solution, we assigned this band to the charge-transfer transition in the solid state. However, the intensity of this band is rather weaker than that of Na^+ *p*-Chloranil$^-$ (see below).

Na^+ *p*-Chloranil$^-$ (Fig. 3, Curve b). Unlike K^+ *p*-Chloranil$^-$, the solid-state spectrum of this salt shows a high-energy band at 26.5 kK and a shoulder beyond 30 kK. The charge-transfer band is located at 11.6 kK. Although this value is coincident with that of K^+ *p*-Chloranil$^-$, the charge-transfer band for Na^+ *p*-Chloranil$^-$ was found to be very much intensified. In accordance with this view, the high-energy band at 23.3 kK for K^+ *p*-Chloranil$^-$ is shifted to the band at 26.5 kK for Na^+ *p*-Chloranil$^-$, which is, therefore, assigned to the shifted band of the $^2B_{3g} \rightarrow {}^2B_{1u}$ transition for the anion-radical monomer. The π-π transitions of the monomer will be perturbed in the field of the other anion-radicals when the anion-radicals come close enough together for the π orbitals to overlap.

K^+ *p*-$QBr_2Cl_2^-$ (Fig. 4, Curve a). Obviously, in spite of weak low-energy absorptions at 11.5 kK and at 17.4 kK, the solid-state spectrum of this salt is almost identical with that of the anion-radical monomer in an acetone solution. The strong band at 23.3 kK of the solid-state spectrum corresponds well to the $^2B_g \rightarrow {}^2A_u$ transition at 22.1 kK of the monomer spectrum. The shoulder around 30 kK of the solid salt corresponds to the place where the band at 30.2 kK appears in the monomer spectrum. The intensity of the charge-transfer band of this salt located at 11.5 kK is very much decreased in comparison with that at 11.8 kK of K^+ *p*-Chloranil$^-$. The origin of the other weak absorption, at 17.4 kK, of K^+ *p*-$QBr_2Cl_2^-$ remains in question. From the above-mentioned results, the anion-radicals in this salt appear to interact more weakly than those in K^+ *p*-Chloranil$^-$. It seems that the *p*-QBr_2Cl_2 anion-radicals exist almost as monomers in the solid state.

Na^+ *p*-$QBr_2Cl_2^-$ (Fig. 4, Curve b). Unlike K^+ *p*-$QBr_2Cl_2^-$, this salt shows strong absorptions at 12.2 kK and at 26.3 kK, and a slight shoulder around 22 kK. These features seem to be similar to those of Na^+ *p*-Chloranil$^-$. Figure 4 shows that the intensity of the charge-transfer band for Na^+ *p*-$QBr_2Cl_2^-$ is very much increased compared

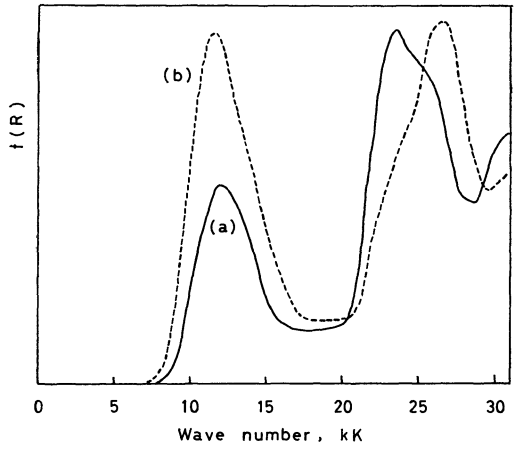

Fig. 3. The solid-state spectra of (a) K^+ *p*-Chloranil$^-$ and (b) Na^+ *p*-Chloranil$^-$.

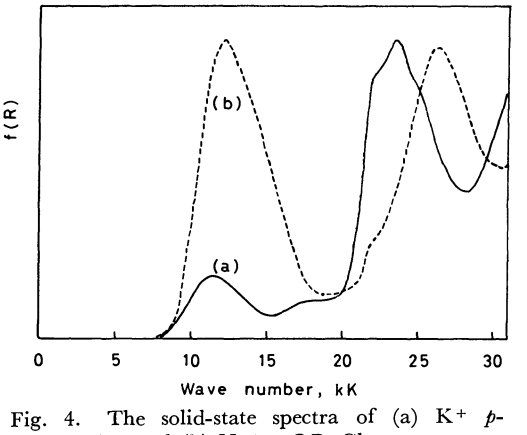

Fig. 4. The solid-state spectra of (a) K^+ *p*-$QBr_2Cl_2^-$ and (b) Na^+ *p*-$QBr_2Cl_2^-$.

to that for K^+ p-$QBr_2Cl_2^-$. In accordance with this view, the band at 23.3 kK due to the $^2B_g \rightarrow {}^2A_u$ transition for K^+ p-$QBr_2Cl_2^-$ is appreciably shifted to 26.3 kK for Na^+ p-$QBr_2Cl_2^-$. Judging from these results, the situation of the solid state of this salt seems to be very analogous to that of Na^+ p-Chloranil$^-$.

K^+ p-Bromanil$^-$ (Fig. 5, Curve a). The solid-state spectrum of this salt shows weak low-energy bands at 10.9 kK and at 17.5 kK, and a strong high-energy band at 23.0 kK. The locations of the band peaks for this salt coincide with those of K^+ p-$QBr_2Cl_2^-$. The high-energy band at 23.0 kK corresponds well with the band due to the $^2B_{3g} \rightarrow {}^2B_{1u}$ transition at 22.2 kK for the p-bromanil anion-radical monomer. The intensity of the low-energy band is as weak as that of K^+ p-$QBr_2Cl_2^-$. These spectroscopic features clearly indicate that the situations in these two substances are very much alike.

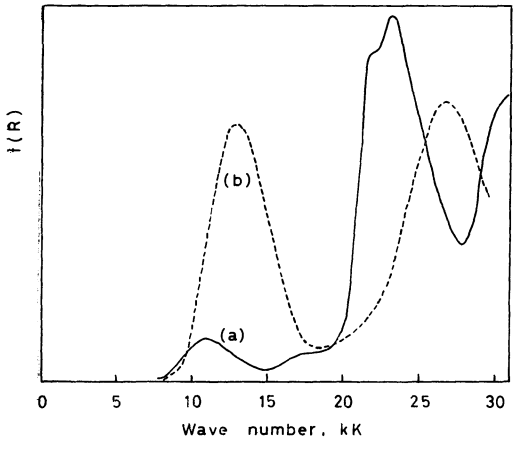

Fig. 5. The solid-state spectra of (a) K^+ p-Bromanil$^-$ and (b) Na^+ p-Bromanil$^-$.

Na^+ p-Bromanil$^-$ (Fig. 5, Curve b). Unlike K^+ p-Bromanil$^-$, this salt shows a solid-state spectrum comprising a strong band at 13.0 kK and a strong high-energy band at 26.8 kK. It is interesting to see that these spectral differences between Na^+ p-Bromanil$^-$ and K^+ p-Bromanil$^-$ are very analogous to those between Na^+ p-$QBr_2Cl_2^-$ and K^+ p-$QBr_2Cl_2^-$. Therefore, the mode of the charge-transfer interaction in Na^+ p-Bromanil$^-$ seems to be very similar to that in Na^+ p-$QBr_2Cl_2^-$.

Discussion

The experimental results of the solid-state spectra clearly indicate that these anion-radical salts can be classified into the following three groups (this classification is based on the mode of the charge-transfer interaction between the anion-radical molecules):

(I) K^+ p-$QBr_2Cl_2^-$ and K^+ p-Bromanil$^-$ belong to this group, in which the solid-state spectra are almost identical with the spectrum of the anion-radical monomer. This means that the anion-radical molecules exist as monomers in the solid state. Hence, the magnetic properties of these salts may be expected to exhibit nearly the behaviour due to free-spin paramagnetism. In this case, the temperature variation of the paramagnetic susceptibility may be approximated by the Curie law.

(II) Na^+ p-Chloranil$^-$, Na^+ p-$QBr_2Cl_2^-$, and Na^+ p-Bromanil$^-$ belong to this group. In these cases, the intensity of the low-energy charge-transfer band is remarkably strong, and the high-energy band, originating from the monomer band, is blue-shifted. A strong charge-transfer interaction between the anion-radicals is expected to cause such behaviour. Therefore, the intermolecular overlap between the molecular orbitals of the anion-radicals is quite large in the crystal of these salts. For this reason, the anion-radicals seem to be stacked in the solid salts one flat upon another to form parallel chains. On the other hand, such a crystal system is considered to be a linear-chain antiferromagnet, since the charge-transfer interaction leads to a considerable stabilization of the state where the spins are antiparallel.[2-4] It can, therefore, be expected that the salts in this group may be diamagnetic or, at most, weakly paramagnetic at room temperature.

(III) Only K^+ p-Chloranil$^-$ belongs to this group. The spectrum of this salt shows a low-energy charge-transfer band. However, the high-energy band is similar to the monomer band. Therefore, the charge-transfer interaction for this group is intermediate between those for the (I) and (II) groups. Such an intermediate case may be observed only when the temperature of the measurement is comparable with the interaction. McConnell and Lynden-Bell have discussed the electronic structures for such systems composed of the linear chains of $S=1/2$ ion-radical molecules.[10] According to their discussion, at temperatures which are large compared to the exchange interaction, the spin of any one individual radical interacts equally strongly with two others, while at temperatures comparable to or less than the exchange interaction the linear chains are unstable with respect to the distortions that produce an alternation in the distances between the interacting units. At this time, since this effect is cooperative, a sharp decrease in the magnetic susceptibility may be expected. In accordance with this view, Andre *et al.* have found a sharp decrease in the paramagnetic susceptibility for K^+ p-Chloranil$^-$ around 250°K when the temperature is

10) H. M. McConnell and R. Lynden-Bell, *J. Chem. Phys.*, **36**, 2393 (1962).

lowered.[11] We consider that this "magnetic" anomaly may be attributed to the phase-transition that has been discussed by McConnell and Lynden-Bell.*3

Summarizing the above-mentioned results, we have to note that the charge-transfer interaction in these anion-radical salts is largely affected not only by the kinds of the halogen substituents in the anion-radical molecules, but also by the species of the counter cations. In the case of the potassium cation, the interaction of the salt is markedly decreased compared to that of the sodium salt. In this respect, the crystal structure of the potassium salt is expected to be quite different from that of the sodium salt. This difference may be related to the difference in the ion radii between these two cations. It is obvious that the charge-transfer interaction is decreased when the substituted chlorine for the anion-radical molecule is replaced by bromine.

In conclusion, the existence of charge-transfer interaction between ion-radical molecules is not limited to Würster cation-radical salts or TCNQ anion-radical salts, but is regarded as of the nature of ion (cation and anion) radical salts in general.

11) J. J. Andre, J. Clementz, R. Jesser and G. Weill, *C. R. Acad. Sci. Paris*, **t. 266**, 1057 (1968).

*3 Similar anomalies in the magnetic susceptibilities of ion-radical salts have previously been observed with *N,N,N',N'*-tetramethyl-*p*-phenylenediamine (Würster's Blue) perchlorate at 189°K and with $[(C_6H_5)_3PCH_3]^+$-$(TCNQ)_2^-$ at 315°K. See W. Duffy, Jr., *J. Chem. Phys.*, **36**, 490 (1962); K. Okumura, *J. Phys. Soc. Japan*, **18**, 69 (1963); R. G. Kepler, *J. Chem. Phys.*, **39**, 3528 (1963); Y. Iida, M. Kinoshita, M. Sano and H. Akamatu, This Bulletin, **37**, 428 (1964).

BULLETIN OF THE CHEMICAL SOCEITY OF JAPAN VOL. 43 2776—2785 (1970)

Molecular Structure and the Effect of Large-Amplitude Vibration of Carbon Suboxide as Studied by Gas Electron Diffraction

Mitsutoshi TANIMOTO,*1 Kozo KUCHITSU and Yonezo MORINO*1

Department of Chemistry, Faculty of Science, The University of Tokyo, Hongo, Bunkyo-ku, Tokyo

(Received May 4, 1970)

The molecular structure of carbon suboxide, C_3O_2, has been studied by the sector-microphotometer method of gas electron diffraction. The C=O and C=C distances (r_g) have been determined to be $1.163_2 \pm 0.001_3$ Å and $1.289_4 \pm 0.002_2$ Å, respectively, where the uncertainties represent estimated limits of error. The observed mean amplitudes for three nonbonded atom pairs and their shrinkages are found to be much larger than those expected for ordinary molecules with linear framework. A usual harmonic approximation up to the quadratic terms of displacements cannot account for the observed values in this molecule. This indicates that the π_u bending vibration ν_7 has a very low frequency (an *effective* frequency being about 68 cm^{-1}) and that this vibration is essentially a bending motion of the valence angle of the central carbon atom, in agreement with recent spectroscopic studies. The effect of the large-amplitude vibration on mean amplitudes and shrinkages has been studied in detail by using a model, which assumes that atomic motions take curvilinear paths in the ν_7 vibration with the valley in the potential surface running along the loci of fixed bond lengths. The potential function for this bending motion has been estimated by a least-squares analysis on the observed structural parameters. The potential function is given by $V(Q_7) = (23 \pm 5)Q_7^4 - (100 \pm 31)Q_7^2$ (cm^{-1}), where the uncertainties representing random standard errors take the upper and lower signs in the same order and $Q_7 = \sin\alpha/0.145$ ($amu^{1/2}$ Å). The potential rises steeply with increasing angle of bending, $\alpha = 1/2[180° - \angle(C=C=C)]$, and appears to have a small hump at $\alpha = 0$. This "quasi-linear" potential function is consistent with the recent experimental estimates by Seip *et al.* within experimental errors, but the double-minimum nature of the potential is subject to a further critical examination by other experimental methods.

Carbon suboxide has presented a number of problems with regard to its structure and spectra. From a naive valence consideration, this molecule should have a linear equilibrium structure. However, no definite conclusion about its structure has been drawn in spite of various spectroscopic in-

*1 Present address: Sagami Chemical Research Center, 3100 Ohnuma, Sagamihara, Kanagawa.

vestigations.[1-5] The infrared and Raman spectra of this molecule were so complex that they were once regarded as evidence for a nonlinear structure.[1-3] Lafferty *et al.*[5] reported that their high-resolution vibration-rotation spectrum in the 3170 cm^{-1} region could be assigned satisfactorily as a linear symmetric structure. Their analysis also indicated that the lowest bending fundamental mode was very low, probably between 25—70 cm^{-1}. This was consistent with the entropy measurements by McDougall and Kilpatrick;[6] they estimated ν_7 to be 61.6 ± 2.6 cm^{-1} on the assumption of a rigid rotor and harmonic vibrations. The first successful detection of ν_7 was reported in 1965 by Miller *et al.*,[7] who observed a very weak and broad absorption band with a maximum around 63 ± 2 cm^{-1}.

The finding of the ν_7 band, however, by no means answered all the problems in the infrared spectrum of carbon suboxide. In order to explain a number of anomalous features in the spectra, Pitzer and Strickler[8] and later Miller *et al.*[7] suggested that this CCC bending vibration may be highly anharmonic like the low-frequency bending mode in diazomethane. On the other hand, Bell *et al.*[9] claimed that the anharmonicity constant x_{77} must be small, although the interaction with other fundamental vibrations may be large. With regard to the details of the CCC bending potential function, controversial remarks have been made. Redington[10] fitted a two-term potential function for this bending motion to the spectra observed by Miller *et al.*[4,7] using the theory of Thorson and Nakagawa[11] and suggested that the potential was relatively flat-bottomed, being characteritic of a quasi-linear molecule. Almenningen *et al.*[12] favored a potential with a barrier at a linear structure on the basis of their analysis of electron-diffraction data.

The interatomic distances in carbon suboxide were determined by the Norwegian group by electron diffraction at three different temperatures (237°K, 290°K, 508°K).[12] Their results at room temperature were $r(C=C)=1.2898\pm0.0036$ Å and $r(C=O)=1.1655\pm0.0021$ Å, which are consistent with the earlier results of Livingston and Rao,[13] and of Mackle and Sutton,[14] both by the visual method. These earlier results were used by Lafferty *et al.*[5] to prefer one of their assignments on the π-π transitions in a vibration-rotation band.

The presence of a low-frequency vibration should have a significant influence on some of the structural parameters observed by gas electron diffraction. The study of such anomalous vibrational effects by a diffraction method should supply useful information, which is hard to obtain by other methods, on the potential function. Accordingly, the present study aims to make a precise analysis of the mean amplitudes and shrinkages so as to shed light on this problem.

Experimental

The sample of carbon suboxide was prepared by the dehydration of malonic acid in vacuum[15] using glass tubes and stopcocks with KEL-F stopcock grease. Twenty grams of malonic acid, 200 g of fresh powdered phosphorus pentoxide and 40 g of roasted sand were mixed in a 1*l* flask, which was attached to a vacuum system with a sample holder and a U-tube of 20 mm diameter. Towers packed with glass-wool and with calcium oxide were inserted between the U-tube and the sample holder. The flask was heated for two hours on an oil-bath at 140 to 150°C under about 10^{-2} mmHg, and volatile products (carbon suboxide, carbon dioxide, and acetic acid) were condensed in a U-tube cooled to liquid-nitrogen temperature. The U-tube was then put in a dry ice-acetone bath, and the gaseous mixture of carbon dioxide and carbon suboxide was allowed to pass into a sample holder cooled at liquid-nitrogen temperature. Carbon dioxide was then distilled off at dry ice-acetone temperature until the vapor pressure decreased to about 6 mmHg, the pressure of carbon suboxide measured by Stock and Stolzenberg.[15] A gas-chromatographic analysis of the product showed that the sample was more than 99% pure. It was possible to store the sample at liquid-nitrogen temperature for over a month without decomposition.

Diffraction photographs were taken on Fuji Process Hard plates at 20°C with an apparatus equipped with an r^3-sector.[16] The sample stored in a 2*l* flask with a pressure of about 40 mmHg at 20°C was introduced into the diffraction chamber through a nozzle of 0.2 mm diamter. The camera lengths used were measured

1) H. D. Rix, *J. Chem. Phys.*, **22**, 429 (1954).
2) D. A. Long, F. S. Murfin and R. L. Williams, *Proc. Roy. Soc.* (London), **A223**, 251 (1954).
3) B. P. Stoicheff, *Advan. Spectry.*, **1**, 124 (1959).
4) F. A. Miller and W. G. Fateley, *Spectrochim. Acta*, **20**, 253 (1964).
5) W. J. Lafferty, A. G. Maki and E. K. Plyler, *J. Chem. Phys.*, **40**, 224 (1964).
6) L. A. McDougall and J. E. Kilpatrick, *ibid.*, **42**, 2311 (1965).
7) F. A. Miller, D. H. Lemmon and R. E. Witkowski, *Spectrochim. Acta*, **21**, 1709 (1965).
8) K. S. Pitzer and S. J. Strickler, *J. Chem. Phys.*, **41**, 730 (1964).
9) S. Bell, T. S. Varadarajan, A. D. Walsh, P. A. Warsop, J. Lee and L. Sutcliffe, *J. Mol. Spectry.*, **21**, 42 (1966).
10) R. L. Redington, *Spectrochim. Acta*, **23A**, 1863 (1967).
11) W. R. Thorson and I. Nakagawa, *J. Chem. Phys.*, **33**, 994 (1960).
12) A. Almenningen, S. P. Arnesen, O. Bastiansen, H. M. Seip and R. Seip, *Chem. Phys. Lett.* **1**, 569 (1968).
13) R. L. Livingston and C. N. R. Rao, *J. Amer. Chem. Soc.*, **81**, 285 (1959).
14) H. Mackle and L. E. Sutton, *Trans. Faraday Soc.*, **47**, 937 (1951).
15) A. Stock and H. Stolzenberg, *Ber.*, **50**, 498 (1917).
16) Y. Murata, K. Kuchitsu and M. Kimura, *Japan. J. Appl. Phys.*, **9**, 591 (1970).

to be 107.78±0.02 mm and 243.22±0.02 mm. The beam current was about 0.16 μA. The exposure times were about 1 and 3 minutes for the longer and shorter camera lengths, respectively. The accelerating voltage was stabilized within 0.1% during the experiment and was measured by the method of Rymer and Wright[17] to be about 39.4 kV. The wavelength of the electron beam was calibrated to within 0.07% with reference to the r_a(C=O) bond length of carbon dioxide, 1.1646 Å.

The photographic densities were measured using an integrating digital voltmeter along the diameter of the diffraction pattern at integral q values.[18] Several readings on both sides for 4 sec each were averaged. The optical densities were regulated below 0.6, where a linear relation for the conversion of optical density into electron intensity is applicable. The electron intensity was divided by a theoretical background function in order to make the background nearly flat. A slight uniform fogging observed in the region of larger scattering angles was ascribed to the reflection of scattered electrons by the sector race[16] and was subtracted from the observed total intensity.*2 No significant systematic deviations were observed among the intensities taken from different photographic plates nor from different camera lengths.

Analysis

The molecular intensity curve was obtained by drawing a smooth background through the intensity curve corrected for the imperfection in the sector opening and for the effect of non-nuclear scattering.[19] The background was revised with the aid of Karles' criterion of minimum ghosts in the radial distribution curve.[20] The atomic scattering factors, F, of carbon and oxygen were calculated from the Hartree-Fock potential expressed analytically by Strand and Bonham.[21] The inelastic scattering factors, S, and the phase shift, $\Delta\eta_{CO}=\eta_C-\eta_O$, were taken from the tables of Pohler and Hanson[22] and those of Ukaji and Bonham,[23] respectively.

The molecular parameters were determined by a least-squares fit of the observed molecular intensity (Fig. 1) to the following theoretical expression with a preestimated weight function:[24]

$$qM(q) = k\sum_{i\neq j} A_{ij}\mu_{ij}\cos\Delta\eta_{ij}\sin\frac{\pi}{10}q \times\left[r_{aij}-\left(\frac{\pi}{10}q\right)^2\kappa_{ij}\right]\exp\left[-\frac{1}{2}\left(\frac{\pi}{10}ql_{ij}\right)^2\right], \quad (1)$$

where the symbols have their usual significance. The parameters representing asymmetry, κ, for the bonded C=O and C=C atom pairs were fixed in the analysis to the values estimated by assuming the Morse potential functions.[25] The anharmonicity parameters, a_3, were assumed to be 2.39 $Å^{-1}$ and 2.13 $Å^{-1}$, respectively.[26] The κ parameters for all the nonbonded pairs were ignored. Despite the presence of a low-frequency bending vibration, the present assumption for the O_1–C_4

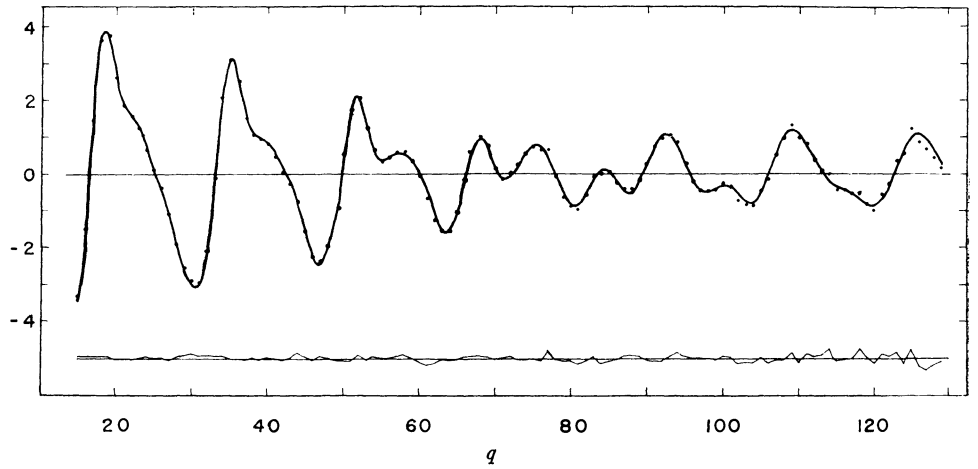

Fig. 1. Reduced molecular intensity curves (dots for observed values and the solid curve calculated from the best-fit model). The residual is shown below.

17) T. E. Rymer and K. H. R. Wright, *Proc. Roy. Soc.* (London), **A215**, 550 (1952).

18) Y. Morino, K. Kuchitsu and T. Fukuyama, This Bulletin, **40**, 423 (1967).

*2 The correction for this fogging made the calculated and observed mean amplitude for carbon dioxide and other molecules agree within the experimental error of 0.002 Å.

19) L. S. Bartell, L. O. Brockway and R. H. Schwendeman, *J. Chem. Phys.*, **23**, 1854 (1955).

20) J. Karle and I. L. Karle, *ibid.*, **18**, 957 (1950).

21) T. G. Strand and R. A. Bonham, *ibid.*, **40**, 1686 (1964).

22) R. F. Pohler and H. P. Hanson, *ibid.*, **42**, 2347 (1965).

23) R. A. Bonham and T. Ukaji, *ibid.*, **36**, 72 (1962).

24) Y. Morino, K. Kuchitsu and Y. Murata, *Acta Crystallogr.*, **18**, 549 (1965).

25) K. Kuchitsu, This Bulletin, **40**, 498 (1967).

26) K. Kuchitsu and Y. Morino, *ibid.*, **38**, 805 (1965).

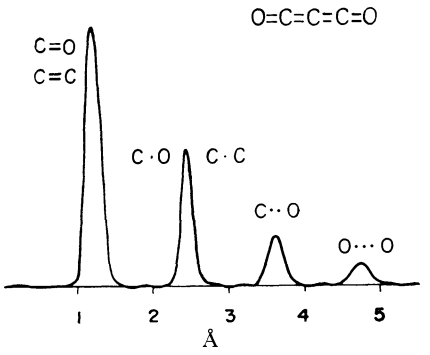

Fig. 2. Radial distribution curve calculated with an artificial damping factor, $\exp(-0.00138s^2)$.

and O_1–O_5 pairs is justified by the approximate symmetry of their radial distribution peaks (Fig. 2), which are found to fit to Gaussian functions within experimental error. It is hard to make analogous tests for the C_2–C_4 and C_3–O_1 distributions, since they overlap each other. Nevertheless, their κ parameters are possibly within the range of $\pm 10^{-6}$ Å[3,25] and hence, the systematic errors in their distances and shrinkages due to the neglect of their κ are certainly within their quoted uncertainties.

Six atomic distances r_a, six mean amplitudes l, and the index of resolution k were determined in the analysis as variable parameters. The most probable values of the parameters with their limits of error are given in Tables 1 and 2.*3 The mean value of an internuclear distance averaged over the probability distribution function, $\langle r \rangle$ or r_g, is related to r_a as[25] $r_g = r_a + l^2/r_a$. The shrinkages, δ_g,[27] for nonbonded atom pairs are given in Table 3. The observed mean amplitudes and the shrinkages for the C_2–C_4, O_1–C_4, and O_1–O_5 atom pairs are much larger than for the other atom pairs, as expected from the low frequency of the ν_7 vibration. This effect is discussed in detail in the following section.

Table 1. Observed values of bond lengths in carbon suboxide at room temperature (in Å units)

	r_a	r_g	ε[a]
$O_1=C_2$	1.162_0	1.163_2	0.001_3
$C_2=C_3$	1.288_1	1.289_4	0.002_2
O_1-C_3	2.444_1	2.444_8	0.005_0
C_2-C_4	2.48_2	2.48_5	0.01_7
O_1-C_4	3.629_0	3.630_8	0.004_9
O_1-O_5	4.75_3	4.75_5	0.01_3

a) Estimated limits of error.

*3 Numerical experimental data of the leveled total intensity and their error matrix have been deposited with the Chemical Society of Japan (Document No. 7005). A copy may be secured by citing the document number and by remitting, in advance, ¥200 for photoprints. Payment by check or money order payable to: Chemical Society of Japan.

27) Y. Morino, J. Nakamura and P. W. Moore, *J. Chem. Phys.*, **36**, 1050 (1962).

Table 2. Observed and calculated values of mean amplitudes for carbon suboxide at room temperature (in Å units)

	$l_{obs.}$	$l_{calc.}$ (a)	$l_{calc.}$ (b)
$O_1=C_2$	$0.036_8 \pm 0.001_3$	0.034_9	0.034_9
$C_2=C_3$	$0.041_2 \pm 0.002_2$	0.038_5	0.038_5
O_1-C_3	$0.042_1 \pm 0.002_1$	0.042_0	0.043_4
C_2-C_4	$0.07_6 \pm 0.01_9$	0.042_4	0.071_3
O_1-C_4	$0.080_9 \pm 0.007_1$	0.045_1	0.084_4
O_1-O_5	$0.09_9 \pm 0.01_0$	0.047_3	0.095_3

(a) Harmonic approximation with ω_7 assumed to be 63 cm^{-1}.
(b) Large-amplitude analysis for ν_7 (see text).

Table 3. Observed and calculated values of shrinkages for carbon suboxide at room temperature (in Å units)

	$\delta_{g\ obs.}$	$\delta_{g\ calc.}$ (a)	$\delta_{g\ calc.}$ (b)
O_1-C_3	$0.007_8 \pm 0.005_5$	0.007_1	0.007_0
C_2-C_4	$0.09_4 \pm 0.01_7$	0.072_3	0.087_8
O_1-C_4	$0.111_1 \pm 0.005_9$	0.105_2	0.111_2
O_1-O_5	$0.15_0 \pm 0.01_4$	0.162_7	0.151_0

(a) Harmonic approximation with ω_7 assumed to be 63 cm^{-1}.
(b) Large-amplitude analysis for ν_7 (see text).

Vibrational Effects

Conventional Calculations. *Mean Amplitudes.* If a linear equilibrium structure and small amplitudes of bending vibrations are presupposed for this molecule, the mean-square amplitudes for bonded and nonbonded atom pairs are related in the first approximation to the stretching vibrations only, namely Q_1 through Q_4. Provided the force constants representing the interactions between non-adjacent bonds are ignored and the normal frequencies are approximated by the fundamental frequencies, the force constants for the stretching vibrations can be determined uniquely, and the mean amplitudes can be calculated by a conventional method.[28] Table 2 lists the values derived in this way; they agree with those calculated by Brunvoll *et al.*[29] In striking contrast to the ex-

28) Y. Morino, K. Kuchitsu and T. Shimanouchi, *ibid.*, **20**, 726 (1952).

29) J. Brunvoll, S. J. Cyvin, I. Elvebredd and G. Hagen, *Chem. Phys. Lett.*, **1**, 566 (1968).

perience for ordinary molecules, where the present approximation is known to be valid,[30] the calculated values for the atom pairs C_2–C_4, O_1–C_4, and O_1–O_5 cannot account for the observed values. This implies that a higher-order effect due to the bending vibrations is important for the above-mentioned atom pairs.

Shrinkage Effects. The linear shrinkage effect is given by:[27]

$$\delta_g = \boldsymbol{D}[r_g], \tag{2}$$

where $\boldsymbol{D}$ stands for the operation of taking a difference of the quantity in brackets for a nonbonded atom pair and a sum of those for the component bonded pairs. If one assumes that the vibrations are *harmonic*, then the shrinkage may be approximated by the following expression:[27]

$$\delta_g = \boldsymbol{D}[(1/2r_e)\langle\Delta\rho^2\rangle], \tag{3}$$

where r_e is the corresponding bonded or nonbonded equilibrium distances and $\Delta\rho^2=\Delta x^2+\Delta y^2$ is linearly related to the squares of bending coordinates, Q_5^2, Q_6^2 and Q_7^2. The perpendicular amplitudes $\Delta\rho^2$ were calculated by the usual *GF* method,[31] with the quadratic force constant for the CCO bending transferred from the out-of-plane CCO bending constant of ketene.[32] Since the calculated shrinkages are insensitive to the differences of several wave numbers in ν_5 and ν_6, the observed fundamental frequencies ν_5 and ν_6 were used in place of the normal frequencies ω_5 and ω_6, respectively. On the other hand, the position of the maximum absorption (63 cm^{-1})[7] was tentatively substituted for the effective ω_7 frequency in order to estimate the shrinkages. Table 3 shows that the above harmonic approximation roughly accounts for the observed shrinkages.

The above conventional procedure thus fails to predict the observed mean amplitudes, although the agreement is fair for the shrinkages. The principal origin of the discrepancies in the mean amplitudes lies in the ν_7 bending vibration; the instantaneous displacements of certain nonbonded distances caused by this vibration should be much larger than those caused by the parallel vibrations ν_1 through ν_4 as a result of the large amplitude of the ν_7 vibration.

If the average values of the mass-adjusted bending coordinate ($\langle Q_7^2\rangle$ and $\langle Q_7^4\rangle$) and the ratio of the perpendicular amplitudes, $\Delta\rho_{CC}/\Delta\rho_{CO}$, are taken as parameters, one can analyze the observed mean amplitudes and shrinkages without assuming any explicit form of the potential function for the ν_7 vibration. According to a preliminary analysis of this kind,[33] the average value $\langle Q_7^2\rangle$ turns out to be about 3.0 amu Å^2, which corresponds to an effective normal frequency of *ca.* 68 cm^{-1}, being compatible with the thermodynamic and infrared results. Furthermore, the ratio $\langle Q_7^4\rangle/\langle Q_7^2\rangle^2$, which should be equal to 2 if the potential were harmonic,[*4] is estimated to be about 1.36. Thus the problem is to find a potential function that satisfies the above average values.

Large-amplitude Analysis for the ν_7 Vibration. *Hamiltonian Operator.* For ordinary triatomic molecules the potential function is expanded in terms of the normal coordinates, and the average values of interatomic displacements are calculated by a perturbation method.[34,35] However, this method is not suitable for the present problem because the large vibrational amplitude deteriorates the convergence. Thus it is simpler to use a curvilinear coordinates for this vibration at the expense of a more complicated expression for the kinetic energy. The mean amplitudes and shrinkages were calculated by the following model: The ν_7 mode is regarded as a set of doubly-degenerate slowly-varying coordinates, since this vibration has much lower frequency than the other vibrations. The atoms take curvilinear paths holding the bond distances (averaged over the vibrations ν_1 through ν_6) constant. This is equivalent to assuming that the effective force field characterizing the small-amplitude vibrations (ν_1 through ν_6) is independent of the ν_7 displacement.

Being analogous to the case of puckering motions in ring compounds[36] and that of quasi-linear molecules,[11] the reduced mass for this vibration depends on the ν_7 displacement coordinate. This was taken into account when the kinetic energy was set up in classical dynamics and converted into an operator representing the quantum-mechanical kinetic energy.

After the separation of translational motions, the ν_7 motion is described by a molecule-fixed coordinate system xyz, where the z axis corresponds to the equilibrium molecular axis, and the bending motion takes place in the xz plane, because the coupling between the ν_7 vibration and other bending modes has been ignored.

According to the above assumptions the in-

30) Y. Morino and T. Iijima, This Bulletin, **35**, 1661 (1962).

31) Y. Morino and E. Hirota, *J. Chem. Phys.*, **23**, 737 (1955).

32) G. B. Moore and G. C. Pimentel, *ibid.*, **38**, 2816 (1963).

33) M. Tanimoto, Thesis, The University of Tokyo (1969).

*4 For a doubly-degenerate harmonic oscillator, $Q_7^2=Q_{7a}^2+Q_{7b}^2$, it follows that $\langle Q_7^4\rangle=2\langle Q_7^2\rangle^2$.

34) L. S. Bartell, *J. Chem. Phys.*, **38**, 1827 (1963). A. Reitan, Thesis, Trondheim (1958).

35) Y. Morino and T. Iijima, This Bulletin, **36**, 412 (1963).

36) D. O. Harris, H. W. Harrington, A. C. Luntz and W. D. Gwinn, *J. Chem. Phys.*, **44**, 3467 (1966).

stantaneous coordinates of the atoms, $x(=\rho)$ and z, are given to a good approximation in terms of a mass-adjusted bending coordinate Q_7.

$$\left.\begin{array}{ll} O_1\ (d_1Q_7,\ -D_{12}-D_{23}) & C_2\ (d_2Q_7,\ -D_{23}) \\ C_3\ (d_3Q_7,\ 0) & C_4\ (d_2Q_7,\ D_{23}) \\ O_5\ (d_1Q_7,\ D_{12}+D_{23}) & \end{array}\right\} \quad (4)$$

where the constants d_i are equal to the $(i, 7)$ elements of the L_x matrix, usually defined for infinitesimal displacements around the linear position, and D_{ij} is defined as

$$D_{ij} = [r_{ij}^2 - (d_i - d_j)^2Q_7^2]^{1/2}. \quad (5)$$

The constants r_{12} and r_{23} represent the C=O and C=C distances, respectively, averaged over the normal modes ν_1–ν_6. Equation (4) shows that the ratio of the relative displacements of the C=C and C=O bonds in the direction of the ρ axis, $\Delta\rho_{CC}/\Delta\rho_{CO}$, assumes a constant value for the ν_7 vibration.

The kinetic energy for this motion is given by

$$2T = \sum m_i\boldsymbol{v}_i^2 + \sum m_i(\omega\times\boldsymbol{r}_i)^2 + 2\omega\cdot\sum m_i(\boldsymbol{r}_i\times\boldsymbol{v}_i), \quad (6)$$

where $\boldsymbol{v}_i$ and ω are the velocity of the atom i and the angular momentum of the molecule-fixed frame, respectively. Substitution of the coordinates $\boldsymbol{r}_i$ in Eq. (4) and their derivatives into (6) leads to

$$2T = M_7\dot{Q}_7^2 + I_{xx}\omega_x^2 + I_{yy}\omega_y^2 + I_{zz}\omega_z^2, \quad (7)$$

where M_7 is the reduced mass for the ν_7 vibration and I_{xx}, I_{yy} and I_{zz} are instantaneous moments of inertia. They are expressed in terms of Q_7 in the following way

$$\left.\begin{array}{l} M_7 = 1 + [2m_O\{(d_1-d_2)^2/D_{12} + (d_2-d_3)^2/D_{23}\}^2 + 2m_C(d_2-d_3)^4/D_{23}^2]Q_7^2 \\ I_{xx} = 2[m_O(D_{12}+D_{23})^2 + m_CD_{23}^2] \\ I_{yy} = 2[m_O(D_{12}+D_{23})^2 + m_CD_{23}^2] + Q_7^2 \end{array}\right\} \quad (8)$$

and

$$I_{zz} = Q_7^2.$$

In terms of the momenta P_m the kinetic energy takes the following form,

$$2T = \sum G^{mn}P_mP_n \qquad (P_m = P_x, P_y, P_z, P_7) \quad (9)$$

The coefficient G^{mn} is given by a diagonal matrix with elements I_{xx}^{-1}, I_{yy}^{-1}, I_{zz}^{-1} and M_7^{-1}.

The corresponding quantum-mechanical operator is given by the relation[37]

$$2T'_{QM} = G^{1/2}\sum P_mG^{mn}G^{-1/2}P_n, \quad (10)$$

where G is the determinant of G^{mn} and the wavefunction is normalized in the Cartesian coordinate system as in the case of a degenerate bending motion in a linear triatomic molecule.[38] Since the reduced mass depends on Q_7, the density factor defined in Ref. 37 contains contributions from higher powers of Q_7, whereas the resulting differential equation is equal to that for a two-fold degenerate vibration[39] as far as the zeroth-order terms are concerned.

In order to make the density factor proportional to Q_7, the following substitution is made

$$G^{-1/2} = I_0Q_7g^{-1/2}, \quad (11)$$

where I_0 is the moment of inertia about the x-axis in the equilibrium structure and

$$g^{-1/2} = 1 + FQ_7^2 \quad (12)$$

where the coefficient F is a function of the constants A, B, and C given in Appendix 1. When the factor $g^{-1/2}$ is taken into the kinetic energy operator, the resulting operator is given by

$$\left.\begin{array}{l} T_{QM} = g^{-1/4}T'_{QM}g^{1/4} \\ \quad = \dfrac{1}{2}g^{-1/4}G^{1/2}\sum P_mG^{mn}G^{-1/2}P_ng^{1/4} \\ \quad = T_{rot} + T_{vib}, \end{array}\right\} \quad (13)$$

where the rotational energy is

$$2T_{rot} = P_x^2/I_{xx} + P_y^2/I_{yy}. \quad (14)$$

The vibrational part

$$2T_{vib} = P_7^2 - \frac{i\hbar P_7}{Q_7} + \frac{P_z^2}{I_{zz}} + 6i\hbar AQ_7P_7 - 2AQ_7^2P_7^2 - F(8A-3F)\hbar^2Q_7^2 + F^2(2A+F)\hbar^2Q_7^4 \quad (15)$$

can be expanded in terms of a dimensionless coordinate $q_7=(2\pi c\nu/\hbar)^{1/2}Q_7$, where a constant ν, which has a dimension of frequency, can be chosen arbitrarily since it does not appear in the result of the analysis. Thus $2T_{vib}$ is divided into two parts,

$$2T_{vib} = 2T^0_{vib} + 2T'_{vib}, \quad (16)$$

where

$$2T^0_{vib} = -hc\nu\left[\frac{\partial^2}{\partial q_7^2} + \frac{1}{q_7}\frac{\partial}{\partial q_7} + \frac{1}{q_7^2}\frac{\partial^2}{\partial\chi^2}\right]$$

and

$$2T'_{vib} = 6\hbar^2Aq_7\frac{\partial}{\partial q_7} + 2\hbar^2Aq_7^2\frac{\partial^2}{\partial q_7^2} - F(8A-3F)\hbar^3q_7^2/2\pi c\nu + F^2(2A+F)\hbar^4q_7^4/(2\pi c\nu)^2$$

The operator T^0_{vib} leads to a differential equation for a two-fold degenerate vibration, where χ represents the angular coordinate. Following the treatment of puckering motions in a number of ring compounds,[40] the potential function is assumed to have the following form

$$V(Q_7) = aQ_7^4 + bQ_7^2 \quad (17)$$

37) E. C. Kemble, "The Fundamental Principles of Quantum Mechanics," McGraw-Hill, New York (1937), Sec. 35b.

38) D. M. Dennison, *Rev. Mod. Phys.*, **3**, 280 (1931).

39) W. H. Shaffer, *ibid.*, **16**, 245 (1944).

40) S. I. Chan, T. R. Borgers, J. W. Russell, H. L. Strauss and W. D. Gwinn, *J. Chem. Phys.*, **44**, 1103 (1966); J. Laane and R. C. Lord, *ibid.*, **47**, 4941 (1967).

Thermal Average Values of Normal Coordinates. With the approximate Hamiltonian operator obtained above, the thermal average values of even powers of the normal coordinate q_7 can be calculated in a straightforward way. The Hamiltonian matrix is set up with the orthonormal set of functions which diagonalize the Hamiltonian for the two-dimensional harmonic oscillator, and the matrix is diagonalized by Jacobi's method.*5 The anharmonic mean values of q_7 are calculated by a weighted sum,

$$\langle q_7^{2m}\rangle = \sum_{n,l}\langle n,l|q_7^{2m}|n,l\rangle \times \exp(-E_{n,l}/\boldsymbol{k}T)/\sum_{n,l}\exp(-E_{n,l}/\boldsymbol{k}T) \quad (18)$$

where $\langle n,l|q_7^{2m}|n,l\rangle$ denotes the expectation values for a transformed function numbered with n and l.

The harmonic mean values for q_1 through q_6 are calculated by[28]

$$\left.\begin{aligned}\langle q_i^{2m}\rangle &= \frac{(2m)!}{4m!}\left(\coth\frac{\boldsymbol{hc}\omega_i}{2\boldsymbol{k}T}\right)^m \quad (i=1-4)\\ \text{and}\\ \langle q_i^{2m}\rangle &= m!\left(\coth\frac{\boldsymbol{hc}\omega_i}{2\boldsymbol{k}T}\right)^m \quad (i=5,6)\end{aligned}\right\} \quad (19)$$

Mean Amplitudes and Shrinkage Effects. An instantaneous distance of an atom pair is expressed in terms of its Cartesian displacements up to the sixth power as

$$r = r_e + \Delta z + \frac{\Delta\rho^2}{2r_e} - \frac{\Delta z\Delta\rho^2}{2r_e^2} + \frac{\Delta z^2\Delta\rho^2}{2r_e^3} - \frac{\Delta\rho^4}{8r_e^3} - \frac{\Delta\rho^2\Delta z^3}{2r_e^4} + \frac{3\Delta z\Delta\rho^4}{8r_e^4} - \frac{\Delta\rho^6}{16r_e^5} - \frac{3\Delta\rho^4\Delta z^2}{4r_e^5} + \frac{\Delta\rho^2\Delta z^4}{2r_e^5} \quad (20)$$

The parallel displacement, Δz, may essentially be divided into two parts, $\Delta z_{\mathrm{I}}+\Delta z_{\mathrm{II}}$, where the first and second terms represent the changes in the projected bond length due to stretching and bending vibrations, respectively.[26] The Δz_{I} term may be expanded in terms of q_1 through q_4, while the Δz_{II} term may be expanded in terms of the perpendicular amplitudes $\Delta\rho$; by assumption the average values of the bond lengths are unchanged in the bending vibrations, so that the constraint, $\langle r\rangle = r_g$, exists for the bending vibrations. It therefore follows that

$$\Delta z_{\mathrm{II}} = (r_g^2 - \Delta\rho^2)^{1/2} - r_g = -\frac{\Delta\rho^2}{2r_g} - \frac{\Delta\rho^4}{8r_g^3} - \frac{\Delta\rho^6}{16r_g^5} + \cdots \quad (21)$$

for bonded atom pairs, and

$$\Delta z_{\mathrm{II}}(ij) = \Delta z_{\mathrm{II}}(ik) + \Delta z_{\mathrm{II}}(kl) + \cdots + \Delta z_{\mathrm{II}}(nj) \quad (22)$$

for nonbonded atom pairs i-k-$l\cdots j$. Thus, it is possible to express an instantaneous distance in terms of q_1 through q_7, and its thermal average value can be calculated by Eqs. (18) and (19).

The mean amplitudes l_g^2 may be calculated by the relation:[25]

$$l_g^2 = \langle r^2\rangle - \langle r\rangle^2 \quad (23)$$

and the shrinkages, δ_g, are calculated by the use of Eqs. (2) and (20).

Least-squares Analysis on Mean Amplitudes and Shrinkages. Two parameters a and b in the potential function, Eq. (17), and the ratio $\Delta\rho_{\mathrm{CC}}/\Delta\rho_{\mathrm{CO}}$, by which the shape of the ν_7 mode is specified, were used to adjust the calculated values of mean amplitudes and shrinkages. A least-squares method was applied with statistical weights estimated from the errors of their observed values. The HITAC 5020E in the Computer Centre of the University of Tokyo was used for this analysis. Thermal averages of the q_7 coordinate were calculated by solving a matrix of 30×30. The parameters a, b, and $\Delta\rho_{\mathrm{CC}}/\Delta\rho_{\mathrm{CO}}$ were refined until the deviations of the calculated values for the mean amplitudes and shrinkages were in the limits of their experimental errors. The final values of the determined parameters are listed in Table 4 with their estimated standard errors[41] and the parameters representing the vibrational coordinate.*6 The mean amplitudes and shrinkages calculated from the parameters are listed in the last columns of Tables 2 and 3, respectively. The $\Delta\rho$ ratio is estimated to be 1.30 ± 0.10. If the C=O and C=C bonds stay colinear in the ν_7 mode, the ratio should be equal to $r_{23}/r_{12}=1.10$. Thus the CCO angle does not deviate far from 180° in the ν_7 mode. The half bending angle,[19] $\alpha=1/2[180°-\angle(\mathrm{C{=}C{=}C})]$, is related to Q_7 as $\sin\alpha=\Delta\rho_{\mathrm{CC}}/r_{\mathrm{CC}}=0.145\ Q_7$.

*5 Perturbing terms involved in T'_{vib} do not mix states with different values of l, and hence, a separate matrix can be set up for each l value. Since v and l have the same parity, the rows and columns of a matrix for a given l are labeled by a series of either even or odd v numbers according to whether the l is even or odd.

41) Y. Morino and T. Nakagawa, *J. Mol. Spectry.*, **26**, 496 (1968).

*6 In our preliminary analysis, where the perturbing terms in the kinetic energy operator, T'_{vib}, were ignored and a first-order perturbation method was used, the potential function was estimated to be $V=1.35Q_7^4+43.6Q_7^2$ (cm^{-1}). This potential function was cited by Pickett and Strauss[42] in their calculation of the statistical entropy (61.94 cal/deg·mol). However, a subsequent, more rigorous procedure described in this article has shown that the first-order treatment is not accurate enough and the T'_{vib} terms make a significant contribution to $\langle Q_7^2\rangle$ and $\langle Q_7^4\rangle$. The values listed in Table 4 replace the above estimates. The presented study still ignores stretching-bending interactions, by which the C=O and C=C stretching force constants may change slightly with angle deformation.

42) H. M. Pickett and H. L. Strauss, *J. Chem. Phys.*, **51**, 952 (1969); H. L. Strauss, private communication (1970).

TABLE 4. POTENTIAL CONSTANTS AND DYNAMICAL PARAMETERS CHARACTERIZING THE ν_7 BENDING MODE[a)]

a	b	$\Delta\rho_{CO}/\Delta\rho_{CO}$	V_0[c)]	
23 ± 5[b)] $cm^{-1}\,amu^{-2}Å^{-4}$	-100 ± 31[b)] $cm^{-1}\,amu^{-1}Å^{-2}$	1.30 ± 0.10	110 ± 47[d)] cm^{-1}	
$\langle Q_7^2\rangle$	$\langle Q_7^4\rangle$	d_1	d_2	d_3
2.98 ± 0.10[d)] $amuÅ^2$	$12.0_9\pm0.7_7$[d)] $amu^2Å^4$	-0.110[e)] $amu^{-1/2}$	0.035[e)] $amu^{-1/2}$	0.222[e)] $amu^{-1/2}$

a) Derived from a least-squares analysis on the observed mean amplitudes and shrinkages. The potential function is expressed as: $V(Q_7)=aQ_7^4+bQ_7^2$ cm^{-1}, where $\sin\alpha=0.145Q_7$.
b) Random standard errors. The upper and lower signs should be taken in the same order because of the correlation of the parameters a and b.
c) Potential hump. See Fig. 3.
d) Evaluated from the standard deviations with allowance for the correlation among the parameters (Ref. 41). The uncertainties represent standard deviations. No systematic error due to the assumption made in the analysis is included.
e) Coefficients of the atomic ρ coordinates. Eq. (4).

Discussion

Bond Length. The r_a distances for the C=O and C=C atom pairs agree with the distances reported in earlier investigations within their limits of error.[12-14] The C=O bond length (r_g=(C=O)=1.163_2 Å) is shorter than that in carbon dioxide ($r_g=1.165_1$ Å) and is nearly the same as that in ketene ($r=1.16_1$ Å).[43] The distance between adjacent carbon atoms linked with a double bond, r_g(C=C)$=1.289_4$ Å, is appreciably shorter than 1.311_6 Å in allene[44] and nearly equal to 1.283 Å of the central C=C bond in butatriene.[45] A general rule, suggested by Stoicheff *et al.*[46] for the estimation of CC bond lengths from the number of adjacent atoms, leads to 1.282 Å in this case, in good agreement with the experimental r_g value.

Potential Function. The potential function for the bending mode ν_7, calculated with the values of a and b obtained above, is illustrated in Fig. 3. The potential energy rises steeply with increasing angle of bending, and possibly a small potential hump of the order of 100 cm^{-1} exists at the linear position. The potential nimimum appears at the α angle of about 12°. The random standard errors in the parameters listed in Table 4, not including systematic errors originating from the assumptions on which the present analysis is based, result in the uncertainties indicated as vertical bars in the figure. There is little doubt as to the quasi-linearity of the potential function for the ν_7 mode in spite of the above assumptions, whereas the double-minimum nature of the function, which is obscured appreciably by random and systematic uncertainties, is subject to a further critical examination by other experimental methods.

This potential function is consistent with those reported by Almenningen *et al.*,[12] who first suggested a double-minimum potential with humps ranging from 40 to 255 cm^{-1}. The mean amplitudes and shrinkages for 237°K and 508°K, calculated from the potential function given in Table 4, are found to be consistent with their observed values within their experimental uncer-

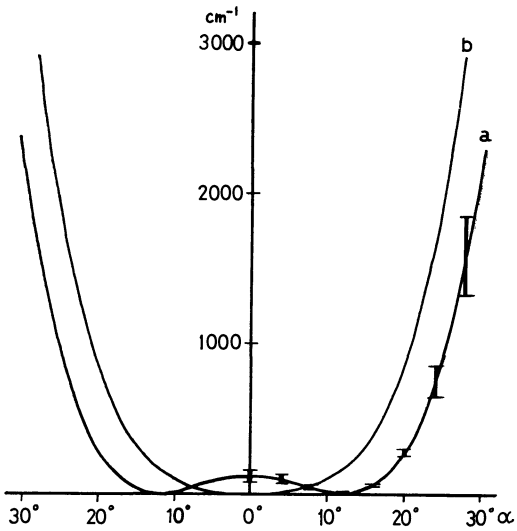

Fig. 3. Potential function for the ν_7 bending vibration in terms of the half bending angle $\alpha=(1/2)[180°-\angle(C=C=C)]$.
(a) Present study (Vertical bar represents random standard uncertainty estimated from the standard deviations in the potential constants a and b given in Table 4.
(b) Potential estimated by Redington (Ref. 10).

43) A. P. Cox, L. F. Thomas and J. Sheridan, *Spectrochim. Acta*, **51**, 542 (1959).
44) A. Almenningen, O. Bastiansen and M. Traetteberg, *Acta Chem. Scand.*, **13**, 1699 (1959).
45) A. Almenningen, O. Bastiansen and M. Traetteberg, *ibid.*, **15**, 1557 (1961).
46) C. C. Costain and B. P. Stoicheff, *J. Chem. Phys.*, **30**, 777 (1959); B. P. Stoicheff, *Tetrahedron*, **17**, 135 (1962).

tainties.*7

On the other hand, Redington[10] calculated the low-lying energy levels by the WKB method and determined the force constants on the assumption that $\nu_7(n,\ l=0,1\leftarrow 0,0)=63\ cm^{-1}$ and $\nu_7\ (1,1\leftarrow 0,0)=214\ cm^{-1}$. The frequencies of these transitions have not been established, however, because the observed absorption bands are evidently composed of many hot bands ($\Delta l=1$). His potential function shown in Fig. 3, $V(\alpha)=1500\alpha^2+45000\alpha^4$ (cm^{-1}) (the half bending angle α in radians), has no hump and rises moer steeply than the potential determined in the present study.

Centrifugal Effect. A comment should be made on the recent work of Smith.[47] He suggested that the excess in the O_1–O_5 vibrational amplitude observed by Almenningen *et al.*[12] over that calculated by an ordinary method was due to an oscillatory displacement of the nuclei as a result of the centrifugal force generated by the large-amplitude bending motion. If this were the case, the effective force balancing the centrifugal stretching should correspond to the force constants for the C=C and C=O bond stretching, because the centrifugal force acts in the bond direction and is most effective near the zero bending displacement, where the atoms have the largest angular velocities. The effect of the centrifugal force on the O_1–O_5 amplitude, calculated with a set of stretching force constants, turns out to be an order of magnitude smaller than that needed to account for the observed anomaly. Thus the centrifugal force cannot be the essential source of the anomaly. It is not permissible to estimate the centrifugal effect with a much smaller force constant representing "effective stretch-bend interactions" as he assumed in his calculation, because the physical significance of the equation is then lost. As the present analysis has shown, the observed O_1–O_5, O_1–C_4 and C_2–C_4 amplitudes can be explained by a large-amplitude model for the ν_7 vibration.

Statistical Entropy. The entropy due to the ν_7 vibration has been calculated using the potential function determined in the present study. In order to take account of the anharmonicity, the partition function is calculated by a direct summation over all the vibrational levels. The statistical entropy for 230°K and 1 atm is found to be 61.87 cal/deg·mol. This compares with the experimental values,[8] 62.12 ± 0.15 and 61.37 ± 0.11 cal/deg·mol; the ambiguity arises from alternative measurements of the heat of vaporization. According to the recent calculations of Pickett and Strauss,[42] the entropy is insensitive to the various bending potentials which have been suggested to fit the electron-diffraction data.

Infrared Spectra. A series of sharp band heads were observed by Milionis[48] in a high-resolution spectrum in the far-infrared region (20 to 300 cm^{-1}). The spectrum was interpreted in terms of a linear equilibrium structure and a strongly anharmonic vibration with a large increase in the rotational constant B with increasing values of the vibrational quantum number. Since the spectrum was analyzed parametrically, the shape of the potential function for the ν_7 vibration was not determined.

The shape of the ν_7 band has been estimated by the use of the potential function given in Table 4. According to Thorson and Nakagawa,[11] who discussed the characteristic features of the infrared spectrum of a quasi-linear molecule, the band intensities for the bending mode resemble those for a linear molecule, whereas the frequencies approach those for a bent molecule. As the potential hump at the linear position, if present, is estimated to be less than the thermal energy at room temperature, levels above the hump are densely populated. Therefore, the band intensities are calculated by using the band strength S corresponding to the transition in a linear molecule. The band strength is given for a molecule with no nuclear spins by the relation[49]

$$S = K\nu_0[1 - \exp(-\boldsymbol{h}\nu_0/\boldsymbol{k}T)]\,|R|^2 G \exp(-E/\boldsymbol{k}T) \tag{24}$$

where K is a constant, E is the energy of the lower state, R is the transition moment, ν_0 is the transition frequency, and G is a weight factor dependent on the transition (1 for transitions between a $\sum$-state and any other state, and 2 for all other transitions). The transition moment was calculated by the use of perturbed wavefunctions. The intensities of a series of the transitions $\Delta l=1$, $\Delta n=0$, which are analogous to the "pure rotational spectrum" of a bent molecule, are found to be much stronger than the other transitions. The calculated band contour has its absorption maximum at about 70 cm^{-1}, in contrast to the observed peak around 63 cm^{-1}.[7,48] Both observed and calculated bands have absorption peaks well below 63 cm^{-1}, but the calculated band has much fewer absorption maxima than the observed spectrum. The reason for this discrepancy is unknown. Should the present calculation be responsible for this discrepancy, possible sources are that the n dependence of B has been ignored and that the intensities of the

*7 After the present manuscript had been submitted to this Bulletin, the authors received a preprint from Dr. H. M. Seip (A. Clark and H. M. Seip, *Chem. Phys. Lett.*, **6**, in press (1970)). Their estimate of the potential is in good agreement with that of the present study.

47) W. H. Smith, *Chem. Phys. Lett.*, **3**, 430 (1969).

48) C. C. Milionis, Thesis, Massachusetts Institute of Technology (1969).

49) D. F. Eggers, Jr., and B. L. Crawford, Jr., *J. Chem. Phys.*, **19**, 1554 (1951).

P and R branches have been calculated jointly with those of the Q branches using Eq. (24).

Rotational Constant. The rotational constant B_0 has been determined to be 0.073206 ± 0.00002 cm^{-1} by Lafferty *et al.*[5] from the analysis of a $\Sigma_g^+ - \Sigma_g^+$ transition around 3170 cm^{-1}. This constant should be contrasted with the molecular geometry determined in the present study. For a system having a large-amplitude vibration, no theory is available by which one can calculate the "average" rotational constant B_z from B_0*8. If one assumes that the conventional second-order theory is applicable, the B_z constant is calculated from the above B_0 to be 0.07330 cm^{-1}. On the other hand, the average rotational constant can also be estimated from the observed r_g distances provided the approximate procedure of the r_g to r_α^0 conversion[50] is permissible. The B_α^0 constant estimated in this way is 0.0738 ± 0.0002 cm^{-1}. The two constants, B_z and B_α^0, which agree with each other for most nonlinear molecules,[51] thus seem to differ significantly. The origin of this discrepancy is left for a future study.

The authors wish to thank Professors O. Bastiansen, R. C. Lord, F. A. Miller, H. M. Seip and H. L. Strauss for their helpful comments and discussions. They are also indebted to Dr. T. Itoh of the Department of Physics for his valuable advice in deriving the quantum-mechanical Hamiltonian operator.

*8 *Added in proof:* After the present article was submitted for publication, the following paper has come to our attention: J. T. Hougen, P. R. Bunker and J. W. C. Johns, *J. Mol. Spectry.*, **34**, 136 (1970).

50) K. Kuchitsu, *ibid.*, **49**, 4456 (1968).

51) Y. Morino, K. Kuchitsu and T. Moritani, *Inorg. Chem.*, **8**, 867 (1969).

Appendix 1

The constants F and A in Eqs. (12) and (15) are given by the following relations:

$$F = A - B - C + 1/2I_0$$

$$A = m_O[(d_1 - d_2)^2/r_{12} + (d_2 - d_3)^2/r_{23}]^2 + m_C(d_2 - d_3)^4/r_{23}^2$$

where

$$B = 2m_O(r_{12} + r_{23})(d_1 - d_2)^2/r_{12}I_0$$

$$C = 2(d_2 - d_3)^2[m_O(r_{12} + r_{23}) + m_C r_{23}]/r_{23}I_0$$

and other parameters are defined in the text.

Appendix 2

The nonvanishing matrix elements of $q\frac{d}{dq}$ and $q^2\frac{d^2}{dq^2}$ are:

$$\left(\sigma, s \left| q\frac{d}{dq} \right| \sigma + 1, s\right) = -[(\sigma + 1)(\sigma - s + 1)]^{1/2}$$

$$\left(\sigma, s \left| q\frac{d}{dq} \right| \sigma, s\right) = -1$$

$$\left(\sigma, s \left| q\frac{d}{dq} \right| \sigma - 1, s\right) = [\sigma(\sigma - s)]^{1/2}$$

$$\left(\sigma, s \left| q^2\frac{d^2}{dq^2} \right| \sigma + 2, s\right) = [(\sigma + 1)(\sigma + 2)(\sigma - s + 1)(\sigma - s + 2)]^{1/2}$$

$$\left(\sigma, s \left| q^2\frac{d^2}{dq^2} \right| \sigma + 1, s\right) = 3[(\sigma + 1)(\sigma - s + 1)]^{1/2}$$

$$\left(\sigma, s \left| q^2\frac{d^2}{dq^2} \right| \sigma, s\right) = 1 - [(\sigma - s)(2\sigma + 1) + \sigma]$$

$$\left(\sigma, s \left| q^2\frac{d^2}{dq^2} \right| \sigma - 1, s\right) = -3[\sigma(\sigma - s)]^{1/2}$$

$$\left(\sigma, s \left| q^2\frac{d^2}{dq^2} \right| \sigma - 2, s\right) = [\sigma(\sigma - 1)(\sigma - s)(\sigma - s - 1)]^{1/2}$$

BULLETIN OF THE CHEMICAL SOCIETY OF JAPAN VOL. 43 2786—2795 (1970)

Photoreduction of Phenazine in Alcohols and by EDTA in the Aqueous Solution

Teiki IWAOKA, Shigeya NIIZUMA and Masao KOIZUMI

Department of Chemistry, Faculty of Science, Tohoku University, Katahira-cho, Sendai

(Received May 4, 1970)

By the combined use of the steady-light experiment and a flash technique, photoreduction of phenazine in methanol, ethanol, isopropanol and by EDTA in the aqueous solution and also the related elementary processes have been studied. The photoproduct has been identified as dihydrophenazine of which the absorption spectrum has been measured for the first time. It has been concluded that the lowest triplet, $T(\pi-\pi^*)$ is not a reactive state. Most probably the reactive state is a higher $T(n-\pi^*)$. The quantum yields of photoreduction in methanol, ethanol, and isopropanol are respectively 0.023, 0.037 and 0.050. Singlet-Triplet transition probability (Φ_{ST}) has been found to be >0.33 in the aqueous solution. Semiquinone produced in alcohols disappears by disproportionation reaction with almost the diffusion controlled rate constant while in the aqueous solution the disproportionation is much slower and at high EDTA concentrations, semiquinone is further reduced by EDTA. The absorption due to a molecular compound consisting of phenazine and dihydrophenazine has been detected in the visible region. It has been suggested that a certain equilibrium exists between three compounds and that a rather stable radical species, the existence of which has been proved by an ESR spectroscopy, participates in this equilibrium.

This paper is an extension of our photochemical investigation of acridine[1-5] and reports the general feature of the photoreduction of phenazine in alcohols and by EDTA in the aqueous solution all dearated which was elucidated by the steady light experiment and by flash photolysis.[6] At the time when we commenced this work, there was no work on the photoreduction of phenazine other than that of Toromanoff.[7] He reported that the deaerated 2-propanol solutions of phenazine (ϕ), when exposed to sunlight, yield two types of molecular compound, 3 phenazine-1 dihydrophenazine (violet) and 1 phenazine-1 dihydrophenazine (blue) but the final product obtained by the prolonged irradiation is dihydrophenazine (ϕH_2) (colourless). The interrelation of the molecular compound with the eventual photoreduction was unknown and even the electronic spectrum of dihydrophenazine was not found in literature.

A little later after we have finished the present work, a report by Bailey *et al.*[8] appeared. They studied mainly in acidic methanol and concluded that the photoproduct in weakly acidic solutions is dihydrophenazine while in strong acidic solutions the final product is a radical cation, ϕH_2^+. They also proposed that a reactive state is the excited singlet (n-π^*) state. But unambigous evidence for the formation of molecular complex was not given and the product in the weakly acidic solution, *i.e.* dihydrophenazine was not identified in any way.

We have investigated the photoreduction in pure methanol, ethanol and isopropanol and by EDTA in the aqueous solution. The results obtained agree with Bailey's in some points but not in others. This is natural partially because the experimental conditions are different. Firstly, we have demonstrated unequivocally, that the photoproduct is dihydrophenazine by comparing its absorption spectrum with that of chemically prepared dihydrophenazine. Secondly, strong evidence has been obtained for the view that a molecular complex consisting of ϕ and ϕH_2 is produced in solution in equilibrium with ϕ and

1) S. Niizuma, Y. Ikeda and M. Koizumi, This Bulletin, **40**, 2249 (1967).

2) A. Kira and M. Koizumi, *ibid.*, **40**, 2486 (1967).

3) M. Koizumi, Y. Ikeda and H. Yamashita, *ibid.*, **41**, 1056 (1968).

4) S. Niizuma and M. Koizumi, *ibid.*, **41**, 1090 (1968).

5) A. Kira and M. Koizumi, *ibid.*, **42**, 625 (1969).

6) It has already been reported previously that the photoreduction of phenazine by EDTA in the aqueous solution occurs most likely in a higher $T(n-\pi^*)$ state. M. Koizumi, Y. Ikeda and T. Iwaoka, *J. Chem. Phys.*, **48**, 1869 (1968).

7) C. Dufraisse, A. Etienne and E. Toromanoff, *Compt. Rend.*, **232**, 2379 (1951); **235**, 759 (1952); E. Toromanoff, *Ann. Chim.*, **1**, 115 (1956).

8) D. N. Bailey, D. K. Roe and D. M. Hercules, *J. Amer. Chem. Soc.*, **90**, 6291 (1968).

ϕH_2. A radical cation reported by Bailey *et al.* has also been detected by ESR in pure methanol but in a very small quantity. Thirdly, it has been concluded that our kinetic results cannot be consistently interpreted unless a higher $T(n\text{-}\pi^*)$ is a reactive state.

Before entering the experimental part, it will be convenient to write down the reaction scheme in alcohol (RH_2) which we would like to propose. The processes underlined are the main ones.

$$\underline{\phi \xrightarrow{h\nu} {}^1\phi^*} \quad (1)$$

$$\underline{{}^1\phi^* \longrightarrow {}^3\phi(n\text{-}\pi^*)} \quad (2)$$

$${}^3\phi(n\text{-}\pi^*) \longrightarrow {}^3\phi(\pi\text{-}\pi^*) \quad (3)$$

$$\underline{{}^3\phi(n\text{-}\pi^*) + RH_2 \longrightarrow \phi H\cdot + RH\cdot} \quad (4)$$

$${}^3\phi(n\text{-}\pi^*) + O_2 \longrightarrow \phi + O_2 \quad (5)$$

$${}^3\phi(n\text{-}\pi^*) + \phi \longrightarrow 2\phi \quad (6)$$

$${}^3\phi(\pi\text{-}\pi^*) + \phi \longrightarrow 2\phi \quad (7)$$

$${}^3\phi(\pi\text{-}\pi^*) + RH_2 \not\longrightarrow \quad (8)$$

$$\underline{2\phi H\cdot \longrightarrow \phi H_2 + \phi} \quad (9)$$

$$\phi H_2 + \phi \longrightarrow (\phi H_2 \cdots \phi) \quad (10)$$

In the case of the aqueous solution, (4) and (9) are replaced by

$${}^3\phi(n\text{-}\pi^*) + EDTA \longrightarrow \phi H\cdot + EDTA' \quad (4)$$

$$2\phi H\cdot \longrightarrow \phi H_2 + \phi \quad (9)$$

$$\phi H\cdot + EDTA \longrightarrow \phi H_2 + EDTA' \quad (9')$$

Experimental

Materials and Procedures. Phenazine rom Tokyo Kasei was purified by recrystallization from ethanol two times. Methanol, ethanol, isopropanol and tetrahydrofuran used as solvents were of Wako Junyaku and were distilled before use. Disodium ethylenediaminetetraacetate (EDTA) of Wako Junyaku G. R. grade was used without further purification. Palladium charcoal was kindly supplied by Professor Nakanishi.

An apparatus for the steady-light illumination and a flash apparatus are the ordinary ones used in our laboratory. The exciting light for the steady-light experiments was 365 nm from a Toshiba SHL-100UV mercury lamp monochromatized with suitable filters. The reaction temperature was always 25°C.

Results from the Steady-light Experiments

Photoreduction in Alcohols. Figures 1a, b, c, d give the spectral changes when the solutions of phenazine in methanol, ethanol, isopropanol and tetrahydrofuran were irradiated by 365 nm. Broadly speaking, they are similar in that the 362 nm peaks of phenazine decline monotonously with more or less shift to shorter wavelengths and with isosbestic points around 340 nm. The ultimate absorption spectra obtained by prolonged illumination are different from solvent to solvent; the peak positions are 345 nm (methanol), 358 nm (ethanol), 360 nm (isopropanol) and 320 nm (tetrahydrofuran). At first sight, these results led us to suspect that the photoproduct might not be dihydrophenazine, because dihydro compounds with the similar type of structure such as acridan in general, have no absorption in this wavelength region. Hence the hydrogenation of phenazine by two other methods were attempted. One is the reduction by treating the ethanol solution of

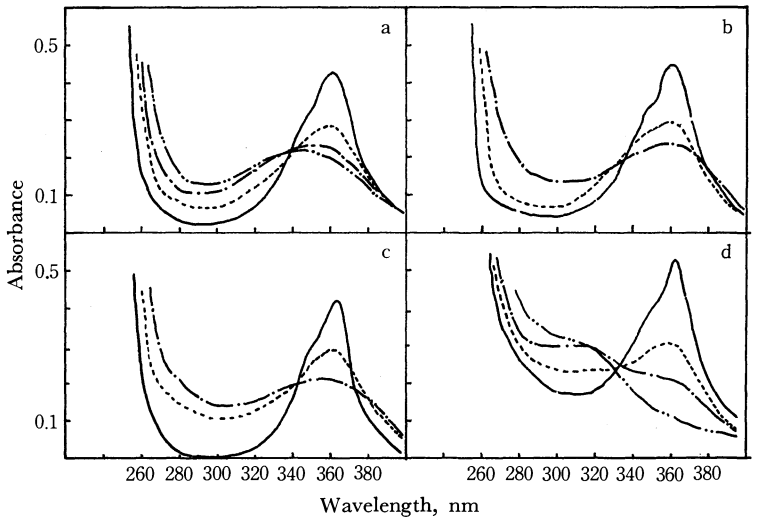

Fig. 1. Spectral change of phenazine in the deaerated solutions.
a: Methanol $[\phi]=3.3\times10^{-5}$ M. ——, 0 sec; - - -, 9 min; —·—, 27 min; —··—, 115 min
b: Ethanol $[\phi]=3.4\times10^{-5}$ M. ——, 0 sec; - - -, 7 min; —·—, 87 min
c: Isopropanol $[\phi]=3.9\times10^{-5}$ M. ——, 0 sec; - - -, 10 min; —·—, 24 min
d: Tetrahydrofuran $[\phi]=3.1\times10^{-5}$ M. ——, 0 sec; - - -, 2.5 min; —·—, 7 min; —··—, 60 min

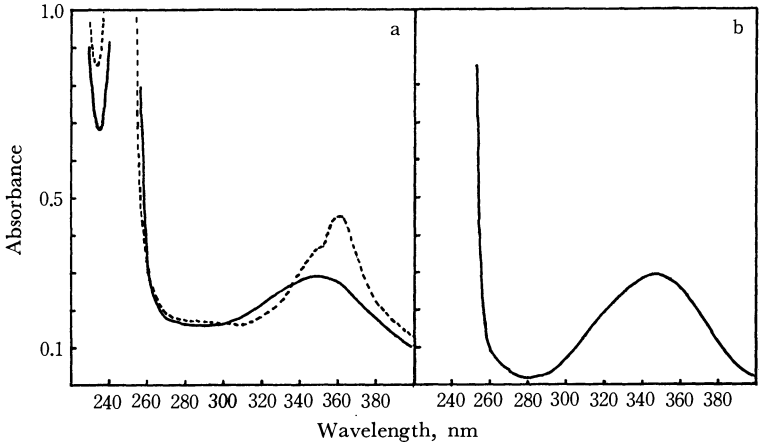

Fig. 2. Ultraviolet spectra of the chemically prepared dihydrophenazine.
a: By reduction with amalgamated sodium *in vacuo*. - - -, after air introduction.
b: By catalytic hydrogenation.

phenazine with amalgamated sodium *in vacuo*, and the other is the catalytic hydrogenation using palladium charcoal as a catalyst. As seen from Figs. 2a, and 2b, the absorption spectra of both products dissolved in ethanol agree with that of the photoproduct except for the lack of a slight absorption around ~280 nm. The difference may be due to the presence of aldehyde or some other photoproduct resulting from alcohol in the irradiated sample. Upon introduction of air, the chemically prepared dihydrophenazine was oxidized quantitatively to phenazine as shown in Fig. 2a, while the photoproduct gave some unknown substance in addition to phenazine, as judged from a slight shift of the absorption peak to the longer wavelength. Apart from these minor points, the agreement between the photoproduct and chemically prepared dihydrophenazine verifies that the photoproduct is dihydrophenazine and that it gives the absorption band near 340 nm. This may be due to the participation of lone pairs on nitrogen atoms in the π-electron system of the molecule.

Quantum Yields of Photoreduction in Alcohols. Figure 3 gives a typical example for photobleaching curves, which indicates that the photoreduction rate is simply proportional to the absorption of light. But in order to get the correct values of quantum yield, a certain correction should be made because the photoproduct absorbs the exciting 365 nm light to some extent. By assuming that the photoproduct merely acts as an inner filter, the following relation can easily be derived,

$$\ln(e^{2.303A}-1)-\ln(e^{2.303A_0}-1) = 2.303\Phi I_0\varepsilon\left\{t-\varepsilon' C_0\int_0^t (1/A)dt\right\}\times 10^3 \qquad (1)$$

where I_0, ε and ε' are respectively the incident light intensity (mol/cm^2 sec), molar extinction coefficients of phenazine and of the photoproduct

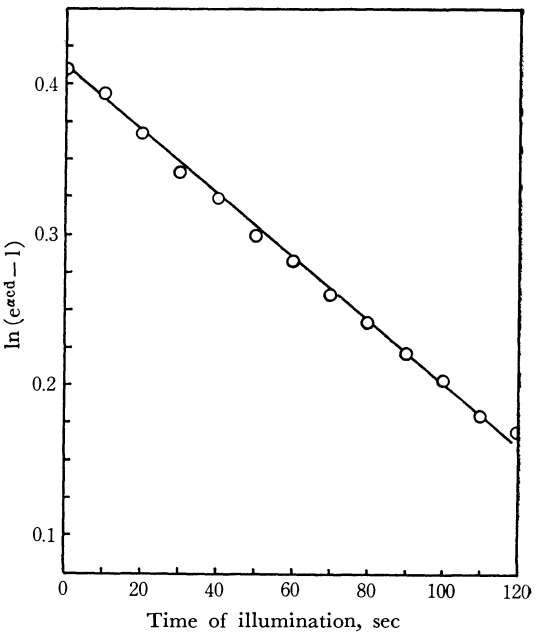

Fig. 3. Photobleaching curve of phenazine in the deaerated methanol solution.
$[\phi]=3.3\times10^{-5}$ M. α, absorption coefficient.
c, phenazine concentration
d, optical path length.

(both at 365 nm). The evaluation of the correction terms $\varepsilon' C_0\int_0^t (1/A)dt$ is a simple matter, and these corrections made on the time axis for the similar plots as in Fig. 3 give the corrected values of quantum yield. The quantum yields for the four solvents, corrected and uncorrected are given in Table 1. The quantum yield increases in the order, methanol<ethanol<isopropanol; this is the same as the order of easiness with which α-hydrogen is detached from alcohols.

TABLE 1. QUANTUM YIELD (Φ) OF PHOTOREDUCTION

	Concn. of phenazine (M)	Φ, uncorrected	Φ, corrected
CH_3OH	3.3×10^{-5}	0.0094	0.023
C_2H_5OH	3.4×10^{-5}	0.016	0.037
$(CH_3)_2CHOH$	3.1×10^{-5}	0.020	0.050
Tetrahydrofuran	3.7×10^{-5}	0.031	0.062

Retarding Effect of Oxygen on the Photoreduction of Phenazine in Methanol and Ethanol. Since dihydrophenazine is sensitive to oxygen, the photoreduction does not occur in the aerated solutions. This is in sharp contrast to acridine which is reduced to acridan by a molecular mechanism even in the presence of oxygen. When the aerated solutions of phenazine in methanol or in ethanol are irradiated by 365 nm for a long time, the original peak of phenazine at 362 nm gradually shifts to red and attains to 370 nm and 375 nm in the case of methanol and ethanol respectively. These shifts may perhaps be due to some oxidation reaction which yields, for instance, phenazine oxide. Along with these shifts, a new small band appeared at about 510 nm, the assignment of which is still unknown. The above spectral changes, however, proceed at very slow rates and no appreciable spectral change was observed by several minutes' irradiation. In such a short time illumination, oxygen is considered as a mere quencher on the photoreduction and the retarding effect of a small quantity of oxygen is expected to afford the information about the intermediate which is attacked by oxygen. From such a viewpoint, the photoreduction of phenazine in methanol and ethanol containing oxygen in the order of 10^{-5} M were investigated. It was really found that the spectral change is not essentially different from that of the completely deaerated solution. Some typical photobeaching curves are shown in Fig. 4. The plots are somewhat similar to those obtained in the case of acridine[3] in the point that the bleaching occurs at much slow rate in the initial stage and after a certain time interval the rate increases rather rapidly to the final value which is 70—90% of the rate in the deaerated solution. These results imply that in the initial stage oxygen prevents the photoreduction by attacking some intermediate, and that the final rate is attained after oxygen is consumed by the reaction, for instance, with semiquinone. Figure 5 shows the dependence of Φ (obtained from the initial slopes in Fig. 4) on the oxygen concentration. Presuming tentatively that oxygen*1 attacks $^3\phi$-

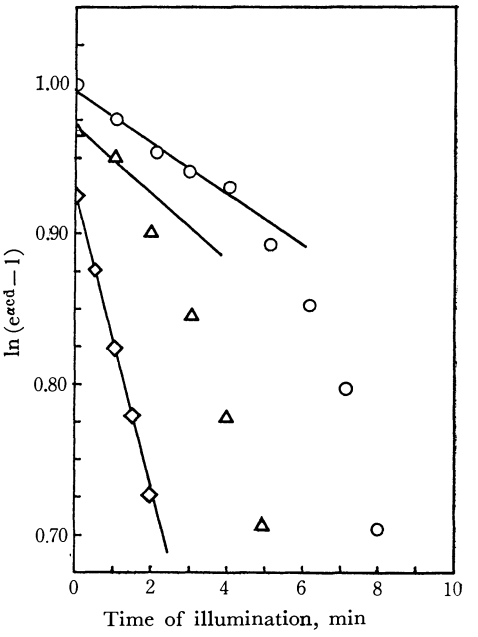

Fig. 4. Photobleaching curve of phenazine methanol solution, dissolving a small amount of oxygen.
○: $[O_2]=2.05\times10^{-5}$ M, △: 1.38×10^{-5} M,
◇: $[O_2]=0$ M

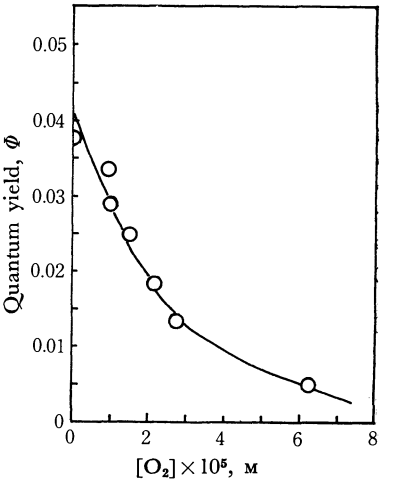

Fig. 5. Dependence of the quantum yields on the oxygen concentration in ethanol solution.
$[\phi]=3—6\times10^{-5}$ M

(n-π^*), the data can be treated simply by the following equation,

$$1/\Phi = (1/\Phi_0)\times(1+k_5[O_2]/k_3) \quad (2)$$

where Φ_0 and Φ are the quantum yields in the absence and in the presence of oxygen respectively. Assuming that the quenching process is diffusion controlled, and putting $k_5=10^{10}$ M^{-1} sec^{-1}, the estimated lifetime of the intermediate in methanol and ethanol was 8×10^{-6} and 5×10^{-6} sec respectively.

*1 It will be demonstrated later that this intermediate is neither semiquinone nor the excited singlet state. (See Discussion.)

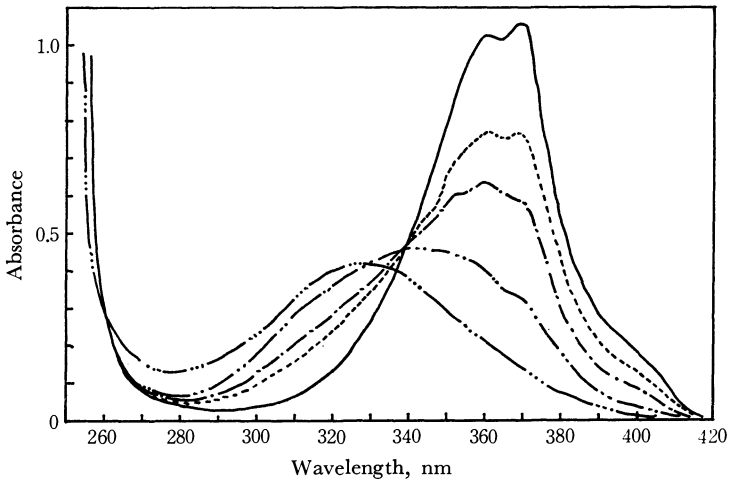

Fig. 6. Spectral change of phenazine in the aqueous solution involving EDTA.
$[\phi]=8.4\times10^{-5}$ M. $[EDTA]=7.9\times10^{-3}$ M.
Time of illumination,
—— before illumination, - - - 40 sec, —·— 80 sec, —··— 270 sec,
—···— 165 min

Photoreduction of Phenazine by EDTA in the Aqueous Solution. To get a better insight into the mechanism of the photoreduction in question, the reaction with a reducing agent (EDTA) dissolved as a solute in an inert solvent (H_2O) was investigated. pH of the solution containing EDTA is *ca.* 6. A typical example of the spectral change caused by 365 nm irradiation is shown in Fig. 6. It is seen that the reaction proceeds in a simple way with a higher rate than in organic solvents. The spectrum for 165 min irradiation shows a slight deviation from the isosbestic point, perhaps due to the decomposition of dihydrophenazine. In contrast to alcoholic solutions, there is no sign of the superposition of the absorption band due to some other photoproduct. Upon introduction of air, phenazine was recovered almost quantitatively unless the illumination period was not so long.

Dependence of the Quantum Yield on the Concentration of Phenazine and of EDTA in the Aqueous Solution. The phenazine concentration effect was investigated because it is well known that the triplet states of some substances are often quenched by the same substances in the ground state. Fixing the concentration of EDTA at 7.9×10^{-3} M, the concentration of phenazine was changed from 3×10^{-5} to 1×10^{-4} M. The results are shown in Fig. 7. It is to be added that a small absorption becomes observable at 450 nm at higher concentrations of phenazine; this may be

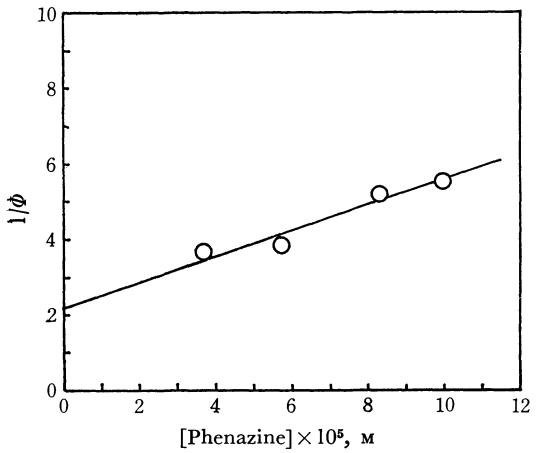

Fig. 7. Dependence of the quantum yield on the phenazine concentration in the aqueous solution involving EDTA as a reducing agent.
$[EDTA]=7.9\times10^{-3}$ M

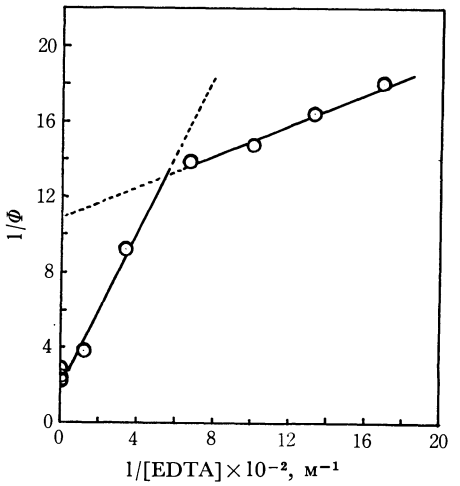

Fig. 8. Dependence of the quantum yield on the concentration of EDTA in the aqueous solution.
$[\phi]=5.0\times10^{-5}$ M

attributed to the formation of a certain molecular complex as will be described later. Since the absorption spectrum is not essentially affected by the above change in the phenazine concentration, decrease in the quantum yield with increasing phenazine concentrations is due to deactivation of a certain reactive state by phenazine in the ground state.

The quantum yield increases with the increase of EDTA concentration but becomes practically constant above 3×10^{-2} M. Figure 8 gives the plot of $1/\Phi$ against 1/[EDTA]. It is apparent that the plot consists of two linear portions. This is due to the processes (9) and (9′) as will be more fully established later. Assuming that the entire reaction consists of (1), (2), (3), (4), (6), (9) and (9′), the lower limit of the intersystem crossing probability, Φ_{ST} was evaluated from the intercept of the plot in Fig. 8 as 0.33. If this is a true value for Φ_{ST}, the values of k_6/k_4 and k_3/k_4 are calculated from the slope of the plot in Fig. 7 and the slope/intercept of the plot in Fig. 8 as follows,

$$k_4/k_3 = 2.7\times10^{2}\ \text{M}^{-1}$$
$$k_4/k_6 = 1.3\times10^{-2}$$

Investigation by a Flash Technique

Transient Spectra in Various Media. Figure 9 shows the transient spectra in various media and at various time points after flashing. Since

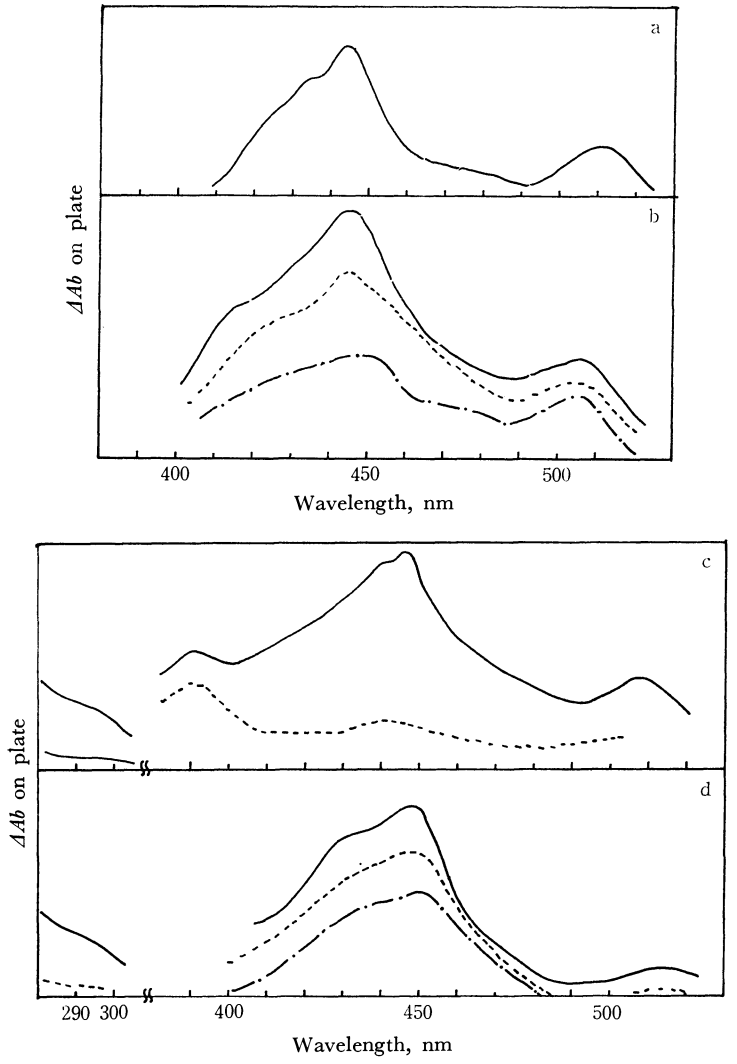

Fig. 9. Transient absorption spectra in the deaerated various solutions of phenazine.
a: Cyclohexane, —— 30 μsec after flashing.
b: Water, —— during photolysis; - - - after 17 μsec; —·— 30 μsec.
c: Methanol, —— 65 μsec after flashing; - - - 365 μsec.
d: Water involving EDTA, [EDTA]=3.2×10^{-2} M; —— during photolysis; - - - 17 μsec after flashing; —·— 1200 μsec

photoreduction does not occur in the plain aqueous solution, the transient spectra observed in these cases are safely assigned as $T(\pi-\pi^*)$. In the case of the reactive media on the other hand, two transient species can be discriminated, short lived and relatively long lived ones. The comparison with the results for inert media leads to the assignment that the former is $T(\pi-\pi^*)$ and the latter is most likely semiquinone. These assignments will be further substantiated by the findings described later. The characteristic bands for $T(\pi-\pi^*)$ are

490—525 nm (510), 410—470 nm (~445), <300 nm

and are essentially the same in different solvents. The numbers in parentheses are for the peak positions. The results are consistent with those of Bailey *et al.*[8]

The absorption of semiquinone in the aqueous solution was investigated in some details. From Fig. 9d it is evident that there is a prominent absorption in the 400—480 nm (~450 nm) region in agreement with the spectrum given by Bailey *et al.*[8] The assignment of this band to semiquinone is supported by the fact that the absorbance at 320 nm due to dihydrophenazine increases in a parallel way with the decrease in absorbance at 445 nm. The transient increase in absorbance occurs in the neighborhood of 360 nm and this means that the gain in absorption by semiquinone supersedes the loss due to the disappearance of phenazine. At 340 nm *i.e.* at the isosbestic point of the steady light reaction, the opposite phenomenon is observable. Although the exact measurement of the absorption spectrum of semiquinone was not attempted, the tentative values of extinction coefficient at some selected wavelengths were determined in the following way. Assuming that dihydrophenazine is exclusively produced by disproportionation of semiquinone in methanol and that in the aqueous solution, semiquinone is further reduced by EDTA (when its concentration is high) (see below), the yield of the semiquinone was estimated from the decrease in the phenazine concentration by one flash. The ε-values thus obtained are given in Table 2. Although these values are not very reliable but may be used for the semiquantitative discussion on the kinetic data.

Table 2. ε-Values of semiquinone

	390 nm	400 nm	430 nm	450 nm
in methanol	2.1×10^4	1.2×10^4	1.4×10^4	1.7×10^4
in water	$(6.0\pm1)\times10^3$ at 445 nm			

Kinetics for the Elementary Reactions. The decay of semiquinone in methanol was measured at 390 nm where the absorption of other species does not exist. As shown in Fig. 10, the

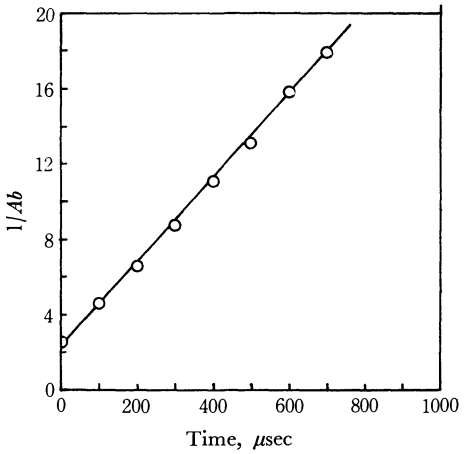

Fig. 10. Second order decay of phenazine semiquinone in the deaerated methanol solution observed at 390 nm.

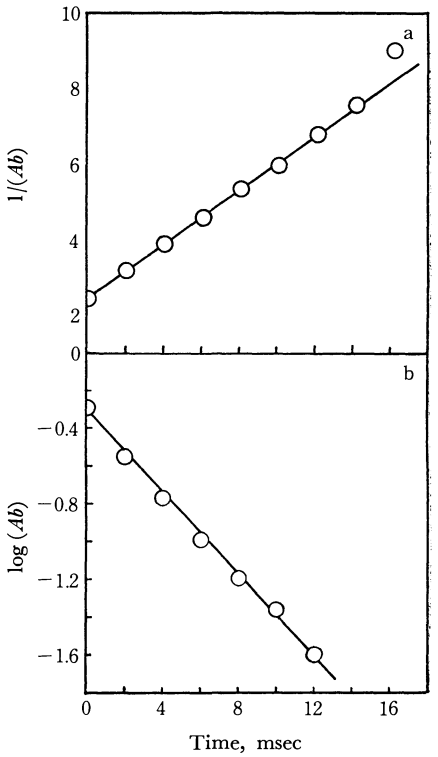

Fig. 11. Decays of phenazine semiquinone in the aqueous solutions involving EDTA as a reducing agent, observed at 445 nm.
a: Second order decay at low EDTA concentration, [EDTA]$=7.9\times10^{-3}$ M
b: First order decay at high EDTA concentration, [EDTA]$=7.7\times10^{-2}$ M

decay was found to be satisfactorily reproduced by the second order plot throughout the entire stage beginning from the end of flashing. This is one of the strongest evidences that $T(\pi-\pi^*)$ still surviving after flashing, does not participate in

the reaction. It can also be concluded that the semiquinone does not react with alcohol nor with alcoholic radical produced in the preceeding process. The analysis was also made at 445 nm where the triplet absorption superposes, by making use of the data in the later stage. The results obtained are moderately satisfactory and the ultimate value for the disproportionation rate constant is $(3.0\pm 0.5)\times 10^9$ M^{-1} sec^{-1}. The semiquinone in the aqueous solution survives a longer time than in alcohol. This made it possible to measure the decay rate at 445 nm. It has been found that the decay consists of two processes, disproportionation reaction and the reaction with EDTA. Of course the former prevails in low concentrations of EDTA while the latter is predominant in the opposite condition. This is shown in Fig. 11. In general the decay can be treated by the following equation which takes into account the above two processes.

$$-\mathrm{d}[\phi\mathrm{H}]/\mathrm{d}t = 2k_9[\phi\mathrm{H}]^2 + k_{9'}[\phi\mathrm{H}][\mathrm{EDTA}] \quad (3)$$

From this equation the following relation can easily be derived.

$$\log A - \log (A + k_{9'}[\mathrm{EDTA}]\varepsilon \cdot d/2k_9) = -k_{9'}[\mathrm{EDTA}]t/2.303 \quad (4)$$

This relation fits the decay curve quite satisfactorily. By making experiments at various EDTA concentrations, the ultimate values of k_9 and $k_{9'}$ were evaluated as follows.

$$k_9/\varepsilon d = (1.8\pm 0.2)\times 10^2, \quad k_9 = 1.1\times 10^7 \text{ M}^{-1}\text{ sec}^{-1},$$
$$k_{9'} = \sim 3\times 10^3 \text{ M}^{-1}\text{ sec}^{-1}$$

These values are not so much reliable, particularly so for the disproportionation reaction because of the uncertainty of the ε-value.

The decay of $T(\pi\text{-}\pi^*)$ in methanol was measured at 280 nm, where the absorption of semiquinone is small, though not negligible. The decay is neither first order nor second order. Assuming that $T(\pi\text{-}\pi^*)$ is not a reactive state, the analysis was made by the following formula

$$\ln (A - A(\phi\mathrm{H})) = -kt + \text{const} \quad (5)$$

where $A(\phi\mathrm{H})$ is the absorbance of semiquinone and can be evaluated from the extrapolation of the later stage of the $1/A$ - t plot in case of methanol. In the aqueous media the similar procedure was allowed for low EDTA concentrations but the log A - t plot must be used for high EDTA concentrations. The first order rate constant obtained for methanol is $\sim 10^4$ sec^{-1}. Figure 12 gives the dependence of the decay rate on the concentration of EDTA in the aqueous solution. Figure 12 definitely shows that the addition of EDTA does never increase the decay constant of $T(\pi\text{-}\pi^*)$. The effect is rather opposite and may be due to the difference in physical properties of the solutions such as pH or ionic strength. The dependence of the decay rate on the phenazine concentration was similarly investigated, in order to know whether the triplet state $T(\pi\text{-}\pi^*)$ is deactivated by the ground state molecule or not. The result as shown in Fig. 3, clearly demonstrates the occurrence of such a process. The k_7-value was estimated to be $\sim 4\times 10^7$ M^{-1} sec^{-1}.

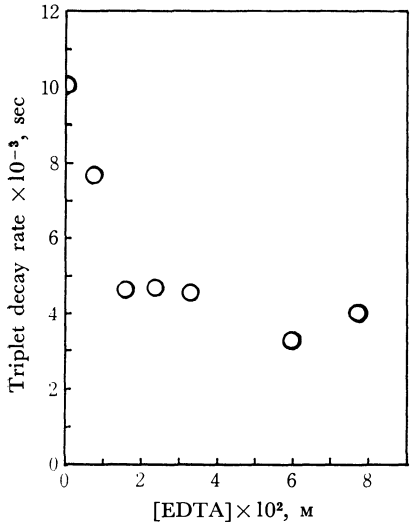

Fig. 12. Dependence of the decay rate of phenazine triplet, $T(\pi\text{-}\pi^*)$ on the concentration of EDTA in the aqueous solution.
[ϕ]=5×10^{-5} M

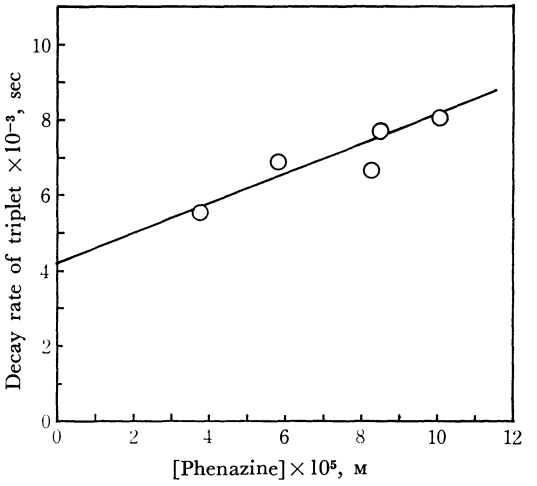

Fig. 13. Dependence of the apparent first order decay constant of phenazine triplet, $T(\pi\text{-}\pi^*)$ on the phenazine concentration.
[EDTA]=7.9×10^{-3} M

The Formation of Molecular Complex and a Radical Species related with it

In the course of the steady light experiment, a remarkable fact was found that in the illuminated solutions of rather high phenazine concentrations (from 10^{-4} to 10^{-2} M), a new small absorption band appears in the $\sim$450 nm region, as shown in

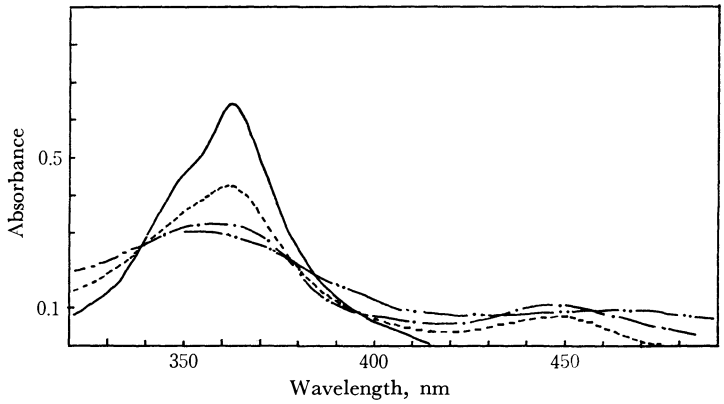

Fig. 14. Spectral change of the deaerated methanol solution in the high phenazine concentration. $[\phi]=1.7\times10^{-4}$ M. —— 0 min, - - - 6 min, —·— 12 min, —··— 199 min

Fig. 14. This band with a peak at 450 nm gradually grows with the time of illumination and in about 30 minutes attains its maximum and then declines slowly accompanied with a shift to the longer wavelength. The ultimate position of the peak is usually about 500 nm. The quantum yields of the photoreduction in the case that the above band was observed, were not essentially different and the spectral changes from 300 to 400 nm region was the same as that in other cases. All these facts are understandable if one assumes that the visible absorption is due to the complex formation occuring between phenazine and dihydrophenazine and the equilibrium exists between them with a rather small equilibrium constant for the complex formation.

Since the complex consisting of 3 phenazine-1 dihydrophenazine and 1 phenazine-1 dihydrophenazine has been reported by Toromanoff *et al.*,[7] the molecular weight of the photoproduct was examined by mass spectrometry. Thus the deaerated ethanol solution of phenazine was illuminated for about three hours, and then the solid mixture obtained by distilling off the solvent, was submitted to mass spectrometry. A fragment with a molecular weight about two times that of phenazine was really detected but most of the fragments are of the molecular weight near that of phenazine. No fragment of larger molecular weight was not detected. The solid mixture consisting of the complex, phenazine and dihydrophenazine was found to display the ESR signal. When the degassed methanol solution of phenazine 1×10^{-3} M was illuminated in a capillary cell for ESR with a light of 365 nm, the signal was clearly detected and it increased in intensity with the time of irradiation. The signal intensity was found to remain constant for a long time after the irradiation was stopped. Hence the signal is due to a certain stable paramagnetic species different from neutral semiquinone radical which is not so stable. The complex itself may be paramagnetic, but some other radical species might be formed in the equilibrium system $\phi+\phi H_2 \rightleftarrows (\phi\cdots\phi H_2)$ in solutions. In the former case a molecular complex may be of a charge transfer type or the dimer of the semiquinone radical. However, we have some evidence for identifying the paramagnetic species as the radical cation reported by Bailey *et al.*,[8] though it is not clear how it is formed. Further studies are now in progress.

General Discussion

As to the reactive state of phenazine, the results obtained exclude definitely the possibility of the lowest $T(\pi\text{-}\pi^*)$ being a reactive state. Evidence in addition to the one already described are as follows. Firstly, in alcohols the decay constant of $T(\pi\text{-}\pi^*)$, $k\lesssim10^4$ sec^{-1} is too small for considering it as a reactive state because this value cannot compete with the quenching action of $\sim10^{-5}$ M oxygen. If the reactive state were $T(\pi\text{-}\pi^*)$, the reaction would have to be retarded by oxygen far more efficiently than was observed. Secondly, in the aqueous solution, the decay rate of $T(\pi\text{-}\pi^*)$ does not increase by the addition of EDTA in the amount which is enough to make the steady reaction to occur.*2 Thus the remaining possible states are certain higher $T(n\text{-}\pi^*)$ or the singlet excited state. But the latter is not likely in view of the result that the quantum yield becomes constant at and above the EDTA concentration of $\sim3\times10^{-2}$ M. Furthermore, the inhibiting action of oxygen of 10^{-5} M in methanol cannot be understandable if the reactive state is the excited singlet.

The view that a $T(n\text{-}\pi^*)$ is a reactive state is

*2 Baiely *et al.* concluded from somewhat similar argument as above, that the lowest $T(\pi\text{-}\pi^*)$ is not a reactive state. But their argument does not seem to be strong enough to support the excited singlet mechanism and to reject the $T(n\text{-}\pi^*)$ state.

further supported by the following consideration about the intermediates attacked by oxygen. At first sight it seems reasonable to consider that oxygen attacks only semiquinone in addition to the final product, ϕH_2. But this is highly improbable because semiquinone would have a much longer lifetime than $5—8\times10^{-6}$ sec (the value of lifetime estimated for the intermediate attacked by oxygen). One must therefore consider another shorter-lived intermediate attacked by oxygen and there is no other state conceivable than a certain higher $T(n–\pi^*)$. The exact lifetime of $T(n–\pi^*)$ however, cannot be evaluated, since the deactivation process of $T(n–\pi^*)$ by oxygen is superposed by the reaction between semiquinone and oxygen. Hence the above value $5—8\times10^{-6}$ sec is an overestimation. The real value may be $\lesssim1\times10^{-6}$ sec.

The result that the quantum yield is much less in alcohols than the Φ_{ST} value obtained for the aqueous solution, 0.33 (lower limit) can be attributed to the difference of reactivity of alcohol molecules and EDTA. The exact value of Φ_{ST} will be determined in near future.

As for the semiquinone, it disappears in methanol only by disproportionation and its rate constant approximates the diffusion controlled value. This differs from Bailey's result in acidic medium where the disproportionation is rather slow. In the aqueous solution on the other hand, the reaction with EDTA occurs in addition to the disproportionation. The rate constant for the former is $\sim3\times10^3$ M^{-1} sec^{-1} and for the latter $\sim1\times10^7$ M^{-1} sec^{-1}. The result that the $1/\Phi$ - 1/[EDTA] plot consists of two linear portions is related with these two reactions. Thus the overall quantum yield when the semiquinone disappears by disproportionation is expected to be half that when it is reduced to dihydrophenazine by EDTA. The result in Fig. 8 is qualitatively consistent with this expectation. Much smaller rate constant of disproportionation in the aqueous solution may be due to the liquid state.*3 If one assumes that the lifetime of $T(n–\pi^*)$ in the aqueous solution, is the same as that in alcohol, then the rate constants k_4 and k_6 in the aqueous solutions are evaluated as $k_4=3\times10^8$ M^{-1} sec^{-1}, $k_6=2\times10^{10}$ M^{-1} sec^{-1}, from the values of $k_4/k_3=2.7\times10^2$ M^{-1} and $k_4/k_6=1.3\times10^{-2}$ obtained by the steady light experiments. The value of k_6 is compared with the rate constant, 4×10^7 M^{-1} sec^{-1} for the reaction $T(\pi–\pi^*)+\phi\rightarrow2\phi$.

The determination of the exact Φ_{ST} value, the dependence of the stability of semiquinone on the solvent property, especially the dependence on pH, and more decisive evidence for $T(n–\pi^*)$ as a reactive state by means of the triplet energy transfer await further studies. In particular, further investigations on the molecular complex and the radical species related with it will be most interesting.

*3 It is well comprehended that Bailey's result in acidic media is rather similar to the present one in the aqueous solutions.

BULLETIN OF THE CHEMICAL SOCIETY OF JAPAN VOL. 43 2796—2800 (1970)

Photochromic Reaction of *N*-Nitroso-*N*-alkylaniline in the Aqueous Solution—A Contribution to the Photochemistry of Nitrosamine

Mikio Hoshino, Hiroshi Kokubun and Masao Koizumi

Department of Chmistry, Faculty of Science, Tohoku University, Katahira, Sendai

(Received May 8, 1970)

It has been found that the aqueous solution of *N*-nitroso-*N*-methylaniline when irradiated by 253.7 nm shows photochromism. The unstable photoproduct reconverts to the original compound photochemically as well as thermally. The quantum yields for the forward and backward reaction are respectively 0.23 and 0.58. *N*-Nitroso-*N*-ethylaniline also reacts in the similar way. In the alcoholic solutions, different types of reaction occurred; in the absence of oxygen the reaction is mainly the formation of *N*-methylaniline. It has been suggested that the present photochromism is due to the *cis-trans* isomerization.

Photochemical reactions of nitrosamines have attracted much attention in recent years because of various and interesting types of reaction. One type is a splitting of nitrous oxide, an example of which is $(CH_3)_2N-NO \rightarrow (CH_3)_2N\cdot + NO$ studied by Banford in the gaseous state.[1] Another type of reaction is a photoaddition of *N*-nitrosodialkylamine to olefines followed by the C–C double bond cleavage.[2] The third is an intramolecular rearrangement of the following type studied extensively by Chow,[3-5] and by others,[6,7] from the organic viewpoint,

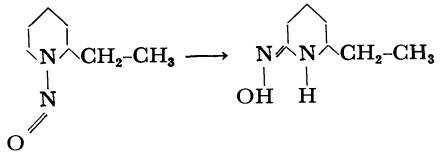

Chow in one of his papers, mentioned the non-reactivity of *N*-nitroso-*N*-methylaniline (NMA) even in the acidic mixture of water and alcohol. We have found, however, that this compound shows an interesting type of photochromism in the aqueous solution although the eventual reaction does not occur. The present paper reports on this newly discovered photochromism and some observations related with it.

Experimental

Materials. NMA was prepared by a usual method from *N*-methylaniline and nitrous acid and purified by vacuum distillation.

Procedures. A light source is a 6 W germicidal mercurs lamp. The absorption spectrum was measured by a Hitachi EPS-3T spectrophotometer. The gradual change of the optical density with time was followed at several fixed wavelengths on the same instrument.

Results

Photochromism and the UV Spectrum of the Product. When the aqueous solution of 1.32×10^{-4} M NMA was irradiated by 253.7 nm for about five minutes, the UV spectrum displayed a change as shown in Fig. 1. Further it was found

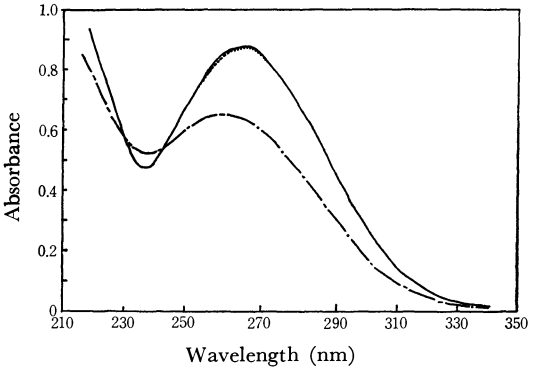

Fig. 1. Spectral change.
—— Spectrum of NMA in the aqueous solution(a)
—·— after irradiation at 253.7 nm for 5 min(b)
····· after being kept in dark for 30 min

that the original spectrum was almost completely recovered by keeping the irradiated solution in dark for thirty minutes. This photochromism was observed in quite the same way in the degassed solution indicating the non-participation of oxygen in the reaction. When one plots the decrease

1) C. H. Banford, *J. Chem. Soc.*, **1939**, 12.
2) Y. L. Chow, *J. Amer. Chem. Soc.*, **87**, 4642 (1965).
3) Y. L. Chow, *Can. J. Chem.*, **45**, 53 (1967).
4) Y. L. Chow, *Tetrahedron Lett.*, **1964**, 2333.
5) Y. L. Chow, *ibid.*, **1964**, 2473.
6) E. M. Burgass and J. M. Lavanish, *ibid.*, **1964**, 1221.
7) T. Axenrod and G. W. A. Milne, *ibid.*, **1967**, 4443.

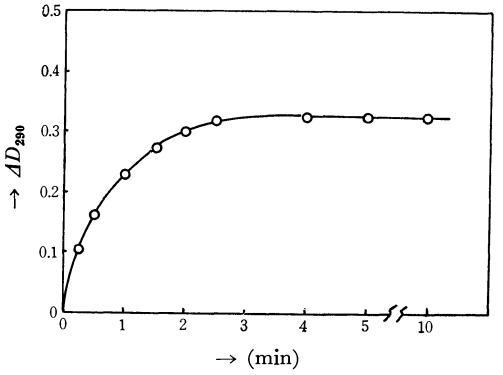

Fig. 2. Change of D (at 253.7nm) with time of irradiation.

in the optical density, ΔD at 290 nm against the time of irradiation, ΔD reaches a certain limiting value in about four minutes as shown in Fig. 2. This indicates that the photoproduct which absorbs the exciting light (see below) is not transformed photochemically to any other compound than NMA and that the photostationary state holds between the forward and backward reaction.

The absorption spectrum of the photoproduct was obtained in the following way. The ratios of the optical density of the absorption spectrum a and b in Fig. 1 were evaluated at various wavelengths and were found to be constant beyond 290 nm. This means that the photoproduct has no absorption in this region. On the basis of this assumption, the absorption of the photoproduct can easily be obtained. The result is shown in Fig. 3.

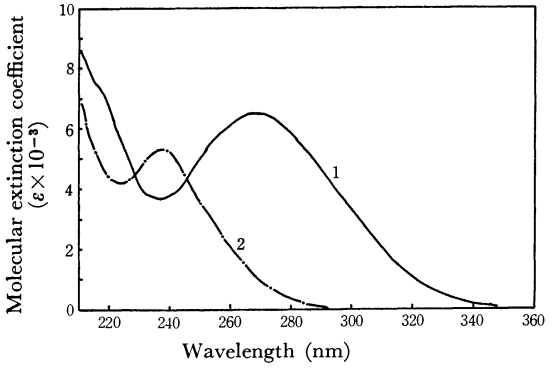

Fig. 3. Spectrum of the photoproduct.
——— Spectrum of NMA
—·— unstable photoproduct in the aqueous solution

Kinetics of the Recovery Reaction. As shown in Fig. 4, the recovery of the initial spectrum proceeds in a simple manner with isosbestic points at 320 nm and 243 nm.

The reaction is interpreted by the following most simplest scheme,

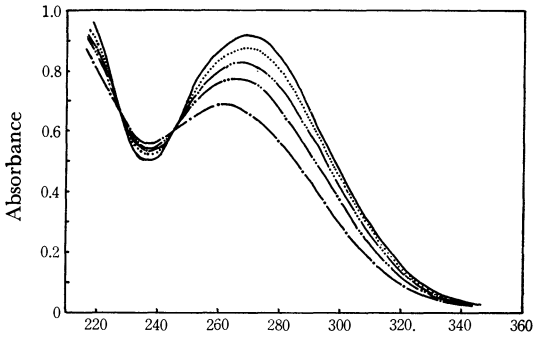

Fig. 4. Thermal recovery of spectrum.
——— before irradiation
—·—· after irradiation for 5 min
—··— kept in dark for 2 min
—···— kept in dark for 4 min
····· kept in dark for 10 min

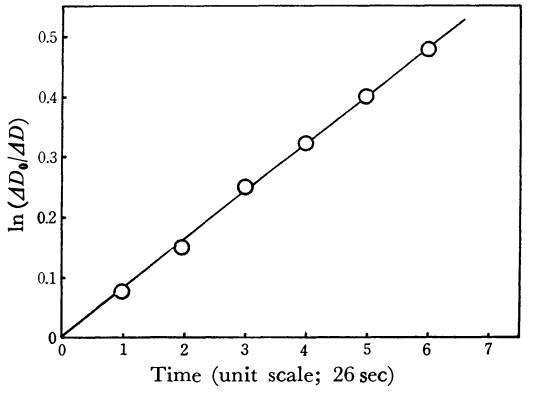

Fig. 5. Plot of $\ln(\Delta D_0/\Delta D)$ (at 290 nm) against time of irradiation.

$$\mathrm{B} \longrightarrow \mathrm{A}$$

where B is the photoproduct and A is the original compound. From the above scheme the following equations hold,

$$D = \varepsilon_A C_A + \varepsilon_B C_B$$

$$\Delta D = \varepsilon_A C_A^0 - (\varepsilon_A C_A + \varepsilon_B C_B) = (\varepsilon_A - \varepsilon_B) C_B$$

$$-\frac{d\Delta D}{dt} = k\Delta D$$

where D is the optical density of the sample at time t, $\Delta D = D_0 - D$ and C_A^0 is the original concentration of NMA. The other notations are the usual ones. Figure 5 gives the plot of $\ln(\Delta D_0/\Delta D)$ against time. From the slope of the plot one obtains the value of the rate constant at 17°C as 3.08×10^{-3} sec^{-1}. Thus the lifetime of the photoproduct at this temperature is about 5.5 min.

The Effect of Light Intensity on the Steady State and the Evaluation of the Quantum Yields for the Two Opposed Reactions. Since the backward reaction in photochromism often proceeds photochemically, the dependence of the steady state on the light intensity was examined.

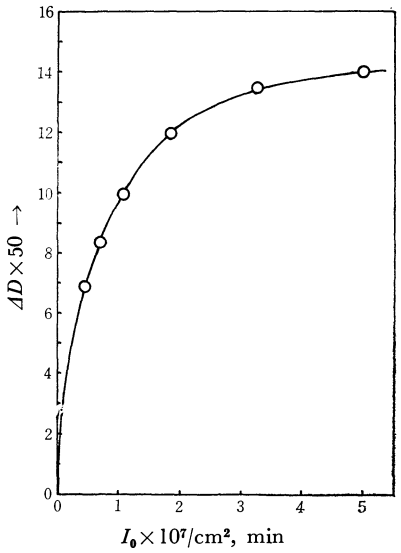

Fig. 6. Dependence of ΔD_∞ (at 290 nm) on light intensity.

As seen from Fig. 6, the limiting value of ΔD_∞ at 290 nm increases appreciably with the increase in light intensity when it is low but gradually tends to a constant value which is only a fraction of the original optical density. This indicates that the backward reaction involves the photochemical reaction in addition to the thermal one.

On the basis of the following scheme,

$$A \underset{k}{\overset{h\nu}{\rightleftarrows}} B \quad (h\nu)$$

the result given in Fig. 6 was analysed in the following way. The rate of the forward reaction is

$$\frac{dC_B}{dt} = \Phi_{AB} I_0 (1 - e^{-2.303D}) \left(\frac{D_A - \alpha D_B}{D} \right) - kC_B$$

where D, D_A and D_B are the optical densities of the sample, A- and B- species at time t and Φ_{AB} and $\alpha\Phi_{AB}=\Phi_{BA}$ are respectively the quantum yields for the forward and backward reactions. In the photostationary state, the relation

$$\Phi_{AB} I_0 (1 - e^{-2.303D}) \frac{D_A - \alpha D_B}{D} = kC_B$$

holds, and this equation can be rewritten as follows.

$$\Phi_{AB}(1 - (D_B/D_A)\alpha) = (1/I_0)(1/1 - e^{-2.303D})(D/D_A)kC_B \quad (= \Gamma)$$

Since all the quantities involved on the right hand term are known experimentally, the values of Γ at various light intensities can easily be obtained. Then the Γ *vs.* (D_B/D_A) plot should be linear with an intercept Φ_{AB} and the slope $\Phi_{AB}\alpha=\Phi_{BA}$. Figure 7 shows the result obtained when the light intensities were changed at the constant concentration

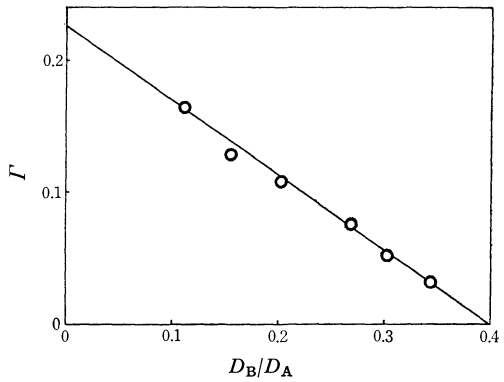

Fig. 7. Plots of Γ *vs.* D_B/D_A.
$\Gamma=(1/I_0)(1/1-e^{-2.303D})(D/D_A)kC_B$

of NMA, 1.56×10^{-4} M, at 17°C. It was checked that the rate of the thermal backward reaction always remained constant. The values of quantum yield for the forward and backward reactions thus obtained are

$$\Phi_{AB} = 0.23, \qquad \Phi_{BA} = 0.58$$

The intercept of the abscissa which corresponds to the infinite light intensity gaves the values of Φ_{AB}/Φ_{BA}, because the relation $\Phi_{AB}D_A=\Phi_{BA}D_B$ holds under this condition. The value of Φ_{AB}/Φ_{BA} evaluated by this method is 0.4 in complete agreement with 0.39_4 calculated from the values of Φ_{AB} and Φ_{BA} obtained above.

Photoreaction of Other Related Nitrosamines in the Aqueous Solution. Some other nitroso-compounds were investigated in order to know whether they show the similar photochromism or not. It was found that *N*-nitroso-*N*-ethylaniline (NEA) displays quite the same photochromism as shown in Fig. 8. On the other hand, *N*-nitrosodiethylamine 10^{-3} M in the aqueous solution decomposed photochemically without any sign of pnotochromism. *N*-nitrosodiphenylamine 5.3×10^{-5} M in the aqueous solution also did not

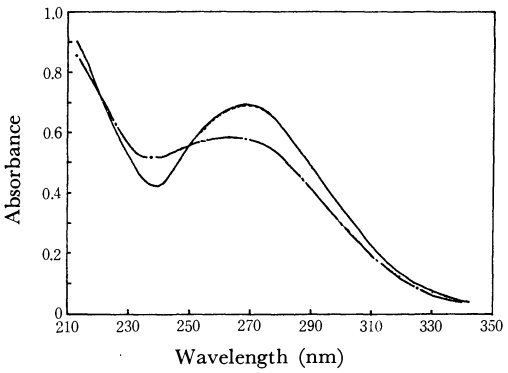

Fig. 8. Spectral change of NEA in the aqueous solution.
—— Spectrum of NEA
—·— after 5 min irradiation (at 253.7 nm).

show photochromism and only the formation of carbazole was observed.

Reaction in Ethanol. In order to know whether the similar photochromism occurs in other solvents, the reaction of NMA and NEA in alcohols were investigated preliminarily. When the degassed ethanol solution of 1.08×10^{-4} M of NMA was irradiated by 253.7 nm, the absorption spectrum changed quite rapidly with two distinct isosbestic points, as shown in Fig. 9. But in this case the final product was found to be stable. It was identified as *N*-methylaniline for the following reason. Firstly, NMA in ethanol gives no emission, while the sample irradiated for 25 minutes gives the fluorescence spectrum with two peaks at 345 nm and 430 nm, and the measurement of the excitation spectra clearly showed that these two peaks belong to the two different emitting species. The excitation spectrum for the 345 nm peak agrees with that of *N*-methylaniline, and moreover, the fluorescence spectrum of this compound coincides almost exactly with the shorter wavelength part of the spectrum of the irradiated sample (Fig. 10). The absorption spectrum also supports this identification.

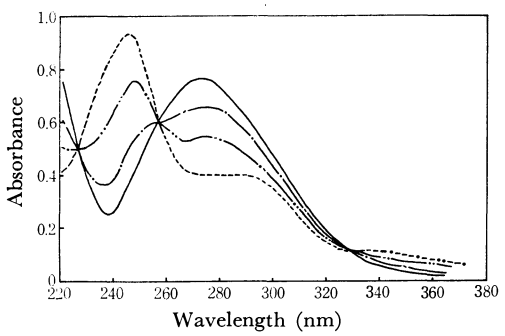

Fig. 9. Spectral change of NEA in degassed ethanol solution.
——— before irradiation
—·—· 4 min irradiation
—··— 8 min irradiation
····· 12 min irradiation

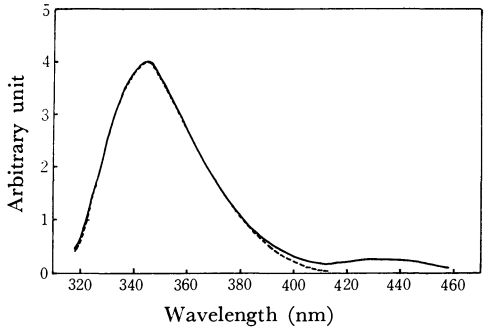

Fig. 10. Fluorescence spectrum of the photoproduct when the degassed ethanol solution of NMA was irradiated at 253.7 nm for 12 min.
——— solid line
– – – *N*-Methylaniline in ethanol

On the other hand, the aerated ethanol solution when irradiated, gave a quite different absorption spectrum, which is shown in Fig. 11. The photoproduct in this case has not yet been identified although there is no doubt that it is not *p*-nitroso-*N*-methylaniline. Somewhat similar spectral change was also observed upon irradiation of the aerated ethanol and cyclohexane solutions of *N*-nitroso-*N*-ethylaniline.

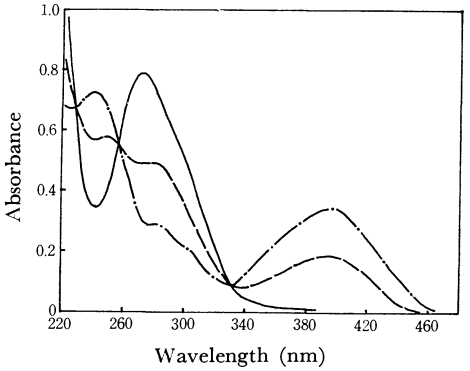

Fig. 11. Spectral change of NEA in the aerated ethanol on the irradiation at 253.7 nm.
——— before irradiation
— — after 6 min
—·— after 12 min

Discussion

The unstable photoproduct produced in the present photochromism has not yet been fully identified. Here, a plausible interpretation will be given by taking into consideration the results reported in literature. Chow in his study on photochemical isomerization reaction of nitrosamines, presumes the formation of a ring of the –N–C– type, as follows,

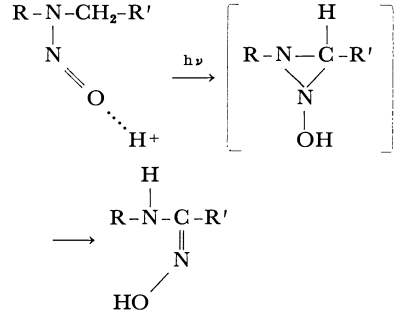

If one considers as a possible interpretation, that the present photoproduct has such an annular structure, then the C–N bond instead of the N–N bond should be broken for the present photochromism to occur. This, however, is not reasonable in view of the bond strength of C–N and N–N. As another possibility, *cis-trans* isomerization is conceivable and this is very plausible. Karabatsos

et al.[8] in their studies on the structure of *N*-nitroso-*N*-alkylamines by means of NMR, proposed the existence of the following *cis-trans* isomerization in *N*-nitroso-*N*-alkylamines,

8) G. J. Karabatsos and R. A. Taller, *J. Amer. Chem. Soc.*, **86**, 4373 (1964).

According to them, only the *cis*-form exists in case that *R* is methyl, while in ethyl and isopropyl, *trans-form* can also be existent in equilibrium with the *cis-form*. They proposed that the absorption of the *trans-form* is located in the shorter wavelength than that of the *cis-form*. In view of these results it is very likely that the present photochromism is the *cis* to *trans* isomerization. The non-occurrence of photochromism in alcoholic solution may be due to the preponderance of other types of reaction.

BULLETIN OF THE CHEMICAL SOCIETY OF JAPAN VOL. 43 2800—2804 (1970)

The Precise Coulometric Titration of the Acidic Primary Standard using Amperometric End-point Detection

Takayoshi Yoshimori and Ikuko Matsubara

Faculty of Engineering, Science University of Tokyo, Shinjuku-ku, Tokyo

(Received November 5, 1969)

The sensitive amperometric end-point procedure (*Anal. Chem.*, **23**, 1662 (1951)) with an antimony electrode is used in the titrations of acids. The cyclic voltammetric curves of the electrode indicate the possibility of the use of the above method for the titration of acids. The purities of potassium biphthalates (primary standard substances) are determined directly by precise coulometric titration with this end-point location. The standard deviations of the results (99.999%) are 0.007 or 0.008%. The purity of the benzoic acid prepared as the standard material for the calorimeter is also determined by this method. The standard deviation of these results (99.993%) is 0.009%.

Many investigations have indicated that coulometric titration is the most precise and accurate method in analytical chemistry. The purities of several primary standard substances have been directly determined by this method.[1-5]

Although the relative standard deviation by this method has been 0.003% in the most accurate studies, there are several problems in obtaining this value in ordinary laboratories without atmospheric control. Among these problems, the location of the end-point of the titration is the most important, especially in the titration of an acid or a base.[6] A pH meter with a glass electrode has been preferably used in locating the end-point of the titration. This potentiometric method has, however, several disadvantages because of the very high impedance of the electrode.

In the direct determination of the bulk material in a sample, a large amount of the sample should be taken in order to decrease the error in weighing. This causes the need to use a correspondingly large electrolytic current; otherwise, the electrolysis cannot be finished within a reasonable time interval. The electric field in the titrating cell caused by such a large electrolytic current then interferes with the high impedance circuit, that is say, the indication of the pH meter for end-point detection. After the current is cut off, it is necessary to wait several minutes in order to measure the pH value of the titrating solution. Furthermore, it is also necessary to measure many pH values in order to draw the titration curve clearly.

On the other hand, the circuit for the amperometric end-point location has a low impedance. Therefore, the disturbance caused by the electrolytic current disappears; also, only a few measurements are enough to locate the end-point. Chris-

1) J. K. Taylor and S. W. Smith, *J. Res. Nat. Bur. Stand.*, *A*, **63**, 153 (1959).
2) G. Marinenko and J. K. Taylor, *ibid.*, *A*, **67**, 31; 453 (1963).
3) E. L. Eckfeldt and E. W. Shaffer, Jr., *Anal. Chem.*, **37**, 1534 (1965).
4) G. Marinenko and J. K. Taylor, *ibid.*, **39**, 1568 (1967).
5) J. Knoeck and H. Diehl, *Talanta*, **16**, 181 (1969).
6) T. Yoshimori and I. Hikawa, *Bunseki Kagaku*, **16**, 927 (1967).

tian[7] has already recommended the use of the amperometric method in locating the end-point of a coulometric titration, and the present authors have had the same experience. However, only a few amperometric methods have yet been used in the case of the titration of an acid or a base.

The present authors have now tried to use an antimony electrode with the aid of a sensitive amperometric end-point procedure,[8] they have obtained fairly satisfactory results.

Experimental

Apparatus and Reagents. The apparatus used for the amperometric titration with an antimony electrode and that used for the coulometric generation of hydroxyl ions are shown in Fig. 1. The generating

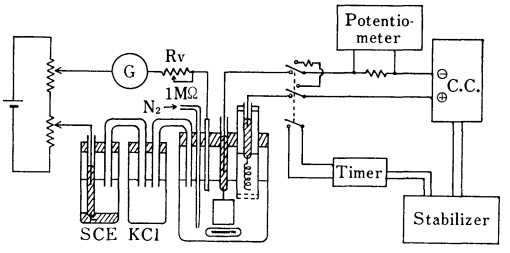

G: Galvanometer (2×10^{-9} A) C.C.: Constant current source

Fig. 1. Apparatus.

current was measured with a standard resistor and a potentiometer. The error in the measurement of the current had a standard deviation of less than 0.005%. As the Faraday constant, 96487.2 coulomb was used. The generating current was kept constant by the following method; the fine adjuster of the constant-current source was regulated so as to keep as small as possible the deflection of the galvanometer (Sens. 10^{-6} V) connected to the potentiometer in the electrolytic circuit.

The 50-Hz oscillator of a quartz crystal and a cycle counter were used to measure the time interval of the electrolysis.[9]

The potential between the antimony electrode and a saturated calomel electrode was 0.50 volt for the titration of potassium biphthalate and 0.58 volt for benzoic acid. According to the character of the electrode, and also according to the pH value at the end-point, this potential should be chosen from the titration curve obtained by a preliminary potentiometric titration of the sample.

All the weights were corrected to standard weights. A weighing bottle of nearly the same weight as that containing the sample was used as a counterpoise. A lipless beaker made from polystyrene (about 200 m*l*) was used as the cell. An auxiliary electrode compartment, made from a polyethylene tube with an agar-agar diaphragm,[6] was installed through a silicone rubber stopper. About a 100-mg portion of barium carbonate was added into the compartment in order to neutralize the acid produced by the anodic reaction.

All the reagents were of an analytical grade, and all were used without further purification. For the purity determination of potassium biphthalate, a 0.5 M potassium chloride solution was used as the electrolyte, while for benzoic acid a 30% v/v ethanolic solution of 0.7 M potassium chloride was used.

Procedure. *Drying of the Sample.* Potassium biphthalate was heated at 120°C for 4 hr and then cooled in a desiccator containing concentrated sulfuric acid for 1.5 hr.

Benzoic acid was dried by the following two methods. First, the acid was dried in the desiccator containing concentrated sulfuric acid for 72 hr. Secondly, it was melted in a platinum crucible at 135°C,[10] cooled under the same conditions as above for 1.5 hr, and then weighed and introduced into the cell.

Coulometric titration. Place an electrolytic cell containing 100 m*l* of a potassium chloride solution (0.5 M) in a thermostat. Introduce nitrogen (free from carbon dioxide) for more than 40 min; then neutralize the solution with electrolytically-generated hydroxyl ions until the galvanometer in the indicator circuit shows zero. At this point, the potential of the antimony electrode (*vs.* SCE) coincides with the voltage of the potentiometer in the indicator circuit.

A weighed sample is introduced into the solution, and nitrogen is allowed to flow through for about 10 min. The solution is then electrolyzed with a constant current until it is neutralized to the previous pH value. The end-point of the electrolysis can be located by the point at which the galvanometer in the indicator circuit reaches zero. During the electrolysis, nitrogen must be allowed to flow over the electrolyte (not through the solution). Early in the titration, the indicator current through the galvanometer must be regulated with a variable resistor (1 MΩ).

Results and Discussion

Before the practical use of the antimony electrode, the cyclic voltammetric curves of the electrode were recorded with the instrument named Electroscan 30 (Beckman Instrument Co.). Typical cyclic voltammetric curves thus obtained at pH 4.0, 7.0, and 9.0 are shown in Fig. 2 (a).

Figure 2 (b) is an example of the curve obtained at pH 4.0. Identical curves were obtained at pH 7.0 and 9.0. This figure shows that the potentials of the zero-current point in cathodic curves (from the positive to the negative direction) coincide with one another. Since the pH of the electrolyte changes from acidic to basic near the end of the titration, the good reproducibility of the zero-current potential of the electrode from the positive to the negative direction demonstrates

7) G. D. Christian, *J. Electroanal. Chem.*, **11**, 94 (1966).

8) W. D. Cooke, C. N. Reilley and N. H. Furman, *Anal. Chem.*, **23**, 1662 (1951).

9) T. Miwa, T. Yoshimori and T. Takeuchi, *Kogyo Kagaku Zasshi*, **67**, 2045 (1964).

10) I. M. Kolthoff and E. B. Sandell, "Textbook of Quantitative Inorganic Analysis," 3rd. Ed., MacMillan Co., New York (1952), p. 529.

that the electrolyte has the same pH value when the indicator current becomes zero (galvanometer zero). Thus, the titration of acid with electrolytically-generated hydroxyl ions will be possible with the antimony electrode and a sensitive amperometric end-point procedure.

Determination of the Purities of Potassium Biphthalates. The results obtained for the analyses of potassium biphthalates are shown in Table 1. In this case, the samples were weighed with a semimicrobalance; the error in the measurement of the electricity was less than 0.01% as a standard deviation. These accuracies are the same as those of the potentiometric method reported previously.[6]

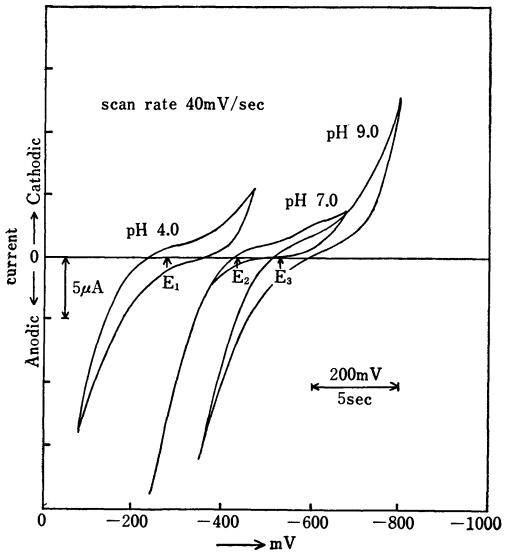

Fig. 2(a). Current-voltage curves of antimony electrode
$E_1 \sim E_3$: equilibrium potentials of the electrode measured by the very high impedance circuit.

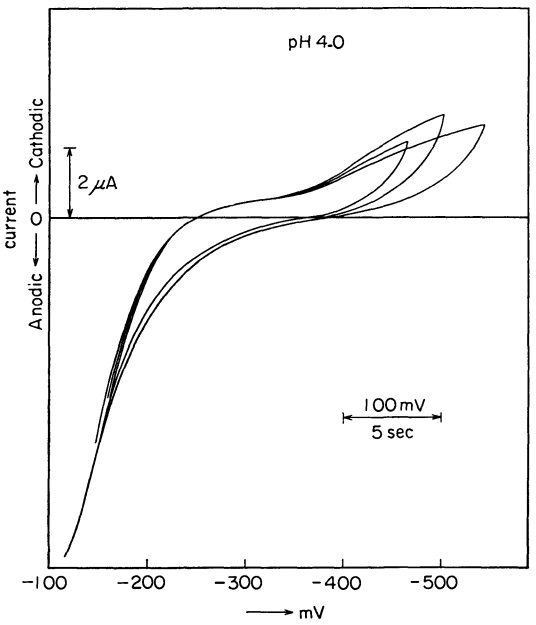

Fig. 2(b). Cyclic voltammetric curves of antimony electrode.

When the relative standard deviation in Table 1 is compared to that of the previous potentiometric method,[6] it is seen to be considerably decreased (nearly one-half). In this case, the time necessary for a single determination does not exceed

Table 1. Purity test of potassium biphthalate
(Current = about 210 mA)

Sample	Sample taken (mg)	Current of electrolysis (mg)	$KHC_8H_4O_4$ found (mg)	Purity (%)	Deviation from mean (%)
NBS standard sample	481.38	210	481.28	99.97_9	-0.01_2
	425.95		425.92	99.99_3	$+0.00_2$
	499.37		499.32	99.99_0	-0.00_1
	522.88		522.99	100.02_1	$+0.03_0$
	465.62		465.49	99.97_2	-0.01_9
				Mean 99.991%	R = 0.049%
					$\hat{\sigma}$ = 0.021%
Standard sample 100.00%*	545.94	200	545.77	99.96_9	-0.02_1
	518.89		518.74	99.97_1	-0.01_9
	388.83		388.91	100.02_1	$+0.03_1$
	411.76		411.85	100.02_2	$+0.03_2$
	382.21		382.08	99.96	-0.02_4
				Mean 99.990%	R = 0.056%
					$\hat{\sigma}$ = 0.024%

* Certificated value by Industrial Inspection Institute (Japan).

1 hr. By the potentiometric method, more than 3 hr are needed.

Next, the error due to the measurements of the electricity decreased to about 0.005% as the standard deviation, and the samples were weighed with a microbalance. In order to verify the error in the weighing of the sample, the following experiment was carried out. The potassium biphthalate in a weighing bottle (0.5 g) was dried at 110°C for 4 hr, cooled in the desiccator for 1.5 hr, and then weighed with the microbalance. This procedure was repeated 6 times.

Table 2. Error of weighing

Weight of sample (mg)
433.429
433.429
433.412
433.414
433.416
433.406
Mean 433.418
$\hat{\sigma}=9.12\,\mu g$

Table 3. Purity test of potassium biphthalate
(Current: about 160 mA)

Sample	Sample taken (mg)	$KHC_8H_4O_4$ found (mg)	Purity (%)	Deviation from mean (%)
NBS Standard sample	279.323	279.317	99.998	−0.001
	421.849	421.860	100.003	+0.004
	402.995	403.025	100.007	+0.008
	353.535	353.545	100.003	+0.004
	393.055	393.009	99.988	−0.011
	407.154	407.167	100.003	+0.004
	403.716	403.672	99.989	−0.010
			Mean 99.999%	$\hat{\sigma}=0.007\%$
Standard sample 100.00%*	494.551	494.555	100.001	+0.002
	491.758	491.738	99.996	−0.003
	505.377	505.435	100.011	+0.012
	457.803	457.766	99.992	−0.007
	506.761	506.724	99.993	−0.006
			Mean 99.999%	$\hat{\sigma}=0.008\%$

* Certificated value by Industrial Inspection Institute (Japan).

Table 4. Purity test of benzoic acid
(Calorimetric standard sample)

Sample	Sample taken (mg)	C_6H_5COOH found (mg)	Purity (%)	Deviation from mean (%)
Stored in the desiccator containing conc. H_2SO_4 for 72 hr	265.140	265.119	99.992	+0.001
	218.390	218.367	99.989	−0.002
	236.576	236.579	100.001	+0.010
	262.040	262.032	99.997	+0.006
	265.032	264.974	99.978	−0.013
			Mean 99.991%	$R=0.023\%$
				$\hat{\sigma}=0.010\%$
Melted at 135°C	256.173	256.129	99.983	−0.010
	323.689	323.695	100.002	+0.009
	234.715	234.697	99.992	−0.001
	245.042	245.054	100.005	+0.012
	287.920	287.875	99.984	−0.009
			Mean 99.993%	$R=0.022\%$
				$\hat{\sigma}=0.009\%$

The results thus obtained are shown in Table 2; there may be some problems in the above method for drying, because it seems that the weight of the sample decreased gradually. The decrease is, however, very small, and may be considered at a later time. When the overall difference is regarded as the error of drying and weighing of the sample, the standard deviation of the error does not exceed 0.003%.

The results obtained by the procedure described previously are shown in Table 3. The standard deviation of these results was 0.007%, somewhat larger than the value to be expected from the errors in samplings and in coulometric titration. The difference may be based on the errors connected with the location of the end point. Material transference through the diaphragm used should also be considered. Taylor's method[1] is very time-consuming, and the diaphragm proposed by Eckfeldt and Shaffer[3] is not suitable either because the condition of the electrolyte at the end-point does not coincide with that at the beginning of the electrolysis. Although the diaphragm used here does not have as many advantages as the above two types, it is simple and useful when the electrolysis is finished within one hour.

Determination of the Purity of Benzoic Acid. The purity of the benzoic acid was determined by the proposed method. The acid was prepared as a standard material for a calorimeter and could be obtained from the Resources Research Institute (Japan). Two drying methods shown previously were used here.

The results obtained are shown in Table 4. These results indicate that there are not much difference between the above methods for drying; the purity of the acid was somewhat lower than 100% when the acid was evaluated as the "acidic" standard.

BULLETIN OF THE CHEMICAL SOCIETY OF JAPAN VOL. 43 2805—2807 (1970)

Dielectric Relaxation of Esters in Benzene Solutions

KRISHNAJI, S. C. SRIVASTAVA and DINA NATH

Physics Department, Allahabad University, Allahabad-2, India

(Received January 5, 1970)

Dielectric relaxation times and distribution parameters of three esters in benzene solutions have been evaluated using three methods, *viz.*, Cole-Cole arc plot method, Higasi's single frequency method and the Gopal Krishna method. Three microwave frequencies have been used to determine a' and a'' apart from the static and optical frequencies for a_0 and a_∞. The distribution parameters obtained from Cole-Cole arc plot and Higasi's method are in good agreement showing that the sploes a' and a'' have been determined accurately. In these esters the values of the distribution parameter are high. Since the dipole-dipole interactions are negligible in dilute solutions, the higher values of the distribution parameter suggests the existence of multiple relaxation processes.

Earlier[1] measurements on a few esters have been carried out in the pure liquid. In order to reduce the effect of dipolar fields we have studied the esters in solutions. In this paper three esters *viz.*, ethyl capronate, ethyl α-bromobutyrate and ethyl α-bromoisobutyrate have been studied in benzene solutions at three microwave frequencies apart from the static and optical frequencies. Because of the interesting results obtained by other workers on different esters it seemed desirable to determine their dielectric relaxation.

Method of Measurement and Analysis of Data. Static permittivity was measured at the frequency 1 MHz by means of a dipolemeter based on the principle of heterodyne beat method. The cell used for the purpose was calibrated with standard liquids. Refractive indices of all the solutions were measured with the help of an Abbe's refractometer and the square of the refractive index gave the values of optical permittivity ($\varepsilon_\infty = n_D^2$).

The permittivity and dielectric loss at microwave frequencies were determined using Smyth's method[2] and the shorted standing wave technique.

The compounds were obtained from M/s Fluka AG, Switzerland. Benzene, Analar Grade (B.D.H.), was used for making the solutions and was distilled twice before use.

It has been observed by earlier workers[3] that permittivity and dielectric loss in solutions are linear functions of the concentration. Thus one can represent the permittivity and dielectric loss by the equations,

$$\begin{aligned} \varepsilon_0 &= \varepsilon_{10} + a_0 c_2 \\ \varepsilon' &= \varepsilon_1 + a' c_2 \\ \varepsilon'' &= a'' c_2 \\ \varepsilon_\infty &= \varepsilon_{1\infty} + a_\infty c_2 \end{aligned} \qquad (1)$$

where ε_0 is static permittivity and $\varepsilon_\infty = n_D^2$ is optical permittivity. Subscript 1 refers to the pure solvent, c_2 is the molar concentration of polar solute and a's are the slopes of the straight lines obtained by plotting the dielectric quantity against concentration. These graphs have been plotted and the slopes determined from these plots are given in Table 1.

Cole-Cole[4] semi-empirical relation for the complex permittivity, $\varepsilon^* = \varepsilon' - j\varepsilon''$ is given by

$$\varepsilon^* = \varepsilon_\infty + \frac{\varepsilon_0 - \varepsilon_\infty}{1 + (j\omega\tau)^{1-\alpha}} \qquad (2)$$

TABLE 1. SLOPES OF THE PLOTS OF CONCENTRATION *vs.* PERMITTIVITY AT DIFFERENT FREQUENCIES

Substance	Frequency	a'	a''
Ethylcapronate	1.0 MHz	$a_0=2.41$	—
	3.4 GHz	2.40	0.07
	9.9 GHz	1.70	0.73
	27.2 GHz	1.16	0.90
	Optical	$a_\infty=-0.27$	—
Ethyl α-bromobutyrate	1.0 MHz	$a_0=3.46$	—
	3.4 GHz	3.28	0.14
	9.9 GHz	2.25	0.90
	27.2 GHz	0.83	0.84
	Optical	$a_\infty=-0.12$	—
Ethyl α-bromoisobutyrate	1.0 MHz	$a_0=3.29$	—
	3.4 GHz	3.20	0.15
	9.9 GHz	2.46	0.85
	27.2 GHz	1.14	0.98
	Optical	$a_\infty=-0.11$	—

1) P. L. McGeer, A. J. Curtis, G. B. Rathmann and C. P. Smyth, *J. Amer. Chem. Soc.*, **74**, 3541 (1952).
2) W. M. Heston, Jr., A. D. Franklin, E. J. Hennelly and C. P. Smyth, *ibid.*, **72**, 3443 (1950).
3) A. D. Franklin, W. M. Heston, Jr., E. J. Hennelly and C. P. Smyth, *ibid.*, **72**, 3447 (1950).

where τ and α are the relaxation time and the distribution parameter respectively and ω is the angular frequency. Substituting equations (1) into (2) we obtain

$$a^* = a' - ja'' = a_\infty + \frac{a_0 - a_\infty}{1 + (j\omega\tau)^{1-\alpha}} \tag{3}$$

The plot of a' *vs.* a'' is an arc of a circle with its centre below the abscissa. The angle which the line joining the centre with the a_∞ point makes with the abscissa is equal to $\alpha\pi/2$. The values of τ and α can thus be determined from the Cole-Cole are plot of a' *vs.* a''.

Higasi[5] has proposed that the values of relaxation time and the distribution parameter may be determined from a measurement of a' and a'' at a single frequency in the dispersion region. The equations for τ and α are

$$\tau = \frac{1}{\omega}\left(\frac{A^2+B^2}{C^2}\right)^{1/2(1-\alpha)} \tag{4}$$

$$1 - \alpha = (2/\pi)\tan^{-1}(A/B) \tag{5}$$

where

$$\begin{aligned} A &= a''(a_0 - a_\infty) \\ B &= (a_0 - a')(a' - a_\infty) - a''^2 \\ C &= (a' - a_\infty)^2 + a''^2 \end{aligned} \tag{6}$$

For the three esters studied here, we have calculated τ and α from Eqs. (4) and (5) using the data at 9.9 GHz.

Relaxation times have also been determined by the Gopal Krishna method.[6] In this method ε' and ε'' of a solution are determined at a single frequency at many concentrations. A graph is then plotted between X and Y. The parameters X and Y are related to the observed quantities as follows:

$$X = \frac{\varepsilon' + \varepsilon''^2 + \varepsilon'' - 2}{\varepsilon''^2 + (\varepsilon'+2)^2} \tag{7}$$

$$Y = \frac{3\varepsilon''}{\varepsilon''^2 + (\varepsilon'+2)^2} \tag{8}$$

and $$X = P + \frac{1}{\omega\tau}Y, \quad \text{where } P = \frac{\varepsilon_\infty - 1}{\varepsilon_\infty + 2}.$$

The slope of the straight line plot is equal to $(1/\omega\tau)$ and thus the relaxation time τ can be determined. The distribution parameter α cannot be determined by this method.

The values of τ and α determined by the above three methods are compared in Table 2.

Discussion

The values of the distribution parameter α obtained from Cole-Cole and Higasi's method are in good agreement. In the Cole-Cole method α is evaluated from the semi-circular plot of a' *vs.* a'' (Figs. 1, 2 and 3) at different frequencies and then the most probable value of the relaxation time is calculated over the whole frequency region used, while in the Higasi method α is calculated from the slopes a', a'', a_0 and a_∞ and the value of the relaxation time is calculated at the single frequency of measurement. Since the values of the distribution parameter α calculated from both the methods are in good agreement, we can say that the values of the slopes obtained at the single frequency of observation in Higasi's method are quite accurate and hence the value of τ will also be accurate.

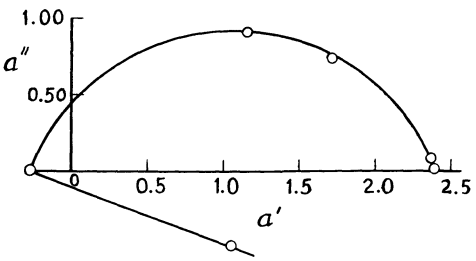

Fig. 1. Plot of a' *versus* a'' for ethyl capronate in benzene solutions.

TABLE 2. VALUES OF RELAXATION TIME AND THE DISTRIBUTION PARAMETER AT 30°C

Substance	τ and α from Cole-Cole arc plot	τ and α from Higasi method at 9.9 GHz	τ from Gopal Krishna method at 9.9 GHz
Ethyl capronate	$\tau = 7.42 \times 10^{-12}$ sec	$\tau = 5.98 \times 10^{-12}$ sec	$\tau = 6.1 \times 10^{-12}$ sec
$CH_3(CH_2)_4COOC_2H_5$	$\alpha = 0.23$	$\alpha = 0.27$	——
Ethyl α-bromobutyrate	$\tau = 9.69 \times 10^{-12}$ sec	$\tau = 7.14 \times 10^{-12}$ sec	$\tau = 6.5 \times 10^{-12}$ sec
$CH_3CH_2CHBrCOOC_2H_5$	$\alpha = 0.34$	$\alpha = 0.36$	——
Ethyl α-bromoisobutyrate	$\tau = 8.46 \times 10^{-12}$ sec	$\tau = 5.07 \times 10^{-12}$ sec	$\tau = 4.5 \times 10^{-12}$ sec
$(CH_3)_2CBrCOOC_2H_5$	$\alpha = 0.27$	$\alpha = 0.29$	——

4) K. S. Cole and R. H. Cole, *J. Chem. Phys.*, **9**, 341 (1941).
5) K. Higasi, This Bulletin, **39**, 2157 (1966).
6) K. V. Gopal Krishna, *Trans. Faraday Soc.*, **53**, 767 (1957).
7) A. J. Curtis, P. L. McGeer, G. B. Rathmann and C. P. Smyth, *J. Amer. Chem. Soc.*, **74**, 644 (1952).

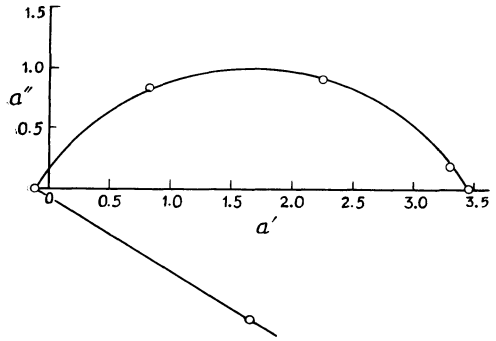

Fig. 2. Plot of a' *versus* a'' for ethyl α-bromo butyrate in benzene solutions.

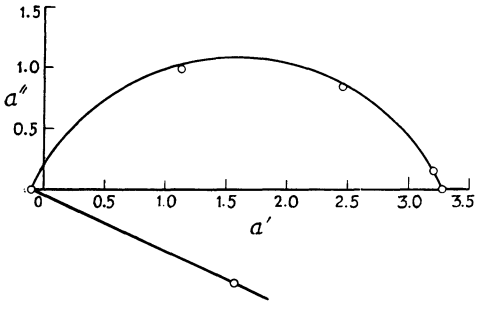

Fig. 3. Plot of a' *versus* a'' for ethyl α-isobromo butyrate in benzene solutions.

We have obtained, invariably, low values of relaxation time from the Gopal Krishna method. In this method, it has been assumed that the Debye equation of a single relaxation time holds good and the value of α is nearly zero. It means that this method is not applicable to the systems showing large distribution of relaxation times. It will give correct values of τ only in the case where α is zero or nearly zero, and smaller values of τ where α is large. The Gopal Krishna method does not give correct values also because the parameter P is not a constant as the concentration is changed.

The distribution of relaxation times obtained for these esters is large. It has been observed by some workers[8,9] that the distribution parameter in solution are larger than in pure liquid. In any liquid the distribution in the relaxation time is due to two basic causes. One factor is the variation in the local field about the individual molecule due to random field fluctuations; and the other is due to possible multiple relaxation processes in the molecule. The latter phenomenon depends on how the internal energy is distributed in the various possible ways of the motion of the molecule. In an actual case both these factors are significant in determining the value of the distribution parameter. In dilute solutions the distribution due to field fluctuations is small, and so if the distribution parameter in solution is large it indicates the existence of multiple relaxation processes.

The values of relaxation times are, however, not very high presumably due to the fact that the dipole-dipole interactions are reduced to a greater extent in dilute solutions. The value of the relaxation time of ethyl α-bromoisobutyrate is less than that of ethyl α-bromobutyrate, though both the compounds have nearly the same molar volume. Ethyl α-bromobutyrate has larger free volume of rotation than ethyl α-bromoisobutyrate, hence the volume swept away by ethyl α-bromobutyrate in the dipole rotation will be larger than the volume swept away by ethyl α-bromoisobutyrate. This explains the larger value of τ in ethyl α-bromobutyrate than in ethyl α-bromoisobutyrate.

One of us (Dina Nath) is thankful to the Atomic Energy Commission for financial support in the form of a Senior Research Fellowship.

8) E. J. Hennelly, W. M. Heston, Jr., and C. P. Smyth, *ibid.*, **70**, 4102 (1948).

9) V. K. Agarwal and P. Kumar, *Indian J. Pure Appl. Phys.*, **7**, 702 (1969).

BULLETIN OF THE CHEMICAL SOCIETY OF JAPAN VOL. 43 2808—2811 (1970)

Radiolysis of Aqueous Solution of Potassium Periodate

S. N. BHATTACHARYYA and D. K. BARDHAN

Saha Institute of Nuclear Physics, Nuclear Chemistry Division, Acharya Prafulla Chandra Road, Calcutta-9, India

(Received March 16, 1970)

Aqueous solutions of potassium periodate in neutral medium were irradiated with X-rays and with Cobalt-60 gamma rays. It was observed that the periodate on radiolysis is reduced only to iodate and no other reduction product was detected. A mechanism for the radiation induced reduction of periodate in aqueous solution is proposed and discussed. Effect of methanol on the course of radiolysis has also been studied.

Radiation induced reduction has been studied[1] in a number of cases of oxidizing agents. It is difficult, however, to make any definite correlation between such studies. Moreover, there are systems where the effect of radiation is little understood or has not been studied at all. Iodate and periodate, though well known as classical oxidizing agents, comprise such systems where not enough studies have been made to get a clear understanding of the mechanism of the radiation induced reduction. Radiolysis of iodate in acid or alkaline solution has been studied by earlier workers.[2-4] However, no study has yet appeared on the radiolysis of periodate. Radiation induced reduction of potassium periodate in aqueous solution in neutral medium forms the subject matter of the present investigation.

Experimental

Materials. Reagents such as potassium periodate, methanol, sodium bicarbonate, potassium iodide, *etc.* used in the investigation were all of analytical grade. Triply distilled water was used for preparing solutions for irradiation.

Irradiation. Irradiation with ^{60}Co γ-rays was carried out at 29°C at the Bhabha Atomic Research Centre, Trombay. The dose rate was determined with the Fricke dosimeter taking $G(Fe^{3+})=15.5$ and measuring absorbances due to Fe^{3+} at 305 mμ. The dose rate was also determined by using ceric sulphate-sulphuric acid solutions. The Ce^{3+} yield was computed by measuring the depletion in absorbances due to Ce^{4+} at 315 mμ. The temperature dependence[5] of Ce^{3+} yield was taken into consideration and $G(Ce^{3+})$ was accordingly taken as 2.34.

Exposures to X-rays were done at the Biophysics Division of the Institute by using unfiltered X-rays in a Mullard MG 150 tube operated at 80 KV and 9 mA. Average energy of the X-ray beam at the irradiation position as determined through aluminium absorption curves was found to be 27 keV. The dose rate was again measured with the help of the Fricke dosimeter. $G(Fe^{3+})$ was, however, taken from Allen's mean curve[6] as 14.5 molecules per 100 eV. Deaeration of solutions was carried out by means of nitrogen gas containing less than 10 ppm of oxygen. The nitrogen gas, which was procured from Messrs. Indian Oxygen Limited, was washed with alkaline pyrogallol and then passed through the solutions for about half an hour.

Analytical Procedures. Periodate was determined[7] iodometrically in $NaHCO_3$ solutions. When periodate is added to iodide solution which is 1 M in $NaHCO_3$, the following reaction takes place:

$$IO_4^- + 2I^- + 2H^+ = IO_3^- + H_2O + I_2$$

Iodate was also determined iodometrically by using the usual reaction in acid medium:

$$IO_3^- + 5I^- + 6H^+ = 3I_2 + 3H_2O$$

Iodine liberated in both cases was extracted with benzene and the optical density of the benzene layer was measured spectrophotometrically at the absorption maxima, 297 mμ.

H_2O_2 was determined with the help of titanium sulfate reagent.[8] All spectrophotometric measurements were carried out in a Hilger Uvispek photoelectric spectrophotometer.

Results and Discussion

Figure 1 shows the amount of decomposition of periodate as a function of absorbed dose due to γ- or X-irradiation. It is thus observed that the amount of decomposition is linear with dose up

1) A. O. Allen, "The Radiation Chemistry of Water and Aqueous Solutions," D. Van Nostrand Co., Princeton, New Jersey (1961).

2) G. L. Clark and W. S. Coe, *J. Chem. Phys.*, **5**, 97 (1937).

3) N. R. Todd and S. L. Whitcher, *ibid.*, **20**, 1172 (1952).

4) M. Haissinsky, J. Jove and W. Szymanski, *J. Chim. Phys.*, **61**, 572 (1964).

5) C. J. Hochanadel and J. A. Ghormley, *Radiat. Res.*, **16**, 653 (1962).

6) Ref. 1, p. 54.

7) W. L. Lockhart and M. M. Jones, *J. Inorg. Nucl. Chem.*, **28**, 2619 (1966).

8) G. M. Eisenberg, *Ind. Eng. Chem.*, **15**, 327 (1943).

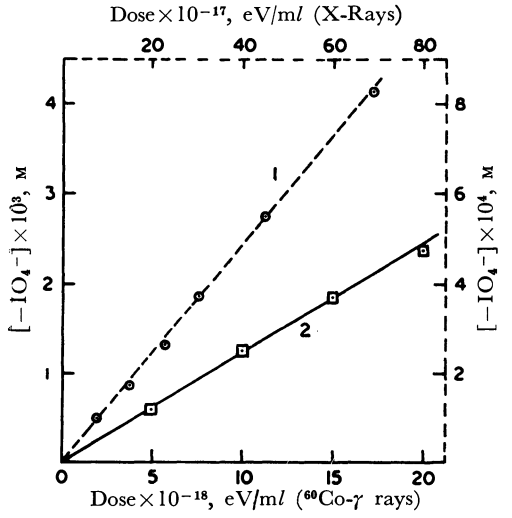

Fig. 1. Radiolysis of 5 mM KIO_4 solution in neutral medium with X-rays (1) and ^{60}Co γ-rays (2).

to an absorbed dose of about 10^{19} eV/m*l* and the radiolytic reduction yield, $G(-IO_4^-)$ was accordingly calculated from the slope. Both aerated and N_2-saturated solutions were irradiated and the decomposition yields in both cases were determined and $G(-IO_4^-)$ value was found to remain constant either in the presence or absence of dissolved oxygen.

It should be pointed out here that the radiolytic yield of the decomposition of periodate was ascertained by determining the concentration of periodate iodometrically both before and after radiolysis. In the iodometric procedure, as has already been mentioned, periodate is reduced only to iodate state, and if it is assumed that radiation induced degradation of periodate also leads to the formation of iodate only, then the molar concentration of iodate, as determined after reduction of periodate by iodide in $NaHCO_3$ medium and the removal of the liberated iodine from the system, should be equivalent to the molar concentration of periodate as taken initially before radiolysis. It is evident from Fig. 2, where the observed concentration of iodate is plotted as a function of absorbed dose, that the concentration of iodate is identical with that of initial periodate and that it remains fairly constant in the initial stages of radiolysis. When the absorbed dose, however, exceeds 60×10^{18} eV/m*l*, the observed iodate concentration is characterized by its linear decrease, which indicates that iodate is possibly undergoing radiolysis. It should also be pointed out that no periodate could be detected at such high doses, *i.e.*, all periodate ions that were present have been radiolysed. Moreover, the reduced states, such as I^- and I_2, which happen to be the characteristic products in the radiolysis of iodate, appear only at such high doses. But prior to such a limiting high dose no such reduction product could be detected. Therefore, the aforesaid linear decrease of iodate concentration with absorbed dose may in all probability be due to the radiolysis of iodate only, and if the dose corresponding to the point at which the straight line showing the linear decrease in observed iodate concentration meets on extrapolation the straight line showing its constant behavior, is taken as the point initiation of the process, then the iodate decomposition yield, $G(-IO_3^-)$, is found to have a value of 0.34 molecules per 100 eV which agrees well with our observed value in the case of radiolysis of iodate in neutral medium. However, this study on the radiolysis of iodate will, form the subject matter of a separate investigation. From what has been discussed above it can be concluded that periodate on radiolysis is reduced to iodate only.

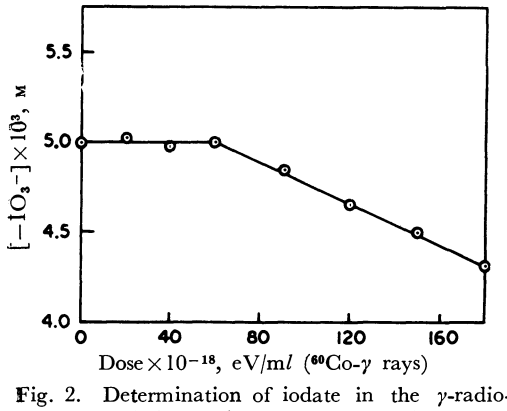

Fig. 2. Determination of iodate in the γ-radiolysed periodate solution after reduction of the periodate with KI in $NaHCO_3$ medium and removal of the liberated iodine through extraction with benzene. 5 mM KIO_4 solution was always initially taken before radiolysis.

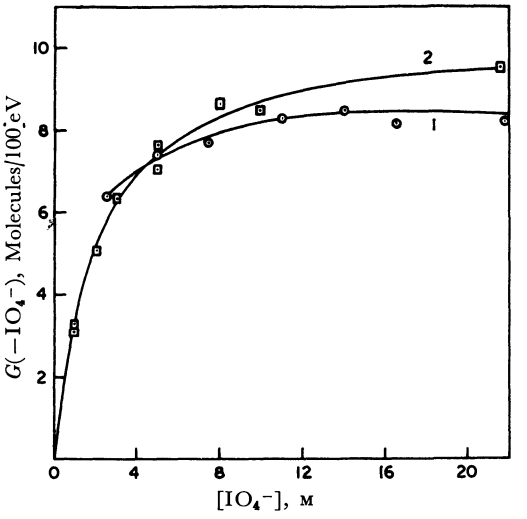

Fig. 3. Effect of initial concentration of periodate on $G(-IO_4^-)$. 1: irradiation with X-rays; 2: irradiation with ^{60}Co γ-rays.

Figure 3 shows the decomposition yield values as a function of solute concentration in cases where radiolysis is initiated by γ- or X-rays. It is evident from the figure that in the case of X-irradiation the decomposition yield, $G(-IO_4^-)$, initially increases but easily attains a steady value of 8.30 molecules per 100 eV. In the case of γ-radiolysis, however, the yields are strongly dependent on the initial concentration of periodate, and they have a tendency to attain a limiting value with increase of the solute concentration. It is therefore necessary to find the limiting G value where all the radicals generated in the solution are supposed to be swept away by the scavenger so that the stoichiometric explanation of the decomposition yields may be made easier. The limiting G value can be evaluated[9] by plotting reciprocals of G value against reciprocals of solute concentration and by extrapolating the straight line to zero reciprocal concentration. The results are shown in Fig. 4 and the limiting $G(-IO_4^-)$ value for γ-irradiation has thus been found to be 11.11 molecules per 100 eV.

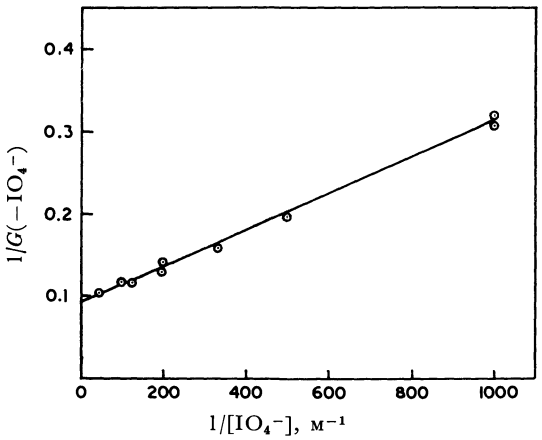

Fig. 4. Plot of the reciprocals of $G(-IO_4^-)$ against the reciprocals of $[IO_4^-]$ in case of γ-radiolysis.

It is well known [10] that water on absorption of γ-radiation gives rise to radical and molecular products as:

$$H_2O \text{ -}\!\!\wwave\!\!\rightarrow H, OH, e_{aq}^-, H_2, H_2O_2 \qquad (1)$$

and the radiolysis of a dilute aqueous solution is initiated by an attack of the solute by these radical and molecular products.

It should be pointed out that no hydrogen peroxide could be detected in the solutions after irradiation. It can therefore be presumed that hydrogen peroxide takes part in some form of reaction during radiolysis. In fact, it is known[11] that hydrogen peroxide in neutral medium reacts with periodate. Although gaseous hydrogen was not determined in the solutions after irradiation, it is assumed that such a small amount of molecular hydrogen that is formed as a result of absorption of radiation by water, will not play any important role in affecting the course of radiolytic reduction taken under consideration.

Amongst the water radiolysis products, H or e_{aq}^- has a reducing action. If it takes part in one electron reduction process in the radiolysis of periodate, unstable IO_3 will be produced and this will immediately disproportionate itself into IO_3^- and IO_4^-. In that case the observed high reduction yield cannot be accounted for. Periodate is, however, known to be reduced to iodate very easily. If, on the other hand, it is assumed that H atom reduces IO_4^- to IO_3^-, then an equivalent amount of OH radicals will be produced in the system.

Now, as regards the mode of reaction of OH radicals in the system, one is naturally immediately inclined to treat them as oxidizing entities. But since a very high reduction yield has been observed in the system, one is tempted to think that OH radicals also take part in some sort of reduction processes. If the reduction of IO_4^- by OH comprises a two-electron process, as has been assumed for H atom reaction, then IO_3^- and an equivalent amount of HO_2 radical will be produced. It has already been stated that the reduction yield is not affected by the presence or absence of dissolved oxygen, which is clearly indicative of the fact that both H and HO_2 are equally effective in reducing periodate. If HO_2 is produced in the reaction of OH with IO_4^-, it will give rise to the development of a chain reaction. But a study of the dose rate dependence on the reduction yield does not, however, conform to such a view. Another possibility is that OH may reduce by an one-electron process. Then IO_3 and an equivalent amount of HO_2^- will be produced which in turn will reduce more periodate.

In the light of the observed results the following reaction sequences together with reaction (1) may be proposed for the radiolytic mechanism, e_{aq}^- for simplicity being represented by H:

$$IO_4^- + H \rightarrow IO_3^- + OH \qquad (2)$$

$$IO_4^- + H_2O_2 \rightarrow IO_3^- + H_2O + O_2 \qquad (3)$$

$$IO_4^- + OH \rightarrow IO_3 + HO_2^- \qquad (4)$$

$$2IO_3 + H_2O \rightarrow IO_3^- + IO_4^- + 2H^+ \qquad (5)$$

$$IO_4^- + HO_2^- \rightarrow IO_3^- + OH^- + O_2 \qquad (6)$$

From the proposed mechanism it follows that the reduction yield, $G(-IO_4^-)$, at the steady state will be expressed by the relation:

9) N. Matsuura, N. Shinohara and M. Takigawa, *Sci. Papers Coll. Gen. Educ., Univ. Tokyo*, **13**, 179 (1963).
10) H. A. Schwarz, "Advances in Radiation Biology," Vol. 1, Academic Press, New York (1964), p. 1.
11) I. M. Kolthoff and P. J. Elving, "Treatise on Analytical Chemistry," Part II, Vol. 7, Interscience Publishers, New York (1961), p. 375.

$$G(-IO_4^-) = \frac{5}{2}G_H + \frac{3}{2}G_{OH} + G_{H_2O_2}$$

Taking[12] $G_H=2.80$, $G_{OH}=2.22$ and $G_{H_2O_2}=0.71$ for γ-rays, the yield is calculated to be 11.04. Taking[13] again $G_H=2.09$, $G_{OH}=1.42$ and $G_{H_2O_2}=0.98$ for X-ray induced radiolysis in neutral solution, the decomposition yield, according to the above relation, comes out to be 8.33. The observed limiting yield values in cases of γ- and X-irradiation have, however, been found to be as 11.11 and 8.30 respectively. Thus it is evident that the observed decomposition yields are in good agreement with the values calculated in terms of the yields of the primary radical and molecular products.

If radiolysis of periodate is carried out in the presence of small amounts of methanol, the periodate decomposition yield is found to be significantly large. When methanol is present during radiolysis, the OH radicals will naturally compete for both CH_3OH and IO_4^- ions. By the reaction of OH with CH_3OH another reducing radical, CH_2OH, will be produced which in turn may reduce more periodate.

$$CH_3OH + OH \rightarrow CH_2OH + H_2O \quad (7)$$

$$IO_4^- + CH_2OH \rightarrow IO_3^- + CH_2O + OH \quad (8)$$

Any possibility that formaldehyde that is produced in reaction (8) may react with undecomposed periodate in neutral medium has been tested separately, but no such reaction within the concentration limits of the present investigation could be detected. Radiolysis of periodate in the presence of methanol will then comprise the reactions (1) through (8) and the reduction yield will accordingly be expressed by the relation:

$$G(-IO_4^-) = \frac{5}{2}G_H + \frac{3}{2}G_{OH} + G_{H_2O_2} \div (G_H \div G_{OH})\frac{K_7[CH_3OH]}{K_4[IO_4^-]}$$

12) J. W. T. Spinks and R. J. Woods, "An Introduction to Radiation Chemistry," John Wiley & Sons, New York (1964), p. 259.

13) Ref. 1, p. 58.

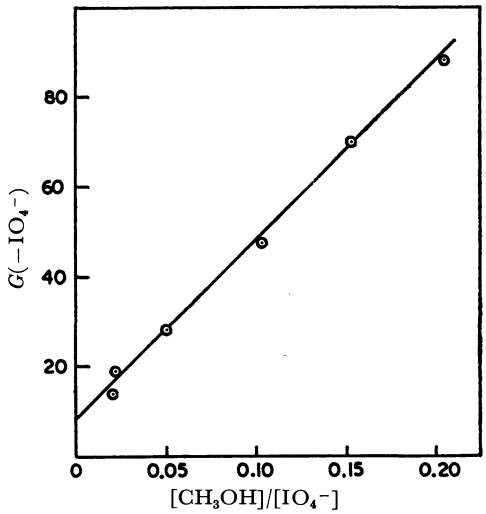

Fig. 5. Effect of methanol on X-ray induced radiolysis of potassium periodate in deaerated neutral solution.

A plot of $G(-IO_4^-)$ against $[CH_3OH]/[IO_4^-]$ will therefore yield a straight line. As has been stated previously, the intercept in case of the X-ray induced radiolysis will be equal to 8.33. Figure 5 shows the variation in the radiolytic decomposition yields with the ratios of the concentrations of methanol and periodate in the medium. A smooth straight line is thus obtained with an intercept of 8.3 which agrees well with the calculated value. This confirms the assumed kinetic behaviour in the proposed radiolytic mechanism. From the slope, the ratio of the rate constants K_7/K_4 is found to be 1.12×10^2.

The authors are grateful to Professor B. C. Purkayastha of this Division for discussion and encouragement and to Dr. S. B. Bhattacharjee of the Biophysics Division for the facilities of irradiation with X-rays. For the irradiation facilities with cobalt-60 gamma rays the authors are highly indebted to the Bhabha Atomic Research Centre, Trombay.

BULLETIN OF THE CHEMICAL SOCIETY OF JAPAN VOL. 43 2812—2815 (1970)

Spectrophotometric Determination of Mercury(II) by Solvent Extraction with Variamine Blue B*[1]

Masahiro TSUBOUCHI

Faculty of Education, Tottori University, Tottori

(Received February 5, 1970)

A new rapid, sensitive and selective method is proposed for the spectrophotometric determination of a trace of mercury(II) by solvent extraction. The method is based on the formation of an ion-pair complex between the tribromo-mercury(II) complex anion and the dyestuff cation obtained by oxidation of variamine blue B. The optimum pH range for the color reaction is 2.5—4. The blue complex can be extracted into nitrobenzene and has a maximum absorption at 605 mμ in the organic solvent. Beer's law holds in the range $3.2\times10^{-6}-2.2\times10^{-5}$ M of mercury(II) in the aqueous layer before the extraction, with a molar absorptivity of 4.03×10^{4} $mol^{-1}cm^{-1}$ l at 605 mμ. The color reaction is instantaneous and the complex remains stable 15 mintes in the nitrobenzene layer. Of the 22 cations and 11 anions examined, tin(II), tin(IV), antimony(III), iodide, cyanide, and thiocyanate showed serious interferences.

Many investigations[1] have been made on the spectrophotometric determination of mercury(II). The standard method based on the reaction with dithizone has been considered unsatisfactory because of its extreme sensitivity to variations in laboratory conditions, while the diphenylcarbazone method has serious drawbacks because of its extreme sensitivity to changes in acidity. A spectrophotometric method using thiocyanate has also been reported.[2] The method is limited by interference of halide and pseudohalide ions as well as such as silver.

Recently, rhodamine B,[3] phthalein complexone[4] and xylenol orange[5] were described as spectrophotometric reagents for mercury(II). The methods are sensitive, but suffer from a number of interferences. Another method based on the complex formation between mercury(II) ions and iodide ions has been described by Pappas and Powell.[6] A molar absorptivity of about 2.34×10^{4} is claimed. 2,2′-dipyridyl-iron(II) chelate[7,8] was proposed for the spectrophotometric determination of mercury(II) by solvent extraction. Although this method is more reliable than the dithizone method, it is not sufficiently sensitive. The method proposed here has even greater sensitivity than the above techniques which have employed iodide ions or 2,2′-dipyridyl-iron(II) chelate.

Variamine blue B[9,10] (VBB) is known to be oxidized to form the blue dyestuff cation (VBB^+) as follows:

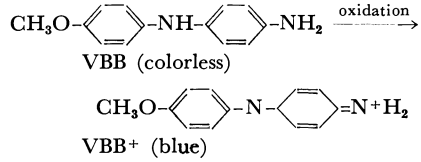

The tribromo-mercury(II) complex anion can be extracted into nitrobenzene with the VBB^+. This system was studied in detail to establish a method for the determination of mercury(II).

Experimental

Apparatus. Absorbance measurements were made using a Shimadzu Beckman Model QR-50 spectrophotometer with matched 1 cm quartz cells. A Toa Denpa Model HM-5A pH meter was used for pH measurements. An Iwaki Model KM shaker was used for the

*1 Presented at 18th Annual Meeting of the Japan Society for Analytical Chemistry, Hokkaido, October, 1969.

1) E. B. Sandell, "Colorimetric Determination of Traces of Metals," Interscience Pub. Inc., New York (1965), p. 621.
2) G. E. Markle and D. F. Boltz, *Anal. Chem.*, **26**, 488 (1954).
3) H. Imai, *Nippon Kagaku Zasshi*, **90**, 275 (1969).
4) S. Komatsu and T. Nomura, *ibid.*, **88**, 542 (1967).
5) S. Komatsu, T. Nomura and M. Saito, *ibid.*, **88**, 1124 (1967).
6) A. J. Pappas and H. B. Powell, *Anal. Chem.*, **39**, 579 (1967).
7) K. Kotsuji, This Bulletin, **38**, 402 (1965).
8) Y. Yamamoto, S. Kikuchi, Y. Hayashi and T. Kumamaru, *Bunseki Kagaku*, **16**, 931 (1967).
9) L. Erdey and G. Rady, *Z. Anal. Chem.*, **149**, 250 (1956).
10) L. Erdey, *Chemist Analyst*, **48**, 106 (1959).

extraction.

Reagents. Guaranteed grade of mercuric chloride was dissolved in dilute sulfuric acid and diluted with deionized water to a concentration of 1.0×10^{-3} M of mercury(II). This standard solution was then diluted to the concentration required for the experiments.

Variamine blue B (VBB) solution, 10^{-3} M, was prepared by dissolving variamine blue B hydrochloride in deionized water.

A buffer solution was made 0.2 M from reagent grade sodium citrate and dilute sulfuric acid.

All the other reagents of a reagent grade were used without further purification.

Recommended Procedure. A solution was prepared by pipetting 2 m*l* of 0.1 M potassium bromide solution, 7 m*l* or less of a sample solution containing less than 0.016 g of mercury(II) per liter, 5 m*l* of 0.2 M citrate buffer solution (pH 2.9), 2 m*l* of 10^{-3} M VBB solution, and 2 m*l* of 0.1 M ammonium persulfate solution into 100-m*l* separatory funnel. This solution was brought to 25 m*l* with water. After adding 10 m*l* of nitrobenzene to the separating funnel, the contents were mixed thoroughly by a shaker for about one minute. After standing for five minutes, the nitrobenzene layer was drawn off into a glass tube with a glass stopper containing about 1 g of anhydrous sodium sulfate, and shaken to remove droplets of water. The absorbance of the extract is measured immediately at 605 mμ against a reagent blank or nitrobenzene.

Results and Discussion

Absorption Spectra. The absorption spectra shown in Fig. 1 were obtained for 0 and 1.6×10^{-5} M of mercury(II) solution through the recommended procedure. The presence of mercury(II) leads to a considerable increase in the absorbance (curve 1). The curve has a maximum value at 600 mμ. The absorbance maximum of the reagent blank (curve 2) in the nitrobenzene was at 500 mμ. The shift in the organic layer may be attributed to the effect of the association between the dyestuff cation and the complex anion. The maximum difference in the absorbance between curves 1 and 2 is found at 605 mμ. The absorbance is propotional the mercury(II) concentration at this wavelength.

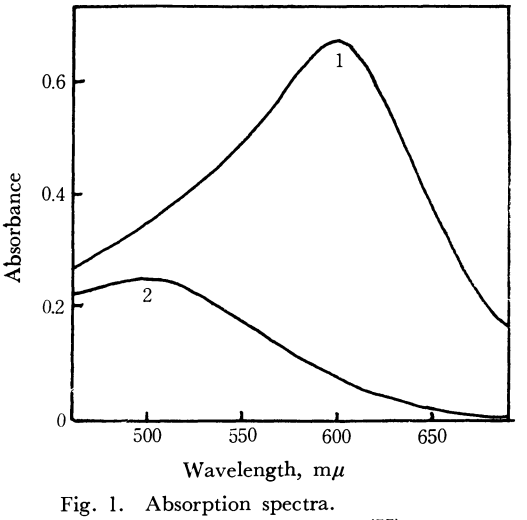

Fig. 1. Absorption spectra.
1: 1.6×10^{-5} M of Mercury(II)
2: Reagent blank
Reference: Nitrobenzene

Effect of pH. Figure 2 shows the typical pH dependence of the extraction system. The study was made by extracting 1.6×10^{-5} M of mercury(II) through the recommended procedure. The optimum pH was from 2.5 to 4.0. The pH of the solution was adjusted to 2.9 in this work.

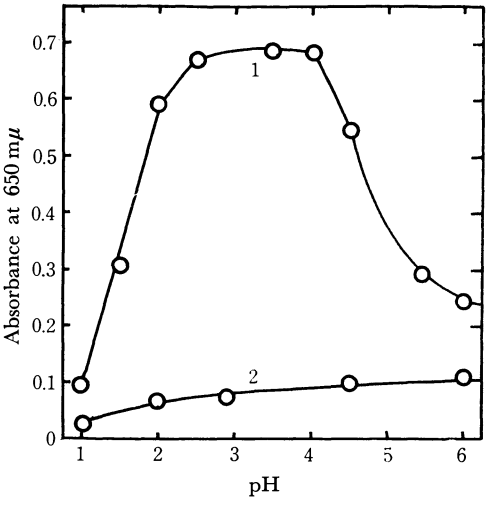

Fig. 2. Effect of pH.
1: 1.6×10^{-5} M of mercury(II)
2: Reagent blank
Reference: Nitrobenzene

A sodium citrate buffer was effective in keeping the solution at pH 2.9 as well as in masking metal ions. When the citrate concentration was less than 0.01 M in the aqueous layer, it took too long to separate the two layers. 0.01—0.08 M of citrate had no influence on the absorbance of the extract. At pH 2.9 no citrate-mercury(II) complex formation was apparent from this experiment.

Solvent for Extraction. Several organic solvents have been examined for their ability to extract the bromo-mercury(II)-dyestuff ternary complex. The solvents investigated were benzene, butyl acetate, carbon tetrachloride, chloroform, cyclohexane, 1,2-dichloroethane, ether, ethyl acetate, *n*-hexane, isoamylalcohol, methyl isobutyl ketone, monochlorobenzene, nitrobenzene, and toluene. Among the solvents tested, only nitrobenzene was capable of extracting the complex while in the other cases a blue precipitate was slightly observed at the interface.

Effect of Reagents. In aqueous solution the tribromo-mercury(II) complex anion is in equilibrium with the mercury bromide and tetrabromo-

mercury(II) complex anion. The distribution of the tribromo-mercury(II) concentration in the 8×10^{-3} M of potassium bromide is about 60%, from the formation constant ($\log\beta_1$: 9.05, $\log\beta_2$: 17.3, $\log\beta_3$: 19.7, $\log\beta_4$: 21.0). The absorbance in the nitrobenzene layer of a series of 1.6×10^{-5} M mercury(II) solution remained unchanged when the potassium bromide concentration was varied from 1.0×10^{-3} to 1.6×10^{-2} M. Mercury(II) seemed to be extracted as tribromo-mercury(II) through the equilibrium shift against the changes of bromide concentration.

Several kinds of oxidizing agents were tested to obtain the colored dyestuff cation. They were ferric sulfate, hydrogen peroxide, ammonium persulfate, potassium permanganate, ceric sulfate, potassium dichromate, manganic sulfate, potassium bromate, potassium iodate, calcium hypochlorite, chloramine T, and iodine. Of these, ammonium persulfate was chosen for the present work because it is the most effective in oxidizing the VBB and gives a lower absorbancy of the reagent blank. Maximum and constant color development required about a 5-fold molar excess of the ammonium persulfate to the VBB concentration. 2 m*l* of 0.1 M ammonium persulfate solution used in this work supplies the oxidizing reagent in a ratio of 100 to 1 against the 8×10^{-5} M of VBB.

Samples containing 1.6×10^{-5} M of mercury(II) were treated by the recommended procedure, except that the concentration of VBB was varied. Maximum color development in the nitrobenzene layer required more than about a 3-fold molar excess of VBB to mercury(II). 2 m*l* of 10^{-3} M VBB solution used in the procedure supplies a ratio of 5 to 1 if the sample contains 1.6×10^{-5} M of mercury(II).

Other Variable. In order to confirm complete extraction with nitrobenzene, a sample containing 1.6×10^{-5} M of mercury(II) was treated according to the procedure. The first extraction yielded an absorbance of 0.605 using a reagent blank as a reference. The aqueous solution was then extracted with another 10 m*l* portion of nitrobenzene. The measured absorbance of this organic layer was 0.003 against a reagent blank. From this experiment, it seems that the extraction rate using 10 m*l* of nitrobenzene is not less than 95%.

The stability of the color of the extracted organic layer was studied. Little or no error will be introduced if the absorbance is measured within fifteen minutes after extraction. After an hour, the absorbance decreased by 6.3%.

Color development in the nitrobenzene layer varied with the shaking time. For the condition in the present work, full color development took about thirty seconds. Continued shaking up to five minutes produced no further change in absorbance.

Calibration and Reproducibility. The system followed Beer's law in the range 3.2×10^{-6}—2.2×10^{-5} M of mercury(II). The molar absorptivity can be calculated to be 4.03×10^{4} $mol^{-1}\,cm^{-1}l$.

Ten identical samples, each with a final mercury(II) concentration of 1.6×10^{-5} M, were treated and their absorbance were measured at 605 mμ using a reagent blank as a reference. The mean absorbance was 0.605, with a standard deviation of 0.007 absorbance unit.

Method of Continuous Variations. In order to investigate the structure of this colored complex, continuous variations plots were employed. The total concentration of mercury(II) plus VBB was 4×10^{-5} M. The continuous variations plots at 605 mμ and 560 mμ have a maximum 0.5 mole fraction of mercury(II), indicating a 1 to 1 mercury(II)-VBB ratio. The overall molar ratio of the mercury(II) : bromide : VBB is 1 : 3 : 1, and its formula can be suggested as $VBB^{+}\cdot[HgBr_3]^{-}$.

Effect of Diverse Ions. The effect of diverse ions was studied for a sample containing 1.6×10^{-5} M of mercury(II). The tolerance to a given ion was defined as the maximum concentration which could be present without causing a deviation of 0.025 for the absorbance of the sample. Tolerances for diverse ions tested are listed in Table 1. Anions were added as solutions of their sodium, potassium or ammonium salts. Cations were added as solutions of their chlorides or sulfates. The citrate used as a buffering agent is also useful.

Table 1. Effect of diverse ions

Ion	Tolerance (M)	Ion	Tolerance (M)
Ag^{+}	1×10^{-3}	Sn^{2+}	5×10^{-7}
Al^{3+}	2×10^{-3}	Sn^{4+}	1×10^{-6}
Ba^{2+}	5×10^{-3}	Th^{4+}	1×10^{-4}
Be^{2+}	5×10^{-3}	Tl^{+}	1×10^{-4}
Bi^{3+}	2×10^{-4}	Zn^{2+}	5×10^{-3}
Ca^{2+}	5×10^{-3}	CH_3COO^{-}	2×10^{-3}
Cd^{2+}	5×10^{-4}	SO_4^{2-}	5×10^{-3}
Co^{2+}	1×10^{-3}	F^{-}	5×10^{-3}
Cr^{3+}	2×10^{-3}	I^{-}	1×10^{-5}
Cu^{2+}	2×10^{-3}	Cl^{-}	2×10^{-3}
Fe^{2+}	2×10^{-4}	NO_3^{-}	2×10^{-4}
Fe^{3+}	5×10^{-3}	$H_2PO_4^{-}$	5×10^{-3}
Mn^{2+}	5×10^{-4}	VO_3^{-}	1×10^{-3}
Mg^{2+}	5×10^{-3}	CN^{-}	5×10^{-7}
Ni^{2+}	2×10^{-3}	HCO_3^{-}	5×10^{-3}
Pb^{2+}*	1×10^{-3}	SCN^{-}	1×10^{-6}
Sb^{3+}	1×10^{-5}		

Mercury: 1.6×10^{-5} M. * Added as acetate.

11) Assoc. of Offic. Agr. Chemists, "Official Methods of Analysis," 8th ed., Washington (1955), p. 76.

Table 2. Application of the method

Sample No.	Mercury content (%)		Difference
	Proposed method	Official method	
1	2.21	2.14	+0.07
2	2.23	2.10	+0.13
3	2.20	2.09	+0.11

as a masking agent for many cations. Antimony(III) formed insoluble precipitates under these conditions, and only tin(II), (IV) among the cations tested showed serious effects.

Application of the Method. By following the official method,[12] three solutions were prepared from agricultual medicines contained ethylmercuric phosphate. These solutions were analyzed by the official method and the proposed method. The results obtained are summarized in Table 2.

Appreciation is expressed to Professor Yuroku Yamamoto of Hiroshima University for valuable advice.

BULLETIN OF THE CHEMICAL SOCIETY OF JAPAN VOL. 43 2815—2820 (1970)

Nickel(II) Complexes of Ethylenediaminemonoacetic Acid (EDMA). The Preparation and Thermal Decomposition of Nickel(II)-EDMA Complexes

Yuki FUJII

Department of Chemistry, Ibaraki University, Bunkyo-cho, Mito, Ibaraki

(Received March 4, 1970)

The following nickel(II) complexes containing ethylenediaminemonoacetate anion(s) (edma) were newly prepared from an aqueous solution containing nickel(II) ion and edma: $[Ni(edma)(H_2O)_3]X$ (X=Cl and Br), $[Ni(edma)I]_4$, and $[Ni(edma)_2]\cdot 2H_2O$. By the thermal decomposition of $[Ni(edma)(H_2O)_3]X$, $[Ni(edma)X]_4$-type complexes (X=Cl and Br) were also prepared. By absorbing three molecules of water in an atmosphere, two new, mixed complexes containing a halogen anion and water molecule(s), $[Ni(edma)Cl(H_2O)_2]\cdot H_2O$ and $[Ni(edma)Br(H_2O)]_2\cdot 4H_2O$ (dimer), were prepared from $[Ni(edma)X]_4$. By the measurements of the absorption spectra, the magnetic moments, and the dehydrations, their structures were all assigned to octahedral. The $[Ni(edma)X]_4$ complexes (X=Cl, Br and I) were presumed to have the tetramer structure, where four halogen anions are triply bridged to the nickel(II) ion. The difference between the $[Ni(edma)(H_2O)_3]X$, $[Ni(edma)Cl(H_2O)_2]\cdot H_2O$, and $[Ni(edma)Br(H_2O)]_2\cdot 4H_2O$ complexes were clearly observed on the basis of their derivatographic behavior. The mechanisms of the dehydrations were also discussed.

In the previous paper, the stability constants of nickel(II)-EDMA complexes with 1-to-1 and 1-to-2 compositions were reported.[1] From the spectrophotometric evidence, it was concluded that the formation of a mixed complex containing chloride ions could be ruled out in an aqueous solution. This conclusion is reasonable because it is known that the formation constant of a nickel(II)-hexaquo complex with chloride ions is very small.[2] However, it can not always be said that the information obtained by the solution equilibrium study safely holds for solid-state chemistry. Therefore, in order to obtain much information concerning the complex formation reaction, it would be necessary to prepare the complexes and characterize them.

In these circumstances, in order to obtain information on mixed nickel(II)-EDMA complexes containing halogen anions and in order to compare the properties in the solution state and those in the solid state, the preparation and thermal decomposition of nickel(II)-EDMA complexes were examined.

Experimental

Preparation of the Complexes. *1) Ethylenediaminemonoacetatotriaquonickel(II) Chloride,* [Ni(edma)-

1) M. Kodama, Y. Fujii and T. Ueda, This Bulletin, **43**, 2085 (1970).

2) L. G. Sillén and A. E. Martell, "Stability Constants of Metal-Ion Complexes," The Chemical Society, London (1964), p. 282.

$(H_2O)_3]Cl$ (I). To an aqueous solution containing 2.4 g (0.01 mol) of nickel(II) chloride hexahydrate, 2.5 g (0.012 mol) of ethylenediaminemonoacetic acid dihydrochloride monohydrate (EDMA·2HCl·H_2O)[3] were added, and the solution was warmed at 70—80°C. After adjusting the solution's pH to 6—7 by adding sodium bicarbonate, the resulting solution was concentrated to about 15 m*l*. Three or four volumes of alcohol were then added to the solution, and the resulting solution was cooled to 0°C for a day. Light blue crystals were separated out. They were recrystallized from water-alcohol. Yield, about 2.0 g (75%). Found: C, 18.81; H, 5.93; N, 10.97; H_2O, 20.6%. Calcd for $C_4H_{15}NiN_2O_5Cl$: C, 18.55; H, 5.62; N, 10.67; H_2O, 20.37%.

2) Tetramer of Ethylenediaminemonoacetatochloronickel(II), $[Ni(edma)Cl]_4$ (II). The complex I was heated at about 180°C for half an hour. A light green powder was thus obtained. This complex was cooled and preserved in a desiccator with silica gel. Found: C, 22.41; H, 4.26; N, 12.58%. Calcd for $C_4H_9NiN_2O_2Cl$: C, 22.11; H, 4.18; N, 12.89%.

3) Ethylenediaminemonoacetatochlorodiaquonickel(II) Monohydrate, $[Ni(edma)Cl(H_2O)_2]\cdot H_2O$ (III). The complex II was allowed to stand in an atmosphere for two or three days at room temperature. The color thus changed gradually from light green to light blue. Found: C, 18.40; H, 5.92; N, 10.44; H_2O, 20.2%. Calcd for $C_4H_{13}NiN_2O_4Cl\cdot H_2O$: C, 18.55; H, 5.62; N, 10.67; H_2O, 20.37%.

4) Ethylenediaminemonoacetatotriaquonickel(II) Bromide, $[Ni(edma)(H_2O)_3]Br$ (IV). To an aqueous solution of the complex I (7 g, 0.0264 mol), an aqueous solution of silver nitrate (5.1 g, 0.03 mol) was added. The silver chloride which resulted was filtered off, and then potassium bromide (9.4 g, 0.07 mol) was added to the filtrate. The precipitate of silver bromide was filtered off, and the resulting solution was concentrated to about 15 m*l*. Three or four volumes of alcohol were added to the solution, which was then cooled to 0°C for a day. After filtering off the potassium bromide thus precipitated, the filtrate was concentrated to a volume of about 25 m*l*. When it was cooled to 0°C, light blue crystals were separated out. They were recrystallized from water-alcohol. Yield, about 5 g (61%). Found: C, 15.75; H, 4.78; N, 9.27; H_2O, 17.7%. Calcd for $C_4H_{15}NiN_2O_5Br$: C, 15.51; H, 4.89; N, 9.04; H_2O, 17.45%.

5) Tetramer of Ethylenediaminemonoacetatobromonickel(II), $[Ni(edma)Br]_4$ (V). This compound was prepared from the complex IV by the same way as was employed for the complex II. Found: C, 18.58; H, 3.77; N, 10.49%. Calcd for $C_4H_9NiN_2O_2Br$: C, 18.35; H, 3.47; N, 10.70%.

6) Bis(ethylenediaminemonoacetato)diaquo-μ-dibromodinickel(II) Tetrahydrate, $[Ni(edma)Br(H_2O)]_2\cdot 4H_2O$ (VI). This compound was prepared from the complex V in the same manner as has been described for the complex III. Found: C, 15.92; H, 4.44; N, 9.45; H_2O, 17.1%. Calcd for $C_4H_{11}NiN_2O_3Br\cdot 2H_2O$: C, 15.51; H, 4.89; N, 9.04; H_2O, 17.45%.

7) Tetramer of Ethylenediaminemonoacetatoiodonickel(II), $[Ni(edma)I]_4$ (VII). An aqueous solution of the complex I (7 g, 0.0264 mol) was treated with a silver nitrate solution. After filtering off the silver chloride thus precipitated, potassium iodide was added to the filtrate. The resulting solution was treated in the same manner as in the case of the complex IV. When the alcoholic solution was then concentrated to about 30 m*l* and allowed to stand for a day, light green crystals were separated out. They were washed with 50% alcohol. Yield, about 2 g (24%). Found: C, 15.76; H, 2.92; N, 9.47%. Calcd for $C_4H_9NiN_2O_2I$: C, 15.56; H, 2.94; N, 9.08%.

8) Bis(ethylenediaminemonoacetato)nickel(II) Dihydrate, $[Ni(edma)_2]\cdot 2H_2O$ (VIII). To an aqueous solution of nickel(II) chloride hexahydrate (2.4 g, 0.01 mol), 8.4 g (0.08 mol) of ethylenediaminemonoacetic acid dihydrochloride monohydrate were added. The solution was warmed to about 80°C, and the solution's pH was adjusted to 10—11 by adding a 6 N sodium hydroxide solution. The resulting solution was concentrated to about 10 m*l*. The sodium chloride thus precipitated was filtered off. About 60—70 m*l* of alcohol were added to the filtrate, and the resulting solution was allowed to stand in a refrigerator for 2—3 weeks. Blue crystals could thus be separated out. They were washed with 80% alcohol. Yield, about 1.0 g (34%). Found: C, 29.39; H, 6.91; N, 16.94%. Calcd for $C_8H_{18}NiN_4O_4\cdot 2H_2O$: C, 29.20; H, 6.75; N, 17.03%.

Measurements. The visible and far-infrared absorption spectra of aqueous solutions were recorded on a Hitachi EPS-3 pen-recording spectrophotometer. The reflection spectra were measured with a Hitachi Perkin-Elmer 139 spectrophotometer with a standard Hitachi reflection attachment. The infrared absorption spectra were taken on Nujol mulls between sodium chloride or on potassium bromide disks using a Hitachi EPI-S2 spectrometer. The TGA, DTA, and DTG curves were automatic-photographically recorded with a single sample by means of a Metrimpex Derivatograph, type-OD-102. The magnetic susceptibility was determined with a Gouy balance at room temperature. The elemental analyses were performed by the conventional combustion method, using a Yanagimoto C.H.N. Corder, MT-1.

Results and Discussion

IR Spectra. The infrared absorption spectra were measured in order to confirm whether or not the carboxylate group was coordinated to the nickel(II) ion. All the spectra of the complexes showed the νCOO-Ni band in the range from 1585 to 1660 cm^{-1} (Table 1). Therefore, it is clear

Table 1. Infrared absorption spectra (in cm^{-1}) and mangetic moments

Complex	νCOO-Ni asym. str.	νN-H def.	μ (B.M.)
I	1645	1575	3.26
II		1585 (overlapped)	3.26
III	1650	1570	3.27
IV	1645	1570	3.08
V		1585 (overlapped)	3.15
VI		1585 (overlapped)	3.06
VII		1605 (overlapped)	3.10
VIII	1660	1575	3.06

3) Y. Fujii, E. Kyuno and R. Tsuchiya, This Bulletin, **43**, 786 (1970).

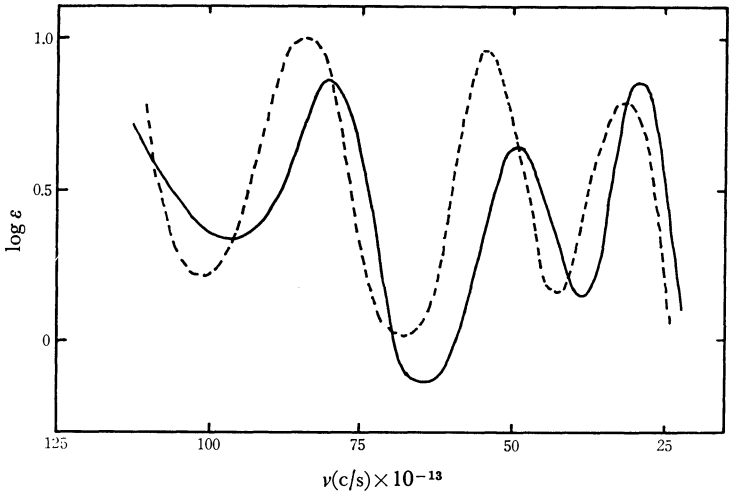

Fig. 1. Absorption spectra: complexes I and IV (——), VIII (----).

that the carboxylate group is coordinated to the nickel(II) ion.[4] In the cases of the complexes II, V, VI, and VII, the νCOO–Ni band is shifted to lower energy sites than those of the other complexes. This fact may indicate that the COO–Ni bonds of the complexes II, V, VI, and VII are slightly weakened as compared with those of the other complexes because of the distortion of their structures. On the other hand, the complexes I, III, IV, and VIII, in which they take the monomer structure, showed the νCOO-Ni band at higher energy sites than those of the complexes II, V, VI, and VII. Therefore, though it is difficult to distinguish the difference in the structure between the complexes III and VI on the basis of their absorption spectra (shown in the next paragraph), it can be suggested from their clearly different νCOO–Ni bands that the complex VI has a different structure than the complex III.

Electronic Spectra. The absorption spectra in an aqueous solution and those obtained by the diffuse-reflectance method are shown in Figs. 1, 2, and 3. The numerical values are summarized in Table 2, together with those of the related compounds.

The spectra of the complexes I and IV in an aqueous solution are similar to those which are characteristic for the octahedral Ni–N_2O_4-type complexes.[5] The aqueous solutions of the complexes I and IV were adsorbed by a cation exchanger, but not by an anion exchanger. Therefore, in an aqueous solution, the complexes I and IV must be cationic and the coordination of the halogen anion to the nickel(II) ion can be ruled out. This result agrees well with the finding obtained in the previous study.[1] In the solid state,

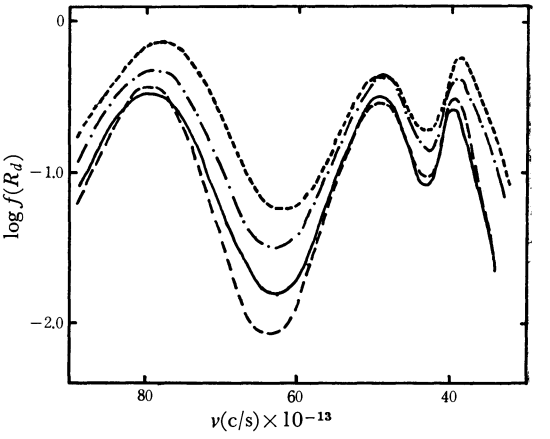

Fig. 2. Absorption spectra by the diffuse-reflectance method: I (——), III (—·—·—), IV (— — —), VI (----).

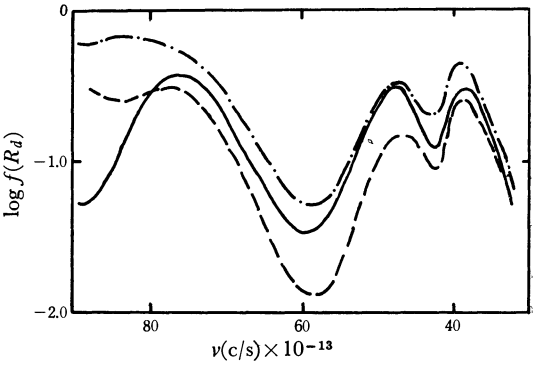

Fig. 3. Absorption spectra by the diffuse-reflectance method: II (——), V (—·—·—), VII (———).

the diffuse-reflectance spectra of the complexes I and IV also show spectra similar to those in an aqueous solution, although the peak near 30×

4) T. Sakaguchi and K. Ueno, "Metal Chelates," Vol. II, Nankodo, Tokyo (1963), p. 43.

5) H. Ito, *Nippon Kagaku Zasshi*, **77**, 1383 (1956).

Table 2. Absorption spectra for the complexes

Complex	ν (log ε)	ν (log ε)	ν (log ε)
I	80.0 (0.86) 80.0 (−0.47)*	49.2 (0.64) 49.6 (−0.49)*	29.1 (0.85) 40.0 (−0.58)*
II	76.0 (−0.44)*	46.9 (−0.50)*	38.0 (−0.50)*
III	77.9 (−0.33)*	48.8 (−0.35)*	39.5 (−0.38)*
IV	80.0 (0.86) 80.0 (−0.45)*	49.2 (0.64) 49.6 (−0.54)*	29.1 (0.85) 40.0 (−0.51)*
V	83.3 (−1.97)*	46.9 (−0.45)*	39.2 (−0.35)*
VI	77.9 (−0.14)*	48.4 (−0.34)*	39.5 (−0.24)*
VII	76.9 (−0.50)*	46.9 (−0.80)*	39.2 (−0.58)*
VIII	84.0 (1.02)	54.1 (0.97)	30.8 (0.79)
$[Nien(H_2O)_4]SO_4 \cdot H_2O$[5]	81.0 (0.76)	48.5 (0.54), 41.0 (0.25)	30.8 (0.68)
$[Ni(gly)_2(H_2O)_2]$[5]	80.8 (0.90)	48.8 (0.68)	29.3 (0.85)
$[Ni(en)_2(H_2O)_2](ClO_4)_2$[5]	84.0 (1.02)	54.8 (0.81)	33.4 (0.85)

The frequency is given in 10^{13} sec^{-1}.
* Data by the diffused-reflectance method, ( ) is the value of $\log f(R_d)$.

10^{13} c/s observed in an aqueous solution shifts to a shorter wavelength. Though there is a possibility that the halogen anion coordinates to the nickel(II) ion in the case of the solid state, this can be safely ruled out on the basis of the facts that the complexes in which the halogen anion is coordinated to the nickel(II) ion can be isolated by another method (the complexes III and VI) and that the behavior of the dehydration, as measured by the derivatograph, is clearly different between the complexes I, IV and III, VI. Therefore, the complexes I and IV can be concluded to have an octahedral structure, $[Ni(edma)(H_2O)_3]X$ (X= Cl and Br), where three molecules of water are all coordinated to the nickel(II) ion, in both an aqueous solution and a solid crystal.

The reflectance spectra of the complexes II, V, and VII show three peaks with nearly the same intensities in the visible and far-infrared regions. Their magnetic-moment data indicate that their structures are octahedral or tetrahedral (Table 1). If these complexes have a tetrahedral structure, only one peak would be expected in this absorption region.[6-8] The existence of three peaks with nearly identical intensities can, then, be thought to be characteristic of the octahedral nickel(II) complexes.[5] Therefore, on the basis of absorption spectra, the structures of the complexes II, V, and VII can be identified as octahedral.

The reflectance spectra of the complexes III and VI are nearly identical with those of the complexes I and IV, except that all the peaks of the complexes III and VI are shifted to slightly lower energy sites than the peaks of the complexes I and IV. This is thought to be due to the coordination of the halogen anion. Therefore, an octahedral structure can be assigned to them. These explanations were confirmed by the behavior of their dehydrations. The details will be discussed in the next paragraph. Here, it is enough to note that the difference in the coordination between one molecule of water and one molecule of the halogen anion (Cl^- and Br^-) do not show any considerable difference in their absorption spectra.

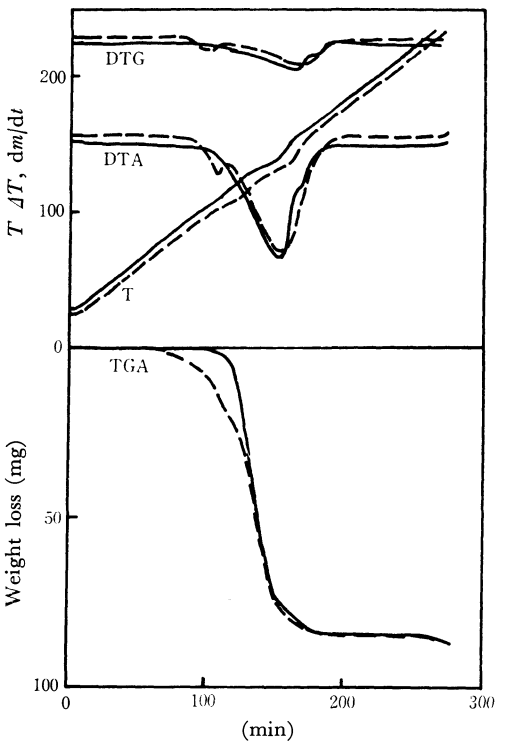

Fig. 4. Derivatogram of I (——) and III (———). The starting weight of sample is 400 mg.

6) G. P. Smith, C. H. Liu and T. R. Griffiths, *J. Amer. Chem. Soc.*, **86**, 4796 (1964).
7) H. A. Weakliem, *J. Chem. Phys.*, **36**, 2117 (1962).
8) C. R. Boston and G. P. Smith, *J. Amer. Chem. Soc.*, **85**, 1006 (1963).

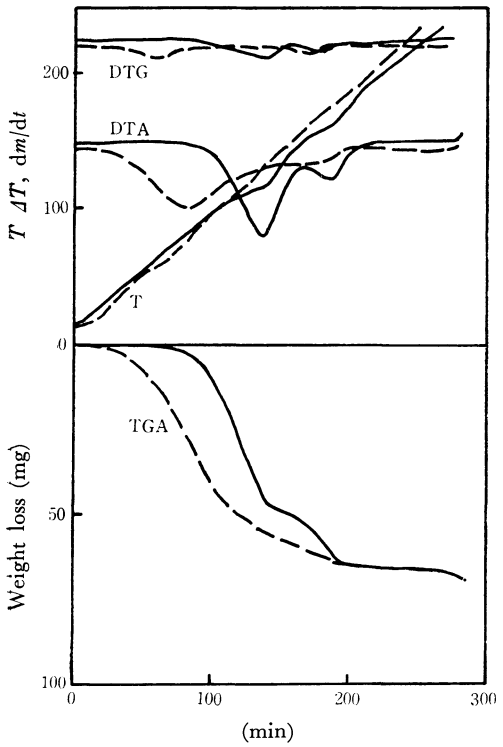

Fig. 5. Derivatogram of IV (——) and VI (— — —). The starting weight of sample is 400 mg.

The 1-to-2-ratio complex, VIII, shows a spectrum similar to those of Ni–N_4O_2-type complexes.[5] Therefore, an octahedral structure can be assigned to the complex VIII, although the configuration of the coordinated edma is not clear in detail.

Derivatogram and Magnetic Moments. From the TGA, DTA, and DTG curves[9] (Figs. 4 and 5), it was observed that two molecules of water dehydrated from 110°C to 140°C, and another molecule of water, from 140°C to 175°C, for the complex I. On the other hand, in the case of the complex III, one molecule of water dehydrated from a very low temperature (from about 50°C to 110°C), and other two molecules of water, from 110°C to 175°C. These facts indicate that the structure of the complex I is clearly different from that of the complex III. The low temperature of the dehydration of one molecule of water for the complex III can be ascribed to the dehydration of crystalline water. Therefore, the structure of the complex III can be presumed to be $[Ni(edma)Cl(H_2O)_2]\cdot H_2O$, where the chloride ion is coordinated to the nickel(II) ion, and the structure of the complex I to $[Ni(edma)(H_2O)_3]Cl$, where the three molecules of water are all coordinated to the nickel(II) ion. The high temperature of the dehydration of one molecule of water for the complexes I and III may suggest that the dehydration proceeds through the intermediate of the dimer structure in which two molecules of the chloride ion are bridged to the nickel(II) ion as is shown in Fig. 6 (A). Further information which gives strong support to the explanation presented above was obtained by the dehydration of the complex IV. The difference in the dehydration between two molecules of water (from 80°C to 125°C) and one molecule of water (from 125°C to 175°C) is clearly distinguished in the case of the complex IV. The high temperature of the dehydration of the last molecule of water clearly indicates that the dehydrations proceed through the intermediate of the dimer structure in which two bromide ions are bridged and in which the two molecules of water are coordinated to the nickel(II) ions, as is shown in Fig. 6 (A).

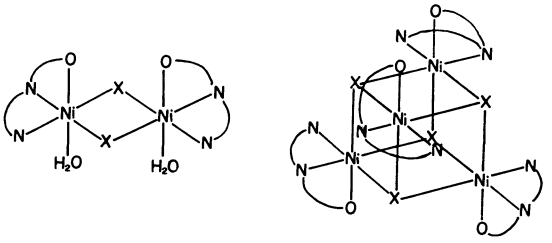

Fig. 6. The probable structure of the dimer and tetramer structures.
A: $[Ni(edma)X(H_2O)]_2$ (X=Cl and Br)
B: $[Ni(edma)X]_4$ (X=Cl, Br and I)

On the other hand, in the case of the complex VI, the dehydration of two molecules of water takes place from a very low temperature (from 35°C to about 100°C) compared with the case of the complex IV, and the last molecule of water dehydrates from about 100°C to 175°C. The low temperature of the dehydration of the two molecules of water is ascribed to two molecules of crystalline water. Therefore, the structure of the complex VI is assigned to the dimer of $[Ni(edma)Br(H_2O)]\cdot 2H_2O$, where the bromide ion is bridged. This assignment agrees well with the suggestion of the IR spectra that the complex VI may take a different structure from that of the complex III.

The values of the effective magnetic moment of the complexes are listed in Table 1. All the complexes show values near 3.10 B.M. These values suggest that all the complexes have an octahedral structure, for the nickel(II) complexes with a tetrahedral structure have been established generally to have the effective magnetic moments from 3.50 to 4.00 B.M.[10]

9) R. Tsuchiya, Y. Kaji, A. Uehara and E. Kyuno, This Bulletin, **42**, 1881, 1886 (1969).

10) D. M. L. Goodgame, M. Goodgame and F. A. Cotton, *J. Amer. Chem. Soc.*, **83**, 4161 (1961).

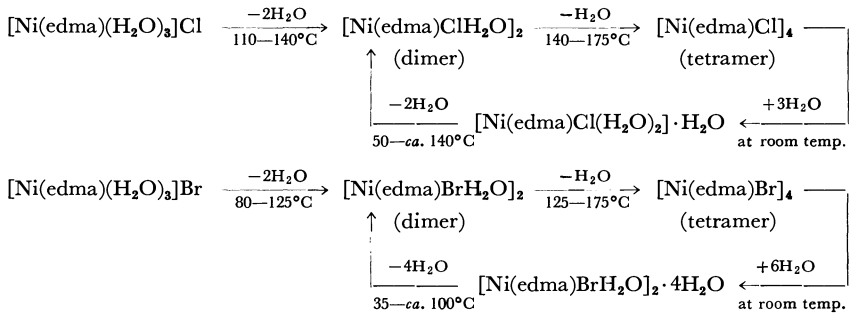

Scheme 1. The mechanism of dehydrations.

On the basis of these results and discussions, as the structure of the complexes II, V, and VII, tetramer in which the four halogen anions are triply bridged to the four nickel(II) ions may be considered reasonable (Fig. 6 (B)). Here, it is established that two nitrogen atoms and one oxygen atom of edma coordinate to the nickel(II) ion, making a facial form.

As the mechanism of the dehydration process, the above scheme can be proposed (Scheme 1).

The author wishes to express his deep thanks to Professor R. Tsuchiya and his co-workers of Kanazawa University for their kind help in measurements using the Derivatograph. He also wishes to thank Professor K. Yamamoto and Dr. M. Kodama of Ibaraki University for their encouragement.

BULLETIN OF THE CHEMICAL SOCIETY OF JAPAN VOL. 43 2820—2823 (1970)

Anodic Process of Thiosulfate at a Dropping Mercury Electrode

Teisuke MURAYAMA, Toshiko SAWAKI and Shukichi SAKURABA

Department of Industrial Chemistry, Faculty of Engineering, Shizuoka University, Hamamatsu

(Received March 13, 1970)

In the anodic process of thiosulfate at a dropping mercury electrode, the formation of a species $Hg(S_2O_3)_3^{4-}$ is considerable even in dilute solution. An equation of current-potential curve is derived with proper consideration for the formation of the species. The successive stability constant of $Hg(S_2O_3)_3^{4-}$ was calculated to be 3×10^2 (at 25°C and an ionic strength of 0.2) by comparing the equation with experimental results.

A few decades ago, Kolthoff and Miller showed that the anodic wave of thiosulfate at a dropping mercury electrode (DME) corresponds to the formation of a complex ion $Hg(S_2O_3)_2^{2-}$.[1] More recently Nyman and Salazar investigated the same process.[2] They found that although a plot of $\log i/(i_d-i)^2$ *vs.* E gave a straight line its reciprocal slope did not remain constant. The slope increased from 30 to 41 mV when the concentration of thiosulfate increased from 2×10^{-4} to 5×10^{-3} M. They attributed the slope increase to the formation of a species $Hg(S_2O_3)_3^{4-}$, which invalidated Eq. (9) in the paper by Kolthoff and Miller. Nyman and Salazar applied DeFord-Hume's method to evaluate stability constants of $Hg(S_2O_3)_2^{2-}$ and $Hg(S_2O_3)_3^{4-}$ from the observed shift in half-wave potential. However, they did not mention whether calculated values of constants were consistent with the behavior of the slope of the plot or not. In the following we have examined the relationship between the reciprocal slope of log plot and stability constants of the complex ions.

1) I. M. Kolthoff and C. S. Miller, *J. Amer. Chem. Soc.*, **63**, 1405 (1941).

2) C. J. Nyman and T. Salazar, *Anal. Chem.*, **33**, 1467 (1961).

Results and Discussion

The potential of the dropping mercury electrode, E, may be written as

$$E = E^0 + \frac{RT}{2F}\ln\gamma_1 + \frac{RT}{2F}\ln[Hg^{2+}] \qquad (1)$$

where E^0 is the standard potential of mercuric-mercury electrode, γ_1 is the activity coefficient of mercuric ion, and R, T, and F are molar gas constant, absolute temperature, and Faraday, respectively. Square brackets indicate the concentration at the surface of DME. Mercuric ions are produced by an electrode process

$$Hg = Hg^{2+} + 2e \tag{2}$$

and consumed by chemical reactions

$$Hg^{2+} + 2S_2O_3^{2-} = Hg(S_2O_3)_2^{2-} \tag{3}$$

$$Hg^{2+} + 3S_2O_3^{2-} = Hg(S_2O_3)_3^{4-} \tag{4}$$

which follow the electrode process. Formation of $Hg(S_2O_3)_4^{6-}$ is not considered here, because its high negative charge forbids it. In the following we assume that reactions (2), (3), and (4) are reversible.

The average anodic current, i, may be written as

$$i = i_2 + i_3 \tag{5}$$

where i_2 and i_3 are the current parts relating to concentration of $Hg(S_2O_3)_2^{2-}$ and $Hg(S_2O_3)_3^{4-}$ at the electrode surface through

$$i_2 = \kappa_2[Hg(S_2O_3)_2^{2-}]$$

$$i_3 = \kappa_3[Hg(S_2O_3)_3^{4-}]$$

where κ_2 and κ_3 are the Ilkovic constants for $Hg(S_2O_3)_2^{2-}$ and $Hg(S_2O_3)_3^{4-}$, respectively. Because $[Hg^{2+}]$ is too small compared with $[Hg(S_2O_3)_2^{2-}]$ and $[Hg(S_2O_3)_3^{4-}]$ at the potential of thiosulfate wave, the current part relating to $[Hg^{2+}]$ is neglected in Eq. (5).

Equation (5) may be rewritten as

$$i = (\beta_2\kappa_2 + \beta_3\kappa_3 x)x^2[Hg^{2+}] \tag{6}$$

where β_2 and β_3 are stability constants of $Hg(S_2O_3)_2^{2-}$ and $Hg(S_2O_3)_3^{4-}$, respectively, and x is the concentration of thiosulfate ions at the surface of DME. After rearrangement, we obtain the equation for $[Hg^{2+}]$:

$$[Hg^{2+}] = \frac{2\kappa_4 y}{\beta_2\kappa_2(1 + rx)x^2} \tag{7}$$

In the above κ_4 is the Ilkovic constant for thiosulfate ion, and

$$r = \frac{\beta_3\kappa_3}{\beta_2\kappa_2} \tag{8}$$

$$y = \frac{i}{2\kappa_4} \tag{9}$$

Combination of Eqs. (1) and (7) gives

$$E = E^0 + \frac{2.303RT}{2F}\log\frac{2\gamma_1\kappa_4}{\beta_2\kappa_2} + \frac{2.303RT}{2F}\log\frac{10^{-3}y}{(1 + rx)x^2} + \frac{6.909RT}{2F} \tag{10}$$

The last term of the right-hand side is added in order to compensate the factor 10^{-3} in the third term, which is introduced to displace the zero point of ordinate of the log plot for convenience. The third term represents the contribution by the current. For construction of a log plot according to Eq. (10) it is necessary to know numerical values of x at given potentials. This can be done as follows.

Fluxes of out-going species, $Hg(S_2O_3)_2^{2-}$ and $Hg(S_2O_3)_3^{4-}$, at electrode surface are given by

$$f_2 = \frac{i_2}{2F} = \frac{\kappa_2[Hg(S_2O_3)_2^{2-}]}{2F} \tag{11}$$

$$f_3 = \frac{i_3}{2F} = \frac{\kappa_3[Hg(S_2O_3)_3^{4-}]}{2F} \tag{12}$$

The flux of in-coming species $S_2O_3^{2-}$ is given by

$$f_4 = \frac{i_d - \kappa_4 x}{F} \tag{13}$$

where i_d is the diffusion current. There is no accumulation of S_2O_3 group at the surface of DME. Hence

$$f_4 = 2f_2 + 3f_3 \tag{14}$$

Substituting Eqs. (11), (12), and (13) into Eq. (14) we obtain

$$i_d - \kappa_4 x = \kappa_2[Hg(S_2O_3)_2^{2-}] + \frac{3}{2}\kappa_3[Hg(S_2O_3)_3^{4-}]$$

$$= \frac{1}{2}\beta_2\kappa_2(2 + 3rx)x^2[Hg^{2+}] \tag{15}$$

Combining this with Eq. (7), we get

$$x_0 - x = \frac{2 + 3rx}{1 + rx}y \tag{16}$$

where $x_0 = i_d/\kappa_4$.

Equation (16) is solved for x.

$$x = \frac{(x_0 - 3y)r - 1 + \sqrt{(x_0 - 3y)^2r^2 + 2r(x_0 - y) + 1}}{2r} \tag{17}$$

Numerical values of x can be calculated by this equation if r is known. However, it is not and we adopted the following procedure as we did previously.[3] First, values of x are calculated by Eq. (17) with a value of r arbitrarily chosen, and $\log 10^{-3}y/(1+rx)x^2$ is plotted against E. With an

Table 1. Reciprocal slopes of log plots constructed according to Eq. (10)
$r = 3\times10^2$

Concentration of thiosulfate ions mM	Reciprocal slope mV	e_0* *vs.* SCE V
0.522	30	0.143
1.044	30	0.143
1.566	30	0.141
2.088	30	0.142
3.17	29	0.145
4.23	30	0.144
5.29	30	0.143

* Potential at which $\log 10^{-3}y/(1+rx)^2$ becomes zero.

3) T. Murayama, *Sci. Rep. Tohoku Univ., Series I*, **45**, 98 (1961).

arbitrary value of r, the plot does not necessarily produce a straight line. Then the whole process is repeated with a slightly different value of r which is chosen to lessen deviation of the plot from a straight line. The process is repeated until the plot yields a straight line. It was found that the plot constructed from polarograms obtained at 25°C gave a straight line when a value of 3×10^2 was substituted for r. The accompanying table shows the reciprocal slope of plots constructed with this value of r and the potential at which log $10^{-3}\cdot y/(1+rx)x^2$ becomes zero. Fair agreement may be considered as an evidence in support of Eq. (10) and underlying assumptions.

The value of r is related to a stability constant ratio β_3/β_2, which is the successive stability constant of the tris complex, through Eq. (8). Evaluation of a ratio κ_3/κ_2 is necessary for calculation of the successive constant. It seems possible to determine the ratio by observing the change of diffusion current of mercuric ion with increasing concentration of thiosulfate ions in supporting electrolyte. However, this is not possible because mercuric ions react with thiosulfate ions to precipitate mercuric sulfide. The difficulty was overcome by substituting mercuric ions by mercuric cyanide in a buffer solution of an appropriate pH. Although the stability constant of mercuric cyanide, having a value of $10^{35.2}$ (activity constant),[4] is much larger than that of bis(thiosulfato)mercurate-(II), it is still possible to convert the most part of mercuric cyanide to the bis complex, without precipitation of mercuric sulfide, by selecting pH of the buffer.

Measurement of diffusion current was carried out for 1 mM mercuric cyanide in the buffer of pH 5.26 with varying thiosulfate concentrations. Results are shown in Fig. 1 as the ratio of the diffusion current to that in the absence of thiosulfate. With a value of $10^{29.27}$ for the stability constant (activity constant) of bis(thiosulfato) complex,[2] the mole ratio of $Hg(S_2O_3)_2^{2-}$ to $Hg(CN)_2$ was calculated to be not less than 100 when the concentration of thiosulfate was 4.5 times as much as that of mercuric cyanide. Accordingly, the decrease of diffusion current beyond this point is due to the formation of tris(thiosulfato) complex. The formation of the tris complex seems incomplete even in the presence of thiosulfate of the highest concentration employed in this experiment (see Fig. 1). Although it is impossible to determine exactly the ratio κ_3/κ_2 from this experiment, it does not seem to deviate much from unity. If it is assumed to be equal to unity, the successive stability constant of tris(thiosulfato)mercurate(II) is calculated to be 3×10^2 (concentration constant). The activity constant was calculated to be $3._4\times10$ from this and activity coefficients estimated by the Debye and Hückel equation without the extended term.[5]

$$\log\gamma_i = -\frac{0.358z_i^2(2\mu)^{1/2}}{1+10^8a_i0.2325(2\mu)^{1/2}}$$

In this equation γ_i, z_i, and a_i are the activity coefficient, the electrovalency, and the ionic parameter, respectively, of the ion i, and μ is the ionic strength of the solution. Values of a_i assumed for thiosulfate ion, and bis- and tris(thiosulfato)mercurate-(II) ions are 4, and 4 and 5 Å, respectively. These values were chosen for respective ions to be in accord with ions listed in Kielland's table with respect to charge type.[5,6]

A value of 3×10 was calculated for the successive stability constant (activity constant) from β's at zero ionic strength given by Nyman and Salazar.[2] This is in good agreement with the value derived from the slope of the log plot in the present study.

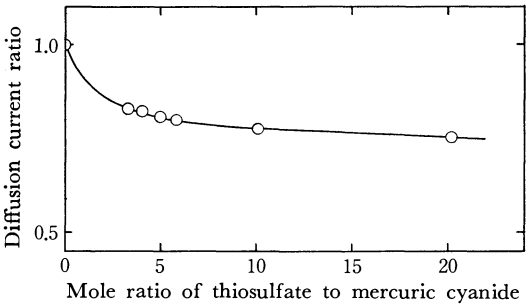

Fig. 1. Change of the ratio of the diffusion current of mercuric cyanide to that in the absence of thiosulfate.
Concentration of mercuric cyanide, 0.983 mM.

Experimental

A manual polarograph was used for the measurement of the current-potential curve. The cell used was of a beaker type with a Hume and Harris type salt bridge.[7] To avoid contamination of chloride ion, the intermediate agar plug saturated with potassium chloride was replaced by one prepared with 1 M potassium nitrate. The dropping mercury electrode used had an m value of 1.865 mg/sec and a drop time of 4.28 sec, being measured in a deaerated 0.2 M sodium nitrate solution at the potential of the saturated calomel electrode with a head of mercury of 90.0 cm.

Stock solutions were prepared from redistilled water with chemicals of guaranteed grade. The sodium thiosulfate stock solutions were standardized against potassium iodate.[8] The mercuric cyanide stock solution

4) T. Murayama, *Sci. Rep. Tohoku Univ., Series I*, **45**, 111 (1961).

5) G. Kortüm and J. O'M. Bockris, "Textbook of Electrochemistry," Vol. II, Elsevier Publishing Co., Amsterdam (1951), p. 680.

6) J. Kielland, *J. Amer. Chem. Soc.*, **59**, 1675 (1937).

7) D. N. Hume and W. E. Harris, *Ind. Eng. Chem., Anal. Ed.*, **15**, 465 (1943).

8) I. M. Kolthoff and E. B. Sandell, "Textbook of Quantitative Analysis," Macmillan Co., New York, N. Y. (1952), p. 594.

was prepared by dissolving a weighed amount of solid salt in known volume of the solution. As supporting electrolyte, 0.2 M sodium nitrate solution was used for anodic wave, and an acetate buffer of pH 5.26, of which ionic strength was controlled to 0.2 with sodium nitrate, for cathodic wave. To the latter 0.005% gelatin was added as a maximum suppressor. The pH of the buffer was measured by a Hitachi-Horiba Model P pH meter.

All measurement were carried out in a thermostat kept at 25.0 ± 0.1°C. All potentials were corrected for the internal resistance (iR drop) across the cell.

BULLETIN OF THE CHEMICAL SOCIETY OF JAPAN VOL. 43 2823—2827 (1970)

An Internal-Reference Method for the Determination of Rubidium by Photon-Activation Analysis with Strontium Used as the Reference Element*[1]

Hui-Tuh TSAI, Toyoaki KATO and Yoshinaga OKA

Department of Chemistry, Faculty of Science, Tohoku University, Katahira-cho, Sendai

(Received March 17, 1970)

We have studied a method for the determination of rubidium by activation analysis with bremsstrahlung photons, with strontium used as the internal-reference element. This method is based on the γ-ray spectrometric measurement of the ^{84}Rb activities produced by the ^{85}Rb(γ,n) reaction and on the comparisons of those activities with that of ^{83}Rb arising from strontium as a result of the (γ,p) reaction. The yields of various photonuclear reactions in rubidium and in strontium have also been examined as a function of bremsstrahlung maximum energies up to 60 MeV, and the best conditions for the determination of rubidium are proposed. When the maximum energy was set at 18 to 20 MeV, no interfering reactions occurred; a rubidium content down to about 2 μg can be determined accurately. A comparison of solid-state and scintillation γ-ray spectrometry in this method has also been included with respect to the sensitivity and the selectivity.

A minute amount of rubidium can be determined by a thermal neutron activation method by inducing ^{86}Rb activity in an irradiated sample; this technique has been applied to the determination of rubidium in a number of materials of geochemical interest[1-3] The contents of rubidium and strontium in terms of the rubidium-to-strontium ratios have been utilized for the age-determination of these materials.[4] An accurate and precise analytical method was required in this work.

The work described here was undertaken for the purpose of establishing an accurate method for the determination of rubidium by photon-activation analysis, using strontium as the internal-reference element. In order to determine the best conditions for the determination of rubidium by this method, some work has also been carried out on the yields of photonuclear reactions over the energy range of bremsstrahlung photons up to 60 MeV. When a maximum energy was set at 18 to 20 MeV, no interfering reactions occurred, and traces of rubidium down to about 2 μg could be determined accurately. A comparison of the solid-state detection by means of the scintillation-detection method is also included with respect to the sensitivity and the selectivity.

Experimental

Materials and Irradiation. The rubidium chloride was a guaranteed reagent grade. Strontium carbonate of a guaranteed reagent grade was further purified by repeated reprecipitations. Synthetic mixtures of these two compounds, with known weight ratios of rubidium to strontium ranging from 1.3×10^{-1} to 5.4×10^{-3}, were prepared in order to examine the sensitivity and the accuracy of the method. Each sample (weight, about 100 mg) was placed in a quartz tube with an internal diameter of 4 mm for bremsstrah-

*1 Study of the Activation Analysis using the Internal-Reference Method. XIV., A part of this work was presented at the 17th Annual Meeting of the Analytical Chemistry Society of Japan, Hiroshima, October, 1968. Part XIII: H-T. Tsai, T. Kato and Y. Oka, This Bulletin, **43**, 2482 (1970).

1) M. J. Cabell and A. A. Smales, *Analyst*, **82**, 390 (1957).

2) A. A. Smales, T. C. Hughes, D. Mapper, C. A. J. McInnes and R. K. Webster, *Geochim. Cosmochim. Acta*, **28**, 209 (1964).

3) K. Tomura, H. Higuchi, H. Takahashi, N. Onuma and H. Hamaguchi, *Anal. Chim. Acta*, **43**, 523 (1968).

4) E. Anders, *Rev. Mod. Phys.*, **34**, 287 (1962).

lung irradiation. All the irradiations were terminated in 1 hr. The linear electron accelerators of Tohoku University and of the Japan Atomic Energy Research Institute were used as the bremsstrahlung sources. The experimental method involving bremsstrahlung-flux monitoring and the details of the irradiation were essentially the same as have been described in detail in a previous paper.[5]

Separation Procedure. The irradiated sample was dissolved in a small amount of 0.1 N hydrochloric acid, along with 20 mg of a rubidium carrier. The solution was evaporated to dryness, and the residue was dissolved with dilute aqueous ammonia (pH 8) and then subjected to cation-exchange separation. The resin used was Dowex 50W×8, 100 to 200 mesh size. This was fed into a column 25 cm long and with an internal diameter of 8 mm. The rubidium was eluted with a 0.5 M ammonium acetate solution and was precipitated by the addition of 0.1 N perchloric acid with ice-cooling. The rubidium perchlorate was filtered and dried in a vacuum.

After the elution of the rubidium, the strontium was eluted from the column with 1 N nitric acid and precipitated as strontium carbonate by means of an aqueous ammonium carbonate solution. The precipitate was filtered and dried at 500°C. Either rubidium perchlorate or strontium carbonate was wrapped with a thin sheet of aluminum in order to determine the chemical yield, if needed, and for γ-counting.

Counting Equipment. A lithium-drifted germanium detector with an active volume of 36 cm^3, ORTEC 8101-30P, was coupled to a TMC 1024-channel pulse-height analyzer. The counting system had a resolution of 4 keV for the 661.6 keV γ-line of ^{137}Cs. The counting efficiency of this detector has been determined as a function of the source distance and the γ-ray energy by counting a series of calibrated sources of known activities. A sample was measured at a fixed position, 9 mm from the active surface of the detector.

A 3″ dia.×3″ NaI(Tl) crystal was also used as the detector. This was coupled to an 800-channel pulse-height analyzer made by the Tokyo Shibaura Electric Co., Ltd. For the determination of the photonuclear yields where a much greater resolving power was required, the Ge(Li) detector was used exclusively; for analytical purposes, both counting systems were employed.

Yield Determination. A yield was defined as the production rate of nuclide due to a certain photonuclear reaction in dps at the end of the irradiation of one mole of a parent nucleous when a standard amount of bremsstrahlung radiation with a given maximum energy has passed through the target during the irradiation period. The initial decay rates of the various activities produced were determined from a decay-curve analysis of the counting rate of the relevant photopeak area. The corresponding saturation rates were computed and normalized for the bremsstrahlung intensity, which was measured by means of the amount of of ^{196}Au activity produced by the $^{197}Au(\gamma,n)^{196}Au$ reaction in a gold foil irradiated together with the sample. After correcting for chemical yields, counting efficiencies, branching ratios,[6] and the internal conversion electrons,[7] the yields were expressed relative to that of the $^{87}Rb(\gamma,n)^{86}Rb$ process or of the $^{84}Sr(\gamma,n)^{83}Sr$ process.

Results and Discussion

Photonuclear Reaction. Rubidium has two naturally-occurring isotopes, ^{85}Rb(72.15%) and ^{87}Rb(27.85%), while strontium has four isotopes, ^{84}Sr(0.56%), ^{86}Sr(9.86%), ^{87}Sr(7.02%), and ^{88}Sr-(82.56%). The experimental results showed that the rubidium nuclides formed in the irradiations of the two elements by bremsstrahlung with maximum energies up to 60 MeV were ^{82m}Rb ($T_{1/2}$= 6.3 hr), ^{83}Rb ($T_{1/2}$=83d), ^{84}Rb ($T_{1/2}$=33.0 d), ^{84m}Rb ($T_{1/2}$=20 min), and ^{86}Rb ($T_{1/2}$=18.66 d). In addition, the production of ^{81}Rb($T_{1/2}$=4.7 hr) was also observed in an irradiated strontium sample. In this experiment, γ-rays from ^{81m}Rb could not be measured because of its lower energies (0.085 MeV with IT) and its relatively short half-life (31 min). The ^{84m}Rb activity could not be detected from strontium since it has decayed away during the separation processes.

From the threshold-energy considerations, the main reactions which can occur in both elements with bremsstrahlung and with maximum energies below 20 MeV are the (γ,n) and (γ,p) reactions. Thus, when irradiated with 17.6 MeV bremsstrahlung, ^{84}Rb, ^{84m}Rb, and ^{86}Rb, the (γ,n) reaction products, were measured. No nuclides other than the above were produced at 20 MeV. Since the ^{84}Rb activity was used in the determination of rubidium, the irradiation conditions leading to the production of ^{84}Rb from strontium had to be avoided. The only possible reaction producing ^{84}Rb in the irradiation with bremsstrahlung below 20 MeV is the $^{86}Sr(\gamma,d)^{84}Rb$ reaction ($-Q$=17.84 MeV). The experimental results showed that the production of ^{84}Rb from strontium with 20 MeV bremsstrahlung could not be observed in any appreciable amount.

The yields of various reactions are given as a function of the bremsstrahlung maximum energy in Figs. 1 and 2. Since an excitation energy beyond 30 MeV covers the giant resonance region well for most nuclei, and since the main nuclear event in this energy region is the emission of one neutron,[8] the yield value of the (γ,n) reaction remains almost unchanged throughout this energy region. The yield of the reaction with the emission of more than one nucleon appeared to be strongly

5) Y. Oka, T. Kato and N. Sato, This Bulletin, **42**, 387 (1969).

6) The decay schemes used were those listed in G. M. Lederer, J. M. Hollander and I. Perlman, "Table of Isotopes," Sixth Ed., John Wiley & Sons, New York (1967).

7) The tables in M. E. Rose, "Internal Conversion Coefficients," North-Holland Publ. Co., Amsterdam (1958), were used.

8) R. Montalbetti, L. Katz and J. Goldenberg, *Phys. Rev.*, **91**, 659 (1953).

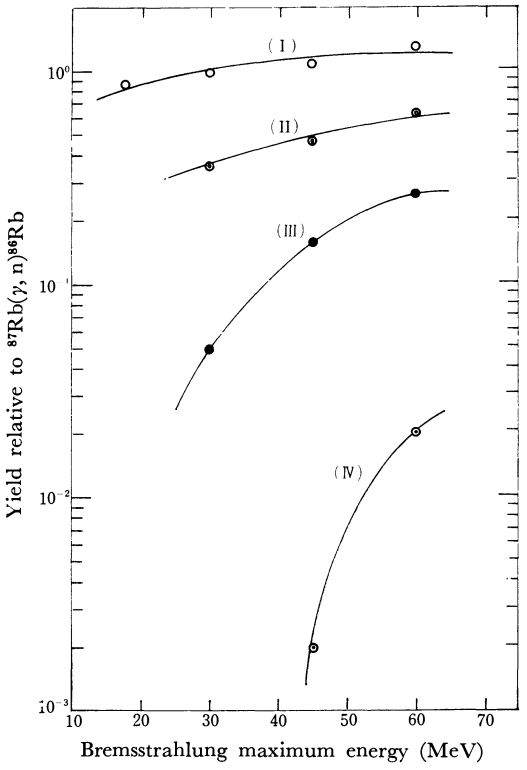

(I): $^{85}Rb(\gamma,n)^{84}Rb$. (III): $^{85}Rb(\gamma,2n)^{83}Rb$.
(II): $^{85}Rb(\gamma,n)^{84m}Rb$. (IV): $^{85}Rb(\gamma,3n)^{82m}Rb$.

Fig. 1. The yield of rubidium nuclides produced from rubidium as a function of bremsstrahlung maximum energy.

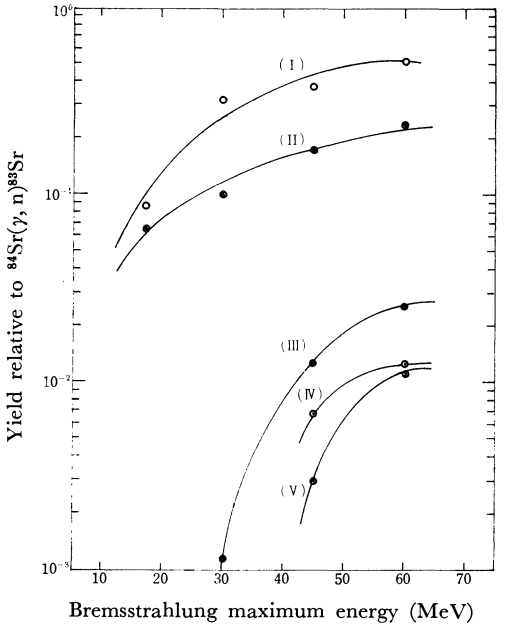

(I): $^{84}Sr(\gamma,p)^{83}Rb$. (IV): $^{84}Sr(\gamma,pn)^{82m}Rb$.
(II): $^{87}Sr(\gamma,p)^{86}Rb$. (V): $^{84}Sr(\gamma,p2n)^{81}Rb$.
(III): $^{86}Sr(\gamma,pn)^{84}Rb$.

Fig. 2. The yield of rubidium nuclides produced from strontium as a function of bremsstrahlung maximum energy.

energy-dependent. In the energy region higher than 45 MeV, the $^{85}Rb(\gamma,3n)^{82m}Rb$ and $^{85}Rb(\gamma,4n)^{81m,81}Rb$ reactions occurred; the ^{81}Rb and ^{82m}Rb activities were also measured from an irradiated strontium sample. An increase in the yields of the (γ,pn) reactions can be seen beyond 45 MeV. The $^{84}Sr(\gamma,pn)^{81}Rb$ reaction contributes mainly to the production of ^{81}Rb from strontium. At 60 MeV, however, the additional contribution to the total production rate comes from the $^{86}Sr(\gamma,p4n)^{81}Rb$ reaction. The main reaction leading to the production of ^{82m}Rb in this energy region is the $^{84}Sr(\gamma,pn)$ reaction.

For analytical purposes, the ^{84}Rb activity as a result of the (γ,n) reaction can be used effectively with respect to the sensitivity at a given maximum energy investigated here. Table 1 shows the photopeak activities of ^{84}Rb, together with those of ^{83}Rb from strontium, as a function of the bremsstrahlung maximum energy. In the determination of rubidium by the use of strontium as a reference, however, it is necessary to avoid interferences due to the production of ^{84}Rb from strontium through the (γ,d) and (γ,pn) reactions. As has been stated earlier, the irradiation by bremsstrahlung with maximum energies below 20 MeV gives no such trouble.

Determination of Rubidium. The 0.880 MeV γ-ray photopeak of ^{84}Rb can be utilized for the determination of rubidium, while the ^{83}Rb activity arising from strontium can be used as a reference. A comparison of the scintillation detection by the solid-state detection method can be discussed in terms of the sensitivity and the selectivity by processing the synthetic mixtures.

When a 3″ dia. × 3″ NaI(Tl) detector was used, we obtained the typical γ-ray spectrum shown in Fig. 3. The sample was irradiated with 20 MeV bremsstrahlung in this case. It can be seen that the photopeak appearing at 0.525 MeV is the compound peak of the 0.511 MeV γ-ray from ^{84}Rb and the 0.521, 0.530, and 0.553 MeV γ-rays of ^{83}Rb. The area under the latter three different γ-rays of ^{83}Rb were determined from these spectra by the following sequences:

1) from the spectrum in Fig. 3, the background activity due to the 1.078 MeV γ-ray of ^{86}Rb was subtracted by the graphical subtraction method;[9]

2) the area under the 0.880 MeV photopeak, A_{detn}(cpm), was obtained;

3) the 0.511 MeV photopeak area due to ^{84}Rb,

9) "Guide to Activation Analysis," ed. by W. S. Lyon, Jr., D. Van Nostrand Co., Princeton, N. J. (1964), p. 104.

Table 1. Photopeak activity of the rubidium nuclides with a Ge(Li) detector

Nuclide	Production reaction	γ-Ray (MeV)	Photopeak activity (cpm/mg)*			
			17.6 MeV	30 MeV	45 MeV	60 MeV
^{84}Rb	^{85}Rb(γ,n)	0.880	5.02×10^{3}	7.71×10^{3}	1.95×10^{4}	1.21×10^{4}
^{83}Rb	^{84}Sr(γ,p)	0.553	5.76×10^{-1}	3.03×10^{0}	4.92×10^{0}	6.02×10^{0}

* cpm at the end of 1 hr-irradiation with a standard dose rate of bremsstrahlung photons with a given maxinum energy incident on 1 mg of the element: With this dose rate, 1.0 μCi ^{196}Au is produced by the (γ,n) process in 1 mg Au.

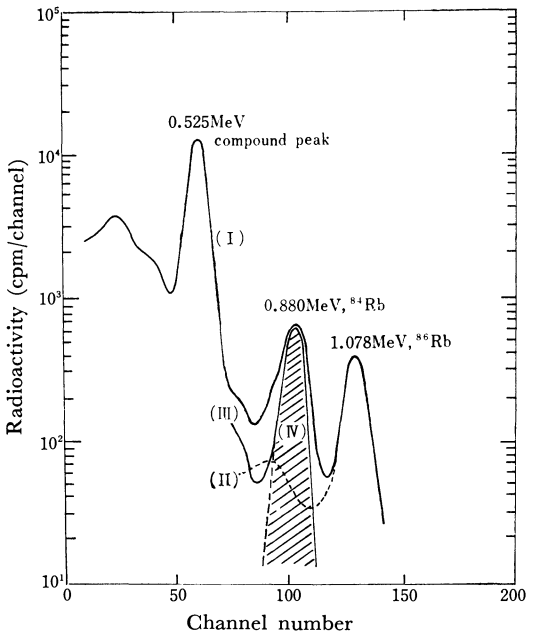

(I): The original compound spectrum.
(II): Compton back ground due to the 1.078 MeV γ-ray.
(III): Photopeak due to the 0.880 MeV γ-ray of ^{84}Rb.
(IV): The area under the 0.880 MeV photopeak.

Fig. 3. γ-Ray spectra of radiorubidium separated from a mixed sample (Rb 7.21 mg+Sr 55.5 mg), 29 days after irradiation with 20 MeV bremsstrahlung with a NaI(Tl) detector.

A(0.511 MeV), was calculated by:

$$A(0.511\ \mathrm{MeV}) = R\,A_{\mathrm{detn}}$$

where R is the activity ratio, $A_{^{84}\mathrm{Rb}}$(0.511 MeV)/$A_{^{84}\mathrm{Rb}}$(0.880 MeV), which has been determined with the aid of ^{84}Rb, and

4) the area under the composite peak of ^{83}Rb used as reference, A_{ref}, was then calculated by:

$$A_{\mathrm{ref}} = A_{\mathrm{m}} - A(0.511\ \mathrm{MeV}) = A_{\mathrm{m}} - R\,A_{\mathrm{detn}}$$

where A_{m} is the observed area under the compound peak at 0.525 MeV. From the spectra obtained from irradiated mixtures, the A_{detn}'s and the A_{ref}'s were determined, and those activity data were corrected for decay to the end of the irradiation through the use of the half-lives of ^{84}Rb and ^{83}Rb respectively. In the present experiment, all separations were performed 12 days after irradiation; all of the 20 min-^{84m}Rb had decayed away to ^{84}Rb.

Table 2 shows the relation between the photopeak activity ratios, $R_{A_0}=(A_{\mathrm{detn}}/A_{\mathrm{ref}})_{t=0}$, and the ratios of the weights, R_W=Rb/Sr. A good

Table 2. R_W *versus* R_{A_0} for rubidium-strontium mixtures with a NaI(Tl) detector

R_W	R_{A_0}	R_W/R_{A_0}
1.30×10^{-1}	21.6	5.99×10^{-3}
6.23×10^{-2}	10.1	6.16×10^{-3}
1.55×10^{-2}	2.61	5.82×10^{-3}
6.87×10^{-3}	1.14	6.04×10^{-3}
2.40×10^{-4}	3.90×10^{-2}	6.16×10^{-3}

Mean: $6.0_3\times10^{-3}$
Std. dev.: $\pm0.1_3\times10^{-3}$

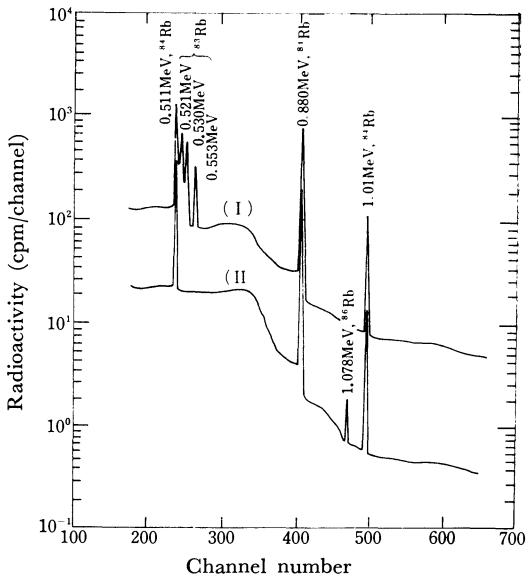

Fig. 4. γ-Ray spectra of radiorubidium with a Ge(Li) detector; (I) separated from a mixed sample (Rb 0.84 mg+Sr 419 mg), 11.9 days after irradiation with 17.6 MeV bremsstrahlung, and (II) of the rubidium sample.

proportionality was held between them, and a relative standard deviation of ±2.1% was obtained under the present experimental conditions:

$$R_W = (6.0_3 \pm 0.1_3) \times 10^{-3} R_{A_0}$$

When the amount of rubidium needed to give a photopeak activity of 10 cpm is selected as the limit of determination, it can be set at 2 μg.

When a 36 cm^3 Ge(Li) detector was used, we obtained the typical γ-ray spectrum shown in Fig. 4, together with that of the rubidium sample. The much greater resolving power of this detector made it feasible to distinguish clearly three different γ-ray photopeaks of ^{83}Rb. The photopeak area under the 0.553 MeV γ-ray was selected as the reference. The ratios of the area under the 0.880 MeV γ-ray to that under the 0.553 MeV γ-ray were computed and corrected for decay to the end of the irradiation. The relation between the R_{A_0}'s and the R_W's was again discussed from these activity data. Table 3 shows the results. The following relationship was obtained:

$$R_W = (1.1_3 \pm 0.0_5) \times 10^{-3} R_{A_0}$$

The relative standard deviation was ±4.8%. A sensitivity of 23 μg for rubidium was obtained in accordance with the definition described earlier.

With a Ge(Li) detector, the method is less sensitive by one order, but the determination of the photopeak areas is quite feasible as compared with scintillation spectrometry. An increase in sensitivity would be expected with a higher bremsstrahlung dose rate and with a longer period of irradiation.

Table 3. R_W *versus* R_{A_0} for rubidium-strontium mixtures with a Ge(Li) detector

R_W	R_{A_0}	R_W/R_{A_0}
5.30×10^{-2}	5.01×10^{1}	1.06×10^{-3}
4.28×10^{-2}	3.86×10^{1}	1.11×10^{-3}
2.95×10^{-2}	2.52×10^{1}	1.17×10^{-3}
1.20×10^{-2}	9.90×10^{0}	1.21×10^{-3}
5.41×10^{-3}	4.90×10^{0}	1.11×10^{-3}

Mean: $1.1_3\times10^{-3}$
Std. dev.: $\pm0.0_5\times10^{-3}$

The general applicability of this method lies in the determination of rubidium in samples of geochemical interest, in biological materials, and in various chemicals. A sample is ready for bremsstrahlung irradiation when it is ground to a powder along with a known amount of strontium carbonate, 100 mg in most cases. Rubidium often accompanies cesium in such samples, and the mutual separation of them can not be performed by the procedure described earlier. Considering the nuclear characteristics of ^{132}Cs ($T_{1/2}$=6.5 d, β^+ 0.6%, γ's), the (γ,n) reaction product, however, does not appear to be a serious source of interference. The γ-ray energies are 0.6678 MeV (96.7%), 0.6303 MeV(0.85%), 0.508 MeV(0.5%), and others (very weak). When a sample contains a large amount of cesium, a lithium-drifted germanium detector may be considered to be superior to a scintillation detector.

BULLETIN OF THE CHEMICAL SOCIETY OF JAPAN VOL. 43 2828—2835 (1970)

Polarography of Halides in Dimethylformamide. V. Bromine and the Tribromide Ion

Yoshihisa MATSUI and Yoshio DATE

Department of Agricultural Chemistry, Shimane University, Nishikawazu-cho, Matsue

(Received March 30, 1970)

The polarographic behavior of bromine and the tribromide ion at the dropping mercury electrode was investigated in dimethylformamide. A freshly-prepared solution of bromine gives two cathodic waves. When the solution is allowed to stand at 25°C in the dark, however, the first wave gradually becomes anodic, independently of the electrolysis. When the first wave is completely anodic, an equilibrium is established. The resulting polarogram coincides with that of hydrogen tribromide. The formation of hydrogen tribromide was ascribed to the chemical reduction of bromine by dimethylformamide. Diffuse sunlight accelerates the decomposition of bromine, which in turn yields hydrogen bromide. It was also suggested that, when the dropping mercury is used as an indicator electrode, bromine and the tribromide ion may react with the dropping mercury prior to being electrolyzed, forming mercuric bromide and the tribromomercurate ion respectively, which may in turn depolarize the indicator electrode.

The halogen-halide systems in non-aqueous solutions have been the subjects of a number of voltammetric studies. The solvents so far used include acetic acid,[1] acetic anhydride,[1] acetonitrile,[2-6] dimethylformamide (DMF),[7-11] dimethyl sulfoxide,[12,13] sulfolane,[14] and tetrahydrofuran.[15] In these solvents the trihalide ion (X_3^-) is so stable that the halogen species give two voltammetric waves, corresponding to the two redox reactions as follows:

$$3X_2 + 2e \rightleftarrows 2X_3^- \quad (1)$$

$$2X_3^- + 4e \rightleftarrows 6X^- \quad (2)$$

On the other hand, X_3^- is unstable in an aqueous solution, and X_2 gives only one reduction wave due to the reaction, as follows:[16]

$$X_2 + 2e \rightleftarrows 2X^- \quad (3)$$

Among the halogen-halide systems, the iodine-iodide system has been studied most extensively.[1-3,5-7,10-15] Fewer studies have been reported about the bromine-bromide[2,4,5,8,13,14] and the chlorine-chloride[2,9,13,14] systems, and none about the fluorine-fluoride system. The electrodes used in these investigations are made of platinum or pyrolytic graphite, each of which is inert to the halogen species. The dropping mercury electrode, which is reactive to the halogen species, has never been used for these studies.

In the present paper, the bromine-bromide system in DMF was investigated as part of a series of polarographic studies of halides in this medium.[17] The dropping mercury electrode was used as the indicator electrode. Sinicki and Bréant[8] have already studied the voltammetric behavior of bromine in DMF, using the platinum electrode. They have reported that a freshly-prepared solution of bromine gives two cathodic waves due to the reactions expressed by Eqs. (1) and (2). Using the dropping mercury electrode,

1) R. Guidelli and G. Piccardi, *Anal. Lett.*, **1**, 779 (1968).
2) I. M. Kolthoff and J. F. Coetzee, *J. Amer. Chem. Soc.*, **79**, 1852 (1957).
3) A. I. Popov and D. H. Geske, *ibid.*, **80**, 1340 (1958).
4) A. I. Popov and D. H. Geske, *ibid.*, **80**, 5346 (1958).
5) G. Dryhurst and P. J. Elving, *Anal. Chem.*, **39**, 606 (1967).
6) V. A. Macagno, M. C. Giordans and A. J. Arvia, *Electrochim. Acta*, **14**, 335 (1969).
7) M. Bréant and C. Sinicki, *C. R. Acad. Sci., Paris, Ser. C*, **260**, 5016 (1965).
8) C. Sinicki and M. Bréant, *Bull. Soc. Chim. Fr.*, **1967**, 3080.
9) C. Sinicki, P. Desportes, M. Bréant and R. Rosset, *ibid.*, **1968**, 829.
10) I. E. Barbasheva, Yu. M. Povarov and P. D. Lukovtsev, *Electrokhimiya*, **3**, 1149 (1967).
11) Yu. M. Povarov, I. E. Barbasheva and P. D. Lukovtsev, *ibid.*, **3**, 1202 (1967).
12) R. T. Iwamoto, *Anal. Chem.*, **31**, 955 (1959).
13) M. Michlmayr and D. T. Sawyer, *J. Electroanal. Chem. Interfacial Electrochem.*, **23**, 387 (1969).
14) R. L. Benoit, M. Guay and J. Desbarres, *Can. J. Chem.*, **46**, 1261 (1968).
15) J. Perichon and R. Buvet, *Bull. Soc. Chim. Fr.*, **1967**, 3707.
16) I. M. Kolthoff and J. Jordan, *J. Amer. Chem. Soc.*, **75**, 1571 (1953).
17) Part IV: Y. Matsui and Y. Date, This Bulletin, **43**, 2052 (1970).

however, we found that the two cathodic waves given by a freshly-prepared solution of bromine may be explained in terms of the electrolytic reduction of the mercuric bromide formed by the reaction between the bromine and the mercury of the electrode prior to the electrolysis. Sinicki and Bréant[8] have also reported that bromine in DMF quantitatively converts to the tribromide ion on standing for a few hours, irrespective of the electrode process:

$$3Br_2 \text{ (in DMF)} \rightarrow 2Br_3^- \quad (4)$$

This reaction is rather unusual in view of the fact that halogens or interhalogen compounds generally undergo disproportionation reactions in electron-donating solvents to yield the trihalide ions and the uni-positive halogen ions:[18-20]

$$2X_2 \rightleftharpoons X_3^- + X^+ \quad (5)$$

They ascribed it to the reduction of bromine by formic acid, which was formed by the hydrolysis of DMF, but no experimental proof was presented. In the present paper, we also will examine the mechanism of the chemical reduction of bromine to the tribromide ion, and will suggest that the reductant may be not formic acid, but DMF.

Experimental

The DMF was purified as has been described previously.[21] The tetraethylammonium perchlorate (TEP) used as a supporting electrolyte was prepared and purified as has been described by Fujinaga *et al.*[22] Polyvinyl chloride (PVC) obtained commercially was used as a maximum suppressor. The bromine was dried over phosphorus pentoxide and was purified by distillation. Bp 57.8—58.1°C. Hydrogen bromide which had been generated from aqueous hydrobromic acid and concentrated sulfuric acid was passed through a glass tube packed with red phosphorus and was then bubbled through concentrated sulfuric acid. The dry hydrogen bromide thus obtained was dissolved in DMF. The resulting solution was standardized by titration against an aqueous sodium hydroxide solution, using phenolphthalein as the indicator. The solution of hydrogen tribromide in DMF was prepared by an equimolar addition of the hydrogen bromide solution to bromine. The solution of hydrogen tribromomercurate in DMF was similarly prepared from the hydrogen bromide and mercuric bromide.

D. c. polarography and conductivity measurements were carried out at 25°C as has been described previously.[23] All the potential measurements were done with reference to the aqueous saturated calomel electrode connected with the cell solution by a DMF-agar salt bridge.[22] The dropping mercury electrode used had the following characteristics in a 0.10 M solution of TEP in DMF (open circuit): m=1.245 mg/sec, t=4.97 sec for h=66.0 cm. The oxygen dissolved in the solution was expelled by passing a stream of dry nitrogen through the cell solution for about 20 min prior to each electrolysis.

Results

Variation in the Polarographic Characteristics of Bromine with the Time. The polarographic characteristics of bromine varied with the time. Figure 1 shows the polarograms recorded at several intervals after the addition of

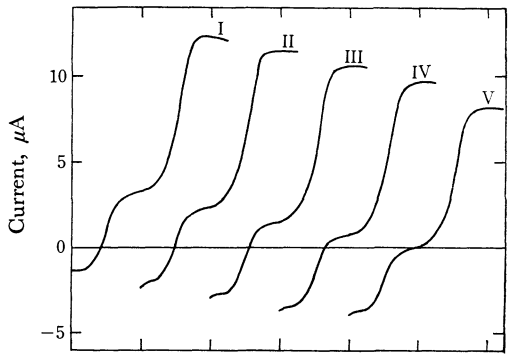

Fig. 1. Change of the polarogram of Br_2 (1.70 mM) with time in the dark. Each recording was started 0.8(I), 8.0(II), 25.0(III), 51.0(IV), or 161(V) minutes after addition of Br_2 to DMF.

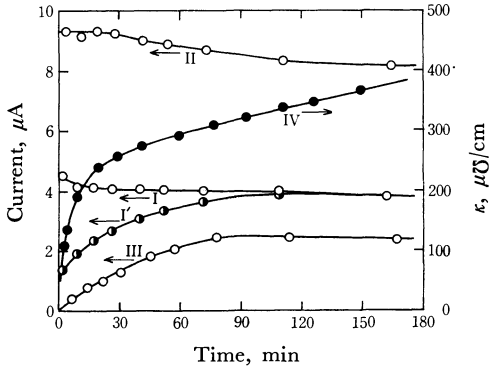

Fig. 2. Plots of the currents and the conductance *vs.* time for a Br_2 solution in the dark.

I, II and III: the limiting currents of the 1st, 2nd, and 3rd waves of Br_2 (1.70 mM), respectively

I': the anodic part of the 1st wave

IV: the conductance of Br_2 (47.9 mM) in DMF

18) C. Reid and R. S. Muliken, *J. Amer. Chem. Soc.*, **76**, 3869 (1954).

19) R. E. Buckels and J. F. Mills, *ibid.*, **76**, 4845 (1954).

20) A. I. Popov and W. A. Deskin, *ibid.*, **80**, 2976 (1958).

21) Y. Matsui, Y. Kurosaki and Y. Date, This Bulletin, **43**, 1707 (1970).

22) T. Fujinaga, K. Izutsu, K. Umemoto, T. Arai and K. Takaoka, *Nippon Kagaku Zasshi*, **87**, 105 (1968).

23) Y. Matsui, R. Kawakado and Y. Date, This Bulletin, **41**, 2913 (1968).

bromine to DMF containing 0.10 M TEP and 0.005% PVC. Since it was found that diffuse sunlight accelerates the change, as will be discussed later, the cell solution was placed in the dark. When the recording of the polarogram was started as soon as possible (45 sec) after the addition of bromine to a DMF solution, most of the two waves obtained were cathodic, although the first wave had already turned anodic in part. The anodic part of the first wave increased with the time at the expense of its cathodic part. When the first wave was completely anodic, an equilibrium was established. Parallel to this change, a new cathodic wave and a maximum arose and grew at about −1.33 and −2.15 V *vs.* SCE respectively (Fig. 6).

Figures 2 and 3 show the plots of the limiting currents and the half-wave potentials respectively *vs.* the time. The height of the second wave was approximately double that of the first wave, and both of them slightly decreased with the time. The height of the third wave increased with an increase in the anodic part of the first wave. An equilibrium was attained about two hours after the addition of bromine to DMF. Throughout these changes, however, the half-wave potential of each wave remained practically constant. The increase in the anodic part of the first wave obeyed good first-order kinetics (Fig. 4). The rate constant was determined to be 0.030 min^{-1} at 25°C.

The conductance of the bromine solution also increased with the time. The mode of increase in the conductance was analogous to that in the anodic current (Fig. 2). If bromine was added to DMF containing excess tetraethylammonium bromide, the conductance of the solution scarecely varied with the time (Fig. 5). No increase in the conductance with the time was observed until the molar concentration of the bromine added was higher than that of the bromide ion. This indicates that bromine rapidly reacts with the bromide ion, forming the tribromide ion, which is stable in DMF in the dark.

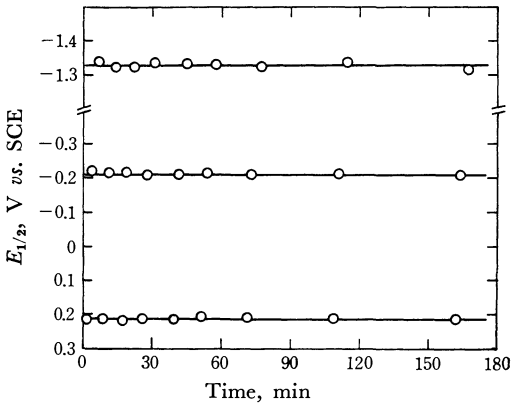

Fig. 3. Plots of the half-wave potentials *vs.* time for the three waves given by Br_2 in the dark.

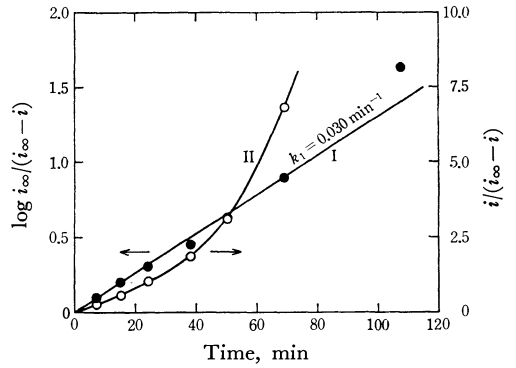

Fig. 4. The 1 st(I)- and 2 nd(II)-order rate plots for the increase of the anodic part of the 1 st wave given by Br_2.

the initial concn. of Br_2=1.70 mM

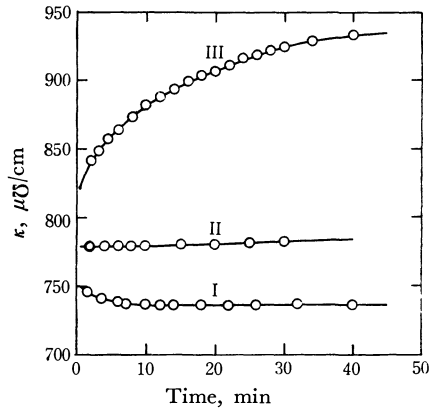

Fig. 5. Plots of the conductances *vs.* time for the various ratio of mixing between Br_2 and Et_4NBr.

$[Br_2]/[Et_4NBr]$=0.5(I), 1.1(II), and 1.8(III), where $[Et_4NBr]$=10.4 mM

Polarographic Behavior of Bromine, the Tribromide Ion, and Related Compounds. The polarogram of 1.0 mM bromine, which was recorded in the dark about two hours after it had been added to DMF, is shown in Fig. 6. The effects of the bromine concentration and of the height of the mercury reservoir on the polarographic characteristics are summarized in Tables 1 and 2 respectively. The heights of both the first and second waves were virtually proportional to the concentrations of the depolarizer and to the square roots of the heights of the mercury reservoir; this indicates that these waves are diffusion-controlled. The ratio between the diffusion-current constants (I_d's) of these waves is about 1.0 : 2.3. The characteristics of the third wave are somewhat more complicated. The height of this wave was practically proportional to the square root of the height of the mercury reservoir, but not to the con-

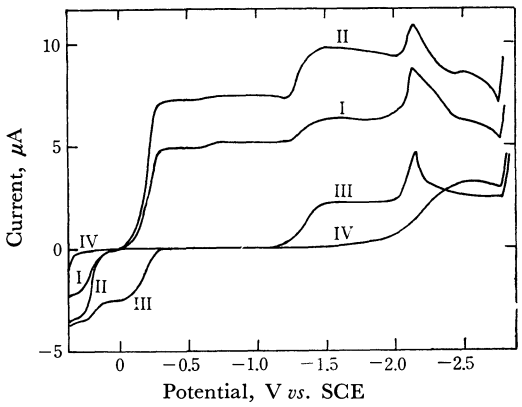

Fig. 6. Polarograms of 1.0 mM depolarizers in DMF containing 0.1 M TEP and 0.005% PVC at 25°C.

I, Br_2 recorded *ca.* 2 hr after the addition to DMF; II, HBr_3; III, HBr; IV, HCOOH

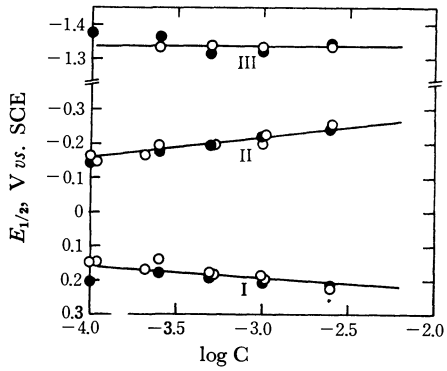

Fig. 7. Plots of the half-wave potentials *vs.* the logarithms of the concentrations of depolarizers.

I, 1 st wave; II, 2 nd wave; III, 3 rd wave; ○, Br_2; ●, HBr_3

centration of bromine. As will be described later, however, the wave is due to the reduction of the hydrogen ion which is formed by the reaction between bromine and DMF. Therefore, the decrease in the diffusion-current constant may be due to the consumption of the hydrogen ion for the neutralization of such bases as dimethylamine present in solution as impurities.

With an increase in the concentration of bromine, the half-wave potential of the first wave shifted to a more positive direction, and that of the second wave, to a more negative direction, while that of the third wave remained virtually constant. Figure 7 shows the relation between the half-wave potentials of the waves ($E_{1/2}$) and the common logarithms of the concentrations of bromine (log C). Approximately linear relations were obtained between them with slopes of 0.030 V for the first wave, −0.060 V for the second wave, and 0.000 V for the third wave.

Figure 6 also shows the polarograms of hydrogen bromide, hydrogen tribromide, and formic acid in DMF. It is notable that hydrogen tribromide gives three polarographic waves closely similar to those of bromine recorded about two hours after it had been added to DMF. Hydrogen tribromomercurate also gave three waves similar to those of hydrogen tribromide. These data indicate that bromine converts to hydrogen tribromide in DMF and that the tribromide ion may react with mercury at the electrode surface, yielding the tribromomercurate ion, which may in turn depolarize the electrode. Formic acid gives no wave at the potential where the hydrogen ion is electrolytically reduced.

The polarographic characteristics of these depolarizers at various concentrations and at various heights of the mercury reservoir are summarized in Tables 3 and 4 respectively. All the heights of the first and second waves given by these depolarizers were practically proportional to the concentrations and to the square roots of the mercury heads; this indicates that they are diffusion-controlled. The height of the third wave of hydrogen bromide or of hydrogen tribromide was also proportional to the square root of the height of the mercury reservoir, but not to the concentration of the depolarizer, as had been observed for bromine. Hydrogen tribromomercurate gave no third wave until the concentration was as high as 2.1 mM. The relation between the half-wave potentials and the common logarithms of the concentration is plotted for hydrogen tribromide in Fig. 7. Approximately linear relations were obtained be-

Table 1. Polarographic characteristics of bromine at various concentrations

Concn. (mM)	$E_{1/2}$ (V *vs.* SCE)			I_d		
	1 st wave	2 nd wave	3 rd wave	1 st wave	2 nd wave	3 rd wave
0.10	+0.147	−0.161	*	1.23	3.17	*
0.25	+0.141	−0.197	−1.332	1.49	3.42	0.11
0.50	+0.176	−0.194	−1.338	1.35	3.06	0.50
1.01	+0.207	−0.198	−1.335	1.36	3.00	0.63
2.52	+0.222	−0.258	−1.337	1.37	3.28	0.84

* No wave appeared.

Table 2. Relation between limiting currents of 0.50 mM of bromine and effective heads of the dropping mercury electrode

$h_{corr.}$ (cm)	i_d, (μA)			$i_d/(h_{corr.})^{1/2}$		
	1 st wave	2 nd wave	3 rd wave	1 st wave	2 nd wave	3 rd wave
34.8	0.70	1.58	0.29	0.12	0.27	0.049
46.5	0.79	1.85	0.32	0.12	0.28	0.048
56.5	0.91	2.09	0.36	0.12	0.28	0.049
66.5	1.04	2.36	0.37	0.13	0.29	0.046
81.5	1.13	2.60	0.43	0.13	0.29	0.048

Table 3. Polarographic characteristics at various concentrations

Depolarizer	Concn. (mM)	$E_{1/2}$ (V *vs.* SCE)			I_d		
		1 st wave	2 nd wave	3 rd wave	1 st wave	2 nd wave	3 rd wave
HBr_3	0.10	+0.202	−0.145	−1.374	1.78	4.68	0.26
	0.26	+0.177	−0.177	−1.361	2.18	4.85	0.74
	0.51	+0.190	−0.194	−1.313	2.14	4.52	1.17
	1.02	+0.206	−0.215	−1.318	2.17	4.48	1.64
	2.55	+0.217	−0.244	−1.346	2.11	4.30	1.26
HBr	0.26	+0.156	−0.155	−1.310	0.67	1.56	0.11
	0.53	+0.175	−0.165	−1.359	0.51	1.39	0.86
	1.05	+0.203	−0.162	−1.317	0.58	1.40	0.86
	2.63	+0.229	−0.184	−1.309	0.60	1.32	1.17
	5.25	+0.233	−0.217	−1.390	0.60	1.31	1.27
$HHgBr_3$	0.25	+0.166	−0.176	*	1.58	4.00	*
	1.00	+0.189	−0.217	*	1.71	4.00	*
	2.50	+0.204	−0.240	−1.365	1.79	3.95	0.84

* No wave appeared.

Table 4. Relation between limiting currents of 1.0 mM of depolarizers and effective heads of the dropping mercury electrode

Depolarizer	$h_{corr.}$ (cm)	i_d (μA)			$i_d/(h_{corr.})^{1/2}$		
		1 st wave	2 nd wave	3 rd wave	1 st wave	2 nd wave	3 rd wave
HBr_3	34.8	2.39	4.22	1.86	0.41	0.75	0.32
	44.8	2.52	5.26	2.11	0.38	0.79	0.32
	54.8	3.05	6.16	2.23	0.41	0.83	0.30
	64.8	3.30	6.90	2.48	0.41	0.86	0.31
	79.8	3.70	7.52	2.75	0.41	0.84	0.31
HBr	34.8	0.72	1.65	1.05	0.12	0.28	0.18
	44.8	0.80	1.86	1.17	0.12	0.28	0.17
	54.8	0.84	2.09	1.27	0.11	0.28	0.17
	64.8	0.93	2.25	1.33	0.12	0.28	0.17
	79.8	1.03	2.50	1.46	0.12	0.28	0.16

tween them, similar to those obtained for bromine.

Figure 8 shows the effect of bromine, as well as those of mercuric bromide and tetraethylammonium bromide, on the electrocapillary curve in DMF containing 0.10 M TEP and 0.005% PVC. The addition of these compounds to DMF apparently caused a decrease in the surface tension of the mercury drop in the potential region between +0.4 and −0.5 V *vs.* SCE.

Effect of Diffuse Sunlight on the Change in the Polarogram of Bromine. Figure 9 shows the manner in which the growth of the anodic

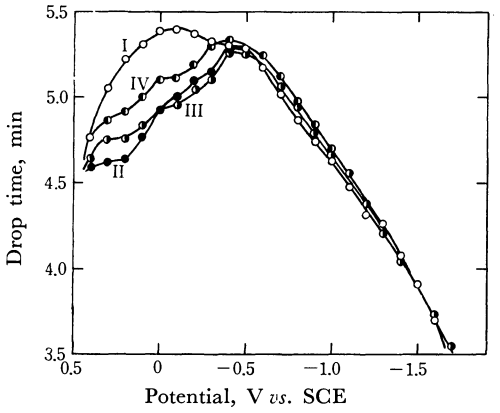

Fig. 8. Electrocapillary curves at 25°C.

I, 0.1 M TEP+0.005% PVC in DMF; II, I+1.0 mM Br_2; III, I+1.0 mM $HgBr_2$; IV, I+1.0 mM Et_4NBr

part of the polarographic wave, as well as the increase in the electric conductivity, of the bromine solution is accelerated by diffuse sunlight. The rate of the current increase abruptly slows down about 15 min after the addition of bromine to DMF. The resulting polarogram coincides with that of hydrogen tribromide. However, the tribromide ion is not so stable in diffuse sunlight as in the dark, and it slowly decomposed hereafter. Equilibrium was not established until both the first and second waves were completely anodic. The polarogram recorded after equilibrium was attained agreed with that of hydrogen bromide, as is shown in Fig. 6.

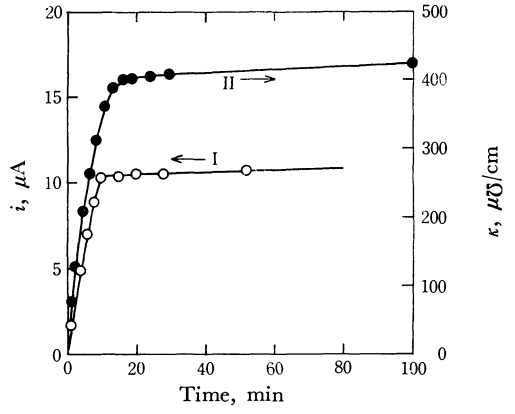

Fig. 9. Plots of the anodic part of the 1 st wave (I) and the conductance (II) *vs.* time for Br_2 solutions in the diffuse sunlight.

the initial concn. of Br_2=5.6 mM (I) or 10.0 mM (II)

Discussion

Mechanism of the Formation of Hydrogen Tribromide from Bromine in DMF in the Dark.

The conversion of the first wave of bromine from cathodic to anodic (Fig. 1) and the excellent agreement of the resulting polarogram with that of hydrogen tribromide (Fig. 6) indicate that bromine in DMF gradually forms hydrogen tribromide. This is supported by the fact that the conductance of the solution increases with an inrecase in the anodic part of the first wave (Fig. 2). The stoichiometry of this reaction is interesting. The height of each wave of 1.0 mM bromine measured about two hours after it is added to DMF is approximately equal to two-thirds of that of the corresponding wave of 1.0 mM hydrogen tribromide, which indicates that three moles of bromine quantitatively yield two moles of hydrogen tribromide in DMF:

$$3Br_2 + 2H\cdot(DMF) \rightarrow 2H^+ + 2Br_3^- \quad (6)$$

This reaction is rather unusual, since it is well known that a disproportionation reaction occurs between two moles of halogen in electron-donating solvents, yielding one mole of the trihalide ion and one mole of the uni-positive halogen ion (Eq. (5)).[18-20] However, Reid and Muliken[18] have also reported that iodine in pyridine (Pr) forms the trihalide ion, together with the uni-positive iodine ion solvated by pyridine (PrI^+), which may in turn decompose to the iodide ion and the cation radical of pyridine ($Pr\cdot^+$) as follows:

$$Pr + PrI^+ \rightarrow I^- + 2Pr\cdot^+ \quad (7)$$

Similar reactions have also been proposed by Zingaro *et al.*[24] Recently, Bist and Person[25] reported that a rapid reaction occurs between iodine and excess triethylamine in dioxane, yielding the iodide ion quantitatively as the end product. The reaction was ascribed to the reduction of the uni-positive iodine ion to the iodide ion by the amine. Thus, it can be considered that the following reaction may occur between bromine and DMF:

$$Br_2 \rightleftharpoons Br^+ + Br^- \quad (8)$$

$$Br^+ + 2DMF \rightarrow Br^- + 2DMF\cdot^+ \quad (9)$$

$$2DMF\cdot^+ \rightarrow 2H^+ + 2R \quad (10)$$

$$2Br_2 + 2Br^- \rightleftharpoons 2Br_3^- \quad (11)$$

The net result would be:

$$3Br_2 + 2DMF \rightarrow 2H^+ + 2Br_3^- + 2R \quad (12)$$

In this reaction mechanism, Br_2 and Br^+ may be strongly solvated by DMF. The electron-transfer reaction from DMF to Br^+ has never been reported, but it is well known that DMF forms charge-transfer complexes with a number of Lewis acids. We have also found that DMF can reduce the simple mercuric ion, yielding metalic mercury.[17] The cation radical ($DMF\cdot^+$) thus formed may

24) R. Zingaro, C. A. VanderWerf and J. Kleinberg, *J. Amer. Chem. Soc.*, **73**, 88 (1951).

25) H. D. Bist and W. B. Person, *J. Phys. Chem.*, **73**, 482 (1969).

rapidly decompose to the hydrogen ion and an unknown radical (R). Among the elemental reactions demonstrated above, either the disproportionation reaction (Eq. (8)) or, more probably, the electron-transfer reaction (Eq. (9)) may be the rate-determining step, for the kinetics of the total reaction is of the first-order (Fig. 4).

Sinicki and Bréant[8] have attributed the quantitative formation of the tribromide ion to the reduction of bromine by formic acid, which had been formed by the hydrolysis of DMF. However, none of the polarograms of the DMF solutions in either the presence or absence of bromine gave any appreciable wave at −2.25 V *vs.* SCE, where formic acid gives a cathodic wave. Accordingly, it is unlikely that the formic acid plays a major role in the reduction of the uni-positive bromine ion. Michlmayr and Sawyer[13] have reported that halogen may react with dimethyl sulfoxide and acetonitrile, yielding hydrogen halide, as follows:

$$X_2 + (CH_3)_2SO \rightarrow CH_2X(CH_3)SO + HX \quad (13)$$

$$X_2 + CH_3CN \rightarrow CH_2XCN + HX \quad (14)$$

However, according to these mechanisms, halogen does not quantitatively form the trihalide ion, but a part of it enters into combination with the carbon atoms of the solvents. Therefore, this is not the present case.

Effect of Diffuse Sunlight on the Reaction of Bromine in DMF. Diffuse sunlight accelerates the increase in the anodic part of the polarographic waves given by bromine. This rapid increase accompanies the rapid increase of the conductance of the solution (Fig. 9). The polarogram obtained after equilibrium is established is in accord with that of hydrogen bromide; this indicates that bromide is quantitatively reduced to the bromide ion in DMF. This behavior may be explained in terms of the following mechanism:

$$Br_2 \rightleftarrows 2Br\cdot \quad (15)$$

$$Br\cdot + DMF \rightarrow H^+ + Br^- + R \quad (16)$$

$$Br^- + Br_2 \rightleftarrows Br_3^- \quad (17)$$

$$Br_3^- \rightleftarrows 2Br\cdot + Br^- \quad (18)$$

The net result would be:

$$Br_2 + 2DMF \rightarrow 2H^+ + 2Br^- + 2R \quad (19)$$

Mechanism of the Electrode Reaction of Bromine and the Tribromide Ion in DMF. The following electrode reaction mechanism has been proposed by Sinicki and Bréant[8] for the reduction of bromine in DMF at the platinum electrode:

$$3Br_2 + 2e \rightleftarrows 2Br_3^- \quad (20)$$

$$2Br_3^- + 4e \rightleftarrows 6\,Br^- \quad (21)$$

A similar mechanism has also been offered by Michlmayr and Sawyer[13] for the oxidation of hydrogen bromide in dimethyl sulfoxide at the platinum electrode. However, in the present study the dropping mercury electrode was used as the indicator electrode, and it is reactive to both bromine and the tribromide ion. If the heterogeneous reactions between mercury and bromine, and between mercury and the tribromide ion, are very rapid, the formation of mercuric bromide and of the tribromomercurate ion may precede the electrode reactions. Thus, the following mechanisms can be considered for bromine:

(Chemical process)

$$Br_2 + Hg \rightarrow HgBr_2 \quad (22)$$

(Electrode process)

$$3HgBr_2 + 2e \rightleftarrows Hg + 2HgBr_3^- \quad (23)$$

$$2HgBr_3^- + 4e \rightleftarrows 2Hg + 6Br^- \quad (24)$$

and for the tribromide ion:

(Chemical process)

$$Br_3^- + Hg \rightarrow HgBr_3^- \quad (25)$$

(Electrode process)

$$2HgBr_3^- + Hg \rightleftarrows 3HgBr_2 + 2e \quad (26)$$

$$2HgBr_3^- + 4e \rightleftarrows 2Hg + 6Br^- \quad (27)$$

These mechanisms are supported by the fact that the polarographic characteristics of bromine and the tribromide ion are closely similar to those of mercuric bromide and the tribromomercurate ion respectively. The electrocapillary curve of the solution of bromine in DMF was also very similar to that of mercuric bromide. Sinicki and Bréant[8] have reported that the tribromide ion in DMF gives two waves, anodic and cathodic, at +0.57 and −0.46 V *vs.* Hg/Hg(II) at the platinum electrode. The difference (1.03 V) in the half-wave potential between these two waves is much greater than that observed at the dropping mercury electrode (0.40 V). This may be caused either by the irreversibility of the electrode reaction at the platinum electrode or, more probably, by the difference between the depolarizers in the two cases.

In any case, however, the relations between the current (i) and the potential of the dropping mercury electrode (E) should be expressed for the first wave of the tribromide ion or of bromine measured after equilibrium is attained as:[23]

$$E_p = C_p + (\boldsymbol{RT}/2\boldsymbol{F}) \ln i^3/(i_d - i)^2 \quad (28)$$

and for the second wave as:

$$E_n = C_n - (\boldsymbol{RT}/2\boldsymbol{F}) \ln i^3/(i_d - i) \quad (29)$$

where i_d is the limiting current and where C_p and C_n are constants. The results of the logarithmic plot for the waves of the tribromide ion, as well as those for bromine (Fig. 10), show that Eqs. (28) and (29) hold for these depolarizers. The reciprocal slopes of the logarithmic plots are equal to 0.032—0.035 V for the first wave and to −0.040 ——0.041 V for the second wave. Both of the values are somewhat larger than the theoretical

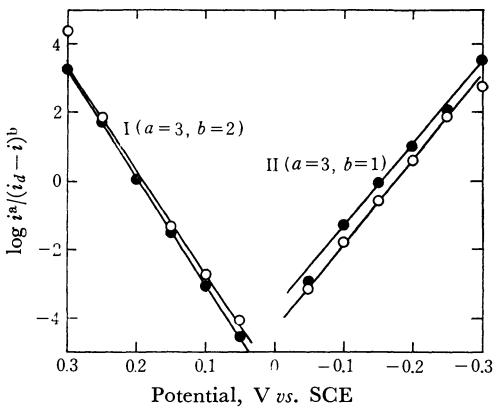

Fig. 10. Analysis of the polarograms of 1.0 mM Br_3^- (●) or of 1.0 mM Br_2 measured *ca.* 2 hr after it was added to DMF (○).

reciprocal slopes; I(●), 0.032 V; II(●), −0.041 V; I(○), 0.035 V; II(○), −0.040 V

value (0.030 V), but virtually agree with those obtained for the waves of the tribromomercurate ion (0.032 and −0.038 V respectively[23]).

From Eqs. (28) and (29), the following relations between the half-wave potentials ($E_{1/2}$) and the limiting currents (i_d), or between $E_{1/2}$ and the concentrations (C) of the tribromide ion or of bromine, can easily be derived for the first wave:

$$E_{p,\,1/2} = C_p' + (\boldsymbol{RT}/2\boldsymbol{F}) \ln C \qquad (30)$$

and for the second wave:

$$E_{n,\,1/2} = C_n' - (\boldsymbol{RT}/\boldsymbol{F}) \ln C \qquad (31)$$

Fig. 5 shows that these relations also hold for the depolarizers.

No close examination was made of the maximum which appeared at −2.15 V *vs.* SCE on the polarograms of hydrogen tribromide and hydrogen bromide. However, it was found that no maximum arose on the polarograms with tetraethylammonium tribromide, but that a maximum appeared on the polarogram with hydrogen perchlorate. This clearly indicates that the hydrogen ion is responsible for the maximum.

BULLETIN OF THE CHEMICAL SOCIETY OF JAPAN VOL. 43 2835—2839 (1970)

The Thermal Annealing Behavior of ^{80}Br Recoils Produced by the Nuclear Isomeric Transitions in Alkali Metal Bromates*[1]

Teikichi SASAKI*[2] and Takanobu SHIOKAWA

Department of Chemistry, Faculty of Science, Tohoku University, Sendai

(Received April 8, 1970)

The transient annealing behavior of bromine recoils produced by isomeric transition was studied in five alkali metal bromates. In the case of ^{80m}Br-labelled potassium bromate, the isothermal annealing curves were characterized by maximum and minimum points. A numerical treatment of them indicated that, at the earlier stage of the thermal treatment, the annealing processes proceeded very fast, which was ascribed to the characteristics of the isomeric transition recoils. A remarkable effect of the cationic components on the thermal annealing was observed and interpreted in terms of their ionization potentials.

Several investigations have been reported into the thermal annealing behavior of bromine recoils produced by the radiative neutron capture.[1-5] However, no detailed work has been made on the thermal annealing effect of isomeric transitions.

Jones[6] found that the retention for ^{80}Br recoils in the ^{80m}Br-labelled sodium bromate increased rapidly for a few minutes and then decreased over a longer period on thermal annealing. Shiokawa and his co-workers[7] have also studied the transient

*1 Presented at The 5th International Hot-Atom Chemistry Meeting, Cambridge, July, 1969.

*2 Present address: Japan Atomic Energy Research Institute, Tokai, Ibaraki.

1) J. E. Boyd, J. W. Cobble and S. Wexler, *J. Amer. Chem. Soc.*, **74**, 237 (1952); J. W. Cobble and G. E. Boyd, *ibid.*, **74**, 1282 (1952).

2) J. Jach and G. Harbottle, *Trans. Faraday Soc.*, **54**, 520 (1958).

3) I. G. Campbell and C. H. W. Jones, *Radiochim. Acta*, **9**, 7 (1968).

4) G. E. Boyd and Q. V. Larson, *J. Amer. Chem. Soc.*, **90**, 254 (1968).

5) T. Andersen, H. B. L. Marsen and K. Olesen, *Trans. Faraday Soc.*, **62**, 2409 (1966).

6) C. H. W. Jones, *Inorg. Nucl. Chem. Lett.*, **3**, 363 (1967).

annealing of the recoils in the ^{80m}Br-labelled potassium bromate. They observed that the annealing curves had maximum and minimum points and that the increase in the retention continued even after the radioactive equilibrium had been reached. The thermal annealing behavior of the recoils produced by isomeric transition depends only on the annealing temperature, while that of the recoils produced by neutron capture is complicated with the secondary effects of gamma radiation during a pile irradiation, for this radiation inevitably produces vacancies, color centers, various defects, etc. Therefore, the transient annealing of ^{80}Br recoils seems to provide us with direct information about the effects of the inherent crystal defects on the thermal annealing.

This paper will describe the annealing behaviors of ^{80}Br recoils produced by the nuclear isomeric transition. A numerical treatment will be given to explain the role of the inherent crystal defects. The effects of the cations, which supports the previous assumptions regarding the thermal annealing of manganese recoils[8], will also be described.

Experimental

Samples. The potassium bromate labelled with ^{80m}Br atoms was prepared by a previously-described method.[7] The other labelled alkali metal bromates were prepared from the potassium bromate by usnig cationic exchange resin. All the samples except for lithium salt were dried at 160°C for 1 hr, while the latter was dried at 110°C for 1 hr.

Thermal Annealing Procedure. After drying, all the samples were stored at the temperature of liquid nitrogen until the radioactive equilibrium was attained. The thermal annealing procedure in the temperature region above 100°C was usually carried out by using an oil bath whose temperature was controlled within ±1°C.

Chemical Separation and Radioactivity Measurements. Although most of the samples were dissolved in redistilled water, in some cases aqueous solutions of methanol or solutions whose pH had been adjusted with nitric acid or sodium hydroxide were used as the solvents. The chemical separations were performed by the extraction method described by Saito *et al.*[9] The radioactive measurements were carried out by means of a multi-channel pulse-height analyser connected with a well-type NaI(Tl) scintillation detector. The 0.62 MeV gamma rays of ^{80}Br were counted for aliquots of the organic and the inorganic fractions. The retention—the yield of the inorganic fraction—was calculated in a manner reported before.[7]

Results and Discussion

Thermal Annealing Processes. The recoil species detected were the bromide and bromate ions, but no evidence for the presence of $^{80}BrO_2^+$ ions found in the ^{80m}Br-labelled bromate solution by Campbell[10,11] was obtained.

The transient annealing curves of ^{80}Br recoils in the labelled potassium bromate are shown in Fig. 1. In these experiments, samples were stored for 3 hr at −196°C to ensure the radioactive equilibrium and were then quickly heated to 184 or 264°C. While the annealing curves have maximum and minimum points in the early stage of the heating, the retentions increase slowly even after the radioactive equilibrium has been attained. In Fig. 2, the retentions for the samples annealed for 3—4 hr are plotted against the annealing temperatures. The retentions are constant for all the bromates in the temperature region below room temperature, while they increase slowly at higher temperatures. All the alkali bromates show different rates of thermal annealing.

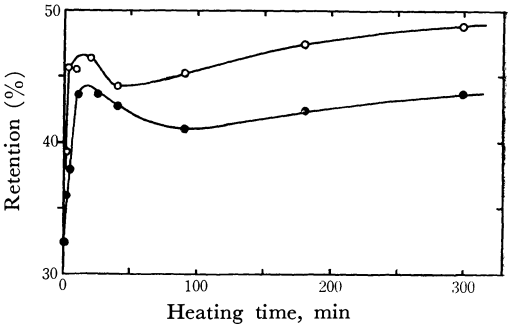

Fig. 1. Isothermal annealing curves for the retention in the labelled potassium bromate.
●: 184°C ○: 264°C

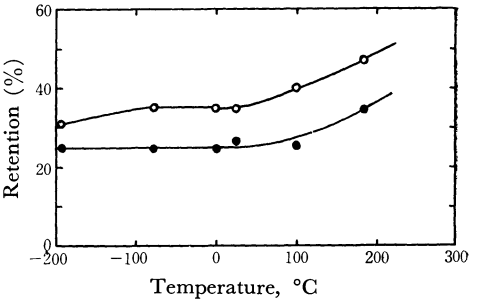

Fig. 2a. The relationships between the retention and the annealing temperature for sodium and rubidium salts.
○: $NaBrO_3$(^{80m}Br) ●: $RbBrO_3$(^{80m}Br)

7) T. Shiokawa, T. Sasaki and S. Takahashi, *Radiochem. Radioanal. Lett.*, **1**, 31 (1969).

8) T. Shiokawa, M. Yagi and T. Sasaki, *Radiochim. Acta*, **12**, 54 (1969); T. Shiokawa and T. Sasaki, This Bulletin, **43**, 801 (1970).

9) N. Saito, F. Ambe and H. Sano, *Radiochim. Acta*, **7**, 131 (1967).

10) I. G. Campbell, *J. Chim. Phys.*, **56**, 480, 665 (1959).

11) I. G. Campbell, *J. Inorg. Nucl. Chem.*, **15**, 46 (1960).

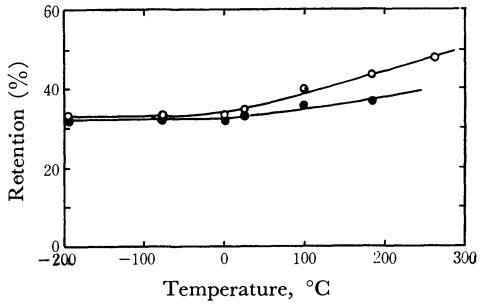

Fig. 2b. The relationships between the retention and the annealing temperature for potassium and cesium salts.

○: $KBrO_3(^{80m}Br)$ ●: $CsBrO_3(^{80m}Br)$

In order to discuss quantitatively the mechanism of the thermal annealing of ^{80}Br recoils, corrections must be made for the radioactive growth and decay of ^{80}Br atoms during the thermal annealing. Their schematic processes and the thermal annealing of ^{80}Br recoils are shown in Fig. 3.

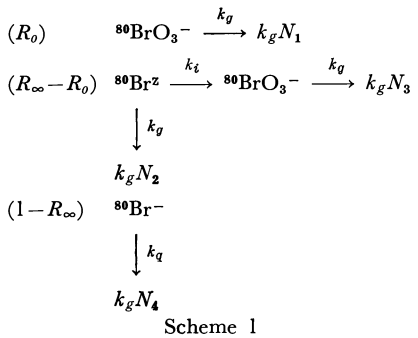

Scheme 1

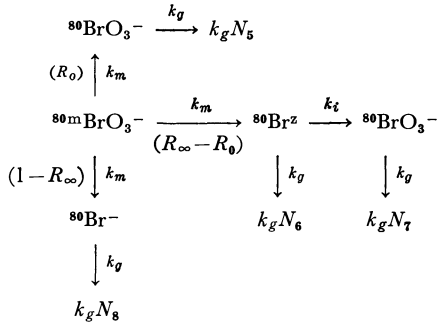

Scheme 2

Fig. 3. Schemes for the radioactive growth and decay of ^{80}Br and for the thermal annealing processes.

In these schemes, k_m and k_g are the decay constants of the metastable and ground states, while k_gN_{2i-1} and $k_gN_{2i}(i=1, 2, 3, 4)$ are the radioactive intensities corresponding to the bromate ions and the bromide ions respectively. R_0 is the initial yield of the recoil species which become precursors of the bromate ion in consequence of the isomeric transition at −196°C, while R_∞ is the plateau or the asymptotic value of the retention in the annealing curve.

Scheme I shows the changes in the initial yield of the recoil species; these species are, respectively, R_0, $(R_\infty - R_0)$, and $(1-R_\infty)$ at the beginning of the thermal treatment. An intermediate species, Br^z, which may be converted by the thermal annealing to a precursor of the bromate ion with a rate constant, k_i, is assumed. Scheme 2 shows the annealing and the decay processes of the recoils which are produced during the thermal treatment of the sample. Thus, considering the radioactive growth and decay of ^{80}Br, the retention, R, is related to the annealing time, t, as follows (see also the Appendix):

$$R = R_0 + [k_i(R_\infty - R_0)\{1 - \exp(-kt)\}]/k$$

where $k = k_g + k_i - k_m$. Since the values of R and R_0 are determined experimentally k_i can be calculated by varying the value of R_∞ as a parameter.

Some of the calculated results are shown in Fig. 4. The constant values of k_i are obtained after the initial rapid decrease in both the annealing temperatures. The changes in k_i show similar trends regardless of the changes in R_∞ at the same annealing temperature.

The results from the transient annealing seem to offer direct information about the role of the inherent crystal defects in the thermal annealing processes of bromine recoils. Campbell[3] has found that the thermal annealing of the ^{82}Br recoils produced by the (n, γ) reaction in the sodium bromate could be prevented by heating the samples prior to the neutron irradiation. This phenomenon was ascribed to the removal of the crystal defects, which might otherwise participate in the annealing processes of the recoils in the non-heated sample. The observations about k_i may, then, be interpreted as follows. The concentration of crystal defects is higher in the early stage of the thermal treatment, and the thermal annealing proceeds very fast. Since it becomes lower after a few hours' heating, the processes of the ^{80}Br recoils produced during the thermal treatment are

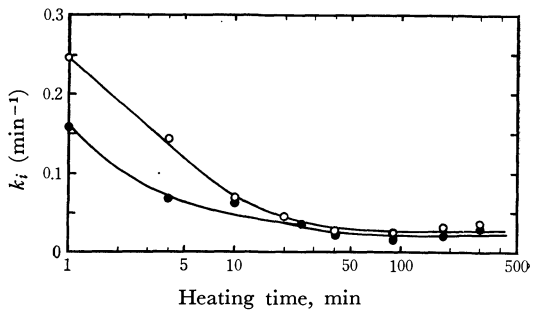

Fig. 4. Variations of k_i calculated from the results in Fig. 1.

●: 184°C, $R_\infty = 0.60$ ○: 264°C, $R_\infty = 0.65$

Table 1. The annealed fractions in the alkali metal bromates

Compound	R (%)		ΔY(%)	ΔR(%)*
	−196°C	184°C		
$LiBrO_3$	25.7±1.3	40.5±1.1	14.8	24.0
$NaBrO_3$	31.4±1.0	47.2±0.8	15.8	—
$KBrO_3$	32.5±1.2	43.6±1.3	11.1	19.5
$RbBrO_3$	25.3±1.2	34.2±1.0	8.9	—
$CsBrO_3$	32.2±1.0	35.5±0.8	3.3	17.8

* The values of ΔR were estimated from the work by Boyd and Larson[4] as follows:
$\Delta R = R$(200°C, 1 hr) − R(room temperature)

suppressed; this corresponds to the rapid decrease in the value of k_t with the lapse of the annealing time.

Effect of the Cations. A remarkable effect of the cations was observed in the thermal annealing behavior of the recoils. Table 1 shows the retentions for the samples stored at −196 and 184°C for 5 hr and the values of ΔY, which are the fractions annealed between these two temperatures. The tabulated values are the means of three determinations. The values of ΔR are the annealed fractions of ^{82g}Br recoils estimated from the work by Boyd and Larson.[4] The values become smaller in the order of the atomic number of the cation, and the tendencies are independent of the type of nuclear transformation.

In a study of the radiolytic decomposition of the alkali metal bromates, Boyd and his co-workers[12] found the relationship between the G-value and the crystal free space. The latter term was introduced by Saito and his co-workers[9] in order to interpret the amount of the retention for bromine recoils produced by the (n,γ) reactions. However, the electrostatic factor seems to influence the annealing behaviors of the recoils more strongly. The relationship between ΔY and the first ionization potential of the alkali metal is shown in Fig. 5.

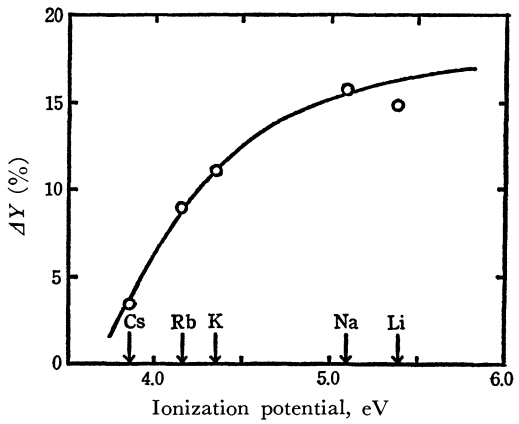

Fig. 5. Relationship between the retention and the ionization potential of alkali metals.

Although the trend is similar to that observed for the annealing behavior of bromine recoils in alkaline earth metal bromates,[13] it is entirely the reverse of the results for the permanganates salts.[8] These observations suggest that the thermal annealing is the more promoted as the polarization of the lattice constituents is larger, or as the electron density of the inactive bromate ion is higher, and that it proceeds through a direct interaction between the bromate ion and the reduced species of bromine recoil. The present conclusions also support the previous considerations regarding the annealing behavior of manganese recoils.[8]

Comparison with the Results for Other Nuclear Transformations. The thermal annealing of bromine recoils produced by the isomeric transition proceeds more rapidly than that of those produced by the (n,γ) reactions.[1-5] Furthermore, the retention for the former nuclear process is higher than those for the other nuclear transformations at room temperature, as Table 2 shows.

Table 2. Retentions for the various nuclear transformations in potassium bromate crystals

Nuclear transformation	Retention (%)	Reference
$^{80m}Br \xrightarrow{IT} {}^{80}Br$	35.5±1.2	present work
$^{79}Br(n,2n)^{78}Br$	12.4±0.4	14)
$^{79}Br(n,\gamma)^{80m}Br$	12±1	9)
$^{81}Br(n,\gamma)^{82m}Br \xrightarrow{IT} {}^{82}Br$	14.6±0.2	9)

A similar effect of the different nuclear processes on the retention was also observed in the case of aqueous solutions of labelled potassium bromate; the retention was 24.6±2.3% for the $^{80m}Br \xrightarrow{IT} {}^{80}Br$ process, whereas it was lower than 5% for the

12) G. E. Boyd, E. W. Graham and Q. V. Larson, *J. Phys. Chem.*, **66**, 300 (1962).

13) T. Shiokawa, T. Sasaki and S. Takahashi, to be published in *Radiochem. Radioanal. Lett.*

14) N. Saito, F. Ambe and H. Sano, *Nature*, **205**, 688 (1965).

$^{79}Br(n,\gamma)^{80m}Br$ reaction. By an approximate calculation, the initial kinetic energy is estimated to be less than 50 eV for the isomeric transition, while it is 220 eV for the (n,γ) reaction and 260 keV for the $(n,2n)$ reaction. Therefore, the disordered region of the ^{80}Br recoil sites may be smaller than those of the recoils produced by the (n,γ) and $(n,2n)$ reactions, and the recovery process for the former may proceed faster than those for the latter in the condensed phase. These properties caused by the isomeric transition account for the characteristic annealing curves shown in Fig. 1.

The authors wish to thank Dr. K. Yoshihara and Dr. T. Omori for their useful discussions. They are also indebted to Dr. K. Kondo for arranging the bremsstrahlung irradiation in the Laboratory of Nuclear Science of Tohoku University.

Appendix

In order to obtain information about the processes of the thermal annealing of ^{80}Br recoils, corrections of the measured radioactivities must be made for the growth and the decay of ^{80}Br atoms. According to the schemes shown in Fig. 3, $^{80m}BrO_3^-$ ions are converted to $^{80}BrO_3^-$, ^{80}BrZ, and $^{80}Br^-$ ions in consequence of the isometic transition at the ratio of R_0, $(R_\infty - R_0)$, and $(1-R_\infty)$ respectively. If these values are taken to be constant regardless of the annealing time, Scheme I under the state of radioactive equilibrium may be expressed as follows:

$$\frac{dN_2}{dt} = -k_g N_2 - k_i N_2 \tag{1}$$

$$\frac{dN_4}{dt} = -k_g N_4 \tag{2}$$

where N_2 and N_4 are, respectively, the numbers of Br^z and bromide ions after the lapse of annealing time, t. Thus, the values of N_2 and N_4 are given by the following equations:

$$\ln N_2 = -(k_g+k_i)t + \ln(R_\infty - R_0)N_g^\circ \tag{3a}$$

or:

$$k_g N_2 = k_g(R_\infty - R_0)N_g^\circ \exp\{-(k_g+k_i)t\} \tag{3b}$$

and:

$$\ln N_4 = -k_g t + \ln(1-R_\infty)N_g^\circ \tag{4a}$$

or:

$$k_g N_4 = k_g(1-R_\infty)N_g^\circ \exp(-k_g t) \tag{4b}$$

Equations for Scheme II are given with the same considerations as for Scheme I:

$$\frac{dN_6}{dt} = k_m N_m - k_i N_6 - k_g N_6 \tag{5}$$

$$\frac{dN_8}{dt} = k_m N_m - k_g N_8 \tag{6}$$

The values of N_6 and N_8 are evaluated from the equations for a transient equilibrium:[15]

$$k_g N_6 = \frac{k_g k_m (R_\infty - R_0)N_m^\circ}{k_g + k_i - k_m} \times [\exp(-k_m t) - \exp\{-(k_g+k_i)t\}] \tag{7}$$

$$k_g N_8 = \frac{k_g k_m (1-R_\infty)N_m^\circ}{k_g - k_m} \times \{\exp(-k_m t) - \exp(-k_g t)\} \tag{8}$$

and:

$$N_g^\circ = \frac{k_m}{k_g - k_m} N_m^\circ \tag{9}$$

In the above equations, N_m° and N_g° denote the total numbers of ^{80}Br and ^{80m}Br atoms at $t=0$. The sum of Eqs. (3b), (4b), (7), and (8) gives the radioactive intensity of the bromide fraction. Therefore, the retention can be related with the annealing time as follows:

$$\begin{aligned} R &= 1 - \frac{\sum_{i=1}^{4}(k_g N_{2i})}{k_g N_g} \\ &= 1 - \frac{(k_g-k_m)(N_2+N_4+N_6+N_8)}{k_m N_m^\circ \exp(-k_m t)} \\ &= R_0 + \frac{k_i(R_\infty - R_0)}{k_g+k_i-k_m}[1-\exp\{-(k_g+k_i-k_m)t\}] \end{aligned} \tag{10}$$

15) G. Friedlander and J. W. Kennedy "Nuclear and Radiochemistry," 4th Ed., John Wiley and Sons, Inc., New York (1960), pp. 129—137.

BULLETIN OF THE CHEMICAL SOCIETY OF JAPAN VOL. 43 2840—2844 (1970)

The Syntheses and Properties of the Benzothiazole or Benzimidazole Derivative Adducts of Tin(II, IV) and Antimony(III) Halides

Akira Ouchi, Toshio Takeuchi and Iwao Taminaga

Department of Chemistry, College of General Education, The University of Tokyo, Komaba, Meguro-ku, Tokyo

(Received April 9, 1970)

The benzothiazole, 2-amino-benzothiazole, benzimidazole-2-thiol, and benzothiazole-2-thiol adducts of tin(II, IV) chlorides, antimony(III) chloride, and antimony(III) bromide with the formulae of $M^{n+}L_mX_n^-$ (where L is the ligand and where X is Cl or Br) were synthesized. From their electronic and infrared spectra, it can be seen that the 2-amino-benzothiazole adducts are more stable than those of other ligands and that the metal–ligand bonds in the former remain even in the ethanolic solution.

Benzothiazole(BT), benzimidazole(BI), and their 2-derivatives (2-amino-benzothiazole (ABT), benzimidazole-2-thiol(BIT), and benzothiazole-2-thiol(BTT), for example) are interesting ligands, and many transition metal complexes have already been synthesized and investigated.[1-8] All of these studies, however, have been confined to the transition metal complexes; the tin(II, IV) and antimony(III) adducts have not yet been reported on. Since we expected that tin and antimony halides could also form adducts with such ligands, we attempted syntheses and thus obtained a series of adducts.

Experimental

Starting Materials. The ligands used were all Tokyo Kasei G. R. grade reagents. The tin(II) chloride, tin(IV) chloride, antimony(III) chloride, and antimony(III) bromide used were all G. R. or E. P. grade reagents of the Wako Chemical Co.; they were all used without any further purification.

The organic solvents used, such as isopropyl ether, acetone, and ethyl alcohol, were all of the E. P. grade and were used after distillation.

The Syntheses of the Adducts. *The synthesis of the Benzothiazole-2-thiol Adduct of Tin(IV) Chloride.* Anhydrous tin(IV) chloride and benzothiazole-2-thiol were dissolved in anhydrous ethyl alcohol in the mole ratio of 1 to 2. (The mole ratio of the starting materials varied between 1 : 2 to 2 : 1, but the same product was always obtained, though in different yields.) The solution was concentrated on a water bath to a syrupy liquid; then it was cooled and kept at room temperature several hours with stirring. The powder product thus obtained was washed well first with an isopropyl ether–acetone mixture, next by pure isopropyl ether, and finally by petroleum ether, washing being done several times with each material. The other adducts were synthesized in the same way. Some of them could be recrystallized by acetone, but the others could not. The products thus obtained were dried in a vacuum desiccator overnight.

Instruments. The magnetic moments were measured using a Gouy balance at room tempetature. The reflectance spectra were obtained with an Ito Model QU-3 spectrophotometer, using the reflectance attachment and a magnesium oxide standard. The electronic absorption spectra were obtained with a Hitachi EPS-2-type automatic recording spectrophotometer, using ethanolic-solution samples as well as nujol-mull samples. The infrared spectra were obtained by means of the nujol or hexachloro-1,3-butadiene mull procedure, using a Japan Spectroscopic Co. 403 G grating infrared spectrophotometer.

Results and Discussion

The analyses of the adducts and their expected chemical formulae are shown in Table 1. They are all diamagnetic at room temperature, and no abnormal valency of the central metal was expected. Therefore, the benzothiazole or benzimidazole derivatives in these adducts seem to be neutral, and the positive charge of the central metal ion is neutralized by halogen ions. The analytical data as well as the results of alkalimetric titration show that the 2-amino-benzothiazole adducts of tin(II, IV) chlorides contain two moles

1) M. Goodgame and L. I. B. Haines, *J. Chem. Soc., A*, **1966**, 174.
2) D. M. L. Goodgane, M. Goodgame and M. J. Weeks, *ibid.*, **1967**, 1125.
3) D. M. L. Goodgame, M. Goodgame and M. J. Weeks, *ibid.*, **1967**, 1676.
4) M. Goodgame and F. A. Cotton, *J. Amer. Chem. Soc.*, **84**, 1543 (1962).
5) T. Takiguchi, M. Abe, K. Kurosaki, E. Asada and M. Nakagome, *Kogyo Kagaku Zasshi*, **70**, 1182 (1967).
6) F. Wilson and P. Merchant, Jr., *J. Inorg. Nucl. Chem.*, **29**, 1993 (1967).
7) B. Milligan, *J. Chem. Soc., A*, **1966**, 34.
8) E. J. Duff, M. N. Hughes and K. J. Rutt, *ibid.*, **1968**, 2354; **1969**, 2101.

TABLE 1. COLORS, ANALYSES AND THE CHEMICAL FORMULAE OF THE ADDUCTS
(Figures are given in %)

		M	C	H	N	S	X
Benzothiazole adducts							
$Sn^{II}(C_7H_5NS)_2Cl_2$	Calcd	25.80	36.56	2.19	6.09	13.94	15.42
(white)	Found	25.12	36.37	2.41	6.00	13.92	14.93
$Sn^{IV}(C_7H_5NS)_2Cl_4$	Calcd	22.36	31.68	1.90	5.28	12.08	26.71
(pale brown)	Found	22.40	30.89	2.09	5.06	12.62	25.73
$Sb^{III}(C_7H_5NS)Cl_3$	Calcd	33.51	23.14	1.39	3.86	8.82	29.28
(pale brown)	Found	33.80	23.21	1.97	3.78	8.16	29.00
$Sb^{III}(C_7H_5NS)Br_3$	Calcd	24.51	16.93	1.01	2.82	6.46	48.27
(pale brown)	Found	24.45	17.01	1.47	2.75	6.50	47.80
2-Amino-benzothiazole adducts							
$Sn^{II}(C_7H_6N_2S)_2Cl_2\cdot 2HCl$	Calcd	21.19	29.88	2.49	9.96	11.36	25.22
(white)	Found	22.22	30.05	2.59	9.83	11.61	24.00
$Sn^{IV}(C_7H_6N_2S)_2Cl_4\cdot 2HCl$	Calcd	18.79	26.48	2.21	8.84	10.03	33.60
(white)	Found	19.23	27.01	2.31	8.83	10.30	33.00
$Sb^{III}(C_7H_6N_2S)Cl_3$	Calcd	32.18	22.22	1.60	7.41	8.47	28.11
(white)	Found	31.90	21.84	1.79	7.12	8.67	28.07
$Sb^{III}(C_7H_6N_2S)_2Br_3$	Calcd	18.40	25.41	1.83	8.47	9.69	36.22
(white)	Found	18.20	25.76	2.17	8.51	10.25	36.04
Benzimidazole-2-thiol adducts							
$Sn^{II}(C_7H_6N_2S)Cl_2$	Calcd	34.93	24.74	1.78	8.24	9.44	20.87
(white)	Found	35.00	24.01	1.86	7.84	9.42	20.06
$Sn^{IV}(C_7H_6N_2S)_2Cl_4$	Calcd	21.16	29.98	2.16	9.99	11.43	25.28
(yellow)	Found	21.90	29.20	2.14	9.36	11.70	24.40
$Sb^{III}(C_7H_6N_2S)Cl_3$	Calcd	32.18	22.22	1.60	7.41	8.47	28.11
(pale yelow)	Found	32.73	22.46	1.71	7.53	9.20	27.88
$Sb^{III}(C_7H_6N_2S)_2Br_3$	Calcd	18.40	25.41	1.83	8.47	9.69	36.22
(yellow)	Found	17.96	25.67	2.16	8.67	9.96	35.30
Benzothiazole-2-thiol adducts							
$Sn^{II}(C_7H_5NS_2)Cl_2$	Calcd	33.26	23.56	1.41	3.93	17.97	19.87
(yellow)	Found	34.02	23.31	1.79	3.75	18.52	19.30
$Sn^{IV}(C_7H_5NS_2)_2Cl_4$	Calcd	19.95	28.26	1.69	4.71	21.55	23.83
(yellow)	Found	20.60	27.50	1.66	4.57	21.97	22.88
$Sb^{III}(C_7H_5NS_2)Cl_3$	Calcd	30.80	21.27	1.28	3.53	16.21	26.90
(yellow)	Found	30.66	20.67	1.43	3.23	16.75	26.20
$Sb^{III}(C_7H_5NS_2)_2Br_3$	Calcd	17.49	24.16	1.45	4.05	18.43	34.44
(yellow)	Found	18.56	23.78	1.84	3.87	18.85	35.10

of hydrogen chloride per mole of the adduct. It is not the adsorbed one, since the content is always constant, but it is not yet known how these molecules are bound in the adducts.

In order to study why the colors of these adducts are sometimes more intense than those of the free ligands (white or light yellow), the absorption spectra of the nujol mulls of the solid adducts were examined. The wave numbers of the maxima of the spectra coincide approximately with those of the surface diffuse-reflectance spectra, although the latter were obtained only in the visible region; moreover, it was difficult to obtain precise data in both measurements because of the experimental difficulties. The results are shown in Table 2. The absorption maximum or a shoulder appears in about the 24—26 kK region in the cases of benzothiazole-2-thiol adducts and at about 28 kK in the cases of benzimidazole-2-thiol adducts. These peaks or shoulders disappear when the substances are dissolved in ethyl alcohol. The electronic absorption spectral data of the adducts and the ligands in ethanolic solutions shown in Table 3 show that the absorption maxima appear only in the ultraviolet region. All the metal complexes of the same ligand show nearly the same spectra; even the ABT adducts of Sn(II, IV) containing hydrogen chloride show almost the same spectra as the Sb(III) adducts which do not contain it. (Therefore, in Table 3 their average values are

Table 2. The maximum wave number of nujol mull absorption spectra of adducts
(Figures are given in kK)

$Sn^{II}(BIT)Cl_2$	28.3	28.9	31.1
$Sn^{IV}(BIT)_2Cl_4$	27.0	33.0	34.3
$Sb^{III}(BIT)Cl_3$	28.5	32.5	35.2
$Sb^{III}(BIT)_2Br_3$	28.5	29.9	33.0
BIT		32.5	
$Sn^{II}(BTT)Cl_2$	24.8	32.4 sh	34.9 sh
$Sn^{IV}(BTT)_2Cl_4$	26.4 sh	30.1	
$Sb^{III}(BTT)Cl_3$	26.7	31.0	
$Sb^{III}(BTT)_2Br_3$	25.3	33.2	
BTT		30.5	35.7 sh

BTT: Benzothiazole-2-thiol.
BIT: Benzimidazole-2-thiol.

shown).

In the cases of BT, BIT, and BTT complexes, each free ligand also shows the same spectra as the respective metal adduct. However, in the case of ABT complexes the absorption peaks of the free ligand is somewhat different from those of the metal adducts.

Duff has reported[8] that, in the cases of nickel, copper, and cobalt complexes of benzothiazole and all its derivatives except 2-amino-benzothiazole, the ligand bonds to the central metal ion by means of the nitrogen hetero-atom of the ring just like pyridine in its complexes and not by means of the sulfur atom of the thiol or the thion group on the 2-carbon, while the 2-amino-benzothiazole shows a different behavior toward metal ions and the amino nitrogen atom seems to act as a donor atom. Probably this is also true in these tin and antimony adducts, since the spectral data indicate that 2-amino-benzothiazole adducts are more stable than the others and that their metal–ligand bonds are kept even in an ethanolic solution. On the other hand, in the cases of benzothizaole, benzimidazole-2-thiol, and benzothiazole-2-thiol adducts, the spectra show that the adducts are perfectly dissociated in the solution. However, the existence of metal-ligand bonds in the solid adducts of these ligands is quite probable (*cf.* the specific colors of the solid products and the characteristic bands in the near-ultraviolet region in the nujol mull of reflectance spectra). Among the bands of the solid adducts observed, the band at 30.5 kK of benzothiazole-2-thiol and that at 32.5 kK of benzimidazole-2-thiol are probably due to the transition of conjugated p_π electrons of the thiazole or imidazole ring. When the ligand coordinates to the metal ion by means of the hetero-atom of the ring, the electronic structure of the conjugated ring π-system changes and there should be a shift of the band. The phenomenon was observed in the cases of several BIT or BTT adducts.

The main peaks of the infrared spectra (1700—400 cm^{-1}) of the ligands and the tin(IV) chloride adducts are shown in Table 4. The general fea-

Table 3. The maximum wave numbers and the absorption coefficients of the electronic spectra of some metal adducts (in ethanolic solution)
Figures are given in kK for wave numbers and log ε (calculated for the concentration of ligand) for intensities (in parentheses)

Benzothiazole						
ligand	34.1 (3.35)	35.3 (3.41)	36.2 sh (3.35)	38.4 (3.83)	40.0 (3.92)	46.0 (4.42)
adducts	34.1 (3.38)	35.3 (3.37)	36.2 sh (3.35)	38.4 (3.78)	40.0 (3.86)	46.0 (4.47)
2-Amino-bezothiazole						
ligand	34.1 (3.38)	35.1 (3.52)		38.2 (4.08)		45.1 (4.53)
adducts	35.2 (3.79)	36.0 (3.77)		39.2 (3.95)		46.3 (4.35)
Benzimidazole-2-thiol						
ligand	32.8 (4.40)	33.6 (4.32)			40.5 (4.13)	45.9 (4.22)
adducts	32.8 (4.41)	33.6 (4.32)			40.5 (4.15)	45.9 (4.27)
Benzothiazole-2-thiol						
ligand	30.8 (4.42)			38.8 (3.73)	41.6 (4.12)	43.5 (4.11)
adducts	30.8 (4.46)			38.8 (3.75)	41.6 (4.12)	43.5 (4.14)

Table 4. Infrared wave numbers of the ligands and their adducts in 1700—400 cm^{-1} region (cm^{-1})

BT	$Sn^{IV}(BT)_2Cl_4$	ABT	$Sn^{IV}(ABT)_2Cl_4 \cdot 2HCl$	BIT	$Sn^{IV}(BIT)_2Cl_4$	BTT	$Sn^{IV}(BTT)_2Cl_4$	Tentative assignments
1691 m	1670 w	1641 s						
1590 m			1629 s	1612 w	1610 w			ν(C=C)
1552 m	1560 w	1586 w	1562 m			1595 w	1593 w	
		1523 s		1508 s	1494 s	1495 s	1485 s	(II)* ν(N-C=S)
1458 s	1462 m		1467 s					
1450 s	1454 m	1444 s		1461 s	1446 m	1451 m	1459 m	aromatic
1424 m	1408 m	1370 w	1365 w	1382 w	1410 m	1420 m	1412 m	
				1355 s	1348 m			C_6H_5-NH
1313 s		(1316 m 1307 m				1319 m		
1290 s	1294 w		1302 w			1280 m	1303 m	
1262 s	1271 m	1281 w	1255 m	1270 w			1261 w	(III)* δNH and others
1195 m	1193 m	1247 w	1242 w	1256 m	1250 m	1242 m		
1154 m	1153 w	1152 w	1153 m	1180 s	1169 w	1153 m	1153 m	(I)* ν(C=S) and others
1121 s	1079 m		1087 br		1075 m	1076 s	1080 s	1,2-disubst C_6H_6
1067 s	1066 m	1064 w				1034 m	1037 w	
1010 s	1022 m	1014 w	1011 w	1012 m	1011 w	1011 m	1025 w	
794 s	787 m						786 m	
757 s	761 s		752 s			753 s	753 s	δ(C-H)
729 s	(727 m 707 m	741 s 720 s	741 s 710 m	741 s	748 s			
668 s	670 w	682 m	694 w	658 s	665 s	668 s	692 m	
			663 m	597 s	597 m	603 s	597 s	
		624 m	646 s			568 m	574 s	
582 w	580 m	564 m	582 s				564 s	
531 m	537 s					524 m	517 w	
505 w	510 m	501 m	490 s	470 s	460 m	502 w	498 m	
423 s	425 s	483 s	479 s	430 s	432 m	425 m	433 m	
		430 s	425 m	418 s	418 w			

* I, II, III, mean first, second and third thioamide-bands respectively.
s: strong, br: broad, m: medium, w: weak, sh: shoulder, BT: benzothiazole, ABT: 2-amino-benzothiazole, BTT: bezimidazole-2-thiol, BTT: benzothiazole-2-thiol.

Table 5. Far-infrared spectra of adducts (400—200 cm^{-1})
Refer Table 4 for the abbreviations

Metal salt	Ligands				Tentative assignment
	BT	ABT	BIT	BTT	
$Sn^{II}Cl_2$	284 m	271 s	258 m	285 s	ν(Sn-Cl)
	247 s	237 s	243 s	245 w	(Sn-L)*
$Sn^{IV}Cl_4$	320 s	313 s	302 s	323 s 310 s	ν(Sn-Cl)
	287 m 263 m	290 s	289 s 280 s	293 s	(Sn-L)*
$Sb^{III}Cl_3$	313 s 293 s	304 s	329 s	320 s	ν(Sb-Cl)
	280 s	271 s	295 s	272 s	(Sb-L)*
$Sb^{III}Br_3$	210 s	212 m	213 s	212 m	ν(Sb-Br)
	302 m 245 s	302 s 253 m	311 w 260 m 248 s	301 m 277 s	(Sb-L)*

* Probably the mixture of ν(M-N) and other ring vibrations.

tures of the spectra of the adducts resemble those of the respective free ligand. As these peaks seem to be mainly caused by the ligands, their tentative assignments are obtained with reference to those of the benzothiazole or benzimidazole derivatives.[9-12]

In the cases of 2-amino-benzothiazole adducts, the bands of the free ligand at 1641, 1523, and 1444 cm^{-1} shift to 1629—1638, 1562—1568, and 1467—1470 cm^{-1} respectively. These bands all correspond to the stretching modes of particular bonds or to conjugated modes of the thiazole ring. Therefore, the shifts seem to be due to the bonding of of the metal, which causes the change in the bonding states in the ring system, such as the prohibition of the tautomeric transition of the ring system. The adducts of the other ligands show only far smaller shifts of the corresponding bands.

The metal-halogen and the metal-ligand stretching bands appear in the 400—200 cm^{-1} region. The metal-halogen stretching bands (Sn(II)-Cl,[13] Sn(IV)-Cl,[14-16] Sb(III)-Cl,[17] and Sb(III)-Br,[17]) have already been reported; they appear as an almost pure group vibration, and do not mix with other modes. Consequently, the bands have been assigned according to the references mentioned above.

On the other hand, the metal-ligand group frequencies are not clear. Only a very few references have yet been published for the pure group-stretching vibration between tin or antimony and nitrogen or sulfur. Duff[8] shows that the metal-nitrogen stretching mode of benzothiazole complexes is apt to mix with some ring-vibrations, as in the cases of pyridine complexes. Therefore, the bands in this region, which appear only in the spectra of the adducts and are not identified as metal-halogen stretching bands, may be assigned tentatively to the metal-ligand vibrations. The results are summarized in Table 5.

Thus, the exact structures of the adducts are not yet clear; the ligand may bond not only by means of -N but, in some cases, also by means of -S, forming a multi-layer polymer structure, as in the cases of some benzothiazole complexes reported by Duff,[8] although all the metal-ligand bonds are certainly not very strong.

The authors wish to express their thanks for the helpful discussions by Professor Yukichi Yoshino and our other colleagues of this laboratory.

9) M. G. Ettlinger, *J. Amer. Chem. Soc.*, **72**, 4699 (1950).
10) M. P. V. Mijovic and J. Walker, *J. Chem. Soc.*, **1961**, 3381.
11) W. Otting and F. Drawert, *Chem. Ber.*, **88**, 1469 (1955).
12) L. J. Bellamy, "The Infrared Spectra of Complex Molecules," 2nd Ed., Methuem Co. Ltd., New York, (1958), p. 374.
13) J. D. Donaldson and D. G. Nicholson, *J. Chem. Soc., A*, **1970**, 145.
14) R. C. Poller and D. L. B. Toley, *ibid.*, **1967**, 1578.
15) M. Webster and H. E. Blayden, *ibid.*, **1969**, 2443.
16) M. F. Farona and J. G. Grasselli, *Inorg. Chem.*, **6**, 1675 (1967).
17) G. E. B. Y. Ahlijah and M. Goldstein, *Chem. Commun.*, **1968**, 1356.

BULLETIN OF THE CHEMICAL SOCIETY OF JAPAN VOL. 43 2845—2850 (1970)

The Hydrated and Anhydrous Copper(II) Complexes with Thioglycolic Acid Derivatives

Yayoi OHASHI, Toshio TAKEUCHI, Akira OUCHI and Yukichi YOSHINO

Department of Chemistry, College of General Education, The University of Tokyo, Komaba, Meguro-ku, Tokyo

(Received April 10, 1970)

The dihydrates and anhydrous copper(II) complexes with methyl, ethyl, *n*-propyl, isopropyl, *n*-butyl, and benzyl thioglycolic acids were synthesized, and their properties were investigated. The magnetic data show that the copper in the complexes is divalent and that the complexes do not have a copper(II) acetate structure. The spectroscopic data show that these ligands bond to the central metal ion as strongly as does amino acid or water. In the case of isopropyl thioglycolato copper(II) dihydrate, the blue and the violet isomers were obtained. The structures of the complexes in the solid state as well as in the solution were discussed.

In a previous paper,[1] solid metal complexes with ETTA(ethanediylidenetetrathiotetraacetic acid) and some alkyl di- or mono-thioglycolic acid derivatives were reported. The copper(II) complex of benzylthioglycolic acid was obtained in the dihydrate form as well as in the anhydrous form; their colors are quite different, the former being light blue, and the latter, dark green. On the other hand, McAuliffe recently studied the structural difference between hydrated and anhydrous nickel complexes of amino acids.[2] Therefore, in order to study the structural difference, hydrated and anhydrous copper complexes of methyl, ethyl, *n*-propyl, isopropyl, *n*-butyl and benzyl thioglycolic acids were synthesized and investigated magnetically as well as spectroscopically. In the course of this study, two isomers of isopropyl thioglycolato copper(II) dihydrate were isolated.

Experimental

Instruments. The magnetic moments of the samples were measured with a Gouy balance at room temperature (15°C). The electronic absorption spectra were obtained by the use of a Hitachi EPS-2 automatic recording spectrophotometer. The reflectance spectra were measured with an Ito QU-3 spectrophotometer, using a reflectance spectra attachment. The infrared spectra were obtained by means of a nujol or hexachloro-1,3-butadiene mull procedure, using a Japan Spectroscopic Co. DS 403 G grating automatic recording infrared spectrophotometer.

The Syntheses of the Metal Complexes. The ligands were obtained by Larsson's method[3] from thioglycolic acid and alkyl halides. The metal complexes were synthesized from the ligands and copper(II) hydroxide. A typical pattern of the process is shown below.

The Synthesis of the Isopropyl Thioglycolato Copper(II). Copper(II) hydroxide, itself produced from one gram of copper(II) chloride dihydrate and sodium hydroxide, was mixed with 2 grams of isopropyl thioglycolic acid, and the mixture was stirred. After the copper(II) hydroxide had been dissolved, the residue was filtered off; the filtrate was kept overnight in a refrigerator. A pale blue dihydrate complex was thus precipitated. The product was filtered off and repeatedly washed with diethyl ether. It could be recrystallized with acetone, but the recrystallized product was found to be an anhydrous green complex and not the dihydrate. After the pale blue dihydrate had been filtered off and the filtrate had been kept several days more in a refrigerator, the violet dihydrate was deposited as black, needle-like crystals. The complex was filtered off and washed with diethyl ether. The yield of the blue complex was 0.6 g (26%), and that of violet one, 0.7 g (31%). The yield was calculated on the basis of copper chloride.

The other complexes in the dihydrate form were synthesized by almost the same procedure, but only those in the pale blue form have thus for been obtained. The isopropyl and the benzyl thioglycolato copper(II) dihydrate were dehydrated by refluxing them with acetone or benzene respectively (the violet and blue isomers of the former gave the same green anhydrous product). However, the anhydrous methyl, ethyl, *n*-propyl, and *n*-butyl complexes could not be obtained by refluxing their dihydrates with any organic solvents; some of them were decomposed. Therefore, their anhydrous complexes were obtained by heated their dihydrate to 40°C on phosphorus pentoxide in a vacuum for about 10 hours.

Results and Discussion

The elemental analysis, the expected chemical formulae, and the magnetic moments of the com-

1) A. Ouchi, Y. Ohashi, T. Takeuchi and Y. Yoshino, This Bulletin, **43**, 1088 (1970).

2) C. A. McAuliffe and W. D. Perry, *J. Chem. Soc., A*, **1969**, 634.

3) E. Larsson, *Ber.*, **63**, 1347 (1930).

Table 1. Analyses and the magnetic moments of the complexes

Chemical formula		Analysis (%) M	C	H	S	Magnetic moment (B.M.)	Method of dehydration
$Cu(MeS_1)_2 \cdot 2H_2O$	Calcd	20.51	23.26	4.55	20.70		
	Found	20.55	23.85	4.20	20.21	1.84	
$Cu(MeS_1)_2$	Calcd	23.21	26.32	3.68	23.42		*
	Found	23.48	25.26	4.20	22.75	1.82	
$Cu(EtS_1)_2 \cdot 2H_2O$	Calcd	18.80	28.44	5.37	18.98		
	Found	18.16	28.76	5.41	17.40	1.73	
$Cu(EtS_1)_2$	Calcd	21.05	31.83	4.68	21.24		*
	Found	20.58	31.40	4.86	20.96	1.79	
$Cu(n\text{-}PrS_1)_2 \cdot 2H_2O$	Calcd	17.36	32.82	6.06	17.52		
	Found	17.62	32.95	5.88	16.54	1.85	
$Cu(n\text{-}PrS_1)_2$	Calcd	19.26	36.41	5.50	19.44		*
	Found	18.57	36.60	4.87	18.50	1.71	
$Cu(i\text{-}PrS_1)_2 \cdot 2H_2O$ (blue)	Calcd	17.36	32.82	6.06	17.32		
	Found	17.29	33.07	5.96	17.05	1.84	
$Cu(i\text{-}PrS_1)_2 \cdot 2H_2O$ (violet)	Calcd	17.36	32.82	6.06	17.32		
	Found	17.52	32.17	6.05	16.30	1.88	
$Cu(i\text{-}PrS_1)_2$	Calcd	19.26	36.41	5.50	19.44		**(acetone)
	Found	19.59	36.25	5.70	19.44	1.87	
$Cu(n\text{-}BuS_1)_2 \cdot 2H_2O$	Calcd	16.13	36.58	6.65	16.28		
	Found	16.27	37.01	6.53	17.40	1.83	
$Cu(n\text{-}BuS_1)_2$	Calcd	17.75	40.26	6.20	17.91		*
	Found	17.80	38.19	6.48	16.90	1.80	
$Cu(BzS_1)_2 \cdot 2H_2O$	Calcd	13.75	46.79	4.80	13.88		
	Found	13.58	46.62	4.85	14.38	1.75	
$Cu(BzS_1)_2$	Calcd	14.92	50.75	4.26	15.05		
	Found	14.87	51.09	4.53	15.47	1.86	**(benzene)

* Dehydrized by Abderhalden exciccator on phosphorus pentoxide at 40°C under reduced pressure.
** Dehydrized by refluxing the hydrate in the written solvents.
MeS_1H=methyl thioglycolic acid, EtS_1H=ethyl thioglycolic acid, $n\text{-}PrS_1H$=*n*-propyl thioglycolic acid, $i\text{-}PrS_1H$=isopropyl thioglycolic acid, $n\text{-}BuS_1H$=*n*-buthyl thioglycolic acid, BzS_1H=benzyl thioglycolic acid.

plexes obtained are shown in Table 1. The sulfur analyses sometimes gave values which were a little low, probably because of the experimental difficulties. However, as the contents of other elements coincided with calculated values well enough, the proposed chemical formulae seem to be supported.

The magnetic moments of these complexes are about 1.75—1.85 B.M. Although many copper(II) compounds show the magnetic moment of 1.9—2.1 B.M., some amine or amino acid complexes give values in the range of 1.8—1.88 B.M.[4-6]. Therefore, Cotton stated that usual copper(II) complexes show magnetic moments of 1.75—2.20 B.M.[7] Some copper(II) complexes show a subnormal magnetic moment (<1.74 B.M.).[8] Copper(II) acetate containing three atom bridges of the carboxyl group has a magnetic moment value of 1.43 B.M., while copper(II) bromide containing monoatomic bridges of halogen atom has a

4) W. E. Hatfield and R. Whyman, "Transition Metal Chemistry," Vol. 5, ed. by R. L. Carlin, Marcel Dekker, New York, N. Y. (1969), p. 84.

5) C. A. McAuliffe, J. V. Quagliano and L. M. Vallarino, *Inorg. Chem.*, **5**, 1996 (1966).

6) S. E. Livingstone and J. D. Nolan, *ibid.*, **7**, 1447 (1968).

7) F. A. Cotton and G. Wilkinson, "Advanced Inorganic Chemistry," 2nd Ed., Interscience Publishers, New York, N. Y. (1966), p. 902.

8) M. Kato, H. B. Jonassen and J. C. Fanning, *Chem. Rev.*, **64**, 99 (1964).

TABLE 2. THE WAVE NUMBERS AND THE MOLAR EXTINCTION COEFFICIENTS OF THE ABSORPTION MAXIMA OF THE ELECTRONIC SPECTRA OF THE COMPLEXES (in kK for the wave numbers and log ε for the extinction coefficients (in parentheses))

Complex	Solvent	Absorption spectra				Reflection spectra	
$Cu(MeS_1)_2$	H_2O	13.9(1.79)	30.6(2.86)	38.5(2.84)		$2H_2O$	15.6 sh 15.9 16.4
	C_2H_5OH	14.7(2.23)	29.9(3.06)	36.4(3.20)		$0H_2O$	14.3 sh 14.9
$Cu(EtS_1)_2$	H_2O	14.3(1.94)	30.4(2.85)	38.5(2.87)		$2H_2O$	15.6
	C_2H_5OH	14.9(2.30)	28.9(3.36)	36.1(3.44)		$0H_2O$	14.5
$Cu(n\text{-}PrS_1)_2$	H_2O	14.5(1.97)	27.0(2.64)	30.3(2.87)	36.8(2.90)	$2H_2O$	15.3 sh 15.1 sh
	C_2H_5OH	14.9(2.17)	28.3(3.47)		36.1(3.35)	$0H_2O$	14.3 sh 14.9 16.4 sh
$Cu(i\text{-}PrS_1)_2$	H_2O	14.5(2.05)	27.0(2.70)	29.9(2.85)	38.5(3.11)	$2H_2O$	14.9 16.1 sh
(blue)	C_2H_5OH	14.5(2.41)	27.4(3.64)	34.9(3.51)		$0H_2O$	14.3 sh 15.9 sh
$Cu(i\text{-}PrS_1)_2$*	H_2O	14.5(2.02)	29.9(2.77)	38.0(2.89)		$2H_2O$	16.1 sh 17.2 18.5
(violet)	C_2H_5OH	14.9(2.38)	27.5(3.55)	35.1(3.49)	46.3(3.78)		
$Cu(n\text{-}BuS_1)_2$	H_2O	14.3(1.99)	27.0(2.70)	30.1(2.90)	38.4(2.91)	$2H_2O$	14.3
	C_2H_5OH	14.9(2.38)	27.6(3.25)	35.5(3.20)	46.1(3.49)	$0H_2O$	14.7 br
$Cu(BzS_1)_2$**	H_2O	13.1	30.7	37.7		$2H_2O$	13.7 sh 14.5
	C_2H_5OH	14.1	30.9	38.0		$0H_2O$	14.5 sh 15.3

The sample solutions for the absorption spectra were obtained by dissolving the anhydrous complexes unless the note is given.

* Solutions were made from the dihydrate.

** As hardly soluble in the solvents, log ε values could not be determined.

sh: shoulder br: broad. refer the other abbreviations in Table 1.

$2H_2O$: dihydrate, $0H_2O$: anhydrous complex.

value of 1.31 B.M. These phenomena are caused by the spin-spin interaction between copper(II) ions. However, the subnormally low magnetic moment is not found in all carboxyl group bridged polymers. Copper(II) benzoate trihydrate, for example, shows a magnetic moment of 1.87 B.M. in spite of its linear polymer structure.[9] These alkyl thioglycolato complexes surely do not have a strong spin-spin interaction between copper(II) ions. It is not probable that they have a structure like copper(II) acetate, but the possibility of some weakly-bonding linear polymer structure of the copper(II)-benzoate type, for example, can not be denied.

The reflectance spectra of the solid dihydrate and anhydrous complexes as well as the absorption spectra of ethanolic or aqueous solutions of the anhydrous complexes are shown in Table 2.*1

All of the complexes studied show one band in the visible region. It has been identified as the *d-d* band ($^2E_g \rightarrow {}^2T_{2g}$) of the octahedral copper(II) ion.[10] As all octahedral copper(II) complexes are apt to be deformed by the Jahn-Teller effect, the band is broadened. These alkyl thioglycolates, do not seem to be in the pure square-planar form. The square-planar copper(II) complexes, bis-(acetylacetonato) copper(II), for example, show two bands of nearly equal intensities in the visible region, at about 15.0 and 18.0 kK; they are identified as the $^2B_{1g} \rightarrow {}^2A_{1g}$ and $^2B_{1g} \rightarrow {}^2E_g$ bands respectively.[11-13] Almost all of these alkyl thioglycolato copper(II) complexes show only one absorption maximum with a relatively low ν_{max} value, although in some cases they are broad or have a shoulder.

Two other bands in the ultraviolet region are probably charge-transfer or ligand-transition bands. By comparing the wave numbers of the *d-d* bands given in Table 2, it can be seen that, for

9) M. Inoue, T. Kishita and S. Kubo, *Nippon Kagaku Zasshi*, **84**, 759 (1963).

*1 The absorption spectra of aqueous solutions of dihydrates are the same as those of the respective anhydrous salts. However, those of ethanolic solutions of both forms are slightly different from each other, although the general features of the spectra are the same and the difference in their maximum wave numbers (ν_{max}) is small. Probably a part of the coordinated water of the solid dihydrate is not removed completely even in the ethanolic solution.

10) C. J. Ballhausen, "Introduction to Ligand Field Theory," McGraw Hill, New York, N. Y. (1962), p. 269.

11) F. A. Cotton and J. J. Wise, *J. Amer. Chem. Soc.*, **88**, 3451 (1966), *Inorg. Chem.*, **6**, 917 (1967).

12) J. P. Fackler, Jr., F. A. Cotton and D. W. Barnum, *ibid.*, **2**, 97 (1963).

13) B. N. Figgis, "Introduction to Ligand Field," Interscience Publishers (Wiley), New York, N. Y. (1966), p. 316.

each complex, the ν_{max} of the aqueous solution is the lowest, and that of the reflectance spectra of the solid dihydrate, which is a little higher, is next. The *d-d* band of the complex in the ethanolic solution always has higher ν_{max} and ε values than those of an aqueous solution. The *d-d* band of the reflectance spectra of the dihydrates shifts to the higher-wave number side in the cases of *n*-butyl and benzyl thioglycolato complexes when they are dehydrated. However, in the cases of methyl, ethyl and propyl thioglycolates, the band shifts to the opposite side.

It seems that these facts can be explained as follows. The alkyl thioglycolic acids generally have a little stronger ligand field effect than water, and the smaller the alkyl group is, the higher the affinity of the ligand is. In the aqueous solution, however, as the concentration of water is predominant, the complex species have four molecules of water and two molecules of ligand working as a monodentate and bonding with the copper ion by means of its carboxyl oxygen only. Therefore, the wave number as well as the intensity of the *d-d* band of the aqueous solution is low, although it is higher than that of $[Cu(H_2O)_6]^{2+}$.

In the cases of solid dihydrates, the complex is also in an octahedral form, but the ligand serves as a bidentate and bond with the central metal ion not only by means of the carboxyl group but also by means of the sulfur atom, although the metal-sulfur bond is probably not strong. The other two bonds of the octahedral copper ion may be linked with each other by means of the bridge of a water molecule, thus forming a linear polymer. The species in an ethanolic solution also seems to be in an octahedral form. Probably only two alcohol molecules bond weakly to the metal ion, and the ligand molecules work as the bidentate. In the case of a solid anhydrous complex, not a simple monomeric square-planar structure, where two molecules of the ligand coordinate to the metal, but a polymeric, distorted octahedral structure bridged with the carboxyl group of the ligand, as with the amino acid complexes of nickel proposed by McAulliffe,[2] is probable.

The violet isomer of isopropyl thioglycolato copper(II) dihydrate gives a different reflectance spectra as well as a different X-ray powder pattern of the solid from those of the blue isomer. Moreover, the violet color is very deep, although the exact measurement of the intensity of the bands is impossible. However, when the violet isomer is dissolved into solvents, its absorption spectra are just the same as those of the pale blue isomer, and when the violet or blue dihydrates were dehydrated by refluxing them with acetone, the same anhydrous complex was obtained. Therefore, the structural difference between them is probably caused only by the bond type of the ligand and the water in the complex. Probably the sulfur atom of the ligand bonds more tightly to the copper ion in the violet dihydrate than in the blue one.

TABLE 3. INFRARED SPECTRA OF THE ISOPROPYL THIOGLYCOLIC ACID AND ITS COPPER(II) COMPLEXES (1700—200 cm^{-1})

i-PrS_1-H	$Cu(i\text{-}PrS_1)_2\cdot 2H_2O$ (blue)	$Cu(i\text{-}PrS_1)_2\cdot 2H_2O$ (violet)	$Cu(i\text{-}PrS_1)_2$	Tentative assignment
1710 s	1588 s	1590 s	1583 s	$\nu_{antisym}$(COOH)
1460 sh 1420 s	1460m	1440 s	1460 1445 w	ν_{sym}(COOH)
	1380 s	1380 1360 s	1352 1342 m	$\delta(CH_3)$
1300 s				
1250w	1251m	1260 s	1243m	
1200w	1231m	1225w	1229m	δ(O-C=O)+others
1152m	1152m	1152m	1154m	
1044 s	1053m	1060m	1059 s	$\rho(CH_3)$
930w	941 s	925 s	930m	δ(O-C=O)+others
	896m	895 s	897 s	
790m	789 s		777 s	$\delta(COO^-)$
	710m	720m		
580m	638m	620 s	630m	
	538m	556m		
465 s	470m	467 s	467 s	δ(OCO) or others
		410 s		
348w	368 s	401 s	370 s 327 s	ν(M-O) or others
	242 s 226 sh	250 s 220m	260 s 192m	ν(M-S)

s: strong, m: medium, w: weak, sh: shoulder. Refer the other abbrevations in Table 1.

A nearly square planar form with two bidentate ligand molecules is probable in the former. The water molecules are only loosely bonded or are held in crystalline interstices.

The infrared spectra (1700—200 cm^{-1}) of the complexes were studied; their tentative assignments, obtained with reference to those of oxalato, acetylacetonato, and amino acid complexes,[2,6,7,14-16] are shown in Table 3.

The antisymmetric COO stretching bands of the complexes appear at about 1580—1590 cm^{-1}. These values correspond to those of glycinato and other amino-acid complexes. The bridging carboxyl groups of metal carboxylato complexes also show the band in this region. Therefore, the low wave number of the band is not necessarily a proof of the ionized carboxyl group. The symmetric COO stretching bands appear at about 1440—1460 cm^{-1}. In the far infrared region, the ν(Cu–O) bands of pyridine-1-oxide complexes are found at about 400 and 450 cm^{-1};[17] that of acetylacetonate, at about 480 cm^{-1},[14] and those of oxalato complexes, at about 420 cm^{-1}. Therefore, the ν(Cu–O) bands of these alkyl thioglycolato complexes should appear near the 400—450 cm^{-1} region. The bands in 360—410 cm^{-1}, which appear only in the spectra of these metal complexes, not in those of the free ligands, are tentatively assigned as ν(Cu–O) bands, although their wave numbers are a little low.

The metal-sulfur stretching band of the first transition metals have been reported to occur over a wide range of wave numbers,[7] the bands of monothio- or dithio-β-diketonates occur at about 350 cm^{-1}, while the bands occur in the range of 205—298 cm^{-1} in the cases of thiourea adducts.[18] A broad band at 205 cm^{-1} was identified as the ν(Cu–S) one in the case of the ethylenethiourea complex of copper(I). Consequently, the bands at about 250 cm^{-1} can be tentatively assigned.

A strong band at about 450—470 cm^{-1} is also observed in the spectra of all metal complexes. However, the free ligands also have the band. Therefore, it is probable that this band is the δ(O-CO) one. As the alkyl thioglycolato complexes are less stable than β-diketonates and such complexes, the bond between the Cu–O and Cu–S of the former are probably weaker and, consequently, their stretching bands appear in the lower-wave number region.

Table 4. Some infrared wave-numbers of the alkyl thioglycolic acids and its copper(II) complexes

Refer the abbreviation in Table 1 and 3.

Chemical formula	Tentative assignments			
	$\nu_{antisym}$(COOH)	ν_{sym}(CCOH)	ν(M–O)+others	ν(M–S)
MeS_1–H	1710 s	1420 s		
$Cu(MeS_1)_2 \cdot 2H_2O$	1600 s	1420w	387 s	248 s
$Cu(MeS_1)_2$	1600 s	1440w	398 s	262 s
EtS_1–H	1710 s	1420 s		
$Cu(EtS_1)_2 \cdot 2H_2O$	1665 s 1614 s	1455m 1443m	382 s	259 s
$Cu(EtS_1)_2$	1550 s	1453w	380 s	260w
n-PrS_1–H	1710 s	1420 s		
$Cu(n\text{-}PrS_1)_2 \cdot 2H_2O$	1590 s	1460m	375 s	245m
$Cu(n\text{-}PrS_1)_2$	1550 s	1438m	398 s	247m
i-PrS_1–H	1710 s	1420 s		
$Cu(i\text{-}PrS_1)_2 \cdot 2H_2O$ (blue)	1588 s	1460 s	368 s	242 s
$Cu(i\text{-}PrS_1)_2 \cdot 2H_2O$ (violet)	1590 s	1440 s	410 s 401 s	250 s
$Cu(i\text{-}PrS_1)_2$*	1583 s	1460 s 1443w	370 s	260 s
n-BuS_1–H	1710 s	1464 s		
$Cu(n\text{-}BuS_1)_2 \cdot 2H_2O$	1590 s	1463 s	370 s	262w 225 s
$Cu(n\text{-}BuS_1)_2$	1560 br	1463m	375 s 253w	249w 228m
BzS_1–H	1690 s	1490w		
$Cu(BzS_1)_2 \cdot 2H_2O$	1590 s	1494m	370 s	253 s 241 s
$Cu(BzS_1)_2$	1590 s	1494m	384 s	247m 231w

* Dehydrized the blue dihydrate.

14) K. Nakamoto, "Infrated Spectra of Inorganic and Coordination Compounds," John Wiley & Sons, New York, N. Y. (1963), pp. 197—225.
15) J. Fujita, A. E. Martell and K. Nakamoto, *J. Chem. Phys.*, **36**, 324, 331 (1962).
16) K. Nakamoto, Y. Morimoto and A. E. Martell, *J. Amer. Chem. Soc.*, **83**, 4528 (1961).
17) D. M. Adams and P. J. Lock, *J. Chem. Soc., A*, **1967**, 620.
18) D. M. Adams and J. B. Cornell, *ibid.*, **1967**, 884.

The characteristic difference in the infrared spectra between the blue and violet dihydrate isomers appears only in about the 200—400 cm^{-1} region. In the spectra of the violet isomer, the 368 cm^{-1} band of the blue isomer shifts to 401 and 410 cm^{-1} and the band near 242 cm^{-1}, to 250 cm^{-1}. In the case of the blue isomer, it is supposed that the sulfur atom of the ligand bonds to the central copper ion more weakly, and the water coordinates more strongly. On the other hand, in the violet form, the ligand works as a bidentate and water molecules bond weakly. Therefore, the shifts of the ν(Cu–O) as well as ν(Cu–S) of the violet isomer to the higher-wave number side are reasonable, and these results are consistent with those from the electronic spectra.

The wave numbers of several infrared bands, and the tentative assignments of other alkyl thioglycolic acids and their copper(II) complexes are summarized in Table 4.

The authors wish to express their gratitude for the helpful discussions of Professor Kunihiko Watanuki, Mr. Iwao Taminaga, Mr. Bokuichiro Takano, Mr. Mitsuhisa Nakatani, and Mr. Yoshiaki Takahashi.

BULLETIN OF THE CHEMICAL SOCIETY OF JAPAN VOL. 43 2850—2858 (1970)

Ion-exchange Chromatographic Analysis on the Chain Length of Polyphosphate Products

Niro MATSUURA, Tsin-ko LIN and Yoshimitsu KOBAYASHI

Department of Pure and Applied Sciences, College of General Education, The University of Tokyo, Komaba, Meguro-ku, Tokyo

(Received April 22, 1970)

The ion-exchange chromatographic technique was used in order to find the average chain number of a polyphosphate product. For the assignment of the *n*th polymer in the obtained chromatogram, the dependence of the distribution coefficient, K_d, on the eluent concentration examined by the use of both 20-cm and 60-cm resin columns. A lower series of polyphosphate was included in a relatively large amount in order that the average chain number based on the chromatographic analysis could be duly appreciated only for the case of basic polymers with lower molecular weights. For a product "Graham Salt" with a number of phosphate links, the higher series of polyphosphate could not be desorbed entirely from the resin column; the accurate estimation of the average number was, then, improbable. The viscosity method is also not advisable to use the computation of a mean polymerization number in the polyphosphate with a low molecular weight. An attempt was made to improve the data on the average chain number by the viscosity measurements together with the chromatographic analysis of the polymer constituent.

Among the wide range of industrial applications of the condensed polyphosphate[1,2] its use as an inorganic high polymer, soluble in water and inert to redox chemical reagents, is of great interest for promise and it holds of a possible improvement in the natural products in both the solid and dispersion phases. In order to have a correct understanding of its polymer structure, the knowledge of the chemical composition of a polyphosphate product is indispensable for physical and chemical research into the characteristic properties of this material. Paper chromatographic analysis is a convenient tool for the detection of the constituent members in a polyphosphate product;[3-5] nevertheless, the obtained result offers only a perspective on qualitative or semi-quantitative analysis. In this work, a microamount of an ingredient in the polyphosphate was examined in the presence of an excess of a major component by the ion-exchange chromatographic technique, which makes it possible to treat several hundred milligrams of the sample in order to obtain more detailed information on the chemical composition.[6] A large number

1) S. Ueda, *Denki Kagaku*, **30**, 798 (1962).
2) Van Wazer, "Phosphorus and Its Compounds, Vol. 1, Interscience Pub., New York, (1958).
3) H. Hettler, *J. Chromatogr.*, **1**, 389 (1956).
4) H. Huhti and P. A. Gartagams, *Can. J. Chem.*, **34**, 785 (1956).
5) S. Ohashi, "Handbook of Inorganic Chem. (Muki Kagaku Zensho)," Maruzen Pub., Tokyo (1965); *Kagaku to Kogyo*, **22**, 878 (1969).

of works have been published on the analytical procedure, studying the conditions to be used in separating the constituent members of polyphosphate by means of ion-exchange chromatography;[5-10] however, few of them have dealt with the distribution of the constituent species. The conventional degree of polymerization in a polyphosphate product is evaluated as a mean value on the basis of the molar ratio in a mixture of the monobasic salt of $M^{I}H_2PO_4$ and the dibasic salt of $M^{I}_2HPO_4$ taken as starting materials, although the true degree of polymerization is far different, depending on the conditions of the synthesis, particularly on the temperature and the time of dehydration.

In the course of our studies of the hot atom and the radiation chemistry of polyphosphate in the aqueous phase and in the solid glassy state,[11] a hundred various samples were dealt with. The data resulting from the analysis of the phosphates, detected as resolved constituent members, will be summarized; they subtantiate, from the analytical point of view, the polymer structure of the condensed phosphate, using its molecular weight and polymerization number as an average.

Experimental

Reagent and Materials. For the purification of sodium triphosphate, a commercial anhydrate product which was 80% pure was used as the starting material. Purification by recrystallization[2] was carried out from an aqueous solution consisting of 20% ethyl alcohol; the procedure was repeated five times. The anhydrate polyphosphates were prepared from a mixture of monophosphates, dibasic sodium dihydrate salt, and monobasic sodium decahydrate salt by pyrosynthesis with a temperature-controlled electric-muffle furnace. A chelate triphosphate of the divalent metallic cation was obtained by the precipitation method. A hot clear solution containing one equivalent of the metallic ion and two equivalents of the triphosphate ion separates out when a chelate salt with the composition of $Na_6M^{II}(H_2P_3O_{10})_2$ is cooled. The ammonium triphosphate was obtained by the cation-exchange method through a column of ammonium-form resin, while the ammonium salt was precipitated by the addition of alcohol, as was in the precipitation of sodium salt. All the other chemical reagents used were of an analytical grade.

Chemical Analysis. For the chemical analysis, from 20 to 1000 mg of the sample were dissolved in 5 to 25 m*l* of distilled water, out of which 1 or 2 m*l* was adsorbed on a Dowex 1×8 anion-exchange resin column. The gradient elution technique described in a published paper[6] was used in the chromatographic development of polyphosphate species. Each 5- or 10-m*l* fraction of the eluates from the resin column was subjected to the colorimetry of the phosphate by the molybdenum blue method using a red filter (Madzuda VR-1 filter). A fractionated aliquot sample should be diluted for color development when the fraction is too concentrated with phosphate.

Viscosity Measurements. An Ubellohde-type viscosimeter of 1 to 5 centi-Stokes was used for the viscosity measurements. The temperature was controlled by a thermostat at 25.00±0.05°C for all the measurements. In order to obtain reproducible data, the hydrolysis of the unstable branch-points in the polyphosphate glass should be completed before the measurements by keeping the sample solution for 12 hr. According to our preliminary examination,[12] the anion species of a supporting electrolyte little affected the reduced viscosity of a sample solution. In the present work, 0.035 N sodium chloride was, therefore, employed in place of bromide. In the medium containing 0.035 N NaCl or NaBr, the reduced viscosity is regarded as constant no matter what the concentration of the phosphate is, and the intrinsic viscosity was determined by the standard of 1 g/100 m*l* phosphate solution according to this equation:

$$[\eta] = K \cdot M$$

where K is a constant based on the light scattering data given by 1.76×10^{-5} M^{-1},[13] and where M is the average molecular weight to be computed.

Results

1. Analysis of Short-chain Members. The chromatographic development of orthophosphate, pyrophosphate, and triphosphate can be effcted in an excellent resolution by using as the eluent a potassium chloride solution whose concentration is raised in an exponential-gradient form. At a certain stage of elution the effluent has a concentration of KCl, C being given by (1).[14]

$$C = C_0 + (C_r - C_0)(1 - \exp[-V_f/V_0]) \quad (1)$$

In Eq. (1) C_0 is the starting concentration of KCl in the mixing bottle of V_0 m*l* and C_r is the concentration of KCl in the reservoir joined to the mixing bottle for the supply of a concentrated eluent solution. For the purpose of the impurity analysis of a purified triphosphate hexahydrate sample, the parameters in Eq. (1) were 2×10^{-3}M HCl for C_0 and 0.6 M KCl for C_r; 500 m*l* was the volume for V_0,[6] and as the sample as much as 100 mg of $NaPO_3$ was taken for the adsorption on

6) N. Matsuura and K. Kyokawa, *Bunseki Kagaku*, **16**, 612 (1967).
7) F. H. Pollard, G. N. Nickless and M. T. Rothwell, *J. Chromatogr.*, **27**, 214 (1967).
8) F. H. Pollard and R. F. Jameson, *J. Chem. Soc.*, **1959**, 752.
9) M. Kobayashi, *Kogyo Kagaku Zashi*, **69**, 2071 (1966); **70**, 1097 (1967).
10) N. Shiraishi and T. Iba, *Bunseki Kagaku*, **13**, 883 (1964).
11) N. Matsuura, N. Shinohara and C. K. Lin, *J. Inorg. Nucl. Chem.*, **24**, 1252 (1969).
12) R. C. Mehrotra and V. S. Gupta, *J. Polym. Sci.*, **55**, 81 (1961).
13) U. P. Strauss, E. H. Smith and P. L. Wineman, *J. Amer. Chem. Soc.*, **75**, 3935 (1953).
14) L. E. Netherton, A. R. Wheath and D. N. Berhart, *Anal. Chem.*, **27**, 214 (1955).

a 20-cm resin column. The developed pattern, as is illustrated in Fig. 1, demonstrates that three peaks are located about equidistantly apart, even though the highest peak of the major component (triphosphate) is present thousand times in excess. In the analysis of a commercial product of triphosphate, a very small amount of the sample is required; for example, two mg or less is sufficient for an accurate analysis. However, for assaying the impurities of polyphosphate present in an orthophosphate sample, the tailing of the precedent peak interferes with the accurate computation of the nearest neighbor, as is shown in Fig. 2. The results of the impurity analysis of

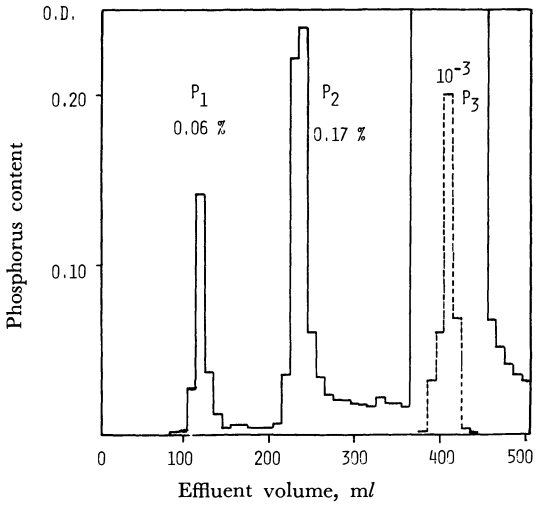

Fig. 1. Impurities in $Na_5P_3O_{10}\cdot 6H_2O$. Chromatogram developed through 20 cm resin column of Dowex 1×8 by KCl solution in exponential gradient concentration of 2×10^{-3} M to 0.6 M Each fraction: 10 ml, sample taken: 53.2 mg.

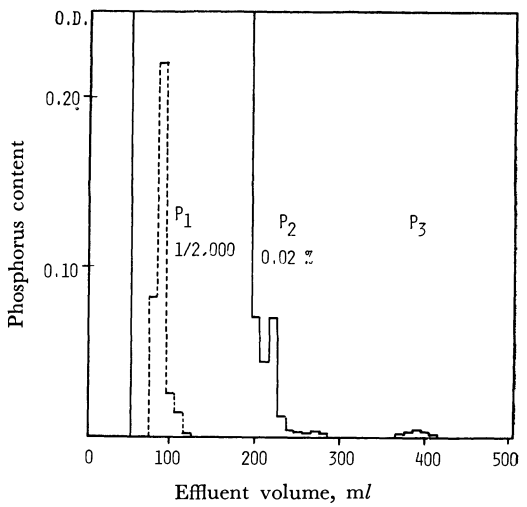

Fig. 2. Ion-exchange chromatogram of $NaHPO_4\cdot 12H_2O$ developed under the same condition as Fig. 1, sample taken: 42 mg.

triphosphate products are summarized in Table 1. A considerable amount of monophosphate is included as an impurity in a variety of triphosphate products, probably because the chemical treatment of repeated dissolutions and precipitations brings about a partial degradation of the triphosphate products.

2. Standardization of Polyphosphate Analysis. The separation of polyphosphates into their components can be achieved by anion-exchange chromatography according to their step-by-step rising negative charge on the $H_2P_nO_{3n+1}^{n-}$ ion. The resolution among them depends on the partition of polyphosphate between the resin and liquid phases, and its distribution coefficient, K_d, is defined by Eq. (2):[15]

Table 1. Composition analysis of tripolyphosphate and pyrophosphate products in P% unit

Sample	Phosphate species				
	P_1, %	P_2, %	P_3, %	$P_{4,5}$, %	$P_{6,\ etc.}$
$Na_5P_3O_{10}\cdot 6H_2O$	0.035	0.163	99.8	0.026	0.011
$Na_5P_3O_{10}$	0.50	8.07	87.25	0.95	3.23
Commercial triphosphate	3.60	47.61	41.77	7.02	0.0
$(NH_4)_5P_3O_{10}$*	0.06	0.19	99.6	0.15	0.02
$Na_8Mn(P_3O_{10})_2$**	0.77	1.05	97.7	0.38	0.08
$Na_8Co(P_3O_{10})_2$**	1.56	5.11	93.0	0.30	0.0
Commercial metaphosphoric acid	13.5	17.4	13.8	24.6	30.7
$Na_4P_2O_7\cdot 10H_2O$	0.10	99.8	0.05	0.03	0.01
$Na_4P_2O_7$	0.20	96.75	1.69	1.36	—

* Prepared by substitution of sodium ion with ammonium ion on the ammonium ion form cation exchange-resin.

** Precipitated from the solution containing 1 mol of manganese chloride and and 2 mol of sodium triphosphate hexahydrate with 20% alcohol and crystallized from hot water.

15) S. Ohashi, K. Koguchi and H. Waki, *J. Chromatogr.*, **25**, 398 (1968).

$$K_d = (V_f - V_m)/(V_b - V_m) \quad (2)$$

The effluent volume, V_f, at a break-through point was determined from the appearance of a concentration peak, while the holding-up volume, V_m, in the column was measured by pouring 2 N hydrochloric acid through the column until the indicator added to the recipient changed color. Since the total resin-bed volume, V_b, is given by our experimental conditions, the net volume of the charged resin is, then found to be $(V_b - V_m)$ by measuring the difference. In our routine work, both 20 cm- and 60-cm columns were employed in comparing the results in detail, assuming $V_m =$ 10 m*l* for the first and 30 m*l* for the second.

As Beukenkampf *et al*,[16] have pointed out, the K_d value of a polyphosphate ion species, $H_2P_nO_{3n+1}^{n-}$, obeys the rule of *n*-power inverse proportionality with regard to the chloride concentration, [Cl$^-$], in the exchange reaction (3):

$$R_n(H_2P_nO_{3n+1}) + Cl^- = n \cdot RCl + H_2P_nO_{3n+1}^{n-} \quad (3)$$

This rule is a valuable guide for determining the polymerization number, $\bar{n}$ of the species found in a chromatogram, particularly in the analysis of a polyphosphate sample lacking several members of an unknown $\bar{n}$. To the first approximation, the activity of the chloride in the resin, [RCl], can be regarded as unity, because a greater part of the resin phase is in the form of RCl; therefore:

$$K_d = [R_n(H_2P_nO_{3n+1})]/[H_2P_nO_{3n+1}^{n-}]$$
$$= [RCl]^n/K \cdot [Cl^-]^n = 1/K \cdot [Cl^-]^n$$

or

$$\log K_d = -\log K - n \cdot \log [Cl^-] \quad (4)$$

where K denotes the ion-exchange selectivity coefficient. In accord with this rule, K_d values were obtained from the data on the gradient elution of a polyphosphate sample with the mean-chain number of ten, as is shown in Table 2. The agreement is surprisingly good; a constant value of 0.15 ± 0.03 was obtained for the sum $(\log K_d + n \cdot \log[Cl^-])$ if a non-integer number of polymerization is allowed to serve for the assignment of the *n*th polymer of a suspicious peak, very close to a distinct maximum, as is shown in Fig. 3.

However, a negative deviation of the calculated *n* in Eq. (4) was observed in the data by the use of a 60-cm column charged with Dowex 1×4, especially for higher members of polyphosphate, even though the agreement is quite excellent for the first three members, ortho-, pyro-, and triphosphates. A picture of the chromatogram pattern of the same sample developed through the use of a 60-cm resin column is shown in Fig. 4. In so far as we have observed, it is likely that the unfavored conditions are related to the incomplete attainment of the exchange equilibrium, involving a shift of the K_d value to the negative side by the use of the 60-cm column.

By taking the polyphosphate sample with a mean chain number of ten as the standard reference, two products of polyphosphate with six and twenty links of phosphate were tested in order to find if the mean chain number coincides with the average composition of polyphosphate obtained from the chromatographic data. As is shown in Figs. 5—7, the largest peak lies at nearly the effluent volume corresponding to its mean chain number, while the distribution of the members is

Table 2. Distribution coefficient, $K_d = (V_f - V_m)/(V_b - V_m)$, of polyphosphates on 20-cm anion exchange resin column Dowex 1×8

Peak number (assumed chain no.)	Retention volume V_f m*l*	K_d	[Cl$^-$] M	$\log K_d + n \cdot \log$ [Cl$^-$] (calculated for assumed chain number)
1	90	8.0	0.17	0.13
2	150	14.0	0.26	0.10
3	245	23.5	0.39	0.14
4	310	30.0	0.46	0.13
5	325	31.5	0.46_2	0.14
6 (5.5)*	345	33.5	0.50	0.27 (0.13)**
7 (6.5)*	380	37.0	0.53	0.07 (0.14)**
8 (7)	395	38.5	0.54_5	0.39 (0.18)
9 (7)	405	39.5	0.55_5	0.70 (0.19)
10 (9)	480	47.0	0.62	0.37 (0.17)
11 (10)	510	50.0	0.64	0.39 (0.20)
12 (10)	535	52.5	0.64	0.38 (0.13)
				mean $(0.15_4 \pm 0.03)$**

* No distinct peaks.
** Calculated for well unresolved peaks under assumption of a half-integer polymer chain number.

16) J. Beukenkampf, W. Rieman and S. Lindenbaum, *Anal. Chem.*, **26**, 505 (1954).

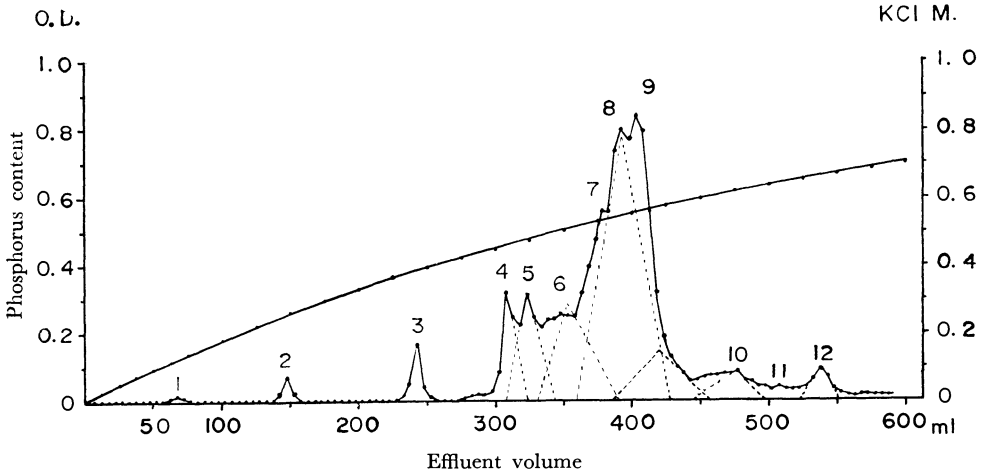

Fig. 3. Chromatogram of sodium polyphosphate with stoichiometric mean chain number of ten, developed through 20 cm resin column of Dowex 1×8.
The peaks, including several inconspicuous ones, are numbered in the order of their appearance and the corresponding *n*th polymer was assigned to a peak on the basis of of K_d value (see Table 2).
Sample under heat treatment at 800°C for 12 hr.

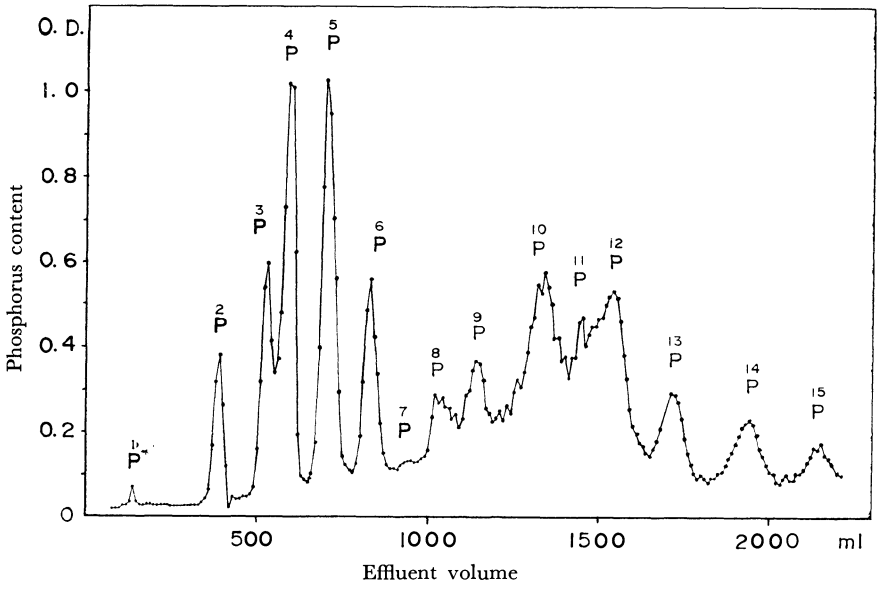

Fig. 4. Chromatogram of sodium polyphosphate with stoichiometric mean chain number of ten, developed through 60 cm column of Dowex 1×4.
Sample prepared under heat at 650°C for 12 hr

not of a Gaussian type. They contained, on the one hand, a considerable amount of low polymers with three to six links and, on the other hand, very high polymers. It should be emphasized here that preparing a polyphosphate with a normalized distribution of polymer components around its mean chain number is very hard, even for a lower polyphosphate product with six to twenty chains which has a melting point lower than long-chain Graham salt.

3. Calculation of the Mean Chain Number from the Chemical Composition. The mean chain number of a polyphosphate product is determined by end-group titration or by the viscosity measurement of its solution as a function of the molecular weight. More directly, the mean $\bar{n}$ can be calculated from the data of chemical analysis. The amount of the constituent members present in a given mean $\bar{n}$ product is evaluated by the colorimetry of Molybdenum-blue in optical-

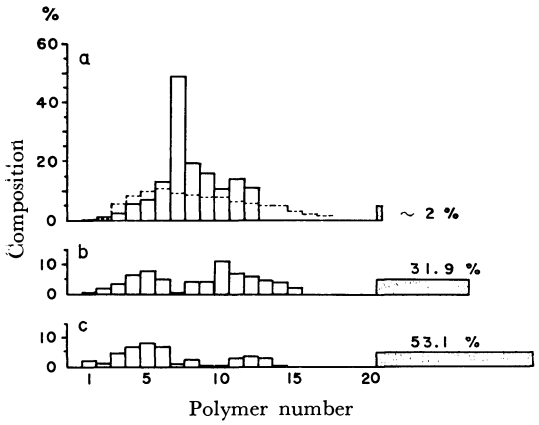

Fig. 5. Comparison of polymer ingredients in polyphosphate products of stoichiometric $\bar{n}=10$, prepared (a) commercial product (b) at 650°C for 12 hr, (c) at 650°C for 1 hr, by chromatographic analysis.

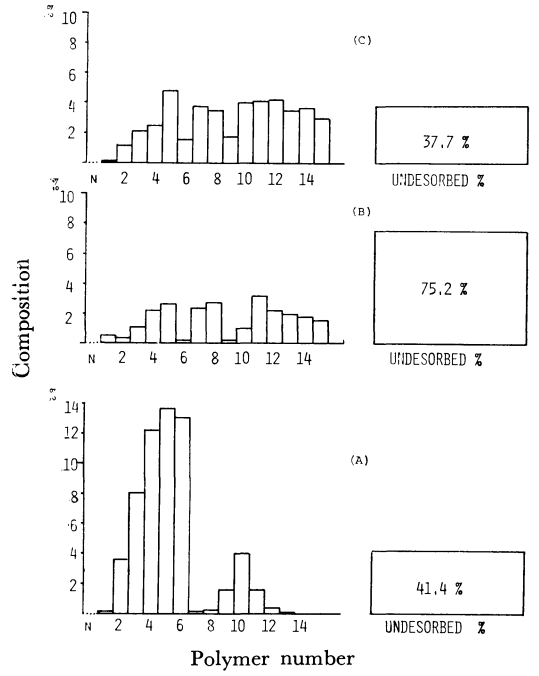

Fig. 6. Composition of polymers in polyphosphate products of $\bar{n}=6$ (A), 20 (B and C), prepared (A) 650°C, 12 hr, (B) 650°C, 1 hr, (C) 650°C 12 hr.

Chromatographic analysis under the same condition as Fig. 5.

density units, denoted here by x_n, which is proportional to the phosphorus content in the resolved nth polymer. The molar abundunce is, then, (x_n/n) for each nth polymer, while the mean value of n for a polyphosphate mixture is described by (5):

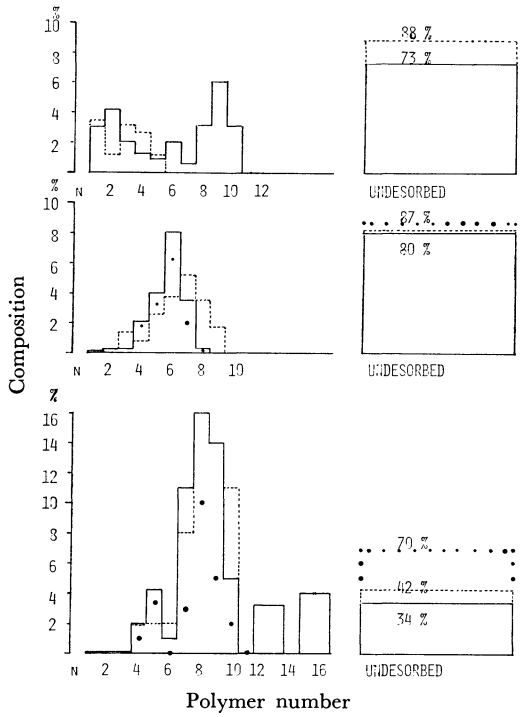

Fig. 7. Composition of polymers in Graham salt, prepared at (A) 800°C 3 hr (B) 850°C 12 hr (C) the sample as (B) irradiated in 2 MW reactor for 20 to 40 min.

Chromatographic analysis under the same condition as Fig. 5 and Fig. 6.

$$\bar{n} = \sum_1^\infty x_n / \sum_1^\infty (x_n/n) = 1/\sum_1^\infty (x_n/n) \qquad (5)$$

In practice, the greater the number of n in (5), the smaller the (x_n/n) value, and the latter value can be ignored in the calculation of the mean $\bar{n}$ value from (5) for uneluted fractions of a very high polymer. This approximation is valid in our case so long as the polyphosphate product has a mean chain length not greater than twenty. However, more than half of the higher members are left uneluted in the analysis of Graham salt. Accordingly, the mean $\bar{n}$ computed from the analysis of a developed chromatogram is surely underestimated, although a lower limit for $\bar{n}$ can be decided by means of the equation expressed in (6), where the suffix below $\bar{n}_l$ indicates the last number of n so far eluted throughout the resin column:

$$\bar{n}_l = \sum_1^l x_n / \sum_1^l (x_n/n) \qquad (6)$$

The calculated $\bar{n}$ values are displayed in Table 3, along with the lower limit, $\bar{n}_l$, as determined by (6), which must serve as a reference for the validity of the estimated $\bar{n}$ values. The difference between the values of $\bar{n}$ estimated under the above assumption and the lower limit, $\bar{n}_l$, is of no problem for a polyphosphate of a small $\bar{n}$, but the disagree-

Table 3. Mean chain number of polyphosphate products

Mixing of (NaH_2PO_4/Na_2HPO_4) molar ratio	Stoichiometric mean no.	Heat °C	Treatment hr	Observed mean number $\bar{n}_c$ chromatography	$\bar{n}$	$\bar{n}_v$ viscosity	Uneluted fraction x_f	Mean $\bar{n}$ calculated by (7)
1/2	3	650	12	2.90	(2.90)	u.m.		
2	6	650	12	7.4	(4.4)	u.m.	0.41	
4	10			6.4	(6.3)	18	0.02	6.5
		650	12	9.6	(8.8)	20	0.32	11.5
		650	1	10	(4.7)		0.53	
9	20	650	12	15.4	(10.2)	26	0.38	18.7
		650	1	20	(9.6)		0.52	
Metaphosphoric acid		800	0.5	9.5	(5.0)	58	0.48	15.8
Graham Salt		800	3	11.2	(7.7)	110	0.31	15.6
		800	3	12.7	(7.2)	98	0.42	20.4
		800	3	15.5	(6.5)	89	0.70	37
		850	12	30.5	(6.0)	100	0.82	82
		850	12	62	(4.5)	100	0.93	96
		750	24	40	(5.5)	100	0.86	83
		750	24	65	(4.5)	100	0.93	96

Table 4. Comparison of K_d of phosphorus oxy-acids on anion-exchange resin, Dowex 1×8 (by column method)

Oxidation state phosphorus oxy-acid (Blaser notation[21])	Acetate method: Retention volume V_f, ml	[Ac^-] M	K_d	$K_d \times$[Ac^-]	Chroride method: Retention volume V_f, ml	[Cl^-] M	K_d	$K_d \times$[Cl^-]	Selectivity coefficient ($K_d \times$[Ac^-]/$K_d \times$[Cl^-])
^{1}P	100±5*	0.28	19	5.3	60±10*	0.10	5.0	0.50	$10._1$
^{5}P	180±10*	0.36	35	12.6	80±10*	0.12	7.0	0.84	15
^{3}P	230±10*	0.40	45	18.0	90±10*	0.16	9.0	1.45	$12._4$
^{4}P–^{4}P	355±10*	0.48	70	33.6	123±5*	0.19	11.3	2.09	16
^{2}P–^{4}P	420±20*	0.52	83	43.2	160±5*	0.23	15	3.45	$12._4$
									mean 13

* Average deviation of V_f for ten experiments.

ment is conceivable for the Graham salt. For the sake of comparison, the mean chain number, $\bar{n}$, of polyphosphate was computed by means of viscosity measurements; the results are represented in the middle column of Table 3. These data indicate that the viscosity measurements are liable to evaluate too highly the mean $\bar{n}$ number for the lower homologue of polyphosphate. This is probably because the viscosity method is based on the interaction between long-chain polymer molecules and because the contribution of lower polymers to the viscosity is disregarded.

4. Analysis of Oxyphosphorus Acid in a Lower Oxidation State. By the use of a Molybdenum(V)+(VI) reagent[17] incorporated with acid sulfite[18] to facilitate the colorimetry of phosphorus, many oxyphosphorus acids with low oxidation numbers can be observed in a chromatogram developed by the usual method described above. The elution order of the lower oxidation species is: hypophosphite($\overset{1}{P}$), phosphite($\overset{3}{P}$), hypophosphate (P_2) and diphosphite($\overset{2\ 4}{P\text{-}P}$), and other polymerized oxyphosphorus acids with low oxidation numbers. all these non-polymerized species without bridged oxygen (P–O–P) behave like a monomer species in the chromatography, as is evidenced by the effluent volumes of hypophosphate and diphosphite, which are located very close to that of orthophosphate in the developed chromatographic pattern.

The distribution coefficients, K_d, of this series are shown in Table 4; they have been obtained from the data obtained both on the 20-cm resin column in the chloride form and on the 10-cm column in the acetate form. As may be seen in Table 4, the K_d values on the acetate resin are found to be several times larger than those on the chloride resin. A favorable condition is anticipated by the use of a resin bed in the acetate form from the point of view of mutual separation; however, the ammonium acetate reagent used for elution proved to cause an unadvisable contamination of phosphorus, which increased the reagent blank in our chromatogram. The radiometric technique used as this occasion has, though, caused no trouble, and has provided good results for computing the phosphorus content by means of the radioactivity of ^{32}P. The difference in K_d values between the ammonium acetate and potassium chloride methods can be interpreted in terms of their selectivity coefficients. The results of the comparison of these two methods, shown in Table 4, indicate that the two K_d values differ by the factor, of 13, which is in good agreement with the selectivity coefficient of the acetate ion to the chloride-form resin of Dowex 1×8.[19]

Discussion

As may be seen in Table 1, the commercial products named metaphosphate and metaphosphoric acid and formulated as MPO_3 and HPO_3 respectively, contain polyphosphate in a diverse composition. No PO_3^- ion is substantiated as a stable anion, taking part in the hydrolysis and condensation reactions, although such an ion is frequently assumed to be a transient intermediate in interpreting the kinetic behavior of phosphate derivatives. In general, the polyphosphate anion, $H_2P_nO_{3n+1}^-$, is characterized as a PO_3^- donor in an aqueous medium, while orthophosphate and lower members of polyphosphate behave like PO_3^- acceptors under limited conditions of a strongly dehydrated and acid medium. The identity of the lower polymers of phosphate with three to six links, appearing in considerable yields throughout the hydrolysis process of Graham salt, has been established by several authors.[11,12] It appears likely that there exists a polymer unit with chain or ring numbers of three to six in the intermediate stage of the alkaline hydrolysis of a long-chain polymer, and that a similarity exists in the dehydration of a single phosphate into a polymer. The quite high yields of the lower members in contrast to the low yields of the middle members of polyphosphate, as established in this work, reflect the important role played by the lower polymer in the condensation process. This means that the growth of the chain length needs a certain amount of phosphates with a low polymerization, one of them three to six. This coincides with the fact that the eutectic mixture has a composition corresponding to hexapolyphosphate, with a (NaH_2PO_4/Na_2HPO_4) ratio around two and with a melting point of 550°C. The contribution of the low-members of polyphosphate to the chemical composition was, thus, emphasized in correctly com puting the average number of links in polyphosphate in relation to the structure and the kinetic behavior of polyphosphate. The viscosity data, on the other hand, underestimate this contribution, since the viscosity is mostly decided by the long-chain polymers alone and is little affected by the presence of a solute with a low molecular weight. In view of the above points, and by a combination of two complimentary contributions, a more accurate evaluation of the mean chain number, $\bar{n}$, is possible on the basis of the data of

17) F. Lucena-Conde and L. Prat, *Anal. Chim. Acta*, **16**, 473 (1957).

18) N. Yoza and S. Ohashi, This Bulletin, **37**, 33, 37 (1964).

19) H. P. Gregor, J. Bell and R. A. Marcus, *J. Amer. Chem. Soc.*, **77**, 2713 (1955).

20) E. J. Grifith and R. L. Buxton, *ibid.*, **89**, 2884 (1967).

21) B. Blaser, *Z. Anor. Allg. Chem.*, **300**, 225 (1959).

the chromatographic analysis as well as those of the viscosity measurement, by the following relation (7):

$$1/\bar{n} = (1-x_f)/\bar{n}_c + x_f/\bar{n}_v \quad (7)$$

Equation (7) can be interpreted in terms of $\bar{n}_c$, the mean chain number as computed by chromatographic analysis, and $\bar{n}_v$, that based on the visocity data, where x_f is the fraction of phosphorus content belonging to the high-polymer group that could not be desorbed by our chromatographic technique. The assumption previously introduced for computing a mean $\bar{n}$ from the chromatographic data was that x_f, the high-polymer fraction, was considered to be. On this assumption, the $\bar{n}$ in (7) is exactly equal to $\bar{n}_c$. The results of the computation of $\bar{n}$, represented in the last column of Table 3, provide a reasonable way to correct the discrepancy in the data between those obtained by chromatographic analysis and those obtained by viscosity measurements.

BULLETIN OF THE CHEMICAL SOCIETY OF JAPAN VOL. 43 2858—2862 (1970)

The Copolymerization of Dimethallylidenepentaerythritol and Dicrotylidenepentaerythritol with Maleic Anhydride*[1]

Tatsuro OUCHI and Masayoshi OIWA*

* *Department of Applied Chemistry, Faculty of Engineering, Kansai University, Senriyama, Suita-shi, Osaka*

(Received October 14, 1969)

Dimethallylidenepentaerythritol (DMAPE) and dicrotylidenepentaerythritol (DCPE) have been copolymerized with maleic anhydride (Manh), using benzoyl peroxide as an initiator. From the results of the UV spectrum concerning the rate of copolymerization, it was found that the copolymerization might proceed on the *pseudo*-terpolymerization of the charge transfer complex-allylidene group-Manh. The following functional group reactivity ratios were calculated at 60°C in these systems:

DMAPE(M_1)-Manh(M_2)
$r_{1c}K=0.77$, $r_{2c}K=0.058$
$r_1=0.05$, $r_2=0.025$
DCPE(M_1)-Manh(M_2)
$r_{1c}K=0.89$, $r_{2c}K=0.057$
$r_1=0.02$, $r_2=0.020$

It has already been pointed out that maleic anhydride (Manh) is copolymerized alternately with various vinyl monomers.[1-10]

In a previous experiment paper,[11] the copolymerization of diallylidenepentaerythritol (DAPE) and Manh was carried out as one of a series of studies of the copolymerization of DAPE; then the behavior of the radical copolymerization was investigated by means of kinetic equations derived by assuming a *pseudo*-tersystem.

On the other hand, 2-vinyl-1,3-dioxolane (VDOL) has been further copolymerized with Manh, and the difference in the copolymerizations between mono- and di-allylidene cyclic acetal compounds with Manh has been studied.[12]

In this paper, the copolymerizations of dimethallylidenepentaerythritol (DMAPE) and dicrotylidenepentaerythritol (DCPE), which are α,α'- and β,β'-substitution products of DAPE respectively, with Manh will be reported; the functional reactivity ratios will be estimated, and the in-

*1 Studies of Polymerization of Diallylidenepentaerythritol. VIII.

1) T. Alfrey and C. C. Price, *J. Polym. Sci.*, **2**, 101 (1947).
2) C. C. Price, *ibid.*, **1**, 83 (1946).
3) C. C. Price, *ibid.*, **3**, 772 (1948).
4) C. C. Price, *Discuss. Faraday Soc.*, **2**, 304 (1947).
5) P. D. Bartlett and K. Nozaki, *J. Amer. Chem. Soc.*, **68**, 1495 (1946).
6) C. Walling, E. R. Briggs, K. B. Woltsirn and F. R. Mayo, *ibid.*, **70**, 1537, 1544 (1948).
7) F. R. Mayo and C. Walling, *Chem. Rev.*, **46**, 191 (1950).
8) F. M. Lewis, C. Walling, W. Cumming, E. R. Briggs and E. R. Mayo, *J. Amer. Chem. Soc.*, **70**, 1519 (1948).
9) S. Iwatsuki and Y. Yamashita, *Makromol. Chem.*, **89**, 205 (1965); **104**, 263 (1967).
10) S. Iwatsuki and Y. Yamashita, *J. Polym. Sci., Part A-1*, **5**, 1753 (1967).
11) T. Ouchi and M. Oiwa, *Kogyo Kagaku Zasshi*, 1713, **73**, (1970).
12) T. Ouchi and M. Oiwa, *ibid.*, **73**, 1717 (1970).

fluence of substituents on the reactivity of copolymerization will be discussed.

Experimental

Materials. The DMAPE and DCPE were synthesized by a previously-reported method.[13] The Manh was purified by the recrystallization and vacuum distillation of a commercial product.

The benzoyl peroxide (BPO) used as an initiator and the solvents were purified by the conventional method.

Copolymerization Procedure. A glass ampoule was charged with prescribed amounts of each monomer, BPO, and benzene in such a way that the concentration of DMAPE or DCPE was kept constant. The ampoule was then sealed off under a vacuum and set in a thermostated water bath at 60±0.1°C, without stirring, for the time necessary to give less than 10% of conversion. A hydroquinone/benzene solution was added to the reaction solution to inhibit further polymerization, and the polymer was precipitated from an excess of dehydrated ether. The polymer thus obtained was washed repeatedly with ether in the Soxhlet extractor and dried under reduced pressure to a constant weight.

Analysis of the Copolymer. The composition of the resulting copolymer was determined by C and H elementary analysis. The residual unsaturation was calculated by the determination of the bromine value of the resulting copolymer according to a previously-described method.[14]

The UV spectrum was measured by means of an Ito Chodenpa apparatus, Model QU-3, in chloroform with a quartz cell over the range of 352—358 mμ and at room temperature.

Results and Discussion

The Ratio of "Charged" to "Reacted" Vinyl Groups. The copolymerizations were carried out at 60°C under various concentrations and ratios of the functional groups in the monomer feed. The relations among the residual unsaturation and the monomer and copolymer compositions are plotted in Figs. 1 and 2. From Figs. 1 and 2, it can be found that the DMAPE or DCPE mole fraction in copolymer increases with an increase in that in the monomer over the range of 0.3—0.4, and also with an increase in the feed concentration of DMAPE or DCPE. On the other hand, the residual unsaturation of the polymer tends to decrease with a decrease in the DMAPE or DCPE mole fraction and in the concentration in the monomer feed.

When all the allylidene-compound units in a copolymer have unreacted pendant double bonds without any cyclization or crosslinking, the ideal bromine values of the copolymer are indicated by BV_{id}; the ratio of the experimental bromine

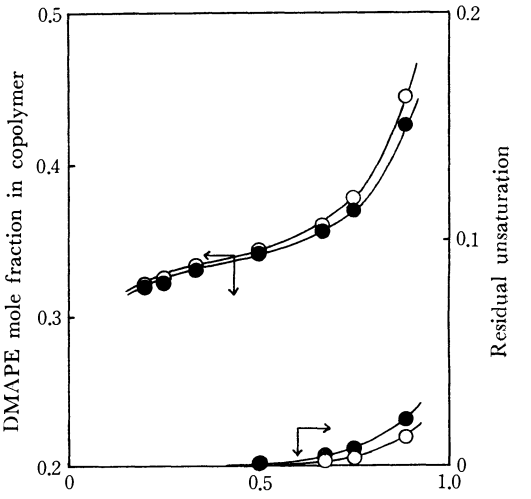

Fig. 1. Relation of the monomer compositions to the copolymer composition and the residual unsaturation.
(DMAPE-Manh)
○: (DMAPE) = 0.208 mol/*l*
●: (DMAPE) = 0.416 mol/*l*

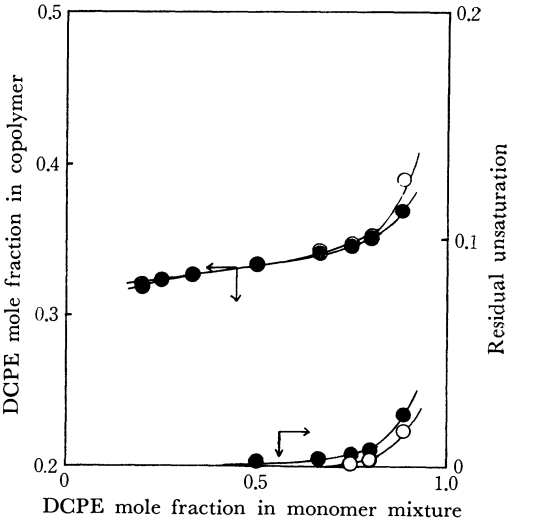

Fig. 2. Relation of the monomer composition to the copolymer composition and the residual unsaturation.
(DCPE-Manh)
○: (DCPE) = 0.277 mol/*l*
●: (DCPE) = 0.555 mol/*l*

value (BV_{ex}) to BV_{id}, that is, BV_{ex}/BV_{id}, indicates the residual unsaturation.

When the concentrations of the allylidene compounds and the Manh in the copolymer are $d(M_1)$ and $d(M_2)$, and when those of the allylidene group and the Manh in it are $d(m_1)$ and $d(m_2)$ respectively, the following relation may be obtained:

$$d(m_1)/d(m_2) = (2-BV_{ex}/BV_{id})d(M_1)/d(M_2)$$

The relations between charged and reacted vinyl

13) T. Ouchi, S. Tatsuno, T. Nakayama and M. Oiwa, This Bulletin, **43**, 2241 (1970).
14) T. Ouchi and M. Oiwa, *Kogyo Kagaku Zasshi*, **72**, 746 (1969).

groups are plotted in Figs. 3 and 4. The reacted methallylidene- or crotylidene-group fraction tends to increase with an increase in the charged methallylidene- or crotylidene-group fraction, and also with a decrease in its concentration. It may be expected that the formation of the CT complex is related to the propagation reaction.

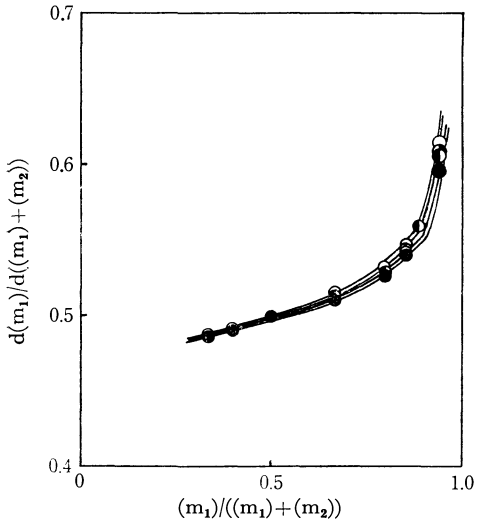

Fig. 3. The relation between charged and reacted vinyl group fraction.
DMAPE(M_1)—Manh(M_2)
○: $(m_1)=0.416$ vinyl group/l
◐: $(m_1)=0.554$ vinyl group/l
◑: $(m_1)=0.666$ vinyl group/l
●: $(m_1)=0.832$ vinyl group/l
—: logical curves

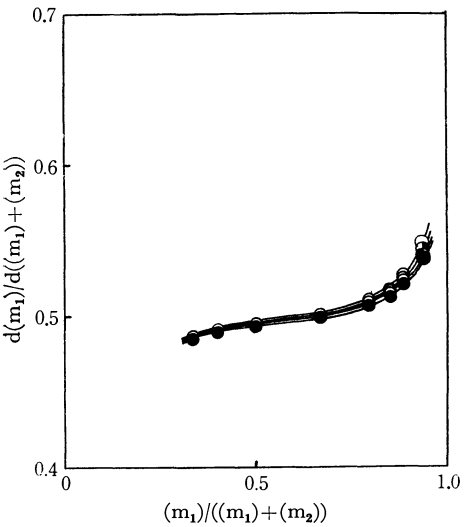

Fig. 4. The relation between charged and reacted vinyl group fraction.
DCPE(M_1)-Manh(M_2)
○: $(m_1)=0.554$ vinyl group/l
◐: $(m_1)=0.668$ vinyl group/l
◑: $(m_1)=0.832$ vinyl group/l
●: $(m_1)=1.110$ vinyl group/l
—: logical curves

The Relation between the Charged Composition and the Rate of Copolymerization. The dependence of the monomer composition and concentration upon the rate of copolymerization is shown in Fig. 5. The rate of copolymerization reaches a maximum at the feed ratio of 1 : 2, regardless of the monomer concentration.

A similar tendency was also recognized in the DCPE-Manh system.

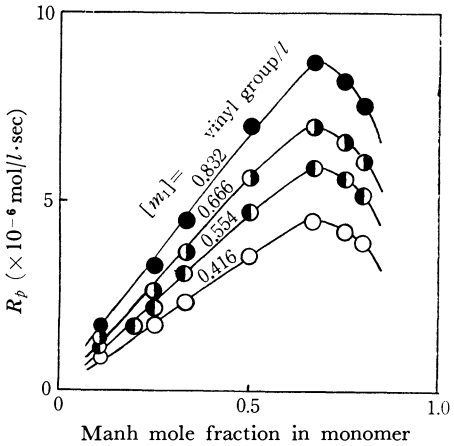

Fig. 5. Plots of the rate of copolymerization against the monomer composition in benzene at 60°C.
DMAPE-Manh

The Continuous-variation Method. The Q and e values for the functional group of DMAPE have already been calculated as 0.05 and −0.48, while those of DCPE have been obtained as 0.01

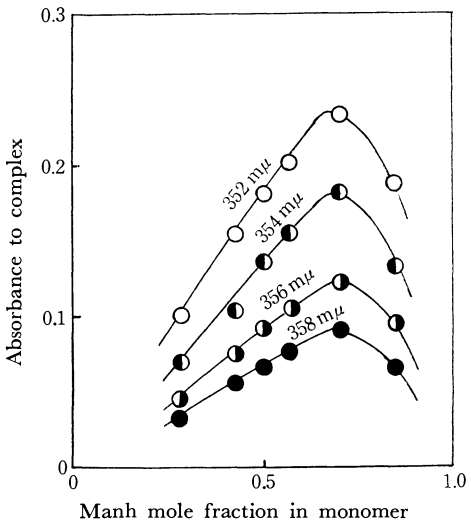

Fig. 6. The continuous variation method.
DMAPE-Manh
Solvent: chloroform, room temp.

and −0.32, respectively.[15] As the Q and e values of Manh are also 0.23 and 2.25,[16] the complex formation between such monomer pairs may be expected. Further, when DMAPE and Manh were mixed, no color appeared, but it was found according to the optical analysis, that is, according to the continuous-variation method, that a 1 : 2 complex formation occurred between the monomer[17] (Fig. 6).

A similar tendency was observed in the DCPE-Manh system.

These molecular complexes are probably CT complexes with the following structure, if we can make an analogy with the results of *p*-dioxen and Manh:[9-10]

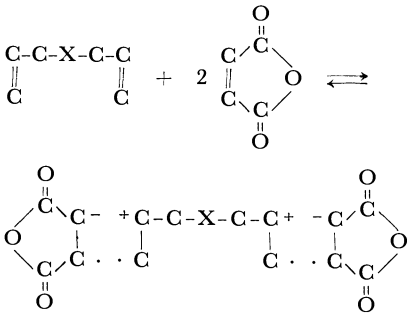

CT Complex

The Kinetic Analysis. The copolymerizations of DMAPE and DCPE with Manh were kinetically investigated by a previously-reported method.[1]

The *pseudo*-terpolymerization of the CT complex-allylidene group-Manh is dealt with assuming that the complex is attacked on the side of Manh, assuming that the active growing chain ends become allylidene radicals. Here, m_1 denotes an allylidene group; m_2, Manh; C or m_1m_2, the complex; $m_1\cdot$, an allylidene radical, and $m_2\cdot$, a Manh radical. The following elementary reactions can then be presumed to hold in the copolymerization of these allylidene compounds and Manh:

		Rate Const.
Complex Formation	$m_1 + m_2 \rightleftarrows m_1m_2(C)$	k_1, k_{-1}
Propagation	$m_1\cdot + C \rightarrow m_1\cdot$	k_{1c}
	$m_1\cdot + m_1 \rightarrow m_1\cdot$	k_{11}
	$m_1\cdot + m_2 \rightarrow m_2\cdot$	k_{12}
	$m_2\cdot + C \rightarrow m_1\cdot$	k_{2c}
	$m_2\cdot + m_1 \rightarrow m_1\cdot$	k_{21}
	$m_2\cdot + m_2 \rightarrow m_2\cdot$	k_{22}

If a steady state is assumed for the radicals and the complex, Eq. (1) can be derived:

$$\frac{F}{1-f} = A\left(\frac{1}{B+F}\right)\left(\frac{f}{1-f}\right) - C \qquad (1)$$

where $r_1=k_{11}/k_{12}$, $r_2=k_{22}/k_{21}$, $r_{1c}=k_{1c}/k_{12}$, $r_{2c}=k_{2c}/k_{21}$, $K=k_1/k_{-1}$, $F=(m_1)/(m_2)$, $f=d(m_1)/d(m_2)$, and

$$A = \frac{r_{2c}K(m_1)+r_2}{r_1},\quad B = r_{2c}K(m_1),\quad C = \frac{r_{1c}K(m_1)+1}{r_1} \qquad (2)$$

The values of A, B, and C can be obtained by the trial-and-error method according to Eq. (1). The relation of $F/(1-f)$ *vs.* $f/(1-f)(B+F)$ is plotted in Fig. 7, when (m_1) is the 0.666 vinyl group/l on the DMAPE-Manh system. It is found that a straight line is obtained when B is 0.04. Therefore, A and C are estimated to be 1.30 and 31.3 respectively from this slope and intercept. A similar example of the DCPE-Manh system is shown in Fig. 8.

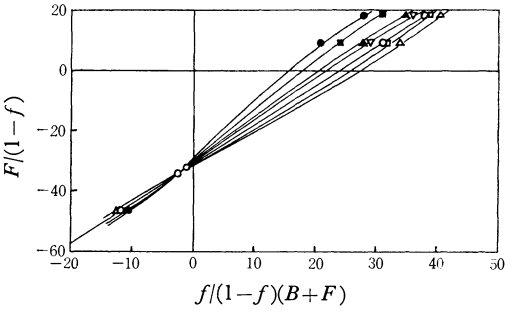

Fig. 7. Plots of $F/(1-f)$ *vs.* $f/(1-f)(B+F)$.
DMAPE-Manh
$[m_1]$=0.666 vinyl group/l
△ B=0, □ B=0.03, ○ B=0.04
▽ B=0.08, ▲ B=0.10, ■ B=0.20
● B=0.30

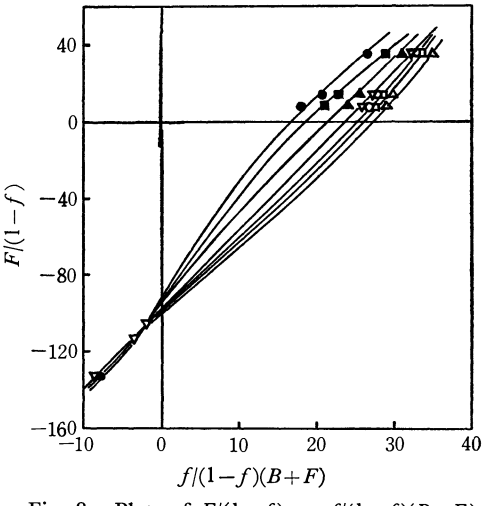

Fig. 8. Plots of $F/(1-f)$ *vs.* $f/(1-f)(B+F)$.
DCPE-Manh
(m_1)=1.110 vinyl group/l
△ B=0, □ B=0.03, ○ B=0.05,
▽ B=0.06, ▲ B=0.10, ■ B=0.20,
● B=0.30

15) T. Ouchi, S. Tatsuno, T. Nakayama and M. Oiwa, *Kogyo Kagaku Zasshi.*, **73**, 607 (1970).
16) G. E. Ham, "Copolymerization," Interscience Pub., New York (1964), p. 859.
17) P. Job, *Ann. Chim.*, **9**, 113 (1928).

By varying the m_1 concentration, the *A*, *B*, and *C* values are obtained by the same procedure; the relations among *A*, *B*, and *C* *vs.* (m_1) are plotted in Figs. 9—11. Straight lines are obtained in every case, as was expected on the basis of Eq. (2).

From these slopes and intercepts, the parameters of copolymerization can be estimated to be as in Table 1.

From Table 1, it can be found that $r_{1c}K$ values became DAPE < DMAPE < DCPE, and that r_1 and r_2 values decreased unlike as in the case of $r_{1c}K$ in the order of DCPE < DMAPE < DAPE.

The values of r_{1c}, r_{2c} were much larger than those of r_1 and r_2 in allylidene compounds-Manh systems because the *K* values were presumed to be very small; therefore, it seemed that the propagation radicals reacted preferentially with the functional groups of the complex rather than with the monomer. If the *K* values are taken to be equal in these systems, such a tendency was observed in the order of DAPE < DMAPE < DCPE; the influence of an α- or β-methyl group on the reactivity of the functional group was thus recognized. Since the $r_{1c}K$ values were larger than $r_{2c}K$, $K_{1c} > K_{2c}$; this suggests that the addition rate of allylidene radicals to the complex is larger than that of Manh radicals, as had been expected.

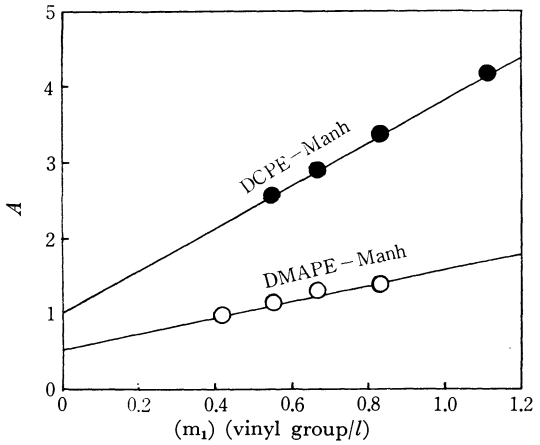

Fig. 9. Plots of *A* *vs.* (m_1).

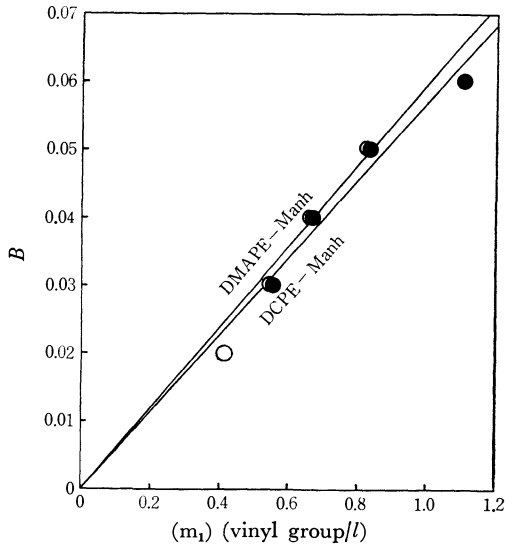

Fig. 10. Plots of *B* *vs.* (m_1).

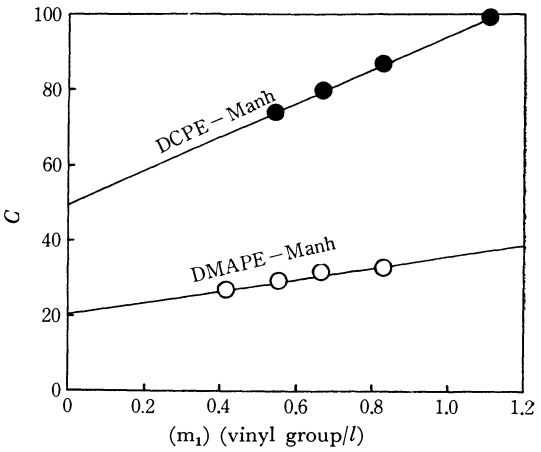

Fig. 11. Plots of *C* *vs.* (m_1).

Table 1. The parameters of copolymerization

M_2	$r_{1c}K$	$r_{2c}K$	r_1	r_2
DMAPE	0.77	0.058	0.05	0.025
DCPE	0.89	0.057	0.02	0.020
DAPE	0.76	0.055	0.08	0.030

The curves of the relation between charged and reacted vinyl group fractions agreed well with the experimental results shown in Figs. 3 and 4.

Summarizing the above results, three significant facts can be pointed out:

1) DMAPE or DCPE and Manh are copolymerized easily with a radical initiator to give the alternating copolymer, whereas neither one can be polymerized with a radical initiator. 2) The rate of copolymerization reaches a maximum at the feed ratio of 1 : 2. 3) The formation of the 1 : 2 CT complex between DMAPE or DCPE and Manh may proceed by way of a *pseudo*-terpolymerization of the allylidene group - Manh - the CT complex.

BULLETIN OF THE CHEMICAL SOCIETY OF JAPAN VOL. 43 2863—2870 (1970)

The Polymerization of Di-(β-methacrylyloxypropionaldehyde)-pentaerythritolacetal*[1]

Tatsuro OUCHI, Yorihiro IMASE and Masayoshi OIWA*

** Department of Applied Chemistry, Faculty of Engineering, Kansai University, Senriyama, Suita-shi, Osaka*

(Received October 18, 1969)

The polymerization of di-(β-methacrylyloxypropionaldehyde)-pentaerythritolacetal (DβMPP) and the copolymerizations of DβMPP with styrene (St) and acrylonitrile (AN) have been carried out at 60°C, using benzoyl peroxide as an initiator. They have then been discussed kinetically from the point of view of cyclopolymerization. The results can be summarized as follows:

1) The relation among the rate of polymerization, R_p, the initiator concentration, (I), and the monomer concentration, (M), can be expressed by the following equations;

$$R_p/(\mathrm{I})^{1/2} = A(\mathrm{I})^{1/2} + B$$
$$R_p/(\mathrm{M}) = C(\mathrm{M}) + D$$

where A, B, C, and D are constant.

2) The ratio of the rate constant of the unimolecular cyclization reaction to that of the bimolecular propagation reaction of the uncyclized radical, k_c/k_p, was 22.0 mol/l.

3) The copolymerization of DβMPP proceeded primarily by means of cyclocopolymerization, and the ratio of the cyclization rate to the vinyl propagation also decreased with an increase in the comonomer fraction in the copolymer.

4) The following reactivity ratios were estimated on the basis of the Smets-Roovers equation:

System	$K_c=k_c/k_{11}$	$K_c'=k_c/k_{12}$	$r_1=k_{11}/k_{12}$	$r_2=k_{22}/k_{21}$	$r_c=k_{c1}/k_{c2}$
DβMPP(M_1)-St(M_2)	12.7	2.54	0.20	0.35	0.32
DβMPP(M_1)-AN(M_2)	12.7	5.08	0.40	0.35	0.61

As one of a series of studies of the polymerization of diallylidenepentaerythritol (DAPE), di-(β-methacrylyloxypropionaldehyde)-pentaerythritol (DβMPP) was prepared from DAPE and methacrylic acid; it was then confirmed to be a pure product. Although a patent has been previously published regarding the synthesis of DβMPP, its method is still far from clear.[1] On the present paper, it is well known that divinyl-compounds undergo cyclopolymerization.[2-4]

In the present paper, the polymerization of DβMPP will be discussed kinetically from the point of view of cyclopolymerization by modifying the Minoura and Mitoh method,[3] and the correlation with the rate constants will be investigated.

The copolymerizations of DβMPP with styrene (St) and acrylonitrile (AN) will also be carried out, and then the reactivity ratios will be estimated according to the Roovers and Smets procedure.[5]

Experimental

Materials. DβMPP was prepared as follows. A mixture of 310 g (1.46 mol) of DAPE, 372 m*l* (4.38 mol) of methacrylic acid, and 0.3 g of *p*-toluenesulfonic acid as an initiator was heated in a flask fitted with a reflux condenser at 55—60°C for 8—10 hr, the mixture was then washed with water to remove any unreacted methacrylic acid. Benzene was added, whereupon two layers formed; the product remaining in the benzene layer was separated and treated with sodium hydrosulfite to remove the dark color. After the benzene had been distilled under reduced pressure, the residual solution was filtered through an activated silica-charcoal layer to remove any haziness and foreign particles. The final product gave 90% of a light brown liquid and was confirmed to be DβMPP by the determination of the infrared spectrum, the molecular weight (MW), the saponification value (SV), and the bromine value (BV). $d_D^{20}=1.1353$, $n_D^{20}=1.4735$.

Found: C, 59.29; H, 7.41%; MW, 382.3; BV, 84.99; SV, 289.9. Calcd for $C_{19}H_{28}O_8$: C, 59.36; H, 7.34%; MW, 384.4; BV, 83.14; SV, 291.9.

St and AN, used as the comonomers, benzoyl per-

*1 Studies of the Polymerization of Diallylidenepentaerythritol. IX.

1) F. Fekete, U. S. 2975156 (1961).
2) C. Aso, T. Nawata and H. Kamao, *Makromol. Chem.*, **68**, 1 (1963).
3) Y. Minoura and M. Mitoh, *J. Polym. Sci., Part-A*, **3**, 2149 (1965).
4) S. G. Matsoyan, *ibid.*, **52**, 189 (1961).
5) J. Roovers and G. Smets, *Makromol. Chem.*, **60**, 89 (1963).

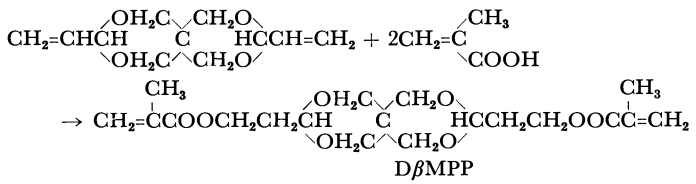

DβMPP

oxide (BPO), and the solvents were purified by the conventional method.

Polymerization Procedure. A glass ampoule was charged with the prescribed amount of each monomer, a solvent, and BPO; it was then degassed, sealed off under a vacuum, and set, without stirring, in a thermostated water bath at 60±0.1°C. The reaction solution was poured into a large amount of petroleum ether, and the polymer which was thus precipitated was centrifuged, filtered, and then dried *in vacuo* until a constant weight was attained. The conversion was less than 10%. The homopolymer was then purified from benzene-petroleum ether. The copolymers obtained on DβMPP-St and DβMPP-AN systems were also reprecipitated from benzene-petroleum ether and acetone-petroleum ether respectively.

Analyses of the Polymer and Copolymer. The polymer was dissolved in benzene, saponified in excess alcoholic potassium hydroxide, and neutralized with hydrochloric acid; then the residual unsaturation of the polymer was determined by the method of Siggia.[6] The molecular weight of the polymer was determined by means of a vapor-pressure osmometer (Hewlett Packard Model-302) at 37°C, using benzene as the solvent.

The composition of the resulting copolymer was determined by C, H, and N elementary analysis. The residual unsaturation of the copolymer was also calculated according to the Siggia method.[6]

The infrared spectra were measured by applying the potassium bromide-pellet technique to the polymer and the salt-plate method to the monomer on a Shimadzu infared spectrophotometer, Model IR-27.

The Kinetics of Polymerization

The preliminary experiment showed that the rate of the cyclization reaction was larger than that of the propagation reaction of the uncyclized radical on the polymerization of DβMPP. Therefore, the kinetics of the polymerization of DβMPP was discussed according to a modification of the Minoura *et al.* procedure.

The kinetic equations on the following reaction scheme were derived by assuming a steady-state condition:

		Rate const.	
Decomposition of initiator	$I \rightarrow 2R\cdot$	k_d	(1)
Initiation	$R\cdot + M \rightarrow M\cdot$	k_i	
Cyclization	$M\cdot \rightarrow M_c\cdot$	k_c	
Propagation	$M\cdot + M \rightarrow M\cdot$	k_p	
	$M_c\cdot + M \rightarrow M\cdot$	k_{cp}	
Termination	$M_c\cdot + M_c\cdot \rightarrow P_c$	$\alpha^2 k_t$	
	$M_c\cdot + M\cdot \rightarrow P_c'$	$\alpha\beta k_t$	
	$M\cdot + M\cdot \rightarrow P$	$\beta^2 k_t$	

where I denotes an initiator; M, a monomer; P_c, P_c', and P, the polymers; R·, the initiator radical; M·, the uncyclized radical, and M_c·, the cyclized radical. α and β are certain constants introduced to simplify the following algebraic treatment; the rate constants of the three termination reactions are, of course, determined by the values of α and β.

Here the crosslinking may be neglected as having been treated with the initial state.

If a steady state is assumed for the different types of radicals, Eqs. (2)—(4) can be obtained:

$$(R\cdot) = fk_d(I)/k_i(M) \tag{2}$$

$$(M\cdot) = \frac{(2/\alpha)(2fk_d/k_t)^{1/2}(I)^{1/2}\{k_{cp}(M)+(\alpha/2)(2fk_dk_t)^{1/2}(I)^{1/2}\}}{k_c+(2\beta/\alpha)\{k_{cp}(M)+(\alpha/2)(2fk_dk_t)^{1/2}(I)^{1/2}\}} \tag{3}$$

$$(M_c\cdot) = \frac{(k_c/\alpha)(2fk_d/k_t)^{1/2}(I)^{1/2}}{k_c+(2\beta/\alpha)\{k_{cp}(M)+(\alpha/2)(2fk_dk_t)^{1/2}(I)^{1/2}\}} \tag{4}$$

or $$\alpha(M_c\cdot) + \beta(M\cdot) = (2fk_d/k_t)^{1/2}(I)^{1/2} \tag{5}$$

Here, f denotes the efficiency of the initiator.

The Rate Polymerization. Consequently, the rate of polymerization is given in Eq. (6);

$$\begin{aligned} R_p &= -\mathrm{d}(M)/\mathrm{d}t \\ &= 2k_p(M\cdot)(M) + 2k_{cp}(M_c\cdot)(M) \qquad (6) \\ &= (2k_{cp}/\alpha)(2fk_d/k_t)^{1/2}(I)^{1/2}(M) \\ &\quad \times \frac{1+(2k_p/k_{cp})\{(k_{cp}/k_c)(M)+(\alpha/2k_c)(2fk_dk_t)^{1/2}(I)^{1/2}\}}{1+(2\beta/\alpha)\{(k_{cp}/k_c)(M)+(\alpha/2k_c)(2fk_dk_t)^{1/2}(I)^{1/2}\}} \qquad (7) \end{aligned}$$

Eqaution (7) can be developed as:

$$R_p = R_o\{1+(a-b)x-b(a-b)x^2+\cdots\cdots\} \tag{8}$$

where:

$$R_o = (2k_{cp}/\alpha)(2fk_d/k_t)^{1/2}(I)^{1/2}(M)$$

$$a = 2k_p/k_{cp},\ b = 2\beta/\alpha$$

and:

$$x = (k_{cp}/k_c)(M) + (\alpha/2k_c)(2fk_dk_t)^{1/2}(I)^{1/2} \tag{9}$$

From the results of the investigation of residual unsaturation, it was found that the rate of cyclization was far faster than that of propagation, namely,

$$k_c(M\cdot) \gg k_p(M\cdot)(M) \tag{10}$$

Therefore,

6) S. Siggia, "Quantitative Organic Analysis *via* Functional Groups," 3rd ed., J. Wiley & Sons, New York and London (1963), p. 301.

$$k_c \gg k_p(\mathrm{M}) \tag{11}$$

Both k_p and k_{cp} may be assumed to be almost of the same order. Equation (11) is, then given by:

$$k_c \gg k_{cp}(\mathrm{M}) \tag{12}$$

The second term of x in Eq. (9) is rewritten as:

$$(\alpha/2k_c)(2fk_dk_t)^{1/2}(\mathrm{I})^{1/2} = (\alpha/2k_c)k_t^{1/2}R_i^{1/2} \tag{13}$$

where R_i is the rate of initiation.

Generally, R_i is of an order of about 10^{-8}, and k_t is about 10^8—10^6; then, $\alpha \leq 1$ in the case of a radical polymerization such as is described in this experiment. Therefore, the second term of x in Eq. (9) is influenced only by $1/k_c$.

As will be described later, the value of k_p/k_c is 0.046 l/mol. The rate constant of the propagation reaction in radical polymerization is in the range of 10—10^3; therefore, the value of $1/k_c$ is very small.

In view of these considerations, x is very small, and x^2, x^3 and other higher terms in Eq. (8) may be neglected.

Considering this approximation, R_p may be indicated as in the following equation:

$$\begin{aligned} R_p &= R_0\{1+(a-b)x\} \\ &= (2k_{cp}/\alpha)(2fk_d/k_t)^{1/2}(\mathrm{M}) \\ &\quad \times [1+\{2k_p/k_{cp}-(2\beta/\alpha)\}\{(k_{cp}/k_c)(\mathrm{M}) \\ &\quad + (\alpha/2k_c)(2fk_dk_t)^{1/2}(\mathrm{I})^{1/2}\}] \end{aligned} \tag{14}$$

Accordingly, if the monomer concentration is kept constant and the initiator concentration is varied, Eq. (14) can be written as follows:

$$R_p/(\mathrm{I})^{1/2} = A(\mathrm{I})^{1/2} + B \tag{15}$$

where:

$$\begin{aligned} A &= (k_{cp}/k_c)(2fk_d)(2k_p/k_{cp}-2\beta/\alpha)(\mathrm{M}) = \text{const.} \\ B &= (2k_{cp}/\alpha)(2fk_d/k_t)^{1/2}(\mathrm{M}) \\ &\quad \times \{(2k_p/k_{cp}-2\beta/\alpha)(k_{cp}/k_c)(\mathrm{M})+1\} = \text{const.} \end{aligned} \tag{16}$$

Similarly, when the initiator concentration is kept constant and the monomer concentration is varied, Eq. (14) can be written as follows:

$$R_p/(\mathrm{M}) = C(\mathrm{M}) + D \tag{17}$$

where:

$$\left.\begin{aligned} C &= (2k_{cp}/\alpha)(2fk_d/k_t)^{1/2}(2k_p/k_{cp}-2\beta/\alpha)(k_{cp}/k_c)(\mathrm{I})^{1/2} \\ &= \text{const.} \\ D &= (k_{cp}/k_c)(2fk_d)(2k_p/k_{cp}-2\beta/\alpha)(\mathrm{I}) \\ &\quad + (2k_{cp}/\alpha)(2fk_d/k_t)^{1/2}(\mathrm{I})^{1/2} = \text{const.} \end{aligned}\right\} \tag{18}$$

The Residual Unsaturation of the Polymer. On the other hand, the rate of the formation of the pendant double bonds in the polymer is given by:

$$\mathrm{d(m)/d}t = 2k_p(\mathrm{M}\cdot)(\mathrm{M}) + 2k_{cp}(\mathrm{M}_c\cdot)(\mathrm{M}) - k_c(\mathrm{M}\cdot) \tag{19}$$

From Eqs. (6) and (19), we obtain:

$$\mathrm{d(m)/d(M)} = 1 - \frac{k_c(\mathrm{M}\cdot)}{2(\mathrm{M})(k_p(\mathrm{M}\cdot)+k_{cp}(\mathrm{M}_c\cdot))} \tag{20}$$

The combination of Eqs. (3), (4), and (20) gives:

$$\frac{1}{(\mathrm{M})(1-\mathrm{d(m)/d(M)})} - \frac{k_p}{k_c} = \frac{k_{cp}}{2k_{cp}(\mathrm{M})+\alpha(2fk_dk_t)^{1/2}(\mathrm{I})^{1/2}}$$

which, on rearrangement, gives:

$$\frac{1}{1-2R_{us}} - \frac{1}{1+E(\mathrm{I})^{1/2}/2(\mathrm{M})} = (2k_p/k_c)(\mathrm{M}) \tag{21}$$

where:

$$2R_{us} = \mathrm{d(m)/d(M)},\quad E = \alpha(2fk_dk_t)^{1/2}k_{cp}$$

Results and Discussion

Polymerization of DβMPP. The conditions and the results of polymerization are summarized in Tables 1 and 2. From these tables, it is obvious that the rate of polymerization is not proportional to the square root nor to the first power of the initiator concentration, nor is it proportional to either the first or the second power of the monomer concentration, as was to be expected from Eqs. (15) and (17).

Table 1. Results of polymerization of DβMPP in benzene at 60°C, (M)=1.48 mol/l

(I) ($\times 10^{-3}$ mol/l)	R_p ($\times 10^{-6}$ mol/l·sec)	BV*	$2R_{us}$*	$\bar{P}_n$*
10.0	12.8	4.24	0.102	107
7.50	11.0	4.28	0.103	124
5.00	9.05	4.32	0.104	155
2.50	6.36	4.45	0.107	223
1.20	4.40	4.53	0.109	310

* The values were obtained by extrapolating to zero for the conversion.

Table 2. Results of polymerization of DβMPP in benzene at 60°C, (I)=5.00×10^{-3}mol/l

(M) (mol/l)	R_p ($\times 10^{-6}$ mol/l·sec)	BV*	$2R_{us}$*	$\bar{P}_n$*
2.95	19.1	7.98	0.192	342
2.22	14.0	6.82	0.164	243
1.48	9.05	4.32	0.104	155
1.03	6.18	2.62	0.063	105
0.738	4.31	2.04	0.049	71

* The value were obtained by extrapolating to zero for the conversion.

Since the value of residual unsaturation, $2R_{us}$, was very small, the rate of the cyclization reaction might be far faster than that of the propagation reaction. That is, the residual unsaturation decreased with a decrease in the monomer concentration.

Influence of the Initiator and Monomer Concentrations on the Rate of Polymerization. When the monomer concentration is varied, it may

be kinetically expected from Eq. (15) that the plots of $R_p/(\mathrm{I})^{1/2}$ *vs.* (I) will be a straight line.

Similarly, if the initiator concentration is kept constant and the monomer concentration is varied, a linear relationship between $R_p/(\mathrm{M})$ and (M) may be expected on the basis of Eq. (17).

The results are plotted in Fig. 1, in which the fit of the experimental data to the linear relationship is fairly good. From the slopes and intercepts of the straight line shown in Fig. 1, *A*, *B*, *C*, and *D* were estimated to be 7.00×10^{-6}, 1.27×10^{-4}, 2.65×10^{-7}, and 5.68×10^{-6} respectively. Thus, the following ratios of the rate constant were calculated from the above values:

$$2fk_d = 6.95\times10^{-5}\ \mathrm{sec}^{-1}$$

$$2k_{cp}/\alpha\sqrt{k_t} = 1.14\times10^{-2}\ l^{1/2}/\mathrm{mol}^{1/2}\cdot\mathrm{sec}^{1/2}$$

$$(2k_p/k_{cp}-2\beta/\alpha)(k_{cp}/k_c) = 4.52\times10^{-2}\ l/\mathrm{mol}$$

Here, $2fk_d$ of the order of 10^{-5} seems to be pertinent when BPO is used as an initiator.

On the other hand, $2k_{cp}/\alpha\sqrt{k_t}$ of the order of 10^{-2} suggests that the termination between two $\mathrm{M}_c\cdot$ may be very fast. Therefore, $(2k_p/k_{cp}-2\beta/\alpha)(k_{cp}/k_c)$ of the order of 10^{-2} may be presumed to be much cyclized by this polymerization.

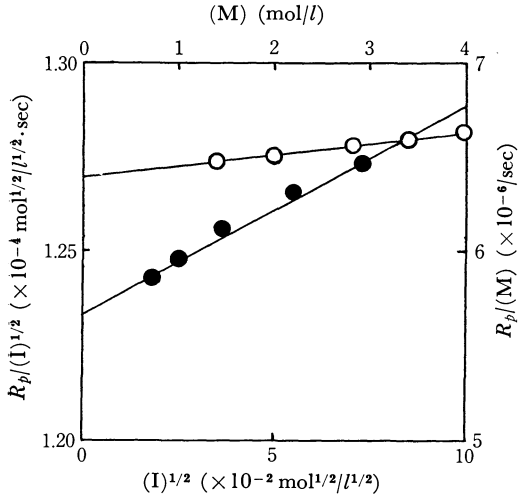

Fig. 1. Plots of $R_p/(\mathrm{I})^{1/2}$ *vs.* (I)$^{1/2}$ and $R_p/(\mathrm{M})$ *vs.* (M).

The Residual Unsaturation. If the monomer concentration is kept constant, the residual unsaturation is almost independent of the initiator concentration; the ratio of cyclization is almost never related to the initiator concentration, as is shown in Table 1. The ratio of the rate constant of the unimolecular cyclization reaction to that of the bimolecular propagation of the uncyclized radical, k_c/k_p, was evaluated by means of Eq. (21). E was then calculated to be 1.46 mol$^{1/2}/l^{1/2}$ on the basis of the previous rate constants. Accordingly, the plots of $\{1/(1-2R_{us})-(1+\mathrm{E(I)}^{1/2}/2(\mathrm{M}))\}$ *vs.* (M) are shown in Fig. 2; there is a good

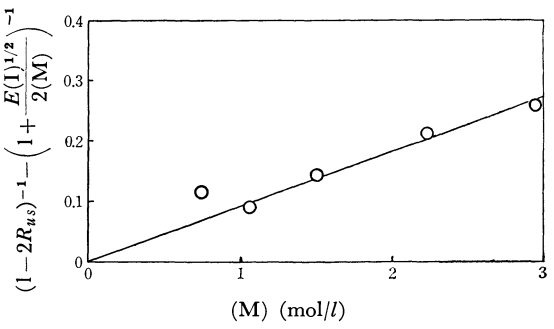

Fig. 2. Plots of $\left\{(1-2R_{us})^{-1}-\left(1+\frac{E(\mathrm{I})^{1/2}}{2(\mathrm{M})}\right)^{-1}\right\}^{-1}$ *vs.* (M).

linear relationship, as was predicted by Eq. (21). The k_c/k_p value was estimated to be 22.0 mol/l from the slope of the straight line.

As the rate of cyclization was larger than the propagation of uncyclized radicals, the previous kinetic equations may be suitable for the polymerization of DβMPP. By combining k_c/k_p and $(2k_p/k_{cp}-2\beta/\alpha)(k_{cp}/k_c)$, the following rate constant could be obtained;

$$(k_{cp}/k_c)(2\beta/\alpha) = 4.58\times10^{-2}\ l/\mathrm{mol}$$

Accordingly, it was presumed that the propagation of the cyclized radical was almost equal to that of uncyclized radicals.

The degree of polymerization, $\bar{P}_n$, is small, and it then decreases with a decrease in the monomer concentration and with an increase in the initiator concentration, as is shown in Tables 1 and 2.

Copolymerization Results. The curves of the monomer and copolymer compositions are shown in Fig. 3. It was found that the azeotropic copolymers were prepared in both systems; Dβ-MPP was copolymerized with St and AN. On the other hand, it might be seen that the rate of copolymerization had a minimum, but was almost

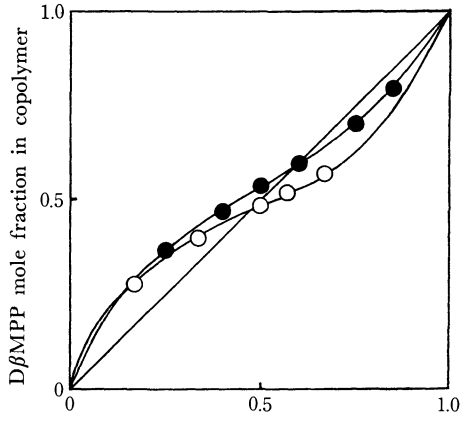

Fig. 3. Monomer - copolymer composition curves.
○: DβMPP-St, ●: DβMPP-AN,
—: calculated curve

independent of the monomer composition.

The Residual Unsaturation of the Copolymer. The ideal bromine value of the copolymer denotes BV_{id} when all the DβMPP units in polymer have pendant double bonds without any cyclization or crosslinking reaction, and the ratio of the experimental bromine value (BV_{ex}) to BV_{id} defines the residual unsaturation. Accordingly, the value of BV_{ex}/BV_{id} becomes 1.0 without any cyclization or crosslinking reaction, and it then decreases with an increase in those reactions.

The relation between the copolymer composition and the residual unsaturation is shown in Fig. 4. It was found that the residual unsaturation decreased with an increase in the DβMPP mole fraction in the copolymer, while the degree of cyclization increased. Such a tendency was more obvious in DβMPP-AN than in DβMPP-St because St was polymerized more easily than AN.

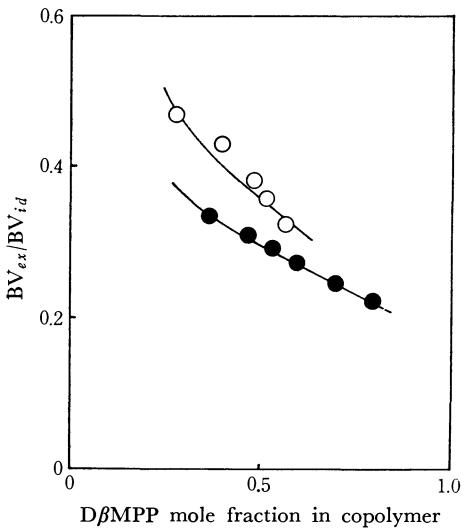

Fig. 4. Correlation of the copolymer composition to the residual unsaturation.
○: DβMPP-St, ●: DβMPP-AN,
—: calculated curve

The Determination of the Reactivity Ratio. The degree of cyclization to propagation was very large in those copolymerizations, as has been described previously.

Although the apparent monomer reactivity ratios could be calculated by the well-known Fineman-Ross method, the true monomer reactivity ratios could not be obtained.

In this experiment, the Smets-Roovers equation was applied to these copolymerizations, and then the reactivity ratios were calculated.

That is, the following reaction scheme was based on these copolymerizations:

$$M_1\cdot + M_1 \rightarrow M_1\cdot \qquad k_{11}(M_1\cdot)(M_1)$$
$$M_1\cdot + M_2 \rightarrow M_2\cdot \qquad k_{12}(M_1\cdot)(M_2)$$

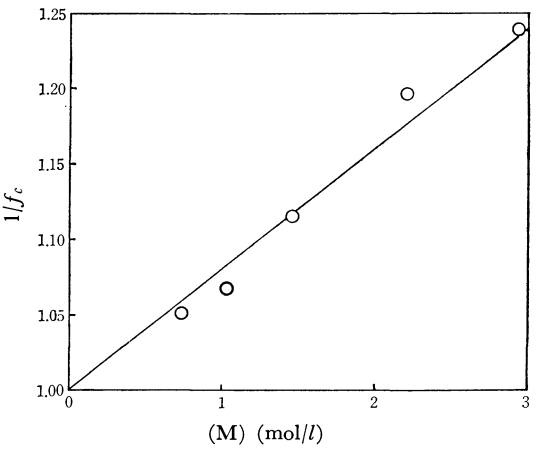

Fig. 5. Plots of $1/f_c$ *vs.* (M) on polymerization of DβMPP at 60°C; $[BPO]=5.00\times10^{-3}$ mol/l.

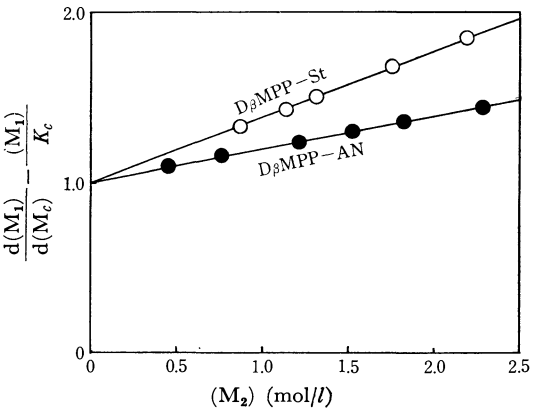

Fig. 6. Plots of $\left(\frac{d(M_1)}{d(M_c)}-\frac{(M_1)}{K_c}\right)$ *vs.* (M_2).

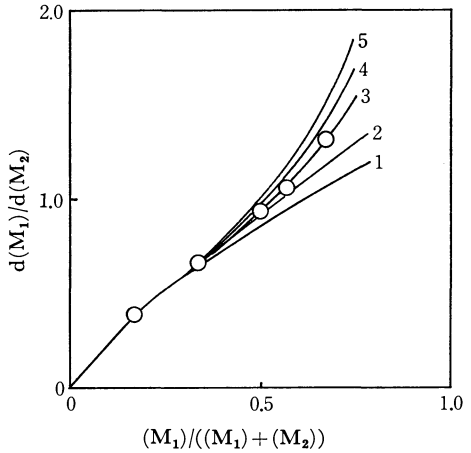

Fig. 7. Plots of $(M_1)/((M_1)+(M_2))$ *vs.* $d(M_1)/d(M_2)$.
DβMPP(M_1)-St(M_2)
$r_2=0.35$ 1: $r_c=0.10$, 2: $r_c=0.20$, 3: $r_c=0.30$
4: $r_c=0.40$, 5: $r_c=0.50$,
○: experimental value

$$M_1\cdot \rightarrow M_c\cdot \qquad k_c(M_1\cdot)$$
$$M_c\cdot + M_1 \rightarrow M_1\cdot \qquad k_{c1}(M_c\cdot)(M_1)$$
$$M_c\cdot + M_2 \rightarrow M_2\cdot \qquad k_{c2}(M_c\cdot)(M_2)$$
$$M_2\cdot + M_1 \rightarrow M_1\cdot \qquad k_{21}(M_2\cdot)(M_1)$$
$$M_2\cdot + M_2 \rightarrow M_2\cdot \qquad k_{22}(M_2\cdot)(M_2)$$

Here M_1 denotes a divinyl monomer; M_2, a comonomer; $M_1\cdot$ and $M_2\cdot$, the uncyclized radical, and $M_c\cdot$, the cyclized radical.

If a stationary state is assumed for the different types of radicals, Eqs. (22)—(24) can be derived:

$$\frac{d(M_1)}{d(M_2)} = \frac{(M_1)}{(M_2)} \times \frac{r_1(M_1)+(M_2)+K_c'}{\left\{r_2(M_2)+(M_1)+K_c'\left[\frac{r_2(M_2)+(M_1)}{r_c(M_1)+(M_2)}\right]\right\}} \quad (22)$$

$$\frac{d(M_1)}{d(M_c)} = 1 + \frac{(M_1)}{K_c} + \frac{(M_2)}{K_c'} \quad (23)$$

$$\frac{d(M_2)}{d(M_c)} = (M_2)\left\{1+r_2\frac{(M_2)}{(M_1)}\right\}\left\{\frac{1}{K_c'}+\frac{1}{r_c(M_1)+(M_2)}\right\} \quad (24)$$

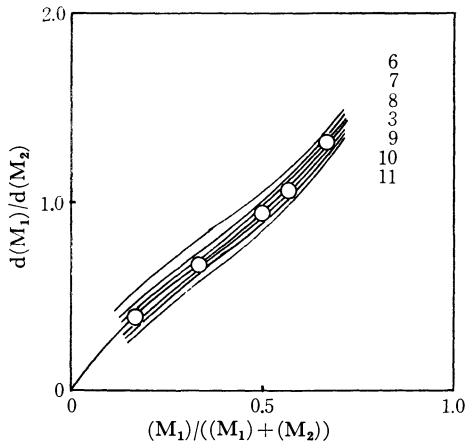

Fig. 8. Plots of $(M_1)/((M_1)+(M_2))$ *vs.* $d(M_1)/d(M_2)$.
DβMPP(M_1)-St(M_2)
$r_c=0.30$ 6: $r_2=0.20$, 7: $r_2=0.25$, 8: $r_2=0.30$
3: $r_2=0.35$, 9: $r_2=0.40$, 10: $r_2=0.45$
11: $r_2=0.50$, ○: experimental value

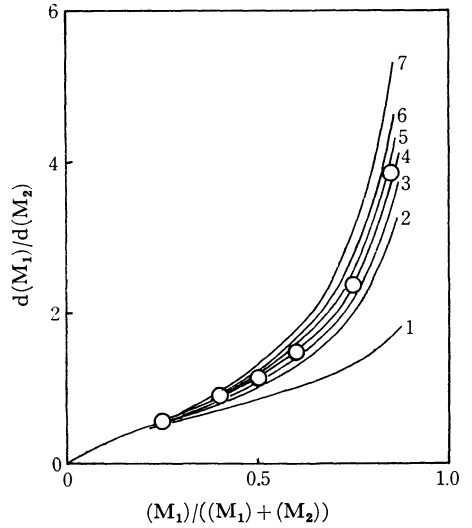

Fig. 9. Plots of $(M_1)/((M_1)+(M_2))$ *vs.* $d(M_1)/d(M_2)$.
DβMPP(M_1)-AN(M_2)
$r_2=0.35$ 1: $r_c=0.10$, 2: $r_c=0.40$, 3: $r_c=0.50$,
4: $r_c=0.60$ 5: $r_c=0.70$, 6: $r_c=0.80$,
7: $r_c=1.00$, ○: experimental value

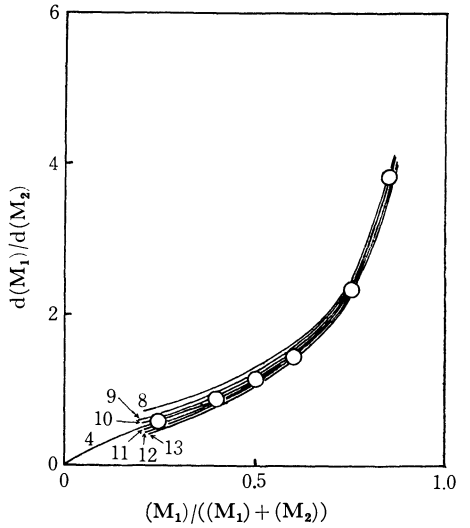

Fig. 10. Plots of $(M_1)/((M_1)+(M_2))$ *vs.* $d(M_1)/d(M_2)$.
$r_c=0.60$ 8: $r_2=0.20$, 9: $r_2=0.25$, 10: $r_2=0.30$,
4: $r_2=0.35$, 11: $r_2=0.40$, 12: $r_2=0.45$,
13: $r_2=0.50$, ○: experimental value

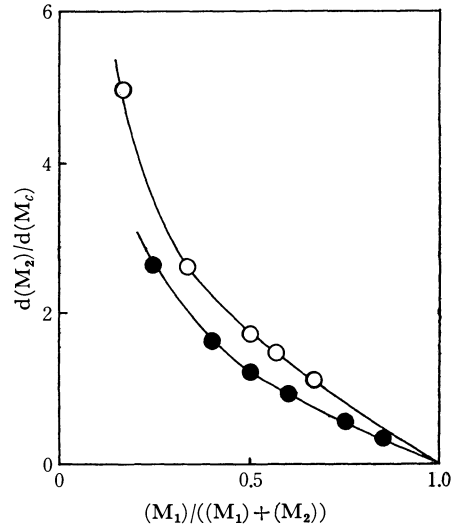

Fig. 11. Plots of $(M_1)/((M_1)+(M_2))$ *vs.* $d(M_2)/d(M_c)$.
○: DβMPP(M_1)-St(M_2)
●: DβMPP(M_1)-AN(M_2)
—: calculated curve

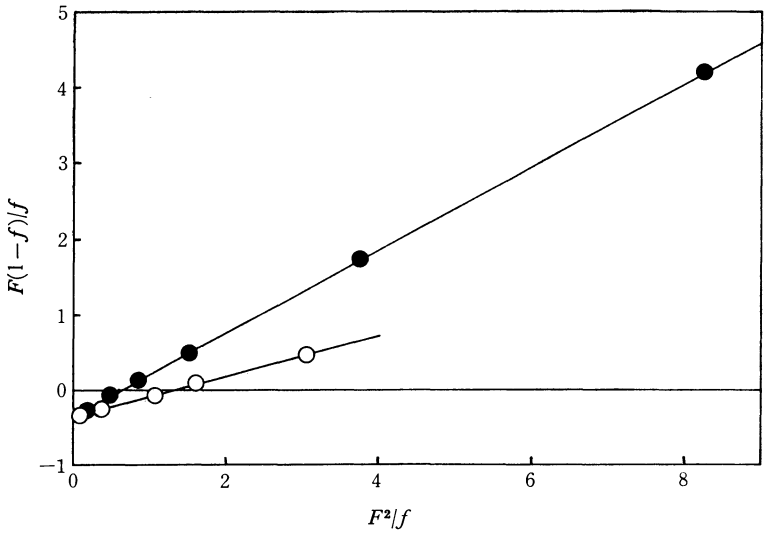

Fig. 12. Fineman-Ross plots.
○: DβMPP(M_1)-St(M_2), ●: DβMPP(M_1)-AN(M_2)

where $r_1=k_{11}/k_{12}$, $r_2=k_{22}/k_{21}$, $r_c=k_{c1}/k_{c2}$, $K_c=k_c/k_{11}$, and $K_c'=k_c/k_{12}$; d(M_1), d(M_2), and d(M_c) then denote M_1, M_2, and M_c respectively in the copolymer.

On the other hand, the relation between the fraction of cyclized units, f_c, and the monomer concentration is given in Eq. (25):

$$1/f_c = 1 + (M)/K_c \qquad (25)$$

The plots of $1/f_c$ *vs.* (M) are shown in Fig. 5 by using the data of the previously-reported homopolymerization of DβMPP; they have a good linear relationship, as was predicted from Eq. (25). K_c was estimated to be 12.7 mol/*l* from the slope of the straight line.

The correlations of $\{d(M_1)/d(M_c)-(M_1)/K_c\}$ to (M_2) are plotted in Fig. 6; they have a good linear relationship, and the K_c' values were calculated to be 2.54 on DβMPP-St and 5.08 on DβMPP-AN from these slopes.

From the values of K_c and K_c', the r_1 values were estimated to be 0.20 on DβMPP(M_1)-St(M_2) and 0.40 on DβMPP(M_1)-AN(M_2).

Then r_2 and r_c were determined from Eqs. (22) and (24) according to the trial-and-error method. The theoretical curves are compared with the experimental results in Figs. 7 and 8 (DβMPP-St) and Figs. 9 and 10 (DβMPP-AN). A good agreement between them is seen at $r_2=0.35$ and $r_c=0.30$ on DβMPP-St and $r_2=0.35$ and $r_c=0.60$ on DβMPP-AN.

By using these values, the relations between $(M_1)/((M_1)+(M_2))$ and $d(M_2)/d(M_c)$ are plotted in Fig. 11. The values calculated from Eq. (24) agreed very closely with the experimental values. Accordingly, the monomer reactivity ratios obtained might be proper for the copolymerizations.

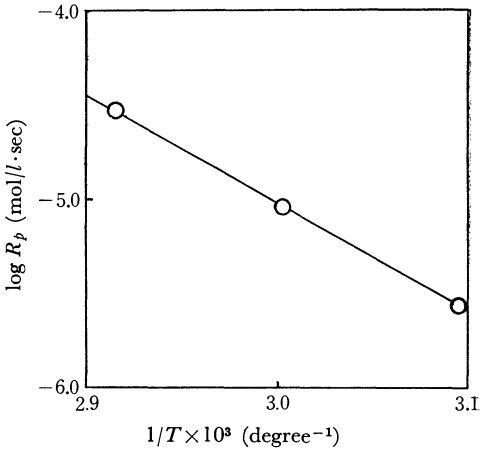

Fig. 13. Arrhenius plots.
(M)=1.48 mol/*l*, (I)=5.00×10⁻³ mol/*l*

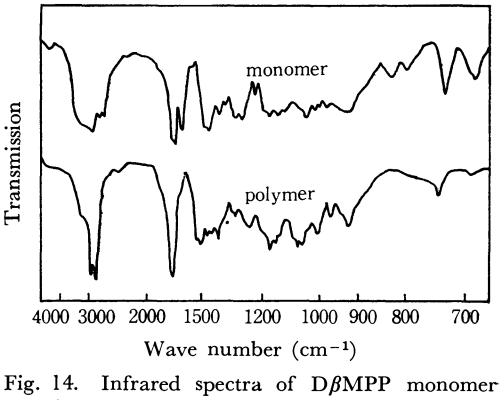

Fig. 14. Infrared spectra of DβMPP monomer and polymer.

If the cyclization and crosslinking reaction are neglected, the apparent monomer reactivity ratios can be obtained by the well-known Fineman-Ross method. The following results were estimated from the slopes and the intercepts of the straight line shown in Fig. 12:

$D\beta MPP(M_1)$-$St(M_2)$ $r_1'=0.27$, $r_2'=0.35$

$D\beta MPP(M_1)$-$AN(M_2)$ $r_1'=0.55$, $r_2'=0.35$

Activation Energy. To determine the overall activation energy, the polymerization of DβMPP was carried out at 50, 60, and 70°C. The plots of the logarithm of R_p *vs.* $1/T$ are shown in Fig. 13. The apparent activation energy was calculated to 26.5 kcal/mol from the slope of the obtained straight line. The value was almost equal to those of the normal vinyl polymerizations.

IR Spectrum. The infrared spectra of the resulting monomer and polymer are shown in Fig. 14. The absorption peaks at 1625, 1740, and 2930 cm^{-1} are assigned to C=C, >C=O, and CH_3 respectively. The absorptions of the cyclic acetal compound are also presented in the range of 1200—1040 cm^{-1}. In spite of the initial state, the C=C band at 1625 cm^{-1} on the polymer almost disappears; therefore, it was found that the cyclization reaction was preferential upon the polymerization of DβMPP.

On the other hand, DβMPP was gelated with a high conversion; we will later report on such crosslinking.

BULLETIN OF THE CHEMICAL SOCIETY OF JAPAN VOL. 43 2870—2873 (1970)

The Reactions of Phosphonium Ylides and Oxosulfonium Methylide with Sulfenamide Derivatives

Teruaki MUKAIYAMA, Takanobu KUMAMOTO, Shinichi FUKUYAMA and Takeo TAGUCHI

Laboratory of Organic Chemistry, Tokyo Institute of Technology, Ookayama, Meguro-ku, Tokyo

(Received November 19, 1969)

It was found that vinyl sulfide derivatives were obtained in good yields by the reactions of carbonyl compounds with α-phenylthioalkylidenetriphenylphosphorane. Phosphorane was prepared by the equimolar reaction of alkylidenetriphenylphosphorane and *N*-phenylthio-*N*-methylacetamide. It was established that, differing from the case of alkylidenetriphenylphosphorane, dimethyloxosulfonium methylide reacted with *N*-phenylthiophthalimide and *N*-phenylthiosuccinimide to give *N*-bis(phenylthio)methylphthalimide and *N*-bis(phenylthio)methylsuccinimide, respecitively.

It was recently reported that unsymmetrical ketones are synthesized in good yields *via* vinyl sulfide derivatives obtained from α-thioalkylidenetriphenylphosphorane and carbonyl compounds.[1] The phosphorane is successfully derived from 2 mol of alkylidenetriphenylphosphorane and 1 mol of sulfenyl chloride as shown in the following equation (1).

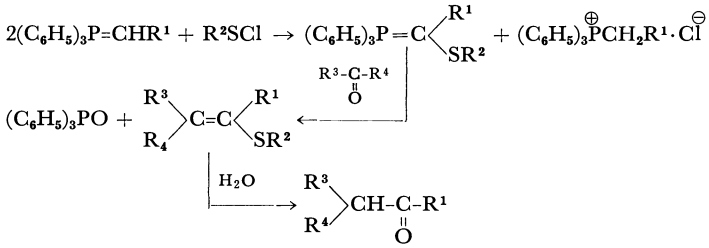

(1)

In this reaction, one mole of alkylidenetriphenylphosphorane is consumed as hydrogen chloride scavenger to form phosphonium chloride.

We studied the reactions of alkylidenetriphenylphosphorane with sulfenamide derivatives with the

1) T. Mukaiyama, S. Fukuyama and T. Kumamoto, *Tetrahedron Lett.*, **1968**, 3787.

expectation that the equimolar reactions may proceed to give α-phenylthioalkylidenetriphenylphosphorane and amine, since the amido anion of initially formed phosphonium salt [I] may carry out the deprotonation from [I] to form corresponding phosphorane [II] (Eq. 2).

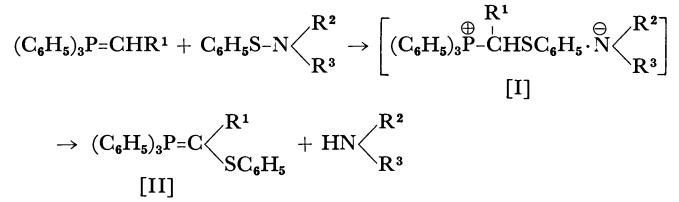

(2)

Benzenesulfenyl diethylamide did not react with ethylidenetriphenylphosphorane even after refluxing them in tetrahydrofuran, and benzenesulfenyl diethylamide was recovered quantitatively. On the other hand, it was established that when *N*-phenylthio-*N*-methylacetamide was treated with ethylidenetriphenylphosphorane at room temperature under nitrogen, a white precipitate deposited soon and β-methyl-β-phenylthiostyrene and triphenylphosphine oxide were obtained in 75% and 82% yields, respectively, by the subsequent reaction with benzaldehyde in refluxing tetrahydrofuran for 3 hr.

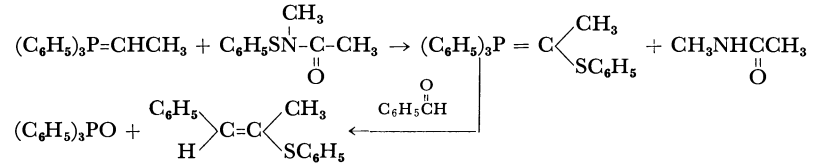

The white precipitate did not disappear in the absence of benzaldehyde even when it was refluxed for 5 hr in tetrahydrofuran. This suggests that the addition of benzaldehyde may shift equilibrium from the initially formed phosphonium salt [III] to the side of the α-phenylthioethylidenetriphenylphosphorane.

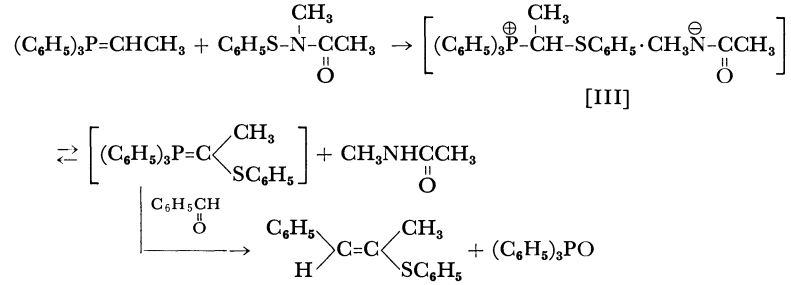

The reactions of α-phenylthioethylidenetriphenylphosphorane with *n*-butyraldehyde and acetophenone were also studied (see Table 1).

Table 1. The reactions of α-phenylthioethylidenetriphenylphosphorane with carbonyl compounds

Carbonyl compound	Thiovinyl ether Yield (%)	Thiovinyl ether Bp (°C/mmHg)	$OP(C_6H_5)_3$ Yield (%)
C_6H_5CHO	75	132/3	82
n-C_3H_7CHO	83	121/11	77
$C_6H_5COCH_3$	22	—*	57

* This compound was isolated by column chromatography.

It was found that bis(phenylthio)methylenetriphenylphosphorane was obtained in 98% yield by treating 1 mole of methylenetriphenylphosphorane with 2 moles of *N*-phenylthio-*N*-methylacetamide in tetrahydrofuran at room temperature under nitrogen.

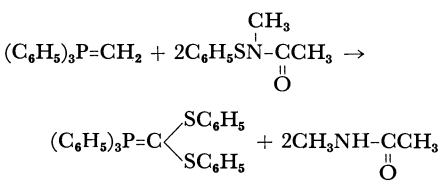

Sulfenamide derivatives were treated with dimethyloxosulfonium methylide in place of alkylidenetriphenylphosphorane. When dimethyloxosulfonium methylide was treated with *N*-phenylthiophthalimide[2] in boiling tetrahydrofuran for 6 hr under nitrogen, *N*-bis(phenylthio)methylphthalimide was obtained in 41% yield instead of dimethyloxosulfonium phenylthiomethylide expected from the reaction of the alkylidenetriphenylphosphorane with sulfenamide mentioned above.

2) M. Behforouz and J. E. Kerwood, *J. Org. Chem.*, **34**, 51 (1969).

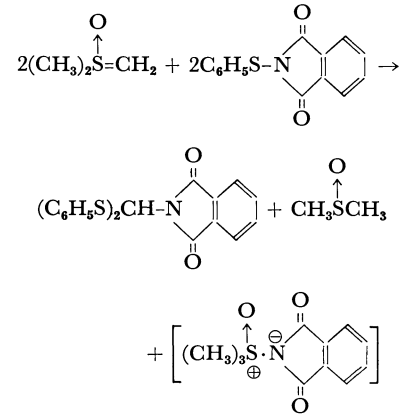

The unexpected formation of *N*-bis(phenylthio)-methylphthalimide may be explained by considering an initial formation of oxosulfonium salt [I] from equimolar amounts of dimethyloxosulfonium methylide and *N*-phenylthiophthalimide. Salt [I] rapidly reacts with one mole of dimethyloxosulfonium methylide and one mole of *N*-phenylthiophthalimide to give oxosulfonium salt [II]. Salt [II] thus formed affords *N*-bis(phenylthio)methylphthalimide and dimethyl sulfoxide by the nucleophilic attack of the phthalimide anion to the α-carbon atom of the salt [II] as sketched below.

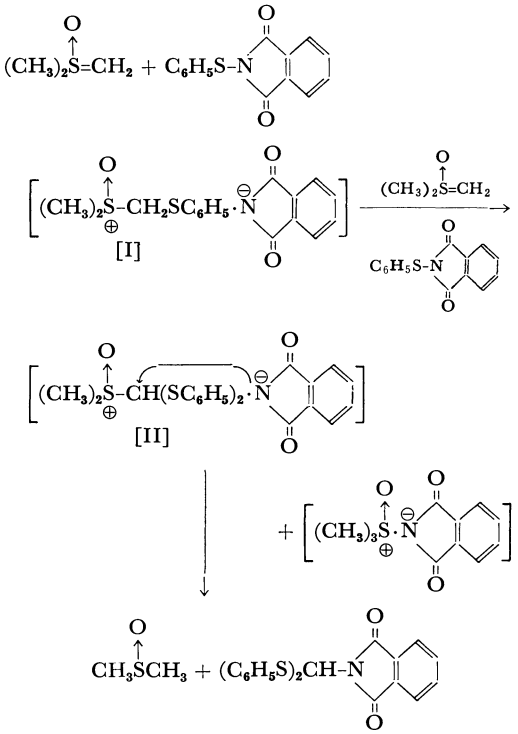

Similarly, *N*-bis(phenylthio)methylsuccinimide was obtained in 42% yield by the reaction of *N*-phenylthiosuccinimide[2] with dimethyloxosulfonium methylide in boiling tetrahydrofuran.

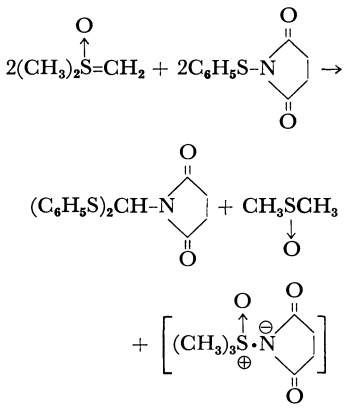

Benzenesulfenyl diethylamide did not react with dimethyloxosulfonium methylide even after refluxing them in tetrahydrofuran for 10 hr and the starting materials were recovered quantitatively.

It was found that the reaction of dimethyloxosulfonium methylide with bis(2-nitrophenyl) disulfide in tetrahydrofuran at room temperature gave tris(2-nitrophenylthio)methane in 77% yield.

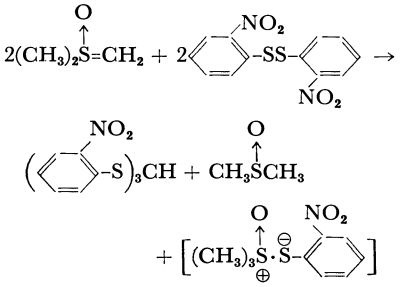

In the reaction of diphenyl disulfide with dimethyloxosulfonium methylide in boiling tetrahydrofuran, bis(phenylthio)methane was obtained in 51% yield.

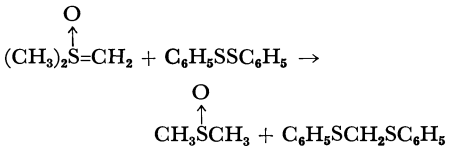

This suggests that the nucleophilic attack of phenylthio anion on the α-carbon atom of the oxosulfonium salt [IV] to form bis(phenylthio)methane is much faster than the reaction of [IV] with the oxosulfonium methylide to form tris(phenylthio)-methane through dimethyloxosulfonium phenylthiomethylide.

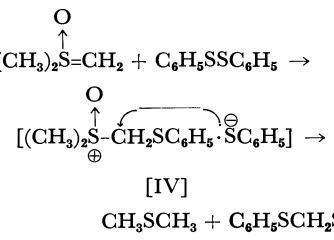

Experimental

Synthesis of *N*-Phenylthio-*N*-methylacetamide. Into a solution of sodium salt of *N*-methylacetamide, formed from *N*-methylacetamide (7.30 g, 0.10 mol) and sodium ethoxide, in tetrahydrofuran, benzenesulfenyl chloride (14.45 g, 0.10 mol) was added dropwise under stirring at room temperature. After stirring for 1 hr at room temperature, the solvent was evaporated under reduced pressure. The residue was added into 100 m*l* of water and the mixture was extracted with ether. After removal of ether, *N*-phenylthio-*N*-methylacetamide was obtained by distillation under reduced pressure, 11.13 g (62%) bp 96°C/2 mmHg.

Reaction of *N*-Phenylthio-*N*-methylacetamide with Ethylidenetriphenylphosphorane. *N*-Phenylthio-*N*-methylacetamide (1.10 g, 0.0065 mol) was added into a solution of ethylidenetriphenylphosphorane, formed from triphenylethylphosphonium bromide (2.41 g, 0.0065 mol) and *n*-butyl lithium (0.0065 mol), in tetrahydrofuran under stirring. Following the addition of *N*-phenylthio-*N*-methylacetamide, a white precipitate was obtained. Into the reaction mixture, benzaldehyde (0.69 g, 0.0065 mol) was added under stirring. The white precipitate disappeared by refluxing for 2 hr. After removal of the solvent, the residue was chromatographed on silica gel with benzene and ether, *β*-phenylthio-*β*-methylstyrene, 1.10 g (75%), bp 130—132°C/3 mmHg and triphenylphosphine oxide, 1.48 g (53%), mp 153—155°C, were obtained from the elute with benzene and ether, respectively.

Similarly, 2-phenylthio-2-hexene and 2-phenylthio-3-phenyl-2-butene were obtained by the reaction of *α*-phenylthioethylidenetriphenylphosphorane with *n*-butyraldehyde and acetophenone, respectively. The results are listed in Table 1.

Reaction of Methylenetriphenylphosphorane (1 mol) with *N*-Phenylthio-*N*-methylacetamide (2 mol). A solution of *N*-phenylthio-*N*-methylacetamide (1.81 g, 0.01 mol) in tetrahydrofuran was added into the solution of methylenetriphenylphosphorane (0.005 mol) in tetrahydrofuran under stirring. The reaction mixture was stirred for 1 hr at room temperature. After removal of the solvent, a crystalline solid precipitate was obtained by the addition of ethanol to the residue. Recrystallization from a mixture of benzene and ethanol gave bis(phenylthio)methylenetriphenylphosphorane, 2.40 g (98%), mp 165°C.

Reaction of Dimethyloxosulfonium Methylide with *N*-Phenylthiophthalimide. Into a solution of *N*-phenylthiophthalimide (2.55 g, 0.01 mol) in tetrahydrofuran, dimethyloxosulfonium methylide[3] (0.01 mol) was added under nitrogen. The reaction mixture was refluxed for 6 hr under stirring. After removal of the solvent, phthalimide (0.84 g, quantitatively) was obtained as white crystalline solid by the addition of a mixture of benzene and ether. The residue was chromatographed on silica gel with benzene. From the elute of benzene, *N*-bis(phenylthio)methylphthalimide was obtained by recrystallization from ethanol, 0.77 g (41%), mp 164—165°C. Found: C, 67.07; H, 3.89; N, 3.82; S, 16.76%. Calcd for $C_{21}H_{15}NO_2S_2$: C, 66.84; H, 4.01; N, 3.71; S, 16.96%.

Similarly, *N*-bis(phenylthio)methylsuccinimide was obtained by the reaction of dimethyloxosulfonium methylide with *N*-phenylthiosuccinimide, 42%, mp 94—95°C.

Found: C, 62.64; H, 4.36; N, 4.17; S, 19.70%. Calcd for $C_{17}H_{15}NS_2O_2$: C, 62.00; H, 4.59; N, 4.25; S, 19.43%.

Reaction of Dimethyloxosulfonium Methylide with Bis(2-nitrophenyl) Disulfide. Dimethyloxosulfonium methylide (0.01 mol) was added to a solution of bis(2-nitrophnyl) disulfide (3.08 g, 0.01 mol) in tetrahydrofuran under stirring. After stirring for 3 hr at room temperature, the solvent was evaporated under reduced pressure. A yellow crystalline was obtained by the addition of a small amount of ether to the residue. Recrystallization of the crystalline solid from ethanol gave tris(2-nitrophenylthio)methane 1.82 g (77%) mp 198—199°C.

Reaction of Dimethyloxosulfonium Methylide with Diphenyl Disulfide. Into a solution of diphenyl disulfide (2.18 g, 0.01 mol) in tetrahydrofuran, dimethyloxosulfonium methylide (0.01 mol) was added under stirring. The reaction mixture was refluxed for 2 hr. After removal of the solvent, the residue was chromatographed on silica gel with benzene. From the elute with benzene, bis(phenylthio)methane was obtained by distillation under reduced pressure, 1.19 g (51%), bp 170—175°C/0.7 mmHg.

3) E. J. Corey and M. Chaykovsky, *J. Amer. Chem. Soc.*, **87**, 1353 (1965).

BULLETIN OF THE CHEMICAL SOCIETY OF JAPAN VOL. 43 2874—2877 (1970)

Studies of Unnatural Amino Acids and Their Peptides. IV. The Syntheses of DL-β-(5-Cytosinyl)-α-alanine Peptides

Mitsuhisa SHIMADA, Kōji TAKEUCHI,*1 Yoshiya ASAI,*2 Shigeru KUWATA and Hiroshi WATANABE

Laboratory of Chemistry, Faculty of Science, Kōnan University, Okamoto, Higashinada, Kobe

(Received December 22, 1969)

DL-β-(5-Cytosinyl)-α-alanine and its dipeptides with glycine were synthesized. The benzyloxycarbonylation of this amino acid afforded the α-*N*-substituted derivative, but all attempts to obtain the diacylated derivative were unsuccessful. The condensation of the benzyloxycarbonyl derivative with glycine ethyl ester by the carbodiimide method afforded the expected dipeptide, though the yield was low (18%); it was accompanied by a large amount of a bicyclic compound, a lactam produced by an intramolecular acylation. The ethyl ester hydrochloride of this amino acid could not be obtained in a pure state, probably because of its ready cyclization to the same lactam structure under weakly acidic conditions. This complication could be avoided by using the tertiary butyl in place of the ethyl ester. Benzyloxycarbonylglycine *p*-nitrophenyl ester was condensed smoothly with this ester, affording the expected dipeptide in a 53% yield. The carbodiimide method could also be used, but it was less effective.

As a part of a series of studies of unnatural amino acids and their peptides, DL-β-(5-cytosinyl)-α-alanine derivatives were investigated. The present authors were interested in this amino acid not only biologically, because cytosine is one of the constituents of nucleic acid, but also chemically, because it had become clear that the usual method a synthesizing peptides was not always applicable to phenylalanine analogs containing such a heterocyclic ring as furan,[1] thiazole,[2] or pyridine.[3]

This amino acid has already been prepared by Blank and Caldwell.[4] The present authors followed substantially the same scheme, with only a few modifications; in place of 4-amino-5-bromomethyl-2-methylthiopyrimidine, the corresponding chloride was used. The starting material, 4-amino-5-ethoxycarbonyl-2-mercaptopyrimidine, was prepared according to the method described by Ulbricht and Price.[5]

In order to synthesize *N*-benzyloxycarbonyl-DL-β-(5-cytosinyl)-α-alanyl-glycine ethyl ester, *N*-benzyloxycarbonyl-DL-β-(5-cytosinyl)-α-alanine (VII) was prepared from DL-β-(5-cytosinyl)-α-alanine (VI) and an equivalent amount of benzyloxycarbonyl chloride by the usual method. The analytical data of this substance showed that it contains only one benzyloxycarbonyl group introduced into the α-amino group, for this compound showed no ninhydrin reaction. The benzyloxycarbonyl derivative VII was coupled with glycine ethyl ester hydrochloride in dry pyridine in the presence of dicyclohexylcarbodiimide. The oily material thus obtained was then solidified by trituration with ethyl acetate, which was separated by extraction with a large amount of water into two components, *i.e.*, a water-insoluble, colorless, amorphous powder, IX, decomposing at 310—312°C, and a water-soluble, colorless, amorphous powder, VIII, decomposing at 254—258°C. When the compound VIII was hydrolyzed with concentrated hydrochloric acid, the hydrolysate gave two spots of cytosinylalanine and glycine on a paper chromatogram. This result, as well as that of its elementary analysis, supports that the compound VIII is a dipeptide derivative : *N*-benzyloxycarbonyl-cytosinylalanyl-glycine ethyl ester.

The molecular formula, $C_{15}H_{14}N_4O_4$, was assigned to the compound IX on the basis of the results of an elementary analysis (C, 57.23; H, 4.88; N, 17.58%) and the molecular weight, 329, determined by the method of Schwyzer and his coworkers.[6] When hydrolyzed with hydrochloric

*1 Present address: Japan Malting Co. Ltd., Koganei 37, Kokubunji-cho, Shimotsuga-gun ,Tochigi-ken.

*2 Present address: Nippon Glass Fiber Co. Ltd., No. 744, Osaka Bldg., 1-Soze-cho, Kita-ku, Osaka.

1) H. Watanabe, S. Kuwata, S. Nakajima, K. Koshida and M. Hayashi, This Bulletin, **38**, 146 (1965).

2) H. Watanabe, S. Kuwata, T. Sakata and K. Matsumura, *ibid.*, **39**, 2473 (1966).

3) H. Watanabe, S. Kuwata, N. Naoe and Y. Nishida, *ibid.*, **41**, 1634 (1968).

4) B. Blank and W. T. Caldwell, *J. Org. Chem.*, **24**, 1138 (1959).

5) T. L. V. Ulbricht and C. C. Price, *ibid.*, **21**, 567 (1956).

6) R. Schwyzer, B. Iselin, W. Rittel and P. Sieber, *Helv. Chim. Acta*, **39**, 881 (1956).

acid, IX gave only one ninhydrin-positive material, one which was identical with cytosinylalanine. On the basis of these facts, the structure of the compound IX was assumed to be 2-hydroxy-6-benzyloxycarbonylamino-5,6,7,8-tetrahydro-7-oxopyrido-[2,3-*d*]pyrimidine; it is probably produced by lactam-formation between the 6-amino group of the pyrimidine and the carboxyl group activated by the carbodiimide. In order to confirm this, the benzyloxycarbonylated amino acid, VII, was treated with the carbodiimide under the same conditions as above except that ethyl glycinate hydrochloride was omitted. The substance thus obtained was found to be identical with IX by elementary analysis and by a comparison of the infrared spectra. Thus, the reactions producing these two compounds may be represented by the following equation:

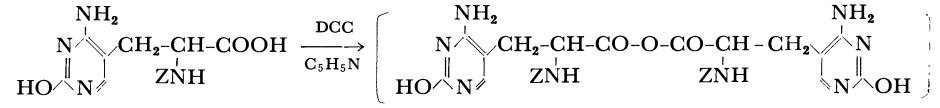

(VII)

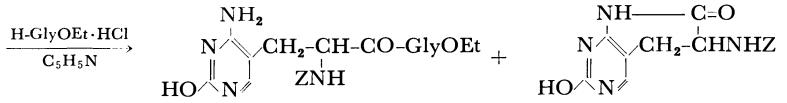

(VIII) (IX)

(Z = benzyloxycarbonyl; DCC = dicyclohexylcarbodiimide; Gly = glycine)

To prevent the lactam formation of the 6-amino group, we attempted to provide protection by the benzyloxycarbonyl group; unfortunately, all the attempts to acylate it with a large excess of benzyloxycarbonyl chloride ended in failure. When, for instance, the further benzyloxycarbonylation of the monobenzyloxycarbonyl derivative was attempted in pyridine at 40°C, the compound IX was obtained in place of the expected one.

In order to esterify cytosinylalanine, hydrogen chloride gas was bubbled into a suspension of the amino acid in ethanol; the reaction was pursued by paper chromatography. When the spot of the free amino acid disappeared and a new spot (R_f = 0.31*[3]) (probably of the desired ester) appeared, the reaction mixture was concentrated to dryness *in vacuo*; the colorless, hygroscopic crystalline residue was then left to stand over sodium hydroxide in a desiccator in order to remove the excess hydrogen chloride. In this step, paper chromatography gave only one spot. When the dried material was dissolved in hot ethanol for recrystallization, however, it gave another spot (R_f = 0.41*[3]). This new spot can probably be attributed to 2-hydroxy-6-amino-5,6,7,8-tetrahydro-7-oxopyrido[2,3-*d*]pyrimidine produced by the cyclization of cytosinylalanine ethyl ester under weakly acidic conditions. This complication was avoided by using the tertiary butyl ester in place of the ethyl ester. It was found that *t*-butyl β-(5-cytosinyl)-α-alaninate could be prepared without any trouble by treating the acid with a large amount of *t*-butyl acetate in the presence of perchloric acid, according to the method of Taschner.[7] When we used five times as much catalyst as in the literature, the transesterification proceeded smoothly; after the raw product has been treated with sodium hydrogen carbonate, the ester was obtained in a 71% yield as perchlorate-monohydrate. The free ester was obtained as a colorless, amorphous powder by treating it with aqueous ammonia or triethylamine. Benzyloxycarbonylglycine *p*-nitrophenyl ester was condensed with *t*-butyl cytosinylalaninate in hexamethylphosphoramide. From

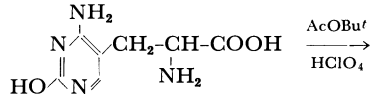

(VI)

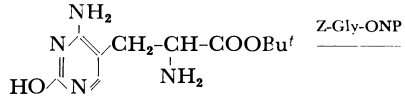

(XI)

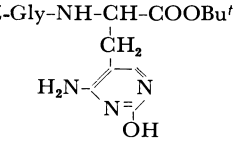

(XIII)

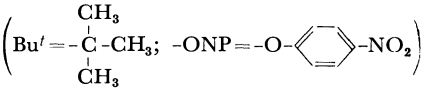

*[3] Circular paper chromatography. Toyo Roshi No. 51. Solvent, *n*-BuOH : AcOH : H_2O = 4 : 1 : 2. (R_f of glycine = 0.34).

7) E. Taschner, A. Chimiak, B. Bartor and T. Sokolowska, *Ann. Chem.*, **646**, 134 (1961).

the reaction mixture, a colorless, amorphous powder decomposing at about 320°C was obtained in a 53% yield. Upon hydrolysis with concentrated hydrochloric acid, it gave cytosinylalanine and glycine. This result and the analytical data support that the substance obtained here is the desired product: benzyloxycarbonylglycyl-DL-β-(5-cytosinyl)-α-alanine *t*-butyl ester. The same compound was also obtained in a lower yield by the use of the carbodiimide method in a mixture of dimethylformamide and dimethyl sulfoxide.

Experimental

4-Amino-5-ethoxycarbonyl-2-mercaptopyrimidine (I). This was prepared in a 79% yield, according to the literature,[5] by condensing ethyl ethoxymethylenecyanoacetate and thiourea in the presence of sodium ethoxide.

4-Amino-5-ethoxycarbonyl-2-methylthiopyrimidine (II). The procedure described in the literature[5] was somewhat modified; into a suspension of I (100 g) in methanol (50—100 m*l*) was stirred aqueous potassium hydroxide (37 g/500 m*l*), and then dimethyl sulfate (67 g) over a 10—15-min period; the mixture was then stirred for 1 hr at room temperature. The pH of the reaction mixture was adjusted to 9.4—9.6 with aqueous potassium hydroxide; the separated crystals were collected by filtration, washed with dilute aqueous potassium hydroxide and then with water, and dried *in vacuo* on a water bath to give 89.5 g (84%) of II; mp 125—129°C. Recrystallization from 50% acetic acid gave tiny, glistening plates. The yield was 69 g (65%); mp 130—131.5°C (lit,[5] mp 130—131°C).

4-Amino-5-Hydroxymethyl-2-methylthiopyrimidine (III). Prepared, according to the literature,[4] in a 73% yield; mp 125—126°C (lit,[4] mp 126—127°C).

4-Amino-5-chloromethyl-2-methylthiopyrimidine Hydrochloride (IV). To a cooled and stirred suspension of III (24 g) in dry ether (600 m*l*), there was added thionyl chloride (40 m*l*) drop by drop. The mixture was refluxed for 3 hr with stirring and then evaporated to dryness. After this procedure had been repeated twice more, the residue was used for the next reaction without purification.

Ethyl 6-Acetamido-5,6,7,8-tetrahydro-2-methylthio-7-oxopyrido[2,3-*d*]pyrimidine-6-carboxylate (V). Prepared by condensing IV with diethyl acetamidomalonate in the presence of sodium ethoxide by a method similar to that in the literature.[4] The reaction period was, however, elongated to 6 hr. The yield was 57% (calculated from the alcohol (III)); mp 186—189°C (lit,[4] mp 187—188°C).

DL-β-(5-Cytosinyl)-α-alanine (VI). Prepared by the method in the literature.[4] The yield was 85%. Crude amino acid was purified by dissolving it in aqueous ammonia, decolorizing it, and acidifying it to pH *ca.* 6 with acetic acid. The yield was 65%; mp above 360°C (decomp.) (turned brown from about 220°C and darkened at 290°C) (lit,[4] mp above 300°C); R_f = 0.23*[3]; $\lambda_{max}^{0.1\ N\ HCl}$ 283 mμ (lit,[4] $\lambda_{max}^{0.1\ N\ HCl}$ 283 mμ).

***N*-Benzyloxycarbonyl-DL-β-(5-cytosinyl)-α-alanine (VII).** Benzyloxycarbonyl chloride (1.10 g) and 2 N sodium hydroxide (3.5 m*l*) were stirred, drop by drop, into a solution of VI (1.08 g) in 0.5 N sodium hydroxide (20 m*l*) over about a 1-hr period under ice-cooling. The solution was kept alkaline throughout the reaction. Stirring was continued further at room temperature until the solution became negative to the ninhydrin test (4—5 hr). After washing with ether, the solution was then acidified to Congo Red with glacial acetic acid. The white crystals thus formed were collected and washed thoroughly with water. The yield was 0.96 g (55%); mp about 310°C (decomp.). Recrystallization from a large amount of methanol gave a white, amorphous powder melting at about 315°C (decomp.). This compound dissolves sparingly in ethyl acetate, acetone, dioxane, methanol, ethanol, acetonitrile, tetrahydrofuran, or chloroform, and forms a viscous emulsion in dimethylformamide and pyridine.

Found: C, 51.32; H, 5.15; N, 15.57%. Calcd for $C_{15}H_{16}N_4O_5 \cdot H_2O$: C, 51.43; H, 5.18; N, 15.99%.

The Reaction of *N*-Benzyloxycarbonyl-DL-β-(5-cytosinyl)-α-alanine with Ethyl Glycinate.

***N*-Benzyloxycarbonyl-DL-β-(5-cytosinyl)-α-alanylglycine Ethyl Ester (VIII).** Glycine ethyl ester hydrochloride (0.35 g) was added to an emulsion of VII (0.84 g) in dry pyridine (20 m*l*). Into the mixture was then stirred a solution of dicyclohexylcarbodiimide (0.57 g) in dry pyridine (5 m*l*) over about a 15-min period under strong cooling (about −10°C). After an additional 2 hrs' stirring in the cold, the mixture was allowed to stand for three days at room temperature. The dicyclohexylurea which was thus separated was filtered off, and the filtrate was concentrated under reduced pressure. To the resulting oil was added ethyl acetate, and the mixture was allowed to stand at room temperature. Meanwhile, the oil solidified; this solid was thoroughly extracted with water. From the extracts the dipeptide derivative, VIII, was separated as an amorphous powder. The yield was 0.18 g (18%); mp 253—262°C (decomp.). Recrystallization from methanol gave a colorless, amorphous powder decomposing at 254—258°C.

Found: C, 54.40; H, 5.42; N, 16.55%. Calcd for $C_{19}H_{23}N_5O_6$: C, 54.67; H, 5.55; N, 16.78%.

2-Hydroxy-6-benzyloxycarbonylamino-5,6,7,8-tetrahydro-7-oxopyrido[2,3-*d*]pyrimidine (IX). The solid material, the residue of the extraction described above, melted at 308—314°C (decomp.). The yield of IX was 0.5 g (66%). Recrystallization from dimethylformamide-methanol gave an amorphous powder; mp 310—312°C (decomp.).

Found: C, 57.23; H, 4.88; N, 17.58%. Calcd for $C_{15}H_{14}N_4O_4$: C, 57.32; H, 4.49; N, 17.83%.

The Reaction of *N*-Benzyloxycarbonyl-DL-β-(5-cytosinyl)-α-alanine with Dicyclohexylcarbodiimide in Pyridine. Into an emulsion of VII (1.05 g) in dry pyridine (35 m*l*) was stirred a solution of dicyclohexylcarbodiimide (0.71 g) in the same solvent (6 m*l*) over about a 20-min period under cooling (about −5°C). The stirring was continued for 2 hr under the same conditions, and then the mixture was allowed to stand for 5 days at room temperature. The crystals which were thus separated were collected by filtration and washed with a large amount of boiling ethyl acetate. The yield of IX was 0.50 g. From the mother liquor some crystals were obtained by adding glacial acetic acid; this also gave an additional 0.21 g of IX. The

total yield was 0.71 g (75%); mp about 316°C. For analysis, it was recrystallized from dimethylformamide.

Found: C, 57.64; H, 4.56; N, 17.46%. Calcd for $C_{15}H_{14}N_4O_4$: C, 57.32; H, 4.49; N, 17.83%.

The same compound was obtained by the action of 3 equivalents of benzyloxycarbonyl chloride on *N*-benzyloxycarbonyl-cytosinylalanine in dry pyridine at 40°C. The yield here was 0.60 g (56%).

DL-β-(5-Cytosinyl)-α-alanine *t*-Butyl Ester Perchlorate Monohydrate (X). Into a suspension of the amino acid, VI (1.08 g), in *t*-butyl acetate (116 m*l*), was stirred, drop by drop, 70% perchloric acid (3.66 g) at about 5°C; the mixture was then stirred at room temperature. After about 3 hr, the amino acid was almost dissolved into the solution and crystals began to separate. After the mixture had stood at room temperature overnight, the crystals were collected, dissolved in chilled water (10 m*l*), and kept in the cold after the pH had been adjusted to 7.6 with sodium hydrogencarbonate. Thus the crude crystalline *t*-butyl ester perchlorate was obtained. The yield was 1.42 g (71%); mp 175—180°C (decomp.). For further purification, it was dissolved in a mixture of acetone and chloroform (2 : 1) and freed from insoluble materials, while the solvent was removed under reduced pressure. To the residue was added a mixture of *t*-butyl alcohol and water (2 : 1), and the separated solid was recrystallized from the same mixture. The purified compound melted at 216—219°C (decomp.); R_f=0.57*[3].

Found: C, 36.04; H, 5.71; N, 15.25%. Calcd for $C_{11}H_{18}N_4O_3 \cdot HClO_4 \cdot H_2O$: C, 35.44; H, 5.68; N, 15.03%.

DL-β-(5-Cytosinyl)-α-alanine *t*-Butyl Ester (XI). Into a solution of the perchlorate, X (1.00 g), in dimethylformamide (5 m*l*), was stirred triethylamine (0.3 g) at −10°C. After the solution had been stirred for 30 min at this temperature, a colorless solid separated; this was filtered, washed with cold water, and dried in a desiccator. The yield was 0.62 g (91%); mp above 320°C (decomp.). (It turned yellow from about 180°C and darkened from about 280°C.) Recrystallization from a mixture of dimethylformamide and dimethyl sulfoxide gave a colorless powder; mp above 320°C (it turned yellow from about 190°C and darkened from about 305°C).

***N*-Benzyloxycarbonyl-glycyl-DL-β-(5-cytosinyl)-α-alanine *t*-Butyl Ester (XII).** To a suspension of XI (0.25 g) in hexamethylphosphoramide (20 m*l*), there was added benzyloxycarbonylglycine *p*-nitrophenyl ester (0.33 g) and triethylamine (0.1 g); the mixture was then stirred at room temperature overnight. To the almost clear solution was added a large quantity of water, and then the solution was left to stand in a refrigerator overnight. The crystals which were thus separated were collected, washed with cold 0.1 N citric acid, water, 0.5 N aqueous sodium hydrogencarbonate, and then with water, and dried in a desiccator. The yield was 0.24 g (53%); mp above 320°C (decomp.). Recrystallization from a mixture of dimethyl sulfoxide and methyl ethyl ketone gave a colorless, amorphous substance; mp above 320°C (decomp.) (sintered at about 93°C). When hydrolyzed with hydrochloric acid, this compound gave glycine and cytosinylalanine, the presence of which was confirmed by paper chromatography.

Found: C, 55.01; H, 6.15; N, 14.93%. Calcd for $C_{21}H_{27}N_5O_6 \cdot H_2O$: C, 54.42; H, 6.31; N, 15.11%.

From XI (355 mg), benzyloxycarbonylglycine (881 mg), and dicyclohexylcarbodiimide (640 mg) in a mixture of dimethylformamide and dimethyl sulfoxide (1 : 1), the same dipeptide was obtained in a lower yield (58 mg; 9%).

BULLETIN OF THE CHEMICAL SOCIETY OF JAPAN VOL. 43 2878—2884 (1970)

Transformation of Progesterone by *Rhizopus nigricans* REF 129 as Influenced by Modification of the Fermentation Medium

Abdel-Monem EL-REFAI, Lotfy SALLAM and Ismail EL-KADY

Microbiological Chemistry Research Lab., National Research Centre, Dokki, Cairo, U.A.R.

(Received January 14, 1970)

Hydroxylation of progesterone with *Rhizopus nigricans* REF 129 at C-11, C-6, C-17, C-21 as well as formation of 11α-hydroxy-5α-pregnane-3,20-dione was investigated when the fermentation medium was modified in a different manner. The various transformation products of progesterone were found to be affected qualitatively and quantitatively by the composition of the medium employed. Mg^{2+}, PO_4^{3-} proved to be indispensable for the transformation processes. Mn^{2+} and Fe^{2+} stimulated the reactions. Similarly, acetate, malate and riboflavin enhanced the transformation processes. Formation of the various derivatives of progesterone, except for 11α-hydroxy-5α-pregnane-3,20-dione and 6β,11α-dihydroxyprogesterone, was also favoured by the addition of adenine, adenosine, uracil and guanine to the fermentation medium.

The very important discovery of the microbiological 11α-hydroxylation of progesterone and other steroids by Peterson and Murray[1] served as a new and vigorous stimulus for studies on microbiological transformation of steroids. By using common industrial microbiological methods, chemical transformation of steroids have now been effected in many different ways.[2] However, the studies made for the elucidation of various physiological and biochemical aspects of the microbiological hydroxylation of steroids are still of fragmentary nature. O'Connell *et al*[3] had studied the effect of the composition of the fermentation media on the conversion of substance S (17α,21-dihydroxy-4-pregene-3,20-dione) to cortisone (17α,21-dihydroxy-4-pregnene-3,11,20-trione) and cortisol (11β,17α,21-trihydroxy-4-pregnene-3,20-dione) by *Cunninghamella blakesleeana*. Zetsche[4] also showed that the enzyme system of *Curvularia lunata*, responsible for the introduction of 6β;7α;11β; 14 α hydroxyl groups to progesterone, was affected by the conditions of the culture.

In a previous communication the authors[5] reported the role of some redox agents and trace elements on the transformation of progesterone with *Rhizopus nigricans* REF 129. It was found that the addition of potassium ferricyanide or cadmium ions to the fermentation medium inhibited the formation of 11α-hydroxy-5α-pregnane-3,20-dione and 6β,11α-dihydroxyprogesterone with the subsequent increase of the yields of 11α-hydroxyprogesterone and 11α,17α,21-trihydroxy derivative. However, the formation of the other transformation products, namely, 17α-hydroxyprogesterone; 21-hydroxyprogesterone and 11α, 17α-dihydroxyprogesterone were unaffected. Identity of the different transformation products of progesterone with this local strain of *R. nigricans* were previously confirmed by the authors.[6]

In this paper, we should like to report our studies on the role of some factors that influence the hydroxylation of progesterone with *R. nigricans* REF 129, in a trial to throw some light on the identification of the required cofactors for hydroxylases systems of microbiological origin.

Experimental

Cultivation. The local strain of *R. nigricans* REF 129 was selected from the centre of culture of the Microbiological Chemistry Research Lab., National Research Centre, Cairo. Cultivation was performed in 250-m*l* Erlenmeyer flasks each containing 75 m*l* of the following medium:[5] glucose, 40.0; KH_2PO_4, 0.74; $MgSO_4 \cdot 7H_2O$, 1.0; asparagine, 1.825 g/*l*. The pH was adjusted to 5.5. The flasks were sterilized at 1 atm for 20 min and inoculated with 2-m*l* spore suspension of 48 hr old culture of the pure organism. The culture flasks were agitated on reciprocal shaker (110 strokes/min, amplitude 7 cm) at 30°C±2 for 48 hr; 100 mg of progesterone dissolved in 2 m*l* ethanol was then added to each flask and fermentation was continued for another 72 hr. Throughout the course of this study, grading of the amount of growth by visual estimation

1) D. H. Peterson and H. C. Murray, *J. Amer. Chem. Soc.*, **74**, 1871 (1952).

2) D. H. Peterson, "Biochemistry of Industrial Microorganisms," Rainbow and Rose (Eds.), Acad. Press, London and N. Y. (1963), Ch. 10, p. 537.

3) P. W. O'Connell, K. M. Mann, E. D. Nielson and F. R. Hanson, *Appl. Microbiol.*, **3**, 16 (1955).

4) K. Zetsche, *Archiv für Mikrobiologie*, **38**, 237 (1961).

5) L. A. R. Sallam, A. H. El-Refai and I. A. El-Kady, *J. Gen. Appl. Microbiol.*, in press.

6) L. Sallam, A. El-Refai and I. A. El-Kady, This Bulletin, **43**, 1239 (1970).

has been a routine observation.

Extraction and Analysis of the Mixture of Transformation Products. At the end of the fermentation period, the contents of each flask (medium+fungus) were homogenized in a blender (16000 rpm) with twice its volume of chloroform(150 m*l*). Extraction was repeated 3 times in order to assure that all the transformation products were extracted. The combined chloroform extracts were washed with half its volume 5% sodium bicarbonate followed by an equal volume distilled water, dried over anhydrous sodium sulphate, filtered, then distilled to give a semi-solid residue which was then dissolved in a measured volume of chloroform: methanol (1 : 1, v/v) mixture. The mixture was referred to as "tested material".

Qualitative analysis of the different transformation products encountered during this work was carried out as previously described.[7] The preparative thin-layer chromatographic analysis using silica gel G and standard equipments were used for quantitative determination of the different components of the transformation mixture. A measured volume of the tested material was applied as a streak across the bottom of the glass plate (20×20 cm) covered with a layer of silica gel G (1 mm thickness). The plates were developed with cyclohexane : acetone : chloroform (75 : 25 : 20, v/v). After development, the bands of the individual steroids were marked, scraped off from the plate and quantitatively eluted with spectroscopic ethanol. The concentration of each compound was determined by UV spectrophotometric measurement. The band corresponding to 11α-hydroxy-5α-pregnane-3,20-dione was eluted and the eluate was evaporated in a tared beaker whereby its exact weight was determined.

Results

Inorganic Constituents. In considering the inorganic ions affecting the transformation of progesterone when *R. nigricans* was grown on the basal medium, certain ones seemed to be indispensable. In order to test this idea and investigate the need for other inorganic ions, the basal medium was modified by the omission of the ion under investigation and the addition of various levels of this ion in different experimental series. The data were compared with yields obtained from incubation in the basal medium from which the compound under investigation was omitted.

Effect of $MgSO_4 \cdot 7H_2O$. Study of the effect of the addition of various levels of $MgSO_4 \cdot 7H_2O$ to the fermentation medium(Table 1) showed that the formation of the different transformation products of progesterone was markedly stimulated by the addition of the magnesium salt. Addition of 1.5 g/*l* $MgSO_4 \cdot 7H_2O$ seemed to be optimal for the formation of 11α-, 17α- and 21-monohydroxyprogesterones, as well as 6β,11α- and 11α,17α-dihydroxy derivatives. Although the concentration of 6β, 11α-dihydroxyprogesterone did not appear to be affected by the addition of higher levels of $MgSO_4 \cdot 7H_2O$, the concentrations of the other products were gradually decreased under these conditions. However, the concentration of 11α,17α,21-trihydroxyprogesterone was markedly increased with the increase of the magnesium salt level.

Effect of KH_2PO_4. Omission of KH_2PO_4 from the medium markedly reduced the amounts of progesterone transformed (Table 2). Thus, about 23% and 82% of the added progesterone was transformed when the experimental organism was grown on the medium without added phosphate and on the medium supplemented with 1.5 g/*l* KH_2PO_4, respectively. Similarly, the formation of the different derivatives of progesterone was enhanced with phosphate addition. Maximal yields of 11α-, 17α- and 21-monohydroxyprogesterones, as well as 11α,17α,21-trihydroxy derivative were obtained with 1.5 g/*l* KH_2PO_4 treatment. However, the optimal level for the formation of 6β,11α- and 11α, 17α-dihydroxyprogesterones seemed to lie at 0.5 g/*l*. On the other hand, the addition of lower concentrations of phosphate exerted no noticeable effect on the formation of 11α-hydroxy-5α-pregnane-3,20-dione. However, inhibition of the formation of this product was observed with higher

Table 1. Hydroxylation of progesterone by *R. nigricans* as influenced by varying the $MgSO_4 \cdot 7H_2O$ level of the fermentation medium

Product (mg/culture)	Control*	$MgSO_4 \cdot 7H_2O$ levels (g/*l*)				
		0.25	0.50	1.00	1.50	2.00
Residual progesterone	82	60	45	27	20	23
21-Hydroxyprogesterone	0.8	1.5	2.1	3.0	3.4	2.4
17α-Hydroxyprogesterone	0.6	1.4	2.7	3.8	4.4	2.0
11α-Hydroxy-5α-pregnane-3,20-dione	0.9	2.5	3.5	4.6	6.6	5.4
11α-Hydroxyprogesterone	4.9	17.2	22	29.5	32	31.4
11α,17α-Dihydroxyprogesterone	1.8	5.1	8.3	11	12.6	10.3
6β,11α-Dihydroxyprogesterone	1.0	3.2	3.6	4.2	4.7	4.7
11α,17α,21-Trihydroxyprogesterone	1.0	4	7.3	11.5	13.2	14.6

* Control medium having the following composition (g/*l*): glucose, 40.0; KH_2PO_4, 0.74; asparagine, 1.825.

7) A. El-Refai, L. Sallam and I. El-Kady, *J. Gen. Appl. Microbiol.*, **15**, 309 (1969).

Table 2. Hydroxylation oe progesterone by *R. nigricans* as influenced by varying the KH_2PO_4 level of the fermentation medium

Product (mg/culture)	Control*	KH_2PO_4 levels (g/*l*)				
		0.25	0.50	1.00	1.50	2.00
Residual progesterone	86.2	47	30	22	18	20
21-Hydroxyprogesterone	0.3	2	3	3	4.8	4
17α-Hydroxyprogesterone	0.3	2	2	3	4	3
11α-Hydroxy-5α-pregnane-3,20-dione	0.6	2.6	3.0	3.0	3.0	2.4
11α-Hydroxyprogesterone	5	22	25	30	38	34
11α,17α-Dihydroxyprogesterone	1	7	14	12	10	8
6β,11α-Dihydroxyprogesterone	1	4	6	5	4	3
11α,17α,21-Trihydroxyprogesterone	0.6	5	8	11	15.9	14.8

* Control medium having the following composition (g/*l*): glucose, 40.0, $MgSO_4 \cdot 7H_2O$, 1.0, asparagine, 1.825.

Table 3. Hydroxylation of progesterone by *R. nigricans* as influenced by varying the $MnSO_4$ level of the fermentation medium

Product (mg/culture)	Control*	$MnSO_4$ levels (g/*l*)				
		0.01	0.05	0.1	0.15	0.2
Residual progesterone	23.6	18.2	15.0	12	10.4	8.8
21-Hydroxyprogesterone	3.3	4.2	4.8	5.5	6.4	7.0
17α-Hydroxyprogesterone	3.3	4.5	5.4	6.6	6.9	6.9
11α-Hydroxy-5α-pregnane-3,20-dione	9.3	4.4	5	5.8	6.4	6.7
11α-Hydroxyprogesterone	30	30.0	30.0	26	24	22.2
11α,17α-Dihydroxyprogesterone	12.5	13.2	13.6	14.4	14.8	15.7
6β,11α-Dihydroxyprogesterone	5.5	5.5	5.9	6.6	6.6	7
17α,21-Dihydroxyprogesterone	—	4.2	4.2	5.3	6.8	7.4
11α,17α,21-Trihydroxyprogesterone	11.1	12	12.6	13.3	14	14.5

* Control medium having the following composition (g/*l*): glucose, 40.0, $MgSO_4 \cdot 7H_2O$, 1.0; KH_2PO_4, 0.74; asparagine, 1.825.

levels of phosphate.

Effect of $MnSO_4$. The data presented in Table 3 show that the addition of $MnSO_4$ to the basal medium stimulated the transformation processes. However, 11α-hydroxylation does not appear to be affected by such addition. The yield of 11α-hydroxyprogesterone was appreciably decreased upon the addition of 0.1—0.2 g/*l* of $MnSO_4$. 17α, 21-Dihydroxyprogesterone, a compound not detected when the experimental organism was grown on the basal medium (control treatment), was detected on the addition of manganous salt. The concentration of this product increased with the increase of the level of the manganous salt.

Effect of $FeSO_4 \cdot 7H_2O$. Addition of the ferrous salt exhibited different effects on the various transformation reactions (Table 4). Hydroxylation at C-17 or C-21 was appreciably enhanced on the addition of the different levels of ferrous salt. On the other hand, the concentration of 11α-hydroxy-5α-pregnane-3,20-dione decreased at the higher levels of $FeSO_4$. The transformation of progesterone to 6β,11α-; 11α,17α- as well as to 11α,17α,21-trihydroxy derivatives did not seem to be appreciably influenced by the addition of ferrous salt to the medium. Hydroxylation into both 17α- and 21-positions was observed when the experimental organism was grown on the basal medium to which ferrous salt was added. Under the experimental conditions employed, the concentration of this product increased with the increase of the level of the ferrous salt.

Organic Acids. The effect of the addition of some organic acids, mostly the intermediates of TCA cycle, to the fermentation medium, on the transformation of progesterone with the experimental organism is presented in Table 5. It was found that the addition of these acids exerted different effects on the transformation reactions. Thus, although the addition of citrate, *cis*-aconitate, fumarate, pyruvate and α-ketoglutarate showed no noticeable effect on the transformation processes, yet malate, succinate, acetate, and oxalate affected the reactions in a different manner. The concentrations of the residual progesterone obtained in the case of malate and acetate were about 46% and

Table 4. Hydroxylation of progesterone by *R. nigricans* as influenced by varying the $FeSO_4 \cdot 7H_2O$ level of the fermentation medium

Product (mg/culture)	Control*	$FeSO_4 \cdot 7H_2O$ levels (g/*l*)				
		0.01	0.05	0.1	0.15	0.2
Residual progesterone	23.6	16.8	12	15	17.2	20
21-Hydroxyprogesterone	3.3	4	5.2	5.2	5.2	6.0
17α-Hydroxyprogesterone	3.3	5.2	5.5	6.2	7.3	7.7
11α-Hydroxy-5α-pregnane-3,20-dione	3.9	3.6	3.4	2.6	2.2	2.2
11α-Hydroxyprogesterone	30	30.0	30.0	25.6	20.7	16.8
11α,17α-Dihydroxyprogesterone	12.5	13.4	12.4	15.6	16.5	17.4
6β,11α-Dihydroxyprogesterone	5.5	5.5	6.4	7.8	7.8	7.8
17α,21-Dihydroxyprogesterone	—	3.3	3.6	4.2	5.6	5.8
11α,17α,21-Trihydroxyprogesterone	11.1	12.2	13.4	14.4	12.2	12.2

* Control medium having the following composition (g/*l*): Glucose, 40.0; $MgSO_4 \cdot 7H_2O$, 1.0; KH_2PO_4, 0.74; asparagine, 1.825.

Table 5. Effect of addition of some organic acids* on the hydroxylation of progesterone by *R. nigricans*

Product (mg/culture)	Control	Citrate	Malate	*cis*-Aconitate	Acetate	Oxalate	Fumarate	Pyruvate	α-Ketoglutarate	Succinate
Residual progesterone	23.6	22.7	11.0	22.0	6.4	36.5	24.4	22.5	24.5	10.5
21-Hydroxyprogesterone	3.3	3.3	3.8	3.3	5.3	2.0	3.0	3.3	3.0	3.2
17α-Hydroxyprogesterone	3.3	3.3	3.6	3.3	6.0	1.8	3.5	3.3	3.0	3.3
11α-Hydroxy-5α-pregnane-3,20-dione	3.9	4.1	4.5	4.1	3.9	3.0	4.3	4.3	3.0	4.2
11α-Hydroxyprogesterone	30.0	32.4	30.8	33.8	36.2	25.5	30.0	32.7	33.0	30.0
11α,17α-Dihydroxyprogesterone	12.5	12.0	17.3	12.0	15.0	10.0	10.8	12.7	12.5	15.2
6β,11α-Dihydroxyprogesterone	5.5	5.5	7.4	5.5	16.2	4.7	5.5	5.8	5.5	5.5
11α,17α,21-Trihydroxyprogesterone	11.2	11.4	16.2	11.5	17.2	10.0	10.6	11.6	11.5	19.2

* These acids in concentration 1 g/*l* of each were added to the fermentation medium. The initial pH value of the medium was adjusted to pH 5.5 in each treatment. Control medium has the same composition as that in Table 4.

Table 6. Effect of addition of some biologically active compounds* on the hydroxylation of progesterone by *R. nigricans*

Product (mg/culture)	Control**	Adenine	Xanthin	Uracil	Guanine	Adenosine
Residual progesterone	23.6	10.8	2.0	6.1	10.7	12.5
21-Hydroxyprogesterone	3.3	6.7	5.2	6.4	8	7.2
17α-Hydroxyprogesterone	3.3	6.9	5	6.4	8	7.7
11α-Hydroxy-5α-pregnane-3,20-dione	3.9	1.2	4	1.0	2	2
11α-Hydroxyprogesterone	3.0	36	38.4	35.3	31.7	32
11α,17α-Dihydroxyprogesterone	12.5	16.2	15.5	20	18.6	16.7
6β,11α-Dihydroxyprogesterone	5.5	2	5.5	2.1	1.2	2.0
11α,17α,21-Trihydroxyprogesterone	11.1	15.3	18.2	17.4	15.6	14.8

* Added in concentrations of 100 mg/*l* each.
** The same composition as in Table 4.

27% of that recorded with basal medium (control treatment). The addition of malate favoured the formation of both 6β,11α- and 11α,17α-dihydroxyprogesterones as well as 11α,17α,21-trihydroxy derivative, rather than the transformation of progesterone to the monohydroxy derivatives. Similar results were recorded in the case of succinate treatment, however, in contrast to malate, the formation of 6β,11α-dihydroxyprogesterone was not stimulated in the case of succinate. On the other hand, the yields of the various transformation products except for 6β,11α-dihydroxyprogesterone and 11α-hydroxy-5α-pregnane-3,20-dione were markedly increased when acetate was added to the basal medium. Oxalic acid appeared to exert an inhibitory effect on the transformation processes.

Biological Bases and Nucleoside. The effect of adding some purine, pyrimidine bases as well as a nucleoside (adenosine) on the different transformation processes of progesterone was also investigated. As shown in Table 6, the addition of xanthin and uracil to the fermentation medium increased the concentrations of the transformed progesterone (compare with control treatment). Addition of adenine, adenosine, guanine and uracil stimulated the formation of 17α- and 21-hydroxyprogesterones. The yields of these two products greatly increased as compared with those recorded with the control treatment. Moreover, a noticeable increase in the concentrations of 11α-hydroxyprogesterone; 11α,17α-dihydroxyprogesterone and 11α,17α,21-trihydroxy derivative was observed. In contrast, the formation of 11α-hydroxy-5α-pregnane-3,20-dione and 6β,11α-dihydroxyprogesterone were greatly reduced in the cases of uracil, guanine and adenosine treatments. The addition of xanthine increased also the concentrations of various transformation products except 11α-hydroxy-5α-pregnane-3,20-dione and 6β,11α-dihydroxyprogesterone.

Vitamins. Addition of some individuals of the vitamin B group, namely, nicotinic acid, thiamine and riboflavin to the fermentation medium proved to enhance the transformation reactions (Table 7). The concentration of the residual progesterone greatly decreased with nicotinic acid and thiamine. Moreover, progesterone was almost completely consumed in the case of riboflavin treatment. An appreciable increase in the yields of the various transformation products was generally observed under these experimental conditions, maximal yields being obtained with riboflavin.

Discussion

The nature of the fermentation medium employed is a decisive factor influencing the microbiological transformation of steroids. We have shown that the transformation of progesterone with a local strain of *Rhizopus nigricans* REF 129 was greatly affected by the composition of the fermentation medium. Various transformation products were found to be affected quantitatively as well as qualitatively by the nature of the fermentation medium. In considering the inorganic ions required for an adequate transformation of progesterone with the experimental organism, certain ions seemed to be indispensable. Only Mg^{2+} and PO_4^{3-} were considered as possibly superfluous constituents of the medium. Omission of either one of these two ions proved to inhibit the transformation processes. The activities assayed when the organism was grown on medium without added Mg^{2+} or PO_4^{3-} might be due to the presence of traces of these two ions as impurities already present in the analytical reagent grade chemical ingradient used in the preparation of the medium. Under these conditions the growth of the fungus was greatly inhibited. Similarly, the addition of Fe^{2+} or Mn^{2+} stimulated the hydroxylation process especially at C-17 and C-21. On the other hand, formation of 11α-hydroxy-5α-

TABLE 7. EFFECT OF SOME VITAMINS OF THE B GROUP ON HYDROXYLATION OF PROGESTERONE BY *R. nigricans*

Product (mg/culture)	Control*	Vitamins**		
		Nicotinic acid	Thiamine	Riboflavin
Residual progesterone	23.6	5.4	7.0	traces
21-Hydroxyprogesterone	3.3	5.0	3.3	3.3
17α-Hydroxyprogesterone	3.3	5.0	3.3	3.6
11α-Hydroxy-5α-pregnane-3,20-dione	3.9	4.6	4.6	6.0
11α-Hydroxyprogesterone	300	37.4	38	40.8
11α,17α-Dihydroxyprogesterone	12.5	14	15.2	16.7
6β,11α-Dihydroxyprogesterone	5.5	7.0	6.1	6.1
11α,17α,21-Trihydroxyprogesterone	11.1	14.3	15	16.2

* The same composition as Table 4.

** Vitamins were added to the Sterile medium under aseptic conditions in 750 μg/75 m*l* each.

TABLE 8. TRANSFORMATION ASSAY OF 21-HYDROXYFROGESTERONE* BY *R. nigricans* WITH THE ADDITION OF Fe^{2+} AND Mn^{2+}** IONS TO THE FERMENTATION MEDIUM

Treatment	Incubation period/hr	Transformation products (mg/culture)			
		21-Hydroxy-progesterone	11α,21-Dihydroxy-progesterone	17α,21-Di-hydroxypro-gesterone	11α,17α,21-Trihydroxy-progesterone
Control***	24	4.5	5.2	—	—
	48	—	9.4	—	—
Control+Fe^{2+}	24	4.2	3.0	2.2	—
	48	—	4.1	3.2	2.1
Control+Mn^{2+}	24	5.0	2.2	2.2	—
	48	—	3.5	2.6	3.2

* 21-Hydroxyprogesterone (10 mg/75 m*l* medium) was charged to 48 hour old culture and fermentation was continued for 24 and 48 hr.
** Fe^{2+} and Mn^{2+} ions were added as 0.1 g/*l*.
*** Control medium: The same composition as in Table 4.

pregnane-3,20-dione decreased on the addition of Fe^{2+} to the medium. A peculiar finding is the presence of 17α,21-dihydroxyprogesterone, in addition to the other derivatives of progesterone, when the experimental organism was grown on the basa lmedium supplemented with Fe^{2+} or Mn^{2+} ions. This product which was not detected on cultivation of the organism on other medium modifications was proposed by the authors[8] to be formed momentarily, by the introduction of 17α-hydroxyl group into 21-hydroxyprogesterone, during the course of transformation to 11α,17α,21-trihydroxyprogesterone. Addition of Fe^{2+} or Mn^{2+} ions to the medium was accompanied with the formation of comparatively lower yields of 11α-hydroxyprogesterone, although the yields of both 17α- and 21-hydroxy derivatives were appreciably increased. It seems, therefore, that the presence of Fe^{2+} or Mn^{2+} stimulated hydroxylation at C-17 and C-21. As a result of the comparatively lower activities of 11α-hydroxylase system, catalyzing the transformation of 17α,21-dihydroxyprogesterone to 11α,17α,21-trihydroxy derivative, the dihydroxylated product was accumulated.

Formation of 17α,21-dihydroxyprogesterone from 21-hydroxyprogesterone was confirmed, however, when 21-hydroxyprogesterone was charged as substrate to fermentation medium supplemented with Fe^{2+} or Mn^{2+} (Table 8). Under these conditions, 21-hydroxyprogesterone was transformed after 24 hr into 11α,21-dihydroxyprogesterone and 17α,21-dihydroxy derivative. After 48 hours of fermentation, 11α,17α,21-trihydroxyprogesterone was detected.

The importance of Mg^{2+}, PO_4^{3-} and Fe^{2+} ions for the microbial hydroxylation of steroids had been reported by some workers.[3,4] Sweat and Bryson,[9] also showed that 11β-hydroxylase of mammalian system is markedly enhanced by the addition of Mn^{2+} and to a lesser extent by Mg^{2+}. Evidence from studies carried out by many workers[10-13] clearly confirms the hydroxylation reaction to be an aerobic reaction requiring conditions for oxidative phosphorylation, and that reduced triphosphopyridine nucleotide (TPNH) is an important cofactor. Diphosphopyridine nucleotide (DPN^+), adenosine triphosphate (ATP), triphosphopyridine nucleotide (TPN^+), nicotinamide, magnesium ions, and intermediates of the Kreb's citric acid cycle were needed as cofactors in the formation and maintenance of TPNH in its reduced state.

In a trial to identify the required cofactors for the hydroxylation processes, the role of intermediates of TCA cycle, some purine and pyrimidine bases and nucleoside as well as some vitamins, on the transformation of progesterone by the experimental organism was investigated. Among the different organic acids tested, acetate, malate and succinate appeared to stimulate the hydroxylation reactions. Similarly, riboflavin, thiamine and nicotinic acids increased the capacity of the organism to transform progesterone. Maximal yields of the various progesterone derivatives were obtained with riboflavin whereby progesterone was practically quantitatively transformed after 3 days of fermentation. Ryan and Engel[14] noted that nicotinic acid amide stimulated the hydroxylation of steroids in mammals presumably because nicotinic acid amide participate in the synthesis of DPNH or TPNH. Zetsche[4] also showed

8) A. El-Refai, L. Sallam and I. El-Kady, *J. Gen. Appl. Microbiol.*, **16**, 137 (1970).

9) M. L. Sweat and M. J. Bryson, *Arch. Biochem. Biophys.*, **96**, 186 (1962).
10) P. Talalay, *Physiol. Revs.*, **37**, 362 (1957).
11) J. K. Grant, *Biochem. J.*, **64**, 559 (1956).
12) H. K. Grant and A. C. Brownie, *Biochem. et Biophys. Acta.*, **18**, 433 (1956).
13) M. L. Sweat and M. D. Lipscomb, *J. Amer. Chem. Soc.*, **77**, 5185 (1955).
14) K. J. Ryan and L. L. Engel, *ibid.*, **78**, 2654 (1956).

that malate and riboflavin the favour hydroxylation of progesterone at 7α,11β and 14α by *Curvularia lunata*.

Addition of adenine, adenosine, xanthin, uracil or guanine to the fermentation medium seemed to enhance the transformation reactions. However, in the cases of adenine, adenosine, uracil and guanine, formation of 11α-hydroxy-5α-pregnane-3, 20-dione as well as 6β,11α-dihydroxyprogesterone was noticeably restricted. Such results are encouraging because the latter two compounds were considered to be undesired products.

We are grateful to Professor Dr. M. Abdel-Aziz, Faculty of Science, Cairo University, Professor Dr. H. G. Osman, and Professor Dr. M.B.E. Fayez, National Research Centre, Cairo, for their encouragement and interest.

Thanks are also due to Dr. D. H. Peterson UpJohn Company, U.S.A., Dr. H. Azfasadour, Organon, Oss. Holland and the Schring group for the in gifts of the steroid compounds.

BULLETIN OF THE CHEMICAL SOCIETY OF JAPAN VOL. 43 2884—2890 (1970)

The Friedel-Crafts Reaction of 2,3-Dimethylbenzofuranyl Ketones and the Corresponding Carboxylic Esters[1]*

Yoshiyuki KAWASE, Tomoko OKADA and Toshio MIWA*

Department of Chemistry, Faculty of Literature and Science, Toyama University, Gofuku, Toyama
** Department of Chemistry, Faculty of Science, Osaka City University, Sumiyoshi-ku, Osaka*

(Received January 21, 1970)

The acetylation of methyl 2,3-dimethyl-4- and -7-benzofurancarboxylates was carried out by the action of acetyl chloride and aluminum chloride in carbon disulfide at room temperature to afford the 6-acetyl compounds; these compounds were converted to keto-acids by hydrolysis, and then to the known dicarboxylic acid or to the known 6-acetylbenzofuran. The alkylation of acetyl and methoxycarbonyl derivatives of 2,3-dimethylbenzofuran was carried out by the action of *n*- or iso-propyl bromide and aluminum chloride in carbon disulfide at reflux temperature, both the bromides furnishing the same isopropylated product. The crude products from the 4-acetyl- and 4-methoxycarbonyl-benzofurans could not be purified, but 2,3-dimethyl-6-isopropyl-4-benzofurancarboxylic acid was obtained by the hydrolysis of the product from the latter. In the cases of 5-acetyl- and 5-methoxycarbonyl-benzofurans, the isopropylation occurred at the 7-position and the products were converted to the same carboxylic acids, while the isopropylation occurred at the 4-position in the cases of 6-acetyl- and 6-methoxycarbonylbenzofurans, and diisopropylation occurred in the case of 7-methoxycarbonylbenzofuran.

In previous papers, one of the present authors and others reported that acetylation by the Fridel-Crafts reaction of acetyl-[1-4] and methoxycarbonyl-2,3-dimethylbenzofurans[4] afforded the acetylated compounds, generally in the *m*-position to the acetyl or methoxycarbonyl group except that methyl 2,3-dimethyl-5-benzofurancarboxylate (**9b**) afforded the 6-acetylated compound; they also reported that the isopropylation of the 2,3-dimethyl-6-benzofuranyl methyl ketone (**5**) furnished the 4-isopropyl compound[1,2] (**18**).

In connection with this, the acetylation of other isomeric methyl benzofurancarboxylates (**8b** and **23b**) and the alkylation of benzofuranyl methyl ketones (**3**, **4** and **5**) by the Friedel-Crafts reaction have been studied further; also, extended studies of the alkylation of methyl benzofurancarboxylates (**8b**, **9b**, **10b** and **23b**) have been carried out.

At first, some examinations of the preparation of starting compounds were carried out[5] (Chart 1);

*1 A major part of this paper was presented at the 21st Annual Meeting of the Chemical Society of Japan, Osaka, March, 1968.

1) Y. Kawase, M. Hubert-Habart, J.-P. Buisson and R. Royer, *Compt. Rend.*, **258**, 5007 (1964).

2) Y. Kawase, R. Royer, M. Hubert-Habart, A. Cheutin, L. René and J.-P. Buisson, *Bull. Soc. Chim. Fr.*, **1964**, 3131.

3) R. Royer, Y. Kawase, M. Hubert-Habart, L. René and A. Cheutin, *ibid.*, **1966**, 211.

4) Y. Kawase and M. Takashima, This Bulletin, **40**, 1224 (1967).

5) Preliminary report: Y. Kawase, *Chem. Ind.* (London), **1970**, 687.

3-(*m*- and *p*-acetylphenoxy)butanones[4,6] (**1** and **2**) were treated with concentrated sulfuric acid at 45 or 60°C for 30 min to give 2,3-dimethyl-4- and -5-benzofuranyl methyl ketones (**3** and **4**) respectively, while **1** and **2** afforded 2,3-dimethyl-6- and -5-benzofuranyl methyl ketones (**5** and **4**) by means of the action of polyphosphoric acid.[4,5] Therefore, the almost pure ketone **3** could be prepared much more easily than by the reported method;[4] however, the product was found by the NMR spectroscopy to contain only a small amount (*ca.* 1%) of the isomeric ketone (**5**). On the other hand, 3-(*m*- and *p*-methoxycarbonylphenoxy)-butanones[4] (**6** and **7**) were treated with polyphosphoric acid at 100°C for 1 hr to give a mixture of 2,3-dimethyl-4- and -6-benzofurancarboxylic acids (**8a** and **10a**) and 2,3-dimethyl-5-benzofurancarboxylic acid (**9a**) respectively, the ester group having been hydrolyzed, while **6** and **7** afforded 4-benzofurancarboxylic acid (**8a**) and methyl 5-benzofurancarboxylate (**9b**) respectively, by the action of concentrated sulfuric acid.[4]

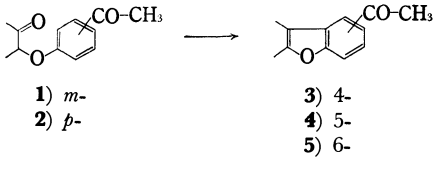

1) *m*- **3**) 4-
2) *p*- **4**) 5-
5) 6-

6) *m*- **8**) 4-
7) *p*- **9**) 5-
10) 6-

In all charts: a) R=H, b) R=Me

Chart 1

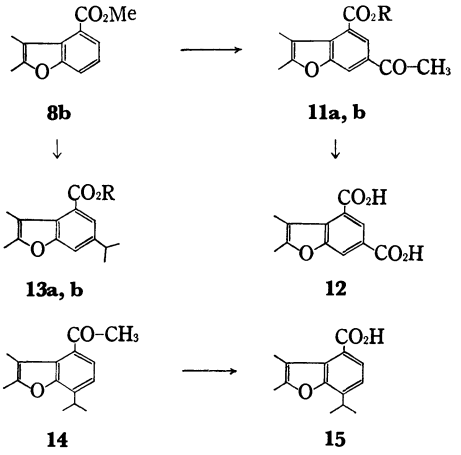

Chart 2

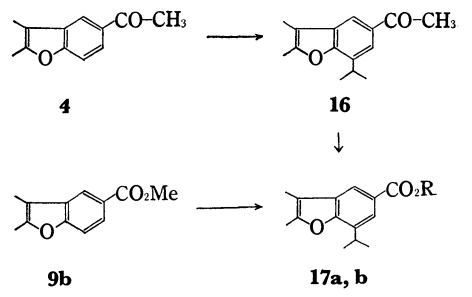

Chart 3

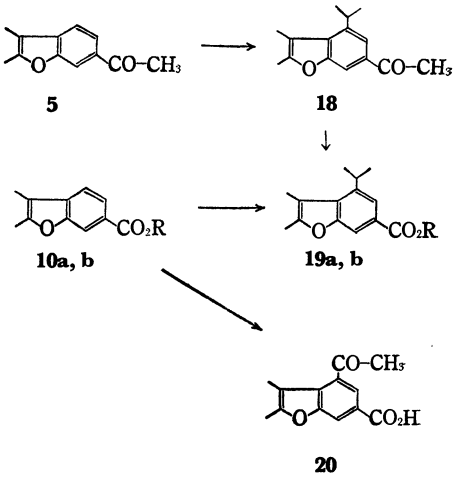

Chart 4

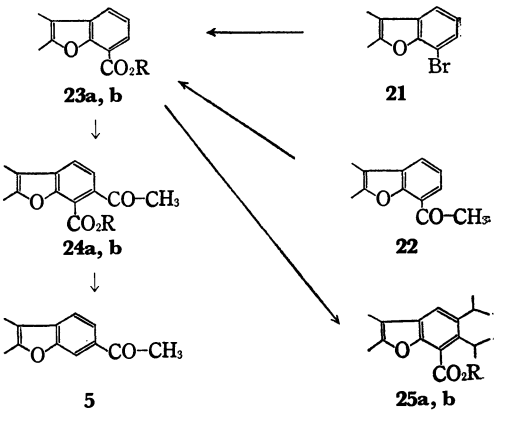

Chart 5

The mixture of 4- and 6-carboxylic acids (**8a** and **10a**) described above could not be separated by crystallization or chromatography, but the ratio of the components was determined by estimating the areas of the peaks corresponding to the 3-methyl protons of **8a** and **10a** (δ=2.22 and 2.17 ppm respectively) in the NMR spectrum of the mixture. The ring closure of **1** and **6** occurred at the ortho position of the acetyl or methoxy-

6) E. Bisagni, J. -P. Marquet, A. Cheutin, R. Royer and M. L. Desvoye, *Bull. Soc. Chim. Fr.*, **1965**, 1466.

carbonyl group by means of sulfuric acid and mainly at the para position by means of polyphosphoric acid. 2,3-Dimethyl-7-benzofurancarboxylic acid (**23b**) was prepared by the action of carbon dioxide on the Grignard reagent prepared from 7-bromobenzofuran[7] (**21**) or by the bromoform reaction of the 7-benzofuranyl methyl ketone[7] (**22**), and methyl 4- and 7-benzofurancarboxylates (**8b** and **23b**) were prepared by the esterification of the corresponding carboxylic acids (**8a** and **23a**).

Therefore, the actylation of the esters **8b** and **23b** was carried out much as has been reported before[4] by the action of acetyl chloride and aluminum chloride in carbon disulfide at room temperature; this gave the acetylated compounds (**11b** and **24b**) (Charts 2 and 5). The position of the acetyl group was determined by NMR spectroscopy and also by converting the keto-esters to known compounds; the keto-esters (**11b** and **24b**) were converted to the corresponding keto-acids (**11a** and **24a**). The keto-acid **11a** was oxidized by the bromoform reaction to the known 2,3-dimethyl 4,6-dicarboxylic acid[4] (**12**); this indicated that the acetylation occurred at the 6-position of the ester **8b**, similarly to the case of the 4-benzofuranyl methyl ketone[4] (**4**). The keto-acid **24a** was decarboxylated to the ketone **5**;[6] this indicated that the acetylation occurred at the 6-position of the ester, **23b**, as in the case of methyl 2,3-dimethyl-5-benzofurancarboxylate[4] (**9b**). The analogous acetylation of 6-carboxylic acid (**10b**) furnished the 4-acetyl compound (**20**), which was identical with the authentic sample prepared by the acetylation of the 6-carboxylic ester (**10b**), followed by hydrolysis[4] (Chart 4).

Next, the alkylation of the ketones (**3**, **4** and **5**) and the esters (**8b**, **9b**, **10b** and **23b**) was carried out by the use of *n*- or iso-propyl bromide and alminum chloride in carbon disulfide at the reflux temperature, whereas the alkylation occurred at room temperature in the cases of the 6-substituted compounds (**5** and **10b**). Normal- and iso-propyl bromide gave the same isopropylated products, probably through the isomerization of the *n*-propyl group, while ethyl bromide or iodide and aluminum chloride or bromide gave no alkylation products.

In the cases of the ketone **3** and the ester **8b** (Chart 2), the crude products could not be purified by usual methods; it was confirmed by gas chromatography that they contained some recovery compounds and two other compounds in each case. The crude product from the ester **8b** was hydrolyzed and then crystallized to give pure 2,3-dimethyl-6-isopropyl-4-benzofurancarboxylic acid (**13b**). The position of the isopropyl group was determined from the fact that the compound was not identical with 2,3-dimethyl-7-isopropyl-4-benzofurancarboxylic acid (**15**), which had itself been prepared by the bromoform reaction of the corresponding ketone[2] (**14**), and from the pattern of the NMR spectrum.

The alkylation of the ketone **4** and the ester **9b** was carried out similarly to give the isopropylated ketone (**16**) and ester (**17b**) (Chart 3); these products were then both converted to the same 2,3-dimethyl-7-isopropyl-5-benzofurancarboxylic acid (**17a**) by the bromoform reaction or by hydrolysis respectively. The ketone **16** was identical with an authentic sample[2] prepared from the 4-hydroxy-3-isopropylphenyl methyl ketone, and the NMR spectra of **16** and **17b** had two doublets (J= 2 Hz) corresponding to the aromatic protons, indicating that the two aromatic hydrogens were at positions meta to each other.

The alkylation of the ketone **5** and the ester **10b** afforded the known 4-isopropyl compounds (**18** and **19b**)[2,8] (Chart 4).

The alkylation of the ester **23b** by a similar procedure afforded a mixture which was proved by gas chromatography to contain the recovery compound and four other compounds. The crude product was hydrolyzed and then crystallized from ethanol to give an acid, the structure of which was confirmed to be 2,3-dimethyl-5,6-diisopropyl-7-benzofurancarboxylic acid (**25a**) from the data of microanalysis and the NMR spectrum (Chart 5). The NMR spectrum of **25a** had a peak corresponding to one aromatic proton and two doublets corresponding to two isopropyl methyl protons, plus a peak corresponding to 3-methyl protons which was in a higher field than in the cases of 4-substituted compounds,[5,8] indicating that **25a** had no substituent in the 4-position.

In conclusion, we can say that in the electrophilic substitution of *bz*-acetyl or *bz*-methoxycarbonyl derivatives of 2,3-dimethylbenzofuran, all position, but especially the 6- and 4-positions, are activated by the effect of the furan ring,[1-4] and that the *m*-position relative to the acetyl or methoxycarbonyl group is less deactivated than the *o*- or *p*-position by the effect of the group. In the cases of the acetylation of **8b** and the alkylation of **5** and **10b**, the reaction occurred at the 6- and 4-positions, favored by both effects, and the effect of the furan ring predominated in the acetylation of **23b**, while the substituent effect dominated in the alkylation of **4** and **9b** and the polyalkylation occurred in the alkylation of **3**, **8b** and **23b**.

Experimental

All the melting points and boiling points are uncorrected, and IR spectra were measured in the form

7) C. Pène, P. Demerseman, A. Cheutin and R. Royer, *Bull. Soc. Chim. Fr.*, **1966**, 586.

8) Y. Kawase, S. Takata and T. Miwa, This Bulletin, **43**, 1796 (1970).

of KBr disks in the case of solid samples, and the gas chromatography was carried out on a Hitachi K23 apparatus, with Silicone DC-11 on Chamelite as a stationary phase, a flow rate, He, of 46 ml/min (0.7 kg/cm^3), and a temperature rise of 5°C/min from 180°C. The NMR spectra were measured on a Nihon Denshi 60 MHz spectrometer in carbon tetrachloride (*ca.* 5% solution), unless otherwise noted, with TMS as the internal standard. The detailed data are summarized in the tables.

Materials. *a) Aryloxybutanones.* The 3-(*m*- and *p*-acetyphenoxy)butanones[4,6] (**1** and **2**) and 3-(*m*- and *p*-methoxycarbonylphenoxy)butanones[4] (**6** and **7**) were prepared following the methods in the references.

b) Benzofuranyl Methyl Ketones. 2,3-Dimethyl-6-[9] and -7-benzofuranyl methyl ketones[7] (**5** and **22**) and 2,3-dimethyl-7-isopropyl-4-benzofuranyl methyl ketone[2] (**14**) were prepared following the methods in the references. 2,3-Dimethyl-4- and -5-benzofuranyl methyl ketones (**3** and **4**) were prepared as follows:

Table 1. Reactions other than alkylation

Starting compd.	Reagent	Prod.	Yield %
	Dehydro-cyclization		
1	H_2SO_4	**3**	62[a]
2	H_2SO_4	**4**	33
6	PPA[b]	**8a**+**10a**	43[c]
7	PPA	**9a**	86
	Grignard Reaction		
21	$Mg+CO_2$	**23a**	58
	Esterification		
8a	$Me_2SO_4+K_2CO_3$	**8b**	74.5
8a	$MeOH+H_2SO_4$	**8b**	93
23a	$Me_2SO_4+K_2CO_3$	**23b**	76
	Acetylation		
8b	$AcCl+AlCl_3$	**11b**	37.5
10a	$AcCl+AlCl_3$	**20**	16
23b	$AcCl+AlCl_3$	**24b**	55
	Hydrolysis		
11b	KOH	**11a**	81
13b[d]	KOH	**13a**	27
17b	KOH	**17a**	69
24b	KOH	**24a**	65
25b[d]	KOH	**25a**	20
	Bromoform Reaction		
11a	NaOBr	**12**	49.5
14	NaOBr	**15**	48
16	NaOBr	**17a**	61
22	NaOBr	**23a**	14
	Decarboxylation		
24a	Cu+quinoline	**5**	42.5

a) This contains about 1% of **5**.
b) Polyphosphoric acid.
c) This consists of 77% of **8** and 23% of **10**.
d) The crude compound.

9) E. Bisagni and R. Royer, *Bull. Soc. Chim. Fr.*, **1962**, 925.

2,3-Dimethyl-5-benzofuranyl Methyl Ketone (4). Concentrated sulfuric acid (5 g) was stirred, drop by drop, into the 3-aryloxybutanone **2** (3 g) with cooling below 60°C, after which the mixture was stirred at 60°C for 30 min. The cooled mixture was then poured into ice water and extracted with ether. The ethereal solution was washed with an aqueous sodium hydroxide solution, and the ether was distilled off. The residual product was distilled, bp 175—183°C/23 mmHg, 1.2 g (44%), and then crystallized to give the pure ketone **4**, mp 78°C, 0.9 g (33%), which was identical with an authentic sample.[6]

2,3-Dimethyl-4-benzofuranyl Methyl Ketone (3). This was also prepared by the same procedure with a reaction temperature of 45°C; the product, bp 157—160°C/20 mmHg, 1.7 g (62%), was confirmed to be identical with an authentic sample[4] by a study of the IR and NMR spectra, by gas chromatography, and preparing 2,4-dinitrophenylhydrazone. However, it was found to contain a small amount (*ca.* 1%) of the isomeric ketone **5** on the basis of the NMR spectrum, in which a low peak corresponding to the 3-methyl protons of **5** appeared at $\delta=2.14$ in addition to high peak corresponding to those of **3** at $\delta=2.11$.[5,8]

c) Benzofurancarboxylic Acids. 2,3-Dimethyl-4- and -6-benzofurancarboxylic acids[4] (**8a** and **10a**) were prepared following the method in the reference, while 2,3-dimethyl-5- and -7-benzofurancarboxylic acid (**9a** and **23a**) were prepared as follows:

2,3-Dimethyl-5-benzofurancarboxylic Acid (9a). A mixture of 3-aryloxybutanone (**7**) (3 g) and polyphosphoric acid ($n=2.5$, 60 g) was heated at 100°C for 1 hr with stirring, after which the cooled mixture was poured into ice water. The crystalline product thus formed was collected and recrystallized from ethanol to give **9a**, mp 239—240°C, 2.2 g (86%), which was identical with an authentic sample.[4]

The 3-aryloxybutanone (**6**) (1.5 g) was also treated similarly to give a crude crystalline product, mp 151—155°C, 0.55 g (43%), which could not be purified by crystallization; the product was found to be a mixture of **8a** (77%) and **10a** (23%) by estimating the area of the peaks, $\delta=2.22$ and 2.17 ppm (in trifluoroacetic acid), corresponding to the 3-methyl protons of **8a** and **10a** respectively.[5,8]

2,3-Dimethyl-7-benzofurancarboxylic Acid (23a). *i) By the Grignard Reaction of the Bromo Compound **21**.* A solution of 2,3-dimethyl-7-bromobenzofuran[7] (**21**) (30 g) in tetrahydrofuran (80 ml) was gradually added to a suspension of magnesium (3.3 g) in tetrahydrofuran (30 ml), with the addition of a small amount of iodine at first. After all of the magnesium had been dissolved (about 40 min), the solution was cooled to −10°C; then a stream of carbon dioxide from dry ice was passed into it with stirring and cooling. Dilute sulfuric acid was added, and the mixture was extracted with ether. The ether was distilled off, and the residue was crystallized from ethanol to give **23a**; mp 192—193.5°C, 14.6 g (58%). The UV[8] and NMR[5,8] spectra were reported previously.

*ii) By the Bromoform Reaction of the Ketone **22**.* A solution of **22** (0.7 g) in dioxane (30 ml) was added with cooling to an aqueous sodium hypobromite solution; this solution had been prepared by adding bromine (0.8 g, 3.8 mol equivalents) to a mixture of sodium hydroxide (1.5 g, 9 mol equivalents), water (5 ml),

and ice (5 g). The mixture was stirred for 30 min with cooling and then for 1.5 hr at 45°C. The cooled mixture was diluted with water, washed with ether, and then acidified after the addition of a small amount of sodium bisulfite. The crystalline product thus formed was collected and recrystallized from ethanol to give **23a**, mp 189—191°C, 0.1 g (14%), which was identical with the other sample.

d) Methyl Benzofurancarboxylates. Methyl 2,3-dimethyl-5- and -6-benzofurancarboxylates[4] (**9b** and **10b**) were prepared following the method of the reference, while the 4- and 7-isomers (**8b** and **23b**) were prepared as follows:

Methyl 2,3-Dimethyl-4- and -7-Benzofurancarboxylates (8b and 23b). *i) By the Action of Dimethyl Sulfate and Potassium Carbonate.* Potassium carbonate (8.5 g, 3 mol equivalents) was added to a solution of the acid **8a** (4 g) and dimethyl sulfate (3.9 g, 1.4 mol equivalents) in acetone (150 m*l*), and the mixture was refluxed for 8 hr. Most of the acetone was distilled off, and the residue was treated with water and then extracted with ether. The ethereal solution was washed with an aqueous sodium hydroxide solution, and the ether was distilled off. The residual product was distilled to give **8b**, bp 162—165°C/16 mmHg, n=1.5660 (21.5°C), 3.2 g (74.5%). The UV[8] and NMR[5,8] spectra of which have been reported previously. The ester **23b** was prepared by the same procedure; mp 58—59°C (from cyclohexane); yield, 76%; its UV[8] and NMR[5,8] spectra have also been reported previously.

ii) By the Action of Methanol and Sulfuric Acid. A mixture of the acid **8a** (7 g), methanol (40 m*l*), and concentrated sulfuric acid (2 g) was refluxed for 4 hr. A half of the methanol was then distilled off, and the mixture was treated with water and then extracted with ether. The ethereal solution was washed with a 5% aqueous sodium hydroxide solution, and the ether was distilled off. The residual product was distilled to give **8b**, bp 163—164°C/20 mmHg, 7 g (93%).

Acetylation of the Esters (8b and 23b) and the Acid (10a). Powdered aluminum chloride (4.5 g, 2.2 mol equivalents) was gradually added, with cooling, to a solution of the ester **8b** (3.1 g) and acetyl chloride (1.5 g, 1.7 mol equivalents) in carbon disulfide (50 m*l*); the mixture was stirred for 4 hr at room temperature and then allowed to stand overnight. The next day, the mixture was poured into ice water and extracted with chloroform. The organic layer was washed with an aqueous sodium hydroxide solution and the solvent was distilled off. The residual product was crystallized from petroleum ether to give methyl 2,3-dimethyl-6-acetyl-4-benzofurancarboxylate (**11b**), mp 106—107°C, 1.4 g (37.5%).

Methyl 2,3-dimethyl-6-acetyl-7-benzofurancarboxylate (**24b**) was obtained by the same procedure from the ester **23b**, and 2,3-dimethyl-4-acetyl-6-benzofurancarboxylic acid (**20**), mp 211—212°C, which was identical with an authentic sample,[4] was also obtained by the same procedure from the acid **10a** by means of the action of acetyl chloride (1.2 mol equivalents) and aluminum chloride (3 mol equivalents) in carbon di-

TABLE 2. ALKYLATION OF KETONES AND ESTERS BY $AlCl_3$ IN CS_2

Starting compd.	RBr	Reac. temp.	Crude product		Pure[b] product (yield %)
			Bp°C/mmHg (yield %)	Peaks in gas chromatogram °C[a] (share %)	
3	*n*-Pr	Reflux	185—190/21 (76)	195[c] (2), 204 (30), 208 (50)	—
3	*i*-Pr	Reflux	178—183/20 (71)	195[c] (2), 204 (30), 208 (50)	—
4	*n*-Pr	Reflux	185—195/20 (74)	193[c] (5), 203[d] (75), 209 (10)	**16** (37)
5	*n*-Pr	Room	180—190/23 (67)	—	**18** (15.5)
5	*n*-Pr	Reflux	193—196/21 (90)	197[c] (2), 205[d] (95)	**18** (70)
5	*i*-Pr	Reflux	185—196/19 (80)	197[c] (2), 205[d] (95)	**18** (30.5)
8b	*i*-Pr	Room	Recovery		
8b	*n*-Pr	Reflux	195—198/23 (73)	195[c] (2), 208[d] (95), 211 (3)	e)
8b	*i*-Pr	Reflux	180—195/21 (57)	195[c] (2), 208[d] (95), 211 (3)	e)
9b	*n*-Pr	Room	Recovery		
9b	*n*-Pr	Reflux	185—190/21 (66)	198[c] (3), 208[d] (90), 213 (7)	**17b** (41.5)
9b	*i*-Pr	Reflux	185—189/20 (58)	198[c] (3), 208[d] (90), 213 (7)	**17b** (21)
10b	*n*-Pr	Room	~187/20 (58)	—	**19b** (16.5)
10b	*i*-Pr	Room	~198/23 (66)	—	**19b** (16.5)
10b	*n*-Pr	Reflux	190—200/21 (75)	198[c] (1), 211[d] (85), 214 (5), 217 (5)	**19b** (25)
10b	*i*-Pr	Reflux	~190/21 (75)	—	**19b** (16.5)
23b	*i*-Pr	Room	Recovery		
23b	*i*-Pr	Reflux	190—205/21 (35)	198[c] (20), 207 (17), 210 (30), 212 (10), 220 (15)	e)

a) The gas chromatography was carried out with temperature rise of 5°C/min from 180°C.
b) Crystallized from the solvent described in references or Table 3.
c) This peak corresponded to the recovery.
d) This peak corresponded to the compound obtained in pure form.
e) The crude product was hydrolyzed to the acid.

Table 3. The mp or bp, IR and analyses of new compounds

Compd.	Mp°C (solv.)[a] or bp°C/mmHg	ν_{CO}^{max} cm^{-1}	Formula	Found C%	Found H%	Calcd C%	Calcd H%
			Esters				
8b	163—164/20	1724	$C_{12}H_{12}O_3$	70.43	6.07	70.57	5.92
11b	106—107 (Pet)	1720 1674	$C_{14}H_{14}O_4$	68.43	5.74	68.28	5.73
17b	84.5—86 (Pet)	1715	$C_{15}H_{18}O_3$	73.22	7.39	73.14	7.37
23b	58—59 (Cy)	1720	$C_{12}H_{12}O_3$	70.64	5.84	70.57	5.92
24b	124.5—125.5 (Cy)	1720 1668	$C_{14}H_{14}O_4$	68.44	5.72	68.28	5.73
			Carboxylic Acids				
11a	178—180 (Et)	1710 1680	$C_{13}H_{12}O_4$	66.70	5.56	67.23	5.21
13a	135—137.5 (DMe)	1695 1672	$C_{14}H_{16}O_3$	72.61	7.19	72.39	6.94
15	180.5—182 (Et)	1700 1685	$C_{14}H_{16}O_3$	72.53	6.73	72.39	6.94
17a	213—215 (Me)	1680	$C_{14}H_{16}O_3$	72.12	6.99	72.39	6.94
23a	192—193.5 (Et)	1685	$C_{11}H_{10}O_3$	70.05	5.10	69.46	5.30
24a	207—208 (Et)	1728 1640	$C_{13}H_{12}O_3$	67.07	5.19	67.23	5.21
25a	242—244 (DMe)	1668	$C_{17}H_{22}O_3$	74.07	8.35	74.42	8.08

a) Pet: petroleum ether, Cy: cyclohexane, Et: ethanol, DMe: dilute methanol, Me: methanol.

Table 4. The NMR spectra (δ-value[a] (ppm))

Compd.	Ph-H	$-CO_2CH_3$	Ph-CH<	$-COCH_3$	2-CH_3	3-CH_3	Ph-C(CH$_3$)$_2$
b)			3.33 (m)		2.28	2.03	1.32 (d)
11b	5-H 7-H 8.02 (d) 7.77 (d) J=2 Hz	3.83		2.52	2.32	2.19	
13a[c]	5-H 7-H 7.83 (d) 7.45 (d) J=2 Hz		3.06 (m)		2.42	2.36	1.31 (d)
14	5-H 6-H 7.28 (d) 6.33 (d) J=7 Hz		3.40 (m)	2.47	2.34	2.12	1.30 (d)
16	4-H 6-H 7.73 (d) 7.63 (d) J=2 Hz		3.40 (m)	2.55	2.40	2.15	1.39 (d)
17b	4-H 6-H 7.83 (d) 7.67 (d) J=2 Hz	3.84	3.39 (m)		2.35	2.11	1.36 (d)
24b	5-H 4-H 7.41 (d) 7.24 (d) J=8 Hz	3.91		2.49	2.39	2.11	
25a	7.54		3.34 (m)		2.20	1.80	1.28 (d) 1.23 (d)

a) Measured on a Nihon Denshi 60 MHz apparatus in CCl_4 (about 5%), unless otherwise noted, using TMS as the internal standard, and (d): doublet and (m): multiplet.
b) 2, 3-Dimethyl-7-isopropylbenzofuran. c) In $CDCl_3$.

sulfide.

Alkylation of the Ketones (3, 4, and 5) and the Esters (8b, 9b, 10b and 23b) (Table 2). Powdered aluminum chloride (2.8 g, 2 mol equivalents) was added, with stirring and cooling, to a solution of the ketone **4** (2 g) and *n*-propyl bromide (1.6 g, 1.2 mol equivalents) in carbon disulfide (50 m*l*); the mixture was then refluxed for 3 hr. The cooled mixture was poured into ice water containing some dilute hydrochloride acid and subsequently extracted with chloroform. The organic layer was washed with a dilute aqueous sodium hydroxide solution, and the solvent was distilled off. The residual product was distilled to give a crude product, bp 185—195°C/20 mmHg, 1.8 g; this crude product was crystallized from petroleum ether to give a pure 2,3-dimethyl-7-isopropyl-5-benzofuranyl methyl ketone (**16**), mp 107—108°C, 0.9 g (37%), which was identical with an authentic sample.[2]

The alkylation was carried out much as in the cases of the ketones (**3** and **5**) and the esters (**8b**, **9b**, **10b**, and **23b**) as is shown in Table 2, but the products could not be purified by distillation, crystallization, or chromatography on alumina in the cases of **3**, **8b**, and **23b**; the crude products from the latter two were directly hydrolyzed to the carboxylic acids. In the cases of the ketone **5** and the ester **10b**, some of the alkylated products were obtained by a reaction at room temperature.

Hydrolysis of the Keto-esters (11b and 24b) and the Esters (13b, 17b and 25b). A mixture of the keto-ester **11b** (1.3 g), methanol (2 m*l*), and a 50% aqueous potassium hydroxide solution (2 m*l*) was refluxed for 3 hr. The cooled mixture was diluted with water and washed with ether. The alkaline solution was then acidified to give a crystalline product; this product was subsequently recrystallized from ethanol to give 2,3-dimethyl-6-acetyl-4-benzofurancarboxylic acid (**11a**), mp 178—180°C, 1 g (81%).

Similarly, 2,3-dimethyl-6-acetyl-7-benzofurancarboxylic acid (**24a**) and 2,3-dimethyl-7-isopropyl-6-benzofurancarboxylic acid (**17a**) were obtained from **24b** and **17b** respectively, and 2,3-dimethyl-6-isopropyl-4-benzofurancarboxylic acid (**13a**) and 2,3-dimethyl-5,6-diisopropyl-7-benzofurancarboxylic acid (**25a**) were obtained from two crude esters, **13b** and **25b** respectively.

The Bromoform Reaction of the Ketones (14 and 16) and of the Keto-acid (11a). In the cases of **14** and **16**, the reaction was carried out to give 2,3-dimethyl-7-isopropyl-4-benzofurancarboxylic acid (**15**) and **17a** respectively, much as has been described for **23a** from **22**. The keto-acid **11a** was treated with an excess of sodium hydroxide to give 2,3-dimethyl-4,6-benzofurandicarboxylic acid (**12**), mp 324°C, which was identical with an authentic sample.[4]

Decarboxylation of the Keto-acid 24a. A mixture of the keto-acid **24a** (0.29 g), copper powder (0.18 g), and quinoline (5 m*l*) was refluxed under a stream of nitrogen until the evolution of carbon dioxide had ceased. The cooled solution was then acidified by the addition of dilute hydrochloric acid, and the mixture was extracted with ether. The ethereal solution was washed with a 5% auqueous sodium hydroxide solution, and the ether was distilled off. The residual product was crystallized from cyclohexane to give the ketone **5**, mp 79—80°C, 0.034 g (42.5%), which was identical with an authentic sample.[9]

The authors are grateful to the members of the Laboratory of Analysis, Faculty of Pharmacology of Toyama University, for their microanalyses.

BULLETIN OF THE CHEMICAL SOCIETY OF JAPAN VOL. 43 2891—2893 (1970)

Photoinduced Reactions. XLI.[1] Stereochemical Course in the Photochemistry of a 2,5-Cyclohexadienone

Katsuyuki OGURA and Teruo MATSUURA

Department of Synthetic Chemistry, Faculty of Engineering, Kyoto University, Kyoto

(Received January 24, 1970)

Mechanism for the photochemical transformation of a 2,5-cyclohexadienone into a bicyclo[3.1.0]hex-3-en-2-one (so-called lumiketone) was discussed. Photolysis of 2,4,6-tri-*t*-butyl-4-methoxy-2,5-cyclohexadienone (VII) gave only one stereoisomer (VIIIa) of the corresponding lumiketones. This fact and the prediction by the Woodward-Hoffmann rule indicate that a biradical-like excited state XI with 3,5-bonding gives rise to a direct rearrangement to lumiketone VIIIa as shown in Path B (Scheme II).

The transformation of 2,5-cyclohexadienone into bicyclo[3.1.0]hex-3-en-2-one, the so-called lumiketone, is a most intriguing photochemical reaction. It was originally postulated[2] that the course of this transformation involves the sequence of events shown in Scheme I (Path A), namely, rebonding of the triplet excited state II to give the bridged excited state III, followed by electron demotion to the ground-state zwitterion IV which finally undergoes rearrangement to the product V. That the immediate precursor to the lumiketone is the zwitterion is generally accepted in recent discussions.[3] However, Schuster and Patel[4] suggested that an alternative pathway, by which rearrangement and electron demotion occur simultaneously without involvement of the zwitterion intermediate (Path B in Scheme I), is favorable in the photochemical transformation of 4-trichloromethyl-4-methyl-2,5-cyclohexadienone (VI) into the corresponding lumiketone (XVII). The latter possibility (Path B) was also supported by Swenton *et al.*[5] We now wish to discuss these possibilities from the stereochemical viewpoint of this photochemical reaction.

In a previous paper,[6] we reported that photolysis of 2,4,6-tri-*t*-butyl-4-methoxy-2,5-cyclohexadienone (VII) underwent the same transformation as mentioned above to yield a lumiketone (VIII), which on further irradiation gave photoketone(IX) and photophenol(X). For the transformation of VII into VIII, two routes, Path A and Path B shown in Scheme II, are also possible. It can be expected that intermediates of steric formulas, XIa for a biradical-like species and XIIa for a zwitterion species, are preferred to the isomeric forms, XIb and XIIb, respectively. It is well known that the preferred conformation of *t*-butylcyclohexane is i. The methoxyl of VII showed its NMR signal at τ 6.88. This value is relatively large compared with that of dimethyl ether (τ 6.76), and may indicate that this methoxyl is located on a shielding area of π-clouds. Therefore, it is reasonable that the preferred conformation of VII is depicted as ii, and that XIa is more easily formed from VII than XIb is formed.

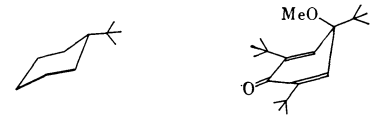

i ii

Zimmerman and Crumrine,[7] and Brennan and Hill[8] have shown that the isomerization of the zwitterions, which were produced by treatment of XIIIa and XIIIb with potassium *t*-butoxide and of XIIIc with zinc, to the corresponding lumiketones follows the "slither" mechanism, involving two 1,2-shifts with C-6 migrating from C-5 to C-4 and then from C-1 to C-5 (Scheme III). There-

1) Photoinduced Reactions. XL. I. Saito, S. Kato and T. Matsuura, *Tetrahedron Letters*, 239 (1970).

2) H. E. Zimmerman and D. I. Schuster, *J. Amer. Chem. Soc.*, **84**, 4527 (1962).

3) a) N. J. Turro, "Molecular Photochemistry," W. A. Benjamin, Inc., New York, N. Y. (1965). b) K. Schaffner, *Advan. Photochem.*, **4**, 81 (1966). c) P. J. Kropp in "Organic Photochemistry," O. L. Chapman, Ed., Marcel Dekker, Inc., New York, N. Y. (1967), p. 1ff. d) H. E. Zimmerman, *Advan. Photochem.*, **1**, 183 (1963); O. L. Chapman, *ibid.*, **1**, 323 (1963).

4) D. I. Schuster and D. J. Patel, *J. Amer. Chem. Soc.*, **90**, 5145 (1968).

5) J. S. Swenton, E. Saurborn, R. Srinivasan and F. I. Sonntag, *ibid.*, **90**, 2990 (1968).

6) T. Matsuura and K. Ogura, *ibid.*, **89**, 3846 (1967).

7) H. E. Zimmerman and D. S. Crumrine, *ibid.*, **90**, 5612 (1968); *ibid.*, **91**, 434 (1969).

8) T. M. Brennan and R. K. Hill, *ibid.*, **90**, 5615 (1968).

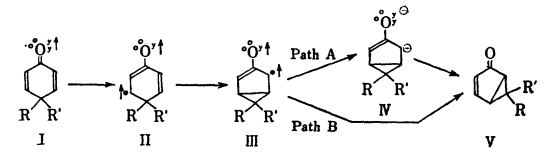

Scheme I

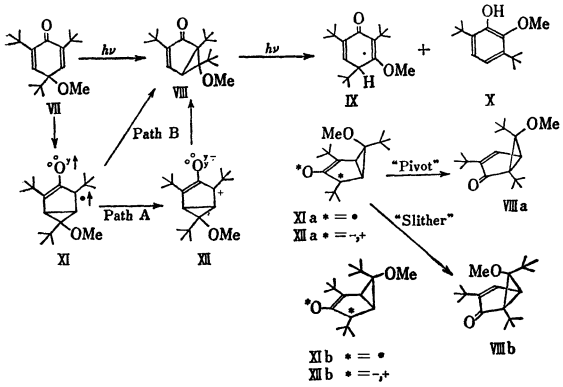

Scheme II

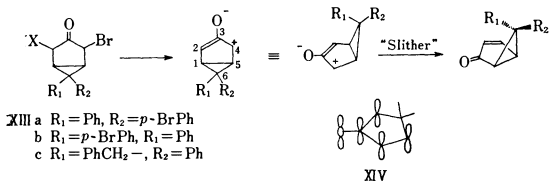

Scheme III

Scheme IV

fore, if the zwitterion XI is involved in the photochemical reaction of VII, VIIIb should be the preferred structure for the lumiketone. The conjugated system, over which 1,4-sigmatropic migration occurs, may be considered as a 2-oxobutadiene skeleton. Calculation of the symmetry properties of the Hückel molecular orbitals of XIV shows that the highest occupied molecular orbital (ψ_2 of butadiene or ψ_3 of 2-oxobutadiene) is antisymmetric irrespective of the effect of the oxygen. Thus it is supported that the transformation of IV to V follows the slither mechanism.[7,8] However, the lowest vacant molecular orbital (ψ_3 of butadiene or ψ_4 of 2-oxobutadiene) is symmetric, and consequently a concerted suprafacial rearrangement in an excited state requires inversion of configuration of the migrating group (the "pivot" mechanism, the orbital at C-6 detaching itself from C-1, then bonding to C-4 as shown in Scheme

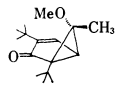

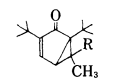

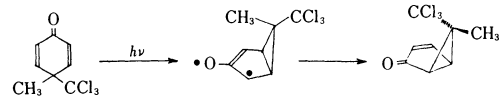

IV).[9] If the photochemical isomerization of VII to VIII follows Path B (Scheme II), the lumiketone with structure VIIIa should be formed predominantly.

Photolysis of VII in petroleum ether with a visible light gave only an isomer of VIII. Furthermore, careful chromatographic analyses of the reaction mixture at various stages of irradiation showed that only one isomer of VIII was formed in addition to recovered VII. The configuration of this lumiketone was deduced by comparing its NMR spectrum with that of 1,3-di-*t*-butyl-6-methyl-6-methoxybicyclo[3.1.0]hex - 3 - en - 2 - one (XV), which was formed on photolysis of 2,6-di-*t*-butyl - 4 - methyl - 4 - methoxy - 2,5 - cyclohexadienone.[10],*1 The resonance of the methoxyl of VIII appeared at τ 6.73, similar to that of dimethyl ether (τ 6.76), while the methoxyl singlet of XV was observed at an unusually high field (τ 6.97). The high-field shift should result from diamagnetic shielding by the enone system of XV. The analogous unusual shifts were also observed in a methoxyl of α-lumicolchicine[11] and C-6 methyl of 1,3-di-*t*-butyl-6-allyl (or *n*-propyl)-6-methylbicyclo[3.1.0]-hex-3-en-2-one (XVI),[12] and it was suggested that the shifts were ascribed to the location of these groups over the π-electron clouds. In the NMR spectra of VII and XV measured in benzene, the methoxyl signal of VIII appeared at a field (τ 6.70) similar to that in $CDCl_3$, while the methoxyl of XV was shifted to a higher field (τ 7.17). This might indicate that the methoxyl group of XV is located over the cyclopentenone ring but not that of VIII.[13]

Both of the *t*-butyl groups of XV at C-1 and C-3 positions were shifted to lower fields by using benzene as a solvent instead of $CDCl_3$. Although two *t*-butyl signals of VIII appeared at lower fields

9) R. B. Woodward and R. Hoffmann, *J. Amer. Chem. Soc.* **87**, 2511 (1965).

10) T. Matsuura, This Bulletin, **37**, 564 (1964).

*1 VPC and TLC analyses showed that only one isomer of XV was not necessarily formed.

11) O. L. Chapman and H. G. Smith, *J. Amer. Chem. Soc.*, **83**, 3915 (1967).

12) B. Miller and H. Margulies, *ibid.*, **89**, 1678 (1967).

13) a) J. Ronayne and D. H. Williams, *Chem. Commun.*, **1966**, 712. b) C. J. Timmons, *ibid.*, **1965**, 576.

in benzene than in $CDCl_3$, other *t*-butyl signal shifted to a higher field. This suggests that the *t*-butyl of VIII at C-6 position may have an endo-configuration. The aliphatic methyl signal of XV appears at τ 8.45, characteristic of an exo-geometry.*2.

Accordingly, formulas VIIIa and XV were given as the stereochemical structures of the "lumi" compounds VIII and XV, respectively. It seems reasonable from the stereochemical structure of VIIIa and the above prediction by the Woodward-Hoffmann rule that Path B (Scheme II) is favorable in the photochemical reaction of VII. It should be also noted that the same stereochemistry is held in the photochemical transformation of VI into its lumiketone XVII.*3 Of course, our conclusion does not necessarily deny the zwitterion intermediate (Path A) in the photochemical transformation of 2,5-cyclohexadienones. It can be expected that the formation of lumiketones predominantly follows Path A (the "slither" mechanism), if electron demotion occurs faster than direct isomerization of III to V (Path B) or if Path B (the "pivot" mechanism) is stereochemically excluded (for example, the photochemical formation of lumisantonine from santonin[2]).

One of the authors (K. O.) is indebted to Fuji Film Co. for a financial support.

*2 Miller and Margulies[12] reported that an exo-methyl at C-6 position of XVI shows its NMR signal at a lowet field (τ 8.60 or 8.65) than an endo-methyl (τ 9.05 or 9.08).

*3 Schuster and Patel[14] reported that this transformation is stereospecific and formula XVII is assigned as the stereochemical structure of this lumiketone. This stereochemical assignment is supported by the fact that the methyl of XVII shows its NMR signal at a field analogous to that of XV.

14) D. J. Patel and D. I. Schuster, *J. Amer. Chem. Soc.*, **90**, 5137 (1968).

BULLETIN OF THE CHEMICAL SOCIETY OF JAPAN VOL. 43 2893—2899 (1970)

Formation and Cycloaddition Reactions of Substituted *N*-Ethoxycarbonyl-1(1*H*)-azepine Derivatives[1]

Tadashi SASAKI, Ken KANEMATSU and Akikazu KAKEHI

Institute of Applied Organic Chemistry, Faculty of Engineering, Nagoya University, Chikusa, Nagoya

(Received February 25, 1970)

The formation of substituted *N*-ethoxycarbonyl-1(1*H*)-azepine derivatives is reinvestigated in the thermal reactions of benzene derivatives with ethyl azidoformate. The rate-determining step in these reactions is determined by kinetic experiments to be the decomposition of the azide. The (4+2) π cycloadducts of these azepine derivatives are obtained by thermal reactions with tetracyanoethylene (TCNE) as a dienophile. The formation of compounds **22**, **23**, **24**, **25**, **26**, and **27** is confirmed by the spectral evidence.

Previously, we reported on the photosynthesis of substituted 1(1*H*),2-diazepines and their reactivities in the cycloaddition reactions.[2] In view of the interest in the theoretical aspects of the cycloaddition reactions of seven-membered cyclic non-benzenoid heteroaromatic hydrocarbons, the above-mentioned new 1(1*H*),2-diazepines would seem to be of timely interest. At the same time, substituted 1(1*H*)-azepines are also considered to comparable with the diazepines in the cycloaddition reactions. Furthermore, recent works[3,4] along these lines have prompted us to report our different preliminary observations concerning the

1) Presented in part at the symposium on Synthetic Organic Chemistry of the Chemical Society of Japan, Tokyo, Nov., 1969. Studies of Heteroaromaticity. XL. Part XXXIX, T. Sasaki, K. Kanematsu and K. Hayakawa, *Chem. Commun.*, **1970**, 82.

2) T. Sasaki, K. Kanematsu, A. Kakehi, I. Ichikawa, and K. Hayakawa, *J. Org. Chem.*, **35**, 426 (1970).

3) Recently, the structures of the adducts from the reactions of *N*-ethoxycarbonyl- and *N*-methoxycarbonylazepines with TCNE have been rigorously established; see a) J. E. Baldwin and R. A. Smith, *J. Amer. Chem. Soc.*, **87**, 4819 (1965); *J. Org. Chem.*, **32**, 3511 (1967). b) A. S. Kende, P. T. Izzo and J. E. Lancaster, *J. Amer. Chem. Soc.*, **87**, 5044 (1965).

4) While this paper was being prepared, a report of the cycloadditions reactions of 1(1*H*)-azepine derivatives has been published: see L. A. Paquette, D. E. Kuhla, J. H. Barrett and L. M. Lwichter, *J. Org. Chem.*, **34**, 2889 (1969).

Table 1. Reaction of ethoxycarbonylnitrene with benzene derivatives

Benzene derivatives	Reaction conditions a) and b)*	(°C)	Absolute yields (%)** Azepines	Urethans
Benzene	a	80	10	0
	b	120	40	0
Toluene	a	110	30	0
	b	120	50	0
o-Xylene	a	120	40—50	0—10
	b	120	20—30	30—40
m-Xylene	a	120	40—50	0—10
	b	120	20—30	30—40
p-Xylene	a	120	40—50	0—10
	b	120	20—30	30—40
Mesitylene	a	120	25	30
	b	120	0	70

* a) in an open flask for 3 hr. b) in a sealed-tube for 2 hr.
** Absolute yields based on ethyl azidoformate.

cycloaddition reactions of 1(1*H*)-azepine derivatives.

This paper will deal with the thermal formation of azepine derivatives from benzene derivatives and ethyl azidoformate under various conditions in both open and sealed-tube systems. To obtain further information concerning the mechanisms for these reactions, we carried out kinetic experiments in the formation of azepines from *p*-xylene and ethyl azidoformate. Subsequently, we investigated the isomeric structures of the reaction adducts between ethyl azidoformate and benzene derivatives in the presence of TCNE.

Results and Discussion

Thermal Reaction of Benzene Derivatives and Ethyl Azidoformate. Although substituted *N*-ethoxycarbonyl-1(1*H*)-azepines have been prepared by the photolysis or pyrolysis of ethyl azidoformate in aromatic substrates such as toluene, anisole, and halobenzenes,[5] we reinvestigated the thermal reaction under various conditions.

When ethyl azidoformate was decomposed in *o*-, *m*- and *p*-xylene in an open flask or in a sealed-tube at 120°C, the corresponding azepines were obtained, together with aromatic urethans. However, when ethyl azidoformate was refluxed in benzene (at 80°C) and toluene (at 110°C) or in a sealed-tube at 120°C, only the corresponding azepines were obtained. On the other hand, when ethyl azidoformate was decomposed in mesitylene at 120°C in an open flask, the corresponding azepines and aromatic urethans were produced in 25 and 30% yields respectively, but at 120°C in a sealed-tube, only the aromatic urethan was produced in about a 60% yield. These results are summarized in Table 1.

These results indicate that ethyl azidoformate was not thermolyzed appreciably at the reflux temperatures of benzene and toluene, as has been reported by Baldwin and Smith.[6]

Substituted aromatic urethans were obtained conveniently by the thermal isomerization of dimethyl and trimethyl-substituted azepines under more drastic conditions. Especially, because of the thermal instability of the tri-substituted azepine skeleton, 1-ethoxycarbonyl-2,4,6-trimethylazepine was readily converted to the aromatic urethans and no seven-membered ring compounds could

Table 2. The number and the ratio of 1(1*H*)-azepines produced

Azepine precusor	Number of azepines	Ratio of azepines* (Comp. No.)
Toluene	3	40 (**9**) : 35 (**8**) : 25 (**10**)
o-Xylene	4	50** : 30** : 15** : 5**
m-Xylene	3	15 (**15**) : 50** : 35**
p-Xylene	2	20 (**18**) : 80 (**19**)

* These ratios were determined by glpc and NMR spectra.
** Structures of isomeric azepines were difficult to determine.

5) a) W. Lwowski and R. L. Jahnson, *Tetrahedron Lett.*, **1967**, 891, and the refs. cited therein. b) R. J. Cotter and W. F. Beach, *J. Org. Chem.*, **29**, 751 (1964). c) K. Hafner, D. Zinser and K. L. Moritz, *Tetrahedron Lett.*, **1964**, 1733. d) R. A. Smith, J. E. Baldwin and I. C. Paul, *J. Chem. Soc., B*, **1967**, 112.

6) Ethoxycarbonylnitrene and ethoxycarbonylcarbene have been generated by the thermal decomposition of ethyl azidoformate and ethyl diazoacetate at 129.6°C in a solution of benzene and anisole, toluene, chlorobenzene or of fluorobenzene in an unreactive perfluorinated polyether: see J. E. Baldwin and R. A. Smith, *J. Amer. Chem. Soc.*, **89**, 1886 (1967).

be detected. The relative ratio of the yielded isomeric ethoxycarbonylazepine derivatives was determined by gas-chromatographic and spectroscopic means. However, the reaction mixture was difficult to separate by means of column chromatography and molecular distillation. These results[7] are shown in Table 2.

In order to obtain kinetic information concerning the above-mentioned reactions, we investigated the reaction of *p*-xylene with ethyl azidoformate in an open flask. The thermolysis of ethyl azidoformate was done at 100, 120, and about 140°C in pure *p*-xylene, and the reactants were then analyzed by glpc. The products were identified as di-substituted *N*-ethoxycarbonylazepines by their retention times and IR and NMR spectra, given in Table 3. The amounts of unchanged ethyl azidoformate at different reaction times were measured by glpc in the reactions of the heating of the mixture of *p*-xylene and ethyl azidoformate at 120°C. These results are shown in Fig. 1. Thus, the following zeroth-order rate constants were determined: $k_{100°}=1.7\times10^{-3}$ min^{-1}; $k_{120°}=6.3\times10^{-3}$ min^{-1}; $k_{138°}=1.7\times10^{-2}$ min^{-1}. On the other hand, the rate of the decomposition of ethyl azidoformate was calculated to be -6.3×10^{-3} min^{-1} at 120°C. These results can be explained in terms of a ethoxycarbonylnitrene which

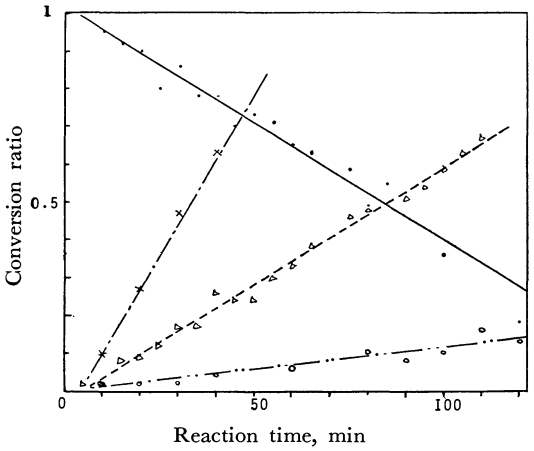

Fig. 1. Kinetic experiments in the reactions of ethyl azidoformate with *p*-xylene.

——— Decomposition curve of ethyl azidoformate at 120°C.
— - — Formation curve of azepines at *ca.* 138°C.
------ Formation curve of azepines at 120°C.
—··— Formation curve of azepines at 100°C.

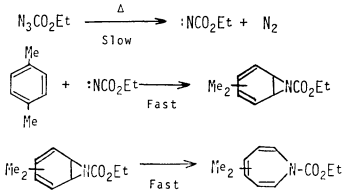

Chart 1.

is generated by the thermal decomposition of ethyl azidoformate in the rate-determing step (slow); it is added to *p*-xylene to form the bicyclic aziridine intermediate, and they converted to the valence-bond isomerization products rapidly (Fig. 1 and Chart 1).

On the basis of the above facts, in summary it can be said that 1*H*-azepines are formed by the kinetically-controlled and aromatic urethans by the thermodynamically-favored reaction pathway shown in Chart 2.

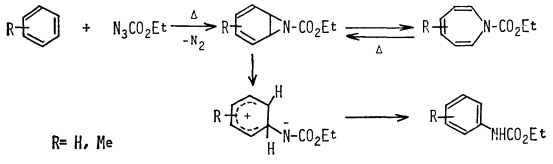

Chart 2.

The structures of a representative number of 1(1*H*)-azepines thus formed from the corresponding benzene substrates are illustrated in Table 3.

The structural assignments for the produced azepines and aromatic urethans were determined by means of their spectral characteristics. In the infrared spectra, the azepines (**7**—**20**) show two strong absorptions due to the carbonyl ester in the ranges of 1700—1720 cm^{-1} and 1320—1340 cm^{-1}, and medium absorptions due to the carbon-carbon double bond in the range of 1610—1660 cm^{-1}. On the other hand, the aromatic urethans exhibit absorptions at 3240—3320 cm^{-1} (NH) and at 1600 cm^{-1} (C_6H_5). More significantly, the isomeric azepine mixture was confirmed by NMR inspection.[8]

From their NMR assignments for substituted 1*H*-azepines, the structures of the isomeric mixture of methyl-substituted 1*H*-azepine derivatives were confirmed. In the 2- and 7-methyl isomers, methyl protons appeared at the lowest field, while in the 3- and 6-methyl isomers, methyl protons appeared at the highest field. The spectrum of a mixture of **18** and **19** showed signals at τ 7.93 (C_2-Me, almost singlet), 8.09 (C_5-Me, almost

7) These results were different from the preliminary observations in the reactions of the ethoxycarbonylnitrene and methoxycarbonylcarbene with substituted benzene derivatives; a) K. Hafner, D. Zinter and K. L. Moritz, *Tetrahedron Lett.*, **1964**, 1733. b) K. Alder, R. Munders and P. Wirtz, *Ann. Chem.*, **627**, 59 (1959).

8) Coincidentally, a general synthetic entry to 1*H*-azepine derivatives has been reported in which structures of substituted 1*H*-azepines have been elucidated by their NMR and Mass spectra: L. A. Paquette, D. E. Kuhla, J. H. Barrette and R. J. Haluska, *J. Org. Chem.*, **34**, 2866 (1969).

Table 3. Structures of 1(1*H*)-azepines from corresponding benzene derivatives

Azepine precursor	Possible structure of formed 1(1*H*)-azepines
Benzene (**1**)	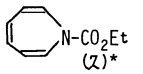 (7)*
Toluene (**2**)	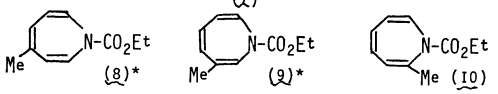 (8)* (9)* (10)
o-Xylene (**3**)	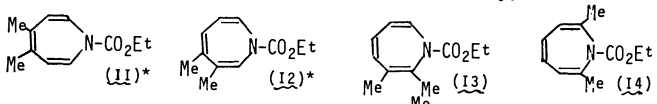 (11)* (12)* (13) (14)
m-Xylene (**4**)	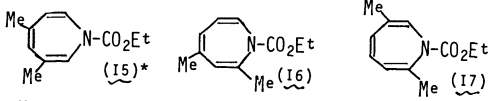 (15)* (16) (17)
p-Xylene (**5**)	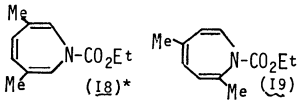 (18)* (19)
Mesitylene (**6**)	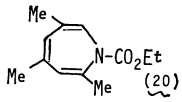 (20)

* The positions of substituents of the 1(1*H*)-azepine derivatives were determined by confirmation of NMR spectra of thier adducts to TCNE.

singlet), and 8.34 (C_3- and C_6-Me, doublet $J=1.5$ Hz) with relative intensities of 2 : 2 : 1. However, the chemical shifts of the C_3- and C_4-Me of the mixture (**8**—**17**) showed approximate values in the range of τ 8.05—8.30, and the signals often overlap. Aromatic urethans, of course, showed a broad signal at about τ 3.60 due to the amino group and at τ 7.65—7.85 attributable to methyl protons attached to the benzene ring.

Thermal Reaction of Ethyl Amidoformate and Aromatic Substrates in the Presence of TCNE. The adducts from tetracyanoethylene and 1-ethoxycarbonylazepines[9] have already been reported to arise from (4+2) π Diels-Alder cyclo addition reactions.[3]

We investigated a series of cycloaddition reactions of ethyl azidoformate and aromatic substrates in the presence of TCNE under thermal conditions (in a sealed-tube at 110°C for 15 hr.).

A dark solution of the reaction mixture was carefully chromatographed in order to obtain the adducts. Thus, four 1 : 1 adducts, **21**,[3] **22**, **26**, and **27**, were isolated. These adducts were structurally elucidated through a consideration of their NMR

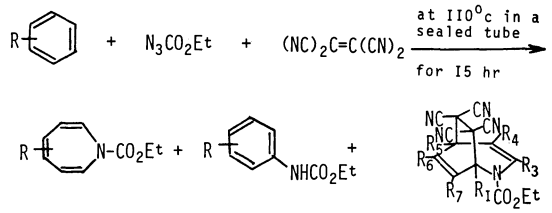

Adduct Comd. No.	R_1	R_3	R_4	R_5	R_6	R_7
21	H	H	H	H	H	H
22	H	H	H	H	Me	H
23	H	H	H	H	H	Me
24	H	H	H	Me	Me	H
25	H	H	H	H	Me	Me
26	H	H	Me	H	Me	H
27	H	H	Me	H	H	Me

Chart 3.

Table 4. Reaction of ethoxycarbonylnitrene and bnzenee derivatives in the presence of TCNE

Benzene derivatives	Absolute yield (%) azepines+Urethans	Cycloadducts (Comp. No.)
Benzene	24*	18 (**21**)
Toluene	20	61 (**22**+**23**)
o-Xylene	16	39 (**24**+**25**)
m-Xylene	20	11 (**26**)
p-Xylene	22	11 (**27**)
Mesitylene	73**	—

* In this case, urethan was not detected.
** In this case, azepine was not detected.

9) The (4+2) π cycloadditions of *N*-substituted azepines to various dienophiles such as tetracyanoethylene,[3] 4-phenyl-1,2,4-triazoline-3,5-dione,[1] *N*-phenylmaleimide,[4] and isobenzofurans,[4] have already been studied. In addition, *N*-carbethoxyhomoazepine and a TCNE adduct were obtained in a similar fashion: T. Sasaki, K. Kanematsu and A. Kakehi, *Chem. Commun.*, in press.

(in $CDCl_3$) and mass spectral menas. The NMR spectrum of the adduct from *m*-xylene shows signals at τ 3.30 (bs, 1H, H_3), 4.03 (bd, 1H, H_7 overlapped with H_1), 4.11 (bs, 1H, H_1 overlapped with H_7), 5.66 (q, 2H, J=7.0 Hz, $COC\underline{H}_2$-), 6.93 (d, 1H, J=7.5 Hz, H_5), 7.90 (d, 3H, J=1.5 Hz, C_6-Me), 8.07 (d, 3H, J=1.5 Hz, C_4-Me), and 8.66 (t, 3H, J=7.0 Hz, $COCH_2C\underline{H}_3$), which was assigned as **26**. Similarly, the spectrum of the adduct from *p*-xylene shows characteristic signals at τ 3.30 (bs, 1H, H_3), 3.59 (bd, 1H, J=7.5 Hz, H_6), 4.30 (bs, 1H, H_1), 5.61 (q, 2H, J=7.0 Hz, $COC\underline{H}_2$-), 6.71 (d, 1H, J=7.5 Hz, H_5), 7.89 (d, 3H, J=1.5 Hz, C_7-Me), 8.06 (d, 3H, J=1.5 Hz, C_4-Me), and 8.62 (t, 3H, J=7.0 Hz, $COCH_2C\underline{H}_3$). The cycloaddition product in this case was then concluded to be **27**. On the other hand, the adduct fraction from toluene afforded a 61% yield of a mixture of **22** and **23**[10] in a 4 : 6 ratio (NMR). The mixture was then recrystallized from chloroform - *n*-hexane to give a 1 : 1 adduct with a mp of 131—133°C (**22**) and which shows signals at τ 3.12 (bd, 1H, J=9.0 Hz, H_3), 3.95 (bd, 1H, J=8.0 Hz, H_7), 4.02 (be, 1H, J=8.0 Hz, H_1), 4.99 (t, 1H, J=9.0 Hz, H_4), 5.66 (q, 2H, J=7.0 Hz, $COC\underline{H}_2$), 6.75 (bd, 1H, J=9.0 Hz, H_5), 7.88 (d, 3H, J=1.5 Hz, C_6-Me), and 8.66 (t, 3H, J=7.0 Hz, $COCH_2C\underline{H}_3$). From the mother liquor, however, **23** was obtained by further recrystallization, but it was still mixed with **22**. The spectrum of the crude adduct, **23**, shows weak signal at τ 3.95, but it exhibited characteristic signals at 3.62 (bd, 1H, J=7.5 Hz, H_6), 4.02 (bs, 1H, H_1), and τ 6.75 (bt, J=7.5 and 8.0 Hz, H_5). For the adducts from *o*-xylene, a mixture of **24** and **25** was produced in a 3 : 7 ratio, but it could not be separated by column chromatography. However, the NMR spectrum of the mixture showed C-methyl groups at τ 8.00 and 8.33 with relative intensities of 17 : 3. Because of the abnormality of the chemical shift

Table 5. NMR Spectral data of cycloadducts at 60 MHz in $CDCl_3$

Cycloadduct	Chemical shifts (τ-value)						$COOCH_2CH_3$	
	R_1	R_3	R_4	R_5	R_6	R_7	$-CH_2-$	$-CH_3$
21	4.23	3.20	5.03	6.60	3.26	3.75	5.71	8.67
22	4.25	3.12	4.99	6.73	7.88	3.95	5.66	8.66
23	4.36	3.18	4.94	6.60	3.62	7.89	5.64	8.65
24	4.32	3.23	5.51	8.33	8.00	4.02	5.71	8.68
25	4.43	3.23	5.03	6.88	8.00	8.00	5.71	8.68
26	4.11	3.30	8.07	6.93	7.90	4.03	5.66	8.66
27	4.30	3.30	8.06	6.71	3.59	7.89	5.61	8.62

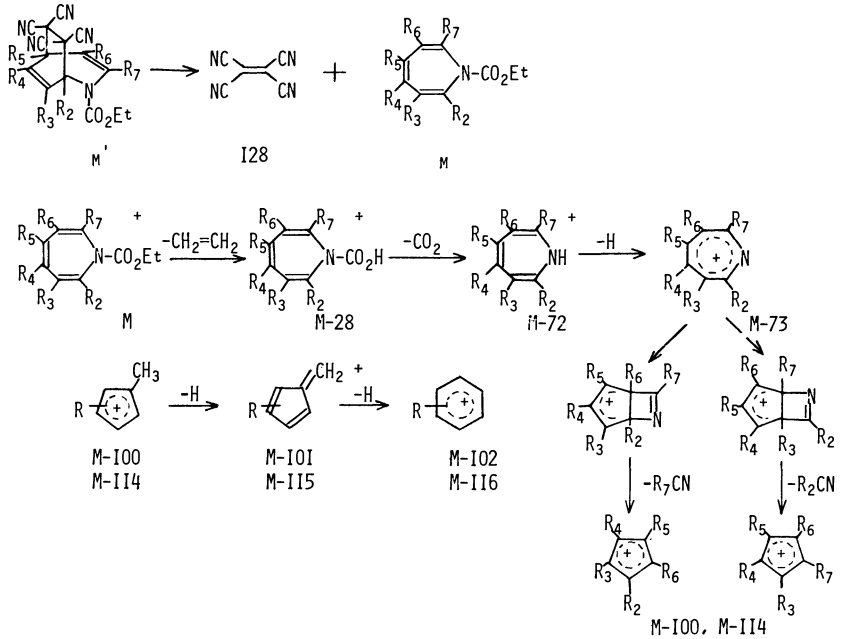

Chart 4.

10) The 4-methyl isomer was observed as a minor product by NMR (τ 8.06, 3H, d, J=1.5 Hz $C\underline{H}_3$)

Table 6. Mass spectral data for various fragment ions and the relative abundance (%) of 1(1*H*)-azepines and its diels-alder adducts

Comp. No.	Ions, rel. int. (%)								
	M′	128	M	M-28	M-72	M-73	M-106	M-101	M-102
7	—	—	58	16	26	100	60	4	5
21	5	19	100	45	41	88	45	23	24
22	20	21	100	55	26	50	51	96	82
26	5	3	100	28	11	56	14	4	9
27	7	5	100	57	28	71	27	10	30

of methyl protons at τ 8.33, the structure of the adduct **24** was tentatively identified as that of a 5,6-dimethyl isomer. The chemical shifts of these compounds are shown in Table 5.

These results suggest the importance of both steric and inductive effects on the 1*H*-azepine reactivity and that it is difficult for the methyl substitution of the adduct to proceed at a bridgehead position excepting that of **24** and at an α-position adjacent to nitrogen.[11] Furthermore, the mass spectra of **21**, **22**, **26**, and **27** show molecular ion peaks, and strong at M′-128 (=M) by the loss of a C_6N_4-molecule from the molecular ion; this fragment may arise from a retro-Diels-Alder fragmentation. Further fragmentations are pararelled to those of substituted azepinium ions,[4] as is shown in Chart 4 and Table 6.

On the basis of the above facts, we could determine the positions of the substituted 1(1*H*)-azepine derivatives (**7**, **8**, **9**, **11**, **12**, **15**, and **18**) by confirming the structures of their adducts (**21**—**27**) with TCNE. Other azepine derivatives (**10**, **13**, **14**, **16**, **17**, **19** and **20**) had been confirmed only partially by spectral and glpc data because of the difficulty of forming their adducts.

Experimental[12]

Preparation of Azepine Derivatives. Method A. A solution of ethyl azidoformate (2.3 g) and an excess of the respective benzene derivatives (10 g) was heated in an oil bath for 3 hr. The solution was then evaporated *in vacuo*, and the residue was separated by chromatography (silica gel), using chloroform as the eluent. The resulting crude red or orange azepine derivatives were purified by fractional distillation.

Method B. Ethyl azidoformate (4.0 g) and an aromatic compound (20 g) were mixed in a 100 m*l* stainless tube. The reaction was carried out in a sealed system at 120°C for 2 hr, after which the reaction mixture was treated much as with method A. These results are summarized in Tables 1 and 2.

These azepine derivatives were isomerized to the aromatic urethans under thermal conditions at 150—200°C in an oil bath for 4—5 hr.[13]

The relative ratio of the produced isomeric *N*-ethoxycarbonylazepine derivatives was determined by glpc and spectroscopic means. Especially, the structures of the mixture of azepine derivatives were determined by the NMR data in the following regions: 3.70—4.65 (olefinic-ring protons), τ 7.90—8.00 (C_2- and C_7-methyl protons), 8.10—8.30 (C_3-, C_4-, C_5- and C_6-methyl protons), and 5.60—6.00 and 8.60—8.90 (ethyl protons of the carbethoxyl group).

2,5-Dimethyl-*N*-ethoxycarbonylaniline. This compound was obtained by the reaction described above when *p*-xylene was employed; mp 95—96°C; NMR τ 2.47 (bs, 1H, H_6), 3.30 and 3.25 (each bd, 2H, J=7.0 Hz, H_3- and H_4), 3.60 (bd, 1H, NH), and 7.69 and 7.81 (each broad singlet, 6H, C_2- and C_5-Me).

Found: C, 68.30; H, 7.95; N, 7.00%. Calcd for $C_{11}H_{15}NO_2$: C, 68.37; H, 7.82; N, 7.25%.

2,4,6-Trimethyl-*N*-ethoxycarbonylaniline. This compound was obtained by the reaction described above when mesitylene was employed; mp 90—92°C (lit,[5c] 90°C); mass *m/e* 207: NMR 3.23 (bs, 2H, H_3 and H_5), 3.63 (bs, 1H, NH), and 7.77—7.83 τ (two singlets, 9H, C_2-, C_4- and C_6-Me).

Kinetics in the Reaction of *p*-Xylene and Ethyl Azidoformate. Solutions for the "nitrene" runs were prepared by adding *p*-xylene (10 g, 0.094 mol) an ethyl azidoformate (2.3 g, 0.02 mol) from a 10-μ*l* syringe to a 20-m*l* volumetric flask at 100, 120, and 138°C (in oil baths). The contents of the reaction solution were then analyzed by glpc. Each analysis was carried out at least three times. The relative rate ratios thus determined are given in Fig 1. The peaks of azepine derivatives were calculated by the half-width method, but the amounts of the side-formed aromatic urethan were not calculated because the yields were low

11) Recently, the adduct of 2-methyl-*N*-methoxycarbonylazepine has been reported to give the 3-methyl compound, but only in a 2.5% yield.[4]

12) The melting points were measured with a Yanagimoto micro-melting-point apparatus and are uncorrected. The microanalyses were performed on a Yanagimoto C.H.N.-Corder, Model MT-1. The NMR spectra were taken with a Japan Electric Optics Lab. Co., Ltd, Model JNN-MH-60 NMR spectrometer and with a Varian A-60 recording spectrometer, with tetramethylsilane as the internal standard. The chemical shifts are expressed in τ values. The mass spectra were obtained on a Hitachi RMU-D double-focussing mass spectrometer operating at an ionization potential of 70 eV. The IR spectra were taken with a JASCO Model IR-S spectrophotometer. The glpc was done isothermally with a Hitachi K-23 Gas Chromatograph on a 3-ft, 5 wt% SE 30 (Chromosorb G NAW) column (flame-ionization detector).

13) *Cf.* L. A. Paquette, D. E. Kuhla and J. H. Barette, *J. Org. Chem.*, **34**, 2879 (1969).

(below 3%).

Reaction of Benzene and Ethyl Azidoformate in the Presence of TCNE. In a stainless steel tube benzene (10 g), ethyl azidoformate (1.15 g, 0.01 mol) and TCNE (0.005 mol) were mixed. The closed tube was heated at 100—110°C in an oil bath for 15 hr and then cooled. After the reaction mixture had been concentrated *in vacuo*, the residue was purified by column chromatography (silica gel) using *n*-hexane, benzene, and chloroform successively as eluents. A red oil (0.51 g, 24%) was obtained from the first fraction; it was identical in all respects with *N*-ethoxycarbonyl-1-(1*H*)-azepine (**7**).[5c] Subsequently, white crystals **21** (0.54 g, 24%) were obtained from the second fraction, mp 156—158°C; they were identical with a specimen prepared by the method of Kende *et al.*[3b]

Reaction of Toluene and Ethyl Azidoformate in the Presence of TCNE. In a closed tube toluene (10 g), ethyl azidoformate (1.15 g), and TCNE (1.28 g, 0.01 mol) were mixed. The reaction was then carried out under the conditions described above. The reaction mixture was concentrated *in vacuo*, and the tarry residue was purified by column chromatography (silica gel). Red, oily compounds (0.35 g, 20%) were obtained from the first fraction, but they were found to consist of azepine derivatives and aromatic urethans (by IR and NMR). On the other hand, a yellow, oily adduct (1.88 g,61%) was obtained from the second fraction; its NMR spectra showed that it consisted of **22** and **23** in a 40 : 60 ratio, together with the 4-methyl isomer as a minor product. However, the mixture was recrystallized from *n*-hexane - chloroform to give colorless crystals, **22**; mp 131—133°C; IR ν_{max}^{KBr} 1645 (C=C), 1710 (C=O), 2280 cm^{-1} (w, C≡N); mass *m/e* 307.

Found: C, 62.60; H, 4.26; N, 22.70%. Calcd for $C_{16}H_{13}N_5O_2$: C, 62.53; H, 4.26; N, 22.79%.

The mother liquor afforded crude **23**, which was still mixed with **22** and the 4-methyl isomer (τ 8.06, d, J=1.5 Hz, 3H, C_4-Me distinguish between C_6- and C_7-methyl protons) even after further purification by recrystallization from benzene.

Reaction of *o*-Xylene and Ethyl Azidoformate in the Presence of TCNE. In a closed tube *o*-xylene (10 g), ethyl azidoformate (0.75 g), and TCNE (0.83 g, 0.065 mol) were mixed. The reaction was then carried out under the conditions described above. After the reaction mixture had been concentrated *in vacuo*, the residue was separated by column chromatography (silica gel), using *n*-hexane and benzene successively as eluents. Red, oily compounds (0.20 g, 16%) were obtained from the first fraction; they were determined by NMR and IR inspections to be mixtures of aromatic urethans (major products) and azepine derivatives (minor products).

The second fraction afforded colorless crystals (0.78 g, 39%) of **24** and **25** in a 30 : 70 ratio, but no further purification was undertaken. On the other hand, when two equimolar portions of ethyl azidoformate were employed in the reaction, a mixture of **24** and **25** was obtained in a 22% yield, while the aromatic urethans were given in a 22% yield.

Reaction of *m*-Xylene and Ethyl Azidoformate in the Presence of TCNE. In a closed tube *m*-xylene (10 g), ethyl azidoformate (2.3 g, 0.02 mol), and TCNE (1.28 g, 0.01 mol) were mixed. The reaction was then carried out under the conditions described above. From the reaction mixture, aromatic urethans and **26** were obtained in 10 and 11% yields respectively. The adduct was recrystallized from benzene; mp 200—201°C; IR ν_{max}^{KBr} 1660 (C=C), 1705 (C=O), 2280 cm^{-1} (w, C≡N); mass *m/e* 321.

Found: C, 63.60; H, 4.75; N, 21.90%. Calcd for $C_{17}H_{15}N_5O_2$: C, 63.54; H, 4.70; N, 21.80%.

Reaction of *p*-Xylene and Ethyl Azidoformate in the Presence of TCNE. In a closed tube *p*-xylene (10 g), ethyl azidoformate (2.3 g, 0.02 mol) and TCNE (1.28 g, 0.01 mol) were mixed, and the reaction was carried out under the conditions described above. From the reaction mixture, 2,5-dimethylethoxycarbonylaniline and **27** were obtained in 22 and 11% yields respectively. **22** was recrystallized from ether - *n*-hexane, mp 147—149°C; ν_{max}^{KBr} 1668 (C=C), 1716 (C=O), 2280 cm^{-1} (w, C≡N); mass *m/e* 221.

Found: C, 63.64; H, 4.56; N, 21.99%. Calcd for $C_{17}H_{15}N_5O_2$: C, 63.52; H, 4.70; N, 21.80%.

Reaction of Mesitylene and Ethyl Azidoformate in the Presence of TCNE. In a closed tube mesitylene (10 g), ethyl azidoformate (2.3 g), and TCNE (0.25 g, 0.002 mol) were mixed, and the reaction was carried out under the conditions described above. After the reaction mixture had been under concentrated *in vacuo*, the residue was recrystallized from benzene to give 2,4,6-trimethyl-ethoxycarbonylaniline (3.04 g, 73%), mp 90—92°C (lit,[5] 90°C), while TCNE (0.25 g) was recovered from the mother liquor.

BULLETIN OF THE CHEMICAL SOCIETY OF JAPAN VOL. 43 2900—2907 (1970)

The Synthesis of Benzoyl-L-arginine-*p*-nitroanilide*[1]

Norio NISHI, Seiichi TOKURA and Junzo NOGUCHI

Department of Polymer Science, Faculty of Science, Hokkaido University, Sapporo

(Recieved February 27, 1970)

Benzoyl-arginine-*p*-nitroanilide (BAPA) is a synthetic substrate for trypsin, papain, and other enzymes, but it has not yet been prepared in the active L-form, although the preparations of DL-form and D-form by the trypsin digestion of the DL-form have been reported. The optically active L-BAPA was prepared by the following route; N^{α}-carbobenzyloxy-N^{ω}-nitro-L-arginine-*p*-nitroanilide was prepared from N^{α}-carbobenzyloxy-N^{ω}-nitro-L-arginine and *p*-nitrophenyl isocyanate, and the subsequent decarbobenzyloxylation and the benzoylation of this compound gave N^{α}-benzoyl-N^{ω}-nitro-L-arginine-*p*-nitroanilide. The removal of the nitro group was followed by Sakakibara's method using hydrogen fluoride. The L-BAPA shows the same melting point and the same reversal optical rotation as those of D-BAPA. When N^{α}-benzoyl derivatives of L-arginine were used as starting materials in the preparation of BAPA, DL-BAPA was always obtained with complete racemization; when N^{α},N^{ω},$N^{\omega'}$-tricarbobenzyloxy-L-arginine as the starting material reacted on *p*-nitrophenyl isocyanate, the product had no racemization, but the desired L-BAPA was not obtained because one of the carbobenzyloxy groups on the guanido group was extraordinally stable to reagents and could not be removed completely.

Benzoyl-arginine-*p*-nitroanilide (BAPA) is a interesting material for use as a synthetic chromogenic substrate of trypsin and papain; DL-BAPA has been used as a substrate because the L-form has not yet been prepared. The synthesis of the L-form is important in order to see whether enzymic activity to the L-form is inhibited by the D-form or not. BAPA has thus far been synthesized from benzoyl-arginine and *p*-nitroaniline using the polyphosphoric ester[1] or phosphorous pentoxide in diethylphosphite[2] as a condensation reagent, but only the racemic compound was obtained in these methods. The optically-active D-form was prepared by the tryptic digestion of the DL-form.[2] The optically-active L-BAPA was prepared after we had examined the several synthetic routes shown in Scheme 1.

The obtained L-BAPA shows the same melting point, the same reversal optical rotation, and the same solubility to water and ethanol as D-BAPA.[2] The carboxyl group of arginine tends to form a six-membered lactam by cyclization with the δ-imino group, and the reactivity of the amino group of *p*-nitroaniline is less than that of amino acid because of its low basicity.

In this paper, *p*-nitrophenyl isocyanate was used to form an amide bond with the carboxyl group of arginine.[3] Generally, it is hard to prepare *p*-nitroanilide of amino acids by other methods, such as the use of dicyclohexyl carbodiimide[4] or Woodward's reagent.[5] When a carbobenzyloxy derivative is used on the coupling step of the carboxyl and isocyanate group, as is shown in Scheme 1-A, no racemization occurs, but when a benzoyl derivative, like N^{α}-benzoyl-N^{ω}-nitro-L-arginine (Scheme 1-B) or N^{α}-benzoyl-N^{δ}-carbobenzyloxy-L-ornithine (Scheme 1-C),[6] is used, the reaction always proceeds with racemization. When N^{α},N^{ω},$N^{\omega'}$-tricarbobenzyloxy-L-arginine is used as the starting material and is coupled with *p*-nitrophenyl isocyanate, the reaction proceeds, producing a high yield without any racemization (Scheme 1-D), but one of the carbobenzyloxy group on the guanido group is not removed by the usual method without a breakdown of the amide bond because of the extraordinally stability.[7]

*1 This work was presented at the 7th Symposium on Peptide Chemistry, Chemical Society of Japan, Tokyo, Nov. 21, 1969.

1) E. A. Bashkir, Ya. I. Lapuk and V. M. Stepanov, *Metody Polucheniya Khim. Reactivov i Preparanov*, **13**, 76 (1965).

2) B. F. Erlanger, N. Kokowsky and W. Cohen, *Arch. Biochem. Biophys.*, **95**, 271 (1961).

3) W. Diekmann and F. Breest, *Ber.*, **309**, 3052 (1906); S. Goldschmidt and M. Wick, *Z. Naturforsch.*, **B, 5** 170 (1950); S. Goldschmidt and M. Wick, *Ann., Chem.*, **575**, 217 (1952).

4) J. C. Sheehan, G. P. Hess and M. Goodman, *J. Amer. Chem. Soc.*, **77**, 1067 (1955); J. C. Sheehan, M. Goodman and G. P. Hess, *ibid.*, **78**, 1367 (1956).

5) R. B. Woodward, R. A. Olofson and H. Mayer, *ibid.*, **83**, 1010 (1961).

6) J. Noguchi and N. Nishi, The 5th Symposium on Peptide Chemistry, (1967), p. 36.

7) N. Nishi and J. Noguchi, The 6th Symposium on Peptide Chemistry, (1968), p. 1.

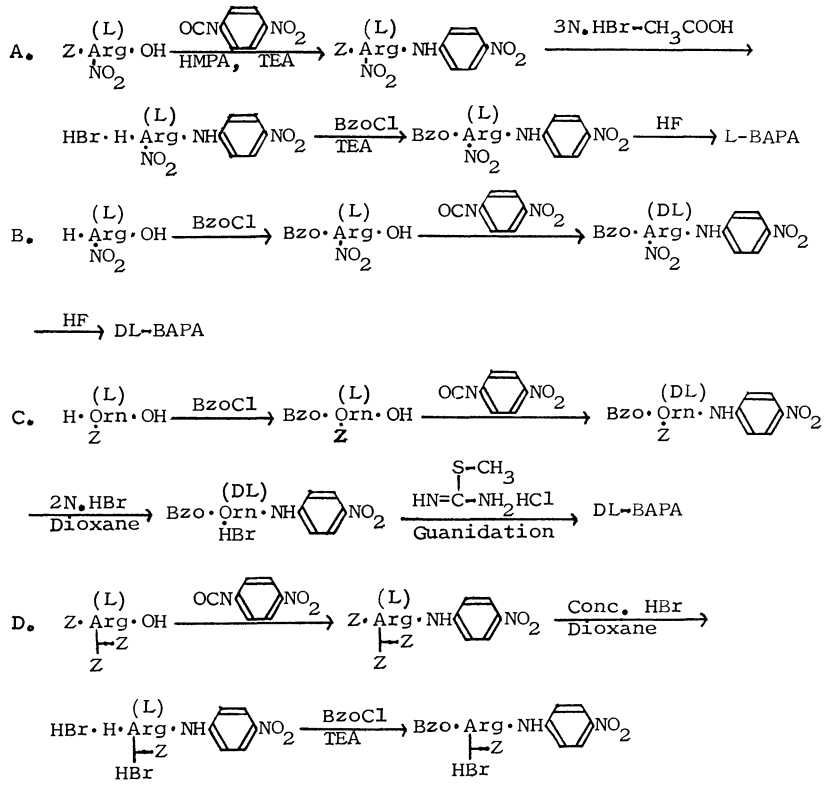

Scheme 1

HMPA: Hexamethyl Phosphoramide; TEA: Triethylamine; Z: Carbobenzyloxy; Bzo: Benzoyl.

Experimental

The melting points for the sample over 220°C were determined with a Mitamura Hot-stage Apparatus. The ultraviolet and visible absorption spectra were measured with a Hitachi 124 Spectrophotometer, while the infrared absorption spectra were measured with a Hitachi Grating Infrared Spectrophotometer, EPI-G2. The optical rotations were measured with a Yanagimoto Direct Reading Polarimeter, Model OR-10, and an Automatic Recording Polarimeter, Model OR-1. Toyo Densitorol #2 was used for the measurement of the concentration after development by ninhydrin. The elemental analysis was carried out by means of a Yanagimoto C.H.N. Corder, Model MT-2, and a Coleman Nitrogen Analyser, Model 29.

N^{ω}-Nitro-L-arginine. N^{ω}-Nitro-L-arginine was prepared according to Hayakawa *et al.*[8]

N^{α}-Carbobenzyloxy-N^{ω}-nitro-L-arginine. This material was prepared by the carbobenzyloxylation of N^{ω}-nitro-L-arginine essentially as has been described by Hofmann *et al.*[9]

***p*-Nitrophenyl Isocyanate.**[10] Hydrogen chloride was introduced into *p*-nitroaniline (20 g, 145 mmol) in dry dioxane (200 ml) until saturation at room temperature, and then phosgene was bubbled into the reaction mixture for 1 hr at 50°C until a clear solution was obtained. After expelling the excess phosgene at room temperature by bubbling with nitrogen for 30 min, the solution was evaporated to dryness below 40°C and the residue was refluxed with dry carbon tetrachloride (120 ml) for 2.5 hr. The insoluble part was removed by filtration at room temperature, the filtrate was concentrated to dryness, and the crystalline *p*-nitrophenyl isocyanate was recrystallized from carbon tetrachloride. Yield, 21.8 g (92.4%). mp 56°C.

Found: C, 51.1; H, 2.23; N, 17.3%. Calcd for $C_7H_4N_2O_3$: C, 51.2; H, 2.44; N, 17.1%.

N^{α}-Carbobenzyloxy-N^{ω}-nitro-L-arginine-*p*-nitroanilide. Into the solution of N^{α}-carbobenzyloxy-N^{ω}-nitro-L-arginine (20.0 g, 56.7 mmol) in dry hexamethylphosphoramide (HMPA) (120 ml), triethylamine (7.92 ml, 56.7 mmol) and *p*-nitrophenyl isocyanate (18.7 g, 114 mmol) were stirred successively at 20°C. The mixture was stirred for 20 hr at room temperature, diluted with 1000 ml of 2% sodium bicarbonate to separate the product, and then cooled. The resulting precipitate was filtered and washed successively with 2% sodium bicarbonate, water, 0.5 N hy-

8) T. Hayakawa, Y. Fujiwara and J. Noguchi, This Bulletin, **40**, 1205 (1967).

9) M. Bergmann, L. Zervas and H. Rinke, *Z. Physiol. Chem.*, **224**, 40 (1934); K. Hofmann, W. D. Peckham and A. Rheiner, *J. Amer. Chem. Soc.*, **78**, 238 (1956).

10) Vittenet, *Bull. Soc. Chim.*, **(3)21**, 586 (1899); V. Hoogstraten, *Rec. Trav. Chim. Pays-Bas*, **51**, 418 (1932); Swartz, *Amer. Chem. J.*, **19**, 318 (1897); Shriner and Cox, *J. Amer. Chem. Soc.*, **53**, 1603 (1931).

drochloric acid and water. The product was extracted twice with 300-ml and 100-ml portions of hot dioxane, and the extract was concentrated to dryness. The residue was washed several times with ether and recrystallized from *n*-butanol (300 ml). The crystal was washed with ether and dried. Yield, 20.4 g (76.2%); mp 178°C, $[\alpha]_D^{29}$ +52.8° (*c* 1.05, HMPA), −1.4° (*c* 1.02, glacial acetic acid).

Found: C, 50.7; H, 4.75; N, 20.4%. Calcd for $C_{20}H_{23}N_7O_7$: C, 50.8; H, 4.87; N, 20.7%.

N^{ω}-Nitro-L-arginine-*p*-nitroanilide Hydrobromide. N^{α}-Carbobenzyloxy-N^{ω}-nitro-L-arginine-*p*-nitroanilide (20.0 g, 42.3 mmol) was treated with 3 N hydrogen bromide in glacial acetic acid (200 ml) for 7 hr at 20—23°C while being stirred. The product was precipitated by the addition of dry ether (1000 ml); after the mixture had stood for 1 hr at 0°C, the precipitate was collected by decantation and washed with dry ether. This precipitate was easily crystallized with water, cooled, filtered, washed with a small amount of cold water, and dried. From the concentration of the mother liquor of acetic acid and ether containing HBr, an additional product was obtained. The combined product was refluxed with dioxane (40 ml) for a few minutes to remove the impurity; then it was cooled, filtered and dried. Yield, 15.8 g (88.8%); mp 174—175°C.

Found: Br, 18.7%. Calcd for $C_{12}H_{18}N_7O_5Br$: Br, 19.0%.

N^{α}-Benzoyl-N^{ω}-nitro-L-arginine-*p*-nitroanilide. N^{ω}-Nitro-L-arginine-*p*-nitroanilide hydrobromide (19.5 g, 46.4 mmol) was dissolved in a mixture of tetrahydrofuran and water (9 : 1, 195 ml) and then cooled to −5—−7°C. After the addition of triethylamine (13.5 ml, 97.5 mmol) to the solution, benzoyl chloride (6.05 ml, 51.1 mmol) was stirred in, drop by drop, over a five-minute period. After standing for 1 hr, it was kept for 1 hr at 0°C and for another 1 hr at room temperature; then the solution was evaporated to dryness at room temperature. The residue was washed with water, dried, and crystallized by refluxing with ethanol. It was recrystallized from dimethyl formamide (DMF) and water. Yield, 15.4 g (75.2%); mp 246°C; $[\alpha]_D^{26}$ +60.7° (*c* 1.12, HMPA).

Found: C, 51.5; H, 4.41; N, 21.9%. Calcd for $C_{19}H_{21}N_7O_6$: C, 51.5; H, 4.73; N, 22.1%.

N^{α}-Benzoyl-L-arginine-*p*-nitroanilide Hydrochloride. N^{α}-Benzoyl-N^{ω}-nitro-L-arginine-*p*-nitroanilide (13 g, 29.4 mmol) was placed in a HF-reaction cylinder containing anisole (13 ml, 120 mmol). Forty milliliters of hydrogen fluoride dried with CoF_3 were collected under cooling with dry ice in the cylinder;[11] the mixture was then allowed to react at 0°C for 40 min while being stirred. The excess HF was removed under reduced pressure, and the residue was kept *in vacuo* for a further 2 hr. The residue was washed with ether, and then hydrofluoride was converted into the hydrochloride by successive treatment with 3 N HCl. It was crystallized with ethanol (100 ml) and ether (300 ml), and then left for 1 hr at 0°C. The crystal was collected by filtration and dried. The yield was 11.0 g. This crude product was extracted four times with hot ethanol (200 ml, 100 ml, 50 ml and 50 ml), and the combined extract was concentrated to dryness and recrystallized from absolute ethanol. Yield, 5.6 g (44.1%); mp 225°C; $[\alpha]_D^{25}$ +14.2° (*c* 1.0, water).

Found: C, 52.4; H, 5.23; N, 19.2; Cl, 8.1%. Calcd for $C_{19}H_{23}N_6O_4Cl$: C, 52.5; H, 5.29; N, 19.3; Cl, 8.2%.

N^{α}-Benzoyl-N^{ω}-nitro-L-arginine. A solution of N^{ω}-nitro-L-arginine (20 g, 91.5 mmol) in 1 N sodium hydroxide (91.5 ml, 91.5 mmol) was cooled to −3—−5°C. 1 N sodium hydroxide (109 ml, 109 mmol) and benzoyl chloride (12.8 ml, 109 mmol) were stirred in alternatively over a 30-min period. After stirring for an additional 90 min, the reaction mixture was extracted three times with ether in order to remove the excess benzoyl chloride. The solution was acidified to pH 1—2 with concentrated hydrochloric acid, and the precipitate was crystallized by trituration. The crystal was collected by filtration, and then washed with diluted hydrochloric acid, water, and ether. It was recrystallized from water. Yield, 27.8 g (94.5%); mp 158—159°C; $[\alpha]_D^{24}$ +1.4° (*c* 1.0, methanol).

Found C, 48.5; H, 5.47; N, 21.3%. Calcd for $C_{13}H_{17}N_5O_5$: C, 48.3; H, 5.26; N, 21.6%.

N^{α}-Benzoyl-N^{ω}-nitro-DL-arginine-*p*-nitroanilide. Into a solution of N^{α}-benzoyl-N^{ω}-nitro-L-arginine (3.2 g, 10 mmol) in 30 ml of dry dioxane, *p*-nitrophenyl isocyanate (1.64 g, 10 mmol) was stirred at 20°C. After the dissolution of *p*-nitrophenyl isocyante in the solution, the mixture was kept for a further 2 hr at 50°C. The crystal which separated out from the solution was filtered and refluxed with methanol (15 ml). It was recrystallized from nitrobenzene and washed with methanol and ether. Yield, 2.5 g (56.4%); mp 236°C; $[\alpha]_D^{25} \fallingdotseq 0$ (*c* 0.5, glacial acetic acid).

Found: C, 51.6; H, 4.78; N, 22.0%. Calcd for $C_{19}H_{21}N_7O_6$: C, 51.5; H, 4.73; N, 22.1%.

N^{α}-Benzoyl-DL-arginine-*p*-nitroanilide Hydrochloride. N^{α}-Benzoyl-N^{ω}-nitro-DL-arginine-*p*-nitroanilide (2.0 g, 4.5 mmol) was treated with hydrogen fluoride in order to remove the nitro group by the same procedure as was used for N^{α}-benzoyl-N^{ω}-nitro-L-arginine-*p*-nitroanilide. The product was recrystallized from 20% acetic acid. Yield, 1.5 g (76.6%); mp 262°C; $[\alpha]_D^{25}=0$ (*c* 0.4, glacial acetic acid).

Found: C, 52.4; H, 5.16; N, 19.2; Cl, 8.1%. Calcd for $C_{19}H_{23}N_6O_4Cl$: C, 52.5; H, 5.29; N, 19.3; Cl, 8.2%.

N^{δ}-Carbobenzyloxy-L-ornithine. N^{δ}-Carbobenzyloxy-L-ornithine was prepared according to the method of Synge.[12]

N^{α}-Benzoyl-N^{δ}-carbobenzyloxy-L-ornithine. Into a cold solution (−1—−2°C) of N^{δ}-carbobenzyloxy-L-ornithine (20.0 g, 75 mmol) in 1 N sodium hydroxide (75 ml, 75 mmol), 4 N sodium hydroxide (22.5 ml, 90 mmol) and benzoyl chloride (10.6 ml, 90 mmol) were stirred alternately over a 20-min period. After the addition of ether (5 ml), the reaction proceeded for a further 3 hr at the same temperature. Then the reaction mixture was extracted three times with ether in order to remove the excess benzoyl chloride. The

11) S. Sakakibara, Y. Shimonishi, Y. Kishida, M. Okada and H. Sugihara, This Bulletin, **40**, 2164 (1967); S. Sakakibara, Y. Kishida, R. Nishizawa and Y. Shimonishi, *ibid.*, **41**, 438 (1968); S. Sakakibara, N. Nakamizo, Y. Kishida and S. Yoshimura, *ibid.*, **41**, 1477 (1968).

12) R. L. M. Synge, *Biochem. J.*, **42**, 99 (1948).

solution was acidified to pH 1—2 with concentrated hydrochloric acid, and the precipitate was crystallized by trituration. The crystals were collected by filtration and washed with diluted hydrochloric acid, water and ether. They were then recrystallized from ethyl acetate. Yield, 26.7 g (96.2%); mp 145°C; $[\alpha]_D^{20}$ −1.4° (*c* 1.0 and 3.0, methanol); $[\alpha]_{508}^{20}$ −1.7° (*c* 3.0, methanol).

Found: C, 64.7; H, 5.60; N, 7.40%. Calcd for $C_{20}H_{22}N_2O_5$: C, 64.8; H, 5.95; N, 7.57%.

N^{α}-Benzoyl-N^{δ}-carbobenzyloxy-DL-ornithine-*p*-nitroanilide. Into a solution of N^{α}-benzoyl-N^{ω}-carbobenzyloxy-L-ornithine (24.0 g, 65 mmol) in dry dioxane (240 m*l*), *p*-nitrophenyl isocyanate (18.0 g, 110 mmol) was stirred at 20°C. After 2 days at 20—23°C, the product which precipitated from the solution was filtered and dried. It was then recrystallized from ethanol. Yield, 25.8 g (81.5%); mp 174°C; $[\alpha]_D^{20} \fallingdotseq 0°$ (*c* 1.3, dioxane).

Found: C, 63.3; H, 5.02; N, 11.5%. Calcd for $C_{26}H_{26}N_4O_6$: C, 63.7; H, 5.31; N, 11.4%.

Dinitrodiphenyl Urea.[6,10] The above-mentioned part which was insoluble in hot ethanol was confirmed to be dinitrodiphenyl urea by the elemental analysis after recrystallization from dimethyl formamide. Yield, 4.8 g; mp 340°C (lit,[10] 360°C).

Found: C, 51.7; H, 3.14; N, 18.3%. Calcd for $C_{13}H_{10}N_4O_5$: C, 51.7; H, 3.31; N, 18.5%.

N^{α}-Benzoyl-DL-ornithine-*p*-nitroanilide Hydrobromide. N^{α}-Benzoyl-N^{δ}-carbobenzyloxy-DL-ornithine-*p*-nitroanilide (10.0 g, 20.4 mmol) was treated with 2 N hydrogen bromide in dioxane (300 m*l*) for 30 min at 20°C, and the N^{δ}-carbobenzyloxy group was removed. The product was then recrystallized from methanol-ethylacetate. Yield, 6.4 g (71.5%); mp 207°C.

Found: C, 49.0; H, 4.55; N, 12.8; Br, 18.5%. Calcd for $C_{18}H_{21}N_4O_4Br$: C, 49.2; H, 4.78; N, 12.8; Br, 18.2%.

The Guanidation of Benzoyl-ornithine-*p*-nitroanilide Hydrobromide. To a methanol solution (500 m*l*) of benzoyl-ornithine-*p*-nitroanilide hydrobromide (8.4 g, 19.1 mmol), 1.08 N sodium methylate in methanol (17.64 m*l*, 19.1 mmol) was added, and the sodium bromide was centrifuged. *S*-Methyl isothiourea hydrochloride (3.9 g, 28.8 mmol) in methanol (10 m*l*) was then added to the solution, and the solution was refluxed for 5 hr. After treatment with charcoal, the reaction mixture was concentrated to dryness and washed with water. The product was recrystallized from 20% acetic acid, washed with hot ethyl acetate (50 m*l*), and recrystallized again with 10% aqueous DMF. Yield, 4.8 g (57.6%); mp 225°C; $[\alpha]_D^{25}=0°$ (*c* 1.0, DMF). The Sakaguchi reaction was positive, and the ninhydrin reaction was negative. $R_f=0.84$ (*n*-butanol: glacial acetic acid : water=4 : 1 : 5). *Cf.* Standard DL-BAPA's R_f is 0.84.

Found: Cl, 8.0%. Calcd for $C_{19}H_{23}N_6O_4Cl$: Cl, 8.2%.

N^{α},N^{ω},$N^{\omega'}$-Tricarbobenzyloxy-L-arginine. This material was prepared according to the method of Zervas *et al.*[13]

N^{α},N^{ω},$N^{\omega'}$-Tricarbobenzyloxy-L-arginine-*p*-nitroanilide. Into a dry dioxane solution (68 m*l*) of N^{α},N^{ω},$N^{\omega'}$-tricarbobenzyloxy-L-arginine (11.3 g, 19.6 mmol), *p*-nitrophenyl isocyanate (4.4 g, 26.8 mmol) was stirred at 20°C. After the mixture had then stood for 20 hr at 20°C, a small excess of water corresponding to the excess isocyanate was added. 150 m*l* of ether were added to the reaction mixture, it was stirred for 1 hr, and the insoluble part was filtered off. The clear filtrate was concentrated to dryness *in vacuo* and the residue was washed with 0.1 N hydrochloric acid and water. The crude product was dissolved in methanol and reprecipitated with water. The precipitate was crystallized with cold water, and the crystals were filtered out, washed with water, and dried. Yield, 13.4 g (97.8%); mp 64°C; $[\alpha]_D^{25}$ +4.1° (*c* 1.0, chloroform). Found: C, 61.8; H, 5.31; N, 12.0%. Calcd for $C_{36}H_{36}N_6O_9$: C, 62.1; H, 5.18; N, 12.1%.

Decarbobenzyloxylation of N^{α},N^{ω},$N^{\omega'}$-Tricarbobenzyloxy-L-arginine-*p*-nitroanilide by Hydrogen Bromide and its Benzoylation. A solution of N^{α},N^{ω},$N^{\omega'}$-tricarbobenzyloxy-L-arginine-*p*-nitroanilide (5 g, 8.7 mmol) in dioxane was saturated with dry HBr and then heated at 50°C for 6 hr. The progress of the reaction was followed by paper chromatography every hour. A spot of the reaction mixture was applied to paper in performing ascending chromatography in a *n*-butanol : glacial acetic acid : water (4 : 1 : 5), and the quantity of the color developed with ninhydrin was measured by means of Densitorol at 563 mμ. The ratio of each spot to the total color is plotted against the time in Fig. 4. After six hr, the reaction mixture was concentrated, treated with dry ether (150 m*l*), washed with water saturated with NaCl, and dried. The product was dissolved in ethanol and precipitated with ether. The precipitate was crystallized from ether. The crystals were centrifuged, washed with ether, and dried. Yield, 2.7 g (63.7%); mp 75—78°C (hygroscopic). Found: Br, 27.4%. Calcd for $C_{20}H_{26}N_6O_5Br_2$ ($N^{\omega'}$-carbobenzyloxy-L-arginine-*p*-nitroanilide dihydrobromide): Br, 27.1%.

The hydrobromide (1 g, 1.7 mmol) was dissolved in 10 m*l* of tetrahydrofuran-water (9 : 1), and the mixture was cooled at −8°C. Triethylamine (0.71 m*l*, 5.1 mmol) and benzoyl chloride (0.20 m*l*, 1.7 mmol) were then stirred in. The solution was allowed to stand for 30 min at −8°C, and then for another hour at room temperature. The reaction mixture was concentrated to dryness, washed with 1 N hydrochloric acid and water, and then dried. The product was recrystallized twice from 20% acetic acid. Yield, 330 mg; mp 157°C. Found: C, 52.2; H, 4.92; N, 13.4; Br, 13.1%. Calcd for $C_{27}H_{29}N_6O_6Br$ (N^{α}-benzoyl-$N^{\omega'}$-carbobenzyloxy-L-arginine-*p*-nitroanilide hydrobromide): C, 52.8; H, 4.73; N, 13.7; Br, 13.0%.

After the hydrolysis of a sample (6.14 mg) with 4 m*l* of 6 N HCl at 110°C for 15 hr, the quantity of arginine was determined by studying ninhydrin color on a paper chromatogram, while that of *p*-nitroaniline was measured by means of the absorption at 380 mμ; Found: Arg. 1.67 mg (27.2%); Calcd for $C_{27}H_{29}N_6O_6Br$: Arg. 1.74 mg (28.4%), Found: *p*-nitroaniline, 1.33 mg (21.7%); Calcd: 1.38 mg (22.5%).

Results and Discussion

North and Young[14] have reported that in acyl

13) L. Zervas, M. Winitz and J. P. Greenstein, *J. Org. Chem.*, **22**, 1515 (1957).

14) M. B. North and G. T. Young, *Chem. Ind.* (London), **1955**, 1597.

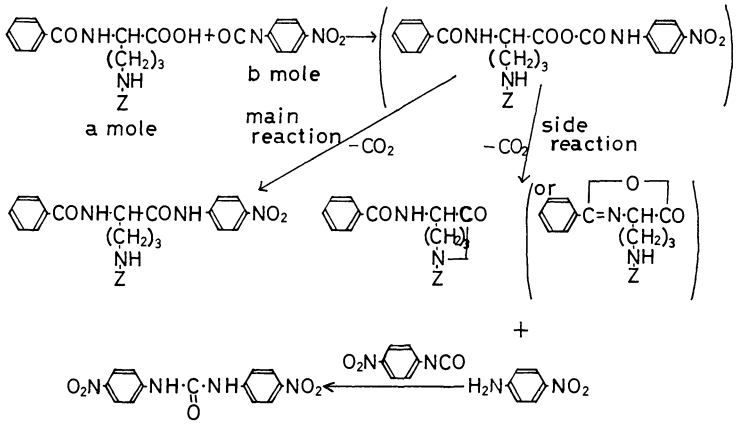

Scheme 2. The main and side reaction during the coupling reaction of N^{α}-benzoyl-N^{ω}-carbobenzyloxy-L-ornithine with *p*-nitrophenyl isocyanate.

amino acids of the urethane type, such as carbobenzyloxy amino acid, no racemization occurs on the coupling of the carboxyl group with an other amino group because the carbobenzyloxy derivative can not form the oxazolone as an intermediate. Recently optically-active acetyl-L-phenylalanine-*p*-nitroanilide[15] and acetyl-D-phenylalanine-*p*-nitroanilide[16] were prepared by Ramenskii and Botovinik *et al.* They used carbobenzyloxy-L- or D-phenylalnine as the starting material, and coupled it with *p*-nitroaniline before the decarbobenzyloxylation and the acetylation. This is consistent with our method. Optically-active L-BAPA could not be prepared by the benzoyl derivatives, but it was successfully prepared by carbobenzyloxylation at the first step and by the displacement of the carbobenzyloxy group with the benzoyl group at the last step.

Formation of *p*-nitroanilide by a Reaction between Carboxyl and Isocyanate Groups. N^{α}-Carbobenzyloxy-N^{ω}-nitro-L-arginine-*p*-nitroanilide was prepared by the reaction of N^{α}-carbobenzyloxy-N^{ω}-nitro-L-arginine and *p*-nitrophenyl isocyanate in hexamethyl phosphoramide (HMPA). When dioxane, pyridine, and *N*-methyl pyrolidone but not HMPA were used as solvents, this reaction did not proceed at all, even upon the addition of triethylamine or acids as a catalyst; only HMPA gave a good result in spite of the fact that N^{α}-benzoyl-N^{ω}-nitroarginine, N^{α}-benzoyl-N^{ω}-carbobenzyloxy-ornithine, and N^{α},N^{ω},$N^{\omega'}$-tricarbobenzyloxy-L-arginine reacted with *p*-nitrophenyl isocyanate in dioxane. By another route, one *via* such benzoyl derivatives as N^{α}-benzoyl-N^{ω}-nitro-L-arginine and N^{α}-benzoyl-N^{δ}-carbobenzyloxy-L-ornithine, as is shown in Scheme 1, DL-BAPA was always prepared with racemization. In the reaction of N^{α}-benzoyl-N^{δ}-carbobenzyloxy-L-ornithine with *p*-nitrophenyl isocyanate, dinitrodiphenyl urea was obtained as its by-product in addition to the main product, N^{α}-benzoyl-N^{δ}-carbobenzyloxy-L-ornithine-*p*-nitroanilide. This dinitrodiphenyl urea seems to be formed through a side reaction, as is shown in scheme 2. Since the *p*-nitroaniline produced by the side reaction reacts with *p*-nitrophenyl isocyanate, the yield of the main product was only 43 percent when equivalent moles (a : b= 1 : 1) of isocyanate were used, but if the reaction was carried out with 1.7 equivalent moles (a : b= 1 : 1.7) of isocyanate, the amount of *p*-nitrophenyl isocyantate was sufficient and the main product was obtained in an 82 percent yield. N^{α},N^{ω},$N^{\omega'}$-

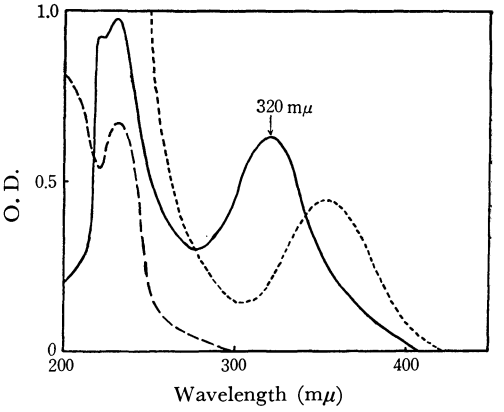

Fig. 1. The absorption spectra of N^{α},N^{ω},$N^{\omega'}$-tricarbobenzyloxy-L-arginine-*p*-nitroanilide, N^{α},N^{ω},$N^{\omega'}$-tricarbobenzyloxy-L-arginine and *p*-nitroaniline in dioxane.
PNA: -*p*-nitroanilide, Z: carbobenzyloxy.
---- *p*-nitroaniline, ——— tri-Z-Arg
—— tri-Z-Arg·PNA

15) E. V. Ramenskii, M. M. Botovinik and R. U. Beisembaeva, *Khim. Prir. Soedin.*, **4(1)**, 23 (1968).
16) M. M. Botovinik and E. V. Ramenskii, *Ber. II*, **21 (5)**, 127 (1966).

tricarbobenzyloxy-L-arginine gave N^{α},N^{ω},$N^{\omega'}$-tri carbobenzyloxy-L-arginine-*p*-nitroanilide in a good yield of 98 percent through a coupling reaction with *p*-nitrophenyl isocyanate. The absorption spectrum in dioxane shows its maximum at 320 mμ, as is shown in Fig. 1.

Removal of the Protected Groups in L-Arginine-*p*-nitroanilide Derivatises. The removal of the carbobenzyloxy group in N^{α}-carbobenzyloxy-N^{ω}-nitro-L-arginine-*p*-nitroanilide was more difficult than that of the usual N^{α}-carbobenzyloxy group; upon standard treatment with 2 N HBr-glacial acetic acid at room temperature for 30 min, the decarbobenzyloxylation of the N^{α}-position did not proceed completely. The treatment of 3 N HBr-glacial acetic acid at 20—23°C for 7 hr was necessary in order to remove it. This is likely to be related to the difficult decarbobenzyloxylation of N^{α},N^{ω},$N^{\omega'}$-tricarbobenzyloxy-L-arginine-*p*-nitroanilide which will be described below. After the benzoylation of nitro-L-arginine-*p*-nitroanilide, benzoyl-L-arginine-*p*-nitroanilide hydrochloride was obtained by the removal of the nitro group through the HF method of Sakakibara *et al.*[11] However, the yield of L-BAPA was about 44 percent on the removal of the nitro group.

It was very much harder to remove two of the three carbobenzyloxy groups of N^{α},N^{ω},$N^{\omega'}$-tricarbobenzyloxy-L-arginine-*p*-nitroanilide in Scheme 3 completely than it was to remove the ordinary N^{α}-carbobenzyloxy group ((I)′ in Scheme 3).

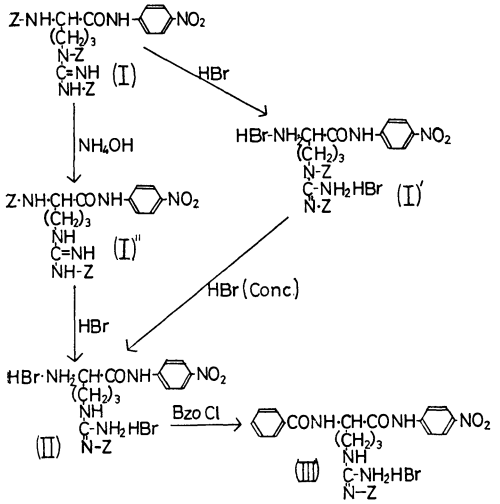

Scheme 3. Decarbobenzyloxylation of N^{α},N^{ω},$N^{\omega'}$-tricarbobenzyloxy-L-arginine-*p*-nitroanilide and its benzoylation.

This might be due to the transfer of a double bond in the guanido group (–N(Z)–C(=NH)–NH–Z→ –N(Z)–C(NH_2HBr)=N–Z) in HBr-dioxane, which stabilises the guanido group to acid, because the carbobenzyloxylated nitrogens are accompanied by no proton. Under even more drastic conditions, one N^{ω}-carbobenzyloxy group was removed ((II) in Scheme 3). The third carbobenzyloxy group was removed in concentrated HBr-glacial acetic acid at a high temperature, the process being accompanied by the cleavage of the amide bond and by the decomposition of the guanido group. When I in Scheme 3 was treated with aqueous ammonia, $>N^{\omega}$–Z, without a proton, was split into I″ without any cleavage of the –NH–Z groups, which were stable in alkaline. By the treatment of I″ in Scheme 3 with HBr, the transfer of the double bond in the guanido group was induced, as is shown in I′ of Scheme 3, and only the N^{α}-carbobenzyloxy group was removed (II). As is shown in Scheme 4, one of the carbobenzyloxy group on the guanido group was made very stable to acid or alkaline by the transformation of guanido group, and the final product was N^{ω}-monocarbobenzyloxy-L-arginine-*p*-nitroanilide. The course of the decarbobenzyloxylation of N^{α},N^{ω},$N^{\omega'}$-tricarbobenzyloxy-L-arginine-*p*-nitroanilide with hydrogen bromide at 50°C is shown in Fig. 2.

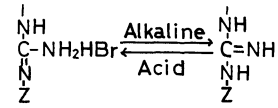

Scheme 4. The transfer reaction of carbobenzyloxylated guanide group with acid and alkaline.

An aliquot of the reaction mixture was spotted on paper (Toyo Roshi No. 51) every hour, used in ascending chromatography in a mixture of *n*-butanol : glacial acetic acid : water (4 : 1 : 5) and developed with ninhydrin. The ratios of the color intensities of the spots, (A) (R_f=0.65), (C) (R_f=0.51) and (B) (several spots in the closed R_f values) to the total spots were then plotted against the reaction time. The (A) spot corresponding to I′ in Scheme 3, disappeared after 4—5 hr. The (C) spot corresponded to II in Scheme 3; it increased with time and reached a constant value after 6 hr. The (B) spot was the side product of the cleavage of the amide bond and the decomposition of the guanido group. At the end of the reaction, the (C) and (B) spots were given instead of the (A) spot and the density of the (C) spot to the total density was 64 percent. From the reaction mixture, a product corresponding to the (C) spot was isolated, it was then benzoylated into compound III. The infrared absorption spectrum III showed a sharp absorption at 1740 cm^{-1} corresponding to the *N*-carbobenzyloxy group, as is shown in Fig. 3.

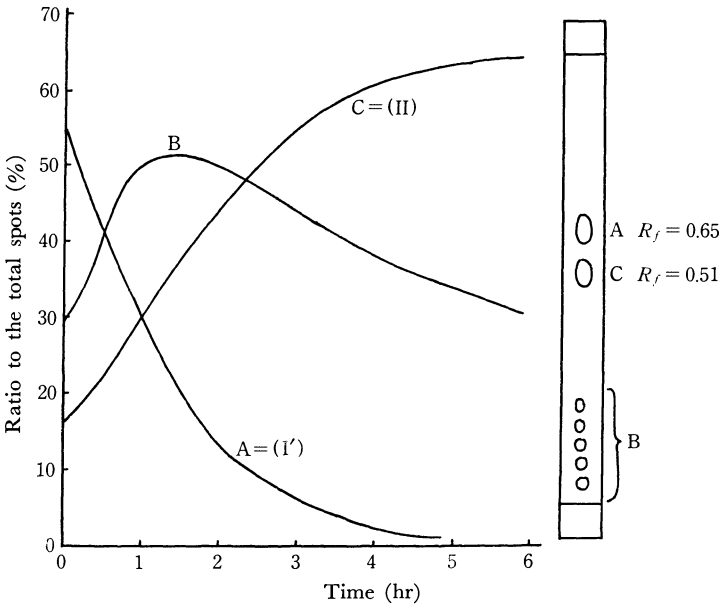

Fig. 2. The time course of decarbobenzyloxy reaction of $N^{\alpha},N^{\omega},N^{\omega'}$-tricarbobenzyloxy-L-arginine-*p*-nitroanilide with HBr saturated dioxane at 50°C.

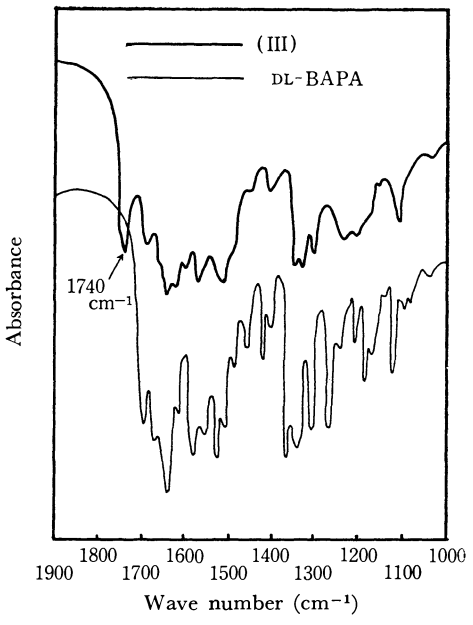

Fig. 3. The infrared absorption spectrum of III and DL-BAPA.

$N^{\alpha},N^{\omega},N^{\omega'}$-tricarbobenzyloxy or N^{α},N^{ω}-dicarbobenzyloxy-L-arginine-*p*-nitroanilide was treated with hydrogen fluoride instead of hydrogen bromide, and the reaction was followed by thin-layer chromatography or by paper electrophoresis. However, one carbobenzyloxy group on the guanido group was too stable to be removed by hydrogen fluoride as it had been by hydrogen bromide. Hayakawa *et al.*[17] succeeded in removing two carbobenzyloxy groups on the guanido group of poly-$N^{\omega},N^{\omega'}$-dicarbobenzyloxy-L-arginine by the treatment of 6 N HBr-glacial acetic acid at 50°C for 90 min, and Sakakibara *et al.*[11] have reported that carbobenzyloxy groups are easily removed from $N^{\alpha},N^{\omega},N^{\omega'}$-tricarbobenzyloxy-L-arginyl-peptide by means of treatment with hydrogen fluoride at 0°C for 30 min. In the case of $N^{\alpha},N^{\omega},N^{\omega'}$-tricarbobenzyloxy-L-arginine-*p*-nitroanilide, the difficulty in completely removing the three carbobenzyloxy groups is due to the steric hindrance of *p*-nitroanilide.

Properties of L-BAPA. The melting point of L-BAPA, 225°C, is the same as that of D-BAPA reported by Cohen *et al.*[2] and is considerably lower than the melting point of 262°C for DL-BAPA. The specific optical rotation of the L-form is +14.2° (*c* 1.0, water, 25°), while that of the D-form is −14.2° under the same conditions.

The absorption spectrum of L-BAPA in water is the same as that of DL-BAPA; it shows its maximum absorption at 312 mμ, as is shown in Fig. 4.

The infrared absorption spectra of the DL-form and the L-form in the solid state (KBr pellet) give almost the same pattern, except for the absorptions of amide I at 1630 cm^{-1} and of the guanido group at 1660 cm^{-1} in DL-BAPA, which shift to the shorter wavelengths of 1640 cm^{-1} and 1680 cm^{-1} respectively in L-BAPA.

These results seem to indicate that DL-BAPA forms a stable racemic compound by means of the

17) T. Hayakawa, Y. Kondo, H. Yamamoto and Y. Murakami, This Bulletin, **42**, 478 (1967).

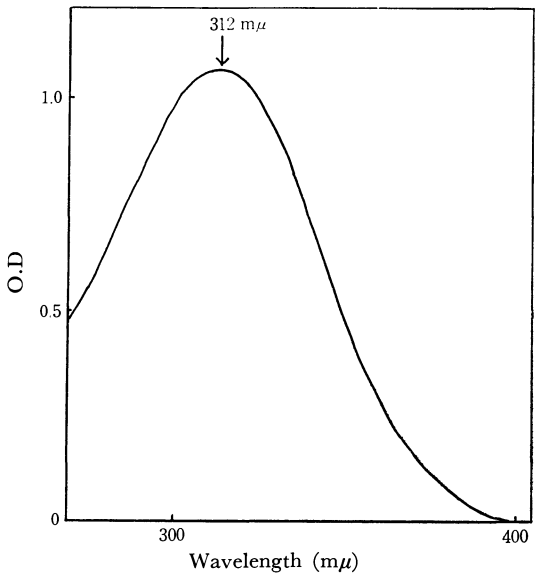

Fig. 4. The absorption spectrum of L-BAPA and DL-BAPA, 8.1×10^{-5} M in water at 22°C, pH 5.60.

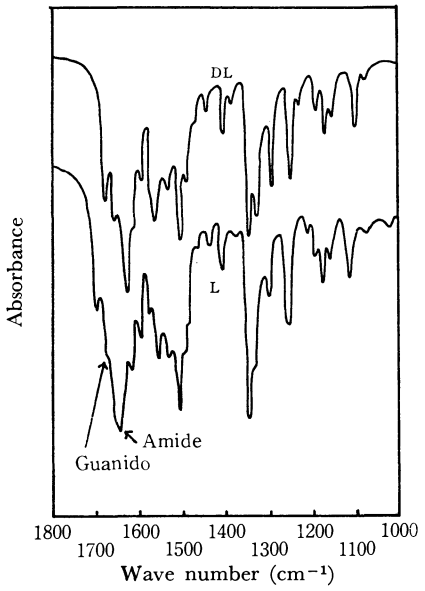

Fig. 5. The infrared absorption spectrum of L- and DL-BAPA.

guanido group; L-BAPA is more easily soluble in water and ethanol than is DL-BAPA.

Conclusions

Optically-active N^{α}-benzoyl-L-arginine-*p*-nitroanilide hydrochloride was synthesized through N^{α}-carbobenzyloxy-N^{ω}-nitro-L-arginine-*p*-nitroanilide, which had been prepared from N^{α}-carbobenzyloxy-N^{ω}-nitro-L-arginine and *p*-nitrophenyl isocyanate in hexamethyl phosphoramide. The N^{α}-carbobenzyloxy group was removed with HBr-glacial acetic acid and converted to the N^{α}-benzoyl derivative, and then the nitro group was removed with hydrogen fluoride. If the benzoyl derivative is used as the starting material, racemization is unavoidable, and so the urethane type of N^{α}-protecting group should be used in order to prevent racemization upon the coupling between carboxyl and isocyanate groups. The coupling reaction proceeded smoothly only in hexamethyl phosphoramide. $N^{\alpha},N^{\omega},N^{\omega'}$-tricarbobenzyloxy-L-arginine-*p*-nitroanilide was prepared from $N^{\alpha},N^{\omega},N^{\omega'}$-tricarbobenzyloxy-L-arginine, but the complete removal of the carbobenzyloxy group into L-arginine-*p*-nitroanilide was unsuccessful. The enzymatic study of trypsin or papain to L-BAPA or DL-BAPA is still in progress.

The authors wish to thank for Dr. Shumpei Sakakibara and Mr. Yasuo Kishida of the Peptide Center, the Protein Research Institute, Osaka University, for permission to use the HF-reaction apparatus and for much useful advice.

BULLETIN OF THE CHEMICAL SOCIETY OF JAPAN VOL. 43 2908—2911 (1970)

Photochemistry of Non-enolizable β-Diketones Containing Cyclopropane Ring in Conjugation

Taiiti OKADA, Koiti KAMOGAWA, Mituyosi KAWANISI and Hitosi NOZAKI

Department of Industrial Chemistry, Kyoto University, Sakyo-ku, Kyoto

(Received March 11, 1970)

Irradiation of bicyclo[3.1.0]hexane-2,4-diones affords isomeric enol lactones retaining the cyclopropane ring. In contrast, photoreaction of 6,6-dimethylspiro[2.5]octane-4,8-dione in ethanol results in the formation of an isomeric benzofuran derivative and dimedone-acetaldehyde condensation product. Cleavage of the cyclopropane ring is characteristic of the behavior of the latter β-diketone.

A compound with a cyclopropane ring in close proximity to a carbonyl group is expected to be photoreactive on account of the unsaturated nature of the three-membered ring. In fact, the photochemical reactions of conjugated cyclopropyl ketones are well-known.[1] In continuation of photochemical studies on non-enolizable β-diketones,[2] we have examined the behavior of two types of this class of compound containing a cyclopropane ring in conjugation of both ketone chromophores, in which the cyclopropane ring is in a different environment with respect to carbonyl groups. One is bicyclo[3.1.0]hexane-2,4-diones (I and II) and the other spiro[2.5]octane-4,8-dione (X). A remarkable difference in the stability of cyclopropane ring has been observed.

Irradiation of I*1 in a benzene solution by means of a Pyrex-filtered mercury arc lamp afforded a single volatile product V in a 98% isolation yield. The structure assigned to V was consistent with spectral data and analyses. Alkaline hydrolysis of V gave a known keto-acid VIII,[3],*2 which was transformed into the known keto-ester IX[3] by means of diazomethane. Epimerization of the *cis*-isomer VII into a thermodynamically stable *trans*-isomer VIII must have occurred during the alkali treatment.*3 UV irradiation of the diketone II[4] also induced the same

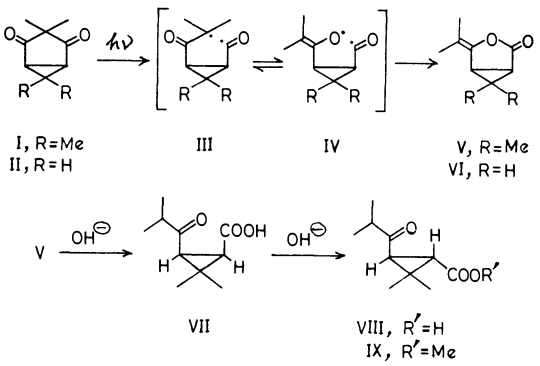

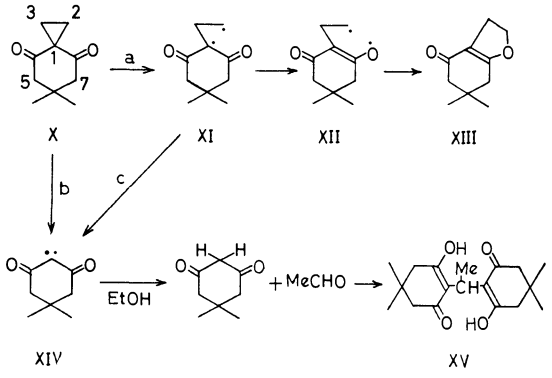

1) a) A. Padwa, "Organic Photochemistry," Vol. 1, ed. by O. L. Chapman, Marcel Dekker Inc., New York, N. Y. (1967), p. 35. b) L. D. Hess and J. N. Pitts, Jr., *J. Amer. Chem. Soc.*, **89**, 1973 (1967). c) W. G. Dauben and G. W. Shaffer, *Tetrahedron Lett.*, **1967**, 4415. d) A. Sonoda, I. Moritani, J. Miki and T. Tsuji, *ibid.*, **1969**, 3187.

2) H. Nozaki, Z. Yamaguti, T. Okada, R. Noyori and M. Kawanisi, *Tetrahedron*, **23**, 3993 (1967). Similar types of rearrangement have been disclosed: R. C. Cookson, A. G. Edwards, J. Hudec and M. Kingsland, *Chem. Commun.*, **1965**, 98; H. U. Hostettler, *Tetrahedron Lett.*, **1965**, 1941; J. Rigaudy and P. Derible, *Bull. Soc. Chim. Fr.*, **1965**, 3047, 3055, 3061; N. J. Turro, W. B. Hammond and P. A. Leermakers, *J. Amer. Chem. Soc.*, **87**, 2775 (1965).

*1 Synthesis and reaction of I are described in Experimental.

3) M. Matsui, H. Yoshioka and H. Hirai, *Agr. Biol. Chem.* (Tokyo), **28**, 456 (1964).

*2 Matsui *et al.* have recently reported the synthesis of *trans*-chrysanthemic acid from VIII in three steps.[3]

*3 *Cf.* Ref. 3, footnote in p. 456.

4) H. Stetter and H.-J. Sandhagen, *Chem. Ber.*, **100**, 2837 (1967).

type of rearrangement to afford lactone VI in an 85% isolation yield. This kind of transformation reminds us of the photochemical rearrangement of 2,2-dimethyl-1,3-cyclohexanediones.[2] The intermediacy of the diradicals III and IV is to be considered.

Irradiation of X[5] was conducted in an ethanolic solution by means of a high pressure mercury arc (quartz vessel). Chromatographic separation on a silica gel column afforded two products, which were found to be 4-oxo-6,6-dimethyl-2,3,4,5,6,7-hexahydrobenzofuran (XIII, 31%) and a dimedone-acetaldehyde condensation product (XV, 5%). Both products were identified by comparison with authentic samples.

Conjugated cyclopropyl ketones such as XVI gives the primary photoproduct XVII under cleavage of the cyclopropane ring.[1a] If the cyclopropane ring is held in a rigid conformation with

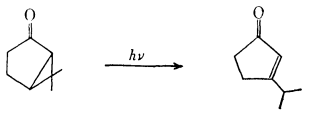

XVI XVII

respect to the carbonyl π system so as to construct optimum geometry for an overlap with the π electrons of the carbonyl group, excitation of an electron into π^* orbital appears to lead to rupture of the cyclopropane bond. Absence of cyclopropane ring cleavage is rather unexpected in the reaction of I and II. Inspection of the molecular model shows the existence of considerable conjugation between cyclopropane ring and carbonyl group. *Gem*-dimethyl groups in the cyclopropane ring should be expected to contribute to the conjugation. However, α-fission is preferred to cyclopropane ring cleavage in the case of I and II. This is because the diradical(s) III and/or IV are stabilized on account of allylic conjugation.

Cleavage at C_1–C_2 position of X affords the diradical XI (path a), which isomerizes to the O-radical XII followed by cyclization to form the furan XIII. As the conversion of X to XIII was also observed thermally (>120°), the precursor of XIII would be either the electronically excited state of X or the vibronically excited one. The formation of XV is rationalized by assuming the intermediacy of cyclic diketocarbene XIV.*4 Carbene XIV abstracts hydrogen from the solvent ethanol to afford dimedone and acetaldehyde, which subsequently condense to form XV. It is not certain whether XIV is derived from X in one step in a concerted manner (path b) or from X by a stepwise mechanism *via* XI (path c). Thus, α-fission is not observed in the case of X. This can be accounted for by the fact that the bond order of C_1–C_4 or C_1–C_8 increases on account of conjugation between the cyclopropane ring and both the carbonyl groups. Cyclopropane ring cleavage is the only observed process, although the result differs greatly from that obtained in the case of XVI.

Experimental

All melting points and boiling points were uncorrected. The IR spectra were obtained in a neat liquid film or in Nujol mull on a Shimadzu IR-27-G spectrophotometer. The NMR spectra were taken with a JEOL C-60-H spectrometer with CCl_4 as a solvent, and chemical shifts are reported in δ values relative to TMS as an internal standard. The NMR data are given in the order of multiplicity (s=singlet, d=doublet, t=triplet, q=quartet and m=unresolved multiplet), integration and assignment. The UV spectra were taken in EtOH on Hitachi EPS-2 recording spectrophotometer. The mass spectra were obtained with a Hitachi RMU-6D spectrometer with a direct inlet (200°) and at 80 eV. Plates of Silica gel G were used for TLC and the spots were visualized with iodine vapor.

Preparation of 4-Bromo-2,2,5,5-tetramethyl-1,3-cyclohexanedione. The method was essentially based on the bromination procedure.[4] A solution of 2,2,5,5-tetramethyl-1,3-cyclohexanedione[7] (40.0 g, 240 mmol) in carbon tetrachloride (150 m*l*) was treated with *N*-bromosuccinimide (50.0 g, 280 mmol), which afforded a bromide (43.0 g, 73%), mp 91°C (from ether). IR (Nujol): 1710 (C=O) and 1685 cm^{-1} (C=O). NMR: δ 1.05 (s, 3, CH_3), 1.20 (s, 3, CH_3), 1.37 (s, 3, CH_3), 1.46 (s, 3, CH_3), 2.77 (s, 1, CH_2), 2.85 (s, 1, CH_2) and 4.75 ppm (s, 1, CH).

Preparation of 3,3,6,6-Tetramethylbicyclo[3.1.0]-hexane-2,4-dione (I). The method was essentially based on the one reported by Stetter in the preparation of 3,3-dimethylbicyclo[3.1.0]hexane-2,4-dione (II).[4] A solution of bromide (15.0 g, 61 mmol) in dry dioxane (150 m*l*) was dropwise added with a solution of potassium *t*-butoxide (f=1.3) (20.0 g, 178 mmol) in *t*-butyl alcohol (50 m*l*) with stirring at reflux. Evaporation

5) K. Ichikawa, O. Itoh and T. Kawamura, This Bulletin, **41**, 1240 (1968).

*4 We have independently found that diketocarbene XIV in triplet state, generated by the benzophenone-sensitized photolysis of 2-diazo-5,5-dimethyl-1,3-cyclohexanedione, abstracts hydrogen from the medium to form dimedone.[6] When ethanol was used as a solvent, dimedone-acetaldehyde condensation product XV was obtained, but in 2-propanol dimedone and acetone were isolated, which do not condense under that condition. In view of these behaviors of diketocarbene XIV, the formation of XV in the photolysis of X reminds us of the intermediacy of XIV.

6) Y. Hayasi, T. Okada and M. Kawanisi, This Bulletin, **43**, 2506 (1970).

7) T. G. Halsall and D. B. Thomas, *J. Chem. Soc.*, **1956**, 2431, 2438.

8) H. E. Simmons, E. P. Blanchard and H. D. Hartzler, *J. Org. Chem.*, **31**, 295 (1966).

*5 The sample of II was kindly supplied by Professor H. Stetter, Technische Hochschule Aachen. The measurement of NMR spectrum was performed in our laboratory (Fig. 2).

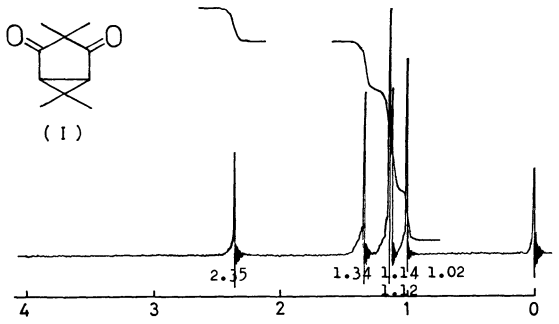

Fig. 1. NMR spectrum of I.

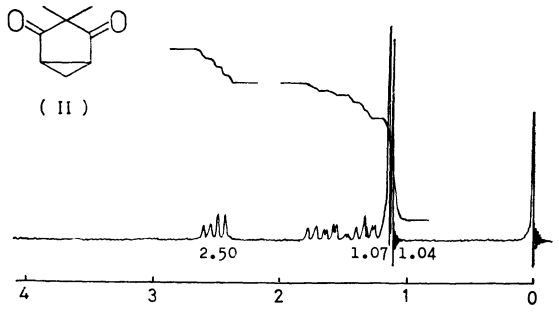

Fig. 2. NMR spectrum of II.

of the solvent, ether extraction, drying ($MgSO_4$), concentration *in vacuo* followed by distillation afforded I (4.50 g, 44%), bp 75°C/5 mmHg, n_D^{20} 1.4681. IR (neat): 3060 (C-H stretching in cyclopropane ring),[8] 1710 (C=O) and 1040 cm^{-1} (cyclopropane ring).[8] NMR: δ 1.02 (s, 3, CH_3), 1.12 (s, 3, CH_3), 1.14 (s, 3, CH_3), 1.34 (s, 3, CH_3) and 2.35 ppm (s, 2, CH). The NMR spectrum of I is shown in Fig. 1. Each methyl signal can be assigned by comparing the spectrum of I with II.*5 UV: λ_{max} (EtOH) 281 nm (log ε 2.01). Mass spectrum consisted of parent peak at *m/e* 166.

Found: C, 72.1; H, 8.2%. Calcd for $C_{10}H_{14}O_2$: C, 72,3; H, 8.5%.

Acid-catalyzed Isomerization of I. A solution of I (4.5 g, 27 mmol) in 18 N hydrochloric acid (120 m*l*) was heated under reflux for 3 hr. After cooling the reaction mixture was extracted twice with ether, and the combined extracts were washed with aqueous sodium carbonate solution and subsequently with water and dried ($MgSO_4$). Removal of the solvent *in vacuo* followed by distillation at 90—92°C/20 mmHg afforded a greenish yellow oil (2.7 g, 60%), which was established to be 1,1-dimethyl-3-isopropyl-3-cyclopentene-2,5-dione, n_D^{20} 1.4667. NMR: δ 0.90 (s, 6, CH_3), 1.04 (d, 6, CH_3), 2.67 (septet, 1, CH) and 6.55 ppm (s, 1, -CH). UV: λ_{max}(EtOH) 232 nm (log ε 4.12).

Found: C, 72.5; H, 8.6%. Calcd for $C_{10}H_{14}O_2$: C, 72.3; H, 8.5%.

Irradiation of 3,3,6,6-Tetramethylbicyclo[3.1.0]-hexane-2,4-dione (I). A solution of I (1.40 g, 8.4 mmol) in benzene (43 m*l*) was irradiated by means of 200 W high pressure mercury arc (Pyrex filter) for 9 hr under nitrogen at room temperature. The progress of the reaction was followed by vpc analysis of the aliquots. Evaporation of the solvent and single distillation afforded 2,2-dimethyl-3-*cis*-(1′-hydroxy-2′-methyl-1′-propenyl)cyclopropanecarboxylic acid γ-lactone (V) (1.37 g, 98%), bp 115—117°C/20 mmHg, n_D^{20} 1.4793. IR (neat): 3050 (C-H stretching in cyclopropane),[8] 1785, 1720 (enol lactone) and 995 cm^{-1}. NMR: δ 1.10 (s, 3, CH_3), 1.23 (s, 3, CH_3), 1.70 (broad s, 6, olefinic CH_3), 2.05 (d, 1, J=6 Hz, CH) and 2.47 ppm (d, 1, J=6 Hz, CH). The NMR spectrum of V is shown in Fig. 3. UV: λ(EtOH) 220 nm (log ε 3.66) and λ(EtOH) 280 nm (log ε 2.42). The mass spectrum consisted of parent peak at *m/e* 166.

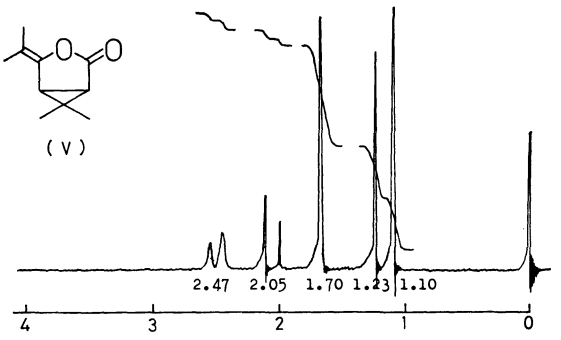

Fig. 3. NMR spectrum of V.

Found: C, 72.2; H, 8.3%. Calcd for $C_{10}H_{14}O_2$: C, 72.3; H, 8.5%.

Hydrolysis of the Enol Lactone V. A solution of V (332 mg, 2 mmol) in alcoholic aqueous potassium hydroxide solution (20 m*l*) was heated under reflux for 2 hr. Work-up afforded 2,2-dimethyl-3-*trans*-isobutyrylcyclopropanecarboxylic acid (VIII) (250 mg, 68%), mp 88—89°C (from *n*-hexane) (lit,[3] mp 86—87.5°C). The IR spectrum was superimposable with that of the authentic spectrum.*6 (Found: C, 65.0; H, 8.6%). 2,4-Dinitrophenylhydrazone of VIII melted at 186—187°C (lit,[3] mp 184—186°C).

Esterification of VIII by means of excess ethereal diazomethane afforded methyl 2,2-dimethyl-3-*trans*-isobutyrylcyclopropanecarboxylate (IX), bp 118—120°C/22 mmHg (lit,[3] bp 126—131°C/38 mmHg). The IR spectrum was superimposable with that of the authentic sample.*6 (Found: C, 65.9; H, 9.0%).

Irradiation of 3,3-Dimethylbicyclo[3.1.0]hexane-2,4-dione (II). A solution of II (100 mg, 0.72 mmol) in benzene (15 m*l*) was irradiated by means of 200 W high pressure mercury arc (Pyrex filter) for 1 hr

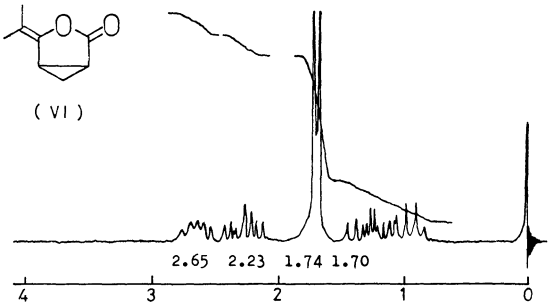

Fig. 4. NMR spectrum of VI.

*6 The IR spectra of VIII and IX were kindly supplied by Professor M. Matsui, The University of Tokyo.

at room temperature. The progress of the reaction was followed by vpc analysis of the aliquots. After the complete disappearance of II, the reaction mixture was concentrated *in vacuo* and the single distillation at 123—125°C/25 mmHg afforded 2-*cis*-(1′-hydroxy-2′-methyl-1′-propenyl)-cyclopropanecarboxylic acid γ-lactone (VI) (85 mg, 85%), n_D^{24} 1.4958. IR (neat): 3100 (C–H stretching in cyclopropane ring),[8] 1795, 1720 cm^{-1} (enol lactone). NMR: δ 0.80—1.50 (m, 2, CH_2), 1.70 (s, 3, CH_3), 1.74 (s, 3, CH_3), 2.23 (m, 1, CH) and 2.65 ppm (m, 1, CH). The NMR spectrum is shown in Fig. 4. UV: λ(EtOH) 220 nm (log ε 3.62) and λ(EtOH) 280 nm (log ε 2.12). The mass spectrum consisted of parent peak at *m/e* 138.

Found: C, 69.5; H, 7.4%. Calcd for $C_8H_{10}O_2$: C, 69.5; H, 7.3%.

Irradiation of 6,6-Dimethylspiro[2.5]octane-4,8-dione (X). A solution of X[5] (1.3 g, 8.2 mmol) in EtOH (20 m*l*) was irradiated by means of 200 W high pressure mercury arc (quartz vessel) for 16 hr under nitrogen at room temperature. The reaction mixture was concentrated *in vacuo* and taken up in benzene (5 m*l*). Polymeric amorphous material undissolved in benzene was removed by filtration and the filtrate was chromatographed on silica gel. The following compounds were isolated: 4-oxo-6,6-dimethyl-2,3,4,5,6,7-hexahydrobenzofuran (XIII) (210 mg, 31%), bp 125—128°C/15 mmHg (lit,[5] bp 109—113°C/4 mmHg). IR (neat): 1630 (broad), 1407, 1223 and 1035 cm^{-1}. The IR spectrum was superimposable with that of the authentic specimen.*[7] The NMR spectrum of XIII was quite similar to the one given in literature.[5] Mass spectrum consisted of parent peak at *m/e* 166. 2,2′-Ethylidenebis(5,5-dimethyl-1,3-cyclohexanedione) (XV) (33 mg, 5%), mp 139—140°C (from H_2O) (lit,[9] mp 140°C). The IR spectrum was superimposable with that of the authentic specimen, which was prepared from dimedone and acetaldehyde.[9] NMR: δ 1.06 (s, 12, CH_3), 1.50 (d, 3, J=7.5 Hz, CH_3), 2.30 (s, 8, CH_2), 4.15 (q, 1, J=7.5 Hz, CH) and 11.45 ppm (broad s, 2, enolic protons). X (638 mg, 50%) was recovered in addition.

Thermal Reaction of X. Neat X (50 mg) was heated at 120°C in a sealed tube for 1 hr. Vpc analysis indicated the formation of XIII (60%) accompanied with the recovered X and unidentified products.

The authors are grateful to Professor K. Sisido for help and encouragement. They are also grateful to Prof. K. Ichikawa for valuable suggestions concerning the preparation of X. They are indebted to the staff of Kao Soap Co., to the sttaff of the Central Research Institute of Toray Industries, and to Dr. M. Nishikawa, Chemical Research Laboratories of Takeda Chemical Industries, Ltd., for determining the mass spectra.

*[7] The IR spectrum of XIII was kindly supplied by Professor K. Ichikawa, Kyoto University.

9) W. Weinberg, *Ind. Eng. Chem. Anal. Ed.*, **3**, 365 (1931).

BULLETIN OF THE CHEMICAL SOCIETY OF JAPAN VOL. 43 2912—2919 (1970)

Synthesis of *N*-Terminal Nonapeptide of Trypsinogen and Its Hydrolysis by Trypsin[1)]

Norio YOSHIDA, Tetsuo KATO and Nobuo IZUMIYA

Laboratory of Biochemistry, Faculty of Science, Kyushu University, Hakozaki, Fukuoka

(Received March 13, 1970)

An *N*-terminal nonapeptide fragment of bovine trypsinogen, H-L-Val-L-Asp-L-Asp-L-Asp-L-Asp-L-Lys-L-Ile-L-Val-Gly-OH, was synthesized *via* two routes and its susceptibility with trypsin was investigated. Protected derivatives, *t*-butyloxycarbonyl protected nonapeptide *t*-butyl ester and benzyloxycarbonyl protected nonapeptide benzyl ester, were prepared by stepwise elongation. Removal of the protecting groups was carried out by treatment with trifluoroacetic acid and hydrogenation respectively. The naked peptide was purified with chromatography on ECTEOLA cellulose column using dilute acetic acid as a solvent. Upon lyophilization the desired nonapeptide was obtained as colorless powder, a portion of the product being digested with trypsin. Rate of tryptic hydrolysis of the peptide was found to be unexpectedly low in the absence of calcium ion, while considerable acceleration of the hydrolysis by calcium ion was noted.

Bovine trypsinogen is activated to trypsin upon cleavage with trypsin. An *N*-terminal hexapeptide of trypsinogen, H-Val-Asp-Asp-Asp-Asp-Lys-OH,[2)] is isolated on the cleavage and a tripeptide sequence of Ile-Val-Gly is found to be a newly generated *N*-terminal protion of trypsin.[3)] A similar tryptic cleavage of chymotrypsinogen furnishes the same Ile-Val-Gly sequence as a new *N*-terminal.[4)] Calcium ions seem to take part in this specific cleavage,[5)] but the mode of action of calcium has not yet been made clear. Savrda and Bricas[6)] prepared a related heptapeptide, H-Val-Asp-Asp-Lys-Ile-Val-Gly-OH, but the rate of tryptic digestion of this peptide was found to be rather low.[7)] As a cluster of four β-carboxylates in a tetra-aspartyl sequence adjacent to the cleaved bond was suggested to be the site of interaction of calcium ions with trypsinogen,[8)] a synthesis of *N*-terminal nonapeptide of trypsinogen, H-Val-$(Asp)_4$-Lys-Ile-Val-Gly-OH (I) was undertaken in order to clarify the role of the tetra-aspartyl carboxyl cluster in tryptic cleavage of the Lys-Ile bond.

Savrda and Bricas[9)] reported recently the synthesis of I and Abita *et al.*[10)] discussed the mode of tryptic digestion of I and related peptides. The rate of tryptic hydrolysis of I was found to be much lower than that of the previous heptapeptide,[7)] but it was raised three to four times by the addition of calcium ion. Radhakrishnan *et al.*[11)] reported that the role of calcium ion is in chelation to the tetra-aspartyl residues. These publications prompt us to disclose the present status of our study which includes synthesis of the nonapeptide I *via* two routes and tryptic digestion of synthesized I.

Reaction sequences employed for synthesis of I are shown in Figs. 1 and 2. In both routes, each protected amino acid was coupled with amino acid ester or peptide esters from *C*-terminus.

In the route of Fig. 1, *Z* group was used as α-amino protecting group of each amino acid other than *N*-terminal valine, and the Z group was selectively hydrogenolyzed in the presence of pal-

1) A part of this work was read at the 20th and 21st Meetings of the Chemical Society of Japan, Tokyo, April, 1967 and Osaka, April, 1968.

2) Abbreviations: Z-, benzyloxycarbonyl; BOC-, *t*-butyloxycarbonyl; Nps-, *o*-nitrophenylsulfenyl; Bz-, benzoyl; -OBu^t, *t*-butyl ester; -OBzl, benzyl ester; DCC, dicyclohexylcarbodiimide; DMF, dimethylformamide; HPT, hexamethylphosphortriamide; *p*-TsOH, *p*-toluenesulfonic acid; DCHA, dicyclohexylamine. Amino acid symbols except Gly denote L-configuration.

3) E. S. Davide and H. Neurath, *J. Biol. Chem.*, **212**, 515 (1955); P. Desnuelle and C. Fabre, *Biochim. Biophys. Acta*, **18**, 29 (1955).

4) M. Rovely, M. Poilroux, A. Yoshida and P. Desnuelle, *ibid.*, **23**, 608 (1957).

5) M. R. MacDonald and M. Kunitz, *J. Gen. Physiol.*, **25**, 53 (1941).

6) J. Savrda and E. Bricas, *Bull. Soc. Chim. Fr.*, **1968**, 2423.

7) M. Delaage, P. Desnuelle and M. Lazdunski, *Biochem. Biophys. Res. Commun.*, **29**, 235 (1967).

8) T. M. Radhakrishnan, K. A. Walsh and H. Neurath, *J. Amer. Chem. Soc.*, **89**, 3059 (1967).

9) J. Savrda and E. Bricas, *Bull. Soc. Chim. Fr.*, **1969**, 883.

10) J. P. Abita, M. Delaage and M. Lazdunski, *Eur. J. Biochem.*, **8**, 314 (1969).

11) T. M. Radhakrishnan, K. A. Walsh and H. Neurath, *Biochemistry*, **8**, 4020 (1969).

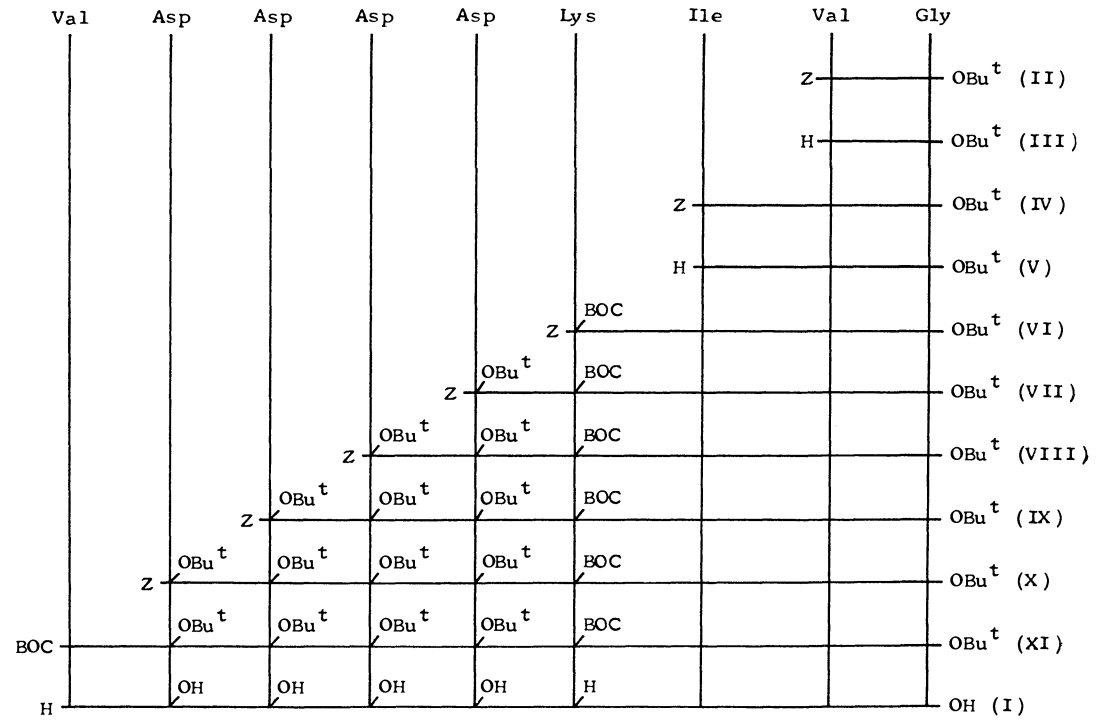

Fig. 1. Synthesis of the nonapeptide I using BOC and OBu^t protecting groups.

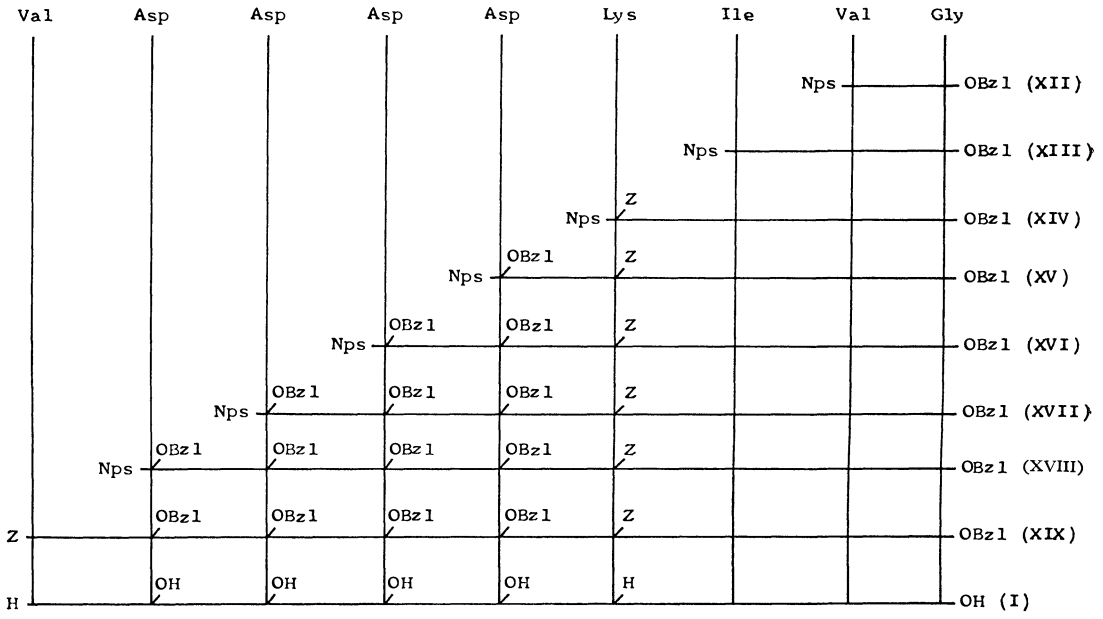

Fig. 2. Synthesis of I using Nps and OBzl groups.

ladium black. The protecting groups related to *t*-butyl alcohol were used for masking the side chain and the terminal functional groups. They are, BOC group for *N*-terminal amino group of valine and *ε*-amino group of lysine, and OBu^t group for *C*-terminal of glycine and *β*-carboxyl groups of four aspartic acid residues. In the coupling of each step, the mixed anhydride method using isobutylchloroformate as a coupling reagent generally gave good results. The use of 10—50% excess of each Z-amino acid brought satisfactory yield as in the cases of VII, VIII, IX and X. Z-

Val-Gly-OBu^t (II) was prepared with the esterification of Z-Val-Gly-OH[12] by the action of isobutylene in the presence of sulfuric acid as a catalyst. After hydrogenolysis of II, furnished dipeptide ester was coupled with the next amino acid, Z-Ile-OH. A similar procedure was repeated to attain the protected nonapeptide, BOC-Val-[Asp-(β-OBu^t)]$_4$-Lys(ε-BOC)-Ile-Val-Gly-OBu^t (XI), which was treated with trifluoroacetic acid to cleave all the protecting groups simultaneously. Although the BOC and OBu^t groups were reported previously to be easily cleavable,[13] all the acidolysis tested failed to give clear results. In addition to trifluoroacetic acid, hydrogen chloride in organic solvent, hydrogen bromide in acetic acid and liquid hydrogen fluoride were used as splitting reagents, but the product after acidolysis gave several ninhydrin-positive spots on their paper chromatograms and electrophoregrams. In order to purify the derived peptide from contaminations, chromatography on ECTEOLA cellulose column was found effective. Upon elution with dilute acetic acid, peptide I was obtained in a yield of about 30%. Anderson *et al.*[14] described the trifluoroacetic acid treatment to split five *t*-butyl esters from a protected macropeptide related to gastrin I and the chromatographic purification of the product, the over-all yield being lowered by the chromatographic procedure to about 10%.

Another route to synthesize the nonapeptide was planned in order to obtain I in better yield. In Fig. 2, Nps group[15] was used as α-amino protecting group except that of *N*-terminal valine. Z group and OBzl group were used to protect α-amino group of *N*-terminal valine, ε-amino group of lysine and all of the carboxyl groups, respectively, in order to hydrogenolyze all the protecting groups at once in the final stage of synthesis. Coupling of each protected amino acid with amino acid ester or peptide esters was accomplished *via* mixed anhydride method for syn-

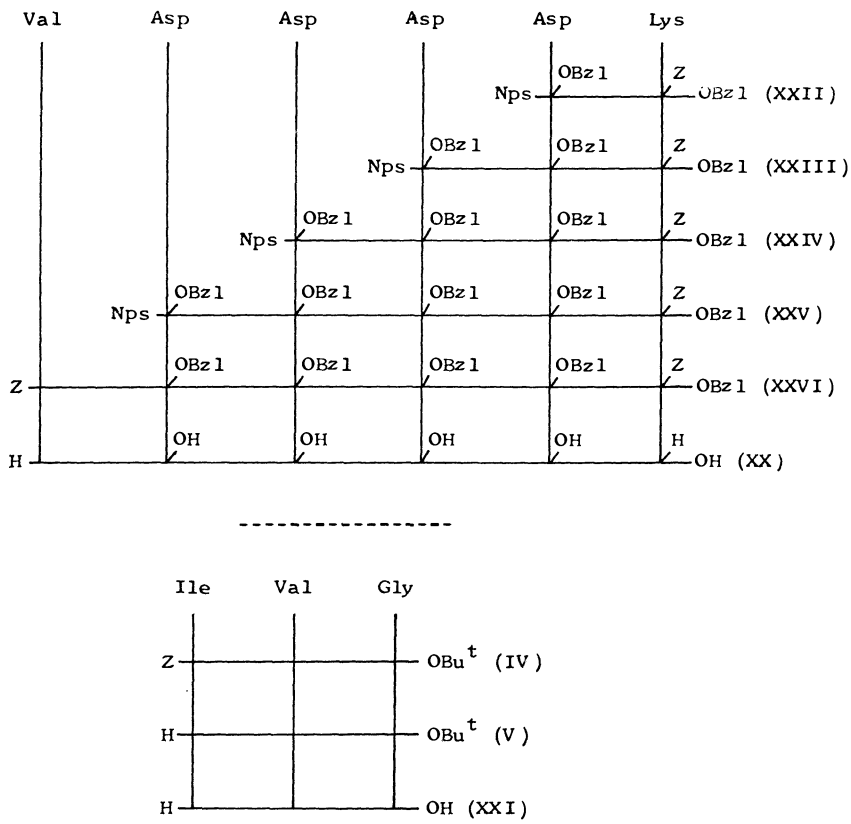

Fig. 3. Synthesis of the hexapeptide XX and tripeptide XXI.

12) E. Wünsch and A. Zwick, *Z. Physiol. Chem.*, **328**, 235 (1962).
13) R. Schwyzer and H. Kappeler, *Helv. Chim. Acta*, **44**, 1136, 1191 (1961).
14) J. C. Anderson, G. W. Kenner, J. K. Macleod and R. C. Sheppard, *Tetrahedron, Suppl.* **8**, part 1, 39 (1966).
15) L. Zervas, D. Borovas and E. Gazis, *J. Amer. Chem. Soc.*, **85**, 3660 (1963); L. Zervas and C. Hamalidis, *ibid.*, **87**, 99 (1965).

thesis of XIV—XIX, and *via* DCC procedure for XII and XIII. In the latter case, the desired acylpeptide ester was obtained easily in good yield by the procedure mixing up each Nps-amino acid DCHA salt with the corresponding amine component, such as H-Gly-OBzl·*p*-TsOH, and DCC. In the case of the mixed anhydride, the use of excess Nps- or Z-amino acid gave satisfactory yield similar to the previous instances. Removal of Nps group was brought about by treatment with N hydrogen chloride in dioxane for XII—XIV, in dioxane-DMF for XV, and in dioxane-dimethylsulfoxide for XVI and XVII.

Protected nonapeptide ester thus obtained, Z-Val-[Asp(β-OBzl)]$_4$-Lys(ε-Z)-Ile-Val-Gly-OBzl (XIX), was applied to a column of Sephadex LH-20 to remove supposed contamination of Nps derivatives. The purified XIX was, then, catalytically hydrogenated and the product was applied to ECTEOLA cellulose column chromatography to give pure peptide I tetrahydrate in a 40% yield. The protected nonapeptide ester was treated with hydrogen fluoride also, but no improvement could be observed compared to the result of hydrogenolysis.

Figure 3 shows syntheses of hexapeptide (XX) and tripeptide (XXI), as authentic samples on enzymic experiment. There was no trouble in synthesis of protected hexapeptide ester, Z-Val-[Asp-(β-OBzl)]$_4$-Lys(ε-Z)-OBzl (XXVI). After purification using Sephadex LH-20 chromatography, hydrogenolysis of XXVI gave peptide XX quantitatively in a pure state. Paper electrophoretic behavior of XX was the same as that of peptide I in citrate buffer at pH 6.7 (Fig. 4). As shown in Fig. 4, crude products from XI and XIX contain several ninhydrin positive components other than I, but these compounds were not identified.

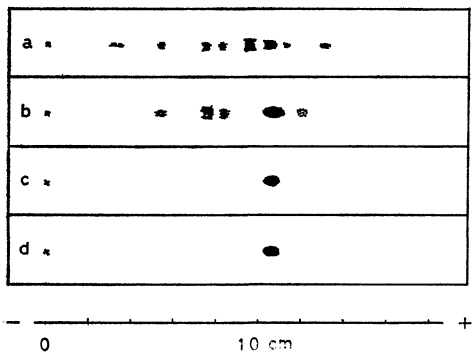

Fig. 4. Paper electrophoregrams of crude and pure peptides. Solvent, 0.01 M citrate buffer, pH 6.7; 600 V/30 cm; 1.5 hr. a, crude product by trifluoroacetic acid treatment on XI; b, crude product by hydrogenolysis of XIX; c, peptide I after ECTEOLA cellulose column chromatography; d, peptide XX.

H-Val-[Asp]$_4$-Lys-Ile-Val-Gly-OH (I)

↓ Trypsin

H-Val-[Asp]$_4$-Lys-OH (XX)

+ H-Ile-Val-Gly-OH (XXI)

Fig. 5. Scheme for tryptic cleavage of I.

Tryptic digestion of I (Fig. 5) was carried out in various conditions, and the progress of the reaction was followed by paper chromatography. In the absence of calcium ion, rate of tryptic hydrolysis of I was unexpectedly low at 30°C and the reaction was apparently inhibited at 47°C. On the contrary, when peptide I was digested with trypsin in the presence of 0.04 M calcium ion, the activating effect of calcium was always observed at 30°, 47° and 0°C, being especially remarkable at 47°C. In addition, susceptibility of I to trypsin was qualitatively compared with that of Bz-Arg-NH$_2$, one of the representative synthetic substrates of trypsin. For example, in a definite experimental condition described in Table 1, peptide I was digested by trypsin in 6 hr, while Bz-Arg-NH$_2$ was digested by one twentieth amount of trypsin in the same 6 hr interval. The results indicate that calcium ion accelerates tryptic digestion of I especially in high temperature as shown by Sipos and Merkel,[16] but the rate of digestion of I was found to be considerably low. This conclusion was compatible with the view given by Abita *et al.*[10] It should be noted that a similar promotion of hydrolysis of *N*-terminal undecapeptide of trypsinogen with calcium ion was also observed by Radhakrishnan *et al.*[11]

Experimental

Melting points were not corrected. Optical rotations were measured on a Yanagimoto Photometric Polarimeter OR-20 type. Paper chromatography and electrophoresis were carried out on Toyo Roshi No. 52 paper. Merck silica gel G was used for thin-layer chromatography. Developing solvents were *n*-butanol-acetic acid-pyridine-water (4 : 1 : 1 : 2, v/v) for paper and chloroform-methanol (5 : 1, v/v) for thin-layer except noted otherwise.

Z-Val-Gly-OBu^t (II). To a solution of Z-Val-Gly-OH[13] (2.53 g, 8.4 mmol) and sulfuric acid (0.3 m*l*) in methylene chloride (100 m*l*), isobutylene (10.7 g) was saturated at 0°C. The mixture in a vessel with a tight stopper was kept to stand for 2 days at room temperature and evaporated *in vacuo*. The residue was diluted with ethyl acetate (100 m*l*) and the solution was washed successively with water, 4% sodium bicarbonate solution and saturated sodium chloride solution, and then dried over sodium sulfate. It was evapo-

16) T. Sipos and J. R. Merkel, *Biochem. Biophys. Res. Commun.*, **31**, 522 (1968).

rated *in vacuo* and the crystals were collected by filtration with the aid of ether and petroleum ether. Recrystallization from ethyl acetate-ether-petroleum ether gave 2.64 g (86%); mp 146°C; $[\alpha]_D^{30}$ −4.2° (*c* 1, DMF), (Found: C, 62.92; H, 7.91; N, 7.68%). Savrda *et al.*[6] prepared II by the coupling of Z-valine *p*-nitrophenyl ester with H-Gly-OBu^t; mp 143.5—144.5°C; $[\alpha]_D^{20}$ −2.5±0.5° (DMF).

H-Val-Gly-OBu^t (III). A solution of II (2.55 g, 7 mmol) in ethanol (80 m*l*) was hydrogenated in the presence of palladium black. After removal of the catalyst, the filtrate was evaporated *in vacuo*; yield of an oil, 1.60 g (99%); R_f 0.90 on paper.

Z-Ile-Val-Gly-OBu^t (IV). This compound was prepared by the coupling of III with a mixed anhydride derived from Z-Ile-OH and isobutylchloroformate as described in literature;[17] yield, 67%; mp 164—166°C, $[\alpha]_D^{20}$ −7.9° (*c* 1, DMF) (Found: C, 62.73; H, 8.29; N, 8.62%). Savrda *et al.* reported essentially the same procedure; mp 169—171°C, $[\alpha]_D^{20}$ −9±0.5° (DMF).[6]

H-Ile-Val-Gly-OBu^t (V). A suspension of IV (1.67 g, 3.5 mmol) in ethanol (30 m*l*) was hydrogenated as described for III. Evaporation of the solvent gave oily product (1.26 g, 105%); R_f 0.95 on paper.

Z-Lys(ε-BOC)-Ile-Val-Gly-OBu^t (VI). Coupling of Z-Lys(ε-BOC)-OH with V *via* mixed anhydride procedure gave VI; yield, 91%; mp 202—203°C; $[\alpha]_D^{30}$ −16.9° (*c* 1, DMF) (Found: C, 61.03; H, 8.59; N, 9.85%); reported values mp 213—215°C and $[\alpha]_D^{22}$ −14.5±0.5° (DMF).[6]

Z-Asp(β-OBu^t)-Lys-(ε-BOC)-Ile-Val-Gly-OBu^t (VII). A mixture of VI (3.25 g, 4.6 mmol) in DMF (15 m*l*) was cooled at 0°C and hydrogenated. After hydrogen was passed for 15 min, chilled 0.39 N hydrogen chloride in methanol (13 m*l*, 5.1 mmol) was added. After the reaction had been completed, the filtrate from the catalyst was evaporated. The condensed DMF solution was used as it was in the next coupling. The hydrogenated tetrapeptide was coupled with 1.2 equivalent of mixed anhydride derived from Z-Asp(β-OBu^t)-OH.[18] Yield of VII, 91%; mp 211—212°C (decomp.); $[\alpha]_D^{30}$ −21.2° (*c* 0.8, DMF) (Found as hemihydrate: C, 59.67; H, 8.27; N, 9.58%); reported values, mp 226—228°C and $[\alpha]_D^{20}$ −17.5±0.5° (DMF).[6]

Z-[Asp(β-OBu^t)]$_2$-Lys(ε-BOC)-Ile-Val-Gly-OBu^t (VIII). A similar coupling procedure using 1.25 equivalent of the mixed anhydride gave VIII (84%); mp 208—212°C, $[\alpha]_D^{30}$ −22.6° (*c* 1, DMF) (Found as hemihydrate: C, 59.02; H, 8.26; N, 9.14%); reported values, 225—226°C and $[\alpha]_D^{18}$ −22.5±0.5° (DMF).[6]

Z-[Asp(β-OBu^t)]$_3$-Lys(ε-BOC)-Ile-Val-Gly-OBu^t (IX). A similar coupling procedure using 1.5 equivalent of the mixed anhydride gave IX (92%); mp 213—214°C (decomp.); $[\alpha]_D^{30}$ −23.4° (*c* 1, DMF) (Found: C, 59.40; H, 8.30; N, 9.28%); reported values mp 222—224°C and $[\alpha]_D^{23}$ −25.7±0.7° (DMF).[9]

Z-[Asp(β-OBu^t)]$_4$-Lys(ε-BOC)-Ile-Val-Gly-OBu^t (X). A similar procedure as described above gave X (93%); mp 211—213°C (decomp.); $[\alpha]_D^{30}$ −25.5° (*c* 1, DMF) (Found as hemihydrate: C, 58.42; H, 8.10; N, 9.17%); reported values, mp 224—225°C and $[\alpha]_D^{22}$ −28.9°±0.5° (DMF).[9]

BOC-Val-[Asp(β-OBu^t)]$_4$-Lys(ε-BOC)-Ile-Val-Gly-OBu^t (XI). A similar procedure using 1.5 equivalent of BOC-Val-OH gave XI (91%); mp 219—221°C (decomp.); $[\alpha]_D^{30}$ −27.8° (*c* 1, DMF) (Found for monohydrate: C, 57.07; H, 8.37; N, 9.66%); reported values, mp 249°C and $[\alpha]_D^{20}$ −29.2±0.5° (DMF).[9]

Homogeneity of XI was ascertained by column chromatography using Sephadex LH-20. A solution of XI (5 mg) in methanol (0.6 m*l*) was applied to a column (1.7×37 cm) of Sephadex LH-20, and the column was eluted with methanol at room temperature with a flow rate of one drop per 6 sec. Two milliliter fractions were collected, and a small amount of eluate in each test tube was spotted on a thin-layer plate. Compound on the plate was detected by spraying 47% hydrobromic acid and then ninhydrin. Only one peak (tube number 20—23) was obtained. The result showed the homogeneity of XI. Several di-Z derivatives of cyclic decapeptide were found to elute at the same position under similar experimental conditions.[19]

Nps-Val-Gly-OBzl (XII). To a chilled solution of Nps-Val-OH·DCHA salt[15] (18.1 g, 40 mmol) and H-Gly-OBzl·*p*-TsOH (13.5 g, 40 mmol) in chloroform (80 m*l*), DCC[20] (8.24 g) was added. The mixture was stirred for 3 hr at 0°C and allowed to stand overnight at room temperature. After removal of precipitate by filtration, the filtrate was evaporated and the residual oil was dissolved in ethyl acetate (100 m*l*). The solution was washed with 4% sodium bicarbonate solution, 10% citric acid and water, and dried over sodium sulfate. The filtrate was evaporated and the oily residue was solidified upon addition of petroleum ether. Recrystallization from ether-petroleum ether gave 15.9 g (96%); mp 97—98°C, $[\alpha]_D^{22}$ +52.5° (*c* 2, DMF); R_f 0.90 on thin-layer.

Found: C, 57.40; H, 5.45; N, 10.09%. Calcd for $C_{20}H_{23}O_5N_3S$: C, 57.55; H, 5.55; N, 10.07%.

Nps-Ile-Val-Gly-OBzl (XIII). A solution of XII (10.4 g, 25 mmol) in dioxane (60 m*l*) was treated with 2.5 N hydrogen chloride in dioxane (40 m*l*) at room temperature. After 1 hr the mixture was evaporated and the crystals were washed with ether by decantation. The dipeptide ester hydrochloride (XIIa) (7.70 g, 103%; R_f 0.65 on thin-layer) obtained was used in the next procedure without further purification. Into a solution of Nps-Ile-OH·DCHA salt[15] (11.7 g, 25 mmol), triethylamine (3.5 m*l*) and XIIa in chloroform (140 m*l*), was added DCC (5.15 g) at 0°C. Usual coupling procedure as described for XII gave crude crystals of XIII. The crystals were collected and recrystallized from DMF-dioxane-ethyl acetate. Yield, 11.4 g (86%); mp 185—186°C; $[\alpha]_D^{22}$ +20.0° (*c* 2, DMF); R_f 0.88 on thin-layer.

Found: C, 58.92; H, 6.45; N, 10.44%. Calcd for $C_{26}H_{34}O_6N_4S$: C, 58.85; H, 6.46; N, 10.56%.

Nps-Lys(ε-Z)-Ile-Val-Gly-OBzl (XIV). Compound XIII (8.50 g, 16 mmol) was treated with 2.5 N hydrogen chloride in dioxane to furnish tripeptide hydrochloride (XIIIa) in a similar manner as described

17) J. R. Vaughan, Jr., and R. L. Osato, *J. Amer. Chem. Soc.*, **74**, 676 (1952).

18) P. M. Bryant, R. H. Moore, P. T. Pimlot and G. T. Young, *J. Chem. Soc.*, **1959**, 3868.

19) M. Waki and N. Izumiya, This Bulletin, **40**, 1687 (1967).

20) J. C. Sheehan and G. P. Hess, *J. Amer. Chem. Soc.*, **77**, 1067 (1955).

for XIII. Into a mixed anhydride of Nps-Lys(ε-Z)-OH[15] (7.51 g, 16.8 mmol) and isobutylchloroformate (2.18 ml) in tetrahydrofuran (100 ml), a solution of XIIIa (6.67 g, 16 mmol; R_f 0.71 on thin-layer) and triethylamine (2.24 ml) in DMF (120 ml) was added at −5°C. After being left overnight at room temperature, the solution was poured into water (1000 ml) and the precipitate deposited was collected by filtration, washed, and recrystallized from DMF-ethyl acetate. Yield, 11.4 g (90%); mp 223—225°C; $[\alpha]_D^{22}$ +23.0° (*c* 2, DMF); R_f 0.81 on thin-layer.

Found: C, 60.71; H, 6.62; N, 10.55%. Calcd for $C_{40}H_{52}O_9N_6S$: C, 60.59; H, 6.61; N, 10.60%.

Nps-Asp(β-OBzl)-Lys(ε-Z)-Ile-Val-Gly-OBzl (XV). Compound XIV (6.28 g, 7.9 mmol) was treated with 2.5 N hydrogen chloride in dioxane to give corresponding hydrochloride (XIVa). A solution of XIVa (4.99 g, 93%; R_f 0.61 on thin-layer) and triethylamine (1.02 ml) in DMF (55 ml) was added to a mixed anhydride of Nps-Asp(β-OBzl)-OH[15] (3.03 g, 8.04 mmol) in tetrahydrofuran (30 ml). The product was treated as described for the preparation of XIV. Recrystallization from DMF-ethyl acetate-ether gave 5.79 g (80%); 231—232°C; $[\alpha]_D^{22}$ −36.0° (*c* 1, HPT); R_f 0.88 on thin-layer.

Found: C, 61.38; H, 6.44; N, 9.77%. Calcd for $C_{51}H_{63}O_{12}N_7S$: C, 61.37; H, 6.36; N, 9.82%.

Nps-[Asp(β-OBzl)]$_2$-Lys(ε-Z)-Ile-Val-Gly-OBzl (XVI). A suspension of XV (4.24 g, 4.25 mmol) in DMF (120 ml) was treated with 2.5 N hydrogen chloride in dioxane (6.7 ml). The pale yellow crystals (3.74 g, 100%; R_f 0.74 on thin-layer) obtained were coupled with Nps-Asp(β-OBzl)-OH (1.93 g, 5.1 mmol) as described above. Recrystallization from dimethylsulfoxide-methanol-ether gave 4.02 g (79%); mp 222—223°C; $[\alpha]_D^{22}$ +15.6° (*c* 1, HPT); R_f 0.79 on thin-layer.

Found: C, 61.77; H, 6.49; N, 9.27%. Calcd for $C_{62}H_{74}O_{15}N_8S$: C, 61.88; H, 6.20; N, 9.31%.

Nps-[Asp(β-OBzl)]$_3$-Lys(ε-Z)-Ile-Val-Gly-OBzl (XVII). A solution of XVI (3.39 g, 2.82 mmol) in dimethylsulfoxide (10 ml) was treated with 2.5 N hydrogen chloride in dioxane (7.0 ml). The hexapeptide ester hydrochloride (3.06 g, 100%; R_f 0.59 on thin-layer) obtained was condensed with a mixed anhydride of Nps-Asp(β-OBzl)-OH (1.37 g, 3.64 mmol) in the usual manner. Recrystallization from dimethylsulfoxide-methanol gave 3.19 g (81%); mp 214—216°C; $[\alpha]_D^{22}$ +21.6° (*c* 1, HPT); R_f 0.88 on thin-layer.

Found: C, 61.97; H, 6.35; N, 9.09%. Calcd for $C_{73}H_{85}O_{18}N_9S$: C, 62.24; H, 6.08; N, 8.95%.

Nps-[Asp(β-OBzl)]$_4$-Lys(ε-Z)-Ile-Val-Gly-OBzl (XVIII). Compound XVII (1.15 g, 0.82 mmol) was treated with 2.5 N hydrogen chloride in dioxane; yield of hydrochloride (XVIIa), 1.06 g, 100%; R_f 0.64 on thin-layer. The crude product obtained from XVIIa and Nps-Asp(β-OBzl)-OH (433 mg, 1.15 mmol) was recrystallized from dimethylsulfoxide-methanol. Yield, 1.19 g (91%); mp 221—224°C; $[\alpha]_D^{22}$ +22.4° (*c* 1, HPT); R_f, 0.74 on thin-layer.

Found: C, 62.20; H, 6.44; N, 8.48%. Calcd for $C_{84}H_{96}O_{21}N_{10}S$: C, 62.52; H, 6.00; N. 8.68%.

Z-Val-[Asp(β-OBzl)]$_4$-Lys(ε-Z)-Ile-Val-Gly-OBzl (XIX). Compound XVIII (1.10 g, 0.68 mmol) was treated with 2.5 N hydrogen chloride as described above. The pale yellow powder (1.02 g, 100%; R_f 0.65 on thin-layer) obtained was coupled with Z-Val-OH (256 mg, 1.02 mmol). Recrystallization from DMF-ethyl acetate gave light yellow product; 1.06 g (92%); mp 241—243°C; $[\alpha]_D^{22}$ +27.6° (*c* 1, HPT); R_f 0.64 on thin-layer.

Found: C, 62.84; H, 6.25; N, 8.41%. Calcd for $C_{91}H_{108}O_{22}N_{10}\cdot 2H_2O$: C, 63.17; H, 6.52; N, 8.09%.

A solution of XIX (80 mg) in DMF (1 ml) was applied to a column (0.9×40 cm) with Sephadex LH-20. Elution was carried out with the same solvent at room temperature. The flow rate was one drop per 7 sec, and 1.5 ml fractions were collected; only one peak (tube number 8—12) was observed.

H-Val-[Asp]$_4$-Lys-Ile-Val-Gly-OH (I). *a. I·4H$_2$O from XIX.* A solution of XIX (100 mg, 59 μmol) in a mixture of acetic acid (12 ml), methanol (6 ml), and water (2 ml) was hydrogenated in the presence of palladium black at room temperature. The progress of the reaction was followed by paper electrophoresis. After some 40 hr, the filtrate from the catalyst was evaporated repeatedly, water being added. The precipitate which formed upon the addition of ethanol was collected and dried. The yield was 67 mg. Forteen milligram of this was dissolved in 0.5 M acetic acid and it was applied to a column (0.9×10 cm) of ECTEOLA cellulose, which had been equilibrated with 0.05 M acetic acid. The column was eluted with 0.05 M (50 ml), 0.1 M (50 ml), 0.2 M (25 ml), 0.3 M (25 ml) and 0.5 M acetic acid. The combined eluate from No. 15—No. 18 tubes (2 ml each) was evaporated repeatedly at room temperature, water being added. After ethanol was added to the residue, the precipitate deposited was collected after standing in a refrigerator for several hours; yield, 4.8 mg (40% from XIX); mp 292—295°C (decomp.); $[\alpha]_D^{22}$ +36.4° (*c* 0.5, water); R_f 0.12 on paper; amino acid ratios in acid hydrolysate, $Asp_{3.86}Gly_{1.03}Val_{1.95}Ile_{1.00}Lys_{1.06}$.[21]

Found: C, 45.91; H, 6.92; N, 13.21%. Calcd for $C_{40}H_{66}O_{18}N_{10}\cdot 4H_2O$: C, 45.88; H, 7.12; N, 13.37%. Savrda *et al.*[9] described the preparation of I without elemental analysis by the action of trifluoroacetic acid on XI.

b. I from XI. A solution of XI (73.6 mg, 50 μmol) in a mixture of trifluoroacetic acid (1 ml) and anisole (0.5 ml) was kept for 2 hr at room temperature and the solution was evaporated *in vacuo*. This procedure was repeated, and the dried residue weighed 61.6 mg. Fifty milligram of this was dissolved in 0.5 M acetic acid (0.8 ml) and the solution was applied to a column of ECTEOLA cellulose (0.9×18 cm) as described for the preparation of I from XIX. The eluate from No. 15—No. 20 tubes was evaporated, and the precipitate was collected with the aid of ethanol. It was recrystallized from water-ethanol; 13 mg (30%); R_f 0.12 on paper.

Nps-Asp(β-OBzl)-Lys(ε-Z)-OBzl (XXII). The compound was prepared from Nps-Asp(β-OBzl)-OH·DCHA salt (1.67 g, 3 mmol) and H-Lys(ε-Z)-OBzl-*p*-TsOH (1.63 g, 3 mmol) using DCC as described for the preparation of XII. Yield, 1.82 g (84%); mp 127—129°C; $[\alpha]_D^{22}$ −17.2° (*c* 1, DMF); R_f 0.91 on thin-layer.

Found: C, 62.58; H, 5.51; N, 7.83%. Calcd for $C_{38}H_{40}O_9N_4S$: C, 62.62; H, 5.53; N, 7.69%.

21) The authors are indebted to Mr. Kosaku Noda of this Laboratory for the amino acid analysis.

Nps-[Asp(β-OBzl)]$_2$-Lys(ε-Z)-OBzl (XXIII). Compound XXII (1.33 g, 1.82 mmol) was treated with N hydrogen chloride in dioxane (7.3 m*l*) for 1 hr. The mixture was evaporated and treated with ether. Colorless crystals (1.07 g, 96%; R_f 0.67 on thin-layer) obtained were coupled with Nps-Asp(β-OBzl)-OH (659 mg, 1.75 mmol) by the mixed anhydride procedure. Recrystallization from ethyl acetate-ether gave 1.40 g (84%); mp 137—138°C; $[\alpha]_D^{22}$ −1.4° (*c* 1, DMF); R_f 0.89 on thin-layer.

Found: C, 62.52; H, 5.42; N, 7.44%. Calcd for $C_{49}H_{51}O_{12}N_5S \cdot 1/2H_2O$: C, 62.41; H, 5.55; N, 7.43%.

Nps-[Asp(β-OBzl)]$_3$-Lys(ε-Z)-OBzl (XXIV). A solution of XXIII (1.78 g, 1.9 mmol) in N hydrogen chloride in dioxane (7.6 m*l*) was allowed to stand for 1 hr to give the tripeptide ester hydrochloride (1.29 g, 86%; R_f 0.79 on thin-layer), which was condensed with Nps-Asp(β-OBzl)-OH (746 mg, 1.97 mmol) as above. Yield, 1.61 g (89%); mp 123—125°C; $[\alpha]_D^{22}$ −25.0° (*c* 1, DMF); R_f 0.94 on thin-layer.

Found: C, 63.22; H, 5.50; N, 7.37%. Calcd for $C_{60}H_{62}O_{15}N_6S$: C, 63.25; H, 5.49; N, 7.38%.

Nps-[Asp(β-OBzl)]$_4$-Lys(ε-Z)-OBzl (XXV). Compound XXIV (365 mg, 0.32 mmol) was treated with hydrogen chloride as described above, and the corresponding hydrochloride (319 mg, 100%; R_f 0.67 on thin-layer) obtained was coupled with Nps-Asp(β-OBzl)-OH (196 mg, 0.52 mmol) as shown for XIV. Recrystallization from dioxane-ether gave 352 mg (82%); mp 143—145°C; $[\alpha]_D^{22}$ −32.0° (*c* 1, DMF); R_f 0.92 on thin-layer.

Found: C, 62.87; H, 5.39; N, 7.27%. Calcd for $C_{71}H_{73}O_{18}N_7S$: C, 63.42; H, 5.47; N, 7.29%.

Z-Val-[Asp(β-OBzl)]$_4$-Lys(ε-Z)-OBzl (XXVI). Nps group of compound XXV (310 mg, 0.23 mmol) was removed with hydrogen chloride in the usual manner, and the pentapeptide ester hydrochloride (XXVa, 250 mg, 0.205 mmol, R_f 0.97 on thin-layer) obtained was coupled with Z-Val-OH (75.4 mg, 0.3 mmol) by the mixed anhydride procedure. Recrystallization from dioxane-ethyl acetate gave pale yellow product; 258 mg (90%). A part (115 mg) of this product was applied to a column of Sephadex LH-20 (0.9×50 cm) using dioxane as a solvent. Fractions No. 7—No. 10 (2 m*l* each) were evaporated, and colorless crystals of XXVI were collected with the aid of ether. Recrystallization from dioxane-ether gave 94 mg (74% from XXVa); mp 151—158°C; $[\alpha]_D^{22}$ −37.0° (*c* 1, DMF); R_f 0.93 on thin-layer.

Found: C, 65.58; H, 5.96; N, 6.80%. Calcd for $C_{78}H_{88}O_{10}N_7$: C, 65.76; H, 6.01; N, 6.88%.

H-Val-[Asp]$_4$-Lys-OH (XX). A solution of XXVI (55 mg, 39 μmol) in a mixture of acetic acid (1.8 m*l*), methanol (0.9 m*l*), and water (0.3 m*l*) was hydrogenated in the presence of palladium black. After some 20 hr, the filtrate from the catalyst was evaporated repeatedly, water being added. The precipitate which formed upon the addition of ethanol was collected. Recrystallization from hot water-ethanol gave 24.7 mg (91%); mp 265—272°C(decomp.); $[\alpha]_D^{22}$ −38.0° (*c* 1, water); R_f 0.11 on paper; amino acid ratios in acid hydrolysate, $Asp_{3.91}Val_{1.00}Lys_{1.02}$[21])

Found: C, 43.16; H, 6.58; N, 12.99%. Calcd for $C_{27}H_{43}O_{15}N_7 \cdot 5/2\,H_2O$: C, 43.19; H, 6.45; N, 13.06%.

H-Ile-Val-Gly-OH (XXI). V from IV (0.5 mmol) was dissolved in trifluoroacetic acid (1.5 m*l*), and the solution was left to stand for 2 hr at room temperature and evaporated *in vacuo*. The residue dissolved in water (0.5 m*l*) was applied to a column of Dowex 50×8 (H^+ form, 0.9×7 cm). It was washed with water and eluted with 2 N ammonium hydroxide solution. The eluate was evaporated and the residue was collected with the aid of acetone. Recrystallization from water-acetone gave 122 mg (84%); mp 297—300°C (decomp.); $[\alpha]_D^{22}$ −16.0° (*c* 1, water); R_f 0.82 on paper.

Found: C, 53.77; H, 8.70; N, 14.53%. Calcd for $C_{13}H_{25}O_4N_3$: C, 54.33; H, 8.77; N, 14.62%.

Enzymatic Experiments. *a. Experimental Conditions.* Table 1 shows composition of reaction mixture used. Proceeding of enzyme reaction was followed

Table 1. Composition of mixture for the enzyme reaction

0.1 M Tris buffer at pH 8.0

Experiment number	Substrate (concentration, 0.01M)	Temperature (°C)	Calcium chloride concentration (M)	Enzyme concentration (mg N/m*l*)
1	peptide I	30	0.04	0.3
2	peptide I	30	0	0.3
3	peptide I	47	0.04	0.3
4	peptide I	47	0	
5	peptide I	0	0.04	0.3
6	peptide I	0	0	0.3
7	Bz-Arg-NH_2	30	0	0.3
8	Bz-Arg-NH_2	30	0	0.1
9	Bz-Arg-NH_2	30	0.04	0.1
10	Bz-Arg-NH_2	30	0	0.03
11	Bz-Arg-NH_2	30	0	0.015
12	Bz-Arg-NH_2	30	0	0.01
13	Bz-Arg-NH_2	30	0	0.0075
14	Bz-Arg-NH_2	30	0	0.006
15	Bz-Arg-NH_2	47	0.04	0.3
16	Bz-Arg-NH_2	47	0	0.3

by means of paper chromatography of each reaction mixture during the course of time. Developing solvent system used was *n*-butanol-acetic acid-pyridine-water (15 : 3 : 10 : 12, v/v).

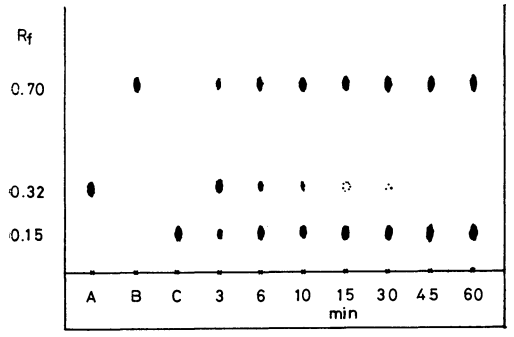

Fig. 6. Paper chromatograms of a reaction mixture of experiment No. 3 in Table 1. A, the nonapeptide I; B, the tripeptide XXI; C, the hexapeptide XX.

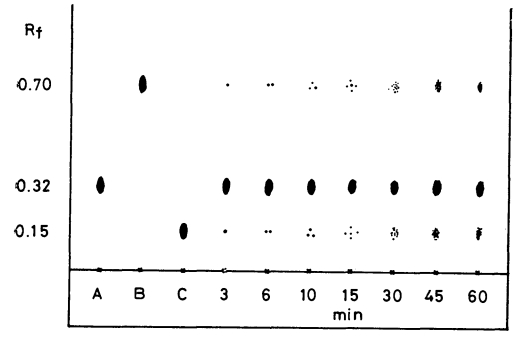

Fig. 7. Paper chromatograms of a reaction mixture of experiment No. 4. in Table 1.

b. Influence of Temperature Variation. Peptide I was digested with trypsin in the presence and absence of calcium ion at various temperatures. A comparison of the results of the experiments of No. 1—No. 6 indicates that the acceleration of hydrolysis with calcium was maximum at 47°C. Trypsin hydrolyzes peptide

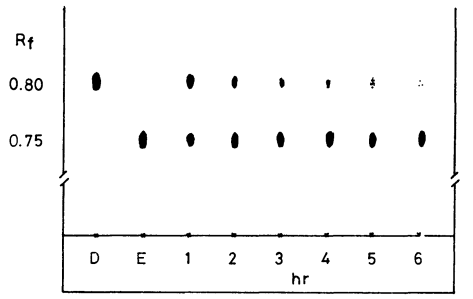

Fig. 8. Paper chromatograms of a reaction mixture of experiment No. 11 in Table 1. D, Bz-Arg-NH_2; E, Bz-Arg-OH.

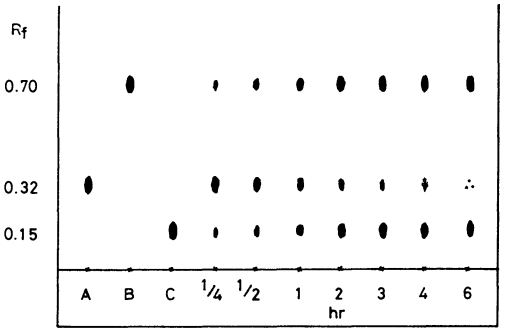

Fig. 9. Paper chromatograms of a reaction mixture of experiment No. 2 in Table 1.

I completely in 30 min with calcium (Fig. 6), but the hydrolysis was nearly inhibited without calcium (Fig. 7). At 30°C, complete digestion of I takes 2 hr and 6 hr in the presence and absence of calcium, respectively. At 0°C, peptide I disappeared after 14 hr with calcium, but it still remained after 19 hr without calcium.

c. Comparison of Hydrolysis Rates of I and Bz-Arg-NH_2. Experiments No. 7—No. 16 were carried out in order to compare the apparent rate of hydrolysis of I and Bz-Arg-NH_2, a typical synthetic substrate for trypsin. Experiment No. 11 (Fig. 8) showed that some one twentieth amount of trypsin was enough to hydrolyze Bz-Arg-NH_2 in the same time interval to hydrolyze I in experiment No. 2 (Fig. 9).

BULLETIN OF THE CHEMICAL SOCIETY OF JAPAN VOL. 43 2920—2924 (1970)

Compounds Related to Acridine. VII.[1] The Synthesis of 9-Ethynylacridine and Its Reaction with *p*-Nitrosodialkylaniline

Otohiko Tsuge and Akiyoshi Torii

Research Institute of Industrial Science, Kyushu University, Hakozaki, Fukuoka

(Received March 13, 1970)

The dehydrobromination of 9-(1,2-dibromoethyl)acridine, which had easily been obtained by the bromination of 9-vinylacridine, to 9-ethynylacridine was attempted by several methods, and it has been established that this transformation can be effected in a 55% yield by the use of methanolic potassium hydroxide in dioxane. It has been found that the reaction of 9-ethynylacridine with *p*-nitrosodialkylaniline under the influence of hydrochloric acid in ethanol leads to the formation of the corresponding 1-(9-acridinyl)-1,2-bis(*p*-dialkylaminophenylimino)ethane N^1,N^2-dioxide. In addition, the configuration of the dioxide has also been proposed on the basis of spectroscopic studies and an inspection of the Dreiding models.

Previously, it has been found that hydrochloric acid (HCl) is an extremely effective catalyst for the condensation of acridine having an active methyl group with an aromatic nitroso compound.[2] Furthermore, even 9-ethylacridine reacts with two moles of *p*-nitrosodimethylaniline under the influence of HCl to give a mixture of 1-(9-acridinyl)-1,2-bis(*p*-dimethylaminophenylimino)ethane and its N^1-oxide.[3]

We decided to investigate the reactions of various acridine derivatives with aromatic nitroso compounds over a wider range. In the present work, several methods of the dehydrobromination of 9-(1,2-dibromoethyl)acridine to 9-ethynylacridine were studied, and a convenient synthetic method was established. It has been found that 9-ethynylacridine reacts with two moles of *p*-nitrosodialkylaniline to give 1-(9-acridinyl)-1,2-bis(*p*-dialkylaminophenylimino)ethane N^1,N^2-dioxide. In addition, the most reasonable configurations for the dioxide and for analogous compounds were decided upon.

Results and Discussion

Dehydrobromination Reactions of 9-(1,2-Dibromoethyl)acridine (I). No information has been available regarding the preparation and properties of 9-ethynylacridine (VI). The preparation of VI from 9-(1,2-dibromoethyl)acridine (I) which had easily been prepared by the bromination of 9-vinylacridine[1], by several manners was investigated, as is shown in Scheme 1.

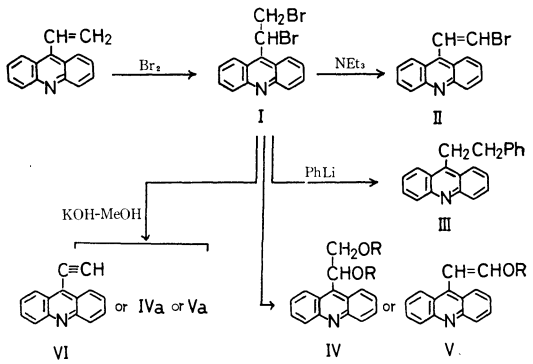

Scheme 1

The acetylene VI was not obtained by the attempted dehydrobromination with triethylamine or phenyllithium. Instead, *trans*-1-(9-acridinyl)-2-bromoethylene (II) or 1-(9-acridinyl)-2-phenylethane (III) was obtained in a 97 or 57% yield in the respective reaction. The structures of II and III were confirmed by spectral studies as well as by elemental analyses.

Mitchell and Sondheimer[4] found that the dehydrobromination of 1,8-bis(1,2-dibromoethyl)-naphthalene to 1,8-diethynylnaphthalene in a 79% yield could be effected by the use of potassium *t*-butoxide in boiling *t*-butyl alcohol and dioxane.

However, the treatment of the dibromide I with several potassium alkoxides in the corresponding boiling alcohol and dioxane did not give the expected acetylene VI, but rather, 9-(1,2-dialkoxy-

1) Part VI: O. Tsuge, A. Torii and T. Tomita, *Nippon Kagaku Zasshi*, **90**, 1263 (1969).

2) O. Tsuge, M. Nishinohara and M. Tashiro, This Bulletin, **36**, 1477 (1963).

3) O. Tsuge, M. Nishinohara and K. Sadano, *ibid.*, **38**, 2037 (1965).

4) R. H. Mitchell and F. Sondheimer, *Tetrahedron*, **24**, 1397 (1968).

ethyl)acridine (IV) or *trans*-1-(9-acridinyl)-2-alkoxyethylene (V) depending on the nature of the alkoxides; the reactions with methoxide, ethoxide, and *n*-propoxide gave the corresponding diether IVa—IVc respectively, while the treatment with *t*-butoxide afforded the vinylether Vb.

Although the dehydrobromination of the dibromide I to the acetylene VI caused such difficulties, it has been found that I reacted with methanolic potassium hydroxide in dioxane to give the corresponding diether IVa, *trans*-vinylether Va, or the expected acetylene VI, depending on the reaction conditions; the results are summarized in Table 1.

Table 1. Conditions and yields of products in the reaction of I with methanolic potassium hydroxide[a)]

MeOH:I mole ratio	Temp. (°C)	Time (min)	Yield (%) IVa	Va	VI
11:1	65	120	80	0	0
9:1	75—80	120	0	75	0
2:1	94—96	120	0	0	27
2:1	94—96	40	0	+[c)]	34
2:1	94—96	20	0	0	55
0[b)]	100	120	0	0	0

a) Mixtures of I (5.0 g), KOH (5.0 g), and specified amounts of MeOH were heated under definite conditions.
b) I was recovered.
c) A plus-sign, +, indicates a trace amount.

The data in Table 1 indicate that differences in the amounts of methanol result in serious differences. As the acetylene VI was proved to be a rather unstable substance, a considerable reduction in reaction time is desirable.

The structures of IV, V, and VI were confirmed by spectral studies as well as by elemental analyses. The infrared spectrum of VI showed the characteristic bands due to the ethynyl group at 3200 and 2130 cm^{-1}, while the NMR spectrum in deuteriochloroform ($CDCl_3$) exhibited signals at τ 5.8 (1H, ethynyl-proton, singlet) and 1.4—2.5 (8H, aromatic protons, multiplet).

Reaction of 9-Ethynylacridine (VI) with the Nitroso Compound VII. The reaction of VI with *p*-nitrosodimethylaniline (VIIa) was investigated under various conditions.

The acetylene VI did not react with VIIa in either the absence or presence of a basic catalyst such as potassium carbonate in ethanol, but the presence of HCl as a catalyst afforded the 1 : 2 adduct (VIIIa) ($C_{31}H_{29}O_2N_5$) as red prisms.

The effects of different amounts of HCl as a catalyst on the yield of VIIIa were also investigated; the results are shown in Table 2.

A similar reaction of VI with *p*-nitrosodiethylaniline (VIIb) gave the corresponding 1 : 2 adduct (VIIIb) as red needles. However, nitrosobenzene, *p*-methyl- or *p*-chloronitrosobenzene did not give the corresponding adduct under similar conditions; resinous materials were obtained exclusively in each case.

Table 2. Conditions and yields of VIIIa in the reaction of VI with VIIa[a)]

VI:VIIa mole ratio	HCl (m*l*)	Yield of VIIIa (%)
1:1	0.1	29
1:2	0.05	38
1:2	0.1	43
1:2	0.1	47[b)]
1:2	0.1	41[c)]
1:2	0.2	29
1:2	0.35	16

a) Reactions of VI (1.0 g) with specified amounts of VIIa and HCl (d^{27} 1.1748) were conducted in ethanol (15 m*l*) at room temperature for 2 hr.
b) Reaction temperature: 0°C.
c) Reaction time: 12 hr.

On the basis of the chemical transformations to the known compounds shown in Scheme 2, and on the basis of the spectroscopic evidence, the 1 : 2 adduct was established to be 1-(9-acridinyl)-1,2-bis(*p*-dialkylaminophenylimino)ethane N^1,N^2-dioxide (VIII).

The hydrolysis of VIIIa with 12% aqueous HCl afforded acridine-9-carbaldehyde (IX)[2)] in a 73% yield. When VIIIa was treated with cold 10% aqueous sulfuric acid, (9-acridinyl)formylmethylene-*p*-dimethylaminoaniline *N*-oxide (X),[3)] which was then subjected to decarbonylation to form (9-acridinylmethylene)-*p*-dimethylaminoaniline *N*-oxide (XI),[2)] was obtained in a 57% yield.

Furthermore, VIIIa was deoxygenated with triethyl phosphite to afford 1-(9-acridinyl)-1,2-bis(*p*-dimethylaminophenylimino)ethane (XII).[3)]

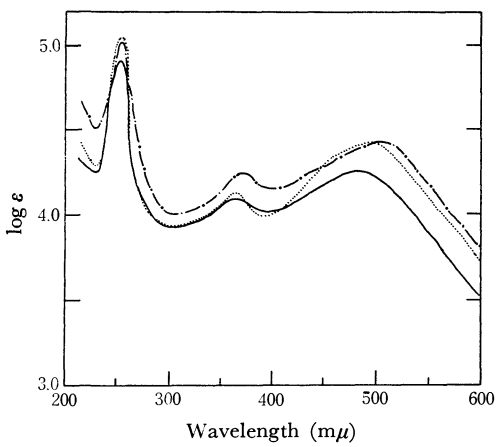

Fig. 1. Ultraviolet spectra in ethanol, VIIIa (——); VIIIb (—·—·); XIII (·····).

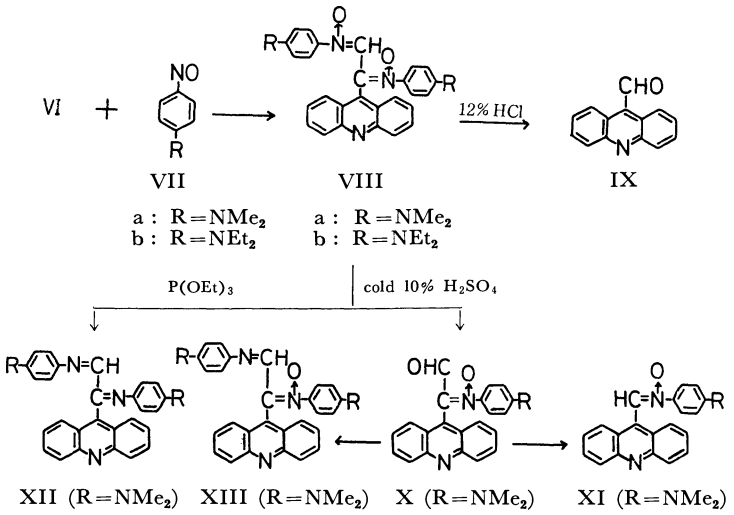

Scheme 2

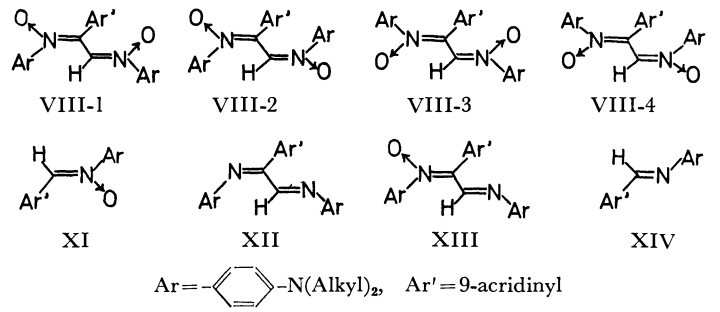

Fig. 2.

The condensation of X and *p*-dimethylaminoaniline gave 1-(9-acridinyl)-1,2-bis(*p*-dimethylaminophenylimino)ethane N^1-oxide (XIII).[3]

The spectral data of VIII are also compatible with the proposed structure. The ultraviolet (Fig. 1) and infrared spectra are very similar to those of XIII. The NMR spectrum of VIIIb in $CDCl_3$ showed signals at τ 9.12 and 8.78 (each 6H, methyl-protons, triplet), at τ 6.95 and 6.65 (each 4H, methylene-protons, quartet), at τ 1.7—4.2 (16H, aromatic protons), and at τ 0.87 (1H, methine proton).

Four geometrical isomers resulting from the *syn*- and *anti*-configurations are, then, possible for the structure of VIII (Fig. 2). An inspection of the Dreiding models for VIII indicates that there is an appreciable interaction between the acridine and phenyl rings in VIII-2—VIII-4, but not in VIII-1. Consequently, it may be thought that VIII-1 is the most favorable configuration for VIII.

Similar inspections of the Dreiding models for XI, XII, XIII, and (9-acridinylmethylene)-*p*-dimethylaminoaniline (XIV) indicate that the most favorable configurations for the above compounds are those shown in Fig. 2.

The NMR spectra in $CDCl_3$ showed the methine proton at τ 0.30, 0.33, 0.32, and 0.30 in XI, XII, XIII, and XIV respectively. Presumably, the appearance of the methine proton at an abnormally low field might be understood in terms of the deshielding effect of aromatic rings.[5] All the ultraviolet spectra of the compounds VIII and XI—XIV exhibited absorptions compatible with a long conjugated system.

The proposed configurations for the above compounds are supported by the above observations as well as by the inspections of the Dreiding models.

Experimental

All the melting points are uncorrected. The infrared spectra were measured in KBr disks, while the NMR spectra were determined at 60 MHz with a Hitachi R-20 spectrometer, using tetramethylsilane as the internal reference. The mass spectra were obtained on a Hitachi RMS-4 spectrometer at an electrode voltage of 70 eV.

5) J. F. King and T. Durst (*Can. J. Chem.*, **40**, 882 (1962)) have reported that the methine proton of benzylidenaniline appears at τ 1.65 in the NMR spectrum (carbon tetrachloride).

9-(1,2-Dibromoethyl)acridine (I). Into a solution of 2.0 g of 9-vinylacridine[1] in 20 m*l* of dry benzene, 1.6 g of bromine was added with stirring at 0°C. After the reaction mixture had then been stirred at room temperature for 20 min, filtration gave 3.45 g (quantitatively) of orange crystals. Recrystallization from ethanol afforded 9-(1,2-dibromoethyl)acridine(I) as orange prisms; mp 156—157°C (decomp.).

Found: C, 49.58; H, 2.72; N, 3.49%. Calcd for $C_{15}H_{11}NBr_2$: C, 49.31; H, 3.01; N, 3.84%.

The mass spectrum was also compatible with the dibromide I: parent peaks (M^+) at *m/e* 367, 365 and 363 (intensity 1 : 2 : 1); $(M-Br)^+$ at *m/e* 286 and 284 (intensity 1 : 1); $(M-2Br)^+$ at *m/e* 205 (base peak).

***trans*-1-(9-Acridinyl)-2-bromoethylene (II).** After a mixture of 1.5 g of the dibromide I in 5 m*l* of triethylamine had been refluxed for 4 hr, it was allowed to stand overnight, thus giving 1.15 g (97%) of yellow crystals. Recrystallization from benzene gave *trans*-1-(9-acridinyl)-2-bromoethylene (II) as pale yellow needles; mp 349—350°C (decomp.).

Found: C, 63.22; H, 3.21; N, 4.62%. Calcd for $C_{15}H_{10}NBr$: C, 63.38; H, 3.52; N, 4.92%. Infrared spectrum: 950 cm^{-1}. NMR spectrum in trifluoroacetic acid: τ 2.7 and 1.9 (each 1H, olefinic proton, doublet, J=14 Hz), 1.2—2.1 (8H, aromatic protons, multiplet).

1-(9-Acridinyl)-2-phenylethane (III). A solution of 3.0 g of the dibromide I and phenyllithium, which had been prepared from 7.5 g of bromobenzene and 0.7 g of lithium in 30 m*l* of diethyl ether, was stirred at 0°C for 40 min. After the reaction mixture had then been decomposed with ice water, the resulting mixture was extracted twice with 50-m*l* portions of benzene. The benzene extract was evaporated *in vacuo* to leave yellow crystals (mp 82—90°C), which were then dissolved in benzene. The benzene solution was chromatographed on alumina, affording 1.3 g (57%) of 1-(9-acridinyl)-2-phenylethane (III) as pale yellow needles; mp 100.5—101.5°C.

Found: C, 89.19; H, 6.14; N, 4.88%. Calcd for $C_{21}H_{17}N$: C, 89.01; H, 6.05; N, 4.94%. Mass spectrum: *m/e* 283 (M^+), 192 $[(M-C_7H_7)^+]$. NMR spectrum in carbon tetrachloride: τ 6.9—7.2 and 6.05—6.45 (each 2H, methylene-protons, multiplet), 1.65—2.8 (13H, aromatic protons, multiplet).

General Method for the Reaction of the Dibromide I with Potassium Alkoxide. *i*) Into a solution of 3.0 g of the dibromide I in 40 m*l* of dioxane was stirred, drop by drop and at room temperature, a methanolic solution of potassium methoxide, prepared from 4.4 g of potassium and 50 m*l* of methanol. After the reaction mixture had then been refluxed for 1 hr, the solvent was evaporated *in vacuo* to leave a residue, which was then quenched with water. The resultant mixture was extracted with 100 m*l* of diethyl ether, after which the ether extract was evaporated to leave a brown oily material which, on the chromatography of the benzene solution on alumina, gave 2.0 g of pale yellow crystals (mp 98.5—100°C). Recrystallization from petroleum benzine (bp 45—60°C) gave 9-(1,2-dimethoxyethyl)acridine (IVa), mp 101.5—102.5°C, as pale yellow prisms.

Found: C, 76.78; H, 6.52; N, 5.21%. Calcd for $C_{17}H_{17}O_2N$: C, 76.38; H, 6.41; N, 5.24%. Mass spectrum: *m/e* 235 $[(M-CH_3OH)^+]$, 220 $[(235-CH_3)^+]$, 192 $[(220-CO)^+]$. NMR spectrum in carbon tetrachloride: τ 6.75 (6H, methyl-protons, singlet), 6.25 (2H, methylene-protons, doublet), 5.3 (1H, methine-proton, triplet), 1.65—2.65 (8H, aromatic protons, multiplet).

A similar reaction of the dibromide I with potassium ethoxide or *n*-propoxide gave the corresponding diether.

9-(1,2-Diethoxyethyl)acridine (IVb): mp 65—66°C; yellow prisms. Yield, 83%. Found: C, 77.08; H, 7.26; N, 4.83%. Calcd for $C_{19}H_{21}O_2N$: C, 77.26; H, 7.17; N, 4.74%.

9-(1,2-Di-*n*-propoxyethyl)acridine (IVc): mp 71—72°C; yellow prisms. Yield, 78%. Found: C, 78.13; H, 8.14; N, 4.58%. Calcd for $C_{21}H_{25}O_2N$: C, 77.98; H, 7.88; N, 4.33%.

ii) Into a solution of 5.0 g of the dibromide I in 50 m*l* of dioxane was stirred, drop by drop and at room temperature, a solution of potassium *t*-butoxide, prepared from 5.5 g of potassium and 250 m*l* of *t*-butyl alcohol. After the reaction mixture had then been refluxed for 1 hr, a treatment similar to that described in *i*) was carried out; *trans*-1-(9-acridinyl)-2-*t*-butoxyethylene (Vb), mp 141.5—142.5°C, was thus obtained as yellow prisms. Yield, 3.4 g (87%).

Found: C, 82.44; H, 6.94; N, 4.97%. Calcd for $C_{19}H_{19}ON$: C, 82.28; H, 6.91; N, 5.05%. Infrared spectrum: 945 cm^{-1}. Mass spectrum: *m/e* 277 (M^+). NMR spectrum in carbon tetrachloride: τ 8.57 (9H, methyl-protons, singlet), 1.5—3.4 (10H, olefinic and aromatic protons).

Reaction of the Dibromide I with Methanolic Potassium Hydroxide. *i*) A solution of 5.0 g of the dibromide I and 5.0 g of potassium hydroxide in a mixture of methanol (7 g) and dioxane (2.5 m*l*) was heated, while being stirred, at 65°C for 2 hr, and then cooled. After water had been added to it, the mixture was extracted three times with 25-m*l* portions of ether. The ether solution was dried over sodium sulfate, and the ether was distilled off, leaving a brown oily material. The benzene solution was chromatographed on alumina, affording 2.9 g (80%) of pale yellow crystals; mp 99—101°C. Recrystallization from petroleum benzine (bp 45—60°C) gave pale yellow prisms, mp 101.5—102.5°C, whose infrared spectrum was identical with that of the diether IVa.

ii) A solution of 5.0 g of the dibromide I and 5.0 g of potassium hydroxide in a mixture of methanol (4 g) and dioxane (10 m*l*) was heated, while being stirred, at 75—80°C for 2 hr. A treatment similar to that described in *i*) gave a reddish-brown oily material from the ether extract. The benzene solution was chromatographed on alumina to give 2.4 g (75%) of yellow crystals, mp 123—125°C, which, on recrystallization from petroleum benzine (bp 45—60°C), afforded *trans*-1-(9-acridinyl)-2-methoxyethylene (Va), mp 125—126°C, as yellow needles.

Found: C, 81.65; H, 5.49; N, 5.64%. Calcd for $C_{16}H_{13}ON$: C, 81.68; H, 5.52; N, 5.95%. Mass spectrum: *m/e* 235 (M^+), 220 $[(M-CH_3)^+]$, 204 $[(M-OCH_3)^+]$. 192 $[(220-CO)^+]$. Infrared spectrum: 940 cm^{-1}.

iii) A solution of 5.0 g of the dibromide I and 5.0 g of potassium hydroxide in a mixture of methanol (1.0 g) and dioxane (2.5 m*l*) was heated, while being stirred, at 94—96°C for 20 min.

A similar treatment gave 1.5 g (55%) of brown crystals, mp 153—155°C (decomp.), from the ether extract. Recrystallization from benzene gave 9-ethynylacridine (VI), mp 157—158°C (decomp.), as yellow needles.

Found: C, 84.43; H, 4.70; N, 6.49%. Calcd for $C_{15}H_9N \cdot \frac{1}{2}H_2O$: C, 84.80; H, 4.71; N, 6.60%. Ultraviolet spectrum λ_{max}^{EtOH} mμ (log ε): 257 (5.3), 371 (4.1). Mass spectrum: *m/e* 203 (M^+).

The results of other reactions under varying conditions are shown in Table 1.

Reaction of the Acetylene VI with *p*-Nitrosodimethylaniline (VIIa). To a mixture of 0.3 g of the acetylene VI and 0.4 g of *p*-nitrosodimethylaniline (VIIa) in 5 m*l* of ethanol was added 0.03 m*l* of HCl at 0°C. The reaction mixture was then stirred at 0°C for 2 hr. Filtration gave 0.35 g (47%) of red crystals which, on recrystallization from pyridine, afforded 1-(9-acridinyl)-1,2-bis(*p*-dimethylaminophenylimino)-ethane N^1,N^2-dioxide (VIIIa), mp 217—218°C, as red prisms.

Found: C, 74.18; H, 5.91; N, 14.10%. Calcd for $C_{31}H_{29}O_2N_5$: C, 73.93; H, 5.80; N, 13.91%. Ultraviolet spectrum λ_{max}^{EtOH} mμ (log ε): 253 (4.9), 367 (4.1), 485 (4.3).

The results of other reactions under varying conditions are summarized in Table 2.

Reaction of the Acetylene VI with *p*-Nitrosodiethylaniline (VIIb). A similar reaction of 0.3 g of the acetylene VI with 0.53 g of *p*-nitrosodiethylaniline (VIIb) in the presence of HCl (0.03 m*l*) at 0°C for 2 hr gave the corresponding N^1,N^2-dioxide VIIIb, mp 190—191°C, as red needles. Yield, 0.41 g (50%).

Found: C, 75.54; H, 6.71; N, 12.16%. Calcd for $C_{35}H_{37}O_2N_5$: C, 75.10; H, 6.66; N, 12.31%. Ultraviolet spectrum λ_{max}^{EtOH} mμ (log ε): 254 (5.2), 368 (4.3), 505 (4.5).

Hydrolysis of the N^1,N^2-Dioxide VIIIa. *i*) A mixture of 0.2 g of the N^1,N^2-dioxide VIIIa in 2 m*l* of 12% aqueous HCl was heated at 90°C for 30 min, and then cooled. The precipitated crystals were collected and washed with ammonium hydroxide, giving 0.6 g (73%) of yellow crystals, mp 143—145°C. Recrystallization from a petroleum benzine-benzene mixture afforded yellow needles, mp 148°C. This compound was proved, by an admixed-mp determination and by a study of its infrared spectrum, to be identical with an authentic sample of acridine-9-carbaldehyde (IX), mp 147°C.[2]

ii) After 10 m*l* of 10% sulfuric acid had been added to 0.5 g of VIIIa under ice cooling, it was allowed to stand at 0°C for 30 min. Filtration gave dark yellow crystals which, when washed with ammonium hydroxide, afforded 0.2 g (57%) of orange crystals. Recrystallization from benzene gave orange needles, mp 206—207°C (decomp.), which were proved, by a study of their infrared spectrum, to be identical with an authentic sample of (9-acridinyl)formylmethylene-*p*-dimethylaminoaniline *N*-oxide (X), mp 208°C (decomp.).[3]

Decarbonylation of (9-Acridinyl)formylmethylene-*p*-dimethylaminoaniline *N*-Oxide (X). A suspension of 0.1 g of X and 1 drop of 20% aqueous sodium hydroxide in 5 m*l* of ethanol was refluxed for 3 hr. After the mixture had then been allowed to stand overnight, filtration gave 60 mg (67%) of red crystals. Recrystallization from pyridine gave red prisms, mp 243°C (decomp.). This compound was proved, by a study of its infrared spectrum, to be identical with (9-acridinylmethylene)-*p*-dimethylaminoaniline *N*-oxide (XI), mp 243°C (decomp.).[2]

Reaction of the N^1,N^2-Dioxide VIIIa with Triethyl Phosphite. A mixture of 0.22 g of VIIIa and 2.0 g of triethyl phosphite was gently refluxed under a nitrogen atmosphere for 10 hr. After the mixture had then been allowed to stand overnight, the precipitated crystals were filtered off and then washed with ethanol to give 0.1 g (50%) of red crystals.

Recrystallization from pyridine gave red prisms, mp 282—283°C (decomp.). These were proved, by a study of their infrared spectrum, to be identical with an authentic sample of 1-(9-acridinyl)-1,2-bis(*p*-dimethylaminophenylimino)ethane (XII), mp 283°C (decomp.).[3]

1-(9-Acridinyl)-1,2-bis(*p*-dimethylaminophenylimino)ethane N^1-Oxide (XIII). A mixture of 0.1 g of X, 0.2 g of *p*-dimethylaminoaniline, and 1 drop of acetic acid in 5 m*l* of ethanol was refluxed for 2 hr, and then cooled. Filtration gave 0.1 g (75%) of red crystals which, on recrystallization from benzene, afforded red prisms, mp 263—264°C (decomp.). This compound was proved, by a study of its infrared spectrum, to be identical with 1-(9-acridinyl)-1,2-bis(*p*-dimethylaminophenylimino)ethane N^1-oxide (XIII), mp 265°C (decomp.).

BULLETIN OF THE CHEMICAL SOCIETY OF JAPAN VOL. 43 2925—2933 (1970)

The Cyclization of Ethyl Cyanoacetate and Salicylaldehyde or 3-Methoxysalicylaldehyde with Ketones by Means of Ammonium Acetate

Akio SAKURAI and Hiroshi MIDORIKAWA

The Institute of Physical and Chemical Research, Yamato-Machi, Saitama

and Yasuo HASHIMOTO

Tokyo Electrical Engineering College, Nishikicho, Chiyoda-ku, Tokyo

(Received March 26, 1970)

Various substituted benz[*f*]isoquinolines were readily prepared by the condensation of ethyl cyanoacetate and salicylaldehyde or 3-methoxysalicylaldehyde with aliphatic ketones (acetone, diethyl ketone, methyl pentyl ketone, methyl isopentyl ketone, *etc.*) or aromatic ketones (acetophenone, *o*-hydroxyacetophenone, *m*-nitroacetophenone, propiophenone, *etc.*) in the presence of ammonium acetate. On the other hand, condensation with cyclic ketones such as cyclopentanone and cyclohexanone gave benz[*f*]cyclopent[*c*]isoquinolines and benzo[*k*]phenanthridines respectively.

Previous papers have shown that ethyl cyanoacetate condensed with ketones[1] (aliphatic methyl, aromatic, cyclic, and α,β-unsaturated) or aldehydes[2] (salicyl and 3-methoxysalicyl) in the presence of ammonium acetate to afford substituted pyridones, quinolines (from ketone), and benzo[*h*]quinazolines (from aldehyde).

The present paper will deal with the syntheses of 6-oxabenz[*f*]isoquinoline, 7-oxabenz[*f*]-2,3-dihydro-1*H*-cyclopent[*c*]isoquinoline, and 8-oxa-1,2,3,4-tetrahydrobenzo[*k*]phenanthridine derivatives by the condensation of ethyl cyanoacetate, salicylaldehyde, or 3-methoxysalicylaldehyde, and a variety of ketones in the presence of ammonium acetate.

The reaction of ethyl cyanoacetate and salicylaldehyde or 3-methoxysalicylaldehyde with ketones was carried out by heating a mixture of ester, aldehyde, ketone, and ammonium acetate (molar ratio 1 : 1 : 1 : 1—1.5) in ethanol. In this case (Scheme 1), the dehydration of the amino group of I and the carbonyl group of ketone, cyclization between the methyl or methylene group of the ketone and the 4-position of the coumarin ring, and subsequent dehydrogenation took place to form 2- or 1,2-disubstituted-4-amino-5-oxo-6-oxabenz[*f*]isoquinolines (II).

When salicylaldehyde was heated with ethyl cyanoacetate and ammonium acetate in ethanol for few minutes, a crystalline product was obtained. Its infrared spectrum exhibited no characteristic absorption for a C≡N group. When dissolved in dilute hydrochloric acid, this substance afforded pale yellow needles. This compound was confirmed as the HCl salt of 3-amidinocoumarin (Ia) on the basis of elemental analysis and its infrared spectrum. Furthermore, when heated with ketones and ammonium acetate in ethanol, crude Ia gave compounds of the types II and V. The cyclization reaction in the present study, therefore, can reasonably be explained in terms of a two-step condensation. Ethyl cyanoacetate and salicylaldehyde condensed to give 3-cyanocoumarin, which in turn converts readily to 3-amidinocoumarin. Then, 3-amidinocoumarin condenses with ketones to give heterocyclic compounds of the types II, IV, and V. When 3-methoxysalicylaldehyde was used instead of salicylaldehyde, the condensation afforded the corresponding methoxy derivatives. The structural assignment of these products was based on the infrared and NMR spectra (Tables 3 and 5). For example, the NMR spectrum of IIa (prepared when acetone was employed as the ketone reactant) showed only a methyl singlet at 2.8 ppm corresponding to three protons in a higher field than the aromatic-ring region. This fact indicated that one methyl group of acetone was involved in this cyclization. In the infrared spectra of II, carbonyl and amino stretching bands shifted to slightly lower frequencies because of the presence of intramolecular C=O···H_2N bonding. The structure of the type II was further supported by the fact that the compound obtained by the condensation of 3-amidinocoumarin (Ia) and methyl *n*-propyl ketone in the presence of ammonium acetate was found to be

1) A. Sakurai and H. Midorikawa, This Bulletin, **40**, 1680 (1967).

2) A. Sakurai and H. Midorikawa, *J. Org. Chem.*, **34**, 3612 (1969).

Table 1. 4-Amino-5-oxo-6-oxabenz[*f*]isoquinoline derivatives and related compounds

Compd.	R	R′	R″	Mp, °C	Yield, %	Formula	Calcd, %			Found, %		
							C	H	N	C	H	N
IIa	H	H	CH_3	241—242	33	$C_{13}H_{10}O_2N_2$	69.01	4.46	12.38	68.92	4.56	12.44
b	H	H	C_2H_5	171—173	13	$C_{14}H_{12}O_2N_2$	69.99	5.03	11.66	70.02	4.82	11.81
c	H	H	*n*-C_3H_7	173—174	24	$C_{15}H_{14}O_2N_2$	70.85	5.55	11.02	71.22	5.57	10.94
d	H	H	iso-C_3H_7	145—147	18	$C_{15}H_{14}O_2N_2$	70.85	5.55	11.02	70.58	5.34	11.03
e	H	H	*n*-C_4H_9	147—148	22	$C_{16}H_{16}O_2N_2$	71.62	6.01	10.44	71.56	5.89	10.57
f	H	H	*s*-C_4H_9	118—120	9	$C_{16}H_{16}O_2N_2$	71.62	6.01	10.44	71.74	5.89	10.44
g	H	H	iso-C_4H_9	155—156	27	$C_{16}H_{16}O_2N_2$	71.62	6.01	10.44	71.48	5.73	10.51
h	H	H	*n*-C_5H_{11}	143—145	24	$C_{17}H_{18}O_2N_2$	72.32	6.43	9.92	72.16	6.27	10.06
i	H	H	iso-C_5H_{11}	149—151	23	$C_{17}H_{18}O_2N_2$	72.32	6.43	9.92	72.15	6.50	9.73
j	H	H	*n*-C_9H_{19}	103—105	10	$C_{21}H_{26}O_2N_2$	74.52	7.74	8.28	74.12	7.55	8.08
k	OCH_3	H	CH_3	233—234	42	$C_{14}H_{12}O_3N_2$	65.62	4.72	10.93	65.47	4.75	11.00
l	OCH_3	H	C_2H_5	186—189	10	$C_{15}H_{14}O_3N_2$	66.65	5.22	10.37	66.83	5.03	10.47
m	OCH_3	H	*n*-C_3H_7	210—212	23	$C_{16}H_{16}O_3N_2$	67.59	5.67	9.85	67.80	5.58	9.86
n	OCH_3	H	*n*-C_4H_9	182—184	26	$C_{17}H_{18}O_3N_2$	68.44	6.08	9.39	68.51	5.89	9.52
o	OCH_3	H	iso-C_4H_9	195—197	33	$C_{17}H_{18}O_3N_2$	68.44	6.08	9.39	68.31	6.11	9.28
p	OCH_3	H	*n*-C_5H_{11}	174—176	30	$C_{18}H_{20}O_3N_2$	69.21	6.45	8.97	69.00	6.23	9.12
q	OCH_3	H	iso-C_5H_{11}	185—187	26	$C_{18}H_{20}O_3N_2$	69.21	6.45	8.97	69.01	6.08	8.97
r	H	CH_3	CH_3	218—220	7	$C_{14}H_{12}O_2N_2$	69.99	5.03	11.66	70.10	5.17	11.75
s	H	CH_3	C_2H_5	167—169	15	$C_{15}H_{14}O_2N_2$	70.85	5.55	11.02	71.04	5.26	10.91
t	H	CH_3	*n*-C_4H_9	163—166	13	$C_{17}H_{18}O_2N_2$	72.32	6.43	9.92	72.40	6.25	10.05
u	OCH_3	CH_3	CH_3	225—228	8	$C_{15}H_{14}O_3N_2$	66.65	5.22	10.37	66.38	5.06	10.26
v	H	H		300—302	32	$C_{18}H_{12}O_3N_2$	71.04	3.98	9.21	71.00	3.83	9.44
w	H	H	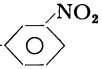	263—266	48	$C_{18}H_{11}O_4N_3$ 1/2 H_2O	63.15	3.51	12.28	62.94	3.71	11.91
x	H	H	-$(CH_2)_2$-Ph	169—171	40	$C_{20}H_{16}O_2N_2$	75.93	5.10	8.86	75.65	4.85	8.90
y	OCH_3	H	-$(CH_2)_2$-Ph	183—185	29	$C_{21}H_{18}O_3N_2$	72.82	5.24	8.09	72.70	5.13	8.20
z	H	CH_3	Ph	242—243	17	$C_{19}H_{14}O_2N_2$	75.48	4.67	9.29	75.22	4.80	9.29
IVa	OCH_3	H	iso-C_4H_9	272—273	7	$C_{17}H_{17}O_4N$	68.21	5.73	4.68	68.01	5.74	4.66
b	H	H	Ph	272—273	38	$C_{18}H_{11}O_3N$	74.73	3.83	4.84	74.33	3.93	4.83
c	OCH_3	H	Ph	303—304	42	$C_{19}H_{13}O_4N$	71.47	4.10	4.39	71.26	4.33	4.55
d	H	H		299—301	35	$C_{19}H_{13}O_4N$	71.47	4.10	4.39	71.27	4.18	4.39
Va	H	$n=1$		249—251	20	$C_{15}H_{12}O_2N_2$	71.41	4.80	11.11	71.73	4.55	11.50
b	H	$n=2$		228—230	18	$C_{16}H_{14}O_2N_2$	72.16	5.30	10.52	72.50	5.39	10.65
c	OCH_3	$n=1$		255—257	30	$C_{16}H_{14}O_3N_2$	68.07	5.00	9.92	68.20	4.97	9.69
d	OCH_3	$n=2$		239—241	21	$C_{17}H_{16}O_3N_2$	68.90	5.44	9.45	68.66	5.34	9.15

Table 2. 4-Acetamino-5-oxo-6-oxabenz[*f*]isoquinoline derivatives and related compounds

Compd.	R	R′	R″	Mp, °C	Yield, %	Formula	Calcd, %			Found, %		
							C	H	N	C	H	N
IIIa	H	H	CH_3	253—255	64	$C_{15}H_{12}O_3N_2$	67.15	4.51	10.44	67.29	4.42	10.58
b	H	H	C_2H_5	200—203	42	$C_{16}H_{14}O_3N_2$	68.07	5.00	9.92	68.39	4.76	10.03
c	H	H	*n*-C_3H_7	216—217	64	$C_{17}H_{16}O_3N_2$	68.90	5.44	9.45	69.14	5.32	9.70
d	H	H	iso-C_3H_7	191—193	69	$C_{17}H_{16}O_3N_2$	68.90	5.44	9.45	69.00	5.33	9.51
e	H	H	*n*-C_4H_9	207—209	87	$C_{18}H_{18}O_3N_2$	69.66	5.85	9.03	69.51	5.76	8.96
f	H	H	*s*-C_4H_9	187—188	60	$C_{18}H_{18}O_3N_2$	69.66	5.85	9.03	69 71	5 85	9.24
g	H	H	iso-C_4H_9	224—226	87	$C_{18}H_{18}O_3N_2$	69.66	5.85	9.03	69.50	5.73	9.04
h	H	H	iso-C_5H_{11}	202—204	72	$C_{19}H_{20}O_3N_2$	70.35	6.22	8.64	69.99	5.99	8.44
i	OCH_3	H	CH_3	273—275	65	$C_{16}H_{14}O_4N_2$	64.42	4.73	9.39	64.29	4.89	9.43
j	OCH_3	H	*n*-C_4H_9	235—237	73	$C_{19}H_{20}O_4N_2$	67.04	5.92	8.23	66.87	5.84	8.22
k	OCH_3	H	*n*-C_5H_{11}	219—221	88	$C_{20}H_{22}O_4N_2$	67.78	6.26	7.91	67.52	6.02	7.97
l	OCH_3	H	iso-C_5H_{11}	229—231	88	$C_{20}H_{22}O_4N_2$	67.78	6.26	7.91	67.53	6.11	8.02
m	H	CH_3	CH_3	210—213	64	$C_{16}H_{14}O_3N_2$	68.07	5.00	9.92	67.93	5.24	9.97
n	H	CH_3	C_2H_5	205—208	70	$C_{17}H_{16}O_3N_2$	68.90	5.44	9.45	68.78	5.42	9.59
o	H	CH_3	*n*-C_4H_9	169—172	65	$C_{19}H_{20}O_3N_2$	70.35	6.22	8.64	70.45	6.30	8.72
p	H	H		231—233	67	$C_{22}H_{16}O_5N_2$	68.03	4.15	7.21	67.79	3.97	7.19
q	H	H		305—307	92	$C_{20}H_{13}O_5N_3$	64.00	3.49	11.20	64.33	3.80	11.60
VIa	H	$n=1$		229—232	74	$C_{17}H_{14}O_3N_2$	69.39	4.80	9.52	69.78	4.78	9.23
b	H	$n=2$		241—242	65	$C_{18}H_{16}O_3N_2$	70.11	5.23	9.09	69.95	5.04	9.17

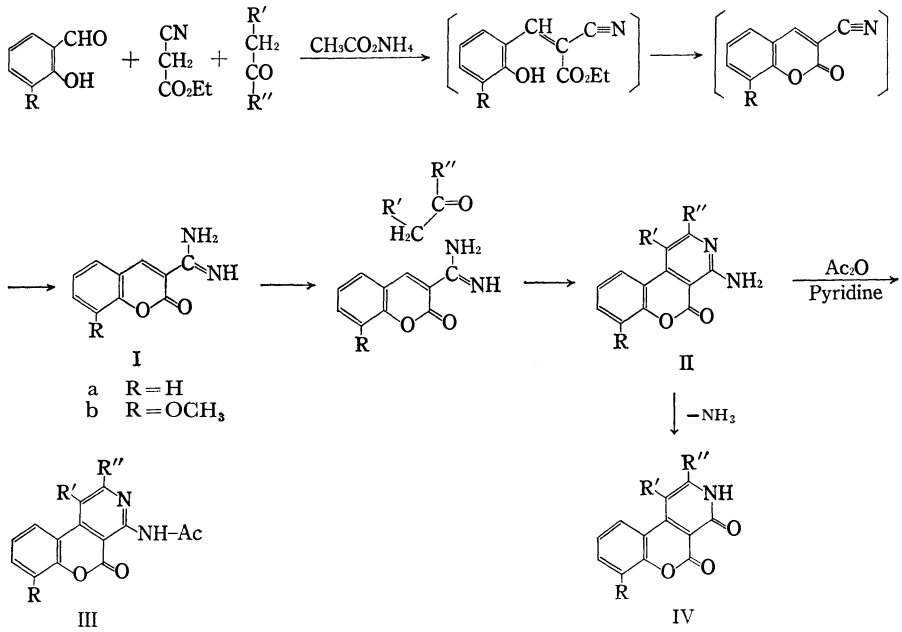

Scheme 1

identical with IIc by a comparison of their melting points and by infrared and elemental analyses.

The reaction of ethyl cyanoacetate and 3-methoxysalicylaldehyde with methyl isobutyl ketone gave a mixture of 4-amino-2-isobutyl-7-methoxy-5-oxo-6-oxabenz[*f*]isoquinoline (IIo) as the main product, plus a small ammount of 2-isobutyl-7-methoxy-5-oxo-6-oxabenz[*f*]-1(2*H*)-isoquinolone (IVa). In the infrared spectrum of IVa, the carbonyl band (5-position) shifted to higher frequencies (1750 cm^{-1}) than that of IIo, and a new, strong band appeared at 1640 cm^{-1}. This band was characteristic of a pyridone- or quinolone-type carbonyl. When methyl ethyl ketone was employed as the ketone reactant, two products, melting at 173 and 218°C, were isolated. Their elemental analyses indicated the formula of $C_{14}H_{12}O_2N_2$. NMR spectrum of the former (mp 173°C) exhibited a triplet corresponding to three protons (CH_3) and a quartet corresponding to two protons (CH_2). On the other hand, the latter (mp 218°C) showed only a singlet corresponding to six protons (CH_3). On the basis of these data, it seemed reasonable to assume the two structures of IIb and IIr for them, as is indicated below. The ratio of the formation of IIb to IIr was about 1 : 0.5, while that of III to IIu was about 1 : 1 (Scheme 2).

Reaction with ketones such as methyl nonyl ketone or methyl *s*-butyl ketone gave products, but in poor yields. However, methyl *t*-butyl, di-*n*-propyl, diisopropyl, or diisobutyl ketones gave no corresponding compounds of the type II.

Reaction with cyclic ketones (Scheme 3) proceeded much as in the case of the reaction with the straight-chain ketones described above. In

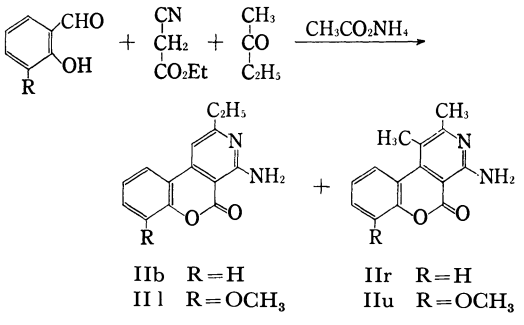

Scheme 2

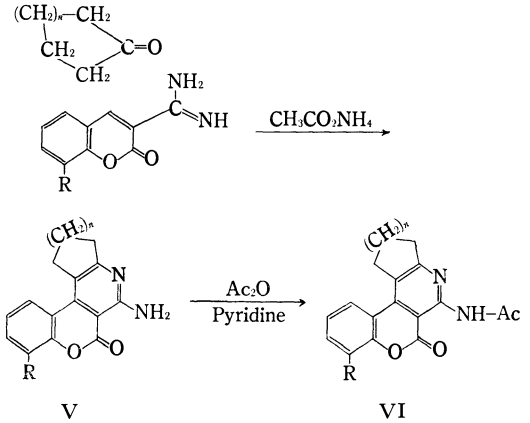

Scheme 3

Table 3. Infrared spectral data[a] for 4-amino-5-oxo-6-oxabenz[*f*]isoquinoline derivatives and related compounds

	νNH_2	$\nu C{=}O$	δNH_2	Aromatic ring	δCH
IIa	3420, 3265, 3120	1700	1630	1610, 1600, 1585, 1550	755
IIb	3420, 3260, 3120	1700	1630	1610, 1600, 1590, 1560	765
IIc	3420, 3280, 3130	1700	1630	1610, 1600, 1580, 1550	765
IId	3420, 3280, 3150	1705	1630	1615, 1580, 1550	760
IIe	3410, 3270, 3150	1705	1625	1610, 1600, 1580, 1545	760
IIf	3400, 3285, 3160	1710	1630	1615, 1600, 1580, 1550	770
IIg	3400, 3260, 3130	1695	1630	1610, 1600, 1585, 1550	765
IIh	3400, 3260, 3130	1700	1625	1610, 1600, 1580, 1545	775
IIi	3410, 3270, 3140	1690	1630	1610, 1600, 1580, 1550	760
IIj	3410, 3270, 3140	1695	1630	1610, 1600, 1585, 1550	760
IIk	3430, 3265, 3140	1705	1635	1625, 1590	790
III	3410, 3270, 3150	1695	1630	1610, 1585, 1550, 1495	785
IIm	3420, 3270, 3150	1690	1630	1615, 1585, 1550, 1550	790
IIn	3410, 3280, 3150	1725	1635	1615, 1585, 1555	780
IIo	3410, 3270, 3150	1695	1625	1615, 1580, 1550, 1495	785, 780
IIp	3410, 3280, 3145	1700	1630	1610, 1580, 1550	788
IIq	3400, 3260, 3130	1700	1630	1615, 1590, 1555	780
IIr	3500, 3380	1680		1610, 1595, 1585, 1535	765
IIs	3500, 3380	1680		1610, 1590, 1580, 1555, 1535	765
IIt	3400, 3260, 3120	1700	1620	1610, 1590, 1550	765
IIu	3400, 3270, 3140	1685	1620	1605, 1580, 1550	790
IIv	3430, 3300	1705	1630	1615, 1600, 1585, 1550	760, 750
IIw	3440, 3360	1700		1610, 1600, 1580, 1525, 1530, 1350 (νNO_2)	768, 755, 738
IIx	3410, 3270, 3150	1710	1630	1615, 1600, 1585, 1555, 1500	770, 760, 700
IIy	3410, 3280, 3150	1705	1630	1610, 1575, 1550	775, 750, 700
IIz	3410, 3270, 3150	1710	1630	1610, 1590, 1550, 1540	765, 710
IVa		1760, 1655		1610, 1595, 1540, 1490	790
IVb		1760, 1640		1615, 1590, 1540, 1510	755
IVc		1745, 1630		1610, 1590, 1575, 1540, 1505	770, 725, 695
IVd		1740, 1625		1610, 1590, 1575, 1535, 1520	825, 770
Va	3470, 3350	1675		1600, 1590, 1580, 1545	765
Vb	3420, 3260, 3130	1690	1620	1610, 1610, 1550	765
Vc	3400, 3260, 3130	1695	1625	1615, 1565, 1555	785
Vd	3430, 3260, 3130	1685	1620	1610, 1590, 1550	785

a) All spectra were taken in potassium bromide disks; cm^{-1}.

Table 4. Infrared spectral data[a] for 4-acetamino-5-oxo-6-oxabenz[*f*]isoquinoline derivatives and related compounds

	νNH	Ring C=O, NH-C=O	Aromatic ring	δCH
IIIa	3240	1695, 1665	1610, 1595, 1560, 1525	770
IIIb	3260	1700, 1675	1610, 1595, 1555	780
IIIc	3250	1700, 1665	1615, 1595, 1555, 1520, 1500	775
IIId	3250	1700, 1665	1615, 1590, 1550, 1520	770
IIIe	3250	1695, 1665	1615, 1595, 1555, 1520, 1500	775
IIIf	3250	1700, 1665	1615, 1595, 1550	765
IIIg	3250	1700, 1670	1615, 1595, 1550, 1515	775, 770
IIIh	3260	1700, 1670	1615, 1595, 1555, 1520	775
IIIi	3240	1700, 1670	1620, 1610, 1600, 1565	790
IIIj	3250	1700, 1670	1620, 1610, 1595, 1560, 1520	790
IIIk	3250	1695, 1665	1620, 1610, 1600, 1555, 1525	790
IIIm	3240	1675	1605, 1595, 1565, 1550, 1500	780
IIIn	3250	1675	1605, 1595, 1570, 1550, 1500	775
IIIo	3240	1670	1605, 1595, 1570, 1550, 1500	775
IIIp	3260	1760, 1700, 1675 (O-Ac)	1610, 1595, 1550, 1520	770
IIIq	3240	1700, 1670	1610, 1595, 1530, 1520, 1550, 1350 (NO_2)	775
VIa	3230	1670	1605, 1595, 1570, 1550, 1500	765
VIb	3240	1700, 1670	1590, 1570, 1550	770

a) All spectra were taken in potassium bromide disks; cm^{-1}.

Table 5. NMR spectral data[a] for 4-amino-5-oxo-6-oxabenz[*f*]isoquinoline derivatives and related compounds

	CH_3	OCH_3	CH_2	-CH-	Ring -CH=	NH
IIa	2.8(s, 3H)				7.5—8.5(m, 6H)	8.9—9.7(br, 1H)
IIb	1.55(t, 3H)		3.1(q, 2H)		7.5—8.7(m, 7H)	8.9—9.6(br, 1H)
IIc[b]	1.02(t, 3H)		2.7(t, 2H) 1.8(sx, 2H)		7.0(s, 1H), 7.15—7.5(m, 5H) 7.85—8.1(m, 1H)	
IId[b]	1.35(d, 6H)			2.5—3.3(sp, 1H)	7.0(s, 1H), 7.15—7.7(m, 5H) 7.85—8.1(m, 1H)	
IIe	1.1(t, 3H)		1.4—2.2(m, 4H) 3.1(t, 2H)		7.4—8.4(m, 5H)	8.8—9.7(br, 1H)
IIf	1.13(t, 3H) 1.6(d, 3H)		1.95(qi, 2H)	3.1(sx, 1H)	7.4—8.4(m, 5H)	8.7—9.6(br, 1H) 11.65(br, 1H)
IIg	1.15(d, 6H)		2.9(d, 2H)	2.0—2.5(m, 1H)	7.4—8.4(m, 6H)	8.9—9.7(br, 1H)
IIh[b]	0.9(t, 3H)		1.2—2.0(m, 6H) 2.68(t, 2H)		6.9(s, 1H), 7.0—7.6(m, 5H) 7.75—8.0(m, 1H)	
IIk	2.8(s, 3H)	4.13(s, 3H)			7.5—8.0(m, 5H)	8.8—9.5(br, 1H)
IIl	1.55(t, 3H)	4.1(s, 3H)	3.08(q, 2H)		7.4—8.0(m, 5H)	
IIm	1.2(t, 3H)	4.1(s, 3H)	2.0(sx, 2H) 3.05(t, 2H)		7.3—8.1(m, 4H)	8.7—8.9(br, 1H)
IIo	1.15(d, 6H)	4.1(s, 3H)	2.9(d, 2H)	2.0—2.5(m, 1H)	7.4—8.1(m, 5H)	
IIr	2.8(s, 6H)				7.5—8.0(m, 4H)	8.5(br, 1H) 8.65(br, 1H)
IIs	1.55(t, 3H) 2.87(s, 3H)		3.17(q, 2H)		7.4—8.0(m, 3H), 8.55(d, 1H)	
IIt	1.1(t, 3H) 2.85(s, 3H)		1.4—2.2(br, 4H) 2.7—3.35(br, 2H)		7.4—8.0(m, 3H), 8.55(d, 1H)	
IIu	2.8(s, 6H)	4.1(s, 3H)			7.4—7.7(d, 2H), 8.0—8.2(t, 1H)	
IIw					7.5—9.0(m, 9H)	9.3—9.9(br, 1H)
IIx			3.3(t, 4H)		7.2—8.2(m, 10H)	8.9—9.5(br, 1H)
IIy		4.12(s, 3H)	3.3(t, 4H)		7.1—7.8(m, 9H)	8.9—9.6(br, 1H)
IIz	2.8(s, 3H)				7.5—8.1, 8.5—8.8(m, 9H)	
IVd		4.07(s, 3H)			7.2—8.6(m, 9H)	
Va			2.3—2.9(m, 2H) 3.1—3.9(m, 4H)		7.5—8.9(m, 5H)	10.9(s, 1H)
Vc		4.1(s, 3H)	2.3—2.8(m, 2H) 3.15—3.8(m, 4H)		7.5—7.7(d, 2H), 7.9—8.2(t, 1H)	
Vd		4.13(s, 3H)	1.8—2.3(br, 4H) 2.9—3.5(br, 4H)		7.53(d, 2H), 8.15(t, 1H)	

a) Parts per million downfield from tetramethylsilane in CF_3CO_2H; s=singlet, d=doublet, t=triplet, q=quartet, qi=quintet, sx=sextet, sp=septet, m=multiplet, br=broad. b) In $CDCl_3$ solution.

Table 6. NMR Spectral data[a] for 4-acetamino-5-oxo-6-oxabenz[*f*]isoquinoline derivatives and related compound

	CH_3	NH-CO-CH_3	OCH_3	CH_2	-CH-	Ring -CH=	NH
IIIa	2.98(s, 3H)	2.66(s, 3H)				7.5—8.5(m, 5H)	12.6(br, 1H)
IIIc	1.2(t, 3H)	2.67(s, 3H)		2.05(sx, 2H) 3.23(t, 2H)		7.5—8.5(m, 5H)	12.55(br, 1H)
IIId	1.6(d, 6H)	2.65(s, 3H)			3.5(sp, 1H)	7.4—8.5(m, 5H)	12.5(br, 1H)
IIIf	1.1(t, 3H) 1.6(d, 3H)	2.68(s, 3H)		2.0(qi, 2H)	3.3(sx, 1H)	7.5—8.5(m, 5H)	12.55(br, 1H)
IIIi	2.98(s, 3H)	2.66(s, 3H)	4.13(s, 3H)			7.5—8.0(m, 3H) 8.2(s, 1H)	12.55(br, 1H)
IIIn	1.65(t, 3H) 2.98(s, 3H)	2.67(s, 3H)		3.38(q, 2H)		7.5—8.6(m, 4H)	12.6(br, 1H)
IIIp		2.72(s, 3H) 2.45(O-CO-CH_3, s, 3H)				7.5—8.6(m, 9H)	12.67(br, 1H)
VIa		2.7(s, 3H)		2.3—2.9(m, 2H) 3.3—4.1(m, 4H)		7.2—8.1(m, 4H)	12.75(br, 1H)

a) Parts per million downfield from tetramethylsilane in CF_3CO_2H; s=singlet, d=doublet, t=triplet, q=quartet, qi=quintet, sx=sextet, sp=septet, m=multiplet, br=broad.

this case, cyclization occured between the methylene group adjacent to the carbonyl group of the ketone and the 4-position of the coumarin ring to form 5-amino-6-oxo-7-oxabenz[*f*]-2,3-dihydro-1*H*-cyclopent[*c*]isoquinoline (Va) (from cyclopentanone) and 6-amino-7-oxo-8-oxa-1,2,3,4-tetrahydrobenzo[*k*]phenanthridine (Vb) (from cyclohexanone). These structures were supported by a study of the infrared and NMR spectra (Tables 3 and 5). In addition, a product obtained by the condensation of Ia and cyclohexanone was identified with Vb. Reaction with methyl aryl ketones (Scheme 1) gave 4-amino-2-aryl-5-oxo-6-oxabenz[*f*]isoquinolines (IIv-y). On the other hand, the use of acetophenone or *p*-methoxyacetophenone as the ketone reactant afforded 2-aryl-5-oxo-6-oxabenz[*f*]-1(2*H*)-isoquinolones (IVb-d) as the main product under the same reaction conditions. The infrared spectra of IVb-d have strong bands at about 1750 and 1640 cm^{-1}. The former band shifted to frequencies higher by from 50 to 60 cm^{-1} than those of the compounds II. This fact shows the absence of intramolecular hydrogen bonding in the structure of the type IV, since the latter band (1640 cm^{-1}) can be attributed to the carbonyl group (4-position) of the quinolone type.

The reaction of ethyl cyanoacetate and salicylaldehyde with propiophenone gave 4-amino-1-methyl-5-oxo-2-phenyl-6-oxabenz[*f*]isoquinoline (IIz). The NMR spectrum revealed only a singlet corresponding to three protons (CH_3) in the high field. It is clear that the cyclization occurred between the methylene group of the ketone and the coumarin ring. The acetylation of the compounds of the types II and V, when treated with acetic anhydride in pyridine, afforded monoacetyl derivatives (III) and (VI) respectively (Table 2), while a diacetamino derivative was obtained from IIz under the same reaction conditions as produced those of the compounds III and VI.

Experimental

All the melting points are uncorrected. The infrared spectra were recorded on a Perkin-Elmer Model 521 grating spectrophotometer by means of potassium bromide pellets. The NMR spectra were obtained using a JNM-C-60 spectrometer; the peak positions are reported in δ values (parts per million downfield from tetramethylsilane).

Reaction of Ethyl Cyanoacetate and Salicylaldehyde. To a solution of ethyl cyanoacetate (4.52 g, 0.04 mol) and salicylaldehyde (4.88 g, 0.04 mol) in ethanol (5 m*l*), ammonium acetate (3.08 g, 0.04 mol) was added and heated for several minutes. The resulting crystals were filtered to give 4.8 g of crude 3-amidinocoumarin (Ia). When this crude Ia (3 g) was dissolved in dilute hydrochloric acid and allowed to stand at room temperature, pale yellow needles were formed. Recrystallization from ethanol afforded 1.5 g of 3-amidinocoumarin hydrochloride melting at 264—266°C (dec); ν_{max}^{KBr} 3390 (=NH), 3320, 3200 (NH_2), 1720 (C=O), 1670 (C=N), 1645 (δ NH_2), 1610, 1575, 1535 (ring); NMR {$(CD_3)_2SO$}, 7.4—8.0 (m, 4H, ring), 8.95 (s, 1H, ring), 9.6 ppm (br, 3H, NH_2 and =NH).

Found: C, 53.35; H, 4.01; N, 12.56; Cl, 16.20%. Calcd for $C_{10}H_8O_2N_2 \cdot HCl$: C, 53.46; H, 4.01; N, 12.47; Cl, 15.80%.

Reaction of Ethyl Cyanoacetate and 3-Methoxysalicylaldehyde. To a solution of ethyl cyanoacetate (2.26 g, 0.02 mol) and 3-methoxysalicylaldehyde (3.04 g, 0.02 mol) dissolved in ethanol (7 m*l*), ammonium acetate (1.51 g, 0.02 mol) was added. After the reaction mixture had been heated for several minutes, 3.4 g of 8-methoxy-3-amidinocoumarin (Ib) were obtained. When this crude Ib (1 g) was dissolved in dilute hydrochloric acid and allowed to stand at room temperature, a pale yellow precipitate was formed. It was then recrystallized from ethanol to afford 0.7 g of 8-methoxy-3-amidinocoumarin hydrochloride; mp 250°C (dec.).

Found: C, 51.53; H, 4.54; N, 10.87; Cl, 13.62%. Calcd for $C_{11}H_{10}O_3N_2 \cdot HCl$: C, 51.89; H, 4.32; N, 11.00; Cl, 13.92%.

Reaction of 3-Amidinocoumarin (Ia) and Methyl *n*-Propyl Ketone. A mixture of Ia (2 g), methyl *n*-propyl ketone (1 g), and ammonium acetate (1 g) in ethanol (3 m*l*) was heated for 1 hr. After cooling, the resulting precipitate was collected and recrystallized from ethanol-glacial acetic acid to give 1.1 g of colorless needles, mp 173—174°C, this substance was found to be identical with IIc by the elemental analyses and by a study of the infrared spectral data.

Reaction of 3-Amidinocoumarin (Ia) and Cyclohexanone. A mixture of Ia (2 g), cyclohexanone (1 g), and ammonium acetate (1 g) in ethanol (3 m*l*) was heated for 1 hr. A pale yellow crystalline matter precipitated out during the reaction; this was collected and recrystallized from glacial acetic acid to afford 0.8 g of pale yellow crystals, mp 225—227°C. This substance was proved to be identical with Vb by a study of their infrared spectra and by the results of elemental analyses.

Reaction of Ethyl Cyanoacetate and Salicylaldehyde or 3-Methoxysalicylaldehyde with Ketones. To a mixture of ethyl cyanoacetate (0.01 mol), salicylaldehyde or 3-methoxysalicylaldehyde (0.01 mol), and ketone (0.01 mol) in ethanol (3 m*l*), ammonium acetate (0.01—0.02 mol) was added, and the new mixture was refluxed for 0.5—2 hr. A crystalline compound precipitated out during the reaction or after the reaction mixture had been allowed to stand at room temperature. The experimental results and spectral data are summarized in Tables 1, 3, and 5. The molecular weight, as determined by means of high-resolution mass spectrometry, exhibited the following values: IIa, 226 (calcd for $C_{13}H_{10}O_2N_2$, 226.23), IIb, 240 (calcd for $C_{14}H_{12}O_2N_2$, 240.25), IId, 254 (calcd for $C_{15}H_{14}O_2N_2$, 254.27), IIr, 240 (calcd for $C_{14}H_{12}O_2N_2$, 240.25), IIs, 254 (calcd for $C_{15}H_{14}O_2N_2$, 254.27), Vb, 266 (calcd for $C_{16}H_{14}O_2N_2$, 266.29), IIv, 304 (calcd for $C_{18}H_{12}O_3N_2$, 304.29), IVb, 289 (calcd for $C_{18}H_{11}O_3N$, 289.28), IVd, 319 (calcd for $C_{19}H_{13}O_4N$, 319.3).

Acetylation of the Compounds II and V by Acetic Anhydride in Pyridine. To a solution of II or V (0.001 mol) dissolved in pyridine (2—4 m*l*), acetic anhydride (4—6 m*l*) was added, after which the

mixture was refluxed for 2—4 hr. After being cooled, the deposited precipitate was collected and washed with dilute methanol. The experimental results and spectral data are summarized in Tables 2, 4, and 6.

Acetylation of IIz. Acetic anhydride (7 m*l*) was added to a solution of IIz (0.5 g) dissolved in pyridine (4 m*l*), after which the mixture was refluxed for 4 hr. After cooling, ice water was added to the reaction mixture to afford a crystalline precipitate. The precipitate was collected, washed with cold dilute methanol, and dried. Recrystallization from glacial acetic acid gave 0.6 g of 4,4-diacetylamino-1-methyl-5-oxo-2-phenyl-6-oxabenz[*f*]isoquinoline, mp 205—207°C; ν_{max}^{KBr} 1740 (O–C=O), 1710, 1695 (CH_3–C=O), 1610, 1590, 1560, 1530 (hetero ring and phenyl), 775, 705 (δ CH); NMR (CF_3CO_2H) peaks at 2.35, 2.65 (s, 3H each, CO–CH_3), 3.0 (s, 3H, CH_3), 7.5—8.0 and 8.55—8.8 ppm (m, 9H, ring).

Found: C, 71.51; H, 4.75; N, 7.31%. Calcd for $C_{23}H_{18}O_4N_2$: C, 71.49; H, 4.70; N, 7.25%.

The authors wish to express their thanks to Dr. Taro Hayashi and Dr. Tatsuo Takeshima for their kind advice. Thanks are also due to Dr. Haruo Homma and his staff for their microanalyses, to Mr. Jun Uzawa for his measurements of the NMR spectra, and to Mr. Hironori Ogawa for his measurements of the infrared spectra.

BULLETIN OF THE CHEMICAL SOCIETY OF JAPAN VOL. 43 2933—2937 (1970)

Oxidation of *N,N'*-Diarenesulfonylhydrazines

Yoshio KOHARA, Michio KOBAYASHI and Hiroshi MINATO

Department of Chemistry, Faculty of Science, Tokyo Metropolitan University, Fukazawa, Setagaya-ku, Tokyo

(Received March 30, 1970)

N,N'-Diarenesulfonylhydrazine was oxidized with several oxidizing regents, but diarenesulfonyl diimide was not isolated. Diarenesulfonyl diimide produced immediately decomposed with evolution of 1 mol of nitrogen, and afforded the corresponding sulfonyl bromide, α-disulfone and sulfonic acid. Plausible mechanisms of decomposition were discussed.

By the analogy with other azo compounds such as azobisisobutyronitrile[1] and dibenzoyl diimide,[2] diarenesulfonyl diimide, $RSO_2N{=}NSO_2R$, is expected to decompose to form sulfonyl free radicals with liberation of nitrogen. Waters *et al.* made a study of the reactions of sulfonyl free radicals generated by photolysis of sulfonyl iodide.[3] Recently, Kwart and Khan reported the isolation of dibenzenesulfonyl diimide (I) by oxidation of the corresponding hydrazine (II).[4] We have been interested in the reactions of sulfonyl radicals, and attempted to produce diarenesulfonyl diimides according to their method. However, our experimental findings differ from theirs, and the diimides formed immediately decomposed in repeated experiments under various conditions. This paper will describe the results of careful products analyses and discuss the plausible mechanisms of its decomposition.

Results and Discussion

Formation of *N,N'*-di-*p*-toluenesulfonyl diimide (III) was attempted by oxidation of *N,N'*-di-*p*-toluenesulfonylhydrazine (IV) with bromine in anhydrous ethyl alcohol or aqueous acetonitrile according to the method of Kwart and Khan.[4] When an excess of bromine was dropped to the solution, 1 mol of nitrogen was instantaneously evolved and III was not isolated. Similarly, the oxidation of II resulted in evolution of 1 mol of nitrogen, and I was not isolated. Even when IV was oxidized at −40°C with bromine, the evolution of nitrogen was instantaneous. These experiments indicate that the azo compounds I and III are too unstable to be isolated as such.

Products of decomposition of I and III were analyzed. Products found were arenesulfonyl bromide, diaryl disulfone, arenesulfonic acid, and, in the case of decomposition in ethyl alcohol, ethyl arenesulfonate, as shown in Scheme 1. Amounts of these products produced under various conditions are shown in Tables 1 and 2.

1) J. P. Van Hook and A. V. Tobolsky, *J. Amer. Chem. Soc.*, **80**, 779 (1958).

2) J. E. Leffler and W. B. Bond, *ibid.*, **78**, 335 (1956).

3) a) C. M. M. da Silva Corrêa, A. S. Lindsay and W. A. Waters, *J. Chem. Soc. C*, **1968**, 1872. b) C. M. M. da Silva Corrêa and W. A. Waters, *ibid.*, **1968**, 1874. c) C. M. M. da Silva Corrêa and W. A. Waters, *ibid.*, **1968**, 1880. d) M. McMillan and W. A. Waters, *J. Chem. Soc., B*, **1966**, 422.

4) H. Kwart and A. A. Khan, *J. Org. Chem.*, **33**, 1537 (1968).

Scheme 1

$$ArSO_2NH\text{-}NHSO_2Ar \xrightarrow[\text{aq. } CH_3CN \text{ or anhyd. EtOH}]{Br_2}$$

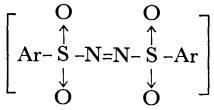

$$\longrightarrow N_2 + ArSO_2Br + ArSO_2\text{-}SO_2Ar$$
$$ArSO_3H + ArSO_2OEt \text{ (in EtOH)}$$

In the oxidation of II with bromine in aqueous acetonitrile and anhydrous ethyl alcohol, diphenyl disulfone was produced. Its melting point was 188—189°C, which is similar to that of diphenylsulfonyl diimide (193—194°C) reported by Kwart and Khan.[4] Diphenyl disulfone absorbed at 1300, 1325, 1345 cm^{-1} ($\nu_{as}SO_2$), 1130 cm^{-1} (ν_s-SO_2), 1580 and 1445 cm^{-1} (phenyl) in the infrared (KBr disc). Its mass spectrum (m/e) was quite similar to that reported for dibenzenesulfonyl diimide.

Various azo compounds, R–N=N–R′, are known; for instance, R=R′= PhCO,[2] R=R′= $(CH_3)_2$-CCN,[1] R=$PhSO_2$, R′=Ph,[5] and R=R′=Ph_2-CH.[6] In general, the more stabilized are the radicals R and R′, the more unstable is the azo compound. Sulfonyl radical is a very stable radical, and its stability is demonstrated by the fact that it does not attack a benzene ring.[3a] In view of these data, it is rather surprising that I is isolated and its melting point is as high as 193°C.

It was not possible to oxidize IV with bromine in anhydrous acetonitrile, and the starting materials were recovered. IV was not oxidized with bromine in acetonitrile under irradiation of light, and the starting materials were also recovered. Therefore, the presence of water is necessary for oxidation of diarenesulfonylhydrazines. The oxidizing species is probably the HOBr formed by the reaction of bromine and water.

IV was oxidized with chloranil, NBS (*N*-bromosuccinimide) or potassium permanganate, and di-*p*-tolyl disulfone was formed with evolution of nitrogen, as shown in Table 3. The presence of water is necessary for the oxidation of IV with NBS, as in the case with bromine. When a solution of IV and BPO (benzoyl peroxide) or AIBN (azobisisobutyronitrile) in acetonitrile was refluxed, IV was recovered. Therefore, dehydrogenation of IV to III could not be accomplished with such radicals as bromine atom, $PhCO_2\cdot$, or $(CH_3)_2\dot{C}CN$.

Waters *et al.* reported that sulfonyl radicals tended to disproportionate according to the equation;

$$6\ ArSO_2\cdot \longrightarrow 2\ (ArSO_2)_2O + ArSSO_2Ar$$

They verified the formation of $ArSO_2\cdot$ radicals by scavenging them with quinones, which converted

Table 1. Oxidation of IV with bromine

Run	Reactions mmol				Products mmol (%)				
	(TsNH–)–$_2$	Br_2	Solvents	Temp.	N_2	TsBr	Ts_2	TsOH	TsOEt
1	2.60	3.15	CH_3CN	r.t.					—[a]
2	1.96	2.81[b]	CH_3CN	r.t.					—[a]
3	2.22	6.71	96% aq. CH_3CN	r.t.	2.32 (104.6)	2.51 (56.6)	0.23 (10.2)	0.87 (19.6)	—
4	2.43	2.68	96% aq. CH_3CN	r.t.	1.30 (53.7)	1.30 (26.9)	0.26 (10.7)	0.67 (13.8)	—[c]
5	2.28	6.15	97% aq. CH_3CN	−40°C	2.20 (96.5)	1.98 (42.3)	0.48 (21.2)	1.03 (22.6)	—
6	1.76	13.23	anhyd. EtOH	r.t.	1.73 (98.3)	0.75 (21.3)	0.56 (31.5)	1.07 (30.2)	0.64 (18.0)

a) The starting materials were recovered.
b) Irradiated with a tungsten lamp for 15 hr.
c) The starting materials were recovered (0.69 mmol, 28.5%).

Table 2. Oxidation of II with bromine at room temperature

Run	Reactants mmol			Products mmol				
	(PhSO$_2$NH–)–$_2$	Br_2	Solvents	N_2	$PhSO_2Br$	(PhSO$_2$–)–$_2$	$PhSO_3H$	$PhSO_2OEt$
1	3.09	6.76	94% aq. CH_3CN	2.85 (92.4)	3.00 (48.7)	0.40 (12.8)	2.42 (39.2)	—
2	2.89	15.85	anhyd. EtOH	2.42 (83.5)	0.98 (16.9)	0.56 (19.5)	1.68 (29.1)	0.42 (7.2)

5) A. J. Rosenthal and C. G. Overberger, *J. Amer. Chem. Soc.*, **82**, 108 (1960); C. G. Overberger and A. J. Rosenthal, *ibid.*, **82**, 117 (1960).

6) S. G. Cohen and C. H. Wang, *ibid.*, **77**, 2457 (1955).

Table 3. Oxidation of IV with various oxidants

Run	Reactants mmol				Products mmol (%)				
	$(TsNH-)_2$	Oxidant	Solvent	Temp.	N_2	TsBr	Ts_2	TsOH	
1	2.55	NBS 4.85	CH_3CN	80°C					a)
2	2.11	NBS 4.01	96% aq. CH_3CN	r.t.	2.19 (104.0)	2.25 (53.3)	0.22 (10.4)	1.04 (24.5)	
3	1.82	$KMnO_4$ 6.37	CH_3CN	r.t.	2.17 (118.6)	—	0.36 (19.5)	1.84 (50.3)	
4	2.06	Chloranil 4.27	CH_3CN	80°C		—	0.58 (27.9)		
5	4.1	BPO 4.1	CH_3CN	80°C		—			a)
6	3.5	AIBN 3.1	CH_3CN	80°C		—			a)

a) The starting materials were recovered.

the radicals into sulfonates of quinols.[3b] However, in our conditions, no thiolsulfonate was found. When IV was oxidized with bromine in the presence of excess *p*-benzoquinone in aqueous acetonitrile, disulfonate of hydroquinone, which was a possible product from sulfonyl radical and *p*-benzoquinone, was not detected. Attempts to scavenge the free sulfonyl radicals by cyclohexane-1-spiro-2'-(4'-oxoimidazolidine-1'-oxyl)-5'-spiro-1'-cyclohexane (V), which was stable under the reaction conditions, was also unsuccessful.

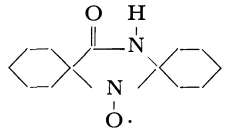

(V)

When IV was oxidized with bromine in aqueous acetonitrile in the presence of benzene or nitrobenzene, *p*-tolyl phenyl sulfone or *p*-tolyl nitrophenyl sulfone was not found. When IV was oxidized with NBS or potassium permanganate in the presence of toluene, neither *p*-tolyl benzyl sulfone nor *p*-toly tolyl sulfone was detected. These findings show that *p*-toluenesulfonyl radical does not attack benzene rings and does not abstract benzyl hydrogens.

When arenesulfonyl radicals were produced by the photolysis of arnenesulfonyl iodide, the reaction between two sulfonyl radicals always yielded a sulfinyl sulfonate (VI) without being accompanied by the formation of a disulfone.[3b] Therefore, the formation of a disulfone in our conditions can be rationalized only in terms of the recombination in a solvent cage. Oxidation of *N*-benzenesulfonyl-*N'*-*p*-toluenesulfonylhydrazine (VII) with bromine in aqueous acetonitrile gave phenyl *p*-tolyl disulfone free from any cross products, namely diphenyl disulfone or di-*p*-tolyl disulfone. This fact also supports our assumption that disulfones are the products of the recombination of the geminate sulfonyl radical pair.

Formation of other products can be explained by the reaction steps shown below.

Mechanism I

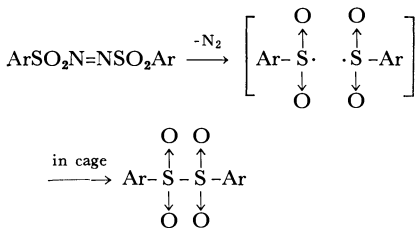

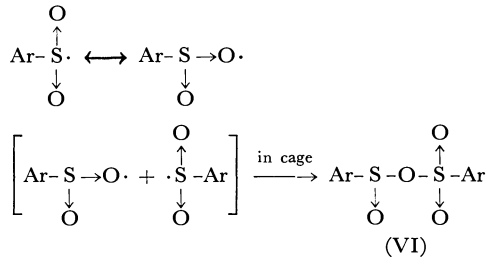

(VI)

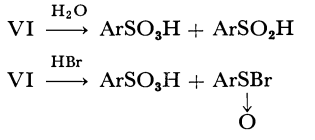

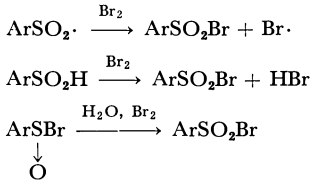

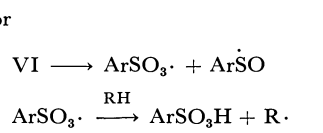

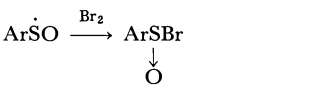

or

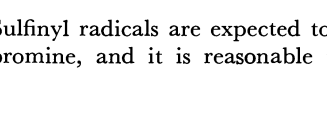

Sulfinyl radicals are expected to react readily with bromine, and it is reasonable that thiosulfonate,

the disproportionation product of sulfinyl radicals, was not found in our conditions. For oxidation of II and IV more than one mole of bromine per mole of disulfonylhydrazines had to be added for evolution of the quantitative amount of nitrogen. Undoubtedly part of bromine added was used for oxidation of species containing sulfinyl sulfur. Ethyl arenesulfonate was formed as below.

$$\mathrm{VI} \xrightarrow{\mathrm{EtOH}} \mathrm{ArSO_3H} + \mathrm{ArSOEt}$$

$$\mathrm{ArSOEt} \xrightarrow{\mathrm{Br_2}} \mathrm{ArSO_2OEt} + \mathrm{ArSO_2Br}$$

$$\mathrm{ArSO_2Br} \xrightarrow{\mathrm{EtOH}} \mathrm{ArSO_2OEt}$$

Ethyl *p*-toluenesulfonate was oxidized with bromine in ethyl alcohol at room temperature to afford *p*-toluenesulfonyl bromide and ethyl *p*-toluenesulfonate, and was produced by ethanolysis of *p*-toluenesulfonyl bromide.

The formation of the diaryl disulfone could be alternatively explained by means of a four-centered transition state:

Mechanism II

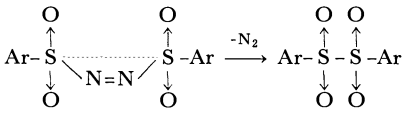

In a similar fashion intermediate VI could arise *via* a five-centered transition state.

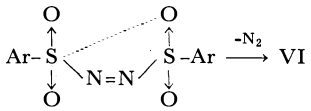

At present it is not possible to determine which of these two mechanisms is correct.

Experimental

Materials. Acetonitrile and ethyl alcohol were purified by the usual method.[7]

Bromine, chloranil and potassium permanganate of first grade were used without further purification. NBS was recrystallized from water.

Synthesis of IV. Twelve grams of *p*-toluenesulfonylhydrazine, prepared from *p*-toluenesulfonyl chloride and hydrazine hydrate, was dissolved in 50 m*l* of ethyl alcohol. To this solution 6.5 g of *p*-toluenesulfinyl chloride was added at 60°C. After 1.5 hr, white crystals precipitated were filtered off, and recrystallized from acetone-water to afford 2.8 g of IV (20%); mp 205°C (decomp.), lit, 218—220°C (decomp.).[8]

Synthesis of II. A solution of 40 g of benzenesulfonylhydrazine and 20 g of benzenesulfonyl chloride in 50 m*l* of ethyl alcohol was refluxed for 4 hr. White crystals obtained were recrystallized from acetone-water; yield, 11 g (31%), mp 218°C (decomp.), lit, *ca.* 245°C.[9]

Synthesis of VII. VII was prepared by a modification of the procedure reported by Munshi *et al.*;[10] mp 185°C, lit, 184°C.[10]

Oxidation of IV with Bromine in Aqueous Acetonitrile. To the solution of 0.754 g of IV in 96% aqueous acetonitrile, 1.073 g of bromine was added. The evolution of nitrogen was measured by use of a gas burette. After reaction was completed, the products were extracted with methylene chloride, and dried over magnesium sulfate. Methylene chloride was removed, and the products were separated with elution chromatography on a silica gel column; *p*-toluenesulfonyl bromide was eluted with hexane-benzene (mp 93°C, lit, 96°C[11]), di-*p*-tolyl disulfone was eluted with benzene (mp 207°C, lit, 210°C[12] or 218—220°C[13]; IR: 1130 and 1340 cm^{-1}). *p*-Toluenesulfonic acid was precipitated as its *S*-benzylisothiuronium salt.

Oxidation of IV with Bromine in Anhydrous Acetonitrile. To a solution of 0.884 g of IV in 50 m*l* of anhydrous acetonitrile, 0.505 g of bromine was added drop by drop at room temperature. No evolution of nitrogen was observed even in 12 hr, and the starting materials were recovered.

Oxidation of IV with Bromine in Anhydrous Ethyl Alcohol. Oxidation was carried out in a similar way. Ethyl *p*-toluenesulfonate was isolated by elution chromatography on a silica gel column with benzene as solvent; IR: 1170 and 1360 cm^{-1}.

Attempt for Oxidation of IV with Bromine under Irradiation. A solution of 0.666 g of IV and 0.449 g of bromine in 50 m*l* of anhydrous acetonitrile was irradiated with a tungsten lamp for 15 hr. When acetonitrile was removed, the starting materials were recovered.

Oxidation of II with Bromine. Oxidation was carried out in a way similar to that of IV. Products were benzenesulfonyl bromide (IR: 1165 and 1365 cm^{-1}), ethyl benzenesulfonate (IR: 1180 and 1355 cm^{-1}), and diphenyl disulfone (mp 188—189°C, lit, mp 193°C[12]; mass spectrum, m/e (relative intensity), 282 (1.2), 250 (0.3), 234 (2.0), 218 (0.5), 154 (0.9), 153 (2.1), 152 (2.5), 151 (0.7), 141 (100), 125 (26.2), 110 (1.1), 109 (2.1), 108 (0.6) and 97 (9.3)). The mass spectrum was measured on a Hitachi mass spectrometer RMU 6E type, operated with 70 eV at 200°C.

Oxidation of IV with NBS. A solution of 0.820 g of NBS in acetonitrile was added drop by drop to a solution of 0.717 g of IV in 50 m*l* of 96% aqueous acetonitrile. The products were separated by elution chromatography.

Oxidation of IV with Potassium Permanganate. When a solution of 0.620 g of IV in 25 m*l* of anhydrous

7) W. Weissberger, "Organic Solvents," Interscience Publishers, Inc., New York (1955).

8) K. F. Jennings, *J. Chem. Soc.*, **1957**, 1172.

9) O. Hinserg, *Ber.*, **27**, 601 (1894).

10) A. A. Munshi, N. M. Shah and J. P. Trivedi, *J. Indian Chem. Soc.*, **40**, (11), 966 (1963).

11) V. O. Lukashevich, *Dokl. Akad. Nauk SSSR*, **103**, 627 (1955); *Chem. Abstr.*, **50**, 5556 (1956).

12) I. M. Damson, A. McL. Mathieson and J. M. Robertson, *J. Chem. Soc.*, **1948**, 322.

13) P. Allen, Jr. and J. W. Brook, *J. Org. Chem.*, **27**, 1019 (1962).

acetonitrile was added drop by drop to a solution of 1.008 g of potassium permanganate in 50 m*l* of anhydrous acetonitrile, 0.110 g of di-*p*-tolyl disulfone was obtained.

Oxidation of IV with Chloranil. A solution of 0.700 g of IV and 1.049 g of chloranil in 85 m*l* of anhydrous acetonitrile was refluxed for 13 hr. Products were separated by chromatography on a silica gel column, and 0.178 g of di-*p*-tolyl disulfone was obtained.

Oxidation of IV with Benzoyl Peroxide. A solution of 1.4 g of IV and 1.0 g of benzoyl peroxide was refluxed for 13 hr in 5 m*l* of acetonitrile. When the solvent was removed, unchanged IV was recovered.

Oxidation of IV with Azobisisobutyronitrile (AIBN). A solution of 1.2 g of IV and 0.5 g of AIBN in 50 m*l* of acetonitrile was refluxed for 15 hr. When the solvent was removed, unchanged IV was recovered.

Oxidation of IV with Bromine in the Presence of *p*-Benzoquinone. When 1.107 g of bromine (6.93 mmol) was added at room temperature to a solution of 0.732 g of IV (2.16 mmol) and 3.1 g of *p*-benzoquinone (28 mmol) in 50 m*l* of aqueous acetonitrile, 39.2 m*l* of nitrogen was evolved. The products were extracted with methylene chloride, and an excess *p*-benzoquinone was removed by sublimation under reduced pressure. The residue was separated by elution chromatography on a silica gel column to afford *p*-toluenesulfonyl bromide, 0.226 g, and quinone mixtures. However no quinol sulfonate was found.

Oxidation of IV in the Presence of V. To a solution of 0.732 g of IV (2.15 mmol) and 1.005 g of V[14] (4.20 mmol) in 50 m*l* of acetonitrile, 0.956 g of bromine (5.98 mmol) was added drop by drop. The products were separated by elution chromatography on a silica gel column, and 0.461 g of *p*-toluenesulfonyl bromide, 0.048 g of di-*p*-tolyl disulfone and 0.750 g of unchanged V were recovered.

Oxidation of IV with Bromine in the Presence of Benzene. To a solution of 0.876 g of IV (2.58 mmol) and 2.080 g of benzene (26.6 mmol) in 50 m*l* of 96% aqueous acetonitrile, 1.353 g of bromine was added drop by drop. The products were separated by elution chromatography on a silica gel column. No *p*-tolyl phenyl sulfone was found.

Oxidation of IV with Bromine in the Presence of Nitrobenzene. To a solution of 0.702 g of IV (2.06 mmol) and 3.091 g of nitrobenzene (25.1 mmol) in 50 m*l* of 96% aqueous acetonitrile, 1.182 g of bromine (7.39 mmol) was added drop by drop. The products were separated by elution chromatography on a silica gel column. No *p*-tolyl nitrophenyl sulfone was found.

Oxidation of IV with NBS in the Presence of Toluene. A solution of 1.383 g of NBS (7.18 mmol) in acetonitrile was added drop by drop to a solution of 1.021 g of IV (3.00 mmol) and 6.6 g of toluene (71.8 mmol) in 50 m*l* of 96% aqueous acetonitrile. The products were separated by elution chromatography on a silica gel column to give 0.020 g of benzyl bromide, 0.741 g of *p*-toluenesulfonyl bromide and 0.106 g of di-*p*-tolyl disulfone, but no *p*-tolyl benzyl sulfone was detected.

Oxidation of IV with Potassium Permanganate in the Presence of Toluene. A solution of 2.197 g of IV and 13 g of toluene (141 mmol) in 50 m*l* of anhydrous acetonitrile was added drop by drop to a solution of 2.0 g of potassium permaganate (12.7 mmol) in 50 m*l* of anhydrous acetonitrile. The products were separated by elution chromatography on an alumina column. No *p*-tolyl benzyl sulfone nor *p*-tolyl tolyl sulfone was found.

Oxidation of VII with Bromine. To the solution of 0.795 g of VII (2.44 mmol) in 50 m*l* of aqueous acetonitrile, 1.066 g of bromine was added. The products were separated with elution chromatography on a silica gel column to give 0.084 g of *p*-tolyl phenyl disulfone (0.28 mmol, 11.5%); mp 162—163°C, lit, 166°C;[15] IR: 1125 and 1345 cm^{-1}. Neither diphenyl disulfone nor di-*p*-tolyl disulfone was detected.

Reaction between Ethyl *p*-Toluenesulfinate and Bromine. A solution of 1.114 g of ethyl *p*-toluenesulfinate (6.05 mmol) and 1.028 g of bromine (6.43 mmol) in 10 m*l* of anhydrous ethyl alcohol was allowed to stand at room temperature for 2 hr. Water was added to the solution and products were extracted with methylene chloride. The products were separated by elution chromatography, and 0.431 g of *p*-toluenesulfonyl bromide (1.95 mmol) and 0.094 g of ethyl *p*-toluenesulfonate (0.47 mmol) were found, and 0.217 g of unchanged ethyl *p*-toluenesulfinate (1.18 mmol) was recovered.

Reaction between *p*-Toluenesulfonyl Bromide and Ethyl Alcohol. A solution of 0.2507 g of *p*-toluenesulfonyl bromide (1.07 mmol) in 25 m*l* of anhydrous ethyl alcohol was allowed to stand at room temperature for 70 min. Water was added to the solution and products were extracted with methylene chloride. The products were separated by elution chromatography and 0.134 g of *p*-toluenesulfonyl bromide (0.57 mmol) and 0.051 g of ethyl *p*-toluenesulfonate (0.26 mmol) were found.

Grateful acknowledgement is made to the donors of the Petroleum Research Fund, administered by the American Chemical Society, for support of this research.

14) K. Murayama, S. Morimura and T. Yoshioka, This Bulletin, **42**, 1640 (1969).

15) E. P. Kohler and M. B. MacDonald, *Amer. Chem. J.*, **22**, 224 (1899).

BULLETIN OF THE CHEMICAL SOCIETY OF JAPAN VOL. 43 2938—2941 (1970)

1,2-Dithiole-3-thione and 1,2,4-Trithiole from α-Cyanodithiocarboxylate

Masataka YOKOYAMA

Department of Chemistry, Faculty of Science, Chiba University, Chiba

(Received March 31, 1970)

1,2-Dithiole-3-thiones and 1,2,4-trithioles were synthesized by the reaction of α-cyanodithiocarboxylate, hydrogen sulfide, and bromine water. The reaction mechanism and the mass spectra of 1,2-dithiole-3-thiones were discussed.

Our attempt to isloate dimercaptomethylenecyanoacetamide (**1a**) from the reaction mixture of di(ammoniomercapto)methylenecyanoacetamide (**2a**) and mineral acid failed. Compound **1a** was unstable, degraded easily along with the evolution of hydrogen sulfide, and changed to 5-amino-4-carbamoyl-1,2-dithiole-3-thione (**3a**).

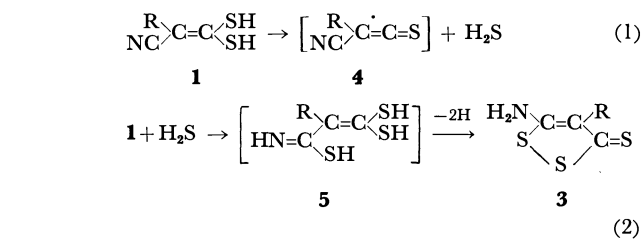

Scheme 1

The reaction mechanism shown in Scheme 1 may be considered to hold for the conversion of **1a** into **3a**. At the very beginning of the conversion, Compound **1a** may be changed into cyanothioketene (**4a**) by splitting off hydrogen sulfide (Eq. (1)). The hydrogen sulfide thus generated attacks the cyano group of **1a** to give an intermediate, **5a**, from which **3a** is produced by the formation of the 1,2-dithiole ring (Eq. (2)).

Resinous material which was considered to be a polymer of (4) was obtained in the above reaction. However, its identification was not achieved. The ammonium salt of **5d** could be prepared by the reaction of di(ammoniomercapto)methylenemalononitrile (diammonium salt of **1d**) and hydrogen sulfide, and then converted quantitatively into **3d** by the addition of acetic acid. The results suggest that the unstable intermediate, **5**, is easily dehydrogenated because of the formation of a stable 1,2-dithiole-3-thione derivative (**3**).[1]

From the decomposition mechanism, syntheses were undertaken for several 1,2-dithiole-3-thione derivatives by the reaction of α-cyanodithiocarboxylate (**2**), hydrogen sulfide, and acetic acid. Bromine water was used in place of acetic acid because of its moderate reactivity. Di(ammoniomercapto)methylenecyanoacetamide (**2a**), methyl di(sodiomercapto)methylenecyanoacetate (**2b**), ethyl di(sodiomercapto)methylenecyanoacetate (**2c**), and di(sodiomercapto)methylenemalononitrile (**2d**) gave 5-amino-4-carbamoyl-1,2-dithiole-3-thione (**3a**, yield 94%), 5-amino-4-methoxycarbonyl-1,2-dithiole-3-thione (**3b**, yield 81%), 5-amino-4-ethoxycarbonyl-1,2-dithiole-3-thione (**3c**, yield 83%), and 5-amino-4-cyano-1,2-

Table 1. UV spectra in 99% EtOH[a]

Compd.	λ_{max}, mμ (log ε)
3a	240.5(3.96), 286(sh, 3.90), 314.5(4.54), 364.3(3.93) 229**, 264 sh**, 282**, 309 sh**, 400**
3b	249(4.06), 290.5(sh, 4.17), 312(4.26), 376(3.78) 248(4.09)***, 292(4.24)***, 311(4.32)***, 374(3.79)***
3c	247.5(4.09), 287.5(sh, 4.17), 311(4.27), 373(3.76) 248(4.11)*, 289(sh, 4.17)*, 311(4.26)*, 373(3.88)*
3d	233.5(4.06), 283(sh, 3.87), 311(4.09), 369(3.68) 235(4.04)*, 280(sh, 3.91)*, 310(4.15)*, 367(3.94)*
6a	244.5(2.96), 320.2(3.98), 336.5(3.68)
6b	241.5(2.76), 323(sh, 4.23), 335(4.27)
6c	238(2.39), 323(sh, 4.28), 335(4.32)

a) Absorbance measurements were made with a Hitachi EPS-3T type spectrophotometer. *, ** show the UV data reported by Mayer *et al.*;[2] * in EtOH, ** in cyclohexane. *** shows the UV data (in MeOH) reported by Gewald.[3]

1) N. Lozac'h and J. Vialle, "Organic Sulfur Compounds," Vol. II, Pergamon Press, Oxford (1966) p. 258.

2) R. Mayer, P. Rosmus and J. Fabian, *J. Chromatogr.*, **15**, 153 (1964).

3) K. Gewald, *J. Prakt. Chem.*, **31**, 214 (1966).

dithiole-3-thione (**3d**, yield 82%) respectively, all in high yields. The UV spectra of **3b**, **3c**, and **3d** coincided with those reported by Mayer and Gewald (see Table 1). This is a new preparative method leading to 1,2-dithiole-3-thione derivatives through the intermediate, **5**. Most of the preparations reported so far have made use of elementary sulfur,[3] phosphorus pentasulfide or a mixture of both.[1]

When the α-cyanodithiocarboxylate (**2**) was mixed with acetic acid, hydrogen sulfide was evolved and **3** was obtained. This reaction was continued until **1** had been degraded completely. On the other hand, bromine water stopped the decomposition of **1** within several hours.

A mixture of α-cyanodithiocarboxylate and bromine water was allowed to stand at room temperature overnight. A small amount of **3** (usually, yield *ca.* 10%) was separated from the reaction mixture. When the filtrate was acidified with acetic acid, hydrogen sulfide was instantly evolved and 1,2,4-trithiole derivative was obtained in a high yield. **2a**, **2b**, and **2c** gave 2,5-di(carbamoylcyanomethylene)-1,2,4-trithiole (**6a**, yield 70%), 3,5-di(methoxylcarbonylcyanomethylene)-1,2,4-trithiole (**6b**, yield 74%), and 3,5-di(ethoxylcarbonylcyanomethylene)-1,2,4-trithiole (**6c**, yield 81%), respectively. An attempt to obtain the compound corresponding to **6d** was unsuccessful.

It seems that the conversion of **2** into **6** proceeds through an intermediate, **7**, which is easily changed to a stable compound, **6**, accompanying elimination of hydrogen sulfide on treatment with acetic acid (see Scheme 2). The IR spectrum of **6b** coincided with that of the compound synthesized from **2b** and ammonium peroxydisulfate by Gompper's method.[4] The UV spectra of **3** and **6** showed several characteristic absorptions (see Table 1).

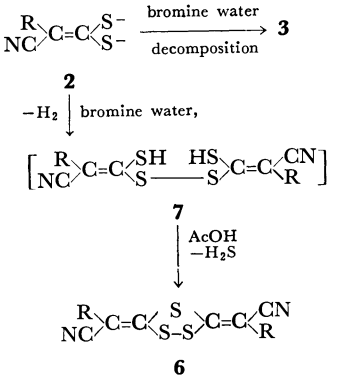

2a, **6a**: R=$CONH_2$; **2b**, **6b**: R=CO_2CH_3; **2c**, **6c**: R=$CO_2C_2H_5$; **2d**: R=CN

Scheme 2

Kirby has proposed that **6** is presumably planar for the conjugation through the **3d** orbitals of sulfur.[5] The strong bands near 320 mμ and 335 mμ may be explained in terms of the through-conjugation. It was considered that **6** existed in a *trans* form with respect to R groups, because the two R groups were shown to be unequivalent from the results of NMR spectra (see Table 2).

Table 2. Chemical shifts and coupling constants for **6***

6a	4.10(br, NH_2)
6b	3.92(s, CH_3), 3.90(s, CH_3)
6c	4.38(q, CH_2, J=7 Hz), 4.36(q, CH_2, J=7 Hz), 1.35(t, $2CH_3$)

* NMR spectra were recorded with a JNM-C-60 high resolution NMR spectrometer operating at 60 MHz. Chemical shift values were shown in δ downfield from tetramethylsilane as an internal standard in deuteriodimethyl sulfoxide as solvent.

Table 3. Mass spectra for **3***, *m/e* (rel. int. %)

3a	**3c**	**3d**
194(23)	223(13)	176(7.5)
192(100) $M^{\cdot+}$	221(100) $M^{\cdot+}$	174(100) $M^{\cdot+}$
176(7)	177(57)	110(99)
148(8.5)	148(40)	83(12)
128(45)	84(73)	64(8.5)
84(33)	72(13)	
64(10)	64(15)	

* Mass spectra were measured with a Nihon Densi JMS-01 SG mass spectrometer. Ionizing energy was maintained at 75 eV and the total ionizing current 200 μA.

Table 3 shows the mass spectra of **3**. Measurement of the fragments revealed different scissions of two sulfur atoms (see Scheme 3). Compound **3c** was changed into fragment (B) through fragment (A) by the removal of group R and then two sulfur atoms. In the case of **3d**, the separation of two sulfur atoms occurred to give fragment (C) from which group R was then separated to give fragment (B). Compound **3a** showed both types of scission.

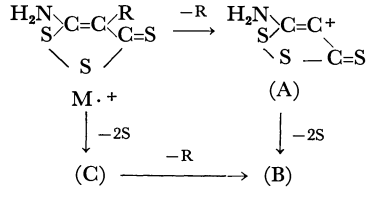

Scheme 3

4) R. Gompper and W. Töpfel, *Chem. Ber.*, **95**, 2861 (1962).

5) A. J. Kirby, *Tetrahedron*, **22**, 3001 (1966).

Experimental

Compound **2a** was prepared by the reaction of ethyl cyanoacetate and carbon disulfide in aqueous ammonia (28%). Compounds **2b**, **2c**, and **2d** were prepared by Soderback's method.[6]

Isolation of Diammonium Salt of 5d. A mixture of malononitrile (25 g, 0.38 mol), carbon disulfide (57 g, 0.75 mol) and *ca.* 200 m*l* of liquid ammonia was stirred for 30 min under cooling with dry ice-methanol. The reaction mixture was then allowed to stand at room temperature. A yellow solid material was recrystallized from methanol-chloroform to give light yellow plates (65.5 g, di(ammoniomercapto)methylenemalononitrile).[7] The light yellow material (8 g) was dissolved in 100 m*l* of ethanol and hydrogen sulfide was passed through for 30 min. The whole was shaken for an additional 3 hr. The yellow material was collected, recrystallized from water, washed with ethanol, and dried: yellow plates (0.5 g, diammonium salt of **5d**), mp 136—137°C (dec.) (slow heating), 153—156°C (dec.) (rapid heating). IR (KBr): 3310 (s, ν NH), 3080, 2960 (s, br, ν NH_4^+), 2180 (s, ν CN), 1590 (s, ν C=N), 1505 (m, ν conj. C=C), 1415 cm^{-1} (s, br, δ NH_4^+). Found: C, 23.23; H, 4.83; N, 26.56; S, 45.36%; mol wt, 214.7 (vapor-pressure osmometer, in acetone). Calcd for $C_4H_{10}N_4S_3$: C, 22.86; H, 4.86; N, 26.66; S, 45.68%; mol wt, 210.15.

The ammonium salt of **5d** was methylated by dimethyl sulfate. Yellow needles (mp 219—220°C) were obtained and from analytical results, and was assigned the structure di(methylmercapto)methylenecyanoacetamide. The NMR spectrum in deuterioacetone revealed signals at δ 7.40 (br, 1, NH) and δ 1.80 (s, 1, SH).

Treatment of Diammonium Salt of 5d with Acetic Acid. To the diammonium salt of **5d** (2 g) in 100 m*l* of water was added acetic acid (4.5 m*l*). This was allowed to stand for 1 hr at 20°C. The crude product was collected and recrystallized from pyridine-water to give yellow prisms quantitatively. The IR spectrum agreed with that of **3d**.

Preparation of 3a. Through the mixture of **2a** (8 g, 0.04 mol) and water (50 m*l*) was passed hydrogen sulfide 30 min at room temperature. The reaction mixture was stirred for 3 hr, and treated under diminishing pressure at 30—40°C in order to remove unchanged hydrogen sulfide. To this was added 50 m*l* of a saturated bromine water and allowed to stand for several hours. The crude yellow material was filtered, washed with water and ether, and recrystallized from pyridine-water: 9.0 g of yellow prisms (**3a**, yield *ca.* 94%), mp 247—248°C. NMR (DMSO-d_6): δ 10.35 (br, $CONH_2$), δ 8.70 (br, NH_2); IR (KBr): 3280, 3260, 3220, 3140, 3020 (w, ν NH_2), 1650 (sh, ν CO), 1638 (s, δ NH_2), 1550 cm^{-1} (s, ν C=C). Found: C, 25.31; H, 2.16; N, 14.47; S, 49.95%; mol wt, 183.1 (vapor-pressure osmometer, in acetone). Calcd for $C_4H_4N_2S_3O$: C, 25.01; H, 2.10; N, 14.58; S, 49.95%; mol wt, 192.09.

Preparation of 3b. Compound **3b** was prepared by the same method as above. 8.1 g of yellow needles was produced from **2b** (15 g, 0.05 mol) and recrystallized from methanol (yield *ca.* 81%): mp 201—202°C (dec.). NMR (acetone-d_6): δ 9.20 (br, NH_2), δ 3.82 (s, CH_3); IR (KBr): 3270, 3150, 3100 (s, ν NH_2), 2950 (m, ν CH_3), 1658 (vs, ν C=O), 1572 (vs, δ NH_2), 1562 (sh, ν conj. C=C), 1332 cm^{-1} (vs, ν C–O–C). Found: C, 29.10; H, 2.62; N, 6.78; S, 46.09%; mol wt, 217.0 (vapor-pressure osmometer, in acetone). Calcd for $C_5H_5NS_3O_2$: C, 28.97; H, 2.44; N, 6.76; S, 46.39%; mol wt, 207.29.

Preparation of 3c. Compound **3c** was prepared as in the case of **3a**. Crude material was prepared from 10.6 g (0.03 mol) of **2c** and recrystallized from pyridine-water to give 6 g of yellow needles (**3c**, yield *ca.* 83%), mp 181°C. NMR (DMSO-d_6): δ 9.20 (br, NH_2), δ 4.32 (q, CH_2, J=6 Hz), δ 1.32 (t, CH_3, J=6 Hz); IR (KBr): 3340, 3200 (s, ν NH_2), 2980 (w, ν CH_3), 1652 (s, ν C=O), 1590 (vs, δ NH_2), 1340 cm^{-1} (s, ν C–O–C). Found: C, 32.80; H, 3.10; N, 6.49; S, 43.26%; mol wt, 226.4 (vapor-pressure osmometer, in acetone). Calcd for $C_6H_7NS_3O_2$: C, 32.59; H, 3.19; N, 6.34; S, 43.60%; mol wt, 221.12.

Another Preparative Method of 3b and 3c. Through the mixture of **2**, water and acetic acid (30 m*l*) was immediately passed hydrogen sulfide. Yellow material was collected and recrystallized. The yield was almost equal to that of the above method.

Preparation of 3d. Preparation was the same as for **3a**. Crude product was obtained from **2** (8.5 g, 0.035 mol) and recrystallized from methanol: 5 g of yellow prisms (**3d**, yield 82%), mp <300°C. NMR (DMSO-d_6): δ 9.58 (br, NH_2); IR (KBr): 3170 (m, br, ν NH_2), 2220 (s, ν CN), 1615 (vs, ν C=N), 1505 cm^{-1} (vs, ν C–C). Found: C, 27.77; H, 0.87; N, 16.35; S, 54.95%; mol wt, 180.0 (vapor-pressure osmometer, in acetone). Calcd for $C_4H_2N_2S_3$: C, 27.60; H, 1.15; N, 16.10; S, 55.00%; mol wt, 174.

Preparation of 6a. To the mixture of **2a** (7 g, 0.036 mol) and water (50 m*l*) was added 50 m*l* of the saturated bromine water. The solution was allowed to stand overnight at 20°C and 0.6 g of light yellow material (**3a**) was filtered off. The filtrate was added with 30 m*l* of acetic acid and kept to stand for 3 hr. Crude yellow material was collected and washed with water and a small amount of methanol. Recrystallization from dioxane gave 3.8 g of light yellow needles (**6a**, yield 70%), mp <300°C. IR (KBr): 3340, 3180 (s, ν NH_2), 2210 (s, ν conj. CN), 1670 (sh, ν C=O), 1655 (vs, δ NH_2), 1450 cm^{-1} (vs, probable ring stretching). Found: C, 33.79; H, 1.31; N, 19.80; S, 34.00%; mol wt, 283.5 (vapor-pressure osmometer, in acetone). Calcd for $C_8H_4N_4S_3O_2$: C, 33.81; H, 1.42; N, 19.72; S, 33.79%; mol wt, 284.14.

Preparation of 6b. Preparation was carried out as above. Crude product was obtained from **2b** (7 g, 0.023 mol) and recrystallized from dioxane: 2.5 g of light yellow needles (**6b**, yield 74%), mp 227—228°C (reported mp 225—228°C[4]). IR (KBr): 2960 (m, ν CH_3), 2220 (s, ν conj. CN), 1675 (vs, ν C=O), 1472 (vs, probable ring stretching), 1300 cm^{-1} (vs, ν C–O–C). Found: C, 38.33; H, 2.05; N, 9.13; S, 30.47%; mol wt, 314 (mass spectrum). Calcd for $C_{10}H_6N_2S_3O_4$: C, 38.22; H, 1.91; N, 8.92; S, 30.63%; mol wt, 314.18.

6) E. Söderbäck, *Acta Chem. Scand.*, **19**, 554 (1965).

7) T. Takeshima, M. Yokoyama, N. Fukada and M. Akano, *J. Org. Chem.*, July (1970), in press: "The Reaction of Malononitrile with Carbon Disulfide in an Aqueous Alkali Medium."

Preparation of 6b. Preparation was carried out as for **6a**. Crude product was obtained from **2c** (7 g, 0.022 mol) and recrystallized from methanol: a light yellow needles (**6c**, 3 g, yield 81%), mp 215—216°C. IR (KBr): 2980 (m, ν CH), 2220 (s, ν conj. CN), 1760, 1655 (vs, ν C=O), 1475 (vs, probable ring stretching), 1305 cm^{-1} (vs, ν C–O–C). Found: C, 41.91; H, 3.14; N, 8.09; S, 28.13%; mol wt, 342 (mass spectrum). Calcd for $C_{12}H_{10}N_2S_3O_4$: C, 42.11; H, 2.95; N, 8.19; S, 28.05%; mol wt, 342.22.

The author is indebted to Professor Dr. Tatsuo Takeshima, Chiba Univ. and Dr. Hiroshi Midorikawa, The Institute of Physical and Chemical Research, for their generous support. Thanks are also due to Dr. Toshio Hayashi and Miss Makiko Akano for their kind advice and assistance.

BULLETIN OF THE CHEMICAL SOCIETY OF JAPAN VOL. 43 2941—2944 (1970)

The Synthesis of a Series of *N*-*t*-Amyloxycarbonyl-oligo-L-proline

Muneji MIYOSHI,*1 Terutoshi KIMURA and Shumpei SAKAKIBARA*2

Peptide Center, Institute for Protein Research, Osaka University, Kita-ku, Osaka

(Received April 1, 1970)

A series of *N*-protected L-proline oligomers, the di-, tri-, tetra-, penta-, hexa- and octamer, were synthesized by conventional methods. The proline imino-group was protected by the *t*-amyloxycarbonyl (Aoc) group, and the carboxyl group was protected as the benzyl ester during the synthesis. These Aoc-oligoprolines were valuable in elucidating the relationship between the conformation and the degree of polymerization of the polyprolines. The Aoc-protecting group was useful in purifying the intermediates and in obtaining crystals of the final compounds.

This paper will report the synthesis of a series of proline oligomers, which have been used in elucidating the relationship between the number of proline residues and the steric structure of the molecules.[1,2] Since a prolyl-prolyl linkage is susceptible to aqueous caustic alkali, the saponification of the ester group was avoided in the synthesis. Generally, the *t*-amyloxycarbonyl (Aoc) group[3] was used to protect an imino group of oligoprolines and the carboxyl groups were protected as benzyl esters. The Aoc-group is known to be stable under the conditions used for the catalytic hydrogenolysis of benzyl esters, and it can be removed by treatment with N hydrogen chloride in an organic solvent or by treatment with trifluoroacetic acid at room temperature for 30 min, the benzyl ester group being unaffected by this treatment.[3] Therefore, each of the protecting group can be removed independently. Furthermore, the use of these lipophilic protecting groups was advantageous in increasing the solubility of the proline oligomers in usual organic solvents and in obtaining many of them as nice crystals. The proline peptides were coupled by the dicyclohexylcarbodiimide (DCC) method, because there is no racemization problem in the activation of proline residues. Since Aoc-derivatives are very soluble in usual organic solvents, as has been mentioned above, urea or ureide compounds could be easily removed from the reaction mixture. Thus, a series of Aoc-oligoprolines were synthesized, as is shown in the following scheme:

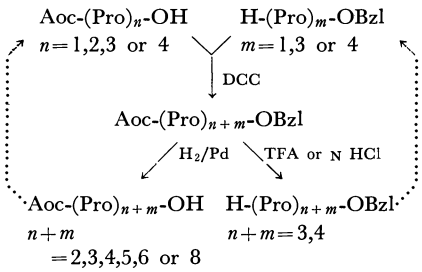

The physical constants and solubilities of the compounds are summarized in Tables 1 and 2.

The molecular rotations of the respective compounds ($n+m$=2—8) seem to conform to the additive rule in this region, as is shown in Fig. 1.

*1 Present address: Chemical Research Laboratory, Tanabe Seiyaku Co., Ltd., Higashiyodogawa-ku, Osaka.

*2 To whom requests for reprints should be addressed.

1) T. Isemura, H. Okabayashi and S. Sakakibara, *Biopolymers*, **6**, 307 (1968).

2) H. Okabayashi, T. Isemura and S. Sakakibara, *ibid.*, **6**, 323 (1968).

3) S. Sakakibara, M. Shin, M. Fujino, Y. Shimonishi, S. Inouye and N. Inukai, This Bulletin, **38**, 1522 (1965).

Table 1. Physical constants and solubilities of Aoc-oligoproline benzyl esters

Aoc-(Pro)$_{n+m}$-OBzl $n+m$	Mp °C	Optical rotation			Solubility		
		$[\alpha]_D$ in ethanol	c	Temp. °C	acetone	ethyl acetate	ethanol
1+1 (III)	oil						
2+1 (V)	93.5—94.5	−171°	2.2	25	soluble	soluble	soluble
3+1 (VII)	101.0—103.0	−211°	2.3	24	soluble	soluble	soluble
2+3 (IX-a)	195.5—197.5	−251°	2.0	24	soluble in hot.	soluble in hot.	soluble
4+1 (IX-b)	197.0—198.5	−254°	2.0	24	soluble in hot.	soluble in hot.	soluble
3+3 (XI)	228.5—230.5	−270°	2.1	24	slightly soluble in hot.	slightly soluble in hot.	soluble
4+4 (XIII)	261.0—262.5	−309°	1.2	22	insoluble	insoluble	soluble

Table 2. Physical constants and solubilities of Aoc-oligoprolines

Aoc-(Pro)$_{n+m}$-OH $n+m$	Mp °C	Optical rotation			Solubility		
		$[\alpha]_D$ in ethanol	c	Temp. °C	acetone	ethyl acetate	ethanol
1+1 (IV)[a]	157.0—159.0	−113°	2.0	25	soluble	soluble	soluble
2+1 (VI)	200.0—201.5	−170°	2.2	25	soluble	slightly soluble in hot.	soluble
3+1 (VIII)	207.5—208.5	−227°	2.1	24	soluble in hot.	insoluble	soluble
2+3 (X-a)	224.5—226.0	−248°	2.3	24	slightly soluble in hot.	insoluble	soluble
4+1 (X-b)	224.5—226.0	−248°	2.3	24	slightly soluble in hot.	insoluble	soluble
3+3 (XII)	240.0—242.0	−291°	2.1	24	insoluble	insoluble	soluble
4+4 (XIV)	280.0	−318°	0.9	22	insoluble	insoluble	soluble in hot.

a) Reported in Ref. 5: mp 155—158°C, $[\alpha]_D^{21}$ −112.8° (c 1, ethanol).

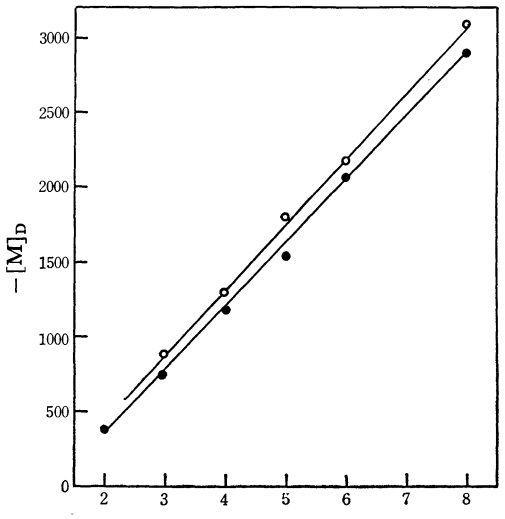

Fig. 1. Molecular rotation change of Aoc-oligo-L-prolines and their benzyl esters.

$$[M]_D = \frac{[\alpha]_D \times (\text{mol wt})}{100}$$

○ Aoc-oligo-L-proline benzyl esters,
● Aoc-oligo-L-proline

4) The separated spots were located by a ninhydrin reaction at 100°C.

Experimental

The physical constants and solubilities of the compounds are shown in Tables 1 and 2. Each compound was dried over phosphorus pentoxide *in vacuo* at 80°C for about 10 hr before being subjected to elementary analysis. All the melting points were determined by the capillary method, and all are given as uncorrected values.

Aoc-L-prolyl-L-proline Benzyl Ester (III). DCC (51.5 g, 0.25 mol) was stirred into a solution of Aoc-L-proline (I) (57.2 g, 0.25 mol) in methylene chloride (150 m*l*) at 0°C. Then, a solution of L-proline benzyl ester hydrochloride (II) (61 g, 0.26 mol) and triethylamine (35 m*l*, 0.25 mol) in methylene chloride (250 m*l*) was added to the reaction mixture. Stirring was continued for 1 hr at 0°C, and then the mixture was left to stand overnight at room temperature. The *N,N*-dicyclohexylurea (DCU) formed during the reaction was removed by filtration. The filtrate was concentrated under reduced pressure, and the residue was dissolved in ethyl acetate. This solution was washed successively with water, 5% sodium bicarbonate, 0.25 N hydrochloric acid, and water. The washed solution was dried over sodium sulfate and concentrated to a syrup, which was then used in the next reaction without any further purification or characterization. The homogeneity of this material was checked by thin-layer chromatography on Silica-gel G using a mixture of chloroform - methanol - acetic acid (95 : 5 : 3 v/v/v) as the solvent.[4]

Aoc-L-prolyl-L-proline (IV).[5] Hydrogen gas was bubbled through a solution of the above syrup (III) in methanol (500 m*l*) in the presence of palladium charcoal (5%, 5 g) for about 10 hr at room temperature. The extent of hydrogenolysis was checked by thin-layer chromatography on Silica-gel G using a mixture of chloroform-methanol-pyridine (95 : 5 : 3 v/v/v) as the solvent.[4] After confirmation that the reaction has been completed, the catalyst was filtered off, and the filtrate was concentrated to a syrup under reduced pressure. The residue was crystallized from a small volume of ethyl acetate in a refrigerator. The product was then collected by filtration and recrystallized from ethyl acetate and *n*-hexane; wt, 67.2 g (yield 82.5%, calcd from I).

Found: C, 58.98; H, 8.02; N, 8.72%. Calcd for $C_{16}H_{26}N_2O_5$: C, 58.88; H, 8.03; N, 8.58%.

Aoc-tri-L-proline Benzyl Ester (V). DCC (24.8 g, 0.12 mol) was stirred into a solution of IV (39.1 g, 0.12 mol) in methylene chloride (150 m*l*) at 0°C. Then, a mixture of II (30.5 g, 0.12 mol) and triethylamine (16.8 m*l*, 0.12 mol) in methylene chloride (150 m*l*) was added to the reaction mixture. Stirring was continued for 1 hr at 0°C, and then the mixture was kept overnight at room temperature. The DCU formed was removed by filtration. The solvent was replaced by ethyl acetate, and a small amount of an insoluble material was filtered off; the ethyl acetate solution was thoroughly washed in succession with water, 5% sodium bicarbonate, 0.25 N hydrochloric acid, and water. The final solution was dried over sodium sulfate and concentrated to a syrup under reduced pressure. The residue was dissolved in acetone, and a small amount of an insoluble material was removed by filtration. The solvent was evaporated off, and the residue was crystallized from ethyl acetate and *n*-hexane. Crystals were collected and recrystallized from ethyl acetate and *n*-hexane as fine needles; wt, 48 g (yield 78%).

Found: C, 65.63; H, 7.70; N, 8.17%. Calcd for $C_{28}H_{39}N_3O_6$: C, 65.47; H, 7.65; N, 8.18%.

Aoc-tri-L-proline (VI). Hydrogen was bubbled slowly through a solution of V (30.8 g, 0.06 mol) in methanol (150 m*l*) in the presence of palladium charcoal (5%, 5 g). After we had confirmed by thin-layer chromatography that the reaction was complete, the catalyst was removed by filtration; the filtrate was then concentrated under reduced pressure. The residue was dissolved in ethyl acetate with the aid of a minimum volume of methanol, and the solution was kept overnight in a refrigerator. The crude product, which separated as crystals, was collected by filtration and then recrystallized as fine needles from a mixture of ethyl acetate and a small volume of methanol; wt, 22.5 g (89.1%).

Found: C, 59.63; H, 7.88; N, 9.75%. Calcd for $C_{21}H_{33}N_3O_6$: C, 59.55; H, 7.85; N, 9.92%.

Aoc-tetra-L-proline Benzyl Ester (VII). Compounds VI (16.9 g, 0.04 mol) and II (11.0 g, 0.04 mol) were treated with DCC (8.3 g, 0.04 mol) in chloroform as has been described for the syntheses of III and V. The DCU formed was removed by filtration, the chloroform was replaced by ethyl acetate, and the solution was thoroughly washed in succession with water, 5% sodium bicarbonate, 0.25 N hydrochloric acid, and water; the washed solution was dried over sodium sulfate and then concentrated to a residue under reduced pressure. The residue was dissolved in acetone, a small amount of an insoluble material was removed by filtration, and the solution was reconcentrated. The final residue was crystallized from ethyl acetate and *n*-hexane. Crude crystals were collected by filtration and recrystallized from ethyl acetate and *n*-hexane; wt, 19.5 g (80.1%).

Found: C, 64.15; H, 7.72; N, 9.02%. Calcd for $C_{33}H_{46}N_4O_7 \cdot \frac{1}{2} H_2O$: C, 63.96; H, 7.59; N, 9.03%.

Aoc-tetra-L-proline (VIII). Compound VII (10 g, 0.016 mol) was subjected to catalytic hydrogenolysis with hydrogen and palladium charcoal in methanol, as with VI. The catalyst was removed by filtration, and the filtrate was concentrated under reduced pressure to obtain the crude product, which was crystallized from ethyl acetate and *n*-hexane. Recrystallization from the same solvent system gave the final product; wt, 7.5 g (90%).

Found: C, 59.71; H, 7.64; N, 10.75%. Calcd for $C_{26}H_{40}N_4O_7$: C, 59.98; H, 7.74; N, 10.76%.

Aoc-penta-L-proline Benzyl Ester (IX). (a) Compound V (5.3 g, 0.011 mol) was dissolved in 10 m*l* of trifluoroacetic acid, after which the mixture was allowed to react for 30 min at room temperature. The excess trifluoroacetic acid was removed by evaporation under reduced pressure, and the residual syrup was dried over sodium hydroxide *in vacuo* for one day. The dried material was then dissolved in chloroform (50 m*l*), and the solution was treated with compound IV (3.6 g, 0.011 mol) and DCC (2.3 g, 0.011 mol) in chloroform, as in the syntheses of III and V. The DCU formed was removed by filtration, and the filtrate was washed successively with 0.25 N hydrochloric acid, 5% sodium bicarbonate, and water, and dried over sodium sulfate. The dried solution was concentrated, and the residue was dissolved in hot ethyl acetate. Crystals formed when this solution was left standing in a refrigerator. The product was collected and recrystallized from ethyl acetate; wt, 5.2 g (74.5%). Found: C, 64.34; H, 7.65; N, 9.77%. Calcd for $C_{38}H_{53}N_5O_8$: C, 64.48; H, 7.55; N, 9.89%. (b) Compound VII (5.2 g, 0.01 mol) was coupled with II (2.6 g, 0.011 mol) in chloroform using DCC (2.1 g, 0.01 mol), and the reaction mixture was treated as has been described above. The product was recrystallized similarly; wt, 5.5 g (78.5%). As is shown in Table 1, the properties of this product were almost the same as those of the compound obtained above.

Found: C, 64.58; H, 7.56; N, 9.92%. Calcd for $C_{38}H_{53}N_5O_8$: C, 64.48; H, 7.55; N, 9.89%.

Aoc-penta-L-proline (X). (a) A solution of compound IX-a (3.6 g, 0.005 mol) in methanol (100 m*l*) was subjected to catalytic hydrogenolysis in the presence of palladium charcoal, as in the syntheses of IV and VI. The catalyst was filtered off, the filtrate was concentrated under reduced pressure, and the residue was recrystallized twice from a minimum volume of methanol and ethyl acetate; wt, 2.55 g (82.7%).

Found: C, 59.95; H, 7.74; N, 11.52%. Calcd for $C_{31}H_{47}N_5O_8$: C, 60.27; H, 7.67; N, 11.34%.

(b) An indistinguishable compound was also obtained from IX-b, as is shown in Table 2.

5) S. Sakakibara and N. Inukai, This Bulletin, **39**, 1567 (1966).

Aoc-hexa-L-proline Benzyl Ester (VI). An Aoc-group was removed from V (5.14 g, 0.01 mol); the triproline benzyl ester thus obtained was coupled with VI (4.24 g, 0.01 mol) in chloroform (50 m*l*) by using DCC (2.1 g, 0.01 mol), as in the synthesis of IX-a. The crude product thus obtained was recrystallized from a mixture of ethyl acetate and methanol (2 : 1 v/v); wt, 5.1 g (69.4%).

Found: C, 63.84; H, 7.54; N, 10.25%. Calcd for $C_{43}H_{60}N_6O_9$: C, 64.16; H, 7.51; N, 10.44%.

Aoc-hexa-L-proline (XII). Compound XI (4.0 g, 0.005 mol) was subjected to catalytic hydrogenolysis in methanol, as with X, VIII, VI, and IV. The catalyst was removed by filtration, and the filtrate was concentrated to a residue which was then triturated with hot ethyl acetate to remove any soluble materials. The insoluble material remaining was dissolved in methanol, and the solution was treated with active charcoal to eliminate any colored impurities. The colorless methanol solution thus obtained was concentrated to a small volume, and the product was precipitated with ethyl acetate. The precipitate was collected by filtration and recrystallized from methanol and ethyl acetate; wt, 3.0 g (84.8%).

Found: C, 60.08; H, 7.48; N, 11.70%. Calcd for $C_{36}H_{54}N_6O_9$: C, 60.48; H, 7.61; N, 11.76%.

Aoc-octa-L-proline Benzyl Ester (XIII). Compound VII (3.05 g, 0.005 mol) was treated with trifluoroacetic acid (5 m*l*) as in the case of IX-a; the tetra-L-proline benzyl ester thus obtained was coupled with VIII (2.6 g, 0.005 mol) in chloroform by using DCC (1.1 g, 0.005 mol), as has been described previously. The DCU thus formed was removed by filtration; the chloroform solution was washed successively with 0.25 N hydrochloric acid, 5% sodium bicarbonate, and water. The solution was then dried over sodium sulfate and concentrated to a residue which was subsequently purified by two precipitations from methanol and ethyl acetate; wt, 2.9 g (59.5%).

Found: C, 63.52; H, 7.50; N, 10.93%. Calcd for $C_{53}H_{74}N_8O_{11}$: C, 63.70; H, 7.47; N, 11.22%.

Aoc-octa-L-proline (XIV). Compound XIII (2.0 g, 0.002 mol) was subjected to catalytic hydrogenolysis in methanol (25 m*l*) with palladium-charcoal, as has been described for the syntheses of similar compounds. After we had confirmed that the reaction was complete, the catalyst was removed by filtration and the solution was concentrated to a residue which was subsequently from methanol and ethyl acetate; wt, 1.5 g (86%).

Found: C, 60.43; H, 7.46; N, 12.16%. Calcd for $C_{46}H_{68}N_8O_{11}$: C, 60.77; H, 7.54; N, 12.33%.

BULLETIN OF THE CHEMICAL SOCIETY OF JAPAN VOL. 43 2944—2948 (1970)

Studies of Peptide Antibiotics. XXI. Synthesis of Tyrocidine C[1)]

Kenji KUROMIZU and Nobuo IZUMIYA

Laboratory of Biochemistry, Faculty of Science, Kyushu University, Hakozaki, Fukuoka

(Received April 3, 1970)

A cyclic decapeptide, *cyclo*-(L-Trp-D-Trp-L-Asn-L-Gln-L-Tyr-L-Val-L-Orn-L-Leu-D-Phe-L-Pro-), having the amino acid sequence of natural tyrocidine C has been synthesized. Chemical and biological properties of this product have been described. An antibiological activity of the product toward Gram positive microorganisms was found to be nearly the same degree as that of tyrocidine B.

In 1952 Battersby and Craig found that a crystalline tyrocidine contained at least three components, tyrocidine A (TA), B (TB) and C (TC), using a countercurrent distribution.[2)] In 1965 Craig and his coworkers isolated a pure crystalline hydrochloride of TC and determined its structure as shown in Fig. 1 by analyses on partial hydrolyzate with hydrochloric acid.[3)] However, they did not describe a quantitative feature of its antibacterial activity and some physical properties. Furthermore, a complete synthesis of TC was not accomplished.

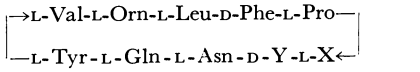

Fig. 1. Structure of TA (X,Y=Phe), TB (X=Trp, Y=Phe) and TC or IX(X, Y=Trp).

This paper will describe the synthesis of a cyclic decapeptide hydrochloride (IX·HCl) having an amino acid sequence of TC (Fig. 1), and the chemical and biological properties of a synthetic product.

Figure 2 indicates the scheme for synthesis of a

1) This work was presented at the 7th Symposium on Peptide Chemistry at the University of Tokyo, Tokyo, November 21 1969, and communicated briefly; K. Kuromizu and N. Izumiya, *Tetrahedron Lett.*, **1970**, 1471.

2) A. R. Battersby and L. C. Craig, *J. Amer. Chem. Soc.*, **74**, 4019 (1952).

3) M. A. Ruttenberg, T. P. King and L. C. Craig, *Biochemistry*, **4**, 11 (1965).

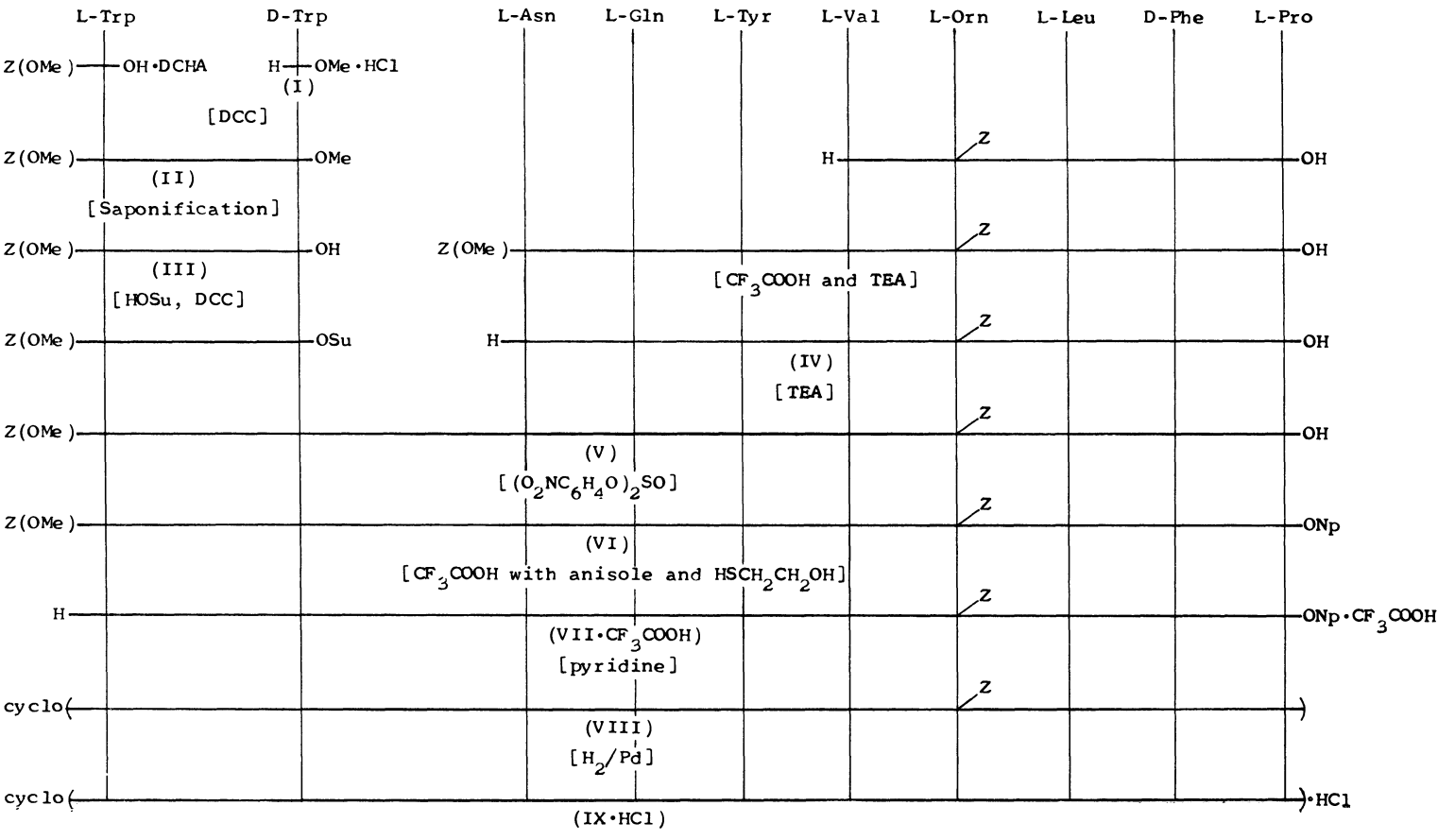

Fig. 2. Synthesis of a cyclic decapeptide hydrochloride (IX·HCl).

TABLE 1. INHIBITORY ACTIVITY OF THE COMPOUNDS ON MICROORGANISMS
Minimum inhibitory concentration, μg/ml

	Staphylococcus aureus	*Bacillus subtilis*	*Escherichia coli*	*Proteus vulgaris*	*Salmonella paratyphi*	*Pseudomonas aeruginosa*	*Shigella sonnea*	*Candida albicans*
IX	>100	6.25	>100	>100	>100	>100	>100	>100
TB	>100	3.13	100	>100	>100	>100	>100	>100
TA	>100	3.13	100	>100	>100	>100	>100	12.5
GS	1.56	0.78	25	>100	50	50	12.5	3.13

desired decapeptide (IX).[4] Some peptide derivatives shown in the scheme had been prepared previously; a pentapeptide H-Val-Orn(δ-Z)-Leu-D-Phe-Pro-OH was prepared during our synthetic studies on TA[5] or tyrocidine E[6] and an octapeptide trifluoroacetate (IV·CF_3COOH) during our synthetic studies on TB.[7]

Strategy for synthesis of decapeptide (IX) is essentially similar as reported for TB synthesis.[7] *p*-Methoxybenzyloxycarbonyldipeptide acid (III) was coupled with a neutral octapeptide (IV) by a method using reagents of HOSu and DCC, and an acyldecapeptide acid (V) was obtained as a crystalline product. It was assumed that no racemization occurred on the D-Trp residue of -L-Trp-D-Trp-L-Asn- sequence in a decapeptide (V or IX) since we had observed[7] that the use of HOSu and DCC in the same condition in the present experiment caused no racemization by an assay technique developed in this laboratory.[8]

A desired decapeptide (IX) was prepared as follows. Acyldecapeptide acid (V) was transformed into a corresponding *p*-nitrophenyl ester (VI), and its *p*-methoxybenzyloxycarbonyl group was removed by trifluoroacetic acid. The cyclization reaction of a decapeptide ester (VII) by the usual way[5,7] gave a benzyloxycarbonyl-substituted cyclic decapeptide (VIII), its molecular weight determination demonstrating that molecular size of VIII corresponds to that of cyclic decapeptide. Hydrogenolysis of VIII in the presence of an equivalent of hydrogen chloride afforded a crystalline cyclic decapeptide hydrochloride (IX·HCl). Its homogeneity was ascertained by thin-layer and paper chromatography, paper electrophoresis and an amino acid analysis. Patterns of ultraviolet spectra on IX, synthetic TA and TB indicated that insertion of one (TB) or two (TC) Trp residues instead of Phe in a TA molecule increased intensities of absorbance at 280.5 mμ.

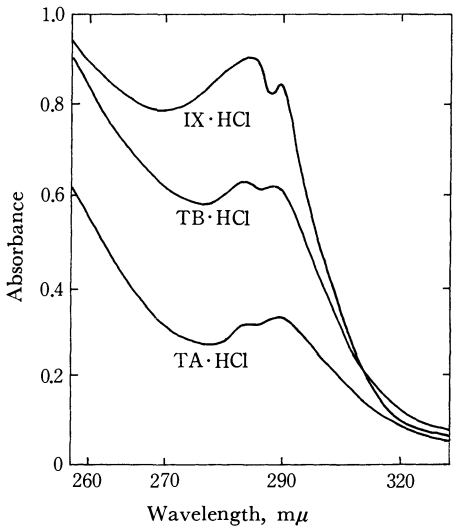

Fig. 3. Ultraviolet spectra of TA, TB and IX in 0.1 N NaOH-EtOH (1:1 v/v). Concentrations of TA·HCl, TB·HCl and IX·HCl; 9.04×10^{-5} M, 9.14×10^{-5} M and 7.05×10^{-5} M.

Antibacterial activities of IX toward several microorganisms are listed in Table 1, that of TA, TB and gramicidin S (GS) as reference compounds also being indicated. It was found that the degree of the activities of decapeptide (IX) was nearly the same as that of TA toward Gram positive (*Staph. aureus* and *B. subtilis*) and Gram negative microorganisms (*E. coli* and others) except for a microorganism, *Candida albicans*. The results indicate that both L- and D-Phe residues in a TA molecule can be replaced by L- and D-Trp residues, respectively, without a remarkable decrease in activity.

Experimental

Thin-layer chromatography was performed on Merck silica gel G with the following solvent systems: $R_f{}^1$, *n*-

4) Abbreviations; Z, benzyloxycarbonyl; Z(OMe), *p*-methoxybenzyloxycarbonyl; ONp, *p*-nitrophenyl ester; HOSu, *N*-hydroxysuccinimide; DCC, dicyclohexylcarbodiimide; TEA, triethylamine; DMF, dimethylformamide. Amino acid symbols denote L configuration otherwise noted.

5) M. Ohno and N. Izumiya, *J. Amer. Chem. Soc.*, **88**, 376 (1966); M. Ohno, T. Kato, S. Makisumi and N. Izumiya, This Bulletin, **39**, 1738 (1966).

6) N. Mitsuyasu and N. Izumiya, *Experientia*, **26**, 476 (1970); This Bulletin, **43**, 1829 (1970).

7) K. Kuromizu and N. Izumiya, *Experientia*, **26**, 587 (1970); This Bulletin, **43**, 2199 (1970).

8) N. Izumiya and M. Muraoka, *J. Amer. Chem. Soc.*, **91**, 2391 (1969).

butanol - acetic acid - pyridine - water 4 : 1 : 1 : 2 *v/v*; R_f^2, chloroform - methanol 5 : 1 *v/v*. Paper chromatography was performed with the following solvent system: R_f^1, the same solvent used for R_f^1.

H-D-Trp-OMe·HCl (I). D-Tryptophan (30 g, 14.7 mmol) and thionyl chloride (22 m*l*) in methanol (300 m*l*) were treated following the same procedure as for the preparation of L-isomer.[9] Yield, 40.8 g (92%); mp 212°C (decomp.); $[\alpha]_D^{20}$ −17.5° (*c* 1, MeOH). Reported values for the L-isomer; mp 216°C (decomp.)[9] and 214°C (decomp.).[10]

Z(OMe)-Trp-D-Trp-OMe (II). To a solution of Z(OMe)-Trp-OH dicyclohexylamine salt[7] (5.5 g, 10 mmol) and I (2.55 g, 10 mmol) in chloroform (40 m*l*) was added DCC (2.06 g, 10 mmol) at 0°C. After stirring had been continued for 3 hr at 0°C, the mixture was left to stand for overnight at room temperature. The mixture was evaporated *in vacuo*, and ethyl acetate was added to the residue. The filtrate from dicyclohexylurea was washed successively with 8% citric acid, 4% sodium bicarbonate solution and water, and dried over sodium sulfate. Evaporation of the filtrate yielded glass-like powder; 5.04 g (*ca.* 90%); mp 85—87°C; R_f^2 0.55; $[\alpha]^{20}$ −7.2° (*c* 1, MeOH).

Z(OMe)-Trp-D-Trp-OH (III). To a solution of II (2.54 g, 4.4 mmol) in methanol (16 m*l*) and dioxane (16 m*l*) was added N sodium hydroxide (8.8 m*l*). The solution was allowed to stand for 1 hr at room temperature. After addition of water (10 m*l*), the solution was concentrated *in vacuo* to remove organic solvent at 10—15°C, and acidified with 0.5 M citric acid under cooling. The oily product was extracted with ethyl acetate and the extract was dried over sodium sulfate. The filtrate was evaporated and the residue was crystallized by addition of ether and petroleum ether. It was recrystallized from ethyl acetate - ether - petroleum ether; yield, 2.10 g (86%); mp 115—116°C; R_f^2 0.34; $[\alpha]_D^{20}$ −21.6° (*c* 0.5, MeOH).

Found: C, 63.06; H, 5.78; N, 9.36%. Calcd for $C_{31}H_{28}O_6N_4 \cdot 2H_2O$: C, 63.25; H, 5.48; N, 9.52%.

H-Asn-Gln-Tyr-Val-Orn(δ-Z)-Leu-D-Phe-Pro - OH (IV). To a mixture of Z(OMe)-Asn-Gln-Tyr-Val-Orn(δ-Z)-Leu-D-Phe-Pro-OH[7] (0.65 g, 0.5 mmol) and anisole (0.5 m*l*) was added trifluoroacetic acid (3 m*l*) at −5°C. When swirled, the reaction mixture turned to a clear solution within some 10 min. After 15 min, the solution was evaporated *in vacuo* at 0°C and the oily residue was dissolved in DMF (5 m*l*). TEA (0.21 m*l*, 1.5 mmol) was added, the solution was evaporated *in vacuo*, and water (20 m*l*) was added to the residue. The precipitate collected was recrystallized from DMF - ethyl acetate - ether; yield, 0.453 g (80%); mp 285—287°C (decomp.); R_f^1 0.74; $[\alpha]_D^{20}$ −19.7° (*c* 0.8, DMF).

Found: C, 60.09; H, 6.86; N, 13.55%. Calcd for $C_{56}H_{77}O_{14}N_{11}$: C, 59.81; H, 6.88; N, 13.66%.

In a previous paper, we reported the preparation of IV trifluoroacetate as powder which was used for the coupling reaction with Z(OMe)-Trp-D-Phe-OH.[7]

Z(OMe)-Trp-D-Trp-Asn-Gln - Tyr - Val - Orn(δ - Z)-Leu-D-Phe-Pro-OH (V). To a chilled solution of III (0.276 g, 0.5 mmol) in ethyl acetate (3 m*l*) were added HOSu (0.067 g, 0.58 mmol) and DCC (0.095 g, 0.46 mmol) at 0°C. After the mixture had been stirred for 3 hr at 0°C, dicyclohexylurea precipitated was filtered off and washed with cold ethyl acetate. The filtrate was evaporated to dryness *in vacuo* at 0°C and the residue was dissolved in cold DMF (3 m*l*). To the solution was added a mixture of IV (0.48 g, 0.385 mmol) and TEA (0.055 m*l*, 0.39 mmol) in DMF (3 m*l*) at 0°C. After stirring had been continued for 5 hr at 0°C and for additional 2 hr at room temperature, the mixture was concentrated *in vacuo* to a small volume and the residue was treated with 0.5 M citric acid solution (10 m*l*). The precipitate collected was recrystallized from DMF - ether; yield, 0.436 g (68%); R_f^1 0.82; mp 208—209°C (decomp.); $[\alpha]_D^{20}$ −23.6° (*c* 1, DMF).

Found: C, 61.89; H, 6.28; N, 12.40%. Calcd for $C_{87}H_{105}O_{19}N_{15} \cdot H_2O$: C, 62.08; H, 6.41; N, 12.48%.

Z(OMe)-Trp-D-Trp-Asn-Gln - Tyr - Val - Orn(δ-Z)-Leu-D-Phe-Pro-ONp (VI). To a solution of V (0.333 g, 0.2 mmol) dissolved in DMF (3 m*l*) and pyridine (3 m*l*) was added di-*p*-nitrophenyl sulfite (0.65 g, 2 mmol). The solution was allowed to stand for 48 hr at room temperature and then evaporated *in vacuo*. After the oily residue was treated with a mixture of ether and petroleum ether, the powder was collected by filtration. The *p*-nitrophenyl ester content of this product (yield, 0.356 g) was estimated to be 104% measuring the optical density at 412 mμ.[7] This product was used for the next reaction without further purification.

***cyclo*-(Trp-D-Trp-Asn-Gln-Tyr-Val-Orn(δ-Z)-Leu-D-Phe-Pro-) (VIII).** To a mixture of VI (0.355 g) and 2-mercaptoethanol (0.05 m*l*)[11] in anisole (0.5 m*l*) was added trifluoroacetic acid (5 m*l*) at −5°C. After 10 min, the solution was evaporated at 0°C and the oily residue was triturated with ether. The powder was collected by filtration and washed with ether (yield of VII·CF_3COOH, 0.556 g). This was dissolved in a mixture of DMF (4 m*l*) and acetic acid (0.2 m*l*). The solution was added to pyridine (50 m*l*) kept at 55—60°C over 5 hr, stirring being continued for additional 3 hr at the same temperature. After evaporation, the residue was dissolved in 15 m*l* of a mixture of methanol - dioxane - water (1 : 2 : 1). The solution was passed successively through columns (0.9×12 cm) of Amberlite IRC-50 (H^+ form) and Amberlite IR-45 (OH^- form), the columns being washed with the same solvent. After the filtrate and washings (total 50 m*l*) were evaporated, the residual product was collected by filtration with the aid of water and recrystallized from DMF - ether; yield, 0.176 g (59% from V); mp 225—228°C (decomp.); R_f^1 0.82; $[\alpha]_D^{20}$ −36.1° (*c* 0.5, MeOH).

Found: C, 60.67; H, 6.63; N, 13.82%; mol wt 1550. Calcd for $C_{87}H_{95}O_{15}N_{15} \cdot 3H_2O$: C, 60.95; H, 6.62; N, 13.68%; mol wt 1537.[12]

***cyclo*-(Trp-D-Trp-Asn-Gln-Tyr - Val - Orn - Leu-D-Phe-Pro-) hydrochloride (IX·HCl).** A solution of VIII (76.8 mg, 0.05 mmol) in 0.02 N methanolic hydrogen chloride (2.5 m*l*) was hydrogenated in the presence of palladium black. After 4 hr, the filtrate from

9) R. A. Boissonnas, St. Guttmann, R. L. Huguenin, P. A. Jaquenoud and Ed. Sandrin, *Helv. Chim. Acta*, **41**, 1867 (1958).

10) E. Abderhalden and M. Kempe, *Z. Physiol. Chem.*, **52**, 207 (1907).

11) J. Blake and C. H. Li, *J. Amer. Chem. Soc.*, **90**, 5882 (1968).

12) Molecular weight was determined on a Hitachi Osmometer, type 115, using methanol as a solvent.

the catalyst was evaporated to dryness *in vacuo* and ether (4 m*l*) was added. Crystals collected were recrystallized from methanol - ethyl acetate - ether; yield of an air-dried product ($IX \cdot HCl \cdot 6H_2O$), 59.7 mg (82%); mp 218—220°C (decomp.); $[\alpha]_D^{20}$ —84.3° (*c* 0.5, MeOH).

Found: C, 56.35; H, 6.86; N, 13.83%. Calcd for $C_{70}H_{89}O_{13}N_{15} \cdot HCl \cdot 6H_2O$: C, 56.30; H, 6.88; N, 14.07%.

Ultraviolet spectra of TA·HCl, TB·HCl and IX·HCl with a Hitachi EPS-2 spectrophotometer are shown in Fig. 3. From the spectra, the characteristic features on each compound are observed; insertion of one (TB) or two (TC) Trp residues in a TA molecule increased intensities of absorbance in reasonable ratio.

Determination of Homogeneity of IX. Homogeneity of compound $IX \cdot HCl \cdot 6H_2O$ was ascertained further as follows. Data of TA·HCl, TB·HCl and GS·2HCl as reference peptides are also indicated.

(a) Thin-layer Chromatography. One spot was detected on IX; R_f^1 0.78 and R_f^2 0.02. That of TA·HCl; R_f^1 0.78 and R_f^2 0.02.

(b) Paper Chromatography. R_f^I 0.96 for IX, R_f^I 0.96 for TA·HCl and TB·HCl.

(c) Paper Electrophoresis.[13] Mobility of IX was found to be nearly the same as that of TA and TB; R_f, 0.60 × GS.

(d) Amino Acid Analysis.[14] Amino acid ratios in acid hydrolyzate were as follows; Asp 0.97, Glu 1.05, Tyr 0.82, Val 1.00, Orn 1.04, Leu 1.07, Phe 0.99, Pro 1.06 and NH_3 2.30. Molar ratios of Trp and Tyr were determined from ultraviolet spectrum of IX in a similar manner as described previously;[7] Trp 1.80, Tyr 1.05.

Microbiological assays.[15] The microorganisms employed are listed in Table 1. In addition to IX, a series of TA, TB and GS were examined as reference compounds. Table 1 indicates that the degree of activities of synthetic IX toward Gram positive (*Staph. aureus* and *B. subtilis*) and Gram negative (*E. coli* and others) microorganisms is nearly the same as that of TB, and TA except for a microorganism, *Candida albicans*.

13) Paper electrophoresis was carried out under the following conditions: solvent, formic acid - acetic acid - methanol - water (1 : 3 : 6 : 10 v/v, pH 1.8); voltage gradient, 20 V/cm.

14) We are indebted to Mr. K. Noda in this laboratory for the amino acid analysis.

15) We are indebted to Meiji Seika Co., Ltd. for microbiological assays.

BULLETIN OF THE CHEMICAL SOCIETY OF JAPAN VOL. 43 2948—2952 (1970)

Hydrazinolysis of Sugar Sulfonates*[1]

Tetsuo SUAMI and Tadao SHOJI

Department of Applied Chemistry, Faculty of Engineering, Keio University, Koganei-shi, Tokyo

(Received April 13, 1970)

Hydrazinolysis of methyl 4,6-di-*O*-acetyl-2,3-di-*O*-tosyl-α-D-glucopyranoside (I) or methyl 2,6-di-*O*-benzoyl-3,4-di-*O*-mesyl-α-D-glucopyranoside (VI), followed by catalytic hydrogenation and acetylation, afforded methyl 2,4-diacetamido-3,6-di-*O*-acetyl-2,4-dideoxy-α-D-idopyranoside (II). Also methyl 2,3-di-*O*-acetyl-4,6-di-*O*-mesyl-α-D-glucopyranoside (VII) was treated analogously as described above to give methyl 4,6-diacetamido-2,3-di-*O*-acetyl-4,6-dideoxy-α-D-galactopyranoside (IX). The structures were studied by means of proton magnetic resonance spectra. And a reaction mechanism was also discussed.

In the previous papers,[1-5] it has been described that hydrazinolysis of inositol sulfonate, followed by catalytic hydrogenation, affords diamino-dideoxyinositol of practical importance. Prior to these reports, Wolfrom and his coworkers described a displacement of sulfonyloxy group in a sugar derivative with hydrazine.[6-9]

Since a diamino-sugar has been found in several antibiotics, such as neomycin B, C,[10] kanamycin

*1 A part of this research has been presented at the 23rd Annual Meeting of the Chemical Society of Japan, Tokyo, April 1970.

1) T. Suami and S. Ogawa, This Bulletin, **40**, 1295 (1967).

2) T. Suami and H. Sano, *Tetrahedron Lett.*, **1968**, 2655.

3) T. Suami, S. Ogawa, Y. Naito and H. Sano, *J. Org. Chem.*, **33**, 2831 (1968).

4) T. Suami and H. Sano, *Tetrahedron Lett.*, **1969**, 1795.

5) T. Suami, S. Ogawa and H. Sano, This Bulletin, **43**, 1843 (1970).

6) D. Horton, M. L. Wolfrom and A. Thompson, *J. Org. Chem.*, **26**, 5069 (1961).

7) M. L. Wolfrom, J. Bernsmann and D. Horton, *ibid.*, **27**, 4505 (1962).

8) M. L. Wolfrom, M. I. Taha and D. Horton, *ibid.*, **28**, 3553 (1963).

9) M. L. Wolfrom, Y. Hung and D. Horton, *ibid.*, **30**, 3394 (1965).

10) K. L. Rinehart, Jr., "The Neomycins and Related Antibiotics," John Wiley & Sons, Inc., New York, N. Y. (1964).

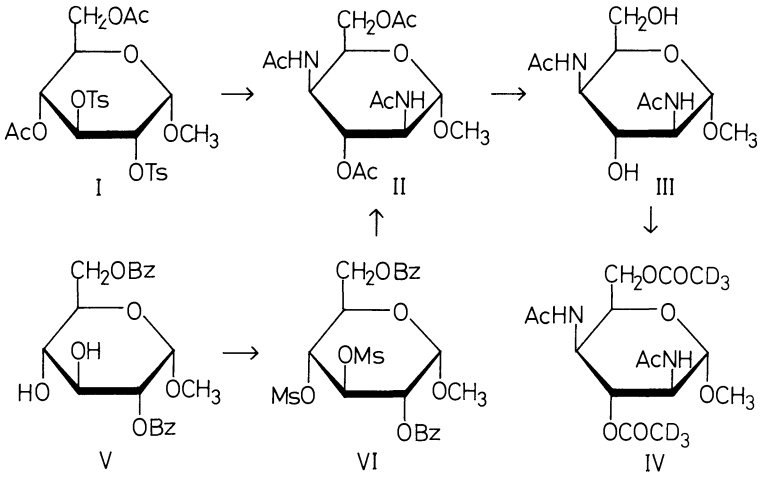

Scheme 1

B[11] and paromomycin,[12] it would be desirable to explore a new process for the synthesis of diaminosugars. For this aim, the above hydrazinolysis of sugar disulfonates seems to be an attractive method.

In the present article, it will be described that methyl 4,6-di-*O*-acetyl-2,3-di-*O*-tosyl-α-D-glucopyranoside (I), methyl 2,6-di-*O*-benzoyl-3,4-di-*O*-mesyl-α-D-glucopyranoside (VI) and methyl 2,3-di-*O*-acetyl-4,6-di-*O*-mesyl-α-D-glucopyranoside (VII) are treated with hydrazine and the reaction products are readily converted to methyl diamino-dideoxyhexosides by the catalytic hydrogenation.

The compound I was prepared by acetylation of methyl 2,3-di-*O*-tosyl-α-D-glucopyranoside which had been prepared by the method of Littmann and Hess.[13] When I was heated with anhydrous hydrazine in 2-methoxyethanol under reflux for 26 hr and the reaction product was hydrogenated in the presence of Raney nickel catalyst, an oily product was obtained. Acetylation of the product afforded methyl diacetamido-di-*O*-acetyl-dideoxyhexoside (II) as crystals of mp 245—247°C in a yield of 43%. A selective de-*O*-acetylation of II yielded methyl diacetamido-dideoxyhexoside (III) of mp 242—244°C in 74% yield.

To establish the structure of II, a proton magnetic resonance (PMR) spectrum was measured with 100 MHz spectrometer. The spectrum of II in deuteriochloroform showed three sharp signals at δ 1.99, 2.00 and 2.09 with a relative intensity of 3 : 3 : 6, which were attributed to four acetyl groups. To find the signal due to the acetamido groups, methyl di-*O*-trideuterioacetyl-diacetamido-dideoxyhexoside (IV) was prepared by trideuterioacetylation of III. The PMR spectrum of IV revealed the signal at δ 2.00 with an intensity of six protons, which was attributed to the two acetamido groups. Hence the signal at δ 2.09(6H) in the spectrum of II was ascribed to the two acetoxy groups. The two acetamido groups were considered to be in axial positions, because their signals appeared in a relatively low field.[14] One of the two acetoxy groups was on C-6, since an acetoxy group on C-6 of methyl α-D-glucopyranoside tetraacetate showed its signal at the same position (δ 2.09).[15] Another acetoxy group seemed to be axial but this was not definitive, because the signal was on an overlapped position of an axial and an equatorial acetoxy group.[14]

A more information on the conformation of II was obtained from the signal pattern of ring protons in a low field (Fig. 1). There were two doublets at δ 7.11 and 7.29 with a same coupling constant of 9.0 Hz, and these signals were removed by adding deuterium oxide to the sample (Fig. 1). Consequently, these signals were ascribed to the two NH protons of acetamido groups.

An anomeric proton should appear as a doublet, since there was only one proton on C-2 to couple with it. This doublet was found at δ 4.76 with a $J_{1,2}$ coupling of 3.5 Hz and the signal was slightly broadened by a long range coupling of less than 1 Hz. The small value of the coupling constant between H-1 and H-2 indicated that H-2 was not anti-parallel to H-1, and accordingly the C1 conformation was supported.

A triplet was observed at δ 4.97 with a coupling

11) H. Schmitz, O. B. Fardig, F. A. O'Herron, M. A. Rousche and I. R. Hooper, *J. Amer. Chem. Soc.*, **80**, 2911 (1958).

12) T. H. Haskell, J. C. French and Q. R. Bartz, *ibid.*, **81**, 3481 (1959).

13) O. Littmann and K. Hess, *Ber.*, **67B**, 519 (1934).

14) F. W. Lichtenthaler and P. Emig, *Tetrahedron Lett.*, **1967**, 577.

15) D. Horton and J. H. Lauterback, *J. Org. Chem.*, **34**, 86 (1969).

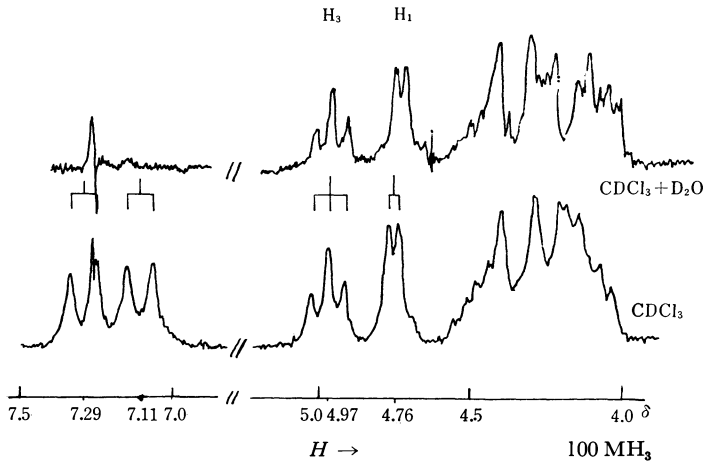

Fig. 1

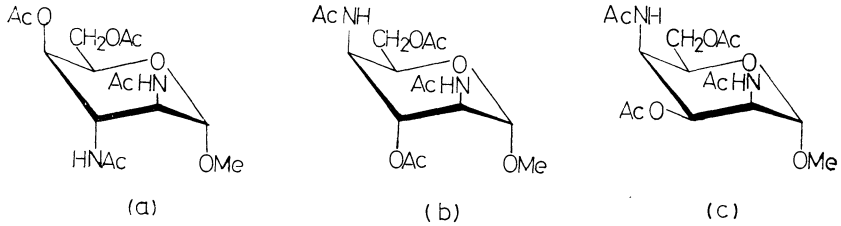

Scheme 2

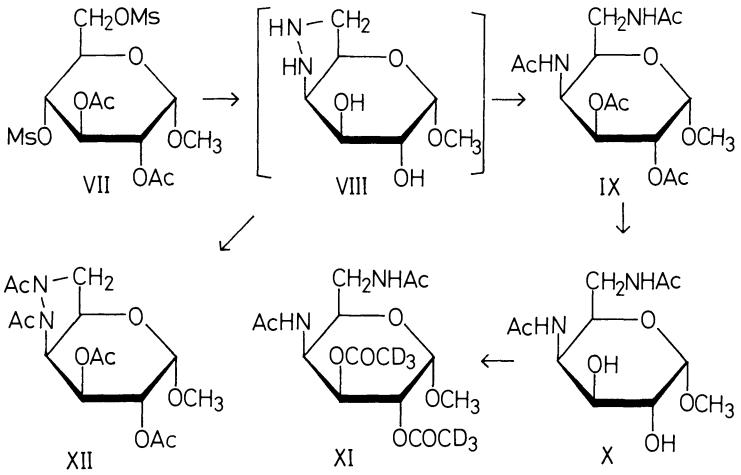

Scheme 3

constant of 5.7 Hz. The fact that a magnitude of the coupling constant was not the same as $J_{1,2}$ showed that the signal was not due to H-2. Also, the triplet was not affected by the addition of D_2O, indicating that the proton was bonded to a carbon atom which held an acetoxy group. If the proton were on C-4, the configuration of II would be (a), and if it were on C-3, the configuration would be (b) or (c).

To establish the configuration, another synthetic study was carried out. When methyl 2,6-di-*O*-benzoyl-3,4-di-*O*-mesyl-α-D-glucopyranoside (VI) was treated with hydrazine and subsequently hydrogenated and acetylated, the compound II was obtained in 26% yield.

In the configuration (a), H-4 should appear as a quartet and therefore, this configuration could be omitted. If it were (c), the intermediary cyclic carbonium ions which were formed in the both reactions (I→II and VI→II) should be opened

in the *cis*-configuration. The *cis*-opening of the cyclic carbonium ion has not been observed in these reaction condition.[16] In the configuration (b), there was no such a contradiction and this configuration was consistent with all respects.

In 1968, Hill and his coworkers[17] described that 4,6-diamino-4,6-dideoxy-D-galactose derivative was prepared by a reaction between methyl 2,3-di-*O*-acetyl-4,6-di-*O*-mesyl-α-D-glucopyranoside (VII) and sodium azide. Very recently, it has been described by Paulsen and Stoye[18] that methyl 2,3-di-*O*-benzyl-4,6-di-*O*-mesyl-α-D-glucopyranoside was treated with hydrazine and subsequently hydrogenated to give the diamino-sugar.

Independently, the present authors have attempted to prepare a diamino-sugar by hydrazinolysis of VII, since hydrazine might induce a different reaction from that of sodium azide. In the present study, hydrazinolysis of VII, followed by catalytic hydrogenation and acetylation, afforded methyl diamino-dideoxyhexoside tetraacetate of mp 220—221°C which was identical with methyl 4,6-diacetamido-2,3-di-*O*-acetyl-4,6-dideoxy-α-D-galactopyranoside (IX) described by Hill *et al.*[17] A selective de-*O*-acetylation of IX yielded methyl 4,6-diacetamido-4,6-dideoxy-α-D-galactopyranoside (X).[18]

The conformation of the product was studied by PMR spectra. The spectrum of IX revealed three sharp signals at δ 2.00, 2.01 and 2.10 with a relative intensity of 3 : 3 : 6, which were ascribed to four acetyl groups. To find out a signal arisen from the acetamido groups, the spectrum of the trideuterioacetyl derivative of X was measured. In the spectrum, two sharp signals at δ 1.99 (3H) and 2.10 (3H) were observed as the two acetamido signals. The latter signal was in a lower field as compared with an acetamido signal given by the group on a pyranose ring, and this signal was thus ascribed to the one on C-6. The former signal was ascribed to an axial acetamido group.[14] Hence, the two signals at δ 2.01 (3H) and 2.10 (3H) were attributed to two equatorial acetoxy groups.

In the lowest field of the spectrum, a signal pattern of two protons appeared as a modified quartet centered at δ 6.5, which were ascribed to two NH protons. These signals were removed step by step by adding deuterium oxide to the $CDCl_3$ solution of the sample. In five minutes after the addition of D_2O, a signal pattern of one proton disappeared to leave a doublet with a coupling constant of 9.8 Hz. This doublet was further removed by warming the sample solution at 40—50°C for 10 min. These facts were not contradictory with the above mentioned structure.

The reaction mechanism was established by isolating the intermediary bicyclic compound (VIII) as the crystalline acetyl derivative (XII). That is, the attack of hydrazine occurred at C-6 of VII and then the hydrazino group on C-6 attacked C-4 to give VIII. The N-N linkage was cleaved by the catalytic hydrogenation to yield the product with the galacto-configuration.

Experimental

The melting points reported were determined on a Mitamura Riken micro hot stage. The melting point marked with an asterisk was measured in a liquid bath and was uncorrected. The PMR spectra of the samples were determined at 60 or 100 MHz in deuteriochloroform with tetramethylsilane as an internal standard. The peak positions are given in δ-values.

Methyl 4,6-Di-*O*-acetyl-2,3-di-*O*-tosyl-α-D-glucopyranoside (I). A 0.85 g portion of methyl 2,3-di-*O*-tosyl-α-D-glucopyranoside which had been prepared by the method of Littmann and Hess[13] was acetylated with acetic anhydride in pyridine at room temperature overnight. The mixture was evaporated under reduced pressure and the residue was crystallized in ethanol. Recrystallization of the crude product from ethanol-ether gave 0.89 g (90%) of I, mp 126—128°C; $[\alpha]_D^{22}$ + 31° (*c* 1, $CHCl_3$).

Found: C, 51.16; H, 5.49; S, 10.77%. Calcd for $C_{35}H_{30}O_{12}S_2$ (586.6): C, 51.19; H, 5.12; S, 10.92%.

Methyl 2,6-Di-*O*-benzyl-α-D-glucopyranoside (V). The product was prepared by the method of Lieser and Schweizer[19] in a yield of 31% from methyl D-glucopyranoside, mp 142°C; $[\alpha]_D^{22}$ + 81.9° (*c* 2, $CHCl_3$). Lit,[19] mp 144°C; $[\alpha]^{23}$ + 80.4° (*c* 4, $CHCl_3$).

Methyl 2,6-Di-*O*-benzoyl-3,4-di-*O*-mesyl-α-D-glucopyranoside (VI). To a solution of 1.78 g of V in 20 m*l* of pyridine, 4.5 m*l* of methanesulfonyl chloride was added under ice cooling. The mixture was settled at room temperature for 48 hr and was poured into a large amount of ice-water. The precipitate was collected by filtration and washed with water. The product was dissolved in ethanol and decolorized with charcoal. The solution was evaporated to give 1.51 g (61%) of amorphous powder: mp 59—64°C. The crude product was recrystallized from isopropanol to give crystals of mp 74—77°C: $[\alpha]_D^{22}$ + 138.0° (*c* 1, $CHCl_3$).

Found: C, 49.38; H, 4.84; S, 11.33%. Calcd for $C_{23}H_{26}O_{12}S_2$ (558.6): C, 49.45; H, 4.69; S, 11.48%.

Methyl 2,4-Diacetamido-3,6-di-*O*-acetyl-2,4-dideoxy-α-D-idopyranoside (II). (a) A mixture of 2.08 g of I and 4.4 m*l* of anhydrous hydrazine in 28 m*l* of 2-methoxyethanol was heated under reflux for 26 hr. The mixture was evaporated *in vacuo* and the residue was dissolved in water. The aqueous solution was treated with Amberlite IRA-400 to remove an acidic substance and then evaporated. The residue was hydrogenated in ethanol under the presence of Raney nickel catalyst in 3.4 kg/cm² of hydrogen atmosphere for 23 hr.

16) E. S. Gould, "Mechanism and Structure in Organic Chemistry," Holt, Rinehart and Winston, Inc., New York (1962), pp. 565—566.

17) J. Hill, L. Hough and A. C. Richardson, *Carbohyd. Res.*, **8**, 7 (1968).

18) H. Paulsen and D. Stoye, *Chem. Ber.*, **102**, 3833 (1969).

19) T. Lieser and R. Schweizer, *Ann.*, **519**, 271 (1935).

After the catalyst was removed by filtration, the filtrate was evaporated to give 1.02 g of an oily residue. Acetylation of the residue with acetic anhydride in pyridine afforded a crystalline product. Recrystallization of the product from ethanol afforded 0.55 g (43%) of crystals: mp* 245—247°C; $[\alpha]_D^{22}$ + 80° (*c* 1, water).

Found: C, 50.10; H, 6.78; N, 7.81%. Calcd for $C_{15}H_{24}N_2O_8$ (360.4): C, 49.99; H, 6.71; N, 7.77%.

(b) A mixture of 7.3 g of methyl 2,3-di-*O*-tosyl-α-D-glucopyranoside[13] and 15 m*l* of anhydrous hydrazine in 80 m*l* of 2-methoxyethanol was heated under reflux for 48 hr and subsequently treated as described in (a) to give 0.84 g (16%) of the product: mp 242—246°C. The product was identified with II by a mixed melting point determination and IR spectra.

(c) A 3.97 g portion of VI was heated with 20 m*l* of anhydrous hydrazine in 50 m*l* of 2-methoxyethanol for 22 hr under reflux. The reaction mixture was treated analogously as described in (a), giving 662 mg (26%) of II: mp 243—245°C.

Methyl 2,4-Diacetamido-2,4-dideoxy-α-D-idopyranoside (III). A 123 mg portion of II was selectively de-*O*-acetylated in 30 m*l* of methanol previously saturated with ammonia. The solution was evaporated under reduced pressure and the residue was washed with ethanol to give 70 mg (73%) of the product: mp 242—244°C. Recrystallization from ethanol afforded an analytically pure sample: mp 242—244°C; $[\alpha]_D^{22}$ +61° (*c* 0.2, water).

Found: C, 47.97; H, 7.32; N, 10.29%. Calcd for $C_{11}H_{20}N_2O_6$ (276.3): C, 47.82; H, 7.30; N, 10.14%.

Methyl 2,4-Diacetamido-3,6-di-*O*-trideuterioacetyl-2,4-dideoxy-α-D-idopyranoside (IV). A 55 mg portion of III was acetylated with 0.2 m*l* of acetic anhydride-d_6 in 0.6 m*l* of pyridine overnight. The mixture was evaporated *in vacuo* and the residue was crystallized in ethanol-ether to give 55 mg (76%) of the product: mp 240—244°C.

Methyl 2,3-Di-*O*-acetyl-4,6-di-*O*-mesyl-α-D-glucopyranoside (VII). The compound was prepared by the method of Hill *et al.*[17]

Methyl 4,6-Diacetamido-2,3-di-*O*-acetyl-4,6-dideoxy-α-D-galactopyranoside (IX). A 2.0 g portion of VII was heated under reflux in a mixture of 6 m*l* of anhydrous hydrazine and 30 m*l* of 2-methoxyethanol for 24 hr. After the mixture was evaporated under reduced pressure, the residue was hydrogenated in ethanol with Raney nickel catalyst at 3.4 kg/cm² of hydrogen stream at 40—50°C for 24 hr. The catalyst was removed by filtration and the filtrate was evaporated. The residue was acetylated with acetic anhydride in pyridine. An excess amount of the reagent was removed by evaporation, and the residue was crystallized from ethanol to give 0.45 g (28%) of the product: mp 220—221°C; $[\alpha]_D^{22}$ +121° (*c* 1, water). Lit,[17] mp 218—219°C; $[\alpha]_D$ +123° (*c* 1, water). Found: C, 50.15; H, 6.86; N, 7.86%.

Methyl 4,6-Diacetamido-4,6-dideoxy-α-D-galactopyranoside (X). A 32 mg portion of IX was selectively de-*O*-acetylated with methanolic ammonia, giving 16 mg (64%) of the product: mp 213.5—214°C; $[\alpha]_D^{24}$ +161° (*c* 1.1, MeOH). Lit,[17] mp 212—213°C; $[\alpha]_D$ +151° (*c* 1.0, water). Lit,[18] mp 215—216°C; $[\alpha]_D^{20}$ +153° (*c* 0.5, MeOH).

Methyl 4,6-Diacetamido-2,3-di-*O*-trideuterioacetyl-4,6-dideoxy-α-D-galactopyranoside (XI). An 89 mg portion of X was acetylated with 0.3 m*l* of acetic anhydride-d_6 in 0.7 m*l* of pyridine overnight. The mixture was evaporated under reduced pressure and the residue was crystallized in ethanol-ether to give 82 mg (70%) of the product: mp 218—219°C.

7,8-Di-*N*-acetyl-4,5-di-*O*-acetyl-3-*O*-methyl-7,8-diaza-2-oxabicyclo[4.3.0]nonane-3,4,5-triol (XII). A 1.3g portion of VII was heated with anhydrous hydrazine (4 m*l*) in 2-methoxyethanol (20 m*l*), and then the mixture was evaporated *in vacuo*. The residue was dissolved in ethanol and an insoluble material was removed by filtration. The filtrate was evaporated and the residue was acetylated with acetic anhydride in pyridine. After an excess reagent was evaporated *in vacuo*, the residue was crystallized in ethanol to give 184 mg (17%) of the product: mp 199—200°C. Recrystallization from ethanol did not raise its melting point. $[\alpha]_D^{22}$ +106° (*c* 0.5, $CHCl_3$); ν_{max}^{KBr} 1740 and 1687 cm^{-1}.

Found: C, 50.40; H, 6.30; N, 7.74%. Calcd for $C_{15}H_{22}N_2O_8$ (358.2): C, 50.27; H, 6.19; N, 7.82%.

This work has been supported financially in part by the grant of the Japanese Ministry of Education. We thank Professor Sumio Umezawa for his helpful advice and Mr. Saburo Nakada for performing elementary analysis.

BULLETIN OF THE CHEMICAL SOCIETY OF JAPAN VOL. 43 2953—2956 (1970)

Aminocyclitols. XXIII. A Synthetic Study of Streptozotocin Analogs*[1]

Tetsuo SUAMI and Tomoya MACHINAMI

Department of Applied Chemistry, Faculty of Engineering, Keio University, Koganei, Tokyo

(Received April 16, 1970)

Streptozotocin is an antibiotic which exhibits wide antimicrobial and antitumor activities, and its structure has been established to be *N*-carbamyl-*N'*-methyl-*N'*-nitroso-D-glucosamine. In the present article, streptozotocin analogs in which the pyranose ring was substituted for a cyclohexane ring were prepared. These compounds showed considerable activities against Ehrlich ascites tumor.

Streptozotocin,[1-4] an antibiotic produced by *Streptomyces achromogenes var.* 128 exhibits wide antimicrobial and antitumor activities *in vitro* and *in vivo*. The structure has been established to be *N*-carbamyl-*N'*-methyl-*N'*-nitroso-D-glucosamine, and this was further confirmed by the syntheses.[5,6]

In the present article, we wish to report a synthesis of *N*-carbamyl-*N'*-methyl-*N'*-nitroso derivatives of *scyllo*-inosamine,[7] *epi*-inosamine-2,[8-10] and *myo*-inosadiamine-1,3.[11,12]

When anisaldehyde was added to a mixture of *scyllo*-inosamine hydrochloride (I)[7] and 1N sodium hydroxide solution, *N*-[*p*-methoxybenzylidene]-*scyllo*-inosamine (II) was obtained in 84% yield. Acetylation of II in a mixture of acetic anhydride and pyridine afforded the pentaacetate (III), which was further converted to penta-*O*-acetyl-*scyllo*-inosamine hydrochloride (IV) by warming in 5N hydrochloric acid.

IV was treated with methyl isocyanate in the presence of silver carbonate to give penta-*O*-acetyl-*N*-carbamyl-*N'*-methyl-*scyllo*-inosamine (V) in a yield of 87%. Nitrosation of V with a mixture of nitrosyl chloride and pyridine afforded penta-*O*-acetyl-*N*-carbamyl-*N'*-methyl-*N'*-nitroso-*scyllo*-inosamine (VI) in 91% yield. An attempted deacetylation of VI in methanolic ammonia resulted in the formation of *N*-carbamyl-*scyllo*-isnosamine (VII) with a loss of diazomethane. Therefore, deacetylation was carried out before the nitrosation to give *N*-carbamyl-*N'*-methyl-*scyllo*-inosamine (VIII) in 64% yield from V.

An alternative method to prepare VIII (64% yield) was successfully carried out by treating I with methyl isocyanate in boiling aqueous acetonitrile in the presence of silver carbonate.

Nitrosation of VIII was achieved with sodium nitrite in aqueous acetic acid to give *N*-carbamyl-*N'*-methyl-*N'*-nitroso-*scyllo*-inosamine (IX) in 72% yield. Acetylation of IX by a conventional method afforded a penta-*O*-acetyl derivative which was identified to be VI.

N-Carbamyl-*N'*-methyl-*N'*-nitroso-*epi*-inosamine-2 (XI) and di-*N*,*N'*-(*N*-methyl-*N*-nitroso-carbamyl)-*myo*-inosadiamine-1,3 (XV) were prepared from *epi*-inosamine-2 hydrochloride (X) and *myo*-inosadiamine-1,3 dihydrochloride (XIII) respectively by analogous reactions described above.

These three compounds: IX, XI and XV, were active against Ehrlich ascites tumor and Hela carcinoma.

Experimental

The melting points reported were determined on a Mitamura Riken micro hot stage. The NMR spectra were determined with a Varian A-60D spectrometer.

***N*-[*p*-Methoxybenzylidene]-*scyllo*-inosamine (II).** To a solution of 949 mg of *scyllo*-inosamine hy-

*1 A part of this study has been presented at the 22nd Annual Meeting of the Chemical Society of Japan, Tokyo, April 1969.

1) J. J. Vavra, C. Deboer, A. Dietz, L. J. Hanka and W. T. Sokolski, *Antibio. Ann.*, **1959—1960**, 230 (1960).
2) W. T. Sokolski, J. J. Vavra and L. J. Hanka, *ibid.*, **1959—1960**, 241 (1960).
3) C. Lewis and A. R. Barbiers, *ibid.*, **1959—1960**, 247 (1960).
4) R. R. Herr, T. E. Eble, M. E. Bergy and H. K. Jahnke, *ibid.*, **1959—1960**, 236 (1960).
5) R. R. Herr, H. K. Jahnke and A. D. Argoudelis, *J. Amer. Chem. Soc.*, **89**, 4808 (1967).
6) E. Hardegger, A. Meier and A. Stoos, *Helv. Chim. Acta*, **52**, 2555 (1969).
7) T. Suami, F. W. Lichtenthaler and S. Ogawa, This Bulletin, **39**, 170 (1966).
8) E. L. May and E. Mosettig, *J. Org. Chem.*, **14**, 1137 (1947).
9) H. E. Carter, R. K. Clark, Jr., B. Lytle and G. E. McCasland, *J. Biol. Chem.*, **175**, 683 (1948).
10) T. Suami, S. Ogawa, Y. Nakashima and H. Sano, This Bulletin, **40**, 2958 (1967).
11) T. Suami and S. Ogawa, *ibid.*, **40**, 1295 (1967).
12) T. Suami, S. Ogawa, S. Naito and H. Sano, *J. Org. Chem.*, **33**, 2831 (1968).

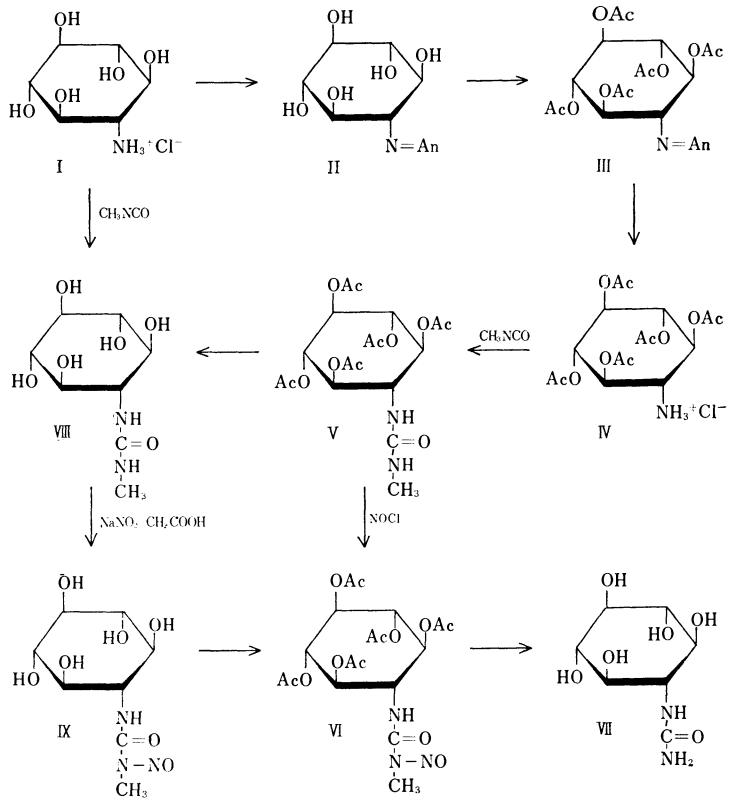

Scheme 1

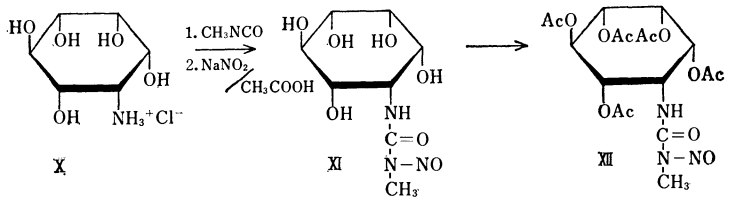

Scheme 2

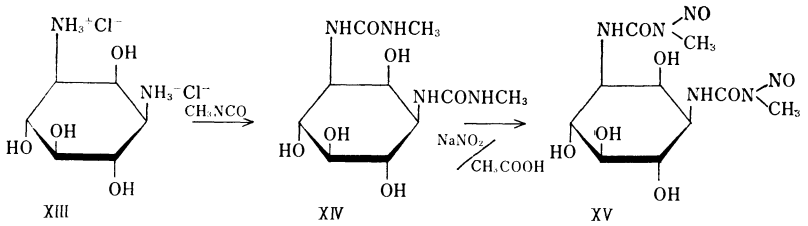

Scheme 3

drochloride (I)[7] in 4.5 m*l* of 1 N sodium hydroxide, 610 mg of anisaldehyde was added with an occasional shaking. After the reaction mixture was settled overnight in a refrigerator, crystals were collected by filtration and washed with a mixture of ethanol and ether (1 : 1). The product (1.087 g) was obtained in a form of fine powder: mp 243—249°C (dec.). A second crop of the product (92 mg) was obtained from the mother liquor. The total yield was 90.6%.

Penta-*O*-acetyl-*N*-[*p*-methoxybenzylidene]-*scyllo*-inosamine (II). A 1.087 g portion of II was acetylated with 3.3 m*l* of acetic anhydride in 5.9 m*l* of pyridine. After the reaction mixture was settled overnight at room temperature, crystals were collected by

filtration and washed with ethanol to give 1.412 g of the product, mp 228°C (dec.). The filtrate was diluted with 20 m*l* of ice-cold water to give 0.205 g of the product. The total yield was 87.2%.

The crude product was recrystallized from ethanol to give crystals, mp 228—229°C.

Penta-*O*-acetyl-*scyllo*-inosamine hydrochloride (IV). To a suspension of 1.412 g of III in 14 m*l* of boiling acetone, 0.57 m*l* of 5 N hydrochloric acid was added. After cooling, 15 m*l* of ethyl ether was added to the mixture and the mixture was stored overnight in a refrigerator. Crystals were collected by filtration and washed with ether to give 1.119 g (94.6%) of the product. The crude product was recrystallized from methanol to give needles melting at 220—222°C (dec.).

Found: C, 45.31; H, 5.93; N, 3.31; Cl, 8.45%. Calcd for $C_{16}H_{24}NO_{10}Cl$: C, 45.13; H, 5.68; N, 3.30; Cl, 8.33%.

Penta-*O*-acetyl-*N*-carbamyl-*N'*-methyl-*scyllo*-inosamine (V). To a suspension of 1.00 g of IV in 20 m*l* of acetonitrile, 1 m*l* of methyl isocyanate and 780 mg of silver carbonate were added. The reaction mixture was refluxed on a steam bath for 35 min. After cooling, precipitates were removed by filtration and the filtrate was evaporated under reduced pressure to give a crystalline residue. The residue was triturated with ethanol to yield 905 mg (86.8%) of the product, mp 255—257°C.

Recrystallizations from ethanol and from chloroform gave an analytically pure sample, mp 255—257°C.

Found: C, 48.71; H, 6.24; N, 6.19%. Calcd for $C_{18}H_{26}N_2O_{11}$: C, 48.43; H, 5.87; N, 6.27%.

Penta-*O*-acetyl-*N*-carbamyl-*N'*-methyl-*N'*-nitroso-*scyllo*-inosamine (VI). To a suspension of 1.00 g of V in 10 m*l* of pyridine, 4.0 m*l* of 1.2 M nitrosyl chloride in acetic anhydride was added drop by drop at 13°C under occasional shaking for 20 min. Then the reaction mixture was poured into 20 m*l* of ice and water. The yellowish crystals which precipitated in the aqueous solution were collected by filtration and washed with water to yield 975 mg (91.5%) of a crude product.

Recrystallization from acetone gave yellow cubic crystals melting at 192—196°C. IR: 1750 (OAc), 1530 (NH) and 1480 cm^{-1} (N–NO).

Found: C, 45.75; H, 5.53; N, 8.81%. Calcd for $C_{18}H_{25}N_3O_{12}$: C, 45.47; H, 5.30; N, 8.84%.

A presence of nitroso group was supported by a positive Liebermann nitroso test.

***N*-Carbamyl-*scyllo*-inosamine (VII).** A 300 mg portion of VI was added to 30 m*l* of methanol previously saturated with dry ammonia under ice cooling, and the mixture was settled in a refrigerator overnight. Colorless crystals which appeared in the mixture were collected by filtration and washed with methanol to give 99 mg of the product, mp 243—245°C, 70.7% yield. Recrystallization from aqueous ethanol did not raise its melting point.

Found: C, 37.59; H, 6.63; N, 12.67%. Calcd for $C_7H_{14}N_2O_6$: C, 37.84; H, 6.35; N, 12.61%.

***N*-Carbamyl-*N'*-methyl-*scyllo*-inosamine (VIII).** (a) A 294 mg portion of V was added to 40 m*l* of ethanol previously saturated with dry ammonia and the mixture was settled in a refrigerator overnight. Crystals which appeared in the mixture were collected by filtration and washed with ethanol to give 99 mg (64.0%) of the product, mp 225—226°C. Recrystallization from aqueous ethanol did not raise its melting point.

Found: C, 40.56; H, 6.98; N, 11.54%. Calcd for $C_8H_{16}N_2O_6$: C, 40.67; H, 6.83; N, 11.86%.

(b) To a solution of 390 mg of I in 10 m*l* of water, a mixture of 100 mg of methyl isocyanate, 20 m*l* of acetonitrile and 295 mg of silver carbonate was added. The reaction mixture was heated under reflux on a steam bath for 50 min. After the reaction mixture was cooled, a precipitate was removed by filtration. The filtrate was evaporated under reduced pressure to give a crystalline residue. The residue was recrystallized from aqueous ethanol to give 271 mg (63.8%) of colorless crystals, mp 225—226°C. The product was identified with the product obtained by the method (a), by a mixed melting point determination and a comparison of IR spectra.

***N*-Carbamyl-*N'*-methyl-*N'*-nitroso-*scyllo*-inosamine (IX).** To a solution of 300 mg of VIII in a mixture of 3.8 m*l* of glacial acetic acid and 5.0 m*l* of water, 17.5 m*l* of 0.1 M sodium nitrite solution was added under ice cooling. The reaction mixture was stored in a refrigerator overnight. Crystals (57 mg) appeared in the solution were collected by filtration and washed with acetone to give the product, mp 122—125°C. The filtrate was treated with Amberlite IR-120 to remove a sodium ion and then freeze-dried. The amorphous powder obtained by freeze-drying was recrystallized from aqueous acetone to give 185 mg of the product, mp 123—126°C. The total yield was 72.2%. IR: 1700 (C=O), 1550 (NH) and 1470 cm^{-1} (N–NO). Liebermann nitroso test was positive. NMR (D_2O): τ 6.77 (N–CH_3).

Found: C, 34.60; H, 6.03; N, 14.65%. Calcd for $C_8H_{15}N_3O_7 \cdot H_2O$: C, 33.90; H, 6.05; N, 14.84%.

Acetylation of IX (42 mg) with acetic anhydride (1.0 m*l*) in pyridine (2.0 m*l*) afforded 53 mg (70.7%) of a product, which was identified to be VI by a comparison of IR spectra.

***N*-Carbamyl-*N'*-methyl-*N'*-nitroso-*epi*-inosamine-2 (XI).** To a solution of 600 mg of *epi*-inosamine-2 hydrochloride (X) in 12 m*l* of water, a mixture of 200 mg of methyl isocyanate, 783 mg of silver carbonate and 24 m*l* of acetonitrile was added and the mixture was heated under reflux for 1 hr. The warm mixture was filtered and the filtrate was evaporated under reduced pressure. The residue was dissolved in a small amount of water and the solution was filtered. The filtrate was again evaporated *in vacuo* to give 720 mg of an oily residue.

The residue was dissolved in a mixture of 1 m*l* of water and 3 m*l* of glacial acetic acid. To the solution, 6.0 m*l* of 0.5 M sodium nitrite solution was added under ice cooling, and the mixture was settled at room temperature overnight. Then the reaction mixture was passed through a column of Amberlite IR-120 to remove a sodium ion, and the aqueous solution was freeze-dried. The crude product was recrystallized from methanol to give 592 mg (81.2%) of nice crystals melting at 104°C (dec.). IR: 1720 (C=O), 1540 (NH) and 1475 cm^{-1} (N–NO).

Found: C, 36.52; H, 6.71; N, 14.50%. Calcd for $C_8H_{15}N_3O_7 \cdot CH_3OH$: C, 36.36; H, 6.40; N, 14.14%.

Penta-*O*-acetyl-*N*-carbamyl-*N'*-methyl-*N'*-nitroso-*epi*-inosamine-2 (XII). Acetylation of XI

(180 mg) with 2 m*l* of acetic anhydride and 2 m*l* of pyridine afforded an oily product. The crude product was crystallized from ethanol to give 265 mg (82.1%) of pale yellow crystals, mp 114—116°C. IR: 1755 (OAc), 1530 (NH) and 1490 cm^{-1} (N–NO).

Found: C, 45.59; H, 5.58; N, 8.71%. Calcd for $C_{18}H_{25}N_3O_{12}$: C, 45.47; H, 5.30; N, 8.84%.

Di-*N*,*N*′-(*N*-methyl-carbamyl)-*myo*-inosadiamine-1,3 (XIV). A mixture of 1.32 g of *myo*-inosadiamine-1,3 dihydrochloride (XIII) and 600 mg of methyl isocyanate in 60 m*l* of 65% aqueous acetonitrile was heated under reflux in the presence of 2.0 g of silver carbonate for 70 min. The warm reaction mixture was filtered and the filtrate was evaporated under reduced pressure to give an oily residue. An insoluble material which was obtained by the filtration was extracted with hot water and from the aqueous extract, 676 mg of the product crystallized out as cubic crystals, mp 230—231°C.

The oily residue was dissolved in a small amount of water and ethanol was added to the solution to give a second crop of the product (222 mg), mp 229—231°C. The total yield was 58.9%.

Recrystallization from aqueous ethanol gave fine crystals, mp 230—231°C.

Found: C, 37.34; H, 7.60; N, 16.90%. Calcd for $C_{10}H_{20}N_4O_6 \cdot 2H_2O$: C, 36.58; H, 7.37; N, 17.07%.

Di-*N*,*N*′-(*N*-methyl-*N*-nitroso-carbamyl)-*myo*-inosadiamine-1,3 (XV). A 202 mg portion of XIV was dissolved in a mixture of 2 m*l* of acetic acid and 15 m*l* of water, and 16.4 m*l* of 0.1 M sodium nitrite solution was added to the solution under ice cooling with an occasional shaking. The mixture was mechanically agitated overnight under ice cooling. Then the clear solution was freeze-dried to give 184 mg (76.4%) of the crude product. Recrystallization from ethanol afforded crystals, mp 158—162°C. IR: 1700 (C=O), 1530 (NH) and 1475 cm^{-1} (N–NO). NMR (D_2O): τ 6.78 (N–CH_3).

Found: C, 34.14; H, 5.71; N, 24.32%. Calcd for $C_{10}H_{18}N_6O_8$: C, 34.28; H, 5.18; N, 23.99%.

Antitumor Activity. A detail of the antitumor activities against Ehrlich ascites tumor and HeLa carcinoma will be published elsewhere.

The authors are grateful to Professor Sumio Umezawa for his helpful advice, Dr. Tomoharu Okuda for a biological assay and Mr. Saburo Nakada for his elementary analyses. This research has been supported financially in part by a grant of the Japanese Ministry of Education, to which the authors' thanks are due.

BULLETIN OF THE CHEMICAL SOCIETY OF JAPAN VOL. 43 2956—2959 (1970)

The Constituents of Hops. IV.[1] The Volatile Composition of *Humulus Lupulus* L. *var. cordifolius* Maxim.

Yoko NAYA and Munio KOTAKE

The Institute of Food Chemistry, Dojimanaka, Kita-ku, Osaka

(Received April 18, 1970)

The steam-volatile constituents of *Humulus Lupulus* L. *var. cordifolius* Maxim. have been studied, and 66 compounds of the oil have been identified. Besides the previously-reported principal hop components (myrcene, β-humulene, caryophyllene, β-selinene, δ- and γ-cadinenes), evidence was found for the presence in an abnormally high concentration of others: zingiberene, α-curcumene together with β-bisabolene, and β-sesquiphellandrene, selina-3,7(11)-diene, and selina-4(14),7(11)-diene. A number of oxygenated sesquiterpenoids were detected. The major one was found to be caryophyllene-oxide. The isolated components were identified by spectroscopic or chemical means.

The steam volatile constituents of the horticultural Japanese hop, "Shinshu-wase" (*Humulus Lupulus* L.), were examined; the characterization of most compounds in the oil has already been reported.[1-5] In the present paper, the isolation and identification of volatile compounds contained in the cone oil of a wild variety, "Karahanaso" (*Humulus Lupulus* L. *var. cordifolius* Maxim.), will be reported for the first time.

Experimental

Separation. The air-dried material (9.2 kg) was distilled with steam, and then the distillate was treated by usual methods to remove any acidic compounds.

1) Previous paper of this series: Y. Naya and M. Kotake, *Nippon Kagaku Zasshi*, **91**, 275 (1970).

2) Y. Naya and M. Kotake, *ibid.*, **89**, 1113 (1968).

3) Y. Naya and M. Kotake, *ibid.*, **88**, 1302 (1967).

4) N. Shigematsu and Y. Kitazawa, *Bull. of Brew. Sci.*, **8**, 23 (1962).

5) R. G. Buttery, R. E. Lundin and L. Ling, *Agri. Food Chem.*, **15**, 58 (1967).

The residual oil (17.8 g)(0.19%) was readily separated into the hydrocarbon and the oxygenated constituents by selective adsorption on neutral alumina. The amount of the hydrocarbon fraction was four times that of the oxygenated fraction. The hydrocarbon fraction was divided into three parts by fractional distillation under a pressure of 3 mmHg. Each part was separated into its constituents by a combination of adsorption chromatography (silica-gel or silica-gel impregnated with silver nitrate) and preparative gas-liquid chromatography (SF 96 and a Carbowax 20 M columns). Similar methods were applied to oxygenated compounds, using appropriate adsorbents and columns.

Apparatus. The analytical GLC was carried out using a Hitachi Model K-53 gas chromatograph provided with a flame-ionization detector. The stainless-steel capillary column (0.25 mm in diameter and 45 m in length) used for the analysis was coated with HB 2000; the column temperature was held isothermally at 100°C, and then it was flushed to 150°C. The nitrogen-carrier gas-inlet pressure was set at 1.5 kg/cm² for the initiation and 2.5 kg/cm² at the end.

For preparative gas chromatography, a Model 90-P Varian Aerograph equipped with a thermal conductivity detector was employed. Usually a 10-ft. × 3/8 in. aluminum column packed with 20% Carbowax 20 M on Chromosorb W (60—80 mesh) was used. Helium was the carrier gas, and the column temperature was 100—220°C.

The NMR spectra were measured in CCl_4, using TMS as an internal reference at 60 MHz on a JEOL Model C-60 spectrometer.

The mass spectra were measured with a Hitachi Model RMU-6 Mass Spectrometer; the operating conditions were as follows: ionization energy, 80 eV; ion-accelerating voltage of 2000 V, at temperatures of 250°C and 150°C in the ionization chamber and the sample injection block respectively.

Table 1. The constituents of hydrocarbons

Peak No. in Fig. 1	Identified compound
1	α-Pinene
2	β-Pinene
3	Myrcene
4	Undecane
6	Limonene
7	β-Phellandrene
8	γ-Terpinene
9	Dodecane
15	Tridecane
19	Tetradecane
23	α-Copaene
27	Pentadecane
27	*trans*-α-Bergamotene
28	Caryophyllene
32	β-Humulene
32	β-Farnesene
34	γ-Muurolene
35-1	Hexadecane
37	α-Selinene
37	β-Selinene
38	Zingiberene
39	β-Bisabolene
40	α-Curcumene
40-1	δ-Cadinene
41	γ-Cadinene
43	β-Sesquiphellandrene
44	Selina-4(14),7(11)-diene
45	Selina-3,7(11)-diene
47	Calamenene
49	Heptadecane
53	Octadecane
58-1	Nonadecane

Results and Discussion

The constituents are listed in Tables 1—3, together with the peak number on the programmed

Table 2. The constituents of oxygenated compounds

Peak No.	Identified compound
1-1	2-Methyl-1-butanol
5	3-Methyl-2-buten-1-ol
7-1	2,2,7,7-Tetramethyl-1,6-dioxaspiro[4.4]-non-3-ene
8	2,2,7,7-Tetramethyl-1,6-dioxaspiro[4.4]-nona-3,8-diene
10	Methyl 4-methyl-2-hexenoate
12	Methyl octanoate
14	*trans*-2-Methyl-2-vinyl-5-hydroxyisopropyl-tetrahydrofuran
16	*cis*-2-Methyl-2-vinyl-5-hydroxyisopropyl-tetrahydrofuran
17	4,4-Dimethylcrotonolactone
18	Linalool
20	β-Fenchol
21	Terpinen-4-ol
23	Methyl 8-methylnonanoate
23-1	Pinocarveol
23-2	2-Undecanone
24	4-Undecen-2-one
24	Methyl decanoate
25	Methyl 4-decenoate
25	Nonanol-1
26	α-Terpineol
26	Borneol
30	Methyl geranate
31	Benzyl alcohol
33-1	Nerol
36	Phenyl ethyl alcohol
38-1	Geraniol
46	2-Tridecanone
52	Caryophyllene-oxide
54	Humulene-epoxide-I
55	Humulene-epoxide-II
56	β-Caryophyllene alcohol
57	Nerolidol
61	T-cadinol
64	α-Bisabolol

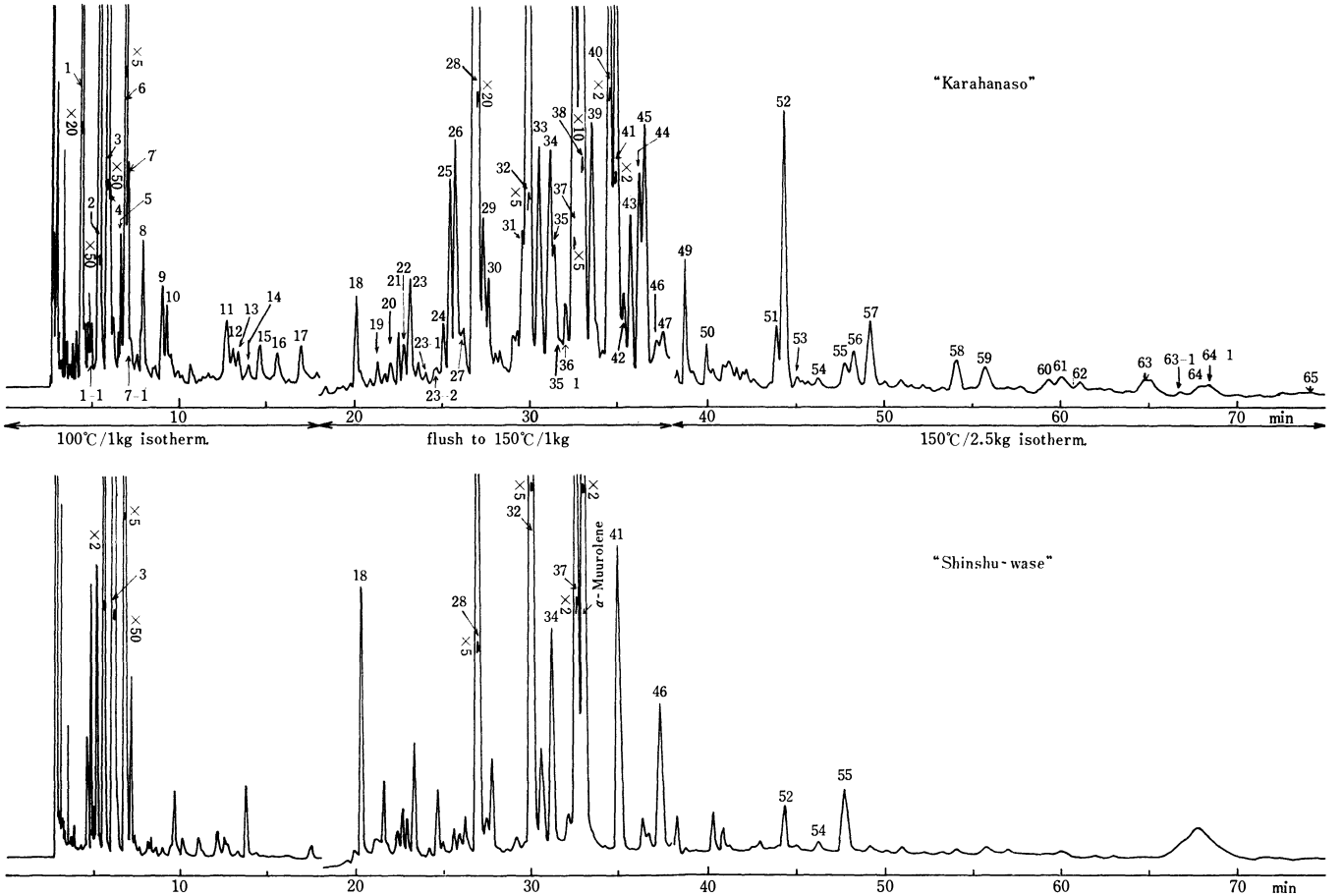

Fig. 1. Comparison of capillary gas-chromatograms obtained for hop oils from "Karahanaso" and "Shinshu-wase". Column 45 m×0.25 mm coated with HB 2000.

Table 3. Tentatively identified or unknown compounds

Peak No.	Compound	Molecular weight	Base peak
10-1	Karahana ether[2]	152	107
	Me-ester $C_{10}H_{20}O_2$	172	74
29	Me-ester $C_{11}H_{18}O_2$	182	85
	Me-ester $C_{12}H_{24}O_2$	200	74
34	Me-ester $C_{12}H_{22}O_2$	198	59
	Me-ester $C_{13}H_{24}O_2$	212	74
	Me-ester $C_{13}H_{22}O_2$	210	79
	Me-ester $C_{14}H_{26}O_2$	226	69
53	Aldehyde $C_{15}H_{24}O$	220	41
	Aldehyde $C_{16}H_{30}O$	238	69
	Aldehyde $C_{17}H_{32}O$	252	41
	Aldehyde $C_{18}H_{34}O$	266	41, 43
	Aldehyde $C_{19}H_{36}O$	280	41, 43
65	Ketone $C_{15}H_{24}O$	220	109
	Ketone $C_{15}H_{26}O$	222	43
	Ketone $C_{17}H_{30}O$	250	43
59	Alcohol $C_{15}H_{26}O$	222	161
63	Bulnesol $C_{15}H_{26}O$	222	59
63-1	Alcohol $C_{15}H_{26}O$	222	166
64	Alcohol $C_{15}H_{26}O$	222	43
64-1	Alcohol $C_{15}H_{24}O$	220	69
65-1	Alcohol $C_{15}H_{24}O$	220	41, 55, 93
32	α-Humulene	204	93
	trans-α-Farnesene	204	69
	Isocaryophyllene	204	93

GLC. Each separated compound was mixed with the original oil, and the peak on the programmed gas-chromatogram was confirmed by an appreciable increase in the height of the particular peak. Authentic compounds were obtained from reliable sources or were prepared by well-established methods. They were purified by GLC separation before use. Identifications are based on at least two physical methods (IR, MS, and NMR). Figure 1 shows a gas chromatogram of the steam volatile oil from "Karahanaso", together with that of the oil from the Japanese "Shinshu-wase," harvested in 1968,*1 for the sake of comparison. Significant differences in the composition are seen in the fingerprinting of GLC analysis. Myrcene, α- and β-humulenes, caryophyllene, β-selinene, α-muurolene, and δ- and γ-cadinenes have been known[1-3] to be major components of "Shinshu wase." In "Karahanaso," myrcene, β-humulene, α- and β-selinenes, and δ- and γ-cadinenes occur in considerable amounts; bisabolane-type sesquiterpene (zingiberene, α-curcumene, together with β-bisabolene, and β-sesquiphellandrene) in an abnormally high concentration, and caryophyllene, in the highest abundance. Unlike the case of "Shinshu-wase", no α-muurolene was detected, whereas evidence was found for the presence of two other selinenes, selina-3,7(11)-diene and selina-4(14),7(11)-diene.

Oxygenated sesquiterpenes occur in relatively small quantities, and caryophyllene-oxide, nerolidol, and β-caryophyllene alcohol have been isolated in certain amounts. The isolation of many GLC peaks with long retention times has shown that each peak is composed of a mixture of several compounds. Most of these appear to be sesquiterpenic alcohols with a molecular weight of 220 or 222.

The authors are deeply indebted to Professor Tsunematsu Takemoto of Tohoku University for supplying "Karahanaso," harvested in 1969 at Miyagi, and to Professor Akira Yoshikoshi for supplying the IR spectrum of synthetic bulnesol.

*1 Previous reports[1-3] have been concerned with "Shinshu-wase" harvested in 1963, the constituests of which were essentially the same as in that harvested in 1968.

BULLETIN OF THE CHEMICAL SOCIETY OF JAPAN VOL. 43 2960—2965 (1970)

Studies on Aminosugars. XXV. The Synthesis of Position Isomers of α-D-Glucopyranosyl-2-deoxystreptamine*[1]

Yoshio NISHIMURA, Tsutomu TSUCHIYA and Sumio UMEZAWA

Department of Applied Chemistry, Faculty of Engineering, Keio University, Koganei-shi, Tokyo

(Received April 27, 1970)

Racemic *O*-isopropylidene derivative of *N,N'*-diethoxycarbonyl-2-deoxystreptamine was glucosidized with 2,3,4,6-tetra-*O*-benzyl-α-D-glucopyranosyl chloride to afford two kinds of position isomers of α-glucoside, which led to 4-*O*-(α-D-glucopyranosyl)- and 6-*O*-(α-D-glucopyranosyl)-2-deoxystreptamine. Structural assignments were made by the determination of Δ[M] of the glucosides in a tetramminecopper(II) sulfate solution.

The preparation of α-glucopyranosides in high yields remains an important problem of carbohydrate chemistry. The Koenigs-Knorr reaction provided a large number of glycopyranosides. However, the reaction leads to the formation of either α- or β-glycoside. In this reaction, the contributing factors for the ratio and the yields of α- and β-glycosides are the stabilities of the anomeric halides, the chemical and stereochemical properties of the group at C-2 in sugars, the interaction of polar substituents with the ring oxygen in sugars, the polar and steric interactions between substituents of both sugar and aglycone molecules in forming the glycosides and the solvent effects. These factors make the reaction complicated.

On the other hand, α-glycosides of 2-deoxystreptamine have received particular attention in recent years in the field of chemistry of antibiotics, since these kinds of glycosides are important components of useful antibiotics such as kanamycins, paromomycins, neomycins, gentamicins, hygromycin B and destomycin.

We have recently reported the total synthesis of kanamycins[1)] as well as the synthesis of paromamine[2)] and neamine[3)]. In relation to these syntheses, we took an interest in the glycosidation reaction between glucose and 2-deoxystreptamine with particular reference to the formation of anomeric *cis* derivatives. The glycosidation reaction involves several interesting problems, such as the difference in reactivity among the three hydroxyl groups of 2-deoxystreptamine for glycosidation, the reaction conditions to force the glucosyl halide into α-glycosidation, the procedure to separate the position isomers formed which are quite similar in their structures, and the method for determination of the position of 2-deoxystreptamine glycosidized. The present paper describes a detailed study of the modified Koenigs-Knorr reaction between 2,3,4,6-tetra-*O*-benzyl-α-D-glucosyl chloride (III) and the racemic *O*-isopropylidene derivative (II) of *N,N'*-diethoxycarbonyl-2-deoxystreptamine (I) as a basic research for the synthesis of more complex α-glycosides of 2-deoxystreptamine.

In order to make the formation of α-linkage favorable, the hydroxyl groups at C-2 and at other carbon atoms of the sugar halide were masked with benzyl groups, which are nonparticipating with the anomeric position and were successfully used in the case of the total synthesis of kanamycins.[1)] Regarding the *O*-isopropylidene derivative of 2-deoxystreptamine, we had already prepared another one, namely, *N,N'*-dicarbobenzoxy-mono-*O*-isopropylidene-2-deoxystreptamine for the synthesis of kanamycins. However, in the present study, the carbobenzoxyl groups were replaced with ethoxycarbonyl groups.

Synthesis of Glucosides. *N,N'*-Diethoxycarbonyldeoxystreptamine (I) was prepared from deoxystreptamine and ethyl chloroformate and acetonated with 2,2-dimethoxypropane in the presence of *p*-toluenesulfonic acid in dimethyl formamide (DMF) to give a racemic mixture (II) of *N,N'*-diethoxycarbonyl-4,5- and 5,6-*O*-isopropylidenedeoxystreptamine in a 71% yield.

*[1] Part XL of "Studies on Antibiotics and Related Substances" by Sumio Umezawa. A part of this paper was read at the 23rd Annual Meeting of the Chemical Society of Japan, Tokyo, April, 1970. (See Abstracts of Papers of the Meeting, Vol. III, p. 1902).

1) S. Umezawa, S. Koto, K. Tatsuta and T. Tsumura, *J. Antibiot.*, **21**, 162 (1968); This Bulletin, **42**, 529 (1969); S. Umezawa, K. Tatsuta and S. Koto, *J. Antibiot.*, **21**, 367 (1968); This Bulletin, **42**, 533 (1969); S. Umezawa, S. Koto, K. Tatsuta, H. Hineno, Y. Nishimura and T. Tsumura, *J. Antibiot.*, **21**, 424 (1968); This Bulletin, **42**, 537 (1969).

2) S. Umezawa and S. Koto, This Bulletin, **39**, 2014 (1966).

3) K. Tatsuta, E. Kitazawa and S. Umezawa, *J. Antibiot.*, **20**, 53 (1967); This Bulletin, **40**, 2371 (1967).

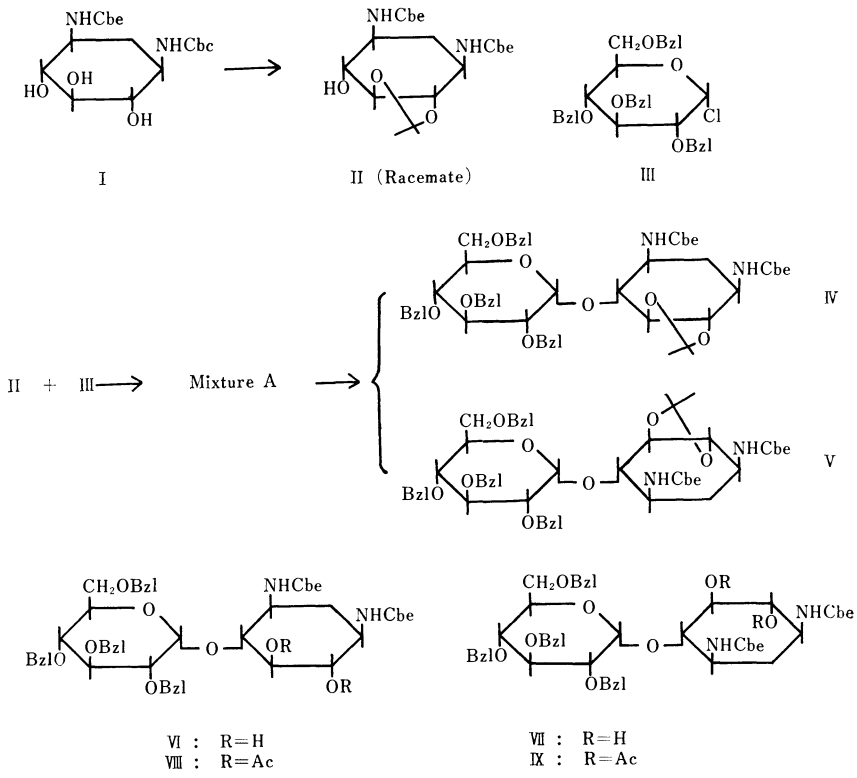

Chart 1. Cbe: $CO_2C_2H_5$ Bzl: $CH_2C_6H_5$

2,3,4,6-Tetra-*O*-benzyl-α-D-glucopyranosyl chloride (III) was prepared by the method of Austin *et al.*[4] The chloride proved to be a homogeneous anomer that was characterized through its NMR spectrum.

The racemic monoisopropylidene derivative (II) was condensed with chloride (III). As in the previous studies on the synthesis of kanamycins,[1] the condensation was similarly effected with the use of mercuric cyanide and Drierite in dioxane-benzene and under an extremely anhydrous condition, which is most important for glycosidation. The crude condensed products (here named mixture A), showed four spots (R_f 0.58, 0.54, 0.46, 0.40) on thin-layer chromatography (TLC). Separation of the mixture A into its components was performed by silica gel column chromatography, and the two products separated (R_f 0.46 and 0.40) were found to be 4-*O*-(2,3,4,6-tetra-*O*-benzyl-α-D-glucopyranosyl)-*N*,*N*′-diethoxycarbonyl-5,6-*O*-isopropylidenedeoxystreptamine (IV) and 6-*O*-(2,3,4,6-tetra-*O*-benzyl-α-D-glucopyranosyl)-*N*,*N*′-diethoxycarbonyl-4,5-*O*-isopropylidenedeoxystreptamine (V), respectively, by their elemental analyses, IR and NMR spectra and also by the fact that they were derivable to 4-*O*- and 6-*O*-(α-D-glucopyranosyl)deoxystreptamine (X and XI), respectively. There is a large difference between IV and V with respect to melting points (62 and 168°C), solubilities in chloroform and the NMR signals assignable to anomeric hydrogens (τ 4.51 and 4.90). This suggests that the products have fairly different conformations as a whole. Another separated, minor product (R_f 0.54) was supposed to be an isomer having β-anomeric configuration.

Compounds IV and V were deisopropylidenated with aqueous acetic acid and gave 4-*O*- and 6-*O*-(2,3,4,6-tetra-*O*-benzyl-α-D-glucopyranosyl)-*N*,*N*′-diethoxycarbonyldeoxystreptamine, respectively (VI and VII).

Separation of mixture A into its components by silica gel column chromatography described above, was, however, troublesome because deisopropylidenation of the compounds took place during chromatography. For this reason, after rough purification by column chromatography with ammonia-treated silica gel, the mixture was subjected to deacetonation by hydrolysis followed by acetylation. Although the hydrolyzate of mixture A showed the presence of products of the same R_f-value and the products could not be separated by chromatography, the acetylated products gave three spots (R_f 0.78, 0.71 and 0.65) on TLC and were successfully separated by column chromato-

4) P. W. Austin, F. E. Hardy, J. G. Buchanan and J. Baddiley, *J. Chem. Soc.*, **1964**, 2128.

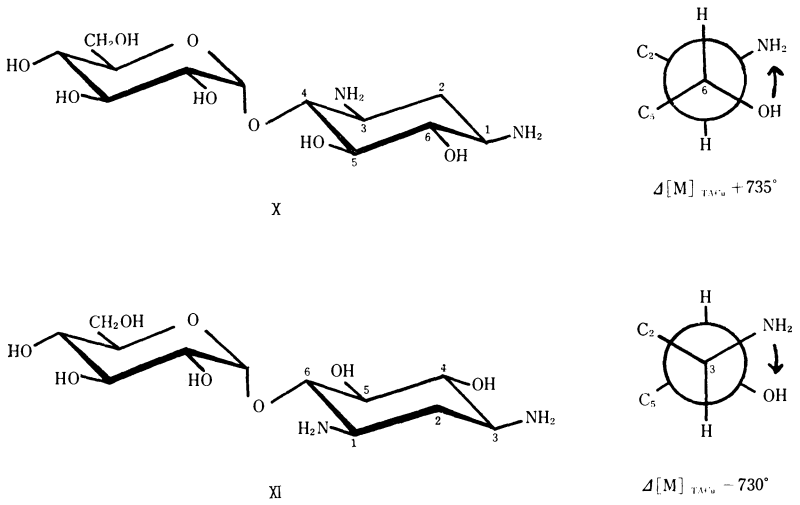

Chart 2.

graphy. The resulting diacetyl derivatives VIII (R_f 0.65) and IX (R_f 0.78) were identical with those derived from the above mentioned pure deisopropylidenation products (VI and VII) by acetylation, and the result indicated that VIII is 5,6-di-*O*-acetyl-4-*O*-(2,3,4,6-tetra-*O*-benzyl-α-D-glucopyranosyl)-*N*,*N*′-diethoxycarbonyldeoxystreptamine and IX is 4,5-di-*O*-acetyl-6-*O*-(2,3,4,6-tetra-*O*-benzyl-α-D-glucopyranosyl)-*N*,*N*′-diethoxycarbonyldeoxystreptamine. The overall yields of VIII and IX from II were 17 and 30%, respectively. It is noteworthy that the hydroxyl group at C-6 in 2-deoxystreptamine is more favorably glycosidated than the hydroxyl group at C-4. This indicates that the unsymmetrical structure of the sugar component greatly influences its approach to the 2-deoxystreptamine component.

VIII and IX were then hydrogenolyzed with palladium black and hydrogen to give debenzylated products, which were then deacetylated and de-*N*-ethoxycarbonylated in a hot barium hydroxide solution to give the final products 4-*O*- and 6-*O*-(α-D-glucopyranosyl)deoxystreptamine (X and XI) in 42 and 57% yield, respectively.

Photolysis of VII was attempted with the aid of bromine according to BeMiller, Meyers and Wing.[5] Removal of benzyl groups proceeded with ease. However, it was found that photolysis was always accompanied by hydrolysis of glycosidic linkage. Addition of powdered potassium hydroxide improved the situation. However, the yield of the product was still variable (95—30%).

Structural Assignment. The problem to differentiate the positional isomers was solved by the determination of Δ[M] in a tetramminecopper (II) sulfate solution (TACu). This reagent was first introduced by Umezawa, Tsuchiya and Tatsuta.[6] Unlike Cupra B[7] or ammoniacal cuprous chloride solution[6] (CuAm), this reagent forms a copper complex with vicinally situated amino and hydroxyl groups without being disturbed by the presence of any other vicinally situated hydroxyl groups. In a six-membered chair-form, a pair of vicinally situated *trans*-diequatorial amino and hydroxyl groups gives a value $\Delta[M]_{TACu}$*2 −900 or +900° according to whether the projection angle*3 between the pair groups (~60°) is clockwise or counterclockwise. X gave $\Delta[M]_{TACu}$ +735°. This value indicates that the copper complex is formed between 1-amino and 6-hydroxyl groups of 2-deoxystreptamine moiety, showing X to be 4-*O*-(D-glucosyl)deoxystreptamine. XI gave $\Delta[M]_{TACu}$ −730°, indicating XI to be 6-*O*-(D-glucosyl)deoxystreptamine.

Experimental

The NMR spectra were measured with a Varian A-60D spectrometer unless otherwise stated. Thin-layer chromatography was carried out on microscope slides coated with silica gel.

***N*,*N*′-Diethoxycarbonyl-2-deoxystreptamine (I).** To a solution of deoxystreptamine dihydrochloride (6 g) and anhydrous sodium carbonate (27 g) in water (150 m*l*) ethyl chloroformate (10.2 m*l*) was added with

5) *C. f.*, *Chem. & Eng. News*, April 24, 51 (1967).

6) S. Umezawa, T. Tsuchiya and K. Tatsuta, This Bulletin, **39**, 1235 (1966).

7) R. E. Reeves, "Advances in Carbohydrate Chemistry," Vol. 6, Academic Press, New York (1951), p. 107.

*2 $\Delta[M]_{TACu} = ([\alpha]_{436}TACu - [\alpha]_{436} \text{ in water}) \times \frac{\text{Mol. wt.}}{100}$

*3 See footnote of Reference 6 on page 1235.

vigorous stirring. The mixture was then stirred at room temperature for 4 hr and allowed to stand overnight. Inorganic precipitate was filtered and washed with methanol. The filtrate and the washings were combined and evaporated to give a residue, which was dissolved in hot dioxane, filtered, and the filtrate was evaporated. The resulting solid was recrystallized from methanol; yield 7.38 g (94%), mp 231—232°C, $[\alpha]_D^{19}$ ~0° (*c* 0.75, water); IR (KBr): 3450 (broad, OH), 3350 (amide, *ν* NH), 1695 (NHCOO), 1545 (amide II), 1470 (w), 1375 (w), 1305, 1240, 1045, 857, 780 cm^{-1}.

Found: C, 47.18; H, 7.26; N, 8.99%. Calcd for $C_{12}H_{22}N_2O_7$: C, 47.02; H, 7.24; N, 9.15%.

Racemic Mixture (II), *N,N'*-Diethoxycarbonyl-4,5 and 5,6-*O*-isopropylidene-2-deoxystreptamine. A solution of I (3.98 g), 2,2-dimethoxypropane (7 m*l*) and fuse-dried *p*-toluenesulfonic acid (82 mg) in DMF (46 m*l*) was heated on a bath (110°C) for 4 hr, cooled, and neutralized with ethanol-washed Amberlite IRA-400 (OH form). A thin-layer chromatogram (benzene-ethanol 5 : 1) of this solution showed that the starting material (I, R_f 0.16) disappeared and II (R_f 0.53) appeared as a single spot. The solution was evaporated *in vacuo* and further coevaporated with water and with a mixture of toluene and ethyl acetate to give a solid, which was recrystallized from ethyl acetate; yield 3.18 g (71%), mp 199—200°C, $[\alpha]_D^{21}$ ~0° (*c* 1, methanol); IR(KBr): ~3400 (broad), 3330; 1725, 1710, 1690 (amide I); 1560 (sh.), 1550, 1540 (amide II); 1450 (w); 1382, 1372 (isopropylidene); 1310, 1220, 1045, 840, 780 cm^{-1}; NMR(methanol-d_4): *τ*: 8.75 (6-p. t., *J* 7.1 Hz, $CH_2C\underline{H}_3$), 8.57 (6-p. s., isopropylidene), 8.2—9.0 (1-p. H_{ax}-2, overlapped with methyl and isopropylidene signals), 7.8 (1-p. doublet of triplets, *J* ~13 and ~3.5 Hz), 6.2—6.7 (5-p. m., H-1,3,4,5,6), 5.87 (4-p. q., $C\underline{H}_2CH_3$). NMR(DMSO-d_6) : *τ*: 8.81 (6-p. t., $CH_2C\underline{H}_3$), 8.62 (6-p. s., isopropylidene), 8.4—9.0 (H_{ax}-2 N), 8.2 (1-p. broad doublet, H_{eq}-2), 6.3—6.8 (5-p. m.), 5.95 (4-p. q., $C\underline{H}_2CH_3$), 4.9 (1-p.), 3.05 (1-p. d.), 2.83 (1-p. d.). NMR(pyridine-d_5): *τ*: 8.87 (6-p. t., CH_2-$C\underline{H}_3$), 8.52 (6-p. s.), 8.05 (1-p. q., *J* ~12 Hz, H_{ax}-2), 7.22 (1-p. doublet of triplets, *J* ~13 and ~3.5 Hz, H_{eq}-2), 5.6—6.3 (5-p. m.), 5.82 (4-p. q., $C\underline{H}_2CH_3$), 3.5 (1-p.), 2.18 (1-p. d., *J* 8 Hz), 1.98 (1-p. d., *J* 8 Hz).

In pyridine-d_5, the signals assignable to H_{ax}-2 appeared without being overlapped with other signals, and H_{ax}-2, H_{eq}-2 and skeleton hydrogens resonated at lower fields than that measured in methanol-d_4 or dimethyl sulfoxide-d_6.

Found: C, 51.83; H, 7.72; N, 8.03%. Calcd for $C_{15}H_{26}N_2O_7$: C, 52.01; H, 7.57; N, 8.09%.

2,3,4,6-Tetra-*O*-benzyl-*α*-D-glucopyranosyl Chloride (III). This compound was prepared by the method of Austin *et al*[4]. except that, in the final step, the product was purified by passing a short column of silica gel with dry benzene-methyl ethyl ketone (10 : 1). Syrup, $[\alpha]_D^{20}$ +116° (*c* 1, benzene)(lit,[4] +95° in benzene), R_f 0.89 (TLC, benzene - methyl ethyl ketone 10 : 1). NMR($CDCl_3$): *τ*: 5.6—6.6 (6-p. skeleton hydrogens), 4.8—5.6 (8-p. m., $C\underline{H}_2C_6H_5$), 3.85 (1-p. d., *J* 3.5 Hz, H-1), 2.5—2.8 (20-p. m., phenyl).

Preparation of Mixture A. To a solution of III (2.4 g) in dry benzene (18 m*l*) and dry dioxane (6 m*l*) II (1.2 g), freshly prepared powder Drierite (2.1 g), and well dried powder mercuric cyanide (2.2 g) were added, and the mixture was refluxed for 4 hr with vigorous stirring. The reaction mixture was filtered with the aid of Celite and the residue was washed with chloroform. The filtrate and the washings were combined and evaporated to give a viscous solid, which was dissolved in chloroform, filtered, and the solution was washed with 2% sodium bicarbonate solution, then with water, dried over sodium sulfate and evaporated to give a solid (3.2 g). On TLC with benzene - methyl ethyl ketone (5 : 1), the solid (mixture A) showed five spots of R_f 0.40 (V), 0.46 (IV), 0.54, 0.58 and 0.71, the last being 2,3,4,6-tetra-*O*-benzyl-D-glucose.

Separation of Mixture A into 4-*O*-(2,3,4,6-Tetra-*O*-benzyl-*α*-D-glucopyranosyl)-*N,N'*-diethoxycarbonyl-5,6-*O*-isopropylidene-2-deoxystreptamine (IV) and 6-*O*-(2,3,4,6-Tetra-*O*-benzyl-*α*-D-glucopyranosyl)-*N,N'*-diethoxycarbonyl-4,5-*O*-isopropylidene-2-deoxystreptamine (V). The chromatographic separation of the crude mixture A into its components with the use of silica gel (Mallinckrodt, or most kinds of silica gel purchased from Kanto-Kagaku, with or without treating with ammonia*[4]) was unsuccessful in most cases owing to de-*O*-isopropylidenation of the components during the procedure; a kind of silica gel purchased from Kanto-Kagaku successfully achieved the separation: The mixture A (3 g) was chromatographed on a silica gel column (Kanto-Kagaku, 300 g, 45×480 mm) with dry benzene - methyl ethyl ketone (9 : 2) and the portions containing pure IV and V, respectively, were separated from overlapping portions; the result of a typical run was as follows: the portion containing the substances of R_f 0.58 and 0.71 weighed 0.13 g; R_f 0.54, 0.25 g (part A); R_f 0.54 and 0.46, 0.32 g; R_f 0.46 (IV), 0.35 g (part B); R_f 0.46 and 0.40, 0.59 g; R_f 0.40 (V), 0.53 g (part C).

Part A was recrystallized from methanol to give crystals; mp 232—234°C, $[\alpha]_D^{19}$ +13° (*c* 1, chloroform); IR (Nujol): 3340 (*ν*NH), 1690, 1550, 1300, 1290, 1145, 1080, 1040, 775; 730, 712, 693 cm^{-1} (phenyl).

Found: C, 68.02; H, 6.96; N, 3.05%. Calcd for $C_{49}H_{60}N_2O_{12}$: C, 67.73; H, 6.96; N, 3.22%.

The substance was supposed to be an isomer having *β*-anomeric configuration.

Part B could not be crystallized from any solvent tested; amorphous solid (IV); mp 60—62°C $[\alpha]_D^{18}$ +31.7° (*c* 1, chloroform); IR(Nujol): 3330; 1725, 1710, 1695 (amide I); 1550 (sh.), 1530 (amide II); 1255, 1220, 1155, 1135, 1065, 1040, 1025, 840, 775; 730, 695 cm^{-1} (phenyl); NMR($CDCl_3$) : *τ* : 8.83 and 8.76 (3-p. t. each, *J* 7.1 Hz, $CH_2C\underline{H}_3$), 8.57 (6-p. s., isopropylidene), 5.9—6.8 (15-p. skeleton hydrogens and $C\underline{H}_2CH_3$), 4.95—5.6 (8-p, $C\underline{H}_2C_6H_5$), 4.51 (1-p. d., *J*~3.5 Hz, H-1′), 2.6—2.9 (20-p. m., phenyl).

Found: C, 67.94; H, 6.90; N, 3.11%. Calcd for $C_{49}H_{60}N_2O_{12}$: C, 67.73; H, 6.96; N, 3.22%.

Part C was recrystallized from methanol to give V; mp 167—168°C, $[\alpha]_D^{19}$ +53° (*c* 1, methanol). This compound, unlike the above compound (IV), is scarcely soluble in cold chloroform. IR(Nujol): 3340; 1690 (amide I); 1550 (sh.), 1530 (amide II); 1275, 1220, 1160, 1065, 1040, 840, 775; 730, 695 cm^{-1} (phenyl); NMR (in warm $CDCl_3$) : *τ* : 8.83 and 8.78 (3-p. t. each, *J* 7.1 Hz, $CH_2C\underline{H}_3$), 8.62 (6-p. s., isopropylidene), 5.7—6.8 (15-p., skeleton hydrogens and ($CH_2C\underline{H}_3$),

*4 See Experimental for the preparation of X and XI.

5.1—5.6 (8-p.) $C\underline{H}_2C_6H_5$), 4.90 (1-p. d., J ~3.5 Hz, H-1'), 2.6—2.9 (20-p. m., phenyl).

Found: C, 67.81; H, 7.16; N, 3.21%. Calcd for $C_{49}H_{60}N_2O_{12}$: C, 67.73; H, 6.96; N, 3.22%.

6-*O*-(2,3,4,6-Tetra-*O*-benzyl-α-D-glucopyranosyl)-*N*,*N*'-diethoxycarbonyl-2-deoxystreptamine (VII). The solution of V (0.30 g) in 80% aqueous acetic acid (4 ml) was heated at 80°C for 5 min. Product (VII) appeared as a single spot (TLC, R_f 0.36 with benzene-ethanol 10 : 1). The solution was poured into water and the resulting precipitates were filtered and washed throughly with water. The soild was recrystallized from acetone; yield 0.23 g (80%); mp 212—213°C, $[\alpha]_D^{18}$ +15° (c 1, chloroform); IR(KBr): 3580 (sh.), 3520, 3360, 1700, 1550, 1457 (w), 1355, 1305, 1270, 1250, 1230, 1110, 1080 (sh), 1065, 1030, 915 (w), 865 (w), 780, 748, 740, 697 cm^{-1}; NMR($CDCl_3$): τ : 8.84 and 8.78 (3-p. t. each, J 7.1 Hz, $CH_2C\underline{H}_3$), 5.92 and 5.87 (2-p. q. each, J 7.1 Hz, $C\underline{H}_2CH_3$), 5.05—5.65 (9-p. $C\underline{H}_2C_6H_5$ and an anomeric hydrogen(?)), 2.6—2.8 (20-p. m., phenyl).

Found: C, 66.81; H, 6.88; N, 3.40%. Calcd for $C_{16}H_{56}N_2O_{12}$: C, 66.65; H, 6.81; N, 3.38%.

4-*O*-(2,3,4,6-Tetra-*O*-benzyl-α-D-glucopyranosyl)-*N*,*N*'-diethoxycarbonyl-2-deoxystreptamine (VI). Compound IV was treated likewise as above and the product was recrystallized from acetone; yield 75%; mp 185—186°C, $[\alpha]_D^{20}$ +28° (c 1, chloroform); IR (KBr): 3580 (sh.), 3450 (broad), 3360, 1695, 1550 (sh.), 1540, 1457 (w), 1362, 1315, 1295, 1285, 1250, 1250, 1225, 1085, 1065, 1040, 1030 (sh.), 865 (w), 780, 745, 735, 697 cm^{-1}; NMR($CDCl_3$): τ : 8.84 and 8.78 (3-p. t. each, J 7.1 Hz, $CH_2C\underline{H}_3$), 5.95 and 5.88 (2-p. q. each, J 7.1 Hz, $C\underline{H}_2CH_3$), 5.05—5.6 (9-p., $C\underline{H}_2$-C_6H_5 and an anomeric hydrogen(?)), 2.6—2.8 (20-p. m., phenyl).

Found: C, 66.76; H, 7.19; N, 3.40%. Calcd for $C_{46}H_{56}N_2O_{12}$: C, 66.65; H, 6.81; N, 3.38%.

5,6-Di-*O*-acetyl-4-*O*-(2,3,4,6-tetra-*O*-benzyl-α-D-glucopyranosyl)-*N*,*N*'-diethoxycarbonyl-2-deoxystreptamine (VIII) and 4,5-Di-*O*-acetyl-6-*O*-(2,3,4,6-tetra-*O*-benzyl-α-D-glucopyranosyl)-*N*,*N*'-diethoxycarbonyl-2-deoxystreptamine (IX). *a*) As the chromatographic separation of mixture A into pure IV and V was troublesome, a mixture mainly consisting of IV and V was first obtained as follows: Mixture A (3.2 g) was chromatographed on a silica gel column (260 g, 33×730 mm) with chloroform ethyl acetate (3 : 1) and the portion (1.5 g) containing mainly IV and V was separated. The mass was again chromatographed by the same procedure to give a solid (1.26 g) which showed three spots (R_f 0.40 (V), 0.46 (IV) and 0.54) on TLC with benzene-methyl ethyl ketone (5 : 1). The silica gel used in this experiment was prepared[8] as follows: Mallinckrodt silica gel in 6N aqueous ammonia was allowed to stand overnight, filtered and activated at 150°C for 3 hr on a flat plate.

b) *Deisopropylidenation.* A solution of the solid (1.26 g) in 50% aqueous acetic acid (20 ml) was heated at 80°C for 1 hr. The products showed the same R_f-value (0.36, TLC with benzene-ethanol 10 : 1) The solution was poured into water and the precipitates were filtered to give a soild, 1.16 g (97%).

c) *Acetylation and Chromatography.* A solution of the solid (1.14 g) in pyridine (5 ml) and acetic anhydride (5 ml) was allowed to stand at 50°C overnight. The reaction mixture showed three spots (R_f 0.78, 0.71 and 0.65) on TLC with chloroform-ethyl acetate (3 : 1). The mixture was poured into water and the resulting syrup was dissolved in chloroform. The solution was washed throughly with water, dried over sodium sulfate and evaporated to give a pale yellow solid. This was chromatographed on a silica gel column (Mallinckrodt, 300 g, 33×750 mm) with chloroform-ethyl acetate (3 : 1), and the eluates containg the substance of R_f 0.78, 0.71 and 0.65 (TLC with the above solvent system) were separated respectively and evaporated to give amorphous solids 0.48 g (IX), 0.11 g and 0.26 g (VIII).

Compound VIII, mp 71—73°C, $[\alpha]_D^{19}$ +25° (c 1, methanol); IR(KBr): 3400; 1745, 1725 (ester); 1705 (amide I); 1540 (amide II); 1455, 1375 (sh.), 1365, 1230, 1150, 1090, 1070, 1035, 910, 850, 775, 735, 695 cm^{-1}; NMR (in $CDCl_3$ with a Japan Electron Optics 4H-100 spectrometer at a frequency of 100 MHz): τ: 8.86 and 8.78 (3-p. t. each, J 7.1 Hz, $CH_2C\underline{H}_3$), 8.18 and 7.98 (3-p. s. each, OAc), 6.1—6.8 (9-p. unresolved m.), 5.93 and 5.88 (2-p. q. each, J 7.1 Hz, $C\underline{H}_2CH_3$), 5.46, 5.30 and 5.15 (2-p. s. each, $C\underline{H}_2C_6H_5$), at τ 5.64, 5.46, 5.25 and 5.07 (2-p. AB quartet, $C\underline{H}_2C_6H_5$, J 11 Hz), 5.0—5.7 (2-p., overlapped with $C\underline{H}_2C_6H_5$; H-5,6), 4.92 (1-p. d., H-1', J~3 Hz), 2.6—2.8 (20-p. m., phenyl).

Found: C, 65.85; H, 6.47; N, 3.19%. Calcd for $C_{50}H_{60}N_2O_{14}$: C, 66.09; H, 6.58; N, 3.39%.

Compound IX, mp 61—63°C, $[\alpha]_D^{19}$ +61° (c 1, methanol); IR(KBr): 3340; 1750, 1725 (ester); 1705 (amide I); 1530 (amide II); 1455, 1375 (sh.), 1365, 1230, 1150, 1070, 1040, 910, 850, 775, 735, 695 cm^{-1}; NMR (100 MHz, in $CDCl_3$): τ : 8.86 and 8.78 (3-p. t. each, J 7.1 Hz, $CH_2C\mathit{H}_3$), 8.03 and 7.98 (3-p. s. each, OAc), 6.9—7.4 (1-p. m., $\underline{H}_{eq}$-2), 6.1—6.8 (9-p. unresolved m., H-1,3,6,2',3',4',5',6',6''), 5.93 and 5.88 (2-p. q. each, J 7.1 Hz, $C\mathit{H}_2CH_3$), 5.50, 5.23 and 5.10 (2-p. s. each, $C\underline{H}_2C_6H_5$), at τ 5.60, 5.42, 5.18 and 5.00 (2-p. AB quartet, $C\underline{H}_2C_6H_5$, J 11 Hz), 5.0—5.7 (2-p., overlapped with $C\underline{H}_2C_6H_5$; H-4,5), 4.90 (1-p. d., H-1', J ~3.5 Hz), 2.6—2.8 (20-p. m., phenyl).

Found: C, 66.31; H, 6.88; N, 3.13%. Calcd for $C_{50}H_{60}N_2O_{14}$: C, 66.09; H, 6.58; N, 3.39%.

The signals which differentiate VIII and IX are those assignable to one of the acetyls (the one lying in the higher field), the benzyls and the phenyls (VIII has one prominent peak and IX has three prominent peaks), and the feature suggests that VIII and IX have conformations differing as a whole from each other. The difference in chemical shifts assignable to the anomeric hydrogens in VIII and IX was unexpectedly small.

Preparation of VII from IX, and VI from VIII. To a solution of IX (444 mg) in methanol (8 ml) 2.4N sodium methylate in methanol (0.2 ml) was added and the solution was allowed to stand for 1 hr, whereupon some crystals deposited. Chloroform was added to the mixture and the resulting solution was treated with Dowex 50 W×8 (H^+ form). The resulting solution was evaporated to give a residue, which was recrystallized from acetone; colorless crystals (350 mg, 87%), mp 212—213°C, $[\alpha]_D^{20}$ +15° (c 1, chloroform). Its IR and NMR spectra were identical with those of the specimen obtained from V.

8) J. G. Buchanan and J. C. P. Schwarz, *J. Chem. Soc.*, **1962**, 4770.

VI was obtained similarly from VIII in 91% yield.

6-*O*-(α-D-Glucopyranosyl)-2-deoxystreptamine (XI). A solution of VII (286 mg) in a mixture of methanol (15 m*l*), water (7 m*l*) and acetic acid (3 m*l*) was hydrogenated with freshly prepared palladium balck and hydrogen at 45°C under 50 lb/inch pressure overnight. The starting material (R_f 1.0, TLC with benzene-ethanol 1 : 1) disappeared and a product having R_f-value of 0.4 appeared. The solution was filtered, the filtrate was evaporated to give a colorless solid which was dissolved in 1 N barium hydroxide (30 m*l*) and the solution was heated at 90°C for 2 hr. After neutralizing the mixture with a slight excess of 2 N sulfuric acid followed by centrifugation, the supernatant layer was treated with a small volume of Dowex 1×2 (OH form), and evaporated to give a solid (100 mg) which gave a single spot on paper chromatography ($R_{f\text{deoxystreptamine}}$ 0.70, with *n*-butanol-pyridine-water-acetic acid 6 : 4 : 3 : 1). An aqueous solution of the solid was then passed through a column of Dowex 1×2 (OH form, 8 m*l*) with water, and ninhydrin-positive fraction (with 0.5% ninhydrin in pyridine) was evaporated to give a colorless solid of XI (75 mg, 66%); mp 231—232°C (decomp.), $[\alpha]_D^{15}$ +102° (*c* 0.1, water), $[\alpha]_{436}^{15}$ +186° (*c* 0.1, water), $[\alpha]_{436}^{15}$ −40° (*c* 0.1, TACu), therefore, $\Delta[M]_{TACu} = -730°$ (Mol. wt. 324.3): IR(KBr): 3400 (broad), 1625 (NH_2), 1145, 1115, 1035, 940, 915 (w), 840, 770 cm^{-1}.

Found: C, 44.21; H, 7.45; N, 8.46%. Calcd for $C_{12}H_{24}N_2O_8$: C, 44.43; H, 7.15; N, 8.64%.

On hydrolysis of XI with 6 N hydrochloric acid at 90°C for 5 hr, paper chromatography (with *n*-butanol-pyridine-water-acetic acid 6 : 4 : 3 : 1) of the hydrolyzate showed two spots corresponding to deoxystreptamine and glucose ($R_{f\text{deoxystreptamine}}$ 3.4).

4-*O*-(α-D-Glucopyranosyl)-2-deoxystreptamine (X). A solution of VIII (150 mg) in a mixture of methanol (10 m*l*), water (5 m*l*) and acetic acid (2.5 m*l*) was hydrogenated likewise as in the preparation of XI. However, in this case, the hydrogenation had to be repeated with fresh catalyst in order to complete the reaction. The resulting product was hydrolyzed with barium hydroxide. The crude product (58 mg) was chromatographed on a cellulose column (10×150 mm) with *n*-butanol-water-ethanol (5 : 2 : 1) and the portion (36 mg) containing X ($R_{f\text{deoxystreptamine}}$ 0.81) was further purified by passing Dowex 1×2 (OH form, 5 m*l*) column to give a hygroscopic solid (27 mg, 46%); $[\alpha]_D^{15}$ +127° (*c* 0.15, water), $[\alpha]_{436}^{15}$ +238° (*c* 0.15, water), $[\alpha]_{436}^{15}$ +465° (*c* 0.15, TACu), $\Delta[M]_{TACu}$ = +735° (Mol. wt. 324.3); IR(KBr): 3300—3400, 1635, 1600, 1145, 1035, 920, 915 (w), 840, 770 cm^{-1}.

Found: C, 44.28; H, 6.90; N, 8.51%. Calcd for $C_{12}H_{24}N_2O_8$: C, 44.43; H, 7.15; N, 8.64%.

On hydrolysis with 6 N hydrochloric acid, X gave glucose and deoxystreptamine.

Preparation of XI by the Photolysis of VII. To a solution of VII (264 mg) in chloroform (15 m*l*) bromine (200 mg) and powered potassium hydroxide (70 mg) were added and the mixture was irradiated with a 60 W lamp from a close distance for 30 min at 0°C under vigorous stirring. More bromine (200 mg) was added and the irradiation was continued for 30 min. The supernatant solution was decanted and the insoluble matter was washed with chloroform. The combined solution and the washings were evaporated to give a solid which was dissolved in 1 N barium hydroxide solution (80 m*l*) and heated at 90°C for 2 hr. After neutralization with a slight excess of 2 N sulfuric acid followed by centrifugation, the supernatant layer was treated with a small volume of Dowex 1×2 (OH form) and the solution was evaporated to give a colorless solid, which showed two spots of $R_{f\text{deoxystreptamine}}$ 0.70 (XI, major) and 1.0 (deoxystreptamine, minor) on paper chromatography with *n*-butanol-pyridine-water-acetic acid (6 : 4 : 3 : 1). An aqueous solution of the solid was chromatographed on a column (10 m*l*) of Dowex 1×2 (OH form) with water and the eluate containing XI was evaporated to give a solid (95 mg, 92%), which was recrystallized from a mixture of ethanol-water-acetone; mp 230°C (decomp.) $[\alpha]_D^{15}$ +102° (*c* 0.3, water). $\Delta[M]_{TACu}$ and IR spectrum were identical with those of the specimen obtained from IX.

The authors wish to thank Mr. Saburo Nakada for carrying out elementary analysis.

BULLETIN OF THE CHEMICAL SOCIETY OF JAPAN VOL. 43 2966—2969 (1970)

Aminosugars. XVIII. Synthesis of 3-Acetamido-3,5-dideoxy-D-ribose*[1]

Hiroaki ANDO and Juji YOSHIMURA

Laboratory of Chemistry for Natural Products, Faculty of Science, Tokyo Institute of Technology, Ookayama, Meguro-ku, Tokyo

(Received April 28, 1970)

3-Acetamido-3,5-dideoxy-1,2-*O*-isopropylidene-α-D-ribofuranose (**5**) was synthesized through two pass-ways: 1) starting from 3-acetamido-3-deoxy-1,2-*O*-isopropylidene-α-D-allofuranose which is obtained from D-glucose, through five steps; periodate oxidation, hydrogenation, 5-*O*-tosylation, 5-iodination and hydrogenation: 2) starting from 1,2-*O*-isopropylidene-3,5-di-*O*-tosyl-α-D-xylofuranose through four steps; 5-iodination, hydrogenation, 3-amination and *N*-acetylation. Total yields in the two pass-ways were 12.7% and 7.6% from the parent aldoses, respectively. Hydrolysis of **5** gave the titled compound as a sirup, which was converted to the crystalline osazone. The structure and conformation of intermediates in these syntheses were examined by NMR spectroscopy.

Since 3-amino-3-deoxy-D-ribose has been found as a component of puromycin[1] and synthesized,[2-4] a numerous homologues of pentoses and hexoses have been reported,[5] but 3-amino-3,5-dideoxy-D-ribose is not yet described in literatures. As an intermediate for a total synthesis of kasugamine,[6] the authors synthesized 3-acetamido-3,5-dideoxy-D-ribose (**9**) by two pass-ways.

Results and Discussion

Lemieux and Chu[3] have synthesized 3-amino-3-deoxy-D-ribose hydrochloride from 3-acetamido-3-deoxy-1,2;5,6-di-*O*-isopropylidene-α-D-allose[7] which is derived from 1,2 ; 5,6-di-*O*-isopropylidene-3-*O*-tosyl-α-D-glucofuranose, by partial hydrolysis to the corresponding 1,2-*O*-isopropylidene derivative (**1**), and followed by periodate oxidation, hydrogenation and hydrolysis. In this process, the authors have improved the condition of partial hydrolysis, and newly isolated 5,6-di-*O*-acetate of **1** and 3-acetamido-3-deoxy-1,2-*O*-isopropylidene-α-D-ribofuranose (**2**) as a crystalline form. Tosylation of **2** in pyridine gave the corresponding 5-*O*-tosylate (**3**) in 68% yield, which was then converted into the 5-iodo-5-deoxy derivative (**4**) in a quantitative yield by heating at 110°C for 2 hr with sodium iodide in acetonitrile. Hydrogenation of **4** in the presence of Raney nickel and triethylamine gave the corresponding 5-deoxy derivative (**5**) in 91% yield.

As another method for the preparation of **5**, 1,2-*O*-isopropylidene-3,5-di-*O*-tosyl-α-D-xylofuranose[8] (**6**) was treated with sodium iodide at 90°C for 20 hr in acetonitrile to give the corresponding 5-iodo-5-deoxy derivative (**7**) in 70% yield. Hydrogenation of **7** in the presence of Raney nickel gave in 70% yield the corresponding 5-deoxy derivative (**8**), which was then converted to **5** by heating with anhydrous hydrazine at 140°C, followed by hydrogenation and *N*-acetylation. Total yield of **5** in the two pass-ways mentioned above were 12.7% and 7.6% from D-glucose and D-xylose, respectively. Treatment of **5** with 60% acetic acid at 95°C for 3 hr gave **9** as a sirup in 95% yield. Crystallization of *N*-phenyl-glycosylamine of **9** was failed, but, further reaction of phenylhydrazine gave the corresponding osazone (**10**) as an yellow crystals.

Lemieux and Chu[3] have corrected the misunderstanding on the configuration of the 3-amino group of **1**[7] by comparison of X-ray powder photograph and IR spectrum of 3-amino-3-deoxy-D-ribose hydrochloride with that of the corresponding natural product, however, the structure of new compounds obtained here were proved by NMR spectra. As representative examples, the spectrum

*1 Part XVII: This Bulletin, **42**, 2352 (1969).

1) C. W. Waller, P. W. Fryth, B. L. Hutchings and J. H. Williams, *J. Amer. Chem. Soc.*, **75**, 2025 (1953).

2) B. R. Baker, R. E. Schaub and J. H. Williams, *ibid.*, **77**, 7 (1955).

3) R. U. Lemieux and Paul Chu, *ibid.*, **80**, 4745 (1958).

4) H. H. Baer and Ivan Furic, *J. Org. Chem.*, **33**, 3731 (1968).

5) L. Hough and A. C. Richardson, "Rodd's Chemistry of Carbon Compounds," Elsevier Publishing Company, Amsterdam, Vol. 1, (1967), Part F, p. 482.

6) Y. Suhara, K. Maeda and H. Umesawa, *J. Antibiotics*, **18A**, 182, 184, 187, 267 (1965); **19A**, 49 (1966).

7) M. L. Wolfrom, F. Shafizadeh and R. K. Armstrong, *J. Amer. Chem. Soc.*, **80**, 4885 (1958).

8) P. Karrer and A. Boëttcher, *Helv. Chim. Acta*, **36**, 837 (1958).

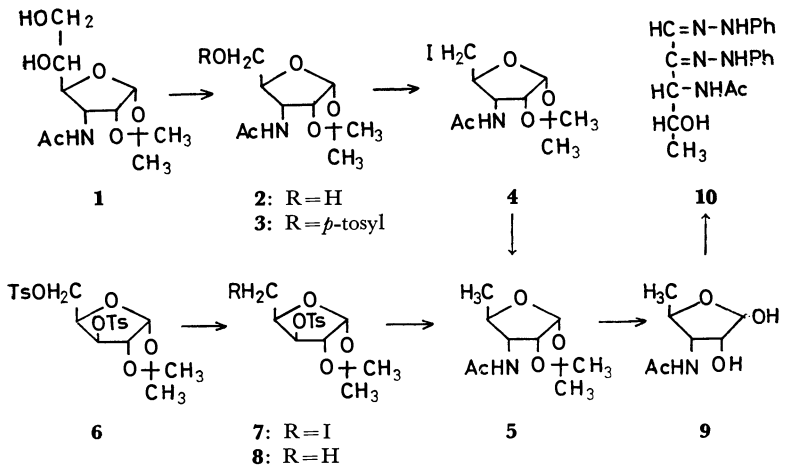

TABLE 1. FIRST-ORDER ANALYSIS OF NMR SPECTRA OF 5-DEOXY-1,2-*O*-ISOPROPYLIDENE-α-D-RIBOSE AND -D-XYLOSE DERIVATIVES

Compound	Chemical shifts (τ), Coupling constants (Hz), and Dihedral angles[13]				
	H_1	H_2	H_3	H_4	H_5
4	4.16 (d) $J_{1,2}$=4.0 (47°)	5.36 (t) $J_{2,3}$=4.7 (43°)	5.82 (sex.) $J_{3,4}$=9.0*2 (161°)	6.27 (sep.) $J_{4,5}$=3.3 $J_{4,5'}$=6.6	6.55 (q.), 6.75 (q) $J_{5,5'}$=11.0
5	4.21 (d) $J_{1,2}$=4.0	5.46 (t) $J_{2,3}$=4.2 (46°)	5.97 (sex.) $J_{3,4}$=8.8*2 (159°)	6.16 (m) $J_{4,5}$=5.8	8.72 (d)
7	4.07 (d) $J_{1,2}$=4.0	5.21 (d) $J_{2,3}$=0 (80°)	5.10 (d) $J_{3,4}$=2.8 (55°)	5.58 (sep.) $J_{4,5}$=6.0*3 $J_{4,5'}$=9.0	6.84 (q), 7.01 (q) $J_{5,5'}$=10.0*3
8	4.15 (d) $J_{1,2}$=4.0	5.39 (d) $J_{2,3}$=0	5.36 (d) $J_{3,4}$=2.8	5.68 (m) $J_{4,5}$=6.4	8.86 (d)

*2 In both cases, $J_{3,NH}$=9.0.
*3 At 80°C, these coupling constants changed to $J_{4,5}$=5.7, $J_{4,5'}$=7.7 and $J_{5,5'}$=10.5.

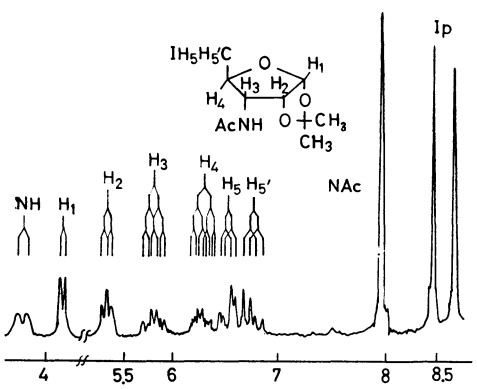

Fig. 1. NMR spectrum of 3-acetamido-3,5-dideoxy-5-iodo-1,2-*O*-isopropylidene-α-D-ribofuranose (**4**) (100 MHz, $CDCl_3$)

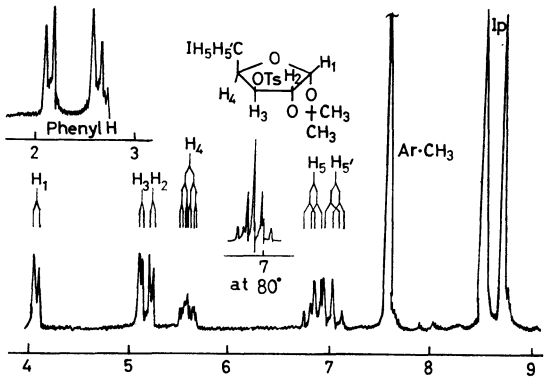

Fig. 2. NMR spectrum of 5-deoxy-5-iodo-5-iodo-1,2-*O*-isopropylidene-3-*O*-(*p*-toluenesulfonyl)-α-D-xylofuranose (**7**) (100 MHz, $CDCl_3$).

of **4** and **7** were shown in Figs. 1 and 2, and some NMR data were summarized in Table 1, in order to compare the conformation of *cis*-fused five-membered ring of 1,2-*O*-isopropylidene-α-D-xylose with that of α-D-ribose. The dihedral angles of ring protons in the both indicate that the conformation of the furanose ring is a twist in which C_2 and C_3 atoms are displaced in opposite senses

from the plane of the other ring atoms, as was shown by several workers by use of α-D-glucofuranose[9,10] and others.[11,12] Comparison of (H_3–H_4) dihedral angle of **4** and **7** with that of the individual planer conformation indicate that the displacement of C_3 in **7** is rather larger than that of **4**. This fact suggests that the nonbonded interaction between *cis*-oriented C_3-*O*-tosyl and C_4-iodomethyl groups effects simply in the former, while that of endo-C_3-acetamido and gauche C_4-iodomethyl or endo-methyl of isopropylidene groups behave reversely in the latter. It is noteworthy that the chemical shift of ring protons in **4** and **7** are to be shifted commonly to lower field than that of **5** and **8**, and that of H_3 in **7** and **8** are markedly shifted due to the inductive effect of the C_3-*O*-tosyl group. The higher shift of H_5 protons in **7** and **8** than that of **4** and **5** will be attributed to the anisotropic effect of the benzene ring.

On the other hand, the remarkable difference in the coupling constant of $J_{4,5}$ and $J_{4,5'}$ between **4** and **7** makes us deduce a hindered rotation of C_4–C_5 bond of **7**. The appearance of H_5 proton signals of **7** measured at 80°C changed markedly as was shown in Fig. 2, and the coupling constants approached to that of **4** (Table 1), while no change was observed in the case of **4**. A more detailed study along with such a line may offer a valuable information on rotational isomers.

Experimental

The solutions were evaporated under diminished pressure at a bath temperature not exceeding 45°C. All melting points are uncorrected. Optical rotations were measured in a 0.5-dm tube, with a Carl Zeiss Photoelectric Precision Polarimeter. The NMR spectra were taken in deuteriochloroform solution with a JNM-4H-100 MHz Spectrometer, using tetramethylsilane as an internal standard.

3-Acetamido-3-deoxy-1,2-*O*-isopropylidene-α-D-allofuranose (1). A solution of 3-acetamido-3-deoxy-1,2;5,6-di-*O*-isopropylidene-α-D-allofuranose[7] (42 g, 139 mmol) in 0.2 N-hydrochloric acid solution (300 m*l*) of acetone-water (1 : 1 in volume) was maintained at 20—23°C for 1.5 hr, and then neutralized with sodium hydrogencarbonate (6 g), concentrated to a sirup. The sirup was extracted with methanol, the methanol solution was treated with active carbon, and then addition of ether to it gave colorless crystals (29.5 g) in 81% yield. $[\alpha]_D^{23}$ + 158.3° (*c* 1.08, methanol); mp 154—155°C (lit,[3] 154—156°C). NMR: τ 8.63, 8.43 (two s, C–CH_3), 7.92 (s, NAc), 5.34 (t, H_2), 4.11 (d, H_1, J=4.0 Hz), 3.60 (d, NH, J=9.0 Hz).

This compound was acetylated to the corresponding di-*O*-acetate by acetic anhydride and pyridine in an usual manner. Mp 163—164°C; $[\alpha]_D^{23}$ + 66.6° (*c* 0.80, chloroform).

Found: C, 52.24; H, 6.51; N, 4.11%. Calcd for $C_{15}H_{23}NO_8$: C, 52.17; H, 6.71; N, 4.06%.

3-Acetamido-3-deoxy-1,2-*O*-isopropylidene-α-D-ribofuranose (2). To a solution of **1** (20.4 g, 75 mmol) in 100 m*l* of water was added sodium periodate (18 g, 84.5 mmol) in water (200 m*l*), and the solution was left to stand at room temperature for 2 hr, concentrated to 50 m*l*, then filtered. The filtrate was treated with sodium borohydride (1.6 g, 42.5 mmol) for 2 hr, and concentrated to a sirup which was crystallized from ethanol. Yield, 16.5 g (94.8%); mp 148—149°C; $[\alpha]_D^{23}$ + 151.2° (*c* 0.915, methanol); NMR: τ 8.65, 8.45 (two s, C–CH_3), 7.95 (s, NAc), 4.16 (d, H_1, J=3.5 Hz), 3.72 (d, NH, J=8.0 Hz).

Found: C, 51.76; H, 7.22; N, 5.83%. Calcd for $C_{10}H_{17}NO_5$: C, 51.94; H, 7.41; N, 6.06%.

This compound was converted to the corresponding 5-*O*-acetate by acetic anhydride and pyridine in an usual manner, which showed mp 132—133°C; $[\alpha]_D^{23}$ + 73° (*c* 1.0, chloroform); NMR: τ 8.66, 8.45 (two s, C–CH_3), 7.97 (s, NAc), 7.93 (s, OAc), 4.17 (d, H_1, J=3.8 Hz), 3.94 (d, NH, J=9.2 Hz).

Found: C, 52.85; H, 7.02; N, 5.20%. Calcd for $C_{12}H_{19}NO_6$: C, 52.74; H, 7.01; N, 5.13%.

3-Acetamido-3-deoxy-1,2-*O*-isopropylidene-5-*O*-(*p*-toluenesulfonyl)-α-D-ribofuranose (3). To a solution of **2** (8 g, 34.6 mmol) in dry pyridine (20 m*l*) was added *p*-toluenesulfonyl chloride (15 g, 78.9 mmol), and the reaction mixture was heated at 60°C for 10 min, allowed to stand overnight at room temperature, then poured into ice-water. The resultant solution was extracted three times with chloroform, and the combined extracts were washed with aqueous sulfuric acid, sodium hydrogencarbonate and then water, dried over anhydrous sodium sulfate, and concentrated to give a pale yellow sirup in 79% (10.5 g) yield. $[\alpha]_D^{23}$ + 52.6° (*c* 1.25, chloroform), NMR: τ 8.70, 8.51 (two s, C–CH_3), 8.02 (s, NAc), 7.57 (s, aromatic CH_3), 4.27 (d, H_1, J=4.0 Hz), 3.55 (d, NH, J=7,5 Hz).

Found: C, 52.86; H, 6.05; N, 3.67%. Calcd for $C_{17}H_{23}NO_7S$: C, 52.98; H, 6.02; N, 3.64%.

3-Acetamido-3,5-dideoxy-5-iodo-1,2-*O*-isopropylidene-α-D-ribofuranose (4). A solution of **3** (10.5 g, 27.3 mmol) and sodium iodide (8 g, 53.3 mmol) in acetonitrile (100 m*l*) was heated in a sealed tube at 110°C for 24 hr, and then concentrated, extracted three times with chloroform. The combined extracts were washed with water, dried over anhydrous sodium sulfate, concentrated to give a pale yellow sirup which crystallized from ether as needles. Yield, 8.0 g (99%); mp 134.5—135.5°C; $[\alpha]_D^{23}$ +38.1° (*c* 0.756, chloroform).

Found: C, 35.14; H, 4.36; N, 4.21%. Calcd for $C_{10}H_{16}INO_4$: C, 35.20; H, 4.69; N, 4.10%.

3-Acetamido-3,5-dideoxy-1,2-*O*-isopropylidene-α-D-ribofuranose (5). a) A solution of **4** (8 g, 26.7 mmol) in ethanol (100 m*l*) was hydrogenated at 40 atm pressure for 20 hr in the presence of Raney nickel (10 g) and triethylamine (2 m*l*). The reaction mixture was filtered, and the filtrate was concentrated to give a sirup which crystallized spontaneously. The crystals were purified two times by crystallization from ether-petroleum ether. Yield, 5.2 g (91%);

9) R. J. Abraham, L. D. Hall, L. Hough and K. A. McLauchlan, *J. Chem. Soc.*, **1962**, 3699.
10) J. Yoshimura and H. Hashimoto, This Bulletin, **41**, 261 (1968).
11) R. Lemieux, *Can. J. Chem.*, **39**, 116 (1961).
12) L. D. Hall, *Chem. Ind.* (London), **1963** 950.
13) R. J. Abraham, *Mol. Phys.*, **5**, 513 (1962).

mp 98—101°C; $[\alpha]_D^{23}$ +87.8° (*c* 2.12, methanol).

Found: C, 55.92; H, 7.70; N, 6.57%. Calcd for $C_{10}H_{17}NO_4$: C, 55.80; H, 7.96; N, 6.51%.

b) A mixture of **8** (14.3 g, 47.3 mmol) and anhydrous hydrazine (150 m*l*) was heated in an oil bath at 140°C for 20 hr, and the solution was evaporated. The residue was dissolved in ethanol (100 m*l*), hydrogenated in the presence of Raney nickel at 40 atm pressure for 10 hr, and then filtered. The filtrate was evapporated to a sirup, and the dried sirup was acetylated with acetic anhydride (10 m*l*) and pyridine (10 m*l*). The reaction mixture was poured into ice-water, concentrated to a sirup, and then extracted three times with chloroform. The combined extracts were washed with a small amount of aqueous sulfuric acid, sodium hydrogen carbonate, and then water, dried over anhydrous sodium sulfate, concentrated to a sirup which crystallized from ether. Yield, 1.7 g (22.6%); mp 98—100°C.

5-Deoxy-5-iodo-1,2-*O*-isopropylidene-3-*O*-(*p*-toluenesulfonyl)-α-D-xylofuranose (7). A Solution of 1,2-*O*-isopropylidene-3,5-di-*O*-(*p*-toluenesulfonyl-α-D-xylofuranose)[8] (92 g, 184 mmol) and sodium iodide (42 g, 280 mmol) in acetonitrile (1 *l*) was refluxed for 150 hr at ordinary atmosphere, concentrated, and then extracted with chloroform. The extracts were washed with water, dried over anhydrous sodium sulfate, concentrated to dryness to give a pale yellow sirup. Yield, 79 g (89%); $[\alpha]_D^{23}$ −65.5° (*c* 2.0, chloroform). This sirup was analyzed without further purification.

Found: C, 40.02; H, 4.44; S, 7.32%. Calcd for $C_{15}H_{19}IO_6S$: C, 39.66; H, 4.22; S, 7.05%.

5-Deoxy-1,2-*O*-isopropylidene-3-*O*-(*p*-toluenesulfonyl)α-D-xylofuranose (8). A solution of **7** (79 g, 174 mmol) in methanol (200 m*l*) was hydrogenated at 100 atm pressure for 24 hr in the presence of Raney nickel(70 g) and triethylamine (12 m*l*). The reaction mixture was filtered, and the filtrate was concentrated to dryness, extracted with chloroform. The extracts were washed with water, dried over anhydrous sodium sulfate, and concentrated to give a sirup which couldn't be crystallized, and therefore, analyzed without further purification. Yield, 37.2 g (65%); $[\alpha]_D^{23}$ −16.8° (*c* 1.70, chloroform).

Found: C, 54.95; H, 6.27; S, 9.46%. Calcd for $C_{15}H_{20}O_6S$: C, 54.87; H, 6.14; S, 9.76%.

3-Acetamido-3,5-dideoxy-D-ribose (9). A solution of **5** (0.9 g, 4.16 mmol) in 60% acetic acid (30 m*l*) was heated at 80°C for 3 hr, decolorized with active carbon, and concentrated to a sirup which couldn't be crystallized. Yield, 0.7 g (96%); $[\alpha]_D^{23}$ +65.1°—+63.2° (*c* 1.09, for 12 hr in methanol).

As an crystalline derivative, the corresponding osazone (**10**) was prepared as follows: the above sirup (0.7 g, 4 mmol) and phenylhydrazine (2 g, 18.5 mmol) in 60% acetic acid (20 m*l*) was heated at 90°C for 2 hr and then concentrated to a sirup which crystallized after two days. The yellow crystals were recrystallized from ethanol-ether. Yield, 1.35 g, (95%); mp 215—216°C; $[\alpha]_D^{23}$ −7.36° (*c* 1.06, methanol).

Found: C, 64,60; H, 6.51; N, 19.35%. Calcd for $C_{19}H_{23}N_5O_2$: C, 64.57; H, 6.56; N, 19.82%.

The authors wish to express their thanks to Mr. Kiyofumi Fukukawa for measurements of NMR spectra, and to members of Laboratory of Organic Analysis for elemental analyses.

NOTES

BULLETIN OF THE CHEMICAL SOCIETY OF JAPAN VOL. 43 2970—2972 (1970)

Alpha-Benzildioxime Complexes of Copper(II) — A Study by Solvent Extraction —

Hisahiko EINAGA and Hajime ISHII

National Institute for Researches in Inorganic Materials, Science and Technology Agency, Hon-komagome, Bunkyo-ku, Tokyo

(Received November 12, 1969)

It is well known that α-benzildioxime forms complexes with nickel(II) and palladium(II), and has been used as a gravimetric or a spectrophotometric reagent for these metals[1] as a substitute for dimethylglyoxime. Studies have also been made on cobalt(II)[2] and iron(II)[3] complexes of α-benzildioxime. However, little has been made on copper(II) complex of α-benzildioxime, except for the determination of the formation constants of the complex in 50% dioxane-water system by the potentiometric method.[4] During the course of studies on the reaction of copper(II) with α-benzildioxime by the solvent extraction method, we found that copper(II) forms two kinds of complexes with α-benzildioxime; one is light brown bis(α-benzildioximato)copper(II) and the other light greenish yellow mono(α-benzildioximato)copper(II). This paper gives some results of the study on the complexes by the solvent extraction method.

Experimental

Reagents. A copper(II) solution (0.618 mg Cu(II)/m*l*) was prepared from copper(II) sulfate pentahydrate with the addition of a small amount of sulfuric acid to prevent the hydrolysis of copper(II). The solution was used with dilution to an appropriate concentration. Alpha-benzildioxime (Wako Pure Chemicals Ind., Ltd.) was recrystallized from methanol and a 0.02% methanolic solution of the purified reagent (mp 237°C) was used. A 2.5 M solution of ammonium nitrate was used as the ammonium salt solution.

Apparatus. Absorption spectra were recorded with a Hitachi automatic recording spectrophotometer, model EPS-3T, and other absorption measurements were carried out with a Hitachi spectrophotometer, model 139, with 10-mm quartz cells. A pH meter of Toa Dempa Co., Ltd., model HM-5A, was used for pH measurements. Solvent extraction was carried out with an Iwaki universal shaker, model V-D, at the rate of 300 rpm. All the experiments were carried out at about 23°C.

Results and Discussion

Absorption spectra of copper(II)-α-benzildioxime complex extracted into benzene are shown

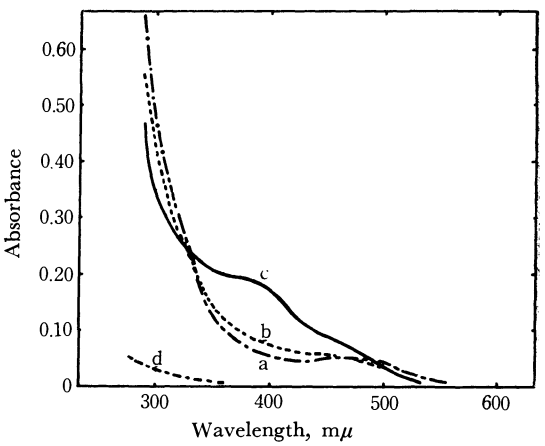

Fig. 1. Absorption spectra of copper(II)-α-benzildioxime complex in benzene.
[α-Benzildioxime]: 3.87×10^{-5} M.
a : [Cu(II)]/[α-Benzildioxime]=0.6 (mole fraction of Cu(II)=0.38).
b : [Cu(II)]/[α-Benzildioxime]=2.5 (mole fraction of Cu(II)=0.67).
c : [Cu(II)]/[α-Benzildioxime]=5.0 (mole fraction of Cu(II)=0.83).
d : α-Benzildioxime alone.
pH value of equilibrated aqueous phase: 8.2.
λ_{max} of curve a: 460 mμ.

1) For example: Y. Uzumasa and S. Washizuka, This Bulletin, **29**, 403 (1956); W. Wawrzyczek, H. Majkowska and J. Soboczynska, *Z. Anal. Chem.*, **188**, 88 (1962).

2) C. Matsumoto, I. Masuda and K. Shinra, *Nippon Kagaku Zasshi*, **88**, 46 (1967).

3) C. Matsumoto, Y. Yamano and K. Shinra, *ibid.*, **89**, 44 (1968).

4) K. Burger and I. Ruff, *Talanta*, **10**, 329 (1963).

in Fig. 1. Curve a in Fig. 1 is a spectrum of the complex obtained with an excess of α-benzildioxime (mole fraction of copper(II): 0.38) and has an absorption maximum at the wavelength of 460 mμ. The complex obtained under these conditions is light brown and moderately soluble in benzene, irrespective of the presence of ammonium salt in the aqueous phase. Curve c in Fig. 1, on the contrary, is a spectrum of the complex obtained with a large excess of copper(II) (mole fraction of copper(II): 0.83) and has no absorption maximum in the near ultraviolet and visible regions. The complex is light greenish yellow, and its solubility in benzene is very low unless ammonium salt is present in the aqueous phase. (Curve b in Fig. 1 can be considered as an intermediate of the above-mentioned two limiting cases).

Figures 2 and 3 show the results obtained by the method of continuous variations and the molar ratio method, respectively. The results indicate that there exists a 1 to 2 (metal to ligand) complex when mole fraction of copper(II) is less than about 0.6 (ratio of copper(II) to α-benzildioxime: about 2), and another kind of copper(II) complex is formed when copper(II) is in a large excess over α-benzildioxime (mole fraction of copper(II) is larger than about 0.8). As we could not determine the composition of the latter complex from these results, chemical analysis of the complex extracted with a large excess of copper(II) was carried out. The results are presented in Table 1. We see that the light greenish yellow complex has a composition of 1 to 1 (metal to ligand).

The extraction equilibrium of bis(α-benzildioxi-

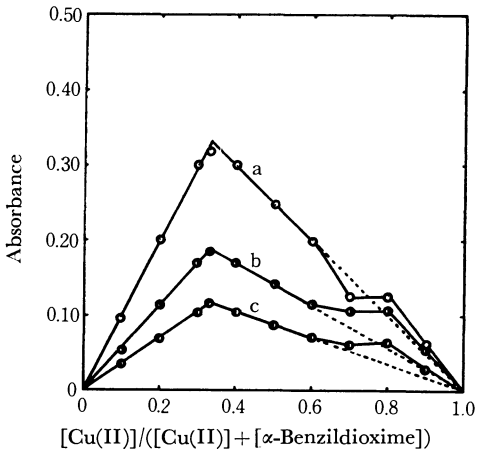

Fig. 2. The method of continuous variations.

λ; a: 350 mμ, b: 380 mμ, c: 430 mμ
[Cu(II)]+[α-Benzildioxime]: 1.54×10^{-4} M
pH value of equilibrated aqueous phase: 8.2
μ=0.15 (NH_4NO_3)

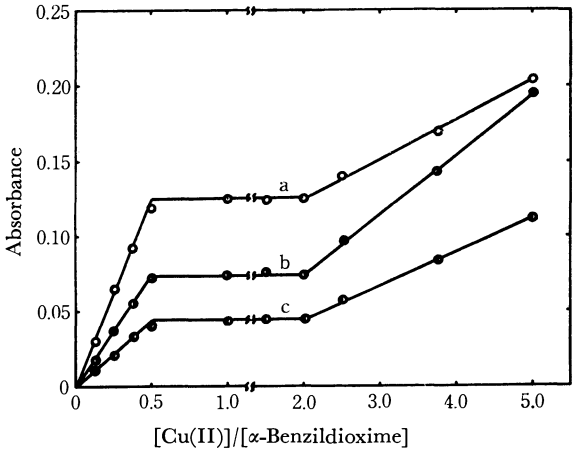

Fig. 3. The molar ratio method.

λ; a: 350 mμ, b: 380 mμ, c: 430 mμ
[α-Benzildioxime]: 3.87×10^{-5} M
pH value of equilibrated aqueous phase: 8.2
μ=0.15 (NH_4NO_3)

TABLE 1. COMPOSITION OF THE COMPLEX EXTRACTED UNDER THE LARGE EXCESS OF COPPER(II) (%)

	Cu	C	H	N
I	19.3	49.5	5.1	17.1
II	19.5	49.8	5.2	16.9
III	18.92	50.06	4.80	16.68

Note I: The complex extracted under 10 times as much as copper(II) against α-benzildioxime and obtained as solid state by evaporation of benzene under vacuum at room temperature.
II: Those extracted under 20 times as much as copper(II) and obtained by the same procedure as described in I.
III: Calcd for $Cu(C_{14}H_{10}N_2O_2)(NH_3)_2$.

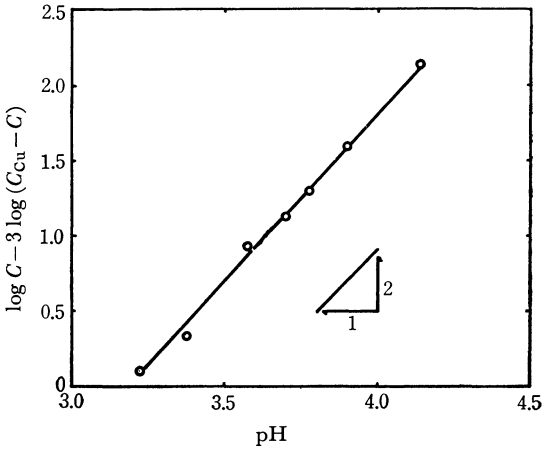

Fig. 4. Reaction between $\log C-3\log(C_{Cu}-C)$ and pH.

($\log C-3\log(C_{Cu}-C)=\log 4K_{ex}+2\cdot pH$)
C_{Cu}: 1.21×10^{-4} M ($C_{H_2L}=2C_{Cu}$)
μ=0.05 (HCl+KCl)
$V/V_{(org)}=1$, ($V_{(org)}=10$ ml)

mato)copper(II) complex might be expressed as follows:

$$Cu^{2+} + 2H_2L_{(org)} \rightleftharpoons Cu(HL)_{2(org)} + 2H^+$$

$$K_{ex} = [Cu(HL)_2]_{(org)} \cdot [H^+]^2/[Cu^{2+}] \cdot [H_2L]^2_{(org)} \quad (1)$$

where H_2L denotes the undissociated α-benzildioxime, K_{ex} the extraction constant of the copper(II) complex, the suffix *org* the organic phase and no suffix the aqueous phase, respectively. To ascertain the validity of the extraction equilibrium represented above, the following considerations were made. Provided that the partition coefficients of α-benzildioxime and its copper(II) complex are sufficiently large and that the equilibrium concentrations of the intermediate species of α-benzildioxime and its copper(II) complex are negligibly low, $[Cu^{2+}]$ and $[H_2L]_{(org)}$ can be expressed in terms of the total concentration of copper(II). C_{Cu}, and that of α-benzildioxime, C_{H_2L}, when volumes of aqueous and organic phases are equal:

$$[Cu^{2+}] = C_{Cu} - [Cu(HL)_2]_{(org)} \quad (2)$$

$$[H_2L]_{(org)} = C_{H_2L} - 2[Cu(HL)_2]_{(org)} \quad (3)$$

When C_{Cu} and C_{H_2L} are taken so as to make $2C_{Cu} = C_{H_2L}$, Eq. (4) can be obtained by inserting Eqs. (2) and (3) into Eq. (1) and writing in logarithmic form:

$$\log C - 3 \log (C_{Cu} - C) = \log 4K_{ex} + 2pH \quad (4)$$

where C denotes the term $[Cu(HL)_2]_{(org)}$. Figure 4 shows the results obtained under the condition $2C_{Cu} = C_{H_2L}$ with varying pH values of the aqueous phase, which reveals that the extraction equilibrium of bis(α-benzildioximato)copper(II) complex can be correctly expressed as represented above.

BULLETIN OF THE CHEMICAL SOCIETY OF JAPAN VOL. 43 2972—2974 (1970)

The Reaction of Bromobenzene with Copper(I) Chloride - Pyridine Complex in Nitrobenzene

Masaru SATO, Izumi MOTOYAMA and Kazuo HATA

Department of Chemistry, Faculty of Science, Tokyo Metropolitan University, Setagaya-ku, Tokyo

(Received November 29, 1969)

The Rosenmund - von Braun nitrile synthesis has been little studied from the viewpoint of its mechanism in spite of its usefulness as a synthetic procedure. Recently Bacon and Hill[1] investigated the substituent effect and the solvent effect in the reaction of aryl halide with copper(I) salts in polar solvents. However, the real reactive species were not elucidated. Ito and Watanabe[2] studied the kinetics of this reaction in nitrobenzene and pointed out an important role of the complexes of copper(I) salt and pyridine bases in the reaction. It was found that pyridine bases and copper(I) salt produced a 1 : 1 complex, and that the structure of pyridine bases affected the rate of the reaction. These results suggest that the Rosenmund - von Braun reaction and its related reactions must be reexamined in view of the reaction between organic halide and metal complex. Thus, the reaction of bromobenzene with copper(I) chloride - pyridine complex in nitrobenzene was investigated from this point of view.

1) R. G. R. Bacon and H. A. O. Hill, *J. Chem. Soc.*, **1964**, 1097.

2) T. Ito and K. Watanabe, This Bulletin, **41**, 419 (1968).

Results and Discussion

It has already been reported that the reaction of bromobenzene with copper(I) cyanide - pyridine complex is second-order, that is, first-order in each of bromobenzene and copper(I) cyanide - pyridine complex.[2] Therefore, we determined the activation parameter of this reaction in order to obtain further information concerning this reaction. The second-order rate constants in the reaction of bromobenzene with copper(I) chloride - pyridine complex*1 were measured in nitrobenzene at several temperatures. The results are summarized in Table 1. The activation enthalpy ($\Delta H^{\neq}$) of the reaction was calculated from the data in the table to be 8.6 kcal/mol, and the activation entropy ($\Delta S^{\neq}$), to be -38.4 e.u. (at 160°C). The activation enthalpy obtained in this study is not an unusual value in comparison with those of other reactions

*1 This complex is insoluble in hydrocarbons and alcohols, but soluble in nitrobenzene, nitromethane, acetonitrile, pyridines, and dimethyl sulfoxide. The halogen-exchange reaction could not take place in nitromethane and acetonitrile at temperatures below their boiling points.

Table 1. The rate constants at various temperatures[a)]

Temperature (°C)	k (l/mol·sec)
155.0	2.29
160.0	3.11
165.0	4.08
170.0	5.45
175.0	7.31

a) Bromobenzene, 1.0 ml; pyridine, 1.0 ml; copper(I) chloride, 0.94 g; nitrobenzene, 40 ml.

between organic halides and metal complexes. For example, the activation enthaply of the reaction of benzyl chloride with chromium(II) salt[3] is 14.0 kcal/mol, and that of the reduction of chloropentaamminechromium(III) complex with chromium(II) salt[4] is 11.1 kcal/mol. The transition these reaction is suggested to be a halogen-bridged state of activated complex (**1**) or (**2**):

$[ArCH_2\cdots Cl\cdots Cr_{aq}]^{2+}$ (**1**) $[(NH_3)_5Cr\cdots Cl\cdots Cr_{aq}]^{2+}$ (**2**)

The activation entropy of the reaction described above is −14.3 e.u. in the former[3] and −23 e.u. in the latter.[4] The larger negative activation entropy obtained in the present study supports the hypothetical four-center type (or double-bridge) transition state previously proposed.[2]

A similar halogen-exhange was observed in the reactions of bromoferrocene with copper(I) halide - pyridine complex.[5] The reactions took place in nitrobenzene, as well as in nitromethane and acetonitrile, at much lower temperatures than those at which the halogen-exchange reactions of bromobenzene could be observed.[6] In the reactions of bromoferrocene, an astonishing solvent effect was observed that can be explained not by the solvation but only in terms of the difference in the coordination-ability of the solvent toward the copper(I) ion.[6]

The Rosenmund - von Braun reaction takes place with ease in pyridine or quinoline,[7] and the halogen-exchange of aryl halide with copper(I) chloride proceeds easily in α-picoline.[8] 3-Halopyridine is converted more easily with copper(I) cyanide to 3-cyanopyridine than is halobenzene.[9]

These facts led us to a detailed investigation of the role of the pyridine base as a ligand in the intermediate complex in the reaction between bromobenzene and copper(I) chloride - pyridine base complex in nitrobenzene. When an equimolar amount of 4-methyl-, 3-methyl-, 2-methyl-, 3-acetyl-, or 4-methoxycarbonylpyridine was added to a mixture of nitrobenzene and copper(I) chloride at 160°C, a clean homogeneous solution was obtained, while 4-cyano-, 3-cyano-, or 3-chloropyridine gave a complex insoluble in nitrobenzene. In the latter cases, the observed second-order rate constants for the halogen-exchange reaction showed considerably deviating results. This is probably due to the insolubility of the copper(I) chloride - pyridine base complex (**3**) caused by the enhanced ionic character of the complex, which is brought about by an N←Cu back donation when an electron-attracting group is introduced to the pyridine nucleus coordinated to the copper atom in the complex. The results of the kinetic measurements using various pyridine bases are shown in Table 2.

Table 2. The effect of substituents on pyridine bases[a)]

Substituent	k (l/mol·min)[b)]	k (l/mol·min)[c)]
4-CH_3	5.2×10^{-2}	
3-CH_3		6.3×10^{-2}
H	4.3×10^{-2}	6.6×10^{-2}
4-$COOCH_3$	3.5×10^{-2}	
3-$COCH_3$		5.4×10^{-2}

a) Bromobenzene, 1.0 ml; nitrobenzene, 40 ml; copper(I) chloride, 0.94 g; pyridine bases, equimolar amount to copper(I) chloride.
b) Temperature, 160.2°C.
c) Temperature, 166.0°C.

The results are quite consistent with the observation by Ito and Watanabe.[2] The relative rate constants are in an almost linear relation to the pK_a's of the bases except for the case of 3-methylpyridine. This suggests that the reaction is accelerated by the strong coordination of pyridine bases to the metal in the complex (**3**).

Contrary to the favorable behavior of 4-methylpyridine, 2-methylpyridine was found to suppress the halogen-exchange reaction of bromobenzene; this fact has been explained in terms of steric hindrance of the methyl group at the 2-position toward the coordination of the pyridine base to copper(I) chloride.[2] A large size of a copper atom will cause a F-strain, proposed by Brown,[10] to the methyl group of 2-methylpyridine. Thus, the nitrogen atom of the pyridine base can be expected to coordinate more weakly to the copper

3) J. H. Kochi and D. D. Davis, *J. Amer. Chem. Soc.*, **86**, 5264 (1964).
4) H. Taube and A. Ogard, *ibid.*, **80**, 1084 (1958).
5) M. Sato, T. Ito, I. Motoyama, K. Watanabe and K. Hata, This Bulletin, **42**, 1976 (1969).
6) M. Sato, I. Motoyama and K. Hata, *ibid.*, **43**, 1860 (1970).
7) N. Akanuma, H. Amemiya, T. Hayashi, K. Watanabe, and K. Hata, *Nippon Kagaku Zasshi*, **81**, 333 (1960).
8) W. B. Hardy and R. B. Fortenbaugh, *J. Amer. Chem. Soc.*, **80**, 1716 (1958).
9) L. C. Craig, *ibid.*, **56**, 231 (1934).
10) H. C. Brown, *J. Chem. Soc.*, **1956**, 1248.

atom in the copper(I) salts - pyridine complex. In any case, it can be concluded that the weak coordination by steric and/or electronic factors brings about a retardation of the reaction of bromobenzene with copper(I) chloride - pyridine complex.

On the other hand, the effect of the substituents in pyridine bases upon the rates of halogen-exchange reactions between bromoferrocene and copper(I) chloride - pyridine complexes was found to be the opposite of that in the reactions of bromobenzene.[6]

The correlation of rate constants with the coordination abilities of pyridine bases may be explicable in terms of the four-center (double-bridge) mechanism which has been proposed in the preceding paper.[2] In the first stage, aryl halide will coordinate to the copper(I) chloride - pyridine complex (**3**) to form a metastable intermediate ($ArX \rightarrow CuY\langle^{Py}_{L_n}$). Such coordination is reasonable, because the complex, in which aryl halide coordinates to a certain transition metal, has been isolated.[11] The intermediate will turn into the final product through a four-center-type transition state (**4**). In the transition state (**4**), the increase in electron density on the copper atom will facilitate the attack of the halogen atom Y on the carbon atom in the aromatic nucleus (Y→C attack). Thus, an electron-releasing substituent on the pyridine base will accelerate the halogen-exchange reaction. The importance of the Y→C attack is also suggested by the fact that the substituent effect in the reaction of the substituted

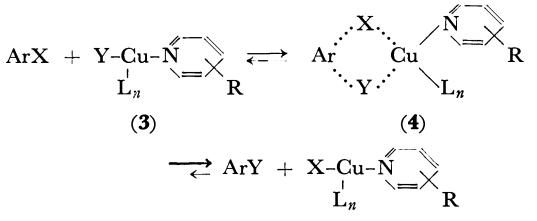

(3) (4)

L=Pyridine base and/or solvent

aryl halide with the copper(I) complex was found to be somewhat nucleophilic.[1,5] On the contrary, the increase in electron density on the copper atom of the complex (**3**) will retard the attack of the halogen atom X on the copper atom in the complex (**3**) (X→Cu attack). Thus, the rate of the halogen-exchange reaction may be regulated by two counteracting factors, that is, the promotion of the Y→C attack and the retardation of the X→Cu attack. The contradiction between these two factors results in the facts that the effect of the substituent on both the aryl halide and pyridine bases upon the reaction rate is not so remarkable as in the ordinary substitution reactions. There would be a certain balance between the Y→C attack and the X→Cu attack. The reactions between bromobenzene and copper(I) chloride - pyridine base complex in nitrobenzene seem to be governed by the ease of the Y→C attack rather than by the X→Cu attack.

Experimental

Materials. Copper(I) chloride was prepared from commercial copper(II) chloride according to the literature.[12] Pyridine bases and nitrobenzene were purified by distillation under reduced pressure.

Kinetic Measurements. A typical procedure was as follows. In a 100-m*l*, three-necked, round-bottomed flask fitted with a sealed stirrer, a thermometer, a nitrogen-inlet tube, and a reflux condenser, were placed 40 m*l* of nitrobenzene, 0.94 g of copper(I) chloride, and 1.0 m*l* of pyridine. The contents were heated to 160°C on an oil bath. When the temperature was regulated to be constant (160±0.1°C), 1 m*l* of bromobenzene was added to the mixture. A small quantity of the reaction mixture was taken out every 5 min and analyzed by gas chromatography. From these measurements, the rate constant was calculated by the usual way.

Gas Chromatography. Apparatus: Ohkura Model 1100; column, 10% Carbowax 1500 on Celite; length, 3.5 m; temperature, 140°C; flow rate, 4 m*l*/min; carrier gas, H_2.

11) W. Reppe and W. J. Schweckendiek, *Ann. Chem.*, **560**, 110 (1948).

12) H. S. Booth, "Inorg. Syntheses," Vol. II, p. 1 (1946).

BULLETIN OF THE CHEMICAL SOCIETY OF JAPAN VOL. 43 2975—2976 (1970)

The Isomer Ratio of the Pentenes Formed by CH_3·-Butenyl Combination

Nobuo YOKOYAMA*1

Department of Chemistry, University of California, Davis, California, U.S.A.

(Received January 31, 1970)

Yokoyama and Brinton[1] studied the gas phase reaction of *cis*-butene-2 with CH_3· which was generated by pyrolysis of di-*t*-butylperoxide. Allylic hydrogen abstraction by CH_3· caused the formation of butenyl radical which gave three pentene isomers when combined with CH_3·. The process is illustrated by the scheme shown below, which includes allylic resonance and *cis-trans* rotation about the center bond.

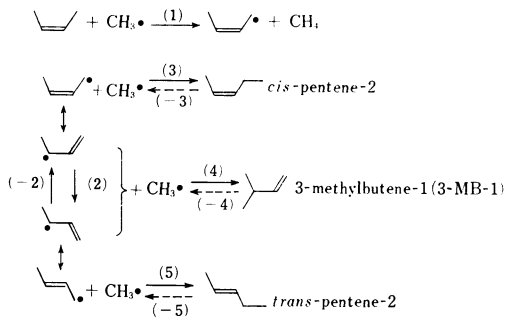

(3) and (5) are the only mechanisms leading to the pentene-2 formation in this system, but 3-MB-1 is also formed by disproportionation of the pentyl radical which is present in the system. However, the quantity of 3-MB-1 formed *via* each route could be distinguished, and the present discussion is limited to 3-MB-1 formed *via* (4) only.

The average ratios of the quantities of pentene isomers were found to be nearly constant at a certain temperature. Their values are shown in Table 1, together with the equilibrium ratios of these pentenes calculated from the generally accepted data.[2]

It should be noted that *trans/cis* ratio exceeded that of the equilibrium in spite of the fact that the reaction was started with *cis*-butene-2. This ratio should have been equal to the equilibrium ratio if there had been the reverse reactions (−3), (−4), and (−5) taking place at sufficient rates. Or it should have been smaller than the equilibrium ratio if (2) had not been sufficiently faster than (3). In fact, the internal rotation (±2) must be much faster than (3), (4), and (5), for the same values were obtained for the isomer ratios when the reaction was started with *trans*-butene-2.

trans/cis equilibrium ratio b may be expressed as

$$b = \frac{k_2}{k_{-2}} \frac{k_{-3}}{k_3} \frac{k_5}{k_{-5}} \tag{6}$$

However, since (−3) and (−5) must be eventually non-existent and (±2) were proved to be sufficiently faster than (3) and (5), the following equation should hold for the observed *trans/cis* ratio

$$a = \frac{k_2}{k_{-2}} \cdot \frac{k_5}{k_3} \tag{7}$$

The following relation should then be valid

$$a/b = k_{-5}/k_{-3} \tag{8}$$

This is the ratio of the rates of bond cleavage to produce butenyl and methyl radicals from *trans*- and *cis*-pentene-2, which could not be directly measured in such temperature range. It is interesting to note that there seems to be a slight difference in the rates of this bond cleavage, *trans* form having a slightly faster rate than *cis*, and that it is not due to the difference in the bond energy. The present data show no evidence for non-zero difference in the activation energy which should be approximately equal to the bond energy itself, because its reverse reaction (radical-radical combination) should have zero or near-zero activation energy.

Exactly the same discussion is applicable to 3-MB-1/*trans*-pentene-2 ratio. In this case the electron density ratio of has a similar role to k_2/k_{-2} in the previous case, and the final result is

$$c/d = k_{-4}/k_{-5} \tag{9}$$

As is seen in Table 1, c/d shows a large divergency from unity, and again no non-zero activation energy difference can be detected. Thus, through this kinetic observation, the bond cleavages of the three pentene isomers (−3), (−4), and (−5) were found to have different rates, (−5) slightly faster than (−3), and (−4) appreciably faster than (−5), not due to the differences in the bond

*1 Present address: Central Technical Research Laboratory, Nippon Oil Company, Ltd. 2-3-2, Yako, Kawasaki-Shi, Kanagawa

1) N. Yokoyama and R. K. Brinton, *Can. J. Chem.*, **47**, 2987 (1969).

2) F. D. Rossini, "Selected values of Physical and Thermodynamic properties of Hydrocarbons and Related Compounds" (API), Carnegie Press, Pittsburgh, Pa. (1953).

Table 1. Pentene ratios

Temp. °C	*trans*-pentene-2/*cis*-pentene-2			3-MB-1/*trans*-pentene-2		
	a observed	*b* equilibrium calculated	*a*/*b*	*c* observed	*d* equilibrium calculated	*c*/*d*
163.0	1.28	1.19	1.1	0.63	0.24	2.6
150.2	1.28	1.22	1.1	0.59	0.24	2.5
136.8	1.35	1.26	1.1	0.59	0.23	2.6
125.8	1.31	1.28	1.0	0.56	0.22	2.5

energies.

It was concluded that the *cis*/*trans* internal rotation of the butenyl radical was fast enough to maintain the equilibrium under the employed conditions, compared with the rates of the competitive chemical reactions. In contrast to this finding, Walling and Thaler[3] reported the complete retention of *cis-trans* configuration of the butenyl radical at 40°C. Although the reaction conditions were entirely different (liquid phase, Cl abstraction as the competitive chemical reaction in their case), this extreme difference between 126—163°C and 40°C is quite interesting. Somewhere between these two temperature regions there might be a certain region in which the internal rotation and the competitive chemical reaction have comparative rates, which would enable one to determine the rate of *cis-trans* rotation of the butenyl radical by comparison with the rate of the competitive reaction, for which no other means of measurement is available at present.

3) C. Walling and W. Thaler, *J. Amer. Chem. Soc.*, **83**, 3877 (1961).

BULLETIN OF THE CHEMICAL SOCIETY OF JAPAN VOL. 43 2976—2977 (1970)

Ionic Dissociation. III. An Extended Hückel Treatment of the Dissociation of Cyclohexanone

Hiroko YAMABE, Hiroshi KATO*1 and Teijiro YONEZAWA

Department of Hydrocarbon Chemistry, Faculty of Engineering, Kyoto University, Sakyo-ku, Kyoto

(Received February 14, 1970)

It is said that the more stable its anion, the more easy is the dissociation of an acid.[1] As for the intermediate of the aldol condensation, Ingraham mentioned[2] that the ionization of the α-hydrogen will be aided: (1) if it is sterically in a favorable position and (2) if the anion can be stabilized. We have discussed these problems in our previous two papers.[3] In this note we will give another example, one concerning the dissociation of cyclohexanone, which should support the above description of the relative stability of a molecule and its anion.

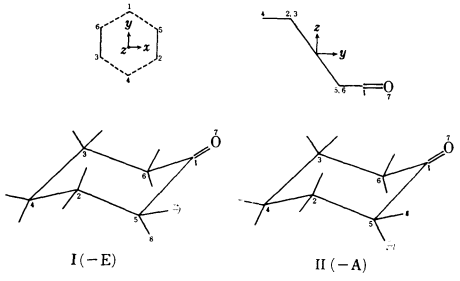

Fig. 1. Coordinate axes adopted and numbering of atoms.

It has been reported by Corey and Sneen[4] that the axial hydrogen of cyclohexane dissociates more readily than the equatorial one, since the former anion is stabilized by the σ-π delocalization. The resonance structure in the transition state is stabi-

*1 Present address: Department of General Education, Nagoya University, Chikusa-ku, Nagoya.

1) M. J. S. Dewar, "The Electronic Theory of Organic Chemistry," The Clarendon Press in the University of Oxford (1949), Chapter VI.

2) L. L. Ingraham, "Biochemical Mechanics," John Wiley and Sons, Inc., New York (1962), Part Two, Condensation.

3) H. Yamabe, T. Yonezawa and H. Kato, "Ionic Dissociation I, and II" (to be published in this Bulletin).

4) E. J. Corey and R. A. Sneen, *J. Amer. Chem. Soc.*, **78**, 6269 (1950).

TABLE 1. TOTAL ELECTRONIC ENERGY AND POPULATION OF SOME ATOMS

I. Dissociation of the equatorial H(−E)

		1C	5C	7O	8H	5C(H.O)*
Atomic orbital population	*S*	1.054	1.274	1.768	0.853	0.018
	x	0.894	1.565	1.967	—	1.097
	y	0.551	1.308	1.730	—	0.386
	z	0.403	0.991	1.766	—	0.002
Atom population		2.902	5.137	7.230	0.853	—
Total electronic energy (eV)				−721.052		

II. Dissociation of the axial H (−A)

		1C	5C	7O	8H	5C(H.O)*
Atomic orbital population	*S*	1.052	1.269	1.767	0.874	0.029
	x	0.900	1.028	1.967	—	0.006
	y	0.552	1.218	1.727	—	0.552
	z	0.624	1.316	1.815	—	0.757
Atom population		3.127	4.831	7.276	0.874	
Total electronic energy (eV)				−721.701		

* 5C(H.O) is an abbreviation of the highest occupied orbital of the 5th carbon.

TABLE 2. ATOMIC ORBITAL BOND POPULATION BETWEEN THE ATOMS 1C AND 5C

(I) Dissociation of the equatorial H (−E)

		1C			
		S	*x*	*y*	*z*
5C	*S*	0.111	0.098	0.038	0.000
	x	0.115	0.111	0.094	0.000
	y	0.079	0.146	−0.006	0.000
	z	0.000	0.000	0.000	0.056

(II) Dissociation of the axial H (−A)

		1C			
		S	*x*	*y*	*z*
5C	*S*	0.105	0.099	0.043	0.000
	x	0.136	0.131	0.096	0.000
	y	0.066	0.106	−0.005	0.000
	z	0.000	0.000	0.000	0.204

(III) Cyclohexanone

		1C			
		S	*x*	*y*	*z*
5C	*S*	0.052	0.043	0.019	0.000
	x	0.067	0.065	0.047	0.000
	y	0.035	0.063	−0.003	0.000
	z	0.000	0.000	0.000	0.028

lized when there is the conjugation between the orbital of the α-carbon, made available by the leaving hydrogen, and the orbital of the carbonyl group is possible. We confirmed their assertion by the Hoffmann's Extended Hückel calculation. The values of the parameters used have been given in a previous paper[3] and will not be repeated here.

In Fig. 1, the coordinate axes adopted and the numbering of the atoms are shown. The 2C, 3C, 5C, and 6C atoms are placed on the X-Y plane. The dissociations of the equatorial and the axial protons are indicated by (-E) and (-A), respectively. Table 1 gives the total energy of the anion, which is derived from the dissociation of a proton from cyclohexanone, and the atomic orbital populations and the atom populations of the several atoms close to the α carbon. From Table 1, it can be seen that anion (II) is more stable than the anion (I) which is in agreement with the experimental suggestion.[4] The atomic orbital population of the P_z AO of the 1C, 5C, and 7O atoms and that of the S orbital of 8H of the anion (II) are larger than the corresponding values of the anion (I). This relation is most prominent in the atomic orbital population of the P_z AO of the 5C atom in the highest occupied MO given in the 7th column of Table 1. That is the conjugation of the anion II is more prevalent than that of the anion I. This also agrees with the previous experimental suggestion.[4] This conclusion can also be deduced from Table 2. In Table 2 the atomic orbital bond populations between the 1C and 5C atoms are given for cyclohexanone and the anions I and II. The atomic orbital bond population in the Z direction increases in the order of cyclohexanone (0.028), the anion I (0.056), and the anion II (0.204). This means that the anion II is more highly conjugated than the anion I.

The calculation was carried out on a HITAC 5020 computer at the computation center of the University of Tokyo.

BULLETIN OF THE CHEMICAL SOCIETY OF JAPAN VOL. 43 2778—2979 (1970)

Polarographic Investigation of Oxidation Reaction of Vanadium(II) by Nitrate Ion

Kazuyoshi TANAKA,* Ken-ichi MORINAGA** and Kunio NAKANO*

* *Department of Chemistry, College of Science, Rikkyo (St. Paul's) University, Nishi-Ikebukuro Toshima-ku, Tokyo*

** *Department of Chemistry, Faculty of Science and Engineering, Saitama University, Shimo-Ohkubo, Urawa-shi, Saitama*

(Received March 17, 1970)

The polarographic behavior of V(II) species in various solutions has been investigated by Lingane and Meites.[1,2] Rates of the oxidation of V(II) by nitrate ion in perchlorate, sulfate, and halide solutions have been determined by means of polarography.[3] The polarographic method was applied because it was possible to measure the-rates at low acidities. It was found that sulfate ion increased the rate of oxidation to some extent. The relationship between the half-wave potentials and the rates of homogenous reactions has been suggested.[4] In the present work, the rates in various supporting electrolytes were determined by the polarographic method. It may be concluded that the difference in the rates was mostly related to that in the half-wave potentials of V(II) in the corresponding media. However, for the systems having similar half-wave potentials, the difference in the rates seems to be related to the polarographic reversibilities of the systems. The relationship will be discussed.

Experimental

All the reagents used were of analytical grade. The preparation and analysis of V(II) solution were reported elsewhere.[3] Ionic strength was adjusted to 0.5 by adding sodium perchlorate.

Measuremnet. An appropriate amount of V(II) perchlorate solution was added to the deaerated solution of a supporting electrolyte, and the polarographic measurements were carried out to obtain the half-wave potential and the reversibility of V(II) ion. While the solution was being stirred by passing N_2 gas, sodium nitrate was added to the solution, and the time dependence of the diffusion current was then recorded at a constant potential. Measurements were performed at 25°C.

Results and Discussion

Calculation of Rate Constants. The overall oxidation of V(II) by nitrate ion was proposed as follows:[3]

$$8V(II) + 2NO_3^- + 10H^+ \rightarrow 8V(III) + N_2O + 5H_2O$$

The reaction between V(II) and nitric oxide was involved in the oxidation paths, but its rate was considerably slow.[3] When excess nitrate ions in relation to V(II) ions are present, the amount of V(II) oxidized by nitrate ions is almost three times as large as that of nitrate ions consumed. Thus, the apparent second-order rate constant, k, corresponding to the decrease in V(II) ions can be calculated from the time dependence of the diffusion current using equation

$$kt = \frac{3}{3[NO_3^-]_i - [V(II)]_i} \times \ln\left\{\left(\frac{[V(II)]_i}{[NO_3^-]_i}\right)\frac{[NO_3^-]_i - X}{[V(II)]_i - X/3}\right\} \quad (1)$$

where X is the increment of reaction at any time, and i denotes the initial concentration. When the rate of oxidation is considerably small, a large excess of nitrate ions over V(II) ions is added to the solution in order to obtain feasible rates. In this case, the rate constant is also calculated from the half time assuming that the rate is pseudo first-order with respect to V(II).

Polarographic Behavior of V(II). The half-wave potentials and the polarographic reversibility as defined by Senda and Tachi[5] are shown in Table 1. From the half-wave potentials, it was concluded that the complex formation of V(II) ions took place in almost all the solutions, except for perchlorate, thiocyanate, and ammonium chloride solutions. In the thiocyanate solution, the concentration of thiocyanate ions was adjusted to 0.05 M in order to prevent the dissolution of mercury of the electrode, but at this concentration

1) J. J. Lingane and L. Meites, *J. Amer. Chem. Soc.*, **69**, 1021 (1947).

2) J. J. Lingane and L. Meites, *ibid.*, **73**, 2165 (1951).

3) K. Tanaka, This Bulletin, **43**, 2030 (1970).

4) A. A. Vlček, "Advances in the Chemistry of the Coordination Compound" Macmillan, New York (1961), p. 590.

5) M. Senda and I. Tachi, *J. Electrochem. Soc. Jap.*, **27**, 83 (1957).

Table 1. Half-wave potentials, reversibility, and rates of oxidation of vanadium (II) at 25°C

Group	Supporting electrolytes	pH	$-E_{1/2}$ V *vs.* SCE	$i_p/i_d\sqrt{\tau}$ $\mho\cdot A^{-1}\cdot sec^{-1}$	k $l\cdot mol^{-1}\cdot sec^{-1}$	Color of solution	
						Reactant	Product
I	0.05 M EDTA	3.79	~1.26	59.6	$\sim 2\times10^2$	yellow brown	brown
	0.25 M potassium oxalate	7.21	1.13	5.3	1.3×10^2	black purple	pale blue
	0.10 M sodium oxalate	7.73	1.00	4.4	1.2×10^2	black purple	pale blue
II	0.10 M sodium citrate	7.08	1.12	2.6	3.8×10	pale brown	colorless
	0.10 M sodium fluoride	6.75	0.67	3.5	2.5×10	colorless	white ppt*
	0.10 M sodium succinate	6.72	0.88	~0	2.2×10	colorless	pale green
	0.10 M sodium tartrate	5.72	0.76	3.5	2.0×10	colorless	blue
III	0.10 M sodium salicylate	4.70	0.69	13.1	7.2	colorless	yellow green
	0.10 M sodium fumarate	6.08	0.72	4.4	3.8	red brown	yellow green ppt*
IV	0.50 M sodium perchlorate	4.38	0.50	8.1	1.4×10^{-1}	colorless	pale green
	0.05 M sodium thiocyanate	4.52	0.53	46.5	1.3×10^{-1}	pink	colorless
	0.25 M ammonium chloride	4.38	0.52	15.8	1.0×10^{-1}	colorless	pale green

* ppt=precipitation

V(II) ions might form a thiocyanato-complex as reported by Biermann and Wong.[6] In this solution, a polarographic minimum was observed at ~−0.05 V *vs.* SCE. From the fact that the half-wave potential shifted to more negative side with increasing oxalate concentration, V(II) ion seems to be able to form a mono-oxalato complex in the range of 0.1—0.25 M oxalate ions as suggested by Lingane and Meites.[2] The polarographic behavior of V(II) ion in fumarate, and succinate solutions were first investigated in this work. In these solutions, two polarographic waves were obtained, the more negative half-wave potentials being listed in Table 1. The a.c. polarographic measurement in fumarate solution indicated that the reversibility of the second wave (more positive) was almost twice as high as that of the first one, and the a.c. polarogram of the first wave was split into two peaks. The same phenomenon was found in a citrate solution.

Rates of Oxidation. A considerable variation in the rate constants was observed for this oxidation reaction. From their magnitudes the results may be divided into four groups as shown in Table 1. It was suggested by Vlček that the more negative the half-wave potential, the faster the rate of oxidation.[4] This relationship may hold among the groups in Table 1, but not always within each group. The difference in the rates between fluoride and succinate solutions, and salicylate and fumarate solutions, could not be related to their half-wave potentials, but probably to their reversibility. It is supposed qualitatively that the difference in the rates of the oxidation is related to the rates of the electrode reaction of V(II) species. For example, the difference in the rates between oxalate and citrate solutions, in which almost the same half-wave potentials were obtained, is considered to be related to their polarographic reversibility. The fastest rate of oxidation and the highest reversibility were obtained in EDTA solution. However, the relationship does not always hold, because the reversibility is easily changed by: (1) polarographic kinetics, and (2) adsorption of supporting electrolytes or depolarizer on mercury electrode. As shown in group IV, the rates in thiocyanate, and ammonium chloride solutions were slow, but their reversibility were higher than that in perchlorate solution. This is thought to be caused by the adsorption of each anion. It has been found that the rate of the oxidation decreased with increasing chloride ion concentration.[3]

No influence of sulfate ion on the rates could be observed in fumarate, and tartrate solutions. However, when 0.05 M sodium sulfate was present in thiocyanate solution, the rate increased about 10%, and after completion of oxidation the solution became pale yellow, indicating that a single two-electron oxidation step might be involved.[3]

As shown in Table 1, the rates of oxidation decreased as: oxalate>citrate>tartrate>thiocyanate. This decreasing order in the rates is in good agreement with the results obtained for the oxidation of Ti(III) by chlorate ion.[7]

6) W. J. Biermann and W-K. Wong, *Can. J. Chem.*, **41**, 2510 (1963).

7) K. Tanaka, K. Morinaga and K. Nakano, *Nippon Kagaku Zasshi*, **90**, 478 (1969).

BULLETIN OF THE CHEMICAL SOCIETY OF JAPAN VOL. 43 2980—2981 (1970)

The Fluorination of Carbon Monoxide, Carbonyl Chloride, and Carbonyl Fluoride*[1]

Shunji NAGASE, Takashi ABE, Hajime BABA and Kazuo KODAIRA

Government Industrial Research Institute, Nagoya, Kita-ku, Nagoya

(Received March 28, 1970)

This paper will deal with the electrochemical fluorination of carbon monoxide, carbonyl chloride, carbonyl fluoride, cyanogen, and hydrogen cyanide. These gaseous compounds have been subjected to fluorination by various methods,[1] but no work has yet been published on their electrochemical fluorination. The primary objective of this work was to extend the scope of the technique of electrochemical fluorination for gaseous compounds,[2] previously used mostly in the fluorination of organic gases,[3] to inorganic gases containing a carbon-oxygen or carbon-nitrogen multiple bond, and to clarify the behavior of these compounds in the fluorination.

The method of the fluorination involves the bubbling of metered starting materials through a bubbler into anhydrous liquid hydrogen fluoride in an electrolytic cell.[2] The fluorinated products were freed from hydrogen fluoride and then analyzed. It was found that carbon monoxide, carbonyl chloride, and carbonyl fluoride were fluorinated to give the anticipated products, while cyanogen and hydrogen cyanide were cleaved extensively by the fluorination. The reaction conditions for the electrochemical fluorination of carbon monoxide, carbonyl chloride, and carbonyl fluoride, and the results obtained are shown in Table 1.

In addition, oxygen difluoride was always found in the products. Small amounts of perfluorodimethyl ether and carbon dioxide were present in the products obtained from carbon monoxide. From carbonyl chloride, a considerable amount of chlorine was identified, besides a trace of chlorotrifluoromethane. This indicates the ease of the removal of chlorine of carbonyl chloride in the electrochemical process.*[2]

The electrochemical fluorination of carbon dioxide was also examined. The bulk of the starting material was recovered unchanged; traces of carbon tetrafluoride, hexafluoroethane, trifluoromethane, and a highly explosive product, which was not identified, were also found.

Table 1. Fluorination of carbon monoxide, carbonyl chloride and carbonyl fluoride

Sample	Sample feed rate ml/min	Total amount of sample fed mol	Electrolysis condition[a]	Product composition %				Total Yield[b] %
				CF_4	COF_2	CF_3OF	CF_3OOCF_3	
CO	51	0.416	A	15	71	8	6	58
$COCl_2$	25	0.201	B	8	82	10	—	72
COF_2	49	0.197	C	10		73	17	74

a) A: HF 1 *l*, NaF 10 g, He 20 ml/min, anodic current density 2.2 A/dm², cell voltage 5.5—6 V, electricity passed 61 A. hr, cell temperature 7—8°C.
B: HF 300 ml, He 20 ml/min, anodic current density 1.7 A/dm², cell voltage 7—8 V, electricity passed 30 A. hr, cell temperature 12—13°C.
C: HF 1 *l*, NaF 10 g, He 20 ml/min, anodic current density 2.2 A/dm², cell voltage 5.5—6 V, electricity passed 30 A. hr, cell temperature 7—8°C.

b) Calculated on the basis of the amount of the starting material fed.

*1 "Electrochemical Fluorination of Gases." Part VII.

1) For example, a detailed study of the catalytic fluorination of carbon monoxide has recently been reported; M. Wechsberg and G. H. Cady, *J. Amer. Chem. Soc.*, **91**, 4432 (1969).

2) Part VI of this series: S. Nagase, T. Abe and H. Baba, This Bulletin, **42**, 2062 (1969).

3) See, for example, S. Nagase, T. Abe and H. Baba, *ibid.*, **40**, 684 (1967).

*2 Under pressure, carbonyl chloride is known to react with anhydrous hydrogen fluoride to yield carbonyl chlorofluoride and carbonyl fluoride, together with hydrogen chloride. [J. H. Simons, D. F. Herman and W. H. Pearlson, *J. Amer. Chem. Soc.*, **68**, 1672 (1946)]. This reaction was examined under the conditions used for the present work. When carbonyl chloride was bubbled into anhydrous hydrogen fluoride in a cell kept at 7°C without passing a current through, small amounts of carbonyl chlorofluoride and hydrogen chloride were produced.

The electrochemical fluorination of cyanogen and hydrogen cyanide resulted in an extensive cleavage of the carbon-nitrogen multiple bond, giving fragmented fluorinated products.[4] We will now give examples of the composition of the products obtained from the electrochemical fluorination of cyanogen and hydrogen cyanide, which was carried out under conditions similar to those described above. Cyanogen (feed rate, 56 m*l*/min; hydrogen fluoride, 1 *l*; temperature, 5—6°C) gave 59% nitrogen trifluoride, 35% hexafluoroethane, and 6% carbon tetrafluoride. From hydrogen cyanide (feed rate, 37 m*l*/min; hydrogen fluoride 1 *l*; temperature, −5°C), 48% nitrogen trifluoride, 42% carbon tetrafluoride, 7% trifluoromethane, and 3% trifluoromethyldifluoroamine were formed. The evolution of nitrogen was also observed.

Experimental

Materials. Carbon monoxide and carbonyl chloride from a commercial cylinder were used. The carbonyl fluoride[5] and cyanogen[6] were prepared by the methods described in the literature. The hydrogen cyanide was synthesized by a conventional method.

Procedures. The fluorination procedures used were essentially the same as those described in a previous paper.[2] Product identification and analysis were performed by means of gas chromatography,[*3] infrared spectroscopy (Hitachi EPI-S2 spectrometer), and mass spectrometry (Hitachi RMU-7 spectrometer).

4) T. Abe, S. Nagase and K. Kodaira, *ibid.*, **43**, 957 (1970).

[*3] Gas chromatography was carried out with a Shimadzu GC-2C model chromatograph using a 0.3 cm i.d. × 6 m column packed with 66% FC 43 (Minnesota Mining & Manufacturing Co.) on 60/80 mesh Celite 545 SK (Gaschro-Kogyo Co.). Column temperature, 0°C; carrier gas, helium.

In preliminary experiments, an attempt was made to analyze the products by a modification of Hempel's gas analysis, but the method was found not to be suitable for this purpose because of the reaction of carbonyl fluoride and trifluoromethyl hypofluorite with glass and with mercury covered with fluorocarbon oil respectively.

5) F. S. Fawcett, C. E. Tullock and D. D. Coffman, *J. Amer. Chem. Soc.*, **84**, 4275 (1962).

6) T. Moeller, "Inorganic Syntheses," Vol. V., p. 43 (1957).

BULLETIN OF THE CHEMICAL SOCIETY OF JAPAN VOL. 43 2981—2983 (1970)

The Syntheses and Properties of the Complexes of Boron with Ethylenediaminetetraacetic Acid Analogs

Mitsuhisa NAKATANI, Yoshiaki TAKAHASHI, Akira OUCHI and Kunihiko WATANUKI

Department of Chemistry, College of General Education, University of Tokyo, Komaba, Meguro-ku, Tokyo

(Received April 9, 1970)

In a previous paper[1] we reported the syntheses of the boron trifluoride complexes with ethylenediaminetetraacetic acid (H_4EDTA), cyclohexanediaminetetraacetic acid (H_4CDTA), and nitrilotriacetic acid (H_3NTA), as well as their infrared and ultraviolet spectroscopic properties. According to the results, the boron trifluoride forms 2 : 1 and 1 : 1 adducts with H_4EDTA and H_4CDTA respectively, and a 1 : 1 adduct, NTA·B, with H_3NTA.

Along the lines of extending this work, the boron trifluoride adducts with other aminocarboxylic acids, such as diethylenetriaminepentaacetic acid (H_5DTPA), iminodiacetic acid (H_2IDA), and *N*-hydroxyethylenediaminetriacetic acid (H_3EDTA-OH), were synthesized. New complexes, H_4DTPA·BF_2·$2H_2O$, HIDA·BF_2·H_2O and H_3EDTA-OH·$(BF_3)_2$, were obtained from boron trifluoride ethyl etherate (BF_3·$(C_2H_5)_2O$) and aminocarboxylic acids in acetonitrile media.

Experimental

Instruments. The infrared spectra were obtained by the nujol and hexachloro-1,3-butadiene mull procedure using a DS-403G infrared spectrophotometer of the Japan Spectroscopic Co., Ltd. The electronic spectra were obtained with a Hitachi EPS-2 automatic recording spectrophotometer.

Syntheses of Complexes. Table 1 shows the results of elemental analyses, the chemical formulae of the products as calculated from the analytical data, and the yields of the products.

Synthesis of H_4DTPA·BF_2·$2H_2O$. 0.8 g (0.002 mol) of H_5DTPA and 5 m*l* (0.017 mol BF_3) of a 45% ether solution of BF_3·$(C_2H_5)_2O$ were mixed with 5 m*l* of acetonitrile containing a small amount of water. The mixture was refluxed on a water bath for 30 min and then cooled to room temperature. A small insoluble

1) M. Nakatani, Y. Takahashi, A. Ouchi and K. Watanuki, This Bulletin, **43**, 2072 (1970).

Table 1. Analyses of complexes

Chemical formulae	Yield* (%)		Analyses C	H	N	B	F
$H_4DTPA \cdot BF_2 \cdot 2H_2O$	50	Calcd	35.24	5.49	8.81	2.27	7.96
		Found	35.13	5.70	9.07	1.71	8.21
$HIDA \cdot BF_2 \cdot H_2O$	20	Calcd	24.15	4.05	7.04	5.43	19.10
		Found	24·43	3.83	7.25	5.55	18.51
$H_3EDTA\text{-}OH \cdot (BF_3)_2$	65	Calcd	29.02	4.38	6.77	5.21	27.55
		Found	29.76	3.97	7.30	4.72	27.41

$H_5DTPA = C_{14}H_{23}O_{10}N_3$: Diethylenetriaminepentaacetic Acid
$H_2IDA = C_4H_7O_4N$: Iminodiacetic Acid
$H_3EDTA\text{-}OH = C_{10}H_{18}O_7N_2$: *N*-Hydroxyethylenediaminetriacetic Acid
* Yields were calculated for H_5DTPA, H_2IDA and $H_3EDTA\text{-}OH$.

residue was separated out, to which solution ether was added in order to obtain a white precipitate. This was filtered off and washed with ether. This product was dissolved in 10 : 1 (v/v) acetonitrile-water, and the mixture was heated under reflux for 45 min and then cooled. To the solution was then added an excess of ether, after which the mixture was kept at room temperature for several days in order to obtain a white crystalline product. This was filtered off, washed with acetonitrile and ether, and freed from the solvent under reduced pressure at room temperature.

Synthesis of $HIDA \cdot BF_2 \cdot H_2O$. 1.33 g (0.01 mol) of H_2IDA and 5 m*l* (0.017 mol BF_3) of a 45% ether solution of $BF_3 \cdot (C_2H_5)_2O$ were dissolved in 20 m*l* of acetonitrile containing a small amount of water at room temperature. After the filtration of the insoluble residue, the filtrate was kept overnight at room temperature to give a white crystalline product.

Synthesis of $H_3EDTA\text{-}OH \cdot (BF_3)_2$. 0.6 g (0.002 mol) of $H_3EDTA\text{-}OH$, 3 m*l* (0.01 mol BF_3) of a 45% ether solution of $BF_3 \cdot (C_2H_5)_2O$, and 10 m*l* of acetonitrile containing a small amount of water were mixed and dissolved by heating. After the solution had been refluxed for 2 hr, the precipitate thus obtained was filtered off.

Results and Discussion

Although the ultraviolet absorption spectra of acetonitrile solutions of these complexes are qualitative due to their low solubilities in common organic solvents, their patterns are closely similar to each other. The spectra of all the complexes show a characteristic absorption maximum at $39.3 \pm 0.1 \times 10^3$ cm^{-1} and two shoulders at 40.0 ± 0.1 and $38.2 \pm 0.1 \times 10^3$ cm^{-1}.

The typical pattern of the infrared spectra of these complexes is shown in Table 2. The tentative assignments of their infrared absorption bands are given with reference to the data about free H_5DTPA, H_2IDA, $H_3EDTA\text{-}OH$, and other BF_3 adducts with nitrogen-containing compounds.[1-6]

Table 2. Infrared spectra of complexes (cm^{-1})

$H_4DTPA \cdot BF_2 \cdot 2H_2O$	$HIDA \cdot BF_2 \cdot H_2O$	$H_3EDTA\text{-}OH \cdot (BF_3)_2$
		1762 s
1725 s	1720 s	1720 sh
1635 s	1560 m	1690 s
		1492
1460	1450	1468
1405	1430	1440
1351	1402	1415
	1375	1375
		1342
1305 w	1320 w	1316 s
1260 s	1290 s	1275 s
1223 w	1255 sh	1241 s
1210 sh	1205 w	1221 w
		1206 w
	1165 sh	
1150	1120 s	1200
~ br	1076 s	~ br
950	1042 s	1000
	1025 s	
		980
	970 s	963
		950
910 w	923 s	913 s
900 m	900 s	
		883 w
857 w	840 s	
845 sh		
801 w		801 m
778 w	766 w	
708 w		

s=strong, m=medium, w=weak, br=broad, sh=shoulder

2) K. Nakamoto, Y. Morimoto and A. E. Martell, *J. Amer. Chem. Soc.*, **84**, 2081 (1962).

3) K. Nakamoto, Y. Morimoto and A. E. Martell, *ibid.*, **85**, 309 (1963).

4) K. Nakamoto, "Infrared Spectra of Inorganic Coordination Compounds," John Wiley & Sons, Inc., New York, N. Y. (1963), p. 205.

5) A. Kreutzberger and F. C. Ferris, *J. Org. Chem.*, **27**, 3469 (1962).

6) W. G. Paterson and M. Onyszchuk, *Can. J. Chem.*, **39**, 986 (1961).

The crystalline H_5DTPA[3] has three strong bands of about the same intensity at 1731, 1700 and 1634 cm^{-1}. The former two correspond to the antisymmetric stretching bands of four $>N-CH_2COOH$-type carboxyl groups, while the last one corresponds to that of the $>NH^+-CH_2COO^-$-type group. $H_4DTPA \cdot BF_2 \cdot 2H_2O$ in the solid state shows antisymmetric stretching bands of the carboxyl group at 1725 and 1635 cm^{-1}, but the band at 1700 cm^{-1} of the free ligand disappears. The band at 1725 cm^{-1} probably corresponds to that of four $>N-CH_2COOH$-type carboxyl groups, as in the case of the free acid, and the band at 1635 cm^{-1} is probably to be identified as the band of the $>NBF_2^+-CH_2COO^-$-type carboxyl group, although the shift is not so great as that of the free ligand. The broad bands in the 1150—950 cm^{-1} region are probably to be identified as those of the B–F stretching mode or of a mixture with another vibration.[5,6]

At pH 2.2, the aqueous solution of H_2IDA shows two bands, at 1721 and 1619 cm^{-1}, which can be identified as the stretching bands of the $-NH_2^+-CH_2COOH$-type and the $-NH_2^+-CH_2COO^-$-type carboxyl groups respectively.[2] The solid metal complex of H_2IDA has antisymmetric carboxyl bands which are shifted to lower wave numbers.[4]

$HIDA \cdot BF_2 \cdot H_2O$ in the solid state has two antisymmetric stretching bands of carboxyl groups at 1720 and 1560 cm^{-1}. They can probably be identified as of the $-NHBF_2^+-CH_2COOH$ carboxyl group and the $-NHBF_2-CH_2COO$ carboxyl group respectively. Several bands appear in the 1150—1000 cm^{-1} region; not only the B–F band but also the B–N, C–N, and other band probably appear in this region.[5-7]

Solid $H_3EDTA-OH$ has bands at 1705 (shoulder), 1667, and 1629 cm^{-1}, all of which are identified as antisymmetric stretching bands of the carboxyl group,[3] while in the case of $H_3EDTA-OH \cdot (BF_3)_2$ the corresponding bands occur at 1762, 1720 (shoulder), and 1690 cm^{-1}. The shift to higher wave numbers of the bands of this complex is probably due to the effect of boron trifluoride, which is coordinated with the nitrogen atom in $H_3EDTA-OH$. As the boron trifluoride is a strong Lewis acid and is expected to take off electrons effectively from the nitrogen atom, the bands shift more. The broad bands appearing in the 1200—1000 cm^{-1} region may include the bands of the B–F band and others.[5,6]

The authors wish to thank Professor Yukichi Yoshino and their other colleagues for their helpful discussions.

7) Y. Tomita and K. Ueno, This Bulletin, **36**, 1069 (1963).

BULLETIN OF THE CHEMICAL SOCIETY OF JAPAN VOL. 43 2984—2985 (1970)

Sesquiterpene Constituents of the Essential Oil of Mitsuba (*Cryptotaenia japonica* Hassk)

Toshiko OKUDE and Shûichi HAYASHI

Department of Chemistry, Faculty of Science, Hiroshima University, Higashisenda-machi, Hiroshima

(Received April 10, 1970)

The chemical constituents of the essential oil of Mitsuba, *Cryptotaenia japonica* Hassk, were investigated by Hirao[1] quite a long time ago; he isolated a sesquiterpene hydrocarbon which produced eudalene on sulfur dehydrogenation and suggested the name "mitsubaene" for it. However, the structure of this component has not yet been established.

As is shown in Fig. 1, a sesquiterpene portion of the essential oil showed eleven peaks on gas chromatography using Diasolid L-Carbowax 6000 (3%). These components, after being isolated upon fractional distillation, preparative gas chromatography, and/or elution chromatography, were characterized by various spectrometries and by gas-chromatographic comparisons with authentic specimens.

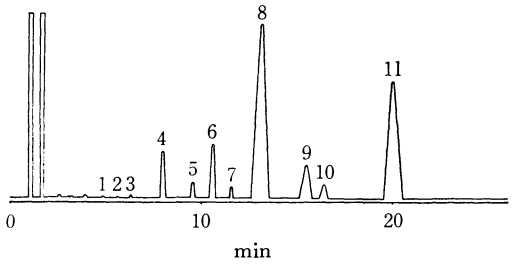

Fig. 1. Gas chromatogram of mitsuba oil (I) at 110°C on Diasolid L-Carbowax 6000.

(+)-α- and (+)-β-Selinenes. The component of the largest peak, 8, isolated by preparative gas chromatography is represented by the molecular formula of $C_{15}H_{24}$ (M^+, *m/e* 204); it was hydrogenated over Adams catalyst in acetic acid to produce a saturated hydrocarbon, $C_{15}H_{28}$ (M^+, *m/e* 208). This evidence indicates the component to be a bicyclic sesquiterpene. The IR spectrum, however, suggested that the component was a mixture of α- and β-selinenes[2]; the further separation into two components was accomplished by eluting it, step by step, over silver nitrate (10%)-coating silica gel with mixed solvents of benzene and *n*-hexane. One component, M^+ *m/e* 204, n_D^{25} 1.5040, $[\alpha]_D^{15}$ +6.31°, which was eluted more easily with a benzene and *n*-hexane-mixed solvent (v/v 10 : 90), exhibited IR and NMR spectra superimposable on those of α-selinene.[3,4] The other, M^+ *m/e* 204, n_D^{25} 1.5013, $[\alpha]_D^{15}$ +43.56°, which was eluted with a benzene and *n*-hexane mixture (v/v 15 : 85), exhibited IR and NMR spectra which were in good agreement with those of β-selinene.[5] Accordingly, the main constituents of the essential oil are (+)-α- and (+)-β-selinenes.

β- and (−)-γ-Elemenes. Both components from the 4 and 5 peaks possess the same molecular formula of $C_{15}H_{24}$ (M^+, *m/e* 204), and each uptook three molar equivalents of hydrogen on catalytic hydrogenation over Adams catalyst in acetic acid to give saturated compounds of $C_{15}H_{30}$ (M^+, *m/e* 210), whose IR spectra both coincided with that of hexahydroelemene.[3] The IR spectra of these components, however, were different from each other in the relative intensity of the absorption bands at 907 and 888 cm^{-1}; the IR spectrum of the component corresponding to the 4 peak was superimposable on that of β-elemene,[3] while that of the 5 peak on that of γ-elemene.[6] This result also agreed with those obtained by NMR and mass spectrometry and/or a gas-chromatographic comparison using an authentic specimen.[7] Although the γ-elemene isolated from this essential oil showed the following constants: n_D^{20} 1.5016, $[\alpha]_D^{20}$ −3.9°, there is some doubt whether these elemenes are natural products or artifacts, for the essential oil was collected by steam distillation. The physical constants of β-elemene were not taken.

α-Ylangene, α- and β-Copaenes, Eremophilene, Cuparene, δ-Elemene and α-Cubebene. In addition to the above components, five

1) N. Hirao, *Kogyo Kagaku Zasshi*, **29**, 48 (1926).

2) The authors wish to thank Professor Shô Itô of Tohoku University for kindly providing the IR and NMR spectra of a mixture of of α- and β-selinenes.

3) M. Horák, O. Molt, J. Plíva and F. Šorm, Die Terpene, s. 81, 22, 24 and 211, Akademie-Verlag, Berlin (1960).

4) G. L. Chetty, G. S. Krishna Rao, S. Dev and D. K. Banerjee, *Tetrahedron*, **22**, 2311 (1966).

5) A. S. Bawdekar and G. R. Kelkar, *ibid.*, **21**, 1521 (1965).

6) J. A. Wenninger, R. L. Yates and M. Dolinsky, *J. Ass. Offic. Anal. Chem.*, **50**, 1304 (1967); *ibid.*, **50**, 1313 (1967).

7) K. Nishimura, N. Shinoda and M. Shiga, The 11th Symposium on the Chemistry of Terpenes, Essential Oils and Aromatics, Matsuyama, October (1967).

Table 1. Sesquiterpene components of *Cryptotaenia japonica*

Peak No.	Component	Content (%)	Means of identification
1	unidentified δ-elemene α-cubebene	0.2	GLC GLC
2	α-ylangene α-copaene	0.3	IR,[3] NMR,[9] mass,[10] GLC IR,[11] NMR,[12] mass, GLC
3	β-copaene	0.5	IR,[13] GLC
4	β-elemene	7.5	IR,[3] NMR,[14,15] mass,[10] GLC
5	(−)-γ-elemene	3.4	IR,[6] NMR, mass, GLC
6	unidentified	8.9	
7	unidentified	2.5	
8	(+)-β-selinene (+)-α-selinene	20.2 18.6	IR,[5] NMR,[5] mass IR,[3] NMR,[4] mass
9	eremophilene	9.1	IR,[16] NMR,[17] mass
10	unidentified	4.6	
11	cuparene	24.2	IR,[18] NMR,[15] mass[18]

components, α-ylangene, α- and β-copaenes, eremophilene, and cuparene, were isolated; they were identified by the methods listed in Table 1. Furthermore, two components of δ-elemene and α-cubebene were tentatively assigned by comparison with the authentic specimens obtained by gas chromatography using Gas Chrom P-Apiezon L.

The relative composition of the sesquiterpene components in the essential oil of mitsuba was calculated to be as shown in Table 1 from the peak areas on the gas chromatogram measured by the use of Carbowax 6000 at 110°C. Hirao's mitsubaene, which was separated by fractional distillation only, seems to be a mixture of these components. This conclusion does not contradict the fact that he obtained eudalene by the sulfur dehydrogenation of mitsubaene.

Experimental

The gas chromatograms were taken with a Shimadzu GC-2B apparatus equipped with a hydrogen-flame ionization detector by using two separation columns (4 mm×3 m), packed with Diasolid L-Carbowax 6000 (3%) and with Gas Chrom P-Apiezon L (4.6%). Preparative gas chromatography was carried out with Celite-Carbowax 6000 (20%) (8 mm×3 m). The NMR spectra were taken in a $CDCl_3$ solution, using tetramethylsilane as the internal standard.

Fractional Distillation of the Essential Oil of Mitsuba. As has been reported in a previous paper on the monoterpene constituents,[8] the essential oil obtained by the steam distillation of the whole herb of Mitsuba was fractionated into thirty-four fractions using a spining-band distillation column under reduced pressure. The fractions (Fr. 1—11), bp 82—140°C/50 mmHg, totaled 26.46 g; they corresponded to the monoterpene constituents used for the previous investigation. The present work was carried out on Fr. 12—34, bp 84.5—168.0°C/3 mmHg, 40.30 g. These fractions were further separated into individual components by means of preparative gas chromatography or elution chromatography over silica gel impregnated with silver nitrate.

NMR of γ-elemene: One tert-methyl (1.05 ppm, 3H, s), three allylic methyls (1.67, 6H, s and 1.71, 3H, d, J=1.2 Hz), and five olefin protons (4.63—5.20, 4H, m and 5.81, 1H, q, J=18 and 10 Hz).

The authors are deeply indebted to Professor Kenji Fukui of Hiroshima University for his kind measurement of the NMR spectra and to Kumiko Morikawa and Yoshimoto Ohta of the Institute of Food Chemistry for the donation of authentic specimens.

8) S. Hayashi, T. Okude and T. Matsuura, This Bulletin, **42**, 3026 (1969).

9) O. Molt, V. Herout and F. Šorm, *Tetrahedron Lett.*, **1965**, 451.

10) G. L. K. Hunter and W. B. Brogden, Jr., *Anal. Chem.*, **36** 1122 (1964).

11) P. de Mayo, R. E. Williams, G. Büchi and S. H. Feairheller, *Tetrahedron*, **21**, 619 (1965).

12) V. H. Kapadia, B. A. Nagasampagi, V. G. Naik and S. Dev, *ibid.*, **21**, 607 (1965).

13) G. L. K. Hunter and W. B. Brogden, Jr., *J. Org. Chem.*, **29**, 2100 (1964); L. Westfelt, *Acta Chim. Scand.*, **21**, 152 (1967).

14) M. Takahashi, K. Isoi, Y. Kimura and M. Yoshikura, *Yakugaku Zasshi*, **84**, 752 (1964).

15) T. Yoshida, K. Endo, S. Itô and T. Nozoe, *ibid.*, **87**, 434 (1967).

16) J. Hochmannová, L. Novotný and V. Herout, *Collect. Czech. Chem. Commun.*, **27**, 1870 (1964).

17) J. Hochmannová and V. Herout, *ibid.*, **29**, 2369 (1964).

18) C. Enzell and H. Erdtman, *Tetrahedron*, **4**, 361 (1958).

BULLETIN OF THE CHEMICAL SOCIETY OF JAPAN VOL. 43 2986—2987 (1970)

The Preparation of 2-Oxo-1,2-dihydro-10*aH*-imidazo[1,2-*a*]-(1,2,5)-oxadiazo[3,4-*b*]indole from Isatin

Masahiko TAKAHASHI

Department of Industrial Chemistry, Faculty of Engineering, Ibaraki University, Hitachi-shi, Ibaraki

(Received April 10, 1970)

There are several studies in the literature concerned with isatin oximes. o-Cyanophenylisocyanate was obtained from isatin-*β*-oxime[1] by treating it with phosphorus pentachloride and also from *N*-asetylisatin dioxime.[2] Previous workers[3] have shown that the pyrolysis of isatin-*β*-oxime resulted in decomposition, yielding o-aminobenzonitrile.

In connection with our continuing interest in the reaction of isatin derivatives,[4] we have obtained a new tetracyclic compound from *N*-acetylisatin dioxime.

N-Acetylisatin dioxime (II), prepared from *N*-acetylisatin (I), was heated in acetic anhydride. A crystallizable compound, accompanied with uncontractable tars, was obtained in a low yield from the reaction mixture. Results of the elemental analysis and the mass spectra of the compound (III) supported the idea of the structure of $C_{10}H_7N_3O_2$ (*m/e* 201). The IR spectra (KBr) showed a C=O stretching frequency at 1810 cm^{-1}, but no NH or OH absorptions. The proton resonance (in DMSO-d_6) was observed at τ 1.7—2.4 (m, 4H), 5.92 (s, 1H), and 7.28 (s, 2H). Thus, the structure of III was established by these data to be the cyclized compound, 2-oxo-1,2-dihydro-10*aH*-imidazo[1,2-*a*]-(1,2,5)-oxadiazo[3,4-*b*]indole, which is a heterocycle with a new ring system.

The treatment of III with potassium hydroxide at room temperature afforded two crystalline compounds. The major product (IV) (45% yield) showed the NMR spectra (in DMSO-d_6) of methyl and oxime protons at τ 7.72 (s, 3H) and −0.18 (s, 1H) respectively, but no NH proton. However, the sharp absorption at 3340 cm^{-1} in the IR spectra (KBr) was apparently due to NH streching, along with the absorption at 3030—2700 cm^{-1} (OH) and 1635 cm^{-1} (C=N). The identification of IV as 3-hydroxyimino-2-methyliminoindoline was based on these data and the analytical value of $C_9H_9N_3O$ (*m/e* 175). IV must be a result of the scission of the imidazole skeleton of III, followed by decarboxylation.

The structure of the minor product (V) (8% yield) was established to be 4-acetyl-(1,2,5)-oxadiazo[3,4-*b*]indole, whose analogous compounds have not yet been synthesized, by the following data; NMR (in DMSO-d_6) τ 1.6—2.5 (m, 4H) and 7.28 (s, 3H); IR (KBr) 1800 cm^{-1} (C=O) 1640 cm^{-1} (C=N) and no NH or OH absorption; elemental analysis $C_{10}H_7N_3O_2$; mass spectral molecular ion at *m/e* 201.

Experimental

2-Oxo-1,2-dihydro-10*aH*-imidazo[1,2-*a*]-(1,2,5)-oxadiazo[3,4-*b*]indole (III). Two grams of *N*-acetylisatin dioxime were added to 20 m*l* of acetic anhydride,

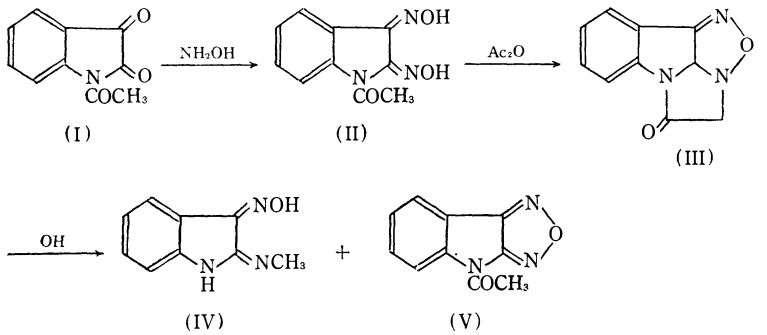

1) W. Borsche and W. Sander, *Ber.*, **47**, 2815 (1914).

2) E. Beckmann and E. Bark, *J. Prakt. Chem.*, [2] **105**, 227 (1923).

3) a) W. Borsche, H. Weussmann and A. Fritzsche, *Ber.*, **57B**, 1149 (1924); b) G. Bargellini and C. J. Turi, *Gazz. Chim. Ital.*, **84**, 157 (1947); c) G. R. Bedford and M. W. Partridge, *J. Chem. Soc.*, **1959**, 1633.

4) a) T. Sasaki and M. Takahashi, This Bulletin, **41**, 1967 (1968); b) T. Sasaki and M. Takahashi, *Yuki Gosei Kagaku Kyokai Shi*, **26**, 899 (1968).

and the mixture was heated at 120°C for 1 hr. Then the solution was poured into 100 m*l* of water, and, after several hours, the aqueous solution was then washed with water, and, after the solvent had been removed, the residue was washed with a small amount of MeOH, giving white solids (31—10% yield). White needles, mp 233—234°C, after recrystallization from MeOH. UV λ_{max}^{EtOH} mμ(ε) 260 (7900), 274 (5900), 284 (5500), 316 (4700), 330 (4400).

Found: C, 59.66; H, 2.99; N, 20.71%. Calcd for $C_{10}H_7N_3O_2$: C, 59.73; H, 3.50; N, 20.90%.

3-Hydroxyimino-2-methyliminoindoline (IV) and 4-Acetyl-(1,2,5)-oxadiazo[3,4-*b*]indole (V). To a stirred solution of 20 m*l* of 5% KOH (H_2O : MeOH–1 : 1), 660 mg of III were added, after which the mixture was stirred for 2 hr at room temperature. Then the solution was neutralized with dilute HCl. After the solution which contained the resulting precipitate had been extracted with 50 m*l* of $CHCl_3$, the materials insoluble in both layers were gathered by filtration to give 262 mg of IV (45% yield), mp 198—201°C; white powder after recrystallization from MeOH. UV λ_{max}^{MeOH} mμ (ε) 252 (57000), 261 (51000), 318 (26000).

Found: C, 61.72; H, 5.11; N, 23.72%. Calcd for $C_9H_9N_3O$: C, 61.75; H, 5.16; N, 24.00%.

The $CHCl_3$ solution was evaporated, and the crude residue was chromatographed on silica gel. Elution with $CHCl_3$ gave 56 mg of V (8% yield), mp 195—197°C, from MeOH. UV λ_{max}^{EtOH} mμ (ε) 236 (17000), 244 (23000), 250 (19000), 294 (4700), 305 (4400), 320 (2900).

Found: C, 59.77; H, 3.64; N, 21.22%. Calcd for $C_{10}H_7N_3O_2$: C, 59.73; H, 3.50; N, 20.90%.

I wish to thank Professor Tadashi Sasaki for his valuable discussions and for the measurement of the NMR and mass spectra.

BULLETIN OF THE CHEMICAL SOCIETY OF JAPAN VOL. 43 2987—2988 (1970)

The Synthesis of Methyl α-Methoxyacrylate

Norio OGATA, Shun-ichi NOZAKURA and Shunsuke MURAHASHI

Faculty of Science, Osaka University, Toyonaka, Japan

(Received April 13, 1970)

In the course of our study of the polymerization of internal olefins, we attempted to prepare methyl β-methoxyacrylate (β-MMOA) and undertook the reaction of sodium methoxide ($NaOCH_3$) with methyl α,β-dibromopropionate (I). It was found, however, that methyl α-methoxyacrylate (α-MMOA) is unexpectedly formed. This is in contrast with the case of α,β-dibromopropionic acid,[1] where it has been shown that α,β-dibromopropionic acid, on treatment with boiling methanolic $NaOCH_3$, yields β-methoxyacrylic acid.

α-MMOA has been prepared either by the reaction of phosphorous pentoxide with methyl α,α-dimethoxypropionate[2] or by the reaction of piperidine with methyl β-bromo-α-methoxypropionate.[3]

In the present study, the reaction of $NaOCH_3$ with compound I at various molar ratios at room temperature was examined, and the course of the reaction leading to the formation of α-MMOA was elucidated.

The reaction paths are summarized in Fig. 1. The reaction of more than 2 mol equivalents of $NaOCH_3$ with compound I gives α-MMOA in good yields. The structure of α-MMOA was

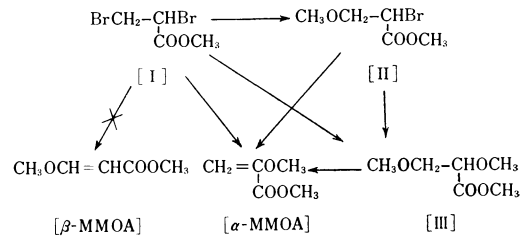

Fig. 1

established by the study of its NMR spectra and that of its hydrogenated product, methyl α-methoxypropionate, and by derivation to a known compound, α-methoxypropionamide. When the reactions were carried out in boiling methanol, similar results were obtained, but in somewhat lower yields.

When an equimolar amount of $NaOCH_3$ is used in the reaction, the main product is compound II, as has been reported in the literature.[4] The structure of compound II was confirmed by a comparison of its NMR and IR spectra with those of authentic methyl α-bromo-β-methoxypropionate prepared by the procedure of Carter.[5]

1) L. N. Owen and H. M. B. Somade, *J. Chem. Soc.*, **1947**, 1030.
2) K. Auwers, *Ber.*, **44**, 3514 (1911).
3) J. W. Baker, *J. Chem. Soc.*, **1942**, 520.
4) J. L. Wood and V. du Vigneaud, *J. Biol. Chem.*, **134**, 413 (1940).
5) a) L. R. Schilz and H. E. Carter, *ibid.*, **116**, 793 (1936). b) H. E. Carter and H. D. West, "Organic Syntheses," Coll. Vol. III, p. 774 (1955).

Table 1. Dependence of product distribution on the molar ratio of $NaOCH_3$ to compound I[a]

$NaOCH_3$/I (molar ratio)	Addition[b] procedure	Yield (%)[c] II	III	α-MMOA
1.15	B	77	19	0
1.20	A	75	24	0
1.48	A	45	52	3
1.82	A	9	62	21
1.85	B	4	53	36
2.05	A	0	8	67
2.31	A	0	7	75
2.38	B	0	6	79
2.99	A	0	5	79

a) After 5 days, at room temperature. Amounts of compound I and methanolic $NaOCH_3$ were 8 m*l* (6.35—6.50 mol) and 50 m*l*, respectively.
b) A: A methanolic $NaOCH_3$ was added to compound I at −4°C.
B: Compound I was added to $NaOCH_3$-methanol solution at −4°C.
c) Determined by gas chromatography using calibration curves.

When the reaction is carried out with 1.50—1.85 mol equivalents of $NaOCH_3$, the main product is methyl α,β-dimethoxypropionate (III). Its structural assignment was based on elementary analysis and its NMR spectrum.

The distribution of the product is remarkably affected by the molar ratio of $NaOCH_3$/I, but only slightly by the addition procedure, as is shown in Table 1. From these data, it seems reasonable to assume that the reaction of $NaOCH_3$ with compound I results in the formation of compound II in the first stage, followed by the formation of compound III and/or α-MMOA. In order to clarify these points, the behavior of compounds II and III in a high concentration of $NaOCH_3$ was examined. The reaction of compound II with methanolic $NaOCH_3$ (the molar ratio of $NaOCH_3$/II=0.98) resulted in the formation of α-MMOA (85%), together with a small amount of compound III (9%). By the reaction of compound III with methanolic $NaOCH_3$ (the molar ratio of $NaOCH_3$/III=1.64), α-MMOA was also obtained (80%). These results suggest that the reaction route is in the order:

$$\text{I}\rightarrow\text{II}\rightarrow\text{III}\rightarrow\alpha\text{-MMOA}.$$

Experimental

Equimolar Reaction of $NaOCH_3$ with Compound I. A solution of 7.7 g (0.34 mol) of sodium in 100 m*l* of dry methanol was added dropwise with mechanical stirring into 80.3 g (0.33 mol) of compound I (bp 97—98°C/24 mmHg) at −2——4°C. At the end of addition, the ice-salt bath was removed and the mixture was stirred at room temperature for 1.5 hr. After dry ice had then been added to neutralize remaining alkali, the precipitate was removed by filtration. Water was added to the filtrate, and it was extracted with chloroform. The chloroform solution was washed with water and dried over anhydrous magnesium sulfate. Distillation gave a product, II; bp 68—70°C/11 mmHg; yield, 48.5 g (76%). Found: C, 30.54; H, 4.69; Br, 40.0%. Calcd for $C_5H_9O_3Br$: C, 30.48; H, 4.60; Br, 40.6%. NMR (CCl_4, 60 MHz): τ= 6.22 (s, $COOCH_3$), 6.63 (s, OCH_3), 5.67—6.42 (m, α and β CH).

Methyl α-Bromo-β-methoxypropionate. Methyl α-bromo-β-methoxypropionate was prepared by the procedure of Carter[5b] from 54 g of methyl acrylate, 120 g of mercuric acetate, 72 g of potassium bromide, and 90 g of bromine. Yield, 54 g. The dibromoester was removed from the reaction mixture by gas chromatography (Apiezon M—Celite 545, 2 m; 130°C). (Found: C, 30.83; H, 4.69; Br, 41.0%).

Reaction of 2 Mol Equivalents of $NaOCH_3$ with Compound I. Compound I (110 g, 0.45 mol) was added to a solution of 21.6 g (0.94 mol) of sodium in 310 m*l* of dry methanol. The mixture was allowed to stand at room temperature overnight and then treated as has been described above. The product (47 g), which boiled at 43.5—54.0°C/7 mmHg, was found by gas chromatography to contain compounds II, III, and α-MMOA in 10, 43, and 47 mol% respectively. Compound III was purified by gas chromatography. Found: C, 48.29; H, 8.08%. Calcd for $C_6H_{12}O_4$: C, 48.62; H, 8.16%. NMR (CCl_4, 60 MHz): τ= 6.29 (s, $COOCH_3$), 6.63 and 6.68 (s, α and β OCH_3, respectively), 6.08—6.67 (m, α and β CH).

Reaction of 2.5 Mol Equivalents of $NaOCH_3$ with Compound I. Compound I (106 g, 0.43 mol) was similarly added to a solution of 25.3 g (1.1 mol) of sodium in 400 m*l* of dry methanol. The mixture was kept at room temperature for 10 days, until there were no peaks of compounds II and III in a gas chromatogram, and then worked up as before. Fractional distillation in the presence of 0.5 g of hydroquinone under a reduced pressure of nitrogen gave α-MMOA. Bp 50.5—51.0°C/10 mmHg (lit, 51.5—52.0°C/11 mmHg[3]). Yield, 38.9 g (78%). Found: C, 51.76; H, 6.94%. Calcd for $C_5H_8O_3$: C, 51.72; H, 6.94%. NMR (CCl_4, 60 MHz): τ=6.23 (s, $COOCH_3$), 6.39 (s, OCH_3), 4.78 and 5.47 d, J=2.4 Hz, $=CH_2$). IR (liq.): 3130 (w, $\nu_{=CH_2}$), 1625) cm^{-1} (vs, $\nu_{C=C}$). The hydrogenationof the ester was performed by Raney nickel to give methyl α-methoxypropionate. Bp 130.5—131.0°C. NMR (CCl_4, 60 MHz): τ=8.67 (d, J=6.8 Hz, CH_3), 6.01—6.37 (q, CH), 6.27 (s, $COOCH_3$), 6.67 (s, OCH_3). α-MMOA was converted by aqueous ammonia into α-methoxyacrylamide. Mp 108—110°C(lit, 109°C[3]), after recrystallization from benzene. The hydrogenation of α-methoxyacrylamide catalyzed by palladium chloride gave α-methoxypropionamide. Mp 83—84°C, after recrystallization from ligroin. NMR ($CHCl_3$, 60 MHz): τ=8.53 (d, J=6.9 Hz, CH_3), 6.00—6.35 (q, CH), 6.51 (s, OCH_3).

Reactions of $NaOCH_3$ with Compounds II and III. Compounds II and III were added to methanolic $NaOCH_3$. The reactions were followed by taking gas chromatograms of the reaction mixtures using calibration curves.

BULLETIN OF THE CHEMICAL SOCIETY OF JAPAN VOL. 43 2989—2990 (1970)

Studies of Heteroaromaticity. XLVI.[1] Syntheses of 2,5-Disubstituted 1,3,4-Oxadiazoles Containing Nitrofuran Nucleus

Tadashi SASAKI and Toshiyuki YOSHIOKA

Institute of Applied Organic Chemistry, Faculty of Engineering, Nagoya University, Chikusa-ku, Nagoya

(Received April 13, 1970)

In a previous paper, we reported that aroyl and ary nitrile oxides have a similar reactivity in the 1,3-dipolar cycloaddition.[2] In continuation of our studies on similar reactivity of the nitrile imines,[3] this paper describes our attempts to prepare *N*-aroyl nitrile imines. 1-α-chlorobenzylidene-2-ethoxycarbonylhydrazine is reported to cyclize by triethylamine to 2-phenyl-5-ethoxy-1,3,4-oxadiazole[4] and in a similar manner, aryhydrazonochloroacetic acids cyclize to 4-aryl-5-oxo-1,3,4-oxadizol-2-ines.[5] Both cyclization reactions might be explained by postulating intermediate *N*-ethoxycarbonyl benzonitrile imine (A) and *C*-carboxynitrile imine (B), respectively.

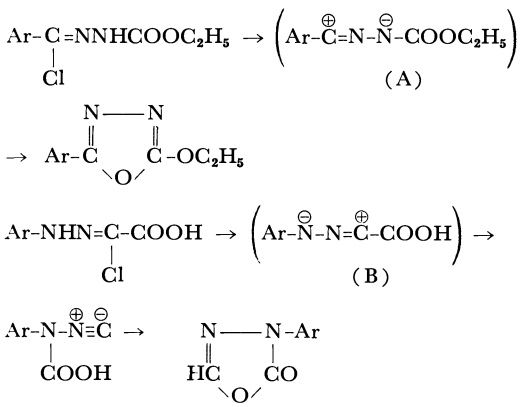

As in the preparation of the nitrile imines,[3] lead tetraacetate-oxidation of the readily available aroylhydrazones (II) from aroylhydrazines (I) was carried out at room temperature. The products were characterized as 2,5-disubstituted 1,3,4-oxadiazoles (III), simple oxidation products of aroylhydrazones which provide general procedure for the preparation of 2,5-disubstituted 1,3,4-oxadiazoles.[6] The recent appearance of an article on a similar subject[7] prompted us to write this note. A sequence of the reaction and the mechanism postulated for the preparation of III are given below.

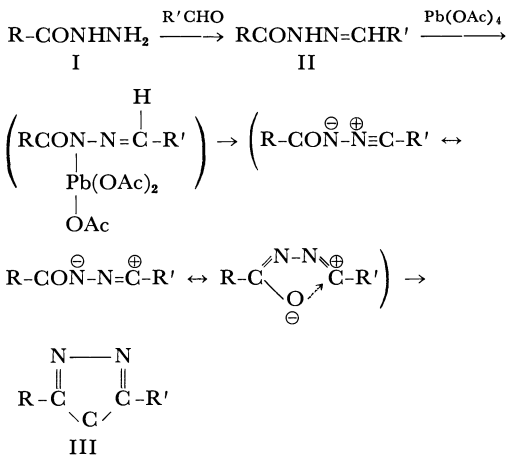

The results are summarized in Tables 1 and 2.

Experimental[8]

Starting Materials. Aroylhydrazines (Ia:[9] 5-nitro-2-furoyl, Ib:[10] 5-nitro-2-furylacroyl, and Ic:[11] benzoylhydrazine) and 5-nitro-2-furylacrolein[12] were prepared by the known procedures. All the other aldehydes were commercial products.

General Procedure. *Conversion of I to II.* A mixture of 0.6 g (3.5 mmol) of 5-nitro-2-furoylhydrazine

1) Part XLV: T. Sasaki, K. Kanematsu and A. Kakehi, *Chem. Commun*, **1970**, 1030.

2) T. Sasaki, T. Yoshioka and Y. Suzuki, This Bulletin, **43**, 2991 (1970).

3) T. Sasaki and T. Yoshioka, *ibid.*, **43**, 1254 (1970).

4) T. Bacchetti, *Gazz. Chem. Ital.*, **91**, 866 (1961).

5) M. O. Losinskii and P. S. Pelkis, *Zh. Obshch. Khim.*, **32**, 526 (1962); **33**, 2231 (1963).

6) A. Hetzheim and K. Mockel, "Advances in 1,3,4-Oxadiazole Chemistry," in "Advances in Heterocyclic Chemistry," Vol. 7, A. R. Katritzky and A. J. Boulton Ed., Academic Press, New York (1966), p. 190.

7) W. A. F. Glaston, J. B. Aylward and R. O. C. Norman, *J. Chem. Soc., C*, **1969**, 2587.

8) The melting points were measured on a micro hot stage and are not corrected. The microanalyses were carried out with a Perkin-Elmer Model 240 Elemental Analyzer. The ultraviolet spectra were obtained on a JASCO ORD/UV-5 and the infrared spectra on a JASCO IR-S spectrometer.

9) M. Amorosa and L. Lipparini, *Ann. Chim.* (Rome), **45**, 724 (1955).

10) T. Sasaki, *Chem. Pharm. Bull.* (Tokyo), **2**, 95 (1954).

11) T. Curtius and H. Franzen, *Ber.*, **35**, 3421 (1902).

12) H. Saikachi and H. Ogawa, *J. Amer. Chem. Soc.*, **80**, 3462 (1958).

Table 1. Acylhydrazones

RCONHN=CHR'

II

R	R'	Product	Mp. °C	Yield %	Found (Calcd) C%	H%	N%	UV λ_{max}^{EtOH} mμ ($\varepsilon \times 10^{-4}$)	IR ν_{CO}^{KBr} cm^{-1}
NF-*	C_6H_5-	IIa	212—214	85	55.58 (55.60	3.58 3.50	16.35 16.21)	322 (1.7), 298 (1.58), 280 (1.7)	1665
NF-	*p*-Cl-C_6H_4-	IIb	226—229	80	48.95 (49.08	2.75 2.72	14.25 14.31)		1665
NF-	*p*-CH_3-C_6H_4-	IIc	210—214	70	57.20 (57.14	4.15 4.06	15.45 15.38)		1670
NFCH=CH-	C_6H_5-	IId	218—220	90	58.85 (58.94	3.95 3.89	14.80 14.73)		1660
C_6H_5-	NF-	IIe	215—219	90	55.55 (55.60	3.65 3.50	16.15 16.21)		1660
C_6H_5-	NFCH=CH-	IIf	233—235	90	59.05 (58.94	3.78 3.89	14.75 14.73)		1640

* NF: 5-nitro-2-furyl

Table 2. Oxadiazoles

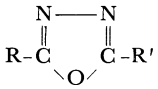

III

R	R'	Product	Mp °C	Yield %	Found (Calcd) C%	H%	N%	UV λ_{max}^{EtOH} mμ ($\varepsilon \times 10^{-4}$)	IR $\nu_{C=N}^{KBr}$ cm^{-1}
NF-	C_6H_5-	IIIa	231—232	80	56.15 (56.03	2.85 2.74	16.45 16.34)	332 (1.55) 266 (1.14)	1610
NF-	*p*-Cl-C_6H_4-	IIIb	216—217	75	49.35 (49.42	2.15 2.06	14.55 14.41)	330 (1.8) 268 (1.4)	1615
NF-	*p*-CH_3-C_6H_4-	IIIc	180—182	85	57.65 (57.56	3.45 3.34	15.55 15.49)	336 (1.68) 268 (1.29)	1610
NFCH=CH-	C_6H_5-	IIId*	216—218	40	59.45 (59.36	3.35 3.20	14.95 14.84)	368 (2.34) 292 (1.06)	1605
C_6H_5-	NF-	IIIa	227—231	70				233 (1.16)	1610
C_6H_5-	NFCH=CH-	IIId	215—217	30					1605

* A. Sugihara and M. Ito, *Yakugaku Zasshi*, **85**, 744 (1965); mp 205—206°C.

(Ia) and 0.4 g (3.5 mmol) of benzaldehyde was refluxed in 40 m*l* of ethanol for 7 hr. After cooling, the precipitates were collected and recrystallized from ethanol to give 0.85 g (85%) of 1-benzylidene-2-(5-nitro-2-furoyl)-hydrazine (IIa). The results of similar reactions using several aroyhydrazines and aromatic aldehydes are summarized in Table 1.

Conversion of II to III. To a stirred suspension of 0.5 g (2 mmol) of IIa in 100 m*l* of dichloromethane was added 1.3 g (3 mmol) of lead tetraacetate at room temperature. The mixture was stirred at room temperature for 2 days. After filtering off the undissolved materials, the solvent was removed under reduced pressure. The residue was recrystallized from ethanol-benzene-tetrahydrofuran to afford 0.38 g (80%) of 2-(5-nitro-2-furyl)-5-phenyl-1,3,4-oxadiazole (IIIa), 231—232°C (decomp.). Analytical and spectral data are summarized in Table 2.

BULLETIN OF THE CHEMICAL SOCIETY OF JAPAN VOL. 43 2991—2993 (1970)

Reactions of Aromatic Hydroxamoyl Chlorides with Benzamidoxime Involving a Novel Synthesis of the 1,4-Dioxa-2,5-diazine Ring System[1]

Tadashi SASAKI, Toshiyuki YOSHIOKA and Yasuyuki SUZUKI

Institute of Applied Organic Chemistry, Faculty of Engineering, Nagoya University, Chikusa-ku, Nagoya

(Received April 16, 1970)

N-Phenylbenzamidoxime is known to react with benzonitrile oxide to afford the *O*-benzoyl oxime as a major product together with small amounts of benzanilide and diphenylfuroxan, but without detailed documentation for the formation mechanism.[2]

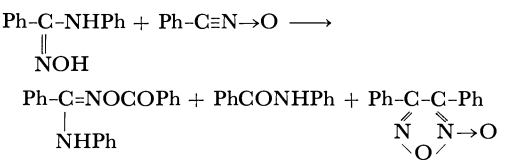

In a previous paper,[3] we have reported the 1,3-dipolar cycloaddition reactions of aromatic hydroxamoyl chlorides, a precursor to the nitrile oxides, with two equivalents amounts of basic dipolarophiles in ether at room temperature leading to the formation of five-membered heterocycles. Under similar conditions, we treated benzhydroxamoyl chloride (**1**) with benzamidoxime (**2**). Two products isolated from the ether-soluble part were characterized as *O*-benzoylbenzamidoxime (**3**) and diphenylfuroxan (**4**) together with benzamide (**5**) from the ether-insoluble part. Compound **3** was alternatively prepared from **2** and benzoyl chloride. When refluxed in toluene, **3** was converted to known 3,5-diphenyl-1,2,4-oxadiazole (**6**).

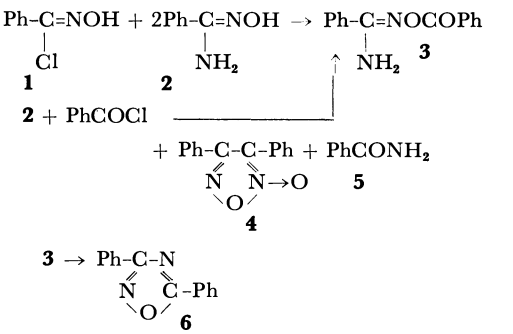

Considering that the types of these products are similar to those from the reaction of benzonitrile oxide with *N*-phenylbenzamidoxime, both reactions are concluded to proceed in the same manner as illustrated in Scheme 1; the nitrile oxide attacks to the hydroxyl, not to the amino group of **2**,[4] leading to the intermediate **7** or **8**, which was hydrolyzed[5] at (a) linkage to give *O*-benzoylbenzamidoxime or **3**, while the hydrolysis at (b) linkage afforded **4** and benzanilide or **5**. The results indicate that both types of the cleavage have occurred competitively.

Expecting similar results, 5-nitro-2-furyl-(**9**), *p*-(**10**) and *m*-nitrobenzhydroxamoyl chloride (**11**) were treated with **2** under similar conditions. From the reaction of **9** and **2**, two crystalline products, **12** and **13**, were isolated from the ether-soluble and insoluble part of the reaction mixture, respectively. The infrared spectrum (KBr) of **12** showed no absorptions due to amino and carbonyl but a strong one at 1200 cm^{-1} presumably due to cyclic ether, and medium ones at 1645 and 1610 cm^{-1} due to –C=N– instead of strong ones at 1600—1625 cm^{-1} characteristic in furoxan structure,[6] while **13** manifested amino (3500), hydroxyl (3225) and carbonyl (1750 cm^{-1}) absorptions, though the first amino absorption was slightly different from that of **3**, in which two amino-absorptions at 3450 and 3400 cm^{-1} indicate the presence of the primary amino group. The analysis of **12** supports a chemical formula $C_{12}H_7O_5N_3$, suggesting the so-called dimer-type structure of the nitrile oxide as expressed by **12′** and **12″**. Recently, Morrocchi *et al.*[7] have reported on the application of mass spectroscopy for distinguishing these isomeric dimers. We adopted this method for determining the structure. As depicted in Fig. 1, the most abundant peak corresponds to benzonitrile ion instead of disubstitued acetylene or aromatic carbonyl ions originated from **12′**

1) Studies on Heteroaromaticity, XLII. Part XLI of this series: T. Sasaki, T. Yoshioka and Y. Suzuki, *Yuki Goseikagaku Kyokai-shi*, **28**, 647 (1970).

2) J. H. Boyer and P. J. A. Frints, *J. Org. Chem.*, **33**, 4554 (1968).

3) T. Sasaki and T. Yoshioka, This Bulletin, **42**, 3335 (1969).

4) N. E. Alexandrou and D. N. Nicoloides, *Tetrahedron Lett.*, **1966**, 2497.

5) Under anhydrous conditions, a hydrolysis cannot occur. We used commercially available ether directly.

6) N. E. Bover and H. R. Snyder, *J. Amer. Chem. Soc.*, **77**, 4238 (1955).

7) S. Morrocchi, A. Ricca and A. Zanarotti, *Gazz. Chim. Ital.*, **99**, 165 (1969).

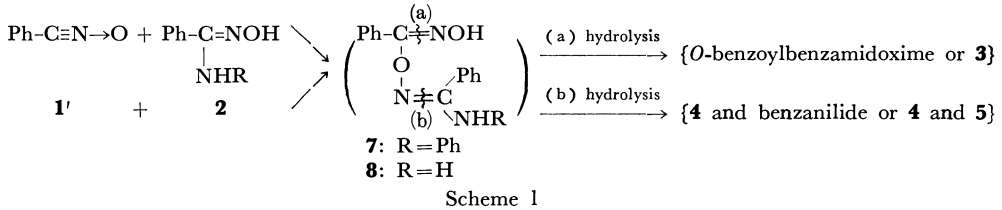

Scheme 1

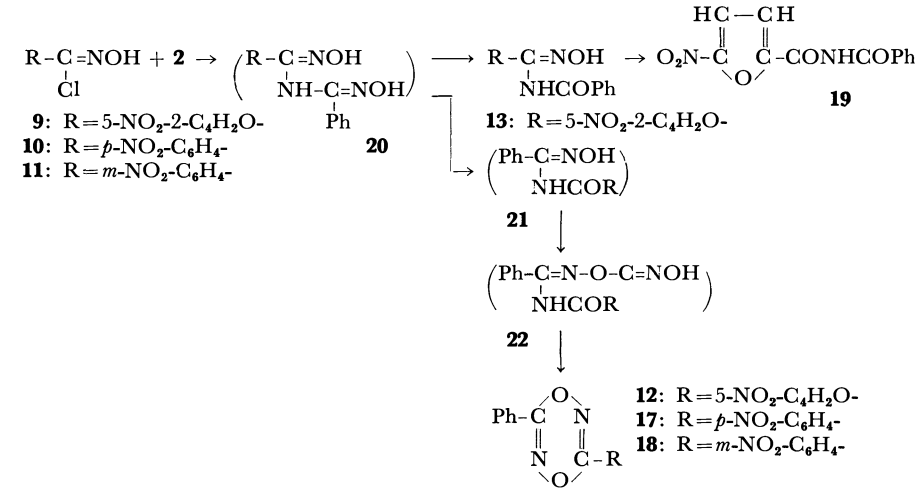

Scheme 2

and **12''** respectively,[7] demonstrating the structure to be **12** having 1,4-dioxa-2,5-diazine structure. When refluxed in toluene for 8 hr, **12** was converted to benzonitrile and 5-nitro-2-furocarbonitrile in 50% conversion with 20% recovery of **12**.

On the other hand, the analysis of **13** indicated a chemical formula $C_{12}H_9O_5N_3$, the same as the corresponding *O*-benzoate **14**. This compound was independently prepared from the amidoxime **15** and benzoyl chloride; the infrared spectrum of **14** was, however, slightly different from **13**. Furthermore, **13** remained unchanged on refluxing in toluene for a long time, while **14** was readily converted to known 3-(5-nitro-2-furyl)-5-phenyl-1,2,4-oxadiazole (**16**) under similar conditions. **13** was hydrolyzed to the benzoyl amide **19**. Finally, we assigned to **13** an *N*-benzoylamidoxime structure. From similar reactions of **10** and **11** with **2**, products **17** and **18** were obtained 50 and 70% yields, respectively. Both products showed the infrared and mass spectral patterns similar to those of **12** (Fig. 2 and Experimental), indicating the presence of 1,4-dioxa-2,5-diazine ring as the common structure. It should be noteworthy that any ring-opened compound corresponding to **13** was not isolated from both reaction mixtures.

The 1,4-dioxa-2,5-diazine has been a ring system of not beyond assumption for a long time[8] until recently the preparation of the *symmetrically* disubstituted dioxadiazines has been reported by Morrocchi *et al.*[7] Our procedure provides the first example for synthesizing *unsymmetrically* disubstituted ones.

The mechanism for the formation is uncertain but may probably be depicted in Scheme 2; the initial attack of the hydroxamoyl chloride to the amino group of **2** at the chlorine atom activated by the electronegative R group, not to the hydroxyl group *via* the nitrile oxide as in Scheme 1, results in the substitution, affording an intermediate **20**, which is convertible to the *N*-benzoylamidoxime **13** upon hydrolysis. Another hydrolysis product **21** reacts with **9** to afford **22** and its cyclization by elimination of amide affords **12**.

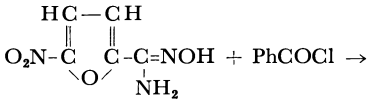

15

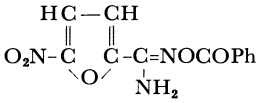

14

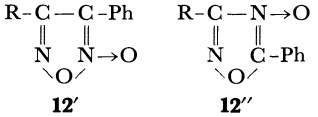

12' **12''**

8) For instance, see C. Grundman, H-D. Frommeld, K. Flory and S. K. Datta, *J. Org. Chem.*, **33**, 1464 (1968); A. Quilico, "The Chemistry of Heterocyclic Compounds," Vol. 17, A. Weissberger Ed., Interscience Publ., New York (1962), p. 21.

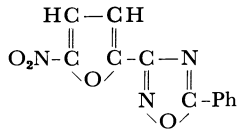

16

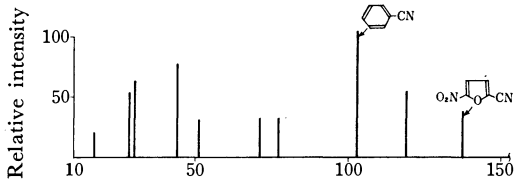

Fig. 1. The mass spectrum of **12**.

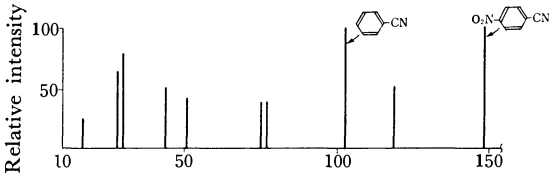

Fig. 2. The mass spectrum of **17**.

Experimental[9]

Reaction of Benzhydroxamoyl Chloride with Benzamidoxime. A solution of 1 g of benzamidoxime in 30 m*l* of ether was added to a solution of 0.5 g of benzhydroxamoyl chloride in 20 m*l* of ether at room temperature with stirring. The reaction mixture was allowed to stand for one month. The resulting precipitates were collected by filtration, washed with a small amount of cold water, and recrystallized from water to give benzamide, mp 130°C. The solvent was removed from the filtrate and the residual oil was extracted with ether (10 m*l*×3). The ether extracts were dried (Na_2SO_4) and evaporated. The residue was chromatographed on silicic acid (Mallinckrodt, 100 mesh), using chloroform as the eluent. The first fraction (150 mg, 30%) was recrystallized from ethanol to give **4**, mp 118°C, which was identified by the infrared spectral comparison with an specimen.[10] The second fraction (300 mg, 40%) was recrystallized from benzene to afford **3** as colorless crystals, mp 153°C.

Found: C, 70.10; H, 4.94; N, 11.71%. Calcd for $C_{14}H_{12}O_2N_2$: C, 69.99; H, 5.03; N, 11.66%.

***O*-Benzoylbenzamidoxime (3).** To a stirred solution of 1.3 g of benzamidoxime and 1.1 g of triethylamine in 60 m*l* of benzene was added dropwise 1.4 g of benzoyl chloride under cooling with ice-water.

After stirring for one day at room temperature, the resulting precipitates were collected by filtration, washed with water and recrystallized from ethanol to give 1.9 g (80%) of **3**, mp 153°C.

3,5-Diphenyl-1,2,4-oxadiazole (6). A solution of 0.7 g of **3** in 30 m*l* of toluene was refluxed for 12 hr. The solvent was removed under reduced pressure and the residue was recrystallized from ethanol to give 0.6 g (85%) of **6**, mp 109°C (lit,[11] mp 109°C).

Reaction of 5-Nitro-2-furylhydroxamoyl Chloride with the Amidoxime. A solution of 0.5 g of 5-nitro-2-furylhydroxamoyl chloride[12] and 1 g of benzamidoxime in 40 m*l* of ether was stirred at room temperature overnight. The precipitates were collected by filtration, washed with water, dried in the air and recrystallized from benzene to give 0.32 g (30%) of **12** as pale yellow crystals, mp 203—205°C (dec.). UV λ_{max}^{EtOH} mμ (ε); 223 (20000) and 308 (8600).

Found: C, 53.19; H, 2.20; N, 15.55%. Calcd for $C_{12}H_7O_5N_3$: C, 52.75; H, 2.58: N, 15.38%.

Ether was removed from the filtrate and the residue was recrystallized from benzene-ethanol to give 0.14 g (15%) of **13**, mp 191—194°C (dec.).

Found: C, 52.59; H, 3.39; N, 15.43%. Calcd for $C_{12}H_9O_5N_3$: C, 52.37; H, 3.30; N, 15.27%.

***O*-Benzoyl-5-nitro-2-furocarbamidoxime (14).** This was prepared in 75% yield from 5-nitro-2-furocarbamidoxime (**15**)[13] and benzoyl chloride as pale yellow crystals, mp 214—217°C.

Found: C, 52.43; H, 3.19; N, 15.05%. Calcd for $C_{12}H_9O_5N_3$: C, 52.37; H, 3.30; N, 15.27%.

3-(5-Nitro-2-furyl)-5-phenyl-1,2,4-oxadiazole (16). Treatment of **14** similar to the preparation of **6** afforded 90% yield of **16**, mp 205°C (lit[11] mp 205°C).

3-(*p*-Nitrophenyl)-6-phenyl-1,4-dioxa-2,5-diazine (17). A solution of 1 g of *p*-nitrobenzhydroxamoyl chloride[3] and 1.4 g of benzamidoxime in 50 m*l* of ether was stirred at room temperature for several days. The resulting precipitates were collected by filtration, washed with water, dried in the air and recrystallized from benzene-ethanol to afford 0.52 g of **17** as yellow needles, mp 208—209°C (dec.). From the ethereal mother liquor, further 0.15 g of **17** was obtained. Total yield was 50%. IR (KBr): 1635 (–N=C–) and 1205 cm^{-1} (–O–).

Found: C, 59.55; H, 3.31; N, 14.88%. Calcd for $C_{14}H_9O_4N_3$: C, 59.36; H, 3.20; N, 14.84%.

3-(*m*-Nitrophenyl)-6-phenyl-1,4-dioxa-2,5-diazine (18). Similarly, 1 g (70%) of **18** was obtained as colorless crystals, mp 195°C (dec.), from *m*-nitrobenzhydroxamoyl chloride[3] (0.8 g) and benzamidoxime (1.5 g). IR (KBr): 1620 (–N=C–) and 1210 cm^{-1} (–O–). Mass Spectrum *m/e* (rel. intensity): 103 (100) and 148 (100).

Found: C, 59.35; H, 2.92; N, 14.93%. Calcd for $C_{14}H_9O_4N_3$: C, 59.36; H, 3.20; N, 14.84%.

Hydrolysis of 13 to *N*-benzoyl-5-nitro-2-furoylamide (19). A solution of **13** in ethanol was refluxed in the presence of 3% hydrochloric acid. The resulting precipitates after cooling were collected by filtration and recrystallized from ethanol-water to give 85% yield of **19**, mp 215°C.

Found: C, 55.45; H, 3.25; N, 10.65%. Calcd for $C_{12}H_8O_5N_2$: C, 55.39; H, 3.10; N, 10.77%.

9) Melting points are uncorrected. Infrared spectra were obtained on a Nippon-Bunko IR-S, ultraviolet spectra on a Nippon-Bunko ORD/UV-5 spectrometer. Mass spectra were measured on a Hitachi RMU-6D mass spectrometer at 70 eV.

10) A. Werner and H. Buss, *Ber.*, **27**, 2199 (1894).

11) T. Sasaki and T. Yoshioka, This Bulletin, **41**, 2206 (1968).

12) H. Rheinboldt, *Ann. Chem.*, **451**, 166 (1927).

13) T. Sasaki and T. Yoshioka, *Yuki Gosei Kagaku Kyokai Shi*, **25**, 665 (1967).

BULLETIN OF THE CHEMICAL SOCIETY OF JAPAN VOL. 43 2994—2995 (1970)

The Photoconductivity in a CCl_4 Solution of *N,N*-Dimethylaniline

Shunsuke MATSUDA, Hiroshi KOKADO and Eiichi INOUE

Imaging Science and Engineering Laboratory, Tokyo Institute of Technology, Ookayama, Meguro-ku, Tokyo

(Received April 14, 1970)

We have examined the photoconductivity in the solution of *N,N*-dimethylaniline in carbon tetrachloride. The carbon tetrachloride used was of a spectrograde and was not purified further. The *N,N*-dimethylaniline was purified by repeated vacuum distillation. The solution showed a remarkable photoconductivity upon ultraviolet irradiation (320—400 nm).

Since carbon tetrachloride is transparent at the wavelength of the exciting light, the photocurrent must be associated with the excited *N,N*-dimethylaniline.

However, since the solution of *N,N*-dimethylaniline in inert solvents such as cyclohexane, *n*-hexane, or benzene was not photoconductive, the photocurrent seems to be caused by an interaction between *N,N*-dimethylaniline and carbon tetrachloride. There are two possibilities in the mechanism of the interaction: energy transfer from the amine to the halide, and charge transfer in the excited states.*1 The latter was proposed by Latowsky in studying the photo-reactions in an ethanolic solution of aromatic amines and aromatic halides.[1]

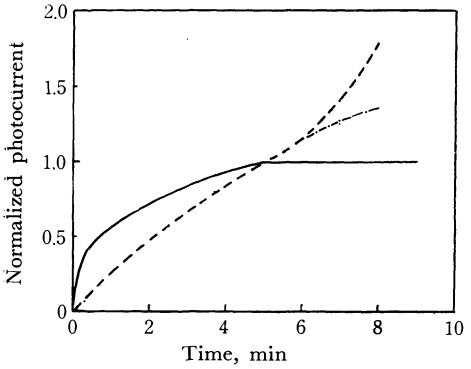

Fig. 1. Photocurrent profiles of solutions of three solutes in CCl_4.
(—·—·) *N,N*-dimethylaniline
(- - - - -) MGCN
(———) MGH.
Exciting light, $\lambda = 320-400$ nm, from a 100 W high pressure Hg lamp. 3 V/cm.

In the charge-transfer mechanism the elementary processes are: (1) light absorption by *N,N*-dimethylaniline, (2) the electron transfer from the excited molecule to a carbon tetrachloride molecule, (3) the dissociation of the carbon tetrachloride anion to the chloride ion and the trichloromethyl radical,[2] and (4) various reactions which are initiated by the radicals.

To get some evidence for the charge-transfer mechanism, leuco malachite green (MGH) and malachite green leuconitrile (MGCN) were studied instead of *N,N*-dimethylaniline. The absorption spectra due to the dimethylanilino group in both materials are similar to those of *N,N*-dimethylaniline.[3]

Both materials, when dissolved in CCl_4, induced a photocurrent, the MGH solution became green, but the MGCN solution did not.

These results can be easily understood by assuming the charge-transfer mechanism for the initial photoinduced processes in these systems. A plausible mechanism for the dye formation is as follows:

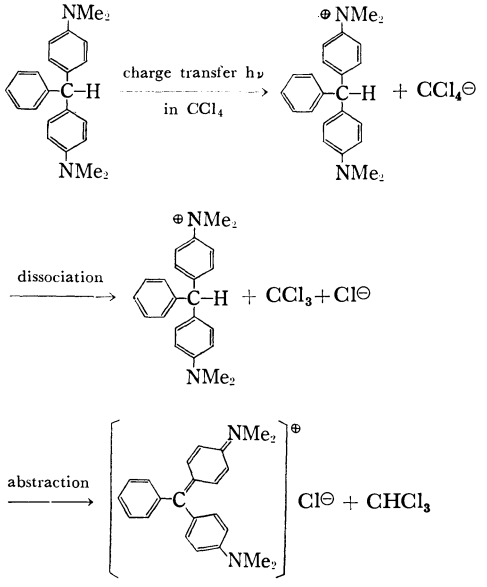

*1 In this system, there is a possibility of a weak charge-transfer interaction even in the ground state. See K. M. C. Davis and M. F. Farmer, *J. Chem. Soc., B*, **1967**, 28

1) T. Latowsky, *Z. Naturforschg.*, **23a**, 1127 (1968).

2) N. R. Daly and R. G. Ridley, *Nature*, **202**, 895 (1964).

3) A. H. Sporer, *Trans. Faraday Soc.*, **57**, 983 (1961).

The failure of color to develop in the MGCN solution indicates that the CN abstraction from the center carbon atom of MGCN is difficult.

By analogy with the results on these leucobases of malachite green, we may deduce that the photoconduction of the system is caused by the charge transfer from excited *N,N*-dimethylaniline molecules to CCl_4 molecules.

BULLETIN OF THE CHEMICAL SOCIETY OF JAPAN VOL. 43 2995—2996 (1970)

Oxidation of Cyclododecane-1,5,9-triol

Shinsaku FUJITA and Hitosi NOZAKI

Department of Industrial Chemistry, Kyôto University, Yoshida, Kyôto

(Received April 15, 1970)

Although transannular reactions of 8-10-membered cyclic compounds have been well investigated,[1] few examples have been reported on cyclododecane derivatives.[2] The present paper deals with a new transannular interaction in the oxidation of *cis,cis,trans*-cyclododecane-1,5,9-triol (I).[3]

Oxidation of I by the Brown procedure (sodium dichromate-sulfuric acid-ether) gave a hemiacetal (II) and an acetal (III) (II : III=43 : 57). The product ratio was considerably changed (II : III= 74 : 26) in the Cornforth oxidation (chromium-(VI) oxide-pyridine-water) of I. No detectable amount of cyclododecane-1,5,9-trione was obtained in each case. Facile formation of six-membered cyclic acetals seems to prevent the oxidation from proceeding to the stage of trione.

Compound II exhibited IR absorptions at 3490 (ν_{O-H}) and 1697 cm^{-1} ($\nu_{C=O}$) and was dehydrated quite easily on distillation and/or gas chromatography to give the corresponding enol ether (IV) (1710 and 1677 cm^{-1}). The reverse hydration of IV afforded the starting compound II. Acetylation of II with acetic anhydride yielded 9-acetoxycyclododecane-1,5-dione (V). The structure of V was shown to be monocyclic, since its NMR spectrum exhibited the signal of a methine proton adjacent to acetoxyl group at δ 4.47 ppm. Consequently, compound II must be the intramolecular hemiacetal of 9-hydroxycyclododecane-1,5-dione (1-hydroxy-13-oxabicyclo[7.3.1]tridecan-5-one), which is in equilibrium with monocyclic hydroxydione II′ affording V on acetylation.

Another oxidation product (III) exhibited IR absorptions between 1250—900 cm^{-1} attributable to ethereal function. The absence of carbonyl group was proved by the IR spectrum. The parent peak at *m/e* 196 in the mass spectrum and the elementary analysis established the molecular formula of $C_{12}H_{20}O_2$. The NMR spectrum in carbon tetrachloride showed the signal of the methylene protons as a complex multiplet. Hence, III was concluded to be the intramolecular acetal of 5,9-dihydroxycyclododecanone (13,14-dioxatricyclo[7.3.1.$1^{1,5}$]tetradecane). Although the stereochemistry of III is not certain at present, the strainless configuration of C_2 symmetry (III′) may be preferred on the basis of the Dreiding model.

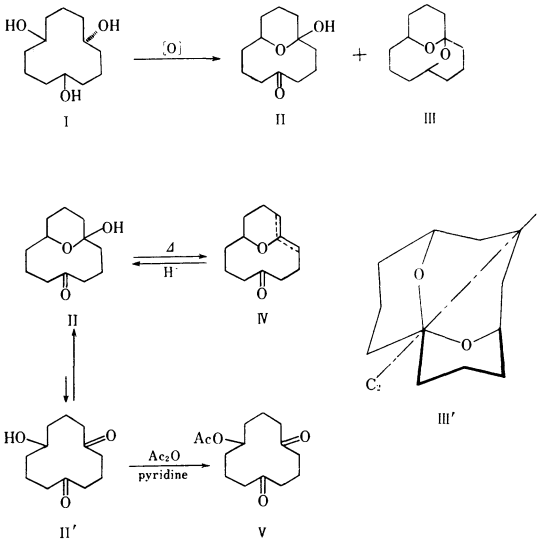

Experimental

Oxidation of *cis,cis,trans*-cyclododecane-1,5,9-triol (I). *(a) Brown's Oxidation.*[4] To a mixture of I (5.41 g, 25 mmol), water (25 m*l*) and ether (100 m*l*)

1) A. C. Cope, M. M. Martin and M. A. McKervey, *Quart. Rev.* (London), **20**, 119 (1966).

2) a) B. Camerino and B. Patelli, *Experientia*, **20**, 260 (1964). b) L. A. Paquette and M. L. Wise, *Tetrahedron*, **24**, 2937 (1968). c) T. Mori, K. Matsui and H. Nozaki, This Bulletin, **43**, 231 (1970).

3) a) G. W. Rotermund and R. Köster, *Ann. Chem.*, **686**, 153 (1965). b) H. C. Brown and W. C. Dickason, *J. Amer. Chem. Soc.*, **91**, 1226 (1969).

4) H. C. Brown and C. P. Garg, *J. Amer. Chem. Soc.*, **83**, 2952 (1961).

a mixture of sodium dichromate dihydrate (5.00 g, 17 mmol), 95% sulfuric acid (3.80 ml) and water (23 ml) was added dropwise for 20 min at 0°C. Stirring was continued for an additional 2 hr. The ether layer was separated and the aqueous layer was extracted twice with ether. The combined extracts were washed with aqueous sodium hydrogen carbonate and then with water, dried over sodium sulfate and concentrated *in vacuo* to give a crude mixture (4.50 g) of II and III. The ratio (II : III=43 : 57) was determined by gas chromatography (High Vacuum Silicone Grease 30% on Celite 545, 190°C). The two components were separated through a silica gel column using benzene as a solvent. The first elute was the acetal (III) (1.39 g, 28%), bp 137°C/21 mmHg. IR (neat): 1220, 1209, 1160, 1124, 1096, 1040, 1006, 962, 934, 899 and 870 cm^{-1}. NMR (CCl_4): δ 4.5—3.6 (2H, multiplet, O–CH) and 2.8—1.1 (18H, fine-structured multiplet). MS *m/e* 196 (M^+).

Found: C, 73.2; H, 10.2%. Calcd for $C_{12}H_{20}O_2$: C, 73.4; H, 10.3%.

The second elute was the hemiacetal(II) (1.21 g, 23%) as large plates, mp 54—56°C. IR (Nujol): 3490, 1697, 1320, 1237, 1206, 1180, 1158, 1141, 1118, 1086, 1046, 1017, 970, 958, 936 and 902 cm^{-1}. NMR (CCl_4): δ 4.1—3.4 (1H, multiplet, O–CH), 3.4—3.1 (1H, broad, OH) and 3.0—1.1 (18H, multiplet).

Found: C, 67.4; H, 9.5%. Calcd for $C_{12}H_{20}O_3$: C, 67.9; H, 9.5%.

Gas chromatographic separation (High Vacuum Silicone Grease, 30% on Celite 545, 198—225°C) of II resulted in dehydration to give IV as an oil, bp 115°C (bath temperature)/1 mmHg. IR (neat): 1710, 1678, 1302, 1225, 1183, 1155, 1082, 1050, 956 and 906 cm^{-1}. NMR (CCl_4): δ 4.5—4.3 (1H, multiplet, OC=CH) and 4.0—1.1 (17H. multiplet). MS *m/e* 194 (M^+).

Found: C, 74.2; H, 9.4%. Calcd for $C_{12}H_{18}O_2$: C, 74.2; H, 9.3%.

5) R. H. Cornforth, J. W. Cornforth and G. Popjàk, *Tetrahedron*, **18**, 1351 (1962).

(b) Cornforth's Oxidation.[5] To cooled pyridine (300 ml) was added an aqueous solution (25 ml) of chromium(VI) oxide (33.0 g, 0.33 mol) and then a solution of I (10.8 g, 0.050 mol) in pyridine (50 ml) during 10 min. Stirring was continued for an additional 30 min at 0°C and the mixture was allowed to stand at room temperature for 2 days. The mixture was poured into water and extracted with ether. The ether extracts were combined, washed successively with water, 5% hydrochloric acid and aqueous sodium hydrogen carbonate, and dried over sodium sulfate. After concentration, the residue (5.18 g) was subjected to gas chromatography (II : III=74 : 26).

Hydration of IV. A solution of IV (0.1 g) in ether (15 ml) and 5% hydrochloric acid (10 ml) were stirred overnight at room temperature. The aqueous layer was extracted with ether and dried over sodium sulfate. Evaporation of the solvent gave hemiacetal II which was identical with the authentic sample.

9-Acetoxycyclododecane-1,5-dione (V). A mixture of II (4.77 g, 22 mmol), acetic anhydride (15 ml) and pyridine (20 ml) was stirred at 100°C for 3 days. The reaction mixture was diluted with water (200 ml) and extracted with ether. The combined ether extracts were washed successively with water, 5% hydrochloric acid, aqueous sodium hydrogen carbonate and water. Drying over sodium sulfate and subsequent concentration gave the crude product (4.14 g) which was subjected to chromatographic separation on a silica gel column with benzene as a solvent. After the recovered hemiacetal (0.52 g, 11%) was eluted, the product (V) (2.03 g, 36%) was obtained as needles (*n*-hexane), mp 81—82°C. IR (CCl_4): 1737, 1711 and 1244 cm^{-1}. NMR (CCl_4): δ 4.6—4.2 (1H, multiplet, AcO-CH), 2.7—1.1 (18H, multiplet+singlet (δ 1.93, OAc)).

Found: C, 66.1; H, 8.9%. Calcd for $C_{14}H_{22}O_4$: C, 66.1; H, 8.7%.

The authors are grateful to Professor Keiiti Sisido for his help. Financial support from Toray Science Foundation is acknowledged.

BULLETIN OF THE CHEMICAL SOCIETY OF JAPAN VOL. 43 2997—2998 (1970)

The Reaction of Aldehydes with Dichloroacetate

Akira TAKEDA, Satosi WADA, Masatosi FUJII and Hideo TANAKA

Department of Synthetics Chemistry, School of Engineering, Okayama University, Tusima, Okayama

(Received April 18, 1970)

Base-catalyzed condensation of aldehydes with dichloroacetic ester has been reported by several workers.[1-3] Martynov and Titov[1] described that the condensation of benzaldehyde with methyl dichloroacetate in the presence of sodium methoxide afforded methyl 2-chloro-2,3-epoxy-3-phenylpropionate (**1**, R=C_6H_5, R′=CH_3). McDonald and Schwab,[2] on the contrary, assigned the structure of methyl chlorophenylpyruvate (**2**, R=C_6H_5, R′=CH_3) instead of **1** to the product of the above reaction suggesting that an anionotropic rearrangement of the intermediate **1** to form **2** has occurred. We also were unsuccessful in isolating aromatic homologs of **1** by the same reaction but obtained the corresponding arylpyruvic esters.[3] Meanwhile, the base-catalyzed cyclization of α,α-dichloro-β-hydroxyalkanecarboxylic esters to yield α-chloroglycidic esters (**1**) has been reported by Castro *et al.* recently.[4] Hence the success of the isolation of intermediate glycidates in these reactions seems largely dependent on their stability. In our attempt to prepare several alkyl-substituted chloropyruvates (**2**, R=alkyl) by the title reaction a mixture of **1** and **2** was formed in the varying ratios of the products depending on the conditions, *e.g.* temperature. In this paper we wish to report the Darzens type condensation of aliphatic aldehydes with dichloroacetic ester to afford **1** and the acid-catalyzed transformation of **1** and **2**.

$$\mathrm{R\text{-}CHO + Cl_2CHCO_2R' \longrightarrow R\text{-}\underset{\backslash O /}{CH}\text{-}\underset{|}{C}\text{-}CO_2R' \longrightarrow R\text{-}\underset{Cl}{CH}\text{-}\underset{O}{\overset{||}{C}}\text{-}CO_2R'}$$

1 **2**

Structural assignments are based on IR spectra, NMR spectra, and analyses. Yields, physical properties, and analyses of the products are summarized in Table 1.

Heptanal, octanal, and nonanal gave only the rearranged products (**2**) in the present reaction, while the aldehydes such as acetaldehyde, propionaldehyde, isobutyraldehyde, and 2-phenylpro-

TABLE 1. PRODUCTS FROM THE REACTION OF ALIPHATIC ALDEHYDES

R-CH(O)-C(Cl)-CO_2R′ (**1**) or R-CH(Cl)-C(=O)-CO_2R′ (**2**)

Compound[a]	Product R	Product R′	Yield, %	Bp, °C/mmHg	Found, % C	Found, % H	Calcd, % C	Calcd, % H
1a	CH_3	CH_3	31.6	75—78/16	39.78	4.39	39.88	4.69
1b	C_2H_5	CH_3	31.6	93—95/24	43.78	5.79	43.78	5.51
1c	C_2H_5	C_2H_5	24.5	94—98/18	46.78	6.26	47.07	6.21
1d and **2a**	n-C_3H_7	C_2H_5	34.8[b]	96—97/12	50.09	6.84	49.88	6.80
1e	$(CH_3)_2CH$	CH_3	67.9	92—93/16	46.94	6.40	47.07	6.21
1f	$(CH_3)_2CH$	C_2H_5	32.6	104—106/20.5	49.74	7.04	49.88	6.80
1g	$CH_3(C_6H_5)CH$	CH_3	45.3	125—127/2	59.72	5.14	59.88	5.44
2b	n-C_6H_{13}	C_2H_5	45.5	134—136/13	56.29	8.37	56.28	8.16
2c	n-C_7H_{15}	C_2H_5	53.3	123—125/4	58.22	8.74	57.94	8.51
2d	n-C_8H_{17}	C_2H_5	50.3	125—128/3	59.20	9.01	59.42	8.82

a) Compounds excepting **1f** are new.

b) The presence of two components (**1d** and **2a**) in equal portions was detected, roughly estimated by the comparison of TLC spot areas [Merck Silica Gel G; Acetone—*n*-Hexane (1 : 5). R_f=0.76 (**1d**); 0.36 (**2a**).].

1) V. F. Martynov and M. I. Titov, *Zh. Obshch. Khim.*, **32**, 319 (1962); *Chem. Abstr.*, **57**, 12373c (1962).

2) R. N. McDonald and P. A. Schwab, *J. Org. Chem.*, **29**, 2459 (1964).

3) A. Takeda, S. Wada, and T. Uno, *Mem. School Eng., Okayama Univ.*, **2**, 80 (1967).

4) B. Castro, J. Villieras and N. Ferracutti, *Compt. Rend., (C)*, **267**, 1502 (1968).

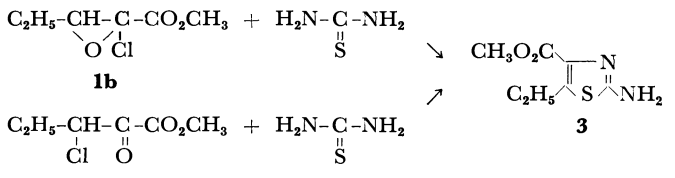

pionaldehyde yielded the intermediate α-chloroglycidic esters (**1**) predominantly. It has been occasionally observed that the conversion of **1** to **2** has occurred partly in the reactions of butyraldehyde, and propionaldehyde with dichloroacetate. α-Chloroglycidic esters (**1**) listed in Table 1 were treated with dry hydrogen chloride in ether at 0°C to investigate the facility of the epoxy-carbonyl rearrangement.[5] Methyl 2-chloro-2,3-epoxyvalerate (**1b**) was thus converted readily to methyl 3-chloro-2-oxovalerate (**2**, $R=C_2H_5$, $R'=CH_3$) in 40.0% yield. On the other hand, an attempt to convert methyl 2-chloro-2,3-epoxy-4-methylvalerate (**1e**) in the same manner resulted in the recovery of the unchanged starting material. The treatment of ketones such as acetone, 3-heptanone, and acetophenone with dichloroacetate gave a small amount of product in each case, but we failed to detect any appreciable amount of either epoxyesters or pyruvates. Sodium methoxide was of no use in effecting the epoxy-carbonyl rearrangement of **1b**.

To establish the correlation in chemical properties of **1** and **2**, methyl 2-chloro-2,3-epoxyvalerate (**1b**) was heated under reflux with equimolar amount of thiourea in methanol. It afforded 2-amino-5-ethyl-4-methoxycarbonylthiazole (**3**) in a yield of 72.6%. This compound was prepared alternatively[6] by the reaction of methyl 3-chloro-2-oxovalerate (**2**, $R=C_2H_5$, $R'=CH_3$) with thiourea under the same condition in 71.4% yield.

Experimental[7]

The following experiments are shown as a typical run.

Methyl 2-Chloro-2,3-epoxyvalerate (1b). Dry powdered sodium methoxide (13.5 g, 0.25 mol) was added gradually to a mixture of propionaldehyde (11.6 g, 0.2 mol) and methyl dichloroacetate (28.4 g, 0.2 mol) dissolved in dry ether (100 m*l*) at 0±1°C. The resulting mixture was stirred at room temperature for 3 hr and treated with water. The ethereal extract was washed several times with water and dried ($MgSO_4$). After removal of the solvent it was distilled giving 9.4 g (31.6%) of **1b**: bp 93—95°C/24 mmHg; IR (cm^{-1}, liquid) 1750 (ester C=O); NMR (τ, $CDCl_3$) 6.60 (t, 1H, J=10 Hz, -CH-CCl).

Methyl 2-Chloro-2,3-epoxy-4-methylvalerate (1e). This product was prepared by the condensation of isobutyraldehyde (14.4 g, 0.2 mol) and methyl dichloroacetate (28.4 g, 0.2 mol) in the presence of dry sodium methoxide (13.5 g, 0.25 mol) in dry ether (100 m*l*), yield 24.2 g (67.9%): bp 92—93°C/16 mmHg; IR (cm^{-1}, liquid) 1750 (ester C=O); NMR (τ, $CDCl_3$) 6.99 (d, 1H, J=15 Hz, -CH-CCl).

Ethyl 3-Chloro-2-oxononanoate (2b). To a mixture of heptanal (11.4 g, 0.1 mol) and ethyl dichloroacetate (15.7 g, 0.1 mol) dissolved in anhydrous ether (50 m*l*) dry sodium ethoxide (8.5 g, 0.125 mol) was added at 0±1°C during the course of 1 hr, with stirring. The stirred mixture was allowed to warm up to room temperature and then refluxed for 2 hr. The ethereal layer was washed with water several times cautiously, dired ($MgSO_4$), and concentrated. The residue was distilled to give 10.7 g (45.5%) of **2b**: bp 134—136°C/13 mmHg; IR (cm^{-1}, liquid) 1760 (shoulder, keto C=O) and 1735 (ester C=O); NMR (τ, $CDCl_3$) 5.06 (t, 1H, J=11.2 Hz, -CHCl-C=O).

Methyl 3-Chloro-2-oxovalerate (**2**, $R=C_2H_5$, $R'=CH_3$). Methyl 2-chloro-2,3-epoxyvalerate (5.0 g, 0.03 mol) was treated for 5 hr with the stream of dry hydrogen chloride in dry ether (50 m*l*) at 0°C. The ethereal layer was washed with water, dried ($MgSO_4$), concentrated, and distilled to give 2.0 g (40.0%) of the product: bp 77—79°C/13 mmHg; IR (cm^{-1}, liquid) 1760 (shoulder, keto C=O) and 1735 (ester C=O).

Found: C, 43.39; H, 5.32%. Calcd for $C_6H_9ClO_3$: C, 43.78; H, 5.51%.

2-Amino-5-ethyl-4-methoxycarbonylthiazole (3). *(a) From* **1b** *and Thiourea.* A mixed solution of **1b** (3.3 g, 0.02 mol) and thiourea (1.5 g, 0.02 mol) in methanol (15 m*l*) was refluxed for 18 hr. The mixture was diluted with water and was made alkaline with aqueous ammonia to yield 2.7 g (72.6%) of the crude product: mp 131—133°C (from benzene); IR (cm^{-1}, nujol) 3400, 3200, 3100, 1690, 1610, 1555, and 1225.

Found: C, 45.36; H, 5.49; N, 14.65%. Calcd for $C_7H_{10}N_2O_2S$: C, 45.14; H, 5.41; N, 15.05%.

(b) From Methyl 3-Chloro-2-oxovalerate and Thiourea. A mixture of methyl 3-chloro-2-oxovalerate (2.5 g, 0.015 mol) and thiourea (1.1 g, 0.015 mol) dissolved in methanol (12 m*l*) was refluxed for 19 hr. The reaction mixture treated similarly as in (a) gave 2.0 g (71.4 %) of the same product as above: mp 131—133°C.

5) M. Mousseron, F. Winternitz, and R. Jacquier, *Compt. Rend.*, **223**, 1014 (1946); *Chem. Abstr.*, **41**, 2008a (1947).

6) H. Erlenmeyer and Ch. J. Morel, *Helv. Chim. Acta*, **25**, 1073 (1942).

7) All the boiling points and the melting points are uncorrected. Elementary analyses were carried out by Mr. Eiichiro Amano and Miss Hiroe Nisino of our laboratory. We are indebted to Dr. Akira Suzuki and Mr. Sigezo Simokawa, both of Hokkaido University, Sapporo, for NMR measurements.

BULLETIN OF THE CHEMICAL SOCIETY OF JAPAN VOL. 43 2999—3002 (1970)

Tris(L-prolinato)nickel(II) Complex

Jinsai HIDAKA and Yoichi SHIMURA

Department of Chemistry, Faculty of Science, Osaka University, Toyonaka, Osaka

(Received April 18, 1970)

Only a few solid nickel(II) complexes of tris-(amino-acidato) type have been reported,[1,2] though the formation in solutions has been well established for many kinds of α-amino acids from stability constant measurements,[3,4] and from studies of $d \rightarrow d$ absorption spectra.[5,6]

Optically active prolinate ligand stands in a unique position among optically active α-amino acids because of its stereospecific coordination to a metal ion. In the case of tris(L-prolinato)cabalt-(III), the *mer(N)-Λ*[7] isomer can not exist[8] because of a large steric interaction between the ligands, and only the *fac(N)-Λ* isomer can be easily prepared because this shows no such steric interaction.[9] The other two Λ-isomers have more or less such steric interaction. However, Denning and Piper have succeeded to isolate these isomers in crystals.[8] As it seems that a similar stereo-specific situation also occurs in the case of tris(L-prolinato)nickel(II), we examined the preparation and optical properties of this complex and some of the related tris(amino-acidato)nickel(II) complexes. The following abbreviations will be used for the amino acid ligand:

gly=$CH_2(COO^-)NH_2$, L-ala=$CH_3CH(COO^-)NH_2$,

L-pro=$CH(COO^-)CH_2CH_2CH_2NH$ and

L-hypro=$CH(COO^-)CH_2CH(OH)CH_2NH$.

Experimental

Potassium Tris(amino-acidato)nickel(II). An aqueous solution containing freshly prepared nickle(II) carbonate, amino acid (L-proline, L-hydroxyproline, L-alanine or glycine) and potassium carbonate (the molar ratio was 1 : 5 : 2.5) was evaporated on a water bath at about 80°C until it became almost syrupy. After the crude product had been cooled to room temperature, the resulting blue precipitate was filtered by suction. Five grams of the blue powder obtained was suspended in 100 m*l* of methanol and it was refluxed for a few hours in order to extract the complex. The color of the solution changed from blue to dark blue. The resulting suspension was filtered and the dark blue filtrate was evaporated to dryness in a vacuum desiccator. The complex obtained was recrystallized from hot methanol and dried in a vacuum desiccator and then analyzed for C, H and N (Table 1).

Bis(amino-acidato)diaquonickel(II). Complexes of this type were prepared by a method similar to that of bis(glycinato)diaquonickel(II).[10] In the case of bis(L-prolinato) complex, dehydration of two moles of coordinated water occurred on heating *in vacuo* at 80°C for 16 hr; Found: 10.73%, Calcd of [Ni(L-$C_5H_8NO_2)_2(H_2O)_2$]: 11.15%. The content of C, H and N was determined after the sample had been dehydrated (Table 1).

The CD curves were obtained by a Roussel-Jouan dichrograph in the region of 800—300 mμ, and a Cary 14R*[1] or a Shimadzu QR-50 spectrophotometer with CD attachments in the region of 1150—800 mμ. The absorption measurements were made by a Beckman DU spectrophotometer. The absorption and CD curves are shown in Fig. 1 and the absorption data are summarized in Table 2.

Discussion

It is easily shown from the reported values of stability constants (*e.g.*, $\log \beta_1 = 5.69$, $\log \beta_2 = 10.50$ and $\log \beta_3 = 13.95$ for Ni(II)--glycinate system[4]) that no nickel(II) complexes of tris(amino-acidato) type dissociate the ligand to any extent. Therefore, the absorption curves of the present tris(amino-acidato)nickel(II) complexes agree well with that of the tris(glycinato) complex reported by Jørgensen[5] which was measured in a solution with

1) C. A. McAuliffe, J. V. Quagliano and L. M. Vallarino, *Inorg. Chem.*, **5**, 1996 (1966).

2) D. R. Stephens and H. G. Drickamer, *J. Chem. Phys.*, **34**, 937 (1961).

3) S. Pelletier, *J. Chim. Phys.*, **57**, 287, 295, 301, 306, 311, 318 (1961).

4) R.-P. Martin and R. A. Paris, *Bull. Soc. Chim. Fr.* **1964**, 3170.

5) C. K. Jørgensen, *Acta Chem. Scand.*, **9**, 1362 (1955); *ibid.*, **10**, 887 (1956).

6) G. R. Brubaker and D. H. Busch, *Inorg. Chem.*, **5**, 211 (1966).

7) The symdols Λ and Λ are used in this paper according to the tentative proposals by the Commission on the Nomenclature of Inorganic Chemistry of the IUPAC: *Inorg. Chem.*, **9**, 1 (1970).

8) R. G. Denning and T. S. Piper, *Inorg. Chem.*, **5**, 1056 (1966).

9) T. Yasui, J. Hidaka and Y. Shimura, This Bulletin, **38**, 2025 (1965).

*1 Thanks are due Professor F. Woldbye and Mag. Sci. G. Borch of Technical University of Denmark for the measurement by the Cary 14R.

10) H. Ito, *Nippon Kagaku Zasshi*, **77**, 1383, 1389 (1956).

Table 1. Analytical results (unit in %)

Complex			C	H	N
$K[Ni(gly)_3]$	deep blue	Calcd	22.52	3.78	13.13
		Found	22.50	3.75	12.96
$K[Ni(L\text{-}ala)_3]\cdot H_2O$	deep blue	Calcd	28.43	5.30	11.05
		Found	28.77	5.11	10.97
$K[Ni(L\text{-}pro)_3]$	sky blue	Calcd	40.93	5.49	9.54
		Found	40.76	5.69	9.39
$K[Ni(L\text{-}hypro)_3]$	sky blue	Calcd	36.90	4.96	8.60
		Found	36.39	5.12	8.22
$[Ni(L\text{-}pro)_2(H_2O)_2]$	marine blue	Calcd	41.86	5.58	9.77
		Found	41.22	5.62	9.63

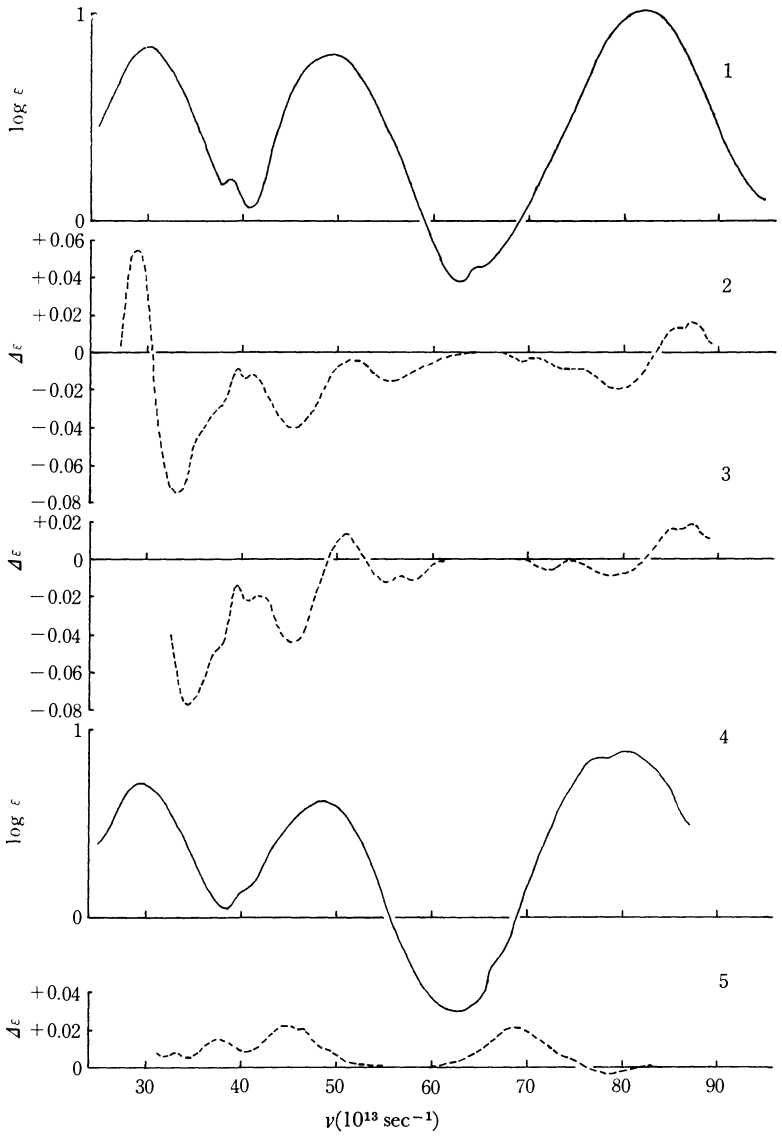

Fig. 1. Absorption curves of (1) $K[Ni(L\text{-}pro)_3]$ and (4) $[Ni(L\text{-}pro)_2(H_2O)_2]$ and CD curves of (2) $K[Ni(L\text{-}pro)_3]$, (3) $K[Ni(L\text{-}hypro)_3]$ and (5) $[Ni(L\text{-}pro)_2(H_2O)_2]$ in aqueous solutions.

TABLE 2. ABSORPTION DATA[a] OF K[Ni(amino-acidato)$_3$] AND [Ni(amino-acidato)$_2$(H_2O)$_2$]

Complex	Solvent	Band I ν_{max} (log ε_{max})	Singlet band ν_{max} (log ε_{max})	Band II ν_{max} (log ε_{max})	Band III ν_{max} (log ε_{max})
K[Ni(gly)$_3$]	H_2O	30.5(1.01)	39.7(0.35)	50.2(0.95)	83.0(1.18)
K[Ni(L-ala)$_3$]	H_2O	30.5(1.03)	39.4(0.40)	50.0(0.99)	82.4(1.20)
K[Ni(L-pro)$_3$]	H_2O	30.0(0.97)	38.8(0.27)	49.2(0.94)	82.2(1.06)
	CH_3OH	30.2(1.01)	39.0(0.32)	50.0(0.99)	82.5(1.12)
K[Ni(L-hypro)$_3$]	H_2O	30.0(0.92)	38.8(0.31)	49.0(0.88)	82.0(1.13)
[Ni(gly)$_2$(H_2O)$_2$]	H_2O	29.5(0.85)	Ca 41 sh	48.8(0.62)	80.8(0.92)
[Ni(L-pro)$_2$(H_2O)$_2$]	H_2O	29.4(0.71)	Ca 40 sh	48.0(0.60)	80.4(0.86)
	CH_3OH	29.6(0.91)	Ca 40 sh	48.4(0.82)	80.8(1.06)

a) The frequencies are given in 10^{13} sec^{-1}.

TABLE 3. CD SIGNS OF NICKEL(II) AND COBALT(III) COMPLEXES IN THE REGION OF THEIR FIRST ABSORPTION BANDS

Complex[a]	Predominant Configuration	Sign of CD Component: Longer wavelength comp.	Sign of CD Component: Shorter wavelength comp.	Ref.
[Ni(*d*-pn)$_3$]$^{2+}$	Λ(lel)	(+)	(−)	13)
[Ni(*d*-2,3-bn)$_3$]$^{2+}$	Λ(lel)		(−)	13)
[Ni(*l*-chxn)$_3$]$^{2+}$	Δ(lel)	(−)	(+)	12)
[Ni(L-pro)$_3$]$^-$	fac(N)-Λ	(+)	(−)	b)
[Ni(L-hypro)$_3$]$^-$	fac(N)-Λ		(−)	b)
Λ(lel)-[Co(*d*-pn)$_3$]$^{3+}$		(+)	(−)	c)
Λ(lel)-[Co(*d*-2,3-bn)$_3$]$^{3+}$		(+)	(−)	13)
Δ(lel)-[Co(*l*-chxn)$_3$]$^{3+}$		(−)	(+)	d)
fac(N)-Λ-[Co(L-pro)$_3$]		(+)	(−)	9)
fac(N)-Λ-[Co(L-hypro)$_3$]		(+)	(−)	9)

a) Abbreviation: pn=propylenediamine, 2,3-bn=2,3-diaminobutane, and chxn=*trans*-1,2-diaminocyclohexane.
b) This work.
c) K. Ogino, K. Murano and J. Fujita, *Inorg. Nucl. Chem. Lett.*, **4**, 351 (1968).
d) T. S. Piper and A. G. Karipides, *J. Amer. Chem. Soc.*, **86**, 5039 (1964).

excess of glycinate, and the absorption spectrum of tris(L-prolinato) complex in methanol is almost the same as that in aqueous solution (Table 2). Recently Katzin and Gulyas[11] reported the circular dichroism (CD) spectra of solution complexes in the systems of nickel(II) and amino acids, but curiously enough excluded the possibility of existence of tris(amino-acidato) complexes. As shown in Fig. 1, the CD spectrum of the tris(L-prolinato) complex differs markedly from that of the bis(L-prolinato)diaquo complex; the CD bands of the latter complex are less intense than those of the former complex. The absorption and CD spectra of the tris(L-hydroxyprolinato) complex are similar to those of the tris(L-prolinato) complex; the only difference is that, in the former complex, the band II ($^3A_{2g}\rightarrow{}^3T_{1g}$(F) transition in an O_h approximation) has a positive component besides two or three negative components while the latter complex has only two negative components in this region.

As mentioned above, four isomers, whose stabilities differ markedly from each other, are possible for a tris(amino-acidato) complex; but, in the case of the tris(L-prolinato)nickel(II) complex, the CD spectrum presented in Fig. 1 is assumed to be predominantly that of the most stable *fac(N)*-Λ isomer because of lability of the nickel(II) complexes. Treptow[12] and Woldbye[13] have already assumed similar situations in the cases of [Ni(*l*-trans-1,2-diaminocyclohexane)$_3$]$^{2+}$ and [(Ni(*d*-2,3-diaminobutane)]$^{2+}$, respectively. Table 3 compares the CD band signs of five nickel(II) complexes, with those of the corresponding cobalt(III) complexes, whose comfigurations are the same as those of the nickel(II) complexes existing predominantly in solutions. It is evident from this Table that the sign characteristics in band I of the nickel(II) complexes ($^3A_{2g}\rightarrow{}^3T_{2g}$ in an O_h

11) L. I. Katzin and E. Gulyas, *J. Amer. Chem. Soc.*, **91**, 6940 (1969).

12) R. S. Treptow, *Inorg. Chem.*, **7**, 1229 (1968).
13) F. Woldbye, "Studies over Optisk Aktivitet," Polyteknisk Forlag, Copenhagen (1069).

approximation) are almost the same as those in band I of the cobalt(III) complexes ($^1A_{1g} \rightarrow {}^1T_{1g}$ in an O_h approximation). The behavior of the CD spectra in the region of bands II and III is rather irregular.

In conclusion, the absolute configuration of a nickel(II) complexes is reflected in the signs of its CD components in the region of the longest wavelength $d \rightarrow d$ absorption band as in the case of cobalt(III) complexes.

BULLETIN OF THE CHEMICAL SOCIETY OF JAPAN VOL. 43 3002—3005 (1970)

The Synthesis of 5-Aminoisoxazolidines by the 1,3-Dipolar Cycloaddition Reaction of Nitrones with Enamines

Yujiro NOMURA, Fumio FURUSAKI and Yoshito TAKEUCHI

Department of Chemistry, College of General Education, The University of Tokyo, Komaba, Meguro, Tokyo

(Received April 24, 1970)

In a preliminary communication[1] it has been shown that 4,5-tetra(or tri)methylene-2,3-diphenyl-5-pyrrolidino(or morpholino)isoxazolidine was formed by the reaction of benzylideneaniline *N*-oxide(diphenylnitrone) (Ia : X=H) with 1-pyrrolidino (or morpholino)-1-cyclohexene (or cyclopentene) in dimethylformamide (DMF) at room temperature. The present note deals with the synthesis of a number of isoxazolidines by the nitrone-enamine cycloaddition in detail.

Isoxazolidines IIb—j with a substituent on 3-phenyl group were synthesized from the corresponding nitrones I and 1-pyrrolidino-1-cyclohexene. The results together with UV spectral data are summarized in Table 1.

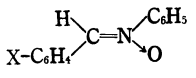

I

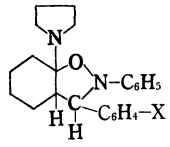

II

The reaction between I and 1-pyrrolidino-1-cyclopentene also gave 2,3-diaryl-4,5-trimethylene-5-pyrrolidinoisoxazolidines IIIa—i. Low yields of III together with the formation of a substantial amount of tar were observed at room temperature. The reaction temperature was controlled to obtain the best results which are tabulated in Table 2.

1-Morpholino-1-cyclopentene was rather sluggish against Ia in DMF at room temperature, and cycloadduct, 4,5-trimethylene-2,3-diphenyl-5-morpholinoisoxazolidine (IVa: X=H) was obtained in 4.2% yield after prolonged heating at 40°C. The main product in this reaction, however, was another isoxazolidine, which was identified as 4,5-trimethylene-2,3-diphenyl-5-(*N*-phenylhydroxyamino)isoxazolidine (Va: X=H, yield 12.9%) from elementary analysis, IR and above all, NMR spectra. Tsuge *et al.*[2] also reported that 4,5-tetramethylene-2,3-diphenyl-5-(*N*-phenylhydroxyamino)isoxazolidine was formed by heating Ia and 1-morpholino-(or 1-piperidino-)1-cyclohexene in boiling benzene.

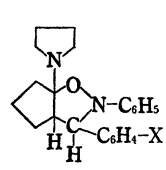

III

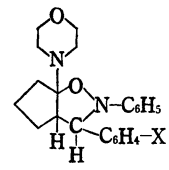

IV

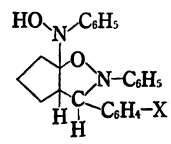

V

Experimental

UV and IR spectra were taken on a Hitachi EPS-2 and a Perkin Elmer 125 spectrophotometer, respectively. NMR spectra were determined in dimethyl sulfoxide-d_6 on a JEOL JNM-4H-100 spectrometer at 100 MHz with tetramethylsilane as the internal standard.

All melting points were uncorrected.

2,3-Diaryl-4,5-tetramethylene-5-pyrrolidinoisoxazolidines (IIa—j). A DMF (30 m*l*) solution of diphenylnitrone (Ia) (5.92 g, 0.03 mol) and 1-pyrrolidino-1-cyclohexene (5.45 g, 0.036 mol) was stirred at room temperature for 72 hr under a nitrogen stream. After removal of the solvent *in vacuo*, the residue was recrystallized from ethanol to afford 4,5-tetramethylene-2,3-diphenyl-5-pyrrolidinoisoxazolidine (IIa) (7.84 g, 74.8%). In a similar manner IIb-j were obtained from the corresponding nitrones and 1-pyrrolidino-1-cyclohexene. The results are summarized in Table 1.

2,3-Diaryl-4,5-trimethylene-5-pyrrolidinoisoxazolidines (IIIa—i). A DMF (30 m*l*) solution of Ia (3.94 g, 0.02 mol) and 1-pyrrolidino-1-cyclopentene (3.30 g, 0.024 mol) was prepared with ice-cooling and

1) Y. Nomura, F. Furusaki and Y. Takeuchi, This Bulletin, **40**, 1740 (1967).

2) O. Tsuge, M. Tashiro and Y. Nishihara, *Tetrahedron Lett.*, **1967**, 3769.

TABLE 1. 2,3-DIARYL-4,5-TETRAMETHYLENE-5-PYRROLIDINOISOXAZOLIDINES(II) OBTAINED BY THE REACTION OF I WITH 1-PYRROLIDINO-1-CYCLOHEXENE

II	X	Reaction time (hr)	Yield (%)	Mp (°C)	Appearance	Elementary analysis	Found	Calcd	Mol. formula	UV: $\lambda_{max}^{ethanol}$ (ε)
a)	H	72	74.8	147—148	Colorless plates*1	C H N	79.32 8.24 7.89	79.27 8.10 8.04	$C_{23}H_{28}N_2O$	251 (11500)
b)	*p*-CH_3	24	31.1	165—167	Colorless needles*1	C H N	79.61 8.40 7.56	79.51 8.34 7.73	$C_{24}H_{30}N_2O$	252.5 (6700)
c)	*p*-CH_3O	67	35.9	131—132	Colorless needles*1	C H N	76.06 8.02 7.32	76.15 7.99 7.40	$C_{24}H_{30}N_2O_2$	229.5 (27100) 253 (10100)
d)	*p*-$(CH_3)_2N$	53	poor	172—174.5	Colorless needles*2	C H N	76.44 8.21 10.77	76.69 8.49 10.73	$C_{25}H_{33}N_3O$	257 (24500)
e)	*p*-Cl	53	51.3	164—166	Colorless needles*1	C H N	72.31 7.17 6.95	72.14 7.11 7.32	$C_{23}H_{27}ClN_2O$	223.5 (15100) 250.5 (11700)
f)	*p*-Br	72	73.3	171—172	Colorless needles*1	C H N	64.31 6.39 6.56	64.63 6.37 6.56	$C_{23}H_{27}BrN_2O$	220 (17100) 249.5 (12100)
g)	*p*-CN	46	54.1	164—165	Colorless needles*1	C H N	77.22 7.32 11.23	77.18 7.29 11.25	$C_{24}H_{27}N_3O$	238.5 (26300)
h)	*p*-NO_2	53	42.0	172—173	Yellow plates*1	C H N	70.07 6.92 10.58	70.20 6.92 10.68	$C_{23}H_{27}N_3O_3$	254 (22000)
i)	*m*-NO_2	65	88.8	180—182	Yellow plates*1	C H N	70.09 6.88 10.67	70.20 6.92 10.68	$C_{23}H_{27}N_3O_3$	251.5 (20200)
j)	*p*-CH_3OCO	42	42.0	142—143	Colorless needles*3	C H N	74.14 7.59 6.82	73.86 7.44 6.89	$C_{25}H_{30}N_2O_3$	245 (33800)

*1 Recrystallized from ethanol.
*2 Purified by column (silica gel) chromatography (benzene-cyclohexane) followed by recrystallization from ethanol.
*3 Purified by column (silica gel) chromatography (dichloromethane) followed by recrystallization from methanol.

TABLE 2. 2,3-DIARYL-4,5-TRIMETHYLENE-5-PYRROLIDINOISOXAZOLIDINES(III) OBTAINED BY THE REACTION OF I WITH 1-PYRROLIDINO-1-CYCLOPENTENE

III	X	Reaction time (hr)	Yield (%)	Mp (°C)	Appearance	Elementary analysis	Found	Calcd	Mol. formula	UV: $\lambda_{max}^{ethanol}$ (ε)
a)	H	34*1	49.9	102.8	Colorless needles	C H N	78.74 7.62 8.28	79.00 7.84 8.38	$C_{22}H_{26}N_2O$	254.5(8900)
b)	*p*-CH_3	43*2	43.1	119.5—121	Colorless needles	C H N	79.08 8.21 8.19	79.27 8.10 8.04	$C_{23}H_{28}N_2O$	254.5(11150)
c)	*p*-CH_3O	49*2	59.5	121.7—123.7	Colorless needles	C H N	75.72 7.79 7.72	75.79 7.74 7.69	$C_{23}H_{28}N_2O_2$	230(17100) 255(7800)
d)	*p*-$(CH_3)_2N$	64*3	8.0	128—130	Reddish crystals*4	C H N	76.42 8.41 10.96	76.36 8.28 11.13	$C_{24}H_{31}N_3O$	264(23750)
e)	*p*-Cl	42*2	63.3	124—125	Colorless needles	C H N	71.95 6.98 7.25	71.63 6.83 7.59	$C_{22}H_{25}ClN_2O$	224(14250) 251(5800)
f)	*p*-Br	43*2	60.2	129—131	Colorless plates	C H N	63.99 6.39 6.66	63.92 6.10 6.78	$C_{22}H_{25}BrN_2O$	224(23000) 249(10200)
g)	*p*-CN	61*3	75.1	162—164	Colorless grains	C H N	76.91 7.15 11.69	76.85 7.01 11.69	$C_{23}H_{25}N_3O$	237(25150)
h)	*p*-NO_2	45*3	12.0	122—123	Yellow crystals	C H N	69.68 6.43 10.86	69.63 6.64 11.08	$C_{22}H_{25}N_3O_3$	264(14700)
i)	*m*-NO_2	41*3	60.6	125—127	Yellow plates	C H N	69.58 6.75 11.00	69.63 6.64 11.08	$C_{22}H_{25}N_3O_3$	256.5(17500)

*1 The reaction mixture was stirred for 10 hr under ice-cooling and then at room temperature.
*2 The reaction mixture was stirred for 4 hr under ice-cooling and then at room temperature.
*3 The reaction mixture was stirred for 24 hr under ice-cooling and then at 8°C.
*4 Purified by column (silica gel) chromatography (benzene-cyclohexane) followed by recrystallization from ethanol.

stirred for 10 hr. The stirring was continued for an additional 24 hr at room temperature. The oil obtained by evaporating the solvent *in vacuo* was taken up in ethanol and the solution was allowed to stand in a refrigerator overnight. The precipitate was collected and recrystallized from ethanol to give 4,5-trimethylene-2,3-diphenyl-5-pyrrolidinoisoxazolidine (IIIa) (3.20 g, 49.9%).

Similarly IIIb—i were obtained from the corresponding nitrones and 1-pyrrolidino-1-cyclopentene. The data together with the reaction conditions are listed in Table 2.

The Reaction between Diphenylnitrone (Ia) and 1-Morpholino-1-cyclopentene. A DMF (30 m*l*) solution of the nitrone Ia (3.94 g, 0.02 mol) and 1-morpholino-1-cyclopentene (3.68 g, 0.024 mol) was stirred at 40°C for 72 hr under a nitrogen stream, and treated as mentioned above. 4,5-Trimethylene-2,3-diphenyl-5-(*N*-phenylhydroxyamino)isoxazolidine (Va : X=H), sparingly soluble in hot ethanol, was isolated as colorless plates, mp 134.5°C (dec.); yield 1.03 g (12.9%).

Found: C, 77.25; H, 6.75; N, 7.54%. Calcd for $C_{24}H_{24}N_2O_2$: C, 77.39; H, 6.49; N, 7.52%.

UV: $\lambda_{max}^{ethanol}$ 247 mμ (ε 11500). IR (KBr): 3320 cm^{-1} (ν OH). NMR: τ 2.6—3.4 (15H, multiplet, aromatic protons); 5.09 (1H, doublet, $J_{3,4}$=8.0, Hz, 3-H); 6.38 (1H, doublet, $J_{3,4}$=8.0 Hz, 4-H); 6.73 (1H, singlet, OH); 7.9—8.8 (6H, multiplet, trimethylene protons).

From the ethanol-soluble fraction, 4,5-trimethylene-2,3-diphenyl-5-morpholinoisoxazolidine (IVa: X=H) was, after purification by chromatography (alumina-benzene), obtained as colorless needles, mp 125—126°C, yield 0.34 g (4.2%).

Found: C, 74.83; H, 7.51; N, 8.00%. Calcd for $C_{22}H_{26}N_2O_2$: C, 75.40; H, 7.48; N, 7.99%.

UV: $\lambda_{max}^{ethanol}$ 254.5 mμ (ε 8100).

The Reaction between *p*-Methoxybenzylideneaniline *N*-Oxide (Ic: X=*p*-CH_3O) and 1-Morpholino-1-cyclopentene. From 6.82 g (0.03 mol) of the nitrone Ic and 5.52 g (0.036 mol) of 1-morpholino-1-cyclopentene in 50 m*l* of DMF, 3-*p*-methoxyphenyl-4,5-trimethylene-2-phenyl-5-(*N*-phenylhydroxyamino)isoxazolidine (Vc: X=*p*-CH_3O) was obtained, mp 136—138°C (dec.) (from ethanol); yield 2.28 g (40.0%).

Found: C, 73.93; H, 6.70; N, 6.85%. Calcd for $C_{25}H_{26}N_2O_3$: C, 74.60; H, 6.51; N, 6.96%.

UV: $\lambda_{max}^{ethanol}$ 230 (ε 22300) and 246 mμ (ε 15800). NMR: τ 2.65—3.35 (14H, multiplet, aromatic protons); 5.15 (1H, doublet, $J_{3,4}$=8.0 Hz, 3-H); 6.32(3H, singlet, CH_3O); 6.47 (1H, doublet, $J_{3,4}$=8.0 Hz, 4-H); 6.72 (1H, singlet, OH); 7.8—8.2 (6H, multiplet, trimethylene protons).

In this reaction, no 5-morpholinoisoxazolidine IVc (X=*p*-CH_3O) could be isolated.

BULLETIN OF THE CHEMICAL SOCIETY OF JAPAN VOL. 43 3005—3007 (1970)

Tungsten-185 and -181 in Atmospheric Precipitations at Niigata in 1968—69

Takeshi SOTOBAYASHI, Toshio SUZUKI and Tomohiko NODA

Department of Chemistry, Faculy of Science, Niigata University, Niigata

(Received April 30, 1970)

For the past five years we have made measurements of the fresh debris resulting from air[1,2] and underground[3–5] nuclear test explosions, and we have had some geochemical discussions of the results obtained. We have recently found unexpected fallout activities with a unique and marked 57.5-keV photon in 16 precipitation samples between December 21, 1968, and May 20, 1969, at Niigata, while a precipitation sample from December 10—20 (86 *l*) as well as earlier ones showed no such radioactivities. All the precipitation samples were γ-spectrometrically analysed by using a 3 in $\times$ 3 in NaI(Tl) scintillation detector equipped with a 800-channel pulse-height analyser. Figure 1 shows a γ-spectrum typical of the 16 precipitation samples in question. The γ-spectra of the samples collected in early January, 1969, had some short-lived fission products, such as ^{131}I, ^{132}Te–^{132}I, and ^{140}Ba–^{140}La, which resulted from the 8th Chinese nuclear test on December 27, 1968, but other samples showed only long-lived fission products, ^{95}Zr–^{95}Nb, ^{137}Cs, and ^{144}Ce–^{144}Pr, originating from other earlier nuclear tests as well as the 8th Chinese test.

In order to identify these unknown radioactivities, we applied a systematic chemical-separation procedure to a precipitation sample (64 *l*) collected on December 25, 1968. The present procedure involves a preliminary 6 M hydrochloric acid leaching in order to prepare a sample solu-

1) T. Sotobayashi, T. Suzuki and S. Koyama, This Bulletin, **42**, 716 (1969).

2) T. Sotobayashi, T. Suzuki and A. Furusawa, *Nature*, **224**, 1096 (1969).

3) S. Koyama, T. Sotobayashi and T. Suzuki, *ibid.*, **209**, 239 (1966).

4) T. Sotobayashi and S. Koyama, *Science*, **152**, 1059 (1966).

5) T. Sotobayashi, T. Suzuki and S. Koyama, This Bulletin, **40**, 1260 (1967).

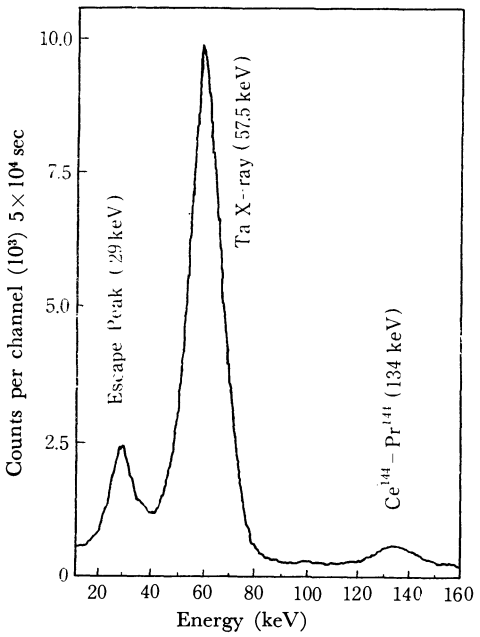

Fig. 1. A γ-ray spectrum of a precipitation sample on December 25, 1968 (64 *l*).

tion for further chemical analysis; it was followed by 3 successive liquid-liquid extractions using mineral acid-xylene solutions of TOA system consisting of 1N sulfuric, 4 N hydrochloric, and 10 N nitric acids, and of 5, 10, and 5% xylene solutions of TOA, respectively. According to the present procedure, one group of elements, V, Mo, Re, Ru, Os, W, and Sb, is expected to remain in the final aqueous phase; the γ-spectrum of the aqueous phase proved to have only a photopeak at 57.5 keV with a half-life of 140 d. As a result, a radionuclide of ^{181}W among the finally-separated 7 elements was expected to correspond to the one emitting such a photon.

For the purpose of reinforcing the present conclusion chemically, the following experiment was made on the residue fraction obtained in the above test. A sample solution for chemical analysis was prepared by the alkali fusion of the residue, followed by hot-water extraction. In this case, sodium tungstate was added to the sample solution as a carrier, and a purified tungsten trioxide was obtained by the usual cinchonine-hydrochloric acid method for tungsten analysis. A nuclide with a 57.5-keV photon was recovered nearly quantitatively, as was found by comparing the photopeak area at 57.5 keV between the residue and the trioxide.

The tungsten trioxide obtained was further submitted to 70-channel β-ray spectrometer equipment, because ^{185}W, a pure β emitter, was expected to be produced by a (n,γ) reaction of ^{184}W with a natural abundance of 30.6%. The trioxide sample proved to have a half-life of 75 d and maximum energy of 0.42 MeV (Fig. 2); these results agreed well with those of ^{185}W listed in the "Table of Isotopes."[6] Thus, it may be concluded that the 57.5-keV photon is a Ta X-ray emitted in the ^{181}W decay process (EC) and that the unknown activities in question originate from radiotungsten isotopes,^{181,185}W.

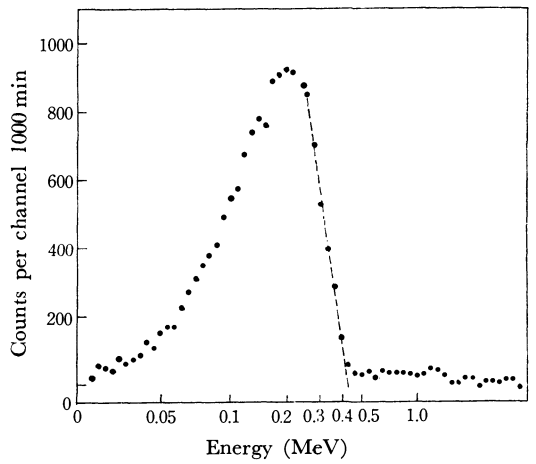

Fig. 2. A β-ray spectrum of a purified tungsten trioxide from a precipitation sample.

The radiotungsten was believed to have occurred in the chemical form of tungsten trioxide on the basis of following chemical behavior of the radiotungsten present in the precipitation samples: (1) Most of the radiotungsten (60—70%) was in the carrier-free state, extracted from precipitation samples into a sodium hydroxide solution (6 M), and when sodium tungstate was added as a carrier the extraction coefficient amounted to more than 95%. (2) No radiotungsten was leached from precipitation samples by distilled water, even in the presence of sodium tungstate as a carrier. (3) Though about 50% of the radiotungsten was leached with hydrochloric acid (6 M) from a precipitation sample in the carrier-free state, the leached radiotungsten was completely precipitated, together with the dehydrated silica produced, when the leachate solution was evaporated to dryness; the solid cake thus obtained was then dissolved in dilute hydrochloric acid.

Table 1 shows the day-to-day variation in the activity concentration of radiotungsten for the precipitation samples from between December 21—30, 1968, together with the averaged values for intervals from 7 to 20 days from December 21, 1968, to May 20, 1969. All the activity values in Table 1 are corrected for decay to the mid-col-

6) C. M. Lederer, T. M. Hollander and I. Perlman, "Table of Isotopes," John Wiley & Sons, N. Y. (1967), p. 108.

Table 1. Radiotungsten in precipitations between December 21, 1968—May 20, 1969

Date of collection	Sample volume (l)	Relative activity (cps)	Relative activity concentration (10^{-3} cps/l)
12/21 1978	64	5.2	81
12/22	64	5.3	83
12/23	64	3.2	50
12/24	64	4.1	64
12/25	64	30.4	457
12/28	60	4.0	67
12/30	43	3.3	77
12/21—28, 1968	75.5	12.4	164
12/29—1/3, 1969	116	0.98	8.4
1/4—16	81	0.77	9.6
1/20—2/1	83	0.60	7.2
2/2—20	52	0.56	10.8
2/21—3/31	160	1.21	7.6
4/1—20	79	0.26	3.3
4/21—30	59.3	—	—
2/1—20	64	0.18	2.8

Relative activity; Photopeak area at 57.5 keV.

lection date. As may be seen, the levels of the radiotungsten concentration in precipitations were kept relatively high for the first 10-day period; then they dropped rapidly to about one-twentieth of the initial levels and remained unchanged until mid-February. Thereafter, the levels continued to decrease gradually. From this decrease rate, the half-time of the removal process for airborne radiotungsten from the atmosphere was roughly estimated to be 33 d. Such atmospheric behavior of airborne radiotungsten seems like that observed in 1965 at Niigata for airborne radiostrontium released by a Soviet underground nuclear test on January 15, 1965.[5]

The radiotungsten fallout was reported to be detected in Italy[7] and Finland.[8] The first arrival at Pisa, Italy (10°E, 44°N), of radioactive clouds with radiotungsten was on December 17, 1968, while it was on December 21 at Niigata (139°E, 38°N). Further, taking into consideration the atmospheric conditions (Niigata had several rain or snow storms, with strong convective activities, for a week before and after the day in question (Dec. 21)), it can possibly be assumed that 4 days were required for the radiotungsten to travel the 10000 km from Italy to Japan and that the radiotungsten travelled at a speed of about 100 km/hr from west to east along the 40th Parallel. This assumed speed was found comparable with that, 110—80 km/hr, observed at Niigata in connection with the recent, fresh Chinese nuclear debris.[9,10] This radiotungsten fraction which at first reached Niigata was probably carried in the jet stream in the tropopause levels. On the other hand, the highest activity concentration of radiotungsten was observed at Niigata on December 25, a week after the appearance of the highest one at Pisa (Dec. 18). This finding suggests that the cloud with the highest concentration of radiotungsten came here at a slower speed of 50 km/hr through relatively lower levels—perhaps about 5 km high—in the atmosphere. Though we found no volatilely-behaving, short-lived fission products in the precipitation samples in question, we may finally make the assumption, from the fallout pattern and the global circulation speed observed, that the radiotungsten in question is attributable to a US underground nuclear test at Nevada on December 8, 1968, which was reported to release radiotungsten-rich radioactivities into the atmosphere by a US Public Health Service report.[11]

7) L. de Franceschi, A. Gentili, G. Gremigni and D. Guidi, *Nature*, **224**, 571 (1969).

8) L. Blomqzist and M. Asikainen, *ibid.*, **225**, 58 (1970).

9) T. Sotobayashi, T. Suzuki and S. Koyama, *ibid.*, **215**, 728 (1967).

10) T. Sotobayashi, T. Suzuki and S. Koyama, This Bulletin, **41**, 2796 (1968).

11) *US Public Health Service, Radiological Health Data and Reports*, **10**, 171 (1969).

BULLETIN OF THE CHEMICAL SOCIETY OF JAPAN VOL. 43 3008—3010 (1970)

The Solvolytic Isomerization and Rearrangement of *cis*-4-*t*-Butylcyclohexyl *p*-Toluenesulfonate

Kunio OKAMOTO, Seiki SAITÔ and Haruo SHINGU

Department of Hydrocarbon Chemistry, Faculty of Engineering, Kyoto University, Sakyo-ku, Kyoto

(Received May 6, 1970)

In a previous paper, we have demonstrated that, during the course of the phenolysis, *cis*- and *trans*-4-*t*-butylcyclohexyl *p*-toluenesulfonates (*cis*- and *trans*-4-ROTs) are isomerized into their respective geometrical isomers, and that they also undergo 1,2-rearrangement to give the 3-*t*-butylcyclohexyl toslyates (*cis*- and *trans*-3-ROTs).[1] Accordingly, such a solvolytic isomerization and rearrangement of these tosylates should occur also in common hydroxylic solvents other than phenol. The interest of the previous investigators with respect to this *t*-butylcyclohexyl system has, however, been confined only rate and product studies;[2] no papers concerned with the solvolytic isomerization and rearrangement of this system have appeared except ours.[1]

To test this prediction, we conducted acetolysis and hydrolysis on *cis*-4-ROTs at 75 and 65°C respectively; after the interruption of the solvolysis at 74 and 70% completion, we identified the four isomeric tosylates, *i.e.*, *trans*-4-, *cis*-4-, *trans*-3-, and *cis*-3-ROTs, in the recovered tosylate mixtures. The results are tabulated in Table 1, along with the results in the phenol solvent.[1] In view of the facile occurrence of the solvolytic isomerization and rearrangement in the three solvent-systems shown in Table 1, one should consider these phenomena to be general in the solvolysis of the *t*-butylcyclohexyl system.

In Fig. 1, the percentages of *trans*-4-, *cis*-3-, and *trans*-3-ROTs in the recovered tosylate mixtures in the acetolysis are plotted against the effective concentration of sodium tosylate, which is designated as one-half of the concentration of the sodium tosylate, increased until the moment when the solvolysis is interrupted.

In a fashion similar to that of the explanation previously presented in the case of the phenolysis,[1] the trend of linear increase in the percentage of *trans*-4-ROTs (Fig. 1) can be explained as reflecting the following two reaction courses for the formation of *trans*-4-ROTs: (1) the S_N2-like attack of the tosylate anion on the *cis*-type ion-pair intermediate (*cis*-4-R^+OTs^-)[1]; (2) the internal return of the *trans*-type ion-pair intermediate (*trans*-4-R^+OTs^-),[1] which is "intramolecularly" formed by the rotation of the carbonium ion (R^+) in the *cis*-type ion-pair intermediate. The occurrence of the latter process is proved by the interception of the *trans*-4-ROTs line on the coordinate axis of Fig. 1. The two courses are illustrated in the following reaction scheme:

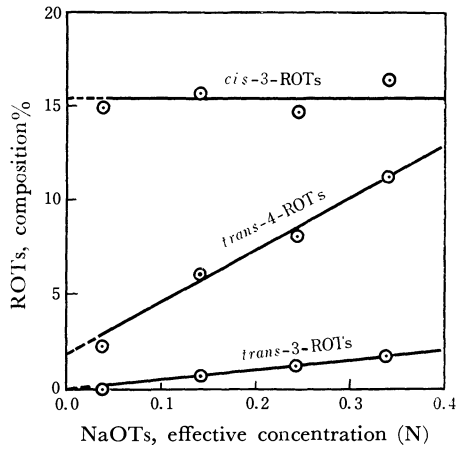

Fig. 1. The composition of the tosylate recovered at 74% completion in the acetolysis conducted in the presence of NaOAc (0.100 N) and of added NaOTs (0.00, 0.10, 0.20, and 0.30 N) at 75.0°C.

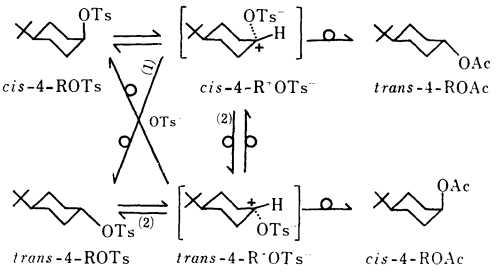

As was explained in the case of the phenolysis,[1] the invariability of the percentage of *cis*-3-ROTs (Fig. 1) indicates that the 1,2-rearrangement is almost intramolecular in nature, namely, that it

1) K. Okamoto, S. Saitô and H. Shingu, This Bulletin, **42**, 3298 (1969).

2) a) S. Winstein and N. J. Holness, *J. Amer. Chem. Soc.*, **77**, 5562 (1955); b) V. J. Shiner, Jr., and J. G. Jewett, *ibid.*, **87**, 1382 (1965); c) N. C. G. Campbell, D. M. Muir, R. R. Hill, J. H. Parish, R. M. Southam and M. C. Whiting, *J. Chem. Soc., B*, **1968**, 355.

Table 1. The composition of the recovered tosylates in the partial solvolysis of *cis*-4-*t*-butylcyclohexyl *p*-toluenesulfonate

Solvent	Temp. °C	Completion %	Recovered ROTs[d] %	Composition%			
				trans-4	*cis*-4	*trans*-3	*cis*-3
Acetic acid[a]	75	74.3	22.1	2.2	82.9	0.0	14.9
60% aq. acetone[b]	65	70	29.4	9.4	72.3	6.7	11.6
Phenol-benzene[c] (1 : 1 by wt)	75	75.5	23.6	1.1	88.3	0.0	10.6

a) In the presence of 0.100 N NaOAc. The initial concentration of *cis*-4-ROTs was 0.100 M.
b) In the presence of 0.048 N Et_3N. The initial concentration of *cis*-4-ROTs was 0.047 M.
c) In the presence of 0.100 N Et_3N; Cited from Ref. 1.
d) Assayed by the solvolysis.

Table 2. Product composition of the partial solvolysis of *cic*-4-*t*-butylcyclohexyl *p*-toluenesulfonate

Solvent and temp.	Cyclohexenes composition			RY (Y=OAc, OH, and OPh) Composition				Ref.
	4-*t*-Bu	3-*t*-Bn	1-*t*-Bu	*trans*-4	*cis*-4	*trans*-3	*cis*-3	
Acetic acid[a] 75.0°C	98.3	1.7	trace	67.5	5.4	25.6	1.5	This paper
Acetic acid[b] 100°C	96.8	3.1	0.1	56.7	5.8	34.2	3.3	Ref. 2c
60% aq. acetone[c] 65°C (reflux temp.)	96.5	1.3	2.2	86.1	2.7	10.3	0.9	This paper
Phenol-benzene[d] (1 : 1 by wt.) 75°C	97.4	2.6	trace	55.0	20.4	13.7	10.9	Previous paper[d]

a) See footnote a in Table 1. Products were assayed by glc.
b) In the presence of 0.05 N NaOAc; the result of the complete acetolysis.
c) See footnote b in Table 1. Products were assayed by glc.
d) In the presence of 0.100 N Et_3N; the result of the complete phenolysis. Cited from our previous paper (K. Okamoto *et al.*, This Bulletin, **42**, 3288 (1969)).

may be caused by the 1,2-hydride shift in the *cis*-type ion-pair intermediate (*cis*-4-R^+OTs^-); the linear increase in the percentage of *trans*-3-ROTs with an increase in the concentration of the added tosylate anion (Fig. 1) indicates that *trans*-3-ROTs is formed mostly by the intermolecular S_N2-like attack of the tosylate anion on the *cis*-3-R^+OTs^--type ion-pair intermediate, which can be formed intramolecularly from the *cis*-4-R^+OTs^--type ion-pair intermediate.

In Table 2, the compositions of the reaction products are presented; they show that, of the three solvents, the phenol solvent is the most effective for the formation of the retained substitution product, *i.e.*, *cis*-4-RY; the composition of olefins is not so much affected by the nature of the solvent.

The hypothesis[2a] that the retained product (*cis*-4-RY) comes from the hydrogen bridged ion-pair intermediate may be considered to be unnecessary, since the considerable solvolytic isomerization of *cis*-4-ROTs into *trans*-4-ROTs clearly indicates that, in these solvolyses, the appreciable part of the retained product (*cis*-4-RY) is actually produced by the course of the inversion of *trans*-4-ROTs or the trans-type ion-pair intermediate (*trans*-4-R^+OTs^-); this is illustrated in the above scheme. Furthermore, the interpretation[2b] that the isotope effect caused by the introduction of the deuterium atom into the 2-positions of *cis*-4-ROBs is to be ascribed to the formation of the hydrogen-bridged ion-pair intermediate seems unreasonable, because the isotope effect measured for *cis*-4-ROBs[2b] is seemingly not the effect of a single *cis*-4-ROBs but the composite effect of a brosylate mixture, *viz.*, a mixture of *cis*-4-, *trans*-4-, *cis*-3-, and *trans*-3-ROBs.

Experimental

Recovery of the Unchanged Tosylate from the Solvolysis Mixture and the Analysis of Its Composition. The solvolysis was interrupted after the desired time; then, after the evaporation of the solvent at 0—10°C, the mixture of the solvolysis product and the unchanged tosylate was distilled under 0.1—0.05 mmHg at room temperature to give the product as the distillate and to leave the tosylate as the residual solid; the IR spectra of the recovered tosylate showed that neither acetate nor alcohol was present (<0.5%). The recovered tosylate was cleaved into the parent al-

cohol using sodium-naphthalene in THF according to the method of Closson *et al.*[3] The alcohol was converted to the corresponding acetate by the method of Rickborn and Quartucci;[4] the analysis of the acetate was performed by glc using a 2 m×4 mm column with 30% PEG 6000 on selite 545 (Yanagimoto) at 130°C.

Product Analysis. The mixture of olefins obtained by the solvolysis was analyzed at 70°C by glc using the column described above. The mixture of the alcohol obtained by the hydrolysis was gas-chromatographically analyzed after its conversion to the corresponding acetate (see above).

3) W. D. Closson, P. Wriede and S. Bank, *J. Amer. Chem. Soc.*, **88**, 1581 (1966); see also Ref. 1.

4) B. Rickborn and J. Quartucci, *J. Org. Chem.*, **29**, 3185 (1964).

BULLETIN OF THE CHEMICAL SOCIETY OF JAPAN VOL. 43 3010—3011 (1970)

The Electron-acceptor Strength of 2,5-Diazido-3,6-dichloro-*p*-benzoquinone

Shigeo KOIZUMI and Yoshio MATSUNAGA

Department of Chemistry, Faculty of Science, Hokkaido University, Sapporo

(Received May 7, 1970)

It has been proposed by Hammond that unsaturated, uncharged compounds contained within the formula $C_wN_xO_yF_z$ comprise a class of organic π-electron acceptors.[1] Here fluorine may be considered as representative of other halogens.[2] He also showed that a high degree of unsaturation is a requisite for large electron affinities. From such a point of view, the evaluation of the effect of the azido group N_3 on the properties of a typical electron acceptor seemed to be of considerable interest. The acceptor strength of 2,5-diazido-3,6-dichloro-*p*-benzoquinone, $C_6N_6O_2Cl_2$, in terms of its complexing properties will be compared with that of *p*-chloranil, $C_6O_2Cl_4$.

The diazidoquinone was prepared by the reaction of sodium azide on chloranil dissolved in methanol and was then recrystallized from benzene.[3] The complexes of the diazidoquinone and *p*-chloranil with the following twenty-nine donors were examined in dichloroethane solutions for the charge-transfer absorptions: (1) phenothiazine, (2) *o*-tolidine, (3) phenoxazine, (4) perylene, (5) 1,5-diaminonaphthalene, (6) dimethyl-*p*-toluidine, (7) dichloro-*o*-tolidine, (8) benzidine, (9) dibromo-*o*-tolidine, (10) *N*-methylphenothiazine, (11) dimethylaniline, (12) phenyl-1-naphthylamine, (13) diphenylamine, (14) anthracene, (15) pyrene, (16) phenoxathiin, (17) *o*-anisidine, (18) 1,2-benzanthracene, (19) 4,4′-dimethoxybiphenyl, (20) *m*-toluidine, (21) *o*-toluidine, (22) *p*-dimethoxybenzene, (23) *p*-chloroaniline, (24) 1-naphthol, (25) aniline, (26) thianthrene, (27) 2-naphthol, (28) *m*-chloroaniline, and (29) triphenylene.

It is well known that one may write, as a good approximation:[4]

$$h\nu_{CT} = I_D - E_A - C, \quad (1)$$

where $h\nu_{CT}$ is the energy of charge-transfer absorption, where I_D is the ionization potential of the donor molecule, where E_A is the electron affinity of the acceptor molecule, and where C represents the electrostatic energy in the dative bond structure and some other minor terms. The difference in $h\nu_{CT}$ for the complexes of a given donor with two acceptors, 1 and 2, is, then:

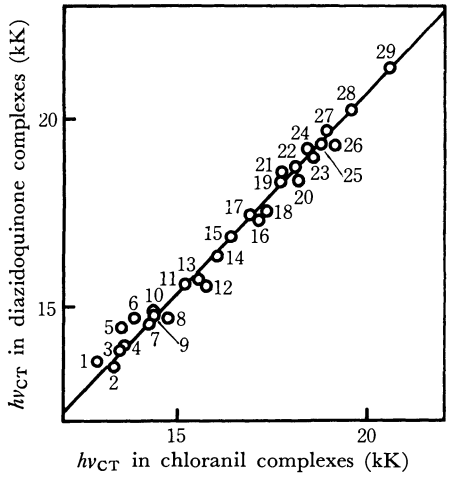

Fig. 1. Plots of wave numbers of maxima of the charge-transfer absorptions in the diazidoquinone complexes against those in the corresponding *p*-chloranil complexes. Point designation corresponds to the numbering of the donors given in the text.

1) P. R. Hammond, *Nature*, **206**, 891 (1965).
2) P. R. Hammond, *J. Chem. Soc., A*, **1968**, 145.
3) K. Fries and P. Ochwat, *Ber.*, **56**, 1291 (1923).
4) J. S. Ham, J. R. Platt and H. M. McConnell, *J. Chem. Phys.*, **21**, 66 (1953).

$$h\nu_{CT_2} = h\nu_{CT_1} + (E_{A_1} - E_{A_2}) + (C_1 - C_2). \quad (2)$$

The term (C_1-C_2) need not be zero, but it may be as large as a few kK if the sizes and shapes of the acceptor molecules are very different.[5] In Fig. 1 the wave numbers of the absorption maxima in the diazidoquinone complexes with each of the above-mentioned donors are plotted against those in the corresponding *p*-chloranil complexes. The line was fitted by the method of least squares. The slope was found to be 1.018, the value is in excellent agreement with that required by Eq. (2). Although the (C_1-C_2) in the complexes of the present quinones is probably small, the intercept, 0.1 kK, is certainly within the limits of uncertainty in this term. Therefore, we may conclude that the electron affinity of 2,5-diazido-3,6-dichloro-*p*-benzoquinone is essentially the same as that of *p*-chloranil, which has been found to be 2.46 eV (19.8 kK) by the magnetron technique.[6] In other words, the azido group appears to be as effective as chlorine in improving the acceptor strength of *p*-benzoquinone.

5) Y. Matsunaga, This Bulletin, **42**, 2490 (1969).

6) A. L. Farragher and F. M. Page, *Trans. Faraday Soc.*, **62**, 3072 (1966).

BULLETIN OF THE CHEMICAL SOCIETY OF JAPAN VOL. 43 3011—3013 (1970)

Some Observations on Ion Exchange Properties of Crystalline Zirconium Phosphate

Yoshitsugu HASEGAWA and Isao TOMITA

Department of Chemistry, Faculty of Science, Tokyo Kyoiku University, Bunkyo-ku, Tokyo

(Received May 13, 1970)

Many synthetic inorganic ion exchangers have been studied because of the fact that they are more stable than organic exchangers under certain conditions, *e.g.* high temperature or the presence of ionizing radiation.[1] Most attentions have been given to zirconium phosphates, gelatious and crystalline, and relation between the structure of the crystalline zirconium phosphate and the mechanism of ion exchange also has been discussed. However, the observations differed among investigators.[2-7] Present study was initiated in order to prepare crystalline zirconium phosphate (c-ZP) which has a constant chemical composition and gives reproducible results of ion exchange experiments, and to apply the product to the separation of alkali metals. Distribution coefficients and pH-titration curves of c-ZP for alkali metal ions were measured and it was found that ion exchange on c-ZP for rubidium and cesium was not ideal when the concentration of metal ions was 1×10^{-3} N.

Experimental

Reagents and Preparation of Crystalline Zirconium Phosphate. The preparation method of c-ZP reported by Clearfield and Stynes[3] has been modified in some points. All reagents used were of reagent grade and not purified further. Details of the preparation procedure are as follows: 100 m*l* of 18 v/v% phosphoric acid and 10 v/v% sulfuric acid solution was added slowly to 100 m*l* of well-stirred 10 v/v sulfuric acid solution of zirconyl chloride octahydrate at 70°C. After standing for two days, the gelatinous suspension was centrifuged and the resulting solid was washed several times with 2% phosphoric acid until free from sulfate ions and then with distilled water. It was dried in air at 110°C. The dried product was suspended in 6.7 M phosphoric acid and refluxed for 120 hr. After refluxing, the solution was stood for another 24 hr, then the precipitate was filtered and washed with 2% phosphoric acid and then with distilled water until free from phosphate ions. It was dried in air at 50°C and microcrystalline zirconium phosphate (c-ZP) was obtained. The dried micro-crystals were made into tablets under pressure of 400 kg/cm^2 and sieved to grain size of 100—200 mesh. This final product was used for further experiments. X-Ray powder patterns and optical microscopic observation showed that the solids obtained have a good crystallinity. The powder patterns were obtained with nickel filtered copper X-Ray using a Geigerflex (Rigaku Denki Co., Ltd.).

Distribution Coefficients. Batch distribution coefficients were measured at 25°C by equilibrating

1) C. B. Amphlett, "Inorganic Ion Exchangers," Elsevier, Amsterdam (1964).
2) C. B. Amphlett, L. A. McDonald and M. J. Redman, *J. Inorg. Nucl. Chem.*, **6**, 220 (1958).
3) A. Clearfield and J. A. Stynes, *ibid.*, **26**, 117 (1964).
4) G. H. Nancollas and V. Pekárek, *ibid.*, **27**, 1409 (1965).
5) J. Albertsson, *Acta Chem. Scand.*, **20**, 1679 (1966).
6) A. Clearfield and G. D. Smith, *J. Colloid Interfac. Sci.*, **28**, 325 (1968).
7) A. Clearfield, R. H. Blessing and J. A. Stynes, *J. Inorg. Nucl. Chem.*, **30**, 2249 (1968).

weighed amounts of c-ZP with a known volume of suitable solutions, followed by analysis of the supernatant. The ratio of solution to solid was usually 100 m*l*/g.

For all alkali metal concentrations studied, the exchange reaction attained to equilibrium within 6 hr. Determination of the batch equilibrium coefficients has been made after reaction mixtures were shaken for at least 24 hr.

Analytical methods employed included the use of radioisotopes such as ^{22}Na, ^{86}Rb and ^{137}Cs as tracers. Measurement of radioactivity was taken on a well-type NaI(Tl) scintillation counter. Flame photometry was used for the determination of potassium.

pH-Titration Curves. 0.5 g of c-ZP was equilibrated with 50 m*l* of a solution containing the appropriate metal chloride and metal hydroxide, the total metal concentration being 0.1 N. pH of the sample solution was measured on a HM-5A pH-meter (Toa Electronics Ltd.). Throughout the measurement the sample was maintained at 25°C in a thermostat and bubbled with nitrogen gas to remove CO_2 gas.

Results and Discussion

X-Ray diffraction powder patterns are given in Table 1. The d values agreed with those reported by Clearfield and Stynes.,[3] though details differ from them. If the c-ZP was dried over P_2O_5 for two months it changed crystalline to amorphous. Hence the drying conditions, temperature and desiccants have to be selected carefully. Distribution coefficients K_d (mequiv/g of exchanger÷mequiv/m*l* solution at equilibrium) for alkali metal ions in neutral solutions on the hydrogen form of c-ZP are shown in Table 2. The K_d values for c-ZP are lower than those for gelatinous zirconium phosphate,[2] but the affinity series is identical *i.e.*, $Na^+ < K^+ < Rb^+ < Cs^+$.

When values of Kd for alkali metal ions as a funtion of acidity are plotted in the form log K_d

Table 1. X-Ray powder patterns of crystalline zirconium phosphate

d	I/I_0	d	I/I_0
7.69	57	2.00	
4.51	34	1.89	5
4.47	18	1.88	
4.08		1.87	
3.59	100	1.83	
3.56	50	1.79	5
3.31		1.77	5
3.23	6	1.73	
3.09		1.72	
2.65	23	1.70	
2.64	22	1.66	5
2.49		1.65	5
2.42	9	1.64	
2.36		1.61	
2.20		1.60	
2.19		1.54	
2.16		1.53	
2.12		1.51	
2.05	9	1.47	
2.02			

I/I_0 values not given in the table indicate that they are less than 5%.

Table 2. Distribution coefficients (K_d values)

[M+]	Na+	K+	Rb+	Cs+
1×10^{-3}	9	—	170	260
	200	—	—	8000
1×10^{-2}	1	3	11	12
	36	84	182	200
1×10^{-1}	0	—	—	0
	6	—	—	12

In each concentration row, upper values are Kd's for c-ZP and lower ones for gelatinous ZP.[2]

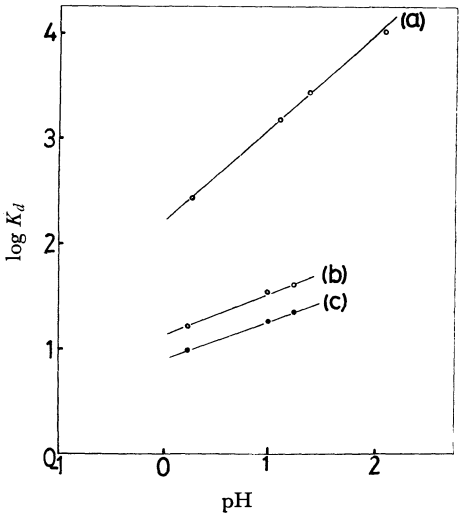

Fig. 1. log K_d *vs.* pH plots.
(a) Cs^+ 1×10^{-5} N
(b) Cs^+ 1×10^{-3} N
(c) Rb 1×10^{-3} N

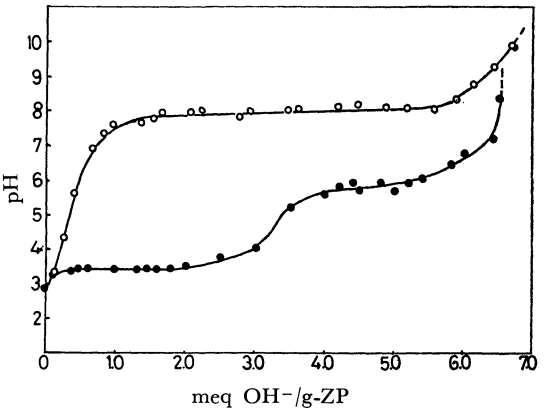

Fig. 2. pH titration curves.
○ Cs^+ ● Na^+

vs. pH, straight lines were obtained (Fig. 1). If ion exchange takes place ideally according to the reaction,

$$H^+ \cdot X^- + M^+ \rightleftarrows M^+ \cdot X^- + H^+,$$

they must show the slope of unity since only univalent cations are involved in ion exchange. The slopes of lines observed were 0.47 for Rb^+ and Cs^+ when $[M^+]=10^{-3}$ N, and 0.94 for Cs^+ when $[M^+]=10^{-5}$ N, respectively. It is apparent that ion exchange on c-ZP is not ideal when $[M^+]$ is 1×10^{-3} N, though it has been reported that ion exchange on gelatinous zirconium phosphate is ideal.[2] The reason why c-ZP and gelatinous zirconium phosphate exhibit the different behaviour may be substantially the structural change of c-ZP during ion exchange. As sodium ion is not exchanged in acid solution, the pH-Kd plot and the ideality of ion exchange can not be discussed for this ion. The pH-titration curves of c-ZP showed that, for sodium ion, hydrogen atoms in c-ZP matrix behave bifunctionally, whereas, for cesium, they appear to behave monofunctionally. The results agreed with those of Albertsson.[5]

The authors express their sincere thanks to Professor Kozo Nagashima of Tokyo Kyoiku University for his continuous interest and encouragement.

BULLETIN OF THE CHEMICAL SOCIETY OF JAPAN VOL. 43 3013—3015 (1970)

A Synthesis of Streptozotocin Derivatives

Tetsuo SUAMI and Tomoya MACHINAMI

Department of Applied Chemistry, Faculty of Engineering, Keio University, Koganei-shi, Tokyo

(Received May 19, 1970)

In connection with a previous paper,[1] biologically active streptozotocin derivatives have been prepared in our laboratory.

Streptozotocin is an antibiotic produced by *streptomyces achromogenes var. 128*, which shows wide antimicrobial and antitumor activities.[2-5] The structure has been established to be *N*-carbamyl-*N'*-methyl-*N'*-nitroso-D-glucosamine.[6-7]

In the present paper, a preparation of methyl glycosides of streptozotocin by a two-step reaction will be described. Methyl β-D-glucosaminide hydrochloride (III) was prepared by the method of Neuberger and Rivers,[8] and then it was treated with methyl isocyanate under the presence of silver carbonate to give methyl *N*-carbamyl-*N'*-methyl-β-D-glucosaminide (IV).

Nitrosation of IV was carried out with sodium nitrite in aqueous acetic acid to give methyl *N*-carbamyl-*N'*-methyl-*N'*-nitroso-β-D-glucosaminide (V) as needle crystals of mp 149°C (dec.) in 70% yield.

Starting from methyl *N*-carbobenzyloxy-α-D-glucosaminide (VII),[8] methyl *N*-carbamyl-*N'*-methyl-*N'*-nitroso-α-D-glucosaminide (X) of mp 133°C was obtained in 33% yield by an analogous reaction process.

A mixture of V and X (XV) was also prepared by an analogous process in 28% yield, beginning with methyl *N*-carbobenzyloxy-D-glucosaminide (XII).

The three compounds: V, X and XV, were fairly active against Ehrlich ascites tumor.

Experimental

A melting point was determined on a Mitamura Riken micro hot stage. A melting point marked with an asterisk was measured in a liquid bath and uncorrected. The infrared spectra were determined in potassium bromide discs. The proton magnetic resonance (pmr) spectra were measured at 60 MHz with a Varian A-60D instrument and the peak position was expressed in τ-values.

Methyl *N*-Carbobenzyloxy-β-D-glucosaminide (II). The compound was prepared by the method of Neuberger and Rivers[8] in a yield of 15.2% from *N*-carbobenzyloxy-D-glycosamine (I).[9] Mp 166—

1) T. Suami and T. Machinami, This Bulletin, **43**, 2953 (1970).

2) J. J. Vavra, C. Deboer, A. Dietz, L. J. Hanka and W. T. Sokolski, *Antibio. Ann.*, **1959—1960**, 230 (1960).

3) W. T. Sokolski, J. J. Vavra and L. J. Hanka, *ibid.*, **1959—1960**, 241 (1960).

2) C. Lewis and A. R. Barbiers, *ibid.*, **1959—1960**, 247 (1960).

5) R. R. Herr, T. E. Eble, M. E. Bergy and H. K. Jahnke, *ibid.*, **1959—1960**, 236 (1960).

6) R. R. Herr, H. K. Jahnke and A. D. Argoudelis, *J. Amer. Chem. Soc.*, **89**, 4808 (1967).

7) E. Hardegger, A. Meier and A. Stoos, *Helv. Chim. Acta*, **52**, 2555 (1969).

8) A. Neuberger and R. P. Rivers, *J. Chem. Soc.*, **1939**, 122.

9) E. Chargaff and M. Bovarnich, *J. Biol. Chem.*, **118**, 421 (1937).

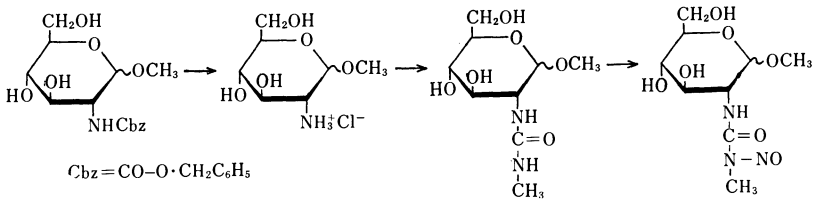

β-Anomer

II III IV V

α-Anomer

VII VIII IX X

Mixture of α- and β-anomers

XII XIII XIV XV

167.5°C, $[\alpha]_D^{25}$ −22.8° (*c* 1.00, pyridine).

Methyl β-D-Glucosaminide hydrochloride (III). The compound was obtained from II by the method of Neuberger and Rivers[8] in 94.3% yield. Mp 188°C (dec.), $[\alpha]_D^{25}$ −24.0° (*c* 1.00, water). The product showed a single spot at R_f 0.48 in a paper chromatogram in a solvent system of *n*-butanol : pyridine : water (6 : 4 : 3). Lit,[8] mp 190°C, $[\alpha]_D$ −24°.

Methyl *N*-Carbamyl-*N'*-methyl-β-D-glucosaminide (IV). A mixture of III (800 mg) and methyl isocyanate (200 mg) in 65% aqueous acetonitrile (60 m*l*) was heated under reflux for 1 hr in the presence of silver carbonate (580 mg). The reaction mixture was filtered to remove an insoluble matter and the filtrate was evaporated under reduced pressure. The residue was digested in ethanol to give 492 mg of the product, mp 239.5 −241°C. From the mother liquor, 63 mg of the product was obtained. The total yield of the crude product was 64.0%. Recrystallization from ethanol gave an analytically pure sample, mp 239.5—241°C.

Found: C, 43.36; H, 7.48; N, 11.52%. Calcd for $C_9H_{18}N_2O_6$: C, 43.19; H, 7.25; N, 11.20%.

Methyl *N*-Carbamyl-*N'*-methyl-*N'*-nitroso-β-D-glucosaminide (V). To a solution of IV (456 mg) in 23% aqueous acetic acid (13 m*l*), 4.3 m*l* of 0.5 M sodium nitrite solution was added dropwise in 20 min under ice cooling. The reaction solution was settled overnight in a refrigerator, and then was treated with Amberlite IR-120(H^+) to remove a sodium ion. After the resin was removed by filtration, the filtrate was freeze-dried to give a crude product. Recrystallization from ethanol afforded 354 mg (69.7%) of needle crystals: mp 149°C (dec.), mp* 118°C (dec.). $[\alpha]_D^{25}$ −23.7° (*c* 0.5, water). IR: 1720(C=O), 1550(NH), 1490(N-NO) and 875 cm^{-1} (β-anomeric C-H).[10]

Found: C, 39.06; H, 6.23; N, 14.87%. Calcd for $C_9H_{17}N_3O_7$: C, 38.71; H, 6.09; N, 15.05%.

Methyl 3,4,6-Tri-*O*-acetyl-*N*-carbamyl-*N'*-methyl-*N'*-nitroso-β-D-glucosaminide (VI). A 140 mg sample of V was acetylated with 2 m*l* of acetic anhydride in 3 m*l* of pyridine at room temperature overnight. The mixture was evaporated under reduced pressure and the residue was recrystallized from aqueous ethanol to give 152 mg (74.9%) of pale yellow crystals, mp 96—99°C. IR: 1745(OAc), 1710(C=O), 1540(NH), 1480(N-NO) and 900 cm^{-1} (β-anomeric C-H).[10]

Pmr (in $CDCl_3$): τ 5.16 (one proton doublet, $J_{1,2}$=8 Hz, H_1); 6.38 ($O-CH_3$)[11]; 6.75 ($N-CH_3$); 7.79, 7.85, 7.89 (singlets, three protons, three protons and three protons, OAc).

Found: C, 44.98; H, 5.86; N, 10.08%. Calcd for $C_{15}H_{23}N_3O_{10}$: C, 44.44; H, 5.72; N, 10.37%.

Methyl *N*-Carbobenzyloxy-α-D-glucosaminide (VII). The compound was prepared by the method of Neuberger and Rivers[8] in a yield of 79.0% from I. Mp 156—158°C, $[\alpha]_D^{25}$ +92.6° (c 2.4, pyridine). Lit,[8] mp 154—155°C, $[\alpha]_D$ +80° (pyridine).

Methyl *N*-Carbamyl-*N'*-methyl-α-D-glucosaminide (IX). A solution of VII (1.0 g) in ethanol (15 m*l*) was hydrogenated with 0.3 m*l* of 12 N hydrochloric acid under the presence of 0.2 g of palladium black at 3.4 kg/cm^2 of hydrogen stream for 21 hr. After the catalyst was removed by filtration, the filtrate was evaporated to give a crude product (735 mg) of methyl α-D-glucosaminide hydrochloride (VIII), which showed a single spot on a paper chromatogram at R_f 0.54 in a solvent system of *n*-butanol : pyridine : water (6 : 4 : 3). R_f of D-glucosamine hydrochloride was 0.41 in the same solvent system. The product was used in a successive synthesis without a further purification.

A mixture of VIII (735 mg), methyl isocyanate (200 mg) and 65% aqueous acetonitrile (45 m*l*) was heated under reflux for 45 min in the presence of silver carbonate (532 mg). After an insoluble matter was removed by filtration, the filtrate was evaporated under reduced pressure. The residue was recrystallized from ethanol to give 494 mg (64.7%) of the product, mp 189—191°C. Recrystallization from *n*-propanol gave crystals melting at 194.5—196°C. $[\alpha]_D^{23}$ +97.5° (*c* 1.0, water).

Found: C, 43.18; H, 7.39; N, 10.91%. Calcd for $C_9H_{18}N_2O_6$: C, 43.19; H, 7.25; N, 11.20%.

Methyl *N*-Carbamyl-*N'*-methyl-*N'*-nitroso-α-D-glucosaminide (X). A 400 mg portion of IX was treated with nitrous acid as described in the preparation of V to give 214 mg (50.5%) of crystals. Mp 129—133°C, mp* 89°C (dec.). $[\alpha]_D^{25}$ +107° (*c* 0.5, water). IR: 1705(C=O), 1540(NH), 1485(N-NO) and 850 cm^{-1} (α-anomeric C-H).[10]

Found: C, 38.81; H, 6.31; N, 14.78%. Calcd for $C_9H_{17}N_3O_7$: C, 38.71; H, 6.09; N, 15.05%.

Methyl 3,4,6-Tri-*O*-acetyl-*N*-carbamyl-*N'*-methyl-

10) S. A. Barker, E. J. Bourne, M. Stacey and D. H. Whiffen, *J. Chem. Soc.*, **1954**, 171.

11) H. H. Baer and T. Neilson, *J. Org. Chem.*, **32**, 1068 (1967).

***N'*-nitroso-α-D-glucosaminide (XI).** A 102 mg portion of X was acetylated analogously as described in the preparation of VI and the reaction mixture was poured into ice and water to give 116 mg (78.3%) of crystals, mp 114—115°C. Recrystallization from ethanol afforded pale yellow crystals melting at 115.5°C. IR: 1750(OAc), 1715(C=O), 1530(NH), 1480(N–NO) and 870 cm^{-1} (α-anomeric C–H).[10] PMR (in $CDCl_3$): τ 5.01 (one proton doublet, $J_{1,2}$=3.7 Hz, H_1); 6.45 (O–CH_3); 6.72 (N–CH_3); 7.77, 7.85, 7.91 (singlets, three protons, three protons and three protons, OAc).

Found: C, 45.04; H, 5.87; N, 10.23%. Calcd for $C_{15}H_{23}N_3O_{10}$: C, 44.44; H, 5.72; N, 10.37%.

Methyl *N*-Carbobenzyloxy-D-glucosaminide (XII). A mixture of I (1.78 g) in methanol (150 m*l*) and dry Amberlite IR-120(H^+) (18 m*l*) was heated under reflux for 2.5 hr. After the resin was removed by filtration, the filtrate was evaporated under reduced pressure. The residue was crystallized from ethanol to give 1.11 g (60.0%) of the product, mp 149—153°C, $[\alpha]_D^{25}$ +33.0° (*c* 2.5, pyridine). The compound consisted of 48% of α-anomer and 52% of β-anomer.

Methyl D-Glucosaminide hydrochloride (XIII). A 400 mg sample of XII was treated analogously as described above to give 162 mg (57.8%) of the product, mp 147—157°C (dec.). The product showed two spots at R_f 0.53 and 0.48 in a paper chromatogram in a solvent system of *n*-butanol : pyridine : water (6 : 4 : 3).

Methyl *N*-Carbamyl-*N'*-methyl-D-glucosaminide (XIV). A 400 mg portion of XIII was treated with methyl isocyanate as described above to give 240 mg (55.3%) of the product, mp 233—235°C. Recrystallization from aqueous ethanol afforded an analytically pure sample, mp 234.5—236°C.

Found: C, 43.39; H, 7.23; N, 11.30%. Calcd for $C_9H_{18}N_2O_6$: C, 43.19; H, 7.25; N, 11.20%.

Methyl *N*-Carbamyl-*N'*-methyl-*N'*-nitroso-D-glucosaminide (XV). A 180 mg sample of XIV was treated with nitrous acid as described above to give 172 mg (88.9%) of the crude product. Recrystallization from ethanol afforded needle crystals, mp 117—121°C (dec.), mp* 59°C (dec.). $[\alpha]_D^{23}$ −19.6° (*c* 0.5, water). The product consisted of 97% of β-anomer, since the β-anomer crystallized preferentially.

Found: C, 39.26; H, 6.26; N, 14.74%. Calcd for $C_9H_{17}N_3O_7$: C, 38.71; H, 6.09; N, 15.05%.

Antitumor activity. A detail of the antitumor activities of V, X and XV against Ehrlich mouse ascites tumor will be reported elsewhere.

The authors are grateful to Professor Sumio Umezawa for his helpful advice and Mr. Saburo Nakada for his elementary analyses.

SHORT COMMUNICATIONS

An Attempt to Estimate the Relative Stability of Tri(hetero)substituted Carbonium Ions*

Takeshi NAKAI, Kazuhisa HIRATANI and Makoto OKAWARA

Research Laboratory of Resources Utilization, Tokyo Institute of Technology, Ookayama, Meguro-ku, Tokyo

(Received May 12, 1970)

In connection with our study on the structures and ambident reactivities of tri(hetero)carbonium ions containing α-alkylthio groups,[1,2] we attempted to estimate the relative stability of tri(hetero)carbonium ions from their electronic spectra and simple HMO calculations. A series of tri(hetero)-carbonium ions shown below were prepared as perchlorates and iodides.[3]

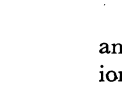

I, X, Y, Z=SMe; II, X, Y=SMe, Z=NMe_2 III, X, Y=NMe_2, Z=SMe; IV, X, Y, Z=NMe_2

In the electronic spectra we observed a well-defined trend, *viz.*, a strong shift of the absorption maxima to shorter wavelengths was observed with the progressive replacement of SMe in (I) by NMe_2.[4] This trend led us to postulate that *there is a linear correlation between the relative stability of the carbonium ion and the transition energy* ($1/\lambda_{max}$). In order to prove this hypothesis we made some attempts described below.

Firstly, it is expected that the stabilizing effect of α-heterosubstituents on carbonium ions concerned might be estimated *relatively* in terms of the Brown-Okamoto's substituent constants (σ_p^+), on the assumption that the additivity rule holds for the series. The observed frequencies of absorption maxima gave a definitely linear correlation with $\sum\sigma_p^+$[5] (Fig. 1), providing a positive criterion for the above hypothesis.

Another criterion for the hypothesis was obtained

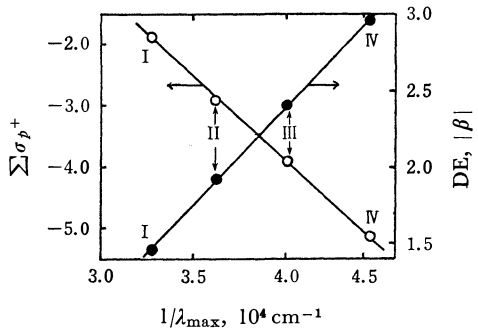

Fig 1. Plots of $1/\lambda_{max}$ (solvent, water) *vs.* $\sum\sigma_p^+$ (○) and DE (●).

from simple HMO calculations. In our calculations,[6] the values assumed for the Coulomb integral and resonance integral are as follows: $\alpha_S=\alpha+\beta$, $\alpha_N=\alpha+1.5\beta$; $\beta_{C-S}=0.6\beta$, $\beta_{C-N}=1.2\beta$[7] Using these parameters, we calculated the energies of the molecular orbitals, the transition energies (ΔE) and the delocalization energies (DE) in the usual manner. A linear correlation between ΔE and $1/\lambda_{max}$ was obtained. Furthermore, a definitely linear correlation of DE with $1/\lambda_{max}$ was obtained (Fig. 1). This correlation provides the second positive criterion.

We suggested that the rates of reactions of various bis(alkylthio)-dialkylaminocarbonium ions with hydroxide ion depend upon the relative stability of the carbonium ions.[2] The logarithms of the rate constants gave a nearly linear correlation with $1/\lambda_{max}$ for the open-chain and cyclic[8] carbonium ions. This may provide a third positive criterion. The relationship between the relative stability and the reactivity of tri(hetero)-carbonium ions will be discussed in full elsewhere.

* Presented at the 3rd Symposium on Organic Sulfur Chemistry, Tokyo, 1969 and at the 23rd Annual Meeting of the Chemical Society of Japan, Tokyo, 1970.

1) T. Nakai and M. Okawara, *Tetrahedron Lett.*, **1967**, 3835; This Bulletin, **43**, 1864 (1970).

2) T. Nakai, K. Hiratani and M. Okawara, 19th Symposium on Organic Reaction Mechanisms, Yamagata, 1968, Abstracts, p. 140, and our previous results cited therein.

3) All carbonium salts gave correct data of elementary analyses and NMR properties in $(CD_3)_2SO$.

4) In all cases, ε_{max} were about 10^4. The values of $\lambda_{max}^{H_2O}$ were dependent slightly upon the nature of the counter anion (±1 mμ).

5) $\sigma_{p-SMe}^+=-0.604$ and $\sigma_{p-NMe_2}^+=-1.70$: H. C. Brown and Y. Okamoto, *J. Amer. Chem. Soc.*, **80**, 4979 (1959).

6) The non-orthogonality integral and the auxiliary inductive parameters for the central carbon atoms were neglected.

7) M. J. Janssen, *Rec. Trav. Chim. Pays-Bas*, **79**, 1066 (1960).

8) For example, 2-dimethylamino-1,3-dithiolanylium ion and 2-methylthio-3-methyl-4,5-dihydrothiazolium ion.

A Study of the Paramagnetic Center in Vanadium Pentoxide

Kozo HIROTA, Keiji KUWATA and Yoshiya KERA

Faculty of Science, Osaka University, Toyonaka, Osaka

(Received March 23, 1970)

ESR studies of the V(IV)ion in vanadium pentoxide have been extensively carried out. The use of a single crystal gives more detailed information regarding the structure of the paramagnetic centers in V_2O_5.[1] In the present paper the esr spectrum of a new center in V_2O_5 is shown, and the mechanism of its formation is discussed.

The single crystal was prepared by the zone-melting method from pure V_2O_5 powder. The *g*-factor and the hyperfine coupling constant were determined at 77°K with DPPH ($g=2.0035$) and the Mn(II) ion in magnesium oxide, respectively.

When the static magnetic field was applied in parallel with the *b*-axis, clear hfs of 27 lines appeared, as is shown in Fig. 1; as the direction of

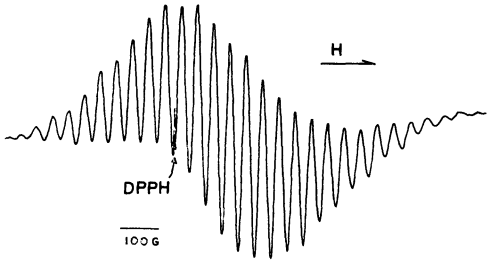

Fig. 1. ESR spectrum of a V_2O_5 single crystal with the static field applied in parallel with the crystallographic *b*-axis.

the field deviated from the *b*-axis on both the *ba*- and *bc*-planes, the hf splitting quickly decreased. On the basis of this finding, one of the principal axes for the hf interaction was estimated to be nearly the *b*-axis, and the maximal principal value was estimated to be 43.3 gauss.

The number of lines in hfs and the polynominal distribution of their intensities indicate the existence of a magnetic center in which four ^{51}V nuclei ($I=7/2$) interact equally with an unpaired electron.

The magnetic center including four ^{51}V atoms has been briefly discussed by Ioffe and Patrina,[1c] but neither detailed experimental results nor discussion was given regarding its structure.

The principal components of the *g*-tensor for this center were $g_{xx}=1.974_9$, $g_{yy}=1.988_7$, and $g_{zz}=1.931_3$, and the *x*, *y*, and *z*-axes nearly accorded with the *a*, *c*, and *b*-axes of the crystal with an orthorhombic symmetry, respectively. The relationship among the components of the *g*-tensor indicates that the V(IV) ion is in the field of fourfold symmetry.[2]

The fourfold symmetry can be obtained when an oxygen ion on the *b*-axis is lost. A pair of V ions formed by the elimination of such an oxygen ion had been proposed by Gillis *et al.*[1] as the paramagnetic center in V_2O_5.

On the basis of the present study, two neighbouring pairs of V ions were assumed to constitute a paramagnetic center containing four V atoms. The removal of the I and II oxygen ions in Fig. 2 produces such pairs (1-2 and 3-4 in Fig. 2). Similarly, 1-2 and 1′-2′ pairs, or 3-4

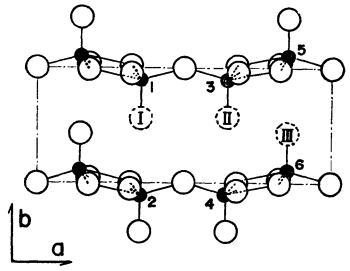

Fig. 2. Arrangements of paramagnetic center in the V_2O_5 crystal, whose structure was taken from Ref. 3. (large circles denote oxygen ions; small circles denote vanadium ions. For example, V atoms of 1′ and 2′ are placed just behind the 1 and 2 V atoms, respectively.)

and 5-6 pairs, can equally form the center. An unpaired electron is assumed to interact equally with the four V ions through fast exchange between these pairs. The center of this kind, as in Eq. (1), can be formed either by the direct elimination of two neibouring oxygen ions, or by the migration of the oxygen vacancy through the crystal lattice to form the two pairs of V ions:

$$2(V^{5+}-O^{2-}-V^{5+}) \rightarrow \begin{matrix} V^{5+}\ldots V^{5+} \\ \vdots \quad\quad \vdots \\ V^{5+}\ldots V^{4+} \end{matrix} + 2O + 3e^- \quad (1)$$

It is worthy of mention that the formation of such a defect could be predicted from the study of catalytic activity of this oxide.[4]

1) a) J. L. Ragle, *J. Chem. Phys.*, **38**, 2020 (1963); b) E. Gillis and E. Boseman, *Phys. Stat. Sol.*, **14**, 337 (1966); c) V. A. Ioffe and I. B. Patrina, *Sov. Phys.-Solid State*, **10**, 639 (1968).

2) H. G. Hecht and T. S. Johnston, *J. Chem. Phys.*, **46**. 23 (1967).

3) A. Byström, K. A. Wilhelmi and O. Brotzen, *Acta Chem. Scand.*, **4**, 1119 (1950).

4) K. Hirota, Y. Kera and S. Teratani, *J. Phys. Chem.* **72**, 3133 (1968).

Syntheses of {Sulfato, *N,N'*-(2-pyridylalkyl)-oxamidatocopper(II)} copper(II)*[1]

Heijiro OJIMA and Kiyoko YAMADA

Department of Chemistry Aichi Kyoiku University, Kariya, Aichi

(Received May 13, 1970)

The present paper reports that the *N,N'*-bis-(2-pyridylalkyl)oxamidatocopper(II) acts as a bidentate ligand coordinating to cupric sulfate to form binuclear complexes with a subnormal magnetic moment: [Cu(PMoxd)-$CuSO_4$] and [Cu(PEoxd)-$CuSO_4$] (*cf.* Fig. 1). The $PMoxdH_2$ ligand was obtained in a 90% yield by the reaction 2 mol of 2-(aminomethyl)pyridine with 1 mol of diethyl oxalate at 150°C for 1 hr. Recrystallized from ethanol, mp 155—156°C. The $PEoxdH_2$ ligand was obtained similarly in a 95% yield using 2-(2-aminoethyl)pyridine and diethyl oxalate. Recrystallized from ethanol, mp 175—176°C. [Cu(PMoxd)-$Cu(OH_2)_2$]$SO_4 \cdot 5H_2O$ (A) was obtained as blue crystals by mixing 1 mol of the ligand and 2 mol of cupric sulfate in an aqueous solution at pH 5—6. Recrystallized from water. This complex was converted into [Cu(PMoxd)-$CuSO_4$] (B) concurrently with the elimination of 7 mol of water, by heating it at more than 80°C under vacuum conditions (*cf.* the change in the IR spectra, Fig. 2). The [Cu(PEoxd)-$CuSO_4$]$\cdot 2.5H_2O$ (C) was isolated as greenish-blue crystals from an aqueous mixture of 1 mol of the $PEoxdH_2$ ligand and 2 mol of cupric sulfate, in which mixture the pH value had been adjusted to 6. Recrystallized from water. It can be understood, considering the analytical data, that the conspicuous spectral change in the SO_4^{2-} region may be due to the change from ionic sulfate to chelated sulfate. The magnetic moment values of the complexes here isolated obviously reflect Cu-Cu interaction. It seems that the Cu-Cu interaction must take place through the π-pathway set up by using $3d_{yz}$(or $3d_{xz}$) orbitals of the cupric ions and $2p_\pi$ orbitals of the bridging oxamide group (*cf.* Fig. 3). When each sulfato complex was dissolved into an aqueous solution, the value of molar conductance fell into the range of 129—133 $\mho/cm^2$. This value reflects that a part of each sulfato complex changes into a divalent complex cation, [Cu(PMoxd)-$Cu(OH_2)_2$]$^{2+}$ or [Cu(PEoxd)-$Cu(OH_2)_2$]$^{2+}$.

TABLE 1. PROPERTIES OF COMPLEX

Complex	Color	Analysis ( ): Calcd			Magnetic Moment		IR-Spectra amide-I[a)]
		Cu %	Nitrogen %	H_2O	μ_{eff} (BM)	T°K	
(A)	blue	22.57 (20.58)	9.14 (9.07)	20.47 (20.42)	0.97	292	1655
(B)	green	25.85 (25.85)			0.88	292	1645
(C)	greenish-blue	22.57 (22.51)	9.76 (9.92)	7.75 (7.98)	1.25	287	1635
(D)	green	24.20 (24.47)			1.15	288	1639

a) Ligand $PMoxdH_2$, amide-I 1645 cm^{-1}; ligand $PEoxdH_2$, amide-I 1659 cm^{-1}. (D): anhydride of (C)

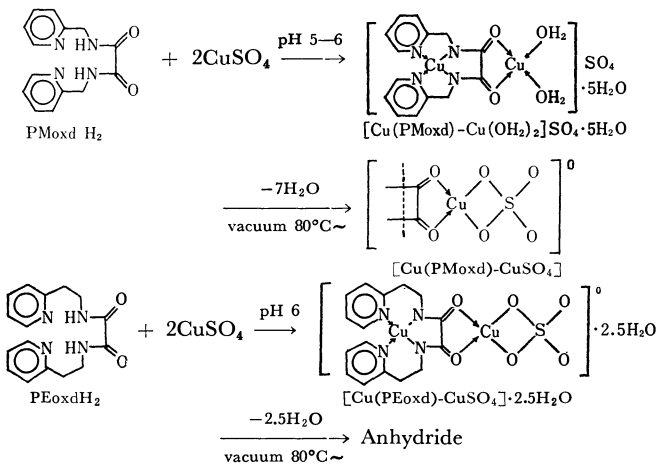

Fig. 1. Formation of copper(II) complexes with a subnormal magnetic moment.

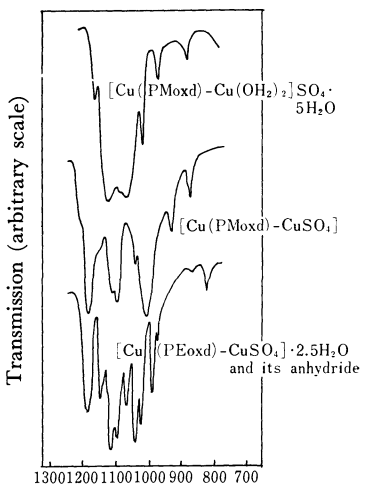

Fig. 2. IR-spectra of SO_4^{2-} region.

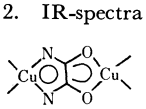

Fig. 3

*[1] Syntheses and Characterization of Metallic Complexes in which the Negative Amide Nitrogen Coordinates. X. Recent note: H. Ojima, K. Yamada, This Bulletin, **43**, 1601 (1970).

Copper(II) Complexes of 3-Formyl-5-methylsalicylaldehyde and Its Schiff Bases with Alkyl Amines

Hisashi OKAWA

Department of Chemistry, Faculty of Science, Kyushu University, Hakozaki, Fukuoka

(Received May 21, 1970)

Two new copper(II) complexes of 3-formyl-5-methylsalicylaldehyde,[1] bis(3-formyl-5-methylsalicylaldehydato)copper(II) (**1**) and dichloro-μ-chloro-μ-(2,6-diformyl-4-methylphenolato)dicopper-(II) (**2**) (Fig. 1), have been prepared by using copper(II) acetate monohydrate and copper(II) chloride dihydrate respectively as metal sources. Both were easily obtained by adding a solution of the copper(II) salt in ethanol to a solution of 3-formyl-5-methylsalicylaldehyde in ethanol.

In addition to these complexes, new series of oxygen-bridged binuclear copper(II) complexes (**3** type) have been synthesized by using the aldehyde, copper(II) chloride dihydrate, and alkyl amines (R-NH_2), in which R represents methyl, ethyl, isopropyl, *t*-butyl, or chclohexyl groups. The method of synthesizing the complexes was as follows. To a warm solution of the aldehyde and copper(II) chloride dihydrate in ethanol we added a solution of an amine in ethanol to give green or brown needles; these needles were collected and washed with ethanol. The results of the molecular-weight determinations of these complexes support the formula given for the complex **3** in Fig. 1. The analytical data of the complexes obtained are given in Table 1.

In the complexes **2** and **3**, the organic moiety acts as a quadridentate chelating agent with the bridging phenolic oxygen, and the copper atoms are held sufficiently close to each other to cause

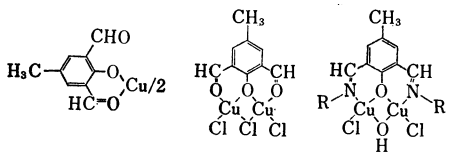

1 **2** **3**

Fig. 1.

antiferromagnetic interactions; the magnetic moments determined for the complexes **2** and **3** at room temperature were 1.58 and 0.80—1.29 B. M. respectively. On the other hand, the complex **1** has a normal magnetic moment of 1.81 B. M.

The reflectance spectra of the complexes **2** and **3** each have one d-d transition band, located at 11,100 cm^{-1} for the complex **2** and at 12,000—14,400 cm^{-1} for the complex **3**; these energies are lower than those expected for mononuclear copper(II) complexes of similar ligands, supporting a binuclear structure and in agreement with the findings of Harris *et al.*[2] It is noteworthy that the complexes also have a binuclear structure in a solution, judging from the spectra in a solution, which are very similar to those measured by the diffuse-reflection method, although the complex **2** is decomposed in the presence of water to the complex **1**.

The details of this work will be reported shortly.

TABLE 1. ANALYTICAL DATA OF COMPLEXES

Complex		Found (%)				Calcd (%)			
		C	H	N	Cu	C	H	N	Cu
1		55.55	3.87		15.96	55.46	3.62		16.30
2		27.28	1.85		31.32	27.26	1.78		32.04
	R								
3	CH_3	32.46	3.24	6.71		32.68	3.49	6.93	
	C_2H_5	36.39	4.01	6.33		36.12	4.20	6.43	
	i-C_3H_7	39.60	4.67	5.73		39.14	4.82	6.09	
	t-C_4H_9	41.65	5.19	5.54		41.81	5.37	5.74	
	C_6H_{11}*	45.97	5.42	4.83		45.90	5.69	5.10	

* It denotes cyclohexyl. With a half molecule of water.

1) D. A. Denton and H. Suschitzky, *J. Chem. Soc.*, **1963**, 4741.

2) C. M. Harris, J. M. James, P. J. Milham and E. Sinn, *Inorg. Chim. Acta*, **3**, 81 (1969); B. Coles, C. M. Harris and E. Sinn, *Inorg. Chem.*, **8**, 2607 (1969).

Effects of Wavelength and Matrix on Four-Center Type Photopolymerization of 2,5-Distyrylpyrazine and Its Photodepolymerization

Masaki HASEGAWA, Yasuzo SUZUKI and Takashi TAMAKI

Research Institute for Polymers and Textiles, Sawatari, Kanagawa-ku, Yokohama, Japan

(Received May 18, 1970)

In previous papers,[1-5] preparative, kinetical and crystallographic studies on four-center type photopolymerization in the solid state have been reported for a series of several diolefine compounds.

As a result, a number of new types of highly crystalline linear polymers with cyclobutane in the main chain has been prepared mostly in quantitative yield.

Recently the polymerization was found to be lattice-controlled, that is, the chain growth is strictly governed by three axes of the monomer crystal and proceeds through a direct rearrangement from monomer crystal to polymer crystal.

For example, crystals of 2,5-distyrylpyrazine (DSP) and poly-2,5-distyrylpyrazine (poly-DSP), belong to the same space group (Pbca).[6]

We have investigated the effects of wavelength and matrix on four-center type photopolymerization of 2,5-distryrylpyrazine and its photodepolymerization.

First, DSP oligomer (average molecular weight $\simeq$900, mp 285—290°C) was obtained from DSP crystals in water-methanol (4 : 6) nearly quantitatively by irradiation of the light with a wavelength longer than 400 mμ for about one hour at room temperature while DSP crystals were converted into a high molecular weight of the polymer (mol wt $>$100000) in a quantitative yield by xenon or high pressure mercury lamp under a similar condition.

DSP oligomer crystals (*as*-polymerized) were converted quantitatively into a high polymer by the irradiation of monochromatic light of 340 mμ from a Shimadzu Bausch & Lomb monochrometer.

DSP crystals show an absorption occurring at 440 mμ with a maximum peak at 380 mμ while DSP oligomer has no absorption of a wavelength longer than 380 mμ. It is presumed that a longer wavelength ($>$400 mμ) can excite only the monomer, and a shorter wavelength ($<$380 mμ) is required for further growth of terminal groups in the oligomer.

On the other hand, DSP oligomer crystals (recrystallized) which differ from the crystals (*as*-polymerized) from X-ray patterns, does not polymerize by the same light (340 mμ).

Moreover, a solution of the DSP oligomer in chloroform promptly returns to the monomer by the same light (340 mμ).

It is noteworthy that the DSP oligomer (*as*-polymerized) consists of thermally irreversible crystals as well as the resulting poly-DSP crystals[7]: DSP oligomer crystal (*as*-polymerized) can never be reproduced after the oligomer becomes amorphous and the oligomer with a different crystal form is reprecipitated from a solution of above oligomer crystal (*as*-polymerized).

DSP oligomer does not grow further into high polymer by the irradiation of 340 mμ without an effective "topotactic assistance", as is the case in the crystalline oligomer (as-polymerized).

It is interesting that chemically the same substance behaves in three different ways according to physical states.

This is a clear-cut example of matrix effect originating in the topochemical procedure.

Amorphous DSP oligomer results from the solution of DSP in chloroform by the prolonged irradiation of light with a wavelength longer than 380 mμ in nitrogen atmosphere. As expected, amorphous oligomer does not polymerize in the solid state and depolymerizes in the solution in the same way as the oligomers from DSP crystals.

A schematical diagram of photochemical interrelationship in DSP, DSP oligomers and poly-DSP is shown below:

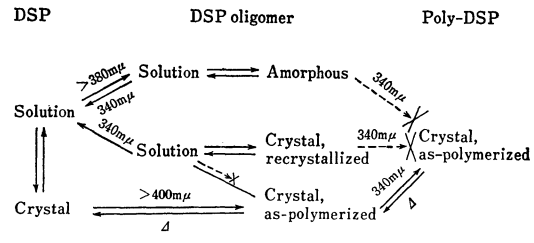

1) M. Hasegawa and Y. Suzuki, *J. Polym. Sci.*, **B5**, 815 (1967).

2) M. Iguchi, H. Nakanishi and M. Hasegawa, *ibid.*, **A6**, 1055 (1968).

3) M. Hasegawa, Y. Suzuki, F. Suzuki and H. Nakanishi, *ibid.*, *A*-1, **7**, 743 (1969).

4) H. Nakanishi, Y. Suzuki, F. Suzuki and M. Hasegawa, *ibid.*, *A*-1, **7**, 753 (1969).

5) F. Suzuki, Y. Suzuki, H. Nakanishi and M. Hasegawa, *ibid.*, *A*-1, **7**, 2319 (1969).

6) Y. Sasada, H. Shimanouchi, H. Nakanishi and M. Hasegawa, to be published.

7) S. Fujishige and M. Hasegawa, *J. Polym. Sci.*, *A*-1, **7**, 2037 (1969).

Bitter Principles of *Picrasma ailanthoides* Planchon. Nigakihemiacetals A and B, and Nigakilactones G and H.

Tatsushi MURAE, Tôru IKEDA, Takahiko TSUYUKI, Tadaaki NISHIHAMA and Takeyoshi TAKAHASHI

Department of Chemistry, Faculty of Science, The University of Tokyo, Bunkyo-ku, Tokyo

(Received June 15, 1970)

In addition to the previously reported nigakilactones A, B, C, D,[1] E and F,[2] four bitter principles (nigakihemiacetals A and B, and nigakilactones G and H) have been isolated from *Picrasma ailanthoides* Planchon (= *P. quassioides* Bennett). Recently, isolation of picrasin B[3] and A[4] from the same plant was recorded by Hikino *et al.*

Nigakihemiacetal A, mp 262—263°C, $C_{22}H_{34}O_7$, M^+ 410, $[\alpha]_D$+20° (*c* 0.22, in EtOH), λ_{max}^{MeOH} 272 nm (ε 5800), IR (nujol): 3560, 3470, 3360, 1668, 1634 cm^{-1}, PMR (Table 1), is a new bitter substance which has a hemiacetal instead of a lactone grouping. On oxidation with Ag_2O, this hemiacetal gave nigakilactone F[2] (I, R_1=OH, R_2=H, R_3=H, R_4=O). Thus, structure I (R_1=OH, R_2=H, R_3=H, R_4=OH, H) is given for nigakihemiacetal A.

Spectral data of nigakihemiacetal B, mp 230.5—231°C, $C_{22}H_{30}O_6$, M^+ 390, $[\alpha]_D$+20° (*c* 0.21, in EtOH), λ_{max}^{MeOH} 256 nm (ε 11400), IR (nujol): 3400, 1690, 1674, 1640, 1621 cm^{-1}, suggest that this substance would be neoquassin. Indeed, nigakihemiacetal B was shown to be identical with neoquassin[5] (II, R=OH, H) by the formation of quassin[5] (II, R=O) on oxidation of this hemiacetal with Ag_2O.

Nigakilactone H, mp 274.5—275.5°C, $C_{22}H_{32}O_8$, M^+ 424, $[\alpha]_D$+67° (*c* 0.14, in EtOH), λ_{max}^{MeOH} 271 nm (ε 4260), IR (nujol): 3450, 1725, 1675, 1640 cm^{-1}, is a new bitter principle containing one hydroxyl group more than nigakilactone F[2]. In the PMR spectrum, C_9-H (1H, δ 2.05) resonates as doublet (J=11 Hz), C_{11}-H (1H, δ 3.96) as quartet (J=11; 9 Hz), C_{12}-H (1H, δ 3.02) as doublet (J=9 Hz), C_3-H (1H, δ 5.51) as doublet (J=2.5 Hz) and C_7-H (1H, δ 4.56) as multiplet. These observations are best interpreted on the basis of the skeletal structure of known nigakilactone F[2] (I, R_1=OH, R_2=H, R_3=H, R_4=O). Nigakilactone H, when treated with $Na_2Cr_2O_7$, afforded a ketone, mp 161—163°C, $C_{22}H_{30}O_8$, M^+ 422, λ_{max}^{MeOH} 264 nm (ε 5920), IR (nujol): 3450, 1720, 1690, 1625 cm^{-1}. The PMR spectrum shows signals due to C_9-H (1H, δ 2.61, singlet), C_{12}-H (1H, δ 3.38, singlet), C_3-H (1H, δ 5.42, doublet, J=2.5 Hz) and C_7-H (1H, δ 4.53, multiplet); no signal due to C_{11}-H is observed. In the PMR spectra of nigakilactone H and its ketone, a signal due to two protons on C_{15} appears as *singlet* at δ 2.67 and at δ 2.89, respectively. This shows that the C_{14}-carbon is tertiary, and leads to the location of an extra hydroxyl group on C_{14} for nigakilactone H. Thus, nigakilactone H and its ketone should be represented by I (R_1=OH, R_2=H, R_3=OH, R_4=O, for nigakilactone H; R_1, R_2=O, R_3=OH, R_4=O, for its ketone) except for absolute configuration.

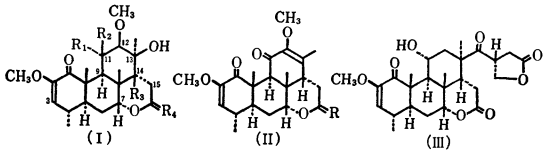

(I) (II) (III)

TABLE 1. PMR SPECTRAL DATA (δ in ppm,* in $CDCl_3$)

	Nigakihemiacetals		Nigakilactones	
	A	B	H	F
s-C$\underline{H}_3$	1.11 d	1.07 d	1.15 d	1.11 d
	J=7	J=6	J=7.5	J=7
t-C$\underline{H}_3$	1.20 s	1.05 s	1.27 s	1.22 s
	1.34 s	1.49 s	1.35 s	1.46 s
	1.44 s		1.50 s	1.46 s
C=C-C$\underline{H}_3$		1.83 s		
$\underline{H}$-C-OCH$_3$	2.98 d		3.02 d	3.03 d
	J=9		J=9	J=9
-O-C$\underline{H}_3$	3.58 s	3.55 s	3.63 s	3.58 s
	3.69 s	3.61 s	3.77 s	3.73 s
$\underline{H}$-C-OH	3.52 q		3.96 q	4.00 q
	J=11; 9		J=11; 9	J=11; 9
C$\underline{H}$-O-	3.88 m	3.95 m	4.56 m	4.13 m
C=C$\underline{H}$	5.40 d	5.25 d	5.51 d	5.43 d
	J=2.5	J=2.5	J=2.5	J=2

* internal standard; TMS

Spectral and some chemical data of nigakilactone G, mp 305—305.5°C, $C_{26}H_{34}O_8$, M^+ 474, $[\alpha]_D$+41° (c 0.29, in EtOH), λ_{max}^{MeOH} 271 nm (ε 5300), IR (Nujol): 3430, 1778, 1734, 1678, 1640 cm^{-1}, suggest that this substance would be identical with picrasin A[4] (III), whose structure was recently determined.[4] Confirmation of this identity is under way.

1) T. Murae, T. Tsuyuki, T. Nishihama, S. Masuda and T. Takahashi, *Tetrahedron Lett.*, **1969**, 3013.

2) T. Murae, T. Ikeda, T. Tsuyuki, T. Nishihama and T. Takahashi, This Bulletin, **43**, 969 (1970).

3) H. Hikino, T. Ohta and T. Takemoto, *Chem. Pharm. Bull.* (Tokyo), **18**, 219 (1970).

4) H. Hikino, T. Ohta and T. Takemoto, *ibid.*, **18**, 1082 (1970).

5) Z. Valenta, S. Papadopoulos and C. Podešva, *Tetrahedron*, **15**, 100 (1961).

The Cation-radical Salts of *p*-Phenylenediamine. A Modified Method of Preparation and the Electrical Resistivity of the Salts

Kei-ichiro HATANO, Yuzaburo FUJITA and Takao KWAN

Faculty of Pharmaceutical Sciences, The University of Tokyo, Hongo, Bunkyo-ku, Tokyo

(Received June 29, 1970)

A method of oxidation using Fe(III) salts was developed for preparing various types of cation radical salts of *p*-phenylenediamine (*p*PD) and its analogue in place of the familiar Br_2-oxidation method.[1,2] As an example, we will briefly describe below the method of preparing $pPD^+Cl^- \cdot H_2O$ and some physico-chemical properties of the salt.

In a cooled methanol solution of *p*PD, a methanol solution containing an equivalent amount of $FeCl_3 \cdot 6H_2O$ was added in small portions, while the reacting system was flushed with nitrogen (or helium) during the mixing. The precipitate formed in the deep green solution was collected, washed repeatedly with a methanol-ether mixture, dried, and stored in an evacuated desiccator. The product thus obtained was a lustrous brownish green powder; it was stable in air, at least at room temperature. Iron was not detected in the product by a colorimetric test. The results of the elemental analysis were as follows:

Found: C, 44.42; H, 6.25; N, 17.14; Cl, 22.03%. Calcd for $C_6H_{10}N_2OCl$: C, 44.59; H, 6.24; N, 17.34; Cl, 21.82%.

Among the observed IR absorption bands of this salt in a KBr disk, the one at 1395 cm^{-1} was characteristic and was common to all the pPD^+ salts prepared. The absorption band can probably be attributed to the C–N stretching in the *p*PD cation radical.

The aqueous solution of this salt ($\sim 10^{-3}$ M) was initially green, but it turned a dark violet within several minutes. The green solution exhibited an esr signal exactly identical to that reported for the cation radical of *p*PD,[3] although the signal soon disappeared as the color changed. The *p*PD cation radical was fairly stable in an ethanolic solution (yellow, $\sim 10^{-4}$ M) and gave rise to an esr signal significantly different in linewidth from that in an aqueous solution, suggesting that the ion-pair was formed between pPD^+ and Cl^-. The UV and visible absorption spectra of this salt in the ethanolic solution almost coincided with those reported by Iida and Matsunaga.[4] Judging from this information, it seems almost certain that the salt of the *p*PD cation radical was formed.

Electrical resistivity measurements were made with a disk of the salt (prepared under 500 kg/cm^2) in an atmosphere of nitrogen. Accordingly, the specific resistivity was $3 \times 10^8\ \Omega$ cm at 20°C, with a negative temperature coefficient of *ca.* 0.7 eV. Other salts, with different cations and counter anions, prepared by this method are listed in Table 1, together with their approximate electrical resistivity data.

TABLE 1. CATION-RADICAL SALTS AND THEIR PROPERTIES

Salts*1	Color of powder	Electrical resistivity at 20°C (Ω cm)
$pPD^+Br^- \cdot H_2O$*2	lustrous brown	10^9
$pPD^+NO_3^- \cdot H_2O$	black	10^6
$pPD^+p\text{-}CH_3\text{-}\phi\text{-}SO_3^- \cdot \frac{1}{2}H_2O$	violet	10^{13}
$Benzidine^+Cl^- \cdot \frac{1}{4}H_2O$	grey	10^{10}
$Benzidine^+Br^- \cdot \frac{1}{4}H_2O$	deep blue	10^6
$(pPD^+)_2[Fe_2(SO_4)_3]^{2-}$	greenish grey	10^{10}
$pPD^+[K_3Fe(CN)_6]^- \cdot nH_2O$*3	deep blue	10^7
pPD^+p-Chloranil$^-$	deep purple	10^7

*1 The chemical compositions were estimated from elemental analyses of C, H and N.
*2 The X-ray analysis of the salt is now in progress.
*3 $n = 1$—3.

1) L. Michaelis and S. Granick, *J. Amer. Chem. Soc.*, **65**, 1747 (1943).
2) G. K. Hughes and N. S. Hush, *J. Proc. Roy. Soc. N. S. W.*, **81**, 48 (1947).
3) M. T. Melchior and A. H. Maki, *J. Chem. Phys.*, **34**, 471 (1961).
4) Y. Iida and Y. Matsunaga, This Bulletin, **41**, 2535 (1968).

Electron Spin Resonance and Cell Division in Silkworm Egg

Shizuo FUJIWARA, Hiroshi TADANO*1 and Makoto NAKAJIMA*2

Department of Chemistry, Faculty of Science, The University of Tokyo, Bunkyoku, Tokyo

(Received June 29, 1970)

Several biological systems have so far been investigated by electron spin resonance (ESR).[1-3] The sources of ESR signals were generally identified and the results of investigation by ESR have presented direct information on the kinetic and chemical behaviors of the sample. ESR can also be used for looking at the free radicals of unknown identity, as this technique can be used as a means of seeing inside the living material without causing any distortion or damage.

Information hitherto given on the commercial silkworm[4] aroused our interest to investigate silkworm eggs by ESR. Studies were carried out on the eggs of six varieties of *Bombyx mori*, including two Japanese (KONJIKI and AOJYUKU), three Chinese (KANSEN, HIKO and SEKKO) and one European (ASCOLI). All showed ESR signal of the same g value, 2.004 ± 0.001, but of different intensity.

All measurements were carried out at room temperature. For the measurements, twenty eggs of each kind were loaded in a glass capillary of about 1 mm I.D. without sealing and placed in the field of ESR spectrometer. All eggs had previously been about one year in diapause. The g-value and signal intensity were measured with two reference substances, *i.e.*, the diphenylpicrylhydrazil and the manganous ions of a known number of spins in magnesium oxide. The g-value, of all six varieties did not change with time, either before incubation, or after the eggs were activated by treatment with hydrochloric acid.

In order to locate the radicals, ESR measurements were carried out on egg fractions of nucleus, mitochondria, and microsome, which were separated from each other according to standard procedures. The shell did not show any signal, and mitochondrial and microsomal fractions showed weak signals. We suspect that these signals are due to contamination with nuclear material. A very strong signal was observed with nucleus. The records of ESR signals are shown in Fig. 1.

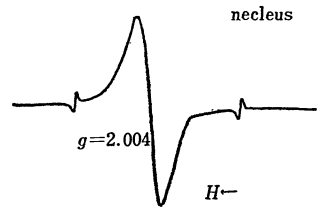

Fig. 1. ESR signal (central peak) in the nucleus of silkworm egg. Satellites in both sides of the central peak refer to the hyperfine signals of Mn^{2+} (in MgO), which has been added to the sample as the reference substance.

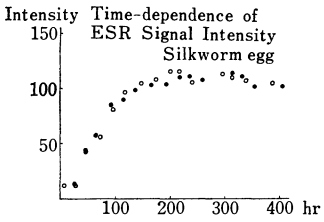

Fig. 2. Time-dependence of ESR signal intensity of silkworm egg.

Figure 2 shows the time dependence of the ESR signal in freshly laid eggs of HIKO. The origin of the time scale in Fig. 2 refers to the time of *OVIPOSITION*. Two sets of measurements were carried out: one was started 3 hr after *OVIPOSITION* (white circles in Fig. 2); the other after 12 hr (black circles).

As shown in Fig. 2, the signal intensity increases linearly during the first 180 hr and then plateaus. The intensity scale in Fig. 2 is arbitrary; after the 180th hour, the number of electron spins in one egg is about 1.4×10^{14}.

If we assume that an egg originally has n spins, and that they increase linearly until equilibrium is achieved, then there is approximately a 60-fold increase during this time.

Further effort has been made in order to locate the spins, *i.e.*, the nuclear material has been separated into DNA and protein by extracting nucleus with 1% Na_2CO_3 or 0.8% NaCl solution. Although a spurious signal is observed in the DNA part, spins are mainly located in that of protein. The principal problem is the source of the ESR signal in these eggs. Whatever the free radicals be, they increase systematically during the early hours of incubation and then stabilize in an equilibrium. Additional studies are being made.

*1 On leave from Rikkyo University, Tokyo.

*2 Tokyo Nōkō University, Fuchū, Tokyo.

1) P. J. E. Ingram, "Spectroscopy at Radio and Microwave Frequencies," 2nd Ed., Butterworth, London, (1967), p. 409.

2) S. Fujiwara, L. Piette ed., "Recent Developments of Magnetic Resonance in Molecular Biology," Hirokawa Pub. Inc., Tokyo (1968).

3) B. Commoner, J. J. Heise, B. B. Lippincott, R. E. Norberg, J. V. Passoneau, J. Townsend, *Science*, **126**, 57 (1957).

4) Kobayashi, "Synthesized Science of Sericulture," Terence Nunes at the Gem Printing Works, Marine Chambers, Marine Lines, Bombay (1962).

Exciton Circular Dichroism of Chromium(III) Complexes Containing Two Nonidentical α-Diimines

Sumio KAIZAKI, Jinsai HIDAKA and Yoichi SHIMURA

Department of Chemistry, Faculty of Science, Osaka University, Toyonaka, Osaka

(Received July 3, 1970)

Application of the exciton theory to the circular dichroism (CD) spectra of tris- or bis-α-diimine metal complexes has been carried out intensively.[1-4] The exciton interaction between the nonidentical long-axis π-π^* transitions of the coordinated 2,2′-dipyridyl (dip) and 1,10-phenanthroline (phen) has been reported in the cases of the CD spectra of $[M(dip)_2(phen)]^{n+}$ and $[M(dip)(phen)_2]^{n+}$ complexes.[1,3] In order to confirm the interaction of this kind, it is most desirable to investigate the simpler mixed complex, $[M(dip)(phen)L_2]^{n+}$, which contains only one each of the nonidentical α-diimines.

A new binuclear μ-diol chromium(III) complex of this kind was prepared by the reaction of $[CrCl_3(dmf)(dip)]$ with phen·HNO_3 in water at 70°C. Found: C, 45.87; H, 4.09; N, 14.73%. Calcd for $C_{44}H_{46}N_{12}O_{20}Cr_2=[(dip)(phen)Cr(OH)_2Cr(dip)(phen)](NO_3)_4\cdot 6H_2O$: C, 45.29; H, 3.97; N, 14.40%. Another new mononuclear oxalato complex was obtained by heating the aqueous solution of the μ-diol complex with oxalic acid. Found: C, 49.25; H, 3.61; N, 11.66%. Calcd for $C_{21}H_{21}N_5O_{9.5}Cr=[Cr(ox)(dip)(phen)]NO_3\cdot 2.5H_2O$: C, 49.41; H, 3.63; N, 12.00%. The μ-diol and oxalato complexes were optically resolved by using resolving agents, potassium di-μ-L-tartrato(4-)diantimonate(III) trihydrate and $(-)_{589}$-$K[Cr(ox)_2(phen)]\cdot 4H_2O$, respectively. The $(-)_{589}$-isomers were isolated and characterized as a nitrate heptahydrate (μ-diol complex) and a perchlorate dihydrate (oxalato complex). As seen in Fig. 1, the absorption spectra of the present μ-diol and oxalato complexes have common bands with μ-diol tetra-dip or -phen complex and oxalato bis-dip or -phen complex, respectively.[3,4] The CD spectra in the ligand absorption band region of the present $(-)_{589}$ complexes show a typical exciton band pattern as in those of $(-)_{589}$-tetra-dip or -phen binuclear complex and of $(-)_{589}$-bis-dip or -phen mononuclear complex.[3,4] That is, from the longer wavelength side, an intense negative and a positive CD band are observed near the long-axis π-π^* transitions of the dip (310 mμ) and phen (275 mμ), respectively. If there were no interaction between the dip and phen transitions in the present complexes, the CD bands at 310 and 275 mμ would have the same sign for the same tris-chelate configuration as in the case of L-tartrato α-diimine chromium(III) complexes.[5] Thus, the present observation confirms the existence of the exciton interaction between the nonidentical π-π^* transitions of the dip and phen in a complex. From the behavior of the exciton CD bands at 310 and 275 mμ, the $(-)_{589}$-isomers of the present complexes are assigned to the $\Lambda(C_2)$ configuration.[1,2] This assignment agrees with the empirical one on the basis of a major CD band in the first *d*-*d* absorption band region.

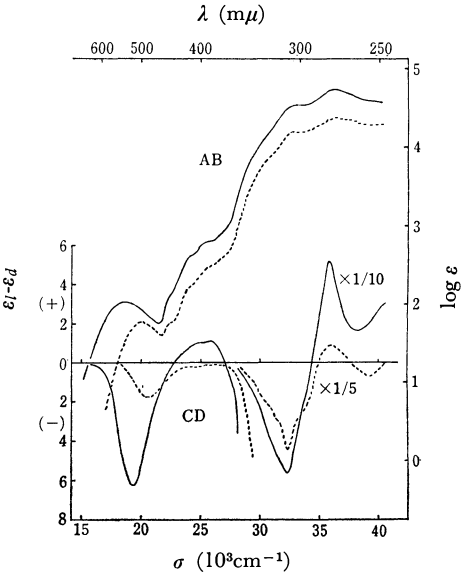

Fig. 1. Absorption (AB) and CD curves of $(-)_{589}$-$[(dip)(phen)Cr(OH)_2Cr(dip)(phen)](NO_3)_4\cdot 7H_2O$ (——) and $(-)_{589}$-$[Cr(ox)(dip)(phen)]ClO_4\cdot 2H_2O$ (----) in water.

1) B. Bosnich, *Inorg. Chem.*, **7**, 2379 (1968).
2) B. Bosnich, *Accounts Chem. Res.*, **2**, 268 (1969).
3) S. F. Mason, *Inorg. Chim. Acta, Rev.*, **2**, 89 (1968).
4) J. Ferguson, C. J. Hawkins, N. A. P. Kane-Magurie and H. Lip, *Inorg. Chem.*, **8**, 771 (1969).
5) S. Kaizaki, J. Hidaka and Y. Shimura, This Bulletin, **42**, 988 (1969).

BULLETIN OF THE CHEMICAL SOCIETY OF JAPAN VOL. 43 3025—3028 (1970)

Chemical Species Produced from Iodine in Stretched PVA Sheets

Harjoto DJOJOSUBROTO*1 and Yoshié TANIZAKI

Department of Chemistry, Faculty of Science, Tokyo Institute of Technology, Meguro-ku, Tokyo

and Toshihiko HOSHI

Department of Chemistry, College of Science and Engineering, Aoyama Gakuin University, Megurisawa-cho, Setagaya-ku, Tokyo

(Received December 24, 1969)

A qualitative dichroism analysis has been made on chemical species produced from iodine in stretched sheets of polyvinyl alcohol. The absorption bands at 290 mμ and 360 mμ have been attributed to the bent triiodine ion, and the transition moments of these bands have been found to be parallel to each other. From the optical density ratio (R_d) curve, the presence of a hidden band at about 420 mμ has been pointed out, and the band has been assigned to the absorption by the linear triiodide ion. Three different chemical species are absorbed in the visible region. By comparing the R_d values, the numbers of iodine atoms in the respective species have been estimated.

The absorption spectra of iodine in polyvinyl alcohol (PVA) sheets or aqueous solutions of PVA consist of several bands in the ultraviolet and visible regions. Two bands at 290 mμ and 360 mμ which may be considered to be due to the triiodide ion always appear, whatever the conditions. From the difference in dichroic properties, Tanizaki *et al.*[1] suggested that these bands originated with different chemical species. The other bands in the visible region are due to the longer polyiodide ions, and either appear or not depending upon the conditions of preparation.[1] Savko and Faerman[2] observed that the blue color (maximum absorption at 600 mμ) does not appear in solutions of PVA and iodine dissolved in aqueous solutions containing iodide ions, but that dried sheets prepared from these solutions show a very strong absorption at 600 mμ. They concluded, therefore, that water prevents the formation of a blue complex, by displacing the polarized configuration of iodine atoms bound to triiodide anions in the polymer network.[2] In the ioidne-PVA mixture, an excess of potassium iodide intensifies the 600 mμ band by completely binding the iodine to form triiodide ions.[3] Mokhnach and Propp[4] suggested that the iodine complex with polyvinyl alcohol absorbs at 600 mμ, and that the appearance of the 288 mμ band is due to triiodide ions, while that at 350 mμ is due to hypoiodite ions.[4]

Triiodide in various solvents shows two absorption bands, at 290 mμ and 360 mμ, the former being always higher in intensity than the latter.[5–7] By the continuous-variation method using mixtures consisting of tetramethylammonium iodide and iodine in ethylene chloride, it is confirmed that the only species which absorbs at 295 mμ and 365 mμ is the triiodide ion.[8] Robin found that the high intensity of the I_3^- bands could be explained using the MO theory only if the ion were bent.[9]

From the X-ray diffraction pattern of iodine in stretched PVA sheets, West[10] concluded that straight chains of polyiodides are formed, all of them parallel to the stretching direction. Rundle[11] pointed out that, in the one-dimensional array,

*1 Present address: Department of Chemistry, Bandung Institute of Technology, Djl. Ganeca 10, Bandung, Indonesia.

1) Y. Tanizaki, T. Kobayashi and N. Ando, *Nippon Kagaku Zasshi*, **80**, 455 (1959).

2) S. S. Savko and G. P. Faerman, *Opt. Spektrosk.*, **22**, 912 (1967); *Chem. Abstr.*, **68**, 50501p (1968).

3) L. G. Tebelev and N. N. Silkina, *Dokl. Akad. Nauk SSSR.*, **161**, (5) 1096 (1965); *Chem. Abstr.*, **63**, 6487c (1965).

4) V.O. Mokhnach and L.N. Propp, *Iodinol Med. Vet. Eksp. Klin. Izsled, Akad. Nauk SSSR., Biol. Inst.*, 1967, 21; *Chem. Abstr.*, **68**, 30450t (1968).

5) A. D. Awtrey and R. E. Connick, *J. Amer. Chem. Soc.*, **73**, 2842 (1951).

6) L. E. Katzen, *J. Chem. Phys.*, **23**, 2055 (1955).

7) A. O. Popov and R.F. Senensen, *J. Amer. Chem. Soc.*, **73**, 3724 (1955).

8) R. E. Buckles, J. P. Yuk and A. I. Popov, *ibid.*, **74**, 4379 (1952).

9) M. B. Robin, *J. Chem. Phys.*, **40**, 3369 (1964).

10) C. E. West, *ibid.*, **15**, 689 (1947).

11) R. F. Rundle, *ibid.*, **15**, 880 (1947).

all of the I-I spacings are identical, and that all are somewhat shorter than the van der Waals separation.

In the present study, the identification of the various species formed from iodine in the stretched PVA sheets was attempted using their linear dichroism. The analysis of the dichroic spectra could not be applied in the present case because the chromophores in the sheet could not be oriented enough to allow the application of the theory.[12] Although quantitative analysis could not be carried out for this reason, useful qualitative information regarding the absorbing species, especially the triiodide ion, could be obtained.

Experimental

The preparation of PVA sheets from polyvinyl alcohol powder has been described elsewhere.[12] In this experiment, sheets about 0.2 mm thick were prepared from commercial PVA powder, whose polymerization degree was 1400. The adsorption of iodine was achieved by hanging the PVA sheet in a bottle with a mouth 500 m*l* wide and containing a few iodine crystals. Under a low humidity, iodine could not be diffused into the dry PVA sheet; therefore, a drop of water was added to the bottle. The sample sheets were prepared as follows:

(1) The iodine was adsorbed on a dry PVA sheet, and its absorption spectrum was measured using unpolarized light. The spectrum is shown as Curve *D* in Fig. 1.

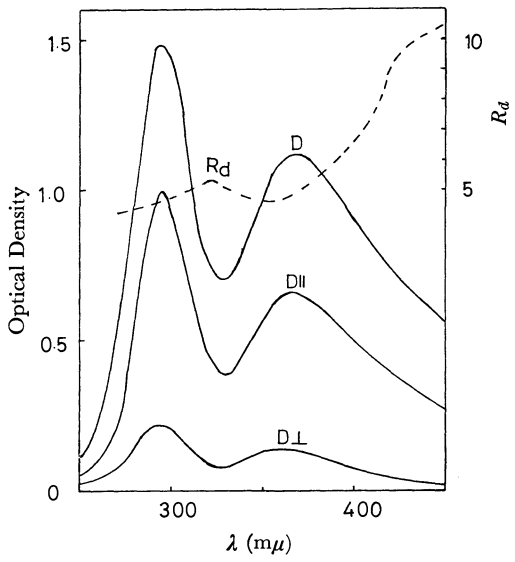

Fig. 1. Absorption spectra of iodine in dry PVA sheet. The *D* curve is the absorption for the non-stretched state. The $D_{||}$ and $D_{\perp}$ curves (dichroic spectra) are the absorptions of the stretched sheet for light with electric vector parallel and perpendicular, respectively, to the stretching direction. R_d means the ratio of $D_{||}$ and $D_{\perp}$.

12) Y. Tanizaki and S. Kubodera, *J. Mol. Spectrosc.*, **24**, 1 (1967).

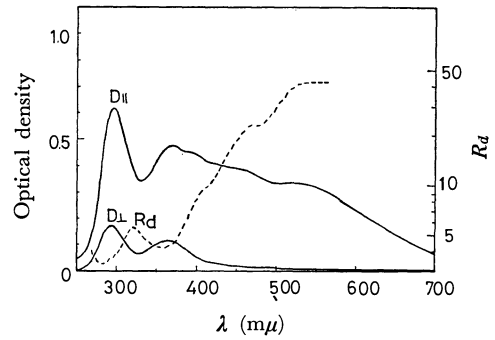

Fig. 2. Dichroic spectra of iodine adsorbed after stretching the dry sheet.

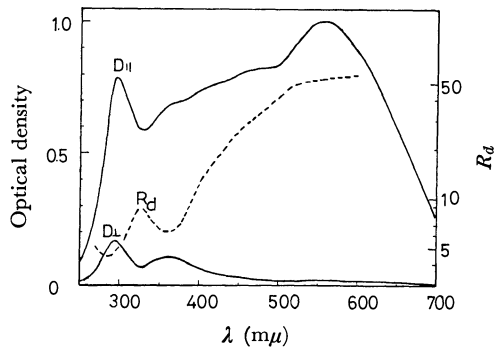

Fig. 3. Dichroic spectra of iodine adsorbed in humid atmosphere after stretching the dry sheet.

(2) After the iodine had been adsorbed, the sheet was stretched. The absorption spectra obtained using plane-polarized light are shown in Fig. 1 ($D_{||}$ and $D_{\perp}$), where $D_{||}$ and $D_{\perp}$ are the absorptions for the light with electric vector respectively parallel and perpendicular to the stretching direction of the sheet.

(3) After stretching, a piece of dry PVA sheet was put in the adsorption bottle. Its dichroic spectra are shown in Fig. 2. Fig. 3 shows the dichroic spectra of a sample sheet prepared in the same way as above, but here more water was added before the iodine adsorption.

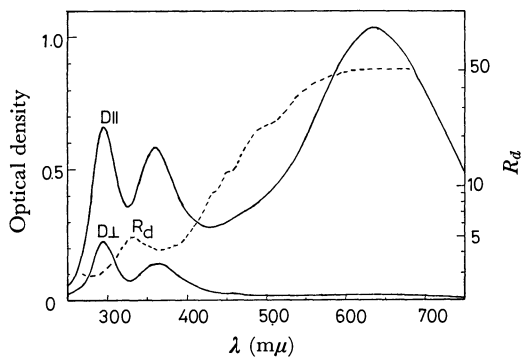

Fig. 4. Dichroic spectra of iodine in the blue-colored state.

(4) PVA sheet was digested in distilled water for at least two hours, and the wet sheet was put in the bottle and then stretched at room temperature. The sheet was air-dried overnight, and then its dichroic spectra were determined (see Fig. 4).

The adsorption of iodine was done at room temperature (about 20°C) until the iodine concentration was sufficient for spectrophotometric measurements. A dry sheet was stretched at 80°C by a stretching machine. The stretched ratio was 9 for the sheet which was stretched in the dry state, while that for the sheet stretched in the wet state was 8 as determined after the sheet became dry. (The stretch ratio was determined by a procedure described elsewhere,[12] but the deformation of the substrate by stretching did not satisfy the conditions required for the dichroism analysis).

The absorption measurements were made with a Shimadzu QR-50 spectrophotometer, equipped with a Glan-Thomson-type polarizer and a simultaneous rotation apparatus for sample and reference sheets.

Results and Discussion

Figure 1 indicates that the stretching does not induce any change in the absorption pattern. In fact, the absorption curve of an unstretched sample sheet coincided completely with the curve, D, obtained by $D=k(D_{\parallel}+2D_{\perp})$, where k is a constant. Moreover, as can be seen in the other figures, the intensity ratio at 290 mμ and 360 mμ of the $D_{\perp}$ curve is always constant at about 1.6. Therefore, both bands must be attributed to only one species, as has been shown by Buckles *et al.*,[8] this species may be considered to be the triiodide ion.

The triiodide ion can be either linear ($D_{\infty h}$) or bent (C_{2v}) in geometry. From the symmetry, the allowed transitions in the linear ion should have only one kind of polarization (long axis, Z), while the strong transitions in the bent ion can have two kinds of polarization (long axis, Z, and short axis, X).

The R_d curve in Fig. 1 is not flat over the region of the two bands, but rises with a sharp inclination from about 350 mμ to 430 mμ and shows a maximum between the two bands. Such a tendency of the R_d curve is also observed at the corresponding part in all the dichroic spectra shown in other figures. This implies that a different kind of absorption band with a higher R_d value (a smaller orientation angle) is hidden near the 360 mμ band.

According to the empirical facts of the dichroism investigation, a long molecule in a stretched PVA sheet will preferentially orient its long axis parallel to the stretching direction of the sheet. Moreover, if there are two bands orthogonal to each other and if the one has a R_d value larger than about 5, then the other must have a value smaller than 0.5. As for the 290 mμ and the 360 mμ bands, therefore, it can safely be said that their polarizations are parallel to each other; besides, they lie along the Z axis. This conclusion is in agreement with the prediction of Robin.[9]

The hidden band with a higher R_d value can be explained only by considering another species. From the point of view of dichroism, a linear molecule will show a higher R_d value than a bent one. Therefore, the hidden band can be attributed to absorption by a linear species. It seems very probable that a linear triiodide ion is another species which can exist besides the bent ion. The only allowed transition for the linear triiodide ion (calculated as a $a_{1g}\rightarrow a^*_{2u}$ by Robin[9]) will lie somewhere near the band region of 290 mμ and 360 mμ. The behavior of the R_d curve of Fig. 1 can be understood in terms of the existence of the linear triiodide ion.

The polarizations of all the absorptions in the visible region are much more parallel to the stretching direction than that of the triiodide ion. The R_d curve in Fig. 2 is complicated; in it the inflective parts correspond well to the shoulders of the $D_{\parallel}$ curve. Such a correspondence seems to indicate that there are absorptions at 450 mμ and 540 mμ. The long tail in the longer-wavelength side of 540 mμ suggests the presence of a hidden band in this region. Figure 3 shows the dichroic spectra of a sample containing more water than is the case in Fig. 2. The increase in the water content results in an intensifying of the 540 mμ band and shifting it to 570 mμ. The dichroic spectra of the sample (Fig. 4) treated in the wet state show a very intense band at 630 mμ and, at the same time, the disappearance of the 450 mμ and 540 mμ bands, though the R_d curve clearly indicates the existence of these bands.

Thus, taking into account the facts that the iodine atoms in a PVA-iodine complex are arranged in a one-dimensional array[10] and that the R_d value reflecting the orientation of the polarization, which should lie on the long axis of a linear species, is different from band to band, it may be considered that all the absorption bands in the visible region are to be attributed to different species. The only difference among the species is in the geometrical length. The longer the length (the larger the number of atoms) of the species, the longer the wavelength of absorption. This consideration is in agreement with the fact that the longer-wavelength bands have the larger R_d values. With respect to the R_d values, this means that the orientation angle (the angle between the orientation axis and the Z axis) becomes smaller as the length of the species increases.

If the orientation angles of the linear polyiodide ions, including the triiodide ion, have some relation to the lengths of the species, the length can be estimated from a comparison of the R_d values, taking the value of the linear triiodide ion as a standard; therefore, the number of iodine atoms in each species may be determined. The method is illustrated with a model in Fig. 5.

Unfortunately, we could not find the distribution

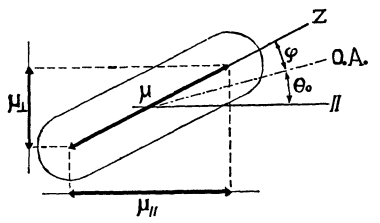

Fig. 5. Schematic illustration of the components ($\mu_\perp$, $\mu_{||}$) of transition moment (μ) of an oriented molecule representative of a species in a distribution state. O.A. represents the orientation axis, and || the stretching direction of the substrate.

function applicable to the present case. Nevertheless, for a stretched state there must be a distribution function which is common to all the species in a stretched sheet. Since the distribution indicates the distribution of an orientation axis (O.A.) of a species, the direction of O.A. must be common to all species. The only difference among species is, therefore, the difference in angle (φ) between O.A. and the transition vectors (μ). The transition vectors of the species are distributed uniformly with the φ around the O.A. axis. If θ_0 is representative of the distribution angle of O.A. to the stretching direction (||), the angle of μ about || can vary from $(\theta_0+\varphi)$ to $(\theta_0-\varphi)$. Allowing θ $(=<\theta_0\pm\varphi>)$ to denote an average angle of μ about the direction, we have:

$$R_d = \frac{D_{||}}{D_\perp} = \mu^2\cos^2\theta/\mu^2\sin^2\theta \qquad (1)$$

As may be seen in Figs. 1—4, the $D_\perp$ of the visible region is very small and is almost constant except for the region affected by the absorption of the bent triiodide ion. Regarding $D_\perp$ as constant for all species under consideration, we can express the ratio of the R_d values for the species A and B as follows:

$$\frac{R_d(B)}{R_d(A)} = \frac{\mu_{||}^2(B)}{\mu_\perp^2(A)} = \frac{\mu_B^2\cos^2\theta_B}{\mu_A^2\cos^2\theta_A} \qquad (2)$$

If we may assume that μ is proportional to the length (L) of the species, then Eq. (2) becomes:

$$R_d(B)/R_d(A) = L_B^2\cos^2\theta_B/L_A^2\cos^2\theta_A \qquad (3)$$

Since θ is very small, we can put $\cos^2\theta$ equal to unity for the first approximation. Using the ratio of the observed R_d values and taking the linear triiodide ion (Species A) as a standard, the lengths of the other species can be estimated. If we take 3.1 Å to be the distance between iodine atoms,[10] the number of atoms of the absorbing species can be estimated to be as is shown in Table 1. In the estimation, we use the value of the R_d curve at around 420 mμ, assuming that an absorption band of the linear triiodide ion is hidden in this region.

It is clear from Fig. 5 that the length-ratio obtained here does not mean the actual ratio of the species, but the ratio of the components parallel to the stretching direction. Naturally, the estimated value presented in Table 1 represents the maximum number of iodine atoms for the species in the PVA sheet; that is, the number of atoms of the actual species should not exceed the number shown in Table 1.

Table 1. Estimation of the number of iodine atoms in the species which have the visible absorption bands

Band	$\sqrt{\frac{R_d}{R_d(I_3^-)}} = \frac{L}{L(I_3^-)}$	Number of atoms
420 mμ	1.0	3
450 mμ	1.4—1.5	4
540 mμ	2.0	5
630 mμ	2.8	7

Several workers have estimated the number of iodine atoms in the species formed in the blue colored amylose-iodine system,[13–15] but their results have not always coincided. The reported values are for starch-iodine systems, so that a direct comparison with the PVA-iodine system is not possible. As has been confirmed by the X-ray diffraction analysis of the halogens incorporated within hydrophilic high polymers (including starch and PVA), the characteristic pattern is independent of the polymer in which the halogens are incorporated. The systems depend only on the type of halogens.[10] This fact suggests that a qualitative comparison is possible. According to the estimated values by Ono *et al.*,[13] for instance, a species consisting of more than one hundred iodine atoms is possible only if the iodine atoms in the polymer are helical or are arranged in a manner similar to that of helical. Since it is known that, in all cases, the iodine atoms are linearly arranged,[10] such large polyiodines are very difficult to understand from the point of view of dichroism.

From the results presented in Table 1, the following mechanism of the formation of polyiodide chains can be proposed, though there is no evidence for the mechanism of the formation of the triiodide ion at the present stage:

$$I_4 : I_2 + I_2 = I_4$$

$$I_5^-: I_3^- + I_2 = I_5^-$$

$$I_7^-: I_3^- + I_4 = I_7^- \text{ and/or } I_5^- + I_2 = I_7^-$$

One of the authors (H.D.) wishes especially to express his gratitude to the Japanese National Commission for UNESCO for the opportunity to study in Japan during the 1968—1969 academic year.

13) S. Ono, S. Tsuchihashi and T. Kuge, *J. Amer. Chem. Soc.*, **75**, 3601 (1953).
14) H. Murakami, *J. Chem. Phys.*, **22**, 367 (1954).
15) G. A. Gilbert, J. V. R. Marriott, *Trans. Faraday Soc.*, **44**, 84 (1948).

BULLETIN OF THE CHEMICAL SOCIETY OF JAPAN VOL. 43 3029—3033 (1970)

Ionic Dissociation. I. A Hückel Molecular-Orbital Treatment of the Dissociation of Carboxylic Acids and Several Azine Compounds

Hiroko YAMABE, Teijiro YONEZAWA and Hiroshi KATO*1

Department of Hydrocarbon Chemistry, Faculty of Engineering, Kyoto University, Sakyo-ku, Kyoto

(Received February 14, 1970)

The relationship between the pK_a value and the change in the electronic energy, ΔE, in the course of the dissociation, and the electronic structure of various mono-carboxylic acids and several azine compounds are discussed on the basis of the calculation by Hückel methods for σ and π electron systems. The parallelism between the pK_a and the calculated ΔE of the acids is observed. The σ electron densities of the -COOH proton and the O^- lone pair, which is constituted by the released electron on the dissociation, run parallel with the pK_a's. The delocalizability of the lone pair for the electrophilic reaction, and that of the proton for the nucleophilic reaction, have a linear relationship with the pK_a's. Similar relations are seen in several azine compounds. Therefore, it may be said that the protonation will take place by means of the electrophilic attack at the lone pair, and that the deprotonation occurs by means of the nucleophilic attack at the proton.

It is said that the strength of an acid depends on the relative stabilities of it and its anion.[1] The dissociation constant, pK_a, of conjugated acids and bases has been related to the change in π electronic energy in the course of the dissociation, and to the charge of the protonated heteroatom in these compounds.[2-4] However, as one of us has pointed out in a previous paper,[5] only a classical electrostatic theory[6] has been proposed in connection with the dissociation of saturated compounds, except for our previous calculation on the α-amino acids.[5] In this paper we will report the relationship between the value of pK_a and the change in the electronic energy, ΔE, and in other quantities of the electronic structures of various mono-carboxylic acids and several bases; our findings are based on the calculation by the Hückel method for σ and π systems.

The distinguishing characteristic of this work is the model it employed; in it the mechanism of the dissociation is taken into account in a simple way. Namely, the carboxylic acid is considered to be dissociated according to Eq. (1):

$$R\text{-}C(=O)\text{-}O\text{-}H \rightleftharpoons R\text{-}C(=O)\text{-}O^- + H^+ \qquad (1)^{*2}$$

The following model is assumed: in the anionic form, electrons released by the dissociation of the proton constitute, in a sense, a new lone pair of the oxygen delocalize over a whole molecule. This will be denoted as "the O^- lone pair" through-out the present paper. A recombination reaction to the left-hand side of Eq. (1) will take place by means of the attack of the dissociated proton (or a hydronium ion) on the O^- lone pair. The electron density of this lone pair is evaluated by the Hückel method for various acids.

After these comparative discussions, the following conclusion was obtained. There is a rough linearity between the pK_a value and the calculated ΔE value. The σ electron density of the O^- lone pair and the delocalizability,[6] D_r^E, for the electrophilic reaction of the O^- lone pair run parallel with the pK_a value, as well as with the σ electron density and the delocalizability,[6] D_r^N, for the nucleophilic reaction of the hydrogen atom of a carboxylic group. Further, similar relations are seen in azine compounds as will be described in detail later. Therefore, the protonation seems to take place by means of the electrophilic attack at the lone pair, while

*1 Present address: Department of General Education, Nagoya University, Chikusa-ku, Nagoya.

1) M. J. S. Dewar, "The Electronic Theory of Organic Chemistry," The Clarendon Press in the University of Oxford (1949), Chapter VI.

2) H. C. Longuet-Higgins, *J. Chem. Phys.*, **18**, 275 (1950); T. Nakajima and A. Pullman, *J. Chim. Phys.*, **1958**, 737.

3) M. T. Reets, *Tetrahedron Lett.*, **1967**, 3549.

4) J. D. Vaughan, D. G. Fullerton and C. A. Chan, *Intern. J. Quantum Chem.*, **II**, 205 (1968).

5) T. Yonezawa, G. Del Re and B. Pullman, This Bulletin, **37**, 985 (1964).

6) K. Fukui, H. Kato and T. Yonezawa, *ibid.*, **34**, 1111 (1961).

*2 The existence of the H_2O molecules and the hydration effect in the dissociation process are not taken into account.

the deprotonation seems to occur by means of the nucleophilic attack at the proton.

Calculations

The electronic energy change, ΔE, in the course of dissociation is due to the difference between the total energy of the final and the initial states in Eq. (1). This equation is adopted for a series of carboxylic acids, and the calculation of ΔE is performed according to the following formulae:[5]

$$\Delta E = E_\sigma(\text{final}) - E_\sigma(\text{initial}) - \sum_\mu \frac{Q_H Q_\mu e^2}{R_{H\mu}}$$
$$\Delta E_\sigma = E_\sigma(\text{final}) - E_\sigma(\text{initial}) \qquad (2)$$

Here, E_σ(initial) and E_σ(final) denote the energies of the protonated compounds and of the conjugate base respectively. The third term corresponds to the electrostatic interactions between the dissociable proton and the other atoms in the protonated compounds. Q_H is the net charge (in e units) of the proton, Q_μ is the net charge of the μ-th atom, and $R_{H\mu}$ is the distance between them. The calculation of $R_{H\mu}$ is carried out using a formula proposed by Eyring[7] and by Kirkwood and Westheimer.[8] The precise interpretation of Eq. (2) was given in a previous paper.[5] In that paper,[5] the variation in the total π electron energy is assumed to be constant. In this work we confirmed this by the performance of the Hückel calculation.*3

For the determination of the electronic energy and the electron distribution of σ and π electron systems, the Hückel approximation is employed. The parameters used in these calculations are tabulated in Table 1.

Results and Discussions

The electronic structures of σ and π electron systems are obtained for various acids. As an example, the σ-electron distribution of the CH_3COOH, CF_3COOH, and C_3H_5COOH molecules and their anions are shown in Fig. 1, together with the π electron distribution. In the anionic form, about 93% of the lone-pair electrons localize at the oxygen atom. Furthermore, the highest occupied orbital localizes largely at the O^- lone pair; that is, it becomes a lone-pair MO.*4 The results of the calculation are listed in Table 2, together with the experimantal values of pK_a for a series of carboxylic acids. In Table 2, ΔE_σ gives the variation in the total σ electronic energies in the course of the dissociation

Table 1. Parameters for the Hückel calculation

Coulomb integrals for σ systems		Resonance integrals for σ systems	
C(sp^3 hybridized)	α	C–C (sp^3-sp^3)	β
C(sp^2 hybridized)	$\alpha+0.1\beta$	C–C (sp^2-sp^2)	1.2β
H	$\alpha-0.2\beta$	C (sp^3) — *	0.34β
=O	$\alpha+0.3\beta$	C (sp^2) — *	0.4β
-O-	$\alpha+0.3\beta$	N — *	0.3β
		O — *	0.3β
N	$\alpha+0.2\beta$	C–N	β
F	$\alpha+0.9\beta$	C–H	1.1β
Cl	$\alpha+0.5\beta$	O–H	1.2β
Br	$\alpha+0.54\beta$	N–H	1.1β
I	$\alpha+0.5\beta$	C=O	1.2β
		C–O	0.7β
		C–F	0.5β
		C–Cl	0.65β
		C–Br	0.58β
		C–I	0.53β

Coulomb integrals for π systems		Resonance integrals for π systems	
C(in -C=O)	$\alpha+0.2\beta$	C=O	1.4β
=O	$\alpha+2\beta$	C–O (in $-COO^-$)	β
-O(in COO^-)	$\alpha+\beta$	C–OH	0.7β
-OH	$\alpha+0.6\beta$	C–NH_2	0.6β
-NH_2	$\alpha+0.4\beta$		

Hyperconjugation is ignored.

* Resonance integrals between two σ orbitals belonging to the same atom.

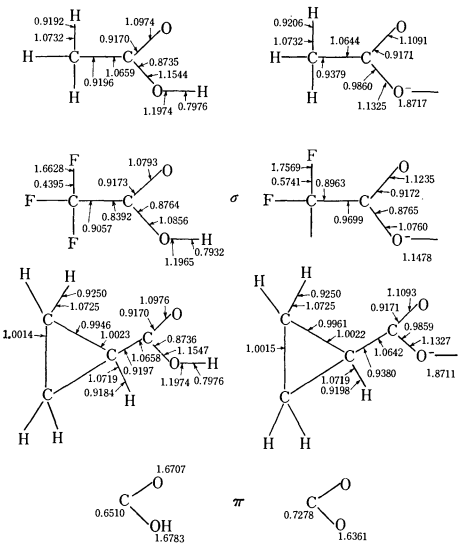

Fig. 1. σ and π electron distribution of some acids.

7) H. Eyring, *Phys. Rev.*, **39**, 746 (1932).

8) J. G. Kirkwood and F. H. Westheimer, *J. Chem. Phys.*, **6**, 506, 513 (1938).

*3 ΔE_π is calculated as 1.1277 β_π for all the acids except benzoic acid, for which the ΔE_π value is 1.1400 β_π.

*4 In the extended Hückel calculation of the CH_3COOH molecule, the highest occupied MO is a σ orbital. Moreover, the atomic orbital population of the x direction, which is one component of the lone pair, of the oxygen atom is considerably increased compared with that of the CH_3COOH molecule. Therefore, this MO has the character of a lone-pair MO.

TABLE 2. CALCULATED RESULTS AND OBSERVED pK_a VALUES

Compound	Obs.[a] pK_a	Calc. ΔE_σ $(-\beta)$	Calc. $\sum_\mu \frac{Q_H Q_\mu e^2}{R_{H\mu}}$ (eV)	Calc. $\Delta E_\sigma - \sum_\mu \frac{Q_\mu Q_\mu e^2}{R_{H\mu}}$ (eV)	Calc. D_r^N	Calc. D_r^E	Calc. Q_H	Calc. Q_L
HCOOH	3.75	1.9004	−0.051	11.454	1.0893	6.4988	0.79786	1.8786
CH_3COOH	4.76	1.8981	−0.075	11.464	1.0951	6.4480	0.79763	1.8717
CH_3CH_2COOH	4.87	1.8980	−0.158	11.546	1.0956	6.4439	0.79761	1.8711
$CH_3(CH_2)_2COOH$	4.82*	1.8980	−0.228	11.616	1.0957	6.4435	0.79761	1.8710
NH_2COCH_2COOH	3.64	1.8977	−0.012	11.398	1.0965	6.4339	0.79757	1.8704
CH_3COCH_2COOH	3.58	1.8977	0.004	11.382	1.0963	6.4358	0.79757	1.8704
FCH_2COOH	2.57	1.8945	0.109	11.258	1.1012	6.3398	0.79725	1.8587
$ClCH_2COOH$	2.87	1.8962	0.073	11.304	1.1014	6.3916	0.79737	1.8655
$BrCH_2COOH$	2.90	1.8960	0.096	11.280	1.1027	6.3847	0.79735	1.8645
ICH_2COOH	3.16	1.8959	0.117	11.258	1.1034	6.3813	0.79734	1.8639
$Cl_2CHCOOH$	1.25	1.8925	0.220	11.135	1.1216	6.2810	0.79695	1.8516
F_3CCOOH	0.23	1.7939	0.668	10.094	1.1070	3.0779	0.79317	1.1478
Cl_3CCOOH	0.66	1.8836	0.376	10.926	2.3693	5.9978	0.79616	1.8084
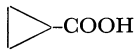 -COOH	4.83*	1.8981	−0.262	11.650	1.0956	6.4474	0.79764	1.8711
-COOH	4.79*	1.8977	−0.330	11.716	1.0966	6.4363	0.79758	1.8701
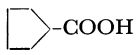 -COOH	4.99*	1.8978	−0.275	11.662	1.0963	6.4395	0.79760	1.8704
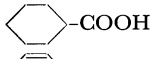 -COOH	4.90*	1.8978	−0.259	11.646	1.0964	6.4386	0.79760	1.8703
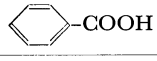 -COOH	4.18*	1.8957	−0.309	11.683	1.0990	6.3542	0.79685	1.8683

pK_a values are observed at the temperature from 18°C to 25°C.

a) A. Albert and E.P. Serjeant "Ionization Constants of Acids and Bases," Methuen & Co. Ltd., London.

* G. Kortum, W. Vogel and K. Andrussow "Dissociation Constants of Organic Acids in Aqueous Solutions," Butterworths, London, 1961. The dissociation constant in this book is converted to pK_a.

in units of $-\beta$ and eV's respectively, where we have chosen 6 eV for $-\beta$.[5),*5] D^N_r indicates the values of delocalizability[6)] for an electrophilic reaction at the hydrogen atom of a -COOH group. D^E_r is the delocalizability[8)] for an electrophilic reaction at the O^- lone pair of a $-COO^-$ group. Q_H and Q_L give the electron densities of the H of a -COOH group and the O^- lone pair of a $-COO^-$ group respectively. From Table 2, a parallelism between the pK_a values and ΔE_σ's is observed, though the values of ΔE_σ's[*5] themselves are not very different for various acids. However, large deviations in CCl_3COOH and CF_3COOH from a linear relationship are seen.

In Fig. 2, the values of pK_a are plotted against ΔE(in eV),[*6] which is given by Eq. (2). Including the electrostatic interaction term[*7] of $Q_H Q_\mu e^2/R_{H\mu}$ the deviation in CCl_3COOH and CF_3COOH is greatly improved, as may be seen in Fig. 2 and Table 2.[*8] This indicates that the CCl_3 and CF_3 groups in these compounds are very electronegative and they attract the dissociable hydrogen, which is in agreement with Dewar's description.[*9] This effect will make an acid weaker than would be expected from the calculated ΔE_σ value. Further-

[*5] Only the relative values of ΔE_σ for the various compounds have meaning. There is some arbitrariness in the selection of the value of $-\beta$.

[*6] The absolute value of ΔE can not be discussed.

[*7] In Table 2, the following relation is noted: as the electrostatic interaction with the dissociable hydrogen, $\sum = Q_H Q_\mu e^2/\mu R_{H\mu}$ increases, the pK_a value decreases.

[*8] CF_3COOH is not included in Fig. 2 because the deviation in CF_3COOH is still large. Possibly this deviation is due to the extraordinarily heteroritic property of the three F atoms.

[*9] Dewar describes in his book (Ref. 1) that "in acids containing a highly polar group in proximity of the dissociable hydrogen, a direct electrostatic attraction or repulsion of the nascent proton may increase or decrease the dissociation energy."

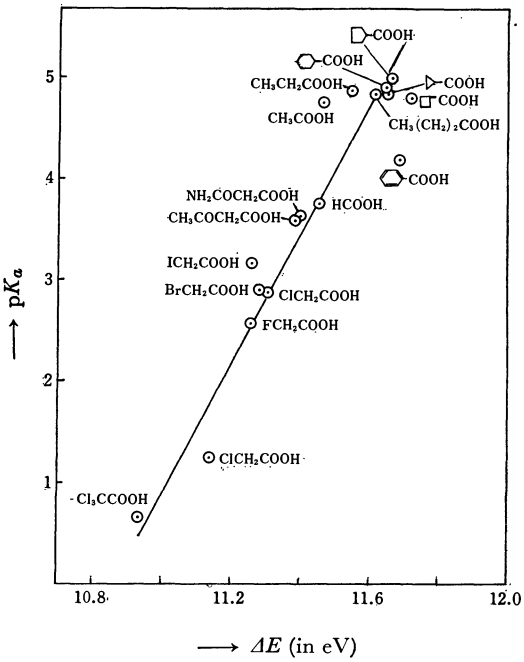

Fig. 2. The dissociation constant pK_a *vs.* ΔE, where $\Delta E=\Delta E_\sigma-\sum_\mu Q_H Q_\mu e^2/R_{H\mu}$.

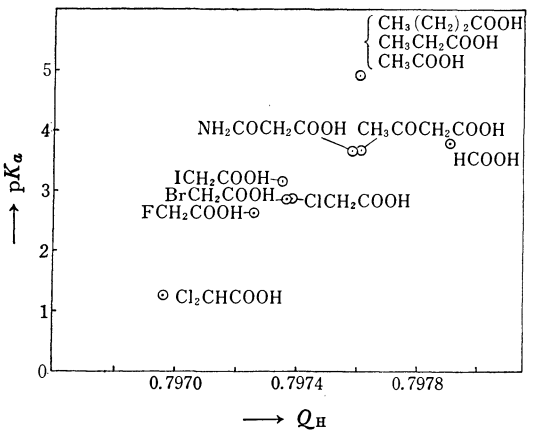

Fig. 3. The dissociation constant pK_a *vs.* Q_H of acids.

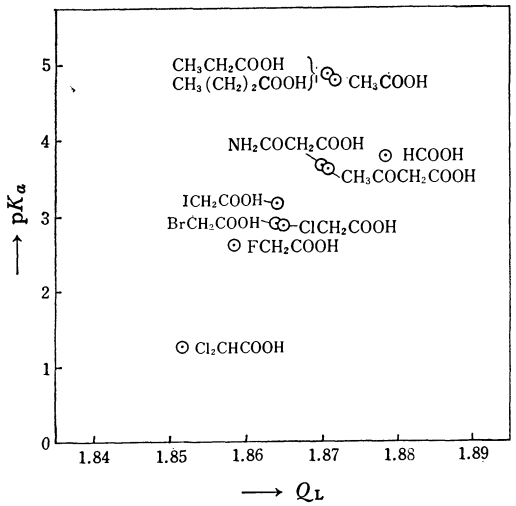

Fig. 4. The dissociation constant pK_a *vs.* Q_L of acids.

more, in Fig. 2 the difference in the values of ΔE for various acids become larger than in the case of ΔE_σ's. That is it may be noted that the electrostatic interaction term contributes to the relative acidity of the acids.

On the basis of these calculations, it may be said that ΔE_σ's calculated by Hückel method run parallel with the pK_a values for the compounds having not so polar a group. As for the molecule having a highly polar group, the contribution of the electrostatic interaction term to its acidity should not be ignored. Furthermore, it may be concluded that the acid dissociates more easily when its anion is more stable than that of the parent acid.

Also, a very rough linear relation is seen between the pK_a and D_r^N and the electron density of the hydrogen, Q_H. It is plotted in Fig. 3.*10 This means that the dissociable hydrogen may be attacked in a nucleophilic fashion by the H_2O molecule to give the $RCOO^-$ and H_3O^+ ions in the dissociation process. Also the D^E_r and the electron density of the O^- lone pair of the anion Q_L run parallen with the pK_a. It is plotted in Fig. 4.*10 This means that the ion recombination takes place by means of the attack on the O^- lone pair by the hydrogen atom of the H_2O molecule. These results suggest that the model employed here is plausible; that is, the electron released on the dissociation constitutes a new lone pair of O^- of the anion and delocalize over the whole molecule.

*10 In Fig. 4 and Fig. 5, CF_3COOH and CCl_3COOH are not included.

Dissociation of Azine Compounds

In the preceding part of this paper we found that, as far as we have treated, the ΔE_σ calculated by the Hückel method runs parallel with the pK_a value for the carboxylic acids having not so highly a polar group. Next, we will examine whether this relation holds in the cases of several azines,*11 though the azines calculated in the present work are few in number.

The dissociation equilibrium is assumed to be in the form of Eq. (3), in which pyridine is taken as an example.

*11 The interrelation between the ΔE_π and the pK_a values of some of these compounds has been discussed by several authors (Ref. 2).

Table 3. Calculated results and the observed pK_a values* for some azine compounds

Compound	pK_a	ΔE_σ (in $-\beta$)	D_H^N	D_L^E	Q_H	Q_L
Pyridine	5.23	1.7544	1.1579	10.8848	0.8345	1.7523
Pyrazine	0.6	1.7378	1.1547	11.2164	0.8351	1.7559
Pyrimidine	1.3	1.7394	1.1521	11.7104	0.8357	1.7581
Pyridazine	2.33	1.7493	1.1347	18.7290	0.8421	1.7708

* A. Albert and E.P. Serjent "Ionizationts of Acids and Bases." Methuen Co. Ltd, London.

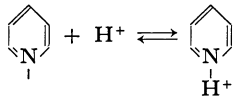

(3)

The value of ΔE_σ is evaluated according to Eq. (4):

$$\Delta E_\sigma = E_\sigma(\text{protonated form}) - E_\sigma(\text{unprotonated form}) \quad (4)$$

The method of the calculation and the parameters employed are similar to those use for the carboxylic acids.

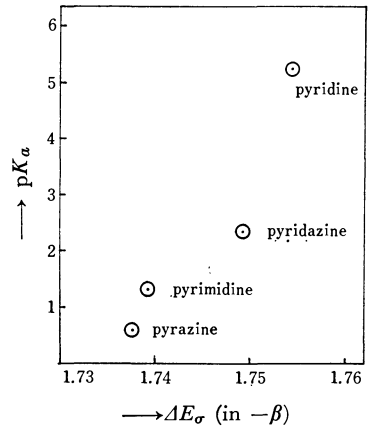

Fig. 5. The dissociation constant pK_a *vs.* ΔE_σ.

The calculated ΔE_σ values are shown in Table 3, together with the observed pK_a values; they are plotted in Fig. 5.*12 A parallelism between ΔE_σ and the pK_a of azines is observed.

In diazines it is observed that, in the anionic form, the electron density of the N lone-pair Q_L and the delocalizability, D_L^E of that lone pair for the electrophilic reaction run parallel with the pK_a.*13 Also, in the protonated form the electron density of the hydrogen, Q_H, and the delocalizability, D_H^N, of that proton for the nucleophilic reaction run parallel with the pK_a in diazines. This means that the protonation takes place by the attack on the N lone pair in Eq. (3) and that the deprotonation is induced by such a molecule as H_2O, which attacks the proton. These circumstances were observed previously in the case of acids.

An approximate linear relation between the pK_a value and the energy change, ΔE, of the acids and bases can naturally be expected. However, the coarse linearity obtained in the present work for some acids and bases seems to be a change result of the appropriate selections of the molecules to be calculated, the method of the approximation, and the various parameters. When the peculiarity of each molecule, which is induced by each substituent, the steric factor, and so on, can not be taken into account in the parameters, the linearity will not be obtained and some corrections for the calculation are needed. An example of the deviation caused by the steric factor has been reported in the calculation of the π energy change in the dissociation of the conjugated acids.[3)]

The calculations were carried out on a HITAC 5020 computer at the computation center of the University of Tokyo.

*12 The σ electron densities of the azines have been presented in one of our previous papers (Ref. 9).

*13 The paralellism between the σ electron density of the N lone pair of diazine and the blue shifts of n–π^* bands, accompanied by the change in the solvent from cyclohexane to aqueous solution, has been reported in our previous paper (Ref. 9).

9) T. Yonezawa, H. Yamabe and H. Kato, This Bulletin, **42**, 76 (1969).

BULLETIN OF THE CHEMICAL SOCIETY OF JAPAN VOL. 43 3034—3036 (1970)

The Mössbauer Effect in Triethyltin Phenyl Derivatives

Noriyuki WATANABE and Eiji NIKI

Department of Industrial Chemistry, Faculty of Engineering, The University of Tokyo, Hongo, Tokyo

(Received February 19, 1970)

Substituent effect of triethyltin phenyl derivatives was investigated by means of the ^{119}Sn Mössbauer effect. The isomer shifts obtained for these compounds fall into the range -0.15—-0.18 mm/sec with respect to $Pd^{119m}Sn$ source. *p*-Cl and *m*-Cl derivatives show broadened spectra, which may be ascribed to an unresolved quadrupole splitting. This small quadrupole interaction may be interpreted in terms of the partial ionicity of the bond formed between tin and carbon in phenyl group.

The Mössbauer effect in organotin compounds provides useful information on the nature of the chemical bond formed by tin atom. The tin atom, which belongs to group IV, may act effectively as a probe embedded in organic compounds. Quadrupole splitting takes place by low symmetric distribution of the valence electron. Thus, it provides a measure of the partially ionic character of sp^3 hybrid bonding. Tin organic compounds have similar values of the isomer shift. A study of the isomer shift for a series of compounds may supply a great deal of information.

In the present paper, the Mössbauer spectra of triethyltin phenyl derivatives ($X\text{-}C_6H_4SnEt_3$, X= H, *p*-CH_3, *m*-CH_3O, *p*-Cl, *m*-Cl) at 80°K and the effects of substituent are described. The compounds showed essentially the same isomer shift. The Mössbauer spectra for *p*-Cl and *m*-Cl derivatives gave single but broadened lines. The broadened line may be decomposed into an unresolved quadrupole doublet, and it seems reasonable to expect that the chlorine atom makes the Sn-C bond character partially ionic through phenyl group due to its inductive effect.

Experimental

The Doppler velocity spectrometer has an electromechanical negative feedback system.[1-4] The circuit for this system is shown in Fig. 1. The velocity signal is 12.5 Hz sawtooth or triangular wave, *viz*, the constant acceleration mode. The velocity scale has been cali-

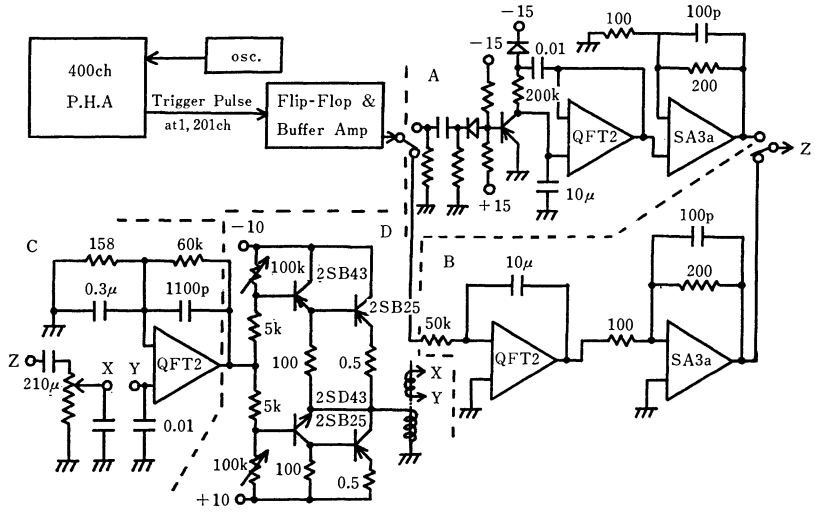

Fig. 1. Electromechanical feedback system for Mössbauer effect experiment.
A; sawtooth wave B; triangular wave C; control circuit D; power circuit

1) D. Rubin, *Rev. Sci. Instrum.*, **33**, 1358 (1962).
2) R. L. Cohen, *ibid.*, **34**, 671 (1963).
3) J. Lipkin, P. G. McMallin and G. K. Wertheim, *ibid.*, **35**, 1336 (1964).
4) E. Niki and N. Watanabe, *J. Fac. Engng. Univ. Tokyo*, **A-7**, 56 (1969).

brated by the isomer shift values of β-Sn and SnO_2. For the triangular wave mode, zero velocity corresponds to the middle of the 100 and 101 channels and also that of the 300 and 301 channels. The isomer shift can be obtained with a good reproducibility within one channel. The source was $Pd^{119m}Sn$ containing about 0.2 mCi ^{119m}Sn. The source was used at room temperature, while the absorber were solidified by cooling with liquid nitrogen in the cryostat shown in Fig. 2. The absorbers are liquid at room temperature and were injected into the cell by a syringe. The cell is made of brass. The windows of the cell are of myler of 25 μ thickness. All of the Mössbauer spectra were obtained with absorber thickness 50—60 mg/cm^2 Sn.

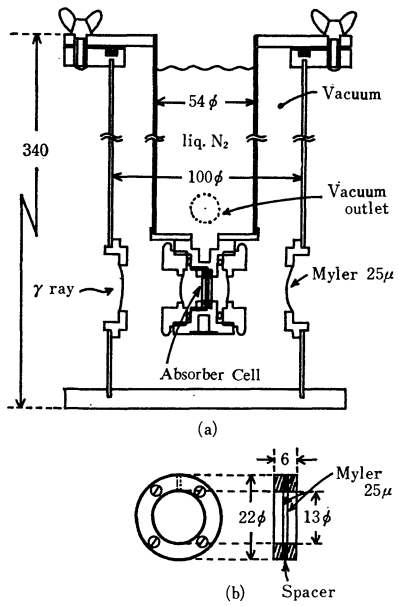

Fig. 2. Cryostat (a) and absorber cell (b). unit; mm

Triethyltin phenyl derivatives were prepared from triethyltin bromide and appropriate phenylmagnesium bromides in dry ether by the Grignard reaction.[5] They were purified by repeated fractional distillation at reduced pressure until GLC showed only one peak. They were identified by means of elementary analysis and infra- and farinfra-red spectra. The compounds can be synthesized easily, but the phenyl derivatives with polar functional group have not been synthesized as yet, for example, Grignard reagent cannot be made in dry ether or dry tetrahydrofuran in the case of m-NO_2 C_6H_4Br.

Results and Discussion

The isomer shifts in organotin compounds such as tetravalent tin fall in a narrow range. Tetravalent tin forms $5sp^3$ hybridization in many cases. An increase in s-electron density at the tin nucleus corresponds to an increase in isomer shift. Difference in s-electron density at the tin nucleus in various compounds mainly depends on the contribution from $5s$-electron density. However, it is important to consider not only $5s$-electron density but also the shielding of the $5s$-electron by the $5p$-electron. It may be considered that the partial ionicity of a bond in a sp^3 hybridization leads not only to a decrease in s-character but also to the compensation of a decrease of s-electron density through the decrease of shielding by the $5p$-electron. For tin compounds, the electric field gradient at the tin nucleus may appear as a result of the asymmetric distribution of the valence electron. Partial ionicity of a bond in sp^3 hybridization leads to an unbalanced state in a p-character of four bonding orbitals. Thus, it is important to obtain a correlation between the isomer shift and quadrupole splitting. A more theoretical treatment is required for this.

It has been suggested that only nonuniformity in dative π-bonding abilities of the atoms bonding to the tin atom can produce an electric field gradient large enough to give an observable quadrupole splitting.[6,7] However, in the Mössbauer spectra of compounds of the type $(C_6F_5)_{4-n}SnX_n$ (X=C_6H_5, CH_3, p-$CH_3C_6H_4$, n=1,2,3), observation of quadrupole splitting has been reported and interpreted in terms of electrostatic inductive and more predominant mesomeric effect of the pentafluoro phenyl group.[8] Similar results for R_3SnX (R=CH_3, C_6H_5, X=CF_3, C_6F_5, C_6Cl_5, C≡CC_6H_5) have shown that the quadrupole splitting can be induced by electrostatic inductive effects alone.[9] Recently, it has been reported that $(CH_3)_3Sn(p$-F-$C_6H_4)$ exhibits a single broader line suggesting unresolved splitting.[10]

We observed that the inductive effect of sub-

Table 1. Mössbauer parameters for triethyltin phenyl derivatives

Compounds[a]	I.S. ($vs.$ $Pd^{119m}Sn$)[b] mm/sec	Q.S. mm/sec
H-$PhSnEt_3$	−0.15	0
p-$CH_3PhSnEt_3$	−0.15	0
m-CH_3O-$PhSnEt_3$	−0.15	0
p-Cl-$PhSnEt_3$	−0.18	0.48±0.05
m-Cl-$PhSnEt_3$	−0.18	0.48±0.05

a) Ph=C_6H_4, Et=C_2H_5
b) ±0.03 mm/sec

5) H. Hashimoto and Y. Morimoto, *J. Organometal. Chem.*, **8**, 271 (1967).

6) T. C. Gibb and N. N. Greenwood, *J. Chem. Soc., A*, **1966**, 43.

7) N. N. Greenwood and J. N. R. Ruddick, *ibid.*, **1967**, 1679.

8) H. A. Stöckler and H. Sano, *Trans. Faraday Soc.*, **64**, 577 (1968).

9) R. V. Parish and R. H. Platt, *Chem. Commun.*, **1968**, 1118.

10) T. Chivers and J. R. Sams, *ibid.*, **1969**, 249.

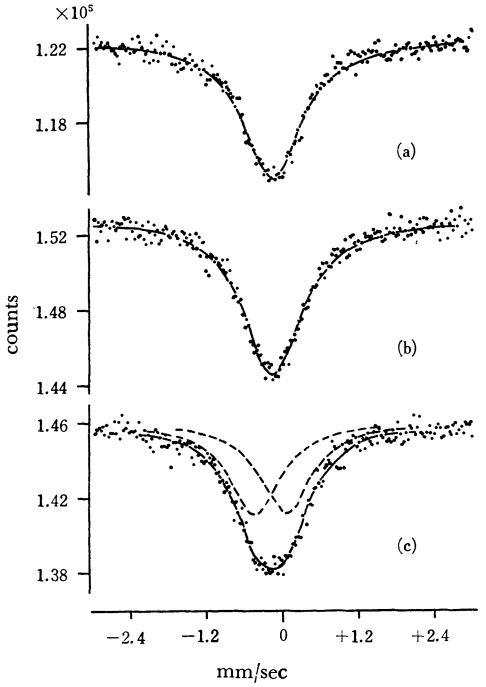

Fig. 3. Mössbauer spectra of triethyltin phenyl derivatives.
(a) $C_6H_5Sn(C_2H_5)_3$
(b) m-$CH_3OC_6H_4Sn(C_2H_5)_3$
(c) p-$ClC_6H_4Sn(C_2H_5)_3$

stituent causes a small quadrupole splitting. The results are summarized in Table 1. The isomer shift and quadrupole splitting are presented in the first and second columns of the table, respectively. A few examples of the spectra are shown in Fig. 3. The isomer shifts are shown relative to $Pd^{119m}Sn$ source, and all the numerical values are given in mm/sec. The isomer shifts of β-Sn and SnO_2 are +1.11 mm/sec and −1.58 mm/sec with respect to $Pd^{119m}Sn$ source, respectively. For X=H, p-CH_3, m-CH_3O in triethyltin phenyl derivatives X-$PhSnEt_3$, sharp, single lines with a half width of 1.14 mm/sec were observed. For p-Cl and m-Cl derivatives, however, apparently about 20 per cent broader, unsplit lines were observed. The isomer shifts were nearly equal within experimental error. The solids lines in Fig. 3(a), (b) are the single Lorentzian best fitted. However, the spectra obtained for p-Cl and m-Cl derivatives are fitted not by the single Lorentzian but by the overlap of two Lorentzians with a half width of 0.96 mm/sec (Fig. 3(c)). The broadened lines for p-Cl and m-Cl derivatives are possibly due to an unresolved quadrupole doublet. The small quadrupole splitting may be attributed to the increased ionicity of the Sn-C bond due to the inductive effect of chlorine atom. The s-character decreases through partially ionic character of the bond, but decreased p-character also compensates the decrease of the s-electron density at the tin nucleus through decreased shielding. Thus the increase of ionicity of the bond may not cause considerable change in isomer shift.

By means of the measurements of the electric dipole moment of the trimethyltin p-phenyl derivatives (p-$XC_6H_4Sn(CH_3)_3$, X=H, CH_3, CH_3O, $N(CH_3)_2$, Cl, Br), it has been concluded that for other derivatives with the exception of halogen derivatives, $d\pi$–$p\pi$ bonding ($(CH_3)_3Sn^-=^+C_6H_4X$), which compensates the contribution due to the difference of electronegativity between tin and carbon ($(CH_3)_3Sn^+-^-C_6H_4X$), may be present, but the negative inductive effect of the halogen atom outweighs the positive mesomeri, *i. e.*, $d\pi$–$p\pi$ bonding is not indicated in the halogen substituted tin compounds.[11,12] For triethyltin phenyl derivatives, the rates of electrophilic cleavage of phenyl-tin bond are rather small for p-Cl and m-Cl derivatives in comparision with those of others.[5]

From a consideration of the inductive effect caused by the substituents, the Mössbauer spectra of the derivatives with polar functional group, *e. g.*, m-$NO_2PhSnEt_3$, p-$NO_2PhSnEt_3$, *etc.*, can be measured, but the preparation of the compounds has not been achieved as yet.

The samples were kindly supplied by Professor H. Hashimoto of Department of Synthetic Chemistry, Tohoku University.[5]

11) H. H. Huang and K. M. Hui, *J. Organometal. Chem.*, **2**, 288 (1964).
12) C. Eaborn and J. A. Waters, *J. Chem. Soc.*, **1961**, 542.

BULLETIN OF THE CHEMICAL SOCIETY OF JAPAN VOL. 43 3037—3043 (1970)

Ultrasonic and Thermodynamic Study on Solute-Solvent Interaction. Binary Mixtures of 1,2-Dichloroethane with Benzene, Toluene, *p*-Xylene and Cyclohexane

Osamu KIYOHARA and Kiyoshi ARAKAWA

Research Institute of Applied Electricity, Hokkaido University, Sapporo

(Received February 19, 1970)

The sound velocity and density of binary mixtures of benzene, toluene, *p*-xylene and cyclohexane with 1,2-dichloroethane (DCE) as a common component were measured at temperature 20—40°C, and the excess molar volume and excess compressibility of these systems were calculated. They were found to be positive. The excess compressibility is independent of temperature in the DCE-benzene system. Thermodynamical properties and the nature of intermolecular interaction in the systems were discussed. It has been shown that there is a certain weak attraction between DCE and aromatic molecules, and that there is no complex formation *viz.*, hydrogen-bonding or change transfer complex. It has been proposed that the interaction between *gauche* form of DCE and aromatic molecules is of electrostatic nature (dipole-induced dipole or hyper-polarizability).

Binary solutions consisting of a halogen-substituted ethane and an aromatic solvent have long been studied from various viewpoints, but complete information is still lacking.

One approach to the liquid structure of the system is in the field of the molecular structure theory by means of Raman and infrared spectroscopy,[1-3] dielectric measurements,[4-7] and NMR.[8] The solvent dependence of the conformational equilibrium in halogen-substituted ethanes in the solution has been studied.[1-8] It has been found that aromatic solvents exhibit an anomaly in the conformational equilibrium of halogen-substituted ethanes in contrast to non-aromatic solvents.[3-8]

In a second approach, *viz.*, a thermodynamical consideration, the 1,2-dichloroethane-benzene system has been regarded as a nearly ideal solution,[9,10] because the excess free energy, enthalpy and entropy resulting from mixing are small. However, excess molar volume is large in comparison with other excess thermodynamical quantities.[11-14] Measurements of thermodynamical quantities have been made on this "pseudo-ideal" solution.[9-16]

By the analysis using the solution theory,[17] it has been shown that this system is not ideal, and that a certain kind of order is present between two components.[17]

As a third approach for the 1,2-dichloroethane-benzene system, ultrasonic studies, which present a useful means for the study of liquid structure in general, have been made by Staveley *et al.*,[18]

1) S. Mizushima "Structure of Molecules and Internal Rotation," Academic Press. Inc., New York (1954).
2) A. Wada, *J. Chem. Phys.*, **22**, 198 (1954).
3) A. Wada and Y. Morino, *ibid.*, **22**, 1276 (1954).
4) O. Kiyohara and K. Higasi, This Bulletin, **42**, 1158 (1969).
5) A. Abadie, C. Michel and P. Mauret, *C. R. Acad. Sci. Paries*, **264**, 1433 (1969).
6) K. Chitoku and K. Higasi, This Bulletin, **40**, 773 (1967).
7) J. Crossley and S. Walker, *J. Chem. Phys.*, **48**, 4742 (1968).
8) R. J. Abraham, L. Cavalli and K. G. R. Pachler, *Mol. Phys.*, **11**, 471 (1966) and papers cited therein.
9) J. H. Hildebrand and R. L. Scott, "The Solubility of Non-Electrolyte," Third Ed., Dover Publications, Inc., New York (1964), Chapt. XIII, pp. 211, 216.
10) J. S. Rowlinson, "Liquids and Liquid Mixtures," 2nd Ed., Butterworth & Co. Ltd., London (1969), p. 137.
11) L. Sieg, J. L. Crutzen and W. Jost, *Z. phys. Chem.*, **198**, 263 (1951).
12) E. A. Coulson, J. L. Hales and E. F. G. Herington, *Trans. Faraday Soc.*, **44**, 636 (1948).
13) H. Tschamler, *Monatsh.*, **79**, 499, 508 (1948).
14) L. H. Ruiter, *Rec. Trav. Chem. Pays-Bas*, **74**, 1131, 1491 (1955).
15) A. Amaya and R. Fujishiro, This Bulletin, **31**, 90 (1958).
16) L. A. K. Staveley, W. J. Tupman and K. R. Hart, *Discuss. Faraday Soc.*, **15**, 130 (1953).
17) K. Arakawa and O. Kiyohara, This Bulletin, **43**, 975 (1970).
18) L. A. K. Staveley, W. J. Tupman and K. R. Hart, *Trans. Faraday Soc.*, **51**, 323 (1955).

Kohler *et al.*[19] and others.[20]

This system is interesting as the object of studies of the interaction between polar molecules and π electrons, as well as that of studies of liquid structure.

We report here the results of an ultrsonic and thermodynamical investigation for the dichloroethane-aromatic systems and the dichloroethane-cyclohexane system which is taken as a reference system, and discuss the nature of the solute-solvent interactions in the systems.

Experimental

Samples of benzene, toluene, *p*-xylene, cyclohexane and 1,2-dichloroethane (DCE) were guaranteed reagents obtained from Wako Pure Chemical Industry Co. Ltd., and used on further purification.[21] The purity was examined by measurements of density at 20°C.

Sample	Density at 20°C	Lit. value[22]
Benzene	0.87904	0.87903
Toluene	0.86703	0.86696
p-Xylene	0.86105	0.68100
Cyclohexane	0.77853	0.77853
DCE	1.25297	1.25294

Sound velocity was measured using a usual crystal interferometer,[23] working at 3 Mc. The cell used is shown in Fig. 1. Measurements were made at 20, 30 and 40°C. The temperature was controlled within ±0.05°C. The measurement of sound velocity was reproducible within ±0.3 m/sec.

In order to test the apparatus, sound velocity was measured at 30°C for pure samples of benzene, *n*-hexane, cyclohexane and carbon tetrachloride. The results obtained were compared with data in literature.

Sample	Sound velocity at 30°C (m/sec)	Lit. value
Benzene	1275.4 (3 Mc)	1276.9,*1 1275.8*2
n-Hexnae	1062.8 (1 Mc)	1055.3*2
Cyclohexane	1228.6 (3 Mc)	1231.3,*3 1229.5*2
Carbon tetrachloride	908.6 (1 Mc)	905.9,*4 908*5

19) a) G. H. Findenegg and F. Kohler, *ibid.*, **63**, 870 (1967). b) E. Wilhelm, R. Schano, G. Becker, G. H. Findenegg and F. Kohler, *ibid.*, **65**, 1443 (1969).

20) R. J. Fort and W. R. Moore, *ibid.*, **61**, 2102 (1965).

21) J. A. Riddick and E. E. Toops, Jr., "Organic Solvent," Vol. II, 2nd Ed., Interscience Publishers, Inc., New York (1967).

22) J. Timmermans, "Physicochemical Constants of Pure Organic Compounds," Elsevier Publishing Co., Vol. I (1950) and Vol. II (1965).

23) H. Nomura and Y. Miyahara, *Nippon Kagaku Zasshi*, **88**, 22 (1967).

*1 Ref. 19a. *2 Ref. 24.
*3 Ref. 19b. *4 Ref. 25.
*5 K. C. Reddy, S. V. Subrahmanyam and J. Bhimasenacher, *J. Phys. Soc. Jap.*, **19**, 559 (1964).

24) W. Wratschko and F. Kohler, *Monatsh.*, **93**, 329 (1961).

25) H. Sackmann and A. Boczek, *Z. Physik. Chem.*, **29**, 329 (1961).

The agreement is satisfactory on the whole.

The merit of this apparatus is that the quantity of samples needed for measurements is small, 15—20 cc.

Density measurements were made using a pycnometer of usual type, whose capacity was about 15 cc. Accuracy of the density obtained was ±0.01%.

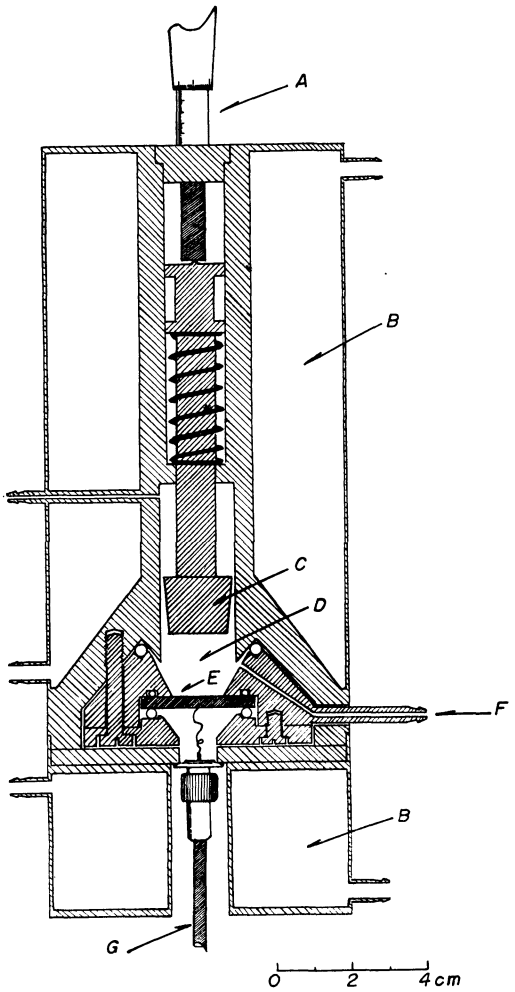

Fig. 1. Interferometer cell.
A: micrometer, B: double jacket, C: reflector, D: sample, E: crystal, F: liquid inlet, G: co-axial cable

Results

Density d and sound velocity v were measured over the whole concentration range at 20, 30 and 40°C for the four systems: DCE-benzene, DCE-toluene, DCE-*p*-xylene and DCE-cyclohexane.

Excess Molar Volume on Mixing. Excess molar volume V^E was calculated from density data which are given in Figs. 2(a), (b), (c) and (d) for each system. Abscissa x represents the mole fraction of DCE. The accuracy of V^E is about ±0.02 cc/mole. V^E values of DCE-benzene system agree

with literature values.[12–14,19a] The trend of its temperature dependence is also in agreement with the data.[13,14,19a] The values of V^E increase in the order: toluene<benzene<*p*-xylene<cyclohexane.

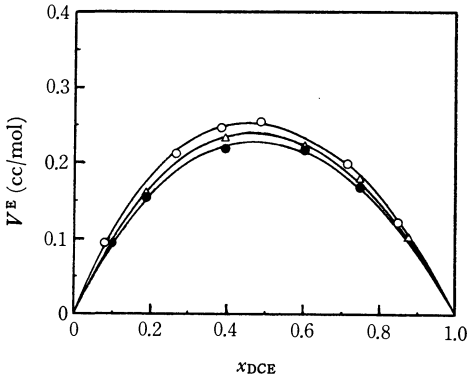

Fig. 2(a). Excess molar volume of DCE-benzene system.
Temperature: ○ 20°C, △ 30°C, ● 40°C

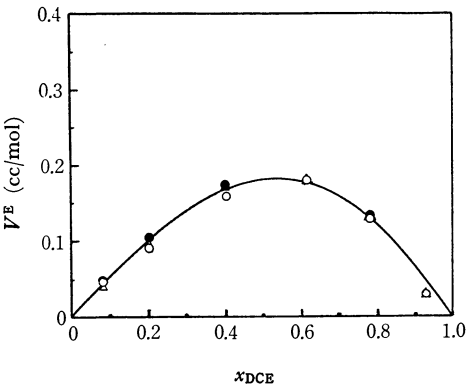

Fig. 2(b). Excess molar volume of DCE-toluene system.
Temperature: ○ 20°C, △30°C, ● 40°C

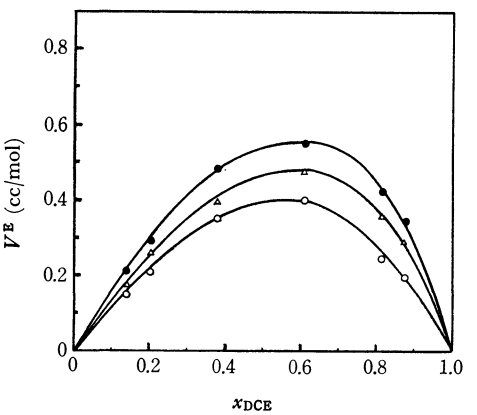

Fig. 2(c). Excess molar volume of DCE-*p*-xlyene system.
Temperature: ○ 20°C, △ 30°C, ● 40°C

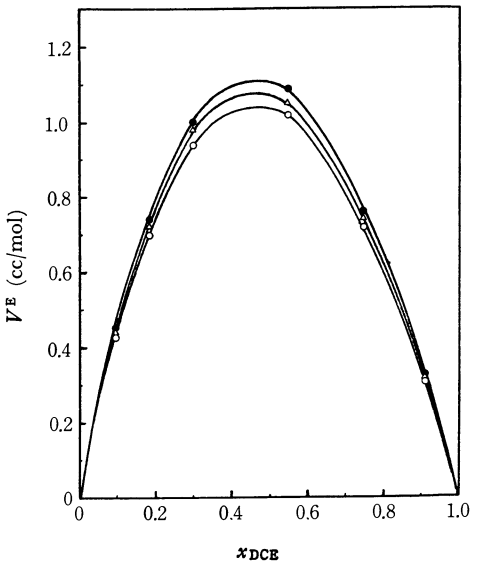

Fig. 2(d). Excess molar volume of DCE-cyclohexane system.
Temperature: ○ 20°C, △ 30°C, ● 40°C

Sound Velocity. Sound velocity v of all these mixtures deviates negatively from linear addivity in mole fraction, and the deviation decreases with rising temperature. Sound velocity *vs.* concentration curve of DCE-xylene system is shown in Fig. 3 as an example. The sound velocity of DCE-benzene system was measured by several workers,[18–20] and that of DCE-cyclohexane system by Kohler *et al.*[19b] Our data for these two systems are in good agreement with those of Kohler *et al.*

Compressibility. From the values of sound velocity v and density d, adiabatic compressibility

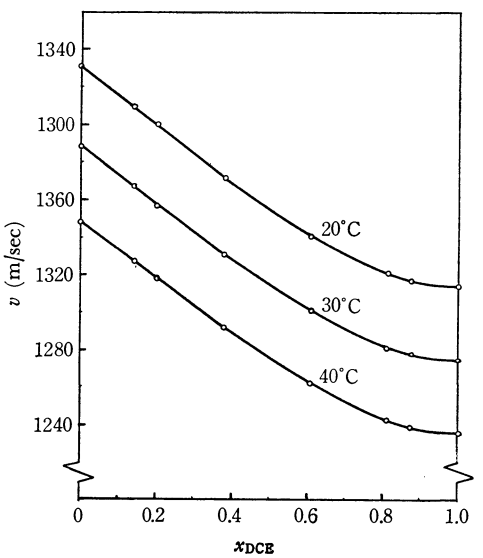

Fig. 3. Sound velocity for DCE-*p*-xylene system.

κ_s has been calculated by means of the relation

$$\kappa_s = \frac{1}{v^2 \cdot d} \tag{1}$$

The κ_s of the pure liquids obtained are given in Table 1. The uncertainty in κ_s is within $\pm 0.1\%$. Values of κ_s of pure liquids are in agreement with the values obtained by Kohler *et al.*[19]

The excess adiabatic compressibility κ_s^E and $(V\kappa_s)^E$ are calculated from κ_s and molar volume V of mixtures and pure components by the equations

$$\kappa_s{}^E = \kappa_s - \frac{1}{V}(x_A V_A \kappa_{s,A} + x_B V_B \kappa_{s,B}) \tag{2}$$

$$(V\kappa_s)^E = V \cdot \kappa_s - (x_A V_A \kappa_{s,A} + x_B V_B \kappa_{s,B}) \tag{2'}$$

$(V\kappa_s)$ becomes linear in mole fraction if a system behaves as an ideal solution.*6 $(V\kappa_s)^E$ *vs.* concentration curves are shown in Figs. 4(a), (b), (c) and (d) for each system.

All κ_s^E and $(V\kappa_s)^E$ are positive. The values increase in the order: benzene$\lesssim$toluene$<$xylene$<$cyclohexane. The temperature coefficients are all positive except for the DCE-benzene system, whose coefficient is found to be zero within experimental error.

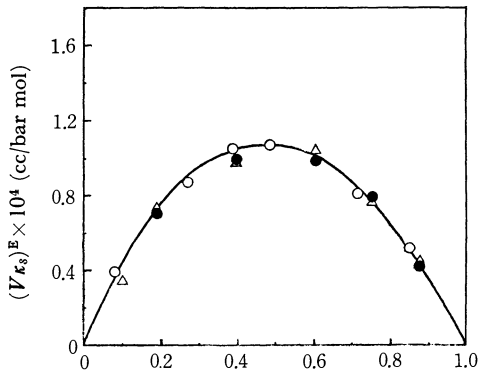

Fig. 4(a). $(V\kappa_s)^E$ for DCE-benzene system. Temperature: ○ 20°C, △ 30°C, ● 40°C

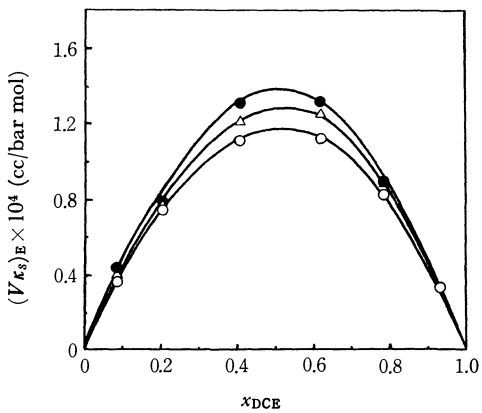

Fig. 4(b). $(V\kappa_s)^E$ for DCE-toluene system. Temperature: ○ 20°C, △ 30°C, ● 40°C

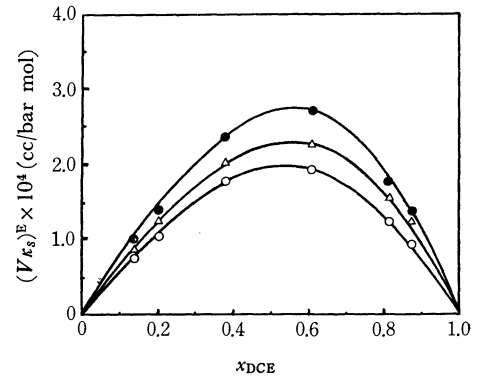

Fig. 4(c). $(V\kappa_s)^E$ for DCE-*p*-xylene system. Temperature: ○ 20°C, △ 30°C, ● 40°C

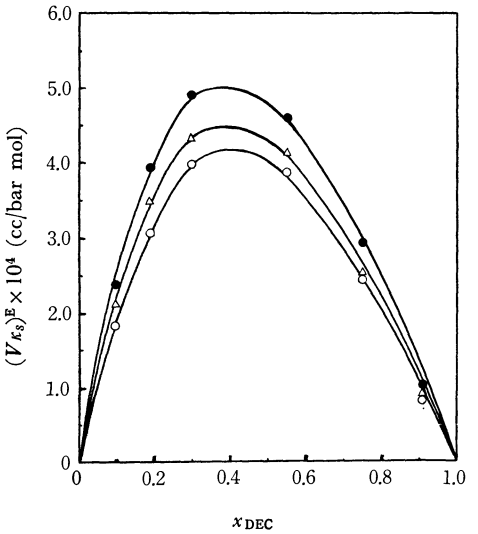

Fig. 4(d). $(V\kappa_s)^E$ for DCE-cyclohexane system. Temperature: ○ 20°C, △ 30°C, ● 40°C

The adiabatic compressibility of DCE-benzene system has been obtained by several workers.[18-20] Stavely *et al.*[18] reported that the temperature coefficient of κ_s^E for this system was slightly positive. However, in our measurements, the coefficient is almost zero within experimental error.

For each system, the data of excess adiabatic compressibility κ_s^E and the excess molar volume V^E

TABLE 1. ADIABATIC COMPRESSIBILITIES κ_s OF PURE LIQUIDS ($bar^{-1} \times 10^{-6}$)

T (°C)	Benzene	Toluene	*p*-Xylene	Cyclo-hexane	DEC
20	64.9_3	65.4_0	65.5_9	78.7_7	54.2_0
30	70.8_0	70.6_6	70.7_0	86.1_3	58.5_4
40	77.1_2	76.5_6	76.1_1	94.4_8	63.3_8

*6 See also Ref. 19a.

Table 2. Values of the coefficients in empirical equations for κ_s^E and V^E

System	T (°C)	A_0	A_1 (bar$^{-1}\times10^{-6}$)	A_2	B_0	B_1 (cm^3/mol)	B_2
DCE-Benzene	20	4.98	0.13	0.17	1.00	0.14	0.17
	30				0.97	0.07	0.05
	40				0.91	0.89	0.17
DCE-Toluene	20	5.01	−1.05	0.52	0.76	−0.03	−0.30
	30	5.44	−0.97	−0.26			
	40	5.49	−0.92	−0.29			
DCE-*p*-Xylene	20	7.80	−3.22	−0.23	1.61	−0.37	−0.21
	30	9.07	−2.80	−0.03	1.84	−0.78	0.50
	40	10.28	−5.03	−0.87	2.16	−0.88	0.55
DCE-Cyclohexane	20	17.32	4.57	−1.25	4.16	0.75	0.17
	30	18.33	5.77	−0.01	4.31	0.78	0.20
	40	20.46	6.66	−0.39	4.44	0.77	0.13

fit with the equation of the type

$$\kappa_s^E = x(1-x)\sum_{i=0}^{2}A_i\cdot(2x-1)^i$$

$$V^E = x(1-x)\sum_{i=0}^{2}B_i\cdot(2x-1)^i$$

where x is the mole fraction of DCE. The coefficients A_i and B_i, which were determined for each system by the method of least squares using FACOM 270—20 Computer, are given in Table 2.

Discussion

Thermodynamical Function. Let us discuss thermodynamical properties of the systems by means of the statistical theory given previously.[17] Excess volume V^E, excess entropy S^E and an interaction energy parameter θ*[7] are calculated for equimolar

Table 3. Molecular parameters of pure liquids

Liquid	T (°C)	V (cc/mol)	$\alpha\times10^3$ (deg^{-1})	V^* (cc/mol)	C_p (cal/deg·mol)
Benzene	20	88.86	1.214	69.09	32.38[a]
	30	89.40	1.223	69.21	32.80[a]
	40	91.07	1.256	69.31	33.38[a]
Toluene	20	106.26	1.055	84.65	36.12[a]
p-Xylene	20	123.29	1.007	98.97	43.07[a]
Cyclohexane	20	108.10	1.180	84.21	36.67[b]
	30	109.41	1.232	84.33	37.48[b]
	40	110.79	1.285	84.51	38.35[b]
DEC	20	78.99	1.141	62.09	30.67[b]
	30	79.92	1.184	62.04	30.79[b]
	40	80.88	1.228	62.01	30.92[b]
DBE	20	86.18	0.943		

a) Ref. 22. b) Ref. 19b.

Table 4. Thermodynamical quantities of equimolar mixtures*

System	T (°C)	$H^E_{obs.}$ (cal/mol)	$V^E_{obs.}$ (cc/mol)	$V^E_{calc.}$ (cc/mol)	$TS^E_{obs.}$ (cal/mol)	$TS^E_{calc.}$ (cal/mol)	$\theta\times10^3$
DCE-C_6H_6	20	21[a]	0.25	−0.04	15[b]	6	3.3
	30	17[a]	0.24	−0.04	12[b]	6	3.6
	40	14[a]	0.23	−0.04	9[b]	5	3.9
DCE-$C_6H_5(CH_3)$	20	−10[c]	0.18	−0.50		4	15.3
DCE-*p*-$C_6H_4(CH_3)_2$	20	−17[c]	0.40	−1.21		9	32.5
DCE-*c*-C_6H_{12}	20	426[c]	1.04	0.86		127	−70.7
DBE-C_6H_6	20	72[d]	0.26[e]	0.01	29[d]	9	− 7.4
C_6H_6-*c*-C_5H_{10}	25	150	0.30	0.49		44	−30.7
C_6H_6-*c*-C_6H_{12}	25	195	0.65	0.50	117	61	−32.1
$C_6H_5(CH_3)$-*c*-C_6H_{12}	25	149	0.57	0.53		41	−25.1
C_6H_5F-*c*-C_6H_{12}	40	212	0.71	0.71	98	67	−36.7

a) Ref. 14.
b) Estimated values (see Ref. 14 and Ref. 11).
c) Ref. 13.
d) A. Neckal and H. Volk, *Monatsh.*, **89**, 754 (1958).
e) Ref. 19b.
* The values given in the 6th to 9th rows are cited from the preceding paper[17] for comparison.

*[7] $\theta=[\varepsilon_{AB}-(\varepsilon_{AA}+\varepsilon_{BB})/2]/\varepsilon_{AA}$, where ε_{AB} is a pair interaction energy between different species, and ε_{AA} and ε_{BB} that between the same species, respectively.

mixtures, using the molecular parameter listed in Table 3. They are given in Table 4, together with the observed values of excess enthalpy H^E (lit. values) and V^E. The values for the 1,2-dibromoethane (DBE)-benzene system and those for the other four binary systems containing an aromatic solvent as a component are also given in Table 4 for comparison.

We see appreciable differences between the three DCE-aromatic solvent systems and others. The values θ for these systems are all positive, and their magnitudes are in the order of aromatic basicity.[26,27] On the contrary, those for six other systems, in which the DCE-cyclohexane and the DBE-benzene systems are included, are all negative. The values of $TS^E_{obs.}$ for the DCE-aromatic solvent systems are found to be less than those for the DBE-benzene system and those for the aromatic-alicyclic systems. This supports the idea that a certain specific but weak attraction is present between DCE and aromatic molecules. The values of $TS^E_{calc.}$ for the aromatic-alicyclic systems are about half as much as $TS^E_{obs.}$. This might be ascribed to the presence of a certain ordered structure in aromatic liquids.[17] The fact that the values of $V^E_{calc.}$ for these DCE-aromatic systems are less than those of $V^E_{obs.}$ in contrast to the good agreement between $V^E_{calc.}$ and $V^E_{obs.}$ for other systems is also attributed to a certain attraction between DCE and aromatic molecules.

Compressibility. The values of κ_s^E obtained for the DCE-aromatic system are found to increase in the order : benzene, toluene, xylene and cyclohexane. The values of $(V\kappa_s)^E$ and κ_s^E of DCE-xylene system are about half as small as those of DCE-cyclohexane system in spite of the fact that molar volume of xylene is larger than that of cyclohexane. This shows that DCE molecules is more interacting with aromatic molecules than with cyclohexane.

Let us compare theoretical values $\kappa^E_{t,calc.}$ with experimental ones, using an approximate formula on excess compressibility[28] derived from the solution theory.[17] We have

$$\kappa_t^E = \frac{1}{3RT}\left[\frac{(V-V^*)^2}{V} - \frac{1}{V}\{(V_A-V^*_{AA})^2x_A+(V_B-V^*_{BB})^2x_B\}\right] \quad (3)$$

where V^* is $V^*_A \cdot x_A + V^*_B \cdot x_B$ and other notations are the same as those in the preceding paper.[17] From the values of sound velocity, we can get the adiabatic compressibility κ_s. κ_s^E can be transferred to excess isothermal compressibility κ_t^E, using the thermodynamical relation

$$\kappa_t = \kappa_s + \frac{V \cdot T \cdot \alpha^2}{C_p} \quad (4)$$

The values of excess specific heat C_p^E are available from literature. The values of κ_t^E obtained for equimolar mixtures are given in column 7 of Table 5, together with the values of $V^E_{obs.}$, $C^E_{p,obs.}$ and $\kappa^E_{s,obs.}$ used (those of pure components are given in Table 3.). On the other hand, κ_t^E can be calculated by Eq. (3) from the observed V^E. The $\kappa^E_{t,calc.}$ are listed in the last column of Table 5, and those for the DBE-benzene system are included for comparison.

The $\kappa^E_{t,obs}$ for all the systems are in good agreement with $\kappa^E_{t,calc.}$. The agreement is good also with respect to its temperature dependence for the DCE-benzene and DCE-cyclohexane system. This supports the idea that the interaction between DCE and aromatic molecules obeys the 6th power rule with respect to intermolecular distance.[17]

TABLE 5. THE EXCESS COMPRESSIBILITIES FOR EQUIMOLAR MIXTURES

System	T (°C)	$V^E_{obs.}$ (cc/mol)	$C^E_{p.obs.}$ (cal/deg·mol)	$\alpha_{obs.}\times10^3$ d) (deg^{-1})	$\kappa_s^E\times10^6$ (bar^{-1}) Obsd	$\kappa_t^E\times10^6$ (bar^{-1}) Obsd	$\kappa_t^E\times10^6$ (bar^{-1}) Calcd
DCE-Benzene	20	0.25	-0.0_7 b)	1.164	1.2_5	1.3	2.5
	30	0.24	-0.0_9 b)	1.195	1.2_5	1.3	2.5
	40	0.23	-0.1_3 b)	1.228	1.2_5	1.3	2.5
DCE-Toluene	20	0.19	-0.4_8 c)	1.089	1.2_5	2.9	4.6
DCE-*p*-Xylene	20	0.40	-0.4_1 c)	1.111	1.9_5	8.0	11.7
DCE-Cyclohexane	20	1.04	-0.6_2 a)	1.191	4.3_3	11.3	12.6
	30	1.08	-0.8_1 a)	1.231	4.5_8	12.1	13.0
	40	1.11	-1.0_1 a)	1.273	5.1_2	13.0	13.4
DBE-Benzene	20	0.26 a)				~-1.5 e)	2.1

a) Ref. 19. b) Ref. 18. c) Ref. 13.
d) Estimated values from the observed dV^E/dT and α of pure liquids (Table 3).
e) Value at 27°C (Ref. 19a).

26) M. Tamres, *J. Amer. Chem. Soc.*, **74**, 3375 (1952).
27) M. R. Basila, E. L. Saier and L. R. Cousins, *ibid.*, **87**, 1665 (1965).
28) O. Kiyohara and K. Arakawa, The 14th Annual Symposium on Ultrasonic and Chemical Physics, Nov. 1969, Tokyo.

Solute-Solvent Interaction. From the consideration on thermodynamical quantities and compressibility it is evident that there is a weak but specific interaction*[8] between DCE and aromatic molecules, which is too small and insufficient for the formation of a complex between solute and solvent molecules.

There have been two interpretations for the nature of this interaction. The first one was given by Ruiter,[14] Neckel and Volk[29] and others.[6,7] They proposed that it is a hydrogen-bonding (proton-donor-acceptor) interaction between the protons of *gauche* form of DCE and π electrons of aromatic molecules. However, the magnitude of $\varepsilon_{AB}-(\varepsilon_{AA}+\varepsilon_{BB})/2$*[8] is evidently too small to support the presence of a hydrogen-bonding between species A and B, where A is DCE and B is an aromatic. The situation is quite similar with respect to the presence of a charge transfer complex (electron-donor-acceptor). The hydrogen-bonding interaction can not explain the presence of "benzene effect" for the 2,3-dihalo-2,3-dimethylbutane-benzene system, in which all hydrogen atoms in DCE or DBE are replaced by methyl groups.[4]

This type of interaction, the so-called "benzene effect", is widely observed in binary mixtures of substituted dihaloethanes and haloketone with aromatic solvents.[5,30,31] The data on the shift of C–H stretching in Raman and infrared spectroscopy[6,32] do not support the presence of hydrogen-bonding in substituted dihaloethane-aromatic solvent systems.

It is concluded that there is no appreciable complex formation between DCE and aromatic molecules, and that the solute-solvent interaction is not ascribed to hydrogen-bonding or charge transfer.

There remains the second interpretation that it is an electrostatic interaction which is of a more general nature. The *gauche* form of DCE molecule has a large dipole moment and aromatic molecules are greatly polarizable. Thus, for the DCE-aromatic system the dipole-induced dipole interaction is considered to play an important role.

As seen in Table 4, the magnitudes of θ for DCE-aromatic systems are positive but at the most of the order of a few %. This shows that the interactions between DCE and aromatic molecules are of a similar nature to those between each identical molecules themselves, and supportes the results that it is the dipole-induced dipole interaction. The same idea was recently presented on the basis of NMR, dielectric and spectroscopy data.[30–33]

It is concluded that the interaction between DCE and aromatic molecules is not hydrogen-bonding and is of electrostatic nature (dipole-induced dipole or hyperpolarizability).

We wish to thank Mr. T. Kabashima for his cooperation in carrying out this study.

29) A. Neckel and H. Volk, *Z. Electrochem.*, **Bd82**, 1104 (1958).

*[8] The magnitude of $\varepsilon_{AB}-(\varepsilon_{AA}+\varepsilon_{BB})/2$ is of the order of several ten calories per mole, which is estimated from the values of θ given in Table 4.

30) C. Altona and H. J. Hageman, *Rec. Trav. Chim. Pays-Bas*, **87**, 279 (1968); H. R. Buys, C. Altona and E. Havinga, *Tetrahedron Lett.*, 3067 (1967).

31) W. F. Reynold and D. J. Wood, *Can. J. Chem.*, **47**, 1295 (1969).

32) N. Oi and J. F. Coetzee, *J. Amer. Chem. Soc.*, **91**, 2478 (1969).

33) T. L. Brown and K. Stark, *J. Phys. Chem.*, **69**, 2679 (1965).

BULLETIN OF THE CHEMICAL SOCIETY OF JAPAN VOL. 43 3044—3048 (1970)

An Application of the Phase-inversion-temperature Method to the Emulsification of Cosmetics. I. Factors Affecting the Phase-inversion Temperature

Takeo MITSUI, Yasuhiko MACHIDA and Fuminori HARUSAWA

Shiseido Research Laboratory, Nippa-cho, Kohoku-ku, Yokohama

(Received February 24, 1970)

Recently, the PIT (phase-inversion-temperature) system was originated and developed by Shinoda and his collaborators as a guide to surfactant selection. In order to apply the PIT system to the cosmetic field, the effects of various factors on the PIT have been reinvestigated using cosmetic materials. POE alkyl ethers, whose distribution of EO chain lengths is broad, are widely used in cosmetics. In such a case, the effect of the distribution of the EO chain lengths is important. When a surfactant with a distribution of EO chain lengths was used, the PIT was lowered by an increase in the concentration of the surfactant, but when a monodisperse surfactant without any distribution was used, the PIT scarcely varied with the concentration of the surfactant. In the case of the surfactant with a distribution of EO chain lengths, however, if the ratio of oil to surfactant was kept constant, the PIT scarcely varied with the ratio of oil phase to water phase. This relationship can be used in estimating the PIT in the case of the practical production of an emulsion.

An emulsion stabilized with a certain non-ionic surfactant changes its type from the oil-in-water type (O/W) to the water-in-oil type (W/O) as the temperature rises. The emulsion tends to form a W/O type because the affinity of the ethylene oxide (EO) chain of the surfactant for water is weakened at higher temperatures.

The phase-inversion temperature (PIT), at which the emulsion inverts its phase, has been adopted by Shinoda[1] as a guide for choosing a suitable type of emulsifier and for estimating the effects of additives because of its precise indication of the characteristics of the emulsion.

The factors which affect the PIT of the emulsion are[1-12]:

1. the nature of the hydrophilic and lipophilic moieties of the surfactant;
2. the mixing of the surfactants;
3. the nature of the oil;
4. the nature of the additives of the oil and water phases;
5. the concentration of the surfactant;
6. the ratio of oil phase to water phase, and
7. the distribution of EO chain lengths in the surfactant.

In the present study the effects of the above-mentioned factors on the PIT were investigated using cosmetic materials in order to establish the application of the PIT system[1] to the emulsification of cosmetics.

Furthermore, as the PIT is greatly affected by the distribution of EO chain lengths in the surfactant when an oil-soluble surfactant on the market is used, a comparison test was carried out with monodisperse surfactants.

Experimental

Samples. Liquid paraffin, whose Saybolt viscosities were 50 sec, 70 sec and 350 sec at 100°F, dodecane (purity: 98.9%), tetradecane (purity: 99.5%), and squalane were used as the oil bases.

POE ($\bar{n}$=3.7, 4.8, 6.2, 6.9, 8.1 mol) oleyl ether, POE ($\bar{n}$=4.8, 5.9, 6.7, 7.5) stearyl ether, POE ($\bar{n}$=4.0, 5.0 mol) lauryl ether (Nihon Emulsion Co.), and POE (n=4.0, 5.0, 6.0, 7.0, 8.0 mol) lauryl ether (Nikko Chemical Co.; purity: 95—98%, a monodisperse surfactant) were used.

Solid paraffin (mp 62.8°C), oleic acid (purity: 88.0%), oleyl alcohol (purity: 79.5%), lauryl alcohol (purity:

1) K. Shinoda, *Nippon Kagaku Zasshi*, **39**, 435 (1968); K. Shinoda, B/O, No. 51, 5th International Congress of Surface Active Substances, Barcelona, Spain (1968).
2) M. Aoki, A. Kamata and T. Matsuzaki, *Yakugaku Zasshi*, **83**, 1132 (1963).
3) K. Shinoda and H. Arai, *J. Phys. Chem.*, **68**, 3485 (1964).
4) H. Arai and K. Shinoda, *Nippon Kagaku Zasshi*, **86**, 299 (1965).
5) M. Aoki and T. Matsuzaki, *Yakugaku Zasshi*, **87**, 761 (1967).
6) M. Aoki and T. Matsuzaki, *ibid.*, **87**, 765 (1967).
7) K. Shinoda, *J. Colloid Interfac. Sci.*, **24**, 4 (1967).
8) H. Arai and K. Shinoda, *ibid.*, **25**, 396 (1967).
9) K. Shinoda and H. Arai, *ibid.*, **25**, 429 (1967).
10) K. Shinoda and H. Takeda, *ibid.*, **32**, 642 (1970).
11) K. Shinoda and H. Saito, *ibid.*, **26**, 70 (1968).
12) K. Shinoda edit. Figs. 9 and 11 in Chapter 2 of "Solvent Properites of Surfactant Solutions," Marcel Dekker Inc., New York (1967).

95.0% or over), 2-octyldodecanol (Dehydag Co.), and castor oil (purity: 86.0%) were studied as additives.

Methods. Oil, water, and surfactant were weighed into the same beaker, and then heated with stirring in order to make an emulsion, the total amount being 100 g. The PIT of the emulsion was determined by an electric conductivity device. The reproducibility of the measurements was within ± 1°C.

Results and Discussion

Effect of the HLB Value of the Surfactant and the Nature of Oil on the PIT. Figure 1

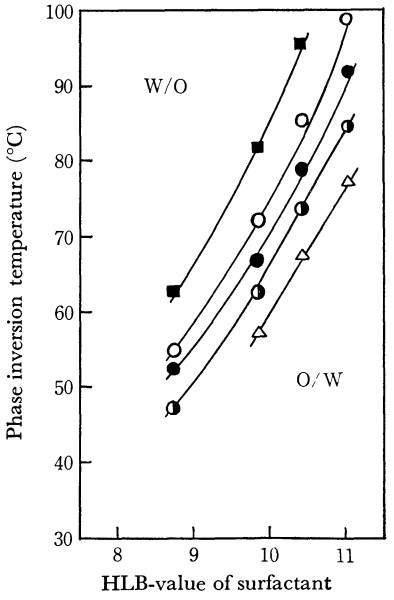

Fig. 1. Effect of different hydrocarbons on PIT *vs.* HLB-value of surfactant.
Surfactant: POE stearyl ether, 5 wt%/system
Phase ratio: 0.5 (wt).
■: squalan, ○, ●, ◑: liquid paraffin (Saybolt vis. 350, 70, 50 at 100°F respectively), △: tetradecane.

shows the effect of the HLB value of the surfactant and the kinds of oils on the PIT. As has already been pointed out by Shinoda and Arai,[3] the PIT's rose almost linearly with the increase in HLB values, and the rising rates were almost identical in all the liquid paraffins used. The PIT's varied with the nature of the oils used, even though surfactants with the same HLB values were used; the greater lipophilic the oil, the higher the PIT. This fact can be explained in terms of the difference in the required HLB values of the oils.

Effect of Additives on the PIT. Shinoda *et al.* studied the effect of added salts in water on the PIT,[10] and Aoki *et al.* studied some oil-soluble components.[6] We have studied the effect of additives on the oil phase because cosmetics always contain several additives in the oil phase. Figure 2 shows

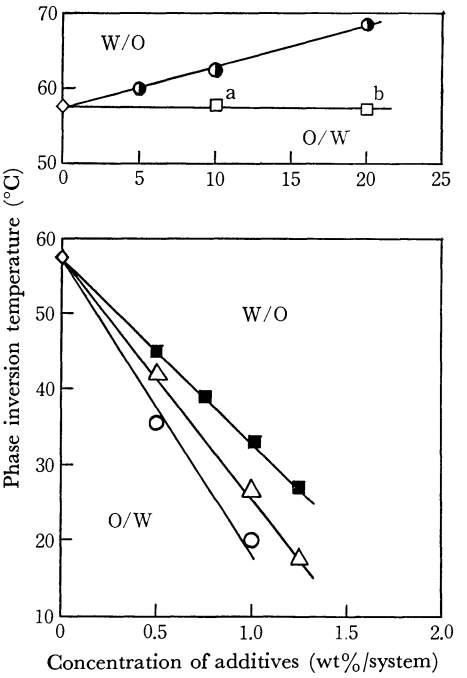

Fig. 2. Effect of different additives on PIT.
Oil: liquid paraffin (Saybolt vis. 70) plus additives.
Surfactant: POE ($\bar{n}$=4.8) oleyl ether, 4 wt%/system.
Phase ratio: 0.5 (wt).
◑: solid paraffin, □: solid paraffin plus oleyl alcohol (a, b: oleyl alcohol 0.23, 0.5 wt%/system respectively), ■: oleyl alcohol, △: lauryl alcohol, ○: oleic acid.

the effects of some oil-soluble additives on the PIT of a three-component system, consisting of liquid paraffin (70 Saybolt viscosity at 100°F), POE (4.8 mol) oleyl ether, and water. When liquid paraffin was replaced with 20% of solid paraffin, which is a non-polar substance, the PIT rose about 10°C. On the contrary, when it was replaced with only 1% of oleyl alcohol, lauryl alcohol, or oleic acid, which are polar substances, the PIT fell about 20—40°C. When a mixture consisting of solid paraffin and oleyl alcohol (the former raises the PIT, while the latter lowers it) in an appropriate ratio was added to the system, it showed the same PIT as the one to which no additive had been added. Thus, when a small quantity of an additive was added to the oil phase, the PIT rose or fell monotonously according to the quantity added. In the cases of 2-octyldodecanol, castor oil, etc., however, as is shown in Fig. 3, the minimum value of the PIT appeared.

Effect of the Concentration of the Surfactant and the Ratio of Oil Phase to the Water Phase on the PIT. The relationship between the concentration of the surfactant and the PIT was in-

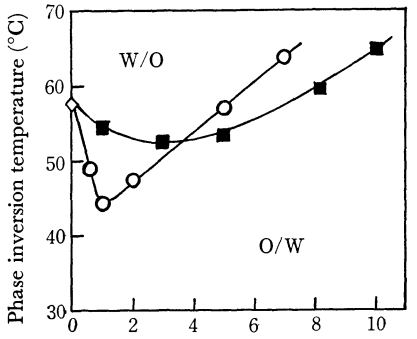

Fig. 3. Effect of castor oil and 2-octyldodecanol on PIT.
Oil: liquid paraffin (Saybolt vis. 70) plus additives.
Surfactant: POE ($\bar{n}$=4.8) oleyl ether, 4 wt%/system.
Phase ratio: 0.5 (wt).
○: castor oil, ■: 2-octyldodecanol.

vestigated by Shinoda *et al.*[3,9,10] using POE alkyl phenyl ether. In the present study, this relationship was reinvestigated using POE alkyl ether, whose distribution of EO chain lengths is broad. The results are shown in Fig. 4. As the concentration of the surfactant increased, the PIT was lowered very steeply compared with the case[3] of POE alkyl

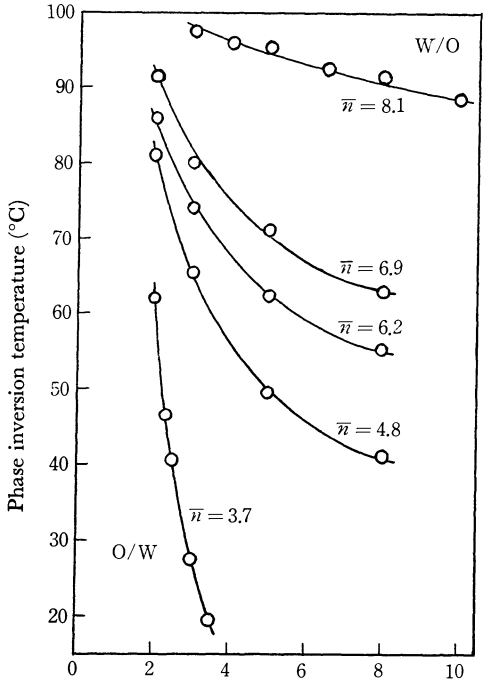

Fig. 4. Effect of ethylene oxide chain length on PIT *vs.* concentration of POE oleyl ether.
Oil: liquid paraffin (Saybolt vis. 70).
Phase ratio: 0.5 (wt).

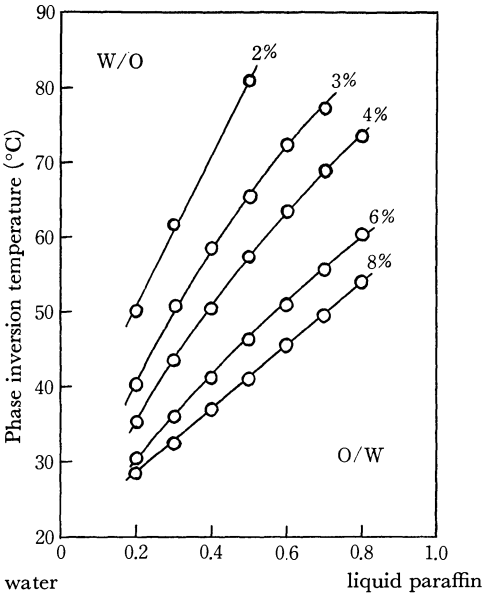

Fig. 5. Effect of concentration of POE ($\bar{n}$=4.8) oleyl ether on PIT *vs.* phase ratio.
Oil: liquid paraffin (Saybolt vis. 70).

phenyl ether. Especially in the case of a surfactant with a shorter EO chain, the falling rate of the PIT was remarkable. It was found that the effect of the distribution of EO chain lengths on the PIT is greater when the average EO chain length is shorter.

The effect of the phase ratio on the PIT was studied using various concentrations of POE oleyl ether, the average EO chain length of which was 4.8 mol. The results are shown in Fig. 5. As the oil-phase ratio became higher, the PIT rose more steeply compared with the case[3] of POE alkyl phenyl ether in a non-polar oil. Furthermore, the lower the concentration of surfactant, the higher the rate of the rise of PIT. However, it can be found from Fig. 5 that when the ratio of the oil to the surfactant is constant, almost the same PIT can be obtained in the same manner as with POE alkyl phenyl ether.[12] For example, the PIT of 50°C is obtained when the oil-phase ratio: concentration of surfactant is 0.2 : 2%, 0.3 : 3%, or 0.4 : 4%.

Therefore, while keeping the ratio of oil to the surfactant fixed, the PIT's were measured at various oil-phase ratios. As is shown in Fig. 6, even though the ratio of oil phase to water phase varied in the range of 0.2—0.8, the PIT was almost constant if the ratio of the oil to the surfactant was fixed. Furthermore, the higher the ratio of the surfactant in the oil phase, the lower the PIT.

In the case of the practical production of emulsion, it would be very convenient if the PIT could be calculated. Therefore, utilizing the above-men-

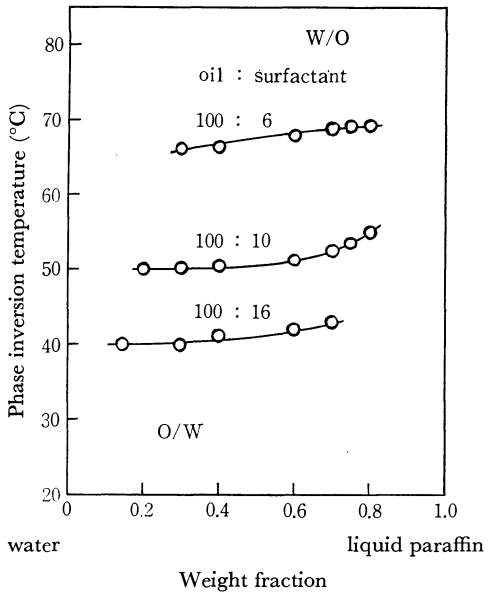

Fig. 6. Effect of phase ratio on PIT in various ratios of surfactant to oil.
Oil: liquid paraffin (Saybolt vis. 70).
Surfactant: POE ($\bar{n}$=4.8) oleyl ether.

tioned relationship, the PIT's were plotted *vs.* the ratio of the oil to the surfactant as well as the ratio of water to the surfactant, as is shown in Fig. 7. It can be found from Fig. 7 that the PIT rises almost linearly with the increase in the ratio of the oil to the surfactant. If such a straight line has been obtained by measuring two PIT's at two different ratios of oil to surfactant, the PIT of a given system can be estimated from its components, *i.e.*, the concentration of the surfactant and the ratio of oil phase to water phase. For example, in the case of a 3% concentration of the surfactant and an oil-phase ratio of 0.3, it can be estimated from Fig. 7 that the PIT is about 50°C.

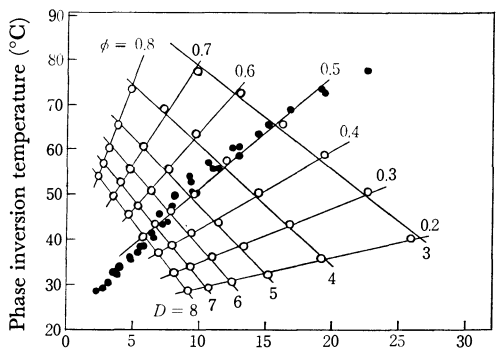

Fig. 7. Correlation between PIT and ratio of oil or water to surfactant.
ϕ: ratio of oil to water (wt).
D: concentration of surfactant (wt%/system).
Oil: liquid paraffin (Saybolt vis. 70).
Surfactant: POE ($\bar{n}$=4.8) oleyl ether.
●: oil/surfactant, ○: water/surfactant.

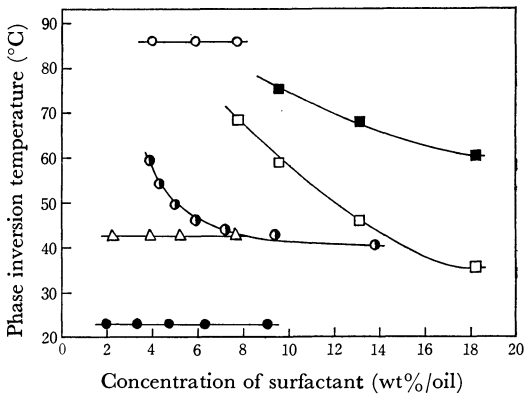

Fig. 8. Effect of distribution of ethylene oxide chain lengths on PIT *vs.* concentration of surfactant.
Oil: dodecane.
Phase ratio: 0.5 (wt.).
Surfactant: POE laurylether.
Monodisperse surfactants: ○: n=8, △: n=5, ●: n=4, ◑: n=8 plus n=4 (1 : 3.4).
Polydisperse surfactants: ■: $\bar{n}$=5, □: $\bar{n}$=4.

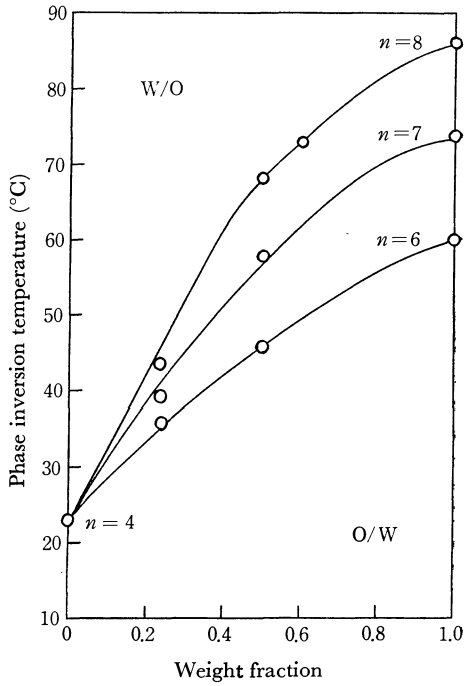

Fig. 9. Effect of mixing of surfactant on PIT.
Oil: dodecane.
Phase ratio: 0.5 (wt).
Surfactant: POE (n) lauryl ether (monodisperse), 4 (wt%/system).

Effect of the Distribution of the EO Chain Lengths in the Surfactant on the PIT. When the concentration of the surfactant was increased, the PIT was lowered, as is shown in Fig. 4. In the case of a surfactant whose average EO chain length is short, the falling rate of the PIT was very high.

Dodecane was used as the oil phase; it was emulsified with POE lauryl ethers with and without the distribution of EO chain lengths. The relationship between the PIT and the concentration of the surfactant is shown in Fig. 8. When a surfactant with a distribution of EO chain lengths was used, the PIT varied greatly with the concentration of the surfactant. However, when a monodisperse surfactant was used, the PIT scarcely varied, though the concentration of surfactant did vary. When a mixed surfactant of POE ($n=8$ mol) lauryl ether and POE ($n=4$ mol) lauryl ether, which are both monodisperse surfactants, was used, the PIT rose upon a decrease in the concentration of the mixed surfactant, as in the case of using a surfactant with a distribution of EO chain lengths. It can be assumed that the ratio of a surfactant with a shorter EO chain to one with a longer EO chain decreased at the interface upon a decrease in the concentration of the mixed surfactant, because the CMC of a nonionic surfactant in oil is far higher that the CMC in water; the average EO chain length of a surfactant affecting phase inversion increased, and the PIT rose.

From the same point of view, the relationship between the PIT and the mixing ratio of the surfactants was investigated using monodisperse surfactants. The results are shown in Fig. 9. The curves are convex, and when the surfactants are mixed the PIT moves to a higher position.

BULLETIN OF THE CHEMICAL SOCIETY OF JAPAN VOL. 43 3048—3053 (1970)

The Structure Theory of Water. III. The Order-Disorder Theory

Kiyoshi ARAKAWA and Katsutaka SASAKI

Research Institute of Applied Electricity, Hokkaido University, Sapporo

(Received April 2, 1970)

Taking into account the cooperative nature of cluster formation, we applied the order-disorder theory, using Bragg and Williams's approximation, to liquid water based on a two state model. The two state model consists of hydrogen-bonded molecules arrayed on α-sites in a tetragonal lattice and non hydrogen-bonded molecules on β-sites in the lattice. A partition function was formulated and calculated. The calculated energy difference, ε, between the molecules on β-sites and those on α-sites decreased continuously with the rise of temperature. Thermodynamic variables of liquid water were calculated at each temperature, where no adjustable parameter was used. Agreement between calculated values and observed ones is fairly good.

The structure of liquid water has been studied by many workers recently,[1,2] but conclusive results are still lacking. In advancing the structure theory of water, the models used are classified into two groups, a multi-state theory and a uniform-state theory. In the former, it has been assumed that liquid water consists of several distiguishable molecular species. Némethy and Scheraga[3] proposed a statistical theory of liquid water based on the model. Eyring and coworkers[4] applied a "significant structure theory" to water. In the preceding paper,[2] we stated that a simple two state theory could explain thermodynamic properties of water. Thus, we pointed out that the principal feature of multi-state theories was described by the two state theory. Existence of two different molecular species in liquid water has been supported experimantally by Luck[5] and Walrafen[6] from spectroscopic data.

Recently, Frank and Franks[7] have discussed the structural change of water caused by the presence of solute in aqueous solutions of urea, using a two state model. The application of two state theory to aqueous solutions has given fairly good results,

1) *Discuss. Faraday Soc.*, pp. 97—148 (1967).
2) K. Arakawa and K. Sasaki, This Bulletin, **42**, 303 (1969).
3) G. Némethy and H. A. Scheraga, *J. Chem. Phys.*, **36**, 3382 (1962).
4) M. S. Jhon, J. Grosh, T. Ree and H. Eyring, *ibid.*, **44**, 1465 (1966).
5) W. A. Luck, *Discuss. Faraday Soc.*, **43**, 115 (1967).
6) G. E. Walrafen, *J. Chem. Phys.*, **48**, 244 (1968).
7) H. S. Frank and F. Franks, *ibid.*, **48**, 4746 (1968).

as Holtzer and Emerson[8] and Ben-Neim and Stillinger[9] have reported. Our data of ultrasonic absorption[10] have shown that a two state model represents the structure of solvent water in aqueous solutions.

Studies based on the uniform-state model have been made since Pople[11] proposed a distored hydrogen-bond model. Einberg and Kauzmann[12] have pointed out the utility of distorted hydrogen-bond models. The "uniform nature" of the structure of water has been emphasized in the interpretation of spectroscopic data by Wall and Hornig,[13] Falk and Ford[14] and Franck and Roth.[15] However, no explanation of the origin of ultrasonic absorption such as made by Hall and others[16] using a two state model has been given by the uniform-state theory.

Though no decisive conclusion has been obtained, various attempts in the field of the structure theory of water have been made. However, one of the most important problems left unsolved at present is the direct introduction of the cooperative nature of the structure formation into theory. Thus, we attemped here an application of order-disorder theory[17] to explain thermodynamic properties of water on the basis of a two state model. The cooperative nature of "cluster" ("open-packed structure") formation are taken directly into account.

Theory

Model. As pointed out recently by Narten *et al.*[18] from X-ray diffraction data, liquid water consists of an ice-like structure and unbonded molecules.[18–20] The ice-like structure is believed to be a partly-broken lattice linked tetragonally by hydrogen bonds. It is seen that the number of first nearest neighbours in liquid water varied from 4.4 to 4.9 at temperatures 1.5—83°C.[21]

In the formulation of the following statistical theory, we assume that all molecules are distributed in a body-centered cubic lattice,[22] and that water is an equilibrium mixture of molecules arranged in two kinds of sites, α and β, in the lattice, as shown in Fig. 1. Hydrogen-bonded molecules occupy α-sites forming a tetragonal sub-lattice, and non-hydrogen-bonded molecules occupy β-sites. The energy level of molecules on β-sites is higher than that on α-sites. At 0°K in a "completely-ordered state" all molecules occupy only α-sites forming an ice-like structure. With the rise of temperature, population of α-sites decreases and that on β-sites increases, causing patial break-down of the ice-I-like structure. At a "completely-disordered state," two kinds of sites are occupied with equal probability.

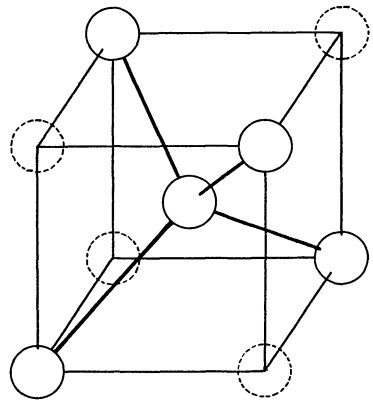

Fig. 1. α and β-site in a body-centered cubic lattice.
○ α-site, ◌ β-site

Application of Order-Disorder Theory. The total partition function, Z, is given by

$$Z = W f_\alpha^{N_\alpha} f_\beta^{N_\beta} \exp(-H/RT) \tag{1}$$

where W is a combinatorial factor, H potential energy, T temperature, N_α and N_β are the number of molecules arranged in each site, and f_α and f_β are the molecular partition functions for molecules in each site, respectively. The combinatorial factor and the potential energy are defined by

$$W = \frac{[\alpha]!}{N_\alpha!([\alpha]-N_\alpha)!} \cdot \frac{[\beta]!}{N_\beta!([\beta]-N_\beta)!} \tag{2}$$

$$H = N_\alpha V_\alpha + N_\beta V_\beta,\ N_\alpha + N_\beta = N \tag{3}$$

where $[\alpha]$ and $[\beta]$ are the number of each kind of lattice site ($[\alpha]=[\beta]=N$), V_α and V_α the potential

8) A. Holtzer and M. F. Emerson, *J. Phys. Chem.*, **73**, 26 (1969).
9) A. Ben-Naim and F. H. Stillinger, *ibid.*, **73**, 900 (1969).
10) K. Arakawa, N. Takenaka and K. Sasaki, This Bulletin, **43**, 636 (1970).
11) J. A. Pople, *Proc. Roy. Soc.*, **A205**, 163 (1951).
12) D. Eisenberg and W. Kauzmann, "The Structure and Properties of Water," Oxford at Clarendon Press (1969).
13) T. T. Wall and D. F. Hornig, *J. Chem. Phys.*, **43**, 2079 (1965).
14) M. Falk and T. A. Ford, *Can. J. Chem.*, **44**, 1699 (1966).
15) E. U. Franck and K. Roth, *Discuss. Faraday Soc.*, **43**, 108 (1967).
16) L. Hall, *Phys. Rev.*, **73**, 775 (1948); T. A. Litovitz and E. H. Carnivale, *J. Appl. Phys.*, **26**, 816 (1955); A. H. Smith and A. W. Lawson, *J. Chem. Phys.*, **22**, 351 (1954).
17) R. H. Fowler and E. A. Guggenheim, "Statistical Thermodynamics," Cambrige University Press (1939).
18) A. H. Narten, M. D. Danford and H. A. Levi, *Discuss. Faraday Soc.*, **43**, 97 (1967).
19) M. D. Danford and H. A. Levi, *J. Amer. Chem. Soc.*, **84**, 3965 (1962).
20) O. Ya. Samoilov and T. A. Nosova, *Zh. Strukt. Khim.*, **6**, 798 (1965).
21) J. Morgan and B. E. Warren, *J. Chem. Phys.*, **6**, 666 (1938).
22) C. M. Davis and T. A. Litovitz, *ibid.*, **42**, 2563 (1965).

energy of molecules on α and β-sites, respectively, and N is the total number of molecules. We define as usual the degree of order, s, in relation to N_α and N_β.

$$N_\alpha = \frac{N(1+s)}{2},\ N_\beta = \frac{N(1-s)}{2} \tag{4}$$

Introducing Eq. (4) into Eq. (2), we obtain the combinatorial factor, *viz.*,

$$W = \left[\frac{N!}{\left\{\frac{N(1+s)}{2}\right\}!\left\{\frac{N(1-s)}{2}\right\}!}\right]^2 \tag{5}$$

The degree of order, s, is determined by minimization of the Helmholtz energy, A, with respect to s. Thus, in equilibrium, we have

$$\frac{\partial A}{\partial s} = 0 \tag{6}$$

where

$$A = -kT\ln Z \tag{7}$$

In carrying out calculation, Bragg and Williams's approximation[17] concerning the relation between the energy for the exchange of molecules on different kinds of sites and the degree of order s is applied.

When the approximation is made as usual, $V_\beta - V_\alpha$ should be proportional to s. Thus, we have

$$V_\alpha = \frac{V^0(1+s)}{2},\ V_\beta = \frac{V^0(1-s)}{2} \tag{8}$$

from the consideration that $V_{\alpha,s=0} = V_{\beta,s=0}$ in the completely-disordered state. This condition is regarded as a special case of $\mu_{\alpha,s=0} = \mu_{\beta,s=0}$ where μ_α and μ_β are chemical potentials of the molecule on each site. Thus, in the present case, $V_{\alpha,s=0} \neq V_{\beta,s=0}$,*1 because the molecular partition function f_α is not identical with f_β.

Let us put

$$V_\alpha = V_\alpha^0\left(\frac{1+s}{2}\right),$$
$$V_\beta = V_\beta^0\left(\frac{1-s}{2}\right) \tag{8'}$$

and $V_\alpha^0 \neq V_\beta^0$.

We assume that at boiling point a complete randomness is realized. Thus, s should vanish at boiling point, and the chemical potential of the molecule on α-site should be equal to that on β-site at that temperature, as follows:

$$\frac{V_\alpha^0}{2} - kT_b\ln(f_\alpha)_{T=T_b} = \frac{V_\beta^0}{2} - kT_b\ln(f_\beta)_{T=T_b} \tag{9}$$

and we have

$$V_\alpha^0 - V_\beta^0 = -2kT_b\ln\left(\frac{f_\beta}{f_\alpha}\right)_{T=T_b} \tag{9'}$$

where a subscript b represents boiling point. When Eqs. (5), (7), (8') and (9') are inserted into Eq. (6), we obtain

$$\ln\left(\frac{1+s}{1-s}\right) = -\frac{1}{4kT}(V_\alpha^0 + V_\beta^0)\,s + \frac{1}{2}\left\{\frac{T_b}{T}\ln\left(\frac{f_\beta}{f_\alpha}\right)_{T=T_b} - \ln\left(\frac{f_\beta}{f_\alpha}\right)\right\} \tag{10}$$

Equation (10) is a fundamental equation which determines s as a function of temperature. The second term on the right hand side of Eq. (10) vanishes at $s=0$ ($T=T_b$) more rapidly with the decrease of s than the first term. The usual procedure in the application of Bragg and Williams's approximation can be used. We have

$$V_\alpha^0 + V_\beta^0 = -8kT_b \tag{11}$$

and

$$V_\alpha^0 = -kT_b\left\{4 + \ln\left(\frac{f_\beta}{f_\alpha}\right)_{T=T_b}\right\} \tag{12}$$

$$V_\beta^0 = -kT_b\left\{4 - \ln\left(\frac{f_\beta}{f_\alpha}\right)_{T=T_b}\right\} \tag{12'}$$

Combining Eqs. (11) and (12) with Eq. (10), we have

$$\ln\left(\frac{1+s}{1-s}\right) = \frac{2T_b}{T}s + \frac{1}{2}\left\{\frac{T_b}{T}\ln\left(\frac{f_\beta}{f_\alpha}\right)_{T=T_b} - \ln\left(\frac{f_\beta}{f_\alpha}\right)\right\} \tag{13}$$

Eq. (13) is used for the calculation of s. Introducing Eqs. (4), (12) and (12') into Eq. (3), we have

$$H = -NkT_b(1+s^2) - \left\{\frac{NkT_b}{2}\ln\left(\frac{f_\beta}{f_\alpha}\right)_{T=T_b}\right\}s \tag{14}$$

Thus, we can calculate the Helmholtz energy A, internal energy E, and entropy S, from the following equations.

$$A = -NkT\{2\ln 2 - (1+s)\ln(1+s) - (1-s)\ln(1-s) + \frac{(1+s)}{2}\ln f_\alpha + \frac{(1-s)}{2}\ln f_\beta\} - NkT_b(1+s^2) - \left\{\frac{NkT_b}{2}\right)\ln\left(\frac{f_\beta}{f_\alpha}\right)_{T=T_b}\Big\}s \tag{15}$$

$$E = \frac{NkT^2}{2}\left\{\left(\frac{1+s}{f_\alpha}\right)\frac{\partial f_\alpha}{\partial T} + \left(\frac{1-s}{f_\beta}\right)\frac{\partial f_\beta}{\partial T}\right\} - NkT_b(1+s^2) - \left\{\frac{NkT_b}{2}\ln\left(\frac{f_\beta}{f_\alpha}\right)_{T=T_b}\right\}s \tag{16}$$

$$S = \frac{(E-A)}{T} \tag{17}$$

The molecular partition function for each site, f_α and f_β, are given by the following equations.[2]

$$f_\alpha = \prod_{i=1}^{6}\left\{1 - \exp\left(\frac{-h\nu_i}{kT}\right)\right\}^{-1} \tag{18}$$

*1 In an ordinary application of Bragg and Williams's approximation the difference between f_α and f_β is not taken into account. Thus, from the equal probability for the occupation of each site at $s=0$, it necessarily follows from the general condition $\mu_{\alpha,s=0} = \mu_{\beta,s=0}$ that $V_{\alpha,s=0} = V_{\beta,s=0}$.

$$f_\beta = \prod_{i=1}^{3} \left\{1 - \exp\left(\frac{-h\nu'_i}{kT}\right)\right\}^{-1} \cdot \frac{(8\pi kT)^{3/2}(\pi ABC)^{1/2}}{2h^3} \quad (19)$$

ν_i is the frequency of intermolecular vibration for α-site which includes translational and rotational ones. ν_i' is the frequency of translational vibrations for β-site. A, B and C are principal moments of inertia of water molecule. In the derivation of Eq. (19), the molecules on β-sites are assumed to be free rotators. In the calculations of f_α and f_β, the contribution from intramolecular vibrations is nearly 1 at temperatures 0—100°C, and thus ignored.

Results

Procedure of Calculation. As seen in Eq. (12), $V_\alpha{}^0$ is the potential energy of water molecules on α-sites at the completely-ordered state ($s=1$, 0°K) so that it is twice the energy for breaking hydrogen bond. The amount of energy can be calculated from Eq. (12) without any additional assumptions. The energy difference, ε, between the molecules on β-sites and those on α-sites is obtained as follows.

$$\varepsilon = V_\beta - V_\alpha = NkT_b\left\{4s + \ln\left(\frac{f_\beta}{f_\alpha}\right)_{T=T_b}\right\} \quad (20)$$

We evaluated the magnitude of ε at $s=1$ to be 4.33 kcal/mol and at $s=0$ 1.36 kcal/mol. The energy difference between two species of molecules for various treatments based on two state model is tabulated in Table 1. The values are distributed within the range 2.4—4.5 kcal/mol. Our value seems to be reasonable on the average compared with those by others.

Table 1. Energy difference between both sites

Authors	Energy (kcal/mol)	Reference
Nemethy and Scheraga	2.64	(a)
Vand and Senior	2.8	(b)
Worley and Klotz	2.4	(c)
Walrafen	2.5	(d)
Scatchard *et al.*	3.4	(e)
Lawson *et al.*	3	(f)
Pauling	4.5	(g)
previous paper of authors	3.0	(h)
present paper $s=1$	4.33	
$s=0.5$	2.85	
$s=0$	1.36	

(a) Reference 3.
(b) Reference 32.
(c) J. D. Worley and I. M. Klotz, *J. Chem. Phys.*, **45**, 2868 (1966).
(d) G. E. Walrafen, *ibid.*, **48**, 244 (1968).
(e) G. Scatchard, G. M. Kavanagh and L. B. Tincknor, *J. Amer. Chem. Soc.*, **74**, 3715 (1952).
(f) A. W. Lawson, R. Lowell and A. L. Jain, *J. Chem. Phys.*, **30**, 643 (1959).
(g) L. Pauling, "The Nature fo the Chemical Bond," 3rd Ed., Cornell, Ithaca, New York (1960).
(h) Reference 2.

The degree of order, s, is within the range of 0—1 at temperatures from 100°C to 0°K. The equilibrium value of s at a given temperarute is determined graphically using Eq. (13) as shown in Fig. 2, where the lines (a), (b) and (c) are the plot of the right hand side of Eq. (13) at 0, 50 and 100°C, respectively. The calculated values of s are plotted against temperature in Fig. 3. The obtained value of s at 0°C is 0.83.

In the assignment of intermolecular vibration of water molecules, there are some ambiguities.[1-3] For the three modes of translational vibrations on

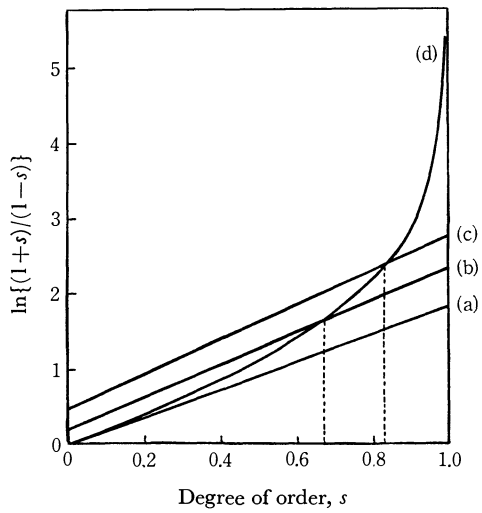

Fig. 2. Determination of the magnitude of s at equilibrium.
(a) 0°C, (b) 50°C, (c) 100°C,
(d) $\ln\{(1+s)/(1-s)\}$

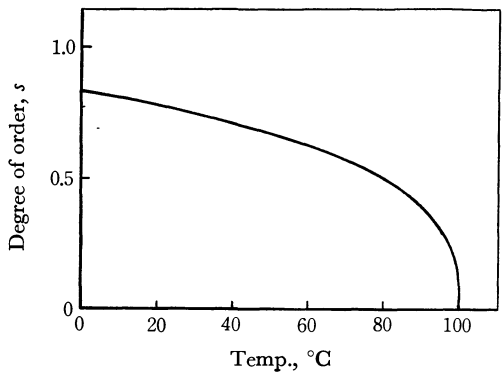

Fig. 3. Temperature dependence of degree of order s.

each site, a common value of 180 cm^{-1} [23] is assigned, and 500, 650 and 750 cm^{-1} are assigned[24,25,2] for each mode of librations for α-site. The principal moments of inertia for a free rotator molecule is the same as in vapor state; $A=1.024\times10^{-40}$, $B=1.921\times10^{-40}$, and $C=2.947\times10^{-40}$ [2,26]

Calculation of Thermodynamic Variables. With the value of s determined graphically, calculation of thermodynamic functions has been made over the temperature range 0—100°C at 10°C intervals. The obtained values of Helmholtz energy A, internal energy E and entropy S are given in Table 2, and are plotted against temperature in Fig. 4—6. The results calculated are compared with the observed data for water.[27] The fraction $x=(1+s)/2$ of the molecules on α-sites is tabulated

TABLE 2. THERMODYNAMIC VARIABLES

Temp. (°C)	$A_{calc.}$ (kcal/mol)	$A_{obs.}$	$E_{calc.}$ (kcal/mol)	$E_{obs.}$	$S_{calc.}$ (cal/deg mol)	$S_{obs.}$	x
0	−0.91	−1.20	1.59	2.75	9.11	14.5	0.915
10	−1.00	−1.35	1.72	2.95	9.60	15.1	0.903
20	−1.10	−1.50	1.87	3.11	10.1	15.7	0.890
30	−1.14	−1.66	2.01	3.29	10.4	16.3	0.875
40	−1.29	−1.83	2.15	3.47	11.0	16.9	0.859
50	−1.41	−2.00	2.35	3.65	11.6	17.5	0.836
60	−1.49	−2.17	2.55	3.83	12.1	18.1	0.806
70	−1.64	−2.36	2.72	4.01	12.7	18.6	0.784
80	−1.77	−2.55	2.94	4.20	13.4	19.1	0.749
90	−1.91	−2.74	3.15	4.36	13.9	19.6	0.713
100	−2.05	−2.94	3.78	4.55	15.6	20.0	0.500

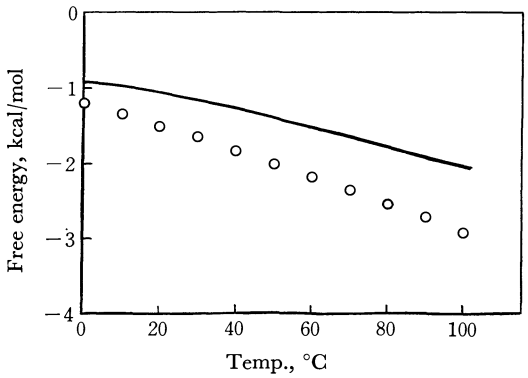

Fig. 4. Free energy, A, for water.
Circle, observed; Solid line, calculated

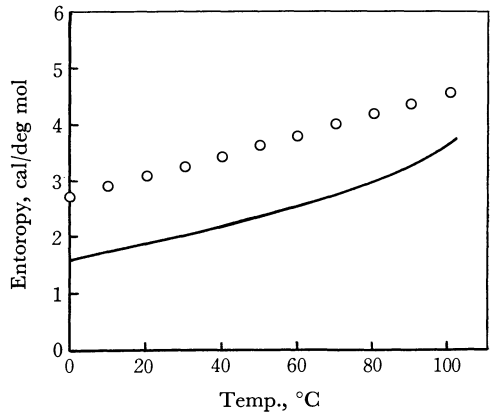

Fig. 5. Internal energy, E, for water.
Circle, observed; Solid line, calculated

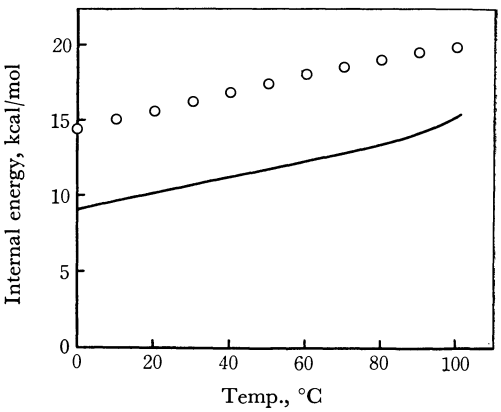

Fig. 6. Entropy, S, for water.
Circle, observed; Solid line, calculated

together with other thermodynamic variables in Table 2. The calculated value of A are satisfactory on the whole. The calculated value of E increases rapidly with increasing temperature at higher temperatures. This can be interpreted by the variation of s with rising temperature, which falls off rapidly near boiling point. But deviation of the calculated results from experimental data is not so large. Agreement of thermodynamic functions calculated with observed values is satisfactory, taking into account the fact that no adjustable parameters are used in the present calculation as in the former theories.

Discussion

Cooperative Formation and Destruction of Ice-like Structure in Liquid Water. From various kinds of relaxational processes in water, Frank and Wen[28] pointed out that the lifetime of ice-like

23) M. Magat, *Discuss. Faraday Soc.*, **43**, 145 (1967).
24) P. A. Giguere and K. B. Harvey, *Can. J. Chem.*, **34**, 798 (1956).
25) G. E. Walrafen, *J. Chem. Phys.*, **40**, 3249 (1964); P. C. Cross, J. Burnham and P. A. Leighton, *J. Amer. Chem. Soc.*, **59**, 1134 (1937).
26) R. P. Marchi and H. Eyring, *J. Phys. Chem.*, **68**, 221 (1964).
27) N. E. Dorsey, "Properties of Ordinary Water Substances," ACS Monograph, No. 81, Reinhold, New York (1940).
28) H. S. Frank and W.-Y. Wen, *Discuss. Faraday Soc.*, **24**, 481 (1957).

structure in liquid water was the order of 10^{-11}—10^{-10} sec. The cooperative nature of the formation and destruction of ice-like structure (clusters) has been pointed out by many workers. However, the cooperative effect itself has never been directly treated theoretically in these studies. Consequently, the clusters in liquid water have been treated like a "solid". Gurikov[29] criticized Némethy and Scheraga's theory, in this respect. Perram and Levine[30] also pointed out an inadequate procedure in Némethy and Scheraga's theory in which geometrically impossible configurations of five species were included for the calculation of the combinatorial factor. In the present situation of the structure theory of water, it is emphasized that the cooperative process of cluster formation should be introduced directly in forming the theory. Thus, we have introduced the cooperative nature of cluster formation through the application of the order-disorder theory on the basis of a two state model.[19,20] This is an essential feature in the present theory.

Parameters used in Theories. In this study, the degree of order, s, has been used as only one parameter, which determines all thermodynamic variables of water. The value of s at equilibrium has been determined by minimizing the free energy. Thus, this theory has no adjustable parameter practically. In Némethy and Scheraga's theory, free volume, v_f, and energy difference, ε, between the tetra-hydrogen-bonded state and the unbonded state were used as adjustable parameters. In our previous paper,[2] v_f and ε were used as adjustable parameters, which were determined to give the best fit to experimental data as made in Némethy and Scheraga's theory. Thus, the present theory has a merit that no adjustable semi-empirical parameters are used.

Weissmann and Blum[31] have recently reported a cell theory in which no adjustable parameter is used. However, their results are far from the observed data. The calculated values in the present theory are seen in fair agreement with observed ones.

Two State Theory and Distorted Hydrogen Bond Theory. The multi-state theories of water have been developed in various forms: Némethy and Scheraga's five species model, Vand and Senior's continuous energy band model[32] and Buijs and Choppin's three state model.[33] We pointed out previously that two state theory could explain most of the observed data as well as multi-state theories. Various multi-state theories are practically reduced to two state theories. The number of states corresponds to the number of parameters which are introduced in the theory. In constructing a theory, the number of parameters is desired to be as small as possible. In this respect, a two state model is superior to a multi-state model consisting of more than two species.

In the discussion of the first report of this series of studies, the authors referred to the presence of a "third state" or "surface state" on the cluster. However, the emphasis of "surface state" has turned out to be inadequate, considering the very short lifetime and the cooperative nature of cluster formation.

On the other hand, various uniform-state models (distorted hydrogen-bonded model) have been proposed by several workers since the presentation of Pople's theory.[11] Eisenberg and Kauzmann[12] have recently claimed that, with rising temperature, hydrogen bonds of water molecules are bent rather than broken. However, concerning the uniform-state model, there are several shortcomings in the explanation of the structure and properties of water. Firstly, the cooperative behavior of cluster formation in liquid water can not be explained by the uniform-state theory. Secondly, the data of ultrasonic absorption have never been explained by the uniform-state theory, while Hall and others[16] succeeded in describing those data using a two state model.

Furthermore, the nature of "hydrophobic interaction" has never been explained by the uniform-state theory, but Némethy and Scheraga succeeded in explaining it by the multi-state theory.[34]

Thus, it may be said that the structure and properties of water have never been described successfully by any uniform-state theory.

The Energy Difference ε between Two States. In our results, the energy difference between both sites continuously decreases as the degree of order decreases with increasing temperature. The magnitude of ε (4.33 kcal/mol at $s=1$ and 1.36 kcal/mol at $s=0$) at each temperature is seem to be reasonable. Up to this time, the energy difference between two structures in the two state theories has been regarded as a constant value in the range of temperature 0—100°C. However, the circumstances of molecules vary with rising temperature, so that the energy difference should decrease as a result of cooperative process. The present theory has succeeded in describing the variation of ε with rising temperature.

29) Yu. V. Gurikov, *J. Struct. Chem.*, (translation of *Zh. Strukt. Khim.*), **6**, 786 (1966).

30) J. W. Perram and S. Levine, *Discuss. Faraday Soc.*, **43**, 131 (1967).

31) M. Weissmann and L. Blum, *Trans. Faraday Soc.*, **65**, 2605 (1969).

32) V. Vand and W. A. Senior, *J. Chem. Phys.*, **43**, 1869, 1873, 1878 (1965).

33) K. Buijs and G. R. Choppin, *ibid.*, **39**, 2035 (1963).

34) G. Némethy and H. A. Scheraga, *ibid.*, **36**, 3401 (1962).

BULLETIN OF THE CHEMICAL SOCIETY OF JAPAN VOL. 43 3054—3063 (1970)

A Nuclear Magnetic Resonance Study of Copolypeptides of L-Proline with γ-Benzyl-L-glutamate*1,1)

Hirofumi Okabayashi,*2 Rume Sakai and Toshizo Isemura

Division of Physical Chemistry, Institute for Protein Research, Osaka University, Kita-ku, Osaka

(Received April 4, 1970)

The nuclear magnetic resonance spectra of the copolymers of L-proline with γ-benzyl-L-glutamate were measured in tetradeuteroacetic acid, deuterochloroform, a mixed solvent (CD_3COOD : $CDCl_3$=4 : 1), and trifluoroacetic acid. The time dependence of the α-CH resonance peaks of copoly-(3 : 1)-(L-proline, γ-benzyl-L-glutamate) and copoly-(1 : 1)-(L-proline, γ-benzyl-L-glutamate) was observed. The NMR spectra of copoly-(1 : 3)-(L-proline, γ-benzyl-L-glutamate) showed no time dependence which can be ascribed to the conformational change in tetradeuteroacetic acid and the mixed solvent. From these experimental facts we concluded that copoly-(3 : 1)-(L-proline, γ-benzyl-L-glutamate) and copoly-(1 : 1)-(L-proline, γ-benzyl-L-glutamate) can assume a poly-L-proline-like helical structure, while copoly-(1 : 3)-(L-proline, γ-benzyl-L-glutamate) can not. Moreover, the ratios of the γ-benzyl-L-glutamate residues which were incorporated into the stable poly-L-proline-II-like helical structure was estimated in copoly-(3 : 1)-(L-proline, γ-benzyl-L-glutamate) and copoly-(1 : 1)-(L-proline, γ-benzyl-L-glutamate).

Poly-L-proline can assume two different conformations, namely, the forms I and II. The structure of poly-L-proline II has been determined by the X-ray diffraction method by Cowan and McGavin[2] and Sasisekharan,[3] who found that the II form has a left-handed helix and that the peptide bonds are in a *trans* configuration. Traub and Shmueli[4] have also found by the X-ray diffraction method that the I form assumes a right-handed helix and that each peptide bond is in a *cis* configuration.

The poly-L-proline takes the I form immediately after the sample is dissolved in organic acids, water, and *m*-cresol. However, it is eventually transformed into the II form.

The first NMR spectra of the poly-L-prolines I and II were reported by Okabayashi, Sakai, and Isemura,[5–7] who observed a marked difference in the magnetic shielding values of the α-CH resonance peaks of the two polymers. The α-CH peaks of the I form appeared at the shielding values of 5.5 ppm in the mixed solvent (deuterochloroform : tetradeuteroacetic acid=8 : 1) and 5.4 ppm in tetradeuteroacetic acid, while that of the poly-L-proline II appeared at 5.2 ppm in tetradeuteroacetic acid. The marked shift of the α-CH resonance peak has been ascribed to the differences in the conformations of the two polymers. During the course of the I→II transition of poly-L-proline in tetradeuteroacetic acid, the two α-CH resonance peaks were observed at 5.2 and 5.4 ppm. However, when the spectrum was measured immediately after the sample has been dissolved in tetradeuteroacetic acid as rapidly as possible, the only α-CH resonance peak of the I form appeared at the magnetic shielding value of 5.4 ppm. The appearance of the α-CH resonance peak of the II form at 5.2 ppm and a gradual increase in the intensity of the resonance peak with the time was observed, whereas the α-CH resonance peak of the I form showed an accompanying decrease in intensity with the time (see Fig. 1).

*1 This paper was presented at the 8th Symposium on Biophysics of the Biophysical Society of Japan, October, 1969, and at the Symposium on Molecular Structures of the Chemical Society of Japan, October, 1969.

*2 Present address: Department of Industrial Chemistry, Nagoya Institute of Technology, Gokiso, Showa-ku, Nagoya.

1) H. Okabayashi and T. Isemura, Abstracts for Symposium on Molecular Structures (October, 1969), p. 199.

2) P. Cowan and S. McGavin, *Nature*, **176**, 501 (1955).

3) V. Sasisekharan, *Acta Cryst.*, **12**, 897 (1959).

4) W. Traub and U. Shmueli, "Aspects of Protein Structure," ed. by G. N. Ramachandran, Academic Press, New York (1963), p. 81.

5) H. Okabayashi, R. Sakai and T. Isemura, Abstract IV, at the 21st Annual Meeting of the Chemical Society of Japan, April, 1968, p. 2685.

6) H. Okabayashi, R. Sakai and T. Isemura, "Abstract", presented at the Symposium on High Polymers of the Chemical Society of Japan, October, 1968, p. 721.

7) R. Sakai, H. Okabayashi and T. Isemura, This Bulletin, **42**, 3028 (1969).

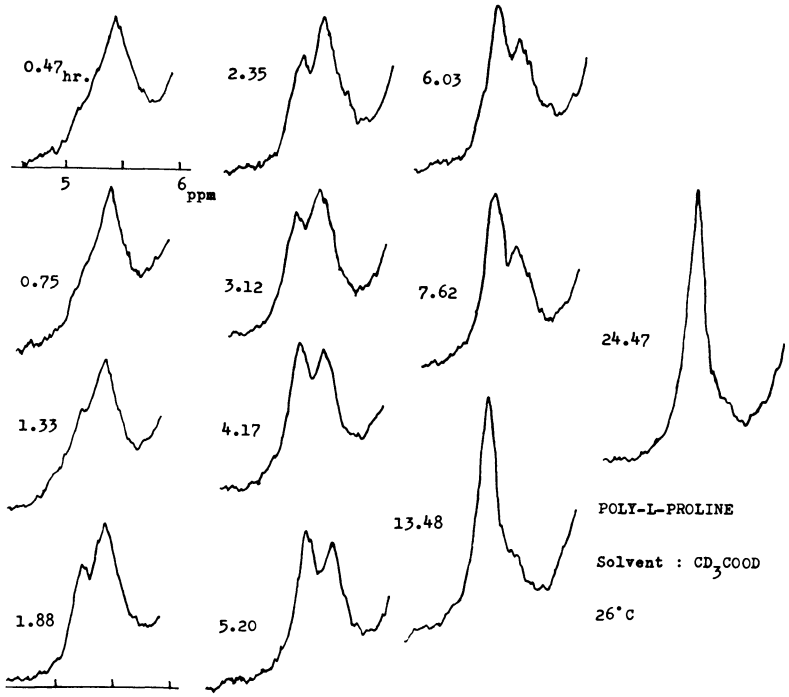

(a) at 26°C

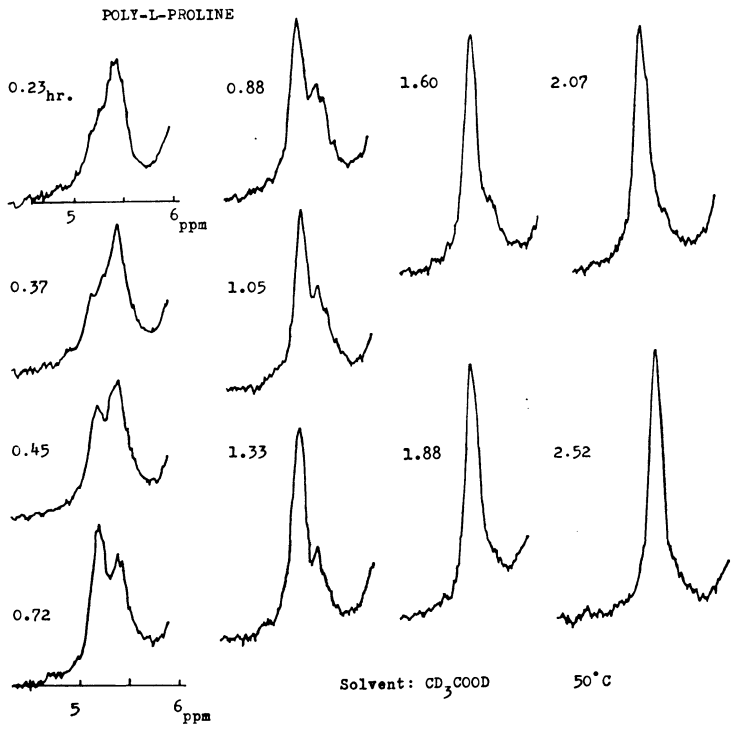

(b) at 50°C

Fig. 1. The time dependence of the NMR spectra of poly-L-proline.

If the temperature is raised, such a transition progresses rapidly. From the ratios of the areas of the α-CH peaks of the I form to those of the II form, the percentages of the I form (or of the II form) during the transition were estimated. The results showed that the α-CH resonance peak of the I form disappeared in thirty hours at 26°C and that the I→II transition was completed within three hours at 50°C. The I→II transition can be concluded to proceed more rapidly than indicated by the measurement by means of the optical rotations.[6]

These studies have now been extended to copolypeptides of L-proline with γ-benzyl-L-glutamate.

In this work the NMR spectra of copoly-(3 : 1)-(L-proline, γ-benzyl-L-glutamate),*3 copoly-(1 : 1)-(L-proline, γ-benzyl-L-glutamate),*3 and copoly-(1 : 3)-(L-proline, γ-benzyl-L-glutamate)*3 were measured and compared with those of the poly-L-prolines I and II and poly-γ-benzyl-L-glutamate.

The steric structures of the copolymers of L-proline with γ-benzyl-L-glutamate in organic solvents have been investigated by Sakai, Ikeda, and Isemura[8] using the methods of the optical rotatory dispersion and the infrared absorption spectra. The results may be summarized as follows.

In 1,2-dichloroethane, which stabilizes the poly-L-proline-I helix and the α-helix of poly-γ-benzyl-L-glutamate, proline residues assume the *cis*-configuration if the copolymers have a proline content of more than 50%. On the other hand, in the copolymers with proline contents of less than 50%, the proline residues tend to take the *trans*-configuration. In an α-helicogenic solvent such as *m*-cresol, the proline residues of the copolymers have the *trans*-configuration, and most benzyl glutamate residues are in random coils in dichloroacetic acid.

Experimental

These copolypeptides, copoly-(3 : 1)-(L-proline, γ-benzyl-L-glutamate), copoly-(1 : 1)-(L-proline, γ-benzyl-L-glutamate), and copoly(1 : 3)-(L-proline, γ-benzyl-L-glutamate), which has been synthesized by one of the present authors, were used in these studies. Table 1 shows the residue mole fractions of the L-proline of the copolymers.[9]

Table 1. Residue mole fraction of L-proline in the copolymers

	A	B	C
Copoly-(3:1)	0.75	0.767	0.756
Copoly-(1:1)	0.50	0.535	0.528
Copoly-(1:3)	0.24	0.274	0.260

A : polymerization ratio,
B : fraction of proline determined from amino acid analysis
C : from absorbance of benzyl residues.

These copolypeptides were synthesized by the copolymerization of *N*-carboxy anhydrides of L-proline and γ-benzyl-L-glutamate in nitrobenzene.

The deuterochloroform (isotopic purity: 99%), tetradeuteroacetic acid (isotopic purity: 99%), trifluoroacetic acid, and tetramethylsilane for spectroscopy were purchased from Merck, Ltd; they were used without further purification.

All the proton magnetic resonance spectra were measured at 100 MHz with the use of a Japan Electron Optics Laboratory (Jeolco), model JNM-4H-100, NMR spectrometer.

A 5% solution of the copolypeptides was used at 26°C in all the experiments.

Results and Discussion

Figure 2 shows the NMR spectra of poly-L-prolines I and II, which were reported in our previous papers.[6,7] All the resonance peaks are fully developed, and their relative areas are proportional to the numbers of protons at the different sites in the polymers. In tetradeuteroacetic

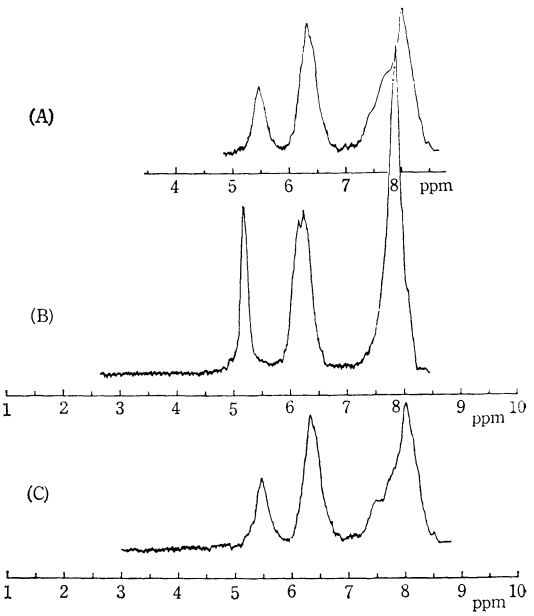

Fig. 2. The NMR spectra of poly-L-prolines I and II in three solvents at 26°C.
(A) Polyproline I
Solvent: CD_3COOD Reference: TMS
(B) Poly-L-proline II
Solvent: CD_3COOD Reference: TMS
(C) Poly-L-proline I
Solvent: $CDCl_3$: CD_3COOD=8 : 1

*3 Abbreviations used: Copoly-(3 : 1), copoly-(3 : 1)-(L-proline, γ-benzyl-L-glutamate); Copoly-(1 : 1), copoly-(1 : 1)-(L-proline, γ-benzyl-L-glutamate); Copoly-(1 : 3), copoly-(1 : 3)-(L-proline, γ-benzyl-L-glutamate).

8) R. Sakai, S. Ikeda and T. Isemura, This Bulletin, **42**, 1332 (1969).

9) R. Sakai, S. Ikeda and T. Isemura, This Bulletin, **39**, 2308 (1966).

acid the α-CH resonance peak of the I form completely disappeared at 26°C in thirty hours, thereafter only the α-CH resonance peak of the II form was observed, at 5.2 ppm. At 45°C the α-CH peak of the I form disappeared within five hours. During the I→II transition of poly-L-proline, no line broadening or decrease in area was observed.

Figure 3 shows the NMR spectra of poly-γ-benzyl-L-glutamate and those of poly-L-proline in trifluoroacetic acid. Table 2 gives the resonance positions of the NMR spectra of two poly-L-prolines and poly-γ-benzyl-L-glutamate. Bovey's data[10] are also listed in this table.

It is of interest to ascertain whether the changes in the α-CH resonance peak found in the NMR spectra of poly-L-proline can be observed in the copolypeptides of L-proline with γ-benzyl-L-glutamate.

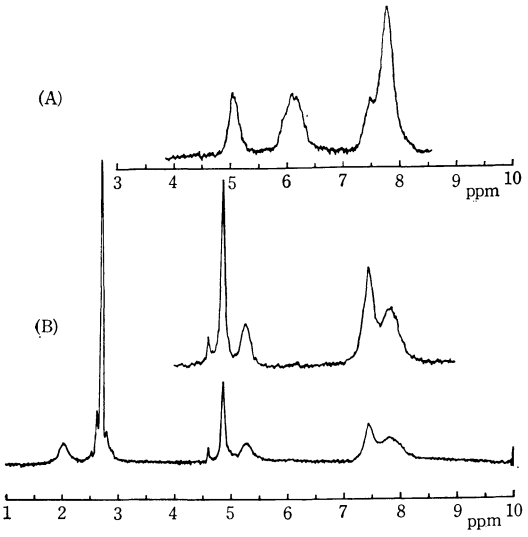

Fig. 3. The NMR spectra of poly-γ-benzyl-L-glutamate and poly-L-proline in trifluoroacetic acid at 26°C.
(A) Poly-L-proline
Solvent: CF_3COOH Reference: TMS
(B) Poly-γ-benzyl-L-glutamate
Solvent: CF_3COOH Reference: TMS

TABLE 2. NUCLEAR MAGNETIC RESONANCE SPECTRA OF POLY-L-PROLINE AND POLY-γ-BENZYL-L-GLUTAMATE AT 26°C

(a) Poly-L-prolines I and II

τ-values relative to internal reference				
CF_3-COOH	CD_3COOD		mixed solvent	assignments
	I*	II	I	
5.05	5.40	5.23	5.50	α-CH
6.15	6.30	6.25	6.30	δ-CH_2
7.50, 7.79	8.0	7.90	7.80, 8.0	β, γ-CH_2

(b) Poly-γ-benzyl-L-glutamate

τ-values relative to internal reference		
CF_3COOH	Bovey's data (CF_3COOH)	assignments
2.05	1.84	NH
2.73	2.54	phenyl group
4.88	4.74	benzylic methylene
5.27	4.98	α-CH
7.45, 7.85	7.50	β, γ-CH_2

Internal reference: TMS
Mixed solvent: (CD_3COOD: $CHCl_3$=4: 1)
* The NMR spectra of the I form in tetradeuteroacetic acid were measured as soon as the sample was completely dissolved.

Figures 4, 5, and 6 show the NMR spectra of copoly-(3 : 1), copoly-(1 : 1) and copoly-(1 : 3) in tetradeuteroacetic acid, deuterochloroform, and a mixed solvent ($CDCl_3$: CD_3COOD=8 : 1). The assignments of the resonance peaks are given in Table 3.

In Fig. 4 especially, the NMR spectra of the copolypeptides in deuterochloroform and tetradeuteroacetic acid are remarkable. In deuterochloroform an α-CH resonance peak of the copoly-

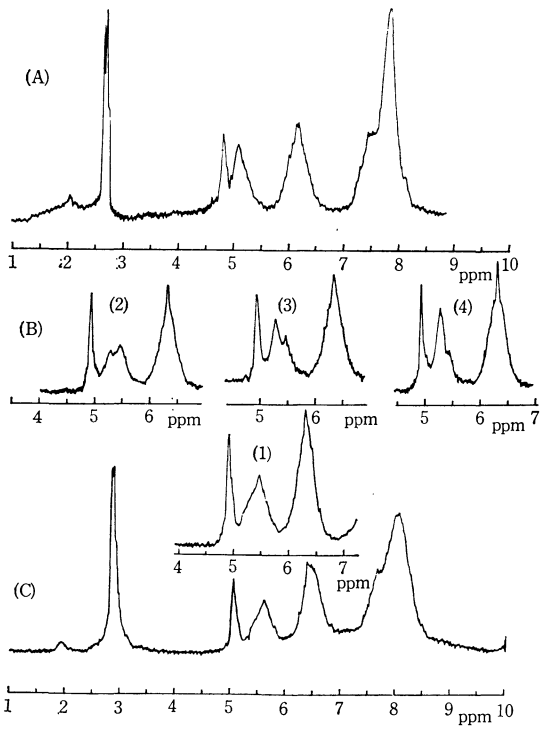

Fig. 4. The NMR spectra of copoly-(3: 1) at 26°C.
(A) Solvent: CF_3COOH
(B) Solvent: CD_3COOD
(1) after 10 min (2) after 30 min
(3) after 90 min (4) after 24 hr
(C) Solvent: $CDCl_3$

10) F. A. Bovey, G. V. D. Tiers and G. Filipovich, *J. Polym. Sci.*, **38**, 73 (1959).

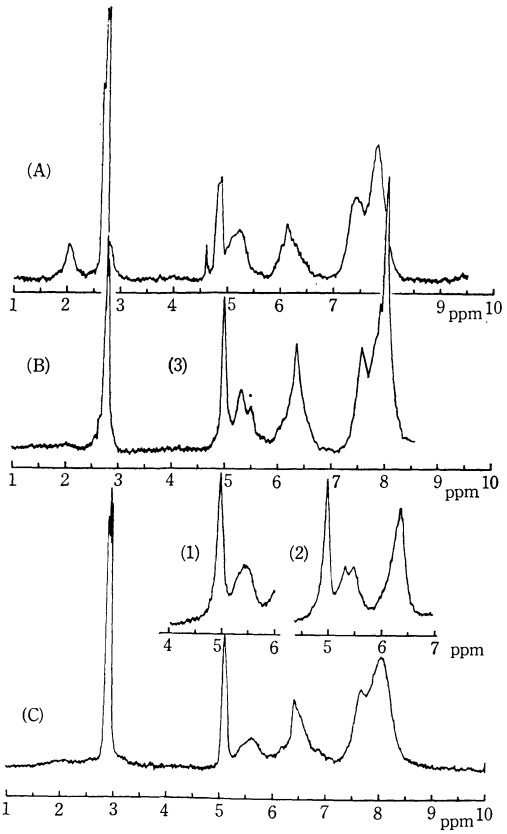

Fig. 5. The NMR spectra of copoly-(1 : 1) at 26°C.
(A) Solvent: CF_3COOH
(B) Solvent: CD_3COOD
(1) after 8 min (2) after 20 min
(3) after 24.85 hr
(C) Solvent: $CDCl_3$

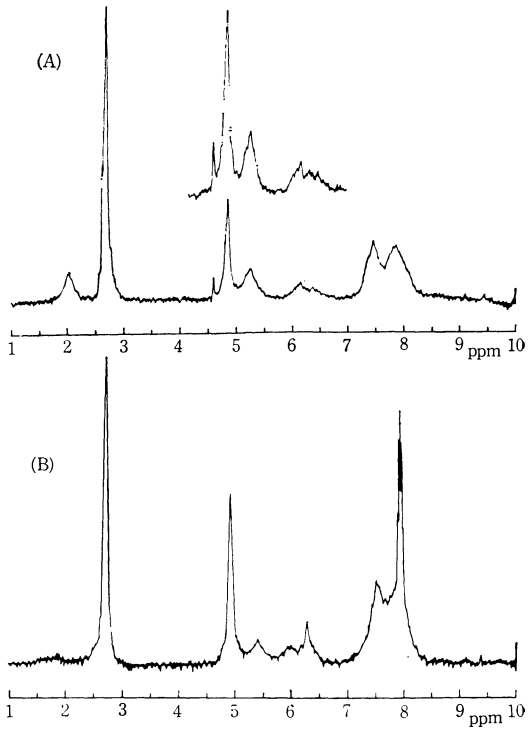

Fig. 6. The NMR spectra of copoly-(1 : 3) at 26°C.
(A) Solvent: CF_3COOH Reference: TMS
(B) Solvent: CD_3COOD : $CDCl_3$=4 : 1
Reference: TMS

(3 : 1) consists of only one component, which shows the agreement between the position of the α-CH resonance peak of the L-proline residues and that of the γ-benzyl-L-glutamate residues. Poly-γ-benzyl-L-glutamate in deuterochloroform has a right-handed α-helical structure, while the conformation of poly-L-proline in the solvent is considered to be a poly-L-proline-I-like helix, since the value of $[\alpha]_{546}$ is +30° in the mixed solvent (CD_3COOD : $CDCl_3$= 1 : 8).

Figure 4 (B) shows the NMR spectra of the copoly-(3 : 1) in the tetradeuteroacetic acid solution. By measuring the spectra immediately after the sample has been completely dissolved as rapidly as possible, the symmetrical α-CH resonance peak was observed. The magnetic shielding value, 5.45 ppm, of the α-CH resonance peak is almost the same as that of the NMR spectra of poly-L-proline I in tetradeuteroacetic acid. After thirty minutes, the NMR spectrum of the copoly-(3 : 1) gives two components of the α-CH resonance peak at 5.2 and 5.45 ppm. The component of 5.2 ppm is in accord with the α-CH peak of the poly-L-proline II in the position. Considering the α-CH peak at 5.2 ppm, the copolypeptide can be said to assume the structure of the poly-L-proline II. The resonance peak at 5.2 ppm increases in intensity with the time, while the peak at 5.45 ppm decreases in intensity with the time, as in the case of the I→II transition of poly-L-proline. Such behavior of the α-CH resonance peak of copoly-(3 : 1) clearly shows that the copolypeptide has the poly-L-proline-like structure. In the NMR spectra of the copoly-(3 : 1), no line broadening or loss of the peak area of the α-CH resonance was observed during the poly-L-proline-I-like→II transition.

In Fig. 5 the α-CH resonance peak of the copoly-(1 : 1) shows a transition of poly-L-proline I→II similar to that in the case of the copoly-(3 : 1). This fact also suggests that the copoly-(1 : 1) partially assumes a helical structure as does poly-L-proline. In the α-CH resonance of the copoly-(1 : 1), a shoulder at 5.2 ppm was observed, with a main peak of the α-CH resonance at 5.4 ppm in tetra-

Table 3. Nuclear magnetic resonance τ-values for copolypeptides of L-proline with γ-benzyl-L-glutamate at 26°C

(a) Copoly-(3:1)-(L-proline, γ-benzyl-L-glutamate)

τ-Values relative to internal reference			assignments
CF_3COOH	CD_3COOD	$CDCl_3$	
—	—	1.95	NH of γ-benzyl-L-glutamate
2.70	2.65	2.88	phenyl group
4.82	4.90	5.06	benzylic methylene
5.10	5.45* 5.40** 5.23	5.60	α-CH
6.51	6.30	6.45	δ-CH_2 of prolyl residues
7.50 7.83	7.52 7.99	7.70 8.05	β, γ-CH_2 of γ-benzyl-L-glutamate and prolyl residues

* Obtained at ten minutes after the dissolution of the sample was completed.
** Obtained at 1.5 hr after the sample was completely dissolved.

(b) Copoly-(1:1)-(L-proline, γ-benzyl-L-glutamate)

τ-Values relative to internal reference			assignments
CF_3-COOH	CD_3-COOD	$CDCl_3$	
2.05	—	—	NH of γ-benzyl-L-glutamate
2.72	2.70	2.91	phenyl group
4.85	4.92	5.08	benzylic methylene
5.20	5.25 5.40	5.60	α-CH
6.15	6.32	6.40	δ-CH_2 of L-proline residues
7.40 7.80	7.56 8.03	7.65 8.03	β, γ-CH_2 of γ-benzyl-L-glutamate and L-proline residues

(c) Copoly-(1:3)-(L-prolin, γ-benzyl-L-glutamate)

τ-Values relative to internal reference		assignments
CF_3COOH	mixed solvent	
2.05		NH of γ-benzyl-L-glutamate
2.75	2.72	phenyl group
4.86	4.92	benzylic methylene
5.28	5.40	α-CH
6.2	6.30	δ-CH_2 of L-proline residues
7.45 7.85	7.52 7.95	β, γ-CH_2 of γ-benzyl-L-glutamate and L-proline residues

Internal reference: TMS
Mixed solvent: (CD_3COOD: $CDCl_3$=4 : 1)

deuteroacetic acid. In deuterochloroform, a shoulder at 5.4 ppm was also found, with a main peak of the α-CH resonance at 5.6 ppm. The shoulder at 5.2 ppm may be interpreted as a function of the helical lengths of the copoly-(1 : 1), in which the short chains of the L-proline residues take a poly-L-proline II-like helical structure, judging from the results of our NMR study[11].

Figure 6 shows the NMR spectra of the copoly-(1 : 3) obtained by using a mixed solvent (CD_3-COOD : $CDCl_3$=4 : 1) solution, since the copolypeptide can not be dissolved in tetradeuteroacetic acid. Although the α-CH resonance peak of the copoly-(1 : 3) appears at the magnetic shielding value of 5.4 ppm, a value which agrees with the position of the α-CH resonance of poly-L-proline I in tetradeuteroacetic acid solution, the α-CH resonance peak of this copolymers can probably be ascribed to that of γ-benzyl-L-glutamate residues, which are contained in ratios of 76% within the copoly- (1 : 3).

However, the poly-L-proline I→II transition could not be observed in the NMR spectra of copoly-(1 : 3). This result suggests that copoly-(1 : 3) can not assume a poly-L-proline-like helical structure. In this copolymer, there are scattered L-proline residues or short chains of L-proline which can not assume a I poly-L-proline-like structure, even the benzyl-L-glutamate assumes a right-handed helix. The shoulder which was observed around 5.2 ppm, with the main peak of the α-CH resonance at 5.4 ppm, should be ascribed to the short chain of L-proline residues.[11]

Further considerations, however, of the NMR spectra of the copoly-(3 : 1) and the copoly-(1 : 1) in tetradeuteroacetic acid are needed; they will be of great importance in ascertaining the ratios of the incorporation of γ-benzyl-L-glutamate residues into the stable II poly-L-proline-like helical structure. The α-CH resonance peak of the two copolypeptides should also be investigated in more detail.

Figure 7 also shows the time dependence of the α-CH resonance peak of the copoly-(3 : 1) and the copoly-(1 : 1) in tetradeuteroacetic acid and the mixed solvent at 26°C. The changes in intensity in the two components of the α-CH resonance peaks of the two copolypeptides seem to stop within five hours, and the resonance peak at 5.45 ppm remains unchanged. This fixing of the site of the α-CH resonance peaks can be ascribed to γ-benzyl-L-glutamate residues which were not incorporated into the poly-L-proline-like helical structure. Assuming that the conformation of the γ-benzyl-L-glutamate residues is independent of that of the L-proline residues in the copoly-(1 : 1), the two components of the α-CH resonance peak can be

11) H. Okabayashi and T. Isemura, This Bulletin, **43**, 359 (1970).

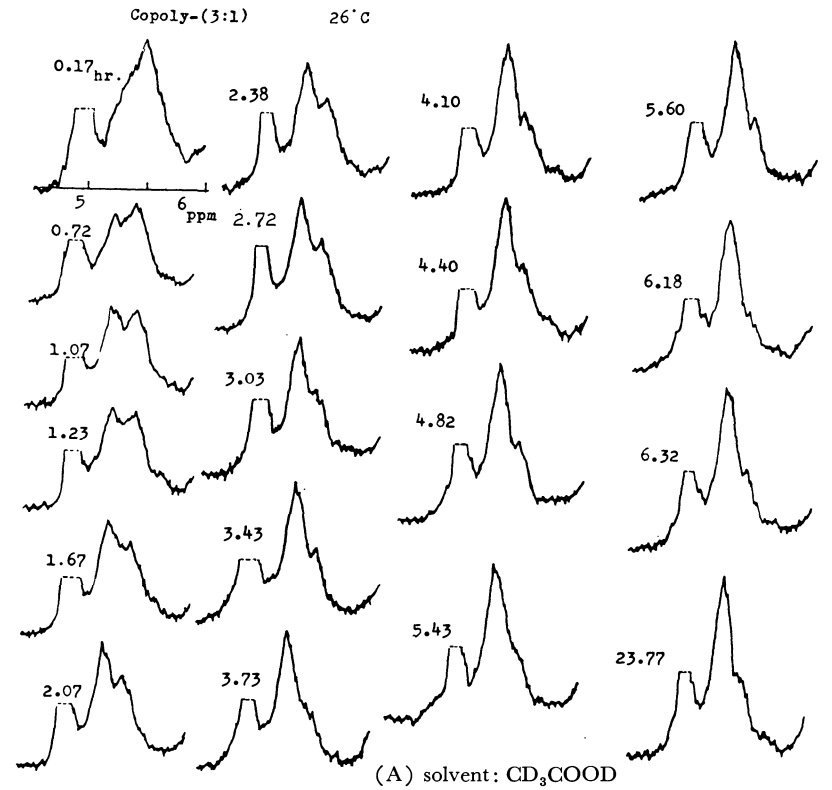

(A) solvent: CD_3COOD

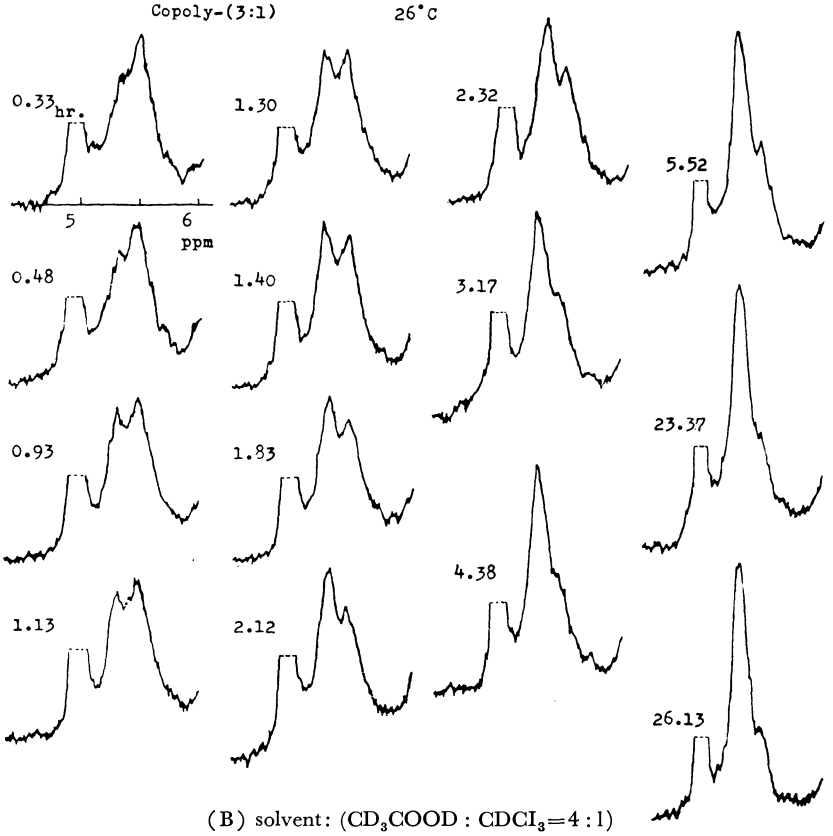

(B) solvent: (CD_3COOD : $CDCl_3$=4 : 1)

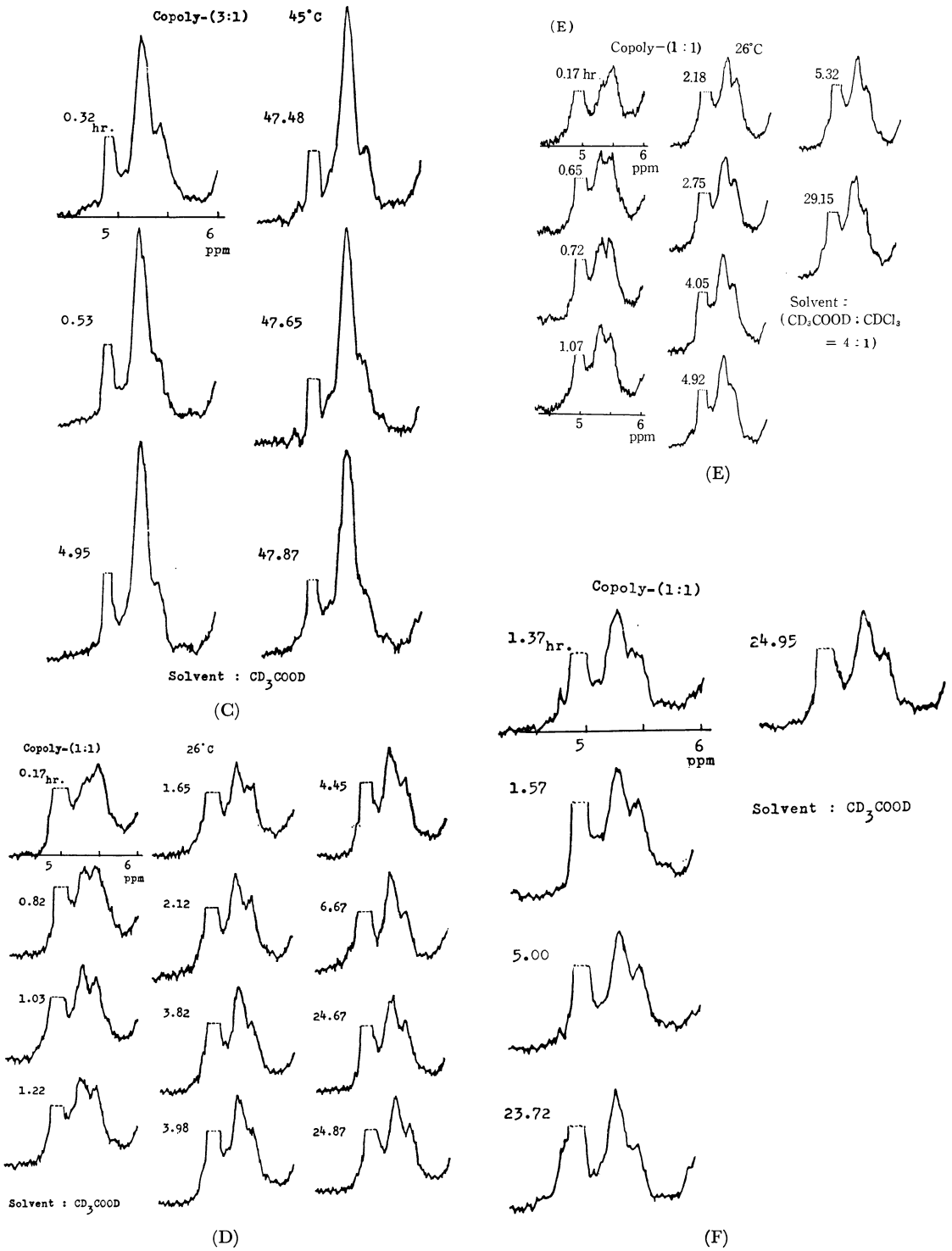

Fig. 7. The time-dependence of the α-CH resonance peak of the copoly-(3 : 1) and the copoly-(1 : 1) in tetradeuteroacetic acid and the mixed solvent (CD_3COOD : $CDCl_3$=4 : 1) at 26°C and 45°C.

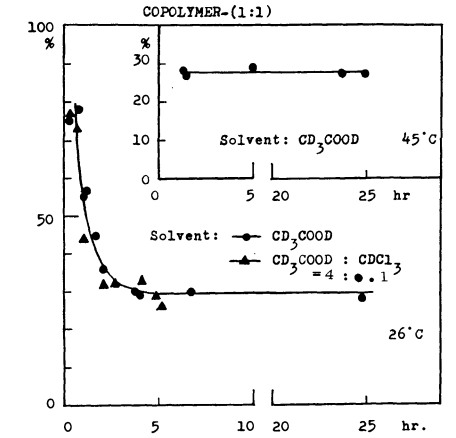

(A) copoly-(1 : 1)

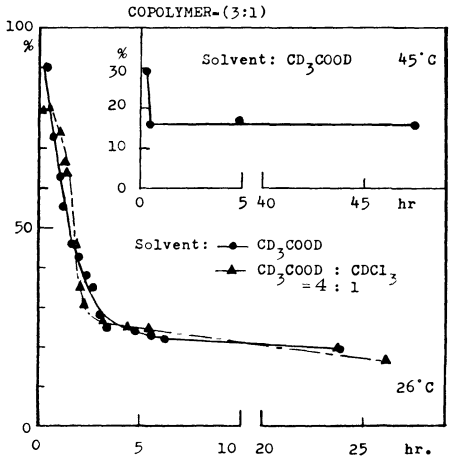

(B) copoly-(3 : 1)

Fig. 8. The time-dependence of the ratios of peak area of the α-CH resonance at 5.40_{ppm} to that of all the α-CH resonance peaks in the NMR spectra of copolypeptides at 26°C and 45°C.

expected to have approximately the same intensity after the transition is completed. However, contrary to our expectations, a great difference in the intensities of the two α-CH resonance peaks was observed. These experiments clearly show the incorporation of parts of the γ-benzyl-L-glutamate residues into the stable II poly-L-proline-like helical structure. The measurement of the areas of the two α-CH resonance peaks can be considered to be a method of estimating the content of the II poly-L-proline-like structure of the γ-benzyl-L-glutamate residues, since hardly no line broadening or decrease in the area of the two α-CH resonance peaks in the copoly-(3 : 1) was observed and since the decrease in the area in the copoly-(1 : 1) is invariable, without any line broadening during the transition in either tetradeuteroacetic acid or the mixed solvent.

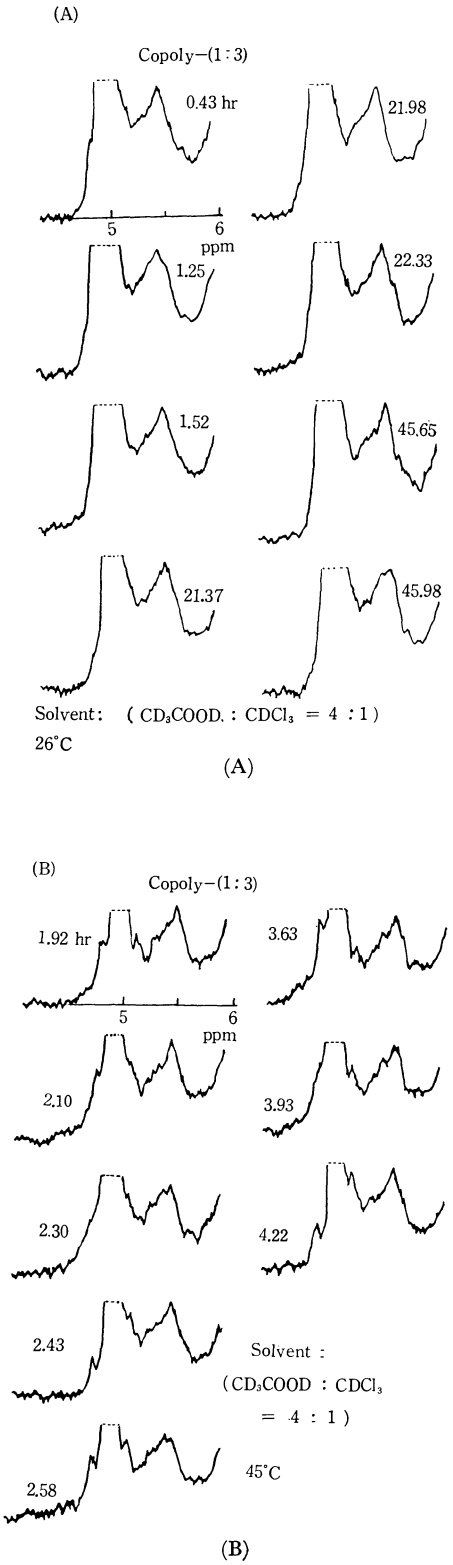

Fig. 9. The time-dependence of the α-CH resonance peak of the copoly-(1 : 3).

Figure 8 shows the time dependence of the ratios of the peak area of the α-CH resonance at 5.45 ppm to that of all the α-CH resonance peaks. These results demonstrate that, in copoly-(3 : 1), 10% of the γ-benzyl-L-glutamate residues were incorporated into the II poly-L-proline-like helical structure of the copolypeptides. Moreover, in copoly-(1 : 1) about 20% of the γ-benzyl-L-glutamate residues were incorporated into the helical structure. The α-CH resonance peak of copoly-(1 : 3) was observed in detail at 26°C and 45°C, as is shown in Fig. 9. However, the transition of copolypeptides such as poly-L-proline was not found. This observation suggests that the poly-L-proline-like structure can not be formed if a sufficient γ-benzyl-L-glutamate ratio exists in the copolypeptide.

BULLETIN OF THE CHEMICAL SOCIETY OF JAPAN VOL. 43 3063—3066 (1970)

Radiotracer Studies on Adsorption of Surface Active Substance at Aqueous Surface. II. The Effect of Excess Salt on the Adsorption of Sodium Dodecylsulfate

Kazuo TAJIMA

Department of Chemistry, Faculty of Science, Tokyo Metropolitan University, Setagaya, Tokyo

(Received April 4, 1970)

The adsorbed amount and the surface tension at the air-solution interface of the solution of tritiated sodium dodecylsulfate in the presence of excess common inorganic salt have been accurately measured at 25°C. The radioactivity of tritium β-rays over the solution was counted with a sheet scintillation counter and the surface tension of the solution was measured by a drop volume method. In the sodium dodecylsulfate solution containing sodium chloride of 0.115 mol/*l*, the adsorbed amount of dodecylsulfate ions was saturated to give 4.33×10^{-10} mol/cm^2 when the bulk concentration was higher than 5.0×10^{-4} mol/1000 g solution. In the presence of the excess inorganic salt common to the ionic surfactant in solution the Gibbs adsorption isotherm has been experimentally proved to be valid for $n=1$. Moreover, it was confirmed that the equation of state for the ionic adsorbed film on the salt-free solution proposed previously is also applicable to the ionic surfactant solution with the excess salt.

The behavior of the surface active substances at the air-solution interface has been studied by many investigators. In spite of the vast amount of studies published up to the present, there are few papers[1-3] which discuss the validity of the Gibbs adsorption isotherm on the basis of reliable data directly obtained for the system of surfactant solution with or without the addition of salt.

In the preceding paper,[4] the adsorbed amount at the air-solution interface was accurately measured by means of a radiotracer method by using the aqueous solution of tritiated sodium dodecylsulfate (TSDS). It was experimentally confirmed for TSDS solution in the absence of added inorganic salt that, if the activity coefficient is taken into account, the adsorption of detergent ions at the air-solution interface takes place in accordance with the Gibbs adsorption isotherm applied for the aqueous binary strong electrolyte solution.

In the present study, the adsorption experiments have been extended to the aqueous solution of TSDS in the presence of excess common inorganic electrolyte. The surface tension of the solution has been measured to check the Gibbs adsorption isotherm and to confirm the equation of state of adsorbed film established in the preceding paper.[4]

Experimental

Materials. The radioactive SDS was synthesized and purified as described in the preceding papers.[4,5] Its specific activity was 12.0 Ci/mol. Sodium chloride used as an inorganic salt was of extra pure grade, which was further purified by recrystallization from the saturated solution by passing HCl gas, by roasting, and then

1) C. P. Roe and P. D. Brass, *J. Amer. Chem. Soc.*, **76**, 4703 (1954).

2) G. Nilsson, *J. Phys. Chem.*, **61**, 1135 (1957).

3) R. Matuura, H. Kimizuka and K. Yatsunami, This Bulletin, **32**, 646 (1959).

4) K. Tajima, M. Muramatsu and T. Sasaki, *ibid.*, **43**, 1991 (1970).

5) M. Muramatsu and K. Tajima, *J. Labelled Compounds*, **2**, 304 (1966).

by ethereal Soxhlet extraction. Such purification was repeated until surface tension of the salt solution reached the constant value. Water used in these experiments was triply distilled. For the preparation of the solution, TSDS was dissolved in the aqueous solution of sodium chloride of constant concentration (0.115 mol/l).

Method. The measurements were made in a glove box with nitrogen atmosphere, which was kept at $98\pm3\%$ humidity and 25 ± 0.2°C. The procedure used for the measurement of the adsorption of TSDS was the same as described in detail in the preceding papers.[4,6] The surface radioactivity was measured by a sheet scintillation counter.

The surface tension measurement was carried out with another portion of the solution used for the adsorption experiment. The drop volume method was adopted with applying the Harkins and Brown corrections.[7] The equilibrium drop volume was obtained within 5 min. The calculation of surface tension was made with the mean volume of 5—10 drops at least. Throughout all experiments, the pH of bulk solutions was controlled at 6 ± 0.2.

Results and Discussion

Figure 1 shows the time dependence of the total surface radioactivity over the solution, A_1, for TSDS solutions of varying concentrations. It was found that the rate of adsorption of dodecylsulfate ion was far greater than the rate of adsorption of salt-free solution, and that time dependence of A_1 did not appear even at concentration below the critical micelle concentration (CMC), except the case of very low TSDS concentration. These phenomena are qualitatively in agreement with the observation on the time dependence in surface tension lowering of the surfactant solution.[8] A_1 value at equilibrium adsorption was obtained as the steady counting rate of each curve in Fig. 1, and given in Fig. 2 as a function of SDS concentration. By subtracting the radioactivity, A_2, due to the bulk of the solution from A_1, surface radioactivity, was obtained and it was converted to surface excess, Γ, by multiplying the conversion factor in the same manner as in the preceding paper.[4]

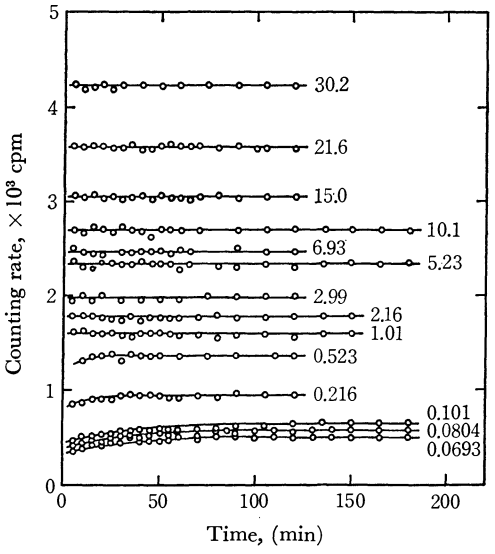

Fig. 1. Time dependence of total radioactivity at solution surface. Figures denote concentration of TSDS in bulk solution, in 10^{-4} mol/1000 g solution.

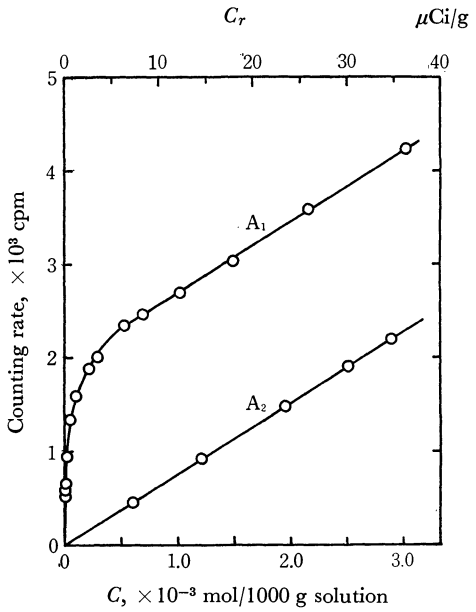

Fig. 2. A_1 and A_2 as a function of concentration of TSDS, C, and radioactive concentration, C_r, respectively.

Figure 3 shows the adsorption isotherm thus obtained at the air-solution interface of the TSDS solution containing excess sodium chloride. The

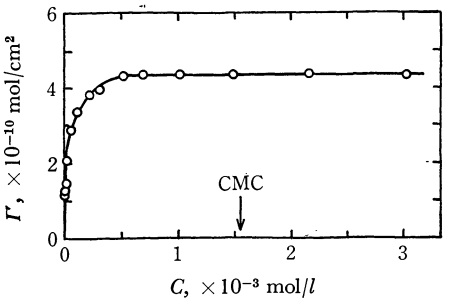

Fig. 3. Adsorption isotherm of TSDS solution in the presence of excess common inorganic electrolyte (25°C).

6) M. Muramatsu, K. Tajima and T. Sasaki, This Bulletin, **41**, 1279 (1968).

7) W. D. Harkins and F. E. Brown, *J. Amer. Chem. Soc.*, **41**, 499 (1919).

8) N. K. Adam and H. L. Shute, *Trans. Faraday Soc.*, **34**, 758 (1938); G. C. Nutting, F. A. Long and W. D. Harkins, *J. Amer. Chem. Soc.*, **62**, 1946 (1940).

adsorbed amount increases rapidly with increasing bulk concentration and to attain the value of saturated adsorption (4.33×10^{-10} mol/cm^2) when the bulk concentration was higher than 5.0×10^{-4} mol/1000 g solution. The saturated adsorption was kept constant even above the CMC within the limit of error. The apparent area per surfactant molecule at saturated adsorption is 38.4 Å^2, while the corresponding value for salt-free solution is 52.0 Å^2 as reported in the previous paper.[4]

Nilsson reported[2] that, in a buffer solution of pH=6.5 and of sodium ion concentration $C_{Na^+}=0.1$ mol/l, the amount of adsorption increases gradually with increasing bulk concentration up to CMC and becomes constant above the CMC, the saturated adsorption of dodecylsulfate ion being nearly 5.3×10^{-10} mol/cm^2 at 25°C. Matuura *et al.*[3] also measured adsorption at the air-solution interface of ^{35}S-labelled SDS containing 0.1 mol/l NaCl, and showed a similar increase in adsorption up to CMC, the adsorbed amounts being somewhat lower than those by Nilsson. The present result does not agree with these results except for the occasional agreement in a region of low SDS concentration.

As to the disagreement of the adsorption isotherms among various investigators, it is pointed out that a 2π windowless gas-flow counter, which Nilsson adopted to measure the adsorption amount, gives much unavoidable influence on the adsorption as described in detail in the previous report.[4] The value obtained by such a method might generally be higher than that of the counter of end-window type. On the other hand, higher accuracy may be expected for the present result than for Matuura's at high SDS concentration, since the radiation from ^{3}H is far softer than ^{35}S. Thus, the results of the present experiment are considered to be most reliable among them.

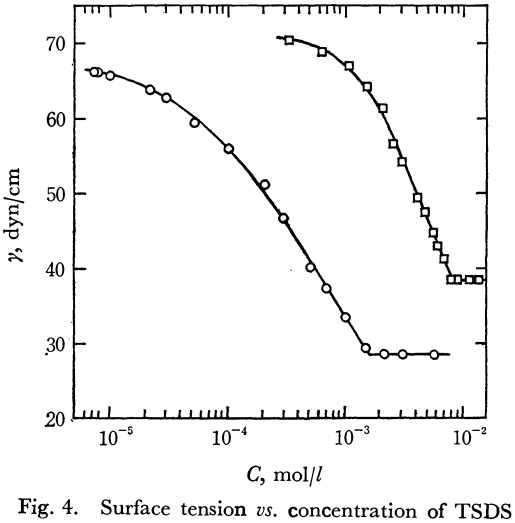

Fig. 4. Surface tension *vs.* concentration of TSDS solution.
—□—: salt-free solution
—○—: excess salt solution

Figure 4 shows the curve of the surface tension *vs.* concentration obtained under the same experimental conditions as reported in the preceding paper.[4] It is noted from Fig. 4 that a constant slope is obtained in the range of TSDS concentration from about 5.0×10^{-4} mol/l to the CMC.

Gibbs Adsorption Isotherm. The Gibbs adsorption isotherm is expressed as follows:

$$-\mathrm{d}\gamma = RT\sum\Gamma_i \mathrm{d}\ln a_i \qquad (1)$$

where γ represents the surface tension, Γ_i and a_i, the surface excess and the activity of ith ionic species in the solution, respectively. Assuming that the bulk solution is neutral and surface hydrolysis is absent (bulk pH was confirmed to be constant, independently of the TSDS concentration), Eq. (1) is rewritten for the TSDS solution containing sodium chloride as,

$$-\mathrm{d}\gamma = RT\Gamma_{Na^+}\mathrm{d}\ln a_{Na^+} + RT\Gamma_{D^-}\mathrm{d}\ln a_{D^-} + RT\Gamma_{Cl^-}\mathrm{d}\ln a_{Cl^-} \qquad (2)$$

where the subscripts Na^+, D^- and Cl^- denote sodium, dodecylsulfate and chloride ions, respectively. In the case of excess and constant concentration of NaCl, we have,

$$\frac{\mathrm{d}C_{Cl^-}}{\mathrm{d}C_{D^-}} = 0, \text{ and } \frac{\mathrm{d}C_{Na^+}}{\mathrm{d}C_{D^-}} \simeq 0 \qquad (3)$$

From Eq. (3) and the mean activity coefficient $f_\pm$, Eq. (2) can be written as,

$$-\frac{\mathrm{d}\gamma}{RT\,\mathrm{d}\ln C_{D^-}} = \Gamma_{D^-} + 2(\Gamma_{D^-}+\Gamma_{Cl^-})\frac{\mathrm{d}\ln f_\pm}{\mathrm{d}\ln C_{D^-}} \qquad (4)$$

The differential term in the right side of Eq. (4) can be evaluated as,

$$2\times\frac{\mathrm{d}\ln f_\pm}{\mathrm{d}\ln C_{D^-}} = 1.17\frac{C_{D^-}}{C_{Na^+}^{1/2}} = 5.27\times10^{-3} \qquad (5)$$

for $C_{NaCl}=0.115$ mol/l and $C_{D^-}=$CMC, with the assumption of the Debye-Hückel limiting law to be held. Thus, the differential term in Eq. (4) is seen to be negligible in this case. Then, Eq. (4) is reduced to

$$\Gamma = -\frac{\mathrm{d}\gamma}{RT\,\mathrm{d}\ln C} \qquad (6)$$

where C is the concentration of the surfactant and is taken to be equal to C_{D^-}, and $\Gamma=\Gamma_{D^-}$. The values of Γ calculated by Eq. (6) from the data of surface tension in Fig. 4 are plotted against SDS concentration in Fig. 5 together with the observed values for comparison. The calculated values are in good agreement with the observed values throughout the whole range of bulk concentration studied. When the surface attains the saturation with adsorbed surfactant at the concentration of 5.0×10^{-4}

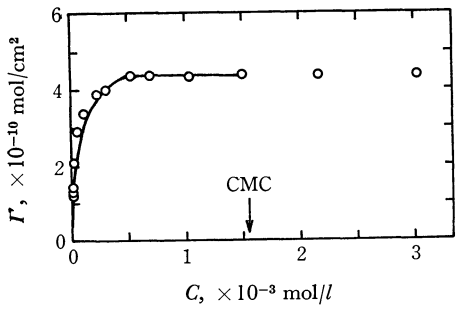

Fig. 5. Adsorption isotherm of SDS solution.
○: observed value
———: Eq. (6)

mol/*l* as shown in this figure, further increase of the bulk surfactant concentration produces no change in the amount of adsorption, while it causes a steady decrease of surface tension. Such a mode of adsorption isotherm was confirmed to persist even above the CMC. Roe and Brass[1] measured the surfate tension lowering of SDS solution of which pH and C_{Na^+} were held constant to 6.5 and 0.1 mol/*l*, respectively, by the use of the buffer solution, and calculated the amount of SDS adsorption by applying the Gibbs equation. They obtained 4.40×10^{-10} mol/cm^2 as the values of saturated adsorption. This value is also in good agreement with that measured in the present radiotracer study as far the saturation value is concerned.

Thus, the Gibbs adsorption isotherm is proved to be valid, when we put $n=1$ in the Gibbs equation[4] for TSDS solution in the presence of excess salt with the common cation.

Equation of State. The relation between the surface pressure, π, and molecular area, A, of the adsorbed film of TSDS on an excess salt solution was calculated from the data of Figs. 3 and 4 by using the following relationships:

$$\pi = \gamma_0 - \gamma$$

$$A = \frac{1}{\Gamma_{D^-} \times N}$$

where γ_0 is the surface tension of water and N Avogadro's number. The result is shown by circles in Fig. 6. In the preceding report[4] we proposed the equation of state for the adsorbed film on the salt-free SDS solution as follows:

$$(\pi + \frac{0.43\,kT}{A} + 6.03\,C_i^{1/2})(A-A_0) = kT \qquad (7)$$

where C_i is the total bulk concentration of ions, A_0 the coarea per molecule, k the Boltzmann constant and T the absolute temperature. In Fig. 6, Eq. (7) is shown by a solid line. An excellent agreement is seen between Eq. (7) and the experimental results. The value of A_0 was found to be about 25.0 Å^2/molecule, which was obtained by the same procedure as that in the preceding paper.[4] This value may be compared with the value of $A_0=38.4$ Å^2/molecule found in the case of salt-free solution. The effects of added salt on A_0 may be interpreted as being due to the shrinkage of diffuse double layers and the dehydration of adsorbed dodecylsulfate ion.

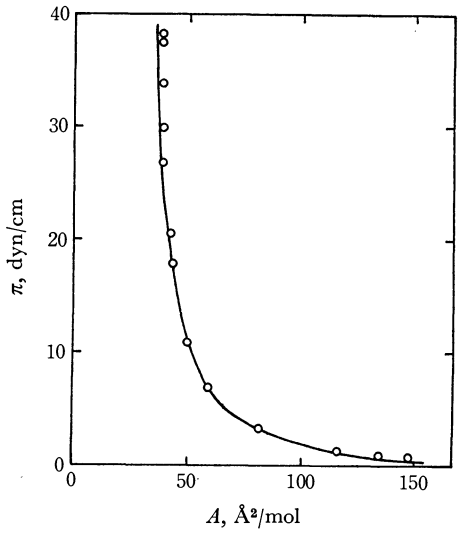

Fig. 6. π *vs.* A plot for adsorbed SDS monolayer on 0.115 mol/*l* NaCl solution at 25°C.
○ : observed value
———: Eq. (7)

It is confimed from Fig. 6 that Eq. (7) expresses satisfactorily behavior of the surface films adsorbed from ionic surfactant solutions with or without excess salts.

The author wishes to express his hearty thanks to Professor T. Sasaki for his encouragement and guidance throughout the experiments. He is grateful also to Assistant Professor M. Muramatsu, for his helpful discussion and advice.

BULLETIN OF THE CHEMICAL SOCIETY OF JAPAN VOL. 43 3067—3069 (1970)

Some Aspects of Gaseous TCNE Complexes Including the Butene-TCNE

Jun-ichi AIHARA,*1 Motoyuki TSUDA*1 and Hiroo INOKUCHI

The Institute for Solid State Physics, The University of Tokyo, Roppongi, Tokyo

(Received April 13, 1970)

The absorption spectra of the gaseous olefin-TCNE complexes were successfully observed for the first time: the absorption maximum of the butene-TCNE complex was found at 28700 cm^{-1}. The CT band of the methyl derivatives was shifted to a higher-energy region because of their steric effect. The systematic collection of the gaseous data made it possible to estimate the magnitude of the steric effect.

1. The Absorption Spectra of the Gaseous Butene-TCNE Complex. Since Lang and Strong first measured the electronic absorption spectra of gaseous diethyl ether-iodine and also gaseous benzene-iodine complexes, various charge-transfer complexes have been investigated in the gas phase.[1-3] We have also measured the spectra of a series of gaseous aromatics-TCNE(tetracyanoethylene) and anthracene-chloranil complexes. These results have been reported in previous papers.[4-6]

Recently, Kroll studied the gaseous charge-transfer complexes, using TCNE as an electron acceptor.[7] However, according to his article, he failed to find the charge-transfer spectra for a gas-phase mixture of ethylene and TCNE, nor did he find the characteristic spectra for a gaseous mixture of butadiene and TCNE. Of course, it is widely known that ethylenic hydrocarbons form charge-transfer complexes with various acceptors in solution.[8,9]

We attempted to detect the charge-transfer band of the gaseous TCNE complex with one of the ethylenic hydrocarbons, *cis*-2-butene, and succeeded in the measurement of its spectrum. The experimental apparatus and procedures were the same as those employed in the previous experiments.[4] The *cis*-2-butene used was a commercial material, while the TCNE was purified by sublimation *in vacuo*. The spectroscopic measurements were made as rapidly as possible in order to observe the clean species. The electric furnace containing the optical cell was maintained at 200°C.

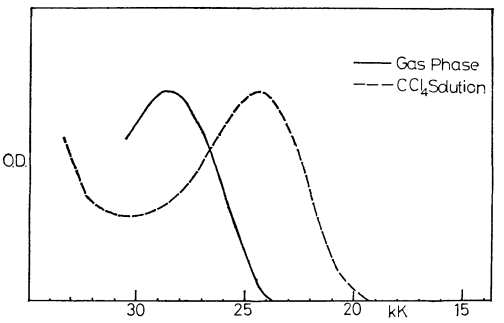

Fig. 1. The CT band of the butene-TCNE complex.

Figure 1 shows the gaseous spectrum of the butene-TCNE complex. The solution spectrum in carbon tetrachloride is added for the sake of comparison. To obtain the solution data, a sufficient amount of gaseous butene was introduced into a solution saturated with TCNE. In the gaseous phase, the characteristic charge-transfer band was observed in the near-ultraviolet region, where neither the vapour of butene nor that of TCNE absorbs. A peak is found at 28700 cm^{-1}; it corresponds to a blue shift of 4300 cm^{-1} from that found when both components are dissolved in carbon tetrachloride. The half-width determined from the long-wavelength part of the band is approximately 2200 cm^{-1}. It can be seen in Fig. 1 that gas and solution bands would coincide almost exactly if

*1 Present address: Hokkaido University, Department of Chemistry, Faculty of Science, Sapporo, Japan.

1) F. T. Lang R. L. Strong, *J. Amer. Chem. Soc.*, **87**, 3245 (1965).
2) J. Prochorov and A. Tramer, *J. Chem. Phys.*, **44**, 4545 (1966).
3) M. Tramer and J. M. Goodenow, *J. Phys. Chem.*, **71**, 1982 (1967).
4) J. Aihara, M. Tsuda and H. Inokuchi, This Bulletin, **40**, 2460 (1967).
5) J. Aihara, M. Tsuda and H. Inokuchi, *ibid.*, **42**, 1824 (1969).
6) J. Aihara, M. Tsuda and H. Inokuchi, *ibid.*, **43**, 2439 (1970).
7) M. Kroll, *J. Amer. Chem. Soc.*, **90**, 1097 (1968).
8) M. A. Muhs and F. T. Weiss, *ibid.*, **84**, 4697 (1962).
9) L. J. Andrews and R. M. Keefer, *ibid.*, **74**, 458 (1952).

TABLE 1. ADDENDUM TO THE LIST OF THE GASEOUS TCNE COMPLEXES

Donor	CT band (cm^{-1})		Gas-to-solution shift (cm^{-1})
	in gas phase	in CCl_4 solution	
cis-2-Butene	28700	24400	−4300
Acenaphthene	18100	15300	−2800

superimposed. In all respects, the nature of the butene-TCNE complex seems like that of usual TCNE complexes.

We also observed the spectra of another TCNE complex, that with acenaphthene at 200°C. These results are summarised in Table 1.

2. Steric Effects of Charge-transfer Complexes in the Gas Phase. Now, a fair amount of data on the gaseous TCNE complexes are available. Therefore, we can survey them from a different point of view. The observed band maxima($h\nu$) of the charge-transfer transition are plotted against the ionization potentials (Ip) of the donor molecules in Fig. 2. As usual, a linear relation between them can be derived:[10]

$$h\nu = aI_p - b \qquad (1)$$

Here, a and b are assumed to be characteristic constants for the complexes of any one acceptor.

The ionization potentials of the donors used were determined by Watanabe, Terenin and Vilessov, and Briegleb.[11–13] We newly determined those of pyrene (7.53±0.03 eV) and acenaphthene (7.66±0.03 eV) by the photoionization method. This simplified equation, which can often be a sufficient approximation, has been used to determine the unknown ionization potential of any donor. In the case of typical polycyclic aromatic hydrocarbons especially, the ionization potentials derived from Eq. (1) coincide well with those obtained from the polarographic oxidation potentials.[14] On the other hand, it is generally admitted that polymethyl-benzenes obey a slightly different equation; that is, they give higher transition energies than the values to be expected from the equation based on typical hydrocarbons.[15,16]

As is illustrated in Fig. 2, we can also broadly classify the gaseous data into two groups; one is the

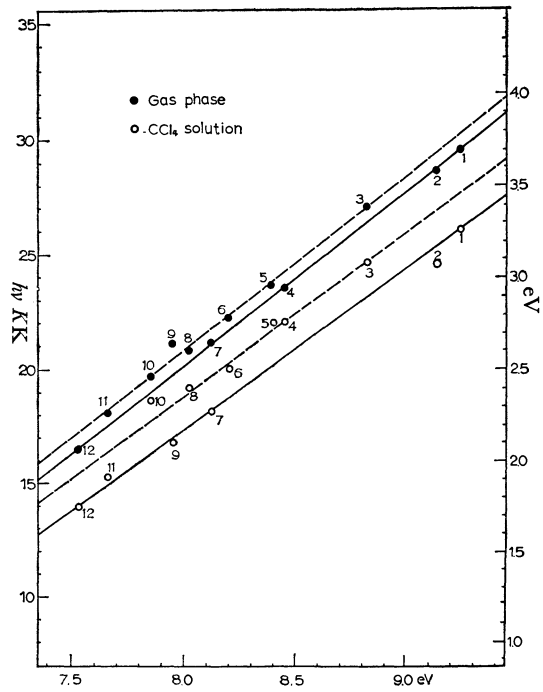

Fig. 2. Plots of CT absorption maxima *versus* ionization potentials of donors.
1. benzene, 2. *cis*-2-butene, 3. toluene, 4. *p*-xylene, 5. mesitylene, 6. diphenyl, 7. naphthalene, 8. durene, 9. stilbene, 10. hexamethylbenzene, 11. acenaphthene, 12. pyrene.
● Gas phase
○ CCl_4 solution

group to which typical aromatic hydrocarbons belong, and the other is that to which their derivatives belong. Benzene, naphthalene, and pyrene can be ascribed to the former, while the other compounds belong mainly to the latter, though there are some exceptions.

For the typical hydrocarbons, we obtained the following relations:

$$h\nu = 0.948I_p - 5.07 \text{ (eV)} \qquad (2)$$

for the TCNE complexes in the gas phase, and

$$h\nu = 0.877I_p - 4.87 \text{ (eV)} \qquad (3)$$

for those in the carbon tetrachloride solution. The complexes with these compounds rigorously maintain a linear relation both in gas and in solution. The coefficient, "a", in the gas phase is almost equal to unity. This means that the charge-transfer transition of the TCNE complexes can be interpreted primarily in terms of a simple electron donation from the donor to the acceptor molecule. In other words, it can be expressed by the ionization potential of the donor minus the electron affinity of the acceptor and minus the Coulomb energy.

10) H. M. McConnell, J. S. Ham and J. R. Platt, *J. Chem. Phys.*, **21**, 66 (1953).
11) K. Watanabe, T. Nakayama and J. Mottl, *J. Quant. Spectry. Radiative Transfer*, **2**, 369 (1962).
12) A. Terenin and F. Vilessov, *Advances Photochem.*, **2**, 385 (1964).
13) G. Briegleb, *Angew. Chem.*, **76**, 326 (1964).
14) E. S. Pysh and N. C. Yang, *J. Amer. Chem. Soc.*, **85**, 2124 (1963).
15) G. Briegleb, "Elektronen-Donator-Acceptor-Komplexe," Springer Verlag, Berlin (1961).
16) M. Kinoshita, This Bulletin, **35**, 1609 (1962).

In the case of complexes with substituted derivatives, the gradients of Eqs. (2) and (3) are not changed. However, the constant terms in them increase by approximately the amounts of 0.075 and 0.19 eV respectively. These situations are shown by the dotted lines in Fig. 2. The data for benzene, *p*-xylene, mesitylene, and hexamethylbenzene are cited from Ref. (7).

In order to explain the above tendencies, it is instructive to consider the steric effect of the substitutents of the donor molecules. Though our information on the stereochemistry of the gaseous complexes is quite deficient, the substitutents should often change the distance between the molecular planes in the complex to some extent.

According to Pauling's idea, the half-thickness of the aromatic ring is 1.85 Å, while the van der Waals radius of the methyl group is about 2.0 Å.[17] Briegleb has suggested that, if the intermolecular distance, R, between the donor and the acceptor increases by 0.01 Å near R=3.2 Å, the Coulombic attraction term contributing to the charge-transfer transition will decrease by 100 cm^{-1}.[15] On the basis of this statement, it may be concluded that the R of the methyl derivatives increases by 0.06 Å on the average. Though R must be interpreted as the distance between the centres of the donor and of the acceptor molecules, the interplanar distance of the complex might be roughly regarded as the same. Exceptionally, *p*-xylene and butene behave as if they are not affected by the steric effect. On the other hand, diphenyl and acenaphthene are apparently affected under these circumstances. This behaviour is reflected in the subsequent polarization energy, P, in the carbon tetrachloride solution. As the dipole moments of the complex are dependent on the ionization potential of the donor, the polarization energy will necessarily depend on it. In fact, the dipole moments in the ground state are 1.28D for the naphthalene-TCNE, 1.35D for the hexamethylbenzene-TCNE, and 2.0D for the pyrene-TCNE complex.[18,19] Theoretical studies have suggested that the dipole moments in the excited state also vary systematically.[15] The actual *Ip* dependence of the polarization energy was derived by Eqs. (2) and (3) for typical complexes:

$$P = 0.071I_p - 0.20 \text{ (eV)} \quad (4)$$

The polarization energy of the complex with the substituted compound is somewhat smaller than that of the typical complex. Supposing that Onsager's approximation is applicable to the dielectric media containing the charge-transfer complex, the solvent shift is inversely proportional to the cube of the cavity radius.[20,21] This assumption has been confirmed by an analysis of the TCNE complex in the solvent, a discussion presented in a previous paper.[5] Therefore, the change in the polarization energy can be shown by the augmentation of the molecular dimensions. The decrease of 30 percent in the polarization energy is equivalent to the increase of 13 percent in the cavity radius. This behaviour is also ascribable to the steric effect of the substitutents.

In the above discussion, we neglected various factors affecting the charge-transfer complex. Accordingly, we must admit that the criterion for the judgement of the steric effects seems somewhat obscure, as the several exceptions show. Such an amount of spectral change may occur by means of the geometrical variation of the complex.[22]

In the case of the stilbene-TCNE, the temperature dependence of the intensity ratio of the first and the second CT bands has been found in a methylene chloride solution.[23] This phenomenon has been explained in terms of geometrical isomerism. This isomerism may cause the location for it to deviate from the linearities. Strictly speaking, we need to examine the individuality of each complex in detail. Therefore, it seems very natural that the gaseous species behave well with fewer exceptions, since they are not influenced by a variety of ways of solvation and so on.

17) L. Pauling, "The Nature of the Chemical Bond," 3rd Ed., Cornell Univ. Press, New York (1960).
18) G. Briegleb, J. Czekalla and G. Reuss, *Z. Physik. Chem.* (Frankfurt), **30**, 333 (1961).
19) H. Kuroda, T. Amano, I. Ikemoto and H. Akamatu, *J. Amer. Chem. Soc.*, **89**, 6056 (1967).
20) Y. Ooshika, *J. Phys. Soc. Jap.*, **9**, 594 (1954).
21) E. G. McRae, *J. Phys. Chem.*, **61**, 562 (1957).
22) R. J. Flurry, Jr., *ibid.*, **73**, 2111 (1969).
23) H. Aiga and T. Matsuo, The 20th Annual Meeting of the Chemical Society of Japan (1967).

BULLETIN OF THE CHEMICAL SOCIETY OF JAPAN VOL. 43 3070—3078 (1970)

The Crystal Structure of a Colored Complex, $C_7H_7OHg \cdot C_7H_6O_2N$, Obtained in the Millon Reaction of *p*-Cresol

Yoshiko KOBAYASHI, Yoichi IITAKA and Yasumasa KIDO

Faculty of Pharmaceutical Sciences, The University of Tokyo, Hongo, Bunkyo, Tokyo

(Received April 27, 1970)

The crystal structure of the complex of 2-mercuri-4-methylphenol and 2-nitroso-4-methylphenol obtained in the modified Millon reaction was determined using three-dimensional X-ray diffraction data. The complex crystallizes in triclinic system, space group $P\bar{1}$, with a unit cell of dimensions $a=10.26$ Å, $b=22.71$ Å, $c=5.61$ Å, $\alpha=97.2°$, $\beta=93.1°$, $\gamma=91.1°$, containing four complex molecules. Each of the two crystallographycally independent complex molecules both having essentially the same structure, forms a dimer with its nearest neighbor related by a center of symmetry through a pair of hydrogen bonds. The mercury atoms adopt a planar four-fold coordination with nitrogen, carbon and two oxygen atoms.

In the modified Millon reaction of *p*-cresol with Hopkins-Cole reagent, three kinds of pigment (pigment 1, 2 and 3) were produced depending upon the reaction condition. Pigment 1 is known as a complex of 2-mercuri-4-methylphenol (MMP) and 2-nitroso-4-methylphenol (NMP).[1,2] In order to determine the structure of the complex, two-dimensional X-ray analysis of pigment 1 was already carried out by Tamura, Iitaka and Kido[2] using the crystal grown from chloroform solution. However, this crystal contained chloroform as a solvent of crystallization and was so small and deteriorative against X-ray irradiation that it was not possible to determine the structure in three dimensions. Later, more stable and larger crystals were obtained from ethanol solutions. The present investigation was therefore undertaken to elucidate the detailed spacial structure of the complex molecule by X-ray diffraction using the new crystals.

Experimental

The crystals of pigment 1 were grown from ethanol solutions as massive aggregates of triclinic prisms elongated along the *c*-axis. They were dark red in color. The lattice constants and space group were determined from the *a*-, *b*- and *c*-axis equatorial precession photographs taken with Cu$K\alpha$ radiation. The density was measured by the floatation method using the mixed solutions of 1,1,2,2-tetrabromoethane and carbon tetrachloride. Unlike the crystals grown from chloroform solutions, the present crystal does not contain the solvent of crystallization.

Crystal Data. 2-Mercuri-4-methylphenol·2-nitroso-4-methylphenol complex $C_7H_7OHg \cdot C_7H_6O_2N$.

Mol wt: 444

Space group: triclinic $P\bar{1}$

Lattice constants:

$a=10.26\pm0.02$, $b=22.71\pm0.03$, $c=5.61\pm0.01$ Å,

$\alpha=97.2\pm0.2$, $\beta=93.1\pm0.2$, $\gamma=91.1\pm0.2°$

Volume of the unit cell: 1297 Å^3

Four structure units in the unit cell

Density measured: 2.25 g·cm^{-3}

Density calculated: 2.27 g·cm^{-3}

Linear absorption coefficient for Cu$K\alpha$ radiation: $\mu=237.6$ cm^{-1}

Three-dimensional intensity data were collected from multiple-film equi-inclination Weissenberg photographs taken with Cu$K\alpha$ radiation of the layers zero to fourth about the *c*-axis and zero to third about [101] axis. The intensities were measured visually with the aid of a calibrated intensity scale and they were corrected for Lorentz and polarization factors. The size of the specimens used for the intensity measurement was about 0.065×0.065 mm in cross section corresponding to the μR value of 1.53, but no absorption correction was applied. The structure factors obtained for the two axes were correlated and scaled to a common base. A total of 2418 independent structure factors was finally derived.

Determination of the Crystal Structure

The three-dimensional Patterson function yielded the positions of two mercury atoms involved in the asymmetric unit. A three-dimensional Fourier map was then calculated on the basis of the contribution of these two atoms which gave the *R* factor of 0.33. Although many spurious peaks were present on the Fourier map especially around the mercury atoms, the locations of the thirty six light atoms forming the two crystallographically independent complex molecules were determined by succesive use of Fourier and difference Fourier syntheses. The

1) Z. Tamura and Y. Kido, *Chem. Pharm. Bull.* (Tokyo), **16**, 1808 (1968).

2) Z. Tamura, Y. Iitaka and Y. Kido, *ibid.*, **17**, 1767 (1969).

refinement of the atomic positional and thermal parameters was first carried out by the block-matrix least-squares method, using the program HBLS.[3] Seven cycles of calculations including isotropic temperature factors for each atom reduced the R factor from 0.30 to 0.15. This factor was further reduced to 0.11 by three cycles of the least-squares calculations including individual anisotropic temperature factor parameters. The weighting system adopted in the calculations was:

$$\sqrt{w}=75/F_o, \text{ when } 75<F_o,$$

$$\sqrt{w}=1, \text{ when } 12<F_o\leq 75,$$

$$\sqrt{w}=0, \text{ when } F_o\leq 12.$$

The final atomic parameters and their standard deviations are listed in Table 1. In Table 2 the observed structure factors are listed. The atomic scattering factors used in the present structure determination were taken from *International Tables for X-ray Crystallography*.[4]

Figure 1 depicts the superposed three-dimensional electron density distribution function calculated on the basis of the atomic parameters listed in Table 1.

Discussion of the Structure

The present crystal contains two crystallographically independent complex molecules I and II. Each of these molecules forms a dimer with its nearest neighbor related by a center of symmetry through a pair of hydrogen bonds.

The bond lengths and angles of the complex molecules calculated from the coordinates given in Table 1 are shown in Fig. 2 along with their standard deviations. It is seen that they resemble each other considering their rather large standard deviations. Furthermore, the c-axis projection of the dimer molecule found in the crystal grown from chloroform solutions (Fig. 1 of the previous paper[2]) closely resembles those found in the present crystal, although the sturucture of the former was solved only in a two-dimensional projection and no detailed spacial arrangement of the atoms was given.

In the previous paper, two resonance forms of the complex were suggested as shown in Fig. 3 of the present paper, but it was not possible to decide which is more predominant. In Table 3, the length of the C–N and N–O bonds reported for various oximes, nitroso compounds and N-oxides are shown. The length of the C–N bonds found in the molecules I and II are both 1.25 Å indicating a strong double bond character. The N–O bond lengths in the molecules I and II differ considerably. In view of the rather large standard deviations, it can not be said that the difference is really significant, but the mean value of the two lengths, 1.27 Å, is nearly of the same order of magnitude as those found in nitroso compounds[12–16] or in N-oxides[17–20] and is clearly shorter than those found in oximes.[5–11]

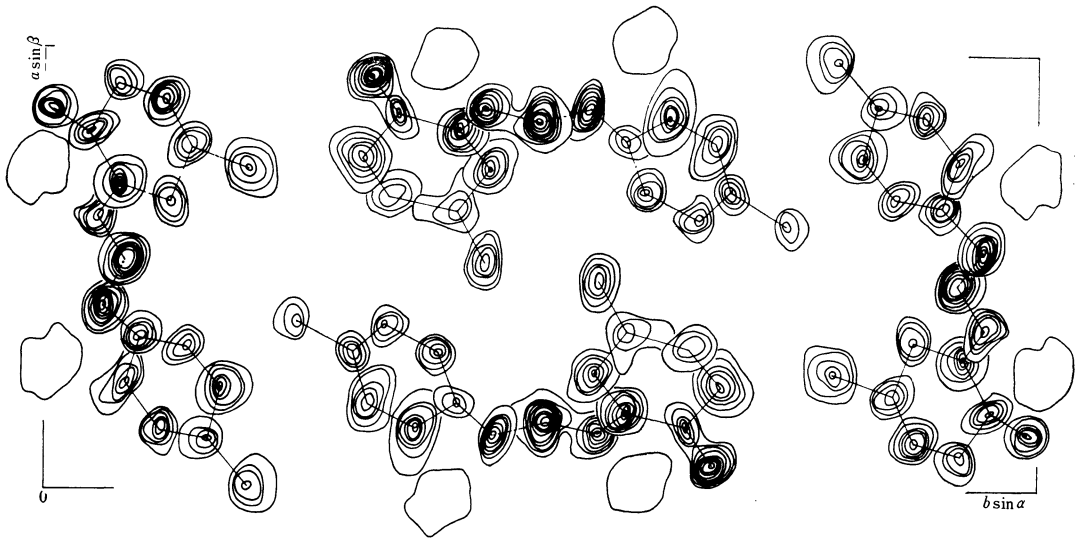

Fig. 1. Composite drawing of the electron density map viewed along the c-axis. Contours are drawn at intervals of 1 e. Å^{-3} starting at 2 e. Å^{-3}. Those for mercury atoms are not shown.

3) Y. Okaya and T. Ashida, HBLS IV, *The Universal Crystallographic Computing System* (I), p. 65, Japanese Crystallographic Association.

4) *International Tables for X-ray Crystallography*, Vol. III, Kynoch Press, Birmingham (1962).

TABLE 1. FINAL ATOMIC PARAMETERS AND THEIR STANDARD DEVIATIONS (e.s.d)

E.s.d.'s are given in parentheses denoting the least significant digits of the corresponding values. x, y, z are the fractional coordinates. The temperature factors are of the form

$$T=\exp\{-(\beta_{11}h^2+\beta_{22}k^2+\beta_{33}l^2+2\beta_{12}hk+2\beta_{13}hl+2\beta_{23}kl)\}$$

ATOM	x	y	z	β_{11}	β_{22}	β_{33}	β_{12}	β_{13}	β_{23}
Hg(1)	0.2514	0.0115	0.1128	0.0093	0.0014	0.0242	0.0007	-0.0006	-0.0013
	(2)	(1)	(1)	(2)	(0)	(8)	(1)	(3)	(1)
Hg(2)	0.0036	0.4983	0.0971	0.0090	0.0015	0.0242	0.0006	-0.0035	-0.0002
	(2)	(1)	(1)	(2)	(0)	(9)	(1)	(3)	(1)
O(1)	0.1243	-0.0155	-0.2448	-0.0014	0.0084	0.0582	-0.0010	-0.0011	0.0011
	(22)	(10)	(60)	(25)	(5)	(158)	(8)	(45)	(20)
O(2)	0.4651	-0.0876	-0.0428	0.0124	0.0025	0.0031	0.0011	-0.0073	-0.0036
	(33)	(15)	(51)	(43)	(8)	(120)	(14)	(51)	(22)
O(3)	0.4129	0.0528	0.0156	0.0140	0.0015	0.0291	0.0017	-0.0114	0.0016
	(33)	(13)	(62)	(47)	(6)	(152)	(14)	(64)	(24)
O(4)	-0.0926	0.4288	-0.2472	0.0114	0.0006	0.0411	0.0002	-0.0147	-0.0060
	(33)	(12)	(62)	(41)	(5)	(159)	(11)	(62)	(22)
O(5)	-0.1800	0.4927	-0.0405	0.0144	0.0012	-0.0002	-0.0018	-0.0077	-0.0040
	(33)	(12)	(48)	(45)	(6)	(113)	(13)	(51)	(19)
O(6)	0.1022	0.4508	0.5900	0.0050	0.0017	0.0331	0.0005	-0.0034	-0.0017
	(27)	(13)	(58)	(29)	(7)	(144)	(11)	(49)	(24)
N(1)	0.3566	-0.0611	-0.1095	0.0011	0.0008	0.0478	0.0006	0.0008	0.0000
	(36)	(13)	(74)	(31)	(6)	(190)	(11)	(58)	(26)
N(2)	-0.1492	0.4430	-0.1104	0.0125	0.0004	0.0161	-0.0000	0.0154	-0.0052
	(41)	(13)	(65)	(56)	(6)	(156)	(14)	(72)	(23)
C(1)	0.1726	-0.0528	-0.3851	0.0097	0.0010	-0.0091	0.0009	-0.0120	-0.0018
	(42)	(16)	(68)	(52)	(7)	(195)	(15)	(63)	(24)
C(2)	0.1141	-0.0723	-0.5886	0.0072	0.0031	0.0248	0.0035	-0.0027	0.0057
	(46)	(24)	(95)	(54)	(14)	(224)	(22)	(82)	(44)
C(3)	0.1535	-0.1226	-0.7334	0.0030	0.0023	0.0312	0.0002	-0.0019	-0.0007
	(42)	(22)	(92)	(46)	(12)	(222)	(18)	(74)	(36)
C(4)	0.2619	-0.1497	-0.6736	0.0116	0.0014	0.0075	0.0022	-0.0008	-0.0045
	(47)	(19)	(76)	(59)	(9)	(178)	(18)	(72)	(29)
C(5)	0.3510	-0.1341	-0.4624	0.0090	0.0017	0.0045	-0.0004	-0.0001	-0.0034
	(40)	(18)	(72)	(46)	(9)	(163)	(16)	(61)	(28)
C(6)	0.2960	-0.0829	-0.3017	0.0098	0.0012	0.0226	0.0001	-0.0164	-0.0058
	(45)	(18)	(83)	(59)	(9)	(214)	(18)	(86)	(34)
C(7)	0.3134	-0.2072	-0.8300	0.0029	-0.0002	0.0970	-0.0028	0.0166	-0.0038
	(41)	(16)	(110)	(45)	(8)	(333)	(14)	(97)	(34)
C(8)	0.3202	0.0940	0.5531	0.0061	0.0015	0.0359	0.0016	0.0034	-0.0055
	(45)	(20)	(93)	(49)	(9)	(227)	(17)	(79)	(35)
C(9)	0.2984	0.1382	0.7155	0.0297	0.0039	-0.0491	0.0006	-0.0002	-0.0018
	(65)	(25)	(72)	(107)	(15)	(172)	(30)	(77)	(31)
C(10)	0.2005	0.1822	0.6437	0.0117	0.0011	0.0395	0.0010	0.0017	-0.0056
	(53)	(20)	(99)	(65)	(9)	(251)	(19)	(95)	(36)
C(11)	0.1232	0.1666	0.4450	-0.0120	0.0003	0.0244	-0.0010	-0.0004	-0.0005
	(28)	(12)	(64)	(30)	(5)	(149)	(9)	(44)	(20)
C(12)	0.1503	0.1197	0.2832	0.0080	0.0015	0.0054	-0.0009	0.0043	-0.0067
	(42)	(18)	(72)	(51)	(9)	(165)	(16)	(65)	(28)
C(13)	0.2450	0.0840	0.3526	0.0019	0.0017	-0.0199	-0.0013	-0.0173	-0.0016
	(35)	(16)	(66)	(37)	(8)	(144)	(13)	(57)	(24)
C(14)	0.0238	0.2106	0.3620	0.0183	0.0024	0.0025	0.0028	-0.0061	-0.0062
	(59)	(23)	(82)	(83)	(12)	(190)	(25)	(88)	(35)
C(15)	-0.1745	0.3522	-0.3634	0.0085	-0.0001	0.0207	-0.0004	0.0039	-0.0030
	(41)	(14)	(74)	(49)	(6)	(175)	(13)	(68)	(23)
C(16)	-0.2257	0.3242	-0.5880	0.0066	0.0011	0.0479	-0.0001	0.0018	0.0025
	(47)	(19)	(104)	(53)	(9)	(261)	(17)	(90)	(37)
C(17)	-0.3093	0.3525	-0.7194	0.0050	0.0042	0.0035	-0.0019	-0.0043	-0.0058
	(44)	(26)	(79)	(50)	(17)	(180)	(22)	(66)	(41)
C(18)	-0.3470	0.4144	-0.6443	-0.0174	0.0027	0.0526	0.0031	-0.0089	0.0059
	(32)	(19)	(85)	(33)	(10)	(215)	(12)	(55)	(36)
C(19)	-0.2918	0.4446	-0.4475	0.0054	0.0015	0.0228	-0.0016	-0.0033	0.0007
	(42)	(19)	(85)	(46)	(9)	(201)	(16)	(71)	(32)
C(20)	-0.2022	0.4147	-0.3035	0.0107	0.0012	-0.0045	0.0000	-0.0078	0.0014
	(47)	(17)	(89)	(68)	(9)	(168)	(19)	(73)	(27)
C(21)	-0.4613	0.4421	-0.7823	0.0024	0.0045	-0.0051	0.0014	-0.0247	0.0187
	(41)	(22)	(88)	(47)	(13)	(208)	(19)	(79)	(47)
C(22)	0.1813	0.4056	0.5250	0.0105	0.0017	-0.0101	-0.0039	-0.0064	0.0021
	(43)	(18)	(67)	(54)	(9)	(149)	(18)	(62)	(26)
C(23)	0.2790	0.3964	0.6654	0.0025	0.0014	0.0284	-0.0012	-0.0100	-0.0064
	(42)	(19)	(88)	(47)	(9)	(215)	(16)	(76)	(35)
C(24)	0.3638	0.3441	0.5864	0.0124	0.0026	0.0567	-0.0024	0.0065	-0.0118
	(63)	(27)	(121)	(83)	(15)	(330)	(28)	(127)	(57)
C(25)	0.3339	0.3129	0.3750	0.0054	0.0016	0.0369	-0.0006	0.0090	0.0078
	(43)	(20)	(94)	(79)	(8)	(169)	(19)	(77)	(27)
C(26)	0.2270	0.3262	0.2247	0.0208	0.0008	-0.0092	0.0003	-0.0036	-0.0059
	(54)	(17)	(75)	(48)	(9)	(234)	(16)	(82)	(39)
C(27)	0.1535	0.3752	0.2952	0.0104	0.0017	0.0140	0.0001	0.0042	0.0055
	(50)	(20)	(88)	(62)	(10)	(208)	(20)	(84)	(36)
C(28)	0.4137	0.2563	0.2818	0.0072	0.0030	0.0656	-0.0022	-0.0058	0.0006
	(56)	(29)	(131)	(65)	(17)	(352)	(26)	(117)	(59)

TABLE 2. OBSERVED STRUCTURE FACTORS

H	K	L	F(OBS)
-10	2	0	40.25
-10	3	0	40.25
-10	5	0	56.44
-10	7	0	34.02
-10	8	0	19.44
-10	9	0	19.06
-10	10	0	45.98
-10	11	0	25.92
-10	14	0	28.28
-10	16	0	20.19
-10	17	0	26.04
-9	1	0	70.40
-9	2	0	35.26
-9	3	0	28.78
-9	4	0	70.52
-9	6	0	67.66
-9	8	0	49.96
-9	9	0	64.17
-9	11	0	63.17
-9	14	0	56.19
-9	16	0	48.84
-8	1	0	51.09
-8	4	0	58.56
-8	5	0	58.94
-8	6	0	34.26
-8	8	0	34.89
-8	9	0	45.23
-8	10	0	57.57
-8	12	0	24.91
-8	13	0	49.72
-8	15	0	59.06
-8	17	0	37.01
-8	18	0	30.53
-8	20	0	40.74
-7	1	0	24.92
-7	2	0	90.33
-7	3	0	64.29
-7	5	0	122.11
-7	7	0	93.57
-7	8	0	105.91
-7	10	0	119.13
-7	11	0	34.51
-7	12	0	57.07
-7	13	0	73.39
-7	15	0	67.53
-7	17	0	34.39
-7	18	0	27.29
-7	20	0	49.59
-7	21	0	23.18
-7	22	0	21.18
-6	1	0	59.06
-6	2	0	27.41
-6	4	0	99.80
-6	5	0	65.79
-6	6	0	94.95
-6	7	0	24.17
-6	8	0	35.01
-6	9	0	107.78
-6	10	0	45.11
-6	11	0	119.37
-6	12	0	27.29
-6	13	0	59.18
-6	14	0	75.01
-6	16	0	84.23
-6	18	0	49.34
-6	19	0	62.18
-6	21	0	65.17
-6	22	0	23.92
-6	23	0	26.91
-6	24	0	36.63
-5	1	0	171.57
-5	2	0	77.75
-5	3	0	40.00
-5	4	0	134.44
-5	6	0	87.59
-5	8	0	143.79
-5	9	0	53.70
-5	10	0	31.90
-5	11	0	146.65
-5	12	0	54.57
-5	13	0	156.62
-5	14	0	62.18
-5	15	0	90.46
-5	16	0	59.31
-5	17	0	60.43
-5	18	0	53.83
-5	20	0	59.56
-5	22	0	31.65
-5	25	0	27.79
-4	1	0	63.85
-4	2	0	41.99
-4	3	0	131.70
-4	4	0	21.93
-4	5	0	227.15
-4	6	0	42.49
-4	7	0	123.98
-4	8	0	122.23
-4	10	0	224.65
-4	12	0	147.78
-4	13	0	105.04
-4	14	0	48.72
-4	15	0	149.03
-4	17	0	72.27
-4	18	0	49.84
-4	20	0	81.11
-4	22	0	57.57
-4	23	0	36.38
-4	25	0	43.49
-3	1	0	13.96
-3	2	0	82.98
-3	3	0	109.15
-3	4	0	97.94
-3	5	0	214.96
-3	6	0	99.56
-3	7	0	86.85
-3	8	0	52.95
-3	9	0	48.97
-3	10	0	110.02
-3	11	0	118.42
-3	12	0	34.89
-3	13	0	17.19
-3	14	0	88.47
-3	15	0	69.65
-3	16	0	59.43
-3	17	0	78.25
-3	18	0	58.82
-3	19	0	78.25
-3	20	0	37.38
-3	21	0	76.63
-3	22	0	61.93
-3	24	0	24.92
-3	26	0	44.11
-2	0	0	119.37
-2	1	0	243.34
-2	2	0	90.33
-2	3	0	93.33
-2	4	0	282.59
-2	5	0	309.01
-2	7	0	112.64
-2	8	0	120.74
-2	9	0	219.06
-2	10	0	46.60
-2	11	0	189.77
-2	12	0	65.29
-2	13	0	102.05
-2	14	0	140.30
-2	15	0	147.40
-2	17	0	20.43
-2	18	u	43.24
-2	19	0	76.50
-2	21	0	90.57
-2	23	0	29.90
-2	24	0	34.14
-1	1	0	196.12
-1	3	0	41.12
-1	5	0	20.06
-1	6	0	114.76
-1	7	0	165.22
-1	8	0	50.21
-1	9	0	181.24
-1	10	0	72.77
-1	11	0	99.68
-1	12	0	93.33
-1	13	0	85.97
-1	15	0	30.28
-1	16	0	127.34
-1	17	0	39.37
-1	18	0	68.41
-1	19	0	220.17
-1	20	0	184.54
-1	21	0	71.89
-1	22	0	238.98
-1	23	0	14.33
-1	24	0	154.63
-1	25	0	78.75
0	0	0	73.02
0	1	0	185.65
0	2	0	43.49
0	3	0	161.61
0	4	0	65.79
0	5	0	142.79
0	6	0	29.28
0	7	0	55.45
0	8	0	39.87
0	9	0	41.99
0	10	0	152.51
0	11	0	194.25
0	12	0	144.91
0	13	0	98.43
0	14	0	140.55
0	15	0	72.39
0	16	0	137.56
0	17	0	51.71
0	18	0	183.66
0	19	0	38.50
0	20	0	102.79
0	21	0	150.77
0	22	0	154.75
0	23	0	80.18
0	24	0	87.59
0	25	0	91.46
0	26	0	48.22
1	1	0	54.45
1	2	0	49.59
1	3	0	103.54
1	4	0	146.90
1	5	0	178.55
1	6	0	47.22
1	7	0	84.98
1	8	0	78.75
1	9	0	79.49
1	10	0	42.74
1	11	0	61.55
1	12	0	178.55
1	13	0	39.87
1	14	0	38.26
1	15	0	75.51
1	16	0	53.08
1	17	0	20.31
1	18	0	120.86
1	19	0	40.00
1	20	0	66.91
1	21	0	30.53
1	22	0	47.85
1	23	0	98.07
1	24	0	69.65
1	25	0	49.22
1	26	0	72.14
1	27	0	78.50
1	28	0	86.72
1	29	0	34.74
2	0	0	108.53
2	1	0	49.96
2	2	0	57.69
2	3	0	61.93
2	4	0	35.26
2	5	0	304.01
2	6	0	112.64
2	7	0	120.74
2	8	0	189.77
2	9	0	133.45
2	10	0	175.55
2	11	0	102.05
2	12	0	140.30
2	13	0	147.40
2	14	0	20.43
2	15	0	157.49
2	16	0	66.30
2	17	0	76.50
2	18	0	90.57
2	19	0	78.50
2	20	0	35.39
2	21	0	86.72
2	22	0	29.90
2	23	0	34.14
2	24	0	196.12
2	25	0	51.58
2	26	0	104.66
2	27	0	78.50
2	28	0	86.72
2	29	0	34.74
3	0	0	158.99
3	1	0	21.68
3	2	0	102.79
3	3	0	98.93
3	4	0	24.17
3	5	0	117.37
3	6	0	93.33
3	7	0	78.75
3	8	0	25.92
3	9	0	68.41
3	10	0	30.28
3	11	0	127.34
3	12	0	39.37
3	13	0	68.41
3	14	0	220.17
3	15	0	119.12
3	16	0	26.42
3	17	0	79.88
3	18	0	238.98
3	19	0	14.33
3	20	0	154.63
3	21	0	78.75
3	22	0	73.02
3	23	0	35.01
3	24	0	185.65
3	25	0	43.49
3	26	0	161.61
3	27	0	78.75
3	28	0	29.28
3	29	0	39.87
4	0	0	282.59
4	1	0	309.01
4	2	0	112.64
4	3	0	120.74
4	4	0	189.77
4	5	0	133.45
4	6	0	175.55
4	7	0	102.05
4	8	0	140.30
4	9	0	147.40
4	10	0	20.43
4	11	0	157.49
4	12	0	66.30
4	13	0	76.50
4	14	0	90.57
4	15	0	78.50
4	16	0	35.39
4	17	0	86.72
4	18	0	29.90
4	19	0	34.14
4	20	0	196.12
4	21	0	51.58
4	22	0	104.66
4	23	0	78.50
4	24	0	86.72
4	25	0	34.74
5	0	0	35.26
5	1	0	309.01
5	2	0	112.64
5	3	0	120.74
5	4	0	189.77
5	5	0	133.45
5	6	0	175.55
5	7	0	102.05
5	8	0	140.30
5	9	0	147.40
5	10	0	20.43
5	11	0	157.49
5	12	0	66.30
5	13	0	76.50
5	14	0	90.57
5	15	0	78.50
5	16	0	35.39
5	17	0	86.72
5	18	0	29.90
5	19	0	34.14
5	20	0	196.12
5	21	0	51.58
5	22	0	104.66
5	23	0	78.50
5	24	0	86.72
5	25	0	34.74
6	0	0	38.00
6	1	0	112.51
6	2	0	54.45
6	3	0	31.77
6	4	0	108.15
6	5	0	34.64
6	6	0	105.79
6	7	0	86.85
6	8	0	59.31
6	9	0	46.48
6	10	0	38.13
6	11	0	53.08
6	12	0	41.49
6	13	0	40.62
6	14	0	39.39
6	15	0	45.85
6	16	0	78.12
6	17	0	28.16
6	18	0	44.11
6	19	0	23.67
6	20	0	38.63
6	21	0	56.57
6	22	0	28.16
6	23	0	44.11
6	24	0	23.67
6	25	0	38.63
6	26	0	56.57
6	27	0	28.16
6	28	0	44.11
6	29	0	23.67
7	0	0	90.32
7	1	0	131.45
7	2	0	127.71
7	3	0	201.35
7	4	0	45.11
7	5	0	81.74
7	6	0	206.96
7	7	0	40.00
7	8	0	198.13
7	9	0	110.38
7	10	0	77.63
7	11	0	75.13
7	12	0	88.22
7	13	0	22.18
7	14	0	157.49
7	15	0	81.74
7	16	0	206.96
7	17	0	40.00
7	18	0	198.13
7	19	0	110.38
7	20	0	77.63
7	21	0	75.13
7	22	0	88.22
7	23	0	22.18
7	24	0	157.49
7	25	0	81.74
7	26	0	206.96
7	27	0	40.00
7	28	0	198.13
7	29	0	110.38
8	0	0	105.79
8	1	0	56.82
8	2	0	171.32
8	3	0	32.89
8	4	0	90.83
8	5	0	134.94
8	6	0	81.49
8	7	0	12.96
8	8	0	94.20
8	9	0	158.74
8	10	0	66.91
8	11	0	59.31
8	12	0	46.48
8	13	0	38.13
8	14	0	53.08
8	15	0	41.49
8	16	0	40.62
8	17	0	39.39
8	18	0	45.85
8	19	0	78.12
8	20	0	22.18
8	21	0	56.57
8	22	0	28.16
8	23	0	44.11
8	24	0	23.67
8	25	0	38.63
8	26	0	56.57
8	27	0	28.16
8	28	0	44.11
8	29	0	23.67
9	0	0	158.74
9	1	0	66.91
9	2	0	151.64
9	3	0	69.78
9	4	0	94.32
9	5	0	66.16
9	6	0	148.90
9	7	0	77.87
9	8	0	100.30
9	9	0	93.82
9	10	0	122.98
9	11	0	97.56
9	12	0	55.82
9	13	0	48.72
9	14	0	93.45
9	15	0	63.67
9	16	0	38.75
9	17	0	34.39
9	18	0	66.91
9	19	0	151.64
9	20	0	69.78
9	21	0	94.32
9	22	0	66.16
9	23	0	148.90
9	24	0	77.87
9	25	0	100.30
9	26	0	93.82
9	27	0	122.98
9	28	0	97.56
9	29	0	55.82
10	0	0	84.73
10	1	0	70.90
10	2	0	32.89
10	3	0	53.33
10	4	0	180.40
10	5	0	29.28
10	6	0	38.75
10	7	0	84.07
10	8	0	115.75
10	9	0	81.36
10	10	0	61.93
10	11	0	65.54
10	12	0	37.50
10	13	0	61.43
10	14	0	37.26
10	15	0	55.32
10	16	0	79.87
10	17	0	43.73
10	18	0	80.37
10	19	0	42.11
10	20	0	69.03
10	21	0	52.63
10	22	0	28.91
10	23	0	43.73
10	24	0	22.91
10	25	0	37.63
10	26	0	55.82
10	27	0	28.16
10	28	0	44.11
10	29	0	23.67
11	0	0	116.13
11	1	0	129.09
11	2	0	60.43
11	3	0	72.27
11	4	0	46.44
11	5	0	38.75
11	6	0	81.36
11	7	0	151.64
11	8	0	37.50
11	9	0	109.27
11	10	0	98.06
11	11	0	61.11
11	12	0	84.07
11	13	0	79.38
11	14	0	101.05
11	15	0	128.84
11	16	0	100.30
11	17	0	93.82
11	18	0	122.98
11	19	0	97.56
11	20	0	55.82
11	21	0	48.72
11	22	0	93.45
11	23	0	63.67
11	24	0	38.75
11	25	0	68.41
11	26	0	55.82
11	27	0	48.72
11	28	0	93.45
11	29	0	63.67
12	0	0	84.73
12	1	0	70.90
12	2	0	32.89
12	3	0	53.33
12	4	0	180.40
12	5	0	29.28
12	6	0	38.75
12	7	0	84.07
12	8	0	115.75
12	9	0	81.36
12	10	0	61.93
12	11	0	65.54
12	12	0	37.50
12	13	0	61.43
12	14	0	37.26
12	15	0	55.32
12	16	0	79.87
12	17	0	43.73
12	18	0	80.37
12	19	0	42.11
12	20	0	69.03
12	21	0	52.63
12	22	0	28.91
12	23	0	43.73
12	24	0	22.91
12	25	0	37.63
12	26	0	55.82
12	27	0	28.16
12	28	0	44.11
12	29	0	23.67
13	0	0	116.13
13	1	0	129.09
13	2	0	60.43
13	3	0	72.27
13	4	0	46.44
13	5	0	38.75
13	6	0	81.36
13	7	0	151.64
13	8	0	37.50
13	9	0	109.27
13	10	0	98.06
13	11	0	61.11
13	12	0	84.07
13	13	0	79.38
13	14	0	101.05
13	15	0	128.84
13	16	0	100.30
13	17	0	93.82
13	18	0	122.98
13	19	0	97.56
13	20	0	55.82
13	21	0	48.72
13	22	0	93.45
13	23	0	63.67
13	24	0	38.75
13	25	0	68.41
13	26	0	55.82
13	27	0	48.72
13	28	0	93.45
13	29	0	63.67
14	0	0	59.43
14	1	0	96.81
14	2	0	76.50
14	3	0	46.85
14	4	0	56.82
14	5	0	51.34
14	6	0	41.87
14	7	0	60.43
14	8	0	41.74
14	9	0	42.49
14	10	0	35.88
14	11	0	43.98
14	12	0	54.08
14	13	0	53.95
14	14	0	54.08
14	15	0	51.71
14	16	0	52.21
14	17	0	49.53
14	18	0	56.82
14	19	0	51.96
14	20	0	43.86
14	21	0	57.69
14	22	0	56.82
14	23	0	41.24
14	24	0	75.26
14	25	0	65.04
14	26	0	37.50
14	27	0	56.82
14	28	0	41.24
14	29	0	75.26
15	0	0	59.43
15	1	0	96.81
15	2	0	76.50
15	3	0	46.85
15	4	0	56.82
15	5	0	51.34
15	6	0	41.87
15	7	0	60.43
15	8	0	41.74
15	9	0	42.49
15	10	0	35.88
15	11	0	43.98
15	12	0	54.08
15	13	0	53.95
15	14	0	54.08
15	15	0	51.71
15	16	0	52.21
15	17	0	49.53
15	18	0	56.82
15	19	0	51.96
15	20	0	43.86
15	21	0	57.69
15	22	0	56.82
15	23	0	41.24
15	24	0	75.26
15	25	0	65.04
15	26	0	37.50
15	27	0	56.82
15	28	0	41.24
15	29	0	75.26
16	0	0	59.43
16	1	0	96.81
16	2	0	76.50
16	3	0	46.85
16	4	0	56.82
16	5	0	51.34
16	6	0	41.87
16	7	0	60.43
16	8	0	41.74
16	9	0	42.49
16	10	0	35.88
16	11	0	43.98
16	12	0	54.08
16	13	0	53.95
16	14	0	54.08
16	15	0	51.71
16	16	0	52.21
16	17	0	49.53
16	18	0	56.82
16	19	0	51.96
16	20	0	43.86
16	21	0	57.69
16	22	0	56.82
16	23	0	41.24
16	24	0	75.26
16	25	0	65.04
16	26	0	37.50
16	27	0	56.82
16	28	0	41.24
16	29	0	75.26
17	0	0	59.43
17	1	0	96.81
17	2	0	76.50
17	3	0	46.85
17	4	0	56.82
17	5	0	51.34
17	6	0	41.87
17	7	0	60.43
17	8	0	41.74
17	9	0	42.49
17	10	0	35.88
17	11	0	43.98
17	12	0	54.08
17	13	0	53.95
17	14	0	54.08
17	15	0	51.71
17	16	0	52.21
17	17	0	49.53
17	18	0	56.82
17	19	0	51.96
17	20	0	43.86
17	21	0	57.69
17	22	0	56.82
17	23	0	41.24
17	24	0	75.26
17	25	0	65.04
17	26	0	37.50
17	27	0	56.82
17	28	0	41.24
17	29	0	75.26
18	0	0	59.43
18	1	0	96.81
18	2	0	76.50
18	3	0	46.85
18	4	0	56.82
18	5	0	51.34
18	6	0	41.87
18	7	0	60.43
18	8	0	41.74
18	9	0	42.49
18	10	0	35.88
18	11	0	43.98
18	12	0	54.08
18	13	0	53.95
18	14	0	54.08
18	15	0	51.71
18	16	0	52.21
18	17	0	49.53
18	18	0	56.82
18	19	0	51.96
18	20	0	43.86
18	21	0	57.69
18	22	0	56.82
18	23	0	41.24
18	24	0	75.26
18	25	0	65.04
18	26	0	37.50
18	27	0	56.82
18	28	0	41.24
18	29	0	75.26
19	0	0	59.43
19	1	0	96.81
19	2	0	76.50
19	3	0	46.85
19	4	0	56.82
19	5	0	51.34
19	6	0	41.87
19	7	0	60.43
19	8	0	41.74
19	9	0	42.49
19	10	0	35.88
19	11	0	43.98
19	12	0	54.08
19	13	0	53.95
19	14	0	54.08
19	15	0	51.71
19	16	0	52.21
19	17	0	49.53
19	18	0	56.82
19	19	0	51.96
19	20	0	43.86
19	21	0	57.69
19	22	0	56.82
19	23	0	41.24
19	24	0	75.26
19	25	0	65.04
19	26	0	37.50
19	27	0	56.82
19	28	0	41.24
19	29	0	75.26
20	0	0	59.43
20	1	0	96.81
20	2	0	76.50
20	3	0	46.85
20	4	0	56.82
20	5	0	51.34
20	6	0	41.87
20	7	0	60.43
20	8	0	41.74
20	9	0	42.49
20	10	0	35.88
20	11	0	43.98
20	12	0	54.08
20	13	0	53.95
20	14	0	54.08
20	15	0	51.71
20	16	0	52.21
20	17	0	49.53
20	18	0	56.82
20	19	0	51.96
20	20	0	43.86
20	21	0	57.69
20	22	0	56.82
20	23	0	41.24
20	24	0	75.26
20	25	0	65.04
20	26	0	37.50
20	27	0	56.82
20	28	0	41.24
20	29	0	75.26
21	0	0	59.43
21	1

TABLE 2. (Continued)

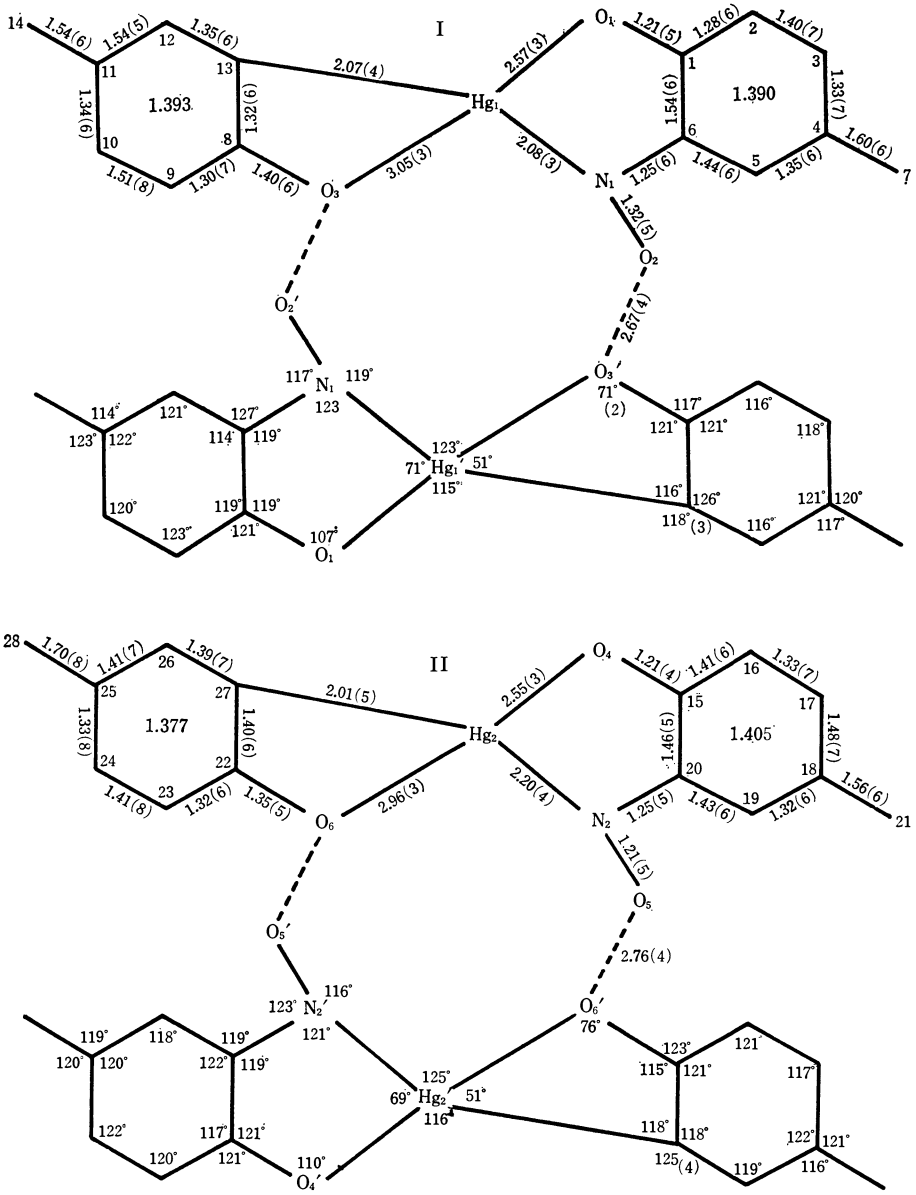

Fig. 2. Bond lengths (Å) and angles (°) found in molecule I and molecule II. E.s.d.'s are shown in parentheses denoting the least significant digits of the corresponding values.

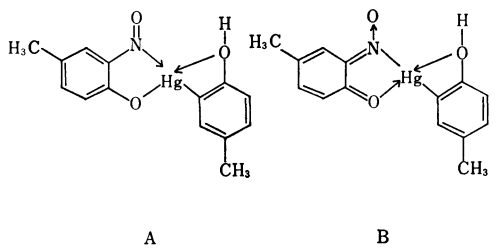

Fig. 3. The structures of the present complex molecule proposed in the previous paper.[2]

Although the location of hydrogen atoms are not shown in the present structure determination, a comparison of the N–O bond lengths in NMP-group which have double bond character and the C–O bond lengths in MMP-group which correspond to the carbon to phenolic oxygen bond lengths (C–OH), indicates that the latter oxygen atoms exist in the form of hydroxyl groups and act as hydrogen donors in the hydrogen bond systems.

From the discussions on the C–N and N–O bond lengths it may be concluded that the structure of the

TABLE 3. COMPARISON OF THE N-O AND C-N BOND LENGTHS AND C-N-O ANGLES OF THE OXIMES, NITROSO AND *N*-OXIDE COMPOUNDS

Compounds	N-O	C-N	C-N-O	Ref.
Oximes				
Bis(salicylaldoximato)copper(II)	1.45 Å	1.25 Å	115°	5
Nickel dimethylglyoxime	1.38 1.37	1.20 1.25	121 121	6
Nickel glyoxime	1.350 1.343	1.277 1.303	121.8 121.1	7
5-Methoxy-2-quinone-2-oxime	1.36	1.22	117	8
N-Methyl-*p*-chlorobenzaldoxime	1.284	1.309	125.2	9
β-5-*n*-Propoxy-*o*-quinone-2-oxime	1.353	1.319	116.8	10
α-5-(2′-Chloroethoxy)-*o*-quinone-2-oxime	1.365	1.306	112.5	11
Nitroso compounds				
(*trans*)	1.25	1.57	125	12
Dinitrosomethane	1.30	1.48	119	13
(*cis*)	1.32	1.45	120	
1-(4-Chlorobenzyl)-1-nitroso-2-(4,5-dihydro-2-imidazolyl) hydrazine monohydrate	1.25			14
p-Methoxyindophenol *N*-oxide	1.266	1.357 1.450	122.7 116.1	15
Nitrosobenzene (dimer)	1.35			16
N-Oxides				
anti-2,5-Dimethyl-4-chloro-*N*-methylbenzene aldoxime	1.298	1.29	124	17
anti-4-Chloro-*N*-methylbenzenealdoxime	1.28	1.30	125	17
Bis-(pyridine *N*-oxide)Copper(II) nitrate	1.362 1.361	1.352 1.337 1.325 1.369	116.8 119.1 120.1 116.9	18
Di-*μ*-(pyridine oxide)-bis(dichloro-copper(II))	1.346	1.341	118.2	19
Pyridine oxide hydrochloride	1.37	1.31 1.36	116.1 117.1	20
Present Compound (mean of the two complexes)	1.27	1.25	120	

present complex is represented as shown in Fig. 3, B.

The mercury atoms adopt planar four-fold coordination if one takes the intramolecular short distances of O(3)–Hg(1), 3.05 Å and O(6)–Hg(2), 2.96 Å as the fourth coordination bonds. Table 4 shows the deviations of atoms from the plane formed by each coordination group.

Figures 4 and 5 show the crystal structure projected along the *c*- and *a*-axis, respectively. Each molecule takes a nearly planar conformation and is inclined to the *c*-axis at an angle of 56° in I and 54° in II. As seen in Fig. 5, the neighboring dimers in the *c* direction overlap strongly and the dimers of each kind, I-I or II-II, are piled up along the *c*-axis forming a columnar unit. The columns are

5) M. A. Jarski and E. C. Lingafelter, *Acta Cryst.*, **17**, 1109 (1964).
6) L. E. Godycki and R. E. Rundle, *ibid.*, **6**, 487 (1953).
7) M. Calleri, G. Ferraris and D. Viterbo, *ibid.*, **22**, 468 (1967).
8) G. W. R. Bartindale, M. M. Crowder and K. A. Morley, *ibid.*, **12**, 111 (1959).
9) K. Folting, W. N. Lipscomb and B. Jerslev, *ibid.*, **17**, 1263 (1964).
10) C. Romers, *ibid.*, **17**, 1287 (1964).
11) J. W. L. van Oijen and C. Romers, *ibid.*, **20**, 169 (1966).
12) M. Van Meerssche and G. Germain, *ibid.*, **12**, 818 (1959).
13) G. Germain, P. Piret and M. Van Meerssche, *ibid.*, **16**, 109 (1963).
14) G. J. Palenik, *ibid.*, **19**, 47 (1965).
15) C. Romers and B. Hesper, *ibid.*, **20**, 162 (1966).
16) J. W. Linnett and R. M. Rosenberg, *Tetrahedron*, **20**, 53 (1964).
17) K. G. Jensen and B. Jerslev, *Acta Cryst.*, **B25**, 916 (1969).
18) S. Šćavničar and B. Matkovic, *ibid.*, **B25**, 2046 (1969).
19) R. S. Sager, R. J. Williams and W. H. Watson, *Inorg. Chem.*, **6**, 951 (1967).
20) G. Tsoucaris, *Acta Cryst.*, **14**, 914 (1961).

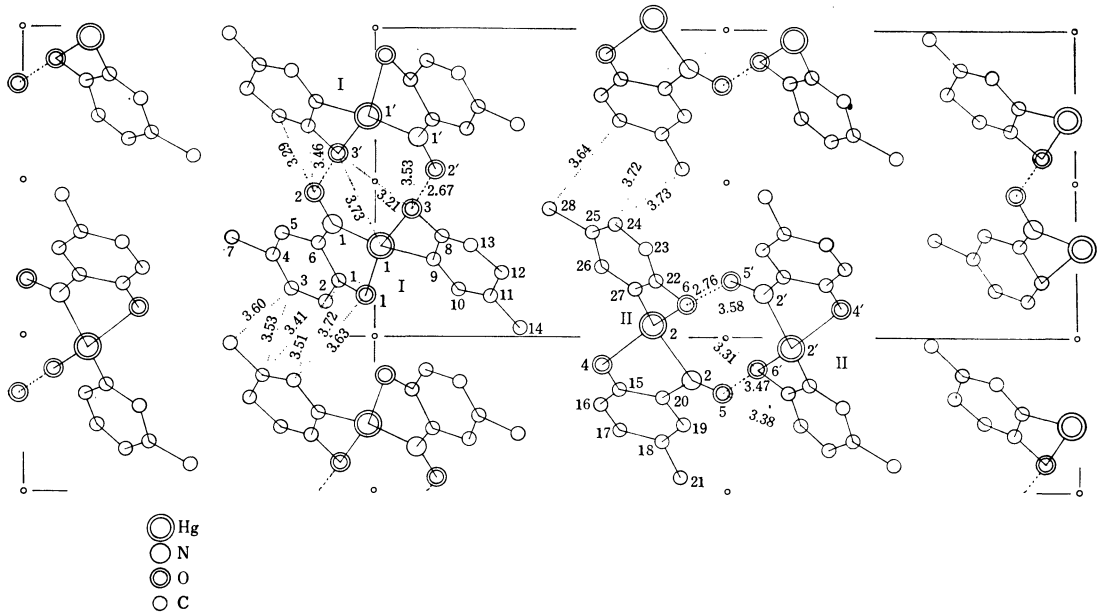

Fig. 4. The *c*-axis projection of the crystal structuere. Hydrogen bonds are shown by broken lines and intermolecular short distances less than 3.75Å are shown by dotted lines.

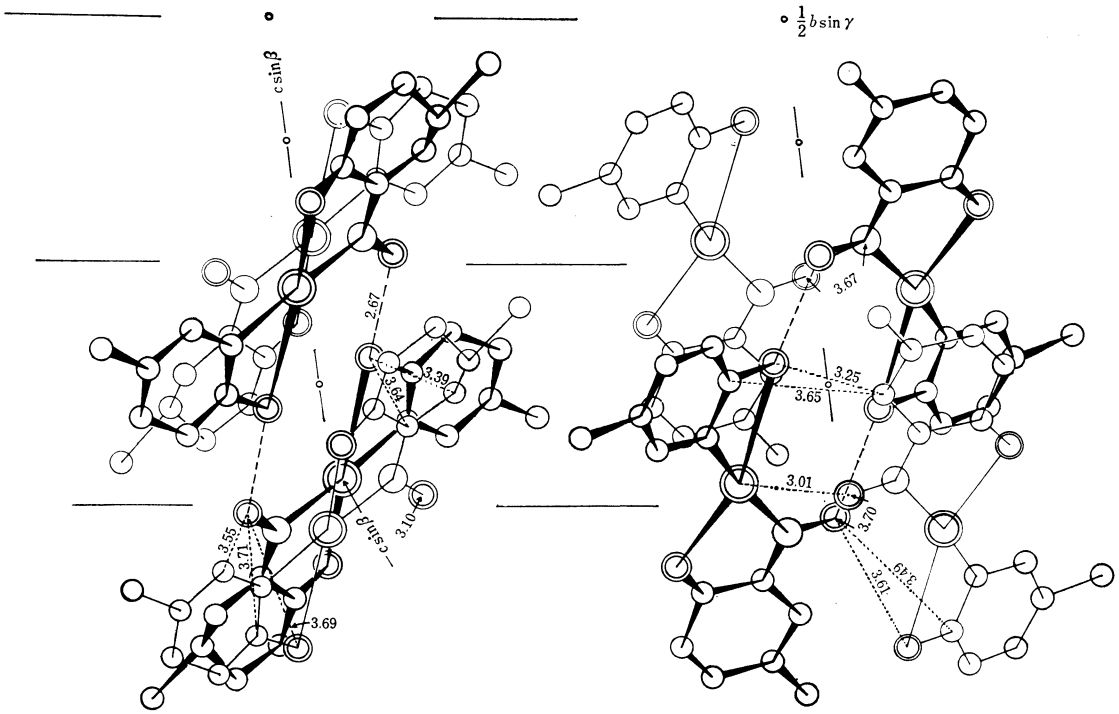

Fig. 5. The *a*-axis projection of the crystal structure showing the stacking of the complex molecules.

Table 4. The deviations of the atoms from the least-squares planes

Molecule I		Molecule II	
Atom	Distances	Atom	Distances
Coordinated group around Hg			
Hg(1)	−0.09 Å	Hg(2)	−0.13 Å
O(1)	0.16	O(4)	0.26
O(3)	0.17	O(6)	0.27
N(1)	−0.09	N(2)	−0.14
C(13)	−0.16	C(17)	−0.26
2-Nitroso-4-methylphenol group			
C(1)	0.01	C(15)	0.05
C(2)	−0.02	C(16)	−0.03
C(3)	0.02	C(17)	−0.01
C(4)	−0.02	C(18)	0.04
C(5)	0.02	C(19)	−0.02
C(6)	0.01	C(20)	−0.03
distance to the plane			
C(7)	0.01	C(21)	0.29
O(1)	0.20	O(4)	−0.04
N(1)	−0.07	N(2)	−0.08
C(2)	−0.09	O(5)	0.01
2-Mercuri-4-Methylphenol group			
C(8)	−0.02	C(22)	0.01
C(9)	0.05	C(23)	0.03
C(10)	−0.07	C(24)	−0.03
C(11)	0.05	C(25)	0.00
C(12)	−0.02	C(26)	0.03
C(13)	0.00	C(27)	−0.04
distance to the plane			
Hg(1)	−0.10	Hg(2)	−0.10
O(3)	0.07	O(6)	0.01
C(14)	−0.09	C(28)	0.17

packed together in the ***a*** direction mainly through the van der Waals interaction between the phenolic groups forming the layers of the dimer molecules. The two kinds of layers each consisting of the dimers I-I or II-II are packed together alternately along the *b*-axis. The packing of the layers in the ***b***-direction is rather loose and no close contact shorter than 3.75 Å is found between the layers.

In Figures 4 and 5 are shown intermolecular short distances less than 3.75 Å. It is to be noted that the dimers I-I and II-II are situated approximately in such positions that they are related by a rotation about the axis parallel to ***c*** followed by a mirror operation with the mirror plane parallel to ***c***. Comparison of Fig. 4 with Fig. 1 of the previous paper[2] indicates that the structure of the present crystal resembles, in some respect, that found in the crystal grown from chloroform solutions. The latter crystal contains chloroform molecules as the solvent of crystallization filling up the spaces between the II-II dimers. These spaces are filled by the dimers I-I in the present crystal.

The authors wish to express their sincere thanks to Professor Zenzo Tamura for his continuous encouragement.

BULLETIN OF THE CHEMICAL SOCIETY OF JAPAN VOL. 43 3079—3082 (1970)

The Fractionation of Tritium in the Crystallization of Inorganic Hydrates from a Tritiated Solution

Haruhiko TANAKA*1 and Hisao NEGITA

Department of Chemistry, Faculty of Science, Hiroshima University, Higashi-sendamachi, Hiroshima

(Received April 27, 1970)

Bennema's theory of crystal growth from a solution was modified and used in explaining fractionations of tritiated water in the crystal-growth processes of several inorganic hydrated salts from concentrated aqueous solutions. It was suggested that some water molecules in the aqueous solutions were free to become growth units which are not necessarily activated for entering the crystal surface. The dilution of tritiated water in the crystal was observed; this was explained in a satisfactory way in terms of the surface-diffusion model originally proposed by Burton, Cabrera, and Frank. On the contrary, the volume diffusion model was inadequate for interpreting the fractionation of tritium.

The theory of crystal growth from the vapor phase has been extensively developed, and there is sufficient experimental evidence supporting the concept of surface diffusion which regulates the growth mechanism.[1] The crystal growth from a solution, however, has been scarcely at all treated from the theoretical point of view. The kinetics of crystallization from a solution becomes more complicated because of the interaction and solvation of constituent ions, although there is no essential difference between the growth from vapor and that from a solution.

The rate of crystal growth from a solution is assumed to depend on the advance velocity of the steps. It is, in turn, a problem whether or not a surface diffusion of growth units plays an essential role in the growth process. This point has been discussed on the basis of the morphological theory of Hartman and Perdok, and the surface diffusion has been found to be an essential process in the crystal growth.[2] Recently Bennema[2,3] has explained his accurate data on the crystal growth by assuming the surface-diffusion model of Burton, Cabrera, and Frank.[1]

On the basis of these works it has come to seem probable that crystal growth from solution at a low supersaturation also occurs with the surface-diffusion process. However, there has thus far been little discussion of the mechanism of the crystal growth of inorganic hydrates, especially those from concentrated aqueous solutions. This is probably due to the complicated behavior of growth units in solutions. The aim of the present paper is to discuss the mechanism of the crystal growth of several inorganic hydrated salts from aqueous solutions in the light of the fractionation of tritiated water.

There have been a few papers studying the fractionations of heavy water (but not that of tritiated water) in the growth processes.[4,5] These results have been discussed from the points of view of the vapor pressures of the ctystal and the solution or from that of the hydrogen bonding of water, but not on the basis of the theory of crystal growth from a solution. On the contrary, it may be possible, under the present experimental conditions, to use the crystal-growth theory from a solution, which is useful at low supersaturations up to *ca.* 20%, in explaining the fractionations of tritiated water. A trace amount of tritiated water was present in a solution of inorganic salt; its fractionation was examined when the salts were crystallized with water of hydration and much attention was paid to the behavior of water crystallized from the solution.

Experimental

Large single crystals of sulfates of cobalt, nickel, and copper were grown from unstirred solutions by evaporating the solvent containing a trace amount of tritiated water (*ca.* 1.0×10^{-6} mol/m*l*). A single crystal of cobalt sulfate was obtained at 30.0°C, while others

*1 Present address: Shinonome Branch School, Faculty of Education, Hiroshima University, Shinonome, Hiroshima.

1) W. K. Burton, N. Cabrera and F. C. Frank, *Phil. Trans. Roy. Soc.*, **243**, 299 (1951).

2) P. Bennema, Thesis, The Technical University of Delft (1965).

3) P. Bennema, *J. Cryst. Growth*, **5**, 29 (1969).

4) R. M. Barrer and A. F. Denny, *J. Chem. Soc.*, **1964**, 4677.

5) M. Johansson and K. E. Holmberg, *Acta Chem. Scand.*, **23**, 765 (1969).

were obtained at 40.0°C. The rates of crystal growth were so slow that only 3 or 4 g of the crystals were obtained in two weeks. The water of hydration was recovered by heating the single crystal until no further dehydration was observed.

The tritium contents in the dehydrated water were compared with those of the mother liquid by observing their activities. The activity measurements were done by a liquid scintillation counter, a Packard Model 2002 Tri-Carb Scintillation Spectrometer. As the scintillant we used a solution composed of toluene, ethylene glycol monomethyl ether, 2,5-diphenyloxazole (PPO), and 1,4-bis-2′-(5′-phenyloxazolyl)benzene (POPOP).

Results and Discussion

The observed fractionations of tritiated water are summarized in Table 1; the table shows that all the separation factors are less than unity, implying the dilution of tritiated water in the hydrate crystal. The separation factor, S, for the equilibrium between solid and liquid phases is usually defined by:

$$S = \{N_s/(1-N_s)\}\{(1-N_l)/N_l\}, \quad (1)$$

where N_s and N_l are the mole fractions of a given isotope (tritiated water, in the present case) in the solid and liquid phases respectively. Since N_s and N_l are extremely small in the present study, Eq. (1) can be simplified to:

$$S = N_s/N_l. \quad (2)$$

Table 1. Separation factor of tritiated water, S, observed in the crystallization of the sulfate from its solution

Crystal	$S_{obs.}$
$CoSO_4 \cdot 7H_2O$	0.979 ± 0.007
$NiSO_4 \cdot 7H_2O$	0.972 ± 0.011[6]
$CuSO_4 \cdot 5H_2O$	0.956 ± 0.012[7]

Theories of Crystal Growth from a Solution. Recently, Bennema has applied the spiral crystal growth model of Burton *et al.*, derived from the vapor phase, to that from a solution.[3] According to his treatment, the rate of crystal growth, R, from a solution at a low supersaturation is given as follows:

$$R = \beta c_0 \Omega (kT/h) A N_0 \exp(-H/kT)(\sigma^2/\sigma_1) \tanh(\sigma_1/\sigma), \quad (3)$$

where the notations are as given below:

β=retarding factor arising if the relaxation time for a growth unit's entry into a kink is small
c_0=retarding factor arising if $x_s \ll x_0$
x_s=mean displacement of a growth unit on the surface
x_0=mean distance between the kinks
Ω=volume of a growth unit in the crystal
k=Boltzmann's constant
T=absolute temperature
h=Planck's constant
A=thickness of the adsorption layer
N_0=equilibrium concentration of growth units per cm^3 in the solution
H=dehydration activation energy for an entry of growth units into the adsorption layer
σ=relative supersaturation
$\sigma_1 = 9.5\ \gamma a/(\varepsilon k T x_s)$
γ=edge free energy of a step of the length of a
a=the shortest distance between growth units
ε=measure of the number of interacting spirals

Equation (3) may be useful in estimating the rate of integration of an ion into the crystal in the case of the growth of an ionic crystal from the aqueous solution.

A modified equation has to be used for estimating the rate of integration of water in the growth of hydrated ionic crystals from aqueous solutions, assuming for the moment that some water molecules integrate independently of ions. For this purpose, the spiral crystal-growth theory from vapor by Burton *et al.*[1] may properly be used. According to this theory, the following relation holds between R and σ, assuming that the diffusion of growth units on the surface determines the growth rate:

$$R = C(\sigma^2/\sigma_1) \tanh(\sigma_1/\sigma). \quad (4)$$

The constant, C, will be given below for a free water molecule integrating from the solution to the crystal surface.

Assuming, further, that the integration occurs without activation, we can use a model for the mobile adsorption layer[8] much like that used for the growth theory from vapor discussed by Bennema.[2] The n_{s0}/N_0 ratio is thus given as follows for the equilibrium between the water molecules (growth units in this case) in the solution and those on the surface:

$$n_{s0}/N_0 = \{h/(2\pi m k T)^{1/2}\} \exp(A/kT), \quad (5)$$

where n_{s0} is the equilibrium concentration of growth units per cm^2 on the surface, m is the mass of a growth unit, and A is the energy difference between growth units in the solution and those on the surface. We should note here that one translational degree of freedom is lost if a growth unit is adsorbed onto the surface from the bulk solution. In Eq. (5) we disregard the fractions of reflected molecules striking the surface and the changes in the degrees of freedom other than the translational.

Accordingly, it follows from Eq. (5) and some lengthy treatments[1,2] that:

$$C = \alpha \beta c_0 \Omega N_0 k T/(2\pi m k T)^{1/2}. \quad (6)$$

The α factor is introduced as a correction for the growth from a solution, which is assumed to be

6) H. Tanaka and H. Negita, *J. Sci. Hiroshima Univ., Ser. A-II*, **32**, 299 (1968).
7) H. Tanaka, K. Hiraga and H. Negita, *J. Sci. Hiroshima Univ., Ser. A-II*, **33**, 243 (1969).
8) S. Glasstone, K. J. Laidler and H. Eyring, "The Theory of Rate Processes," McGraw-Hill Book Co., Inc., New York (1941), P. 350.

independent of the hydrogen isotopes. If the surface diffusion of a growth unit is an essential process in the growth process, Eq. (6) is simplified and combined with Eq. (4) to give rise to:

$$R = \alpha c_0 \Omega N_0 (kT/2\pi m)^{1/2} (\sigma^2/\sigma_1) \tanh(\sigma_1/\sigma), \quad (7)$$

since the value of β becomes unity. On the other hand, if the volume-diffusion model for the growth from a solution is adopted, in which model a growth unit is directly transported from the solution to the kink without any surface diffusion, the rate of the crystal growth is given by:

$$R = \{2\pi\lambda\varepsilon\beta D N_0 \Omega k T/(19\gamma a x_0)\}\sigma^2, \quad (8)$$

where λ is the mean distance between one equilibrium position and a neighboring one in the solution, and where D is the volume-diffusion constant. The volume-diffusion model was discussed extensively by Bennema on the basis of the original theory of Burton *et al.*[2] We may note here that both Eqs. (7) and (8) are adequate in considering the crystal growth from a well-stirred solution at a low supersaturation.

Water and Ions in a Concentrated Solution. In concentrated aqueous solutions of inorganic salts, a given ion can not exist independently of other ions and water molecules; *i. e.*, the system is very complicated due to complex formation and the hydration of ions. The complexes can be divided into two types, outer-sphere and inner-sphere complexes.[9] The process of inner-sphere-complex formation in the sulfates of divalent cations may be formulated as follows, with the successive release of intervening water molecules:

$$M(OH_2)_p^{2+} + SO_4^{2-} \rightleftharpoons M(OH_2)_p^{2+}, SO_4^{2-}$$

$$\rightleftharpoons M(OH_2)_{p-q}^{2+}, SO_4^{2-} + qH_2O,$$

where p is the hydration number of the M^{2+} ion in the dilute aqueous solution and where q is the number of water molecules dehydrated in the inner-sphere-complex formation ($0 \leqq q \leqq p$). In the scheme, the hydration of the anion and any quantum mechanical interaction of the anion with the cation are ignored.

The value of q can be larger than unity; that is, the remaining water molecules in the inner-sphere complex are subject to further dehydration. This point has been discussed by many workers on the assumption that complex formation occurs fundamentally because of coulombic forces between the oppositely-charged ions.[10] Further dehydration seems to be very probable, particularly in the case of the weak hydration of cations, as is the case with the present study. We can thus assume in the succeeding argument that extra water molecules are released from the hydration sheath of cations in the complex under the present conditions.

Estimation of Separation Factors. Recognizing that molecules of the same chemical species but labeled with different isotopes have the same structure and electronic configuration, we can obtain the ratios of R_{HTO}/R_{H_2O} for two cases.

(a) In the case of the surface diffusion, the following relation is derived from Eq. (7):

$$R_{HTO}/R_{H_2O} = (m_{H_2O}/m_{HTO})^{1/2} = 0.949, \quad (9)$$

where R_{HTO}/R_{H_2O} is the ratio of the integration of HTO to that of H_2O molecules into the crystal and where m_{H_2O}/m_{HTO} is the mass ratio of H_2O to HTO molecules.

(b) In the case of the volume diffusion;

$$R_{HTO}/R_{H_2O} = D_{HTO}/D_{H_2O} = 1, \quad (10)$$

where D_{HTO}/D_{H_2O} is the ratio of the diffusion constants of HTO to H_2O molecules in the solution.

Equations (9) and (10) are supported by the following considerations:

(1) σ_1, which is a function of the mean displacement of a growth unit, X_s, may be independent of the mass of water, supposing that growth units in the activated state and those in the non-activated state on the surface have the same degrees of freedom.

(2) The retarding factor, β, in Eq. (8) is a function of relative supersaturations around the steps and the kinks, and the factor, c_0, is a function of both the mean distance between the kinks and the distance between successive turns of the spiral. Therefore, the values of β and c_0 should be unchangeable in a system with a trace amount of tritiated water, though these factors play an important role in determining the mechanism and the absolute value of R in the growth process.

(3) The value of D may be practically independent of the hydrogen isotope of the water molecule, as seen from the work by Wang *et al.*[11]

(4) The other factors in Eqs. (7) and (8) may also be unaffected by the presence of tritiated water.

Accordingly, we can estimate the separation factors from either Eq. (9) or (10), assuming that fractionations of tritiated water occur, if at all, only with free water molecules and not with the hydration water of cations. When hydrated cations

Table 2. Possible growth units and separation factor, S, calculated by Eq. (9)

Crystal	Growth units assumed	$S_{cal.}$
$CoSO_4 \cdot 7H_2O$	$Co(OH_2)_3^{2+}$, SO_4^{2-} and $4H_2O$	0.791
$NiSO_4 \cdot 7H_2O$	$Ni(OH_2)_3^{2+}$, SO_4^{2-} and $4H_2O$	0.971
$CuSO_4 \cdot 5H_2O$	$Cu(OH_2)_2^{2+}$, SO_4^{2-} and $3H_2O$	0.969

9) F. Basalo and R. G. Pearson, "Mechanisms of Inorganic Reactions," John Wiley and Sons, Inc., New York (1967), p. 34.

10) For example; J. E. Prue, *J. Chem. Educ.*, **46**, 12 (1969).

11) J. H. Wang, C. V. Robinson and I. S. Edelman, *J. Amer. Chem. Soc.*, **75**, 466 (1953).

are assumed to be "half-undressed" in the concentrated solutions, the values of S may be given as follows from Eq. (9):
(a) For $CoSO_4 \cdot 7H_2O$ and $NiSO_4 \cdot 7H_2O$ $S = (3 \times 1.000 + 4 \times 0.949)/7 = 0.971$, (b) for $CuSO_4 \cdot 5H_2O$ $S = (2 \times 1.000 + 3 \times 0.949)/5 = 0.969$. Table 2 shows the species of growth units assumed, and the corresponding values of S estimated, as above.

From Eq. (10), which is based on the volume-diffusion mechanism, on the other hand, the values of S become unity, irrespective of the number of free water molecules as well as of the species of the growth units.

Factors Affecting the Separation Factor. There are various factors which affect the separation factor. Among them, those cited below may be most important:

(1) Inner-sphere complexes may be easily formed with an increase in the concentration of the solution, giving rise to more free water molecules and, thus, to a larger fractionation of tritiated water.

(2) The dehydration of ions in a solution should tend to occur at higher temperatures, thus leading to an increase in the fractionation of tritiated water.

(3) The weaker hydration of the cation may favor the release of the molecules from the inner-sphere complex,[12] which will in turn make the fractionation larger.

(4) Rapid crystallization (growth from a highly-supersaturated solution) may result in less fractionation of tritiated water, since it can be assumed that the equilibrium is no longer attained between growth units in the solution and the crystal surface.

(5) The situation becomes complicated at a high concentration of the hydronium ion because of proton transfer through water and proton injection into the crystal.[13] The effect on the fractionation of tritium can be neglected when the concentration of H_2TO^+ is very low.

Fractionation of Tritium and Crystal Growth. (1) Since the agreement between the calculated values of S listed in Table 2 and the experimental values seems to be satisfactory, it may be noted qualitatively that some dilution of tritiated water occurs in the hydrated salts. This ambiguity, however, may be inevitable at this stage, because many assumptions are involved in the preceding argument, especially because the number of free water molecules is adjustable.

(2) The point in our argument is not the absolute value of crystal growth rate, R, but the ratio of R_{HTO}/R_{H_2O}. Although the crystal growth process from an unstirred solution is influenced by the mass-transfer of a growth unit, the ratio of R_{HTO}/R_{H_2O} may be unaffected by the mass-transfer, since the D_{HTO}/D_{H_2O} ratio is nearly equal to unity.

(3) Free water molecules, in fact, can not integrate into the crystal independently, but crystallize accompanying the ion with the lowest relaxation time, since growth units are fixed into the crystal in a stoichiometric way. We presume, however, that it should be possible to obtain the ratio of R_{HTO} to R_{H_2O} either from Eq. (7) or from (8).

(4) Even if the spiral-growth model employed above might be partly disturbed by two-dimensional nuclei formed between steps at a higher supersaturation,[14] it is probable that the surface-diffusion mechanism is not seriously affected by the possible disturbance. We can thus estimate the ratio of R_{HTO} to R_{H_2O} independently of the nucleation, since the growth of the nuclei results from the surface diffusion and the subsequent integration of growth units into the kinks.

(5) It may be generally accepted that water molecules of crystallization come partly from free water in a solution and partly from hydration water in the growth of a hydrated crystal, recognizing that, practically, the latter is not subject to the fractionation of tritiated water.

(6) From the fact that the concept of the surface diffusion for crystal growth from a solution is adequate to explain the experimental results, while the concept of volume diffusion is not, it may be concluded that: (a) some free water must enter the crystal by the surface-diffusion mechanism and (b) inogranic hydrated sulfates probably crystallize, also *via* a process of the surface diffusion of growth units.

The authors gratefully acknowledge Dr. Osamu Yamamoto's help with the tritium analyses. Thanks are also due to Mr. Asao Okinaka for his experiment on $CoSO_4 \cdot 7H_2O$.

12) D. R. Rosseinsky, *J. Chem. Soc.*, **1962**, 785.
13) D. F. Williams, B. Sykes and W. G. Schneider, *Can. J. Chem.*, **45**, 1109 (1967).
14) P. Bennema, R. Kern and B. Simon, *Phys. Status Solidi*, **19**, 211 (1967).

BULLETIN OF THE CHEMICAL SOCIETY OF JAPAN VOL. 43 3083—3086 (1970)

Effect of Pressure on the Solubility of Diketopiperazine in Water*1

Keizo SUZUKI, Masao TSUCHIYA and Hideki KADONO

Department of Chemistry, Faculty of Science and Engineering, Ritsumeikan University, Kita-ku, Kyoto

(Received April 27, 1970)

Diketopiperazine (DKP) was used as a model compound to investigate hydrogen bond interactions between the peptide bond and water under high pressure. The solubility of DKP in water was measured as a function of pressure up to about 6000 atm at 15, 25 and 35°C. It was observed that the solubility decreases with increasing pressure up to about 4500 atm, and then increases above this pressure. The solubility follows a simple exponential dependence upon pressure at least below 4500 atm. The volume change ΔV accompanying the dissolution of DKP in water is obtained from this pressure dependence of the solubility. The values of ΔV are 5.2 and 5.9 ml/mol at 25° and 35°C, respectively. These values coincide well with those obtained from dilatometric measurements at 1 atm. The reason why the solubility is inverted at the pressure above and below 4500 atm is ascribed to the change of water structure brought about by the compression. The effect of pressure on proteins reported in the previous paper is discussed in relation to the present solubility results.

There is evidence that the effect of pressure on proteines is inverted at the pressure above and below 3000 atm.[1] The reason for this curious inversion may be investigated through appropriate model systems. It is well known that hydrogen bonds play a primary role in maintaining the conformation of proteins.

Diketopiperazine (DKP, 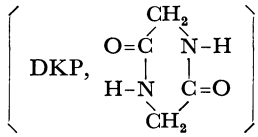) which is a cyclic compound formed through the condensation of 2 molecules of glycine, has been used as a model compound by Gill *et al.*[2] to investigate hydrogen bond interactions. The structure of DKP indicates the possibilities for hydrogen bonds. These possibilities are borne out in the studies of crystal structure[3] and the infrared spectrum using polarized radiation,[4] which show DKP molecules form linear hydrogen bonded polymers in the solid structure. The energy of hydrogen bond maintaining the DKP crystal has been found to be 7 kcal/mol-H bond from the measurements of vapor pressure of DKP by Seki *et al.*[5]

In this report the solubility of DKP in water was measured as a function of pressure to investigate the influence of pressure on the intermolecular forces between DKP-DKP molecules and DKP-water molecules and to gain insight into the behavior of pressure on proteins. The hydrogen bonded interactions between DKP-DKP molecules are analogous to those which maintain the folded structure of proteins. The dissolution of DKP in water is assumed to be analogous to the rupture of the folded structure of proteins.

The solubility measurements of solids under hydrostatic pressure above 1000 atm are seldom found in literatures. Therefore such an experiment is worthwhile to be performed not only for DKP but also for any compound.

The volume changes ΔV that accompany the dissolution of DKP in water were measured at 1 atm by dilatometry, since such a value is a valuable quantity for predicting the initial effect of pressure upon solubility and also for investigating the interactions between DKP-DKP and DKP-water.

Experimental

Sample Preparations. DKP was prepared by the method of Dunn.[6] The product was recrystallized twice from water. The product gave a negative ninhydrin test and was subjected to thin-layer chromato-

*1 Presented at the 21st Annual Meeting of the Chemical Society of Japan, Tokyo, April, 1968, and the 10th Symposium of High Pressure, Kyoto, October, 1968.

1) K. Suzuki, Y. Miyosawa, M. Tsuchiya and Y. Taniguchi, *Rev. Phys. Chem. Japan*, **38**, 63 (1968).

2) S. J. Gill, J. Hutson, J. R. Clopton and M. Dowing, *J. Phys. Chem.*, **65**, 1432 (9161).

3) R. B. Corey, *J. Amer. Chem. Soc.*, **60**, 1598 (1938).

4) R. Newman and R. M. Badger, *J. Chem. Phys.*, **19**, 1147 (1951).

5) S. Seki, K. Suzuki and T. Koide, *Nippon Kagaku Zasshi*, **77**, 346 (1956).

6) M. S. Dunn, *J. Org. Chem.*, **12**, 490 (1947).

graphic analysis. The chromatography indicated no impurity.

Solubility Measurement. For the measurement of solubility of DKP a simple method of residue analysis was used. The solubility data at 25°C and 1 atm with this method was coincident with that obtained by refractive index method.[2]

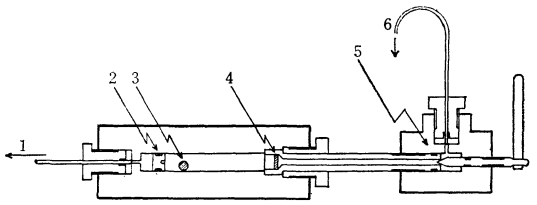

Fig. 1. High pressure equipment for measuring a solubility of solid.
1: To intensifier, 2: Piston, 3: Stainless steel ball, 4: Glass filter, 5: High pressure valve, 6: Outlet

Figure 1 shows the apparatus, which is constructed from a high pressure vessel for obtaining equilibrium solutions and high pressure valve. It is connected to an intensifier with 1/8″ diameter tubing. Glass filter is set at the outlet of the vessel to separate solid DKP from saturated solutions. High pressure measurements were performed with manganin electric-resistance gauge calibrated against Heise's precision pressure gauge of Bourdon type (50 psi scale up to 50000 psi). Paraffin oil was used as a pressure transmitting medium.

To obtain an equilibrium solution, the apparatus was shaken for about 4 hr like a seesaw in a constant temperature bath. The stainless steel ball inserted in the vessel was useful for stirring. Saturated solution was sampled out through high pressure valve by pushing the piston with oil-pump under the pressure as stable as possible. To check the apparatus and the procedures, the solubility of NaCl in water was measured at 25°C and 1000 atm. The accuracy was within ±0.2%, and the solubility data (27.06%) coincided well with that in the reference (27.07%[7]).

Dilatometry. Carlsberg type dilatometer[8] was used to measure the volume change accompanying the dissolution of DKP in water at 1 atm. Kelosine was used as the medium. It was ascertained that kerosine did not attack DKP. Before mixing, the occluded air in DKP sample was thoroughly evacuated. Thermostat was kept within ±0.003°C.

Results and Discussion

Solubility data are listed in Table 1, and are plotted in Fig. 2. These results show that solubility decreases with increasing pressure up to about 4500 atm, but this trend is inverted above this pressure.

In Fig. 3 DKP solubility data at 1 atm is plotted against temperature with the data of Gill *et al.*[2]

Table 1. Solubility of DKP (wt%)

atm / °C	1	1400	2800	4200	5600
15	1.16	0.88	0.68	0.55	0.67
25	1.66	1.25	0.93	0.68	0.82
35	2.32	1.66	1.17	0.90	1.15

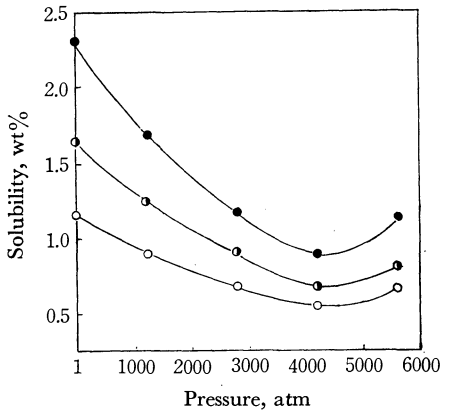

Fig. 2. Solubility of DKP *versus* pressure.
○: 15°C, ◑: 25°C, ●: 35°C

The data when plotted in logarithmic solubility (m_s, molality) *versus* $1/T$, are adequately represented by a straight line. The heat of solution ΔH is calculated from the slope using the relation

$$\left[\frac{\partial \ln m_s}{\partial(1/T)}\right]_p = \frac{-\Delta H}{R} \qquad (1)$$

The value of ΔH determined at 1 atm is 6.2 kcal/mol. This value decreases with increasing pressure, and ΔH value at 4000 atm is 3.3 kcal/mol. That is, the process of DKP dissolution in water is endothermic, and the solubility increases with rising temperature. It is noticed that the pressure effect below 4500 atm on the DKP solubility is opposite

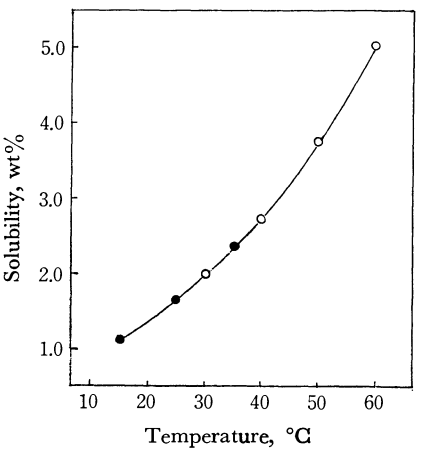

Fig. 3. Solubility of DKP *versus* temperature at 1 atm.
○: Gill *et al.*,[2] ●: This work

7) L. H. Adams, *J. Amer. Chem. Soc.*, **201**, 144 (1956).
8) H. Noguchi, *Tanpakushitsu Kakusan Kōso*, **10**, 1219 (1965).

to the result of temperature.

The effect of pressure on the solubility of solid in liquid is given by the following relation, assuming the activity coefficients of both the solute and solvent are independent of the pressure,

$$\left(\frac{\partial \ln m_s}{\partial p}\right)_T \approx \frac{V'-\bar{V}}{RT} = \frac{-\Delta V}{RT} \qquad (2)$$

where m_s is the molar concentration in the saturated solution, V' the molar volume of the solid, $\bar{V}$ its partial molar volume in the saturated solution and ΔV the volume change accompanying the dissolution of solid in liquid. The DKP solubility decreases with increasing pressure below 4500 atm. This means that $\bar{V}$ is larger than V', that is ΔV is positive. Above this pressure, on the other hand, ΔV changes the sign to negative. The relation between $\ln m_s$ and pressure is almost linear below 4500 atm, and the ΔV values obtained from the slope are listed in Table 2. The ΔV values above this pressure in Table 2 are calculated by Eq. (2).

Table 2. Volume change accompanying dissolution of DKP (ml/mol)

atm / °C	<4500	>4500	1*
15	+4.5	−3.9	—
25	+5.2	−5.3	+5.29
35	+5.9	−6.9	+5.88

* by dilatometric measurements

Figure 4 shows the dilatometric results measured at 1 atm. The ΔV values accompanying the dissolution of DKP at saturated concentration is obtained by extrapolating the straight line to the saturated concentration. The ΔV values thus obtained are also listed in the last column of Table 2, which coincide well with those from $\ln m_s$ *versus* pressure plot.

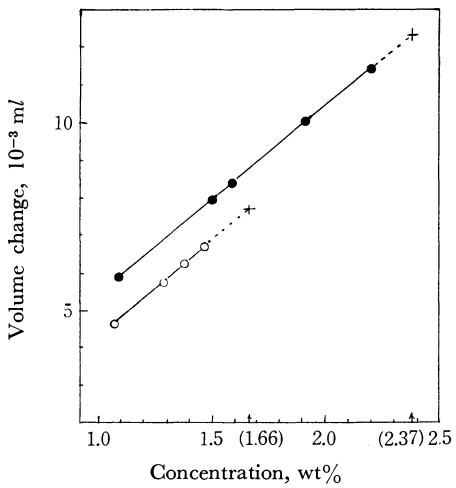

Fig. 4. Volume change accompanying dissolution of DKP.
○: 25°C, ●: 35°C, +: Saturated point

The molar volume of solid DKP is found to be 71.7 and 72.1 ml/mol at 25 and 35°C from our measurements of specific gravity. Therefore the partial molar volume in the saturated solution can be estimated from $\bar{V}=V'+\Delta V$. The $\bar{V}$ values thus calculated are 77.0 and 78.0 ml/mol at 25 and 35°C, respectively. Therefore, the difference between V' and $\bar{V}$ is only 8—9%. This suggests that the DKP dissolution in water is mono-dispersion. In view of the observed linearity of the logarithmic solubility *versus* $1/T$ plot and of the logarithmic solubility *versus* pressure below 4500 atm, mono-dispersion is ascertained over the region investigated.

The intermolecular energy maintaining the DKP crystal is estimated to be 24.83 ± 0.51 kcal/mol from the heat of sublimation, which is the sum of the hydrogen bond energies (14.0 kcal/mol) and van der Waals energies (10.9 kcal/mol).[5] The fact that the DKP crystal dissolves in water can be understood as follows: the intermolecular forces forming the crystal are ruptured and each DKP molecule dissolves in water in hydrated state. As mentioned above, the heat of solution is 6.2 kcal/mol at 1 atm. The difference of both the values, 18.6 kcal/mol (=24.8−6.2) is to be assumed as the heat of interactions between DKP and water molecules when DKP dissolves in water. One kind of the interactions is undoubtedly the hydrogen bond between a DKP molecule and 4 molecules of water as follows:

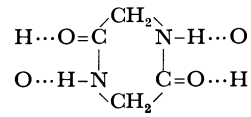

The other kind of interaction between the hydrocarbon moiety of DKP and the surrounding water molecules is supposed when DKP molecule is transferred to water. However, the enthalpy change in the transfer of aromatic hydrocarbons to water has been found to be almost zero.[9] Therefore it will be unnecessary to consider the contribution of this interaction. As mentioned above, one molecule of DKP can interact with 4 molecules of water. Then the binding energy in a set of hydration is 4.7 kcal/mol-H bond as the mean value (18.6 kcal/mol is divided by 4). This seems to be reasonable value as the energy of hydrogen bond.

The volume change accompanying the DKP dissolution is the difference between the partial molar volume $\bar{V}$ and the molar volume of DKP crystal V' as already shown in Eq. (2). Thus, the volume change ΔV reflects the changes of intermolecular forces between DKP-DKP and DKP-

9) W. Kauzmann, *Advances in Protein Chem.*, **14**, 39 (1959).

water. The effect of pressure on V' is assumed to be too small to be neglected as compared to the effect on $\bar{V}$. The partial molar volume $\bar{V}$ is influenced by the hydrogen bonds between DKP and water, that is, NH···O and CO···H, and the interaction between hydrocarbon moiety of DKP and water such as in "icebergs".[10] The positive value of ΔV below 4500 atm means that $\bar{V}$ is larger than V', and the negative value of ΔV above 4500 atm means that V' is larger than $\bar{V}$. This inversion must be ascribed mainly to the decrease of $\bar{V}$ above 4500 atm. This volume contraction might be probably deduced, because the interactions between DKP and water molecules become very strong above 4500 atm owing to the change of water structure brought about by the compression.

It is very interesting to compare the pressure effect on the DKP solubility with the influence of pressure on proteins. The higher pressure above 3000 atm causes the denaturation of proteins, while the lower pressure below 3000 atm retards the heat denaturation of proteins and accelerates the recovery of proteins once denatured by heat and pressure.[1] The denaturation phenomenon in which the folded structure of proteins changes into the unfolded structure is analogous to the dissolution of DKP crystal in water. That is, the folded protein corresponds to the DKP crystal, and the unfolded protein corresponds to the dissolved DKP in the hydrated state. If V' is the molar volume of the folded protein, and $\bar{V}$ is that of the unfolded protein, the sign of the volume change ΔV ($=\bar{V}-V'$) defines the direction of the process: folded protein (native) $\rightleftharpoons$unfolded protein (denatured). It is plausibly supposed that at the higher pressure above 3000 atm where the proteins are denatured, ΔV becomes negative, while at the lower pressure below 3000 atm where the denatured proteins are recovered, ΔV becomes positive as in the case of the DKP dissolution in water. This inversion must be ascribed mainly to the large decrease of $\bar{V}$ above 3000 atm, because the interaction between protein and water molecules becomes so strong due to the change of water structure above this pressure that the interaction maintaining the folded structure of protein is ruptured. The discrepancy in the pressure (4500 atm in DKP and 3000 atm in proteins) where the inversion occurs is not fatal, because at least in proteins this inversion pressure is considerably influenced by the change of the state of medium such as pH, buffer, ionic strength and so on as well as the difference of proteins.

The authors wish to express their thanks to Professor W. Kauzmann of Princeton University for his valuable suggestions, and to Mr. N. Maeda for his assistance in carrying out the measurements. The cost of this research was paid by a Scientific Research Grant of the Ministry of Education.

10) H. S. Frank and M. W. Evans, *J. Chem. Phys.*, **13**, 507 (1945).

BULLETIN OF THE CHEMICAL SOCIETY OF JAPAN VOL. 43 3086—3090 (1970)

Electronic Structures of the Ring-Protonated Aromatic Amines

Tsuguo YAMAOKA*1

The Institute for Solid State Physics, The University of Tokyo, Roppongi, Minato-ku, Tokyo

(Received April 27, 1970)

In order to study the electronic spectra and stabilities of the ring protonated aromatic amines, π-electron structure of nineteen amino-substituted pentadienyl cations were calculated by the composite molecule method. The lower electronic transitions of these ions are assigned to the charge transfer from amino groups to the pentadienyl cation. Stability of the ground state depends on the extent of intramolecular charge transfer, which is determined by the position and number of amino-substitution. The amino group on 1-, 3- or 5-carbon atom greatly stabilizes the ground state while contribution of the amino group on the other position is quite small. Occurrence of the ring or amino protonation for various amino-substituted benzenes is shown to be well predicted by the calculated stabilization energy.

Unlike the ordinary mode of protonation[1] to the aromatic amine, 1,3,5-triaminobenzene in a weakly

*1 Present address: Department of Printing, Faculty of Engineering, Chiba University, Yayoi-cho, Chiba, Japan.

1) E. M. Arnett, "Progress in Physical Organic Chemistry," Vol. 1, Interscience Publishers, New York (1963), p. 223.

acidic solution is singly protonated to the ring carbon atom as well as to the amino group,[2] and the following equilibrium exists among the three components.

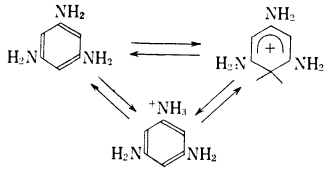

In a previous paper,[3] we reported that in this equilibrium system, ring protonation is predominant at room temperature while the species protonated on the amino group increases its concentration with decreasing temperature. It was demonstrated spectroscopically that ring protonation of this type also takes place for *N,N*-dimethyl-*m*-phenylenediamine in an acidified aqueous solution but not for *N,N*-dimethyl-*p*-phenylenediamine.

The mode of protonation seems to be determined by a slight difference in the stability of the protonated species, and therefore very sensitive to the number and position of the amino-substituent. For discussion on this point, the π-electron structures of several ring-protonated aminobenzenes have been calculated by the so called "composite molecule (CM) method." By this method the stabilization energy due to the transfer of π-electrons from amino groups to the benzene ring can be given. The specificity observed with the protonation to various aminobenzenes is discussed on the basis of the calculated stabilization energies.

Method of Calculation

Let us explain the calculation procedure taking 1,3,5-triaminobenzenium ion as an example. The so-called π-electron approximation is adopted and only the singlet states are considered. First the system was divided into two components, *i. e.*, benzenium ion (or pentadienyl cation with 4 π-electrons) and amino groups (with 2 π-electrons per group). The Hückel orbitals (1, 2,$\cdots$5) of the pentadienyl cation $C_5H_7^+$ were taken as the orbitals for benzenium ion, since they are not appreciably different from the SCF MO by the Pariser-Parr-Pople (PPP) method.[4] The three lone-pair orbitals of the amino groups are represented by n_i's where suffix i indicates the position of the carbon atom to which the respective amino groups are attached. Numbering of the atoms and geometry of the molecule are shown in Fig. 1. The bond distances

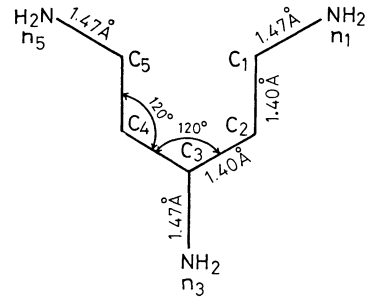

Fig. 1. Geometrical structure and numbering of 1,3,5-triaminopentadienyl cation.

and angles were assumed to be 1.40 Å for C=C bond and 1.47 Å for C–N bond, respectively. All the angles were assumed to be 120°. The two lone-pair orbitals (n_1 and n_5) of the amino groups were combined to give the symmetric n_{s15} and antisymmetric n_{a15} group orbitals

$$n_{s15} = (n_1+n_5)/\sqrt{2}$$
$$n_{a15} = (n_1-n_5)/\sqrt{2}.$$

With the use of the above-mentioned orbitals of the components, ground (G) and several locally-excited (LE's) and charge-transfer (CT's) configurations were constructed, as shown in Fig. 2. The energies of the lowest two locally-excited configurations (LE_1, LE_2) were those estimated from the transition energies of several methylated benzenium ions observed by Hanazaki and Nagakura,[5] while the energy of LE_3 was taken from the value calculated by the same authors. The energies of CT configurations were calculated by the relation, $I-A-\Delta C$, where I, A and ΔC stand for the ionization potential of an amino group (10.15 eV),[6] the electron affinity of the benzenium ion (estimated to be 7.50 eV*[2]) and the electrostatic interaction energy caused by an electron transfer from an amino group to the benzenium ion, respectively. We adopted the Pariser-Parr approximation[8] for evaluating the two-center Coulomb integrals necessary for the calculation of ΔC.

Non-zero off-diagonal matrix elements for the interactions of CT configurations with ground (G)

2) H. Köhler and G. Scheibe, *Z. Anorg. Allg. Chem.*, **285**, 221 (1956).

3) T. Yamaoka, S. Hosoya and S. Nagakura, *Tetrahedron*, **24**, 6203 (1968).

4) H. Hosoya, S. Hosoya and S. Nagakura, *Theoret. Chim. Acta*, **12**, 11, 117 (1968).

5) I. Hanazaki and S. Nagakura, This Bulletin, **38**, 1298 (1965).

6) K. Watanabe, *J. Chem. Phys.*, **26**, 542 (1957).

*2 This value was estimated from the lowest vacant SCF MO energy for the pentadienyl cation after some theoretical corrections presented by Hush and Pople.[7] For CT configurations in which the electron is transferred to the second lowest vacant orbital, the A value was taken to be 4.50 eV considering the difference in orbital energies between the first and the second lowest vacant orbitals obtained by Hanazaki and Nagakura.[5]

7) N. S. Hush and J. A. Pople, *Trans. Faraday Soc.*, **51**, 600 (1955).

8) R. Pariser and R. G. Parr, *J. Chem. Phys.*, **21**, 767 (1953).

TABLE 1. ENERGIES, OSCILLATOR STRENGTHS AND DIRECTIONS OF LOWER ELECTRONIC TRANSITIONS OF 1,3,5-TRIAMINOBENZENIUM ION

Energy (eV)			Oscillator strength (f)			Character	Direction of the moment[a)]
Calcd		Obsd	Calcd		Obsd		
CM	PPP		CM	PPP			
3.87	3.39	3.39	0.03	0.33	0.09	CT $n_{a_{15}} \rightarrow$ ring	$\perp$
4.24	4.49	4.54	0.32	0.44	0.20	CT $n_3 \rightarrow$ ring	$\parallel$
5.96	5.82	5.46	—	—	—	CT $n_{.5a} \rightarrow$ ring	$\parallel$

a) with respect to molecular axis.

TABLE 2. STATE WAVEFUNCTIONS OF 1,3,5-TRIAMINOPENTADIENYL CATION CALCULATED BY THE CM METHOD

Symmetric

Energy (eV)	Coefficient					
	Ψ_G	Ψ_{LE_2}	Ψ_{LE_3}	$\Psi_{CT^3_3}$	$\Psi_{CT^3_{s_{15}}}$	$\Psi_{CT^4_{a_{15}}}$
−2.186	0.8409	−0.0109	−0.0316	−0.2846	0.4020	0.2213
5.206	0.3655	0.5931	0.4142	−0.0774	−0.4412	−0.3774
7.828	−0.2042	0.1268	0.7181	−0.0181	0.1240	0.6410
2.053	0.0027	0.3739	−0.1204	0.7434	0.5409	−0.0219
3.774	−0.2885	0.1722	0.2385	−0.4807	0.5751	−0.5181
6.115	−0.1856	0.6800	−0.4903	−0.3195	−0.0701	0.3590

Antisymmetric

Energy (eV)	Coefficient			
	Ψ_{LE_1}	$\Psi_{CT^3_{a_{15}}}$	$\Psi_{CT^4_3}$	$\Psi_{CT^4_{s_{24}}}$
4.724	0.8262	0.5633	—	—
5.650			1.000	
1.686	−0.5633	0.8262	—	—
5.650	—	—	—	1.000

or *LE* configurations can be represented by the aid of the resonance integral β_{CN} between the neighbouring nitrogen and carbon atoms. The value was determined to be −2.0 eV after several trial calculations.

Results and Discussion

Table 1 shows calculated and observed energies and oscillator strengths for the lower transitions of 1,3,5-triaminobenzenium ion. Results of the Pariser-Parr-Pople type calculation were also cited from the previous paper.[3)] The wavefunctions of the ground and excited states are shown in Table 2 to clarify the nature of each transition. As evident from Table 1, the lowest two transitions at 360 mμ and 273 mμ are undoubtedly assigned to the charge-transfer from the amino groups to the ring, the direction of the transition dipoles being perpendicular and parallel to the molecular axis, respectively. The third transition, though not observed, has also a charge-transfer character (parallel band). The results are in good agreement with those obtained previously by the PPP method.

Figure 2 shows the configuration energies used for the present calculation and also the evaluated state energies. The energy of the ground state, 2.186 eV below zero, corresponds to the π-electron stabilization energy (ΔE) caused by the resonance between the ring and amino groups.

In Table 3 the calculated ΔE values of nineteen aminosubstituted benzenium ions are summarized, together with the lower π-electronic transition energies. For some compounds the calculated oscillator strengths are also given. It is apparent that the larger the number of amino groups, the more the ion is stabilized. On close inspection and least-squares calculation, ΔE is found to be additively increased by the amino groups on the ortho, meta and para positions to the protonated carbon with the following values:

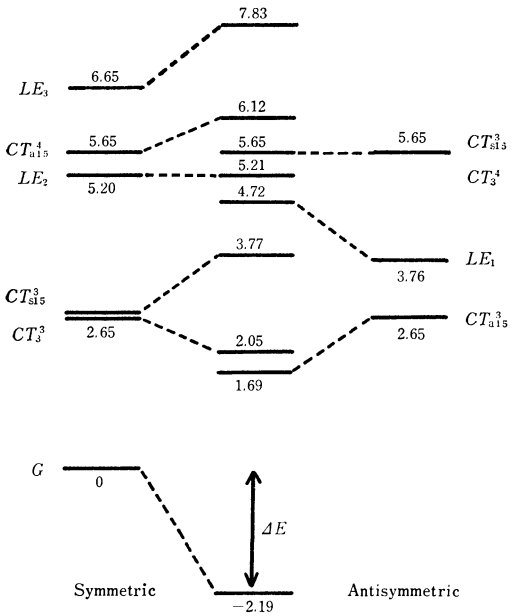

Fig. 2. Configurations used for the CM calculation and the evaluated state energies (eV) of the 1,3,5-triaminopentadienyl cation. Configurations are represented as follows.
$G=|1\bar{1}2\bar{2}n_{s15}\bar{n}_{s15}n_{a15}\bar{n}_{a15}n_3\bar{n}_3|$, $LE_1=\Psi(2\text{—}3)$, $LE_2=\{\Psi(2\rightarrow4)-2\Psi(1\text{—}3)\}/\sqrt{5}$, $LE_3=\{2\Psi(2\rightarrow4)-\Psi(1\text{—}3)\}/\sqrt{5}$, $CT^3{}_{s15}=\Psi(n_{s15}\rightarrow3)$, $CT^3{}_{a15}=\Psi(n_{a15}\rightarrow3)$, $CT_3{}^3=\Psi(n_3\rightarrow3)$, $CT^4{}_{s25}=\Psi(n_{s15}\rightarrow4)$, $CT^4{}_{a15}=\Psi(n_{a15}\rightarrow4)$, $CT_3{}^4=\Psi(n_3\rightarrow4)$, where $\Psi(a\rightarrow b)=\{|\cdots ab\cdots|+|\cdots ba\cdots|\}/\sqrt{2}$ and 1, 2 ··· are the Hückel MO's of the pentadienyl cation.

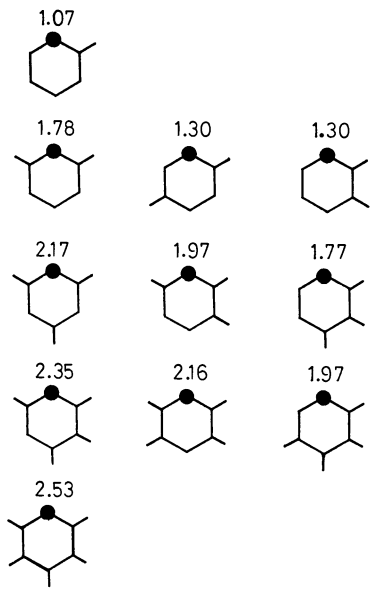

Fig. 3. The most probable sites of the ring-protonation of a series of amino-substituted benzenes are shown by the filled circles. Numbers show the values of ΔE in eV.

Table 3. Stabilization energies, transition energies and oscillator strengths calculated for various amino-substituted benzenium ions

Compound[a)]	Stabilization energy (eV)	Transition energy (eV)	Oscillator strength	Direction[b)]
2-	−0.34	2.29		
		4.51		
2,4-	−0.64	2.35		
		2.71		
3-	−0.82	2.50	0.554	0°
		3.81	0.253	90°
1-	−1.07	3.60		
		5.39		
2,3-	−1.08	2.87	0.111	90°
		3.93	0.022	0°
2,5-	−1.30	3.01		
		3.94		
4,5-	−1.30	2.94		
		4.27		
2,4,3-	−1.31	1.63	0.011	90°
		3.19	0.016	0°
1,2,4-	−1.52	2.97		
		3.55		
3,5-	−1.58	3.51		
		4.79		
1,2,3-	−1.77	3.18		
		4.37		
1,3,4-	−1.77	1.78		
		1.95		
1,5-	−1.78	3.47	0.039	90°
		5.00	0.320	0°
1,2,5-	−1.97	3.29		
		4.37		
1,2,3,4-	−1.97	3.37		
		3.78		
1,2,4,5-	−2.16	2.48	0.140	90°
		5.47	0.036	0°
1,3,5-	−2.17	3.87		
		4.24		
1,2,3,5-	−2.35	3.64		
		4.40		
1,2,3,4,5-	−2.53	2.85	0.081	90°
		4.02	0.529	0°

a) numbers show the position of substitution of the amino group.
b) with respect to molecular axis.

0.81 eV per *o*-NH_2
0.30 eV per *m*-NH_2
0.62 eV per *p*-NH_2.

This simple relationship can be easily explained on the basis of perturbation treatment, if one recalls the shape of the lowest vacant orbital of the

benzenium ion into which the electron migrates from the amino groups. The perturbation of the amino groups on the meta positions might be small because the coefficients of the lowest vacant orbital on these positions are almost zero as shown below.

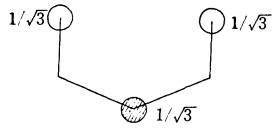

Here we take 1.7 eV as the borderline value of ΔE between the ring and amino protonations, although it is difficult to determine definitely. The filled circles in Fig. 3 indicate the most probable sites of the ring-protonation of a series of amino-substituted benzenes. The fact that a spectrum of a ring-protonated species could be observed for *N,N*-dimethyl-*m*-phenylenediamine ($\Delta E = 1.78$ eV) but not for *N,N*-dimethyl-*p*-phenylenediamine ($\Delta E = 1.30$ eV) can be explained by the borderline value of ΔE. The electronic spectra and the mode of amino-substitution do not seem to be correlated with each other by a simple relation.

The author would like to express his grateful acknowledgment to Professor Saburo Nagakura, the Institute for Solid State Physics, the University of Tokyo for his valuable suggestions and encouragement. His thanks are also due to Professor Haruo Hosoya, Ochanomizu University, for much helpful advice and to Professor Takahiro Tsunoda, Chiba University, for his continued support during this work.

BULLETIN OF THE CHEMICAL SOCIETY OF JAPAN VOL. 43 3090—3095 (1970)

Scavengeable Electron Yield in the Radiolysis of Liquid and Solid Hydrocarbons

Toyoaki KIMURA, Kenji Fueki and Zen-ichiro KURI

Department of Synthetic Chemistry, Faculty of Engineering, Nagoya University, Chikusa-ku, Nagoya

(Received May 1, 1970)

Yields of scavenged electrons have been measured in MCH, 3MP, cumene and *tert*-butylbenzene at 20°C and −196°C. It has been found that the yield of scavenged electrons is considerably lower at −196°C in the glassy state than at 20°C in the liquid state. The temperature effect on electron scavenging indicates that the difference in the yields of scavenged electrons between the liquid and glassy states is attributed to the variation not of temperature but of the physical conditions of the matrix. We have also investigated the effect of composition in MCH-MTHF mixtures and that of the viscosity of the matrix upon the yield of scavenged electrons at −196°C, which has led us to the assumption that the extent of interactions between thermalized electrons and the matrix would affect the yield of scavenged electrons at −196°C. Since such interactions may be related to the mean free path of electrons, we have calculated the contribution of the electron jump distance to the electron scavenging efficiency. The calculated results appear to explain qualitatively the experimental results.

Recent development in the techniques for measurement of reaction intermediates, such as ESR or optical absorption, has brought about very useful information in the field of radiation chemistry. These measurements have usually been made for reaction intermediates in rigid matrices. In order to utilize such information to understand primary processes in radiation chemistry or to correlate it with reaction mechanisms, the application of product analysis to rigid systems is highly desirable.

Our previous studies on the radiolysis of glassy hydrocarbons at −196°C unexpectedly revealed that the scavenged electron yield is much lower than that expected from the liquid phase experiments.[1,2] Shirom and Willard[3] and Shida and Imamura[4] have also reported low scavengeable electron yields in hydrocarbon glasses at −196°C.

1) T. Kimura, T. Miyazaki, K. Fueki and Z. Kuri, This Bulletin, **41**, 2861 (1968).

2) T. Kimura, K. Fueki and Z. Kuri, *ibid.*, **42**, 3088 (1969).

3) M. Shirom and J. E. Willard, *J. Chem. Phys.*, **47**, 206 (1967).

4) T. Shida and M. Imamura, presented at 23rd Annual Meeting of the Chemical Society of Japan, April, 1970, Tokyo.

However, we could little observe effect of irradiation temperature on hydrogen formation for a number of hydrocarbons.[5] These apparently conflicting observations should be clarified to get a complete understanding of radiolysis mechanisms in condensed phases. The question why the yield of scavenged electrons is much lower at −196°C is an important one. In this paper we present factors responsible for the lower yield of scavenged electrons in hydrocarbon glasses at −196°C.

We use bromobenzene or *o*-bromotoluene as an electron scavenger to obtain the yield of scavenged electrons. These substances scavenge an electron to form a phenyl radical, which immediately abstracts an H atom from a solvent molecule to form benzene and a solvent radical:

$$RH \rightsquigarrow RH^+ + e^- \quad (1)$$

$$C_6H_5Br + e^- \longrightarrow C_6H_5\cdot + Br^- \quad (2)$$

$$C_6H_5\cdot + RH \longrightarrow C_6H_6 + R\cdot \quad (3)$$

Benzene formation *via* Br atom abstraction by an H atom can be excluded.[6]

$$H + C_6H_5Br \xrightarrow{\times} C_6H_5\cdot + HBr \quad (4)$$

Thus we can determine the scavenged electron yield from the yield of benzene. To measure the yield of scavenged electrons, N_2O is widely used in the liquid phase, and biphenyl in the glassy state. However, there is ambiguity in the ratio of the nitrogen yield to the scavenged electron yield at −196°C,[1] and biphenyl cannot be used for conventional kinetic studies of liquid phase radiolysis. The merit of the use of halogen substituted benzene (or toluene) are (i) the yield of benzene is equal to the yield of electrons scavenged, and (ii) the method can be applied to both liquid and glassy states.

Experimental

Materials. Methylcyclohexane (MCH) was a product of Tokyo Kagaku Seiki (99.9%) and used without any treatment. Cumene and *t*-butylbenzene were Nakarai guaranteed reagents and fractionally distilled before use. Aldrich 3-methylpentane (3MP) was shaken with concentrated sulfuric acid in a separating flask, and washed with distilled water. After drying over sodium sulfate, 3MP was passed through a silica gel column and then fractionally distilled. Nakarai guaranteed reagent isopentane was used after the same purification as for 3MP. Bromobenzene and *o*-bromotoluene were Nakarai guaranteed reagents, and were fractionally distilled after passing through an activated alumina column. K & K 2-methyltetrahydrofuran (MTHF) was refluxed over potassium hydroxide, fractionally distilled, and passed through an activated alumina column. The middle fraction was used immediately after purification. Tokyo Kasei extra pure reagent biphenyl was used after being recrystallized three times.

Sample Preparation. Each sample was degassed in a 10 mm glass tube by the freeze-pump-thaw technique and then sealed off.

Irradiation. A 3000 Ci ^{60}Co source was used for γ irradiation. Irradiation doses were 2.14×10^{20} eV/g at 20°C, 1.69×10^{20} eV/g at −72°C, 5.05×10^{19} eV/g at −120°C, and 1.71×10^{20} eV/g at −196°C.

Analysis. Yields of benzene and toluene produced were determined by a Hitachi K 53 gas chromatograph with FID. The columns used were *n*-hexatriacontane and TCP. Optical absorption measurements were carried out as follows. Samples were degassed in a glass tube and transferred to a rectangular quartz cell (10 mm × 5 mm). After irradiation in the dark at −196°, absorption measurements were carried out with a Hitachi EPU-2 spectrophotometer. The dose was 9.85×10^{17} eV/g in the experiments.

Results and Discussion

Figure 1 shows benzene yields from bromobenzene-MCH systems γ-irradiated at 20°C and −196°C. Since the ionization potential of MCH is higher than that of bromobenzene, charge transfer from the MCH positive ion to bromobenzene may occur and contribute to benzene formation to some extent. For the sake of confirmations, we added cumene as a positive ion scavenger to the bromobenzene-MCH systems. The results obtained are shown in Fig. 1. The concentration of

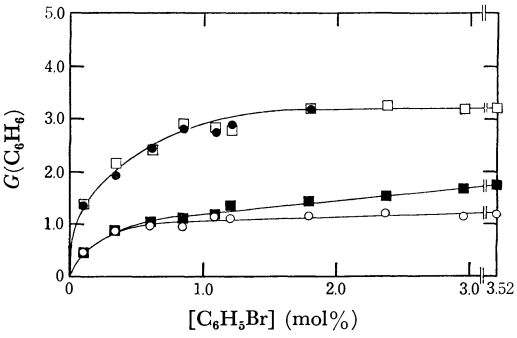

Fig. 1. Yields of benzene from γ-irradiated bromobenzene-MCH systems.
□ at 20°C in the absence of cumene, ■ at −196°C in the absence of cumene, ● at 20°C in the presence of 21.5 mol% of cumene, ○ at −196°C in the presence of 21.5 mol% of cumene

cumene (21.5 mol%) is high enough to scavenge MCH positive ions adequately.[2] Direct benzene formation from cumene was negligible as will be described later. In the liquid state at 20°C the benzene yield was not affected by the presence of cumene, but at −196°C it was lowered slightly at higher bromobenzene concentrations (above ~1 mol%). The reason for this may be that charge

5) T. Kimura, K. Fueki and Z. Kuri, This Bulletin, **43**, 1657 (1970).

6) J. M. Warman, K.-D. Asmus and R. H. Schuler, *J. Phys. Chem.*, **73**, 931 (1969).

transfer from MCH positive ions to bromobenzene molecules occurs both at 20°C and −196°C:*1

$$MCH^+ + C_6H_5Br \longrightarrow MCH + C_6H_5Br^+ \quad (5)$$

Bromobenzene positive ions seem to react with bromide ions at 20°C, but with electrons at −196°C, since more than half of the electrons are scavenged to form bromide ions at 20°C but only a small fraction at −196°C. The reaction of bromobenzene positive ions with electrons might lead to benzene formation, although that with bromide ions does not seem to yield benzene:

$$C_6H_5Br^+ + Br^- \longrightarrow \text{no } C_6H_6 \text{ at } 20°C \quad (6)$$

$$C_6H_5Br^+ + e^- \longrightarrow C_6H_6 \text{ at } -196°C \quad (7)$$

It is expected that cumene supresses reaction (5). Thus, in the presence of cumene the yield of benzene will decrease *via* suppression of reaction (7) at −196°C if reaction (7) occurs at all, but not at 20°C (reaction (6)). It has been found, however, that in the bromobenzene concentration range below 1 mol%, benzene yields from cumene-free systems coincide with those from cumene-added systems at both 20°C and −196°C. Therefore we can say that charge transfer from the MCH positive ion to bromobenzene contributes little to benzene formation in this bromobenzene concentration range and that the positive charge scavenger does not affect the efficiency of electron scavenging. The benzene yields in the presence of cumene shown in Fig. 1 are in agreement with previous results.[1]

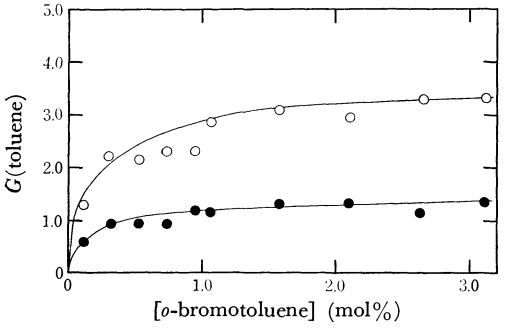

Fig. 2. Yields of toluene from γ-irradiated *o*-bromotoluene-3MP systems.
○ at 20°C, ● at −196°C

Figure 2 shows toluene yields from *o*-bromotoluene-3MP systems γ-irradiated at 20°C and −196°C. Since the limiting value of toluene yield at 20°C is 3.3 G and that at −196°C is 1.3 G, the contribution of positive charge transfer to toluene formation is negligible. The limiting toluene yield in 3MP at −196°C, namely, the scavengeable electron yield agrees well with that by Shirom and Willard.[3]

*1 We previously suggested that positive charge transfer is hardly affected by temperature.[2]

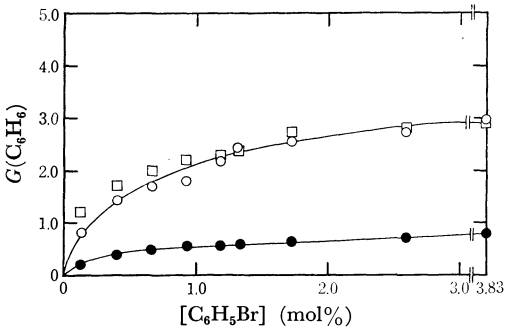

Fig. 3. Yields of benzene from γ-irradiated bromobenzene-cumene systems.
○ at 20°C, □ at −72°C, ● at −196°C.

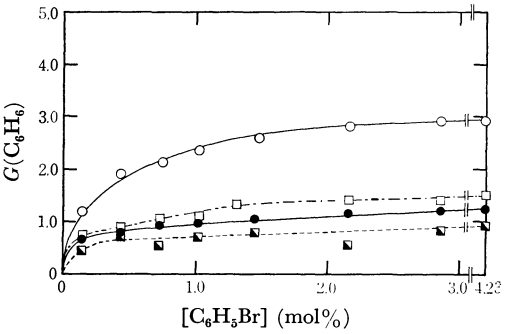

Fig. 4. Yields of benzene from γ-irradiated bromobenzene-*t*-butylbenzene systems: ○ at 20°C, □ at −72°C, ◪ at 120−°C, ● at −196°C.

In both cases of MCH and 3MP, the scavenged electron yields at −196°C are considerably lower than those at 20°C. Such a difference in the yield may be caused by the variation of temperature or the change in physical properties of the system (including phase change). To ascertain this, we investigated the temperature-dependence of electron scavenging. For this purpose we used cumene and *t*-butylbenzene because they form glass at −196°C, and their melting points lie in an experimentally feasible temperature region. Figures 3 and 4 show benzene yields from bromobenzene-cumene and bromobenzene-*t*-butylbenzene systems γ-irradiated at various temperatures. The benzene yield from pure cumene is 0.027 G at 20°C and 0.018 G at −196°C, and that from *t*-butylbenzene is 0.089 G at 20°C and is undetectably low −196°C. Since the ionization potentials of cumene and *t*-butylbenzene are lower than that of bromobenzene, positive charge transfer from solvent positive ions to solute molecules will not be possible. The limiting values of the yield of scavenged electrons in cumene and *t*-butylbenzene at 20°C are slightly lower than those in MCH and 3MP. Only the limiting value in cumene is somewhat lower at −196°C. In both cases of cumene and *t*-butylbenzene, the limiting values of scavenged electrons

at 20°C are considerably different from those at −196°C, as in the cases of MCH and 3MP. The experimental points for the yields of benzene produced from bromobenzene-cumene systems at −72°C and 20°C fit a single curve, though they deviate slightly at lower bromobenzene concentrations. The slight difference might be due to the change in density of cumene. On the other hand, in the case of *t*-butylbenzene, the experimental curve for benzene yield at −72°C is very similar to that at −196°C. Thus it can be concluded that the difference in scavenged electron yield between liquids and solids is not caused by the difference in temperature, but can be ascribed to the change in physical properties of solvents. We calculated the maximum scavengeable electron yield for a better understanding of the above situation. For this purpose the empirical equation proposed by Warman *et al.*[6] was used:

$$G(e^-) = G_{fi} + G_{gi}(\alpha_s[S])^{1/2}/\{1+(\alpha_s[S])^{1/2}\} \quad (8)$$

where G_{fi} is the yield of free electrons, G_{gi} is that of electrons which undergo geminate recombination, [S] is molarity of scavenger and α_s is an empirical parameter. The data were taken from experiments on *t*-butylbenzene systems at 20°C and −196°C (Fig. 4). The results calculated from the equation are plotted in Fig. 5. In the calculation, we assumed that the free electron yield, G_{fi}, is zero at 20°C and −196°C and that the density of *t*-butylbenzene at −196°C is 1.0. Since we have taken $G_{fi}=0$, the value extrapolated to [S]→∞ means the maximum scavengable electron yield. The maximum scavengable electron yields thus obtained are 4.0 G at 20°C and 1.8 G at −196°C.

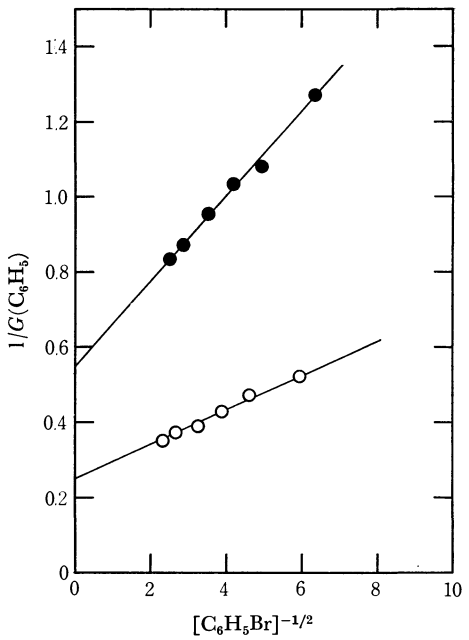

Fig. 5. Plot of $1/G(C_6H_6)$ as a function of $[C_6H_5Br]^{-1/2}$ in bromobenzene-*t*-butylbenzene systems irradiated at 20°C (○), at −196°C (●).

We can cite some possible reasons why the scavengable electron yield is much lower at −196°C: (i) decrease in the reactivity of solutes to electrons, (ii) decrease in the yield of initially ejected electrons, and (iii) recombination of a significant fraction of electrons with positive ions even in the presence of solutes in high concentrations. In order to test whether (i) is acceptable or not, we determined the values of α_s, which corresponds to the reactivity of the solutes to electrons, from the slopes of straight lines in Fig. 5. The values obtained are $\alpha_s=27.1$ at 20°C and $\alpha_s=22.5$ at −196°C. As these values indicate, the reactivity of bromobenzene to electrons at −196°C is not so different from that at 20°C, and so (i) cannot be a dominant factor. It is difficult to determine which is more probable, (ii) or (iii). Though the scavengeable electron yield in hydrocarbons at −196°C is lower, a major fraction of electrons can be scavenged in MTHF at −196°C[7,8]; the yield of biphenyl anion from γ-irradiated MTHF glass containing biphenyl as a solute reaches 2.8—3.0 G. Using the data by Kato *et al.*[8] and assuming $G_{fi}=0.15$, we obtain $G_{gi}=3.9$ in the same manner as that described above. Since the free ion yield in diethylether is 0.19 and that in *n*-butylether is 0.11,[9] the value assumed above for MTHF seems reasonable. Thus, we obtain a value of 4.05 as the total electron yield from γ-irradiated MTHF at −196°C. This indicates that there is no difference in the maximum scavengable electron yield between a liquid at 20°C and glass at −196°C. This contradictory result between MTHF and hydrocarbon glass seemed to suggest a clue to the problem. Thus we determined scavengable electron yields from mixtures of MTHF and a hydrocarbon at −196°C by measuring the yield of biphenyl anion from γ-irradiated MCH-MTHF glass at −196°C. The results are shown in Fig. 6. The absorption spectrum of biphenyl anion has λ_{max} at 409 mμ, and $\varepsilon_{409m\mu}$ 3.7×10^4 *l*/mol·cm.[7] Samples were prepared so as to contain 0.026 mol/*l* of biphenyl at room temperature. It is difficult to measure biphenyl anion in γ-irradiated pure MCH because of the cracking in MCH glass. In order to keep the system in transparent stable glass, 20 vol% of 3MP was added to MCH.

Since the scavenged electron yield in MCH is 1.55 G and that in MTHF is 2.75 G (Fig. 6), and if we assume that reason (ii) is right and that the yield of electrons initially ejected from MCH at

7) J. P. Guarino, M. R. Ronayne and W. H. Hamill, *Radiation Res.*, **17**, 379 (1962).

8) N. Kato, K. Fueki and Z. Kuri, unpublished results.

9) G. R. Freeman and J. M. Fayadh, *J. Chem. Phys.*, **43**, 86 (1965).

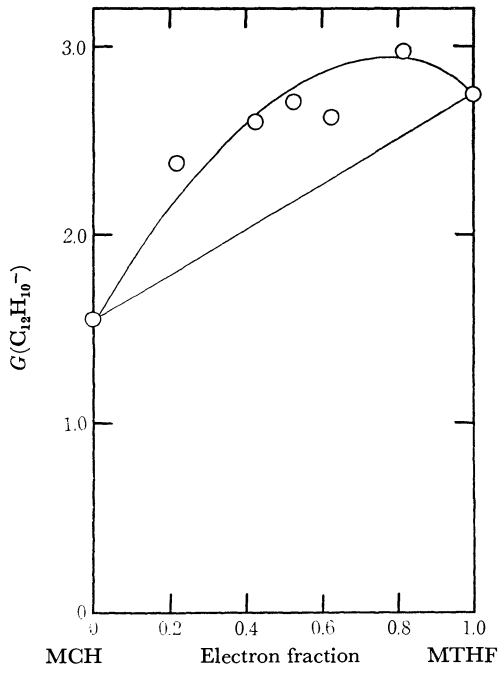

Fig. 6. Yields of biphenyl anion from γ-irradiated MCH-MTHF mixtures at −196°C, which contain 0.026 mol/l of biphenyl.

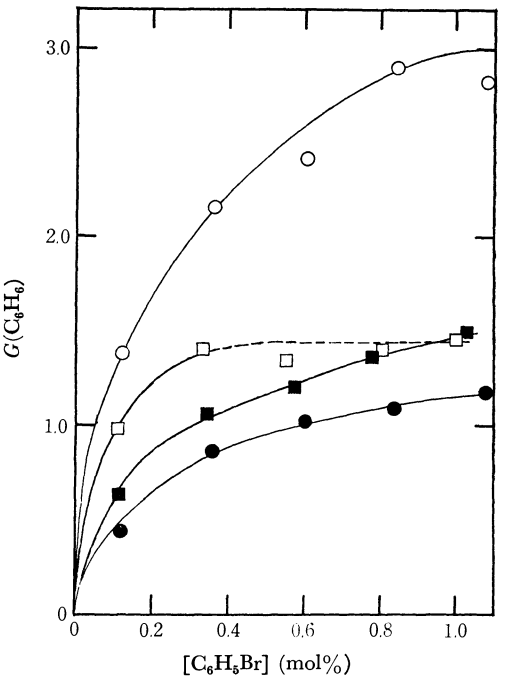

Fig. 7. Yields of benzene from γ-irradiated bromobenzene-hydrocarbon systems with various viscosities.
○ in liquid MCH at 20°C, □ in isopentane-MCH (10 : 1 Vol. ratio) mixed glass at −196 °C, ■ in isopentane-MCH (6 : 5 Vol. ratio) mixed glass at −196°C, ● in MCH glass at −196°C.

−196°C is 2.1 G,[4] about 70% of electrons are scavenged in both matrices. Accordingly, the yield of scavenged electrons from MCH-MTHF mixtures is expected to be proportional to the electron fraction; the experimental points are expected to be on the straight line in Fig. 6. However, all the experimental points for MCH-MTHF mixtures lie well above the straight line. For example, the scavenged electron yield, expected at an electron fraction of MTHF of 0.21, is $1.55(1-0.21)+2.75\times0.21$ G= 1.8G, but the observed yield is 2.38G. Since the yield of electrons initially ejected is $4.05\times0.21+2.1(1-0.21)$ G=2.5G in this case on the basis of the above assumption, it may be said that the efficiency of electron scavenging increases from 70% in MCH to 95% in this mixture. This would be explicable if a positive ion scavenger acts to increase the efficiency of electron scavenging in the region of electron scavenger concentrations studied, but the experimental results of Fig. 1 do not support this explanation. Thus, reason (ii) is not sufficient for the interpretation of our problem.

Finally, let us consider reason (iii). Why a significant fraction of electrons are recombined with positive ions without being scavenged by solutes at higher concentrations at −196°C remains to be answered. The maximum scavengeable electron yield is low in solid hydrocarbons, while it is about 4 in liquid hydrocarbons, and in liquid and solid MTHF. This suggests that interactions between thermalized electrons and solvent molecules affect the yield of scavengeable electrons. In cases of polar solvent, solvated or trapped electrons are observed, indicating strong interactions between electrons and solvents. In the case of liquid hydrocarbons, such interaction must exist to some extent because the motion of themalized electrons is diffusion-controlled. We consider that the electron-solvent interaction would be weaker in the case of solid hydrocarbons.

To develop such a consideration further, we measured the yield of scavenged electrons in hydrocarbon glass with various viscosities, which were prepared by adding isopentane to MCH. The results are shown in Fig. 7, together with the results on liquid and glassy MCH. As the solubility of bromobenzene in isopentane is low, the experimental curve reaches a plateau at lower bromobenzene concentrations in glass with higher concentrations of isopentane (the broken line in Fig.7). We can see that the yield of scavenged electrons depends upon the viscosity of the matrix. This seems to indicate that the electron-solvent interaction depends upon the viscosity of the solvent in hydrocarbon glass.

The interaction may be reflected by the distance of electron jump; the weaker the interaction, the

longer the electron jump distance, λ. Thus, we have calculated the effect of λ on the probability of electron scavenging at -196°C. The procedure of calculation is the same as that reported previously.[1] The probability of electron scavenging, Φ_-, is expressed as

$$\Phi_- = \phi_{fi} + \phi_-(1-\phi_{fi}) \quad (9)$$

$$\phi_{fi} = \exp(-r_c/y) \quad (10)$$

$$\log(1-\phi_-) = \frac{6\varepsilon(y^3-\lambda^3)}{4.32}(b_-/\lambda^2)(kT/e) \times \log(1-f_-N_s) \quad (11)$$

where $r_c=e^2/\varepsilon kT$, e is the charge on an electron, ε is the static dielectric constant, k is Boltzmann's constant, T is the absolute temperature, y is an initially separated distance between positive ion and a thermalized electron, b_- is the number of new neighbors that an electron encounters per diffusive jump, f_- is the encounter efficiency, and N_s is the mole fraction of the scavenger. The probability of electron scavenging at an average positive ion-electron distance at -196°C was calculated as a function of λ, using the values $b_-=6$ and $f_-=1$. The average positive ion-electron distance in liquid cyclohexane is reported to be 50—60 Å[10] and 65.8 Å.[11]

Since the distance between a positive ion and an electron appears to be inversely proportional to the density of the medium,[11] we used the value, $r_{av}=50$ Å, considering the change in density at -196°C. The calculated results at several solute concentrations are shown in Fig. 8. It can be seen that the probability of electron scavenging decreases rapidly with the increase of λ. We cannot obtain the theoretical absolute yield of scavenged electron from the results because we have not calculated the yield integrated over the electron distribution, but we can see how the electron-solvent interaction could contribute to the scavenged electron yield. It is likely that the extent of this interaction plays an important part in ionic processes, especially in the radiolysis of hydrocarbon glass.

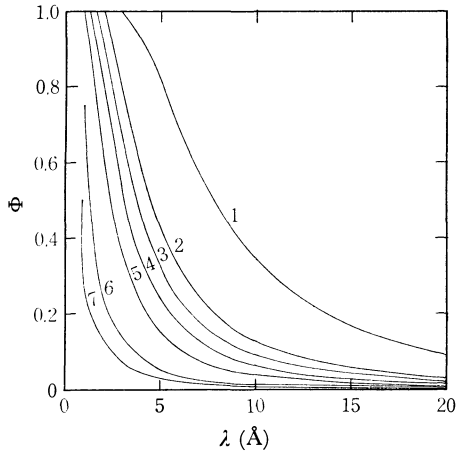

Fig. 8. Probability of electron scavenging as a function of jump distance of electron for $r=50$ Å at -196°C. Mole fraction of electron scavenger: 1) 0.03, 2) 0.01, 3) 0.007, 4) 0.005, 5) 0.003, 6) 0.001, 7) 0.0005

10) S. Sato, This Bulletin, **41**, 304 (1968).
11) W. F. Schmidt and A. O. Allen, *J. Phys. Chem.*, **72**, 3730 (1968).

BULLETIN OF THE CHEMICAL SOCIETY OF JAPAN VOL. 43 3096—3101 (1970)

Nucleation in Liquid Sulfur Droplets

Shuichi HAMADA, Yoshihiro NAKAZAWA and Toshiaki SHIRAI

Department of Chemistry, Faculty of Science, Science University of Tokyo, Kagurazaka, Shinjuku-ku, Tokyo

(Received May 9, 1970)

The freezing behavior of supercooled liquid sulfur droplets were studied by means of a microscopic method. The number fraction of the solidified droplets in the experiments of continuous cooling on well-purified sulfur was only about 15% over the temperature range from 120°C to −70°C at the cooling rate of 0.20°C/min, and no abruptly discontinuous nucleation was found in these supercooling temperatures. The number fractions of the solidified droplets were found to be related to their volumes below −20°C. The nucleations in the well-purified liquid surfur droplets were confirmed to be a homogeneous process under these conditions. The specific nucleation rates per unit of volume were estimated to be 0.450, 1.13, and 1.16 $cm^{-3}sec^{-1}$ at the specified temperatures of −20, −40, and −50°C respectively. The dependences of $(\ln I+\Delta F_A/kT)$ on $1/(\Delta T)^2T$ obeyed the theory of Turnbull and Fisher. The interfacial free energy of sulfur at the liquid-crystal surface was estimated to be 12.1 erg/cm^2; this value was considered to be an appropriate one according to the Zadumkin consideration.

At an initial step of transformation, a nucleation passes through a homogeneous or a heterogeneous process in an unstable phase. In the homogeneous nucleation process, the nuclei grow in number nearly in proportion to the time; therefore, the nucleation rates can be estimated. On the other hand, it is well known that instantaneous crystallizations are observed at low degrees of supercooling or supersaturation in the presence of small amounts of chemical or physical heterogeneities. These instantaneous crystallizations are recognized to be based on the heterogeneous nucleation process. In the heterogeneous nucleation process, the number of nuclei is governed by the amounts of the chemical or the physical heterogeneities; therefore, the rates of crystallization are mainly decided by the growth rates of the nuclei.

Gibbs[1] has introduced a theoretical approach to the homogeneous nucleation in supercooled liquids and in supersaturated, one-component vapors. Frenkel,[2] Volmer,[3] and Becker and Döring[4] developed further the theories of the homogeneous nucleation. Turnbull and Fisher[5] proposed absolute values for the rates of homogeneous nucleation in condensed systems on the basis of the Becker and Döring theory. The first experimental measurements on the nucleation rates were carried out by Vonnegut[6] using the dilatometric technique on a system of supercooled liquid metal droplets. An advantage of the technique using tiny droplets is that the homogeneous nucleation breaking up of heterogeneous nucleating centers is observable. Moreover, experiments concerned with the kinetics of the homogeneous nucleation of many metals, inorganic and organic compounds, and polymers have been reported by Pound[7] and Turnbull.[8,9] The nucleation phenomena in the supercooled liquid sulfur droplets have been reported by Ford *et al.*[10] and by Gorskii.[11] Gorskii has reported a measurable nucleation rate in the supercooled liquid sulfur droplets at a temperature of 50°C, but Ford *et al.* found a very small fraction of solidified droplets even at temperatures as low as −45°C in the aerosol states.

In this work, the rates of the nucleation of the supercooled liquid sulfur droplets were studied by means of the microscopic method.

Experimental

Materials. A guaranteed-grade sulfur was obtained from the Kanto Chemical Company. The sulfur was

1) J. W. Gibbs, *Trans. Conn. Acad.*, **3**, 108 (1876).
2) J. Frenkel, "Kinetics Theory of Liquids," Oxford University Press, New York, N. Y. (1946).
3) M. Volmer, *Z. Elektrochem.*, **35**, 505 (1929).
4) R. Becker and W. Döring, *Ann. Physik*, **24**, 719 (1935).
5) D. Turnbull and J. C. Fisher, *J. Chem. Phys.*, **17**, 71 (1949).
6) B. Vonnegut, *J. Colloid Sci.*, **3**, 563 (1948).
7) G. Pound and V. K. La Mer, *J. Amer. Chem. Soc.*, **74**, 2323 (1952).
8) D. Turnbull, *J. Chem. Phys.*, **20**, 411 (1952).
9) R. L. Cormia, F. P. Price and D. Turnbull, *J. Chem. Phys.*, **37**, 1333 (1962).
10) G. Ford and V. K. La Mer, *J. Amer. Chem. Soc.*, **72**, 1959 (1950).
11) F. K. Gorskii, *J. Expl. Theor. Phys.*, **18**, 45 (1948).

recrystallized six or seven times with freshly-distilled carbon disulfide and then dried *in vacuo*. The carbon disulfide had been shaken with mercury before the distillation in order to remove hydrogen sulfide. The tests of the purification of the recrystallized sulfur were carried out using the following method of continuous cooling.

Procedure. The sample of liquid sulfur droplets was prepared in the following manner; the fine powder of the purified sulfur was dispersed on a clean microscopic cover-glass, and then it was melted in an electric heating block at 120°C for 15 min. The sample was slowly cooled from 120°C to 55°C in the heating block; then it was transferred into a cooling apparatus designed in our laboratory maintained at 55°C. The sample was placed on an aluminum block in contact with a cascade-type semiconductor thermo-module. The temperatures were controlled with an accuracy of ±0.1°C using the thermistor controller. The changes in the sample were microphotographed continuously through the quartz window. The droplets were photographed at specified intervals with the camera mounted on an Olympus reflecting microscope, Model STS, with an object-lens with a long working distance (10×, about 3.8 cm). The temperatures over the range from 120°C to −50°C were measured with a standard thermometer, and those lower than −50°C, with a chromel-alumel thermocouple which was calibrated using materials of known melting points. The errors in the temperature measurements were within the range of ±0.1°C.

The specimens were observed by means of continuous-cooling experiments over the temperature range from 55°C to −70°C for over-all liquid droplets, and by means of isothermal cooling experiments at −20, −40, and −50°C for several droplets classified as to diameter.

In both the experiments, only the nucleation rate is approximately observable, as the growth rate is generally greater than that of nucleation on tiny droplets. Therefore, the number fractions of solidified droplets with respect to the overall droplets or the classified droplets were employed in discussing the nucleation rates.

Results

The droplets were directly observed. Fortunately, the transmittances of the crystalline and the liquid sulfur are sufficiently different for the two kinds of droplets to be easily distinguishable even without the use of polarized light, as is shown in Phot. 1.

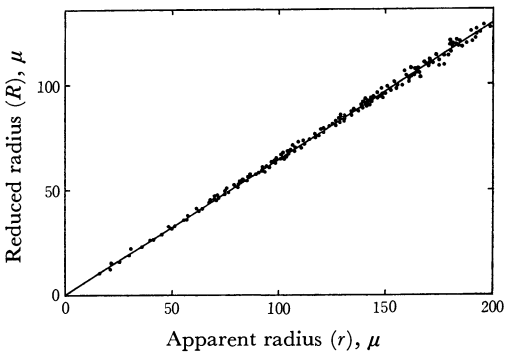

Fig. 1. Plot of reduced radius against apparent radius.

The liquid sulfur droplets on the microscopic cover-glass were regarded as approximately spherical segments, as is shown in Phot. 2. The volumes and the reduced radii of the individual droplets were calculated from the apparent radii and heights. Figure 1 shows the relationship between the apparent radii, r, and the reduced radii, R, of the sphere the volumes of which were the same as in the sulfur droplets. The R is related to the r as in the following equation; $R=0.645r$. The droplets were classified at intervals of 25μ in the apparent diameter, D.

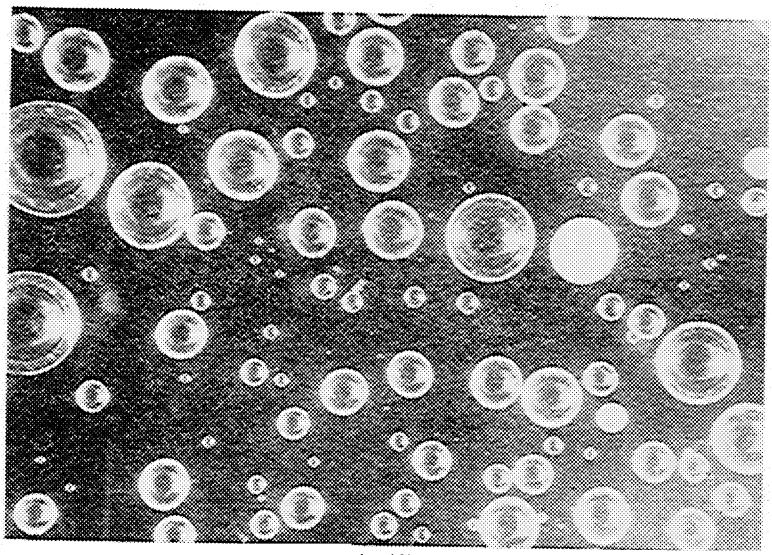

(×40)

Phot. 1. Photograph of liquid sulfur droplets.

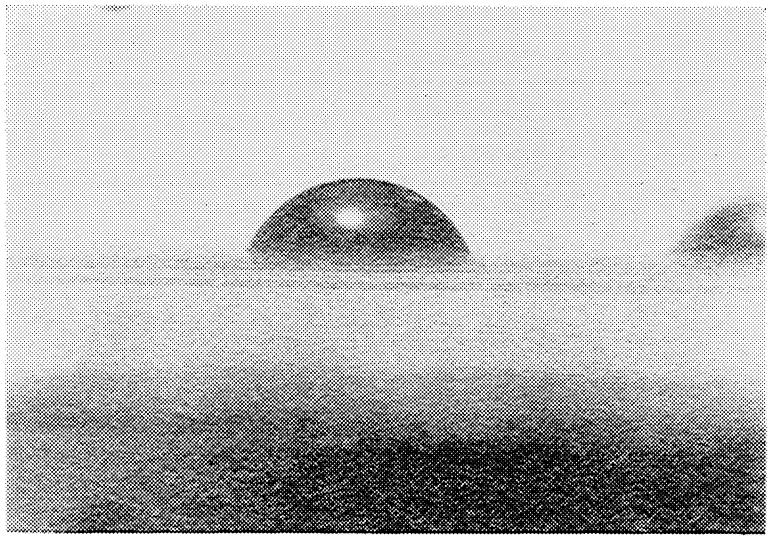

(×100)

Phot. 2. Side view of liquid sulfur droplet.

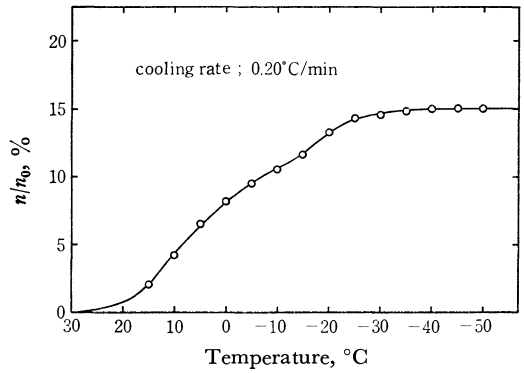

Fig. 2. Plot of number fraction of solidified droplets against temperature.

The Variation in the Number Fraction of the Solidified Droplets by the Continuous Cooling. The results of the continuous-cooling experiment over the size range from 10 μ to 400 μ in the apparent diameter are shown in Fig. 2. The specimen was continuously cooled at the rate of 0.20°C/min. This curve shows the number fractions, n/n_0, of the solidified droplets as a function of the temperatures from 30°C to −60°C. It is shown that the sulfur droplets scarcely crystallized at all at 30°C; moreover, only about 15% of the total droplets solidified even at −60°C —*i. e.*, the temperature of supercooling was 173°C. The crystallization in the whole droplets was not observed under the experimental conditions, while the critical supercooling at which an abruptly discontinuous crystallization occurred was observed to be 55°C in the liquid polyethylene droplets,[9] for example. On the contrary, imperfectly-purified liquid sulfur droplets crystallized entirely at the temperatures from 50°C to 30°C.

The Relationship between the Number Fractions of the Unsolidified Droplets and Radii. The samples were each kept at temperatures from 15°C to −50°C for 2 hr, and the number fractions of the unsolidified droplets were estimated with respect to their radii.

Turnbull[9] expressed the number fraction of the solidified droplets at the specified temperatures as follows:

$$1 - n/n_0 = \sum_{R=0}^{\infty} N_R^0 \exp(-k_R t)$$

where R is the radius of the droplets; N_R^0, the number fraction of the droplets with the radius of R; k_R, the specific nucleation rate of the droplets with the radius of R, and t, the cooling time. If the nucleation takes place throughout the volume of the droplets, *i. e.*, through the homogeneous nucleation process:

$$k_R = v_R I$$

where v_R is the volume of a droplet with the radius of R, and I, the nucleation rate per unit of volume at the specified temperature.

Concerning each droplet's range, the following expression is approximately applicable:

$$1 - (n/n_0)_R = \exp(-k_R t)$$

where $(n/n_0)_R$ is the number fraction of the solidified droplets in the narrow range of droplets with the radius of R. From the expression, the following equation is obtained if the temperature and the cooling time are specified:

$$\log(2 - \log N_{u,R}) = 3 \log R + C$$

where $N_{u,R}$ is the percentage of unsolidified droplets connected with the narrow-range droplets with the radius of R, and C, the constant.

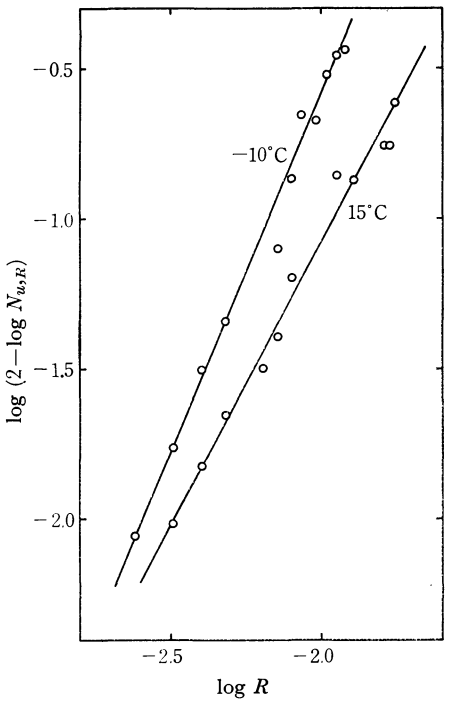

Fig. 3. Relationship between radius and number fraction of unsolidified dropets at 15 and −10°C.

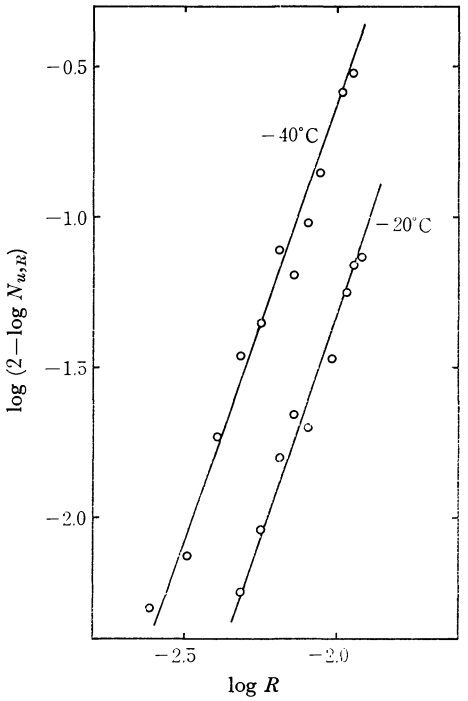

Fig. 4. Relationship between radius and number fraction of unsolidified droplets at −20 and −40°C.

If the nucleation in the sulfur droplets takes place through the homogeneous process, the log (2−log $N_{u,R}$) relation should vary linearly against the log R with the slope of 3 at specified temperatures and cooling times. Figures 3 and 4 show the relationships at 15 and −10°C, and at −20 and −40°C, respectively. At the temperatures of 15 and −10°C, the slopes were roughly estimated to be 2, but those at −20 and −40°C were nearly equal to 3. The slopes of the relationships between log (2−log $N_{u,R}$) and log R at several temperatures are summarized in Table 1.

Table 1. The slopes of the linear relationships between log (2−log $N_{u,R}$) and log R

Temp., °C	Slope	Temp., °C	Slope
15	1.88	−15	2.30
10	2.13	−20	3.00
5	1.94	−40	3.00
−10	2.39	−50	3.00

The slopes were estimated to be approximately 2 above −15°C, while they were close to 3 below −20°C, as is shown in Figs. 3 and 4 and in Table 1 respectively. The nucleations in the sulfur droplets under the conditions below −20°C were confirmed to be homogeneous, while those above −15°C were confirmed to be heterogeneous.

The Nucleation Rates in the Droplets through the Homogeneous Process. The dependences of the cooling times on the isothermal solidification were observed at the temperatures of −20, −40, and −50°C; the temperatures of supercooling were 133, 153, and 163°C respectively.

According to Turnbull's theory, the nucleation rate, k_R, of the droplets with the radius of R is expressed as follows:

$$\ln (n_{u,0}/n_u)_R = k_R t$$

where $(n_{u,0}/n_u)_R$ is the reciprocal of the number fraction of the unsolidified droplets with the radius of R, and t, the cooling time. The results of the experiment at −40°C are shown in Fig. 5. The values of $(n_{u,0}/n_u)_R$ were estimated by eliminating the number of droplets solidified above −15°C, based on the heterogeneous process. The elementary theory would predict that the homogeneous nucleation was a first-order reaction after several times. The figure shows the linear variations in the ln $(n_{u,0}/n_u)_R$ relation to the cooling times, though the variations did not obey the linear relationship before 30 min or 1 hr.

The values of k_R for each of the droplets with the radius of R were estimated from the slopes of the linear relationships. The specific nucleation rates, I, per unit of volume at the specified temperatures were calculated from the k_R values and the volumes of the droplets, as the k_R was expressed as follows: $k_R = v_R I$. The specific nucleation rates, I, were all given as approximately the same value with respect

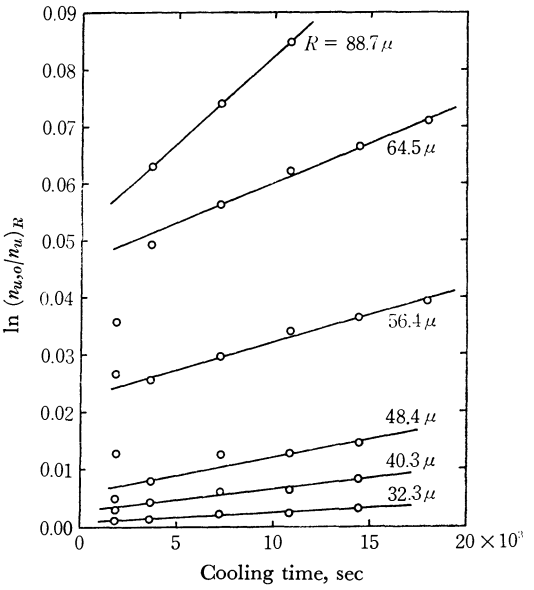

Fig. 5. Plot of $\ln (n_{u,o}/n_u)_R$ against cooling time at -40°C.

to the radii. Table 2 shows the values for k_R and I at -40°C.

TABLE 2. THE VALUES FOR k_R AND I AT -40°C

D, μ	R, μ	k, sec^{-1}	I, $cm^{-3}sec^{-1}$
100	32.3	1.59×10^{-7}	1.13
125	40.3	3.14	1.15
150	48.4	5.75	1.21
175	56.4	9.00	1.20
225	72.6	1.37×10^{-6}	1.09
250	80.6	2.40	1.05
275	88.7	3.06	1.05
		Average	1.13

The values for I were calculated to be 0.450, 1.13, and 1.16 cm^{-3} sec^{-1} at -20, -40, and -50°C respectively. These values were nearly equal to those for some molecular liquids, such as benzoic acid and white phosphorus.[12]

Discussion

The well-purified and imperfectly-purified sulfur droplets showed characteristic behavior in the crystallization phenomena in the experiments of continuous cooling. Gorskii[11] showed a measurable nucelation rate in the sulfur droplets, even at the temperature of 50°C. Presumably the sulfur used in his study contained second-phase impurities, which served to nucleate on the basis of the heterogeneous process, judging from the observations made in the continuous-cooling experiments. It is, therefore, meaningless to discuss the crystallization in Gorskii's temperature range in terms of the homogeneous nucleation processes. There then arises the question of whether the nucleation below 30°C is a heterogeneous or a homogeneous process. The probabilities of the crystallization in individual droplets depend on their sizes. Therefore, the homogeneity of nucleation can be examined from the derivative of Turnbull's theory. Under the conditions of the specified temperatures and the cooling times, the variations in $\log (2-\log N_{u,R})$ against $\log R$ should be linear, with a slope of 3 in the homogeneous process. As is shown in Figs. 3 and 4, the dependences of the number fraction of solidified droplets on the radii show a homogeneity in nucleation at temperatures below -20°C, though a heterogeneity remains at those above -15°C.

Turnbull and Fisher[5] proposed that the rate of the homogeneous nucleation in supercooled liquids was as follows:

$$I = (nkT/h) \exp(-\Delta F_A/kT) \times \exp[-16\pi\sigma^3 T_0^2/3\lambda^2 k(\Delta T)^2 T]$$

where n is the number of atoms or molecules per unit of volume; ΔF_A, the free energy of activation for the short-range diffusion across an interface of liquid and crystal; σ, the interfacial free energy between the liquid and crystalline nuclei; λ, the latent heat of fusion per unit of volume; T_0, the melting point, and ΔT, the difference between the melting point and the nucleating temperature, $T_0 - T$. This expression is derived by assuming the nuclei to be spherical and the entropy change to be independent of the temperature. Turnbull has applied his results to the freezing of supercooled liquid metals using the equation. These results agreed quantitatively with those obtained using the equation when the value of ΔF_A was assumed to be that of the activation energy for viscous flow.

The equation is transformed as follows, since the term of $\ln(nkT/h)$ is almost constant over the temperature range from -20°C to -50°C:

$$\ln I + \Delta F_A/kT = C - (16\pi\sigma^3 T_0^2/3\lambda^2 k)[1/(\Delta T)^2 T]$$

In this work, the value for ΔF_A was estimated to be 5.20 kcal/mol, a value which was obtained from the temperature dependences of the viscous flow in the λ-sulfur.[13] If the homogeneous nucleation is applicable to the liquid sulfur droplets, the variations in $(\ln I + \Delta F_A/kT)$ against $1/(\Delta T)^2 T$ should be linear. Figure 6 shows the relationship between $(\log I + \Delta_A F/2.303\, RT)$ and $1/(\Delta T)^2 T$. An excellent straight line was obtained. The value of the term of $16\pi\sigma^3 T_0^2/2.303\times 3\lambda^2 k$ was estimated to be 1.66×10^7 from the slope of the linear relationship. Assum-

12) D. G. Thomas and L. A. Staveley, *J. Chem. Soc.*, **1952**, 4569.

13) T. Matsushima, *Sci. Res. Inst., Tohoku Univ., Ser.*, **A11**, 474 (1959).

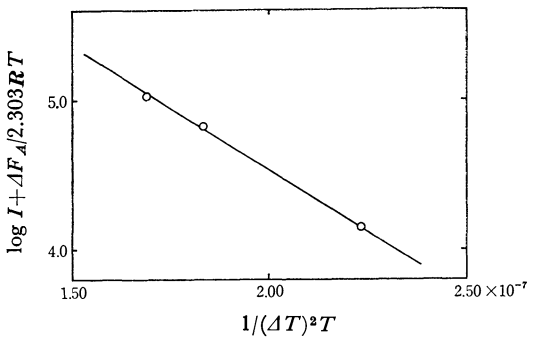

Fig. 6. Plot of (log $I+\Delta F_A/2.303RT$) against $1/(\Delta T)^2T$.

ing the sulfur nuclei to be spherical, the σ was calculated to be 12.1 erg/cm^2 using the value of the melting point of α-sulfur, 386.0°K,[14] and that of the heat of fusion, λ, 9.13×10^8 erg/cm^3.[15]

Zadumkin[16] calculated the interfacial free energies of the melt-crystal for 36 elements involving the chalcogen elements to be 8—15% of the surface tension of their liquids at all the melting points except those of Ge, Si, and Sb. The interfacial free energy of sulfur at the liquid-crystal surface was estimated to be 20% of the surface tension of liquid sulfur at the melting point, 60.5 erg/cm^2. Since the interfacial free energy of selenium, which is an analogous element of sulfur, corresponds to 16% of the surface tension at its melting point,[17] the empirical value of that for sulfur may be considered to be an appropriate one.

14) B. Meyer, "Elemental Sulfur," Interscience Publishers, New York (1965), p. 87.

15) "Handbook of the Physicochemical Properties of the Elements," ed. by G. V. Samsonov, Plenum, New York (1968), p. 250.

16) S. N. Zadumkin, *Akad. Nauk Ukr., SSR*, **1**, 21 (1961).

17) S. Hamada, unpublished.

BULLETIN OF THE CHEMICAL SOCIETY OF JAPAN VOL. 43 3101—3106 (1970)

Organic Charge Transfer Salts; Absorption Spectra of Salts between the Pyrylium or Thiopyrylium Cation and the 1,1,3,3-Tetracyanopropenide or Tricyanomethanide Anion

Hiroshi YASUBA, Tatsuro IMAI, Kenichi OKAMOTO, Shigekazu KUSABAYASHI and Hiroshi MIKAWA

Department of Chemical Technology, Faculty of Engineering, Osaka University, Yamadakami, Suita, Osaka

(Received May 14, 1970)

New organic charge transfer salts composed of an organic cation (pyrylium or thiopyrylium) and an organic anion (1,1,3,3-tetracyanopropenide or tricyanomethanide) were prepared. The absorption spectra were studied both in solution and in a solid. These salts have the charge transfer band in the visible region as a result of the electronic transition from the anion to the cation. The charge transfer bands of these salts in solution are sensitive to the nature of the solvent. The charge transfer band is observed in solvents with a low polarity; this band shifts toward a shorter wavelength in solvents with a high polarity. The increase in the polarity of the solvent causes a decrease in the apparent molar extinction coefficient. The charge transfer band in the solid shifts toward a shorter wavelength compared with that in the solution. In a single crystal, the polarized absorption spectrum shows a remarkable dichroism.

The absorption spectra of heteroaromatic onium iodide salts[1] have been studied in solution, and their features have been understood in terms of the interionic charge transfer. For example, with *N*-alkylpyridinium iodides two new absorption bands were observed in addition to the bands of the component ions in non-polar solvents[2]; the new absorption bands were attributed to the charge transfer from the anion to the cation. The charge

1) S. F. Mason, *J. Chem. Soc.*, **1960**, 2437; E. M. Kosower and P. E. Klinedinst, Jr., *J. Amer. Chem. Soc.*, **78**, 3493 (1956); G. Briegleb, W. Jung und W. Herre, *Z. Phys. Chem.* (Frankfurt), **38**, 253 (1963); A. T. Balaban, M. Mocanu and Z. Simon, *Tetrahedron*, **20**, 119 (1964).

2) E. M. Kosower, J. A. Skorcz, W. M. Schwarz and J. W. Pattor, *J. Amer. Chem. Soc.*, **82**, 2188 (1960).

transfer band was sensitive to the nature of the solvent and shifted toward a shorter wavelength with an increase in the polarity of the solvent.[3]

However, only a few brief studies have been reported concerning the absorption spectra of the organic charge transfer salts between the organic cation and the organic anion.[4] We have, therefore, attempted to make a systematic study of the organic charge transfer salts, and have reported the inter-ionic organic charge transfer band and the crystal structure of the salt between 2-dicyanomethylene-1,1,3,3-tetracyanopropanediide anion and quinolinium cation in previous papers.[5] From our consideration of the crystal structure and the optical studies in this salt, we confirmed that the charge transfer band was due to the electronic transition from the anion to the cation.

The present paper will deal with the charge transfer bands of the salts between the cyanocarbon-acid anion and the pyrylium or thiopyrylium cation.

Experimental

Materials. Tricyanomethanide (TCM) and 1,1,3,3-tetracyanopropenide (TCP) anions were used as the anions, while 2,4,6-triphenylpyrylium (TPP), 2,4,6-triphenylthiopyrylium (TPT), 4-anisyl-2,6-diphenylpyrylium (ADPP) and 4-anisyl-2,6-diphenylthiopyrylium (ADPT) cations were used as the cations.

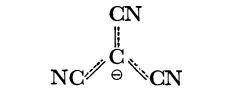

tricyanomethanide anion (TCM)

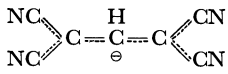

1,1,3,3-tetracyanopropenide anion (TCP)

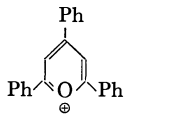

2,4,6-triphenylpyrylium cation (TPP)

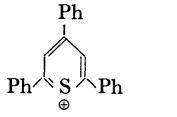

2,4,6-triphenylthiopyrylium cation (TPT)

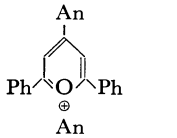

4-anisyl-2,6-diphenyl-pyrylium cation (ADPP)

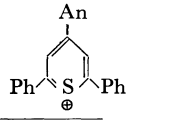

4-anisyl-2,6-diphenylthio-pyrylium cation (ADPT)

3) E. M. Kosower, *J. Amer. Chem. Soc.*, **80**, 3255 (1958).

4) E. L. Goff and R. B. LaCount, *ibid.*, **85**, 1354 (1963).

5) S. Sakanoue, T. Tamamura, S. Kusabayashi, H. Mikawa, N. Kasai, M. Kakudo and H. Kuroda, This Bulletin, **42**, 2407 (1969); S. Sakanoue, N. Yasuoka, N. Kasai, M. Kakudo, S. Kusabayashi and H. Mikawa, *ibid.*, **42**, 2408 (1969).

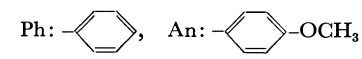

Sodium-TCP (Na-TCP). Pyridinium-TCP (Py-TCP) was prepared by the method described in a previous paper.[6] Na-TCP was obtained from Py-TCP by the use of a cation-exchang resin, Amberlite CG 120 T-1.

Potassium-TCM (K-TCM). This compound was prepared according to Trofimenko's method[7] and was purified by the column chromatography using active carbon as the adsorbent and methanol as the developing solvent.

TPP-perchlorate (TPP-ClO_4), TPT-ClO_4, ADPP-ClO_4 and ADPT-ClO_4. These compounds were prepared according to Ulrich's method.[8]

The following organic charge transfer salts were prepared and used for measurement.

TPP-TCM. This salt was prepared by a double decomposition reaction between TPP-ClO_4 and K-TCM in methanol and was purified by recrystallization from methanol - water (4 : 1) or methanol. Mp 197—199°C. Found: C, 81.05; H, 4.01; N, 10.40%. Calcd for $C_{27}H_{17}N_3O$: C, 81.20; H, 4.26; N, 10.53%.

The other salts were prepared by a similar method.

TPT-TCP. Mp 203—204°C, Found: C, 80.28; H, 3.34; N, 12.56%. Calcd for $C_{30}H_{18}N_4O$: C, 80.00; H, 4.00; N, 12.44%.

TPT-TCM. Mp 156.5—158°C, Found: C, 78.22; H, 3.90; N, 9.77%. Calcd for $C_{27}H_{17}N_3S$: C, 78.07; H, 4.10; N, 10.12%.

TPT-TCP. Mp 142—143°C, Found: C, 77.23; H, 3.40; N, 11.94%. Calcd for $C_{30}H_{18}N_4S$: C, 77.26; H, 3.86; N, 12.02%.

ADPP-TCM. Mp 201—202.5°C. Found: C, 78.39; H, 4.48; N, 9.64%. Calcd for $C_{28}H_{19}N_3O_2$: C, 78.32; H, 4.43; N, 9.78%.

ADPP-TCP. Mp 243—245°C. Found: C, 77.38; H, 4.10; N, 11.67%. Calcd for $C_{31}H_{20}N_4O_2$: C, 77.50; H, 4.18; N, 11.68%.

ADPT-TCM. Mp 65—67°C. Found: C, 72.82; H, 4.56; N, 9.26; S, 6.94%. Calcd for $C_{28}H_{19}N_3OS$: C, 75.51; H, 4.27; N, 9.45; S, 7.19%.

ADPT-TCP. Mp 175—177°C. Found: C, 75.24; H, 3.95; N, 11.36%. Calcd for $C_{31}H_{20}N_4OS$: C, 74.99; H, 4.03; N, 11.29%.

All the solvents used were purified according to the usual method of purification.[9]

Measurements. The absorption spectrum of the solution and the diffuse reflectance spectrum of the solid were measured with a Hitachi spectrophotometer, EPS 3. The diffuse reflectance spectrum was measured using potassium bromide powder as a standard; it was then plotted using the Kubelka-Munk function, $f(R)=(1-R)^2/2R$, where R is the reflectance. The spectrum

6) A. Taniguchi, K. Suzuki and H. Mikawa, *ibid.*, **39**, 1605 (1966).

7) S. Trofimenko, E. L. Little and H. F. Mower, *J. Org. Chem.*, **27**, 433 (1962).

8) R. Winzinger and P. Ulrich, *Helv. Chim. Acta*, **39**, 5 (1956); *ibid.*, **39**, 207 (1956).

9) L. F. Fieser, "Experiments in Organic Chemistry," D. C. Heath and Company, Boston (1957); J. A. Riddick and E. E. Troops, Jr., "Technique of Organic Chemistry," Vol. 7, Organic Solvents, Interscience Publishers, Inc., New York, (1955).

in the single crystal was measured with a Shimadzu multipurpose spectrophotometer, MPS-50, with the use of a microspectrophotometer attachment.

Results and Discussion

The Electronic Absorption Spectra in Solution. The absorption spectrum of TPP-TCP in chloroform has four absorption bands (λ_{max}: 281, 351, 416, and 570 mμ), Na-TCP has one absorption band (λ_{max}: 345 mμ), and TPP-ClO_4 has three absorption bands (λ_{max}: 281, 372, and 414 mμ). The absorption band of Na-TCP is due to the TCP anion, and the absorption bands of TPP-ClO_4 are due to the TPP cation. Three absorption bands (λ_{max}: 281, 351, and 416 mμ) of TPP-TCP can be explained in terms of the superposition of the absorption bands of the parent cation and anion. The other absorption band (λ_{max}: 570 mμ) is characteristic of the TPP-TCP salt, because neither the parent cation nor the parent anion have any absorption in this region, as is shown in Fig. 1.

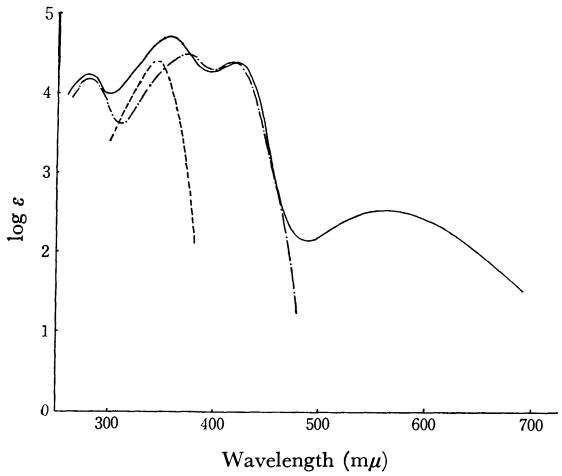

Fig. 1. Absorption spectra of TPP-TCP in chloroform and its component ions.
—— TPP-TCP in $CHCl_3$, — — — TPP-ClO_4 in $CHCl_3$ ------ Na-TCP in CH_3OH

TABLE 1. ABSORPTION MAXIMA OF CHARGE TRANSFER BAND IN CHLOROFORM AND IN SOLID STATE

Salts	λ_{max} in $CHCl_3$ (mμ)	λ_{max} in solid (mμ)
TPP-TCM	538	530
TPP-TCP	570	565
TPT-TCM	566	520 (S)
TPT-TCP	595	540
ADPP-TCM	530 (S)	520 (S)
ADPP-TCP	540 (S)	530 (S)
ADPT-TCM	540 (S)	520 (S)
ADPT-TCP	570 (S)	560 (S)

(S): shoulder

This fact suggests that the new band is an interionic charge transfer band. A new band of this type is also found in the absorption spectra of the other salts. The wavelengths of these new absorption bands are listed in Table 1.

The energies of the new bands in the TCM salts of TPP, TPT, ADPP, and ADPT are 2.30, 2.19, 2.34, and 2.30 eV respectively, while those in the TCP salts of TPP, TPT, ADPP, and ADPT are 2.18, 2.08, 2.30, and 2.18 eV respectively. These two series of energies have a linear relationship, as is shown in Fig. 2. Such a linear relationship has also been observed for usual donor-acceptor complexes between neutral molecules; it has been taken to be evidence of the absorption bands being charge transfer bands.[10] This consideration is thought to be applicable to the present organic salts, also.

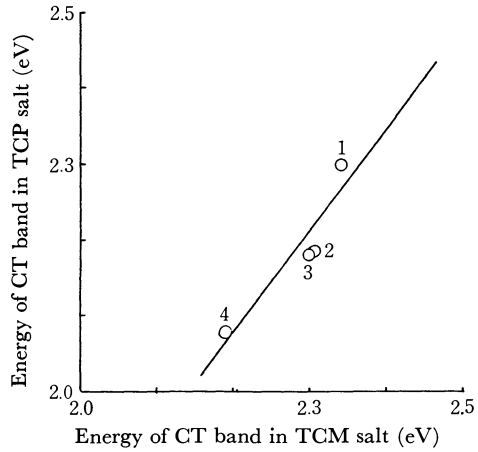

Fig. 2. Energies of charge transfer bands in salts of TCP with the cations: (1) ADPP, (2) ADPT, (3) TPP, (4) TPT, against the energies of the charge transfer bands in the salts of these cations with TCM.
1. ADDP, 2. ADDP, 3. TPP, 4. TPT

The new band is sensitive to the polarity of the solvent. The increase in the polarity of the solvent causes the absorption maximum to shift toward a shorter wavelength and the apparent molar extinction coefficient (ε_{app}) to decrease.

Figure 3 shows the plot of the λ_{max} energies of the new bands of TPT-TCP in various solvents *versus* the *Z*-value,[3] the empirical parameter of the solvent polarity. The linear relationship shows that the absorption maximum shifts to a shorter wavelength with an increase in the solvent polarity. The other salts give similar results. The solvent shift of the absorption bands in these salts can be explained by Kosower's theory presented in his

10) R. Foster, *Tetrahedron*, **10**, 96 (1960); K. Abe, Y. Matsunaga and G. Saito, This Bulletin, **41**, 2852 (1968).

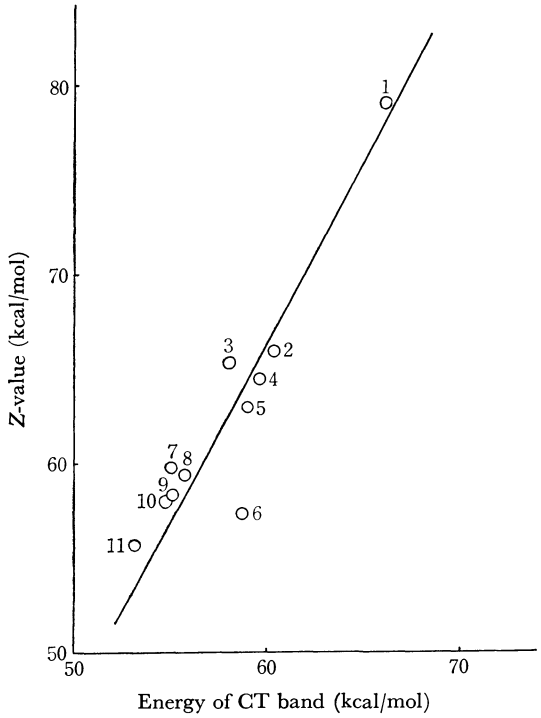

Fig. 3. Energies of the charge transfer bands of TPT-TCP against the *Z*-value for the solvents used.
(1) Acetic acid, (2) Methyl acetate, (3) Anisole, (4) Dichloromethane, (5) Chloroform, (6) Ethyl acetate, (7) Bromobenzene, (8) Chlorobenzene, (9) Dioxane, (10) Toluene, (11) Benzene.

consideration of the solvent effect of the absorption spectrum of organic iodides.[3] That is, the solvent shift of the absorption maximum depends on the stabilization in the ground state and the destabilization in the excited state. From the above results, it can be concluded again that the new bands of these salts are due to the electronic charge transfer from the anion to the cation. The slope in Fig. 3 is associated with the solvent sensitivity of the charge transfer band. If the slope is steep, the solvent sensitivity is low. In these salts, the slope of this straight line is 1.5—2.0. In tropylium iodide[11] and *N*-methylacridinium iodide,[12] the slope of this line is unity. It has been reported that the solvent sensitivity depends on the size of the anion and the delocalization of its charge, the increase in size and the increase in the delocalization of its charge causing the decrease in the solvent sensitivity.[12] In the present case, the size and the delocalization of the charge in TCM or TCP anion are larger than those of the iodide anion. It can, therefore, reasonably be understood that the solvent sensitivity for TCM or TCP is inferior to that of iodides. In ADPP and ADPT systems the new band was observed as a shoulder. It was, therefore, not possible in these salts to investigate the solvent effect in detail.

As these charge transfer bands are due to the interaction between the anion and the cation, both ions must be in the ion-pair form in order to exhibit charge transfer interactions. The salts are in the following equilibrium in solution:

$$AD \rightleftarrows D^- + A^+$$

where DA is an organic charge transfer salt in an ion-pair form and where D^- and A^+ are the component ions. In polar solvents the dissociation of the ion-pair proceeds and the concentration of the ion-pair from decreases, thus decreasing the apparent molar extinction coefficient (ε_{app}). At a certain concentration the ε_{app} values were measured in several different solvents. As is shown in Fig. 4,

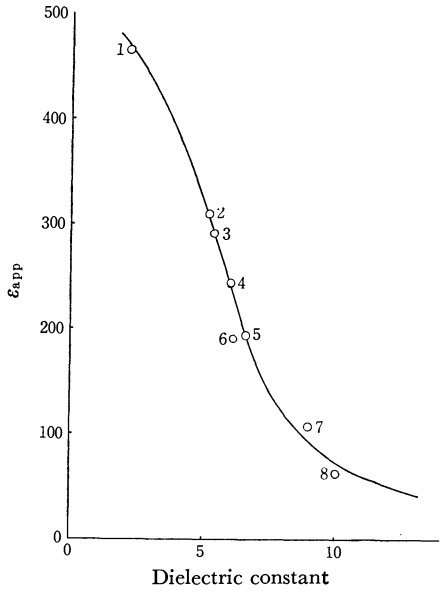

Fig. 4. Apparent molar extinction coefficient of TPT-TCP against the dielectric constants for the solvents used.
(1) Dioxane, (2) Chlorobenzene, (3) Bromobenzene, (4) Methyl acetate, (5) Ethyl acetate, (6) Acetic acid, (7) Dichloromethane, (8) 1,2-dichloroethane.

the ε_{app} values decrease with the increase in the dielectric constant of the solvent. The dissociation constants of these salts were calculated as follows from the concentration dependence of the charge transfer bands by a method similar to that used for *N*-dodecylpyridinium iodide.[13] Provided that the absorbance of the solution at the charge transfer

11) E. M. Kosower, *J. Org. Chem.*, **29**, 956 (1964).
12) T. G. Beaumont and K. M. C. Davis, *J. Chem. Soc., B*, **1968**, 1010.
13) A. Ray and P. Mukerjee, *J. Phys. Chem.*, **70**, 2138 (1966).

band is due entirely to the charge transfer absorption of the ion-pair present, and provided that the absorption due to the component ions is negligible in this wavelength region, the following equation is obtained:

$$D/C_0 = \varepsilon - (K\cdot\varepsilon)^{1/2}\cdot D^{1/2}/C_0$$

where D is the optical density for an optical length of 1 cm; C_0, the total concentration of the salt; ε, the molar extinction coefficient of the ion-pair, and K, the dissociation constant of the salt. The values of K and ε were calculated from the slope and intersection of the plots of D/C_0 *vs.* $D^{1/2}/C_0$; they are shown in Table 2 for chloroform solution. The values of K in Table 2 clearly show that, in chloroform, the anion and the cation exist as an ion-pair form. These results are also supported by the measurement of the conductivity of the solution. In a polar solvent the equivalent conductivity is proportional to $C^{1/2}$, and in a non-polar solvent, to $1/C^{1/2}$, where C is the concentration of the salt. This conductivity behavior suggests that these salts dissociate highly in a polar solvent and do not dissociate so much in a non-polar solvent.

Table 2. Dissociation constant and molar extinction coefficient in chloroform

	K	ε
TPP-TCM	$\sim 10^{-5}$ below	340
TPP-TCP	$\sim 10^{-5}$	310
TPT-TCM	$\sim 10^{-5}$ below	470
TPT-TCP	$\sim 10^{-4}$	370

In conclusion, the solvent shift of the charge transfer band can be explained by the term of Z-values, and the dissociation of the salt is closely related to the dielectric constant of the solvent.

In the interionic charge transfer salts, the following equation is also applicable:

$$E_{ct} = I_p(\mathrm{D}^-) - E_a(\mathrm{A}^+) + E_{coul}$$

where E_{ct} is the energy of the charge transfer transition; $I_p(\mathrm{D}^-)$, the ionization potential of the donor anion; $E_a(\mathrm{A}^+)$, the electron affinity of the acceptor cation, and E_{coul}, the coulomb energy for the separation of ions. The term of the coulomb energy (E_{coul}) is probably nearly the same in different interionic charge transfer salts. For the salts having the same cation, the difference in E_{ct}, therefore, represents the difference in $I_p(\mathrm{D}^-)$, that is, the energy difference between the highest occupied molecular orbitals of the anions. The values of Table 1 suggested that the ionization potential of TCM is larger than that of TCP. The simple Hückel LCAO calculation also supports this suggestion. A similar treatment to the salts composed of the same anion suggested that the electron affinity of TPP is smaller than that of TPT. It has been suggested that the polarographic half-wave potential is correlated with the electron affinity and, hence, with the charge transfer energy.[14] The half-wave potentials of these cations, measured as usual against the saturated calomel electrode, gave the values of -0.24 V for TPP and

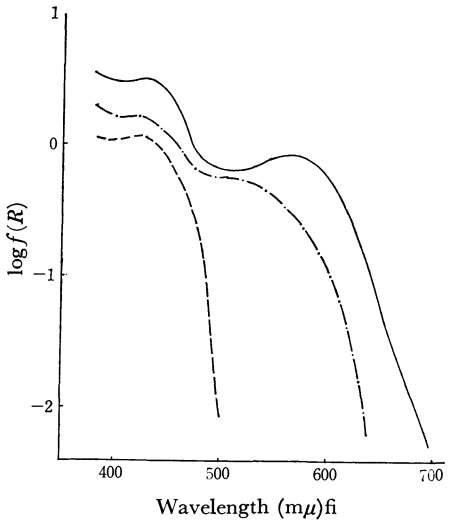

Fig. 5. Diffuse reflectance spectra of TPP-TCP (——), TPP-TCM (— — —) and TPP-ClO_4 (-----).

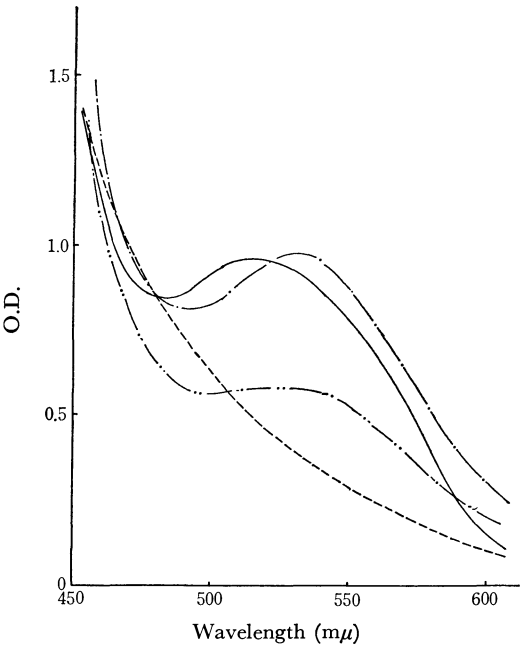

Fig. 6. Polarized absorption spectra of single crystals of TPP-TCP and TPP-TCM.
TPP-TCP: —— 1//, ——— 1⊥
TPP-TCM: —— 1//, ------ 1⊥

14) M. Feldman and S. Winstein, *Tetrahedron Lett.*, **1962**, 853.

−0.17 V for TPT in absolute ethanol. The electron affinity of TPP is, therefore, smaller than that of TPT. From these results, it can reasonably be understood that the charge transfer bands of TPP-TCM and TPP-TCP are in a shorter wavelength region than those of TPT-TCM and TPT-TCP respectively.

The Electronic Absorption Spectrum in Solid. The absorption spectra in a solid were measured by diffuse reflectance spectroscopy. The spectra of TPP-TCM, TPP-TCP, and TPP-ClO_4 are shown in Fig. 5. The absorption band is at 530 mμ in TPP-TCM and at 565 mμ in TPP-TCP. These absorption bands in a solid are considered to correspond to the charge transfer bands in solution. The absorption peaks of other salts in the solid state are shown in Table 1.

The charge transfer band in the solid state lies in a somewhat shorter wavelength region than does the corresponding charge transfer band in the solution, as is shown in Table 1. This suggests that the stabilization by the neighboring ions in the solid state is larger than the stabilization by the neighboring solvent molecules in the solution. The data in Table 1 also suggest that the stabilization of the TPP system is smaller than that of the TPT system. This difference may be due to the differences in the crystal structure and the polarizability of the component ions.

The polarized absorption spectra of the single crystals of TPP salts show a remarkable dichroism in the charge transfer band, the optical density being large in the direction of the crystal growth (Fig. 6). Although the crystal sturcture has not yet been determined in this case, it seems certain that the cation and the anion are stacked in an alternating face-to-face arrangement in the growth direction, and that the charge transfer transition occurs from an anion to the nearest cation in this direction. A similar phenomenon has also been observed in quinolinium 2-dicyanomethylene-1,1,3,3-tetracyanopropanediide (Q_2DMTP). The crystal structure of Q_2DMTP is orthorhombic, and the cation and the anion are stacked alternately along the *a*-axis.[5] The optical density is higher in the *a*-polarization spectrum than in the *c*-polarization spectrum.[5]

All the results show that the new absorption band, both in a solid and in solution, is a charge transfer band between the anion and the cation.

BULLETIN OF THE CHEMICAL SOCIETY OF JAPAN VOL. 43 3107—3115 (1970)

Force Constants and Average Structures of AsF_3 and $AsCl_3$ as Determined by Electron Diffraction and Spectroscopy*1

Shigehiro KONAKA

Department of Chemistry, Faculty of Science, Hokkaido University, Sapporo

(Received May 15, 1970)

The general quadratic potential constants of $AsCl_3$ have been determined by the use of a combination of the mean amplitudes observed by gas electron diffraction and the vibrational frequencies. Those of AsF_3 have been determined from the mean amplitudes, the centrifugal distortion constants given by microwave spectroscopy and the Coriolis coupling constants and the vibrational frequencies given by infrared spectroscopy on the basis of the molecular structure newly-determined by electron diffraction. By using these potential constants, zero-point average structures have been derived from the r_g structures obtained by electron diffraction. The results have been found to be consistent with the average rotational constants, B_z, derived from the effective rotational constants, B_0, observed by microwave spectroscopy according to the theory of vibration-rotation interactions. The final results, obtained by the use of a combination of the electron diffraction and microwave data, are:

$$r_z(\text{As–Cl}) = 2.1621 \pm 0.0009\ \text{Å}, \quad \theta_z(\text{ClAsCl}) = 98°38' \pm 22'$$

$$r_z(\text{As–F}) = 1.7080 \pm 0.0004\ \text{Å}, \text{ and } \theta_z(\text{FAsF}) = 95°58' \pm 17'.$$

Formulas for calculating the sum of perpendicular mean amplitudes for pyramidal XY_3-type molecules have been derived and used to reduce r_g to r_z.

If the anharmonic as well as the harmonic potential constants are known, the equilibrium structures (r_e-structures) of gaseous molecules can be determined by spectroscopy[1] and gas electron diffraction (ED).[2] The r_e-structures derived from ED agreed within the limits of experimental errors with those derived from spectroscopy for CH_4, CD_4,[2–4] and CS_2.[5,6]

Since the anharmonic potential constants are, however, not yet available except for a very limited number of molecules, the r_e-structures have not been obtained for most molecules. Even so, the zero-point average structures (r_z-structures) can be derived from the average rotational constants, B_z, which can themselves be reduced from the effective ground-state rotational constants, B_0, by using only the harmonic potential constants.[7–9] Since the thermal average distances, r_g, observed by ED can also be converted to the r_z distances, it is possible to make an exact comparison between the molecular structures obtained by the two different experimental techniques.[10–15] Furthermore, it is possible to combine both sets of results so as to obtain more precise structures.[16–21]

*1 Main part of this report is included in the doctral thesis presented by the author to the Faculty of Science, Hokkaido University.

1) H. H. Nielsen, *Rev. Mod. Phys.*, **23**, 90 (1951).
2) L. S. Bartell, K. Kuchitsu and R. J. de Neui, *J. Chem. Phys.*, **35**, 1211 (1961).
3) R. A. Olafson, M. A. Thomas and H. L. Welsh, *Can. J. Phys.*, **39**, 419 (1961).
4) K. Kuchitsu and L. S. Bartell, *J. Chem. Phys.*, **36**, 2470 (1962).
5) B. P. Stoicheff, *Can. J. Phys.*, **36**, 218 (1958).
6) Y. Morino and T. Iijima, This Bulletin, **35**, 1661 (1962).
7) T. Oka, *J. Phys. Soc. Jap.*, **15**, 2274 (1960).
8) T. Oka and Y. Morino, *J. Mol. Spectry.*, **6**, 472 (1961).
9) D. R. Herschbach and V. W. Laurie, *J. Chem. Phys.*, **37**, 1668 (1962).
10) Y. Morino, K. Kuchitsu and T. Oka, *ibid.*, **36**, 1108 (1962).
11) K. Kuchitsu, *ibid.*, **44**, 906 (1966).
12) K. Kuchitsu and S. Konaka, *ibid.*, **45**, 4342 (1966).
13) Y. Morino, K. Kuchitsu and S. Yamamoto, *Spectrochim. Acta*, **24A**, 335 (1968).
14) Y. Morino, K. Kuchitsu and T. Moritani, *Inorg. Chem.*, **8**, 867 (1969).
15) M. Tanimoto, K. Kuchitsu and Y. Morino, This Bulletin, **42**, 2519 (1969).
16) K. Kuchitsu, T. Fukuyama and Y. Morino, *J. Mol. Structure*, **1**, 463 (1967—1968).
17) Y. Morino, K. Kuchitsu, Y. Hori and M. Tanimoto, This Bulletin, **41**, 2349 (1968).
18) K. Kuchitsu, *J. Chem. Phys.*, **49**, 4456 (1968).

The r_g-structures of AsF_3 and $AsCl_3$ have been determined by the sector-microphotometer method of gas electron diffraction described in a preceding paper.[22] The ground-state rotational constants, B_0, obtained from the microwave spectra (MW) are 2147.2 ± 0.2 and 2044.7 ± 0.3 Mc for $As^{35}Cl_3$ and $As^{37}Cl_3$ respectively,[23] and 5878.971 ± 0.002 Mc for AsF_3.[24] In the present study, both sets of results have been converted to the r_z-structures or the corresponding average rotational constants, and then compared with each other. Furthermore, more accurate molecular structures have been obtained by the use of a combination of the electron-diffraction and the spectroscopic data.

It is necessary to know the quadratic potential constants for the above purpose. For the pyramidal XY_3-type of molecules, the quadratic potential constants can not be determined from only the observed vibrational frequencies. We must use certain additional physical quantities which can be related to the quadratic potential constants. The mean amplitudes of thermal vibration, which are observed by ED, can be used for such a purpose.[25,26]

There is no published work in which the force constants of $AsCl_3$ have been determined experimentally. In the present study, the intramolecular force field of $AsCl_3$ has been determined by using the observed mean amplitudes given in the preceding paper.[22]

Some investigations have already attempted to determine the force constants of AsF_3 by using the centrifugal distortion constants[27] or the Coriolis constants obtained by spectroscopy.[28,29] However, the bond angles of 98° [27] and 102° [28,29] assumed in these previous studies are appreciably larger than the bond angle of $95.9°\pm0.4°$ which has been determined by our own recent electron-diffraction study.[22] In the present study, the most probable set of the force constants of AsF_3 has been determined from the mean amplitudes,[22] the centrifugal distortion constants, and the Coriolis constants on the basis of the accurate molecular structure.

Determination of the Force Constants

The general quadratic force field for the pyramidal XY_3 molecule can be expressed in terms of the internal coordinates:

$$\begin{aligned}2V = &\sum f_r(\Delta r_i)^2 + 2\sum f_{rr}(\Delta r_i)(\Delta r_j) \\ &+ \sum f_\theta(r_e\Delta\theta_{ij})^2 + 2\sum f_{\theta\theta}(r_e\Delta\theta_{ij})(r_e\Delta\theta_{jk}) \\ &+ 2\sum f_{r\theta}(\Delta r_i)(r_e\Delta\theta_{ij}) + 2\sum f_{r\theta'}(\Delta r_i)(r_e\Delta\theta_{jk}). \quad (1)\end{aligned}$$

Here all the notations except for the equilibrium bond distance, r_e, are those used in Ref. 26.

The symmetry coordinates used are as follows:

$$\begin{aligned}S_1 &= \frac{1}{\sqrt{3}}(\Delta r_1+\Delta r_2+\Delta r_3), \\ S_2 &= \frac{1}{\sqrt{3}}r_e(\Delta\theta_{12}+\Delta\theta_{23}+\Delta\theta_{31}), \\ S_3 &= \frac{1}{\sqrt{2}}(\Delta r_1-\Delta r_2), \\ S_4 &= \frac{1}{\sqrt{2}}r_e(\Delta\theta_{23}-\Delta\theta_{31}), \\ S_5 &= \frac{1}{\sqrt{6}}(\Delta r_1+\Delta r_2-2\Delta r_3), \\ S_6 &= \frac{1}{\sqrt{6}}r_e(\Delta\theta_{23}+\Delta\theta_{31}-2\Delta\theta_{12}), \quad (2a)\end{aligned}$$

which may be written in a matrix form as:

$$\boldsymbol{S} = \boldsymbol{UR}. \quad (2b)$$

The relations between the force constants in the symmetry coordinates and those in the internal coordinates are:

$$\begin{aligned}F_{11} &= f_r + 2f_{rr}, \\ F_{12} &= f_{r\theta'} + 2f_{r\theta}, \\ F_{22} &= f_\theta + 2f_{\theta\theta}, \\ F_{33} &= f_r - f_{rr}, \\ F_{34} &= f_{r\theta'} - f_{r\theta}, \\ F_{44} &= f_\theta - f_{\theta\theta}. \quad (3)\end{aligned}$$

The elements of the $\boldsymbol{G}$ matrix in the symmetry coordinates are given as follows:

A_1 species:

$$\begin{aligned}G_{11} &= \mu_X(1+2c)+\mu_Y, \\ G_{12} &= -2\mu_X(1-c)(1+2c)/s, \\ G_{22} &= 2(1-c)(1+2c)[2(1-c)\mu_X+\mu_Y]/s^2, \quad (4)\end{aligned}$$

E species:

$$\begin{aligned}G_{33} &= G_{55} = \mu_X(1-c) + \mu_Y, \\ G_{34} &= G_{56} = \mu_X(1-c)^2/s, \\ G_{44} &= G_{66} = (1-c)[\mu_X(1-c)^2+\mu_Y(2+c)]/s^2. \quad (5)\end{aligned}$$

Here μ_X and μ_Y are the reciprocals of the atomic masses, m_X and m_Y, respectively, while s and c stand for $\sin\theta$ and $\cos\theta$ respectively.

The formulas for calculating the mean amplitudes of the pyramidal XY_3 molecules, $l(X-Y)$ and

19) T. Fukuyama, K. Kuchitsu and Y. Morino, This Bulletin, **42**, 379 (1969).
20) T. Iijima and M. Kimura, *ibid.*, **42**, 2159 (1969).
21) T. Iijima, *ibid.*, **43**, 1049 (1970).
22) S. Konaka and M. Kimura, *ibid.*, **43**, 1693 (1970).
23) P. Kisliuk and C. H. Townes, *J. Chem. Phys.*, **18**, 1109 (1950).
24) P. Kisliuk and S. Geschwind, *ibid.*, **21**, 828 (1953).
25) Y. Morino, Y. Nakamura and T. Iijima, *ibid.*, **32**, 643 (1960).
26) M. Iwasaki and K. Hedberg, *ibid.*, **36**, 594 (1962).
27) A. M. Mirri, *ibid.*, **47**, 2823 (1967).
28) I. W. Levin and S. Abramowitz, *ibid.*, **44**, 2562 (1966).
29) L. C. Hoskins, *ibid.*, **45**, 4594 (1966).

l(Y–Y), are given as follows:[26]

$$[l(\mathrm{X\text{-}Y})]^2 = \frac{1}{3}(\sum_{11}+2\sum_{33}), \tag{6}$$

$$[l(\mathrm{Y\text{-}Y})]^2 = \frac{2}{3}(2\sum_{11}+\sum_{33})\sin^2\frac{\theta}{2} + \frac{4}{3}(\sum_{12}-\sum_{34})\sin\frac{\theta}{2}\cos\frac{\theta}{2} + \frac{1}{3}(\sum_{22}+2\sum_{44})\cos^2\frac{\theta}{2}. \tag{7}$$

Here $\sum_{ij}$ denotes the thermal average of the product of S_i and S_j. The values of $\sum_{ij}$ can easily be calculated from the force constants.[26]

When the four observed vibrational frequencies are used, the force constants have only two degrees of freedom. For a given value of F_{12}, the other force constants of A_1 species are calculated as:

$$F_{11} = (\gamma \pm \delta)/2G_{11}, \qquad F_{22} = (\gamma \mp \delta)/2G_{22}, \tag{8}$$

where:

$$\gamma = \lambda_1 + \lambda_2 - 2G_{12}F_{12}, \tag{9}$$

$$\delta = [\gamma^2 - 4G_{11}G_{22}(\lambda_1\lambda_2/(G_{11}G_{22}-G^2_{12})+F^2_{12})]^{1/2}, \tag{10}$$

$$\lambda_k = 4\pi^2c^2\nu_k^2. \tag{11}$$

Similar relations hold for the force constants of the E species. The relations in these force constants are shown in Fig. 1. The frequencies used in the calculation are tabulated in Table 1. The bond angles used are 98.5° and 95.9° for $AsCl_3$ and AsF_3 respectively.[22] The solid and dotted curves correspond to the upper sign and the lower sign of Eq. (8) respectively. In the solid curves, the

Table 1. Fundamental frequencies used for the force constant calculation (in cm^{-1} unit)

	ν_1	ν_2	ν_3	ν_4	Ref.
$AsCl_3$	411.8	193.6	386.7	155.3	30
AsF_3	740	336	702	262	28

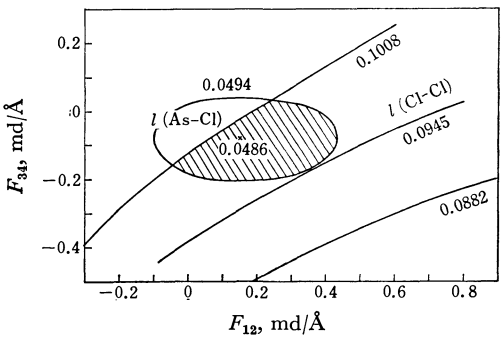

Fig. 2. Force constants of $AsCl_3$ allowed by the observed mean amplitudes at 291°K.

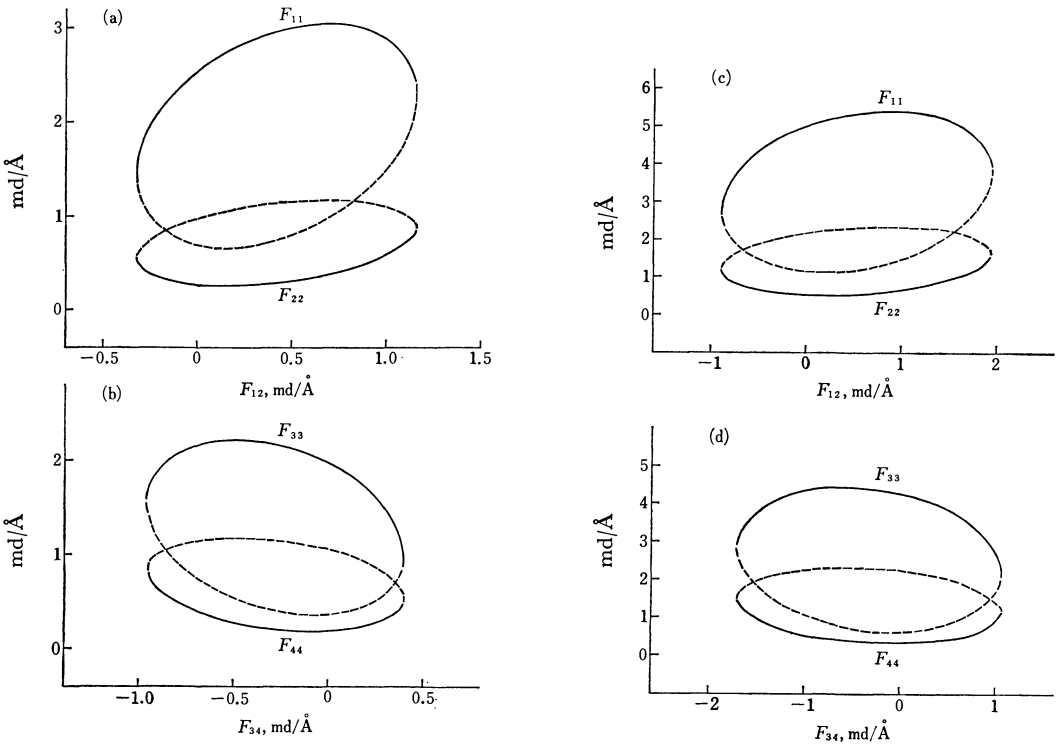

Fig. 1. Correlation curves of force constants (a), (b) $AsCl_3$ and (c), (d) AsF_3.

30) P. W. Davis and R. A. Oetjen, *J. Mol. Spectry.*, **2**, 253 (1958); *ibid.*, **3**, 581 (1959).

TABLE 2. FORCE CONSTANTS OF $AsCl_3$ DETERMINED BY USING THE OBSERVED MEAN AMPLITUDES AND VIBRATIONAL FREQUENCIES (in md/Å unit)

Symmetry coordinate		Internal coordinate	
F_{11}	2.72±0.27	f_r	2.31±0.08
F_{12}	0.19±0.24	f_{rr}	0.22±0.10
F_{22}	0.28±0.02	f_θ	0.22±0.00$_5$
F_{33}	2.05±0.10	$f_{\theta\theta}$	0.03±0.01
F_{34}	−0.08$_5$±0.12	$f_{r\theta}$	0.11±0.07
F_{44}	0.19$_5$±0.00$_5$	$f_{r\theta'}$	0.00±0.13

TABLE 3. FORCE CONSTANTS OF AsF_3 DETERMINED BY EARLIER AUTHORS AND THE SPECTROSCOPIC AND STRUCTURAL DATA USED IN THEIR CALCULATIONS (F, D, ν and r are in md/Å, kc, cm^{-1} and Å units, respectively)

	Levin and Abramowitz[28]	Hoskins[29]	Mirri[27]
F_{11}			4.80 ±0.06
F_{12}			−0.28 ±0.06
F_{22}			0.57 ±0.01
F_{33}	4.20±0.05	4.27±0.04	4.34 ±0.01
F_{34}	0.00±0.05	−0.12±0.06	−0.135±0.006
F_{44}	0.30±0.02	0.29±0.03	0.315±0.001
ζ_3	0.31	0.21	
ζ_4	−0.44	−0.43	
D_J			4.63 ±0.03
D_{JK}			−6.17 ±0.05
ν_1	740		740
ν_2	336		336
ν_3	702	702.2	702
ν_4	262	262.3	262
r_e (As–F)	1.712	1.712	1.708
θ	102°	102°	98°

TABLE 4. EXPERIMENTAL PARAMETERS USED FOR THE FORCE CONSTANT CALCULATION OF AsF_3

l (As–F)	0.0433±0.0022 Å[a]
l (F–F)	0.0689±0.0044 Å[a]
D_J	4.63 ±0.03 kc[b]
D_{JK}	−6.17 ±0.05 kc[b]
ζ_4	−0.35 ±0.02[c]
r_e	1.708 Å[d]
θ	95.9°

a) Ref. 22 b) Ref. 27
c) The error was estimated by the present author.
d) Assumed.

stretching force constants, F_{11} and F_{33}, are larger than the bending force constants, F_{22} and F_{44} respectively. Since such is not necessarily the case for the dotted curves, they should be abandoned. Thus, for a given set of F_{12} and F_{34}, all of the other force constants can be determined uniquely.

The mean amplitudes of $AsCl_3$ were calculated for the various values of F_{12} and F_{34}. The force constants allowed by the two observed mean amplitudes, l(As–Cl)=0.0470±0.0024 Å and l(Cl–Cl)=0.0945±0.0063 Å,[22] and the four vibrational frequencies are shown by the shaded area in Fig. 2. The corresponding values of the other force constants were determined from the solid curves in Figs. 1a and b. The values of the force constants in the symmetry coordinates thus determined are listed in Table 2, along with those in the internal coordinates.

The force constants of AsF_3 reported by earlier authors are listed in Table 3, along with the spectro-

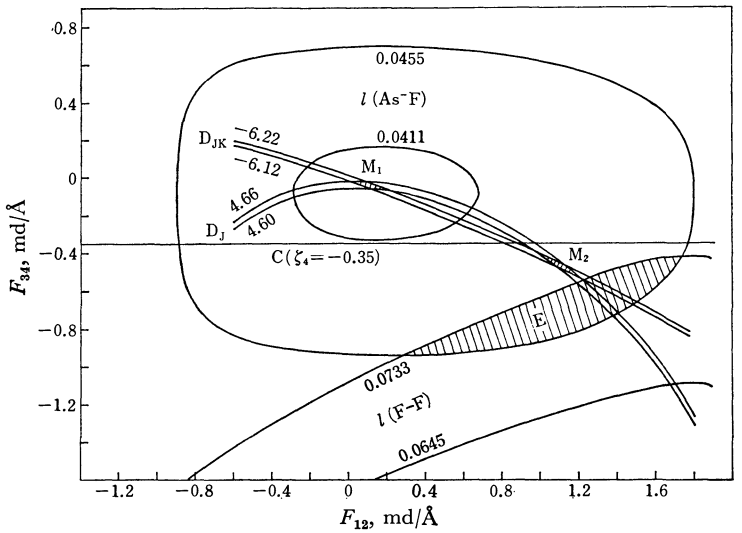

Fig. 3. Comparison of the allowed regions of the force field of AsF_3 which are compatible with the observed values of two mean amplitudes at 292°K (E), two centrifugal distortion constants (M_1 and M_2) and a Coriolis coupling constant (C).

scopic and structural data used in their calculations. The force constants of AsF_3 allowed by the observed mean amplitudes given in Table 4 are shown by the E region of Fig. 3. They are inconsistent with the force constants listed in Table 3.

The force constants reported by Levin and Abramowitz[28] and by Hoskins[29] were obtained by using the Coriolis constants, ζ_3 and ζ_4, which were estimated from the P–R splittings of ν_3 and ν_4 infrared bands respectively. The values of the Coriolis constants thus estimated depend on the assumed values of the bond angles. The value of $(\zeta_3+\zeta_4)$ given by the sum rule[31] also depends on the molecular geometry:

$$\zeta_3 + \zeta_4 = I_c^e/(2I_b^e) - 1. \qquad (12)$$

Here I_c^e and I_b^e are the equilibrium moments of inertia about the symmetry axis and about an axis perpendicular to it respectively. The theoretical values of $(\zeta_3+\zeta_4)$ are -0.22 for the bond angle of 102° and -0.29 for the bond angle of 95.9°.

For the bond angle of 95.9°, the Coriolis constant, ζ_4, was estimated to be -0.35 from the P–R separation of ν_4, 26.7 cm^{-1},[28,29] by the use of the relations given by Edgell and Moynihan.[32] Similarly, the P–R separation of ν_3, 15.4 cm^{-1},[29] led to $\zeta_3=0.32$. However, these values did not satisfy the sum rule. Since the position of the P-branch of the ν_3 band had been very obscure,[29,33] ζ_3 was not included in the present calculation of the force constants. By using the relation between ζ_4 and the force constants,[31] F_{34} was determined to be -0.35 md/Å from the ζ_4 value of -0.35.

The force constants reported by Mirri[27] had been obtained by using the centrifugal distortion constants, D_J and D_{JK}, observed by microwave spectroscopy. Since the bond angle of 98° had been used in her calculation, it was desirable to follow her calculation using the bond angle of 95.9°. The centrifugal constants were calculated from the force constants according to the theory of the semi-rigid rotator.[34,35] The allowed values of the force constants are shown by the two regions, M_1 and M_2, in Fig. 3. It is noticeable that two sets of solutions are present. The force constants reported by Mirri correspond to the M_1 region.

Although there exists no set of force constants compatible with the above five observed quantities, the force constants represented by the M_2 region satisfy all the observed values comparably well.

The final values of the force constants of AsF_3 were determined by the least-squares method.[36] The off-diagonal force constants, F_{12} and F_{34}, are chosen as parameters, while the observed values to be fitted are the l(As–F), l(F–F), D_J, D_{JK}, and ζ_4 values given in Table 4. The weights were taken to be inversely proportional to the squares of errors, ε_j, estimated in Table 4. That is, the most probable set of parameters was determined by the following condition:

$$\boldsymbol{V^*PV} = \sum_{j=1}^{5} \left(\frac{m_j^{obs} - m_j^{calc}}{\varepsilon_j}\right)^2 = \text{minimum}. \qquad (13)$$

The standard errors of parameters were evaluated as:

$$\sigma_i = \sqrt{B_{ii}^{-1}\frac{\boldsymbol{V^*PV}}{3}}\,. \qquad (14)$$

Here the notations correspond to those used in Ref. 36. The most probable set of force constants is given in Table 5, along with the limit of errors.

Table 5. The most probable set of the force constants of AsF_3 with the estimated limits of errors (in md/Å unit)

Symmetry coordinate		Internal coordinate	
F_{11}	5.39±0.03	f_r	4.75±0.03
F_{12}	0.95±0.26	f_{rr}	0.32±0.02
F_{22}	0.64±0.09	f_θ	0.45±0.05
F_{33}	4.42±0.02	$f_{\theta\theta}$	0.10±0.04
F_{34}	−0.39±0.13	$f_{r\theta}$	0.45±0.13
F_{44}	0.35±0.02	$f_{r\theta'}$	0.06±0.17

Table 6. Comparison of the observed values of the mean amplitudes and spectroscopic constants with the calculated values obtained by using the force constants given in Tables 2 and 5
(l and D are in Å and kc units, respectively)

	Obsd	Calcd
(a) $AsCl_3$		
l (As–Cl)	0.0470±0.00024[a]	0.0487±0.0002
l (Cl–Cl)	0.0945±0.0063[a]	0.0989±0.0018
D_J		0.71 ±0.05
D_{JK}		−1.06 ±0.09
ζ_3		0.34 ±0.14
ζ_4		−0.55 ±0.14
(b) AsF_3		
l (As–F)	0.0433±0.0022[a]	0.0422±0.0013
l (F–F)	0.0689±0.0044[a]	0.0761±0.0026
D_J	4.63 ±0.03[b]	4.59 ±0.46
D_{JK}	−6.17 ±0.05[b]	−6.22 ±1.1
ζ_3		0.03_5 ±0.08
ζ_4	−0.35 ±0.02	-0.32_6 ±0.08

a) Ref. 22. b) Ref. 27.

31) J. H. Meal and S. R. Polo, *J. Chem. Phys.*, **24**, 1126 (1956).
32) W. F. Edgell and R. E. Moynihan, *ibid.*, **45**, 1205 (1966).
33) L. C. Hoskins and R. C. Lord, *ibid.*, **43**, 155 (1965).
34) Z. I. Slawsky and D. M. Dennison, *ibid.*, **7**, 509 (1939).
35) D. Kivelson and E. B. Wilson, Jr., *ibid*, **21**, 1229 (1953).

Three times σ_i was taken to be the limit of errors.

The mean amplitudes, the centrifugal distortion constants, and the Coriolis constants of $AsCl_3$ and AsF_3 were calculated from the force constants tabulated in Tables 2 and 5; they are compared with the observed values in Table 6. Agreements are good except for the case of l(F–F). The poor agreement for l(F–F) is perhaps due to some systematic errors in the observed l(F–F) overlooked in the preceding paper.[22]

The correlation of the mean amplitudes with the index of resolution in the analysis of the electron-diffraction data may be considered to be a possible source of systematic errors. However, it is impossible for the observed value of l(F–F) to increase while that of l(As–F) does not as long as a single index of resolution is used in the analysis. An attempt was made to take the two indices of resolution, k(As–F) and k(F–F), as independent variable parameters in the least-squares fitting of molecular scattering intensities instead of assuming that they were equal.[36] The results are compared with those obtained in the previous analysis in Table 7. Both results were consistent within the

TABLE 7. MOLECULAR PARAMETERS OBTAINED BY TAKING TWO INDICES OF RESOLUTION AS INDEPENENT VARIABLE PARAMETERS (COLUMN A) AND THOSE OBTAINED BY ASSUMING THAT THEY ARE EQUAL (COLUMN B)
(r_g and l in Å unit)

	A	*B*
r_g (As–F)	1.7089±0.0016	1.7089±0.0016
r_g (F–F)	2.5370±0.0055	2.5374±0.0055
l (As–F)	0.0429±0.0022	0.0433±0.0022
l (F–F)	0.0748±0.0066	0.0689±0.0044
k (As–F)	0.92 ±0.05	
		0.93 ±0.05
k (F-F)	1.06 ±0.13	

estimated limit of errors, although appreciable changes were found in l(F–F) and k(F–F). The l(F–F) value of Column A is consistent with the calculated value given in Table 6. It is, however, very doubtful that we should prefer the values of Column A to those of Column B, which were obtained in the previous analysis, since there is no sound physical basis for assuming an independent index of resolution for each of the atom-pairs in this molecule.*2

The P–R splitting of the ν_3 band of AsF_3 was estimated to be 22 cm^{-1} from the calculated value of the Coriolis constant, ζ_3. It is about 7 cm^{-1} larger than Hoskins' value.[29] However, it does not seem quite inconsistent with the ν_3 band observed by Hoskins and Lord.[33]

Zero-point Average Structure

Conversion of r_g to r_z. The r_z distance can be derived from the r_g distance observed by ED. The r_g distance has the following relation to the equilibrium distance, r_e:[10]

$$r_g = r_e + \langle \Delta z \rangle + \frac{\langle \Delta x^2 \rangle + \langle \Delta y^2 \rangle}{2r_e} + \delta r_{\text{rot}}, \qquad (15)$$

where the z-axis of the local Cartesian displacement coordinates is taken along the equilibrium positions of the atoms. Here $\langle\ \rangle$ denotes the thermal average, $\langle \Delta z \rangle$ and δr_{rot} are the stretchings due to anharmonic vibration and centrifugal force respectively, and $\langle \Delta x^2 \rangle$ and $\langle \Delta y^2 \rangle$ are perpendicular amplitudes. Since r_z is equal to $r_e + \langle \Delta z \rangle_{0°K}$, it is necessary to calculate the following three terms in order to convert r_g to r_z:

1. Centrifugal stretching, δr_{rot}
2. Stretching due to perpendicular thermal motion, $(\langle \Delta x^2 \rangle + \langle \Delta y^2 \rangle)/2r_e$, and
3. Thermal extension of $\langle \Delta z \rangle$, $\delta\langle \Delta z \rangle \equiv \langle \Delta z \rangle_T - \langle \Delta z \rangle_0$.

The centrifugal terms for $AsCl_3$ and AsF_3 were estimated by using the formulas derived by Iwasaki and Hedberg[37] by balancing the centrifugal force with Hooke's restoring force. The sum of the perpendicular mean amplitudes was calculated by the use of the formula expressed by Cyvin's $\sum$ matrix,[38] which was derived as shown in the Appendix.

The cubic potential constants must be known if we are to calculate the thermal change in $\langle \Delta z \rangle$, but they have not been available for almost all pyramidal XY_3 molecules. For X–Y bonds, however, the Morse potential for diatomic molecules can be used to estimate $\delta\langle \Delta r \rangle$ as:

$$\delta\langle \Delta r \rangle = \frac{3}{2} a_3 \delta\langle \Delta r^2 \rangle, \qquad (16)$$

where a_3 is the anharmonicity parameter of the Morse potential.[39] By using the following relation:

$$\langle \Delta r \rangle = \langle \Delta z \rangle + (\langle \Delta x^2 \rangle + \langle \Delta y^2 \rangle)/2r_e, \qquad (17)$$

the thermal extension of $\langle \Delta z \rangle$ for the X–Y bonds of $AsCl_3$ and AsF_3 was estimated as follows:

$$\delta\langle \Delta z \rangle = \frac{3}{2} a_3 \delta\langle \Delta r^2 \rangle - \delta((\langle \Delta x^2 \rangle + \langle \Delta y^2 \rangle)/2r_e). \qquad (18)$$

36) Y. Morino, K. Kuchitsu and Y. Murata, *Acta Crystallogr.*, **18**, 549 (1965).

*2 Added in Proof: According to a recent electron-diffraction investigation by Clippard and Bartell (*Inorg. Chem.*, **9**, 805 (1970)), the mean amplitudes of AsF_3 are 0.048±0.003 Å and 0.078±0.003 Å for l(As–F) and l(F–F) respectively. The l(F–F) value is in good agreement with the calculated value given in Table 6, while the l(As–F) value is not.

37) M. Iwasaki and K. Hedberg, *J. Chem. Phys.*, **36**, 2961 (1962).

38) S. J. Cyvin, *Spectrochim. Acta*, **15**, 828 (1959).

39) K. Kuchitsu and Y. Morino, This Bulletin, **38**, 805, 814 (1965).

The a_3 parameter was set as approximately equal to 2 Å^{-1}.[40] The above diatomic approximation is, however, not appropriate for non-bonded pairs. The thermal extension of $\langle \Delta z \rangle_{Y-Y}$ for $AsCl_3$ and AsF_3 was estimated by assuming that the thermal change of the average angle was negligible.[14] That is, the following approximation was used:

$$\delta\langle \Delta z \rangle_{Y-Y} = 2\delta\langle \Delta z \rangle_{X-Y} \sin\frac{\theta}{2} . \qquad (19)$$

The values of various correction terms were calculated for $AsCl_3$ and AsF_3 by using the potential constants listed in Tables 2 and 5. The results are tabulated in Table 8.

Table 8. Numerical values of the correction terms for reducing r_g to r_z (in 10^{-4} Å unit)

	$AsCl_3$		AsF_3	
	As–Cl	Cl–Cl	As–F	F–F
$(\delta r_{rot})_T$	6	15	5	6
$\langle \Delta r \rangle_T$	72		53	
$\left(\frac{\langle \Delta x^2 \rangle + \langle \Delta y^2 \rangle}{2r_e}\right)_T$	25	12	20	12
$\langle \Delta z \rangle_T$	47	71	33	49
$(\delta r_{rot})_0$	0	0	0	0
$\langle \Delta r \rangle_0$	54		48	
$\left(\frac{\langle \Delta x^2 \rangle + \langle \Delta y^2 \rangle}{2r_e}\right)_0$	10	5	12	7
$\langle \Delta z \rangle_0$	44	66	36	54
$\langle \Delta z \rangle_T - \langle \Delta z \rangle_0$	3	5	−3	−5
$r_g - r_z$	34 (±3)	32 (±9)	22 (±3)	13 (±9)

Note: T is equal to 291°K and 292°K for $AsCl_3$ and AsF_3, respectively. The values in parentheses are the uncertainties estimated.

Conversion of B_0 to B_z. The average rotational constant, B_z, corresponding to the r_z-structure can be derived by adding some correction terms to the effective constant, B_0.

$$B_z = B_0 + \delta B_{vib} + \delta B_{cent} + \delta B_{elect}. \qquad (20)$$

Here δB_{vib}, δB_{cent} and δB_{elect} are the vibrational, centrifugal, and electronic corrections respectively. For the pyramidal XY_3 molecule, Shaffer[41] and Nielsen[1] derived the relation of the rotational constant, B_0, to the equilibrium rotational constant, B_e, by neglecting the motion of electrons. The first two correction terms, δB_{vib} and δB_{cent} in Eq. (20) can be calculated by using their results.[13]

The last term in Eq. (20) can be estimated if the g tensor of the rotational magnetic moment is known.[7] Since the values of the g tensor were not available for AsF_3 and $AsCl_3$, δB_{elect} was assumed to be zero in the present study. The error caused by this assumption is, however, perhaps negligibly small since δB_{elect} is inferred to be, at most, ten percent of δB_{vib}, judging from the results on formaldehyde.[7] The values of $(B_0 - B_z)$ calculated for $As^{35}Cl_3$, $As^{37}Cl_3$ and AsF_3 are tabulated in Table 9, along with their uncertainties due to those of the force constants.

Table 9. Estimated values of $(B_0 - B_z)$ (in Mc unit)

	$As^{35}Cl_3$	$As^{37}Cl_3$	AsF_3
$B_0 - B_z$	2.70±0.04	2.52±0.04	10.93±0.41

Average Structures. The r_z-structures of $AsCl_3$ and AsF_3 were derived from the observed r_g distances[22] by using the correction values listed in Table 8. The moment of inertia, I_b^z, and the rotational constant, B_z, were calculated from the r_z distances. The results are summarized in Table 10.

The B_z constants were also obtained from the microwave B_0 values and the estimated values of $(B_0 - B_z)$. They are compared with the diffraction values in Table 10. There is no inconsistency between the experimental results of the microwave study and those of the electron-diffraction study.

Table 10. Zero-point average structures and average rotational constants derived from ED and MW data (r_z, I_b^z, and B_z are in Å, amu. Å^2, and Mc units, respectively)

	ED	MW
$r_z(As–^{35}Cl)$	2.1587±0.0034	2.1619±0.0024
$r_z(^{35}Cl–^{35}Cl)$	3.2741±0.0095	3.280±0.022
$\theta_z(^{35}Cl\ As^{35}Cl)$	98°38′±36′	98°43′±1°3′
$I_b^z(As^{35}Cl_3)$	234.93±0.82	235.66±0.03
$B_z(As^{35}Cl_3)$	2151.2±7.5	2144.5±0.3
$I_b^z(As^{37}Cl_3)$	246.72±0.88	247.47±0.04
$B_z(As^{37}Cl_3)$	2048.3±7.3	2042.2±0.3
r_z(As–F)	1.7067±0.0017	
r_z(F–F)	2.5361±0.0056	
θ_z(FAsF)	95°59′±22′	
$I_b^z(AsF_3)$	85.99±0.22	86.1232±0.0061
$B_z(AsF_3)$	5877±15	5868.04±0.41

Table 11. Isotope effects in the r_z distances of $AsCl_3$ (in 10^{-4} Å unit)

	$As^{35}Cl_3$		$As^{37}Cl_3$	
	As–Cl	Cl–Cl	As–Cl	Cl–Cl
$\langle \Delta r \rangle_{0°K}$	54		53	
$\left(\frac{\langle \Delta x^2 \rangle + \langle \Delta y^2 \rangle}{2r_e}\right)_{0°K}$	10		10	
$\langle \Delta z \rangle_{0°K}$	44	66	43	64

$r_z(As–^{35}Cl) - r_z(As–^{37}Cl) = 1(\pm 1)$
$r_z(^{35}Cl–^{35}Cl) - r_z(^{37}Cl–^{37}Cl) = 2(\pm 3)$

40) E. R. Lippincott and R. Schroeder, *J. Chem. Phys.*, **23**, 1131 (1955).
41) W. H. Shaffer, *ibid.*, **9**, 607 (1941).

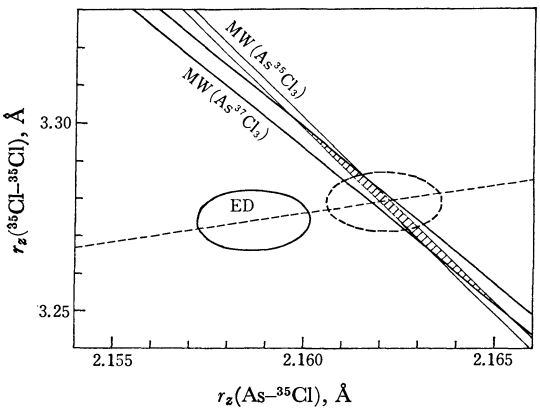

Fig. 4. r_z-Structures of $As^{35}Cl_3$ determined by microwave spectroscopy and electron diffraction. The values allowed by the MW rotational constants are shown by shadows. The ellipse described in solid line shows the ED values, which do not include the error estimated for the scale factor, while the dashed ellipse shows the ED values corrected for the scale factor. The most probable r_z values are obtained from the overlapping regions of the dashed ellipse and the MW region.

In the case of $AsCl_3$, the r_z-structures could be determined from only the microwave data by a tentative estimation of the isotope effects on the r_z distances, as is shown in Table 11. The relations of the r_z distances of $As^{35}Cl_3$ given by the two rotational constants are shown in Fig. 4. The two parallel lines correspond to the limits of errors of a rotational constant. The uncertainties in isotope effects are included as the spread of the curve, $MW(As^{37}Cl_3)$. The structures corresponding to the shaded area are compared with those determined by ED in Table 10. It may be noted that the error of the bond angle is about twice as large as that in the results for ED.

The errors due to the uncertainty of the scale factors are the largest possible systematic errors in the results of ED, so that a more precise structure can be expected if the scale-factor errors are eliminated by using the microwave rotational constants.

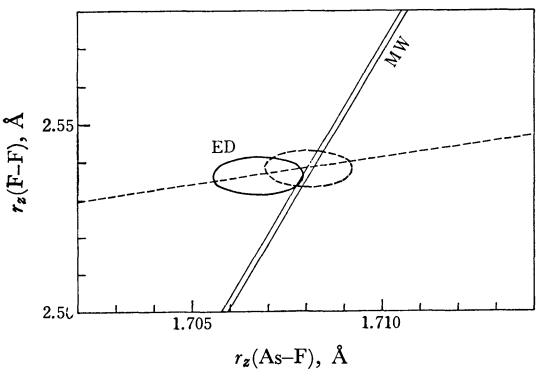

Fig. 5. r_z-Structures of AsF_3 determined by electron diffraction and microwave spectroscopy. See the caption of Fig. 4.

In Figs. 4 and 5, the solid ellipses show the errors associated with the diffraction values, without including the errors for the scale factors. It is mainly because of the scale-factor errors that the centers of the ellipses do not lie on the microwave lines. New ellipses were obtained by shifting the centers of the ellipses along the dashed lines, on which the ratio of r_z(As–Y) to r_z(Y–Y) was kept constant. The most probable average distances were obtained from the overlapping regions of the new ellipses and the microwave lines. They are listed in Table 12, along with the corresponding r_g distances. Because of the steep slopes of the microwave lines, the errors in the As–Y distances became very small.

TABLE 12. r_z AND r_g STRUCTURES OF $As^{35}Cl_3$, $As^{37}Cl_3$ AND AsF_3 OBTAINED BY THE COMBINED USE OF ED AND MW DATA (r in Å unit)

	$As^{35}Cl_3$	$As^{37}Cl_3$	AsF_3
r_z(As–Y)	2.1621 ±0.0009	2.1620 ±0.0009	1.7080 ±0.0004
r_z(Y–Y)	3.2789 ±0.0075	3.2787 ±0.0075	2.5380 ±0.0048
θ_z	98°38′±22′	98°38′±22′	95°58′±17′
r_g(As–Y)	2.1655 ±0.0010	2.1654 ±0.0010	1.7102 ±0.0005
r_g(Y–Y)	3.2821 ±0.0076	3.2819 ±0.0076	2.5393 ±0.0050
θ_g	98°33′±22′	98°33′±22′	95°52′±17′

The author wishes to express his thanks to Professor Masao Kimura and Dr. Takao Iijima for their encouragement and helpful discussions.

Appendix

Calculation of the Perpendicular Mean Amplitudes. For pyramidal XY_3 molecules, the formulas expressed in terms of the $\sum$ matrix[39] for calculating the parallel amplitudes $\langle\Delta z^2\rangle$ $(=l^2)$ have already been derived,[26] but those for the perpendicular amplitudes have not yet been presented. The formulas for calculating the sum of the perpendicular amplitudes, $\langle\Delta x^2\rangle$ and $\langle\Delta y^2\rangle$, can be derived by using the following realtion:

$$(\langle\Delta x^2\rangle + \langle\Delta y^2\rangle)_{ij} = \langle(\rho_i-\rho_j)^2\rangle - \langle\Delta z^2\rangle_{ij}. \quad \text{(A1)}$$

Here ρ_i and ρ_j are the displacement vectors of the i and j atoms respectively.

The internal coordinates can be expressed in terms of the displacement vectors, ρ_i, and the unit vectors, e_{ij}, which start from the i atom and which points to the j atom. The relation was derived in a matrix form as:

$$\boldsymbol{R} = \boldsymbol{T}\boldsymbol{\rho}, \quad \text{(A2)}$$

where:

$$\boldsymbol{\rho} = \begin{bmatrix} \rho_1 \\ \rho_2 \\ \rho_3 \\ \rho_4 \end{bmatrix}, \quad \text{(A3)}$$

and:

$$\boldsymbol{T} = \begin{pmatrix} -e_{14} & 0 & 0 & e_{14} \\ 0 & -e_{24} & 0 & e_{24} \\ 0 & 0 & -e_{34} & e_{34} \\ 0 & \frac{1}{s}e_{34} - \frac{c}{s}e_{24} & \frac{1}{s}e_{24} - \frac{c}{s}e_{34} & \frac{c-1}{s}(e_{24}+e_{34}) \\ \frac{1}{s}e_{34} - \frac{c}{s}e_{14} & 0 & \frac{1}{s}e_{14} - \frac{c}{s}e_{34} & \frac{c-1}{s}(e_{34}+e_{14}) \\ \frac{1}{s}e_{24} - \frac{c}{s}e_{14} & \frac{1}{s}e_{14} - \frac{c}{s}e_{24} & 0 & \frac{c-1}{s}(e_{14}+e_{24}) \end{pmatrix}. \quad \text{(A4)}$$

Here s and c are abbreviations of the sine and the cosine of the bond angle, θ, respectively. With this notation, the $\boldsymbol{G}$ matrix in the symmetry coordinates was expressed as:

$$\boldsymbol{G} = \boldsymbol{UTM}^{-1}\boldsymbol{T}'\boldsymbol{U}', \quad \text{(A5)}$$

where $'$ denotes transposed matrices, where $\boldsymbol{U}$ is a matrix defined by Eq. (2b), and where:

$$\boldsymbol{M}^{-1} = \begin{pmatrix} \mu_Y & & & \\ & \mu_Y & & \\ & & \mu_Y & \\ & & & \mu_X \end{pmatrix}. \quad \text{(A6)}$$

The elements of the $\boldsymbol{G}$ matrix are given in Eqs. (4) and (5).

The ρ_i vectors could be expressed in terms of the symmetry coordinates by using Eqs. (2b), (A2), and (A5):

$$\boldsymbol{\rho} = \boldsymbol{M}^{-1}\boldsymbol{T}'\boldsymbol{U}'\boldsymbol{G}^{-1}\boldsymbol{S}. \quad \text{(A7)}$$

This is essentially equal to the relation derived by Morino and Hirota.[42] By using Eq. (A7), the $<(\rho_i-\rho_j)^2>$ term in Eq. (A1) was expressed in terms of the $\sum$ matrix elements after a rather lengthy manipulation. From the results, the contribution of the parallel amplitudes given in Eqs. (6) and (7) were subtracted, and the following results were obtained:

$$(\langle\Delta x^2\rangle+\langle\Delta y^2\rangle)_{X-Y} = \frac{1}{6}\frac{1+c}{1+2c}\sum_{22} + \frac{2}{3}\frac{1+c}{2+c}\sum_{44} + \frac{2(1-c)(1+2c)}{2+c}\mu_X^2 \cdot P \quad \text{(A8)}$$

$$(\langle\Delta x^2\rangle+\langle\Delta y^2\rangle)_{Y-Y} = \frac{2}{3}\left\{\sin^2\frac{\theta}{2}\sum_{33} - 2\sin\frac{\theta}{2}\cos\frac{\theta}{2}\sum_{34} + \cos^2\frac{\theta}{2}\sum_{44}\right\} + \frac{2}{3}(1+2c)\mu_Y^2 \cdot P, \quad \text{(A9)}$$

where:

$$P = \{(2+c)^2\sum_{33} + 2(2+c)s\sum_{34} + s^2\sum_{44}\}/\{3(1-c)\mu_X + (2+c)\mu_Y\}^2. \quad \text{(A10)}$$

42) Y. Morino and E. Hirota, *J. Chem. Phys.*, **23**, 737 (1955).

BULLETIN OF THE CHEMICAL SOCIETY OF JAPAN VOL. 43 3116—3121 (1970)

The Electron Spin Resonance of the Mn^{2+} Ion in Aqueous Surfactant Solutions*1

Akinori HASEGAWA, Yasuyoshi MICHIHARA and Masaji MIURA

Department of Chemistry, Faculty of Science, Hiroshima University, Higashisenda-machi, Hiroshima

(Received June 8, 1970)

The ESR spectrum of the Mn^{2+} ion in an aqueous solution of a surfactant is affected by its concentration. Sodium dodecyl sulfate and sodium decyl sulfate were employed as surfactants in this study. The linewidth of the Mn^{2+} ion is independent of the concentration of the surfactant in the low-concentration range, but it increases over a certain concentration range and then becomes constant. Two values of CMC were observed by measurements of the conductivity corresponding to the concentrations, where the linewidth of Mn^{2+} changed abruptly with the concentration of the surfactant. The linewidth broadening above the first CMC was interpreted as being due to the formation of an outer-sphere complex of the Mn^{2+} ion with a surfactant micelle. The interaction between the counterion and micelle was also investigated on the basis of the ESR spectra of the Mn^{2+} ion with regard to the effects of the kind of surfactant, the temperature, foreign electrolytes, *etc.*

The manganese ion is a typical paramagnetic ion, and a number of ESR studies of this ion have been published.[1-3] Most of them have dealt with it in solid; trace amounts of cations in a solid are displaced by Mn^{2+} ions, and information with regard to the crystal field, the bond character, *etc.* can be obtained from the ESR spectrum of the Mn^{2+} ion. The method of the spin label of the cation with the Mn^{2+} ion is expected to be informative not only for solids but also for electrolytic solutions.

On the other hand, the formation of a complex ion between the Mn^{2+} ion and halogen ions, SO_4^{2-} ions, or $S_2O_4^{2-}$ ions has been studied by means of the ESR spectra of the Mn^{2+} ion.[4-6] In these studies, a two-step coordination model was proposed to explain the broadening of the ESR spectra of the Mn^{2+} ion and several parameters were estimated for the formation and dissociation of an inner- or outer-sphere complex. The electron-spin relaxation of the Mn^{2+} ion in a liquid solution has been investigated in terms of the solvent fluctuation model[7] and the ESR linewidths of the Mn^{2+} ion have been studied in various solvents.[8,9]

It is well-known that a counterion plays an important role in the formation of a surfactant micelle. In this paper, Mn^{2+} ion was added to an aqueous solution of a surfactant and the ESR spectra of the Mn^{2+} ion were observed. The interactions between the counterion and the surfactant micelle were discussed.

By the magnetic resonance technique, several attempts have been made to investigate the surfactant micelle. Some of them have been NMR studies using a hydrogen[10,11] or a fluorine[12-14] nucleus in a surfactant molecule, and others, ESR studies made by spin-labeling the micelle with a monoradical[15] or a biradical.[16] All of these methods

*1 Briefly communicated by M. Miura, A. Hasegawa and Y. Michihara, This Bulletin, **41**, 534 (1968).

1) M. Miura, A. Hasegawa and M. Watanabe, *ibid.*, **41**, 1035 (1968).
2) R. A. Servay, *Phys. Lett.*, **A 26**, 642 (1968).
3) B. V. R. Chowdari, *J. Phys. Chem. Solids*, **30**, 2747 (1969).
4) R. G. Hayes and R. J. Myers, *J. Chem. Phys.*, **40**, 877 (1964).
5) D. C. McCain and R. J. Myers, *J. Phys. Chem.*, **72**, 4115 (1968).
6) L. Burlamacchi and E. Tiezzi, *ibid.*, **73**, 15 (1969).
7) B. B. Garrett and L. O. Morgan, *J. Chem. Phys.*, **44**, 890 (1966).
8) C. C. Hinckley and L. O. Morgan, *ibid.*, **44**, 898 (1966).
9) S. I. Chan, B. M. Fung and J. Lutje, *ibid.*, **47**, 2121 (1967).
10) T. Nakagawa and K. Tori, *Kolloid Z.*, **194**, 143 (1964).
11) H. Inoue and T. Nakagawa, *J. Phys. Chem.*, **70**, 1108 (1966).
12) N. Muller and R. H. Birkhahn, *ibid.*, **71**, 957 (1967).
13) R. Haque, *ibid.*, **72**, 3056 (1968).
14) R. E. Bailey and G. H. Cady, *ibid.*, **73**, 1612 (1969).
15) A. S. Waggoner, O. H. Griffith and C. R. Christensen, *Proc. Nat. Acad. Aci. U. S.*, **57**, 1198 (1967).
16) S. Ohnishi, T. J. R. Cyr and H. Fukushima, This Bulletin, **43**, 673 (1970).

give information concerning the inner part of the micelle. In contrast to these investigations, the present study offers information with regard to the interactions between the counterion and surfactant micelle.

Theoretical

The theory of the ESR linewidth of the Mn^{2+} ion in a liquid solution has been developed in terms of the relaxation induced by the solvent fluctuation.[7] An outline of the theory will be given here.

The ESR spectra of the aqueous solutions of the Mn^{2+} ion exhibit six hyperfine components due to the electron spin, $S=5/2$, and the nuclear spin, $I=5/2$. Each of the hyperfine components also consists of five transitions for $m_s-1\leftrightarrow m_s$.

The linewidths for these transitions have been investigated in terms of the relaxation induced by solvent fluctuation. The theory was developed from the time-dependent spin-orbit interaction, using the spin density matrix. The resultant linewidths for the five transitions, $m_s-1\leftrightarrow m_s$, are:

$$\begin{aligned} \Delta H_{3/2,5/2} &= \Delta H_{-5/2,-3/2} = 2.633Z \\ \Delta H_{1/2,3/2} &= \Delta H_{-3/2,-1/2} = 2.312Z \\ \Delta H_{-1/2,1/2} &= 1.971Z \end{aligned} \qquad (1)$$

with

$$Z = C^2\tau_c/\hbar^2$$

where C is the trace of the perturbation Hamiltonian; τ_c, the perturbational correlation time, and $\hbar$, Planck's constant.

The spreads theoretically expected for these transitions, $m_s-1\leftrightarrow m_s$, were also demonstrated to depend upon the magnetic quantum number of nuclear spin by the calculation by means of the perturbation theory. The spread is the smallest, *ca.* 5 gauss, for $m_I=+1/2$ and the largest, *ca.* 30 gauss, for $m_I=-5/2$.

The apparent linewidth of $m_I=1/2$, therefore, is proportional to τ_c:

$$\Delta H_{m_I=1/2} \propto \tau_c \qquad (2)$$

Thus, the correlation time of the solvent fluctuation for the Mn^{2+} ion can be estimated from the linewidth of $m_I=1/2$.

In the present system, the linewidth of the Mn^{2+} ion may also result from the relaxation due to the modulation of zero-field splitting induced by the tumbling motion of the complex.[17-19] The linewidth of $m_I=1/2$ can, any event, be a measure of the correlation time, τ_c.

17) B. R. McGarvey, *J. Phys. Chem.*, **61**, 1232 (1957).
18) A. Carrington and G. R. Luckhurst, *Mol. Phys.*, **8**, 125 (1964).
19) A. Hasegawa, *J. Chem. Phys.*, to be published.

Experimental

Sodium dodecyl sulfate (SDS) and sodium decyl sulfate (NaDS) were used as surfactants in this study. The former was synthesized and purified by Nippon Yushi Co. Ltd., and the latter, in our laboratory. Different amounts of surfactants were added to an aqueous solution of 1×10^{-3}M $Mn(NO_3)_2$. The solution thus obtained was sealed in a capillary of glass, and the ESR spectra were measured at different temperatures by using a spectrometer described elsewhere.[20] The conductivity measurements were carried out at 50°C or 25°C. To investigate the effect of electrolytes, 1×10^{-2}M $NaNO_3$ or KNO_3 was added to a surfactant solution containing the Mn^{2+} ion.

Results and Discussion

The ESR spectrum of the Mn^{2+} ion in the aqueous solution was remarkably affected by the con-

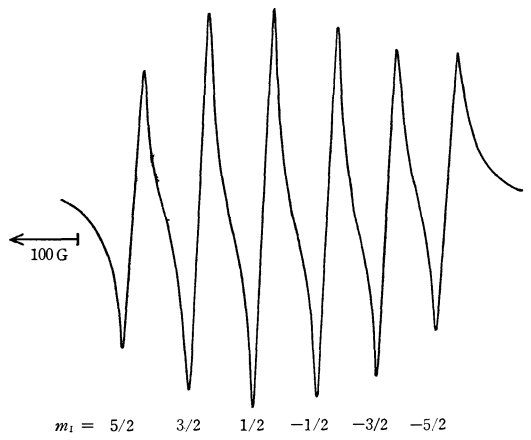

(a)

Fig. 1 (a)

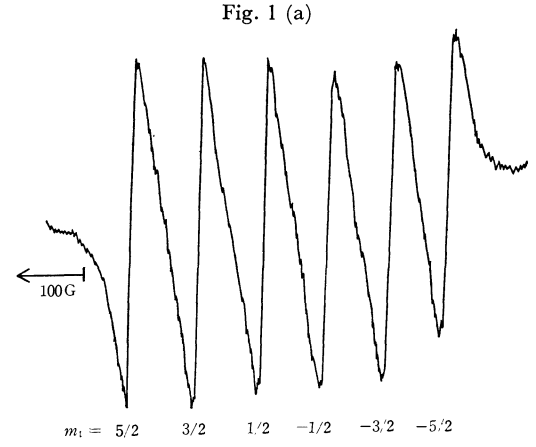

(b)

Fig. 1. ESR spectra of the aqueous solutions of (a) 1×10^{-3}M and (b) 2×10^{-2}M SDS containing 1×10^{-3}M $Mn(NO_3)_2$ at 50°C.

20) A. Hasegawa and M. Miura, This Bulletin, **40**, 2553 (1967).

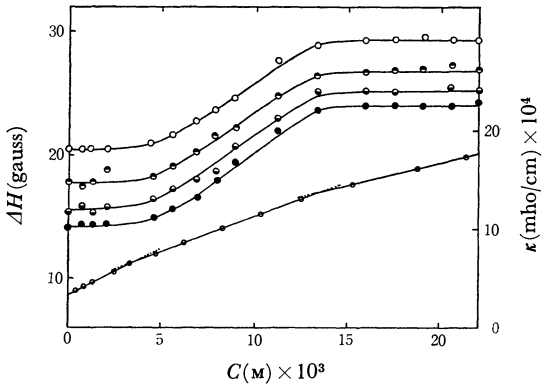

Fig. 2. The dependences of the linewidths (m_I: ○ −5/2, ◓ −3/2, ◒ −1/2 and ● 1/2) and the conductivity (○) on the concentration of SDS at 50°C. The concentration of Mn^{2+} ion is 1×10^{-3}M. Symbols in the following figures have the same meaning as those in this figure except for Fig. 6.

centration of the surfactant, as is shown in Fig. 1. The spectrum consists of six hyperfine structures, corresponding to the states of $m_I=-5/2$, $-3/2$, $-1/2$, $1/2$, $3/2$ and $5/2$ respectively, counting from the side of the lower magnetic field.

The variation in the linewidth is shown in Fig. 2, where the linewidths of four lines in the lower magnetic field are plotted against the concentration of SDS at 50°C. When the concentration of SDS is below 3×10^{-3}M, the linewidth is practically unaffected by the concentration. However, the linewidth increases with the concentration in the range from 3×10^{-3} to 13×10^{-3}M and becomes constant above 13×10^{-3}M. The linewidth of $m_I=1/2$, as is shown in Eq. (2), is proportional to the correlation time, τ_c, of the Mn^{2+} ion resulting from the fluctuation of the solvent shell. In the lower concentration range, the interaction between the Mn^{2+} ion and SDS seems negligibly small, because the correlation time is unaffected by the addition of SDS. The correlation time, however, increases over the concentration range from 3×10^{-3} to 13×10^{-3}M and then takes a constant value, which is 1.7 times that below 3×10^{-3}M.

The conductivity of the aqueous solution of SDS containing Mn^{2+} ions was measured at 50°C; the results are given in Fig. 2. Two broken points were observed, as may be seen in the figure, in the relation between the specific conductivity and the concentration. The concentrations at these broken points, which correspond to the first and the second critical micelle concentrations (CMC) respectively, counting from the lower concentration, are in good agreement with those observed in connection with ESR linewidth of the Mn^{2+} ion.

Similar results were obtained at 25°C, as may be seen in Fig. 3. Both the first and second CMC's decrease with a drop in the temperature, the rate

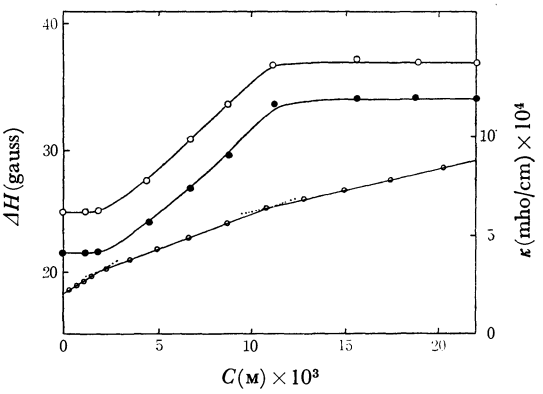

Fig. 3. The dependences of the linewidths and the conductivity on the concentration of SDS at 25°C. The concentration of Mn^{2+} ion is 1×10^{-3}M.

of decrease being larger for the second CMC than for the first. The correlation time of the Mn^{2+} ion takes a higher value at 25°C than at 50°C, and the value below the first CMC at the lower temperature is nearly equal to that above the second CMC at the higher temperature.

A molecule of SDS has a hydrocarbon chain consisting of 12 carbon atoms. The CMC of surfactant generally increases with a decrease in the number of the carbon atom. Thus, sodium decyl sulfate (NaDS), with 10 carbon atoms in a hydrocarbon chain, was investigated. A change in the ESR linewidth of the Mn^{2+} ion was also observed, accompanied by an increase in the concentration of NaDS; the concentrations, where the linewidth abruptly changed, were in excellent agreement with the CMC's determined by the conductivity measurements. The linewidth of $m_I=1/2$ above the second CMC is 22.5 gauss at 50°C, as may be seen in Fig. 4, which is 93% of that in the case of SDS at 50°C. The correlation time, therefore, is short compared with that in the case of SDS.

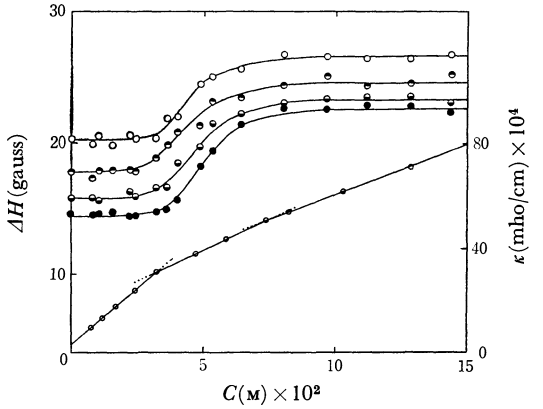

Fig. 4. The dependences of the linewidths and the conductivity on the concentration of NaDS at 50°C. The concentration of Mn^{2+} ion is 1×10^{-3}M.

The effects of the concentration of the Mn^{2+} ion on the two CMC's and on the linewidth of the ESR spectrum were investigated by using an NaDS solution containing Mn^{2+} ion in a concentration of 2×10^{-3}M. The increase in the concentration of the Mn^{2+} ion, as may be seen in Fig. 5, gave rise to the decreases in the CMC's and in the linewidth of the ESR spectrum above the second CMC.

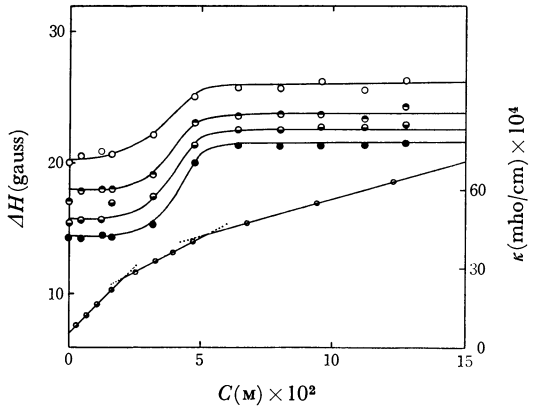

Fig. 5. The dependences of the linewidths and the conductivity on the concentration of NaDS at 50°C. The concentration of Mn^{2+} ion is 2×10^{-3}M.

Frenkel has proposed the following relation with regard to the structural correlation time, τ_c, in terms of the transient lattice model for liquids:[21]

$$\tau_c \propto \rho M/\eta T \tag{3}$$

where η is the viscosity; M, the apparent molecular weight of fluctuating solvent; ρ, the density, and T, the absolute temperature. This relation has been proved by an investigation of the linewidths of the ESR spectra of the Mn^{2+} ion in kinds of solvents.[7]

The equation of viscosity is shown by:[22]

$$\eta = \boldsymbol{h}N_A/v \exp(\Delta F^*/\boldsymbol{R}T) \tag{4}$$

where $\boldsymbol{h}$ is Planck's constant; N_A, Avogadro's number; v, the molar volume, and ΔF^*, the standard free energy of activation per mole in the elemental process of the viscous flow. From Eqs. (2), (3), and (4), the following relation can be obtained:

$$\ln(\rho T\Delta H_{m_I=1/2}) = \Delta F^*/\boldsymbol{R}T + \ln K \tag{5}$$

where K is the constant proportional to M. This equation shows the existence of a linear relation between $\ln(\rho T\Delta H_{m_I=1/2})$ and $1/T$. The ESR spectra of the Mn^{2+} ion in the aqueous solutions of the two surfactants were then measured at different temperatures. The results exhibited linear relations, as was to be expected from Eq. (5), and

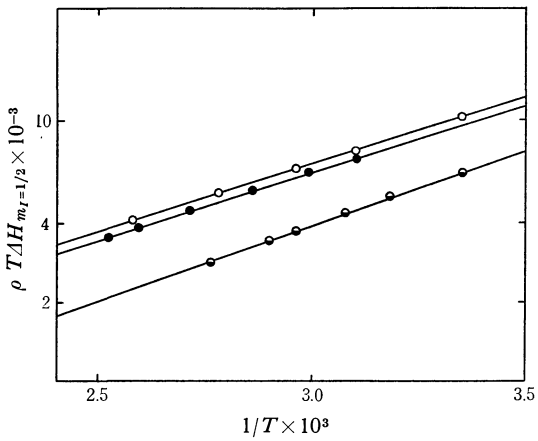

Fig. 6. The relations between $\rho T\Delta H_{m_I=1/2}$ and $1/T$.
◒: below the first CMC for SDS and NaDS
○: above the second CMC for SDS
●: above the second CMC for NaDS

as is shown in Fig. 6. The value of ΔF^* could be obtained from the gradient, and the constant, K, from the intercept. The values of ΔF^* for SDS and NaDS, both below the first CMC and above the second CMC, were determined to be equal to 2.0 kcal/mol in spite of the differences in the kind and concentration of the surfactant. On the other hand, the constant, K, which involves the apparent molecular weight of the solvent bringing about the fluctuation in the Mn^{2+} ion, changes with the kind and concentration of the surfactant. This may be attributed to the change in the apparent molecular weight of the solvent. From Eqs. (2) and (3), the apparent molecular weight of the solvent can be estimated by:

$$M \propto \Delta H_{m_I=1/2}\rho T/\eta \tag{6}$$

By using the ρ and η values of the aqueous solution measured at 25°C, and by assuming that the proportional constant in Eq. (6) is independent of the concentration of the surfactant, the apparent molecular weight of the solvent can be seen to increase over the region from the first CMC to the second CMC, and the ratio of the value above the second CMC to that below the first CMC can be determined to be 1.5 for the aqueous solution of SDS at 25°C.

From the fact that the broadening of the ESR spectrum of the Mn^{2+} ion is observed only above the first CMC, it is expected that the surfactant micelle participates in the solvent fluctuating the Mn^{2+} ion. As the micelle is very large compared with the water molecule, the apparent molecular weight of the solvent in the presence of the micelle might be expected to be much larger than that estimated above. It is, therefore, interesting to speculate about the interactions between the counter-ion and the micelle; one of the interactions is the ion-binding between them. One possible ion-

21) J. Frenkel, "Kinetic Theory of Liquids," Dover Publications, New York (1955), pp. 188—208.
22) S. Glasstone, J. Laidler and J. Eyring, "The Theory of Rate Processes," McGraw-Hill Co., New York (1941), p. 484.

binding is the formation of a complex in which the Mn^{2+} ion largely retains its full hydration sphere, an outer-sphere complex. At the other extreme, ion-binding is accomplished by the formation of an inner-sphere complex in which the Mn^{2+} ion is stripped of its hydration sphere.[5] The two-step process for complex ion formation can be shown by the following reaction equations:[5]

$$Mn^{2+}(H_2O)_n + X^{m-} \rightleftarrows Mn^{2+}(H_2O)_nX^{m-} \quad (I)$$

$$Mn^{2+}(H_2O)_nX^{m-} \rightleftarrows Mn^{2+}X^{m-} \quad (II)$$

where X^{m-} represents the micelle with negative charges. The two-step process has been proved for the Mn^{2+} ion in an aqueous solution containing an ion such as F^-, Cl^-, Br^-, I^-, SO_4^{2-}, or $S_2O_4^{2-}$.[4-6] In these studies, the first process was observed from a broadening of the ESR spectrum of the Mn^{2+} ion near room temperature, and the second one, from a broadening above 100°C. From these results, and from the fact that another broadening was found in an aqueous solution of surfactant near 130°C, the broadening of the ESR spectrum of the Mn^{2+} ion in a surfactant solution near room temperature is interpreted to be due to the process of the formation of an outer-sphere complex. Water molecules mainly, and surfactant micelles partially, participate in the fluctuation of the Mn^{2+} ion.

Accordingly, the "apparent molecular weight" described above is predominantly dependent on the forward and backward rate constants in the reaction (I) rather than an average size of the micelles. Several thermodynamic values for the reaction (I) could be evaluated on the basis of the broadening by the introduction of several assumptions, but that is far from our present purpose.

The broadening of the ESR spectrum above the first CMC may be interpreted in terms of the model in which the amount of the Mn^{2+} ion bound by the surfactant micelle increases with the amount of the micelle. Above the second CMC, no changes in the interaction between the Mn^{2+} ion and the micelle were observed from the ESR spectrum; this may suggest that practically all of the Mn^{2+} ions in the solution participate in the ion-binding with the micelle in the range from the first CMC to the second CMC.

The strength of the ion-binding or the forward rate constant of the reaction (I) is large for SDS as compared with that for NaDS.

The increase in the amount of the added Mn^{2+} ion, as may be seen in Figs. 5 and 6, gave rise to diminutions in both the first and the second CMC's and to a decrease in the correlation time above the second CMC. This may be due to the neutralization of the negative charges of the micelle with Mn^{2+} ions.

Next, the effect of electrolytes on a surfactant solution containing the Mn^{2+} ion was investigated. Numerous authors have reported that the addition of simple electrolytes lowers the CMC of an ionic surfactant and increases the average size of the micelles.[23] Although alkali halides, *e.g.*, NaCl. KCl, and NaBr, are generally used for this purpose, halogen ions are inadequate for the present study because halogen ions give rise to a broadening of the ESR spectrum of the Mn^{2+} ion by forming outer-sphere complexes with the Mn^{2+} ion. Thus, such nitrates as $NaNO_3$ and KNO_3 were used for the following experiments (Figs. 7 and 8), since

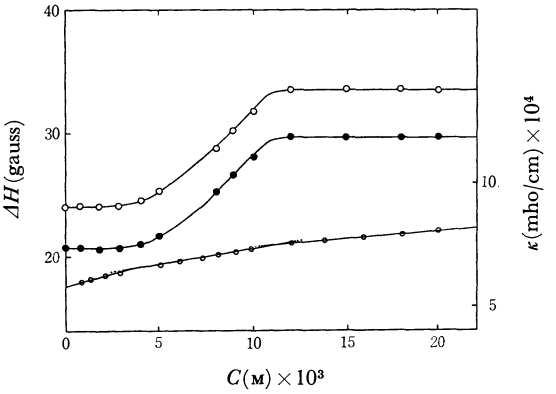

Fig. 7. The dependences of the linewidths and the conductivity on the concentration of SDS in the presence of 1×10^{-2}M $NaNO_3$, at 25°C. The concentration of Mn^{2+} ion is 1×10^{-3}M.

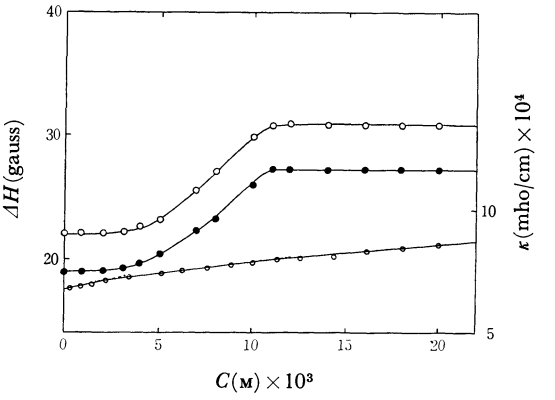

Fig. 8. The dependences of the linewidths and the conductivity on the concentration of SDS in the presence of 1×10^{-2}M KNO_3, at 25°C. The concentration of Mn^{2+} ion is 1×10^{-3}M.

the nitric ion has no appreciable effect on the Mn^{2+} ion. By the addition of 1×10^{-2}M $NaNO_3$ or KNO_3, the broadening of the spectrum is diminished and the effect of KNO_3 on the diminution is superior to that of $NaNO_3$. This may be explained as follows: the added electrolytes weaken the bond between the Mn^{2+} ion and the surfactant micelle. The narrowing of the ESR spectrum of the Mn^{2+}

23) M. J. Shik, *J. Phys. Chem.*, **68**, 3585 (1964).

ion arising from the addition of electrolytes observed below the first CMC corresponds to the fact that a linewidth narrowing was observed upon the initial addition of electrolytes to a solution of the Cr^{3+} ion.[24] This narrowing has been interpreted as being caused by a diamagnetic cation, which decreases the effective charge density of the anions in the outer-sphere.

Thus, by using a paramagnetic ion, the Mn^{2+} ion, as an indicator, several pieces of information with regard to the interaction between the counterion and the surfactant micelle were obtained from our measurements of the ESR spectrum of the ion.

24) K. M. Sancier, *ibid.*, **72**, 1317 (1968).

BULLETIN OF THE CHEMICAL SOCIETY OF JAPAN VOL. 43 3121—3125 (1970)

Luminescence in DNA-Acridine Dye Complexes. I. Phosphorescence and Delayed Fluorescence Due to the Triplet-Triplet Annihilation of Acridine Dyes in the Complexes

Yukio KUBOTA

Department of Chemistry, Yamaguchi University, Yamaguchi

(Received June 15, 1970)

When DNA-acridine dye complexes were excited by a visible light which was not absorbed by DNA, phosphorescence and a delayed fluorescence of the dye were observed. It was found, by comparing the excitation spectra with the absorption spectra, that the monomeric dyes mainly contribute to the fluorescence and phosphorescence emissions. The delayed fluorescence was interpreted as a result of the triplet-triplet annihilation which arises from two triplet dye molecules placed very close together. The decrease in the delayed fluorescence on the denaturation of DNA indicates that the interaction between the two triplets is sensitive to the conformation of the macromolecule.

The interaction of acridine dyes with DNA has been extensively studied by various techniques in connection with the photodynamic and mutagenic actions of these dyes. At present, it is generally accepted that these dyes bind to DNA to form two types of complexes; one (Complex I) results from the dye-dye interaction on the outside of the DNA helix at low P/D[1] values,[2,3] and the other (Complex II) occurs at high P/D values, where the dye-nucleotide interaction is involved.[4] Lerman has proposed that, in Complex II, acridine dye molecules are intercalated in a sandwich-like way between adjacent base pairs in the double-stranded helix.[5] For the understanding of the above biological actions of acridine dyes, therefore, it seems very significant to make clear the mechanism of the interactions between the DNA bases and dye molecules and between the dye molecules in the complexes from the photophysical and photochemical points of view.

In a previous communication,[6] it was shown that the triplet states of acridine dyes play an important role in the photosensitized radical formation in the complexes. In order to obtain further information regarding the excited states of acridine dyes and the energy transfer in the DNA-acridine dye complexes, the luminescence of the complexes was studied in frozen aqueous solutions at 77°K. In this study, proflavine, acridine orange, and acriflavine were used. Recently, the present author reported his preliminary results on the luminescence in the complexes.[7,8] The present paper will describe in detail the luminescence properties of acridine dyes in the complexes upon excitation by visible light.

1) The ratio of the number of nucleotides to that of acridine dye molecules.

2) D. F. Bradley and M. K. Wolf, *Proc. Natl. Acad. Sci. U. S.*, **45**, 94 (1959).

3) A. L. Stone and D. F. Bradley, *J. Amer. Chem. Soc.*, **83**, 3627 (1961).

4) A. R. Peacocke and J. N. H. Skerrett, *Trans. Faraday Soc.*, **52**, 261 (1956).

5) L. S. Lerman, *J. Mol. Biol.*, **3**, 18 (1961); *Proc. Natl. Acad. Sci. U. S.*, **49**, 94 (1963).

6) Y. Kubota and M. Miura, This Bulletin, **40**, 2989 (1967).

7) Y. Kubota, Y. Fujisaki and M. Miura, *Kogyo Kagaku Zasshi*, **72**, 252 (1969).

8) Y. Kubota, Y. Fujisaki and M. Miura, This Bulletin, **42**, 853 (1969).

Experimental

Materials. The acridine orange (Tokyo Kasei) was purified by the method of Zanker.[9] The proflavine sulfate (G. R. of Tokyo Kasei) was precipitated as a free base from an aqueous solution by adding a dilute sodium hydroxide solution. The precipitate was recrystallized three times from an ethanol-water mixture. The acriflavine (Chroma) was purified by the method of Gailliot[10] and was recrystallized twice from methanol. To check the purity, these dyes were subjected to silica-gel thin-layer chromatography; the chromatogram showed only a single colored band for each dye.

Calf thymus DNA (Type I) was obtained from the Sigma Chemical Co. The concentration of the DNA phosphates was determined by analyzing the phosphorus by the method of Chen *et al.*[11] The atomic extinction coefficient per phosphorus was found to be 6700, which is characteristic of a native DNA.

The solutions of the complexes were made up in a 0.01 M phosphate buffer at pH 7.0. Each DNA solution contained 0.01 M sodium chloride to protect it from denaturation. The thermal denaturation of DNA was performed by heating the DNA solutions for 20 min in boiling water and by then rapidly cooling them in ice-water.

Measurements. All the solutions were degassed by the freezing, pumping, and thawing technique under a high vacuum. The glass of the sample solution was made at 77°K in a quartz tube (1.5—2 mm in internal diameter). The emission and excitation spectra at 77°K were measured with a Hitachi MPF-2A fluorescence spectrophotometer; the exciting light source was a 150-W xenon lamp, and the detector was a R-106 photomultiplier. A rotating-shutter phosphoroscope was used to separate the delayed emissions (phosphorescence and delayed fluorescence) from normal fluorescence. No correction of the emission spectra was made for the spectral sensitivity of the detector. The excitation spectra were corrected for the spectral-energy distribution of the exciting light. The intensity of the exciting light was varied by introducing calibrated wire screens. The decay of the delayed emission was generally measured at its maximum wavelength by using a Hitachi V-104 synchroscope.

The absorption spectra were measured with a Shimadzu MPS spectrophotometer at 77°K or at room temperature, using 0.1- and 0.2-cm quartz cells. This apparatus can detect a large fraction of the forward scattered light in addition to the transmitted light; thus, it gives an accurate absorption. We could obtain the reproducible absorption spectra by subtracting the apparent absorption of the reference solution from that of the sample solution, in spite of the development of cracks and translucency in the glass.

The ESR measurements of the lowest triplet state of the acridine dyes in the complexes were made using a JES-3BX ESR spectrometer in an ethylene glycol-water (1 : 1 by volume) mixture at 77°K.

9) V. Zanker, *Z. Physik. Chem.* (Leipzig), **199**, 225 (1952).

10) M. Gailliot, *Quarterly J. Pharm. Pharmacol.*, **7**, 63 (1934).

11) P. S. Chen, Jr., T. Y. Toribara and H. Warner, *Anal. Chem.*, **28**, 1756 (1956).

Results and Discussion

Absorption Spectra of the Complexes. First, the absorption spectra of the complexes were measured at room temperature and at 77°K in order to ascertain the binding states of acridine dyes. It was found that the dye molecules predominantly exist as the monomeric species at a sufficiently high P/D value, and that they tend to associate with a decrease in the P/D value. The associative tendency appears to increase in the order of acridine orange, proflavine, and acrifivine and is more remarkable in the denatured DNA than in the native one. Typical examples of the absorption spectra at 77°K are shown in Figs. 1 and 2. They exhibit a red shift of about 10 nm and are well resolved as compared with those at room temperature.[2,4,12] The absorption band corresponding to the 0—1 transition generally overlaps with the dimer absorp-

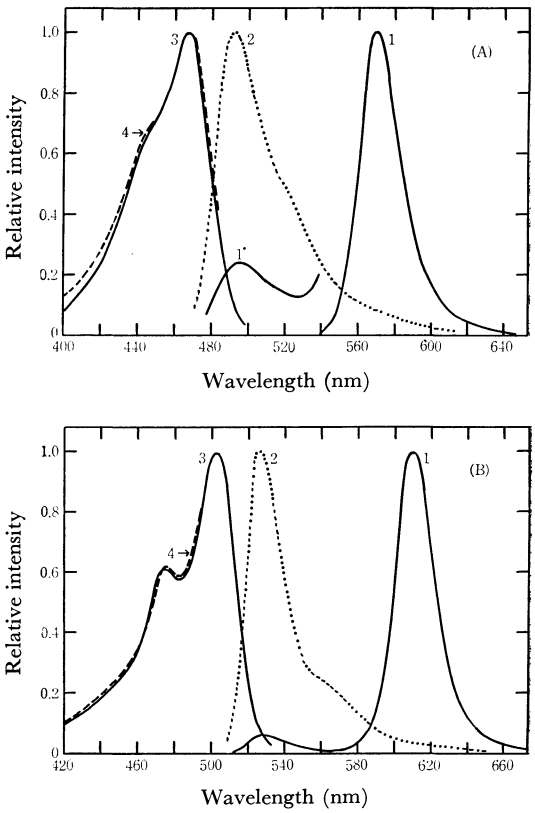

Fig. 1. The emission, excitation, and absorption spectra of (A) proflavine and (B) acridine orange in the complexes ($P/D=100$) at 77°K.
Excitation wavelength: (A) 460 nm, (B) 500 nm
Dye concn.: 5×10^{-5} M
(1) Long-lived emission, (1') higher sensitivity of (1), (2) total emission, (3) absorption, and (4) phosphorescence-excitation spectra.

12) G. Weill and M. Calvin, *Biopolymers*, **1**, 401 (1963).

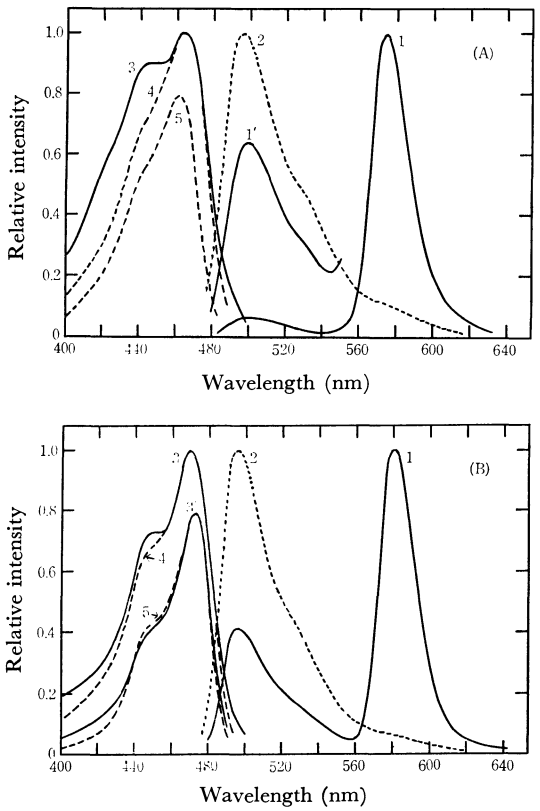

Fig. 2. The emission, excitation, and absorption spectra of (A) proflavine and (B) acriflavine in the complexes ($P/D=5$) at 77°K.
Excitation wavelength: (A) 460 nm, (B) 470 nm
Dye concn.: 5×10^{-5}M
(1) Long-lived emission, (1′) higher sensitivity of (1), (2) total emission, absorption spectra at (3) $P/D=5$ and (3′) $P/D=100$, and the excitation spectra of (4) phosphorescence and (5) delayed fluorescence.

tion band for each dye. In the case of $P/D<5$, absorption due to the aggregation of free dyes develops at wavelengths shorter than the 0—1 band.

Phosphorescence and Phosphorescence-Excitation (PE) Spectra of Acridine Dyes in the Complexes. The total emission and the delayed emission spectra of acridine dyes upon the excitation of the complexes by the visible light are shown in Figs. 1 and 2. The total emission seems to be mainly composed of normal fluorescence. The phosphorescence spectra at low dye concentrations (below 2.5×10^{-5}M) have peaks at 565, 604, and 574 nm for proflavine, acridine orange, and acriflavine respectively. These spectra are similar to those of acridine dyes in organic solvents at 77°K.[13,14] With an increase in the dye concentration, both phosphorescence and fluorescence spectra slightly shift to longer wavelengths; this may be due to self-absorption. The phosphorescence intensity decreases with a decrease in the P/D value; this phenomenon becomes remarkable in the case of denatured DNA.

Next, the PE spectra were measured in order to obtain information on the phosphorescing species by comparing them with the absorption spectra. As Figs. 1 and 2 show, the PE spectra at high and low P/D values are approximately identical and agree well with the absorption spectra at a high P/D value. Further, it was found that the PE spectra are identical with the fluorescence-excitation spectra. These results indicate that the monomeric dyes mainly contribute to the fluorescence and phosphorescence emissions. Thus, the decrease in the phosphorescence intensity with a decrease in the P/D value or in the case of denatured DNA may be interpreted as a result of the increase in the number of dimeric species.

Table 1. Phosphorescence lifetimes of acridine dyes in the complexes at 77°K (sec)

Dye concn. (M)	P/D	Acridine orange (500 nm)*1	Proflavine (460 nm)*1	Acriflavine (470 nm)*1
10^{-4}	100	1.27	1.77	1.89
5×10^{-5}	100	1.34	1.90	1.96
		1.34*2		1.95*2
	50	1.31	1.88	1.94
		1.31*2		1.94*2
	10	1.25*3	1.81*3	1.90*3
	5		1.76*3	1.86*3
2.5×10^{-5}	200	1.50	1.98	2.06
10^{-5}	500	1.60	2.00	2.08

*1 Excitation wavelength.
*2 Denatured DNA.
*3 Slightly deviates from the exponentiality at the initial stage.

Finally, the mean lifetimes of the phosphorescence are summarized in Table 1. In general, these values are a little smaller than those in organic solvents at 77°K (*cf.* Table 2).[13]

ESR of the Lowest Triplet State of Acridine Dyes in the Complexes. The ESR spectra corresponding to the $\Delta M=2$ transitions of acridine dyes in the complexes were observed at a magnetic field of *ca.* 1600 gauss. From the maximum position on the low-field side of the derivative spectrum, one can calculate the root-mean-square zero-field splitting parameter (D^*), which is a measure of the electron spin-spin interaction.[15] As may be seen from Table 2, the D^* value at a high P/D

13) The preliminary results have already been presented; Y. Kubota and M. Miura, This Bulletin, **42**, 2763 (1969).

14) R. W. Chambers and D. R. Kears, *J. Phys. Chem.*, **72**, 4718 (1968); *Photochem. Photobiol.*, **10**, 215 (1969).

15) J. H. van der Waals and M. S. de Groot, *Mol. Phys.*, **2**, 333 (1959); *ibid.*, **3**, 190 (1960).

TABLE 2. ESR RESULTS OF THE TRIPLET STATE OF ACRIDINE DYES IN THE COMPLEXES AT 77°K

DNA (M in phosphate unit)	Acridine orange		Proflavine	
	D^* (cm^{-1})	τ (sec)	D^* (cm^{-1})	τ (sec)
0	0.0714	1.8	0.0795	2.2
1.25×10^{-2}	0.0726	1.9		
2.5×10^{-2}	0.0728	1.9	0.0805	2.2

τ: lifetime of the triplet state
Dye concn.: 5×10^{-4}M
Solvent: ethylene glycol-phosphate buffer (1 : 1 by volume, pH 7.0) mixture

value is in good agreement with those corresponding to the monomeric dyes in organic solvents.[13] Therefore, the ESR results also support the idea that the monomeric dyes mainly contribute to the phosphorescence emission.

Delayed Fluorescence Due to the Triplet-Triplet Annihilation of Acridine Dyes in the Complexes. As Figs. 1 and 2 show, a delayed fluorescence of the dye was also observed. The peak of the delayed fluorescence shifts to a slightly longer wavelength, but this is trivial; this may be attributed to self-absorption. This delayed fluorescence has not yet been reported in the DNA-acridine dye complexes; an effort will be made hereinafter to investigate its nature.

The excitation spectrum of the delayed fluorescence coincides well with the absorption spectra at a high P/D value, where most of the dye molecules exist as the monomeric species (see Fig. 2). Therefore, it may be concluded that the excitation process of the delayed fluorescence is identical with that of the fluorescence or phosphorescence of the monomeric dyes.

Since the thermal excitation from the lowest triplet to the first excited singlet state is actually impossible at 77°K for acridine dyes, the delayed fluorescence observed cannot be interpreted as an α-phosphorescence; this phenomenon was found to become remarkable at temperatures above 200°K.

Following the method of Azumi and McGlynn,[16] we plotted the intensity of the delayed fluorescence against the square of the phosphorescence intensity; this gave a straight line, as is shown in Fig. 3. Further, as is shown in Fig. 4, the growth of the delayed fluorescence was observed to depend on the initial triplet concentration and to be nearly equal to the growth of the triplet concentration after a long period of darkness.[17] In view of these results, it seems reasonable to conclude that two triplets are involved in the phenomenon of the delayed fluorescence—that is, two neighboring

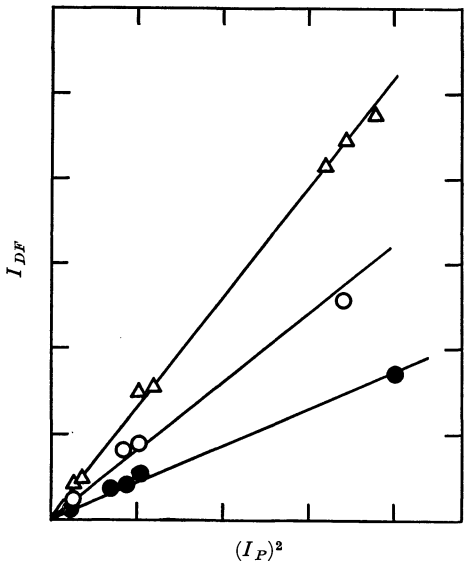

Fig. 3. A relationship between the intensity of delayed fluorescence (I_{DF}) and the square of the phosphorescence intensity (I_P).
△, acriflavine; ○, proflavine; ●, acridine orange

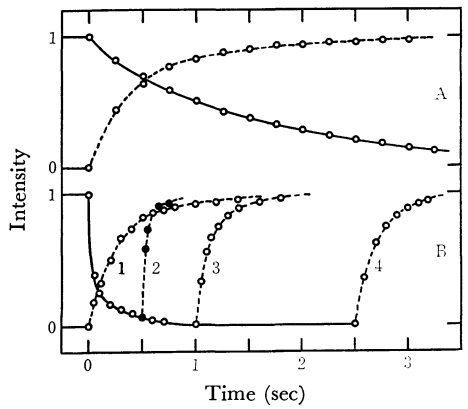

Fig. 4. The decay (solid line) and growth (dashed line) curves of (A) phosphorescence and (B) delayed fluorescence of acriflavine in the complexes at 77°K excited at 470 nm.
Acriflavine concn.: 5×10^{-5}M, P/D: 5
Period of darkness: (1) longer than 60 sec, (2) 0.5 sec, (3) 1 sec, and (4) 2.5 sec

triplet molecules produce one singlet molecule, which is then responsible for the delayed fluorescence. Moreover, the first period of the decay of phosphorescence shows deviations from the exponentiality (Fig. 5); these deviations may be related to the existence of the triplet-triplet annihilation process.[16,18]

16) T. Azumi and S. P. McGlynn, *J. Chem. Phys.*, **39**, 1186 (1963).
17) C. A. Parker, *Trans. Faraday Soc.*, **60**, 1998 (1964).
18) H. Sternlicht, G. C. Nieman and G. W. Robinson, *J. Chem. Phys.*, **38**, 1326 (1963); **39**, 1610 (1963).
19) *e.g.*, R. K. Tubbs, W. E. Ditmars, Jr., and Q. van Winkle, *J. Mol. Biol.*, **9**, 545 (1964).

It is well known that the probability of the triplet-triplet annihilation falls off rapidly with an increase in the triplet-state separation. As may be seen in Fig. 1, the delayed fluorescence can be observed even at P/D values higher than 100. If the dye binding is homogeneous, the interaction between two triplets is unlikely to occur at $P/D \geq 100$. Consequently, it may be thought that the binding is heterogeneous and that, thus, the assembly of dye molecules is partly formed in the double-stranded helix. This is consistent with the results previously obtained.[19]

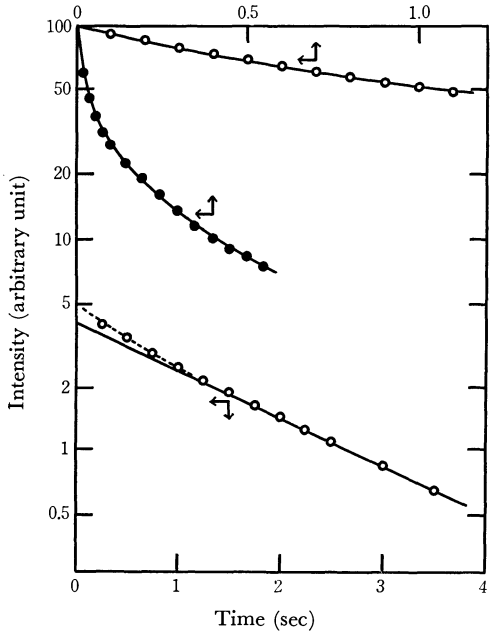

Fig. 5. The decay curves of phosphorescence (○) and delayed fluorescence (●) of acriflavine (5×10^{-5}M) in the complexes ($P/D=5$) at 77°K excited at 470 nm.
Phosphorescence decay in two parts: 0—1 sec and 1—4 sec.

On the other hand, if the triplet molecules are uniformly distributed and if the second-order processes are negligible, the delayed fluorescence will decay exponentially with twice the rate constant of phosphorescence decay.[16,18] In fact, as is shown in Fig. 5 in connection with the DNA-acriflavine complex, the decay of delayed fluorescence is not exponential; it decays very fast at the begining and then gradually becomes slower. The decay mode of the delayed fluorescence was independent of the P/D value and was similar to those of other acridine dyes. As has been mentioned above, a random distribution of dye molecules in the complexes is somewhat unlikely. Therefore, the initial rapid decay of the delayed fluorescence may be ascribed to the strong interaction between triplet molecules spaced very close together.

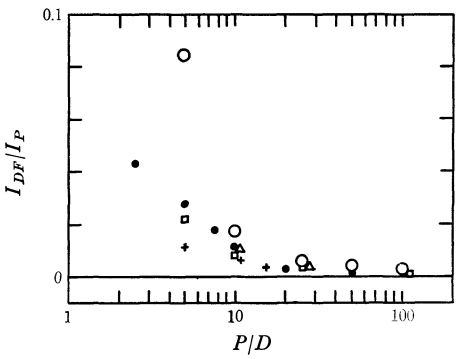

Fig. 6. The ratio of the intensity of delayed fluorescence to that of phosphorescence of the dye (I_{DF}/I_P) as a function of P/D. Both intensities are corrected for the spectral sensitivity of the detector.
○: acriflavine (5×10^{-5}M, I_{DF}/I_P values are 0.10 and 0.16 at $P/D=4$ and 2.5 respectively)
●: acriflavine (10^{-4}M)
+: acriflavine (10^{-4}M, denatured DNA)
□: proflavine (5×10^{-5}M)
△: acridine orange (5×10^{-5}M)

As may be seen in Fig. 6, the phenomenon of the delayed fluorescence seems to depend on the P/D value, the dye concentration, the kind of acridine dye, and the conformation of the macromolecular complex. First, the delayed fluorescence becomes remarkable with a decrease in the P/D value; this may be expected from the decrease in the mean distance between dye-dye molecules—that is, between two triplets. Second, the delayed fluorescence becomes weak with an increase in the dye concentration at a constant P/D value; this may be expected from the fact that dye association becomes more pronounced as the dye concentration increases. Third, the delayed fluorescence is observed most remarkably for acriflavine; this may be understood on the basis of the fact that acriflavine associates less than proflavine and acridine orange do. Finally, the denaturation of DNA leads to a marked diminution in the delayed fluorescence; this may be due to the difference between the conformations of the native and denatured DNA, where dye molecules associate remarkably. In the case of RNA, the delayed fluorescence is greatly decreased. Further, no triplet-triplet annihilation was found in the nucleotide-dye systems. Therefore, the double helical structure seems suitable for producing the annihilative process.

The author wishes to thank Professor Masaji Miura, Hiroshima University, for his helpful discussions and suggestions during this work. Thanks are also due to Professor Yasuo Fujisaki, Yamaguichi University, for his continuing interest and encouragement.

BULLETIN OF THE CHEMICAL SOCIETY OF JAPAN VOL. 43 3126—3130 (1970)

Luminescence in DNA-Acridine Dye Complexes. II. Sensitized Delayed Fluorescence in the Complexes

Yukio KUBOTA

Department of Chemistry, Yamaguchi University, Yamaguchi

(Received June 15, 1970)

When frozen aqueous solutions of DNA-acridine dye complexes or nucleotide-dye mixtures were excited by ultraviolet light, a sensitized delayed fluorescence of the dye was observed. This delayed fluorescence was interpreted by means of a mechanism in which the excitation energy is transferred from the triplet state of the nucleotides to the first excited singlet state of the dye. The efficiency and decays of the sensitized delayed fluorescence revealed that the energy transfer depends greatly on the separation between the energy donor and acceptor and that donor-acceptor pairs spaced very closely are important in the energy transfer. In DNA-acridine dye complexes, the thymine triplet seems to play the most important role as an energy donor. The decrease in the delayed fluorescence on the denaturation of DNA indicates that the energy transfer is sensitive to the conformation of the macromolecule.

In the preceding paper,[1] the luminescence properties of acridine dyes upon the excitation of DNA-acridine dye complexes by visible light have been reported. According to Lerman's intercalation model,[2] in which the dye molecules are in close proximity with purine-pyrimidine base pairs in the double-stranded helix, the electronic excitation-energy transfer between DNA bases and dye molecules may be expected to occur efficiently. Recently, three types of energy transfer, singlet-singlet,[3] triplet-singlet,[4] and triplet-triplet,[5] have been shown to occur in the complexes; DNA bases served as the energy donors, and the bound dye, as the energy acceptor. In order to obtain further information on the energy transfer between DNA bases and dye molecules, our investigations have now been extended to the luminescence properties of the complexes with excitation in the region of DNA absorption. A sensitized delayed fluorescence was observed for various acridine dyes in frozen aqueous solutions of the complexes;[6,7] this was interpreted in terms of energy transfer from the triplet state of the DNA bases to the singlet state of the dye, as was first suggested by Isenberg *et al.*[4] Further, a sensitized delayed fluorescence due to the triplet-singlet energy transfer has also been observed in frozen aqueous solutions of the nucleoside-, nucleotide-, and polynucleotide-acridine dye systems.[8] This paper will present the details of our further investigation of the DNA-proflavine and nucleotide-proflavine systems.

Experimental

Materials. Calf thymus DNA (Type I) and yeast RNA (Type XI) were obtained from the Sigma Chemical Co. The nucleotides*1 were purchased from either Sigma or Miles Laboratories, Inc. These materials were generally used without further treatment. The proflavine was the same as that described in Part I.[1]

Measurements. The emission and absorption measurements were described in Part I.[1] The measurements were carried out at 77°K in frozen aqueous solutions (0.01M phosphate buffer, pH 7.0). No correction of the emission and excitation spectra was made. Unless otherwise stated, all the luminescence data presented

1) Y. Kubota, This Bulletin, **43**, 3121 (1970).
2) L. S. Lerman, *J. Mol. Biol.*, **3**, 18 (1961); *Proc. Natl. Acad. Sci. U. S.*, **49**, 94 (1963).
3) G. Weill and M. Calvin, *Biopolymers*, **1**, 401 (1963).
4) I. Isenberg, R. B. Leslie, S. L. Baird, Jr., R. Rosenbluth and R. Bersohn, *Proc. Natl. Acad. Sci. U. S.*, **52**, 379 (1964).
5) W. C. Galley, *Biochemistry*, **6**, 1279 (1968).
6) Y. Kubota, Y. Fujisaki and M. Miura, *Kogyo Kagaku Zasshi*, **72**, 252 (1969).
7) Y. Kubota, Y. Fujisaki and M. Miura, This Bulletin, **42**, 853 (1969).
8) Y. Kubota, to be published.

*1 The 5'-monophosphates of adenosine, guanosine, cytidine, thymidine, and uridine are abbreviated as AMP, GMP, CMP, TMP, and UMP respectively.

in this paper were obtained by means of the excitation of the complexes or nucleotide-dye mixtures by 280 nm; the total nucleotide concentration was 5×10^{-3}M in phosphate units, and the proflavine concentration, 5×10^{-5}M. In general, the maximum intensity of the sensitized delayed fluorescence was obtained at a dye concentration of *ca.* 5×10^{-5}M.

Results and Discussion

Figure 1 shows the delayed emission spectra of the DNA-proflavine complex in a frozen aqueous solution. With an increase in the dye concentration, the DNA phosphorescence diminishes and two emissions appear; one, having a spectrum identical with the dye fluorescence, is identified as a delayed fluorescence of the dye, and the other, peaking at *ca.* 570 nm, as a phosphorescence of the dye.

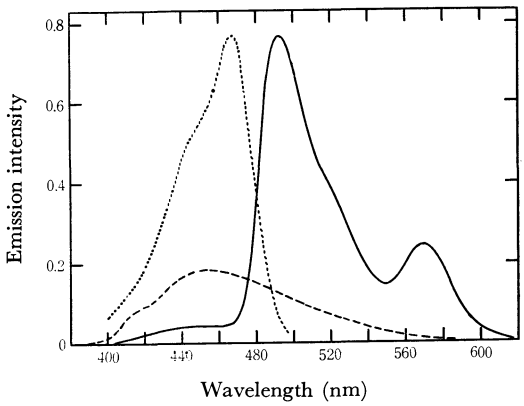

Fig. 1. Delayed emission spectra of DNA (----) and the DNA-proflavine complex (———) and absorption spectrum of the complex (---------). The scale of ordinates is the same on Figs. 1 and 5.

As is shown in Fig. 2, the excitation spectrum of the delayed fluorescence is not similar to that of the dye fluorescence or the phosphorescence, but it is identical with that of the DNA phosphorescence. Therefore, it may be concluded that the excitation of the DNA phosphorescence is responsible for the production of the delayed fluorescence; hereafter, this will be called a *sensitized delayed fluorescence*. The intensity of the sensitized delayed fluorescence is proportional to the intensity of the exciting light. Furthermore, the decay of the DNA phosphorescence is remarkably affected by the addition of the dye; it becomes faster than in the absence of the dye (see Fig. 3). This means that an additional pathway is introduced for the decay of the DNA triplet. In view of these results, it is reasonable to assume that the sensitized delayed fluorescence arises from the triplet-singlet energy transfer,[4] in which the

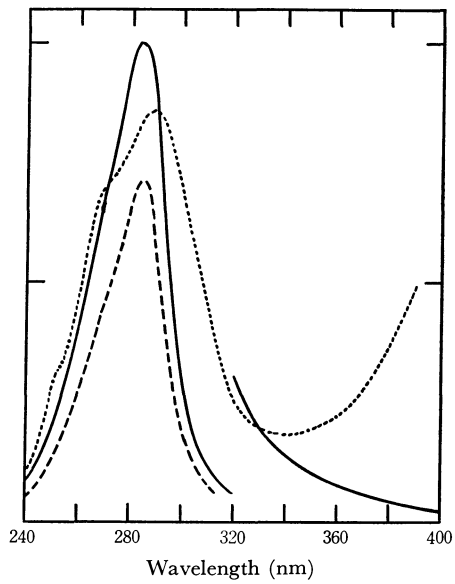

Fig. 2. Excitation spectra of delayed emissions of the DNA-proflavine complex.
----- DNA phosphorescence
——— Sensitized delayed fluoresncne
--------- Proflavine fluoresence or phosphorescence

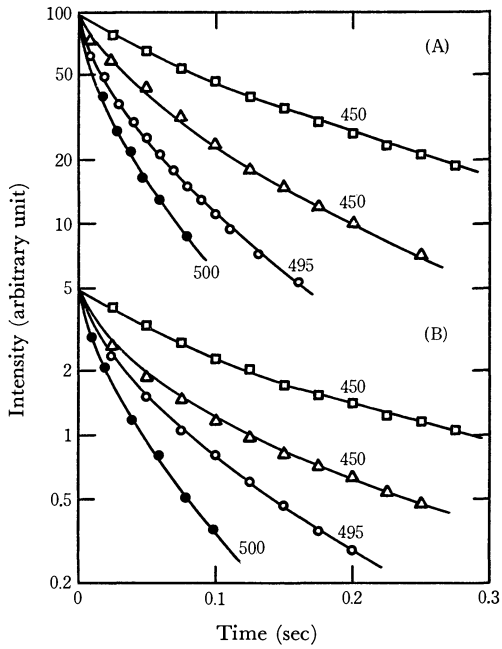

Fig. 3. The decay curves of the delayed emissions of (A) native DNA-proflavine and (B) denatured DNA-proflavine complexes. Each figure represents the wavelength at which the decay was measured.
DNA phosphorescence in the absence (□) and in the presence (△) of proflavine (5×10^{-5}M), sensitized delayed fluorescence of proflavine (○: 5×10^{-5}M, ●: 10^{-4}M)

DNA bases are the triplet donors and the bound dye is the singlet acceptor.

The phenomenon of the sensitized delayed fluorescence was also found in the cases of denatured DNA and RNA. In both cases, the intensity of the sensitized delayed fluorescence greatly decreased with a decrease in the P/D value, the ratio of the number of nucleotides to that of dye molecules. Figure 4 shows that the ratio of the intensity of the

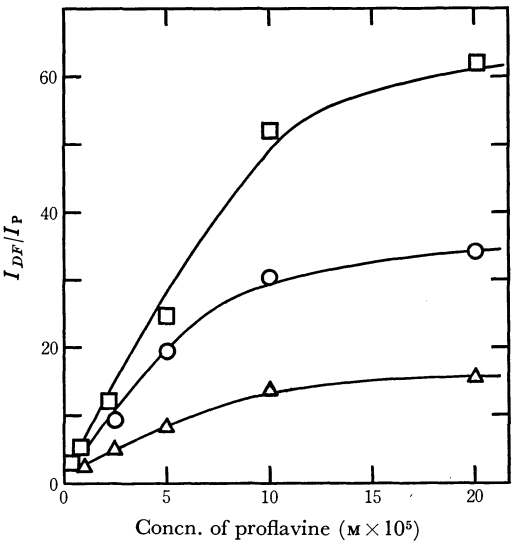

Fig. 4. The ratio of the intensity of sensitized delayed fluorescence to that of donor phosphorescence (I_{DF}/I_P) *vs.* dye concentration. Both intensities are corrected for the spectral sensitivity of the detector.
□, native DNA-proflavine; ○, denatured DNA-proflavine △, RNA-proflavine

sensitized delayed fluorescence to that of the donor phosphorescence (I_{DF}/I_P) increases with an increase in the dye concentration, and then reaches a limiting value. In the case of denatured DNA or RNA, this value is smaller than that in the native DNA. In other words, the energy in the denatured DNA cannot be efficiently transferred to the bound dye in spite of a considerable enhancement of the DNA phosphorescence on denaturation.[9] This means that the energy transfer is sensitive to the conformation of the macromolecular complex; that is, the double helical structure is essential for the energy transfer to occur efficiently.

Next, our investigations were extended to the luminescence properties of the nucleotide-dye systems in order to ascertain how the DNA constituent bases contribute to the energy transfer. Some typical results are shown in Fig. 5. The sensitized delayed fluorescence was also observed in frozen

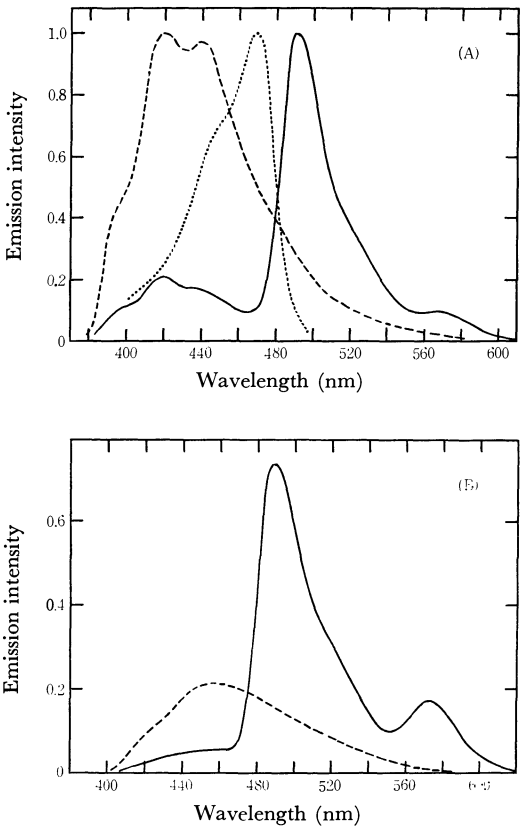

Fig. 5. Delayed emission spectra of (A) AMP-proflavine and (B) TMP-proflavine systems.
----- Nucleotide phosphorescence in the absence of proflavine
——— Delayed emissions in the presence of proflavine
--------- Absorption spectrum of proflavine in the presence of nucleotide

aqueous solutions of nucleotide-proflavine systems. This delayed fluorescence can also be interpreted in terms of the triplet-singlet energy transfer on the basis of the following observations: (1) the excitation spectrum of the sensitized delayed fluorescence is identical with the phosphorescence-excitation spectrum of each nucleotide, (2) the intensity of the sensitized delayed fluorescence varies linearly with the intensity of the exciting light, (3) the addition of the dye greatly quenches the phosphorescence of nucleotide, but has little effect on the fluorescence, and (4) the initial decay of the nucleotide phosphorescence becomes rapid upon the addition of the dye (see Fig. 6) and becomes more and more faster as the dye concentration increases. Furthermore, it is expected that the transfer proceeds with a high probability, since the dye absorption well overlaps with the phosphorescence spectrum of each nucleotide (Fig. 5).[10]

9) R. O. Rahn, R. G. Shulman and J. W. Longworth, *J. Chem. Phys.*, **45**, 2955 (1966).

10) Th. Förster, *Discuss. Faraday Soc.*, **27**, 7 (1959).

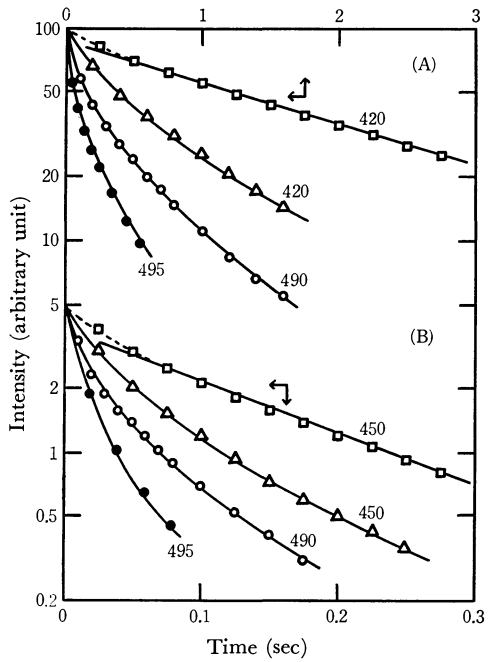

Fig. 6. The decay curves of delayed emissions from (A) AMP-proflavine and (B) TMP-proflavine systems. Each figure represents the wavelength at which the decay was meausred.
Nucleotide phosphorescence in the absence (□) and in the presence (△) of proflavine (5×10^{-5}M), sensitized delayed fluorescence of proflavine (○: 5×10^{-5}M, ●: 10^{-4}M)

As Figs. 3 and 6 show, the decays of both the nucleotide phosphorescence in the presence of the dye and the sensitized delayed fluorescence deviate remarkably from simple exponentials; they decay rapidly at the first stage, and then gradually become slower. The rapid decay at the first stage reflects the strong interaction between the energy donor and acceptor, located very close together. Further, in the frozen aqueous solutions, relatively low dye concentrations (below 5×10^{-6}M) are needed to observe the sensitized delayed fluorescence. On the other hand, the addition of alcohols before freezing the nucleotide-dye solutions resulted in a marked decrease in the sensitized delayed fluorescence despite the observation of a considerable enhancement in the nucleotide phosphorescence. However, the DNA-proflavine complexes exhibited a considerable sensitized delayed fluorescence, even in an alcohol-water mixed solvent. In the freezing of an aqueous solution, nucleotide molecules are considered to be excluded from the ice crystal and to form aggregates.[11] Proflavine also forms aggregates in the absence of a nucleotide, while it exists as the monomeric species in its presence (Fig. 5). Therefore, it seems likely that dye and nucleotide molecules form the stacked aggregates in which dye molecules are placed between nucleotide molecules by the face-to-face arrangement as well as at room temperature.[12,13] The decrease in the sensitized delayed fluorescence upon the addition of alcohols may be ascribed to the destruction of the aggregates. In conclusion, these results suggest that (1) the energy transfer depends greatly on the separation between the energy donor and acceptor; (2) most of donor and acceptor molecules are not distributed uniformly, but are spaced very closely; (3) the energy transfer takes place with a high efficiency between such molecules, and (4) the intercalation is most favorable for the efficient transfer.

The decay behavior of sensitized delayed fluorescence was independent of the kind of acridine dye (proflavine, acridine orange, acriflavine, *etc.*); that is, it appears that the rate constant of energy transfer is almost the same for these dyes. A meaningful transfer rate cannot be obtained because of the non-exponentiality of the decay, but the half-life ($\tau_{1/2}$) will serve as a qualitative measure of the transfer rate. In Table 1, the $\tau_{1/2}$ values are summarized, together with the lifetimes of the nucleotide phosphorescence (τ_P). It may be seen from Table 1 that $\tau_{1/2}$, which is dependent on τ_P, is about one tenth of τ_P, and that $\tau_{1/2}$ in the case of DNA is almost the same as that in the case of TMP. The phosphorescence spectrum of DNA resembles that of TMP. Its decay is composed of two exponen-

Table 1. Decays of nucleotide phosphorescence and sensitized delayed fluorescence of proflavine

Nucleotide	τ_P (sec)	$\tau_{1/2}$ (msec)
AMP	2.30*	135
GMP	1.15*	110
CMP	0.4*	30
UMP	0.3*	25
TMP	0.2*	20
native DNA	non-exponential	
	{fast (0.18) 95% {slow (1.6) 5%	18
denatured DNA	non-exponential	
	{fast (0.18) 90% {slow (1.7) 10%	23
RNA	non-exponential	34

Nucleotide: 5×10^{-3}M in phosphate unit
Proflavine: 5×10^{-5}M
* Slightly deviates from the exponentiality at the initial stage.

11) C. Hélene, *Biochem. Biophys. Res. Commun.*, **22**, 237 (1966).

12) G. Tomita, *Biophysik*, **4**, 118 (1967).

13) F. E. Hruska and S. S. Danyluk, *Biochim. Biophys. Acta*, **161**, 250 (1968).

tials; the major component is the fast one, which has the same lifetime as that of TMP. Therefore, the triplet in DNA appears to reside mainly at the thymine residue; this is consistent with the recent observations by the optical and ESR measurements.[14,15] This phenomenon seems to be achieved by energy transfer to thymine from other bases; this is possible, since thymine has the lowest triplet.[11,16] Hence, the data of the sensitized delayed fluorescence in the complexes can tentatively be interpreted as follows: first, the base-to-base energy transfer produced the thymine triplet, and then a part of the excitation energy is efficiently transferred to the dye placed closest to it.

The author wishes to thank Professor Masaji Miura, Hiroshima University, for his helpful discussions and suggestions during this work. Thanks are also due to Professor Yasuo Fujisaki, Yamaguchi University, for his continuing interest and encouragement.

14) A. A. Lamola, M. Guéron, T. Yamane, J. Eisinger and R. G. Shulman, *J. Chem. Phys.*, **47**, 2210 (1967).
15) K. Imakubo, *J. Phys. Soc. Japan*, **24**, 143 (1968).
16) M. Guéron, J. Eisinger and R. G. Shulman, *J. Chem. Phys.*, **47**, 4077 (1967).

BULLETIN OF THE CHEMICAL SOCIETY OF JAPAN VOL. 43 3130—3136 (1970)

The Interaction of Oxygen with Organic Molecules. II.[1] Oxygen Quenching of the Excited States of Adsorbed Aromatic Hydrocarbons

Hideyuki ISHIDA, Hiroshi TAKAHASHI and Hiroshi TSUBOMURA

Department of Chemistry, Faculty of Engineering Science, Osaka University, Toyonaka, Osaka

(Received June 16, 1970)

Quenching of phosphorescence and fluorescence of aromatic hydrocarbons adsorbed on powdered porous glass or silica gel have been examined as a function of oxygen pressure. It has been found that the phosphorescence quenching at low temperature can be explained mostly by assuming that only those aromatic molecules having an oxygen molecule or molecules within an effective interaction radius are nonphosphorescent (static quenching model). The fluorescence quenching occurs only at much higher oxygen pressures and it has been proposed that contact pairs between aromatic and oxygen molecules, which have shorter intermolecular distances compared to the distances effective for the phosphorescence quenching and give rise to the charge-transfer absorption bands, are relevant. It has been observed that the excimer fluorescence of naphthalene appearing at a higher sample concentration is more strongly affected by oxygen than the monomer fluorescence. The emission spectra from naphthalene-porous glass adsorbate immersed in liquid oxygen and nitrogen have also been examined. The formation of the singlet oxygen ($^1\Delta_g$ or $^1\Sigma_g^+$) through the interaction of oxygen with triplet molecules has been confirmed by use of the peroxidation reaction of adsorbed anthracene.

The interaction of oxygen with electronically excited organic molecules is associated with a number of interesting phenomena.[2] For example, it is well known that molecular oxygen quenches both the excited singlet and triplet states of organic molecules. Theoretical investigation of the quenching of organic triplet states by oxygen indicated that singlet-state oxygen are formed by the intermolecular energy transfer.[3] This mechanism has now been supported by the results of recent experiments.[4-6] The oxygen quenching has been studied mainly in fluid media where the bimolecular quenching is controlled by the diffusion of oxygen and organic

1) Part I of this series; H. Ishida, H. Takahashi, H. Sato and H. Tsubomura, *J. Amer. Chem. Soc.*, **92**, 275 (1970).

2) P. Pringsheim, "Phosphorescence and Fluorescence," Interscience Publisher, Inc., New York (1965).

3) K. Kawaoka, A. U. Khan and D. R. Kearns, *J. Chem. Phys.*, **47**, 1842 (1967); **48**, 3272 (1968).

4) D. R. Snelling, *Chem. Phys. Lett.*, **2**, 346 (1968).

5) D. R. Kearns, A. U. Khan, C. K. Duncan and A. H. Maki, *J. Amer. Chem. Soc.*, **91**, 1039 (1969).

6) E. Wasserman, V. J. Kuck, W. M. Delavan and W. A. Yager, *ibid.*, **91**, 1041 (1969).

molecules.[7–10] It has not been possible to estimate intrinsic quenching efficiencies from such diffusion-controlled reactions. Siegel and Judeikis have recently determined the relative interaction radius for the oxygen quenching of naphthalene triplet-state in rigid matrices where material diffusion is minimized.[11] Oxygen quenching of phosphorescence of aromatic molecules has been used to measure the diffusion rates of oxygen in polymer matrices.[12,13]

It is well known that molecules adsorbed on solid surface have relatively long lifetimes in their triplet states even at room temperature. The luminescent properties of adsorbed molecules have been extensively investigated in the presence of oxygen.[14–17] Previous investigations of oxygen quenching have almost extensively dealt with dye molecules adsorbed on silica gel. In the preceding paper, we have reported the extra charge-transfer absorption spectra caused by the interaction between adsorbed oxygen and organic molecules.[1] The present paper is mainly concerned with the effective quenching interaction between oxygen and electronically excited aromatic hydrocarbons adsorbed on porous glass or silica gel.

Experimental

Materials. Oxygen and naphthalene were purified in the same way as described in the preceding paper. Commercially available α-chloronaphthalene was distilled under reduced pressure. Anthracene and biphenyl were purified by recrystallization from benzene and ethanol, respectively, and by sublimation in vacuum. The particle sizes of silica gel and powdered porous glass[1] used here were 30—42 mesh, and were treated in the same way as described in the preceding paper. It was confirmed that no luminescence was detectable from porous glass itself by excitation in the near ultraviolet region even at liquid nitrogen temperature (77°K). The phosphorescence of silica gel itself at 77°K was negligible in comparison with that of adsorbed molecules.

Procedure. Naphthalene, α-chloronaphthalene and biphenyl were adsorbed from the vapor phase in the same way as described before.[1] Anthracene was adsorbed from the chloroform solution and the adsorbate was dried and thoroughly evacuated at 100—150°C. Sample concentrations ranged from 1×10^{-7}—5×10^{-6} mol/g of the adsorbent for the study of the fluorescence and phosphorescence quenching by oxygen. In this range we detected no luminescence characteristic of the aggregates or microcrystals of adsorbed molecules. However, when sample concentrations were increased (above 5×10^{-5} mol/g), a new band ascribable to excimer fluorescence was detected besides monomer fluorescence in the case of naphthalene or α-chloronaphthalene.

After adsorption, the sample in the ampoule was distributed into several cylindrical quartz cells, 4 mm in diameter, previously attached to the ampoule. Then oxygen was introduced into the vacuum system at room temperature and the quartz cells were sealed off carefully from the ampoule at desired oxygen pressure. Pressures below 5 Torr were read with a McLeod gauge. An ordinary mercury manometer was used for reading higher pressures.

The emission spectra were measured with an Aminco-Bowmann Spectrophotofluorometer. The lifetimes of the phosphorescence were determined from the decay curves traced on an osciloscope. Fluorescence decay curves were measured by exciting the samples with a device for producing nanosecond flash light.[18] The absorption spectra of adsorbed molecules was measured by the reflection method with a Shimadzu MPS-50L Recording Spectrometer as described in the preceding paper.

Results

Phosphorescence and Fluorescence of Adsorbed Aromatic Hydrocarbons. Phosphorescence spectra of the adsorbed molecules at 77°K were found to be nearly in agreement with those

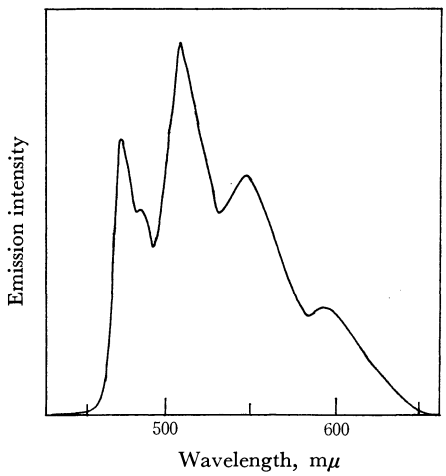

Fig. 1. Phosphorescence spectrum of naphthalene adsorbed on porous glass at 77°K.
Sample concentration: 1×10^{-6} mol per gram of porous glass.

7) W. R. Ware, *J. Phys. Chem.*, **66**, 455 (1962).
8) B. Stevens and B. E. Algar, *ibid.*, **72**, 2582 (1968).
9) A. D. Osborne and G. Porter, *Proc. Roy. Soc.*, **A284**, 9 (1965).
10) C. S. Parmenter and J. D. Rau, *J. Chem. Phys.*, **51**, 2242 (1969).
11) S. Siegel and H. S. Judeikis, *ibid.*, **48**, 1613 (1968).
12) G. Shaw, *Trans. Faraday Soc.*, **63**, 2181 (1967).
13) B. A. Baldwin and H. W. Offen, *J. Chem. Phys.*, **49**, 2933 (1968).
14) H. Kautsky, *Trans. Faraday Soc.*, **35**, 216 (1939).
15) S. Kato, This Bulletin, **30**, 34 (1957).
16) R. F. Weiner and H. H. Seliger, *Photochem. Photobiol.*, **4**, 1207 (1965).
17) J. L. Rosenberg and F. S. Humphries, *J. Phys. Chem.*, **71**, 330 (1967).
18) N. Mataga, M. Tomura and H. Nishimura, *Mol. Phys.*, **9**, 367 (1965).

measured for the same molecules dissolved in rigid matrices, although the spectra showed slight broadening of their vibrational structures in the adsorbed state. As an example, phosphorescence spectrum of naphthalene adsorbed on porous glass is shown in Fig. 1. The similar broadening was found also for fluorescence spectra. This broadening can be interpreted to be due to the wide energy distribution of the adsorbed molecules in the variety of the field of the polar adsorbent.

No difference in the luminescent properties of aromatic molecules have been found between silica gel and porous glass adsorbates. The phosphorescence lifetimes (τ_p) of adsorbed biphenyl, naphthalene and α-chloronaphthalene at 77°K were 4.0, 2.3 and 0.2 sec, respectively, at negligible oxygen pressures. These values also agree very closely with those in rigid matrices at 77°K.[19]

The band maxima of fluorescence show a slight blue shift when cooled down to 77°K. The fluorescence lifetime of naphthalene adsorbed on porous glass was 100 ns at room temperature, in good agreement with the values in the solutions.[18] Increase of the concentrations of naphthalene and α-chloronaphthalene resulted in the appearance of new broad bands almost identical with the corresponding excimer fluorescence in solutions.[20] The intensity ratio of this new band to the monomer fluorescence band depends on the wavelength of the exciting light as shown in Fig. 2 for the case of naphthalene. This ratio increases with increasing the sample concentration. The lifetimes of the new fluorescence band of naphthalene were found to

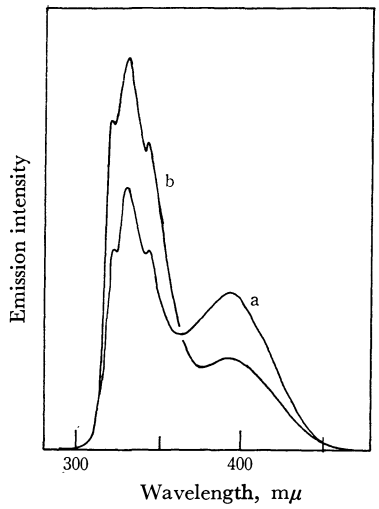

Fig. 2. Fluorescence spectra of naphthalene adsorbed on porous glass at 77°K.
Sample concentration: 5×10^{-5} mol per gram of porous glass; excitation wavelength: (a) 275 mμ and (b) 300 mμ.

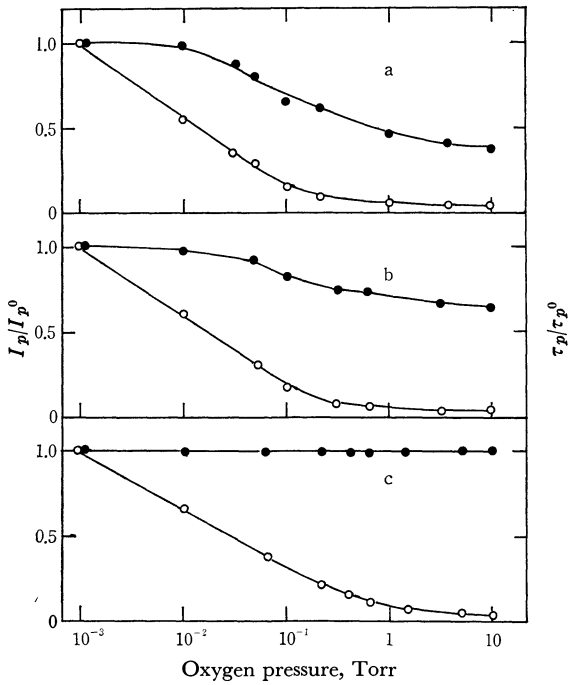

Fig. 3. The relative phosphorescence intensities I_p/I_p° (○) and lifetimes τ_p/τ_p° (●) of aromatic-porous glass adsorbates as a function of oxygen pressure at 77°K. (a), for biphenyl; (b), for naphthalene; (c), for α-chloronaphthalene. I_p° and τ_p° are, respectively, the phosphorescence intensity and lifetime at negligible oxygen pressures. The value of I_p/I_p° was normalized to be 1 at 10^{-3} Torr oxygen pressure. τ_p° at 77°K is 4.0 sec for biphenyl, 2.3 sec for naphthalene and 0.2 sec for α-chloronaphthalene.

be 65 and 100 ns at 300°K and 77°K, respectively, in good agreement with the long lifetimes characteristic of excimer fluorescence.[21] It is therefore concluded that, with increasing the sample concentration, adsorbed naphthalene molecules are forced to form loosely bound dimers on the surface and when this dimer is excited as well as monomer, the dimer is led to the configuration favorable to excimer formation.[22] The effect of oxygen on excimer fluorescence as well as monomer fluorescence is of considerable interest.

Quenching of Phosphorescence by Oxygen. The phosphorescence of the samples prepared in the way described in the experimental section was too weak at room temperature to examine the effect of oxygen quantitatively. Therefore, most of the studies were made at low temperature. The quenching effect of oxygen at 77°K is shown by the curves in Fig. 3, in which the values of the

19) D. S. McClure, *J. Chem. Phys.*, **17**, 905 (1949).
20) C. A. Parker, *Spectrochemica Acta*, **19**, 989 (1963).
21) N. Mataga, Y. Torihashi and Y. Ota, *Chem. Phys. Lett.*, **1**, 385 (1967).
22) E. A. Chandross, J. Ferguson and E. G. McRae, *J. Chem. Phys.*, **45**, 3546 (1966); **45**, 3554 (1966).

relative phosphorescence intensities I_p/I_p^0 and the relative phosphorescence lifetimes τ_p/τ_p^0 are plotted as a function of oxygen pressure. I_p^0 and τ_p^0 are, respectively, the phsophorescence intensity and lifetime of the sample containing negligible amounts of oxygen. The phosphorescence decays at various oxygen pressures were found to obey the first order kinetics. The dependence of the phosphorescence lifetime on oxygen pressure was also examined at 203°K (−70°C) in the case of biphenyl. The temperature was obtained by dropping liquid nitrogen into the Dewar containing 99% ethanol. This curve, being different from that at 77°K, showed a rapid decrease in the lifetime with increasing the oxygen pressure. Although the absolute amount of adsorbed oxygen at each oxygen pressure is unknown, qualitative discussion on the interaction of oxygen with excited molecules can be made from these quenching curves.

Although oxygen pressure above 10 Torr is sufficient to quench phosphorescence totally, weak emission was detected from the naphthalene-porous glass adsorbate immersed in liquid oxygen at 77°K. This emission was observed to lie in almost the same region as the phosphorescence of naphthalene and could not be detected using a sector presumably because of the extremely short lifetime ($<10^{-3}$ sec). The phosphorescence of naphthalene from the naphthalene-porous glass adsorbate immersed in liquid nitrogen was strong and the lifetime was 1.4 sec. This short lifetime in liquid nitrogen compared to the original value (τ_p^0, 2.3 sec) may be due to impurities, such as oxygen, possibly contained in liquid nitrogen.

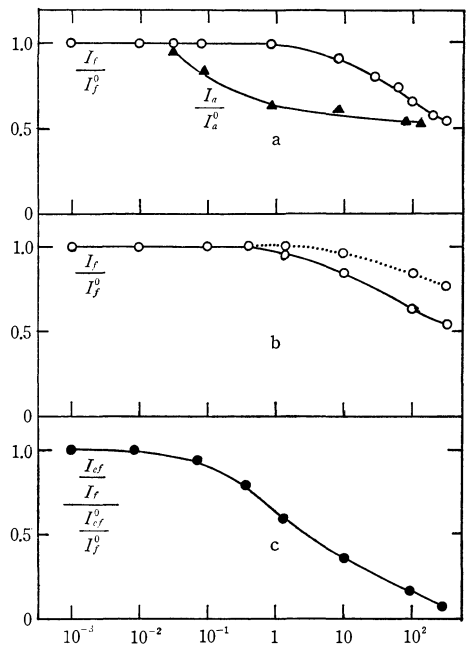

Fig. 4. The relative fluorescence intensities I_p/I_p° (○) and the relative ratios of the intensity of excimer fluorescence versus monomer fluorescence $(I_{ef}/I_f)/(I_{ef}^\circ/I_f^\circ)$ (●) of aromatic-porous glass adsorbates as a function of oxygen pressure at room temperature (———) and 77°K (-----). (a), for anthracene; (b) and (c), for naphthalene. I_f° and I_{ef}° are, respectively, the fluorescence intensities of monomer and excimer at negligible oxygen pressures. The relative absorption intensities I_a/I_a° (▲) of adsorbed anthracene are shown in (a) as a function of oxygen pressure, when the sample containing a known pressure of oxygen is irradiated. I_a° is the absorption intensity of adsorbed anthracene before irradiation.

Quenching of Fluorescence by Oxygen. The quenching effect of oxygen was examined mainly at room temperature. The quenching effect of oxygen on monomer fluorescence is shown in Fig. 4 (a) and (b) in cases of naphthalene and anthracene. The values of the relative fluorescence intensities I_f/I_f^0 are plotted as a function of oxygen pressure. It is found from the curves in Fig. 4 that the quenching curve of naphthalene is almost the same as that of anthracene in spite of the large difference between the fluorescence lifetimes (4.2 ns for anthracene[23] and 100 ns for naphthalene), and the quenching by oxygen is less effective at 77°K than at room temperature. No fluorescence quenching is found at oxygen pressures below 1 Torr where phosphorescence is quenched to some extent. Fluorescence quenching occurs gradually at oxygen pressures above 1 Torr where phosphorescence is quenched to a great extent. No difference was found between the quenching curves of anthracene for both porous glass and silica gel adsorbates.

The quenching effect of oxygen on excimer fluorescence is shown in Fig. 4 (c) in the case of naphthalene (5×10^{-5} mol naphthalene per gram of porous glass). The wavelength of the excitation was fixed at 275 mμ. The relative ratio of the intensity of excimer fluorescence versus monomer fluorescence is plotted as a function of oxygen pressure. It is found from this curve that excimer fluorescence is more strongly affected by oxygen than monomer fluorescence, though the lifetime of excimer fluorescence (65 ns) is rather short compared to monomer fluorescence (100 ns). The flourescence of monomer and excimer was little quenched by nitrogen gas admitted to the sample instead of oxygen.

Liquid oxygen also showed a remarkable effect on the fluorescence of naphthalene. The fluorescence intensity of the naphthalene-porous glass adsorbate immersed in liquid oxygen condensed at 77°K was roughly 1/7 of the original intensity (I_p^0). Liquid nitrogen showed no effect on the fluorescence of adsorbed naphthalene.

23) W. R. Ware and B. A. Baldwin, *ibid.*, **40**, 1703 (1946).

Discussion

Quenching of Phosphorescence by Oxygen. As shown in Fig. 3 the dependence of I_p/I_p^0 on oxygen pressure is obviously different from that of τ_p/τ_p^0 and the curves of I_p/I_p^0 for the three compounds show almost common behavior. I_p/I_p^0 decreases rapidly with increasing the oxygen pressure and approaches to zero at oxygen pressures above 10 Torr. The lifetimes of biphenyl and naphthalene are affected a little by oxygen, but do not decrease indefinitely with increasing the oxygen pressure in such a way as the intensities do, and the values approach approximately to 1.6 and 1.4 sec, respectively, so far as we could detect the phosphorescence. On the other hand, the lifetime of α-chloronaphthalene, naturally having a short lifetime (0.2 sec), is almost constant irrespective of oxygen presure.

In the case where the quenching of phosphorescence of adsorbed organic molecules is assumed to take place by the collision of these organic molecules with oxygen (dynamic quenching model), the lifetime of phosphorescence should be shortened in the presence of oxygen. Under such a condition, the curve of the relative phosphorescence intensity, I_p/I_p^0, should be almost in accord with that of the relative phosphorescence lifetime, τ_p/τ_p^0. On the other hand, in the absence of such collisional processes, the lifetime of the observed phosphorescence should be independent of oxygen pressure. In that case, it should be assumed that only those molecules that have oxygen molecules within an effective interaction radius before excitation are nonphosphorescent (static quenching model). Our results indicate that in the case of α-chloronaphthalene, the phosphorescence quenching is due to static quenching alone and in the cases of naphthalene and biphenyl, having naturally longer lifetimes compared to the former, there exists a slight contribution from the dynamic quenching as well as the static quenching. From these results, it is suggested that the dynamic quenching process is considerably slow at 77°K in the adsorbed state, although the quantitative interpretation of the curves of τ_p/τ_p^0 is impossible because of the inhomogeneity of the surface condition. As the dynamic process is controlled by the diffusion of oxygen, the observed behaviors of τ_p/τ_p^0 should be explained by the slow surface diffusion of oxygen at 77°K. This conclusion is supported by the result of the lifetimes of biphenyl phosphorescence measured at 230°K where the diffusion of oxygen must be faster than at 77°K.

As described in the preceding paper, we have found the existence of the contact pairs between the adsorbed oxygen and organic molecules at high oxygen pressures, which give rise to the charge-transfer absorption spectra. From the absence of any observed effect of oxygen on the absorption spectra at low oxygen pressures where phosphorescence quenching occurs to a large extent, it should be concluded that no contact pairs are formed at such oxygen pressures. It may be worthwhile to add that the effect of oxygen on the phosphorescence quenching is easily removed by evacuation. As it is reported that the binding energy between oxygen and aromatics is negligible in the ground state,[3,24] it is expected that oxygen is physically adsorbed at random on the aromatic-porous glass adsorbate at low oxygen pressures and the aromatic molecules form pairs with some of the adsorbed oxygen which can have an effective interaction for the phosphorescence quenching. The amount of these pairs is considered to increase with increasing the oxygen pressure, in agreement with the observed monotonous decrease of I_p/I_p^0 at low oxygen pressures. The relative situations between the adsorbed aromatic and oxygen molecules are illustrated schematically in Fig. 5.

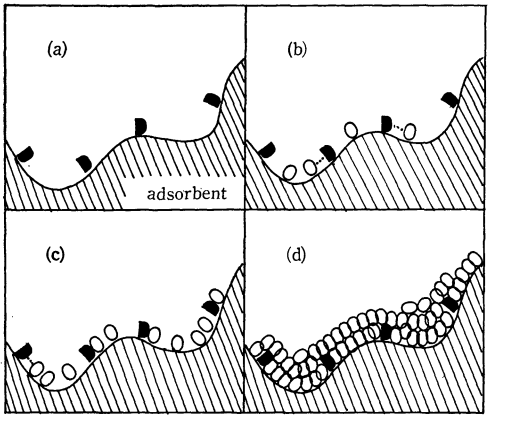

Fig. 5. Schematic illustrations indicating the relative situation between aromatic (◗) and oxygen (O) molecules in the adsorbed state. (a), before admitting oxygen; (b), at low oxygen pressures where phosphorescence quenching occurs; (c), at high oxygen pressures where contact pairs responsible for fluorescence quenching are formed between them; (d), when immersed in liquid oxygen.

Figure 6 shows the schematic potential curves for the states caused between aromatic and oxygen molecules versus the distance between them. Kearns *et al.*,[3] have suggested theoretically that a significant binding energy is expected through the interaction of triplet-state organic molecules with oxygen (curve b in Fig. 6). At a low oxygen pressure where effective phosphorescence quenching, but not the fluorescence quenching, occurs, we assume that most of the oxygen molecules are at distance r_2, or

24) H. Tsubomura and R. S. Mulliken, *J. Amer. Chem. Soc.*, **82**, 5966 (1960).

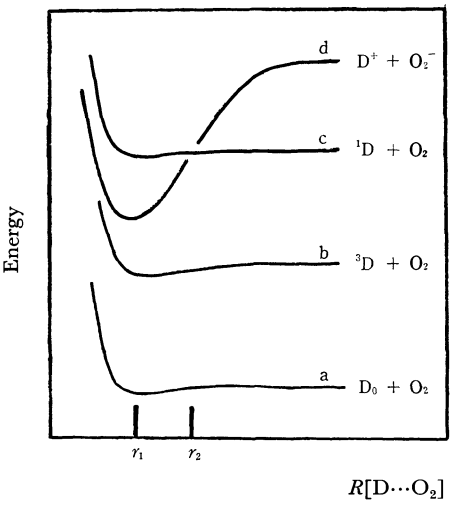

Fig. 6. Schematic potential curves for the states caused between aromatic (D) and oxygen (O_2) molecules versus the distance (R) between D and O_2. D_0 indicates the ground state of aromatic molecule. ^1D and ^3D indicate, respectively, the excited singlet and triplet states. In the adsorbed state, the intermolecular distance R is throught to decrease with increasing oxygen pressure.

larger, from the aromatic molecule D_0. When the aromatic molecule is excited to a ^3D level at such a distance, the interaction between ^3D and oxygen at that distance is thought to be sufficiently strong to cause a radiationless decay process which competes with the slow natural radiative decay process of the phosphorescent state, leading to the quenching of the phosphorescence.

Rosenberg and Humphries[17] have studied the phosphorescence quenching of acriflavine adsorbed on silica gel and suggested the existence of relatively nonphosphorescent complex between the dye and oxygen. Recently, Siegel and Judeikis[11] have investigated the oxygen quenching of naphthalene triplet state in 3-methylpentane glass at 77°K and found a slight contribution from the dynamic quenching process in addition to the static quenching process. They have also determined the effective interaction distance for the quenching to be 10.5 Å. These results seem to be consistent with our conclusion.

We have reported in the preceding paper that the S→T absorption spectrum of naphthalene is enhanced to a great extent when the naphthalene-porous glass adsorbate is immersed in liquid oxygen. The weak emission observed under such an environment may be assigned to the phosphorescence of naphthalene having a shortened lifetime, one possible explanation for this being that the T→S radiative decay process as well as the radiationless decay process is enhanced remarkably by the strong perturbation due to liquid oxygen (see Fig. 5d). The natural radiative lifetime of naphthalene triplet state, which can be calculated in the same way as described by McGlynn and Azumi[25] using the observed S→T absorption, was 9×10^{-4} sec. This value is very short compared to the unperturbed one, 11 sec,[26] in agreement with the observed shortlived emission.

Quenching of Fluorescence by Oxygen. Our results of fluorescence quenching show no difference in the characteristics between the two curves for naphthalene and anthracene despite of the large difference in their fluorescence lifetimes. This indicates that the decreases in I_f/I_f^0 are due to the static quenching alone at room temperature (21°C), and seems to indicate the surface diffusion of oxygen to be much slow compared to the decay of fluorescence. As described in the preceding paper, the extra charge-transfer absorption spectra caused through the interaction between adsorbed oxygen and organic molecules have been detected at high oxygen pressures where fluorescence quenching is observable. It can therefore be concluded that the fluorescence quenching occurs between oxygen and organic molecules in such a close contact as giving rise to the charge-transfer absorption bands, because of the fast decay of fluorescence (for example, at a distance r_1 in Fig. 6). The amount of contact pairs formed on the surface is thought to increase with increasing the oxygen pressure as Fig. 5 shows. From the results obtained for naphthalene fluorescence in liquid oxygen and at 77°K, it seems to be reasonable to assume that the radiationless decay process in contact pair becomes slow when cooled down to the low temperature and becomes comparable to the decay processes of fluorescence.

We have also found that the excimer fluorescence of naphthalene is affected more strongly by oxygen than the monomer fluorescence. This result is consistent with the earlier qualitative report on oxygen quenching of aromatic-hydrocarbon excimers in liquid solutions.[27] Chandross and Ferguson[28] found a very marked heavy-atom effect on the excimer fluorescence which can be explained by the increase in the intersystem crossing to the nearby triplet state of the excimer. Recently, the excimer phosphorescence of naphthalene has been observed in liquid solutions at low temperature.[29,30]

25) S. P. McGlynn and T. Azumi, *J. Chem. Phys.*, **40**, 507 (1964).
26) E. H. Gilmore, G. E. Gibson and D. S. McClure, *J. Chem. Phys.*, **23**, 399 (1955).
27) N. S. Bazilevskaya and A. S. Cherkason, *Opt. Spectry.*, **18**, 77 (1965).
28) E. A. Chandross and J. Ferguson, *J. Chem. Phys.*, **45**, 397 (1966).
29) J. Langelaar, R. P. H. Rettschnick, A. M. F. Lambooy and G. J. Hoytink, *Chem. Phys. Lett.*, **1**, 609 (1968).
30) G. Briegleb, H. Shuster and W. Here, *ibid.*, **4**, 53 (1969).

One possible explanation for the remarkable quenching of excimer fluorescence by oxygen is to take account of the smaller energy difference of excimer between the lowest singlet and triplet states compared to that of monomer.

The Relationship between the Oxygen Quenching and Peroxidation Reaction of Adsorbed Anthracene. Here we present the evidence for the formation of singlet oxygen ($^1\Delta_g$ or $^1\Sigma_g^+$) during the course of oxygen quenching by use of the well-established peroxidation reaction of anthracene with the singlet oxygen.[31] Anthracene adsorbed on silica gel was exposed to a known pressure of oxygen and irradiated with a 250 W high pressure Hg-lamp for five minutes at the wavelength of the first absorption band. The decrease in the first absorption band of anthracene due to the formation of anthracene peroxide was measured by use of the reflection method[1] as a function of oxygen pressure. The result is shown in Fig. 4 (a). The decrease of the anthracene absorption is seen to occur at low oxygen pressures where no fluorescence quenching is observed, although no decrease was observed by the irradiation of the sample without oxygen. This result has thus provided a rigorous experimental proof for the formation of singlet oxygen through the interaction between oxygen and triplet-state anthracene. The rate of peroxidation reaction showed a tendency to become independent of oxygen pressure in the region of high oxygen pressures where the fluorescence quenching begins to be observed and, no characteristic relationship was obtained between the rate of the peroxidation and the fluorescence quenching by oxygen. This seems to indicate that the singlet oxygen is not formed through the interaction with anthracene in the singlet excited state. However, further detailed experimental and theoretical investigations are necessary in order to establish the mechanism of fluorescence quenching by oxygen.

The authors are indebted to Professor N. Mataga and Mr. H. Ohari for the measurement of fluorescence lifetimes by use of a nanosecond flash apparatus.

31) B. Stevens and B. E. Algar, *J. Phys. Chem.*, **72**, 3468 (1968).

BULLETIN OF THE CHEMICAL SOCIETY OF JAPAN VOL. 43 3136—3142 (1970)

The Effect of Intramolecular Hydrogen Bonding on the Polarographic Reduction Potentials of Azomethines[1)]

Miyoshi UEHARA and Jun-ichi NAKAYA

Department of Chemistry, Faculty of Liberal Arts and Sciences, University of Osaka Prefecture, Mozu-Umemachi, Sakai-shi, Osaka

(Received January 16, 1969)

The effects of intramolecular hydrogen bonding on the polarographic reduction potentials ($E_{1/2}$) of several azomethines, such as *N*-salicylidenemethylamine, *N*,*N'*-bis(salicylidene)ethylenediamine, *N*-salicylideneaniline, *N*-salicylidene-*o*-aminophenol, and *N*-benzylidene-*o*-amino-*p*-substituted phenols, have been studied in aqueous and non-aqueous solutions. Contrary to expectations, a larger negative shift of $E_{1/2}$ was observed in the case of *o*-OH-substituted azomethines than in that of unsubstituted azomethines in buffer solutions. On the other hand, the $E_{1/2}$ of the substituted compounds shifted 0.3—0.4V toward the positive side in dimethylformamide or acetonitrile. The relative strengths of hydrogen bonds, as estimated from the positive shifts of $E_{1/2}$, were 6—10 kcal/mol. It has been proposed, from the hydrogen bond strength, the UV spectra, and the *p*-substituent effects, that the introduction of an *o*-OH group into the phenylimino ring provides not a periperpendicular conformation, but a coplanar configuration, by means of the formation of the O–H···N hydrogen bond.

The effects of intramolecular hydrogen bonds due to an *o*-OH substituent on the polarographic reduction potentials indicate a positive shift in contrast to the case with unsubstituted compounds because of the electron-withdrawing character of its substituent. These effects have actually been observed

1) Presented partly at the 16th Annual Meeting of the Chemical Society of Japan, Tokyo, April, 1963 and the 19th Symposium of Polarography, Osaka, Nov., 1967. Paper IV in a series of "Polarography of Azomethine Compounds."

with respect to *o*-nitrophenol by Astle,[2-4] Page,[5] and Pearson[6] in a buffer solution (pH<9). On the other hand, in the case of salicylaldehyde[7] or *o*-hydroxyacetophenone,[7] a negative potential shift of 50—70 mV was obtained for $E_{1/2}$, the potential shift by *o*-OH substituent in this case appears as an electron-donating effect. Doubts regarding the effects of hydrogen bonds on $E_{1/2}$[8] have recently been discussed by Zuman.[9]

We have first investigated polarographically the effects of intramolecular hydrogen bonding with several azomethines in aqueous solutions, in order to interpret the contradictory results for *o*-OH substituent and unsubstituted azomethines in previous works. It is believed that *o*-hydroxyazomethines probably form stronger hydrogen bonds than those of nitrophenol and salicylaldehyde because their O–H···N bond is more stable than the O–H···O bond, this is because of their larger polarizable structure between hetero atoms.

Secondly, we investigated the effect of intramolecular hydrogen bonding in an aprotic solvent, such as dimethylformamide (DMF) and acetonitrile (AN). Since the polarographic electrode reduction process of azomethine is accompanied by proton participation,[10] the study of such an aprotic solvent may be useful for estimating the relative strengths of hydrogen bonds.

Lastly, it has been shown that several interpretations can be made on the basis of the findings on hydrogen-bond strengths and UV spectra, especially at the N-side *o*-OH hydrogen bond of azomethines. If a "periperpendicular conformation[11-13]" can be assumed for *N*-benzylidene-*o*-aminophenols, it can be expected that the substituent effect will not appear at the *N*-side of the –CH=N– bond. These effects on $E_{1/2}$ were investigated in an aprotic solvent.

It can be considered that, together with spectroscopic data such as the IR and NMR data, the polarographic reduction potentials obtained in an aprotic solvent are useful values for studying hydrogen bonds.

Experimental

Materials. The azomethines used as samples were synthesized by the condensation of the corresponding aldehydes and amines in absolute ethanol. The bps and mps of the azomethines used were as follows: (I) *N*-salicylidenemethylamine bp 229°C, (II) *N*-benzylidenemethylamine bp 185°C, (III) *N,N'*-bis(salicylidene)ethylenediamine mp 125—126°C, (IV) *N,N'*-bis(benzylidene)ethylenediamine mp 53—54°C, (V) *N*-salicylideneaniline mp 50—51°C, (VI) *N*-benzylideneaniline mp 52°C, (VII) *N*-salicylidene-*o*-aminophenol mp 184—186°C, (VIII) *N*-benzylidene-*o*-aminophenol mp 89—90°C, (IX) *N*-benzylidene-*o*-amino-*p*-chlorophenol mp 94.2°C, (X) *N*-benzylidene-*o*-amino-*p*-methylphenol mp 88—88.5°C, (XI) *N*-(*o*-methoxybenzylidene)-aniline bp 91°C/5 mmHg, (XII) pyridinealdehyde-(2)-phenylhydrazone(syn-form) mp 88°C, and (XIII) pyridinealdehyde-(2)-phenylhydrazone(anti-form) mp174°C. The other samples, nitro- and aldehyde- compounds, were purified by the distillation or recrystallization of commercial guaranteed reagents. The DMF and AN were purified as has been described by Hatano[14] and by Coetzee[15] respectively. The water content of the DMF, as determined by Karl Fisher titration, was 0.03%.

Apparatus. All the polarograms were obtained by using a Yanagimoto pen-recording polarograph, Model PA-102. The dropping mercury electrode had the following characteristics on an open circuit: a value of $m^{2/3}t^{1/6}=0.99$ $mg^{2/3}sec^{-1/2}$ was obtained at $h=49$cmHg in distilled water, or under the same capillary conditions, a value of $m^{2/3}t^{1/6}=1.18$ $mg^{2/3}sec^{-1/2}$ was obtained in DMF. An aqueous saturated calomel electrode (SCE) was used as the external reference. The electric connection between the SCE and the non-aqueous solution in the polarographic cell was made by means of a DMF-methylcellulose bridge. The IR drop was corrected by measuring the ohmic resistance between the cathode and the anode with a Yokogawa universal bridge, Type BV-Z-13B. All the potentials were corrected with a Shimazu DC potentiometer, Type 3P. The UV spectra were obtained with a Hitachi, Type EPU-2A, spectrophotometer. The pH measurement was done with a Hitachi Model P glass electrode pH meter.

Procedure. The polarographic measurements were carried out with a 0.5 mmol/*l* depolarizer concentration in DMF or AN in which 0.1 mol/*l* n-Bu_4NClO_4 had been dissolved or in a Britton-Robinson buffer solution containing 50% ethanol and at a constant temperature of 20±0.5°C.

In a buffer solution, we used a method in which the hydrolysis of azomethines was avoided. Nitrogen was

2) M. J. Astle and W. V. McConell, *J. Amer. Chem. Soc.*, **65**, 35 (1943).
3) M. J. Astle and W. P. Cropper, *ibid.*, **65**, 2395 (1943).
4) M. J. Astle and S. P. Stephenson, *ibid.*, **65**, 2399 (1943).
5) J. E. Page, J. W. Smith and J. G. Waller, *J. Phys. and Colloid Chem.*, **53**, 545 (1949).
6) J. Pearson, *Trans. Faraday Soc.*, **45**, 199 (1949).
7) D. M. Coulson, W. R. Crowell and S. K. Tendick, *J. Amer. Chem. Soc.*, **79**, 1354 (1957).
8) S. F. Dennis, A. S. Powell and M. J. Astle, *ibid.*, **71**, 1484 (1949).
9) P. Zuman, "Substituent Effects in Organic Polarography," Plenum Press, New York, N.Y. (1967), p. 94.
10) L. Holleck and B. Kastening, *Z. Elektrochem.*, **60**, 127 (1956).
11) N. Ebara, This Bulletin, **33**, 534 (1960).
12) V. A. Izmailskii and E. A. Smirnov, *Zh. Obshch. Khim.*, **26**, 3042 (1956); *Chem. Abstr.*, **51**, 7145 (1957).
13) E. Haselbach, E. Heilbronner, *Helv. Chim. Acta*, **51**, 16 (1968).
14) M. Hatano, T. Yasukawa and M. Yoneyama, *Bull. Chem. Res. Inst. Non-aq. Sol. (Tohoku Univ.)*, **18**, 155 (1968).
15) J. F. Coetzee, G. P. Cunningham, D. K. McGuire and G. R. Padmanabhan, *Anal. Chem.*, **34**, 1139 (1962).

passed through a base solution of 4.5 m*l* in the polarographic cell in order to remove the dissolved oxygen; to this we then added 0.5 m*l* of a sample stock solution which had previously been deaerated with nitrogen, the polarogram was recorded immediately after the solution had become homogeneous by bubbling in nitrogen.

Results and Discussion

Half-wave Potentials in a Buffer Solution. The half-wave potentials of the first reduction waves on *o*-OH substituted and unsubstituted azomethines were measured in a neutral pH range from 7 to 9, because their hydrolysis rates are large in an acidic medium[16] and because OH substituents dissociate in an alkaline medium.[17] The results are given in Fig. 1. The effect of the *o*-OH group on potentials between *N*-salicylidenemethylamine (I) and *N*-benzylidenemethylamine (II) proved to be a negative shift; this was contrary to the expectation of the positive shift as a result of intramolecular hydrogen bond formation, and the shifted value was 110—120 mV. This value is approximately equal to the negative shift of 90 mV for *p*-hydroxybenzylideneaniline[18] or to that of 120 mV for *p*-hydroxybenzaldehyde.[7] Thus, in the case of (I), the function of the *o*-OH substituent is not electron acceptance but electron donation; similar observations were made in the cases of salicylaldehyde and *o*-hydroxyacetophenone.[7] Most of the similar negative ortho shifts are shown in the data concerning the other compounds in Fig. 1, but in the case of III the reverse shift appears partly at low pH values.

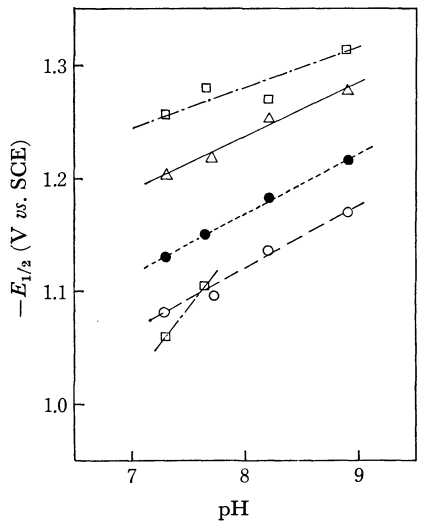

Fig. 1-a. $E_{1/2}$ in buffer solution. Triangle: *N*-salicylidenemethylamine, White Circle: *N*-benzylidenemethylamine, Square: *N,N'*-bis(salicylidene)-ethylenediamine, Filled Circle: *N,N'*-bis(benzylidene)ethylenediamine.

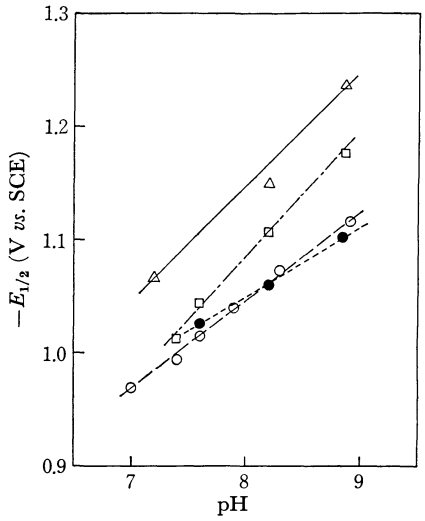

Fig. 1-b. $E_{1/2}$ in buffer solution. Triangle: *N*-salicylideneaniline, White Circle: *N*-benzylideneaniline, Square: *N*-salicylidene-*o*-aminophenol, Filled Circle: *N*-benzylidene-*o*-aminophenol.

It can be considered that there are two different types of intramolecular hydrogen bonds formed by the *o*-OH substituent. As the half-wave potentials of functional groups, such as $-NO_2$, $>C=O$, and $-CH=N-$, depend upon the hydrogen-ion concentration in an aqueous solution, the participation of a proton which accompanies the electron-transfer process in an electrode double layer should not be ignored. However, the participation of a proton

Table 1. The effects of OH group on $E_{1/2}$ Sample: 0.5 mmol/*l* in DMF

Compound	$E_{1/2}$ (V *vs.* SCE)	$\Delta E_{1/2}$ *o*-	*m*-	*p*-
$C_6H_5-CH=N-C_6H_5$	−1.90	+0.31*1		−0.05
		−0.01*2		
		+0.34*3		
		+0.32*4		
$(C_6H_5-CH=N-CH_2)_2$	−2.27	+0.45		
$C_6H_5-CH=N-CH_3$	−2.27	+0.38		
$C_6H_5-NO_2$	−1.13	+0.25	−0.01	−0.05
C_6H_5-CHO	−1.83	+0.20	+0.01	−0.05
		−0.01*5		

The values marked * represent the data in the following substitution.
*1 *o*-OH on benzylidene
*2 *o*-OCH_3 on benzylidene
*3 *o*-OH on phenylimino
*4 *o*-OH groups on both phenyl rings
*5 *o*-OCH_3 group on phenyl

16) B. Kastening and L. Holleck, *Z. Elektrochem.*, **60**, 130 (1956).
17) R. L. Reeves, *J. Org. Chem.*, **30**, 3129 (1965).
18) M. Uehara, *Nippon Kagaku Zasshi*, **86**, 901 (1965).

in the case of $-NO_2$ may be less active than that of >C=O and -CH=N- because of its stronger resonance effect. Thus, the hydrogen bond in *o*-nitrophenol is probably held in a favorable form for its reduction transition state. On the other hand, it is considered that the hydrogen bond in salicylaldehyde or salicylidenemethylamine is first replaced by proton addition in the diffusion layer and that the *o*-OH substituent acts as an electron donor.

Half-wave Potentials in a Non-aqueous Solvent. The effects of intramolecular hydrogen bonds on polarographic half-wave potentials were investigated under condition in which the potentials could be determined simply by the electron-transfer process. Therefore, the effects of hydrogen bonds on salicylideneamines and also on salicylaldehyde and nitrophenol were observed in DMF, an aprotic solvent, by comparing the difference in $E_{1/2}$'s between *o*-, *m*-, *p*-hydroxy-, or methoxy- substituted and unsubstituted compounds. In Table 1, the $E_{1/2}$ and $\Delta E_{1/2}$ values for these compounds are given, where $\Delta E_{1/2}$ is the difference in $E_{1/2}$ between *o*-, *m*-, and *p*-substituted and unsubstituted compounds. The effects of the *o*-OH substituent on $E_{1/2}$ appear as a uniform positive potential shift in the range of 0.20—0.45 V; this shift is considerably larger than the usual *m*- and *p*- substituent effect on $E_{1/2}$ which has been known in polarography.[18] In the case of the introduction of an OH group into the *m*- or *p*-position, and when it is impossible for a hydrogen bond such as OCH_3 to be formed even in the *o*-position, the negative shift of $E_{1/2}$ takes place because of the effect of their electron donor. The same behavior was observed in the AN (Table 2) used as an aprotic solvent.

Table 2. The effects of OH group on $E_{1/2}$ Sample: 0.5 mmol/*l* in AN

Compound	$E_{1/2}$ (V *vs.* SCE)	$\Delta E_{1/2}$		
		o-	*m*-	*p*-
C_6H_5-CH=N-C_6H_5*	−1.87	+0.31		−0.04
C_6H_5-NO_2	−1.09	+0.23	+0.06	+0.01
C_6H_5-CHO	−1.78	+0.19	−0.01	−0.02

* OH substituent on benzylidene

For most of the compounds investigated in DMF, the polarographic Nernstian slopes (α) were similar to each other concerning the *o*-OH substituted compounds and the unsubstituted ones: α=62 mV (*N*-salicylideneaniline), 65 mV (*N*-benzylideneaniline), 58 mV (*N*-salicylidene-*o*-aminophenol), 65 mV (*N*-salicylidenemethylamine), 68 mV (*N*-benzylidenemethylamine), 63 mV (salicylaldehyde), 60 mV (benzaldehyde), 57 mV (*o*-nitrophenol), and 60 mV (nitrobenzene). The above facts suggest that the contribution of the irreversible process in the polarographic reduction may be approximately the same between the *o*-OH substituted compound and the unsubstituted compound. Concerning the polarographic reduction in the aprotic medium, it was expected that $E_{1/2}$ would be determined entirely by the electron-transfer process.

As for the reduction mechanism, it has recently been shown that the azomethines are reduced irreversibly to secondary amines in an aprotic medium through the stage of the formation of free radicals.[19,20] About the half-wave potentials of irreversible systems, the following relationship was derived by Delahay:[21]

$$E_{1/2} = \frac{RT}{\alpha nF} \ln 0.87\, k_f \sqrt{\frac{l}{D}}$$

The reduction mechanism and the values of the transfer coefficient, α, are similar when these compounds are compared, and these substances do not differ substantially in molecular shape or weight. Therefore, the influence of the substituent on the $E_{1/2}$ may be accounted for by the change in the free-activation-energy increment.[22,23]

$$\Delta E_{1/2} \sim \Delta\Delta F^{\pm}$$

The bulk of the azomethine molecules having *o*-OH groups must have been little changed by the formation of the intramolecular hydrogen bond. Therefore, the difference between the entropy change terms ($T\Delta S^{\pm}$) may be neglected compared with that of the enthalpy change ($\Delta H^{\pm}$).
Hence,

$$\Delta E_{1/2} \sim \Delta\Delta H^{\pm}$$

where $\Delta\Delta H^{\pm}$ is regarded as the difference in the lowest vacant MO energy[24] between the hydrogen bonding molecule in the *o*-OH substituted azomethine and the non-hydrogen bonding one. The strengthening of the hydrogen bond due to the electrostatic and mesomeric effects[25] may be considered to result in a lowering of the lowest vacant MO energy. The quite positive shifts of $E_{1/2}$ upon the introduction of an *o*-OH group can be attributed to the decrease in the electron density of the reducible position due to the formation of an intra-

19) L. V. Kononenko, V. D. Bezuglyi and V. N. Dmitrieva, *J. Gen. Chem.*, **38**, 2087 (1968); *Zhur Obshch. Khim.*, **38**, 2153 (1968).
20) S. Ono and M. Uehara, *Denki Kagaku*, **27**, 93 (1959).
21) P. Delahay, *J. Amer. Chem. Soc.*, **75**, 1480 (1953), **76**, 5417 (1954).
22) P. Zuman, "Substituent Effects in Organic Polarography," Plenum Press, New York, N. Y. (1967), p. 25.
23) P. Zuman, *Rev. Polarography*, **11**, 103 (1963).
24) S. Koide, "Polarography," Vol. 3, Nankodo, Tokyo (1965), p. 83.
25) L. N. Ferguson, "The Modern Structural Theory of Organic Chemistry," Translated ed. by M. Ōki, M. Hirota, H. Iwamura and K. Mutai, Tokyo Kagaku Dōjin, Tokyo (1965), p. 128.

molecular hydrogen bond. The facts in Table 1 suggest that the increase in $\Delta E_{1/2}$ may be caused by a strengthening of the hydrogen bond, and the $\Delta E_{1/2}$ is probably related to the relative hydrogen bond strength. Effects other than those of the hydrogen bond in the above case, *i.e.*, the contribution of an inductive effect as a usual electron donor of the OH group, is quite small, as is observed in the case of the $\Delta E_{1/2}$ of the *m*-OH and *o*-OCH_3 groups.

It was confirmed by the invariability of $E_{1/2}$ with the change in sample concentration that the hydrogen bond in this case is not intermolecular, but intramolecular. The invariability of $E_{1/2}$ at varying *N*-salicylideneaniline concentrations is shown in Table 3. In addition, the linear relationship between the concentration of sample and the limiting current seems to show that the diffusion coefficient resulting from the formation of an intermolecular hydrogen bond has not decreased (Table 3).

Table 3. Influence of concentration of hydrogen bonding molecule on $E_{1/2}$
Sample: *N*-Salicylideneaniline in DMF

Concn. mmol/*l*	$E_{1/2}$ V *vs.* SCE	i_d μA
0.1	−1.58	0.13
0.2	−1.58	0.25
0.3	−1.58	0.39
0.5	−1.58	0.62
0.7	−1.58	0.90
1.0	−1.57	1.21

Effects of Proton Donors on Half-wave Potentials in a Non-aqueous Solvent. The effects of several proton donors in a non-aqueous solvent on $E_{1/2}$ were investigated in order to study the intramolecular hydrogen bond in detail. When phenol, a proton donor, was added to *N*-benzylideneaniline (VI) in DMF, a new wave (*ba*°) appeared at the (−1.77 V) potential, a little more positive than the half-wave potential (−1.90 V) of the wave (*ba*) of VI (Fig. 2). An increase in the phenol concentration caused the (*ba*°) wave to increase at the expense of the (*ba*) wave. The addition of excess phenol to VI caused the (*ba*) wave to be replaced by the (*ba*°) wave. The effect of the addition of phenol on the reduction of VI may be attributed to the formation of the hydrogen-bonded complex that is reduced at a potential more positive than that of VI (wave (*ba*)). Similar behavior was observed regarding the influence of benzoic acid, as is shown in Fig. 3. However, no such effect of the acid was found with relation to the wave of *N*-salicylideneaniline (V) under the same conditions, and the $E_{1/2}$ (−1.58 V) of V remained constant. It may, therefore, be considered that the intramolecular hydrogen bond of the *o*-OH group in (V) prevents phenol from going close to the nitrogen atom. It seems reasonable to consider that the above facts support the existence and functions of the intramolecular hydrogen bond in V and the intermolecular hydrogen bond be-

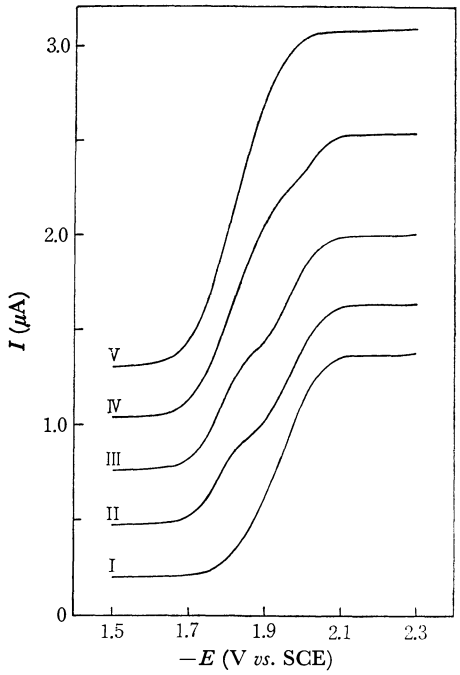

Fig. 2. Influence of phenol on the $E_{1/2}$ of *N*-benzylideneaniline. Sample: 0.5 mmol/*l*. Phenol (mmol/*l*): I) 0; II) 0.1; III) 0.2; IV) 0.5; V) 2.0.

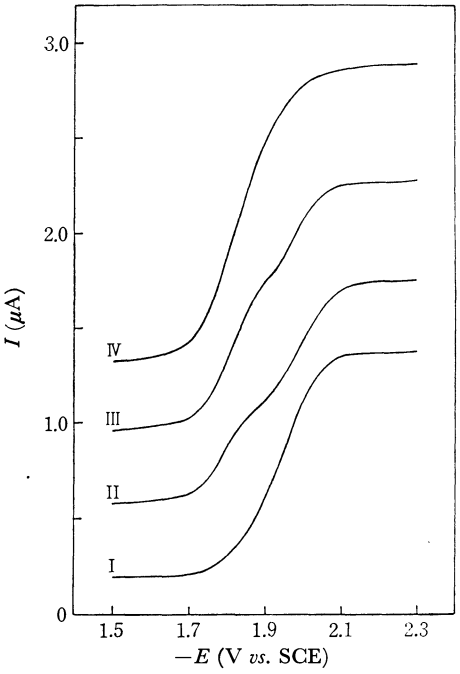

Fig. 3. Influence of benzoic acid on the $E_{1/2}$ of *N*-benzylideneaniline. Sample: 0.5 mmol/*l*. Phenol (mmol/*l*): I) 0; II) 0.1; III) 0.2; IV) 0.5.

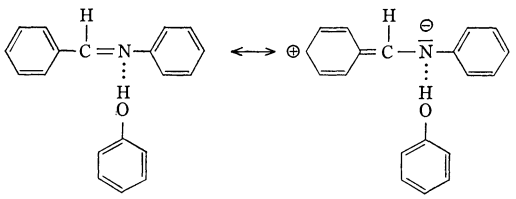

tween VI and phenol.

Some Interpretations Regarding the Relative Hydrogen-bond Strength. As has been explained in detail above, the effect of a positive shift of $E_{1/2}$ on several azomethine hydrogen bonds was evaluated to be from 0.31 to 0.45 V. In order to obtain some information on a six-membered ring hydrogen bond for azomethines, the $E_{1/2}$ of pyridinealdehyde-(2)-phenylhydrazone was measured in DMF. As a result it was found that it was −2.03 V for the *anti*-form (XIII) and −1.99 V for the *syn*-form (XII); the shifted values were so small as to be negligible. Thus, the structure required for a positive shifts as the effect of a hydrogen bond seems to be one in which the hydrogen bond is formed adjacent to the polarographic functional group, -CH=N-.

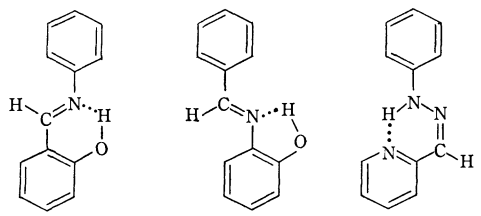

It can be understood from the data of the controlled potential electrolysis[19,20] and the electron paramagnetic resonance spectra[26] that the first step in the polarographic reduction of azomethines is due to a one-electron reduction corresponding to the formation of their anion radical. Therefore, if it is assumed that the $\Delta E_{1/2}$ of *N*-salicylideneaniline obtained from the measurement in DMF is 0.31 eV, the relative strength of the hydrogen bond can be estimated to be 7.1 kcal/mol for this molecule; this agrees with the value of 7 kcal/mol as the mean energy of the O-H···N hydrogen bond.[25] On the other hand, the relative hydrogen bond strength for the *o*-nitrophenol (5.8 kcal/mol), as estimated from the $\Delta E_{1/2}$, agrees with the mean energy, 6 kcal/mol, of the O-H···O hydrogen bond.[25] The relative strengths of the hydrogen bonds obtained from $\Delta E_{1/2}$ can be considered as being appropriate values because they agree with the values in the literature.[25]

Some increase in $\Delta E_{1/2}$ resulted from the introduction of a strong electron-donating substituent into the N-side of such azomethines as *N*-salicylidenealkylamines. It can thus be inferred that the O-H···N hydrogen bond is tightly bound by electrostatic attraction between nitrogen and hydrogen, and that the larger the electron density at N, the larger is the bond energy. The relative strength of the hydrogen bond in *N*-salicylidenemethylamine estimated from $\Delta E_{1/2}$ was about 8.8 kcal/mol.

The strength of the hydrogen bond in *N*-benzylidene-*o*-aminophenol etsimated from $\Delta E_{1/2}$ is much larger than the usual O-H···π hydrogen-bonding energy of 2 kcal/mol.[25] Therefore, it is entirely impossible to suppose an O-H···π hydrogen bond in the molecule; the O-H···N hydrogen bond should be supposed in this case.

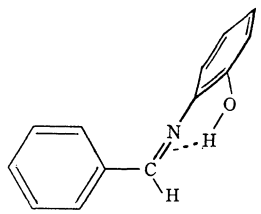

Coplanarity of the Molecular Structure due to Hydrogen Bonding. It has been reported in detail that the azomethine molecule exists as a stable non-planar conformation in which the dihedral angle between the N-side phenyl and the rest of the molecule plane is distorted (periperpendicular conformation[11,12]). This interpretation was recently supported by Haselbach *et al.*[13] They showed that the absorption maxima on *trans*-stilbene and on *trans*-azobenzene were situated at wavelengths of about 230 and 320 mμ, while those of *N*-benzylideneaniline were at 262 and 315 mμ in cyclohexane. Moreover those data indicated that the absorption maximum of *N*-benzylideneaniline in concentrated sulfuric acid shifted to the longer wavelength of 340 mμ; this value agreed with that of 3,3-dimethyl-2-phenyl-indolenine. We have also measured some azomethines in absolute ethanol; the results are listed in Table 4.

In the case of *N*-benzylideneaniline (VI), the absorption maximum of the longer wavelengths (306—310 mμ) agrees approximately with the previ-

Table 4. UV spectra of azomethines in absolute ethanol

Azomethines	λ (mμ)	ε ($\times 10^3$)	λ' (mμ)	ε' ($\times 10^3$)
I	253—255	11.6	320—322	3.6
II	244	14.9	280	1.0
III	254—257	21.7	316	8.8
IV	247—248	30.0	280	3.6
V	269	14.3	338	13.1
VI	262	16.9	306—310	8.8
VII	266	10.3	346	11.6
VIII	261	12.8	344	7.2

26) J. M. W. Scott and W. H. Jura, *Can. J. Chem.*, **45**, 2375 (1967).

ous datum (315 mλ) and also with that of *N*,*N*′-bis(salicylidene)ethylenediamine (III) (316 mμ). It should also be noted that the maximum of the longer wavelength of VI was observed to be 344 mμ in the case of *N*-benzylidene-*o*-aminophenol (VIII). It is possible to give a new interpretation of this compound on the basis of these phenomena; *i.e.*, the two phenyl-rings are probably not distorted because of the hydrogen bond. In this compound, the value of 7.8 kcal/mol estimated to be the relative strength of the hydrogen bond from the $\Delta E_{1/2}$ value of 0.34 eV is slightly larger than that of *N*-salicylideneaniline (V).

Table 5. Half-wave potentials of *N*-benzylidene-*o*-amino-*p*-substituted phenols in DMF

Substituent	$E_{1/2}$ (V *vs.* SCE)	$\Delta E_{1/2}$
Cl	−1.45	+0.11
H	−1.56	
CH_3	−1.58	−0.02

ρ=0.30 V

The effect of *N*-phenyl-substituents on $E_{1/2}$ was investigated for *N*-benzylidene-*o*-aminophenols. As is shown in Table 5, the substituent effect appeared as the potential shift to negative upon the introduction of an electron donor, and as the shift to positive upon the introduction of an electron acceptor. The reaction constant that was obtained from a linear correlation between the reduction potentials and Hammett's substituent constants was 0.30V, similar to those of substituted benzaldehydes (0.31V), benzophenoneoximes (0.30V), stilbenes (0.25V), *etc.* The above results could not be interpreted by periperpendicular conformation. Therefore, the phenyl-ring of the N-side becomes a structure completely co-planar with the rest of the molecular plane, and the effect on $\Delta E_{1/2}$ seems to be one in which a special conjugation effect has been added to the usual hydrogen-bonding effect.

In Table 4, the hypsochromic shifts of the longest wavelength bands upon the introduction of an *o*-OH substituent were obtained with the following values: *N*-salicylideneaniline, 30 mμ; *N*-benzylidene-*o*-aminophenol, 35 mμ; and *N*-salicylidenealkylamines, 36—40 mμ; these values are directly proportional to the relative strengths of the hydrogen bonds of 7.1, 7.8, and 8.8—10.4 kcal respectively as calculated from the polarographic half-wave potentials.

The authors wish to thank Mr. Yasumichi Nakamura for his technical assistance.

BULLETIN OF THE CHEMICAL SOCIETY OF JAPAN VOL. 43 3143—3149 (1970)

An ESR Study of Monomeric Cobalt Oxygen Complexes in Solutions

Seiichiro KODA, Akira MISONO and Yasuzo UCHIDA

Department of Industrial Chemistry, Faculty of Engineering, University of Tokyo, Hongo, Bunkyo-ku, Tokyo

(Received January 12, 1970)

Several mononuclear cobalt oxygen complexes in solutions have been investigated by means of ESR measurements. When a pyridine (and also substituted pyridines, *N*,*N*-dimethylformamide, dimethyl sulfoxide, and hexamethylphosphoramide) solution of a bis-salicylaldehyde-imine cobalt(II) complex (*N*,*N*′-ethylene-bis(salicylideneiminato)cobalt(II), and *N*,*N*′-ethylene-bis(3-methoxysalicylideneiminato)cobalt(II)) was exposed to oxygen, there appeared a reversible ESR signal, in which a hf structure of eight lines caused by a mononuclear cobalt was observed. This spectrum could be analysed by considering the species to be essentially a superoxide cobalt(III). We tried to explain the deviations in the A_{Co} and the *g* values of the species from solvent to solvent by considering that the solvent coodinates to the cobalt complex in the *trans* position against the coodinated oxygen. As a comparative study, the mononuclear oxygen adduct of di(salicylal)-3,3′-diimino-di-*n*-propylamine-cobalt(II) was also studied in the above solvents.

Though cobalt complexes carrying molecular oxygen have long been known, most of these are 2 : 1 cobalt oxygen adducts. Only recently have several examples of 1 : 1 reversible O_2 adducts been reported;[1-8] these reports have kept pace with the study of the present authors, who have investigated the possibility of obtaining mononuclear cobalt oxygen complexes and the physico-chemical properties of the obtained complexes for the past several years. Some of these results have already been reported.[1-3]

In this paper, the authors wish to report an ESR study of mononuclear cobalt oxygen complexes which may exist equilibrially ($Co \overset{O_2}{\rightleftharpoons} Co\text{–}O_2 \overset{Co}{\rightleftharpoons} Co\text{–}O_2\text{–}Co$) in some solutions. Several bis-salicylaldehyde-imine cobalt(II) complexes were dissolved in certain solvents under oxygen. The equilibrially-obtained mononuclear cobalt oxygen complexes were analysed by means of ESR measurements, though no reliable quantitative studies could be carried out because most of the solvents used were such as absorbed considerable microwave energies.

Results

The attempted complexes were *N*,*N*′-ethylene-bis(salicylideneiminato)cobalt(II)(Co(salen)), *N*,*N*′-ethylene-bis(3-methoxysalicylideneiminato)cobalt(II) (Co(3-MeOsalen)), bis(salicylaldimino)cobalt(II) (Co(sa)), and di(salicylal)-3,3′-diimino-di-*n*-propylamine-cobalt(II) (Co(salprtr)).

From the point of view of the solubility, Co(3-MeOsalen) was mainly investigated. When Co-(3-

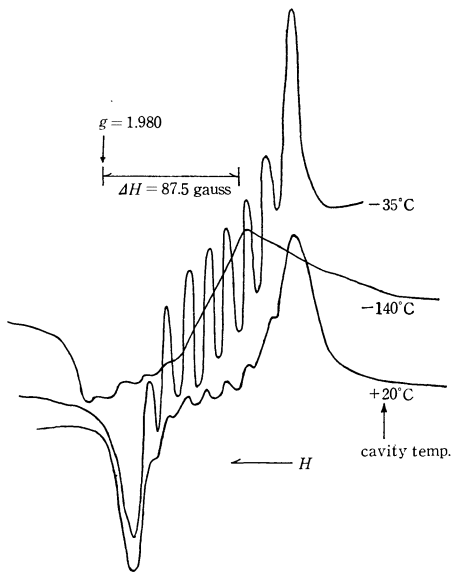

Fig. 1. ESR spectra of Co(3-MeOsalen) in pyridine under oxygen.
complex concn. = 1.4×10^{-2} mol/*l*
oxygen pressure = 1 atm

1) A. Misono, S. Koda and Y. Uchida, This Bulletin, **42**, 580 (1969).
2) A. Misono, S. Koda and Y, Uchida, *ibid.*, **42**, 3470 (1969).
3) A. Misono and S. Koda, This Bulletin, **42**, 3048 (1969).
4) H. Kon and N. E. Sharpless, *Spectrosc. Lett.*, **1**, 49 (1968).
5) J. H. Bayston, F. D. Looney and M. E. Winfield, *Aust. J. Chem.*, **16**, 557 (1963).
6) J. H. Bayston, N. K. King, F. D. Looney and M. E. Winfield, *J. Amer. Chem. Soc.*, **91**, 2775 (1969).
7) C. Floriani and F. Calderazzo, *J. Chem. Soc., A*, **1969**, 946.
8) A. L. Crumbliss and F. Basolo, *Science*, **164**, 1168 (1969).

MeOsalen) was dissolved in pyridine under nitrogen, a transparent red solution was obtained. The solution under nitrogen showed no ESR signal at room temperature.

When oxygen was added to the solution (oxygen was bubbled in or the nitrogen atmosphere above the solution was purged by pure oxygen), the red color of the solution under nitrogen was strengthened to some degree. The solution under oxygen showed an ESR signal which had an eight-line structure, as is shown in Fig. 1. The eight-line structure, all the lines of which had almost the same strength, could be considered to be caused by a certain interaction of a free spin with one cobalt nucleus, because the nuclear spin of ^{59}Co is 7/2. Spectra which were a little more resolved were observed at lower temperatures. When the solution was frozen, the spectrum changed to an anisotropic spectrum, but it was not so well resolved. This signal was observed to be rather stable. In fact, the strength of the signal did not decrease very much within several hours under oxygen at room temperature.

The ESR signal decreased when the solution was exposed to nitrogen, and increased again when the solution was again exposed to oxygen. The signal was suspected, therefore, to be due to a certain oxygen complex which was formed reversibly in the solution from oxygen and the cobalt complex.

Similar spectra could be observed in substituted pyridines, *N,N*-dimethylformamide (DMF), dimethyl sulfoxide (DMSO), and hexamethylphosphoramide (HMPT).

The ESR characteristics are summarized in Table 1. The A_{sol} caused by a cobalt nucleus is the mean interval between two adjacent lines among the eight lines (observed in solutions). The best resolved isotropic spectra were observed in the neighborhood of the cavity temperature described in the table. Some observed results in mixed solvents are shown in Table 2. In these mixed solvents, similar spectra were observed.

TABLE 1. ESR SPECTRA OF THE COMPLEXES IN SEVERAL SOLVENTS UNDER OXYGEN

Complex	Solvent (10^{-2} mol/l)	g_{sol}	A_{sol} (gauss)	Cavity temp. (°C)
Co(salen)	pyridine (2.3)	2.023	12.9	−37
Co(3-MeO-salen)	pyridine (1.4)	2.023	12.8	−35
	4-Mepyridine (1.7)	2.022*	13*	+20
	4-Etpyridine (1.7)	2.022	12.8	−10
	DMF (1.4)	2.028	17.0	−15
	DMSO (1.7)	2.028	17.3	+20
	HMPT (2.0)	2.022	19.0	+20
	toluene-PPh_3 (2.2, PPh_3/Co=17/1)	2.024	15.3	−35
Co(salprtr)	pyridine (1.6)	2.033	14.4	+20
	DMF (2.5)	2.033	14.4	+10
	HMPT (2.0)	2.030*	13.6*	+20

*: not well resolved, P_{O_2}=1 atm

TABLE 2. ESR SPECTRA OF Co(3-MeOsalen) IN MIXED (1/1 vol) SOLVENTS UNDER OXYGEN

Solvent (10^{-2} mol/l)	g_{sol}	A_{sol} (gauss)	Cavity temp. (°C)
pyridine - DMF (0.9)	2.023	12.8	−10
pyridine - HMPT (2.2)	2.023	13.2	− 5
DMF - HMPT (1.6)	2.026	17.7	+ 7
cf.			
pyridine (1.4)	2.023	12.8	−35
DMF (1.4)	2.028	17.0	−15
HMPT (2.0)	2.022	19.0	+20

P_{O_2}=1 atm

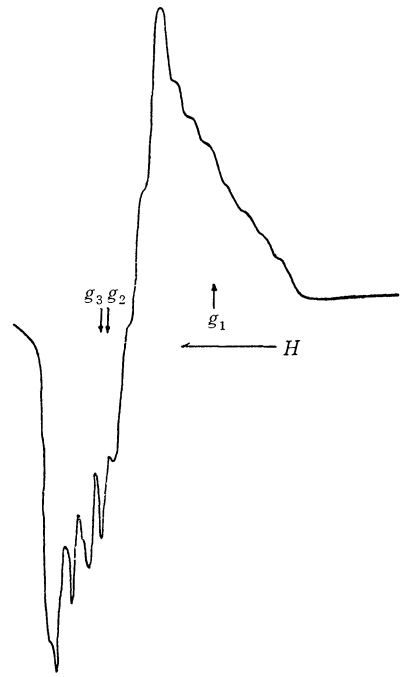

Fig. 2. Co(3-MeOsalen)–O_2 in frozen pyridine-HMPT (about −160°C).

g_1=2.076 A_1=16.0 gauss
g_2=2.008 A_2=14.7
g_3=2.004 A_3=14.7
cf. g_{sol}=2.023 A_{sol}=13.2

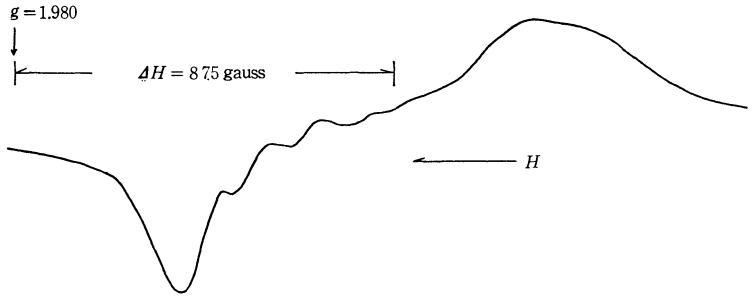

Fig. 3. ESR spectrum of Co(salprtr) in HMPT under oxygen (20°C).
complex conc. $=2.0\times10^{-2}$ mol/l oxygen pressure $=1$ atm

A rather well-resolved anisotropic ESR spectrum was observed for the species in a frozen mixed solvent of pyridine and HMPT (Fig. 2). The anisotropic g values and the corresponding A_{Co} values were roughly estimated, according to the method for randomly-orientated particles in a fixed position.[9]

The solution of Co(3-MeOsalen) in toluene (and benzene) showed no ESR signal under nitrogen; the situation was the same under oxygen at room temperature (the solubility of the complex in these solvents was not very large). When triphenylphosphine (PPh_3) was added to the solution (17 moles of PPh_3 *vs.* 1 mole of Co(3-MeOsalen)), however, a similar spectrum with an eight-line structure could be observed under oxygen.

Co(salen) behaved much like Co(3-MeOsalen) (investigated in a pyridine solution).

Kon *et al.*[4] have already reported on the ESR spectra of Co(salprtr) coordinated with oxygen in several solvents. The present authors investigated them in some other solvents (Fig. 3) in order to compare the spectra with those of Co(3-MeOsalen) (and Co(salen)) under oxygen. The signal shapes did not fully resemble those of Co(3-MeOsalen) under oxygen. This might well indicate the existence of some differences in geometrical structures and in electronic structures between the two kinds of cobalt mononuclear oxygen complexes.

When a red-colored solution of Co(sa) in pyridine was exposed to oxygen, the solution turned brown instantly. On the other hand, no ESR signal could be observed at room temperature several minutes after the exposure to oxygen. For comparison, it may be noted that no ESR spectra were observed when Co(3-MeOsalen) was dissolved in a mixed solvent of pyridine and methanol under oxygen at room temperature.

Discussion

It is naturally expected that some interactions may exist between such complexes as Co(salen), Co(3-MeOsalen), and Co(salprtr) and oxygen in some solvents. Calvin *et al.*[10] reported that two moles of activated Co(salen) absorbed one mole of oxygen and that one mole of Co(salprtr) absorbed one mole of oxygen in the solid state. The present authors have previously reported a reversible formation of mononuclear cobalt oxygen adducts from these complexes mixed in poly(4-vinylpyridine).[1,2] Floriani *et al.*[7] tried to isolate some oxygen complexes derived from these cobalt complexes which might be formed in some solvents. They isolated some binuclear oxygen adducts, such as $[Co(salen)\cdot DMF]_2\cdot O_2$, $[Co(salen)\cdot DMSO]_2\cdot O_2$, $[Co(salen)\cdot pyridine]_2\cdot O_2$, and $[Co(3\text{-}MeOsalen)]_2\cdot O_2\cdot DMSO$. Moreover, they could isolate $[Co(3\text{-}MeOsalen)]\cdot pyridine\cdot O_2$. The 1 : 1 oxygen adduct was isolated in only this case.

On the other hand, the present authors observed an ESR signal with an eight-line structure in both Co(3-MeOsalen) and Co(salen) solution (pyridine, DMF, DMSO, and HMPT) under oxygen, though no quantitative studies were pursued. The ESR signal at the position of a g_{sol} value of about 2 with an eight-line structure showed that the paramagnetic species was a certain radical containing one unpaired electron which interacted with one cobalt nucleus, because the nuclear spin of ^{59}Co is 7/2. In fact, a paramagnetic binuclear cobalt complex bridged by oxygen shows an ESR spectrum with a fifteen-line structure.*1, [11–14]

In view of the facts that the ESR signal appeared reversibly under oxygen, and that the A_{sol} value of the signal and that of a paramagnetic binuclear

9) F. K. Kneubühl, *J. Chem. Phys.*, **33**, 1074 (1960).

10) A. E. Martell and M. Calvin, "Chemistry of the Metal Chelate Compounds," Prentice Hall, N. J. (1956), p. 337.

*1 $2\times2\times(7/2)+1\rightarrow15$ lines.

11) E. A. V. Ebsworth and J. A. Weil, *J. Phys. Chem.*, **63**, 1890 (1959).

12) M. Mori, J. A. Weil and J. K. Kinnaird, *ibid.*, **71**, 103 (1967).

13) J. A. Weil and J. K. Kinnaird, *ibid.*, **71**, 3341 (1967).

14) D. L. Duffy, D. A. House and J. A. Weil, *J. Inorg. Nucl. Chem.*, **31**, 2053 (1969).

cobalt oxygen complex were in the same range (for example,[12] A_{sol} of $[(NH_3)_5CoO_2Co(NH_3)_5](NO_3)_5$ in an acidic solution is 11.4 gauss), and also from a comparative consideration of the previously-published studies of similar complexes,*2,4-6) the signal which was observed under oxygen in the above solutions of Co(3-MeOsalen) (and Co(salen)) was considered to be due to some cobalt oxygen complexes. The ratio of 1 mole of cobalt *vs.* 1 mole of oxygen could also be said to be true, in view of the fact that the signal had an eight-line structure and by naturally assuming that the reversibly-produced binuclear cobalt oxygen complexes were diamagnetic. In fact, the binuclear complex, $[Co(salen)\cdot DMF]_2\cdot O_2$, and some similar complexes have been reported to be intrinsically diamagnetic, though with some temperature-independent paramagnetism.[7] Apparently, a 1 : 2 adduct could be identified as $Co(III)-O_2^{2-}-Co(III)$, which had no free spin, and a 1 : 1 adduct could be schematically considered to be $Co(III)-O_2^-$ or $Co(II)-O_2$, each of which has one unpaired electron.

Therefore, a mononuclear cobalt oxygen complex has been proved to exist equilibrially in these Lewisbase solvents of Co(salen) and Co(3-MeOsalen).*3

The observation that no ESR signal could be found in a toluene solution of Co(3-MeOsalen) under oxygen agrees with the reports of Ueno *et al.*,[7,15] who reported that oxygen could not interact to yield some stable oxygen adducts with Co(salen)'s in such solvents. That is, the coordination of a Lewis base such as pyridine may be necessary for the stable existence of mononuclear (and also binuclear) oxygen complexes. The idea is also supported by the experimental finding that an ESR signal appeared when PPh_3 was added to the solution.

Some decompositional reactions may proceed on the oxygen adducts when some protic solvents coexist. This seems to be a probable reason why no ESR signal could be observed in a pyridine solution of Co(3-MeOsalen) with some methanol under oxygen. In fact, Costa *et al.*[16] supposed that $Co(III)-OR^-$ might be produced from such systems. The same situation might hold in the case of Co(sa) in pyridine, because Co(sa) has protonic hydrogens in the ligands.

The Dependence of ESR Characteristics on Solvents. Let us now discuss the variation in g_{sol} and A_{sol} values from solvent to solvent.

The data in Table 1 show that the g_{sol} and A_{sol} values of the adducts of Co(3-MeOsalen) in pyridine, 4-methylpyridine, and 4-ethylpyridine are almost all the same. The g_{sol} and A_{sol} values of the adducts of Co(3-MeOsalen) are, however, considerably different in pyridine, DMF, DMSO, and HMPT. On the contrary, the difference are very small in the case of those of Co(salprtr), in which the *trans* position of the coordinated oxygen may not be occupied by the solvent (as a ligand) because of steric hindrances caused by the imine ligand. This situation is different from that of Co(3-MeOsalen). In fact, an X-ray analytical study of $[Co(salen)\cdot DMF]_2\cdot O_2$ by Calligaris *et al.*[17] has shown that the DMF's exist in the *trans* positions of the bridge-oxygen.

On the basis of the above discussion, the variation in the g_{sol} and A_{sol} values of the adducts of Co(3-MeOsalen) (and Co(salen)) can be explained by considering that the solvent behaves as the fifth ligand in a *trans* position relative to the coordinated oxygen acting as the sixth ligand. The solvent might possibly affect the coordinated oxygen in a direct way, but the effect on A_{sol} and g_{sol} values may be quite small in comparison with the effect of the solvent in the *trans* position, judging from the observation that the g_{sol} and A_{sol} values of the adducts of Co(salprtr) are almost independent of the solvent.

The data of Table 2 show that the stabilities of the oxygen adduct are in this order: HMPT$\approx$DMF$<$pyridine.*4 On the other hand, the A_{sol} values are in this order: HMPT$>$DMF$>$pyridine, and the g_{sol} values are in this order: HMPT$\approx$pyridine$<$DMF.

The *Dq* values of the solvents may be considered

*2 Recently, $[Co(BAE)\cdot pyridine]\cdot O_2$ and some similar oxygen adducts (Co(BAE)=bis(acetylacetone)-ethylenediiminecobalt(II)) were isolated.[8] ESR studies were attempted on superoxocobalamines ($Co/O_2=1/1$)[6] and also on $[Co(CN)_5O_2]^{3-}$.[5] These ESR spectra very much resemble those in this paper.

*3 Of course, the non-oxygenated complex and the corresponding binuclear oxygen adduct may exist simultaneously; moreover, the amounts of the latter may be larger than those of the mononuclear adduct in many cases (*cf.* the lit.[7]).

15) K. Ueno and A. E. Martell, *J. Phys. Chem.*, **60**, 1270 (1956).

16) G. Costa, G. Mestroni and G. Pellizer, *J. Organometal. Chem.*, **15**, 187 (1968).

17) M. Calligaris, G. Nardin and L. Randassio, *Chem. Commun.*, **1969**, 763.

*4 The g_{sol} and A_{sol} values of the adduct in a mixed solvent of pyridine and DMF (and that of pyridine and HMPT) prove that the existing paramagnetic species in the mixed solvent is not a DMF (nor HMPT)-oxygen adduct, but a pyridine-oxygen adduct. The characteristic values of the paramagnetic species in the mixed solvent of DMF and HMPT (the volume ratio is 1/1; the mole ratio is, then, 2 moles of DMF *vs.* 1 mol of HMPT) may be explained if the species in the solvent is a mixture of a DMF-oxygen adduct and a HMPT-oxygen adduct (in the mole ratio of about 2/1). The observed g_{sol} (and also A_{sol}) value in the mixed solvent is considered to be the weighted mean value of that of the DMF-oxygen adduct and that of the HMPT-oxygen adduct.

to be in this order: HMPT$<^{?}$DMF<pyridine.*5

The above comparison shows that close relationships may exist among the stability, the A_{sol} (caused by the cobalt nucleus) value, and the *Dq* value of the solvent.*6

It seems that the larger the crystal field strength of the *trans* ligand (the solvent), the more stable the oxygen adduct. The A_{sol} value seems to decrease with the increase in the *Dq* value. The changes in g_{sol} values seem to be more complicated than those in A_{sol} values. The description by Crumbliss[8] that the adduct [Co(BAE)·DMF]·O_2 is less stable than [Co(BAE)·pyridine]·O_2 also agrees with the above discussion.

The Properties of the Coordinated Oxygen. It is very important and interesting to clarify the electronic structure of the mononuclear oxygen complexes. The ESR characteristics shall be analysed from this point of view.

Such investigations as have been pursued on paramagnetic species formed on the surfaces of some metal oxides from molecular oxygen by means of ESR spectroscopies[23,24] may be worthy of attention. It is regretable that no ESR studies seem to have been made on the oxygen complexes of so-called low valent transition metal complexes, such as $IrO_2X(CO)(PPh_3)_2$,[25] because of their diamagnetism.

There are two ways of analysing the ESR signals of the mononuclear cobalt oxygen complexes. The first one is based on the electronic structure, Co(II)–O_2 (in this structure, the unpaired electron is considered to be localized in metal orbitals. A low-spin d^7 cobalt(II) is coordinated by a diamagnetic oxygen (for example, a $^1\Delta_g$ oxygen)), while the other is based on the electronic structure, Co(III)–O_2^- (in this structure, the free spin is considered to be localized in an oxygen molecular orbital. A diamagnetic d^6 cobalt(III) is coordinated with a paramagnetic superoxide anion).

There are several low-spin cobalt(II) complexes which have been studied by means of ESR spectroscopy, for example, cobalt phthalocyanine(CoPc),[26,27] $Co(CH_3NC)_5^{2+}$,[28,29] and $Co(CN)_5^{3-}$.[28,29] These low-spin cobalt(II) complexes have *g* values which are relatively close to 2 (for example, $g_{||}=2.000$, and $g_\perp=2.117$ for $Co(CH_3NC)_5^{2+}$, and $g_{||}=1.992$, and $g_\perp=2.157$ for $Co(CN)_5^{3-}$). In general, however, the *A* values caused by the cobalt atom of these complexes are relatively large (for example, $A_{||}=78$ gauss and $A_\perp=57$ gauss for $Co(CH_3NC)_5^{2+}$, and $A_{||}=87$ gauss and $A_\perp=28$ gauss for $Co(CN)_5^{3-}$). From a consideration of these results, the *A* values of the oxygen cobalt complexes should be much larger than the measured values if the electronic structure of the adduct is considered to be mainly Co(II)–O_2. Of course, the smallness of the measured A_{sol} values does not mean necessarily the smallness of the individual anisotropic principal components of the *A* hf tensor (for example, $A_{||}$ and $A_\perp$). The individual anisotropic components are considered, however, not to be very large, as will be discussed later.

The finding that such small differences exist in the A_{sol} values of the adduct of Co(3-MeOsalen) in pyridine, 4-methylpyridine, and 4-ethylpyridine seems rather unacceptable if the unpaired electron exists mostly in the cobalt orbitals. For example, the $A_{||}$ value caused by the cobalt nucleus of a pyridine adduct of CoPc has been reported to be 78×10^{-4} cm^{-1}, and that of a 4-methylpyridine adduct of CoPc, 84×10^{-4} cm^{-1}.[27] If the situation is the same in the oxygen adduct of Co(3-MeOsalen), about 0.3 gauss*7 is expected to be the difference

*5 This order seems to be true in view of the generally-accepted spectrochemical series[18] ($Br^-<Cl^-\sim N_3^-<(NH_2)_2CO<H_2O<NH_3\sim$pyridine) and the results of Donoghue *et al.*[19] ($Cl^-\sim$HMPT$<N_3^-$). The relation between HMPT and DMF is not clear, but the *Dq* of HMPT may be the smaller, for the *Dq* of DMF may be in the neighborhood of that of $(NH_2)_2CO$. Their donor ability against a protic species may be in this order: HMPT>DMF (by $\Delta\tau_{CHCl_3}$),[20] DMF<pyridine (by $\Delta\nu_D$)[21] ($\Delta\tau_{CHCl_3}$ is the deviation of the τ value of the proton signal of $CHCl_3$ in a given solvent from that in a reference solvent: $\Delta\nu_D$ is the deviation of the O–D stretching wave number of CH_3OD in the given solvent from that in a reference solvent). Which has the larger donor ability, HMPT or pyridine, is not clear.

*6 PPh_3 should be omitted, because the properties of this ligand are rather complicated because of the existence of a strong π-ability. The DMSO seems not to be very different from DMF.[22]

*7 0.3 gauss$\fallingdotseq$(84×10^{-4} cm^{-1}—78×10^{-4} cm^{-1})×(13 gauss/84×10^{-4} cm^{-1})×(1/3); the contribution of the $A_{||}$ to the A_{sol} may be one-third of the total.

18) F. Basolo and R. G. Peason, "Mechanisms of Inorganic Reactions," Second Ed., John Wiley & Sons. Inc., New York (1967), p. 67.
19) J. T. Donoghue and D. S. Drago, *Inorg. Chem.*, **1**, 866 (1962).
20) H. Normant, *Angew. Chem., Int. Ed.*, **6**, 1046 (1967).
21) T. Kagiya, Y. Sumida and T. Inoue, This Bulletin, **41**, 767 (1968).
22) D. W. Meek, "The Chemistry of Non-Aqueous Solvents," ed. by J. J. Lagowski, Academic Press, New York (1966), p. 1.
23) P. H. Kasai, *J. Chem. Phys.*, **43**, 3322 (1965).
24) K. M. Wang and J. H. Lunsford, *J. Phys. Chem.*, **73**, 2069 (1969).
25) Y. Saito, *Yuki Gosei Kagaku Kyokai Shi*, **26**, 943 (1968).
26) J. M. Assour and W. K. Kahn, *J. Amer. Chem. Soc.*, **87**, 207 (1965).
27) J. M. Assour, *ibid.*, **87**, 4701 (1965).
28) M. E. Kimball, D. W. Pratt and W. C. Kaska, *Inorg. Chem.*, **7**, 2006 (1967).
29) J. J. Alexander and H. B. Gray, *J. Amer. Chem. Soc.*, **89**, 3356 (1967).

between the A_{sol} value of the cobalt oxygen complex in pyridine and that in 4-methylpyridine. Therefore, we suspect that the unpaired electron does not interact with the cobalt nucleus in a direct way. Very small differences were also observed between the signal characteristics of Co(3-MeOsalen) and that of Co(salen) in pyridine.

In due course, the analytical method based on the Co(III)–O_2^- electronic structure is expected to be more fruitful. This idea is also compatible with the fact that the A_{sol} value of the paramagnetic binuclear complex, $[(NH_3)_4Co(\mu\text{-}O_2)(\mu\text{-}NH_2)Co(NH_3)_4]^{4+}$,[12] the oxygen of which is considered to be superoxide-like as a result of analysing the A_{O17} values,[13] is in the neighborhood of those of the mononuclear oxygen complexes.

The superoxide anion can be analysed as having the following g values, according to Känzig *et al.*,[30,31] who derived the equations for superoxides of alkali metal ions:

$$g_1 = g_e + 2\left(\frac{\lambda^2}{\lambda^2+\Delta^2}\right)^{1/2} l$$

$$g_2 = g_e\left(\frac{\Delta^2}{\lambda^2+\Delta^2}\right)^{1/2} - \left(\frac{\lambda}{E}\right)\left[-\left(\frac{\lambda^2}{\lambda^2+\Delta^2}\right)^{1/2} - \frac{\Delta}{(\lambda^2+\Delta^2)^{1/2}} + 1\right]$$

$$g_3 = g_e\left(\frac{\Delta^2}{\lambda^2+\Delta^2}\right)^{1/2} - \left(\frac{\lambda}{E}\right)\left[\left(\frac{\lambda^2}{\lambda^2+\Delta^2}\right)^{1/2} - \frac{\Delta}{(\lambda^2+\Delta^2)^{1/2}} - 1\right]$$

The E and Δ values are shown in Fig. 4. The splitting, Δ, is caused by the crystal field constructed by surrounding ions. l is a correction to the angular momentum about the oxygen molecular axis caused by the crystal field. λ is the spin-orbit coupling constant. It has been reported that some superoxide anions adsorbed on metal oxides can be analysed by the above equations.[23,24] Theoretically speaking, these equations can be used in the case of the mononuclear cobalt oxygen complex, Co(III)–O_2^-, as the first approximation. The splitting, Δ, may be caused by the parent cobalt chelate (the parent cobalt chelate means the part of the cobalt oxygen adduct except the coordinated oxygen), which serves as a certain crystal field against the superoxide anion.

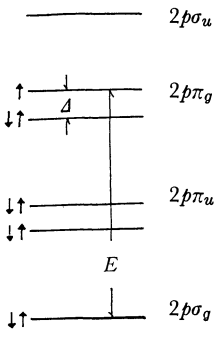

Fig. 4. The electronic levels of O_2^-.

Providing that l is equal to 1.00, that λ/E is negligibly small (the energy internal between $2p\pi_g$ and $2p\sigma_g$ is calculated to be 2.25 Rdg[32]), and that λ is 223 cm^{-1} [30] (or 115 cm^{-1} [24]),*8 the g_1 value of the 2.076 of the oxygen adduct in the mixed solvent of pyridine and HMPT (in Fig. 2; also, g_2, $g_3 \fallingdotseq 2.00$—2.01) is explainable if Δ is 6100 cm^{-1} (or 3050 cm^{-1}). The actual λ value is thought to be between the above two values.[33] This value of Δ (several thousand cm^{-1}) is comparable with those of adsorbed superoxide anions on some metal oxides;[24] it is also comparable with the theoretically-calculated value for an oxygen coordinated with iron phthalocyanine (with its molecular axis parallel to the complex plain).[34]

The g_{sol} value may be also calculated by using the relation:

$$g_{sol} = (1/3)(g_1+g_2+g_3)$$

The derivation in g_{sol} values of the adducts of Co(3-MeOsalen) from solvent to solvent seems not to correspond to the change in the Dq values of the solvent (acting as the *trans* ligand). There may be some complicated mechanism in the transport of the crystal-field effect of the *trans*-position ligand to the coordinated oxygen. It is also probable that there is some deviation of the individual l value from 1.00 and a change in the λ values.

As a summary of the preceding discussions about g values, it can be claimed that the coordinated oxygens in the mononuclear cobalt oxygen complexes can be considered to be rather superoxide-like.

An analysis of the A_{sol} and anisotropic components of the hf tensor is expected to clarify the electronic structure of the oxygen adduct more precisely. An exact analysis based only on the observed results is now, however, very difficult, because of our little knowledge about the geometrical structure and because of the probable disagreement of the directions of the g tensor with those of the A tensor. Therefore, only a rough analysis was attempted according to the method used by Kon *et al.*,[4] by assuming the geometrical structure to

30) W. Känzig and M. H. Cohen, *Phys. Rev. Lett.*, **3**, 509 (1959).

31) R. T. Shuey and H. R. Zeller, *Helv. Phys. Acta*, **40**, 873 (1967).

32) T. Shimanouchi, "Kozo-Kagaku Kogi-Shiryo," Shokabo Co,. Ltd., Tokyo (1965), p. 35.

*8 The value of 223 cm^{-1} was used in the first report of Känzig *et al.*[30]; the value of 115 cm^{-1} was used by Wang *et al.*[24]

33) H. R. Zeller and W. Känzig, *Helv. Phys. Acta*, **40**, 845 (1967).

34) M. Zerner, M. Gouterman an H. Kobayashi, *Theoret. Chim. Acta*, **6**, 363 (1966).

be the one in which the oxygen molecule is coordinated to the parent chelate with its molecular axis oblique (the angle is θ; θ was assumed to be 60°) against the principal axis of the parent cobalt chelate.*9 The A characters used were: $|A_{sol}|=13.2$ gauss, $|A_1|=16.0$ gauss, and $|A_2|=|A_3|=14.7$ guass (for the oxygen adduct in the mixed solvent of pyridine and HMPT).

When it was assumed that the unpaired electron was in d_{z^2} and that $A\fallingdotseq-P(\kappa-4/7)$, $B\fallingdotseq-P(\kappa+2/7)$ (A and B are the probable principal components of the hf tensor under an axis symmetry. These equations are quite rough[36]). The dipolar part, $|A_d|$, was estimated to be 10.4 gauss.

When it was assumed that the unpaired electron was in d_{xz} (or d_{yz}) and that $A\fallingdotseq-P(\kappa+4/7)$, $B\fallingdotseq-(\kappa-2/7)$;[36] the $|A_d|$ was calculated to be 18 gauss.

Though the above assumptions and calculations are quite rough and insufficient, it may be possible to state that the unpaired electron density in the cobalt d orbital (ρ) is rather small, considering that $|A_d|=(4/7)P\rho$ and that the P value for cobalt is 0.022—0.025 cm^{-1}.[4,37]

The above conclusion agrees well with the intended analysis based on the Co(III)–O_2^- structure. It is likely that the larger the A_{sol} value (though it is not necessarily parallel to the A_d value), the more the spin density in cobalt d orbitals.

The observations that such a small deviation exists in the A_{sol} values of the adducts of Co(3-MeOsalen) in pyridine, 4-methylpyridine, and 4-ethylpyridine, and that the ESR characteristics of the oxygen adduct of Co(salen) are almost the same as those of Co(3-MeOsalen), seem to be acceptable in view of the fact that a small part of the unpaired electron is considered to exist in the cobalt orbitals.

Though many considerations should be pursued further, if we are to understand the electronic structure of the individual oxygen adduct exactly (for example, by drawing the molecular orbital energy diagram quantitatively), the coordinated oxygen in these mononuclear cobalt oxygen complexes can be safely stated to be a kind of superoxide anion which is modified by the parent cobalt chelate, and the properties of these oxygens can be changed in some degree by selecting the solvent (or the *trans* ligand). The deviation can be estimated according to the character of the solvent.

Experimental

Reagents. *N,N'-Ethylene-bis(salicylideneiminato)cobalt-(II).* This chelate was obtained according to the method in the literature[38] and was recrystallized from methanol.

Found: C, 58.85; H, 4.08; N, 8.62%. Calcd for $C_{16}H_{14}CoN_2O_2$: C, 59.10; H, 4.30; N, 8.63%.

N,N'-Ethylene-bis(3-methoxysalicylideneiminato)cobalt(II). This chelate was synthesized as a monohydrate by mixing cobalt(II) acetate tetrahydrate (commercially obtained, and recrystallized from aqueous acetic acid) and *N,N'*-ethylene-bis(3-methoxysalicylideneimine) (synthesized from ethylenediamine and 3-methoxysalicylaldehyde) in the mole ratio of 1/1 in a mixed solvent of DMF and water at 60°C.

Found: C, 53.41; H, 5.33; N, 7.07% Calcd for $C_{18}H_{18}CoN_2O_4\cdot H_2O$: C, 53.61; H, 5.00; N, 6.95%.

The monohydrate was dehydrated at 170—185°C for 1.5 hr *in vacuo*. The decrease in the weight: Found: 4.1%. Theoretical: 4.4%. The chelate was stored in dried nitrogen.

Bis(salicylaldimino)cobalt(II). This chelate was synthesized according to the method of Endo.[39] At first as a dihydrate:

Found: C, 50.94; H, 4.86; N, 7.91%. Calcd for $C_{14}H_{12}CoN_2O_2\cdot 2H_2O$: C, 50.16; H, 4.81; N, 8.36%.

Then, it was dehydrated at 130°C for 2.5 hr *in vacuo*.

Found: C, 56.18; H, 3.93%. Calcd for $C_{14}H_{12}CoN_2O_2$: C, 56.20; H, 4.04%.

As for this complex, *cf.* the literature.[1,2]

Di(salicylal)-3,3'-diimino-di-n-propylamine-cobalt(II). This chelate was synthesized according to the method in the literature[38] and was purified by reprecipitating it, by water from an ethanol solution, as a monohydrate.

Found: C, 57.81; H, 6.21; N, 10.21%. Calcd for $C_{20}H_{23}CoN_3O_2\cdot H_2O$: C, 58.00; H, 6.09; N, 10.14%.

Pyridine, 4-Methylpyridine, 4-Ethylpyridine, DMF, DMSO, and HMPT. Commercially obtained solvents were distilled under purified nitrogen or under reduced pressure, and were stored under purified nitrogen.

Methanol, Benzene and Toluene. Commercially obtained solvents were dehydrated by appropriate methods and were distilled under purified nitrogen.

Triphenylphosphine. The commercial product of a guaranteed reagent grade was used without further purification.

The Measurements of the ESR Spectra. In general, a cobalt complex was dissolved in a given solvent under purified nitrogen. A part of the solution was then injected into a slender tube ($\phi=1$ mm), and the ESR spectrum was measured under purified nitrogen. The remaining solution was then exposed to oxygen (from a commercially obtained bomb), and a part of it was injected into a tube which was kept under oxygen. The oxygen atmosphere above the solution could be changed to nitrogen, and *vice versa*.

The ESR spectra were observed with a Japan Optics Laboratory Co., Ltd., ESR spectrometer, Model JES-3BS-X. A manganese marker was used for the calibration. The cavity temperature could be changed over a wide range by means of an attached apparatus for the temperature control.

*9 Similar structures are common in the cases of binuclear cobalt oxygen complexes.[35] A similar structure has been also claimed in the case of [Co(BAE)·ligand]·O_2's, on the basis of their infrared spectra.[8]

35) Lit. 20, p. 641.

36) A. H. Maki, N. Edelstein, A. Davison and R. H. Holm, *J. Amer. Chem. Soc.*, **86**, 4580 (1964).

37) J. M. Assour, *J. Chem. Phys.*, **43**, 2477 (1965).

38) R. H. Bailes and M. Calvin, *J. Amer. Chem. Soc.*, **69**, 1886 (1947).

39) J. Endo, *Nippon Kwagaku Kwaisi*, **65**, 424 (1944).

BULLETIN OF THE CHEMICAL SOCIETY OF JAPAN VOL. 43 3150—3155 (1970)

On the Preparations of Metal Complexes. V. The Preparations of Cholatoamminecomplexes of Cobalt(III) and Chromium(III)

Masayoshi NAKAHARA, Akio URUSHIYAMA, Yasuo SATOH and Yukio KONDO

Department of Chemistry, Faculty of Science, Rikkyo University, Nishi-ikebukuro, Toshima-ku, Tokyo

(Received March 23, 1970)

The mono-, di- and tricholatocobalt(III) and chromium(III) complexes and cobalt complex cholates, including the following new compounds, have been prepared: [Co chol $(NH_3)_5$] X_2 (X =chol, Cl), [M $chol_2$ en_2]Cl (M=Co, Cr), [Co $chol_3$ $(NH_3)_3$] and [Co en_3]$chol_3$. The absorption spectra of these complexes in the visible, ultraviolet, and infrared regions have been measured and compared with those of the corresponding acetato- or acido-complexes.

A number of Werner-type complexes of cobalt(III) and chromium(III) which contain alkyl carboxylic acids are known at present. Two series of complexes, [M $(RCOO)_2$ en_2]$^+$ (M=Co(III) and Cr(III), R=CH_3 to $C_{17}H_{35}$) have been prepared by Linhard and Stirn[1] and by Nakahara.[2] The diacido-type [Co $(RCOO)_2$ $(NH_3)_4$]$^+$,[3] the monoacido-type [Co RCOO $(NH_3)_5$]$^{2+}$,[4] and the triacido-type [Cr $(CH_3COO)_3$ $(NH_3)_3$][5] have also been prepared. One of the present authors (M.N.) has prepared the diacido-type complexes, [M-$(RCOO)_2$ en_2]$^+$ (M=Co(III), Cr(III)), containing fatty acids of various chain lengths (R=C_9H_{19} to $C_{17}H_{35}$) and has studied the *cis-trans* isomerisations.[2] It was found, in this investigation, that, in the case of the fatty acids, C>10, even though the *trans*-form complexes were used as the starting materials, the *cis*-form products were always obtained. This phenomenon has been explained in terms of the attraction between the long chains of the saturated fatty acids.

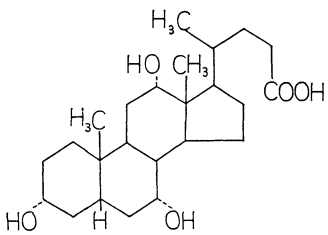

Fig. 1. Cholic acid (abbrev. cholH).

In the present work, cholic acid ($C_{24}H_{40}O_5$, cholH) (Fig. 1) is used as the carboxylic acid. This acid resembles the long-chain fatty acids mentioned above because the steroid skelton may be considered to be a condensed paraffin. However, it is rather different from the fatty acids in that the condensed part of the molecule is fairly bulky. Thus, it seemed that it would be interesting to compare the properties of cholatocomplexes with those of the fatty-acid complexes. For this purpose, three types of cholato complexes, [M chol $(NH_3)_5$]$^{2+}$, [M $chol_2$-en_2]$^+$, and [M $chol_3$ $(NH_3)_3$] (M=Co(III), Cr(III)) are prepared and their properties are investigated.

Experimental

Preparations. *1) Cholic Acid*, $C_{24}H_{40}O_5$. Reagent-grade cholic acid was dissolved in ethanol, and then, after active carbon had been added to the solution, it was recrystallized several times.

2) Sodium Cholate, $NaC_{24}H_{39}O_5$. Purified cholic acid was dissolved in water containing an equivalent amount of sodium hydroxide, and then the solution was evaporated to dryness on a water bath.

3) Silver Cholate, $AgC_{24}H_{39}O_5$. The sodium cholate was dissolved in water at about 50°C, and an aqueous solution of silver nitrate was added to this solution. The precipitate of the silver cholate was filtered, washed several times with water, acetone, and ether successively, and air-dried.

4) Tris(ethylenediamine)cobalt(III) Chloride, [Co en_3]-Cl_3,[6] *Chloropentaamminecobalt(III) Perchlorate*, [Co Cl $(NH_3)_5$] $(ClO_4)_2$,[7] *trans-Dichlorobis(ethylenediamine)cobalt-(III) Chloride*, *trans*-[Co Cl_2 en_2]Cl,[6] *cis-Dichlorobis-(ethylenediamine)cobalt(III) Chloride*, *cis*-[Co Cl_2 en_2]Cl,[7] *Trichlorotriamminecobalt(III)*, [Co Cl_3 $(NH_3)_3$],[8] *trans-Dichlorobis(ethylenediamine)chromium(III) Chloride*, *trans*-[Cr

1) M. Linhard and G. Stirn, *Z. Anorg. Allg. Chem.*, **268**, 105 (1952).
2) M. Nakahara, This Bulletin, **35**, 901 (1962).
3) M. Linhard and M. Weigel, *Z. Anorg. Allg. Chem.*, **260**, 65 (1949).
4) M. Linhard and M. Weigel, *ibid.*, **264**, 321 (1951).
5) M. Nakahara, This Bulletin, **35**, 782 (1962).
6) "Inorganic Syntheses," Vol. 2, (1946), p. 221.
7) *Ibid.*, Vol. 2, (1946), p. 223.
8) M. Mori, M. Shibata, K. Hirota, K. Masuno and Y. Suzuki, *Nippon Kagaku Zasshi*, **79**, 1251 (1958).

Cl_2 en_2]Cl,[9] *cis-Dichlorobis(ethylenediamine)chromium(III) Chloride*, *cis*-[Cr Cl_2 en_2]Cl.[10] These complexes were synthesized according to the method for each.

5) Tris(ethylenediamine)cobalt(III) Cholate, [Co en_3]-$chol_3$. Into a small amount of water we dissolved 0.4 g of [Co en_3]Cl_3, and then the solution was treated with freshly-precipitated silver oxide. The precipitate thus produced was filtered off, and 40 m*l* of methanol were added. One and a half grams of cholic acid in 40 m*l* of methanol were added to the solution, and the mixture was stirred. Then, after a large amount of ether had gradually been poured into the mixed solution, the solution was stirred vigorously with a glass rod until a yellow product was precipitated; this product was filtered, dissolved into methanol again, reprecipitated with ether, filtered, washed with ether, and then air-dried. Yield, 0.8 g (44%).

Found: Co, 4.21; C,*1; H, 9.66; N, 5.50%. Calcd: Co, 4.34; C,*1; H, 9.72; N, 5.75%.

Yellow powder, soluble in methanol, and insoluble in ether.

6) Chloropentaamminecobalt(III) Cholate, [Co Cl-$(NH_3)_5$]$chol_2$. One and a half grams of [Co Cl $(NH_3)_5$]-$(ClO_4)_2$, 2 g of sodium cholate, and 2 g of cholic acid were suspended in methanol, after which the solution was gently heated on a water bath using a reflux condenser. After an hour, the unreacted materials were filtered off from the red solution. A large amount of acetone was added to the filtrate, and the red product which was thus immediately precipitated was filtered, washed with acetone, and air-dried. It was dissolved in methanol again and reprecipitated with acetone for purification. Yield, 2.4 g (45%).

Found: Co, 5.85; C,*1; H, 9.65; NH_3, 8.30%.

Calcd: Co, 5.92; C,*1; H, 9.42; NH_3, 8.56%.

Red powder, soluble in methanol, slightly soluble in ethanol, and insoluble in water, acetone, and ether.

7) Cholatopentaamminecobalt(III) Cholate, [Co chol-$(NH_3)_5$]$chol_2$. In methanol we suspended 2.4 g of [Co-Cl $(NH_3)_5$]$chol_2$, 1 g of sodium cholate, and 1 g of cholic acid, after which, the solution was heated on a water bath with a reflux condenser. The fine purple-red crystals ([Co Cl $(NH_3)_5$]Cl_2) which separated out after an hour were filtered off. To the filtrate we then added 1 g of sodium cholate and 1 g of cholic acid, refluxing the mixture continuously. Then, after about 2 hr, when the solution had began to change its color from red to purple, the reflux condenser was removed and the solution was gently heated on a water bath in order to evaporate the solvent gradually. After a while, a beautiful purple precipitate (Co $chol_2 \cdot 1.5$cholH) was formed; when the purple color of the solution was changed to a light red-orange, the purple precipitate was filtered off. A large volume of ether was poured into the filtrate to precipitate pinkish products. Because they still contained a considerable amount of cholic acid, the crude products were dissolved into 50 m*l* of methanol; with the addition of 200m*l* of ether they were precipitated as a red-orange product which was then filtered, washed with ether, and dried in air. For further purification, the product was reprecipitated with acetone. Yield, 0.2 g (6%).

Found: Co, 4.18; C,*1; H, 9.48; NH_3, 6.21%.

Calcd: Co, 4.38; C,*1; H, 9.73; NH_3, 6.22%.

Red-orange powder, soluble in methanol and ethanol, insoluble in acetone, ether, and water.

8) Cholatopentaamminecobalt(III) Chloride, [Co chol-$(NH_3)_5$]Cl_2. Into 200 m*l* of methanol we dissolved 0.6 g of [Co chol $(NH_3)_5$]$chol_2$. After 10 m*l* of water had then been added to the solution, a few drops of concentrated hydrochloric acid were added and the mixture was stirred vigorously; then an appropriate amount of ether was poured into the solution to form a red-orange precipitate. This precipitate was filtered off and dissolved into 200 m*l* of methanol again, then, after the water and the concentrated hydrochloric acid had been added as before, it was reprecipitated with ether, filtered, washed with ether several times, and dried in air. Yield, 0.2 g (73%).

Found: 9.71; C,*1; H, 8.39; NH_3, 13.05%.

Calcd: 9.47; C,*1; H, 8.74; NH_3, 13.65%.

Red-orange powder, soluble in water, methanol, and ethanol, and insoluble in acetone and ether.

9) cis-Dicholatobis(ethylenediamine)cobalt(III) Chloride, *cis*-[Co $chol_2$ en_2]Cl. In 60 m*l* of ethanol we suspended 0.65 g of *trans*-[Co Cl_2 en_2]Cl or *cis*-[Co Cl_2 en_2]Cl and 2 g of sodium cholate; the solution was gradually heated on a water bath, using a reflux condenser. After about 3 hr, the red solution produced was filtered to remove the unreacted materials, and then about 4 volumes of ether were poured into the filtrate to form a pale red precipitate, which was filtered off and washed with ether. The precipitation from ethanol solution with ether was repeated several times in order to purify it. Yield, 1.7 grams (66%).

Found: Co, 5.65; C,*1; H, 9.17; ,N 5.49%.

Calcd: Co, 5.73; C,*1; H, 9.20; N, 5.44%.

Pale red powder, very soluble in methanol, ethanol, *n*-butanol and anhydrous acetic acid, and insoluble in acetone and ether.

10) cis-Dicholatobis(ethylenediamine)chromium(III) Chloride, *cis*-[Cr $chol_2$ en_2]Cl. Prepared by the same method as that described under 9) using 0.6 g of *trans*-[Cr Cl_2-en_2]Cl or *cis*-[Cr Cl_2 en_2]Cl and 2 g of sodium cholate. Yield, 1.5 g (63%).

Found: Cr, 4.79; C,*1; H, 9.17; N, 5.45%.

Calcd: Cr, 5.09; C,*1; H, 9.26; N, 5.48%.

Pale red powder, very soluble in methanol, ethanol, *n*-butanol, and anhydrous acetic acid, and insoluble in acetone and ether.

11) Tricholatotriamminecobalt(III), [Co $chol_3$ $(NH_3)_3$]. In a mortar we crushed 2.6 g of silver cholate, 0.4 g of [Co Cl_3 $(NH_3)_3$], and 0.3 g of cholic acid; the mixture was then warmed up to about 50°C by the use of hot air. Then a few drops of water was added to it, and the mixture was ground vigorously by the use of a pestle. After the bluish-green color of the mixture had turned

9) P. Pfeiffer, P. Koch, G. Lando and A. Trieschmann, *Ber.*, **37**, 4255 (1904).

10) "Inorganic Syntheses," Vol. 2 (1946), p. 200.

*1 The found values of carbon were always less than the calculated values; for example, [Co Cl $(NH_3)_5$]-$chol_2$: Found 54.09; Calcd 57.09, [Co chol $(NH_3)_5$]-$chol_2$: Found 56.78; Calcd 63.23, [Co chol $(NH_3)_5$]Cl_2: Found 38.77; Calcd 46.31, [Co $chol_2$ en_2]Cl: Found 55.29; Calcd 60.65, [Cr $chol_2$ en_2]Cl: Found 54.18; Calcd 61.07. It was found that a considerable amount of carbon was contained in the residue whenever the sample was burned. Because of the high carbon-to-metal atomic ratios in the complexes, carbide or carbonate may be produced when they were burned.

to red-violet and the reaction was over, a soluble part was extracted from the mixture with 50 m*l* of ethanol and the insoluble silver chloride was filtered off. The red-violet precipitate which appeared as the appropriate amount of ether was poured into the filtrate was filtered, washed with ether, and dried in air. The product was reprecipitated twice from an ethenol solution with ether. Yield, 1.5 g (67%).

Found: Co, 4.56; C, 64.08; H, 9.58; NH_3, 3.96%.

Calcd: Co, 4.43; C, 64.80; H, 9.47; NH_3, 3.83%.

Red-violet powder, soluble in methanol and ethanol, and insoluble in acetone and ether.

Analysis. For the analysis of cobalt, the sample was first slowly burned with sodium hydrogensulfate in a crucible in order to change all the cobalt into $CoSO_4$, after which, the burned solid was dissolved into diluted hydrochloric acid. Then the cobalt was precipitated from the solution with α-nitroso-β-naphthol.

The chromium was determined as follows; the sample was decomposed, in a hot aqueous solution of sodium hydroxide, to chromium(III) hydroxide, which was oxidized by potassium peroxodisulfate to chromate(VI) ions, then, after the pH of the solution had been adjusted to 10, the intensities of the absorption at 348, 356, 388, and 396 mu were measured.

The nitrogen, carbon, and hydrogen were analyzed by ordinary microanalysis, except that the nitrogen which was contained as NH_3 was analyzed by Kjehldahl's method. The found values were in good agreement with the calculated values except in the case of carbon.

Infrared Absorption Spectra. The infrared absorption spectra were measured by Nujol mull method using a JASCO 301 (Japan Spectroscopic Co.) infrared spectrophotometer. The characteristic absorption maxima are listed in Table 1.

Visible and Ultraviolet Absorption Spectra. The visible and ultraviolet absorption spectra in solution were obtained with a Hitachi 139 spectrophotometer.

TABLE 1. INFRARED ABSORPTION MAXIMA OF COMPLEXES (cm^{-1})

	COO^- antisym. str.	N-H str.	O-H str.
[Co en_3]$chol_3$	1545	3195	3415
[Co chol $(NH_3)_5$]$chol_2$	1537	3290	3400 sh
[Co chol $(NH_3)_5$]Cl_2	1642	3190	3390 sh
[Co $chol_2$ en_2]Cl	1567	3265	3395
[Cr $chol_2$ en_2]Cl	1584	3250	3380
[Co $chol_3$ $(NH_3)_3$]	1560	3300	3400 sh
cholH	1712		

Results and Discussion

The authors succeeded in the preparation of various kinds of cholato-complexes, as has been described in the Experimental section. These are all red fine powders, insoluble in water and soluble in an organic solvent such as ethanol. We attempted to prepare [Cr chol $(NH_3)_5]^{2+}$ and [Cr-$chol_3$ $(NH_3)_3$] but neither of the pure products were obtained. For example, for the purpose of obtaining [Cr chol $(NH_3)_5]^{2+}$, when we employed method by which the corresponding cobalt complex had successfully been prepared, [Cr Cl $(NH_3)_5$]-$chol_2$ could be obtained, but further treatment was

TABLE 2. ABSORPTION MAXIMA OF COMPLEXES (Absorption maxima are given in cm^{-1} and intensities, log ε in parentheses)

Complex	I	II	III	IV	
[Co en_3] $chol_3$	21500 (1.94)	29400 (1.90)		46500 (4.15)	*
[Co en_3] Cl_3	21300 (1.94)	29470 (1.90)			
[Co chol $(NH_3)_5$] $chol_2$	19800 (1.88)	28400 (1.95)	42600 (3.90)	46500 (~3.94)	*
[Co chol $(NH_3)_5$] Cl_2	19800 (1.90)	28200 (1.99)	42500 (3.97)		*
[Co$(CH_3COO)(NH_3)_5](ClO_4)_2$	19900 (1.88)	28400 (1.77)			4)
[Co $chol_2$ en_2] Cl	19600 (1.99)	~27500 (~2.0)	42500 (4.15)		*
cis-[Co$(C_{17}H_{35}COO)_2en_2$] ClO_4	19800 (2.18)	27600 (1.98)			1)
[Cr $chol_2$ en_2] Cl	19500 (1.86)	26200 (1.66)	46000 (3.74)		*
cis-[Cr$(C_{17}H_{35}COO)_2en_2$] ClO_4	19800 (1.99)	26600 (1.65)			1)
[Co $chol_3(NH_3)_3$]	19000 (1.85)	~27000	42600 (3.74)		*
fac-[Co$(NH_2CH_2COO)_3$]	19200 (2.2)	26700 (2.14)			13)

* present work

not useful. That is, $[Cr\ Cl\ (NH_3)_5]^{2+}$ was easily decomposed and a ligand-exchange reaction between Cl^- and $chol^-$ was not performed smoothly. These phenomena are consistent with the fact that Co $chol_2$ was produced as the cholatopentaamminecobalt(III) salt was prepared. A very small amount of an impure $[Cr\ chol_3\ (NH_3)_3]$ was obtained by the reaction of Ag chol upon $[Cr\ Cl_3\ (NH_3)_3]$ because of the incomplete reaction.

It was found that, in the reaction of $[Co\ Cl(NH_3)_5](ClO_4)_2$ with Nachol, $[Co\ Cl\ (NH_3)_5]chol_2$ was first obtained, while in the case of $[M\ Cl_2\text{-}en_2]Cl$ (M=Co, Cr) the ligand substitution took place immediately and a cholate was not prepared. This fact aroused our interest in its reaction mechanism.

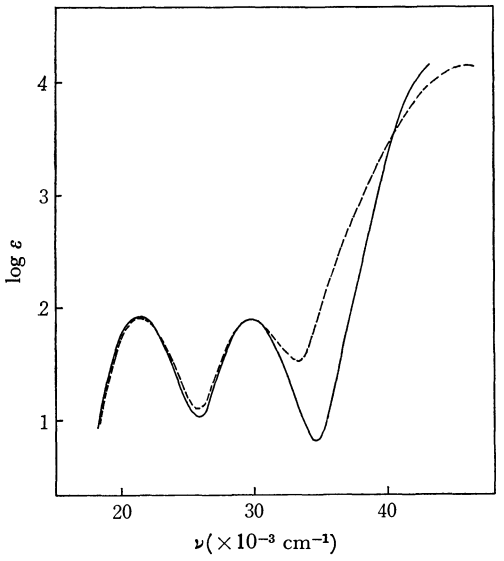

Fig. 2. Absorption spectra of trisethylendiamine complexes.
——— $[Co\ en_3]Cl_3$, ----- $[Co\ en_3]chol_3$

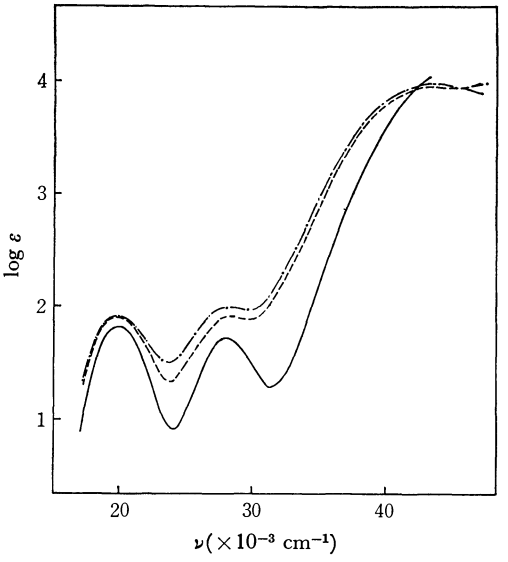

Fig. 3. Absorption spectra of monocholatocomplexes.
——— $[Co(CH_3COO)(NH_3)_5]^{2+}$,*----- $[Co\text{-}chol(NH_3)_5]chol_2$, (in methanol), — - — $[Co\text{-}chol(NH_3)_5]Cl_2$ (in methanol).
* M. Linhard, M. Weigel, *Z. Anorg. Allg. Chem.*, **264**, 321 (1951).

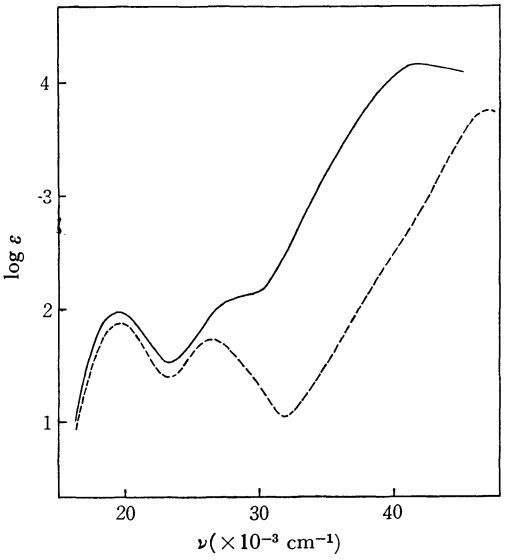

Fig. 4. Absorption spectra of dicholatocomplexes.
——— $[Co\ chol_2\ en_2]Cl$ (in ethanol), ----- $[Cr\ chol_2\ en_2]Cl$ (in ethanol).

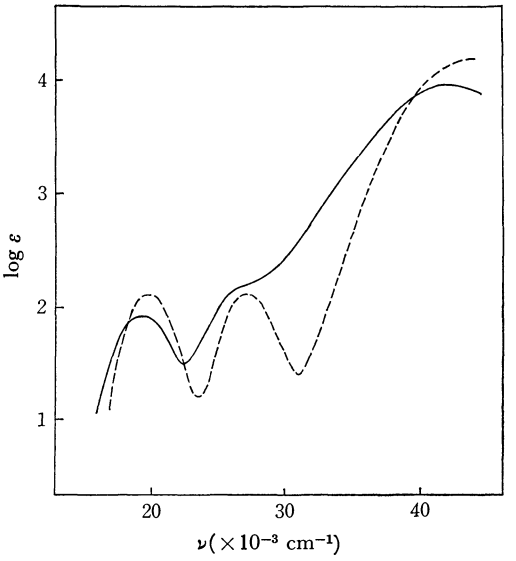

Fig. 5. Absorption spectra of tricholatocomplex.
——— $[Co\ chol_3\ (NH_3)_3]$ (in ethanol), ----- *fac*-$[Co\ gly_3]$.

As is shown in Table 2 and Figs. 2,3,4 and 5, each complex shows two spin-allowed bands which are characteristic of d^3 or low-spin d^6 complexes. An intense absorption band due to cholate ions was also seen in each case. The absorption band at 46500 cm^{-1} in [Co en_3]$chol_3$ coincides with the absorption band which is considered to be due to free cholate ions. Thus, in this case, the cholate ions are not at all coordinated. The spin-allowed bands of [Co en_3]$chol_3$ coincide with those of [Co en_3]Cl_3; this result confirmes that the compound must be a cholate salt of $[Co\ en_3]^{3+}$. However, in all the complexes except [Co en_3]$chol_3$ the cholate bands shifted to 42500 cm^{-1}; this shift suggests that it must be a specific absorption band of coordinated cholate ions. A similar result is also found in the case of $[Co\ chol\ (NH_3)_5]^{2+}$ (Fig. 3); either two ligand-field bands or a specific absorption band due to the cholate ion of [Co chol $(NH_3)_5$]$chol_2$ coincides well with that of [Co chol $(NH_3)_5$]Cl_2 in both the position and the intensity of the absorption maximum; furthermore, the absorption spectra of [Co chol $(NH_3)_5$] $chol_2$ have a band due to uncoordinated cholate ions at 46500 cm^{-1}, much like [Co en_3]-$chol_3$, while no such band is seen in [Co col $(NH_3)_5$]-Cl_2. The so-called "first" and "second" absorption bands of $[Co\ chol\ (NH_3)_5]^{2+}$ coincide with those of $[Co\ (CH_3COO)\ (NH_3)_5]^{2+}$ with respect to position and pattern. The intensity of the first band is slightly higher, and that of second band of $[Co\ chol\ (NH_3)_5]^{2+}$ is considerably higher, than that of the corresponding band of $[Co\ (CH_3COO)\ (NH_3)_5]^{2+}$. The increase in intensity in the case of the second band is evidently due to the overlap of the intense cholate band and the second band. Thus, the ligand-field bands of $[Co\ chol\ (NH_3)_5]^{2+}$ are essentially equal to those of $[Co\ (CH_3COO)\text{-}(NH_3)_5]^{2+}$, which means that the cholate ion coordinates to the cobalt through the carboxyl group.

The spin-allowed bands of [Co $chol_2$ en_2]Cl are similar to those of the corresponding *cis*-distearatocobalt(III)-complex. That is, the patterns and the positions of the absorption band of the two complexes agree well except for the intensity of the second absorption band of the cholato complex, which is again influenced by the specific absorption. Similarly, the absorption spectrum of [Cr $chol_2$ en_2]Cl is consistent with that of the corresponding complexes, $[Cr\ (C_{17}H_{35}COO)_2\ en_2]ClO_4$, in position and pattern. These two cholato cobalt(III) and chromium(III) complexes have the first absorption band characteristic of *cis*-diacido complexes. That is, the band does not show any splitting characteristic of *trans*-diacido-complexes. Thus, the complexes should have the *cis* structures.[11,12] The starting materials used here are [Co Cl_2 en_2]Cl and [Cr Cl_2 en_2]Cl respectively, and the *cis*- and *trans*- or complexes give the same product in each case. In other words, even though the *trans* complex is used as the starting material, the *cis* complex is obtained. The isomerisation reaction from *trans* to *cis* must take place. The situation is similar to the case of long-chain fatty acid complexes reported previously[2]; the reason for this isomerisation must be similar. That is, as the cholate ion is bulky, then the interaction between the cholate ion as ligand in this complex must strongly affect the *trans-cis* isomerisation reaction.

The absorption spectrum of [Co $chol_3$ $(NH_3)_3$] has two ligand-field bands and one specific absorption band (Fig. 5). The latter agrees well with the bands of the mono- and di-cholato complexes with respect to position. However, its intensity is fairly low, and its half-width is quite large. Moreover, there is a large shoulder on the longer-wavelength side of the specific absorption band. The specific absorption band covers the second absorption band and makes it obscure. The position of the maximum absorption of the second band was estimated to be at 27000 cm^{-1}, and the molar extinction coefficient was estimated to be about 100. These absorption bands agree with the absorption bands of *fac*-[Co $(NH_2CH_2COO)_3$], which possesses a similar *cis*-Co N_3O_3 configuration.[13] The complex obtained here should have a *fac*-configuration.

The infrared spectra are rather complicated in each case. However, many bands are associated with cholic acid. The characteristic absorptions are summarized in Table 1. It is observed that the absorptions assigned to the antisymmetric vibrations of COO^- are the considerably shifted to the lower-wave number side compared with the corresponding absorptions in free cholic acid. The absorption at 1537 cm^{-1} of [Co chol $(NH_3)_5$]$chol_2$ is fairly intense and has a small shoulder at 1640 cm^{-1} which is not listed in the table. Consequently, the absorption bands at 1537 cm^{-1} and 1545 cm^{-1} must be associated with the uncoordinated cholate ions in [Co chol $(NH_3)_5$]$chol_2$ and [Co en_3 $chol_3$] respectively. It is also found that the wave numbers of the COO^- antisymmetric vibration in the order; [Co chol $(NH_3)_5$]Cl_2, [Co $chol_2$ en_2]Cl, [Co $chol_3$-$(NH_3)_3$], and [Co en_3]$chol_3$. It is generally known that the absorption of a free carboxylic group should be at 1700—1730 cm^{-1} (in the free cholic acid at 1712 cm^{-1}), and that the absorption of a COO^- group coordinated to Co(III) or Cr(III) should be at 1620—1650 cm^{-1} and should be shifted to the lower-wave number side as the coordinate bond increases in ionic character.[14] These inter-

11) M. Linhard and M. Weigel, *Z. Anorg. Allg. Chem.*, **267**, 121 (1951).

12) Y. Shimura, This Bulletin, **25**, 49 (1925).

13) Y. Shimura and R. Tsuchida, *ibid.*, **29**, 311 (1956).

14) K. Nakamoto, "Spectroscopy and Structure of Metal Chelate Compounds," John Wiley & Sons, New York (1960), p. 277.

pretations were supported by the above results. That is, in the free cholic acid the maximum is at 1712 cm^{-1}; in the monocholato complex, at 1642 cm^{-1}; in the dicholato complex, at 1567 cm^{-1} (Co complex) and at 1584 cm^{-1} (Cr complex), and in the tricholato complex, at 1569 cm^{-1}. The absorption maxima of the monocholato complex are comparable with those of the monoacetato complexes. However, when there is such a large steric hindrance on the *cis* configuration as *cis*-dicholato and *fac*-tricholato complexes, the Co-O bond length may be lengthened by the hindrance and ionic character of the bonds may increase.

BULLETIN OF THE CHEMICAL SOCIETY OF JAPAN VOL. 43 3155—3158 (1970)

The Hydrolysis of the Copper(II) Ion in Heavy Water*1

Hidetake KAKIHANA, Toshihiko AMAYA and Masunobu MAEDA*2

Research Laboratory of Nuclear Reactor, Tokyo Institute of Technology, Ookayama, Meguro-ku, Tokyo

(Received March 26, 1970)

The hydrolysis equilibria of the copper(II) ion in heavy water have been studied at 25°C by measuring the deuterium-ion concentration by means of a commercial glass electrode. The total copper(II) concentration was varied between 50 and 90 mM, while the concentration of the perchlorate ion was held constant at 3M by the addition of $NaClO_4$. A hydrolyzed copper(II) perchlorate solution was gradually acidified up to the point where hydrolysis was negligible by the use of constant-current coulometry. The experimental data, which indicate a slight hydrolysis in the log d range from -4.0 to -5.26, can be explained by assuming these equilibria;

$$Cu^{2+} + D_2O = CuOD^+ + D^+, \log \beta_{1,1} = -7.71 \pm 0.07;$$
$$2Cu^{2+} + 2D_2O = Cu_2(OD)_2^{2+} + 2D^+, \log \beta_{2,2} = -11.46 \pm 0.04.$$

It has been found that the hydrolytic reactions of metal ions in heavy water can be studied with the same accuracy as in light water.[1] We have previously reported on our studies of the hydrolysis of the beryllium ion and the uranyl ion in heavy water.[2-4]

The present work was carried out in order to obtain information on the hydrolysis species of the copper(II) ion in heavy water and to estimate their stability constants.

The hydrolysis equilibria of the copper(II) ion in light water have been studied by a number of investigators,[5-9] using glass electrodes. It has been concluded that the main product is the binuclear complex, $Cu_2(OH)_2^{2+}$, but the minor one is not yet precisely known.

Symbols

- B total concentration of copper(II)
- b concentration of free copper ions
- D analytical excess of deuterium ions $=[ClO_4^-]-2B-[Na^+]$
- d concentration of free deuterium ions
- h concentration of free hydrogen ions
- Z average number of deuterium ions set free per copper atom
- p number of OD groups bound to hydrolyzed species
- q number of Cu groups present in hydrolyzed species
- $\beta_{p,q}$ stability constant of the following reaction: $q\,Cu^{2+} + p\,D_2O = Cu_q(OD)_p^{(2q-p)+} + p\,D^+$
- v number of μF passed through the test solution
- E emf
- v volume of a test solution, ml
- [ ] concentration of the relevant species

Experimental

Reagents and Analysis. *The reagents used* were, unless otherwise stated, prepared and analyzed as has

*1 Ionic Equilibria in Heavy Water (Part 5).

*2 Present address: Department of Inorganic Chemistry, The Royal Institute of Technology, Stockholm.

1) H. Kakihana, M. Maeda and T. Amaya, This Bulletin, **43**, 1377 (1970).

2) H. Kakihana and M. Maeda, *ibid.*, **42**, 1458 (1969).

3) H. Kakihana and M. Maeda, *ibid.*, **43**, 109 (1970).

4) H. Kakihana and M. Maeda, *ibid.*, **43**, 1097 (1970).

5) H. Hagisawa, *Rikagaku Kenkyusho Iho*, **18**, 275 (1939).

6) K. J. Pedersen, *Kgl. Danske Videnskab. Selskab, Mat. Fys. Medd.*, **20** (7), 1 (1943).

7) C. B. Biedermann, *Arkiv Kemi*, **9**, 175 (1956).

8) D. D. Perrin, *J. Chem. Soc.*, **1960**, 3189.

9) H. Ohtaki, *Inorg. Chem.*, **7**, 1205 (1968).

been described in Ref. 2.

The copper(II) perchlorate solution was prepared by dissolving copper(II) oxide of a commercial *p. a.* reagent in an excess of hot $HClO_4$ (*p. a* 70%) and by then recrystallizing it twice. The H_2O was expelled by evaporating the solution under an infrared lamp until crystals had formed, whereupon D_2O was added. No chloride or sulfate ions could be detected in the stock solution. The copper content of the stock solutions was measured by electrodeposition,[10] and the total perchlorate concentration was determined by neutralization after passing a definite amount of the solution through a column of the cation exchange resin, Dowex 50W-12, of the H^+ form.

Apparatus. All the apparatuses used were the same as those described in Ref. 3.

Procedures. Earlier investigations[7,9] have indicated that the hydrolysis becomes appreciable at log $h<-4.0$, and that only a small part of Cu^{2+} can be transformed to hydrolysis products before precipitation starts. Under such conditions, it is imperative to avoid contamination of the solutions to be studied by foreign protolytes. Furthermore, it has been pointed out that copper hydroxide precipitates slowly with a small excess of alkali.[7]

In the present work, in order to avoid contamination by foreign protolytes and the formation of any precipitates during titration, a "*back titration*" technique[9,11,12] was employed: a test solution saturated with copper(II)-hydrolyzed products was prepared and acidified by generating D^+ ions coulometrically.

The saturated solutions were prepared by employing apparatuses similar to those described in Refs. 9 and 12. A copper(II) perchlorate solution containing 3M ClO_4^- was put into a vessel. Then a NaOD solution prepared by the electrolysis of a 3M $NaClO_4$ solution was added until pale blue precipitates of copper(II) hydroxides were formed. The solution was stirred at least 40 hr by the use of a magnetic stirrer and filtered through G4 glass filters into a flask.

The turbidity was examined for several months with an aliquot of the filtered solution, but no suspended particles could be detected. Another portion was used for potentiometric titration.

All the preparations were carried out under a nitrogen atmosphere. Nitrogen gas was presaturated by passing it through D_2O and $NaClO_4$ in D_2O.

Emf Measurements. The general composition of a test solution is written as: BM Cu(II), DM D^+, $(3-2B-D)$M Na^+, 3M ClO_4^-, where D may be negative. For each titration, a definite volume of the test solution (v ml) was taken and the value of D was increased in a step-by-step fashion by constant-current coulometry, using the cell assembly reported as in Refs. 3 and 13.

After $v\mu F$ have been passed through the test solution, D is equal to:[13]

$$D = D_0 + (v/v) \times 10^{-3} \qquad (1)$$

where D_0 is the analytical excess of the deuterium-ion concentration in the starting test solution.

The deuterium ion concentration, d, was measured by the use of the cell assembly described in Ref. 3.

The emf of the cell may be written as follows:[1]

$$E = E_0 + 59.15 \log d \text{ (at 25°C)} \qquad (2)$$

where E_0 is the constant which includes the standard potential for the glass electrode and the term for the activity factor of the D^+ ion.

Each of the potentiometric titrations may be divided into two parts. In the first part, D_0 and E_0 were determined by measuring the emf in the region where log-$d>-3.5$; they were calculated by means of the Gran plot,[14] $10^{E/59.15}$ *vs.* v. In the second part, measurements were made at log $d<-3.5$, where the hydrolysis becomes appreciable. Then $Z=(d-D)/B$, the average number of OD groups bound per copper atom, was calculated by the use of Eqs. (1) and (2).

All the emf measurements were carried out at 25.00± 0.01°C in a paraffin oil thermostat, and the test solution was stirred by nitrogen gas presaturated by passing it through D_2O and $NaClO_4$ in D_2O.

Results and Calculations

The $Z(\log d)_B$ data are shown graphically in Fig. 1. The experimental data were analyzed by the graphical method. At first, the analysis was made in order to obtain information on the composition of the hydrolysis species and the approximate stability constants, then, on the basis of the

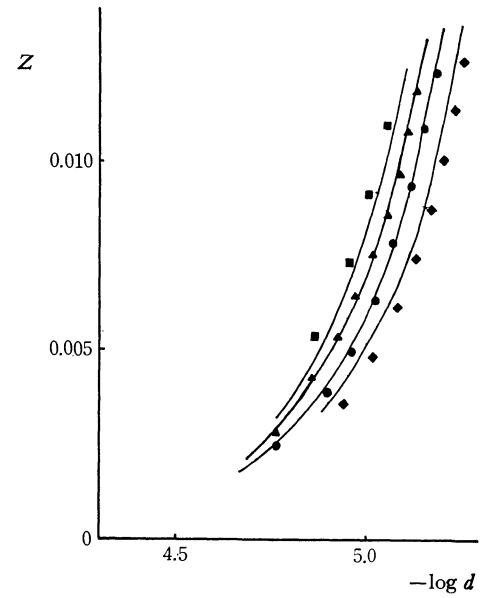

Fig. 1. Average number, Z, of OD bound per Cu, as a function of $-\log d$. Drawn curves were calculated with the stability constants given in Table 1.

B			
■	90.58 mM	▲	76.20
●	62.12	◆	47.65

10) E. P. Treadwell and W. T. Hall, "Analytical Chemistry," Vol. 2, John Wiley & Sons, New York (1955), p. 156.

11) G. Biedermann and S. Hietanen, *Acta Chem. Scand.*, **14**, 711 (1960).

12) G. Biedermann and L. Ciavatta, *ibid.*, **16**, 2221 (1962).

13) L. Ciavatta, *Arkiv Kemi*, **20**, 417 (1962).

14) G. Gran, *Analyst*, **77**, 661 (1952).

information thus obtained, the accurate stability constants were determined.

1) The Evaluation of the Composition of the Hydrolysis Species. When we take into account the fact that, in test solutions, the maximal value of Z never exceeds 0.015, then, without introducing any appreciable error, we may simplify the preliminary calculations by using the approximation:

$$[Cu^{2+}] = b \cong B = \text{constant.} \quad (3)$$

The concentration of the deuterium ions set free by hydrolysis, BZ, is expressed by the equation:

$$BZ = \sum_p \sum_q p\,[Cu_q(OD)_p^{(2q-p)+}] = \sum_p \sum_q p\,\beta_{p,q}\,b^q d^{-p}. \quad (4)$$

Using Eq. (3), Eq. (4) can be written:

$$Zd = \sum_p \sum_q p\,B^{q-1}\beta_{p,q}d^{-(p-1)} = \sum_p p\,d^{-(p-1)}K_p. \quad (5)$$

where:

$$K_p = \sum_q B^{q-1}\beta_{p,q}. \quad (6)$$

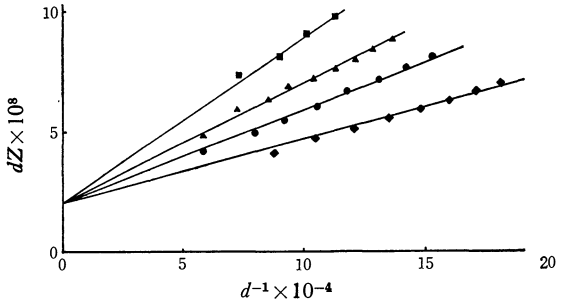

Fig. 2. dZ as a function of d^{-1} (see Eq. (5)). The straight lines are given by the stability constants; $\log\beta_{1,1}=-7.69$ and $\log\beta_{2,2}=-11.47$.

B

■ 90.58 mM ▲ 76.20

● 62.12 ◆ 41.65

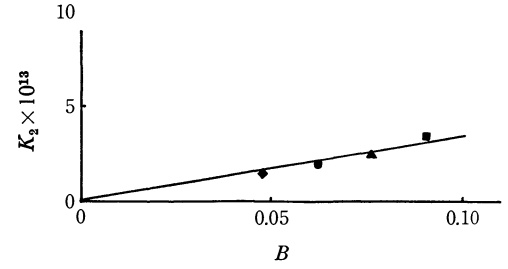

Fig. 3. K_2 as a function of B (Eq. (6)). The straight line represents the equation $K_2=3.42\times10^{-12}B$.

B

■ 0.09058 M ▲ 0.07620

● 0.06212 ◆ 0.04765

In order to find the prevailing values of p, plots of Zd against d^{-1} were constructed;[9] they are shown in Fig. 2. The plots closely approximate a set of straight lines with a common intercept. This result indicates that the prevailing values of p are 1 and 2.

Next, to determine the values of q, the data were compared at different values of B. The common intercept, $K_1=\sum_q B^{q-1}\beta_{1,q}$, of the previous plots shows that one of the prevailing values of q is 1. The other values were obtained from their slopes. The slope of the line is represented as $2K_2=2(\beta_{2,1}+B\beta_{2,2}+\cdots)$ at each value of B. Figure 3 shows a plot of these K_2 values against B, which gives a straight line passing through the point of

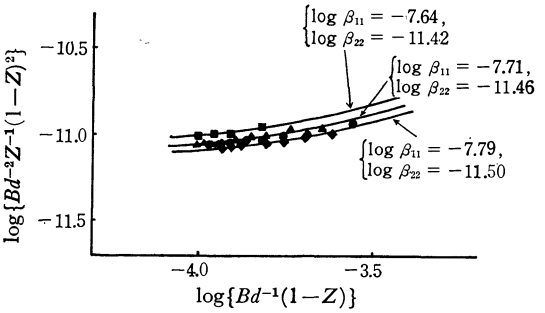

Fig. 4. $-\log\alpha$ as a function of $-\log\omega$, see Eq. (9). The curves were calculated with the $\log\beta_{1,1}$ and $\log\beta_{2,2}$ values given in the figure.

B

■ 90.58 mM ▲ 76.20

● 62.12 ◆ 47.65

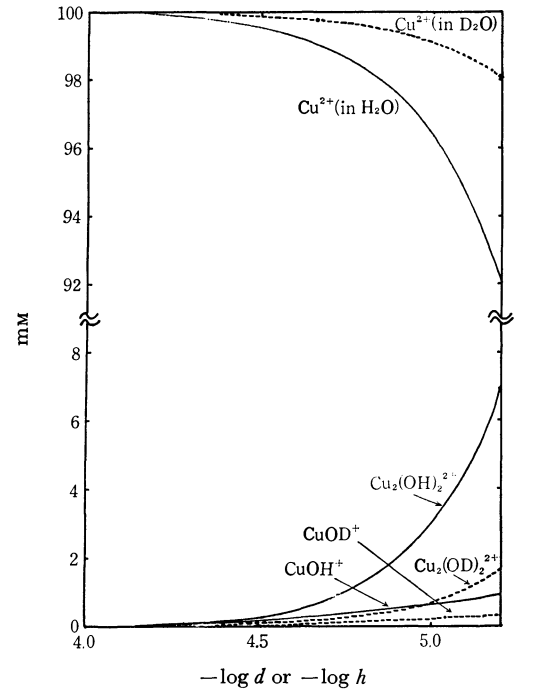

Fig. 5. The calculated distribution of the hydrolytic species in heavy water and in light water at total copper(II) concentrations of 100 mM. Dotted curves represent the distribution of the species in heavy water and full curves in light water.

origin. This indicates that another value of q is 2.

From the results, it can be concluded that the compositions of the hydrolysis species of the copper(II) ion are $CuOD^+$ and $Cu_2(OD)_2^{2+}$, and the approximate stability constants can be estimated to be $\log \beta_{1,1} = -7.69$ and $\log \beta_{2,2} = -11.47$.

2) The Evaluation of the Stability Constants of the Hydrolysis Species. The above analysis involved some approximation. It is, therefore, desirable to compare the data directly with the normalized function similar to that described in Ref. 15. We start from the fundamental equations:

$$Z = (\beta_{1,1}d^{-1}+2\beta_{2,2}bd^{-2})/(1+\beta_{1,1}d^{-1}+2\beta_{2,2}bd^{-2}) \quad (7)$$

$$B = b(1+\beta_{1,1}d^{-1}+2\beta_{2,2}bd^{-2}). \quad (8)$$

From Eqs. (7) and (8), and by eliminating $b=B\times(1-Z)$, the following equation is obtained:

$$\alpha = Zd^2B^{-1}(1-Z)^{-2} = \beta_{2,2}(2+\beta_{1,1}\beta_{2,2}^{-1}dB^{-1}(1-Z)^{-1}) = \beta_{2,2}(2+\beta_{1,1}\beta_{2,2}^{-1}\omega) \quad (9)$$

If we set $\alpha_1=\alpha\beta_{2,2}^{-1}$ and $\omega_1=\omega\beta_{1,1}\beta_{2,2}^{-1}$, Eq. (9) may be compared with the normalized function:

$$\log \alpha_1 = \log (2+\omega_1). \quad (10)$$

A plot of the log $\{Bd^{-2}Z^{-1}(1-Z)^2\}$ against log $\{Bd^{-1}(1-Z)\}$, which will be independent of B, can be fitted to a plot of α_1 against log $(2+\omega_1)$ at the particular values of $\beta_{1,1}$ and $\beta_{2,2}$. As shown in Fig. 4, we can obtain the following values:

$$-\log \beta_{1,1} = 7.71\pm0.07 \text{ and } -\log \beta_{2,2} = 11.46\pm0.04$$

These values are listed in Table 1, together with the values obtained by us in light water.

Table 1. The values for the stability constants of the hydrolysis species of copper(II) ion in heavy water and in light water containing 3M $NaClO_4$ as an ionic medium

	in heavy water	in light water
$\log \beta_{1,1}$	-7.71 ± 0.07	-7.22 ± 0.03
$\log \beta_{2,2}$	-11.46 ± 0.04	-10.75 ± 0.02

3) Distribution of the Species. The distribution of the hydrolysis species in heavy water and in light water, calculated at the total copper(II) concentration of 100 mM and assuming the values of the stability constants obtained by us, is shown in Fig. 5.

As has been mentioned earlier,[3,4] the species are less hydrolyzed in heavy water than in light water.

A more detailed discussion must be postponed until other hydrolytic reactions of metal ions have been investigated.

15) G. Biedermann, N. C. Li and J. Yu, *Acta Chem. Scand.*, **15**, 555 (1961).

BULLETIN OF THE CHEMICAL SOCIETY OF JAPAN VOL. 43 3159—3164 (1970)

The Photometric Determination of Micro Amounts of Bromine in Silicate Rocks by Means of Its Catalytic Effect

Kazuyoshi TAKAHASHI, Minoru YOSHIDA, Takejiro OZAWA and Iwaji IWASAKI

Laboratory of Analytical Chemistry and Geochemistry, Faculty of Science, Tokyo Institute of Technology, Ookayama, Tokyo

(Received March 31, 1970)

The catalytic action of bromide on the oxidation of to iodine iodate by potassium permanganate in sulfuric acid solution has been utilized for the microdetermination of bromine in silicate rocks. The method described consists of decomposing the silicate-rock sample by fusion with potassium hydroxide, leaching the melt with water, oxidizing bromide to bromine with potassium permanganate, extracting by benzene, and finally determining the bromine by the catalytic method. By this method, the bromine in samples with more than 0.04 ppm can be determined rapidly and accurately, using only 0.25—0.5 g of samples.

Data on the halogen contents of igneous rocks are important in discussing the relation between igneous rocks and magmatic emanations. The fluorine and chlorine contents have been reported by many investigators, but the data on bromine and iodine are rather scanty on account of the lack of a suitable analytical method. The results of a systematic investigation of bromine in rocks made by Behne[1] were long accepted as reliable, but the sensitivity of his analytical method (titrimetric) is too low to determine as low a bromine content as 1 ppm or less. In 1964, Filby[2] reported that the bromine content of two standard rocks collected by the U.S.Geological Survey, as determined by neutron activation analysis, was appreciably lower than Behne's average value. Recently, Sugiura[3] determined the bromine content of igneous rocks by a photometric method using rosaniline and molybdate after distillation. His values were also lower than those of Behne. Sugiura's method is applicable to rocks with more than 0.2 ppm bromine, but its sensitivity is not yet enough for many igneous rocks.

The sensitivities of usual photometric methods are too low for them to be used in the determination of bromine in igneous rocks. The neutron activation method has, indeed, a very high sensitivity, but it requires special equipment and time-consuming irradiation procedures.

One of the present authors (I.I.) and others[4] have previously reported a photometric method for the determination of bromide, a method based on the catalytic effect of bromide on the oxidation of iodine to iodate by potassium permanganate in a sulfuric acid solution. This method has an excellent sensitivity and sufficient accuracy and does not need any expensive equipment.

The present authors have first investigated in detail the iodine-potassium permanganate reaction in the presence of Br^- or Cl^- as a catalyst and have established optimum conditions for the microdetermination of bromine by means of its catalytic effect.

Although the catalytic action itself is highly selective, the method is affected by various coexisting substances. Because of the chemical complexity of usual silicate rocks, the isolation of bromine is necessary before using the catalytic method. We have established a rapid, sensitive, and accurate method for the determination of very small amounts of bromine (>0.04 ppm) in common silicate rocks.

Experimental

Apparatus. A Hirama photoelectric-colorimeter with a 460 filter (with maximum transmission at 460 mμ) and 10-mm cells was used to measure the absorbance.

The reactions were carried out in a water bath kept at 25.0±0.1°C with a Taiyo Thermo Unit.

Reagents. All the chemicals used were of analytical-reagent quality. Redistilled water was used for the reagent preparation and throughout the procedure.

Potassium Iodide Solution. Dissolve 1.31 g of potassium iodide and 2 g of sodium carbonate in water and dilute to 1 *l*; this yields 1 mg/m*l*.

Potassium Permanganate Solution (0.04M).

Potassium Bromide Solution. Prepare a 0.1M potassium bromide solution. The solution is standardized by Volhard's method.[5] Prepare the working solution by

1) W. Behne, *Geochim. Cosmochim. Acta*, **3**, 186 (1953).
2) R. H. Filby, *Anal. Chim. Acta*, **31**, 434 (1964).
3) T. Sugiura, This Bulletin, **41**, 1133 (1968).
4) M. Shiota, S. Utsumi and I. Iwasaki, *Nippon Kagaku Zasshi*, **80**, 753 (1959).
5) F. P. Treadwell and W. T. Hall, "Analytical Chemistry," Vol. II, John Wiley & Sons, Inc., New York (1935), p. 657.

diluting this solution adequately.

Sodium Chloride Solution. Dissolve 1.649 g of sodium chloride in water and dilute to exactly 1 *l*. This solution contains 1 mg of chloride per m*l*. The working solution is prepared by successive dilutions.

Sulfuric Acid Solution (1 : 1).

Ferric Ammonium Sulfate Solution. Dissolve 6 g of ferric ammonium sulfate in 100 m*l* of a 6N nitric acid solution. The solution is then stored in a brown glass bottle.

Mercuric Thiocyanate Solution. Solid mercuric thiocyanate was prepared as has been described by Utsumi.[6] Dissolve 0.3 g of mercuric thiocyanate in 100 m*l* of absolute ethyl alcohol.

Sodium Sulfite Solution (0.1M). Dissolve 1.26 g of anhydrous sodium sulfite in 100 m*l* of water. This solution is prepared afresh each week.

Potassium Dichromate Solution (0.01M).

Benzene. Wash guaranteed benzene with a 1N sodium hydroxide solution, a 1N sulfuric acid solution, and finally three times with water.

Procedure and Calibration Curve. 0.25 to 0.5 g of a finely-powdered sample is placed in a 30-m*l* nickel crucible. Add 3.0 g of potassium hydroxide pellets to the crucible. Cover the crucible, and heat it to about 500°C on an electric heater for 15 min. Leach the resulting fused cake with 35 m*l* of water. Centrifuge the resulting suspension in a 50-m*l* centrifuge tube. Transfer the supernatant liquid to a 100-m*l* separatory funnel. Add 10 m*l* of water to the residue, shake, and centrifuge again. Transfer the supernatant liquid to the above-mentioned separatory funnel.

To the solution in the separatory funnel add 1.5 m*l* of the sodium sulfite solution, and then 6.4 m*l* of the sulfuric acid solution (1 : 1).

After the solution has stood for about 10 min, add the potassium dichromate solution until the yellow color of the dichromate ion persists. After the subsequent addition of 30 m*l* of benzene, immerse the separatory funnel in a water bath kept at 25°C for about 15 min. Start shaking (360 strokes/min, using a shaker) immediately after adding 1.2 m*l* of the potassium permanganate solution. After 20 min's shaking, discard the aqueous layer. Shake the organic layer with 5 m*l* of 1.8N sulfuric acid for one minute. Discard the aqueous phase. To the organic layer, add 3.0 m*l* of a 1N sodium hydroxide solution and 16.8 m*l* of water, and shake the separatory funnel for 3 min. After the phase separation, transfer the aqueous layer to a 50-m*l* separatory funnel. Care must be exercised to completely exclude benzene, since even a small amount of benzene disturbs the subsequent procedure.

To the aqueous layer, add 3.2 m*l* of the sulfuric acid solution (1 : 1) and 1.0 m*l* of the potassium iodide solution, and then mix. Place the separatory funnel in a water bath at 25.0±0.1°C for about 15 min. Start the reaction by adding 0.5 m*l* of the potassium permanganate solution (at the same temperature). Swirl to mix thoroughly and let the separatory funnel stand in the water bath. Exactly 3 min after the addition of the potassium permanganate solution, add 10 m*l* of cold (about 0°C) carbon tetrachloride and immediately shake the separatory funnel for 15 sec.

After the phase separation, transfer the organic layer to a 50-m*l* separatory funnel. To the organic layer, add 10.0 m*l* of water, 2.0 m*l* of the ferric ammonium sulfate solution, and 1.0 m*l* of the mercuric thiocyanate solution, and shake the separatory funnel for about one minute. The aqueous layer is thus colored with ferric thiocyanate. Measure the absorbance of this aqueous layer at 460 mμ using a 10-mm cell and against water used as a reference.

The calibration curve shown in Fig. 1 was obtained by the procedure described above, using 45 m*l* of standard bromide solutions (or bromate solutions) of known concentrations and 3 g of solid potassium hydroxide.

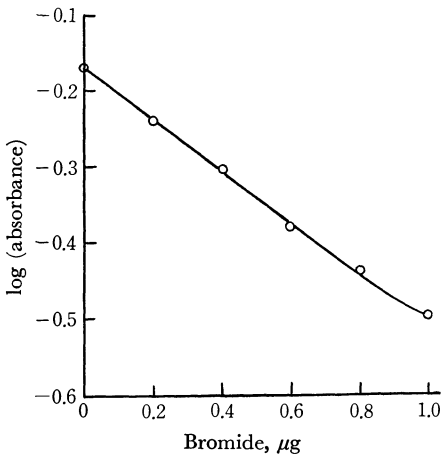

Fig. 1. Calibration curve.

Results and Discussion

The Catalyzed Oxidation Reaction of Iodine by Permanganate. The oxidation reaction between iodide and potassium permanganate in an acid medium is shown in Eqs. (1) and (2).

$$10\,I^- + 2MnO_4^- + 16H^+ \rightarrow 5I_2 + 2Mn^{2+} + 8H_2O \quad (1)$$

$$I_2 + 2MnO_4^- + 4H^+ \xrightarrow[\text{catalyst}]{Br^-,\ Cl^-} 2IO_3^- + 2Mn^{2+} + 2H_2O \quad (2)$$

The reaction (1) is very fast compared to the reaction (2), which is the rate-determining step. The rate of the reaction (2) was followed by the photometric determination of the change in the concentration of the unreacted iodine as a function of the time.

One of the present authors (I.I.) and others[7] have previously reported a photometric method for the determination of iodide by using ferric ammonium sulfate and mercuric thiocyanate. In order to examine the relationship between the amounts of unreacted iodine and the absorbance, a series of reaction mixtures containing various amounts of iodine was prepared. Into each separatory funnel, 20-m*l* portions of iodide solutions of known con-

6) S. Utsumi, *Nippon Kagaku Zasshi*, **73**, 835 (1952).

7) I. Iwasaki, S. Utsumi, A. Tomonari and I. Morita, *ibid.*, **80**, 749 (1959).

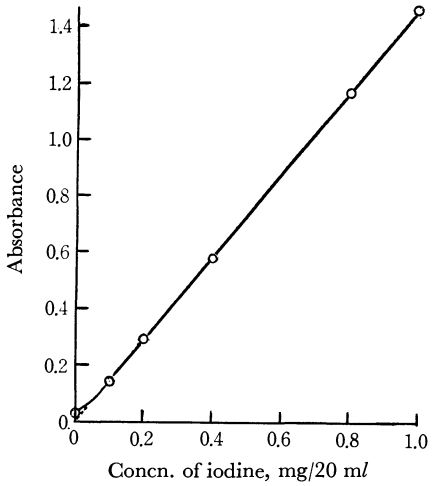

Fig. 2. Relationship between concentration of iodine and absorbance at 460 mμ.

centrations, 3 m*l* of sulfuric acid (1 : 1), and 3 m*l* of a 3% hydrogen peroxide solution were introduced. The resulting iodine was extracted with 10 m*l* of carbon tetrachloride and was colored with ferric thiocyanate as in the analytical procedure.

As is shown in Fig. 2, there is a linear relationship between the absorbance at 460 mμ and the concentration of iodine, but not at low concentrations. In order to exclude the nonlinear portion of the curve, absorbance readings were subsequently confined to the range of from 0.1 to 1 mg of iodine.

The concentration of sulfuric acid suitable for the oxidation reaction was first sought. The reaction proceeds smoothly when 3 m*l* of the sulfuric acid solution (1 : 1) are added to 20 m*l* of a sample.

After the most satisfactory conditions of acidity had been determined, the effect of potassium permanganate on the oxidation reaction in the absence of bromide or chloride was investigated by adding 0.5-m*l* portions of potassium permanganate solutions with various concentrations.

The plots of the log absorbance *vs.* the time yield fairly good straight lines, indicating a first order relationship with respect to iodine. From the slopes of the straight lines, the rate constants, *K*, were calculated; they were then plotted as a function of the initial concentration of potassium permanganate (Fig. 3). The direct proportionalities between the rate constants and the initial concentration of potassium permanganate indicate that the reaction is again first order with respect to potassium permanganate. (Variations in the ionic strength in this range produce no effect on the reaction rate; the rate did not change even in the presence of 0.1 mol/*l* of sodium sulfate).

The reaction rate increases sharply with an increase in the concentration of potassium permanganate, as is shown in Fig. 3. Consequently, the higher the concentration of potassium permanganate, the lower the accuracy of the present kinetic method because of the inevitable variation in the rate of the noncatalytic reaction. It is best to use 0.5 m*l* of a 0.04M potassium permanganate solution, because the reaction proceeds relatively slowly under these conditions.

The catalyst may influence the rate constant without altering the kinetic order of the noncatalytic reaction. Accordingly, using solutions containing bromide or chloride we carried out catalyzed reactions between iodine and potassium permanganate with 0.5 m*l* of a 0.04M potassium permanganate solution.

The reaction rate curves, II, III, and IV, in Fig. 4 were obtained by using 0.02- and 0.05-ppm bromide solutions and a 5-ppm chloride solution. The curve I was obtained by using redistilled water. The differences in absorbances among the three curves (I, II, and III) are largest after 3 minutes. A reaction time of 3 min is adequate for

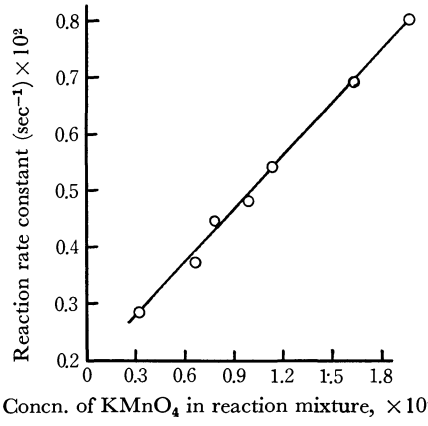

Fig. 3. Effect of potassium permanganate on the reaction rate constant.

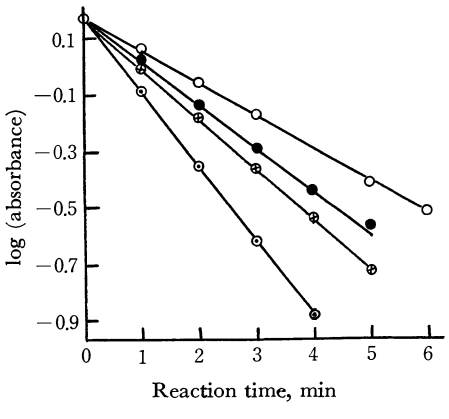

Fig. 4. Effects of bromide and chloride on the reaction rate.
○ redistilled water (I) ⊗ 0.02 ppm Br^- (II)
⊙ 0.05 ppm Br^- (III) ● 5 ppm Cl^- (IV)

the determination of bromide because of the high sensitivity. As can be seen in Fig. 4, the reaction follows approximately (pseudo) first order kinetics at each catalyst concentration, and the first order rate constant increases with the quantity of the catalyst. If the reaction is first order with respect to the catalyst, for the same initial concentration of potassium permanganate the log absorbance and the catalyst concentration should yield a linear relationship at a constant reaction time.

In order to confirm this point, experiments on a series of reaction mixtures containing various amounts of catalysts were carried out. In Fig. 5,

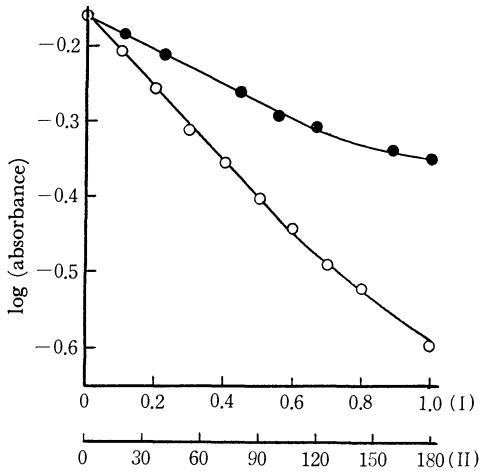

Fig. 5. Effects of amounts of bromide and chloride.
○ Br^- (I) ● Cl^- (II)

the resulting log absorbance are plotted against the catalyst concentration. At a low concentration of the catalyst, the linear relationship was recognized, but at a high concentration there was a departure from linearity. It seems that the catalyst dependence is first order at a low concentration. The catalytic effect of chloride is smaller than that of bromide. The abundance of chlorine in silicate rocks is, however, considerably greater than that of bromine.

Extraction. Utsumi *et al.*[8] have discussed the extraction of small amounts of bromine (order of 100 μg) by carbon tetrachloride in the determination of bromide in natural waters. Their procedure was based on the selective oxidation of bromide to bromine by potassium permanganate. In this investigation the present authors examined the extraction procedure of less than 1 μg of bromine. Bromide was oxidized to bromine by employing various oxidizing agents. The resulting bromine was extracted by benzene, stripped from the organic layer by a sodium hydroxide solution, and determined by the catalytic method. The use of carbon tetrachloride as the solvent was not suitable, because a minute amount of carbon tetrachloride retained in the aqueous layer remarkably promoted the iodine-potassium permanganate reaction in the subsequent procedure.

It was found that the oxidation of bromide to bromine by potassium dichromate or ceric ammonium sulfate is very slow and that the oxidation reaction by potassium permanganate proceeds fairly smoothly. However, the recovery of added bromide decreased with an increase in the standing time for the oxidation by permanganate, and satisfactory results were not obtained.

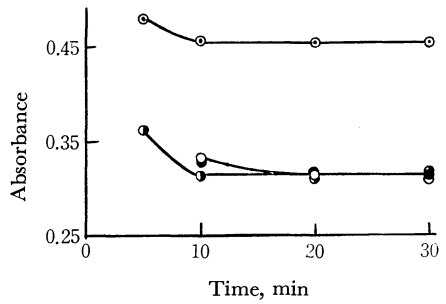

Fig. 6. Effect of shaking time on oxidation and extraction.
25°C, Volume of sample solution: 50 ml
○ 18N H_2SO_4 2 ml, Br^- 1 μg
◑ 18N H_2SO_4 4 ml, Br^- 1 μg
0.04M $KMnO_4$ 1 ml
● 18N H_2SO_4 6.4 ml, Br^- 1 μg, KOH 3 g
⊙ 18N H_2SO_4 6.4 ml, Br^- 0.5 μg, KOH 3 g
0.04M $KMnO_4$ 1.2 ml

Table 1. Recovery of added bromide after extraction

Br^- added, μg	0.20	0.40	0.60	0.80	1.00
Br^- found, μg	0.14	0.28	0.43	0.57	0.71
Recovery, %	70	70	72	71	71

Subsequently, the oxidation of bromide to bromine by permanganate and the extraction of the resulting bromine by benzene were made simultaneously. The extraction was carried out at 360 strokes/min using a shaker. As can be seen in Fig. 6, the absorbance at first changes rapidly with the shaking time, and then, after about 20 min, it does not change very much. In order to ascertain the recovery of added bromide after oxidation and extraction, some experiments were made using solutions containing various quantities of bromide.

The results listed in Table 1 show that recovery is about 70%, regardless of the amount of bromide. It was also found that the recovery of bromide increases slightly with an increase in the shaking

8) I. Iwasaki, S. Utsumi, I. Morita and M. Shiota, *nippon Kagaku Zasshi*, **80**, 744 (1959).

Table 2. Effect of diverse ions

Ion	Added as	Amount μg	Absorbance	
			Reagent blank	0.6 μg Br^-
None			0.681	0.420
Fe^{3+}	$Fe_2(SO_4)_3(NH_4)_2SO_4 \cdot 24H_2O$	10^5	0.680	0.422
Mg^{2+}	$MgSO_4 \cdot 7H_2O$	5×10^4	0.685	0.420
Al^{3+}	$K_2Al_2(SO_4)_4 \cdot 24H_2O$	5×10^4	0.680	0.420
Silicate ion	SiO_2+KOH	4×10^5	0.675	0.423
Cl^-	NaCl	3×10^2	0.680	0.420
		5×10^2	0.672	0.416
		10^3	0.650	0.405
Hg^{2+}	$HgSO_4$	1	0.678	0.422
		2	0.689	0.465
		10	—	0.420*
Ag^+	Ag_2SO_4	5	0.685	0.425
		10	0.685	0.450
I^-	KI	40	0.690	0.421

* The procedure of potassium hydroxide fusion was carried out.

rate. Even when bromine once extracted into benzene is shaken with a washing solution of 1.8N sulfuric acid, appreciable amounts of bromine do not move to the aqueous layer. Bromine extracted in benzene is stripped into the aqueous layer by shaking it for about 2 min with a sodium hydroxide solution.

The Effect of Diverse Ions. The effect of diverse ions on this method was studied, some experiments being made in the presence of 0.6 μg of bromide and in its absence. The experimental results given in Table 2 were obtained without fusion. Magnesium, iron, aluminum, and silicate do not interfere, even at high concentrations. Chloride interferes slightly at 500 μg. However, even if the sample contains a large amount of chloride, the bromine can be determined by decreasing amounts of the sample to be weighed, for fortunately, the bromine-to-chlorine ratios in igneous rocks are rather constant.[3],*1 Iodide does not interfere at 40 μg. As silver and mercuric ions react with bromide, they interfere even at low concentrations. However, the interference of mercury can be completely removed by fusion with potassium hydroxide. Most igneous rocks do not contain silver in concentrations which cause any serious interference.[9,10]

Table 3. Determination of bromine in some silicate rocks

Sample	Amount of sample, g	Br added μg	Br found μg		Br found in washed residue μg	Concn. of Br ppm (Average)
I (Basalt)	0.5	—	0.82	0.84	(0.00)	1.66
II (Andesite)	0.5	—	0.71	0.78	(0.01)	
			0.73	0.71	(0.00)	1.45
			0.70			
	0.25	—	0.36	0.35		
			0.37	0.40		1.48
	0.25	0.50	0.85	0.85		
III (Liparite)	0.25	—	0.64	0.63	(0.02)	
			0.61		(0.01)	2.51
	0.25	0.30	0.90	0.93		

*1 The results of the determination of bromine and other halogens in igneous rocks will be reported in a forthcoming paper.

9) K. Rankama and Th. G. Sahama, "Geochemistry," University of Chicago Press, Chicago (1950), p. 702.

10) M. Fleischer, *Geochim. Cosmochim. Acta*, **29**, 1263 (1965).

In practice, many metal ions occurring in silicate rocks are removed as precipitates by potassium hydroxide fusion. The amounts of bromine retained in the washed residue of fused silicate rock samples is small enough to be neglected. The amounts of bromine found in the washed residue are given in Table 3. These results were obtained by dissolving the washed residue with sulfuric acid (1.8N) and sodium sulfite solutions and using the method described under "Procedure and Calibration Curve."

The Results of Determination. The reproducibility of the method was tested by taking 0.25 to 0.5-g samples of various silicate rock samples and by then following the procedure described above. The method was also checked by adding known amounts of bromide to rock samples. The results shown in Table 3 demonstrate the reliability of the method.

According to these results, it may be concluded that the present method is satisfactory for the determination of bromine in rocks. By this method, bromine in samples with more than 0.04 ppm can be determined rapidly using only 0.25 to 0.5-g portions of the sample. The error in this method is about ± 0.03 μg at bromine of 0.50 μg and less at lower amounts.

The authors wish to express their sincere thanks to the Research Fund of the Kawakami Memorial Foundation for a research grant partly used in support of this work.

BULLETIN OF THE CHEMICAL SOCIETY OF JAPAN VOL. 43 3164—3166 (1970)

Spectrophotometric Determination of Diphenhydramine in Pharmaceutical Preparations

Masahiro TSUBOUCHI

Faculty of Education, Tottori University, Tottori

(Received May 29, 1970)

A spectrophotometric method is proposed for the determination of diphenhydramine in pharmaceutical preparations. The method is based on an addition-compound formation between diphenhydramine and the tetrabromophenolphthalein ethyl ester in 1,2-dichloroethane. Beer's law is obeyed over the range of 2.0×10^{-6}—1.0×10^{-5}M of diphenhydramine at 594 mμ. Optimum conditions are described. The effect of diverse substances and the composition of the colored species were also investigated.

The titrimetric method[1] has been used for the determination of diphenhydramine, which is widely used as antihistaminate. Cobalt nitrate - potassium thiocyanate - sulfuric acid[2] and nitric acid -sulfuric acid[3] have been described as spectrophotometric reagents for diphenhydramine. A fluorometric method[4] based on the oxidation of diphenhydramine has also been described.

Recently, plasmocorinth B[5] was proposed for the spectrophotometric determination of diphenhydramine by solvent extraction. This method can not, however, be used in the analysis of injections because it suffers from the interference of halide and calcium ions.

This paper will report the results of a study designed to develop a new spectrophotometric method for diphenhydramine by means of solvent extraction. The tetrabromophenolphthalein ethyl ester forms an addition compound with colorless diphenhydramine in 1,2-dichloroethane. In the absence of diphenhydramine, a yellow color was observed, while in its presence a red-violet color was developed.

Experimental

Apparatus. The spectrophotometric measurements were made with a Shimadzu QR-50 spectrophotometer, equipped with 10-mm cuvettes. An Iwaki Model KM shaker with a time switch was used for the extraction. The pH measurements were carried out with a Toa Denpa Model HM-5 pH meter.

Reagents. *Tetrabromophenolphthalein Ethyl Ester (TEE)*

1) J. P. VII-1, Part II, Nankodo (1965), p. 594.
2) G. Sekules and G. Guadagnini, *Boll. Chim. Farm.*, **103**, 432 (1964); *Chem. Abstr.*, 11853 (1964).
3) L. Molle, *J. Pharm. Belg.*, **5**, 339 (1950).
4) R. E. Jensen and R. T. Pflaum, *J. Pharm. Sci.*, **53**, 835 (1964).
5) H. Koike, K. Ohashi, M. Matsuo and A. Kawasaki, *Bunseki Kagaku*, **17**, 603 (1968).

Solution. Weighed amounts of tetrabromophenolphthalein ethyl ester potassium salt were dissolved in ethyl alcohol.

Standard Diphenhydramine Solution. A stock solution was prepared by dissolving 2.919 g of diphenhydramine hydrochloride (dried at 105°C) and diluting it to 1 *l* with water to make the solution 1.0×10^{-2}M. The stock solution was used to prepare the standard solution in the desired concentration.

Buffer Solution. The pH 8 buffer was prepared by mixing a 0.4M potassium dihydrogen phosphate solution and a 0.4M disodium hydrogen phosphate solution.

All the chemicals were of a reagent grade, and the water used was passed through an ion-exchange resin.

Procedure. *Standard Procedure.* Pipette 5 m*l* of a diphenhydramine solution (less than 5×10^{-5}M), 5 m*l* of a TEE solution (10^{-3}M), and 5 m*l* of the buffer solution into a 100-m*l* separatory funnel. Dilute the mixture to 25 m*l* with water and shake the solution for 2 min with 10 m*l* of 1,2-dichloroethane. After the separation of the two layers, run off the extract into a glass tube through filter paper to remove any droplets of water. Measure the absorbance of the extract at 594 mμ, using a reagent blank as a reference.

Injection. Dilute a sample with water and treat the solution in the same manner as with the standard procedure.

Powder and Tablet. Dissolve a sample containing about 5 mg of diphenhydramine in 50 m*l* of 0.01N sulfuric acid. Filter the solution with a glass filter and dilute the filtrate to 500 m*l* with water. Treat the solution in the same manner as with the standard procedure.

Ointment. Place a sample containing about 5 mg of diphenhydramine in a separatory funnel, and add 15 m*l* of ether. Extract the diphenhydramine three times with 30-m*l* portions of 0.03N sulfuric acid. Put all the extracts together into a 500-m*l* volumetric flask and make up to the mark with water. Treat the solution in the same manner as with the standard procedure.

Results and Discussion

Absorption Spectra. Figure 1 shows the visible absorption spectra of extracts treated as with the standard procedure. It can be seen that the presence of diphenhydramine leads to a considerable increase in the absorbance. The absorbance maximum of the extracts is at 594 mμ. This red-violet color in the organic layer may be attributed to the effect of the association between the TEE and the diphenhydramine.

Effect of pH. The absorbance of the extract is constant over the 7—9 pH range. In a more acidic or a more alkaline solution, the absorbance decreases, presumable because the TEE is not extracted into an organic solvent from a strong alkaline solution and because the diphenhydramine is not extractable from an acidic solution.

Effect of Reagents. Excess amounts of the phosphate buffer had no influence on the absorbance of the extract. When the buffer concentration was less than 0.05M in the aqueous layer, a good separation of the two layers was not observed.

The absorbance of the extract was constant if the TEE concentration was more than the 1.2×10^{-4}M initially present in the aqueous layer when the concentration of diphenhydramine was 1.0×10^{-5}M. With smaller amounts of TEE, low absorbances were obtained.

Solvent for Extraction. The behavior of various solvents in the extraction was studied. The solvents tested were benzene, butyl acetate, carbon tetrachloride, chloroform, cyclohexane, 1,2-dichloroethane, ether, ethyl acetate, *n*-hexane, isoamyl alcohol, methyl isobutyl ketone, monochlorobenzene, and toluene. Of these, dichloroethane was chosen for the present work because it gave the deepest color.

The Other Variables. Full color development took about 1 min of shaking. Continued shaking up to 5 min product no further change in the absorbance. The color intensity of the dichloroethane extracts remained constant for 1 hr. Normal room temperature fluctuations (14—26°C)

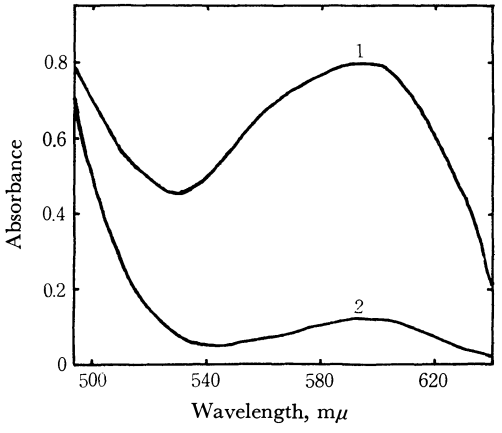

Fig. 1. Absorption spectra.
1: 1.0×10^{-5}M of diphenhydramine
2: Reagent blank
Reference: water

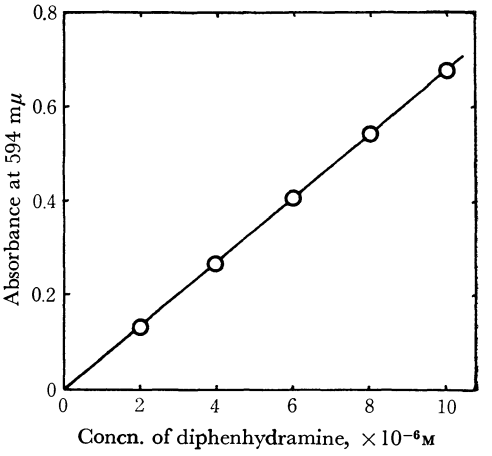

Fig. 2. Calibration curve.
Reference: Reagent blank

TABLE 1. EFFECT OF FOREIGN SUBSTANCES

Substance	Mole Ratio	Recovery (%)
Ammonium sulfate	1000	104.3
Calcium chloride	1000	99.0
Sodium carbonate	1000	102.1
Sodium chloride	1000	100.0
Sodium nitrate	1000	98.8
Potassium bromide	1000	100.0
Aniline	1000	99.7
Aminopyrine	5	125.1
Antipyrine	20	115.5
Benzyl alcohol	1000	99.6
Caffeine	10	117.7
Ethoxybenzamide	50	119.2
Glucose	1000	100.0
Lactose	1000	100.1
Noscapine	1	112.3
Phenacetine	5	116.5
Phenol	1000	93.8
Sodium acetate	1000	100.0
Sodium cirate	1000	100.2
Sodium salicylate	1000	99.8
Sodium tannate	1000	100.2
Vitamine C	1000	99.4
Starch	0.4 %	100.0

Diphenhydramine taken : 1.0×10^{-5}M

were without measurable effect on the absorbance.

Calibration and Precision. Figure 2 shows the calibration curve obtained according to the standard procedure.

The reproducibility of the proposed method was setimated from the results for ten sample solutions, each with a final diphenhydramine concentration of 1.0×10^{-5} M. The mean absorbance was 0.675, with a standard deviation of 0.006 absorbance unit.

Composition of the Colored Species. A sample (25 m*l*) containing 1.0×10^{-5}M of diphenhydramine was extracted with 10 m*l* of dichloroethane at pH 8. Then the amounts of diphenhydramine in the aqueous layer and organic layer were determined according to the proposed method. The extraction rate was about 94% in the absence of TEE, and 95% in its presence. These results indicate that diphenhydramine is extracted independently of TEE and is then associated with TEE in the organic solvent.

TABLE 2. ANALYSIS OF DIPHENHYDRAMINE IN COMMERCIAL SAMPLES

Sample	Diphenhydramine content	
	Titrimetric method	Proposed method
Injection*	9.98 mg/m*l*	9.97 mg/m*l*
Tablet*	91.0 mg/g	90.6 mg/g
Powder	99.7 mg/g	99.4 mg/g
Ointment	9.84 mg/g	9.87 mg/g

* Contained as diphenhydramine hydrochloride
All samples were obtained from a drugstore.

Continuous-variation plots were employed in order to investigate the composition of the colored species. The total concentration of TEE and diphenhydramine was kept constant at 1.6×10^{-5}M. The resulting curves at 594 and 560 mμ, in which the reagent blank has been subtracted, have a maximum at 0.5 mol fraction of diphenhydramine. It may, therefore, be suggested that a 1 : 1 addition compound is formed in the dichloroethane phase between TEE and diphenhydramine.

Effect of Foreign Substances. Table 1 shows the effect of diverse substances on the determination of diphenhydramine. Sodium chloride, tannate, benzyl alcohol, and starch, all of which are apt to be present in a pharmaceutical preparation with diphenhydramine, do not interfere.

Analysis of Practical Samples. Commercial samples used as antihistaminates were analyzed according to the proposed method and the titrimetric method.[1] The results obtained are summarized in Table 2.

The author would like to express his appreciation to Professor Y. Yamamoto of Hiroshima University for his valuable advice.

BULLETIN OF THE CHEMICAL SOCIETY OF JAPAN VOL. 43 3167—3170 (1970)

Synthesis of Chelating Agents. VII.*1 Synthesis and Chelating Behavior of 2,3-Dinitrilo-1,2,3,4-tetrahydronaphthalene-*N*,*N*,*N*′,*N*′-tetraacetic Acid*2

Tairoku YANO, Hiroshi KOBAYASHI and Keihei UENO

Department of Organic Synthesis, Faculty of Engineering, Kyushu University, Hakozaki, Fukuoka

(Received June 1, 1970)

trans-2,3-Dinitrilo-1,2,3,4-tetrahydronaphthalene-*N*,*N*,*N*′,*N*′-tetraacetic acid was synthesized by the carboxymethylation of *trans*-2,3-diaminotetrahydronaphthalene. The acid dissociation constants as well as the chelate stability constants for alkaline earth metal ions were determined by a potentiometric method. The results were compared with the values of other complexane ligands of the cycloalkane family.

Extensive investigations have been carried out on the relationship between the structures of complexane type ligands and their chelate stability constants.[1] In our previous paper, we reported on the effect of phenyl substitutions on the ethylenic carbons of ethylenedinitrilo-*N*,*N*,*N*′,*N*′-tetraacetic acid (EDTA) upon the chelate stability constants.[2] It was pointed out that the ease of taking a skew configuration with regards to the nitrilodiacetate groups plays an important role in governing the chelate stability constants of EDTA analogous ligands. In this connection, we have been interested in the synthesis of the derivatives of 1,2-cyclohexanedinitrilo-*N*,*N*,*N*′,*N*′-tetraacetic acid (C_yDTA) in which the ease of taking a skew configuration is controlled by fusing an additional cyclohexane or benzene ring to 4,5-position. This paper deals with the synthesis as well as the chelating behaviour of a new ligand, 2,3-dinitrilo-1,2,3,4-tetrahydronaphthalene-*N*,*N*,*N*′,*N*′-tetraacetic acid (THDTA). *trans*-THDTA was obtained by the carboxymethylation of *trans*-2,3-diamino-1,2,3,4-tetrahydronaphthalene, whereas *cis*-THDTA could not be obtained from the corresponding *cis*-diamine as in the case of *meso*-1,2-diphenyl ethylenedinitrilotetraacetic acid.[2] The acid dissociation constant and the chelate stability constants for alkaline earth metal ions of *trans*-THDTA, which were measured by the direct potentiometric titration method, were interpreted in relation to those of complexane ligands of the cycloalkane family.

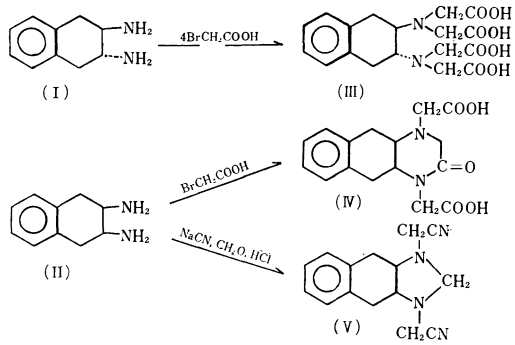

Scheme

Experimental

IR spectra were measured with a Nippon Bunko Model DS 301 spectrophotometer, and NMR spectrum was obtained with a Varian A-60 spectrophotometer with tetramethylsilane as an internal standard.

Synthesis of Ligand. *trans-2,3-Dinitrilo-1,2,3,4-tetrahydronaphthalene-N, N, N′, N′-tetraacetic Acid (trans-THDTA) (III).* Tetraacetic acid was synthesized by the alkaline condensation of bromoacetic acid with *trans*-2,3-diamino tetrahydronaphthalene.*3 The condition of a typical run was as follows.

In a 100 m*l* reaction vessel, a solution of 1.8 g (0.008 mol) of *trans*-2,3-diamino tetrahydronaphthalene dihydrochloride in 30 m*l* of 50% ethanol was placed. The solution was neutralized to phenolphthalein with 7N aqueous sodium hydroxide. Into this solution, a solution of 6.86 g (0.046 mol) of bromoacetic acid in 10 m*l* of water which had been neutralized with sodium hydroxide solution below 10°C was added with stirring,

*1 Paper VI: Y. Moriguchi, M. Miyazaki and K. Ueno, This Bulletin, **41**, 1344 (1968).

*2 Contribution No. 208 from the Department of Organic Synthesis, Kyushu University.

1) For example, H. Kroll and M. Gordon, *Annals of New York Academy of Sciences*, **88**, 341 (1960).

2) N. Okaku, Y. Toyoda, Y. Moriguchi and K. Ueno, This Bulletin, **40**, 2326 (1967).

*3 *trans*-Diamine (I) and *cis*-diamine (II) are new compounds, and the details of the synthetic procedures and the structural proof will be reported elsewhere along with the other new 1,2-diamines such as 2,3-diaminodecahydronaphthalenes.

and the temperature of the mixture was raised to 40°C. The pH of the reaction mixture was maintained at 9—10 (red to phenolphthalein) with an occasional addition of 7N aqueous sodium hydroxide. After adding 0.032 mole of sodium hydroxide, the resulting mixture was acidified with concentrated hydrochloric acid to pH 1.6—1.8. Monosodium salt of *trans*-THDTA was obtained as colorless precipitates. The free acid of THDTA was prepared by dissolving the sodium salt into hot water, followed by the readjustment of the pH of the solution to 1.8. The crude acid was recrystallized from hot water, to give the pure *trans*-THDTA, which was dried over phosphorous pentoxide in vacuum at 60°C for 10 hr. Yield 40%. It decomposed at 245°C. IR: ν_{CO}, 1740. 1620 cm^{-1}.

Found: C, 54.90; H, 5.69; N, 6.98%; mol. wt. (Neutrl. equiv.) 391. Calcd for $C_{18}H_{22}N_2O_8$: C, 54.82; H, 5.62; N, 7.10%; mol. wt. 394.

Attempted Synthesis of cis-THDTA. In order to obtain the *cis* isomer of tetraacetic acid, various reactions such as the alkaline condensation of bromoacetic acid with *cis*-diamine (II),*3 the alkaline condensation of ethyl bromoacetate with diamine in ethanol, or the cyanomethylation of diamine using hydrocyanic acid and formaldehyde, were tried. However, the isolated products were, instead of *cis*-THDTA, a ketopiperazine derivative and an imidazolidine derivative which were the cyclocondensation products of the reaction intermediates.

In the case of the alkaline condensation of bromoacetic acid, which is carried out under a similar condition to that described in the synthesis of the *trans* isomer, white precipitates (IV) were obtained from the acidified reaction mixture. The pure material which was recrystallized from hot water, melted at 205—217°C with decomposition. Yield 63%. The result of elementary analysis and infrared spectrum confirmed that the product (IV) is 1,4-diaza-2-keto-1,2,3,4,4a,9,9a,10-octahydroanthracene-1,4-diacetic acid (IV). IR (KBr): ν_{CO}, 1760, 1680, 1620 cm^{-1};

Found: C, 60.43; H, 5.63; N, 8.69%. Calcd for $C_{16}H_{18}N_2O_5$: C, 60.63; H, 5.67; N, 8.80%.

In the case of the cyanomethylation, 1.3 g (0.016 mol) of 36% formaldehyde and 0.77 g (0.016 mol) of sodium cyanide were successively added into a cold solution of 1 g (0.004 mol) of the *cis*-diamine in 11 m*l* of 1.2N hydrochloric acid, and the resulting mixture was kept in a pressure bottle. It was allowed to stand for 45 hr at 40°C with occasional stirring. The white precipitates (V) from the reaction mixture was recrystallized from ethanol. Mp 180—183°C. From the result of elementary analysis, infrared spectrum and NMR spectrum, the product was proved to be 1,3-diaza-1,3-cyanomethyl-5,6-benzo-3a,4,7,7a-tetrahydroindane (V). IR (in Nujol): ν_{CN} 2220 cm^{-1}. NMR ($CDCl_3$): δ: 7.16 (strong singlet, 4H), 3.81 (doublet, J=3.5 Hz, 1H), 3.68 (strong singlet, 4H), 3.41 (doublet, J=3.5 Hz, 1H), 3.31 (broad band with fine structure, 2H), 2.73 (appreciable quartet, 4H).

Found: C, 71.49; H, 6.13; N, 22.69%. Calcd for $C_{15}H_{16}N_4$: C, 71.43; H, 6.35; N, 22.22%.

Determination of Acid Dissociation Constants and Chelate Stability Constants. The same apparatus as that described in a previous paper was employed.[4] Measurements were carried out at 25.0± 0.1°C in aqueous solutions under the ionic strength, μ, of 0.10 with potassium nitrate. For the determination of acid dissociation constants, 100 m*l* of a 0.8—0.9×10^{-3}M solution of the ligand was titrated with a solution of 0.1M potassium hydroxide freed from carbonate ion. For the determination of chelate stability constants with alkaline earth metal ions, the direct pH titration method was employed on 100 m*l* of a solution (8×10^{-4}M in ligand and in metal ions).

Calculations

Calculation of the Acid Dissociation Constants. The titration curve of *trans*-THDTA is shown in Fig. 1. The acid dissociation scheme of the ligand can be expressed as follows:

$$H_4Y \rightleftarrows H_3Y^- + H^+$$
$$Ka_1 = [H_3Y^-][H^+]/[H_4Y]$$
$$H_3Y^- \rightleftarrows H_2Y^{2-} + H^+$$
$$Ka_2 = [H_2Y^{2-}][H^+]/[H_3Y^-]$$
$$H_2Y^{2-} \rightleftarrows HY^{3-} + H^+$$
$$Ka_3 = [HY^{3-}][H^+]/[H_2Y^{2-}]$$
$$HY^{3-} \rightleftarrows Y^{4-} + H^+$$
$$Ka_4 = [Y^{4-}][H^+]/[HY^{3-}]$$

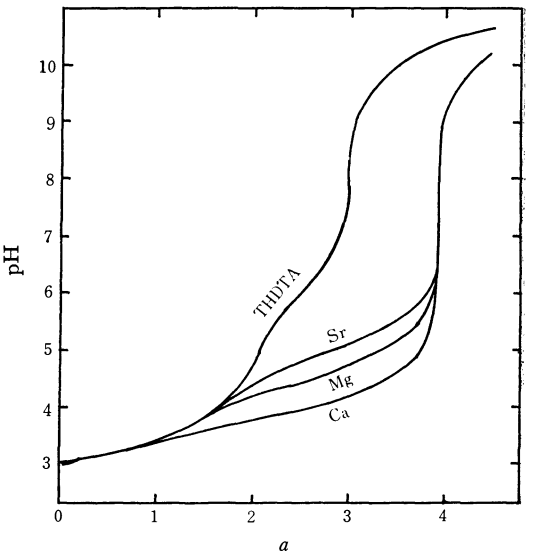

Fig. 1. Titration curves of THDTA.
Concn. of ligand and metal ions: 0.8×10^{-3}M
For the titration of ligand only: 0.9×10^{-3}M

It can be seen from Fig. 1 that the titration curve is essentially the same as that of EDTA and dissociation of the first two steps, third step and fourth step is clear. The acid dissociation constants of the ligand were calculated by two different methods; *i. e.*, the method of Schwarzenbach,[3] except that

3) G. Schwarzenbach, A. Willi and R. O. Bach, *Helv. Chim. Acta*, **30**, 1303 (1947).
4) T. Ando, This Bulletin, **36**, 1593 (1963).

an algebraic method of solution was used instead of a graphical one, and the method of Bjerrum as modified by McIntyre.[5]

a) Schwarzenbach's Method. The final equations for the first two dissociation steps are:

$$K_{a_2}[(2-a)C_A-[H^+]] - (aC_A+[H^+])[H^+]^2/K_{a_1} = [(a-1)C_A+[H^+]][H^+] \quad (1)$$

For the calculation of K_{a_3} and K_{a_4}, the following equations were used:

$$K_{a_3} = \{[H^+]\{(a-2)C_A+[H^+]-[OH^-]\}\}/\{C_A-\{(a-2)C_A+[H^+]-[OH^-]\}\} \quad (2)$$

$$K_{a_4} = \{[H^+](a-3)C_A-K_W\}/\{(4-a)C_A+[OH^-]\} \quad (3)$$

where a represents the moles of alkali added per mole of the ligand, C_A, the total ligand concentration and K_W, the ionic product of water.

b) Bjerrum's Method. The final equations for the first three dissociation steps are:

$$\bar{n} = J_1/K_{a_3} + J_2/K_{a_2}\cdot K_{a_3} + J_3/K_{a_1}\cdot K_{a_2}\cdot K_{a_3} \quad (4)$$

$$\bar{n}' = J_1'/K_{a_3} + J_2'/K_{a_2}\cdot K_{a_3} + J_3'/K_{a_1}\cdot K_{a_2}\cdot K_{a_3} \quad (5)$$

$$\bar{n}'' = J_1''/K_{a_3} + J_2''/K_{a_2}\cdot K_{a_3} + J_3''/K_{a_1}\cdot K_{a_2}\cdot K_{a_3} \quad (6)$$

where $\bar{n}$ represents the mean number of protons attached to the ligand, and

$$J_n = (n-\bar{n})[H^+]^n \quad (7)$$

For the calculation of K_{a_4}, equation (3) was used.

The results of both calculations are summarized in Table 1. The values for K_{a_2}, K_{a_3} and K_{a_4} are in fairly good agreement for both methods.

Calculation of the Chelate Stability Constants. By analogy with C_yDTA, THDTA will form almost exclusively the 1 : 1 chelate with multivalent metal ions.

$$M + Y \rightleftarrows MY \quad K_{MY} = [MY]/[M][Y] \quad (8)$$

Therefore, the calculation of the chelate stability constant K_{MY} can be carried out according to Bjerrum's standard procedure.[6] The final equation can be written as follows:

$$K_{MY} = \{C_A-\alpha[Y^{4-}]\}/\{C_M-C_A+\alpha[Y^{4-}]\}\cdot[Y^{4-}] \quad (9)$$

where C_A and C_M represent the total concentration of the ligand and the metal ion, respectively, and

$$\alpha = [H^+]^4/K_{a_1}\cdot K_{a_2}\cdot K_{a_3}\cdot K_{a_4} + [H^+]^3/K_{a_2}\cdot K_{a_3}\cdot K_{a_4} + [H^+]^2/K_{a_3}\cdot K_{a_4} + [H^+]/K_{a_4} + 1 \quad (10)$$

$$[Y^{4-}] = \{(4-a)C_A-[H^+]+[OH^-]\}/\{4[H^+]^4/K_{a_1}\cdot K_{a_2}\cdot K_{a_3}\cdot K_{a_4} + 3[H^+]^3/K_{a_2}\cdot K_{a_3}\cdot K_{a_4} + 2[H^+]^2/K_{a_3}\cdot K_{a_4}+[H^+]/K_{a_4}\} \quad (11)$$

The K_{MY} value was determined as a mean of K_{MY} values which were computed by Eq. (9) using Bjerrum's pK_a values, and a series of experimental values of a and $[H^+]$ during the course of titration. The results are summarized in Table 2.

Table 2. Chelate stability constants of THDTA and related complexanes
25±0.1°C μ=0.10 (KNO_3)

Metal ion	log K_{MY}		
	trans-THDTA	*trans*-C_yDTA[8]	*trans*-CPDTA[9]
Mg(II)	10.28±0.01	10.97	9.05
Ca(II)	11.63±0.03	13.15	11.08
Sr(II)	9.56±0.03	10.45	9.45

Table 1. Acid dissociation constants of THDTA and related complexanes
25±0.1°C μ=0.10 (KNO_3)

	pK_{a_1}	pK_{a_2}	pK_{a_3}	pK_{a_4}	t, °C	Ref.
trans-THDTA	2.2[a]	3.48±0.02	5.96±0.03	10.26±0.01	25	
	1.9[b]	3.54±0.03	5.99±0.01	10.30±0.05		
trans-C_yDTA	2.43	3.52	6.12	12.35	20	7, 8
cis-C_yDTA	2.44	3.50	5.21	10.70	20	9
trans-CPDTA	1.75	2.63	7.44	10.26	20	10

a) Schwareznbach method
b) Bjerrum method
trans-C_yDTA : *trans*-Cyclohexane-1,2-diaminetetraacetic acid
cis-C_yDTA : *cis*-Cyclohexane-1,2-diaminetetraacetic acid
trans-CPDTA : *trans*-Cyclopentane-1,2-diaminetetraacetic acid

5) B. P. Block and G. H. McIntyre, Jr., *J. Amer. Chem. Soc.*, **75**, 5667 (1953).
6) J. Bjerrum, "Metal Ammine Formation in Aqueous Solution," P. Hasse & Son, Copenhagen (1941).
7) G. Schwarzenbach and H. Ackelman, *Helv. Chim. Acta*, **32**, 1682 (1949).
8) G. Anderegg, *ibid.*, **46**, 1834 (1963).
9) H. Kroll, *A E C Contract* (**30**—1) 2096, Annual Report (1960).
10) H. Kroll and M. Gordon, *Federation Proceedings*, **20**, 51 (1961).

Results and Discussion

Acid Dissociation Constants. It may be convenient to discuss the acid dissociation constants and chelate stability constants of *trans*-THDTA in comparison with those of *trans*-C_yDTA which has a similar skeletal structure to *trans*-THDTA. As shown in Table 1, the pK_{a_1} and pK_{a_2} values are quite different from pK_{a_3} and pK_{a_4} values. Thus, *trans*-THDTA is expected to exist as zwitter ions in an aqueous solution as in the case of *trans*-C_yDTA, where the acid dissociations of the first two and the last two steps are known to correspond to the dissociation of carboxylic protons and ammonium protons, respectively.

In an aqueous solution, *trans*-C_yDTA is considered to exist as the skew form with regard to the nitrilodiacetate groups, as this form is more stable thermodynamically than the trans form because of the steric repulsions of axial protons at 3 and 5 positions and the axial nitrilodiacetate group at 1 position. On the other hand, the trans form is more stable than the skew form for EDTA because of the electrostatic repulsion of the two nitrilodiacetate groups. It is easily recognized from Table 3 that the smaller ΔpK_{2-1} (pK_{a_2}–pK_{a_1}) values are obtained for the ligands having the trans configuration, while the larger ΔpK_{2-1} values are obtained for the ligands having the skew configuration. This result may be explained as follows. After the dissociation of the first carboxylic proton, the second carboxylic proton will be bound by two carboxylic groups in the ligand of the trans form. On the other hand, the proton will be bound by four carboxylic groups in the ligand of a skew form. Therefore, the second proton is more difficult to dissociate in the skew form ligands, resulting in the larger ΔpK_{2-1} values. This situation is schematically shown in Fig. 2. Thus, *trans*-THDTA is also considered to take the skew configuration with regard to the nitrilodiacetate groups.

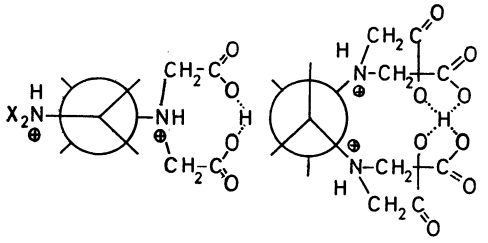

trans skew

Fig. 2. Hydrogen bonding in carboxylic groups.

TABLE 3. ΔpK_{2-1} AND ΔpK_{4-3} VALUES OF RELATED LIGANDS

Ligand	ΔpK_{2-1}	Favorable configuration of two nitrilodiacetate groups.
trans-THDTA	1.29	skew
trans-C_yDTA	1.15	skew
cis-C_yDTA	1.06	skew
EDTA[11]	0.67	trans
MEDTA[12]	0.43	trans
trans-CPDTA	0.51	trans

MEDTA: 1-Methylethylenedinitrilo-*N,N,N',N'*-tetraacetic acid.

The ease of dissociation of the third proton is usually correlated with the electrostatic repulsion of protonated nitrogens, and that of the fourth proton with the basicity of nitrogen as well as the ease of hydrogen bond formation between the two nitrogen atoms. It is seen from Table 1 that the smallest pK_{a_3} is observed for *cis*-C_yDTA and the largest for *trans*-CPDTA in cycloalkane derivatives. Kroll explained the differences of pK_{a_3} values by estimating the N–N distances of these ligands as 2.0 Å for *cis*-C_yDTA and 3.5 Å for *trans*-CPDTA.[1] However, his estimation for *cis*-C_yDTA does not seem to be reasonable. According to our estimation, the N–N distance of *cis*-C_yDTA, *trans*-(e,e)-C_yDTA as well as *trans*-THDTA have about the same value 2.8 Å. Therefore, the electrostatic repulsion of protonated nitrogens may be the same order for these ligands. It is likely that pK_{a_3} of these ligands are influenced by some other factors.

The values of pK_{a_4} are approximately the same except for *trans*-C_yDTA, and the result can not clearly be correlated with the effect caused by the fusion of aromatic ring to cyclohexane ring.

Chelate Stability Constants. The stability constants of the alkaline earth chelates of *trans*-THDTA are listed in Table 2, along with those of *trans*-C_yDTA and *trans*-CPDTA. Although the values for *trans*-THDTA lie in between those for *trans*-C_yDTA and *trans*-CPDTA, not much difference is found among those values. We should wait for more detailed discussion on the chelate stability constants, until we get other ligands of the cycloalkane family.

Thus, the fusing of benzene ring to the cyclohexane ring does not influence greatly the acid dissociation constants and the chelate stability constants. It is necessary to compare these results with that of the complexanes derived from trans decahydronaphthalene, where the puckering of cyclohexane ring is not allowed.

11) G. Schwarzenbach, R. Gut and G. Anderegg, *Helv. Chim. Acta*, **37**, 936 (1954).

12) J. H. Grines, A. J. Huggard and S. P. Wilford, *J. Inorg. Nucl. Chem.*, **25**, 1225 (1963).

BULLETIN OF THE CHEMICAL SOCIETY OF JAPAN VOL. 43 3171—3175 (1970)

A Spectrophotometric Study of Indoferron as a Color Reagent for Zirconium(IV) and Iron(III)*1

Takayoshi SAKAI

Hachinohe Technical College, Tamonoki, Hachinohe, Aomori

(Received June 10, 1970)

Indoferron is shown to be a useful spectrophotometric reagent for the determination of zirconium(IV) and iron(III). An excess reagent reacts with zirconium(IV) and iron(III) to form blue complexes, which have absorption maxima at 605 and 590 mμ respectively against the reagent blank. The maximum absorbances of the solutions containing the complexes are obtained in the pH range from 3.6 to 3.7 for zirconium(IV), and in that from 3.9 to 4.1 for iron(III). The former complex is stable for 1 hr, and the latter, for 4 hrs. The color systems obey Beer's law in 25 m*l* over the ranges up to 40 μg Zr and up to 50 μg Fe respectively. The molar absorptivities of the complexes are calculated to be 3.18×10^4 for zirconium(IV) and 1.81×10^4 for iron(III). The sensitivities of the reactions are 0.0038 μg Zr/cm^2 and 0.0039 μg Fe/cm^2 for an absorbance of 0.001. As for composition, the complexes used have a metal-to-ligand ratio of 1:3 for zirconium(IV) and 1:2 for iron(III). The apparent formation constant of the complex for iron(III) is calculated to be $7.81\times10.^{10}$

Indoferron [2,6-dibromo-3′-methyl-5′-*N*,*N*-di(carboxymethyl)aminomethyl-indophenol] was prepared by Körbl *et al.*[1] as a chromogenic dye-stuff. They studied the complex formation between this reagent and such metal cations as bismuth(III), thorium(IV), scandium(III), and iron(III), and discussed the molar absorptivities of the complexes thus formed. Recently, the spectrophotometric determination of scandium(III) with the reagent has been described by Shimizu and Ogami.[2]

A preliminary investigation was undertaken to evaluate the usefulness of indoferron as a spectrophotometric reagent for various metal cations: bismuth(III), thorium(IV), iron(III), zirconium(IV), vanadium(IV), gallium(III), indium(III), and copper(II). The reagent reacts with those metal cations in a slightly acidic medium (~pH 5.5) to form colored complexes. The results show that indoferron may be useful as a color reagent for the spectrophotometric determination of these metal cations; in every case, the chelation occurs instantaneously at room temperature; all the complexes formed are water-soluble; and their molar absorptivities are of the order of 10^4.

This paper will describe the fundamental conditions for the spectrophotometric determinations of zirconium(IV) and iron(III). Indoferron is not a very good reagent for these elements, but the properties of these complexes are worth being analysed.

Experimental

Reagents and Apparatus. *Indoferron* (abbreviated IF; MW, 560.12 as Na_2 salt) *Solution.* A 1×10^{-3}M IF solution was prepared by dissolving the Dotite IF reagent in water; fresh solutions were used for each set of experiments.

Zirconium(IV) Solution. A 1×10^{-2}M zirconium(IV) solution was prepared by dissolving a guaranteed zirconyl nitrate dihydrate in about 2N perchloric acid. The solution was standardized by EDTA titration, using xylenol orange as the indicator.[3]

Iron(III) Solution. About a 1×10^{-2}M iron(III) solution was prepared by dissolving purified iron(III) hydroxide in 1N perchloric acid. The solution was standardized by EDTA titration, using Cu-PAN as the indicator.[4]

Stock solutions of diverse ions were prepared from their reagent-grade chemicals in appropriate concentrations.

A 0.25 or 2M acetic acid - sodium acetate buffer solution was used for the pH adjustment.

A Hitachi recording spectrophotometer with 1-cm cells, Model 124, was used for the absorbance measurements. A Hitachi-Horiba glass-electrode pH meter,

*1 Presented in part at the Hokkaido Branch Meeting of the Chemical Society of Japan, Muroran, August, 1969 (for zirconium(IV)), and at the Tohoku Branch Meeting of the Chemical Society of Japan, Iwaki, October, 1969 (for iron(III)).

1) J. Körbl and V. Svoboda, *Chem. Ind.* (London), **1958**, 1233: V. Svoboda, L. Dorazil and J. Körbl, *Collection Czech. Chem. Commun.*, **25**, 1037 (1960).

2) T. Shimizu and K. Ogami, *Talanta*, **16**, 1527 (1969).

3) K. Ueno, "Kireto Tekitei (Chelatometric Titration)" (in Japanese), Nankodo, Tokyo (1960), p. 325.

4) *Idem, ibid.*, p. 256.

Model M-5, was used for the pH measurments.

All the measurements were made at 25±0.5°C.

Results and Discussion

Absorption Curves. *Indoferron.* Measurements were made as a function of the pH. As is shown in Fig. 1, below pH 4, the solution has an absorption maximum at about 485 mμ. Between pH 5 and 9, however, the solution has an absorption maximum at about 617 mμ. Above pH 9, this absorption maximum shifts towards a lower wavelength; it is at 580 mμ in the pH range from 11 to 14.

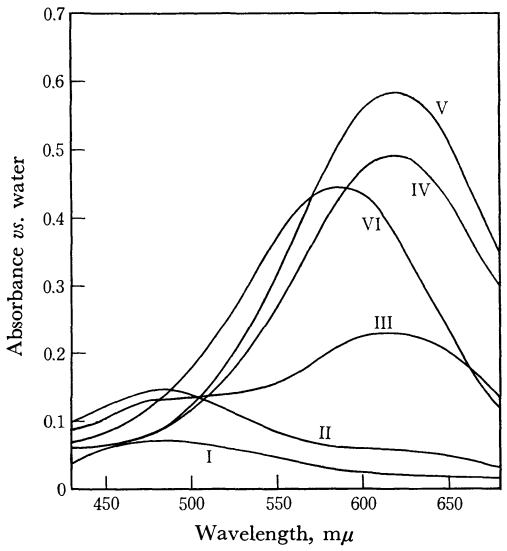

Fig. 1. Absorption curves of IF.
IF: 4.0×10^{-5}M, μ=01, pH—I: 2.0, II: 4.0, III: 4.9, IV: 6.1, V: 9.0, VI: 11—14.

Some Metal-IF Complexes. An attempt was made to evaluate the usefulness of indoferron as a spectrophotometric reagent for several metal cations. To a solution containing a 2.0×10^{-5}M (finally) metal cation in a 25-m*l* volumetric flask, we added 2 m*l* of a 1×10^{-3}M IF solution and 10 m*l* of a 0.25M acetate buffer solution adjusted in the pH range from 2.0 to 5.5 (at intervals of 0.5). The solution was then diluted to the mark with water. The absorbances of the colored complexes were measured against the reagent blanks. The data thus obtained are summarized in Table 1.

Zirconium(IV)-IF Complex. A colored solution containing 23.0 μg of zirconium(IV) was measured in the same way. In this case, 10-m*l* portions of a 2M acetate buffer solution adjusted to various pHs were used. As Fig. 2 shows, the maximum absorption is found at 625 mμ below pH 2.5, at 605 mμ between pH 3 and 3.5, and at 590 mμ at pH 4.5. From the viewpoint of the sensitivity of the reaction, the complex with its absorption maximum at about 605 mμ was used for the determination of zirconium(IV).

Table 1. Properties of metal-indoferron complexes

Metal Cations: each 2.0×10^{-5}M, IF: 8.0×10^{-5}M, μ=0.1

Metal	pH	λ^*_{max} mμ	M: L**	$\varepsilon^{***}\times10^{-4}$	Color
Th(IV)	3.0	615	1 : 2	1.75	Blue
	4.0	648	1 : 3	3.95	Blue-green
V(IV)	3.5	603	1 : 2	1.85	Blue
Bi(III)	3.0	575	1 : 2	1.01	Purple
Ga(III)	3.0	585	1 : 2	1.29	Blue
In(III)	4.0	605	1 : 2	1.57	Blue
Cu(III)	5.5	670	1 : 2	1.74	Blue-green
Sc(III)[2]	4.1	600	1 : 2	0.96	

* Wavelength of maximum absorbance
** Composition of the complex measured by the method of continuous variation
*** Molar absorptivity of the complex

Iron(III)-IF Complex. A colored solution containing 32.2 μg of iron(III) was measured in a manner similar to that used for the zirconium. In this case, 1 m*l* of a 1×10^{-3}M IF solution and 10 m*l* of a 0.25M acetate buffer solution were used. The curves were characterized by an absorption maximum at 590 mμ in the pH range from 2.5 to 4.5. Some of the results are shown in Fig. 3.

The Effect of pH. The absorbances of the solutions containing the complexes were measured

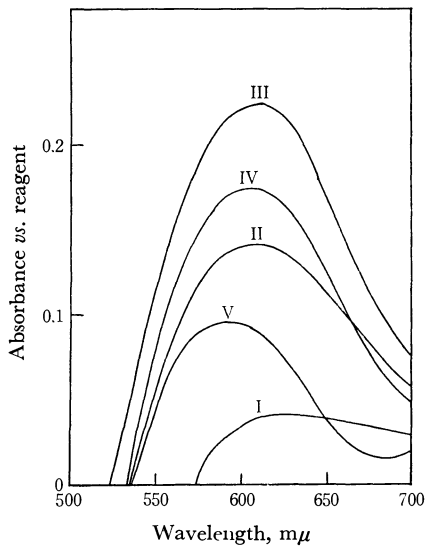

Fig. 2. Absorption curves of the solution containing complex in the presence of an excess of reagent over zirconium.
Zr: 23.0 μg (1.00×10^{-5}M), IF: 8.00×10^{-5}M, pH—I: 2.50, II: 3.00, III: 3.50, IV: 4.00, V: 4.50, μ=1.44.

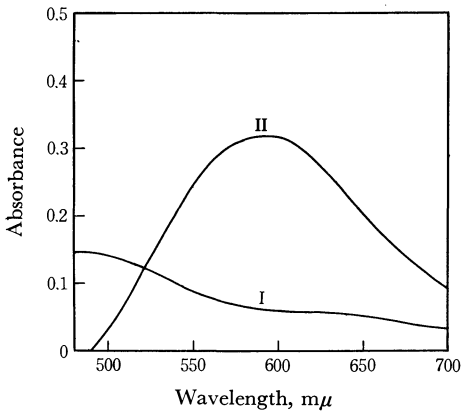

Fig. 3. Absorption curves of IF and its iron complex in the presence of an excess of reagent.
Fe(III): 32.2 μg (2.31×10^{-5}M), IF: 4.00×10^{-5}M
I: IF *vs.* water
II: Fe(III)—IF complex *vs.* reagent
μ: 0.1, pH 4.0.

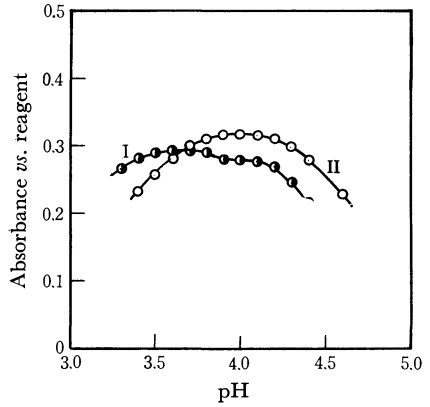

Fig. 4. Effect of pH.
I: Zr(IV); 25.1 μg, IF; 6.06×10^{-5}M, 605 mμ, μ; 1.44
II: Fe(III); 32.2 μg, IF; 4.00×10^{-5}M, 590 mμ, μ; 0.1

as a function of the pH. The ranges in which the highest absorbance was obtained were found to be pH 3.6—3.7 for zirconium(IV) and pH 3.9—4.1 for iron(III) (Fig. 4).

The Effect of the Reagent Concentration. A volume of 1.9—2.0 m*l* of a 1×10^{-3}M IF solution suffices for the complete development of color with less than 40 μg of zirconium, while 1.5—2.1 m*l* of a 1×10^{-3}M IF solution suffices with less than 50 μg of iron. The addition of more reagent decreased the absorbances.

Color Stability. The color of the zirconium system prepared at pH 3.65 was stable for 1 hr, while that of the iron system prepared at pH 4.0 was stable for 4 hr. Both color systems reached their maximum absorbances immediately after preparation.

Calibration Curves. From the foregoing results, the optimum conditions for determining zirconium and iron were derived. The procedures for preparing the calibration curves for these metal cations were as follows.

Zirconium(IV): To a sample solution containing up to 40 μg of zirconium in a 25-m*l* volumetric flask, we added 2.0 m*l* of a 1×10^{-3}M IF solution and 15 m*l* of a 2M acetate buffer solution with a pH of 3.65. After the solution had then been diluted to the mark with water, its absorbance was measured at 605 mμ against the reagent blank.

Iron(III): To a sample solution containing up to 50 μg of iron in a 25-m*l* volumetric flask, we added 1.8 m*l* of a 1×10^{-3}M IF solution and 10 m*l* of a 0.25M acetate buffer solution with a pH of 4.0. After the solution had then been diluted to the mark with water, its absorbance was measured at 590 mμ against the reagent blank.

The zirconium and iron systems obey Beer's law over the 2—40 and 1.5—50 μg ranges respectively in 25 m*l*. The optimum concentration ranges, as obtained from the curves drawn according to Ringbom,[5] are 10—30 μg for zirconium and 9—21 μg for iron. The molar absorptivities are 3.18×10^4 for zirconium and 1.81×10^4 for iron, while the sensitivities calculated[6] for $\log I_0/I=0.001$ are 0.0038 μg/cm² for zirconium and 0.0039 μg/cm² for iron. The reproducibilities of the methods, using 10 samples, each containing 20.94 μg of zirconium, and 9 samples, each containing 22.34 μg of iron, were then examined. The standard deviation were found to be 0.0028 absorbance unit, or 2.1%, for zirconium, and 0.0010, or 2.1%, for iron. The proposed method is comparable in sensitivity with the xylenol orange method[7] for zirconium and with the methylthymol blue method[8] for iron.

Considering the high sensitivity of zirconium(IV)-, iron(III)-, and others-IF complexes (Table 1), indoferron may well be considered a useful reagent for the spectrophotometric determination of these metal cations.

Effect of Diverse Ions. The effect of 29 cations and 12 anions on the zirconium(IV) and iron(III) determinations was examined separately. Many bi-, ter-, and quadrivalent metals and chelating agents interfered with both determinations, indicating that indoferron is not a selective reagent for zirconium and iron, in spite of its high sensitivity to these metals.

Composition of the Complexes. The compositions of the zirconium(IV) and the iron(III) complexes were determined by the method of con-

5) A. Ringbom, *Z. Anal. Chem.*, **115**, 332 (1938/9).
6) E. B. Sandell, "Colorimetric Determination of Traces of Metals," Interscience Publishers, New York (1950), p. 49.
7) K. L. Cheng, *Talanta*, **2**, 61, 266 (1956).
8) K. Tonosaki, This Bulletin, **39**, 425 (1966).

tinuous variation and by the mole-ratio method.

Zirconium(IV)-IF Complex. In the case of the former method, the maximum absorbance corresponded to a complex of the $Zr(Ligand)_3$ type at all the wavelengths investigated. The same results were also obtained by the mole-ratio method: the curves show sharp breaks at a zirconium(IV): ligand mole ratio of 1 : 3 (Fig. 5).

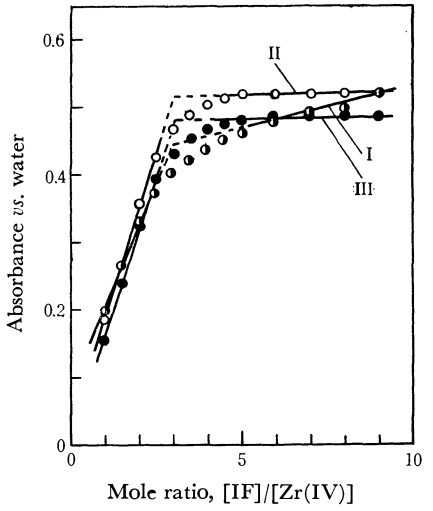

Fig. 5. Mole ratio method.
Zr(IV): 2.0×10^{-5}M, μ: 1.2, I: 565 mμ, II: 605 mμ III: 625 mμ, pH 3.65

Considering the ionic species of zirconium(IV) and the possibility of forming polymerized complexes, it is speculative to postulate a structure for the zirconium(IV)-IF complex. Therefore, no calculation of the formation constant was made.

Iron(III)-IF Complex. According to the method of continuous variation, the maximum absorbance corresponded to a complex of the $Fe(Ligand)_2$ type. Some of the results are shown in Fig. 6. The same results were also obtained by the mole-ratio method.

The apparent formation constant, K', was calculated from the curves shown in Fig. 6, using the relations:[9]

$$K' = C(1-\alpha)/(\alpha C)(2\alpha C)^2$$

$$\alpha = (E_m - E_s)/E_m$$

where C is the total concentration of the complex in moles per liter, α is the degree of dissociation, E_m is the maximum absorbance indicating that all the iron is present as a complex, and E_s is the absorbance at the stoichiometric molar ratio. The apparent formation constant at pH 4.0 was found to be 7.81×10^{10}.

Comparing the formation constants of the acetatocomplexes with those of hydroxocomplexes of iron(III),[10] it may be said that the latter complexes are not formed under the conditions investigated. Assuming that the indoferron serves as a terdentate ligand, the acetate ion in the acetatoiron(III) complexes may be eliminated by the chelate formation between iron(III) and indoferron. In other words, the coordination atoms of indoferron are found to be phenolic oxygen, nitrogen, and one of the two carboxyloxygens, and these atoms will coordinate with iron to form five- and six-membered rings.

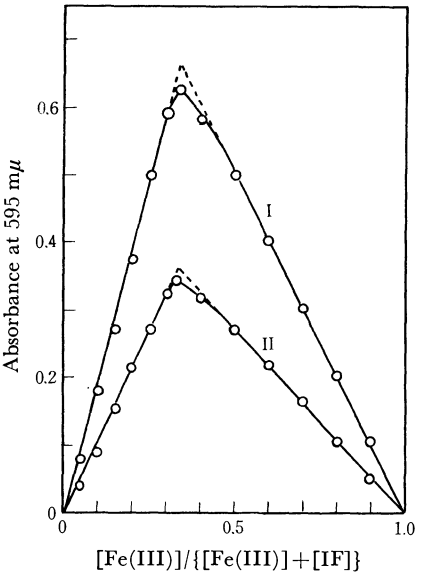

Fig. 6. Continuous variation method at pH 4.0.
[Fe(III)]+[IF]: I; 1.2×10^{-4}M, II; 0.6×10^{-4}M, μ: 0.5

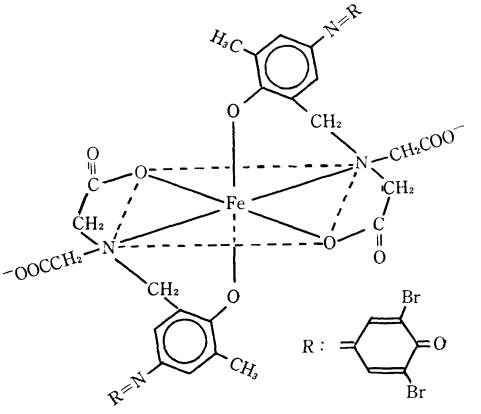

Fig. 7. Postulated structure for the complex Fe(III)$(Ligand)_2$.

9) A. E. Harvey, Jr., and D. L. Manning, *J. Amer. Chem. Soc.*, **72**, 4488 (1950).

10) A. Ringbom, "Complexation in Analytical Chemistry," Interscience Publishers, New York (1963), pp. 298, 320: log $\beta_1=11.0$ ($\mu=3$) for hydroxoiron(III) complex, log $K_1=3.4$ ($\mu=0.1$) for acetatoiron(III) complex.

Thus, this structure for the complex may be postulated:

The author wishes to express his hearty thanks to Professor Kôichi Tonosaki of Hirosaki University for his kind advice and instruction throughout this study, to Dr. Makoto Otomo for his helpful discussions, and also to Mr. Yoshinobu Wakamatsu and Mr. Keizo Demachi for their laboratory work.

BULLETIN OF THE CHEMICAL SOCIETY OF JAPAN VOL. 43 3175—3181 (1970)

Tri(hetero)substituted Carbonium Ions. III. Ring-size Effects on the Dual Reactivities of 2-Dimethylamino-1,3-dithiolanylium Ion and Its Ring Analogs as Ambident Electrophiles*1

Takeshi NAKAI, Yoshio UENO and Makoto OKAWARA

Research Laboratory of Resources Utilization, Tokyo Institute of Technology, Ookayama, Meguro, Tokyo

(Received January 17, 1970)

The following ring analogs of 2-dimethylamino-1,3-dithiolanylium perchlorate (Ia) were prepared: 2-dimethylamino-1,3-dithianylium perchlorate (IV), 2-dimethylamino-1,3-dithiepanylium perchlorate (V) and an open-chain analog, bis(methylthio)dimethylaminocarbonium perchlorate (VI). In order to investigate the structural effect on the reactivities of the tri(hetero)-carbonium ions at two reactive sites, *i. e.*, the centered carbon (sp^2) (a) and the *S*-methylene carbon (sp^3) atoms (b), the reactions of these carbonium ions with hydroxide ion (mode A) and with *N,N*-dimethyldithiocarbamate ion (mode B), respectively, were studied at 30°C. The rates of mode A of these carbonium ions, relative to that of Ia, are 1 : 15.0 (IV) : 32.5 (V) : 1.06×10^4 (VI), and of mode B are 1 : 6.5 : 23.5 : $\approx2.0\times10^4$. In their electronic spectra a definite trend that as the ring-size increases there is a strong shift of absorption maxima toward the lower energies was observed. The fact suggests that the stability of the carbonium ion decreases with an increase in ring-size. On the basis of the schematic energy profiles for the two modes as well as the structural and kinetical aspects, it has been assumed that one of common factors contributing to the ring-size effect on both reactivities would be the stability of the carbonium ion.

In the preceding paper[1] we have reported that 2-dialkylamino-1,3-dithiolanylium ion (I) is an ambident electrophile with two reactive sites, (a) and (b), and reacts with the nucleophile ($^-$Nu) *via* reaction mode A and B to give cyclic product II (or its pyrolytic product) and ring-opening product III, respectively, according to the nucleophilicity of the attacking reagent used.

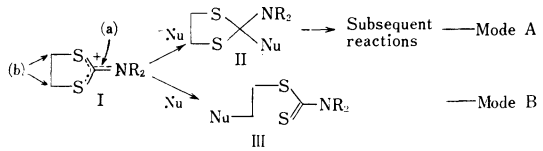

Furthermore, it has been assumed[1] that the reaction course is decided by the relative stability of the cation I to the kinetical adduct II. Thus, it is anticipated that both reaction course and dual reactivities of this type of tri(hetero)substituted carbonium ions would depend largely upon the structure of the carbonium ions.

In the present paper we will describe the ring-size effect on the dual reactivities of 2-dimethylamino-1,3-dithiolanylium ion (Ia) and its ring analogs as ambident electrophiles and discuss structural factors controlling the reactivities of these carbonium ions.

Results

Preparations of Carbonium Salts. Tri(hetero)substituted carbonium ions studied here are 2-dimethylamino-1,3-dithiolanylium ion (Ia) (five-membered), 2-dimethylamino-1,3-dithianylium ion (IV) (a six-membered analog), 2-dimethylamino-1,3-dithiepanylium ion (V) (a seven-membered analog) and bis(methylthio)-dimethylamino-

*1 Presented at the 18th Symposium on Organic Reaction Mechanisms, Kyoto, October, 1967.

1) Part II: T. Nakai and M. Okawara, *Tetrahedron Lett.*, **1967**, 3835; This Bulletin, **43**, 1864 (1970).

carbonium ion (VI) (an open-chain analog).[2] All these carbonium ions were isolated as perchlorates.

Cyclic carbonium perchlorates, Ia, IV and V, were prepared by the equimolar reaction of the corresponding α,ω-dichloroalkane with sodium *N,N*-dimethyldithiocarbamate in ethanol followed by treatment with sodium perchlorate (Eq. (1)).[3] In all cases the reaction was accompanied by the formation of the corresponding bis(dithiocarbamate) (VII), arising mainly from the interaction between the cyclic carbonium ion formed and the dithiocarbamate anion *via* mode B.[4] The yield of disubstituted product VII under the equimolar condition increases with the ring-size *n* (Table 1). The fact suggests that with an increase in ring-size participation of the dithiocarbamate function might be favorably involved in the second substitution process from the monosubstituted intermediate to the disubstituted VII.[4,5]

Open-chain carbonium perchlorate (VI) was prepared by methylation of *S*-methyl *N,N*-dimethyldithiocarbamate with dimethyl sulfate[6] followed by treatment with sodium perchlorate (Eq. (2)).

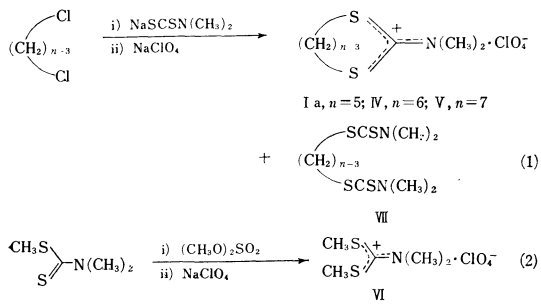

(1)

(2)

These carbonium ions were identified by elemental analyses and NMR spectra. Characterization and spectral data of carbonium perchlorates obtained are summarized in Table 1, along with yields of disubstituted product VII.

Reactions as Ambident Electrophiles. It has been reported that the reaction of five-membered cation Ia with hydroxide ion yielded β-mercaptoethyl *N,N*-dimethylthiolcarbamate (VIII, $n=5$).[1] Similarly six-membered IV and open-chain VI gave γ-mercaptopropyl thiolcarbamate (VIII, $n=6$)[3] and methyl thiolcarbamate, respectively. These hydrolytic products are best explained as the result of initial attack of hydroxide ion at the reactive site (a) followed by proton transfer (Eq. (3)). On the other hand, it has been shown that the reaction of Ia with *N,N*-dimethyldithiocarbamate anion yielded ethylene bis(dithiocarbamate) (VII, $n=5$) in the quantitative yield.[1] Similarly reactions of other cyclic carbonium ions and open-chain VI with the dithiocarbamate anion afforded the corresponding bis(dithiocarbamate) (VII) and methyl *N,N*-dimethyldithiocarbamate, respectively. The formation of these products may be explained by attack of the dithiocarbamate anion at site (b) presumably through the SN2-like mechanism (Eq. (4)).[1,4]

Thus, in order to estimate both reactivities at the two sites of each carbonium ion, the rates of reactions of the carbonium ion with hydroxide and the dithiocarbamate ions selected as typical reactions of mode A and B, respectively, were measured.

The reactions of the carbonium salt with hydrox-

Table 1. Carbonium perchlorates

Cation	Ring-size *n*	Yield %	Mp °C	UV (H_2O)[a] λ_{max} (mμ)	NMR,[b] δppm			VII[c] Yield, %
					-S-CH_2-	N-CH_3	-CH_2-CH_2-CH_2	
Ia	5	61	179—181	249	4.06(s)	3.58(s)		8
IV	6	27	97—99	262	4.43(t)[d]	3.55(s)	2.27(t)[d]	23
V	7	*ca.* 10	58—60	275	3.47(m)[e]	3.61(s)	2.10(m)[e]	48
VI	∞	76	84—86	276	2.85(s)[f]	3.70(s)		—

a) Accurate molar extinction coefficients (ε) could not be obtained due to occurrence of partial hydrolyses during measurements; however, the observed values were $0.70—1.42\times10^4$.
b) Multiplicity: s=singlet, t=triplet, m=multiplet.
c) The disubstituted product isolated as a by-product (see the text).
d) J=7.0 Hz. e) The center of the multiplet. f) The *S*-methyl protons.

2) The cation may be also termed *N,N*-dimethyl-*S,S'*-dimethyldithiocarbamidium ion: J. L. Richards, D. S. Tarball and E. H. Hoffmeister, *Tetrahedron*, **24**, 6485 (1968). For the nomenclature on other cations, see Ref. 3 in the preceding paper.[1]

3) K. C. Kennard and J. A. VanAllan [*J. Org. Chem.*, **24**, 470 (1959)] have prepared *p*-toluene sulfonates of the five- and six-membered carbonium ions by the reactions of ω-hydroxyalkyl *N,N*-dimethyldithiocarbamates with *p*-toluenesulfonyl chloride in benzene or DMF.

4) T. Nakai, Y. Ueno and M. Okawara, *Tetrahedron Lett.*, **1967**, 3831; This Bulletin, **43**, 156 (1970).

5) T. Nakai, H. Kawaoka and M. Okawara, This Bulletin, **42**, 508 (1969).

6) H. V. Rinteln and O. Riester [*Mitt. Forshungslab. Agfa Leverkusen-München*, **1**, 65 (1955); *Chem. Abstr.*, **51**, 7013 (1957)] have reported the formation of the methyl sulfate salts of bis(alkylthio)dialkylaminocarbonium ions, but no carbonium salts were isolated.

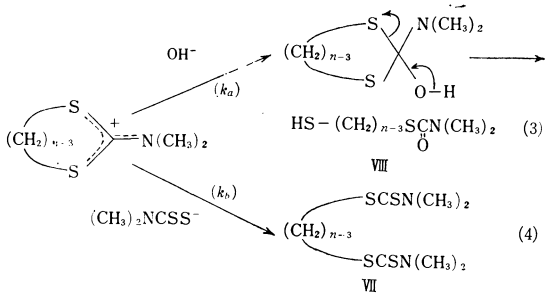

ide ion and water in aqueous solutions were undertaken in buffer solutions at 30°C under pseudo-first-order conditions. The rate of disappearence of the carbonium ion was followed by spectrophotometry. As the hydroxide concentration is essentially constant, the rate equation may be represented as

$$k_{obs} = k_{H_2O} + k_a[OH^-]$$

where $[OH^-]$ and k_{obs} refer to the hydroxide concentration and the observed pseudo-first-order rate constant, respectively. The plots of k_{obs} against $[OH^-]$ for these carbonium ions were linear in the ranges of the hydroxide concentrations studied. From the slopes and intercepts of these plots, we obtained the values of the second-order rate constant (k_a) for reaction with hydroxide ion and the pseudo-first-order rate constant (k_{H_2O}) for reaction with water (Table 2).

Table 2. Hydrolyses of carbonium perchlorates

Cation	Ring-size n	$[OH^-]$, mol/l	$10^5\,k_{obs}$ sec^{-1}	$10^6\,k_{H_2O}$ sec^{-1}	k_a $mol^{-1}l$ sec^{-1}
Ia	5	6.31×10^{-6}	0.397		
		12.3	0.650	3.5	0.51
		16.6	0.825		
IV	6	0.603×10^{-6}	0.617		
		2.00	1.39	1.0	7.60
		3.02	2.25		
		5.25	3.33		
V	7	0.407×10^{-6}	0.650		
		2.00	3.30	0.5	16.6
		3.02	5.05		
VI	∞	5.13×10^{-9}	8.4		
		6.46	9.0		
		7.94	10.4	56	5.4×10^3
		12.6	12.3		

On the other hand, the reaction of the carbonium ion with sodium *N,N*-dimethyldithiocarbamate was studied in dimethylformamide (DMF) at 30°C under the equimolar condition. The rate of reaction was measured by following the disappearance of the dithiocarbamate anion using the previously-reported method.[4] From the slopes of the second-order rate plots (Fig. 1), we obtained the values of the rate constant (k_b) for reaction of the cyclic cations with the dithiocarbamate ion. The rate of reaction of open-chain VI with the anion was too large to be accurately measured by this method. The value of k_b for VI was found to be approximately 26.0 $mol^{-1}l\ sec^{-1}$. The values of the relative k_b obtained are shown in Table 3 together with those of the relative k_a.

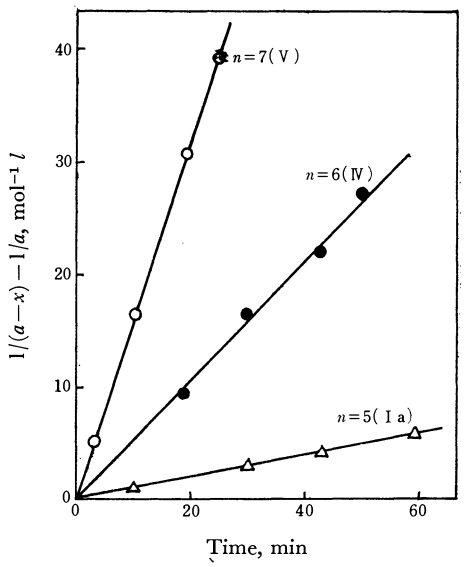

Fig. 1. Second-order rate plots for the cyclic carbonium ions at 30°C under the equimolar condition; a=0.03 mol/l.

Table 3. The relative k_a and k_b for the carbonium ions at 30°C

Cation	Ring-size n	Mode A Rel. k_a	Mode B Rel. k_b
Ia	5	1.0	1.0
IV	6	15.0	6.5
V	7	32.5	23.8
VI	∞	1.06×10^4	$\approx2.0\times10^4$

Discussion

Structural Aspects. The carbonium ions concerned are strongly stabilized by accepting electrons from α-hetro atoms, and so the positive charge is widely delocalized as expressed in formula IX.

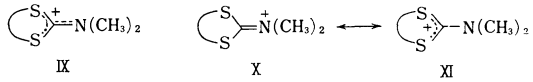

The *exo*-iminium structure X would be more important rather than the sulfonium XI if the cation is not subject to any steric requirements as in the case of open-chain VI, since the electron-donating power of the dimethylaminogroup is much larger

than the alkylthio groups. In the electronic spectra of these carbonium salts (Table 1), there is a definite trend that as the ring-size increases there is a strong shift of absorption maxima (λ_{max}) toward the lower energies (the longer wavelengths) (Fig. 2).

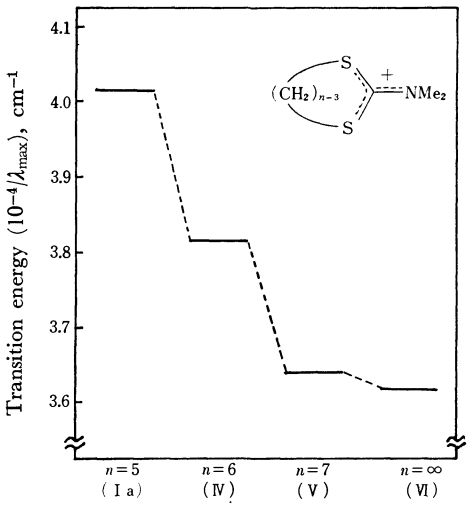

Fig. 2. The ring-size effect on the transition energy of the carbonium ions.

A similar trend has also been observed in the electronic spectra of a series of cyclic alkenylcarbonium ions.[7] This observation has been interpreted by the idea that one of factors contributing to the ring-size effect on a band shift may be that 1,3-π-overlap will be progressively more significant as the bond angle between the three conjugating carbon atoms decreases. The ring-size effect on band shifts is implicit in Mulliken's[8] and Walsh's[9] treatment of bonding in triatomic systems.

Appling the idea to the tri(hetero)carbonium ions concerned, the spectral trend suggests that α-hetero atoms stabilize the ground state more than the excited state[10] and, hence, as the ring-size decreases, the ground state is more stabilized presumably due to the more developed 1,3-overlap in the ring system, *i. e.*, $\overset{+}{\overbrace{S\cdots C\cdots S}}$, as found experimentally. In other words, contribution of the sulfonium structure XI to stabilization of the carbonium ion progressively increases with decrease in ring-size.

The ring-size effect on stabilization described above is also implicit in the NMR spectra (Table 1). A change in ring-size appears to affect the chemical shifts of the *S*-methylene protons in the ring more greatly rather than those of the *N*-methyl protons. The *S*-methylene protons of five-membered Ia are deshielded more than those of other ring analogs presumably due to more favorable contribution of the sulfonium structure.

Ring-size Effects on Reactivities. The kinetical results obtained indicate that reactivities of these carbonium ions at the two reactive sites are progressively enhanced as the ring-size increases (Fig. 3). In the light of these results our task is now to consider factors contributing to the ring-size effects on reactivities.

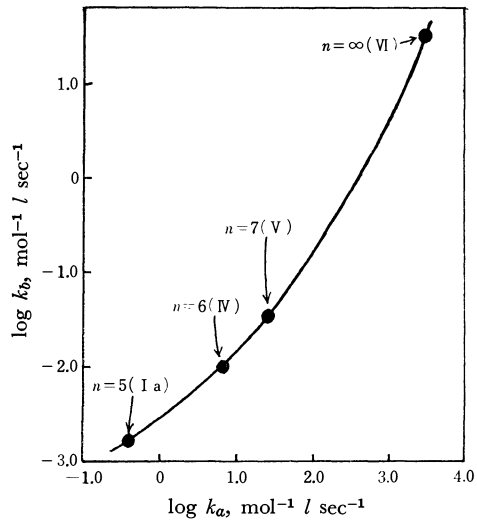

Fig. 3. Plot of log k_a (mode A) *vs.* log k_b (mode B).

As has been assumed,[1] the mode A process initially yields a kinetically-controlled product and the activation free energy ($\Delta F_A^{\neq}$) is small since the primary process of mode A involves an association between a cation and an anion. Thus, the reaction of the carbonium ion with hydroxide ion might be a expressed as follows:

$$R^+ + OH^- \overset{K}{\rightleftharpoons} ROH \underset{\text{(fast)}}{\longrightarrow} \text{VIII}$$

where R^+ and ROH are the carbonium ion concerned and the carbinol, respectively. The overall rate constants (k_a) would be proportional to the equilibrium constant (K). Consequently the rate of mode A should depend upon the relative position between R^+ and ROH in the energy diagram.

7) G. A. Olah, C. U. Pittman, Jr., and M. C. R. Symons, "Carbonium Ions," Vol. 1, G. A. Olah and P. von R. Schleyer, Ed., Interscience Publishers, New York (1968), Chapter 5.

8) R. S. Mulliken, *Can. J. Chem.*, **36**, 10 (1958).

9) A. D. Walsh, *J. Chem. Soc.*, **1953**, 2266.

10) Another definite evidence for this idea has been presented that as the methylthio group in tris(methylthio)carbonium ion is progressively replaced by the dimethylamino group, there is a strong shift of absorption maxima to the higher energies (the shorter wavelengths): T. Nakai, K. Hiratani and M. Okawara, the 3rd Symposium on Organic Sulfur Chemistry, Tokyo, 1969. Furthermore, this idea has been confirmed by simple HMO calculations: T. Nakai and M. Okawara, the 23rd Annual Meeting of the Chemical Society of Japan, Tokyo, 1970.

Although it is easy to estimate the stability of ROH, the relative stability of R^+ may be evaluated in terms of the absorption maximum (λ_{max}) as described above.

The kinetical result shows that increasing k_a-values are paralleled by increasing ring-sizes, *i. e.*, by decreasing stabilities of the carbonium ions; this fact suggests that an increase in ring-size would lower the stability of the carbonium ion, at least to a more extent, rather than that of the carbinol. On the basis of the schematic energy profile for mode A (Fig. 4),[11] the free energy gap between

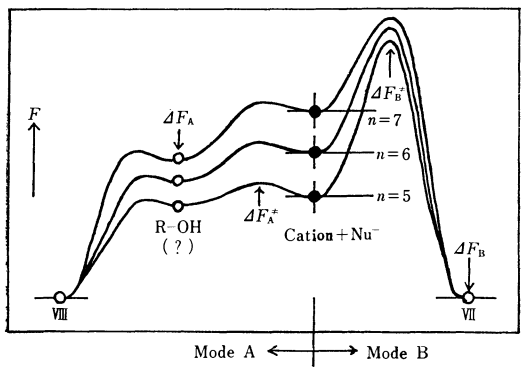

Fig. 4. Schematic energy profiles for mode A and B. Strictly speaking, the energy content of the initial system, cation and Nu^-, depends on the nature of Nu^-. However, since the nucleophile remains constant, this energy content of the respective mode is determined solely by the nature of the cation.

the cation and the carbinol (ΔF_A) increases as the ring-size increases. In short, it may be noted that the rate of mode A depends upon the stability of the carbonium ion varying mainly with ring-size.

On the other hand, the reaction of mode B is irreversible. Accordingly it can be assumed[1,11] that in contrast to mode A the rate of reaction with the dithiocarbamate ion is determined by the magnitude of the activation free energy ($\Delta F_B^{\neq}$) rather than that of ΔF_B in the schematic energy profile for mode B (Fig. 4). The kinetical result shows that the rate of mode B increases in the same order as that of mode A (Fig. 3); this fact suggests that an increase in ring-size would lower the stability of the carbonium ion, at least to a more extent, rather than that of the transition state. In consequence an increase in ring-size results in a stepwise lowering of the energy gap ($\Delta F_B^{\neq}$), as found experimentally. However, large differences in rate (k_a and k_b) between seven-membered V and open-chain VI, of which stabilities appear to be almost the same from their absorption maxima, cannot reasonably explained in the present stage.

In any case, these considerations permit only a qualitative conclusion that one of significant factors controlling both reactivities may be the stability of the ground state of the carbonium ion varying with the extent of 1,3-overlap in the ring system.

11) For similar considerations, *e. g.*, see S. Hünig, *Angew. Chem. Internat. Ed.*, **3**, 548 (1964) and Ref. 14 in the preceding paper.[1]

Experimental

General. Melting and boiling points are uncorrected. The IR and UV spectra were recorded with Hitachi EPI-S2 and EPS-2 spectrometers, respectively. The NMR spectra were determined with a Varian Associates A-60 spectrometer. Chemical shifts are reported in parts per million (ppm) from tetramethylsilane as an internal standard.

2-Dimethylamino-1,3-dithiolanylium Perchlorate (Ia). The carbonium perchlorate was prepared by the procedure reported in the previous paper[1]: mp 179—180°C.

2-Dimethylamino-1,3-dithianylium Perchlorate (IV). 1,3-Dichloropropane (12.3 g, 0.11 mol) was added to a solution of 20.0 g (0.11 mol) of sodium *N,N*-dimethyldithiocarbamate in 75 m*l* of ethanol. The mixture was stirred at 60°C for 6 hr. The mixture was concentrated in reduced pressure and then poured into 100 m*l* of cold water giving 2.4 g (23%) of disubstituted product VII ($n=6$): mp 108—109°C (ethanol).

Found: C, 38.25; H, 6.61; N, 9.87%. Calcd for $C_9H_{18}N_2S_4$: C, 38.26; H, 6.42; N, 9.92%.

The filtrate was extracted with ether and an excess of a saturated aqueous solution of sodium perchlorate was added to the aqueous layer giving 8.0 g (27%) of white precipitates of IV: mp 97—99°C (methanol).

Found: C, 27.73; H, 4.68; N, 5.59%. Calcd for $C_6H_{12}ClNO_4S_2$: C, 27.53; H, 4.62; N, 5.32%.

2-Dimethylamino-1,3-dithiepanylium Perchlorate (V). 1,4-Dichlorobutane (26.5 g, 0.21 mol) was added to a solution of 36.0 g (0.20 mol) of sodium *N,N*-dimethyldithiocarbamate in 75 m*l* of ethanol. The mixture was stirred at 60°C for 6 hr. The mixture was concentrated in reduced pressure and poured into cold water giving 12.4 g (48%) of disubstituted product VII ($n=7$): mp 112—113°C.

Found: C, 40.09; H, 6.95; N, 9.71%. Calcd for $C_{10}H_{20}N_2S_4$: C, 40.54; H, 6.80; N, 9.46%.

To the filtrate there was added 100 m*l* of a saturated aqueous solution of sodium perchlorate. The mixture was cooled in an ice box for a few days giving about 4.0 g (10%) of very hygroscopic white precipitates of V. These precipitates were washed several times with ether and dried *in vacuo*: mp 58—60°C.

Found: C, 29.94; H, 4.72; N, 4.97%. Calcd for $C_7H_{14}ClNO_4S_2$: C, 30.49; H, 5.12; N, 4.97%.

Bis(methylthio)-dimethylaminocarbonium Perchlorate (VI). *S*-Methyl *N,N*-dimethyldithiocarbamate (13.5 g, 0.01 mol) was dissolved in 12.6 g (0.01 mol) of dimethyl sulfate. When the mixture was heated to 60°C a vigorous exothermic reaction occurred. The reaction temperature was kept below 100°C. After the exothermic reaction ceased the mixture was further stirred at 90°C for 1 hr. The mixture was poured into 100 m*l* of a

saturated aqueous solution of sodium perchlorate giving 19.0 g (76%) of pale yellowish precipitates. The precipitates were washed with ether and recrystallized from methanol giving white precipitates: mp 84—86°C.

Found: C, 23.73; H, 4.68; N, 5.13%. Calcd for $C_5H_{12}ClNO_4S_2$: C, 24.05; H, 4.85; N, 5.61%.

Products. A. Hydrolyses of Carbonium Perchlorates. 2-Dimethylamino-1,3-dithiolanylium perchlorate (Ia) was hydrolyzed to afford β-mercaptoethyl *N,N*-dimethylthiolcarbamate.[1] Similarly 2-dimethylamino-1,3-dithianylium perchlorate (IV) gave γ-mercaptopropyl *N,N*-dimethylthiolcarbamate.[3] No attempt was made to isolate the hydrolytic product of V.

Bis(methylthio)-dimethylaminocarbonium perchlorate (VI) (12.5 g, 0.05 mol) was added to a solution of water (1.0 g, 0.05 mol) and triethylamine (5.0 g, 0.05 mol) in 50 m*l* of dioxane. The mixture was stirred at 80°C for 6 hr, then poured into water. The ethereal extract was dried over sodium sulfate and the solvent evaporated *in vacuo*. Distillation of the residue gave 3.7 g (62%) of *S*-methyl *N,N*-dimethylthiolcarbamate: bp 91—92°C/31 mmHg; n_D(21°C) 1.4964 (lit.[12] bp 115—116°C/89 mmHg; n_D(30°C) 1.4932); IR (neat): 1650 cm^{-1} (C=O). The IR spectrum of the distillate was in agreement with that of the authentic sample.

B. Reactions of Carbonium Perchlorates with Sodium *N,N*-Dimethyldithiocarbamate. The reaction of Ia with sodium *N,N*-dimethyldithiocarbamate afforded ethylene bis(*N,N*-dimethyldithiocarbamate) (VII(n=5)) in the quantitative yield.[1]

Six-membered IV (0.50 g, 2 mmol) and sodium *N,N*-dimethyldithiocarbamate (0.37 g, 2 mmol) were dissolved in 5 m*l* of DMF. The mixture was stirred at 60°C for 4 hr, then poured into water giving 0.48 g (78%) of white precipitates of disubstituted product VII (n=6). The IR spectrum of the product was in agreement with that of the authentic sample. Similarly seven-membered V gave disubstituted product VII (n=7) in the quantitative yield.

Bis(methylthio)-dimethylaminocarbonium perchlorate (VI) (2.5 g, 0.01 mol) and sodium *N,N*-dimethyldithiocarbamate (1.8 g, 0.01 mol) were dissolved in 20 m*l* of DMF. The mixture was stirred at 70°C for 3 hr, then poured into cold water giving 1.1 g (41%) of white precipitates of *S*-methyl *N,N*-dimethyldithiocarbamate: mp 44—46°C (lit.[13] 47°C). The IR spectrum of the product was in agreement with that of the authentic sample. The low yield would be due to partial dissolution of the product in the solvents.

Kinetic Runs. A. Rates of Hydrolyses of Carbonium Salts (Mode A). A Hitachi EPS-2 spectrophotometer equipped with a thermostated cell holder was used to record spectral data. The thermostated cell holder consisted of a brass block through which thermostated water was circulated. A spectrometer cell of 1.0 cm fits into a bore of the block. The rates of all reactions of these carbonium salts with water and hydroxide ion were studied in aqueous solutions buffered with the Clark-Lubs systems. A solution of the desired pH, which initially contained *ca.* 10^{-4} mol/*l* carbonium salt, was prepared in the cell and placed in the holder thermostated at 30±0.3°C. At various time intervals decreases in absorbance at the respective maximum absorption band (λ_{max}) were followed. The semilogarithmic plots of A_0/A_t against time were linear and yielded the observed first-order rate constants (k_{obs}). A typical example of the first-order rate plot is shown in Fig. 5. The second-order rate constants (k_a) for reactions with hydroxide ion, and the pseudo-first-order rate constants (k_{H_2O}) for reactions with water were determined from the slopes and intercepts, respectively, of plots of k_{obs} *vs.* concentrations of hydroxide ion. The values of pH studied ranged from 7.5 to 9.5 and from 5.7 to 6.1 for the cyclic and open-chain carbonium perchlorates, respectively. Results of these experiments are summarized in Table 2.

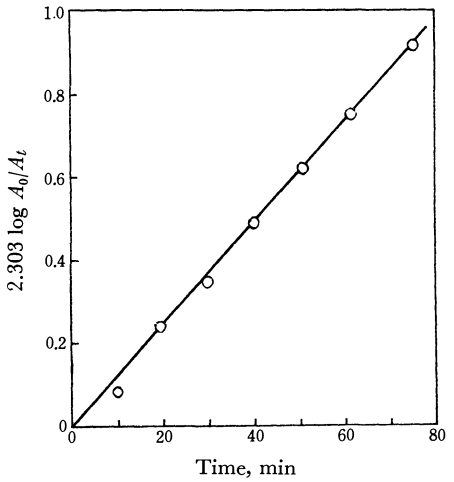

Fig. 5. An example of kinetic runs of carbonium ion IV at 262 mμ; pH=8.48.

Table 4. Reactions of IV with sodium *N,N*-dimethyldithiocarbamate

Time, min	N-salt formed, g	$1/a-x$, $mol^{-1}l$
0	0.122	30.6
15	0.105	35.5
30	0.081	45.9
40	0.074	50.5
50	0.065	57.5

B. Rates of Reactions of Carbonium Salts with Sodium *N,N*-Dimethyldithiocarbamate (Mode B). The rates of reactions with sodium *N,N*-dimethyldithiocarbamate were measured according to the procedures reported in our previous paper.[4] At various time intervals the remaining dithiocarbamate ion was gravimetrically determined from quantities of the nickel chelate precipitated by treatment of the aqueous solution of the sample with an excess of a saturated aqueous solution of nickel chloride. All reactions were carried out at 30°C in DMF solutions under the equimolar condition. The initial concentration was 0.03 mol/*l* for all reactions.

The carbonium perchlorate (0.15 mol) was dissolved in a solution of 0.805 g (0.15 mol) of sodium *N,N*-dimethyldithiocarbamate in 150 m*l* of DMF. The re-

12) H. Tilles, *J. Amer. Chem. Soc.*, **81**, 714 (1959).
13) J. v. Braun, *Ber.*, **35**, 3368 (1902).

action vessel was placed in a constant-temperature bath at 30±0.2°C. At various time intervals a 25.0-m*l* aliquot was removed and poured into cold water (*ca.* 100 m*l*) giving white precipitates of disubstituted product VII. The precipitates were filtered off and the aqueous filtrate was treated with an excess of a saturated aqueous solution of nickel chloride giving green precipitates of the nickel chelate. The nickel chelate was collected in a glass filter. The glass filter was completely dried *in vacuo*. An example of results is given in Table 4.

All plots of $1/a-x$ against time were linear and yielded the second-order rate constants (k_b) for reactions with the dithiocarbamate ion. The reaction of open-chain VI with the anion under these conditions was so fast that accurate measurements could not be made. A very rough estimate for the second-order rate constant for the open-chain analog was 26.0 $mol^{-1}l\ sec^{-1}$. Results of these experiments are shown in Fig. 1 and Table 3.

BULLETIN OF THE CHEMICAL SOCIETY OF JAPAN VOL. 43 3181—3187 (1970)

Photoinduced Reactions. XLII.[1] Homolytic Expulsion of 4-Substituent in the Photochemical Reaction of 2,5-Cyclohexadienones

Katsuyuki OGURA and Teruo MATSUURA

Department of Synthetic Chemistry, Faculty of Engineering, Kyoto University, Sakyo-ku, Kyoto

(Received January 24, 1970)

Irradiation of 2,4,6-tri-*t*-butyl-4-bromo-2,5-cyclohexadienone (X) in various solvents yielded 2,4,6-tri-*t*-butylphenol (XIII) in high yields. It was shown that 2,4,6-tri-*t*-butylphenoxy radical (XII) was formed as an intermediate and that the light of shorter wavelengths than 450 mμ accelerated the hydrogen abstraction of XII. The rate of the photochemical decomposition of X decreased in the order: *n*-hexane, *N*,*N*-dimethylformamide and acetic acid. This and the sensitized reaction suggest that the formation of XII from X may result from the n-π^* triplet state of X. On the other hand, irradiation of 2,4,6-tri-*t*-butyl-4-nitro-2,5-cyclohexadienone (XI) afforded 2,6-di-*t*-butyl-*p*-quinone (XV) and 2,4,6-tri-*t*-butylphenol (XIII), indicating a homolytic cleavage of the C–NO_2 bond.

2,5-Cyclohexadienones have been found to undergo two basic types of transformation on irradiation in neutral media; *i. e.*, (a) skeletal rearrangement, which furnishes bicyclo[3.1.0]hex-3-en-2-ones (the so-called "lumiketone"), and (b) expulsion of one of the 4-substituents followed by phenol formation.[2] Warszawski *et al.*[3] found that photolysis of 3-oxo-10β-hydroxy-17β-acetoxy-$\Delta^{1,4}$-oestradiene (Ia) and 3-oxo-10β,17β-diacetoxy-$\Delta^{1,4}$-oestradiene (Ib) resulted in the cleavage of the 10-substituent (hydroxyl and acetoxyl, respectively) and afforded the corresponding phenol II. It was also reported by Schuster and Polowczyk[4] that a spirodienone (III), photochemically, gave a biradical (IV), which abstracted hydrogen from the solvent to yield *p*-ethylphenol and an ether (V) as major products.

Recently, Schuster and Patel[5] reported the typical photochemical reaction of 2,5-cyclohexadienone, 4-methyl-4-trichloromethyl-2,5-cyclohexadienone (VI), which isomerizes in benzene to form predominantly 6-methyl-6-trichloromethylbicyclo[3.1.0]hex-3-en-2-one (VII) and affords *p*-cresol as the main product in ethyl ether, and two possible mechanisms for *p*-cresol formation were postulated. If such a species as VIII is involved, it seems possible that cleavage of one of the substituents at the C-4 position would give *p*-methylphenoxy radical, leading to *p*-cresol (path A). A mechanistic alternative to the formation of *p*-cresol is hydrogen abstraction from the solvent by VIII to give the dienone ketyl radical IX (path B). Schuster and Patel suggested from their experimental data that the latter mechanism is favorable.

The present paper reports on the photochemical

1) Part XLI: K. Ogura and T. Matsuura, This Bulletin, **43**, 2891 (1970)

2) For example, K. Schaffner, *Advan. Photochem.*, **4**, 81 (1966).

3) a) R. Warszawski, K. Schaffner and O. Jeger, *Helv. Chim. Acta*, **43**, 500 (1960); b) C. Ganter, R. Warszawski, H. Wehril, K. Schaffner and O. Jeger, *ibid.*, **46**, 320 (1963).

4) D. I. Schuster and C. J. Polowczyk, *J. Amer. Chem. Soc.*, **86**, 4502 (1964).

5) a) D. J. Patel and D. I. Schuster, *ibid.*, **90**, 5137 (1968); b) D. I. Schuster and D. J. Patel, *ibid.*, **90**, 5145 (1968).

reactions of 2,4,6-tri-*t*-butyl-4-bromo-2,5-cyclohexadienone (X)[6] and 2,4,6-tri-*t*-butyl-4-nitro-2,5-cyclohexadienone (XI),[7] in which the process *via* path A seems preferable for the formation of 2,4,6-tri-*t*-butylphenol.

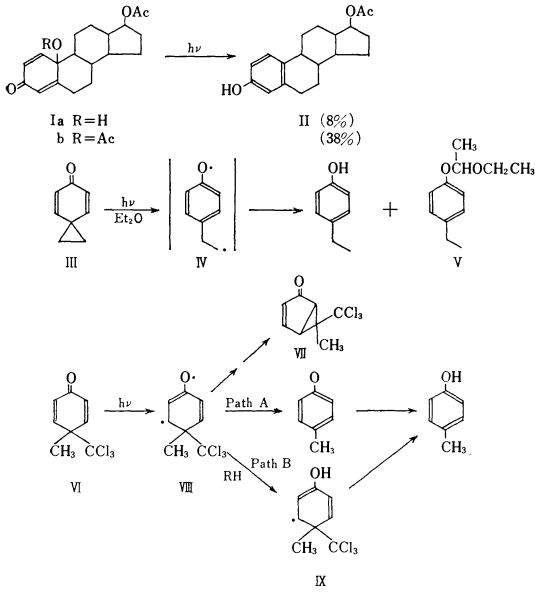

Results and Discussion

Irradiation of X in various solvents with a high-pressure mercury arc lamp filtered through Pyrex yielded 2,4,6-tri-*t*-butylphenol (XIII) in high yields (88% in ethyl ether; 81% in *n*-hexane; 56% in *N*,*N*-dimethylformamide; 56% in benzene). On photolysis of X in *N*,*N*-dimethylformamide, the solution became blue soon after the irradiation had been started. The color was extinguished by continued irradiation for a longer period of time or by bubbling oxygen. This blue solution showed a UV absorption at 630 mμ and an ESR spectrum (triplet, $a_H = 1.8$). Comparison of these spectra with those of 2,4,6-tri-*t*-butylphenoxy radical (XII), which was produced by the oxidation of XIII with lead dioxide, led us to the conclusion that the color was attributed to XII. Ultraviolet analysis indicated that the yield of the radical at a photostationary state amounted to 15%. The blue color also appeared, although weakly, on photolysis of X in *n*-hexane and benzene.

In order to see whether the recombination of the phenoxy radical XII and a bromine atom, which were produced by photolysis of X, occurs or not, X was irradiated under bubbling oxygen.

Table 1. Photolysis of X in various solvents[a]

Solvent	Irrad. time (min)	Bubbled gas	Yield (%)[b] X	XIII	XV
n-Hexane	45	N_2	—	81(81)	—
n-Hexane	13	N_2	63	27	1
n-Hexane	14	O_2	—(6)	—	56(50)
DMF	62	N_2	—	56	7
DMF	15	N_2	77	14	—
DMF	15	O_2	59(68)	—	13(24)
Benzene[c]		N_2		(56)	
Ether	40	N_2		(88)	
Acetic acid	60	N_2	53	15	5
DMSO	30	N_2	77	—	10

a) A solution (500 mg in 70 m*l*) of X was irradiated with a 100-W high-pressure mercury arc lamp (Pyrex filter).
b) Yields in parenthesis were obtained by VPC analysis.
c) A solution (2.00 g in 70 m*l*) of X was irradiated for 6.75 hr and bromobenzene was detected in a 4.5% yield (by VPC analysis).

It is well known that in the presence of oxygen the phenoxy radical XII was easily converted into a peroxide (XIV)[6] and that XIV was photochemically decomposed to afford 2,6-di-*t*-butyl-*p*-quinone (XV) in a high yield.[8] When a solution of X in *n*-hexane was irradiated for a short period of time with a high-pressure mercury arc lamp under bubbling oxygen, a mixture of the products, which was shown by VPC analysis to contain XV (50%) and X (6%), was obtained. However, XIII, which was formed on irradiation of X in *n*-hexane under nitrogen for the same period of time (see Table 1), could not be detected in the reaction mixture. It should be noted that the yield of the recovered X decreased remarkably in the presence of oxygen, compared with that under nitrogen. This suggests that the recombination of the phenoxy radical XII and a bromine atom may take place in *n*-hexane under nitrogen. On the other hand, it was shown that recombination was slower in *N*,*N*-dimethylformamide than in *n*-hexane (Table 1). This conclusion was also confirmed by the fact that the

Table 2. Photolysis of X[a]

Additive	Conversion of X (%)[b]
—	82
Naphthalene (0.203M)	84
Benzophenone (0.275M)	100

a) A solution of X in ether (0.0147M) was irradiated externally by the light of the longer wavelengths than 318 mμ.
b) by NMR analysis.

6) E. Müller, K. Ley and W. Kiedaisch, *Chem. Ber.*, **87**, 1605 (1954).
7) C. D. Cook and R. C. Woodworth, *J. Amer. Chem. Soc.*, **75**, 6242 (1953).

blue color of the phenoxyl XII produced on photolysis of X in *N,N*-dimethylformamide (15% of the amount of the starting material X) was extinguished very slowly under bubbling nitrogen.*1 These facts and the results shown in Table 1 indicate that the primary decomposition rate of X decreases in order of *n*-hexane, *N,N*-dimethylformamide, and acetic acid. Since the photochemical decomposition of X was sensitized by benzophenone as shown in Table 2, it may be reasonable to assume that the photochemical dissociation of X to XII and bromine results from a n-π^* triplet state of X.

There is another question concerning how the intermediary phenoxyl XII, which is known to be very stable in the dark, abstracts a hydrogen to afford XIII. Irradiation of the solution of the phenoxyl XII in benzene and petroleum ether with a high-pressure mercury arc lamp through a pyrex filter under bubbling nitrogen gave XIII in 47 and 71% yields, respectively. The photochemical disappearance of the phenoxyl XII in various solvents was followed by the decrease of the ultraviolet maximum at 630 mμ. The result shown in Fig. 2 indicates that the reaction rate of

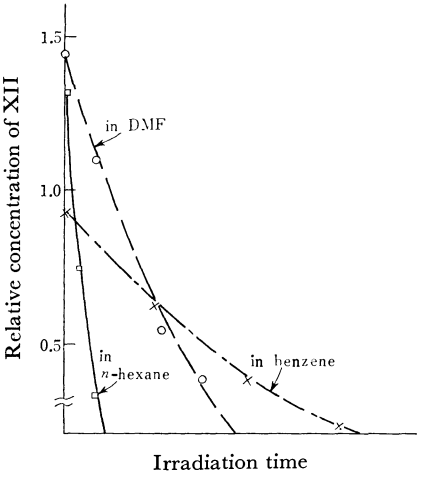

Fig. 2

XII increases in the order: benzene, *N,N*-dimethylformamide and *n*-hexane. Analogous phenomena have been observed in the photolysis of a stable radical, diphenylpicrylhydrazyl (DPPH), in various solvents. Pitts *et al.*,[9] reported that hydrogen abstraction of DPPH afforded diphenylpicrylhydrazine. The ultraviolet spectrum of the phenoxyl XII showed a maximum at 625 mμ and a minimum at 450 mμ in benzene. A light at 625±7 mμ did not accelerate the hydrogen-abstraction of XII, but that at shorter wavelengths than 450 mμ did.*2

*1 A kinetic consideration supports the conclusion that XII reacts with a bromine molecule. The mechanism shown in the following scheme is adequate to describe the disappearance of XII which was formed by irradiation of X in *N,N*-dimethylformamide.

$$XII + Br_2 \xrightarrow{k_1} X + Br \quad (1)$$

$$XII + Br \xrightarrow{k_2} X \quad (2)$$

$$XII \xrightarrow{k_3} \text{products} \quad (3)$$

$$2Br \xrightarrow{k_4} Br_2 \quad (4)$$

where, k_1 and k_2 are the rate constants for reactions (1) and (2), and k_3 for the first-order decomposition of XII (3). The disappearance of XII follows the next equation.

$$-\frac{d[XII]}{dt} = k_1[XII][Br_2] + k_2[XII][Br] + k_3[XII]$$

In the early stages, it is inferred that $1/2[XII]=[Br_2]$ and the fourth equation was neglected ($k_2[Br]=k_1[Br_2]$). In this case, the above-mentioned equation may be written as

$$-\frac{d[XII]}{dt} = k_1[XII]^2 + k_3[XII]$$

Integration of this equation gives the equivalent expression

$$\log\frac{[XIII]_0}{[XII]_0+k_3/k_1} - \log\frac{[XII]}{[XII]+k_3/k_1} = k_3t$$

where $[XII]_0$=the concentration of XII at time $t=0$. Supposing that k_3/k_1 is 0.05, a plot of log (XII/XII+k_3/k_1) against time is linear in the early stage (Fig. 1).

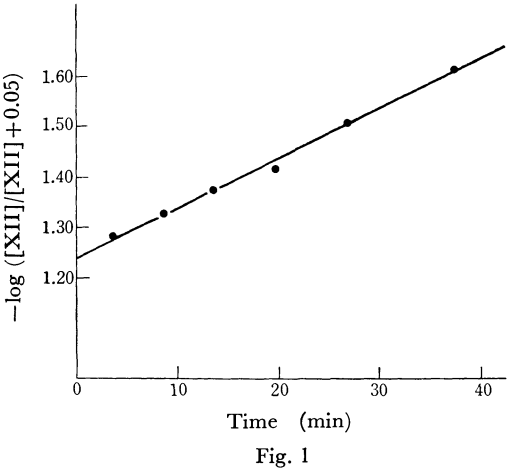

Fig. 1

This indicates that the disappearance of the phenoxyl XII may be largely attributed to its reaction with bromine molecules.

8) T. Matsuura, This Bulletin, **37**, 564 (1964).

9) J. N. Pitts, Jr., E. A. Schuck and J. K. S. Wan, *J. Amer. Chem. Soc.*, **86**, 296 (1964).

*2 The selected light was obtained by a concave radiation monochromator (Japan Spectroscopic Co., Model CRM-50). For its performances see Ref. 10.

10) a) T. Matsuura and K. Ogura, *ibid.*, **89**, 3846 (1967); b) Y. Yamada, H. Uda, and K. Nakanishi, *Chem. Commun.*, **1966**, 423.

When a solution of 2,4,6-tri-*t*-butyl-4-nitro-2,5-cyclohexadienone (XI) in benzene was irradiated with a 450-W high-pressure mercury arc lamp (Pyrex filter) under bubbling nitrogen, the reaction mixture, was shown to contain 2,4,6-tri-*t*-butylphenol (XIII, 6%), 2,6-di-*t*-butyl-*p*-benzoquinone (XV, 11%) and 2,4,6-tri-*t*-butyl-4-hydroxy-2,5-cyclohexadienone (XX, trace). Irradiation (>318 mμ) of XI in petroleum ether yielded XV (17%), XX (10%) and 3,5-di-*t*-butyl-*o*-benzoquinone (XXI, 5%) along with a trace of XIII. On the other hand, XIII was formed as the main product of the photolysis of XI in polar solvents such as *N*,*N*-dimethylformamide (28%) and methanol (43%). The results are summarized in Table 3.

TABLE 3. PHOTOLYSIS OF XI

Solvent	Yield (%)[c]	
	XIII	XV
DMF[a]	28	—
Methanol[a]	35 (43)	—
Ether[b]	(8)	(11)
Benzene[a]	11 (6)	(11)
Petroleum ether[b]	trace	(17)

a) >280 mμ (Pyrex filter)
b) >318 mμ (through a 0.08 M solution of naphthalene in benzene)
c) Yields in parenthesis were obtained by VPC analysis.

The formation processes of these products may be rationalized as shown in Scheme II. In the first step, XI suffers homolytic decomposition to give XII and nitrogen dioxide, which has two resonance structures, O-radical and N-radical forms. The recombination of the radical XII and nitrogen dioxide (as the O-radical form) produces two isomeric nitrites (XVI and XVII). These nitrites undergo further photochemical cleavage of O–NO bond give XVIII and XIX, which are de-*t*-butylated to the corresponding benzoquinones, XV and XXI, respectively. The compound XX may be formed by hydrogen abstraction of XVIII or by hydrolysis of XVI during working up. Since XII and bromine recombine slowly in polar solvents, as mentioned already, it is expected that the recombination of XII and nitrogen dioxide is also a slow process. In fact, XIII was a major product in photolysis of XI in methanol and *N*,*N*-dimethylformamide, but XV could not be detected. Furthermore, it may be reasonable that the recombination of XII and nitrogen dioxide is a faster process in non-polar solvents, and that the formation of XV is predominant over the hydrogen abstraction of XII to afford XIII.

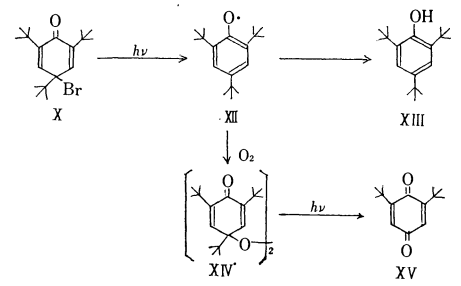

Scheme I

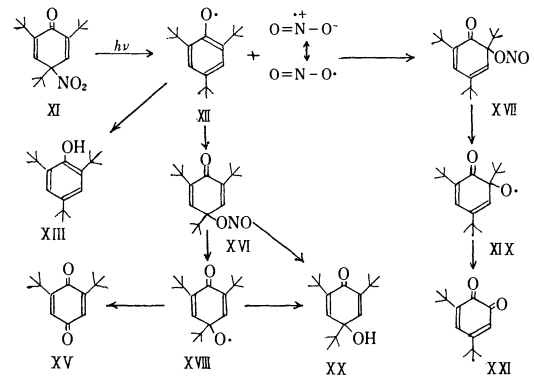

Scheme II

Experimental

Reaction of X in the Dark. Bromodienone X[6] was very unstable on silica gel and neutral alumina, but considerably stable in refluxed benzene. A solution of X (400 mg) in 10 m*l* petroleum ether was adsorbed on 20 g of silica gel and then allowed for half an hour at room temperature. Elution with 50 ml of petroleum ether gave 179 mg (56%) of colorless crystals which were identified as 2,4-di-*t*-butyl-6-bromophenol[6] (by IR). Further elution with 150 m*l* of petroleum ether afforded 110 mg (36%) of colorless crystals which were identified as 2,4,6-tri-*t*-butylphenol (XIII) (by IR). Elution with 50 m*l* of benzene yielded 3 mg of a yellow oil which was not further investigated. Continuous elution with 50 m*l* of benzene gave 28 mg (11%) of orange crystals which were identified as 2,6-di-*t*-butyl-*p*-benzoquinone (XV)[11] (by IR). The results were reproducible.

After X (300 mg) was adsorbed on 30 g of neutralized alumina (Woelm Co., Act. I), elution with 200 m*l* of petroleum ether and 100 m*l* of benzene gave 8 mg of a yellow oil which was not further investigated. Further elution with 150 m*l* of chloroform afforded 199 mg (83%) of pale yellow crystals which were identified as 2,4,6-tri-*t*-butyl-4-hydroxy-2,5-cyclohexadienone (XX)[11] (by IR).

A solution containing 200 mg of X in 20 m*l* of benzene was refluxed for 6 hr. The reaction mixture was evaporated under reduced pressure to yield pale yellow crystals which exhibited the same IR spectrum as that of X and were shown by TLC analysis not to contain

11) E. Müller and K. Ley, *Chem. Ber.*, **88**, 601 (1955).

2,4-di-*t*-butyl-6-bromophenol.

Photolysis of X. Since the starting material X was very unstable on silica gel and had a similar retention time on VPC to that of XIII to make VPC analysis difficult, the yield of the recovered X was estimated from the amount of 2,4-di-*t*-butyl-6-bromophenol which could be shown by TLC analysis not to exist in the photolysis mixture of X and which might be derived from the decomposition of X on silica gel.

a) In n-Hexane for a Long Period of Time under Bubbling Nitrogen. A solution containing 500 mg of X in 60 m*l* of *n*-hexane was irradiated for 45 min with a 100-W high-pressure mercury arc lamp surrounded by a Pyrex jacket under bubbling nitrogen. After addition of *n*-hexane (100 m*l*), the reaction mixture was washed with water and evaporated under reduced pressure. The residue was chromatographed on 20 g of silica gel. Elution with 200 m*l* of petroleum ether gave 309 mg (81%) of colorless crystals which were identified as XIII (by IR). In another run, VPC analysis of the reaction mixture (silicon DC 550, 1.5 m; 180°C; carrier gas: H_2, 1.5 kg/cm^2) showed that the yield of XIII was 81%.

b) In n-Hexane for a Short Period of Time under Bubbling Nitrogen. A solution containing 500 mg of X in 60 m*l* of *n*-hexane was irradiated for 13 min under the same conditions as described above. After evaporation of the solvent under reduced pressure, the residue was chromatographed on 20 g of silica gel. Elution with 50 m*l* of petroleum ether gave 41 mg of colorless crystals which were identified as 2,4-di-*t*-butyl-6-bromophenol (by IR). Further elution with 50 m*l* of petroleum ether afforded 153 mg of colorless crystals which were shown by IR analysis to consist of 101 mg of 2,4-di-*t*-butyl-6-bromophenol and 52 mg of XIII. Elution with 250 m*l* of petroleum ether yielded 134 mg of colorless crystals which were identified as XIII (by IR). Elution with 100 m*l* of benzene - petroleum ether (1 : 1) gave 20 mg of a yellow oil which was not further investigated. Continuous elution with 100 m*l* of benzene afforded 27 mg of orange crystals which were identified as XV. The yields of X, XIII and XV were 63, 27 and 2%, respectively.

c) In n-Hexane under Bubbling Oxygen. A solution containing 500 mg of X in 60 m*l* of *n*-hexane was irradiated for 14 min with a 100-W high-pressure mercury arc lamp (Pyrex filter) under bubbling oxygen. After evaporation of the solvent under reduced pressure, the residue was chromatographed on 20 g of silica gel. Elution with 300 m*l* of petroleum ether gave 12 mg of a colorless oil which was not further investigated. Further elution with 150 m*l* of benzene afforded 179 mg (56%) of orange crystals which were identified as XV (by IR).

d) In Benzene. A solution containing 2.00 g of X in 70 m*l* of benzene was irradiated for 6.75 hr under the same conditions mentioned in a). After removal of the solvent under reduced pressure, the residue was shown by VPC analysis to contain XIII and bromobenzene in 56 and 4.5% yields, respectively.

e) In Ether. A solution containing 500 mg of X in 60 m*l* of ether was irradiated under the same conditions described in a). The reaction mixture was evaporated under reduced pressure and the residue was shown by VPC analysis to contain XIII in a 88% yield.

f) In N,N-Dimethylformamide for a Long Period of Time. A solution containing 500 mg of X in 60 m*l* of *N,N*-dimethylformamide was photolyzed for 62 min under the same conditions mentioned in a). After addition of 200 m*l* of water, the reaction mixture was extracted with three 100-m*l* portions of ether. The ethereal layer was washed with water and dried on anhydrous sodium sulfate. After removal of the solvent under reduced pressure, the residue was shown by VPC analysis to contain XIII and XV in 56 and 7% yields, respectively.

g) In N,N-Dimethylformamide for a Short Period of Time. A solution containing 500 mg of X in 60 m*l* of *N,N*-dimethylformamide was irradiated for 15 min under the same conditions described in a). The resulting blue solution was allowed to stand for 2 hr under bubbling nitrogen to give a yellow solution. After addition of 150 m*l* of ether, the reaction mixture was washed with water and dried on anhydrous sodium sulfate. After evaporation of the solvent under reduced pressure, the residue, which was shown by TLC analysis not to contain 2,4-di-*t*-butyl-6-bromophenol, was chromatographed on 20 g of silica gel. Elution with 50 m*l* of petroleum ether gave 144 mg of colorless crystals which were identified as 2,4-di-*t*-butyl-6-bromophenol (by IR). Further elution with 50 m*l* of petroleum ether afforded 94 mg of colorless crystals which were shown by IR analysis to consist of 32 mg of 2,4-di-*t*-butyl-6-bromophenol and 62 mg of XIII. Elution with 250 m*l* of petroleum ether yielded 91 mg of colorless crystals which were identified as XIII (by IR). Elution with 200 m*l* of benzene - petroleum ether (1 : 1) gave 5 mg of a yellow oil which was not further investigated. The continuous elution with 100 m*l* of benzene - petroleum ether (1 : 1) afforded 25 mg of orange crystals which were identified as XV (by IR). The yields of X and XIII were 77 and 14%, respectively.

h) In N,N-Dimethylformamide under Bubbling Oxygen. A solution containing 500 mg of X in 60 m*l* of *N,N*-dimethylformamide was irradiated for 15 min under the same conditions mentioned in c). After addition of ether (150 m*l*), the mixture was washed with water and dried on anhydrous sodium sulfate. The ethereal solution was evaporated under reduced pressure and the residue, which was shown by TLC analysis not to contain 2,4-di-*t*-butyl-6-bromophenol, was chromatographed on 20 g of silica gel. Elution with 50 m*l* of petroleum ether gave 134 mg of colorless crystals which were identified as 2,4-di-*t*-butyl-6-bromophenol (by IR). Further elution with 200 m*l* of petroleum ether afforded 84 mg of colorless crystals which were identified as XIII (by IR). Elution with 50 m*l* of benzene - petroleum ether (1 : 1) yielded 10 mg of a yellow oil which was not further investigated. Continuous elution with 130 m*l* of benzene - petroleum ether (1 : 1) gave 62 mg of orange crystals which were identified as XV (by IR). The yields of X and XV were estimated to be 59 and 13%, respectively. In another run, the photolyzed mixture was shown by VPC analysis to contain X and XV in 68 and 24% yields, respectively.

i) In Dimethyl Sulfoxide. A solution containing 500 mg of X in 60 m*l* of dimethyl sulfoxide and 10 m*l* of benzene was irradiated for 30 min under the same conditions described in a). During photolysis, the solution did not show a blue color, but a deep yellow. After addition of ether (100 m*l*), the reaction mixture was washed with water and dried on anhydrous sodium sulfate. Evaporation of the solvent under reduced

pressure gave a yellow oil which was shown by IR and TLC analyses to contain mainly X. The oil was chromatographed on 20 g of silica gel. Elution with 150 m*l* of petroleum ether afforded 175 mg of pale yellow crystals which were identified as 2,4-di-*t*-butyl-6-bromophenol (by IR). Further elution with 150 m*l* of petroleum ether yielded 94 mg of colorless crystals, which were identified as XIII (by IR). Elution with 100 m*l* of benzene - petroleum ether (1 : 1) gave 10 mg of a yellow oil which was not further investigated. Continuous elution with 200 m*l* of benzene - petroleum ether (1 : 1) afforded 67 mg of orange crystals which were identified as XV (by IR). It was estimated from these results that the yields of X and XV were 77 and 10%, respectively.

j) In Acetic Acid. A solution containing 500 mg of X in 100 m*l* of acetic acid was irradiated for 1 hr under the same conditions mentioned in a). After addition of ether (200 m*l*), the reaction mixture was washed with water and an aqueous bicarbonate solution and dried on anhydrous sodium sulfate. Evaporation of the solvent afforded a yellow oil which was chromatographed on 20 g of silica gel. Elution with 50 m*l* of petroleum ether gave 120 mg of colorless crystals which were identified as 2,4-di-*t*-butyl-6-bromophenol (by IR). Further elution with 150 m*l* of petroleum ether yielded 128 mg of colorless crystals which were identified as XIII (by IR). Elution with 100 m*l* of petroleum ether and 70 m*l* of benzene afforded 30 mg of a pale yellow oil which was not further investigated. Elution with 50 m*l* of benzene gave 33 mg of orange crystals which were identified as XV (by IR). The estimated yields of X, XIII and XV were 53, 15 and 5%, respectively.

Photolysis of the Phenoxyl Radical XII. *a) In Petroleum Ether.* A solution of the phenoxy radical XII in 400 m*l* of petroleum ether, prepared from 4.00 g of 2,4,6-tri-*t*-butylphenol (XIII) according to the known method,[12] was irrradiated with a 450-W high-pressure mercury arc lamp surrounded by a Pyrex water-cooled jacket under bubbling nitrogen until the blue color of the solution disappeared (irradiation time: 15 hr). The reaction mixture was evaporated under reduced pressure and the residue was shown by VPC analysis to contain XIII and XV in 71 and 13% yields, respectively. Eight-ninths of the reaction mixture was chromatographed on 50 g of silica gel. Elution with 200 m*l* of petroleum ether gave 1.90 g of pale yellow crystals which were identified as XIII (by IR).

b) In Benzene. A solution of XII in 400 m*l* of benzene, prepared from 4.00 g of XIII, was irradiated for 43 hr under similar conditions to those described in a) to afford a yellow solution. The reaction mixture was shown by VPC analysis to contain XIII and XV in 47 and 7%, respectively. The mixture was evaporated under reduced pressure to give a brown oil which, by crystallization from methanol, yielded 155 mg of pale yellow crystals, identified as XIII (by IR and mixture mp).

c) With a Selected Light. The selected light was obtained by a concave radiating monochromator (Japan Spectroscopic Co., Model CRM-50).[8] A solution of XII was prepared from 150 mg of XIII in 50 m*l* of benzene, which was treated with 1.30 g of lead dioxide followed by filtration of the reaction mixture under nitrogen atmosphere.[6] Each 4 m*l* of the solution was placed in a quartz cell (1 cm square) and irradiated with the selected light. The solution completely absorbed the incident light of wavelengths longer than 570 mμ and shorter than 410 mμ. The progress of the reaction was followed by decrease of the absorbances at 550 and 530 mμ. The relative rates of disappearance of XII with various wavelength lights were 1.0 at 305±7 mμ, 0.6 at 341±7 mμ, 0.6 at 377±7 mμ, 0.3 at 413±7 mμ, 0.2 at 449±7 mμ, 0.0 at 485±7 mμ, and 0.0 at 625±7 mμ.

Photolysis of XI. *a) In Methanol.* A solution containing 1.00 g of XI in 60 m*l* of methanol was irradiated for 1.5 hr with a 100-W high-pressure mercury arc lamp through a Pyrex filter under bubbling nitrogen. Evaporation of the solvent under reduced pressure gave a brown oil which was chromatographed on 20 g of silica gel. Elution with 410 m*l* of petroleum ether afforded 310 mg (35%) of colorless crystals which were identified as XIII (by IR).

A solution containing 500 mg of XI in 60 m*l* of methanol was also irradiated for 52 min under the same conditions as described above. The reaction mixture was shown by VPC analysis (Silicon DC 550, 1.5 m, 170°C. carrier gas: H_2, 1.5 kg/cm^2) to contain XIII in 43%.

b) In N,N-Dimethylformamide. A solution containing 500 mg of XI in 60 m*l* of *N,N*-dimethylformamide was irradiated for 45 min under the same conditions mentioned in a). After addition of ether (150 m*l*), the reaction mixture was washed with water and dried on anhydrous sodium sulfate. Evaporation of the solvent under reduced pressure afforded a brown oil which was chromatographed on 20 g of silica gel. Elution with 130 m*l* of petroleum ether gave 121 mg (28%) of colorless crystals which were identified as XIII (by IR).

c) In Ether. A solution containing 1.00 g of XI in 400 m*l* of ether was irradiated for 4 hr and 11 min with a 100-W high-pressure mercury arc lamp under bubbling nitrogen through the filter solution, which contained 1 g of naphthalene in 100 m*l* of benzene and absorbed completely the incident light of wavelength shorter than 318 mμ. The reaction mixture was shown by VPC analysis to contain XV in 11%. Three-fourths of the reaction mixture was evaporated under reduced pressure and chromatographed on 20 g of silica gel. Elution with 30 m*l* of benzene - petroleum ether (1 : 1) yielded 53 mg of pale yellow crystals which were identified as XIII (by IR).

d) In Benzene. A solution containing 500 mg of XI in 60 m*l* of benzene was irradiated for 52 min under the same conditions described in a). The reaction mixture was shown by VPC analysis to contain XIII and XV in 6 and 11%, respectively. A solution containing 2.00 g XI in 60 m*l* of benzene was also photolyzed for 5.5 hr under the same conditions mentioned above. After removal of the solvent under reduced pressure, the residue was chromatographed on 60 g of silica gel. Elution with 25 m*l* of benzene - petroleum ether (1 : 1) gave 188 mg of pale yellow crystals which was shown by IR analysis to consist mainly of XIII. Further elution with 365 m*l* of benzene- petroleum ether afforded 350 mg of a brown oil which was not further investigated. Elution with 100 m*l* of the same solvent yielded 89 mg of orange crystals which were identified

12) E. Müller and K. Ley, *Chem. Ber.*, **87**, 922 (1954).

as XV (by IR). Elution with 350 m*l* of petroleum ether-benzene gave 190 mg of a orange oil which was not further investigated. Continuous elution with 150 m*l* of benzene afforded 46 mg of a pale yellow oil containing a small amount of colorless crystals (8 mg), which were separated by filtration and identified as XX (by IR).

e) In Petroleum Ether. A solution containing 1.00 g of XI in 400 m*l* of petroleum ether was irradiated for 3.5 hr under the same conditions as described in c). The reaction mixture was shown by VPC analysis to contain XV in 17%. Three-fourths of the reaction mixture was evaporated under reduced pressure and chromatographed on 30 g of silica gel. Elution with 500 m*l* of petroleum ether gave 29 mg of a yellow oil which was shown by TLC analysis to contain a trace of XIII. Further elution with 130 m*l* of petroleum ether - benzene (1 : 1) afforded 88 mg of a yellow oil which was not further investigated. Elution with 100 m*l* of petroleum ether - benzene (1 : 1) yielded 95 mg of orange crystals which were identified as XV (by IR). Elution with 150 m*l* of the same solvent gave 71 mg of pale yellow crystals which were identified as XX (by IR). Elution with 430 m*l* of benzene afforded 114 mg of a brown oil which was not further investigated. Continuous elution with 300 m*l* of benzene and with 100 m*l* of methylene chloride yielded 99 mg of purple crystals which were further purified by preparative TLC to give 27 mg of XXI[13] (identified by IR).

One of the authors (K. O.) is indebted to Fuji Film Co. for financial support.

13) W. Flay, T. Ploetz and H. Biergans, *Ann. Chem.*, **597**, 196 (1955).

BULLETIN OF THE CHEMICAL SOCIETY OF JAPAN VOL. 43 3187—3194 (1970)

Photoinduced Reactions. XLIII. Photochemical Reactions of 4-Hydroxy-2,5-cyclohexadienones[1]

Katsuyuki OGURA and Teruo MATSUURA

Department of Synthetic Chemistry, Faculty of Engineering, Kyoto University, Sakyo-ku, Kyoto

(Received January 24, 1970)

Irradiation of 2,4-di-*t*-butyl-4,5-dihydroxy-2,5-cyclohexadienone (V) in methanol afforded a *β*-diketone (VIII) in a 68% yield. Diketone VIII was also formed on photolysis of a suspension of V in petroleum ether (62%) and an aqueous alkaline solution of V (56%). Photolysis of 2,4-di-*t*-butyl-4-hydroxy-5-methoxy-2,5-cyclohexadienone (VI) in various solvents yields IXa as a main product. On irradiation of VI in methanol, XI which might be formed by the addition of methanol to IXb was also isolated. Irradiation of 2,4,6-tri-*t*-butyl-3-methoxy-4-hydroxy-2,5-cyclohexadienone (VII) in a variety of solvents gave a cyclopentadienone (XIII) in high yields. It is reasonable to assume that the cyclopentadienone XIII is formed by elimination of methanol from a 2-cyclopentenone derivative (XII). The formation of XIII from VII was sensitized by benzophenone and acetophenone, and quenched by piperylene. The mechanisms of these reactions are discussed.

In the photochemical reaction of a 2,5-cyclohexadienone in neutral media, isomerization to a bicyclo[3.1.0]hex-3-en-2-one, the so-called lumi-type ketone, is the most common process (Eq. 1).[2] On the other hand, photolysis of certain 4-hydroxy-2,5-cyclohexadienones was reported to afford 4-acyl-2-cyclopentenones and two reaction pathways were proposed (paths 1 and 2 in Scheme 1). Ganter *et al.* found that the photochemical rearrangement of 3-oxo-10*β*-hydroxy-17*β*-acetoxy-$\Delta^{1,4}$-estradiene affords a 4-acyl-2-cyclopentenone derivative along with 17-*O*-acetylestradiol, and they proposed a zwitterion intermediate leading to the acylcyclopentenone *via* path 1 (Eq. (2)).[3] Altwicker and Cook[4] showed that irradiation of 2,6-di-*t*-butyl-4-hydroxy-4-phenyl-2,5-cyclohexadienone gives 2,5-di-*t*-butyl-4-benzoyl-2-cyclopentenone, and they considered the possibility of path 2 for its formation (Eq. (3)). Furthermore, Burkinshaw *et al.*[5] reported the photolysis of several 4-

1) Part XLII: K. Ogura and T. Matsuura, This Bulletin, **43**, 3181 (1970).

2) For example, K. Schaffner, *Advan. in Photochem.*, **4**, 81 (1966).

3) C. Ganter, R. Warszawski, H. Wehrli, K. Schaffner and O. Jeger, *Helv. Chim. Acta*, **46**, 320 (1963).

4) E. R. Altwicker and C. F. Cook, *J. Org. Chem.*, **29**, 3087 (1964).

5) G. F. Burkinshaw, B. R. Favis and P. C. Woodgate, *Chem. Commun.*, **1967**, 607.

hydroxy-2,5-cyclohexadienones to give 4-acyl-2-cyclopentenone derivatives, some of which undergoes further photochemical rearrangement to form Δ^1-butenolides (*e.g.*, Eq. (4)). Recently, we showed[6],*1 that the photolysis of 2,4,6-tri-*t*-butyl-4-hydroxy-2,5-cyclohexadienone (I) in non-polar media affords the products A and B which are unequivocally formed *via* a bicyclo[3.1.0]hex-3-en-2-one (II), a 4-acyl-2-cyclopentenone derivative IIIa and the further transformed product IVa. The photolysis of I in polar solvents gave the product (IVb) as the main product.

In the present study photochemical reactions of 2,4-di-*t*-butyl-4,5-dihydroxy-2,5-cyclohexadienone (V),[8] 2,4-di-*t*-butyl-4-hydroxy-5-methoxy-2,5-cyclohexadienone (VI),[8] and 2,4,6-tri-*t*-butyl-3-methoxy-4-hydroxy-2,5-cyclohexadienone (VII)[9] were examined in order to investigate the substituent effect upon the course of the photochemical reaction of 4-hydroxy-2,5-cyclohexadienones and to discuss the validity of two possible mechanisms (paths 1 and 2 in Scheme 1) for the formation of 4-acyl-2-cyclopentenones.

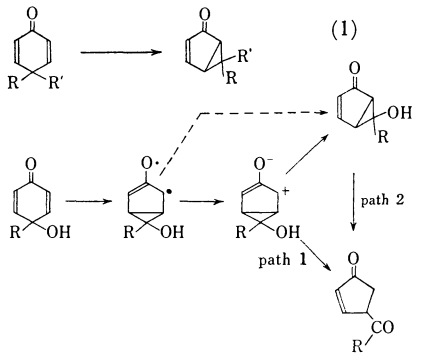

Scheme 1

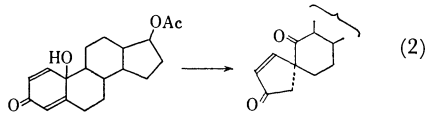

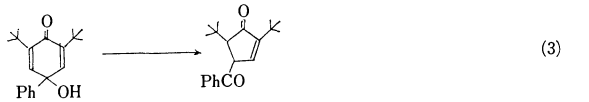

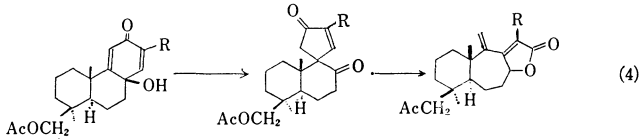

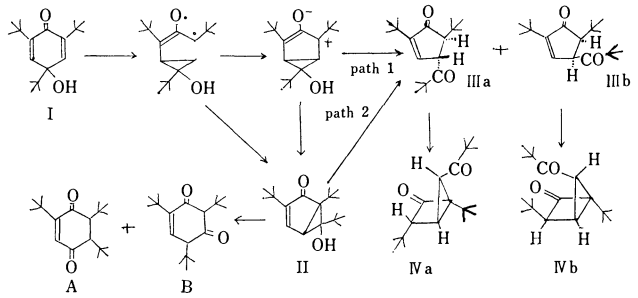

6) T. Matsuura and K. Ogura, *Tetrahedron*, **24**, 6167 (1968).

*1 Recently Plank *et al.* reported that a vinylcyclobutenone (i) had been isolated from the photolysis of I in benzene.[7]

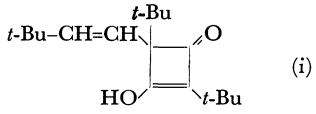

(i)

7) D. A. Plank, J. C. Floyd and W. H. Starnes, Jr., *Chem. Commun.*, **1969**, 1003.

8) H. Musso and D. Maassen, *Ann. Chem.*, **689**, 93 (1965).

9) T. Matsuura and K. Ogura, *J. Amer. Chem. Soc.*, **89**, 3846 (1967).

Results and Discussion

Photolysis of V. Irradiation of V in methanol with a high-pressure mercury arc lamp (Pyrex filter) afforded a β-diketone (VIII) in a 68% yield. The product was also obtained by the photolysis of a suspension of V in petroleum ether (62%) and of an aqueous alkaline solution of V (56%). The IR spectrum of VIII showed broad bands at 3500—2200, 2100—1750, and 1675—1400 cm^{-1}, indicating the presence of strong hydrogen bonding between a hydroxyl group and a carbonyl group. The UV absorption of VIII (λ_{max}^{EtOH} 248.5 mμ) suggests that VIII has an enone system. In the NMR spectrum of VIII, four singlets appear at τ 1.45 (1H), 4.91 (1H), 8.74 (9H), and 9.00 (9H), and two doublet signals at τ 5.80 and 7.20 (J=2 Hz). These data are consistent with formula VIII, which is the structure expected from the mechanism analogous to the photochemical reaction of 4-hydroxy-2,5-cyclohexadienones (Scheme 1). Since β-diketone VIII is unchangeable on treatment with a base*2 and the coupling constant (J=2 Hz) between C-4 and C-5 protons of VIII is similar to that of IIIa,[10] it is suggested that the steric relation between the *t*-butyl and pivaloyl groups of VIII is *trans*. The structure VIII for β-diketone was further supported from the spectral data of its methyl ethers. Treatment of a solution of VIII in absolute methanol with dry hydrogen chloride gave two 3-methoxy-2-cyclopentenone derivatives, IXa (mp 57—61°C) and Xa (mp 35—36°C). Both of them showed similar spectral data which were consistent with the structures IXa and Xa. 3-Methoxy-2-cyclopentenone with a higher melting point (57—61°C) exhibits its IR absorptions at 1705 (2-cyclopentenone), 1693 (pivaloyl) and 1627 cm^{-1} (strong, >C=C–O–), and its UV band at 240 mμ (ε 9200). The NMR spectrum of the cyclopentenone (mp 57—61°C) showed three singlets at τ 6.24 (3H, =C–OCH_3), 8.75 (9H, =C-*t*-Bu)[10] and 9.00 (9H, >C-*t*-Bu),[10] two doublets at τ 4.71 (1H, J=1 Hz) and 7.56 (1H, J=2 Hz), and a quartet at τ 5.83 (1H, J=1 and 2 Hz). On the other hand, in the NMR spectrum of the 3-methoxy-2-cyclopentenone with a lower melting point (35—36°C), six signals appeared at τ 4.79 (1H, singlet), 5.84 (1H, doublet, J=2 Hz), 6.14 (3H, singlet, =C–OCH_3), 6.99 (1H, doublet, J=2 Hz), 8.73 (9H, singlet, =C-*t*-Bu)[10] and 9.03 (9H, singlet, C-*t*-Bu).[10] The singlet (τ 4.79) and the doublet (τ 6.99) couple slightly with each other. The compound showed its IR bands at 1712 (2-cyclopentenone), 1685 (pivaloyl) and 1596 cm^{-1} (strong, >C=C–O–) and its UV absorption at 240 mμ (ε 16100). Formula IXa was assigned to the structure of the 2-cyclopentenone with a higher melting point, because the 2-cyclopentenone (IXa) was also obtained by photolysis of VI which is expected to give IXa (Scheme 1). Thus the lower melting 2-cyclopentenone is represented as formula Xa. It should be noted that a methoxyl signal of IXa appeared at a higher magnetic field (τ 6.26) than that (τ 6.14) of Xa. This may be due to the location of the methoxyl group of IXa in the deshielding area of its pivaloyl group.

Photolysis of VI. Irradiation of VI in methanol with a high-pressure mercury lamp through a Pyrex filter gave the 2-cyclopentenone IXa and a dimethoxycyclopentanone (XI) in 39 and 32% yields, respectively. Dimethoxycyclopentanone XI was shown from its IR bands at 1748 and 1694 cm^{-1} to have two carbonyl groups. The NMR spectrum of XI exhibits four singlets at τ 6.67 (3H, >C–OCH_3), 6.83 (3H, >C–OCH_3), 8.76 (9H, =C-*t*-Bu)[10] and 9.00 (9H, >C-*t*-Bu),[10] a doublet of doublet at τ 5.80 (1H, J=1 and 7 Hz), a multiplet at τ 7.50 (3H), and no signal at fields lower than τ 5.5. This compound was converted into IXa by mild treatment with a base. These data suggest that dimethoxycyclopentanone is formulated as XI. It is considered[6] that the hydrogen at C-5 position of IXa is derived from a solvent or the hydroxyl hydrogen at C-4 position of VI (*via* an intermolecular or intramolecular hydrogen transfer), and that therefore deuterated compounds IXc and XIa corresponding to IXa and XI should be formed on photolysis of VI in methanol-*O*-d_1.[6] In fact, irradiation of VI in methanol-*O*-d_1 afforded the products IXc and XIa. Deuteriocyclopentenone IXc showed its NMR signals corresponding to those of IXa except for the disappearance of the signal of IXa at τ 7.56. This indicates that, in the NMR spectrum of IXa, the proton at C-5 position is coupled with the C-4 proton (J=2 Hz) and the proton at C-2 with the C-4 proton (J=1 Hz). In the NMR spectrum of XIa, the signal at τ 5.80 appeared as a diffused singlet and the intensity of the multiplet signal at τ 7.50 was reduced as compared with that of XI. This supports the observation that the signal of XI at τ 5.80 is attributed to the C-4 proton and the coupling constant between the C-4 and C-5 protons is 7 Hz.

Photolysis of VII. Irradiation of VII in various

Table 1. The sensitized reaction of VII[a]

exp. No.	VII[b]	Additive	XIII Yield (%)	Rel. rate
1	62 mg	—	24	1.0
2	62 mg	benzophenone (1.95 g)	15	0.61
3	62 mg	acetophenone (1.30 g)	10	0.41

a) Done with a merry-go-round apparatus using a high-pressure mercury arc lamp.
b) Diluted to 20 ml with benzene.

*2 It is known that IIIb (*cis*) is easily converted to IIIa (*trans*) by a mild treatment with a base.[10]

10) T. Matsuura and K. Ogura, *ibid.*, **89**, 3850 (1967).

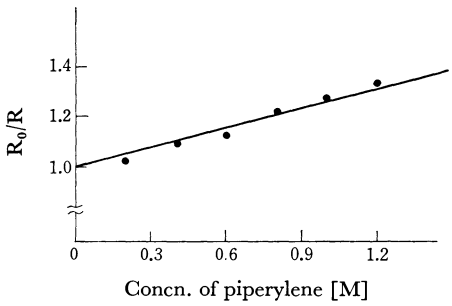

Fig. 1. Photolysis of VII in benzene.
R=the formation rate of XIII
R_0=R in the absence of piperylene

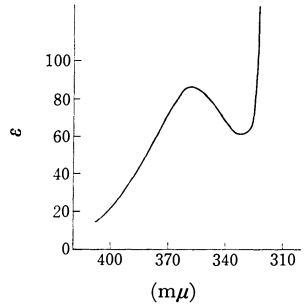

Fig. 2. n-π^* absorption of VII in cyclohexane.

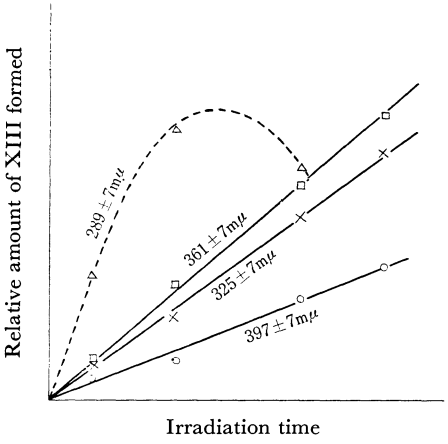

Fig. 3. Photolysis of VII in cyclohexane with selected lights.

solvents with a high-pressure mercury arc lamp (Pyrex filter) gave an orange crystalline product XIII in yields of 76% in petroleum ether, 78% in benzene, 36% in methanol, 33% in acetic acid-ethanol - water (2 : 2 : 1) and 62% in *N*,*N*-dimethylformamide. The NMR spectrum of XIII showed four singlets at τ 8.77 (9H), 8.85 (9H), 8.90 and 3.71 (1H). The product XIII exhibited UV bands at 404 and 262 mμ and IR absorption at 1713 cm^{-1}, characteristic of a cyclopentadienone.[11]

11) E. N. Garbisch, Jr., and R. F. Sprecher, *J. Amer. Chem. Soc.*, **88**, 3433 (1966); **88**, 3434 (1966) and the references cited therein.

Reduction of XIII with zinc in acetic acid afforded cyclopentenones IIIa and IIIb.[10] This led us to assign structure XIII for the orange product.

Since the formation of XIII was sensitized by benzophenone and acetophenone (Table 1) and quenched by piperylene as shown in Fig. 1 (Stern-Volmer plot), it is concluded that XIII is formed *via* the triplet state of VII. The n-π^* absorption of VII in cyclohexane showed its maximum at 360 mμ as shown in Fig. 2. Photolysis of VII with the selected lights (see Experimental) was performed, the results of which are summarized in Fig. 3. It follows from the experiments with the selected lights that both the n-π^* and π-π^* excitations are responsible for the formation of XIII.

Photolysis of 4,6-Di-*t*-butyl-3-hydroxy-4-acetoxy-2,5-cyclohexadienone (XV). The starting material was prepared by partial acetylation of V with acetic anhydride and pyridine. Irradiation of XV in methanol with a high-pressure mercury arc lamp through a Pyrex filter yielded a methyl ester in 30% yield, for which we assigned structure XVI. The ester showed its IR bands at 1750 (vinyl acetate), 1713 (ester) and 1680 cm^{-1}. In the NMR spectrum, five singlets appeared at τ 6.29 (3H, $COOCH_3$), 6.48 (2H, $-CH_2-$), 7.80 (3H, =C-OCO-CH_3), 8.93 (9H, =C-*t*-Bu)[10] and 9.05 (9H, >C-*t*-Bu),[10] and two doublets at τ 4.81 (1H, J=11 Hz) and 7.03 (1H, J=11 Hz) indicating the presence of a >CH–CH= group. These data are in accord with structure XVI. The formation of XVI can be explained by the addition of methanol to a ketene intermediate XVII which was produced by the photochemical ring fission from a tautomeric form of 2,4-cyclohexadienone (XVb).*3 Photolysis of XV in *N*,*N*-dimethylformamide or benzene gave a complex mixture of products.

Mechanistic Consideration. The photochemical formation of XI from VI in methanol can be explained by methanol addition to 2-cyclopentenone IX. Considering the facts that XI was not formed by the photolysis of IXa in methanol and that a larger coupling constant (7 Hz) was observed*4 between the C-5 and C-4 protons in XI, it is reasonable to assume that XI is formed by the addition of methanol to *cis*-2-cyclopentenone IXb. However, we cannot distinguish the two following possibilities; *viz.*, methanol addition to IXb is easier than to IXa because of (1) the presence of a less-hindered site in IXb and (2) the decrease of the steric repulsion between the *t*-butyl and the pivaloyl groups by the

*3 Although it was reported[8] that only one tautomeric form V is predominant in solution, the UV spectrum of XV in ethanol showed two absorption bands at 285 and 249 mμ indicating the presence of, at least, two tautomeric forms, one of which might be XVb.

*4 *Cf.* The coupling constant between the C-4 and C-5 protons in IIIa is 2 Hz and that in IIIb 5 Hz.[10]

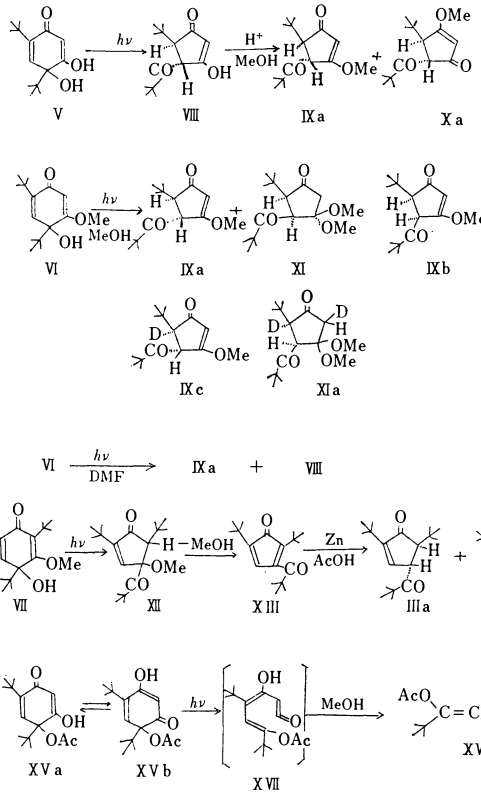

Scheme 2

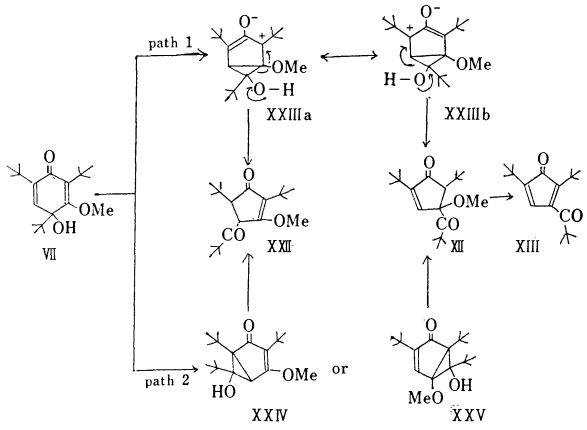

Scheme 3

transformation of IXb in to XI. Formation of VIII on photolysis of VI in *N*,*N*-dimethylformamide can be also attributed to the addition of water to IXb followed by the elimination of methanol. It is probable that the formation of cyclopentadienone XIII arises from elimination of a methanol molecule from an intermediate XII, which is the product expected from the known transformation of 4-hydroxy-2,5-cyclohexadienones (Scheme 1).

For the formation of VIII from V, IX from VI and XIII from VII, two reaction routes, "path 1" and "path 2", as shown in Schemes 2 and 3 can be written. In the photochemical reactions of V and VI, we cannot explain the predominant formation of VIII and IX, respectively, by the "path 1" mechanism, because it appears reasonable that the resonance structure XIXb is more stabilized by the inductive effect of a *t*-butyl group than XIXa.

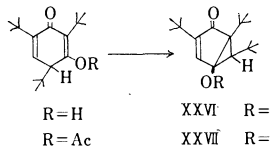

We cannot expect a large enough difference between the stabilities of XXIIIa and XXIIIb to control the reaction courses, XXIIIa→XXII and XXIIIb →XII, and the photochemical formation of XXIV from VII has an analogy in the photochemical reactions of 2,4,6-tri-*t*-butyl-3-hydroxy-2,5-cyclohexadienone[6] and 2,4,6-tri-*t*-butyl-3-acetoxy-2,5-cyclohexadienone[6] which were photochemically isomerized to form the corresponding lumiketones (XXVI and XXVII). Therefore, the "path 2" mechanism seems preferable in the photochemical reaction of VII.

Experimental

Photolysis of 2,4-Di-*t*-butyl-4,5-dihydroxy-2,5-cyclohexadienone (V). *(a) In Methanol.* A solution containing 4.00 g of V[8] in 500 m*l* of methanol was irradiated for 3.5 hr with a 450-W high-pressure mercury arc lamp (Ushio UM 450) surrounded by a Pyrex jacket under bubbling nitrogen. After removal of the solvent under reduced pressure, the residue was crystallized from petroleum ether to give 2.52 g of pale yellow crystals, which, by recrystallization from benzene-petroleum ether afforded β-diketone VIII as colorless crystals, mp 188—189°C: $\lambda_{max}^{cyclohexane}$ 245 mμ (log ε 4.24); λ_{max}^{EtOH} 248.5 mμ (log ε 4.10); $\lambda_{max}^{EtO\text{-}OH^-}$ 265 mμ (log ε 4.25); ν_{max}^{KBr} 3500—2200, 2100—1750, 1705 and 1675—1400 cm^{-1}; the NMR spectrum: τ^{CDCl_3} 1.45 (1H, singlet), 4.91 (1H, singlet), 5.80 (1H, doublet, J=2 Hz), 7.20 (1H, doublet, J=2 Hz), 8.74 (9H, singlet) and 9.00 (9H, singlet).

Found: C, 70.31; H, 9.61%. Calcd for $C_{14}H_{22}O_3$: C, 70.55; H, 9.31%. The mother liquor was evaporated and the residue was chromatographed on 60 g of silica gel. Elution with 300 m*l* of benzene and then with 800 m*l* of chloroform gave 991 mg of a pale yellow oil which was not further investigated. Elution with 100 m*l* of ether afforded 990 mg of semicrystals which, by recrystallization from benzene - petroleum ether yielded 205 mg of colorless crystals. These crystals were identified as β-diketone VIII (by IR). Total yield of VIII amounted to 68%.

(b) In Petroleum Ether. A suspension containing 1.00 g of V in 200 m*l* of petroleum ether was photolyzed for 10.5 hr with a 100-W high-pressure mercury arc lamp (Pyrex filter) under bubbling nitrogen. The reaction mixture was evaporated under reduced pressure and the residue was chromatographed on 40 g of silica gel. Elution with 450 m*l* of petroleum ether - benzene (1 : 1), 200 m*l* of benzene, 200 m*l* of chloroform and 90 m*l* of chloroform - acetone (19 : 1) gave 311 mg of a yellow oil containing a small amount of crystals which was not further investigated. Further elution with 100 m*l* of acetone - chloroform (1 : 9) afforded 616 mg of yellow crystals, which, on washing with petroleum ether and recrystallization from benzene, yielded colorless crystals, mp 185—187°C. These crystals were identified as β-diketone VIII (by IR and mixture mp).

(c) In an Alkaline Solution. A solution containing 1.00 g of V and 2.00 g of potassium hydroxide in 200 m*l* of water was irradiated for 10.5 hr under the same conditions as mentioned above. The reaction mixture was acidified with concentrated hydrochloric acid and extracted with three 150-m*l* portions of ether. After washing with water and drying on anhydrous sodium sulfate, the ethereal layer was evaporated under reduced pressure. Recrystallization of the residue from petroleum ether gave 560 mg of pale yellow crystals, mp 187—188°C, which were identified as β-diketone (by IR and mixture mp).

Etherification of VIII. A solution containing 2.29 g of VIII in 30 m*l* of absolute methanol was saturated with hydrogen chloride and allowed to stand for 3 hr at room temperature. After removal of the solvent under reduced pressure, the residue was chromatographed on 80 g of silica gel. Elution with 500 m*l* of chloroform gave 17 mg of a pale yellow oil which was not further investigated. Further elution with 500 m*l* of chloroform afforded 517 mg of a pale brown oil which soon crystallized. It was purified by a short-path distillation (100°C/3 mmHg) to yield cyclopentenone Xa as colorless crystals, mp 35—36°C: λ_{max}^{EtOH} 240 mμ (log ε 4.21); ν_{max}^{KBr} 1712, 1685 and 1596 cm^{-1}; the NMR spectrum: τ^{CDCl_3} 4.79 (1H, singlet), 5.84 (1H, doublet, J=2 Hz), 6.14 (3H, singlet), 6.99 (1H, J=2 Hz), 8.73 (9H, singlet) and 9.03 (9H, singlet).

Found: C, 71.11; H, 9.33%. Calcd for $C_{15}H_{24}O_3$: C, 71.39; H, 9.59%. Elution with 100 m*l* of chloroform gave 257 mg of a pale brown oil which was shown by TLC analysis to be a mixture of IXa and Xa. Continuous elution with 200 m*l* of chloroform afforded 638 mg of pale brown crystals, mp 56—59°C, which were identified as cyclopentenone IXa, the photolysis product of VI described below (by IR, VPC and mixture mp). Elution with 500 m*l* of chloroform yielded 118 mg of a pale brown oil which was not further investigated. Further elution with 300 m*l* of chloroform-acetone (9 : 1) gave 622 mg of colorless crystals which were identified as VII (by IR).

Photolysis of VI. *a) In Methanol.* A solution containing 500 mg of VI[8] in 180 m*l* of methanol was irradiated for 6 hr with a 100-W high pressure mercury arc lamp (Pyrex filter) under bubbling nitrogen. After evaporation of the solvent under reduced pressure, the residue was chromatographed on 15 g of silica gel. Elution with 200 m*l* of benzene gave 57 mg of a pale yellow oil which was not further investigated. Further elution with 150 m*l* of benzene and 280 m*l* of chloroform yielded 143 mg of colorless crystals, which, on recrystallization from petroleum ether, afforded dimethoxycyclopentanone XI as colorless crystals, mp 97—98°C: ν_{max}^{KBr} 1748 and 1694 cm^{-1}; the NMR spectrum: τ^{CDCl_3} 5.80 (1H, doublet of doublet, J=1 and 7 Hz), 6.67 (3H, singlet), 6.83 (3H, singlet), 7.50 (3H, multiplet), 8.76 (9H, singlet) and 9.00 (9H, singlet).

Found: C, 67.35; H, 9.89%. Calcd for $C_{16}H_{28}O_4$: C, 67.57; H, 9.93%. Elution with 50 m*l* of chloroform gave 115 mg of a yellow oil which was shown by VPC analysis to contain mainly IXa. Continuous elution with 50 m*l* of chloroform afforded 114 mg of a yellow oil, which was purified by a preparative VPC and a short-path distillation (130°C/3 mmHg) to yield cyclopentenone IXa as colorless crystals, mp 57—61°C: λ_{max}^{EtOH} 240 mμ (log ε 3.96); ν_{max}^{KBr} 1705, 1693 and 1627 cm^{-1}; the NMR spectrum: τ^{CDCl_3} 4.71 (1H, doublet, J=1 Hz), 5.83 (1H, quartet, J=1 and 2 Hz), 6.24 (3H, singlet), 7.56 (1H, doublet, J=2 Hz), 8.75 (9H, singlet) and 9.00 (9H, singlet).

Found: C, 71.69; H, 9.76%. Calcd for $C_{15}H_{24}O_3$:

C, 71.39; H, 9.59%.

b) In N,N-Dimethylformamide. A solution containing 500 mg of VI in 80 m*l* of *N,N*-dimethylformamide was irradiated for 6 hr under the same conditions as described in a). Ether (150 m*l*) was added into the reaction mixture, and then the solution was washed with water and dried on anhydrous sodium sulfate. After removal of the solvent under reduced pressure, the residue was chromatographed on 10 g of silica gel. Elution with 225 m*l* of chloroform gave 164 mg of a pale yellow oil which was not further investigated. Further elution with 30 m*l* of chloroform afforded 174 mg of a pale brown oil which was re-chromatographed on 10 g of silica gel and yielded 99 mg of IXa (identified by IR and VPC). Elution with 100 m*l* of chloroform gave 43 mg of pale yellow crystals which were identified as V (by IR).

c) Quantitative Analysis by VPC. A Pyrex tube (10 mm diameter) containing 100 mg of VI and 5 m*l* of a solvent was externally irradiated with a 450-W high-pressure mercury arc lamp, after the atomosphere was replaced with nitrogen. The reaction mixture was analyzed by VPC (silicon DC 550, 1.5 m; column temperature, 210°C. carrier gas; helium, 1.5 kg/cm^2). The yields of IXa were 28% in *n*-hexane, 32% in benzene, 44% in *N,N*-dimethylformamide and 39% in methanol. The yield of XI in methanol was 32%.

Treatment of XI with a Base. Forty mg of XI was added to 3 m*l* of 1 N methanolic potassium hydroxide and the mixture was allowed to stand for 1 hr at room temperature. After addition of 100 m*l* of water, the reaction mixture was extracted with two 15-m*l* portions of ether. The ethereal layer was washed with water and dried on anhydrous sodium sulfate. After evaporation of the solvent, the residue was purified by a short-path distillation (95°C/3 mmHg) to yield 32 mg of colorless crystals, mp 55—61°C, which were identified as IXa (by IR, VPC and mixture mp).

Photolysis of VII. *a) In Methanol.* A solution containing 500 mg of VII[9] in 150 m*l* of methanol was irradiated for 1.5 hr with a 100-W high-pressure mercury arc lamp surrounded by a Pyrex jacket under bubbling nitrogen. After evaporation of the solvent under reduced pressure, the residue was chromatographed on 15 g of silica gel. Elution with 20 m*l* of petroleum ether - benzene (7 : 3) gave 8 mg of a yellow oil which was not further investigated. Further elution with 40 m*l* of the same solvent afforded 160 mg (36%) of orange crystals, which, on recrystallization from methanol, yielded cyclopentadienone XIII as orange crystals, mp 75—76°C: λ_{max}^{KBr} 404 (log ε 2.66) and 262 mμ(3.30); ν_{max}^{KBr} 1713, 1683 and 1593 cm^{-1}; the NMR spectrum: τ^{CCl_4} 3.71 (1H, singlet), 8.77 (9H, singlet), 8.85 (9H, singlet) and 8.90 (9H, singlet); the mass spectrum: *m/e* 276 (parent peak).

Found: C, 77.22; H, 10.12%. Calcd for $C_{18}H_{28}O_2 \cdot 1/4CH_3OH$: C, 77.06; H, 10.28%.

b) In Petroleum Ether. A solution containing 500 mg of VII in 150 m*l* of petroleum ether was irradiated for 1 hr and 50 min under the same conditions as described above. After removal of the solvent under reduced pressure, the residue was chromatographed on 15 g of silica gel. Elution with 10 m*l* of petroleum ether - benzene (7 : 3) gave 6 mg of a yellow oil which was not further investigated. Further elution with the same solvent afforded 340 mg (76%) of orange crystals, which were purified by recrystallization from methanol to yield 207 mg of orange crystals, mp 74—76°C. These crystals were identified as cyclopentadienone XIII (by IR).

c) In Benzene. A solution containing 1.10 g of VII in 180 m*l* of benzene was irradiated for 3 hr under the same conditions as mentioned in a). The reaction mixture was evaporated under reduced pressure and the residue was chromatographed on 30 g of silica gel. Elution with 20 m*l* of petroleum ether - benzene (7 : 3) gave 7 mg of a yellow oil which was not further investigated. Further elution with 110 m*l* of the same solvent afforded 765 mg (78%) of orange crystals which were identified as XIII (by IR).

d) In N,N-Dimethylformamide. A solution containing 500 mg of VII in 80 m*l* of *N,N*-dimethylformamide was irradiated for 1 hr under the same conditions as described above. Ether (150 m*l*) was added to the reaction mixture and the ethereal solution was washed with water. After drying on anhydrous sodium sulfate and evaporating the solvent under reduced pressure, the residue was chromatographed on 20 g of silica gel. Elution with petroleum ether - benzene (1 : 1) gave 279 mg (62%) of orange crystals which were identified as XIII (by IR).

e) In Acetic Acid - Ethanol - Water. A solution containing 500 mg of VII in 80 m*l* of acetic acid - ethanol - water (2 : 2 : 1) was photolyzed for 1 hr under the same conditions as mentioned above. After ether (300 m*l*) was added, the reaction mixture was washed with water and then with aqueous bicarbonate solution. After being dried on anhydrous sodium sulfate and the solvent evaporated under reduced pressure, the residue was chromatographed on 30 g of silica gel. Elution with 100 m*l* of petroleum ether - benzene (7 : 3) gave 19 mg of a yellow oil which was not further investigated. Further elution with 80 m*l* of the same solvent afforded 146 mg (33%) of orange crystals which were identified as XIII (by IR).

f) Quenching Experiment. Seven samples were prepared as shown in Table 2 and the atmospheres were replaced with nitrogen. The samples were irradiated for 20 min with a 450-W high-pressure mercury arc lamp surrounded by a Pyrex water-cooled jaket using a merry-go-round apparatus.[12]

Table 2.

Exp. No.	VII (mg)	Solution A[a] (m*l*)	Benzene (m*l*)
1	62	—	20
2	62	1	19
3	62	2	18
4	62	3	17
5	62	4	16
6	62	5	15
7	62	6	14

a) Solution A was prepared by diluting 6.87 g of freshly distilled piperylene to 25 m*l* with benzene.

The yield of XIII in each sample was determined

12) A. A. Lamola and G. S. Hammond, *J. Chem. Phys.*, **43**, 2129 (1965).

by VPC analysis (silicon DC 550, 1.5 m; 210°C; Carrier gas; helium, 1.0 kg/cm²). The results are summarized in Fig. 1.

g) With Selected Light. Selected light was obtained by a concave radiating monochromator (Japan Spectroscopic Co., Model CRM-50).[9,13] The experiment was carried out with a solution of 0.167 mg of VII in 3 m*l* of cyclohexane. The progress of the reaction was followed by the increase of a maximum at 406 mμ attributed to the absorption of XIII. The results are summarized in Fig. 2.

Reduction of XIII with Zinc in Acetic Acid. Zinc dust (6.0 g) was added to a solution of XIII (222 mg) in 20 m*l* of acetic acid. The reaction mixture was warmed at 50°C until the orange color disappeared. After removal of the deposited solid by filtration, 60 m*l* of water was added to the filtrate and the mixture was extracted with two 100-m*l* portions of ether. After the ethereal layer was washed with water and with aq. bicarbonate solution and dried on anhydrous sodium sulfate, the solvent was evaporated under reduced pressure. The residue was chromatographed on 7 g of silica gel. Elution with 30 m*l* of petroleum ether - benzene (1 : 1) gave 14 mg of a yellow oil which was not further investigated. Further elution with 45 m*l* of the same solvent afforded 73 mg of pale yellow crystals which, on recrystallization from methanol, yielded 13 mg of colorless crystals, mp 76—77.5°C, identified as IIIb[10] (by IR). Elution with 175 m*l* of petroleum ether - benzene (1 : 1) gave 48 mg of pale yellow crystals, which was purified by recrystallization from methanol to yield 13 mg of colorless crystals, mp 75—78°C, identified as IIIa[10] (by IR and mixture mp).

Preparation of XV. A solution containing 4.00 g of V in 30 m*l* of acetic anhydride and 15 m*l* pyridine was allowed to stand overnight at room temperature. After 150 m*l* of ice was added, the deposited crystals were separated by filtration and purified by recrystallization from ether - petroleum ether to afford colorless crystals, mp 52—53°C (with very slow heating). The mp was raised by rapid heating to 82.5—84°C. This behavior of the mp may be due to thermal tautomerization of XV. ν_{max}^{KBr} 3500—2600, 1745, 1730, 1685, 1655, 1625, 1595 and 1555 cm^{-1}; $\nu_{max}^{CHCl_3}$ 1735, 1685 and 1740 (sh) cm^{-1}; λ_{max}^{EtOH} 285 (log ε 3.02) and 249 mμ (3.59); $\lambda_{max}^{cyclohexane}$ 251 mμ (3.51); the NMR spectrum: τ^{CDCl_3} 3.60 (1H, singlet), 6.50 (1H, doublet, J=21 Hz), 6.63 (1H, doublet, J=21 Hz), 7.91 (3H, singlet), 8.75 (9H, singlet) and 8.99 (9H, singlet).

Found: C, 64.03; H, 8.96%. Calcd for $C_{16}H_{24}O_4 \cdot H_2O$: C, 64.40; H, 8.78%.

Photolysis of XV. A solution containing 530 mg of XV in 170 m*l* of methanol was irradiated for 10 hr with a 100-W high-pressure mercury arc lamp (Pyrex filter) under bubbling nitrogen. After removal of the solvent under reduced pressure, the residue was chromatographed on 20 g of silica gel. Elution with 180 m*l* of chloroform gave 155 mg of a pale yellow oil which was not further investigated. Further elution with 250 m*l* of chloroform afforded 176 mg (30%) of pale yellow crystals, which, on recrystallization from petroleum ether, gave ester XVI as colorless crystals, mp 52.5—53°C: ν_{max}^{KBr} 1750, 1712 and 1680 cm^{-1}; λ_{max}^{EtOH} 255 mμ (log ε 3.50); the NMR spectrum: τ^{CDCl_3} 4.81 (1H, J=11 Hz), 6.29 (3H, singlet), 6.48 (2H, singlet), 7.03 (1H, doublet, J=11 Hz), 7.80 (3H, singlet), 8.93 (9H, singlet) and 9.05 (9H, singlet).

Found: C, 65.25; H, 9.29%. Calcd for $C_{17}H_{28}O_5$: C, 65.36; H, 9.03%.

13) Y. Yamada, H. Uda and K. Nakanishi, *Chem. Commun.*, **1966**, 403.

One of the authors (K. O.) is indebted to Fuji Film Co., for financial support.

BULLETIN OF THE CHEMICAL SOCIETY OF JAPAN VOL. 43 3195—3198 (1970)

The Carbon-13 NMR Spectra of Alkyl Vinyl Ethers, and Their Structures and Reactivities

Koichi HATADA, Kazuhiko NAGATA and Heimei YUKI

Department of Chemistry, Faculty of Engineering Science, Osaka University, Toyonaka, Osaka

(Received January 26, 1970)

The ^{13}C NMR spectra of alkyl vinyl ethers were investigated at 22.5°C with neat liquid at 15.09 MHz. When the alkyl group of the ether becomes more electron-donating, the chemical shift of the α-carbon of the vinyl group shifts to a higher field, and that of the β-carbon, to a lower field. From these results, it was concluded that the contribution of the resonance form, $\bar{C}H_2-CH=\overset{+}{O}-R$, in the ether decreases in the order of the increasing electron-repelling power of the alkyl group. Good correlations were obtained between the chemical shifts of the vinyl group and the reactivity of vinyl ether in the cationic reaction. When the ether becomes more reactive, the chemical shift of the α-carbon shifts to a higher field, and that of the β-carbon to a lower field. This fact clearly shows that the attack of the proton on the β-carbon is not the rate determining step in the cationic reaction of the vinyl group. Linear relations were obtained between the chemical shifts of β-methylene protons and of β-carbon, but no correlation was obtained between the chemical shifts of the α-methine proton and of the α-carbon.

Carbon-13 chemical shifts (δ_c) have been reported for several olefinic compounds.[1-3] However, few data have been obtained on alkyl vinyl ethers.[3,4] In our preceding paper[5] we measured the ^1H NMR spectra of alkyl vinyl ethers and studied the resonance contribution in the ether. In this work, we will investigate the ^{13}C NMR spectra of alkyl vinyl ethers and will obtain direct evidence for the previous conclusions. The relationships between the reactivity of alkyl vinyl ether and the ^{13}C chemical shift of the vinyl group were also studied.

Experimental

The methyl vinyl ether was commercially obtained. The other vinyl ethers were prepared from methyl vinyl ether and alcohols by an ether-exchange reaction catalyzed by $Hg(OAc)_2$ in the presence of molecular sieves.[6] All the ethers were purified by refluxing them over lithium aluminum hydride and by subsequent distillation under a high vacuum.

The ^{13}C NMR spectrum was taken at 22.5°C on a JEOL C-60HL spectrometer with a 15.09 MHz RF unit and using a neat liquid in an 8 mmϕ sample tube. The signal to noise ratio of the spectrum was enhanced by the ^{13}C–H noise decoupling. The spectrum of *t*-butyl vinyl ether was also obtained by means of the accumulation over 16 scans using a JEOL JRA-1 accumulator. The chemical shift measurements were done with a nuclear resonance single side band technique;[7] their accuracies were within ± 0.2 ppm. Carbon disulfide was used as an external standard, the high field shifts being shown as positive values.

Results and Discussion

^{13}C Chemical Shifts of Alkyl Vinyl Ethers. The chemical shifts of alkyl vinyl ethers are given in Table 1, in which the vinyl ethers are arranged in increasing order of the electron-repelling power of their alkyl groups from the top to the bottom. When the alkyl group becomes more electron-donating, the chemical shift of the α-carbon shifts to a higher field, and that of the β-carbon, to a lower field.

The ^{13}C chemical shift of the vinyl group has been reported to be mainly controlled by the π-electron density and shows an upfield shift when the π-electron density on the carbon atom increases.[3,8] Therefore, the results in Table 1 show that the electron density of the α-carbon is mainly determined

1) R. A. Friedel and H. L. Retcofsky, *J. Amer. Chem. Soc.*, **85**, 1300 (1963).
2) G. B. Savitsky and K. Namikawa, *J. Phys. Chem.*, **68**, 1956 (1964).
3) G. E. Maciel, *J. Phys. Chem.*, **69**, 1947 (1965).
4) T. Higashimura, S. Okamura, I. Morishima and T. Yonezawa, *Polymer Lett.*, **7**, 23 (1969).
5) K. Hatada, M. Takeshita and H. Yuki, *Tetrahedron Lett.*, **1968**, 4621.
6) H. Yuki, K. Hatada and K. Nagata, This Bulletin, **42**, 3546 (1969).
7) M. Takeuchi and K. Nakagawa, "Magnetic Resonance and Relaxation," ed. by R. Blinc, North-Holland, Amsterdam, 1967.
8) M. Karplus and J. A. Pople, *J. Chem. Phys.*, **38**, 2803 (1963).

TABLE 1. ^{13}C NMR SPECTRA OF ALKYL VINYL ETHERS ($H_2C_\beta=C_\alpha HOR$)

R	Chemical shift from CS_2 (ppm)					
	α	β	c	d	e	f
$-C_cH_3$	40.5	109.6	141.2			
$-C_cH_2C_dH_3$	39.7	108.5	131.4	180.7		
$-C_cH_2C_dH_2C_eH_2C_fH_3$	40.6	108.1	126.8	162.8	174.9	180.7
$-C_cH_2C_dH(C_eH_3)_2$	40.8	108.7	120.5	167.0	175.8	
$-C_cH(C_dH_3)_2$	42.3	106.2	123.3	172.7		
$-C_c(C_dH_3)_3$	46.9	103.5	118.9	166.7		

by the electron-repelling power of the alkyl group.

On the contrary, the electron density of the β-carbon decreases when the electron-repelling power of alkyl group becomes stronger. Alkyl vinyl ether takes the following resonance form: $\bar{C}H_2-CH=\overset{+}{O}-R$.[9] Our inspection of ^1H NMR spectra of alkyl vinyl ethers suggested that the resonance contribution decreases in the order of the arrangement shown in Table 1, from the top to the bottom.[5] The contribution of such a resonance form would lead to an increase in the π-electron density of β-carbon. Therefore, the results in Table 1 are considered to be direct evidence for the above suggestion.

The resonance will be most favorable when the olefinic π-orbital and the lone-pair p-orbital on the oxygen atom overlap. Therefore, the degree of this resonance contribution is considered to depend on the conformation of alkyl vinyl ether. If the oxygen atom is assumed to have essentially sp^3 hybridization and, hence, a tetrahedral disposition of its bonds and lone-pair electrons, the probable conformations are *cis*, *trans* and *gauche* forms. From the inspection of molecular models, the *cis* and *trans* forms are most favorable for the resonance,

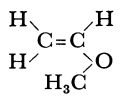

cis

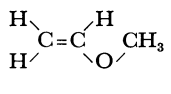

trans

while in the *gauche* form the resonance is almost entirely hindered. Infrared study[10] showed that, in methyl vinyl ether, the *cis* form is more stable at room temperature. As the alkyl group of vinyl ether is bulkier, the *cis* and *trans* forms become unstable because of the steric interaction between the alkyl group and α- or β-hydrogen of the vinyl group and the proportion of the gauche form gradually increases. Therefore, the degree of resonance contribution in alkyl vinyl ether is mainly controlled by the steric effect and decreases with an increase in the bulkiness of its alkyl group.

9) J. Feeney, A. Ledwith and L. H. Sutcliffe, *J. Chem. Soc.*, **1962**, 2021.

10) N. L. Owen and N. Shepherd, *Trans. Faraday Soc.*, **60**, 634 (1964).

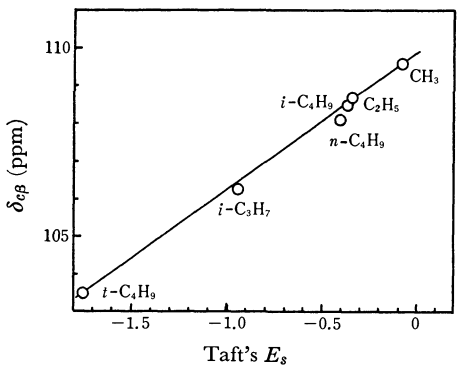

Fig. 1. Plots of $\delta_{c\beta}$ *vs.* E_s.

The order of the arrangement of the ether shown in the table is also in accordance with the increasing order of bulkiness of the alkyl group. By plotting the ^{13}C chemical shifts of β-carbon ($\delta_{c\beta}$) against the Taft steric parameter, E_s, of the alkyl group, a good linear relation was obtained; it is shown in Fig. 1, where the E_s value for R in the ether is that for the RCH_2 of RCH_2COOR'. These results clearly indicate the validity of the above theory.

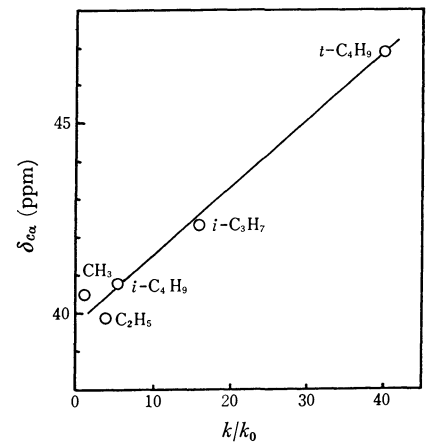

Fig. 2. Plots of $\delta_{c\alpha}$ *vs.* the relative rate of hydrolysis. The hydrolysis was carried out in acetone-water mixture (95/5 vol/vol) at 25°C using HCl catalyst.[11] The relative rate is represented by the ratio of the rate coefficient of respective vinyl ether to that of methyl vinyl ether.

^{13}C Chemical Shift and Reactivity of Alkyl Vinyl Ether. The carbon-13 NMR spectrum of alkyl vinyl ether may also give important information concerning its reaction mechanism. Therefore, let us now briefly discuss the mechanism of the cationic reaction of alkyl vinyl ether.

Alkyl vinyl ether is readily hydrolysed by dilute aqueous acids, and the relative rate of hydrolysis falls in the sequence;

$$CH_2{=}CHOR + H_2O \xrightarrow{H^+} ROH + CH_3CHO$$

R=t-C_4H_9>i-C_3H_7>i-C_4H_9>C_2H_5>CH_3. From their inspection of the ^1H NMR spectra of alkyl vinyl ethers, Ledwith and Woods[11] suggested that the electron release to the double bond of alkyl vinyl ether falls in the sequence: CH_3>i-C_3H_7>t-C_4H_9 and that, therefore, a simple, slow proton transfer to the terminal methylene group cannot be the rate-determining step in the acid-catalyzed hydrolysis.

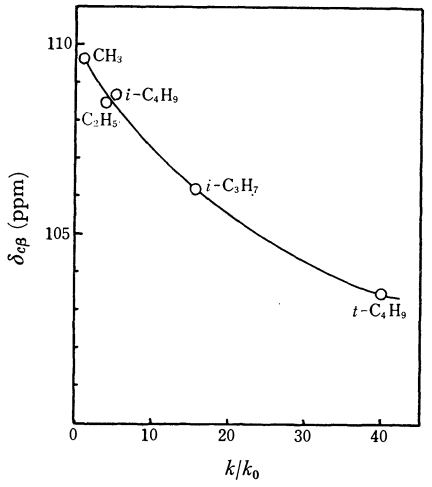

Fig. 3. Plots of $\delta_{c\beta}$ *vs.* the relative rate of hydrolysis.

As is shown in Figs. 2 and 3, a good correlations was obtained between the relative rate of hydrolysis[11] and the ^{13}C chemical shift of α- or β-carbon. These results show that the lower the electron density of β-carbon, and the higher that of α-carbon, the higher the reactivity in acid hydrolysis. This clearly indicates that the attack of the proton on the β-carbon is not the rate-determing step in this reaction. The π-electron density of α-carbon may play an important role in the rate-determining process in the hydrolysis.

The relative reactivity of alkyl vinyl ether in the cationic polymerization falls in the same order as that in the acid-catalyzed hydrolysis. In Figs. 4 and 5 the α- and β-carbon resonances are plotted against the relative reactivities of the ethers. Linear

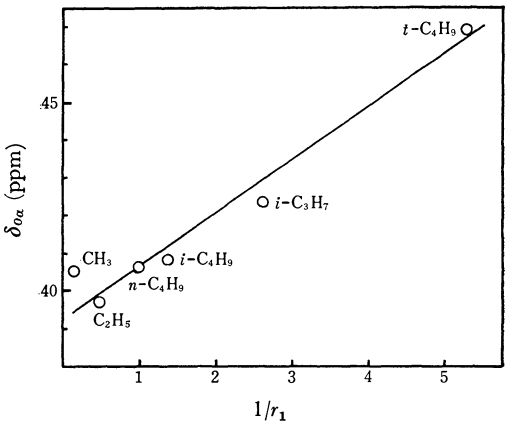

Fig. 4. Plots of $\delta_{c\alpha}$ *vs.* $1/r_1$ for alkyl vinyl ether.

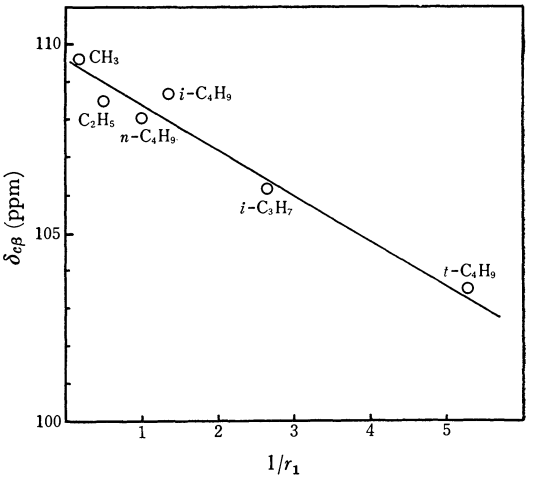

Fig. 5. Plots of $\delta_{c\beta}$ *vs.* $1/r_1$ for alkyl vinyl ether.

relations similar to those in Figs. 2 and 3 were obtained. The reactivities are represented by $1/r_1$, which was determined in the copolymerization of the respective vinyl ether (M_2) with n-butyl vinyl ether (M_1) at -78°C in toluene by the use of an $EtAlCl_2$ catalyst.[12]

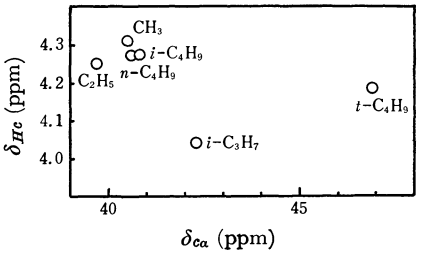

Fig. 6. Plots of $\delta_{H\alpha}$ *vs.* $\delta_{c\alpha}$.
The proton chemical shift was referred to the methyl signal of solvent toluene, low field shift being shown as positive value.

11) A. Ledwith and H. J. Woods, *J. Chem. Soc., B*, **1966**, 753.

12) H. Yuki, K. Hatada and M. Takeshita, *J. Polym. Sci., Part A-1*, **7**, 667 (1969).

Higashimura and his collaborator[13] studied the ^{13}C NMR spectra of *n*-butyl, isopropyl, and 2-chloroethyl vinyl ethers and found that the reactivity of vinyl ethers is not related to their chemical shifts. From this results, they concluded that the attack of the carbonium ion on the β-carbon is not the rate-determining step in the cationic polymerization of vinyl ether.

The results in Figs. 4 and 5 may give a strong evidence for Higashimura's suggestion, and may also suggest that the interaction of the carbonium ion with the α-carbon is an important consideration in determining the transition state of the rate-determining step.

Correlation of ^{1}H Chemical Shifts with ^{13}C Chemical Shifts. The chemical shift of the α-methine proton of alkyl vinyl ether has been reported to be independent of the electron-repelling power of the alkyl group.[5] No correlation was obtained between the chemical shifts of the α-methine proton and of the α-carbon (Fig. 6). These facts suggest that the chemical shift of this proton is controlled not only by the electron density at the α-carbon, but also by the diamagnetic shielding effect of an O–C bond in the OR group. On the other hand, linear relations were obtained between the chemical shifts of β-methylene protons and of the β-carbon, as is shown in Fig. 7. These relations show that the chemical shifts of β-methylene protons

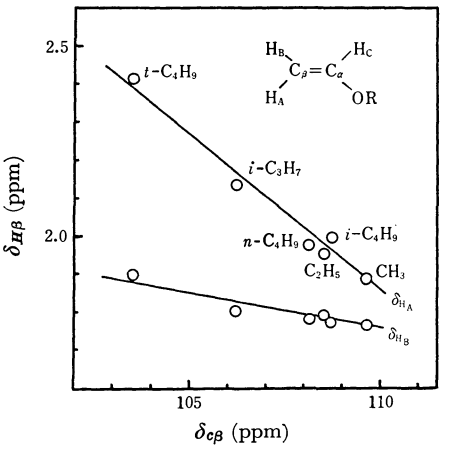

Fig. 7. Plots of $\delta_{H\beta}$ *vs.* $\delta_{c\beta}$.

shift to a higher field when the π-electron density of β-carbon increases. The diamagnetic shielding may have little effect on these protons; the chemical shifts are mainly controlled by the electron density at the β-carbon.

The authors are very grateful to Dr. M. Takeuchi and Dr. K. Gotoh of the Japan Electron Optics Laboratory Co., Ltd., for their measurements of the ^{13}C NMR spectra, and also to Mrs. F. Yano for her clerical assistance in preparing the manuscript.

One of the authors (K. H.) is grateful to the Matsunaga Science Foundation for a grant in support of this work.

13) T. Higashimura, S. Okamura, I. Morishima and T. Yonezawa, *Polymer Lett.*, **7**, 23 (1969).

BULLETIN OF THE CHEMICAL SOCIETY OF JAPAN VOL. 43 3199—3205 (1970)

Studies of Tritylated Sucrose. I. Mono-*O*-tritylsucroses

Toshiki OTAKE

Nippon Electric Varian, Ltd., Azabu, Iigura-machi, Minato-ku, Tokyo

(Received February 2, 1970)

Two isomeric mono-*O*-tritylsucroses were isolated from a mixture of tritylated sucrose which had been obtained by the reaction of sucrose and trityl chloride in the ratio of 1 : 1.2 by mole. The structures of these two isomers were established by the application of gas chromatography and NMR spectroscopy to appropriate derivatives. One of the two substances is 6′-mono-*O*-tritylsucrose, and the other is 6-mono-*O*-tritylsucrose, which is crystallized as white needles. The detritylation of mono-*O*-trityl-*O*-acetylsucroses yielded hepta-*O*-acetylsucroses, which were confirmed by a study of their NMR spectra to be 2,3,4,6,1′,3′,4′- and 2,3,4,1′,3′,4′,6′-hepta-*O*-acetylsucrose. No migration of the acetyl group on the sucrose molecule was observed during the detritylation procedure.

Several works on tritylated sucrose have been reported during the past forty years. Josephson[1] in 1929 reported the synthesis of "tri-*O*-tritylsucrose" with 3 mol of trityl chloride. Later, McKeown and his co-workers[2] described that the product obtained by the Josephson's route was a mixture of tri-*O*-tritylsucrose, products with a lower trityl content, reducing sugar, and tritanol. McKeown reported also that tri-*O*-trityl-penta-*O*-acetylsucrose was conveniently prepared in a crystalline form, after the tritylation of sucrose in pyridine, by acetylation in the same solution. The detritylation of this crystalline substance by graded hydrolysis with acetic acid, followed by methylation and deacetylation, yielded 1′,6′,4-tri-*O*-methylsucrose. The structure of this tri-*O*-methylsucrose was established by the production of the corresponding *O*-methyl ethers of glucose and fructose.

However, according to McKeown,[3] his deacetylation of the same crystalline substance, followed by methylation and detritylation, gave a syrupy penta-*O*-methylsucrose, which was concluded to consist of 2,3,4,3′,4′-penta-*O*-methyl derivatives of sucrose by the specific rotation measurement and by the paper chromatography of the corresponding *O*-methyl ethers of glucose and fructose. Accodingly, McKeown and his co-workers concluded that the original positions of trityl groups were at the three primary carbons in the sucrose molecule and that the acetyl migration from C_4 to C_6 occurred during the detritylation or methylation reaction.

Subsequently, Bredereck and his co-workers[4] reported a crystalline tri-*O*-trityl-penta-*O*-acetylsucrose with a melting point equal with that of the crystalline substance prepared by McKeown. The mild detritylation of the tri-*O*-trityl-penta-*O*-acetylsucrose with hydrobromic acid in a cold acetic acid solution yielded 2,3,4,3′,4′-penta-*O*-acetylsucrose, which turned into 2,3,6,3′,4′-penta-*O*-acetyl derivative when treated with sodium bicarbonate. The structure of the penta-*O*-acetylsucrose was established by periodate oxidation.

Scanning through these reports, one cannot help noticing how often treacherous conclusions were obtained from chemical reactions alone; thus, McKeown and his co-workers were first beguiled with the position of trityl groups and speculated on migration during deacetylation or methylation, and later confirmed the structure through a complex reaction route and a purely chemical determination, leaving ambiguities inherently connected with the chemical analyses.

Our present objective is the synthesis and structural determination of mono- and di-*O*-tritylsucroses obtained through various separation techniques. Studies of these products with a lower trityl content by a direct physical method such as NMR spectroscopy will give a further confirmation of the structure of the tri-*O*-trityl derivative of sucrose by eliminating the ambiguity which would otherwise arise from the analysis of the chemical procedures. The hepta-*O*-acetylsucroses prepared from the mono-*O*-tritylsucroses will be compounds for the synthesis of oligosaccharides, such as raffinose and planteose. This paper will deal with two isomeric mono-*O*-tritylsucroses and hepta-*O*-acetylsucroses derived from these isomers.

1) K. Josephson, *Ann. Chem.*, **472**, 230 (1929).
2) G. McKeown, R. Serenius and L. Hayward, *Can. J. Chem.*, **35**, 28 (1957).
3) G. McKeown and L. D. Hayward, *ibid.*, **35**, 992 (1957).
4) H. Bredreck, H. Zimmer, A. Wagner, G. Faber, W. Greiner and W. Huber, *Chem. Ber.*, **91**, 2824 (1958).

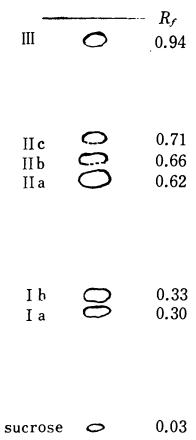

Fig. 1. The thin layer chromatogram of a reaction mixture of tritylation, effected on silica gel G with 20 : 20 : 3 : 57 (V/V/V/V) methanol-acetone-water-chloroform. Zones were located with 50% sulfuric acid.

Results and Discussion

The thin-layer chromatogram of a reaction mixture obtained from the treatment of sucrose with slightly overdosed trityl chloride in a pyridine solution is shown in Fig. 1. The chromatogram, which was detected by spraying with 50% sulfuric acid and by subsequent heating at 120°C, shows at least six kinds of tritylated sucroses, observable in the form of dark green spots. The tritylated sucroses, Ia and Ib, corresponding to the R_f values of 0.30 and 0.33 respectively, have been identified as mono-*O*-tritylated sucroses by UV spectroscopy, as will be described later. The tritylated sucroses, IIa, IIb and IIc, corresponding to the R_f values of 0.62, 0.66, and 0.71, are confirmed to be di-*O*-tritylsucroses by UV spectroscopy.

Of the total tritylated sucroses obtained, 47% by weight consisted of the combined yields of the di- and tri-*O*-tritylsucroses, this was quite a large figure in comparison with the overdosage of trityl chloride, in the molar ratio of 1.2 : 1, used for the treatment of sucrose. It is also noteworthy that the reaction mixture was about 10% free sucrose.

The reaction mixture was resolved in 1-butanol, and the butanol solution was washed with water to remove the free sucrose; the subsequent evaporation of the organic layer produced a mixture of tritylated sucroses as colorless glass. It was found that this mixture could conveniently be separated into mono-*O*-tritylsucrose and a mixture of substances with higher trityl contents by a counter-current distribution using a solvent system such as trichloroethylene - methanol - water; thus, the evaporation of the polar layer, consisting of methanol and water, yielded the mono-*O*-tritylsucrose 53% of the total tritylated sucroses, while the non-polar layer contained the remaining 47% the di- and tri-*O*-tritylsucroses.

Mono-*O*-tritylsucrose, Ib, was separated as white needles from a solution of 80% ethanol (mp 99—101°C; $[\alpha]_D^{20}$ +51.7° (*c* 4, *N*,*N*-dimethylformamide). The other isomeric mono-ether, Ia, was obtained as an amorphous powder from the concentrate of the mother liquid after Ib had been removed by means of recycling column chromatography.[5] The amorphous powder Ia softens at 149°C and has $[\alpha]_D^{22}$ +31.9° (*c* 4, *N*,*N*-dimethylformamide). A small amount of Ib was further recovered in a crystalline form from a fraction with a higher Ib content by recycling column chromatography; the total yield for the crystalline Ib was 35% as against 36% for Ia, relative to a mixture of mono-*O*-tritylsucroses.

The IR spectra of Ia and Ib, while each shows essentially the same pattern as that of free sucrose between 1400 and 800 cm^{-1}, both exhibited characteristic phenyl absorptions at 1600, 1495, and 1450 cm^{-1}. On the UV spectra of trityl chloride, Ia and Ib have also identical absorption patterns (λ_{max}=260 mμ) and assume almost the same values in the molar extinction coefficients (ε_{max}: Ia, 725; Ib 715; trityl chloride, 720). These spectroscopic observations confirm that Ia and Ib are mono-*O*-tritylsucroses.

The tritylated sucroses with higher R_f values, IIa, IIb, and IIc, take molar extinction coefficients of 1415—1460, which are twice as much as those of mono-*O*-tritylsucroses; this proves that IIa, IIb, and IIc, are di-*O*-trityl derivatives.

The methylation of both the mono-*O*-tritylsucroses according to the Kuhn procedure,[6] followed by column-chromatographic purification, produced mono-*O*-trityl-hepta-*O*-methylsucroses, IVa and IVb, in 77% and 83% yields respectively. Both the products were colorless glass, and IVb was crystallized from 80% ethanol as white plates, melting at 84°C. They showed a single spot of a dark green color in a thin-layer chromatogram and no hydroxy absorption in IR spectra, revealing that the methylation was completed in both IVa and IVb.

The NMR spectrum of IVa shows all seven methoxyl-group signals separately defined (δ 3.33 (3H), 3.36(3H), 3.41(3H), 3,43(3H), 3.47(3H), 3.54(3H), and 3.56(3H)). In IVb, two of the methoxyl-group signals overlap to give five 3-proton singlets and a coincident resonance of six protons (δ 3.30(3H), 3.32(6H), 3.39(3H), 3.42(3H), 3.50 (3H) and 3.62(3H)). These spectra further confirm that both products are hepta-*O*-methyl derivatives. The IVa and IVb products were then detritylated by Bredereck's procedure.[4] After column-chromatographic purification, hepta-*O*-methylsucroses, Va and Vb, were obtained as a colorless oil in yields

5) T. Otake and E. Tamate, *Nippon Kagaku Zasshi*, **90**, 388 (1969).

6) R. Kuhn, H. Trischmann and I. Low, *Angew. Chem.*, **67**, 32 (1955).

of 74% and 78% respectively. The phenyl absorptions were not observed, but the absorptions due to the hydroxy group were noticed in the IR spectra and the thin-layer chromatograms showed a single black spot each.

The detritylated products, Va and Vb, were subjected to methanolysis with 5% methanolic hydrochloric acid to yield a mixture of the fully and the partially-methylated methyl fructoside and methyl glucoside. These methanolysis products did not reduced Fehling's solution, and unreacted hepta-*O*-methylsucrose was not observed by thin-layer chromatography. The products of methanolysis were subsequently analyzed by gas chromatography, using the diethyleneglycol succinate polyester as the liquid phase. The gas chromatogram of the methanolysate of Va (Fig. 2) showed six peaks. Among

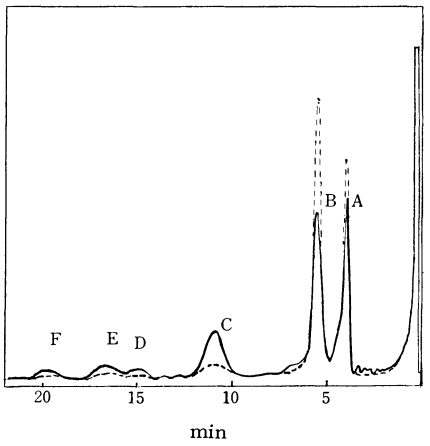

Fig. 2. The gas chromatogram of the methanolysis products of the hepta-*O*-methylsucrose derived from Ia. Conditions: 5′×1/8″, 20% diethyleneglycol succinate polyester on Chromosorb W 100/120 mesh at 170°, N_2 at 20 ml/min. Ditector: FID. ———, methanolysis products; -----, methanolysis products+permethylglucose.

these peaks, A and B were assigned to methyl 2,3,4,6 tetra-*O*-methyl β-, and α-D-glucopyranoside respectively, for they had the same retention volumes as authentic samples. The peaks with higher retention volumes, C, D, E, and F, may be assumed to be partially-methylated fructosides, but the assignment of each peak still remains to be done. The gas-chromatographic analysis reveals, however, that the trityl group of the original compound, Ia, is at the fructose moiety of the sucrose molecule.

All five peaks were observed in a gas chromatogram of the methanolysis product of Vb (Fig. 3). The peaks A′ and B′ which did not correspond to the permethyl glucose, were identified as methyl 1,3,4,6-tetra-*O*-methyl α- and β-D-fructofuranoside respectively by referring to Gee's data.[7] The D′

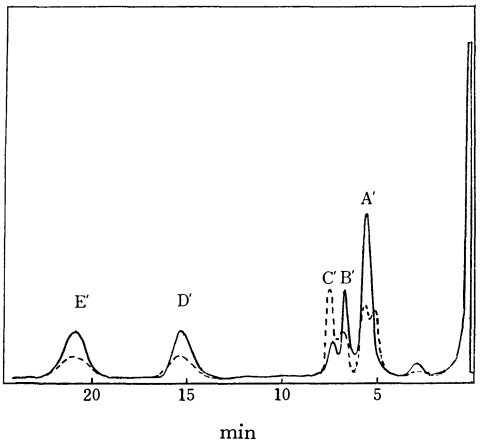

Fig. 3. The gas chromatogram of the methanolysis products of the hepta-*O*-methylsucrose derived from Ib. Conditions are same as for Fig. 2, except the column temperature ,which is 108°C. ———, methanolysis product; -----, methanoysis product+permethylglucose.

and E′ peaks were assigned to methyl 2,3,4-tri-*O*-methyl β- and α-D-glucopyranoside respectively by comparing them with authentic samples.

The relatively low peak, C′, was assigned to methyl 1,3,4,5-tetra-*O*-methyl-α-D-fructopyranoside, again by referring to Gee's results, in which both the anomeric isomers were assumed to be contained in the peak E′.

The two methyl glucosides of the peak E′ were actually separated into compounds by gas chromatography using a Chromosorb W-neopentyl-glycol-succinate-polyester (10% W/W) glass column. Though the route of the formation of the minor fructopyranosides is not clear, it may be concluded that the original compound, Ib, has a trityl group combined at the glucose moiety of the sucrose molecule. Mono-*O*-tritylsucroses (Ia and Ib) were acetylated with acetic anhydride in pyridine at room temperature; these products were then purified by chromatography on silica gel to obtain mono-*O*-trityl-hepta-acetylsucroses (VIa and VIb). The product VIb was crystallized from 80% ethanol as white prisms (mp 103—104°C). The thin-layer chromatograms of the products (VIa and VIb) showed a single spot of a dark green color on each, and no hydroxy absorption was observed in the IR spectra.

The mass spectra of the two products were identical on all the fragments with respect to the mass numbers. Both parent peaks were of a very low intensity, and the only prominent peaks appearing close to the parent peaks were at *m/e* 801 (M−77). There were, however, some differences in the mass spectra as regards the pattern coefficients of the two products; for example, the intensities of the M−77 ions of VIa and VIb relative to the peak

7) M. Gee and H. G. Wlker, Jr., *Anal. Chem.*, **34**, 650 (1962).

at *m/e* 243 were 2.4% and 0.8% respectively. It should be remembered that *m/e* 243 and M−77 are considered as coming mainly from the trityl cation and from the phenyl radical dissociation of the products respectively.

Turning to NMR spectroscopy, the integrated intensities of the acetyl, trityl, and other protons of VIa and VIb agreed with the theoretical values of the assumed mono-*O*-trityl-hepta-*O*-acetyl-derivatives.

The observed chemical shifts of the acetyl-group protons of VIa and VIb have low δ values, with certain differences between them (VIa: δ 1.93(3H), 1.99(3H), 2.00(3H), 2.07(9H) and 2.10(3H); VIb: δ 1.75(3H), 2.01(6H), 2.09(3H), and 2.12(9H), while the signals arising from the methine and the methylene protons fall in the region between δ 2.8—5.9; each spectrum can be subdivided into three non-overlapping regions, the region A (δ 2.7—3.5, 2H), the region B (δ 3.6—4.5, 6H), and the region C (δ 4.5—5.8, 6H).

The NMR spectrum of octa-*O*-acetylsucrose[8] shows no signal in the region A, but it does show signals in the region B which arise from eight protons assigned to the overlapped signal of H-5, of H-5′, and of the protons of the methylene groups to which *O*-acetyl groups are attached. The signals in the region C correspond to six protons, the number of protons in the region C of VIa and VIb, all of which can be assigned to the ring protons of sucrose other than H-5 and H-5′.

When we compare the NMR spectra of mono-*O*-trityl-hepta-*O*-acetylsucroses and octa-*O*-acetylsucrose, the signals of the region A in the spectra of VIa and VIb may be assigned to the protons of the methylene group to which an *O*-trityl group is directly attached. The acetyl derivatives, VIa and VIb, show apparent seven-line and eight-line signals respectively in the region A. Each of these

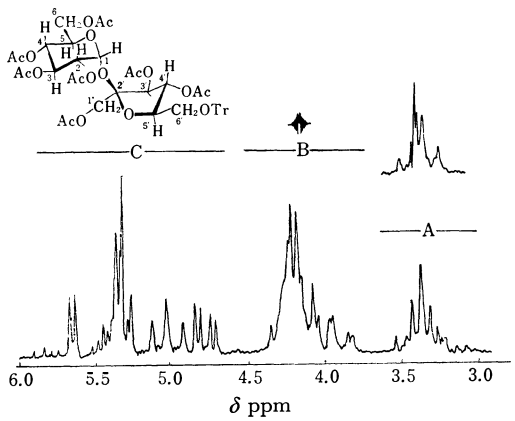

Fig. 4. Partial NMR spectra at 100 MHz of VIa in $CDCl_3$.

8) W. W. Binkly, D. Horton and N. S. Bhacca, *Carbohyd. Res.*, **10**, 245 (1969).

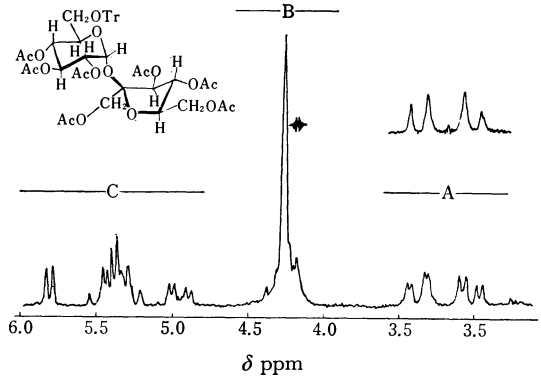

Fig. 5. Partial NMR spectra of 100 MHz of VIb in $CDCl_3$.

signals is considered to consist of the AB part in an ABX system. This assumption has been confirmed for both the products by irradiating them near δ 4.0 and by then observing the perturbation of the signals in the region A as it gives rise to the signals with four transitions, as is shown in Figs. 4 and 5. The following simulation spectra were obtained by a computer, thus confirming the proposed spin systems defined thus: for VIa δ (1) 3.30, (2) 3.43, (3) 4.16 and (4) 5.36 with J(1,2) −10.2, J(1,3) 5.4, J(2,3) 6.0 and J(3,4) 5.5Hz; for VIb δ (1) 3.01, (2) 3.36, (3) 4.16 and (4) 5.28 with J(3,4) −10.6, J(1,4) 3.6, J(2,3) 2.0 and J(3,4) 10.0Hz.

	1	2	3	4	5	6	7	8
VIa								
Observed	3.21	3.27	3.31		3.37	3.43	3.47	3.53
Generated	3.20	3.26	3.30		3.36	3.42	3.47	3.53
VIb								
Observed	2.93	2.97	3.04	3.07	3.31	3.33	3.41	3.43
Generated	2.94	2.98	3.05	3.08	3.31	3.33	3.42	3.43

On the basis of these observations, the signals in the region A can be assigned to the methylene protons of H-6 and H-6′. Combined with the data of gas chromatography, it can be concluded that the original compounds, Ia and Ib, are 6′-mono-*O*-trityl-sucrose and 6-mono-*O*-tritylsucrose respectively.

The products VIa and VIb were detritylated by Bredereck's method, using hydrobromic acid in an acetic acid solution. The oily chloroform extracts then separated from the trityl bromide and the unreacted mono-*O*-trityl-hepta-*O*-acetyl derivatives by column chromatography on silica gel, thus producing hepta-*O*-acetylsucroses, VIIa and VIIb, as colorless glass in 69% and 63% yields respectrively. The product VIIa was crystallized from 80% ethanol as white prisms which melted at 93—94°C.

The thin-layer chromatogram confirmed that both products were homogeneous and untritylated com-

pounds generating a single black spot. Their IR spectra noted to have absorptions in the O–H stretching region, and no phenyl absorption was observed. The NMR spectra of each of the products showed acetyl-group signals of the anticipated 21 protons (VIIa: δ 2.01(3H), 2.04(3H), 2.11(9H), 2.13(3H) and 2.21(3H); VIIb: δ 2.02(3H), 2.06(3H), 2.09(3H), 2.10(3H), 2.21(6H) and 2.20(3H)). The NMR spectrum of VIIa shows an apparent 2-proton octet between δ 3.5—4.0. The chemical shift of the octet consists of directly connecting the methylene group to the hydroxy group. The irradiation at δ 4.1 brings about the collapse of the octet to a four-line pattern (one line showing beat perturbation), as Fig. 6 shows. This 8-line pattern may be recognized as the AB part of an ABX system. The spectrum of VIIb appeared as a wide doublet of 2-protons, between δ 3.55—3.75, which reduces to a wide singlet with a half-width of 7Hz upon irradiation at δ 4.0 (Fig. 7).

Inasmuch as the chemical shift is almost identical to that of the above-mentioned octet, the observed wide doublet can also be assigned to the methylene protons of the hydroxymethyl group. Because the protons of the methylene group are practically equivalent, there are no other signals which appear on both sides of the wide doublet.

On the basis of the NMR data, the hydroxymethyl groups of VIIa and VIIb may be said to be those of the 6′- and 6-positions respectively. Thus, the detritylated products, VIIa and VIIb, must be 2,3,4,6,1′,3′,4′- and 2,3,4,1′,3′,4′,6′-hepta-*O*-acetylsucrose respectively.

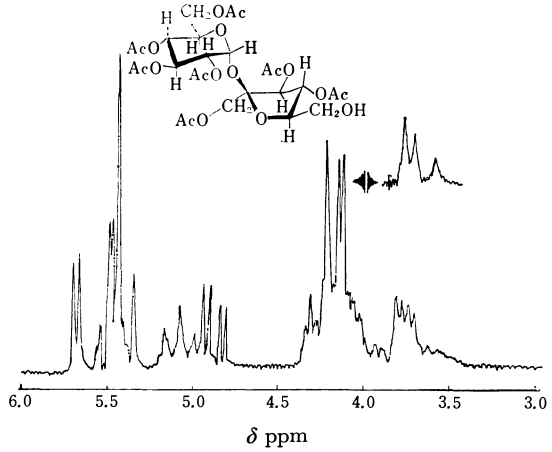

Fig. 6. Partial NMR spectra at 100 MHz of VIIa in $CDCl_3$.

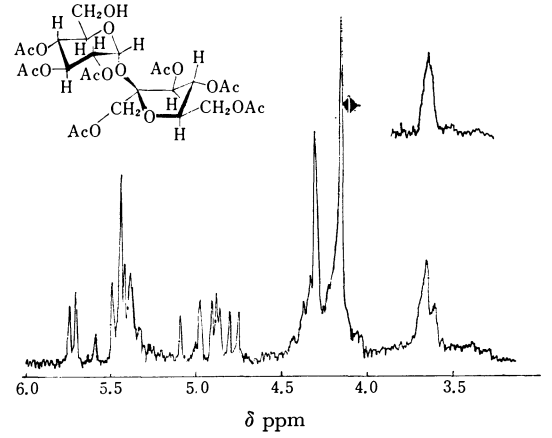

Fig. 7. Partial NMR spectra at 100 MHz of VIIb in $CDCl_3$.

Experimental

General Methods. Thin-layer chromatography was effected using Merck silica gel G as the adsorbent in a thickness of 0.25 mm and with these solvent systems: (A) methanol - water - acetone - chloroform (20 : 4 : 20 : 56) for tritylated sucrose and (B) methyl ethyl ketone (MEK)-toluene for the *O*-methyl and *O*-acetyl derivatives of sucrose. The developed plates were sprayed with 50% sulfuric acid and heated at 120°C. The column chromatography was performed using silica gel, 60—80 mesh, prepared by the Kanto Chemical Co., Japan.

The IR and the UV spectra were measured with a Hitachi EPI-II IR spectrometer and a Cary Model 14R recording spectrophotometer respectively. The mass spectra were recorded with a Varian M-66 mass spectrometer. The gas-liquid chromatography were performed with a Varian-Aerograph Model 1200 instrument with a hydrogen-flame ionization detector. The NMR spectra were recorded with a Varian HA-100D (100 MHz) spectrometer using chloroform-d, with tetramethylsilane as an internal lock; the signal positions were expressed in δ values. The NMR simulations were accomplished by a Varian Spectro System SS-100 equipped with a Varian 620/i computer.

Tritylation of Sucrose. Commercial granulated sucrose (34.2 g) was reacted with recrystallized trityl chloride (33.4 g) in dry pyridine (1 *l*) at room temperature. The reaction was assisted by the agitation of the reaction solution on a magnetic stirrier for 96 hours. At the end of the reaction period, the solution was dried *in vacuo* on a rotary evaporator. The residue was dissolved in 1-butanol (200 m*l*) and then washed with a McKirrvin buffer (pH 7.0) and water in order to remove the free sucrose. The evaporation of the butanol solution under reduced pressure left 59.5 g of tritylated sucrose as colorless glass.

6-Mono-*O*-tritylsucrose (Ib). A mixture of tritylated sucrose (55.1 g) was subjected to a counter-current distribution of six steps using an equilibrated system with methanol (1.75 *l*), a McKirrvin buffer (pH 7.0) (0.75 *l*), and trichloroethylene (2.5 *l*).

The polar layer, consisting of methanol and water, was dried *in vacuo* to yield 28.54 g of a mixture of mono-*O*-tritylsucroses. The evaporation of the combined polar layer under reduced pressure yielded 24.98 g of a glassy product which contained di- and tri-*O*-tritylsucrose.

A mixture of mono-*O*-tritylsucroses (25.92 g) was dissolved in 50% ethanol (200 m*l*); 7.5 g of 6-mono-*O*-tritylsucrose (Ib) were crystallized from this solution as white needles. Further, 2.8 g of Ib were separated

from the evaporated residue of the mother liquid by recycling column chromatography. After repeated recrystallizations from 70% ethanol, Ib had a mp of 99—101°C, $[\alpha]_D^{20}$ +51.7° (*c* 4, dimethylformamide (DMF)). The thin-layer chromatogram developed by the A solvent showed the crystalline product to be homogeneous with the R_f value of 0.33.

Found: C, 63.23; H, 6.62%. Calcd for $C_{31}H_{36}O_{17}$: C, 63.78; H, 6.16%.

6′-Mono-*O*-tritylsucrose (Ia). After the crystallization of Ib, the mother liquid was dried *in vacuo* to yield 16.56 g of the residue, which contained Ia as the major component.

The residue was chromatographed on silica gel (160 g) by means of graded elution with 1.6-*l* portion of 8, 12, and 16% methanol/chloroform solutions. The eluent was divided into twelve 400-m*l* fractions; after all the solvent had then passed through the column, the fractions were gradually returned to the column. The column was then washed with 800 m*l* of the 16% methanol/chloroform solution. The recycling procedure was repeated again to give 16 fractions of the eluent.

Each of the fractions was dried *in vacuo*, and each residue was chromatographed on thin-layer plates; this indicated that the residues of the 13th, 14th, 15th, and 16th fractions consisted of almost pure Ia. The admixture of the residues from those four fractions weighed 9.06 g and had a softening point of 149°C and $[\alpha]_D^{20}$ +31.9° (*c* 4, DMF). The spots on a thin-layer chromatogram (solvent A) of the combined residues were very faint for a R_f value of 0.33, while they were distinct for a R_f value of 0.30.

Found: C, 63.00; H, 6.58%. Calcd for $C_{31}H_{36}O_{17}$: C, 63.70; H, 6.16%.

6- and 6′-Mono-*O*-trityl-hepta-*O*-methylsucrose (IVa and IVb). Each of the mono-*O*-tritylsucroses, Ia and Ib (0.584 g) was methylated in dry *N,N*-dimethylformamide (DMF) (10 m*l*) with methyl iodide (10 m*l*) and silver oxide (5 g). Finely-divided anhydrous barium oxide (5 g) was added to each of the reaction solutions to ensure anhydrous conditions, and the reaction was assisted by the vigorous agitation of the reaction solution on a magnetic stirrer for 24 hr. At the end of the reaction period, the solution was filtered to remove any solids, and the residues were washed with an admixture of toluene and DMF (1 : 1 vol/vol) (10 m*l*). The combined filtrate and washings were then evaporated to yield a syrupy product. The product was resolved in an admixture of methyl ethyl ketone (MEK) and toluene (1 : 1 vol/vol) (20 m*l*), after which the solution was filtered to remove any insoluble matter. The filtrate was then dried *in vacuo* to yield a colorless glass.

Each of the products was resolved in 5 m*l* of toluene and chromatographed on a column of silica gel (5 g). The column was eluted with 5% MEK/toluene (100 m*l*) and 8% MEK/toluene (100 m*l*). The evaporation of the latter solvent yielded 0.447 g of IVa and 0.480 g of IVb in both cases as colorless glass. The IVb was crystallized from 90% methanol as white plates which melted at 84°C.

A thin-layer chromatogram with MEK/toluene (3 : 7 vol/vol) showed both IVa and IVb to be homogeneous, and both R_f values were 0.50 .

Found, IVa: C, 65.72; H, 7.76%. Found, IVb: C, 66.10; H, 7.28%. Calcd for $C_{38}H_{50}O_{17}$: C, 66.90; H, 7.34%.

2,3,4,6,1′,3′,4′- and 2,3,4,1′,3′,4′,6′-Hepta-*O*-methylsucrose (Va and Vb). Each of the methylation products (IVa and IVb) (200 mg) was detritylated in 0.6 m*l* of acetic acid with hydrogen bromide, which was added as a saturated acetic acid solution (0.06 m*l*) under ice cooling. The reaction solution was then allowed to remain for two minutes while being vigorously agitated. At the end of the reaction period, the solution was poured into iced water (10 m*l*) and the detritylation products were extracted from the suspension with 10 m*l* of chloroform. The chloroform solution was allowed to stand for three hours after calcium chloride (1 g) had been added, and then it was filtered to remove any solids. The filtrate was evaporated under reduced pressure, and the residue was chromatographed on 5 g of silica gel to free it from trityl bromide and the unreacted IVa or IVb.

The column was washed with 10 m*l* of 10% MEK/toluene and then with 100 m*l* of 15% MEK/toluene to elute the hepta-*O*-methylsucrose. The evaporation of the latter washing *in vacuo* yielded 103 mg of Va and 108 mg of Vb as colorless oil. A thin-layer chromatogram with MEK/toluene (6 : 4) showed both products, Va and Vb, to be homogeneous; they had R_f values of 0.25 and 0.21 respectively.

Methanolysis of Hepta-*O*-methylsucroses. Approximately 100 mg of each hepta-*O*-methylsucrose was methanolized at 60°C with 3 m*l* of 5% methanolic hydrochloric acid in a sealed tube for one hour. At the end of the reaction period, the reaction solution was passed through an anion exchanger column, *e.g.*, IRA 410 (Amberlite Rohm & Haas) (5 m*l*). Then the column was washed with approx. 50 m*l* methanol. The combined mixture of the eluent and the wasing was dried, and the evaporation residue was submitted to gas chromatography.

Mono-*O*-trityl-hepta-*O*-acetylsucroses (VIa and VIb). Each of the mono-*O*-tritylsucrose (Ia and Ib) (1.168 g, each) was dissolved in 10 m*l* of dry pyridine and then acetylated with acetic anhydride (2.8 m*l*). The solution was allowed to stand for 24 hr and then evaporated to yield a syrupy product. Each of the products was chromatographed on silica gel (10 g) column; the column was washed with 200 m*l* of toluene and then with 200 m*l* of 10% MEK/toluene to elute mono-*O*-trityl-hepta-*O*-acetylsucroses. The evaporation of the MEK-toluene fractions yielded 1.39 g of VIa and 1.42 g of VIb respectively, as both a white amorphous powder. Thin-layer chromatography with MEK/toluene (9 : 6) showed both products, VIa and VIb, to be homogeneous and to have R_f values of 0.55. One of the acetyl derivatives, VIb, was crystallized from 80% ethanol as white prisms with a mp of 103—104°C.

Found, VIa: C, 62.01; H, 6.08.% Found, VIb: C, 59.49; H, 5.86%. Calcd for $C_{45}H_{50}O_{24}$: C, 61.49; H, 5.69%.

Hepta-*O*-acetylsucroses (VIIa and VIIb). 0.878 g-portions of VIa and VIb were dissolved in 3 m*l* of glacial acetic acid saturated with hydrogen bromide under ice cooling. The reaction solution was allowed to stand with vigorous agitation for 5 min and then poured into cold water (20 m*l*). The reaction products were extracted twice with 20 m*l* of chloroform from the water suspension by washing the chloroform layers with water after which the combined chloroform solution was dried. The

evaporation residue was chromatographed on a silica-gel (10 g) column. The column was then washed with 200 m*l* of 10% MEK/toluene to elute trityl bromide and unreacted mono-*O*-trityl derivatives, and each hepta-*O*-acetylsucrose sample was eluted with 200 m*l* of the 20% MEK/toluene from the column. The evaporation of the 20% MEK/toluene fractions yielded 439 mg of VIIa and 401 mg of VIIb respectively, in both cases as colorless glass. Thin-layer chromatography with MEK/toluene (4 : 6) showed the final products to be homogeneous, with a R_f value of 0.25. VIIa was crystallized from 80% ethanol as white prisms which melted at 93—94°C.

Found, VIIa: C, 49.19; H, 5.80%. Found, VIIb: C, 49.16; H, 5.66%. Calcd for $C_{26}H_{36}O_{18}$: C, 49.06; H, 5.66%.

The author wishes to thank Professor Tetsuo Suami for his helpful advice and Mr. Iwao Miura for the determination of the NMR spectra.

BULLETIN OF THE CHEMICAL SOCIETY OF JAPAN VOL. 43 3205—3209 (1970)

The Photoreaction of 2,6-Diphenyl-4*H*-thiopyran-4-one and Its Related Compounds

Noboru SUGIYAMA, Yoshiaki SATO and Choji KASHIMA

Department of Chemistry, Tokyo Kyoiku University, Otsuka, Tokyo

(Received February 16, 1970)

The irradiation of 2,6-diphenyl-4*H*-thiopyran-4-one (**1**) or 2,6-diphenyl-4*H*-pyran-4-one (**2**) in an alcohol in the presence of oxygen gave benzoic acid and a benzoylacetic acid ester, while that of **2** in benzene or 2,6-dimethyl-4*H*-thiopyran-4-one (**5**) in various solvents gave the corresponding cage dimer, (**9**) or (**10**). No photoreaction could be observed in case of the irradiation of 1,2,6-trimethyl-4-pyridone (**3**) and 6-methyl-1,2-diphenyl-4-pyridone (**4**). A reaction mechanism *via* the triplet state of the substrate was also proposed.

Previously we have reported that the irradiation of 2,6-diphenyl-4*H*-thiopyran-4-one (**1**) in non-polar solvents gave a head-to-tail, antidimer (**8**),[1] while that of 6-methyl-1,2-diphenyl-2,3-dihydro-4-pyridone (**6**) gave 6-methyl-2,5-diphenyl-2,3-dihydro-4(1*H*)-4-pyridone, 5-methyl-2,6-diphenyl-2,3-dihydro-4(1*H*)-4-pyridone and 2-anilino-6-phenyl-2,5-hexadiene-4-one.[2] Now we have found that the irradiation of **1** in polar solvents gave photooxidized products. For comparison, the photoreactions of **1** and its related compounds have been examined.

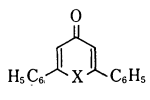

1 X=S
2 X=O

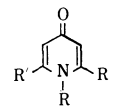

3 R=R′=CH$_3$
4 R=C$_6$H$_5$, R′=CH$_3$

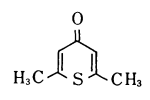

5

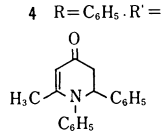

6

Results and Discussion

The irradiation of **1** in methanol or ethanol by means of a high-pressure mercury lamp with a Pyrex filter gave benzoic acid and methyl or ethyl benzoylacetate (**7a** or **b**), but in the reaction mixture **8** was not detected. The results of irradiation reactions of **1** under various conditions are summarized in Table 1.

In order to ascertain whether or not this reaction is characteristic of thiopyrones, we studied the photoreaction of 2,6-diphenyl-4*H*-pyran-4-one (**2**),[3] 1,2,6-trimethyl-4-pyridone (**3**)[4] and 6-methyl-1,2-diphenyl-4-pyridone (**4**),[5] in which the sulfur atom in the thiopyrone ring is replaced by an oxygen or nitrogen atom. When **2** in methanol was irradiated under the same conditions as **1**, similar

1) N. Sugiyama, Y. Sato, H. Kataoka, C. Kashima and K. Yamada, This Bulletin, **42**, 3005 (1969); anti-type structure is also supported by the fact that the the further irradiation of this dimer does not give a cage dimer.

2) C. Kashima, M. Yamamoto, Y. Sato and N. Sugiyama, *ibid.*, **42**, 3596 (1969).

3) R. J. Light and C. R. Hauser, *J. Org. Chem.*, **25**, 538 (1960).

4) S. Garratt, *ibid.*, **28**, 1886 (1963).

5) S. Boatman, R. E. Smith, G. E. Morris, W. G. Kofron and C. R. Hauser, *ibid.*, **32**, 3817 (1967).

TABLE 1. PHOTOOXIDATION OF **1** AND **2**

Substrate	Solvent (0.01 mol/*l*)	Conditions	Time (hr)	Yield (%)		
				Benzoic Acid	**7a** or **b**	Unreacted **1** or **2**
1	Benzene	P[a]	48	—	—	90
1	Ethanol	P	48	33	8(b)	51
1	Ethanol		26	49	14(b)	—
1	Methanol	P	48	48	8(a)	8
1	Methanol	P N_2 bubbling[b]	48	33	13(a)	21
1	Methanol	P O_2 bubbling	48	32	9(a)	12
1	Methanol	P N_2 sealed[c]	48	—	—	93
1	Methanol (Piperylene 0.02 mol/*l*)	P	48	18	4(a)	65
1	Methanol		26	48	9(a)	—
1	Methanol	O_2 bubbling	24	50	10(a)	—
2	Methanol	P N_2 sealed	168	—	—	98
2	Methanol	P	48	34	8(a)	24

a) Pyrex filter was used. The atmosphere was air.
b) Nitrogen gas was passed through the reaction vessel.
c) Nitrogen gas was passed for an hour before the irradiation and the reaction vessel was sealed with a rubber stopper.

results of photooxidation were obtained, as is shown in Table 1. However, **3** or **4** under various conditions did not show any change, in contrast to the photolysis of **6**.[2]

The mechanism of these photooxidation was examined in detail. It was found that this reaction did not take place when an alcoholic solution of **1** or **2** was sealed in a nitrogen atmosphere before irradiation. Also, the photooxidation was not observed when the **1** in an alcohol was irradiated with a tungsten lamp, using methylene blue or rose bengal as a sensitizer. When **1** was treated with sodium hypochlorite and hydrogen peroxide,[6] no reaction occurred. This fact excluded the possible participation of O_2 in the above photooxidation. When oxygen or nitrogen gas was passed through an alcoholic solution of **1**, the UV absorption of **1** did not show any change; this suggests no participation of the charge-transfer complex at the ground state in this reaction.[7,8] Considering that oxygen seems to quench the excited state of **1**, as can be seen by comparing the disappearance rate of **1** under nitrogen with that under oxygen (Table 1), it can be speculated that the triplet state of **1** is an reactive species. This is also supported by the quenching effect with piperylene. The irradiation of **7** under the same conditions as in case of **1** or **2** did not give benzoic acid. All the above facts are in accord with the mechanism shown in Scheme 1, except that there is no clear evidence for the presence of dioxetane or keto-aldehyde intermediates.

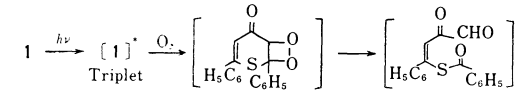

Scheme 1

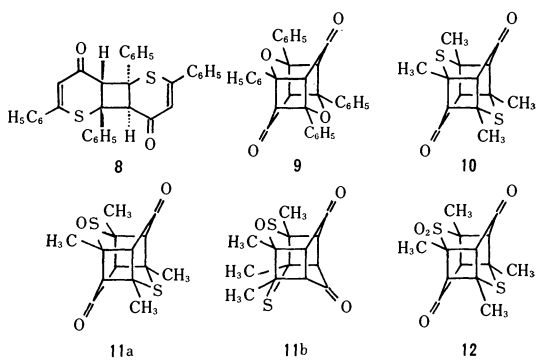

On the other hand, when a benzene solution of **2** was irradiated under a nitrogen atmosphere for a week, a dimer (**9**) was obtained in a 37% yield. The structure of **9** seems to be a head-to-tail cage dimer, judging from the following data. The results of elemental analysis and the mass spectrum [*m/e* 391 ($M^+-C_6H_5-C{\equiv}O^+$)] confirm that **9** is a dimeric compound. The UV, IR, and NMR spectra indicate a saturated carbonyl compound. The ther-

6) E. Mckeown and W. A. Waters, *J. Chem. Soc., B*, **1966**, 1040.
7) K. Wei, J.-C. Mani and J. N. Pitts, Jr., *J. Amer. Chem. Soc.*, **89**, 4225 (1967).
8) K. S. Wei and A. H. Adelman, *Tetrahedron Lett.*, **1969**, 3297.

mal decomposition of **9** afforded only **2**.[9,10] The mass spectrum of **9** shows a strong monomeric peak (*m/e* 248, 36%).

Furthermore, we studied the photoreaction of 2,6-dimethyl-4*H*-thiopyran-4-one (**5**)[11,12] in a benzene, ether, or methanol solution. The irradiation of **5** under a nitrogen atmosphere for 72 hr gave a dimer (**10**) in about a 1% yield in each case. The structure of **10** was determined to be a head-to-tail cage dimer on the basis of the following data.

The results of elemental analysis, the mass (*m/e* 280), UV, IR, and NMR spectra, and the thermal decomposition support the idea that **10** is a cage dimer. The head-to-tail form of **10** is unequivocally confirmed by the NMR spectrum of **11a** as follows. The oxidation of **10** by hydrogen peroxide at room temperature gave monosulfoxide **11a** and monosulfone (**12**). The structures of **11a** and **12** are supported by the results of elemental analysis and and the UV, IR, NMR, and mass spectra. In the NMR spectrum of **12** methine protones show a singlet signal at τ 6.73, while in that of **11a** they show two singlet signals at τ 7.00 and 6.94, indicating that **11a** has a head-to-tail form, for the head-to-head form (**11b**) may be expected to show an AB quartet pattern.

Since the photodimerization of **2** or **5** is strongly inhibited in the presence of oxygen, it seems reasonable to deduce that the triplet state of **2** or **5** is responsible for the photodimerization. Moreover, the photoreaction of **2** or **5** gives a head-to-tail cage dimer, and that of **1** or **2** in the presence of oxygen gives oxidation products, *via* the triplet state.

The theory that the photoreaction depends on the electron density in this pyrone ring has been proposed with regard to the photoreaction of **1** in various solvents.[1] The UV spectra of **2** and **5** in benzene, ether, ethanol, and methanol show little difference compared with that of **1** as will be shown in the Experimental Section. Therefore, it is expected that the photoreaction of **2** or **5** in those solvents would show the similar reaction. Indeed, the same photodimer was isolated in the photoreaction of **5** in benzene, ether, and methanol, but the photolysis of **2** in benzene gave a dimeric product, while that of **2** in methanol gave no product.

Moreover, we found interesting facts in the UV spectra of **9** and **10** and the mass spectra of **10**, **11a**, and **12**. The UV absorption of the 2,6-dimethyl-4*H*-pyran-4-one cage dimer shows a strong charge-transfer absorption at 233 nm (ε 2410).[13] That of **9** shows an absorption at 220 nm (ε 26000, sh), and that of **10** shows an absorption at 240 nm (ε 345). These are very similar to that of 9-thiabicyclo[3.3.1]-non-6-en-2-one (240 nm, ε 290)[14] and that of tetrahydro-4*H*-thiopyran-4-one (233 nm, ε 507).[15] The mass spectrum of **10** does not show any fragments of *p*-benzoquinone (*m/e* 108) or tetramethyl-1,4-dithiahexadiene (*m/e* 172), but it does show that of the correspondine monomer, **5** (*m/e* 140, 80%), as well as those of 2,5-dimethylthiophene (*m/e* 112, base peak), *m/e* 97 (25%) and *m/e* 59 (17%).[16] In addition to the fragment of the monomer **5**, the mass spectra of **11a** and **12** show a desulfoxide or desulfone fragment at *m/e* 148 (3 or 23% respectively), accompanied by decarbonylation, demethylation, decarbonylation and fission to the 1,2-dimethylcyclobutadiene cation radical[16] (Fig. 1, Scheme 2).

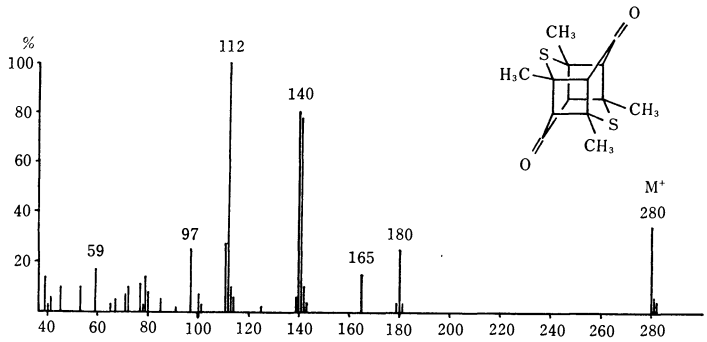

Fig. 1-a. The mass spectrum of **10**.

9) W. Flaig, J.-C. Salfeld and A. Llanos, *Angew. Chem.*, **72**, 110 (1960).

10) R. C. Cookson, D. A. Cox and J. Hudec, *J. Chem. Soc.*, **1961**, 4499.

11) M. Rolla, G. Traverso and M. Sanesi, *Ann. Chim.* (Rome), **42**, 515 and 673 (1952); *Chem. Abstr.*, **42**, 4178i (1948).

12) Ishibe, Kotani and Teramura reported the photoreaction of 4*H*-thiopyran-4-one which gave small amount of a cage dimer at the 22th Annual Meeting of the Chemical Society of Japan, April, 1969, Proceedings III, p. 1363.

13) P. Yates and M. J. Jorgenson, *J. Amer. Chem. Soc.*, **85**, 2956 (1963).

14) A. Padwa, A. Battisti and E. Shefter, *ibid.*, **91**, 4000 (1969).

15) N. J. Leonard, T. L. Brown and T. W. Milligan, *ibid.*, **81**, 504 (1959).

16) H. Budzikiewicz, C. Djerassi and D. H. Williams, "Mass Spectrometry of Organic Compounds," Holden-Day, Inc., San Francisco, p. 527, 625 (1967).

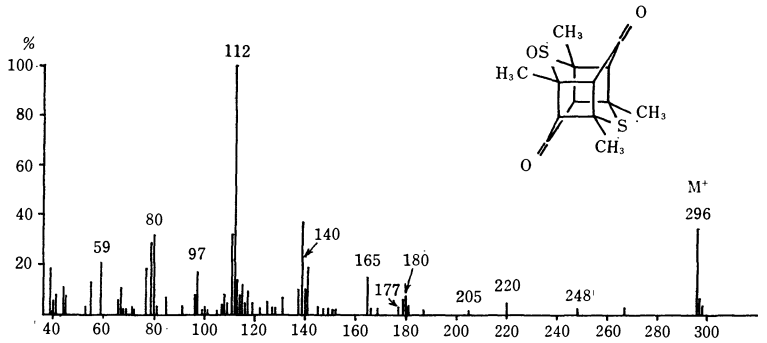

Fig. 1-b. The mass spectrum of **11a**.

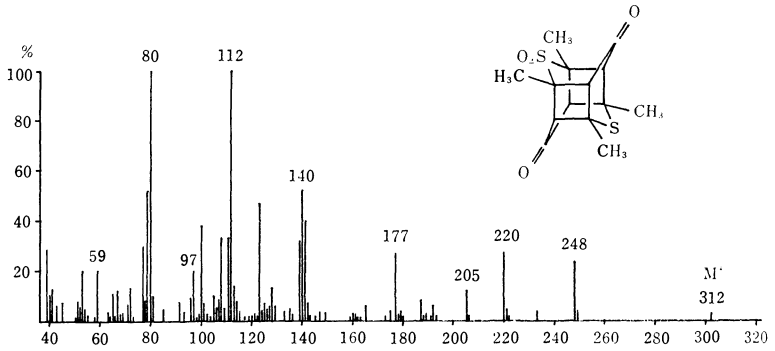

Fig. 1-c. The mass spectrum of **12**.

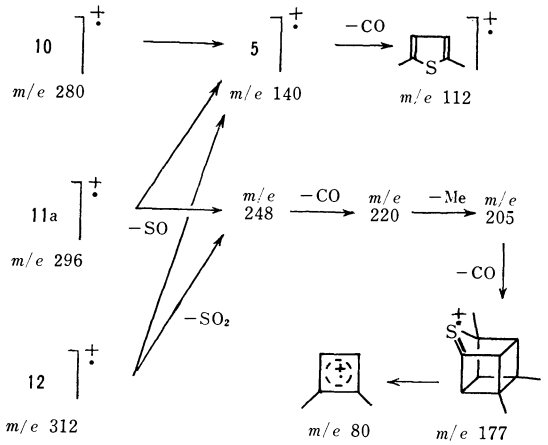

Scheme 2

Experimental

All the melting points are uncorrected. A Taika H-type 125 W high-pressure mercury lamp and a Toshiba 110 V, 200 W tungsten lamp were used as light sources. The UV, IR, NMR, and mass spectra were measured by means of a Hitachi EPS-3T-type spectrophotometer, a Hitachi EPI-S2-type spectrometer, a Hitachi H-60-type spectrometer, and a Hitachi RMU-6E-type spectrometer, respectively.

Photooxidation of 2,6-Diphenyl-4*H*-thiopyran-4-one (1). After a methanol solution (240 m*l*) of **1** (620 mg) has been irradiated by means of a high-pressure mercury lamp with a Pyrex filter while being stirred at room temperature for 48 hr, the methanol was removed and the residue was chromatographed on silica gel. From the benzene, benzene - ethyl acetate (1 : 1, v/v), and an ethyl acetate eluate, methyl benzoylacetate (**7a**) (33 mg, 8%), unreacted **1** (48 mg, 8%) and benzoic acid (270 mg, 48%) were obtained respectively. Each product was identified with the corresponding authentic sample by comparing the UV, IR, and NMR spectra as well as the R_f value on thin-layer chromatography on silica gel. The results of the photoreaction of **1** under various conditions are summarized in Table 1.

All the starting material was recovered when a methanol solution (30 m*l*) of **1** (100 mg) was treated with sodium hypochlorite (7 m*l*, containing 10—14% chlorine) and hydrogen peroxide (11 m*l*, 3%) by a previously-reported procedure,[6] or when a methanol solution (70 m*l*) of **1** (100 mg) containing methylene blue (5 mg) or rose bengale (5 mg) was irradiated with a tungsten lamp for 30 hr.

Preparation and Photolysis of Methyl Benzoylacetate 7a. By Hauser's method,[17] **7a** was prepared, as copper salt; mp 197—200°C (lit, mp 200—201°C). When a methanol solution (50 m*l*) of **7a** (200 mg) in a Pyrex tube was irradiated under the same conditions as have been described above, the formation of benzoic acid could not be observed.

Preparation of 2,6-Diphenyl-4*H*-pyran-4-one (2).

17) R. Leving and C. R. Hauser, *J. Amer. Chem. Soc.*, **66**, 1768 (1944).

By Hauser's method[3] **2** was prepared; mp 140—141.5°C (lit, mp 138.5—141.5°C). UV: $\lambda_{max}^{Benzene}$ nm (ε) 278 (24500), λ_{max}^{Ether} nm (ε) 257 (23600), 279 (26900), $\lambda_{max}^{Ethanol}$ nm (ε) 257 (22900), 283 (25800), $\lambda_{max}^{Methanol}$ nm (ε) 257 (22100), 285 (24000). IR: (KBr, cm^{-1}) 1645, 1600, 1380. NMR: (τ in $CDCl_3$) 3.19 (s, 2H), 2.53—2.3 (m, 6H), 2.3—2.04 (m, 4H).

Photooxidation and Photodimerization of 2. A methanol solution (240 m*l*) of **2** (600 mg) was irradiated; the photoproducts listed in Table 1 were obtained. After a benzene solution (2 m*l*) of **2** (300 mg) in a Pyrex tube had been irradiated at room temperature under a nitrogen atmosphere for a week, the solvent was removed and the reaction mixture was treated in chloroform to give undissolved white precipitates (**9**) (110 mg (37%)). Reprecipitation from chloroform afforded white powders; mp 268—274°C.

Found: C, 67.54; H, 4.37%. Cacld for $C_{34}H_{24}O_4$–$CHCl_3$: C, 68.35; H, 4.10%.

Recrystallization from methanol afforded colorless cubes; mp 271—278°C.

Found: C, 78.53; H, 5.49%. Calcd for $C_{34}H_{24}O_4$–CH_3OH: C, 79.52; H, 5.34%.

MS: *m/e* 391 (7%), 348 (4%), 248 (36%), 220 (100%), 149 (100%), 105 (40%), 102 (39%). UV: $\lambda_{max}^{Ethanol}$ nm (ε) 220 (26000) sh., 254 (2400) sh., 260 (1950) sh., 266 (1370), sh., 295 (186) sh. IR: (KBr, cm^{-1}) 1700, 1110, 1070. NMR: (τ in Pyridine-d_5) 5.61 (s, 4H), 3.0—2.7 (m, 12H), 2.6—2.2 (m, 8H).

The irradiation of **2** (300 mg) in a methanol solution (30 m*l*) for a week gave no product. When **9** was heated in a test tube, **9** turned quantitatively to **2** at 200°C, with a half life of 5 min, while it turned immediately at the melting point. Below 180°C, even at 10^{-4} mmHg **9** did not sublime at all. The 2,4-dinitrophenylhydrazone of **9** was an orange powder; mp 261—263°C (decomp.).

Found: C, 64.73; H, 3.98; N, 12.67%. Calcd for $C_{46}H_{32}O_{10}N_8$: C, 64.48; H, 3.76; N, 13.08%. UV: $\lambda_{max}^{Ethanol}$ nm (ε) 222 (44100), 256 (27200) sh., 366 (52800). IR: (KBr, cm^{-1}) 1615, 1593, 1510, 1335.

Preparation and Irradiation of 1,2,6-Trimethyl-4-pyridone (3) and 6-Methyl-1,2-diphenyl-4-pyridone (4). By Garratt's method[4] **3** was prepared; mp 245—247°C (lit, 247—248°C). By Hauser's method[5] **4** was prepared; mp 240—243°C (lit, 242—243°C). The irradiation of **3** or **4** in methanol, benzene, or aqueous hydrogen chloride (10%) in a Pyrex tube gave no product.

Preparation of 2,6-Dimethyl-4*H*-thiopyran-4-one (5). To a cold acetic acid solution (236 m*l*) of 2,6-dimethyl-4*H*-thiopyran-4-thione[18] (12 g), hydrogen peroxide (30%, 143 m*l*) and sodium acetate (23.6 g) were added. After the reaction mixture had then been stirred at room temperature for an hour, it turned dark blue; it was then poured into water (500 m*l*), extracted with chloroform, washed with water, and dried. The removal of the solvent gave a crude precipitate, which was recrystallized from water to afford colorless needles; 7.8 g (72%); mp 103—105°C (lit,[11] 104°C). UV: $\lambda_{max}^{Benzene}$ nm (ε) 288 (17700), 296 (13200) sh., λ_{max}^{Ether} nm (ε) 288 (15500), 296 (17700), $\lambda_{max}^{Ethanol}$ nm (ε) 288 (18200), 297 (18200), $\lambda_{max}^{Methanol}$ nm (ε) 288 (17800), 297 (17800). IR: (KBr, cm^{-1}) 1610, 1535. NMR: (τ in $CDCl_3$) 7.63 (s, 6H), 3.28 (s, 2H).

Irradiation of 5. After the irradiation of **5** in benzene (0.5 mol/*l*), ether (0.5 mol/*l*) or methanol (1 mol/*l*) in a Pyrex tube under a nitrogen atmosphere for 72 hr, the solvent was removed and the residue was chromatographed on silica gel with chloroform. The concentration of the eluted fraction gave crude products as pale yellow crystals; the crystals were collected, washed with methanol to afford colorless cubes (**10**) in a 1.3—0.9% yield in each case; mp 340—341°C (decomp.).

Found: C, 59.99; H, 5.75%. Calcd for $C_{14}H_{16}O_2S_2$: C, 60.23; H, 5.82%.

MS: *m/e* 280 (M^+). UV: $\lambda_{max}^{CH_3CN}$ nm (ε) 240 (345), 281 (319). IR: (KBr, cm^{-1}) 1693. NMR: (τ in $CDCl_3$) 8.35 (s, 12H), 6.83 (s, 4H).

In each case, most of the unreacted material (about 96%) was recovered. In the irradiation in the presence of oxygen, all of the starting material was recovered. When the photodimer **10** was heated above 220°C in a pressure tube under an atmosphere of nitrogen, the **10** was sublimed. When the **10** was heated at the melting point, the monomer **5** was obtained (R_f 0.25 on silica-gel thin-layer chromatography with ethyl acetate). Refluxing the photodimer **10** (5 mg) in ethanol (4 m*l*) and aqueous hydrogen chloride (10%, 2.5 m*l*) for an hour gave no other product.

Oxidation of the Photodimer 10 to the Monosulfoxide Dimer (11a) and the Monosulfone Dimer (12). To a cold acetic acid solution (10 m*l*) of **10** (48 mg), we added hydrogen peroxide (30%, 600 m*l*). After the reaction mixture had then been stirred at room temperature for an hour, the mixture was poured into water (50 m*l*) and extracted with chloroform. A procedure similar to that used for the isolation of **10** gave colorless cubes, (**11a**, 22 mg) and (**12**, 20 mg). **11a**; mp 335—340°C (decomp.).

Found: C, 56.47; H, 5.58%. Calcd for $C_{14}H_{16}O_3S_2$: C, 56.75; H, 5.44%.

MS: *m/e* 296 (M^+). UV: $\lambda_{max}^{CH_3CN}$ nm (ε) 223 (2840), 280 (170) sh. IR: (KBr, cm^{-1}) 1695, 1055. NMR: (τ in $CDCl_3$) 8.25 (s, 6H), 8.19 (s, 6H), 7.00 (s, 2H), 6.94 (s, 2H). **12**: mp 354—356°C (decomp.).

Found: C, 53.93; H, 5.22%. Calcd for $C_{14}H_{16}O_4S_2$: C, 53.84; H, 5.16%.

MS: *m/e* 312 (M^+). UV: $\lambda_{max}^{CH_3CN}$ nm (ε) 264 (367), 310 (42) sh. IR: (KBr, cm^{-1}) 1704, 1310, 1106. NMR: (τ in $CDCl_3$) 8.23 (s, 6H), 8.20 (s, 6H), 6.73 (s, 4H).

18) H. Kato, T. Ogawa and M. Ohta, This Bulletin, **33**, 1467 (1960).

BULLETIN OF THE CHEMICAL SOCIETY OF JAPAN VOL. 43 3210—3214 (1970)

Studies of the Reissert-Kaufmann-type Reaction of 4-Nitropyridine *N*-Oxide and Its Homologues

Eizo MATSUMURA, Masahiro ARIGA and Takahiko OHFUJI

Department of Chemistry, Osaka Kyoiku University, Tennoji-ku, Osaka

(Received March 2, 1970)

The Reissert-Kaufmann-type reaction of substituted *N*-methoxy-4-nitropyridinium methylsulfates gave the corresponding 2-cyano-4-nitropyridines in satisfactory yields. When 3-methyl-4-nitropyridine *N*-oxide was used as the starting material, a cyano group was introduced not into the 6-position, but into the 2-position. This preference may be explained by proposing a hyperconjugation effect of the 3-methyl group. The resulting nitriles were quantitatively hydrolyzed to the corresponding 4-nitropicolinic acids. These reactions provided a new route for the preparation of nitropyridinecarboxylic acids from pyridine homologues. Further, some nucleophilic substitution reactions of the products were carried out.

It has recently been established that the nitration of pyridine *N*-oxides with fuming nitric acid alone provides a convenient method for the preparation of 4-nitropyridine *N*-oxides.[1]

As is commonly known, the Reissert-Kaufmann reaction has offered a general synthetic method for heterocyclic nitriles in condensed heteroaromatic compounds such as quinoline and isoquinoline since it was reported by Reissert[2] and by Kaufmann *et al.*[3-6] Ochiai and Nakayama reported an example of the formation of a cyanopyridine by the nucleophilic attack of a cyanide ion on a pyridinium salt.[7] Thus, 4-chloro-2-cyanopyridine was obtained from 4-chloropyridine *N*-oxide. Further, Feely and Beavers[8] and Okamoto and Tani[9,10] independently extended the reaction to include various derivatives of pyridine *N*-oxides.

Tani also reported the reaction of 4-nitropyridine *N*-oxide,[11] but the reported neither a detailed investigation of the product nor the reaction of other homologues of 4-nitropyridine *N*-oxide.

In the present study, the Reissert-Kaufmann-type reaction of 4-nitropyridine *N*-oxide and its homologues was performed in order to prepare 2-cyano-4-nitropyridines and in order to clarify the electronic effects of the 4-nitro group in the reaction. The hydrolysis of 2-cyano-4-nitropyridines led to the corresponding acids, and the nucleophilic reactivity of the 4-nitro group of the nitriles and the carboxylic acids, were also examined.

Results and Discussion

The *N*-oxides used as starting materials were 4-nitropyridine *N*-oxide (**1a**), 2-methyl-4-nitropyridine *N*-oxide (**Ib**), 3-methyl-4-nitropyridine *N*-oxide (**Ic**), and 5-ethyl-2-methyl-4-nitropyridine *N*-oxide (**1d**). The *N*-oxides were treated at 65—70°C with 1—1.2 equivalents of dimethyl sulfate to form *N*-methoxypyridinium salts (**2**). But above this temperature the salts were liable to decompose, with the evolution of nitrogen dioxide. The resulting salts were hygroscopic crystals; they were used for subsequent reactions without purification. The

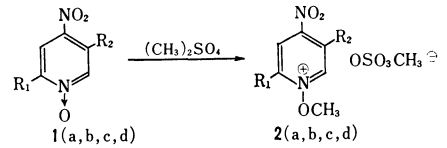

1(a,b,c,d) 2(a,b,c,d)

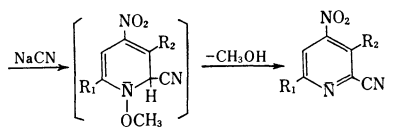

3(a,b,c,d) 4(a,b,c,d)

a: $R_1=R_2=H$ c: $R_1=H$, $R_2=CH_3$
b: $R_1=CH_3$, $R_2=H$ d: $R_1=CH_3$, $R_2=C_2H_5$

1) E. Matsumura, unpublished results.
2) A. Reissert, *Ber.*, **38**, 1603, 3415 (1905).
3) A. Kaufmann and A. Albertini, *ibid.*, **42**, 3776 (1909).
4) A. Kaufmann and R. Widmer, *ibid.*, **44**, 2058 (1911).
5) A. Kaufmann and H. Peyer, *ibid.*, **45**, 1805 (1912).
6) A. Kaufmann, *ibid.*, **51**, 116 (1918).
7) E. Ochiai and I. Nakayama, *Yakugaku Zasshi*, **65**(**ko**), 7 (1945).
8) W. E. Feely and E. M. Beavers, *J. Amer. Chem. Soc.*, **81**, 4004 (1959).
9) T. Okamoto and H. Tani, *Chem. Pharm. Bull.* (Tokyo), **7**, 130, 925 (1959).
10) H. Tani, *ibid.*, **7**, 930 (1959).
11) H. Tani, *Yakugaku Zasshi*, **80**, 1418 (1960).

aqueous solution of the salts was treated with an aqueous solution of sodium cyanide under a nitrogen atmosphere in an ice-salt mixture in order to avoid any violent reaction and excessive tar formation. From the reaction mixture, the nitriles (**4**) were obtained, in the cases of (**a**), (**b**), and (**c**), as crystals (which were subsequently purified by recrystallization), and, in the case of (**d**), as an oil (which was subsequently purified by vacuum distillation).

The infrared spectra of all of the products indicated the presence of a nitro group (1350—1360, 1530 cm^{-1}), a nitrile group (2200 cm^{-1}), and no *N*-oxide group. The results of the micro analyses of the products were in good agreement the findings on the mono cyano derivatives of 4-nitropyridine and its homologues. In order to ascertain the position of the introduced cyano group, each of the products was converted to the corresponding pyridinecarboxylic acid; **4a** was converted to picolinic acid; **4b**, to 6-methyl-4-nitropicolinic acid; **4c**, to quinolinic acid, and **4d**, to 6-methylquinolinic acid. The acids were identified by a mixed-melting-point determination and by a comparison of the infrared spectra with those of authentic samples. From the above facts, the products are identified as 2-cyano-4-nitropyridine (**4a**), 2-cyano-6-methyl-4-nitropyridine (**4b**), 2-cyano-3-methyl-4-nitropyridine (**4c**), and 2-cyano-3-ethyl-6-methyl-4-nitropyridine (**4d**) respectively. The elementary analyses and some properties of the products are summarized in Table 1.

The fact that the nucleophilic attack of the cyanide ion on the methylsulfates occurred at the 2-position to form 1,2-dihydro intermediates (**3**), which then led to the corresponding nitriles with the elimination of a molecule of methanol, can be explained by presuming that the inductive and electromeric effects of quaternary nuclear nitrogen on the methylsulfates (**2**) are greater than those of the 4-nitro group.

With the reaction of 3-methyl-4-nitropyridine *N*-oxide (**1c**), a cyano group was introduced into the 2-position, this was contrary to the expectation that the inductive and steric effects of the 3-methyl group would tend to direct the entering cyano group to the 6-position of the pyridine nucleus. Analogous results have been reported with 3-methylpyridine *N*-oxide.[8,9] The result may rationally be explained as follows. Considering the hyperconjugation of the 3-methyl group in the dihydro-type structure (**3**), which is assumed to be an intermediate, the electron density is more extensively delocalized when a cyano group is introduced into the 2-position (**A**) than when it is introduced into the 6-position (**B**), as is shown in Fig. 1. Therefore, the **A** intermediate is preferentially formed to give the 2-cyano derivative.

The hydrolysis to 4-nitropicolinic acids (**5**) was successfully carried out, and the 4-nitro group was held, by heating with 90% sulfuric acid followed by treatment with sodium nitrite. The results

Table 1. Substituted 2-cyano-4-nitropyridines

Product	Mp (bp) °C	Yield %	ν_{NO_2} cm^{-1}	ν_{CN} cm^{-1}	Formula	C% Found	C% Calcd	H% Found	H% Calcd	N% Found	N% Calcd
4a	73—74*	56.9	1360 1530	2200	$C_6H_3N_3O_2$	48.57	48.33	1.78	2.03	28.02	28.18
4b	76.5—77.5	67.1	1360 1530	2200	$C_7H_5N_3O_2$	51.45	51.53	2.91	3.09	25.90	25.76
4c	64—65	85.7	1350 1530	2200	$C_7H_5N_3O_2$	51.89	51.53	3.01	3.09	25.76	25.76
4d	(94/0.05 mmHg)	82.4	1350 1530	2200	$C_9H_9N_3O_2$	56.42	56.56	4.63	4.72	21.68	21.98

* Lit, (Ref. 11) mp 72—74°C.

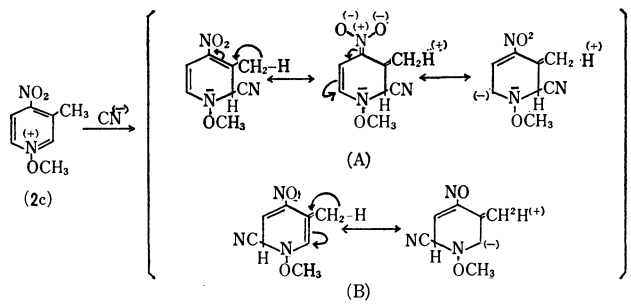

Fig. 1

and analytical data are summarized in Table 2. The sequence of the reactions starting with pyridine homologues, *N*-oxidation, nitration with fuming nitric acid alone, cyanation, and hydrolysis, provides a new rout for the preparation of 4-nitropyridine-2-carboxylic acids, which attract our attention by their antibacterial and antifungal activities[12] and which have been scarcely obtained by other methods.

These cyanonitropyridines and their carboxylic derivatives were anticipated to undergo a nucleophilic substitution at the 4-position because of the strong electron-withdrawing property of the 2-cyano or the 2-carboxyl group. A concurrent substitution of the nitro group by the chloride ion has been observed on the hydrolysis of 2-cyano-4-nitropyridine with hydrochloric acid in a sealed tube.[11]

We obtained 4-chloropicolinic acids from 4-nitropicolinic acids in good yields under milder conditions by heating them with hydrochloric acid. The results and the analytical data are summarized in Table 3. It also became clear that the substitution of 2-cyano-4-nitropyridines by sodium ethoxide at the 4-position occurred more easily than that of 4-nitropyridine which was observed on heating.[13] Thus, 2-cyano-4-ethoxypyridines (**7**) were yielded from 2-cyano-4-nitropyridines (**4**) when they were treated with ethanolic sodium ethoxide in an ice-salt mixture. The results and analytical data are

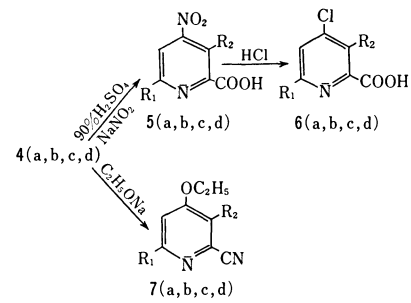

a: $R_1=R_2=H$ b: $R_1=CH_3$, $R_2=H$
c: $R_1=H$, $R_2=CH_3$ d: $R_1=CH_3$, $R_2=C_2H_5$

TABLE 2. SUBSTITUTED 4-NITROPICOLINIC ACIDS

Product	Mp °C	Yield %	ν_{NO_2} cm^{-1}	ν_{COOH} cm^{-1}	Formula	C% Found	C% Calcd	H% Found	H% Calcd	N% Found	N% Calcd
5a	154—155*	97.6	1360 1530	1700	$C_6H_4N_2O_4$	42.88	42.87	2.16	2.40	16.70	16.67
5b	129—130	98.5	1360 1530	1710	$C_7H_6N_2O_4\cdot H_2O$	41.94	42.00	4.00	4.03	13.85	14.00
5c	148	97.6	1360 1530	1710	$C_7H_6N_2O_4$	46.28	46.16	3.22	3.32	15.30	15.38
5d	76—77	98.1	1350 1530	1710	$C_9H_{10}N_2O_4$	51.60	51.42	4.84	4.80	13.24	13.30

* Lit, (Ref. 12) mp 152°C (decomp.).

TABLE 3. SUBSTITUTED 4-CHLOROPICOLINIC ACIDS

Product	Mp °C	Yield%	ν_{COOH} cm^{-1}	Formula	C% Found	C% Calcd	H% Found	H% Calcd	N% Found	N% Calcd
6a	186—187*	85.3	1700	$C_6H_4NO_2Cl$	45.85	45.71	2.48	2.52	8.78	8.89
6b	123—124	90.5	1710	$C_7H_6NO_2Cl$	48.81	49.00	3.62	3.52	7.98	8.16
6c	163—164	98.0	1710	$C_7H_6NO_2Cl$	48.75	49.00	3.26	3.52	7.97	8.16
6d	43—44	95.0	1710	$C_9H_{10}NO_2Cl\cdot 1/2H_2O$	52.08	51.80	5.20	5.33	6.95	6.71

* Lit, mp 183—183.5 °C; T. Kato, *Yakugaku Zasshi*, **83**, 352 (1963).

TABLE 4. SUBSTITUTED 2-CYANO-4-ETHOXYPYRIDINES

Product	Mp °C	Yield %	ν_{CN} cm^{-1}	Formula	C% Found	C% Calcd	H% Found	H% Calcd	N% Found	N% Calcd
7a	66—67*	91	2200	$C_8H_8N_2O$	64.75	64.85	5.36	5.44	18.66	18.91
7b	87—88	95	2200	$C_9H_{10}N_2O$	66.36	66.65	6.22	6.22	17.14	17.27
7c	128—129	90	2200	$C_9H_{10}N_2O$	66.65	66.65	6.32	6.22	17.46	17.27
7d	89—90	92	2200	$C_{11}H_{14}N_2O$	69.37	69.44	7.52	7.42	14.49	14.73

* Lit, mp 70—72°C; Y. Nishijima, *Yakugaku Zasshi*, **82**, 1267 (1962).

12) E. V. Brown, U. S. 2766251 (1956).

13) M. Katada, *Yakugaku Zasshi*, **67**, 20 (1947).

summarized in Table 4. The fact that nucleophilic substitution at the 4-position proceeds with such ease shows that the activity of the 4-nitro group as a leaving group toward the nucleophilic substitution and the reactivity are favoured by the inductive effects of the 2-substituents.

Experimental

All the melting points and boiling points are uncorrected. The infrared spectra were recorded on a Hitachi infrared spectrophotometer, Model EPI-S 2, as Nujol mulls.

2-Cyano-4-nitropyridine (4a). A mixture of 20.0 g of 4-nitropyridine *N*-oxide (**1a**) and 18.0 g of dimethyl sulfate was placed in a three-necked flask, equipped with a sealed stirrer, a thermometer, and a silica-gel tube. The mixture was heated at 65—70°C for 2 hr. Upon cooling, the salt crystallized out; it was then collected and dissolved in 50 m*l* of water, and the silica-gel tube was replaced by a dropping funnel. A solution of 14.6 g of sodium cyanide in 100 m*l* of water was added from the dropping funnel at −7—−8°C with vigorous stirring in a slow stream of nitrogen over a period of 7 hr. After standing overnight, the crystalline precipitates were collected and recrystallized from isopropyl ether to give 12.1 g (56.9%) of 2-cyano-4-nitropyridine (**4a**).

2-Cyano-6-methyl-4-nitropyridine (4b). Twenty grams of 2-methyl-4-nitropyridine *N*-oxide (**1b**) were worked up as in the foregoing experiment with 19.7 g of dimethyl sulfate and 14.0 g of sodium cyanide to give 14.2 g (67.1%) of 2-cyano-6-methyl-4-nitropyridine (**4b**).

2-Cyano-3-methyl-4-nitropyridine (4c). The treatment of 20.0 g of 3-methyl-4-nitropyridine *N*-oxide (**1c**) with 16.4 g of dimethyl sulfate and 12.7 g of sodium cyanide in the manner as described above gave 18.1 g (85.7%) of 2-cyano-3-methyl-4-nitropyridine (**4c**).

2-Cyano-3-ethyl-6-methyl-4-nitropyridine (4d). Twenty grams of 5-ethyl-2-methyl-4-nitropyridine *N*-oxide (**1d**) were treated with 15.6 g of dimethyl sulfate and 11.9 g of sodium cyanide according to the above procedure, and the resulting mixture was extracted with chloroform. The extract was worked up in the usual manner, and the residual oil was distilled *in vacuo* to give 17.3 g (82.4%) of 2-cyano-3-ethyl-6-methyl-4-nitropyridine (**4d**).

4-Nitropicolinic Acid (5a). A solution of 5 g of 2-cyano-4-nitropyridine (**4a**) in 50 g of 90% sulfuric acid was heated at 120°C for 2 hr. Into the reaction mixture, 5.6 g of sodium nitrite in 10 m*l* of water were added dropwise with stirring at 20—25°C over a period of 30 min. The mixture was kept at 20—25°C for an hour and then heated at 80°C for an additional hour. The resulting solution was poured onto 100 g of cracked ice and neutralized to pH 1.6 with sodium carbonate. The crystalline precipitates were then separated and recrystallized from acetone to give 5.4 g (97.6%) of 4-nitropicolinic acid (**5a**).

Other 4-Nitropicolinic Acids. 6-Methyl- (**5b**) (monohydrate), 3-methyl- (**5c**), and 3-ethyl-6-methyl-4-nitropicolinic acid (**5d**) were obtained by procedure described above.

4-Chloropicolinic Acid (6a). A solution of 5.0 g of 4-nitropicolinic acid (**5a**) in 50 m*l* of concentrated hydrochloric acid was heated at 100°C for 2 hr. The reaction mixture was then evaporated to dryness under reduced pressure and neutralized to pH 2.0 with sodium carbonate. The crystalline precipitates were collected and recrystallized from methanol - water to give 4.1 g (95.3%) of 4-chloropicolinic acid (**6a**).

Other 4-Chloropicolinic Acids. 4-Chloro-6-methyl- (**6b**) and 4-chloro-3-methylpicolinic acid (**6c**) were obtained by the above method, and both of them were recrystallized from benzene. 4-Chloro-3-ethyl-6-methylpicolinic acid (**6d**) was obtained as follows. 3-Ethyl-6-methyl-4-nitropicolinic acid (**5d**) was treated with concentrated hydrochloric acid, and the reaction mixture was neutralized as above. Evaporation to dryness, the extraction of the residue with benzene, and the removal of the solvent gave 4-chloro-3-ethyl-6-methylpicolinic acid (**6d**).

2-Cyano-4-ethoxypyridine (7a). A solution of 1 g of 2-cyano-4-nitropyridine (**4a**) in 30 m*l* of absolute ethanol was placed in a three-necked flask, equipped with a sealed stirrer, a dropping funnel, a thermometer, and a silica-gel tube. A solution of sodium ethoxide prepared from 0.18 g of sodium and 20 m*l* of absolute ethanol was added dropwise with stirring at −5—0°C over a period of an hour. After having been stirred for an additional hour, the reaction mixture was filtered and the filtrate was evaporated under reduced pressure. The residue was extracted with benzene, and from the extract 0.9 g (91%) of 2-cyano-4-ethoxypyridine (**7a**) was obtained. This was then recrystallized from petroleum benzine.

Other 2-Cyano-4-ethoxypyridines. 2-Cyano-4-ethoxy-6-methyl- (**7b**), 2-cyano-4-ethoxy-3-methyl- (**7c**), and 2-cyano-4-ethoxy-3-ethyl-6-methylpyridine (**7d**) were obtained by the same procedure.

Picolinic Acid. The catalytic reduction of 4-chloropicolinic acid (**6a**) with 5% Pd–C in methanol at room temperature gave picolinic acid in a 90.6% yield; mp 136°C; IR 1700 cm^{-1} (COOH); (Found: C, 58.38; H, 3.92; N, 11.35%). It was identified by a mixed-melting-point determination and by a comparison of the infrared spectra with those of an authentic sample.

6-Methyl-4-nitropicolinic Acid (Monohydrate). By applying the method for the preparation of 5-ethyl-4-nitropicolinic acid,[14] authentic 6-methyl-4-nitropicolinic acid melting at 129—130°C was prepared from 6-methyl-4-nitropicolinaldehyde, which had itself been obtained according to the directions of Furukawa.[15]

Quinolinic Acid. 3-Methylpicolinic acid melting at 114—115°C was obtained from 4-chloro-3-methylpicolinic acid (**6c**) by the same method as was used for picolinic acid in a 95.8% yield. 3-Methylpicolinic acid was oxidized with aqueous potassium permanganate at 90°C to give quinolinic acid in a 74.1% yield; decomp. 187; 229—230°C; IR 1700 cm^{-1} (COOH); (Found: C, 50.50; H, 2.84; N, 8.21%). It was identified by a mixed-melting-point determination and by a comparison of the infrared spectra with those of an authentic sample prepared by the oxidation of quinoline with

14) M. Endo and T. Nakajima, *Yakugaku Zasshi*, **80**, 875 (1960).

15) S. Furukawa, *ibid.*, **77**, 11 (1957).

aqueous potassium permanganate.

6-Methylquinolinic Acid. 3-Ethyl-6-methylpicolinic acid boiling at 83—84°C (0.05 mmHg) was obtained from 4-chloro-3-ethyl-6-methylpicolinic acid (**6d**) in a 97.7% yield by the procedure described above. It was oxidized with aqueous potassium permanganate at 20°C to give 6-methylquinolinic acid in an 81.2% yield; mp 166—167°C; IR 1720 cm^{-1} (COOH); (Found: C, 53.04; H, 3.90; N, 7.77%). It was identified by means of a mixed-melting-point determination and by a comparison of the infrared spectra with the authentic sample prepared from 8-hydroxyquinaldine.[16]

16) Anchor Chemical Co., Ltd., and H. N. Rydon, Brit. 838015 (1960).

BULLETIN OF THE CHEMICAL SOCIETY OF JAPAN VOL. 43 3214—3219 (1970)

Studies of the Thiocarbonyl Compounds. II. Syntheses and Thermal Rearrangement of Aryl Thionobenzoates*1

Yoshiaki ARAKI and Aritsune KAJI*2

Department of Chemistry, Faculty of Science, Kyoto University, Sakyo-ku, Kyoto

(Received March 6, 1970)

Various aryl thionobenzoates were prepared. When maintained at elevated temperatures, they rearranged smoothly to aryl thiolbenzoates. The mechanism of this rearrangement was kinetically investigated. The rearrangement rates were correlated with the first-order kinetic equation, and the rearrangement was found to be facilitated by substitution with an electron-withdrawing group in the migrating aromatic rings. The Hammett ρ value was found to be 2.11 in diphenyl ether at 200.5°C. The entropies of activation were negative. A linear free-energy relationship existed between this rearrangement and the rearrangement of *O,S*-diaryl dithiocarbonates. From these observations, a four-membered cyclic structure can be suggested as the transition state for this rearrangement. The present results indicate that the existence of hetero atoms directly bound to the thiocarbonyl group is not essential for the thermal rearrangement with intramolecular 1,3 aryl migration from oxygen to sulfur.

In a previous paper,[1] the intramolecular thermal rearrangement of *O,S*-diaryl dithiocarbonates (Ia) to *S,S*-diaryl dithiocarbonates (IIa) at elevated temperatures was reported. In addition to this rearrangement, of the thermal rearrangements with intramolecular 1,3 aryl migration from oxygen to sulfur, the thermal rearrangement of aryl *N,N*-disubstituted thionocarbamates (Ib) to aryl *N,N*-disubstituted thiolcarbamates (IIb) (Miyazaki-Newman-Kwart rearrangement)[2–6] and the thermal rearrangement of diaryl thionocarbonates (Ic) to diaryl thiolcarbonates (IIc) (Schönberg rearrangement)[3,7–10] are known. All of the compounds I

$$\underset{\text{I}}{\text{R-C(=S)-O-Ar}} \xrightarrow{\Delta} \underset{\text{II}}{\text{R-C(=O)-S-Ar}} \qquad (1)$$

a: R=Ar'S- b: R=R_1R_2N- c: R=Ar'O-

have hetero atoms with lone-pair electrons, such as sulfur, nitrogen, and oxygen, in the R group. In order to ascertain the nature of this kind of thermal rearrangement, it is necessary to examine whether hetero atoms, which are connected to the thiocarbonyl group, are required in the R group for rearrangement. Accordingly, the thermal rearrangement of aryl thionobenzoates (III), which

*1 Presented at the 22nd Annual Meeting of the Chemical Society of Japan, Tokyo, April, 1969.

*2 To whom inquiries should be addressed.

1) Y. Araki, This Bulletin, **43**, 252 (1970).

2) J. D. Edwards and M. Pianka, *J. Chem. Soc.*, **1965**, 7338.

3) H. Kwart and E. R. Evans, *J. Org. Chem.*, **31**, 410 (1966).

4) M. S. Newman and H. A. Karnes, *ibid.*, **31**, 3980 (1966).

5) K. Miyazaki, *Tetrahedron Lett.*, **1968**, 2793.

6) H. M. Relles and G. Pizzolato, *J. Org. Chem.*, **33**, 2249 (1968).

7) A. Schönberg and L. Vargha, *Ber.*, **63**, 178 (1930).

8) A. Schönberg, L. Vargha and W. Paul, *Ann. Chem.*, **483**, 107 (1930).

9) H. R. Al-Kazimi, D. S. Tarbell and D. Plant, *J. Amer. Chem. Soc.*, **77**, 2479 (1955).

10) D. H. Powers and D. S. Tarbell, *ibid.*, **78**, 70 (1956).

have no hetero atom in the R group, to aryl thiolbenzoates (IV) was investigated.

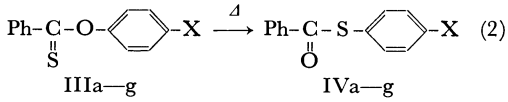

(2)

IIIa—g IVa—g

X = {a: OCH_3 b: CH_3 c: H d: Cl; e: $COCH_3$ f: CN g: NO_2}

In regard to the thermal rearrangements of thionobenzoates to thiolbenzoates, the thermal rearrangements of dialkylaminoalkyl thionobenzoates[11-13] (an anchimerically-assisted rearrangement), allyl thionobenzoates[14,15] (an allylic rearrangement), and benzhydryl thionobenzoates[16] (a rearrangement through an intimate ion-pair) have been reported. Of the thermal rearrangement of aryl thionobenzoates, however, an example has been reported[4] in which the thermal rearrangement of *p*-*t*-butylphenyl thionobenzoate was qualitatively tested. The present authors have now studied the kinetics of the thermal rearrangement of aryl thionobenzoates in order to establish the reaction mechanism and in order to compare it with the thermal rearrangement of other compounds with the formula I which have hetero atoms in the R group.

Results

The various aryl thionobenzoates (III) were synthesized by the reaction of a *p*-substituted phenol with a thiobenzoyl chloride (Eqs. (3) and (4)). The results are shown in Table 1.

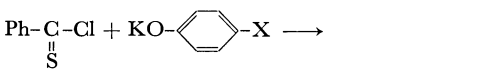

(3)

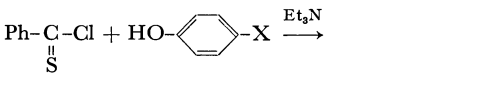

(4)

When maintained at 200°C without any solvent under a nitrogen atmosphere, the compounds III gradually rearranged to aryl thiolbenzoates (IV). The compounds thus obtained were identified by a mixed-melting-point test and by a comparison of the infrared spectra with those of the corresponding authentic samples prepared by the reaction of a *p*-substituted thiophenol with a benzoyl chloride (Eq. (5)).

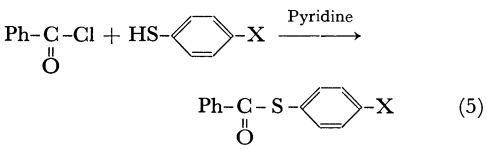

(5)

In order to clarify the influence of the substituents upon the rates of the rearrangement, the kinetics of the rearrangement were studied in a diphenyl ether solution. The reaction rates were followed by the ampoule technique and were determined by ultraviolet spectrophotometric measurements. It was found that the rearrangement reaction

Table 1. Aryl thionobenzoates

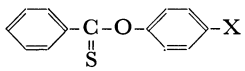

Compd. No.	X	Appearance	Mp[a] °C	Formula	Analysis Found C(%)	Found H(%)	Found S(%)	Calcd C(%)	Calcd H(%)	Calcd S(%)
IIIa	OCH_3	yellow needles[b]	65.5—66.0	$C_{14}H_{12}O_2S$	69.10	4.93	12.88	68.84	4.95	13.10
IIIb	CH_3	yellow needles[b]	44.0—44.5	$C_{14}H_{12}OS$	73.43	5.48	13.96	73.67	5.30	14.02
IIIc	H	yellow needles[b]	40.0—40.5[c]	$C_{13}H_{10}OS$	73.16	4.58	14.87	72.89	4.71	14.94
IIId	Cl	yellow prisms[b]	53.0—55.0	$C_{13}H_9ClOS$	62.78	3.79	13.14	62.79	3.65	12.87
IIIe	$COCH_3$	yellow needles[b]	97.0—98.0	$C_{15}H_{12}O_2S$	70.10	4.72	12.44	70.30	4.72	12.49
IIIf	CN	yellow prisms[d]	112.0—113.0	$C_{14}H_9NOS$	70.56	3.90	13.67	70.29	3.79	13.38
IIIg	NO_2	yellow needles[b]	108.0—109.0[e]	$C_{13}H_9NO_3S$	60.40	3.43	12.19	60.23	3.50	12.35

a) All melting points are uncorrected. b) Recrystallized from *n*-hexane. c) Y. Sakurada, *Mem. Coll. Sci. Kyoto*, [A] **10**, 71 (1927); bp 155—160°C/40 mmHg. R. Mayer and St. Scheithauer, *J. Prakt. Chem.*, **21**, 214 (1963); bp 92°C/0.1 mmHg. d) Recrystallized from benzene-*n*-hexane. e) Ref. 4; mp 98—100°C.

11) S. A. Karjala and S. M. McElvain, *ibid.*, **55**, 2966 (1933).
12) T. Taguchi, Y. Kawazoe, K. Yoshihira, H. Kanayama, M. Mori, K. Tabata and K. Harano, *Tetrahedron Lett.*, **1965**, 2717.
13) K. Yoshihira and T. Taguchi, *Yakugaku Zasshi*, **89**, 1225 (1969).
14) S. G. Smith, *J. Amer. Chem. Soc.*, **83**, 4285 (1961).
15) K. D. McMichael, *ibid.*, **89**, 2943 (1967).
16) S. G. Smith, *Tetrahedron Lett.*, **1962**, 979.

Table 2. Rearrangement of *p*-cyanophenyl thionobenzoate (IIIf) at 200.5±0.1°C

Time (sec)	% of IIIf remaining	$k\times10^6$ (sec^{-1})
0	100	
3600	79.8	6.28
7200	65.3	5.92
10800	51.8	6.08
14400	41.7	6.07
18000	34.6	5.90

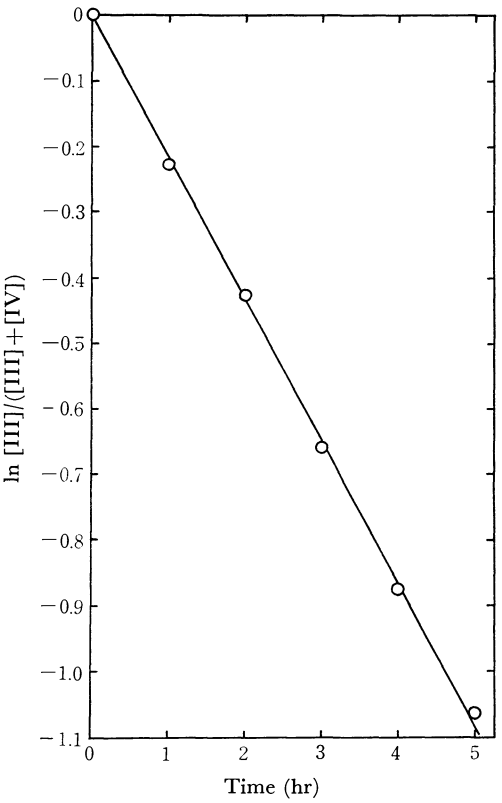

Fig. 1. Rate plot for the rearrangement of *p*-cyanophenyl thionobenzoate at 200.5±0.1°C.

Table 3. First-order rate constants and activation parameters of the rearrangement

Compd. No.	$k\times10^6$ (sec^{-1}) 200.5°C	230.0°C	*Ea* (kcal/mol)	$\Delta S^{\neq}$ (e.u.)
IIIa	0.542	7.07	41.2	−3.2
IIIb	1.46	17.2	39.5	−4.8
IIIc	2.87	30.0	37.6	−7.4
IIId	3.66	38.5	37.7	−6.7
IIIe	28.9	263	35.4	−7.5
IIIf	60.5	504	34.0	−9.0
IIIg	118	946	33.4	−8.9

obeyed first-order kinetics fairly well. A typical run is shown in Table 2 and Fig. 1; there do not seem to be any drifts in the rate constants. The first-order rate constants were derived from the slopes of the straight lines obtained by plotting ln [III]/([III]+[IV]) against the time. The rate constants found for the rearrangement are summarized in Table 3. From these data, the energies and entropies of activation were calculated. These results are also shown in Table 3.

Discussion

As is shown in Table 3, the rearrangement is accelerated by the electron-withdrawing substituents at the *p*-position on the migrating group. The plot of the logarithms of the first-order rate constants at 200.5°C against Hammett's σ values showed a good linear relationship (Fig. 2). The value of the reaction constant, ρ, determined by the least-squares method is 2.11 (the correlation coefficient is 0.987).

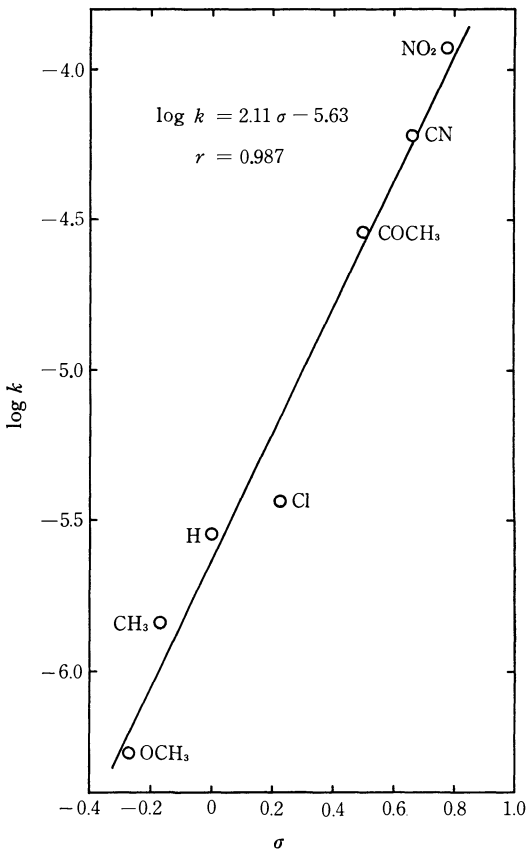

Fig. 2. Hammett plot for the rate of the rearrangement of 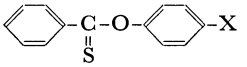 at 200.5±0.1°C.

This result indicates that the rearrangement of aryl thionobenzoates is a nucleophilic reaction which may involve a nucleophilic attack of the thiocarbonyl sulfur atom in the rate-determining step.

The intermolecular reaction mechanism which involves a rate-determining initial ionization[16] (Eq. (6)) can be ruled out. In such a case, the rate should depend on the stability of the aryl cation which is stabilized by the electron-donating substituents.

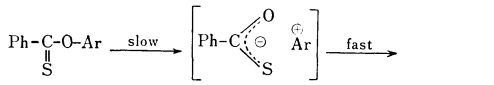

Ph-C-S-Ar (6)
‖
O

The fact that all of the *p*-substituted compounds III rearranged to only the *p*-substituted products, IV, with no accompanying *m*-substituted product, eliminates the benzyne mechanism (Eq. (7)).

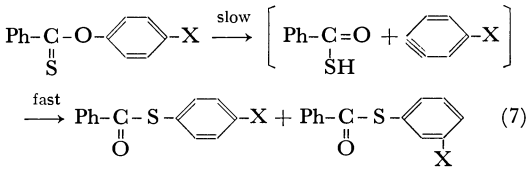

The isokinetic temperature, β, was calculated to be 1300°K from the data in Table 3 (the correlation coefficient is 0.96). This shows that the rearrangement may be governed by the enthalpy of activation at temperatures near 200°C.

In addition to these results, the first-order kinetics and the negative entropies of activation (Table 3) lead to the conclusion that the rearrangement of aryl thionobenzoates may proceed *via* a four-membered cyclic transition state (Scheme 1) formed by a nucleophilic attack of the thiocarbonyl sulfur atom on the migrating aromatic ring.

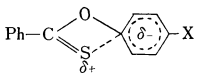

Scheme 1

A very good linear free-energy relationship was found between the rearrangement of aryl thionobenzoates and the rearrangement of *O*-aryl *S*-phenyl dithiocarbonates, as is shown in Fig. 3 (the correlation coefficient is 0.999). The slope of the straight line is 1.12. This was rather astonishing considering the absence, in aryl thionobenzoates, of any hetero atoms, which may promote the rearrangement of this sort.

The present results indicate that the existence of hetero atoms in the R group of the formula I at the α position of the thiocarbonyl group is not essential for the thermal rearrangement with intramolecular 1,3 aryl migration from oxygen to sulfur. The rearrangements described above may all proceed analogously by means of an "intramolecular S_N-Ar" mechanism.

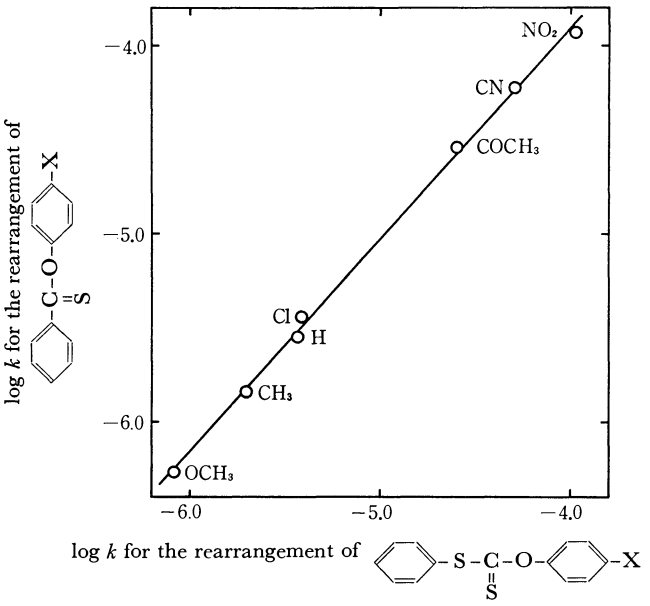

Fig. 3. Free-energy relationship between the rearrangement of aryl thionobenzoates and the rearrangement of *O*-aryl *S*-phenyl dithiocarbonates.

Experimental*3

Thiobenzoyl Chloride. This material was prepared by the method of Staudinger.[17]

Aryl Thionobenzoates (III). These compounds were prepared by two methods (Eqs. (3) and (4)). Method A (Eq. (3)) was generally employed, but Method B (Eq. (4)) was also used to prepare the compounds bearing electron-withdrawing substituents because of its convenience. The results are listed in Table 1.

Method A. To 20 m*l* of cold absolute methanol was added, in small portions, 0.78 g (0.02 mol) of potassium. After hydrogen evolution had ceased, 0.02 mol of *p*-substituted phenol was added. The resulting solution was then evaporated to dryness on a rotary evaporator. To the potassium *p*-substituted phenolate thus obtained was added 25 m*l* of dry acetone. This solution was cooled to 0°C in an ice-water bath, and then a solution of 3.13 g (0.02 mol) of freshly-distilled thiobenzoyl chloride in 20 m*l* of dry acetone was added all at once. The resulting mixture was then stirred for 3 hr at 5—10°C, after which the cooling bath was removed. After additional, overnight stirring at room temperature, the reaction mixture was poured into *ca.* 500 m*l* of cold water and then extracted with ether. The ethereal extract was washed with water, dried over anhydrous magnesium sulfate, and freed of solvent on a rotary evaporator. The crude product thus obtained was chromatographed on a silica-gel column, using benzene and/or *n*-hexane as the elution solvent, and then recrystallized from *n*-hexane, giving yellow crystals.

Method B. To a cold solution of 0.02 mol of *p*-substituted phenol and 3.13 g (0.02 mol) of freshly-distilled thiobenzoyl chloride in 40 m*l* of dry acetone in an ice-water bath, there was added, all at once, 2.03 g (0.02 mol) of triethylamine with vigorous agitation. The cooling bath was then removed, and stirring was continued overnight at room temperature. The reaction mixture was then poured into *ca.* 500 m*l* of cold water and extracted with ether. The ethereal extract was washed with water, dried over anhydrous magnesium sulfate, and freed of solvent on a rotary evaporator. The crude product thus obtained was chromatographed on a silica-gel column, using benzene and/or *n*-hexane as the elution solvent, and then recrystallized from *n*-hexane, giving yellow crystals.

Aryl Thiolbenzoates (IV). The following general procedure was employed for the synthesis of these compounds.

To a cold solution of 0.01 mol of *p*-substituted thiophenol and 1.41 g (0.01 mol) of benzoyl chloride in 20 m*l* of dry acetone in an ice-water bath, there was added, all at once, 0.79 g (0.01 mol) of dry pyridine with vigorous agitation. The cooling bath was then removed, and stirring was continued for two more hours at room temperature. The reaction mixture was poured into *ca.* 300 m*l* of cold water; colorless crystals were thus obtained quantitatively. These were recrystallized from a suitable solvent: IVa, colorless needles (from *n*-hexane), mp 100.0—100.5°C (lit,[18] mp 99—100°C). IVb, colorless prisms (from *n*-hexane), mp 76.0—76.5°C (lit,[19] mp 75—76°C). IVc, colorless prisms (from *n*-hexane), mp 56.0—57.0°C (lit,[19] mp 55—56°C). IVd, colorless prisms (from *n*-hexane), mp 75.5—76.0°C (lit,[20] mp 75—76°C). IVe, colorless needles (from benzene–*n*-hexane), mp 134.0—134.5°C (Found: C, 70.05; H, 4.65; S, 12.45%. Calcd for $C_{15}H_{12}O_2S$: C, 70.30; H, 4.72; S, 12.49%). IVf, colorless plates (from benzene–*n*-hexane), mp 101.0—102.0°C (Found: C, 70.00; H, 3.90; S, 13.35%. Calcd for $C_{14}H_9NOS$: C, 70.29; H, 3.79; S, 13.38%). IVg, pale yellow needles (from benzene–*n*-hexane), mp 125.0 — 126.0°C (lit,[21] mp 126—127°C).

Thermal Rearrangement of III. About 500 mg of III was placed in a test tube without any solvent and was heated at 200°C under a slow stream of nitrogen. The progress of the reaction could be followed by thin-layer chromatography on silica gel, with development by benzene and/or *n*-hexane. As a result, it was shown that the compound III was gradually converted to another compound. After the compound III had changed completely, the reaction mixture was chromatographed on a silica-gel column, using benzene and/or *n*-hexane as the elution solvent. After the solvent had been removed under reduced pressure, the product was recrystallized and identified by means of its IR spectrum and by a mixed-melting-point test with an authentic sample.

Kinetic Measurements. The rates were followed by the ampoule technique. That is, approximately 10 mg of III was dissolved in diphenyl ether, giving a final volume of 5 m*l*. This corresponds to *ca.* a 0.01 M solution. About a 0.8-m*l* portion of this solution was transferred to each of six ampoules. These ampoules were flushed with nitrogen and sealed. Five of these ampoules were then immersed in a constant-temperature bath controlled within ±0.1°C. These ampoules, taken out from the bath at appropriate intervals, were cooled immediately by immersion in cold water. From each run thus obtained, a 0.5-m*l* portion was accurately removed into a 5-m*l* measuring flask. The solution was made up to volume with chloroform, and then, further, the solution was diluted twenty times with chloroform to make it suitable for use as the sample for the ultraviolet spectrophotometric measurements.*4 The optical densities for each run were measured at 300—320 mμ.*5 The composition of III could be determined directly by substitution in the following equation:

$$\frac{[\mathrm{III}]}{[\mathrm{III}]+[\mathrm{IV}]} = \frac{\varepsilon_{\mathrm{III}}A_t-\varepsilon_{\mathrm{IV}}A_0}{\varepsilon_{\mathrm{III}}A_0-\varepsilon_{\mathrm{IV}}A_0}$$

where $\varepsilon_{\mathrm{III}}$ and $\varepsilon_{\mathrm{IV}}$ are the molar extinction coefficients of III and IV respectively at a stated wavelength, and

*3 All melting points are uncorrected.

17) H. Staudinger and J. Siegmant, *Helv. Chim. Acta*, **3**, 824 (1920).

18) M. F. Taboury, *Bull. Soc. Chim. Paris*, [3] **33**, 836 (1905).

19) K. Miyaki and S. Yamagishi, *Yakugaku Zasshi*, **76**, 436 (1956).

20) M. F. Taboury, *Bull. Soc. Chim. Paris*, [3] **31**, 646 (1904).

21) G. Cilento, *J. Amer. Chem. Soc.*, **75**, 3748 (1953).

*4 A Hitachi Perkin-Elmer 139 UV-VIS spectrophotometer was used for the ultraviolet spectrophotometric measurements.

*5 In this range, the absorption of diphenyl ether could be negligible.

where A_t and A_0 are absorption intensities at the same wavelength, observed at time t and time 0 respectively. In all cases, a plot of the logarithms of [III]/([III]+[IV]) against the time gave a straight line, indicating the reaction to be of first-order (Fig. 1). The results of a typical kinetic run are illustrated in Table 2. From these data, the rate constants were calculated (Table 3).

The authors wish to express their sincere thanks to Dr. Jun-ichi Hayami for his invaluable discussions.

BULLETIN OF THE CHEMICAL SOCIETY OF JAPAN VOL. 43 3219—3223 (1970)

The Synthesis and Reaction of α,β-Unsaturated α-Nitrocarboxylic Esters[1]

Chung-gi SHIN,[2] Mitsuo MASAKI and Masaki OHTA

Laboratory of Organic Chemistry, Tokyo Institute of Technology, Ookayama, Meguro-ku, Tokyo

(Received March 7, 1970)

Synthetic studies of α,β-unsaturated α-nitrocarboxylic esters and the corresponding α-amino compounds are described. When α,β-unsaturated carboxylic ester was treated with fuming nitric acid, two products, α,β-unsaturated α-nitrocarboxylic ester and α-hydroxy-β-nitrocarboxylic ester, were formed. The former was converted into β-methoxy-α-nitrocarboxylic ester by treatment with methanol in the presence of a base such as sodium methoxide or sodium acetate. Reduction of β-methoxy-α-nitrocarboxylic esters with aluminum amalgam and the subsequent distillation of the products afforded α,β-unsaturated α-aminocarboxylic esters and α-hydroxyamino-β-methoxycarboxylic esters, which were confirmed by their *N*-phthaloylglycyl derivatives.

It was previously reported that the reduction of methyl and ethyl esters of β-methyl-α-nitrocrotonic acid (I: $R=R'=CH_3$) with aluminum amalgam gave the corresponding α-aminocarboxylic esters (enamines), while α-oximinocarboxylic esters were formed in the reduction of β-monosubstituted α,β-unsaturated α-nitrocarboxylic esters.[3,4]

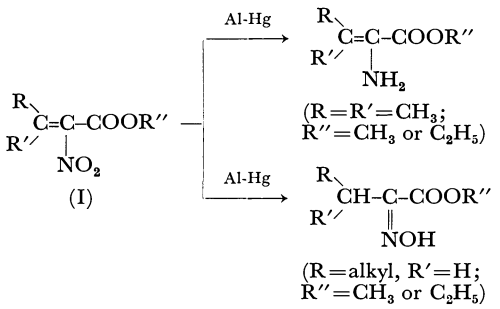

In the present paper, we report detailed studies on the preparation of α,β-unsaturated α-nitrocarboxylic esters (I), and the synthesis of α,β-unsaturated α-aminocarboxylic esters (VI) by the reduction of β-methoxy-α-nitrocarboxylic esters (III).

Nitration of α,β-unsaturated carboxylic esters with fuming nitric acid was reported by Bouveault[5] and Tatsuoka.[6] The reaction was reinvestigated under various conditions and it was found that two products were formed in the reaction. When methyl 4-methyl-2-pentenoate was treated with fuming nitric acid (sp.gr., 1.52) with vigorous stirring at about 30°C for more than 5 hr, methyl 4-methyl-2-nitro-2-pentenoate (Ie) and methyl 2-hydroxy-4-methyl-3-nitropentanoate (IIe) were obtained in 33 and 39% yields, respectively.

The nitroolefincarboxylic ester Ie was characterized by elementary analysis and infrared spectrum. The structure was also supported by the reduction with aluminum amalgam giving methyl 4-methyl-2-oximinopentanoate.[4]

In place of methyl 2-hydroxy-4-methyl-3-nitro-

1) Presented at 19th and 20th Annual Meetings of the Chemical Society of Japan, Tokyo (April, 1966), Osaka (April, 1967).

2) Present Address: Laboratory of Organic Chemistry, Kanagawa University, Rokkakubashi, Kanagawa-ku, Yokohama.

3) C. Shin, M. Masaki and M. Ohta, This Bulletin, **39**, 858 (1966).

4) C. Shin, M. Masaki and M. Ohta, *J. Org. Chem.*, **32**, 1860 (1967).

5) L. Bouveault and A. Wahl, *C. R. Acad. Sci. Paris*, **131**, 687, 1212 (1900); L. Bouveault and A. Wahl, *Bull. Soc. Chim. Fr.*, **25**, 801, 913 (1901).

6) S. Tatsuoka, M. Murakami and T. Tamura, *Yakugaku Zasshi*, **70**, 230 (1950).

TABLE 1. α,β-UNSTATURATED α-NITRO- AND α-HYDROXY-β-NITROCARBOXYLIC ESTERS

Compd	Yield (%)	Bp °C/mmHg	Formula	Found % C	Found % H	Found % N	Calcd % C	Calcd % H	Calcd % N	IR Spectrum[a] ν_{max}, cm^{-1}
Ia	32	88—92/4	$C_5H_7NO_4$	41.12	4.81	9.42	41.38	4.86	9.65	1740, 1640, 1560, 1350
Ib	39	85—87/3	$C_7H_{11}NO_4$			7.99			8.09	1735, 1650, 1540, 1370
Ic	31	91—107/4	$C_7H_{11}NO_4$	48.68	6.65	8.32	48.55	6.40	8.09	1740, 1660, 1540, 1380
Id	24	98—105/3[b]	$C_8H_{13}NO_4$	51.83	7.19	6.99	51.34	6.95	7.49	1740, 1665, 1560, 1380
Ie	33	84—86/4	$C_7H_{11}NO_4$	48.84	7.11	7.93	48.55	6.40	8.09	1740, 1660, 1540, 1380
If	38	91—95/2.5	$C_8H_{13}NO_4$	51.51	7.12	7.58	51.34	6.95	7.49	1740, 1660, 1560, 1380
IIb	18	108—109/3	$C_7H_{13}NO_5$	44.44	6.58	7.59	43.97	6.85	7.33	3450, 1740, 1560, 1375
IIc	27	104—110/5	$C_7H_{13}NO_5$	44.08	6.66	7.48	43.97	6.85	7.33	3450, 1740, 1560, 1370
IId	32.5	120—121/2	$C_8H_{15}NO_5$	46.51	6.99	6.76	46.82	7.37	6.83	3450, 1740, 1555, 1370
IIe	39	120—121/2	$C_7H_{13}NO_5$	44.21	6.67	7.21	43.97	6.85	7.33	3450, 1740, 1560, 1375
IIf	28	107—110/2	$C_8H_{15}NO_5$	46.61	7.08	7.18	46.82	7.37	6.83	3450, 1740, 1650, 1380

a) In NaCl. b) lit,[7] bp 72.5—79.5°C/0.7 mmHg.

pentanoate, an alternative 3-hydroxy-2-nitro structure might be also possible from elementary analysis and infrared spectrum. However, methyl 3-hydroxy-4-methyl-2-nitropentanoate prepared by an authentic method[7] showed bp 102—114°C/3 mmHg, while compound IIe obtained from the above nitration method has bp 120—121°C/2 mmHg.

Thus the most probable structure for IIe was concluded to be methyl 2-hydroxy-4-methyl-3-nitropentanoate.

Nitration of analogous olefinic carboxylic esters afforded the corresponding α-nitrocarboxylic esters (Ia—d and If) and 2-hydroxy-3-nitrocarboxylic esters (IIb—d and IIf) under similar experimental conditions; results of the elementary analyses and infrared spectra of the products are shown in Table 1.

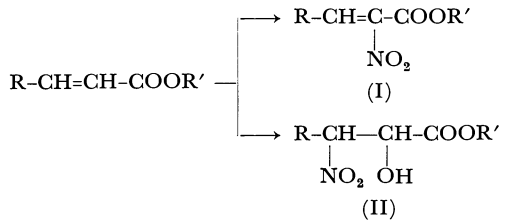

(I) (II)

a) R=CH_3, R′=CH_3
b) R=C_2H_5, R′=C_2H_5
c) R=n-C_3H_7, R′=CH_3
d) R=n-C_3H_7, R′=C_2H_5
e) R=i-C_3H_7, R′=CH_3
f) R=i-C_3H_7, R′=C_2H_5

Infrared spectrum of I showed bands of carbon-carbon double bond at 1640—1665 cm^{-1}, and of nitro group at 1540—1560 and 1350—1380 cm^{-1} regions. On the other hand, II showed infrared absorption bands of hydroxyl group at 3450 cm^{-1}, and of nitro group at 1555—1560 and 1370—1380 cm^{-1} regions.

The nitration method is useful for the preparation of α,β-unsaturated α-nitrocarboxylic esters (I), while Dornow and Menzel[8] and other workers[7,9] reported the preparation of I by a three-step reaction starting from aldehydes and nitroacetic ester *via* the route illustrated below.

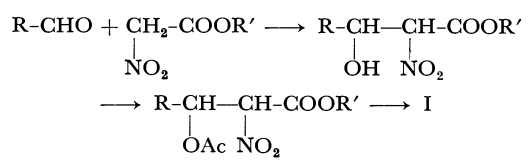

When ethyl 4-methyl-2-nitro-2-pentenoate (If) was treated with methanol in the presence of sodium methoxide or sodium acetate below −10°C, ethyl 3-methoxy-4-methyl-2-nitropentanoate (IIIf) was obtained in a good yield. Other 3-methoxy-2-nitrocarboxylates (IIIb, IIIc and IIId) were also obtained from I under similar experimental conditions in good yields; the results are summarized in Table 2. When compounds III were heated at 150—160°C for 6 hr, the methoxyl group in the 3-position was eliminated to afford I.

Reduction of IIIf with aluminum amalgam in ether and the subsequently distillation of the resulting product under reduced pressure gave a small amount of ethyl 2-amino-4-methyl-2-pentenoate (VIf) as a lower boiling point fraction and ethyl 2-hydroxyamino-3-methoxy-4-methylpentanoate (IVf) as a higher boiling fraction in a 70% yield. The infrared spectrum of VIf exhibits two absorption bands at 1650 and 1735 cm^{-1} in carbonyl region and a broad band at 3350 cm^{-1} in amino region. The absorption pattern is essentially the

7) S. Umezawa and S. Zen, This Bulletin, **36**, 1143 (1963).

8) A. Dornow and H. Menzel, *Ann. Chem.*, **588**, 40 (1959).

9) I. S. Ivanova, Yu. V. Konnova and S. S. Novikov, *Izv. Akad. Nauk SSSR, Otd. Khim. Nauk*, **1962**, 1677.

Table 2. β-methoxy-α-nitro- and β-methoxy-α-hydroxyaminocarboxylic esters

Compd	Yield (%)	Bp °C/mmHg	Formula	Found % C	Found % H	Found % N	Calcd % C	Calcd % H	Calcd % N	IR Spectrum[a] ν_{max}, cm^{-1}
IIIb	66	72—85/2	$C_8H_{15}NO_5$	46.13	7.34	6.97	46.82	7.37	6.83	1750, 1570, 1375, 1030
IIIc	92	95—97/2.5	$C_8H_{15}NO_5$	47.14	7.09	7.10	46.82	7.37	6.83	1750, 1565, 1370, 1100
IIId	70	99—103/3	$C_9H_{17}NO_5$	49.77	7.82	6.76	49.30	7.82	6.39	1750, 1570, 1380, 1100
IIIe	65	96—97/5	$C_8H_{15}NO_5$	47.50	7.02	7.27	46.82	7.37	6.83	1750, 1570, 1375, 1090
IIIf	78.4	88—93/2	$C_9H_{17}NO_5$	49.87	7.63	7.27	49.30	7.82	6.39	1750, 1570, 1380, 1100
IVb	87.8	105—110/4	$C_8H_{17}NO_4$	50.72	9.27	7.45	50.25	8.96	7.33	3350, 3250, 1735, 1075
IVc	52	96—101/4	$C_8H_{17}NO_4$			7.49			7.33	3350, 3250, 1735, 1080
IVd	59	105—108/2	$C_9H_{19}NO_4$			6.75			6.82	3400, 3250, 1735, 1095
IVe	50	109—111/4	$C_8H_{17}NO_4$			7.72			7.33	3400, 3250, 1735, 1095
IVf	74.5	98—100/4	$C_9H_{19}NO_4$			7.36			6.82	3350, 3250, 1735, 1095

a) In NaCl.

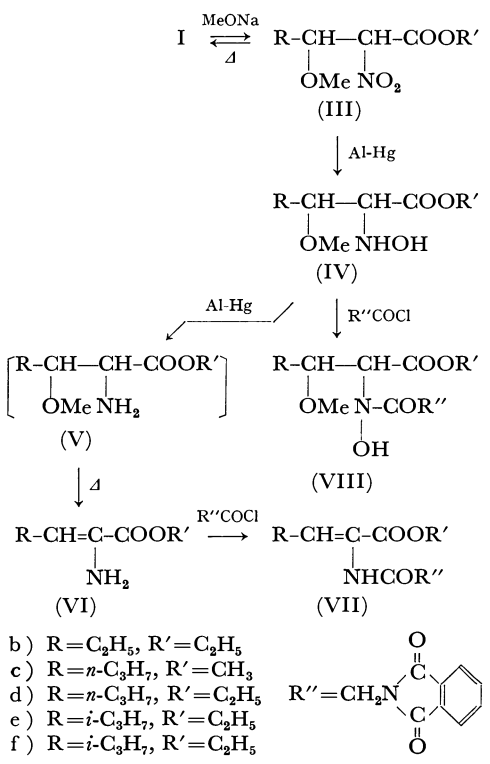

b) R=C_2H_5, R′=C_2H_5
c) R=n-C_3H_7, R′=CH_3
d) R=n-C_3H_7, R′=C_2H_5
e) R=i-C_3H_7, R′=C_2H_5
f) R=i-C_3H_7, R′=C_2H_5

same as that of α,β-unsaturated α-aminocarboxylic ester.[4] Reduction of other β-methoxy-α-nitro compounds (IIIb—e) afforded also enamines (VIb—e) as minor products and α-hydroxyamino-β-methoxycarboxylic esters (IVb—e) as main products. Formation of enamines could be explained by the fact that elimination of methoxyl group in the 3-position as methanol occurred during the distillation of α-amino-β-methoxycarboxylic esters (V) which were the further reduced products of the initially formed hydroxyamino esters (IV). Compounds VI were unstable and gradually polymerized at room temperature. In order to establish the structure, the new enamines were converted into their *N*-phthaloylglycyl derivatives. When ethyl 2-amino-2-pentenoate (VIb) was treated with phthaloylglycyl chloride in benzene in the presence of pyridine at room temperature, ethyl 2-(phthaloylglycyl)amino-2-pentenoate (VIIb) was obtained as a colorless crystalline product in a 9% yield. Analogous treatment of other enamines (VIc—f) with phthaloylglycyl chloride afforded (phthaloylglycyl)amino derivatives (VIIc—f); the results are summarized in Table 4. The structures of these phthaloylglycyl derivatives were confirmed by elementary analyses and their infrared absorption spectra which are very similar to alkyl esters of 3-methyl-2-(phthaloylglycyl)aminocrotonic acid.[3,4] On the other hand, treatment of IVf with phthaloylglycyl chloride under similar conditions, afforded ethyl 3-methoxy-4-methyl-2-*N*-(phthaloylglycyl)hydroxyaminopentanoate (VIIIf). Analogous acylation of other α-hydroxyaminocarboxylic esters (IVb and IVe) afforded the corresponding (phthaloylglycyl) hydroxyamino derivatives (VIIIb and VIIIe) in a poor yield; the results are summarized in Table 4. All these (phthaloylglycyl)hydroxyamino derivatives gave red coloration with methanolic ferric chloride. The structures of these esters were assigned on the basis of elementary analysis and infrared spectrum.

When methyl 2-hydroxyamino-3-methoxy-4-

Table 3. α,β-unsaturated α-aminocarboxylic esters

Compd	Yield (%)	Bp °C/mmHg	IR Spectrum[a] ν_{max}, cm^{-1}
VIb	16	62—66/4	3400, 1740, 1620
VIc	15.4	65—71/4	3300, 1730, 1650
VId	8.4	83—86/3	3350, 1740, 1650
VIe	18	57—65/4	3350, 1740, 1650
VIf	15.8	61—65/3	3350, 1735, 1650

a) In NaCl.

TABLE 4. *N*-PHTHALOYLGLYCYL DERIVATIVES OF ENAMINE (VI) AND HYDROXYAMINOCARBOXYLATES (IV)

Compd	Yield (%)	Mp °C	Formula	Found %			Calcd %			IR Spectrum[d] ν_{max}, cm^{-1}		
				C	H	N	C	H	N			
VIIb	9	245—247	$C_{17}H_{18}N_2O_5$	61.48	5.66	8.62	61.81	5.49	8.48	3250,	1730,	1670
VIIc	13	202—203[a]	$C_{17}H_{18}N_2O_5$			7.84			8.48	3250,	1730,	1670
VIId	8.4	196—197[b]	$C_{18}H_{20}N_2O_5$			7.72			8.14	3250,	1720,	1660
VIIe	26	164—165	$C_{17}H_{18}N_2O_5$	61.45	5.70	8.64	61.81	5.49	8.48	3300,	1730,	1670
VIIIb	20.2	146—147	$C_{18}H_{22}N_2O_7$	57.06	6.02	7.67	57.13	5.86	7.40	3450,	1750,	1690
VIIIe	31	189—190[c]	$C_{18}H_{22}N_2O_7$			7.54			7.40	3500,	1720,	1660
VIIIf	52	119—120	$C_{19}H_{24}N_2O_7$	58.14	6.22	7.30	58.15	6.17	7.14	3470,	1730,	1670

a, b) Recrystallized from ethanol (colorless needles). c) Recrystallized from ligroin (colorless needles).
d) In KBr.

methylpentanoate (IVe) was allowed to stand at room temperature for two weeks, cyclic condensation took place and 1,4-dihydroxy-3,6-diisobutylidene-2,5-dioxopiperazine (IX) was obtained. Formation of the 2,5-dioxopiperazine ring supports 2-hydroxyamino structure of the reduction product and also the position of nitro group in the parent ester, methyl 4-methyl-2-nitro-2-pentenoate (Ie).

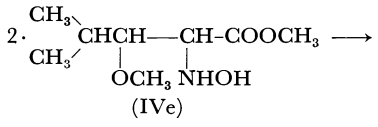

(IVe)

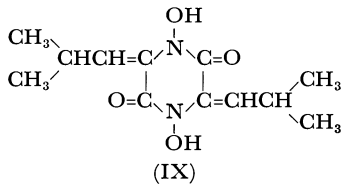

(IX)

Experimental

All melting and boiling points are uncorrected. The IR spectra were recorded with a Hitachi EPI-S2 Spectrometer.

Nitration of Methyl 4-Methyl-2-pentenoate with Fuming Nitric Acid. Methyl 4-methyl-2-pentenoate (20 g) was added drop by drop, with vigorous stirring, to fuming nitric acid (36 m*l*, sp.gr. 1.52) below 5°C. After addition of the ester had been completed, the mixture was stirred for several hr, while being allowed to warm to room temperature, and stirring was continued for additional 5 hr at 30°C. The mixture was added to ice water (200 m*l*) and then extracted several times with ether. The combined ethereal extracts were washed successively with water, saturated aqueous solution of sodium carbonate and finally with water. The extracts were dried over anhydrous sodium sulfate and then evaporated. Distillation of the residual oil afforded two fractions, as pale yellow oils, which were identified as methyl 4-methyl-2-nitro-2-pentenoate (Ie) and methyl 2-hydroxy-4-methyl-3-nitropentanoate (IIe).

Under analogous conditions, nitration of other olefinic carboxylic esters was performed and the corresponding α-nitro esters (Ia—d and If) and β-nitro esters (IIb—d and IIf) were obtained.

Ethyl 3-Methoxy-4-methyl-2-nitropentanoate (IIIf). The procedure was modified from the method of Yamagishi and Ishibiki.[10] A solution of ethyl 4-methyl-2-nitro-2-pentenoate (11 g) in methanol (70 m*l*) was added, with vigorous stirring, to 5% methanolic solution of sodium methoxide (from 4.8 g of sodium in methanol (70 m*l*)) cooled below −10°C. The temperature of the reaction mixture rose up to 15°C, at which stirring was continued for 20 min, and then a small amount of crushed dry ice was added portionwise. The cooled mixture was poured into water (500 m*l*), and the resulting solution was acidified with glacial acetic acid, whereby an oily product was separated out. The product was extracted several times with ether. The combined ethereal extracts were washed with water, dried over anhydrous magnesium sulfate, and then evaporated. Distillation of the residual oil afforded ethyl 3-methoxy-4-methyl-2-nitropentanoate as an almost colorless oil.

Analogous treatment of other α-nitroolefinic carboxylic esters with sodium methoxide afforded the corresponding β-methoxy-α-nitrocarboxylic esters (IIIb—e).

Reduction of Ethyl 3-Methoxy-4-methyl-2-nitropentanoate. A solution of IIIf (6 g) in ether (50 m*l*) was added drop by drop with vigorous stirring to a suspension of aluminum amalgam (from 4 g of aluminum) in ether (120 m*l*) at room temperature. In a few minutes ether began to reflux. During the addition of the above solution a few drops of water was added at 10-min intervals to maintain refluxing. After addition of the solution had been completed stirring was continued for additional 2 hr. The mixture was extracted thoroughly several times with ether. The combined ethereal extract was dried over anhydrous sodium sulfate and then evaporated. Distillation of the residual oil afforded two fractions, as pale yellow oils, which were identified as ethyl 2-amino-4-methyl-2-pentenoate (VIf) and ethyl 2-hydroxyamino-3-methoxy-4-methylpentanoate (IVf).

Analogous reduction of other α-nitrocarboxylic esters (III) afforded the corresponding enaminocarboxylic (VIb—e) and hydroxyaminocarboxylic esters (IVb—e).

Ethyl 2-(Phthaloylglycyl)amino-2-pentenoate (VII). Phthaloylglycyl chloride (0.65 g) was added

10) K. Yamagishi and Y. Ishibiki, *Nippon Kagaku Zasshi*, **81**, 971 (1960).

portionwise with vigorous stirring to ethyl 2-amino-2-pentenoate (VIb, 0.5 g) suspended in a solution of sodium hydrogencarbonate (0.3 g) in water (10 m*l*) at room temperature. After stirring for 30 min a syrup was precipitated. After one day the viscous syrup crystallized. The crystals were collected, washed well with water and recrystallized from a small quantity of ethanol to afford colorless needles. The product was characterized by the data given in Table 4.

Methyl 4-Methyl-2-(phthaloylglycyl)amino-2-pentenoate (VIIe). A solution of phthaloylglycyl chloride (2.5 g) in dry benzene (20 m*l*) was added drop by drop with vigorous stirring to a solution of methyl 4-methyl-2-amino-2-pentenoate (VIe, 1.8 g) at 20°C. After stirring for 3 hr, 30 m*l* of water was added to the resulting mixture and the insoluble substance was filtered off. The benzene layer was washed with water, dried over anhydrous sodium sulfate, and then evaporated. The residual viscous syrup crystallized gradually. Recrystallization from a small quantity of ethanol gave colorless needles, which were characterized as the expected phthaloylglycylamino compound by the data given in Table 4.

In an analogous manner, acylation of other α-aminocarboxylic esters (VIc and VId) was performed, and the corresponding α-phthaloylglycylamino esters (VIIc and VIId) were obtained in poor yields (Table 4).

Ethyl 3-Methoxy-2-*N*-(phthaloylglycyl)hydroxyaminopentanoate (VIIIb). Phthaloylglycyl chloride (0.65 g) was added portionwise with vigorous stirring to ethyl 2-hydroxyamino-3-methoxypentanoate (IVb, 0.6 g) suspended in a solution of sodium hydrogencarbonate (0.3 g) in water (10 m*l*) at room temperature. After stirring for 30 min, a viscous syrup began to separate. On being allowed to stand overnight at room temperature, the syrup became crystalline. The crystals were collected and washed with water. Recrystallization from ethanol afforded colorless prisms (Table 4).

Ethyl 3-Methoxy-4-methyl-2-*N*-(phthaloylglycyl)-hydroxyaminopentanoate (VIIIf). A solution of phthaloylglycyl chloride (1.1 g) in dry benzene (10 m*l*) was added drop by drop, with vigorous stirring, to a solution of ethyl 2-hydroxyamino-3-methoxy-4-methylpentanoate (IVf, 1 g) in dry benzene (10 m*l*) in the presence of pyridine (0.42 g) at room temperature. After stirring for 2 hr, 30 m*l* of water was added to the resulting mixture. The mixture was allowed to stand overnight at room temperature and the insoluble substance was filtered off. The benzene layer of the filtrate was washed with water, dried over anhydrous sodium sulfate, and then evaporated. The residual viscous syrup was crystallized by successive treatment of a small quantity of ether and di-*n*-butyl ether. Recrystallization from petroleum ether (bp 70—120°C) afforded the expected acylated compound as colorless needles.

In an analogous manner, α-hydroxyaminocarboxylic ester (IVe) was treated with phthaloylglycyl chloride to afford the corresponding α-(phthaloylglycyl)hydroxyaminocarboxylic ester (VIIIe) in a poor yield (Table 4).

1,4-Dihydroxy-3,6-diisobutylidene-2,5-dioxopiperazine (IX). Methyl 2-hydroxyamino-3-methoxy-4-methylpentanoate (IVe, 8 g) was allowed to stand for two weeks at room temperature, during which the ester became viscous, and then a small amount of crystals separated out gradually. The mixture was treated with ether and the crystalline product was collected. Recrystallization from a small quantity of methanol afforded colorless prismatic needles (2.1 g, 42%), mp 250—251°C (decomp.), which turned dark purple with methanolic ferric chloride. ν_{max}^{KBr} 3250, 1775, 1720, 1635 and 1610 cm^{-1}. λ_{max}^{EtOH} 221.5 mμ (ε=3500), 265.5 (4800) and 349 (9000).

Found: C, 56.29; H, 7.58; N, 11.09%. Calcd for $C_{12}H_{18}N_2O_4$: C, 56.68; H, 7.14; N, 11.02%.

The authors are indebted to Miss Toshiko Aoyagi for elementary analyses.

BULLETIN OF THE CHEMICAL SOCIETY OF JAPAN VOL. 43 3224—3226 (1970)

Sugars Containing a Carbon-phosphorus Bond. II. Syntheses of Phosphinyl Sugars by the Michaelis-Arbuzov Reaction of Halogenated Sugars

Saburo INOKAWA, Yoshimi TSUCHIYA, Hiroshi YOSHIDA and Tsuyoshi OGATA*1

Department of Synthetic Chemistry, Faculty of Engineering, Shizuoka University, Johoku, Hamamatsu

(Received April 20, 1970)

3,5-*O*-Benzylidene-6-deoxy-6-diethoxyphosphinyl-1,2-*O*-isopropylidene-α-D-glucofuranose was prepared in an 80% yield by heating a solution of 3,5-*O*-benzylidene-6-deoxy-6-iodo-1,2-*O*-isopropylidene-α-D-glucofuranose (**1**) in an excess of triethyl phosphite (**5**). Similarly, 6-deoxy-6-diethoxyphosphinyl-1,2;3,4-di-*O*-isopropylidene-α-D-galactopyranose was prepared in a 95% yield from 6-deoxy-1,2;3,4-di-*O*-isopropylidene-α-D-galactopyranose (**2**), and (**5**); 5-deoxy-5-ethoxyphenylphosphinyl-1,2-*O*-isopropylidene-3-*O*-methyl-α-D-xylofuranose was prepared in a 90% yield from 5-bromo-5-deoxy-1,2-*O*-isopropylidenne-3-*O*-methyl-α-D-xylofuranose and diethyl phenylphosphonite; 3,5-*O*-benzylidene-6-deoxy-1,2-*O*-isopropylidene-6-(*N*,*N*′-tetraethyldiaminophosphinyl)-α-D-glucofuranose was prepared in a 44% yield from **1** and ethyl *N*,*N*′-tetraethylphosphorodiamidite (**7**); 6-deoxy-1,2;3,4-di-*O*-isopropylidene-6-(*N*,*N*′-tetraethyldiaminophosphinyl)-α-D-galactose was prepared in a 70% yield from **2** and **7**.

In the previous investigation,[1] sugars containing a carbon-phosphorus bond were synthesized by the photochemical addition of the phosphonates to the unsaturated sugars. This time, the Michaelis-Arbuzov reaction has been used in the preparation of the phosphorus sugars; the results will be reported here. As the halogenated sugars, 3,5-*O*-benzylidene-6-deoxy-6-iodo-1,2-*O*-isopropylidene-α-D-glucofuranose (**1**), 6-deoxy-6-iodo-1,2;3,4-di-*O*-isopropylidene-α-D-galactose (**2**), 5-bromo-5-deoxy-1,2-*O*-isopropylidene-3-*O*-methyl-α-D-xylofuranose (**3**), and 1-bromo-1-deoxy-2,3;4,5-*O*-isopropylidene-β-D-fructopyranose (**4**) were used, and as the phosphorus compounds, triethyl phosphite (**5**), diethyl phenylphosphonite (**6**), and ethyl *N*,*N*′-tetraethylphosphorodiamidite (**7**) were used. The structures of the products were determined by studying the NMR spectra and by elementary analyses.

Experimental

The infrared spectra were measured on a Hitachi-Perkin-Elmer 337 spectrophotometer. The nuclear magnetic resonance spectra were taken at 60 MHz on a Hitachi-Perkin-Elmer R-20 spectrometer, using tetramethylsilane as the internal reference. The thin-layer chromatogram were run on a silica-layer G[2]; phosphorus compounds were detected by spraying the plates with a cobalt chloride solution[3] and then by heating them. Periodic sampling and examination by thin-layer chromatography permitted the determination of the suitable reaction conditions for the preparation runs.

Materials. The 3,5-*O*-benzylidene-6-deoxy-6-iodo-1,2-*O*-isopropylidene-α-D-glucofuranose (**1**) was prepared by the method of Meyer and Reichstein;[4] mp 142°C. The 6-deoxy-6-iodo-1,2;3,4-di-*O*-isopropylidene-α-D-galactopyranose (**2**) was prepared by the method of Schmidt;[5] mp 72°C. The 5-bromo-5-deoxy-1,2-*O*-isopropylidene-3-*O*-methyl-α-D-xylofuranose (**3**) was prepared by the method of Inokawa *et al.*;[6] bp 67°C/0.2 mmHg. The 1-bromo-1-deoxy-2,3;4,5-*O*-isopropylidene-β-D-fructopyranose (**4**) was prepared in a 65% yield by heating 2.5 g of 2,3;4,5-di-*O*-isopropylidene-1-*O*-(*p*-toluenesulfonyl)-α-D-fructopyranose[7] and 2.0 g of lithium bromide in 20 ml of dimethylformamide at 150°C for 55 hr; mp 49—50°C[8] after sublimation. The triethyl phosphite (**5**)[9] was used after distillation. The diethyl phenylphosphonite (**6**)[10] and ethyl *N*,*N*′-tetra-

*1 This work was presented at the 23rd Annual Meeting of the Chemical Society of Japan, Tokyo, April 4, 1970.

1) K. Kumamoto, H. Yoshida, T. Ogata and S. Inokawa, This Bulletin, **42**, 3245 (1969).

2) Nakarai Chemicals, Ltd., Kyoto.

3) R. Donner and K. Lohs, *J. Chromatogr.*, **17**, 349 (1965).

4) A. S. Meyer and K. Lohs, *Helv. Chim. Acta*, **29**, 139 (1946).

5) O. Th. Schmidt, "Methods in Carbohydrate Chemistry," Vol I, ed. by R. L. Whistler and M. L. Wolfrom, Academic Press, New York and London (1962), p. 191.

6) S. Inokawa, H. Yoshida, C.-C. Wang and R. L. Whistler, This Bulletin, **41**, 1472 (1968).

7) S. B. Baker, *Can. J. Chem.*, **33**, 1460 (1955).

8) L. K. Dalton, *Aust. J. Chem.*, **19**, 445 (1966).

9) It was offered by Nippon Kagaku Kogyo, Ltd.

10) R. Schliebs, Ger. 1088955 (1959).

ethylphosphorodiamidite (**7**)[11] were prepared in the usual way.

3,5-*O*-Benzylidene-6-deoxy-6-diethoxyphosphinyl-1,2-*O*-isopropylidene-α-D-glucofuranose (8). A solution of 2.0 g of **1** in 20 ml of **5** was heated at 150°C for 5 hr under a stream of nitrogen. The solution was then concentrated *in vacuo*; the residue was dissolved in ether, washed with water, dried over sodium sulfate, and concentrated *in vacuo* to give, in an 80% yield (1.6 g), a pale yellow oil (practically pure). An analytical sample was obtained by the use of a high vacuum at 125°C/10^{-2}—10^{-3} mmHg; $[\alpha]_D^{29}$ +17.4° (*c* 13.3, carbon tetrachloride).

Found: C, 55.0; H, 6.98%. Calcd for $C_{19}H_{29}O_8P$: C, 54.8; H, 7.02%. The PMR data (carbon tetrachloride) were as follows: 2.7 (five-proton multiplets, C_6H_5–), 4.1 (one-proton doublet, $J_{1,2}$=3.7 Hz, H_1), 4.4 (one-proton singlet, Ph–CH=), 5.4—6.3 [eight-proton multiplets, H_2, H_3, H_4, H_5, (P–O–CH_2–)$_2$], 7.7 (two-proton quartet, $J_{6,P}$=18 Hz, $J_{5,6}$=8.0 Hz, $H_{6,6'}$), 8.6, 8.8 [six-proton singlets, overlapping with (P–O–C–CH_3)$_2$; C(CH_3)$_2$], and 8.8 [six-proton triplets, overlapping with C(CH_3)$_2$; (P–O–C–CH_3)$_2$].

6-Deoxy-6-diethoxyphosphinyl-1,2;3,4-di-*O*-isopropylidene-α-D-galactopyranose (9). A solution of 2.0 g of **2** in 20 ml of **5** was heated at 160° for 3 hr under a stream of nitrogen. The resulting solution was treated as has been described above to give, in a 95% yield (1.9 g), a pale yellow oil (practically pure). An analytical sample was obtained by high-vacuum distillation at 110°C/10^{-2}—10^{-3} mmHg; $[\alpha]_D^{19}$ −48.0° (*c* 10, carbon tetrachloride).

Found: C, 50.0; H, 7.81%. Calcd for $C_{16}O_8H_{29}P$: C, 50.2; H, 7.62%. The PMR data (chloroform-*d*) were as follows: 4.7 (one-proton doublet, $J_{1,2}$=4.0 Hz, H_1), 5.3—6.4 (eight-proton multiplets, H_2, H_3, H_4, H_5, (P–O–CH_2–)$_2$], 7.8—8.3 (two-proton qualtet, $J_{6,P}$=18 Hz, $J_{5,6}$=6.8 Hz, $H_{6,6'}$), and 8.4—8.9 (twelve-proton multiplets, C(CH_3)$_2$, (P–O–C–CH_3)$_2$].

5-Deoxy-5-ethoxyphenylphosphinyl-1,2-*O*-isopropylidene-3-*O*-methyl-α-D-xylofuranose (10). A solution of 10 g of **3** in 30 ml of **6** was heated at 160°C for 5 hr. The resulting solution was treated as has been described above, and the oil thus obtained was distilled *in vacuo* to give, in a 90% yield, a colorless oil; bp 160—161°/0.1 mmHg, $[\alpha]_D^{25}$ −45.3° (*c* 10, chloroform).

Found: C, 57.7; H, 7.05%. Calcd for $C_{17}H_{25}O_6P$: C, 57.3; H, 7.07%. The PMR data (carbon tetrachloride) were as follows: 2.0—2.7 (five-proton multiplets, C_6H_5–), 4.3 (one-proton doublet, $J_{1,2}$=3.4 Hz, H_1), 5.5—6.5 (five-proton multiplets, H_2, H_3, H_4, P–O–CH_2–), 6.8 (three-proton doublet, –OCH_3), 7.4—8.0 (two-proton multiplets, $H_{5,5'}$), 8.6, 8.8 [six-proton singlets, overlapping with P–O–C–CH_3; C(CH_3)$_2$], and 8.8 (three-proton triplets, overlapping with C(CH_3)$_2$, P–O–C–CH_3).

3,5-*O*-Benzylidene-6-deoxy-1,2-*O*-isopropylidene-6-(*N*,*N*′-tetraethyldiaminophosphinyl)-α-D-glucofuranose (11). A solution of 1 g of **1** in 10 ml of **7** was heated at 140°C for 24 hr under a stream of nitrogen, and the solution was then concentrated *in vacuo*; the residue was dissolved in chloroform, washed with an aqueous sodium carbonate solution and water, dried over sodium sulfate, and concentrated *in vacuo*; the residue was extracted with petroleum ether under reflux, and the extract was evaporated *in vacuo* to give, in a 44% yield (0.5 g), a brown oil. High-vacuum distillation gave a pale yellow oil, pure enough for a NMR measurement but not enough for an elementary analysis; bp 120—130°C/10^{-2}—10^{-3} mmHg, $[\alpha]_D^{15}$ −55.5° (*c* 0.9, chloroform). The PMR data (chloroform-*d*) were as follows: 2.4—2.8 (five-proton multiplets, C_6H_5–), 4.0 (one-proton doublet, $J_{1,2}$=3.8 Hz, H_1), 4.4 (one-proton singlet, Ph–CH=), 5.3—5.6 (four-proton multiplets, H_2, H_3, H_4, H_5), 6.7—7.3 [eight-proton multiplets, [N–(CH_2–)$_2$]$_2$], 7.5—8.0 (two-proton multiplets, $H_{6,6'}$), 8.5, 8.7 [six-proton singlets, overlapping with [N–(C–CH_3)$_2$]$_2$; C(CH_3)$_2$], and 8.9 [twelve-proton triplets, overlapping with C(CH_3)$_2$; [N–(C–CH_3)$_2$]$_2$].

6-Deoxy-1,2;3,4-di-*O*-isopropylidene-6-(*N*,*N*′-tetraethyldiaminophosphinyl)-α-D-galactopyranose (12). A solution of 1 g of **2** in 10 ml of **7** was heated at 150—160°C for 5 hr under a stream of nitrogen. The resulting solution was treated as has been described above to give, in a 70% yield (0.7 g), a brown oil. High-vacuum distillation gave a pale yellow oil, pure enough for a NMR measurement but not enough for an elementary analysis; bp 90—100°C/10^{-2}—10^{-3} mmHg, $[\alpha]_D^{15}$ +18.5° (*c* 1.2, chloroform). The PMR data were as follows: 4.6 (one-proton doublet, $J_{1,2}$=4.4 Hz, H_1), 5.4—6.0 (four-proton multiplets, H_2, H_3, H_4, H_5), 6.7—7.3 [eight-proton multiplets, [N-(CH_2–)$_2$]$_2$], 7.7—8.3 (two-proton multiplets, $H_{6,6'}$), and 8.4—9.1 [eighteen-proton multiplets, C$(CH)_{32}$, [N–(C–CH_3)$_2$]$_2$].

Results and Discussion

The Michaelis-Arbuzov reaction is one of the most important reactions making a phosphorus-carbon bond, but the application of this reaction to carbohydrate chemistry has been made in only a few reports.[12] When a solution of the halogenated sugars, **1, 2, 3,** or **4** in an excess of **5** was heated at 150—160°C for several hr under a stream of nitrogen, **1, 2,** and **3** gave the corresponding phosphonyl sugars, **8, 9,** and **10,** in a good yield.

In the case of **4**, however, the reaction did not proceed practically.[13] The reason for this seems to be the steric effect of two isopropylidene groups and the electron-withdrawing effect from the anomeric acetal group, which would hinder the cleavage of the C-Br bond. For the same reason, the formation of **4** from the corresponding tosyl compounds with lithium bromide in dimethylformamide was very slow, as has been shown in the Experimental part. The reaction of **3** with **8** was also carried out with ease to give **10** in a good yield. The structures of **8**, **9**, and **10** were established by elementary analyses and by studies of the NMR

11) A. Michaelis, *Ann. Chem.*, **326**, 160 (1903).

12) R. L. Whistler and C.-C. Wang, *J. Org. Chem.*, **33**, 4455 (1968); A. Holy, *Tetrahedron Lett.*, **1967**, 881.

13) H. Muller and T. Reichstein, *Helv. Chim. Acta*, **21**, 263 (1938); J. M. Williams, "Rodd's Chemistry of Carbon Compounds," Vol. I-F, ed. by S. Coffey, Elsevier Publishing Co., Amsterdam, London, New York (1967), p. 403.

TABLE 1. THE FORMATATION OF SUGARS CONTAINING A CARBON-PHOSPHORUS BOND BY THE MICHAELIS-ARUBUZOV REACTION

Sugar moieties	Halogenated sugars	Phosphorus compounds	Products	Yields (%)	$[\alpha]_D$ (temp.)
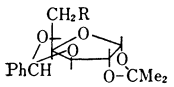	[1] (R=I)	$(EtO)_3P$ [5]	[8] (R=P(O)(OEt)$_2$)	80	+17.4° (29°C) (c 13.3, CCl_4)
	[1] (R=I)	$EtOP(NEt_2)_2$ [7]	[11] (R=P(O)(NEt$_2$)$_2$)	44	+18.5° (15°C) (c 1.2, $CHCl_3$)
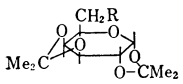	[2] (R=I)	[5]	[9] (R=P(O)(OEt)$_2$)	95	−48.0° (19°C) (c 10, CCl_4)
	[2] (R=I)	[7]	[12] (R=P(O)(NEt$_2$)$_2$)	70	−55.5° (15°C) (c 0.9, $CHCl_3$)
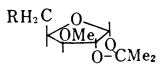	[3] (R=Br)	$PhP(OEt)_2$ [6]	[10] (R=PPh(OEt))	90	−45.3° (25°C) (c 10, $CHCl_3$)
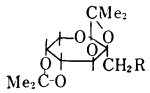	[4] (R=Br)	[5]	no reaction		

spectra. The resonance of $H_{6,6'}$ in **8** and **9** was shifted to a higher field and showed a characteristic multiplet-shape upon P–H coupling. It was the same concerning the resonance of $H_{5,5'}$ in **10**. When a solution of **1**, or **2** in an excess of **7** was heated at 140—160°C for several 1 hr under a stream of nitrogen, the solution became brown, but **11** or **12** was afforded in a moderate yield. The structures were established by studies of the NMR spectra. The results described above are summarized in Table 1.

The authors express their sincere thanks to Professor R. L. Whistler of Purdue University for his continued interest in this work. They are also greateful to Nippon Kagaku Kogyo Ltd. for supplying them phosphorus compounds.

BULLETIN OF THE CHEMICAL SOCIETY OF JAPAN VOL. 43 3227—3231 (1970)

Intramolecular Hydrogen Bonds. XV.[1] Intramolecular Interaction in *N*-Alkylaminoalkanonitriles

Nobuo Mori, Yoshihiro Asabe, Junko Tatsumi and Yojiro Tsuzuki

Department of Chemistry, Science University of Tokyo, Shinjuku-ku, Tokyo

(Received April 27, 1970)

The ν_{NH} values of monomeric alkylmethylamines in carbon tetrachloride solutions are associated with the rotational isomerism about the N–C bond. In the series of *N*-alkylaminoalkanonitriles, the intramolecular hydrogen-bonding interaction of the NH group with the π-electrons of the CN group was deduced on the basis of the ν_{NH} values and a model examination; in the α-series, the NH group probably interacts exclusively, and in the β-series it partially interacts, but in the γ-series it shows no interaction.

There have been many reports on the intramolecular hydrogen bondings in which a hydroxyl group participates;[2] this subject has, indeed, hitherto been dealt with in this series of studies. The results have prompted us to investigate the intramolecular hydrogen bonding in which an amino group parcipitates, since the situation should be very similar in the two series of compounds.

The literature contains scant information on the intramolecular hydrogen bonding involving a secondary amino group. Several reports have, however, recently been published on the rotational isomerism around the N–C bond in *N*-alkylanilines[3] and on the intramolecular interaction between the NH group and the π-electrons in ω-secondary amino-alkylbenzenes;[3,4] the results are essentially omparable with those of the corresponding hydroxyl compounds.

The present paper will report on the rotational isomerism in alkylmethylamines and the intramolecular interaction between the NH group and the π-electrons of the CN group in *N*-alkylaminoalkanonitriles, and the results will be compared with those of the corresponding ω-hydroxyalkanonitriles previously reported on.[5]

Experimental

Samples. The dimethylamine was liberated from commercial aqueous dimethylamine, and the other alkylmethylamines were obtained by the reported method.[6] The α-*N*-alkylaminoalkanonitriles were prepared from the corresponding cyanohydrines by treating them with monoalkylamines in methanol.[7] The β-*N*-alkylaminopropionitriles were synthesized by the reaction of acryronitrile with alkylamines in methanol.[8] The γ-*N*-methylaminobutyronitrile was obtained by the reaction of γ-bromobutyronitrile with methylamine.[9] All the samples were purified through fractional distillation in an atmosphere of nitrogen; their physical constants agreed with those reported in the literature, and their purity was further proved by their gas chromatograms and/or NMR spectra. Compounds **7**, **8**, **9**, **10**, and **15** have not been reported previously; their analytical data are summarized in Table 2.

The carbon tetrachloride was fractionally distilled over phosphorus pentoxide.

Infrared Measurement. This was carried out at *ca.* 20°C, unless otherwise noted, in the same manner as has previously been described,[1] using a grating infrared spectrometer, Model DS-403G, of the Japan Spectroscopic Co.; the spectrometer was equipped with cells with a path-length of 5.0 cm. Each amine was weighed and dissolved in carbon tetrachloride in a concentration of 0.005 mol/*l* or less immediately before the measurement. The NMR examination of some amine solutions at a higher concentration indicated that no significant reaction of the amines with the solvent occurred during the period required for the infrared measurement.

Results and Discussion

The NH stretching absorption spectra of four alkylmethylamines are shown in Fig. 1A. The spectrum of ethylmethylamine is unsymmetric, with a widely-broadened part being centered at 3347

1) Part XIV: N. Mori, Y. Asano and Y. Tsuzuki, This Bulletin, **42**, 488 (1969).

2) M. Tichy, "Advances in Organic Chemistry, Method and Results," Interscience Publishers, New York (1965), Vol. 5, p. 115.

3) M. Ōki and K. Mutai, This Bulletin, **33**, 784 (1960).

4) M. Ōki and K. Mutai, *ibid.*, **38**, 387 (1965); **39**, 809 (1966); **38**, 393 (1965).

5) N. Mori, S. Omura, H. Yamakawa and Y. Tsuzuki, *ibid.*, **38**, 1627 (1965).

6) E. H. Woodruff, J. P. Lambooy and W. E. Burt, *J. Amer. Chem. Soc.*, **62**, 922 (1940).

7) A. H. Cooke and S. F. Cox, *J. Chem. Soc.*, **1949**, 2334.

8) D. S. Tarbell, N. Shakespeare, C. J. Claus and J. F. Bunnett, *J. Amer. Chem. Soc.*, **68**, 1217 (1946).

9) W. Keil, *Hoppe-Seyler's Z. Physiol. Chem.*, **171**, 245 (1927).

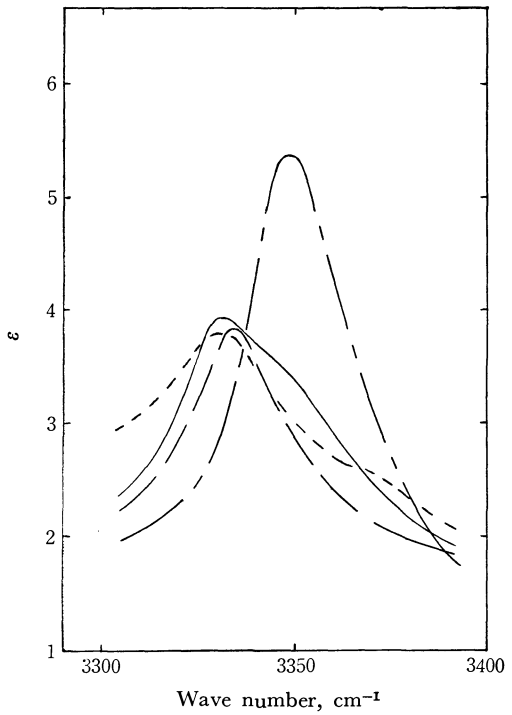

Fig. 1(A). NH spectra of alkylmethylamines.
Alkyl: methyl (— — —), ethyl (———), isopropyl (— —) and *t*-butyl (-----)

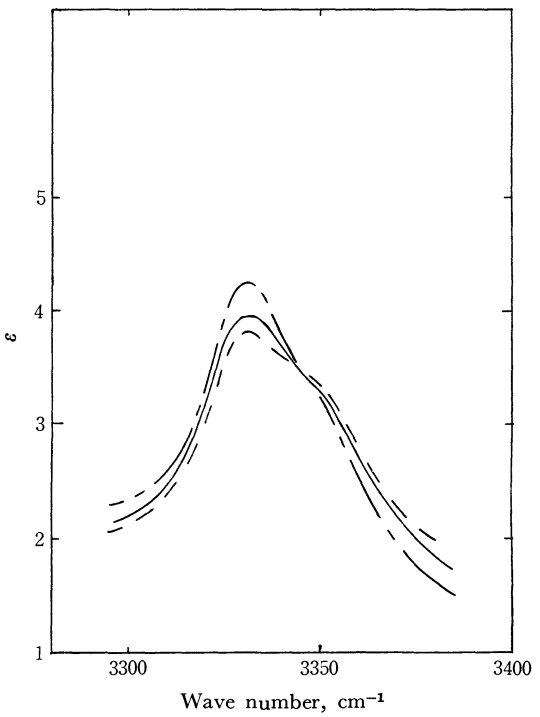

Fig. 1(B). Temperature dependence of the NH spectrum of ethylmethylamine.
10°C: — — — 20°C: ——— 36°C: -----

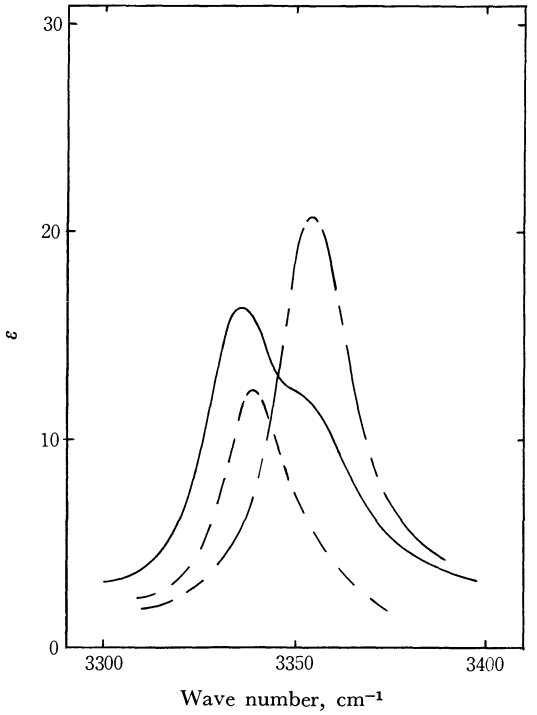

Fig. 1(C). NH spectra of α-(*N*-alkylamino)-acetonitriles.
Alkyl: methyl (— — —), ethyl (———) and isopropyl (-----).

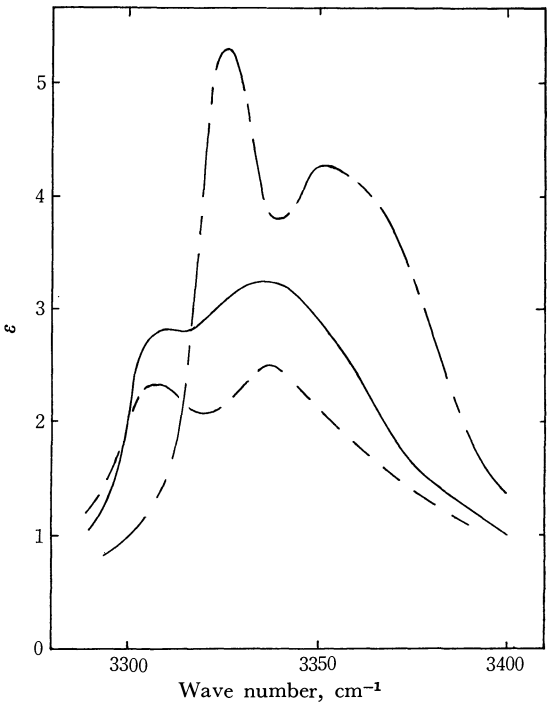

Fig. 1(D). NH spectra of β-(*N*-alkylamino)-propionitriles.
Alkyl: methyl (— — —), ethyl (———) and isopropyl (-----).

cm^{-1}, while those of dimethylamine and isopropylmethylamine are almost symmetrical. *t*-Butylmethylamine shows a broad adsorption.

A more detailed inspection of the band-shape was not performed because of the very low ε values. Moreover, even if it were made, it would not permit a confident discussion of the results. Accordingly, we will mainly discuss the peak frequencies, insofar as there is no intense shoulder or broadening. The apparent spectral data are summarized in Table 1.

Table 1. The spectral properties of ν_{NH} of alkylmethylamines, R-NH-CH_3

No.	R	ν^{a}_{max}, cm^{-1}	ε^{a}
1	CH_3	3348	5.4
2	C_2H_5	3347* 3331	3.9
3	$(CH_3)_2CH$	3334	3.8
4	$(CH_3)_3C$	3330	3.8

* Value at the center of the broadened part.

The unsymmetry of the spectrum of ethylmethylamine can not be caused by any molecular association, since no association explains the symmetry of the spectra of the other amines examined under the same conditions. The peak frequencies and the shapes of the spectra vary with the type of alkyl substituent (R); hence, the concept of the rotational isomerism about the C-N axis may be valid in explaining these facts, as has been made for a similar phenomenon observed in aliphatic alcohols[10] and in *N*-alkylanilines.[3]

According to the projection along the C_R-N bond (C_R is the carbon atom of an alkyl group, R, attached to the nitrogen atom), there are three possible types of steric environment around the N-H group, one or two of which can be taken by each amine depending on the type of R and on the rotational position to be favored. Fig. 2 shows the so-called Newman projection along the C_R-N bond, in which the nitrogen atom is described on the upper side, the circle denoted the C_R atom, and C is the methyl group.

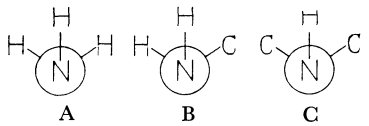

Fig. 2. Three types of steric environment around the NH group in alkylmethylamines.

In this model examination, the following three assumptions were made; (1) the tricovalently-bound nitrogen atom has a tetrahedron-like structure, with the N atom at the center of the tetrahedron and with the four electron orbitals pointing towards the vertices, since such a structure is generally seen in most aliphatic, sterically-uncrowded amines; (2) the steric size of the lone pair of electrons on the nitrogen atom is expected to be much smaller than that of any alkyl group, and almost equal to that of the hydrogen atom, on the basis of the conformational analysis of piperidine compounds,[11] and (3) the molecule takes a skew form, but not an eclipsed one. Hence, the hydrogen atom of the NH group in dimethylamine and also in *t*-butylmethylamine must be in the same steric environment, A or C respectively, because it always exists between two of the three hydrogen atoms or methyl groups on C_R, no matter in what rotational position it exists.

When the R group is ethyl, on the other hand, there are two possible steric environments, A and B. Similarly, two environments, B and C, are possible for the NH group of isopropylmethylamine. The spectral data seem to indicate that the NH group of ethylmethylamine exists in the environment B in a major proportion. This can probably be attributed to the steric effect of the methyl group for the following reasons: in Fig. 3, which shows the Newman projection along the N-C_R bond in each amine, dimethyl- and *t*-butylmethylamine can take only one conformation, I or IV respectively. Ethylmethylamine can exist in three conformations, IIa—c; IIa corresponds to the environment B and may be sterically preferable, while IIb and IIc may be less preferable. This interpretation can be suppoted by measuring the temperature dependence of the relative intensity of the two observed band-components. As Fig. 1B shows, the intensity of the maximum absorption relative to the broadened part decreases with an increase in the temperature. This phenomenon agrees with the thermodynamical generalization that the proportion of a stable conformation becomes higher at a lower temerature. On the other hand, isopropylmethylamine can exist in three conformations, IIIa—c. The two of them,

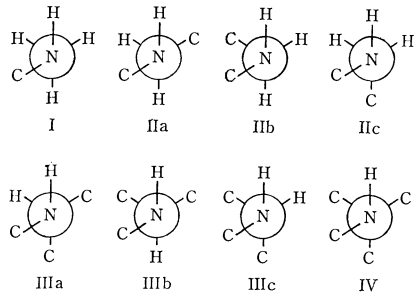

Fig. 3. Conformations about the N-C_R bond in alkylmethylamines.

10) M. Ōki and H. Iwamura, This Bulletin, **32**, 950 (1959).

11) N. L. Allinger and J. C. Tai, *J. Amer. Chem. Soc.*, **87**, 1277 (1965); N. L. Allinger, J. G. D. Carpenter and F. M. Karkowski, *ibid.*, **87**, 1232 (1965); J. B. Lambert and R. G. Keske, *ibid.*, **88**, 620 (1966); J. B. Lambert, R. G. Keske, R. E. Carhart and A. P. Jovanovich, *ibid.*, **89**, 3761 (1967).

Table 2. Physical properties, nitrogen-analytical data and NH-spectral data of *N*-alkylaminoalkanonitriles

No.	RNH-CR_1R_2-CN			Bp, °C/mmHg	n_D^{18}	N % Found (Calcd)	ν_{NH}^a, cm^{-1}	$\Delta\nu_{1/2}^a$, cm^{-1}	ε^a
	R	R_1	R_2						
5	CH_3	H	H	60/18	1.4221		3355	26	21
6	C_2H_5	H	H	69/19	1.4260		3355* 3336	49	17
7	$(CH_3)_2CH$	H	H	74/20	1.4264	29.05 (28.55)	3338	29	13
8	CH_3	CH_3	H	61/28.5	1.4193	33.52 (33.30)	3353* 3343	32	13
9	C_2H_5	CH_3	H	68/24	1.4224	28.90 (28.55)	3343* 3328	37	10
10	$(CH_3)_2CH$	CH_3	H	64/19	1.4229	25.11 (24.98)	3329	30	10
11	CH_3	CH_3	CH_3	59/24	1.4186		3347	30	7
12	C_2H_5	CH_3	CH_3	60/19	1.4217		3324	28	7
	RNH-$(CH_2)_n$-CN								
	R		n						
13	CH_3		2	79/20	1.4328		3356 3326		4.3 5.3
14	C_2H_5		2	81/19	1.4336		3336 3307		3.2 2.8
15	$(CH_3)_2CH$		2	88/20	1.4325	24.86 (24.98)	3337 3307		2.5 2.3
16	CH_3		3	97—98/60			3371	52	5.1

* Value at the center of the broadened part.

IIIa and IIIb, may be indistinguishable in steric preference from each other and correspond to the environments, B and C respectively. Therefore, the observed single NH bond seems to be due to the NH species in both environments, rather than in either of them. In fact, the band has been essentially identical with those observed at 10 and 40°C.

α-(*N*-Alkylamino)-alkanonitriles. Some NH spectra are shown in Fig. 1C, and the apparent spectral data are summarized in Table 2. The spectra of *N*-alkylaminoacetonitriles (**5**—**7**) are similar in general shape to, but are somewhat different in peak frequency from, those of the alkylmethylamines. When the alkyl group, R, is methyl or isopropyl, they show a single, almost symmetrical NH spectrum. When R is ethyl, the spectrum is widely broadened on the higher-frequency side. This may be explained in terms of the same alkyl effect as has been suggested as the origin of a similar phenomenon observed in alkylmethylamines, since the rotational isomerism about the C_R–N bond can be illustrated by Fig. 3, in which N–CH_3 is replaced by N–CH_2CN. On the other hand, in the projection along the C_α–N bond, all the acetonitriles predominantly prefer the same conformation, V, containing R and CN in a *trans* relationship, as is shown in Fig. 4. This conformer would involve an additional stabilization, one which should result from an attractive interaction which is probable between the NH group and the π-electrons of the CN group. As for the presence of the interaction, no evidence can be obtained from the spectral data of ν_{NH} and ε, and it can not, of course, be ascertained whether the interaction is of the usual charge-transfer type or of the electrostatic-attraction type. The observed ε values, much higher than those of alkylmethylamines, can not provide decisive evidence for the presence of the interaction, because both types of interaction and also the electron-attractive CN group would serve to increase the N–H bond moment and, thereby, to increase the ε value. The presence of the interaction is yet suggested in view of a situation similar to that in α-cyanohydrines, in which the interaction between the OH and the CN group results in no significant lowering of the OH stretching frequency.[5]

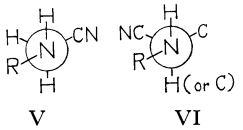

Fig. 4. Projection along the C_α–N bond in α-*N*-alkylaminoalkanonitirles.

In α-(*N*-alkylamino)-propionitriles (**8**—**10**) and -isobutyronitriles (**11** and **12**), the peak frequencies are lower by *ca.* 10 cm^{-1}, irrespective of the number of α-methyl groups, than those of the corresponding

alkylaminoacetonitriles. This lowering seems to be attributable to the steric effect of the α-methyl groups, and its independence of the number of methyl groups seems to suggest that both series of nitriles involve an essentially equal steric environment around the N–H group when they contain the same R. These suggestions can be supported by an examination of their models; in the rotation around the C_R–N bond, the steric environment around the NH group is again as is shown in Fig. 2. On the other hand, the conformation, VI, about the C_α–N bond, which is shown in Fig. 4, may be preferable for both nitriles, if it is assumed that; (1) the CN group is much smaller in steric size than the methyl,[12] and that, hence, CH_3 and R are preferably *trans*, and (2) the interaction between the NH group and the π-electrons of the CN group is possible. This conformation contains one more methyl group skew to the NH group than does the conformation V of the alkylaminoacetonitriles. If the presence of this methyl group is responsible for the lowering of *ca.* 10 cm^{-1} in the NH frequency, the conformation VI may contribute to a major component of the band. Consequently, the above assignments can be summarized as in Table 3; the combination of the forms A and D, for example, gives the ν_{NH} of 3355 cm^{-1}.

Table 3. Relationship between the NH frequencies and the steric and/or interacting conditions

Projection along the N–C_R Bond / Projection along the N–C_α Bond		A	B
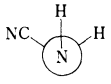	D	3355	3336
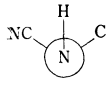	E	3345	3328

12) N. L. Allinger and W. Szkryblo, *J. Org. Chem.*, **27**, 460 (1962); B. Rickborn and F. R. Jensen, *ibid.*, **27**, 4606 (1962).

β-(*N*-Alkylamino)-propionitriles (13—15) and γ-(*N*-Methylamino)-butyronitrile (16). The NH spectra of the former contain apparently two resolved bands with a spacing of *ca.* 30 cm^{-1}, independent of the type of alkyl, as Fig. 1D shows; the lower and the higher frequency bands may be due to the interacted and the free NH species respectively. In the projection along the C_α—C_β bond, the CN and the NH group can be in a skew (VII) or *trans* relationship (VIII), as is shown in Fig. 5. In the skew form VII, the NH group can interact with the CN group, while most of the free NH species should exist in the sterically preferable *trans* form VIII.

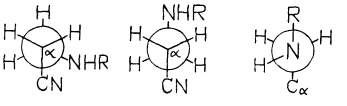

VII VIII IX

Fig. 5. Projection along the C_α–C_β bond (forms VII and VIII) and along the N–C_β bond (form IX).

On the other hand, the projection along the N–C_β bond shows that the both interacted and free NH groups must be located in a position skew to the C_α atom in Form IX, which is sterically preferable. Accordingly, the difference in frequency among the alkylaminopropionitriles depends mainly on the type of R and may again be explained in terms of the same steric effect of R as that which has been mentioned above in the case of the α-alkylaminonitriles.

Finally, the γ-methylamino group does not interact with the nitrile group, probably because of the thermodynamically more difficult formation of a largering through interaction. The same phenomenon was observed in γ-hydroxybutyronitrile.[5]

BULLETIN OF THE CHEMICAL SOCIETY OF JAPAN VOL. 43 3232—3236 (1970)

Reactions between β-Propiolactone and Dialkyl Dimethylphosphoramidite-Ambident Character of β-Propiolactone and of Dialkyl Dimethylphosphoramidite

Jugo KOKETSU,*1 Seiji Kojima and Yoshio ISHII

Department of Synthetic Chemistry, Faculty of Engineering, Nagoya University, Nagoya

(Received April 30, 1970)

The reactions between dialkyl dimethylphosphoramidite, $Me_2NP(OR)_2$, and β-propiolactone were carried out in various solvents at 80°C. Two kinds of reaction products were separated on a silica gel by elution with benzene-ethanol (4 : 1 v/v). The first species eluted was *N,N*-dimethyl-*O*-alkyl 2-alkoxycarbonylethylphosphoramidate, $(RO)P(O)(NMe_2)CH_2CH_2CO_2R$. The fraction having lower R_f value contained dialkyl 2-*N,N*-dimethylcarbamoylethylphosphonate, $(RO)_2P(O)CH_2CH_2CONMe_2$. The reaction mechanism is discussed from kinetic study.

During the course of studies on the reactions of aminophosphines, we found that aminophosphines showed an ambident nature in their reactions with various kinds of electrophilic reagents, such as phenyl cyanate,[1] alkyl benzenesulfonate,[2] dialkyl sulfates,[2] acetic anhydride,[3] and cyclic carbonate esters.[4] On the other hand, β-propiolactone is well known to be cleaved through either alkyl-oxygen bond or acyl-oxygen bond in the reactions with various nucleophilic reagents. The mode of ring-opening of β-propiolactone depends upon the nature of nucleophiles. Therefore, in the reaction between aminophosphine and β-propiolactone, several reaction products would be obtained.

McConnell and Coover[5] reported that β-propiolactone reacted with trialkyl phosphite to give dialkyl 2-alkoxycarbonylethylphosphonate. This results from the attack of the trivalent phosphorus atom on the β-carbon atom of β-propiolactone followed by Arbuzove-like rearrangement, as shown by the following equation.

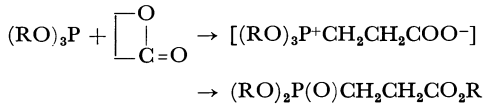

$$(RO)_3P + \text{β-propiolactone} \rightarrow [(RO)_3P^+CH_2CH_2COO^-] \rightarrow (RO)_2P(O)CH_2CH_2CO_2R \quad (1)$$

They also found[6] that acyl-oxygen bond fission occured in the reaction with dialkylphosphite:

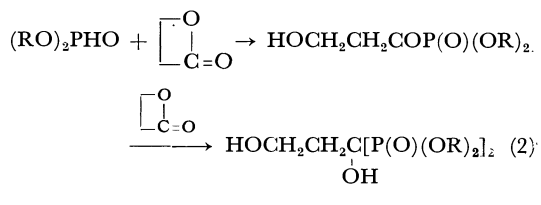

$$(RO)_2PHO + \text{β-propiolactone} \rightarrow HOCH_2CH_2COP(O)(OR)_2 \xrightarrow{\text{β-propiolactone}} HOCH_2CH_2C[P(O)(OR)_2]_2 \quad (2)$$

As regards the reaction of β-propiolactone with dialkyl dialkylphosphoramidite and alkyl tetraalkylphosphorodiamidite, they disclosed in U. S. Patent[7] that the products obtained were *N,N*-dialkyl-*O*-alkyl 2-alkoxycarbonylethylphosphoramidate ($n=2$ in Eq. (3)) and *N,N,N',N'*-tetraalkyl 2-alkoxycarbonylethylphosphonic diamide ($n=1$ in Eq. (3)), respectively, and that the P–N bond was not cleaved at all.

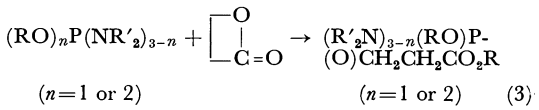

$$(RO)_nP(NR'_2)_{3-n} + \text{β-propiolactone} \rightarrow (R'_2N)_{3-n}(RO)P(O)CH_2CH_2CO_2R \quad (n=1 \text{ or } 2) \quad (n=1 \text{ or } 2) \quad (3)$$

However, we found that diphenyl dimethylphosphoramidite reacted with β-propiolactone to give *N,N*-dimethylacrylamide and undistillable polymer containing P(O), P–O–Ph, and P–O–P groups, and that in the reaction of β-propiolactone with *N,N*-dimethyl diphenylphosphinous amide, poly-β-propiolactone was obtained quantitatively.[8]

*1 Present address: Department of Synthetic Chemistry, Faculty of Engineering, Nagoya University, Furocho, Chikusa-ku, Nagoya.

1) J. Koketsu, S. Sakai and Y. Ishii, *Kogyo Kagaku Zasshi*, **72**, 2503 (1969).

2) J. Koketsu and Y. Ishii, This Bulletin, **34**, 2527 (1970).

3) J. Koketsu, S. Sakai and Y. Ishii, *Kogyo Kagaku Zasshi*, **73**, 205 (1970).

4) J. Koketsu, S. Sakai and Y. Ishii, *ibid.*, **73**, 201 (1970).

5) R. L. McConnell and H. W. Coover, Jr., *J. Amer. Chem. Soc.*, **78**, 4453 (1956).

6) R. L. McConnell and H. W. Coover, Jr., *ibid.*, **78**, 4450 (1956).

7) R. L. McConnell, H. W. Coover, Jr., and K. Tenn, U.S. 3121105 (1964).

8) J. Koketsu, S. Sakai and Y. Ishii, Preprint of Autumn Meeting of the Chem. Soc. of Japan, (Nagoya, 1969), p. 136.

$$(PhO)_2PNMe_2 + \begin{bmatrix} -O \\ | \\ -C=O \end{bmatrix} \rightarrow [(PhO)_2POCH_2CH_2\text{-}CONMe_2]$$

$$\rightarrow Me_2NCOCH{=}CH_2 + \text{"polymer"} \quad (4)$$

$$Ph_2PNMe_2 + \begin{bmatrix} -O \\ | \\ -C=O \end{bmatrix} \rightarrow [Ph_2P^+(NMe_2)CH_2CH_2CO_2^-]$$

$$\rightarrow -(CH_2\,CH_2CO_2)-_n \quad (5)$$

It seemed worthwhile to reinvestigate the reaction between β-propiolactone and dialkyl dimethylphosphoramidite in order to elucidate the discrepancies between the above results.

Experimental

Commercial β-propiolactone was distilled before use. All the solvent were thoroughly dried over calcium hydride and distilled before use. The reactions and measurements of physical constants of the products were carried out under dry nitrogen. Infrared and NMR spectra were measured on a Nippon Bunko IR 403G Spectrometer and a Japan Electron Minimer spectrometer. Thin-layer chromatography was carried out on 250 mμ thick silica gel layer by using benzene - ethanol (4 : 1 v/v). Column chromatography was performed in a column 50 cm long (ratio of column length to diameter=20 : 1). Into the column filled with 40 g of 100 mesh silica gel (Mallinckrodt Chemical Works) was put 1—2 g of samples by the wet method and eluted by benzene - ethanol (4 : 1 v/v).

Synthesis of Dialkyl Dimethylphosphoramidites. To a solution of lithium alkoxide, prepared from the corresponding alcohol and *n*-butyllithium in petroleum ether, an equimolar amount of Me_2NPCl_2 was added slowly with ice-cooling. After stirring for 30 min at room temperature, the mixture was refluxed for 1 hr. Separation of lithium chloride and removal of the solvent gave crude phosphoramidite which was purified by column-distillation. Boiling points and the yields of the phosphoramidites are shown in Table 1.

Table 1. Dialkyl dimethylphosphoramidites

Compound		Bp (°C/mmHg)	Yield (%)
$(i\text{-PrO})_2PNMe_2$	Ia	62—65/7.0	75.5
$(s\text{-Bu})_2PNMe_2$	Ib	47—52/3.5	78.4
$(n\text{-PrO})_2PNMe_2$	Ic	75—84/5.4	73.0
$(EtO)_2PNMe_2$	Id	40—48/12.0	55.6

Reaction of $(i\text{-PrO})_2PNMe_2$ (Ia) with β-Propiolactone. β-Propiolactone (1.5 g, 21 mmol) was added to a solution of Ia (40 g, 20.9 mmol) in 40 m*l* of benzene, and the mixture was allowed to stand for 30 hr at 80°C. Completion of the reaction was confirmed by means of IR absorption spectrum. After removal of the solvent, a fraction having boiling point range of 50—100°C/0.007 mmHg was obtained in 75% yield (4.28 g). The fraction showed two spots on thin-layer chromtography at R_f=0.62 and 0.50. By column chromatographic treatment on silica gel, two species II and III were obtained. The first species II was identified as *N,N*-dimethyl-*O*-isopropyl 2-isoproxycarbonylethylphosphoramidate, yield 2.60 g (45% based on Ia), and the other III as diisopropyl 2-*N,N*-dimethylcarbamoylethylphosphonate, yield 1.67 g (29% based on Ia), by their NMR and IR spectra, respectively, shown in Tables 2 and 3, and by their elemental analyses.

II: Found: C, 49.26; H, 9.30; P, 11.53%. Calcd for $C_{11}H_{24}NO_4P$: C, 49.80; H, 9.12; P, 11.67%. III: Found: C, 49.74; H, 9.38; P, 11.59%. Calcd for $C_{11}H_{24}NO_4P$: C, 49.80; H, 9.12; P, 11.67%.

Reaction of $(s\text{-BuO})_2PNMe_2$ (Ib) with β-Propiolactone. The reaction betwene Ib (3.60 g, 16.2 mmol) and β-propiolactone (1.17 g, 16.2 mmol) was carried out in a similar way by refluxing their mixture in 30 m*l* of benzene for 46 hr. After the reaction was over, the reaction mixture was distilled under reduced pressure to give a fraction having the boiling point range of 39—110 °C/0.01 mmHg. By column chromatographic treatment on silica gel, two species IV and V were obtained. The first species IV eluted was proved to be *N,N*-dimethyl-*O*-*s*-butyl 2-*s*-butoxycarbonylethylphosphoramidate, yield 2.41 g (49% based on Ib), and the other V to be di-*s*-butyl 2-*N,N*-dimethylcarbamoylethylphosphonate, yield 1.52 g (31% based on Ib), by their spectral data shown in Tables II and III, and by elemental analyses.

IV: Found: C, 52.64; H, 10.19%. Calcd for $C_{13}H_{28}NO_4P$: C, 53.23; H, 9.62%. V: Found: C, 52.43; H, 9.82; P, 10.49%. Calcd for $C_{13}H_{28}NO_4P$: C, 53.23; H, 9.62; P, 10.91%.

Reactions of $(n\text{-PrO})_2PNMe_2$ (Ic) and $(EtO)_2PNMe_2$ (Id) with β-Propiolactone. The reaction between Ic (4.00 g, 21 mmol) and β-propiolactone (1.50 g, 20 mmol) was carried out by refluxing the benzene solution (40 m*l*) for 51 hr. Distillation of the reaction mixture gave a fraction which had a boiling point range of 39—119°C/0.02 mmHg (4. 91 g, 85% based on Ic). This distillate exhibited strong IR absorption at 1740 and 1658 cm^{-1} in equal intensity, which could be assigned to the stretching frequencies of an ester carbonyl and an amide carbonyl group, respectively. Other strong absorption bands appeared at 1245 (P=O) and 990 cm^{-1} (P–O–C). In the NMR spectrum, there were a doublet at τ 7.50 (J=10 Hz) which could be ascribed to P–NMe_2 protons, and two singlets at τ 7.45 and τ 7.60 assignable to –$CONMe_2$. However, when the reaction product was chromatographed on silica gel, it decomposed to various species such as di-*n*-propyl phosphite, a polymer which contained phosphoryl group and unidentified substances.

The same phenomenon as that of the above experiment was observed in the reaction of $(EtO)_2PNMe_2$ (Id) with β-propiolactone, and no identified product was obtained.

Reaction of II, III, IV and V with Elementary Sulfur. Equimolar amounts of elementary sulfur were added to a solution of II in ethyl ether. Even after refluxing this solution for two days, sulfur did not react, and phosphonamidate II was recovered quantitatively. In the cases of III, IV and V also, sulfur addition reaction did not occur at all.

Kinetic Study on the Reaction between Ib and β-Propiolactone. A solution containing 0.1807 mol/*l* of Ib and 0.2070 mol/*l* of β-propiolactone was prepared and divided into several ampoules filled with nitrogen and then sealed. The sealed ampoules were heated in a bath kept at 80±0.5°C. At an appropriate time interval, an ampoule was broken and the concentrations

of IV and V were determined from the intensity of the absorptions at 1743 and 1658 cm^{-1}, respectively.

Results and Discussion

Contrary to the results of McConnell *et al.*,[7] two kinds of products were obtained in the reaction between dialkyl dimethylphosphoramidite and β-propiolactone. The two products were identified to be *N,N*-dimethyl-*O*-alkyl 2-alkoxycarbonylethylphosphoramidate (II and IV) and dialkyl 2-*N,N*-dimethylcarbamoylethylphosphonate (III and V) by their chemical behavior and spectral data. None of them reacted with elementary sulfur. Thus, it is likely that they have a quinquevalent phosphorus atom rather than the trivalent phosphorus atom. In the NMR spectrum of II, shown in Table 2, the methyl protons of isopropyl group of II showed two doublets at τ 8.73 and 8.42, and in the case of IV, those of *s*-butyl group showed complex multiplets at τ 8.50—9.45. The results indicate that each of the two alkoxy groups attaches itself to different sites of the molecules. In addition, the β-substituted ethyl protons were observed over the range of τ 7.20—8.40 as a complex multiplet, which could be explained by the fact that the ethyl group attaches itself to the phosphorus atom.

In IR spectra, shown in Table 3, there were strong absorptions at 1740 and 1240 cm^{-1} in both II and IV, which could be assigned to the carbonyl stretching frequency of ester group and to P=O group, respectively. Thus, the structures of II and IV were confirmed as phosphoramidate.

By similar chemical and spectral evidence as that of the above discussion, it could be assumed that III and V have phosphonate structures. Therefore, it would be reasonable to assume that there are two routes to give different reaction products as visualized in the following equation.

$$(RO)_2PNMe_2 + \begin{array}{c} \\ \\ \text{—O—C(=O)—} \end{array} \begin{array}{l} \xrightarrow{\text{route(a)}} \text{ROP(O)(NMe}_2\text{)CH}_2\text{CH}_2\text{CO}_2\text{R} \\ \quad \text{II: R=}i\text{-Pr, IV: R=}s\text{-Bu} \\ \xrightarrow{\text{route(b)}} (RO)_2\text{P(O)CH}_2\text{CH}_2\text{CONMe}_2 \\ \quad \text{III: R=}i\text{-Pr, V: R=}s\text{-Bu} \end{array} \quad (6)$$

In order to elucidate the reaction mechanism, kinetic study on the reaction between Ib and β-propiolactone was carried out in various solvents by determining the absorbances of IR frequencies at 1743 and 1658 cm^{-1}, which are characteristic absorptions of IV and V, respectively. The rates of the formation of IV and V in the initial stage of the reaction satisfied typical first order kinetics. The first order rate constants [k_1(phosphoramidate) and k_1(phosphonate)] obtained in five solvents are sum-

TABLE 2. NMR SPECTRA OR THE ADDITION PRODUCTS; $(RO)P(O)(NMe_2)CH_2CH_2CO_2R$ (II, R=*i*-Pr; IV, R=*s*-Bu) AND $(RO)_2P(O)CH_2CH_2CONMe_2$ (III, R=*i*-Pr; V, R=*s*-Bu)[a]

Compound	assignment (τ)		POR and CO_2R
	NMe_2	$-CH_2CH_2-$	
II	7.60 (d, J=9.0 Hz)	7.20—8.50 (m)	5.26 (m), 8.35 (d), 8.42 (d).
III	7.32, 7.66	7.20—8.40 (m)	5.30 (m), 8.80 (d),
IV	7.55 (d, J=9.0 Hz)	7.20—8.40 (m)	5.10 (m), 5.54 (m), 8.75 (d), 9.15 (t)
V	7.31, 7.64	7.20—8.40 (m)	5.48 (m), 8.55 (m), 8.50—9.45 (m)

a) In 15% benzene solution.

TABLE 3. IR SPECTRA OF THE ADDITION PRODUCTS (II, III, IV and V) IN 3% BENZENE SOLUTION

Compound	Absorptions
II	2990 (m), 2970 (m), 2870 (w), 1738 (vs), 1430 (m), 1383 (m), 1370 (m), 1240 (s), 1176 (s), 1139 (w), 1108 (s), 983 (vs), 886 (m), 812 (w), 772 (w), 672 (w).
III	2985 (m), 2920 (m), 2880 (w), 1650 (vs), 1500 (m), 1468 (m), 1455 (m), 1418 (m), 1403 (m), 1388 (m), 1377 (m), 1342 (s), 1242 (s), 1178 (m), 1108 (s), 985 (vs), 890 (m), 782 (m), 685 (m).
IV	2970 (m), 2800 (w), 1743 (vs), 1460 (m), 1420 (m), 1380 (m), 1243 (s), 1170 (m), 1122 (m), 1112 (m), 1092 (w), 1025 (m), 970 (vs), 810 (m).
V	2980 (w), 2900 (w), 1658 (vs), 1450 (m), 1394 (m), 1379 (m), 1325 (vs), 1242 (s), 1200 (m), 1170 (w), 1125 (m), 1100 (m), 1025 (m), 975 (vs), 955 (m), 850 (w), 810 (w), 760 (w).

Table 4. First order rate constants; k_1 (phosphoramidate), k_1 (phosphonate) for the formation of IV and V at 80±0.5°C[a]

Solvent	Dielectric constant (ε)	$10^5 k_1$ (phosphoramidate) (sec^{-1})	$10^5 k_1$(phosphonate) (sec^{-1})
Acetonitrile	3.75	very fast[b]	very fast[b]
o-Dichlorobenzene	9.93	5.43	1.73
Tetrahydrofuran	7.93	3.57	2.11
Tetralin	2.76	1.07	0.74
Benzene	2.28	0.75	0.67

a) $[Ib]_0=0.1807$ mol/*l*, $[\beta$-Propiolactone$]_0=0.2070$ mol/*l*.
b) The reaction was completed within 30 min.

marized in Table 4.

A fairly good linear relationship exists between the logalithms of the rate constants and the Kirkwood parameter $(\varepsilon-1)/(2\varepsilon+1)$, as shown in Fig. 1.

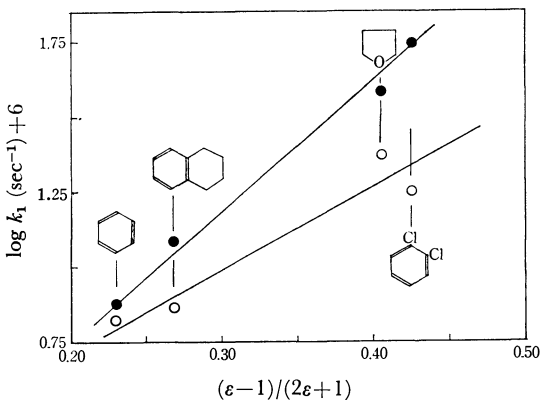

Fig. 1. Effect of solvent polarity on the rate constant; k_1 (phosphoramidate) —●— and k_1 (phosphonate) —○—.

Relative amounts of IV/V were determined in some solvents at the end point of the reaction by their IR absorption. The results are summarized in Table 5.

Table 5. Relative amount (IV/V) in various solvents at the termination of the reaction

Solvent	Dielectric constant (ε)	IV/V
Acetonitrile	37.5	5.77
o-Dichlorobenzene	9.93	2.31
Tetrahydrofuran	7.93	2.15
Benzene	2.28	1.58

It is clear from Fig. 1 and Table 5 that the overall rate of the reaction is more accelerated in polar solvent than in nonpolar solvent and that the relative amounts (IV/V) increase with increasing polarity of the solvent. This indicates that V was formed *via* the intermediate (VI) in which large charge-separation occurs. The mechanism of this reaction could be rationalized as follows: In the reaction of route(a) in Eq. (6), the sp^3 carbon of β-propiolactone is attacked by the phosphorus atom of the phosphoramidite to give betaine intermediate, and succeeding Arbuzov-like rearramgement of alkyl group gives phosphoramidate (II and IV) as shown in the following.

$$(RO)_2PNMe_2 + \begin{bmatrix} -O \\ | \\ -C=O \end{bmatrix} \downarrow [(RO)_2P^+(NMe_2)CH_2CH_2COO^-] \quad \text{VI} \quad \downarrow (RO)P(O)(NMe_2)CH_2CH_2CO_2R \quad (7)$$

II: R=*i*-Pr
IV: R=*s*-Bu

On the other hand, in the reaction of route (6) in Eq. (6). the sp^2 carbon of β-propiolactone is attacked by the nitrogen atom of the phosphoramidite with synchronous interaction between the oxygen atom of the ester group and the phosphorus atom as visualized by the following equation.

$$(RO)_2PNMe_2 + \begin{bmatrix} -O \\ | \\ -C=O \end{bmatrix} \rightarrow \left[\begin{array}{l} \quad\quad O \\ Me_2N\cdots C \\ (RO)_2P\cdots O \end{array} \right] \quad \text{VII} \quad \downarrow [Me_2NCOCH_2CH_2\cdots P(OR)_2] \quad (8)$$

$$\downarrow Me_2NCOCH_2CH_2P(O)(OR)_2$$

III: R=*i*-Pr
V: R=*s*-Bu

This four-centered mechanism explains the fact that the formation of V is less influenced than that of IV by solvent polarity.

In our former study on the reaction of aminophosphine with acetic anhydride[3] and cyclic carbonate esters,[4] the analogous four-centered mechanism was adopted.

According to Pearson, the sp^3 carbon atom may be a softer acid than the sp^2 carbon atom and also the phosphorus atom would be a softer base than the nitrogen atom. Therefore, it is relevant to as-

sume that in this reaction the softer phosphorus atom would attack preferably the sp^3 carbon atom of β-propiolactone, whereas the harder nitrogen atom interacts with the sp^2 carbon atom of β-propiolactone.

In this reaction, the rate determining step might be assumed from the solvent effect on the reaction to be the formation of betaine VI or four-centered intermediate VII. The fact that this reaction satisfied first order kinetics shows the existense of "complex" equilibrating quikly between phosphoramidite and β-propiolactone before the rate determing step:

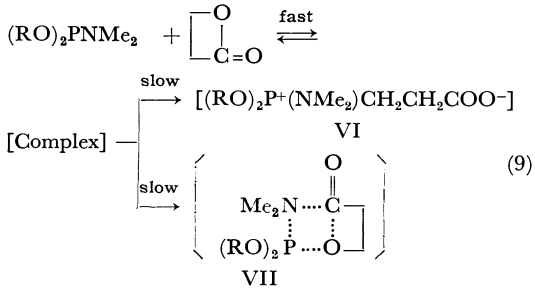

(9)

Existence of this complex could not be identified spectroscopically or by other methods.

BULLETIN OF THE CHEMICAL SOCIETY OF JAPAN VOL. 43 3236—3238 (1970)

Synthesis of 5-Styryltropolones

Hidehiro HIGASHI,*1 Kazu KUROSAWA and Hisashi MATSUMURA

Department of Chemistry, Faculty of Science, Kumamoto University, Kurokami-machi, Kumamoto

(Received May 1, 1970)

5-Styryl-, 5-(*p*-bromostyryl)-, 5-(*p*-chlorostyryl)-, 5-(*p*-methoxystyryl)-, 5-(*p*-methylstyryl)-, 5-(*m*-chlorostyryl)- and 5-(*m*-methylstyryl)tropolone were synthesized by the Wittig reaction of 5-formyltropolone. Their UV and NMR spectra were determined.

In connection with the studies on syntheses and chemical properties of 4-styryltropolones[1] in our laboratory, we also investigated on the synthesis of 5-stytyltropolenes by means of the Wittig reaction with *p*- and *m*-substituted benzylidenetriphenylphosphorane on 5-formyltropolone (III). Seven 5-styryltropolones (IVa—g) have been synthesized and the results are described in this paper.

5-Styryltropolone (IVa) has firstly been synthesized by Matsumura[2] through the abnormal substitution reaction of 2-tosyloxy-4-styryltropolone. When this synthetic scheme was applied to *p*-methoxystyryl- and *p*-nitrostyryltropolone, we found that the separation of 2-tosyloxy-4-(substituted styryl)-tropolone from 2-tosyloxy-6-(substituted styryl)-tropolone was extremely difficult.

It would be expected that the Wittig reaction of substituted benzylidenetriphenylphosphorane with III, which has been obtained by the Reimer-Tiemann reaction of tropolone,[3] could introduce a styryl group at the position in tropolone nucleus. The Wittig reagents were formed with *m*- and *p*-substituted benzyltriphenylphosphonium halides[4–9] on treatment with sodium ethoxide in anhydrous ethanol. The Wittig reaction usually took 4 to 25 hr depending upon the nature of the substituent of the ylids used and gave 5-styryltropolones in excellent yield. It was strange, however, that *p*-nitrobenzylidenetriphenylphosphorane did not react with III.

Yields and melting points of the 5-styryltropolones are listed in Table 1.

UV spectra of the 5-styryltropolones are shown in Table 2. The absorption in the region of 380—405 mμ could be correlated to the electronic effects

*1 Present address: Shokubai-Kasei Kogyo Co., Ltd., Wakamatsu-ku, Kitakyushu.

1) K. Imafuku and H. Matsumura, *Tetrahedron*, **26**, 1821 (1970).

2) H. Matsumura, *Nippon Kagaku Zasshi*, **81**, 1763 (1960).

3) J. W. Cook, *J. Chem. Soc.*, **1952**, 4416.

4) M. Grayson and P. T. Keough, *J. Amer. Chem. Soc.*, **82**, 3919 (1960).

5) H. Hoffman, *Ann. Chem.*, **634**, 1 (1959).

6) R. A. Jones and M. A. Talmet, *Aust. J. Chem.*, **18**, 903 (1965), *Chem. Abstr.*, **63**, 12517e (1965).

7) A. W. Johnson and V. L. Kyllingstad, *J. Org. Chem.*, **31**, 334 (1966).

8) S. Cabiddu, A. Maccioni and M. Secci, *Ann. Chim.* (Roma), **54**, 1153 (1964); *Chem. Abstr.*, **63**, 4190e (1965).

9) C. E. Griffin and M. Gordon, *J. Organometal. Chem.*, **3**, 414 (1965), *Chem. Abstr.*, **63**, 465a (1965).

Table 1. The Wittig synthesis of 5-styryltropolones

Reagent	Mp (°C)	Lit. mp	Reaction conditions: Mol ratio of I : III	Temp. (°C)	Time (hr)	Product	Yield (%)	Mp (°C)	Lit. mp
Ia	288	274—275[4]	3 : 1	50	18	IVa	68	132—133	131—133[2]
Ib	282—283	278 [5]	3 : 1	60	12	IVb*	80	239	—
Ic	289—290	[6]	2.9 : 1	50	22	IVc**	53	241—242	—
Id	241—242	236—238[7]	3.3 : 1	50	24	IVd**	88	198	—
Ie	262	267 [8]	2.9 : 1	30	24	IVe**	80	136	—
If	>300	310 [5]	3.5 : 1	50	25	IVf*	60	142—144	—
Ig	>300	[9]	3.3 : 1	47	6	IVg*	81	145—146	—

* Recrystallized from benzene-light petroleum.
** Recrystallized from benzene.

Table 2. UV absorption spectral data for 5-styryltropolones

Compound	λ_{max} mμ (ε)
IVa	235(30400), 260(20300), 270(23800), 277(inf.)(22000), 382(35000), 400(inf.)(34000)
IVb	237(26000), 262(16300), 274(21500), 281(20900), 384(36100), 405(35600)
IVc	237(28100), 261(inf.)(17600), 273(23300), 280(inf.)(23000), 384(38000), 405(inf.)(37200)
IVd	237(inf.)(26400), 261(inf.) (14500), 277(inf.)(11200), 390(inf.)(28000), 418(31200)
IVe	236(27200), 262(17300), 272(17800), 382(30200), 400(30000)
IVf	236(28600), 261(inf.)(19800), 271(24200), 278(inf.)(22200), 382(39800), 400(inf.)(37400)
IVg	236(28000), 261(inf.)(19000), 272(21000), 278(inf.)(19300), 382(36000), 400(inf.)(35500)

inf: inflection.

Table 3. NMR spectral data for 5-styryltropolones in $CDCl_3$ at 60 MHz

Compound	δ Value: OH	H_3,H_7*	H_4,H_6*	-CH=CH-	Phenyl or substituted phenyl	CH_3
IVa	7.9	7.40	7.60	7.06	7.45	
IVc	—	7.39	7.61	7.03	7.45	
IVe	8.1	7.33	7.61	7.04 7.36	7.25	2.43 2.35
IVf	7.9	7.36	7.61	7.00	7.32	
IVg	7.8	7.34	7.56	7.01	7.30	2.40

* $J_{3,4}=J_{6,7}=12$ Hz, analysed as an AB system.

Table 4. Analytical data for 5-styryltropolones

Compound	Formula	Found (%) C	Found (%) H	Calcd (%) C	Calcd (%) H
IVb	$C_{15}H_{11}O_2Br$	59.37	3.75	59.42	3.66
IVc	$C_{15}H_{11}O_2Cl$	69.31	4.27	69.64	4.29
IVd	$C_{16}H_{14}O_3$	75.36	5.69	75.57	5.55
IVe	$C_{16}H_{14}O_2$	80.47	6.29	80.64	5.92
IVf	$C_{15}H_{11}O_2Cl$	69.75	4.36	69.64	4.29
IVg	$C_{16}H_{14}O_2$	80.50	6.05	80.64	5.92

of *p*- and *m*-subtituents: *p*-CH_3O-, *p*-Br- and *p*-Cl- cause a bathochromic shift, while *m*-Cl- and *m*-CH_3- cause a little or none.

An absorption band at 950 cm^{-1} appeared in the IR spectra of all the 5-styryltropolones may indicate that the ethylenic double bond has a *trans* configuration.

NMR spectra of the 5-styryltropolones recorded in $CDCl_3$ are summarized in Table 3.

The ethylenic protons appeared as a sharp singlet and failed to show whether the configuration of the double bond is *trans* or *cis*. It was also observed that IVe showed two methyl protons and two

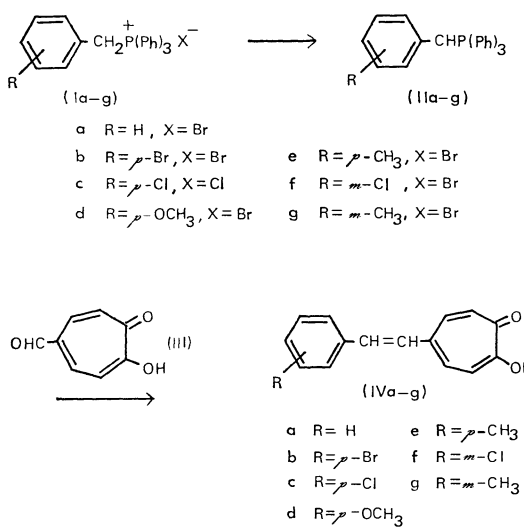

ethylenic protons, the intensities being 4 : 1. This indicates that the IVe is a mixture of *trans*- and *cis*-isomers. The presence of a band at 950 cm^{-1} in its IR spectrum is in favor of the *trans*-isomer being predominant.

pK_a measurements and a study of the correlation of pK_a values to the Hammett equation are now in progress.

Experimental

Measurements. IR spectra were determined in chloroform with a grating infrared spectrometer, Model DS 403G (Japan Spectroscopic Co. Ltd.). UV spectra were obtained in methanol with a recording spectrophotometer, Model EPS-2 (Hitachi Ltd.). NMR spectra were recorded in deuteriochloroform with TMS as an internal reference using a JNM C 60H (Japan Electron Optics Lab.). Melting points were determined with a Yanagimoto melting point apparatus.

5-Formyltropolone (III). 5-Formyltropolone was prepared according to the reference.[3] The work up procedure was, however, conveniently shortened by chloroform extraction of the products in place of continuous ether extraction and by chromatographic separation of III from the unchanged tropolone on silica (Wakogel C100) column.

Preparation of 5-Styryl- and 5-(*m*- and *p*-Substituted-styryl)tropolones (IVa—g). Phosphonium salt (I) (5.2 mmol) was treated with sodium ethoxide, prepared from metallic sodium (5.2 mmol) and anhydrous ethanol (13 m*l*). To the solution, there was added 5-formyltropolone (III) (1.67 mmol) and the mixture was stirred at a temperature between 30° and 60°C for a period of time shown in Table 1. The mixture was acidified with 2N sulfuric acid and extracted with chloroform. The chloroform was evaporated and the residue was chromatographed with chloroform on a silica column (Wakogel C100 (36 g) plus B10 (4 g)). The first fraction (100 m*l*) was taken and the chloroform was evaporated. The resulting solid was recrystallized from benzene or from a mixture of benzene and light petroleum (bp 30—70°C), giving 5-styryltropolone (IV) in 53—88% yield.

The authors wish to thank Professor Tetsuo Nozoe for his helpful discussions and encouragements throughout this work and Sankyo Co., Ltd., for supplying tropolone to us. The authors were also gratefully acknowledged to Professor Shin-ichi Sasaki and Mr. Hidetsugu Abe, of Miyagi University of Education for the measurements of the NMR spectra. We appreciate the Ministry of Education for the support by a grant to buy a grating infrared spectrometer, Model DS 403G (Japan Spectroscopic Lab.).

BULLETIN OF THE CHEMICAL SOCIETY OF JAPAN VOL. 43 3239—3241 (1970)

The Acid-Catalyzed Ring-Opening of Cyclooctenimine Derivatives

Shinsaku FUJITA, Tamejiro HIYAMA and Hitosi NOZAKI

Department of Industrial Chemistry, Kyôto University, Yosida, Kyôto

(Received, May 1, 1970)

The acid-catalyzed ring-opening of 9-ethoxycarbonyl-9-aza-bicyclo[6.1.0]nonane (**1**) and -4-nonene (**2**) is reported to give normal products **3a** and **11a**, respectively, together with several transannular products.

The ring opening of cyclooctene oxide is well known,[1] and treatment of cyclooctenimine with perchloric acid results in recovery of the starting material.[2] We wish to report the acid-catalyzed aziridine ring cleavage of 9-ethoxycarbonyl-9-aza-bicyclo[6.1.0]nonane (**1**) and -4-nonene (**2**).

The reaction of **1** with perchloric acid gave ethyl *trans*-2-hydroxycyclooctane-1-carbamate (**3a**) along with two transannular products, **4** and **5**. The structure of **3a** was determined on the basis of spectral data and the following chemical correlation. Oxidation of **3a** with chromic acid gave the corresponding ketone **6** which was identical with the product prepared by the DMSO-oxidation of aziridine **1**.[3] The *trans*-configuration of **3a** was determined by hydrolysis which gave *trans*-2-aminocyclooctanol. Sodium borohydride reduction of **6** afforded **3a** as well as the *cis*-isomer (**3b**) whose configuration was established by conversion to *cis*-2-aminocyclooctanol. Heating **3b** at 170°C under reduced pressure afforded *cis*-4,5-hexamethylene-2-oxazolidone (**9**). The same compounds was obtained by thermolysis of *trans*-β-iodocarbamate (**10**). The formation of 2-oxazolidones from *N*-alkoxycarbonyl-β-aminoalcohols has not been reported.

The transannular product **4** was oxidized to the corresponding ketone (**7**) which exhibited an IR band at 1705 cm^{-1} characteristic of a medium-sized cyclic ketones. The elementary analysis and spectral data indicated that **4** was the isomer of **3a** and **3b**. The structure of **4** was tentatively assigned to be ethyl 4-hydroxycyclooctane-1-carbamate on the analogy of the formation of cyclooctane-1,4-diol in the solvolysis of cyclooctene

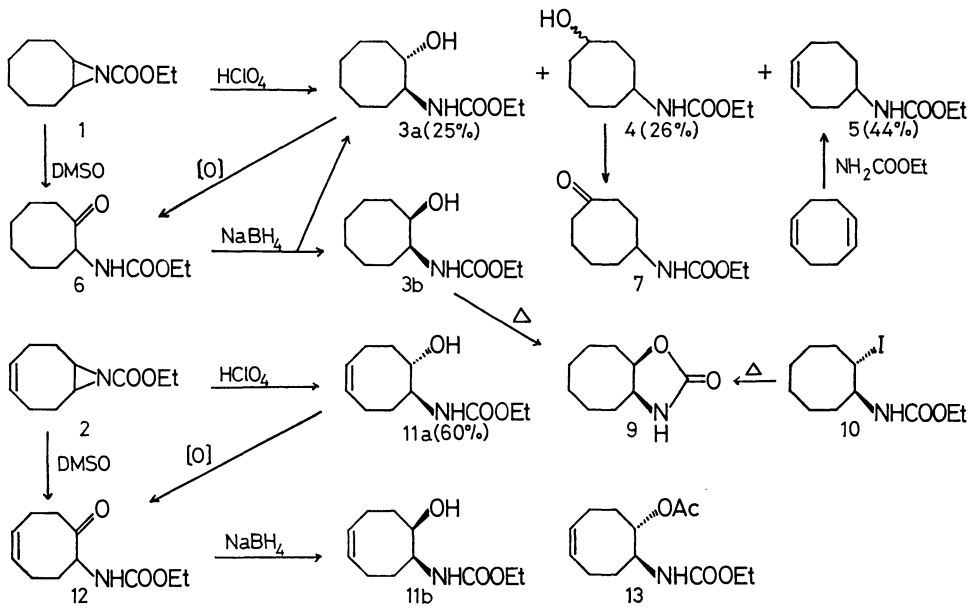

1) A. C. Cope, M. M. Martin and A. M. McKervey, *Quart. Rev.* (London), **20**, 119 (1966).

2) D. V. Kashelikar and P. E. Fanta, *J. Amer. Chem. Soc.*, **82**, 4927 (1960).

3) S. Fujita, T. Hiyama and H. Nozaki, *Tetrahedron Lett.*, **1969**, 1677; *Tetrahedron*, in press.

oxide.[1] The olefinic product (**5**) was identical with the authentic ethyl 4-cyclooctene-1-carbamate prepared by the acid-catalyzed addition of urethane to 1,5-cyclooctadiene.[3]

The acid-catalyzed cleavage of **2** in aqueous phase gave ethyl *trans*-8-hydroxy-4-cyclooctene-1-carbamate (**11a**), together with a small amount of transannular by-products whose structures have not been determined. The *trans*-configuration of **11a** was established by the fact that **11a** absorbed 1 molar equivalent of hydrogen to afford **3a**. Chromic acid oxidation of **11a** yielded the corresponding ketone (**12**) which was also prepared by the DMSO-oxidation of **2**.[3] Reduction of **12** with sodium borohydride afforded ethyl *cis*-8-hydroxy-4-cyclooctene-1-carbamate (**11b**) exclusively, which on catalytic hydrogenation gave **3b**. The difference between **6** and **12** in borohydride reduction should be ascribed to the rigidity[4] of the ring of **12** as compared with that of **6**. Ethyl *trans*-8-acetoxy-4-cyclooctene-1-carbamate (**13**) was obtained by treatment of **2** with dry acetic acid along with several bicyclic minor products.

Apparently, the acid-catalyzed aziridine ring-cleavage is favored by the presence of alkoxycarbonyl group on nitrogen. Initial protonation on carbonyl oxygen[5] would account for this rather unusual activation. Formation of the transannular products may be explained by intramolecular hydride shift analogous to the solvolysis of cyclooctene oxide.[1]

The normal addition products **3a** and **11a** have *trans* configuration, where the so-called "borderline" S_N2 mechanism should be involved in a stereochemical sence.[6]

Experimental

Acid-catalyzed Hydrolysis of 1. A solution of aziridine (**1**)[3] (1.27 g, 65 mmol) in ether (12 m*l*) was added dropwise for 5 min at room temperature to a mixture of water (0.80 g), ether (15 m*l*) and 60% perchloric acid (0.30 g). After being stirred for 6.5 hr, the reaction mixture was neutralized with aqueous sodium bicarbonate, extracted with ether and dried over sodium sulfate. Concentration and separation through a Silica gel column (benzene - ether (4 : 1) as a solvent) afforded ethyl 4-cyclooctene-1-carbamate (**5**) (0.56 g, 44%), which was identical with the authentic sample.[3]

Subsequent elution with ether gave ethyl *trans*-2-hydroxycyclooctane-1-carbamate (**3a**) (0.35 g, 25%), bp 140—145°C/0.05 mmHg, mp 42—43°C (*n*-hexane - acetone). IR (neat): 3450—3300 (broad), 1690, 1535, 1300, 1250—1235, 1090, 1035 cm^{-1}. NMR (CCl_4): δ 5.7—5.3 (broad, 1H, NH), 4.09 (q, 2H, $OC\underline{H}_2CH_3$), 4.0—3.3 (m, 3H, methines and OH), 2.4—1.0 (m, 12H, methylenes), 1.28 (t, 3H, $OCH_2C\underline{H}_3$).

Found: C, 61.4; H, 10.0; N, 6.8%. Calcd for $C_{11}H_{21}NO_3$: C, 61.4; H, 9.8; N, 6.5%.

The third eluent was ethyl 4-hydroxycyclooctane-1-carbamate (**4**) (0.36 g, 26%) bp 150—155°C/0.05 mm Hg IR (neat): 3450—3330 (broad), 1685, 1530, 1300, 1235, 1090, 1059, 1028 cm^{-1}. NMR (CCl_4): 6.0—5.3 (broad, 1H, NH), 4.3—3.4 (m+q, 5H, methines, OH and $OC\underline{H}_2CH_3$), 2.5—1.3 (m, 12H, methylenes), 1.25 (t, 3H, $OCH_2C\underline{H}_3$).

Found: C, 61.4; H, 10.0; N, 6.5%. Calcd for $C_{11}H_{21}NO_3$: C, 61.4; H, 9.8; N, 6.5%.

Oxidation of 4. (0.12 g, 0.56 mmol) by the Brown procedure[7] and subsequent preparative thin-layer chromatography (TLC) afforded ethyl 4-cyclooctanone-1-carbamate (**7**), bp 110—115°C/0.5 mm. IR (neat): 3350, 1705, 1675, 1530, 1380, 1340, 1225, 1040 cm^{-1}. NMR (CCl_4): δ 4.87 (s, 1H, NH), 4.14 (q, 2H, $OC\underline{H}_2CH_3$), 3.9—3.4 (m, 1H, methine), 2.7—1.0 (t+m, 15H, $OCH_2C\underline{H}_3$ (δ 1.30) and methylenes).

Found: C, 62.5; H, 9.1; N, 6.6%. Calcd for $C_{11}H_{19}NO_3$: C, 61.9; H, 9.0; N, 6.6%.

Oxidation of 3a. (0.12 g, 0.56 mmol) by the Brown procedure[7] gave ethyl 2-oxocyclooctane-1-carbamate (**6**), whose IR and NMR spectra were identical with those of the sample prepared by the DMSO-oxidation of **1**.[3]

Reduction of 6 with Sodium Borohydride. Sodium borohydride (0.10 g) was added in one portion to a solution of **6** (0.15 g, 0.70 mmol) in methanol at 0°C. After being stirred for 4 hr, and suspension was acidified to pH 4 by dilute hydrochloric acid, poured into water, extracted with ether and dried. Concentration and separation by preparative TLC afforded **3a** (0.025 g, 17%) as well as ethyl *cis*-2-hydroxycyclooctane-1-carbamate (**3b**) (0.040 g, 26%), bp 160°C/1 mmHg. IR (neat): 3450—3350 (broad), 1685, 1520—1510, 1310, 1248, 1107, 1090, 1060, 1035 cm^{-1}. NMR (CCl_4): δ 5.7—5.2 (broad, 1H, NH), 4.2—3.5 (m+q, 4H, methines and $OC\underline{H}_2CH_3$), 3.4—3.0 (broad, 1H, OH) 2.0—1.0 (m+t, 13H, methylenes and $OCH_2C\underline{H}_3$) (δ 1.20)).

Found: C, 61.3; H, 9.9; N, 6.2%. Calcd for $C_{11}H_{21}NO_3$: C, 61.4; H, 9.8; N, 6.5%.

Hydrolysis of 3a. A mixture of **3a** (0.26 g, 1.2 mmol), sodium hydroxide (1.5 g), methanol (10 m*l*) and water (10 m*l*) was refluxed under nitrogen atmosphere for 25 hr. Usual work-up gave *trans*-2-aminocyclooctanol (0.18 g) quantitatively, mp 72.6—73°C (lit,[8] mp 73—74°C).

Hydrolysis of 3b. (0.050 g, 0.23 mmol) with methanolic sodium hydroxide yielded *cis*-2-aminocyclooctanol (0.030 g, 90%) as a solid, whose IR spectrum was identical with that of the sample prepared from the oxazolidone (**9**).

***cis*-4,5-Hexamethylene-2-oxazolidone (9).** A solution of β-iodocarbamate **10**[3] (5.0 g, 15 mmol) in xylene (40 m*l*) was heated for 20 hr. Concentration and recrystallization gave the oxazolidone (**9**) (2.57 g) quantitatively, mp 106.5—107.5°C (acetone). IR (Nujol): 3260, 3170, 1745, 1725, 1260, 1235, 1090, 1080, 1042,

4) M. St. Jacques, M. A. Brown and F. A. L. Anet, *Tetrahedron Lett.*, **1966**, 5947.

5) G. A. Olah and P. J. Szilagyi, *J. Amer. Chem. Soc.*, **91**, 2949 (1969).

6) R. E. Parker and N. S. Isaacs, *Chem. Rev.*, **59**, 737 (1959).

7) H. C. Brown and C. P. Garg, *J. Amer. Chem. Soc.*, **83**, 2952 (1961).

8) J. Sicher and M. Svoboda, *Chem. Listy*, **52**, 1560 (1958); *Chem. Abstr.*, **53**, 1185 (1959).

974 cm^{-1}. NMR (CCl_4): δ 7.4—7.1 (broad, 1H, NH), 4.8—4.2 (m, 1H, CH-O), 4.1—3.5 (m, 1H, CH-N), 2.4—1.0 (m, 12H, methylenes).

Found: C, 63.7; H, 9.1; N, 8.2%. Calcd for $C_9H_{15}NO_2$: C, 63.9; H, 8.9; N, 8.3%.

The same oxazolidone (**9**) was obtained by distillation of **3b** at 170°C/1.5 mmHg.

Hydrolysis of 9. (1.69 g, 10 mmol) with alcoholic potash afforded *cis*-2-aminocyclooctanol (1.40 g, 98%), mp 45—47°C (*n*-hexane - benzene) (lit,[8] mp 52—54°C).

Acid-catalyzed Hydrolysis of 2. Aziridine **2**[3] (4.68 g, 24 mmol) was treated with perchloric acid as described above. Recrystallization of the crude solid (5.6 g) gave ethyl *trans*-8-hydroxycyclooct-5-ene-1-carbamate (**11a**) (2.38 g), mp 98.8—99.5°C (ethyl acetate – *n*-hexane). IR (Nujol): 3420, 3290, 3090, 3040, 1690, 1550, 1260, 1329, 1154, 1130, 1060, 1042 cm^{-1}. NMR ($CDCl_3$): δ 5.8—5.5 (m, 2H, olefinic), 5.4—5.0 (broad, 1H, NH), 4.3—3.5 (m+q, 4H, methines and $OC\underline{H}_2CH_3$), 2.80 (s, 1H, OH), 2.7—1.3 (m, 8H, methylenes), 1.26 (t, 3H, $OCH_2C\underline{H}_3$).

Found: C, 61.7; H, 9.0; N, 6.5%. Calcd for $C_{11}H_{19}NO_3$: C, 61.9; H, 9.0; N, 6.6%.

The mother liquor was submitted to chromatography on Silica gel. Elution with benzene - ether (3 : 1) gave an isomerization product (0.68 g, 15%), bp 100—110°C/0.04 mmHg. IR (neat): 3320, 1690, 1525, 1230, 1080, 1045 cm^{-1}. NMR (CCl_4): δ 5.9—5.2 (m, 4H, olefinic and NH), 4.07 (q, 2H, $OC\underline{H}_2CH_3$), 2.7—1.3 (m, 8H, methylenes), 1.23 (5, 3H, $OCH_2C\underline{H}_3$). MS *m/e* 195 (M^+). The compound was tentatively assigned as ethyl 1,5-cyclooctadiene-1-carbamate.

Found: C, 67.4; H, 8.8; N, 7.0%. Calcd for $C_{11}H_{17}NO_3$: C, 67.7; H, 8.8; N, 7.2%.

Further elution with benzene - ether (1 : 1) gave additional **11a** (0.70 g, totally 3.08 g, 60%). The third component was an oil (0.24 g, 5%), bp 120—130°C/0.05 mmHg. IR (neat): 3450—3330, 1688, 1535, 1288, 1240, 1098, 1070, 1046 cm^{-1}. NMR (CCl_4): δ 5.7—5.4 (broad, 1H, NH), 4.9—4.5 (m, 1H, methine), 4.3—3.5 (m+q, methine and $OC\underline{H}_2CH_3$), 2.93 (s, 1H, OH), 2.6—0.8 (m+t, 13H, methylenes and $OCH_2C\underline{H}_3$). MS *m/e* 213 (M^+). The compound was tentatively assigned as ethyl 6-hydroxybicyclo [3.3.0] octane-2-carbamate, since the corresponding ketone obtained by its oxidation exhibited an IR band at 1735 cm^{-1} characteristic of a five-membered cyclic ketone.

Oxidation of 11a (0.43 g, 2.0 mmol) with chromic acid[7] gave an oil (0.37 g, 88%), which was identical with the sample of **12** prepared by the DMSO-oxidation of **2**.

Sodium Borohydride Reduction of 12 (0.75 g, 3.5 mmol) and subsequent chromatography on Silica gel column gave ethyl *cis*-8-hydroxy-4-cyclooctene-1-carbamate (**11b**) (0.63 g, 83%), mp 93.5—94.5°C (acetone). IR (Nujol): 3420, 3280, 1690, 1550, 1255, 1235, 1060, 1040 cm^{-1}. NMR ($CDCl_3$): δ 5.8—5.4 (m, 3H, olefinic and NH), 4.3—3.6 (m+q, 5H, OH, methines and $OC\underline{H}_2CH_3$), 2.9—1.5 (m, 8H, methylenes), 1.26 (t, 3H, $OCH_2C\underline{H}_3$).

Found: C, 61.8; H, 9.1; N, 6.4%. Calcd for $C_{11}H_{19}NO_3$: C, 61.9; H, 9.0; N, 6.6%.

Hydrogenation of 11a. A mixture of **11a** (0.50, 2.4 mmol), Raney's nickel (*ca.* 0.3 g) and ethanol (10 m*l*) was stirred under hydrogen atmosphere at room temperature until 1 molar hydrogen was absorbed (*ca.* 24 hr). The catalyst was filtered, washed exclusively with ether and the combined washings were evaporated *in vacuo*, yielding **3a** as an oil (0.51 g, quantitatively).

Hydrogenation of 11b. (0.26 g, 1.2 mol) gave **3b** (0.23 g, 90%) as a colorless oil, which was identical with the sample obtained by reduction of **6**.

Solvolysis of 2 in Acetic Acid. A solution of **2** (1.56 g, 8 mmol) in glacial acetic acid (5 m*l*) was added dropwise under nitrogen atmosphere to a mixture of acetic acid (8 m*l*), acetic anhydride (3 drops) and BF_3-etherate (10 drops) at 50—55°C. After stirring for 3 hr and usual work-up, chromatography on Silica gel gave the isomerization product (0.22 g, 14%) which was identical with the one obtained by the hydrolysis of **2**. The second eluent was ethyl *trans*-8-acetoxy-4-cyclooctene-1-carbamate (**13**) (0.92 g, 45%), bp 110—120°C/0.05 mmHg. IR (neat): 3350, 1724, 1700, 1530—1510, 1230, 1050, 1032 cm^{-1}. NMR (CCl_4): δ 5.8—5.5 (m, 2H, olefinic), 5.1—4.5 (m, 2H, methine and NH), 4.3—3.7 (m+q, 3H, methine and $OC\underline{H}_2CH_3$), 2.5—1.4 (m+s, 11H, methylenes and AcO (δ 2.00)), 1.22 (t, 3H, $OCH_2C\underline{H}_3$).

Found: C, 60.9; H, 8.3; N, 5.5%. Calcd for $C_{13}H_{21}NO_4$: C, 61.2; H, 8.3; N, 5.5%.

The authors are indebted to Professor Keiiti Sisido for his kind help. Financial support from the Ministry of Education, Japanese Government, and from Toray Science Foundation is acknowledged.

BULLETIN OF THE CHEMICAL SOCIETY OF JAPAN VOL. 43 3242—3245 (1970)

Syntheses of Some Derivatives of D-Glucuronic Acid*1

Takeshi IRIMAJIRI, Hiroshi YOSHIDA, Tsuyoshi OGATA
and Saburo INOKAWA

Department of Synthetic Chemistry, Faculty of Engineering, Shizuoka University, Johoku, Hamamatsu

(Received May 6, 1970)

The syntheses of some derivatives of D-glucuronic acid from D-glucofuranurono-6→3-lactone have been investigated. That is, 5-bromo-5-deoxy-1,2-*O*-isopropylidene-β-L-idofuranurono-6→3-lactone (**2**) and 5-bromo-5-deoxy-1,2-*O*-isopropylidene-α-D-glucofuranurono-6→3-lactone (**3**) were prepared by heating 1,2-*O*-isopropylidene-5-*O*-(*p*-toluenesulfonyl)-α-D-glucofuranurono-6→3-lactone (**1**) with lithium bromide in dimethylformamide (DMF); methyl 5-*O*-(*p*-toluenesulfonyl)-β-D-glucofuranurono-6→3-lactone, 5-bromo-5-deoxy-α-L-idofuranurono-6→3-lactone, and 5-bromo-5-deoxy-β-D-glucofuranurono-6→3-lactone were prepared by heating **1**, **2**, and **3** respectively in methanol in the presence of strong acidic ion-exchange resins; 5-deoxy-1,2-*O*-isopropylidene-α-D-glucofuranurono-6→3-lactone (**7**) was prepared by the reaction of **2** with thiolacetic acid of benzylmercaptan in pyridine or by the reaction of **2** with triethyl phosphite; 5-bromo-5-deoxy-1,2-*O*-isopropylidene-β-L-*ido*-hexodialdo-3,6-furanoid(6S)-1,4-furanose (**8**) was prepared by the reduction of **2** with lithium aluminum hydride; 1,2-*O*-isopropylidene-5-*O*-(*p*-toluenesulfonyl)-α-D-*gluco*-hexodialdo-3,6-furanoid-1,4-furanose and 1,2-*O*-isopropylidene-5-*O*-(*p*-toluenesulfonyl)-α-D-glucofuranose (**10**) were prepared by the reduction of **1** with lithium aluminum hydride, and 1,2;3,6-di-*O*-isopropylidene-5-*O*-(*p*-toluenesulfonyl)-α-D-glucofuranose and 3,6-di-*O*-acetyl-1,2-*O*-isopropylidene-5-*O*-(*p*-toluenesulfonyl)-α-D-glucofuranose were prepared by the acetonation and the acetylation of **10** respectively.

D-Glucuronic acid is of considerable biological importance; moreover, it is easily obtained as a commercial sugar. Therefore, it seemed that it would be interesting to investigate the preparation of its deribatives. The present paper will report on the syntheses of compounds derived from 1,2-*O*-isopropylidene-5-*O*-(*p*-toluenesulfonyl)-α-D-glucofuranurono-6→3-lactone (**1**). When a solution of **1** and lithium bromide in dimethylformamide (DMF) was heated and the progress of the reaction was monitored by thin-layer chromatography in a solvent (ethyl acetate and petroleum ether, 1 : 4), it was found that the starting compound **1**, R_f 0.2, was initially transformed into a product **2** having R_f 0.5, and that then another product **3** with R_f 0.3 appeared. After the **1** was gone, fractional recrystallization gave **2** and **3** in 34 and 28% yields respectively. The compound **2** was identified as 5-bromo-5-deoxy-1,2-*O*-isopropylidene-β-L-idofuranurono-6→3-lactone and **3**, as 5-bromo-5-deoxy-1,2-*O*-isopropylidene-α-D-glucofuranurono-6→3-lactone. The structures of **2** and **3** were established by elementary analyses and by studies of the NMR spectra. The coupling constants, $J_{4,5'}$ in **1** and **3** were 4.1 and 4.0 Hz respectively. The coupling constants of 3,6-anhydro-1,2-*O*-isopropylidene-α-D-glucofuranose and 3,6-anhydro-5-*O*-(*p*-toluenesulfonyl)-1,2-*O*-isopropylidene-α-D-glucofuranose have been reported to be 4.1 and 3.9 Hz[1] respectively. It seems reasonable to say that the structure of **3** is a D-*gluco*-form. In the case of **2**, however, the $J_{4,5}$ is about zero. As the conformation of the lactone ring in **2** is considered to be an envelope form (E_4), the structure of **2** must be L-*ido*-form. The compound **3** seems to be produced by the inversion of the initial product **2** by a displacement reaction with lithium bromide, as the tracing by TLC showed.

The treatment of **1**, **2**, and **3** in methanol with strong acidic ion-exchange resins[2,3] afforded methyl 5-*O*-(*p*-toluenesulfonyl)-β-D-glucofuranuronoside-6→3-lactone (**4**), methyl 5-bromo-5-deoxy-α-L-idofuranuronoside-6→3-lactone (**5**), and methyl 5-bromo-5-deoxy-β-D-glucofuranuronoside-6→3-lactone (**6**) respectively, all in good yields. The structures of **4**, **5**, and **6** were established by elementary analyses and/or by studies of the NMR spectra. The

*1 This work was presented at the 23rd Annual Meeting of the Chemical Society of Japan, Tokyo, April 4, 1970.

1) R. J. Abraham, L. Hall, L. Hough and K. A. McLauchlan, *J. Chem. Soc.*, **1962**, 3702.
2) E. M. Osman, K. C. Hobbs and W. E. Walton, *J. Amer. Chem. Soc.*, **73**, 2726 (1951).
3) J. E. Cadotte, F. Smith and D. Spriestersbath, *ibid.*, **74**, 1501 (1952).

values of $J_{1,2}$ in **4** and **5** were near zero; therefore, the anomeric structures should be β-glucofuranoside and α-idofuranoside forms.[4] The structure of **6** also seems to be the same form, although the low solubility of **6** in chloroform-*d* did not give a clear NMR spectrum by which we could observed $J_{1,2}$.

The reaction of **2** in pyridine with thiolacetic acid or benzylmercaptan did not give the expected product having a carbon-sulfur bond at the C-5 position; instead, it gave 5-dioxy-1,2-*O*-isopropylidene-α-D-glucofuranurono-6→3-lactone (**7**)[5] with an uncertain mechanism. The reaction of **2** with triethyl phosphite also gave **7**, probably *via* the route of the Perkow reaction.[6]

The reduction of **2** in ether with lithium aluminum hydride (LAH) at −15°C gave 5-bromo-5-deoxy-1,2-*O*-isopropylidene-β-L-*ido*-hexodialdo-3,6-furanoid(6S)-1,4-furanose (**8**) in a 20% yield. The structure of **8** was established by elementary analysis and by studies of the NMR and IR spectra. The IR spectrum of **8** showed the absorption of a hydroxy group at 3400 cm^{-1} in place of the absorption of a carbonyl group at 1780 cm^{-1} in **2**. In the NMR spectrum of **8**, the coupling constants, $J_{4,5}$ and $J_{5,6'}$ were about zero. These values probably show that the conformation of C-6 is S-form, because the conformation of the γ-lactone seems to be an envelope conformation (E_4).[1] The reduction of **1** in tetrahydrofuran (THF) with LAH at −10°C gave 1,2-*O*-isopropylidene-5-*O*-(*p*-toluenesulfonyl)-α-D-*gluco*-hexodialdo-3,6-furanoid-1,4-furanose (**9**) in a 70% yield. The structure of **9** was established by elementary analysis and by studies of the NMR and IR spectra. The coupling constant, $J_{5,6'}$ was 3.0 Hz in its NMR spectrum. The conformation of C-6 remained uncertain. The

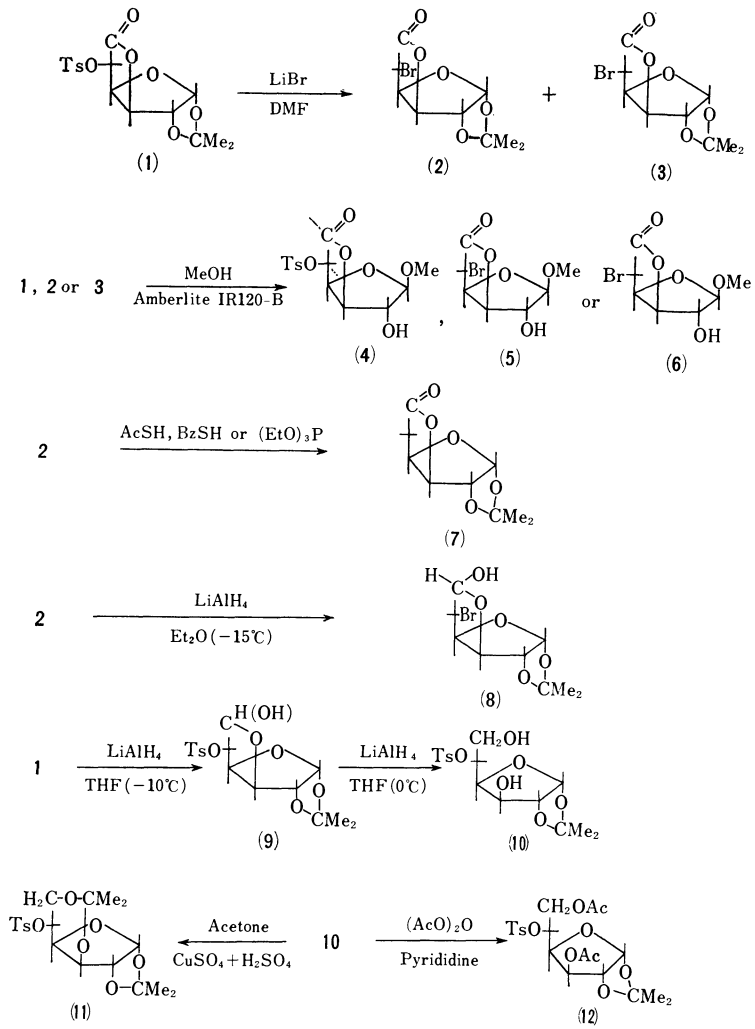

4) S. J. Angyal, *Angew. Chem.*, **81**, 179 (1969).

5) H. Paulsen and D. Stoy, *Chem. Ber.*, **99**, 908 (1966).

6) R. F. Hudson, "Structure and Mechanism in Organophosphorus Chemistry," Academic Press, London and New York (1965), p. 153.

further reduction of **9** in THF with LAH at 0°C gave 1,2-*O*-isopropylidene-5-*O*-(*p*-toluenesulfonyl)-α-D-glucofuranose (**10**) in a 48% yield based on **1**. The structure of **10** was established by elementary analysis and by a study of the NMR spectrum.

The acetonation and acetylation of **10** gave 1,2;3,6-di-*O*-isopropylidene-5-*O*-(*p*-toluenesulfonyl)-α-D-glucose (**11**) and 3,6-di-*O*-acetyl-1,2-*O*-isopropylidene-5-*O*-(*p*-toluenesulfonyl)-α-D-glucofuranose (**12**) in a 33% and a quantitative yield respectively. The structures of these compounds were established by elementary analyses and by studies of the NMR spectra.

Considering that **12** was prepared in a 25% overall yield, and in only three steps, from D-glucuronolactone, the route through **12** from D-glucuronolactone seems to be an atractive one for the synthesis of 5-thio-D-glucopyranose.

Experimental

The infrared spectra were measured on a Hitachi-Perkin-Elmer 337 spectrophotometer. The nuclear magnetic resonance spectra were measured at 60 Mc on a Hitachi-Perkin-Elmer R-20 spectrometer, using tetramethylsilane as the internal reference. The thin-layer chromatograms were run on a silica-layer G[7] using various mixtures of ethyl acetate and petroleum ether, while sugars were detected by spraying the plates with a methanolic 20% sulfuric acid solution and then heating them. Periodic sampling and examination by thin-layer chromatography permitted the determination of the most suitable reaction conditions for the preparative runs.

Materials. The 1,2-*O*-isopropylidene-5-*O*-(*p*-toluenesulfonyl)-α-D-glucofuranurono-6→3-lactone (**1**), mp 185—187°C, was prepared in an 89% yield by a modification of the method of Hall *et al.*,[8] while 1,2-*O*-isopropylidene-α-D-glucofuranurono-6→3-lactone, mp 121.5—122.5°, was prepared in an 85% yield by the acetonation of D-glucuronolactone using the method of Schmidt.[9] The thiolacetic acid, bp 87—88°C and the benzylmercaptan, bp 111—112°C/54 mmHg were prepared by the method of Ellingboe[10] and by the method of Shishido *et al.*[11] respectively.

5-Bromo-5-deoxy-1,2-*O*-isopropylidene-β-L-idofuranurono-6→3-lactone (2) and 5-Bromo-5-deoxy-1,2-*O*-isopropylidene-α-d-glucofuranurono-6→3-lactone (3). A solution of 20 g of **1** and 5 g of lithium bromide in 50 m*l* of DMF was heated at 100°C for 8 hr. The solution was then concentrated *in vacuo*; the residue was dissolved in chloroform, washed with water, dried over sodium sulfate, and concentrated *in vacuo* to give a solid. After fractional recrystallization from ether and acetone, **2** was obtained in a 34% yield from the acetone solution and **3** was obtained in a 28% yield from the ether solution. The compound **2** had mp 146.5—147.0°C and $[\alpha]_D^{16}$ +35° (*c* 1.54, chloroform).

Found: C, 38.48; H, 3.90; Br, 27.8%. Calcd for $C_9H_{11}BrO_5$: C, 38.73; H, 3.97; Br, 27.7%. PMR (in carbon tetrachloride): τ 4.1 (one-proton doublet, $J_{1,2}$= 3.5 Hz, H_1), 5.0—5.3 (three-proton doublets, $J_{2,3}$=0.5, $J_{3,4}$=3.4 Hz, $H_{2,3,4}$), 5.9 (one-proton singlet, $J_{4,5}\fallingdotseq 0$, H_5), and 8.5, 8.7 [six-proton singlets, $C(CH_3)_2$]. The compound **3** had mp 135.0—137.5°C and $[\alpha]_D^{16}$ +68° (*c* 1.03, chloroform).

Found: C, 38.99; H, 4.06; Br, 26.9%. Calcd for $C_9H_{11}BrO_5$: C, 38.73; H, 3.96; Br, 27.7%. PMR (in carbon tetrachloride): τ 4.0 (one-proton doublet, $J_{1,2}$= 4.0 Hz, H_1), 5.1—5.0 (three-proton multiplets, $J_{2,3}\fallingdotseq 0$, $H_{2,3,4}$), 5.5 (one-proton doublet, $J_{4,5}$=4.0 Hz, H_5), and 8.5, 8.7 [six-proton singlets, $C(CH_3)_2$].

Methyl 5-*O*-(*p*-Toluenesulfonyl)-β-D-glucofuranuronoside-6→3-lactone (4). A solution of 2 g of **1** and 10 m*l* of methanol was refluxed with 3 g of acidic Amberlite IR-120B for 10 hr. The solution was then filtered, and the filtrate was concentrated *in vacuo* to give a sirup of **4** in an almost quantitative yield. The sirup was pure enough for the measurement of the NMR spectrum; $[\alpha]_D^{16}$ +21° (*c* 3.4, chloroform).*2 PMR (in chloroform-*d*): τ 2.1—2.7 (four-proton multiplets, $-C_6H_4-$), 4.8—5.3 (two-proton multiplets, $H_{4,5}$), 5.7 (one-proton singlet, $J_{1,2}\fallingdotseq 0$, H_1), 6.3—6.8 (two-proton multiplets, overlapping with $-OCH_3$, $H_{2,3}$), 6.8 (three-proton singlet, overlapping with $H_{2,3}$, $-OCH_3$), 6.9 (one-proton singlet, disappearing upon the addition of D_2O, –OH), and 7.6 (three-poroton singlet, Ar–CH_3).

Methyl 5-Bromo-5-deoxy-α-L-idofuranuronoside-6→3-lactone (5). A solution of 1 g of **2** in 5 m*l* of methanol was refluxed with 1.5 g of acidic Amberlite IR-120B for 3 hr. The solution was then concentrated *in vacuo* to give colorless needles (from ethyl acetate–petroleum ether) in a 90% yield; mp 116—117°C, $[\alpha]_D^{16}$ −87° (*c* 0.92, chloroform).

Found: C, 33.21; H, 3.66%. Clacd for $C_7H_9BrO_5$: C, 33.23; H, 3.58%. PMR (chloroform-*d*): τ 4.8—5.1 (three-proton multiplets, $H_{1,3,4}$), 5.5 (one-proton singlet, $J_{1,2}\fallingdotseq 0$, H_2), 5.7 (one-proton singlet, $J_{4,5}\fallingdotseq 0$, H_5), 6.8 (three-proton singlet, $-OCH_3$), and 7.0 (one-proton singlet, disappearing upon the addition of D_2O, –OH).

Methyl 5-Bromo-5-deoxy-β-D-glucofuranuronoside-6→3-lactone (6). The compound **3** was treated as has been described above. Recrystallization from ethyl acetate gave colorless needles in a 90% yield; mp 192—194°C, $[\alpha]_D^{16}$ −0.86° (*c* 1.2, methanol).

Found: C, 33.40; H, 3.60%. Calcd for $C_7H_9BrO_5$: C, 33.23; H, 3.58%.

5-Deoxy-1,2-*O*-isopropylidene-α-D-glucofuranurono-6→3-lactone (7). *a) The Reaction of* **2** *with Thiolactic Acid.* A solution of 1 g of **2** and 0.4 g of thiolacetic acid in 10 m*l* of pyridine was heated at 100°C for 3 hr under a nitrogen atmosphere; the solution was then concentrated *in vacuo*. The residue was extracted with chloroform; the solution was then washed with water, dried over sodium sulfate, and evaporated *in vacuo* to give cololess needles (from petroleum ether)

7) Nakarai Chemicals, Ltd. Kyoto.

8) L. D. Hall, L. Hough and R. A. Pritchard, *J. Chem. Soc.*, **1961**, 1953.

9) O. T. Schmidt, "Methods in Carbohydrate Chemistry," Vol. II, ed. by R. L. Whistler and M. L. Wolfrom, Academic Press, New York and London (1963), p. 318.

10) E. K. Ellingboe, "Organic Syntheses," Coll. Vol. IV, p. 928 (1963).

11) K. Shishido, H. Nozaki and Y. Arido, "Yukikagobutsu Goseiho," ed. by the Society of Synthetic Organic Chemistry, Japan, Tokyo (1960), p. 11.

*2 Containing a small amount of an impurity.

in a 40% yield; mp 90—90.5°C, $[\alpha]_D^{16}$ +104° (*c* 0.89, chloroform).[5]

Found: C, 54.27; H, 6.15%. Calcd for $C_9H_{12}O_5$: C, 54.00; H, 6.04%. PMR (in chloroform-*d*): τ 4.1 (one-proton doublet, $J_{1,2}$=3.5 Hz, H_1), 4.9—5.3 (three-proton multiplets, $H_{2,3,4}$), 7.32 (one-proton singlet, $J_{4,5}\fallingdotseq 0$, H_5), 7.34 (one-proton doublet, $J_{4,5'}$=2.8 Hz, $H_{5'}$), and 8.5, 8.7 [six-proton singlets, $C(CH_3)_2$].

b) The Reaction of **2** *with Benzylmercaptan.* A solution of 1 g of **2** and 0.5 g of benzylmercaptan in 10 m*l* of pyridine was heated at 90°C for 6 hr under a nitrogen atmosphere, and then treated as has been described above to give **7** in a 30% yield.

c) The Reaction of **2** *with Triethyl Phosphite.* A solution of 1 g of **2** and 10 m*l* of triethyl phosphite was heated at 150°C for 3 hr and then treated as has been described above to give **7** in a 10% yield.

5-Bromo-5-deoxy-1,2-*O*-isopropylidene-β-L-*ido*-hexodialdo-3,6-furanoid(6S)-1,4-furanose (8). A solution of LAH in ether was added, drop by drop, into a solution of 1 g of **2** in 20 m*l* of ether at 15°C until the spot of **2** disappeared on TLC with a solvent (ethyl acetate–petroleum ether, 1 : 4; R_f=0.3); the excess of LAH was then destroyed water-containing ether; the solution was filtered, and the filtrate was concentrated *in vacuo*. The residue was extracted with hot ether, the ether solution was concentrated *in vacuo*, and the residue was recrystallized from petroleum ether to give **7** in a 20% yield; mp 75.0—76.0°C; $[\alpha]_D^{16}$ +1.9 (*c* 1.07, chloroform).

Found: C, 38.46; H, 4.79. Calcd for $C_9H_{13}BrO_5$: C, 38.45; H, 4.66%. PMR (in chloroform-*d*); τ 4.1 (one-proton doublet, $J_{1,2}$=3.5 Hz, H_1), 4.5 (one-proton doublet, $J_{6,OH}$=9.0 Hz, H_6), 5.1—5.4 (three-proton doublets, $J_{2,3}$=0.5, $J_{3,4}$=4.0 Hz, $H_{2,3,4}$), 5.9 (one-proton singlet, $J_{5,6}\fallingdotseq 0$, H_5), 6.8 (one-proton doublet, disappearing upon the addition of D_2O, C_6–OH), and 8.6, 8.7 [six-proton singlets, $C(CH_3)_2$].

1,2-*O*-Isopropylidene-5-*O*-(*p*-toluenesulfonyl)-α-D-*gluco*-hexodialdo-3,6-furanoid-1,4-furanose (9). A solution of LAH in THF was added, drop by drop, into a solution of 2 g of **1** in 20 m*l* of THF at −10°C until the spot of **1** disappeared on TLC. The excess of LAH was destroyed with water-containing THF; the solution was then filtered, and the filtrate was concentrated *in vacuo*. The residue was extracted with hot ether; the ether solution was concentrated *in vacuo*, and the residue was recrystallized with ethyl acetate–petroleum ether to give **9** in a 70% yield; mp 141—143°C, $[\alpha]_D^{16}$ +54°(*c*1.5, chloroform).

Found: C, 51.47; H, 5.50%. Calcd for $C_{16}H_{20}O_8S$: C, 51.61; H, 5.41%. PMR (in chloroform-*d*): τ 2.1—2.7 (four-proton multiplets, $-C_6H_4-$), 4.1 (one-proton doublet, $J_{1,2}$=3.5 Hz, H_1), 4.6 (one-proton doublet, $J_{5,6}$=3.0 Hz, H_6), 5.1—5.5 (four-proton multiplets, $H_{2,3,5}$), 6.4 (one-proton broad, disappearing upon the addition of D_2O, C_6–OH), 7.5 (three-proton singlet, Ar–CH_3), and 8.5, 8.7 [six-proton singlets, $C(CH_3)_2$]. TLC: R_f 0.6 (ethyl acetate–petroleum ether, 1 : 1).

1,2-*O*-Isopropylidene-5-*O*-(*p*-toluenesulfonyl)-α-D-glucofuranose (10). To a solution of 0.2 g of LAH in 20 m*l* of THF, 5 g of **1** were added at −10°C under stirring; then a solution of LAH in ether was further added at 0°C untill the spots of **1** and **9** disappeared on TLC. The solution was then treated as has been described above. The recrystallization of the residue from ether gave **10** in a 48% yield; mp 124.0—125.5°C; $[\alpha]_D^{16}$ +11.6° (*c* 1.55, chloroform).

Found: C, 51.47; H, 6.04. Calcd for $C_{16}H_{22}O_8S$: C, 51.32; H, 5.92%. PMR (in chloroform-*d*): τ 2.1—2.7 (four-proton multiplets, $-C_6H_4-$), 4.1 (one-proton doublet, $J_{1,2}$=3.5 Hz, H_1), 5.1 (one-proton doublet of triplets, $J_{4,5}$=8.5, $J_{5,6}=J_{5,6'}$=3.5Hz, H_5), 5.5 (one-proton doublet, H_2), 5.6—5.9 (two-proton multiplets, $H_{3,4}$), 6.2 (two-proton triplet, $H_{6,6'}$), 6.6 (one-proton doublet, disappearing upon the addition of D_2O, $J_{3,OH}$= 4.5 Hz, C_3–OH), 7.4 (one-proton triplet, disappearing upon the addition of D_2O, $J_{6,OH}=J_{6'OH}$=6.0 Hz, C_6–OH), 7.7 (three-proton singlet, Ar–CH_3), and 8.5, 8.7 [six-proton singlets, $C(CH_3)_2$].

The acetonation of **10** by the usual method[9] gave 1,2; 3,6-di-*O*-isopropylidene-5-*O*-(*p*-toluenesulfonyl)-α-D-glucofuranose (**11**) in a 33% yield; mp 133.0—133.5°C (from ethyl acetate–petroleum ether); $[\alpha]_D^{15}$ +25° (*c* 0.73, chloroform).

Found: C, 54.78; H, 6.44%. Calcd for $C_{19}H_{26}O_8S$: C, 55.06; H, 6.32%. PMR (in chloroform-*d*): τ 2.1—2.8 (four-proton multiplets, $-C_6H_4-$), 4.2 (one-proton doublet, $J_{1,2}$=3.5 Hz, H_1), 5.2—5.6 (two-proton multiplets, $H_{2,5}$), 5.8—6.1 (three-proton multiplets, $H_{3,4,6}$), 6.5 (one-proton quartet, $H_{6'}$), 7.6 (three-proton singlet, Ar–CH_3), 8.6—8.7 [twelve-proton singlets, $[C(CH_3)_2]_2$].

The acetylation of **10** by the usual method[12] gave 3,5-di-*O*-acetyl-1,2-*O*-isopropylidene-5-*O*-(*p*-toluene-sulfonyl)-α-D-glucofuranose (**12**) in a quantitative yield; mp 131.5—132.5°C (from methanol); $[\alpha]_D^{16}$ −15° (*c* 2.9, chloroform). Found: C, 52.12; H, 5.88%. Calcd for $C_{20}H_{26}O_{10}S$: C, 52.39; H, 5.72%. PMR (in chloroform-*d*): τ 2.2—2.7 (four-proton multiplets, $-C_6H_4-$), 4.1 (one-proton doublet, $J_{1,2}$=3.5 Hz, H_1), 4.7—5.0 (two-proton multiplets, $H_{3,5}$), 5.3—6.0 (four-proton multiplets, $H_{2,4,6,6'}$), 7.6 (three-proton singlet, Ar–CH_3), 7.9, 8.0 [six-proton singlets, $(OCOCH_3)_2$], and 8.5, 8.7 [six-proton singlets, $C(CH_3)_2$].

The authors wish to express their deep gratitude to Professor R.L. Whistler of Purdue University for his continued interest in this work. They are also grateful to the Yodogawa Pharmaceutical Co., Ltd., for supplying them with D-glucuronolactone.

12) M. L. Wolfrom and A. Thompson, "Methods in Carbohydrate Chemistry," Vol. II, ed. by R. L. Whistler and M. L. Wolfrom, Academic Press, New York and London (1963), p. 221.

BULLETIN OF THE CHEMICAL SOCIETY OF JAPAN VOL. 43 3246—3251 (1970)

Studies on Hydroxy Amino Acids. III.*1 The Synthesis of Cyclic Peptide Containing L-Serine

Michio Iwai, Kiichiro Nakajima, Akio Uno,*2 Satoe Hase,*3
Ikuko Takeuchi*4 and Kenji Okawa

Department of Chemistry, Faculty of Science, Kwansei Gakuin University, Nishinomiya

(Received May 6, 1970)

Modified gramicidin S peptides, *cyclo*(Ser-Orn-Ser-D-Phe-Pro)$_2$ and *cyclo*(Ser-Orn-Ser-D-Phe-Pro), were synthesized in order to clarify the correlation between the component amino acids and the antibiotic activity. To obtain the cyclic peptides, we examined several sets of conditions for cyclization reactions. The antibiotic activity of these peptides could not be found against some microorganisms *in vitro*. It was concluded that the lipophilic amino acids residues are the essential groups contributing to gramicidin S activity.

Many works concerning the synthesis of gramicidin S analogues have been investigated by several workers, especially Izumiya *et al.*, in order to study the correlation between the component amino acids and their biological activities.[1)]

We have been studying the synthesis of modified gramicidin S peptides, in which the lipophilic amino acids are replaced by hydrophilic amino acid, such as serine or threonine.

In the present work, the authors have studied the synthesis of a cyclic decapeptide containing L-serine, 1,1′,3,3′-L-seryl gramicidin S, and also cyclic pentapeptide, *cyclo* Ser-Orn-Ser-D-Phe-Pro (Fig. 1).*5

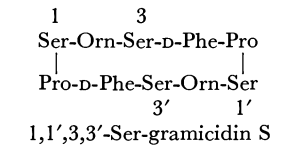

1,1′,3,3′-Ser-gramicidin S
(XIX)

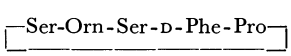

(XXIV)

Fig. 1

The synthetic scheme of 1,1′,3,3′-L-seryl gramicidine S is shown in Fig. 2. The blocking groups were used as follows: the δ amino group of the ornithine was protected by the Z group, the carboxyl groups of the C terminus amino acids were blocked by the methyl ester, while the hydroxyl group of serine was protected by the benzyl and the BOC group was used as a protecting group for the amino group of serine.

The BOC-pentapeptide methyl ester (XI) was prepared by the usual coupling methods, DCCD, mixed anhydride, and the azide method, mp 138.5—139°C, $[\alpha]_D^{24}$ −40.8° (*c* 1.0, AcOH). The ester of pentapeptide (XI) was converted into the hydrazide (XII) by hydrazinolysis in methanol, while XI was also converted into the free ester (XIII) by the acid-catalyzed cleavage of the BOC group. These two components could be coupled by means of the azide method to form the BOC-decapeptide methyl ester (XIV) as a white powder in a 75.5% yield; $[\alpha]_D^{24}$ −47.8° (*c* 0.5, AcOH).

The BOC-decapeptide ester (XIV) was converted into the BOC-decapeptide *p*-nitrophenyl ester (XVI) by hydrolysis with sodium hydroxide in a methanol solution, followed by esterification with *p*-nitrophenol and *N*,*N*′-dicyclohexylcarbodiimide. The active ester (XVI) was confirmed by thin-layer chromatography on silica gel and by a study of its IR spectra at 1760 cm^{-1} (ester) and 1350 cm^{-1} (C–NO$_2$); it was used immediately for the next reaction. The *N*-terminal protecting group (BOC) of the decapeptide active ester (XVI) was removed by treatment with anhydrous trifluoroacetic acid. The

*1 Part II: K. Okawa, K. Hori, K. Hirose, and Y. Nakagawa, This Bulletin, **42**, 2720 (1969).

*2 Deceased 30 June, 1968.

*3 Present address: Peptide Center, Institute for Protein Research, Osaka University, Kita-ku, Osaka.

*4 Present address: Toyo Institute of Food Technology, Kawanishi.

1) H. Aoyagi, T. Kato, M. Ohno, M. Waki, S. Makizumi and N. Izumiya, This Bulletin, **38**, 2139 (1965); H. Aoyagi and N. Izumiya, *ibid.*, **39**, 1747 (1966); H. Aoyagi, M. Kondo, T. Kato, S. Makizumi and N. Izumiya, *ibid.*, **40**, 1685 (1967).

*5 The abbreviations used for the amino acid residues, peptides and other abbreviations are based on the proposals by: E. Schröder and K. Lübke "The Peptides." Academic Press, New York, 1965. E. Bricas (ed.) "Peptides 1968" Proceedings of the Ninth European Peptide Symposium, Orsay, France, April 1968., North-Holland Publishing Company, Amsterdam.

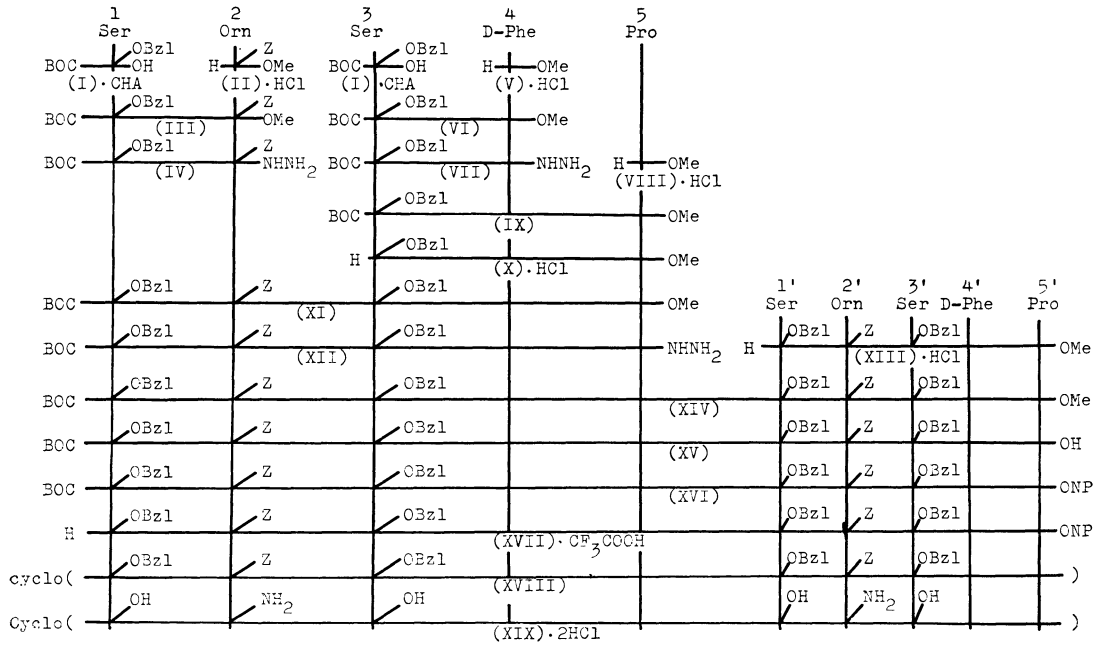

Fig. 2. Synthetic route of 1,1′,3,3′-Ser-gramicidin S (XIX).

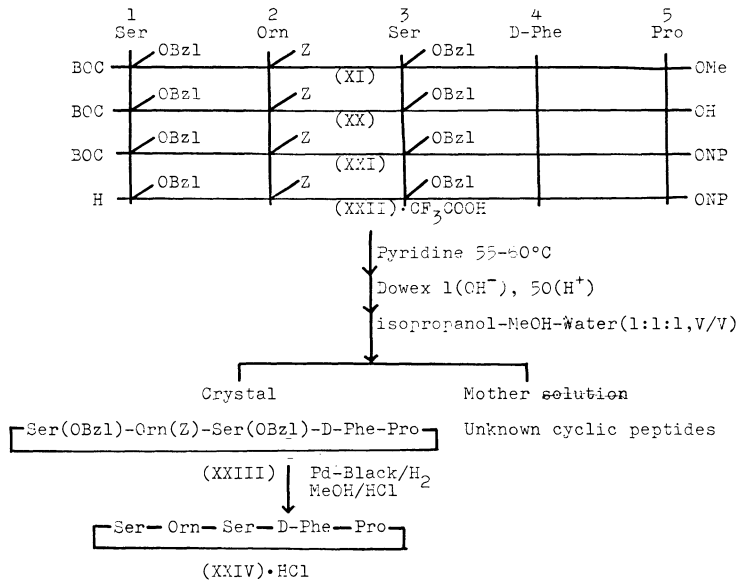

Fig. 3. Cyclization of linear pentapeptide.

cyclization of the free decapeptide *p*-nitrophenyl ester (XVII) trifluoroacetate was accomplished by means of Schwyzer's high-dilution method.[2] It was carried out by the drop-by-drop addition (4 hr 57°C) of XVII trifluoroacetate in DMF to a large amount of anhydrous pyridine (5×10^{-4}M solution). The crude product in methanol-water (10:1 V/V) was treated with Dowex 1(OH^-) and 50(H^+) to remove the linear peptide fractions. From the neutral part, *cyclo* (Ser(OBzl)-Orn(Z)-Ser(OBzl)-D-Phe-Pro)$_2$ (XVIII) was obtained as crystal in a 44.6% yield (mp 246—247°C, $[\alpha]_D^{24}$ −185.0° (*c* 0.2, AcOH)); it was confirmed by molecular-weight measurements. The protecting groups of XVIII were removed by catalytic hydrogenation, and the resulting 1,1′,3,3′-L-seryl gramicidin S (XIX) dihydrochloride was crystallized from methanol-ether

2) R. Schwyzer and P. Sieber, *Helv. Chim. Acta*, **40**, 624 (1957).

in a 75.7% yield; mp 320°C (dec.), $[\alpha]_D^{25}$ −126° (*c* 0.1, AcOH). This analogue (XIX) of gramicidin S has almost the same mobility on paper electrophoresis as the native gramicidin S (Fig. 4).

As an alternative approach to the synthesis of gramicidin S, Schwyzer and Sieber have reported that gramicidin S can be synthesized by the dimeric cyclization of the linear pentapeptide active ester.[3] Izumiya and Waki reported, however, that the linear pentapeptide active ester does not cyclize in the dimeric form exclusively, but that monomeric cyclization occurs.[4] The present authors have also at tempted the dimeric cyclization reaction of our pentapeptide (Fig. 3).

The BOC-pentapeptide methyl ester (XI) was saponified and then converted into the BOC-pentapeptide *p*-nitrophenyl ester (XXI) by estirification using DCCD. After the cleavage of the BOC group by treatment with anhydrous trifluoroacetic acid, the cyclization reaction were carries out as has been described above in the case of anhydrous pyridine. The molar concentrations of the pentapeptide active ester (XXII) trifluoroacetate in pyridine, 0.26×10^{-3} mol, 1.3×10^{-3} mol and 6.5×10^{-3} mol, were employed for the cyclization reactions. The resulting crude product was treated in methanol-water (5 : 1 v/v) with Dowex 1 (OH^-) and Dowex 50(H^+) to remove any linear peptide fractions. Cyclic pentapeptide (XXIII), *cyclo* Ser(OBzl)-Orn-(Z)-Ser(OBzl)-D-Phe-Pro, could be isolated as crystals from a solution of isopropanol-methanol-water (1 : 1 : 1 v/v) and was confirmed by molecular-weight measurements; mp 118—119°C, $[\alpha]_D^{24}$ −93.4° (*c* 0.7, AcOH). The resulting *cyclo* Ser-Orn-Ser-D-Phe-Pro (XXIV) hydrochloride was crystallized from methanol-ether in an 82.3% yield, mp 250°C (dec.), $[\alpha]_D^{24}$ −156.8° (*c* 0.5, AcOH), and was shown to have a smaller mobility than either the native gramicidin S or the cyclic decapeptide (XIX) on paper electrophoresis, as is shown in Fig. 4.

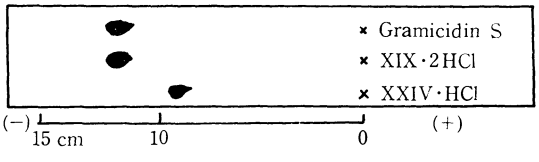

Fig. 4. Paper electrophoresis: solvent system AcOH 1M HCOOH 0.6M (pH 1.8) 600 V/30 cm 2 hr Toyo Roshi No. 50.

In the mother solution of XXIII, the presence of cyclic decapeptide (XVIII) and two other products was confirmed on thin-layer chromatography in each case, but no crystalline cyclic peptides other than cyclic decapeptide could be isolated. Under different concentrations of the cyclization, the yields of the cyclic pentapeptides were 76.3% (0.26×10^{-3} mol), 50.2% (1.3×10^{-3} mol), and 13.4% (6.5×10^{-3} mol) respectively.

The above results confirmed that the yield of the cyclic pentapeptide decreases proportionally to the increase in the reaction concentration, and that the monomeric cyclization proceeded predominantly more than the dimeric cyclization when the high-dilution method was used.

The biological activities of cyclic pentapeptide (XXIV) hydrochloride and 1,1',3,3'-L-seryl-gramicidin S (XIX) dihydrochloride against several microorganisms were investigated by the paper-disk method. No antibiotic activity could be found against *B. subtilis*, *St. albus*, *M. lysodakius*, and *E. coli*. From the above results, it may be concluded that the lipophilic amino acid residues are essential groups in contributing to gramicidin S activities.

Experimental

All the melting points are uncorrected.

***N*-*t*-Butyloxycarbonyl-*O*-benzyl-L-serine (I) Cyclohexylamine salt.** I was prepared from *O*-benzyl-L-serine[5] according to Anderson's method[6] in an 80% yield; mp 156—157°C, $[\alpha]_D^{24}$ +29.5° (*c* 1.3, MeOH).

Found: C, 63.78; H, 8.62; N, 7.14%. Calcd for $C_{21}H_{34}O_5N_2$: C, 63.93; H, 8.69; N, 7.10%.

N^{δ}-Benzyloxycarbonyl-L-ornithine Methyl Ester (II) Hydrochloride. II hydrochloride was prepared by the method of Boissonnas[7] in a 92.4% yield. N^{α},N^{δ}-dibenzyloxycarbonyl-L-ornithine[8] was treated with thionyl chloride in anhydrous ether-tetrahydrofuran (9 : 1 v/v), and with anhydrous methanol; mp 140—142°C, $[\alpha]_D^{24}$ +2.2° (*c* 1.0, AcOH).

Found: C, 53.30; H, 6.63; N, 8.86; Cl, 11.32%. Calcd for $C_{14}H_{21}O_4N_2Cl$: C, 53.08; H, 6.68; N, 8.84; Cl, 11.19%.

BOC-Ser(OBzl)-Orn(Z)-OMe(III). II (from the hydrochloride; 9.5 g, 0.03 mol) was treated with *N,N'*-dicyclohexylcarbodiimide (6.8 g, 0.03 mol) and I (from cyclohexylamine salt 11.8 g, 0.03 mol) in methylene chloride (200 m*l*) at 5°C for 1 hr. After the reaction mixture had then been allowed to stand overnight at room temperature, acetic acid (3 m*l*) was added and the reaction mixture was stirred for 15 min. The precipitate thus produced was filtered off; after the filtrate had been washed with 0.1N hydrochloric acid, N sodium bicarbonate, and water successively, it was dried over anhydrous sodium sulfate and then concentrated under reduced pressure. III was obtained from ethyl acetate - petroleum ether in a 90% (15 g) yield. The product was recrystallized from ethyl acetate - petroleum ether; mp 86—88°C, $[\alpha]_D^{24}$ +2.8° (*c* 1.1, AcOH).

3) R. Schwyzer and P. Sieber, *Helv. Chim. Acta*, **41**, 2186 (1958).

4) M. Waki and N. Izumiya, This Bulletin, **40**, 1687 (1967).

5) K. Okawa, *ibid.*, **29**, 486 (1956).

6) G. W. Anderson and A. C. Mc Gregon, *J. Amer. Chem. Soc.*, **79**, 6180 (1957).

7) R. A. Boissonnas, S. Guttmann, R. L. Huguenin, P. A. Jaquenoud and E. Sandrin, *Helv. Chim. Acta*, **41**, 1867 (1958).

8) R. L. M. Synge, *Biochem. J.*, **42**, 99 (1948).

Found: C, 62.47; H, 6.79; N, 7.44%. Calcd for $C_{29}H_{39}O_8N_3$: C, 62.46; H, 7.04; N, 7.53%.

BOC-Ser(OBzl)-Orn(Z)-NHNH$_2$ (IV). To III (54.64 g, 1.00 mol) in ethanol (200 m*l*), we added 80% hydrazine hydrate (63 g, 1.25 mol) in ethanol (100 m*l*) and then stirred the mixture for 1 hr in an ice-bath. After the reaction mixture had been kept at room temperature for 3 days, white crystals were formed; these were collected (45.50 g), and another crop of the hydrazide (8.29 g) was obtained from the mother liquor. The total yield was 53.79 g (98%). They were recrystallized from ethanol - water; mp 152—154°C, $[\alpha]_D^{24}$ −9.5° (*c* 1.0, AcOH).

Found: C, 60.39; H, 7.14; N, 12.60%. Calcd for $C_{28}H_{39}O_7N_5$: C, 60.31; H, 7.03; N, 12.56%.

BOC-Ser(OBzl)-D-Phe-OMe (VI). I (from cyclohexylamine salt (7.89 g, 0.02 mol)) was treated with ethyl chloroformate (2.17 g, 0.02 mol) and triethylamine in THF at −5°C. After the solution had stood for 20 min, D-phenylalanine methyl ester (V) (from hydrochloride[9] (4.31 g, 0.02 mol)) was added, drop by drop, to the above solution at −5°C. After the reaction mixture had then been allowed to stand overnight at room temperature, the precipitate thus produced was filtered off. The solvent was replaced by ethyl acetate (70 m*l*); after the solution had then been washed with water, 4% sodium bicarbonate, 0.5N hydrochloric acid, and water successively, it was dried over anhydrous sodium sulfate and concentrated under reduced pressure. VI was obtained from ethyl acetate – *n*-hexane in a 76.8% (7.03 g) yield. Recrystallization from ethyl acetate–*n*-hexane gave a pure material; mp 81.5—82°C, $[\alpha]_D^{13}$ −18.7° (*c* 1.1, AcOH).

Found: C, 65.82; H, 6.97; N, 6.13%. Calcd for $C_{25}H_{32}O_6N_2$: C, 65.77; H, 7.06; N, 6.14%.

BOC-Ser(OBzl)-D-Phe-NHNH$_2$ (VII). VI (6.7 g, 0.01 mol) was treated with 80% hydrazine hydrate (1.5 g, 0.03 mol) in anhydrous methanol (12 m*l*). After the reaction mixture had then been allowed to stand for 46 hr at room temperature, it was concentrated to dryness. The precipitate was recrystallized from ethyl acetate–*n*-hexane. The yield was 6.0 g (89.5%). Mp 114—115°C, $[\alpha]_D^{13}$ −6.3° (*c* 1.1, AcOH).

Found: C, 63.17; H, 7.04; N, 12.28%. Calcd for $C_{24}H_{32}O_5N_4$: C, 63.14; H, 7.06; N, 12.28%.

BOC-Ser(OBzl)-D-Phe-Pro-OMe (IX). Into a solution of VII (2.29 g, 5 mmol) in acetic acid (25 m*l*) and N hydrochloric acid (10 m*l*), we added N sodium nitrite (5 m*l*) drop by drop under cooling at −5——10°C. After stirring for 10 min, sodium bicarbonate (1.5 g) and ice-cold water (50 m*l*) were added to the above solution and the product was extracted with ice-cold ethyl acetate (50 m*l*). The organic layer was washed with ice-cold 0.5N sodium bicarbonate, and then immediately cooled to under −5°C. To this, the L-proline methyl ester (VIII) (from hydrochloride;[9] 0.94 g, 5.65 mmol) was stirred in, drop by drop; the stirring was thereafter continued for 3 hr at 0°C. After the reaction mixture had been allowed to stand overnight in a refrigerator, it was washed with 0.1N hydrochloric acid, N sodium bicarbonate, and water. The solution was dried over anhydrous sodium sulfate and then concentrated under reduced pressure. IX was obtained from ether–*n*-hexane in the theoretical yield; mp 62—63°C, $[\alpha]_D^{24}$ −46.6° (*c* 1.0, AcOH).

Found: C, 64.79; H, 7.22; N, 7.56%. Calcd for $C_{30}H_{39}O_7N_3$: C, 65.08; H, 7.10; N, 7.59%.

H-Ser(OBzl)-D-Phe-Pro-OMe (X) Hydrochloride. Through an ethyl acetate (45 m*l*) solution of IX (5.54 g, 0.01 mol) dry hydrogen chloride was bubbled for 30 min in an ice-bath. After the reaction mixture had then been allowed to stand at room temperature for 30 min, the solution was concentrated under reduced pressure. The addition of ether gave 4.65 g (95%) of a white powder; mp 189.5—190°C.

Found: C, 61.20; H, 6.52; N, 8.53; Cl, 7.32%. Calcd for $C_{25}H_{32}O_5N_3Cl$: C, 61.28; H, 6.58; N, 8.58; Cl, 7.24%.

BOC-Ser(OBzl)-Orn(Z)-Ser(OBzl)-D-Phe-Pro-OMe (XI). IV (12.27 g, 22 mmol) (5 m*l*) was coupled with X (from hydrochloride (10.47 g, 22 mmol)) in ethyl acetate (300 m*l*) by the azide method described in connection with compound IX. The subsequent crystallization from ethyl acetate gave 19.1 g of XI (88.8%); mp 138.5—139°C, $[\alpha]_D^{24}$ −40.8° (*c* 1.0, AcOH).

Found: C, 64.72; H, 6.92; N, 8.43%. Calcd for $C_{53}H_{66}O_{12}N_6$: C, 65.01; H, 6.79; N, 8.58%.

BOC-Ser(OBzl)-Orn(Z)-Ser(OBzl)-D-Phe-Pro-NHNH$_2$ (XII). Hydrazine hydrate (80%) (5.1 g, 102 mmol) in anhydrous methanol (10 m*l*) was added to an anhydrous methanol solution (40 m*l*) of XI (5 g, 5.1 mmol). The reaction mixture was then kept at 35—40°C for 3 days. After the excess hydrazine had then been removed under reduced pressure, a large amount of cold water was added. The product was soon solidfied; it was collected as a white powder, and dried in a desiccator over sulfuric acid to yield 4.80 g (96%). $[\alpha]_D^{23}$ −37.3° (*c* 0.7, AcOH).

Found: C, 63.85; H, 6.92; N, 11.21%. Calcd for $C_{52}H_{66}O_{11}N_8$: C, 63.78; H, 6.80; N, 11.45%.

H-Ser(OBzl)-Orn(Z)-Ser(OBzl)-D-Phe-Pro-OMe (XIII) Hydrochloride. Through an anhydrous dioxane (20 m*l*) solution of XI (2 g, 2.04 mmol), dry hydrogen chloride was bubbled for 20 min under cooling in an ice-bath. The reaction mixture was then allowed to stand room temperature for 1 hr. After the evaporation of the solvent and hydrogen chloride under reduced pressure, ether was added to the residual oil. The crude product was recrystallized from methanol–ether; yield, 1.72 g (92.4%); mp 168°C.

Found: C, 62.67; H, 6.78; N, 9.05; Cl, 4.11%. Calcd for $C_{48}H_{59}O_{10}N_6Cl$: C, 62.97; H, 6.50; N, 9.18; Cl, 3.87%.

BOC-(Ser(OBzl)-Orn(Z)-Ser(OBzl)-D-Phe-Pro)$_2$-OMe (XIV). XII (2.94 g, 3 mmol) and XIII (from hydrochloride (2.75 g, 3 mmol)) were coupled by the azide method in the same way as was used in the case of the synthesis of compound IX. The resulting oily material was chromatographed over silica gel using ethy acetate as a solvent. A white powder was subsequently obtained by the addition of *n*-hexane. Yield, 4.14 g (75.5%); $[\alpha]_D^{23}$ −47.8° (*c* 0.5, AcOH).

Found: C, 65.50; H, 6.67; N, 9.29%; mol wt,*6 1875. Calcd for $C_{100}H_{120}O_{21}N_{12}$: C, 65.77; H, 6.62; N, 9.20%; mol wt, 1826.

9) B. F. Erlanger, H. Sachs and E. Brand, *J. Amer. Chem. Soc.*, **76**, 1806 (1954).

*6 Knauer Vapour Pressure Osmometer; solvent: methanol, standard curve; the solution of BOC-Ser-(OBzl)-D-Phe-OMe (VI) in methanol.

BOC-(Ser(OBzl)-Orn(Z)-Ser(OBzl)-D-Phe-Pro)$_2$-OH (XV). XIV (1.83 g, 1 mmol) in anhydrous methanol (20 ml) was treated with 2N sodium hydroxide (2 ml, 4 mmol) at room temperature. The solution was kept at 37°C until no turbidity appeared upon the addition of one drop of water (8 hr) After the solution had then been adjusted to pH 2 with N hydrochloric acid (about 4 ml) in an ice-bath, water (100 ml) was added to give a precipitate; yield, 1.54 g. Recrystallization from methanol - water yielded 1.32 g (73%) of pure crystals; mp 113—115°C, R_f 0.15*7 $[\alpha]_D^{23}$ −39.3° (*c* 0.9, AcOH).

Found: C, 65.66; H, 6.54; N, 9.34%; mol wt, 1820.*6 Calcd for $C_{99}H_{118}O_{21}N_{12}$: C, 65.62; H, 6.56; N, 9.28%; mol wt, 1820.

BOC-(Ser(OBzl)-Orn(Z)-Ser(OBzl)-D-Phe-Pro)$_2$-ONP (XVI). XV (500 mg, 0.27 mmol) and *p*-nitrophenol (70 mg, 0.5 mmol) were dissolved in methylene chloride (5 ml), and then a methylene chloride solution of *N,N'*-dicyclohexylcarbodiimide (62 mg, 0.30 mmol) was added, drop by drop, to the solution at 0—5°C. The reaction mixture was allowed to stand overnight in a refrigerator. After the addition of acetic acid (one drop), the dicyclohexylurea thus produced was filtered off and washed with cold ethyl acetate. The filtrate was concentrated under reduced pressure, and the resulting oily material was dissolved in a cold ethyl acetate solution. It was washed with N sodium bicarbonate and water to remove the excess *p*-nitrophenol, and then dried over anhydrous sodium sulfate. XVI was obtained from ethyl acetate–ether in the yield of 460 mg (88%); mp 110—112°C, R_f 0.89*7 ν_{max}^{Nujol} 1760 (ester), 1350 cm^{-1} (C–NO$_2$).

Found: C, 63.98; H, 6.26; N, 9.42%. Calcd for $C_{105}H_{121}O_{23}N_{13}\cdot 2H_2O$: C, 64.04; H, 6.39; N, 9.25%.

***Cyclo* (Ser(OBzl)-Orn(Z)-Ser(OBzl)-D-Phe-Pro)$_2$ (XVIII).** The BOC-decapeptide active ester (XVI) (200 mg, 0.1 mmol) was dissolved in anhydrous trifluoroacetic acid (3 ml), after which the solution was kept at 0°C for 1 hr. The trifluoroacetic acid was subsequently evaporated under reduced pressure at room temperature. The residual decapeptide *p*-nitrophenyl ester (XVII) trifluoroacetate was immediately dissolved in dimethylformamide (10 ml) without purification. A DMF solution containing 5 drops of acetic acid was added, drop by drop, to pyridine (200 ml) at 57°C over a 4 hr period, after which the stirring was continued for an additional 2 hr. The solution was then evaporated under reduced pressure and water was added to give a crude product. This colored product was collected, washed with water, and dissolved in a mixed solvent of methanol and water (5 : 1 v/v). After the insoluble substance had been filtered off, the filtrate was treated with a Dowex 1 (OH^-) column (1.5×20 cm) and a Dowex 50 (H^+) column (1.5×20 cm). The effluent (300 ml) was evaporated; the subsequent addition of water yielded a white powder which gave a negative ninhydrin reaction; 75.5 mg (44.6%). Purification with Sephadex LH-20 and recrystallization from ethanol - water yielded 50.7 mg (30% from XVI) of XVIII; mp 246—247°C, R_f 0.88,*7 $[\alpha]_D^{24}$ −185.0° (*c* 0.2, AcOH).

Found: C, 65.64; H, 6.46; N, 9.90%. Calcd for $C_{94}H_{112}O_{20}N_{12}$: C, 65.26; H, 6.53; N, 9.72%; mol wt,*6 1710, Calcd for $C_{94}H_{108}O_{18}N_{12}$; mol wt, 1694.

*7 Thin-layer chromatography with Merck silica gel; solvent system; water saturated ethyl acetate.

***Cyclo* (Ser-Orn-Ser-D-Phe-Pro)$_2$ (XIX) Dihydrochloride.** A methanol solution (5 ml) of XVIII (84.7 mg, 0.05 mmol) containing N hydrochloric acid (0.05 ml) was hydrogenated, by the use of palladium black (300 mg) as the catalyst, at room temperature for 42.5 hr. After the catalyst had been filtered off and the solvent had been evaporated under reduced pressure, the addition of methanol - ether gave needle crystals (43.1 mg (75.7%)); mp 320°C (dec.), $[\alpha]_D^{25}$ −126° (*c* 0.1, AcOH), R_f 0.55.*8

Found: C, 47.69; H, 6.36; N, 13.58%. Calcd for $C_{50}H_{83}O_{19}N_{12}Cl_2$: C, 48.89; H, 6.89; N, 13.69%.

Amino acid ratios in acid hydrolyzate: Ser 1.94, Orn 0.89, Phe 1.00, Pro 1.03.

BOC-Ser(OBzl)-Orn(Z)-Ser(OBzl)-D-Phe-Pro-OH (XX). XI (4.9 g, 5 mmol) in dioxane (5 ml) was treated with N sodium hydroxide (5.25 ml) at room temperature for 2 hr. The reaction mixture was then adjusted to pH 2 with N hydrochloric acid, the reaction products were extracted with methylene chloride, and the organic layer was dried over anhydrous sodium sulfate. The solvent was evaporated under reduced pressure, and the residuals were crystallized from ethyl acetate–*n*-hexane (4.35 g (90.1%)). Recrystallization from methanol–water gave a pure material; mp 135.5—136°C, R_f 0.10,*7 $[\alpha]_D^{24}$ −35.2° (*c* 1.0, AcOH).

Found: C, 64.82; H, 6.94; N, 8.54%. Calcd for $C_{52}H_{64}O_{12}N_6$: C, 64.71; H, 6.68; N, 8.71%.

BOC-Ser(OBzl)-Orn(Z)-Ser(OBzl)-D-Phe-Pro-ONP (XXI). A solution of XX (9.7 g, 10 mmol) and *p*-nitrophenol (2.8 g, 20 mmol) in methylene chloride (30 ml) was treated with *N,N'*-dicyclohexylcarbodiimide (2.27 g, 11 mmol) at 0°C for 4 hr with stirring. After the dicyclohexylurea thus produced had been filtered off, the reaction mixture was washed with 10% citric acid, N sodium bicarbonate, and water successively, and then dried over anhydrous sodium sulfate. The solvent was evaporated under reduced pressure. The residual crystals were recrystallized from ethyl acetate–ether (8.99 g (82.6%)); mp 151—152°C, $[\alpha]_D^{24}$ −35.8° (*c* 1.0, AcOH), ν_{max}^{Nujol} 1770 (ester), 1345 cm^{-1} (C–NO$_2$).

Found: C, 63.35; H, 6.41; N, 9.23%. Calcd for $C_{58}H_{67}O_{14}N_7$: C, 64.13; H, 6.22; N, 9.03%.

***Cyclo* Ser(OBzl)-Orn(Z)-Ser(OBzl)-D-Phe-Pro (XXIII).** XXI (1.09 g, 1 mmol) was suspended in anhydrous trifluoroacetic acid (2.5 ml) containing anisole (0.25 ml), after which the mixture was allowed to stand at 0°C for 1 hr. After the solvent had been removed under reduced pressure at room temperature, the addition of absolute ether gave a white powder of XXII trifluoroacetate (1.03 g (93.6%)). This active ester was used immediately in the following cyclization procedure.

XXII trifluoroacetate (768 mg, 0.698 mmol), dissolved in DMF (10 ml) containing 6 drops of acetic acid, was stirred, drop by drop, into anhydrous pyridine (2685 ml, 0.26×10^{-3} molar concentration of XXII·CF_3COOH) at 55—60°C for 4 hr. After the stirring had been continued for 2 hr, the solvent was evaporated under reduced pressure. The residual oil was dissolved in methanol–water (5 : 1 v/v) and then treated with Dowex 1 (OH^-) and 50 (H^+). After elution with the same solvent (300 ml), the effluent was concentrated

*8 Thin-layer chromatography with Merck silica gel; solvent system; *n*-butanol: acetic acid: water: pyridine 4 : 1 : 2 : 1 (v/v).

under reduced pressure and the residuals were treated with isopropanol–methanol–water (1 : 1 : 1 v/v). *Cyclo* Ser(OBzl)-Orn(Z)-Ser(OBzl)-D-Phe-Pro (XXIII) was thus obtained as fine crystals; yield, 451 mg (76.3%), R_f 0.53*[7], mp 118—119°C $[\alpha]_D^{24}$ −93.4° (*c* 0.7, AcOH).

Found: C, 65.52; H, 6.45; N, 10.17%; mol wt*[6], 867. Calcd for $C_{47}H_{56}O_{10}N_6$: C, 65.24; H, 6.53; N, 9.72%; mol wt, 847.

In other cases using different concentrations of the active ester (1.3×10^{-3} mol and 6.5×10^{-3} mol), XXIII was also obtained as crystals, but in different yields (50.2% and 13.4% respectively). From the mother solution, cyclic decapeptide (XVIII), R_f 0.88*[7] and two other cyclic peptides, R_f 0.77*[7] and 0.85*[7] confirmed in each case on thin-layer chromatography, but no crystalline cyclic peptides have yet been isolated except for cyclic decapeptide (XVIII).

***Cyclo* Ser-Orn-Ser-D-Phe-Pro (XXIV) Hydrochloride.** XXIII (169 mg, 0.2 mmol) was hydrogenated in methanol (10 m*l*) with N hydrochloric acid (0.2 m*l*), using palladium black (200 mg) as the catalyst at room temperature for 13.5 hr. After the catalyst had then been filtered off and the solvent removed under reduced pressure, the addition of methanol–ether gave needle crystals (80 mg (75%)); mp 250° (dec.), $[\alpha]_D^{25}$ −156.8° (*c* 0.6, AcOH), R_f 0.55.*[8]

Found: C, 52.75; H, 6.61; N, 14.63; Cl, 6.47%. Calcd for $C_{25}H_{37}O_7N_6Cl$: C, 52.76; H, 6.55; N, 14.77; Cl, 6.23%. Amino acid ratios in acid hydrolyzate: Ser 1.93, Orn 0.87, Phe 1.00, Pro 0.94.

The authors wish to express their deep thanks to Mr. Kiyotaka Hori and his staff of the Fuji Photo Film Co., Ltd., for their amino acid analyses, and to the staff of the Toyo Jozo Co., Ltd., for their elemental microanalyses. They are also indebted to Dr. Homare Kuwana, Kwansei Gakuin University, Department of Biology, for the bioassays.

BULLETIN OF THE CHEMICAL SOCIETY OF JAPAN VOL. 43 3251—3255 (1970)

The Synthesis of a Partial Sequence of Proinsulin Using the A-Chain of Natural Insulin

Yasutsugu SHIMONISHI

The Institute of Scientific and Industrial Research, Osaka University, Suita-shi, Osaka

(Received May 23, 1970)

Elongation reactions of the *S*-sulfonate of the A-chain of bovine insulin were carried out with acylamino acid-active esters or with acylpeptide azide; the following derivatives of the A-chain were thus synthesized: *S*-sulfonates of N^G-nitro-L-arginyl-, L-lysyl-N^G-nitro-L-arginyl-, and L-prolyl-L-prolyl-L-glutaminyl-N^ε-benzyloxycarbonyl-L-lysyl-N^G-nitro-L-arginyl-A-chain. Thus, this was demonstrated to be a useful procedure for the partial synthesis of proinsulin.

Insulin has been successfully synthesized by binding a synthetic A-chain with a natural B-chain[1] or *vice versa*.[2] This is one so-called half-synthesis of complicated polypeptides. The possibility that natural peptide fragments may be used in the synthesis of longer molecules has already been suggested by Goldberger and Anfinsen,[3] and by Offord.[4] However, no examples of successful re- or half-syntheses of natural linear polypeptides from natural or synthetic fragments have yet been reported. Nevertheless, this type of synthesis can be an important preliminary step in the total synthesis of complicated natural polypeptides. The difficulties in this procedure stem from the structure of the peptide fragments involved: when a natural peptide fragment is used as an amino component, all the amino groups except that to be acylated must be protected with suitable groups, and when it is used as a carboxyl component, all functional groups with active hydrogen except that to be activated should be protected.

Recently, proinsulins, the single-chain precursor of insulin, have been isolated from several sources,[5–7]

1) P. G. Katsoyannis, A. Tometsko and K. Fukuda, *J. Amer. Chem. Soc.*, **85**, 2863 (1963).

2) C.-i. Niu, Y.-t. Kung, W.-t. Huang, L.-t. Ke, C.-c. Chen, Y.-c. Chen, Y.-c. Du, R.-q. Jiang, C.-l. Tsou, S.-c. Hu, S.-q. Chu and K.-z. Wang, *Scientia Sinica*, **14**, 1386 (1965).

3) R. F. Goldberger and C. B. Anfinsen, *Biochemistry*, **1**, 401 (1962).

4) R. E. Offord, *Nature*, **221**, 37 (1969).

5) R. E. Chance, R. M. Ellis and W. W. Bromer, *Science*, **161**, 165 (1968).

6) D. F. Steiner, O. Hallund, A. H. Rubenstein, S. Cho and C. Bayliss, *Diabetes*, **17**, 725 (1968).

7) J. L. Clark, S. Cho, A. H. Rubenstein and D. F. Steiner, *Biochem. Biophys. Res. Commun.*, **35**, 456 (1969).

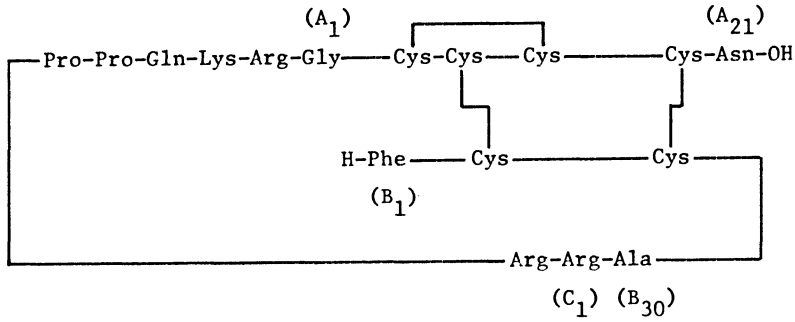

Fig. 1. Structural model of proinsulin from pig[5] and ox.[8]

and the primary structures of those of pig[5] and ox[8] have been elucidated. As is shown in Fig. 1, proinsulin is a linear polypeptide in which the amino terminus of the A-chain of insulin is linked to the carboxyl terminus of its B-chain by a connecting peptide (C-peptide). The A-chain of insulin has only one active amino group at the amino end of its peptide chain, and is readily obtainable from natural insulin. Thus, the natural A-chain seems to be a suitable starting material for the half-synthesis of proinsulin.

In the present study, the reactivities of the natural A-cain of insulin with acylamino acids and with acylpeptide were examined in the preliminary studies of the synthesis of proinsulin. First, the reactivity of A-chain *S*-sulfonate[9] was tested with acylamino acid-active esters. This *S*-sulfonate seemed suitable not only for the protection of the thiol functions, but also for the solubilization of the A-chain in an alkaline medium. Those properties should favor the use of this peptide in the coupling reactions. Next, the author attempted the azide coupling of an acylpeptide with A-chain *S*-sulfonate. The C-terminus of the connecting peptide in proinsulin is arginine, and the coupling of an acylpeptide, having an arginyl residue in the C-terminus, with the natural A-chain by the azide procedure seemed likely to be difficult. Therefore, the author attempted fragment condensation by the azide procedure after a one-step elongation of the A-chain with an N^G-nitro-L-arginine residue.

When this study had almost been completed, the author realized that Zahn *et al.*[10] had published a paper on the syntheses of three A-chain peptides; L-lysyl-, L-histidyl-, and L-arginyl-A-chain. Especially, Zahn *et al.* used DES-glysine-A-chain, obtained by the Edman-degradation of the A-chain, as a starting peptide for the synthesis of L-arginyl-A-chain. Their procedure may have advantages, since the acylated peptide, which is intended to be coupled with DES-glycine-A-chain, should have a glycine residue in the carboxyl terminus, and it may be activated by various coupling methods. However, this procedure seems unnecessarily complicated if the direct elogation of the A-chain with acylated peptide is possible. The possibility of the direct elongation of the A-chain received special attention in the present investigation.

Experimental

Crystalline bovine insulin was obtained from the Chemical Research Laboratories, Takeda Chemical Industries, Ltd. (Osaka), by the courtesy of Dr. M. Fujino. The *S*-sulfonate of the A-chain was prepared from insulin as has been described in the literature.[9,11-12] The dialysis tubing 24/32 was a product of the Visking Co. (Chicago). Sephadex G-25 fine was purchased from the Pharmacia Co. (Uppsala). The chemicals used were of a reagent grade and were used without further purification. Paper electrophoresis was performed at pH 2.1 in a 4M urea-3M formic acid buffer.[11] The purity of the A-chain derivatives thus synthesized was confirmed by paper electrophoresis and by the recovery of the constituent amino acids from acid hydrolysates upon amino-acid analysis. All the melting points given are uncorrected.

***S*-Sulfonate of N^G-Nitro-L-arginyl-A-chain.** The *S*-sulfonate of the A-chain (413 mg) was dissolved in water (3 ml) with sodium bicarbonate (0.16 g), and then a solution of the N^α-*p*-methoxybenzyloxycarbonyl-N^G-nitro-L-arginine pentachlorophenyl ester[13] (1.27 g) in dioxane (6 ml) was added. The mixture was mechanically agitated for 2 days at room temperature, washed with ethyl acetate, and then concentrated *in vacuo*. The residue was then again treated with the fresh N^α-*p*-methoxybenzyloxycarbonyl-N^G-nitro-L-arignine pentachlorophenyl ester (0.63 g) in the same way as has been described above, and the mixture was stirred for one day more at room temperature. Then the reaction mixture was washed with ethyl acetate, concentrated *in vacuo*, and dried over phosphorus pentoxide. The residual powder was dissolved in trifluoroacetic acid

8) C. Nolan and E. Margoliash, unpublished data (1969).

9) J. L. Bailey and R. D. Cole, *J. Biol. Chem.*, **234**, 1733 (1959).

10) M. Weinert, D. Brandenburg and H. Zahn, *Hoppe-Seyler's Z. physiol. Chem.*, **350**, 1566 (1969).

11) H. Zahn and E. Drechsel, *ibid.*, **349**, 359 (1968).

12) Y. Shimonishi and H. Zahn, *Biochim. Biophys. Acta*, **154**, 598 (1968).

13) S. Sakakibara, unpublished.

(15 ml) together with anisole (0.7 ml), and the solution was allowed to stand for 30 min at room temperature. Then it was concentrated *in vacuo*, and the oily residue was dried over phosphorus pentoxide. It was then dissolved in 2% aqueous sodium bicarbonate and dialyzed against distilled water (500 ml) for 60 min at room temperature. The dialyzed solution was lyophilized. The lyophilizate was dissolved in a small volume of a 0.1M ammonium bicarbonate solution, charged on a column of Sephadex G-25 (2×50 cm), and eluted using the same buffer solution. The first peak in the eluate, with an absorption at 280 mμ (see Fig. 3), was collected and lyophilized to obtain the *S*-sulfonate of N^G-nitro-L-arginyl-A-chain as a solid; wt. 393 mg.

N^α,N^ε-Di-*t*-butyloxycarbonyl-L-lysine *N*-Hydroxysuccinimide Ester. N^α,N^ε-Di-*t*-butyloxycarbonyl-L-lysine[14,15] (1.38 g, 4.0 mmol) and *N*-hydroxysuccinimide (0.46 g, 4.0 mmol) were dissolved in absolute tetrahydrofuran (20 ml), after which the solution was cooled to −10°C. A solution of *N*,*N'*-dicyclohexylcarbodiimide (0.82 g, 4.0 mmol) in absolute tetrahydrofuran (10 ml) was added to the chilled solution. The solution was stirred for an hour at the same temperature and then for 24 hr at room temperature; the urea thus formed was filtered off and washed with ethyl acetate. The filtrate and washings were combined and concentrated to a syrup *in vacuo*, which was crystallized by trituration with petroleum ether; wt. 1.70 g. The crude material was recrystallized from ethyl acetate and petroleum ether; wt. 1.54 g (87.0%); mp 92—96°C, $[\alpha]_D^{18}$ −30.6° (*c* 2, ethanol).

Found: C, 54.18; H, 7.96; N, 9.19%. Calcd for $C_{20}H_{33}O_8N_3$: C, 54.16; H, 7.50; N, 9.48%.

S-Sulfonate of L-Lysyl-N^G-nitro-L-arginyl-A-chain. The *S*-sulfonate of N^G-nitro-L-arginyl-A-chain (104 mg) was dissolved in water (1.5 ml) containing sodium bicarbonate (0.04 g) and allowed to react with the N^α,N^ε-di-*t*-butyloxycarbonyl-L-lysine *N*-hydroxysuccinimide ester (0.22 g) dissolved in dioxane (2 ml). The reaction mixture was then treated as has been described for the synthesis of the *S*-sulfonate of N^G- nitro-L-arginyl -A-chain. The yield of the *S*-sulfonate of L-lysyl-N^G -nitro-L-arginyl-A-chain was 93.8 mg. This material had a slower mobility on paper by electrophoresis at pH 2.1 than the *S*-sulfonate of N^G-nitro-L-arginyl-A-chain.

***t*-Amyloxycarbonyl-L-prolyl-L-proline *N*-Hydroxysuccinimide Ester.** A solution of *t*-amyloxycarbonyl-L-prolyl-L-proline[16] (3.26 g, 10 mmol) and *N*-hydroxysuccinimide (1.15 g, 10 mmol) in absolute tetrahydrofuran (30 ml) was cooled to 0—5°C, and then *N*,*N'*-dicyclohexylcarbodiimide (2.06 g, 10 mmol) was added to the chilled solution. The mixture was stirred for an hour at the same temperature and then for 20 hr at room temperature, and the precipitate thus formed was removed by filtration. The filtrate was concentrated to a syrup *in vacuo*; crystals formed on storage in a refrigerator. The crude product was collected by filtration with petroleum ether; wt. 4.29 g. It was recrystallized from ethyl acetate and petroleum ether; wt. 4.04 g (95.5%), mp 111.5—112.5°C, $[\alpha]_D^{29}$ −103.8° (*c* 2, ethanol).

Found: C, 56.52; H, 7.91; N, 9.72%. Calcd for $C_{20}H_{29}O_7N_3$: C, 56.72; H, 6.90; N, 9.92%.

***o*-Nitrophenylsulfenyl-L-glutaminyl-N^ε-benzyloxycarbonyl-L-lysine Methyl Ester.** N^ε-Benzyloxycarbonyl-L-lysine methyl ester hydrochloride[17] (2.68 g, 8.09 mmol) and triethylamine (1.13 ml) were dissolved in dimethylformamide (25 ml), and then the *o*-nitrophenylsulfenyl-L-glutamine *N*-hydroxysuccinimide ester[18] (2.67 g, 6.74 mmol) was added to the solution. After having been stirred for 2 days at room temperature, the reaction mixture was diluted with ethyl acetate (*ca.* 200 ml). The solution was washed successively with 0.1N hydrochloric acid, 5% sodium bicarbonate, and water, and dried over anhydrous sodium sulfate. The dried solution was concentrated to obtain green crystals, which were then collected with ethyl acetate and petroleum ether; wt. 3.11 g. The crude product was recrystallized from methanol and water; wt. 3.00 g (77.3%), mp 155—157°C.

Found: C, 54.33; H, 5.60; N, 12.00; S, 5.47%. Calcd for $C_{26}H_{33}O_8N_5S$: C, 54.25; H, 5.78; N, 12.17; S, 5.57%.

***t*-Amyloxycarbonyl-L-prolyl-L-prolyl-L-glutaminyl-N^ε-benzyloxycarbonyl-L-lysine Methyl Ester.** The *o*-nitrophenylsulfenyl-L-glutaminyl-N^ε-benzyloxycarbonyl-L-lysine methyl ester (6.34 g, 11 mmol) was suspended in distilled dioxane (40 ml), and then treated with 4N HCl in dioxane (15 ml) for 15 min. The clear solution thus formed was concentrated to a syrup and dried over sodium hydroxide *in vacuo*. Then it was thoroughly washed with a mixture of acetone and ether. The residue was dissolved in dimethylformamide (40 ml), and triethylamine (1.6 ml) and the *t*-amyloxycarbonyl-L-prolyl-L-proline *N*-hydroxysuccinimide ester (3.95 g, 9.35 mmol) were added to the solution. After having been stirred for 2 days at room temperature, the reaction mixture was diluted with ethyl acetate (*ca.* 300 ml). The diluted solution was washed successively with 0.1N hydrochloric acid, 5% sodium bicarbonate, and water, and dried over anhydrous sodium sulfate. The dried solution was concentrated *in vacuo* to a syrup; wt. *ca.* 5.6 g. This material has not yet been crystallized.

***t*-Amyloxycarbonyl-L-prolyl-L-prolyl-L-glutaminyl-N^ε-benzyloxycarbonyl-L-lysine Hydrazide.** The syrupy material of the *t*-amyloxycarbonyl-L-prolyl-L-prolyl-L-glutaminyl-N^ε-benzyloxycarbonyl-L-lysine methyl ester (*ca.* 5.6 g) was dissolved in ethanol (80 ml), and then 100% hydrazine hydrate (8 ml) was added to the solution. After standing for 24 hr at room temperature, the mixture was concentrated to a syrup; crystals were obtained by rubbing the syrup with petroleum ether; wt. 5.40 g. The crude product was recrystallized from ethanol and ether; wt. 4.82 g (70.5% of the theoretical yield based on the content of the *t*-amyloxycarbonyl-L-prolyl-L-proline *N*-hydroxysuccinimide ester); mp 104°C, $[\alpha]_D^{18}$ −68.5° (*c* 2, ethanol).

Found: C, 57.47; H, 7.55; N, 15.04%. Calcd for

14) L. Bernardi, G. Bosisio, R. De. Castiglione, O. Goffredo and F. Chillemi, *Gazz. Chim. Ital.*, **94**, 853 (1964).

15) K. Hofmann, R. Schmiechen, R. D. Wells, Y. Wolman and N. Yanaihara, *J. Amer. Chem. Soc.*, **87**, 611 (1965).

16) S. Sakakibara and N. Inukai, This Bulletin, **39**, 1567 (1966).

17) R. A. Boissonnas, S. Guttmann, R. L. Huguenin, P. A. Jaquenoud and E. Sandrin, *Helv. Chim. Acta*, **41**, 1867 (1958).

18) C. Meyers, R. T. Havran, I. L. Schwartz and R. Walter, *Chem. Ind.* (London), **1969**, 136.

$C_{35}H_{54}O_9N_8$: C, 57.52; H, 7.54; N, 15.33%.

***S*-Sulfonate of L-Prolyl-L-prolyl-L-glutaminyl-N^{ε}-benzyloxycarbonyl-L-lysyl-N^{G}-nitro-L-arginyl-A-chain.** *t*-Amyloxycarbonyl-L-prolyl-L-prolyl-L-glutaminyl-N^{ε}-benzyloxycarbonyl-L-lysine hydrazide (366 mg) was dissolved in dimethylformamide (3 m*l*) and cooled to −40°C. The solution was mixed with 1N HCl in tetrahydrofuran (1.0 m*l*) and then with isoamylnitrite (70 mg) dissolved in tetrahydrofuran (1.0 m*l*) at the same temperature.[19] After 30 min, triethylamine (0.17 m*l*) and a solution of the *S*-sulfonate of N^{G}-nitro-L-arginyl-A-chain (280 mg) and sodium bicarbonate (0.12 g) dissolved in water (2 m*l*) were added to the solution. The mixture was stirred mechanically at −20°C for 2 days, and then dialyzed against distilled water (500 m*l*) for 60 min at room temperature and lyophilized. The residue was dried over phosphorus pentoxide *in vacuo* and then treated with trifluoroacetic acid (15 m*l*) at 5°C for 30 min. The solution was concentrated *in vacuo*, and the residual oil was dried over phosphorus pentoxide. This was dissolved in 2% aqueous sodium bicarbonate at room temperature. After 30 min, the solution was dialyzed against distilled water and lyophilized. The residue was dissolved in a small volume of a 0.1M ammonium bicarbonate solution and fractionated on a column of Sephadex G-25 (2×50 cm) using the same buffer solution. The first peak in the eluate with an absorption at 280 mμ, as has been described in the synthesis of the N^{G}-nitro-L-arginyl derivative, was collected and lyophilized. Thus L-prolyl-L-prolyl-L-glutaminyl-N^{ε}-benzyloxycarbonyl-L-lysyl-N^{G}-nitro-L-arginyl-A-chain *S*-sulfonate was obtained as a powder; wt. 163 mg.

Results and Discussion

The coupling reaction was, first, carried out by mixing an aqueous solution of A-chain *S*-sulfonate with a solution of the N^{α}-*p*-methoxybenzyloxycarbonyl-N^{α}-nitro-L-arginine pentachlorophenyl ester in dioxane under the standard conditions used in peptide synthesis.[20] A large molar excess of the N^{α}-*p*-methoxybenzyloxycarbonyl-N^{G}-nitro-L-arginine pentachlorophenyl ester was employed, since it was thought that the quantitative acylation of the A-chain *S*-sulfonate would facilitate the purification procedure. When a 10—15 fold molar excess of this reagent was allowed to react with A-chain *S*-sulfonate for 2 days at room temperature, a little unreacted A-chain was detected in the reaction mixture by paper electrophoresis using a formic acid buffer solution at pH 2.1. However, the repeated addition of 5—7 fold molar excesses of the pentachlorophenyl ester to the reaction mixture resulted in the quantitative acylation of the A-chain *S*-sulfonate, as is shown in Fig. 2. After removing the protective group with trifluoroacetic acid, the reaction product

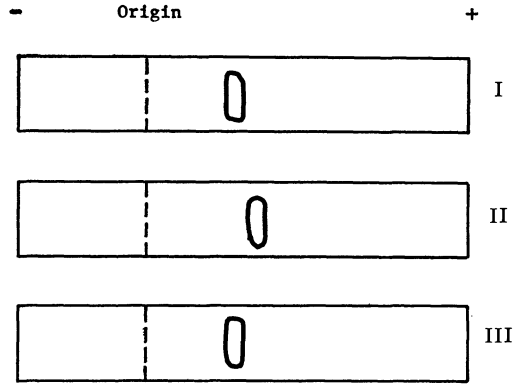

Fig. 2. Diagram of paper electropherogram stained with Pauly reagent (urea-formic acid buffer, pH 2.1, 7.5 V/cm). Bands I, II and III correspond to the *S*-sulfonate of A-chain, reaction mixture after reaction of the *S*-sulfonate of A-chain with N^{α}-*p*-methoxybenzyloxycarbonyl-N^{G}-nitro-L-arginine pentachloropyenyl ester, and the *S*-sulfonate of N^{G}-nitro-L-arginyl-A-chain, respectively.

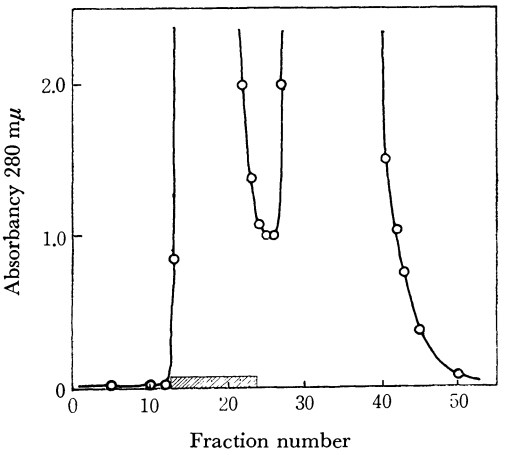

Fig. 3. Gel-filtration of mixture after reaction of the *S*-sulfonate of A-chain and N^{α}-*p*-methoxybenzyloxycarbonyl-N^{G}-nitro-L-arginine pentachlorophenyl ester and removing the *N*-terminal protective group by treatment with trifluoroacetic acid on Sephadex G-25 (2×50 cm).

was purified by gel-filtration on Sephadex G-25, using ammonium bicarbonate buffer as a solvent, as is shown on Fig. 3. The first fraction of the eluate, N^{G}-nitro-L-arginyl-A-chain *S*-sulfonate, was collected and lyophilized to yield a cotton-like residue. This compound was identified by paper electrophoresis and by an amino-acid analysis of its acid hydrolysate, as is shown in Fig. 2 and Table 1 respectively.

Second, the N^{G}-nitro-L-arginyl-A-chain *S*-sulfonate obtained above was allowed to react with the N^{α},N^{ε}-di-*t*-butyloxycarbonyl-L-lysine *N*-hydroxysuccinimide ester. The reaction was car-

19) J. Honzl and J. Rudinger, *Collect. Czech. Chem. Commun.*, **26**, 2333 (1961).

20) G. W. Anderson, J. E. Zimmerman and F. M. Callahan, *J. Amer. Chem. Soc.*, **86**, 1839 (1964).

ried out in the same way in dioxane-water under weakly alkaline conditions. The extent of the coupling reaction was also monitored by paper electrophoresis at pH 2.1, and L-lysyl-N^G-nitro-L-arginyl-A-chain *S*-sulfonate was isolated similarly. The amino-acid analysis of its acid hydrolysate also gave satisfactory results, as is shown in Table 1.

Table 1. Amino acid compositions of various derivatives of the A-chain[a)]

Amino acid	*S*-Sulfonate of A-chain[b)]	I[c)]	II[c)]	III[c)]
Asp	1.88 (2)	1.88	1.80	1.94
Ser	1.67 (2)	1.62	1.57	1.69
Glu	4.15 (4)	4.06	3.68	4.88
Pro				2.19
Gly	1.09 (1)	1.00	1.00	1.00
Ala	1.00 (1)	1.00	1.00	1.00
Cys	1.69 (2)	1.35	1.53	1.50
Val	1.67 (2)	1.56	1.63	1.69
Ile	0.55 (1)	0.53	0.61	0.66
Leu	2.00 (2)	1.91	1.98	2.03
Tyr	1.85 (2)	1.41	1.49	1.28
Arg+Lys[d)]		1.06	1.78	1.81

a) Samples were hydrolyzed in 6N hydrochloric acid without added phenol in sealed tubes, for 24 hr, at 110°C, and analyzed in a Hitachi KLA-3B analyzer. All values shown are uncorrected.
b) This compound was analyzed for comparison with the synthesized compounds.
c) Compounds I, II and III mean *S*-sulfonates of N^G-nitro-L-arginyl-, L-lysyl-N^G-nitro-L-arginyl-, and L-prolyl-L-prolyl-L-glutaminyl-N^ε-benzyloxycarbonyl-L-lysyl-N^G-nitro-L-arginyl-A-chain, respectively.
d) Total values of lysine and arginine are showed, because lysine was not separated from ornithine derived from nitroarginine in this analysis.

Third, N^G-nitro-L-arginyl-A-chain *S*-sulfonate was coupled with *t*-amyloxycarbonyl-L-prolyl-L-prolyl-L-glutaminyl-N^ε-benzyloxycarbonyl-L-lysine by the azide procedure described in the introduction. In this case, the reaction product could not be detected by paper electrophoresis at pH 2.1, because it did not separate distinctly from unreacted *S*-sulfonate. The reaction was allowed to proceed for 2 days at −20°C, and then the product was isolated after removing the *N*-terminal protective group by treatment with trifluoroacetic acid. The product was found to migrate slower than A-chain *S*-sulfonate at pH 2.1, and seemed to be almost pure L-prolyl-L-prolyl-L-glutaminyl-N^ε-benzyloxycarbonyl-L-lysyl-N^G-nitro-L-arginyl-A-chain *S*-sulfonate. The amino-acid analysis of the hydrolysate also gave good results, as is shown in Table 1. This compound will be used as material for further elongation reactions, since the ε-amino group of the lysyl residue and the thiol group of cysteinyl residues are still suitably protected.

The above results clearly show that the natural A-chain of insulin can be used as a starting material in the partial synthesis of proinsulin, in which acylamino acid-active esters are used for step-by step elongation reactions and fragment condensation by means of the azide procedure can be applied the to N^G-nitro-L-arginyl-A-chain. The success of azide coupling with N^G-nitro-L-arginyl-A-chain is especially noteworthy. Thus, the use of Des-glycine-A-chain for the elongation reactions does not seem always to be necessary. Attempts at direct condensation with the A-chain by the azide procedure remain unsuccessful.

The author wishes to express his thanks to Professor S. Sakakibara of Osaka University and to Professor H. Zahn of the Deutsches Wollforschungsinstitut, Technischen Hochschule Aachen, for their encouragement throughout this investigation.

BULLETIN OF THE CHEMICAL SOCIETY OF JAPAN VOL. 43 3256—3259 (1970)

Structure and Reactivity of α,β-Unsaturated Ethers. X. The Acid-Catalyzed Hydrolysis of Ring-Substituted Styryl Ethyl Ethers

Tadashi OKUYAMA and Takayuki FUENO

Faculty of Engineering Science, Osaka University, Toyonaka, Osaka

and Junji FURUKAWA

Department of Synthetic Chemistry, Kyoto University, Yoshida, Kyoto

(Received June 1, 1970)

The acid-catalyzed hydrolysis of *cis*- and *trans*-styryl ethyl ethers (SEE) and several of their ring-substituted derivatives has been kinetically investigated in 80% aqueous dioxane. It has been found that these ethers are less reactive than vinyl ethyl ether by a factor of *ca.* 500 and that all the *cis* isomers studied are about twice as reactive as the corresponding *trans* isomers. The hydrolysis of the substituted ethers at 35°C has proved to obey the Hammett relation with the reaction constants $\rho=-1.07$ and -0.70 for the *cis* and the *trans* isomers, respectively. All these results appear to be interpretable at least qualitatively in terms of the reaction scheme involving the rate-determining protonation to the β-carbon atom.

It is generally accepted that the acid-catalyzed hydrolysis of α,β-unsaturated ethers involves irreversible protonation to the unsaturated bond. In a previous paper[1] of this series, the kinetic courses of hydrolysis of various alkenyl alkyl ethers were investigated and direct evidence that the protonation step is rate-determining was given. It was also shown that the effects of β-alkyl substitutions on the reactivity of vinyl ether can best be interpreted in terms of the conjugative stabilities of the intermediate carbonium ions which are formed on transfer of a proton from the hydronium ion to the ethers. Further, it was demonstrated both experimentally and theoretically that the electronic effect of α-alkoxyl groups is an important contribution to the rates of hydrolysis of ring-substituted phenyl vinyl ethers.[2]

In order to gain a deeper insight into the electronic factors of β-substituents influencing the vinyl ether hydrolysis, we have investigated the effect of ring substituents in the hydrolysis rates of *cis*- and *trans*-styryl ethyl ethers (SEE). The results were interpreted in terms of the reaction scheme involving the rate-determining protonation:

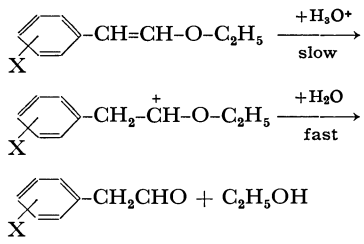

(1)

Experimental

Materials. Styryl ethyl ether (SEE) and its ring-substituted derivatives were prepared by the method of Dufraisse and Chaux[3,4] from diethyl acetals of appropriate substituted phenylacetaldehydes, which were obtained by the Grignard method[5] from benzyl bromides or chlorides. Methyl-, chloro-, and fluorobenzyl bromides were prepared by bromination of corresponding substituted toluenes.[6] *p*-Methoxybenzyl chloride was obtained by the solvolysis of *p*-anisyl alcohol. *p*- and *m*-fluorotoluenes were prepared from *p*- and *m*-toluidines, respectively, according to the procedure of Roe.[7]

The unsaturated ethers thus obtained were nearly equimolar mixtures of geometrical isomers, and their boiling points were as follows: H, 112—115°C/20 mmHg; *p*-CH_3O, 110—113°C/3 mmHg; *p*-CH_3, 87—89°C/5 mmHg; *m*-CH_3, 90—93°C/5 mmHg; *p*-F, 115—116°C/22 mmHg; *m*-F, 82—83°C/5 mmHg; *p*-Cl, 77—78°C/2 mmHg; *m*-Cl, 97—100°C/5 mmHg. Purities were checked by gas chromatography (>99%).

Dioxane, tetralin and carbon tetrachloride were obtained as described previously.[1]

Kinetic Measurements. Hydrolysis was carried

1) T. Okuyama, T. Fueno, H. Nakatsuji and J. Furukawa, *J. Amer. Chem. Soc.*, **89**, 5826 (1967).
2) T. Fueno, I. Matsumura, T. Okuyama and J. Furukawa, This Bulletin, **41**, 818 (1968).
3) C. Dufraisse and R. Chaux, *Bull. Soc. Chim. France*, [4] **39**, 905 (1926).
4) S. I. Miller, *J. Amer. Chem. Soc.*, **78**, 6091 (1965).
5) C. E. Wood and M. A. Comley, *J. Soc. Chem. Ind.* (London), **42**, 429T (1923).
6) S. S. Jenkins, *J. Amer. Chem. Soc.*, **55**, 2896 (1933).
7) A. Roe, "Organic Reactions," Vol. **5**, p. 193 (1949).

out in 80% aqueous dioxane containing *ca.* 0.2N hydrochloric acid at a specified temperature between 25 and 45°C. Each SEE derivative was hydrolyzed as a mixture of *cis* and *trans* isomers, but the kinetic courses were followed for each isomer separately by simultaneous determination of the isomers by gas chromatography. A Shimadzu Model 4APT gas chromatograph with a 3-m column packed with Apiezon Grease L was operated at a column temperature of *ca.* 130°C with hydrogen as carrier gas. In all cases, the *trans* isomers had a greater retention time. The initial total concentration of the reactant ethers was typically *ca.* 0.15M. Tetralin or dichlorobenzene was used as internal standard. The internal standard method coupled with the half-height width evaluation of the peak areas was sufficient for the determination of the ethers. Other details of the procedures for the rate measurements were the same as those described previously.[1,2] Each rate constant was obtained as an average of three to five independent runs and accurate to within 5%.

Results

It is known that the acid-catalyzed hydrolysis of α,β-unsaturated ethers is first order in both ether and acid.[1,2] Although most of the kinetic courses investigated here were pursued with the mixture of geometrical isomers, the first-order decay was found to hold for each isomer separately over the range up to 80% conversion. Figure 1 shows an example.

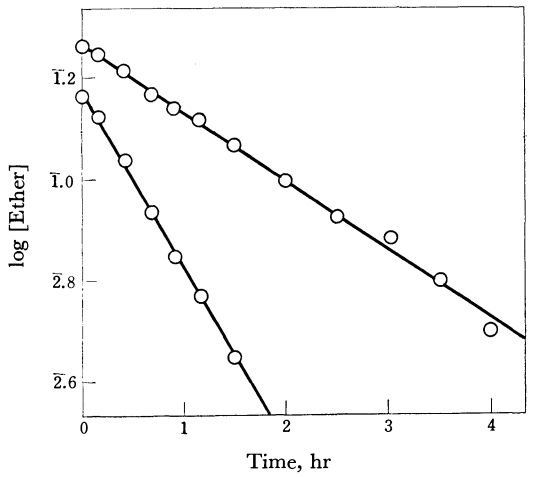

Fig. 1. First-order plots for the hydrolysis of *cis*- and *trans*-*p*-methylstyryl ethyl ethers.
[HCl], 0.189M. Temperature, 35°C.

The situation is in agreement with the previous observation that geometrical isomerization does not take place during the hydrolysis of alkenyl alkyl ethers.[1] This in turn endorses the conclusion that the hydrolysis involves the rate-determining protonation to an olefinic carbon atom. Formation of the products as expected from Eq. (1) was confirmed for the nonsubstituted compounds; the gas-chromatographic retention times of the products measured with the use of two different columns, polyethylene glycol and Apiezon Grease L, both exactly coincided with those of the authentic samples.

Table 1. Second-order rate constants for the acid-catalyzed hydrolysis of ring-substituted styryl ethyl ethers at 35°C

Substituent	10^4k_2, $M^{-1}sec^{-1}$	
	cis	*trans*
p-CH_3O	10.4_2	5.43
p-CH_3	11.8_4	4.72
m-CH_3	9.39	4.22
H	1.99[a]	1.14[a]
	7.33	3.85
	25.2[b]	13.8[b]
p-F	3.90	2.28
p-Cl	3.37	2.12
m-Cl	3.16	2.07

a) At 25°C.
b) At 45°C.

In Table 1 are summarized the second-order rate constants, $k_2=k_1/[HCl]$. In all the cases studied, *cis* isomers were *ca.* twice more reactive than the *trans* isomers, and their reactivities diminished with increasing electron-attracting ability of the ring substituents. From temperature dependence data, the heats and the entropies of activation, $\Delta H^{\neq}$ and $\Delta S^{\neq}$, were calculated for the unsubstituted SEE's: *cis*-SEE, $\Delta H^{\neq}=23.3$ kcal mol^{-1} and $\Delta S^{\neq}=2.7$ e.u.; *trans*-SEE, $\Delta H^{\neq}=21.4$ kcal mol^{-1} and $\Delta S^{\neq}=-4.9$ e.u.

Discussion

It has been reported[1] that the acid-catalyzed hydrolysis of vinyl ethyl ether in 80% aqueous dioxane at 25°C is $k_2=7.51\times10^{-2}M^{-1}\,sec^{-1}$. The reactivity of styryl ethyl ether toward proton is thus smaller than that of vinyl ethyl ether by a factor of *ca.* 500. This effect of the β-phenyl group in lowering the vinyl ether reactivity is far greater than that of a β-methyl group, which reduces the reactivity only by a factor of *ca.* 5.[1]

The effect of the β-phenyl group may be interpreted qualitatively from the greater stability of styryl ether in the ground state as compared with vinyl ether. Because of the excessive ground-state stability due to the conjugation between phenyl group and the olefinic bond, the π-electronic energy required for localizing an electron pair on the β-carbon ought to be greater for the styryl ether than for the vinyl ether. Simple calculations of the Hückel type readily confirm the above view. The difference in localization energy between the two ethers must reflect itself in the difference in

the activation energies for their hydrolysis.[8]

All the *cis*-SEE's are more reactive than the corresponding *trans* isomers in the temperature region studied here. Nonetheless, the heat of activation for *cis*-SEE was found to be greater than that for *trans*-SEE. Hence, the relative reactivities of *cis*- and *trans*-SEE's are entropy-controlled at the ordinary temperature region. The isomerization equilibrium experiments showed that *cis*-SEE is thermochemically less stable than *trans*-SEE in the liquid phase, and it was deduced that the former isomer is in a non-planar conformation in contrast to the planar structure for the latter.[9] This structural irregularity may have some bearing with the unusual entropy effect found between the activation profiles of *cis*- and *trans*-SEE's. A similar trend was also found in the cationic polymerization of SEE.[10]

As has been stated above, the reactivity of SEE is enhanced by electron-donating substituents and is lowered by electron-attracting substituents. As is seen in Fig. 2, the effects of the ring substituents obey the Hammett $\rho\sigma$ relationship for the *cis* and *trans* isomer series separately, although a relatively

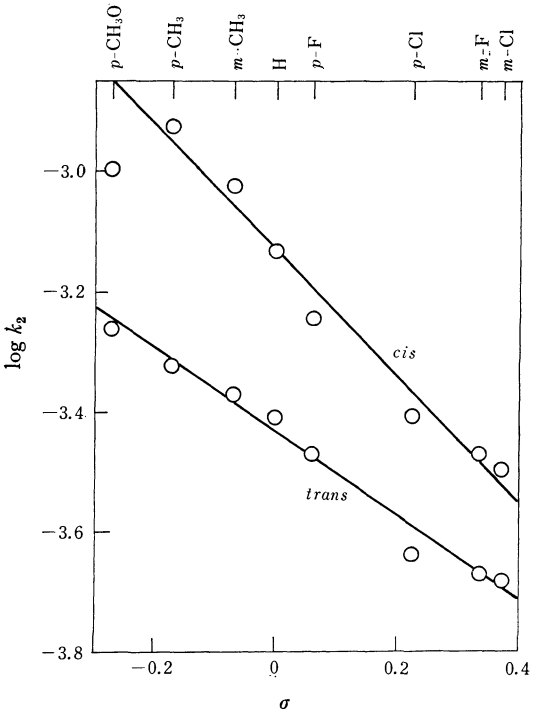

Fig. 2. The Hammett relationships of the hydrolysis rates of ring-substituted styryl ethyl ethers. Temperature, 35°C.

large deviation from the line was found for the *cis*-*p*-methoxy derivative. The reaction constants, ρ, are -1.07 ($r=0.990$, excluding a point for the *p*-methoxy compound) and -0.70 ($r=0.991$) for the *cis* and *trans* series, respectively.

That an electron-donating ring substituent enhances the rate of the acid-catalyzed reaction of SEE has by no means been intuitively obvious. In fact, Winterfeldt[11] observed that the *p*-$N(CH_3)_2$ group lowers the rate of the acid-catalyzed methanolysis of styryl ether and interpreted this rate lowering in terms of the "opposing" electron donation of the *p*-$N(CH_3)_2$ group. His observation thus conflicts with our present results on hydrolysis and, therefore, his interpretation is greatly dubious. It appears that, in the acidic medium where his measurement was carried out, the $N(CH_3)_2$ group was actually in the form of $N^+(CH_3)_2H$, which retarded the methanolysis rate.[12]

The ρ values (-1.07 and -0.70) for the SEE hydrolysis are somewhat small as compared with those for the usual electrophilic addition reactions to styryl compounds. For instance, the acid-catalyzed hydration of styrenes[13] and the chlorination of cinnamic acids[14] were reported to have the values of -3.42 and -4.01, respectively. These reactions occur with an electrophilic attack on the *beta* carbon atom with respect to the phenyl group.[15] In contrast to these reactions, the hydrolysis of styryl ether occurs with an *alpha*-attack of hydronium ion, as is shown in Eq. (1). The lower sensitivity of the present reaction to the ring substituents is undoubtedly due to the fact that the primary reaction center is the *alpha*-position. This is easily understandable considering that, in the intermediate carbonium ions, the cationic center is insulated out of the π-conjugation involving the phenyl group which carries a substituent.

8) The activation papameters for vinyl ethyl ether are $\Delta H^{\neq}=17.5$ kcal mol^{-1} and $\Delta S^{\neq}=-4.9$ e.u.

9) T. Okuyama, T. Fueno and J. Furukawa, *Tetrahedron*, **25**, 5409 (1969); Part IX of this series.

10) T. Okuyama, N. Asami and T. Fueno, This Bulletin, in press.

11) E. Winterfeldt, *Chem. Ber.*, **96**, 3346 (1963).

12) The ammonium groups are electron-attracting in nature, as may be judged from their σ-values [D. H. McDaniel and H. C. Brown, *J. Org. Chem.*, **23**, 420 (1958)]. Besides, part of the catalyst acid must have been consumed for the ammonium ion formation. These would have combined to act as a drawback of the electronic effect of the *p*-$N(CH_3)_2$ group which would otherwise have enhanced the rate of protonation to the olefinic carbon atom.

13) W. H. Schubert, B. Lamm and J. R. Keefe, *J. Amer. Chem. Soc.*, **86**, 4272 (1964).

14) H. P. Rothbaum, I. Ting and P. W. Robertson, *J. Chem. Soc.*, **1948**, 980.

15) It is expedient to regard SEE as a derivative of styrene when chemical characteristics are to be compared between the two compounds. Thus, when we refer to those carbon atoms at the positions α and β with respect to the phenyl group, we make use of the word *alpha* and *beta* in order to avoid confusion with the α- and β-carbon atoms of an α,β-unsaturated ether. This expedience will be used whenever we discuss the properties of SEE in comparison with those of styrene.

Electrophilic reactions of styryl compounds involving the rate-determining *alpha*-attack do not seem to be very familiar at present. The only example that has been reported in connection with the substituent effects is the acid-catalyzed geometrical isomerization of substituted *cis*-stilbenes,[16] where the ρ value was noted to be -0.96 or -3.30, depending on whether the primary reaction center is the *alpha*- or the *beta*-carbon with respect to the phenyl group that carries the substituents to be examined. The present studies provide another example of the electrophilic *alpha*-attack reactions of styryl compounds which should have a ρ value relatively small in magnitude.

16) D. S. Noyce, D. R. Hatter and F. B. Miles, *J. Amer. Chem. Soc.*, **90**, 4633 (1968).

BULLETIN OF THE CHEMICAL SOCIETY OF JAPAN VOL. 43 3259—3262 (1970)

Properties of Vinyl Chlorides-Ethylene Copolymers

Akira MISONO and Yasuzo UCHIDA

Department of Industrial Chemistry, Faculty of Engineering, The University of Tokyo, Hongo, Tokyo

and Kunikazu YAMADA

Research Institute, Sekisui Chemical Co., Shimamoto-cho, Mishima-gun, Osaka

(Received May 14, 1970)

Properties of vinyl chloride-ethylene copolymers rich in vinyl chloride have been studied by means of infrared as well as NMR spectroscopy and dynamic mechanical testing. The infrared and NMR spectra of the copolymer indicate that crystallinity decreases with decreasing sequence length of the vinyl chloride segment. The copolymer containing more than 80 mol % vinyl chloride shows optical melting point, a plot of which *versus* logarithmic composition satisfies Flory's relationship. Temperature dispersion curve of elastic modulus E′ of the copolymer also indicates that the crystalline region of vinyl chloride segments disappears as the ethylene content increases. Glass transition temperature as determined by loss modulus E″ fits Gordon-Taylor's relationship well provided the coefficient k equals unity.

From the results of crystallographic,[1-3] mechanical[4-6] and thermal studies,[7] it is considered that polyvinyl chloride can be regarded as a semi-crystalline polymer, though its crystalline region is very small. On the other hand, Flory[8] has shown that the crystallinity of an original polymer decreases regularly depending on the amount of the comonomer incorporated. Many copolymer systems have been examined in relation to the melting point depression predicted by Flory.[9] Few vinyl chloride copolymers, however, have been studied in this respect probably because of their poor crystallinity. We reported the syntheses[10-12] and some aspects of structural problems[13,14] of vinyl chloride-ethylene copolymers. It has been suggested that the copolymer is more or less crystalline on the basis of our recent investigation. We wish to report on the results of a preliminary study on the properties of the copolymers.

1) G. Natta and P. Coradini, *J. Polymer Sci.*, **20**, 251 (1956).
2) T. Shimanouchi, S. Tsuchiya and S. Mizushima, *Kobunshi*, **8**, 202 (1959).
3) M. Asahina and S. Enomoto, *Nippon Kagaku Zasshi*, **81**, 1374 (1960).
4) L. E. Nielsen, R. Buchdahl and R. Levreault, *J. Appl. Phys.*, **21**, 607 (1950).
5) A. V. Tobolsky, D. Carlson and N. Indicator, *J. Appl. Polymer Sci.*, **7**, 393 (1963).
6) R. B. Taylor and A. V. Tobolsky, *ibid.*, **8**, 1563 (1964).
7) Y. Watanabe, Y. Kondo and E. Iida, *Kogyo Kagaku Zasshi*, **69**, 1781 (1966).
8) P. J. Flory, *J. Chem. Phys.*, **17**, 223 (1949).
9) M. L. Miller, "The Structure of Polymers," Reinhold, New York (1966).
10) A. Misono, Y. Uchida and K. Yamada, This Bulletin, **39**, 2458 (1966).
11) A. Misono, Y. Uchida and K. Yamada, *ibid.*, **40**, 2366 (1967).
12) A. Misono, Y. Uchida, K. Yamada and T. Saeki, *ibid.*, **41**, 2995 (1968).
13) A. Misono, Y. Uchida and K. Yamada, *ibid.*, **40**, 2696 (1967).
14) A. Misono, Y. Uchida and K. Yamada, *ibid.*, in contribution.

Experimental

Copolymer samples were prepared by using the catalyst system consisting of tri-*n*-butylboron and *t*-butyl hydroperoxide in a water-methanol mixture (1 : 1 by volume).[1] The composition of the copolymer was determined from the results of elementary analysis of C and Cl. The infrared spectrum of the copolymer was measured with a JASCO 201 infrared spectrometer by the KBr disk method. The NMR spectrum of the copolymer was measured by a Japan Electron Optics high resolution NMR spectrometer, model JNM-60, in a 10 wt/vol% monochlorobenzene solution of the copolymer at 60 MHz and 110°C using tetramethylsilane as internal standard. The melting point of the copolymer was measured by a Yanagimoto hotstage polarizing microscope. The dynamic viscoelasticity of the copolymer was measured by Toyo Measuring Instruments Vibron viscoelastometer, model DDV-II, at 11 Hz using a sheet of sample prepared by hot-pressing at 100°C for 5 min under a pressure of 70 kg/cm².

Results and Discussion

In the region 700 to 600 cm^{-1} of the infrared spectrum of polyvinyl chloride, four absorption bands were observed at 690, 635, 615 and 603 cm^{-1}.[2] They are denoted by α, β, γ and δ, respectively. The δ-band cannot be observed in the spectrum measured by the KBr disk method. The four bands were assigned to the C–Cl streching modes from comparison with the spectrum of olyvinyl bromide. β- and δ-bands were assigned to the crystalline bands.[2,3] In Fig. 1 are shown the infrared spectra of vinyl chloride-ethylene copolymers together with that of polyvinyl chloride, observed in the KBr region. The α-band observed in polyvinyl chloride shifts to somewhat lower frequency and its intensity decreases as the vinyl chloride content of the copolymer decreases. Intensity of β-band also decreases with decreasing vinyl chloride content and, completely disappears in the spectrum of the copolymers containing less than 60 mol% vinyl chloride. In

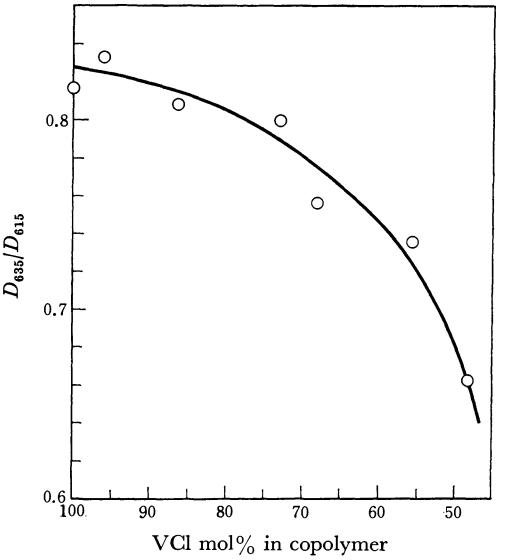

Fig. 2. D_{635}/D_{615} as a function of copolymer composition.

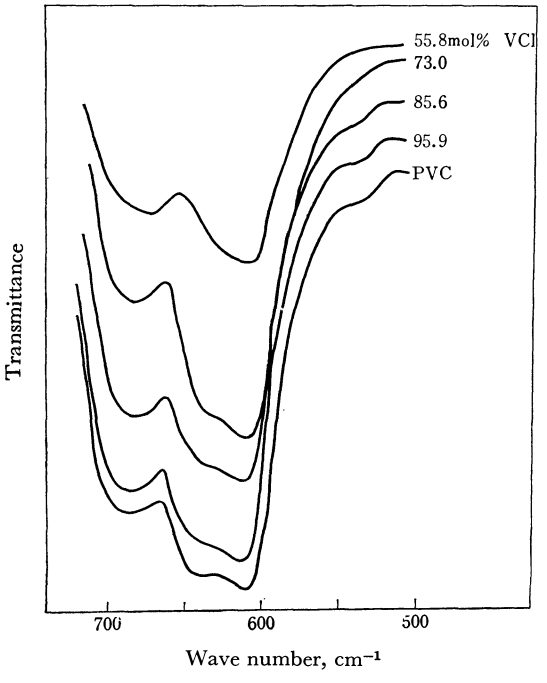

Fig. 1. Infrared spectra of polymers in KBr region.

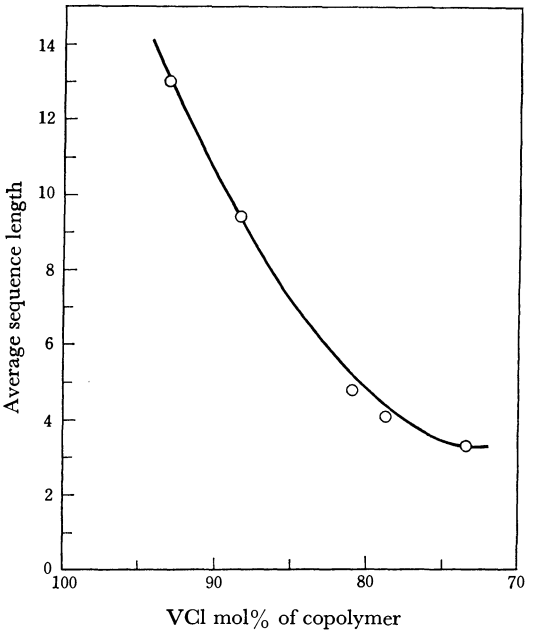

Fig. 3. Average sequence length of vinyl chloride unit of copolymer as a function of their composition.

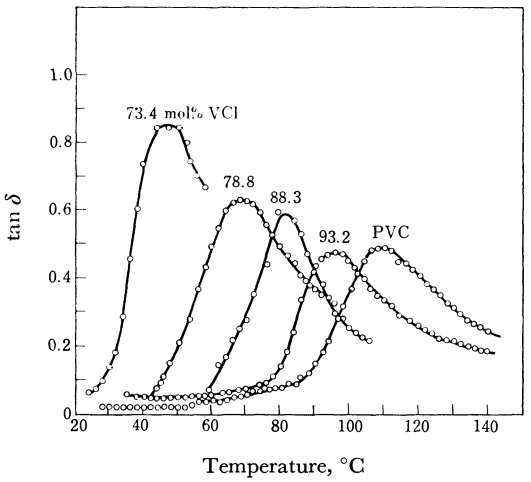

Fig. 4. Mechanical damping of polymers.

Fig. 2 the change in the ratio of optical densities of β- and γ-bands are shown. It may be seen that the crystallinity of the copolymer decreases with the decreasing vinyl chloride content. In Fig. 3 is shown the average sequence length of vinyl chloride units determined by NMR technique.[14] The decrease in the average sequence length of vinyl chloride units with the decreasing vinyl chloride content may be correlated with the decressing crystallinity observed in the infrared spectra.

The loss tangent curves of the copolymers are shown in Fig. 4. The temperature of the maximum loss tangent decreases linearly with the decreasing vinyl chloride content. This seems to correspond to the change in glass transition temperature according to the change in copolymer composition. Glass transition temperature of the copolymer will be discussed later on the basis of the temperature dependence of loss modulus E″. Decrease in the temperature of the maximum loss tangent with the decreasing vinyl chloride content seems to be analogous with what has been observed in plasticized polyvinyl chloride.[4] Increase in magnitude and decrease in half-height width of loss tangent with the increasing ethylene content, however, are in contrast with the increase in half-height width with the increasing amount of plasticizer in plasticized polyvinyl chloride.[4] The difference may reflect the mechanism of plasticizing functioning in each polymer. The plasticizer plasticizes polyvinyl chloride by decreasing the intermolecular interaction between chloride atoms located on each polymer chain, whereas the ethylene unit incorporated into the copolymer plasticizes the polymer by diminishing the number of chlorine atoms distributed along the polymer chain. We need to investigate the behavior of loss tangent in lower temperature regions, in order to see more closely the mechanism of plasticization. However, the viscoelastometer used in this study was not equipped with a low temperature bath, and no study was carried out.

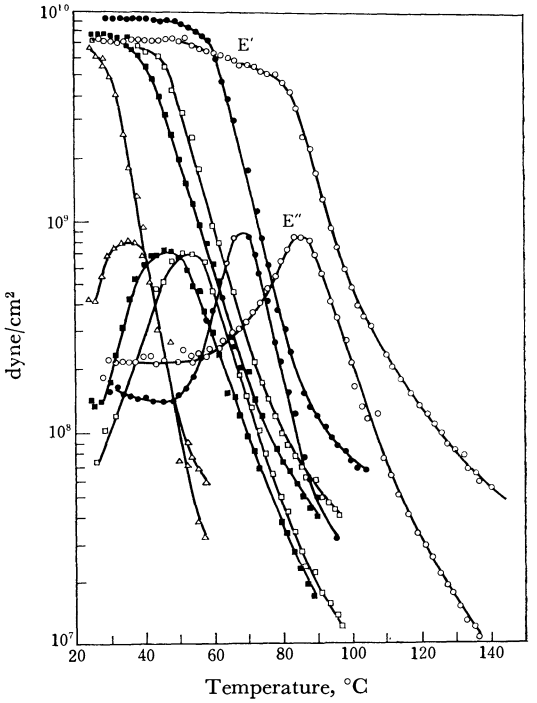

Fig. 5. Elastic and loss moduli of polymers.
○ PVC, ● 93.2 mol% VCl, □ 88.3 mol% VCl
■ 78.8 mol% VCl △ 73.4 mol% HCl

Dynamic elastic and loss moduli of the copolymers are shown in Fig. 5. The temperature where glass transition begins decreases with the increasing ethylene content of the copolymer and, the width of the transition region also decreases in the same manner. This is different from the behavior of plasticized polyvinyl chloride in which the width of transition region increases with the increasing amount of plasticizer.[4] The temperature dependence of elastic modulus of polyvinyl chloride has been studied, and the existence of the rubbery region continuing from the transition region has been elucidated in terms of microcrystallites occurring in vinyl chloride segments.[5,6] In our polymers, a part of such rubbery region is observed as a curvature of elastic modulus E′ continuing from the high temperature-end of the transition region. Such a curvature, however, disappears when the ethylene content exceeds about 10 mol%, where the average sequence length of vinyl chloride units is estimated as about 10. These results might indicate that more than about 10 monomer units of vinyl chloride are required appreciable crystallinity of the copolymer. Nambu[15] has concluded that as least 20 to 30 monomer units are necessary for the crystallization of vinyl chloride segments from the results

15) K. Nambu, *Kobunshi Kagaku*, **20**, 131 (1963).

of investigation on vinyl chloride-diethylfumarate copolymers, in which the bulky side group of the comonomer seems to render the vinyl chloride segment more difficult to crystallize than in vinyl chloride-ethylene copolymers.

It is established that the main dispersion of polyvinyl chloride, which is associated with glass transition, can be attributed to the motion of long segments of main chain. The peak temperature of loss modulus E″ varies monotonously according to the change in copolymer composition as shown in Fig. 6, and this relationship fits Gordon-Taylor's equation provided the coefficient k equals unity.[16]

$$c_2=(T_g-T_{g1})/\{k(T_{g2}-T_g)+(T_g-T_{g1})\}$$

where T_g, T_{g1} and T_{g2} are the glass transition temperatures of the copolymer, homopolymer 1 and homopolymer 2 respectively, c_2 the weight fraction of the comonomer 2 in the copolymer, and k is the ratio of the difference of expansion coefficients of the homopolymer 1 and 2 above and below the glass transition temperature. Glass transition temperatures thus determined are in good consistency with diatometrically observed ones.[17]

The copolymer containing more than about 80 mol% vinyl chloride shows appreciable birefringence under polarized light. The birefringence does not disappear on annealing the copolymer a little below melting point, hence cannot be due to internal strain of the sample. Birefringence was hardly observed in the copolymer containing less than 80 mol% vinyl chloride. The melting points of the copolymers are shown as a function of their composition in Fig. 6. Figure 7 shows a plot reciprocal melting point *versus* logarithmic compossition. This relationship can be expressed by Flory's equation[8]

$$1/T_m-1/T_m^0=-(R/\Delta H_u)\ln N$$

where T_m is the copolymer melting point, T_m^0 that of the crystallizable homopolymer, N the mole fraction of crystallizable units in the copolymer, and ΔH_u the heat of fusion per mole of repeating unit. The slope of the straight line gives about 3900 cal/mol as the heat of fusion, which is in good agreement with the reported value of 3040 cal/mol.[18]

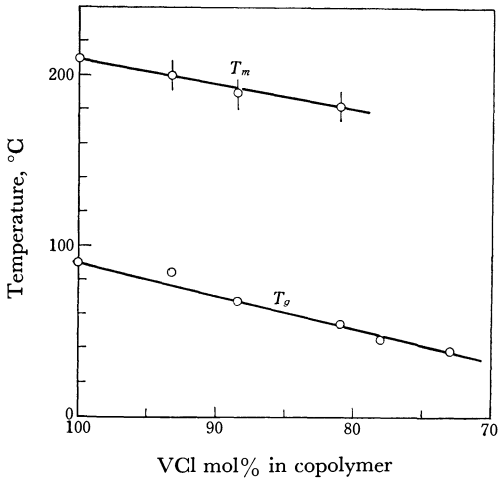

Fig. 6. Glass transition temperature and melting point of copolymers as a function of their composition.

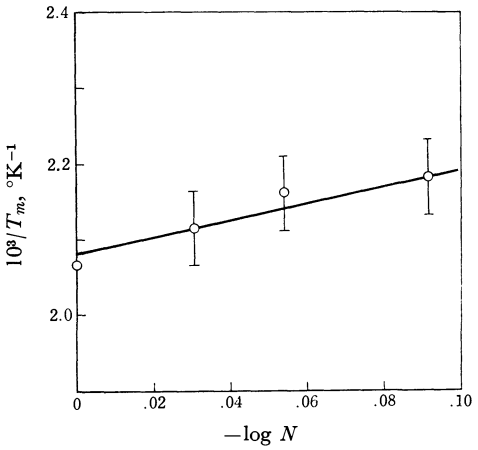

Fig. 7. Melting point depression of copolymer.

The results on the copolymer melting point, together with those on the infrared study and dynamic mechanical testing, prove that vinyl chloride-ethylene copolymers rich in vinyl chloride are more or less crystalline. From the linearity of Flory's plot the crystal structure of the original vinyl chloride segments does not seem to undergo change by copolymerization caused by the introduction of ethylene unit.

16) M. Gordon and J. S. Taylor, *J. Appl. Chem.*, **2**, 494 (1952).

17) S. Koyanagi, *Kobunshi Kagaku*, **19**, 431 (1962).

18) L. E. Nielsen, "Mechanical Properties of Polymers," Reinhold, New York (1962).

NOTES

BULLETIN OF THE CHEMICAL SOCIETY OF JAPAN VOL. 43 3263—3264 (1970)

Some Thermal Properties of Deuterated Copper(II) Sulfate Pentahydrate

Hisaya Oki,*1 Eishin Kyuno and Ryokichi Tsuchiya

Department of Chemistry, Faculty of Science, Kanazawa University, Kanazawa

(Received October 25, 1969)

Few papers can be found on the thermal behavior of the deuterated copper(II) sulfate pentahydrates except for that by Heinzinger and Rao,[1] who pointed out that the ratio of the quantity of the deuterium to that of hydrogen gradually increased as dehydration proceeded in partially deuterated copper(II) sulfate pentahydrates. The effect of deuteration in copper(II) salt hydrates upon thermochemical functions has been fully investigated so far.

The present work was undertaken to determine the thermochemical functions in the dehydration of copper(II) sulfate pentahydrates deuterated to different extents in order to find difference in thermal properties of hydrates.

Experimental

Preparation. Copper(II) sulfate pentahydrates, $CuSO_4\cdot 4H_2O\cdot D_2O$, $CuSO_4\cdot 3H_2O\cdot 2D_2O$, $CuSO_4\cdot 2H_2O\cdot 3D_2O$, $CuSO_4\cdot H_2O\cdot 4D_2O$ and $CuSO_4\cdot 5D_2O$ deuterated to different extents, were prepared according to the following schemes:

$$CuSO_4\cdot 5H_2O \begin{cases} \xrightarrow{50^\circ C} CuSO_4\cdot 3H_2O \xrightarrow{D_2O} CuSO_4\cdot 3H_2O\cdot 2D_2O \\ \xrightarrow{150^\circ C} CuSO_4\cdot H_2O \xrightarrow{D_2O} CuSO_4\cdot H_2O\cdot 4D_2O \\ \xrightarrow{260^\circ C} CuSO_4 \xrightarrow{D_2O} CuSO_4\cdot 5D_2O \end{cases}$$

$$CuSO_4\cdot 5D_2O \begin{cases} \xrightarrow{53^\circ C} CuSO_4\cdot 3D_2O \xrightarrow{H_2O} CuSO_4\cdot 2H_2O\cdot 3D_2O \\ \xrightarrow{150^\circ C} CuSO_4\cdot D_2O \xrightarrow{H_2O} CuSO_4\cdot 4H_2O\cdot D_2O \end{cases}$$

Each formula is reasonable for the preparation of respective hydrates.

Heavy water from Merck Co., Germany was used.

Measurements. Thermal analysis was carried out with a Metrimpex Derivatograph MOM Type-OD-102 made in Hungary, and the enthalpy changes and the activation energies on each step of dehydration were calculated by analyzing the DTA curves in the same manner as described previously.[2]

Infrared absorption spectra of these salts were measured in the Nujol mull state with a Nippon-Bunko DS-301 IR-Spectrophotometer. The X-ray powder patterns were obtained with a Rigaku-Denki Geiger-Flex X-ray Analyser.

Results and Discussion

Thermal Analyses. Dehydration of copper(II) sulfate pentahydrate and those deuterated partially or completely was found by derivatography to proceed in the following three distinct steps: the first and the second steps indicate liberation of each two moles of water from the hydrates and the DTA peaks in both steps are, to some extent, overlapped. The third one corresponds to the liberation of the last one mole of water.

The values of the weight loss percent due to the liberation of all the five moles of water determined from the derivatograms for the hydrates and the corresponding values calculated on the basis of each formula are listed in the second column of Table 1, together with the thermochemical data. We see that the above values of the two groups are almost consistent with each other in the respective hydrates. This supports the validity of the formulas for the hydrates.

The temperatures at which dehydration begins to take place are given in the third column of Table 1, where the values under I, II, and III deal with the first, second and third steps of dehydration, respectively. The activation energies, $E^{\neq}$, and enthalpy changes, ΔH, calculated by

*1 Present address: Department of Chemistry, Faculty of Education, Fukui University, Fukui.

1) K. Heinzinger and T. S. Rao, *Z. Naturforschg.*, **22a**, 2111 (1967).

2) R. Tsuchiya, Y. Kaji, A. Uehara and E. Kyuno, This Bulletin, **42**, 1881 (1969).

Table 1. Thermal data for the deuterated copper(II) sulfate pentahydrates

	Total weight loss		The dehydration temperature (°C)			Activation energy E^* (kcal/mol)			Enthalpy change ΔH (kcal/mol)		
	obsd (%)	calcd (%)	I	II	III	I	II	III	I	II	III
$CuSO_4 \cdot 5H_2O$	36.0	36.1	45	82	201	19	45	30	14	14	17
$CuSO_4 \cdot 4H_2O \cdot D_2O$	36.6	36.6	45	82	212	21	44	49	14	14	17
$CuSO_4 \cdot 3H_2O \cdot 2D_2O$	37.0	37.1	49	82	213	24	44	47	14	14	17
$CuSO_4 \cdot 2H_2O \cdot 3D_2O$	37.5	37.6	52	83	212	26	43	48	14	14	17
$CuSO_4 \cdot H_2O \cdot 4D_2O$	38.0	38.0	53	82	214	29	43	53	14	14	17
$CuSO_4 \cdot 5D_2O$	38.6	38.5	55	84	214	33	43	53	14	14	17

analyzing the DTA curves are also included in both the forth and fifth columns of Table 1.

From these values the following information can be obtained. The temperatures at which the first step of dehydration begins are gradually elevated as the ratio of amounts of heavy water to those of ordinary water contained increases in the series of the hydrates except for $CuSO_4 \cdot 5H_2O$ and $CuSO_4 \cdot 4H_2O \cdot D_2O$ which have comparable data with each other, and the activation energies thereof also increase more and more in the same order. The results suggest that the liberation of ordinary water predominates in the first step of dehydration in both $CuSO_4 \cdot 5H_2O$ and $CuSO_4 \cdot 4H_2O \cdot D_2O$, whereas the ratio of heavy water against ordinary water liberated in the dehydration step becomes progressively greater in the order of $CuSO_4 \cdot 3H_2O \cdot 2D_2O$ through $CuSO_4 \cdot 5D_2O$.

On the other hand, the corresponding temperatures and the activation energies in the second step of dehydration are not so remarkably different from each other. The reason is not clear because of the ambiguity in the structure of each intermediate hydrates.

In the last step, the temperatures and activation energies of dehydration do not differ from each other as remarkably as in the first step, except for the especially smaller values for $CuSO_4 \cdot 5H_2O$. The results can be explained by assuming that the last one mole of water liberated is that of ordinary water in $CuSO_4 \cdot 5H_2O$, whereas in other hydrates, the last one mainly consists of heavy water, because the contribution of heavy water on dehydration becomes larger in the order of $CuSO_4 \cdot 4H_2O \cdot D_2O$ through $CuSO_4 \cdot 5D_2O$.

The enthalpy changes of dehydration do not differ sufficiently from each other in each step to give data for a discussion on dehydration.

X-Ray Powder Pattern. The X-ray powder patterns in several, stepwise deuterated copper sulfate pentahydrates were compared with each other in order to determine whether or not the structures of the salts differ depending upon the ratio of the amounts of heavy water to ordinary water. Their patterns are almost the same, however, and it seems that there is no appreciable structure deformation from the original according to the replacement of water by heavy water.

Infrared Absorption Spectra. Infrared absorption spectra of these copper(II) sulfate pentahydrates are shown Fig. 1. Despite the fact that the X-ray diffraction patterns of the sulfates are almost the same, the splitting of IR band assigned to SO_4 asymmetric vibration is complicated in the cases of $CuSO_4 \cdot 2H_2O \cdot 3D_2O$ and $CuSO_4 \cdot 3H_2O \cdot 2D_2O$. The reason is not clear. The ratio of the wave number of the absorption peak measured as the assignment to the stretching vibration of OH (3280 cm^{-1}) against that of OD (2410 cm^{-1}) was calculated to be 1.36, which is in good agreement with that generally accepted.

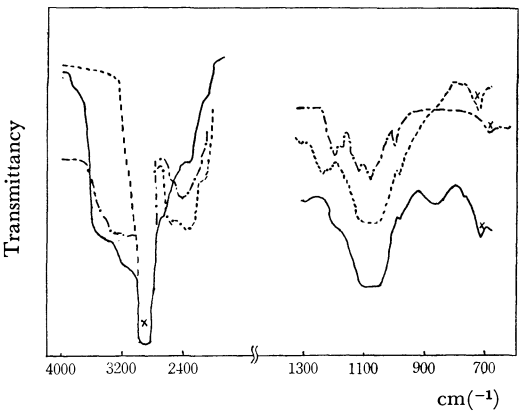

Fig. 1. IR-spectra of $CuSO_4$–$5H_2O$ (———), $CuSO_4 \cdot 2H_2O \cdot 3D_2O$ (— — —) and $CuSO_4 \cdot 5D_2O$ (– – – – –). × is absorption of nujol.

BULLETIN OF THE CHEMICAL SOCIETY OF JAPAN VOL. 43 3265—3267 (1970)

Syntheses of 4-Styryltropolones

Shunsuke NAKAMA,*1 Kimiaki IMAFUKU and Hisashi MATSUMURA

Department of Chemistry, Faculty of Science, Kumamoto University, Kurokami-machi, Kumamoto

(Received October 25, 1969)

The syntheses of colchicine and its derivatives led to the syntheses of many derivatives of 4-styryltropolone.[1-4] In order to examine the chemical reactivities of 4-styryltropolone, one of us (H. M.) investigated its reactions with various nucleophilic reagents.[5]

It was reported that the substituent on the tropolone ring affects the dissociation of tropolone derivatives.[6] It is of interest to know the extent of the effect of the substituent in the benzene ring of styryltropolones.

The present communication deals with the syntheses of 4-styryltropolones having *p*-methyl, *p*-chloro, *m*-chloro and *m*-nitro groups in the benzene ring.

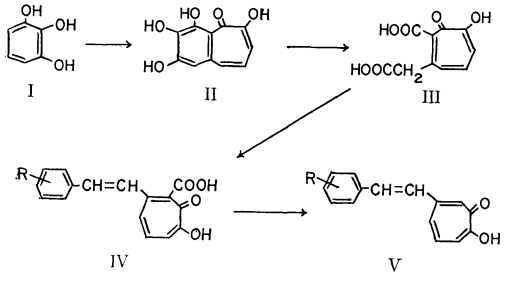

IVa R=H Va R=H
IVb R=*p*-CH_3 Vb R=*p*-CH_3
IVc R=*p*-Cl Vc R=*p*-Cl
IVd R=*m*-Cl Vd R=*m*-Cl
IVe R=*m*-NO_2 Ve R=*m*-NO_2

Scheme 1

Syntheses

The starting material, 3-carboxy-4-carboxymethyltropolone (III), was prepared from pyrogallol (I) *via* purpurogallin (II).[7] Condensation of *p*-methyl-, *p*-chloro-, *m*-chloro- and *m*-nitrobenzaldehydes with III under a similar condition used for the synthesis of 4-styryltropolone[3] gave the substituted 3-carboxy-4-styryltropolones, IVb, IVc, IVd and IVe, respectively. 3-Carboxy-4-styryltropolones were heated under reduced pressure to afford the corresponding 4-styryltropolones, Vb, Vc, Vd and Ve, respectively.

Properties

Ultraviolet Absorption Spectra. The ultraviolet absorption spectra of 4-styryltropolones are shown in Fig. 1. The positions and molecular extinction coefficients of the maximum absorptions are listed in Table 1.

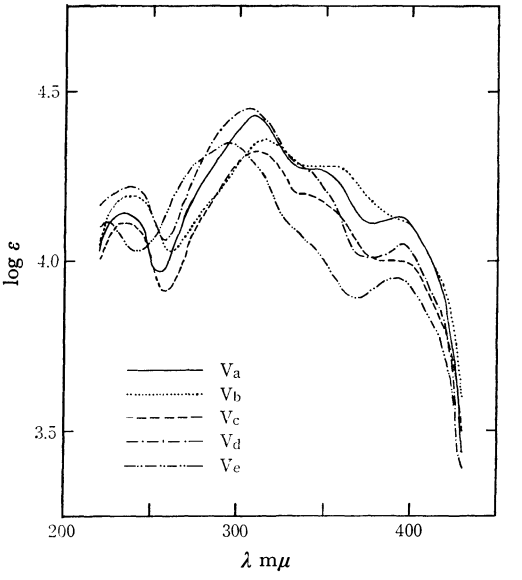

Fig. 1. Ultraviolet absorption spectra of 4-styryltropolones in methanol solution.
Va ———, Vb ·····, Vc – – – –, Vd — — —, Ve — · — · —

*1 Present address: Idemitsu Petrochemical Co. Ltd., Tokuyama.

1) W. D. Crow, R. D. Haworth and P. R. Jefferies, *J. Chem. Soc.*, **1952**, 3705.
2) D. S. Tarbell, R. F. Smith and V. Boekelheide, *J. Amer. Chem. Soc.*, **76**, 2470 (1954).
3) T. Nozoe, Y. Kitahara, K. Doi, S. Masamune, M. Endo, M. Ishii and J.-K. Shin, *Sci. Repts. Tohoku Univ., I*, **38**, 257 (1955).
4) D. S. Tarbell, K. I. H. Williams and E. J. Sehm, *J. Amer. Chem. Soc.*, **81**, 3443 (1959).
5) H. Matsumura, *Nippon Kagaku Zasshi*, **77**, 300 (1956); **78**, 669 (1957); **81**, 1763 (1960); **82**, 623, 775 (1961); H. Matsumura and S. Nagamura, *ibid.*, **85**, 901 (1964).
6) N. Yui, *Sci. Repts. Tohoku Univ., I*, **40**, 102, 114 (1956).
7) R. D. Haworth and J. D. Hobson, *J. Chem. Soc.*, **1951**, 561.

Table 1. UV Data of 4-styryltropolones: λ_{max}^{MeOH} mμ (log ε)

Va	236(4.14)	308(4.43)	338(sh.)	395(4.13)
Vb	239(4.19)	314(4.36)	352(sh.)	—
Vc	232(4.14)	310(4.33)	340(sh.)	390(4.00)
Vd	236(4.22)	306(4.45)	—	396(4.05)
Ve	223(4.11)	295(4.35)	—	394(3.95)

The pattern of all the absorption bands is very similar to that of 4-styryltropolone.[3,5] The absorption maxima in the 280—330 mμ region shift toward the long and short wavelengths with the presence of electron-donating and electron-attracting substituents, compared with that of 4-styryltropolone (308 mμ).

Infrared Absorption Spectra. The infrared spectral data of 4-styryltropolones are summarized in Table 2. As characteristic absorption bands, there are the $\nu_{C=O}$ and δ_{CH} (in *trans* –CH=CH–) absorption bands in 1610—1595 and 960—955 cm^{-1}, respectively.

Table 2. IR Data of 4-styryltropolones (in cm^{-1}; chloroform solution)

Va	Vb	Vc	Vd	Ve
3200(w)	3200(w)	3200(w)	3200(w)	3200(w)
3000(m)	3000(m)	3000(m)	3000(m)	3000(m)
1609(s)	—	1609(s)	1610(s)	1609(s)
1598(s)	1599(s)	1595(s)	1600(s)	1599(s)
1547(m)	—	1545(m)	1549(m)	—
—	—	—	—	1529(s)
—	1512(s)	—	1512(s)	—
1488(s)	1485(s)	1492(s)	1482(s)	1483(s)
1472(s)	1471(m)	1471(s)	1474(s)	1470(sh)
1401(m)	—	1405(m)	—	—
—	—	1350(s)	—	—
1260(s)	—	1262(s)	1260(s)	1261(m)
—	1251(s)	1251(s)	1255(s)	1251(m)
1205(s)	—	1202(m)	1204(m)	1200(s)
—	1172(s)	—	—	—
1148(w)	1146(m)	1145(w)	1148(s)	—
—	1030(m)	1090(m)	—	—
959(s)	958(s)	959(m)	959(s)	957(m)
816(m)	827(m)	822(m)	815(w)	—
688(s)	—	—	680(m)	—
—	658(w)	569(m)	661(m)	659(m)

The ethylenic linkage which connects benzene ring with tropolone ring is found to be a *trans* configuration, because there is a very sharp absorption band in the 960—955 cm^{-1} region. This is also found in 3-carboxy-4-styryltropolones. It is found that the $\nu_{C=O}$ values are little affected by the substituents in the benzene ring.

Dissociation Constants. The dissociation constants were measured in 50% aqueous methanol. These values are listed in Table 3, and give the Hammett equation:

$$pK_a = 7.83 - 0.13\sigma$$

The details are described in another paper.[8]

Table 3. Dissociation constants of 4-styryltropolones

Compound	R	pK_a
Va	H	7.83
Vb	*p*-CH_3	7.85
Vc	*p*-Cl	7.81
Vd	*m*-Cl	7.76
Ve	*m*-NO_2	7.74

Experimental

Elementary analyses were performed in the Elementary Analyses Center of Kyushu University. All the melting points were measured on a Yanagimoto micro-melting point apparatus and are uncorrected. The infrared absorption spectra were taken on a JASCO DS-403G grating spectrophotometer in chloroform, and the ultraviolet absorption spectra on a Hitachi EPS-2 spectrophotometer in methanol.

3-Carboxy-4-styryltropolones (IVb—e). 3-Carboxy-4-carboxymethyltropolone (III) (10 mmol) was dissolved in acetic acid (30 ml) on gentle heating, and acetic anhydride (1.5 ml) was added to the solution at 50°C. After the solution was maintained at 80°C for 30 min, the solution was cooled down to 40°C, substituted benzaldehydes (10 mmol) and pyridine (0.7 ml) were added, and the mixture was kept at 40—45°C for 1 hr. The mixture was further heated up to 60°C, and stirring was continued for 3 hr after removal of the source of heat. The reaction mixture was poured into 10% hydrochloric acid (50 ml) which was cooled with ice to afford IVb—e. The yields and melting points are listed in Table 4.

Table 4. 3-Carboxy-4-styryltropolones

Compound	R	Yield (%)	Mp* (°C)
IVb	*p*-CH_3	83.1	196—199
IVc	*p*-Cl	85.5	204—206
IVd	*m*-Cl	81.5	169—172
IVe	*m*-NO_2	53.7	215—218

* Decomposition points.

4-Styryltropolones (Vb—e). 4-(Substituted styryl)-tropolones were obtained from IVb—e (5 mmol) by decarboxylation at 160—200°C/5 mmHg in a sublimation flask. The substances obtained were recrystallized from methanol. The yields, melting points and data of analyses are shown in Table 5.

8) K. Imafuku, S. Nakama and H. Matsumura, *Tetrahedron*, **26**, 1821 (1970).

Table 5. 4-Styryltropolones

Compound	R	Yield (%)	Mp (°C)	Elementary analyses (%) Found C	Found H	Found N	Calcd C	Calcd H	Calcd N
Vb	*p*-CH_3	37.8	156—156.5	80.34	5.90	—	80.64	5.92	—
Vc	*p*-Cl	31.6	151—151.5	69.57	4.28	—	69.62	4.26	—
Vd	*m*-Cl	44.5	138.5—139	68.98	4.27	—	69.62	4.26	—
Ve	*m*-NO_2	34.9	142—143	66.74	4.07	5.19	66.91	4.12	5.20

The authors wish to express their gratitude to Professor Emeritus Tetsuo Nozoe for his kind encouragement and to Dr. Kazu Kurosawa of Kumamoto University for his helpful suggestions. The authors' thanks are due to the Ministry of Education for financial support.

BULLETIN OF THE CHEMICAL SOCIETY OF JAPAN VOL. 43 3267—3268 (1970)

The Carbon-13 NMR Spectra and *e*-Values of Vinyl Compounds

Koichi HATADA, Kazuhiko NAGATA and Heimei YUKI

Department of Chemistry, Faculty of Engineering Science, Osaka University, Toyonaka, Osaka

(Received February 2, 1970)

The Q—e scheme has been proposed by Alfrey and Price[1] for systematizing large amounts of copolymerization data. In this scheme the Q value is associated with the resonance stabilization, and e is correlated with the polarity of the double bond or of free redical. Although these values have been determined for a wide variety of monomers and they agree fairly well with general chemical knowledge concerning the effect of substituents on resonance stabilization and on polarity,[2,3] direct evidence for their significance have not yet been obtained. In this paper we have correlated the e values of various monomers with the ^{13}C chemical shifts of their vinyl groups and have obtained additional support for the interpretation of the e values as a measure of polarity.

The ^{13}C chemical shifts of the vinyl group have been reported for several vinyl compounds (H_2C_β=$C_\alpha H$–X).[4-9] By plotting the ^{13}C chemical shifts of the β-carbon of the vinyl monomers, $\delta_{C\beta}$, against their e values, a fairly good straight line was ob-

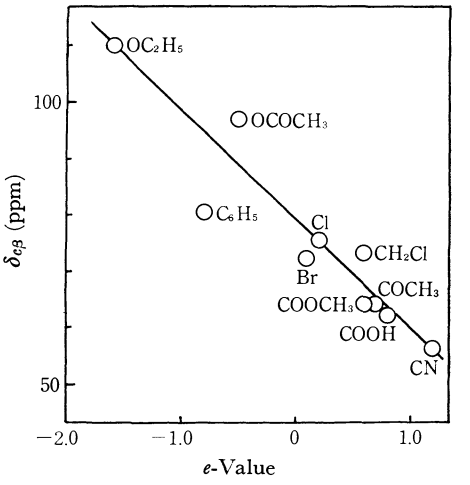

Fig. 1. $\delta_{C\beta}$ *vs.* e value.
δ is referred to CS_2, the high field shift being shown as the positive value.

1) T. Alfrey, Jr., and C. C. Price, *J. Polymer Sci.*, **2**, 101 (1947).
2) A. F. Roche and R. M. Price, paper presented at Cleveland, 1951 Spring Meeting of American Chemical Society.
3) J. Furukawa and T. Tsuruta, *J. Polymer Sci.*, **36**, 275 (1959).
4) R. A. Friedel and H. L. Retcofsky, *J. Amer. Chem. Soc.*, **85**, 1300 (1963).
5) G. E. Maciel, *J. Phys. Chem.*, **69**, 1947 (1965).
6) G. B. Savitsky and K. Namikawa, *J. Phys. Chem.*, **68**, 1956 (1964).
7) T. Higashimura, S. Okamura, I. Morishima and T. Yonezawa, *Polymer Lett.*, **7**, 23 (1969).
8) K. Hatada, K. Nagata and H. Yuki, This Bulletin, **43**, 3193 (1970).
9) G. Miyazima and K. Takahashi, Preprint of the 8th Symposium on NMR Spectroscopy in Japan (1969), p. 121.

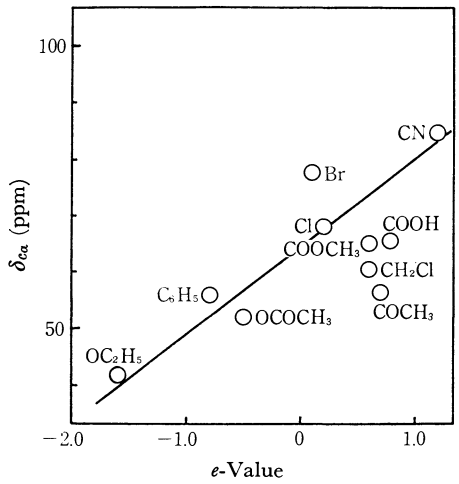

Fig. 2. $\delta_{C\alpha}$ *vs.* *e* value.

tained, as is shown in Fig. 1. The $\delta_{C\beta}$ value shifts to a lower field when the *e* value of the monomer becomes larger. A linear relationship was also obtained between the ^{13}C chemical shifts of α-carbon, $\delta_{C\alpha}$, and the *e* value, although the slope of the straight line was the reverse of that in Fig. 1 (Fig. 2). The ^{13}C chemical shift of the vinyl group has been reported to be mainly controlled by the π-electron density,[5,7,10] although it may also depend, to some extent, on some other factor such as the bond order or the average excitation energy. Therefore, it will show an upfield shift when the π-electron density on the carbon atom increases. Therefore, the results in Figs. 1 and 2 show that as the *e* value of the monomer increases, the π-electron density of the β-carbon decreases, and that of the α-carbon increases.

The vinyl compound with a positive *e* value generally has an electron-withdrawing substituent, and the π-electron in the double bond is drawn toward the substituent, so that the β-carbon is more electropositive. The reverse is the case with the monomer having a negative *e* value, and the β-carbon of the monomer of this type is more electronegative. The *e* value has been proposed as the measure of this polarity in the double bond. Therefore, the results mentioned above may be considered to be a convincing proof for the validity of the *e* value as a measure of the polarity.

One of the authors (K. H.) is grateful to the Matsunaga Science Foundation for a grant in support of this work.

10) M. Karplus and J. A. Pople, *J. Chem. Phys.*, **38**, 2803 (1963).

BULLETIN OF THE CHEMICAL SOCIETY OF JAPAN VOL. 43 3268—3271 (1970)

The Acetylation of Acetamino-2,3-dimethylbenzofurans and the Synthesis of Furoquinolines*1

Yoshiyuki KAWASE and Shigeo KONDÔ

Department of Chemistry, Faculty of Literature and Science, Toyama University, Gofuku, Toyama

(Received February 17, 1970)

The acetylation of 2,3-dimethylbenzofuran derivatives has previously been reported in the cases of alkyl,[1–3] methoxyl,[4] hydroxyl,[5] halo,[6] acetyl,[7–9] and methoxycarbonyl[9] compounds. In the cases of the methoxyl, hydroxyl, and acetyl compounds, the acetylation occurred at the position under the influence of the substituent; it occurred at the 6-position under the influence of the furan ring in the cases of the methoxycarbonyl compounds, while it occurred at various positions in the cases of the alkyl compounds. It has also been reported that the nitration of the 5-acetamino-2,3-dimethyl-

*1 The major part of this work was presented at the 22nd Annual Meeting of the Chemical Society of Japan, Tokyo, April, 1969.

1) E. Bisagni and R. Royer, *Bull. Soc. Chim. Fr.*, **1962**, 925.

2) R. Royer, M. Hubert-Habart, L. René and A. Cheutin, *ibid.*, **1964**, 1259.

3) Y. Kawase, R. Royer, M. Hubert-Habart, A. Cheutin, L. René and J.-P. Buisson, *ibid.*, **1964**, 3131.

4) R. Royer, E. Bisagni, A.-M. Laval-Jeantet and J.-P. Marquet, *ibid.*, **1965**, 2607.

5) Y. Kawase, M. Nanbu and F. Miyoshi, This Bulletin, **41**, 2676 (1968).

6) C. Goldenberg, F. Binon and C. Gillyus, *Chim. Ther.*, **1966**, 221.

7) Y. Kawase, M. Hubert-Habart, J.-P. Buisson and R. Royer, *Compt. Rend.*, **258**, 5007 (1964).

8) R. Royer, Y. Kawase, M. Hubert-Habart, L. René and A. Cheutin, *Bull. Soc. Chim. Fr.*, **1966**, 211.

9) Y. Kawase and M. Takashima, This Bulletin, **40**, 1224 (1967).

benzofuran afforded the 6-nitro derivative.[10]

Now, in the present experiments, the Friedel-Crafts acetylation of 4-, 5-, 6-, and 7-acetamino-2,3-dimethylbenzofurans[11] (**1**, **4**, **8**, and **12**) was carried out. The acetylated products (**2**, **5**, **9**, and **13**) obtained were hydrolyzed to the corresponding amino-ketones (**3**, **6**, **10**, and **14**), the structures of which were determined by the NMR data (see Table 2) and by converting the amino-ketones (**6**, **10**, and **14**) to the known 2,3-dimethyl-6- and -4-acetylbenzofurans (**7** and **11**) (see Chart 1). The coupling constants and δ-values in the NMR spectra indicate that **3** and **10** have aromatic *meta* protons, that **6** has *para* protons, and that **14** has *ortho* protons.

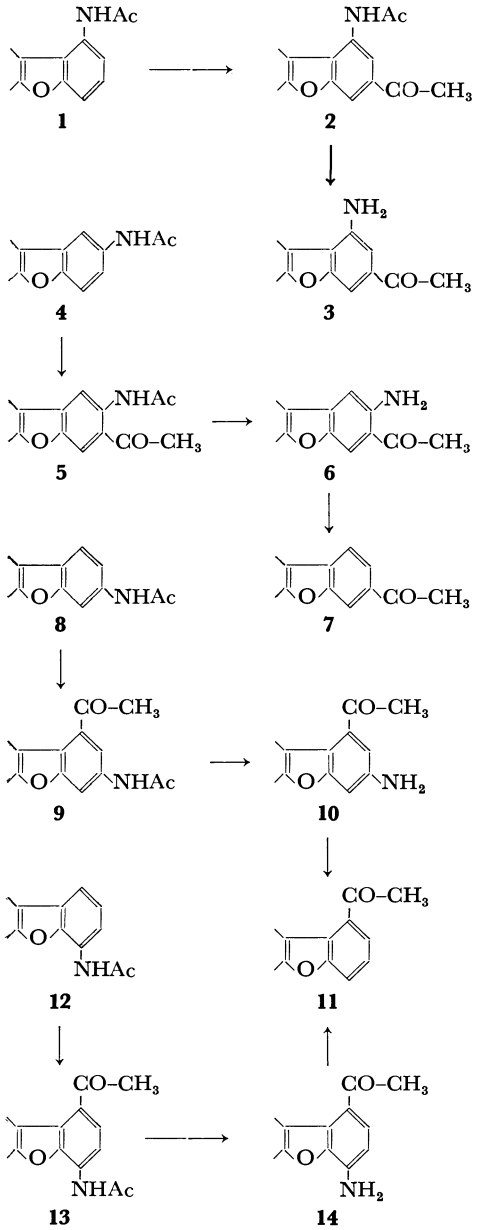

Chart 1

In conclusion, it may be considered that, in the electrophilic substitution, every position on the benzene ring of 2,3-dimethylbenzofuran, especially the 6-position, are activated by the furan ring, and that the acetylation of the compound **4** occurred at the 6-position, which is activated by both the furan ring and the acetamino group, while the compound **1** was acetylated at the 6-position, which is activated by the furan ring. Further, the compound **8** was acetylated at the 4-position, which seems to be fairly well activated by the furan ring, and the compound **12** was acetylated at the 4-position, which is activated by both the acetamino group and the furan ring.

Acetamino-ketone (**5**) was heated with an aqueous sodium hydroxide solution in ethanol to give a compound the structure of which was considered to be 2,3,8-trimethylfuro[2,3-*g*]-6(5*H*)-quinolone (**15**) on the basis of the data of elemental analysis and UV spectrum and on the basis of the analogous formation of 4-methyl-2(1*H*)-quinolone[12] by a similar reaction of *o*-acetaminophenyl methyl ketone (**17**). The treatment of **5** with polyphosphoric acid afforded a compound the structure of which was considered to be 6-(5-acetamino-2,3-dimethyl-6-benzofuranyl)-2,3,8-trimethylfuro[2,3-*g*]quinoline (**16**) on the basis of the data of elemental analysis and UV spectrum and on the basis of the analogous formation of 2-(*o*-acetaminophenyl)-4-methylquinoline (**18**) by a similar reaction of the acetamino-ketone (**17**). The quinoline (**18**) was also obtained by the acetylation of the corresponding amine (**20**), while the compounds **18** and **20** have been prepared by Camps[12] by the action of sodium hydroxide on **17** and amino-ketone (**19**) respectively. The quinoline (**16**) was also obtained in a low yield by the use of acetic acid and polyphosphoric acid on the acetaminobenzofuran (**4**) (see Chart 2).

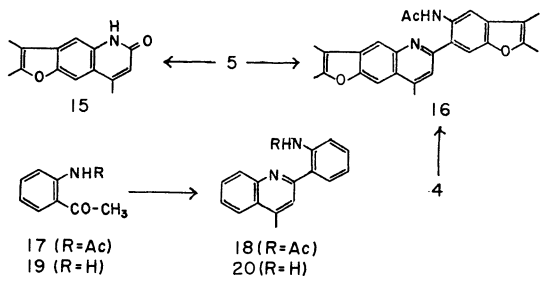

Chart 2

10) C. Pène, P. Demerseman, A. Cheutin and R. Royer, *Bull. Soc. Chim. Fr.*, **1966**, 586.

11) Y. Kawase, S. Takata and E. Hikishima, This Bulletin, to be published.

12) R. Camps, *Ber.*, **32**, 3230 (1899); *Arch. Pharm.*, **237**, 670 (1899).

Table 1. The MP and analyses of the new compounds

Compd.	Mp (°C)[a]	Formula	Found (%)			Calcd (%)		
			C	H	N	C	H	N
Acetamino-ketones								
2	181—182	$C_{14}H_{15}O_3N$	68.32	6.03	5.73	68.55	6.16	5.71
5	181.5—182	$C_{14}H_{15}O_3N$	68.47	6.24	5.75	68.55	6.16	5.71
9	180—181	$C_{14}H_{15}O_3N$	68.62	6.17	5.61	68.55	6.16	5.71
13	169—171	$C_{14}H_{15}O_3N$	68.35	6.21	5.78	68.55	6.16	5.71
Amino-ketones								
3	138—140	$C_{12}H_{13}O_2N$	70.66	6.28	6.67	70.91	6.45	6.89
6	144—145.5	$C_{12}H_{13}O_2N$	70.98	6.20	6.65	70.91	6.45	6.89
10	114.5—115.5	$C_{12}H_{13}O_2N$	70.93	6.46	6.62	70.91	6.45	6.89
14	142—143	$C_{12}H_{13}O_2N$	71.19	6.27	6.64	70.91	6.45	6.89
Furoquinolines								
15	318—319 (dec.)	$C_{14}H_{13}O_2N$	73.93	5.63	6.06	73.99	5.77	6.16
16	298	$C_{26}H_{24}O_3N_2$	75.84	5.79	6.68	75.70	5.89	6.79

a) From ethanol.

Experimental

All the melting points are uncorrected; the NMR spectra were measured on a JEOL Model JNM-C-60H (60 MHz) spectrometer, while the UV spectra were measured on a Hitachi Model 139 spectrophotometer. The melting points and elemental analyses are summarized in Table 1.

Acetylation of Acetaminobenzofurans. *a) By AcCl-$AlCl_3$.* Powdered aluminum chloride (1.3 g) was stirred into a mixture of **1**[11] (1 g), acetyl chloride (0.45 g), and carbon disulfide (20 m*l*); the new mixture was stirred for 3 hr at room temperature and then allowed to stand overnight. The mixture was poured into dilute hydrochloric acid and extracted with chloroform. The organic layer was washed with an aqueous sodium hydroxide solution. The residual product from the organic layer was crystallized from ethanol to give 4-acetamino-2,3-dimethyl-6-benzofuranyl methyl ketone (**2**); mp 181—182°C; 0.25 g (21%). Similarly, 5-acetamino-2,3-dimethyl-6-benzofuranyl methyl ketone (**5**) and 6- and 7-acetamino-2,3-dimethyl-4-benzofuranyl methyl ketones (**9** and **13**) were also obtained from acetaminobenzofurans (**4**, **8**, and **12**) in yields of 50, 58, and 20% respectively.

b) By Ac_2O-$AlCl_3$. Aluminum chloride (2.6 g) was added to a mixture of **1** (1 g), acetic anhydride (0.5 g), and carbon disulfide (20 m*l*), and the mixture was treated much as has been described in a) to give **2** in a yield of 50%. The other acetamino-ketones (**5**, **9**, and **13**) were also obtained in yields of 76, 71, and 35%.

Hydrolysis of the Acetamino-ketones. The acetamino-ketones (**2**, **5**, **9**, and **13**) were hydrolyzed by refluxing them for 1 hr with dilute hydrochloric acid in ethanol to give the corresponding 4- and 5-amino-2,3-dimethyl-6-benzofuranyl methyl ketones (**3** and **6**) and 6- and 7-amino-2,3-dimethyl-4-benzofuranyl methyl ketones (**10** and **14**) in yields of 41, 90, 85, and 41% respectively.

Deamination of the Amino-ketones. The amino-ketones (**6**, **10**, and **14**) were diazotized and then decomposed in the presence of copper powder by the usual procedure[13] to give 6-[1] and 4-benzofuranyl methyl ketones[9] (**7** and **11**) in yields of 57, 73, and 42% respectively.

Table 2. The NMR spectra of the amino-ketones[a]

Compd.	Ph-H[b]	NH_2	COMe	2-Me	3-Me
3	7-H 7.43(d), 5-H 7.03(d); J=2 Hz	3.93	2.55	2.33	2.33
6	7-H 7.58, 4-H 6.48	5.73	2.58	2.31	2.02
10	5-H 6.83(d), 7-H 6.78(d); J=2 Hz	3.67	2.56	2.31	2.11
14	5-H 7.42(d), 6-H 6.47(d); J=8 Hz	4.02	2.58	2.39	2.29

a) δ (ppm) values measured in $CDCl_3$ (*ca.* 5% solution), with TMS as the internal standard.
b) d: Doublet.

2,3,8-Trimethylfuro[2,3-*g*]-6(5*H*)-quinolone (15). An aqueous sodium hydroxide solution (30%, 16 m*l*) was added, drop by drop, to a hot solution of **5** (2 g) in ethanol (80 m*l*), after which the mixture was refluxed for 5 hr. Most of the ethanol was then distilled off, and the residue was steam-distillated. The residual crystalline precipitates were recrystallized from ethanol to give the furoquinolone (**15**); mp 318—319°C; 1.55 g (84%); λ_{max}^{EtOH} mμ (log ε): 227 (4.66), 252 (4.03), 322 (4.29), and 342 (4.23).

6-(5-Acetamino-2,3-dimethylbenzofuranyl)-2,3,8-trimethylfuro[2,3-*g*]quinoline (16). *a) From the*

13) *Cf.* L. A. Bigelow, J. R. Johnson and L. T. Sandborn, "Organic Syntheses," Coll. Vol. 1, p. 133 (1956).

Acetamino-ketone (**5**). A mixture of **5** (2 g) and polyphosphoric acid (n=2.5, 40 g) was heated at 100°C for 1 hr. The cooled mixture was poured into ice water and extracted with ethyl acetate, and the residual product from the organic layer was crystallized from ethyl acetate or benzene to give **16**; mp 298°C; 1.37 g (81%); λ_{max}^{EtOH} mμ (log ε): 258 (4.34), 304.5 (4.34), and 363 (4.05).

b) From the Acetaminobenzofuran (**4**). A mixture of **4** (1 g), acetic acid (0.45 g), and polyphosphoric acid n=1.5, 20 g) was heated at 100°C for 1 hr. The cooled mixture was then treated much as has been described in a) to give **16** (mp 290°C; 0.05 g (5%)), which was identical with the above sample.

2-(2-Acetaminophenyl)-4-methylquinoline (18). *a) From Acetamino-ketone* (**17**). The compound **17** (2 g) was treated with polyphosphoric acid (n=2.5, 40 g), much as has been described in the case of **16**, to give **18**; mp 138.5—139°C (lit,[12] mp 138°C); 1.2 g(77%); λ_{max}^{EtOH} mμ (log ε): 244 (4.40), 259.5 (4.21), and 338 (3.74).

b) By Acetylation of Amine (**20**). The amine **20**[12] (0.09 g) was acetylated with acetic anhydride - acetic acid to give **18**, mp 134—136°C; 0.05 g (47%), which was identical with the above sample.

The authors are grateful to the members of the Laboratory of Analysis, Faculty of Pharmacology, Toyama University, for their microanalyses and NMR spectroscopy.

BULLETIN OF THE CHEMICAL SOCIETY OF JAPAN VOL. 43 3271—3273 (1970)

The Catalytic Hydrogenation of 2,5-Diphenylfuran

Yutaka INAMURA

Department of Chemistry, Fukushima Medical College, Fukushima

(Received February 18, 1970)

The reductions of *trans*-1,2-dibenzoylethylene and its derivatives have been studied, and the reaction mechanisms have been discussed.[1)]

In the following experiment, the hydrogenation of 2,5-diphenylfuran, which was often obtained by these reductions, was carried out over several kinds of catalysts.

Experimental

2,5-Diphenylfuran (I). I was prepared from *trans*-1,2-dibenzoylethylene or 1,2-dibenzoylethylene oxide by the method of Lutz and Rowlett[2)] or by that of the present author.[1)]

Catalysts. The catalysts used were palladium-charcoal-A (5%), palladium-charcoal-B (5%), Raney nickel W-5, and Adams' platinum oxide, all of which were prepared by known methods.[3-6)]

Solvents. When Raney nickel was the catalyst, ethanol was used as the solvent, while in the case of the other catalysts, glacial acetic acid was used. One milliliter of concentrated hydrochloric acid or 0.05 g of sodium hydroxide was used as the additive.

Hydrogenation. I (1.1 g, 1/200 mol) was dissolved in 100 m*l* of a solvent, and reduction was then carried out over a catalyst (0.5 g, of Pd–C, 0.1 g of platinum oxide, or 0.5—1.5 g of Raney nickel) under atmospheric hydrogen pressure and at room temperature. After the reduction had been completed and the catalyst had been filtered out, the solvent was distilled off under reduced pressure. The residue was then recrystallized from 15 m*l* of ethanol. After the filtration of I, which was recovered as crystals, the filtrate was condensed to about 5 m*l*; the solution was subsequently kept below 0°C. After the substance, mp 54—55°C, had crystallized, it was filtered and the solvent of the filtrate was distilled off completely. This residue was recrystallized from *n*-hexane. A substance with a mp of 48—49°C was thus obtained. When platinum oxide was used as a catalyst, the raw reduction product was recrystallized from *n*-hexane after the filtration of the catalyst and the complete distillation of the solvent. The crystals thus obtained melted at 82—83°C. When the hydrogen uptake was stopped at less than 8 mol over platinum oxide, an oily substance, perhaps be a mixture of several intermediates, was produced.

1,4-Diphenyl-1-butanol (II) and 1,4-diphenyl-1-butanone (III), which had been prepared by the method of Stoemer and Schenck,[7,8)] were also reduced by the

1) Y. Inamura, *Nippon Kagaku Zasshi*, **85**, 905 (1964); *ibid.*, **88**, 648 (1967); *ibid.*, **87**, 734 (1966); *ibid.*, **89**, 208 (1968).

2) R. E. Lutz and R. J. Rowlett, Jr., *J. Amer. Chem. Soc.*, **70**, 1359 (1948).

3) R. Mozingo, "Organic Syntheses," Vol. 26, p. 77. (1964),

4) S. Mitsui and H. Saito, *Nippon Kagaku Zasshi*, **83**, 390 (1961).

5) H. Adkins and H. R. Billica, *J. Amer. Chem. Soc.*, **70**, 695 (1948).

6) R. Adams, V. Voorhees and R. L. Schriner, "Organic Syntheses," Coll. Vol. 1, 2nd Ed., p. 463 (1948),

7) R. Stoemer and Fr. Schenck, *Ber.*, **61**, 2320 (1928).

8) H. Rupe and J. Bürgin, *ibid.*, **43**, 172 (1910).

same method as that described above.

Results

The results of the experiments are shown in Tables 1, 2, and 3. In the reduction of I, the maximum quantity of absorbed hydrogen was 3 mol when palladium-charcoal or Raney nickel was the catalyst, and 9 mol when Adams' platinum oxide was used. No effect was observed on the reduction products by the addition of an acid or an alkaline substance.

The substance (mp 48—49°C) yielded by the reaction of I with 2—3 mol of hydrogen with palladium-charcoal-B or Raney nickel as a catalyst was identified by a mixed-melting-point determination with 1,4-diphenyl-1-butanol, an authentic sample which had been synthesized by the method described in previous papers.[7,8] The IR spectrum of this substance showed an absorption at 3300 cm^{-1}.

The IR spectrum of the substance (mp 54—55°C) yielded by the reaction of I of 2 or 3 mol of hydrogen with palladium-charcoal-A, or that of the substance yielded by the reaction of 3 mol of hydrogen with palladium-charcoal-B or Raney nickel, showed no absorption of the hydroxyl group or the carbonyl group. The mixed-melting-point determination confirmed that this substance was 1,4-diphenylbutane (IV). The authentic sample of IV was prepared by the method of Freund[9] or by the hydrogenation of *trans*-1,2-dibenzoylethylene with 5 mol of hydrogen.[10]

The IR spectrum of the substance (mp 82—83°C) obtained in the hydrogenation of I over the Adams' platinum oxide catalyst showed an absorption at 3400 cm^{-1}. The chromic anhydride oxidation of this compound in glacial acetic acid gave an oily substance. The 2,4-dinitrophenylhydrazone made from it melted at 80—81°C. Moreover, the data of the elementary analysis of this substance (mp 82—83°C) proved it to be 1,4-dicyclohexyl-1-butanol (V).

Found: C, 80.51; H, 12.73%. Calcd for $C_{16}H_{30}O$: C, 80.61; H, 12.68%.

The ketone III was not obtained under any of the following conditions: that is, when large quantities of I were used, when the absorption period was shortened, when a small quantity of hydrogen was absorbed, or when the solvents were changed.

Table 1. The yields of products in the hydrogenation of I (%)

Catalyst	Additive	Quantity of absorbed hydrogen (mol/mol)	Recovered (I)	(II)	(IV)	(V)
Pd-C-A	—	1	91	—	—	—
Pd-C-A	—	2	23	—	19	—
Pd-C-A	—	3	—	—	41	—
Pd-C-A	HCl	3	—	—	46	—
Pd-C-B	—	1	67	—	—	—
Pd-C-B	—	2	41	5	—	—
Pd-C-B	—	3	—	—	62	—
Pd-C-B	HCl	3	—	—	50	—
Raney Ni	—	1	78	5	—	—
Raney Ni	—	2	32	14	—	—
Raney Ni	—	3	—	14	28	—
Raney Ni	NaOH	1.5	50	14	—	—
PtO_2	—	9	—	—	—	55
PtO_2	HCl	9	—	—	—	30

Table 2. The yields of products in the hydrogenation of II (%)

Catalyst	Quantity of absorbed hydrogen (mol/mol)	Recovered (II)	(IV)
Pd-C-A	1	12	55
Pd-C-B	1	—	55
Raney Ni	1	32	19

Table 3. The yields of products in the hydrogenation of III (%)

Catalyst	Quantity of absorbed hydrogen (mol/mol)	Recovered (II)	(IV)
Pd-C-A	1	14	48
Pd-C-A	2	—	80
Pd-C-B	1	64	—
Pd-C-B	2	—	50
Raney Ni	1	69	—
Raney Ni	2	32	19

Discussion

The hydrogenation of furan derivatives has been well examined,[11] and the reductions of 2-phenylfuran and 2-phenyltetrahydrofuran have been reported on by Mitsui and his co-workers.[12] These reports indicate that hydrogenation mainly occurs when palladium-charcoal or Raney nickel is used as the catalyst, while hydrogenation and hydrogenolysis occur competitively over the platinum oxide catalyst.

The present results show that 2,5-diphenylfuran also undergoes hydrogenolysis to give II and IV

9) M. Freund and P. Immerwahr, *Ber.*, **23**, 2845 (1890).
10) Y. Inamura, *Nippon Kagaku Zasshi*, **84**, 416 (1963).
11) H. A. Smith and J. F. Fuzeck, *J. Amer. Chem. Soc.*, **71**, 415 (1949); H. A. Smith, J. B. Conley and W. H. King, *ibid.*, **73**, 4633 (1951).
12) S. Mitsui, Y. Ishikawa, Y. Takeuchi, H. Saito and H. Mamuro, *Nippon Kagaku Zasshi*, **81**, 286 (1960); S. Mitsui and H. Saito, *ibid.*, **81**, 289 (1960).

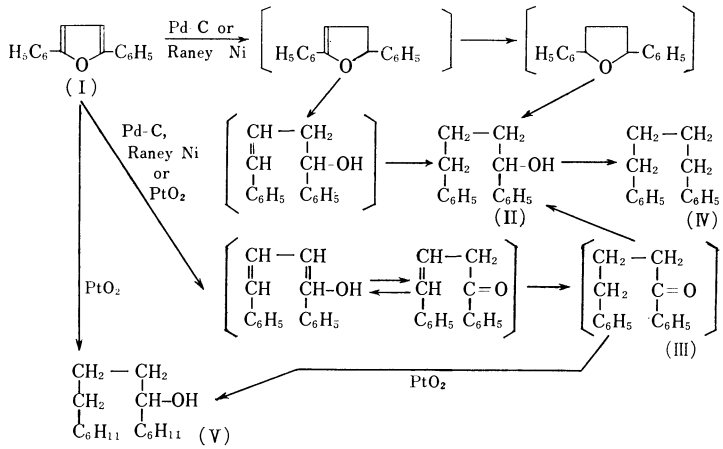

Fig. 1

over the palladium-charcoal or the Raney nickel catalyst.

Some possible courses of the reduction of I are shown in Fig. 1. The hydrogenation of I over Raney nickel gave more II than that over the palladium-charcoal catalyst. The results presented above and those of Table 2 show that the hydrogenation of I took the course: I→II→IV and that the II→IV course was more difficult over the Raney nickel catalyst than over the palladium-charcoal catalyst.

It is well known that the benzene ring is hydrogenated over the platinum catalyst.[13] In the present experiment, too, after the cleavage of the furan ring and the saturation of the benzene ring of I, V was produced. Though III easily gave II and IV, as is shown in Table 3, III was not obtained at all in the reduction of I.

The compounds described in brackets in Fig. 1 were not isolated; therefore, it is uncertain which course of those shown in Fig. 1 is mainly taken in this reaction. However, from the fact that III which, if present, is expected to crystallize easily, was not obtained under any of the conditions described above, and from the fact that 2-aryltetrahydrofuran is easily hydrogenated,[12] it can be said that the hydrogenation of I seems to take the reaction course of, first, the reduction of the furan ring, and then the reaction II→IV.

The author wishes to express his cordial thanks to Professor Sekio Mitsui, Faculty of Engineering, Tohoku University.

13) R. H. Baker and R. D. Schuetz, *J. Amer. Chem. Soc.*, **69**, 1259 (1947).

BULLETIN OF THE CHEMICAL SOCIETY OF JAPAN VOL. 43 3274—3276 (1970)

The Electron Spin Resonance Spectra of Dicyanobiphenyl Radical Anions

Hideo SHIKATA,*1 Kazuhiko ISHIZU,*1 Yasuo DEGUCHI and Hideo TAKAKI

Department of Chemistry, Faculty of Science, Kyoto University, Sakyo-ku, Kyoto

(Received February 19, 1970)

Some of the radical anions of biphenyl and its derivatives, produced by the reduction with alkali metals, show ESR spectra which can be interpreted in terms of the pairing of the alkali metal cation with the anion. As a remarkable case, the dinitrobiphenyl radical anions[1] have their unpaired electron localized only one of the nitrophenyl rings. In the course of several previous studies,[1-3] the ESR spectra have been observed for the radical anions of several dicyanobiphenyls, substances which possess substituents with a weaker electron-withdrawing tendency than that of the nitro groups.

Experimental

Dicyanobiphenyls were synthesized by the following procedures:

2,2′-Dicyanobiphenyl. Diphenic acid[4] obtained from anthranilic acid with a Sandmeyer reaction was converted to its diamide by repetition of the anhydration with acetic anhydride and by treatment with ammonium hydroxide,[5] the diamide was finally anhydrated with acetic anhydride to its dinitrile, 2,2′-dicyanobiphenyl,[6] mp 177°C.

3,3′-Dicyanobiphenyl. 3,3′-Dinitrobiphenyl[7] was synthesized from *m*-iodonitrobenzene[8] by Ullmann's method. It was then reduced to 3,3′-diaminobiphenyl in the presence of Raney nickel. 3,3′-Diaminobiphenyl was tetrazotized and added to the hot $KCN-CuSO_4$ solution to obtain 3,3′-dicyanobiphenyl, mp 201°C.

4,4′-Dicyanobiphenyl. 4,4′-Dicyanobiphenyl[9] was prepared from benzidine by the same procedures as those used in the last step used in obtaining 3,3′-dicyanobiphenyl, mp 221°C.

All the final products were purified by vacuum sublimation or by recrystallization from ethanol several times.

The radical anions were prepared by reduction with potassium, sodium, lithium, or cecium in some solvent such as 1,2-dimethoxyethane, tetrahydrofuran, or tetrahydropyran. The reduction of 4,4′-dicyanobiphenyl gave a fairly stable radical anion at room temperature, whereas 2,2′-dicyanobiphenyl and 3,3′-dicyanobiphenyl radical anions were found to be stable only at the temperature of an acetone-dry ice bath. Therefore, the ESR spectra were examined in detail for only the 4,4′-diycanobiphenyl radical anions.

The ESR spectra were measured using a JEOL-3B X-band-type ESR spectrometer with a 100 kc/sec field modulation.

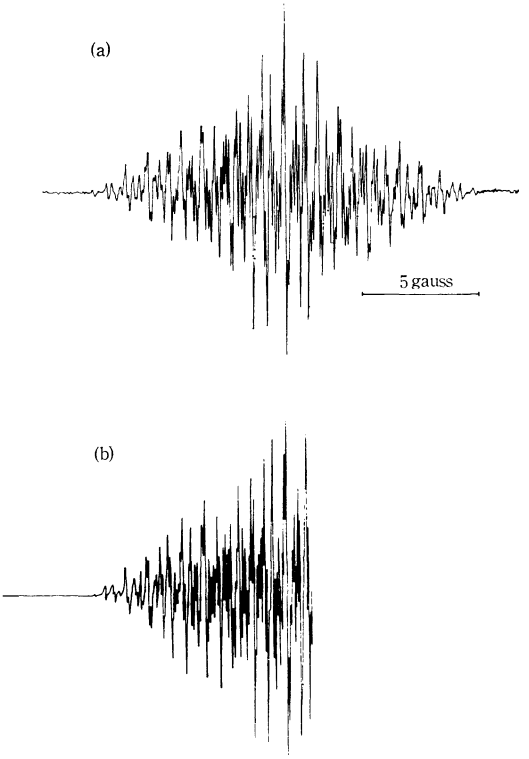

Fig. 1

(a) (2,2′-dicyanobiphenyl)$^-$ K^+ in DME
(b) the simulated spectrum of (a),

*1 Present address: Department of Chemistry, Faculty of Science, Ehime University, Matsuyama.

1) Y. Nakai, K. Nakamura, K. Ishizu, Y. Deguchi and H. Takaki, This Bulletin, **39**, 847 (1966).
2) K. Ishizu, *ibid.*, **36**, 938 (1963); **37**, 1093 (1964); **42**, 2808 (1969).
3) H. Nishiguchi, Y. Nakai, K. Nakamura, K. Ishizu, Y. Deguchi and H. Takaki, *J. Chem. Phys.*, **40**, 241 (1964); H. Nishiguchi, Y. Nakai, K. Nakamura, K. Ishizu, Y. Deguchi and H. Takaki, *Mol. Phys.*, **9**, 153 (1965).
4) E. R. Atkinson and H. J. Lawler, "Organic Syntheses," Coll. Vol. I, p. 222 (1941).
5) Underwood and Kochmann, *J. Amer. Chem. Soc.*, **46**, 2075 (1924).
6) Underwood and Kochmann, *ibid.*, **51**, 584 (1929).
7) R. C. Fuson and E. A. Cleveland, "Organic Syntheses," Coll. Vol. III, p. 339 (1955).
8) Ferriss and Turner, *J. Chem. Soc.*, **117**, 1149.
9) Dannett and Turner, *ibid.*, **1926**, 480.

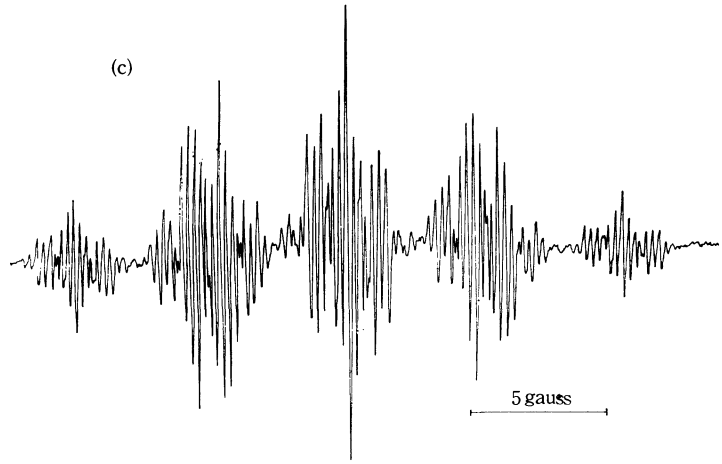

Fig. 1. (c) (3,3′-dicyanobiphenyl)$^-$ K^+ in DME.

TABLE 1. THE HYPERFINE SPLITTING CONSTANTS AND THE EXPERIMENTAL AND THE THEORETICAL SPIN DENSITIES

Position*	h.f.s.c. (gauss)	ρ_{exp}	$\rho_{Hückel}$	$\rho_{McLachlan}$
4,4′-Dicyanobiphenyl				
1			0.1059	0.1174
2	1.86	0.0785	0.0658	0.0767
3	0.26	0.011	0.0315	0.0075
4			0.1288	0.1591
7			0.0271	0.0143
8	1.05	0.0528	0.0437	0.0409
3,3′-Dicyanobiphenyl				
1			0.1026	0.1058
2	0.91	0.039	0.0333	0.0238
3			0.0387	0.0258
4	5.59	0.236	0.1672	0.2113
5	0.52	0.022	0.0064	−0.0489
6	4.69	0.1965	0.1258	0.1649
7			0.0108	0.0065
8	0.26	0.013	0.0153	0.0113
2,2′-Dicyanobiphenyl				
1			0.1151	0.1263
2			0.1174	0.1470
3	1.41	0.0595	0.0002	−0.0459
4	3.39	0.143	0.1112	0.1455
5	0.57	0.024	0.0471	0.0357
6	0.84	0.035	0.0408	0.0394
7			0.0267	0.0139
8	0.91	0.046	0.0415	0.0384

parameter values: $\alpha_N=\alpha+1.0\beta$, $\beta_{CN}=2.0\beta$, $\beta_{CC'}=0.9\beta$, $\lambda=1.2$

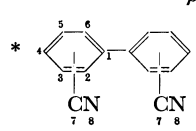

Results and Discussion

The observed spectra for dicyanobiphenyls are shown in Fig. 1. Rieger *et al.*[10] have reported that the radical anion produced by the electrolytic reduction of *p*-cyanoaniline showed the ESR spectrum of the 4,4′-dicyanobiphenyl radical anion. Our observation for synthesized 4,4′-dicyanobiphenyl supports their interpretation.

The hyperfine splitting constants for the proton summarized in Table 1, were assigned by taking into account the results of the McLachlan MO calculation, though those results are not unarbitrary. The experimental spin density for the ring carbon atoms is calculated from the McConnell relation, $a_H=Q\rho_C$, where $Q=23.7$ gauss, while for the nitrogen atom of the cyano group, $A_N=K\rho_N$ is used (according to Rieger and Fraenkell[11]), where $K=19.8$ gauss. The experimental spin density is then compared with that obtained from either the simple Hückel MO or the McLachlan MO calculation.

In contrast to the dinitrobiphenyl ion pairs, no alkali metal splitting was found for the 4,4-dicyanobiphenyl radical anion, though we repeatedly observed solutions with a variety of solvents, using different alkali metal and at temperatures from 20°C to −90°C. Moreover, the unpaired spin distribution was found to be symmetrical for two cyanophenyl rings of dicyanobiphenyl. These results suggest that the ion pairing, if any, is rather weaker in this case. The difference may be the weaker electron-withdrawing tendency of the cyano group than that of the nitro group.

When terephthalonitrile, which has a structure analogous to 4, 4′-dicyanobiphenyl, is reduced with lithium, it is known that the ESR spectrum

10) P. H. Rieger, I. Bernal, W. H. Reinmuth and G. K. Fraenkel, *J. Amer. Chem. Soc.*, **85**, 683 (1963).

11) P. H. Rieger and G. K. Fraenkel, *J. Chem. Phys.*, **37**, 2795 (1962).

shows an extra-hyperfine splitting of lithium and results in an asymmetric spin distribution of the anion.[12] In order to explain the difference in the ion pairing between the two cases, the π electron energy of these anions was estimated by the Hückel MO method on the following assumption: the accession of the alkali metal to one of the cyano groups leads to the variation of the Coulomb integral parameter, h_N, at its nitrogen atom, where $\alpha_N=\alpha+h_N\beta$. As the result of the calculations,

$$\left[\frac{\partial E}{\partial h_N}\right]_{h_N=1.0}(\text{terephthalonitrile}) - \left[\frac{\partial E}{\partial h_N}\right]_{h_N=1.0}(\text{4,4'-dicyanobiphenyl}) = 0.042\beta,$$

where E is the total π electron energy of the anion and where β is the resonance integral. This may mean that the 4,4'-dicyanobiphenyl radical anion is less stabilized by the ion-pair formation than is the terephthalonitrile radical anion. Though no consideration was made of the energy of the lone-paired electrons and of the solvation, this calculation can explain the experimental results qualitatively.

The authors are grateful to Drs. Kazuo Nakamura, Hiroaki Nishiguchi, and Kazuo Mukai for their kind discussions throughout the work. The authors also wish to thank Mr. Hideo Hasegawa for his simulation of the spectra.

12) K. Nakamura, This Bulletin, **40**, 1019 (1967).

BULLETIN OF THE CHEMICAL SOCIETY OF JAPAN VOL. 43 3276—3278 (1970)

Synthetic Studies of the Flavone Derivatives. XVIII.*1 The Syntheses of 5,7,3′-Trihydroxy-3,8,4′,5′-tetramethoxyflavone and Related Compounds

Mitsuru NAKAYAMA and Kenji FUKUI

Department of Chemistry, Faculty of Science, Hiroshima University, Higashisenda-machi, Hiroshima

and Tokunaru HORIE and Mitsuo MASUMURA

Department of Applied Chemistry, Faculty of Engineering, University of Tokushima, Tokushima

(Received March 3, 1970)

Recently, a new pigment isolated from *Beyeria brevifolia* (Muell Arg.) Benth.[1] was identified as 5,7,3′-trihydroxy-3,8,4′,5′-tetramethoxyflavone (I).

The present paper will describe the syntheses of I and its related compounds from 3,ω-dimethoxy-2,4,6-trihydroxyacetophenone (II)[2] by a modification of a procedure reported earlier.[2–6]

According to the method of Allan-Robinson's flavone synthesis, the condensation of the ketone II with 3-benzyloxy-4,5-dimethoxybenzoic anhydride and potassium 3-benzyloxy-4,5-dimethoxybenzoate, followed by treatment with alcoholic potassium hydroxide, was expected to afford a mixture of 3′-benzyloxy-5,7-dihydroxy-3,6,4′,5′-tetramethoxyflavone (III) and the 3′-benzyl ether (IV) of I. The reaction mixture could be separated into two crystals, A (mp 159.5—160.5°C) and B (mp 126—127 and 135—135.5°C), by a fractional partition. The catalytic hydrogenolysis of A over Pd–C gave the 5,7,3′-trihydroxyflavone derivative (V), which was then converted into the triacetate (VI), triethyl (VII), and trimethyl ether (VIII) with usual methods. The properties of VIII were superimposable upon those of 3,5,6,7,3′,4′,5′-heptamethoxyflavone.[7,8] Further, in the NMR spectra data*2

*1 Part XVII of this series: K. Fukui, M. Nakayama and T. Horie, This Bulletin, **43**, 1524 (1970).

1) P. W. Chow and P. R. Jefferies, *Aust. J. Chem.*, **21**, 2529 (1968).

2) K. Fukui, T. Matsumoto, S. Nakamura, M. Nakayama and T. Horie, *Experientia*, **24**, 108 (1968); This Bulletin, **41**, 1413 (1968).

3) K. Fukui, M. Nakayama and T. Horie, *Experientia*, **24**, 417 (1968); This Bulletin, **41**, 2805 (1968).

4) K. Fukui, M. Nakayama and T. Horie, *Experientia*, **24**, 769 (1968); This Bulletin, **42**, 1649 (1969).

5) T. Horie, *Experientia*, **24**, 880 (1968); This Bulletin, **42**, 2701 (1969).

6) K. Fukui, T. Matsumoto, M. Nakayama and T. Horie, *Experientia*, **25**, 349 (1969); *J. Sci. Hiroshima Univ. Series A-II*, **33**, 221 (1969).

7) P. R. Jefferies, J. R. Knox and E. J. Middleton, *Aust. J. Chem.*, **15**, 532 (1962).

8) D. L. Dreyer, *J. Org. Chem.*, **33**, 3574 (1968).

*2 The NMR spectra were measured with a Hitachi R-20 spectrometer (60 MHz) in $CDCl_3$, using tetramethylsilane as the internal standard (δ, ppm): s, singlet; m, multiplet.

of VII and VIII, the chemical shift (δ *ca.* 6.70) of the singlet peak (1H) was very similar to that due to the C-8 proton of some flavones reported in the literature.[2-9] From the above results, A and V may be formulated as III and 5,7,3′-trihydroxy-3,6,4′,5′-tetramethoxyflavone respectively. On the other hand, the singlet peak at δ 6.46 (1H) of B can be assigned to the C-6 proton of the flavone nucleus. Thus, B is identified as the benzyl derivative (IV) of I. The hydrogenolysis of IV gave the desired flavone, I, which was then easily derived to triacetate (IX) and triethyl ether (X). The properties of the synthetic flavones (I, IX and X) were consistent with those described in an earlier report.[1]

By a similar method, 5,7-dihydroxy-3,6,3′,4′,5′-pentamethoxyflavone (XI), which was easily converted into diacetate (XII) and diethyl ether (XIII), was prepared from II and 3,4,5-trimethoxybenzoic anhydride. XIII was also prepared by the reaction of the 4,6-diethoxy-5,ω-dimethoxy-2-hydroxyacetophenone (XIV)[2] with 3,4,5-trimethoxybenzoic anhydride. The dimethyl ether of XI was found to be identical with VIII by a direct comparison.

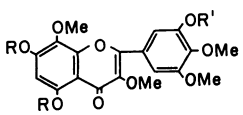

I R=R′=H
IV R=H R′=C6H5CH2
IX R=R′=CH3CO
X R=R′=Et

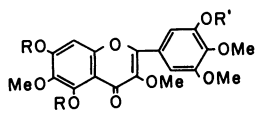

III R=H R′=C6H5CH2
V R=R′=H
VI R=R′=CH3CO
VII R=R′=Et
VIII R=R′=Me
XI R=H R′=Me
XII R=CH3CO R′=Me
XIII R=Et R′=Me

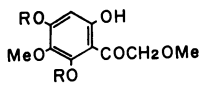

II R=H
XIV R=Et

Experimental*3

3′-Benzyloxy-5,7-dihydroxy-3,6,4′,5′-tetramethoxyflavone (III) and 3′-Benzyloxy-5,7-dihydroxy-3,8,4′,5′-tetramethoxyflavone (IV). A mixture of II (2.5 g),[2] 3-benzyloxy-4,5-dimethoxybenzoic anhydride (25 g), and potassium 3-benzyloxy-4,5-dimethoxybenzoate (9 g) was heated at 175—180°C under reduced pressure for 10 hr; the mixture was then treated by a method analogous with those of previous reports[2-6] to give an oily flavone mixture (*ca.* 3.5 g).

The mixture was dissolved with a 5% aqueous potassium hydroxide solution (50 m*l*) and then allowed to stand in a refrigerator. The precipitate thus separated was collected to give potassium salt of flavone. After the mother liquor had been acidified with hydrochloric acid, the resulting oily material was repeatedly treated with a solution of potassium hydroxide (1.2 g) and potassium carbonate (3.0 g) in water (20 m*l*). The second crop of the potassium salt was thus obtained.

The mother liquor was acidified with hydrochloric acid and extracted with ether. After the solvent had been removed, the residue was dissolved with absolute ether (*ca.* 10 m*l*) and then allowed to stand in a refrigerator. The crystals thus separated were collected and recrystallized from aqueous methanol to give a hydrate of IV as pale yellow needles; mp 95—100°C (67—68°C sinter); yield, 240 mg (4.5%). This was recrystallized from absolute ether to give yellow needles; mp 126—127°C and 135—135.5°C. UV: λ_{max} mμ (log ε); (EtOH) 278 (4.33), 314 (4.17), 370$_{sh}$ (4.05);*4 (EtOH–AcONa) 286 (4.39), 364 (3.99); (EtOH–$AlCl_3$) 288.5 (4.27), 314 (4.17), 349 (4.18), 420 (3.87). NMR:*2 6.46$_s$ (C_6–H), 7.40—7.60$_m$ (7H; $C_{2'}$–H, $C_{6'}$–H and $C_6\underline{H}_5CH_2$).

Found: C, 64.90; H, 5.18%. Calcd for $C_{26}H_{24}O_9$: C, 64.99; H, 5.04%.

The combined potassium salt of flavone was treated with diluted hydrochloric acid and extracted with ether. After the solvent had then been removed, the residue was recrystallized from ethanol to give III as pale yellow needles; mp 159.5—160.5°C; yield, 700 mg (13%). UV: λ_{max} mμ (log ε); (EtOH) 275 (4.21), 339 (4.29); (EtOH–AcONa) 277.5 (4.35), 304 (4.12), 352 (4.14); (EtOH–$AlCl_3$) 258 (4.09). 284 (4.17), 355 (4.27). NMR:*2 6.57$_s$ (C_8–H), 7.35—7.60$_m$ (7H; $C_{2'}$–H, $C_{6'}$–H $C_{6'}$–H and $C_6\underline{H}_5CH_2$).

Found: C, 64.75; H, 4.94%. Calcd for $C_{26}H_{24}O_9$: C, 64.99; H, 5.04%.

5,7,3′-Trihydroxy-3,6,4′,5′-tetramethoxyflavone (V). A solution of III (325 mg) dissolved in a mixture of ethyl acetate and methanol (1 : 1 : 100 m*l*) was shaken with Pd–C (10% : 140 mg) in hydrogen. The product was recrystallized from methanol to give V as yellow needles; mp 163.5—164.5°C; yield, 237 mg (90%). UV: λ_{max} mμ (log ε); (EtOH) 275 (4.21), 343 (4.28); (EtOH–AcONa) 277 (4.45), 304 (4.14), 378 (4.22); (EtOH–$AlCl_3$) 283 (4.20), 358 (4.29).

Found: C, 58.70; H, 4.82%. Calcd for $C_{19}H_{18}O_9$: C, 58.46; H, 4.65%.

Triacetate (VI). Mp 126—127°C (colorless prisms from ether). UV: λ_{max}^{EtOH} mμ (log ε); 248 (4.31), 327 (4.31).

Found: C, 58.23; H, 4.76%. Calcd for $C_{25}H_{24}O_{12}$: C, 58.14; H, 4.68%.

Triethyl Ether (VII). Mp 111.5—112.5°C (colorless needles from ether). UV: λ_{max}^{EtOH} mμ (log ε); 267$_{sh}$ (4.19), 328 (4.39). NMR:*2 6.72$_s$ (C_8–H), 7.37$_s$ (2H; $C_{2'}$–H and $C_{6'}$–H).

Found: C, 63.19; H, 6.43%. Calcd for $C_{25}H_{30}O_9$: C, 63.28; H, 6.37%.

Trimethyl Ether (3,5,6,7,3′,4′,5′-Heptamethoxyflavone) (VIII). Mp 153—154°C (colorless needles from methanol) (lit, mp 155—156°C,[7] 156—157°C[8]). UV: λ_{max}^{EtOH} mμ (log ε); 267$_{sh}$ (4.22), 327.5 (4.35). NMR:*2 6.74$_s$ (C_8–H), 7.38$_s$ (2H; $C_{2'}$–H and $C_{6'}$–H).

Found: C, 60.90; H, 5.51%. Calcd for $C_{22}H_{24}O_9$:

9) C. A. Henrick and P. R. Jefferies, *Aust. J. Chem.*, **17**, 934 (1962); J. Massicot and J-P. Marthe, *Bull. Soc. Chim. Fr.*, **1962**, 1962; **1963**, 2712.

*3 All the melting points are uncorrected.

*4 sh=shoulder.

C, 61.10; H, 5.59%.

5,7,3′-Trihydroxy-3,8,4′,5′-tetramethoxyflavone (I). IV (195 mg) was debenzylated by the method described for III; mp 213—214°C (yellow prisms from methanol) (lit, mp 214—216°C[1]); yield, 140 mg (91%). UV: λ_{max} mμ (log ε); (EtOH) 279 (4.38), 314 (4.21), 355_{sh} (4.15); (EtOH–AcONa) 286 (4.55), 310_{sh} (4.27), 395 (4.11); (EtOH–$AlCl_3$) 284 (4.34), 314 (4.23), 350 (4.25), 407 (3.93).

Found: C, 58.35; H, 4.66%. Calcd for $C_{19}H_{18}O_9$: C, 58.46; H, 4.65%.

Triacetate (IX). Mp 126—127°C (colorless needles from methanol). UV: λ_{max}^{EtOH} mμ (log ε); 246.5 (4.31), 338 (4.20).

Found: C, 58.05; H, 4.56%. Calcd for $C_{25}H_{24}O_{12}$: C, 58.14; H, 4.68%.

Triethyl Ether (X). Mp 115—116°C (colorless needles from absolute ether). UV: λ_{max}^{EtOH} mμ (log ε); 275 (4.30), 313 (4.16), 350 (4.22).

Found: C, 63.39; H, 6.15%. Calcd for $C_{25}H_{30}O_9$: C, 63.28; H, 6.37%.

5,7-Dihydroxy-3,6,3′,4′,5′-pentamethoxyflavone (XI). A mixture of II (1.8 g), 3,4,5-trimethoxybenzoic anhydride (13 g), and potassium 3,4,5-trimethoxybenzoate (5.3 g) was heated at 180°C under reduced pressure for 8 hr. The product was recrystallized from methanol to give XI as yellow needles; mp 189—190°C; yield, 260 mg (8%). UV: λ_{max} mμ (log ε); (EtOH) 275 (4.12), 340 (4.29); (EtOH–AcONa) 278 (4.41), 371 (4.14); (EtOH–$AlCl_3$) 284 (4.17), 358 (4.25).

Found: C, 59.21; H, 4.94%. Calcd for $C_{20}H_{20}O_9$: C, 59.40; H, 4.99%.

Diacetate (XII). Mp 148.5—149.5°C (colorless prisms from methanol). UV: λ_{max}^{EtOH} mμ (log ε); 252_i (4.18).*[5] 356 (4.04).

Found: C, 58.82; H, 4.74%. Calcd for $C_{24}H_{24}O_{11}$: C, 59.01; H, 4.95%.

Dimethyl Ether. Mp 153—154°C. It was undepressed on admixture with the sample of VIII.

Diethyl Ether (XIII). *a) From XI.* Mp 144—145°C (colorless needles from methanol). UV: λ_{max}^{EtOH} mμ (log ε); 265 (4.20), 342 (4.22).

Found: C, 62.37; H, 5.81%. Calcd for $C_{24}H_{28}O_9$: C, 62.60; H, 6.13%.

b) From XIV. A mixture of XIV (1.0 g), 3,4,5-trimethoxybenzoic anhydride (3.5 g), and triethylamine (2 ml) was heated at 170°C for 8 hr under a stream of nitrogen. The mixture was then treated by a usual method; mp 144.5—145.5°C; yield, 500 mg (31%). It was undepressed on admixture with the sample of a).

*[5] i=inflection point.

BULLETIN OF THE CHEMICAL SOCIETY OF JAPAN VOL. 43 3278—3280 (1970)

Laser-induced Chemical Reactions. IV. Reactions of Carbon Vapor with Hydrogen at Various Pressures

Ko TAKI, Pil Hyon KIM and Susumu NAMBA

The Institute of Physical and Chemical Research Yamato-machi, Saitama

(Received March 12, 1970)

In previous papers,[1-3] the present authors have described the reaction of carbon vapor produced by the irradiation of a focused laser beam with hydrogen and low hydrocarbons. In this paper the effect of the hydrogen pressure in the reaction of the carbon vapor from graphite carbon is investigated; the reactions of hydrogen with the carbon vapor from silicon carbide and boron carbide are also investigated. The experimental procedures were almost the same as those described in the previous papers. The ruby laser used was a normal laser, the output energy and pulse duration of which were 3 J and 0.5 msec respectively. The laser beam was focused by a lens 35 mm in focal length upon the carbon target. The surface temperature[4] of the carbon target was estimated to be 3000—4000°K. After 2—5 pulse irradiations, the products were analysed by gas chromatography.

Results and Discussion

In the reaction of carbon vapor with hydrogen, the main products are acetylene and methane, as has previously been shown. In order to examine the reaction in detail, experiments were carried out at various hydrogen pressures; the representative product yields per pulse were 0.0063×10^{-7} mol for methane and 1.8×10^{-7} mol for acetylene at 20 Torr H_2, and 0.12×10^{-7} mol for methane and 4.7×10^{-7} mol for acetylene at 350 Torr H_2. The ratio of the acetylene to the methane varied with the

1) K. Taki, P. H. Kim and S. Namba, This Bulletin, **42**, 823 (1969).

2) K. Taki, P. H. Kim and S. Namba, *ibid.*, **42**, 2377 (1969).

3) K. Taki, P. H. Kim and S. Namba, *ibid.*, **43**, 1450 (1970).

4) S. Namba, P. H. Kim and A. Mitsuyama, *J. Appl. Phys.*, **37**, 3330 (1966).

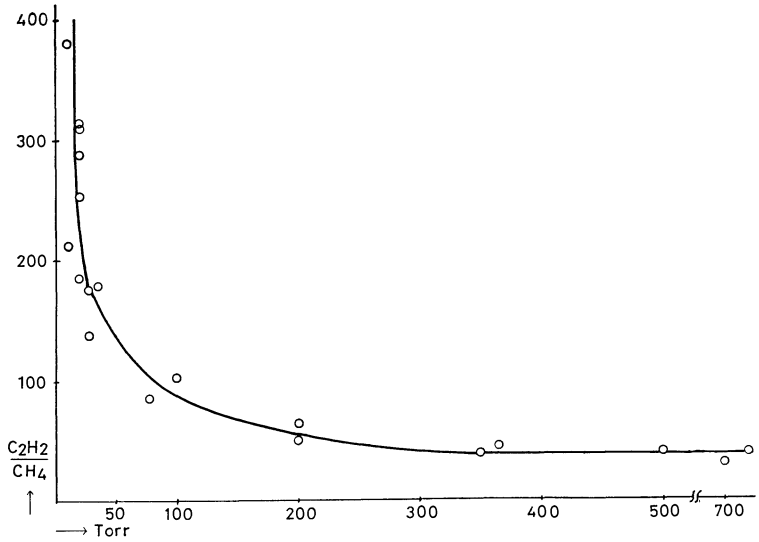

Fig. 1. Ratio of C_2H_2/CH_4 *vs.* hydrogen pressure.

hydrogen pressure, as is shown in Fig. 1. At a low hydrogen pressure, the methane yield is extremely small as compared with the acetylene yield, and the ratio of acetylene to methane increases. Such a variation was also observed in mixtures of helium or nitrogen: the C_2H_2/CH_4 ratio was about 150/1 at 30 Torr H_2 and 730 Torr He. From the above results, it may be considered that the ratio does not depend on the total pressure, but on the hydrogen concentration.

A pulse laser irradiated on a carbon target produces about a 10^{-6} mol carbon atom as a jet stream, which then reacts with the substrate*1 to form products. The volume of the carbon stream is estimated to be about 1 cm^3, as is shown in Fig. 2. A high hydrogen pressure (300—760 Torr)

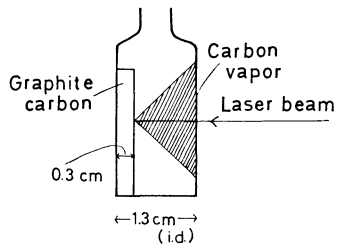

Fig. 2. Reaction cell for irradiation.

contains about 10^{-5} mol hydrogen molecules in each 1 cm^3 volume; therefore, the concentration of hydrogen in the reaction region is much higher than that of carbon vapor. On the other hand, at hydrogen pressures less than 100 Torr, the concentration of hydrogen is equivalent to or less than that of carbon vapor.

The reaction in a differently-designed cell*2 having a long passage (2.0 cm from the carbon target to the glass wall) gave a slightly smaller ratio of C_2H_2/CH_4 than in the former cell; the ratio of C_2H_2/CH_4 was about 200/1 at 20 Torr H_2. In this case, as the volume of carbon stream is larger than in the former cell, the concentration of carbon vapor is lower than in the former.

The above experimental facts indicate that acetylene and methane may not be produced from a common precursor. The acetylene and methane precursors may be C_2 and C_1 respectively, as has previously been shown.[1,2] Acetylene and methane are produced throughout several reaction steps. The details of the formation processes of acetylene and methane are not yet clear, and the rate constant of each step is also unknown, but the reaction may be as follows. In a low concentration of hydrogen, both the C_1 and C_2 species may react with hydrogen competitively. In this case, acetylene may be formed more easily than methane, because two hydrogen molecules are necessary for the formation of methane, while one molecule is enough for the formation of acetylene. It may also be considered that acetylene is formed by the reaction of the methane precursor with C_1, consequently increasing the C_2H_2/CH_4 ratio.

Similar experimental results were obtained in the C_3-compound formations. The ratio of C_4/C_3*3

*1 This reaction has been called an energetic carbon plasma-type reaction by Wiley and Veeravagu.[5]

5) R. H. Wiley and P. Veeravagu, *J. Phys. Chem.*, **72**, 2417 (1968).

*2 At pressures of less than 100 Torr of hydrogen, the reaction cell was contaminated by the deposited carbon vapor, but the long cell was less contaminated.

*3 The yields of C_3 and C_4 compounds were determined by the measurement of the yields of the propane and butane which are formed by the catalytic hydrogenation of products. The main C_4 compounds are diacetylene, and the main C_3 compounds are propylene and allene.

Table 1. Product yield of C_2, C_3 and C_4 compounds at various pressure of hydrogen in graphite carbon

Pressure of H_2 (Torr)	Number of irradiation	Product yield ($\times 10^{-7}$ mol)			Ratio	
		C_2-comp.	C_3-comp.	C_4-comp.	C_4/C_2	C_4/C_3
350	2	13	0.17	0.74	0.057	4.4
350	2	15	0.17	0.63	0.042	3.7
350	1	6.0	0.077	0.25	0.042	3.2
20	4	11	0.045	0.87	0.079	19
21	2	6.0	0.023	0.40	0.067	17

increases at a low hydrogen pressure, but the ratio of C_4/C_2 is almost constant, as is shown in Table 1. C_3 compounds need much more hydrogen than C_4 compounds need hydrogen.

Another experimental finding also supports the above discussion. When the power density of the irradiated beam was lowered by defocusing, the decrease in methane as compared with that in acetylene was not remarkable at hydrogen pressures of 20 Torr and 350 Torr, as is shown in Table 2. This result may be explained by the fact that the concentration of the carbon vapor produced by such weakened beam is lower than that of hydrogen.

Table 2. Product yield of methane and acetylene produced by the weakenned laser beam in graphite carbon

Power density	Pressure of H_2 (Torr)	Number of irradiation	Product yield ($\times 10^{-7}$ mol)		Ratio C_2H_2/CH_4
			CH_4	C_2H_2	
1/4 of the focused beam	350	2	0.078	3.0	38.0
	20	5	0.019	2.6	137
1/10 of the focused beam	350	4	0.16	6.5	40.6
	20	10	0.063	3.8	60.3

Moreover, from the fact that the product yields[2] were not affected by such radical scavengers as NO and O_2, it may be considered that the reaction is brought about in a jet stream of carbon vapor, and that, because of the high concentration of carbon vapor, all the scavengers react mainly with carbon vapor and do not react with the acetylene and methane precursors.

The carbon vapor from silicon carbide and boron carbide[*4] also gave acetylene and methane in the reaction with hydrogen. However, the product yields were about one-tenth as much as in the reaction of carbon vapor from graphite carbon. This may be explained by the fact that the concentration of the carbon vapor produced from silicon carbide and boron carbide is less than that from graphite carbon. The data are listed in Table 3. Spectroscopically, the Swan bands were also observed in the carbon vapor from silicon carbide, as had been observed in that from graphite carbon. In the reaction of the carbon vapor from silicon and boron carbide with hydrogen, no pressure dependence such as that described above was observed. These experimental results also support the explanation of the pressure dependence in acetylene and methane formation. The reaction occurs in a jet carbon stream.

Table 3. Product yield of methane and acetylene in silicon carbide(SiC) and boron carbide ($B_{12}C_3$)

Target	Pressure of H_2 (Torr)	Number of irradiation	Product yield ($\times 10^{-7}$ mol)		Ratio C_2H_2/CH_4
			CH_4	C_2H_2	
SiC	700	3	0.078	5.1	65.4
	350	3	0.044	4.6	105
	100	5	0.016	1.8	113
	20	10	0.013	trace	
$B_{12}C_3$	760	6	0.047	0.53	11.3
	20	6	0.028	0.26	9.3
	20	6	0.026	0.35	13.5

The authors are grateful to Miss K. Motegi for her valuable assistance in the course of this work.

*4 The silicon carbide (SiC) was purchased from the Siliconit Konetsu Kogyo Co., while the boron carbide ($B_{12}C_3$) was kindly provided by Dr. Atoda of this Institute.

BULLETIN OF THE CHEMICAL SOCIETY OF JAPAN VOL. 43 3281—3282 (1970)

Reaction of 1-*t*-Butyl-2-cyanoazetidine with Silver Nitrate or Silver Perchlorate

Takayoshi MASUDA, Akiko CHINONE and Masaki OHTA

Department of Chemistry, Faculty of Science, Tokyo Institute of Technology, Ookayama, Meguro-ku, Tokyo

(Received March 30, 1970)

Studies on the syntheses and reactions of azetidine derivatives having functional substituent at 2-position are very few. Recently Rodebaugh and Cromwell[1] have reported the syntheses of methyl 1-alkylazetidine-2-carboxylates by the reaction of primary amines with methyl α,γ-dibromobutyrate, and these azetidine-2-carboxylates are suitable for our studies on the preparation and reactions of various azetidine derivatives.

We wish to report on the synthesis of 1-*t*-butyl-2-cyanoazetidine and its reactions with silver nitrate or silver perchlorate in ethanol anticipating the intermediacy of 1-*t*-butyl-1-azetinium salt.

When methyl 1-*t*-butylazetidine-2-carboxylate (I) was allowed to react with liquid ammonia in a sealed tube at room temperature for a week, 1-*t*-butylazetidine-2-carboxamide (II) was obtained in good yield. Reaction of II with triphenylphosphine dibromide in the presence of two equivalents of triethylamine gave 1-*t*-butyl-2-cyanoazetidine (III) in 71% yield.

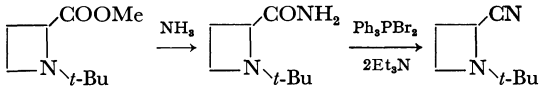

I II III

It is known that α-aminonitriles afford iminium salts by silver nitrate.[2] Treatment of III, which is cyclic α-aminonitrile, with silver nitrate or silver perchlorate in absolute ethanol gave *t*-butyl-(3,3-diethoxypropyl)ammonium nitrate (VIa) or perchlorate (VIb) instead of the expected 1-*t*-butyl-1-azetinium nitrate or perchlorate (IV). The structure of VI was determined by means of elementary analysis, infrared spectrum and NMR spectrum.

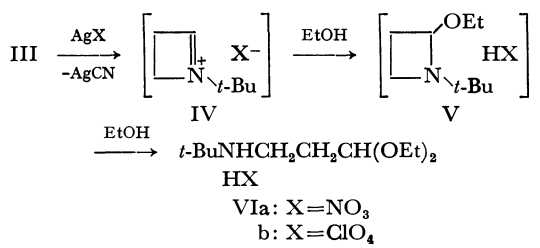

VIa: X=NO_3
b: X=ClO_4

In this reaction, silver cyanide was obtained almost quantitatively, which suggests the formation of azetinium salt (IV) as an intermediate. However, IV is highly strained and reacts easily with ethanol affording VI, presumably *via* 1-*t*-butyl-2-ethoxyazetidinium nitrate (Va) or perchlorate (Vb) as shown above. This mechanism is strongly supported by the fact that 1-phenyl-2-methoxy-3,3-dimethylazetidine is unstable and reacts with methanol to give anilinoacetal.[3] We found that 1-*t*-butyl-2-cyanoaziridine gave only adduct with silver perchlorate,[4] probably due to the difference of ring strain between azetidines and aziridines. Attempts to isolate IV by using aprotic solvents such as acetonitrile or methylene chloride were unsuccessful and gave only resinous product in spite of the formation of silver cyanide.

Experimental

1-*t*-Butylazetidine-2-carboxamide (II). A mixture of methyl 1-*t*-butylazetidine-2-carboxylate (8.6 g), liquid ammonia (50 m*l*) and aqueous methanol (1 : 1, 5 m*l*) was stirred in a sealed tube at room temperature for a week. Ammonia was evaporated by standing overnight at room temperature. Methanol and water were removed by vacuum distillation to give an oily residue which crystallized on standing for several hours. Recrystallized from *n*-hexane. Mp 80—81°C. Yield, 7.5 g (94%).

Found: C, 61.61; H, 10.02; N, 18.21%. Calcd for $C_8H_{16}ON_2$: C, 61.50; H, 10.32; N, 17.93%.

Picrate: mp 186.5—187.5°C.

Found: C, 43.91; H, 5.25; N, 18.11%. Calcd for $C_{14}H_{19}O_8N_5$: C, 43.64; H, 4.97; N, 18.18%.

1-*t*-Butyl-2-cyanoazetidine (III). To a solution of triphenylphosphine dibromide (prepared from 27.5 g of triphenylphosphine, 16.8 g of bromine and 21.2 g of triethylamine) in acetonitrile (120 m*l*) was added a solution of amide (II) in acetonitrile (30 m*l*). After heating for 20 min, acetonitrile was removed in a vacuum and the residue was extracted with petroleum ether, dried over anhydrous sodium sulfate and the solvent was removed by distillation. The residual oil was distilled under reduced pressure. Bp 55—56.5°C/2.5 mmHg. Yield, 8.6 g (71%). NMR ($CDCl_3$, τ): 8.98 (9H, singlet), 7.38—7.92 (2H, multiplet), 6.72—6.92 (2H, multiplet), 6.02 (1H, triplet).

1) R. M. Rodebaugh and N. H. Cromwell, *J. Heterocycl. Chem.*, **5**, 309 (1968).

2) H. G. Reiber and T. D. Stewart, *J. Amer. Chem. Soc.*, **62**, 3026 (1940).

3) F. Nerdel, P. Weyerstahl and K. Zabel, *Chem. Ber.*, **102**, 1606 (1969).

4) K. Ichimura, Ph. D. Thesis, Tokyo Institute of Technology (1968).

Found: C, 69.57; H, 9.98; N, 20.00%. Calcd for $C_8H_{14}N_2$: C, 69.52; H, 10.21; N, 20.27%.

Picrate: mp 158—159°C (decomp.).

Found: C, 46.01; H, 4.43; N, 19.05%. Calcd for $C_{14}H_{17}O_7N_5$: C, 45.78; H, 4.69; N, 19.07%.

Perchlorate: mp 170—171°C (decomp.).

Found: C, 40.23; H, 6.04; N, 11.81%. Calcd for $C_8H_{15}O_4N_2Cl$: C, 40.26; H, 6.34; N, 11.74%.

Reaction of III with Silver Nitrate in Ethanol. To a suspension of silver nitrate (2.84 g) in 15 m*l* of ethanol, was added dropwise a solution of III in ethanol (5 m*l*). After stirring for 3 hr at room temperature, silver cyanide was filtered off, the filtrate was concentrated in a vacuum and absolute ether was added to give 2.9 g of VIa. Recrystallized from ethyl acetate–ligroin; mp 71.5—73°C.

Found: C, 49.36; H, 9.65; N, 10.71%. Calcd for $C_{11}H_{26}O_5N_2$: C, 49.60; H, 9.84; N, 10.52%. IR (KBr): 2700—2300, 2030, 1575 cm^{-1} (NH_2^+), 1405, 1370, 830 cm^{-1} (NO_3^-), 1135, 1110, 1075 cm^{-1} (C–O–C). NMR ($CDCl_3$, τ): 8.81 (6H, triplet), 8.60 (9H, singlet), 7.92 (2H, quartet), 6.87 (2H, broad singlet), 6.25—6.60 (4H, multiplet), 5.37 (1H, triplet), 1.55 (2H, broad singlet).

Reaction of III with Silver Perchlorate in Ethanol. The procedure was the same as described above. Starting from 2.76 g of III, 4.7 g of VIb was obtained; mp 89.5—90°C (ethyl acetate–ligroin).

Found: C, 43.64; H, 8.35; N, 4.85%. Calcd for $C_{11}H_{26}O_6NCl$: C, 43.49; H, 8.63; N, 4.61%.

BULLETIN OF THE CHEMICAL SOCIETY OF JAPAN VOL. 43 3282—3284 (1970)

Preparation of 5-Acetyl-8-quinolinol Derivatives

Konomu MATSUMURA, Hisashi OKUMA, Miyoko ONISHI and Akiko IKEMURA

Department of Chemistry, Kitasato University, Minato-ku, Tokyo

(Received April 9, 1970)

It has been reported[1,2] that 5-acetyl-8-quinolinol (I) was obtained by the Friedel-Crafts reaction of 8-quinolinol and when heated with formalin in the absence of base, I gave 1,5-bis-(8-hydroxy-5-quinolyl)-1,5-dioxopentane (V) instead of the expected methylol compound VI.

In the present experiments, it was found that 8-acetoxyquinolinium chloride on treating with aluminum chloride in nitrobenzene gave 5-acetyl-8-quinolinol (I) with a comparable yield as in the case of the Friedel-Crafts reaction.

The reaction of 5-acetyl-8-quinolinol (I) with formaldehyde as well as bromination of I were investigated.

It was found that reaction of I with formaldehyde in the presence of aqueous sodium hydroxide at room temperature led to the formation of 2,4-bis(8-hydroxy-5-quinolylcarbonyl)-1,5-pentanediol (II). In accordance with the structure II, strong intramolecular hydrogen bond was observed in the region on 3000 cm^{-1} in the IR spectrum of II.

On heating it in crystals at 180°C or in the concentrated sulfuric acid solution at water bath temperature, II was converted into 3,5-bis(8-hydroxy-5-quinolylcarbonyl)tetrahydropyrane (III). On the other hand, on heating of the solution in 30% sulfuric acid on a water bath, II afforded 2,4-bis(8-hydroxy-5-quinolylcarbonyl)-1,4-pentadiene (IV) in a good yield. On heating of ethanol or 6N hydrochloric acid solution of II at water bath temperature, a part of II was converted into

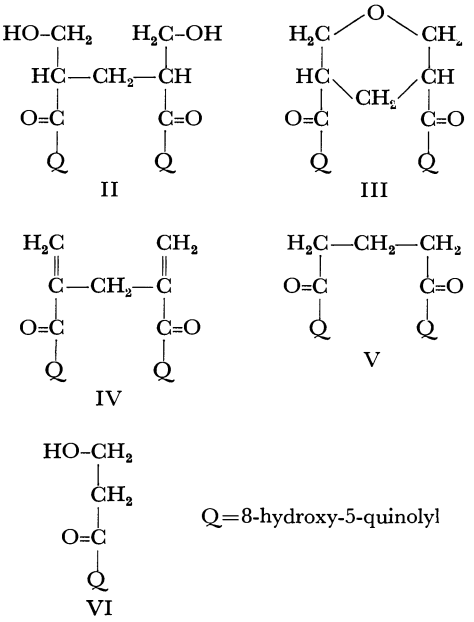

1) K. W. Rosenmund and G. Karst, *Arch. Pharm.* (Weinheim), **279**, 154 (1941); W. Borsche and H. Groth, *Ann. Chem.*, **549**, 238 (1941); K. Matsumura, *J. Amer. Chem. Soc.*, **52**, 4433 (1930).

2) K. Matsumura and C. Sone, *J. Amer. Chem. Soc.*, **53**, 1490 (1931).

III, whereas II could be safely recrystallized from hot benzene without any conversion into III showing that II is unstable to hot protic solvent. It was thought that II might have been formed through V[2] which was obtained through the reaction between 5-acetyl-8-quinolinol (I) and formalin in the absence of base. When V was treated with a mixture of formalin and sodium hydroxide solution, because of its insolubility to the mixture, V was recovered unaltered. From this the formation of II through V is not probable and II may be formed through the condensation of two moles of the methylol compound (VI) with one mole of formaldehyde. To these condensation products, the structures II, III and IV were assigned respectively in consideration of the analytical figures of the free bases, their hydrochlorides and acetyl derivatives.

When brominated with two equivalent atoms of nascent bromine, I gave 5-acetyl-7-bromo-8-quinolinol (VII) which on further bromination produced 5,7-dibromo-8-quinolinol[3] (VIII) in quantitative yield and the expected 7-bromo-5(α-bromoacetyl)-8-quinolinol could not be obtained. VII and VIII exhibited a deep red color with diazotized sulfanilic acid and alkali, showing that these bromines are easily displaced by arylazo group. 5-Acetyl-7-iodo-8-quinolinol,[4] on treating with iodine-potassium iodide or sodium hypoiodite solution at 10°C, no further iodination took place and the initial material was recovered.

Experimental

2,4-Bis(8-hydroxy-5-quinolylcarbonyl)-1,5-pentanediol (II). 5-Acetyl-8-quinolinol (1.87 g, 0.01 mol) was dissolved in a mixture of formalin (37%, 8.1 g, 0.05 mol) and 2.5N sodium hydroxide solution (5 g) with stirring at room temperature. After standing overnight, the solution was acidified (B.T.B. pH 3.6) with dilute acetic acid. A resinous material which soon turned to crystals separated from the solution. It formed orange yellow leaflets containing water of crystallization which was removed on standing *in vacuo* over potassium hydroxide at room temperature or on recrystallization from benzene. Yield, 1.8 g (67%).

Found: H_2O (water of crystallization), 5.21%. Calcd for $C_{25}H_{22}O_6N_2 \cdot 1.5H_2O$: H_2O, 5.71%.

On recrystallization from benzene, it formed light yellow prisms, melting at about 145°C, turning to a solid up to 180°C and unaltered at 300°C. IR (cm^{-1}, KBr) 3500, 3075, 2850 (OH), 1650 (>CO), 1280 (C_6H_5–CO–).

Found: C, 67.42; H, 4.99; N, 6.32%. Calcd for $C_{25}H_{22}O_6N_2$: C, 67.26; H, 4.93; N, 6.28%.

The Hydrochloride of II crystallized as colorless prisms from 3N hydrochloric acid, mp 255°C.

Found: C, 57.15; H, 4.71; N, 5.63%. Calcd for $C_{25}H_{22}O_6N_2 \cdot 2HCl$: C, 57.80; H, 4.62; N, 5.39%.

The Sulfate of II crystallized as columns from 30% sulfuric acid, mp 115—123°C.

Found: C, 43.82; H, 4.72; N, 4.55%. Calcd for $C_{25}H_{22}O_6N_2 \cdot 2H_2SO_4 \cdot H_2O$: C, 44.25; H, 4.43; N, 4.30%.

Tetraacetyl Derivative of II. A mixture of II (100 mg), fused sodium acetate (100 mg) and acetic anhydride (200 mg) was allowed to stand for 7 days at room temperature and then poured into ice water. The product crystallized as glistening colorless plates from ether, mp 115°C.

Found: C, 64.30; H, 5.16; N, 4.59%. Calcd for $C_{33}H_{30}O_{10}N_2$: C, 64.50; H, 4.89; N, 4.56%. The product obtained by heating a mixture of II and acetic anhydride for 3 hr at 130°C formed thick plates when crystallized from ether, mp 108—112°C (Found: N, 4.60%). From the estimated nitrogen content, it is evident that on heating at 130°C with acetic anhydride, dehydration which might be expected to take place between the two primary alcohols did not occur.

Treatment of II with Hot Ethanol. A solution of II (400 mg) in ethanol (20 m*l*) was heated at 80°C for one half hr and the crystals (9 mg), mp 298°C, which separated on cooling, were identified as III by comparison of the IR spectrum with the sample described below.

Treatment of II with 6N Hydrochloric Acid. A solution of II (200 mg) in 6N hydrochloric acid (2 m*l*) was heated at 98°C for 4 hr. The solid, which appeared on addition of sodium acetate to the cooled solution, was collected by filtration and repeatedly washed with hot ethanol. The crystals (10 mg), mp 300°C, which remained undissolved in ethanol were identified as III by comparison of the IR spectrum with that of the sample described below.

3,5-Bis(8-hydroxy-5-quinolylcarbonyl)tetrahydropyran (III). Method A. II (300 mg) was heated at 180° for one hr and the product crystallized as colorless plates from nitrobenzene. Mp: unaltered at 300°C. Yield, 200 mg. IR (cm^{-1}, KBr) 3075 (OH), 1660 (>CO), 1280 (C_6H_5–CO–), 1110, 480 (C–H_2–O–CH_2–).

Found: C, 70.27; H, 4.51; N, 7.11%; mol wt (Mass), 428. Calcd for $C_{25}H_{20}O_5N_2$: C, 70.01; H, 4.67; N, 6.54%; mol wt 428.

Method B. A solution of II (220 mg) in concentrated sulfuric acid (2.2 g) was heated at 100°C for one hr, poured into ice water. The resultant solution was made alkaline with sodium carbonate and then acidified with acetic acid. The separated solid (170 mg) was recrystallized as colorless leaflets from nitrobenzene, mp 300°C. The IR spectrum was identical with that of the product obtained by method A.

The Hydrochloride of III formed long needles on crystallization from 3N hydrochloric acid. The crystals were unaltered at 300°C and completely hydrolysed in water.

Found: C, 54.53; H, 4.85; N, 5.26%. Calcd for $C_{25}H_{20}O_2N_2 \cdot 2HCl \cdot 2.5H_2O$: C, 54.93; H, 4.95; N, 5.13%.

Diacetyl Derivative of III was prepared by heating a mixture III (80 mg), fused sodium acetate (80 mg) and acetic anhydride (400 mg) at 110°C for 3 hr. The product crystallized as colorless needles from acetone, mp 231—234°C.

3) A. Claus and H. Howitz, *J. Prakt. Chem.* [2], **44**, 444 (1891); K. Matsumura and M. Ito, *J. Amer. Chem. Soc.*, **77**, 6672 (1955).

4) K. Matsumura and M. Ito, *J. Org. Chem.*, **25**, 853 (1960).

Found: C, 68.18; H, 4.58; N, 5.55%. Calcd for $C_{29}H_{24}O_7N_2$: C, 67.97; H, 4.69; N, 5.47%.

2,4-Bis(8-hydroxy-5-quinolylcarbonyl)-1,4-pentadiene (IV). A solution of II (1.8 g) in 30% sulfuric acid (18 g) was heated at 95°C for 2 hr and, after cooling, poured into ice water and the solid (1.63 g) which appeared on addition of excess sodium acetate was collected by filtration and dissolved in hot 3N hydrochloric acid. After cooling, the separated fine needles (A) was collected and washed with water. On addition of sodium acetate to the combined filtrate and washings (charcoal), a yellow solid 1.38 g (84%), mp 155°C separated. On recrystallization from benzene (charcoal), it formed colorless prisms, mp 162—165°C (decomp.). IR (cm^{-1}, KBr) 3300 (OH), 1660 (—CO), 1280, 1240 C_6H_5-CO-, 1630 (CH_2=CH–).

Found: C, 73.21; H, 4.75; N, 7.57%. Calcd for $C_{25}H_{18}O_4N_2$: C, 73.17; H, 4.39; N, 6.83%.

(A) was treated with aqueous sodium acetate and the resultant needles, mp 300°C, was identified as III (Found: C, 73.21; H, 4.75; N, 7.57%) by comparison of IR spectrum with that of the sample prepared by another method.

The Hydrochloride of IV. It was prepared by dissolving IV in 3N hydrochloric acid, evaporating the solvent at room temperature to dryness and recrystallizing the residue from ethanol. It formed plates, mp 250°C (decomp.). Found: C, 56.52; H, 4.65; N, 5.79%. Calcd for $C_{25}H_{18}O_4N_2 \cdot 2HCl \cdot 2.5H_2O$:*1 C, 56.82; H, 4.73; N, 5.30%.

Found: C, 61.85; H, 4.27; N, 6.55%. Calcd for $C_{25}H_{18}O_4N_2 \cdot 2HCl$:*2 C, 62.11; H, 4.14; N, 5.80%.

The Diacetyl Derivative of IV. A mixture of IV (150 mg), acetic anhydride (200 mg) and fused sodium acetate (200 mg) was heated at 92°C for 2.5 hr. The product on recrystallization from ether, formed colorless prisms, mp 160—162°C (decomp. with foaming).

Found: C, 69.85; H, 4.99; N, 5.98%. Calcd for $C_{29}H_{22}O_6N_2$: C, 70.45; H, 4.45; N, 5.67%.

Fries Reaction with 8-Acetoxyquinoline.

8-Acetoxyquinolinium Chloride. A mixture of 8-hydroxyquinolinium chloride (1.83 g, 0.01 mol) and acetic anhydride (1.2 g, 0.01 mol) was heated on a water bath for 1.5 hr until complete dissolution resulted. After standing overnight the separated crystals were collected by filtration and dried at room temperature over potassium hydroxide *in vacuo*. Yield 1.9 g (85%). Mp 166—168°C.

Found: C, 58.51; H, 4.58; N, 6.47%. Calcd for $C_{11}H_9O_2N \cdot HCl$: C, 59.06; H, 4.47; N, 6.26%.

5-Acetyl-8-quinolinol. A mixture of 8-acetoxyquinolinium chloride (11.2 g, 0.05 mol), nitrobenzene (50 m*l*) and aluminum chloride (18 g) was gently shaken until complete dissolution resulted. The solution was heated at 75°C for 6 hr, then 85°C for 4 hr and finally 95°C for 5 hr (Calcium chloride tube). After cooling, ice (50 g) and 6N hydrochloirc acid (50 m*l*) were added to the solution. After the nitrobenzene was driven off with steam, the solution (charcoal) was concentrated if necessary and the separated hydrochloride was collected by filtration and washed with 3N hydrochloric acid. The hydrochloride was treated with an excess of aqueous sodium acetate to give the free base (I), yield 5.8—6.2 g (62—66%), mp 108—110°C. It formed colorless needles from benzene, mp 113°C. The identity with that obtained by Friedel-Crafts reaction[1] was established by comparison of IR spectra.

Fries reaction with 8-benzoyloxyquinolinium chloride failed to afford benzoyl-8-quinolinol.

5-Acetyl-7-bromo-8-quinolinol. To the solution of 5-acetyl-8-quinolinol (0.19 g, 0.001 mol) in 0.1N hydrochloric acid (36 m*l*), 0.1N bromate-bromide solution (20 m*l*) was added dropwise with stirring at 5°C. After standing for one hr sodium sulfite was added (iodide-starch paper) to the reaction mixture and the resultant solid was recrystallized from benzene as needles, mp 176°C. It exhibited a deep red color with diazotized sulfanilic acid and dilute sodium carbonate solution. On reaction of one mole of bromine in the form of either bromate-bromide solution or molecular bromine, it gave 5,7-dibromo-8-quinolinol[3] in quantitative yield and its identity was established by comparison of IR spectrum with that of authentic sample.

Found: C, 49.50; H, 3.28; N, 5.22%. Calcd for $C_{11}H_8O_2NBr$: C, 49.64; H, 3.01; ,N 5.26%.

*1 Dried at room temperature *in vacuo* over potassium hydroxide overnight.

*2 Dried at 110°C *in vacuo* over phosphorus pentoxide until constant weight.

BULLETIN OF THE CHEMICAL SOCIETY OF JAPAN VOL. 43 3285—3286 (1970)

Effect of Solvent Acidity on the Rate of Nitric Acid Oxidation of Cumene*1

Yoshiro OGATA and Hiroshi TEZUKA

Department of Applied Chemistry, Faculty of Engineering, Nagoya University, Chikusa-ku Nagoya

(Received April 15, 1970)

It is known that the nitric acid oxidation of cumenes gives acetophenones,[1] but the reaction scheme is unknown. Cumene is oxidized in our hands with 3.0M nitric acid for 6 hr at 90°C in 60% dioxane to give acetophenone as a major product in a yield of 70—76% together with benzoic acid (*ca.* 30%). The products were identified by means of UV and GLC. In view of these products, the intermediate may be dimethylphenylcarbinol, since, in our previous study, it has been observed that the nitric acid oxidation of triphenylmethane gives triphenylcarbinol quantitatively under the similar conditions to the present reaction.[2] The formation of acetophenone is considered to be the result of the oxidative demethylation of an intermediary dimethylphenylcarbinol. If *t*-alkoxy radical is formed, ketone is generally obtained.[3] In fact, under the present conditions, dimethylphenylcarbinol gave acetophenone in a yield of 71% together with benzoic acid after 6 hr. Also acetophenone was oxidized to benzoic acid with nitric acid under the present conditions.

Thus the pathway for the nitric acid oxidation of cumene is considered as follows:

$$PhCH(CH_3)_2 \rightarrow PhC(CH_3)_2OH \rightarrow PhCOCH_3 \rightarrow PhCOOH$$

Here, hydrogen atom abstraction from cumene is of interest in connection with the oxidation of triphenylmethane.[2] In excess nitric acid, the rate of consumption of cumene should be in agreement with that of hydrogen abstraction from cumene. The reaction mixture was extracted with chloroform at appropriate time intervals as described before,[2] and the rate was followed by measuring the consumption of cumene by means of GLC with a column of 1 m packed with Apiezon grease L 15% on Celite 545 at 100—160°C, using chlorobenzene as an internal standard.

In the nitric acid oxidation of diphenylmethane, triphenylmethane[2] and benzoin,[4] the rate was explained in terms of the ionization potential and bond-dissociation energy of the C–H bond which is cleaved, where the attacking species were considered to be both HNO_2^+ and NO_2. Since cumene is more reactive than toluene, the methyl group of cumene facilitates the oxidation in the present reaction. In order to disclose the attacking species in the oxidation of cumene, it is intended to measure the effect of acidity of solution on hydrogen abstraction.[2,4]

The first-order rate constants measured in excess nitric acid are shown in Table 1. As obvious in Table 1, the rate is first-order in cumene. The rate is independent of the amount of sodium nitrite added, but when a considerable amount of urea (a scavenger of nitrous acid) was added, a fairly long induction period was observed (Table 1).

Nitrous acid is an initiator but it does not affect the oxidation rate, *i. e.*, the concentration of NO_2 is constant at the stationary state as reported before;[4-6] hence, the rate is expressed as follows: $v=k$[cumene].

The acidity effect on the rate is shown in Fig. 1.

Table 1. Effect of initial concentrations of reactants in nitric acid oxidation of cumene in 60% dioxane at 90°C[a]

[PhCH-$(CH_3)_2$], M	[$NaNO_2$], M	Induction period, min	$10^4\,k$, sec^{-1}
0.058	0.01	10—20	2.1
0.034	0.01	10—20	2.1
0.059	0	~20	2.0
0.058	0.005	10—20	2.0
0.056	0.015	10—20	2.0
0.059	0.2[b]	>150	—

a) Initial concentration, $[HNO_3]=3.0$M.
b) $CO(NH_2)_2$ was added instead of sodium nitrite.

*1 Contribution No. 152.

1) J. A. Weigner, V. Kudlacek and R. Pavlickova, *Chem. Abstr.*, **55**, 9327 (1961). W. F. Tuley and C. S. Marvel, "Organic Syntheses," Coll. Vol. III, p. 822 (1955).

2) Y. Ogata, H. Tezuka and T. Kamei, unpublished results.

3) D. G. Alder, M. W. T. Pratt and P. Gray, *Chem. Ind.* (London), **1955**, 1517; A. D. Yoffe, *ibid.*, **1954**, 963; A. A. Zavitsas and S. Seltzer, *J. Amer. Chem. Soc.*, **86**, 3836 (1964).

4) Y. Ogata and H. Tezuka, unpublished results.

5) Y. Ogata and Y. Sawaki, *J. Amer. Chem. Soc.*, **88**, 5832 (1966).

6) Y. Ogata, H. Tezuka and Y. Sawaki, *Tetrahedron*, **23**, 1007 (1967).

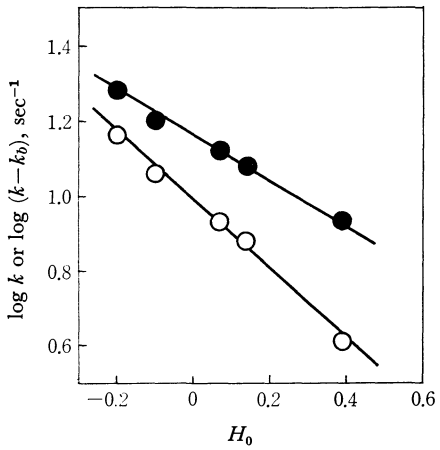

Fig. 1. Acidity effect of the solution on the rate for nitric acid oxidation of cumene in 60% dioxane at 90°C.
Initial concentration: $[HNO_3]=2.0$M, $[NaNO_2]=0.01$M, $[PhCH(CH_3)_2]=0.059$M, $[H_2SO_4]=0-1.0$M. ●, Plot of log k *vs.* H_0; ○, Plot of log $(k-k_b)$ *vs.* H_0.

The plot of log k *vs.* H_0 gave a line with a slope of a fractional number (−0.5), which is analogous to that for triphenylmethane, *etc.* (Fig. 1). Hence, k may be expressed as follows: $k=k_a h_0+k_b$. The plot of $10^5 k$ *vs.* h_0 gives the value of k_b to be 4.5×10^{-5}. The plot of $\log(k-k_b)$ *vs.* H_0 gave a straight line with a slope of *ca.* −1 as expected.

These facts suggest a mechanism involving simultaneous attack of both HNO_2^+ and NO_2 as in the case of diphenylmethane and triphenylmethane.

$$HNO_3 + HNO_2 \rightleftarrows 2NO_2 + H_2O \quad (1)$$

$$H^+ + NO_2\cdot \rightleftarrows HNO_2^+ \quad (2)$$

$$PhCH(CH_3)_2 + HNO_2^+ \xrightarrow{\text{slow}} \underset{\text{I}}{PhC(CH_3)_2} + H_2NO_2^+ \quad (3)$$

$$PhCH(CH_3)_2 + NO_2\cdot \xrightarrow{\text{slow}} \text{I} + HNO_2 \quad (4)$$

$$\text{I} + NO_2\cdot \rightarrow \underset{\text{II}}{PhC(ONO)(CH_3)_2} \quad (5)$$

$$\text{II} + H_2O \rightarrow PhC(CH_3)_2OH + HNO_2 \quad (6)$$

$$PhC(CH_3)_2OH \xrightarrow{HNO_3} PhCOCH_3 \xrightarrow{HNO_3} PhCOOH$$

It is known that alkyl nitrite is easily hydrolyzed even at 0°C.[7] Therefore, II may be rapidly hydrolyzed to dimethylphenylcarbinol, but the direct formation of acetophenone may not be excluded.

$$\underset{\text{II}}{PhC(ONO)(CH_3)_2} \rightarrow PhC(O\cdot)(CH_3)_2 + NO\cdot \rightarrow$$

$$PhCOCH_3 + CH_3NO$$

This mechanism leads to the rate equation:

$$v = (k_3[HNO_2^+]+k_4[NO_2\cdot])[\text{cumene}]$$
$$= (k_3K_2[H^+]+k_4)[NO_2\cdot][\text{cumene}]$$

Here, k and K are rate and equilibrium constants of subscripted steps, respectively.

The methyl group of cumene may facilitate the oxidation due to both lowering the ionization potential of C–H bond[8] and the stability of intermediate radical (I). Hence, two kinds of attacking species, NO_2 and HNO_2^+, should participate in the oxidation as observed in the case of di- and triphenylmethanes,[2] and benzoin.[4]

7) A. D. Allen, *J. Chem. Soc.*, **1954**, 1968.
8) A. G. Harrison, P. Kebarle and F. P. Lossing, *J. Amer. Chem. Soc.*, **83**, 777 (1961); J. B. Farmer, I. H. S. Henderson, C. A. McDowell and F. P. Lossing, *J. Chem. Phys.*, **22**, 1948 (1954); K. Watanabe, *ibid.*, **26**, 542 (1957).

BULLETIN OF THE CHEMICAL SOCIETY OF JAPAN VOL. 43 3287—3288 (1970)

Ring Expansion of Azetidines to Pyrrolidines*1

Takayoshi MASUDA, Akiko CHINONE and Masaki OHTA

Department of Chemistry, Faculty of Science, Tokyo Institute of Technology, Ookayama, Meguro-ku, Tokyo

(Received April 16, 1970)

Many examples are reported in which nucleophilic participation by amino group both in acyclic and cyclic haloamines lead to ring expansion, contraction or cleavage *via* cyclic quaternary salts.[1,2]

We were interested in the behavior of ring-nitrogen atom of azetidine as a neighboring group, since azetidine is highly strained and one of the strongest bases in cyclic amines. Methyl 1-*t*-butylazetidine-2-carboxylate (I), synthesized recently by Rodebaugh and Cromwell,[3] seems to be the best starting material for the studies.

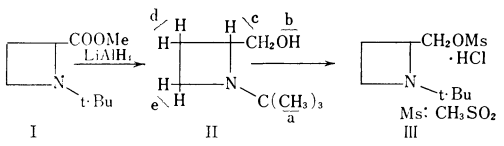

Reduction of I by lithium aluminum hydride afforded 1-*t*-butyl-2-hydroxymethylazetidine (II) in good yield. II was treated with methanesulfonyl chloride in anhydrous pyridine to give 1-*t*-butyl-2-methanesulfonyloxymethylazetidine hydrochloride (III) almost quantitatively. III was carefully neutralized with triethylamine or aqueous potassium carbonate in methylene chloride, the temperature being kept below 10°C. From the organic layer a crude base was obtained which gave a picrate. The NMR spectrum of the picrate shows that the crude base is 1-*t*-butyl-2-methanesulfonyloxymethylazetidine (IV). However, IV is unstable and readily undergoes rearrangement to 1-*t*-butyl-3-methanesulfonyloxypyrrolidine (VI) by standing for a few hours at room temperature, probably *via* bicyclic quaternary salt (V).

Owing to an insufficient amount of VI for purification, its structure was deduced on the basis of the elementary analysis and NMR spectrum of

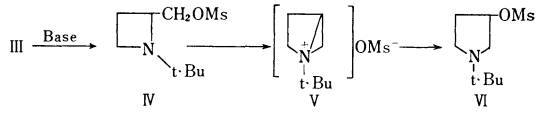

the picrate prepared from the crude rearrangement product. The driving force for the rearrangement of IV to VI is probably due to the release of ring strain and the easiness of internal quaternization to V due to the strong basicity of azetidine.

Treatment of III with triphenylphosphine dibromide in the presence of equimolar amount of triethylamine gave 1-*t*-butyl-3-bromopyrrolidine (VII). The structure of VII is supported by the result of elementary analysis and NMR spectrum. Formation of VII might proceed either *via* bicyclic quaternary salt (pathway A) or *via* quaternary phosphonium salt (pathway B).

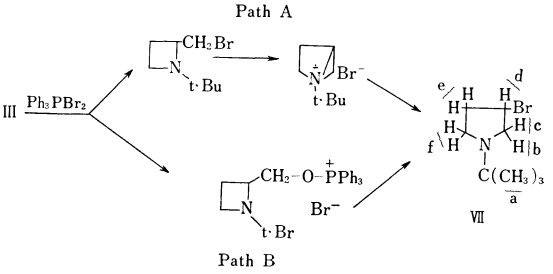

Experimental*2

1-t-Butyl-2-hydroxymethylazetidine (II). To a suspension of lithium aluminum hydride (2.28 g, 0.06 mol) in anhydrous ether (75 m*l*) was added dropwise a solution of methyl 1-*t*-butylazetidine-2-carboxylate (8.6 g, 0.05 mol) in anhydrous ether (50 m*l*) with stirring and cooling with ice-water. Stirring was continued for further 4 hr and the reaction mixture was left standing overnight. Sodium hydroxide (1 g), ether (55 m*l*) and water (3—5 m*l*) were then added successively with cooling with ice-water. After filtration with sintered glass filter, the ethereal solution was dried over potassium hydroxide and the solvent was distilled off to give a colorless oil which was distilled in a vacuum: bp 50—53.5°C/2.5 mmHg, yield 6.3 g (88%).

Found: C, 67.29; H, 11.95; N, 9.70%. Calcd for $C_8H_{17}ON$: C, 67.13; H, 11.89; N, 9.79%.

*1 Presented at the 23rd Annual Meeting of the Chemical Society of Japan, Tokyo, April, 1970.

1) J. F. Kerwin, G. E. Ullyot, R. C. Fuson and C. L. Zirkle, *J. Amer. Chem. Soc.*, **69**, 2961 (1947); E. M. Schultz and J. M. Sprague, *ibid.*, **70**, 48 (1948).

2) R. C. Fuson and C. L. Zirkle, *ibid.*, **70**, 2760 (1948); R. H. Reitsema, *ibid.*, **71**, 2041 (1949); E. G. Brain, F. P. Doyl and M. D. Mehta, *J. Chem. Soc.*, **1961**, 633; V. R. Gaertner, *Tetrahedron Lett.*, **1968**, 5919; J. A. Deyrup and C. L. Moyer, *ibid.*, **1968**, 6179.

3) R. M. Rodebaugh and N. H. Cromwell, *J. Heterocycl. Chem.*, **5**, 309 (1968).

*2 All melting points were determined on a micro hot stage and are not corrected.

The NMR spectrum of II shows signals at τ 9.1 (H_a, singlet), 7.8—8.2 (H_d, multiplet), 6.8—7.1 (H_e, multiplet), 6.3—6.7 (H_c, multiplet) and 5.9 (H_b, singlet).

Picrate: mp 194—195°C (decomp.).

Found: C, 45.42; H, 5.26; N, 15.29%. Calcd for $C_{14}H_{20}O_8N_4$: C, 45.16; H, 5.41; N, 15.05%.

1-*t*-Butyl-2-methanesulfonyloxymethylazetidine Hydrochloride (III). To a stirred solution of II (7.15 g, 0.05 mol) in anhydrous pyridine (60 m*l*) was added dropwise methanesulfonyl chloride (6.5 g), the temperature being kept at 0—5°C by cooling. The mixture was stirred for 4—5 hr, kept in a refrigerator overnight and then anhydrous ether (200 m*l*) was added to precipitate the hydrochloride which was collected by filtration and washed with petroleum ether to remove pyridine. Recrystallized from ethyl methyl ketone: mp 108.5—109.5°C, yield 12.7 g.

Found: C, 41.98; H, 8.06; N, 5.44%. Calcd for $C_9H_{20}O_3NSCl$: C, 41.93; H, 7.82; N, 5.43%. IR (KBr): 2390—2670 cm^{-1} (ammonium salt).

Picrate: mp 148.5—149.5°C (decomp.). (CH_3CN–EtOH).

Found: C, 40.43; H, 4.82; N, 12.36; S, 7.05%. Calcd for $C_{15}H_{22}O_{10}N_4S$: C, 40.00; H, 4.92; N, 12.44; S, 7.12%. The NMR spectrum of the picrate exhibits at τ 8.67 (9H, singlet, *t*-butyl), 7.45—7.87 (2H, multiplet, methylene at 3-position of azetidine ring), 6.97 (3H, singlet, methyl of methanesulfonyl group), 5.83—6.15 (2H, multiplet, methylene at 4-position), 5.31—5.62 (3H, multiplet, methine at 2-position and methylene of methanesulfonyloxymethyl group) and 1.33 (2H, singlet, phenyl).

Reaction of III with Triphenylphosphine Dibromide. To a solution of triphenylphosphine dibromide in acetonitrile (50 m*l*) (prepared from 13.1 g of triphenylphosphine and 8.8 g of bromide) was added dropwise triethylamine (5.6 g, 0.055 mol) at 0—5°C and after 20 min 7.15 g (0.05 mol) of III was added below 10°C. The solution was stirred for 1 hr, heated up to 60—70°C and kept at this temperature for 20 min when the solution turned dark brown. After cooling, acetonitrile was distilled off under reduced pressure and the residue was extracted with petroleum ether. The extract was dried over magnesium sulphate and distilled to remove the solvent. The residual oil was distilled under reduced pressure and 6.5 g (63%) of III, bp 83.5—84°C/13 mmHg was obtained.

Found: C, 46.97; H, 7.78; N, 7.06%. Calcd for $C_8H_{16}NBr$: C, 46.62; H, 7.82; N, 6.80%.

Picrate: mp 193.5—195.5°C (decomp).

Found: C, 38.50; H, 4.27; N, 13.00%. Calcd for $C_{14}H_{19}O_7N_4Br$: C, 38.63; H, 4.40; N, 12.87%.

The NMR spectrum of VII shows signals at τ 8.91 (H_a, singlet), 7.40—8.05 (H_e, multiplet), 7.14—7.35 (H_f, multiplet), 7.09 (H_b, doublet of doublet), 6.67 (H_c, doublet of doublet) and 5.54—5.77 (H_d, multiplet).

BULLETIN OF THE CHEMICAL SOCIETY OF JAPAN VOL. 43 3288—3290 (1970)

Excess Compressibility of Binary Liquid Mixtures

Osamu KIYOHARA and Kiyoshi ARAKAWA

Research Institute of Applied Electricity, Hokkaido University, Sapporo

(Received April 16, 1970)

Excess compressibility is an important quantity related to intermolecular forces between unlike molecules.[1)]

The formulas of compressibility based on statistical theories have been derived by Prigogine,[2)] Flory[3)] and others. Flory's formula is very simple, and the values for nonpolar liquid mixtures calculated by the formula showed a fairly good fit with the observed data. Three parameters are included in Flory's solution theory and were determined experimentally.

A statistical thermodynamic theory for binary liquid mixtures based on the cell method and the Sutherland type potential function for pair interactions, has been successfully applied to nonpolar solutions.[*1,4)] From the theory, the excess compressibility equation has been derived for the relation between the compressibility and intermolecular energy. It is believed that the compressibility data gives a severe test to the statistical theory of solution.

The equation of state for a binary mixture consisting of nonpolar rigid spherical molecules (A and B) differing in size is given by the following equation.

$$-p = \frac{2\pi}{3}\frac{N^2}{V^2}\left[(\gamma\varepsilon^*)_A \cdot r_A^{*3} \cdot x_A + (\gamma\varepsilon^*)_B \cdot r_B^{*3} \cdot x_B\right] - RT\left[\frac{x_A}{\beta a_A^2 \cdot (a_A - r_A^*)} + \frac{x_B}{\beta a_B^2 \cdot (a_B - r_B^*)}\right] \quad (1)^{*2}$$

1) G. H. Findenegg and F. Kohler, *Trans. Faraday Soc.*, **63**, 870 (1967); R. J. Fort and W. R. Moore, *ibid.*, **61**, 2102 (1965).

2) I. Prigogine, "The Molecular Theory of Solutions," North-Holland Publishing Co., Amsterdam (1957).

3) A. Abe and P. J. Flory, *J. Amer. Chem. Soc.*, **87**, 1838 (1965).

*1 In the following, this paper is referred to as paper I and the number of the equation given in paper I is superscripted with a prime.

4) K. Arakawa and O. Kiyohara, This Bulletin, **43**, 975 (1970).

All notations used in the present note are the same as those in paper I.

Differentiating Eq. (1) with respect to pressure at constant temperature, we have

$$\left(\frac{\partial V}{\partial p}\right)_T = 1/\left[\frac{4\pi}{3}\cdot\frac{N^2}{V^3}\{(\gamma\varepsilon^*)_A\cdot r_A^{*3}\cdot x_A + (\gamma\varepsilon^*)_B\cdot r_B^{*3}\cdot x_B\} - RT(k_A\cdot x_A + k_B\cdot x_B)\right], \quad (2)$$

where

$$k_A = \left(\frac{1}{a_A^2\cdot(a_A-r_A^*)\cdot\beta}\right)^2\cdot\left(\frac{3a_A-2r_A^*}{3a_A}\right) \text{ and}$$

$$k_B = \left(\frac{1}{a_B^2\cdot(a_B-r_B^*)\cdot\beta}\right)^2\cdot\left(\frac{3a_B-2r_B^*}{3a_B}\right),$$

and, using the same approximate equation (Eqs. (17′)—(20′)), the isothermal compressibility κ_T for a binary mixture is expressed as follows.

$$\kappa_T^{(I)} = \frac{1}{3RT}\cdot\frac{(V-V^*)^2}{V\cdot\left[\frac{1+3\rho_A}{1+\rho_A}\cdot x_A + \frac{1+3\rho_B}{1+\rho_B}\cdot x_B\right] - 2\cdot(V-V^*)}. \quad (3)$$

For a pure liquid A, we have

$$\kappa_{T,A}^{(I)} = \frac{1}{3RT}\cdot\frac{(V_A^0-V_{AA}^*)^2}{V_A^0\left[\frac{1+3\rho_{AA}}{1+\rho_{AA}}\right]-2\cdot(V_A^0-V_{AA}^*)} \quad (4)$$

where

$$\rho_A = \frac{V-V^*}{3V_A^*},\ \rho_B = \frac{V-V^*}{3V_B^*},$$

$$V^* = V_A^*\cdot x_A + V_B^*\cdot x_B,\ x_A+x_B=1.$$

x_A and x_B are the mole fraction for each species, V_A^* and V_B^* are the "*hard core volume*"[3,4] for each species in solution, and V_{AA}^* and V_{BB}^* are those in pure liquid, respectively. V and V^0 are the volume of solution and pure liquid each.

The excess compressibility κ^E is given by the equation

$$\kappa^E = \kappa - \frac{1}{V}(V_A^0\kappa_A^0 x_A + V_B^0\kappa_B^0 x_B) \quad (5)$$

where κ_A^0 and κ_B^0 are the compressibility for each pure liquid. The $\kappa_T^{E,(I)}$ calculated*3 from the observed excess molar volume V^E (the 3rd column of Table 1) using Eqs. (3), (4) and (5) are compared with experimental results in the 5th column of Table 1. As the values of molecular parameters (molar volume and thermal expansion coefficient of pure liquid), those listed in paper I have been used.

The agreement between calculated and observed results is satisfactory on the whole.

Equation (3) can be simplified further, and we have an extremely simplified formula

Table 1. Excess compressibility for equimolar mixtures

System	T (°C)	V^E (cc/mol) Obsd	$\kappa_T^E\times10^3$ (cc/cal·mol) Obsd	Calcd (I)	Calcd (II)
CCl_4–$C(Me)_4$	0	−0.5[a]	−0.95[b]	−0.57	−0.33
CCl_4–$SiCl_4$	20	0.05[c]	−0.02[d]	−0.03	−0.01
CCl_4–$TiCl_4$	20	0.08[c]	−0.03[d]	0.07	0.05
CCl_4–$SnCl_4$	20	0.46[c]	0.06[d]	0.24	0.15
$SiCl_4$–$TiCl_4$	20	−0.36[c]	−0.48[d]	−0.24	−0.14
$SiCl_4$–$SnCl_4$	20	0.13[c]	−0.12[d]	0.04	0.03
$TiCl_4$–$SnCl_4$	20	0.08[c]	−0.01[d]	0.01	0.01
C_6H_6–CCl_4	25	0.01[e]	0.04[f]	0.01	0.01
	40	0.04[e]	0.04[f]	0.02	0.01
	70	0.11[c]	0.05[f]	0.05	0.03
C_6H_6–c-C_6H_{12}	25	0.65[g]	0.14[f]	0.30	0.19
	40	0.66[g]	0.17[f]	0.30	0.19
	70	0.67[g]	0.24[f]	0.31	0.18
CCl_4–c-C_6H_{12}	25	0.16[h]	0.04[h]	0.08	0.05
	40	0.16[h]	0.04[h]	0.08	0.05
	70	0.16[h]	0.05[h]	0.08	0.05

a) A. Englert-Chwoles, *J. Chem. Phys.*, **23**, 1168 (1955).
b) J. Jeener, *J. Chem. Phys.*, **25**, 584 (1956).
c) H. Sackmann and H. Arnold, *Z. Electrochem.*, **63**, 565 (1959).
d) H. Sackmann and A. Boczek, *Z. Physik. Chem.*, **29**, 329 (1961).
e) S.E. Wood and J.P. Brusie, *J. Amer. Chem. Soc.*, **65**, 189 (1943).
f) A. Abe and P.J. Flory, *ibid.*, **87**, 1838 (1965).
g) S.E. Wood and A.E. Austin, *ibid.*, **67**, 480 (1945).
h) M. D. Peña and M. L. McGlashan, *Trans. Faraday Soc.*, **57**, 1511 (1961).

$$\kappa_T^{(II)} = \frac{1}{3RT}\cdot\frac{(V-V^*)^2}{V}. \quad (6)^{*4}$$

Inserting Eq. (6) into Eq. (5), we obtain a simplified formula of excess compressibility as

$$\kappa_T^{E,(II)} = \frac{1}{3RT}\cdot\frac{1}{V}[(V-V^*)^2 - \{(V_A^\circ-V_{AA}^*)^2\cdot x_A + (V_B^\circ-V_{BB}^*)^2\cdot x_B\}] \quad (7)^{5)}$$

The formula of $\kappa_T^{E,(II)}$ has been tested by the same procedure as described above, and the results are shown in the 6th column of Table 1. The agreement between the observed and calculated is

*2 Eq. (1) is easily derived by differentiation of Eq. (16′).

*3 The values κ_T^E can also be calculated using $V_{calc.}^E$ calculated from the observed excess enthalpy H^E (see Eq. (30′)).

*4 Eq. (6) is derived from Eq. (3) by assuming $\rho_A<1$ and $\rho_B'<1$, and thus, by ignoring $V-V^*$ compared with V.

5) O. Kiyohara and K. Arakawa, *ibid* **43**, 3037 (1970). The 14th Annual Symposium on Ultrasonic and Chemical Physics, Nov. 1969, Tokyo.

as good as one can expect from a simple equation.

It is to be noted that Eqs. (3)—(7) are functions of volume and temperature.

BULLETIN OF THE CHEMICAL SOCIETY OF JAPAN VOL. 43 3290 (1970)

Reactions of Acetoin and Benzoin with Malononitrile

Toshio HAYASHI and Masahiro KAGAWA

The Institute of Physical and Chemical Research, Yamato-machi, Saitama

(Received April 20, 1970)

Although the Knoevenagel reactions of aldehydes and ketones have been investigated by numerous workers,[1] little is known about the reactions involving acyloins and benzoins. The only reported examples involve the reaction of ethyl cyanoacetate with benzoin[2] and acetoins[3] in the presence of sodium ethoxide to give α,β-disubstituted γ-lactones.

The present paper deals with the reactions of malononitrile with acetoin (**1a**) and benzoin (**1b**) under the conditions used by Cope[4] to give 2-amino-3-cyano-4,5-disubstituted furans (**2**) in good yield. The structure of **2a** was inferred from elementary analysis and spectral studies. The NH_2 stretching

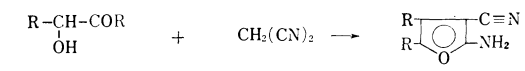

1a, R=Me **2a**, R=Me
1b, R=Ph **2b**, R=Ph

bands appeared at 3488 and 3400 cm^{-1}, and the conjugated CN group occurred at 2200 cm^{-1}. The NMR spectrum ($CDCl_3$) showed the broad NH_2 signal at 4.68 ppm and the two methyl at 1.92 and 2.07 ppm, which are just in the range expected for methylfurans.[5] The fact that the methyl protons show a sharp singlet suggests that **2a** is present almost completely in the amino form shown. This conclusion may be supported by the fact that the IR spectrum shows no imino absorption.

Recently, 2-amino-3-cyano-4,5-diphenylfuran (**2b**) has been synthesized by Russian workers from desyl chloride and malononitrile in the presence of sodium ethoxide.[6] The melting point of **2b** obtained in the present investigation agreed with that reported. The IR and NMR spectra suggest that **2b** is also present in the amino form.

Experimental

NMR spectra were obtained on a JNM-C-60 high-resolution NMR spectrometer at 19—20°C. Tetramethylsilane was used as an internal standard. IR spectra were determined in the chloroform solution using a Perkin-Elmer 521 spectrophotometer.

Reaction of Acetoin (1a) with Malononitrile. In a 200 m*l* round bottomed flask attached to a constant water separator,[4] were placed 11.4 g (0.12 mol) of acetoin, 6.6 g of malononitrile, 3.0 g of ammonium acetate, 2.0 m*l* of acetic acid, snd 60 m*l* of benzene. The solution was refluxed at 120°C in an oil bath till the formation of water ceased. After the solution had been cooled to room temperature, deposited crystals were recrystallized from ethanol-benzene. The yield of **2a**, melting at 167.5—168.5°C, was 7.4 g (54.4% based on malononitrile).

Found: C, 61.87; H, 6.08; N, 20.20%. Calcd for $C_7H_8N_2O$: C, 61.75; H, 5.92; N, 20.58%.

IR ($CHCl_3$) 3488 (m, NH), 3400 (m, NH), 2200 (s, C≡N), 1640 cm^{-1} (s, δNH_2); NMR ($CDCl_3$) 1.92 (s, CH_3), 2.07 (s, CH_3), and 4.68 ppm (broad, NH_2).

Reaction of Benzoin (1b) with Malononitrile. A mixture of 11.0 g of benzoin, 4.5 g of malononitrile, 3.0 g of ammonium acetate, and 2.0 m*l* of acetic acid in 60 m*l* of benzene was refluxed for 5 hr in an apparatus of the same type as used above. After the solvent had been removed, solid product was recrystallized from toluene and then from ethanol, giving 5.0 g of pale yellow needles (**2b**), melting at 205—206°C (uncor., lit,[6] 207—208°C), yield, 28% based on malononitrile.

Found: C, 78.28; H, 4.65; N, 10.79%. Calcd for $C_{17}H_{12}N_2O$: C, 78.44; H, 4.65; N, 10.76%.

IR ($CHCl_3$) 3490 (m, NH), 3400 (m, NH), 2200 (s, C≡N), and 1638 cm^{-1} (s, δNH_2); NMR (DMSO-d_6) 7.25 (s, Ph), 7.44 (s, Ph), and 7.79 (broad, NH_2).

The authors wish to thank Drs. Hiroshi Midorikawa and Isaburo Hori of this Institute for helpful discussions.

1) G. Jones "Organic Reactions" Vol. 15, ed. by A. C. Cope, Wiley and Sons, Inc., New York, N. Y. (1967), p. 204.

2) J. A. McRae and A. L. Kuehner, *J. Amer. Chem. Soc.*, **52**, 3377 (1930).

3) I. Hori, *Sci. Papers Inst. Phys. Chem. Res.*, **56**, 178 (1962).

4) A. C. Cope, C. M. Hofmann, C. Wyckoff, and E. Hardenbergh, *J. Amer. Chem. Soc.*, **63**, 3452 (1941).

5) L. M. Jackman and S. Sternhell, "Applications of Nuclear Magnetic Resonance Spectroscopy in Organic Chemistry," Pergamon, N. Y., (1969), p. 173.

6) T. I. Temnikova and Y. A. Sharanin, *Zh. Org. Khim.*, **2**, 2018 (1966); *Chem. Abstr.*, **66**, 7061 (1967).

BULLETIN OF THE CHEMICAL SOCIETY OF JAPAN VOL. 43 3291—3292 (1970)

The Preparation of Highly-oriented Carbon Fiber from Pitch Material

Sugio Ōtani, Yukio Kokubo and Teruyo Koitabashi

Faculty of Technology, Gunma University, Kiryu, Gunma

(Received May 6, 1970)

In our previous papers[1-3] it was shown that carbon fiber can be prepared from pitch materials, moreover, Araki and Gomi[4] have succeeded in the production of carbon fiber from pitch material on a pilot-plant scale.

In the earlier reports[1,2] it was pointed out that the carbon fibers obtained from pitch had an isotropic structure and were "nongraphitizable." Recently, two methods for the preparation of highly-oriented carbon fiber from pitch material have been developed in our laboratory. One is a technique using a high-temperature treatment under stress in a range of temperature above 1800°C, while the second is a technique using a specific pitch-like material, such as pitch prepared from tetrabenzophenazine.

The object of this communication is to report some results obtained by the former method.

Experimental and Results

The original carbon fiber used in this work was prepared at 1000°C, on a pilot-plant scale, from a pitch which is a by product of the naphtha cracking process.[4] The high-temperature treatment was carried out under stresses ranging from 0.1 to 0.5 g per denier by the use of 2000—3000-denier bundles. The samples were heated by the use of a graphite-tube furnace in a stream of nitrogen and a rate of 125°C per minute up to 2500°C, which last temperature was maintained for about three minutes. A change in the length of the carbon fiber was clearly observed at temperatures over 1800°C, and it increased with increase in both the stress and the temperature applied. These results are shown in Fig. 1. The diameter of the carbon fiber finally obtained under a stress of 0.5 g per denier is 4.5—6.5 μ.

Stresses below 0.2 g per denier do not effectively improve the preferred orientation of crystallines. Improvement, however, gradually becomes clear with increase in the tension applied over 0.3 g per denier. In Fig 2, the intensity of the X-ray reflexion, $I(\phi)$, is plotted against ϕ, the angle between the C-axis of the reflecting crystallite and the fiber axis.

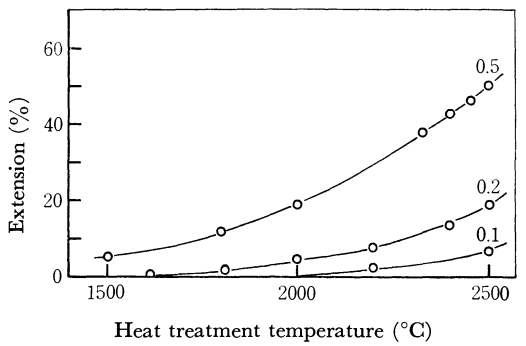

Fig. 1. Relation between the change in length and the stress applied at the heating process.
The numerals in the figure indicate the stress applied (g/denier).

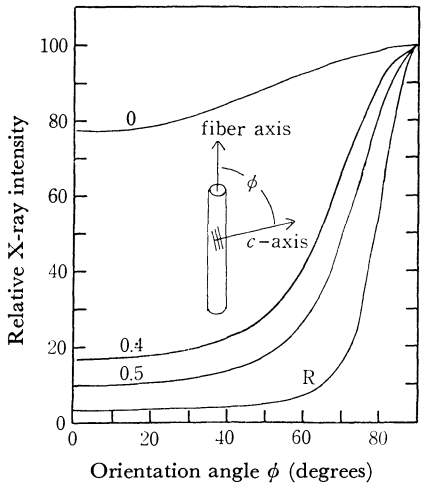

Fig. 2. Relation between the stress applied at the heating process up to 2500°C and the orientation of crystallites.
0: free from stress
0.4: stress of 0.4 g/denier
0.5: stress of 0.5 g/denier
R: RAE carbon fiber Type I (Control)
Royal Aircraft Establishment

1) S. Ōtani, *Carbon*, **3**, 31 (1965).
2) S. Ōtani, *ibid.*, **3**, 213 (1965).
3) S. Ōtani and K. Yamada, *Kogyo Kagaku Zasshi*, **69**, 626 (1966).
4) T. Araki and S. Gomi, *Applied Polymer Symposia*, No. 9, 331 (1969).

The results shown in Fig 2 indicate that the majority of the layer planes in the fiber treated under a stress of 0.5 g per denier are oriented within 30° of the fiber axis. The interlayer spacing and the crystallite size of the filament are 3.45 Å and about 45 Å respectively.

Heat treatment under stress improves the tensile strength and the modulus of the carbon fiber. The average tensile strength and the average modulus of the original carbon fiber are 9.5×10^6 g/cm^2 and 650×10^6 g/cm^2 respectively. The average values of the carbon fiber prepared at 2500°C under a stress of 0.5 g per denier are 18.3×10^6 g/cm^2 in strength and 2100×10^6 g/cm^2 in the modulus.

Discussion

These findings on the mechanical properties are not satisfactory when compared with those from the best high-modulus or high-strength carbon fiber obtained from other materials. It was, however, confirmed that a high-temperature treatment under stress is effective in causing a preferred orientation of carbon crystallites, even when the carbon fiber is prepared from pitch materials. In general, the structure and properties of carbon fiber prepared from pitch materials vary with the type of raw pitch material used, the temperature and the period of preoxidation, the oxidizing atmosphere, *etc.* For example, when a pitch material prepared from tetrabenzophenazine, which possesses highly-oriented molecules,[5] is used as the raw material, the application of stress at the heating stage is not necessary to prepare a highly-oriented carbon fiber. On the contrary, when using pitch fiber spun at a low speed from PVC pitch, it is unlikely that a high orientation can be obtained even when the heat-treatment is carried out under stress.[6]

In these experiments, the application of the higher temperatures and the greater stresses was not possible because of the design of the furnace. However, from the results described above and from general information concerning high-modulus carbon fiber from PAN and rayon,[7] it is likely that further improvements can be expected by the use of a higher treatment temperature and a greater stress.

5) S. Ōtani and S. Watanabe, 9th Conference on Carbon at Boston, June, 1969, Summary of Papers (1969), p. 29.

6) S. Ōtani, A. Yokoyama and A. Nukui, *Applied Polymer Symposia*, No. 9, 325 (1969).

7) H. M. Ezekel, 9th Conference on Carbon at Boston, June, 1969.

BULLETIN OF THE CHEMICAL SOCIETY OF JAPAN VOL. 43 3292—3294 (1970)

The Iodine Affinity of Polyvinyl Acetate and Its Derivatives

Sadao HAYASHI, Takashi NAKABAYASHI and Kumiko YOSHIDA

Faculty of Fiber Science and Technology, Shinshu University, Tokiiri, Ueda

(Received May 9, 1970)

Polyvinyl acetate (PVAc)[1] and its derivatives, such as partially saponified PVAc[2], and polyvinyl alcohol (PVA),[3] are known to form colored complexes with iodine. The complex reaction of PVA with iodine has been reported on by several investigators, and various mechanisms have been suggested to explain the reaction. Zwick[4] proposed a helical complex structure, such as has been described in the case of amylose.[5] On the other hand, Tebelev *et al.* pointed out that complex iodine is taken up into the interstices between the aggregated PVA molecules.[6] In order to clarify the mechanism of the complex formation between these polymers and iodine, stoichiometric studies of the binding of iodine to the polymers are required. In the present paper, accordingly, we will attempt to clarify whether or not it is possible to determine the iodine affinity of PVAc and its derivatives by the potentiometric titration method.

Experimental

Materials. Both of the PVA's used were commercial products from the Nippon Synthetic Chemical Industry

1) F. D. Hartley, *J. Polym. Sci.*, **34**, 397 (1959).
2) S. A. Miller and A. Bracken, *J. Chem. Soc.*, **1951**, 1933.
3) K. Imai and M. Matsumoto, *J. Polym. Sci.*, **55**, 335 (1961).
4) M. M. Zwick, *J. Appl. Polym. Sci.*, **9**, 2393 (1965).
5) R. S. Stein and R. E. Rundle, *J. Chem. Phys.*, **16**, 195 (1948).
6) L. G. Tebelev, G. F. Mikulskii, E. P. Korchagina and S. A. Glikman, *Visokomolekul. Soedin.*, **7**, 128 (1965).

Co., Ltd. The NL-05 was used as perfectly saponified PVA, while the GL-05 was used as partially saponified PVAc. The residual acetyl content in the partially saponified PVAc was 11.32 mol%. A PVAc suspension was used as the PVAc sample. The PVAc suspension was prepared both by the suspension polymerization of vinyl acetate and by the addition of the PVAc solution obtained by methanol-solution polymerization to water. The suspension polymerization of vinyl acetate was carried out at 70°C for 1.5 hr, using potassium peroxydisulfate as the initiator. The solid content thus obtained was 14.26%, and the mean particle diameter of the PVAc suspension, as determined by means of an electron microscope, was 0.17 μ. The excess initiator, the by-products formed by the decomposition of the initiator, and the residual vinyl acetate were removed by dialysis. The degree of polymerization of PVAc was calculated by measuring the intrinsic viscosity in acetone at 30°C, using the following equation first proposed by Nakajima;[7] $[\eta]=7.94\times10^{-4}P^{0.62}$. 0.5 g of commercial starch was dissolved in 100 m*l* of water, and its supernatant solution was used as the starch sample.

Measurements. A Yanagimoto potentiometric titrimeter equipped with a calomel cell and a bright platinum electrode, type KY-5, was used for the measurement of the iodine affinity of PVAc and its derivatives. The potentiometric titration was carried out as follows at room temperature according to the procedure reported by Bates *et al.*[8] The sample solution (50 m*l*) containing potassium chloride (0.3728 g) and potassium iodide (0.8300 g) was titrated with a 0.001N iodine solution prepared by dissolving iodine (0.1269 g), potassium iodide (8.3003 g), and potassium chloride (3.7278 g) in distilled water (1000 m*l*).

Results and Discussion

PVAc Derivatives. Figure 1 shows the potentiometric titration curves for PVAc derivatives. A blank curve was also obtained in the absence of the polymer sample. The PVA used in our experiment did not exhibit any color reaction with iodine in a dilute aqueous solution. The titration curve for the PVA was the same as that for a blank. The color reaction of the partially saponified PVAc with iodine was red-violet, and the complex solution possessed an absorption peak at 480—490 mμ. The iodine potentials of the titration curves for the partially saponified PVAc decreased with the increase in the concentration of the polymer, and the titration curves were all similar in type to those of amylopectin reported by Bates *et al.*[8] Consequently, the increase in iodine bound to partially saponified PVAc appears to be proportional to the increase in the concentration of free iodine.

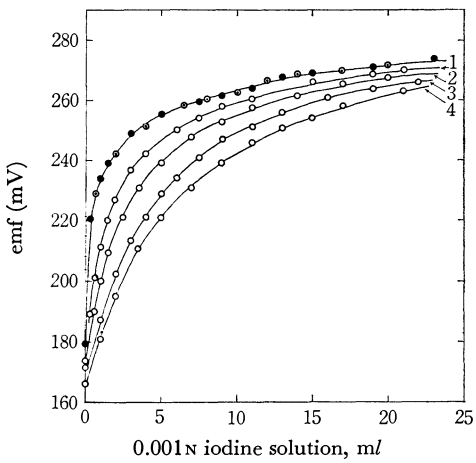

Fig. 1. Titration curves for PVA and partially saponified PVAc.
●: Blank, ⊙: PVA, 0.1500 g, ○: Partially saponified PVAc, 1: 0.0500 g, 2: 0.1000 g, 3: 0.1500 g, 4: 0.2000 g.

PVAc Suspension. The color of the iodine-PVAc suspension complex was the same red-violet as that of the iodine-partially saponified PVAc complex, and the absorption maximum was at 490—500 mμ. Figure 2 shows the potentiometric titration curves for the PVAc suspension, together with those for starch. The curves in Fig. 2 were obtained by the titration of PVAc and of starch in varying amounts. The curves for PVAc, as well as those for amylose, had horizontal parts for the iodine potentials, indicating that all the added iodine was consumed in the complex formation. Therefore, according to the calculation method of the iodine affinity suggested by Bates *et al.*,[8] it is possible to determine the amounts of iodine consumed in the complex formation with PVAc. As is shown in

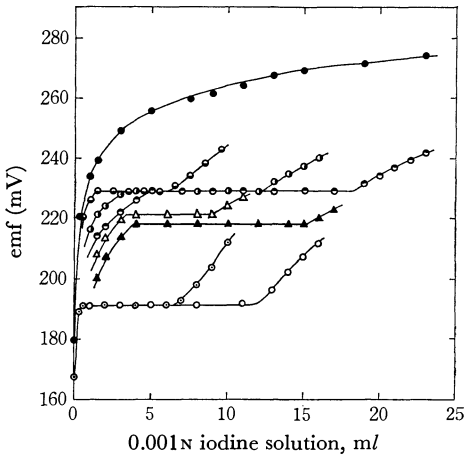

Fig. 2. Titration curves for PVAc and starch.
●: Blank.
PVAc sample of suspension polymerization: ($\bar{P}$=3640)
◒: 0.0100 g, ◑: 0.0200 g, ◓: 0.0300 g.
PVAc sample suspended polymer in water ($\bar{P}$=510): △: 0.0150 g, ▲: 0.0250 g.
Starch: ⊙: 0.0158 g, ○: 0.0252 g.

7) A. Nakajima, *Kobunshi Kagaku*, **6**, 451 (1949).
8) F. L. Bates, D. French and R. E. Rundle, *J. Amer. Chem. Soc.*, **65**, 142 (1943).

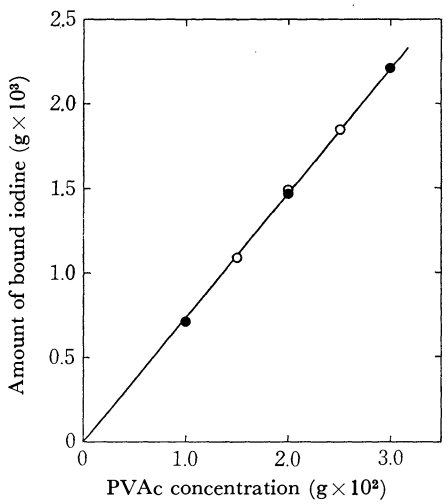

Fig. 3. Relationship between PVAc concentration and amount of bound iodine.
●: PVAc sample of suspension polymerization ($\bar{P}=3640$)
○: PVAc sample suspended polymer in water ($\bar{P}=510$)

Fig. 3, a linear relationship was obtained between the amount of iodine bound to PVAc and the PVAc concentration, regardless of the form of PVAc suspended in water, and the iodine affinity of PVAc (grams of iodine consumed by 100 g of PVAc) was found to be 7.3. All the iodine potentials of the horizontal parts for PVAc were higher than those for starch. It is already clear from the experimental results that amylose of a low molecular weight requires a higher iodine potential for a complex formation. However, there have not yet been any reports concerning the reason for this. In the case of PVAc, it is impossible to consider the relationship between the potential of a horizontal part and the degree of polymerization, because the spectrum of the complex is not influenced by the degree of polymerization.[9] Since the complex reaction of the partially saponified PVAc with iodine is also based on the number of the vinyl acetate units existing continuously in the polymer chain,[10] the mechanism of the complex formation of the partially saponified PVAc must be essentially identical with that of PVAc. When we compare Figs. 1 and 2, PVAc and partially saponified PVAc can be seen to indicate a remarkable difference in the titration curves. This seems to be because only PVAc among the samples examined was a heterogeneous system, since water is a nonsolvent for PVAc. Further, more detailed studies will be necessary to confirm the above results.

9) S. Hayashi, C. Kawamura and M. Takayama, This Bulletin, **43**, 539 (1970).
10) S. Hayashi, C. Nakano and T. Motoyama, *Kobunshi Kagaku*, **20**, 303 (1963).

BULLETIN OF THE CHEMICAL SOCIETY OF JAPAN VOL. 43 3294—3296 (1970)

Intrinsic Electrical Conductivity of Violanthrene, $C_{34}H_{18}$

Yasurō Hori, Satoshi Iwashima*1 and Hiroo Inokuchi

The Institute for Solid State Physics, The University of Tokyo, Roppongi, Tokyo

(Received May 9, 1970)

Since 1948, the electrical conductivity of aromatic crystals has been reported on by many workers. However, the conduction mechanism is still ambiguous because the measurement of the intrinsic conductivity is very difficult experimentally. In this study, we measured the electrical resistivity of high-purity violanthrene under a high vacuum.

The material used in the present study was violanthrene A (VEA). The VEA was synthesized from 16,17-dioxyviolanthrene by reduction.[1] The samples were two kinds of VEA. One of them was recrystallized from a 1,2,4-trichlorobenzene solution of the above-synthesized VEA three times and was sublimed once *in vacuo*. This sample will be denoted as VEA (I). In obtaining the second sample, further purification was applied to VEA (I): the sample was recrystallized once from trichlorobenzene and sublimed three times repeatedly. This further-purified sample will be denoted as VEA (II). The concentration of impurities, including that in these samples, was estimated to be 10^{-4} mol/mol for VEA (I) and less than 10^{-5} mol/mol for VEA (II). The single crystal of VEA (II), 5 mm × 8 mm × 70—100 μ in dimensions, was made by means of a sublimation method. Three sorts of specimens, the VEA (I) thin film, the VEA (II) thin film, and the VEA (II) single crystal, were used in the conductivity measurements.

*1 Present address: Department of Science and Technology, Meisei University, Hino, Tokyo, Japan.

1) J. Aoki, This Bulletin, **37**, 1356 (1964).

The resistivity of these specimens was measured at 10^{-7} Torr (of air) and 760 Torr in a high-vacuum bell-jar system; the details of the experimental procedure have been reported in a previous paper.[2] To make the surface-type cell, evaporated aluminum electrodes were attached on the thin film of VEA prepared by evaporation in a high vacuum. The preliminary X-ray analysis showed that, in the evaporated thin film of VEA (II), the *ab*-plane was parallel with the surface of the quartz substrate. Therefore, we established that the observed resistivity is that along the *ab*-plane.

For the single crystal specimen of VEA(II), silver paste was painted on both sides of that as electrodes. Silver wires, 0.1 mm in diameter, were stuck to the electrodes with the silver paste and connected with the resistivity measurement apparatus. The growth plane of the single crystal of VEA was the *ab*-plane; therefore, for the single crystal specimen, we observed the resistivity perpendicular to the *ab*-plane, this direction being denoted as the *c'*-axis.

The resistivity was measured in the temperature range from 20°C to 150°C, and a Cary 31-type vibrating-reed electro meter was employed for the high-resistivity measurements.

Table 1. The electrical resistivity and the apparent band gap of various types* of violanthrene A

Type	ρ_{15}** (Ωcm)	$\Delta\varepsilon$** (eV)
Powder	2.1×10^{14}	0.85
Surface-type	$\sim10^{9}$	0.9
Sandwich-type	$\sim10^{14}$	0.9

* H. Inokuchi, H. Kuroda and H. Akamatu, This Bulletin, **34**, 749 (1961).

** $\rho=\rho_0\exp(\Delta\varepsilon/2kT)$, at $T=288°$ K, $\rho=\rho_{15}$.

Some previous results concerning the resistivity of VEA are listed in Table 1. The present results show a large discrepancy from the previous ones; particularly, the effects of ambient oxygen and impurities are extraordinarily great. Table 2 illustrates the present results.

The resistivity of the evaporated VEA (I) thin film, observed at 760 Torr, was of the same order as the previous one. The value of the $\Delta\varepsilon$, derived from the equation in Table 1, of VEA (I), under a pressure of 10^{-7} Torr, was nearly nil; this was very different from the previous value. The resistivity at 10^{-7} Torr was, however, of the same order as that at 760 Torr.

The resistivity of the evaporated VEA (II) thin film could not be observed at a high vacuum because the resistivity was very large ($>10^{15}\Omega$ between 20—150°C) compared with that of the VEA (I) thin film and that of the VEA (II) at 760 Torr.

Further, the resistivity of the evaporated VEA (II) thin film at 760 Torr, was three orders higher than the previous ones and that observed for the VEA (I) thin film, and $\Delta\varepsilon$ was probably larger as well.

The results on the VEA (II) single crystal specimen were that the resistivity at 10^{-7} Torr was three orders higher than that at 760 Torr; further, the $\Delta\varepsilon$-value under a high vacuum, 1.95 eV, was the largest one ever observed. The resistivity and $\Delta\varepsilon$ at 760 Torr were larger than those of the evaporated VEA (II) thin film.

We concluded that the $\Delta\varepsilon$-value of the VEA (II) single crystal at 10^{-7} Torr, 1.95 eV, was the intrinsic value of violanthrene A, because the threshold value of the absorption spectrum of the violanthrene evaporated film was 2.0 eV and the threshold value of the spectral response of the photoconductivity was about 1.8 eV*[2]: However, we understand that this $\Delta\varepsilon$-value is not coincident with that of the band-gap energy. We presume that the electrical conduction of violanthrene A is produced through excitonic-carrier generation, because the 500 mμ-peak of the absorption spectrum of evaporated thin film may not be the conduction band absorption and is identified as the exciton level, for a very similar band has been found in a violanthrene A solution.*[2]

The nearly zero of $\Delta\varepsilon$-value of the evaporated VEA (I) thin film was interpreted as indicating that

Table 2. The electrical resistivity of violanthrene A *in vacuo* and in air

	in vacuo		in air	
Specimen	ρ_{15} (Ωcm)	$\Delta\varepsilon$ (eV)	ρ_{15} (Ωcm)	$\Delta\varepsilon$ (eV)
VEA (I) thin film	8.5×10^{8}	0.094	8.5×10^{8}	1.06
VEA (II) thin film	—	—	3.7×10^{12} 1.6×10^{13}	1.10 (<55°C) 1.65 (>55°C)
VEA (II) single crystal	3.8×10^{18}	1.95	6.5×10^{15}	0.99

*2 The details of these measurements, the photoconduction, and the absorption spectra of violanthrene A will be reported elsewhere by Y. H. and H.I.

2) Y. Maruyama and H. Inokuchi, This Bulletin, **39**, 1418 (1966).

the decrease in resistivity with the increase in temperature compensated for the increase in resistivity by the desorption of oxygen from the VEA (I) thin film with the increase in temperature; therefore, the $\Delta\varepsilon$-value apparently become nearly zero.

The $\Delta\varepsilon$-value of the VEA (II) single crystal, however, was not nearly zero. This may be for two reasons; the purity of VEA (II) was higher than that of VEA (I), so the number of active sites was less and oxygen was adsorbed more easily with the thin film than the single crystal. After all, the VEA (II) single crystal kept in a high vacuum (10^{-7} Torr) adsorbs so little oxygen that the increase in the resistivity by the desorption with an increase in the temperature does not appear. At an atmospheric pressure, the resistivity of the VEA (II) single crystal was three orders larger than that of the VEA (II) evaporated thin film. This was interpreted as indicating that the resistivity of the c'-axis was larger than that of the *ab*-plane. These phenomena also appeared in previous works on several kinds of polycyclic aromatic hydrocarbons.

The authors wish to thank Professor Junji Aoki, Toho University, and Dr. Yusei Maruyama of our Institute for their kind advice and discussion. They are also indebted to Professor Mizuka Sano, The University of Electro-Communications, for his preparation of the violanthrene A single crystals.

BULLETIN OF THE CHEMICAL SOCIETY OF JAPAN VOL. 43 3296—3297 (1970)

Electronic Absorption Spectrum of Tris(2,2′-bipyridine)-cobalt(I) Complex

Youkoh KAIZU, Yasuo TORII and Hiroshi KOBAYASHI

Department of Chemistry, Tokyo Institute of Technology, Ookayama, Meguro-ku, Tokyo

(Received May 11, 1970)

Very recently electronic absorption spectral studies have appeared on the lower valent tris-(2,2′-bipyridine)-complexes.[1-3] In these lower valent complexes, 'metal to ligand' charge-transfer bands are observed in the near infrared and visible region. In previous papers,[2,3] it was shown that the charge-transfer transitions can be identified since they give rise to a different spectral behavior from those of the (π,π^*) transition of the coordinating ligand or the (d,d^*) transition in the central metal ion, when a small perturbation such as methyl-substitution is introduced into the system of bipyridine.

In this note, a small perturbation technique was applied for assignment of the lower wave number absorption bands.[2,3] Figure 1 shows absorption spectra of the tris-bipyridine complexes of cobalt(I). The absorption bands were observed at 7200, 16400 and 26200 cm^{-1}. The 16400 cm^{-1} band is the same as the result of qualitative measurement by Waind and Martin,[4] who overlooked the 7200 and 26200 cm^{-1} bands and reported quite different ultraviolet spectrum[5] from ours. The lowest wave number band observed at 7200 cm^{-1} behaves as 'ligand to metal' charge-transfer band upon the dimethyl-substitutions. The band at 7200 cm^{-1} is shifted in the order: 4dmbip*1 (6700 cm^{-1}), bipy (7200 cm^{-1}), 5dmbip*1 (7500 cm^{-1}). On the contrary, the ultraviolet band is shifted in the order: 5dmbip (33200 cm^{-1}), bipy (34200 cm^{-1}), 4dmbip (34300 cm^{-1}). This indicates that the band observed at *ca.* 34000 cm^{-1} should be assigned to a (π,π^*) transition of the coordinating bipyridine. Martin *et al.*[5] reported the lowest (π,π^*) transition of the coordinating bipyridine at 35200 cm^{-1}. However, we observed the band at 34200 cm^{-1} when the solution of higher concentration was measured in a 0.1 cm quartz cell, otherwise the band appeared at 35300 cm^{-1}. The spectrum given by Martin *et al.* might be apparently shifted due to some contamination of free bipyridine. As a matter of fact, free bipyridine shows a band at 35500 cm^{-1}.

We showed that low energy charge-transfer bands are observed when electrons are trapped by the central metal ion upon the reduction of a complex,

1) E. König and S. Herzog, *J. Inorg. Nucl. Chem.*, **32**, 585, 601, 612 (1970).

2) Y. Kaizu, T. Yazaki, Y. Torii and H. Kobayashi, This Bulletin, **43**, 2068 (1970).

3) I. Fujita, T. Yazaki, Y. Torii and H. Kobayashi, *ibid.*, to be published.

4) G. M. Waind and B. Martin, *J. Inorg. Nucl. Chem.*, **8**, 551 (1958).

5) B. Martin, W. R. McWhinnie and G. M. Waind, *ibid.*, **23**, 207 (1961).

*1 4,4′-dimethyl- and 5,5′-dimethyl-2,2′-bipyridine are abbreviated to 4dmbip and 5dmbip, respectively.

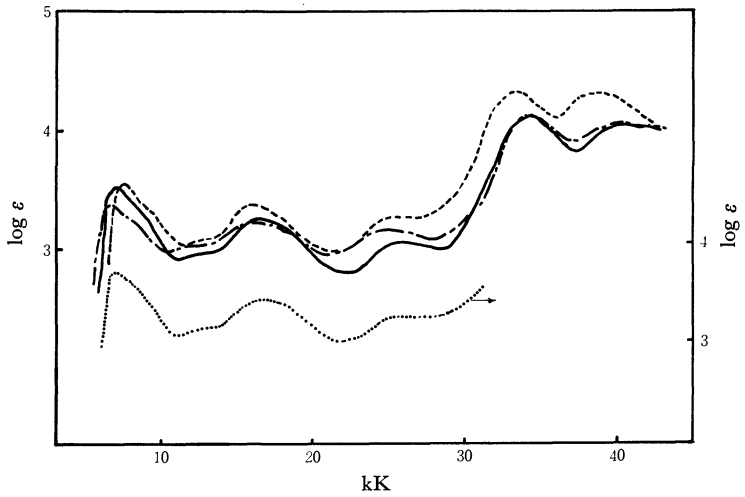

Fig. 1. Absorption spectra of the bipyridine complexes of cobalt(I) in methanol solution.
———: $[Co(bipy)_3]ClO_4$, — — —: $[Co-(4dmbip)_3]ClO_4$, – – – – –: $[Co(5dmbip)_3]ClO_4$, ·····: $Co(bipy)_2ClO_4$. The symbol (→) indicates the right ordinate.

while low energy (π,π^*) bands of the coordinating negative ion are observed when electrons are captured by the coordinating ligand.[2] Since we observed low energy charge-transfer bands, majority population of the electron furnished by reduction is concluded to localize at the central cobalt ion. The oxidation number of cobalt is +1. Since univalent cobalt has eight electrons in *d*-orbitals, two unpaired electrons are expected under the ligand field of D_3 symmetry. This is in good agreement with our observed magnetic moment 2.53 B.M.

In addition to tris(2,2′-bipyridine)cobalt(I) complex, it is well known that bis(2,2′-bipyridine)cobalt-(I) complex exists.[6] The bis-complex shows an intense and diffuse spectrum very similar to that of the tris-complex. From the fact that tris(2,2′-bipyridine)nickel(II) complex, an isoelectronic system of tris(2,2′-bipyridine)cobalt(I) complex, gives rise to (d,d^*) transitions in the visible region, the low energy absorption band observed in the bis-complex has been assigned to (d,d^*) transitions by Császár.[7] We are convinced from our data that the bands in the near infrared and visible region should be assigned to 'metal to ligand' charge-transfer transitions.

6) A. A. Vlecek, *Nature*, **180**, 753 (1957).
7) J. Császár, *Naturwissenschaften*, **46**, 488 (1959).

Experimental

Tris(2,2′-bipyridine)- and bis(2,2′-bipyridine)cobalt(I) perchlorates were prepared by the same method as given in the literature.[4,6] Tris(4,4′-dimethyl-2,2′-bipyridine)- and tris(5,5′-dimethyl-2,2′-bipyridine)-cobalt(II) perchlorate were prepared by the same method with some modifications. The four compounds are deep blue. Tris(2,2′-bipyridine)cobalt(I) perchlorate we prepared showed a magnetic moment of 2.53 B.M. at room temperature. Waind and Martin, however, reported that the tris-complex was diamagnetic.[4,8] The bis-complex gave a moment of 2.71 B.M. The results of elemental analysis are shown in Table 1.

Table 1.

Complex	Analysis Co (%)	
	Calcd	Found
$[Co(bipy)_3]ClO_4$	9.4	9.7
$[Co(4dmbip)_3]ClO_4$	8.3	8.8
$[Co(5dmbip)_3]ClO_4$	8.3	8.5
$Co(bipy)_2ClO_4$	12.5	12.3

Measurement of the electronic absorption spectra of such air-sensitive compounds was described previously.[9] Spectra were measured using a Shimadzu automaticrecording spectrophotometer Model MPS-50.

8) B. Martin and G. M. Waind, *Proc. Chem. Soc.*, **1958**, 169.
9) Y. Torii, T. Yazaki, Y. Kaizu, S. Murasato and H. Kobayashi, This Bulletin, **42**, 2264 (1969).

BULLETIN OF THE CHEMICAL SOCIETY OF JAPAN VOL. 43 3298 (1970)

Infrared and Raman Spectra of Chlorosulfonyl Isocyanate

Isao KANESAKA and Kiyoyasu KAWAI

Faculty of Literature and Science, Toyama University, Gofuku, Toyama

(Received May 20, 1970)

Chlorosulfonyl isocyanate, $ClSO_2NCO$, was first prepared by Graf,[1] and the presence of -NCO and $>SO_2$ groups in this compound was shown by Onodera[2] in his study of the infrared spectra of this compound. Detailed studies of the infrared and Raman spectra of this compound are of interest not only in themselves, but also in comparison with those of such related compounds with -NCO or $>SO_2$ groups as sulfonyl diisocyanate, sulfuryl chloride, or sulfamide.

By using a liquid cell arranged so as to prevent the compound from hydrolysis, the infrared spectra were recorded in the NaCl region. The Raman spectra were observed photographically using Hg-e and -k lines for excitation. The polarization ratios were not determined, however. The frequencies of the infrared and Raman spectra are expected to be accurate to within ± 2 and ± 5 cm^{-1} respectively; their tentative assignments are listed in Table 1.

$ClSO_2NCO$ may be formed by replacing a Cl atom of SO_2Cl_2 with an NCO group; it belongs to the point group *Cs*, in which the plane containing the Cl-S-NCO group is perpendicular to that containing the SO_2 group. Accordingly, the fifteen normal vibrations of this compound are reduced to $\Gamma = 10A' + 5A''$ and are active in both infrared and Raman spectra.

All the strong and medium Raman bands, except for two medium bands, one at 85 cm^{-1} which is present as the anti-Stokes line from Hg-k, and one at 1412 cm^{-1}, are assigned to A′ modes of vibration. A strong band at 130 cm^{-1} could be assigned to the bending vibration of the S-N=CO group, and the band at 85 cm^{-1} to the torsional virbation of this group. The S-N stretching frequency of this compound, 741 cm^{-1}, is lower than those of $SO_2(NH_2)_2$,[3] 904 and 931 cm^{-1}. On the basis of these assignments, it is clear that the S-N=CO group does not have a linear form like $S^-=N^+=CO$, but a bent form. By comparing the normal frequencies of SO_2Cl_2,[4-10] $SO_2(NCO)_2$,[11] and $SO_2(NH_2)_2$[3] with those of $ClSO_2NCO$, the assignments of the observed frequencies listed in Table 1 may be seen to be probable.

TABLE 1. THE ASSIGNMENT OF THE INFRARED AND RAMAN SPECTRA OF $ClSO_2NCO$ (cm^{-1})

Infrared	Raman	Assignment
3590 m		2258+1353=3611
3230 vw		1412+1353+482=3247
2998 m		2258+741=2999
2823 vw		1412×2=2824
2704 w		1353×2=2706
2580 w		1412+1182=2594
2258 vs	2258 m(e)	N=C=O asym. str. A′
1998 w		1412+586=1998
1797 w		1182+623=1805
1496 w		1412+85=1497
1412 vs	1412 m(e,k)	SO_2 asym. str. A″
1353 vs	1357 m(e,k)	N=C=O sym. str. A′
1218 w,sh		741+482=1223
1182 vs	1186 s(e,k)	SO_2 sym. str. A′
1094 vw		482×2+132=1096
1060 vw		482+302+278=1062
989 vw		586+403=989
871 w		438+302+132=872
741 vs	744 s(e,k)	S-N str. A′
	632 vw(e,k)	N=C=O bend. A″
	586 s(e,k)	SO_2 bend. A′
	482 s(e,k)	N=C=O bend. A′
	438 w(e,k)	SO_2 rock. A″
	403 vs(e,k)	S-Cl str. A′
	302 m(e,k)	N-S-Cl bend. A′; SO_2 twist. A″
	278 m(e,k)	SO_2 wag. A′
	130 s(e,k)	S-N=CO bend. A′
	85 m(k+)	-NCO tors. A″.

1) R. Graf, *Chem. Ber.*, **89**, 1071 (1956).
2) N. Onodera, *Kogyo Kagaku Zasshi*, **65**, 790 (1962).
3) T. Uno, K. Machida and K. Hanai, *Spectrochim. Acta*, **22**, 2065 (1966).
4) R. Vogel-Hogler, *Acta Phys. Austriaca*, **1**, 311 (1947).
5) D. E. Martz and R. T. Langeman, *J. Chem. Phys.*, **22**, 1193 (1954).
6) K. C. Schreiber, *Anal. Chem.*, **21**, 1168 (1949).
7) H. Ziebert, *Z. Anorg. Alleg. Chem.*, **257**, 210 (1954).
8) R. J. Gillespie and E. A. Robinson, *Can. J. Chem.*, **39**, 2171 (1961).
9) G. R. Hunt and M. K. Wilson, *Spectrochim. Acta*, **18**, 959 (1962).
10) H. Toyuki and K. Shimizu, This Bulletin, **39**, 2364 (1966).
11) K. Kawai and I. Kanesaka, to be published.

BULLETIN OF THE CHEMICAL SOCIETY OF JAPAN VOL. 43 3299—3301 (1970)

Chloromethylation with Chloromethyl Methyl Ether and 60%-Fuming Sulfuric Acid. A Simple Synthesis of Some Nitropolymethylbenzyl Chlorides and Dihalopolymethylbenzyl Chlorides[1]

Hitomi SUZUKI

Department of Chemistry, Faculty of Science, Kyoto University, Sakyo-ku, Kyoto

(Received May 29, 1970)

A common method to introduce chloromethyl group directly into aromatic nucleus is to treat an aromatic compound with formaldehyde and hydrogen chloride in the presence of a Lewis acid catalyst like zinc chloride.[2] However, nitropolymethylbenzenes and dibromopolymethylbenzenes were found to remain mostly unchanged in the attempted chloromethylation according to the ordinary procedure. The presence of the three or four activating methyl groups was not sufficient to counterbalance the deactivating effect of a nitro or two halogen atoms. The reported procedures[3] for the chloromethylation of deactivated aromatic systems generally requires a quite long reaction time to obtain a moderate yield. The use of stronger catalyst led to the extensive resinification of the substrate as well as the partial migration of bromine atom.

An excellent result of chloromethylation was obtained by dissolving these deactivated aromatic compounds in an excess of chloromethyl methyl ether and adding dropwise with shaking 60%-fuming sulfuric acid. The active reaction immediately took place. After standing for some minutes, the dark brown mixture was diluted with water to precipitate the desired benzyl chloride in good yield. Neither charring nor polymerization was observed under these conditions. The use of a large excess of chloromethyl methyl ether (bp 55—60°C) prevents the temperature of the system from rising too much and thus the reaction from going too far to form polymeric products. This modification also suppresses the formation of undesirable diarylmethane derivatives, which are often a major product in the chloromethylation of deactivated aromatic compounds under drastic conditions.[4]

With increasing amounts of fuming sulfuric acid and extended reaction time, or with the use of smaller amounts of chloromethyl methyl ether, the reaction proceeded very vigorously and the second chloromethylation giving bis(chloromethyl)benzenes as well as the condensation leading to polymeric substances became a prominent process. Owing to poor solubility and high melting point, bischloromethylated products readily separated as a crystalline mass from the hot reaction mixture.

In contrast to the case of lower alkyl homologs, the action of nitrating agent upon tri- or tetramethylbenzyl chlorides usually gives a complicated mixture of side-chain substituted products.[5] Thus, the present method provides the most simple direct route for the highly alkylated nitrobenzyl chlorides in high state of purity. Nine benzyl chlorides and four bis(chloromethyl)benzenes were prepared from nitro and dihalo derivatives of some polymethylbenzenes, and their physical properties are summarized in Table 1.

Experimental

Melting points were determined with a hot stage and are uncorrected. IR spectra were recorded on Nujol mulls with a Jasco DS-402G spectrophotometer and only prominent peaks are given. NMR spectra were determined in carbon tetrachloride solutions (TMS as internal standard) at 60 MHz with a JEOL JNM-3H 60 spectrometer. A commercial chloromethyl methyl ether of ordinary grade was used without purification.

2,5-Dibromo-3,6-dimethylbenzyl Chloride. 2,5-Dibromo-*p*-xylene (10 g) was dissolved in chloromethyl methyl ether (20 g) and 60%-fuming sulfuric acid (*ca.* 8—9 g) was added carefully with stirring. The dark hot mixture was stood for some minutes and then diluted with water. The oily precipitate soon solidified, which was collected by filtration, washed, and dissolved into a mixture of methylene chloride and ligroin. The solution was dried over anhydrous calcium chloride, and removal

1) The Reaction of Polysubstituted Aromatics. Part XIX; Part XVIII; H. Suzuki, *Nippon Kagaku Zasshi*, **91**, 484 (1970).

2) R. C. Fuson and C. H. McKeever, "Organic Reactions," Vol. 1, John Wiley & Sons. Inc., New York (1942), p. 63.

3) a) L. Wals and W. Th. Nauta, *Rec. Trav. Chim. Pays-Bas*, **87**, 65 (1968);b) V. M. Berezovskii, V. A. Kurdyukova and N. A. Preobrazhenskii, *Zh. Obshch. Khim.*, **21**, 1163,1269 (1951).

4) T. Matsukawa, T. Matsuno and K. Shirakawa, *Yakugaku Zasshi*, **63**, 1 (1943).

5) *Cf.* H. Suzuki and K. Nakamura, This Bulletin, **43**, 477 (1970), line 51 on the right column.

Table 1. Physical properties of some polysubstituted benzyl chlorides and fully substituted bis(chloromethyl)benzenes

Compound	Mp or bp*1 (°C)	NMR spectra (τ) ArH	CH_2	CH_3	IR spectra (cm^{-1})*2	Elementary analysis Calcd	Found	Yield (%)
Benzyl Chlorides								
5,6-Dibromo-2,3-dimethyl-	118—120	2.55	5.11	7.58(1)*3 7.68(1)	723, 748, 873 934, 1019, 1174 1200, 1259	C: 34.60% H: 2.90	34.62% 3.17	72
2,6-Dibromo-3,5-dimethyl-*4	123—125 (162—163/ 8 mmHg)	2.81	4.89	7.46(2)	749, 871, 903 948, 984, 1033 1045, 1258, 1303	C: 34.60% H: 2.90	34.51% 2.92	58
2,5-Dibromo-3,6-dimethyl-	94—96 (154—156/ 6 mmHg)	2.50	5.09	7.33(1) 7.50(1)	746, 872, 920 953, 1015, 1114 1168, 1261	C: 34.60% H: 2.90	34.62% 2.97	63
3,5-Dichloro-2,4,6-trimethyl-	104—106		5.35	7.44(2) 7.52(1)	718, 796, 886 1012, 1175, 1255	C: 50.55% H: 4.67	50.63% 4.82	—
5,6-Dichloro-2,3,4-trimethyl-	95—97		5.22	7.56(1) 7.60(1) 7.72(1)	686, 908, 942 1208, 1260	C: 50.55% H: 4.67	50.47% 4.87	72
3-Nitro-2,4,6-trimethyl-	61—62	3.02	5.39	7.53(1) 7.66(1) 7.72(1)	686, 793, 839 873, 1034, 1186 1256, 1519, 1610	C: 56.20% H: 5.66	55.91% 5.70	75
6-Nitro-2,3,4,5-tetramethyl-	123—125		5.51	7.53(1) 7.63(2) 7.76(1)	688, 727, 828 846, 1074, 1255 1300, 1524	C: 58.02% H: 6.15	57.79% 6.15	73
5-Nitro-2,3,4,6-tetramethyl-	119—120		5.27	7.47(1) 7.58(2) 7.67(1)	706, 835, 853 1228, 1261, 1523	C: 58.02% H: 6.15	58.25% 6.26	58
4-Nitro-2,3,5,6-tetramethyl-	112—113		5.35	7.57(2) 7.79(2)	711, 842, 1023 1225, 1258, 1270 1298, 1532	C: 58.02% H: 6.15	57.93% 6.22	66
*Bis(chloromethyl)benzenes*5								
5,6-Dibromo-2,3-dimethyl-1,4-	217—219		5.04	7.52(2)	731, 887, 909 943, 1155, 1202 1258	C: 33.28% H: 2.79	33.15% 2.85	74
3,5-Dibromo-2,6-dimethyl-1,4-	208—210		4.89 5.28	7.39(2)	732, 809, 879 998, 1165, 1255	C: 33.28% H: 2.79	33.01% 2.77	51
2,5-Dibromo-3,6-dimethyl-1,4-	213—215		5.06	7.33(2)	710, 730, 838 928, 1010, 1128 1189, 1262	C: 33.28% H: 2.79	32.71% 2.83	66
5-Nitro-2,4,6-trimethyl-1,3-	168—169		5.05	7.66(3)	699, 726, 828 856, 1027, 1255 1253, 1266	C: 50.39% H: 5.00	50.54% 4.85	88

*1 Bp in parentheses.
*2 Principal peaks in the regions, 650—1350 and 1500—2000 cm^{-1}.
*3 Numerals in parentheses refer to the number of methyl groups.
*4 The appearance of a methylene proton peak at lower field and of a ring proton peak at higher field than those of the two isomers favors this orientation over the alternative one, 2,6-dimethyl-3,5-dibromobenzyl chloride.
*5 NMR spectra were determined in deuteriochloroform solutions.

of the solvent, followed by fractional distillation under reduced pressure gave the unchanged starting material (2.9 g) at 110—112°C/7 mmHg and the chloride (5.3 g, 63%) at 154—156°C/6 mmHg. Crystallization of the latter fraction from light petroleum gave white fine needles, mp 94—96°C (lit,[3a] 96—97°C).

When a warm solution of dibromo-*p*-xylene (5 g) in chloromethyl methyl ether (5 g) was treated with 60%-fuming sulfuric acid (*ca.* 4—5 g), the reaction proceeded with vigorous evolution of heat and the mixture soon turned into a black crystalline mass. The product was washed with water, dissolved into a mixture of methylene chloride and ligroin, and freed from the colored polymeric substances through chromatography on a short alumina column. Removal of the solvent, followed by recrystallization of the product (4.5 g, 66%) from chloroform gave **1,4-bis(chloromethyl)-2,5-dibromo-3,6-dimethylbenzene** as colorless fine needles, mp 213—215°C. It sublimes on heating.

5,6-Dichloro-2,3,4-trimethylbenzyl Chloride. 4,5-Dichloro-1,2,3-trimethylbenzene (1 g) was dissolved in chloromethyl methyl ether (3 g) and 60%-fuming sulfuric acid (*ca.* 3 g) was carefully added with shaking. The mixture became dark brown and the active reaction immediately started. After the end of the reaction, the mixture was diluted with water and the precipitate

was collected by filtration, washed, and chromatographed on a short alumina column using a mixture of light petroleum and methylene chloride as eluant. Evaporation of the solvent from the eluate gave colorless prisms (0.9 g, 72%), mp 95—97°C.

3-Nitro-2,4,6-trimethylbenzyl Chloride. Nitromesitylene (3 g) was dissolved in chloromethyl methyl ether (3 g), to which was added dropwise and with frequent shaking 60%-fuming sulfuric acid (*ca.* 2—3 g). After the cease of the active reaction, the mixture was quenched with water. Working up as above, followed by crystallization from light petroleum gave colorless prisms, mp 61—62°C. Yield, 2.9 g (75%).

When a further amount (*ca.* 2—3 g) of fuming sulfuric acid was added to the above mixture, a vigorous exothermal reaction followed and the content soon solidified to a dark crystalline mass, which was washed with water, taken up into hot benzene, and decolorized through chromatography on a short alumina column. Evaporation of the solvent from the eluate gave **2,4-bis(chloromethyl)-6-nitro-1,3,5-trimethylbenzene** (4.2 g, 88%) as colorless prisms, mp 168—169°C.

BULLETIN OF THE CHEMICAL SOCIETY OF JAPAN VOL. 43 3301—3302 (1970)

Homolytische aromatische Benzoyloxylierung bei der Prévost-Reaktion

Tadashi SUEHIRO, Mikio HIRAI und Machiko NIITSU

Chemisches Institut, Gakushuin Universität, Mejiro, Tokyo

(Eingegangen am 1. Juni, 1970)

Olefine werden bei der Umsetzung mit benzoesaurem Silber und Jod in Dibenzoyloxy-Verbindungen übergeführt.[1] Wenn aber die Reaktion in benzolischer Lösung durchgeführt wird, entstehen nebenbei Benzoesäure-phenyl-ester.[2] Weiter ist es auch bekannt, daß das Olefin, das einen phenolischen Ring im Molekül trägt, sich nicht nur an der Doppelbindung hydroxylieren sondern auch an dem aromatischen Kern jodieren läßt.[3] Diese aromatische Jodierung geschieht wahrscheinlich elektrophil wie bei der Hansdiecker-Reaktion, aber die mechanistischen Untersuchugen über die Ester-Bildung in benzolischer Lösung sind noch nicht vollzogen. Wir arbeiten seit einiger Zeit über die homolytische Tritylierung der Aromaten und über den Zusammenhang zwischen Tritylierung und Benzoyloxylierung.[4] In dieser Beziehung nahmen wir Interesse an dem Verhältnis zwischen Jodierung und Ester-Bildung in der Prévost-Reaktion.

Um die Benzyloxylierung zu klären, haben wir die Prévost-Reaktion in einer Mischung von Toluol und Benzol untersucht. Die Ergebnisse der Umsetzung bei 80—160°C sind in der Tabelle aufgestellt.

Tabelle 1. Isomere-Verhältnisse und relative Reaktivität des Toluols in a) Benzoyloxylierung und b) Jodierung bei der Prévost-Reaktion

Reakt. Nr.	Temp. °C	Isomere-Verhältnis %			Ausb. %	k_{PhCH_3}/k_{PhH}
		o-	*m*-	*p*-		
a) 1	80	46.2	24.1	29.7	9.1—10.7	3.01
2	80	42.8	29.8	27.4	—	—
3	100	47.5	27.5	24.0	—	—
4	120	46.5	29.0	24.5	—	—
5	140	46.6	32.5	20.9	—	—
6	160	43.8	29.2	27.0	—	—
b) 1	80	~32	~0	~68	36—46	17

Nr. 1: Ansatz von 30 mMol benzoesaurem Silber, 30 mMol Jod in 60 m*l* Toluol-60 m*l* Benzol, 4 Stunden im Dunkel.

Nr. 2—6: Ansätze von 1.3 mMol benzoesaurem Silber, 1.3 mMol Jod in 5 m*l* Toluol in Einschlußrohr im Dunkel.

Die Umsetzungen sind alle unter Stickstoff-Atmosphäre durchgeführt. Toluol und Jod gaben in Abwesenheit des Silber-Salzes das Jodtoluol in einer Ausbeute weniger als 0.24%.

Neben Jodtoluolen und Benzoesäure-estern von Kresolen entstehen bei der Umsetzung bei 80°C *o*-, *m*- und *p*-Methylbiphenyle und Bibenzyl insgesammt in *ca.* 10% Ausbeute, und in rein toluolischer Lösung nur wenig Jodbenzol (weniger als 0.2%). Im letzteren Fall wurde überhaupt kein Benzoesäure-phenyl-ester gefunden.

1) C. Prévost und R. Lutz, *Compt. Rend.*, **198**, 2264 (1934); C. V. Wilson, "Organic Reactions," Vol. 9, 350 (1957).

2) C. Prévost und J. Wiemann, *Compt. Rend.*, **204**, 989 (1937).

3) M. Sletzinger und C. R. Dawson, *J. Amer. Chem. Soc.*, **68**, 345 (1946); *J. Org. Chem.*, **14**, 671 (1949).

4) T. Suehiro, S. Igeta, O. Kuwabara und M. Hirai, *Tetrahedron*, **26**, 963 (1970).

Die Isomere-Verhältnisse der Benzoesäure-ester von Kresolen (*o*/*m*/*p*=46/24/30) ähneln denen der Produkte von Benzoyloxylierung des Toluols mettels Benzoylperoxyds in Gegenwart von Kupfer(II)-chlorid[5] (56/18/26) bzw. in Gegenwart von Jod[6] (53/16/31). Die relative Reaktivität k_{PhCH_3}/k_{PhH}= 3.01 steht im guten Einklang mit derjenigen Werte der entsprechenden Reaktionen, d.h. 2.51[5] bzw. 2.85[6] und 2.82[4]. Die homolytische Natur des Zerfalls von Benzoylperoxyd in Gegenwart von Kupfer(II)chlorid,[5] Jod[6] und Trityl[4] ist zweifellos klar und demnach verläuft die Benzoyloxylierung bei der Prévost-Reaktion sehr wahrscheinlich über das Benzoyloxy Radikal.

Homolytischer Zerfall von benzoesaurem Silber-Jod Komplex ist in einigen Beispielen angedeutet worden, z.B. in der Bildung von α-Methyl-β-phenyl-propionsäure-α-methylphenäthyl-ester aus α-Methyl-β-phenylpropionsaurem Silber und Jod.[7] Zu der Bildung von Benzcoumarin aus Biphenyl-*o*-carbonsaurem Silber und Jod[8] gaben aber die Autoren auf Grund der Abhängigkeit der Ausbeute von der Substituenten vielmehr elektrophile Substitution. Diese Abhängigkeit der Ausbeute kann man jedoch besser der elektrophilen Eigenschaft des freien Aroyloxy Radikals zuschreiben, genau so wie es in der abnehmenden Tritylierung bei der Aromaten mit Elektronen anziehenden Substituenten der Fall ist.[4]

Jodierung des Toluols bei der Prévost-Reaktion ist *o*- und *p*-orientierend und die relative Reaktivität k_{PhCH_3}/k_{PhH} ist 17. Das ist viel großer als 3 bei der Benzoyloxylierung. Dies weist auf die heterolytische Jodierung hin.

Jodbenzol kann auch aus Phenyl Radikal und Jod gebildet werden, weil wärend der Prévost-Reaktion Benzoyloxy Radikal auftritt, welches thermisch in Phenyl Radikal zerfallen kann. Man kann dies aber übersehen, weil die Bildung des Jodbenzols aus Phenyl Radikal höchstens nur 0.2% beträgt.

Was dem Wert 17 betrifft, ist er, obwohl er bei 80°C bestimmt wurde, viel kleiner als 344 für Cl_2-[9] bzw. 605 für Br_2-[10] Halogenierung. Immernoch ist er kleinier als 60 für Cl^+-[11] bzw. 36 für Br^+-[12] Halogenierung (alle bei 25°C). Einen etwas größeren Wert, mehr als 140, kann man für die Jodierung mit JCl-Zinkchlorid[13] errechnen. Die Jodierung bei der Prévost-Reaktion muß also durch J^+ oder durch ein analoges reaktionsfähiges Reagens hervorgerufen worden sein. Ein Beispiel der Prévost-Reaktion, wo J^+ Rolle spielt, findet man bei der Umsetzung von 3,3,3-Triarylpropen,[14] deren Zwischenprodukt, d.h. Carboniumion, Aryl-Umlagerung erleidet.

Beschreibung der Versuche

Bestimmung der Benzoesäure-ester von Kresolen. Man entfernt Jod und Silber Salz von der Reaktionsmischung und untersucht die neutrale Produkte gaschromatographisch. Die Analyse wurde bei 210°C mit einer Kolonne von Apiezon L 25%, 3 m, mit Helium 15 ml/15 Sek durchgeführt. Der innere Standard war *o*-Nitrotoluol.

Bestimmung der Jodtoluole. Man destilliert zunächst die Reaktionsmischung mit Wasserdampf ab und nimmt NMR-Spektrum von dem eingeengten Destillat in Tetrachlorkohlenstoff mit dem inneren TMS Standard auf. Die Signale in τ-Wert für *o*-Jodtoluol, 2.27d (8 Hz), 7.61s; *m*-Jodtoluol, 2.58s, 3.09s, 7.72s; *p*-Jodtoluol, 2.52d (8 Hz), 3.20d (8 Hz), 7.72s.

Methyl-Protonen von Jodtoluolen wurden durch Vergleich mit denen von *o*-Nitrotoluol als innerem Standard gestimmt. Weil die Signale der Methyl-Protonen von *m*- und *p*-Jodtoluolen sich übereinander lagern, wurde der *m*-Isomer aus den Signalen im Bereich τ 2—3 ermittelt, wo keine bei τ 2.58 und bei 3.09 gefunden wurden. Die Ausbeuten von Jodbenzol und Jodtoluolen wurden gaschromatographisch mit einer 3 m Kolonne von Apiezon L bei 155°C ermittelt.

5) M. E. Kurz und P. Kovacic, *J. Org. Chem.*, **33**, 1953 (1968).

6) S. Hashimoto, W. Koike und M. Yamamoto, gelesen for der 10. Diskuss. Tagung über Org. freie Radikale Reaktionen, Osaka, Okt. 1969.

7) S. Oae, T. Kashiwagi und S. Kozuka, Dieses Bulletin, **39**, 2441 (1966).

8) D. J. Chalmers und R. H. Thomson, *J. Chem. Soc., C*, **1968**, 848.

9) H. C. Brown und L. M. Stock, *J. Amer. Chem. Soc.*, **79**, 5175 (1957).

10) H. C. Brown und L. M. Stock, *ibid.*, **79**, 1421 (1957).

11) P. B. D. de la Mare, J. T. Harvey, M. Hassan und S. Varmar, *J. Chem. Soc.*, **1958**, 2756.

12) P. B. D. de la Mare und J. T. Harvey, *ibid.*, **1956**, 36.

13) R. M. Keefer und L. J. Andrews, *J. Amer. Chem. Soc.*, **78**, 5623 (1956).

14) R.O.C. Norman und C. B. Thomas, *J. Chem. Soc., B*, **1967**, 604.

BULLETIN OF THE CHEMICAL SOCIETY OF JAPAN VOL. 43 3303—3304 (1970)

Zur Reaktionsgeschwindigkeit bestimmenden Stufe der homolytischen aromatischen Triphenylmethylierung (der Wielandschen Reaktion)

Tadashi SUEHIRO, Shinichi IGETA, Osamu KUWABARA, Mikio HIRAI, Mototoshi ISHIDA und Junji YAMAZAKI

Chemisches Institut, Gakushuin Universität, Mejiro, Tokyo

(Eingegangen am 3. Juni 1970)

Die Tritylierung der Aromaten verläuft in folgender Weise:[1)]

$$(C_6H_5COO)_2 + Ph_3C\cdot \longrightarrow C_6H_5COOCPh_3 + C_6H_5COO\cdot \quad (1)$$

$$C_6H_5COO\cdot + Ph_3C\cdot \longrightarrow C_6H_5COOCPh_3 \quad (2)$$

$$C_6H_5COO\cdot + C_6H_6 \longrightarrow C_6H_5COO(H)C_6H_5\cdot \quad (3)$$

$$(I) + Ph_3C\cdot \longrightarrow C_6H_5COO(H)C_6H_5(H)CPh_3 \quad (II) \quad (4)$$

$$(II) \longrightarrow C_6H_5CPh_3 + C_6H_5COOH \quad (5)$$

Die Reaktion (2) läuft mit (3)—(5) nebeneinander. Wir haben festgestellt, dass Reaktion (3) die Geschwindigkeit bestimmende Stufe der Tritylierung ist. Dieser Schluss beruhte auf der Übereinstimmung der Reaktivität Toluols in Tritylierung mit der dessen Benzoyloxylierung.[2)] Die Charakterisierung der Geschwindigkeit bestimmenden Stufe wurde weiter verfolgt.

a) Einfluss der Konzentration Trityls auf die Ausbeute an Tetraphenylmethan. Wenn die Konzentration von Trityl kleiner wird, muss die Reaktion (2) verlangsamt werden, dagegen muss Reaktion (3) genau so schnell wie früher verlaufen. Die Ausbeute an Tetraphenylmethan nimmt also zu, wenn (3) Geschwindigkeit bestimmend ist. Bei der Tabelle 1 ersieht man die Zunahme der Ausbeute und daraus rechnet man die Herabsetzung der Geschwindigkeit von (2) bis zur Hälfte. Aus dem Verdünnen von Hexaphenyläthan von 3.3×10^{-2} bis zu 2.1×10^{-3} Mol/l wird die Abnahme der Geschwindigkeit der Reaktion (2) bis zu ein fünftel berechnet. Falls die Reaktion (4) bzw. (5) Geschwindigkeit bestimmend ist, muss die Ausbeute an Tetraphenylmethan unverändert bleiben.

b) Einfluss der Polarität des Lösungsmittels auf die Ausbeute an Tetraphenylmethan. Die Ausbeute wird durch Verdünnen der Aromaten mittels Nitrobenzols vermindert. Nitrobenzol spielt hier zuerst als unwirksames Lösungsmittel gegen

TABELLE 1. ABHÄNGIGKEIT DER AUSBEUTE AN TETRAPHENYLMETHAN VON DER KONZENTRATION TRITYLS UND VON POLARITÄT DES LÖSUGSMITTELS

Lösungsmittel			Konz. $(Ph_3C)_2$ Mol/l	Ausbeute an $ArCPh_3$		
	ml	Nitrobenzol ml		mMol*	%	Berechnete** %
Benzol	90	—	3.3×10^{-2}	1.208±0.026	40	—
	45	45	3.2×10^{-2}	0.746±0.016	26	(25)
Benzol	900	—	2.0×10^{-3}	0.950±0.019	55	—
	450	450	2.1×10^{-3}	0.808±0.017	42	(38)
Anisol	500	—	1.4×10^{-2}	3.631±0.110	52	—
	250	250	1.5×10^{-2}	3.787±0.110	50	(37)
Toluol	90	—	1.6×10^{-2}	0.978±0.049	67	—
	45	45	1.6×10^{-2}	0.867±0.047	60	(50)
Chlorbenzol	90	—	1.6×10^{-2}	0.512±0.039	36	—
	45	45	1.6×10^{-2}	0.398±0.039	29	(22)

* Durch Isotopie-Verdünnungsmethode bestimmt.

** Berechnet unter der Annahme, dass die Konz. der Atomaten durch Verdünnen bis zur 1/2 vermindert wird.

1) T. Suehiro, S. Igeta, O. Kuwabara und M. Hirai, *Tetrahedron*, **26**, 963 (1970).

2) M. E. Kurz, P. Kovacic, A. K. Bose und I. Kugajevsky, *J. Amer. Chem. Soc.*, **90**, 1819 (1968).

Tritylierung[3] und die berechnete Ausbeute sind im Klammer aufgestellet. Die experimentelle Ergebnisse stehen in erster Annäherung im Einklang mit der berechneten, aber sind, genauer gesagt, etwa grösser als sie. Nitrobenzol muss zweitens als polares Lösungsmittel zur Erhöhung der Polarität des Mediums beitragen.

Die Geschwindigkeit der Reaktion kann je nach der Eigenschaft des Übergangszustandes durch die Polarität des Lösungsmittels beschleunigt werden.[4] Wenn man als Model des Übergangszustandes der Reaktionen (2), (3) und (4) oder (5) jeweils Benzoesäuretritylester (1.06D),*1 Benzoesäurephenylester (1.96D)*1 und Benzoesäure-*p*-tritylphenylester (1.36D)*1 wählt und r^* durch Molgewicht ersetzt, so erhält man für μ^{*2}/r^{*3} 3.03×10^{-3}, 1.94×10^{-2} und 4.20×10^{-3}. Daraus ergibt sich, dass die Reaktion (3) durch die Polarität mehr beschleunigs wird als (2), (4) und (5).

c) Isotopie-Effekt der Tritylierung. Die Isomere-Verhältnisse der Methyltetraphenylmethanen bei der Tritylierung Toluols hängt von den *o*-Substituenten der Aroyloxy Radikale ab (Tabelle 2). Dass die Zunahme des *m*-Isomern nicht einfach von den räumlichen Bedingungen der *o*-Substituenten herbeigeführt wird, ist aus der Reihenfolge, CH_3O–, Br–>Cl–>CH_3–, NO_2–, CH_3SO_2–, klar.

Tabelle 2. Die Isomere-Verhältnisse der *o*-, *m*- und *p*-Methyltetraphenylmethane bei der Tritylierung Toluols (25°C)

Peroxyd	Methyltetraphenylmethanen %		
	o-	*m*-	*p*-
Bis-*o*-methoxybenzoyl	4.8	92.0	3.2
Bis-*o*-methylbenzoyl	9.9	83.4	5.7
Bis-*o*-chlorbenzoyl	5.4	90.5	4.1
Bis-*o*-brombenzoyl	3.7	91.9	4.4
Bis-*o*-methylsulfonylbenzoyl	11.3	84.8	3.9
Bis-*o*-nitrobenzoyl	10.4	83.5	6.1
Bis-*o*-phenylbenzoyl	Keine Methyltetraphenylmethanen, sondern eine Carbonsäure vom Schmp. 254°C**		
Bis-α-naphthoyl	6.2	87.0	6.8
Bis-α-thenoyl	10.9	81.6	7.5
Bis-*p*-methoxybenzoyl	13.6	74.0	12.4
Benzoyl	13.0	74.8	12.2
Bis-*p*-nitrobenzoyl	10.5	77.5	12.0

* Bestimmt durch NMR-Spektrum,[1] Fehlergrenze ±2.

** Analyse, Gef: C, 87.34; H, 5.78%. Ber. für 2-(3'-Tritylphenyl)benzoesäure $C_{32}H_{24}O_2$: C, 87.24; H, 5.49%.

Isotpie-Effekte k_H/k_D der Tritylierung waren 1.03 beim Bis-*o*-methoxybenzoylperoxyd und 1.04 beim Bis-*o*-methylbenzoylperoxyd. Dies bedeutet, dass die Geschwindigkeit bestimmende Stufe nicht in (5) liegt und dass Benzoyloxy Radikale durch *o*-Methoxy- oder *o*-Halogen-Gruppe so stabilisiert werden, dass sie immermehr spezifisch an die *o*- und *p*-Stellungen Toluols angreifen können.

Aus diesen Befunden wird festgestellt, dass die Stufe (3) in der Tritylierung Geschwindigkeit bestimmend ist.

Beschreibung der Versuche

Die Umsetzungen von Trityl mit Benzoylperoxyden wurden alle wie früher[1] bei 25°C unter Stickstoff im Dunkel durchgeführt.

Isotopie-Effekt. Die Isotopie-Effekte wurden aus der Konzentration deuterierten Benzols und Tetraphenylmethans berechnet. Als Lösungsmittel verwendet man eine Mischung von Benzol und Benzol-d_6 und reinigt durch Vakuum Destillation (Probe 1). Man destilliert aus der Reaktionsmischung das Lösungsmittel im Vakuum zurück (Probe 2), nimmt den Rückstand in Benzol auf, zersetzt den Überschuss Peroxyd mit Natriumjodid, zieht Carbonsäure aus und chromatographiert den neutralen Teil an Florisil (Benzol-Petroläther). Die rohe Kristalle Tetraphenylmethans sublimiert man im Vakuum und isoliert das Sublimat bei 200°C. Man kristallisiert das Produkt aus Benzol um bis konstanter Schmp. 285.5—286.5°C (Einschlussrohr) erreicht wird (Probe 3). Die Kristalle aus der Mutterlauge chromatographiert man nochmals und reinigt wie oben (Probe 4). Die Fehlergrenze der massenspektrometrischen Analyse war ±1%. Für die massenspektrometrische Bestimmung danken wir Herrn Dr. Y. Moriyama der Universität Tokyo herzlichst.

Umsetzung mit	(H-Verbindung)/(D-Verbindung)				k_H/k_D
	Probe 1	2	3	4	
Bis-*o*-methoxybenzoylperoxyd	1.046	1.035	1.071	1.068	1.03
Bis-*o*-methylbenzoylperoxyd	0.965	—	1.007	—	1.04

Peroxyde. Die Peroxyde wurden nach der Methode von Blomquist und Buselli[5] hergestellt. Bis-*o*-brombenzoylperoxyd, Schmp. 108°C, z. Gef: C, 42.44; H, 1.88%. Ber: C, 42.03; H, 2.02%. Bis-*o*-methylsulfonylbenzoylperoxyd, Schmp. 151°C, z. Gef: C, 48.18; H, 3.23%. Ber: C, 48.23; H, 3.54%.

3) R. A. Benkeser, R. B. Gosnell und W. Schroeder, *J. Am. Chem. Soc.*, **79**, 2339 (1957).

4) J. G. Kirkwood, *J. Chem. Phys.*, **2**, 351 (1934).

*1 Die Werte sind von Herrn Prof. T. Shimozawa der Universität Saitama bei 25°C in Benzol Lösung ermittlet, dem sind wir zum Dank verpflichtet.

5) T. Blomquist und A. J. Buselli, *J. Amer. Chem. Soc.*, **73**, 3883 (1951).

BULLETIN OF THE CHEMICAL SOCIETY OF JAPAN VOL. 43 3305—3306 (1970)

Study on Oxazolopyrimidines. IV. The Preparation of 7-Aminooxazolo[5,4-*d*]pyrimidine 6-Oxide

Yozo Ohtsuka and Kikuo Sugimoto

Sagami Chemical Research Center, Onuma, Sagamihara, Kanagawa

(Received June 8, 1970)

Various *N*-oxides of nitrogen-containing heteroaromatic compounds have been prepared, and several purine *N*-oxides have been shown to exhibit biological activities.[1,2] Although amino-substituted purines[3] and 7-aminothiazolo[5,4-*d*]pyrimidine[2] have been known to yield the corresponding *N*-oxides with peroxyacetic acid, the treatment of 7-aminooxazolo[5,4-*d*]pyrimidine under similar oxidizing conditions led to the formation of 6,8-dihydroxypurine.[4] Another way to *N*-oxide has recently been provided by the preparation of adenosine 1-oxides by the treatment of 5-amino-4-cyanoimidazole derivatives with ethyl orthoformate, followed by hydroxylamine.[5] A similar approach was previously used for the synthesis of hypoxanthine 1-oxide.[6]

The synthesis of 7-aminooxazolo[5,4-*d*]pyrimidine 6-oxide (II) has now been accomplished in a 61% yield by the treatment of 4-cyano-5-ethoxymethyleneaminooxazole (I)[7] with hydroxylamine. By the same treatment, 4-cyano-5-ethoxymethyleneaminoimidazole[8] gave adenine 1-oxide.

The structure of the *N*-oxide (II) was supported by the results of elementary analysis, its spectroscopic data, and its rearrangement to hypoxanthine 3-oxide (III) when stirred in an aqueous alkali for 2 days, but an attempt to obtain 7-aminooxazolopyrimidine by catalytic hydrogenation with Pt/C was unsuccessful.

The present method for the preparation of the *N*-oxide of the pyrimidine derivative by the cyclization of cyanoethoxymethyleneamino compound with

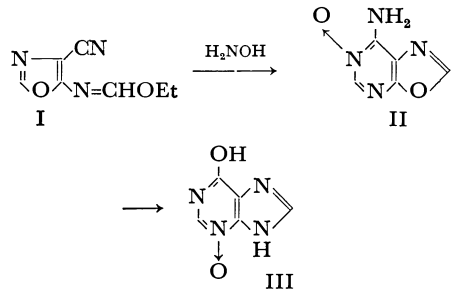

hydroxylamine can generally be applied to a variety of systems, including a relatively unstable system such as oxazolopyrimidine.

Experimental

Preparation of 7-Aminooxazolo[5,4-*d*]pyrimidine 6-Oxide (II). 4-Cyano-5-ethoxymethyleneaminooxazole (I)[7] (1.65 g) was added to an ice-cooled solution of hydroxylamine hydrochloride (0.70 g) and sodium hydroxide (0.4 g) in water (5 m*l*). A precipitate was formed at an early stage of the reaction. When the mixture was stirred at room temperature, it gradually dissolved and then crystals deposited again. The product (0.92 g) was collected after 15 min and washed with water and ethanol. Recrystallization from water gave colorless needles, mp>300°C.

This compound gave a positive $FeCl_3$ test (violet) and a negative TTC (triphenyltetrazolium chloride) test. Its mass spectrum showed a pattern identical with that of 7-aminooxazolopyrimidine[7] except for the peak of the molecular ion, $m/e=152$ (14.4% in intensity relative to the peak, $m/e=136$). The relatively small pH-dependence of the UV spectra seems to support the oxazolopyrimidine structure (λ_{max} (mμ), logε; 231, 4.45; 256, 3.94; 300, 3.34 (pH=2.9): 230, 4.52; 259, 3.96; 301, 3.40 (pH=8.5): 226, 4.41; 259, 3.85; 289, 3.63 (pH=12.0)). This compound possessed paper chromatographic R_f values of 0.53 and 0.27 in solvents A and B[9] respectively.

Found: C, 39.45; H, 2.93; N, 36.73%. Calcd for $C_5H_4N_4O_2$: C, 39.48; H, 2.65; N, 36.84%.

Adenine 1-Oxide. 4-Cyano-5-ethoxymethyleneaminoimidazole[8] (0.22 g) was treated by the same procedure as has been described above. The product (0.10 g) was identified as adenine 1-oxide[3] from its IR spectrum

1) K. Sugiura and G. B. Brown, *Cancer Res.*, **27**, 925 (1967).

2) G. B. Brown, G. Levin, S. Murphy, A. Sele, H. C. Reilly, G. S. Tarnowski, F. A. Schmid, M. N. Teller and C. C. Stock, *J. Med. Chem.*, **8**, 190 (1965).

3) M. A. Stevens, D. I. Magrath, H. W. Smith and G. B. Brown, *J. Amer. Chem. Soc.*, **80**, 2755 (1958); M. A. Stevens and G. B. Brown, *ibid.*, **80**, 2759 (1958).

4) Y. Ohtsuka and K. Sugimoto, This Bulletin, **43**, 2281 (1970).

5) A. Yamazaki, I. Kumashiro and T. Takenishi, *Chem. Pharm. Bull.* (Tokyo), **17**, 1128 (1969).

6) E. C. Taylor, C. C. Cheng and O. Vogl, *J. Org. Chem.*, **24**, 2019 (1959).

7) Y. Ohtsuka, This Bulletin, **43**, 187 (1970).

8) K. Suzuki and I. Kumashiro, Brit. 1134974 (1968).

9) Solvent A; BuOH–HOAc–H_2O (60 : 15 : 25 v/v): solvent B; *i*-PrOH–NH_4OH–H_2O (7 : 1 : 2 v/v): solvent C; 5% disodium phosphate - *i*-AmOH (3 : 2 v/v).

and R_f value.

Conversion of the Oxide II to Hypoxanthine 3-Oxide (III). The *N*-oxide (II, 0.8 g) was stirred in a 4N aqueous NaOH solution (10 m*l*) at room temperature for 2 days. After this period, the reaction mixture was acidified with acetic acid. The product was collected and purified by reprecipitation from an aqueous alkali with acetic acid. The yield was 42% (0.52 g). The structure of the compound was identified as hypoxanthine 3-oxide[10] on the basis of its UV spectra at various pH (pH=3, 8.5 and 12) and R_f values in solvents A, B, and C.[9]

10) I. Scheinfeld, J. C. Parham, S. Murphy and G. B. Brown, *J. Org. Chem.*, **34**, 2153 (1959).

BULLETIN OF THE CHEMICAL SOCIETY OF JAPAN VOL. 43 3306—3307 (1970)

On the Precipitation of Siderite and Magnetite from Homogeneous Solutions as Observed by Means of Visual Autoclaving

Tominosuke KATSURAI* and Masayuki UDA

Pilot Laboratory, Hiratsuka-Kanagawa and The Institute of Physical and Chemical Research, Yamato-machi, Saitama

(Received June 11, 1970)

Visual autoclaving was worked out for the purpose of following the hydrothermal changes which take place during the course of autoclaving.[1] The method is useful not only in the sense seeing is believing, but it also makes it possible for us to observe the change taking place in a homogeneous solution above 100°C.[2] Precipitation from homogeneous solutions has been extensively studied in the field of analytical chemistry for obtaining compact, easily filtrable precipitates. However, it seems that the studies were restricted to temperatures below 100°C. We would like to describe the results which we obtained with homogeneous ferrous and ferrous-ferric solutions. The solutions were subjected to visual autoclaving in the presence of urea, and the structures of the resulting precipitates were confirmed by means of X-ray diffraction. Commercial reagents of the best grade were used in the experiments. The results were found to be of interest in relation to mineral synthesis.

Formation of Siderite. Preparation of pure siderite is known to be difficult. However, we found that it can be obtained by autoclaving a solution of ferrous ammonium sulfate in the presence of urea. A solution containing ferrous ammonium sulfate (0.1M) and urea (0.4M) was used. A white bulky precipitate appears at 150°C. It begins to coagulate at 170°C and at 200°C becomes compact. This snow-white precipitate contains a small amount of dark magnetic particles which can easily be removed by a magnet. It was found that the white precipitate is siderite ($FeCO_3$) and the dark particles magnetite. The magnetite is derived from the ferric compound contained in ferrous ammonium sulfate in a small amount as an impurity. This can be illustrated by the formation of magnetite from a ferrous-ferric solution in the presence of urea.

Formation of Magnetite. The following solutions (a) and (b) were subjected to autoclaving at 200°C for 1 hr. For the sake of comparison, a ferrous-ferric solution (c) was also studied.

Solution (a): 0.05M in $FeSO_4 \cdot (NH_4)_2SO_4$, 0.1M in $FeCl_3$ and 1M in $CO(NH_2)_2$. A brown precipitate

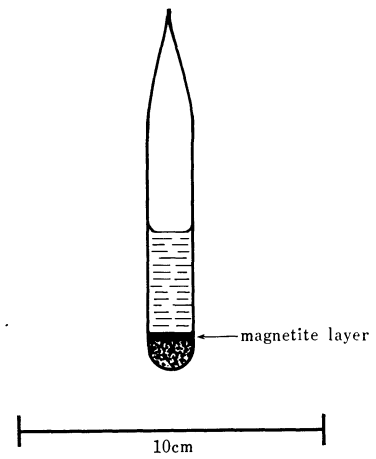

Fig. 1. Formation of magnetite.

* Present address: The Chemical Society of Japan, Kanda Surugadai, Chiyoda-ku, Tokyo.

1) For the technique of autoclaving, *cf.* T. Katsurai and K. Sone, *Kolloid-Z.*, **163**, 70 (1959); T. Katsurai, *ibid.*, **170**, 57 (1960).

2) T. Katsurai, *Kolloid-Z. Z. Polym.*, **204**, 126 (1965).

Table 1

No.		Composition of solution	Autoclaving product
1		0.1M in $FeSO_4 \cdot (NH_4)_2SO_4$ 0.4M in $CO(NH_2)_2$	Siderite ($FeCO_3$) Magnetite (Fe_3O_4), small amount
2	(a)	0.05M in $FeSO_4 \cdot (NH_4)_2SO_4$ 0.1M in $FeCl_3$ 1M in $CO(NH_2)_2$	Magnetite (Fe_3O_4) Siderite ($FeCO_3$), small amount α-FeO·OH, small amount Hematite (α-Fe_2O_3), trace
	(b)	0.2M in $FeSO_4 \cdot (NH_4)_2SO_4$ 0.04M in $FeCl_3$ 1M in $CO(NH_2)_2$	Magnetite (Fe_3O_4) Siderite ($FeCO_3$), small amount
	(c)	0.05M in $FeSO_4 \cdot (NH_4)_2SO_4$ 0.1M in $FeCl_3$	Hematite (α-Fe_2O_3)

is formed at about 100°C. It turns to brick red at 150°C. The upper liquid turns colorless at 160°C. The surface of the precipitate turns black above 170°C. The black layer thickens with the rise of temperature. The principal constituent of the autoclaving product is magnetite. Siderite, αFeO·OH and a trace of hematite are found as minor constituents.

Solution (b): 0.2M in $FeSO_4 \cdot (NH_4)_2SO_4$, 0.04M in $FeCl_3$ and 1M in $CO(NH_2)_2$. The process of the formation of magnetite could be demonstrated more clearly than for (a). At 100°C a brown precipitate is formed and the upper liquid phase becomes turbid. With temperature rise up to 140°C, the precipitate turns brick red and the contact surface of precipitate with the liquid phase begins to blacken. The thickness of the black layer gradually increases in a downward direction (Fig. 1). At 170°C two distinct phases are formed, *viz.*, an almost colorless, clear upper liquid phase and a compact, black precipitate. The gradual formation of magnetite in two steps, *viz.*, formation of hematite and that of magnetite by the interaction between hematite and the ferrous ion in solution, could be followed.

Solution (c): 0.05M in $FeSO_4 \cdot (NH_4)_2SO_4$ and 0.1M in $FeCl_3$. In contrast to cases (a) and (b), hematite only and no magnetite was obtained. The same formation of hematite as in the autoclaving of $FeCl_3$ solution only takes place.[3] This is in line with the previous results in which no magnetite was formed by the autoclaving of the solutions containing various pairs of ferrous and ferric salts.[4] For the sake of illustration, the results are summarized in a table (Table 1).

3) T. Katsurai and T. Watanabe, *Sci. Papers Inst. Phys. Chem. Research* (Tokyo), **13**, 89 (1930).

4) T. Katsurai, T. Okubo and H. Mikawa, *Kolloid-Z.*, **154**, 56 (1957).

BULLETIN OF THE CHEMICAL SOCIETY OF JAPAN VOL. 43 3308—3309 (1970)

Far Infrared Spectra of Glucose and Saccharose

Masakazu HINENO and Hiroshi YOSHINAGA

Department of Applied Physics, Faculty of Engineering, Osaka University, Osaka

(Received June 13, 1970)

Infrared spectra of sugars have been measured and internal vibrations in the ring have been analysed by Barker *et al.*[1] However, the observed spectra are limited to the mid-infrared region down to 400 cm^{-1}. Absorption bands caused by inter-ring interactions are expected to appear in the far infrared region. To obtain information about inter-ring interactions glucose and saccharose seem to be suitable compounds as considered from their structural formulae. In this note far infrared absorption spectra of glucose and saccharose are reported.

Samples were powdered and suspended in the Nujol null, and were then inserted between thin polyethylene sheets. The samples were checked by measuring infrared absorption spectra from 4000 to 400 cm^{-1}.

Far infrared spectra were measured in the region from 500 to 50 cm^{-1} by using a vacuum single beam grating spectrometer constructed in our laboratory.[2] The results are shown in Figs. 1 and 2. In order to determine the wavenumbers of the far infrared bands precisely, the scale of the logarithm in wavelength is used in the spectral chart of this

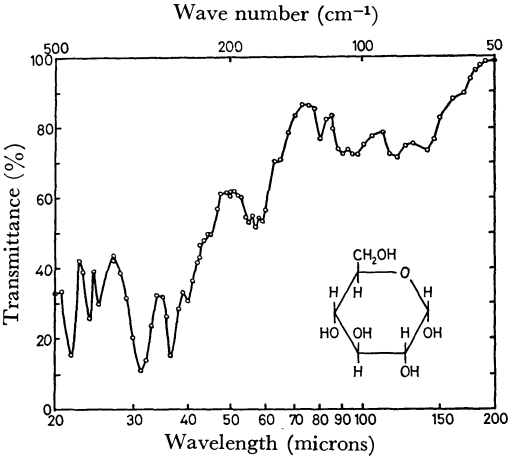

Fig. 1. Far infrared absorption spectrum of glucose in the region from 500 to 50 cm^{-1}.

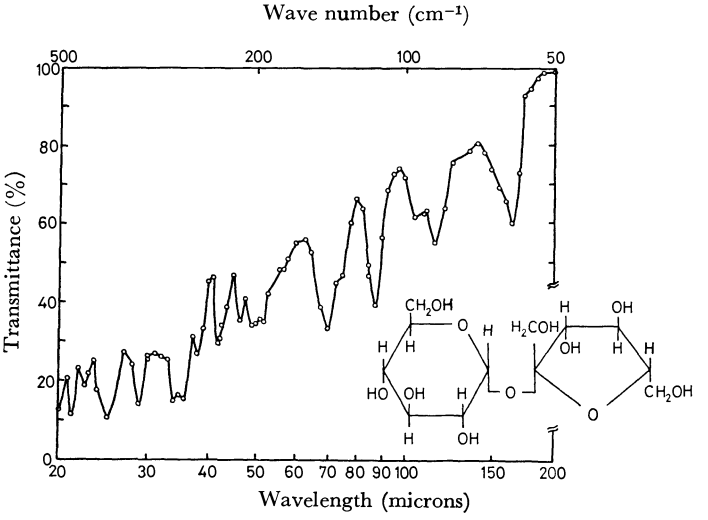

Fig. 2. Far infrared absorption spectrum of saccharose in the region from 500 to 50 cm^{-1}.

1) S. A. Barker, E. J. Bourne, M. Stacey and D. H. Whiffen, *J. Chem. Soc.*, **1954**, 171; S. A. Barker, E. J. Bourne, R. Stephens and D. H. Whiffen, *ibid.*, **1954**, 3468; S. A. Barker, E. J. Bourne, R. Stephens and D. H. Whiffen, *ibid.*, **1954**, 4211; S. A. Barker and R. Stephens, *ibid.*, **1954**, 4550.

2) H. Yoshinaga, S. Fujita, S. Minami, A. Mitsuishi, R. A. Oetjen and Y. Yamada, *J. Opt. Soc. Amer.*, **48**, 315 (1958).

TABLE 1. FAR INFRARED ABSORPTION BANDS OF GLUCOSE AND SACCHAROSE

Glucose cm^{-1} (μm)				Saccharose cm^{-1} (μm)			
459	(21.8) (m)	113	(88.1) (w)	472	(21.2) (m)	215	(46.5) (w)
420	(23.8) (m)	106	(93.9) (w)	444	(22.5) (w)	204	(49.0) (w)
400	(25.0) (m)	84.0	(119) (w)	401	(24.9) (s)	195	(51.3) (w)
320	(31.3) (s)	70.7	(141) (w)	345	(29.0) (m)	143	(70.0) (s)
274	(36.5) (s)			294	(34.0)(m)	114	(87.4) (s)
250	(40.0) (w)			280	(35.7) (m)	94.8	(106) (m)
175	(57.0) (m)			263	(38.0) (w)	87.0	(115) (s)
124	(80.9) (m)			235	(42.5) (m)	61.0	(164) (s)

(s), (m), and (w) indicate strong, medium, and weak in relative intensity, respectively.

spectrometer. In this measurement interference fringes which cause trouble to find weak absorption bands were not observed.

Observed bands of glucose and saccharose are listed in Table 1. Strong absorption bands which are observed in the region below 100 cm^{-1} may arise from inter-ring modes. It is considered that absorption bands of 87.0 and 61.0 cm^{-1} are caused by inter-ring deformation modes such as twisting and bending vibrations between two rings of saccharose, because the bands appear in saccharose but not in glucose.

BULLETIN OF THE CHEMICAL SOCIETY OF JAPAN VOL. 43 3309—3310 (1970)

Reactions of Group IV Organometallic Compounds. XXI.[1] Addition and Decomposition Reactions of Arenesulfonyl Iso(thio)-cyanates with Trimethylsilyl Ethyl Sulfide and Bis(trimethylsilyl) Sulfide

Kenji Itoh, Nobukatsu Kato and Yoshio Ishii

Department of Synthetic Chemistry, Faculty of Engineering, Nagoya University, Chikusa, Nagoya

(Received June 16, 1970)

In our previous report,[1] the addition reactions of arenesulfonyl isocyanates with trimethylsilylamines or *N*-methyldisilazane were found to occur exothermically at room temperature, giving the 1 : 1 adducts quantitatively, along with the pyrolysis results (150°C, 72 hr) of these adducts, as is shown in Eq. (1).

$$p\text{-X-C}_6\text{H}_4\text{SO}_2\text{-N=C=O} + (\text{Me}_3\text{Si})_2\text{NMe} \longrightarrow$$

$$p\text{-X-C}_6\text{H}_4\text{SO}_2\text{-N(SiMe}_3\text{)-C=O} \xrightarrow{\Delta}$$

$$\text{Me}_3\text{Si-NMe}$$

$$p\text{-X-C}_6\text{H}_4\text{SO}_2\text{N(SiMe}_3\text{)}_2 + \text{Me-N=C=O} \quad (1)$$

In continuation of the paper,[1] this note deals with new reactions between arenesulfonyl isocyanates or isothiocyanates and trimethylsilyl ethyl sulfide or bis(trimethylsilyl) sulfide. Formerly, we found that in the case of the reaction between phenyl isocyanate and bis(trimethylsilyl) sulfide,[2] it was necessary to heat the mixture at 80°C for 24 hr to give the 1 : 1 aduct in 80% yield, due to relatively low reactivity of bis(trimethylsilyl) sulfide.

Results and Discussion

The equimolar mixtures of *p*-X-substituted benzenesulfonyl isocyanate (X=H, Me and Cl) and trimethylsilyl ethyl sulfide were allowed to react at 30—40°C in glass ampoules, and the characteristic absorption at 2240 cm^{-1} ($\nu_{SO_2N=C=O}$) in their IR spectra disappeared completely after ten days. The adducts were thermally unstable and were readily decomposed into starting compounds when heated above 80°C on vacuum distillation (Eq. (2)).

1) Part XX of this series: K. Itoh, N. Kato and Y. Ishii, *J. Organometal. Chem.*, **22**, 49 (1970).

2) K. Itoh, K. Matsuzaki and Y. Ishii, *J. Chem. Soc., C*, **1968**, 2709.

$$p\text{-X-C}_6\text{H}_4\text{SO}_2\text{-N=C=O} + \text{Me}_3\text{Si-SEt} \xrightarrow[80°\text{C}]{30—40°\text{C, 10 days}}$$

Ia—c

(Ia X=H, b X=Me, c X=Cl)

$$p\text{-X-C}_6\text{H}_4\text{SO}_2\text{-N(SiMe}_3\text{)-CO-SEt} \quad (2)$$

IIa—c

These adducts (IIa—c) could be obtained solely as residues by distilling off the unreacted starting compounds under 0.03 mmHg, and their IR and NMR spectral data are shown in Experimental. In the case of the reaction with phenyl isocyanate,[2] rather drastic conditions (80°C, 80 hr) was necessary and the 1 : 1 adduct could be isolated on vacuum distillation. The reaction of Me_3SiNEt_2 with benzoyl isocyanate took place at 80°C for 24 hr, giving the 1 : 1 adduct, bp 72—79°C/0.002 mmHg.[3]

On the other hand, the reactions of arenesulfonyl isocyates (Ia—c) with bis(trimethylsilyl) sulfide did not occur at 30—40°C. These reactions did take place when the equimolar mixtures were heated at 110—120°C for 16 hr in glass ampoules filled with dry argon gas. However, the obtained were *N,N*-bis(trimethylsilyl) arenesulfonamides (IIIa—c) and carbonyl sulfide, which are the decomposition products of the 1 : 1 adducts (Eq. (3)).

$$p\text{-X-C}_6\text{H}_4\text{SO}_2\text{-N=C=O} + (\text{Me}_3\text{Si})_2\text{S} \longrightarrow$$

Ia—c

$$\left[p\text{-X-C}_6\text{H}_4\text{SO}_2\text{-N(SiMe}_3\text{)-C(=O)-S-SiMe}_3 \right] \longrightarrow$$

$$p\text{-X-C}_6\text{H}_4\text{SO}_2\text{N(SiMe}_3\text{)}_2 + \text{COS} \quad (3)$$

IIIa—c

We tried to isolate the 1 : 1 adducts under various conditions, but in vain. Bp and yields of IIIa—c are shown in Experimental.

On the other hand, the reaction of phenyl isocyanate with bis(trimethylsilyl) sulfide occurred at 80°C for 24 hr to give a colorless needle-like crystalline 1 : 1 adduct (mp 54°C) in 79% yield.

The reactions between benzenesulfonyl or *p*-toluenesulfonyl isothiocyanate (IVa, b) and bis-(trimethylsilyl) sulfide were quite similar to those reactions as are formulated in Eq. (3). The products obtained were *N,N*-bis(trimethylsilyl)arenesulfonamides (IIIa, b) and carbon disulfide (Eq. (4)).

$$p\text{-X-C}_6\text{H}_4\text{SO}_2\text{-N=C=S} + (\text{Me}_3\text{Si})_2\text{S} \longrightarrow$$

IVa, b

(IVa X=H, b X=Me)

$$\left[p\text{-X-C}_6\text{H}_4\text{SO}_2\text{-N(SiMe}_3\text{)-C(=S)-S-SiMe}_3 \right] \longrightarrow$$

$$p\text{-X-C}_6\text{H}_4\text{SO}_2\text{N(SiMe}_3\text{)}_2 + \text{CS}_2 \quad (4)$$

IIIa b,

In conclusion, the results obtained in this note and in the previous paper[1] confirmed the enhanced acceptor power of arenesulfonyl isocyanate, due to the electron-withdrawing property of sulfonyl group, compared with phenyl of benzyl isocyanate.

3) I. Matsuda, K. Jinda, K. Itoh and Y. Ishii, unpublished results.

Experimental

Three arenesulfonyl isocyanates and two isothiocyanates were prepared as described in the previous paper.[1] IR and NMR spectra were measured using Nippon-Bunko IR-S and JEOL Minimar MH-60, respectively. Microanalyses were carried out with Yanagimoto apparatus.

Ethylthiol Ester of *N*-(Benzenesulfonyl)-*N*-trimethylsilyl Carbamate (IIa). The mixture of 10 mmol of benzenesulfonyl isocyanate and 10.5 mmol of trimethylsilyl ethyl sulfide was heated at 30—40°C for ten days. Then, the reaction product showed no ν_{SO_2NCO} absorption at 2240 cm^{-1} in IR spectrum, and was evacuated under 0.03 mmHg to remove unreacted starting compounds. The adduct IIa had IR (CCl_4) cm^{-1}: 1710 (CO), 1360 (SO_2, as), 1185 (SO_2, s) and 1253 ($SiMe_3$) and NMR (CCl_4) τ: 9.70 (s, Me_3Si), 8.72 (t, CH_3), 7.12 (q, CH_2) and 2.25—2.88 (C_6H_5).

Ethylthiol Ester of *N*-(*p*-Toluenesulfonyl)-*N*-trimethylsilyl Carbamate (IIb). The reaction was carried out analogously as was described above. The adduct IIb had IR (CCl_4) cm^{-1}: 1710 (CO), 1360 (SO_2, as), 1177 (SO_2, s) and 1250 ($SiMe_3$) and NMR (CCl_4) τ: 9.70 (s, Me_3Si), 8.72 (t, CH_3), 7.60 (s, *p*-CH_3), 7.12 (q, CH_2) and 2.25—2.89 (C_6H_4).

Ethylthiol Ester of *N*-(*p*-Chlorobenzenesulfonyl)-*N*-trimethylsilyl Carbamate (IIc). IIc had IR (CCl_4) cm^{-1}: 1710 (CO), 1360 (SO_2, as), 1180 (SO_2, s) and 1252 ($SiMe_3$) and NMR (CCl_4) τ: 9.70 (s, Me_3Si), 8.72 (t, CH_3), 7.12 (q, CH_2) and 2.25—2.88 (C_6H_4).

Reactions of Bis(trimethylsilyl) Sulfide with Three *p*-X-Benzenesulfonyl Isocyanates (Ia—c). The equimolar amounts of $(Me_3Si)_2S$ (0.50—0.52 g) and *p*-X-substituted benzenesulfonyl isocyanate (0.50—0.52 g) were allowed to react at 110—120°C for 1 hr in glass ampoules filled with argon. The products obtained were the pyrolysis products of the 1 : 1 adducts, *i.e.*, *N,N*-bis(trimethylsilyl)arenesulfonamides (IIIa—c) and COS. The bp and yields of IIIa—c were as follows: IIIa (X=H) 106—110°C/0.35 mmHg, 79%; IIIb (X=Me) 121—122°C/0.4 mmHg, 72%; IIIc (X=Cl) 120—122°C/0.5 mmHg, 61%. The other product, COS, was confirmed by its characteristic IR absorption at 2030 cm^{-1} (CCl_4). IIIa—c were identified by their IR and NMR spectral data (which were reported in our previous paper[1]), together with the confirmation of mixed mp and IR spectra of their hydrolysis products.

Reactions of Bis(trimethylsilyl) Sulfide with Benzenesulfonyl Isothiocyanate (IVa) or *p*-Toluenesulfonyl Isothiocyanate (IVb). The equimolar amount of benzenesulfonyl isothiocyanate (IVa) 0.52 g and bis(trimethylsilyl) sulfide 0.46 g were heated in a glass ampoule filled with argon gas at 110—120°C for 16 hr. The products obtained were *N,N*-bis(trimethylsilyl)benzenesulfonamide (IIIa) and CS_2 in 60% and 55% yields, respectively.

The reaction of *p*-toluenesulfonyl isothiocyanate (IVb) with bis(trimethylsilyl) sulfide at 110—120°C for 16 hr gave *N,N*-bis(trimethylsilyl)-*p*-toluenesulfonamide (IIIb) and CS_2 in 55% and 61% yield, respectively.

These products IIIa and IIIb coincided completely with those products obtained in the reactions between $(Me_3Si)_2S$ and Ia or Ib.

BULLETIN OF THE CHEMICAL SOCIETY OF JAPAN VOL. 43 3311—3312 (1970)

The Synthesis of Desmethylencecalin

Mitsuru NAKAYAMA, Mikoto OHNO, Shûichi HAYASHI and Kenji FUKUI

Department of Chemistry, Faculty of Science, Hiroshima University, Higashisenda-machi, Hiroshima

(Received July 3, 1970)

Recently, desmethylencecalin[1] (eupatoriochromene)[2] was isolated along with several acetophenone derivatives from the roots of *Helianthella uniflora* and some *Eupatorium* species. Its structure was identified as 6-acetyl-7-hydroxy-2,2-dimethyl-2H-chromene (I) on the basis of the spectral evidence.[1,2] Encecalin (methyl ether of I) (II) was also isolated from *Encelia californica*.[3]

The present paper will describe the synthesis of I from 7-hydroxy-2,2-dimethylchroman (III) *via* the corresponding acetophenone (IV).

The Hoesch reaction of III[4] with acetonitrile afforded a hydroxy-acetophenone derivative, which was then easily converted into an acetate and may be expected to have one of two structures (IV or V). The NMR spectrum of the acetophenone shows two proton signals, at δ 7.50 and 6.35 ppm (each 1H, singlet) (para positions at C-5 and C-8 on the aromatic ring). Therefore, it can be formulated as 6-acetyl-7-hydroxy-2,2-dimethylchroman (IV). The dehydrogenation of IV with 2,3-dichloro-5,6-dicyano-*p*-quinone in anhydrous benzene gave the desired chromen I. Then, the I was easily converted into acetate (VI) and methyl ether (II) by the usual methods.

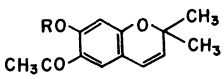

I R = H

II R = CH_3

VI R = CH_3CO

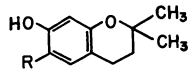

III R = H

IV R = $COCH_3$

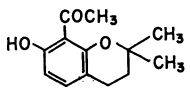

V

The properties of the synthetic I and II were superimposable upon those recorded for natural desmethylencecalin and encecalin.[1-3]

Experimental*1

6-Acetyl-7-hydroxy-2,2-dimethylchroman (IV). A mixture of III[4] (2.0 g), acetonitrile (0.7 g), and anhydrous zinc chloride in anhydrous ether (50 m*l*) was saturated with dried hydrogen chloride in an ice bath and then allowed to stand for 24 hr. After the ether layer had been decanted, the ketimine hydrochloride was washed with anhydrous ether and then hydrolyzed with water (100 m*l*) on a steam bath for 1 hr. The precipitates were then collected and recrystallized from methanol to give IV as colorless plates; mp 119.5—120°C; yield, 0.6 g (24%). IR: 1649 (C=O) cm^{-1}. UV: λ_{max} mμ (log ε); 236 (3.98), 242_{sh} (3.93),*2 283 (4.18), 327 (3.85). NMR: 1.36_s (6H) ($(CH_3)_2C<$); 1.82_t, 2.76_t (each 2H, J=7.0 Hz) ($-CH_2-CH_2-$); 2.54_s (3H) (CH_3COC); 6.35_s (C_8–H); 7.50_s (C_5–H); 12.38_s (OH).

Found: C, 70.80; H, 7.43%. Calcd for $C_{13}H_{16}O_3$: C, 70.89; H, 7.32%.

Acetate. Mp 141.5—142°C (colorless needles from ethanol). IR: 1768, 1671 (C=O) cm^{-1}. UV: λ_{max} mμ (log ε); 230 (4.17), 275 (4.16). NMR: 1.36_s (6H) ($(CH_3)_2C<$); 1.83_t, 2.80_t (each 2H, J=7.0 Hz) ($-CH_2-CH_2-$); 2.34_s (3H) (CH_3COO); 2.49_s (3H) (CH_3COC); 6.52_s (C_8–H); 7.67_s (C_5–H).

Found: C, 68.76; H, 6.83%. Calcd for $C_{15}H_{18}O_4$: C, 68.68; H, 6.92%.

Desmethylencecalin (6-Acetyl-7-hydroxy-2,2-dimethyl-2H-chromene) (I). A mixture of IV (0.1 g) and DDQ (0.1 g) in anhydrous benzene (30 m*l*) was refluxed for 1.5 hr. After the solution had then been cooled, the precipitated hydroquinone derivative was filtered off and the solvent was removed as far as possible. The chromatography of the resulting viscous oil on silica gel (8 g) with benzene gave a pale yellow solid, a soild which crystallized from ethanol as pale yellow needles,

*1 The melting points are uncorrected. The infrared spectra were measured in Nujol, while the ultraviolet spectra were measured in an ethanol solution. The NMR spectra were measured with a Hitachi R-20 spectrometer (60 MHz), using tetramethylsilane as the internal standard (δ-value in $CDCl_3$): s, singlet; d, doublet; t, triplet. The mass spectra were measured with a Hiatchi RMS-4 mass spectrometer.

*2 sh=shoulder.

1) F. Bohlmann and M. Grenz, *Chem. Ber.*, **103**, 90 (1970).

2) T. Anthonsen, *Acta Chem. Scand.*, **24**, (1970), in press.

3) L. F. Bjeldanes and T. A. Geissman, *Phytochem.*, **8**, 1293 (1970).

4) W. Bridge, A. J. Crocker, T. Cubin and A. Robertson, *J. Chem. Soc.*, **1937**, 1530.

I; mp 80.5—81°C (lit, mp 77°C,[1] mp 76°C[2]); yield, 54 mg (54%). IR: 1650 (C=O) cm^{-1}. UV: λ_{max} mμ (log ε); 234.5 (3.95), 257.5 (4.23). NMR: 1.44$_s$ (6H) ($(CH_3)_2C<$); 2.54$_s$ (3H) (CH_3COC); 5.59$_d$, 6.32$_d$ (J=10 Hz) (–CH=CH–); 6.37$_s$ (C_8–H); 7.38$_s$ (C_5–H); 12.78$_s$ (OH). MS: M^+ *m/e* 218.

Found: C, 71.57; H, 6.44%. Calcd for $C_{13}H_{14}O_3$: C, 71.54; H, 6.47%.

Acetate (VI). Mp 80—81.5°C (colorless needles from ethanol). IR: 1768, 1685 (C=O) cm^{-1}. UV: λ_{max} mμ (log ε); 251.5 (4.55), 300 (4.12). NMR: 1.46$_s$ (6H) ($(CH_3)_2C<$); 2.34$_s$ (3H) (CH_3COO); 2.50$_s$ (3H) (CH_3–COC); 5.64$_d$, 6.36$_d$ (J=10 Hz) (–CH=CH–); 6.51$_s$ (C_8–H); 7.53$_s$ (C_5–H).

Found: C, 68.95; H, 6.23%. Calcd for $C_{15}H_{16}O_4$: C, 69.21; H, 6.20%.

Methyl Ether (II). Viscous oil. IR: 1675 (C=O) cm^{-1}. UV: λ_{max} mμ (log ε); 255 (4.43), 335 (3.77). NMR: 1.44$_s$ (6H) ($(CH_3)_2C<$); 2.56$_s$ (3H) (CH_3COC); 3.87$_s$ (3H) (CH_3O); 5.52$_d$, 6.34$_d$ (J=10 Hz) (–CH=CH–); 6.41$_s$ (C_8–H); 7.57$_s$ (C_5–H). MS: M^+ *m/e* 232. Oxime; mp 137—138°C (lit,[3] mp 140°C).

BULLETIN OF THE CHEMICAL SOCIETY OF JAPAN VOL. 43 3312—3313 (1970)

Organophosphorus Compounds. XI. Action of Trialkyl Phosphites on *p*-Quinoneimines

M. M. SIDKY and M. F. ZAYED

National Research Centre, Dokki, Cairo, U.A.R.

(Received October 20, 1969)

Although the action of trialkyl phosphites on *p*-quinones is well established,[1] their action on *p*-quinoneimines has hitherto not been investigated. We have found that trimethyl phosphite and triethyl phosphite react with *p*-quinoneimines (Ia, b) to give the corresponding phosphoramidate derivatives (IIa—d).

The IR spectrum of IIa, taken as example, revealed the absence of NH absorption and its NMR spectrum showed the following assignments:

(a) $\tau=7.04$ and $\tau=6.76$ (for protons of SO_2CH_3 groups, 2 singlets), (b) $\tau=6.6$ (for N–CH_3 protons, singlet), (c) $\tau=6.2$ (for protons of $P(O)(OCH_3)_2$ groups, doublet with $J_{HP}=11.4$ Hz), (d) $\tau=2.63$ (for aromatic protons, singlet). The integration ratio is 6 : 3 : 6 : 4.

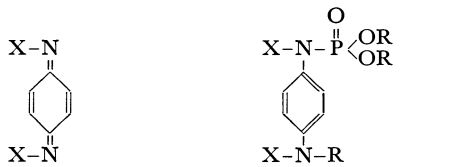

Ia, X=SO_2CH_3
b, X=$SO_2C_6H_5$
c, X=COC_6H_5

IIa, R=CH_3; X=SO_2CH_3
b, R=C_2H_5; X=SO_2CH_3
c, R=CH_3; X=$SO_2C_6H_5$
d, R=C_2H_5; X=$SO_2C_6H_5$

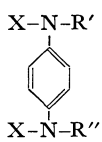

IIIa, R′=X=H; R″=CH_3
b, R′=H; R″=CH_3; X=SO_2CH_3
c, R′=R″=CH_3; X=SO_2CH_3
d, R′=R″=H; X=$SO_2C_6H_5$
e, R′=R″=H; X=COC_6H_5

Adduct IIa, when treated with alcoholic alkali yielded IIIb. The identity of the latter compound was established by an unequivocal synthesis, namely by the methanesulphonylation of *N*-methyl-*p*-phenylenediamine (IIIa) in pyridine. Compound IIIb reacted with diazomethane to give IIIc, in contrast to compound IIa which is stable towards this reagent. When treated with concd. H_2SO_4, IIIb afforded IIIa. This reaction represents a new route for the preparation of *N*-alkyl-*p*-phenylenediamines when the adducts II are subjected to hydrolysis.

From the above results, it appears that *p*-quinoneimines (Ia, b) add trimethyl and/or triethyl phosphite in a 1 : 6 pattern with the creation of a new phosphorus-nitrogen bond, in a similar way to that for *p*-quinones[1] where a phosphorus-oxygen bond is likewise formed.

Quinoneimine Ic is reduced mainly to *p*-phenylenedibenzamide (IIIe), when treated with trialkyl phosphites under similar conditions. This disparity in behaviour of quinones Ia, b on the one hand and Ic on the other towards trialkyl phosphites is in accord with the differences in their behaviour towards a number of various reagents.[2]

1) F. Ramirez and S. Dershowitz, *J. Amer. Chem. Soc.*, **81**, 587 (1959); F. Ramirez, E. H. Chen and S. Dershowitz, *ibid.*, **81**, 4338 (1959); F. Ramirez, O. P. Madan and C. P. Smith, *J. Org. Chem.*, **30**, 2284 (1965); F. Ramirez, O. P. Madan and C. P. Smith, *Tetrahedron*, **22**, 567 (1966).

2) R. Adams and W. Reifschneider, *Bull. Soc. Chim. Fr.*, **1958**, 23.

Experimental

All melting points are uncorrected. The IR spectra were taken as KBr wafers in a Perkin-Elmer 237B Grating Spectrophotometer. The NMR spectra were run in $CDCl_3$ at 60 Mc, with TMS as internal reference.

Dimethyl [*p*-(*N*-Methylmethanesulphonamido)-phenyl](methanesulphonyl)phosphoramidate (IIa). A mixture of Ia[3] (0.001 mol), trimethyl phosphite[4] (0.001 mol) and dry bezene (10 m*l*) was kept under N_2 for 48 hr at 20°C. The crystalline product obtained was filtered and recrystallized from benzene to give IIa as colourless crystals, mp 150—152°C, yield 85%. (Found: C, 34.22; H, 4.91; N, 7.28; P, 7.95; S, 16.50%. Calcd for $C_{11}H_{19}N_2O_7PS_2$: C, 34.19; H, 4.95; N, 7.25; P, 8.01; S, 16.59%.) [IR: 7.81 (P=O),[5] 8.51 and 9.62 μ ($POCH_3$)[5]]

Similarly, triethyl phosphite[4] reacted with quinone Ia (in benzene at reflux for 6 hr) to give IIb as colourless crystals from chloroform - petrolerum ether (bp 40—60°C), mp 142—143°C, yield 80%. (Found: C, 39.21; H, 6.11; N, 6.47; P, 7.15; S, 14.90%. Calcd for $C_{14}H_{25}N_2O_7PS_2$: C, 39.24; H, 5.89; N, 6.53; P, 7.23; S, 14.96%.

***N*-Methyl-*N*,*N*′-dimethanesulphonyl-*p*-phenylenediamine (IIIb).** Compound IIa (0.1 g) was treated with 10% alcoholic NaOH (10 m*l*) and the mixture was refluxed for 6 hr. Alcohol was evaporated and the mixture was cooled and acidified with 10% aq. HCl. The precipitate was filtered off and crystallized from acetic acid to give IIIb as colourless crystals, mp 175—176°C, yield 90%. Compound IIIb proved to be identical (mixed mp), with that obtained by the following procedure: To a cold solution of IIIa[6] (1.2 g) in pyridine (5 m*l*), was added methanesulphonyl chloride (2.3 g) and the reaction mixture was left overnight at room temperature. Acidification with 10% aq. HCl precipitated IIIb, mp 175—176°C (from acetic acid). (Found: C, 38.94; H, 5.16; N, 10.19; S, 23.03%. Calcd for $C_9H_{14}N_2O_4S_2$: C, 38.83; H, 5.07; N, 10.06; S, 23.03%.) [IR: 3.12 μ (N-H)].

***N*-Methyl-*p*-phenylenediamine (IIIa).** A solution of IIIb (0.5 g) in concd. H_2SO_4 (sp. gr. 1.98) was kept at room temperature for 24 hr. The resulting solution was cooled, made alkaline with 15% aq. NaOH, and extracted with two 25 m*l* portions of ether. The combined extracts were dried over $MgSO_4$ (anhydrous) and evaporated to dryness. The oily residue thus formed was crystallized from pentane to give IIIa as colourless crystals, mp 35—36°C.[6]

***N*,*N*′-Dimethyl-*N*,*N*′-dimethanesulphonyl-*p*-phenylenediamine (IIIc).** To a suspension of IIIb (0.1 g) in dry ether (10 m*l*), was added an ethereal solution of diazomethane. Methanol (1 m*l*) was added and the reaction vessel was kept in a refrigerator for 72 hr. The ethereal solution was evaporated and the solid residue thus obtained (*ca.* 90%) was crystallized from acetic acid to give IIIc, mp 220°C, yield 80%. (Found: C, 40.98; H, 5.44; N, 9.49; S, 21.85%. Calcd for $C_{10}H_{16}N_2O_4S_2$: C, 41.07; H, 5.51; N, 9.58; S, 21.93%.) [IR: N-H absent.]

Dimethyl [*p*-(*N*-Methylbenzenesulphonamido)-phenyl](benzenesulphonyl)phosphoramidate (IIc). A mixture of Ib[3] (0.001 mol), trimethyl phosphite (0.001 mol) and dry benzene (10 m*l*) was kept under N_2 at room temperature for 24 hr. The ppt (A) thus formed was filtered. The colourless oil that remained after evaporation of the volatile materials was solidified in a refrigerator. Crystallization from benzene - petroleum ether (bp 40—60°C) gave IIc as colourless crystals, mp 78°C, yield 70%. (Found: C, 49.34; H, 4.49; N, 5.42; P, 6.11; S, 12.51%. Calcd for $C_{21}H_{23}N_2O_7PS_2$: C, 49.40; H, 4.54; N, 5.48; P, 6.07; S, 12.56%.) Spectral characteristics: bands at 7.78 (P=O), 8.55 and 9.62 ($POCH_3$), and 10.1 μ (P–N);[7] a $3H^1$ singlet at 6.88, a $6H^1$ doublet (J_{HP}=11.4 Hz) at 6.25, and a $14H^1$ multiplet at 2.66 τ.

Compound (A) upon recrystallization from acetic acid gave *p*-phenylenedibenzenesulphonamide (IIId),[3] mp 243°C, yield 15%.

IId was obtained similarly, together with a small amount of IIId (*ca.* 10%), by the action of triethyl phosphite on quinone Ib. Compound IId was crystallized from benzene - petroleum ether mp 85°C, yield 60%. (Found: C, 52.10; H, 5.24; N, 5.07; P, 5.59; S, 11.55%. Calcd for $C_{24}H_{29}N_2O_7PS_2$: C, 52.16; H, 5.29; N, 5.07; P, 5.60; S, 11.60%.)

Action of Trimethyl Phosphite on Quinone Ic. To a solution of quinone Ic[8] (0.32 g) in dry benzene (10 m*l*) was added trimethyl phosphite (0.13 g) and the mixture was refluxed for 10 hr. After cooling a colourless crystalline product was separated. It was filtered off, washed with ethanol, dried, crystallized from dimethylformamide and proved to be *p*-phenylenedibenzamide (IIIe), mp 340°C,[8] yield 95%.

3) R. Adams and A. S. Nagarkatti, *J. Amer. Chem. Soc.*, **72**, 4601 (1950).

4) T. Milobendzki and A. Sachnowski, *Chem. Polski*, **15**, 34 (1917); *Chem. Abstr.*, **13**, 2865 (1919); A. H. Ford-Moore and B. J. Perry, Organic Synthese, Vol. 31, p. 111 (1951).

5) L. W. Daasch and D. C. Smith, *Anal. Chem.*, **23**, 853 (1951).

6) A. Bernthsen and A. Goske, *Ber.*, **20**, 924 (1887).

7) N. B. Colthup, L. H. Daly and S. E. Wiberely, "Introduction to Infrared and Raman Spectroscopy," Academic Press, New York (1964), pp. 304, 405.

8) R. Adams and J. L. Anderson, *J. Amer. Chem. Soc.*, **72**, 5154 (1950).

SHORT COMMUNICATIONS

Mechanism of Benzene Formation in the Radiation-Induced and Photochemical Reactions of Acetylene

Shoji SHIDA, Masao TSUKADA, Noboru FUJISAKI and Takefumi OKA

Laboratory of Physical Chemistry, Tokyo Institute of Technology, Meguro-ku, Tokyo

(Received July 17, 1970)

It is known that acetylene polymerizes to give benzene and solid polymers in radiation-induced and photochemical reactions. For the formation of benzene, radical mechanism[1-4] and excited molecule mechanism[5-11] have been proposed, but no decisive conclusion has been reached.

Table 1 shows the distribution of isotopic benzenes formed in equimolar C_2H_2-C_2D_2 mixtures. In mercury photosensitization[10] and direct photolysis,[11] the distribution is almost constant above 20 mmHg of acetylene pressure. In Table 1, distributions for photolyses are given by average values within this pressure range.

The distribution in radiolysis[12] may be regarded as constant within the acetylene pressures applied and is almost the same as that in the mercury-photosensitized reaction and the direct photolysis at 1849 Å.

It has been shown that the distribution could be explained by a modified excited molecule mechanism[10,11] as well as, or more favourably, by the free radical mechanism, for the photolytic reactions.

The results suggests that benzene is formed in the same mechanism irrespective of the kind of active rays. Detailed studies are in progress.

TABLE 1. DISTRIBUTIONS OF ISOTOPIC BENZENES FORMED IN MERCURY PHOTOSENSITIZATION, DIRECT PHOTOLYSIS AT 1849 Å AND THE GAMMA-RAY-INDUCED REACTION OF ACETYLENE

Acetylene initial press. mmHg	Radiolysis							Photolysis	
	20	40	69	105	299	503	Av.	Av.[a]	Av.[b]
C_6H_6	9.5%	9.5%	9.2%	9.0%	9.4%	9.5%	9.4%	9.4%	9.5%
C_6H_5D	6.7	6.7	6.8	6.9	6.4	6.4	6.7	6.5	6.7
$C_6H_4D_2$	28.5	28.6	28.2	28.0	28.8	28.9	28.5	26.6	27.3
$C_6H_3D_3$	12.3	12.3	12.9	13.3	12.1	12.1	12.5	12.2	13.0
$C_6H_2D_4$	28.0	28.0	28.0	27.8	28.2	28.4	28.1	28.4	27.5
C_6HD_5	5.8	5.8	6.0	6.3	5.8	5.7	5.9	6.8	6.6
C_6D_6	9.1	9.0	8.9	8.7	9.3	9.2	9.0	10.3	9.4

a) Photolysis at 1849 Å, see Ref. 11.
b) Mercury photosensitization, see Ref. 10.

1) G. J. Mains, H. Niki and M. H. J. Wijnen, *J. Phys. Chem.*, **67**, 11 (1963).
2) J. H. Futrell and L. W. Sieck, *ibid.*, **69**, 892 (1965).
3) D. J. LeRoy and E.W.R. Steacie, *J. Chem. Phys.*, **12**, 117 (1944).
4) D. J. LeRoy, *ibid.*, **45**, 3482 (1966).
5) L. M. Dorfman and A. C. Wahl, *Radiation Res.*, **10**, 680 (1959).
6) F. H. Field, *J. Phys. Chem.*, **68**, 1039 (1964).
7) M. Zelikoff and L. M. Aschenbrand, *J. Chem. Phys.*, **24**, 1034 (1956).
8) S. Shida, Z. Kuri and T. Furuoya, *ibid.*, **28**, 131 (1958).
9) S. Shida, M. Tsukada and T. Oka, *ibid.*, **45**, 3483 (1966).
10) S. Shida and M. Tsukada, This Bulletin, **43**, 2740 (1970).
11) M. Tsukada and S. Shida, to bepublished in this Bulletin.
12) Isotopic exchange between acetylene and benzene formed was not considered to occur since the radiolysis of C_2H_2-C_6D_6 mixtures gave only C_6H_6.

The Singlet Sensitized Decomposition of Benzoyl Peroxide

Toshio NAKATA and Katsumi TOKUMARU

Department of Chemistry, Faculty of Science, The University of Tokyo, Hongo, Bunkyo-ku, Tokyo

(Received July 17, 1970)

In spite of recent investigations by several groups of workers,[1-5] the mechanism of the photochemical decomposition of benzoyl peroxide remains puzzling. We wish to present clear evidence that irradiation of benzoyl peroxide in benzene in the presence of aromatic hydrocarbons such as chrysene, anthracene, pyrene, naphthalene or phenanthrene, under nitrogen with light of 366 nm or over 300 nm at room temperature leads to the sensitized decomposition of the peroxide (denoted by P) by the added hydrocarbons (denoted by S) in their excited singlet states through the following mechanism.

$$S^*(S_1) + P(S_0) \xrightarrow{k_t} X \quad (1)$$

$$X \xrightarrow{k_r} S(S_0) + \text{Decomposition Fragments} \quad (2)$$

$$X \xrightarrow{k_d'} S(S_0) + P(S_0) \quad (3)$$

Thus, the excited singlet sensitizer, on interaction with the peroxide, forms an exciplex (process 1), which subsequently undergoes either decomposition leading to products (process 2) or deactivation (process 3).

The above mechanism for the singlet sensitization is supported by the following findings. First, the quantum yield of the decomposition of the peroxide (0.02M) in the presence of chrysene or phenanthrene was scarcely reduced by the addition of 1,3-pentadiene. For example, the quantum yield observed with added chrysene (0.0064M) was 0.38 and 0.37 in the absence and in the presence (0.08M) of 1,3-pentadiene, respectively. Secondly, fluorescence of the aforementioned hydrocarbons in benzene was effectively quenched by benzoyl peroxide,*1 obeying the following Stern-Volmer equation: $I_0/I = 1 + k_t\tau_0[P]$, with $k_t\tau_0$ 105, 39, 171 and 160 $mol^{-1}\ l$ for chrysene, anthracene, pyrene and naphthalene respectively, where I_0 and I represent the intensities of the fluorescence of the hydrocarbons in the absence and in the presence of the peroxide in the concentration [P], respectively, and τ_0 denotes the average life time of the excited singlet state in the absence of the peroxide. Thirdly, plots of the reciprocals of the quantum yields for the decomposition of the peroxide (Φ) measured in the presence of a constant concentration(0.007M) of chrysene irradiated with 366 nm light were shown to be linear with the reciprocals of varying concentrations of the peroxide, and were analyzed according to the following Stern-Volmer equation, which is derived from the aforementioned mechanism: $1/\Phi = (1 + k_d'/k_r) \cdot (1 + 1/k_t\tau_0[P]))$. The value for k_d'/k_r was shown to be 0.98 and that for $k_t\tau_0$ to be $1.87 \times 10^2\ mol^{-1}l$. The latter value agrees satisfactorily with the aforementioned value for $k_t\tau_0$, $1.05 \times 10^2\ mol^{-1}l$, obtained from the quenching of the fluorescence of chrysene. Fourthly, the experimental values for $k_t\tau_0$ for the hydrocarbons examined, on being divided by the reported values for τ_0,[6] give the values for k_t in the range of 10^9—$10^{10}\ mol^{-1}l\ sec^{-1}$ (for example, $9.8 \times 10^9\ mol^{-1}l\ sec^{-1}$ for anthracene, with τ_0 reported to be 4×10^{-9} sec[6]), nearly equal to the magnitude of the diffusion-controlled rate constant. The fluorescence spectra of the above hydrocarbons do not overlap with the absorption spectrum of the peroxide, the former being in longer wave length region than the latter. These facts rule out the possibility that the excited singlet hydrocarbon undergoes energy transfer to the peroxide by resonance mechanism[7] or by simple collisional mechanism,[7] therefore supporting the mechanism shown in the above scheme in which the energy transfer takes place through the formation of the exciplex.[7]

The present conclusion together with previous results[1-5] clearly demonstrates that, among sensitizers, aromatic hydrocarbons act in their excited singlet states, and aromatic ketones (if they act at all) in their excited triplet states to sensitize the decomposition of benzoyl peroxide.

*1 Fluorescence was measured without exclusion of atmospheric oxygen, with exciting light of 366 nm except for naphthalene which was excited with 300 nm.

1) T. Nakata, K. Tokumaru and O. Simamura, *Tetrahedron Lett.*, **1967**, 3303.

2) J. C. Bevington and T. D. Lewis, *Trans. Faraday Soc.*, **54**, 1340 (1958).

3) I. N. Vasil'ev and V. A. Krongauz, *Kinet. Katal.* **4**, 204 (1963).

4) C. Walling and M. J. Gibian, *J. Amer. Chem. Soc.*, **87**, 3413 (1965).

5) W. F. Smith, Jr., *Tetrahedron*, **25**, 2071 (1969); W. F. Smith, Jr., and B. W. Rossiter, *ibid.*, **25**, 2059 (1969).

6) The average life times in the aerated condition are taken from I. B. Berlman, "Handbook of Fluorescence Spectra of Aromatic Molecules," Academic Press, New York (1965).

7) For general features of the energy transfer process, see, for example, A. A. Lamola, "Technique of Organic Chemistry," Vol. 14, ed. by P. A. Leermakers and A. Weissberger, Interscience Publishers, New York (1969), p. 17.

Photoionization of *s*-Tetracyanobenzene - Toluene Complex in Its Lowest Excited Singlet State

Hiroshi MASUHARA, Motoo SHIMADA and Noboru MATAGA

Department of Chemistry, Faculty of Engineering Science, Osaka University, Toyonaka, Osaka

(Received July 18, 1970)

The electron donor-acceptor interactions in *s*-tetracyanobenzene (TCNB) - aromatic hydrocarbon complexes in their lowest excited singlet state have been studied in detail by Mataga and Murata[1] by means of fluorescence measurements. They showed clearly that there is a considerable difference in energy as well as structure between the excited Franck-Condon state and equilibrium state. This difference was considered to originate from the large difference between the electronic structures in the ground and excited states of the complex including the surrounding solvent, and the electronic structure in the excited equilibrium state way supposed to be quite polar.

Another useful way for investigating the behaviors of excited EDA complexes might be the measurements of the absorption spectra of these species by means of the laser photolysis method.[2] In this paper, we report the results of measurements on the TCNB-toluene-acetonitrile system. We might expect for this system the ionic dissociation of the complex at the lowest excited singlet state, since the excited complex seems to have a quite polar electronic structure and the radical ions can be stabilized strongly in a polar solvent. Although there are many examples[3] of the ion radical formation in the excited singlet state when the electron donor and the acceptor are not associated with each other in the ground state, we have hardly any results for the photo-excitation of the EDA complex which is stable in the ground state. Moreover, in many cases, the electron transfer reaction, $D^*+A \rightarrow D_s^+ + A_s^-$ or $D+A^* \rightarrow D_s^+ + A_s^-$, in a strongly polar solvent does not seem to proceed *via* the intermediate EDA complex having a definite structure, but occurs due to a very weak interaction in a loose encounter complex.[4] The TCNB-toluene system, though it is a weak complex, seems to have a definite structure. Accordingly, the electron transfer in this system may be considered as a rearrangement relaxation process from the excited Frank-Condon state to the ion-pair state and dissociated ion-radical state. However, the problem whether the electron transfer and ionic dissociation occur at all in the lowest excited singlet state of an EDA complex, when it is excited by light absorption exclusively at the CT band, does not seem to have been elucidated yet. The present study will give a more or less clearcut information on this problem.

We have used a Q-switched ruby laser with an output power of *ca.* 1 J. The exciting light pulse was produced by an ADP frequency doubler with conversion efficiency of about 8%. The light pulse has a duration of 15—20 nsec. The transient absorption spectra were measured photographically or by means of photomultiplier and synchroscope. The laser breakdown sparks produced in O_2 and Xe was used as spectroflashes.

The absorption spectra of the transient species at room temperature obtained by exciting the TCNB-toluene complex to its lowest excited singlet state in acetonitrile solution are very similar to those of the TCNB anion.[5]

Our kinetic analysis showed that the light-induced production of the transient species was completed rapidly(during the time range smaller than a few 10 nsec). Thus, the observed spectra may be ascribed to the dissociated TCNB anion or to the solvated ion-pair A_s^----D_s^+, although it was not possible to identify the transient spectra of toluene cation. It is also possible that the transient spectra are assigned to the excited singlet-singlet absorption of the complex in view of its polar structure in the excited equilibrium singlet state.[1]

In order to identify the transient species, we have measured the photoconductivity induced by laser photolysis.[6] The rise and decay curves of the photoconductivity were practically the same as those of the absorbance of transient spectra. This kinetic relation is an evidence for the ionic dissociation of the complex at the lowest excited singlet state.

1) N. Mataga and Y. Murata, *J. Amer. Chem. Soc.*, **91**, 3144 (1969).

2) J. R. Novak and M. W. Windsor, *Proc. Roy. Soc.*, **A308**, 95 (1968).

3) H. Leonhardt and A. Weller, *Ber. Bunsenges. Phys. Chem.*, **67**, 791 (1963); H. Knibbe, D. Rehm and A. Weller, *ibid.*, **72**, 257 (1698); M. Koizumi and H. Yamashita, *Z. Phys. Chem. N.F.*, **57**, 103 (1968); K. Kawai, N. Yamamoto and H. Tsubomura, This Bulletin, **42**, 369 (1969); T. Okada, H. Oohari and N. Mataga, *ibid.*, in press.

4) N. Mataga and O. Tanimoto, *Theor. Chim. Acta*, **15**, 111 (1969).

5) M. Sofue and S. Nagakura, This Bulletin, **38**, 1048 (1965).

6) Details of the apparatus and measurements on various donor-acceptor systems will be described in a forthcoming paper by A. Taniguchi and N. Mataga.

pH and Temperature Pulses during the Periodic Decomposition of Hydrogen Peroxide

Isao MATSUZAKI,*1 John H. WOODSON*2 and Herman A. LIEBHAFSKY

Department of Chemistry, Texas A & M University, College Station, Texas 77843, U.S.A.

(Received June 1, 1970)

Among the large number of homogeneous, liquid-phase, and non-enzymic reactions only two are so far known to be periodic in nature; they are the decomposition of H_2O_2 by IO_3^- and I_2[1-4] and of malonic acid by Ce^{3+}, Ce^{4+}, and BrO_3^-.[5-7] Owing to their complexity, neither reaction has so far been given a satisfactory mechanism; only one aspect of the former reaction, *i.e.* the periodic change in $[I_2]$ ([ ] means mol/*l*), has been qualitatively reproduced[8] *via* computer for a hypothetical mechanism.

In our reinvestigation[9] of the $IO_3^- - I_2 - H_2O_2$ system, we have found pulses in $[I^-]$ that are closely related to previously discovered pulses[1,3,4] in $[I_2]$ and dO_2/dt (rate of oxygen evolution). We have now succeeded in finding pulses also in pH and in temperature. To find these new pulses, it was necessary to have sensitive measuring instruments and to choose the proper reaction conditions. As evidence for this, we mention that Peard and Cullis,[3] apparently the first to look for pH pulses, failed to find them.

Reaction mixtures (140 cc) consisting of approximately 0.6M KIO_3, 0.052M $HClO_4$, and 0.5M H_2O_2 were subjected to both pH and temperature measurements. The reaction vessel, which was surrounded by a water jacket at 50°C, was equipped as needed with instruments for the measurements. Recording of pH was by means of a glass electrode connected to a mV recorder *via* a digital pH/mV meter. Temperature recording was by means of Cu-constantan thermocouple connected to a mV recorder *via* a microvoltometer. Supplementary measurements of $[I_2]$, pI, and dO_2/dt were made with a spectrophotometer, an iodide selective electrode,[10] and a mass flowmeter, respectively.

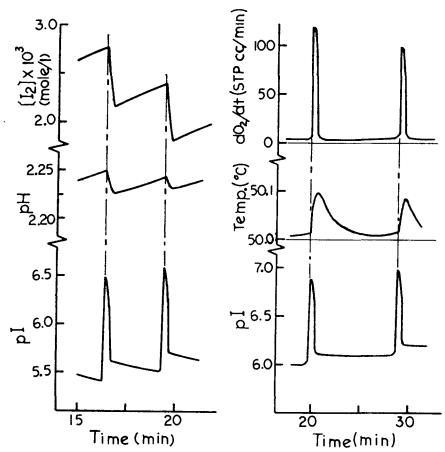

Fig. 1. Pulses in pI, pH, $[I_2]$, temperature, and dO_2/dt. pH pusles were perceptible for the first hour. Replenishment of 0.3M H_2O_2 at time= 150 min resulted in their reappearance at time= 180 min.

Figure 1 shows the observed pulses in pH and temperature and the concomitant pulses in $[I_2]$, pI, and dO_2/dt. Preliminary analysis of the data supports the view that the pH decrease results mainly from the reaction $I_2 + 5H_2O_2 = 2H^+ + 2IO_3^- + 4H_2O$, the incomplete dissociation of HIO_3 being considered. The heat evolved during the temperature pulses appears to result from the reaction just given (responsible for the $[I_2]$ decrease) and from $H_2O_2 = H_2O + \frac{1}{2}O_2$ (responsible for the oxygen evolution). Work is continuing on the relationship of the pulses and their interpretation in terms of known reactions.

*1 On leave from Dept. of Chem., Faculty of Science, Hokkaido Univ., Sapporo, Japan.

*2 Present address: Dept. of Chem., San Diego State College, San Diego, Calif. 92115, U.S.A.

1) W.C. Bray, *J. Amer. Chem. Soc.*, **43**, 1262 (1921).
2) W. C. Bray and H. A. Liebhafsky, *ibid.*, **53**, 38 (1931).
3) M. G. Peard and C. F. Cullis, *Trans. Faraday Soc.*, **47**, 616 (1951).
4) H. Degn, *Acta Chem. Scand.*, **21**, 1057 (1967).
5) B. P. Belousov, Sborn. referat. radiats. med. za 1958, Medgiz, Moscow, 1959.
6) A. M. Zhabotinskij, *Biofizika*, **9**, 306 (1964).
7) H. Degn, *Nature*, **213**, 589 (1967).
8) P. Lindblad and H. Degn, *Acta Chem. Scand.*, **21**, 791 (1967).
9) J. H. Woodson and H. A. Liebhafsky, *Nature*, **224**, 690 (1969).
10) J. H. Woodson and H. A. Liebhafsky, *Anal. Chem.*, **41**, 1894 (1969).

Unusual Solvent Effects on the *ortho*:*para* Ratio in the Chlorination of Anisole*[1]

Kazuyoshi SEGUCHI, Tsutomu ASANO, Akira SERA and Ryozo GOTÔ

Department of Chemistry, Faculty of Science, Kyoto University, Kyoto

(Received June 8, 1970)

In the uncatalyzed molecular chlorination of aromatic compounds, no relationship has been observed between the *ortho*:*para* ratio and the dielectric constants of the media.[1] However, the present authors wish to report an interesting correlation between the dielectric constants of the solvents and the *ortho*:*para* ratios in the chlorination of anisole. Anisole was chlorinated[2] in a series of solvents; the logarithms of the *ortho*:*para* ratios are plotted against $1/\varepsilon$ in Fig. 1.

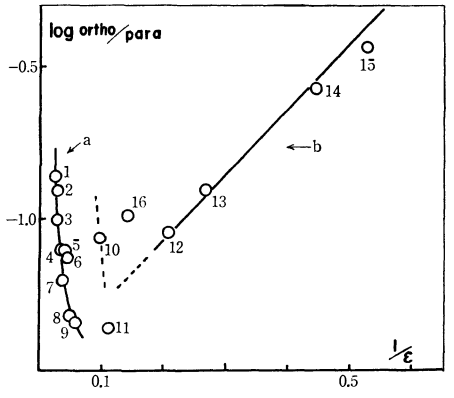

Fig. 1. Plot of log *o*/*p* against $1/\varepsilon$.
a: in alkyl cyanides and nitroalkanes; 1, $MeNO_2$; 2, MeCN; 3, DMF; 4, $EtNO_2$; 5, *iso*-$PrNO_2$; 6, *n*-$PrNO_2$; 7, EtCN; 8, *n*-PrCN; 9, *n*-BuCN.
b: in halogenated hydrocarbons; 10, $(CH_2Cl)_2$; 11, CH_2Cl_2; 12, $CHCl_3$; 13, $CHCl_2CCl_3$; 14, CCl_4; 15, *n*-C_6H_{14}; 16, *s*-BuCl.

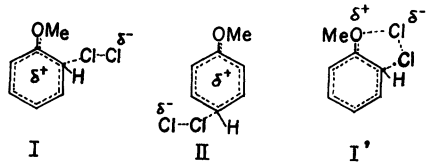

The results show that: (1) in the aprotic media with relatively high dielectric constants, the *ortho*: *para* ratio decreases with a decrease in the dielectric constant, and (2) in the aprotic media with relatively low dielectric constants, the ratio increases unexpectedly with a decrease in the dielectric constant. These results can be interpreted qualitatively in terms of the following two factors; that is, (a) the difference in the solvation of the cationic moiety, $Ar^{\delta+}$, in I and II, and (b) the interaction of $-Cl^{\delta-}$ with $-O^{\delta+}-CH_3$ in the *ortho*-transition state, as in I'. In the chlorination of anisole, the positive charge generated during the activation process will delocalize more extensively in the transition state II than in I. Accordingly, I will be solvated more strongly than II, and the difference in solvation in these two species will become larger with an increase in the polarity of the medium. The observed increase in the *ortho*:*para* ratio with increase in the dielectric constant (curve a) may be mainly ascribable to this difference in solvation between I and II. The effect of pressure on the *ortho*:*para* ratio in aprotic solvents supports this suggestion.[3] The *ortho*:*para* ratios increase with an increase in the pressure in acetonitrile and DMF.[4] This means that the activation volume in *ortho* substitution is smaller than that in *para* substitution ($\delta\Delta V^{\neq} = -1.6 \sim -2.4$ ml/mol[5]). This difference in the activation volumes must result from the difference in solvation between I and II.[6]

On the other hand, the *ortho*: *para* ratio decreases with an increase in the dielectric constants of media in halogenated hydrocarbons (curve b). This fact suggests that, in less polar solvents in this series, an additional stabilization of the *ortho*-transition state arises from an interaction between positively and negatively charged atoms in the molecule (I'). Such stabilization will become less important in more polar solvents. In the medium with a dielectric constant of about 9, the two effects, the difference in the solvation of $Ar^{\delta+}$ and the stabilization by the interaction between $-Cl^{\delta-}$ and $-O^{\delta+}-CH_3$ are balanced and the *ortho*: *para* ratio reaches its minimum value.[7]

*1 Organic Reactions under High Pressure. V.

1) L. M. Stock and A. Himoe, *Tetrahedron Lett.*, No. 13, 9 (1960).

2) The molar ratio of anisole to chlorine was kept at *ca.* 2 in order to prevent disubstitution.

3) Unpublished results.

4) Iodobenzene dichloride was employed as a chlorine source; *cf.* R. M. Keefer and L. J. Andrews, *J. Amer. Chem. Soc.*, **80**, 277 (1958).

5) $\delta\Delta V^{\neq} = \Delta V^{\neq}_{(ortho)} - \Delta V^{\neq}_{(para)}$, at 1 atom.

6) See T. Asano, This Bulletin, **42**, 2005 (1969).

7) Such a minimum was not observed in the chlorination of toluene in halogenated hydrocarbons.[3]

Lilac Alcohol-a and -b, New Naturally Occurring Odorous Ingredients

Seiji WAKAYAMA and Satoshi NAMBA

Chemical Laboratory, Hokkaido University of Education, Sapporo

and Masaji OHNO

Basic Research Laboratory, Toray Industries, Inc., Kamakura

(Received June 16, 1970)

No constituents of lilac flower oil, *Syringa vulgaris* L. are known.[1] We could isolate and identify eighteen constituents from the oil obtained by steam distillation of the concrete (*n*-hexane extract of flowers). The main components which amount to 70 per cent of the oil have been found to be four new stereoisomeric terpene alcohols named lilac alcohol-a, -b, -c, and -d. They have the most exquisite floral fragrance. Lilac alcohol-a and -b have been assigned to the diastereomers of (2R, 5R)-β,5-dimethyl-5-vinyl-2-tetrahydrofuranethanol (I).

Lilac alcohol-a $[\alpha]_D^{25}+15.5°$ ($c=0.515$ in $CHCl_3$) and -b, $[\alpha]_D^{25}-2°$ ($c=0.535$ in $CHCl_3$) have the same molecular formula $C_{10}H_{18}O_2$ (M^+, 170). The close similarity of their spectroscopic evidence such as IR, NMR and MS suggests that they are stereoisomers. The IR spectra show the presence of hydroxy (3520 cm^{-1}) and vinyl group (1640, 990, 920 cm^{-1}), and ether linkage (1015 cm^{-1}). The hydroxyl function has been shown to be primary by a prominent peak at *m/e* 31 (C^+H_2OH), and the presence of tetrahydrofuran ring has been shown by the characteristic α-fission of α-substituted tetrahydrofuran derivatives[2] (*m/e*, 155 ($M-CH_3$)$^+$; 143 [$M-(-CH=CH_2)$]$^+$; 111 [$M-(-CH-Me-CH_2OH)$]$^+$; 43 $CH_3{}^+C=O$). The NMR spectra (Table 1) of lilac alcohol-a and -b are reasonably consistent with the proposed structure (I).

A clear proof of the structure has been achieved by the transformation of lilac alcohols and *trans*-linalool oxide[3,4] (II) into the same derivative as shown below. Hydrogenation of II over Pt followed by acetylation and pyrolysis afforded 5-ethyl-2-isopropenyl-5-methyl-tetrahydrofuran (III), which gave a mixture of diastereomers of 5-ethyl-β,5-dimethyl-2-tetrahydrofuranethanol (IV) by hydroboration. Dihydrolilac alcohol-a and -b obtained by catalytic hydrogenation of I were confirmed to be identical with one diastereomer (Rt, 12.6 min) and another (Rt, 9.8 min) respectively.

TABLE 1. NMR SPECTRAL DATA
(δ in ppm, in $CDCl_3$)*

Lilac alcohol		a	b
s-CH_3		0.94 d $J=6.0$	0.80 d $J=6.0$
t-CH_3		1.31 s	1.30 s
$-CH_2-CH_2-$ $-C-$ $H/\ \backslash CH_3$		1.82m	1.80m
$>C(H)-CH_2OH$		3.66 (ABX)	3.62 (A_2X)
$>C(H)-O-$		4.12m	3.80m
$H_3\backslash\ /H_1$ $C=C$ $/\ \backslash H_2$	H_1* H_2 H_3	4.99 5.17 5.87	5.01 5.19 5.89

* The signals of alcohols appear at 2.96—2.60 δ, depending on the concentration, and typical signals of a vinyl group are observed with $J_{1,2}=1.6$ Hz, $J_{1,3}=8.0$ Hz and $J_{2,3}=18$ Hz.

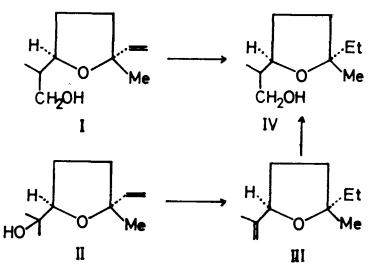

1) E. Guenther, "The Essential Oils," Vol. V, D. Nostrand Company, New York (1952), p. 338; E. Gildemeister, "Die Aetherischen Oele," B. VI, Akademie-Verlag, Berlin (1961), p. 554; W. A. Poucher, "Perfume, Cosmetics and Soaps," Vol. 1, Chapman and Hall Ltd., London (1959), p. 151.

2) H. Budzikiewicz, C. Djerassi and D. H. Williams, "Structure Elucidation of Natural Products by Mass Spectrometry," Vol II, Holden-Day, Inc., San Francisco (1964), p. 270.

3) D. Felix, A. Melera, J. Seibe and E. sz. Kovats, *Helv. Chim. Acta*, **46**, 1513 (1963); *ibid.*, **47**, 918 (1964).

4) E. Klein, H. Farnow and W. Rojahn, *Ann. Chem.*, **675**, 73 (1964).

Functional Group Analysis by Gas Chromatography. III.[1] Pyrolysis of Organic Compounds in Sulfur Vapor

Tadashi HARA and Susumu ITO

Faculty of Engineering, Doshisha University, Kamikyo-ku, Kyoto

(Received July 9, 1970)

Many papers have been published on the reactions between gaseous sulfur and organic compounds.[2] However, they have never been utilized in analytical chemistry. This paper deals with the pyrolysis of organic compounds in sulfur vapor, with special reference to the relationship between the pyrolytic products and functional groups.

Two grams of sulfur was placed in a quartz tube 10 mm dia. × 180 mm (Fig. 1) and melted on the tube wall under helium atmosphere. Either a glass boat or a capillary tube containing 10—30 mg solid or liquid sample was inserted into the reaction tube. The tube was then filled with helium, and heated at 850—880°C by means of a movable electric furnace. The time required for the reaction was about 10 min. The stroke pump was then driven and the sample was gas-chromatogramed under the following conditions: column 2 m, charged with silica gel (60—80 mesh); column temp. 100°C; and carrier gas He, 40 ml/min.

The results are shown in Table 1, and a typical pyrogram of sulfanilic acid in Fig. 2.

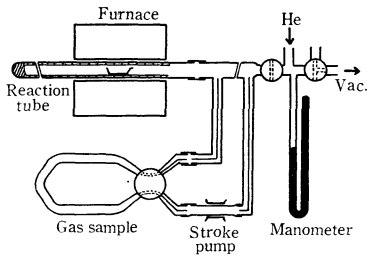

Fig. 1. Apparatus.

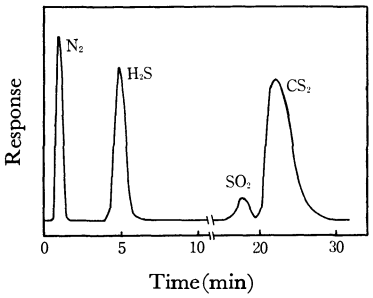

Fig. 2. Pyrogram of sulfanilic acid.

TABLE 1. RELATIONSHIP BETWEEN THE TYPE OF COMPOUND AND PYROLYTIC PRODUCTS

Type of compounds	Compounds	Products found	CO/CO_2 mol ratio
R–COOH	Stearic-, Fumaric-, Cinnamic- and Adipic-acids, Potassium acetate	CO_2 H_2S	
Ar–COOH	Benzoic- and Terephthalic-acids	CS_2	
R–CO–R′	Acetylacetone		>1
R(Ar)–CO–R′	Acetophenone, Benzophenone		<1
(Ring C)=O	Cyclohexanone		<1
Ar–CHO	Benzaldehyde	CO	>1
R(Ar)–O–Ar	Anisol, Diphenyl ether	CO_2	>1
R–COOR′	Ethyl acetate, *n*-Butyl acetate	H_2S	<1
Ar–COOR	Methyl benzoate, Dimethyl terephthalate	CS_2	<1
R–OH	Ethylene glycol, Diethylene glycol, Benzyl alcohol		>1
Ar–OH	Phenol, Hydroquinone, Pyrogallol		<1
Ar–NO_2	Nitrobenzene, 2,4-Dinitrophenylhydrazine	N_2, H_2S, SO_2, CS_2	
R(Ar)–NH_2	Hexamethylenediamine, *o*-, *p*-Phenylenediamines	N_2, H_2S, CS_2	
R(Ar)–CN	Adiponitrile, Phthalonitrile	N_2, H_2S, CS_2	
Ar–SO_3H	Sulfanilic-, Sulfosalicylic-, *m*-Sulfobenzoic- and *p*-Toluenesulfonic acids	(N_2, CO, CO_2), H_2S, SO_2, CS_2	

1) Part II: S. Ito, S. Aikawa and T. Hara, *Nippon Kagaku Zasshi*, **91**, 251 (1970).

2) For example: W. J. Thomas and R. F. Strickland-Constable, *Trans. Faraday Soc.*, **53**, 972 (1957); W. A. Bryce and Sir Cyril Hinschelwood, *J. Chem. Soc.*, **1949**, 3379; C. M. Thacker and E. Miller, *Ind. Eng. Chem.*, **36**, 182 (1944); H. O. Folkins, E. Miller and H. Henning, *ibid.*, **42**, 2202 (1950); G. W. Nabor and J. M. Smith, *ibid.*, **45**, 1272 (1953).

Synthesis and Reactivities of 1-Carbobenzoxy-3-substituted-aziridinones

Muneji MIYOSHI

Chemical Research Laboratory, Tanabe Seiyaku Co., Ltd., Higashiyodogawa-ku, Osaka

(Received July 13, 1970)

Interest in aziridinones has increased since Baumgarten[1] first proved the existence of *N*-*t*-butyl-3-phenylaziridinone by spectral studies. Recently, some analoges were obtained in crystalline forms and their chemical properties were reported.[2-6]

I wish to report a new synthetic route and the reactivities of 1-carbobenzoxy-3-substituted-aziridinones (I) derived from the corresponding carbobenzoxy-L-amino acids (ZAA). Dehydration of ZAA was carried out successfully in THF at −20°C, with the aid of dehydrating agents containing two reactive halogen atoms in the molecule ($COCl_2$, $SOCl_2$, $POCl_3$, *etc.*), and subsequently by dropwise addition of triethylamine (TEA) exactly to neutralize. 1-carbobenzoxy-3-benzylaziridinone (Ia) was obtained as crystalline needles, mp 73.0—73.5°C. $[\alpha]_D^{20}$ −36.0° ($c=1$, THF), mass M^+ 281. NMR ($CDCl_3$, δ): 7.21 (*bs*, 5H), 7.37 (*bs*, 5H), 5.30 (*s*, 2H), 4.55 (*t*, 1H), 3.26 (*dd*, 2H), 3.03 (*dd*, 2H). Found: C, 72.60; H, 5.33; N, 5.11%. Calcd for $C_{17}H_{15}NO_3$: C, 72.58; H, 5.37; N, 4.98%. I showed 1840 cm^{-1} band in IR (Fig. 1) which was characteristic of aziridinones.[1,2]

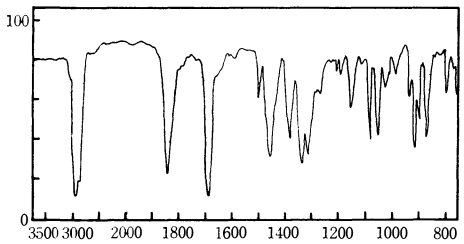

Fig. 1. IR spectrum of Ia.

I was found to be quite sensitive to the nucleophiles and ring opening took place always between N and C=O bond selectively. Typical reactions with I are as follows.

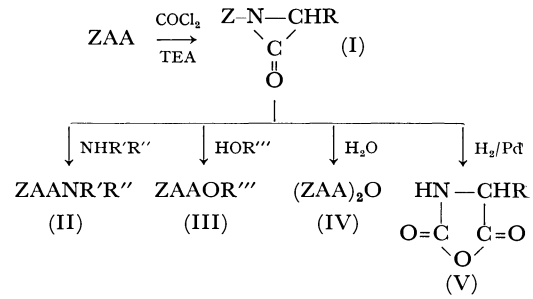

Usually it was convenient for I to be treated directly with the desired nucleophile at −20°C without isolation from the reaction mixture. So far, no racemization has been observed (Table 1).

Table 1. Results of reactions with I

R	Nucleophile	Product	Yield (%)	mp (°C)	$[\alpha]_D^{20}$ ($c=1$)
$CH_2C_6H_5$	H·Gly·OEt	(II)	83.8	111	−16.8 (EtOH)
$CH_2C_6H_5$	$NHCHCO_2CH_3$ $H_3C\ CH(CH_3)_2$	(II)	81.0	81	−70.0 (MeOH)
$CH_2C_6H_5$	*t*-BuOH	(III)	83.3	82	− 6.0 (EtOH)
$CH_2C_6H_5$	H_2O	(IV)	47.2	146	+14.6 (Dioxan)
$CH(CH_3)_2$	H·Gly·OEt	(II)	81.7	164	−27.0 (EtOH)
$CH(CH_3)_2$	MeOH	(III)	81.9	56	−18.9 (MeOH)
$CH(CH_3)_2$	H_2O	(IV)	45.6	98	+10.7 (THF)
CH_3	H·Gly·OEt	(II)	71.1	101	−22.2 (EtOH)
CH_3	H_2O	(IV)	45.2	122	−11.0 (THF)
$CH_2CO_2CH_2C_6H_5$	H·Phe·OMe	(II)	72.4	116	−14.8 (DMF)

1) H. E. Baumgarten, R. L. Zey and U. Krolls, *J. Amer. Chem. Soc.*, **83**, 4469 (1961); H. E. Baumgarten, *ibid.*, **84**, 4975 (1962); H. E. Baumgarten and J. F. Fuerholzer, *ibid.*, **85**, 3303 (1963).

2) J. C. Sheehan and I. Lengyel, *ibid.*, **86**, 1356 (1964); J. C. Sheehan and J. H. Beeson, *ibid.*, **89**, 362 (1967); J. C. Sheehan and M. M. Nafissi-V, *ibid.*, **91**, 1176 (1969).

3) I. Lengyel and D. B. Uliss, *Chem. Commun.*, **1968**, 1621.

4) K. Bott, *Tetrahedron Lett.*, **1968**, 3323.

5) E. R. Talaty and A. E. Dupuy, Jr., *Chem. Commun.*, **1968**, 790; E. R. Talaty and C. M. Utermoehlen, *ibid.*, **1970**, 473.

6) J. C. Sheehan and I. Lengyel, *Angew. Chem.*, **80**, 27 (1968).

A New Protective Group Suitable for Masking Specific Amino Groups during Peptide Synthesis

Shumpei SAKAKIBARA, Tsunehiko FUKUDA, Yasuo KISHIDA and Ichiro HONDA

Peptide Center, Institute for Protein Research, Osaka University, Kita-ku, Osaka

(Received July 14, 1970)

The benzyloxycarbonyl (Z) group is considered to be stable under conditions necessary for the removal of a *t*-butyloxycarbonyl (Boc) group, and a combination of these two protective groups has been widely used in syntheses of lysine-peptides. For instance, N^{α}-Boc-N^{ε}-Z-lysine was used in the solid-phase synthesis of lysine-peptides.[1] However, on the repeated removal of Boc-groups with N HCl/AcOH or with trifluoroacetic acid, a partial cleavage of the ε-Z-groups has been noted, and it has been claimed that the resulting unprotected ε-amino groups cause the branching of the peptide bonds.[2] The present communication is concerned with the use of the diisopropylmethyloxycarbonyl (Dipmoc)-group as a new amino-protecting group. The introducing reagents were synthesized by keeping a mixture of diisopropylcarbinol[3] (0.5 mol) and phosgene (70 m*l*) in tetrahydrofuran (70 m*l*) at −20°C for 3 days. The excess phosgene was removed by evaporation under reduced pressure at room temperature, and the remaining tetrahydrofuran solution was used as the Dipmoc-Cl solution without further purification. Dipmoc-hydrazide was synthesized by a procedure previously used for the synthesis of *t*-amyloxycarbonyl-hydrazide;[4] mp 62.5—64.5°C; yield 78% (Found: N, 15.80%. Calcd: N, 16.08%). The hydrazide was converted to the azide by a method which has been reported before,[4] and this was used without purification. ε-Dipmoc-L-lysine was synthesized with the copper-lysine complex using Dipmoc-Cl or Dipmoc-N_3; the same ε-Dipmoc-L-lysine was thus obtained in a 57—58% yield; mp 198.5—200.5°C (decomp); $[\alpha]_D^{25}$ +22.3° (*c* 1.0, N-HCl) (Found: N, 9.78%. Calcd: N, 9.71%). Z-L-Pro-L-Lys(Dipmoc)-Gly-NH_2 (I) was synthesized by conventional methods; mp 174.5—176.5°C, $[\alpha]_D^{26}$ −39.9° (*c*, 1.0, EtOH). The stability of the protective group against N HCl/AcOH is shown in Fig. 1 in comparison with those of the Z group and of the *p*-chlorobenzyloxycarbonyl [Z(Cl)] group.[5] The Dipmoc-group could be removed completely by treatment with HF[6] in the presence of anisole at 20°C for 60 min. This cleavage was demonstrated with Compound I; L-Pro-L-Lys-Gly-$NH_2 \cdot 2HCl \cdot \frac{1}{2}H_2O$ was thus obtained in a 92.3% yield as an amorphous powder; $[\alpha]_D^{26}$ −40.0° (*c* 1.8, H_2O) (Found: C, 41.25; H, 7.58; N, 17.87%. Calcd: C, 40.94; H, 7.40; N, 18.36%). Thus, the usefulness of this procedure was confirmed.

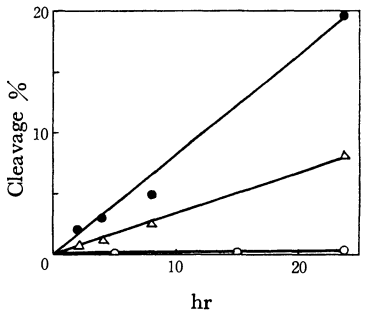

Fig. 1. Cleavage of ε-protective groups of lysine in N HCl-acetic acid at 20°C.
-●- ε-Z-L-Lysine; -△- ε-Z(Cl)-L-Lysine;
-○- ε-Dipmoc-L-Lysine.

1) A. Marglin and R. B. Merrifield, *J. Amer. Chem. Soc.*, **88**, 5051 (1966); B. Gutte and R. B. Merrifield, *ibid.*, **91**, 501 (1969).

2) A. Yaron and S. F. Schlossman, *Biochemistry*, **7**, 2673 (1968).

3) J. B. Conant and A. H. Blatt, *J. Amer. Chem. Soc.*, **51**, 1227 (1929).

4) I. Honda, Y. Shimonishi and S. Sakakibara, This Bulletin, **40**, 2415 (1967).

5) ε-Z(Cl)-L-Lysine was synthesized by the conventional method; mp 255—258°C (decomp), $[\alpha]_D^{16}$ +14.2° (*c* 0.51, 50% AcOH); (Found: N, 8.92%. Calcd: N, 8.90%).

6) S. Sakakibara, Y. Shimonishi, Y. Kishida, M. Okada and H. Sugihara, This Bulletin, **40**, 2164 (1967).

Absorption Spectra of Charge-Transfer Complexes in the Molten State

Jun-ichi AIHARA, Akira SASAKI and Yoshio MATSUNAGA

Department of Chemistry, Faculty of Science, Hokkaido University, Sapporo

(Received July 15, 1970)

Since Mulliken set forth the distinguished charge-transfer theory, a considerable amount of effort has been devoted to explaining the various interactions responsible for the actual charge-transfer complexes.[1,2] However, as previous investigations were interested in the interactions around room temperature for the sake of convenience, our knowledge of the complexes is necessarity confined to those in solution and, to lesser degree, those in the solid state.

In our previous papers, we overcame the experimental difficulties due primarily to the thermal instability of the complexes and succeeded in measuring the gaseous absorption spectra of typical TCNE complexes.[3,4] On the other hand, attempts to detect the liquid-phase complex have been completely lacking. The observation of the spectra in the molten state might be useful for the analysis of the liquid-phase structure.

Recently, we investigated the charge-transfer complexes in the molten state and, for the first time, succeeded in the optical detection of the fused complexes. The absorption spectra were derived from the diffuse reflection spectra. The measurements were made at temperatures considerabley higher than the melting points, using a Beckman DK-2A spectroreflectometer.

We first prepared the *N,N*-dimethylaniline-*s*-trinitrobenzene 1:1 complex from an *N,N*-dimethylaniline solution of *s*-trinitrobenzene. The observation in the liquid phase was made at 150°C, which is higher by 50°C than the melting point of the complex. Figure 1 shows the liquid-phase absorption specrtum of the *N,N*-dimethylaniline-*s*-trinitrobenzene complex. The spectra in the solid state and in the *n*-heptane solution are added for the sake of comparison. In the solid, two characteristic charge-transfer bands were observed at 19300 and at 23300 cm^{-1}. However, the second band was missing in the other phases. The absorption maximum in the molten state was found at 21100 cm^{-1}, which corresponds to a blue shift of 1800 cm^{-1} from that found in the crystal. On the other hand, it was located at 21400 cm^{-1} in the *n*-heptane solution. It can be easily seen therein that, though each band-width is somewhat different, the absorption bands in the liquid phase and in the solution are almost superimposed upon each other. The naphthalene-TCNE complex also has similar tendencies in the liquid-phase spectrum.

It is widely known that, in the crystal, the presence of nearby charge-transfer complexes markedly alters the properties of the isolated complex. The complexes generally from an $\infty:\infty$ complex instead of distinct 1:1 complexes. Though we can expect such situations in the liquid phase, at least in view of the optical absorption, we can not characterize them in the spectra. However, this fact dose not preclude the possibility that interactions inducing such phenomena as the liquid-phase exciton and the quite high conductivity exist in the liquid-phase complexes.[5,6]

We are now continuing to examine other type of charge-transfer complexes in the molten state.

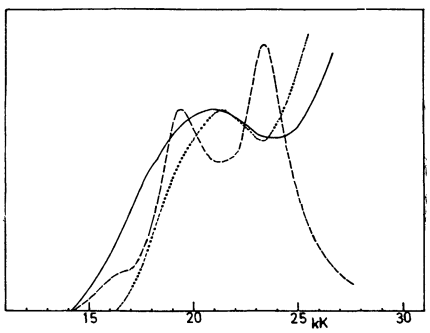

Fig. 1. Absorption spectra of the *N,N*-dimethylaniline-*s*-trinitrobenzene complex in various phases.
—— liquid-phase
------ *n*-heptane solution and
----- solid-state spectra

1) G. Briegleb, "Elektron-Donator-Acceptor-Komplexe," Springer-Verlag, Berlin (1961).

2) L. J. Andrews and R. M. Keefer, "Molecular Complexes in Organic Chemistry," Holden-Day Inc., San Francisco (1964).

3) J. Aihara, M. Tsuda and H. Inokuchi, This Bulletin, **40**, 2460 (1967).

4) J. Aihara, M. Tsuda and H. Inokuchi, *ibid.*, **42**, 1824 (1969).

5) S. A. Rice and J. Jortner, *J. Chem. Phys.*, **44**, 4470 (1966).

6) J. Kommandeur, C. J. Korinek and W. G. Schneider, *Can. J. Chem.*, **36**, 513 (1958).

Transition in Solution of Polyvinyl Acetate in Toluene

Satoru MASHIMO, Yoshio OTSUBO and Keniti HIGASI

School of Science and Engineering, Waseda University, Shinjuku, Tokyo

(Received July 29, 1970)

The dielectric properties of polyvinyl acetate in toluene were studied over a frequency range of 1—150MHz at various temperatures. Molecular weights of the polyvinyl acetate were determined by intrinsic viscosities to be 7900, 17200, 43000, 165000, and 387000. Dielectric measurements[1] on these five samples were carried out at the same concentration, *viz.*, 5% by weight.

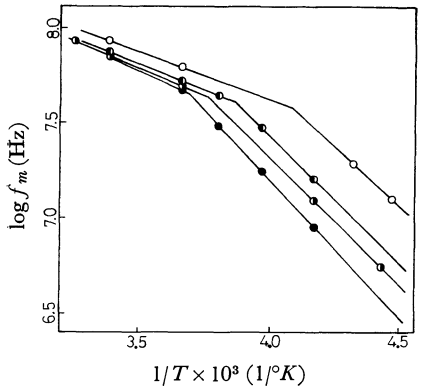

Fig. 1. Plot of $\log f_m$ *vs.* $1/T$.
○: 5%M 7900; ◐: 5%M 17200; ◑: 5%M 43000
●: 5%M 165000, 5%M 387000.

When the logarithm of the frequency of maximum dielectric absorption is plotted against the reciprocal of absolute temperature, two straight lines are obtained (Fig. 1). The point at which two lines intersect is taken tentatively as transition temperature. The apparent activation energy is 2.8 kcal/mol above this temperature, and 6.3 kcal/mol below it. The dielectric behavior of the sample changes at this temperature. This is similar to the transition temperature of solid hydrogen halides[2] or of solid polymers.[3] The values of ε_0, ε_∞ obtained from the Cole-Cole plot change at this temperature; above it Cole's distribution parameter α decreases with increasing temperature, while it remains constant below.

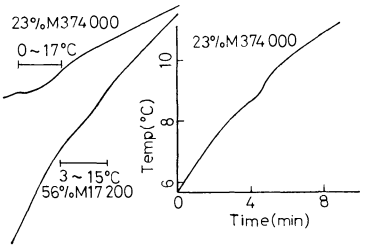

DTA Heating curve

Fig. 2. Results of heat capacity measurements.

The results of differential thermal analysis are shown in Fig. 2. A small but abrupt change of heat capacity could be observed in all the samples having sufficiently high concentrations. The change is detected also in the heating curve (Fig. 2).

The transition temperature determined from heat capacity measurements slightly differs that of dielectric measurement. However, it appears certain that they would approach each other, if the solution of the same concentration could be employed for the two sorts of measurements.

The transition phenomenon thus depends on the concentration and also the molecular weight of the solute. When the transition temperature is plotted against $1/M$, the following equation for a straight line appears to be valid:

$$T_{\text{transition}} = 272 - 2.2 \times 10^5/M \quad (^\circ\text{K}) \qquad (1)$$

This equation is very similar to that between the glass transition temperature T_g and the molecular weight M of polyvinyl acetate in the solid state

$$T_g = 310 - 1.8 \times 10^5/M \quad (^\circ\text{K}) \qquad (2)$$

which is obtained from studies on nuclear magnetic resonance.[4]

1) S. Mashimo and K. Higasi, to be published.
2) S. Havriliak, Jr., and R. H. Cole, *Discuss. Faraday Soc.*, **23**, 78 (1957).
3) S. Saito and T. Nakajima, *J. Appl. Polymer Sci.*, **2**, 2455 (1959).
4) K. Hattori and A. Nojiri, unpublished results. Regarding polystyrene *cf.* T. G. Fox, Jr., and P. J. Flory, *J. Appl. Phys.*, **21**, 581 (1950).

BULLETIN OF THE CHEMICAL SOCIETY OF JAPAN VOL. 43 3325—3331 (1970)

The Crystal and Molecular Structure of Bromoanhydrotetrodoic Lactone Hydrobromide

Akio FURUSAKI, the late Yujiro TOMIIE and Isamu NITTA

Faculty of Science, Kwansei Gakuin University, Nishinomiya

(Received February 26, 1970)

The absolute configuration of bromoanhydrotetrodoic lactone, $C_{11}H_{14}O_7N_3Br$, has been determined on the basis of an X-ray study of its hydrobromide. The crystals are orthorhombic, with four chemical units in a unit cell of these dimensions: $a=10.88\pm0.04$, $b=15.95\pm0.05$, and $c=8.55\pm0.03$ Å; the space group is $P2_12_12_1$. The observations for Bijvoet inequalities were made on equi-inclination integrating Weissenberg photographs taken with Cu$K\alpha$ radiation around the a axis. On the other hand, the calculations were carried out with the parameters at the stage of the R factor of 11.9% and with anomalous dispersion correction of -0.9 for $\Delta f'_{Br}$ and 1.5 for $\Delta f''_{Br}$. The observed and calculated inequalities for ten pairs of reflections were all in agreement with each other, so the absolute configuration was determined without any uncertainty. In addition to the X-ray determination of the absolute configuration mentioned above, the present paper will describe the details of the crystal and molecular structure.

Tetrodotoxin is well-known as a highly poisonous principle of the puffer fish, but, to say nothing of its molecular structure, even its chemical formula remained uncertain till quite recently. In 1964, through independent investigations, Tsuda *et al.*, Hirata *et al.*, and Woodward *et al.* arrived at the same molecular structure for this poison.[1-3] All their results were based on X-ray structure analyses of halogen-containing derivatives of tetrodotoxin.[3-6] In cooperation with the organic chemical investigation by Hirata *et al.*, the structure of one of the derivatives, bromoanhydrotetrodoic lactone hydrobromide, was studied in our laboratory by means of X-ray methods, an outline of the results having already been published at the stage when the R factor was 15.4%.[6] Although very delayed in publication due partly to the unexpected death of one of the authors, Yujiro Tomiie, the present account will describe the X-ray determination of the absolute structure, which had been already reported at the Third International Symposium on the Chemistry of Natural Products held in Kyoto in 1964, and will discuss in detail the molecular and crystal structure thus obtained.

Structure Determination

The crystal data obtained from the oscillation and Weissenberg photographs taken with Cu$K\alpha$ radiation are summarized in Table 1. The crystal structure was elucidated by means of the minimum-function and Fourier methods, using the 1860 structure factors which were obtained from equi-inclination integrating Weissenberg photographs taken around the a and c axes. The approximate atomic coordinates thus obtained were refined at first by the diagonal-matrix least-squares method, assuming isotropic thermal motions for all the atoms, and then by the block-diagonal-matrix least-squares method, assuming anisotropic thermal motions only for the bromine atoms. The latter

Table 1. Crystal data

Formula	$C_{11}H_{14}O_7N_3Br\cdot HBr$
Orthorhombic	$a=10.88\pm0.04$Å
	$b=15.95\pm0.05$
	$c=8.55\pm0.03$
Space Group	$P2_12_12_1$
Z	4
D_m	2.03 g/cm³
D_x	2.06 g/cm³

1) K. Tsuda, S. Ikuma, M. Kawamura, R. Tachikawa, K. Sakai, C. Tamura and O. Amakasu, *Chem. Pharm. Bull.*, **12**, 1357 (1964).

2) T. Goto, Y. Kishi, S. Takahashi and Y. Hirata, *Tetrahedron Lett.*, **1964**, 779.

3) R. B. Woodward, "Special Lectures presented at the Third International Symposium on the Chemistry of Natural Products," ed. by IUPAC (1964), p. 49.

4) K. Tsuda, C. Tamura, R. Tachikawa, K. Sakai, O. Amakasu, M. Kawamura and S. Ikuma, *Chem. Pharm. Bull.*, **11**, 1473 (1963); C. Tamura, O. Amakasu, Y. Sasada and K. Tsuda, *Acta Cryst.*, **21**, 219 (1966).

5) K. Tsuda, C. Tamura, R. Tachikawa, K. Sakai, O. Amakasu, M. Kawamura and S. Ikuma, *Chem. Pharm. Bull.*, **12**, 643 (1964); C. Tamura, O. Amakasu, Y. Sasada and K. Tsuda, *Acta Crystallogr.*, **21**, 226 (1966).

6) Y. Tomiie, A. Furusaki, K. Kasami, N. Yasuoka, K. Miyake, M. Haisa and I. Nitta, *Tetrahedron Lett.*, **1963**, 2102.

Table 2. The final atomic parameters

Atom	x/a	y/b	z/c	B	Atom	x/a	y/b	z/c	B
Br(1)	0.2079	0.1744	0.2944	*	C(2)	−0.1126	0.1345	0.3222	2.29
Br(2)	−0.1065	−0.0752	−0.4579	*	C(4)	−0.0114	0.2161	0.1129	1.97
O(5)	0.2536	0.1175	−0.0839	3.65	C(4a)	0.0963	0.1509	0.1216	2.34
O(6)	−0.0510	0.2097	−0.0427	2.63	C(5)	0.1520	0.1651	−0.0321	2.15
O(7)	0.0675	0.0156	−0.2135	3.04	C(6)	0.0347	0.1588	−0.1323	2.47
O(8)	−0.0588	−0.0461	0.0207	2.95	C(7)	−0.0146	0.0720	−0.1419	2.71
O(9)	0.2305	−0.0112	0.1058	3.37	C(8)	−0.0563	0.0432	0.0153	2.32
O(10)	0.0598	−0.1542	0.0822	5.09	C(8a)	0.0344	0.0634	0.1565	1.84
O(11)	0.1230	0.2674	−0.2987	3.26	C(9)	0.1147	−0.0172	0.1670	2.94
N(1)	−0.0425	0.0720	0.2955	2.99	C(10)	0.0383	−0.0790	0.0745	3.80
N(2)	−0.1944	0.1343	0.4329	3.03	C(11)	0.0461	0.1989	−0.2910	2.67
N(3)	−0.1071	0.2023	0.2215	2.59					

*	B_{11}	B_{22}	B_{33}	B_{12}	B_{23}	B_{31}
Br(1)	0.00532	0.00490	0.00917	−0.00157	−0.00228	−0.00280
Br(2)	0.00661	0.00287	0.01098	−0.00069	−0.00113	0.00132

refinement was carried out using a program devised by Yoshiharu Okaya, IBM Thomas Watson Research Center.*1 Thus, the R factor reached a value of 11.9%. The final atomic parameters are given in Table 2. Tables of the observed and calculated structure factors are preserved by the Chemical Society of Japan.*2

Determination of the Absolute Configuration

The absolute configuration of the present crystal structure was determined by using the anomalous dispersion effects of bromine atoms for Cu$K\alpha$ radiation. For the present point group 222, $|F(h\bar{k}l)|^2$ should be equal to $|F(\bar{h}\bar{k}\bar{l})|^2$ even if the anomalous dispersion effects are taken into account. Accordingly, the intensities of the hkl reflections were compared with those of $h\bar{k}l$ instead of with those of $\bar{h}\bar{k}\bar{l}$ on integrating Weissenberg photographs around the a axis. The observed signs of $\Delta|F(hkl)|^2$'s for ten reflections are listed in Table 3, together with the values calculated, using $\Delta f'_{Br}=-0.9$ and $\Delta f''_{Br}=1.5$, from the final atomic parameters in Table 2. Table 3 clearly shows that the atomic coordinates which have been so far used correspond exactly to the actual absolute configuration.

Table 3. Bijvoet inequalities

h	k	l	$\Delta\|F_o\|^2$	$\Delta\|F_c\|^2$	$\|F_c\|^2$	$\|\Delta\|F_c\|^2/\|F_c\|^2\|$
1	1	5	−	−93	819	0.114
1	2	3	−	−62	396	0.157
1	2	6	−	−76	386	0.197
1	5	5	−	−176	512	0.344
1	9	1	+	+210	1083	0.194
2	1	4	−	−323	1439	0.224
3	9	2	−	−66	231	0.286
3	11	1	−	−131	327	0.401
4	3	5	+	+81	546	0.148
5	3	5	+	+191	1601	0.119

*1 Present address: Department of Chemistry, State University of New York at Stony Brook, Stony Brook, Long Island, N. Y., U. S. A.

*2 The complete data of the F_o-F_c table are kept as Document No. 7006 at the office of the Bulletin of the Chemical Society of Japan. A copy may be secured by citing the document number and by remitting, in advance, ¥500 for photoprints. Pay by check or money order, payable to: The Chemical Society of Japan.

Results and Discussion

Molecular Structure. The framework of the molecular ion of bromoanhydrotetrodoic

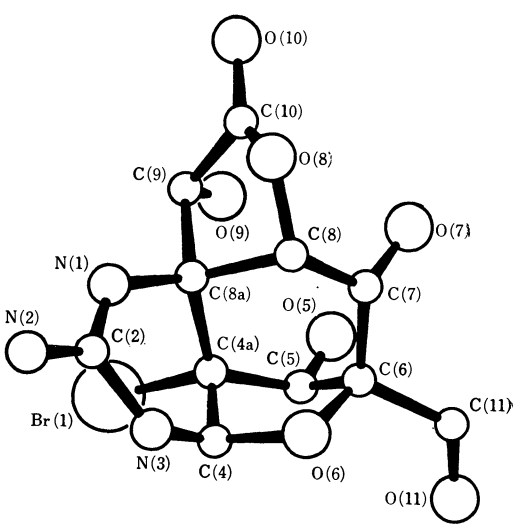

Fig. 1. The framework of the bromoanhydrotetrodoic lactone ion.

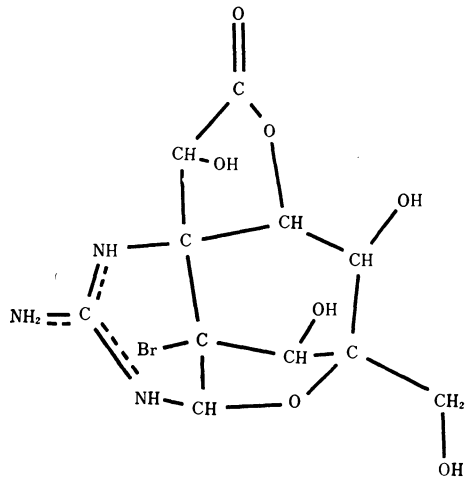

Fig. 2. The structural formula corresponding to Fig. 1.

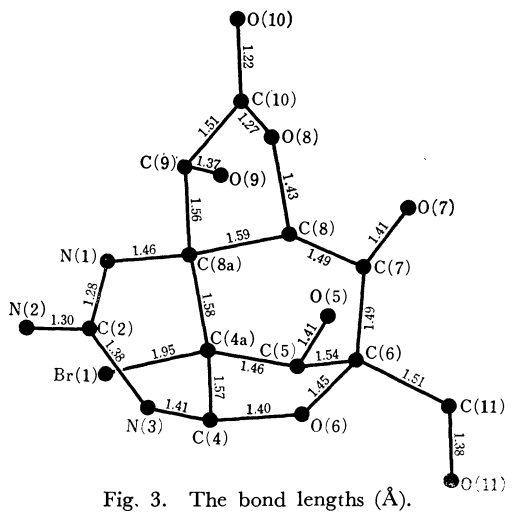

Fig. 3. The bond lengths (Å).

lactone and the corresponding structural formula are shown in Figs. 1 and 2 respectively. The bond lengths and angles calculated from the final atomic coordinates are given, respectively, in Fig. 3 and Table 4. The average standard deviations of the interatomic distances are 0.016 Å for C–Br, 0.021 Å for C–O, 0.022 Å for C–N, and 0.023 Å for C–C. Considering these standard deviations, the molecular dimensions calculated are all reasonable, except for the C(10)–C(8) bond distance (1.27 Å).

The skeleton of the present molecular ion is composed of two six-membered and two five-membered rings. One of the first two rings is heterocyclic, with two nitrogen atoms of a guanidinium group, while the other is homocyclic, with a somewhat distorted chair form. These two rings are joined to each other in the *cis* configuration. On the other hand, both of the five-membered rings are heterocyclic; one of them is a γ-lactone ring attached in the *cis* configuration to the second of the six-membered rings mentioned above, while the other contains an ethereal oxygen atom which bridges, additionally, the two fused six-membered rings. Since, moreover, a bromine atom, a hydroxymethyl group, and three hydroxyl groups are connected to the skeleton, the molecular ion assumes quite a complicated stereostructure and includes very close interatomic contacts. Such intramolecular contacts are listed in Table 5, together with the distances.

Table 4. The bond angles (°)

N(1)-C(2)-N(2)	122	C(6)-C(7)-O(7)	113
N(1)-C(2)-N(3)	118	C(8)-C(7)-O(7)	113
N(2)-C(2)-N(3)	119	C(7)-C(8)-C(8a)	116
N(3)-C(4)-C(4a)	115	C(7)-C(8)-O(8)	110
N(3)-C(4)-O(6)	113	C(8a)-C(8)-O(8)	101
C(4a)-C(4)-O(6)	103	C(8)-C(8a)-N(1)	106
C(4)-C(4a)-C(5)	99	C(8)-C(8a)-C(4a)	107
C(4)-C(4a)-C(8a)	106	C(8)-C(8a)-C(9)	103
C(4)-C(4a)-Br(1)	112	C(9)-C(8a)-N(1)	110
C(5)-C(4a)-C(8a)	119	C(9)-C(8a)-C(4a)	120
C(5)-C(4a)-Br(1)	113	C(4a)-C(8a)-N(1)	108
C(8a)-C(4a)-Br(1)	107	C(8a)-C(9)-C(10)	101
C(4a)-C(5)-C(6)	98	C(8a)-C(9)-O(9)	116
C(4a)-C(5)-O(5)	121	C(10)-C(9)-O(9)	111
C(6)-C(5)-O(5)	116	C(9)-C(10)-O(8)	112
C(5)-C(6)-C(7)	113	C(9)-C(10)-O(10)	120
C(5)-C(6)-C(11)	114	O(8)-C(10)-O(10)	126
C(5)-C(6)-O(6)	102	C(6)-C(11)-O(11)	115
C(7)-C(6)-C(11)	112	C(4)-O(6)-C(6)	110
C(7)-C(6)-O(6)	109	C(8)-O(8)-C(10)	114
C(11)-C(6)-O(6)	107	C(2)-N(1)-C(8a)	124
C(6)-C(7)-C(8)	110	C(2)-N(3)-C(4)	124

Table 5. Intramolecular non-bonded distances (Å)

Br(1)···O(5)	3.39	O(7)···C(11)	3.01
Br(1)···O(9)	3.38	O(8)···N(1)	3.02
Br(1)···N(1)	3.18	O(9)···C(5)	3.17
Br(1)···N(3)	3.50	O(11)···C(5)	2.82
Br(1)···C(9)	3.40	N(1)···C(4)	2.80
O(5)···O(7)	2.82	N(1)···C(10)	3.18
O(5)···O(9)	2.63*	N(3)···C(8a)	2.75
O(5)···C(8a)	3.26	C(2)···C(8)	3.06
O(5)···C(9)	3.39	C(2)···C(4a)	2.86
O(5)···C(11)	3.15	C(4)···C(8)	2.92
O(6)···O(11)	3.03	C(4a)···C(9)	2.72
O(6)···C(8a)	3.03	C(5)···C(8)	3.01
O(7)···O(8)	2.62	C(5)···C(9)	3.39
O(7)···O(9)	3.28	C(6)···C(8a)	2.90
O(7)···C(8a)	3.27	C(7)···C(9)	3.31
O(7)···C(9)	3.33	C(7)···C(10)	3.09
O(7)···C(10)	2.90		

* hydrogen-bonded

The guanidinium group is almost planar, and C(4) and C(8a) are apart from the mean plane of this group by about 0.23 and 0.22 Å respectively; C(4) is on the same side of the plane as the C(4a) atom, while C(8a) is on the opposite side.

The hydroxyl oxygen atoms, O(5) and O(7), are both attached in the axial orientation to the cyclohexane ring of the chair form; consequently, these atoms are very close to each other, their distance being about 2.82 Å. Though this distance may be taken numerically to correspond to the hydrogen bonding, it is not so, as will be described later. Further, O(5) and O(7) approach closely to the hydroxyl oxygen O(9) and the lactone oxygen O(8) respectively. The former contact occurs at a distance of 2.63 Å and corresponds to an intramolecular hydrogen bond. On the other hand, the latter contact, although the distance is also very small, 2.62 Å, and although the azimuthal angle between C(7)-O(7) and C(8)-O(8) around C(7)-C(8) is only about 31° which is small considering that O(7) and O(8) occupy roughly the axial and equatorial positions of the cyclohexane ring, is not due to hydrogen-bond formation, but to the distortion of the ring. This point will be explained later.

The lactone ring deviates considerably from a planar structure. The distances of the atoms from the mean plane through the four atoms, C(9), C(10), O(8), and O(10), are given in Fig. 4. From this figure, it is found that the lactone ring takes a conformation close to the half-chair form. In this molecule, such a ring conformation seems to favor to some degree the relaxation of the repulsions between Br(1) and O(9) and between O(7) and O(8).

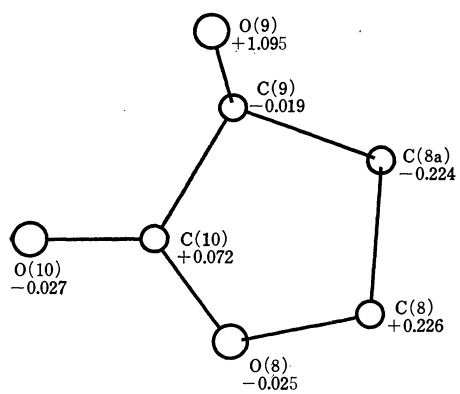

Fig. 4. The deviations from the mean plane through C(9), C(10), O(8) and O(10).

The five-membered ethereal ring takes a conformation of the envelope type; C(4), C(4a), C(6), and O(6) are nearly coplanar, and the remaining C(5) is considerably apart from the mean plane of the first four atoms. The deviations of the atoms from the plane are shown in Fig. 5.

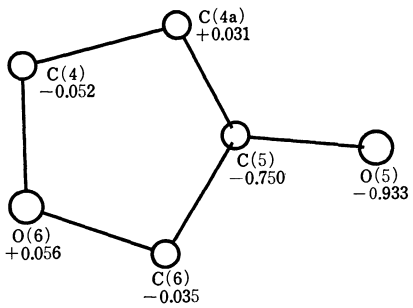

Fig. 5. The deviations from the mean plane through C(4), C(4a), C(6) and O(6).

The hydroxymethyl group is linked to the C(6) of the cyclohexane ring in the equatorial orientation. The C(11)-O(11) bond makes azimuthal angles of about 32° with C(5)-C(6) and 100° with C(6)-O(6) around C(6)-C(11). Consequently, O(11) is much closer to C(5) than to O(6), in spite of the larger van der Waals radius of the former, the O(11)—C(5) distance being only about 2.82 Å.

Crystal Structure. The projections of the present crystal structure along the *a* and *c* axes are shown in Figs. 6 and 7 respectively. The molecular and bromide ions are connected by several hydrogen bonds, forming a three-dimensional hydrogen-bonded structure. Each bromide ion makes three hydrogen bonds with its adjacent molecular ions; one is formed with O(7) at a distance of 3.17 Å; another, with O(11) at 3.34 Å, and the remaining one, with N(1) at 3.23 Å. Besides these, each molecular ion forms four additional hydrogen bonds; one of them is the O(5)-H···O(9) intramolecular bond, as has already been mentioned. The remaining three hydrogen bonds, N(2)-H···O(11′), N(3)-H···O(10″), and O(9)-H···O(7‴), connect molecular ions around screw axes along the *a*, *b*, and *c* axes respectively, their distances being 2.78, 2.88, and 2.69 Å respectively. As for the first two of these, if the protons of the nitrogen atoms are in the plane of the guanidinium group, it follows that they are considerably off the hydrogen bond directions.

It has been mentioned already, without any explanation, that neither of the intramolecular close approaches, O(7)···O(8) and O(5)···O(7), is due to hydrogen bonding. This may be explained as follows. As for the former approach, since O(7) donates its proton to the bromide ion to form the O(7)-H···Br(2) hydrogen bond, while O(8) has no proton, these two oxygen atoms can not make a hydrogen bond with each other. On the other hand, as for the latter approach, if O(5) forms a hydrogen bond with O(7), the proton donor in this bond should be the former oxygen for the same reason. Therefore, in this case, the O(5)···O(9) approach can not be accepted as a

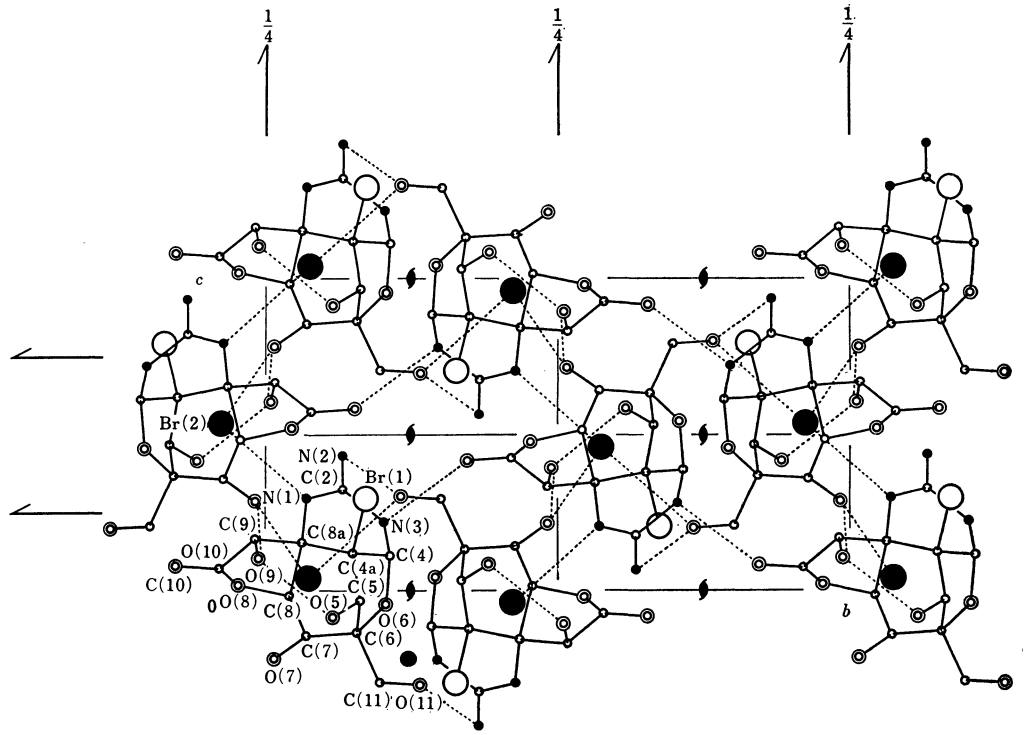

Fig. 6. The crystal structure viewed down along the *a* axis.

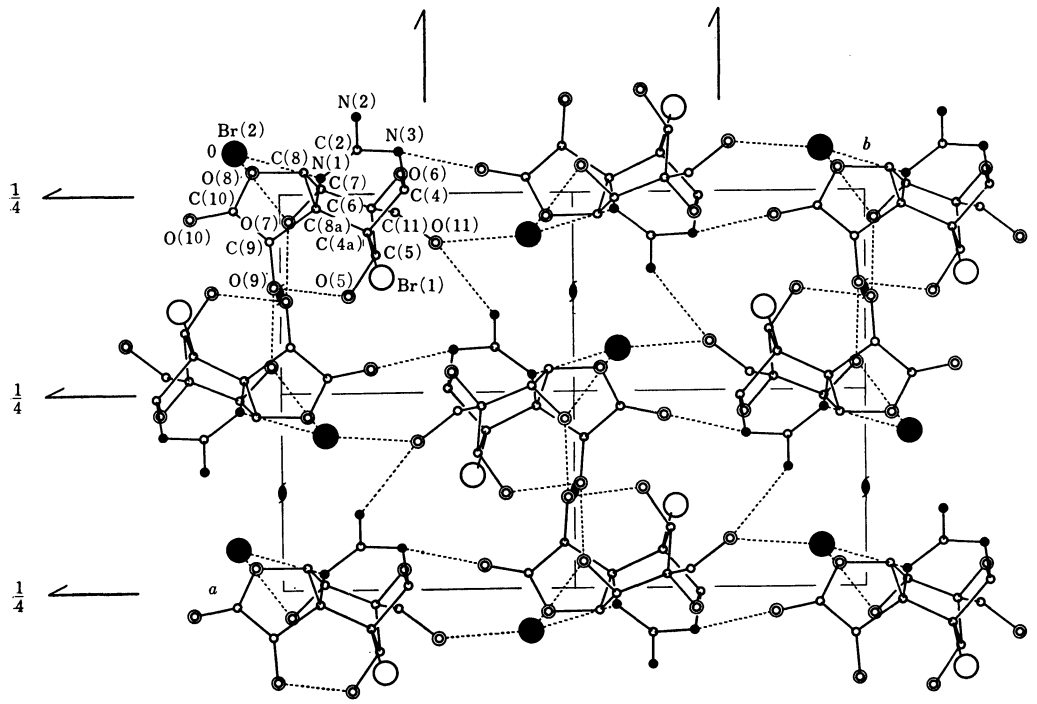

Fig. 7. The crystal structure viewed down along the *c* axis.

Table 6. Intermolecular distances (Å) smaller than 4.0 Å

Atom of I	Atom	Molecule	Distance	Atom of I	Atom	Molecule	Distance
Br(1)	O(6)	IV (0, 1, 0)**	3.86		C(11)	III (0, 0, −1)	3.61
	O(7)	II	3.89	O(11)	Br(1)	I (0, 0, −1)	3.89
	O(9)	II	3.78		Br(2)	III (0, 1, −1)	3.34*
	O(10)	II	3.54		O(8)	III (0, 1, −1)	3.60
	O(11)	I (0, 0, 1)	3.89		O(10)	III (0, 1, −1)	3.37
	N(2)	IV (0, 1, 1)	3.98		N(2)	IV (0, 1, 0)	2.78*
	C(10)	II	3.96		N(3)	IV (0, 1, 0)	3.05
	C(11)	I (0, 0, 1)	3.97		C(2)	IV (0, 1, 0)	3.28
Br(2)	O(6)	III (0, 0, −1)	3.83		C(10)	III (0, 1, −1)	3.83
	O(7)	I	3.17*	N(1)	Br(2)	I (0, 0, 1)	3.23*
	O(11)	III (0, 0, −1)	3.34*	N(2)	Br(1)	IV (−1, 1, 1)	3.98
	N(1)	I (0, 0, −1)	3.23*		Br(2)	I (0, 0, 1)	3.60
	N(2)	I (0, 0, −1)	3.60		O(8)	II (−1, 0, 0)	3.12
	C(2)	I (0, 0, −1)	3.84		O(10)	III (0, 1, 0)	3.68
	C(2)	II (−1, 0, −1)	3.99		O(11)	IV (−1, 1, 0)	2.78*
	C(4)	III (0, 0, −1)	3.80		C(8)	II (−1, 0, 0)	3.98
	C(7)	I	3.71		C(11)	I (0, 0, 1)	3.67
	C(8)	II (−1, 0, −1)	3.71	N(3)	O(5)	IV (−1, 1, 0)	3.45
O(5)	O(6)	IV (0, 1, 0)	3.64		O(10)	III (0, 1, 0)	2.88*
	O(9)	II (0, 0, −1)	3.15		O(11)	IV (−1, 1, 0)	3.05
	O(10)	II (0, 0, −1)	3.55		C(5)	IV (−1, 1, 0)	3.74
	N(3)	IV (0, 1, 0)	3.45		C(10)	III (0, 1, 0)	3.97
	C(4)	IV (0, 1, 0)	3.69	C(2)	Br(2)	I (0, 0, 1)	3.84
	C(9)	II (0, 0, −1)	3.02		Br(2)	II (−1, 0, 0)	3.99
	C(10)	II (0, 0, −1)	3.74		O(10)	III (0, 1, 0)	3.51
O(6)	Br(1)	IV (−1, 1, 0)	3.86		O(11)	IV (−1, 1, 0)	3.28
	Br(2)	III (0, 1, −1)	3.83		C(11)	I (0, 0, 1)	3.87
	O(5)	IV (−1, 1, 0)	3.64	C(4)	Br(2)	III (0, 1, −1)	3.80
	C(5)	IV (−1, 1, 0)	3.85		O(5)	IV (−1, 1, 0)	3.69
O(7)	Br(1)	II (0, 0, −1)	3.89		O(10)	III (0, 1, 0)	3.37
	Br(2)	I	3.17*	C(5)	O(6)	IV (0, 1, 0)	3.85
	O(9)	II (0, 0, −1)	2.69*		N(3)	IV (0, 1, 0)	3.74
	C(9)	II (0, 0, −1)	3.60	C(7)	Br(2)	I	3.71
O(8)	O(11)	III (0, 0, −1)	3.60		O(9)	II (0, 0, −1)	3.89
	N(2)	II (−1, 0, −1)	3.12	C(8)	Br(2)	II (−1, 0, 0)	3.71
O(9)	Br(1)	II (0, 0, −1)	3.78		N(2)	II (−1, 0, −1)	3.98
	O(5)	II	3.15	C(9)	O(5)	II	3.02
	O(7)	II	2.69*		O(7)	II	3.60
	C(7)	II	3.89	C(10)	Br(1)	II (0, 0, −1)	3.96
	C(11)	II	3.95		O(5)	II	3.74
O(10)	Br(1)	II (0, 0, −1)	3.54		O(11)	III (0, 0, −1)	3.83
	O(5)	II	3.55		N(3)	III	3.97
	O(11)	III (0, 0, −1)	3.37	C(11)	Br(1)	I (0, 0, −1)	3.97
	N(2)	III	3.68		O(9)	II (0, 0, −1)	3.95
	N(3)	III	2.88*		O(10)	III (0, 1, −1)	3.61
	C(2)	III	3.51		N(2)	I (0, 0, −1)	3.67
	C(4)	III	3.37		C(2)	I (0, 0, −1)	3.87

I: x, y, z (given in Table 2)
II: $a/2-z, -y, c/2+z$
III: $-x, -b/2+y, c/2-z$
IV: $a/2+x, -b/2-y, -z$
* These are corresponding to a hydrogen-bonded approach.
** (l, m, n) shows a translational transformation, $(la+x, mb+y, nc+z)$, to be further applied to I, II, III or IV.

hydrogen bond, because, if it is so assumed, O(9) would donate a proton to O(5) and, consequently, could not form the O(9)···O(7‴) intermolecular hydrogen bond. If, on the contrary, O(5) forms a hydrogen bond with O(9), it follows that O(5) does not form one with O(7). Thus, it is the key to the present problem which of the two hydroxyl oxygens, O(7) and O(9), forms a hydrogen bond with O(5). Considering the facts that the distance between O(5) and O(9) is much smaller than that between O(5) and O(7), and that the C(5)-O(5)··· O(9) angle, 99°, is closer to the H-O-H angle, 104.5°, of a water molecule in the gas phase than to that of C(5)-O(5)···O(7), 83°, the latter possibility, *i.e.*, O(5)-H···O(9), seems to be more probable, though the evidence is not quite conclusive.

Intermolecular distances smaller than 4.0 Å in the present crystal are listed in Table 6. These values are all reasonable except for the distance of 3.02 Å between C(9) of the I molecule and O(5) of II. This approach may be called a kind of hydrogen bonding, since C(9) is expected to carry a considerable amount of positive charge because of the existence of two more electronegative groups, a hydroxyl and a lactone group. This view is also supported by the fact that the estimated position of the hydrogen atom at C(9) is not far off the C(9)···O(5) line; the C(9)-H bond and the C(9)···O(5) line make an angle of only about 28°, and hence the atomic distance between H and O(5) is no more than 2.12 Å.*3 As may be seen from Table 6, each bromide ion Br(2) is surrounded by four molecular ions. Of these four, three approach the anion by hydrogen bonds, as has already been mentioned. As for the remaining one, the smallest interatomic distance, 3.71 Å, is found between Br(2) and C(8). This value is somewhat smaller than the sum of the van der Waals radii, 3.95 Å.

In conclusion, the authors would like to express their hearty thanks to Professor Yoshimasa Hirata, Nagoya University, for providing them with the samples. The authors also wish to express their thanks to Professor Yoshiharu Okaya, State University of New York at Stony Brook, for his kind help in the structure refinement.

*3 In the estimation of the position of the H atom, it was assumed that the four unit vectors from C(9) to C(8a), C(10), O(9), and H are in tetrahedral directions and that the atomic distance between C(9) and H is 1.09 Å.

BULLETIN OF THE CHEMICAL SOCIETY OF JAPAN VOL. 43 3332—3341 (1970)

The Crystal and Molecular Structure of Tetrodotoxin Hydrobromide

Akio FURUSAKI, the late Yujiro TOMIIE and Isamu NITTA

Faculty of Science, Kwansei Gakuin University, Nishinomiya

(Received February 26, 1970)

The crystal and molecular structure of the hydrobromide of tetrodotoxin itself, $C_{11}H_{17}O_8N_3 \cdot HBr$, have been studied by means of three-dimensional X-ray analysis. The crystals are triclinic, with two formula units in a unit cell of the dimensions; $a=8.79$, $b=9.02$, $c=9.51$ A, $\alpha=106°51'$, $\beta=88°1'$, and $\gamma=96°23'$; the space group is $P\bar{1}$. The intensities of reflections were recorded on equi-inclination Weissenberg photographs taken with Cu$K\alpha$ radiation around the b and c axes, and were measured visually with a calibrated intensity scale. The structure was elucidated by means of the Fourier and least-squares methods, and was refined by the block-diagonal-matrix least-squares method, the anisotropic thermal motion being assumed only for bromine atoms. The stereostructures of the two crystallographically-independent molecules of tetrodotoxin thus obtained are almost identical and correspond to that deduced by Tsuda *et al.*, by Hirata *et al.*, and by Woodward *et al.*, all in 1964. It is noteworthy that, in both of the two molecules, the C–O distance for the free hydroxyl group in the ortho-ester part (1.36 and 1.39 Å) is somewhat smaller than the ordinary aliphatic C–O distance, 1.43±0.01 Å, and that it is rather closer to the phenolic C–O distance, 1.36±0.01 Å.

The molecular structure of tetrodotoxin, one of the most poisonous natural substances, had remained unknown for a long time in spite of extensive organic chemical investigations, until it was, in 1964, at last elucidated independently by Tsuda *et al.*, by Hirata *et al.*, and by Woodward *et al.*[1-3] All of these three groups derived the same structure for the poison from those structures determined by X-ray crystal analyses for its different derivatives.[3-6] The X-ray determination of one of the derivatives, bromoanhydrotetrodoic lactone hydrobromide, was carried out in our laboratory in cooperation with Hirata *et al.* of Nagoya University.[6,7] Since Professor Yoshimasa Hirata kindly provided us also with single crystals of the hydrobromide of tetrodotoxin itself, a three-dimensional X-ray crystal analysis was later undertaken in order to confirm directly the molecular structure deduced from those of the derivatives.

Experimental

The crystal data were obtained from oscillation and Weissenberg photographs taken with Cu$K\alpha$ radiation around the three principal axes; the results are summarized in Table 1. The intensities were recorded on equi-inclination Weissenberg photographs taken with Cu$K\alpha$ radiation for 0—8 layers around the b axis and for 0—3 layers around the c axis, and were measured visually with a calibrated intensity scale. No absorption correction was applied, though the

TABLE 1. CRYSTAL DATA OF TETRODOTOXIN HYDROBROMIDE

Formula	$C_{11}H_{17}O_8N_3 \cdot HBr$
Triclinic	
	$a=8.79\pm0.04$ Å
	$b=9.02\pm0.04$
	$c=9.51\pm0.04$
	$\alpha=106°51'\pm15'$
	$\beta=88°1'\pm15'$
	$\gamma=96°23'\pm15'$
Space Group	$P\bar{1}$
Z	2
D_x	1.86 g/cm^3

1) K. Tsuda, S. Ikuma, M. Kawamura, R. Tachikawa, K. Sakai, C. Tamura and O. Amakasu, *Chem. Pharm. Bull.*, **12**, 1357 (1964).

2) T. Goto, Y. Kishi, S. Takahashi and Y. Hirata, *Tetrahedron Lett.*, **1964**, 779.

3) R. B. Woodward, "Special Lectures presented at the Third International Symposium on the Chemistry of Natural Products," ed. by IUPAC (1964), p. 49.

4) K. Tsuda, C. Tamura, R. Tachikawa, K. Sakai, O. Amakasu, M. Kawamura and S. Ikuma, *Chem. Pharm. Bull.*, **11**, 1473 (1963); C. Tamura, O. Amakasu, Y. Sasada and K. Tsuda, *Acta Cryst.*, **21**, 219 (1966).

5) K. Tsuda, C. Tamura, R. Tachikawa, K. Sakai, O. Amakasu, M. Kawamura and S. Ikuma, *Chem. Pharm. Bull.*, **12**, 643 (1964); C. Tamura, O. Amakasu, Y. Sasada and K. Tsuda, *Acta Cryst.*, **21**, 226 (1966).

6) Y. Tomiie, A. Furusaki, K. Kasami, N. Yasuoka, K. Miyake, M. Haisa and I. Nitta, *Tetrahedron Lett.*, **1963**, 2102.

7) A. Furusaki, Y. Tomiie and I. Nitta, The preceding paper.

samples used were not sufficiently small (about 0.5 mm in diameter). After the Lorentz and polarization correction, these data were put on an absolute scale by means of Wilson's method. The overall temperature factor obtained at this stage was 2.08 Å^2. Thus, the absolute values of the structure factors of 2839 independent reflections were derived.

All the photographs used for the present study were taken in the Crystallography Laboratory, University of Pittsburg, when one of the authors (Y. T.) was there (1963).

Structure Determination

A Patterson function, $P(u, v, w)$, was calculated at intervals of 1/30 for u, for v and for w. The resulting map showed that if one of two bromine atoms in a unit cell, Br(a), was placed at the point of origin (0, 0, 0), the other Br(b) should be situated close to the (1/2, 1/2, 1/2) position. In order to refine the latter position, the diagonal-matrix least-squares method was applied. After three cycles, the R factor dropped from the initial value of 0.554 to 0.345, and the bromine position became (0.5180, 0.5276, 0.4900). On the other hand, we tried to estimate the positions of light atoms from the Patterson map on the basis of the proposed molecular structure of tetrodotoxin. In this way, out of the positions of forty-four independent light atoms present in an asymmetric unit, twenty were found. Using the two bromine positions and these positions, and assuming all the light atoms to be carbon, the first Fourier synthesis was carried out; the calculated R factor was 0.312. The map thus obtained had many maxima; out of these forty-eight higher maxima were taken as temporary atomic positions and were tested for the divergence of temperature factors.[8] After three cycles of the least-squares method, nine positions were found to be inadequate. Then, using the thirty-nine remaining positions, the second Fourier map was calculated. From the map drawn, forty-seven maxima were chosen again as positions of the light atoms and were tested again by the least-squares method. The results after three cycles are given in Table 2, which shows that, out of the forty-seven positions, the three marked with asterisks may be inadequate. However, from a comparison of these positions with the structure determined on the basis of the chemical evidence, it turned out that not all the forty-four light-atom positions which seemed adequate before, in view of the results of the least-squares test, were actually cor-

Table 2. The result of the second structure test

No.	Atom	x/a	y/b	z/c	B(Å^2)	No.	Atom	x/a	y/b	z/c	B(Å^2)
1	Br(a)	0.000	0.000	0.000	2.19	24	Br(b)	0.518	0.528	0.490	2.32
2	O(A1)	0.260	0.513	1.137	0.07	25	O(B1)	0.773	0.030	0.640	0.66
3	O(A2)	0.520	0.613	1.147	−0.14	26	O(B2)	1.033	0.183	0.653	0.75
4	O(A3)	0.360	0.727	1.327	1.13	27	O(B3)	0.863	0.227	0.820	0.92
5	O(A4)	0.080	0.553	0.917	2.38	28	O(B4)	0.577	0.060	0.413	0.69
6	O(A5)	0.443	0.283	0.803	0.98	29	O(B5)	0.977	−0.167	0.313	0.49
7	O(A6)	0.783	0.693	0.820	0.38	30	O(B7)	0.887	0.440	0.643	0.37
8	O(A7)	0.433	0.897	1.113	0.41	31	O(B8)	1.143	−0.213	0.543	1.63
9	O(A8)	0.377	0.147	1.020	0.73	32	N(B1)	1.040	0.393	0.317	0.67
10	N(A1)	0.583	0.853	0.817	1.53	33	N(B2)	0.787	0.317	0.350	0.36
11	N(A2)	0.333	0.770	0.813	1.38	34	N(B3)	0.830	0.497	0.240	1.51
12	N(A3)	0.430	0.953	0.683	0.80	35	C(B1)	0.873	0.413	0.300	1.14
13	C(A1)	0.450	0.863	0.780	2.95	36	C(B2)	0.847	0.203	0.430	1.58
14	C(A2)	0.350	0.700	0.940	1.59	37	C(B3)	0.727	0.037	0.380	1.88
15	C(A3)	0.233	0.530	0.890	1.17	38	C(B4)	0.787	−0.047	0.483	1.28
16	C(A4)	0.267	0.423	0.983	2.14	39	C(B5)	0.953	−0.097	0.447	2.68
17	C(A5)	0.447	0.380	0.960	1.22	40	C(B6)	1.047	0.080	0.497	1.12
18	C(A6)	0.537	0.550	0.997	3.06	41	C(B7)	1.000	0.187	0.403	1.16
19	C(A7)	0.513	0.640	0.897	1.33	42	C(B8)	1.110	0.323	0.400	1.54
20	C(A8)	0.627	0.773	0.897	2.74	43	C(B9)	0.807	0.293	0.607	1.32
21	C(A9)	0.337	0.763	1.083	0.44	44	C(B10)	0.867	0.167	0.673	1.70
22	C(A10)	0.373	0.657	1.177	1.16	45	**	0.270	0.267	0.160	2.01
23	C(A11)	0.473	0.277	1.043	1.62	46	**	0.420	0.933	0.603	1.24
						47	*	0.060	0.663	0.713	11.30
						48	*	0.907	0.673	0.667	8.22
						49	*	0.173	0.747	0.663	10.30

8) M. Nishikawa, K. Kamiya, M. Tomita, Y. Okamoto, T. Kikuchi, K.Osaki, Y. Tomiie, I. Nitta and K. Coto, *J. Chem. Soc., B*, **1968**, 652.

rect for the two of them marked with a double asterisk were inadequate.

The reason why the temperature factors corresponding to the two positions do not diverge remains unknown, but this fact seems to warn against the formal use, without criticism, of the divergence of the temperature factors as a structure test.

The two remaining atomic positions were obtained from the third Fourier map. The coordinates of the forty-six atoms thus obtained were refined by the block-diagonal-matrix least-squares method using isotropic temperature factors for all the atoms. After four cycles, the R factor dropped to 0.150. Next, the atomic coordinates were further refined by the above-mentioned method, using anisotropic temperature factors only for the bromine atoms; the final R factor was 0.130. The atomic parameters thus obtained and the electron density distribution calculated with these parameters are given in Table 3 and Fig. 1 respectively. Tables of the observed and calculated structure factors are preserved by the Chemical Society of Japan.*1

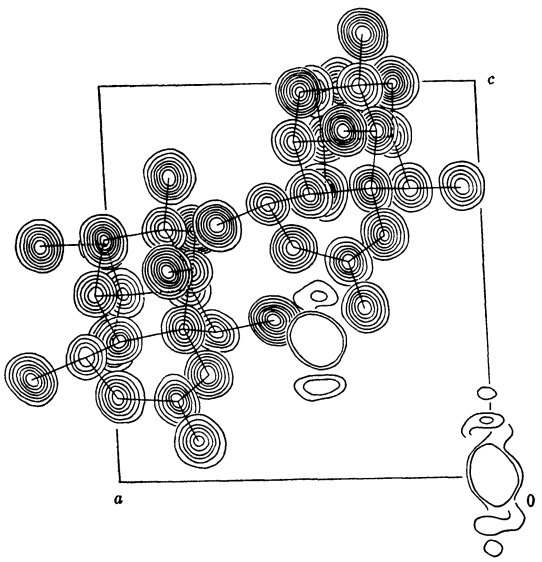

Fig. 1. The final electron density distribution. Contours are at intervals of 2.0 e/Å^3 for the oxygen, nitrogen, and carbon atoms, beginning at the 2.0 e/Å^3 level.

Table 3. The final atomic parameters

Atom	x/a	y/b	z/c	B(Å^2)	Atom	x/a	y/b	z/c	B(Å^2)
Br(a)	−0.0020	0.0025	0.0000	*	Br(b)	0.5163	0.5271	0.4900	*
O(A1)	0.2708	0.5256	1.1370	1.038	O(B1)	0.7710	0.0284	0.6364	1.316
O(A2)	0.5337	0.6112	1.1424	1.075	O(B2)	1.0232	0.1551	0.6494	1.113
O(A3)	0.3761	0.7299	1.3196	1.501	O(B3)	0.8536	0.2354	0.8321	1.834
O(A4)	0.0913	0.5792	0.9029	1.587	O(B4)	0.5693	0.0677	0.4169	1.269
O(A5)	0.4500	0.2931	0.8076	1.579	O(B5)	0.9775	−0.1688	0.3057	1.546
O(A6)	0.7856	0.6889	0.8314	1.072	O(B6)	1.2454	0.2650	0.3298	1.838
O(A7)	0.4532	0.9060	1.1256	1.206	O(B7)	0.8947	0.4328	0.6432	1.384
O(A8)	0.3712	0.1355	1.0229	1.684	O(B8)	1.1523	−0.2069	0.5400	2.013
N(A1)	0.6033	0.8575	0.8159	0.946	N(B1)	1.0401	0.4066	0.3192	1.406
N(A2)	0.3412	0.7754	0.8219	0.826	N(B2)	0.7852	0.3071	0.3486	0.991
N(A3)	0.4264	0.9448	0.6843	1.308	N(B3)	0.8320	0.5014	0.2345	2.217
C(A1)	0.4561	0.8578	0.7766	0.788	C(B1)	0.8852	0.4018	0.3052	0.833
C(A2)	0.3629	0.6742	0.9162	0.531	C(B2)	0.8297	0.2064	0.4340	0.927
C(A3)	0.2459	0.5316	0.8792	1.025	C(B3)	0.7306	0.0505	0.3881	0.646
C(A4)	0.2734	0.4350	0.9849	1.226	C(B4)	0.7835	−0.0518	0.4787	1.176
C(A5)	0.4385	0.3722	0.9575	1.115	C(B5)	0.9559	−0.0842	0.4558	1.057
C(A6)	0.5481	0.5234	0.9925	1.000	C(B6)	1.0459	0.0839	0.4966	1.121
C(A7)	0.5235	0.6229	0.8862	0.413	C(B7)	0.9979	0.1722	0.3961	0.772
C(A8)	0.6475	0.7524	0.8965	0.819	C(B8)	1.1076	0.3198	0.4028	1.453
C(A9)	0.3504	0.7663	1.0814	0.726	C(B9)	0.8139	0.2836	0.5999	1.046
C(A10)	0.3801	0.6611	1.1720	0.934	C(B10)	0.8626	0.1766	0.6807	1.095
C(A11)	0.4716	0.2771	1.0590	1.315	C(B11)	0.9906	−0.1801	0.5506	1.401

*	B_{11}	B_{22}	B_{33}	B_{12}	B_{23}	B_{31}
Br(a)	0.00532	0.00971	0.00966	−0.00279	0.00690	0.00400
Br(b)	0.00541	0.00744	0.00774	0.00625	0.00618	0.00557

*1 The complete data of the F_o-F_c table are kept as Document No. 7007 at the office of the bulletin of the Chemical Society of Japan. A copy may be secured by citing the doqument number and by remitting, in advance, ¥1200 for photoprints. Pay by check or money order, payable to: The Chemical Society of Japan.

Results and Discussion

Molecular Structure. The bond lengths and angles of the two crystallographically-independent tetrodotoxin molecules, A and B, are listed in Tables 4 and 5, together with the arithmetical means of the corresponding values of the two. The average standard deviations of the atomic distances are estimated to be 0.033 Å for C–C, 0.031 Å for C–N, and 0.029 Å for C–O. If these deviations are taken into consideration, the dimensions of the two independent molecules are in good agreement with each other. Thus, from the present results, it may be concluded that the stereostructures of the two tetrodotoxin molecules, A and B, are almost identical and that they correspond to that derived from the organic chemical investigations.[1–3] In Figs. 2 and 3, the framework of one of the two independent molecules and the corresponding structural formula are, respectively, drawn with reference to the absolute configuration based on that of the derivative of the poison, bromoanhydrotetrodoic lactone hydrobromide.[7]

The molecules are characterized by an ortho-ester system rarely found in natural products. This system makes a part of an adamantane-like cage structure and might have some close connection with the powerful toxicity. It has been reported by Tamura *et al.* that the remarkable system in the molecule is still preserved in the derivative, diacetylanhydrotetrodotoxin hydroiodide.[5] The geometry of the ortho-ester part found in the present molecule is shown in Fig. 4, as is that in the derivative.*2

Table 4. The bond distances (Å)

Bond	Mol. A	Mol. B	Mean
C(2)-C(3)	1.52	1.52	1.52
C(3)-C(4)	1.55	1.55	1.55
C(4)-C(5)	1.60	1.57	1.59
C(5)-C(6)	1.54	1.58	1.56
C(5)-C(11)	1.52	1.48	1.50
C(6)-C(7)	1.57	1.51	1.54
C(7)-C(8)	1.49	1.54	1.52
C(2)-C(7)	1.53	1.55	1.54
C(2)-C(9)	1.56	1.54	1.55
C(9)-C(10)	1.50	1.50	1.50
C(1)-N(1)	1.36	1.37	1.36
C(1)-N(2)	1.32	1.30	1.31
C(1)-N(3)	1.38	1.39	1.39
C(2)-N(2)	1.48	1.47	1.48
C(8)-N(1)	1.47	1.45	1.46
C(3)-O(4)	1.46	1.45	1.46
C(4)-O(1)	1.44	1.47	1.46
C(5)-O(5)	1.40	1.43	1.41
C(6)-O(2)	1.42	1.43	1.42
C(8)-O(6)	1.44	1.44	1.44
C(9)-O(7)	1.43	1.40	1.42
C(10)-O(1)	1.43	1.44	1.44
C(10)-O(2)	1.46	1.46	1.46
C(10)-O(3)	1.36	1.39	1.37
C(11)-O(8)	1.43	1.46	1.45

Table 5. The bond angles (°)

Angle	Mol. A	Mol. B	Mean
N(1)-C(1)-N(2)	122	124	123
N(1)-C(1)-N(3)	119	117	118
N(2)-C(1)-N(3)	119	118	119
N(2)-C(2)-C(3)	111	109	110
N(2)-C(2)-C(7)	107	109	108
N(2)-C(2)-C(9)	110	111	111
C(3)-C(2)-C(7)	109	107	108
C(3)-C(2)-C(9)	110	110	110
C(7)-C(2)-C(9)	109	110	109
C(2)-C(3)-C(4)	107	107	107
C(2)-C(3)-O(4)	110	112	111
C(4)-C(3)-O(4)	109	109	109
C(3)-C(4)-C(5)	111	115	113
C(3)-C(4)-O(1)	112	110	111
C(5)-C(4)-O(1)	106	104	105
C(4)-C(5)-C(6)	103	104	103
C(4)-C(5)-O(5)	108	108	108
C(4)-C(5)-C(11)	113	109	111
C(6)-C(5)-O(5)	109	112	111
C(6)-C(5)-C(11)	110	114	112
C(11)-C(5)-O(5)	114	109	112
C(5)-C(6)-C(7)	112	110	111
C(5)-C(6)-O(2)	111	108	109
C(7)-C(6)-O(2)	111	115	113
C(6)-C(7)-C(8)	113	113	113
C(2)-C(7)-C(6)	107	108	107
C(2)-C(7)-C(8)	115	113	114
C(7)-C(8)-N(1)	110	108	109
C(7)-C(8)-O(6)	109	106	108
N(1)-C(8)-O(6)	109	109	109
C(2)-C(9)-C(10)	108	109	109
C(2)-C(9)-O(7)	114	112	113
C(10)-C(9)-O(7)	109	113	111
C(9)-C(10)-O(1)	110	110	110
C(9)-C(10)-O(2)	110	109	110
C(9)-C(10)-O(3)	114	114	114
O(1)-C(10)-O(2)	109	110	109
O(1)-C(10)-O(3)	109	108	109
O(2)-C(10)-O(3)	105	105	105
C(5)-C(11)-O(8)	109	111	110
C(1)-N(1)-C(8)	122	122	122
C(1)-N(2)-C(2)	123	122	122
C(4)-O(1)-C(10)	114	113	113
C(6)-O(2)-C(10)	111	111	111

*2 Since, for both the present substance and the derivative, the crystals contain two crystallographically-independent molecules, the respective mean values are given in Fig. 4.

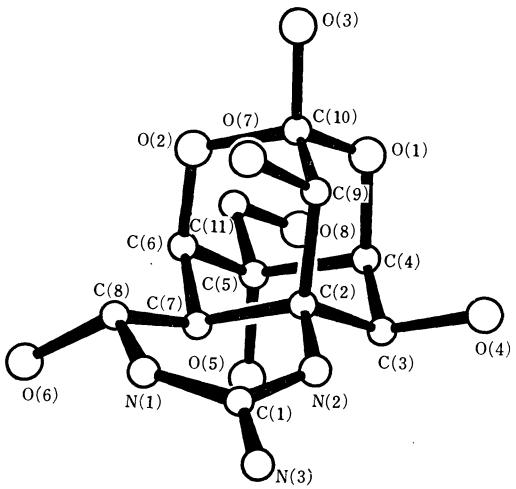

Fig. 2. The framework of the tetrodotoxin ion (A).

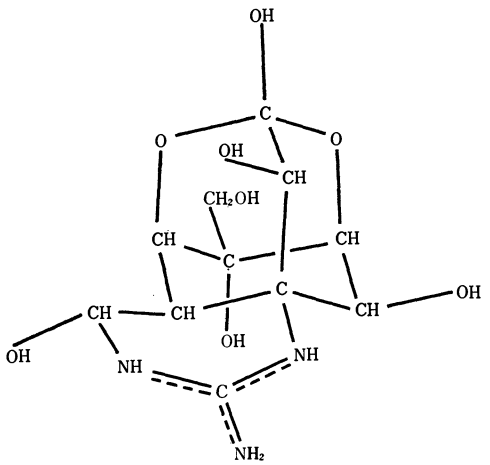

Fig. 3. The structural formula corresponding to Fig. 2.

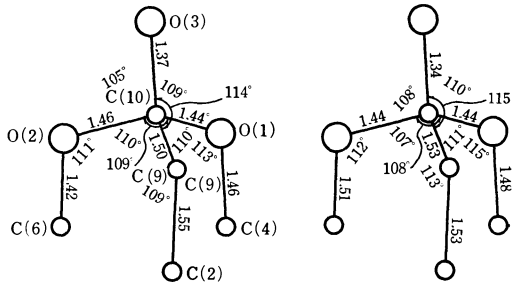

Fig. 4. The geometry of the ortho-ester parts.
II: in tetrodotoxin.
II: in diacetylanhydrotetrodotoxin.

Though neigher of the analyses has a sufficiently high accuracy for a detailed discussion, the two results show some common characteristics. For example, the bond distance between the free hydroxyl oxygen atom and the central carbon atom of the ortho-ester is 1.37 Å in the present molecule and 1.34 Å in the derivative; both of these values are considerably smaller than the ordinary aliphatic C–O distance, 1.43±0.01 Å, and rather closer to the phenolic C–O distance, 1.36±0.01 Å.[9]

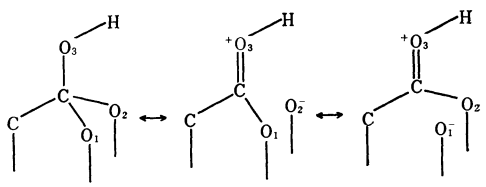

Fig. 5. The resonance of the ortho-ester.

This shortening of the C–O bond may be explained by the resonance, shown in Fig. 5. In this resonance, in addition to the ortho-ester structure, I, two ionic structures of the ordinary ester type, II and III, take part, and both of these contribute to the shortening of the C–O bond under consideration. In an acidic solution where the free hydroxyl oxygen O(3) has a proton, the structures

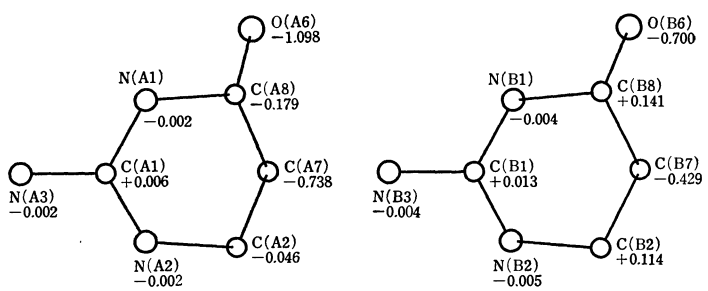

Fig. 6. The deviations from the guanidinium planes.

9) "Tables of Interatomic Distances and Configuration in Molecules and Ions," ed. by L. E. Sutton *et al.*, Burlington House, London (1958).

II and III may contribute only a little to the resonance. However, in an alkaline solution where O(3) loses a proton and where it becomes easy to feed electrons to C(10), the contribution of structures corresponding to II and III would increase and, consequently, the molecules would become more unstable with respect to C(10)–O(1) and C(10)–O(2). As another of the common characteristics, it is further found that the bond angle C(9)–C(10)–O(3) and the corresponding angle in the derivative are 114° and 115° respectively, both larger than the tetrahedral angle, 109.5°.

It is of interest to compare the two independent molecules of tetrodotoxin with each other. Though almost identical, strictly speaking, these two may be conformational isomers since they appear, so far as the present results are concerned, to be different only in conformation and different only in part. Thus, appreciable conformational differences are found in two parts of the molecules; one of them is the hydroxymethyl group, and the other is the six-membered ring containing a guanidinium group. The former part is different in respect to the conformation of the hydroxyl oxygen O(8) around C(5)–C(11); in one of the molecules, A, O(8) is *trans* to C(6), while, in the other, B, it is *trans* to C(4). Since the potential energy curve for the internal rotation of O(8) around the C(5)–C(11) bond seems to be approximately symmetrical with respect to the plane through C(5), C(11), and O(5), the two observed conformations which are almost related to each other by the mirror plane may not be appreciably different in energy. Accordingly, which of the two conformations the molecule takes seems to

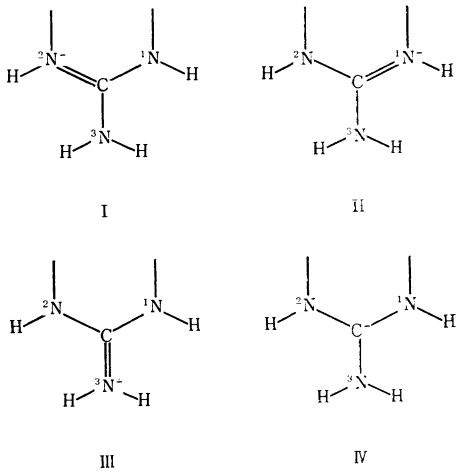

Fig. 7. The four predominant formulae for the resonance of the guanidinium group.

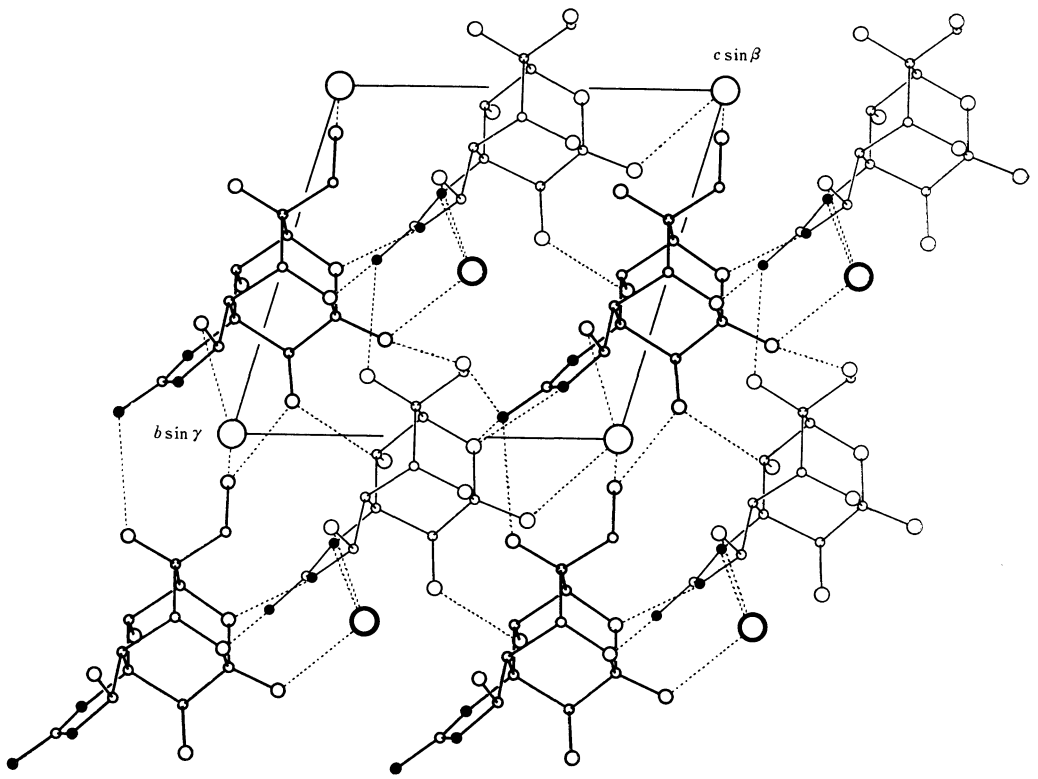

Fig. 8. The crystal structure viewed along the *a* axis.

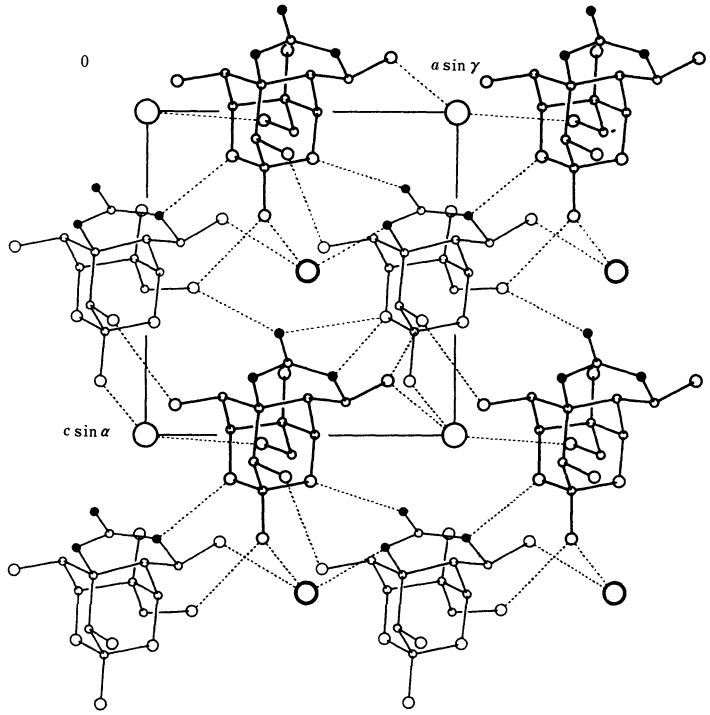

Fig. 9. The crystal structure viewed along the *b* axis.

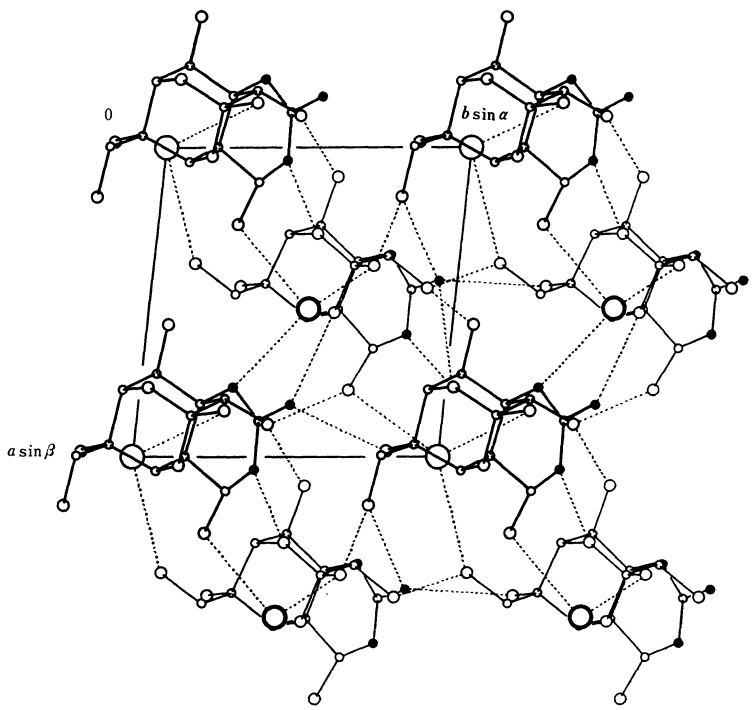

Fig. 10. The crystal structure viewed along the *c* axis.

depend on the intermolecular rather than on the intramolecular interactions. On the other hand, the six-membered rings with a guanidinium group are different in overall form; in A, the ring is in rather the boat form, while, in B, it is in the chair form, though, in either case, the five atoms, C(2), N(2), C(1), N(1), and C(8), lie roughly on a plane. The guanidinium group itself is almost planar in both of the molecules. The deviations of the atoms from the mean plane of the group are shown in Fig. 6 for the respective molecules. In A, C(2) and C(8) deviate from the guanidinium plane in the same sense as C(7), while, in B, the two atoms are on the opposite side of the plane to C(7). This shows that the two corresponding rings take different conformations, as has already been mentioned.

Considering the resonance of the guanidinium group, the two molecules have parallel characteristics, as may be seen from the bond distances in Table 4. To this resonance, the four formulae given in Fig. 7 seem to contribute mainly. In view of the bond distances, in both molecules, out of the three formulae containing a double bond, I would seem to be the most predominant, and III, the least. That I is superior to II is consistent with the fact that, in both molecules, C(8) deviates more considerably from the guanidinium plane than does C(2); in other words, the twisting of the bond C(1)–N(1) is larger than that of the C(1)–N(2) bond.

Crystal Structure. The projections of the crystal structure viewed along the *a*, *b*, and *c* axes are shown in Figs. 8, 9, and 10 respectively. Further, in Table 6, possible hydrogen bonds are listed, together with the distances, in consideration of the correspondence between the two independent molecules. Since the present molecules have many proton donors and acceptors, the crystal takes quite a complicated three-dimensional hydrogen-bonded structure; for A molecules, each makes fourteen hydrogen bonds with adjacent molecules and bromide ions, while, B molecules make thirteen.

Both of the bromide ions, Br(a) and Br(b), form three hydrogen bonds with their adjoining tetrodotoxin molecules. For the former bromide ion, the three hydrogen bonds are all of the O–H···Br^- type; the distances are 3.23 Å for O(A6)–H···Br(a) and 3.36 Å for O(B3)–H···Br(a) and O(A8)–H···Br(a). On the other hand, for the latter, out of the three hydrogen bonds, two are O–H···Br^- and the other is N–H···Br^-; the distances are 3.14 Å for O(A3)–H···Br(b), 3.24 Å for O(B6)–H···Br(b), and 3.26 Å for N(B2)–H···Br(b). So far as only the atomic distances smaller than 4.0 Å are concerned, Br(b) is surrounded merely by the three molecules which make hydrogen bonds with it, while Br(a) is approached by two additional molecules as well.

In some of the hydrogen bonds found in the present crystal, the proton seems to be, to a considerable degree, off the line joining the proton donor and acceptor. Since, for the four protons of the guanidinium grouping, their approximate positions can be estimated on reasonable assumptions,*3 the deviations of the N–H bond directions from the respective donor-acceptor lines have been calculated; the results are listed in Table 7. The maximum deviation is found for N(B2)–H···Br(b), the angle being no less than about 47°. Nevertheless, the approach between N(B2) and Br(b) may be taken as hydrogen-bonded because the proton at N(B2) is separated from Br-

Table 6. Possible hydrogen bonds

O(A3)–H···Br(b)	3.14 Å	O(B3)–H···Br(a)	3.35 Å
O(A6)–H···Br(a)	3.23	O(B6)–H···Br(b)	3.24
O(A8)–H···Br(a)	3.36	——	
——		N(B2)–H···Br(b)	3.26
O(A4)–H···O(B7)	2.95	O(B4)–H···O(A7)	2.89
O(A7)–H···O(A8)	2.70	——	
——		O(B7)–H···O(A6)	2.73
——		O(B8)–H···O(A3)	2.80
O(A5)–H···N(A3)	3.00	——	
N(A1)–H···O(B1)	2.88	N(B1)–H···O(A1)	2.94
N(A3)–H···O(B8)	2.82	——	
——		N(B3)–H···O(A2)	3.14
N(A3)–H···O(B1)	3.09	——	
——		N(B3)–H···O(B5)	3.00

*3 The proton positions were estimated on the following assumptions: the N–H bond distances are 1.01 Å; for H at N(1), ∠C(8)–N(1)–H=∠C(1)–N(1)–H and these four atoms are coplanar; for H at N(2), ∠C(2)–N(2)–H=∠C(1)–N(2)–H and these four atoms lie on a plane; for the two H atoms at N(3), ∠C(1)–N(3)–H=120° and the H atoms are coplanar with, respectively, N(1), C(1), and N(3), and N(2), C(1), and N(3).

Table 7. The deviations of the guanidinium protons from the hydrogen bond directions

N-H···X	N···X (Å)	H···X (Å)	∠H-N···X (°)	N-H···X	N···X (Å)	H···X (Å)	∠H-N···X (°)
N(A1)-H···O(B1)	2.88	1.98	22	N(B2)-H···Br(b)	3.26	2.68	47
N(A3)-H···O(B1)	3.09	2.26	29	N(B3)-H···O(A2)	3.14	2.25	24
N(A3)-H···O(B8)	2.82	1.99	28	N(B3)-H···O(B5)	3.00	2.28	37
N(B1)-H···O(A1)	2.94	1.97	14				

Table 8. Intermolecular contacts except hydrogen-bonded

Br(a)	N(A1)	I	3.86 Å	O(A7)	C(A11)	V	3.57 Å
	C(A8)	I	3.60		O(B6)	XI	3.88
	O(B2)	V	3.95		C(B3)	VIII	3.42
	O(A4)	IV	3.83	O(A8)	N(A1)	III	3.51
	N(A2)	IV	3.90		N(A2)	III	3.24
	O(B5)	VIII	3.66		N(A3)	III	3.23
	O(B6)	VIII	3.90		C(A1)	III	3.04
	C(B7)	VIII	3.63		C(A2)	III	3.98
Br(b)	O(A2)	VII	3.59		C(A9)	III	3.52
	O(A6)	XII	3.91		O(B6)	IX	3.03
	N(A1)	XII	3.66	N(A1)	O(B3)	V	3.81
	N(A2)	XII	3.70		C(B4)	V	3.79
	N(A3)	XII	3.84		C(B10)	V	3.95
	C(A1)	XII	3.48	N(A2)	O(B8)	X	3.25
	C(A7)	XII	3.61	N(A3)	C(A5)	V	3.97
	C(A8)	XII	3.95		C(A11)	V	3.93
	C(A10)	VII	3.84		O(B4)	V	3.22
	O(B7)	XII	3.95		C(B4)	V	3.64
	N(B3)	XII	3.61	C(A1)	C(A11)	V	3.94
	C(B1)	XII	3.76		O(B1)	V	3.43
	C(B8)	VIII	3.86		O(B8)	X	3.44
	C(B9)	XII	3.94	C(A3)	O(B2)	II	3.83
O(A1)	O(B5)	XI	3.94		O(B7)	II	3.75
	O(B6)	IX	3.36	C(A4)	O(B6)	IX	3.99
	N(B3)	IX	3.93		N(B1)	IX	3.78
	C(B1)	IX	3.89	C(A6)	O(B3)	I	3.91
	C(B8)	IX	3.71		N(B3)	VI	3.51
O(A3)	N(A3)	VI	3.46	C(A8)	O(B7)	I	3.98
	O(B4)	VIII	3.22	C(A9)	O(B4)	VIII	3.94
	O(B5)	XI	3.73		O(B5)	XI	3.85
	N(B1)	IX	3.91	C(A10)	O(B4)	VIII	3.95
	C(B3)	VIII	3.94		O(B8)	XI	3.91
O(A4)	O(A6)	II	3.13	C(A11)	O(B6)	IX	3.22
	O(B2)	II	3.88		N(B2)	VI	3.90
	O(B3)	II	3.45		N(B3)	VI	3.73
	C(B9)	II	3.99	O(B3)	N(B3)	VI	3.89
	C(B10)	II	3.99	O(B4)	O(B6)	II	3.76
O(A5)	C(A1)	III	3.86	O(B5)	N(B1)	III	3.97
	O(B1)	I	3.90		C(B1)	III	3.87
	O(B3)	I	3.67	O(B7)	C(B11)	V	3.84
	O(B4)	I	3.86	O(B8)	N(B1)	III	3.56
	C(B9)	I	3.70	N(B1)	C(B11)	V	3.80
	C(B10)	I	3.94	N(B3)	C(B5)	V	3.78
O(A6)	C(B9)	I	3.71		C(B11)	V	3.69
	C(B11)	V	3.58	C(B1)	C(B11)	V	3.85

I: x/a, y/b, z/c (given in Table 3); II: $-1+x/a$, y/b, z/c; III: x/a, $-1+y/b$, z/c; IV: $1+x/a$, y/b, z/c; V: x/a, $1+y/b$, z/c; VI: x/a, y/b, $1+z/c$; VII: $1+x/a$, $1+y/b$, z/c; VIII: x/a, $1+y/b$, $1+z/c$; IX: $-1+x/a$, y/b, $1+z/c$; X: $-1+x/a$, $1+y/b$, z/c; XI: $-1+x/a$, $1+y/b$, $1+z/c$; XII: $1+x/a$, $1+y/b$, $1+z/c$.

(b) by only 2.68 Å; this distance is much smaller than the sum of the van der Waals radii, 3.15 Å. That such large deviations of the hydrogen bond directions are found in the present crystal is probably related with the fact that the molecules make extremely numerous hydrogen bonds.

As has been found for Br(a) and Br(b), for the two independent molecules also the hydrogen bond natures are different in some respects. The most interesting of these differences is that, in the O(5)···N(3) hydrogen bond, for the A molecule the proton seems to be donated by the former atom, while, for the B, it seems to be donated by the latter. As for the A molecule, the estimated positions of the two protons at N(A3) are separated from O(B1) and O(B8) respectively by only 2.26 and 1.99 Å, and hence the two approaches to N(A3) are considered hydrogen-bonded. On the other hand, since O(A5) is sufficiently separated from both of the protons (2.70 and 3.17 Å), these two protons have little relation with the close approach between O(A5) and N(A3). Considering the facts that the O(A5)···N(A3) direction makes a relatively small angle of about 33° with the normal of the guanidinium plane and that the π-electrons are localized to some extent at N(A3), since, out of the three important formulae for the resonance of the guanidinium group, III is the least predominant, as has been mentioned above, O(A5) and N(A3) seem to make a hydrogen bond of the O–H···N type. On the other hand, as for the B molecules, since O(B5) is only 2.28 Å apart from the proton at N(B3), the O(B5)··· N(B3) approach would seem to be due to a hydrogen bond of the N–H···O type.

All the small intermolecular atomic distances except the hydrogen-bonded ones are listed in Table 8. These distances nearly correspond to the van der Waals contacts, though some of them are somewhat smaller than the ordinary values because of the intermolecular approach due to hydrogen bonding and other forces.

In conclusion, the authors wish to express their thanks to Professor Yoshimasa Hirata, Nagoya University, for providing them with the samples. The authors would also like to express their thanks to the staff of the X-ray group, University of Pittsburgh, for their kind help in the collection of the intensity data.

BULLETIN OF THE CHEMICAL SOCIETY OF JAPAN VOL. 43 3341—3344 (1970)

Pyrolysis-Gas Chromatographic Investigation of Chlorinated Polystyrenes

Shin TSUGE, Hajime ITO and Tsugio TAKEUCHI

Department of Synthetic Chemistry, Faculty of Engineering, Nagoya University, Chikusa-ku, Nagoya

(Received April 22, 1970)

The distribution of chlorine atoms in radically chlorinated polystyrenes was studied by means of pyrolysis gas chromatography. Degradation products such as styrene, benzene, toluene and chlorobenzenes are related to different structures of the chlorinated polymers. The sequence distribution of each structure was discussed over a wide range of degree of chlorination. Chlorine atoms are first substituted with α- then β-hydrogen in the main chain of polystyrene. The first ring substitution of chlorine occurs competitively at *p*-position even before both α- and β-hydrogens are substituted.

Many types of chlorinated polymers have been synthesized in a search for improved thermal characteristics such as flammability, heat-distortion temperature and thermal stability. Thermal properties are closely associated with the microstructres of polymers, especially with the distribution of chlorine atoms.

Chlorinated polystyrenes have been synthesized by both ionic and radical mechanisms and their structures have been studied by various methods.[1-3]

Bachmann *et al.*[1] reported on the depolymerization of some ionically chlorinated polystyrenes to elucidate their structures. They identified halogenated styrenes such as *p*-chlorostyrene and 3,4-dichlorostyrene after fractional distillation of the depolymerized mixture.

Teyssie *et al.*[2] also carried out an ionic chlori-

1) G. B. Bachman, H. Hellman, K. R. Robinson, R. W. Finholt, E. J. Kahler, L. J. Filar, L. L. Lewis and D. D. Micucci, *J. Org. Chem.*, **12**, 108 (1947).

2) Ph. Teyssie, M. C. de Wilde and G. Smets, *J. Polym. Sci.*, **16**, 429 (1955).

3) R. K. Jenkins, N. R. Byrd and J. L. Lister, *J. Appl. Polym. Sci.*, **12**, 2059 (1968).

nation of polystyrene and characterized the resulting structure by chemical and infrared spectrometric analysis. The chlorination reaction takes place concurrently on the aromatic nucleus and on the main chain. The chlorine, which is substituted on the aromatic nucleus, is preferentially bonded to the para position and secondarily to the ortho position. The second chlorine is then introduced mainly in 3 position with respect to *p*-chlorostyrene unit and in 5 position with respect to *o*-chlorostyrene unit to form 3,4- and 2,5-dichlorostyrene units, respectively.

Jenkins *et al.*[3] prepared chlorinated polystyrenes by means of the radical method using ultraviolet radiation and determined the changes in the infrared spectrum, glass transition temperature and molecular weight of the polymers. In contrast to the ionic reaction, the radical chlorination reaction proceed mainly by substitution at the α-hydrogen position in the main chain. Main chain scission also took place as the chlorination reaction proceeded.

In our previous work, we characterized chlorine containing polymers such as vinyl chloride-vinylidene chloride copolymers,[4] chlorinated polyethyrenes[5] and chlorinated polyvinylchlorides[6] by means of pyrolysis-gas chromatography (PGC).

The purpose of the present work is to characterize the distribution of chlorine atoms in radically chlorinated polystyrenes with the use of PGC. Degradation products of the polymers at 455°C were separated chromatographically and identified to be styrene monomer, benzene, toluene, chlorobenzenes. Benzene and toluene, which are related with the structures produced by substituting the main chain, are observed concurrently with chlorobenzenes which are originated from the structures of substituted aromatic rings. The sequence distribution of each structure was discussed as a function of degree of chlorination.

Experimental

Chlorination. Polystyrene (PSt) was dissolved in chloroform and filtered. The polymer was chlorinated by slowly passing Cl_2 gas into the solution (55 g/*l*) under the illumination of a mercury lamp. Samples of the solution (30 m*l*) were removed from the reaction flask, neutralized and precipitated in sodium hydroxide-methanol solution. The samples were dried in a vacuum oven.

Pyrolysis-Chromatography. The gas chromatograph was a GCG-550F with flame ionization detectors and the pyrolysis apparatus a GP-1000, both supplied by Yanagimoto Co., Ltd. The sample holder and the precut portion of the pyrolysis apparatus were modified to increase the precision of the data and to trap hydrogenchloride gas evolved at the pyrolysis, respectively.[4,5] Operating conditions were as follows.

Column: 3 mm×2 m copper column packed with Diasolid L(80—100 mesh) coated with PEG 6000 (10 wt% to the support)

Carrier gas: nitrogen gas flowing at the rate of 20 cc/min

Pyrolysis temperature: 455°C

Infrared Spectrometry. Infrared spectra were obtained on a Nihon Bunko IR-S by the KBr disc methoed.

The chlorine content of the polymers were chemically determined. In the following, the degree of chlorination D is defined as the number of chlorine atoms per styrene monomer unit.

Results and Discussion

The pyrograms of the polymers with various *D* are shown in Fig. 1. Raw PSt yields nearly quantitatively styrene monomer. As the chlorine content increases, peaks for benzene, toluene and

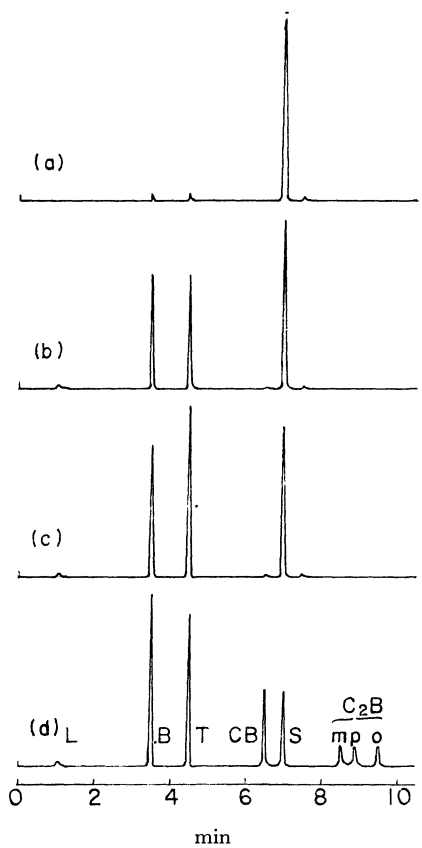

Fig. 1. Typical programs of PSt and chlorinated PSt at 455°C.
(a): PSt, (b)—(d): chlorinated PSt; (b): D=0.57, (c): D=1.50, (d): D=2.25, where D is the degree of chlorination (the number of chlorine atoms per monomer unit).

4) S. Tsuge, T. Okumoto and T. Takeuchi, *Makromol. Chem.*, **123**, 123 (1969).

5) S.Tsuge, T. Okumoto and T. Takeuchi, *Macromol.*, **2**, 200 (1969).

6) S. Tsuge, T. Okumoto and T. Takeuchi, *ibid.*, **2**, 277 (1969).

chlorobenzenes appear on the pyrograms, while the yield of styrene monomer decreases.

The relationships between the relative yields among the aromatic products and D are shown in Fig. 2, where a small amount of low boiling point products appearing in the earliest retention time is neglected for the sake of simplicity.

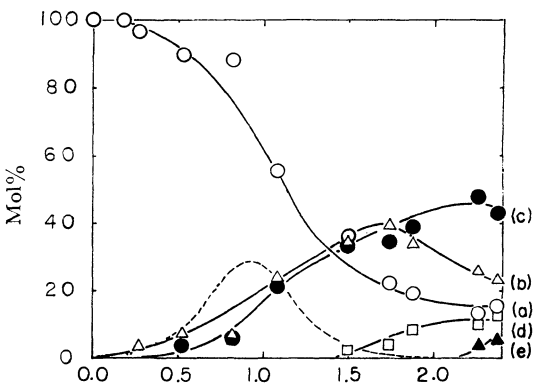

Fig. 2. Relationships between the degree of chlorination (D) and the yield of the degradation products from chlorinated PSt.
A: styrene monomer, B: toluene, C: benzene, D: chlorobenzene, E: dichlorobenzenes.
Dotted curve is calculated from Eq. (2) for $n=3$.

The yield of styrene monomer decreases monotonously as a function of D. The yield of toluene is first observed at $D=0.27$ and shows a maximum (40 mol%) at $D=1.74$. On the other hand, benzene, which first appears at $D=0.53$, increases monotonously up to $D=2.26$. The appearance of chlorobenzene starts at $D=1.50$. Dichlorobenzenes are observed above $D=2.26$.

Each characteristic product is closely related to the structure of the polymers as follows:

Styrene Monomer. PSt with molecular weight higher than ten thousand was depolymerized nearly completely to monomer.[7] PSt with lower molecular weight, however, yielded such additional products as toluene and benzene. Thus the relative yield of styrene monomer decreases with the decrease of molecular weight.

In the case of chlorination of PSt, we must consider competitive reactions such as substitution of the hydrogen atoms in the main chain of PSt or in the aromatic ring of PSt and simple scission of the main chains. Each reaction causes shorter sequences of styrene unit than that of the raw PSt and accordingly is responsible for the reduction of the yield of styrene monomer.

Toluene. The chlorination reaction of PSt proceeds mainly by substituting at the α-hydrogen in the main chain.[3] For chlorinated PSt with D above 1.0, some monomer units have two chlorine atoms at both α- and β-positions, since no ring protons are substituted until $D=1.5$ as described below.

The relative yield of toluene in the pyrolysis products of PSt increases rapidly with the decrease of its degree of polymerization.[7] Thus we consider the apparent reduction of the sequence of unsubstituted styrene unit in chlorinated PSt as follows.

For the sake of simplicity, it is assumed that chlorination reaction takes place almost at rondom at α- or β-hydrogen, but that of α-substitution occurs in preference to β-one.[3] The substitution of ring protons is not taken into consideration.

Sequences (I), (II) and (III) are formed with the probabilities of ac^na, ac^nb+bc^na and bc^nb, respectively, where a and b are the probabilities of substitution of only α- and both α- and β-hydrogens, respectively, and c is that of non-substitution and n is sequence number of styrene unit. Consequently, the following equation is expected to hold for the total number of the unstubstituted styrene units.

$$N=\sum_{k=1}^{n} Pc^k(a^2+2ab+b^2)$$

where P is the degree of polymerization of PSt and $a+b+c=1$. The number of the hydrogen atoms that can be substituted is $2P$, provided that the substitution reactions take place at α-hydrogen and one of β-hydrogens. On the other hand, the number of chlorine atoms contained in chlorinated PSt is $D\times P$. When we assume random substitution, the probability of introduction of one chlorine atom is $D\times P/2P=D/2$ and that of non-substitution is $\{1-(D/2)\}$. Consequently, we have $a=2(D/2)\{1-(D/2)\}$, $b=(D/2)^2$ and $c=\{1-(D/2)\}^2$.

Thus, N can be shown as a function of D, where we have only to consider relatively small n value (at most $n=10$).

$$N=\sum_{k=1}^{n} P\{1-(D/2)\}^{2k}[4(D/2)^2\{1-(D/2)\}^2 +4(D/2)^3\{1-(D/2)\}+(D/2)^4] \quad (2)$$

As shown in Fig. 2 with a dotted curve, the function always passes through a maximum between $D=0$ and 2.0. The observed yield of toluene shows a maximum value between $D=0$ and 2.0 ($D\sim1.6$).

7) S. Tsuge, T. Okumoto and T. Takeuchi, *J. Chromatogr. Sci.*, **7**, 250 (1969).

The results suggest that toluene may be closely associated with the short sequences mentioned above. However, the fact that the theoretical curve deviates at high D may be attributed to the rough assumptions, where the substitution of ring protons and reduction of molecular weight during chlorination are neglected. Strictly speaking, reduction of molecular weight of PSt during chlorination also leads to the yield of toluene. However, if this had been predominant, the yield of toluene should have had a monotonously increasing inclination as the rise of D.

Benzene. The yield of benzene, which is very small even in PSt with low molecular weight,[7] increases almost monotonously up to $D=2.25$ as the rise of D. This suggests that the mole fraction of both α- and β-disubstituted styrene unit increases as chlorination proceeds. However, the fact that the yield exhibits a decreasing tendency above $D=2.26$ implies that a substitution of the hydrogen atoms considerably participates in the aromatic ring of PSt.

Chlorobenzenes. Chlorobenzene is first observed at $D=1.50$. The infrared spectrum of chlorinated PSt with $D=1.50$ has an absorption band near 1080 cm^{-1}, which is characteristic for *p*-substituted styrene unit.[2] It is very interesting that the substitution of ring protons begins at $D=1.50$, where α- and β-hydrogens in the main chain are not completely substituted. The first ring substitution occurs at *p*-position, but the second one seems to proceed at random since *o*-, *m*- and *p*-dichlorobenzenesappear almost at the same time above $D=2.25$.

One of the authors (S.T.) wishes to thank the Sakkokai Foundation for financial aid.

BULLETIN OF THE CHEMICAL SOCIETY OF JAPAN VOL. 43 3344—3353 (1970)

The π-Electronic Structures of Five-membered Heterocycles Containing Two or Three Heteroatoms and Their Benzo-derivatives

Mamoru KAMIYA

Shizuoka College of Pharmacy, Oshika, Shizuoka

(Received May 13, 1970)

The semiempirical Pariser-Parr-Pople SCF method combined with configuration-interaction has been applied for calculation of the electronic spectrum, ionization potential and electron affinity, π-electron distribution and total π-energy of such heterocycles as oxazole, isoxazole, oxadiazoles, imidazole, pyrazole, triazoles and their monobenzo-derivatives, and the theoretical results have been compared with the available spectral data and miscellaneous chemical properties including the position-dependency on substitution reactions, novel photochemical isomerization of several compounds and so forth.

The π-electronic structures and chemical properties of the titled compounds are of interest because the parent five-membered heterocycles are known as small aromatic molecules exhibiting unique chemical behaviour, and it is only recently that the chemistry of these compounds has made a remarkable progress. Several molecular orbital calculations have been performed for such compounds; Hückel-type calculations, both simple and modified, have been applied chiefly for evaluating dipole moment, reactivity index and resonance energy,[1-7] and an extended Hückel method including all valency electrons has also been used for the calculation of charge distribution of imidazole, pyrazole, *v*-triazole, and the four possible oxadiazoles,[8] which indicates that the calculated σ-polarizations are almost independent of the π-electron distributions. SCF calculations have also been performed for explanation of electronic spectra and dipole moments of the several molecules and have given good agreement with the experimental data by adopting proper semiempirical para-

1) L. E. Orgel, T. L. Cottrell, W. Dick and L. E. Sutton, *Trans. Faraday Soc.*, **47**, 113 (1951).

2) V. I. Minkin, O. A. Osipov, A. D. Garnovskii and A. M. Simnov, *Z. Fiz. Khim.*, **36**, 469 (1962).

3) H. Hamano and H. F. Hameka, *Tetrahedron*, **18**, 985 (1962).

4) G. Del Re, *J. Chem. Soc.*, **1962**, 3324.

5) G. Berthier and G. Del Re, *ibid.*, **1965**, 3109.

6) B. Zurawski, *Bull. Acad. Polon. Sci. Ser. Sci. Chim.*, **14**, 481 (1966).

7) W. Woznicki and B. Zurawski, *Acta Phys. Pol.*, **31**, 95 (1967).

8) W. Adam and A. Grimson, *Theor. Chim. Acta*, **7**, 342 (1967).

meters.[9-13]

It seems, however, that no attempts have been made for SCF calculations which systematically treat both the electronic spectra and chemical properties of the molecules mentioned above. In this work the standard Pariser-Parr-Pople SCF method with configuration-interaction procedure has been carried out for all the molecules in the title, such as oxazole, isoxazole, oxadiazoles, imidazole, pyrazole, triazoles, and their benzo-derivatives.

Calculation Method

Calculations have been performed on the basis of the Pariser-Parr-Pople method[14] with configuration-interaction including all singly excited configurations. The elements of F matrix are taken as

$$F_{\mu\mu} = -I_\mu + (1/2)q_\mu\gamma_{\mu\mu} + \sum_{\nu\neq\mu}(q_\nu - n_\nu)\gamma_{\mu\nu},$$

$$F_{\mu\nu} = \beta_{\mu\nu} - (1/2)p_{\mu\nu}\gamma_{\mu\nu},$$

where q_μ and $p_{\mu\nu}$ are the diagonal and off-diagonal elements, respectively, of the bond order-charge density matrix, and n_ν is the number of electrons donated to the π-electron system by the νth atom. The values of valence-state ionization potential (I) and electron affinity (A) are determined as follows referring to the paper of Hinze and Jaffe.[15]

I (eV): 11.16 (-C=), 14.12 (-N=), 26.70 (-N(H)-), 32.90 (-O-)

A (eV): 0.03 (-C=), 1.78 (-N=), 9.26 (-N(H)-), 11.37 (-O-)

The two-center repulsion integral ($\gamma_{\mu\nu}$) is computed according to the Nishimoto-Mataga approximation. The core-resonance integral ($\beta_{\mu\nu}$) is evaluated using the equation $\beta_{\mu\nu} = -1/2\, S_{\mu\nu}(I(\mu)+I(\nu))$, where the overlap integral ($S_{\mu\nu}$) is calculated using Slater-type atomic orbital.[16] For comparison the calculation is performed both including and neglecting the $\beta_{\mu\nu}$ over non-neighbouring atomic pairs.

The comparison is meaningful in view of the present purpose of explaining both electronic spectra and chemical properties at the ground state; it is well-known that a good description of the ground state by using semiempirical parameters, in particular the core-resonance integral $\beta_{\mu\nu}$ adjusted to experimental spectral data is difficult, since the ground state which can be represented by a single Slater determinant does not mix with any of the corresponding singly excited states.

Molecular structures of all the heterocycles studied herein are tentatively approximated as a regular hexagon and pentagon with a bond length of 1.395 Å on account of lack in enough available expermental data.

The present calculations have been performed using HITAC 5020-E computer at the University of Tokyo.

Results and Discussion

Optical Properties. The calculated results of singlet π–π* transition energy, corresponding oscillator strength and polarization direction, and excitation energy of the lowest $^3(\pi, \pi^*)$ state are summarized in Table 1(a) and 1(b), the experimental spectral data being collected in Table 2.

In the case of the five-membered heterocyclic molecules the predicted values of the first π–π* transition energy are remarkably (0.4—1.0 eV) lowered by the calculation including the $\beta_{\mu\nu}$ over non-neighbouring atomic pairs (This procedure will be denoted as method I and the other as method II), and these values tend to be slightly smaller than those observed. It is of interest to note that the predicted first π–π* transitions of vicinal-triazoles are more bathochromic and stronger in intensity than those of symmetrical-ones. It is also known that the direction of the first transition moment tends to be of a positive angle for isoxazole and pyrazole, and of a negative angle for oxazole and imidazole.

As for the benzo-derivatives, such as 1,2-benzisoxazole (indoxazene), 2,1-benzisoxazole (anthranil) and benzimidazole, fairly good agreement is found between the calculated (by method I) and experimental spectra, even though the core-resonance integral ($\beta_{\mu\nu}$) is not chosen so as to reproduce individual transition energy. The observed spectrum of indazole is in better agreement with the calculated one (by method I) of 1*H*-tautomer rather than that of 2*H*-tautomer for the relative intensities of the lowest two bands. In the case of benzotriazole also, the observed transition energies of the lowest two bands seem to be in better agreement with the calculated values (by method I) of the 1*H*-tautomer rather than those of the 2*H*-

9) M. K. Orloff and D. D. Fitts, *Tetrahedron*, **19**, 1691 (1963).
10) W. C. Mackrodt, A. Wardley, P. A. Curnuck, N. L. Owen and J. Sheridan, *Chem. Commun.*, **1966**, 692.
11) D. W. Davies and W. C. Mackrodt, *ibid.*, 345 (1967).
12) L. Paoloni and M. Cignitti, *Tetrahedron*, **24**, 485 (1968).
13) R. D. Brown and B. A. W. Coller, *Theor. Chim. Acta*, **10**, 435 (1968).
14) R. Pariser and R. G. Parr, *J. Chem. Phys.*, **21**, 466, 767 (1953); J. A. Pople, *Trans. Faraday Soc.*, **49**, 1375 (1953).
15) J. Hinze and H. H. Jaffe, *J. Amer. Chem. Soc.*, **84**, 540 (1962).
16) R. S. Mulliken, C. A. Rieke, D. Orloff and H. Orloff, *J. Chem. Phys.*, **17**, 1248 (1949).

TABLE 1 (a)

	Spectral data calculated by Method I					
	ΔE_s (eV)	f	α (°)		ΔE_s (eV)	f	α (°)
Oxazole	5.26	0.24	−16	Imidazole	5.64	0.20	−23
	6.31	0.11	28		6.41	0.12	19
	8.26	0.79	66		7.93	0.51	23
	2.13* (eV)				2.73*		
Isoxazole	5.74	0.33	3	Pyrazole	5.95	0.17	19
	6.29	0.07	−26		6.42	0.19	−25
	7.90	0.90	81		7.66	0.76	71
	2.07*				2.59*		
1, 2, 3-Oxadiazole	5.07	0.30	−8	1, 2, 3-Triazole	5.44	0.25	−9
	6.41	0.06	17		6.46	0.06	39
	7.80	0.92	73		7.59	0.87	68
	1.53*				2.18*		
1,2,4-Oxadiazole	5.68	0.21	7	1,2,4-Triazole	5.95	0.01	26
	6.01	0.11	−7		6.24	0.23	−2
	7.79	0.68	75		7.36	0.58	56
	2.19*				2.64*		
1,2,5-Oxadiazole	5.78	0.13	90	1,2,5-Triazole	5.62	0.19	90
	5.95	0.40	0		6.29	0.29	0
	7.81	0.80	90		7.72	0.64	90
	1.69*				2.28*		
1,3.4-Oxadiazole	5.65	0.27	0	1,3,4-Triazole	5.78	0.09	90
	5.73	0.08	90		6.10	0.22	0
	7.77	0.19	0		7.37	0.40	0
	2.19*				2.70*		
Benzoxazole	4.69	0.13	−4	Benz-imidazole	4.70	0.08	−8
	5.13	0.26	−27		5.11	0.18	−65
	5.69	0.24	37		5.94	0.65	9
	6.25	0.15	54		6.35	0.34	26
	6.73	0.52	44		6.57	0.50	40
	2.13*				2.40*		
Indoxazene	4.59	0.09	66	1*H*-Indazole	4.47	0.18	84
	5.07	0.37	−29		4.88	0.13	−48
	5.99	0.71	31		6.11	0.94	7
	6.42	0.04	−43		6.22	0.56	18
	6.61	0.46	6		6.53	0.36	−16
	1.84*				1.84*		
Anthranil	3.99	0.35	89	2*H*-Indazole	4.36	0.32	89
	4.75	0.00_2	44		4.78	0.02	59
	5.54	0.01	−14		5.80	0.01	23
	6.02	0.04	−41		6.28	1.61	−4
	6.37	1.89	−1		6.37	0.18	10
	1.04*				1.59*		
Benzofurazan	3.84	0.26	90	2*H*-Benzo-triazole	4.25	0.26	90
	4.60	0.11	0		4.60	0.13	0
	5.61	0.16	90		5.91	0.09	90
	6.10	0.00_1	90		5.94	0.86	0
	6.12	1.29	0		6.33	0.09	90
	0.69*				1.31*		
1,2,3-Benzo-xadiazole	4.34	0.17	39	1*H*-Benzo-triazole	4.47	0.18	52
	4.58	0.35	−25		4.66	0.24	−43
	5.61	0.29	21		5.85	0.71	8
	6.23	0.01	56		6.10	0.01	51
	6.72	0.33	34		6.64	0.64	64
	1.29*				1.56*		

ΔE_s = singlet π-π^* transition energy.

* = excitation energy of the lowest $^3(\pi$-$\pi^*)$ state.

f = oscillator strength, where the transition moment of $i \rightarrow j$ singly excited transition is obtained as $(\boldsymbol{m}_{i\rightarrow j})_x = \sqrt{2}\sum_r C_r^i C_r^j \bar{x}_{rr}$, $(\boldsymbol{m}_{i\rightarrow j})_y = \sqrt{2}\sum_r C_r^i C_r^j \bar{y}_{rr}$ and $(\boldsymbol{m}_{i\ j})_z = 0$.

α = polarization direction measured counterclockwise to the x-axis.

Table 1 (b)

	Spectral data calculated by method II						
	ΔE_s (eV)	f	α (°)		ΔE_s (eV)	f	α (°)
Oxazole	6.32	0.28	−11	Imidazole	6.68	0.19	−20
	7.10	0.13	1		7.35	0.14	1
	8.68	1.02	78		8.65	0.94	62
	2.97*				3.64*		
Isoxazole	6.35	0.32	15	Pyrazole	6.63	0.21	27
	6.96	0.21	−36		7.24	0.26	−31
	8.68	0.89	83		8.63	0.82	76
	2.72*				3.35*		
1,2,3-Oxadiazole	5.75	0.33	−1	1,2,3-Triazole	6.14	0.27	−3
	6.97	0.14	−44		7.13	0.14	−57
	8.35	0.88	75		8.32	0.84	69
	2.18*				2.87*		
1,2,4-Oxadiazole	6.52	0.02	35	1,2,4-Triazole	6.69	0.01	29
	6.55	0.36	2		7.04	0.27	−1
	8.32	0.85	83		8.18	0.74	64
	2.75*				3.34*		
1,2,5-Oxadiazole	6.20	0.19	90	1,2,5-Triazole	6.26	0.21	90
	6.47	0.44	0		6.89	0.35	0
	8.61	0.81	90		8.58	0.71	90
	2.23*				2.93*		
1,3,4-Oxadiazole	6.45	0.05	90	1,3,4-Triazole	6.57	0.09	90
	6.64	0.36	0		7.09	0.20	0
	8.29	0.27	0		8.09	0.56	0
	2.91*				3.47*		
Benzoxazole	5.23	0.06	8	Benzimidazole	5.26	0.06	1
	5.62	0.35	−45		5.52	0.27	−72
	6.60	0.96	21		6.81	1.69	7
	7.01	0.09	38		7.08	0.03	19
	7.28	0.25	22		7.34	0.24	76
	2.65*				2.77*		
Indoxazene	5.01	0.13	82	1*H*-Indazole	4.97	0.23	86
	5.52	0.37	−32		5.41	0.16	−46
	6.61	1.10	24		6.71	1.30	5
	6.99	0.05	−59		6.96	0.53	18
	7.10	0.27	−17		7.14	0.06	−28
	2.27*				2.32*		
Anthranil	4.49	0.41	88	2*H*-Indazole	4.86	0.37	89
	5.21	0.04	24		5.31	0.04	49
	6.09	0.06	−20		6.44	0.14	7
	6.56	0.02	−58		6.84	1.39	−5
	6.78	1.73	−2		6.87	0.32	5
	1.52*				2.10*		
Benzofurazan	4.22	0.31	90	2*H*-Benzotriazole	4.71	0.33	90
	4.95	0.15	0		5.08	0.12	0
	5.99	0.17	90		6.35	0.09	90
	6.54	1.23	0		6.56	1.15	0
	6.57	0.00_0	90		6.79	0.00_3	90
	1.10*				1.80*		
1,2,3-Benzoxadiazole	4.81	0.16	64	1*H*-Benzotriazole	4.94	0.24	69
	5.10	0.38	−23		5.17	0.23	−38
	6.29	0.57	19		6.54	1.08	7
	6.71	0.04	83		6.62	0.03	−37
	7.08	0.22	8		7.07	0.16	7
	1.77*				2.04*		

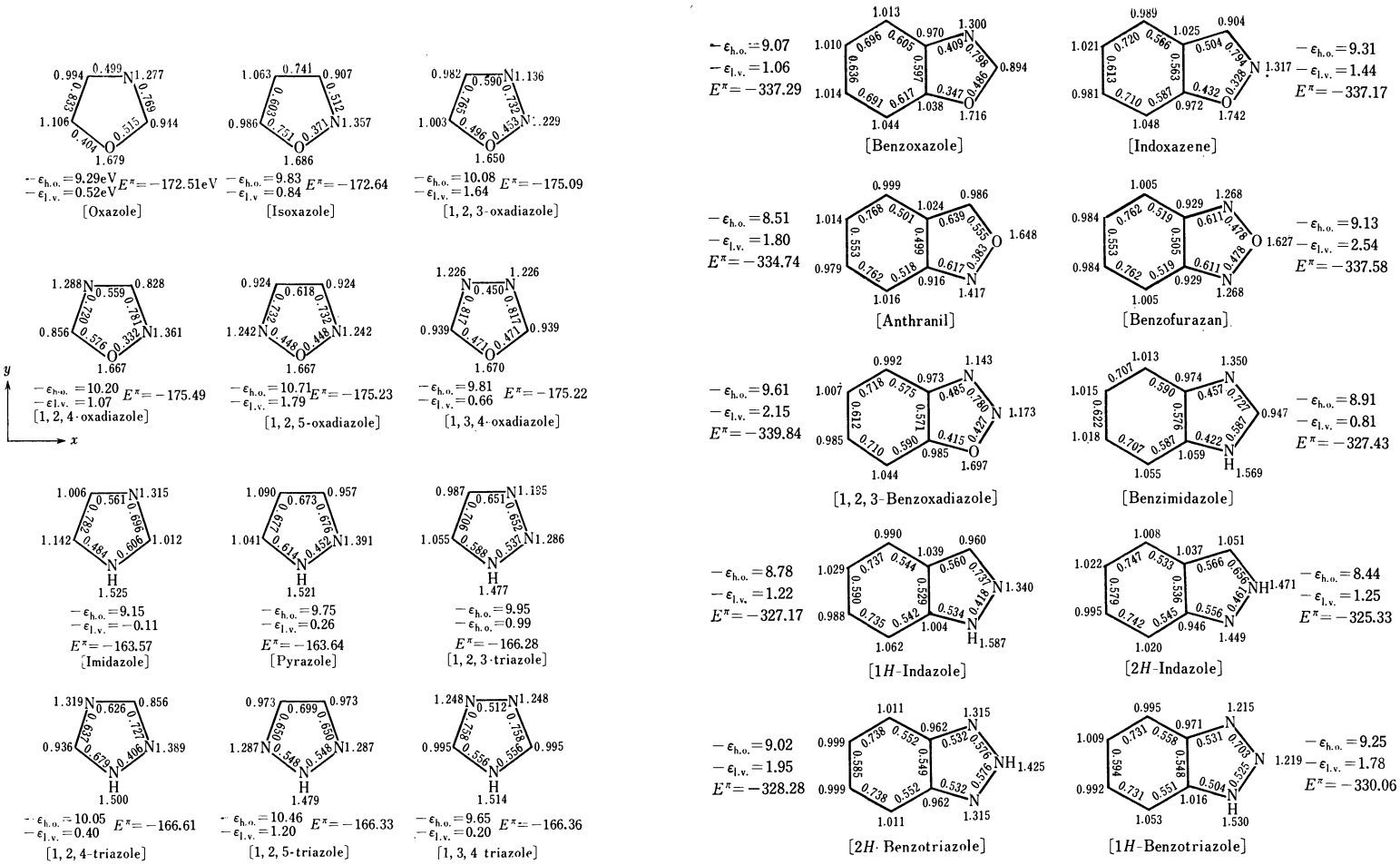

(a)—1

(a)—2

Fig. 1(a). Molecular diagrams at the ground state calculated by method I.

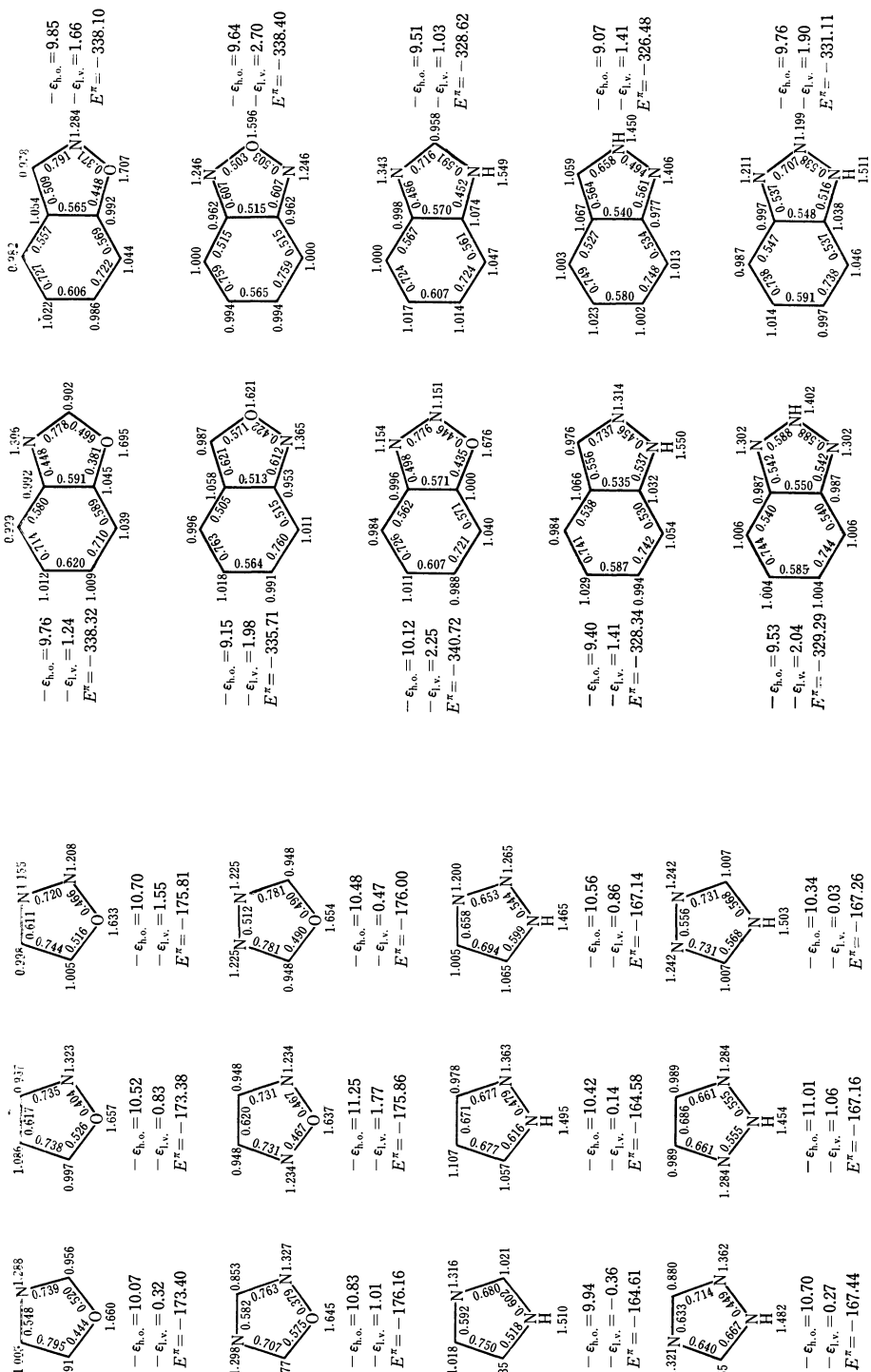

(b)—1 (b)—2

Fig. 1(b). Molecular diagrams at the ground state calculated by method II.

TABLE 2. EXPERIMENTAL SPECTRAL DATA

Oxazole	6.05 eV (3.59=log ε)	*1
Isoxazole	5.88 (3.60)	*2
1,2,5-Oxadiazole	Only end absorption	*3
Imidazole	5.99 (3.70)	*2
Pyrazole	5.90 (3.5)	*2
s-Triazole	5.79	*4
v-Triazole	5.90 (3.6)	*5
Benzoxazole	4.49—4.59 (3.51—3.53) 4.71 (3.38) 5.37 (3.90)	*6
Indoxazene	4.43 5.06	*7
Anthranil	4.04 4.77	*8
Benzimidazole	4.55 (3.83) 5.08 (3.74) 6.14 (4.6)	*2
Indazole	4.19—4.37 (3.61) 4.90 (3.64) 5.60	*9
Benzotriazole	4.42—4.56 (3.80—3.74) 4.66 (3.58) 5.08 (3.77)	*2

*1 H. Bredereck, R. Gompper and F. Reich, *Chem. Ber.*, **93**, 1389 (1960).
*2 G. Leandri, A. Mangani, F. Montanari and R. Passerini, *Gazz. Chim. Ital.*, **85**, 769 (1955).
*3 R. A. Olofson and J. S. Michelman, *J. Org. Chem.*, **30**, 1854 (1965).
*4 M. R. Atkinson, E. A. Parkes and J. B. Polya, *J. Chem. Soc.*, **1954**, 4256.
*5 L. W. Hartzel and F. R. Benson, *J. Amer. Chem. Soc.*, **76**, 667 (1954).
*6 R. Passerini, *J. Chem. Soc.*, **1954**, 2256.
*7 P. Grammaticakis, *Bull. Soc. Chim. Fr.*, **8**, 101 (1941).
*8 R. Ramart-Lucas and M. Grumez, *ibid.*, **17**, 317 (1950).
*9 J. M. Barclay, N. Campbell and G. Dodds, *J. Chem. Soc.*, **1941**, 113.

tautomer. Experimentally, it is reported[17] that the first π–π^* band of benzotriazole is characteristic of a quinoid chromophore and its second band is characteristic of a benzenoid chromophore.

The polarization direction of the initial three transitions are much affected by introducing benzene ring, but the general trends of variation are not affected appreciably by the replacement of the pyrrole-nitrogen with the furan-oxygen. In this case also, the first π–π^* transition of the molecules with NH (O)-N bond tends to polarize along the bond, in contrast to the other-type molecule in which the corresponding transition polarizes in remarkably different directions. As to benzimidazole, indazole and benzotriazole it has been revealed[18] from fluorescence polarization data that the polarization directions of the lowest two absorptions are remarkably different to each other, and the first and third bands of benzimidazole have moderately close polarization directions. The calculated angle (by method I) between the two transition moments is 57° in benzimidazole, 48° (40°) in indazole and 85° (90°) in benzotriazole, the angle between the first and third transition moments in benzimidazole being 17°. According to method II the calculated angle is 73° in benzimidazole, 48° (40°) in indazole and 73° (90°) in benzotriazole, the angle between the first and third transition moments in benzimidazole being 6°. Such results are in line with the experimental facts.

The excitation energy of the lowest triplet state has been given for benzimidazole, indazole and benzotriazole as about 2.8, 2.6 and 2.8 eV, respectively.[18] The calculated excitation energy of the lowest triplet state of these molecules is by 0.4—1.2 eV (by method I) and 0.5—1.0 eV (by method II) lower as compared to the experimental values.

It may be said that the present calculations by method I on spectroscopic properties are in rather good correlation with the experimental results, although no specific adjustment of the core-resonance integral to the experimental transition energy is made. This encourages us to predict various chemical properties on the basis of the presently obtained π-electron distributions.

Chemical Properties. The calculated results on the π-electron distributions at the ground state, such as π-electron density and π-bond order, and the orbital energies of the highest occupied and lowest vacant ($\varepsilon_{h.o.}$ and $\varepsilon_{l.v.}$) are presented in Fig. 1(a), and for comparison the similar results evaluated by method II are also given Fig. 1(b). Comparative survey of the whole system will be useful especially for recognizing the effect of atom-rearrangements since the standardization of molecular geometry may remove complicated perturbations on the semiempirical integrals accompanied by geometrical variations.

As concerns oxazole and isoxazole molecules several features are eminent in the given molecular diagrams; the π-bond order of the N–O bond in isoxazole is very low as compared to those of the neighbouring bonds (particularly by method I), and the largest localized dipole is associated with the N–O bond. This predicts that the bond may be a preferred point of attack for any hydrolytic reagent. This bond, in fact, undergoes nucleophilic cleavage in sodium ethylate solution, differently from other azoles, and the cleavage is more facilitated in the state with a free 3-position than that with a free 5-position.[19] This preference of the position is also predicted by the presently given order of $q^{\pi}_{(C-3)} < q^{\pi}_{(C-5)}$. The present result indicates that oxazole gives less contribution of a shortly polarized ionic structure to hybrid resonance than isoxazole. The calcu-

17) J. E. Fagel and G. W. Ewing, *J. Amer. Chem. Soc.*, **73**, 4360 (1951).
18) H. U. Schuett and H. Zimmerman, *Ber. Bunsenges. Phys. Chem.*, **67**, 54 (1963).
19) A. Quilico, *Atti. accad. nazl. Lincei, Rend. Classe sci. fis., mat. e nat.*, **15**, 357 (1953).

lated total π-energy of isoxazole is close to that of oxazole, and it seems probable that the π-energy stabilization in isoxazole is caused by the electrostatic interaction of the two oppositely polarized N and O atoms in spite of the reduced cyclic conjugation.

The relation of $q^{\pi}_{(c-4)} > q^{\pi}_{(c-2)}$ in oxazole is different from the result of a previous SCF calculation using the furan- and imidazole-type parameters for the empirical parameters.[9] The present result predicts that among the carbon atoms in oxazole ring the 5-atom has the largest π-electron density which is in line with a remark of other workers.[20] There is, however, a claim that the 2-atom should be expected to have a larger q^{π} than the other two carbon atoms.[21] Electrophilic substitution on isoxazole is normally predicted to occur selectively at the C-4 position analogously to the β-position substitution in pyridine. This indicates that the influence of the nitrogen atom is predominant.

From comparison of the molecular diagrams of the four possible oxadiazole it is known that the π-electron density on the oxygen atom is almost invariant for all the molecules. This may indicate that with the same regular pentagon geometry the ionic structure with O(+) is equally predominant for all the molecules. It is of interest to note that the accepted mechanism for nucleophilic fission of the N–O bond in 1,2,4-oxadiazole is also accounted for by the low N–O π-bond order and π-electron density at the C-3. Electrophilic substitution such as nitration, halogenation or Friedel-Crafts' reaction are known not to occur at the C-3 or C-5 position of mono-substituted 1,2,4-oxadiazole.[22] This is in harmony with the present result which shows that these positions are markedly electron-deficient to favour nucleophilic substitutions.

In the case of the benzo-derivatives of oxazole, isoxazole and oxadiazoles the following effects of fused benzene-ring upon the π-electron distribution in each heterocyclic ring are known from the given molecular diagrams; in benzoxazole π-electrons on the hetero-ring are smoothly attracted toward the delocalized benzene-ring. In anthranil and benzofurazan the similar π-electron-migration occurs selectively along the O–N–C and O–N linkages, respectively. In 1,2,3-benzoxadiazole and indoxazene in which the π-dipole of the polar O(+)–N(−) bond is in direction against the fused benzene-ring, such migration is prohibitive. Electrophilic (nucleophilic) substitutions on indoxazene are predicted to occur in the increasing order of 7>5 (3>4,6), while the C-5 is assigned from experiment to the preferred point of electrophilic attack such as nitration[23] and bromination,[24] and the C-3 to the site of the initial nucleophilic attack in the N–O bond fission in alkaline solution,[25] respectively. Electrophilic (nucleophilic) substitution on anthranil is predicted to occur in the order of 5≈7 (3,6>4), and electrophilic halogenation[26] and nitration[27] are reported to occur at the 5-position. The corresponding orders in 1,2,3-benzoxadiazole and benzoxazole are 7>5 (6>4 by method I and 4>6 by method II), and 7>4,5,6 (2), respectively. The hydrolysis of benzoxazole in alkaline solution is possibly due to a nucleophilic attack on the C-2, but its electrophilic substitution such as nitration is known to occur at the C-6.

Concerning the negatives of the highest occupied orbital and lowest vacant orbital energies which represent ionization potential and electron affinity, respectively, it is of interest to note that the presence of the polar N–O bond in the benzo-derivatives as well as the five-membered heterocycles tends to increase both values so as to justify the contribution of the electrostatic interaction to π-energy stabilization. However, few experimental data are available to check the predicted tendency.

It is known[28] that indoxazene undergoes photochemical isomerization into benzoxazole and at the same time ring-cleavage into the nitrile of salicylic acid. The present calculation indicates that excitation into the lowest $^1(\pi, \pi^*)$ and/or $^3(\pi, \pi^*)$ state induces decrease of the π-bond orders in the O–N–C linkage of indoxazene and favours bond-lability (See the corresponding molecular diagrams in Fig. 2(a) and 2(b).).

More discussions will be made for the nitrogen-containing heterocycles; firstly, the experimental basic pK_a values of five-membered heterocycles (6.95(imidazole), 2.53 (pyrazole), 2.55 (1,2,4-triazole))[29a] are found in bad correlation with the ordering of the π-electron density on the pyridine-type nitrogen. It is probable that the present disagreement is partly due to difference in the protonation energy except π-energy term, since a recent CNDO-type calculation of the total

20) A. R. Katritzky and J. M. Lagowsky, "Heterocyclic Chemistry," John Wiley, New York (1961), p. 221.
21) I. M.Basset, R. D. Brown and A. Penfold, *Chem. Ind.*, **1956**, 892.
22) J. H. Bayer, "Heterocyclic Compounds," Vol. 7, Chap. 6, Ed. by R. C. Elderfield, John Wiley, New York (1961).
23) H. Lindemann and H. Thiele, *Ann. Chem.*, **449**, 63 (1926).
24) W. Ried and H. Gutjahr, *Chem. Ber.*, **86**, 1096 (1953).
25) G. Del Re, *Tetrahedron*, **10**, 81 (1960).
26) E. Bamberger and L. Lublin, *Ber.*, **42**, 1676 (1909).
27) K.-H. Wünsch, H. Linke, A. J. Boulton and Altaf-ur-Rahman, *Chem. Commun.*, **1965**, 408.
28) H. Göth and H. Schmidt, *Chimia*, **20**, 148 (1966).
29a) G. Leandri, A. Mangani, F. Montanari and R. Passerini, *Gazz. Chim. Ital.*, **85**, 769 (1955).
29b) J. D. Vaugham, *Tetrahedron Lett.*, **1968**, 3237.

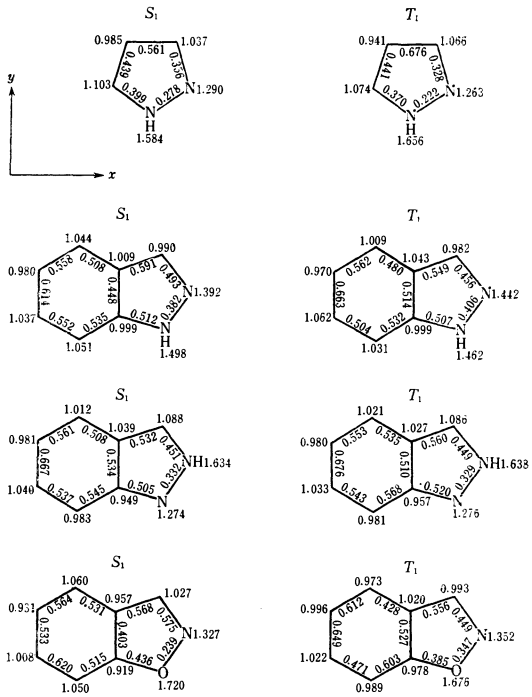

Fig. 2(a). Molecular diagrams at the lowest $^1(\pi, \pi^*)$—S_1— and $^3(\pi, \pi^*)$—T_1— states calculated by method I.

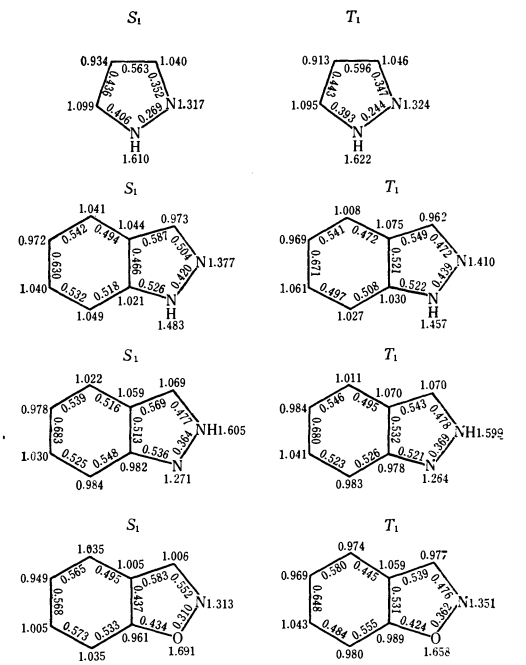

Fig. 2(b). Molecular diagrams at the lowest $^1(\pi, \pi^*)$—S_1— and $^3(\pi, \pi^*)$—T_1— states calculated by method II.

molecular protonation energy assuming the same regular pentagon geometry[29b] can predict correctly the experimental order of pK_a. Also, the predicted relations, $q^{\pi}_{=N-}$(pyrazole)$>q^{\pi}_{=N-}$(imidazole) and $q^{\pi}_{-\underset{H}{N}-}$(pyrazole)$\sim q^{\pi}_{-\underset{H}{N}-}$(imidazole) appear as incompatible with the observed order[30] of strength of the autoassociating hydrogen-bond in these molecules, indicating that the autoassociation involves complicated polymerization as usually accepted.

In the case of pyrazole the charge distribution predicts that electrophilic substitution occurs in the order of $4>5>3$, in agreement with the accepted fact that the ordinary electrophilic substitutions proceed readily at the 4-position. But the theoretical prediction for pyrazole should be modified because it is known that there is a tautomeric exchange of the position of the N–H bond so that the 3- and 5-positions should be considered as equivalent. As for imidazole the predicted order of electrophilic substitution is $5>2>4$, while nitration[31] and sulfonation[32] occur at the 5- and 4-positions. This may also be due to the equivalence of both positions associated with tautomerism. It should be mentioned here that diazonium coupling has been found to occur at the 2-position in imidazole, in disagreement with the predicted ordering. Electrophilic substitution on benzimidazole, 2*H*-indazole and 1*H*-indazole is predicted to occur in the order of $7\geqq6\geqq5\geqq4$ (by method I) and $7\geqq5\geqq6\geqq4$ (by methodII), $3>5>7>4$, and $7>5$, respectively, while it is known that nitration of benzimidazole occurs at the 5(6)-position,[33] and nitration[34] and halogenation[35] of indazole occur at the C-5 and C-3(5), respectively.

Electrophilic substitution on 1,2,3-triazole is predicted to occur at the 5-position, while actual bromination is known to give the 4,5-dibromoderivative.[36] In the case of 1,2,4-triazole with π-electron-deficient C atoms, such electrophilic substitutions as halogenation, sulfonation and Friedel-Crafts' alkylation of the nucleus are unknown. Electrophilic substitution on 1*H*-benzotriazole is predicted to occur at the C-5 and C-7 positions, while nitration[37] and chlorination[38] are known to occur at the 4,7- and 4,5,6,7-positions,

30) V. Lorenzelli and G. Randi, *Atti. accad. nazl. Lincei, Rend. Classe sci. fis., mat. e nat.*, **36**, 646 (1964).
31) R. G. Fargher and F. L. Pyman, *J. Chem. Soc.*, **1919**, 217; R. G. Fargher, *ibid.*, **1920**, 668.
32) F. L. Pyman and L. A. Ravald, *ibid.*, **1920** 1429.
33) G. M. Van der Want, *Rec. Trav. Chim. Pays-Bas*, **67**, 45 (1948).
34) K. v. Auwers and H. Kleiner, *J. Prakt. Chem.*, **118**, 75 (1928).
35) K. v. Auwers and H. Lange, *Ber.*, **55**, 1139 (1922).
36) R. Hüttel and A. Gebhardt, *Ann. Chem.*, **558**, 34 (1947).
37) N. L. Miller and E. C. Wagner, *J. Amer. Chem. Soc.*, **76**, 1847 (1954).
38) R. H. Wiley, K. H. Hussung and J. Moffat, *ibid.*, **77**, 5105 (1955).

respectively.

It is known that the calculated ionization potential becomes higher by the increase of π-electron localization; among the five-membered diazoles and triazoles the largest value is found in 1,2,5-triazole with a polar N–NH–N linkage, and in the case of the molecules with one NH–N bond it is enhanced most for 1,2,4-triazole with alternate arrangement of plus and minus charges. The calculated electron affinity is in parallel relation with the corresponding ionization potential except for the case of 1,2,3- and 1,2,4-triazoles. So far as the present result is concerned, the effect of atom-rearrangement upon the relative orderings of both value is not affected by the replacement of pyrrole-nitrogen with furan-oxygen. On fusing the benzene-ring the ionization potential tends to be lowered, and the difference of the ionization potential and electron affinity is minimized at benzo-1,2,5-triazole in which the pyrrole-nitrogen mostly donates its π-electron to the whole conjugated system. Now, the lower ionization potentials calculated by method I are higher by $\sim$0.5 eV than those evaluated by a generalized free-electron model.[7]

It is known, by analogy with indoxazene, that 1*H*-indazole and pyrazole undergo photoisomerization into benzimidazole and imidazole, respectively.[39] But the mechanism in detail is unknown excepting that the presence of quinoid-type tautomer and the introduction of electron-donating group into the 5- or 6-position appears to favour the isomerization of 1*H*-indazole. For reference the π-electron distributions for the lowest $^1(\pi, \pi^*)$ and $^3(\pi, \pi^*)$ which were calculated with the CI procedure are given in Fig. 2(a) and 2(b). The result indicates that such excitations on 1*H*-indazole and pyrazole give rise to increased convertibility of 1*H*-indazole into 2*H*-tautomer as expected from the photoexcited change in the π-electronic state on the –NH–N–C– system, and to the increased lability of the pyrazole ring as expected from the much reduced π-bond orders.

39) H. Tieffenthaler, W. Dörschein, H. Göth and H. Schmid, *Tetrahedron Lett.*, **1964**, 2999; H. Göth, H. Tieffenthaler and W. Dörschein, *Chimia*, **19**, 596 (1965).

BULLETIN OF THE CHEMICAL SOCIETY OF JAPAN VOL. 43 3353—3357 (1970)

The Distribution of the Acid Strength on Zeolite Catalyst — Estimation from the Heats of Adsorption —

Yasuaki OKAMOTO, Toshinobu IMANAKA and Shiichiro TERANISHI

Department of Chemical Engineering, Faculty of Engineering Science, Osaka University, Machikaneyama, Toyonaka, Osaka

(Received May 15, 1970)

The distribution of the acid strength on two zeolites, 13X and 10X, and on the copper form of X-type zeolite were estimated from the differential heats of *n*-butylamine adsorption in a benzene solution. The acid sites on these zeolites were revealed to have two kinds of acid strengths, that is, the cation-dependent one and the cation-independent one. The former corresponds to the stronger acid strength, and the latter, to the weaker. The IR spectra of the residual surface OH groups on these catalysts were also investigated. The strongest acid sites on each zeolite were considered to be those of the cation-dependent OH group which has the lowest frequency. The interaction between surface OH groups and immersed benzene was assumed to be a π-type hydrogen bond.

It is expected that the properties of catalytic reaction on an acidic catalyst can be explained in terms of the distribution of acid strength on it. The distribution of surface acid strength has usually been measured by means of the indicator method[1] and the volumetric-base adsorption method.[2,3] The former method, however, is incapable of measuring the acid strength of colored solids which include many cation-exchanged zeolites and other useful acidic catalysts. The number of useful indicators is limited, and their pKa values lie only between -8.2 and $+6.8$

1) H. A. Benesi, *J. Phys. Chem.*, **61**, 970 (1957).

2) G. A. Mills, E. R. Boedecker and A. G. Oblad, *J. Amer. Chem. Soc.*, **72**, 1554 (1950).

3) R. G. Richardson and S. W. Benson, *J. Phys. Chem.*, **61**, 405 (1957).

discontinuously. Therefore, this method has disadvantages for obtaining a continuous value and for providing both the stronger and weaker acid strengths. From the fraction of the base which desorbs slowly, the latter method allows some estimation of the number of effective acid sites and the average acid strength of the sites, as measured by the activation energies for desorption. As this method gives only the average acid strength, however, it is not effective in discussing the relation between the acid properties and the acid catalytic reactions. Consequently, the distribution of the differential adsorption heats of base must be measured in order to clarify the behavior of acidic catalysts of varying activities in terms of a site-energy distribution, that is, the number of acid sites and their individual strength.

Direct measurements of the adsorption heat of a base on acidic catalysts have been carried out by several workers. Richardson and Benson[3] measured the heat of adsorption of trimethylamine on Davison DA-1 cracking catalysts at 300°C with a crude adiabatic calorimeter, but gave only average values. Chessick and Zettlemoyer[4,5] determined quantitatively the site-energy distributions on attapulgite, silica-aluminas, and kaoline cracking catalysts on the basis of immersional heats in butylamine.

In this paper, the differential heats of the adsorption of *n*-butylamine in benzene are used for the elucidation of the acid-strength distributions on zeolites. Moreover, the relation between the acid strength and the frequencies of the IR adsorption bands of the residual surface OH group is discussed.

Experimental

Materials. The molecular Sieves, 13X and 10X, were supplied by the Union Carbide Company. In order to prepare copper-form X-type zeolite (CuX), sodium ions in 13X zeolite were 48.1% exchanged in a conventional method for Cu(II) with a copper sulfate solution. The *n*-butylamine was of a commercial grade and was used in adsorption experiments as a benzene solution. The benzene was purified by dehydration with sodium metal and subsequent distillation. The concentration of *n*-butylamine in benzene was determined in the following manner. *n*-Butylamine in benzene was extracted from the benzene phase to the water phase by pouring water into it, and then it was neutralized with a dilute aqueous HCl solution in the water phase, using phenolphthalein as an indicator. The normality of the amine solution was in the range of 0.165—0.0025 N.

Procedure. After zeolite had been treated in a glass ampoul at 400°C for several hours under a vacuum, it was used in the adsorption experiments. The over-all heat, which evolved when the treated zeolite was immersed in a benzene solution of *n*-butylamine at 25°C, was measured with a micro calorimeter manufactured by the Applied Electric Lab., Ltd. The amount of amine adsorbed on zeolite was elucidated by washing the immersed zeolite with benzene several times and then by using the neutralization method described in the previous section in connection with a material balance.

The amounts of *n*-butylamine adsorbed on zeolite from the gas phase were determined with a thermanobalance at different temperatures. Zeolite was dehydrated to a constant weight in a flowing stream of nitrogen at 400°C and then cooled to an adsorption temperature in it. *n*-Butylamine was introduced on the dehydrated, constant-weight zeolite at that temperature by the passage of nitrogen gas through a saturator containing *n*-butylamine. The increase in weight in comparison with that of the dehydrated zeolite is due to the physically- and chemically-adsorbed *n*-butylamine. In order to determine the amount of *n*-butylamine chemisorbed, the zeolite saturated with *n*-butylamine was flushed with nitrogen gas in order to remove the physically-adsorbed *n*-butylamine. After this treatment, the increase in weight was considered to reflect the amount of *n*-butylamine chemisorbed at that temperature.

The behavior of the residual OH groups on these zeolites was observed by means of studying the infrared spectra with a Hitachi IR spectrometer. The disks of zeolites were heated at 200—300°C in an IR cell under a vacuum. The disks were prepared by pressing zeolites between two polished stainless steel plates to a pressure of about 5 ton/cm^2.

The H-D exchange reaction of OH groups on the zeolites used was carried out with D_2O (supplied by the Merck Co.) in an IR cell at 400—500°C.

Results and Discussion

The surface properties of zeolite are assumed to be dependent on the amount of water on the surface. Figure 1 shows that the heats of immersion for 13X and 10X zeolites in benzene vary with the preheating temperature. The value for 13X

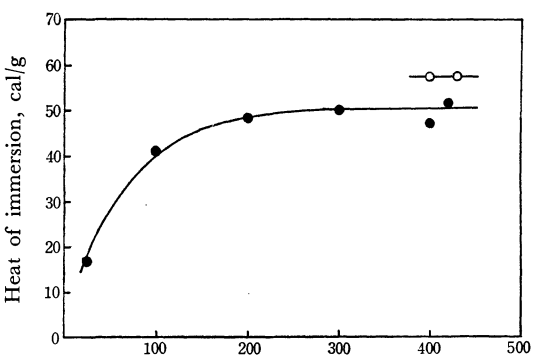

Fig. 1. Dependency of immersion in benzene on preheating temperature.
● 13X, ○ 10X

4) J. J. Chessick and A. C. Zettlemoyer, *J. Phys. Chim.*, **62**, 1217 (1958).

5) A. C. Zettlemoyer and J. J. Chessick, *ibid.*, **64**, 1131 (1960).

gradually increases up to about 300°C and then becomes constant at about 400°C. The heats of immersion contain the surface energy of the solid and liquid and the energy of interaction between the surfaces of the solid and molecules in a liquid. Thus, it may be supposed, from the constancy of the heats of immersion, that the interaction between them is not dependent upon the preheating temperature beyond about 300°C. When these catalysts are dehydrated in a flowing stream of nitrogen gas at an incremental temperature, the change in their weights becomes constant beyond about 300°C. It is revealed by the IR spectra that the change in their weights is due to the adsorbed water. The amount of water adsorbed depends on the treating temperature as does the heat of immersion. The results suggest that the properties of the surfaces of the 13X and 10X zeolites are dependent mainly on the amount of adsorbed water and that they remain almost constant beyond 300°C.

The distribution of the acid strength on an acidic catalyst is expressed as that of the differential heats of adsorption of a base on its acid site. In our experiments, the acid-strength distribution of zeolites is determined from both the differential heats of the adsorption of *n*-butylamine in benzene and the amount of *n*-butylamine chemisorbed from the benzene phase.

The total heat which evolved in the system when zeolite was immersed in a benzene solution of *n*-butylamine includes the heat of the immersion of zeolite in benzene and the adsorption heats of *n*-butylamine on the acidic sites. When the sum of the coverage of the immersed benzene and that of the adsorbed base is assumed to be unity, the following equations can be derived;

$$\theta_A + \theta_B = 1 \quad (1)$$

$$Q_T(\theta_A, \theta_B) = Q_A(\theta_A, \theta_B) + Q_B(\theta_A, \theta_B) \quad (2)$$

where θ_A and θ_B are the coverages of the adsorbed *n*-butylamine and the immersed benzene respectively; Q_T, the total heat evolved in the system (cal/g); Q_A, the evolved heat due to adsorbed *n*-butylamine, that is, the integral heats of adsorption (cal/g), and Q_B, the evolved heat due to immersed benzene (cal/g). If the interactions between adsorbed *n*-butylamine and immersed benzene are neglected, $Q_B(\theta_A, \theta_B)$ is $Q_B^\circ \times \theta_B$ and $Q_A(\theta_A, \theta_B)$ is $Q_A(\theta_A)$, where Q_B° is the heat of immersion in the absence of adsorbed *n*-butylamine. Therefore,

$$Q_T(m_A) = Q_A(m_A) + Q_B^\circ \times [1-(m_A/m_A^\circ)]$$
$$\theta_A = m_A/m_A^\circ \quad (3)$$

where m_A is the amount of *n*-butylamine adsorbed on acid sites on zeolite (mol/g) and m_A°, the saturated amount of it. Figure 2 shows the $Q_T(m_A)$ values of 13X, 10X, and CuX.

The m_A° value of each catalyst is deduced from the amount of *n*-butylamine adsorbed on zeolite from the gas phase, as determined with a thermanobalance at 25°C. The m_A° values are 2.7 mmol/g, 3.2 mmol/g, and 2.7 mmol/g for 13X, 10X, and CuX respectively. Figure 3 shows clearly that $Q_A(m_A)$ consists of two straight lines. The differential heat of the adsorption of *n*-butylamine is obtained from Eq. (3):

$$dQ_A(m_A)/dm_A = dQ_T(m_A)/dm_A + Q_B^\circ/m_A^\circ \quad (4)$$

On the basis of the value of $dQ_A(m_A)/dm_A$ calculated from Eq. (4), Figure 4 shows the acid-strength distribution on these zeolites in terms of the differential heats of adsorption; that is, the acid strength and the ordinate show the acidity corresponding to each acid strength. It is interestingly found that acid sites of each zeolite have a distinct distribution of differential heats of adsorption with two peaks, indicating two kinds of acid strengths. The stronger acid site varies with the

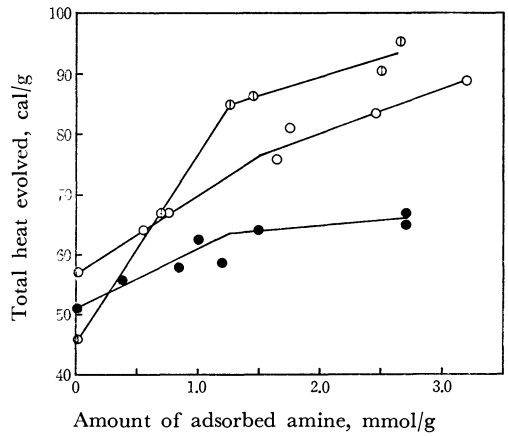

Fig. 2. Total heat evolved in system *vs.* amount of adsorbed *n*-butylamine.
● 13X, ○ 10X, ⊕ CuX

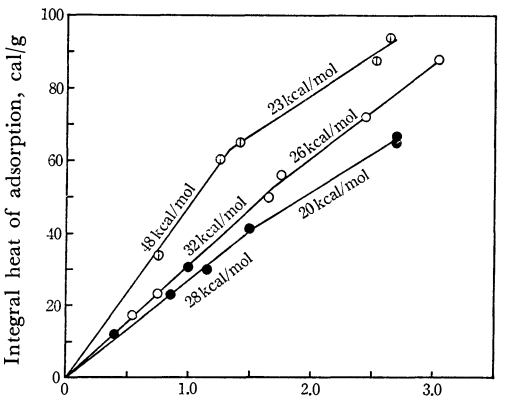

Fig. 3. Integral heat of adsorption of *n*-butylamine *vs.* amount of adsorbed amine. Numerical values are differential heats of adsorption calculated from Eq. (4).
● 13X, ○ 10X, ⊖ CuX

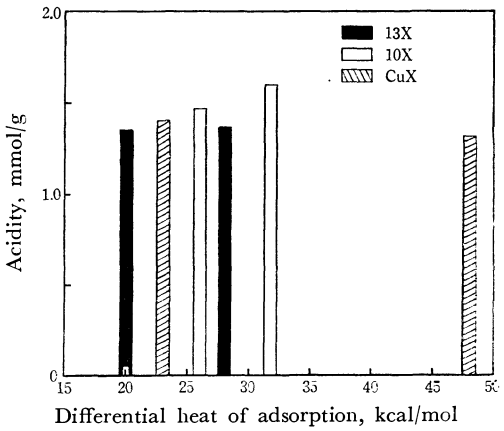

Fig. 4. Distributions of acid strength.

three zeolites used, but the weaker one is about constant. Therefore, the stronger acid site is cation-dependent, and the weaker one is cation-independent. It is considered that the reaction activities of these catalysts are dependent on the stronger one rather than on the weaker one. Thus, it is well and quantitatively shown that the activity of a reaction on cation-exchanged zeolite changes with the kind of the cation on zeolite.

The distribution of acid strength is estimated from the amount of *n*-butylamine adsorbed from the gas phase at an incremental temperature. Figure 5 shows the amounts of *n*-butylamine chemisorbed at various desorption temperatures. The curves are divided into two parts; one is in the region of desorption temperatures lower than about 150°C, while the other is in a higher temperature region than this. This behavior of the adsorbed amine also suggests that the acid sites on the zeolites have two kinds of acid strengths. This result is in agreement with that from the calorimetric method.

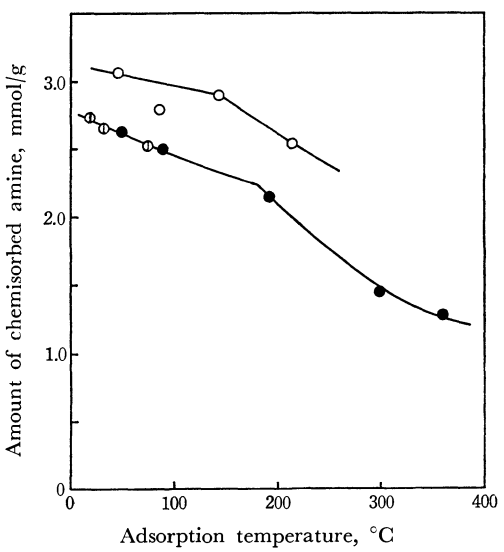

Fig. 5. Temperature dependency of chemisorbed amount of *n*-butylamine.

● 13X, ○ 10X, ⓘ CuX

It has been reported[6] that the acid sites of zeolite which is pretreated under a vacuum at 400°C consist almost entirely of Brönsted acid, that is, of residual surface OH groups. Therefore, the distribution of acid strength which is estimated here from the calorimetric method corresponds to that of the acid strength of the Brönsted acid sites. The acid strength of the Brönsted sites is deduced to be depend on the frequency of the residual OH group. It has previously been shown [7-9] that each zeolite has a few kinds of residual surface OH groups. It is interesting, therefore, to clear up the relation between the distribution of acid strength and that of the frequencies of the surface residual OH groups on zeolites. In this paper, the IR spectra of zeolites were investigated. The stretching vibrations of surface OH groups appear in the region of 3750 cm^{-1}—3600 cm^{-1}, but in this region

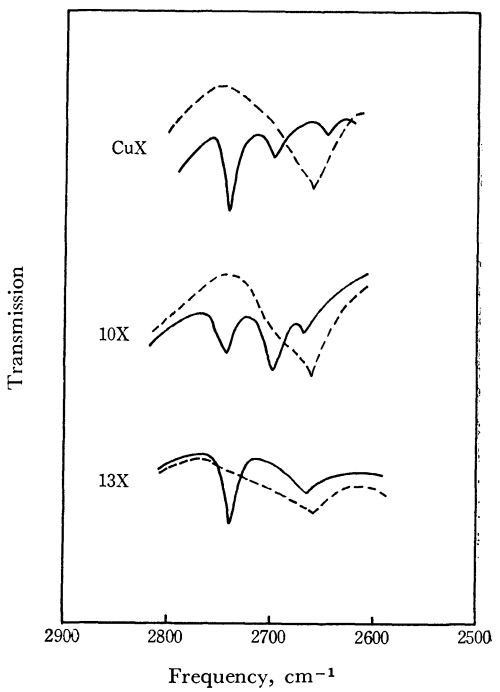

Fig. 6. Effect of adsorbed benzene on zeolite, solid line; IR spectra of residual surface OD groups on zeolite, dotted line; after introduction of benzene.

6) J. W. Ward, *J. Cat.*, **11**, 251 (1968).
7) L. Bertsh and H. W. Habgood, *J. Phys. Chem.*, **67**, 1621 (1963).
8) J. L. Carter, P. J. Lucchesi and J. C. Yates, *ibid.*, **68**, 1385 (1964).
9) C. L. Angell and P. C. Schaffer, *ibid.*, **69**, 3463 (1965).

of the spectrum, the stretching vibrations of OH groups of water adsorbed on KBr windows appear also and the transmission of infrared rays is small because of their large divergence. Thus, the surface residual OH groups were turned into OD groups with D_2O. The solid lines in Fig. 6 show the IR spectra of the OD groups on the zeolites used. 10X and CuX have three species of residual OD groups, while 13X has only two. These OD groups are classified into two groups according to the dependency on the cation of the zeolite; that is, group (I) contains OD groups which are independent of the kind of the cation, while in group (II) they are dependent on it. Group (I) contains the 2733-cm^{-1} band on 13X, 10X, and CuX, and the 2699-cm^{-1} band on 10X and CuX, while group (II) includes the 2645-cm^{-1}, 2665-cm^{-1}, and 2668-cm^{-1} bands on CuX, 10X, and 13X respectively. It is shown above that the acid sites of zeolites have two kinds of acid strengths, namely, the cation-independent and cation-dependent acid strengths. The relation between the distribution of the acid strength and the behavior of residual surface OD groups can be obtained on the basis of these observations. Figure 7 shows that the differential heat of the adsorption of *n*-butylamine on the stronger acid sites depend linearly upon the frequency of the OD group which is lowest one on each zeolite. Therefore, it may be concluded that the stronger acid sites, which are cation-dependent, correspond to the cation-dependent OH group which has the lowest frequency. It may also be deduced that the reaction activity on zeolite generally depends on the lowest frequency of the residual OH group.

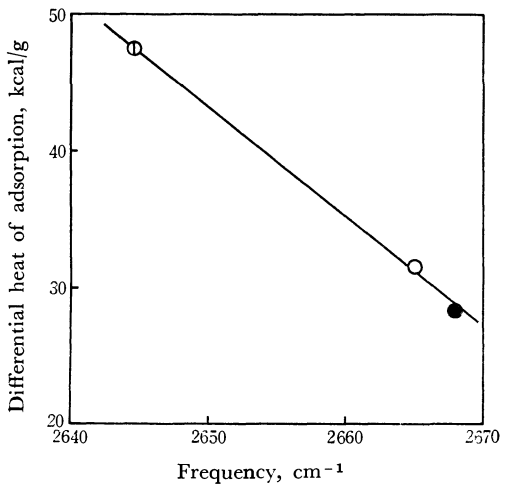

Fig. 7. Relation between differential heats of adsorption on *n*-butylamine and frequencies of residual surface OD groups.
● X, ○ 10X, ⓘ CuX

As the heats of the adsorption of *n*-butylamine were measured in benzene, the surface OH groups were affected by the immersed benzene. The influence of the immersed benzene can be estimated from the change in the IR spectra of the OH group due to adsorbed benzene. The dotted lines in Fig. 6 show that the spectra of surface OH groups are broadened and that these groups are shifted to lower frequencies. The behavior of these group is the reverse of the adsorption and desorption of benzene molecules. When the surface OH group is hydrogen-bonded, the spectrum shows a similar behavior. On the basis of this fact and the properties of benzene, it may be concluded that the changes in the spectrum are due to the interaction between the π-electron system of the benzene molecule and the surface OH groups, that is, the π-type hydrogen bond.[10]

Conclusions

The acid-strength distribution of zeolite was estimated from the differential heats of *n*-butylamine adsorption in benzene. The acid strengths of the zeolites used were of two kinds, cation-dependent and cation-independent. The residual surface OH groups are classified into two groups, the cation-dependent group, which has the lowest frequency, and the cation-independent one. The stronger acid site, whose strength is dependent on the cation corresponds to the cation-dependent OH groups on zeolites which have the lowest frequencies. The π-electron system of the benzene molecule adsorbed on zeolite interacts with residual surface OH groups; this interaction are estimated to consist of a π-type hydrogen bond.

10) G. A. Galkin, A. V. Kiselev and V. I. Lygin, *Trans. Faraday Soc.*, **60**, 431 (1964).

BULLETIN OF THE CHEMICAL SOCIETY OF JAPAN VOL. 43 3358—3363 (1970)

Electron Spin Resonance Study on Radical Anions of Acridine and Its Halogen Derivatives

Shiro KONISHI, Shigeya NIIZUMA and Masao KOIZUMI

Department of Chemistry, Faculty of Science, Tohoku University, Katahira, Sendai

(Received May 16, 1970)

ESR spectra of radical anions produced by bringing 9-chloro-, 2,7-dibromo-9-chloro-, and 2,4,5,7-tetrabromo-9-chloroacridine into contact with alkali metal (sodium and potassium) in tetrahydrofuran were measured at room temperature and/or at lower temperatures, and the analysis of them was made by means of a simulation method. Hyperfine coupling constants of acridine anion radicals, produced by the similar method in tetrahydrofuran and also by the electrolytic reduction in acetonitrile with the flow method, were determined, taking those of halogen derivatives into consideration. ESR spectra of acridine and 9-chloroacridine anion radical were found to involve the coupling of sodium, showing that these radicals were in the form of ion pair. The coupling constants of bromoacridine anion radicals did not give any difference between the sodium and the potassium reduction. The couplings of halogen atoms were not observed. Good agreement was obtained between the coupling constants calculated from spin densities and those determined experimentally. In general, the solution of radical anions of halogenides gradually yields brownish aggregates at lower temperatures (−20∼−30°C), their ESR spectra becoming weaker and unresolved. The temperature change is reversible and qualitatively resembles the behavior of acridine anion radical.

In a previous paper,[1] the physicochemical behavior of the radical anions of acridine paired with alkali cations in THF was investigated in detail. It was found that the paramagnetic monovalent anion transforms to the diamagnetic dianion in the presence of excess alkali metal and that a certain association reaction of the $n(A^-Na^+) \rightleftarrows (A^-Na^+)_n$ type (n, perhaps 2) occurs in THF. It was further found that this equilibrium shifts to right with lowering the temperature. Furthermore, we obtained the ESR spectrum consisting of more than fifty lines most plausibly attributable to the radical anion of acridine, but an attempt for analysis was postponed.

When we succeeded in taking the ESR spectrum with hyperfine structure, there was no such work found in literature. But in the course of our investigation, two papers dealing with the ESR of acridine radical anion appeared. One is Hoeve and Yeranos's[2] and the other, Szwarc *et al.*'s.[3] The hfs constants of the acridine radical anion produced by electrolysis in pyridine were determined by the former workers, while by the latter workers the similar determination was made for the radical anion produced by the alkali metal method in hexamethylphosphoramide.

In continuance of our study we have succeeded in obtaining the ESR spectrum of acridine radical anion produced electrolytically in acetonitrile. Although the radical anion thus produced was rather unstable, its hfs could be studied successfully by employing the flow method. Further, we have taken the ESR spectra of radical anions originating from a few halogen substituted acridines which also displayed good hfs. As is well known, the substitution of halogen atoms for aromatic ring protons generally makes the analysis of the spectrum easier because of the disappearance of the proton coupling[4] at the substitution positions (there is some line broadening, however, and in the case of chlorine substitution there are some papers reporting on the resolution of hfs coupling of chlorine,[5,6] which is rather remarkable).

The results for the radical anions of (I) have been found to be in good agreement with those in literature except for the case of sodium reduction, in which the sodium coupling was observed and other coupling constants were somewhat different from those in other cases. This implies that the radical anion in the latter cases exists

1) S. Niizuma, M. Okuda and M. Koizumi, This Bulletin, **41**, 795 (1968).

2) H. G. Hoeve and W. A. Yeranos, *Mol. Phys.*, **12**, 597 (1967).

3) J. Chandhuri, S. Kume, J. Jagur-Grodzinski and M. Szwarc, *J. Amer. Chem. Soc.*, **90**, 6421 (1968).

4) M. Bruin, F. Bruin and F. W. Heineken, *J. Chem. Phys.*, **37**, 135 (1962).

5) T. C. Hollocher, N. M. Tooney and R. Adman, *Nature*, **197**, 74 (1963).

6) B. T. Allen and W. Vanneste, *ibid.*, **204**, 991 (1964).

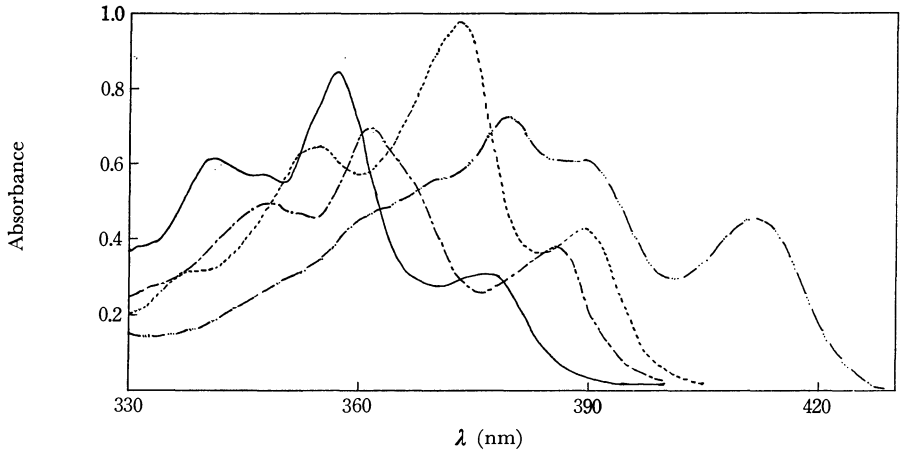

Fig. 1. Electronic absorption spectra of acridine and its halogen derivatives.
ca. 7×10^{-5} M in tetrahyrofuran.
——; I, —·—; II, ----; III, —···—; IV

essentially as free (at least from the viewpoint of ESR) while with sodium cation the formation of ion pair occurs. It has been established that the coupling constants obtained, satisfy McConnell's relation moderately well.

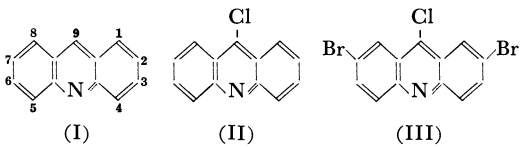

(I) (II) (III)

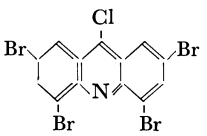

(IV)

Experimental

A JEOL P-10 type ESR spectrometer was used. Its characteristics and the apparatus for temperature control are the same as descrived in the previous paper.[1]

Materials. THF was purified in the same way as in the previous paper.[1] First grade acetonitrile from Wako Junyaku was distilled, dried on calciumhydride and then stored in vacuo. (I) was purified in the way described in the previous paper.[7] (II) was synthesized from *N*-phenylanthranylic acid after Albert and Ritchie,[8] (III) and (IV) from acridon after Acheson and Robinson[9] and recrystalized from THF. Mass spectra of these halogenides were in good agreement with the theoretical distribution. Electronic spectra of these compounds are shown in Fig. 1.

Procedure. Anion radicals were prepared by bringing 2 m*l* degassed THF solutions containing several mg of acridines into contact with a sodium mirror deposited by vacuum evapolation. In the case that an anion was unstable at room temperature, the contact was carried out in dry ice methanol bath. A flow method apparatus as shown in Fig. 2 was devised for the steady current electrolysis. The flow was controlled by cock C, and checked by the time interval necessary for one drop to fall down from the tip of capillary, F. The optimum flow rate was 10.3 sec/one drop. 5 to 6 V was applied between anode and cathod, A and B.

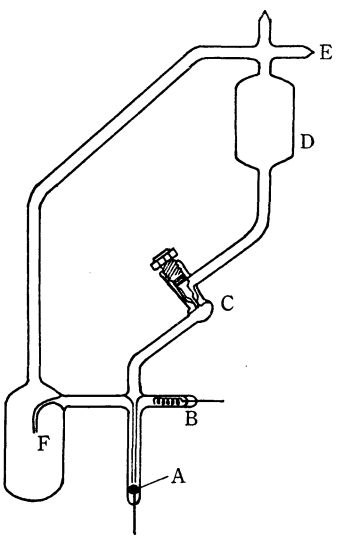

Fig. 2. The apparatus for the flow method electrolytic reduction.
A; Mercury anode
B; Platinum cathode
C; Teflon greeseless cock
D; Reservoir for the solution
E; A diffusion pump
F; Capillary for checking the flow rate

7) S. Niizuma and M. Koizumi, This Bulletin, **36**, 1629 (1963).
8) Albert and Ritchie, *Org. Synthesis*, **22**, 5 (1942).
9) R. M. Acheson and M. J. T. Robinson, *J. Chem. Soc.*, **1954**, 232; *ibid.*, **1953**, 4142.

Spin Density Calculation and Simulation of ESR Spectrum. The spin densities on nitrogen, carbon and halogen atoms of acridines were calculated by a simple LCAO-MO method. For simulation of ESR spectra, the simulation program was composed in our laboratory. The calculation and the simulation were carried out on the NEAC-2200 Model 500 Electronic Computer in the Calculation Center of Tohoku University.

Results and Discussion

2,4,5,7-Tetrabromo-9-chloroacridine (IV). ESR spectrum obtained by making contact with sodium mirror at room temperature, is shown in Fig. 3(a). The spectrum changes from (a) to (d) as the temperature is lowered and this temperature change is reversible. It is seen that the signal is more resolved at lower temperature, and at room temperature it becomes highly broadened with no apparent reduction in intensity. Any difference was not observed between sodium and potassium as a reducing agent. This means that the two anion radicals have the similar structures, suggesting that they exist as free ions. But these two ion pairs which are equally unstable at room temperature show quite different modes of destruction.

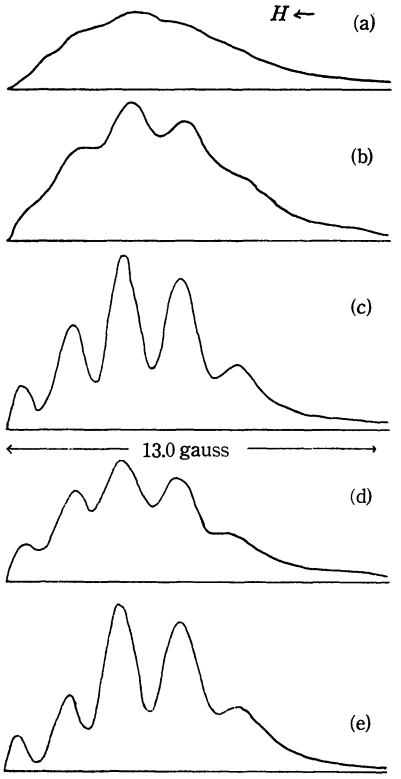

Fig. 3. ESR spectra of radical anion of IV. (a); at +15°C, (b); at −16°C, (c); at −55°C, (d); at −70°C, (e); Simulated spectrum, corresponding to (c).

Thus the ion pair with sodium cation decays according to the first order rate formula with a half life of 180 min (at 22°C) while the potassium ion pair obeys the second order (Fig. 4a, b). Furthermore the solution after reaction becomes yellowish brown in the former case while in the latter it is colorless and the electronic absorption spectrum strongly suggests the destruction of acridine frame.

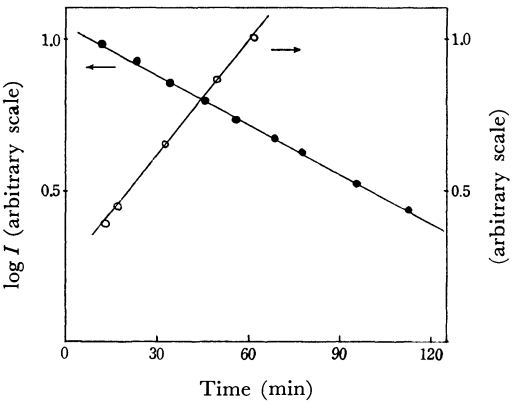

Fig. 4. The decay curve of ESR signal intensity for radical anion of IV.
● Sodium reduction, at 22°C
○ Potassium reduction, at 0°C

By assuming that the coupling of halogen atoms is not resolved and by neglecting the coupling of sodium, hfs was analysed satisfactorily. The simulation spectrum obtained by taking only a nitrogen atom and two pairs of magnetically equivalent protons, is shown in Fig. 3(e) which corresponds to the observed one (c). The parameters used for simulation and the calculated spin densities are listed respectively in Tables 1 and 2 given later, together with those for the other compounds.

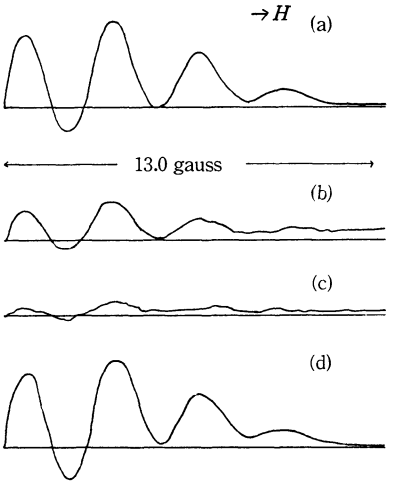

Fig. 5. ESR spectra of radical anion of III. (a) at +22°C, (b) at −51°C, (c) at −78°C, (d) Simulated spectrum, corresponding to (a).

TABLE 1.

Anion radical	Method of reduction	Temp.	Coupling constant (gauss) H_1	H_2	H_3	H_4	H_9	N	Metal	Δh (gauss)	Total width (gauss)
Acridine	Sodium (THF)	room temp.	2.59	1.13	2.14	2.03	8.78	4.17	0.56	0.10	34.6
	Potassium (THF)	room temp.	2.83	0.57	2.31	1.36	7.74	3.79		0.34	29.5
	Electrolytic (CH_3CN)	room temp.	2.75	0.79	2.23	1.57	7.60	3.40	——	0.34	29.1
	Electrolytic[2] (pyridine)	10°C	2.73	0.81	2.19	1.60	7.74	3.48	——		29.4
	Sodium[3] (HMPA)	room temp.	2.78	0.91	2.02	1.82	7.60	3.72			30.1
	Calcd*		2.65	0.75	1.90	1.60	7.60	3.60			28.6
9-Chloro-acridine	Sodium (THF)	−55°C	2.90	0.80	2.30	1.60	——	3.90	0.80	0.60	25.4
	Calcd*		2.71	0.64	1.93	1.56	——	3.24			20.2
2,7-Dibromo-9-chloro-acridine	Sodium and potassium (THF)	room temp.	3.00	——	2.60	0.87	——	3.10		1.00	19.1
	Calcd*		2.48	——	2.04	1.59	——	3.37			19.0
2,4,5,7-Tetra-bromo-9-chloroac-ridine	Sodium (THF)	−55°C	2.20	——	2.00	——	——	3.42		1.45	15.2
	Potassium (THF)	−58°C									
	Calcd*		2.23	——	1.76	——	——	3.62			15.2

* The values calculated by a simple LCAO-MO method (see text).

TABLE 2. UNPAIRED SPIN DENSITY

Compound	C_1	C_2	C_3	C_4	C_9	N	C_N*
Acridine	0.0947	0.0268	0.0679	0.0570	0.2716	0.1507	0.0368
9-Chloroacridine	0.0969	0.0229	0.0690	0.0558	(0.2648)**	0.1338	0.0377
2,7-Dibromo-9-chloroacridine	0.0886	(0.0225)	0.0729	0.0569	(0.2569)	0.1391	0.0368
2,4,5,7-Tetrabromo-9-chloroacridine	0.0795	(0.0237)	0.0629	(0.0579)	(0.2440)	0.1495	0.0408

* C_N carbon atom adjacent to nitrogen.
** The value in the parenthesis is the spin density at the position substituted by halogen.

2,7-Dibromo-9-chloroacridine (III). The radical anion originating from this compound has four sets of atoms which are responsible for hfs, *i.e.*, a nitrogen and three pairs of magnetically equivalent protons. The anion radical produced from III by using sodium as a reducing agent was stable at room temperature and gave a ESR spectrum shown in Fig. 5(a). Signal intensity decreased with lowering temperature, as is shown in in Fig. 5(b) and (c). This change was reversible and qualitatively the same as observed in the acridine radical anion.[1] The similar ESR signal was obtained by using potassium as a reducing agent and the values of hfs constants were equal to the ones for the sodium reduction. The simulated spectrum, (d) in Fig. 5, corresponds to the observed one, (a) in Fig. 5.

9-Chloroacridine (II). The anion radicals of II were stable at room temperature. Their ESR spectra were measured in the best condition at −55°C for the sodium reduction and at −66°C for the potassium reduction and are shown in Fig. 6(a) and (b) respectively. The analysis of the spectrum for the sodium reduction was accomplished by taking account of sodium coupling, 0.80 gauss as shown in Fig. 6(c). It may be due to the absence of metal coupling that the ESR spectrum for the potassium reduction differs from that for the sodium reduction.

By the prolonged contact with alkali metal, the THF solution of II turned red and ESR signal disappeared. This diamagnetic species is considered to be a dianion by analogy with I.

Acridine (I). ESR spectra of anion radicals

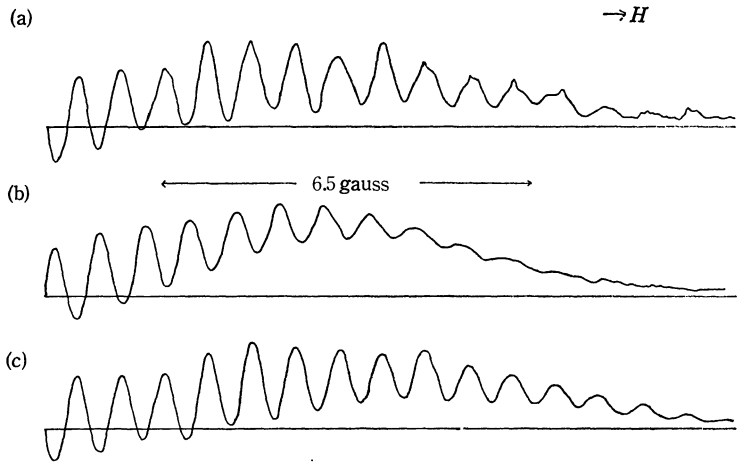

Fig. 6. ESR spectra of radical anions of II.
(a) Sodium reduction, at −55°C
(b) Potassium reduction, at −66°C
(c) Simulated spectrum, corresponding to (a)

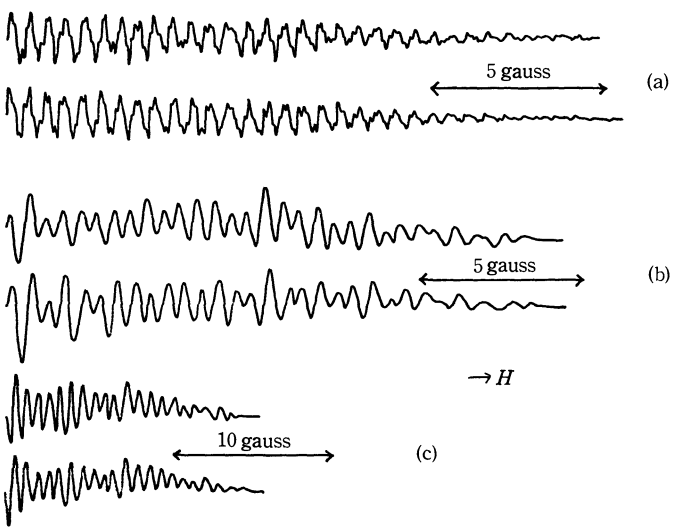

Fig. 7. ESR spectra of radical anions of I.
(a) Sodium reduction, (b) Potassium reduction (c) Electrolytic reduction
For each the upper spectrum; observed, the lower; simulated.

produced from I with the sodium reduction and with the potassium reduction, although they were already given in the previous paper,[1] are shown again in Fig. 7 in order to make a comparison with the simulated spectra and with the spectrum of the anion produced by electrolytic reduction.

The anion radical produced by electrolysis of the acetonitrile solution of I was so unstable that we could not make the ESR measurement under the static condition. In the initial stage of electrolysis, the green layer appeared in the solution close to the anode surface, but in several minutes after electrolysis the solution turned pink and proved to be diamagnetic. Therefore we had to use the technique of flow method. By employing the apparatus shown in Fig. 2 and by electrolyzing the acetonitrile solution containing ~1 mM acridine and 30 mM tetra-*n*-propyl ammonium perchlorate we could obtain the ESR spectrum which is shown in Fig. 7.

From Fig. 7 it is evident that only for the sodium reduction, there exists the effect of counter ion (metal cation) on the ESR spectrum. The hfs constant was determined to be 0.56 guass. In spite of the difference in solvent, coupling constants for the potassium reduction are in good

agreement with the ones for the electrolytic reduction. Only the values for the sodium reduction are different, and this is certainly due to the formation of ion pair.

The parameters which correspond to the coupling constants and line widths used are listed in Table 1. These values are reliable within ± 0.05 gauss. The assignment was made by taking the spin density from a molecular orbital calculation into consideration. The data in Table 2 are electron densities of the lowest vacant orbital for the four compounds under consideration. In the calculation according to the simple LCAO-MO method, the values of the Coulombic integrals and of the resonance integrals were assumed as follows:

$$\alpha_N = \alpha + 0.7\beta, \quad \alpha_{C'-N} = \alpha + 0.1\beta, \quad \beta_{C-N} = \beta$$
$$\alpha_{Cl} = \alpha + 1.8\beta, \quad \alpha_{C'-Cl} = \alpha + 0.18\beta, \quad \beta_{C-Cl} = 0.8\beta$$
$$\alpha_{Br} = \alpha + 1.4\beta, \quad \alpha_{C'-Br} = \alpha + 0.14\beta, \quad \beta_{C-Br} = 0.7\beta$$

α and β are the Coulombic integral of carbon atom and the resonance integral of the C–C bond respectively. The subscripts N, Cl and Br imply the values for nitrogen, chlorine and bromine atom, C'–N *etc.* for carbon atom connecting with nitrogen atom *etc.*, and C–N *etc.* for C–N bond etc.

Spin densities (given in Table 2) *vs.* hfs constants (given in Table 1) are plotted in Fig. 8 to give a linear relation. From its slope, the McConnell's Q-value is obtained as 28 gauss. The coupling constant of nitrogen, a_N was calculated from the following equation,

$$a_N = Q_N \rho_N + \sum Q_{C_i} \rho_{C_i}$$

where ρ_N and ρ_{C_i} are the unpaired spin density on nitrogen and carbon atoms adjacent to nitrogen, C_i. As the values of Q_N and Q_{C_i}, 20 gauss and 7 gauss were used, which had been proposed by Smid.[10]

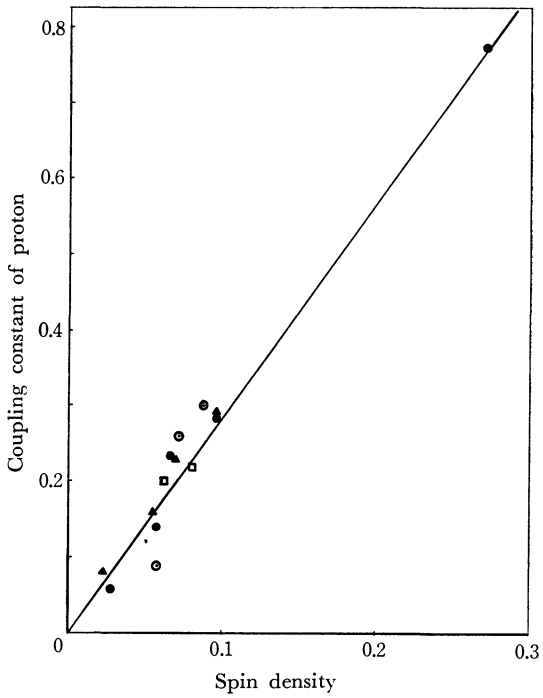

Fig. 8. Plot of spin densities *vs.* hfs constants of protons.
- ● I (Potassium reduction)
- ▲ II (Sodium reduction)
- ⊙ III (Sodium and potassium reduction)
- □ IV (Sodium and potassium reduction)

The authors wish to thank Mr. Katubumi Kumano and Mr. Katsumi Nakamaru for supplying the samples.

10) T. E. Hogen-Esch and J. Smid, *J. Amer. Chem. Soc.*, **88**, 307 (1966).

BULLETIN OF THE CHEMICAL SOCIETY OF JAPAN VOL. 43 3364—3372 (1970)

ζ-Potentials of Synthetic Fibers in Aqueous Solutions of Sodium Alkyl Sulfates and Viscosities of Their Solutions*1,*2

Yoshio IWADARE

Department of Applied Chemistry, Faculty of Engineering, Hiroshima University, Senda-machi, Hiroshima

(Received May 23, 1970)

In order to study the surface-adsorption behavior of anionic surfactants on fibers, the ζ-potentials of some synthetic fibers in aqueous solutions of sodium alkyl sulfates and their mixtures mainly above the critical micelle concentration (CMC), were measured. Further, the viscosities of aqueous solutions of pure surfactants were determined. Consequently, it can be presumed, on the basis of the viscosity data, that the structure of the micelles of these agents varies at the break of the η_{sp}/c_m *vs.* c_m curve. The ζ-potentials (negative) of fibers in aqueous solutions of the agents rapidly changed with an increase in the agent concentrations, but it remained nearly constant above the CMC. At much higher concentrations, the ζ values gradually changed; thereafter, passing a break or a minimum, they became approximately constant again. The concentration at the break or the minimum observed nearly corresponded to that at the break of the η_{sp}/c_m *vs.* c_m curve. It may, therefore, be suggested that the change in ζ-potentials at high concentrations is connected with that in the structure of the micelles. The ζ-potentials (negative) of fibers in aqueous mixed solutions changed sharply with an increase in the concentration of the mixtures and thereafter, passing a maximum in the vicinity of the CMC, complicatedly changed as the total concentrations and mixing ratios changed.

The determination of the adsorption behavior of surfactants on solid surfaces, especially on fiber surfaces, is of fundamental importance in a study of the mechanism of the detergent action. A few investigators[1-4] previously attempted to elucidate the adsorption behavior of surfactants on fiber surfaces, mainly below the critical micelle concentration (CMC), by measuring the ζ-potential of the fiber-solution interface, but little work was done in systems above the CMC.[1,2]

The present author has, therefore, tried to make clear the adsorption behavior of anionic surfactnats on the surfaces of several fibers, mainly near and above the CMC. In a previous experiment,[5] in order to ascertain the surface-adsorption properties of sodium dodecyl sulfate (SDS) on fibers, the ζ-potentials of natural and synthetic fibers in aqueous solutions of the agent were measured, and then the amounts of SDS adsorbed per unit of area of the fiber surfaces were calculated from the ζ values thus obtained. In another investigation,[6] the viscosities of aqueous solutions of SDS and sodium tetradecyl sulfate (STS) were determined as part of a study of the structure of the micelles of these agents. Further, the relation between the change in the ζ-potentials of fibers and that in the structure of SDS micelle was discussed in detail.[7]

In this investigation, in order to clarify the structure of micelles of aqueous sodium alkyl sulfates, the viscosities of aqueous solutions of sodium hexadecyl sulfate (SHS) were determined in a manner similar to that mentioned previously.[6] The ζ-potentials of some synthetic fibers in aqueous of the pure surfactants were measured, and then the relation between the change in the ζ-potentials of these fibers and that in the structure of the surfactant micelles was discussed. In addition, the ζ-potentials of fibers in aqueous solutions of

*1 This paper is Part X in a series on "Surface Adsorption Properties and ζ-Potentials of Fibrous Materials in Surfactant Solutions," Part IX: Y. Iwadare, M. Sasaki and T. Suzawa, *Kogyo Kagaku Zasshi*, **73**, 1927 (1970).

*2 Presented at the 21st Symposium on Colloid and Interface Chemistry, Kyoto, Nov. 2, 1968; at the 22nd Annual Meeting of the Chemical Society of Japan, Tokyo, April 7, 1969; at the Meeting on Oil Chemistry of Japan Oil Chemists' Society, Osaka, Nov. 6, 1969, and at the 23rd Annual Meeting of the Chemical Society of Japan, Tokyo, April 5, 1970.

1) J. S. Stanley, *J. Phys. Chem.*, **58**, 533 (1954).
2) M. v. Stackelberg, W. Kling, W. Benzel and F. Wilke, *Kolloid-Z.*, **135**, 67 (1954).
3) T. Suzawa, *Kogyo Kagaku Zasshi*, **65**, 2042 (1962).
4) T. Suzawa, *ibid.*, **66**, 1002 (1963).
5) Y. Iwadare, M. Sasaki and T. Suzawa, *ibid.*, **73**, 1927 (1970).
6) Y. Iwadare and T. Suzawa, *Nippon Kagaku Zasshi*, **90**, 1106 (1969).
7) Y. Iwadare and T. Suzawa, This Bulletin, **43**, 2326 (1970).

mixtures of the two surfactants (that is, SDS-STS and STS-SHS mixtures) were measured and compared with those obtained in pure surfactant solutions.

Experimental

Apparatus and Procedures. *ζ-Potential.* The ζ-potential was determined by the method of the streaming potential, which has been described previously.[5,8] The streaming potential was measured by using a Transistorized Dynamic-Condenser Electrometer, Model UFE 26301 H (Tokyo Shibaura Electric Co., Ltd.). The conductance of the solutions was obtained from a Yanagimoto Conductivity Outfit, Model MY-7 (Yanagimoto MFG. Co., Ltd.).

The streaming potential was accurately proportional to the pressure in the range from 30 to 60 mmHg above the CMC, as well as below it,[7] regardless of the kinds of the fibers, the kinds, mixing ratios and concentrations of the surfactants, and the temperatures. Actually, the streaming potential measurements were carried out at 50 mmHg and at 25±0.02°C for SDS and the SDS-STS mixture, at 40±0.02°C for STS, and at 45±0.02°C for SHS and the STS-SHS mixture. The solutions examined contained 10^{-4} mol/*l* of sodium chloride.

Viscosity. Viscosity measurements were made with an Ostwald viscometer, as has been described in a previous paper.[6] The flow time for the water was 448.2 sec at 45±0.02°C. The Reynolds' number was about 65. The kinetic energy correction was less than 1 part in 1000 over the whole concentration range investigated. From three to five flow-time measurements were made on each solution. The solution contained 10^{-4} mol/*l* of sodium chloride.

Critical Micelle Concentration (CMC). The critical micelle concentration was determined by measuring the surface tension, the conductance, and the viscosity of aqueous surfactant solutions in the presence of 10^{-4} mol/*l* of sodium chloride, as has been described previously.[7]

Materials. *Fibers.* The polypropylene Pylen, polyamide Nylon 6, polyacrylonitrile Cashimilon, and polyvinyl alcohol Vinylon fibers were the same as those used in previous works.[5,7]

Surface Active Agents. The sodium dodecyl (SDS) and tetradecyl (STS) sulfate used were the same as in a previous study.[6] The sodium hexadecyl sulfate (SHS) was prepared from hexadecyl alcohol which contained 0.6% C_{14} and 1.2% C_{18} alcohols as impurities.

This substance was twice recrystallized from ethanol and then carefully extracted with petroleum ether for 50 hr in order to remove unreacted alcohol. The purified substance had a purity of at least 99.85%; most of the impurity was moisture. The surface tension *vs.* log concentration curve was free of a minimum. The CMC values obtained are given in Table 1.

Table 1. The CMC of sodium alkyl sulfates of 10^{-4} mol/*l* of sodium chloride

Surfactants	CMC (mol/*l*)×10^3		
	Surface tension	Conductivity	Viscosimetry
SDS (25°C)	7.1	7.61	7.0
STS (40°C)	2.13	2.20	2.0
SHS (45°C)	0.61	0.71	0.6

8) T. Suzawa, T. Saito and H. Shinohara, This Bulletin, **40**, 1596 (1967).

Results and Discussion

Viscosities and Structure of Micelles of Aqueous Sodium Alkyl Sulfates

Viscosities of SDS and STS Solutions and Change in the Structure of SDS and STS Micelles. The viscosities of aqueous SDS and STS solutions were reported in a previous paper.[6] The reduced viscosities for the micelles of these agents, η_{spm}/c_m (c_m: the micellar concentration),*3 increased rapidly with the c_m as long as the c_m was small; thereafter, passing a break, they gradually increased with the increase in c_m. The break was observed in the (20—25)×10^{-3} mol/*l* concentration range for SDS and at (8—10)×10^{-3} mol/*l* for STS. The intrinsic viscosity,[11] the hydration,[11,12] and the hydrodynamic volume[12] for the micelle observed in the higher concentration range, above the break, were much larger than those of the lower concentration range, below it.

From Guth and Simha's equation,[13-15] the effective specific volumes,[14,15] of these agents including hydrated water were calculated. They increased with the agent concentrations, but thereafter, passing a break, remained nearly constant. The break nearly corresponded to that of

*3 As has been shown in previous papers, the following operations were performed[9,10]

$$c_m = c_s - c_{c(1)}$$

$$\eta_{spm}/c_m = \{(\eta_r/\eta_{rc(1)}) - 1\}/(c_s - c_{c(1)})$$

where;

c_s: surfactant concentration.

$c_{c(1)}$: the 1st CMC.

η_{spm}/c_m: reduced viscosity for the micelle.

$\eta_{rc(1)}$: relative viscosity at $c_{c(1)}$.

9) N. Sata and K. Tyuzyo, *ibid.*, **26**, 177 (1953); H. Okuyama and K. Tyuzyo, *ibid.*, **27**, 259 (1954); K. Tyuzyo, *ibid.*, **31**, 117 (1958); K. Tyuzyo, *Kolloid-Z.*, **175**, 40 (1961).

10) N. Nakagaki and Y. Ninomiya, This Bulletin, **37**, 817 (1964).

11) P. Mukerjee, *J. Phys. Chem.*, **66**, 1733 (1962).

12) R. J. Vetter, *J. Phys. & Colloid Chem.*, **51**, 262 (1947).

13) E. Guth and R. Simha, *Kolloid-Z.*, **74**, 266 (1936).

14) K. Shinoda, T. Nakagawa, B. Tamamushi and T. Isemura, "Collidal Surfactants," Academic Press Inc., New York (1963), p. 115.

15) D. C. Robins and I. L. Thomas, *J. Colloid Interfac. Sci.*, **26**, 415 (1968).

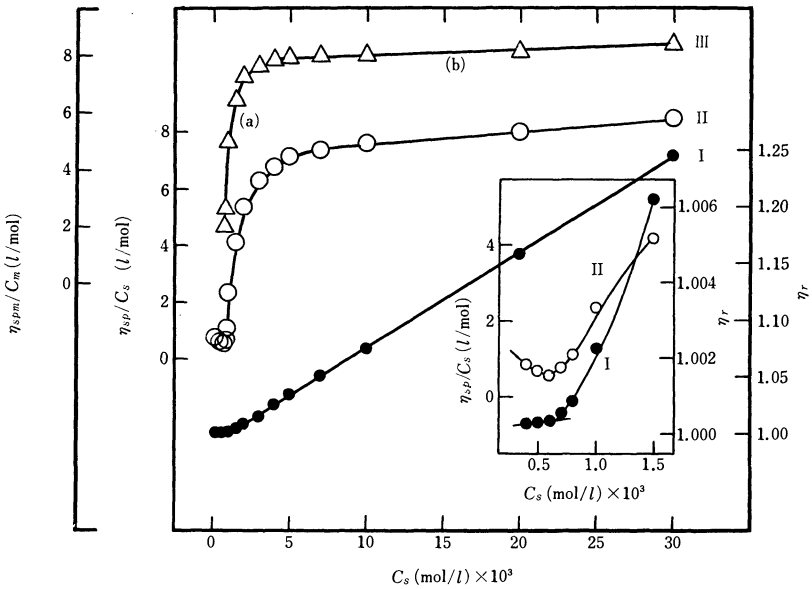

Fig. 1. Viscosity of aqueous SHS solution (45°C).
curve I: η_r *vs.* c_s, curve II: η_{sp}/c_s *vs.* c_s, curve III: η_{spm}/c_m *vs.* c_m
Inset: enlarged in the vicinity of the CMC.

the η_{spm}/c_m *vs.* c_m curve.

The results calculated from the experimental data using Jones and Dole's equation[11,16,17] showed two distinct breaks. The first break corresponded to the 1st CMC of these agents, while the second corresponded approximately to the break in the η_{spm}/c_m *vs.* c_m curve.

From these results, it may be presumed that the structures of the micelles of these surfactants in an aqueous solution would vary at the break of the η_{spm}/c_m *vs.* c_m curve.

Viscosity of SHS Solution and Change in the Structure of SHS Micelle. *i) Viscosity of Aqueous SHS Solution.* The results of viscosity measurements for an aqueous SHS solution are shown in Fig. 1. Curve I clearly breaks at the concentration of 0.6×10^{-3} mol/*l* (*cf.* inset). The gentle upward curvature with η_r above the break seems to result from mutual interference between micelles in motion during the flow.[12] Curve II shows a minimum at the break of curve I. The minimum point is believed to correspond to the CMC[9,10] and agrees well with the CMC value obtained by surface-tension measurements (*cf.* Table 1). The behavior of η_{spm}/c_m was similar to those in SDS[6] and STS[6] micelles. A break of its curve was observed in the concentration range of $(3\text{—}4)\times10^{-3}$ mol/*l*. The intrinsic viscosity of the SHS micelle obtained from the higher concentration range, above the break, was much larger than that of the lower concentration range below it.

On the other hand, Grindley and Bury[12,18] and Suzuki and Sasaki[19] have indicated that the size of the micelles increases to a maximum over a narrow transition range of concentration. From the results mentioned above, it may be presumed that the size of the SHS micelle increases to some extent with an increase in the agent concentration on the portion (a).

As the solution becomes more concentrated, the counter-ion concentration steadily increases, with a resulting decrease in the degree of ionization of the micelle; the stability of the micelles is thereby enhanced.[20] It can, therefore, be assumed that the micellar properties remain unchanged over a relatively wide range of concentration on the portion (b), suggesting that the size and shape of micelles remains constant.[15,21]

ii) Effective Specific Volume. Guth and Simha's equation[13–15] was used for the calculation of the effective specific volume of the surfactant, including hydrated water.[14,15] The results obtained are shown in Fig. 2. The concentration at the break in the curve corresponded well to that at

16) G. Jones and M. Dole, *J. Amer. Chem. Soc.*, **51**, 2950 (1929).

17) L. Gargallo, L. Sepulveda and J. Goldfarb, *Kolloid-Z. Z. Polym.*, **229**, 51 (1969).

18) J. Grindley and C. R. Bury, *J. Chem. Soc.*, **1929**, 679.

19) H. Suzuki and T. Sasaki, Preprints for the 22nd Annual Meeting of the Chemical Society of Japan, separate volume 1, Tokyo (1969), p. 188.

20) K. A. Wright and H. V. Tartar, *J. Amer. Chem. Soc.*, **61**, 544 (1939).

21) T. Ito and H. Mizutani, *Yukagaku*, **17**, 246 (1968).

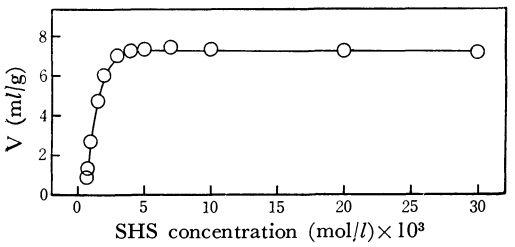

Fig. 2. Effective specific volume (V) of SHS (45°C).

the break of curve III in Fig. 1. The constancy of the effective specific volume is indicative of a spherical micelle.[14,15] Therefore, the shape and size of SHS micelle must remain unchanged in the range of concentration above the break, but is not unchanged below it.

iii) Change in the Structure of the SHS Micelle Observed from Jones and Dole's Equation. The results calculated from the experimental data using Jones and Dole's equation[11,16,17] are shown in Fig. 3. It is recognized that there are two distinct breaks, at points a and b. Point a corresponds to the 1st CMC of this agent, while point b corresponds well to the break of curve III in Fig. 1.

It is suggested that the formation of the micelle is attended by a change in the structure of the solvent, that is, by an interaction between the micelle and the solvent.[12] Therefore, if the change in the structure of micelle is attended by a change in the structure of water, the coefficient B in the equation will be variable.*4 It is noticed that the coefficient B evidently changes at point b.

From these results it may be presumed that the structure of the SHS micelle in an aqueous solution would change at point b in Fig. 3, that is, at the break of curve III in Fig. 1.

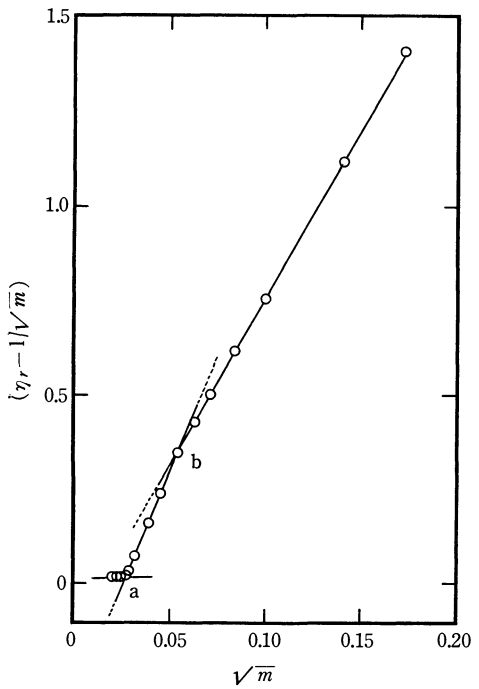

Fig. 3. Behavior of viscosity of aqueous SHS solution observed from Jones and Dole's equation (45°C).

ζ-Potentials of Fibers in Aqueous Solutions of Pure Sodium Alkyl Sulfates

ζ-Potentials of Synthetic Fibers in an Aqueous SDS Solution. The ζ-potentials of natural and synthetic fibers in an aqueous SDS solution were reported in detail in a previous paper.[7] As an example, the ζ-potentials of four synthetic fibers are shown in Fig. 4.

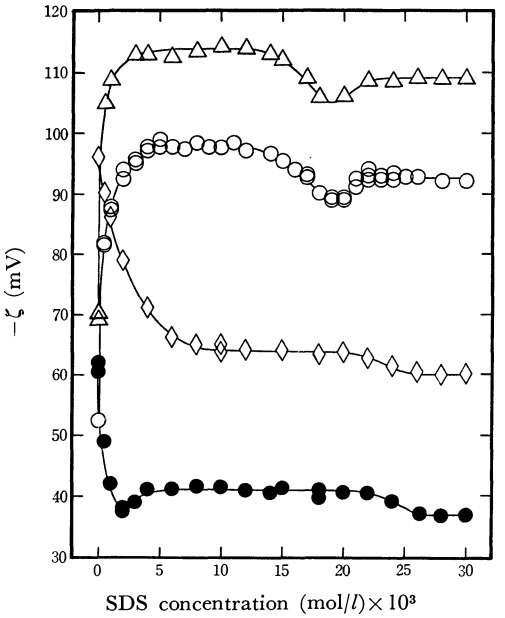

Fig. 4. ζ-Potentials of synthetic fibers in SDS solution (25°C).
(△) Pylen; (○) Nylon 6; (◇) Cashimilon; (●) Vinylon.

The ζ values obtained were all negative and changed rapidly with an increase in the SDS concentration, but remained approximately constant near and above the CMC. As the solution became more concentrated, they gradually changed again and thereafter, passing a minimum or a

*4 It is believed that the coefficient B for a particle in water is a positive quantity, indicating a structure-forming tendency. On the other hand, if the electrolyte particle tended to destroy the structure of water and produce disorder, then the coefficient B would be a negative quantity.[17,22]

22) M. Abu-Hamdiyyah, *J. Phys. Chem.*, **69**, 2720 (1965).

break, became nearly constant again. The concentration of the minimum or the break at high concentrations roughly corresponded to that of the break of the η_{spm}/c_m *vs.* c_m curve (*cf.* Fig. 1 in Ref. 6). It was, consequently, suggested that the change in ζ-potentials at high concentrations may be connected with that in the structure of the SDS micelle.[7]

ζ-Potentials of Synthetic Fibers in an Aqueous STS Solution. *i) ζ-Potentials below the CMC.* The results obtained are shown in Fig. 5.

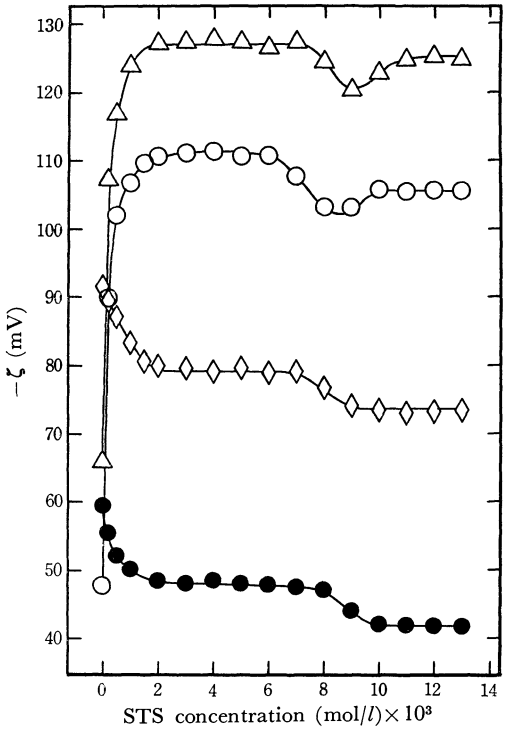

Fig. 5. ζ-Potentials of synthetic fibers in STS solution (40°C).
(△) Pylen; (○) Nylon 6; (◇) Cashimilon; (●) Vinylon.

The ζ-potentials (negative) for Pylen and Nylon 6 fibers increased sharply with an increase in the STS concentration below the CMC. This fact suggests that the amounts of STS adsorbed on the surfaces of these fibers rapidly increase with an increase in the agent concentration. The absolute ζ values of this system were considerably larger than those of the SDS system. It may, therefore, be suggested that the interaction between the hydrocarbon chain of the anionic surfactant and the hydrophobic part of fibers is important for the adsorption of the agent on the fibers.[3]

On the other hand, the ζ-potential (negative) for Cashimilon fiber decreased with an increase in the STS concentration. The decrease in ζ values with an increase in the concentration may be due to the compression of the diffuse double layer, because the total ionic strength in solutions increases with an increase in the concentration. The behavior of the ζ-potential for Vinylon fiber was similar to that obtained for Cashimilon fiber.

ii) ζ-Potentials above the CMC. The ζ values of the fibers examined remained nearly constant for some distance above the CMC. It can, therefore, be presumed that the surface adsorptions of STS on the fibers remain approximately constant in the range of concentrations larger than the CMC.

As the solution became more concentrated, the ζ values gradually changed again and thereafter, passing a minimum or a break, became constant once more. It is worth noting that the concentration of the minimum or the break observed corresponds roughly to those of the break of the η_{spm}/c_m *vs.* c_m curve (*cf.* Fig. 4 in Ref. 6) and of point β (*cf.* Fig. 6 in Ref. 6).

From these facts, it may be assumed that if the structure of the STS micelle in an aqueous solution changed at the concentration for the break or at that for point β, the structure of the diffuse double layer would be variable, resulting in a change of the ζ-potentials of the fibers.

In the more concentrated solutions, the properties of the STS micelle are invariable over a relatively wide range of concentration, suggesting that the size and the shape of the micelle remain nearly constant, as is shown by the viscosity data.[6] It can, therefore, be understood that the ζ-potentials of fibers are kept constant again at a high concentration, for the structure of the double layer is stable.

ζ-Potentials of Synthetic Fibers in an Aqueous SHS Solution. *i) ζ-Potentials below the CMC.* As is shown by Fig. 6, the variations in the ζ-potential (negative) with the concentration for Pylen and Nylon 6 fibers in an aqueous SHS solution were depicted by curves similar to those of SDS and STS systems. The absolute values of the ζ of the SHS system were appreciably larger than those of the latter. It may, therefore, be suggested that these fibers combine mainly with the SHS anion by means of the van der Waals force.[3]

On the other hand, the ζ-potential (negative) of Cashimilon or Vinylon fiber increased with an increase in the SHS concentration and thereafter, passing a maximum, gradually decreased with the concentration. This behavior was fairly different from that of the SDS and STS systems. The difference seems to result from the fact that the adsorption properties of the SHS anion on the fiber are superior to those of the SDS and STS anions.[3]

ii) ζ-Potentials above the CMC. The relation between the ζ-potentials and the surfactant concentrations of this system was very similar to those of the SDS and STS systems. The constancy of the ζ-potentials, therefore, implies that the sur-

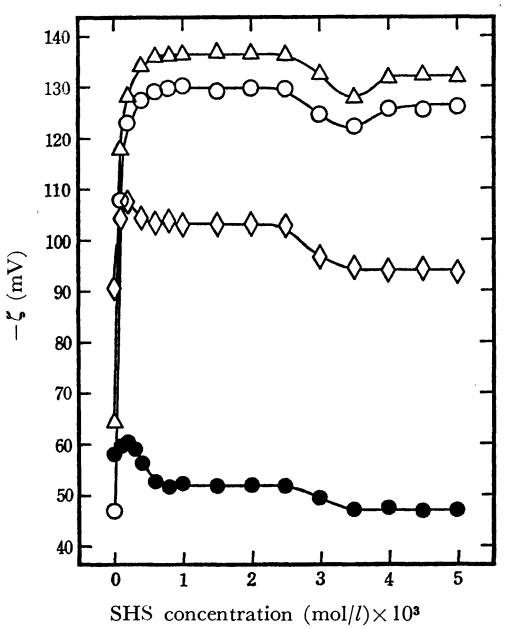

Fig. 6. ζ-Potentials of synthetic fibers in SHS solution (45°C).
(△) Pylen; (○) Nylon 6; (◇) Cashimilon; (●) Vinylon.

face SHS adsorptions on the fibers are unchanged in the range of concentration of $(0.6—2.5)\times10^{-3}$ mol/*l*. It may also be suggested that the surface-surfactant adsorptions of this system are considerably larger than those of the SDS and STS systems, because the absolute ζ values of this system are considerably larger than those of the latter above the CMC, as well as below it. The surfactant concentration corresponding to a minimum or a break in the ζ *vs.* concentration curves is very consistent with that of the break in the η_{spm}/c_m *vs.* c_m curve and that of point b in Fig. 3. It can, consequently, be presumed that the change in ζ-potentials above the CMC is connected with that in the structure of the SHS micelle.

In more concentrated solutions, the ζ values again became constant. This fact may be correlated with the stable structure of the diffuse double layer, as has been mentioned for SDS[7] and STS systems.

Mixed Micelle Compositions and CMC of Mixed Sodium Alkyl Sulfates

Mysels and Otter[23] suggested, from the conductivity data on aqueous solutions of pure sodium decyl and dodecyl sulfates and their mixtures, that the micelles initially formed are strongly enriched by the higher homolog, that the micellar compositions continue to change even after the CMC has been exceeded severalfold, and that, at higher concentrations, they tend to return to the initial composition. Tokiwa *et al.*[24] and Shedlovsky *et al.*[25] determined the mixed micelle compositions of the SDS-STS system. Their results were similar to those of Mysels and Otter.

In this study, the mixed micelle compositions of the SDS-STS and STS-SHS systems were determined in the same way as was used by Mysels and Otter; the results are shown in Figs. 7—10. It can be seen from Figs. 8 and 10 that the results are similar to those of Mysels and Otter. It can, consequently, be understood why some conclusions drawn from these results show a marked resemblance to those of Mysels and Otter.

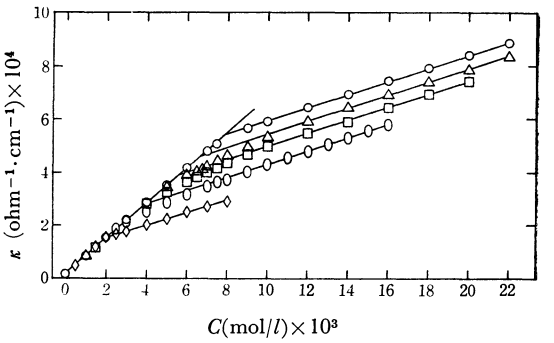

Fig. 7. Relation of specific conductivities (κ) to surfactant concentration (*c*) in SDS-STS mixed system (25°C).
mole% of lower homolog:
(○) 100; (△) 85; (□) 75; (0) 50; (◇) 0.

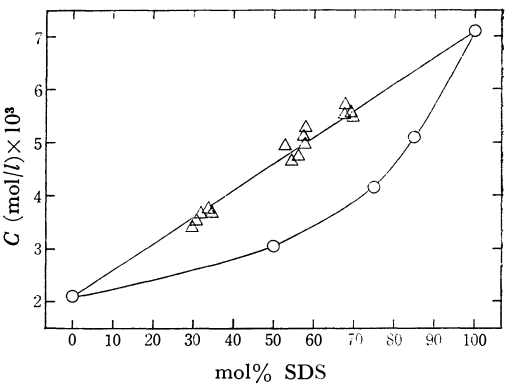

Fig. 8. Mixed micelle compositions (upper line) and CMC values (lower curve) in SDS-STS mixed system (25°C).

23) K. J. Mysels and R. J. Otter, *J. Colloid Sci.*, **16**, 462 (1961).

24) F. Tokiwa, K. Ohki and I. Kokubo, This Bulletin, **41**, 2845 (1968).

25) L. Shedlovsky, C. W. Jakob and M. B. Epstein, *J. Phys. Chem.*, **67**, 2075 (1963).

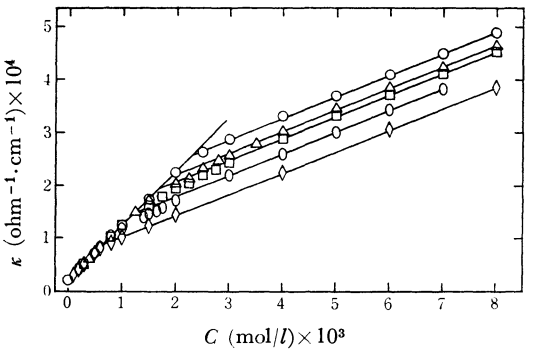

Fig. 9. Relation of specific conductivities (κ) to surfactant concentration (C) in STS-SHS mixed system (45°C).
mole % of lower homolog:
(○) 100; (△) 85; (□) 75; (o) 50; (◇) 0.

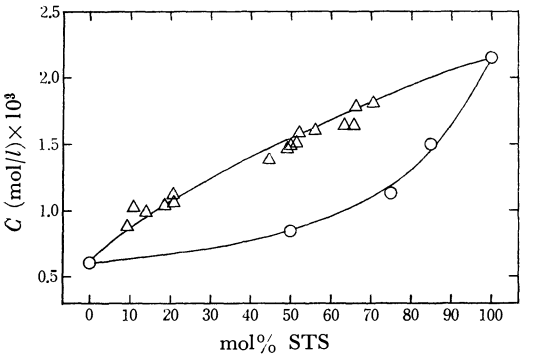

Fig. 10. Mixed micelle compositions (upper curve) and CMC values (lower curve) in STS-SHS mixed system (45°C).

ζ-Potentials of Fibers in Aqueous Solutions of Mixed Sodium Alkyl Sulfates

ζ-Potentials of Synthetic Fibers in an Aqueous Solution of the SDS-STS Mixture. *i) Mixed System Containing 85 mol% SDS.* The results obtained are shown in Fig. 11. The ζ-potential (negative) for Nylon 6 fiber rapidly increased with an increase in the concentration of the mixture below the CMC. This behavior was similar to that of the pure SDS and STS systems. However, the absolute ζ values of this mixed system were considerably larger than those of the pure SDS system, but smaller than those of the pure STS system. It can, therefore, be noted that the surface-adsorption properties of the higher homolog on the fiber are superior to those of the lower homolog.

On the other hand, the ζ-potential (negative) for Cashimilon fiber quickly decreased with an increase in the concentration and thereafter, passing a minimum, gradually increased. This behavior is different from that of the pure SDS and STS systems. It may be suggested that the decrease in the absolute ζ values is due to the compression of the double layer and that the increase is due to a preferential uptake of the higher homolog anions on the fiber. In the vicinity of the CMC, the ζ-potentials showed a maximum for each of the fibers. This may be due to the adsorption of the STS anion in preference to that of the SDS anion, because the concentration of the monomeric anion of the higher homolog reaches a maximum at the CMC.[23] Further, it may be due to the change in the mixed-micelle compositions.[23] However, it is not clear why the maximum appears in the vicinity of the CMC.

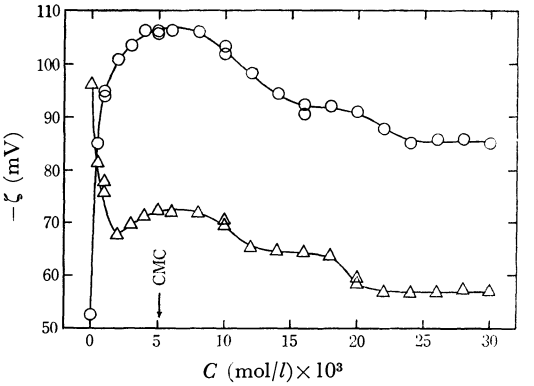

Fig. 11. ζ-Potentials of synthetic fibers in SDS-STS mixed system containing 85 mol% SDS (25°C).
(○) Nylon 6; (△) Cashimilon.

As the solution became more concentrated, the absolute ζ values of both the fibers decreased, step by step. This may be associated with the change in the compositions of the mixed micelles or with that in the compositions of the monomeric ions of the mixtures.

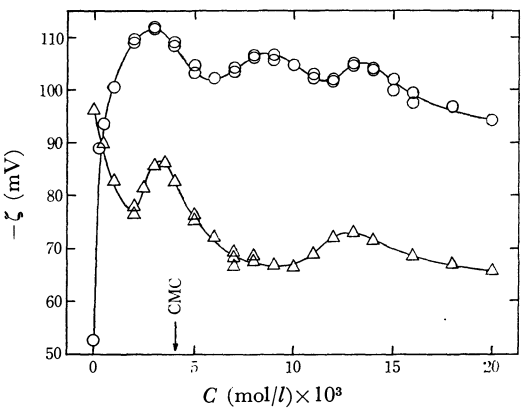

Fig. 12. ζ-Potentials of synthetic fibers in SDS-STS mixed system containing 75 mol % SDS (25°C).
(○) Nylon 6; (△) Cashimilon.

26) D. W. Fuerstenau, *J. Phys. Chem.*, **60**, 981 (1956).

ii) Mixed System Containing 75 mol% SDS. The ζ-potentials of this system changed in a complicated fashion, showing a few maxima, with an increase in the concentration of the mixtures, as is shown by Fig. 12. The first maximum, in the vicinity of the CMC, seems to be due to the cause described in the previous section. The maximum observed at a slightly lower concentration than the CMC may at least partly be interpreted as follows: with an increase in the concentration, sufficient surfactant anions diffuse into the fiver-solution interface and are condensed there because of the increased adsorption; consequently, the adsorbed ions reach a certain critical concentration at the interface in the concentration range below the CMC.[26] A maximum corresponding to the second maximum of Nylon 6 fiber was not observed in the case of Cashimilon fiber. This may result from the difference between the adsorption properties of mixtures on the two fibers.

The third maximum of Nylon 6 fiber corresponds to the second of Cashimilon fiber. It is, however, not clear why these maxima appear in the high concentration range.

iii) Mixed System Containing 50 mol% SDS. The ζ-potentials (negative) of both the fibers also showed a small maximum in the vicinity of the CMC, and thereafter decreased, step by step, with an increase in the concentration, as is shown in Fig. 13. The maximum was observed at a lower concentration than that of the former mixed system because of the decrease in the CMC. This is due to the cause mentioned in connection with the mixed system containing 85 mol% SDS. Further, it shifted somewhat to a lower concentration than the CMC. This partly results from the same cause, as has been described above. The step-by-step decrease in the ζ-potentials is connected with the change in the compositions of mixed micelles or with that in those of monomeric ions of the mixtures.

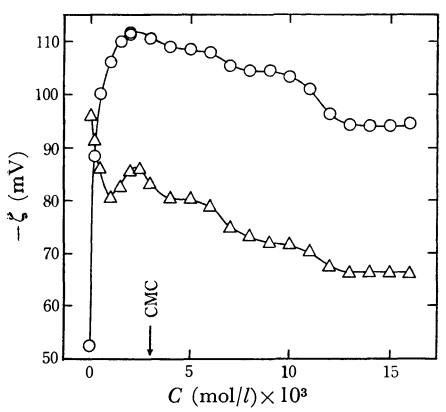

Fig. 13. ζ-Potentials of synthetic fibers in SDS-STS mixed system containing 50 mol% SDS (25°C).
(○) Nylon 6; (△) Cashimilon.

ζ-Potentials of Synthetic Fibers in Aqueous Solutions of STS-SHS Mixtures. The ζ-potentials of two synthetic fibers in mixed systems containing 85, 75 and 50 mol% STS are shown in Figs. 14, 15, and 16 respectively. The behavior of ζ-potentials for Nylon 6 fiber below the CMC was similar to those obtained in the pure STS and SHS systems, but the absolute values of ζ, which increased in the order of the composition: 85,

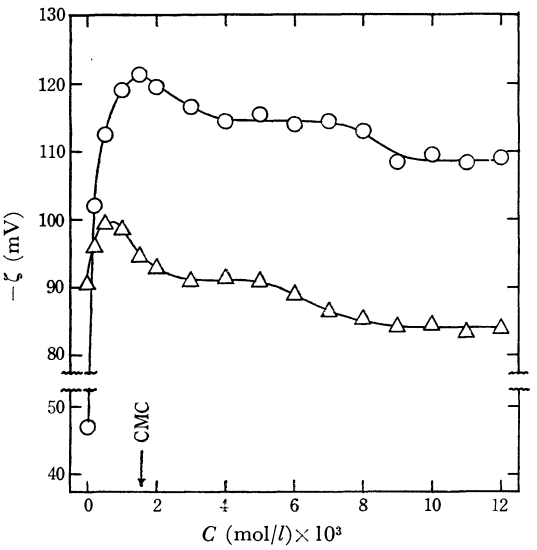

Fig. 14. ζ-Potentials of synthetic fibers in STS-SHS mixed system containing 85 mol % STS (45°C).
(○) Nylon 6; (△) Cashimilon.

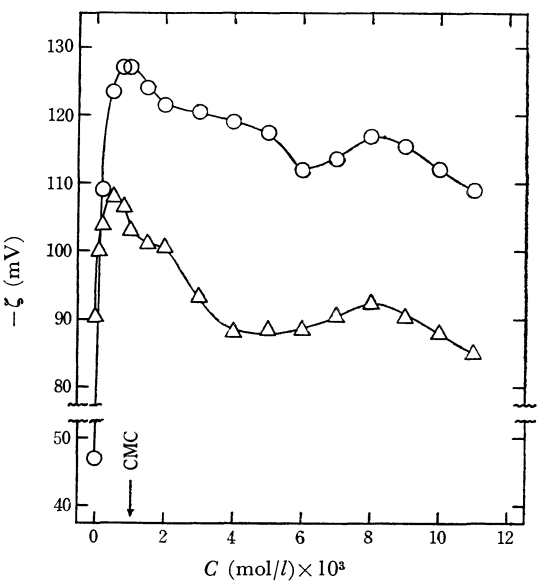

Fig. 15. ζ-Potentials of synthetic fibers in STS-SHS mixed system containing 75 mol % STS (45°C).
(○) Nylon 6; (△) Cashimilon.

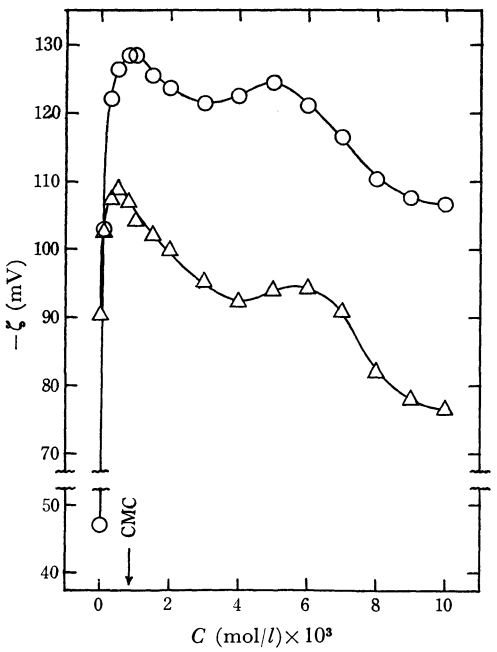

Fig. 16. ζ-Potentials of synthetic fibers in STS-SHS mixed system containing 50 mol % STS (45°C).
(○) Nylon 6; (△) Cashimilon.

75 and 50 mol% STS, were intermediate between those of the pure systems. The results suggest that the surface adsorptions of the higher homolog on the fiber are larger than those of the lower homolog.

On the other hand, the behavior of ζ-potentials for Cashimilon fiber below the CMC is similar to that of the pure SHS system, and different from that of the pure STS system. This results from the preferential adsorption of the SHS anion on the fiber.

In the vicinity of the CMC, a maximum of ζ-potentials for both the fibers was observed in all the mixed systems studied. The maximum shifted to low concentrations in the order of the composition: 85, 75 and 50 mol% STS, because of the decrease in the CMC. This may be attributed to the same cause as has been mentioned in connection with SDS-STS mixed systems.

As the solution became more concentrated, the absolute values of ζ for the mixed system containing 85 mol% STS decreased, step by step. This behavior was similar to that obtained for the mixed system containing 85 mol% SDS. It is connected with the change in the mixed micelle compositions or with that in the monomeric ion compositions of mixtures. On the other hand, the ζ-potentials of both the fibers in the mixed systems containing 75 and 50 mol% STS changed in an intricate manner, showing a maximum and a minimum, with an increase in the concentration of the mixtures. The behavior of the ζ-potentials is roughly analogous to that observed for the mixed system containing 75 mol% SDS.

The author wishes to thank Professor T. Suzawa, Faculty of Engineering of Hiroshima University, for many helpful discussions and suggestions during this work. Thanks are also due to Professor M. Miura, Faculty of Science of Hiroshima University, for his continuing interest and encouragement. In addition, the author wishes to thank the Toray Co., Ltd., the Kurashiki Rayon Co., Ltd., and the Asahi Chemical Industry Co., Ltd., for providing him with the fibers, and the Nippon Oils & Fats Co., Ltd., and the Nikko Chemicals Co., Ltd., for providing him with the surfactants.

BULLETIN OF THE CHEMICAL SOCIETY OF JAPAN VOL. 43 3373—3376 (1970)

The Phosphorescence Bands of Anthraquinone in Crystalline Solvents at 77°K

Akira KUBOYAMA

Government Chemical Industrial Research Institute, Tokyo, Shibuya-ku, Tokyo

(Received May 23, 1970)

The phosphorescence bands of anthraquinone in the solvents used in this work are all safely assigned to the $\pi^*\rightarrow n$ bands on the basis of their short lifetimes. In *n*-paraffins (*n*-hexane, *n*-heptane, and *n*-octane), two phosphorescence bands which are close to each other are found. Considering the dependence of the relative intensities of these two phosphorescence bands on the carbon-numbers of the *n*-paraffins, it is assumed that the longer- and the shorter-wavelength bands are due to the anthraquinone molecules with the C–O bond axis parallel to and perpendicular to the longitudinal axis of the planar zig-zag form of the *n*-paraffin molecules in the *n*-paraffin crystals respectively. In chloroform and dioxane, a broad phosphorescence band shows a blue-shift relative to the corresponding band in the alkane solvents. In chloroform a sharp phosphorescence band was also observed for a solution which was rapidly cooled. This sharp band is assumed to be due to the anthraquinone molecules with a certain geometry relative to the surrounding chloroform molecules.

In a previous work,[1] we studied the phosphorescence bands of various *o*- and *p*-quinones and α-diketones in solutions and in fine crystals at 77°K. All the solutions studied there were glassy. However, valuable information on the properties of phosphorescence bands, on solute-solvent interactions, and on the arrangements of solutes in solvents is expected to be obtained from the study of the phosphorescence bands in crystalline solutions at low temperatures.[2,3] From this point of view, the phosphorescence bands of anthraquinone in solutions at 77°K have been studied by using various kinds of solvents, all of which form a crystalline state at 77°K.

Experimental

Measurements. The phosphorescence spectra and their lifetimes have been measured in the manner described in our previous paper.[1] The exciting light used was a mercury 313-mμ line emitted from a Hanovia xenon mercury lamp of 150 W. The solvents used were *n*-hexane, *n*-heptane, *n*-octane, 3-methylpentane, isooctane, methylcyclohexane, chloroform, and dioxane. The concentrations used ranged from 10^{-4}—10^{-5} M. The measurements were carried out at the liquid-nitrogen temperature (77°K) in air. Two kinds of cooling speeds, fast and slow, were used. For the rapid cooling, capillary quartz or Pyrex cells were plunged in liquid nitrogen. On the other hand, for the slow cooling the capillary cells were steeped in liquid nitrogen after having been hung immediately above the surface of liquid nitrogen for about 15 min. The solutions used were in polycrystalline states at 77°K except for methylcyclohexane and 3-methylpentane solutions, which were glassy at 77°K.

Materials. Commercially-available anthraquinone was purified by recrystallization. The melting point of the purified sample agreed with that reported in the literature. As for solvents, commercially-available spectro-grade *n*-hexane, *n*-heptane, *n*-octane, isooctane, methylcyclohexane, and chloroform were used without further purification. Aromatic impurities in commercially-available 3-methylpentane were removed with silica gel. After the treatment, the 3-methylpentane was distilled. Dioxane of a special grade was dried over sodium and distilled.

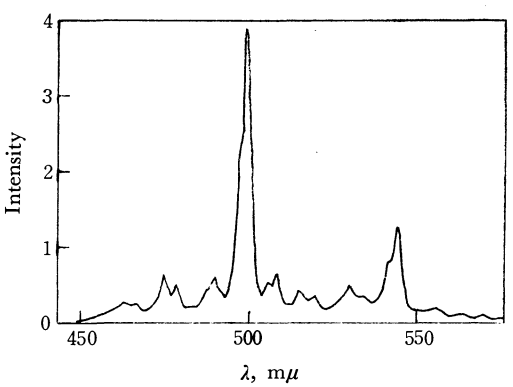

Fig. 1. Solvent: *n*-hexane, slow-cooling.

1) A. Kuboyama and S. Yabe, This Bulletin, **40**, 2475 (1967); *Rep. Gov. Chem. Ind. Res. Inst., Tokyo*, **64**, 105 (1969).

2) E. V. Shpol'skii, *Sov. Phys. Usp.*, **3**, 372 (1960); *ibid.*, **5**, 522 (1962).

3) E. J. Bowen and B. Brocklehurst, *J. Chem. Soc.*, **1955**, 4320; R. Shimada, *Spectrochim. Acta*, **17**, 14 (1961).

Results

The phosphorescence spectra obtained are shown in Figs. 1—6. All the spectra are uncorrected

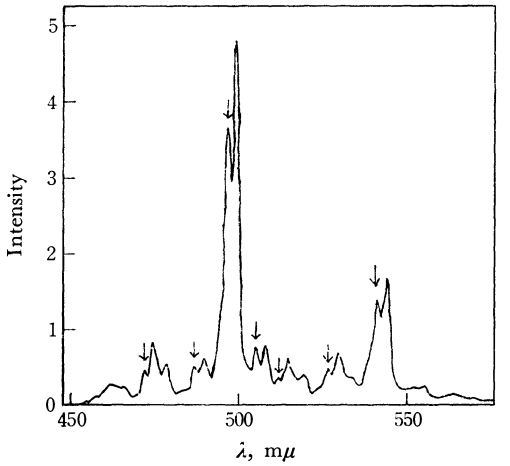

Fig. 2. Solvent: *n*-heptane, slow-cooling.

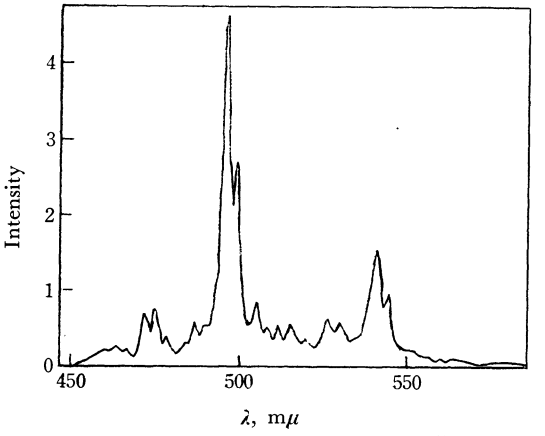

Fig. 3. Solvent: *n*-octane, slow-cooling.

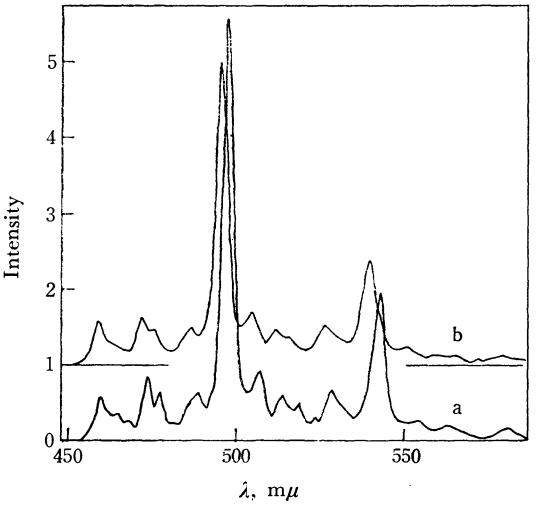

Fig. 4. Solvent: methylcyclohexane, slow-cooling.
a: crystalline state, b: rigid glass state

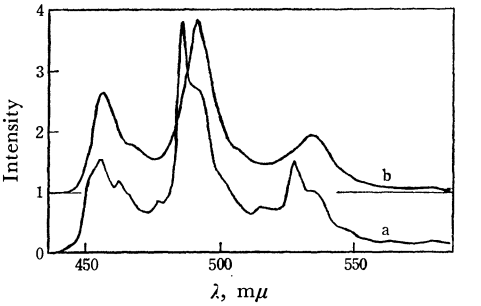

Fig. 5. Solvent: chloroform.
a: rapid-cooling, b: slow-cooling

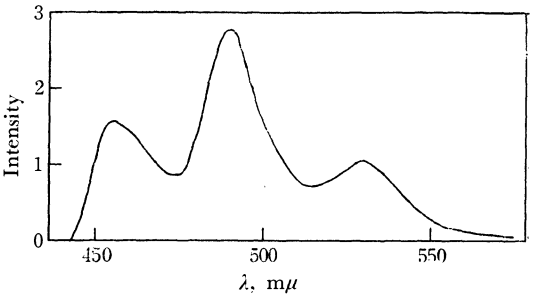

Fig. 6. Solvent: dioxane, slow-cooling.

TABLE 1. STRONGEST-PEAK WAVELENGTHS IN VARIOUS SOLVENTS

Solvent	Wavelengths (mμ)
n-Hexane	499
n-Heptane	499
n-Octane	496
Methylcyclohexane (Crystalline state)	497
Methylcyclohexane	495
3-Methylpentane	495
Isooctane	495
Chloroform	492
Chloroform (Rapid-cooling)	486
Dioxane	490

for the response of the photomultiplier, and the scales of the ordinates are arbitrary. In Table 1, the wavelengths of the strongest peaks near 500 mμ in the phosphorscence spectra in various solvents are given. The observed lifetimes of the phosphorescence bands were all close to that (3.3 msec) in methylcyclohexane and methanol-ethanol (1 : 4) mixture obtained in our previous work.[1)]

Discussion

The phosphorescence bands in the solvents used in this work can all saelfy be assigned to the $\pi^* \rightarrow n$ band on the basis of their short lifetimes.

As is shown in Figs. 1—3, the phosphorescence spectra in the *n*-paraffins show sharp, fine struc-

tures. Previously, Shpol'skii[2] found that, when the longitudinal dimention of the planar zig-zag form of an *n*-paraffin molecule used as a solvent is close to the molecular dimension of a solute aromatic hydrocarbon, for example, anthracene (7.5 Å) in *n*-heptane (7.6 Å),[4] the fluorescence spectrum of the solution shows a very sharp, fine structure. This Shpol'skii effect has been generally observed for the electronic absorption and emission spectra of various aromatic compounds which have a rigid molecular structure. Anthraquinone has a rigid molecular structure, and the dimension (7.4 Å) of its long axis (perpendicular to the C–O bond axis) is close to that of *n*-heptane, while that (5.3 Å) of its short axis (parallel to the C–O bond axis) is relatively close to that (6.3 Å) of *n*-hexane. That of *n*-octane is 8.9 Å.[4] Therefore, it may be surmised that the sharp phosphorescence band in the *n*-paraffins mentioned above are due to the Shpol'skii effect. In *n*-heptane (Fig. 2), the peaks corresponding to the two main peaks near 500 and 540 mμ in methylcyclohexane (Fig. 4) have doublet structures. Similar doublet structures are also found in *n*-hexane and *n*-octane (Figs. 1, 3). In *n*-hexane the intensity of the shorter wavelength peak relative to that of the longer wavelength one in each doublet structure is considerably weaker than that in *n*-heptane. On the other hand, in *n*-octane the intensity of the longer-wavelength in each doublet structure is considerably weaker than that of the corresponding shorter-wavelength peak, contrary to the cases of *n*-heptane and *n*-hexane.

The effect of the cooling speed on the doublet structures is as follows. The relative intensity of the weaker peak (shorter-wavelength peak) to that of the stronger peak in each doublet structure increases in the case of *n*-hexane (Fig. 1), and decreases in the case of *n*-heptane (Fig. 2), for solutions which are rapidly cooled. On the other hand, in the case of *n*-octane (Fig. 3), the intensity of the weaker peak (longer-wavelength peak) relative to that of the stronger peak in each doublet structure becomes considerably stronger for solutions which are rapidly cooled. In these paraffins the wavelengths of peaks in the phosphorescence band are all the same, irrespective of the cooling speed. Though the reproducibility of the doublet structures in each case is not very good, the difference in the relative intensity of the two peaks of the doublet structure among the three paraffins is always definite.

From these facts it may be concluded that, in these paraffins, two phosphorescence bands closely overlap,[5] and that, in *n*-hexane, the longer-wavelength phosphorescence band and, in *n*-octane, the shorter-wavelength band appear more intensely. The energy difference between these two phosphorescence badns is *ca.* 100 cm^{-1}. On the basis of a comparison of the phosphorescence spectra in these paraffins, the peaks identifiable with the shorter-wavelength band are denoted with an arrow in Fig. 2. These two phosphorescence bands in these paraffins are assumed to be due to the anthraquinone molecules incorporated in two different ways in the paraffin crystals.

Since no complete single-crystal X-ray-analysis has been made for these paraffin crystals, precise structural details are unknown. However, considering the crystal data[6] for other *n*-paraffins, it may be assumed that, in the paraffin crystals used in this work, the paraffin molecules with the planar zig-zag form are arranged in parallel rows.[2] As for the anthracene in *n*-heptane crystals, mentioned before, it may be assumed that the anthracene molecules are arranged with their long axis parallel to the longitudinal axis of *n*-heptane molecules in *n*-heptane crystals.[2] It may analogically be assumed that, in the three paraffin crystals, anthraquinone molecules are incorporated in two different ways, namely, with their C–O bond axis parallel to and perpendicular to the longitudinal axis of the paraffine molecules, and that the above two phosphorescence bands are due to the anthraquinone molecules arranged in these two ways. If so, the difference in the relative intensities of the two phosphorescence bands between *n*-hexane and *n*-octane, mentioned before, can be explained on the reasonable presumption that, in *n*-hexane, most anthraquinone molecules are situated with their C–O bond axis parallel to the longitudinal axis of *n*-hexane molecules, while in *n*-octane most quinone molecules direct the C–O bond axis perpendicular to the longitudinal axis of *n*-octane molecules, and that the longer- and the shorter-wavelength phosphorescence bands are due to the anthraquinone molecules with the C–O bond axis parallel to and perpendicular to the longitudinal axis of the paraffin molecules. The situation in *n*-heptane can be assumed to be intermediate between those in *n*-hexane and *n*-octane. It can also be assumed that, in *n*-heptane, a majority of the anthraquinone molecules direct the C–O bond axis (short axis) parallel to the longitudinal axis of the *n*-heptane molecules, unlike as in the case of anthracene. This situation may be mainly due to the dipole-induced dipole interaction between the polar carbonyl groups of the quinone molecules and the *n*-heptane molecules, which may be stronger in the case of the anthraquinone molecules directing the C–O bond axis parallel to the

4) In obtaining these data, hydrogen atoms are neglected. The value for anthracene is that of the long axis.

5) The similar conclusion was obtained by D. N. Shygorin *et al.* ("Advances in Spectroscopy," Vol. 1 (1957), p. 672).

6) J. M. Robertson, "Organic Crystals and Molecules," Cornell Univ. Press. Ithaca (1953), p. 165.

longitudinal axis of the *n*-heptane molecules than in the other case because of the anisotropy of the polarizability of the *n*-heptane molecules.

Methylcyclohexane solutions at 77°K usually form glassy states and show the same phosphorescence band, irrespective of the cooling speed. When the solution is cooled slowly, it occasionally becomes polycrystalline, and the phosphorescence band in the crystalline solution is different from that in the glassy solution. The phosphorescence band in the crystalline solution shifts toward wavelengths longer by *ca.* 80 cm^{-1} and becomes sharper than that in the glassy solutions (Fig. 4). Both in polycrystalline isooctane and in glassy 3-methylpentane the phosphorescence band is unaffected by the cooling speed and is very similar to that in the methylcyclohexane glass.

In chloroform (Fig. 5), a broad phosphorescence band appears for the slowly-cooled solutions. On the other hand, the rapidly-cooled solutions exhibit a sharp phosphorescence band, accompanied by a weak, broad band on its longer wavelength side. The weaker band situated at the same position as the broad band observed for the slowly-cooled solutions. It may be assumed that the sharp band is due to the anthraquinone molecules incorporated in the crystalline part of the chloroform matrix and that the broad band is associated with the anthraquinone molecules in the amorphous part of chloroform.

Generally speaking, the solvent effects on the energies of an absorption band and the corresponding emission band of solutions at 77°K are expected to be similar, since both the solute and solvent molecules can hardly move at 77°K. As a result, the solvent effects on the energies of the $\pi^* \rightarrow n$ phosphorescence band at 77°K and the corresponding $n \rightarrow \pi^*$ absorption band at room temperature can also be expected to be similar to some extent. Therefore, the blue shift of the phosphorescence bands in chloroform relative to those in the saturated hydrocarbons may be attributed to the hydrogen-bond formation between anthraquinone and chloroform.

In dioxane (Fig. 6), the same broad phosphorescence band is found for both the slowly- and rapidly-cooled solutions. This broad band may also be due to the anthraquinoe molecules in the disordered crystals of dioxane. A blue shift of the phosphorescence band in dioxane relative to those in the saturated hydrocarbons may be due to the π-*n*-type charge-transfer interaction between anthraquinone and dioxane molecules.[7]

7) A. Kuboyama, This Bulletin, **33**, 1027 (1960); *Gov. Chem. Ind. Res. Inst., Tokyo*, **57**, 1 (1962).

BULLETIN OF THE CHEMICAL SOCIETY OF JAPAN VOL. 43 3377—3382 (1970)

The Electron Spin Resonance of the Mn^{2+} Ion on the Surface of Magnesium Oxide

Takemi YAMAMURA,*1 Akinori HASEGAWA, Yoshio YAMADA and Masaji MIURA

Department of Chemistry, Faculty of Science, Hiroshima University, Higashisenda-machi, Hiroshima

(Received June 1, 1970)

The behavior of the Mn^{2+} ion on the surface of MgO was studied by using the ESR technique. The powder of MgO, the surface of which was doped with the Mn^{2+} ion, was calcined at different temperatures from 100 to 1000°C in a vacuum, and then the ESR spectra were observed at room temperature. It was noticed that the spectral intensity showed a minimum at about 500°C, that the zero-field splitting parameter, D, increased with the temperature, and that the hyperfine coupling constant, A, decreased enormously at about 700°C. The environments around the Mn^{2+} ion on the surface of MgO were discussed on the basis of these results. When H_2, CO, or O_2 was added after the calcination, the D and A values changed in the temperature range above 500°C. Especially when O_2 was introduced, the D value fell to zero upon treatment at 1000°C. The crystal field around the Mn^{2+} ion and the bonding between the Mn^{2+} ion and its environments were discussed by taking into account the results of the magnetic-susceptibility measurements of the manganese ion on MgO.

Many studies have been done on the ESR of the Mn^{2+} ion doped in the bulk of solids. These have dealt with the phase transition,[1] the defects,[2] the crystal field of solids,[3] *etc.* Several studies have also been done on the ESR of the Mn^{2+} ion on the surfaces of ion-exchange resin[4] and zeolite.[5-7] The character of the bonding between the Mn^{2+} ion and the adsorbent, the kind of adsorption site,[5,6] and the crystal field around the Mn^{2+} ion[7] have been discussed in these studies.

In this paper, the Mn^{2+} ion is selected as a probe for the surface of magnesium oxide in the expectation that information about the Mn^{2+} ion and its environments on the surface will be obtained from the ESR spectrum of the ion. The information, if any is obtained, may also be useful in discussing the surface reactivity of magnesium oxide doped with transition metal ions.[8,9] The ESR spectrum of the Mn^{2+} ion offers several parameters: the spectral intensity, the hyperfine coupling constant, and the zero-field splitting parameter. The intensity of the spectrum, which is proportional to the concentration of the Mn^{2+} ion, can be taken as a measure of the oxidation or reduction of the manganese ion, because the ion takes different valencies. The hyperfine coupling constant, as revealed by van Wieringen[10] and Matsumura,[11] is correlated with the ionic character in the bond between the Mn^{2+} ion and its environments. The zero-field splitting parameter gives information about the crystal field, that is, the symmetry of the environments around the Mn^{2+} ion.

Changes in the valence state and in the environment of the manganese ion on the surface of magnesium oxide, resulting from the thermal treatment and the introduction of various gases, were investigated by the ESR technique and by magnetic-susceptibility measurements.

Experimental

The powder of magnesium oxide was prepared by the calcination of magnesium hydroxide, which had itself been obtained from the methylation of magnesium

*1 Present address: Ube Industries Ltd., Polymer Research Laboratory, 8-2 Minamikaigan, Goi, Ichihara-shi, Chiba.

1) J. G. Chambers, W. R. Datars and C. Calvo, *J. Chem. Phys.*, **41**, 806 (1964).

2) K. N. Shrivastava and Putcha Venhateswarlu, *Proc. Indian Acad. Sci.*, **63**, 284 (1966).

3) M. Miura, A. Hasegawa and M. Watanabe, This Bulletin, **41**, 1035 (1968).

4) R. J. Faber and M. T. Mogress, *J. Amer. Chem. Soc.*, **81**, 1849 (1959).

5) T. I. Barry and L. A. Lay, *J. Phys. Chem. Solids*, **27**, 1821 (1966).

6) T. I. Barry and L. A. Lay, *ibid.*, **29**, 1395 (1968).

7) L. G. Dzhashiashvili, N. N. Tikhomirova and G. V. Tsitsishvili, *Zh. Strukt. Khim.*, **10**, 443 (1969).

8) D. Cordischi, R. L. Nelson and A. J. Tench, *Trans. Faraday Soc.*, **65**, 2740 (1969).

9) V. Grecu and D. Barb, "Magnetic Resonance and Relaxation," ed. by R. Blinc, North-Holland Publishing Co., Amsterdam (1967), p. 805.

10) J. S. van Wieringen, *Discuss. Faraday Soc.*, **19**, 118 (1955).

11) O. Matsumura, *J. Phys. Soc. Jap.*, **14**, 108 (1959).

metal, followed by the hydrolysis of the methylate, in an atmosphere of oxygen for 4 hr at 700°C. The magnesium metal (99.9999%) was supplied by the Material Research Corporation (U. S. A.). The calcination temperature is sufficiently high to bring about the complete dehydration of magnesium hydroxide.[12,13] The resulting magnesium oxide gave none of the ESR spectrum of paramagnetic species.

Silica gel was prepared from water glass and sulfuric acid and was calcined at 500°C for 5 hr.[14]

The powders of magnesium oxide and silica gel were immersed into an aqueous solution of manganese nitrate, and the products were dried at 110°C for 24 hr in air. The amount of the adsorbed Mn^{2+} ion is 0.3 wt% of the Mg^{2+} ion. As the surface area of the magnesium oxide is determined to be 69 m^2/g by the B. E. T. method from the nitrogen adsorption, the mean distance between Mn^{2+} ions is estimated to be about 11.4 Å when the Mn^{2+} ions are distributed homogeneously. If the latter situation is granted, the contribution of the dipole-dipole interaction between Mn^{2+} ions is assumed to be negligible in the ESR spectra and the features of the spectra may be treated on the basis of the crystal field around the Mn^{2+} ion.

These specimens were calcined at various temperatures from 100 to 1000°C for 4 hr in a vacuum and were exposed to such gases as oxygen, hydrogen, and carbon monoxide at each temperature and at 0.5 atm. Oxygen gas was also introduced under the same conditions as above after the magnesium oxide containing the Mn^{2+} ion on its surface had been calcined at 1000°C.

The specific susceptibilities of the manganese ion on the magnesium oxide (Mn/Mg=0.03 by weight, ten times the concentration in the case of the ESR measurement), treated at room temperature and at 500, 800, and 1000°C for 4 hr in a vacuum (10^{-4}—10^{-5} Torr), were measured to give information as to the valence state of the manganese ion. The specific susceptibility of the manganese oxide prepared by heating manganese nitrate at 110°C for 24 hr was also determined after treatment under the same conditions. The measurements of the specific susceptibility were carried out at room temperature by the Faraday method, using a Cahn RG electrobalance.

Estimation of the *D* Value and the Ionicity.

Since the Mn^{2+} ion has $S=5/2$ and $I=5/2$ and since its ground state is ^6S, the hyperfine and fine structures are expected to occur in the ESR spectrum. However, since the specimen used is in a powder state and has a small zero-field splitting, the observed spectrum of the Mn^{2+} ion on the surface of magnesium oxide consists of six hyperfine structures due to the allowed transition, $\Delta m_I=0$, and the weak lines, observed between hyperfine structures, due to the forbidden transitions, $\Delta m_I=\pm 1$, as may be seen in Fig. 1.

The following two methods have been proposed for the estimation of the zero-field splitting parameter, *D*, or the distortion of the crystal field from cubic symmetry on the basis of the ESR spectrum of the Mn^{2+} ion. One is Allen's method,[15] which utilizes the relation, shown in Fig. 2, between the value of *D* and the ratios of the intensity of the hyperfine line of $m_I=-5/2$ to those of $m_I=-1/2$ and $m_I=-3/2$. An alternative method is to use the intensity ratio of the forbidden lines to the allowed lines; this method has been proposed by Bleaney and Rubins[16] and by de Wijn and van Balderen.[17] Though the value estimated by this method is in considerable agreement with that ob-

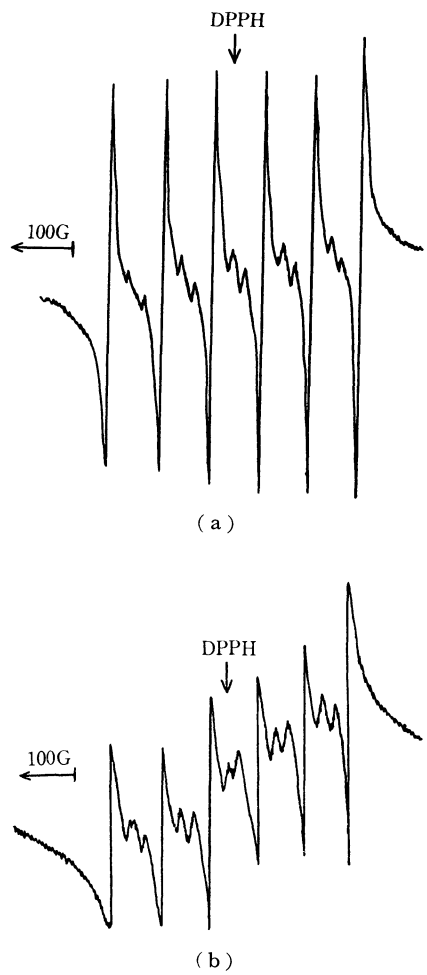

Fig. 1. ESR spectra of Mn^{2+} ion on magnesium oxide, treated (a) at 110°C for 24 hr in air and (b) 1000°C for 4 hr in a vacuum.

12) R. I. Razouk and R. Sh. Mikhail, *J. Phys. Chem.*, **61**, 886 (1957).

13) S. J. Gregg and R. K. Packer, *J. Chem. Soc.*, **1955**, 51.

14) M. Miura, A. Hasegawa and Y. Yamada, This Bulletin, **41**, 1320 (1968).

15) B. T. Allen, *J. Phys. Chem.*, **43**, 3820 (1965).

16) B. Bleaney and R. S. Rubins, *Proc. Phys. Soc.* (London), **77**, 103 (1961).

17) H. W. de Wijn and R. F. van Balderen, *J. Chem. Phys.*, **46**, 1381 (1967).

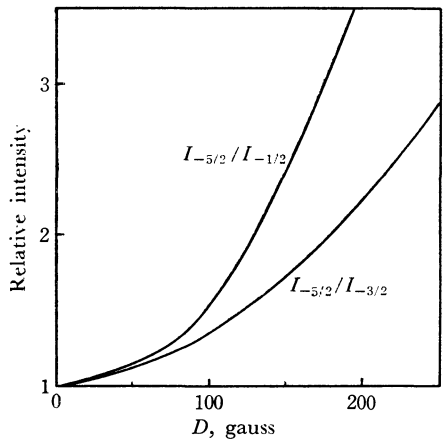

Fig. 2. The relations between relative intensity and D value proposed by Allen.[15]

tained by Allen's method, this method is not adopted in the present study since the estimation of the intensities of the forbidden lines is accompanied by a rather large error.

An almost linear relation between the coupling constant of the hyperfine structure, A, and the ionicity of the bonds between the Mn^{2+} ion and the environments has been proposed by Matsumura. It is shown in Fig. 3,[11] where the ionicity has been calculated from the electronegativities of the Mn^{2+} ion and the surrounding negative ions and the number of the latter ions, after Pauling.[18] The ionicity of the bonds was. therefore, estimated in terms of this relation.

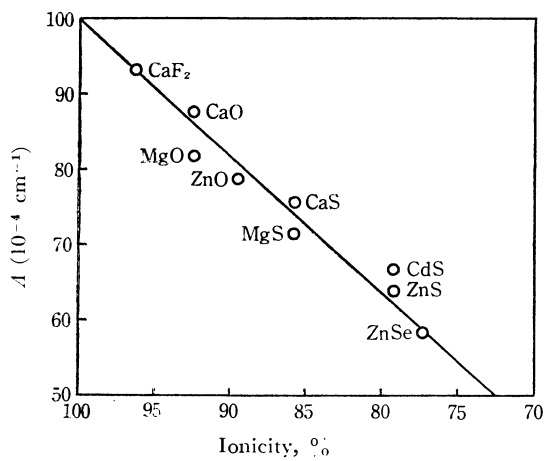

Fig. 3. The relation between A value and ionicity proposed by Matsumura.[11]

Results and Discussion

ESR Spectra of the Mn^{2+} Ion on the Surface of MgO in Air at Room Temperature. After the magnesium oxide containing the Mn^{2+} ion on its surface had been dried at 110°C for 24 hr in air, the ESR spectrum was measured at room temperature (Fig. 1). The zero-field splitting parameter, D, was evaluated to be 46 gauss from the relative intensities of their spectral lines by using the relations shown in Fig. 2. The ionicity was estimated to be 90% from the observed value of the hyperfine coupling constant, A, (89.4 gauss) and Fig. 3. The value of g was also determined to be 2.0022.

Effect of the Calcination Temperature in a Vacuum on the ESR Spectrum of the Mn^{2+} Ion on MgO. The intensity of the ESR spectrum of the Mn^{2+} ion on magnesium oxide changed with the calcination temperature, as is shown in Fig. 4,

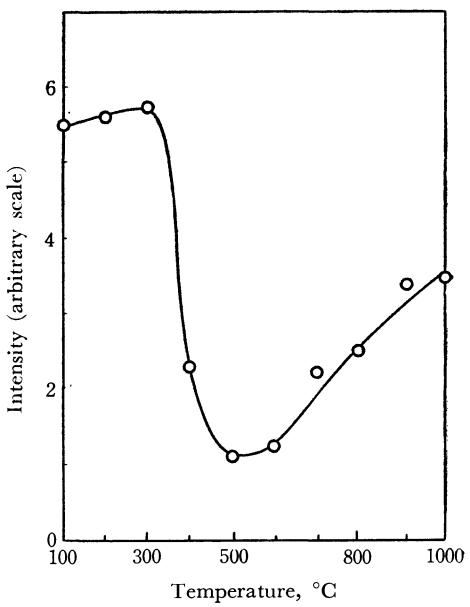

Fig. 4. The variation in ESR spectral intensity of Mn^{2+} ion by the treatment at different temperatures.

while the g value hardly changed at all from 2.0022. The intensity should be proportional to the concentration of the Mn^{2+} ion, since the Mn^{3+} ion does not participate in the ESR spectrum because of the strong spin-lattice interaction and since the spectrum of the Mn^{4+} ion, with $g=1.9980$ and $A=76$ gauss, is considerably different from those obtained here.[19-21] Accordingly, the concentration of the Mn^{2+} ion falls remarkably with a rise in the temperature, reaches a minimum at about 500°C,

18) L. Pauling, "Nature of the Chemical Bond," Cornell Univ. Press, Ithaca. New York (1940), p. 69.

19) Y. Miyako and M. Date, *J. Phys. Soc. Jap.*, **19**, 784 (1964).

20) M. Nakada, K. Awazu and S. Ibuki, *ibid.*, **19**, 781 (1964).

21) B. Henderson and T. P. P. Hall, *Proc. Phys. Soc.*, **90**, 511 (1967).

and then increases to some extent with a further rise in the temperature. On the other hand, the calcination up to 1000°C brings about a small decrease in the surface area of the magnesium oxide, from 69 to 60 m^2/g.

Specific Susceptibility. The specific susceptibilities of magnesium oxide containing the Mn^{2+} ion on the surface and of manganese oxide prepared from manganese nitrate were measured after the samples had been calcined at 500, 800, and 1000°C. The results are shown in Table 1.

TABLE 1. SPECIFIC SUSCEPTIBILITY OF MANGANESE OXIDE TREATED AT VARIOUS TEMPERATURES IN A VACUUM

	χ*			
	Room temp.	500°C	800°C	1000°C
Manganese on MgO	120.88	87.50	134.66	151.51
Manganese oxide	30.03	80.46	55.03	50.81

* unit of χ: 10^{-6} cgs emu

TABLE 2. SPECIFIC SUSCEPTIBILITY OF VARIOUS MANGANESE OXIDES

	χ*	Ref.
MnO	75.9	22
Mn_3O_4	55.8	22
Mn_2O_3	69.0	22
MnO_2	38.4	22
^{55}Mn	9.9	22
8MnO-5MgO	91.63	23
2MnO-11 MgO	126.87	23

* Unit of χ: 10^{-6} cgs emu

The value of the former is considerably decreased by the calcination at 500°C and then increased by the treatment in the higher-temperature range; the values at 800 and 1000°C are rather higher than that at room temperature. On the other hand, the value of the latter exhibits a remarkable increase at 500°C and then decreases with a further rise in the temperature. For comparison with these results, the values of various manganese oxides and of manganese oxide in magnesium oxide (mMnO–nMgO) are presented in Table 2.[22,23]

The electronic configurations of various manganese ions are as follows:

$Mn^{1+}\cdots(3d)^5(4s)$ $\quad$ $Mn^{3+}\cdots(3d)^4$

$Mn^{2+}\cdots(3d)^5$ $\quad$ $Mn^{4+}\cdots(3d)^3$

The specific susceptibility, therefore, should decrease with the increase in the valence of the manganese ion.

The data in Tables 1 and 2 and the results shown in Fig. 4 lead us to the following speculation: the manganese ions on magnesium oxide are mainly bivalent at room temperature, but some of them are oxidized to a higher valence state, namely Mn_2O_3, by calcination at 500°C in a vacuum, and these oxidized ions are in turn reduced to bivalence or, further, to univalence when treated at 800 and 1000°C. On the other hand, as may be seen from these tables, the manganese ion in manganese oxide may be Mn^{4+} at room temperature, and it may then be reduced to Mn^{2+} by heating at 500°C in a vacuum. This discrepancy may be attributed to the influence of the ground.

Variations in *D* and *A* Values. The values of D and A of the Mn^{2+} ion on magnesium oxide were estimated to be as is shown in Figs. 5 and 6 after calcination at 100, 300, 500, 800, and 1000°C in a vacuum, followed by the addition of hydrogen, carbon monoxide, or oxygen at each temperature.

The D value increases with the temperature, particularly abruptly from 500°C. When hydrogen is added after the calcination, the value also increases with the calcination temperature above 500°C, but the value is low as compared with that in the absence of hydrogen. The introduction of carbon monoxide causes the value to reach a maximum near 500°C. In the case of oxygen, it changes slightly from room temperature to 500°C, but thereafter it falls to almost zero at 1000°C.

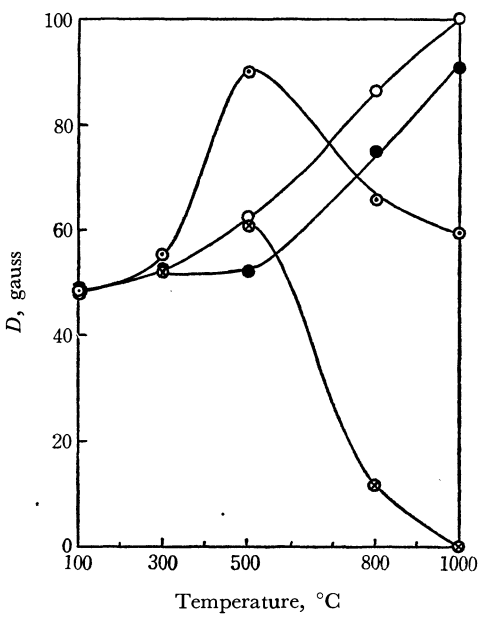

Fig. 5. The variations in D value by the addition of gases at different temperatures; ○: in a vacuum, ●: H_2, ⊙: CO, and ⊗: O_2.

22) International Critical Tables, **6**, 355, 357.

23) H. Bizette and B. Tasai, *Compt. Rend.*, **217**, 444 (1943).

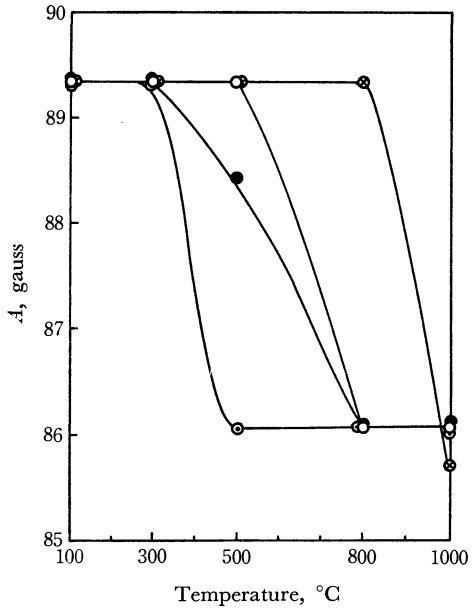

Fig. 6. The variations in A value by the addition of gases at different temperatures. Symbols in this figure have the same meaning as those in Fig. 5.

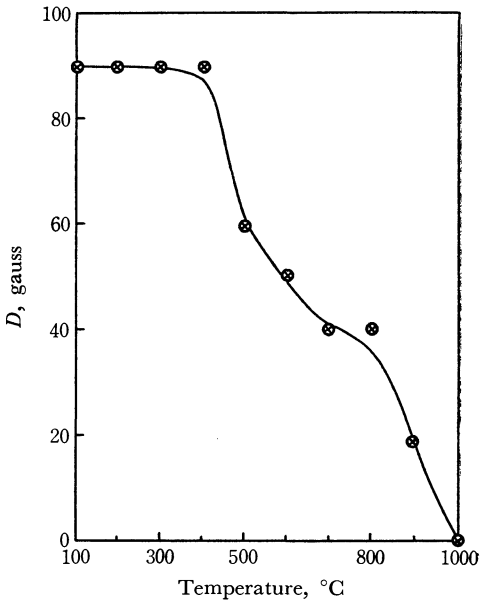

Fig. 7. The variations in D value by the addition of O_2 at different temperatures for the specimen precalcined at 1000°C.

Upon calcination in a vacuum, the value of A decreases remarkably above 500°C and remains constant, 86.2 gauss, at temperatures higher than 800°C. The bonding between the Mn^{2+} ion and its surroundings, accordingly, has a high degree of covalent character in the temperature range above 500°C. When hydrogen is added, the A value is steadily reduced by the treatments from 300 to 800°C, and then it remains constant, 86.2 gauss. By the addition of carbon monoxide, however, the A value already reaches to 86.2 gauss at 500°C and remains unchanged when treated at higher temperatures. When oxygen was introduced, the A value hardly changes till 800°C, but it reaches its lowest value, 85.7 gauss, at 1000°C.

Two effects are entangled with each other in the results of these experiments; one is due to the calcination, and the other, to the introduction of gas at different temperatures. Therefore, we attempted to remove the former effect by precalcining the magnesium oxide with the Mn^{2+} ion at 1000°C for 4 hr in a vacuum. The zero-field splitting parameter, D, was estimated when oxygen was added at different temperatures from 100 to 1000°C, as is shown in Fig. 7. The value falls abruptly to zero upon treatment at a temperature above 500°C. From the results, it is conceivable the oxygen is coordinated to the Mn^{2+} ion and that the crystal field around the ion is less distorted and becomes almost cubic-symmetrical at 1000°C. Such a cubic symmetry may be attributed to the cubic bulk structure of magnesium oxide.

The Mn^{2+} Ion on the Surface of Silica Gel. The ESR spectrum of the Mn^{2+} ion on the surface of silica gel was also investigated. The values of D, A, and ionicity are, respectively, 72 gauss, 98 gauss, and 95%, these values being obtained from the spectrum (Fig. 8) of the sample dried at 110°C for 24 hr in air. By a comparison of these values with those on magnesium oxide under the same conditions, it may be concluded that, on the surface of silica gel, the bonding between the Mn^{2+} ion

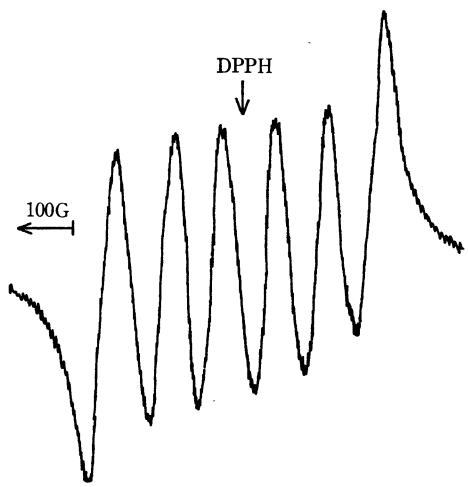

Fig. 8. ESR spectrum of Mn^{2+} ion on silica gel treated at 110°C for 24 hr in air.

and its environments has a higher degree of ionic character and that the crystal field around the Mn^{2+} ion is more distorted from the cubic symmetry than on the surface of magnesium oxide. The calcination of the sample in the same way as in the case of magnesium oxide brings about a complete disappearance of the six hyperfine structures of the Mn^{2+} ion above 300°C. This may be attributed to the fact that the signal becomes broad and smeared out with a rise in the temperature because of an increase in the D value. Even when hydrogen, carbon monoxide, and oxygen were introduced, the six hyperfine structures did not come out again.

Behavior of the Mn^{2+} Ion on MgO. We will discuss the behavior of the adsorbed manganese ion on the basis of the results of the ESR and susceptibility measurements. When the sample is treated up to 300°C, the coupling constant, A, is comparatively large, which means that the bonding between the Mn^{2+} ion and the environments has a high degree of ionic character, and the zero-field splitting parameter, D, is relatively small. The Mn^{2+} ion, therefore, combines weakly with magnesium oxide and surface hydroxyl groups. Upon treatment at 500°C, however, the distortion of the crystal field increases and the A value decreases; that is, the bonding of Mn^{2+} has a low degree of ionic character. Furthermore, both the ESR spectral intensity shown in Fig. 4 and the susceptibility measurement shown in Table 1 show that the concentration of the Mn^{2+} ion reaches a minimum. This may be interpreted as follows: the Mn^{2+} ion combines with oxygen as a result of the removal of the surface hydroxyl groups by a condensation dehydration, and some Mn^{2+} ions assume a higher valence state, Mn^{3+}. With the treatments at higher temperatures, the distortion of the crystal field increases and the bonding of the Mn^{2+} ion comes to take a much lower ionic character, thus reflecting the strong covalent bonding with oxygen. The increase in both the intensity of the ESR spectrum and the specific susceptibility above 500°C is caused by the elimination of oxygen, accompanied by the reduction of Mn^{3+} to Mn^{2+} or, partially, that of Mn^{2+} to Mn^{1+}. The possibility of the existence of Mn^{1+} may be speculated from the higher value of the susceptibility and the lower intensity of the ESR spectrum at 1000°C than those at room temperature. The presence of the Mn^{2+} ion may also mean that there is little oxygen on the surface of magnesium oxide at 1000°C.

It is somewhat doubtful that the information with regard to the surface of magnesium oxide obtained from the ESR spectra of Mn^{2+} ion can be directly applied to a discussion of its clean surface. Nevertheless, the cationic site, namely, the Mg^{2+} ion, on the surface of magnesium oxide doped with transition metal ions may be in a situation analogous to that of the Mn^{2+} ion observed in the present study, since the adsorption capacity of magnesium oxide increases remarkably upon the addition of a trace of transition metal ions to the bulk of magnesium oxide.[8,9]

The addition of hydrogen after the calcination in a vacuum leads to an increase in the distortion of the crystal field above 500°C, as is shown in Fig. 5. The value of A falls steadily above 300°C, as is shown in Fig. 6. This may be interpreted as follows: a part of the added hydrogen combines with the oxygen adjacent to the Mn^{2+} ion to form water, and then the Mn^{2+} ion enters into combination with the water molecules and the oxygen atoms of magnesium oxide in such a manner that the distortion of the crystal field around the Mn^{2+} ion is relatively small and the bonding bears a high degree of covalent character.

When carbon monoxide is introduced into the system, the A value decreases and the D value reaches a maximum at 500°C. The carbon monoxodie, having a greater reduction ability than hydrogen, easily draws out the oxygen coordinated weakly to the Mn^{2+} ion, and the ion, in turn, combines strongly with the oxygen on the surface of magnesium oxide and is subject to a large distortion of the crystal field from cubic symmetry. Such a distortion may be reduced by a coordination of carbon monoxide or carbon dioxide to the Mn^{2+} ion resulting from treatment at a higher temperature.

On the addition of oxygen, the A value shows no change below 800°C, but it abruptly decreases at 1000°C, while the D value decreases gradually above 500°C and becomes almost zero at 1000°C. It may, therefore, be suggested that oxygen atoms around the ion is slightly distorted from the cubic symmetry below 800°C, and that the bonding is strengthened by the thermal treatment, with the result that the oxygen atoms surrounding the Mn^{2+} ion have a cubic symmetry in the same manner as in the bulk of magnesium oxide.

On the other hand, none of the effects of gases are observed in the case of silica gel; this may indicate that the effect of the gas conceals itself behind the strong influence of the silica-gel surface. As to the manganese ion on the surface of magnesium oxide, the information obtained through the ESR spectrum may also be characterized by the cationic lattice point, Mg^{2+}, activated by the addition of the Mn^{2+} ion. It may, therefore, be mentioned that the manganese ion plays a significant role as a probe for the surface of magnesium oxide and, at the same time, contributes to the surface reactivity of the magnesium oxide in reaction to gases.

BULLETIN OF THE CHEMICAL SOCIETY OF JAPAN VOL. 43 3383—3390 (1970)

Measurement of Negative Ions Formed by Electron Impact. VII. Negative Ion Mass Spectra from Alkyl Cyanides

Satoru TSUDA, Akira YOKOHATA and Toshikatsu UMABA

Department of Chemistry, Faculty of Engineering, University of Hiroshima, Senda-machi, Hiroshima

(Received June 4, 1970)

The negative ion mass spectra from alkyl (methyl, ethyl, *n*- and *iso*-propyl) cyanides with electron energies of 80 eV, 40 eV and 9.5 eV were measured by a Hitachi RMU-6D mass spectrometer with emphasis on the relative abundance of negative ions to positive ions with electron energies of 80 eV, 40 eV and 15 eV. In every sample, the electron impacts with 80 eV and 40 eV gave almost the same distribution of *m/e* for negative ion mass spectra. Then, the peak of *m/e* 26(CN^-) ions was the most intense and also the relatively strong peak of 25(C_2H^-) ions was found through all samples. On the other hand, the formations of 38(C_2N^-), 39($CHCN^-$) and 41(CH_3CN^-) ions from methyl cyanide, of 50(C_3N^-) ions from ethyl cyanide, *n*- and *iso*-propyl cyanides, of 40(CH_2CN^-) ion from *n*-propyl cyanide were characteristic of each sample. The ratio of the yield of negative ions to positive ions was respectively of the order of $\sim 10^4$ for CH_3CN^+/CN^- (CH_3CN), $C_2H_4^+/CN^-$ (C_2H_5CN), $C_3H_5^+/CN^-$ (*n*-C_3H_7CN) and $C_3H_6^+/CN^-$ (*iso*-C_3H_7CN) at 80 eV and 40 eV electron energies. At 9.5 eV, *m/e* 26 (CN^-) ions predominated over other negative ions for all the samples and a much larger peak of 40 (CH_2CN^-) ions in *n*-C_3H_7CN than in *iso*-C_3H_7CN was also observed. Then, we got the values of 19$\sim$65 for CH_3CN^+/CN^-, $C_2H_4^+/CN^-$, $C_3H_5^+/CN^-$ and $C_3H_6^+/CN^-$ (15 eV for positive ions). This work also gave linear relationship of the yield of each negative ion to the pressure in the range used for an usual chemical analysis.

Collisions of electrons of low velocity with molecules may produce charged fragments of the molecules. The data on the minimum electron energy necessary to produce these fragments, their identification, and the processes involved may permit one to determine the electron affinity of fragments and the heat of dissociation of the molecule. The relative abundance of ion products and the probability of a process as a function of the electron energy are also of interest.

If the kinetic energy of the electron in a gaseous medium is below the ionization potential of the molecules, the electron would lose energy to electronic excitation as long as its kinetic energy is above the first excitation potential of the medium. When the electron energy is below the first excitation potential, moderation occurs through elastic and inelastic collisions leading to vibrational and rotational excitation of the molecules. A subexcitation electron may lose energy also through various types of electron attachment processes and the excitation of compound negative ion states. Compound negative ion states can decay purely elastically, give vibrationally excited molecules, or lead to dissociative attachment.[1-6]

Especially, of interest and practical importance are the processes which result in the formation of negative ions. As described frequently,[7] they are classified into the following types: a) resonance capture, b) dissociative resonance capture and c) ion pair formation. Under the normal operating conditions (80—40 eV) of a mass spectrometer, all processes may occur. As they are pressure dependent, the relative ion intensities in negative ion mass spectra would change with the sample pressure. In the formation of $CH_2NO_2^-$ ions from *n*- and *iso*-nitropropanes,[8] the authors reported the linear relationship of their yield to the pressure in the region used for an usual analysis, and also their yield is $\sim$100 times greater in *n*-nitropropane than in isonitropropnane. This shows clearly the usefulness of the measurement of

1) G. J. Schulz and R. E. Fox, *Phys. Rev.*, **106**, 1179 (1957).
2) G. J. Schulz, *Phys. Rev. Lett.*, **10**, 104 (1963).
3) C. R. Bowman and W. D. Miller, *J. Chem. Phys.*, **42**, 681 (1965).
4) H. G. M. Heideman, C. E. Kuyatt and G. E. Chamberlain, *J. Chem. Phys.*, **44**, 440 (1966).
5) M. G. Menedez and H. K. Holt, *ibid.*, **45**, 2743 (1966).
6) R. N. Compton, L. G. Christophorou and R. H. Huebner, *Phys. Lett.*, **23**, 656 (1966).
7) C. E. Melton in "Mass Spectrometry of Organic Ions," ed. by F. W. McLafferty, Academic Press Inc., New York, N. Y. (1963), Chapter 4.
8) S. Tsuda, A. Yokohata and M. Kawai, This Bulletin, **42**, 607 (1969).

negative ions for chemical analysis. Also, the formation of molecular anions by resonance capture would permit the determination of the molecular weight, and in some cases might be useful for structural and stereochemical problems.[9]

Unfortunately, however, a very little has been published on negative ion mass spectrometry. There also appear to be discrepancies in the published experimental results which calls for further work. For the purpose of gathering the data of negative ions and establishing their pattern in comparison with positive ions under various electron energies, this series of studies[10] has been begun. This work is an extension to alkyl cyanides, with emphasis on a comparative study of negative and positive ions.

Experimental

Experiments were performed on a Hitachi RMU-6D mass spectrometer equipped with the T-2M ion source having a rhenium filament. The ion detection circuit consisted of a ten stage electron multiplier having Ag–Mg dynode and of a Faraday collector. All the spectra were measured with a total emission current of 20 μA, an accelerating voltage of 3.6 kV and an electron multiplier voltage of 2.5 kV, under the electron energies of 80 eV, 40 eV, 9.5 eV (80 eV, 40 eV and 15 eV for positive ions) and a pressure of $\sim 10^{-6}$ mmHg in the source. An ionizing current showed a constant value of 10.5 μA down to $\sim$10 eV. The energy scale was calibrated in every measurement by the vanishing current method as compared to the ionization potential of argon or the appearance potential of m/e 16(O^-) ions

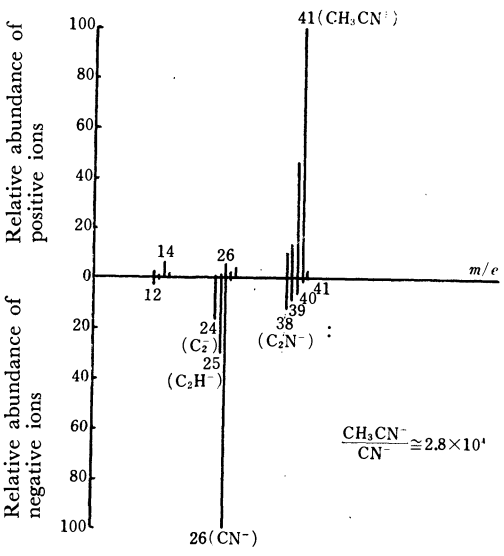

1a

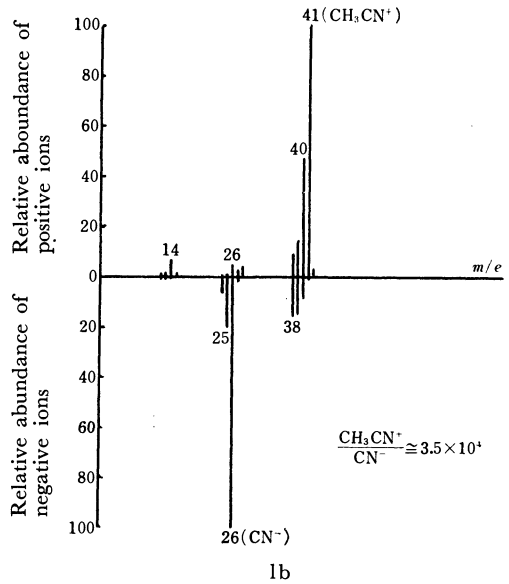

1b

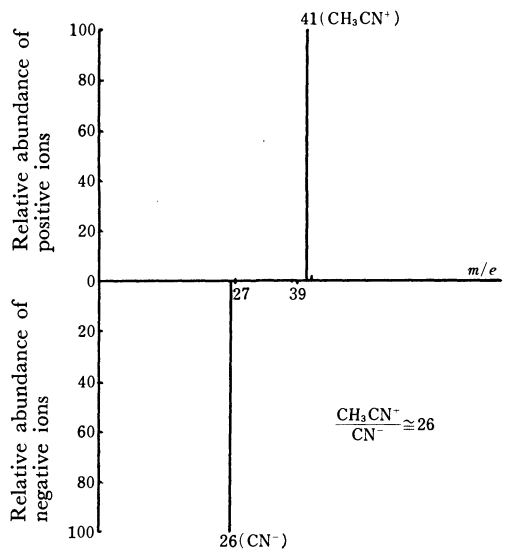

1c

Fig. 1. Positive and negative ion mass spectra of CH_3CN.
a 80 eV, b 40 eV, c 15 eV for positive ions, 9.5 eV for negative ions

from carbon monoxide, carbon dioxide and oxygen as described previously.[10] The repeller voltage was adjusted respectively to the best condition to collect the ions in positive and negative ion measurements. All chemicals were of research grade.

Results and Discussion

Negative Ion Mass Spectra. *Methyl Cyanide.* In 80 eV electron impact experiments (Fig. 1a), the foregoing spectra were observed where they are shown in decreasing order of yield; m/e 26

9) R. T. Aplin, H. Budzikiewiez and C. Djerassi, *J. Amer. Chem. Soc.*, **87**, 3180 (1965).
10) S. Tsuda, A. Yokohata and M. Kawai, This Bulletin, **42**, 614, 1515, 2514 (1969).

(CN^-), 25 (C_2H^-), 24 (C_2^-), 38 (C_2N^-), 39 ($CHCN^-$), 40 (CH_2CN^-), 12 (C^-), 27 (HCN^-), 13 (CH^-), 41 (CH_3CN^-) and 14 (CH_2^-). The comparison of the yield of CN^- ion with that of CH_3CN^+ (*m/e* 41, the most intense peak among the positive ions) gave a value of $\sim 2.8 \times 10^4$ for CH_3CN^+/CN^-.

For 40 eV electron energies (Fig. 1b) the pattern of the negative ions was almost the same as that for 80 eV except for a small change in the relative abundance of C_2H^-, C_2^- and $CHCN^-$ ions, and the ratio of CH_3CN^+ to CN^- was $\sim 3.5 \times 10^4$.

For 9.5 eV electron energies (Fig. 1c) CN^- ions predominated over other negative ions. A value of ~26 for CH_3CN^+/CN^- was obtained where 15 eV electron energies are used for positive ions.*1. Table 1 shows the yield of minor negative ions for 80 eV, 40 eV and 9.5 eV.

Table 1. Minor negative ions from CH_3CN

m/e	Relative intensities at electron energies of		
	80 eV	40 eV	9.5 eV
12	2.56	1.07	
13	1.24	1.34	
14	0.17	0.40	0.05
15		trace	0.09
27	1.47	1.89	1.31
38	12.00	15.80	0.24
39	8.66	15.00	1.03
40	6.18	8.67	0.23
41	0.83	1.08	

Normalized to CN^- (yield=100)

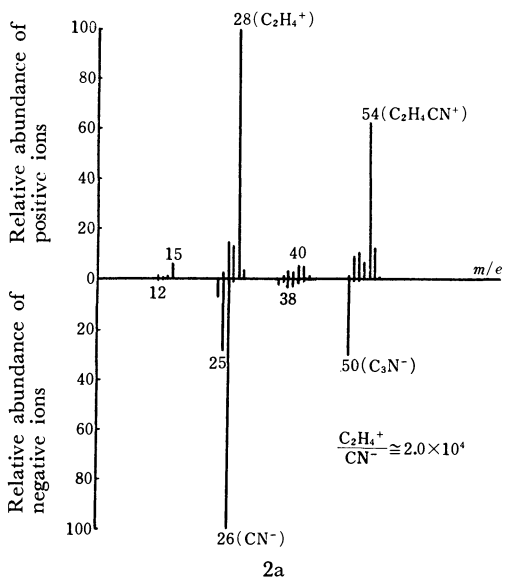

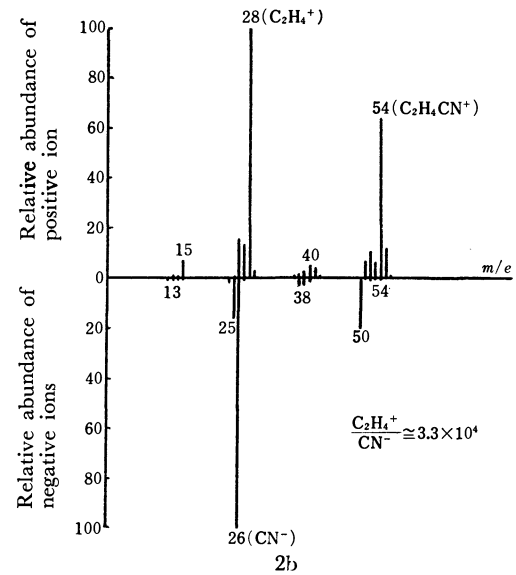

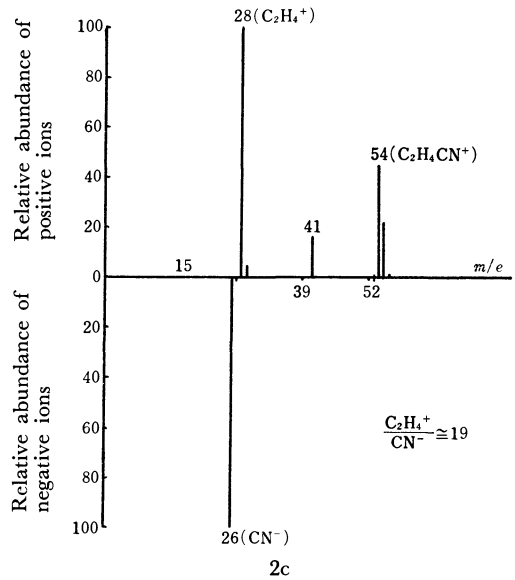

Fig. 2. Positive and negative ion mass spectra of C_2H_5CN.
a 80 eV, b 40 eV, c 15 eV for positive ions, 9.5 eV for negative ions

Then, the formation of parent negative ion, CH_3CN^- at 80 eV and 40 eV was observed while at 9.5 eV it was not. It is noticed[11] that the appearance potential, AP_{obs} value of CH_3CN^- ions from methyl cyanide is ~23 eV and the effect of an additive xenon suggests the possibility of the occurrence of the reaction; $Xe^* + CH_3CN \rightarrow Xe^+ + CH_3CN^-$. Also, the formation of C_2H^- and C_2^-

*1 Since at 9.5 eV electron energies the positive ions are not observed, the energy of 15 eV was substitutionally used.

11) T. Sugiura and T. Arakawa, presented at the annual meeting of 22nd Chemical Society of Japan, Tokyo (1969).

ions from the compounds containing two carbon atoms besides hydrogen atoms may be regarded to be a general phenomenon as found in ethane,[7] nitroethane[10] and ethyl chloride.[12] Furthermore, in the case of compounds containing cyano group, CN^- and C_2N^- ions should be added to them. These are qualitatively understood on the basis of EA(C_2)$\simeq$3.1 eV[13] and EA (CN)$\simeq$ 3.4 eV[8] while a value of $\gtrsim$2.3 eV is expected for EA (C_2N).[14] The data on EA (HCN), EA (CHCN) and EA (CH_2CN) will be reported in the next paper.

Ethyl Cyanide. The 80 eV electron impact gave the following spectra (Fig. 2a), being shown in the decreasing order of yield: *m/e* 26 (CN^-), 50 (C_3N^-), 25 (C_2H^-), 24 (C_2^-), 38 (C_2N^-), 39 ($CHCN^-$), 36 (C_3^-), 40 (CH_2CN^-), 51 (HC_3N^-), 27 (HCN^-), 12 (C^-), 13 (CH^-), 52 ($H_2C_3N^-$), 37 (C_3H^-), 14 (CH_2^-), 53 ($H_3C_3N^-$) and 54 ($H_4C_3N^-$). The comparison with $C_2H_4^+$ ions (*m/e* 28, the most intense peak among the positive ions) gave a value of $\sim 2.0\times10^4$ for $C_2H_4^+/CN^-$.

For 40 eV electron energies (Fig. 2b), almost the same pattern as 80 eV was observed except for a relatively small change in the yield of C_2H^-, C_2^-, and C_3N^- ions, and a value of $C_2H_4^+/CN^-$ was estimated to be $\sim 3.3\times10^4$.

For 9.5 eV electron energies (Fig. 2c), CN^- ions predominated over other negative ions, where

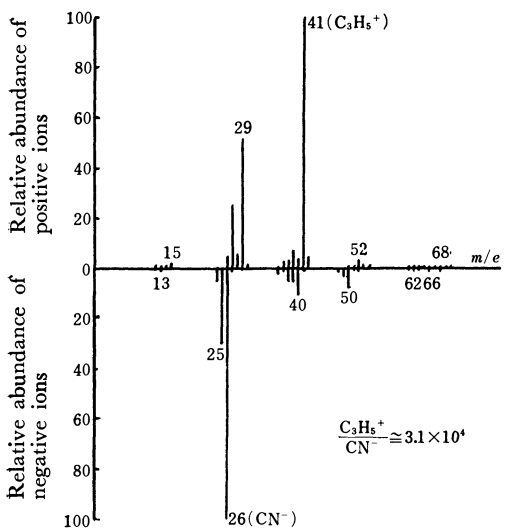

3a

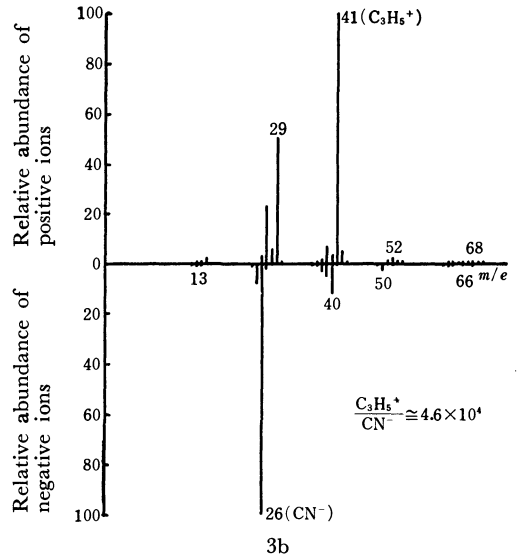

3b

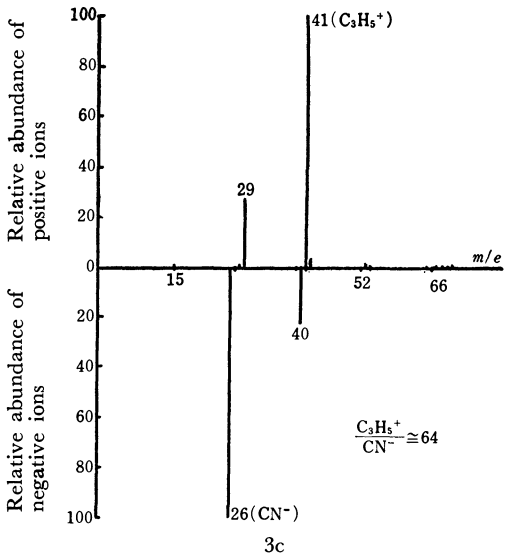

3c

Fig. 3. Positive and negative ion mass spectra of n-C_3H_7CN.
a 80 eV, b 40 eV, c 15 eV for positive ions, 9.5 eV for negative ions

a value of $C_2H_4^+/CN^-\simeq 19$ was found. Table 2 shows the yield of minor negative ions for 80 eV, 40 eV and 9.5 eV.

It is of interest to note that a relatively strong peak of C_3N^- ions was observed. This can be understood on the basis of a relatively high value (55 kcal/mol) of EA(C_3N) obtained by Dibeler *et al.*[14] in a mass spectrometric study of cyanogen and cyanoacetylenes, in which the measurement of appearance potentials of positive ions was made mainly. On the other hand, C_2N^- ions decrease in a considerable amount when compared with those in methyl cyanide. Another difference

12) S. Tsuda, A. Yokohata and M. Kawai, This Bulletin, to be published.

13) V. I. Vedeneyev, L. V. Gurvich, V. N. Kondrat'yev, V. A. Medvedev and Ye. L. Frankevich, "Bond Energies, Ionization Potentials and Electron Affinities," Edward Arnold Ltd., London (1966), p. 192. EA: electron affinity.

14) V. H. Dibeler, R. N. Reese and J. L. Franklin, *J. Amer. Chem. Soc.*, **83**, 1813 (1961).

Table 2. Minor negative ions from C_2H_5CN

m/e	Relative intensities at electron energies of		
	80 eV	40 eV	9.5 eV
12	1.23	0.51	
13	0.92	0.64	trace
14	0.25	0.59	0.01
15		0.22	0.02
24	7.07	2.21	
25	30.70	16.10	0.04
27	1.25	1.40	1.37
36	2.07	0.11	
37	0.37	0.24	
38	3.64	3.49	0.04
39	2.65	2.76	0.30
40	1.88	1.66	0.13
50	30.80	20.20	0.02
51	1.30	0.93	trace
52	0.57	0.97	1.23
53	trace		0.12
54	trace	0.19	0.04

Normalized to CN^- (yield=100)

from methyl cyanide is that there is no formation of parent negative ion, $C_2H_5CN^-$, which was not observed throughout the whole range of electron energies used.

n- and iso-Propyl Cyanides. For the impacts of 80 eV and 40 eV electron energies (Figs. 3a, 4a and 3b, 4b), the two samples gave almost the same negative ions; *m/e* 26 (CN^-), 25 (C_2H^-), 50 (C_3N^-), 24 (C_2^-), 39 ($CHCN^-$), 38 (C_2N^-), 49 (C_4H^-), 36 (C_3^-), 27 (CHN^-), 48 (C_4^-), 37 (C_3H^-), 13 (CH^-), 62 (C_4N^-), 63 (C_4HN^-), 12 (C^-), 64 ($C_3H_2CN^-$), 66 ($C_3H_4CN^-$), 52 ($C_2H_2CN^-$), 51 (C_2HCN^-), 14 (CH_2^-), 41 (CH_3CN^-), 68 ($C_3H_6CN^-$), and 65 ($C_3H_3CN^-$), except for a relatively

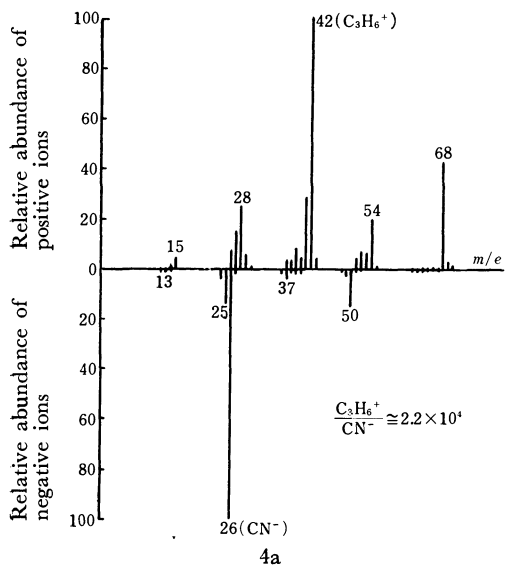

4a

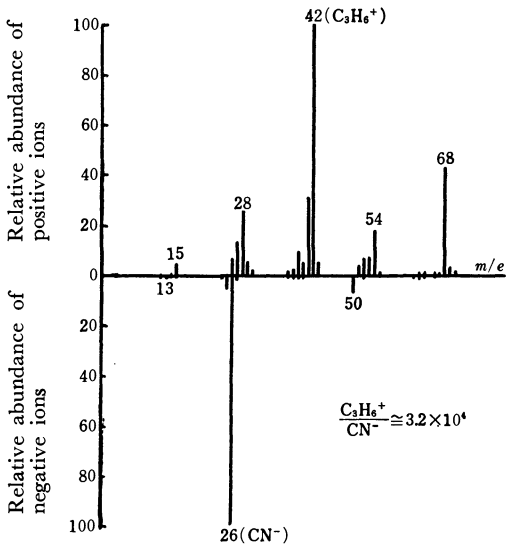

4b

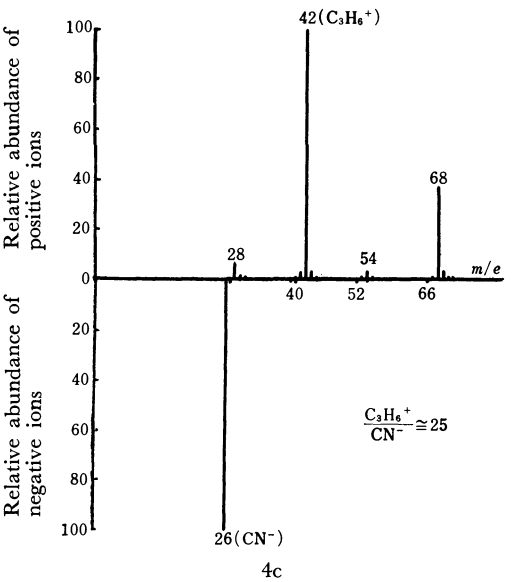

4c

Fig. 4. Positive and negative ion mass spectra of *iso*-C_3H_7CN.
a 80 eV, b 40 eV, c 15 eV for positive ions, 9.5 eV for negative ions

large peak of 40 (CH_2CN^-) ion in *n*-C_3H_7CN. The parent ion, *m/e* 69 ($C_3H_7CN^-$) was not observed for both compounds.

It is of great interest to note that a relatively strong peak of *m/e* 25 (C_2H^-) ion has been observed among the negative ions arising from the propyl group. This is consistent with the situation in propyl alcohol[7] and nitropropane.[8] Also, *m/e* 50 (C_3N^-) ion was observed to be comparatively strong as in the case of C_2H_5CN.

Especially, we should like to emphasize here

that a relatively strong peak of *m/e* 40 (CH_2CN^-) was found only in *n*-C_3H_7CN, the situation being very similar to that[8] of *m/e* 60 ($CH_3NO_2^-$) obtained from nitropropanes. The comparison of the yield of CN^- ion with that of $C_3H_5^+$ and $C_3H_6^+$ ions (*m/e* 41 and 42, the most intense peaks among the positive ions from *n*- and *iso*-propyl cyanides) gave the following values for $C_3H_5^+/CN^-$ and $C_3H_6^+/CN^-$; $\sim 3.1\times10^4$ and $\sim 2.2\times10^4$ at 80 eV respectively, $\sim 4.6\times10^4$ and $\sim 3.2\times10^4$ at 40 eV, respectively.

At 9.5 eV, *m/e* 26 (CN^-) ions predominated over other negative ions (Fig. 3c and Fig. 4c). Moreover, a relatively large yield of *m/e* 40 (CH_2CN^-) from *n*-C_3H_7CN is very characteristic, while in *iso*-C_3H_7CN it is found only as a relatively small peak. This finding would be useful for one of the identification methods of *n*-C_3H_7CN. The reason for a small cross section of CH_2CN^- ion formation from *iso*-C_3H_7CN would probably be that it is the rearrangement ion. The ratio of the yield of $C_3H_5^+$ and $C_3H_6^+$ to CN^- gave values of $\sim$64 and $\sim$25, respectively. Tables 3 and 4 show the yields of minor negative ions from *n*- and *iso*-propyl cyanides in relation to the electron energy.

Table 3. Minor negative ions from *n*-C_3H_7CN

m/e	Relative intensities at electron energies of		
	80 eV	40 eV	9.5 eV
12	0.82	0.48	
13	1.33	0.97	trace
14	0.40	0.40	trace
15			0.11
24	5.83	1.33	
25	30.28	8.19	0.07
27	1.58	1.72	1.56
36	2.49	0.37	
37	1.38	0.53	
38	5.12	3.48	0.04
39	5.30	5.28	0.33
40	11.00	12.00	23.00
41	0.38	0.39	0.76
48	1.53		
49	3.37	0.26	
50	7.97	2.91	0.04
51	0.47	0.21	
52	0.48	0.62	0.69
53			0.05
62	1.17	0.40	
63	1.10	0.66	
64	0.66	0.62	0.02
65	0.04	0.06	
66	0.52	0.75	1.34
67		trace	0.15
68	0.28	0.61	0.08

Normalized to CN^- (yield=100)

Table 4. Minor negative ions from *iso*-C_3H_7CN

m/e	Relative intensities at electron energies of		
	80 eV	40 eV	9.5 eV
12	0.65	0.44	
13	1.04	0.91	
14	0.41	0.57	0.04
15	0.10	0.20	0.10
24	4.01	1.08	
25	13.99	5.61	0.03
27	1.53	1.18	1.34
36	1.53	0.40	
37	2.46	0.50	
38	1.20	1.50	
39	1.62	1.48	0.17
40	1.17	1.14	0.28
41	trace	trace	trace
42			trace
48	1.06	trace	
49	2.12	0.05	
50	15.22	6.15	trace
51	0.61	0.28	
52	0.36	0.93	0.69
53			0.1
54			0.12
62	0.64	0.28	
63	0.49	0.26	
64	0.29	0.42	
66	trace	0.11	0.36
67			0.03
68			0.02

Normalized to CN^- (yield=100)

Effect of Pressure. Figure 5 shows the relation between the yields of *m/e* 26 (CN^-), 38 (C_2N^-), 39 ($CHCN^-$), 40 (CH_2CN^-) and 50 (C_3N^-) ions and the pressure for each sample (5a for *m/e* 26 ion, 5b for *m/e* 38 ion, 5c for *m/e* 39 ion, 5d for *m/e* 40 ion and 5e for *m/e* 50 ion) under the electron energy of 80 eV. All the results show good linearities against the pressure under given experimental conditions. Also, this linear relationship was independent of the electron energy as shown in Fig. 6, where the *m/e* 26 (CN^-) ion from CH_3CN is shown as an example. A similar linear relationship had been reported for the *m/e* 1 (H^-) ion produced from hydrogen[15] under the electron energies of 6.8 eV, 10.0 eV and 14.2 eV in the range of pressure from 1×10^{-4} mmHg to 4×10^{-4} mmHg, for the *m/e* 39 (CH_3CC^-) ion[16] from methylacetylene in the range of pressure up to about 5×10^{-5} mmHg and for *m/e* 46 (NO_2^-), 16 (O^-), 26 (CN^-) and 42 (CNO^-) ions[8] from nitroalkanes in the range of pressure used for usual analysis. Of course,

15) G. J. Schulz, *Phys. Rev.*, **113**, 816 (1959).
16) T. Sugiura, T. Seguchi and K. Arakawa, This Bulletin, **40**, 2992 (1967).

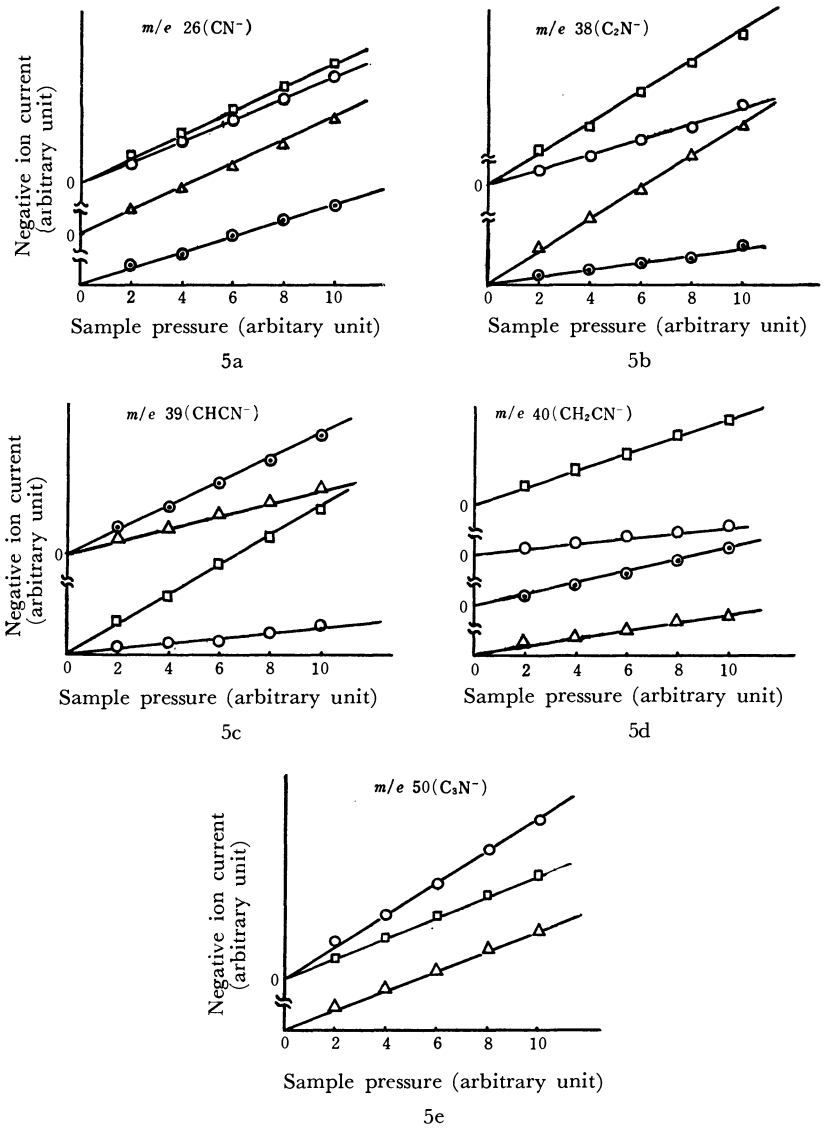

Fig. 5. Plot of negative ion current against pressure (electron energy ; 80 eV).
○ *iso*-C_3H_7CN, □ *n*-C_3H_7CN, △ C_2H_5CN, ⊙ CH_3CN

the pressure dependency may become complicated at higher pressures because of the occurrence of ion-molecule reactions. In the present work, however, such a study was not made because of instrumental difficulty.

The Formation of Negative Ions. As mentioned above, the yield of negative ions is dependent on electron energies and cross sections of formation processes which are very different from those of positive ions, especially in their behaviors in the low energy region. Here, we should like to add a few words on the formation of parent negative ions and the excitation of negative ions.

It is generally accepted that a parent negative ion is formed by the capture of a free electron by a molecule, with the vibrational excitation of the molecular ion and its subsequent stabilization in a collision with another molecule ($e^- + AB \rightarrow [AB^-]^*$; $[AB^-]^* + X \rightarrow [AB^-] + X +$ kinetic energy.[17] However, we should not overlook that electron attachment may be significantly impeded when the formation of a stable negative ion requires a substantial deformation from the neutral geometry. For example, although N_2O containing 16 valence electrons is linear in the ground electronic state,[18] a compound with 17 electrons is bent in the ground

17) E. W. McDaniel, "Collision Phenomena in Ionized Gases," John Wiley & Sons, Inc., New York (1964), p. 368.

18) E. E. Ferguson, F. C. Fehsenfeld and A. L. Schmeltekopf, *J. Chem., Phys.*, **47**, 3085 (1967).

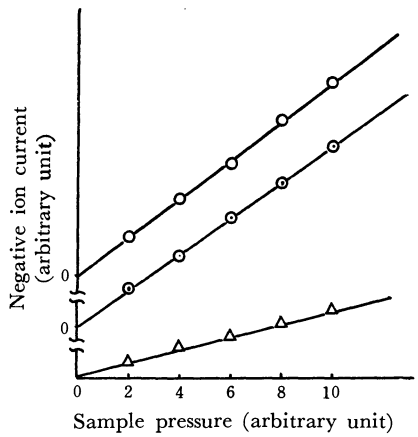

Fig. 6. Plot of negative ion (CN^-) current against pressure in CH_3CN.
△ 9.5 eV, ⊙ 40 eV, ○ 80 eV

state, *e.g.*, NO_2 with $\alpha=134.1°$. The energy necessary to bend N_2O from 180° to 134° can be estimated to be about 1 eV, using a harmonic bending force constant. On the other hand, the appearance potential of the reaction; $e^-+N_2O\rightarrow O^-+N_2$, is said to be ~0.21 eV on the basis of $D(N_2-O)=1.677$ eV and $EA(O)=1.465$ eV. Thus, energetic electrons do not attach to N_2O but rather cause dissociative attachment. The failure to form N_2O^- by a simple transfer of an electron*2 could be understood on this basis. Very recently, Chantry[19] showed that the prominent peak of O^- ion via dissociative attachment in N_2O occurs at or very close to zero (0—0.05 eV) in the high temperature (1050°K). This leads us to conclude that the cross section increases very rapidly with increasing vibrational excitation of the initial molecule. It seems to be a feature of many dissociative attachment processes.

MacNeil *et al.*[20] also report that production of negative ions is clearly influenced by the size, symmetry and bonding of the molecule being bombarded with electrons; in general, large, symmetrical molecules containing multiple linkages tend to undergo less fragmentation and consequently to form larger negative ions, sometimes including the molecular ion.

Next, let us discuss on the excitation of the negative ion. It is known that it is unlikely that negative ions with stable discrete excited states exist with appreciable binding energy. For example, in the case of CN^- ions it seems reasonable to assume that the electron attaching to the CN radical will go into the $(x\sigma)$ orbital*3 of N_2^+ or CO^+ ions which is isoelectronic with the CN radical.[21] Then, it leads to a molecule which is isoelectronic with the N_2 and CO molecules. Examination of the energy level diagrams of these molecules shows that the first excited singlet levels are between 8 and 9 eV above the ground state. Thus, it would seem improbable that it could be produced in a low-lying electronically excited state. Of course, the production in the vibrational excited state would be possible.

*2 The possibility of formation of N_2O^- via ion-molecule reactions in N_2O cannot be excluded. (P. J. Chantry, *J. Chem. Phys.*, **51**, 3380 (1969)).

19) P. J. Chantry, *J. Chem. Phys.*, **51**, 3369 (1969).

20) K. A. G. MacNeil and J. C. J. Thynne, *Trans. Faraday Soc.*, **64**, 2112 (1968).

*3 The electron configuration is shown to be $kk(z\sigma)^2(y\sigma)^2(w\pi)^4(x\sigma)^1$.

21) J. D. Craggs, C. A. McDowell and J. W. Warren *Trans. Faraday Soc.*, **48**, 1093 (1952).

BULLETIN OF THE CHEMICAL SOCIETY OF JAPAN VOL. 43 3391—3399 (1970)

Structure of Polynucleotide Complex with Non-Complementary Nucleosides. I. Poly A,G+Poly U

Hideo AKUTSU and Masamichi TSUBOI

Faculty of Pharmaceutical Sciences, The University of Tokyo, Hongo, Bunkyo-ku, Tokyo

(Received June 4, 1970)

Copolymers of riboadenylic and riboguanylic acids (poly A,G) with guanylic acid contents of 8.5—29.6% were prepared. The ultraviolet and infrared absorptions were examined of aqueous solutions of mixtures of poly A,G and polyribouridylic acid (poly U) of various mole ratios. It has been shown that in a solvent with 0.1 M Na^+ a triple-helical structure is formed with a A$\begin{matrix}\cdot\cdot U\\ \cdot\cdot U\end{matrix}$ type inter-base binding as well as a double-helical structure with a A···U type binding, while in a solvent with 0.01 M Na^+ only double-helical structure is formed. A guanine residue in the copolymer remains within the helix structure when its neighbors are mostly adenine residues, whereas it rotates out when there are many guanine residues in its vicity. On heating the solution, the structures just mentioned were found to be broken. The process of such a breaking down was followed also by means of the ultraviolet and infrared absorption measurements.

Polyriboadenylic acid (poly A) and polyribouridylic acid (poly U) are known to form a double- or triple-stranded helical structure in aqueous solution (see Figs. 1 (a) and 1(b)).[1,2] In such a structure, adenosine (A) and uridine (U) residues are considered to be strongly bound with each other through specific hydrogen bonds; A and U are considered to be complementary. In the present work, we have introduced the guanosine residue (G), which is not complementary to U, into the poly A chain, to examine its effect upon the structure. The question is whether the structure becomes like Fig. 1(c), 1(d), 1(e), or 1(f). In the structure Fig. 1(c) or 1(d), the G residues remain within the interior of the helix. They merely replace the A residues, and the outline of the structure here remains almost the same with that without the G residues (Fig. 1 (a) or 1 (b)). While, in the structure Fig. 1 (e) or 1 (f), the G residues rotate out of the helix in such a manner as to enable complementary A···U binding in the the subsequent regions of the polynucleotide chains.

As was shown previously,[3-8] the structures (c), (d), (e), and (f) in Fig. 1 can be distinguished by examining the mixing curve—*i.e.*, by examining the mole ratio poly A, G/poly U (on the basis of the phosphorus analysis), at which the maximum hypochromicity (minimum absorbance) appears for a proper ultraviolet radiation (at 259 mμ, for example). The mole ratio should be 50/50 for (c), 33.3/66.7 for (d), $100/x$ for (e), and $100/2x$ for (f), where x(%) is the mole % of A in the copolymer of A and G (poly A, G) now in question. On the other hand, the hydrogen-bonded A···U and A$\begin{matrix}\cdot\cdot U\\ \cdot\cdot U\end{matrix}$ structures are known to give characteristic infrared absorptions in D_2O solution which are distinguished from each other and from A and U residues free from hydrogen-bonds.[9] We attempted the ultraviolet and infrared absorption measurements of our poly A, G+poly U in aqueous solutions, keeping these previous demonstrations in mind.

Preparation of the Polynucleotide Samples

The polynucleotide samples used were prepared by the use of polynucleotide phosphorylase obtained from *Micrococcus lysodeikticus* or from *Azotobacter vinelandii*. The compositions of the reaction mixtures and the incubation times are given

1) A. Rich and D. R. Davies, *J. Amer. Chem. Soc.*, **78**, 3548 (1956).
2) G. Felsenfeld, D. R. Davies and A. Rich, *ibid.*, **79**, 2023 (1957).
3) J. R. Fresco and B. M. Alberts, *Proc. Nat. Acad. Sci. U. S.*, **46**, 311 (1960).
4) R. F. Steiner, *J. Biol. Chem.*, **235**, 2946 (1960); **236**, 342 (1961).
5) W. Szer and D. Shugar, *Acta Biochim. Pol.*, **8**, 235 (1961).
6) M. N. Lipset, L. A. Heppel and D. F. Bradley, *J. Biol. Chem.*, **236**, 857 (1961).
7) T. Ichikawa, H. Fujita, K. Matsuo and M. Tsuboi, This Bulletin, **40**, 2272 (1967).
8) M. Tsuboi, K. Matsuo, and M. Nakanishi, *Biopolymers*, **6**, 123 (1968).
9) H. T. Miles and J. Frazier, *Biochem. Biophys. Res. Commun.*, **14**, 21 (1964).

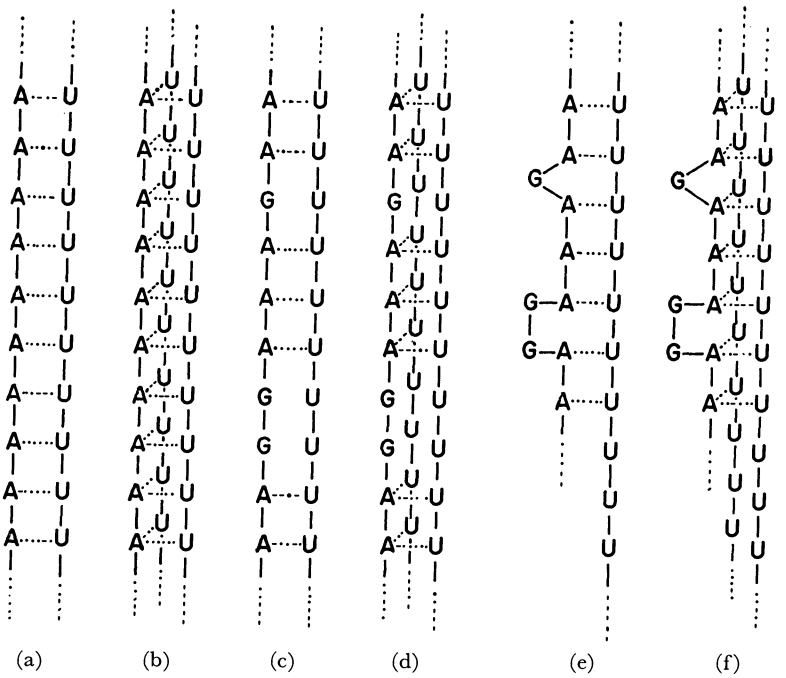

Fig. 1. Schematic drawings of possible structures of polynucleotide complexes.
(a) Complete double-helix.
(b) Complete triple helix.
(c) Double-helix with the G residues inside.
(d) Triple-helix with the G residues inside.
(e) Double-helix with the G residues looping out.
(f) Triple-helix with the G residues looping out.

Table 1. An example of reaction mixture in enzymatic preparation of polynucleotide

Buffer solution[a)]	1.0 m*l*
Enzyme solution	1.5[b)]
Adenosine-5′-diphosphate (21 mg/m*l*)	1.1
Adenosine-5′-triphosphate (25 mg/m*l*)	0.5
Guanosine-5′-diphosphate (11 mg/m*l*)	0.9
$(NH_4)_2SO_4$ solution (saturated)	1.25
Total	6.25 m*l*

a) This buffer solution was prepared by mixing 1.25 m*l* of 2 M Tris, 3 g of urea, and 2 m*l* of 2 M $MgSO_4$, by adding 12 M HCl to reach pH 9, and then by adding 0.5 M mercaptoethanol so that the total volume become 25 m*l*.

b) Usually this amount contains 10—20 units of enzyme. 1 units=amount of enzyme which can liberate 1 μmol of orthophosphate in the enzymatic reaction of 15 min. The most efficient amount of enzyme was determined by several trial experiments with smaller scale (1/200 of that described here).

in Tables 1 and 2. The incubation temperature was 37°C for the enzyme from *M. lysodeikticus* and 30°C for that from *A. vinelandii*. After the enzymatic reaction, the product was precipitated with perchloric acid or with ethanol and then purified by the method of phenol extraction and by dialysis.

Base Composition and Some Other Characterization of the Copolymers

The base composition of each poly A,G sample was determined by hydrolyzing it with 1 N HCl, by the paper-chromatographic separation of the resulting adenine and guanine, and by ultraviolet absorption measurements of them. The composition thus determined is given in Table 2. The base sequences in these copolymers are not known, but it is probable that they are nearly random. Saigo, Uchida and Egami (private communication) made an analysis of the products obtained by a digest of a poly A,G in which G content is 30% with ribonuclease T_1. In a DEAE-Sephadex column chromatography with 7M urea they found more than ten peaks, each of which corresponds to $(A_p)_nG_p$ where $n=0,1,2,\cdots$. The relative amounts of these oligonucleotides were not found to be greatly different from what are expected for the random sequence.

The degrees of polymerization of the polymers prepared were not determined, but they are considered to be sufficiently high on the basis of the

Table 2. Enzymatic preparation of homopolymers of uridylic acid and copolymers of adenylic and guanylic acids

Polymer	Substrate[a] ADP mg	Substrate[a] GDP mg	Enzyme from	Incubation time hr	Product[d] Yield mg	A %	G %	Sedimentation coefficient S_{20}
Poly A,G(1)	18.0	2.0	*A.v.*	14.5	4.6	91.5	8.5	6.3
Poly A,G(2)	17.0	3.0	*A.v.*	14.5	6.5	85.5	14.5	3.7
Poly A,G(3)[b]	—	—	*M.l.*	—	—	80.0	20.0	7.7
Poly A,G(4)	23.2	9.9	*M.l.*	3.0	7.5	76.0	24.0	5.6
Poly A,G(5)	17.1	15.9	*M.l.*	3.0	3.9	70.4	29.6	6.2
Poly U	UDP 10 mg		*A.v.*	3.0	2.0	—	—	6.5
Poly U	UDP 40 mg		*A.v.*	3.0	11.7	—	—	5.2

a) ADP: adenosine-5′-diphosphate. GDP: guanosine-5′-diphosphate.
b) Prepared by Drs. T. Saigo, T. Uchida and F. Egami and kindly placed at our disposal by them.
c) *A.v.*: *Azotobacter vinelandii*. *M.l.*: *Micrococcus lysodeikticus*.
d) A: adenine residue content. G: guanine residue content.

sedimentation constants given in the last column of Table 2. These were measured in distilled water with no salt except for poly A,G(4) and poly A,G(5). The sedimentation constants of the latter two were examined in 0.1 M NaCl+0.01 M Na-cacodylate buffer (pH 6.5).

Experimental

Ultraviolet absorption measurements were made with an Ito spectrophotometer Model QU-3. The temperature of the samples was controlled as previously described.[10] The polynucleotide concentration was determined by measuring phosphorus content.[11]

Infrared absorption measurements were made of D_2O solutions by the use of a Perkin-Elmer 621 spectrometer. Each D_2O solution was placed in a cell with CaF_2 windows and of 50 μ in optical path length. The temperature of the solution was controlled by an electric heating device constructed by ourselves, and the temperature was measured by the use of a thermocouple.

UV Mixing Curves: Effect of Salt

Solutions of poly A,G and poly U of various mole ratios were made, and their ultraviolet absorbance at 259 mμ recorded. The results are shown in Figs. 2—6. From such an absorbance versus mole-ratio profile, we may judge whether the two polymers in question have no interaction or whether they form a complex. When a complex is formed, its stoichiometric ratio may also be determined from the observed profile of the mixing curve.

As may be seen in Figs. 2—6, every poly A,G shows evidence of interaction with poly U. Each of the mixing curves consists of two straight lines which intersect at a proper mole ratio. As has been stated in the introduction of this paper, the intersection should take place at poly A,G/poly U = 50/50, 33.3/66.7, 100/x, or 100/2x if the structure of the cmplex is respectively like (c), (d), (e), or (f) of Fig. 1. Actually, however, the intersection does not always take place exactly at one of these four expected mole ratios (see Figs. 2—6).

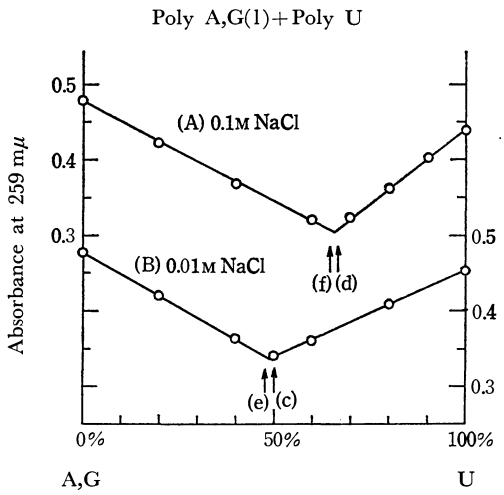

Fig. 2. Mixing curves for poly A,G(1) and poly U.
Abscissa: mol% (determined by measuring phosphorus contents) of poly U, ordinate: absorbance at 259 mμ. Total nucleotide concentration in the solution was kept at 0.48×10^{-4} M. (A) In 0.1 M NaCl plus 0.01 M Na-cacodylate buffer, pH 7.0; at 21.7°C. (B) In 0.01 M NaCl plus 0.001 M Tris buffer, pH 8.0; at 24.5°C. The vertical arrows indicate the positions of minimum expected for complexes with structures (c), (d), (e) and (f) given in Fig. 1.

10) K. Matsuo and M. Tsuboi, This Bulletin, **39**, 347 (1966).
11) B. N. Ames and D. T. Dubin, *J. Biol. Chem.*, **235**, 769 (1960).

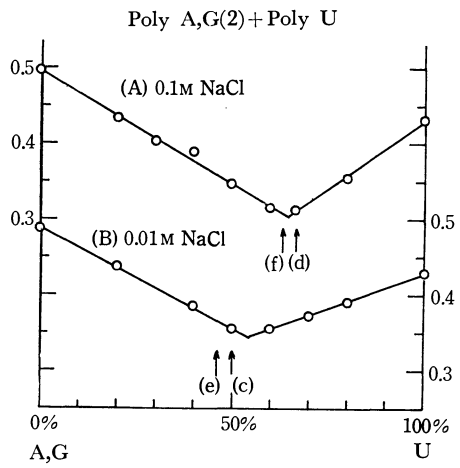

Fig. 3. Mixing curves for poly A,G(2) and poly U.
Abscissa: mol% of poly U, ordinate: absorbance at 259 mμ. Total nucleotide concentration in the solution was kept at 0.48×10^{-4} M. (A) In 0.1 M NaCl plus 0.01 Tris buffer, pH 8.0; at 23.6°C. (B) In 0.01 M NaCl plus 0.001 M Tris buffer, pH 8.0; at 23.6°C.

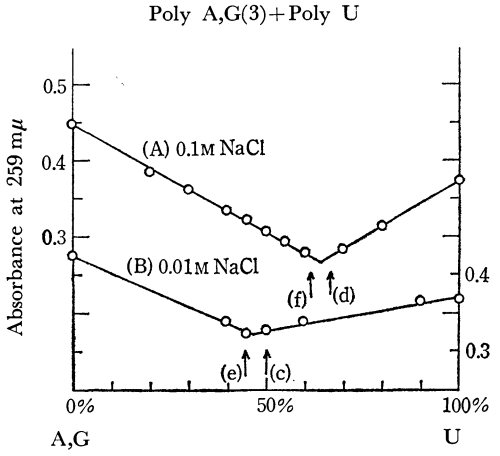

Fig. 4. Mixing curves for poly A,G(3) and poly U.
Abscissa: mol% of poly U, ordinate: absorbance at 259 mμ. Total nucleotide concentration in the solution was kept at 0.43×10^{-4} M. (A) In 0.1 M NaCl plus 0.01 M Na-cacodylate buffer, pH 6.5; at 9.8°C. (B) In 0.01 M NaCl plus 0.001 M Na-cacodylate buffer, pH 6.5; at 10.6°C.

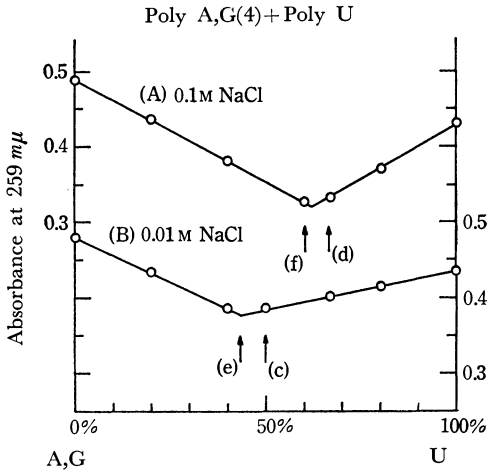

Fig. 5. Mixing curves for poly A,G(4) and poly U.
Abscissa: mol% of poly U, ordinate: absorbance at 259 mμ. Total nucleotide concentration in the solution was kept at 0.48×10^{-4} M. (A) In 0.1 M NaCl plus 0.01 M Tris buffer, pH 8.0; at 12.9°C. (B) In 0.01 M NaCl plus 0.001 M Na-cacodylate buffer, pH 7.0; at 12.6°C.

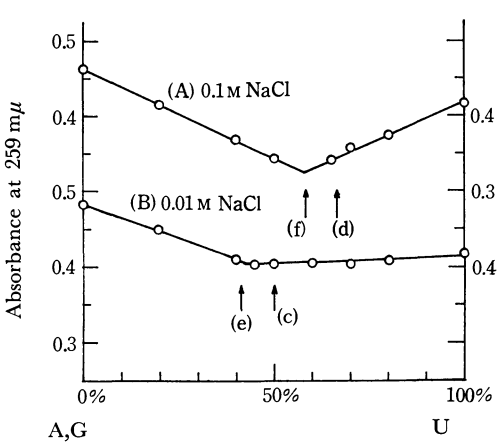

Fig. 6. Mixing curves for poly A,G(5) and poly U.
Abscissa: mol% of poly U, ordinate: absorbance at 259 mμ. Total nucleotide concentration in the solution was kept at 0.48×10^{-4} M. (A) In 0.1 M NaCl plus 0.01 M Na-cacodylate buffer, pH 7.0; at 13.0°C. (B) In 0.01 M NaCl plus 0.001 M Na-cacodylate buffer, pH 7.0; at 16.7°C.

This is in contrast to the case of poly A, U + poly U, where the stoichiometric ratio of the complex was found to be always $100/x$ or $100/2x$[3] (x= mole % of A in the copolymer of A and U).

The intersection appears always in the vicinity of poly A, G/poly U = 33.3/66.7 for solutions with 0.1 *M* NaCl, and in the vicinity of 50/50 for solutions with 0.01 *M* NaCl (with one exception). When the guanine content in poly A, G is smaller, the intersection appears at a point between those expected for (d) and (f) or between those expected for (c) and (e) (see Figs. 2, 3, and 4). When the guanine content in poly A, G is higher, on the other hand, the intersection appears at a point which is very near to that expected for (f) or (e) (see Figs. 5 and 6). These facts indicate that in a solvent with 0.1 *M* Na^+ a triple-helical structure is formed

Table 3. Observed and calculated minima in the mixing curve of poly A,G and poly U

Copolymer	Total G %	G in A_pG_pA %	Minimum point in the mixing curve with poly U	
			Expected (% of U)	Observed (% of U)
Poly A,G(1)	8.5	7.4	66.4	66.0
Poly A,G(2)	14.5	10.8	65.7	65.0
Poly A,G(3)	20.0	12.8	65.0	64.5
Poly A,G(4)	24.0	13.9	64.2	62.5
Poly A,G(5)	29.6	14.7	62.9	58.0

with a A⋮U type inter-base hydrogen bonding, while in a solvent with 0.01 *M* Na^+ a double-helical structure is formed with a A···U type hydrogen-bonding. These facts also show that some of the guanine residues in the copolymer remain within the helix structure and some rotate out of the helix; in other words, some parts of the structure are like Fig. 1 (c) or (d) and some parts like (e) or (f). When the guanine content in the copolymer becomes greater the parts like (e) or (f) predominate. This may be taken as indicating that an isolated guanine residue is incorporated into the helix whereas a guanine cluster is looped out of the helix.

By assuming the random sequence, the amount of the isolated guanylic acid residue (that is the guanylic acid whose two neighbors are both adenylic acids, like $A_pG_pA_p$) was calculated from the total amount of the guanylic acid residue in each copolymer (Table 3). By assuming further that only such an isolated guanine residue is incorporated into the helix and that other guanine residues rotate out of the helix, the stoichiometric ratios poly A,G/poly U were calculated for poly A,G-poly U complexes. The results are given in Table 3. As may be seen here, the calculated ratio is always slightly higher than the observed ratio, and the discrepancy becomes greater as the guanylic acid content in the copolymer becomes higher. Thus, it is probable that a guanine residue is incorporated into the helix only when there are some adenine residues in its vicinity, and that the number of such adenine residues requires in its vicinity is *greater* than two.

Copolymer A,G(2) is found to be somewhat anomalous. Even in a solvent with 0.01 *M* Na^+ the minimum of the mixing curve (with poly U) does not appear in the vicinity of the mole ratio 50/50. Instead, the minimum is found with a good reproducibility at poly A, G/poly U = 45/55 (see Fig. 3). No explanation is yet given for this fact, but it may be pointed out here that, when a homopolymer poly A (instead of poly A,G) was mixed with poly U, the minimum of the mixing curve was always observed at poly A/poly U = 33.3/66.7, and never at 50/50.[12] Therefore, it is probable that copolymer A, G (2) happens to have a long···$A_pA_pA_p$···cluster in it, which behaves like a homopolymer poly A.

UV Mixing Curves: Effect of Temperature

The profile of the mixing curve just mentioned changes not only with the ionic strength but also with the temperature of the solution. As has been already described, the minimum in the mixing curve appears in the vicinity of poly A,G/poly U = 1/2 at a lower temperature in a higher ionic strength. As may be seen in Figs. 7 and 8, the minimum is shifted into the vicinity of poly A,G/poly U = 1/1 at an elevated temperature. This fact indicates that a triple-helical complex poly A,G–poly U–poly U first decomposes into double-

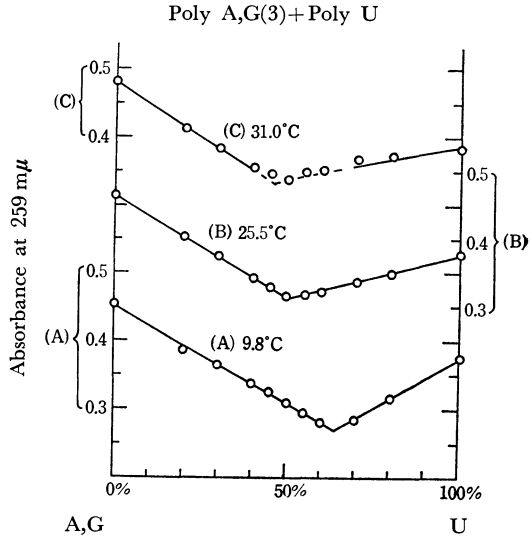

Fig. 7. Mixing curves for poly A,G(3) and poly U.
Abscissa: mol% of poly U, ordinate: absorbance at 259 mμ. Total nucleotide concentration in the solution was kept at 0.43×10^{-4} M. Solvent: 0.1 M NaCl plus 0.01 M Na-cacodylate buffer, pH 6.5. (A) At 9.8°C. (B) At 25.5°C. (C) At 31.0°C.

12) S. Higuchi and M. Tsuboi, This Bulletin, **39**, 1886 (1966).

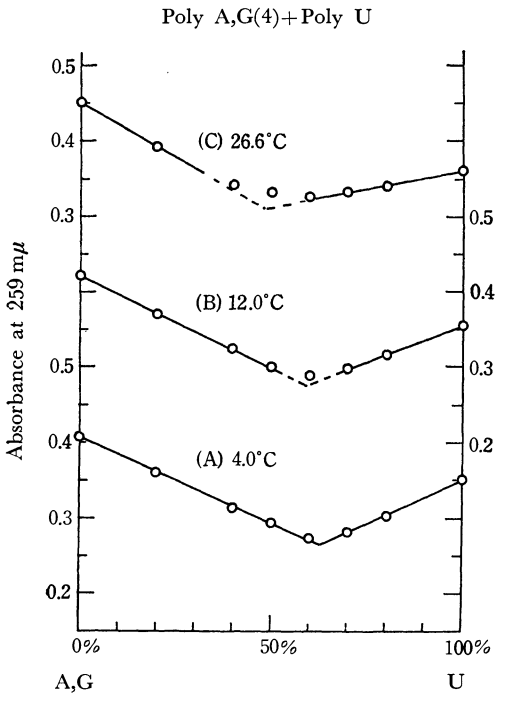

Fig. 8. Mixing curves for poly A,G(4) and poly U.
Abscissa: mol% of poly U, ordinate: absorbance at 259 mμ. Total nucleotide concentration in the solution was kept at 0.48×10^{-4} M. Solvent: 0.05 M NaCl plus 0.005 M Na-cacodylate buffer, pH 7.0. (A) At 4.0°C. (B) At 12.0°C. (C) At 26.6°C.

helical complex poly A,G–poly U and single-stranded poly U, before it completely melts into single-stranded random coils. Thus, the melting process is given as

$$\text{poly A,G·poly U·poly U} \longrightarrow \text{poly A,G·poly U + poly U} \longrightarrow \text{poly A,G + poly U + poly U} \quad (1)$$

This is similar to the melting process known of the the triple-helical complex without G, *i.e.*, poly A–poly U–poly U.[12–14]

As is illustrated in Fig. 8, the minimum in a mixing curve observed at a higher temperature is often less sharp than that a at lower temperature. In the curve obtained at 12.0°C or at 26.6°C given in Fig. 8, the angle is rounded off at the minimum. For this, the last course of the melting process (1) is considered to be responsible. Thus, if a certain fraction of helices melts into random coils, a hyperchromicity takes place whose amount should be proportional to the amount of helices. The amount of hyperchromicity should be greatest at the minimum where the amount of helices is greatest. At an extremely high temperature, at which all the helices melt into random coils, the mixing curve should be a single straight line and have no minimum.

UV Heating Curves

Absorbance-temperature profiles of each of the 1 : 2 (molar) mixtures of poly A,G and poly U are shown in Figs. 9 and 10.

The triple-helical complex poly A,G(1)–poly U–poly U shows a two-step melting (at 43 and 51°C) in a solvent with 0.1 *M* Na^+ (Fig. 9(A)), whereas it shows a single-step sharp melting (at 34.5°C) in 0.01 *M* Na^+ (Fig. 10 (A)). Similar melting profiles were observed of the triple-helical complex without G, *i.e.* poly A–poly U–poly U.[12–14] For the latter, however, every melting temperature is found slightly higher than the corresponding melting temperature observed here for the complex with poly A,G(1). For the system of 1 : 2 (molar) mixture of poly A and poly U, a phase diagram shown in Fig. 11 was constructed.[12–14] For the system of 1 : 2 (molar) mixture of poly A,G(1) and poly U, now in question, a similar phase diagram would be valid. On the basis of the melting profiles just described (Figs. 9 (A) and 10 (A)), such a phase diagram is drawn with the broken lines in Fig. 11. The difference of the two phase diagrams (full and broken lines in Fig. 11) is considered to be caused by the 8.5% guanine residues in poly A,G(1).

As is shown in Figs. 9 and 10, the melting temperature becomes lower as the guanine content in

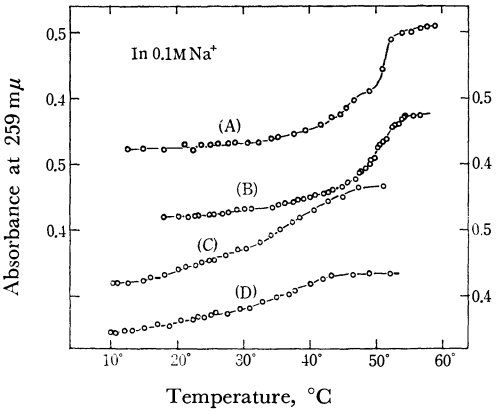

Fig. 9. Variation of the absorbance at 259 mμ with temperature of mixture solutions of poly A,G and poly U.
Mole ratio, poly A,G/poly U, was always 1/2. Solvent: 0.1 M NaCl plus buffer. (A) Poly A,G(1)+poly U. (B) Poly A,G(2)+poly U. (c) Poly A,G(4)+poly U. (D) Poly A,G(5)+poly U.

13) J. R. Fresco, In "Informational Macromolecules," ed. by H. J. Vogel, V. Bryson and J. Q. Lampen, Academic Press, New York (1963), p. 121.
14) C. L. Stevens and G. Felsenfeld, *Biopolymers*, **2**, 293 (1964).

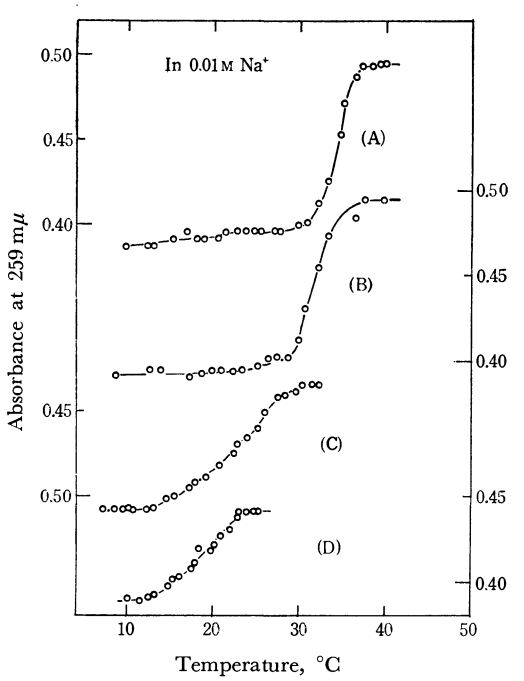

Fig. 10. Variation of the absorbance at 259 mμ with temperature of mixture solutions of poly A,G and poly U.
Mole ratio, poly A,G/poly U, was always 1/2. Solvent: 0.01 M NaCl plus buffer. (A) Poly A,G(1)+poly U. (B) Poly A,G(2)+poly U. (C) Poly A,G(4)+poly U. (D) Poly A,G(5)+poly U.

the copolymer poly A,G becomes higher. At the same time, the melting region becomes broader and total amount of hyperchromicity in the melting becomes smaller. These facts show that the secondary structure of a complex with poly A, G with a higher G content is less definite.

Infrared Spectra

Poly A,G(1) in heavy water solution (with 0.2 M Na^+) gives a strong absorption band at 1624 cm^{-1} at pD=7.0 and at 36°C (Fig. 12). This band is assignable to a double-bonds stretching vibration in the deuterated adenine ring.[15] On heating the solution this band is shifted slightly towards lower frequency (1620 cm^{-1} at 75°C).

Figure 13 shows the infrared spectrum of a 1 : 1 (molar) mixture of poly A,G(1) and poly U. At 38°C, it shows strong absorption peaks at 1689, 1671, and 1630 cm^{-1}. These are assigned respectively to $C_2=O$ stretching vibration of uracil, $C_4=O$ stretching vibration of uracil, and double-bonds stretching vibration of adenine residues involved in the Watson-Crick type A···U base pair.[15,16] This is definitely different from the infrared spectrum expected from A⋱U type interbase bonding plus free adenine residue.[15-17]

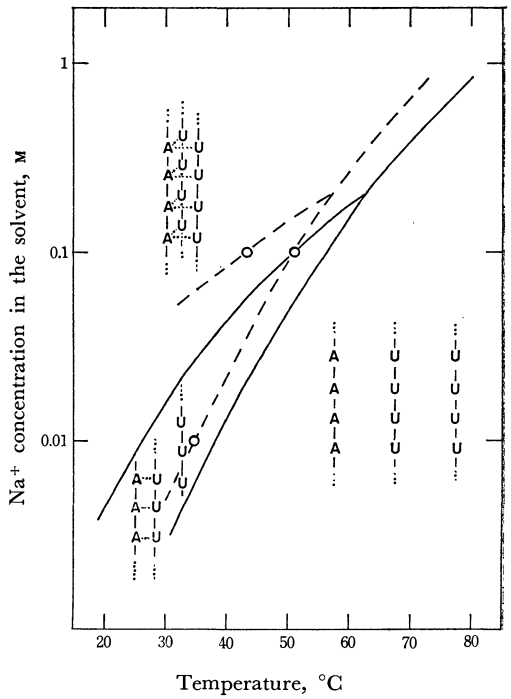

Fig. 11. Equilibrium diagram for 1:2 (molar) mixtures of poly A and poly U (full lines).
Broken lines show the effect of introduction of the guanine resideue into poly A. The small circles indicate melting temperatures observed for 1:2 complex of poly A,G(1) and poly U.

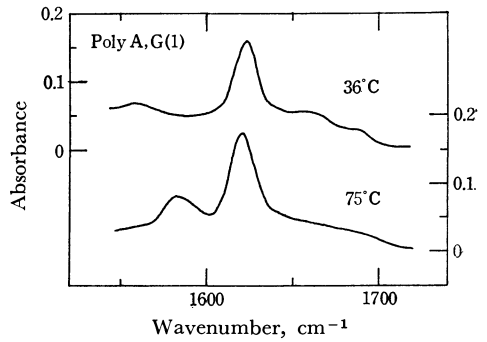

Fig. 12. Infrared absorption spectrum of poly A,G(1) in D_2O + 0.2 M NaCl + 0.01 M Nacacodylate buffer, pD 7.0.
Approximate concentration of poly A,G(1) is 0.02 M.

15) See, for example, M. Tsuboi, Applied Spectroscopy Reviews (Marcel Dekker), Vol. 3, 45—90 (1969).
16) H. T. Miles and J. Frazier, *Biochem. Biophys. Res. Commun.*, **14**, 21 (1964).
17) S. Higuchi, Doctor Thesis, Tokyo University, 1968.

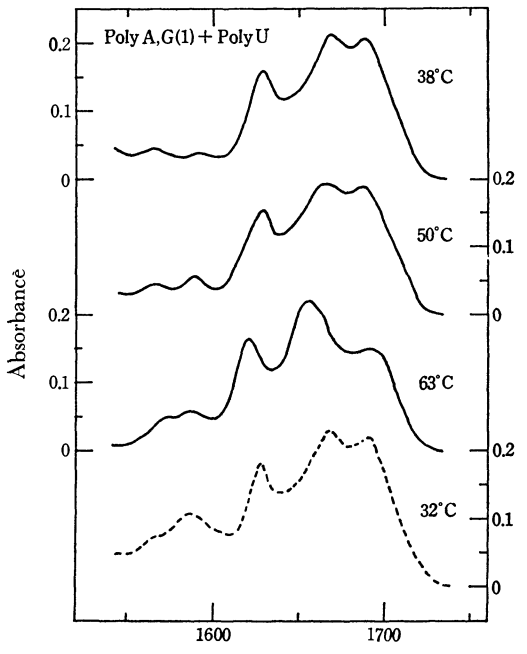

Fig. 13. Infrared absorption spectrum of 1:1 (molar) mixture of poly A,G(1) and poly U.
Solvent: D_2O + 0.2 M NaCl + 0.01 M Na-cacodylate buffer, pD 7.0. Total concentration of nucleotides: about 0.04 M. The lowest curve was obtained when the solution heated up to 63°C was cooled again to 32°C.

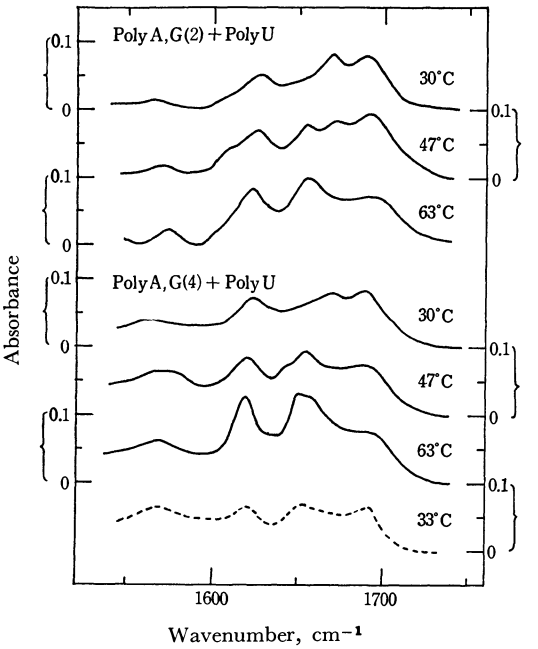

Fig. 14. Infrared absorption spectra of 1:1 (molar) mixtures of poly A,G(2)+poly U and of poly A,G(4)+poly U.
Solvent: D_2O + 0.2 M NaCl + 0.01 M Na-cacodylate buffer, pD 7.0. Total concentration of nucleotide: about 0.02 M. The lowest curve was obtained when the poly A,G(4)+poly U solution heated up to 63°C was cooled again to 33°C.

Therefore, it is evident that 1 : 1 (molar) mixture of poly A,G(1) and poly U forms a double-helical complex, poly A,G(1)–poly U, in 0.2 M Na^+ at 38°C. The ultraviolet (259 mμ) mixing curve shown in Fig. 2 (A) does not show any bend in the vicinity of the mole ratio 1/1, and therefore this might be taken as indicating that a 1 : 1 (molar) mixture of poly A,G(1) and poly U consists of a triple-helical poly A,G(1)–poly U–poly U and single-stranded poly A,G(1) in the solvent with 0.1 M or more Na^+. By means of the infrared absorption measurement, however, this is not found to be actually the case. We consider that here is a double-helical complex, poly A,G(1)–poly U, and that this is not distinguishable from the triple-helix plus single poly A,G(1) by the ultraviolet absorbance at 259 mμ. Similar situation was already found for 1 : 1 (molar) mixture of poly A and poly U in high-salt solution.[12,14,16]

Infrared spectra of 1 : 1 (molar) mixtures of poly A,G(2) & poly U and of poly A,G(4) & poly U are given in Fig. 14. Both of these show the characteristic bands (1690, 1670, and 1630 cm^{-1}) of Watson-Crick type A···U structure in 0.2 M Na^+ and at 30°C.

The melting process of these double-helical complex, poly A,G–poly U, was examined by means of the infrared absorption measurement, and the results are shown also in Figs. 13 and 14. At this salt concentration (0.2 M Na^+), the double-helical structure seems to decompose directly into single-stranded poly A,G and poly U. These give strong bands at 1692 cm^{-1} (C_2=0 stretching of uracil), 1657 cm^{-1} (C_4=0 stretching of uracil), and 1621 cm^{-1} (double-bonds stretching of adenine). On lowering the temperature of the solution again to 32 or 33°C, the A···U base-pair is reformed for poly A,G(1) + poly U (see the lowest curve in Fig. 13), but not for poly A, G (4) + poly U (lowest curve in Fig. 14).

The guanine residues involved in the copolymer should give absorptions in the 1600—1550 cm^{-1} region. There is certainly an absorption band observed in this spectral region in every spectrum of poly A, G (Fig. 12) and of poly A, G + poly U (Figs. 13 and 14). It appears at 1565 cm^{-1} for lower temperatures, and on elevating the temperature it is shifted to higher frequency (at about 1590 cm^{-1}). On lowering the temperature, however, the band does not come back to 1565 cm^{-1} even when the absorption bands (at 1689, 1671, and 1630 cm^{-1}) due to the A···U base-pair are restored (see the lowest curve in Fig. 13). This fact shows that the environment of the G residues

changes on breaking down the double-helical structure of the complex molecule and that this change is not easily reversed even when the A···U base-pairs are reformed. No interpretation however is yet given of the spectral change (1565→1590 cm^{-1}).

Discussion

Present ultraviolet and infrared spectroscopic data are well explained by postulating the following items:

(1) In the solvent with 0.1 M or more Na^+, both of the double-helical complex, poly A,G–poly U, with the Watson-Crick type A···U base-pair and the triple-helical complex, poly A,G–poly U–poly U, with the A⋮U⋱U type inter-base binding are to be formed at 10°C. What are formed depend upon the mol % of poly U in the solution:

0 to 50%	single poly A,G and double helix
50%	double-helix
50 to 66%	double-helix and triple-helix
66%	triple-helix
66 to 100%	triple-helix and single poly U.

(2) On heating such a solution, the triple-helical complex first decomposes into double-helix and single poly U, and then at a higher temperature melts into three single-stranded random coils.

(3) In the solvent with Na^+ concentration as low as 0.01 M, only double-helical complex is formed at 10°C.

(4) A guanine residue in the copolymer poly A,G remains within the helical structure when its neighbors are mostly adenine residues. Otherwise, it rotates out from the helix so that the complementary A···U binding can be formed in the subsequent region of the polynucleotide chains.

What is described in item (4) here may be related with the "wobble hypothesis" of Crick.[18] It has now been established that three base-pairs are formed between the "codon" of a messenger RNA and the "anticodon" of a transfer RNA in a certain step of translation of a genetic code in a biological system. Crick[18] suggested that while the standard base-pairs (A···U and G···C) are used rather strictly in the first two positions of the three codon-anticodon pairings, there may be some wobble in the pairing of the third base. He pointed out several possible base-pairs for the third position, and among them the G···U pair is included. It may also be pointed out here that guanine and uracil residues are often located in a primary structure of a transfer RNA molecule at a position in which we usually postulate a strong A···U or G···C base pair in other transfer RNA molecules.[19] Our present experiment indicated that such a "G···U base-pair" certainly takes place if there are a number of standard base-pairs formed in its neighborhood. Our experiment also indicated, however, that such "G···U base-pairs" are not stable enough to support a helical structure by themselves.

We wish to express our thanks to Professor Makoto Ishimoto and Mr. Kaoru Saigo for their instruction in our preparation of polynucleotides by the use of the enzyme from *Micrococcus lysodeikticus*, to Professor Sanae Mii for her providing wet cells of *Azotobacter vinelandii*, and to Dr. Kimiko Matsuo for her valuable advices. This work was supported by a grant from the Ministry of Education of Japan and by a grant from the United States Public Health Service (GM 10024—06).

18) F. H. C. Crick, *J. Mol. Biol.*, **19**, 548 (1966).
19) See, for example, G. R. Philipps, *Nature*, **223**, 374 (1969).

BULLETIN OF THE CHEMICAL SOCIETY OF JAPAN VOL. 43 3400—3404 (1970)

The Effect of Chloromethanes on Hydrogen Formation in the Radiolysis of Methylcyclohexane and 3-Methylpentane at −196°C

Toyoaki KIMURA, Mitsuharu FUKAYA, Minoru HADA, Terunobu WAKAYAMA, Kenji FUEKI and Zen-ichiro KURI

Department of Synthetic Chemistry, Faculty of Engineering, Nagoya University, Chikusaku, Nagoya

(Received June 4, 1970)

The effect of chloromethanes (CH_2Cl_2, $CHCl_3$ and CCl_4) on hydrogen formation from γ-irradiated methylcyclohexane (MCH) and 3-methylpentane (3MP) at −196°C was investigated. It was found that the decrease in hydrogen yield by the presence of CH_2Cl_2 was almost the same as that caused by an electron scavenger such as N_2O, *n*-butyl chloride, SF_6 or iodobenzene, but the hydrogen yield was much lower in the presence of $CHCl_3$ or CCl_4 than other electron scavengers. Although the yield of $CCl_3\cdot$ radicals formed from dissociative electron attachment to CCl_4 in CCl_4-MCH systems was ~1.4 *G*, the decrease in hydrogen yield was ~3 *G*. A similar result was obtained for $CHCl_3$-MCH systems. Thus we have ascribed the effect of CH_2Cl_2 on hydrogen formation to electron scavenging and that of $CHCl_3$ or CCl_4 to excitation transfer as well as electron scavenging. ESR studies on radical formation from these systems also support the above interpretation.

It is not easy to determine the role of excited molecules in radiolysis. Energy transfer from cyclohexane to benzene, originally proposed by Manion and Burton,[1] does not seem to be excitation transfer, but positive charge transfer in the light of recent studies.[2-7] Though excitation transfer was proposed for quenching of fluorescence from a γ-irradiated cyclohexane system,[8] some ionic process was recently suggested for this phenomenon.[4-7] A study which clearly demonstrated excitation transfer was that by Collinson *et al.*,[9] who found a sudden increase in the reduction yield of $FeCl_3$ in benzene when the temperature of the system was lowered below the melting point and ascribed it to excitation transfer.

We have shown in a previous work[10] that carbon tetrachloride lowers the yields of hydrogen and of solvent radicals from γ-irradiated methylcyclohexane (MCH) at −196°C much more than electron scavengers, such as SF_6 or N_2O, and ascribed the effect of carbon tetrachloride to excitation transfer as well as electron scavenging. We have extended the previous study of CCl_4 in MCH to other chloromethanes ($CHCl_3$ and CH_2Cl_2) in order to investigate their effects on the hydrogen yield from MCH γ-irradiated at −196°C. We also examine the effect of these chloromethanes on the radiolysis of 3-methylpentane (3MP) systems. In order to examine the possibility of excitation transfer from 3MP to chloromethanes, it was necessary to investigate the effect of electron scavengers on hydrogen yields from 3MP. Though 3MP has been widely used as a matrix for measurements of reaction intermediates, only a few studies on hydrogen formation have been reported.[11,12] Thus we attempted to investigate the effect of N_2O as an electron scavenger on the hydrogen formation from γ-irradiated 3MP.

Experimental

Materials. MCH was Tokyo Kagaku Seiki 99.9% and used as received. Aldrich 3MP was shaken with concentrated sulfuric acid in a separating flask, washed with distilled water, and then dried over sodium sulfate. After passing through a silica gel column, 3MP was fractionally distilled before use. Carbon tetrachloride, chloroform and methylene dichloride were

1) J. M. Manion and M. Burton, *J. Phys. Chem.*, **56**, 560 (1952).
2) W. V. Dusen and W. H. Hamill, *J. Amer. Chem. Soc.*, **84**, 3648 (1962).
3) S. Z. Toma and W. H. Hamill, *ibid.*, **86**, 1478 (1964).
4) M. Burton, *Mol. Cryst.*, **4**, 61 (1968).
5) P. K. Ludwig and M. M. Huque, *J. Chem. Phys.*, **49**, 805 (1968).
6) R. R. Hentz and R. J. Knight, *J. Phys. Chem.*, **72**, 1783 (1968).
7) T. Saito and S. Sato, This Bulletin, **42**, 2228 (1969).
8) R. A. Holroyd, *J. Phys. Chem.*, **72**, 759 (1968).
9) E. Collinson, J. J. Conlay and F. S. Dainton, *Discuss. Faraday Soc.*, **1963**, 1531.
10) T. Wakayama, T. Kimura, T. Miyazaki, K. Fueki and Z. Kuri, This Bulletin, **43**, 1017 (1970).
11) M. G. Robinson and G. R. Freeman, *J. Chem. Phys.*, **48**, 983 (1968).
12) T. Kimura, K. Fueki and Z. Kuri, This Bulletin, **43**, 1657 (1970).

Nakarai Kagaku specially prepared reagent and used as received. N_2O was Takachiho Shoji Co. 99.9% and used as received.

Sample preparation. Amounts of liquid materials were measured volumetrically. Usually 1 m*l* of MCH or 3MP was used for a sample. Solutions in irradiation cells equipped with a break-seal (usually 2 m*l*) were degassed by the freeze-pump-thaw technique and then sealed off. N_2O was introduced into a bulb of known volume to the desired pressure and then condensed into the irradiation cell.

Irradiation. A 3000 Ci ^{60}Co source was used for γ-irradiation. Irradiation doses were 2.51×10^{20} eV/g at 20°C, 1.97×10^{20} eV/g at −72°C and 2.23×10^{20} eV/g at −196°C.

Analysis. Gaseous products noncondensable at liquid nitrogen temperature were collected by a Toepler pump and their quantities were determined by the PVT method. To convert hydrogen into water, the gas was circulated about 20 times through a cupric oxide furnace, heated at 220—260°C, and a liquid nitrogen trap, and then the residual gas was recollected and its quantity was measured. Yields of solvent and solute radicals were determined by ESR technique in the same manner as reported[10] previously.

Results and Discussion

Figures 1, 2 and 3 show the effect of N_2O on hydrogen formation from γ-irradiated 3MP at 20°C, −72°C and −196°C, respectively. The decrement of hydrogen yield with increasing N_2O concentration at −196°C is lower than at 20°C and −72°C, while the nitrogen yield at 20°C is somewhat lower than those at −72°C and −196°C. It has been proposed that the nitrogen yield is twice the yield of scavenged electrons in the radiolysis of cyclohexane at room temperature.[13] It can be seen from Fig. 1 that the ratio of the nitrogen yield to the decrease in hydrogen yield is about 3 in N_2O-3MP systems at 20°C. The difference in the ratio, $G(N_2)/\Delta G(H_2)$, between cyclohexane and 3MP may be explained in terms of the difference in the decomposition pattern between branched and non-branched hydrocarbons[12]; a part of energy which is consumed in C–H bond cleavage in the case of non-branching hydrocarbons is spent for C–C bond cleavage in the case of branching hydrocarbons. Recently Asmus *et al.* have suggested that the efficiency of hydrogen formation from ion recombination is 0.6 in the case of 3MP.[14] With this value, the yield of electrons scavenged by N_2O at 20°C is given by $(1/0.6)\Delta G(H_2)$. Thus the ratio of the nitrogen yield to the yield of scavenged electrons is $G(N_2)/\{(1/0.6)\Delta G(H_2)\}=\sim2$. Such

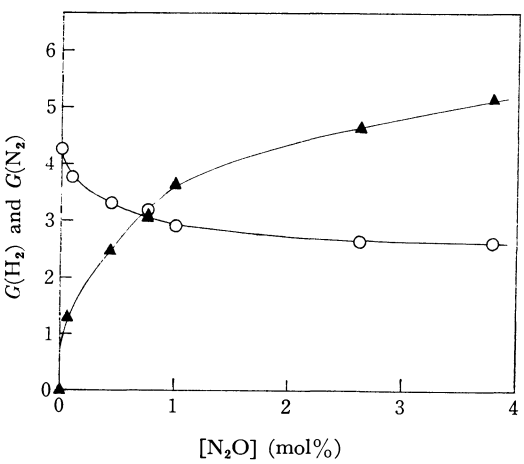

Fig. 1. Yields of hydrogen and nitrogen from γ-irrddiated N_2O-3MP systems at 20°C.
○; $G(H_2)$, ▲; $G(N_2)$

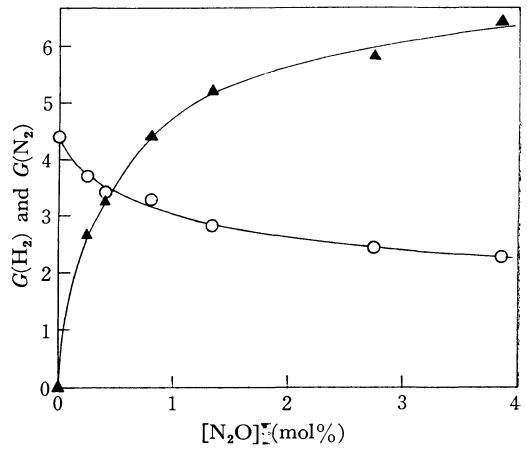

Fig. 2. Yields of hydrogen and nitrogen from γ-irradiated N_2O-3MP systems at −72°C.
○; $G(H_2)$, ▲; $G(N_2)$

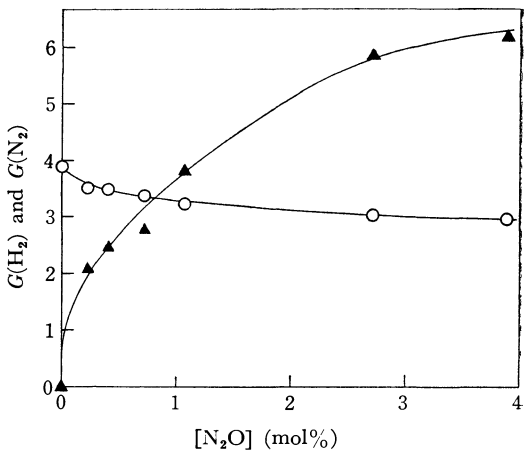

Fig. 3. Yields of hydrogen and nitrogen from γ-irradiated N_2O-3MP systems at −196°C.
○; $G(H_2)$, ▲; $G(N_2)$

13) S. Sato, R. Yugeta, K. Shinsaka and T. Terao, *ibid.*, **39**, 156 (1966).

14) K. D. Asmus, J. M. Warman and R. H. Schuler, *J. Phys. Chem.*, **74**, 246 (1970).

argument may be applied to the case of N_2O-3MP systems at $-72°C$, although the nitrogen yield at $-72°C$ is slightly higher than that at 20°C. The nitrogen yield at $-196°C$ is almost the same as that at 20°C and $-72°C$, but we do not think that the yields of scavenged electrons in these three cases are the same. We have shown that the ratio of the nitrogen yield to the decrease in hydrogen yield in N_2O-MCH systems γ-irradiated at $-196°C$ depends upon the N_2O concentration and it increases from 1 to 4 with increasing N_2O concentration, and that the neutralization of an MCH positive ion with an electron leads to the formation of one hydrogen molecule.[15] Our result in which the efficiency of hydrogen formation from ion recombination is $\sim$1 is in rough agreement with that by Asmus *et al.*[14] Thus we have estimated the ratio of the nitrogen yield to the yield of electrons scavenged by N_2O in N_2O-MCH systems at $-196°C$ $\sim$4 at higher N_2O concentrations. Using the result by Asmus *et al.*,[14] the ratio of the nitrogen yield to the yield of scavenged electrons, $G(N_2)/G(e^-)$, in 3MP at $-196°C$ is $G(N_2)/\{(1/0.6)\cdot \Delta G(H_2)\}=\sim 4$. The process of nitrogen formation other than Eq. (1) is not clear, but the relation $G(N_2)/G(e^-)=\sim 4$ holds for 3MP as well as MCH at $-196°C$.

$$N_2O + e^- \longrightarrow N_2O^- \longrightarrow N_2 + O^- \qquad (1)$$

The mechanism of nitrogen formation other than Eq. (1) may be short chain reactions,[16] excitation transfer[17] or negative charge transfer from O^- to N_2O.[15] Considering the relation $G(N_2)/G(e^-)=\sim 4$ in 3MP and MCH, it seems that nitrogen is formed via negative ion processes such as Eq. (1). Assuming that $G(N_2)/G(e^-)$ is 4 in 3MP at $-196°C$, $G(e^-)$ is estimated to be 1.57 at the highest N_2O concentration studied, which is considerably lower than that at 20°C. Such a low yield of scavenged electrons in 3MP at $-196°C$ has been reported by us.[18] Therefore we can say that the hydrogen yield and the yield of scavenged electrons at $-196°C$ are lower than those at 20°C in the case of 3MP as well as MCH.

Hydrogen yields from γ-irradiated MCH and 3MP at $-196°C$ in the presence of CH_2Cl_2, $CHCl_3$ or CCl_4 are shown in Figs. 4 and 5, respectively. The yield of hydrogen was calculated using the following equation:*1

$$G(H_2) = \frac{P - G'(H_2)\cdot D'\cdot W_s}{D\cdot W} \qquad (I)$$

where P is the number of hydrogen molecules produced, $G'(H_2)$ is the yield of hydrogen from pure solute, D and D' are the doses absorbed by solvent of unit weight and that by solute of unit weight, respectively, and W and W_s are the weights of solvent and solute, respectively. The values of $G'(H_2)$ were 0.186 for CH_2Cl_2 and 0.109 for $CHCl_3$. Although the solubility of CH_2Cl_2 at $-196°C$ is poor compared with that of $CHCl_3$ or CCl_4, solutions of CH_2Cl_2 in MCH form a transparent glass in the concentration range below 3 mol%. The dashed lines in Figs. 4 and 5 indicate that the solutes are not adequately soluble. The decrement of the hydrogen yield from CH_2Cl_2-MCH systems in Fig. 4 agrees well with that from N_2O-MCH

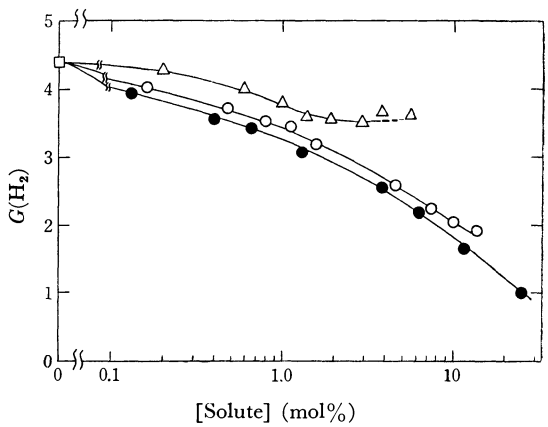

Fig. 4. Yields of hydrogen from γ-irradiated pure MCH (□), MCH in the presence of CH_2Cl_2 (△), $CHCl_3$ (○) and CCl_4 (●) at $-196°C$.

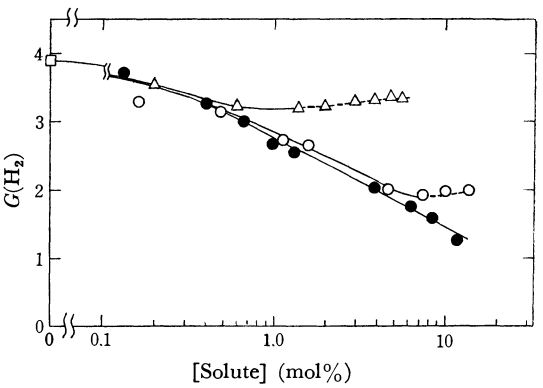

Fig. 5. Yields of hydrogen from γ-irradiated pure 3MP (□), 3MP in the presence of CH_2Cl_2 (△), $CHCl_3$ (○) and CCl_4 (●) at $-196°C$.

15) T. Kimura, T. Miyazaki, K. Fueki and Z. Kuri, This Bulletin, **41**, 2861 (1968).

16) W. J. Holtslander and G. R. Freeman, *Can. J. Chem.*, **45**, 1649 (1967).

17) R. A. Holroyd, *J. Phys. Chem.*, **72**, 759 (1968).

18) T. Kimura, K. Fueki and Z. Kuri, presented at 23rd Annual Meeting of the Chemical Society of Japan, April, 1970, Tokyo; This Bulletin, **43**, 3090 (1970).

*1 The G value usually employed in a binary system (A-B), *viz.*, the number of product molecules per 100 eV of the energy absorbed by both A and B, is useful only for knowing whether there is an interaction between A and B. The merit of Eq. (I) is that we can see the extent of the interaction; if there is no interaction, G value from Eq. (I) is constant but if there is an interaction it varies corresponding to the extent of the interaction.

systems.[15] Thus the effect of CH_2Cl_2 on the hydrogen formation can be regarded as the same as that of an electron scavenger such as N_2O or SF_6. However, both $CHCl_3$ and CCl_4 suppress the hydrogen formation much more than CH_2Cl_2. The effects of these chloromethanes in 3MP (Fig. 5) are similar to that for MCH.

We now examine the reason for the abnormal suppression of hydrogen formation by $CHCl_3$ or CCl_4. We previously suggested the possibility of excitation transfer.[10] It was shown that H atoms abstract chlorine atoms from $CHCl_3$ or CCl_4 in cyclohexane at room temperature.[19,20] Further, Teplý and Janovský reported the suppression of hydrogen formation by CCl_4 in γ-irradiated glassy methanol at -196°C and ascribed it to Cl atom abstraction from CCl_4 by H atoms in addition to the suppression of charge neutralization.[21] However, Stone denied Cl atom abstraction by H atoms at -196°C.[22] We have shown that the hydrogen yields from thermal H atoms at -196°C are 0.5 G in MCH and 0.65 G in 3MP.[12] Thus, the decrements of hydrogen yield from MCH and 3MP at -196°C in Figs. 4 and 5 cannot be explained only by Cl atom abstraction by thermal H atoms.

The abnormal suppression of hydrogen yield by $CHCl_3$ or CCl_4 is explicable if the yield of electrons scavenged by $CHCl_3$ or CCl_4 is higher than that by other electron scavengers. If this is true, the yield of scavenged electrons in MCH should be $\sim$3 G at the highest CCl_4 concentration studied because the decrement of the hydrogen yield is $\sim$3 G. Thus, the yield of $CCl_3\cdot$ radicals in MCH produced by Reaction (2) is expected to be $\sim$3 G. For the sake of confirmation, we attempted to determine the yields of $CCl_3\cdot$ radicals in MCH by ESR and the results are shown in Fig. 6. The yield of $CCl_3\cdot$ radicals in MCH increases with increasing CCl_4 concentration and reaches a constant value at CCl_4 concentrations above 2 mol %. The experimental curve for the yield of $CHCl_2\cdot$ radicals produced by Reaction (3) was very similar to that for $CCl_3\cdot$ radicals although the former was somewhat lower in the lower solute concentration range.

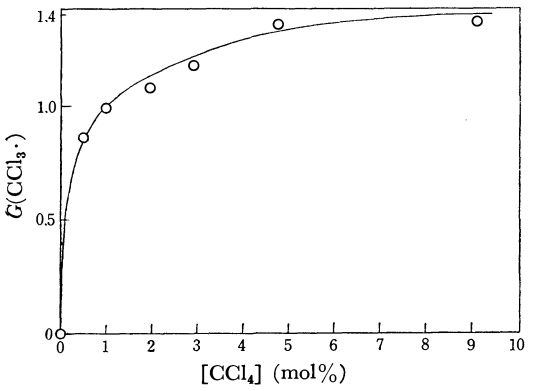

Fig. 6. Yields of $CCl_3\cdot$ radicals from γ-irradiated CCl_4-MCH systems at -196°C.

$$CCl_4 + e^- \longrightarrow CCl_3\cdot + Cl^- \quad (2)$$

$$CHCl_3 + e^- \longrightarrow CHCl_2\cdot + Cl^- \quad (3)$$

The limiting value of $CCl_3\cdot$ radicals in Fig. 6 is 1.4 G which agrees well with the yield of scavenged electrons in MCH glass obtained by the different procedures.[18,23] Thus the yield of $CCl_3\cdot$ radicals produced from Cl atom abstraction by H atoms seems to be very low, if produced at all. We are inclined to ascribe the abnormal suppression of hydrogen yield by $CHCl_3$ or CCl_4 to the excitation transfer from excited solvent molecules to solutes.

Another support for the excitation transfer mechanism was obtained from ESR experiments. We determined the yields of MCH· radicals in γ-irradiated MCH glasses containing CH_2Cl_2, $CHCl_3$ or CCl_4. The results are shown in Fig. 6.

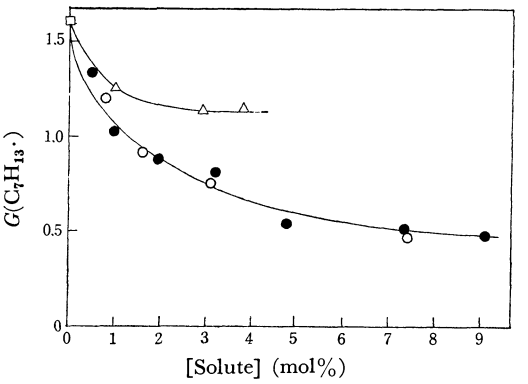

Fig. 7. Yields of MCH· radicals from γ-irradiated pure MCH (□) containing CH_2Cl_2 (△), $CHCl_3$ (○) and CCl_4 (●) at -196°C.

In a previous work we have shown that electron scavengers such as SF_6 or n-butyl chloride suppress the formation of MCH· radicals by $\sim$25% at a solute concentration of about 5 mol%.[10] This implies that the suppression of neutralization of solvent positive ions with electrons leads to the decreases in solvent radical yield of about 25%. Thus, the origin of solvent radicals seems to be mainly the decomposition of directly excited molecules and only partly the neutralization of positive

19) L. J. Forrestal and W. H. Hamill, *J. Amer. Chem. Soc.*, **83**, 1535 (1961).
20) J. Roberts and W. H. Hamill, *J. Phys. Chem.*, **67**, 2446 (1963).
21) J. Teplý and I. Janovský, *Int. J. radiat. Phys. Chem.*, **1**, 117 (1969).
22) J. A. Stone, *Can. J. Chem.*, **46**, 1267 (1968).
23) T. Shida and M. Imamura, presented at 23rd Annual Meeting of the Chemical Society of Japan, April, 1970, Tokyo.

ions with electrons. Since the decrement of MCH· radical yield by the addition of CH_2Cl_2 is nearly equal to that by SF_6 or *n*-butyl chloride,[10] the effect of CH_2Cl_2 on radical formation can be ascribed to electron scavenging, which is consistent with the result on hydrogen formation. We can see from Fig. 7 that both $CHCl_3$ and CCl_4 suppress the formation of solvent radicals to a greater extent than CH_2Cl_2. Thus, we can ascribe the effect of $CHCl_3$ or CCl_4 on the radical formation to excitation transfer in addition to electron scavenging.

If we exclude the role of excitation transfer for the abnormal suppression of the yields of hydrogen and solvent radicals, the only possible cause for this will be electron scavenging by $CHCl_3$ and CCl_4 which is nondissociative.

$$CHCl_3 + e^- \longrightarrow CHCl_3^- \quad (4)$$

$$CCl_4 + e^- \longrightarrow CCl_4^- \quad (5)$$

Suppression of radical formation by these solutes can be explained by Reactions (4) and (5), if radicals are mainly formed by neutralization of positive ions with electrons. At present, however, we have no evidence for nondissociative electron capture by these solutes in condensed systems. Thus it appears reasonable to ascribe the abnormal suppression of hydrogen and radical formation by $CHCl_3$ or CCl_4 to excitation transfer.

BULLETIN OF THE CHEMICAL SOCIETY OF JAPAN VOL. 43 3404—3409 (1970)

The Diffuse Reflection Spectra of 1-Arylazo-2-naphthols Diluted with Sodium Chloride

Chihiro DEHARI, Yoshio MATSUNAGA*1 and Kensuke TANI

Department of Chemistry, Faculty of Science, Hokkaido University, Sapporo

(Received June 8, 1970)

The diffuse reflection spectra of sixteen 1-arylazo-2-naphthols diluted with sodium chloride were measured at concentrations of 1, 0.1, and 0.01% in the range from 350 to 700 mμ. The spectra indicate the coexistence of the azo and hydrazone tautomers in this solid, two-component system. Moreover, the spectra were found to be markedly modified in many cases by elevating the temperature, especially at a concentration of 0.01%. These changes were shown to be thermally reversible and were attributed to the movement of the tautomeric equilibrium. The direction depends upon the kind and position of the substituents, *e.g.*, towards the hydrazone tautomer in the case of the *p*-Cl and *o*-NO_2 derivatives and towards the azo tautomer in the case of the *p*-NO_2 and *o*-OH derivatives. It was suggested that the present systems are not simple mixtures of pulverized 1-arylazo-2-naphthols and sodium chloride, but that some fraction of the organic components is well dispersed and adsorbed on the highly polar surface of the alkali halide.

A large number of studies have been carried out to elucidate the structure of 1-arylazo-2-naphthols,*2 which may exist as true azo compounds (I) or as β-naphthoquinone hydrazones (II).[1]

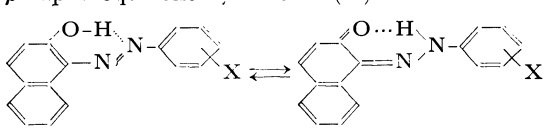

(I) (II)

On the basis of the electronic spectra in various solvents, Burawoy *et al.* have clearly demonstrated that they exist in solution as tautomeric equilibria.[2] For example, the spectrum of 1-phenylazo-2-naphthol in hexane shows an absorption region consisting of two coalescent bands at about 420 and 460 mμ, whereas in alcohol, chloroform, and 50% alcohol the intensity of the former band is consistently reduced, and that of the latter, increased. The two bands correspond to the azo and the hydrazone tautomers respectively, the former being present in an appreciable quantity only in a hexane solution.

A few years later Hadzi discovered that the electronic spectrum of solid 1-phenylazo-2-naphthol

*1 To whom inquiries may be addressed.

*2 This designation is used throughout this paper for convenience; it is not intended to define the structure of the compounds.

1) H. Zollinger, "Azo and Diazo Chemistry," Interscience, New York (1961), p. 322.

2) A. Burawoy, A. G. Salem, and A. R. Thompson, *J. Chem. Soc.*, **1952**, 4793.

pressed with potassium bromide into a disc consists of two bands, at 410 and 486 mμ.[3] The first maximum was assigned to the azo tautomer, and the second, to the hydrazone tautomer. His finding was rather surprising, as Hadzi himself noted. To the best of our knowledge, compounds exhibiting tautomerism in solution are known to be in one form only in the crystalline state. Therefore, Hadzi suggested that the two types of molecules have very similar bond lengths, that the proton changes its position from oxygen to nitrogen with time, and that thus the two types of molecules give, on the time-average, a single set of bond dimensions. It is noteworthy that the general character of the electronic spectrum of the solid corresponds to that of solutions in polar solvents. Recently Bansho *et al.* extended the spectral measurement by the same technique to cover a number of derivatives.[4] By comparing the extinctions in the regions from 410 to 420 mμ and from 480 to 500 mμ, they concluded that 60 to 70% of the molecules in the solids exist as hydrazones. Further evidence for the presence of the tautomerism in solid 1-arylazo-2-naphthols has been provided by the infrared spectra examined by Morgan and also by the fluorescence studied by Rau.[5,6]

If the compounds exist as tautomeric equilibria in solids, the temperature dependence of the electronic spectra may be observed. To confirm this expectation, we started measurements of the diffuse reflection spectra. As our preliminary attempts indicated that the spectra, which are much better resolved than the transmission spectra presented by Hadzi, depend appreciably on the degree of dilution, concentrations of 1, 0.1, and 0.01% were used throughout this work.

Experimental

Materials. The compounds were prepared by the usual diazo-coupling reactions with 2-naphthol. The derivatives carrying one of the following substituents in the *o*-, *m*-, or *p*-position on the phenyl ring were included in the present work: methyl, chloro, hydroxy, methoxy, and nitro. They were recrystallized twice from appropriate solvents selected from among methanol, benzene, toluene, and acetic acid, and were finally sublimed in *vacuo*.

Measurements. The compounds were diluted with dried sodium chloride in the desired concentrations. The well-ground mixture was mounted on a brass block in which a 60-W heater is embedded. The temperature near the surface of the mixture was monitored by a copper-constantan thermocouple and was kept constant with the aid of a Chino temperature-indicating controller, Type E 500. The difference in reflectance between the mixture heated to a desired temperature and pure sodium chloride kept at room temperature was recorded in the range from 350 to 700 mμ by a Beckman DK 2A spectroreflectometer. The spectra were then plotted using the Kubelka-Munk function $f(R)=(1-R)^2/2R$, where R is the reflectance. The measurements were carried out at three different temperatures, namely, room temperature (about 20°C), the highest temperature selected (at least 50°C below the melting point of each compound), and one between these two. As the reflectance is strongly affected by the thermal dispersion of the compound as the temperature rises, only the spectra measured as the temperature fell were employed in our considerations. The room-temperature spectra are those recorded after cooling by storage in a desiccator over silica gel. Even with these precautions, the absorption intensity depends somewhat upon how the mixture was heated and cooled; therefore, the maximum was arbitrarily taken as 1.00 in each spectrum.

Results and Discussion

1-Phenylazo-2-naphthol (Fig. 1). The room-temperature spectra at concentrations of 1, 0.1, and 0.01% are presented in Fig. 1. There are a broad band covering the region from 350 to 425 mμ and a sharp strong doublet appearing at 480 and 525 mμ. The former band is assigned to the azo tautomer, and the latter, to the hydrazone tautomer. In the present case, the spectra at the three concentrations are rather similar to each other. As the compound is strongly absorbing, the deviation from the Kubelka-Munk theory due to regular reflection may be considered to be the cause of the apparent flattening of the spectra at high concentrations. However, the spectral change observed in the case of the *p*-NO_2 derivative (shown in Fig. 9) undoubtedly indicates that the deviation from the theory cannot be the sole cause of the concentration dependence of the spectra. The marked depression in the relative

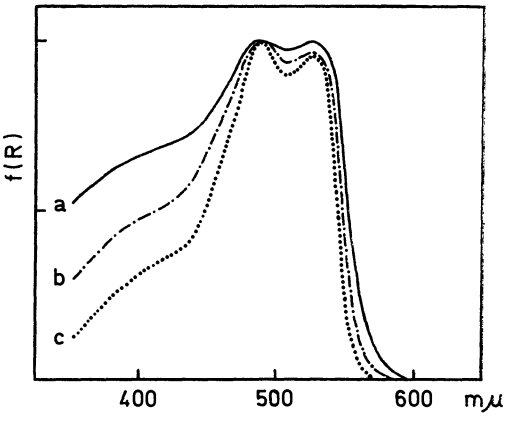

Fig. 1. Spectra of 1-phenylazo-naphthol diluted with sodium chloride; (a) 1%, (b) 0.1% and (c) 0.01% at room temperature.

3) D. Hadzi, *ibid.*, **1956**, 2143.
4) I. Saito, Y. Bansho, and A. Kakuta, *Kogyo Kagaku Zasshi*, **70**, 1715 (1967).
5) K. J. Morgan, *J. Chem. Soc.*, **1961**, 2151.
6) H. Rau, *Ber. Bunsenges. Phys. Chem.*, **72**, 637 (1968).

intensity of the broad band by dilution found in Fig. 1 may be partially attributed to the movement of the equilibrium towards the hydrazone tautomer. We do not expect such movements if the samples are simple mixtures of pulverized substances. Therefore, the contribution from the molecules adsorbed on the surface of the diluent to the observed spectra should be taken into consideration. Even if the concentration is as high as 1%, the spectrum may still not be that of a true solid, but, on the other hand, it may not be far from that. Our spectrum at a concentration of 0.01% is in good agreement with the one reported by Rau, who measured it by the same technique and at the same concentration.

When the temperature was raised to 75°C, no change occurred in the spectrum at any of the concentrations examined except for a small broadening of the doublet.

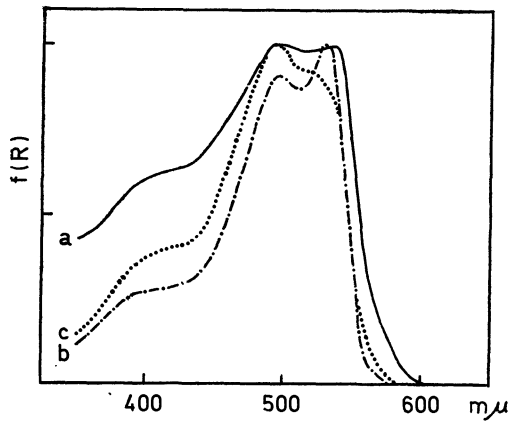

Fig. 2. Spectra of 1-(*o*-tolylazo)-2-naphthol diluted with sodium chloride; (a) 1%, (b) 0.01% at room temperature and (c) 0.01% at 75°C.

1-Tolylazo-2-naphthols (Fig. 2). The spectra of these compounds are almost identical with that of 1-phenylazo-2-naphthol (presented in Fig. 1). Although the relative intensity in the region from 350 to 450 mμ cannot be directly correlated with the amount of the azo tautomer, it is interesting to note that the intensity at a concentration of 1% increases in this order of substituents: *o*-Me∼H<*m*-Me<*p*-Me. This order is nearly the same as that found in an ethanolic solution by Burawoy *et al.*: *o*-Me<*m*-Me∼H<*p*-Me.[2]

A change in the spectrum upon an elevation of the temperature was observed in the case of the *o*-Me derivative, most clearly at 0.01%. As is shown in Fig. 2, the intensities in the region from 350 to 500 mμ measured at 75°C are higher than those at room temperature. This observation indicates that the equilibrium moves towards the azo tautomer at high temperatures. The change in the spectrum upon dilution is also illustrated in this figure. In the case of the *m*-Me derivative, none of the spectra recorded at 75°C were found to be different from those at room temperature. The spectrum of the *p*-Me derivative is modified a little bit only at 0.01% when the temperature is raised to 75°C. The direction of the change is the same as that found in the *o*-Me derivative.

1-Chlorophenylazo-2-naphthols (Figs. 3 and 4). The spectra of the *o*-Cl and *m*-Cl derivatives are shown in Fig. 3. No temperature dependence was observed in these cases; however, a movement of the equilibrium towards the hydrazone tautomer upon heating to 75°C was found in the *p*-Cl derivative. It must be added that this movement is in the direction opposite to that observed in the *o*-Me and *p*-Me derivatives. At a concentration of 1%, the presence of a doublet due to the hydrazone tautomer is clearly noted only in the *m*-Cl derivative. In the other two cases, the

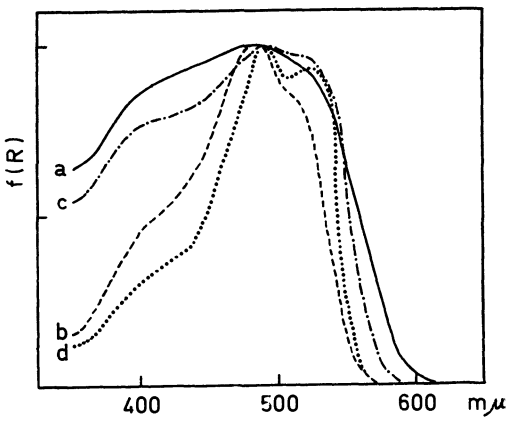

Fig. 3. Spectra of 1-(*o*-chlorophenylazo)-2-naphthol; (a) 1% and (b) 0.01% and those of 1-(*m*-chlorophenylazo)-2-naphthol; (c) 1% and (d) 0.01% at room temperature.

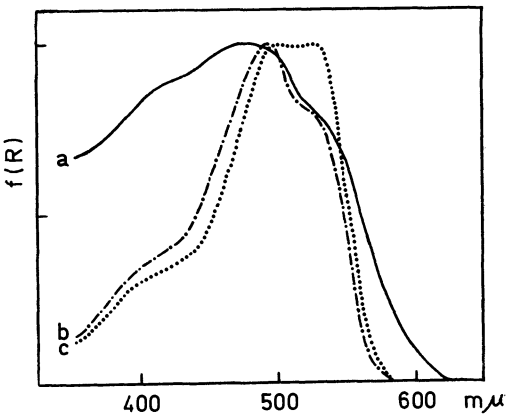

Fig. 4. Spectra of 1-(*p*-chlorophenylazo)-2-naphthol diluted with sodium chloride; (a) 1%, (b) 0.01% at room temperature and (c) 0.01% at 75°C.

absorptions in the region from 350 to 450 mμ are so high that the sharp peaks due to the hydrazone tautomers cannot be resolved. The relative intensities measured at 1% in the above-mentioned region increase in this order: H<*m*-Cl<*p*-Cl~*o*-Cl, an order which is not in accordance with that drawn from the data obtained in an ethanolic solution: *o*-Cl<*m*-Cl<*p*-Cl~H.[2] When the compounds are much more diluted with sodium chloride, the relative intensities in the region from 350 to 450 mμ are drastically decreased, as is generally found in a solid, two-component system. Nevertheless, the order remains essentially the same: H<*m*-Cl<*o*-Cl<*p*-Cl. Therefore, the effect of chlorine substitution on the tautomeric equilibrium in our system is apparently very different from that observed in solution by Burawoy *et al.*

1-Hydroxyphenylazo-2-naphthols (Figs. 5 and 6). The *o*-OH derivative is one of the compounds showing a very pronounced temperature dependence in the spectra. In Fig. 5 the spectra measured at room temperature and at 100°C are presented. The room-temperature spectrum at 1% is very similar to that of 1-phenylazo-2naphthol examined under the same conditions. However, the whole spectrum is shifted to the long-wavelength side. The doublet to be assigned to the hydrazone tautomer is located at 500 and 540 mμ. It is apparent that the equilibrium moves towards the azo tautomer when the temperature is elevated. Contrary to the case of the *o*–OH derivative, the absorption due to the azo tautomer is dominant in the spectrum of the *m*–OH derivative at a concentration of 1%. A small movement of the equilibrium towards the hydrazone tautomer is noted upon heating to 100°C only at 0.01%. The spectra of the *p*–OH derivative shown in Fig. 6 bear some similarity to those of the *o*–OH derivative, but the change upon an elevation of the temperature is in the opposite direction.

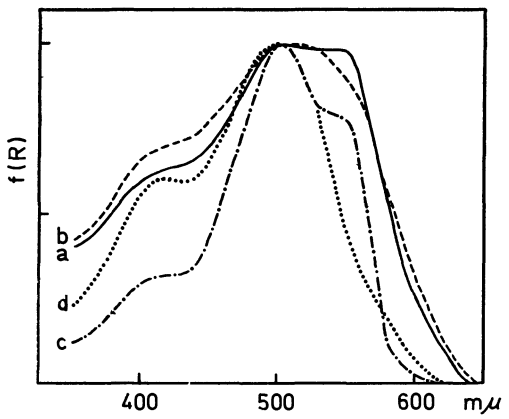

Fig. 5. Spectra of 1-(*o*-hydroxyphenylazo)-2-naphthol diluted with sodium chloride; (a) 1% at room temperature, (b) 1% at 100°C, (c) 0.01% at room temperature and (d) 0.01% at 100°C.

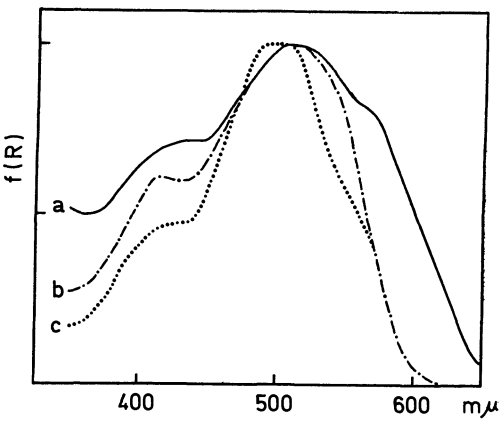

Fig. 6. Spectra of 1-(*p*-hydroxyphenylazo)-2-naphthol diluted with sodium chloride; (a) 1%, (b) 0.01% at room temperature and (c) 0.01% at 100°C.

1-Anisylazo-2-naphthols (Fig. 7). The doublet to be assigned to the hydrazone tautomer is located at 500 and 540 mμ in the spectrum of the *o*–MeO derivative. By heating to 100°C, the peak at the longer wavelength disappears. The equilibrium seems to move slightly towards the azo tautomer upon an elevation of the temperature. The *m*–MeO derivative shows a spectrum similar to that of the *o*-MeO derivative; however, no temperature dependence was detected in this case. The spectrum of the *p*-MeO derivative shown in Fig. 7 suggests that a fairly large amount of the azo tautomer is present, even at a concentration of 0.01%. The change caused by heating discloses that high temperatures favor the hydrazone tautomer. The spectrum examined as a potassium bromide disc by Bansho *et al.* is like ours measured at 0.01%. The concentration of the azo tautomer in solution was reported by Burawoy *et al.* to increase in this order: *o*-MeO

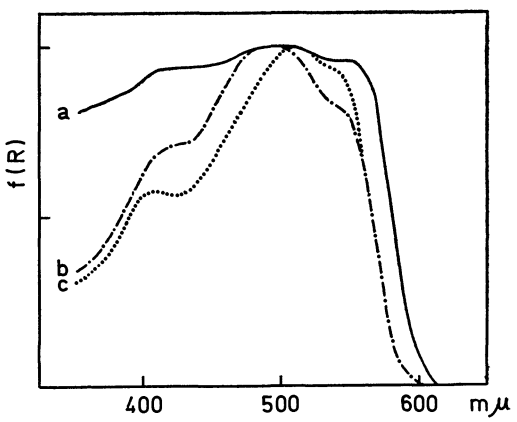

Fig. 7. Spectra of 1-(*p*-anisylazo)-2-naphthol diluted with sodium chloride; (a) 1%, (b) 0.01% at room temperature and (c) 0.01% at 75°C.

$<m$-MeO$<$H$<p$-MeO.[2] In our solid, two-component system, the effect of the substituent on the equilibrium is quite different from theirs. The relative intensity in the region between 350 and 450 mμ is found to be in this order: H$<$ m-MeO$\sim o$-MeO$<p$-MeO at a concentration of 1%.

1-Nitrophenylazo-2-naphthols (Figs. 8 and 9). As is shown in Fig. 8, the spectrum of the o-NO_2 derivative at room temperature is dominated by the broad absorption assigned to the azo tautomer. The change upon an elevation of the temperature is well demonstrated, even at a concentration of 1%. Apparently the amount of the hydrazone tautomer increases at high temperatures. In the spectra of the m-NO_2 derivative, the doublet due to the hydrazone tautomer can be seen in this case, but only weakly, at a concentration of 1%. As the absorption assigned to the azo tautomer at 100°C is stronger than that at room temperature, the hydrazone tautomer appears to be more stable than the azo tautomer.

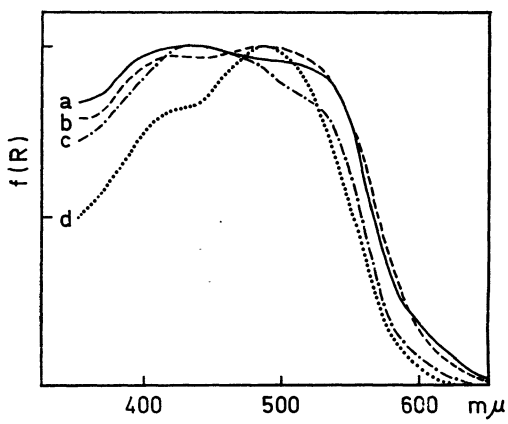

Fig. 8. Spectra of 1-(o-nitrophenylazo)-2-naphthol diluted with sodium chloride; (a) 1% at room temperature, (b) 1% at 125°C, (c) 0.01% at room temperature and (d) 0.01% at 125°C.

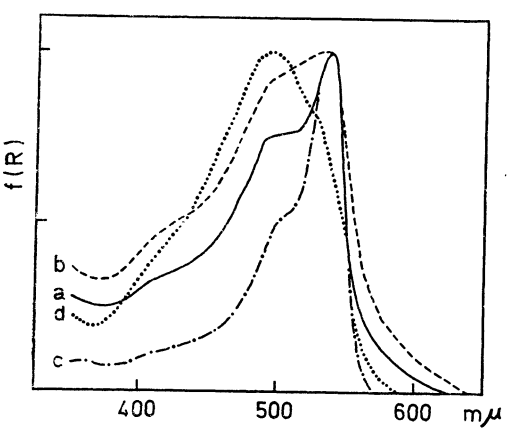

Fig. 9. Spectra of 1-(p-nitrophenylazo)-2-naphthol diluted with sodium chloride; (a) 1% at room temperature, (b) 1% at 150°C, (c) 0.01% at room temperature and (d) 0.01% at 150°C.

The most pronounced temperature dependence of the spectrum has been observed with the p-NO_2 derivative. There is a sharp peak at 538 mμ, with a shoulder around 500 mμ. Upon heating to 150°C, the shoulder is appreciably intensified. Especially at a concentration of 0.01%, the change is quite remarkable. The peak at 538 mμ, which is supposed to be assigned to the hydrazone tautomer, is nearly completely obscured by a strong absorption appearing at 500 mμ. The latter may be assigned to the azo tautomer. Our high-temperature spectrum obtained at 0.01% closely resembles the one reported by Bansho *et al.*[4] It must be pointed out that the high-temperature spectrum at 0.01% differs greatly from that at 1%. This observation confirms the dependence of the tautomeric equilibrium on the degree of dilution. Burawoy *et al.* stated that the concentration of the hydrazone tautomer in these nitro derivatives is the highest among the 1-arylazo-2-naphthols examined.[2] However, the spectra of the o-NO_2 derivative given in Fig. 8 are not consistent with their finding.

General Remarks. Since the true maxima and intensities of the bands of the individual tautomers are not known, a quantitative analysis of the equilibria cannot be made. Bansho *et al.* reported that 60 to 70% of the molecules in solid 1-arylazo-2-naphthols exist as hydrazone tautomers, regardless of the kind and position of the substituents examined, *i.e.*, Me, MeO, Cl, and NO_2.[4] In their estimations, the relative intensities of the bands due to the azo and hydrazone tautomers were assumed to be constant throughout the derivatives examined and were taken to be equal to those of 4-(o-chlorophenylazo)-1-naphthol in solution. The temperature dependence of the electronic spectra reported in the present work indicates that some of the Bansho estimations are too high.

The effects of the temperature on the tautomeric equilibria are summarized in Table 1. There are five derivatives for which the temperature dependence of the electronic spectra could not be detected. Such cases may occur when the azo and hydrazone tautomers have nearly the same energy or when the energy difference between the two tautomers is so large that the amount of the minor one is too small to affect the spectrum. In the present system, the former situation seems to be likely. If the magnitude of the energy difference is in the order of thermal energy, the electronic spectrum may be modified by the temperature change. The direction of the movement of the equilibrium upon an elevation of the temperature should be towards the minor tautomer. Thus, more than 50% of the molecules in the o-Me, p-Me, o-OH, o-MeO, m-NO_2, and p-NO_2

Table 1. The movement of the equilibrium by elevating temperature; towards the azo tautomer (+) or the hydrazone tautomer (−)
The number in parenthesis is Hammett substituent constant.

Substituent	Position		
	ortho	meta	para
None		not detectable (0.00)	
Methyl	+	not detectable (−0.07)	+ (−0.17)
Chloro	not detectable	not detectable (0.37)	− (0.23)
Hydroxy	++	− (0.12)	− (−0.37)
Methoxy	+	not detectable (0.12)	− (−0.27)
Nitro	−−	+ (0.71)	++ (0.78)

derivatives are expected to exist as hydrazone tautomers in the present two-component system. On the other hand, the situation must be reversed in the *p*-Cl, *m*-OH, *p*-OH, *p*-MeO, and *o*-NO_2 derivatives. This conclusion is in serious conflict with the estimations made by Bansho *et al.* On the basis of this disagreement, we have to conclude that the relative intensities of the bands of the tautomers are not independent of the kind and position of the substituents. Although the distribution of the substituents in the above-discussed three groups reveals the general tendency for the hydrazone tautomer to be favored in the derivatives carrying substituents with large Hammett constants, no simple correlation can be established in the present system.

The electronic and vibrational spectra examined as potassium bromide discs have been considered like those of solid samples.[3-5] However, our observation that the spectra depend greatly upon the degree of dilution casts some suspicion on the technique. As has been mentioned earlier, the spectral changes caused by dilution may be attributed not only to a decreasing deviation from the Kubelka-Munk theory, but also, at least in part, to the movement of the equilibrium towards the hydrazone tautomer. As a matter of fact, Rau has considered his spectrum of 1-phenylazo-2-naphthol, measured at a concentration of 0.01%, as that of the species adsorbed on the diluent.[6] These pieces of evidence suggest that the spectra obtained by the potassium-bromide-disc method are also not free from the influence of the diluent. It has been pointed out by Burawoy *et al.* that the relative stability of the hydrazone tautomer increases in this order of the solvents: hexane< ethanol<chloroform<water.[2] The observed trend of the movement of the equilibrium upon dilution with sodium chloride seems reasonable, since more and more molecules of 1-arylazo-2-naphthol are dispersed and adsorbed on the highly polar surface of the alkali halide. As has been discussed earlier, measurements at higher concentrations may provide the spectra of true solids, but they will be very much distorted. At a maximum concentration of 1% or higher, the reflectance spectra are expected to be flattened because of an increasing regular reflection.

The authors wish to express their thanks to Mr. Nobuhiko Miyajima for his collaboration throughout the course of this work.

BULLETIN OF THE CHEMICAL SOCIETY OF JAPAN VOL. 43 3410—3414 (1970)

Catalytic Activity and Reactivity of Aromatic Nitrile and Alkali Metal Ion Radical Salt. I. Homogeneous and Heterogeneous Catalysis of Benzonitrile-Cesium Ion Radical Salt

Motoyuki TSUDA*1 and Hiroo INOKUCHI

The Institute for Solid State Physics, The University of Tokyo, Roppongi, Tokyo

(Received June 13, 1970)

Homogeneous and heterogeneous mechanisms of parahydrogen conversion and hydrogen-deuterium exchange reactions were investigated in the presence of benzonitrile–cesium ion radical salt. Studies of their activation energies and rate constants showed that the heterogeneous reaction on the solid-ion radical salt occurs mainly through the "chemisorption mechanism" and the "exchange mechanism", but the homogeneous reaction over the salt solution in benzonitrile takes place only through the "physical mechanism." According to these results, it was concluded that the catalytic activity and reactivity of the ion-radical salt must be due to the nature of its solid phase, not to that of its aromatic anion or free-ion radical pair.

Since tetracyanopyrene-cesium ion radical salt was found to catalyze the hydrogen-deuterium exchange reaction,[1] the catalytic activities for various aromatic–alkali metal ion radical salts[2–7] and charge-transfer complexes[8,9] have been studied. The results of these works may be summarized as follows: (1) the aromatic–aromatic charge-transfer complexes have only a weak catalytic activity for para-orthohydrogen conversion through the physical mechanism[8,10] (see Appendix 1); (2) the aromatic-halogen charge-transfer complexes, for instance, the violanthrene-iodine complex, catalyze the isomerization of 1-butene⇌2-butene, but no H_2-D_2 equilibration takes place over the complexes,[9] and (3) aromatic-alkali metal ion radical salts catalyze the hydrogen-deuterium equilibration. Further, over these ion radical salts it is found that deuterium exchanges with the hydrogen of the bulk aromatic anion.[1–7]

Recently, some assumptions about the catalytic mechanism on these ion salts were proposed, mainly on the basis of the electronic properties of the acceptor aromatic molecule, that is, the electron affinity,[7] the charge density of the lowest unoccupied orbitals,[4,7] the valency,[5] the reduction potential, and the effect of substitution on the aromatic skeleton,[4] but not on the basis of the properties of the bulk complex. Accordingly, no findings have been reported on whether the nature of isolated molecules or that of molecular aggregates is decisive in the catalytic activity.

In this paper, we will present the results of our study of homogeneous and heterogeneous catalyses over benzonitrile*2-alkali metal ion salts. Because the melting point of benzonitrile is fairly low (−13°C), the homogeneous reaction*3 on the ion salts dissolved in a benzonitrile solution with hydrogen was observed satisfactorily.

Experimental

Purification of Samples. Commercial benzo-

*1 Present Adress: Department of Chemistry, Faculty of Science, Hokkaido University, Sapporo.

1) T. Kondow. H. Inokuchi and N. Wakayama, *J. Chem. Phys.*, **43**, 3766 (1965).

2) H. Inokuchi, N. Wakayama, T. Kondow and Y. Mori, *ibid.*, **46**, 837 (1967).

3) H. Inokuchi, Y. Mori and N. Wakayama, *J. Catal.*, **8**, 288 (1967).

4) N. Wakayama and H. Inokuchi, *ibid.*, **11**, 143 (1968).

5) N. Wakayama, Y. Mori and H. Inokuchi, *ibid.*, **12**, 15 (1968).

6) M. Tsuda, G. Inokuchi and H. Suzuki, *J. Phys. Chem.*, **73**, 1595 (1969).

7) M. Ichikawa, M. Soma, T. Onishi and K. Tamaru, *ibid.*, **70**, 2069 (1966); *J. Catal.*, **6**, 336 (1966); *Trans. Faraday Soc.*, **63**, 997 (1967); *ibid.*, **63**, 2529 (1967); This Bulletin, **41**, 1739 (1968).

8) H. Inokuchi, M. Tsuda and T. Kondow, *J. Catal.*, **8**, 91 (1967).

9) M. Tsuda, T. Kondow, H. Inokuchi and H. Suzuki, *ibid.*, **11**, 81 (1968).

10) M. Tsuda, M. Sc. Thesis, Waseda University (1967).

*2 The electronic spectra and also the ESR spectra show that only the mononegative anion (benzonitrile$^-$) in the ion salt is stable, though other aromatic anions have multivalencies.

*3 We demonstrated a homogeneous catalysis for para-orthohydrogen conversion in the presence of a gaseous anthracene-*syn*-trinitrobenzene charge-transfer complex under illumination.[8] However, no ion-radical salts in the gaseous phase could be obtained.

nitrile was refluxed with diphosphorus pentoxide in a sealed glass vessel to eliminate a trace of water and was subsequently degassed by alternate boiling under a vacuum and repeated distillations. The cesium metal was prepared by reduction between its chloride and calcium metal, that is, $2CsCl+Ca=CaCl_2+2Cs$; it was distilled several times *in vacuo* in order to purify it.

Preparation of the Benzonitrile-Alkali Metal Ion Radical Salts. The benzonitrile-cesium ion radical salt used in this study was prepared as follows. A known amount of benzonitrile was placed in a glass vessel cooled with a dry ice-ethanol mixture, on which a measured volume of purified cesium metal had previously been evaporated. The vessel was then sealed off and heated at 60°C for 40 hr in order to complete the formation of the complex; a deep red-coloured ion radical salt solution was thus obtained. To separate the solid-phase salt aggregates from the solution, if any existed, the solution was passed through a fine glass filter. The solution was then submitted to a homogeneous catalytic reaction. The excess benzonitrile in the solution was completely evaporated at 60°C *in vacuo* in order to obtain the solid specimen.

Experimental Procedure. For the investigation of the homogeneous catalysis of the hydrogen conversion in the ion-radical salt solution, a cylindrical, thermostated glass vessel containing the solution was agitated with a magnetic stirrer arrangement, as is shown in shown in Fig. 1. A known amount of the salt solution was placed in the vessel and sealed off at the point indicated by the arrow ↓ in Fig. 1. Para-rich-hydrogen (80% p-H_2) was admitted into the vessel under a pressure of 100 Torr (at room temperature), and the system was sealed off by a greaseless stopcock. The temperature of the reaction system (surrounded by a broken line in Fig. 1) was controlled at temperatures between 33—90°C.

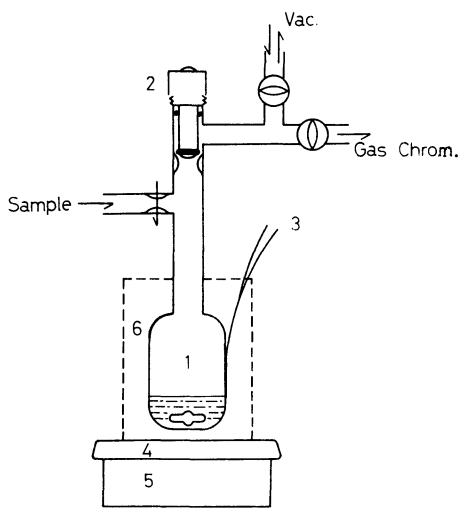

Fig. 1. The schematic diagram of the reaction system.
1. reaction vessel containing a piece of magnet, 2. greaseless stopcock, 3. chromel-alumel thermocouple, 4. electrical heater controlled at appropriated temperature, 5. magnetic stirrer and 6. air bath.

In order to keep the condition of the homogeneous catalytic reaction constant, after finishing each procedure the ion-salt solution was degassed in order to remove the converted hydrogen by alternate boiling under a vacuum.

In the heterogeneous reaction, the exchange of gaseous deterium with the hydrogen of the aromatic anion occurred. Therefore, after measuring the hydrogen–deuterium equilibration on the solid specimen, the hydrogen gas was admitted into the vessel to replace the deuterium in the aromatic ring of the anion and/or the chemisorbed deuterium of the salt at 70°C. This procedure was repeated until no D_2 (or HD) was detected in the gas phase. By this method, the solid specimen could be reproduced repeatedly.

The compositions of the various orthohydrogen–parahydrogen or hydrogen-deuterium mixtures were measured successfully by means of gaschromatography. A mixture was separated quantitatively by passing it through a heat-treated alumina column at the temperature of liquid nitrogen.[11,12] The electronic spectrum of the benzonitrile-cesium ion radical salt in a benzonitrile solution and that of the solid-ion salt film were measured with a Cary recording spectrophotometer, Model 14. The preparation of the radical anion and the measurement of the electronic absorption spectra were made in a vacuum system, as is shown in Fig. 2.

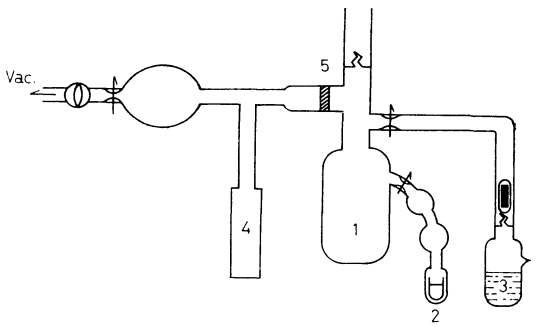

Fig. 2. The apparatus for preparation ion radical salt.
1. reaction vessel, 2. iron cell contained CsCl+Ca, 3. purified benzonitrile, 4. optical cell for electronic absorption spectra measurement and 5. glass filter.

Results

The kinetics of the heterogeneous and homogeneous reactions of the benzonitrile-cesium ion radical salt were investigated as a function of the hydrogen pressure and of the temperature. The experimental results on the heterogeneous reaction will first be shown, while those of the homogeneous reaction will be described later.

Heterogeneous Reaction. *Pressure Dependency.* The para-orthohydrogen conversion on

11) W. R. Moore and H. W. Ward, *J. Amer. Chem. Soc.*, **80**, 2909 (1958).

12) S. Ohkoshi, Y. Fujita and T. Kwan, This Bulletin, **31**, 771 (1958).

the solid-ion radical salt was investigated as a function of the partial pressure of parahydrogen under a constant pressure (110 Torr) and at a constant temperature (87°C). Figure 3 shows the results, in which the rate was found to be a first-order reaction concerning the partial pressure of parahydrogen. Hence, the experimental rate constant, k_e^H, was derived from the following equation:

$$k_e^H = \frac{1}{t} \ln \frac{C_p(t) - C_p(\infty)}{C_p(0) - C_p(\infty)} \quad (1)$$

where $C_p(0)$, $C_p(\infty)$, and $C_p(t)$ are the concentration of parahydrogen at the initial point, in equilibrium, and after t min respectively.

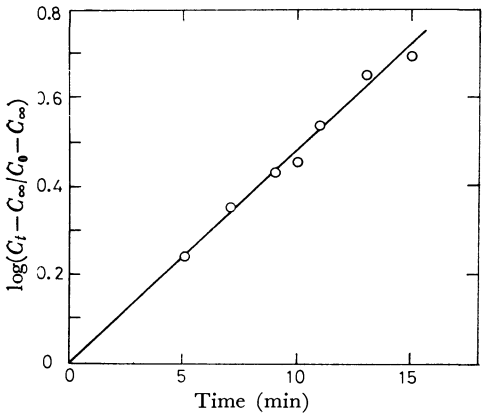

Fig. 3. The reaction velocity of ortho-parahydrogen conversion under constant pressure for determining the order of rate constant.

Temperature Dependency. The kinetics of the hydrogen conversion were studied over the temperature range between 0°C and 100°C under a constant pressure of hydrogen. The experimental rate constant was also given by Eq. (1); the progression of the para-orthohydrogen conversion is plotted against the reaction time in Fig. 4.

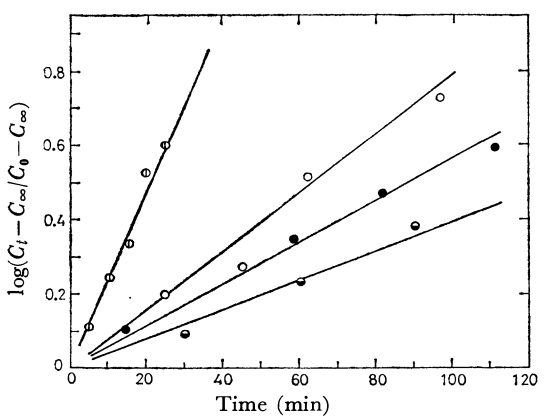

Fig. 4. The progression of the para-orthohydrogen conversion on the solid of the benzonitrile-cesium ion radical salt.
—◑— at 80°C, —○— at 41°C,
—●— at 20°C, and —◒— at 0°C.

On the other hand, when deuterium gas was placed in contact with the benzonitrile-cesium solid film, it was found that exchange took place between the admitted deuterium and the hydrogen of the aromatic anion. In the reaction, denoted as the exchange mechanism, the decay of the concentration of deuterium in the gas phase obeyed the first-order law.*4 The rate constant, k_e^D is:

$$k_e^D = -\frac{1}{t} \ln \frac{D(t)}{D(0)} \quad (2)$$

where $D(0)$ and $D(t)$ represent, respectively, the concentrations of deuterium in the gas phase at the initial point and t min later. The experimentally-determined rate constants, k_e^H and k_e^D, are shown in Fig. 5 as functions of the temperature. On the basis of the temperature dependence of the rate constant, we could determine an apparent activation energy, E^D or E^H, for these two reactions:

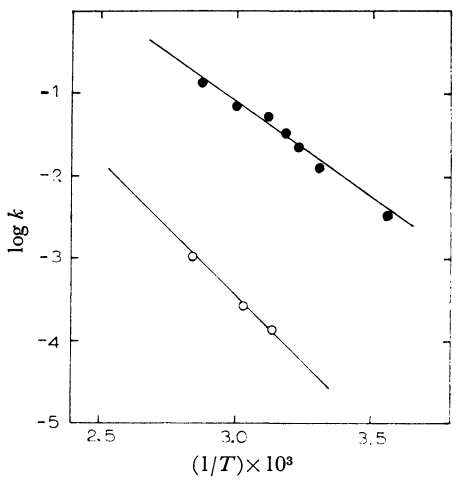

Fig. 5. The rate of the conversion at various temperatures for the solid of the benzonitrile-cesium ion radical salt.
-●- the rate of the para-othohydrogen conversion, -○- the rate of $D_2 + \phi H \rightleftarrows HD + \phi D$ reaction.

$$k_e^H = S^H A^H \exp(-E^H/\boldsymbol{k}T) \quad (3a)$$

$$k_e^D = S^D A^D \exp(-E^D/\boldsymbol{k}T) \quad (3b)$$

where S^H and S^D are the areas of the catalyst and where A^H and A^D are the factors which depend hardly at all upon the temperature. Experimentally, we obtained $E^H = 10.2$ kcal/mol, and the value of E^D was 14.3 kcal/mol.

Homogeneous Reaction. The catalytic activity and the reactivity of benzonitrile-cesium ion salt dissolved in benzonitrile were also investigated by means of the para-orthohydrogen con-

*4 This reaction rate will be analyzed in Part II.

version and the hydrogen-deuterium exchange reaction. As was shown in the previous section, the solid film of the ion radical salt has a good catalytic activity. On the contrary, the hydrogen conversion with the salt solution occurred very slowly. Further, we could not detect any H_2-D_2 exchange reaction even after a long time, 1320 hr.*5 These facts suggest that the hydrogen conversion in the homogeneous system is caused by the paramagnetic mechanism,[13] but not by the chemical mechanism.

The rate constant, $[k_e^H]_L$, which was found to be first order, as given by Eq. (1) for the solid system, was investigated at a series of temperatures between 33—90°C under a constant pressure of hydrogen (100 Torr).

The concentration of parahydrogen is plotted against the reaction time in Fig. 6. From these

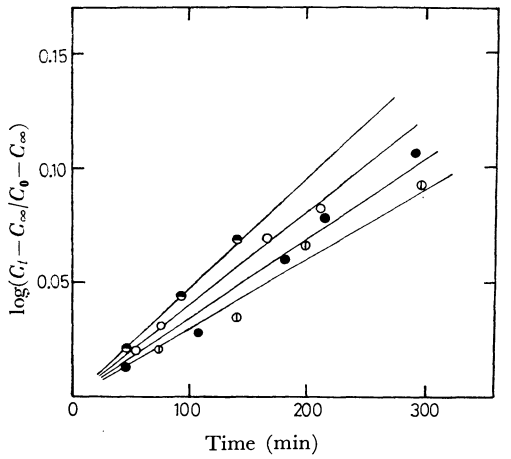

Fig. 6. The progression of the para-orthohydrogen conversion in the presence of the benzonitrile-cesium ion radical salt solution.
-◒- at 90°C, -○- at 70°C,
-●- at 40°C, and -◑- at 33°C.

results, it seems that the apparent rate constant, $[k_e^H]_L$, is enhanced with the increase in the temperature. To obtain the intrinsic rate constant, k_L, however, we must eliminate the term of the temperature dependency of the solubility of hydrogen in the solution, as is described in the following equation:[14]

$$[k_e^H]_L = \frac{a(T)V_L}{V_G + a(T)V_L} k_L \qquad (4)$$

where $a(T)$ is the solubility*6 and where V_G and V_L are the volumes of the gas and the solution in the reaction vessel. Figure 7 shows an Arrhenius plot for the k_L and $[k_e^H]_L$. The intrinsic activation energy, $[E^H]_L$, was found to be 0.1 kcal/mol though the apparent activation energy was 1.0 kcal/mol. When we compare these values with the value of $E^H = 10.2$ kcal/mol for the solid film, the mechanism of hydrogen conversion for these two systems may be assumed to be different.

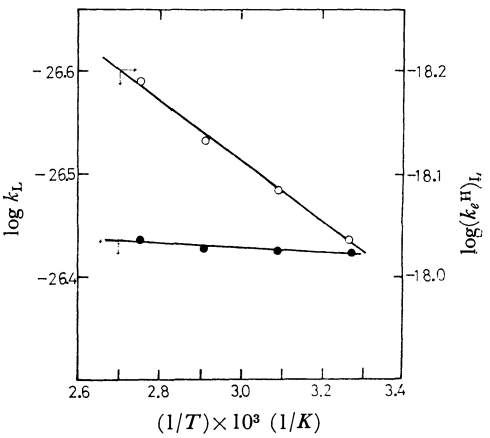

Fig. 7. The rate of the conversion at various temperatures for the benzonitrile-cesium ion radical solution.
-○- apparent rate, -●- intrinsic rate.

Discussion

In the last five years, the mechanism of the hydrogen conversion of the aromatic-alkali metal ion radical salt and the reaction of deuterium with the hydrogen of the aromatic anion have been investigated extensively, and some assumptions have been proposed based on the electronic structure of the aromatic *molecule* or the aromatic *anion*. However, the compounds used in those studies were in a solid state. Accordingly, the question was still left whether the nature of the isolated molecule or that of solid state is decisive in the catalytic activity.

The essential point is the fact that the isolated ion and/or ion pair shows no catalytic activity caused by the chemical mechanism; rather, a slow para-orthohydrogen conversion occurs in the presence of the ion and/or ion pair through the

*5 No apparent change in the activity for para-orthohydrogen conversion with the solution was found between before and after the long reaction; that is, the ion-radical salt solution was stable under these conditions.

*6 Because of various experimental difficulties, the solubility, $a(T)$, of hydrogen in benzonitrile has not yet been measured, but the solubilities of hydrogen in benzene ($a = 5.8\times10^{-2} + 5\times10^{-4}$T) and in chlorobenzene ($a = 5.5\times10^{-2} + 3.5\times10^{-4}$T) have been observed.[15] For the present system, the solubility of hydrogen is assumed to be of the same order as that of benzene or chlorobenzene.

13) L. G. Harrison and C. A. McDowell, *Proc. Roy. Soc.*, (London), **A220**, 77 (1953).
14) H. Sachsse, *Z. Phys. Chem.*, **B24**, 429 (1933).
15) "Solubilities of Inorganic and Organic Compounds," Vol. 1, ed. by H. Stephen and T. Stephen, Pergamon Press, London (1963).

physical mechanism. This conclusion is supported by the following two reasons.

First, the ratio of the rate constant of the hydrogen conversion to that of the deuterium exchange reaction is very different in the cases of the solid film and the liquid phase at the same temperature. The empirically-determined rate constant of each case at 90°C is given as: $k_e^H = 2.6 \times 10^{-1}$/min and $k_e^D = 2.1 \times 10^{-3}$/min for the solid phase and $[k_e^H]_L = 1.8 \times 10^{-5}$/min and $[k_e^D]_L \simeq 0$ for the liquid phase. Assuming that the catalytic mechanism for hydrogen is the same for both states and that the large difference in the absolute value of k_e^H and $[k_e^H]_L$ originates only from the difference in collision efficiency in the two states, the following relation must be satisfied:

$$\frac{k_e^H}{k_e^D} = \frac{[k_e^H]_L}{[k_e^D]_L} \tag{5}$$

Equation (5) requires the value of 2.22×10^{-3}/min for $[k_e^D]_L$ instead of nearly zero, in view of the experimental results for k_e^H, k_e^D and $[k_e^H]_L$; for instance, 4.8% of HD must be detected for a hydrogen-deuterium exchage reaction at 90°C after 1320 hr. However, we could not find any trace of HD content during that long period, as has been menitoned above.

Second, the catalytic mechanism is recognized from the activation energies of the para-ortho-hydrogen conversion for the two states. Figure 5 shows $E^H = 10.2$ kcal/mol; the hydrogen conversion on solid film occurs with the chemical mechanism. In the case of the molecular state, however, the activation energy is $[E^H]_L \simeq 0$; this means that the hydrogen conversion occurs through the physical process.[13]

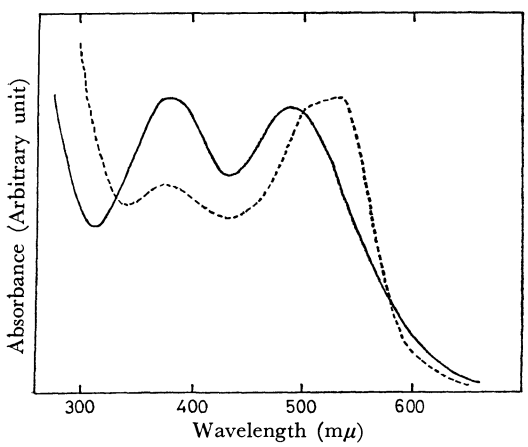

Fig. 8. The electronic spectra of the benzonitrile-cesium ion radical salt.
—— solid film, ---- solution.

The mechanism of the chemisorption of hydrogen on the aromatic-alkali metal ion radical salt is not clear at present. However, we may conclude that the mechanism can not be explained only in terms of the electronic structure of the isolated aromatic anion.

The electronic absorption spectra of the solid and liquid phases are both similar to the spectrum of the benzonitrile mononegative anion,[16] as is shown in Fig. 8. However, the wavelengths of the peaks are shifted from 375 mμ and 510 mμ in the solution to 380 mμ and 488 mμ in the solid, and the ratio of the extinction coefficients, ε, varies from $\varepsilon_{488m\mu}/\varepsilon_{380m\mu} = 1.06$ in the solution to $\varepsilon_{510m\mu}/\varepsilon_{375m\mu} = 2.01$ in the solid. These changes suggest that the benzonitrile anion in the solid-ion radical salt is strongly perturbed by the neighbouring cesium cations and the other benzonitrile anions. Therefore, in order to analyze the chemical mechanism of the hydrogen conversion on the ion salts, the structure of aromatic anion-alkali metal cation pairs perturbed strongly by neighbouring ions must be considered.

The authors wish to thank Drs. N. Wakayama and Y. Mori for their helpful discussion. One of us (M.T) also wishes to express his thanks to Professor S. Okamoto and Professor H. Suzuki of Waseda University for helpful discussion and for continuous encouragement. Thanks are due to Kawakami Foundation for financial support.

Appendix 1

The catalytic activity of a number of aromatic-aromatic charge transfer complexes, mentioned below, has been examined by means of the hydrogen-deuterium exchange reaction by us. (T. Kondow, N. Wakayama, Y. Mori, Y. Matsunaga and the authors) However, no exchange reaction occurred over these complexes.

Donor	Acceptor	Donor	Acceptor
DAD[a]	Chloranil (1 : 1)	TTN	TCNE (3 : 2)
DAD	9-Dicyanomethylene-2,4,7-Trinitrofluorene (1 : 1)	Dibenzo-Phenothiazine	DDQ[e] (2 : 1)
DAD	Dicyanonaphthoquinone (1 : 1)	Dibenzo-phenothiazine	DDQ (1 : 1)
DAD	TCNE[b] (1 : 1)	Tetramethylbenzidine	TCNE (1 : 1)
DAD	TCNQ[c] (1 : 1)	Tetramethylbenzidine	TCNQ (1 : 1)
TTN[d]	*o*-Chloranil (3 : 1)		

a) diaminodurene, b) tetracyanoethylene, c) tetracyanoquinodimethane, d) tetrathionaphthacene
e) dichlor-dicyano-*p*-benzoquinone

16) A. Ishitani and S. Nagakura, *Theor. Chem. Acta*, **4**, 236 (1966).

BULLETIN OF THE CHEMICAL SOCIETY OF JAPAN VOL. 43 3415—3419 (1970)

Catalytic Activity and Reactivity of Aromatic Nitrile and Alkali Metal Ion Radical Salt. II. Hydrogen Exchange on Benzonitrile Ion Salt as a Function of Alkali Metals

Motoyuki TSUDA*1

The Institute for Solid State Physics, the University of Tokyo, Roppongi, Tokyo
and Department of Physics, School of Science and Engineering, Waseda University, Tokyo

(Received June 13, 1970)

The para-orthohydrogen conversion (rate constant k_e^H and the deuterium exchange reaction (rate constant k_e^D) over the benzonitrile-alkali metal ion radical salt were investigated as functions of the donor component—alkali metal. The sort of alkali metals in the ion radical salts greatly affected the catalytic activity and the reactivity. The activation energies obtained from the temperature dependence of k_e^H and k_e^D, E^H and E^D, and the value of α(depending on the ratio of k_e^H to k_e^D monotonously decreased as Na→K→Rb, but those values showed an irregular trend for the Cs-complex. The results suggest that the catalytic activity cannot be understood only in terms of the nature of the components; must also be considered the structural nature of the solid phase of the ion radical salt.

In a previous paper,[1] we reported that the benzonitrile-cesium ion radical salt has a strong catalytic activity in the solid phase, but that the salt solution in a benzonitrile solvent does not possess any catalytic activity for hydrogen-deuterium equilibration. Thus, we concluded that the catalytic activity on the ion radical salts can be explained not by the electronic structure of the isolated aromatic anion, but by the structure of the solid ion radical salt which is perturbed strongly by neighbouring ions.

In this report, we wish to discuss mainly the catalytic activity on benzonitrile-alkali metal ion radical salts as a function of their donor metals in order to clarify the role of the metallic cations in the ion salt with regard to the catalytic activity. Further, we will discuss the mechanism of hydrogen-deuterium equilibration on the ion radical salt.

Experimental

The preparation of the benzonitrile-alkali metal ion radical salts has already been reported.[1] In this work, four sorts of alkali metals—Na, K, Rb and Cs— were used as electron-donor components. Their preparations and purifications were carried out carefully.*2 The purified alkali metal was first evaporated onto the surface of a glass reaction vessel *in vacuo* and then the purified benzonitrile was introduced. A dark red-coloured ion radical salt solution was obtained immediately. The excess benzonitrile was completely evaporated from the salt solution by heating *in vacuo* about 8 hr, since no catalytic activity was found for the ion radical salt solution or the wet ion salt.

The hydrogen mixtures (p-H_2+o-H_2 and H_2+HD+D_2) were analyzed by gaschromatography using a heat-treated alumina column at the temperature of liquid nitrogen, as has been described in a previous paper.[2]

The electronic spectra of benzonitrile-alkali metal ion radical salt in a benzonitrile solvent and the solid film of the salt were observed with a Cary recording spectrophotometer, Model 14.

Results

As has been mentioned in the previous papers,[1-4] the aromatic-alkali metal ion radical salts show two chemical reactivities for hydrogen molecules; one is the "chemisorption mechanism", and the other is the "exchange mechanism."*3 To make clear the mechanisms of these two reactions, the

*1 Present Address: Department of Chemistry, Faculty of Science, Hokkaido University, Sapporo.

*2 The sodium and potassium, obtained commercially, were purified by a distillation procedure under a vacuum free from hydrogen and carbohydrates. The rubidium and cesium were prepared from their chloride by reduction with calcium metal in an evacuated glass tube: $2MCl+Ca \rightarrow 2M+CaCl_2$

1) M. Tsuda, and H. Inokuchi, This Bulletin, **43**, 3410 (1970).

2) T. Kondow, H. Inokuchi and N. Wakayama, *J. Chem. Phys.*, **43**, 3766 (1965); H. Inokuchi, N. Wakayama, T. Kondow and Y. Mori, *ibid.*, **46**, 837 (1967).

3) H. Inokuchi, Y. Mori and N. Wakayama, *J. Catalysis*, **8**, 288 (1967).

4) M. Tsuda, H. Inokuchi and H. Suzuki, *J. Phys. Chem.*, **73**, 1595 (1969).

*3 The chemisorption mechanism and exchange mechanism proceed by way of a hydrogen-deuterium equilibration over the catalyst and by way of an exchange reaction between gaseous deuterium and the hydrogen atom of the aromatic anion respectively.

para-orthohydrogen conversion (p-$H_2 \rightleftarrows o$-H_2) and the deuterium-exchange reaction ($D_2+H\text{-}\phi \rightleftarrows HD+D\text{-}\phi$) were employed.

Hydrogen Conversion and Deuterium-Exchange Reaction. The kinetic analysis of these two reactions was done over the temperature range from 0°C to 80°C under a constant pressure of hydrogen (100 Torr). The rate constant, k_e^H, for the hydrogen conversion was found to obey a first-order law, as has been shown in Part I. The rate constant for the deuterium exchange reaction, k_e^D, obeys a first-order law for a fresh sample (curve a in Fig. 1), but the value of k_e^D for the salt washed with hydrogen seems to deviate a first-order law (curve b in Fig. 1). In the Fig. 1, where the progression of the decay of deuterium on the ion radical salt is plotted against the reaction time, a sharp kink is found at the initial stage (region I of curve b) of the reaction. This behaviour suggests that both the two different mechanisms for hydrogen exchange occur on the hydrogen-exposed ion radical salt.*4

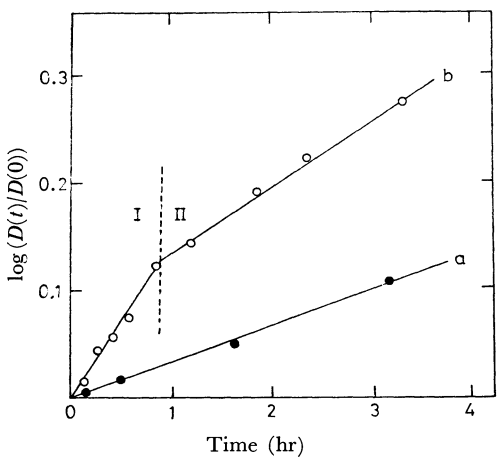

Fig. 1. The progression of deuterium exchange reaction with the benzonitrile-cesium ion radical salt.
—●— for fresh film
—○— for hydrogen exposed film

The progression of the reaction on the fresh salt was similar to that of the later stage (region II of curve b) of the reaction on hydrogen-exposed film. Therefore, the rate constant for the deuterium exchange reaction was obtained from the analysis of the reaction of region II of curve b at various temperatures, as is shown in Fig. 2 (see "Discussion").

*4 Whenever the deuterium-exchange reaction was carried out over the salt, the species were washed with hydrogen gas completely in advance in order to eliminate the exchanged and/or chemisorbed deuterium of the proceeding reaction from the salt, and the hydrogen was evacuated for about 3 hr.

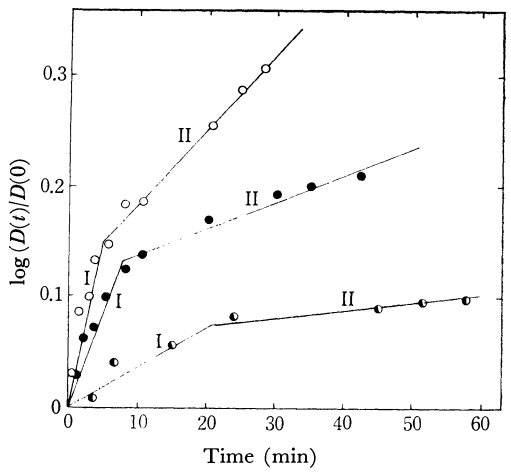

Fig. 2. The progression of deuterium exchange reaction with the benzonitrile-cesium metal film as a function of temperature.
—○— at 80°C
—●— at 60°C
—◐— at 40°C

Table 1. Activation energy for benzonitrile-alkali-metal ion radical salts

Donor metal	E^H (kcal/mol)	E^D (kcal/mol)
Na	8.2	12.7
K	6.6	9.3
Rb	5.5	7.1
Cs	10.2	14.3

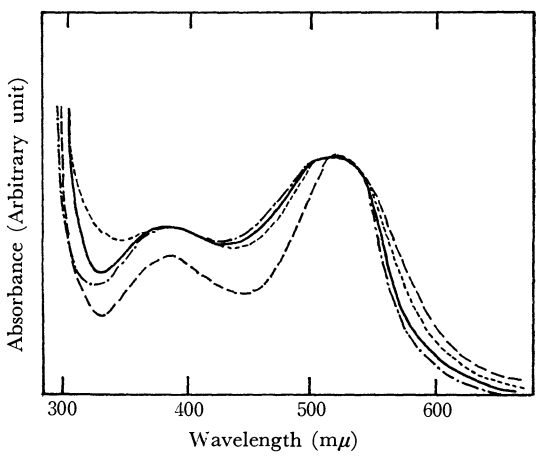

Fig. 3. Electronic spectra of benzonitrile-alkali metal ion radical salt in benzonitrile solvent as sorts of donor metals.
——— Sodium salt
— — — Potassium salt
——— Rubidium salt
----- Cesium salt

From the temperature dependency (0°C—80°C) of k_e^H and k_e^D for the benzonitrile-alkali metal ion

radical salts under a constant pressure (100 Torr), the activation energies for four alkali metal ion radical salts were obtained; they are summarized in Table 1.

Spectroscopic Survey. The results presented in the previous section show that the catalytic activity of the salt is greatly affected by a variation in the component—alkali metal. These findings suggest that the electronic state of the ion radical salt is influenced by the change in the donor metals. Figure 3 shows the electronic spectra of the benzo-

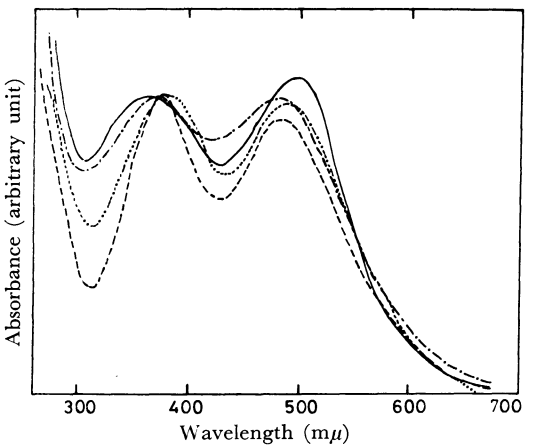

Fig. 4. Electronic spectra of solid film of benzonitrile-alkali metal ion radical salt as sorts of donor metals.
- · · · — Sodium salt
- — — Potassium salt
- ——— Rubidium salt
- ----- Cesium salt

nitrile solutions of the above four ion radical salts while Fig. 4 illustrates the patterns for their solid films. The spectral responses of the salt solutions resembled those of the benzonitrile mononegative ion reported by Ishitani and Nagakura.[5] The sort of donor metals in the salt solution did not strongly affect the response curve. For the solid films, however, the positions of the absorption peaks and also their extinction coefficients changed as a function of the donor metals. As the atomic weight of the alkali metals increased, the 380 mμ absorption peak shifted to the longer-wavelength side and the 480 mμ absorption peak shifted to the shorter-wavelength side. Moreover, the ratio of the extinction coefficient of the 380 mμ-peak to that of the 480 mμ-peak decreased.

Discussion

In the studies of the catalytic behaviour of the ion radical salts, the mechanism has often been interpreted in terms of the nature of the acceptor molecules[6,7]—aromatics. Among the various types of aromatic complexes,[8,9] however, only the aromatic-alkali metal (or alkali earth metal) ion radicals show catalytic activity in relation to hydrogen-deuterium equilibration. This suggests that the donor metal plays an important role in the reactivity of the ion radical salt. Therefore, we will discuss the relation between the catalytic activity and the sort of alkali metal in the salt.

First, the mechanism of the deuterium-exchange reaction on the hydrogen-exposed film will be discussed. Then, the role of the donor metal in the catalytic activity of the salt will be investigated. Finally, the electronic state of the salt is surveyed by means of the spectroscopical method.

Deuterium-Exchange Reaction. As has been mentioned in the section on "Results," two different mechanisms for deuterium exchange occur on the hydrogen-exposed ion radical salt. These mechanisms may be supposed to be as follows. One is that deuterium gas (D_2) exchanges with chemisorbed hydrogen ($\overset{*}{H}$) [Mechanism A]. The other is that deuterium gas chemisorbs on the salt surface ($D_2+2*\rightarrow 2\overset{*}{D}$), and that the chemisorbed deuterium ($\overset{*}{D}$) exchanges with the hydrogen of the aromatic anion (H-ϕ) and that the chemisorbed hydrogen thus produced reacts with D_2 ($\overset{*}{D}+$ H-$\phi\rightarrow\overset{*}{H}+$D-$\phi$; $D_2+\overset{*}{H}\rightarrow HD+\overset{*}{D}$) [Mechanism B].

The procedures are illustrated as:

$$D_2 + \overset{*}{H} \rightarrow HD + \overset{*}{D} \qquad \text{[Mechanism A]*5}$$

$$\left.\begin{aligned} &D_2 + 2* \rightarrow 2\overset{*}{D} \\ &\overset{*}{D} + H\text{-}\phi \rightarrow \overset{*}{H} + D\text{-}\phi \\ &D_2 + \overset{*}{H} \rightarrow HD + \overset{*}{D} \end{aligned}\right\} \qquad \text{[Mechanism B]*5}$$

It is assumed that the rate-determining process for the initial stage (region I of curve b in Fig. 1) of the exchange reaction is "Mechanism A," and that for the later stage (region II of curve b in Fig. 1) is the chemisorption of deuterium on the complex salt ($D_2+2*\rightarrow 2\overset{*}{D}$) of "Mechanism B." The above assumptions require that the deuterium exchange on the fresh sample occur through Mechanism B (curve a in Fig. 1). The fact that the region II of curve b (Fig. 1) has a similar inclination to that of curve a for the fresh sample supports this assumption. Therefore, in order to obtain

5) A. Ishitani and S. Nagakura, *Theoret. Chem. Acta*, **4**, 236 (1966).

6) M. Ichikawa, M. Soma, T. Onishi and K. Tamaru, *Trans. Faraday Soc.*, **63**, 997, 2528 (1967).

7) N. Wakayama and H. Inokuchi, *J. Catalysis*, **11**, 143 (1968).

8) H. Inokuchi, M. Tsuda and T. Kondow, *ibid.*, **8**, 91 (1967).

9) M. Tsuda, T. Kondow, H. Inokuchi and H. Suzuki, *ibid.*, **11**, 81 (1968).

*5 Here, * indicates a site of salt for chemisorption.

the rate constant for deuterium exchange with the hydrogen of the aromatic anion over the hydrogen-exposed salt film, the behaviour in the region II must be adopted.

The Role of the Donor Metal in the Catalytic Activity. As has been described in previous papers,[1-4] there are two processes which occur over the complexes: the chemisorption mechanism and the exchange mechanism. The para-ortho-hydrogen conversion (its rate constant: k_e^H) takes place through both these mechanisms,*6 but the deuterium-exchange reaction (the rate constant: k_e^D) takes place only through the exchange mechanism. The ratio k_e^H/k_e^D,*7 therefore, indicates the quantity of the contribution of the chemisorption mechanism to the hydrogen conversion. When we introduce the value of $\alpha(k_e^H/k_e^D=\alpha I_{HD}$, where I_{HD} is as described in the Appendix), we can eliminate the hydrogen-deuterium isotope effect on the exchange reaction. Accordingly, the value of α is unity when the hydrogen conversion takes place through only the exchange mechanism, and the increasing value of α shows the increasing contribution of the chemisorption mechanism to the hydrogen conversion. The experimentally-determined values were about 1—10[2]. The α-values are plotted against the reciprocal of the temperature for each alkali metal ion radical salt in Fig. 5. This behaviour shows that the contribution of the chemisorption mechanism to the hydrogen conversion increases as the temperature decreases.

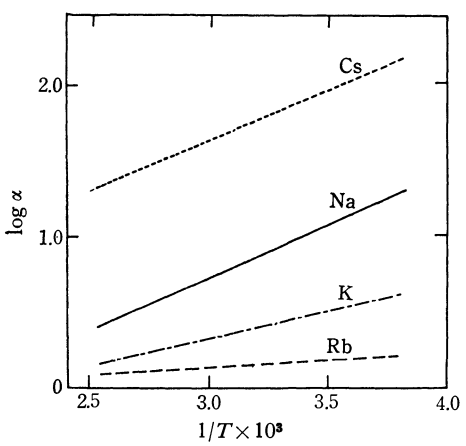

Fig. 5. log α is ploted as a function of temperature.
——— for benzonitrile-Na complex
— — — for benzonitrile-K complex
———— for benzonitrile-Rb
----- for benzonitrile-Cs

From Table 1 and Fig. 5, two parameters for the reactivity of the salt—the activation energy, E^H and E^D, and the α-value—seem to be influenced by the sort of donor metal in the salt. In this section, therefore, the catalytic activity (E and α) of the ion radical salt will be discussed as a function of alkali metals—Na, K, Rb and Cs. The nature of the alkali metals—the ionization potential, the electron affinity, the ion radius and so on—changes monotonously with their atomic numbers. Among these characteristics, the cation radius of the alkali metal is adopted as a parameter for the reactivity for two reasons. An ESR study of the ion radical salt has shown that the cation radius correlates with the magnitude of the alkali metal splittings and with that of the spin density at the carbon of the aromatic anion.[10] Further, the location of the metal cation in the salt crystal or the interionic separation depends on the metal ion radius.

The activation energies, E^H and E^D, are first compared with the cation radius. Figure 6 shows the values of E^H and E^D plotted as functions of the cation radius. There is a regular trend for the E^H and E^D values to decrease with an increase in the size of the metal cations with the exception of cesium-benzonitrile ion radical salt. Similar phenomena are observed in the relation between the value of α and the ion radius, as is illustrated in Fig. 7. The value of α decreases in this order: Na→K→Rb, but for the Cs salt the value shows an irregular tendency.

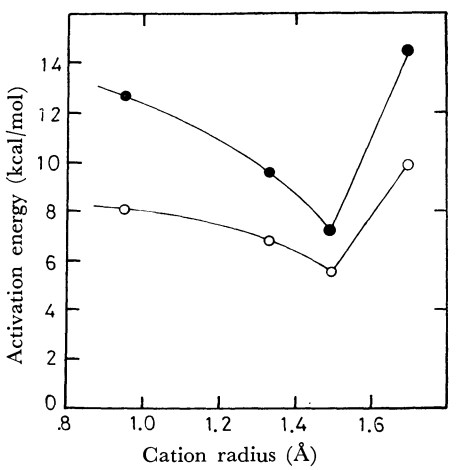

Fig. 6. Activation energies E^H for para-ortho-hydrogen conversion and E^D for deuterium exchange reaction plotted against the size of ion radius of donor metals.
—○— for E^H
—●— for E^D

*6 The contribution of the paramegnetic mechanism to the ortho-parahydrogen conversion is negligible.

*7 As the rate constants, k_e^H and k_e^D, are studied with relation to the same specimen, the two surface areas, S^H and S^D, may be assumed to be equivalent (see Eq. (3a) and (3b) in Part I). Therefore, the ratio (k_e^H/k_e^D) includes only A (enthropy factor) and E (activation energy) belongs to the nature of the catalyst.

10) N. Hirota, *J. Amer. Chem. Soc.*, **90**, 3603 (1968); N. Hirota, R. Carraway and W. Schook, *ibid.*, **90**, 3611 (1968).

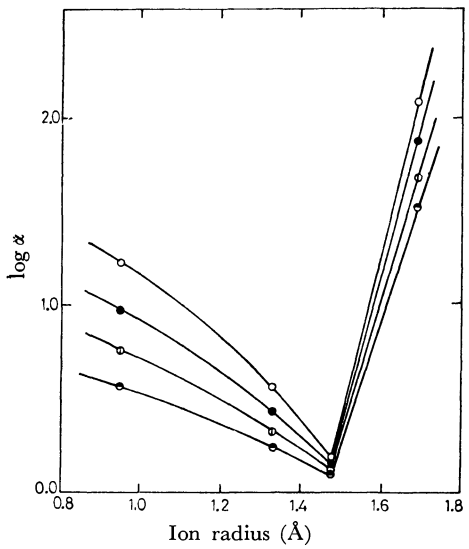

Fig. 7. log α ploted against the size of ion radius of donor metals at a various temperature.
—○— 0°C
—●— 30°C
—◑— 60°C
—◓— 90°C

Mori *et al.*[11] proposed that the reactivity of the ion radical salt could be understood from the ionization potential of the donor metals. The present result does not, however, support their assumption.

As the activation energy and the α-value show a monotonous tendency to change in the orders: Na→K→Rb, the reactivity of the ion radical salt seems to be influenced by the metal-cation field. However, the irregularity in the cesium ion radical salt suggests that the reactivity of the salt can not be understood only in terms of the nature of the donor metals; also, the nature of the salt in the solid phase must be taken into consideration. To analyze the nature of the salt in the solid phase, the crystal structure must be considered, but the structure of the benzonitrile-alkali metal ion radical salt has not yet been reported.

Sometimes, the crystal structure of ion radical salts changes with the kind of their donor metal; for instance, the structure of *p*-chloranil-alkali metal salt shows a difference between the Li (or Na)-salt and the K (or Rb)-salt.[12] Accordingly, the crystal structure of the benzonitrile ion radical salt must be studied in order to ascertain the mechanism of the catalytic reaction.

Spectroscopical Analysis

Figure 3 illustrates that the patterns of the spectral response of the ion radical salt solutions scarcely change at all with the kind of metal cation. In the solution, the salt is stable as a free-anion or a loose-ion pair, as has been established by Carrington and Todd.[13] Therefore, the spectra of the ion radical salt in a solution is almost the same as that of a free anion. On the other hand, the spectral response curves of the solid film (illustrated as Fig. 4) vary with the kind of alkali metal. The interionic separation in the solid ion radical salt would be smaller than that in solution, and the perturbation of the neighbouring ionic field seems to affect the electronic state of the aromatic anion strongly. Figure 6 shows that the metal dependency of the parturbation increases monotonously in this order: Na<K<Rb, and the Cs salt seems to be tremendously perturbed compared with the other three metal salts. As a tentative explanation for these irregularities, it is assumed that the Cs-benzonitrile ion radical salt has a unique structure, because the cesium ion, Cs^+, has an enormously large ion radius as comparison with those of the other alkali metal cations.

The author wishes to express his thanks to Professor H. Inokuchi for his valuable advice, his many stimulating discussion, and his reading of the manuscript. He also wishes to express his thanks to Dr. N. Wakayama and Dr. Y. Mori for their helpful discussion.

Appendix

As shown in Part I, the rate constant, k_e^H, for the hydrogen conversion and that, k_e^D, for the deuterium-exchange reaction are expressed as:

$$k_e^H = S^H A^H \exp(-E^H/\boldsymbol{k}T) \quad \text{(A1)}$$

$$k_e^D = S^D A^D \exp(-E^D/\boldsymbol{k}T) \quad \text{(A2)}$$

The ratio between k_e^H and k_e^D can be described as:

$$\frac{k_e^H}{k_e^D} = \alpha I_{HD} \quad \text{(A3)}$$

where I_{HD} is the kinetic isotope effect in the activated complex and is given as a function of the temperature:

$$I_{HD} = I_0 \exp(-\varepsilon/\boldsymbol{k}T) \quad \text{(A4)}$$

I_0 and ε have the following values:[14,15] Theoretically $I_0=1.15$ and $\varepsilon=1.08$ kcal/mol, and experimentally $I_0=1.10$ and $\varepsilon=1.3$ kcal/mol. From Eqs. (A1)—(A4), α is given as;

$$\alpha = \frac{1}{I_0}\frac{A^H}{A^D}\exp\left(-\frac{E^H-E^D-\varepsilon}{\boldsymbol{k}T}\right), \quad \text{(A5)}$$

assuming that the surface areas, S^H and S^D, are equivalent. Thus, the value of α of Eq. (A5) can be estimated experimentally.

11) Y. Mori, N. Wakayama and H. Inokuchi, *J. Catalysis*, **14**, 1 (1969).
12) I. Shirotani and N. Sakai, private communication.
13) A. Carrington and P. F. Todd, *Mol. Phys.*, **6**, 161 (1963).
14) K. B. Wiberg and E. L. Motell, *Tetrahedron*, **19**, 2009 (1963).
15) W. K. Wilmarth Jr., and C. F. Baes, *J. Chem. Phys.*, **20**, 116 (1952).

BULLETIN OF THE CHEMICAL SOCIETY OF JAPAN VOL. 43 3420—3424 (1970)

Determination of Ion Activity Coefficients from the Measurement of Membrane Concentration Potentials—Activity Behavior of Alkali-metal Cations in Aqueous Solutions at 25°C

Reita TAMAMUSHI

The Institute of Physical and Chemical Research, Yamato-machi, Kita-adachi-gun, Saitama

and Shojiro GOTO*

Department of Physics and Chemistry, Gakushuin University, Tokyo

(Received July 2, 1970)

The membrane concentration potentials across a permselective sulfonated polystyrene collodion-base membrane were measured with aqueous solutions of alkali-metal salts at 25.0°C. By assuming the ideal behavior of the membrane, the activity coefficients of the critical cations were determined from the membrane concentration potentials at ionic strengths higher than 0.01. The ion activity coefficients of alkali-metal cations were found to follow the order $Li^+ > Na^+ > K^+$ for the chlorides, nitrates, perchlorates, and sulfates. The order of activity coefficients of Na^+ in different halide solutions was bromide > chloride > fluoride. Considerable differences were observed between the individual and mean activity coefficients at ionic strengths higher than 0.01. The individual ion activity coefficients determined from the experimental data were analysed by means of the extended Debye-Hückel equation.

The application of permselective membranes, *i.e.*, membranes of highest ionic selectivity and high permeability, to the determination of ion activities has been suggested and demonstrated by Sollner and his collaborators.[1-3] Among various ion-selective membranes, some of them being available on market, Sollner's permselective collodion-base membranes seem to be the best for theoretical activity studies because of their ideal characteristics over a considerable range of concentration.

This study deals with the measurement of membrane concentration potentials with aqueous solutions of some alkali-metal salts across a permselective sulfonated polystyrene collodion-base membrane, and shows the applicability of the method to the study of ion activity behavior. The individual activity coefficients of the critical cations determined from the membrane concentration potentials will be discussed on the basis of theoretical activity equations.

Experimental

Permselective Sulfonated Polystyrene Collodion-base Membrane. Test-tube-shaped sulfonated polystyrene collodion-base membranes were prepared by the method proposed by Sollner and Neihof,[4,5] and a membrane of the best quality was employed throughout this study. The ohmic resistance of the membrane, being measured in a 0.1 M potassium chloride solution at 1000 Hz, was 50 ohms cm^2. The ionic selectivity of the membrane was examined by measuring the rates of exchange of critical and non-critical ions across the membrane.[5,6] The anion leak after five hours was found to be less than 0.5% of actual cation movement in a 0.5 M KNO_3/membrane/0.5 M NH_4Cl system whose bi-ionic potential was about 5.2 mV.

Solutions. All solutions were made from analytical reagent grade chemicals and redistilled water.

Measurement of Membrane Concentration Potentials. For the determination of membrane concentration potentials, the electromotive force of a cell,

SCE(I)/sat. KCl-agar bridge/soln. (c)/membrane/
soln. (c')/salt. KCl-agar bridge/SCE(I') (1)

was measured by a precision potentiometer (Model P-1, Yokogawa Electric Works). The concentration ratio $c : c' = 2 : 1$ was used. In each experimental run, the solutions were renewed after 20 min from the

* Present address: Research Div., Research Laboratory, Asahi Glass Co., Ltd., Hazawa-cho, Kanagawa-ku, Yokohama.

1) K. Sollner, *Ann. N. Y. Acad. Sci.*, **57**, 177 (1953).

2) K. Sollner, S. Dray, E. Grim and R. Neihof, "Ion Transport Across Membranes," ed. H. T. Clarke, Academic Press, New York (1954), p. 144.

3) K. Sollner, *Ann. N. Y. Acad. Sci.*, **148**, 154 (1968).

4) K. Sollner and R. Neihof, *Arch. Biochem. Biophys.*, **33**, 166 (1951).

5) R. Neihof, *J. Phys. Chem.*, **58**, 916 (1954).

6) H. P. Gregor and K. Sollner, *ibid.*, **50**, 53 (1946).

construction of the cell, and then several readings of the electromotive force were made at a 10 min-interval. Stable electromotive forces were established within 10 min with the membrane which had been saturated with the critical ions by prior ion exchange. The reproducibility of the individual measurements was better than ± 0.05 mV, except at the ionic strengths lower than 0.01. All measurements were carried out in a a water thermostat of 25.0 ± 0.1°C.

Results and Discussion

The electromotive force, E, of the concentration cell represented by (1) is given by

$$E = E_M + \Delta E_{SCE} + E_L \qquad (2)$$

where E_M is the membrane concentration potential, ΔE_{SCE}, the asymmetry of electrode potentials of the two saturated calomel electrodes, and E_L, the sum of liquid junction potentials at sat. KCl-agar bridge/soln. (c) and soln. (c')/sat. KCl-agar bridge. In order to obtain the membrane concentration potential from the raw experimental data, the electromotive force of the cell should be corrected for ΔE_{SCE} and E_L.[3] The value of ΔE_{SCE} was determined directly from the electromotive force measurement of a cell, SCE (I)/sat. KCl-agar bridge/sat. KCl/sat. KCl-agar bridge/SCE (I'), while the liquid junction potentials were calculated by using Henderson's equation[7] and ionic mobility data. The accuracy of E_M thus obtained is considered to be of the order of ± 0.1 mV because of the uncertainty in estimating liquid junction potentials. Table 1 presents the membrane concentration potentials with aqueous solutions of alkali-metal salts at various concentrations.

The following analysis of the membrane concentration potentials is based upon the assumption of virtually ideal selectivity of the membrane. The extremely small leak of anions across the membrane provides a strong evidence to support the fulfilment of this assumption in the present systems.

Theoretically, the membrane concentration potential of a concentration chain, soln. (c)/membrane/soln. (c'), with an ideal negative membrane is given by a Nernst-type equation,

$$E_M = \frac{RT}{z_+F} \ln \frac{a_+}{a_+'} = \frac{RT}{z_+F}\left(\ln \frac{c_+}{c_+'} + \ln \frac{y_+}{y_+'}\right) \qquad (3)$$

where z_+, a_+, c_+ and y_+ are the valency, activity, molar concentration, and activity coefficient on the molarity basis, respectively, of the critical cation. Thus the ratio of activity coefficients of the critical cation at two different concentrations, c and c', can be determined from the membrane concentration potential:

$$\ln \frac{y_+}{y_+'} = \frac{z_+F}{RT} E_M - \ln \frac{c_+}{c_+'} \qquad (4)$$

Figures 1—5 show the experimental relationship between log (y_+/y_+^{st}) and $I^{1/2}$, where I is the ionic strength on the molarity scale, y^+, the ion activity coefficient at a given value of I, and y_+^{st}, the ion activity coefficient at the ionic strength I^{st} chosen for standard; in the present study, I^{st} being equal to 0.01 for 1 : 1 electrolytes and 0.015 for 1 : 2 electrolytes, respectively. The behavior of mean ionic activity coefficients, $y_\pm$, of the salts[8] is also

Table 1. Membrane concentration potentials, E_M (mV),* with aqueous solutions of alkali-metal salts across the permselective sulfonated polystyrene collodion-base membrane at 25.0°C
(Concentration ratio, $c : c' = 2 : 1$)

Salt	$c : c'$ (M)							
	0.01: 0.005	0.02: 0.01	0.04: 0.02	0.08: 0.04	0.16: 0.08	0.32: 0.16	0.64: 0.32	1.28: 0.64
LiCl	16.8**	16.3**	16.5	16.7	16.5	16.6	17.0	17.5
NaCl	16.9**	16.6	16.6	16.4	16.2	16.0	16.1	16.1
KCl	16.7**	16.6	16.5	16.2	15.9	15.2	15.0	14.3
NaF	16.2**	16.4**	16.4	16.2	15.9	15.4	14.7	—
NaBr	17.0**	16.8	16.5	16.6	16.3	16.4	16.4	16.7
$LiNO_3$	16.7**	16.4**	16.9	17.0	17.2	17.7	18.5	19.9
$NaNO_3$	16.9**	16.8	16.8	16.4	16.4	16.1	15.6	14.6
KNO_3	16.8**	16.6	16.6	15.8	15.8	14.6	13.4	11.6
$NaClO_4$	16.8**	16.8**	16.7	16.6	16.4	—	—	—
$KClO_4$	17.0**	17.0	16.1	15.8	—	—	—	—
Na_2SO_4	16.4	16.3	16.0	15.8	15.4	14.9	14.1	—
K_2SO_4	16.1**	16.1	16.0	15.6	15.1	14.5	—	—

* Corrected for ΔE_{SCE} and E_L; accuracy, ± 0.1 mV.
** Accuracy, ± 0.2 mV.

7) D. A. MacInnes, "The Principles of Electrochemistry," Reinhold, New York (1939), Chap. 13.

shown in the figures for comparison. The data at ionic strengths below 0.01 are not subject to the discussion because of their relatively low accuracy.

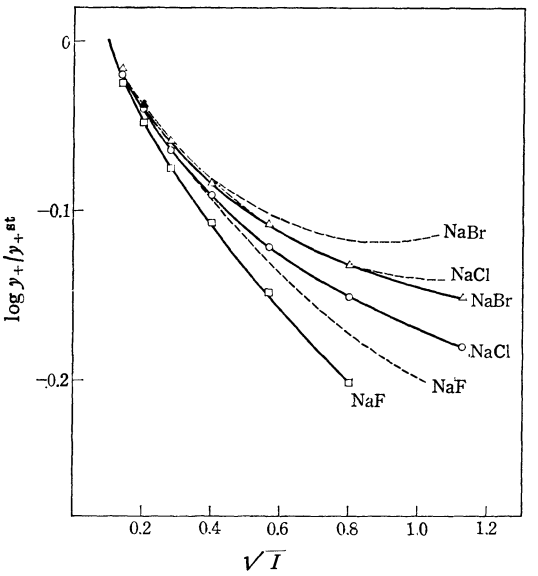

Fig. 1. Behavior of individual and mean activity coefficients with changing ionic strength at 25.0°C: solid lines for $\log(y_+/y_+^{st})$ and broken lines for $\log(y_\pm/y_\pm^{st})$; —□— (NaF), —○— (NaCl), —△— (NaBr). The ionic strength chosen for standard: $I^{st}=0.01$.

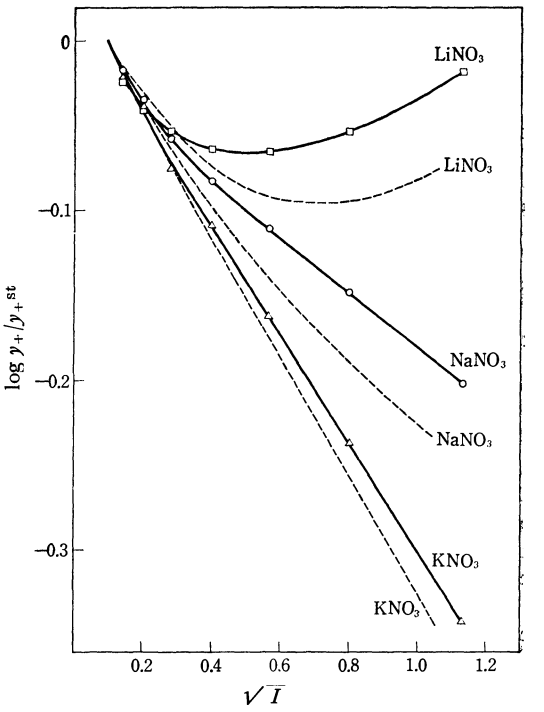

Fig. 3. Behavior of individual and mean activity coefficients with changing ionic strength at 25.0°C: solid lines for $\log(y_+/y_+^{st})$ and broken lines for $\log(y_\pm/y_\pm^{st})$; —□— ($LiNO_3$), —○— ($NaNO_3$), —△— (KNO_3). The ionic strength chosen for standard: $I^{st}=0.01$.

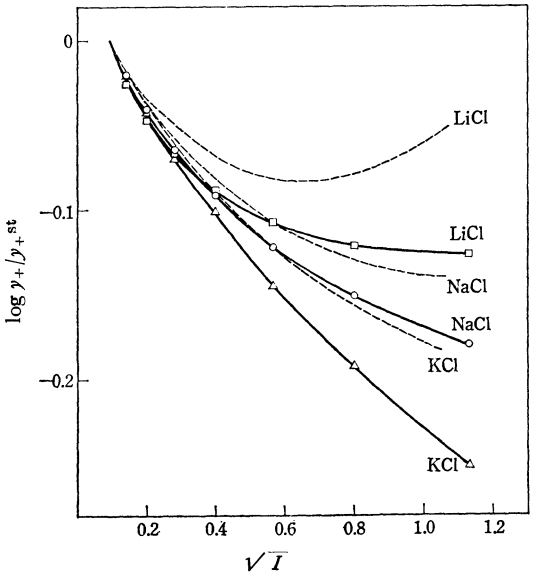

Fig. 2. Behavior of individual and mean activity coefficients with changing ionic strength at 25.0°C: solid lines for $\log(y_+/y_+^{st})$ and broken lines for $\log(y_\pm/y_\pm^{st})$; —□— (LiCl), —○— (NaCl), —△— (KCl). The ionic strength chosen for standard: $I^{st}=0.01$.

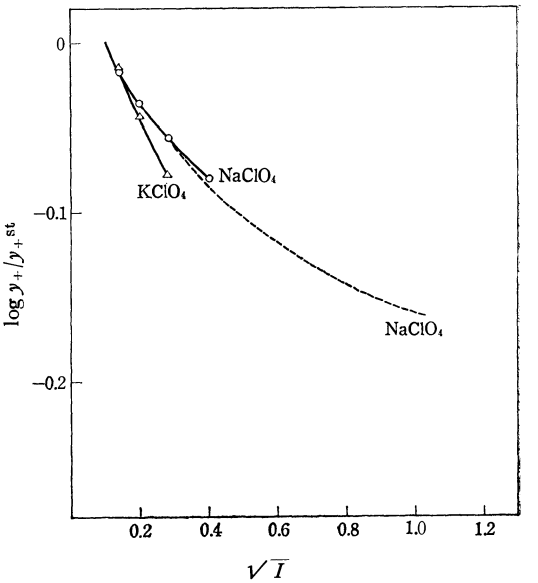

Fig. 4. Behavior of individual and mean activity coefficients with changing ionic strength at 25.0°C: solid lines for $\log(y_+/y_+^{st})$ and broken lines for $\log(y_\pm/y_\pm^{st})$; —○— ($NaClO_4$), —△— ($KClO_4$). The ionic strength chosen for standard: $I^{st}=0.01$.

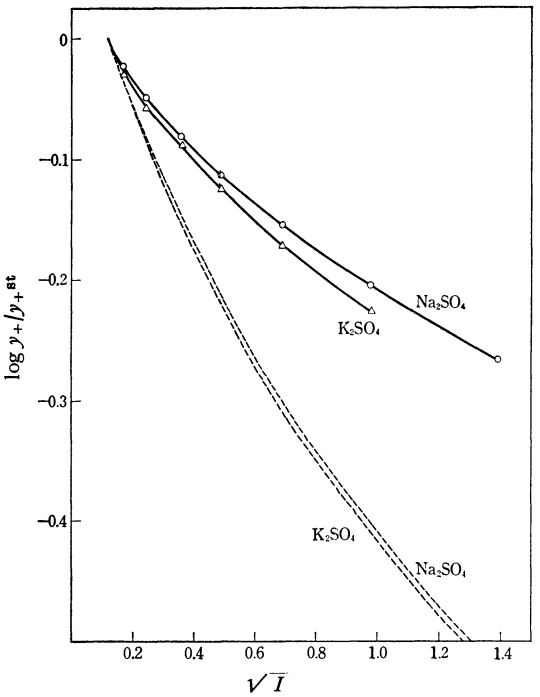

Fig. 5. Behavior of of individual and mean activity coefficients with changing ionic strength at 25.0°C: solid lines for $\log(y_+/y_+^{st})$ and broken lines for $\log(y_\pm/y_\pm^{st})$: —○— (Na_2SO_4), —△— (K_2SO_4). The ionic strength chosen for standard: $I^{st}=0.015$.

From these figures the following remarks can be made about the behavior of the individual ion activity coefficients with changing ionic strength.

(i) The individual activity coefficient curves of the cations follow the order of $Li^+>Na^+>K^+$ for the chlorides, nitrates, perchlorates, and sulfates. The order of the curves for Na^+ of different halides is bromide>chloride>fluoride. These sequences are consistent with those observed for the mean ionic activity coefficients of alkali-metal salts.[9]

(ii) Considerable differences between the individual and mean activity coefficients arise at ionic strengths higher than 0.01, which indicates the specific effect of individual ions on their activity behavior.

The determination of individual ion activity coefficients requires the introduction of a non-thermodynamic assumption. The activity coefficients of the critical cations at relatively low ionic strengths ($I\lesssim 0.01$) can be given with reasonable accuracy by the Debye-Hückel equation (5),

$$\log y_+ = \frac{-z_+^2 A\sqrt{I}}{(1+Ba_+^\circ\sqrt{I})} \tag{5}$$

where A and B are the Debye-Hückel constants, and a_+° is the ion-size parameter. Estimating y_+^{st} by Eq. (5) with suitable values of a_+°, we can determine the individual activity coefficients of the critical cations at higher ionic strengths from the experimental data according to the following relation,

$$\log y_+ = \log\frac{y_+}{y_+^{st}} - \frac{z_+^2 A\sqrt{I^{st}}}{(1+Ba_+^\circ\sqrt{I^{st}})} \tag{6}$$

The numerical values used in the calculation are as follows: $A=0.5116$ and $B=0.3292\times 10^8$ on the molarity basis at 25°C; $a_+^\circ=6$, 4.5 and 3 (10^{-8} cm) for Li^+, Na^+ and K^+, respectively.[10] The individual ion activity coefficients, y_+, of Li^+, Na^+ and K^+ thus obtained for various salts are summarized in Table 2. The uncertainty in the y_+-values is estimated to be ±1%.

In most cases the deviation of the experimentally determined activity coefficients, y_+, from the Debye-Hückel values, $(y_+)_{DH}$, calculated by Eq. (5) increases with increasing ionic strength as shown in Fig. 6. It is expected that the experimental

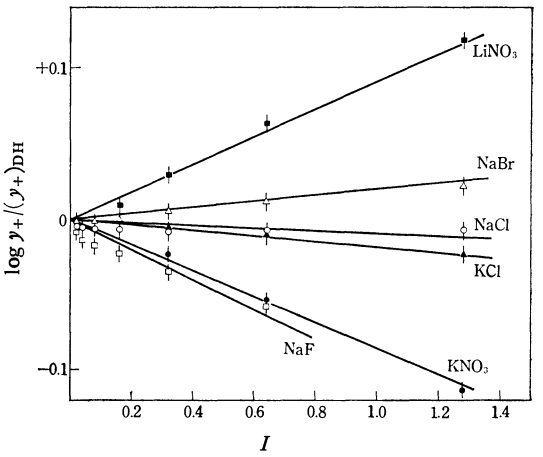

Fig. 6. Deviation of the experimentally determined activity coefficients, y_+, from the Debye-Hückel values, $(y_+)_{DH}$, as a function of ionic strength: —□— (NaF), —○— (NaCl), —△— (NaBr), —▲— (KCl), —●— (KNO_3), —■— ($LiNO_3$).

results at higher ionic strengths can be reproduced with smaller deviations by using the extended Debye-Hückel equation (7) with a linear term,

$$\log y_+ = \frac{-z_+^2 A\sqrt{I}}{(1+Ba_+^\circ\sqrt{I})} + b_+ I \tag{7}$$

8) For example: R. Parsons, "Handbook of Electrochemical Constants," Table 19, Butterworths, London (1959).

9) R. A. Robinson and R. H. Stokes, "Electrolyte Solutions," Butterworths, London (1965), p. 219.

10) G. Kortüm and J. O'M. Bockris, "Textbook of Electrochemistry," Vol. II, Elsevier, Amsterdam (1951), p. 680.

Table 2. Individual activity coefficients of the critical cations in aqueous solutions of alkali-metal salts at different concentrations (25.0°C)

Salt	Concn. (M)								
	0.005	0.01	0.02	0.04	0.08	0.16	0.32	0.64	1.28
LiCl	—	0.91* (0.91)	0.86 (0.88)	0.81 (0.85)	0.78 (0.81)	0.74 (0.77)	0.71 (0.73)	0.69 (0.69)	0.68 (0.66)
NaCl	—	0.90* (0.90)	0.86 (0.87)	0.82 (0.83)	0.78 (0.79)	0.73 (0.74)	0.68 (0.69)	0.64 (0.64)	0.60 (0.59)
KCl	—	0.90* (0.90)	0.86 (0.86)	0.82 (0.82)	0.77 (0.77)	0.71 (0.71)	0.64 (0.64)	0.58 (0.57)	0.50 (0.50)
NaF	—	0.90* (0.90)	0.85 (0.87)	0.81 (0.83)	0.76 (0.78)	0.71 (0.72)	0.64 (0.65)	0.57 (0.56)	—
NaBr	—	0.90* (0.90)	0.87 (0.87)	0.82 (0.83)	0.79 (0.79)	0.74 (0.76)	0.70 (0.71)	0.67 (0.67)	0.64 (0.65)
$LiNO_3$	—	0.91* (0.91)	0.86 (0.88)	0.83 (0.85)	0.80 (0.82)	0.78 (0.80)	0.78 (0.78)	0.80 (0.79)	0.87 (0.86)
$NaNO_3$	—	0.90* (0.90)	0.87 (0.87)	0.83 (0.83)	0.79 (0.79)	0.75 (0.74)	0.70 (0.69)	0.64 (0.63)	0.57 (0.57)
KNO_3	—	0.90* (0.90)	0.86 (0.86)	0.82 (0.82)	0.76 (0.76)	0.70 (0.69)	0.62 (0.61)	0.52 (0.52)	0.41 (0.41)
$NaClO_4$	—	0.90*	0.87	0.83	0.79	0.75	—	—	—
$KClO_4$	—	0.90*	0.87	0.81	0.75	—	—	—	—
Na_2SO_4	0.89* (0.89)	0.84 (0.85)	0.79 (0.80)	0.74 (0.75)	0.68 (0.70)	0.62 (0.63)	0.55 (0.56)	0.48 (0.47)	—
K_2SO_4	0.88* (0.88)	0.82 (0.84)	0.77 (0.79)	0.72 (0.73)	0.66 (0.66)	0.59 (0.59)	0.52 (0.51)	—	—

* $y_{\pm}^{st}$ determined by Eq. (5) with the ion-size parameters given in Table 3.
The values in parentheses are the activity coefficients calculated by Eq. (7) with the parameters given in Table 3.

Table 3. Ion-size parameter, $a_+°$, and b_+-parameter of the extended Debye-Hückel equation (7) for the critical cations of various salts (25°C)

Critical cation	Salt	$10^8 a_+°$ (cm)*	b_+**	Range of I examined
Na^+	NaF	4.5	−0.10	0.01—0.64
	NaCl		−0.01	0.01—1.28
	NaBr		+0.02	0.01—1.28
	$NaNO_3$		(−0.02)***	0.01—1.28
	$NaClO_4$		****	0.01—0.16
	Na_2SO_4		−0.05	0.015—1.92
K^+	KCl	3.0	−0.02	0.01—1.28
	KNO_3		−0.09	0.01—1.28
	$KClO_4$		****	0.01—0.08
	K_2SO_4		−0.04	0.015—0.94
Li^+	LiCl	6.0	(0)***	0.01—1.28
	$LiNO_3$		+0.09	0.01—1.28

* Assumed.
** Determined from the plot of $[\log y_+ - \log(y_+)_{DH}]$ *vs.* I.
*** The $[\log y_+ - \log(y_+)_{DH}]$ *vs.* I plot was not linear.
**** Not determined because of a narrow range of I.

where b_+ is another adjustable parameter. Rough estimates of parameters b_+ for each cation of given salts were obtained from the slope of the plot of $[\log y_+ - \log (y_+)_{DH}]$ against I (Fig. 6), and are presented in Table 3.

The individual ion activity coefficients calculated by Eq. (7) with $a_+°$- and b_+-parameters given in Table 3 are presented in parentheses in Table 2. The agreement between the experimental and calculated values is reasonable except for the LiCl-system in which an appreciable deviation of the $[\log y_+ - \log (y_+)_{DH}]$ *vs.* I plot from linearity was observed. A better fit may be expected by adjusting both parameters, $a_+°$ and b_+; such a trial, however, will be meaningless unless more accurate data are available for analysis.

BULLETIN OF THE CHEMICAL SOCIETY OF JAPAN VOL. 43 3425—3434 (1970)

Chemi-ionization of Cs*($8^2P_{1/2}$) with Cs and Foreign Gases

Yoko ONO, Inosuke KOYANO, Yuji MORI and Ikuzo TANAKA

Laboratory of Physical Chemistry, Tokyo Institute of Technology, Ohokayama, Meguro-ku, Tokyo

(Received July 2, 1970)

Chemi-ionization has been studied by the collision of the excited atom of cesium ($8^2P_{1/2}$), whose energy is lower by 0.7 eV than its ionization energy, with cesium, rare gases or simple molecules. The mechanisms for the chemi-ionization, and quenching processes occurring simultaneously were set up and the cross sections of the processes have been determined. Since the pressure effects of added gases to the absorption coefficient of Cs at 3888 Å from the He lamp could not be neglected, suitalbe corrections were made.

It has long been known that the vapor of cesium or rubidium[1] can be photoionized by the light in the discrete region of its atomic spectrum. This ionization has been known[2,3] to take place by absorption of the light at the principal series of cesium (6S→*n*P). Their observation suggested that the mechanism of the ionization processes was

$$Cs + h\nu \rightarrow Cs^*(nP) \qquad n \geq 8 \qquad (1)$$

$$Cs^* \rightarrow Cs + h\nu \qquad (2)$$

$$Cs^* + Cs \rightarrow Cs_2^+ + e \qquad (3)$$

From the measurement of the mobility of the ions Lee and Mahan[4] showed that another process

$$Cs^* + Cs \rightarrow Cs^+ + Cs^- \qquad (4)$$

can not be excluded for the state above 12P. On the basis of the energetic relation the old[2,5] and recent[4,6] data have indicated that the one-electron bond in such ions as Cs_2^+ is stronger than the two-electron bond in Cs_2. Another paper[7] of Mohler and Boeker showed the effects of the foreign gases on the photoionization of cesium at line absorption. They obtained the value of σ (collision radius) between 1.4 and 4×10^{-8} cm for foreign gases, N_2, H_2, He, and Ar, while the value for Cs-Cs collision was about ten times larger. Recent work[8] by Williams has shown the effect of Cs using a Kingdom Cage or space-charge ion collector. The addition of ammonia has altered the photoionization at the principal series lines of cesium by attenuating the wavelength peaks longer than 3440 Å and intensifying the shorter wavelength peaks. They suggested the two processes, one is quenching and the other is ionization.

$$Cs^* + NH_3 \rightarrow Cs + NH_3 \qquad (5)$$

$$Cs^* + NH_3 \rightarrow Cs(NH_3)^+ + e \qquad (6)$$

The latter is similar to the molecular ion formation by collisions between Cs* and normal Cs. The present authors have reported the mass spectrometric identification of Cs_2^+ ion produced by line absorption at 3888 Å.[9] In this paper we report detailed measurements for the chemi-ionization of Cs at 3888 Å and the effects of foregin gas atoms on the chemi-ionization.

Experimental

Reaction System. In the static system, the cesium vapor was irradiated with the 3888 Å light from a microwave discharge He lamp. Figure 1 illustrates the reaction system used in this work. The quartz cell contained platinum parallel-plate electodes of 1.5×4 cm dimension separated by 2 cm. The cell with a window for light irradiation, a small tube for cesium supply and a side-arm to a vacuum system through two grease-free valves was placed in a constant temperature oven. Another small oven around the Cs tube was heated independently in order to control the Cs vapor pressure. Light from the He lamp passed through a chopper, a filter, a collimating lens, a slit, and the photoionization cell. Care was was taken to prevent scattered light or photoexcited atoms from striking the electrodes. The helium discharge lamp emitted the two intense lines at 3888 and 3188 Å in the region between 3000 and 4000 Å. The longer wavelength lines than 4000 Å could not be absorbed by Cs and the shorter ones than 3000 Å could not be through a pyrex window. The 3188 Å line was re-

1) E. O. Lawrence and N. Edlefsen, *Phys. Rev.*, **34**, 233 (1929). K. Freudenberg, *Z. Physik*, **67**, 417 (1931).

2) F. Mohler and C. Boecker, *J. Res. Natl. Bur. Std.*, **5**, 51 (1930).

3) F. Mohler, P. Foote and R. Chenault, *Phys. Rev.*, **27**, 37 (1926).

4) Y. T. Lee and B. H. Mahan, *J. Chem. Phys.*, **42**, 2893 (1965).

5) H. M. James, *ibid.*, **3**, 9 (1935).

6) R. F. Barrow, N. Travis and C. V. Wright, *Nature*, **187**, 141 (1960).

7) F. L. Mohler and C. Boeker, *J. Res. Natl. Bur. Std.*, **5**, 399 (1930).

8) R. A. Williams and S. Naiditch, *J. Chem. Phys.*, **41**, 343 (1967).

9) Y. Ono, I. Koyano and I. Tanaka, *ibid.*, **52**, 5969, (1970).

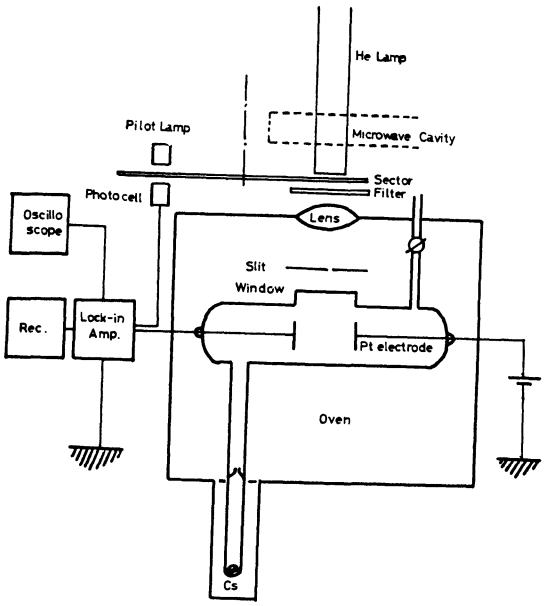

Fig. 1. Schematic diagram of reaction system.

moved by a filter and the essentially monochromatic 3888 Å light was then modulated by a chopper to form the 20 Hz square-wave. The total ions arriving to the cathode were detected by a lock-in amplifier tuned to 20 Hz. Dc voltage from mercury dry cells was applied between the electrodes.

Materials. An ampule of Cs metal from Merck Ltd. was opened in an evacuated tube and the metal was distilled into the tube with a break-off seal and the tube was sealed off. The rare gases such as He, Ne, Ar, Kr, and Xe, inorganic gases such as NH_3, H_2 and N_2, saturated hydrocarbons such as CH_4, C_2H_6, C_3H_8 and n-C_4H_{10} and unsaturated hydrocarbons such as C_2H_4, C_3H_6, *cis*-2-butene, and 2-pentene were supplied from Takachiho Co., Ltd.

Procedure. Before the experiment, the reaction cell was heated at 400°C and evacuated to less than 10^{-6} Torr for at least a few days. The metal vapor was introduced into the cell through the break seal from the Cs tube, and the foreign gas was introduced through a tube containing Cs getter to remove a trace of impurities in the gas after the gas pressure was measured by an oil manometer. During the experiments the vapor pressure of Cs was controlled by the temperature of the Cs supply tube. The temperature of the reaction cell was maintained about 350°C in order to avoid the condensation of Cs in the reaction cell.

Since the electrodes were always covered by adsorbed Cs metal, a current due to surface ionization followed by detachment from the surface by electric field was detected. In a new cell this ion current was 10^{-9} amp/cm² at 350°C with 1.3 V collecting potential and became larger as the cell aged. Since this ion current was always much larger than the expected photoionization current, the latter could only be detected by chopping the incident light beam and using a lock-in amplifier. By using this technique the limit of detection for photoionization current was 10^{-13} A, and 10^{-14} A with a narrow-band preamplifier. In most runs the collecting voltage was fixed at 1.3 V dc for the reason which will be described later. The sector was so designed that the light was irradiated during 1/120 sec by a hysteresis motor of 10 Hz.

At first the photoionization for Cs vapor without foreign gases was measured, and then the variation of the ion current by the addition of foreign gases was measured. The pressure of foreign gas introduced was measured by an oil manometer through a tube of getter of Cs to remove a trace of impurities. Since the pressure effect of the absorption lines of Cs atoms due to foreign gases can not be ignored, a correction was made as described in the appendix.

Results

i) Collecting Efficiency of Chemi-ionization Current. In order to confirm the saturation of the ion collecting efficiency by the electrodes the ion current was examined by changing the collecting voltage. The plots of the ion current *versus* the voltage were shown in Fig. 2. Curve 1 shows the variation of the ion current for Cs vapor only, curve 2 that for the addition of N_2 gas at 4 Torr, and curve 3 that for the addition of Xe gas at 6 Torr. All curves indicated that the collecting voltage of about 1.3 V was suitable for measuring the ion current. The output of the lock-in amplifier used depends on the input signal form, therefore the values of ion currents measured by the lock-in amplifier must be corrected by a suitable method. In our experiments this correction was made by the use of dc amplifier.

ii) Chemi-ionization of Cs*($8\,^2P_{1/2}$) with Cesium Atom. The vapor pressure of cesium was calculated from the relation given by Langmuir and Kingdon.[10] In order to interpret these experimental results, the reaction mechanisms can be assumed as follows:

$$Cs(6S) + h\nu(3888\,Å) \rightarrow Cs^*(8^2P_{1/2}) \quad (7)\ I_{abs}$$

$$Cs^*(8^2P_{1/2}) \rightarrow Cs'(7S, 6S, etc.) + h\nu' \quad (8)\ 1/\tau$$

$$Cs^*(8^2P_{1/2}) + Cs(6S) \rightarrow Cs_2^+ + e \quad (9)\ k_i$$

$$Cs^*(8^2P_{1/2}) + Cs(6S) \rightarrow Cs_2 \text{ or } Cs + Cs \quad (10)\ k_g$$

where I_{abs}, the light intensity absorbed by Cs(6S), is nearly equal to $\varepsilon l I_0[Cs]$, ε is the absorption coefficient of Cs at 3888 Å He line which was determined to be 1.4×10^{-19} cm²/molecule as described in the appendix, l is the absorption path length, 15 mm, I_0 is the intensity of the incident light which was measured to be 1×10^{15} photons/sec, τ is the radiative life time of Cs*($8\,^2P_{1/2}$), k_i and k_q are the rate constants of the collisional ionization with Cs and of the quenching process by Cs, respectively. The possibility of the ion pair formation was neglected because the electron affinity of Cs is about 0.19 eV[4] whose energy is insufficient to produce Cs^+ ion and also the ion except Cs_2^+ was not detec-

10) I. Langmuir and K. H. Kingdon, *Proc. Roy. Soc.*, **107A**, 61 (1925).

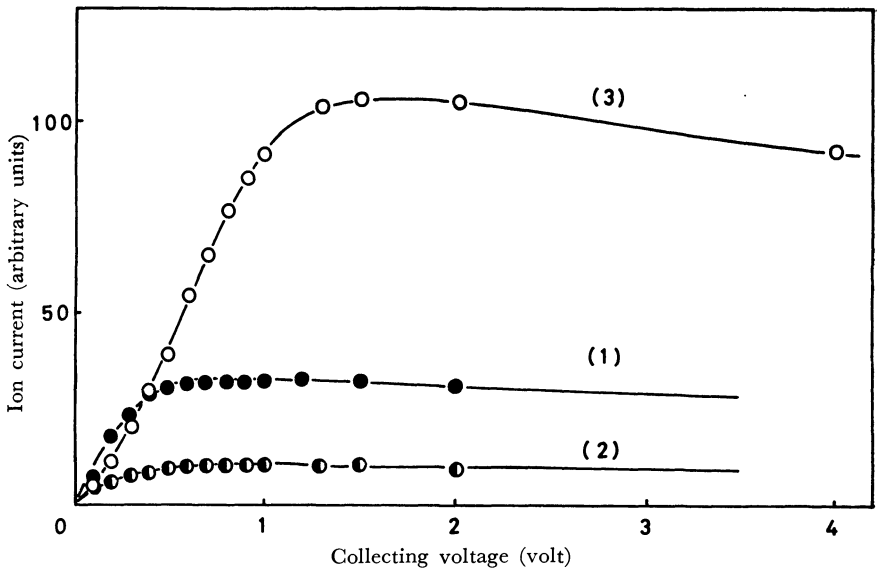

Fig. 2. Ion-current *versus* collecting voltage.
curve (1): ● Cs vapor (10^{-2} Torr)
curve (2): ◐ Cs vapor (10^{-2} Torr) + N_2(4 Torr)
curve (3): ○ Cs vapor (10^{-2} Torr) + Xe(6 Torr)

ted by the mass spectrometer as has been described in the previous paper.[9] The rate equation for the concentration of Cs*($8\ ^2P_{1/2}$) is

$$\frac{d[Cs^*]}{dt} = \varepsilon l I_0[Cs] - \frac{1}{\tau}[Cs^*] - (k_i + k_q)[Cs^*][Cs] \tag{11}$$

Since the apparent life time of Cs* is much shorter than the duration of irradiation pulse, *i.e.*, 1/120 sec, the stationary concentration would be maintained during the irradiation. In this case the concentration of Cs* is obtained as follows:

$$[Cs^*] = \frac{\varepsilon l I_0[Cs]}{1/\tau + (k_i + k_q)[Cs]} \tag{12}$$

Now the equation for the ion current of Cs_2^+ ion is

$$I = k_i[Cs][Cs^*] \tag{13}$$

Substituting Eq. (12) into Eq. (13) we obtain

$$I = \frac{\varepsilon l I_0 k_i[Cs]^2}{1/\tau + (k_i + k_q)[Cs]} \tag{14}$$

and

$$\frac{[Cs]}{I} = \frac{1}{\varepsilon l I_0}\left\{\frac{1}{\tau k_i} \cdot \frac{1}{[Cs]} + \frac{k_i + k_q}{k_i}\right\} \tag{15}$$

The values of P/I were plotted against $1/P$ and then a straight line was obtained as shown in Fig. 3. These experimental results indicated that the reaction mechanisms (7)—(10) were reasonable, and the values of τk_i and τk_q were determined from the intercept and the slope of these linear plots. τk_i was calculated to be 1.3×10^{-15} mol^{-1} cm^3 and τk_q was 1.6×10^{-15} mol^{-1} cm^3. Using the following relation between the reaction rate k and

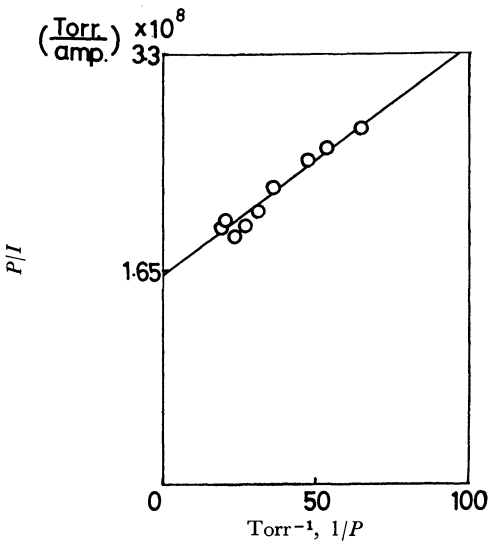

Fig. 3. Plot of the ratio of the pressure of Cs to the chemi-ionization current against the reciprocal value of the pressure according to Eq. (15) for cesium.

the cross section σ^2, $k=\sigma^2(8\pi RT/\mu)^{1/2}$, the products of the life-time τ of Cs* and the cross sections for photo-ionization σ_i^2, and quenching, σ_q^2, have been calculated to be

$$\tau\sigma_i^2 = 9.5\times10^{-21}\ \text{cm}^2\cdot\text{sec}$$

and

$$\tau\sigma_q^2 = 1.17\times10^{-20}\ \text{cm}^2\cdot\text{sec}$$

respectively.

iii) Chemi-ionization of Cs*($8^2P_{1/2}$) with Foreign Gas. The gases used were a) rare gases such as He, Ne, Ar, Kr, and Xe, b) simple inorganic gases NH_3, H_2, and N_2, c) saturated hydrocarbons CH_4, C_2H_6, C_3H_8, and *n*-C_4H_{10} and d) unsaturated hydrocarbons C_2H_4, C_3H_6, *cis*-2-butene, and 2-pentene. The results were described qualitatively as follows. The addition of rare gas except He increased the ion current, while the He gas decreased it. The H_2, NH_3, and N_2 gases decreased the ion current. The saturated hydrocarbon increased the ion current but the unsaturated hydrocarbons C_2H_4, C_3H_6, and 2-pentene except *cis*-2-butene decreased it.

From these qualitative results, the following processes should be added to the previous four processes (7)—(10).

$$Cs^*(8^2P_{1/2}) + M \rightarrow CsM^+ + e \qquad (16)\ k_i'$$

$$Cs^*(8^2P_{1/2}) + M \rightarrow Cs + M \qquad (17)\ k_q'$$

where k_i' and k_q' are the rate constants of the collisional ionization between Cs* and a foreign gas M, and of the collisional quenching process by M, respectively. Since the electron affinities of atoms and molecules used in this experiment are considered to be less than 0.7 eV, the ion pair formation ($Cs^*+M \rightarrow Cs^+ + M^-$) seems to be impossible so that the ion pair formation can be excluded. Therefore the rate equation for the excited Cs* atom is

$$d[Cs^*]/dt = \varepsilon l I_0[Cs] - (1/\tau)[Cs^*] - (k_i + k_q)[Cs^*][Cs] - (k_i' + k_q')[Cs^*][M] \qquad (18)$$

The stationary state treatment leads to the following equation for the concentration of the Cs*,

$$[Cs^*] = \frac{\varepsilon l I_0[Cs]}{1/\tau + (k_i + k_q)[Cs] + (k_i' + k_q')[M]} \qquad (19)$$

The ion current for the total ionic species is

$$I' = k_i[Cs^*][Cs] + k_i'[Cs^*][M] \qquad (20)$$

Substituting Eq. (19) into Eq. (20), the following equation is derived,

$$I' = \frac{\varepsilon l I_0\{k_i[Cs] + k_i'[M]\}[Cs]}{1/\tau + (k_i + k_q)[Cs] + (k_i' + k_q')[M]} \qquad (21)$$

The ratio of the ion current in the presence of a foreign gas to that in the absence of foreign gas is

$$\frac{I'}{I} = \frac{k_i[Cs] + k_i'[M]}{1/\tau + (k_i + k_q)[Cs] + (k_i' + k_q')[M]} \cdot \frac{1/\tau + (k_i + k_q)[Cs]}{k_i[Cs]} \qquad (22)$$

Changing this equation to the suitable form to analyse the data, the following equation can be derived,

$$\frac{[M]}{Y-1} = \frac{(k_i' + k_q')[M]}{k_i'(\beta-\alpha) - k_q'\alpha} + \frac{\alpha\beta}{\{k_i'(\beta-\alpha) - k_q'\alpha\}\tau} \qquad (23)$$

where $Y = I'/I$,

$\alpha = \tau k_i[Cs]$,

and

$\beta = \tau(k_i + k_q)[Cs] + 1$.

Since for a series of measurements the vapor pressure of cesium was kept constant, α and β have the constant values. The plots of $[M]/(Y-1)$ *versus* [M] gave straight lines as shown in Figs. 4—7. These results suggested that the mechanisms considered for chemi-ionization and quenching of cesium with M should be reasonable. From the slopes and the intercepts of these lines the values of $\tau k_i'$ and $\tau k_q'$ could be determined. Utilizing the values of $\tau k_i'$ and $\tau k_q'$, the values of $\tau\sigma'_i{}^2$ and $\tau\sigma'_q{}^2$ could be obtained. The values of $\tau\sigma'_t{}^2 = \tau(\sigma'_i{}^2 + \sigma'_q{}^2)$, $\tau\sigma'_i{}^2$ and $\tau\sigma'_q{}^2$ were summarized in Table 1. The value of collisional cross

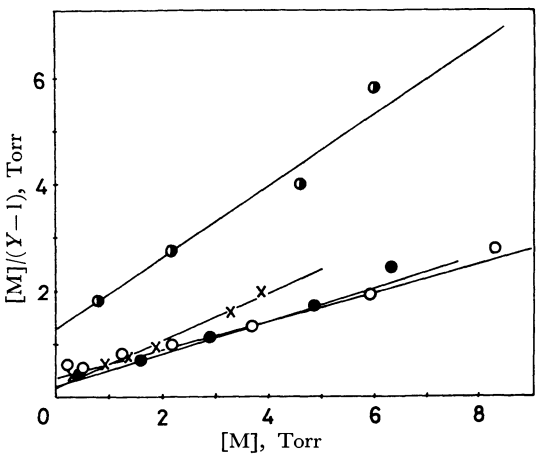

Fig. 4. Plot of $[M]/(Y-1)$ against [M] according to Eq. (23).
◑ Neon, ● Krypton, ○ Argon, × Xenon

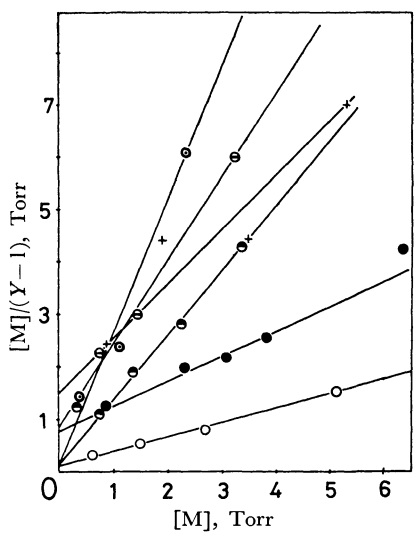

Fig. 5. Plot of $[M]/(Y-1)$ against [M] according to Eq. (23).
⊖ CH_4, + C_2H_6, ○ C_3H_8, ⊙: cyclo-C_3H_6, ◓ *n*-C_4H_{10}, ● *cis*-2-butene

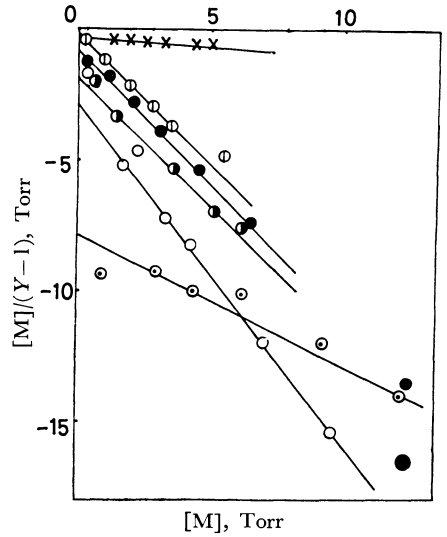

Fig. 6. Plot of [M]/($Y-1$) against [M] according to Eq. (23).
○ C_3H_6, ◑ He, ⊙ C_2H_4, ● N_2, ◫ H_2, × NH_3

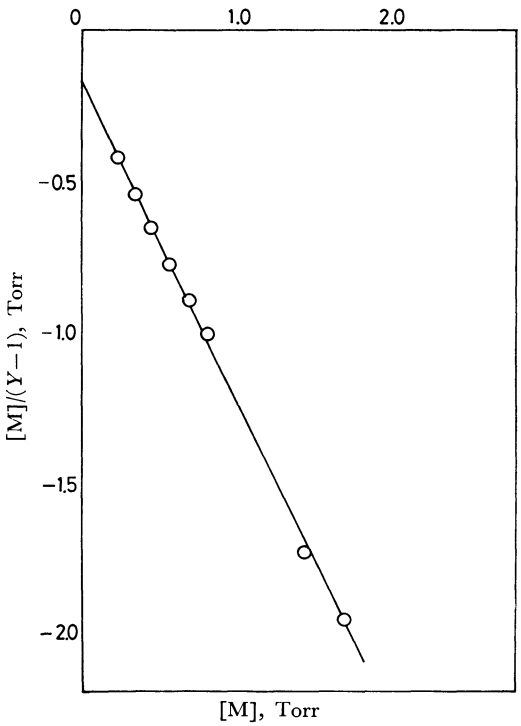

Fig. 7. Plot of [M]/($Y-1$) against [M] according to Eq. (23).
○: 2-pentene

section was nearly equal to $2.2\times10^{-20}/\tau$ cm²/sec obtained by Mohler using the space charge method. This coincidence is surprising, considering the two quite different experimental techniques. If the life time of Cs*($8^2P_{1/2}$) is assumed to be the order of 10^{-6} sec, the value of collisional radius is estimated to be $1-3\times10^{-7}$ cm for Cs–Cs collision. This value remarkably large compared with the kinetic radius obtained from the viscosity data. The collisional cross sections for excited cesium with foreign gases, are reduced by two or three orders. The radii for collisions with foreign gases agree in magnitude with the kinetic radii. For the Cs–Cs collision, the ionization and the quenching cross sections are almost equal.

Discussion

Figure 8 shows the schematic potential energy curves for Cs–M system relevent to the ionization quenching processes from the system Cs*($8^2P_{1/2}$)+M. It is to be seen in Fig. 8 that $Cs^+ + M^-$ and $Cs^+ + M + e$ curves both interact with the curve for the Cs*($8^2P_{1/2}$)+M, and also the repulsive curves (Π state) of the lower excited states of Cs with M (for example, Cs**($7^2P_{1/2}$)+M) cross the curve of Cs*+M in the $\sum$ state. The quenching of Cs*($8^2P_{1/2}$) by M can be interpreted by cross over from Cs*+M to Cs**+M. The chemi-ionization of Cs*($8^2P_{1/2}$) with M can be interpreted by transfer from the Cs*+M curve to the $CsM^+ + e$ curve.

As predicted in the theories of inelastic collisions[11] between alkali and rare gas atoms concerning the spin-orbit relaxation of alkali atoms, cross section should depend on the attractive force between the atoms, and increase monotonically with the polarizabilities of rare gas atoms from helium to xenon. The total cross section equal to the sum of the quenching and ionization cross sections should follow exactly the predicted sequence. The plots of $\tau\sigma_t^2/r_0^2$ *versus* $\alpha\mu^{1/2}$ gave a straight

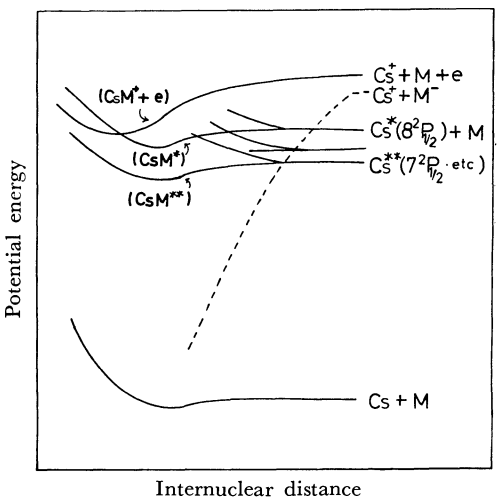

Fig. 8. The schematic potential energy curves for Cs-M system.

11) L. Krause, *Applied Optics*, **5**, 1375 (1966).

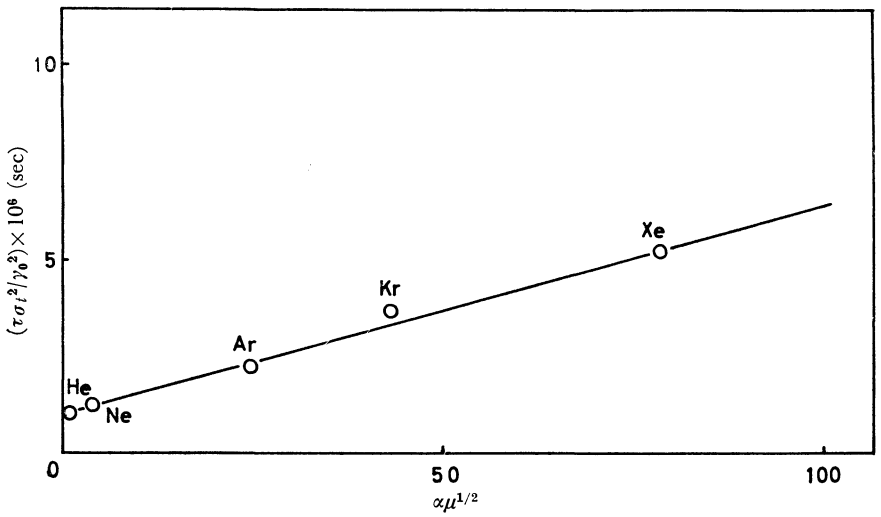

Fig. 9. Correlation the ratio of the total cross section to the kinetic collision cross section *versus* $\alpha\mu^{1/2}$.

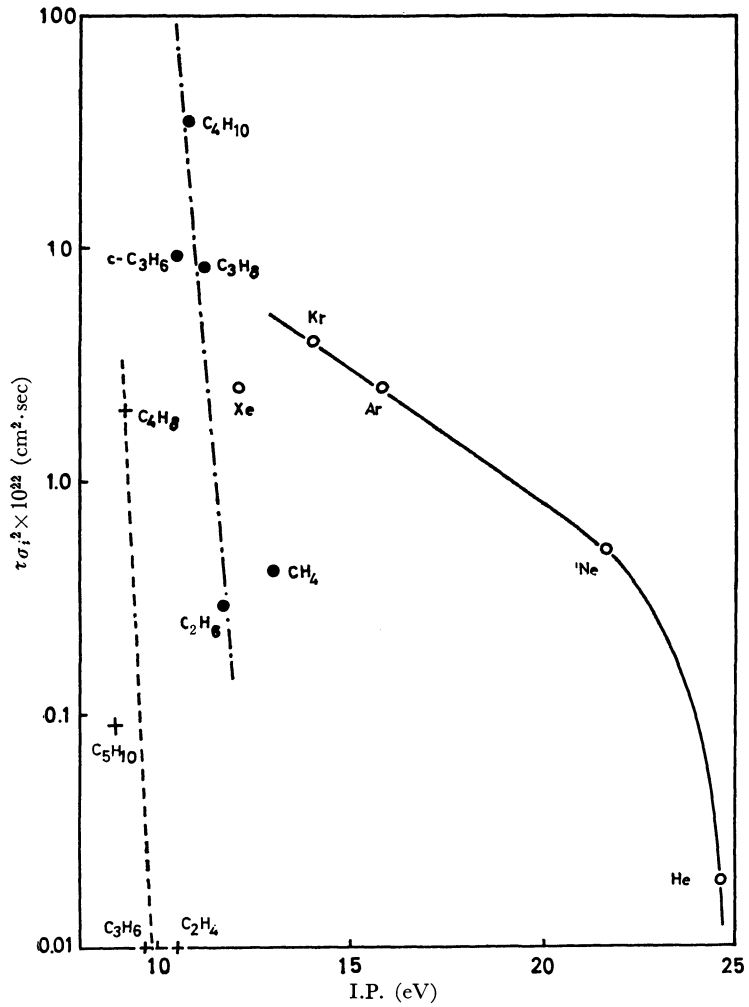

Fig. 10. Correlation $\tau\sigma_i^2$ *versus* the ionization potential.

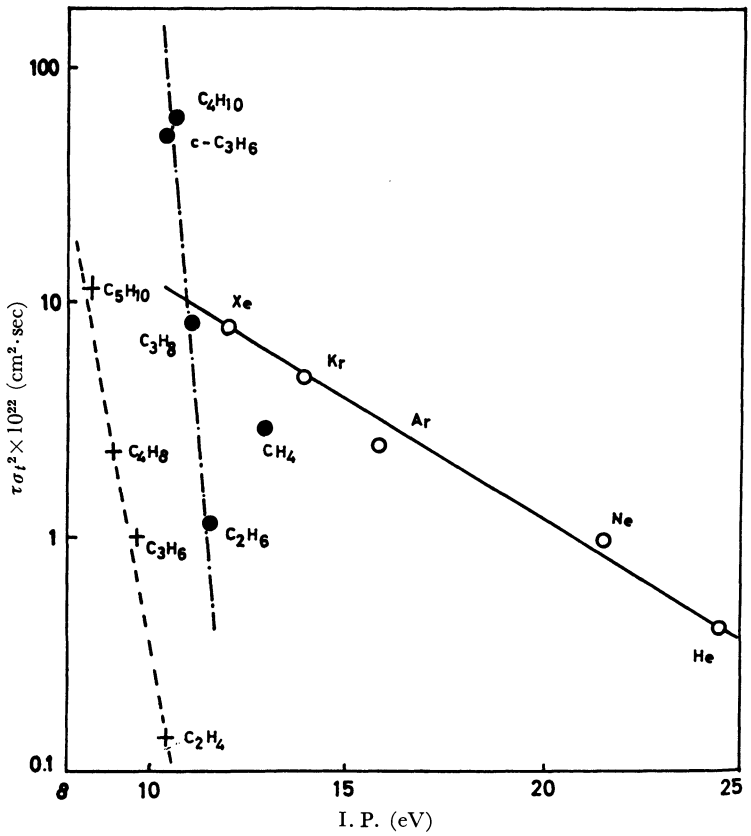

Fig. 11. Correlation $\tau\sigma_t^2$ *versus* the ionization potential.

line as shown in Fig. 9, where r_0 is the kinetic collision diameter between the Cs atom and the rare gas atoms, α is the polarizability of each rare gas atom, and μ is the reduced mass of cesium and each rare gas atom. This relation indicated that the total cross section ($\sigma_t'^2$) divided by kinetic cross section (πr_0^2) corresponding to the easiness of making collision complex should be related with the $\alpha\mu^{1/2}$ which means the effective intermolecular attractive force. H_2, N_2 and NH_3 have larger cross sections than rare gases, and H_2 has the largest one. In the case of hydrocarbons, the cross section decreases from CH_4 to C_2H_6 and then shows a rather steep rise to n-C_4H_{10}. The cross sections of unsaturated hydrocarbons have smaller values than those of rare gases and those of corresponding saturated hydrocarbons. This tendency seems to be reverse to that for the physical quenching cross sections of Na*(3^2P) by hydrocarbons.[12] This difference may be caused by the different processes from excited states of atoms.

Since we can exclude the ion pair formation in the reaction of Cs*($8^2P_{1/2}$) with the foreign gases as described before, the increase of ion current by the foreign gases should be explained by the occurrence of chemi-ionization reaction

$$Cs^* + M \rightarrow CsM^+ + e$$

Herman and Cermak[13] confirmed the presence of ions $CsAr^+$ and $CsKr^+$ in the reactions

$$Ar^* + Cs \rightarrow ArCs^+ + e$$

and

$$Kr^* + Cs \rightarrow KrCs^+ + e$$

A recent work by Williams and Naiditch[8] suggested the molecular ion $Cs(NH_3)^+$, from the reaction

$$Cs(nP) + NH_3 \rightarrow CsNH_3^+ + e \quad (n \geq 12)$$

On the energetic basis for the possibility of the chemi-ionization reaction between Cs*($8^2P_{1/2}$) and M, the value of bond energy of molecular ion CsM^+ should be greater than 0.7 eV. The bond energy of CsM^+ strongly depends on the polarizability and/or ionization potential of foreign gases. If the ionization potential of M is lower, the energy of the molecular ion becomes lower. It is expected that the ionization cross section with M may be correlated with the ionization of M. This correlation is found in the series of foreign gases such as rare gases and saturated hydrocarbons

12) R. G. W. Norrish and W. MacF. Smith, *Proc. Roy. Soc.*, **A176**, 295 (1940).

13) V. Cermak and Z. Herman, *Collect. Czech. Chem. Commum.*, **30**, 169 (1965).

Table 1. The values of $\tau\sigma_t'^2$, $\tau\sigma_i'^2$, $\tau\sigma_q'^2$ and relative ionization efficiency η for inert gases and simple molecules with cesium atom
(Prime of collisional radius is removed in this Table)

Gas M	Cross section $\tau\sigma_t^2$ ($\times 10^{22}$)	$\tau\sigma_i^2$ ($\times 10^{22}$)	$\tau\sigma_q^2$ ($\times 10^{22}$)	Relative ionization efficiency $\eta = \frac{\sigma_i^2}{\sigma_t^2}$
He	0.41	0.019	0.39	0.046
Ne	0.98	0.51	0.47	0.52
Ar	2.5	2.5	0	1.00
Kr	4.8	3.9	0.90	0.81
Xe	7.8	2.5	5.3	0.33
H_2	6.5	0.060	6.4	0.0093
N_2	3.3	0.026	3.3	0.008
NH_3	2.7	0	2.7	0
CH_4	2.9	0.41	2.5	0.14
C_2H_5	1.2	0.29	0.88	0.25
C_3H_8	8.2	8.2	0	1.00
C_4H_{10}	62	35	27	0.56
c-C_3H_6	51	9.1	42	0.18
C_2H_4	0.14	0	0.14	0
C_3H_6	1.0	0	1.0	0
C_4H_8	2.3	2.0	0.32	0.86
C_5H_{10}	12.6	0.06	12.5	0.007
Cs	212	95	117	0.18

except for Xe and CH_4 as shown in Fig. 10. Compared with the ionization cross section, $\tau\sigma_i^2$, it is interesting to note that the plots of $\log \tau\sigma_t^2$ *versus* the ionization potential give three straight lines for three groups of foreign gases; rare gases, saturated hydrocarbons, and unsaturated hydrocarbons as shown in Fig. 11.

In Fig. 12 the quenching cross sections listed in Table 1 are plotted against atomic weight in cesium-rare gas system. The plots show a minimum at argon. Similar behavior of the cross sections was observed in the cases of the collisional spin-orbit relaxation of $Cs(6^2P_{1/2} \rightarrow 6^2P_{3/2})$ by rare gases.[11] It was demonstrated that there was a good correlation between the spin-orbit relaxation cross sections for $Cs(6^2P_{1/2})$-rare gas collisions and the elastic scattering cross sections of electrons by the rare gases with the electron velocity assumed as equal to that of the valence electron of cesium. However the complete theoretical interpretation of this behavior of rare gases has not been given.

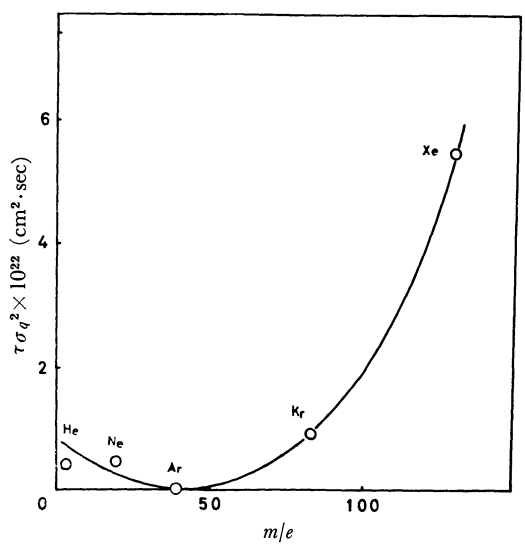

Fig. 12. Correlation $\tau\sigma_q^2$ *versus* atomic weight.

Figure 13 shows that the plots of $\eta(\sigma_i^2/\sigma_t^2 = \sigma_i^2/(\sigma_i^2+\sigma_q^2))$, relative ionization efficiency, *versus* the mass weight gave the same configuration for each group of gases. For rare gases they have a maximum at arogn, and the saturated hydrocarbons at C_3H_8 and the unsaturated at C_4H_8. The increases in η from He to Ar, CH_4 to C_3H_8 and C_2H_4 to C_4H_8, can then be ascribed to the increase in the ionization probability owing to the decrease in ionization potential of M which lowers the $CsM^+ + e$ curve. The decrease from Ar to Xe for rare gases can be interpreted by the rapid increase in the quenching probability owing to the increasing spin-orbit interaction which will be evidenced from the experimental results shown in Fig. 12. However, for the saturated and unsaturated hydrocarbons, the increase in the number of potential curves which cross the CsM* curve to dissipate the electronic energy to various vibrational energies may play an important role for the decreases in η from C_3H_8 to n-C_4H_{10} and from

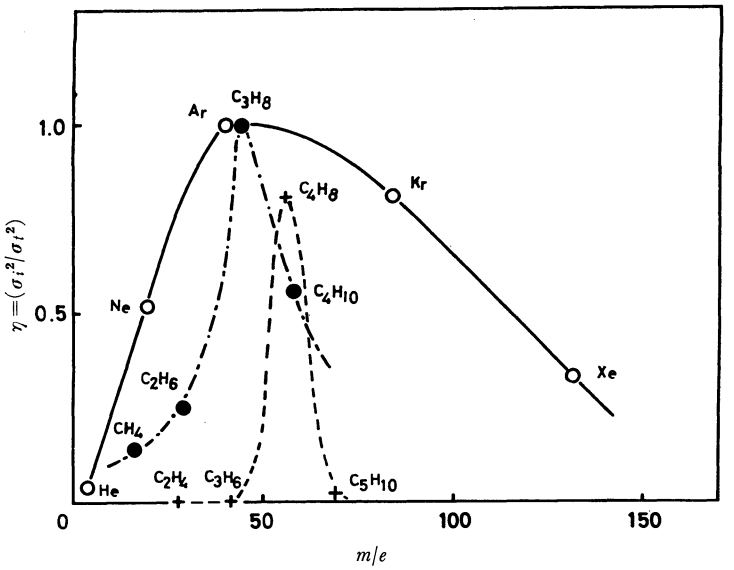

Fig. 13. Correlation ionization efficiency of chemi-ionization for Cs-M system *versus* atomic and molecular weight.

C_4H_8 to C_5H_{10}.

Appendix

Effects of Foreign Gases on the Line Absorption of Cs. The modification of the spectral lines of emitting or absorbing atom due to collisions with other atoms and molecules is exhibited by broadening, shift and symmetry of lines and the occasional appearance of a certain diffuse band. The emission line 3888 Å from the He lamp used is substantially broader than the absorption line of cesium, and also the peak of He line does not coincide with that of cesium line. Since the added gas pressure was varied up to about 10 Torr in this experiment, the pressure effect on the absorption of the light at 3888 Å could not be neglected for the quantitative discussion.

The absorption cell consists of 150 cm length and 1.5 cm diameter pyrex tube with pyrex windows at both ends, a small tube for supply of Cs vapor and a tube connected with a gas inlet system through the two grease-free valves. The cell was mounted in a constant temperature oven. Before measurement the cell was evacuated to less than 10^{-6} Torr by heating at 400°C for a few days, and kept at 350°C during the measurement. In the experiment the slit width of the monochrometer 0.1 mm was enough to cover the whole emission line at 3888 Å line. After the absorption of the light by Cs vapor only was measured, a foreign gas purified by a getter was introduced into the cell and the variation of the intensity by adding a foreign gas was measured.

The Apparent Absorption Coefficient. The logarithmic plots of the transmitted light intensity, I, *versus* the cesium pressure can give the apparent absorption coefficient. The value of the apparent absorption coefficient calculated from Fig. 14 was 1.4×10^{-19} cm²/molecule.

Pressure effects of foreign gases on the absorption line of Cs. Relative measurements of the

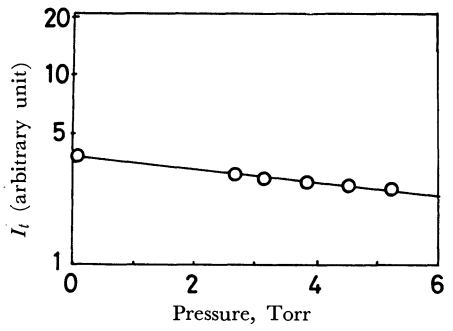

Fig. 14. Plot of the transmitted light against the vapor pressure of Cs.

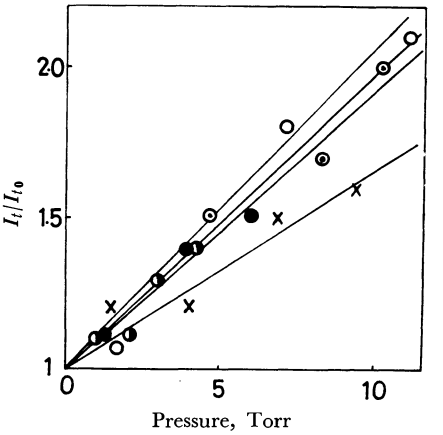

Fig. 15. Pressure effects of foreign gases on the absorption line of Cs.
⊙ He, × Ne, ● Ar, ○ Kr, ◑ Xe

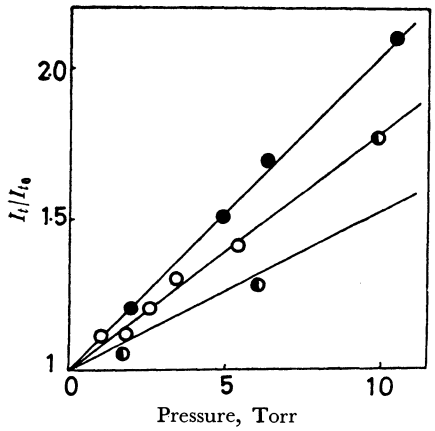

Fig. 16. Pressure effects of foreign gases on the absorption line of Cs.
● H_2, ○ NH_3, ◐ N_2

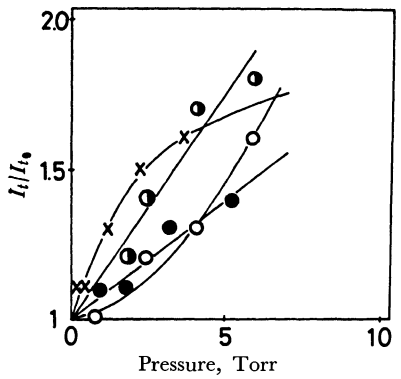

Fig. 17. Pressure effects of foreign gases on the absorption line of Cs.

absorption of the line at 3888 Å from He lamp with and without foreign gases were made to correct the effects of gases on the chemi-ionization of Cs. The

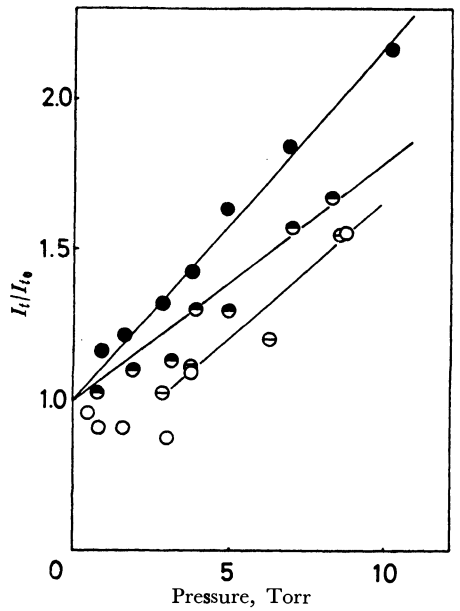

Fig. 18. Pressure effects of foreign gases on the absorption line of Cs.
● n-C_4H_{10}, ◓ C_3H_8, ○ C_4H_8, ⊖ C_3H_6

effects of rare gas atoms in the pressure region, 0 to 10 Torr were shown in Fig. 15. The results for simple inorganic gases such as H_2, N_2, and NH_3 were shown in Fig. 16, the results for CH_4, C_2H_4, C_2H_6, and cyclo-C_3H_6, for C_3H_6, C_3H_8, and n-C_4H_{10}, and for C_5H_{10} are shown in Fig. 17, 18, and 19, respectively. For each foreign gas plots of the relative absorption *versus* the pressure of gas yield almost a straight line. In order to evaluate the pressure effect of the foreign gas on the chemi-ionization of Cs, the ion current of chemi-ionization is corrected by multiplying the factor I_{t_0}/I_t at each foreign gas pressure, where I_t and I_{t_0} are the transmitted light intensities with and without foreign gases, respectively.

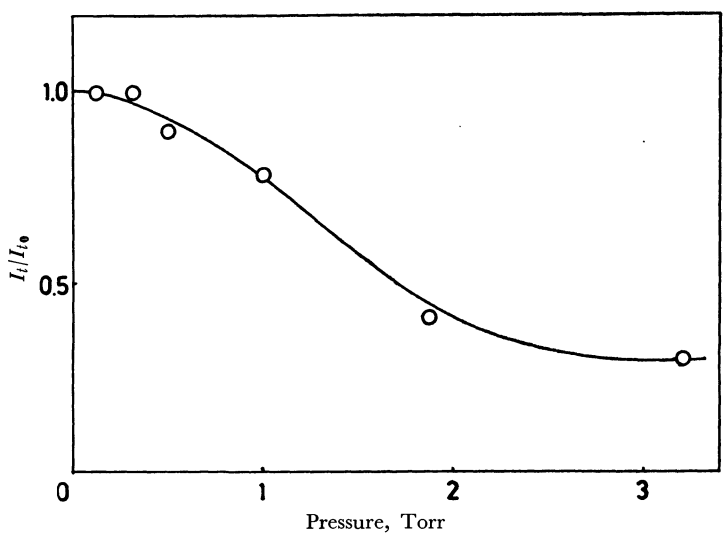

Fig. 19. Pressure effects of 2-pentene on the absorption line of Cs.

BULLETIN OF THE CHEMICAL SOCIETY OF JAPAN VOL. 43 3435—3443 (1970)

Reactive States of Acridine for the Photoreduction in Tetrahydrofuran

Yoshikatsu MIYASHITA, Shigeya NIIZUMA, Hiroshi KOKUBUN and Masao KOIZUMI

Department of Chemistry, Faculty of Science, Tohoku University, Katahira, Sendai

(Received July 6, 1970)

The photoreduction of acridine in tetrahydrofuran (THF) has been investigated by the steady light experiment and also by the flash technique. The quantum yields in the aerated and deaerated solution were 0.12 and 0.36 respectively. The former value is referred to molecular mechanism while the difference of the two, 0.24, to radical mechanism. It was established that the sensitized reaction occurs with biacetyl ($T(n\text{-}\pi^*)$, 19700 cm^{-1}) as a triplet energy donor. The probability factor β with which the produced $T(\pi\text{-}\pi^*)$ of acridine (15840 cm^{-1}) reacts with THF was found to be $\gtrsim 0.6$. Anthracene ($T(\pi\text{-}\pi^*)$, 14700 cm^{-1}) was found to act as a triplet energy acceptor and to reduce the photoreduction. From the decrease of the quantum yield caused by the addition of anthracene, the quantum yield *via* the lowest $T(\pi\text{-}\pi^*)$ of acridine was evaluated as 0.06. By combining this value with the above β-value, the apparent φ_{ST} has proved to be $\lesssim 0.1$. This very small value compared with the φ_{ST} values presented for other solvents (benzene $\gtrsim 0.25$, water $\gtrsim 0.24$, ethanol $\gtrsim 0.29$) leads to the conclusion that in THF, $T(n\text{-}\pi^*)$ is also a reactive state for the photoreduction. Further, an interesting aspect of the radical mechanism was elucidated from the comparison of Φ_R (quantum yield due to radical mechanism) and Φ_{O_2} (quantum yield of oxygen consumption).

There is at present some disagreement as to the reactive state of acridine for the photoreduction in alcohols. In 1965, Kellmann and Dubois[1] reported that in methanol, the $T(n\text{-}\pi^*)$ state in addition to the singlet excited state may participate in the reaction but the lowest $T(\pi\text{-}\pi^*)$ does not. On the other hand, Vander Donkt and Porter[2] concluded that in isopropanol, only the singlet excited state is reactive. That this discrepancy in methanol and in isopropanol really exists was verified by our group[3] using biacetyl as a T-energy acceptor. This was further reconfirmed from the study on the pH dependence of the photoreduction quantum yield.[4] But a little later, Wilkinson and Dubois[5] proposed that only $^1L_a(\pi\text{-}\pi^*)$ is a reactive state in ethanol on the basis of the experiments involving external heavy atom effects.

Recently Zanker and Prell asserted that for the photoreduction of 9-methylacridine in ethanol, the singlet ($n\text{-}\pi^*$) instead of $^1L_a(\pi\text{-}\pi^*)$, is a reactive state.[6] According to our results, the quantum yields of photoreduction *via* $T(n\text{-}\pi^*)$ in methanol, ethanol, *n*-propanol and isopropanol are 0.063, 0.019, 0.022 and 0.00 respectively. These results may perhaps be interpreted in terms of the number of α-H atoms and of the steric factors in the reaction. Some workers however seem to have the opinion that the higher T states of short duration are unable to participate in the reaction. One purpose of the present paper is to show another example opposite to such a view.

The second point which we would like to stress is that although all the above workers agree in the point that the lowest $T(\pi\text{-}\pi^*)$ is not reactive in the photoreduction in alcohols, this can not be true in general. For instance, Koizumi *et al.*[7] established that the photoreaction between acridine and acridan in benzene occurs *via* the lowest $T(\pi\text{-}\pi^*)$ of the former. It is expected therefore, that such a possibility exists also in the photoreduction of acridine in some suitable solvents. The second object of the present paper is to demonstrate such an example. We found that the photoreduction of acridine in tetrahydrofuran (THF) occurs with a high quantum yield and now the lowest $T(\pi\text{-}\pi^*)$ has been established to be reactive in this solvent, and most likely, the higher

1) A. Kellmann and J. T. Dubois, *J. Chem. Phys.*, **42**, 2518 (1965). A. Kellmann, *J. Chim. Phys.*, **63**, 936 (1966).

2) E. Vender Donkt and G. Porter, *J. Chem. Phys.*, **46**, 1173 (1967).

3) a) M. Koizumi, Y. Ikeda and T. Iwaoka, *J. Chem. Phys.*, **48**, 1869 (1968). b) M. Koizumi, Y. Ikeda and H. Yamashita, This Bulletin, **41**, 1056 (1968).

4) K. Nakamaru, S. Niizuma and M. Koizumi, *ibid.*, **42**, 255 (1969).

5) F. Wilkinson and J. T. Dubois, *J. Chem. Phys.*, **48**, 2651 (1968).

6) V. Zanker and G. Prell, *Ber. Bunsenges. Phys. Chem.*, **73**, 791 (1969).

7) a) S. Niizuma, Y. Ikeda and M. Koizumi, This Bulletin, **40**, 2249 (1967). b) A. Kira and M. Koizumi, *ibid.*, **40**, 2486 (1967).

$T(n\text{-}\pi^*)$ takes part in the photoreduction.

In addition, an interesting feature of the radical process has been elucidated from the review of all our data so far obtained on the quantum yields for photoreduction and for oxygen consumption.

Experimental

Apparatus for the flash photolysis and the steady light experiment, procedures and samples are all essentially similar as in our previous papers. All the steady light experiments were carried out at 25°C. The light intensity for the steady light experiment was usually $2\text{—}3\times10^{-9}$ mol cm^{-2} sec^{-1}. As an exciting light, 365 nm was used for the direct photoreduction and 435.8 nm for the sensitized reaction by biacetyl. The reaction was followed by measuring the change in optical density at 365 nm ($\varepsilon=3.75\times10^3$). A Hitachi MPF-2 spectrofluorometer was used for the measurement of the emission spectra. The concentration of oxygen in THF was decided by the manometric method using Bunsen absorption coefficient. The solubility of oxygen in THF, being not found in literature, was measured with an apparatus specially constructed for the present purpose. See Appendix.

Results and Discussion

Broadly speaking, the photoreduction of acridine in THF occurs in the similar way as in alcohol. Thus as shown in Fig. 1, the absorption maximum at 357 nm declines upon irradiation with 365 nm, and a new peak rises at 285 nm with an isosbestic point at 324 nm. Since the absorption maximum of acridan lies at 290 nm, the photoproducts may contain some acridan derivatives and possibly diacridan in addition to acridan. It was established further, that as in alcohols, the photoreduction occurs even in the aerated solution. The quantum yields in the aerated and in the deaerated solutions were respectively 0.12 and 0.36.

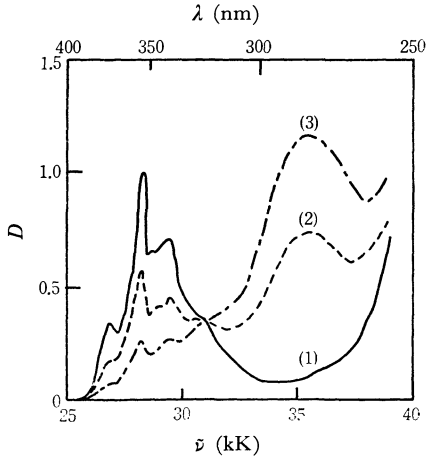

Fig. 1. Change of absorption spectra due to illumination at 365 nm (air-saturated THF solution of acridine).
[A] $=1\times10^{-4}$ M
1) before illumination
2) 4 min 50 sec illumination
3) 10 min 50 sec illumination

The Effect of Oxygen Concentration on the Quantum Yield. Figure 2 shows the plots of $\ln(e^{2.303D}-1)$ against time (D, the optical density at 365 nm) for various concentrations of oxygen up to 2×10^{-3} M. It is seen that the runs for low concentrations of oxygen consist of two linear portions, the earlier portion with almost the same slope as that in the aerated solution and the later one with the slope approaching that in the deaerated solution. These results are similar to those in alcohols,[8] and can be interpreted as follows.

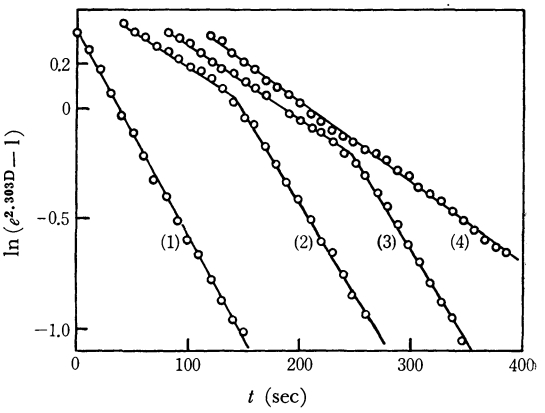

Fig. 2. Plots of $\ln(e^{2.303D}-1)$ *vs.* time for acridine.
[A] $=1\times10^{-4}$ M
(1) Deaerated soln.
(2) [O_2] $=3.4\times10^{-4}$ M
(3) [O_2] $=5.8\times10^{-4}$ M
(4) Aerated soln.

Firstly, the reaction proceeds in proportion to the absorption of light. Secondly, the first linear portion corresponds to the period during which the reaction proceeds *via* molecular mechanism, *i.e.*, proceeds as an elementary process or the like, and not *via* semiquinone which, as has already been fully established, is oxidized by oxygen. A sharp breaking point on each run corresponds to the time point where oxygen has been almost exhausted. After the breaking point, the reaction proceeds essentially in the same way as in the deaerated solution, where the molecular and radical mechanisms (the mechanism *via* semiquinone) occur. As shown in Fig. 3, the decrease in acridine concentration during the first period, $-\Delta$[A] is proportional to the initial oxygen concentration. This implies that as long as the oxygen concentration is above a certain critical value which is very small, only the molecular mechanism occurs

8) S. Niizuma and M. Koizumi, This Bulletin, **36**, 1629 (1963).

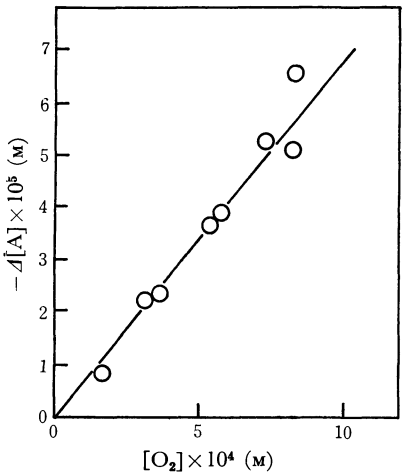

Fig. 3. Plot of the decrease of acridine concentration at the breaking point of the decay curve *vs.* the initial dissolved oxygen concentration.

Table 1. Quantum yields for the photoreduction of acridine in THF

$[O_2]\times10^4$ (M)	Φ_{air}	mean	Φ	mean
20	0.12_1			
20	0.11_5	0.12		
20	0.12_3			
0			0.34_3	
0			0.36_4	0.36
0			0.36_4	

$[O_2]\times10^4$ (M)	Φ_1	Φ_2	$-\Delta[A]\times10^5$ M
1.02	—	0.36_2	—
1.83	0.13_1	0.34_5	0.8_8
3.37	0.11_8	0.30_5	2.2_2
3.95	0.12_4	0.33_1	2.3_3
5.84	0.12_7	0.29_7	3.6_9
6.25	0.12_4	0.29_2	3.9_4
7.91	0.10_0	0.17_5	5.2_9
8.98	0.10_0	0.17_3	5.0_8
9.04	0.09_8	0.19_9	6.5_5
11.3	0.10_0	—	—

and accordingly, $-\Delta[A]$ is the decrease of acridine due to this mechanism during the first stage. The critical value lies in the region, 1.02—1.83$\times10^{-4}$ M. Table 1 gives the values of $-\Delta[A]$, the quantum yields for the aerated (Φ_{air}) and deaerated solution (Φ) and those for the various concentrations of oxygen. In the latter cases, the quantum yields for the early stage Φ_1 and for the later stage Φ_2 are tabulated separately.

The quantum yields of oxygen consumption, Φ_{O_2} can be evaluated simply from the following relation,

$$\frac{-d[O_2]}{dt}\Big/\frac{-d[A]}{dt}=\frac{\Phi_{O_2}}{\Phi_1}=\frac{-\Delta[O_2]}{-\Delta[A]} \qquad (3)$$

where $-\Delta[O_2]$ can be equated to the initial concentration of oxygen. From the plot of Fig. 3 the value of Φ_{O_2}/Φ_1 was evaluated as 16 and accordingly Φ_{O_2}, as $\sim$2.0. This value suggests the occurrence of chain mechanism for the disappearance reaction of oxygen.

Reaction Sensitized by Biacetyl. In order to know whether the lowest $T(\pi\text{-}\pi^*)$ can participate in the reaction, the photosensitized reaction by triplet energy transfer using biacetyl as a donor was attempted at first. The T-levels of biacetyl $T(n\text{-}\pi^*)$ and acridine $T(\pi\text{-}\pi^*)$ are respectively 19700 cm^{-1} [9] and 15840 cm^{-1}.[10] The lifetime of biacetyl $T(n\text{-}\pi^*)$ in methanol is 0.2×10^{-3} sec[3b] and the diffusion controlled rate constant in THF estimated from the Stokes-Einstein relation is 1.4×10^{10} $M^{-1}sec^{-1}$. Therefore, it is expected that 10^{-4} M of acridine is enough for the complete energy transfer to occur from biacetyl to acridine. This was really verified by the complete quenching of biacetyl phosphorescence in the solution containing 10^{-4} M of acridine. This is shown in Fig. 4.

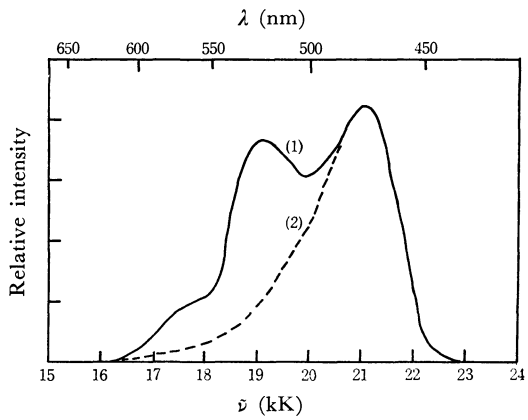

Fig. 4. Emission spectra of biacetyl in the deaerated THF solution (exciting light, 420 nm).
(1) [B]$=1\times10^{-1}$ M
(2) [B]$=1\times10^{-2}$ M, [A]$=1\times10^{-4}$ M

Hence the photosensitized reaction was investigated with the THF solutions containing 10^{-2} M biacetyl and 1×10^{-4} M acridine. The exciting light was chosen at 435.8 nm where there is no absorption of acridine. It is to be noted however, that biacetyl undergoes some unknown reaction in THF gradually when kept in dark for a long time. Hence the sample solution was always prepared immediately before each measurement.

In the aerated solution, the reaction did not occur at all. This is natural since the triplet biacetyl is expected to be quenched completely by $\sim2\times10^{-3}$ M of oxygen.

9) H. L. J. Bäckström and K. Sandros, *Acta Chem. Scand.*, **14**, 48 (1960).
10) D. F. Evans, *J. Chem. Soc.*, **1957**, 1351.

In the deaerated solution the reaction occurred as shown in Fig. 5. In Fig. 6, the relation between the decrease of acridine, $-\Delta$[A] as measured by the optical density at 357 nm and the increase of

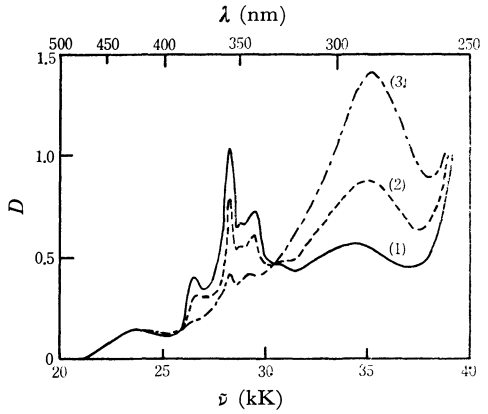

Fig. 5. Change of absorption spectra upon excitation of biacetyl at 435.8 nm (deaerated THF solution).
[A] = 1×10^{-4} M [B] = 1×10^{-2} M
(1) before illumination
(2) 1 min illumination
(3) 4 min illumination

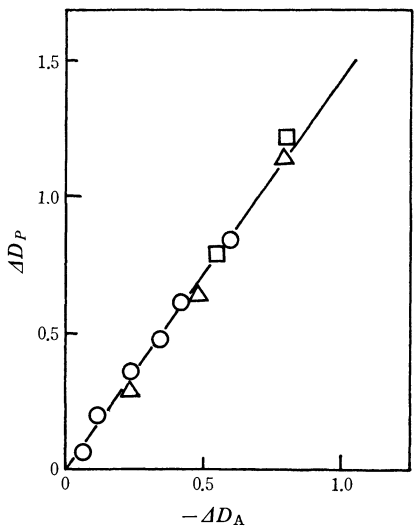

Fig. 6. The relation between the decrease of acridine and the increase of photoproducts.
□ Direct reaction (aerated soln.)
△ Direct reaction (deaerated soln.)
○ Sensitized reaction

photoproducts, Δ[P] measured by the optical density at 285 nm in the present sensitized reaction, is compared with that for the direct reaction. The agreement between the two cases supports that the similar reaction is occurring in the two cases. If one assumes the following scheme,

$$B + h\nu \longrightarrow {}^1B^* \qquad I_{abs}$$
$${}^1B^* \longrightarrow {}^3B \qquad \varphi_{ST}^B I_{abs}$$
$${}^1B^* \xrightarrow{k_1} B + h\nu_f$$
$${}^3B \xrightarrow{k_2} B + h\nu_p$$
$${}^3B \xrightarrow{k_3} B$$
$${}^3B + A \xrightarrow{k_4} B + {}^3A$$
$${}^3A + RH_2 \xrightarrow{k_5} Prod$$
$${}^3A \xrightarrow{k_6} A$$

where $^1B^*$, ^3B and ^3A are respectively the singlet excited state of biacetyl, the n–π^* triplet of biacetyl and the π–π^* triplet of acridine. RH_2 stands for THF which acts as a reducing agent. The steady state method gives the following equation,

$$-d[A]/dt = \varphi_{ST}\cdot\chi\cdot\beta\cdot I_{abs} \qquad (4)$$
$$\chi = k_4[A]/(k_2+k_3+k_4[A])$$
$$\beta = k_5[RH_2]/(k_5[RH_2] + k_6)$$

Putting $\varphi_{ST}^B \simeq 1$[9] and $\chi = 1$, the following zeroth order rate formula is expected to hold, which enables us to evaluate the value of β.

$$[A] = [A]_0 - \beta I_{abs} t \qquad (5)$$

In reality however, this does not hold satisfactorily as shown in Fig. 7. Perhaps it may be due to the occurrence of some side reactions involving biacetyl. Thus the exact value of β could not be decided and only its lower limit was estimated as $\beta \gtrsim 0.6$.

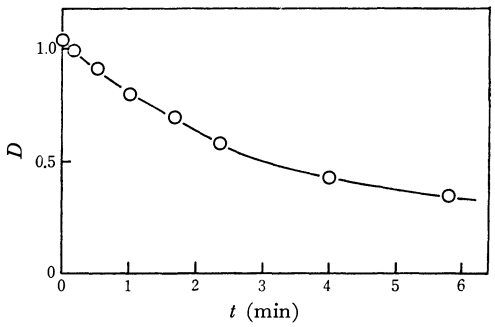

Fig. 7. Plot of D at 357 nm *vs.* time for the biacetyl sensitized reaction.

The Effect of the Addition of Anthracene as a *T*-Energy Acceptor. Although the above results support the occurrence of photoreduction at the lowest $T(\pi$–$\pi^*)$ of acridine, there still remains some suspicion that the reaction is not due to *T–T* energy transfer but due to some other type of sensitization, for instance, a reaction involving half-reduced biacetyl.[2] To get further evidence, the effect of the addition of a triplet energy acceptor on the photoreduction was examined. As such a substance, anthracene $T(\pi$–$\pi^*)$ of which is located at 14700 cm^{-1} [11] was employed. Anthracene has

11) J. Nag-Chaudhuri, L. Stoessell and S. P. McGlynn, *J. Chem. Phys.*, **38**, 2027 (1963).

however, the absorption in the region common to acridine, and care should be paid on its inner filter effect.

Generally, the information on the energy transfer can be obtained directly by the flash technique. But before doing this, the feature of the transient species produced by the flash illumination in THF solutions of acridine alone, anthracene alone and of the two, were examined preliminarily. The transient spectra of acridine, 1×10^{-4} M in THF, resemble those obtained in ethanol[12] and in benzene[7b] very well, and the peaks at 440 nm and at 520 nm are safely assigned to the T–T absorption and to semiquinone. The first order decay constant of the former could not be measured very accurately but was estimated about $\sim1\times10^{4}$ sec^{-1}. The second order decay constant of semiquinone measured at 520 nm was $\sim4\times10^{5}$ ε M^{-1} sec^{-1}. The transient absorption for anthracene alone 1×10^{-5} M and for the mixture of anthracene 1×10^{-5} M and acridine 1×10^{-4} M were compared. The former agrees very well with T–T absorption in literature,[13] and its decay is of the second order in agreement with Linschitz *et al.*[14] The decay constant was measured at 425 nm and was decided as 8.1×10^{4} ε M^{-1} sec^{-1}. The agreement of the main peak position in the two solutions suggested the almost complete energy transfer from acridine to anthracene.

Quantitative Investigation on the Energy Transfer. The energy transfer from acridine $T(\pi\text{–}\pi^*)$ to anthracene was investigated quantitatively under various conditions using the flash technique involving the emission measurement.[15] For this purpose, the yields of triplet anthracene $[^3An]_0$ were investigated at a fixed acridine concentration, $[A]=1\times10^{-4}$ M and at various anthracene concentrations up to 2×10^{-5} M. Under such a condition, the inner filter effect of anthracene may be neglected to a first approximation. The yield of triplet anthracene $[^3An]_0$ for which conventionally the quantity 50 μsec after flashing was taken,[15] consists in general of the two portions, the one due to the direct excitation of anthracene, $[^3An]_d$ and the other due to energy transfer from acridine, $[^3An]_e$. Thus,

$$[^3An]_0 = [^3An]_d + [^3An]_e \qquad (6)$$

Under the above assumption the efficiency of energy transfer can be studied from the effect of anthracene concentration on $[^3An]_e$, and to do this it is necessary to know the magnitude of $[^3An]_d$. This was performed as follows. $[^3An]_d$ which is equated to $\varphi_{ST}^{An}\int I_{abs}^{An}dt$, is proportional to the integrated fluorescence intensity during a flash because of the following relation,

$$\int I_F\,dt \propto \phi_F \int I_{abs}^{An}\,dt$$

in which ϕ_F is the fluorescence quantum yield. The fluorescence of anthracene was measured at 405 nm where there is no absorption of acridine and of anthracene. Figure 8 gives the relationship between $\int I_F\,dt$ (at 405 nm) and D_0 (at 425 nm) measured at various flash intensities for the solution of anthracene alone. It is obvious that the relation

$$D_0 = \gamma\int I_F\,dt \qquad (7)$$

holds satisfactorily and that the parameter γ can be evaluated correctly from the plot. This relation can be used to know the quantity of $[^3An]_d$ for the mixed solution of acridine and anthracene, because acridine is nonfluorescent in THF.

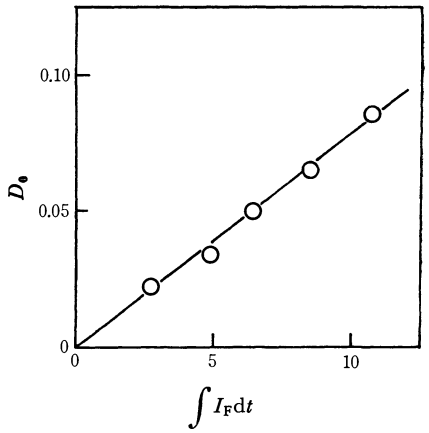

Fig. 8. Plot of D_0 at 425 nm *vs.* $\int I_F dt$ at 405 nm for the THF solution of anthracene.

Now in practice, it is more convenient to make argument in terms of the optical densities, and for this purpose equation (6) is to be rewritten as follows using eq. (7).

$$D_0 = D_0^A + D_{0e}^{An} + \gamma\int I_F\,dt \qquad (8)$$

where D_0, D_{0e}^{An} and D_0^A are respectively the entire optical density at 425 nm, that due to anthracene produced by energy transfer and that due to acridine. The values of $D_0^A+D_{0e}^{An}$ thus obtained are in general written as follows,

$$D_0^A + D_{0e}^{An} = \{\varepsilon_{^3A}[^3A]_0 + \varepsilon_{^3An}[^3An]_e\}d \qquad (9)$$

12) A. Kira, S. Kato and M. Koizumi, This Bulletin, **39**, 1221 (1966).

13) M. W. Windsor and J. R. Novak, "The Triplet State," ed. A. B. Zahlan, Cambridge University Press, Cambridge (1967), p. 229.

14) H. Linschitz, C. Steel and J. A. Bell, *J. Phys. Chem.*, **66**, 2574 (1962).

15) K. Kikuchi, H. Kokubun and M. Koizumi, This Bulletin, **49**, 1545 (1968).

In the special case that [An]=0,

$$D_{00}^{A} = \varepsilon_{^3A}[^3A]_{00}d \tag{10}$$

From these two equations and using the relation $[^3A]_{00}=[^3A]_0+[^3An]_0$, one gets

$$\Delta D_{0e} = D_0^A + D_{0e}^{An} - D_{00}^A = \{(\varepsilon_{^3An}-\varepsilon_{^3A})[^3An]_e\}d \tag{11}$$

which shows that ΔD_{0e} is a measure of $[^3An]_e$.

Figure 9 gives the plot of ΔD_{0e} *vs.* [An]. It can be concluded from Fig. 9 that the energy transfer occurs completely above 5×10^{-6} M of anthracene. It is to be added that the decay of triplet anthracene in the mixed solution is $\sim0.8\times10^4$ sec^{-1} and is very much larger than that in the solution of anthracene alone. This may suggest the attack of some intermediates originating from acridine upon triplet anthracene, but this does not invalidate the above treatment.

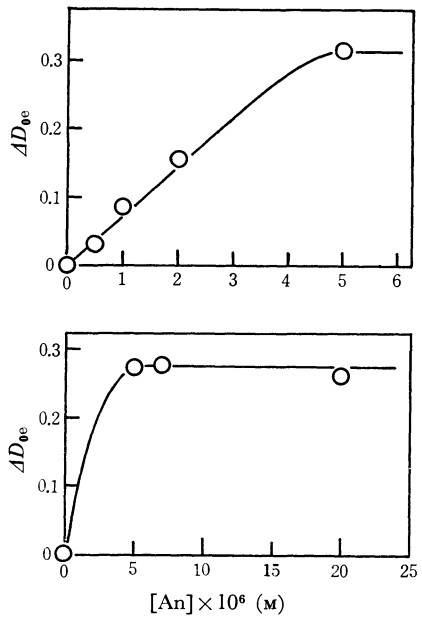

Fig. 9. Plots of ΔD_{0e} *vs.* [An].
upper: lower concentration region
lower: higher concentration region

Dependence of the Quantum Yield on the Anthracene Concentration. This was investigated by varying the concentration of anthracene from 5×10^{-7} to 1.4×10^{-4} M and by fixing the concentration of acridine at 1×10^{-4} M. It was found that the solution of anthracene alone undergoes the photoreaction but the quantum yield is less than 10^{-2} and can be neglected in the present case. The inner filter effect was corrected on the basis of the following equation,

$$\ln(e^{2.303D_0}-1) - \ln(e^{2.303D}-1) = \Phi I_0\alpha\left(t-\int_0^t \frac{D_{An}}{D}dt\right)\times10^3 \tag{12}$$

where α is the molar absorption coefficient of acridine at 365 nm, where D and D_0 are the optical densities at t and $t=0$ and where D_{An} is the optical density of anthracene. The other notations are the usual ones. Thus the correct value of Φ can be obtained only by changing the time axis by $-\int_0^t D_{An}/D\cdot dt$. It was checked that this correction was very satisfactory. The quantum yields at various anthracene concentrations are given in Table 2.

TABLE 2. QUANTUM YIELDS AT VARIOUS ANTHRACENE CONCENTRATIONS

[An] (M)	Φ	$-\Delta\Phi$
0	0.36	—
5×10^{-7}	0.35_7	0.00_3
1×10^{-6}	0.33_0	0.03_0
2×10^{-6}	0.31_4	0.04_6
5×10^{-6}	0.29_8	0.06_2
5×10^{-6}	0.31_2	0.04_8
7×10^{-6}	0.30_6	0.05_4
1×10^{-5}	0.32_1	0.03_9
2×10^{-5}	0.30_2	0.05_8
2.5×10^{-5}	0.29_3	0.06_7
5×10^{-5}	0.28_5	0.07_5
9×10^{-5}	0.26_8	0.09_2
1.4×10^{-4}	0.25_1	0.10_9

It is obvious that the addition of anthracene causes a decrease in the quantum yield. Assuming that this decrease is due to the energy trnasfer from acridine $T(\pi\text{-}\pi^*)$ to anthracene, the analysis can be made on the following scheme,

$$A + h\nu \longrightarrow A^* \qquad I_{abs}$$
$$A^* + RH_2 \longrightarrow Prod \qquad \Phi^* I_{abs}$$
$$A^* \longrightarrow {}^3A \qquad \varphi_{ST} I_{abs}$$
$${}^3A \xrightarrow{k_1} A$$
$${}^3A + RH_2 \xrightarrow{k_2} Prod$$
$${}^3A + An \xrightarrow{k_3} A + {}^3An$$
$${}^3An \xrightarrow{k_4} An$$

where ^3A is the lowest $T(\pi\text{-}\pi^*)$ of acridine and A* stands conventionally for the other reactive states (singlet excited state and $T(n\text{-}\pi^*)$) and where ^3An is the anthracene triplet state. The total quantum yield consists of two parts, one due to A^* (Φ^*) and the other due to ^3A (Φ_T). In the absence of anthracene,

$$\Phi_0 = \Phi^* + \Phi_T^0$$

and in the presence of anthracene (assuming that anthracene quenches only $T(\pi\text{-}\pi^*)$),

$$\Phi = \Phi^* + \Phi_T$$

Then,

$$-\Delta\Phi = \Phi_0 - \Phi = \Phi_T^0 \frac{k_3[\mathrm{An}]}{k_1+k_2[\mathrm{RH_2}]+k_3[\mathrm{An}]} \quad (13)$$

and

$$1/-\Delta\Phi = 1/\Phi_T^0(1+1/(k_3[\mathrm{An}]\tau)) \quad (14)$$
$$(1/\tau = k_1+k_2[\mathrm{RH_2}])$$

Since the flash experiment has already demonstrated that the energy transfer is complete above 5×10^{-6} M of anthracene, it is desirable to apply the above equation at lower concentrations. But in such a region the effect was so small that the reliable data could not be obtained. In fact, Table 2 shows that the values of $-\Delta\Phi$ in the region 5×10^{-6}—2.5×10^{-5} M of anthracene, are almost constant and are 0.06. The further decrease in the higher concentration of anthracene might be due to the quenching of $T(n\text{-}\pi^*)$. Figure 10 gives the plot of $1/\Phi$ *vs.* log [An] and the plot of $1/-\Delta\Phi$ *vs.* [An] which was drawn under the assumption that Φ_T^0 is equal to 0.06. The value of $k_3\tau$ obtained from the latter plot is 3.5×10^6 M^{-1} and by putting $k_3=1.4\times10^{10}$ M^{-1} sec^{-1}, one gets $\tau=2.5\times10^{-4}$ sec. Although these values are not very reliable, the latter value is compared with the result obtained by the flash experiment.

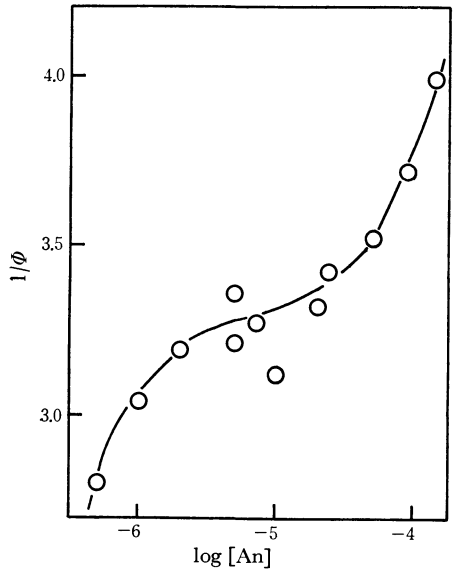

Fig. 10a. Plot of $1/\Phi$ *vs.* log [An].

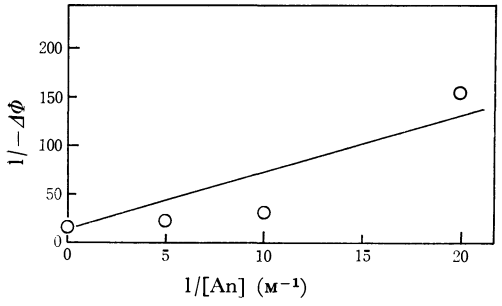

Fig. 10b. Plot of $1/-\Delta\Phi$ *vs.* 1/[An].

Conclusion

The present work has established that the quantum yields of the photoreduction of acridine in the aerated and in the deaerated THF solution are respectively 0.12 and 0.36. The former occurs by molecular mechanism, and the latter by radical mechanism in addition to molecular one. The contribution of radical mechanism is thus 0.24. We have not yet succeeded in deciding the contribution of different excited states to the above two processes. But it has been demonstrated that a certain portion is due to the reaction involving $T(\pi\text{-}\pi^*)$. Thus firstly, the sensitized reaction has been found to occur by using biacetyl as a sensitizer, of which the triplet level is lower than acridine $T(n\text{-}\pi^*)$ but higher than its $T(\pi\text{-}\pi^*)$. Furthermore, it has been shown by the flash technique that anthracene above 5×10^{-6} M, deactivates $T(\pi\text{-}\pi^*)$ of acridine completely and that the quantum yield of photoreduction of acridine decreases by about 0.06 ($=\Phi_T$) by the addition of anthracene of the same concentration. Combining the value of Φ_T with the probability factor $\beta\gtrsim0.6$ with which the $T(\pi\text{-}\pi^*)$ state reacts with THF, it can be concluded that the φ_{ST} value in the present system appears to be $\lesssim0.1$.

On the basis of this value, further conclusion

Table 3. Quantum yields in various solvents

	Φ_{total}	Φ_M (%)	Φ_R (%)	$\Phi_{T(\pi-\pi^*)}$ (%)	Φ_{O_2}
THF	0.36	0.12 (33)	0.24 (67)	0.06 (17)	2
Methanol	0.128	0.033 (25) (S 0.027, T 0.006)	0.096 (75) (S 0.039, T 0.057)	0	0.096
Ethanol	0.129	0.043 (30) (S only)	0.086 (70) (S 0.067, T 0.019)	0	0.086
n-Propanol	0.088	0.030 (35) (S only)	0.058 (65) (S 0.036, T 0.022)	0	—
Isopropanol	0.089	0.031 (35) (S only)	0.058 (65) (S only)	0	0.16

S: Singlet excited state, T: $T(n\text{-}\pi^*)$ state.

can be made on the reactive states in the present system. Table 3 lists the present result with those obtained by our group in the past. From the results in alcohols, one may say that molecular mechanism occurs mainly at singlet excited state. This may perhaps be true for THF. Then the Φ_R value of 0.24 includes 0.06 of $\Phi_{T(\pi-\pi^*)}$ and the remaining part 0.18 may be due to the reaction at both singlet excited and $T(n-\pi^*)$ states. It is highly unlikely that this is due only to singlet excited state in view of the φ_{ST} values estimated from the previous work. Thus the value of φ_{ST} in benzene and in water was estimated respectively as $\gtrsim 0.25$[7a] and $\gtrsim 0.24$.[16] Furthermore it has been decided recently by Kikuchi that the φ_{ST} value in ethanol is 0.27.[17] This value, however, is concerned with the $T(\pi-\pi^*)$ state which is produced under the condition that the reaction *via* $T(n-\pi^*)$ is occurring as shown in the above table. Thus the true φ_{ST} value in ethanol is $\gtrsim 0.27+0.019=0.29$. At any rate, it seems that the φ_{ST} value does not vary so much according to solvents, and it lies in the range 0.25—0.3. Hence, it is very unlikely that the true φ_{ST} value in THF is so small as $\lesssim 0.1$. It may be concluded that this low value is due to the participation of $T(n-\pi^*)$ in the reaction to some considerable extent. Further decrease in the quantum yield by the addition of anthracene $> 2\times 10^{-5}$ M, is also consistent with this conclusion. Determination of the reliable φ_{ST} values of acridine in various solvents are now in progress.

At the end, some consideration will be added on the quantum yields of the oxygen consumption, Φ_{O_2}. In table 3 are added the Φ_{O_2} values in THF and in alcohols, the values in alcohols being recalculated from the old data.[8] It is remarkable that the values of Φ_{O_2} in methanol and ethanol do agree exactly with the Φ_R values. This is interpreted very satisfactorily as follows. Acridine semiquinone AH and the solvent radical RH produced by radical mechanism in these solvents mainly undergo disproportionation reaction separately, as has been substantiated to some extent in the previous paper.[12] Oxygen when existent, is considered to be consumed mainly by the following processes,

$$AH + (O_2) \longrightarrow A + HO_2,\quad 2HO_2 \longrightarrow H_2O_2 + O_2$$

where (O_2) denotes the oxygen involved in the oxidative species.

Then for each two semiquinone molecules, one acridan molecule is produced in the absence of oxygen while in the presence of oxygen, one oxygen molecule is exhausted. Thus the material balance is in excellent agreement with the above data. On the other hand, for isopropanol and especially for THF, the Φ_{O_2} values are much larger than those of Φ_R. It is suggested that in these solvents, the following reactions may occur as proposed by Stockhausen *et al.*,[18] in the presence of oxygen.

$$RH + O_2 \longrightarrow RHO_2 \quad (1)$$

$$RHO_2 + RH_2 \longrightarrow RHO_2H + RH \quad (2)$$

$$RHO_2 + RHO_2 \longrightarrow \text{Prod} \quad (3)$$

If process (2) predominates over process (3) then the chain type-reaction will become possible. In fact, it really occurs in THF, as has been clearly demonstrated by the Φ_{O_2} value larger than unity.

Appendix

Measurement of the Solubility of Oxygen in THF. Since no data on the solubility of oxygen in

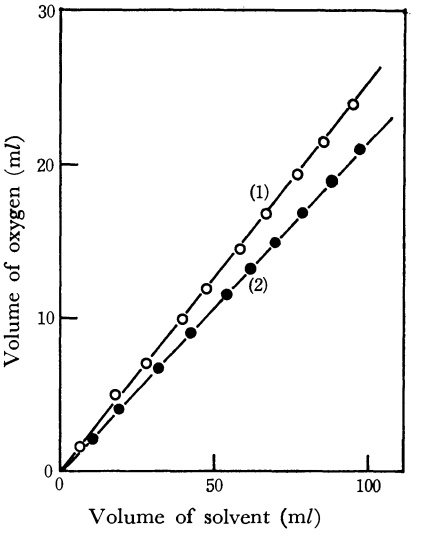

Fig. 11. The relation between the volume of solvent and that of oxygen dissolved in it.
(1) THF (2) Benzene

TABLE 4. SOLUBILITY DATA OF OXYGEN

	Rate of dropping (ml/min)	α	mean	α in literature
Methanol	0.75	0.229	0.229	0.227[20]
	1.5	0.228		
	2.0	0.229		
Benzene	1.5	0.203	0.204	0.205[21]
	2.0	0.205		
THF	1.0	0.236	0.235	—
	1.9	0.234		
	2.5	0.236		

16) K. Uchida and M. Koizumi, This Bulletin, **35**, 1875 (1962).

17) K. Kikuchi, H. Kokubun and M. Koizumi, The 23rd Annual Meeting of Chem. Soc. Japan, April in 1970.

18) K. Stockhausen, A. Henglein and G. Beck, *Ber. Bunsenges. Phys. Chem.*, **73**, 567 (1969).

THF are found in literature, the measurement was made with an apparatus constructed according to the direction recommended by Morrison and Billet,[19] which in principle is based on the saturation method.

Result. The measurement was made at 25°C. The analysis was made by plotting the volume of dissolved gas against that of solvent. Some examples are shown in Fig. 11. From the slope of the plot, the solubility, L was evaluated and Bunsen coefficient was obtained from the following relation.

$$\alpha = L\frac{273}{273+t}$$

As a check Bunsen coefficients of oxygen in methanol and benzene were measured. The results are given in Table 4, together with the data in literature.

19) T. J. Morrison and F. Billet, *J. Chem. Soc.*, **1948**, 2033. R. Battino and H. L. Clever, *Chem. Rev.*, **66**, 395 (1966).

20) C. B. Kretschmer, J. Nowakowska and R. Wiebe, *Ind. Eng. Chem.*, **38**, 506 (1946).

21) J. Horiuchi, *Sci. Pap. Inst. Phys. Chem. Res. (Tokyo)* **17**, 125 (1931).

BULLETIN OF THE CHEMICAL SOCIETY OF JAPAN VOL. 43 3443—3449 (1970)

Electronic Structures of Aromatic Ketyl Radicals and Related Hydrocarbon Radicals

Nobuaki KANAMARU*1 and Saburo NAGAKURA

The Institute for Solid State Physics, The University of Tokyo, Roppongi, Minato-ku, Tokyo

(Received July 7, 1970)

The π-electron structures of neutral aromatic ketyl radicals and their related hydrocarbon radicals were studied theoretically by combining the open-shell SCF MO method with the configuration-interaction calculation. The observed absorption bands of these radicals were well explained by the present theoretical study. From a comparison of the calculated transition energies and intensities with the observed values, it was concluded that the longest and second longest wavelength bands of the benzyl radical and the second longest wavelength band of the diphenylmethyl radical shift to shorter wavelengths upon hydroxy substitution. This may be regarded as characteristic of the substituent effect upon the absorption bands of aromatic radicals. The calculated spin densities were found to be consistent with the reactivity of the ketyl radicals in the formation of pinacols.

Neutral aromatic ketyl radicals and related hydrocarbon radicals are known to be prepared by the photo-reduction of the parent aromatic carbonyl compounds[1-4] and by the photo-decomosition of the parent hydrocarbons,[5,6] respectively. Their electronic spectra have been studied experimentally by several authors and the absorption bands pertinent to each radical have been observed. However, there have been rather few theoretical studies of the electronic structures of the ketyl radicals.

We are interested in the correlation in electronic absorption bands between hydrocarbon radicals and the corresponding ketyl radicals. This is because the latter can be regarded as the hydroxy derivatives of the former and therefore the comparison of their absorption bands may give some information on the substituent effect upon the electronic absorption spectra of radicals. On this line, we have undertaken to study theoretically the electronic absorption spectra of some ketyl radicals and the corresponding hydrocarbon radicals.

Theoretical

The π-electron structures of aromatic ketyl radicals and related hydrocarbon radicals were studied by the method combining the open-shell SCF MO procedure of Longuet-Higgins and

*1 Present address: Research Institute of Applied Electricity, Hokkaido University, Sapporo.

1) G. Porter and F. Wilkinson, *Trans. Faraday Soc.*, **57**, 1686 (1961).
2) A. Beckett, A. D. Osborne and G. Porter, *ibid.*, **60**, 873 (1964).
3) N. Kanamura and S. Nagakura, *J. Amer. Chem. Soc.*, **90**, 6905 (1968).
4) W. A. Bryce and C. H. J. Wells, *Can. J. Chem.*, **41**, 2723 (1963).
5) E. J. Land and G. Porter, *Trans. Faraday Soc.*, **59**, 2027 (1963).
6) I. Norman and G. Porter, *Proc. Roy. Soc.*, **A230**, 399 (1955).

Pople[7] with the configuration-interaction (abbreviated hereafter to CI) calculation. The CI calculation was made by taking at most 50 configurations of lower energies constructed by putting $2m+1$ π electrons into the lower molecular orbitals represented by the linear combination of atomic orbitals. They include the ground configuration and also the singly and doubly-excited configurations.

The Coulomb repulsion integrals of the type of (pp|qq) were calculated according to the Pariser-Parr approximation,[8] the radii of the electron clouds being evaluated with the aid of the effective nuclear charge determined by the Slater rule, and the ionization potentials (I) and electron affinities (A) of the appropriate valence states being taken from Pilcher and Skinner's Table.[9] The I_C, A_C, I_{O^+} and A_{O^+} values are 11.22 eV, 0.62 eV, 34.43 eV and 14.97 eV, respectively. The core Coulomb integral, α_p, was evaluated as the sum of the ionization potential of the π electron on the p-th atom and the Coulomb attraction terms due to the other atomic cores. The penetration integrals were disregarded.

A planar structure was assumed for the radicals under consideration, all the C-C bond lengths and all the bond angles being taken to be equal to 1.39 Å and 120°, respectively. The C-O bond length was taken to be equal to that of 1,4-dimethoxybenzene, 1.36 Å.[10] The core resonance integral, β_{CC}, for the neighbouring carbon atoms was taken to be -2.39 eV, the value for benzene. The core resonance integral, β_{CO}, for the neighbouring carbon and oxygen atoms was taken to be -3.42 eV on the basis of its proportionality to the overlap integrals taken from the table of Mulliken *et al.*[11]

The actual calculation was carried out by an electronic computer HITAC 5020E located at the Computer Centre, The University of Tokyo.*2 The energies and wave functions of the ground and excited states, the spin densities in the ground state, and also the transition moments (in Å) were evaluated for the benzyl, diphenylmethyl and ketyl radicals.

Results and Discussion

Concerning the π-electron structures, the benzophenone (a) and anthrone (b) ketyl radicals may be regarded as equal to each other and as the hydroxy derivative of the diphenyl-methyl radical (c). The situation is same for the benzaldehyde and acetophenone ketyl radicals, the hyperconjugation effect of the methyl group being disregarded.

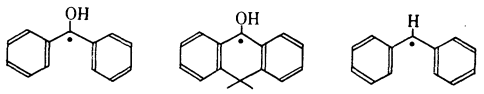

(a) (b) (c)

Hydrocarbon Radicals. The energies of the ground and lower excited states are shown in Table 1. This table also shows the percentages of the configurations mainly contributing to each state. The effect of CI upon the energy levels is shown in Fig. 1. An inspection of Table 1 and Fig. 1 shows that the CI procedure has a great effect upon the energy values and wave functions and is indispensable for this kind of calculation. The excitation energies, the oscillator strengths, and the directions of the transition moments obtained theoretically for the benzyl and diphenylmethyl radicals are shown in Table 2, together with the observed excitation energies and molar extinction coefficients.

From the consideration of the transition energies and oscillator strengths given in Table 2a), the 453 mμ and 318 mμ bands observed for the benzyl radical[5] are assigned to the $E_1{}^B \leftarrow G^B$ and $E_3{}^B \leftarrow G^B$ transitions, respectively. The band corresponding to the $E_2{}^B \leftarrow G^B$ transition may be too weak to be observed and may be covered by the $E_1{}^B \leftarrow G^B$ transition band.

Longuet-Higgins and Pople[7] made a calculation on the benzyl radical, taking only the first-order CI among five configurations. According to their result, the lower excited states corresponding to $E_1{}^B$ and $E_3{}^B$ in our calculation can be represented as follows:

	State function	Excitation energy (eV)
$E_1{}^{B'}$	$\frac{1}{2}(\psi_{3-4}+\psi_{4-5})$	3.46
$E_3{}^{B'}$	$\frac{1}{2}(\psi_{3-4}-\psi_{4-5})$	4.18

The present calculation greatly improves the agreement between the observed and theoretical transition energies compared with the Longuet-Higgins and Pople calculation.

A similar consideration was made of the diphenylmetyl radical, with the results given in Table

7) H. C. Longuet-Higgins and J. A. Pople, *Proc. Phys. Soc.*, **A68**, 591 (1955).

8) R. Pariser and R. G. Parr, *J. Chem. Phys.*, **21**, 466 (1953).

9) G. Pilcher and H. A. Skinner, *J. Inorg. Nucl. Chem.*, **24**, 937 (1962).

10) "Tables of Interatomic Distances and Configuration in Molecules and Ions," ed. by L. E. Sutton, The Chemical Society, London (1958).

11) R. S. Mulliken, C. A. Rieke, D. Orloff and H. Orloff, *J. Chem. Phys.*, **17**, 1248 (1949).

*2 A program written by Dr. Suehiro Iwata, The Institute of Physical and Chemical, Research, was used for the calculation. The authors' thanks are due to his kind help in the calculation.

TABLE 1. THEORETICAL RESULTS OF THE GROUND AND THE LOWER EXCITED STATES OF THE HYDROCARBON RADICALS

a) Benzyl

State*	Energy**	Configurations mainly contributed to each state***
$G^{B}(a)$	−0.612	g (94)
$E_1^{B}(b)$	2.333	4—5(42), 3—4(44)
$E_2^{B}(a)$	2.401	4—6(42), 2—4(43), 4—7(5)
$E_3^{B}(b)$	3.442	4—5(45), 3—4(43), $(2—5)_{\alpha}(5)$
$E_4^{B}(a)$	4.075	$(3—5)_{\alpha}(53)$, $(3—5)_{\beta}(18)$, 1—4(9), 4—7(9)
$E_5^{B}(a)$	4.304	4—6(37), 2—4(38), $(3—5)_{\beta}(12)$

b) Diphenylmethyl

State*	Energy**	Configurations mainly contributed to each state***
$G^{D}(a)$	−0.275	g (96)
$E_1^{D}(b)$	2.447	7—8(45), 6—7(43)
$E_2^{D}(b)$	2.803	7—9(41), 5—7(40), $(4—8)_{\alpha}(6)$
$E_3^{D}(a)$	2.899	4—7(41), 7—10(42), $(6—9)_{\beta}(5)$, $(5—8)_{\alpha}(7)$
$E_4^{D}(a)$	3.358	7—11(37), 3—7(38), $(6—8)_{\beta}(5)$, $(6—8)_{\alpha}(14)$
$E_5^{D}(b)$	3.562	7—8(5), 6—7(5), 7—9(37), 5—7(38)
$E_6^{D}(a)$	3.671	4—7(41), 7—10(40), $(6—9)_{\alpha}(6)$
$E_7^{D}(b)$	3.793	7—8(38), 6—7(40), 7—9(5), 5—7(5)

c) Acetophenone (benzaldehyde) ketyl

State	Energy**	Configurations mainly contributed to each state***
G^{Ak}	−0.444	g (94)
E_1^{Ak}	2.391	5—6(76), 4—5(11)
E_2^{Ak}	2.544	5—7(61), 3—5(26)
E_3^{Ak}	3.869	5—6(12), 4—5(71)
E_4^{Ak}	4.273	$(4—6)_{\alpha}(51)$, $(4—6)_{\beta}(15)$, 5—8(18), 2—5(7)
E_5^{Ak}	4.456	5—7(21), 3—5(51), $(4—6)_{\alpha}(7)$, $(4—6)_{\beta}(8)$, $(3—7)_{\alpha}(6)$

d) Benzophenone (anthrone) ketyl

State*	Energy**	Configurations mainly contributed to each state***
$G^{Bk}(a)$	−0.260	g (96)
$E_1^{Bk}(b)$	2.320	8—9(72), 7—8(15)
$E_2^{Bk}(a)$	2.692	8—10(73), 5—8(11)
$E_3^{Bk}(b)$	2.699	8—11(73), 6—8(10), $(7—10)_{\beta}(5)$
$E_4^{Bk}(a)$	3.242	8—12(45), 4—8(31), $(7—9)_{\alpha}(12)$
$E_5^{Bk}(b)$	3.788	8—11(11), 7—8(18), 6—8(49), $(5—9)_{\alpha}(10)$
$E_6^{Bk}(a)$	3.861	8—10(13), 5—8(63), $(7—10)_{\alpha}(13)$
$E_7^{Bk}(b)$	3.932	8—9(16), 7—8(47), 6—8(16), $(4—9)_{\alpha}(6)$

* The signs a and b represent the symmetry of each state.

** The energy values are indicated in the unit of eV, the ground configuration being taken as the standard.

*** In this column, the notations g and $n—m$ are used for representing the ground configuration and the excited configuration caused by the electron excitation from ϕ_n to ϕ_m, respectively. Here ϕ_n and ϕ_m represent the nth and mth SCF MO's of each radical. The number in parenthesis represents the contribution (in %) of a corresponding configuration to each state. Furthermore, suffixes α and β represent the spin state for each doublet configuration.

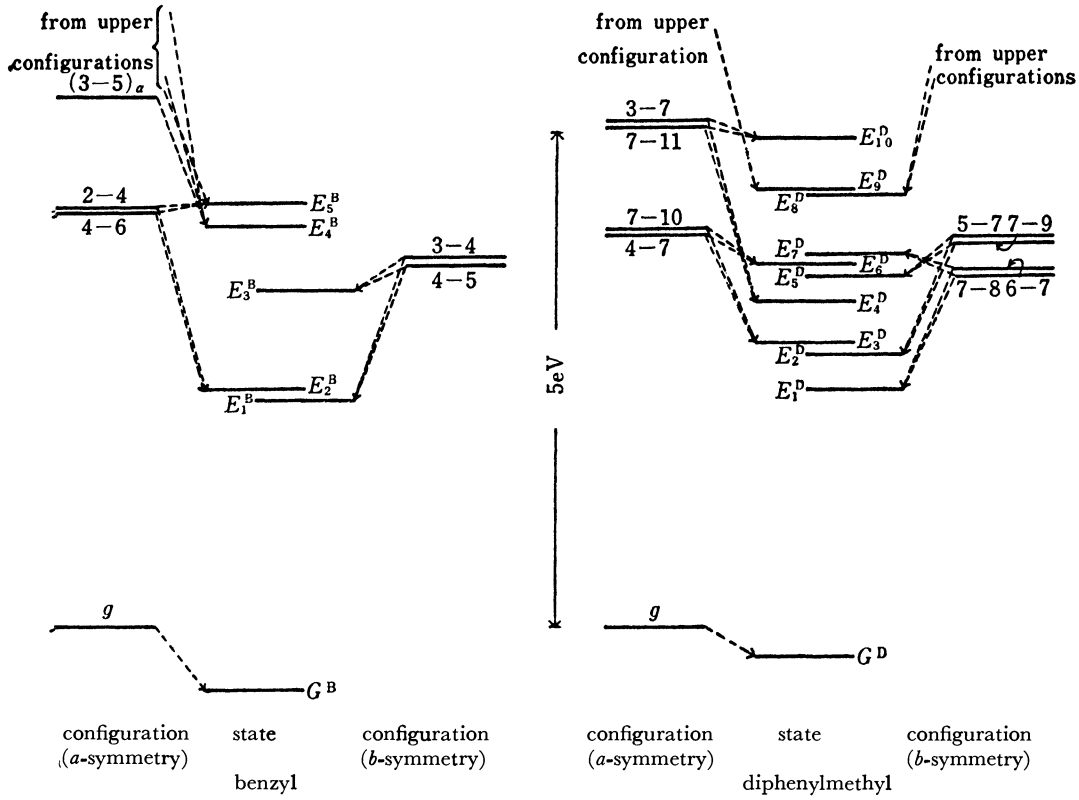

Fig. 1. The CI diagrams of the hydrocarbon radicals. The symbols of the configurations are explained in the footnote of Table 1.

TABLE 2. OBSERVED AND CALCULATED RESULTS FOR THE ABSORPTION SPECTRA OF THE HYDROCARBON RADICALS

a) Benzyl

Transition	Observed[5]		Calculated		
	E (eV)	ε	E (eV)	f	Direction of transition moment*
$E_1^B \leftarrow G^B$	2.74	230	2.945	6.4×10^{-5}	Y
$E_2^B \leftarrow G^B$			3.013	7.0×10^{-7}	X
$E_3^B \leftarrow G^B$	3.90	1100	4.053	5.9×10^{-2}	Y
$E_4^B \leftarrow G^B$			4.687	4.2×10^{-6}	X
$E_5^B \leftarrow G^B$			4.916	2.2×10^{-1}	X

b) Diphenylmethyl

Transition	Observed[6,12]		Calculated		
	E (eV)	ε (ratio)	E (eV)	f	Direction of transition moment*
$E_1^D \leftarrow G^D$	2.70	1	2.722	1.4×10^{-4}	Y
$E_2^D \leftarrow G^D$			3.078	7.5×10^{-6}	Y
$E_3^D \leftarrow G^D$			3.174	1.1×10^{-5}	X
$E_4^D \leftarrow G^D$			3.633	3.0×10^{-6}	X
$E_5^D \leftarrow G^D$			3.837	1.7×10^{-2}	Y
$E_6^D \leftarrow G^D$			3.946	5.7×10^{-2}	X
$E_7^D \leftarrow G^D$	3.70	150	4.068	5.6×10^{-1}	Y

* X is the symmetry axis of the radical.

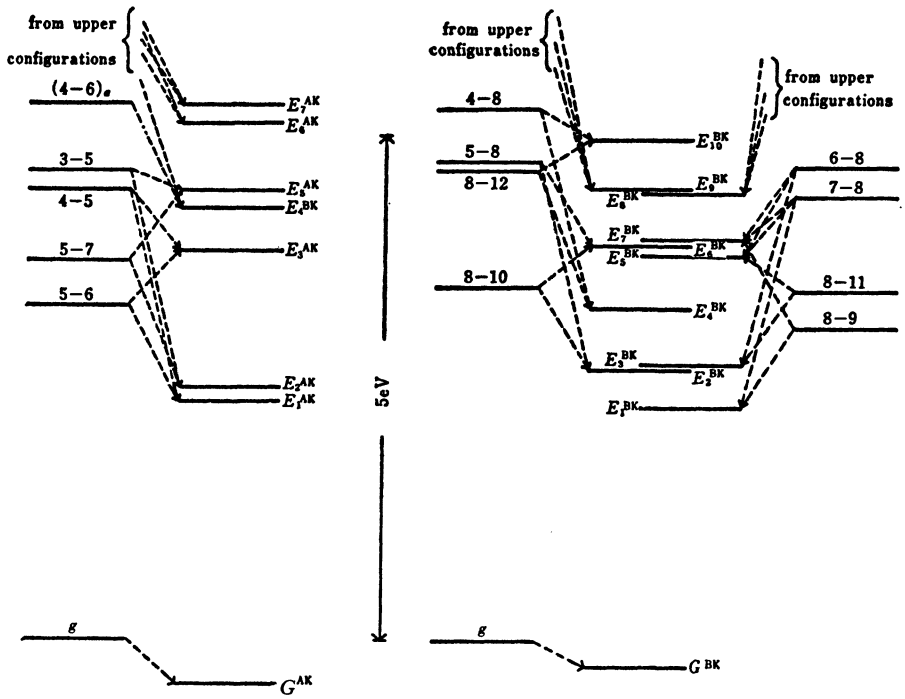

Fig. 2. The CI diagrams of the ketyl radicals. The symbols of the configurations are explained in the footnote of Table 1.

TABLE 3. OBSERVED AND CALCULATED RESULTS FOR THE ABSORPTION SPECTRA OF THE KETYL RADICALS

a) Acetophenone (benzaldehyde) ketyl

Transition	Observed[2]		Calculated	
	E (eV)*	ε (ratio)	E (eV)	f
$E_1^{Ak}\leftarrow G^{Ak}$			2.835	5.3×10^{-3}
$E_2^{Ak}\leftarrow G^{Ak}$	2.99(2.99)	0.05	2.988	2.2×10^{-2}
$E_3^{Ak}\leftarrow G^{Ak}$			4.313	3.8×10^{-2}
$E_4^{Ak}\leftarrow G^{Ak}$			4.717	2.0×10^{-2}
$E_5^{Ak}\leftarrow G^{Ak}$	4.48(4.59)	0.5	4.900	2.2×10^{-1}

b) Benzophenone (anthrone) ketyl

Transition	Observed[1,3]		Calculated		
	E (eV)*	f	E (eV)	f	Direction of transition moment**
$E_1^{Bk}\leftarrow G^{Bk}$	2.28(2.25)	0.065	2.580	8.0×10^{-2}	Y
$E_2^{Bk}\leftarrow G^{Bk}$			2.952	5.3×10^{-3}	X
$E_3^{Bk}\leftarrow G^{Bk}$			2.959	2.1×10^{-3}	Y
$E_4^{Bk}\leftarrow G^{Bk}$			3.502	5.9×10^{-4}	X
$E_5^{Bk}\leftarrow G^{Bk}$			4.048	2.2×10^{-2}	Y
$E_6^{Bk}\leftarrow G^{Bk}$			4.121	4.0×10^{-2}	X
$E_7^{Bk}\leftarrow G^{Bk}$	3.76(3.65)	0.32	4.192	4.2×10^{-1}	X

* The values in the parentheses are concerned with the benzaldehyde or anthrone ketyl radical.
** X is the symmetry axis of the benzophenone (anthrone) ketyl radical.

2b). A weak band was observed by Shida[12] at 460 mμ in addition to the strong band at 335 mμ. The absorbance ratio of the former to the latter is about 1:150. From the comparison of the calculated transition energies and intensities with those obtained experimentally, the observed bands at 460 mμ and at 335 mμ can be assigned to the $E_1^D \leftarrow G^D$ and $E_7^D \leftarrow G^D$ transitions, respectively. The $E_5^D \leftarrow G^D$ and $E_6^D \leftarrow G^D$ transitions also contribute to the 335 mμ band. The weak bands due to the $E_2^D \leftarrow G^D$, $E_3^D \leftarrow G^D$ and $E_4^D \leftarrow G^D$ transitions may be covered by the two bands.

Ketyl Radicals. The energies of the ground and lower excited states calculated for the ketyl radicals are shown in Table 1. This table also gives the percentages of the configurations mainly contributing to each state. The effects of CI upon the energy levels are shown in Fig. 2. The calculated transition energies and oscillator strengths are given in Table 3, together with the observed values.

From the comparison of the observed and calculated transition energies given in Table 3a), the 415 and 277 mμ bands of the acetophenone ketyl radical may be assigned to the $E_2^{Ak} \leftarrow G^{Ak}$ transition overlapped by the weak $E_1^{Ak} \leftarrow G^{Ak}$ transition and to the $E_5^{Ak} \leftarrow G^{Ak}$ transition overlapped by the $E_3^{Ak} \leftarrow G^{Ak}$ and $E_4^{Ak} \leftarrow G^{Ak}$ transitions, respectively.

An inspection of Table 3b) shows that the longer and shorter wavelength bands of the benzophenone ketyl radical can be ascribed to the $E_1^{Bk} \leftarrow G^{Bk}$ and $E_7^{Bk} \leftarrow G^{Bk}$ transitions, respectively. The latter band may be overlapped by the $E_6^{Bk} \leftarrow G^{Bk}$ and $E_5^{Bk} \leftarrow G^{Bk}$ transition bands, and the weak bands corresponding to the $E_2^{Bk} \leftarrow G^{Bk}$, $E_3^{Bk} \leftarrow G^{Bk}$ and $E_4^{Bk} \leftarrow G^{Bk}$ transitions may be covered by the two bands.

Substituent Effects upon the Absorption Bands of Hydrocarbon Radicals. First let us compare the absorption bands of the benzophenone ketyl radical with those of the diphenylmethyl radical. The observed longer wavelength band of the former shifts to longer wavelengths upon hydroxy substitution, as is usually observed with substituted aromatic hydrocarbons. On the other hand, the shorter wavelength band shows the reverse tendency. That is to say, the band corresponding to the 335 mμ band of the diphenylmethyl radical appears at 330 mμ for the benzophenone ketyl radical. The calculated transition energies given in Tables 2b) and 3b) can well explain the above-mentioned substituent effect on the two bands.

Concerning the benzyl and acetophenone radicals, either the longer or the shorter wavelength band was observed to shift to shorter wavelengths upon hydroxy substitution. This tendency is the opposite of the ordinary substituent effect observed for absorption bands of aromatic molecules like benzene and its derivatives; it may be regarded as characteristic of the aromatic radicals. According to the present calculation, the energies for the $E_5^{Ak} \leftarrow G^{Ak}$ and $E_2^{Ak} \leftarrow G^{Ak}$ transitions corresponding to the 277 mμ and 415 mμ bands of the acetophenone ketyl radical are greater than those

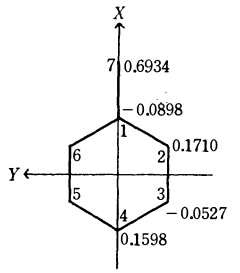

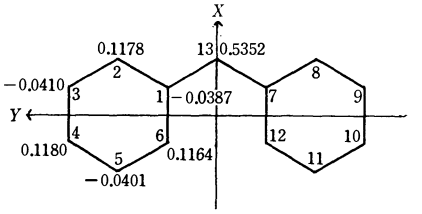

Fig. 3. Spin densities calculated for the benzyl and diphenylmethyl radicals.

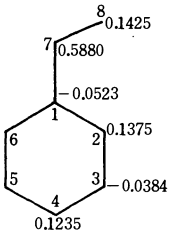

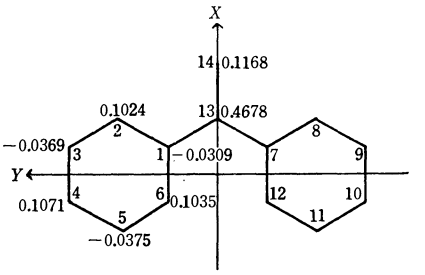

Fig. 4. Spin densities calculated for the acetophenone (benzaldehyde) and benzophenone (anthrone) ketyl radicals.

12) Private communication from Dr. Tadamasa Shida, The Institute of Physical and Chemical Research.

for the $E_3^{B}\leftarrow G^{B}$ and $E_1^{B}\leftarrow G^{B}$ transitions corresponding to the 318 mμ and 453 mμ bands of the benzyl radical, respectively. Therefore, the substituent effect upon the longest and second longest wavelength bands of the benzyl radical can be explained by the present theory.

Since the characters of the wave functions of the E_1^{B} and E_2^{Ak} states are similar to each other, the 415 mμ band of the acetophenone ketyl radical may be regarded as a shifted band of the 453 mμ band of the benzyl radical. This is the real blue shift phenomenon due to the hydroxy substitution. On the other hand, the E_3^{B} state does not correspond to the E_5^{Ak} state, but to the E_3^{Ak} state. Therefore, the 277 mμ band of the acetophenone ketyl radical can not be regarded as a shifted band of the 318 mμ band of the benzyl radical. In this sense, this band may be interpreted as apparently exhibiting the blue shift.*3

Spin Densities. The electron spin densities of the radicals under consideration were calculated with the results shown in Figs. 3 and 4. According to the results, the electron spin densities of the acetophenone and benzophenone ketyl radicals are greatest at the 7 th and 13 th positions, respectively. This is consistent with the fact that the formation of pinacol occurs at the above positions. A similar tendency holds for the hydrocarbon radicals.

The authors are greatly indebted to Dr. Tadamasa Shida, The Institute of Physical and Chemical Research, for his kindness in informing them of his unpublished results on the absorption spectrum of the diphenylmethyl radical.

*3 According to the present calculation, the transition energy for the $E_3^{Ak}\leftarrow G^{Ak}$ is greater than for the $E_3^{B}\leftarrow G^{B}$. This means that the 318 mμ band of the benzyl radical shows the real blue shift upon the substitution of the hydroxy group. In view of this, it may be interesting to carry out detailed experimental studies of the 277 mμ band of the acetophenone ketyl radical, if possible, and to separate it into the three components due to the $E_3^{Ak}\leftarrow G^{Ak}$, $E_4^{Ak}\leftarrow G^{Ak}$ and $E_5^{Ak}\leftarrow G^{Ak}$ transitions.

BULLETIN OF THE CHEMICAL SOCIETY OF JAPAN VOL. 43 3449—3452 (1970)

The Chemical Behavior of Low Valence Sulfur Compounds. VI. Decomposition of Tetrasulfur Tetranitride in Aqueous Ammonia Solution

Mu-Chang SHIEH, Kenichi KATABE and Taijiro OKABE

Department of Applied Chemistry, Faculty of Engineering, Tohoku University, Sendai

(Received April 10, 1970)

The decomposition of tetrasulfur tetranitride in an aqueous ammonia solution has been investigated. Ammonolysis of tetrasulfur tetranitride gives thiosulfate, sulfite, sulfate and sulfamate through the intermediate compound of trithionate. An increase in the concentration of ammonia raises the yield of sulfamate and lowers that of sulfate, but gives no remarkable change in the yield of thiosulfate. Besides this, in a concentration of ammonia higher than 15 N at 100°C an explosive reaction takes place. Addition of copper ion improves the yield of sulfamate, and the sulfite ion reacts with tetrasulfur tetranitride in an ammonia aqueous solution to form sulfate and sulfamate ion quantitatively.

In a previous paper[1] describing the reaction of low valence sulfur compounds, such as elemental sulfur, thiosulfate, sulfide, tetrathionate and trithionate in aqueous ammonia solution, it was shown that sulfate and sulfamate were finally formed in the oxidation of sulfur under oxygen pressure through polythionates as intermediate compounds, when the concentration of ammonia was restricted to about 16 N. On the other hand, it was reported[2] that the reaction of sulfur in an anhydrous ammonia gives tetrasulfur tetranitride:

$$10S + 4NH_3 = S_4N_4 + 6\,H_2S^{*1} \quad (1)$$

In this reaction, if a highly concentrated solu-

1) M. C. Shieh, H. Otsube and T. Okabe, This Bulletin, **38**, 1596 (1965).

2) F. W. Bergstrom, *J. Amer. Chem. Soc.*, **48**, 2319 (1926).

*1 The reaction is reversible, and the following reaction can take place according to the molar ratio of ammonia to sulfur.

$$H_2S + 2NH_3 = (NH_4)_2S$$
$$S_4N_4 + 2NH_3 = 2\,S(NH)_2 + S_2(NH)_2$$
$$(NH_4)_2S + xS = (NH_4)_2S_{x+1}$$
$$(NH_4)_2S_{x+1} = (NH_4)_2S_x + S$$

tion of ammonia is used for sulfur oxidation, tetrasulfur tetranitride can be regarded as an important intermediate compound. Thus we studied the decomposition of tetrasulfur tetranitride in aqueous ammonia solution in order to clarify the behavior of tetrasulfur tetranitride in the solution.

The decomposition of tetrasulfur tetranitride in aqueous sodium hydroxide solution has been studied by Meuwsen,[3] Goehring,[4] and Nair,[5] and it was revealed that the reactions depend on the alkalinity of solution as follows.

In a weak alkaline solution:

$$2S_4N_4 + 6OH^- + 9H_2O = S_2O_3^{2-} + 8NH_3 + 2S_3O_6^{2-} \quad (2)$$

In a strong alkaline solution:

$$S_4N_4 + 6OH^- + 3H_2O = S_2O_3^{2-} + 4NH_3 + 2SO_3^{2-} \quad (3)$$

Thiosulfate, trithionate and ammonia were formed in the former, and thiosulfate and ammonia in the latter. When the reaction, however, was carried out in aqueous ammonia, sulfite, sulfate, thiosulfate and sulfamate were produced through trithionate.

Experimental

Materials. Tetrasulfur tetranitride was prepared by the reaction of ammonia with sulfur chloride as described by Meuwsen.[3]

$$6S_2Cl_2 + 16NH_3 = S_4N_4 + 8S + 12NH_4Cl \quad (4)$$

The crude product was recrystallized from benzene, washed with carbon disulfide and dried over silica gel. The final product has a 99.5% purity and is free from sulfur.

Procedure. Known weights of finely ground tetrasulfur tetranitride and ammonium hydroxide were put into a 100 m*l* flask at 50°C or in a 30 m*l* pressure glass tube at 100°C. The flask or tube was kept in a heated glycerol bath regulated within ±0.5°C, withdrawn at regular intervals and the contents were analyzed in the same manner as described previously. Since the solubility of tetrasulfur tetranitride in the aqueous ammonia solution is low and the rate of reaction is determined merely by the dissolution of tetrasulfur tetranitride, no kinetic research was undertaken.

Results

When aqueous ammonia is added to finely ground tetrasulfur tetranitride, the solution gradually becomes slightly yellowish brown. Colora-

TABLE 1. DECOMPOSITION OF TETRASULFUR TETRANITRIDE AT 50°C

React. time (hr)	S_4N_4 taken (g)	Ammonia		Products (S-g·atom %)				
		concn. (N)	taken (m*l*)	SO_3^{2-}	$S_2O_3^{2-}$	SO_4^{2-}	$SO_3NH_2^-$	$S_3O_6^{2-}$
24	0.4439	0.1	100.0	1.89	49.62	17.57	2.06	28.86
	0.8572	0.5	100.0	3.87	53.80	15.70	3.44	23.19
	1.0015	1.0	100.0	3.53	56.28	15.91	4.15	20.13
	1.1910	3.0	100.0	3.75	60.24	11.35	8.08	16.58
	1.4734	6.0	40.0	3.21	56.48	8.70	12.08	18.81
	1.2988	15.0	20.0	1.25	62.22	6.65	15.80	14.17
96	0.9848	0.5	80.0	1.65	75.25	20.73	3.52	
	0.9985	1.0	60.0	0.51	74.80	19.58	6.24	
	1.0267	3.0	50.0	0.77	75.38	14.01	10.88	
	1.0081	6.0	40.0	0.55	73.60	10.01	14.17	
	1.0034	12.0	30.0	0.06	75.90	6.03	19.26	
	1.0024	15.0	20.0	0.05	76.62	4.91	19.31	

TABLE 2. DECOMPOSITION OF TETRASULFUR TETRANITRIDE AT 100°C

React. time (hr)	S_4N_4 taken (g)	Ammonia		Products (S-g·atom %)			
		concn. (N)	taken (m*l*)	SO_3^{2-}	$S_2O_3^{2-}$	SO_4^{2-}	$SO_3NH_2^-$
1/3	0.9766	3.0	20.0	1.88	75.74	12.51	8.53
1	0.9856	3.0	20.0	2.17	77.64	11.93	9.02
3	0.9761	3.0	20.0	1.53	76.38	12.18	9.02
5	0.9765	3.0	20.0	2.09	77.43	12.58	9.22
1	0.9681	12.0	10.0	1.30	78.79	5.03	15.91
3	0.9989	12.0	10.0	1.03	78.96	5.16	17.11
5	0.9936	12.0	10.0	0.88	78.18	4.97	16.02

3) A. Meuwsen, *Ber.*, **62**, 1959 (1929).

4) W. L. Jolly and M. Goehring, *Inorg. Chem.*, **1**, 76 (1961).

5) C. G. R. Nair and A. R. V. Murthy, *J. Inorg. Nucl. Chem.*, **25**, 453 (1963).

tion is caused by a slight dissolution of tetrasulfur tetranitride and fades away to a colourless state in less than 10 min, producing a large amount of thiosulfate. The results of the decomposition of tetrasulfur tetranitride at 50°C and 100°C are presented in Tables 1 and 2, respectively. The products of the reaction are thiosulfate, sulfite, sulfate and sulfamate and the conversions of sulfur in tetrasulfur tetranitride are $S_2O_3^{2-}$ 50—80 mol%, $SO_3NH_2^-$ 2—19 mol%, SO_4^{2-} 20—5 mol%, and SO_3^{2-} 1—4%.

Figs. 1 and 2 show the effect of ammonia concentration on the yield. An increase in the concentration of ammonia raises the yield of sulfamate and lowers that of sulfate, but gives no remarkable effect on the yield of thiosulfate.

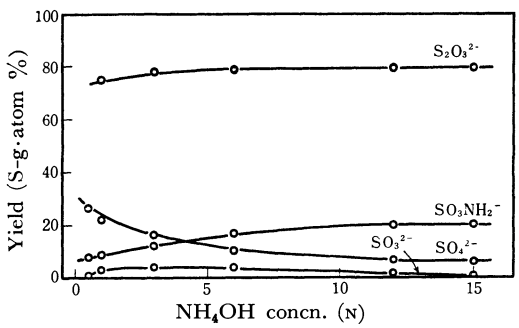

Fig. 1. Effect of ammonia concentration on the yeild of products.
React. temp.: 15°C React. time: 17 hr

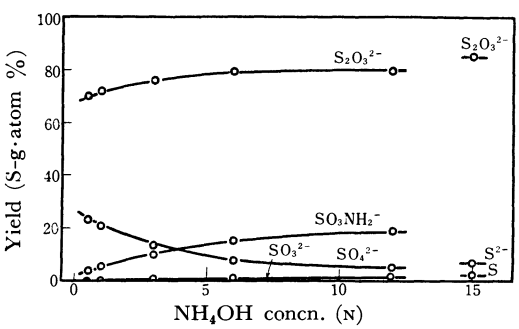

Fig. 2. Effect of ammonia concentration on the yield of products.
React. temp.: 100°C React. time: 3 hr

The effect of reaction temperature on the yield of products is slight as is shown in Fig. 3 and Fig. 4. When the concentration of ammonia is greater than 15 N, an explosive reaction occurs at 100°C with a flash producing a large amount of thiosulfate, a small amount of elemental sulfur and sulfide, and traces of sulfate and sulfamate.

Figs. 5 and 6 give the results of the decomposition of tetrasulfur tetranitride in the presence of sulfite ion and copper ion, respectively. Sulfite reacts with tetrasulfur tetranitride in an aqueous ammonia solution to form sulfate and sulfamate ion, quantitatively.

Addition of copper ion improves the yield of sulfamate but depresses that of thiosulfate. Fig. 7 shows the results of thin layer chromatographic analyses of tetrasulfur tetranitride in aqueous

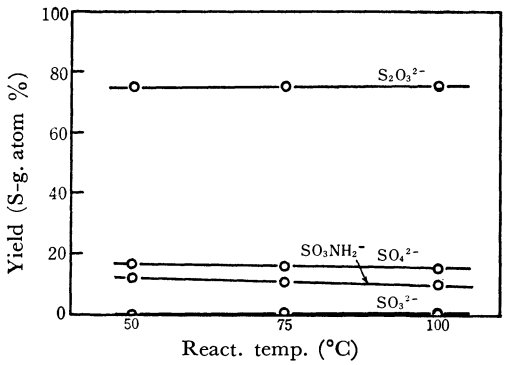

Fig. 3. Effect of reaction temperature on the yield of the products.
Ammonia concn.: 3 N

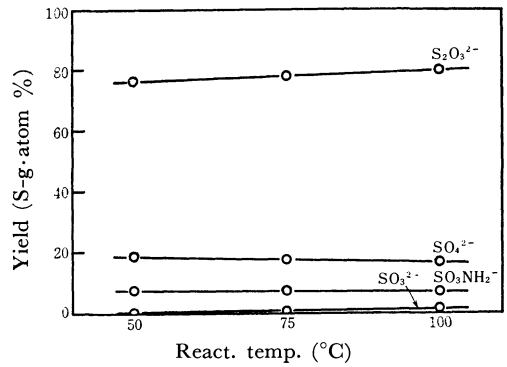

Fig. 4. Effect of reaction temperature on the yield of products.
Ammonia concn.: 12 N

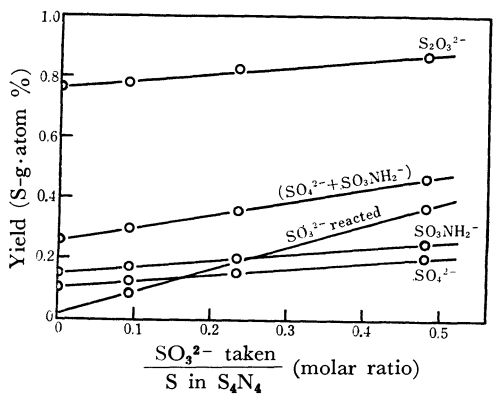

Fig. 5. Decomposition of tetrasulfur tetranitride in the presence of an excess sulfite ion.
React. temp.: 75°C React. time: 17 hr

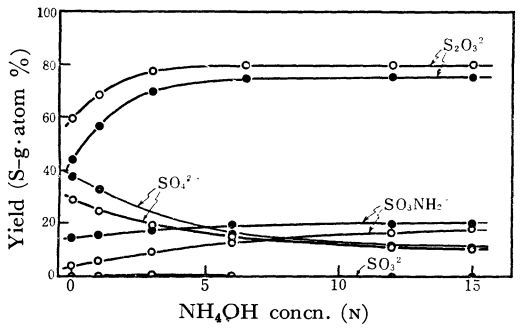

Fig. 6. Decomposition of tetrasulfur tetranitride in the presence of copper ion.
React. temp.: 75°C React. time: 17 hr

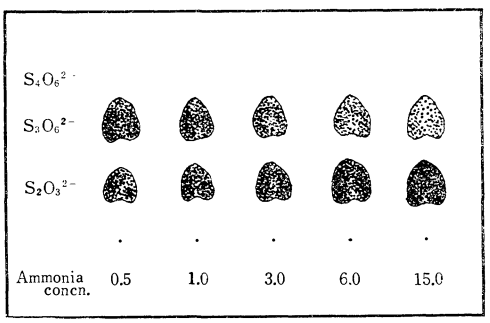

Fig. 7. Thin layer chromatographic analysis of the solution of tetrasulfur tetranitride ammonolysis.
React. temp.: 50°C React. time: 24 hr
Elution solvent: Ethanol—*n*-Butanol—1 mol/*l* of ammonium acetate—conc. ammonia solution =75 : 75 : 40 : 10
Adsorbent: Silica gel (Wako gel B-O)
Thin layer chromatographic analysis following the improved method of Seiler and Erlenmeyer.[6]

ammonia solution. Thiosulfate and trithionate were present in the decomposition of tetrasulfur tetranitride, but no higher polythionate was observed.

Discussion

From the reactions

$$S_4N_4 + 20HI = 4H_2S + 4NH_3 + 10I_2 \quad (5)$$

$$S_4N_4 + 6(O) + 10H_2O = 4H_2SO_4 + 4NH_3 \quad (6)$$

we see that the oxidation states of sulfur and nitrogen in tetrasulfur tetranitride are +3 and −3, respectively. The electropositive nature of sulfur in tetrasulfur tetranitride is in agreement with Pauling's electro-negativity scale (N 3.0, S 2.5).

Nair and Murthy[5] assumed the derivative of S^{3+} *viz.* "sulfur trihydroxide" $S(OH)_3$ to be a primary product in the alkaline hydrolysis of tetrasulfur tetranitride. Such a compound will be extremely unstable and will have only a transient existence, being transformed into sulfoxylic acid and sulfurous acid:

$$S_4N_4 + 12H_2O = 4S(OH)_3 + 4NH_3 \quad (7)$$

$$4S(OH)_3 = 2S(OH)_4 + 2S(OH)_2 \quad (8)$$

$$S(OH)_4 = H_2SO_3 + H_2O \quad (9)$$

Sulfoxylic acid which is not isolated in a pure state or in solution, is known to be a highly reactive species as is seen from studies on its derivatives.[7] Formation of various compounds in the hydrolysis of tetrasulfur tetranitride can be easily explained by the secondary reactions as follows:

$$S(OH)_2 + 2H_2SO_3 = H_2S_3O_6 + 2H_2O \quad (10)$$

$$2S(OH)_2 = H_2S_2O_3 + H_2O \quad (11)$$

$$2S(OH)_2 = H_2S + H_2SO_4 \quad (12)$$

$$3S(OH)_2 = H_2S + 2H_2SO_3 \quad (13)$$

$$S_3O_6^{2-} + OH^- = S_2O_3^{2-} + SO_4^{2-} + H^+ \quad (14)$$

$$2S_3O_6^{2-} + 6OH^- = S_2O_3^{2-} + 4SO_3^{2-} + 3H_2O \quad (15)$$

From results obtained so far, it is apparent that the mechanism of the decomposition of tetrasulfur tetranitride in an aqueous ammonia solution is partly in conformity with the above reaction except for the explosive reaction which occurs at high temperature and high ammonia concentration. The result differs in the following aspects as compared with alkaline hydrolysis: no formation of sulfide ion, formation of trace sulfite ion and formation of sulfamate ion in the reaction of tetrasulfur tetranitride ammonolysis. Thus, we might conclude that the reactions (12) and (13) do not occur in tetrasulfur tetranitride ammonolysis.

Formation of sulfamate is caused by the ammonolysis of trithionate:

$$S_3O_6^{2-} + NH_3 + OH^- = S_2O_3^{2-} + SO_3NH_2^- + H_2O \quad (16)$$

Trithionate is known to be hydrolysed in the presence of sodium hydroxide in two ways as shown in Eqs. (14) and (15) depending upon the concentration of hydroxyl ion, but in an aqueous ammonia solution Eq. (16) will take place instead of Eq. (14).

The abundant presence of sulfite increases the yields of thiosulfate, sulfate and sulfamate. This can be explained by the fact that the formation of trithionate is improved by the addition of sulfite as indicated by Eq. (10), and that trithionate decomposes to thiosulfate, sulfate and sulfamate according to Eq. (16).

6) H. Seiler and H. Erlenmeyer, *Helv. Chem. Acta*, **47**, 264 (1964).

7) M. Goehring, *Z. Anorg. Allg. Chem.*, **253**, 304 (1947).

BULLETIN OF THE CHEMICAL SOCIETY OF JAPAN VOL. 43 3453—3456 (1970)

The Effect of Impurities upon the Physical Properties of Silica Gel by the Heat-Treatment

Masaaki MUROYA

Osaka Electro-Communication University, Hatsumachi, Neyagawa, Osaka

and Seiichi KONDO

Osaka University of Education, Tennoji-ku, Osaka

(Received May 18, 1970)

The effects of various kinds of inorganic salts upon the physical properties of silica gel heated in the range up to 1200°C were studied. We measured the polymorphic behavior by means of X-ray diffraction, the simultaneous measurement of the differential thermal analysis, and the thermogravimetric analysis, and the specific surface area by means of the BET N_2 method and by means of studying the water-adsorption capacity. The cationic impurities which were found to have strong effects upon the physical properties mentioned above are Na^+, K^+, Ca^{2+}, Pb^{2+}, Cd^{2+}, Zn^{2+}, and Sb^{3+}. Cations such as Al^{3+}, Cr^{3+}, Mn^{3+}, and Co^{2+} were shown to have weak but positive effects upon the physical properties of silica gel.

The physical properties, such as the specific surface area and the water-adsorption capacity, of silica gel are known to be changed by heating at high temperatures. For instance, the specific surface area of silica gel is decreased by heating, as has been shown by Bastik,[1] and crystal growth was observed by Hirata[2] upon heating the precipitated silica. These changes seem partly due to the presence of impurities in silica gel. Also, Imelik and others[3] have studied the effects of sodium, potassium, calcium, and several other metal hydroxides upon the specific surface area, the pore volume, the mean pore radius, and crystallization by the high-temperature treatment of silica gel. However, the role of impurities was not made clear enough in these experiments. Moreover, quite a number of investigations of silica gel seem to have more or less ignored the effects of impurities when this material was subjected to high temperatures. Therefore, the influence of impurities upon the properties of silica gel heated at elevated temperatures was studied and will be described in this report.

Experimental

The material used in this study was Japan Industrial Standard Type-A and Fuji-Davison Co. Type-RD silica gel; it was purified by repeated washing with dilute hydrochloric acid and distilled water. The physical and chemical properties of the samples before and after purification are shown in Table 1, where the methods of measurements of these values are the same as those previously described.[4]

TABLE 1. SOME OF PHISICAL AND CHEMICAL PROPERTIES OF SILICA GEL USED IN THIS REPORT

Type of silica gel	Surface area (m^2/g)	Water adsorption capacity (wt %)		Na_2O (wt %)
		20% RH	90% RH	
RD as received	720	12.2	38.2	0.03
RD purified	720	12.2	38.2	0.007
A as received	650	11.0	35	0.2
A purified	650	11.0	35	0.01

The experimental procedures of impregnating various impurities and of pH adjustment are as follows; silica gel was suspended in aqueous solutions of various inorganic salts at given pH values at 50°C for 24 hr; then, after the mother liquid had been thoroughly removed from silica gel, it was used for further heat treatment at temperatures ranging from 200°C to 1200°C in air for 24 hr. The degree of the crystallization of amorphous silica as a function of the temperature was estimated from the ratio of the intensities of the X-ray diffraction lines of the (111) plane of β-cristobalite, the (101) and (100) planes of α-quartz, and the (101) planes of β-tridymite relative to that of the (211) plane of the precipitated calcium carbonate used as an inner standard (by mixing the latter material of 10% by weight with the samples). Flame spectroscopy was used for the determination of the Na^+, K^+, and Ca^{2+} ions, while photometric chelate titration was used for the deter-

1) J. Bastik, *Bull. Soc. Chim. France*, **20**, 437 (1953).
2) Y. Hirata, *J. Japan Rubber Assoc.*, **31**, 920 (1958).
3) D. H. Everett Ed., "The Structure and Properties of Porous Materials," Butterworths, London, (1958), p. 266.
4) S. Kondo and M. Muroya, This Bulletin, **42**, 1165 (1969).

mination of the other metal cations. All data per unit weight of silica were obtained by heating silica gel at 1100°C.

Results and Discussion

(1) Polymorphism. In order to see the effect of the pH upon the thermal behavior of silica gel, X-ray diffraction patterns were taken on powder samples which had been adjusted to pH values of 3, 6, and 9 with acids and bases, such as hydrochloric, sulfuric, phosphoric, and boric acids and ammonium and sodium hydroxide, and which had then been heated at 1000°C for 24 hr. Marked diffraction lines of β-cristobalite, α-quartz, and β-tridymite were observed on the sample adjusted to pH 9 with sodium hydroxide, the rest of these samples showed very weak diffraction lines, except for the one adjusted to pH 3 with hydrochloric acid, which showed no diffraction lines. Figure 1 shows the X-ray powder diffraction lines of the samples prepared by suspending

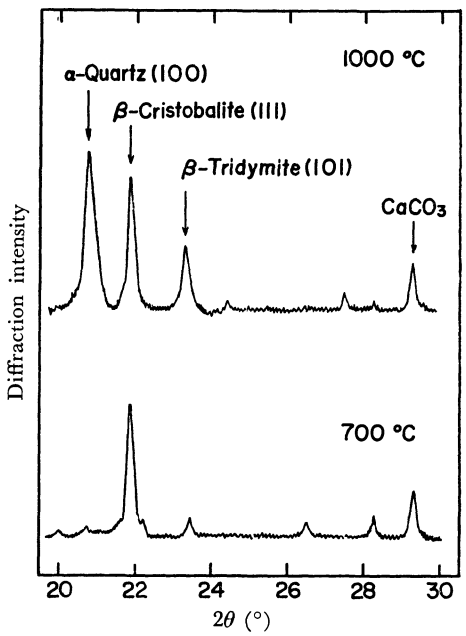

Fig. 1. X-Ray powder diffraction lines of silica gel containing 870 ppm Na^+ cation and heated at 700° and 1000°C for 24 hr.

silica gel in an aquous solution of sodium hydroxide (1% by weight (870 ppm Na^+)) and by then heating it at 700° and 1000°C for 24 hr respectively. At temperatues as low as 700°C, the crystallization from the amorphous state to β-cristobalite was seen very clearly, and α-quartz and β-tridymite seem to have grown at 1000°C. Well-shaped crystals were observed under the electron microscope on these samples. It seems clear from the

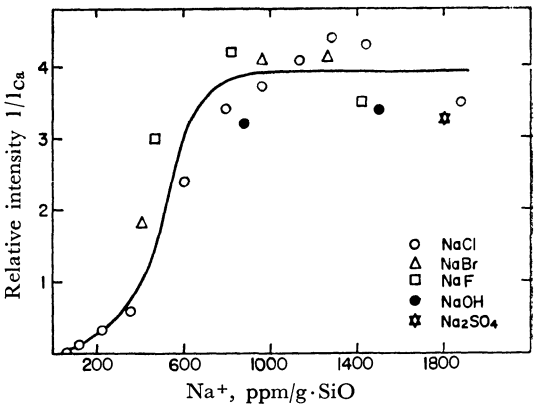

Fig. 2. The curve for plot of the relative intensity of X-ray diffraction lines of (111) planes of β-cristobalite grown by heating silica gel at 1000°C against the concentration of Na^+ cation contained in silica gel.

results mentioned above that only sodium hydroxide had a marked effect on crystallization, but had little effect on the pH adjustment. Since Na^+ and/or OH^- ions seem to play a major role in crystallization, the effects of other sodium salts with various anions, such as F^-, Cl^-, Br^- and SO_4^{2-}, of varied concentrations were examined under the same experimental conditions as above. The relative diffraction intensities of the (111) planes of β-cristobalite which appeared on these samples were dependent upon the concentration of the Na^+ cation, but not on the kind of anion, within the range of experimental error. Figure 2 shows the relation between the relative diffraction intensities of the (111) planes of β-crystobalite and the concentration of the Na^+ cation in the form of various sodium salts. As may be seen in this figure, crystal growth becomes remarkable in the presence of more than about 800 ppm of Na^+ cations, but is almost negligible in the presence of less than 100 ppm of Na^+ cations. The reason for the absence of diffraction lines on the sample adjusted to pH 3, mentioned previously, in that the sample was purified in that preparation.

(2) Differential Thermal Analysis and Thermogravimetric Analysis. The DTA and TGA measurements were carried out on the sample containing 600 ppm of a Na^+ cation in the form of NaCl, as may be seen in Fig. 3, in order to ascertain the thermal behavior of silica gel accompanied by the phase transition from the amorphous to the crystalline phase or from one crystalline phase to another crystalline phase. The experimental conditions for DTA and TGA measurements were the same as have been described before.[5] As may be seen in this figure, four endothermic peaks accompanied by a weight decrease in TGA and two exthothermic peaks with no discontinuous change in TGA were observed. The mechanisms

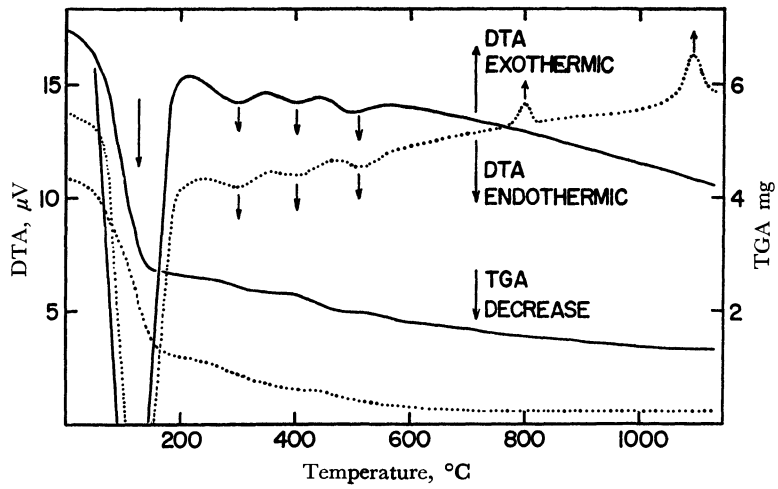

Fig. 3. DTA and TGA curves of silica gel. Full lines and dotted lines show those of silica gel containing 50 and 600 ppm Na^+ cation respectively.

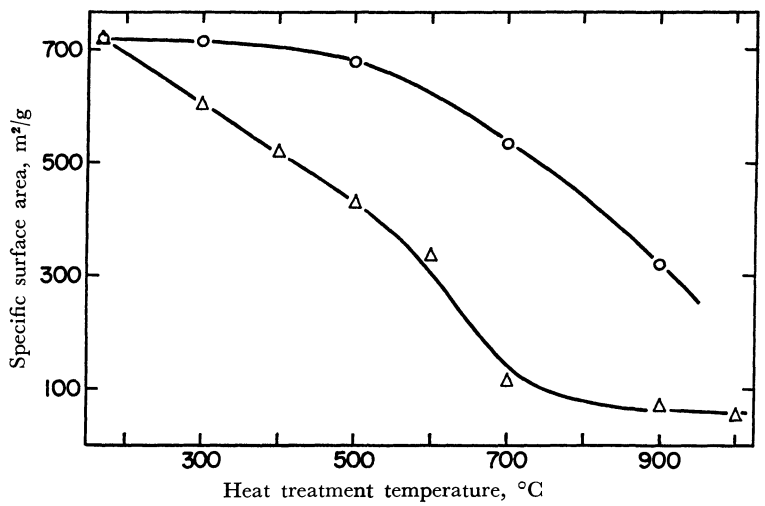

Fig. 4. Curves of the specific surface area *versus* heat-treatment temperature of RD type silica gel. Circles and triangles show results of the sample containing 50 and 600 ppm of Na^+ cation respectively.

of these four endothermic reactions were discussed in a previous paper[5] from the point of view of the dehydration of surface silanol. Since the two exothermic reactions had no discontinuous weight change, the one at 800°C can be attributed to the phase change to β-cristobalite, and the other, at 1100°C, to the phase change to α-quartz and/or β-tridymite; this is supported by the results of the X-ray diffraction experiments described above. On the other hand, no exothermic peak was observed in this temperature range on the sample containing 50 ppm of the Na^+ cation. Since it is now clear that the Na^+ cation has a major effect upon the crystal growth of silica gel, the effects of the salts of other cations, such as chlorides, sulphates, and nitrates of cations such as K^+, Ca^{2+}, Mn^{2+}, Ni^{2+}, Co^{2+}, Cd^{2+}, Zn^{2+}, Pb^{2+}, Fe^{3+}, Al^{3+}, Cr^{3+}, and Sb^{3+}, were tested by the procedures described above. The results of these experiments can be summerized as follows.

1) The influence on the growth of β-cristobalite was marked in the cases of cations such as Na^+, K^+, Pb^{2+}, and Sb^{3+}, and very weak but positive in the cases of cations such as Cr^{3+} and Al^{3+}; 2) the growth of α-quartz was influenced strongly by cations such as Ca^{2+}, Cd^{2+}, and Zn^{2+}, and less strongly by cations such as Mn^{2+}, and Co^{2+}, and 3) the rest of the cations tested had no observable effect upon the growth of either crystal. The combination of group 3) cations with those of group 1) or 2) did not also have an observable

5) S. Kondo and M. Muroya, This Bulletin, **43**, 2657 (1970).

effect on the crystal growth.

(3) Specific Surface Area and Water-adsorption Capacity. In the above section it was shown that many of the cationic impurities had a strong influence on the crystal growth at higher temperatures; this was studied by means of X-ray diffraction. Therefore, it is interesting to see the effect of those ions not only at high temperatures, but also over a wider temperature range, upon other properties of silica gel, such as the specific surface area (SA) and the water-adsorption capacity. The SA values of the RD-type samples containing 50 and 600 ppm of the Na^+ cation as a function of the temperature of heating for 24 hr are shown in Fig. 4. The SA of the sample containing 600 ppm of the Na^+ cation shows a big decrease in the range from 200°C to 700°C, and becomes almost constant at higher temperatures. On the other hand, that of a relatively pure sample remains almost constant up to 500°C and starts to decrease gradually at higher temperatures. Figure 5 shows the influence of the Na^+ cation concentration upon the SA of RD-type samples heated at 700°C for 24 hr. In this figure, the effect of the Na^+ cation becomes bigger at concentrations of approximately more than 100 ppm. These results indicate the remarkable effect of some of the impurity ions on the decrease of SA, even at relatively low temperatures.

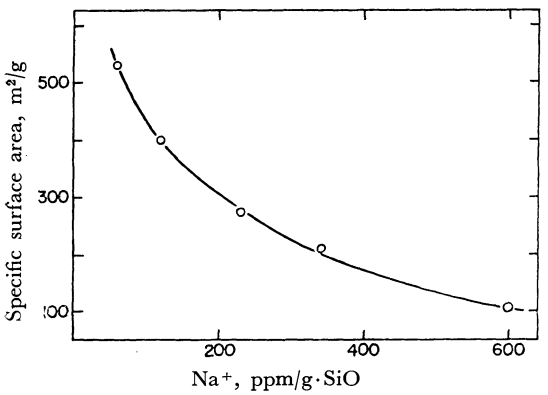

Fig. 5. The relation between the specific surface area and the concentration of Na^+ cation contained in RD type silica gel heated at 700°C for 24 hr.

Figure 6 shows the curves of the plot of the water-adsorption capacities at relative humidities (RH) of 20 and 90% at 23°C against the heat-treatment temperatures on the samples discussed in the above section. In Fig. 6, the values of the purer samples are much higher than those of the less pure samples. The general tendency of the curves of 20% RH is similar to that of the SA-temperature curves. Since the amount of water adsorbed at 20% RH corresponds approximately

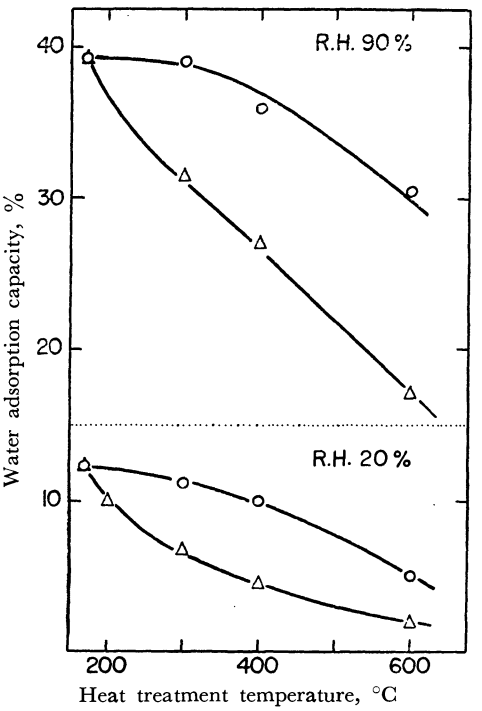

Fig. 6. Curves of the water adsorption capacity *versus* the temperature of heat-treatment. Circles and triangles show those of RD type samples containing 50 and 600 ppm Na^+ cation respectively.

to an amount a little more than a monomolecular layer, it is reasonable to see a close similarity between the curve of 20% RH in Fig. 6 and that in Fig. 4. Because the adsorption capacity at 90% RH is usually compared with the pore volume, the big decrease in the value at 90% RH at higher temperatures of heat-treatment can be interpreted as a decrease in pore volume or as the effect of sintering.

Summary

Such physical properties as the polymorphic behavior, the thermal properties, the specific surface area, and the water-adsorption capacity of silica gel are largely changed when it is heated in the presence of cationic impurities such as Na^+, K^+, Pb^{2+}, Ca^{2+}, Cd^{2+}, Zn^{2+}, and Sb^{3+}. Weak effect upon the physical properties mentioned above were observed in the cases of such cationic impurities as Al^{3+}, Cr^{3+}, Mn^{3+}, and Co^{2+}.

Thanks are due to Miss Fumiko Matsuyama and Messes. Minori Yabuno, Yukio Betsuyaku, and Osamu Tsukide for their experimental help and interest.

BULLETIN OF THE CHEMICAL SOCIETY OF JAPAN VOL. 43 3457—3461 (1970)

The Stability of Fused Rings in Metal Chelates. VII. Copper(II) Complexes of Schiff Bases Derived from 2-Acetylpyridine or Pyridine-2-aldehyde and Dipeptides Containing Glycine, β-Alanine and/or α-Aminoisobutyric Acid

Yasuo NAKAO, Hiroyuki ISHIBASHI and Akitsugu NAKAHARA

Institute of Chemistry, College of General Education, Osaka University, Toyonaka, Osaka

(Received May 25, 1970)

Eight new copper(II) complexes of Schiff bases derived from 2-acetylpyridine or pyridine-2-aldehyde and dipeptides containing glycine, β-alanine and/or α-aminoisobutyric acid have been prepared, and their relative stability was discussed on the basis of numerical data obtained by spectrophotometric, polarographic and other measurements. As a result, it was found that the stability of fused-ring systems decreases in the order 5-5-6-≃5-6-5->5-5-5->5-6-6-system (the first number represents the number of ring members containing pyridine derivatives and the second and third numbers represent those of ring members containing dipeptide moieties). The conclusion proposed previously that Schiff base chelates of aldehydes are generally less stable than those of corresponding ketones, has been proved to be valid also for the copper(II) chelates. It was found that transamination reactions take place in the copper(II) chelates of Schiff bases with pyridine-2-aldehyde and glycylglycine or glycyl-β-alanine.

In a previous paper,[1] it was pointed out that a fused-ring system with two six-membered rings is less stable than that with one six- and one five-membered ring or two five-membered rings in the case of copper(II) chelates of dipeptides. We also investigated the relative stability of copper(II) chelates with various multidentate aldehyde- and ketone-Schiff bases.[2,3]

As an extension of the investigations dealing with the relative stability of metal-multidentate-chelates, the isolation of eight copper(II) complexes of Schiff bases derived from 2-acetylpyridine or pyridine-2-aldehyde and dipeptides containing glycine and/or β-alanine have been performed. Structural formulae of these compounds are illustrated in Fig. 1, (I—VIII). This paper describes the preparations and the relative stabilities of the metal chelates. The temperature of decomposition, absorption maxima for the *d-d* transition band in aqueous solution and the half-wave potentials for the reduction of copper(II) at the dropping mercury electrode of the chelate compounds are tabulated in Tables 3 and 4. The relative stability of copper(II) chelates has been determined on the basis of the numerical data.

We have found that there occur transamination reactions in pyridine-2-aldehyde-glycylglycine- and pyridine-2-aldehyde-glycyl-β-alanine-Cu(II) systems. The correlation between the transamination reaction and the structure of fused-ring system is also described.

Copper(II) Complexes of Schiff Bases derived from 2-Acetylpyridine and Glycylglycine, Glycyl-β-alanine, β-Alanylglycine or β-Alanyl-β-alanine(I—IV). The new compounds have been prepared by the ordinary reaction[2-4] between equimolar amounts of each components. They have been concluded to have the structures, I—IV on the basis of analytical data and the quadricoordinating character of copper(II) complexes. As is clear from their structural formulae, the central copper(II) links, in all cases, to the Schiff base ligand through the pyridine-nitrogen, Schiff base-nitrogen, peptide-nitrogen and carboxylate-oxygen, forming copper(II) tetradentate chelates. Thus the four chelates I—IV differ from one another only in the size of ring containing the peptide moieties. The skeletal structure of I consists of 5-5-5-*1 membered fused rings, and in the same way II, III and IV consist of 5-5-6-, 5-6-5- and 5-6-6-membered fused rings, respectively. Table 3 shows that the polaro-

1) O. Yamauchi, Y. Hirano, Y. Nakao and A. Nakahara, *Can. J. Chem.*, **47**, 3441 (1969).

2) Y. Nakao, K. Sakurai and A. Nakahara, This Bulletin, **39**, 1471 (1966).

3) Y. Nakao, N. Nonagase and A. Nakahara, *ibid.*, **42**, 452 (1969).

4) A. Nakahara, H. Yamamoto and H. Matsumoto, *ibid.*, **37**, 1137 (1964).

*1 The abbreviation 5-5-5 indicates the fused-chelate-ring structure containing 5,5 and 5-membered rings in a counter-clockwise direction in the expression of structural formula I.

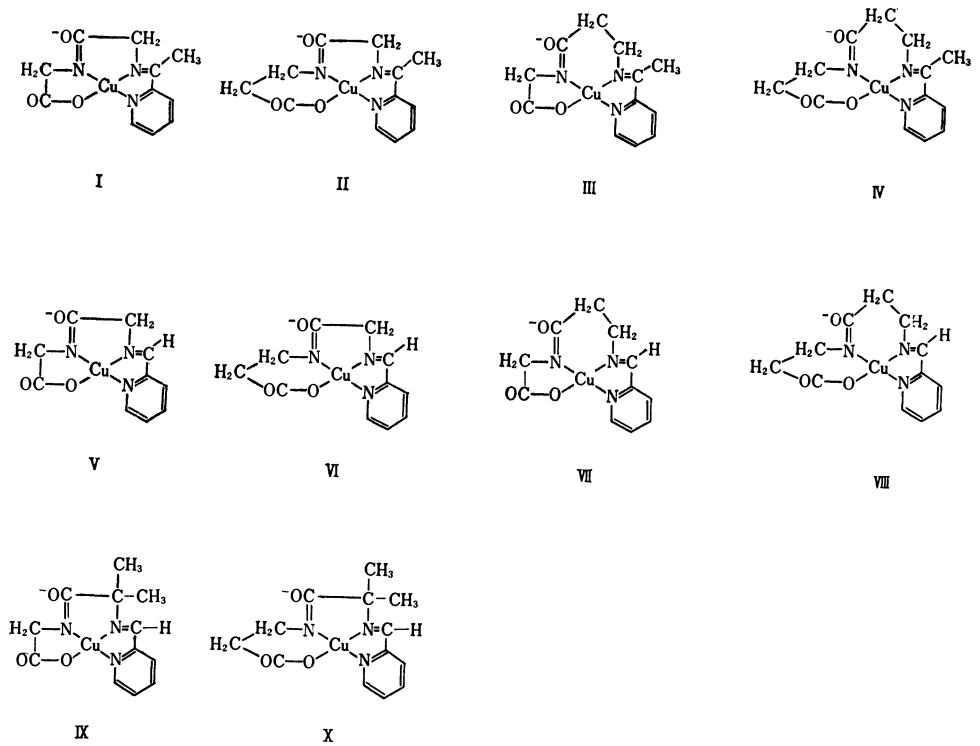

Fig. 1. Structural formulae of copper(II) chelates of aldehyde- and ketone-Schiff bases.

graphic half-wave potentials for the reduction of copper(II) in all the chelates(I—IV) are nearly independent of pH in the region 6–9.5. Only at about pH 11, the half-wave potential becomes slightly more negative. It can also be seen from Table 3 that there is no remarkable difference between the half-wave potential of chelates, II and III. On the other hand, the half-wave potential of I is a little less negative and that of IV is even less negative compared with those of II and III. It may be concluded from the above polarographic data that the stability of chelates I–IV decreases in the order II(5-5-6)$\simeq$III(5-6-5)$>$I(5-5-5)$>$IV(5-6-6). The numerical data for the decomposing temperatures and the maxima of absorption bands due to the ligand field splitting of *d*-orbitals also support the order in the stability of chelates I—IV. In the case of the copper(II) chelates of dipeptides (apart from the Schiff base chelates), copper(II) glycylglycinate is determined to be most stable[1]; but in complexes I—IV, copper(II)-2-acetylpyridine-glycylglycine fused-chelate ring system is less stable than either 2-acetylpyridine-glycyl-*β*-alanine- or -*β*-alanylglycine-Cu(II) systems. This is considered as due to the increasing strain in the 5-5-5-fused ring system.[4] It is of interest that the chelates produced from copper(II), 2-acetylpyridine and *β*-alanyl-*β*-alanine can easily be isolated as stable crystals, whereas the copper(II) *β*-alanyl-*β*-alaninate cannot be isolated.[1]

Copper(II) Complexes of Schiff Bases derived from Pyridine-2-aldehyde and Glycylglycine, Glycyl-*β*-alanine, *β*-Alanylglycine or *β*-Alanyl-*β*-alanine(V—VIII). Preparation of copper(II) complexes of Schiff bases containing pyridine-2-aldehyde instead of 2-acetylpyridine (V—VIII) was carried out. Isolation in the crystalline state was achieved only in cases of chelates with pyridine-2-aldehyde-*β*-alanylglycine(VII) and pyridine-2-aldehyde-*β*-alanyl-*β*-alanine (VIII). The half-wave potentials for the reduction of copper(II), temperatures of decomposition and absorption maxima in the visible region of the chelates VII—VIII are shown in Tables 3 and 4, from which a similar conclusion as in the preceding section is easily obtained: VII(5-6-5)$>$VIII(5-6-6). It can also be concluded from the comparison of III and VII, or IV and VIII, that if the skeletal structure is the same, ketone-Schiff base chelates are more stable than the corresponding aldehyde-Schiff base chelates(III$>$VII; IV$>$VIII). Apart from the relative stability of fused-chelate-rings, it has been found that transamination reactions take place as shown in Fig. 2 in the cases of copper(II) chelates with pyridine-2-aldehyde-glycylglycine- or pyridine-2-aldehyde-glycyl-*β*-alanine. Transamination has been observed by paper chromatographic test of the reaction solutions containing copper(II), pyridine-2-aldehyde, and glycylglycine or glycyl-*β*-alanine. Existence of 2-aminomethylpyridine in the paper chromatogram was distinctly observed

Fig. 2. The transamination reaction of pyridine-2-aldehydeglycine-Cu(II) system.

in the above reaction mixture as is clear from Fig. 2. On the other hand, no transamination was observed in the reaction solution for VII and VIII. Difficulty in isolating complexes V and VI might be elucidated by taking this tendency in transamination reaction into account. Investigation of transamination reactions between oligopeptides and various aldehydes is now under way.

Copper(II) Complexes of Schiff Bases derived from Pyridine-2-aldehyde and α-aminoisobutyrylglycine or α-Aminoisobutyryl-β-alanine(IX—X). In order to isolate copper(II) chelate which consists of 5-5-5- or 5-5-6-fused-ring system and at the same time possesses pyridine-2-aldehyde as carbonyl moiety in Schiff base ligand, the syntheses of pyridine-2-aldehyde-α-aminoisobutyrylglycine- and pyridine-2-aldehyde-α-aminoisobutyryl-β-alanine-copper(II) complexes, IX and X, have been carried out. As is clear from structural formulae IX—X, the transamination reaction cannot be expected in these systems. Thus it was possible to obtain both the chelates in crystalline state. Some properties of the compounds are tabulated in Tables 3 and 4. From the numerical data, it is concluded that X is a little more stable as compared to IX(X(5-5-6)> IX(5-5-5)). The conclusion is consistent with the result obtained through a comparison of I and II.

Experimental*2

Preparation of dipeptides. *Glycylglycine* and *glycyl-β-alanine* were prepared according to the diketopiperazine method[5,6] and chloroacetyl chloride method,[7] respectively.

Carbobenzoxy-β-alanine and -α-Aminoisobutyric Acid. There are several papers on the preparation of these compounds.[8,9] The present procedure is a slightly modified one by Winitz *et al.*[10] One-fifth mole each of β-alanine or α-aminoisobutyric acid were dissolved in 100 m*l* of 2N sodium hydroxide solution. To this was alternately added 52 m*l* of 4N NaOH and 34 m*l* of carbobenzoxy chloride over a period of 30—40 min, under constant stirring and cooling in an ice bath. After completion of the reaction, the reaction mixtures were extracted with ether and the aqueous fraction acidified with 6N HCl to pH 2—3. This was further extracted by ethyl acetate; the ethyl acetate fraction was dried over anhydrous magnesium sulfate. The filtrates were concentrated *in vacuo* to crystalline or oily residues. Recrystallization was carried out by using ethyl acetate and petroleum benzine.

β-Alanine Benzyl Ester p-Toluenesulfonate was prepared from β-alanine, benzyl alcohol and *p*-toluenesulfonic acid monohydrate according to the direction of Izumiya and Makisumi.[11]

Glycine Benzyl Ester p-Toluenesulfonate[12] was prepared by a similar procedure as that for the β-alanine derivative, except that chloroform was used as the solvent. The four materials described above were identified by comparing their melting points with those in literature.

Carbobenzoxy-β-alanylglycine Benzyl Ester. This was prepared in a similar procedure as that reported by Winitz *et al.*[10] To a solution of 15.6 g of carbobenzoxy-β-alanine, 23.6 g of glycine benzyl ester *p*-toluenesulfonate and 9.8 m*l* of triethylamine in 160 m*l* of chloroform was added 14.5 g of dicyclohexylcarbodiimide. The reaction mixture was stirred at 25°C overnight. After removal of white precipitated dicyclohexylurea, the filtrate was washed with water, dilute HCl, saturated $NaHCO_3$ aqueous solution and water. After the chloroform fraction had been dried over anhydrous magnesium sulfate, the filtrate was evaporated to dryness. The crystalline materials obtained were recrystallized from ethyl acetate and petroleum benzine. mp 107—109°C. Found: C, 64.57; H, 5.98; N, 7.97%. Calcd for $C_{20}H_{22}O_5N_2$: C, 64.84; H, 6.00; N, 7.56%.

Carbobenzoxy-β-alanyl-β-alanine Benzyl Ester. This was prepared from carbobenzoxy-β-alanine and β-alanine benzyl ester *p*-toluenesulfonate in the same way as described for carbobenzoxy-β-alanylglycine benzyl ester. mp 99—100°C.

Found: C, 65.96; H, 6.38; N, 7.32%. Calcd for $C_{21}H_{24}O_5N_2$: C, 65.60; H, 6.30; N, 7.29%.

Carbobenzoxy-α-aminoisobutyrylglycine Benzyl Ester and Carbobenzoxy-α-aminoisobutyryl-β-alanine Benzyl Ester were also prepared by the same method as described above. Z-α-NH_2-isoBu-GlyOBz. mp 91—92°C.

Found: C, 65.57; H, 6.45; N, 7.32%. Calcd for $C_{21}H_{24}O_5N_2$: C, 65.60; H, 6.30; N, 7.29%. Z-α-NH_2-isoBu-β-AlaOBz. mp 102—104°C.

Found: C, 66.32; H, 6.70; N, 6.90%. Calcd for $C_{22}H_{26}O_5N_2$: C, 66.30; H, 6.59; N, 7.03%.

β-Alanylglylcine, β-Alanyl-β-alanine, α-Aminoisobutyryl-glycine and α-Aminoisobutyryl-β-alanine were obtained by catalytic reduction of the corresponding carbobenzoxypeptide benzyl ester using palladium black catalyst. In all cases, methanol containing a small volume of glacial acetic acid was used as solvent. The peptides obtained by the procedure described above were re-

*2 Melting points and decomposing temperatures were determined on a micro melting point apparatus and uncorrected.

5) C. Sannie, *Bull. Soc. Chim. Fr.*, **9**, 487 (1942).
6) E. Fischer and E. Fourneau, *Ber.*, **34**, 2868 (1901).
7) H. T. Hanson and E. L. Smith, *J. Biol. Chem.*, **175**, 833 (1948).
8) R. H. Sifferd and V. Vigneaud, *ibid.*, **108**, 753 (1935).
9) M. Bergmann, L. Zervas, J. S. Fruton, F. Schneider and H. Schleich, *ibid.*, **109**, 325 (1935).
10) M. Winitz, L. B. Frankenthal, N. Izumiya, S. M. Birnbaum, C. G. Baker and J. P. Greenstein, *J. Amer. Chem. Soc.*, **78**, 2423 (1956).
11) N. Izumiya and S. Makisumi, *Nippon Kagaku Zasshi*, **78**, 1768 (1957).
12) N. Izumiya and S. Makisumi, *ibid.*, **78**, 662 (1957).

TABLE 1. ANALYTICAL DATA FOR [Cu 2-acetpy=peptide]*

Compound	C, %		H, %		N, %	
	Calcd	Found	Calcd	Found	Calcd	Found
[Cu 2-acetpy=Gly·Gly]·H_2O	42.00	41.72	4.13	4.35	13.35	13.38
[Cu 2-acetpy=Gly·β-Ala]·3.5H_2O	38.55	38.61	5.39	5.49	11.24	11.44
[Cu 2-acetpy=β-Ala·Gly]·3.5H_2O	38.55	38.66	5.39	5.31	11.24	11.76
[Cu 2-acetpy=β-Ala·β-Ala]·3H_2O	41.22	41.07	5.55	5.71	11.10	10.99

* 2-acetpy = 2-acetylpyridine

TABLE 2. ANALYTICAL DATA FOR [Cu py-2-al=peptide]*

Compound	C, %		H, %		N, %	
	Calcd	Found	Calcd	Found	Calcd	Found
[Cu py-2-al=β-Ala·Gly]·3H_2O	37.66	37.64	4.89	4.87	11.98	12.27
[Cu py-2-al=β-Ala·β-Ala]·4H_2O	37.64	37.53	5.53	5.07	10.98	11.12
[Cu py-2-al=α-AIBA·Gly]·2.5H_2O	40.51	40.94	5.06	4.91	11.81	11.96
[Cu py-2-al=α-AIBA·β-Ala]·3H_2O	41.22	40.82	5.55	5.66	11.10	11.02

* py-2-al = pyridine-2-aldehyde, α-AIBA·Gly = α-aminoisobutyrylglycine

crystallized from water and ethanol. β-Alanylglycine, β-alanyl-β-alanine and α-aminoisobutyrylglycine were identified by means of elementary analysis and melting points. Melting point and analytical data of α-aminoisobutyryl-β-alanine are as follows: mp 209—212°C. Found: C, 47.75; H, 8.29; N, 15.80%. Calcd for $C_7H_{14}O_3N_2$: C, 48.25; H, 8.12; N, 16.08%.

Preparation of Metal Chelates. *Copper(II) Chelates of Schiff Bases derived from 2-Acetylpyridine and Dipeptides (I—IV).* To a mixture of 0.005 mol each of 2-acetylpyridine and dipeptide in 10 m*l* of aqueous ethanol(one-to-one volume mixture) was added 0.005 mol of copper(II) acetate monohydrate. The pH-values of each reaction solution were adjusted to 9—11 by using concentrated NaOH solution. The reaction mixture was then stirred at room temperature for half an hour. It was allowed to stand for a few hours in a refrigerator; hereupon crystals were deposited. The products were filtered and recrystallized from aqueous ethanol(seven-to-three by volume mixture). The results of elementary analyses are shown in Table 1.

Copper(II) Chelate of Schiff Base derived from Pyridine-2-aldehyde and β-Alanylglycine (VII). Into 10 m*l* of a water : ethanol mixture(one-to-one by volume) were dissolved 0.37 g of β-alanylglycine and 0.27 g of pyridine-2-aldehyde, and then 0.5 g of copper(II) acetate monohydrate. The reaction mixture was adjusted to pH 8—9 by sodium ethoxide, and was then kept at room temperature for an hour under constant stirring. Bluish violet crystals were precipitated from the reaction solution. After it had been filtered, recrystallization from aqueous ethanol(one-to-one by volume) was carried out. Analytical data are given in Table 2.

Copper(II) Chelate of Schiff Base derived from Pyridine-2-aldehyde and β-Alanyl-β-alanine (VIII). A mixture of 0.40 g of β-alanyl-β-alanine and 0.27 g of pyridine-2-aldehyde was dissolved in 8 m*l* of aqueous ethanol (one-to-one by volume). To the solution was added 0.5 g of copper(II) acetate monohydrate, and the pH was adjusted to about 8—9 by powdered sodium carbonate. After it had been stirred at room temperature for one hour, the reaction mixture was allowed to stand overnight in a desiccator equipped with phosphorous pentoxide; thereupon blue crystals were obtained. The precipitates were collected by filtration and washed several times with an ethanol : acetone mixture (four-to-one by volume). Analytical data are given in Table 2.

Copper(II) Chelate of Schiff Base derived from Pyridine-2-aldehyde and α-Aminoisobutyrylglycine(IX). To a solution of 0.64 g of α-aminoisobutyrylglycine in 6 m*l* of a water : ethanol mixture (1 : 1 by volume) were added 0.43 g of pyridine-2-aldehyde and 0.80 g of cupric acetate monohydrate. The resulting mixture was adjusted to pH 7—8 by sodium hydroxide solution and stirred at 25°C for half an hour. After filtration, the filtrate was allowed to stand in a desiccator equipped with silica gel under reduced pressure until syrupy material was obtained. The material was recrystallized from ethanol containing a small amount of water. Analytical data are given in Table 2.

Copper(II) Chelate of Schiff Base derived from Pyridine 2-aldehyde and α-Aminoisobutyryl-β-alanine (X). A similar procedure to that in the preparation of complex IX was adopted. Compound X was isolated in crystalline state over silica gel. The crystal was washed by a water : ethanol mixture (1 : 4 by volume) and then with acetone. The result of elementary analysis is shown in Table 2.

Transamination Study. The following procedure was employed to estimate the transamination reaction in the fused-ring systems of chelates. To a mixture of 0.0025 mol each of pyridine-2-aldehyde and the dipeptide in 10 m*l* of aqueous ethanol (1 : 1 by volume mixture) was added 0.5 g (0.0025 mol) of copper(II) acetate monohydrate. The reaction mixture was adjusted to pH 9—11 by sodium hydroxide solution and was stirred at 25°C for an hour. After it had been filtered, cupric ion was precipitated as sulfide and filtered. The filtrate was used as a sample solution for the paper-chromatographic test for which the solvent system, *n*-butanol : acetic acid : water (4 : 2 : 1) and Toyo filter paper No. 50 were used. Spots of 2-aminomethylpyridine were detected by spraying a ninhydrine

TABLE 3. HALF-WAVE POTENTIALS OF [Cu 2-acetpy=dipeptide] AND [Cu py-2-al=dipeptide]

	Complex	pH	Half-wave potential, *vs.* SCE, 25°C
I.	[Cu 2-acetpy=Gly·Gly]	6.5	−0.34 V.
		9.5	−0.34
		11.0	−0.36
II.	[Cu 2-acetpy=Gly·β-Ala]	6.5	−0.40
		8.0	−0.40
		10.5	−0.40
III.	[Cu 2-acetpy=β-Ala·Gly]	6.0	−0.37
		9.0	−0.38
		10.5	−0.41
IV.	[Cu 2-acetpy=β-Ala·β-Ala]	7.5	−0.32
		9.5	−0.32
		11.0	−0.34
VII.	[Cu py-2-al=β-Ala·Gly]	6.6	−0.31
		9.0	−0.32
		11.0	−0.35
VIII.	[Cu py-2-al=β-Ala·β-Ala]	7.1	−0.25
		9.4	−0.25
		11.0	−0.26
IX.	[Cu py-2-al=α-AIBA·Gly]	6.0	−0·32
		10.1	−0.32
X.	[Cu py-2-al=α-AIBA·β-Ala]	5.6	−0.36
		11.0	−0.35

TABLE 4. PROPERTIES OF COPPER(II) SCHIFF BASE COMPLEXES

	Complex	Appearance of crystals	Absorp. max. ν_{max} 10^{13} sec^{-1} (log ε)	Decomp. temp.
I.	[Cu 2-acetpy=Gly·Gly]	violet	52.2 (2.21)	158—166°C
II.	[Cu 2-acetpy=Gly·β-Ala]	violet	52.6 (2.20)	203—212
III.	[Cu 2-acetpy=β-Ala·Gly]	red-violet	53.3 (1.89)	205—215
IV.	[Cu 2-acetpy=β-Ala·β-Ala]	blue-violet	51.2 (1.89)	150—158
VII.	[Cu py-2-al=β-Ala-Gly]	blue-violet	50.7 (1.79)	190—200
VIII.	[Cu py-2-al=β-Ala·β-Ala]	grey-violet	49.6 (1.89)	150—190
IX.	[Cu py-2-al=α-AIBA·Gly]	violet	52.0 (2.26)	249—260
X.	[Cu py-2-al=α-AIBA·β-Ala]	violet	52.7 (2.23)	193—196 (melt)

solution.

Spectroscopic Measurements. Visible absorption spectra were obtained with a Shimadzu Spectrophotometer MPS-50L and QR-50 at room temperature. Water was used as a solvent. The concentration of the solutions was 5×10^{-3} M. The numerical data for absorption band are listed in Table 3.

Polarographic Measurements. Measurements were carried out by the same method as described previously.[2] Water was used as a solvent. Concentration of the copper(II) complexes was 5×10^{-4} M. The supporting electrolyte used was 0.1 M potassium nitrate. Triton X-100 (0.002%) was used as a maximum suppressor. The pH-values of each solution were adjusted by potassium hydroxide solution.

The authors express their sincere thanks to Dr. Toshishige Inui for his helpful suggestions in synthesizing peptides.

A part of the expenses for this work was defrayed by a grant from the Ministry of Education.

Bulletin of the Chemical Society of Japan Vol. 43 3462—3467 (1970)

Spectroscopic Studies of Polynuclear Complexes. II.[1] Preparation and Optical Resolution of μ-Amido-μ-superoxo and μ-Amido-μ-peroxo Tetrakis(α-di-imine)dicobalt(III) Ions

Yoichi Sasaki, Junnosuke Fujita and Kazuo Saito

Department of Chemistry, Faculty of Science, Tohoku University, Sendai

(Received June 15, 1970)

New binuclear cobalt(III) complexes of the type, $[L_2Co(\mu\text{-}NH_2,O_2)CoL_2](ClO_4)_n$, where L is 1,10-phenanthroline or 2,2′-bipyridyl, and $n=3$ and 4, correspond to the so-called μ-peroxo and μ-superoxo form, respectively, were prepared and resolved into their optical isomers. Their absorption spectra have been compared with those of analogous ethylenediamine complexes and the structures have been discussed. The absolute configuration of these complexes has been determined by their circular dichroism spectra. The μ-peroxo complexes seem to be more stable than the corresponding μ-superoxo complexes in aqueous solution.

It is well known that cobalt(II) salts in aqueous ammonia solutions react with molecular oxygen to form diamagnetic brown complex,[2] $[(NH_3)_5Co(\mu\text{-}O_2)Co(NH_3)_5]^{4+}$, which can be oxidized to paramagnetic green complex,[3] $[(NH_3)_5Co(\mu\text{-}O_2)Co(NH_3)_5]^{5+}$. Recently, House *et al.*[4,5] prepared many oxygen-bridged complexes of these types containing polyamines such as ethylenediamine (en) and triethylenetetramine. We have studied those complexes which have μ-amido group as a second bridge, and reported on optically active $[(l\text{-pn})_2Co(\mu\text{-}NH_2,O_2)Co(l\text{-pn})_2]^{4+}$ (*l*-pn=*l*-propylenediamine) and its derivatives.[1]

This paper concerns the preparation and optical resolution of $[(\alpha\text{-di-imine})_2Co(\mu\text{-}NH_2,O_2)Co(\alpha\text{-di-imine})_2](ClO_4)_n$ ($n=3$ and 4, α-di-imine=2,2′-bipyridyl (bip) and 1,10-phenanthroline (phen)), and their geometrical and optical structures were determined by absorption (AB) and circular dichroism (CD) spectroscopy. These are first examples of cobalt(III) binuclear complexes which contain oxygen bridge and aromatic ligands, and their optical spectra will provide useful information in elucidating the electronic state of binuclear complexes.

Experimental

Preparation of the complexes. (1) *μ-Amido-μ-superoxo-octaammine-dicobalt(III) Perchlorate.* $[(NH_3)_4Co(\mu\text{-}NH_2,O_2)Co(NH_3)_4](ClO_4)_4$ (**1**). This complex was prepared from the corresponding sulfate dihydrate.[6] To a suspension containing 10 g of the sulfate dihydrate in 50 m*l* of water was added 50 m*l* of 60% perchloric acid slowly with frequent stirrings. The crude complex was precipitated by cooling in an ice bath, filtered off, washed with methanol-ether (1 : 1) and ether, and dried *in vacuo*. Dark green crystals, recrystallized from warm water acidified with perchloric acid, are soluble in water, methanol, ethanol and acetone, but insoluble in ether.

Nitrogen analysis of this complex gave always 1—2% over than the expected value, probably because of the instability of the complex. The dark green crystals changed into an unknown black product in a week. However, the absorption spectrum of this perchlorate in water was identical with that of the corresponding nitrate.[1]

(2) μ-Amido-μ-peroxo-tetrakis(1,10-phenanthroline)-dicobalt(III) Perchlorate Monohydrate, $[(phen)_2Co(\mu\text{-}NH_2,O_2)Co(phen)_2](ClO_4)_3\cdot H_2O$ (**2**). A mixture of 8 g of freshly prepared **1** and 10 g of 1,10-phenanthroline in 300 m*l* of methanol was warmed at 60°C for 10 hr with stirring and cooled in an ice bath. Brown precipitate obtained by adding 2 g of sodium perchlorate was filtered off, washed with cold methanol and ether, and air dried. The product was recrystallized from warm water (60°C) by adding sodium perchlorate. Yield: about 8 g.

Found: C, 47.75; H, 2.72; N, 10.29%. Calcd for $C_{48}H_{36}N_9O_{15}Co_2Cl_3$: C, 47.76; H, 3.01; N, 10.44%.

(3) μ-Amido-μ-peroxo-tetrakis(2,2′-bipyridyl)dicobalt(III) Perchlorate Dihydrate, $[(bip)_2Co(\mu\text{-}NH_2,O_2)Co(bip)_2](ClO_4)_3\cdot 2H_2O$ (**3**). This complex was prepared by the same method as that for **2** by use of 8 g of 2,2′-bipyridyl instead of 1,10-phenanthroline. Yield: about 8 g.

Found: C, 42.99; H, 3.31; N, 11.45%. Calcd

1) Part I of this series, Y. Sasaki, J. Fujita and K. Saito, This Bulletin, **42**, 146 (1969).

2) A. Werner and A. Mylius, *Z. Anorg. Chem.*, **16**, 245 (1898).

3) A. Werner, *Ber.*, **41**, 3915 (1908).

4) A. R. Gainsfeld and D. A. House, *Inorg. Nucl. Chem. Lett.*, **4**, 621 (1968).

5) D. L. Duffy, D. A. House and J. A. Weil, *J. Inorg. Nucl. Chem.*, **31**, 2053 (1969).

6) M. Mori, J. A. Weil and M. Ishiguro, *J. Amer. Chem. Soc.*, **90**, 615 (1968).

for $C_{40}H_{38}N_9O_{16}Co_2Cl_3$: C, 42.71; H, 3.41; N, 11.21%.

(4) μ-Amido-μ-superoxo-tetrakis(1,10-phenanthroline)dicobalt(III) Perchlorate Dihydrate, $[(phen)_2Co(\mu\text{-}NH_2,O_2)Co(phen)_2](ClO_4)_4\cdot 2H_2O$ (**4**). To a solution of 2 g of **2** in 50 ml of 7 N nitric acid was added 3 g of solid sodium perchlorate, and the solution was cooled in an ice bath for an hour. Brown fine crystals were filtered off, washed with aqueous sodium perchlorate solution, cold methanol and ether, and dried. Yield: 1—1.5 g.

Found: C, 43.60; H, 2.94; N, 9.34%. Calcd for $C_{48}H_{38}N_9O_{20}Co_2Cl_4$: C, 43.66; H, 2.90; N, 9.55%.

This complex is unstable in water and gives the μ-peroxo complex **2** and other unidentified materials.

(5) μ-Amido-μ-superoxo-tetrakis(2,2′-bipyridyl)dicobalt(III) Perchlorate Monohydrate, $[(bip)_2Co(\mu\text{-}NH_2,O_2)Co(bip)_2](ClO_4)_4\cdot H_2O$ (**5**). This complex was obtained as green crystalline powder from the μ-peroxo complex **3** by a similar method to that for **4**. This complex also unstable in water, as **4**. Yield: 1—1.5 g.

Found: C, 39.69; H, 3.11; N, 10.50%. Calcd for $C_{40}H_{36}N_9O_{19}Co_2Cl_4$: C, 39.82; H, 3.10; N, 10.45%.

(6) $(+)_D$*-μ-Amido-μ-peroxo-tetrakis(1,10-phenanthroline)dicobalt(III) Perchlorate Hexahydrate,* $(+)_D$-$[(phen)_2Co(\mu\text{-}NH_2,O_2)Co(phen)_2](ClO_4)_4\cdot 6H_2O$ (**6**). Ten grams of **2** was converted into chloride with 50 ml of water and Dowex CG 400 ion-exchange resin in the chloride form by a batch method. The resin was filtered off, and washed with a small amount of water. To the filtrate silver antimonyl *d*-tartrate (12 g) was added, stirred for half an hour, and then silver chloride was filtered off. The filtrate was poured into 100 ml of methanol and stored in a refrigerator with occasional stirring. Addition of methanol to the solution gave an oily product which could not be crystallized. After a day, the precipitated crude antimonyl *d*-tartrate of $(+)_D$-isomer was filtered off, washed with a small amount of cold water, methanol and ether, and dried. The filtrate was stored to obtain $(-)_D$-isomer (filtrate *a*).

Pure perchlorate of $(+)_D$-isomer was obtained as follows; the aqueous solution of the antimonyl *d*-tartrate salt was treated with a small amount of solid sodium perchlorate, and stirred for an hour in an ice bath. At this stage, the other enantioisomer was precipitated as less soluble racemate and filtered off. The $(+)_D$-isomer was obtained by adding excessive sodium perchlorate to the filtrate. This procedure was repeated to give a constant rotation.

Found: C, 44.63; H, 3.19; N, 9.49%. Calcd for $C_{48}H_{46}N_9O_{24}Co_2Cl_4$: C, 44.58; H, 3.59; N, 9.74%.

The $(-)_D$-isomer was obtained from the filtrate *a*. The filtrate was evaporated to 50 ml at about 40°C, and then a small amount of sodium perchlorate was added to remove less soluble racemate as stated above. Pure perchlorate of $(-)_D$-isomer was obtained from the filtrate by adding excessive sodium perchlorate.

(7) $(+)_D$*-μ-Amido-μ-peroxo-tetrakis(2,2′-bipyridyl)dicobalt(III) Perchlorate Trihydrate,* $(+)_D$-$[(bip)_2Co(\mu\text{-}NH_2,O_2)Co(bip)_2](ClO_4)_3\cdot 3H_2O$ (**7**). This isomer was prepared from **3** by a similar procedure to that for **6**. The antimonyl *d*-tartrate of $(+)_D$-isomer was precipitated by cooling at 0°C for 5 hr without adding methanol.

Found: C, 42.03; H, 3.53; N, 11.03%. Calcd for $C_{40}H_{40}N_9O_{17}Co_2Cl_3$: C, 41.96; H, 3.49; N, 10.83%.

The $(-)_D$-isomer was obtained also by the procedure as described for the $(-)_D$-isomer of the (phen) complex.

(8) $(+)_D$*-μ-Amido-μ-superoxo-tetrakis(1,10-phenanthroline)dicobalt(III) Perchlorate,* $(+)_D$-$[(phen)_2Co(\mu\text{-}NH_2,O_2)Co(phen)_2](ClO_4)_4$(**8**), *and* $(+)_D$*-μ-Amido-μ-superoxo-terakis(2,2′-bipyridyl)dicobalt(III) Perchlorate Monohydrate,* $(+)_D$-$[(bip)_2Co(\mu\text{-}NH_2,O_2)Co(bip)_2](ClO_4)_4\cdot H_2O$ (**9**). These $(+)_D$-isomers were prepared from **6** and **7**, by the procedures for **4** and **5**, respectively.

Found: C, 45.22; H, 3.05; N, 10.33%. Calcd for $C_{48}H_{34}N_9O_{18}Co_2Cl_4$: C, 44.88; H, 2.67; N, 9.81%. Found: C, 39.88; H, 3.27; N, 10.33%. Calcd for $C_{40}H_{36}N_9O_{19}Co_2Cl_4$: C, 39.82; H, 3.01; N, 10.45%.

Measurements. Visible and ultraviolet absorption spectra were obtained with a Hitachi 124 recording spectrophotometer. The CD curves were recorded with a Model ORD/UV-5 spectrophotometer of Japan Spectroscopic Co. with its CD attachment. The μ-peroxo complexes were measured in water, and the μ-superoxo complexes in 60% perchloric acid to avoid decomposition. Magnetic susceptibilities were measured with a magnetic balance of the Gouy type. The balance was calibrated with $HgCo(NCS)_4$. The effective magnetic moment, μ_{eff}, per one molecule was calculated from the expression $\mu_{eff}=2.83\sqrt{\chi_M\cdot T}$ B.M., where χ_M is the molar susceptibility corrected using Pascal's constant[7] and T absolute temperature.

All the measurements were made at room temperature.

Results and Discussion

Synthetic Method and the Structure of the Complexes. As stated in the experimental section, the complexes **2** and **3** of the type, $[(\alpha\text{-diimine})_2Co(\mu\text{-}NH_2,O_2)Co(\alpha\text{-diimine})_2]^{3+}$, can be prepared easily from $[(NH_3)_4Co(\mu\text{-}NH_2,O_2)Co(NH_3)_4](ClO_4)_4$ (**1**) and 1,10-phenanthroline and 2,2′-bipyridyl, respectively, by substitution reactions in methanol. The complex **1** is useful for a reaction in a non-aqueous solution, since it is soluble in organic solvents such as methanol or ethanol. The reaction in water always produced a large amount of tris-(phen) or -(bip) complex. It will be interesting to note, however, that the reaction between phenanthroline and nitrate of the complex **1** in water gives an insoluble dark green crystalline product with the formula $[Co_2(phen)_2(NH_3)_4(\mu\text{-}NH_2,O_2)](NO_3)_4$ in a few minutes. Detailed studies of this product will be published later.

Table 1. Magnetic moment of the complexes (solid)

Complex	Magnetic moment
2	diamag.
3	diamag.
4	1.92 B. M.
5	1.80 B. M.

7) B. N. Figgis and J. Lewis, "Modern Coordination Chemistry," ed. by J. Lewis and R. G. Wilkins, Interscience Publishers, New York (1960), p. 400.

Table 2. Numerical data of absorption (AB) and circular dichroism (CD) $\tilde{\nu}$ in 10^3 cm^{-1}, ($\log \varepsilon$) and ($\varepsilon_l - \varepsilon_r$)

Complex		$\tilde{\nu}$	$\tilde{\nu}$	$\tilde{\nu}$	$\tilde{\nu}$	$\tilde{\nu}$
$(+)_D$ form of **2**	AB	15.4(2.78)			37.0(4.99)	
(in water)	CD	15.6(−10.6)	21.5(+39.4)	27.9(+23.8)	34.7(−158)	44.1(−119)
					37.0(+111)	
$(+)_D$ form of **3**	AB	15.6(2.67)			32.6(4.62)	40.0(4.74)
(in water)	CD	15.9(−8.6)	21.8(+34.5)	28.6(+9.5)	31.5(−34.5)	45.5(−68)
					36.8(+50.9)	
$(+)_D$ form of **4**	AB	14.4(2.71)	20.7(3.07)		36.2(5.08)	46.1(5.18)
(in 60% $HClO_4$)	CD		19.5(−11.8)	28.5(+58.0)	35.0(−138)	43.5(−150)
					36.0(+96)	
					37.9(−59)	
$(+)_D$ form of **5**	AB	14.5(2.64)	20.9(2.98)		32.7(4.84)	45.5(5.19)
(in 60% $HClO_4$)	CD		20.3(−11.9)	29.9(+54.5)	32.3(+68.0)	45.5(−123)
					34.3(−53.5)	
					38.8(+46.3)	

As Table 1 shows, the μ-superoxo complexes have a magnetic moment corresponding to one unpaired electron, while the μ-peroxo complexes are diamagnetic. The elementary analyses and the fact that the formers derived from the latters by oxidation with nitric acid are paramagnetic indicate that all the complexes contain bridging μ-dioxygen group.[8,9]

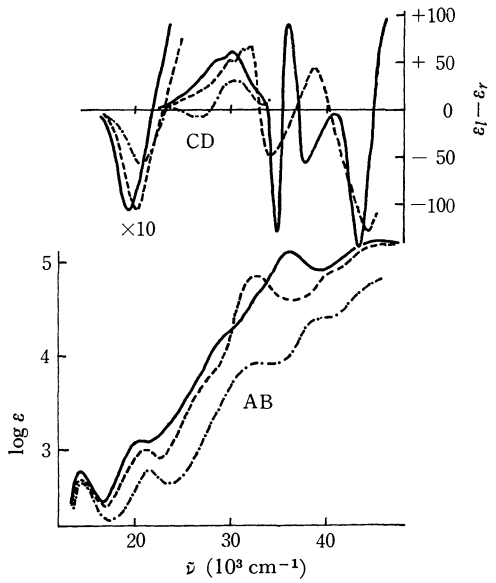

Fig. 1. The AB and CD spectra of $(+)_D$-$[(phen)_2Co(\mu\text{-}NH_2, O_2)Co(phen)_2](ClO_4)_4$ (——), $(+)_D$-$[(bip)_2Co(\mu\text{-}NH_2, O_2)Co(bip)_2](ClO_4)_4 \cdot H_2O$ (----) in 60% perchloric acid and $\Delta\Delta$-$[(en)_2Co(\mu\text{-}NH_2, O_2)Co(en)_2](NO_3)_4$ (—·—·) in water.

Figure 1 shows that the AB spectra of the μ-superoxo complexes (**4**, **5**) in the visible region are very similar to that of the ethylenediamine analog reported previously.[1] This result suggests that these complexes have a similar structure to one another. On the other hand, such a similarity in spectral pattern is not seen among the μ-peroxo complexes (**2**, **3**) and ethylenediamine analog, as shown in Fig. 2. The present μ-peroxo complexes exhibit a distinct absorption maximum at about 15500 cm^{-1}, whereas the ethylenediamine analog does not. Further consideration with

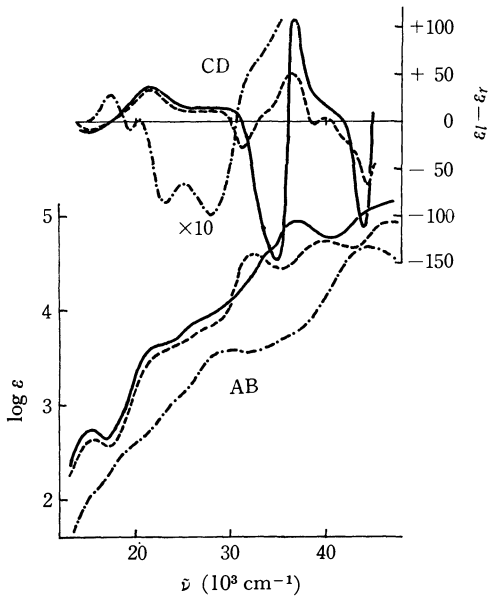

Fig. 2. The AB and CD spectra of $(+)_D$-$[(phen)_2Co(\mu\text{-}NH_2, O_2)Co(phen)_2](ClO_4)_3 \cdot 6H_2O$ (——), $(+)_D$-$[(bip)_2Co(\mu\text{-}NH_2, O_2)Co(bip)_2](ClO_4)_3 \cdot 3H_2O$ (----) and $\Delta\Delta$-$[(en)_2Co(\mu\text{-}NH_2, O_2)Co(en)_2]I_3$ (—·—·) in water.

8) L. R. Thompson and W. K. Wilmarth, *J. Phys. Chem.*, **56**, 5 (1952).

9) M. Mori and J. A. Weil, *J. Amer. Chem. Soc.*, **89**, 3732 (1967).

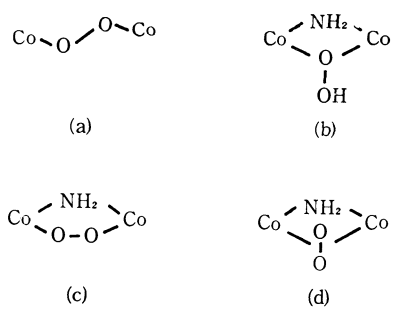

Fig. 3. Possible structures of μ-peroxo bridges.

reference to the structure of the bridge part would be needed.

Although no X-ray analysis has been made on a double bridged complex containing μ-peroxo group, the result for $[(NH_3)_5Co(\mu\text{-}O_2)Co(NH_3)_5](SO_4)_2\cdot 4H_2O$[10] revealed that each oxygen atom of the μ-peroxo group coordinates to each cobalt ion forming the σ-type bonding as shown in Fig. 3(a).

Mori and Weil,[9] on the basis of kinetic and spectroscopic measurements, inferred the isomerization scheme as shown in Fig. 4 for the $[(en)_2Co(\mu\text{-}NH_2,O_2)Co(en)_2]^{3+}$ ion. In this figure, [B] corresponds to the ordinarily prepared brown μ-amido-μ-peroxo-tetrakis-ethylenediamine complex. The [AH] was isolated as red nitrate[9,11] and its structure was determined by X-ray analysis.[12] This complex involves three bonded oxygen atom, as shown in Fig. 3(b). For the brown [B] form, Mori and Weil suggested the σ-type structure which is similar to that in $[(NH_3)_5Co(\mu\text{-}O_2)Co(NH_3)_5]^{4+}$ (Fig. 3(c)), They further considered that the [BH] and the [A] were intermediate species, and that their bridging structures would be similar to those of the [B] and [AH], respectively. In these arguments, however, there remain some ambiguities about the bridging structure of [A], for which a possibility of the π-type bonding structure (Fig. 3(d)) can not be excluded, since the interconversion between the Fig. 3(c) type and the π-type (Fig. 3(d)) seems to be easy.

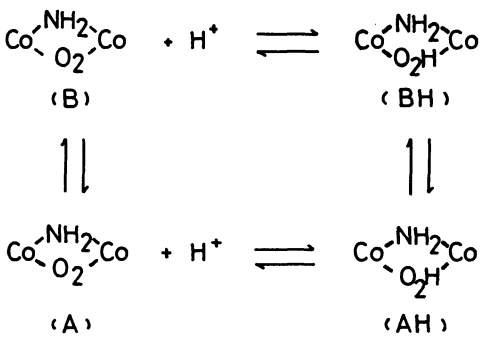

Fig. 4. Reaction scheme of μ-peroxo dicobalt ions. (From Ref. 9).

From the analysis of kinetic data, Mori and Weil[9] obtained absorption spectra of the three species, [B], [BH] and [AH]. The spectra of the present μ-peroxo complexes (**2**, **3**) in water do not seem to correspond to any of these species.

In order to make clear the structure of the present μ-peroxo complexes, we have measured the spectra in the solid state and in various solvents at different pH's. As Fig. 5 shows, the solid spectra of the μ-peroxo complexes (**2**, **3**) show a peak at about 15400 cm^{-1} which seems to correspond to the band at about 15500 cm^{-1} in aqueous solution. No significant difference was either observed between the spectra in water and in a basic solution. These results may indicate that each complex ion exists as a single chemical species under the given conditions, in solid state and in neutral and basic solutions. In acid solutions, on the other hand, the spectra vary remarkably according to the acid concentration, and have no isosbestic point. (Fig. 6). At acid concentrations

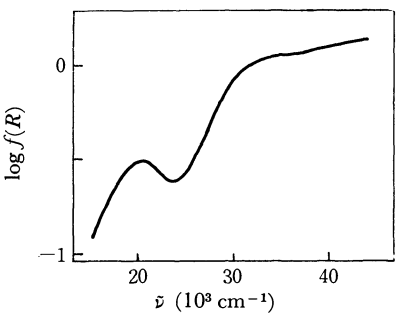

Fig. 5. Diffuse reflectance spectrum of $[(bip)_2Co(\mu\text{-}NH_2, O_2)Co(bip)_2](ClO_4)_3\cdot 2H_2O$ diluted with magnesium oxide.

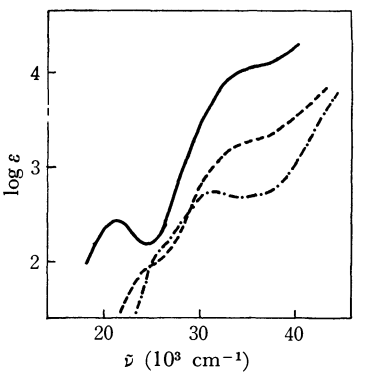

Fig. 6. The AB spectra of $[(bip)_2Co(\mu\text{-}NH_2, O_2)Co(bip)_2](ClO_4)_3\cdot 2H_2O$.
(——) in water and in 0.1 N KOH
(----) in 30% $HClO_4$
(·—·) in 60% $HClO_4$ and in 60% H_2SO_4.

10) W. P. Schaefer, *Inorg. Chem.*, **7**, 725 (1968).
11) A. Werner, *Ber.*, **46**, 3674 (1913).
12) U. Thewalt and R. Marsh, *J. Amer. Chem. Soc.*, **89**, 6364 (1967).

over 12 N, a constant curve is observed with an absorption maximum at 20400 cm^{-1}, and is similar to that of the μ-hydroperoxo ethylenediamine complex, [AH] (Fig. 1 in Ref. 9). Therefore, we can conclude that the complexes exist as μ-hydroperoxo form corresponding to the [AH] in strong acid solutions.

If the complexes had a structure corresponding to the [A] form in the solid state and in basic solutions, the predominant species in acid solutions should be two, [A] and [AH], and the spectra at various acid concentrations should have isosbestic points. Thus, the most probable bridging structure in the present μ-peroxo complexes (**2**, **3**) will be the σ-type as shown in Fig. 3(c), although their spectra in the visible region are different from that of ethylenediamine analog. More detailed studies, however, would be necessary to elucidate the structure of such μ-dioxygen complexes.

Chemical Behavior of the Complexes. The present μ-superoxo complexes, (**4**, **5**) decompose gradually in water and in basic solutions, giving the μ-peroxo complexes in 60—70% yield. The other 30—40% products were not characterized. The yield of the μ-peroxo ions was determined by their absorption intensities at 15500 cm^{-1}. The reduction with iodide ions in water produced the μ-peroxo complexes almost quantitatively. Thompson and Wilmarth[8] considered that $[(en)_2Co(\mu\text{-}NH_2,O_2)Co(en)_2]^{4+}$ in a basic solution is reduced to the μ-peroxo complex by hydroxide ion. Garbett and Gillard[13] examined the yield of this reduction and gave about 60%. However, the fact that the present μ-superoxo complexes are reduced in a neutral aqueous solution, in which the concentration of hydroxide ions is only 10^{-7} mol/*l*, suggests that in our case, the hydroxide ion would not be a main reducing agent. This suggestion will be supported further by the results that the yields of the μ-peroxo complex reduced in a neutral and in a basic solution are almost equal, 60—70%, but the reduction with another reducing agent such as the iodide ion proceeds almost quantitatively. However, we could not give a definite conclusion about such reductions at present.

It should be noted that when the reduction of racemic μ-superoxo complexes (**4**, **5**) is caused to proceed in water containing a large excess of potassium antimonyl *d*-tartrate, the resulting solution shows similar CD spectra to those of the $(-)_D$-μ-peroxo complexes. From their CD intensites, the optical purity of the products is known to be about 10%. The aqueous solutions of racemic μ-peroxo complexes containing potassium antimonyl *d*-tartrate exhibit very weak CD which originates probably from the second sphere coordination.[14,15] Therefore, such a phenomenon may suggest that the antimonyl *d*-tartrate ion interacts with reaction species stereoselectively in the reduction process.

d-Tartaric acid and *d*-bromocamphorsulfonate ions have no such effect.

Spectra and Absolute Configurations of the Complexes. The AB spectra of the μ-superoxo complexes (**4**, **5**) in the visible region are similar to that of ethylenediamine analog, as stated previously. The band at about 14000 cm^{-1} which is characteristic of μ-superoxo complexes might owe to the charge transfer transitions between the μ-superoxo group and the cobalt(III) ions.[1] The band at about 21000 cm^{-1} may correspond to the first band of a uninuclear cobalt(III) complex.[1] These bands, however, are located from the longer to shorter wavelength in the order of phenanthroline, bipyridyl and ethylenediamine complex (Fig. 1). This order is the reverse order of the spectrochemical series.[16] On the other hand, the location of the bands in the ammine and ethylenediamine analogs is in accord with this series.

As Fig. 1 shows, the $(+)_D$-μ-superoxo complexes show a fairly strong negative CD band in the first band region, which can be compared well with that of the $\Delta\Delta$*1 isomer of ethylenediamine analog. This result indicates that these isomers have $\Delta\Delta$ configuration. Both $(+)_D$-isomers of the μ-peroxo complexes, from which the $\Delta\Delta$-μ-superoxo complexes were prepared, therefore, should have also $\Delta\Delta$ configuration, since it is very unlikely that inversion would take place during the oxidation. The CD spectra of these μ-peroxo complexes in the *d-d* transition region are very similar to each other, but are entirely different from that of the $\Delta\Delta$ isomer of ethylenediamine analog.[1]

All the complexes prepared here show strong absorption bands in the region 30000 to 40000 cm^{-1}, which can be assigned to the long-axis π–π^* transitions of the coordinated aromatic ligands.[17,18] It is known that these transitions are not largely modified from those of the free ligands.[18] According to the theory,[19–22] when two or three such

13) K. Garbett and R. D. Gillard, *J. Chem. Soc.*, *A*, **1968**, 1725.

14) S. F. Mason and B. J. Norman, *Chem. Commun.*, **1965**, 335.

15) K. Ogino and U. Saito, This Bulletin, **40**, 826 (1967).

16) Y. Shimura and R. Tsuchida, *ibid.*, **29**, 311 (1956).

*1 We use the symbols Δ and Λ in the sense of Piper's designation, in accord with the recommendation of IUPAC (1968); *Inorg. Chem.*, **9**, 1 (1970).

17) A. J. McCaffery, S. F. Mason and B. J. Norman, *Proc. Chem. Soc.*, **1964**, 259.

18) J. Hidaka and B. E. Douglas, *Inorg. Chem.*, **3**, 1180 (1964).

19) B. Bosnich, *ibid.*, **7**, 178 (1968).

20) J. Ferguson, C. J. Hawkins, N. A. P. Kane-Maguire and H. Lip, *ibid.*, **8**, 771 (1969).

21) A. J. McCaffery, S. F. Mason and B. J. Norman, *J. Chem. Soc., A*, **1969**, 1428.

conjugated ligands are present in an octahedral complex, the CD spectrum corresponding to their transitions consists of two strong components with different signs. For a Δ configuration, their signs are minus and plus from longer to shorter wavelength. As Fig. 1 shows, the $(+)_D$-μ-superoxo-(phen) complex exhibits two strong, sharp CD peaks with minus and plus sign from longer to shorter wavelength in the π–π^* transition region, indicating that the absolute configuration around each cobalt(III) ion is Δ. This result agrees with the previous assignment obtained from the sign of CD band in the *d-d* transition region. The $(+)_D$-μ-peroxo-(phen) complex shows also such a CD pattern in this region, although the bands are somewhat broader than those of the μ-superoxo complex.

Neither $(+)_D$-isomer of the bipyridyl complexes, on the other hand, gives such a CD for the bands corresponding to the π–π^* transitions. In the bipyridyl complexes, the bands due to these transitions are at a longer wavelength region as compared with those of the phenanthroline complexes, and overlap with the so-called polynuclear bands.[1] Accordingly, it is supposed that the CD bands due to the π–π^* transitions of coordinated bipyridyl might be cancelled by overlapping or interacting with the other CD bands due to such polynuclear bands.

All the $(+)_D$-(bip) and -(phen) complexes exhibit strong negative CD bands at about 45000 cm^{-1}. In particular, those of (phen) complexes are strong and sharp. Mason and Norman[23] measured the CD spectrum of $(+)_D$-$[Co(phen)_3]^{3+}$ and claimed to have only a weak CD in this region. As Fig. 7 shows, however, this tris complex shows a strong negative CD band at 44600 cm^{-1}. Although the origin of such a discrepancy is not clear at present, there seems to be an optically active transition in this region for a cobalt(III) complex containing two or three phenanthroline molecules.

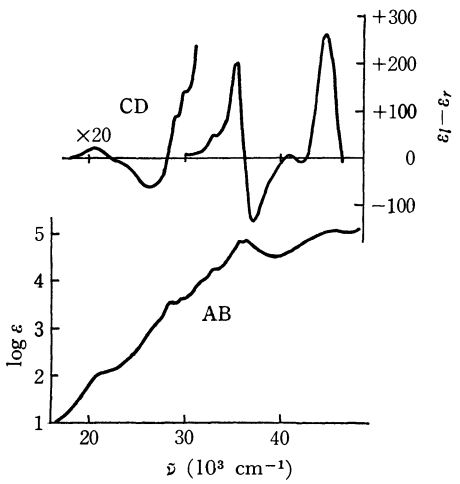

Fig. 7. The AB and CD spectra of $(+)_D$-$[Co(phen)_3](ClO_4)_3 \cdot 2H_2O$ in water.

We thank the Ministry of Education for financial support granted to this research.

22) B. Bosnich, *Accounts Chem. Res.*, **2**, 266 (1969).

23) S. F. Mason and B. J. Norman, *Inorg. Nucl. Chem. Lett.*, **3**, 285 (1967).

BULLETIN OF THE CHEMICAL SOCIETY OF JAPAN VOL. 43 3468—3471 (1970)

The Thermal Decomposition of $CuBr_2 \cdot 2NH_3$ and $CuBr_2$

Nobuyuki TANAKA and Masahiro KAGAWA*

Department of Chemistry, Faculty of Science, Tohoku University, Katahira, Sendai

(Received July 8, 1970)

The thermal decomposition of $CuBr_2 \cdot 2NH_3$ has been examined at the constant temperature, about 220°C. Copper(II) was reduced to copper(I), when bromine gas was found as one of the decomposition products, indicating that bromide anion may be the reducing agent for copper(II). The decomposition reaction of $CuBr_2$ has been investigated by measuring the weight loss under the condition of the constant temperature. In a closed system, the reaction,

$$CuBr_2(s) \leftrightarrows \gamma\text{-}CuBr(s) + \frac{1}{2}Br_2(g)$$

attained to equilibrium, and ΔG° for this reaction was determined in the range from 160°C to 220°C to be given by the equation,

$$\Delta G^\circ(\text{cal.}) = 1.10 \times 10^4 - 19.3\ T\ (160°C—220°C).$$

While the pressure of bromine gas was kept zero, $CuBr_2$ decomposed following a first-order rate law in the beginning of the decomposition, and the activation energy was found to be 25.4 kcal/mol.

When hexammine-[1-3] or aquopentammine-copper(II)[4] halides are heated, they lose ammonia or ammonia and water to form diammine complexes, $CuX_2 \cdot 2NH_3$ (X=Cl, Br and I). At higher temperatures, diammine complexes decompose with an electron transfer reaction and produce copper(I) halides, ammonia and other decomposition products. Smith and Wendlandt[3] showed that the primary reducing agent for copper(II) was ammonia in the case of the bromide and the chloride. There is, however, still left the possibility that halide anion may take part in reducing copper(II). In this investigation, therefore, the electron transfer reaction of $CuBr_2 \cdot 2NH_3$ was reexamined carefully. In addition, the thermal decomposition of $CuBr_2$ was studied as a simpler case of the electron transfer reaction of copper(II) complexes.

Experimental

The Thermal Decomposition of $CuBr_2 \cdot 2NH_3$. Figure 1 shows the apparatus used in this experiment. $CuBr_2$ was put into a crucible, and ammonia gas (about 1 atm.) was introduced into the reaction tube with checking a manometer. $[Cu(NH_3)_6]Br_2$ was formed one or two days later. The reaction tube was heated at about 220°C by an electric furnace. In heating, the pressure of ammonia was kept 1 atm., because ammonia was evolved from $[Cu(NH_3)_6]Br_2$. Then, $CuBr_2 \cdot 2NH_3$ was formed. A trap was cooled with the freezing mixture, alcohol-dry ice. Ammonia gas was rapidly removed from the reaction tube by operating a vacuum pump and opening the cock A. The pyrolysis products were condensed in a cooled trap.

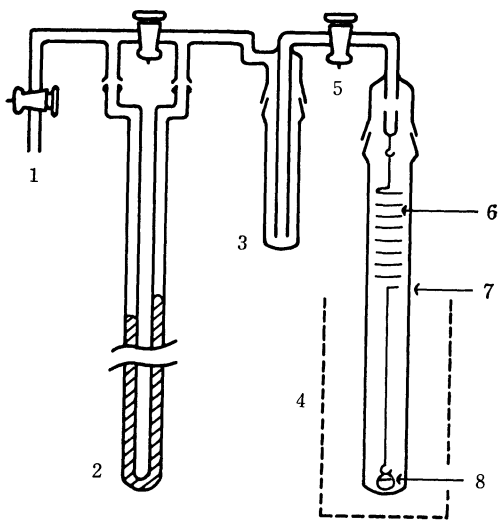

Fig. 1. Apparatus used for the manometric measurement of decomposition reactions.
(1) Outlet to vacuum pump, (2) mercury manometer, (3) trap, (4) electric furnace, (5) cock A, (6) spring balance, (7) reaction tube and (8) crucible.

* Present address: The Research Institute for Iron, Steel and Other Metals, Tohoku University, Katahira, Sendai.

1) W. Biltz, H. Bröhan and W. Wein, *Z. Anorg. Allg. Chem.*, **148**, 207 (1925).
2) F. Ephraim, *Ber.*, **52**, 940 (1919).
3) J. P. Smith and W. W. Wendlandt, *J. Inorg. Nucl. Chem.*, **26**, 1157 (1964).
4) G. G. Urazov, A. K. Kirakosyan and V. D. Galustyan, *Zh. Neorg. Khim.*, **2**, 1094, 1104 (1957).

The Thermal Decomposition of $CuBr_2$. The same apparatus as shown in Fig. 1 was used. The manometer was detached when $CuBr_2$ was treated, because mercury reacts with bromine gas evolved from $CuBr_2$. $CuBr_2$ was put into a quartz crucible (121 mg), which was hung on a quartz spring balance (4.10 mg/mm in sensitivity). The contraction due to the weight loss of the sample was measured with a cathetometer (0.05 mm in accuracy). The reaction tube of Pyrex glass was kept at a constant temperature in the range of ± 1°C with the electric furnace. As bromine gas reacts with mercury even at room temperature, the pressure of bromine gas cannot be directly measured with a mercury manometer. It, however, could be calculated from the equation, $PV=nRT$, P being the pressure of bromine gas, V, the volume of the reaction tube (0.162 l), n, moles of bromine gas calculated from the observed weight loss, T, absolute temperature, and R, gas constant. As the upper part of the reaction tube, however, was left at room temperature, the correction due to this difference in temperature must be considered in calculating the pressure. The values for this correction were obtained experimentally as follows. The trap was removed and the manometer was directly connected to the reaction tube so that the volume between the reaction tube and the manometer could be made as small as possible. From the weight loss at t°C, the pressure of bromine gas, P_{25} was calculated when the whole part of the reaction tube was supposed to be at room temperature, 25°C. Nitrogen gas, the pressure of which was P_{25} was introduced at the room temperature into the reaction tube with checking the manometer. When the reaction tube was heated under the same experimental condition as in the treatment of $CuBr_2$, the pressure of nitrogen gas increased to P_t. From P_t and P_{25}, the correction coefficient, γ_t, characteristic to only this apparatus was obtained as,

$$\gamma_t = P_t/P_{25} \text{ (1.12 at 160°C, 1.14 at 215°C).}$$

Assuming that γ_t was applicable to the case of bromine gas, P_{Br_2} which means the pressure of bromine gas at t°C is given by

$$P_{Br_2} = \gamma_t \times P_{25}$$

In this correction, the volume change of the reaction tube due to heating and the quantity of adsorbed bromine on the wall of the reaction tube were neglected.

After the reaction,

$$CuBr_2(s) \rightleftharpoons CuBr(s) + \frac{1}{2}Br_2(g),$$

had reached to the equilibrium completely, a vacuum pump was operated and the cock A was opened. The reaction proceeded to the right side. The time when the cock A was opened was defined as time zero, and the weight loss was followed. The weight loss was converted to the degree of decomposition, α (α equals 0 when the sample was $CuBr_2$, and 1 when the reaction finished and $CuBr_2$ was changed completely to CuBr), and, then, α *vs.* t(time) curves were obtained. Though α at time zero was different according to the temperature, the largest value of α in this experiment was 0.05, which was found in the measurement at 134°C. The sample taken for the measurement ranged from 15 to 25 mg. $CuBr_2$ used in the kinetic investigation had been pulverized as small as possible using an agate mortar in the room where relative humidity was kept under 40%, because $CuBr_2$ was very deliquescent.

Results and Discussion

The Thermal Decomposition of $CuBr_2 \cdot 2NH_3$. $CuBr_2 \cdot 2NH_3$ did not decompose in a closed system as long as ammonia coexisted. It, however, decomposed when the pressure of ammonia was suddenly reduced, and bromine was found to condense on the wall of the cooled trap. These results indicate that the equilibrium has established between ammonia gas and solid $CuBr_2 \cdot 2NH_3$ before the electron transfer reaction occurs, and that bromide anion takes part in reducing copper(II). The latter result is inconsistent with that of Smith and Wendlandt.[3] They reported that, as the temperature was raised, higher ammine complexes such as $[Cu(NH_3)_6]Cl_2$, $[Cu(NH_3)_6]Br_2$ and $[Cu(NH_3)_4]I_2$ reversibly dissociated ammonia, and diammine complexes, $CuX_2 \cdot 2NH_3$ (X=Cl, Br and I) were formed. Upon further heating, the irreversible reduction of copper(II) to copper(I) took place, of which stoichiometries were

$$6CuX_2 \cdot 2NH_3 \rightarrow 6CuX + 6NH_4X + N_2 + 4NH_3 \quad (X=Cl, Br)$$

$$2CuI_2 \cdot 2NH_3 \rightarrow 2CuI + I_2 + 4NH_3$$

These equations indicate that iodide anion reduces copper(II) in the case of the iodide whereas ammonia does in the case of the chloride and the bromide.

Some questions, however, arose about their discussion on the electron transfer reactions, and a new explanation will be given to their results.

(1) The above stoichiometries may be explained from the standpoint that halide anions reduce copper(II). After the halide anion donates an electron to copper(II), it reaches to the active state of atom or forms halogen gas, which in turn reacts with ammonia. Consequently, nitrogen and ammonium halide are formed by the following reaction.

$$8NH_3 + 3X_2 \text{ (or X*)} \rightarrow 6NH_4X + N_2$$

X=Cl, Br; X*=active atom

Really this reaction proceeds very fast at room temperature.

(2) The temperature at which the reduction of copper(II) took place was found to increase in the following order:

the iodide < the bromide < the chloride

As this order is consistent with that of the depolarizability, halide anions are suggested to be the reducing agent for copper(II).

(3) If ammonia reduces copper(II), the electron transfer reaction is expected to take place easily at the state of hexammine complexes where copper(II) is coordinated with six ammonia molecules. It, however, took place after $CuX_2 \cdot 2NH_3$

was formed in which halide anions were coordinated with copper(II).

(4) Gažo[5] has already discussed the effect of coordinated ammonia on the reduction of copper (II). CuI_2 does not exist at room temperature whereas $CuI_2 \cdot 2NH_3$ is stable even when it is heated at 100°C in ammonia atmosphere. Usually the reduction temperature of $CuX_2 \cdot 2NH_3$ (X=Cl, Br) is higher than that of CuX_2. These facts suggest that coordinated ammonia can not promote the reduction of copper(II), but can hinder the electron transfer from halide anion to copper(II).

These explanations suggest that the coordinated halide anion can have more chance to reduce copper(II) than the coordinated ammonia. Although the results obtained in this investigation cannot completely deny that ammonia is reducing agent, its possibility might be considered less. Therefore, the following reactions may be the main paths of the decomposition.

$$CuBr_2 \cdot 2NH_3 \rightleftharpoons CuBr_2 \cdot NH_3 + NH_3 \quad (1)$$

$$CuBr_2 \cdot NH_3 \rightleftharpoons CuBr_2 + NH_3 \quad (2)$$

$$CuBr_2 \rightarrow CuBr + \frac{1}{2}Br_2 \quad (3)$$

$$CuBr_2 \cdot NH_3 \rightarrow CuBr \cdot NH_3 + \frac{1}{2}Br_2 \quad (4)$$

$$CuBr \cdot NH_3 \rightarrow CuBr + NH_3 \quad (5)$$

$$8NH_3 + 3Br_2 \rightarrow 6NH_4Br + N_2 \quad (6)$$

The equilibrium reactions (1) and (2) well explain the fact shown by Smith and Wendlandt[3] that the reduction temperatures observed with mass spectrometry were lower than those obtained by thermomagnetic analysis; the former was carried out in vacuum while the latter was in ammonia atmosphere.

The Thermal Decomposition of $CuBr_2$. When $CuBr_2$ was heated in vacuum after the cock A was closed, bromine gas was evolved and the weight loss was observed. The weight loss reached to a constant value within one or two hours, which did not change even after twenty four hours. When the evolved bromine was evacuated from the system, the weight loss began again and arrived at a new constant value. When $CuBr_2$ was heated in vacuum, the weight loss reached to a value which would be obtained when all of $CuBr_2$ was assumed to change completely to CuBr. This suggests that there must be the equilibrium reaction

$$CuBr_2(s) \rightleftharpoons CuBr(s) + \frac{1}{2}Br_2(g)$$

The weight loss in equilibrium was measured under the following conditions: (1) The quantity and the grain size of $CuBr_2$ were changed, (2) inert gas, N_2, was introduced into the system, (3) the equilibrium was made to establish from the side of $CuBr_2$ or from that of $CuBr + 1/2\ Br_2$. As the result, the weight loss was found to be independent of these conditions, but dependent only on temperature. This means that the pressure of bromine gas is constant provided that the temperature is given, *i.e.*, the equilibrium of the electron transfer of $CuBr_2$ is dependent on the pressure of bromine gas or temperature.

The weight loss was measured at various temperatures and it was converted to the pressure by following the procedure described in the experimental section. The linearity was obtained between $\log P_{Br_2}$ and $1/T$ as shown in Fig. 2, which is represented by

$$\log P_{Br_2} = 8.43 - \frac{4.79 \times 10^3}{T}$$

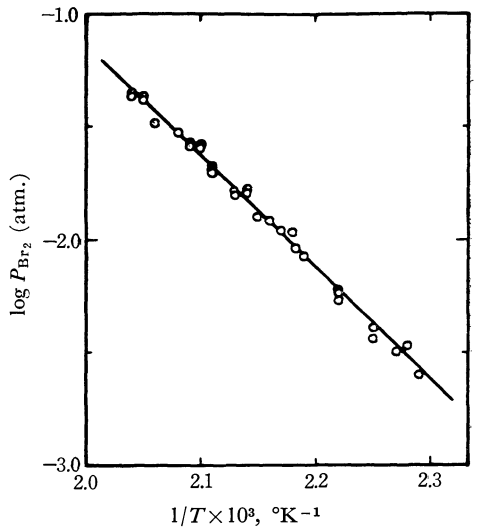

Fig. 2. Temperature dependence of the equilibrium pressure of bromine gas.

As the standard free energy change, $\Delta G°$, is expressed by

$$\Delta G° = -RT \ln K_p = -RT \ln P_{Br_2}^{1/2}$$

where K_p is the equilibrium constant, $\Delta G°$ for the reaction is given by

$$\Delta G° \text{ (cal.)} = 1.10 \times 10^4 - 19.3\ T$$

in the range from 160°C to 220°C.

The structural investigations of $CuBr_2$[6] and CuBr[7] have been reported. $CuBr_2$ has the polymeric chain structure in which a bromine atom bridges two copper(II) atoms and a copper(II) atom is coordinated with four bromine atoms. The bond Cu–Br largely bears covalency. CuBr has three modifications of α-, β- and γ-forms, and transition temperatures are 385°C for γ to

5) J. Gažo, *Chem. Zvesti*, **15**, 20 (1961).

6) L. Helmholz, *J. Amer. Chem. Soc.*, **69**, 886 (1947).

7) S. Hoshino, *J. Phys. Soc. Jap.*, **7**, 560 (1952).

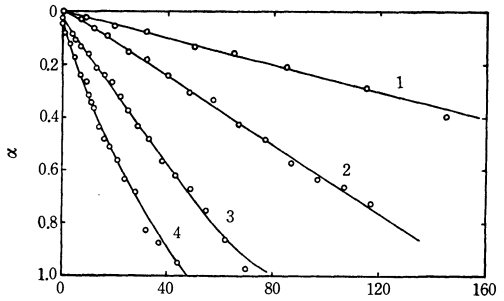

Fig. 3. Typical decomposition curves of $CuBr_2$ *in vacuo* obtained at (1) 105°, (2) 115°, (3) 125° and (4) 134°C.

β and 470°C for β to α. γ-CuBr is of a zinc-blend type, but it shows an anomalous change with temperature. In this investigation, as the temperature was lower than 220°C, CuBr belonged to γ-type. The reaction, therefore, must be expressed as,

$$CuBr_2(s) \rightleftarrows \gamma\text{-}CuBr(s) + \frac{1}{2}Br_2(g)$$

Figure 3 shows the plots of α, *vs.* t. The decomposition reaction was found to follow a first-order rate law expressed by

$$d\alpha/dt = k_1 (1-\alpha)$$

at the beginning of the reaction, and a second-order rate law given by

$$d\alpha/dt = k_2\alpha (1-\alpha)$$

at the intermediate stage of the reaction. This result indicates that the reaction in the beginning may be controlled only by the process of the electron-transfer reaction, while the reaction at the intermediate period may be affected by the formation of decomposition product, CuBr.

This may be well understood by the consideration of the structure of $CuBr_2$. As $CuBr_2$ has polymeric chain structure and covalent bond, the structure change in the formation of Cu(I) might give a great effect to its neighboring chains successively. In view of this, the reaction in the beginning will be discussed so that some informations on the electron-transfer reaction can be obtained.

Since the integral form of the equation

$$d\alpha/dt = k_1 (1-\alpha)$$

is expressed by

$$-\ln(1-\alpha) = k_1 t + C$$

where C is constant, k_1 can be obtained from the slope of the plots of $-\log(1-\alpha)$ *vs.* t. Really, these plots gave straight lines in the beginning of the reaction as shown in Fig. 4. The value of k_1 was independent of the quantity and the grain

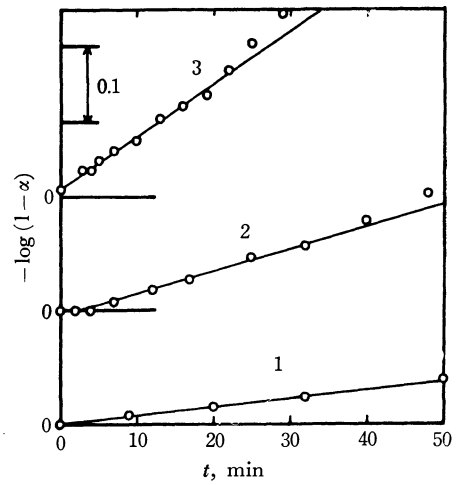

Fig. 4. Linear relationship between $-\log(1-\alpha)$ and time obtained at (1) 105°, (2) 115° and (3) 125°C.

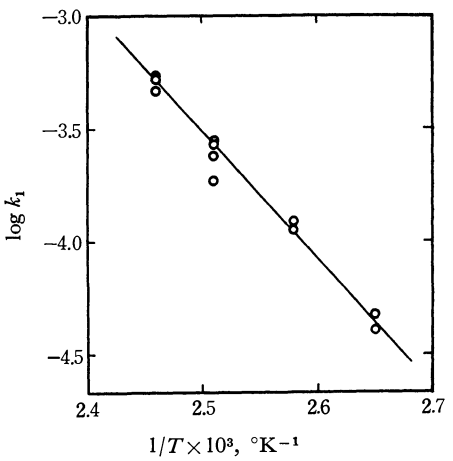

Fig. 5. Arrhenius plots of the first-order reaction rates for the decomposition reaction of $CuBr_2$ *in vacuo*.

size of $CuBr_2$ within the experimental error. Figure 5 shows the plots of $\log k_1$ *vs.* $1/T$, from which activation energy (E) and the frequency factor (A) were calculated to be 25.4 kcal/mol and $10^{10.4}$, respectively. Both of the values are almost the same as those of hexamminecobalt(III) complexes.[8] Though $CuBr_2$ had a polymer structure while hexamminecobalt(III) complexes had a monomer one, the difference could not be distinguished by the kinetic investigation.

The authors wish to thank the Ministry of Education for the financial support granted for this research.

8) N. Tanaka and K. Nagase, This Bulletin, **41**, 1143 (1968).

BULLETIN OF THE CHEMICAL SOCIETY OF JAPAN VOL. 43 3472—3474 (1970)

Competitive Inhibition of Pepsin by Carboxylic Acids

Hong Dae SHIN

Department of Chemistry, College of Liberal Arts and Sciences, Pusan National University, Pusan, Korea

(Received July 25, 1969)

In order to obtain evidence for Tang's hypothesis that pepsin (EC 3.4.4.1) forms a hydrophobic bond with the nonpolar side chain or its substrates, the inhibitory effect of carboxylic acids (from formic acid to isobutyric acid) on the activity of pepsin to the synthetic dipeptide, *N*-carbobenzoxy-L-glutamyl-L-tyrosine, was studied. Kinetic study showed that the inhibition by carboxylic acids was of competitive type. The inhibitor constant K_i decreased with an increase in the size of the inhibitor molecule. The free energy change of formation of complex between pepsin and hydrocarbon chain of carboxylic acid, $-\Delta F_{HC}$, increased linearly with the increase in the number of carbon atoms in the hydrocarbon chain of the inhibitor. It was suggested that the hydrophobic interaction between the side chain of amino acid residues in the binding region of the active center of pepsin and the hydrocarbon side chain of the inhibitor was the cause of the inhibition.

A theory[1,2] that a part of the binding region of their active center is hydrophobic was presented for various proteolytic enzymes. In pepsin (EC 3.4.4.1), it is known that substrates are bound to pepsin through hydrophobic bond.[2] The data given by Tang[1] indicated that pepsin exhibits preference for aromatic amino acid residues on both sides of the susceptible peptide bond. Judging from the fact that phenylalanyl residues are bound to pepsin more strongly than tyrosyl residues, binding of substrates with pepsin is supposed to be hydrophobic in nature. In this communication, the effect of carboxylic acids with aliphatic side chain on pepsin-catalyzed hydrolysis is described in order to examine the hydrophobic character of binding. If the hypothesis is correct, the hydrocarbon group of carboxylic acids and the substrate will bind competitively to the hydrophobic region of the active center of pepsin. Thus the carboxylic acids will act as competitive inhibitor against pepsin-catalyzed hydrolysis. In fact, the competitive inhibition of aliphatic alcohols against pepsin was observed by Tang.[2] Moreover, it was reported by Cann[3] that the formation of the enzyme-substrate complex between serum alubumin and pepsin is inhibited by a long chain fatty acid.

The inhibition of carboxylic acids ranging from formic acid to butyric acid on the pepsin-catalyzed hydrolysis of *N*-carbobenzoxyl-L-glutamyl-L-tyrosine (Z-Glu-Tyr) was studied to see the effect of hydrocarbon side chain of the carboxylic acids.

Experimental

Materials. Ninhydrin and methylcellosolve were obtained from E. Merck, and were purified by the E. Zeffren method.[4] Crystalline porcine pepsin and α-chymotrypsin (twice crystallized) were obtained from Worthington Biochemical Corp. *N*-Carbobenzoxyl-L-glutamyl-L-tyrosine substrate, *N*-benzoyl-L-arginine amide and *N*-acetyl-L-tyrosine amide were obtained from the Institute for Protein Research, Osaka University (Japan), and boving hemoglobin from Difco Laboratory. Carboxylic acids of highest purity were used.

Purification of Enzyme. Purification was carried out following Tang's method.[1,2]

Enzyme Activity. The activity of pepsin was measured with bovine hemoglobin by the Rajagopalan method.[5] The optical density was measured with a spectrophotometer (Unicam SP 500) at 280 mμ. From the results, the specific activity of pepsin was found to be 2505 ± 125 units/mg (mean of five determinations), when assayed with denatured hemoglobin (1.77%) as substrate at pH 1.8 and 30°C. One pepsin unit was defined as the amount of enzyme that produces (in the assay) an increase in the optical density of 0.01 above the blank. The increase in optical density was proportional to enzyme concentration, within the range of pepsin concentration used in the assay with hemoglobin as the substrate. In calculating the molar pepsin concentration, a molecular weight of 35000 was assumed (1 mg=0.0286 μmole). The activity of trypsin was measured with *N*-benzoyl-L-arginine amide as substrate by the Laskowski method[6]. The activity of α-chymotrypsin was also measured with *N*-

1) J. Tang, *Nature*, **199**, 1094 (1964).
2) J. Tang, *J. Biol. Chem.*, **240**, 3810 (1965).
3) J. Cann, *J. Biol. Chem.*, **237**, 707 (1962).
4) E. Zeffren and E. T. Kaiser, *J. Amer. Chem. Soc.*, **88**, 3129 (1966).
5) T. G. Rajagopalan, S. Moore and W. H. Stein, *J. Biol. Chem.*, **241**, 4940 (1966).
6) M. Raskowski, S. P. Coliwick and N. O. Kaplan (Ed.), "Methods in Enzymology," Vol. 11. Academic Press, Inc., New York (1955). pp. 22, 26.

Table 1. Inhibition constant, K_i, of carboxylic acids

Carboxylic acids	$S_0 \times 10^3$ (M)	$i \times 10^3$ (M)	$K_i \times 10^3$ (M)	Average $K_i \times 10^3$ (M)
Acetic acid	1.2	48 ; 90	96	87.3
	2.3	48 ; 90	87	
	3.5	48 ; 90	79	
Propionic acid	1.2	35 ; 71	64	64.3
	2.3	35 ; 71	72	
	3.5	35 ; 71	57	
n-Butyric acid	1.2	36 ; 70	48	46.3
	2.3	36 ; 70	51	
	3.5	36 ; 70	40	
Isobutyric acid	1.2	35 ; 69	50	44.0
	2.3	35 ; 69	38	
	3.5	35 ; 69	44	

acetyl-L-tyrosine amide as substrate by the Laskowski method.[6]

Kinetic Measurements. The rate of enzyme action was measured by modified Moore's method.[7] In order to observe the effect of inhibition, the solution of reactant was incubated at various concentrations of the carboxylic acids added. Incubation mixtures consisted of 1.0 m*l* of inhibitor solution at pH 3.5, 1.0 m*l*, of stock substrate solution*, 0.2 m*l*, of stock enzyme solution**, and 0.1 m*l* of HCl in order to adjust the pH of final mixture to 3.5. Ionic strength of incubation mixture was adjusted to 0.1 with 0.1 M KCl. (*, **, Each stock solution was prepared with 0.2 M sodium citrate buffer, pH 3.5).

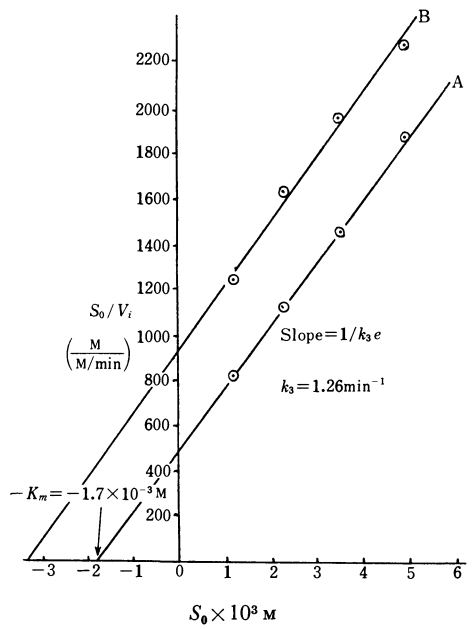

Fig. 1. Hofstee plots for the pepsin-catalyzed hydrolysis of Z-Glu-Tyr with or without the inhibition by acetic acid. The inhibitor concentrations are; A, no inhibitor; and B, 90 mM acetic acid.

7) S. Moore and W. H. Stein, *J. Biol. Chem.*, **176**, 367 (1948).

Results

Effect of Carboxylic Acids on Pepsin Action. The inhibitory effect of the carboxylic acids from formic acid to butyric acid upon the pepsin activity was observed with the use of Z-Glu-Tyr as substrate. The result shows that the degree of inhibition is roughly proportional to the increase in the molecular weights of carboxylic acids as shown in Table 1. However, in the case of formic acid, inhibition was non-competitive. For the purpose of comparing the inhibitory effects of carboxylic acids upon different proteolytic enzymes, the same study was carried out with α-chymotrypsin and trypsin. With α-chymotrypsin was observed such

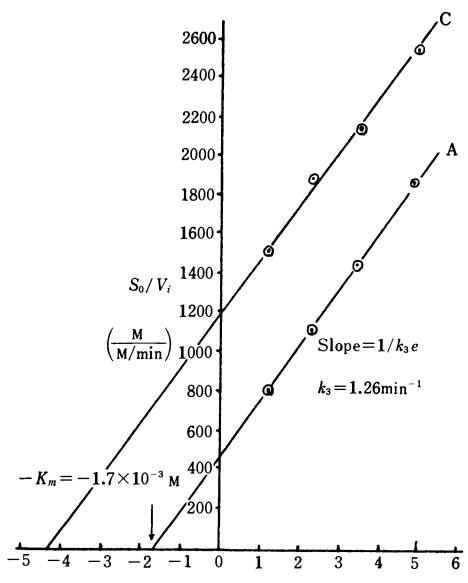

Fig. 2. Hefstee plots for the pepsin-catalyzed hydrolysis of Z-Glu-Tyr with or without the inhibition by *n*-butyric acid. The inhibitor concentrations are; A, no inhibitor, and C, 70 mM *n*-butyric acid.

an inhibitory effect by carboxylic acids as the in case of pepsin. The inhibitory effect on trypsin did not appear up to 1.4% concentration of carboxylic acids. Reversibility of inhibition was confirmed by the removal of carboxylic acids by dialysis.

Kinetics. The Hofstee plot for the hydrolysis of Z-Glu-Tyr showed straight lines as shown in Figs. 1 and 2 in accordance with the Michaelis-Menten equation (1).

$$\text{Pepsin} + \text{Z-Glu-Tyr} \underset{k_2}{\overset{k_1}{\rightleftharpoons}} \overset{\text{Pepsin}}{\dot{\text{Z}}\text{-Glu-Tyr}} \xrightarrow{k_3} \text{Pepsin} + \text{Z-Glu}\cdot\text{COOH} + \text{Tyr}\cdot\text{COOH} \quad (1)$$

$$S_0/V_0 = S_0/V_{max} + K_m/V_{max} \quad (2)$$

$$S_0/V_i = S_0/V_{max} + K_m/V_{max}(1+i/K_i) \quad (3)$$

$$V_0/V_i = 1 + K_m/K_i[i/(K_m+S_0)] \quad (4)$$

where

S_0=initial substrate concentration
V_0=initial velocity of the reaction without inhibitor
V_i=initial velocity of the reaction with inhibitor
V_{max}=maximum velocity without inhibitor
K_m=Michaelis constant without inhibitor
K_i=inhibitor constant
i=inhibitor concentration

The results with acetic acid and *n*-butyric acid as inhibitor, are shown in Figs. 1 and 2 as the plot S_0/V_i *vs.* S_0 according to Eqs. (2) and (3). It is obvious that the two kinds of acid were competitive inhibitors within the concentration range

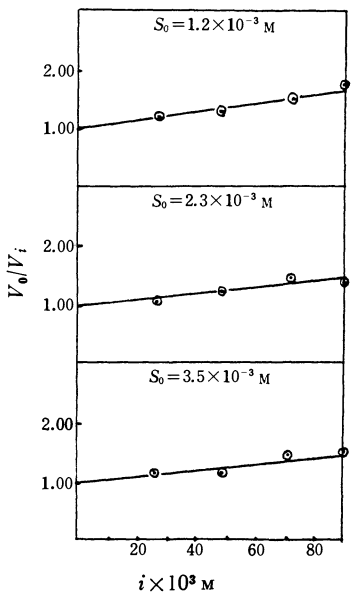

Fig. 3. V_0/V_i *vs.* i plots for the hydrolysis of Z-Glu-Tyr by pepsin inhibited by acetic acid at pH 3.5 (0.2 M sodium citrate buffer); temperature, 37°C.

TABLE 2. VALUES FOR $-\Delta F_i^{0a)}$, $-\Delta F_{HC}^{0b)}$

Carboxylic acids	average $K_i\times10^3$ (M)	$-\Delta F_i^0$ kcal/mol	$-\Delta F_{HC}^0$ kcal/mol
Acetic acid	87.3	1.5	
Propionic acid	64.3	1.8	0.3
n-Butyric acid	46.3	1.9	0.4
Isobutyric acid	44.0	1.9	0.4

a) ΔF_i^0: Standard free energy change of formation of pepsin-inhibitor complex, calculated from the equation, $-\Delta F_i^0=2.303\boldsymbol{R}T\log 1/K_i$.
b) ΔF_{HC}^0: Standard free energy change of formation of complex between pepsin and the hydrocarbon chain of carboxylic acid. The date was obtained by subtracting ΔF_i^0 of acetic acid from all the values of ΔF_i^0.

studied. It has been observed that *n*-butyric acid is a stronger competitive inhibitor than acetic acid. The competitive inhibition did not appear up to 90 mM concentration of acetic acid and 71 mM concentration of *n*-butyric acid. In Fig. 3 plots V_0/V_i *vs.* i by Eq. (4) shows the inhibitory effect at different concentrations of each acid. From the plots, K_i of each competitive inhibitor was determined, and the result is shown in Table 1. We see in Tables 1 and 2, that K_i decreases as the number of carbon atoms in the carboxylic acid molecule increases, as was observed with a series of aliphatic alcohols.[2]

Discussion

The results of the present study show that the pepsin clearly underwent competitive inhibition by carboxylic acids. Since the concentration of carboxylate ion does not affect the rate of pepsin-catalyzed reaction,[8] it is not likely that the observed competitive inhibition is caused by the carboxyl group of carboxylic acids. Thus, it is probable that the effect of competitive inhibition by acid is caused by the hydrocarbon group in the acid molecule. This is supported by the fact that the degree of the inhibition increases with the increase in the number of the carbon atoms in the acid molecule (*cf.* Table 1). Thus the binding site of the active center of enzyme may be considered to be hydrophobic, in line with Tang's result.[1,2] In other words, inhibition by carboxylic acid depends on the competition between the hydrocarbon group of carboxylic acid molecule and the substrate on the hydrophobic binding site of enzyme. It is likely that hydrophobic bond is formed between the side chain of amino acid residue in the substrate molecule and the hydrophobic region of the binding site of the active center of enzyme.

8) K. Inoyue, I. M. Voynick, G. R. Delpierre and J. S. Fruton, *Biochemistry*, **5**, 2473 (1966).

BULLETIN OF THE CHEMICAL SOCIETY OF JAPAN VOL. 43 3475—3479 (1970)

Acid-Catalyzed Oxidation of Olefins with Selenium Dioxide

Khan A. JAVAID, Noboru SONODA and Shigeru TSUTSUMI

Department of Chemical Technology, Faculty of Engineering, Osaka University, Yamadakami, Suita-shi, Osaka

(Received August 25, 1969)

A drastic deviation from the usually accepted reaction path was observed when oxidation of olefins was carried out in acetic acid with selenium dioxide in the presence of concentrated sulfuric acid. Oxidation of cyclohexene gave a mixture of *cis*- and *trans*-1,2-diacetoxycyclohexane. It was shown that in the oxidation of cyclohexene the organoselenium intermediate which produced 3-acetoxy-1-cyclohexene on pyrolysis, is not the intermediate in the present reaction. A study on reaction variables, such as effect of molar ratio of cyclohexene to selenium dioxide, amount of sulfuric acid, and water, reaction time and temperature, was undertaken. The reaction was extended to 1-octene and 1-hexene. A general structure for the organoselenium compound produced in the oxidation of terminal olefins in acetic acid without sulfuric acid, has been proposed. On the basis of our data and some previous concepts a reaction scheme has also been given.

It is generally accepted that oxidation of olefins with selenium dioxide essentially takes place at α position in the most substituted end of the double bond leading to an allylic product that is a function of the solvent used, and order of preference for oxidation is $CH_2 > CH_3$. In a previous paper[1] we reported that addition of two acetoxyl groups to the double bond occurs when the olefins without α-methyl or α-methylene carbon atom are oxidized with selenium dioxide in acetic acid. It is also accepted now that the oxidation follows an ionic path resulting from the electrophilic attack of selenium dioxide or conjugate acid of selenium dioxide on the double bond of the olefin.[2-4] Thus it was thought that addition of a strong acid might either increase the rate of the reaction or change its course by changing the active species. Actually both phenomena were observed. In the oxidation of cyclohexene and 1-octene, the course of the reaction deviated drastically from the generallized path when a small of concentrated sulfuric acid as catalyst was added. We wish to report this new trend in the selenium dioxide oxidation of olefins.

The structure of the organoselenium intermediate resulting from the non-catalytic oxidation of a terminal olefin with selenium dioxide in acetic acid has not been determined. We have proposed a structure for it.

Results and Discussion

Oxidation of Cyclohexene Cyclohexene was selected as a model olefin. Oxidation of cyclohexene has been studied by several researchers. It has been reported that 3-acetoxy-1-cyclohexene is produced in a yield of 48—50% when cyclohexene is treated with selenious acid in acetic anhydride at 80—85°C.[5] 3-Acetoxy-1-cyclohexene is obtained in a yield of 32% together with a trace of 3,6-diacetoxy-1-cyclohexene, when cyclohexene is treated with selenium dioxide in a mixture of acetic acid and acetic anhydride at 80—85°C.[6]

Cyclohexene was oxidized with equimolar amount of selenium dioxide in glacial acetic acid at 110°C for 10 hr in a 200 m*l* glass autoclave in the presence of a small amount of concentrated sulfuric acid to give mainly 1,2-diacetoxycyclohexane in a yield of 32%, as a mixture of *cis* (56%) and *trans* (44%) isomers. Cyclohexenone and cyclohexyl acetate were obtained as minor products. It was interesting to note that no 3-acetoxy-1-cyclohexene was produced and no organoselenium compound could be characterized. Metallic selenium was produced as the final reduced state of the oxidant. This reaction revealed two important features:

i) Addition to the double bond, instead of the allylic oxidation, took place.

ii) *Cis* addition as much as 56% was observed whereas electrophilic additions to cyclohexene molecule are known to give *trans* isomers generally.

1) K. A. Javaid, N. Sonoda and S. Tsutsumi, This Bulletin, **42**, 2056 (1969).

2) J. P. Schaefer, B. Horvath and H. P. Klein, *J. Org. Chem.*, **33**, 2647 (1968).

3) K. Wiberg and S. D. Neilson, *ibid.*, **29**, 3353 (1964).

4) J. L. Huguet, *Advan. Chem. Ser.*, **76**, 345 (1968).

5) Yu. A. Arbuzov, N. D. Zelinskii and N. I. Shuikin, *Bull. Acad. Sc. U. S. S. R. Classe Sci. Chim.*, 163 (1945).

6) E. Schwerk and E. Borgwardt, Ger. 584373 (*Chem. Zentr.*, **11**, 3481 (1933)).

Study of the Reaction Variables. The reaction was very sensitive to the change in the molar ratio of olefin to selenium dioxide and the amount of sulfuric acid. Hardly any reaction took place when molar ratio of cyclohexene to selenium dioxide was 3. The yield of 1,2-diacetoxycyclohexene and the rate of the reaction increased with the decrease in the molar ratio of cyclohexene to selenium dioxide. The amount of sulfuric acid was important since it controlled the stereospecificity of the reaction. The increase in the amount of sulfuric acid increased the *trans* isomer (expts. 2, 4). Explanation for this effect is shown in the reaction scheme. Use of the large amount of catalyst resulted in decomposition of the products. The effect of water is also shown in Table 1. The monoacetate formed in each experiment was found to be almost all *cis* isomer, a part of which turns into the *trans* isomer on acid-catalyzed esterification during the reaction. Thus increase in the amount of water increased the *cis* monoacetate and consequently increased the *trans* diacetate (expts. 2 and 7, 4 and 6). The effects of the reaction time and reaction temperature were not so remarkable. The best results were obtained at 110—115°C. The reaction was very slow at 90—100°C and the residue remained in a large amount after distillation of the products at high temperatures. Some results from the study of the different reaction variables are given in Table 1.

Organoselenium Compounds in the Oxidation of Cyclohexene. We were interested in why the addition of a strong acid changes the reaction path of selenium dioxide oxidation of olefins so much. Two explanations can be given: 1) It is known that oxidation of cyclohexene without sulfuric acid first produces an organoselenium compound which on pyrolysis gives 3-acetoxy-1-cyclohexene.[3] The same organoselenium compound might also have been produced in the present reaction and the subsequent acid catalyzed decomposition may have given 1,2-diacetoxycyclohexene.

2) Addition of strong acid changed the active species at an early stage of the reaction, leading to different products.

A detailed study of organoselenium compounds was undertaken. The organoselenium compound from cyclohexene, responsible for the allylic oxidation products, was prepared by the method given by Arbuzov *et al.*[5] and purified by column chromatography. Wiberg and Neilsen[3] proposed two structures (Ia and Ib) for the compound emphasizing the probability in favor of Ia. The infrared spectrum of the compound purified by column chromatography showed it to be an acetate and absorptions for –OH or C=C were not found. NMR spectrum indicated the presence of –CHOAc. No absorption peak for the olefinic proton could be detected. These spectroscopic data confirm the structure Ia.

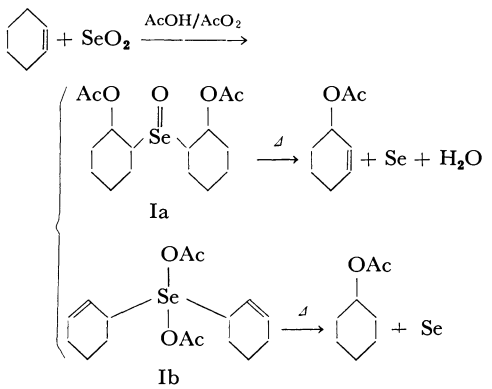

To investigate whether Ia is also an intermediate in the acid-catalyzed oxidation of cyclohexene or not, the compound was decomposed in acetic acid containing a small amount of sulfuric acid under similar conditions as those applied for the acid-catalyzed oxidation of cyclohexene. A large amount of metallic selenium was produced. Among the products, 3,6-diacetoxy-1-cyclohexene and a small amount of 1,2-diacetoxycyclohexane could be detected. The former product was considered to be formed by further oxidation of 3-acetoxy-1-cyclohexene. The discrepancies in the nature of the products, and the percentage composition

Table 1. Oxidation of cyclohexene

	Reaction conditions						Products %		Isomers % of diacetate	
	mol	SeO_2 mol	H_2SO_4 m*l*	H_2O m*l*	Time hr	Temp. °C	OAc OAc	OAc OH	*cis*	*trans*
1	0.146	0.072	0.27	—	9	110	2.5	—	—	—
2	0.098	0.072	0.27	—	9	110	20.0	3.6	50	50
3	0.098	0.098	0.27	—	9	110	30.0	2.0	50	50
4	0.098	0.072	0.18	—	9	110	21.0	2.0	56	44
5	0.098	0.072	0.13	2.5	9	110	18.0	4.0	44	56
6	0.098	0.072	0.18	5.0	12	110	15.2	6.8	37	63
7	0.098	0.072	0.27	18.0	9	110	14.5	9.0	25	75

of the stereoisomers obtained from the direct acid-catalyzed oxidation of cyclohexene and acid-catalyzed decomposition of the organoselenium compound from cyclohexene, lead us to the conclusion that the compound Ia is not the intermediate in the acid-catalyzed oxidation of cyclohexene, and that the addition of sulfuric acid has changed the active species at an early stage of the reaction.

Oxidation of 1-Octene. On the basis of the results obtained from the oxidation of cyclohexene, studies were extended to some terminal olefins such as 1-octene and 1-hexene to investigate the scope of the reaction. Oxidation of 1-octene with equimolar amount of selenium dioxide in acetic acid at 115°C for 10 hr in the presence of concentrated sulfuric acid as a catalyst, gave 1,2-diacetoxyoctane (35%) and a trace of 1-acetoxy-2-octene. When 1-octene was oxidized with selenium dioxide in a mixture of acetic acid and acetic anhydride without sulfuric acid, an organoselenium compound was produced as a major product with a small amount of 1-acetoxy-2-octene. Thermal decomposition of the organoselenium compound gave again 1-acetoxy-2-octene. The acid-catalyzed decomposition of the organoselenium compound in acetic acid containing a small amount of sulfuric acid under similar conditions to those subjected to the acid-catalyzed oxidation of 1-octene, also produced 1-acetoxy-2-octene as a major product and a small amount of 3-acetoxy-1-octene. The result indicates that the organoselenium compound also, is not the intermediate in the acid-catalyzed oxidation of 1-octene.

Organoselenium Compounds in the Oxidation of 1-Octene. Recently oxidation of 1-octene was studied by bubbling air through the reaction mixture, and the formation of two organoselenium compounds IIa and IIb with a small amount of 1-acetoxy-2-octene was reported.[7]

$$CH_3\text{-}(CH_2)_5\text{-}CH{=}CH_2 + SeO_2 + AcOH \xrightarrow{Air}$$

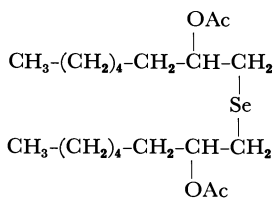

IIa

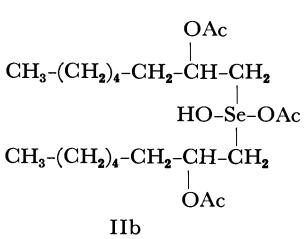

IIb

Decomposition of IIa and IIb in acetic acid containing a small amount of sulfuric acid under similar conditions to those used for the acid-catalyzed oxidation of 1-octene produced again 1,2-diacetoxyoctane. Reaction conditions and stoichiometric calculations indicate that this may be formed from IIb. We assume from the results that in the direct formation of 1,2-diacetoxyoctane from 1-octene, active species resembling IIb may be involved, but IIb can not be considered as the major intermediate in the acid-catalyzed oxidation of 1-octene because of the difference in the yield of the products from the two cases. We can also conclude that organoselenium compound formed in the oxidation of 1-octene is different when (a) air is bubbled, and (b) air is not bubbled. The decomposition in (a) leads to diacetate formation while that in (b) leads to allylic oxidation products. No structure has been assigned to the organoselenium compound resulting from the non-catalytic oxidation of the terminal olefins. In the present work it was purified by column chromatography and its structure III was assigned on the basis of its infrared and NMR spectral data and the results of thermal and acid-catalyzed decompositions. Thermal decomposition of III should be facile and may proceed through a cyclic transition state to give the allylic oxidation product. (Scheme 1)

The effect of air is not understood except that bubbling of it reduced the selenium deposition.[7] It was thought that the following reaction takes place.

$$Se \xrightarrow{Air} SeO$$

$$III \longrightarrow IIa + SeO_2$$

Oxidation of 1-Hexene. Almost the same results as obtained in the oxidation of cyclohexene or 1-octene, except that considerable amounts of allylic oxidation products were obtained along with the addition products, were observed. Thus, oxidation of 1-hexene with an equimolar amount of selenium dioxide in acetic acid at 105°C for 10 hr in the presence of a small amount of concentrated sulfuric acid produced 1,2-diacetoxyhexane (35%), 3-acetoxy-1-hexene, (12%) and 1-acetoxy-2-hexene (5%). Identification of the products was carried out by infrared and NMR spectral analyses and GLC.

In order to compare the reaction with a known one, 1-hexene was oxidized with selenium dioxide following the procedure of Guillemonat[8] to give mainly the organoselenium compound which on pyrolysis and acid-catalyzed decomposition in acetic acid separately produced a mixture of 1-

7) K. Takaoka and Y. Toyama, *Nippon Kagaku Zasshi*, **89**, 618 (1968).

8) A. Guillemonat, *Ann. Chim.* (Paris), **11**, 143 (1939).

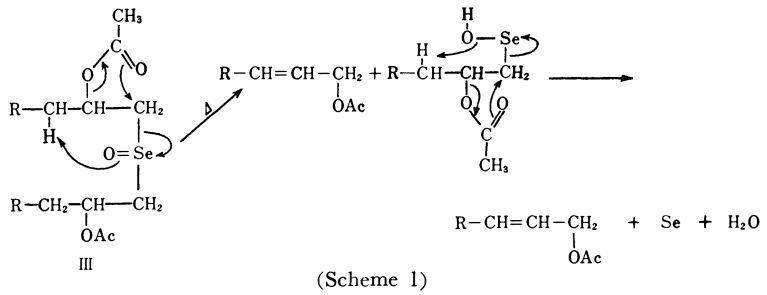

(Scheme 1)

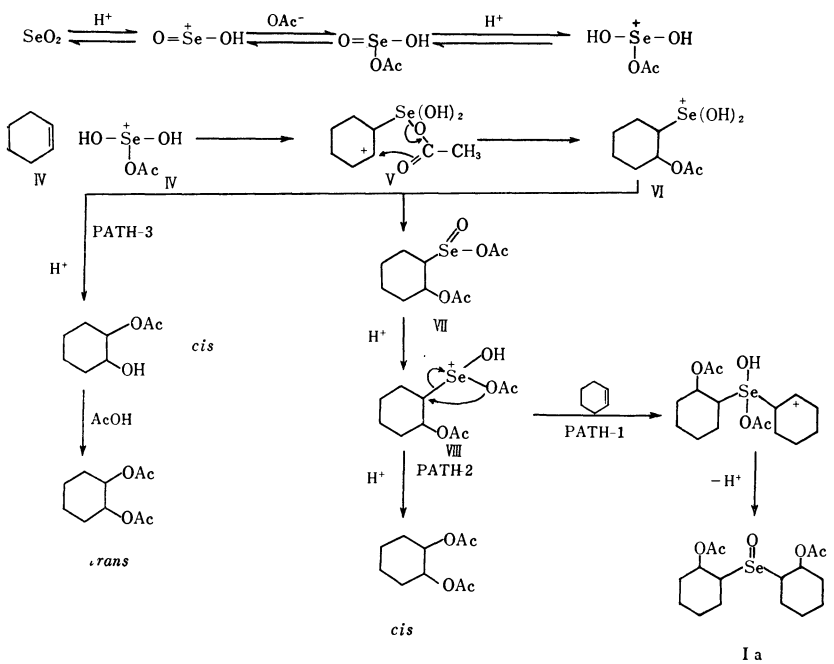

(Scheme 2)

acetoxy-2-hexene and 3-acetoxy-1-hexene.

Reaction Scheme. Schaefer *et al.*[2] suggested a reaction mechanism for the oxidation of olefins. Olson[9] gave a modified mechanism for the oxidation of ethylene. In view of the basic concepts postulated by these workers, a reaction scheme may be given from the consideration of the data presented above and our previous results indicating the *exo-cis* addition of acetoxyl groups to the double bond of norbornene molecule.[1]

According to the reaction scheme (Scheme 2), if no catalyst the reaction will follow path 1 to give there is the organoselenium compound which consequently leads to the allylic oxidation products. In the presence of a small amount of sulfuric acid as the catalyst the reaction will mainly deviated to path 2, whereas the large amount of the catalyst will tend to change the reaction path to 3. The production of the *cis* isomers may be attributed to the interamolecular acetoxylation through a cyclic transition state (VIII) formed by the addition of sulfuric acid as a strong proton donor. The scheme also explains the production of monoacetates as primary products.

Experimental

All the reactions were conducted in a 250 m*l* graduated glass autoclave with a mechanically operated stainless steel stirrer, which can be operated up to a pressure of 15 kg/cm^2. Infrared spectra were taken with a Shimadzu IR-27C spectrophotometer. The proton NMR spectra were taken on a Japan Electron Optics Lab. JNM C-60 spectrometer in deuteriochloroform with TMS as an internal standard. For mass spectral analysis, a Hitachi RMU-60 mass spectrometer was employed with the electron beam energy at 80 eV.

Acid-catalyzed Oxidation of Cyclohexene. A typical example is given here to cover the general reaction procedure. Selenium dioxide (11 g) was suspended in 50 m*l* of glacial acetic acid in the glass autoclave, cyclohexene (8 g) was diluted with a small amount of

9) D. H. Olson, *Tetrahedron Lett.*, **1966**, 2053.

acetic acid and transferred to the autoclave, 0.18 m*l* of concentrated sulfuric acid was added as a catalyst and the total volume was made up to 150 m*l* with acetic acid. The autoclave was heated at 110°C for 10 hr with stirring preventing the settling of selenium dioxide. The color of the reaction mixture changed from yellow to brown and ultimately to black due to the deposition of metallic selenium. After the reaction was over, selenium was filtered off and acetic acid was removed by vacuum distillation. The distillate collected at 40°C/3 mmHg, was found to be a mixture of cyclohexyl acetate and cyclohexenone by GLC. The second fraction boiling at 95°C/3 mmHg was characterized as 1,2-diacetoxycyclohexane (5.5 g). NMR spectrum: τ 5.1 (multiplet, 2H, >CH–OAc), 7.95 (singlet, 6H, $-OCOCH_3$), 7.9—8.8 (multiplet, 8H, ring methylenes).

Non-catalytic Oxidation of Cyclohexene. The procedure given by Arbuzov *et al.*[5] was followed to give a small amount of 3-acetoxy-1-cyclohexene and an organoselenium compound mainly as residue. The residue was divided into three parts. One part was subjected to pyrolysis in a distillation flask at 250°C under the reduced pressure of 20 mmHg to give 3-acetoxy-1-cyclohexene and a small amount of 3,6-diacetoxy-1-cyclohexene. Second part of the residue (about 10 g) was dissolved in 120 m*l* of acetic acid in the glass autoclave, and thermal decomposition was carried out at 110°C for 8 hr in the presence of 0.18 m*l* of concentrated sulfuric acid. Metallic selenium was filtered off and acetic acid was removed by vacuum distillation. The distillate at 95—100°C/3 mmHg was characterized as a mixture of 3,6-diacetoxy-1-cyclohexene, *trans* 1,2-diacetoxycyclohexane and an unknown product. Silica gel column chromatography was employed for the purification of the organoselenium compound. The residue (about 1 g) was diluted with 4 m*l* of *n*-hexane and transfered to a 35 cm×2.5 cm column containing 40 g of silica gel in 80 m*l* of *n*-hexane. The eluents used were *n*-hexane, a mixture of 50% *n*-hexane and 50% benzene, pure benzene and a mixture of 95% benzene and 5% ether. On the basis of its infrared and NMR spectra and the results of thermal and acid-catalyzed decompositions, the structure Ia was confirmed. NMR: τ 5.2 (multiplet, 2H, >CHOAc), 7.1 (multiplet, 2H, >CH–SeO–), 7.95 (singlet, 6H, $-OCOCH_3$), 7.9—8.8 (multiplet, 16H, ring methylenes).

Acid-catalyzed Oxidation of 1-Octene. Selenium dioxide (8 g) was suspended in 50 m*l* of acetic acid in the glass autoclave and 1-octene (8 g) was added. The total volume was made up to 140 m*l* with acetic acid and 0.18 m*l* of concentrated sulfuric acid was added as a catalyst. The reaction was carried out at 115°C for 10 hr. After metallic selenium was removed by filtration, acetic acid was distilled off under the reduced pressure. The distillate boiling at 105—110°C/3 mmHg was almost pure 1,2-diacetoxyoctane (6.5 g). Redistillation of the fraction gave pure 1,2-diacetoxyoctane, 107°C/3 mmHg. NMR: τ 5.1 (multiplet, 1H, –CHOAc), 5.9 (multiplet, 2H, $>CH_2OAc$), 7.95 (singlet, 6H, $-OCOCH_3$), 8.2—9.5 (multiplet, 13H, $-C_6H_{13}$).

Non-catalytic Oxidation of 1-Octene. Selenium dioxide (5 g) was suspended in 120 m*l* of glacial acetic acid and 15 m*l* of acetic anhydride in the glass autoclave and 1-octene (10 g) was poured in. The autoclave was heated at 100—105°C for 8 hr. No deposition of metallic selenium was observed. The solvents and the unreacted 1-octene were removed by vacuum distillation. A small amount of product was obtained at 55°C/3 mmHg and a dark brown residue remained. The product was identified as 1-acetoxy-2-octene by GLC. The residue was pyrolysed in a distillation flask to give 1-acetoxy-2-octene. The acid-catalyzed decomposition of the residue in acetic acid at 115°C for 8 hr in the presence of 0.18 m*l* of concentrated sulfuric acid gave 1-acetoxy-2-octene and a small amount of 3-acetoxy-1-octene. The organoselenium compound was purified by silica gel column chromatography. The method applied was the same as that used for the purification of the organoselenium compound (Ia) from cyclohexene. Structure III was assigned on the basis of its infrared and NMR analyses. NMR spectrum: τ 5.15 (multiplet, 2H, >CHOAc), 7.25 (doublet, 4H, $-CH_2$–SeO–), 7.95 (singlet, 6H, $-OCOCH_3$), 8.2—9.3 (multiplet, 26H, $-C_6H_{13}$).

Acid-catalyzed Oxidation of 1-Hexene. Selenium dioxide (5.5 g) was suspended in 50 m*l* of acetic acid in the glass autoclave and 1-hexene (4 g) was added. The total volume was made up to 140 m*l* with acetic acid and 0.14 m*l* of concentrated sulfuric acid was added as a catalyst. Oxidation was carried out at 105°C for 10 hr with stirring. The deposited metallic selenium was filtered off and acetic acid was removed by vacuum distillation. The fraction boiling at 40—45°C/3 mmHg was found to be a mixture of 1-acetoxy-2-hexene (5%) and 3-acetoxy-1-hexene (12%) by GLC. The second distillate collected at 85°C/2 mmHg was found to be 1,2-diacetoxyhexane (35%). Its structure was confirmed by comparison with an authentic sample. NMR spectrum: τ 5.1 (multiplet, 1H, –CHOAc), 5.9 (multiplet, 2H, $-CH_2OAc$), 7.95 (singlet, 6H, $-OCOCH_3$), 8.2—9.2 (multiplet, 9H, $-C_4H_9$).

Non-catalytic Oxidation of 1-Hexene. The procedure of Guillemonat[8] was followed. Organoselenium compound was the major product. Pyrolysis of the compound at 250°C/23 mmHg in a distillation flask gave a mixture of 1-acetoxy-2-hexene and 3-acetoxy-1-hexene in the ratio 3 to 1. The acid-catalyzed decomposition of the organoselenium compound (10 g) in 120 m*l* of acetic acid containing 0.14 m*l* of concentrated sulfuric acid at 105°C for 8 hr gave 1-acetoxy-2-hexene and 3-acetoxy-1-hexene in the ratio 2 to 1.

Khan A. Javaid expresses his thanks to the Ministry of Education of Japan, for a scholarship.

BULLETIN OF THE CHEMICAL SOCIETY OF JAPAN VOL. 43 3480—3485 (1970)

Aromatic Metalation Reactions by Palladium(II) and Platinum(II) on Aromatic Aldoximes and Ketoximes

Hiroshi ONOUE, Kyoji MINAMI and Kunio NAKAGAWA

Shionogi Research Laboratory, Shionogi & Co., Ltd., Fukushima-ku, Osaka

(Received September 25, 1969)

Ortho metalation by palladium(II) was observed in the reaction of lithium tetrachloropalladate(II) with various aromatic aldoximes and ketoximes in methanol in the presence of sodium acetate. The obtained chloro-bridged complexes(**7**) possessed both *ortho*-attached palladium-carbon σ-bonding and palladium-nitrogen coordinate bonding to oximes. Reactions of *O*-acyl and *O*-methyl oximes with lithium tetrachloropalladate(II) were also carried out. An *ortho* metalation was observed in the former case, but dichlorobis(*O*-methyl oxime)palladium(II) type complexes containing no palladium-carbon σ-bonds were predominantly formed in the latter case. The bridge-splitting reaction of chloro-bridged complexes with triphenylphosphine and the metathetic reaction with sodium bromide in acetone were carried out. In the case of potassium tetrachloroplatinate(II), an *ortho* metalation reaction was observed giving the complexes(**10**) but chloro-bridged complexes could not be isolated.

It has recently been shown that direct electrophilic aromatic substitution reactions by nickel(II), palladium(II), and platinum(II) on azobenzene,[1,2] *N,N*-dimethylbenzylamine,[3] 2-phenylpyridine,[4] and benzylidenaniline[5] gave the following complexes (**1**—**5**), respectively.

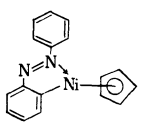

1

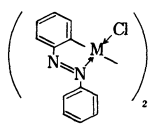

2

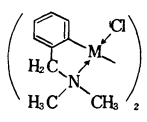

3

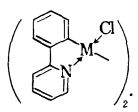

4

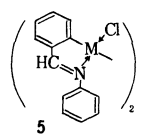

5

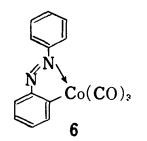

6

M=Pd, Pt

Transition metal complexes containing carbon-metal σ-bonds are usually very unstable[6] but the above complexes are surprisingly stable against air and heat. On the other hand, palladium-aromatic ring σ-bonded complexes may be regarded as intermediates in the reactions,[7-11] although they are unstable and not isolated.

Heck[12] prepared complex **6** and considered it to be the reaction intermediate of the carbonylation of azobenzene catalyzed by dicobalt octacarbonyl; this reaction was first discovered by Horiie and Murahashi.[13] Tsuji *et al.* obtained 2-(dimethylaminomethyl)stilbene by the reaction of complex **3** with styrene in acetic acid.[14]

From the above arguments, transition metal-aromatic ring σ-bonded complexes are important for studying the mechanism of aromatic substitution reactions and the study of the properties of these complexes will help to find out new synthetic methods.

Here we report a new metalation reaction by palladium(II) and platinum(II) on aromatic aldoximes and ketoximes.[15]

1) J. P. Kleiman and M. Dubeck, *J. Amer. Chem. Soc.*, **85**, 1544 (1963).
2) A. C. Cope and R. W. Siekman, *ibid.*, **87**, 3272 (1965).
3) A. C. Cope and E. C. Friedrich, *ibid.*, **90**, 909 (1968).
4) A. Kasahara, This Bulletin, **41**, 1272 (1968).
5) S. P. Molnar and M. Orchin, *J. Organometal. Chem.*, **16**, 196 (1969).
6) G. E. Coates, M. L. H. Green and K. Wade, "Organometallic Compounds," Vol. 2, Methuen & Co., Ltd., London (1968), p. 203.
7) R. van Helden and C. Verberg, *Rec. Trav. Chim. Pays-Bas*, **84**, 1263 (1965).
8) I. Moritani and Y. Fujiwara, *Tetrahedron Lett.*, **1967**, 1119.
9) Y. Fujiwara, I. Moritani, S. Danno, R. Asano and S. Teranishi, *J. Amer. Chem. Soc.*, **91**, 7166 (1969).
10) T. Sakakibara, S. Nishimura, Y. Odaira and T. Yoshida, *Tetrahedron Lett.*, **1969**, 1061.
11) R. F. Heck, *J. Amer. Chem. Soc.*, **90**, 5518, 5526, 5531, 5535, 5538, 5542 (1968).
12) R. F. Heck, *ibid.*, **90**, 313 (1968).
13) S. Horiie and S. Murahashi, This Bulletin, **33**, 88 (1960).
14) H. Takahashi, K. Ohno and J. Tsuji, Abstract III, the 22nd Annual Meeting of the Chemical Society of Japan, Tokyo, April, 1969, p. 1595.

Results and Discussion

It was found that benzophenone oxime gave 3-phenylphthalimidine by carbonylation in the presence of dicobalt octacarbonyl[19] or palladium chloride[20] in benzene. We studied the reaction benzophenone oxime with palladium chloride in the absence of carbon monoxide.

The reaction of benzophenone oxime with lithium tetrachloropalladate(II) in methanol at room temperature gave dichlorobis(benzophenone oxime) palladium(II) having no palladium-carbon σ-bondings. When the reaction was carried out by adding sodium acetate, we obtained complex **7a** ($R^1=H$, $R^2=C_6H_5$, X=Cl) and a small amount of complex **8**. The structure of **7** will be discussed in detail later. Complex **8** was tentatively assigned as follows by analysis and molecular weight determination. This complex seems to be obtained from **7a** and benzophenone oxime by eliminating hydrogen chloride. A similar reaction of opening the palladium-chlorine bond in π-allylic palladium(II) chloride with cyclohexanone oxime was reported by Imamura *et al.*[17]

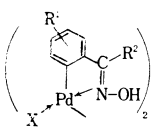

7a—j

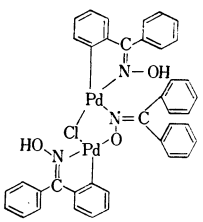

8

The procedure of adding sodium acetate as an acceptor of hydrogen chloride formed by the reaction was successfully applied to various aromatic aldoximes and ketoximes. The resulting complexes analogous to **7a** are shown in Table 1. The corresponding bromo-bridged complexes were obtained by the metathetic reaction of the chloro-complexes with sodium bromide in acetone. All the complexes were stable against air and heat, and complexes except for those from benzophenone, *n*- and isobutyrophenone oxime were insoluble in the usual organic solvents. The reaction product was deposited from the reaction mixture, but in some cases it was necessary to add water to isolate a complex. In the case of acetophenone oxime and its derivatives, their complexes were also obtained in the absence of sodium acetate but the yields were lower and the rate of the reaction slower judging from the disappearing rate of the black-red color of lithium tetrachloropalladate(II). Although *syn*- and *anti*-isomers exist in general in oximes, we used stable *syn*-aldoximes

Table 1. Aromatic metalation by palladium (II) on various aromatic oximes 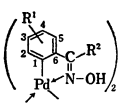

Compound	R^1	R^2	X	Yield (%)	Mp (°C)	ν_{O-H} (cm^{-1})*1	$\nu_{C=N}$ (cm^{-1})*1
7a	H	C_6H_5	Cl	67.8	150—152	3343	1625
7a'	H	C_6H_5	Br	91	190—197(d)*2	3345	1621
7b	H	CH_3	Cl	95.1(53.1)*3	210—(d)	3426	1640
7b'	H	CH_3	Br	88	259—260(d)	3423	1638
7c	3-CH_3O	CH_3	Cl	91.3	245—250(d)	3460, 3433	1629
7d	3-NO_2	CH_3	Cl	79.3	>270	3447	1630
7e	H	$CH_2CH_2CH_3$	Cl	92.8	188—205(d)	3425	1625
7f	H	$CH(CH_3)_2$	Cl	84.2	189—191(d)	3370	1627
7g	3,4-Benzo	CH_3	Cl	98.3	>270	3420	1617
7h	4,5-Benzo	CH_3	Cl	32.5	238—239(d)	3370	1615
7i	H	H	Cl	77.1	200—(d)	3410	1622
7j	3-CH_3O	H	Cl	56.8	195—197(d)	3415	1628

*1 Measured in Nujol mulls or KBr disks.
*2 d: decomposition.
*3 Reaction was carried out in the absence of sodium acetate for 20 hr at room temperature.

15) It has been reported in several papers that monoximes form stable dichlorobis(oxime)palladium(II) type complexes having no palladium-carbon σ-bonds.[16-18]

16) A. V. Babaeva and M. A. Mosyagina, *Dokl. Akad. Nauk SSSR*, **89**, 293 (1953); *Chem. Anst.*, **47**, 10392 (1953).

17) S. Imamura, T. Kajimoto, Y. Kitano and J. Tsuji, This Bulletin, **42**, 895 (1969).

18) T. Takiguchi, K. Kurosaki and M. Abe, *Kogyo Kagaku Zasshi*, **72**, 1549 (1969).

19) A. Rosenthal, R. F. Astbury and A. Hubscher, *J. Org. Chem.*, **33**, 1037 (1958).

20) H. Onoue, unpublished result.

and *anti*-phenylalkyl ketoximes. In the case of isobutyrophenone oxime, both isomers were stable and the isolated isomers were tested for the reaction. As suggested by the structure of the complexes, and *anti*-isomer gave an expected complex (**7f**) in good yield, but the *syn*-isomer gave a different complex, which was not studied further.

The structure of the complexes was established by the following data. The molecular weights of complexes **7a**, **7e** and **7f** in chloroform coincided well with the values calculated for the chloro-bridged dimers. The IR spectra showed the characteristic O–H stretching frequency in the 3310—3460 cm^{-1} region and the C=N stretching frequency in the 1615—1640 cm^{-1} region as shown in Table 1. On the other hand, the C=N stretching frequency in conjugated oximes in solution is known to fall in the range 1630—1660 cm^{-1}, with slightly lower values for solides.[21] It was concluded therefore that the coordination of oximes to palladium in the complexes was established through the lone pair of nitrogen but not through the C=N π-system.[5,22] The NMR spectrum of complex **7f** was in good agreement with the proposed structure, showing a doublet at 1.38 (J= 7 Hz, 6H), a septet at 3.35 (J=7 Hz, 1H), two multiplets at 6.76—7.13 (3H) and 7.23—7.46 (1H) and a singlet at 8.20 ppm (1H), each corresponding to a, b, c, d and e, respectively. This result shows that one aromatic ring proton *ortho* to the C=N group was substituted by palladium(II).

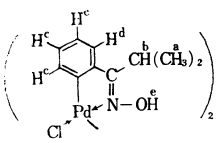

7f

Lithium aluminum deuteride reduction[23] of the acetophenone oxime-palladium(II) chloride complex gave deuterated *dl*-α-phenylethylamine.[24] Its NMR spectrum showed that the incorporation of deuterium had occurred in the phenyl ring and the methine group, a triplet at 1.32 ppm corresponding to methyl protons (J=1 Hz, 3H) and a singlet at 7.25 ppm corresponding so phenyl protons (4H). After treatment with water to exchange deuterium of the amino group with proton, its acetyl derivative was prepared. It was determined by mass spectrometry that the acetyl derivative contained 2% of d_0, 18% of d_1 and 80% of d_2 species.

Although the *ortho* metalation by palladium(II) was confirmed, there are two positions in 2-acetonaphthon oxime, 1 and 3, susceptible to metalation by palladium(II), giving the following complexes, **A** and **B**, respectively.

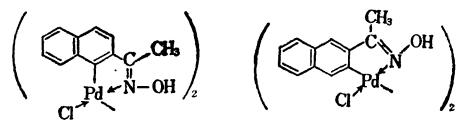

A **B**

The obtained complex was reduced with lithium aluminum deuteride to give deuterated 2-(α-aminoethyl)naphthalene. From the ratio of α- to β-protons on the naphthalene ring calculated from its NMR spectrum, it was established that **B** was the correct one. The structure of the 1-acetonaphthon oxime complex (**7h**) was confirmed by the same method.

The chloro-bridged complexes (**7**) reacted with triphenylphosphine to give the corresponding bridge-splitted complexes (**9**). In contrast to the other complexes, complex **7i** reacted with a theoretical amount of triphenylphosphine to give complex **9c**,

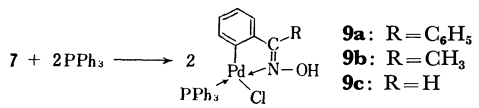

9a: R=C_6H_5
9b: R=CH_3
9c: R=H

but with an excess of triphenylphosphine to give a new complex containing two moles of triphenylphosphine per palladium.

The metalation reaction by palladium(II) was extended to the reaction of oximes with platinum(II). However, the reaction of one-molar quantity of acetophenone oxime and sodium acetate with potassium tetrachloroplatinate(II) in aqueous methanol gave only an intractable black material which deposited platinum metal on dissolving in dichloromethane. When the reaction was carried out in the absence of sodium acetate, complex **10a** was obtained. The IR spectrum was the same as that of the palladium analogue which was prepared from complex **7b** by a bridge-splitting reaction with acetophenone oxime. Complex **10a** reacted with triphenylphosphine giving complex **11**. *anti*-Isobutyrophenone oxime gave also complex **10b**.

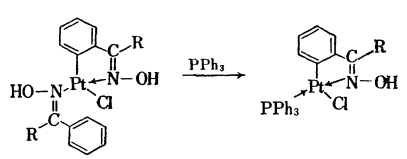

10a: R=CH_3
10b: R=$CH(CH_3)_2$
11: R=CH_3

21) L. J. Bellamy, "The Infra-red Spectra of Complex Molecules," John Wiley & Sons, New York, (1957), p. 270.
22) M. Orchin and P. J. Schmidt, *Coord. Chem. Rev.*, **2**, 345 (1968).
23) Metal hydride reduction of carbon-metal σ-bonds was often tried. See Ref. 3 and the references cited.
24) Reduction of oxime to amine is a well-known reaction.

Thus the electrophilic attack by platinum(II) on the aromatic ring of oximes could occur but the chloro-bridged complexes could not be obtained. It is probable that the differences observed in the case of palladium(II) and platinum(II) are partly attributed to the poor reactivity of platinum(II) compared to palladium(II).

These reactions by palladium(II) and platinum(II) on aromatic oximes would probably proceed through an initial coordination of nitrogen to the metal followed by an electrophilic substitution by the metal at an *ortho* position on the aromatic ring. In fact, the following metalation reaction occurred in boiling tetrahydrofuran yielding complex **12**.

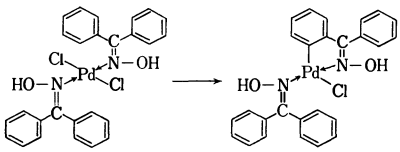

12

Thus it can be expected that if nitrogen coordinates strongly to the metal, dichlorobis(oxime)-metal type complexes are formed and no metalation reaction can take place. We studied the reaction of *O*-methyl and *O*-acyl derivatives with lithium tetrachloropalladate(II).

O-Methyl oxime of benzophenone and acetophenone yielded predominantly dichlorobis(*O*-methyl oxime)palladium(II) even in the presence of sodium acetate. It may be concluded that the strong coordination to palladium with nitrogen due to the presence of the electron donating methyl group reduced the formal charge of palladium(II), preventing its electrophilic attack on the aromatic ring.

On the other hand, *O*-acetyl and *O*-benzoyl acetophenone oxime, in which the coordinating power of nitrogen would be reduced by the presence of electron withdrawing acyl groups, gave complex **7b** in the absence of sodium acetate. In addition, methyl benzoate was isolated in the reaction of *O*-benzoyl acetophenone oxime. It is uncertain whether the methanolysis of *O*-acyl groups occurred before or after the formation of a palladium-carbon σ-bond.

Experimental

Melting points were determined on a Yanagimoto micro-stage apparatus and uncorrected. IR spectra were recorded with Nippon Bunko IR-S and Nippon Bunko Model DS-402G Spectrometers. NMR spectra were determined at 60MHz with a Varian A-60 Spectrometer in deuteriochloroform using tetramethylsilane as an internal standard. Molecular weights were determined with a Mechrolab Model 301A vapor pressure osmometer in a chloroform solution.

Materials. Anhydrous palladium chloride was obtained from Nippon Engelhard, Ltd. Potassium tetrachloroplatinate(II) was obtained from Wako Pure Chemicals Industries, Ltd. Lithium aluminum deuteride was obtained from Metal Hydrides, Inc. A lithium tetrachloropalladate(II) solution in methanol (0.5 M) was prepared by stirring two equivalents of anhydrous lithium chloride and one equivalent of anhydrous palladium chloride in methanol until a homogeneous solution was formed. Each oxime was prepared from the corresponding aldehyde or ketone, hydroxylamine hydrochloride and sodium hydroxide in the usual manner and purified by recrystallization or distillation before use. *Syn-* and *anti*-isobutyrophenone oximes were separated from the mixture by fractional crystallization from *n*-hexane.[25]

Reaction of Benzophenone Oxime with Lithium Tetrachloropalladate(II). When a solution containing 3.95 g (0.02 mol) of benzophenone oxime and 0.01 mol of Li_2PdCl_4 in 40 m*l* of methanol was allowed to stand for 5 days at room temperature, 2.86 g of red-yellow crystals, mp 180°C dec., was obtained. IR spectrum (Nujol): 3280 and 3200 cm^{-1} (ν_{O-H}); 1629 cm^{-1} ($\nu_{C=N}$).

Found: C, 54.45; H, 4.03; N, 5.05; Pd, 18.53%. Calcd for $C_{26}H_{22}N_2O_2PdCl_2$: C, 54.61; H, 3.89; N, 4.90; Pd, 18.61%.

A solution of 2.00 g of the complex in 30 m*l* of tetrahydrofuran was boiled for 1 hr and cooled to give 0.84 g of the starting complex. Upon addition of *n*-hexane to the filtrate, 0.13 g of the complex was further recovered. Pale yellow solids were then formed from this filtrate by a further addition of *n*-hexane followed by standing for 2 days. Solids were recrystallized from chloroform-*n*-hexane to give 0.71 g of complex **12**, mp 192—200°C. IR spectrum (Nujol): 3245 sh, 3160 and 3105 cm^{-1} (ν_{O-H}); 1619 cm^{-1} (broad, $\nu_{C=N}$).

Found: C, 58.04; H, 4.18; Cl, 6.81%. Calcd for $C_{26}H_{21}N_2O_2PdCl$: C, 58.33; H, 3.96; Cl, 6.62%. The complex was also prepared from complex **7a** by a bridge-splitting reaction with benzophenone oxime.

Preparation of Halogen-Bridged Complexes. All complexes were prepared as yellow or orange-yellow solids by the following general procedures. Complexes **7a**, **7a'**, **7e** and **7f** were soluble in dichloromethane, chloroform, acetone and tetrahydrofuran, but other complexes were insoluble in ordinary organic solvents. The yields and physical properties and analytical data are summarized in Tables 1 and 2.

(a) Complexes **7a**, **7d**, **7f**, **7h**, **7i** and **7j**. To a solution containing 0.02 mol of Li_2PdCl_4 in 40 m*l* of methanol, a methanol solution of 0.02 mol of oxime and 0.02 mol of oxime and 0.02 mol of sodium acetate trihydrate was added. When the solution was allowed to stand for one or two days at room temperature, small amounts of precipitates were formed and the black-red colour of the solution turned pale yellow. The mixture was filtered and water was added to the filtrate to give yellow solids. Other oximes except for benzophenone, anisaldehyde, and 1-acetonaphthon oxime gave analytically pure complexes **7d**, **7f** and **7i**.

Yellow solids obtained in the case of benzophenone

25) H. M. Kissman and J. Williams, *J. Amer. Chem. Soc.*, **72**, 5323 (1950).

Table 2. Analytical data for complexes **7a—j**

Compound	Formula	Analyses found (Calcd.) (%) C	H	N	Cl	Pd
7a[*1]	$C_{26}H_{20}N_2O_2Pd_2Cl_2$	46.26 (46.18)	3.13 (2.99)	3.87 (4.14)		
7a'	$C_{26}H_{20}N_2O_2Pd_2Br_2$	41.12 (40.81)	2.76 (2.64)			27.86 (27.81)
7b	$C_{16}H_{16}N_2O_2Pd_2Cl_2$	34.85 (34.81)	2.97 (2.93)	4.88 (5.08)	12.39 (12.84)	
7b'	$C_{16}H_{16}N_2O_2Pd_2Br_2$	30.33 (29.98)	2.62 (2.52)			
7c	$C_{18}H_{20}N_2O_4Pd_2Cl_2$	35.41 (35.32)	3.33 (3.30)	4.43 (4.58)	11.29 (11.58)	
7d	$C_{16}H_{14}N_4O_6Pd_2Cl_2$	30.05 (29.93)	2.31 (2.20)	8.43 (8.73)	11.26 (11.04)	
7e[*2]	$C_{20}H_{24}N_2O_2Pd_2Cl_2$	39.99 (39.50)	3.99 (3.99)	4.58 (4.61)		35.01 (34.99)
7f[*3]	$C_{20}H_{24}N_2O_2Pd_2Cl_2$	39.70 (39.50)	4.02 (3.99)			
7g	$C_{24}H_{20}N_2O_2Pd_2Cl_2$	44.25 (44.20)	3.26 (3.10)	4.17 (4.30)		32.25 (32.63)
7h	$C_{24}H_{20}N_2O_2Pd_2Cl_2$	43.85 (44.20)	3.14 (3.10)	3.96 (4.30)		32.43 (32.63)
7i	$C_{14}H_{12}N_2O_2Pd_2Cl_2$	32.68 (32.08)	2.34 (2.34)			39.93 (40.61)
7j	$C_{16}H_{16}N_2O_2Pd_2Cl_2$	32.96 (32.90)	3.01 (2.77)			35.45 (36.44)

[*1] mol wt, 732 (676.18). [*2] mol wt, 622 (608.16). [*3] mol wt, 597 (608.16).

oxime were separated into two complexes **7a** and **8** by fractional crystallization from dichloromethane-*n*-hexane. Complex **8** was obtained as pale yellow crystals, 0.97 g, mp 200—216°C dec.

Found: C, 56.39; H, 3.78; N, 4.99; Cl, 4.82%; mol wt, 806. Calcd for $C_{39}H_{30}N_3O_3Pd_2Cl$: C, 55.96; H, 3.62; N, 5.02; Cl, 4.24%; mol wt, 836.97.

Yellow solids from anisaldexime were dissolved in dichloromethane. When the solution was concentrated, complex **7j** was obtained which, once isolated, was insoluble in most organic solvents.

Treatment of yellow solids from 1-acetonaphthon oxime with boiling chloroform left pure complex **7h**.

(b) Complexes **7b**, **7c**, **7e** and **7g**. Reactions were carried out according to the same procedure as above, but in these cases the expected complexes precipitated from the solution. The reaction mixtures were then filtered, washed with methanol and water and dried to give pure complexes.

(c) Complexes **7a'** and **7b'**. Complex **7a** or **7b** reacted with sodium bromide in aqueous acetone for an hour at room temperature or by refluxing on a water bath. The yellow solution was concentrated and water was added to give yellow solids.

Preparation of Complexes (9). To a suspension of complex **7a** (0.10 g) in dichloromethane (0.5 m*l*) was added triphenylphosphine (0.10 g). The resulting solution was diluted with *n*-hexane, whereupon complex **9a** was obtained as pale yellow crystals (0.159 g, 89%), mp 203—210°C dec. Purification was accompanied by recrystallization from dichloromethane-*n*-hexane. IR spectrum (Nujol): 3180 cm^{-1} (ν_{O-H}).

Found: C, 62.00; H, 4.26; Cl, 6.07%; mol wt, 558. Calcd for $C_{31}H_{25}NOPPdCl$: C, 62.01; H, 4.21; Cl, 5.90%; mol wt, 600.39.

Similarly complex **9b** was prepared from complex **7b** as yellow crystals, mp 205—211°C dec. IR spectrum (Nujol): 3195 cm^{-1} (ν_{O-H}); 1266 cm^{-1} (CH_2Cl_2). Found: C, 53.39; H, 4.20%. Calcd for $C_{26}H_{23}NOPPdCl\cdot 3/4CH_2Cl_2$: C, 53.37; H, 3.88%.

Complex **9c** was similarly prepared from complex **7i**, as orange crystals, mp 173—174°C dec. IR spectrum (Nujol): 3220 cm^{-1} (ν_{O-H}).

Found: C, 56.88; H, 4.34%. Calcd for $C_{25}H_{21}NOPPdCl$: C, 57.27; H, 4.04%.

Reaction of Complex (7i) with an Excess of Triphenylphosphine. A suspension of 0.262 g (0.5 mmol) of complex **7i** in 1 m*l* of chloroform turned to a yellow solution on adding 0.577 g (2.2 mmol) of triphenylphosphine. Addition of *n*-hexane to the solution gave 0.720 g (93%) of pale yellow crystals, melting at 188—192°C and then solidifying, followed by decomposition at 196—197°C. The complex was found to be completely dissociated in solution from its IR spectrum in chloroform and the molecular weight. IR spectrum (ν_{O-H}): 3390 cm^{-1} (in Nujol); 3220 cm^{-1} (chloroform).

Found: C, 65.03; H, 4.59%; mol wt, 395. Calcd for $C_{43}H_{36}NOP_2PdCl$: C, 65.05; H, 4.62%; mol wt, 786.59.

Reduction of Complexes (7) with Lithium Aluminum Deuteride. To a mixture of 1.00 g of the complex to be reduced in 20 m*l* of absolute tetrahydrofuran was added 0.50 g of lithium aluminum deuteride with stirring. After stirring for 30 min at room temperature, the resulting black mixture was worked up by careful addition of 2 m*l* of deuterium oxide followed by the addition of anhydrous sodium sulfate. The

mixture was filtered and washed well with tetrahydrofuran. Removal of tetrahydrofuran gave crude amine. This was purified by distillation or by transformation to its hydrochloride or acetyl derivative.

Reaction of Oxime with Potassium Tetrachloroplatinate (II). A solution of 2.41 mmol of oxime in 10 m*l* of methanol was added to a solution of 2.41 mmol of K_2PtCl_4 in 20 m*l* of water. The initially clear red solution became lighter in colour and dark yellow solids precipitated. After standing for 2 days, the solids were filtered and purified by passing a short silica gel column with dichloromethane followed by recrystallization from dichloromethane-*n*-hexane.

Complex **10a** was obtained from acetophenone oxime, as yellow crystals (0.158 g), mp 190—193°C. IR spectrum (Nujol): 3310 and 3230 cm^{-1} (ν_{O-H}); 1644 and 1633 cm^{-1} ($\nu_{C=N}$).

Found: C, 38.48; H, 3.53; Pt, 38.69%. Calcd for $C_{16}H_{17}N_2O_2PtCl$: C, 38.44; H, 3.43; Pt, 39.03%.

Complex **10b** was obtained from *anti*-isobutyrophenone oxime, as yellow crystals (0.045 g), mp 178—180°C. IR spectrum (Nujol): 3360 and 3230 cm^{-1} (ν_{O-H}); 1630 sh and 1623 cm^{-1} ($\nu_{C=N}$).

Found: C, 43.11; H, 4.59; Pt, 34.57%. Calcd for $C_{20}H_{25}N_2O_2PtCl$: C, 43.20; H, 4.54; Pt, 35.09%.

A solution of complex **10a** (0.050 g) in 0.5 m*l* of dichloromethane was treated with triphenylphosphine (0.050 g) and *n*-hexane was added, whereupon complex **11** (0.058 g, 92%) was obtained as yellow crystals, mp 254—256°C. Its IR spectrum was consistent with that of the palladium analogue (**9b**) and showed a band at 1266 cm^{-1} due to dichloromethane. Found: C, 47.40; H, 3.82; Cl, 10.60%. Calcd for $C_{26}H_{23}NOPPtCl \cdot 1/2CH_2Cl_2$: C, 47.55; H, 3.62; Cl, 10.59%.

Reaction of *O*-Methyl Benzophenone Oxime with Lithium Tetrachloropalladate (II). Reaction was carried out in the same manner as the preparation of complex **7a** using 0.01 mol of *O*-methyl benzophenone oxime and other reactants. After standing for 16 hr, the resulting yellow solids were filtered. More solids were obtained from the filtrate by extracting with chloroform. The solids were separated into two kinds of compounds by fractional crystallization from chloroform-*n*-hexane. Dichlorobis(*O*-methyl benzophenone oxime)palladium(II), the more soluble compound in chloroform, was obtained as yellow-brown crystals (1.94 g, 71.3%), melting at 174—175°C and then solidyfying, followed by decomposition at 248°C. IR spectrum in the range 800—650 cm^{-1} (Nujol): 799, 773, 749 and 696 cm^{-1}.

Found: C, 55.99; H, 4.37; Pd, 17.63%; mol wt, 524. Calcd for $C_{28}H_{26}N_2O_2PdCl_2$: C, 56.06; H, 4.38; Pd, 17.74%; mol wt, 599.86. The less soluble compound in chloroform was obtained as yellow crystals, 0.26 g, mp 254—258°C dec. IR spectrum (Nujol): 1212 cm^{-1} ($CHCl_3$); 789, 770, 749, 723 and 699 cm^{-1} (in the range 800—650 cm^{-1}).

Found: C, 46.67; H, 3.41; N, 3.68; Cl, 13.19%. Calcd for $C_{28}H_{24}N_2O_2Pd_2Cl_2 \cdot 1/8CHCl_3$: C, 46.21; H, 3.33; N, 3.82; Cl, 13.28%.

Reaction of *O*-Methyl Acetophenone Oxime with Lithium Tetrachloropalladate (II). In the same manner, we obtained 2.13 g (89.2%) of dichlorobis (*O*-methyl acetophenone oxime)palladium(II) as yellow crystals, mp 204°C dec.

Found: C, 45.62; H, 4.74; Pd, 22.07%; mol wt, 466. Calcd for $C_{18}H_{20}N_2O_2PdCl_2$: C, 45.44; H, 4.67; Pd, 22.37%; mol wt, 475.72.

Reaction of *O*-Acetyl and *O*-Benzoyl Acetophenone Oxime with Lithium Tetrachloropalladate (II). A methanol solution of 0.01 mol of each oxime was mixed with 20 m*l* of 0.5 M Li_2PdCl_4 in methanol. After standing for 20 hr, yellow crystals were formed and more solids were obtained by adding water. The yield of complex **7b** was about 80%. In the case of *O*-benzoyl acetophenone oxime, the filtrate was extracted with ether. After ether was removed, the residue was distilled *in vacuo* to give 0.88 g of colorless liquid. This was identified to be methyl benzoate by comparing its IR spectrum with that of an authentic sample.

BULLETIN OF THE CHEMICAL SOCIETY OF JAPAN VOL. 43 3486—3489 (1970)

4-Alkyloxazolidinedione. VI. The Polymerization of α-Amino Acid *N*-Carboxy Anhydride

Masanao Oya and Mayumi Tomizawa,*1

College of Technology, University of Gunma, Tenjin-cho, Kiryu-shi, Gunma

and Keikichi Uno and Yoshio Iwakura

Department of Synthetic Chemistry, Faculty of Engineering, The University of Tokyo, Hongo, Bunkyo-ku, Tokyo

(Received May 14, 1970)

The relationships between the polymerization solvents and the conformation of the polypeptides formed were studied on the basis of the infrared absorption spectra and the X-ray diffraction diagrams of the polymers. Poly-L-α-amino-*n*-butyric acid and poly-L-*n*-valine, prepared in dimethylsulfoxide (DMSO) as a polymerization solvent, formed a β-conformation, but the respective polypeptides obtained in acetonitrile had an α-conformation. The conformational structure of poly-L-α-amino-*n*-butyric acid changed from β to α upon reprecipitation from a solution in dichloroacetic acid with ether. On the other hand, the conformational structure of poly-DL-α-amino-*n*-butyric acid did not change upon reprecipitation from a solution in formic acid and dichloroacetic acid.

In our previous papers in this series, we reported the solvent effect in the polymerization of DL-and L-alanine NCA on the conformation of the formed polypeptides.[1-3] The conformation of the polypeptides was influenced by the polymerization solvent: the polyalanine obtained in acetonitrile had an α-conformation, but the polyalanine obtained in DMSO had a β-conformation.[2] Further relationships between the conformation of the growing chains of poly-L-alanine and poly-L-leucine in DMSO during the polymerization of L-alanine NCA and L-leucine NCA and the polypeptides isolated from DMSO have also been discussed.[4]

The present study will report on the relationships between the conformations of the polypeptides obtained by the polymerization of several kinds of NCA's and the solvents used.

Results and Discussion

Infrared Spectra of L- Configurational polypeptides. The infrared absorption frequencies of the L-configurational polypeptides obtained in acetonitrile and DMSO are shown in Table 1. The spectra of poly-L-α-amino-*n*-butyric acid, poly-L-*n*-valine, poly-L-*n*-leucine, and poly-L-leucine obtained in acetonitrile all gave absorption bands at 1660 cm^{-1}, such bands are characteristic of α-polypeptides.[5] However, the spectra of poly-L-α-amino-*n*-butyric acid and poly-L-*n*-valine obtained in DMSO gave absorption bands at 1635 cm^{-1} and 1535 cm^{-1}, these bands are characteristic of β-conformational polypeptides.[5] These results showed that the L-configurational polypeptides obtained in acetonitrile had an α-conformation, while those obtained in DMSO had a β-conformation. Similar results have been obtained in the polymerization of DL- and L-alanine NCA's. On the other hand, the spectra of each poly-L-valine obtained in acetonitrile and in DMSO gave an absorption band at 1635 cm^{-1} which is characteristic of β-conformational polypeptides.

IR Spectra of DL-Configurational polypeptides. It has been reported that the conformation of poly-DL-alanine obtained in acetonitrile had an α-form and that the one obtained in DMSO had a β-form.[2] However, many polypeptides obtained in acetonitrile and DMSO, such as poly-DL-α-amino-*n*-butyric acid, poly-DL-*n*-valine, poly-DL-*n*-leucine, and poly-DL-valine, showed absorption bands at 1635 cm^{-1} and 1535 cm^{-1}. In the case of the poly-DL-leucine obtained in acetonitrile and DMSO, though,

*1 Present address: Kureha Synthetic Fiber Co., Ltd., Mibu, Tochigi-ken.

1) Y. Iwakura, K. Uno and M. Oya, *Kogyo Kagaku Zasshi*, **69**, 741 (1966).

2) Y. Iwakura, K. Uno and M. Oya, *J. Polym. Sci.*, *A*-1, **5**, 2867 (1967).

3) Y. Iwakura, K. Uno and M. Oya, *ibid.*, *A*-1, **6**, 2165 (1968).

4) Y. Iwakura, K. Uno and M. Oya, This Bulletin, in press.

5) M. Tsuboi, T. Shimanouchi and S. Mizushima, *J. Phys. Chem.*, **59**, 322 (1955).

Table 1. IR spectra of L-conformational polypeptides

Polymer	Polymerization solvent	$\eta_{sp/c}$ (c=0.5 g/100 cc)	IR absorption bands (cm^{-1})	
			Amide I	Amide II
Poly-L-α-amino-*n*-butyric acid	Acetonitrile (ACN)	0.76 (DCA)	1660	1550
Poly-L-α-amino-*n*-butyric acid	Dimethylsulfoxide (DMSO)	0.43 (DCA)	1635	1535
Poly-L-*n*-valine	ACN	0.18 (DCA)	1660	1545
Poly-L-*n*-valine	DMSO	0.20 (DCA)	1635	1535
Poly-L-valine	ACN	0.11 (TFA)	1635	1545
Poly-L-valine	DMSO	0.13 (TFA)	1635	1545
Poly-L-leucine	ACN	1.20 (H_2SO_4)	1655	1550
Poly-L-*n*-leucine	ACN	0.44 (TFA)	1660	1545

DCA: Dichloroacetic acid. TFA: Trifluoroacetic acid.

the absorption bands of the polymers were found at 1655 and 1545 cm^{-1}.

The IR spectra of polyglycine obtained in acetonitrile was very similar to that of the polyglycine obtained in DMSO. These results are shown in Table 2.

X-Ray-Diffracion Diagrams. The X-ray diffraction pattern of oriented poly-γ-methyl-L-glutamate and poly-L-alanine have been extensively studied.[6-8] The diffraction pattern of oriented poly-γ-methyl-L-glutffmate of the α-form shows very strong peaks at 10.35 Å ($d_{10\bar{1}0}$) and around 4.4 Å. The diffraction diagram of this polymer obtained by the powder method showed strong peaks at 2θ=7.9° (d=10.25 Å) and 19.6° (d=4.4 Å), as is shown in Fig. 1. These peaks agreed with the peaks in the pattern of the oriented polymer, but the other peaks in the diagram were not observed clearly. The X-ray-diffraction pattern of oriented poly-L-alanine of the α-form showed strong peaks at 7.4 Å ($d_{10\bar{1}0}$) and 4.4 Å which belong to the flexible side chain in the polymer.[7] On the other hand, peaks at 4.37 Å (d) and 5.35 Å ($b/2$) have been observed in the poly-L-alanine of the β-form (d is the back-bone

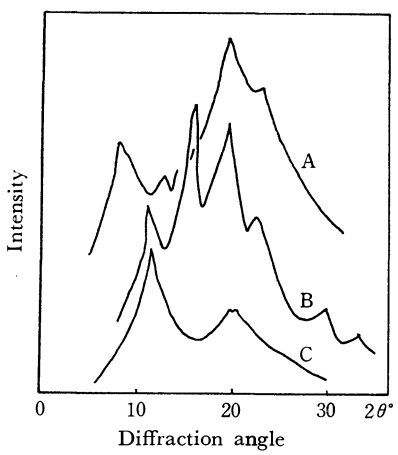

Fig. 1. X-ray diffraction diagrams of poly-γ-methyl-L-glutamate and poly-L-alanine.
A: Poly-γ-methyl-L-glutamate
B: Poly-L-alanine obtained in DMSO
C: Poly-L-alanine obtained in acetonitrile

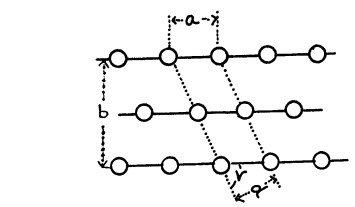

Fig. 2. Diagram showing in plan the packing of hydrogen bonded sheets of poly-L-alanine.

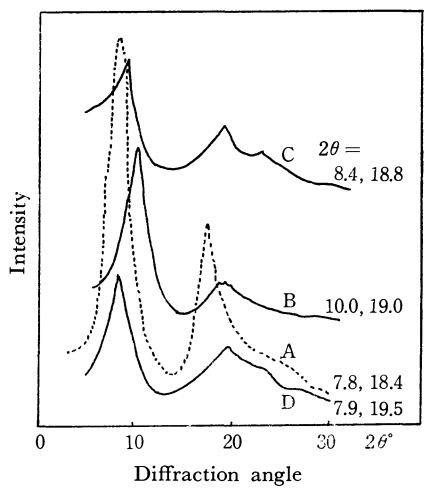

Fig. 3. X-Ray diffraction diagrams of L-conformational polypeptides obtained in acetonitrile.
A: Poly-L-leucine
B: Poly-L-α-amino-*n*-butyric acid
C: Poly-L-*n*-valine
D: Poly-L-*n*-leucine

6) S. J. Ambrose, *Proc. Roy. Soc.*, *A*, **205**, 47 (1955).
7) C. H. Bamford, *Nature*, **173**, 27 (1954).
8) L. Brown and I. F. Trotter, *Trans. Faraday Soc.*, **52**, 539 (1956).

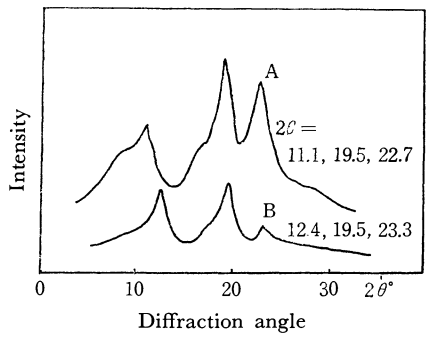

Fig. 4. X-ray diffraction diagrams of poly-L-α-amino-*n*-butyric acid and poly-L-*n*-valine obtained in DMSO.

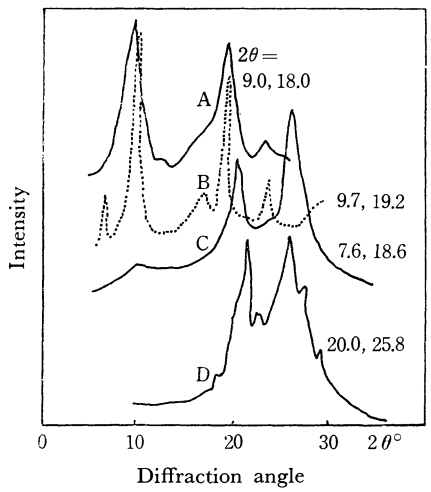

Fig. 5. X-Ray diffraction diagrams of polyglycine and poly-L-valine obtained in DMSO and ACN.
A: Poly-L-valine (ACN)
B: Poly-L-valine (DMSO)
C: Polyglycine (DMSO)
D: Polyglycine (ACN)

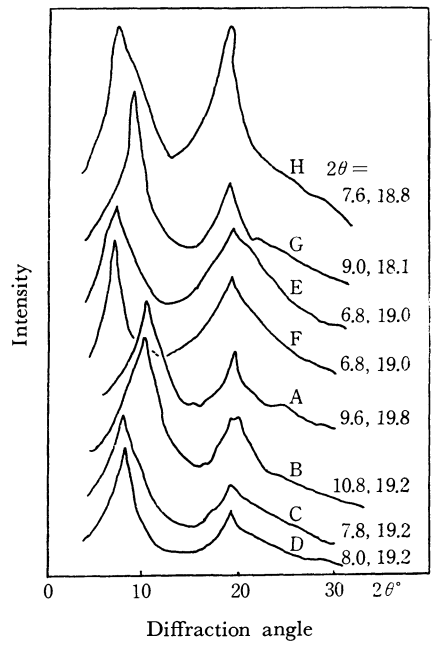

Fig. 6. X-Ray diffraction diagrams of DL-conformational polypeptides.
A: Poly-DL-α-amino-*n*-butyric acid (ACN)
B: Poly-DL-α-amino-*n*-butyric acid (DMSO)
C: Poly-DL-*n*-valine (ACN)
D: Poly-DL-*n*-valine (DMSO)
E: Poly-DL-*n*-leucine (ACN)
F: Poly-DL-*n*-leucine (DMSO)
G: Poly-DL-valine (ACN)
H: Poly-DL-valine (DMSO)

spacing and *b* is twice the side-chain length, as is shown in Fig. 2.[8]) The diffraction diagram of the poly-L-alanine obtained by the powder method (Fig. 1) also showed peaks at $2\theta=11.9°$ ($d=7.4$ Å) and 19.9° in the α-form and at $2\theta=16.6°$ ($d=5.35$ Å), 20.3° ($d=4.37$ Å) and 11.9° in the β-form.

The Diagrams of L-Configurational Poly-

Table 2. IR spectra of DL-configurational polypeptides

Polymer	Polymerization solvents	$\eta_{sp/c}$ ($c=0.5$ g/100 cc)	IR absorption bands (cm^{-1})	
			Amide I	Amide II
Poly-DL-α-amino-*n*-butyric acid	ACN	0.92 (DCA)	1635	1535
Poly-DL-α-amino-*n*-butyric acid	DMSO	0.22 (DCA)	1635	1535, 1515
Poly-DL-*n*-valine	ACN	0.20 (DCA)	1640	1535
Poly-DL-*n*-valine	DMSO	0.20 (DCA)	1640	1535
Poly-DL-*n*-leucine	ACN	0.40 (DCA)	1635	1545
Poly-DL-*n*-leucine	DMSO	0.23 (DCA)	1635	1545
Poly-DL-leucine	ACN	0.23 (DCA)	1655	1545
Poly-DL-leucine	DMSO	0.23 (DCA)	1655	1545
Poly-DL-valine	ACN	0.11 (DCA)	1635	1535
Poly-DL-valine	DMSO	0.11 (DCA)	1635	1515
Polyglycine	ACN	0.30 (TFA)	1635	1515
Polyglycine	DMSO	0.31 (TFA)	1635	1515

peptides. X-Ray–diffraction diagrams obtained by the powder method of poly–peptides consisting of L-configurational α-amino acid obtained by polymerization in acetonitrile are shown in Fig. 3. All these diagrams showed two peaks like those of poly-DL- and poly-L-alanine obtained in acetonitrile. On the other hand, the diagrams of poly-L-α-amino-*n*-butyric acid and poly-L-*n*-valine obtained in DMSO showed three or four peaks, like those of poly-L-alanine obtained in DMSO with the β-form.[2] These patterns are shown in Fig. 4. The diagram of poly-L-α-amino-*n*-butyric acid showed peaks at $2\theta=12.4°$, 19.5,° and $2\theta=23.3°$, while that of poly-L-*n*-valine showed peaks at $2\theta=11.1°$, 19.5°, and $2\theta=22.7°$.

For polyglycine and poly-L-valine, the infrared spectra were not affected by the polymerization solvent used, but the diagrams of both these polymers were different from each other (Fig. 5). Diffraction diagrams obtained by the powder method of almost DL-configurational polypeptides showed two strong peaks in spite of the fact that these polypeptides showed β-conformational spectra. These results are shown in Fig. 6.

Reprecipitation Treatment of the polymers. It has been reported that poly-DL- and L-alanine are changed from the α- to the β-form when treated in dichloroacetic acid and in formic acid.[2] Poly-L-α-amino-*n*-butyric acid was changed from the β- to the α-form by treatment in dichloroacetic acid. However, poly-DL-α-amino-*n*-butyric acid did not change its conformation upon treatment with formic acid and dichloro acetic acid. These conclusions are based on the infrared spectra and X-ray-diffraction diagrams.

Experimental

The NCA's used in this study were prepared in a high purity (chlorine content less than 0.02%) by a method reported previously.[1] The polypeptides were also prepared by a method reported previously.[1] The results are shown in Tables 1 and 2.

The X-ray-diffraction diagrams and IR spectra were obtained as has been reported previously.[2]

The authors wish to thank the Ajinomoto Co., Ltd. for its gift of α-amino acids.

BULLETIN OF THE CHEMICAL SOCIETY OF JAPAN VOL. 43 3490—3495 (1970)

A Study of the Partial Catalytic Oxidation of Hydrocarbons. V. The Effect of Phosphorus Addition to the Vanadium Catalyst on the Oxidation of Butene, Butadiene, and Furan

Mamoru Ai

Research Laboratory of Resources Utilization, Tokyo Institute of Technology, Ookayama, Meguro-ku, Tokyo

(Received February 18, 1970)

In the present investigation, the vapor-phase partial oxidation of *cis*-2-butene, butadiene, and furan was carried out over V_2O_5 and V_2O_5-P_2O_5, (1 : 1.6 atomic ratio), with various contact times, at 350°C, and at the concentration of 0.6—1.6% in air, in order to elucidate the effect of phosphorus addition to V_2O_5, on the selectivity and mechanism of butene oxidation. Oxidation activity decreased remarkably with an increase in the phosphorus content. In the presence of phosphorus (P/V=1.6), selectivity for the $C_4H_8 \rightarrow C_4H_6$ step and $C_4H_6 \rightarrow C_4H_4O$ step were considerably increased, from 46 to 88 and from 72 to 93 mol% respectively, while selectivity for the $C_4H_4O \rightarrow$maleic anhydride (MA) step fell from 60 to 50 mol%, due to the increase in polymer formation. From the results, it was concluded that V_2O_5 and V_2O_5-P_2O_5 catalysts show similar oxidation activity with regard to butene, butadiene, and furan, and that the quantities of the intermediate products are fairly much affected by the activity of the catalyst as well as by the difference in reactivity between the starting material and the intermediate over the catalyst.

Previous papers have studied the mechanism of the partial catalytic oxidation of butene, butadiene, crotonaldehyde, furan, (C_4H_4O), *etc.* over V_2O_5, V_2O_5-P_2O_5 and V_2O_5-MoO_3 catalysts,[1-4] and it has been proposed that, on V_2O_5-P_2O_5 (1 : 1.6 atomic ratio), the main reaction pathway for the catalytic oxidation of butene to maleic anhydride (MA) proceeds through the following successive steps:

$$C_4H_8 \rightarrow C_4H_8\ \text{ads.} \rightarrow C_4H_6\ \text{ads.} \rightarrow C_4H_4O\ \text{ads.} \rightarrow \text{MA}$$

Moreover, side reactions destined to complete combustion proceed parallel to the main pathway in each consecutive step, and the selectivity and the rate of maleic anhydride formation are determined by the steps after furan.[1]

By the addition of phosphorus to the V_2O_5 catalyst, the selectivity for maleic anhydride formation from butene was considerably increased; this may attributed to the increase in selectivity for the $C_4H_8 \rightarrow C_4H_4O$ steps, not for the $C_4H_4O \rightarrow$MA steps.[2]

In the present work, we attempted to ascertain how the phosphorus addition to the V_2O_5 catalyst affects each reaction step in the step-by-step oxidation of butene to maleic anhydride formation, and to elucidate this effect on the mechanism and the selectivity of the partial catalytic oxidation of butene, butadiene, and furan.

Experimental

The vapor-phase air oxidation of butene, butadiene, and furan was carried out over vanadium and vanadium-phosphorus (V : P=1 : 1.6 atomic ratio) oxide catalysts in an ordinary flow-type reaction system at atmospheric pressure as has been shown in previous papers.[1,2] The reactor was a steel tube (1.8 cm id) whose surface was coated with aluminium; it was immersed in a molten lead bath.

The volume concentrations of the reactants were 0.6—1.0% in air, the flow rate (at 25°C) was kept at 1.5 *l*/min, and the contact time, which was defined as the ratio of the catalyst volume (m*l*) to the flow rate, was varied from 0.006 to 1.8 sec. The reaction temperature was always kept at 350°C. The exit gases leaving the reactor passed first through a series of three hot, and then four cold, packed water scrubbers in order to recover the solid and volatile acids and carbonyl compounds. At the end of 2 hr, the contents of the scrubbers were collected and a sample was titrated with 0.1 N NaOH, using a pH meter. The yields of maleic and other acids were calculated from the titration curves. The reactant gas, the exit gas, and a sample of the water-scrubber contents were analyzed by means of gas chromatography.

The following method was employed to prepare the catalysts. V_2O_5 catalyst: NH_4VO_3 was disolved in hot water by using oxalic acid, and then pumice, with a mesh size of from 10 to 20, was added; the solution was then evaporated with constant stirring, and finally dried in an oven at 130°C. The amount of pumice was 400 m*l*/g atom of vanadium. V_2O_5-P_2O_5 catalyst:

1) M. Ai, K. Harada and S. Suzuki, *Kogyo Kagaku Zasshi*, **73**, 524 (1970).
2) M. Ai, T. Niikuni and S. Suzuki, *ibid.*, **73**, 165 (1970).
3) M. Ai, *ibid.*, **73**, 946 (1970).
4) M. Ai, *ibid.*, **73**, 950 (1970).

NH_4VO_3 and H_3PO_4 were dissolved in water (P/V= 1.6 atomic ratio), and the solution was heated with constant stirring. After it had evaporated nearly to dryness, the paste-like substance remaining was molded into pellets 3×3 mm in size, and finally these were dried at 130°C. The activation of the catalysts was performed under flowing air, at 500°C, for 5 hr.

In an earlier paper dealing with the oxidation of butene[2], we used a series of unsupported V_2O_5-P_2O_5 catalysts and learned that P_2O_5-poor catalysts show a failure in mechanical strength. Therefore, in this work, we used pumice for the V_2O_5 catalyst in order to increase its mechanical strength. It was confirmed that this supported V_2O_5 catalyst showed the same catalytic performance as the unsupported V_2O_5 catalyst prepared by the simple evaporation of the NH_4V_3O-$C_2H_2O_4$ solution.[2] It can be considered, therefore, that the external surface of the pumice is coated with a thick layer of V_2O_5 that there is no practical difference in surface structure between supported and unsupported V_2O_5 catalysts.

Results and Discussion

Effects of Phosphorus Addition on the Oxidation Activity. The rates of the oxidation of butene, butadiene, and furan over V_2O_5 or V_2O_5-P_2O_5 catalysts can be considered to be of the first order*1 for the reactant concentration under the reaction conditions used here. The rate constants at 350°C (k sec^{-1}) over both V_2O_5 and V_2O_5-P_2O_5 were calculated for each reactant from the conversion-contact time data, they are shown as functions of the phosphorus content in Fig. 1. The oxidation activity of the catalyst decreased markedly upon the addition of phosphorus to V_2O_5, even when the quantity added was very small. The reactivities of all these reactants on these catalysts were of about the same magnitude. For example, the activity of V_2O_5-P_2O_5 (1 : 1.6 atomic ratio) catalyst was about one-thirtieth that of the V_2O_5 catalyst alone. However, the extent of the deactivation by phosphorus addition was about the same for the butene, butadiene, and furan oxidations. The results are listed in Table 1.

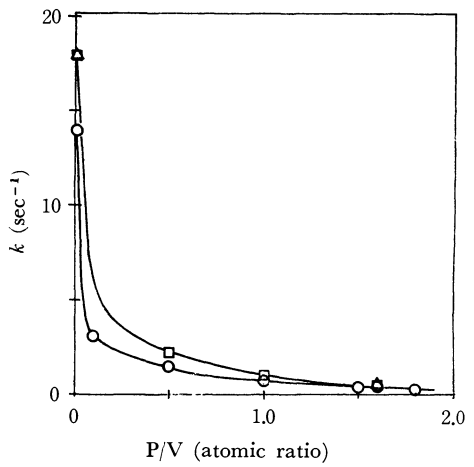

Fig. 1. Oxidation rate constant at 350°C (k sec^{-1}) as a function of P_2O_5/V_2O_5 ratio.
○: butene △: butadiene □: furan

*1 log (C_0/C) is proportional to the contact time (W/F).

Table 1. Oxidation rate constant at 350°C: k (sec^{-1})

Reactant	C_4H_8	C_4H_6	C_4H_4O
$k^{I}(V_2O_5)$	14	18	18
$k^{II}(V_2O_5$-$P_2O_5)$	0.4	0.6	0.6
k^{II}/k^{I}	1/35	1/35	1/30

Effects of Phosphorus Addition on the Maleic Anhydride Formation. The formation of maleic anhydride from butene, butadiene, and furan over V_2O_5 and V_2O_5-P_2O_5 catalysts at 350°C is shown is a function of the reactant conversion in Figs. 2 and 3. Selectivities to maleic anhydride are given as a slope of the curves.

The V_2O_5 catalyst has a high oxidation activity in comparison with V_2O_5-P_2O_5, but it showed only a poor selectivity to maleic anhydride: less than 20%. When butene conversion was more than 70%, the formation of maleic anhydride decreased; therefore, it did not exceed 15 mol%. In the case of butadiene oxidation, however, the selectivity to maleic anhydride was 43%, fairly good in comparison with that from butene. From

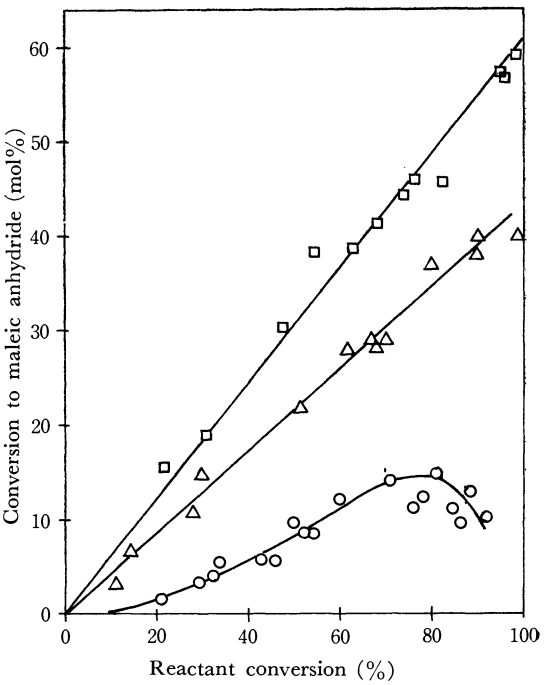

Fig. 2. Effect of reactants on maleic an hydride formation over V_2O_5 catalyst.
○: butene △: butadiene □: furan

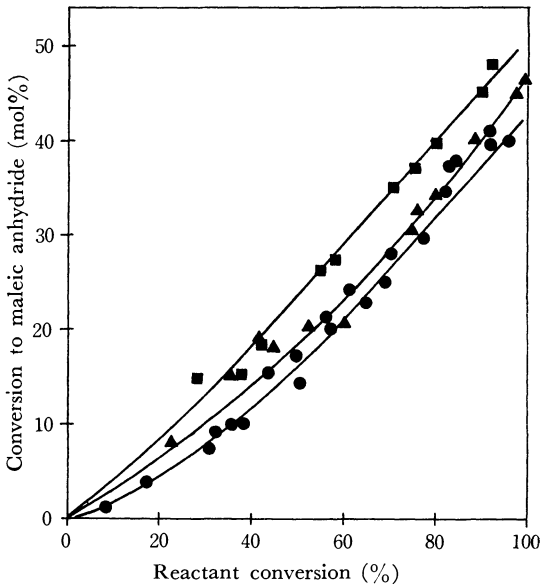

Fig. 3. Effect of reactants on maleic anhydride formation over V_2O_5-P_2O_5 (1 : 1.6).
●: butene ▲: butadiene ■: furan

furan oxidation, the selectivity to maleic anhydride became higher, as was expected, and reached 60 mol%. The decrease in selectivity to maleic anhydride at high conversion may be caused by the destruction of the maleic anhydride formed (Fig. 6); this tendency was more remarkable in the case of butene oxidation than in the cases of butadiene and furan. This phenomenon is probably to be attributed at least in part, to the fact that the reactivity of butene is lower than that of butadiene or furan, *i.e.*, the oxidation of butene requires severer condition, but for a more definite explanation, more studies will be required.

On the other hand, the V_2O_5-P_2O_5 (1 : 1.6) catalyst, whose activity was fairly low, showed a good selectivity, for butene to maleic anhydride (42%), while, in the selectivity to maleic anhydride, no marked difference was observed among the butene, butadiene, and furan oxidations, although it increased slightly in this order, as had been expected. The results are summairzed in Table 2.

Table 2. Selectivity to maleic anhydride (%)

Catalyst	Reactant		
	C_4H_8	C_4H_6	C_4H_4O
V_2O_5	20	43	60
V_2O_5-P_2O_5 (1 : 1.6)	42	46	50

Effect of Phosphorus Addition on the Reaction Pathway. From a perusal of the data in Table 2, the selectivities towards the main reaction pathway in each consecutive step, such as $C_4H_8 \rightarrow C_4H_6 \rightarrow C_4H_4O \rightarrow MA$, were calculated; for example, the selectivity in the $C_4H_6 \rightarrow C_4H_4O$ step over the V_2O_5 catalyst was found to be that, from 100 mol of C_4H_6, 43 mol of MA are formed. As the selectivity in the $C_4H_4O \rightarrow MA$ step is 60%, the portion destined to become by-products in the $C_3H_4O \rightarrow MA$ step is $40/60 \cdot 43 = 29\%$. The sum $(43+29=72)$ corresponds to the selectivity in the $C_4H_6 \rightarrow C_4H_4O$ step. In the same manner, the selectivity in $C_4H_8 \rightarrow C_4H_6$ step can also be obtained. The results are shown in Table 3.

Table 3. Selectivities of the steps (%)

Steps	$C_4H_8 \rightarrow C_4H_6$	$C_4H_6 \rightarrow C_4H_4O$	$C_4H_4O \rightarrow MA$
V_2O_5	46	72	60
V_2O_5-P_2O_5	88	93	50

On the other hand, the portions of the main and the side reactions in each consecutive step, based on 100 mol of reacted butene, can be calculated from the value of the selectivity in each step (Table 3). From the results obtained, the probable scheme of butene oxidation over V_2O_5 and V_2O_5-P_2O_5 catalysts may be proposed to be as follows (the notations in brackets mean selectivity):

V_2O_5 catalyst

$$100\ C_4H_8 \xrightarrow[(54/46)]{46} C_4H_6 \xrightarrow[(28/72)]{33}$$
$$\downarrow 54 \qquad \downarrow 13$$

$$C_4H_4O \xrightarrow[(40/60)]{20} MA$$
$$\downarrow 13 \leftarrow \text{by-products}$$

V_2O_5-P_2O_5 catalyst (P/V=1.6)

$$100\ C_4H_8 \xrightarrow[(12/88)]{88} C_4H_6 \xrightarrow[(7/93)]{83}$$
$$\downarrow 12 \qquad \downarrow 5$$

$$C_4H_4O \xrightarrow[(50/50)]{42} MA$$
$$\downarrow 41 \longrightarrow \text{by-products}$$

The results reveal that:

(1) With the V_2O_5 catalyst, the selectivity to maleic anhydride from butene oxidation is mainly determined by the low selectivity of the $C_4H_8 \rightarrow C_4H_4O$ step (33%), especially in the $C_4H_8 \rightarrow C_4H_6$ step (46%).

(2) In the case of butene oxidation, selectivity to the side pathway destined to form by-products was twice that in the butadiene oxidation.

(3) The presence of phosphorus in V_2O_5 increases the selectivities of both the $C_4H_8 \rightarrow C_4H_6$ and $C_4H_6 \rightarrow C_5H_4O$ steps: from 46 to 88% and from 72 to 93% respectively, while in the $C_4H_4O \rightarrow MA$ step, on the other selectivity to maleic anhydride falls from 60 to 50%.

(4) The incorporation of phosphorus with

V_2O_5 has little effect on the selectivity of butadiene to maleic anhydride. It may be considered that, even over the V_2O_5 catalyst, the selectivity to the side pathway in the $C_4H_6 \rightarrow C_4H_4O$ step is not very important (28%), that the favorable effect of phosphorus addition is not very efficient in this step, and that it is cancelled by its unfavorable effect in the $C_4H_4O \rightarrow$MA step.

Side Reaction in the $C_4H_4O \rightarrow$MA Step. On both V_2O_5 and V_2O_5-P_2O_5 catalysts, the major products from furan oxidation were maleic anhydride, CO_2, CO, the polymer, and a small amount of acetic acid (3—5% for the maleic anhydride formed). Since the reactivity of acetaldehyde, ketones, *etc.* were not great in these reaction conditions, they had to be found in the product gases, if they existed at all. Thus, it can be considered that furan was oxidized directly to maleic anhydride, CO, CO_2, and the polymer, without proceeding *via* some stable intermediate products. The selectivities in this process may be listed as follows:

	Catalyst	V_2O_5	V_2O_5-P_2O_5
Furan →	MA	60%	50%
	$CO + CO_2$	30%	30%
	polymer	10%	20%

The amount of the polymer was obtained as the remainder in the mass-balance of the products (Fig. 4).

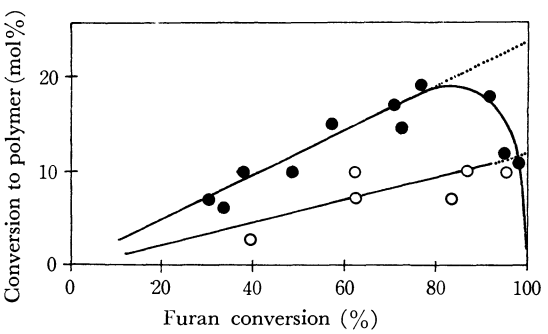

Fig. 4. Polymer formation *verses* furan conversion.
○: V_2O_5 ●: V_2O_5-P_2O_5 (1 : 1.6)

With the addition of phosphorus in V_2O_5, the formation of the polymer doubled at the expense of a decrease in the maleic anhydride formation. It may be considered that polymer formation is promoted by phosphorus, which probably produces some acid species in the catalyst.

Side Reaction in $C_4H_8 \rightarrow C_4H_4O$ Steps. Many sorts of products from butene, butadiene, and furan oxidation on the V_2O_5-P_2O_5 catalyst have been already reported in the previous paper[1], while on the V_2O_5 catalyst, the major by-products were CO and CO_2, with the others being almost negligible except for small quantities of acetone and acrolein (2—3%). From butene oxidation on V_2O_5, very much acetaldehyde (AcH) and acetic acid (AcOH) were formed (Fig. 5). We have represented here the value of the conversion AcH+AcOH, assuming that two moles of AcOH+AcH are formed from one mole of butene, although it is not clear if two moles are formed or only one mole.

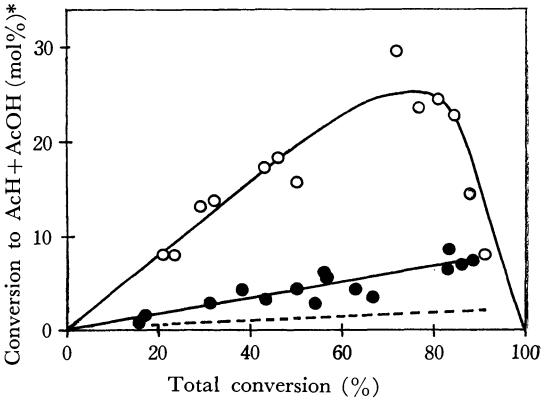

Fig. 5. Conversion to AcH+AcOH* *versus* total conversion.
* basing on the assumption that 2 mol of AcH+AcOH are formed from 1 mol of C_4 compound.
solid line: butene oxidation (○: V_2O_5, ●: V_2O_5-P_2O_5)
dashed line: butadiene oxidation on V_2O_5 or V_2O_5-P_2O_5

The results reveal that:

(1) On both V_2O_5 and V_2O_5-P_2O_5 catalysts, about one half of the side reaction in the $C_4H_8 \rightarrow C_4H_6$ step leads to AcOH+AcH formation, and the other half, to complete combustion: CO, CO_2, *etc.*

(2) Selectivity to the side reaction of butene is twice as much as that of butadiene, a difference which may be attributed to the tendency to scission of a double-bond of butene. Therefore, it may be concluded that the selectivities to complete combustion are of about the same magnitude between butene and butadiene.

CO and CO_2 formation are shown as functions of the maleic anhydride formed in Figs. 6 and 7. The selectivity ratio of CO or CO_2 formation to maleic anhydride is described as a slope of the curve. Over the V_2O_5-P_2O_5 catalyst, the CO_2 formation was independent of the sort of reactants; this indicates that the sources of the CO_2 formation are the $C_4H_4O \rightarrow$MA steps. Moreover, the selectivity ratio of CO_2 to maleic anhydride decreased with an increase in the reactant conversion. In the $C_4H_8 \rightarrow C_4H_4O$ steps, only CO was formed as a complete combustion product, and the ratio increased with the reactant conversion. On the other hand, on the V_2O_5 catalyst, CO_2 is formed also in the $C_4H_8 \rightarrow C_4H_4O$

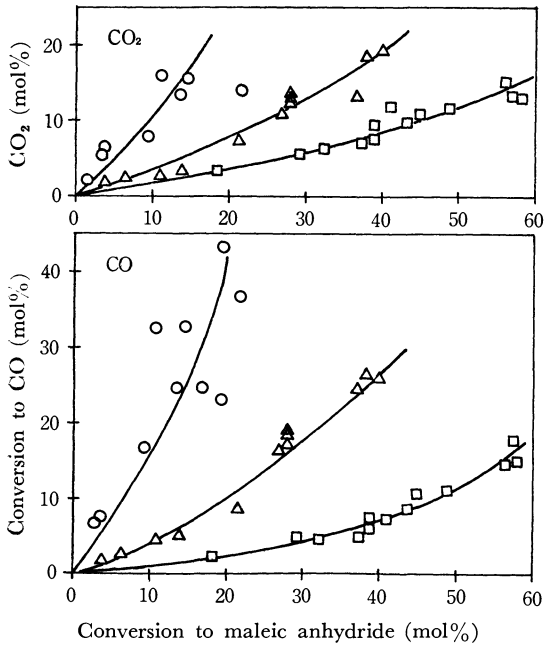

Fig. 6. Conversion* to CO and CO_2 as a function of maleic anhydride formation on V_2O_5.
* 1/4 of the real amount of the formation
○: butene △: butadiene □: furan

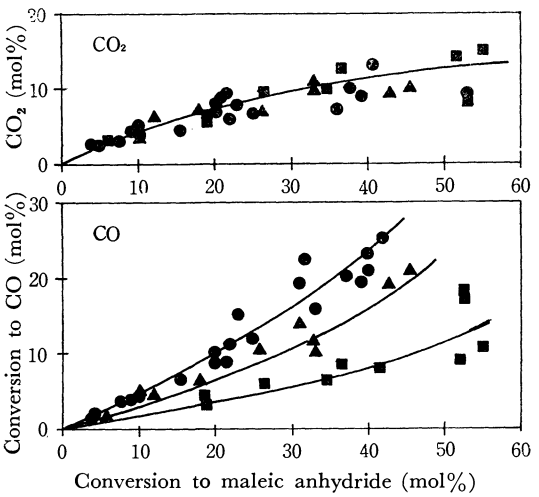

Fig. 7. Conversion* to CO and CO_2 as a function of conversion to maleic anhydride on V_2O_5–P_2O_5.
* 1/4 of the real amount of the formation
●: butene ▲: butadiene ■: furan

steps, but CO is still predominant.

Amounts of Intermediate Products. The amounts of the intermediates formed in the oxidation of butene and butadiene to maleic anhydride are plotted as a function of the reactant conversion (Figs. 8 and 9). In all the cases investigated, they passed through a maximum at a reactant conversion of about 50%.

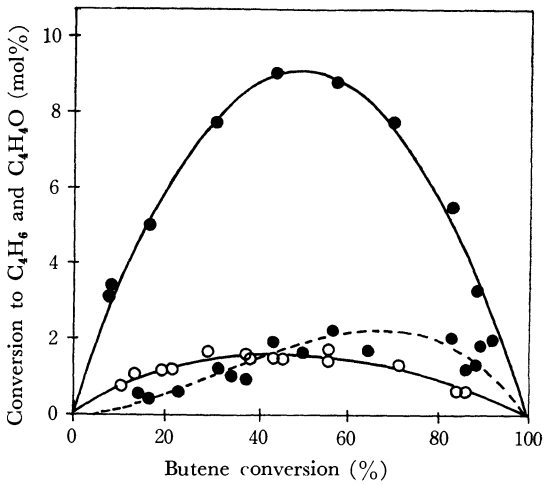

Fig. 8. Conversion to C_4H_6 and C_4H_4O *versus* butene conversion.
solid line: formed butadiene
dashed line: formed furan
○: V_2O_5 ●: V_2O_5–P_2O_5 (1 : 1.6)

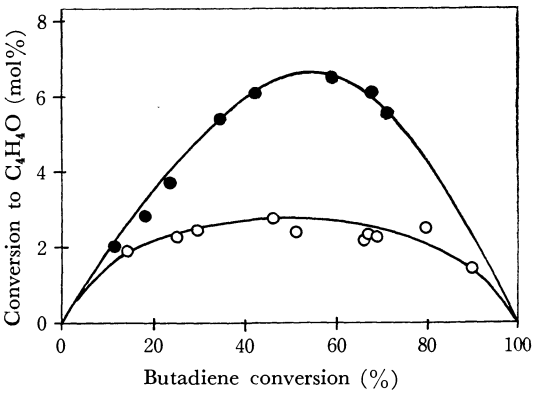

Fig. 9. Conversion to C_4H_4O *versus* butadiene coversion.
○: V_2O_5 ●: V_2O_5–P_2O_5 (1 : 1.6)

The consecutive reaction on the catalyst surface can be explained by the following reaction scheme[5]:

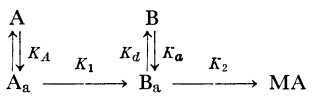

where A is the starting material; B, the intermediate, and MA, the fully-oxygenated compound (maleic anhydride), and where the subscript "a" means "adsorbed."

A steady-state treatment based on the assumption that A_a is in equilibrium with A results, after the elimination of the time and integration[5], in:

5) J. H. de Boer and R. J. A. M. van der Borg, Actes du Deuxieme Congres Internationale de Catalyse, Editions Thechiq, Paris, (1961), p. 919., and P. Zwietering and F. Hartog, *J. Catal.*, **2**, 79 (1963).

$$B = \frac{S}{r-1}(A-A^r)$$

where:

$$r = \frac{K_a K_2}{K_1 K_A (K_2+K_d)}, \quad S = \frac{K_d}{K_2+K_d}$$

A and B are the mole fractions of the starting material and the intermediate in the reaction product. K_a is adsorption equilibrium constant; K_1 and K_2, the reaction rate constants, and K_a and K_d, the adsorption and desorption rate constants.

The values of r and S for butene and butadiene oxidation over both V_2O_5 and V_2O_5-P_2O_5 were calculated from the maximum amount of the primary intermediate products (butadiene from butene and furan from butadine) and the reactant conversion at this point. They are shown in Table 4.

Table 4. r and S values

Steps	$C_4H_8 \rightarrow C_4H_6 \rightarrow$		$C_4H_6 \rightarrow C_4H_4O \rightarrow$	
Catalyst	V_2O_5	V_2O_5-P_2O_5	V_2O_5	V_2O_5-P_2O_5
r	2	2	2	2
S	0.14	0.41	0.13	0.31
k*	18	0.6	18	0.6

* for intermediate oxidation at 350°C

The results reveal that the value of r, which represents the reactivity ratio of feed to the primary intermediate, remains almost unchanged with the variation in reactants and catalyst composition, and that V_2O_5 and V_2O_5-P_2O_5 catalysts show similar oxidation activities for butene, butadiene and furan. It can be concluded that a satisfactory yield of oxygenated intermediates can not be expected from these vanasium-type catalysts.

On the other hand, the value of S, which represents the portion of the intermediate that leaves the surface, increases with a decrease in the oxidation activity of the catalyst; this means that the higher the catalyst activity becomes, that is, the stronger the intermediate adsorption becomes, the larger the portion of the adsorbed intermediate species which goes directly into the next step, without desorbing to the gas phase.

The amount of the intermediate products was considerably affected by the activity of the catalyst as well as by the difference in reactivity between the starting material and the intermediate over the catalyst. Therefore, a mild catalyst is indispensable in order to obtain good yields of intermediate products.

BULLETIN OF THE CHEMICAL SOCIETY OF JAPAN VOL. 43 3496—3500 (1970)

The Acetylation of 2,3-Dimethyl-*bz*-halobenzofurans and Some Reactions of the Products*[1]

Yoshiyuki KAWASE and Sachiko HORI

Department of Chemistry, Faculty of Literature and Science, Toyama University, Gofuku, Toyama

(Received March 12, 1970)

The acetylation of *bz*-chloro- and *bz*-bromo-2,3-dimethylbenzofurans with acetyl chloride and aluminum chloride in carbon disulfide at room temperature was studied; it was found that the acetylation occurred at the 6- or 4-position, which is activated by the furan ring, regardless of whether the halogen atom is at the *o*-, the *m*-, or the *p*-position. In the cases of 7-halo compounds, diacetylation occurred to give the 4,6-diacetyl compounds, and the migration of the bromine atom of 6-acetyl-5-bromo-2,3-dimethylbenzofuran and of the methyl ester of the corresponding carboxylic acid occurred, as a result of the action of aluminum bromide in carbon disulfide at room temperature, to give the 4-bromo compounds. The haloketones thus obtained were then converted to the corresponding carboxylic acids by the bromoform reaction.

The acetylation of 2,3-dimethylbenzofuran and its derivatives, which have various substituents, *e.g.*, hydroxyl,[1] methoxyl,[2] alkyl,[3–5] acetamide,[6] methoxycarbonyl,[7] and acetyl[7–9] groups on the benzene ring, has previously been reported. It has been reported that the acetylation of 7-chloro-2,3-dimethylbenzofuran (**18a** afforded the 4-acetyl compound[10] (**19a**).

Now, in the present experiments, the acetylation of several halo-2,3-dimethylbenzofurans (**5a**, **8a**, **11a**, **11b**, **18a**, and **18b**) was carried out, the acetyl group of the compounds was converted to the carboxyl group, and the bromine atom of 5-bromo-6-acetyl and -6-methoxycarbonyl compounds (**12b** and **16**) migrated to the 4-position as a result of the action of aluminum bromide.

2,3-Dimethyl-5-[11] and -7-halobenzofurans[10,12] (**11a**, **11b**, **18a**, and **18b**) were prepared readily by the reported method through the cyclodehydration of 3-aryloxybutanones, but the 4- and 6-halo compounds (**5a**, **5b**, **8a**, and **8b**) could not be prepared by a similar procedure; the cyclization of 3-(*m*-halophenoxy)butanones (**2a** and **2b**) by sulfuric acid or polyphosphoric acid afforded only crude products, which were found by NMR spectroscopy to be mixtures of the 4- and 6-halo compounds (**5a** and **8a** or **5b** and **8b**). Therefore, the pure 4- and 6-chloro-2,3-dimethylbenzofurans (**5a** and **8a**) were prepared by the Sandmeyer reaction of the corresponding amino compounds[13] (**1** and **3**) (see Chart 1). In the NMR spectra, the 4-halo compounds have the peaks corresponding to the 3-methyl protons in the field lower by about 0.3 ppm than the isomeric 6-halo compounds have; the ratio of the 4- and 6-halo compounds of the mixtures was determined by estimating areas of the peaks.

The acetylation of 4- and 6-chlorobenzofurans (**5a** and **8a**) with acetyl chloride and aluminum chloride in carbon disulfide at room temperature afforded the 6- and 4-acetyl compounds (**6** and **9**) respectively, in which the positions of the acetyl groups were determined by NMR spectroscopy. They have two doublets of $J=1$—3 Hz corresponding to aromatic, two-meta protons. The

*1 The major part of this work was presented at the 21st Annual Meeting of the Chemical Society of Japan, Osaka, March, 1968.

1) Y. Kawase, M. Nanbu and F. Miyoshi, This Bulletin. **41**, 2676 (1968).
2) R. Royer, E. Bisagni, A. -M. Laval-Jeantet and J. -P. Marquet, *Bull. Soc. Chim. Fr.*, **1965**, 2607.
3) E. Bisagni and R. Royer, *ibid.*, **1962**, 925.
4) R. Royer, G. Hubert-Habart, L. René and A. Cheutin, *ibid.*, **1964**, 1259.
5) Y. Kawase, R. Royer, M. Hubert-Habart, A. Cheutin, L. Rene and J. -P. Buisson, *ibid.*, **1964**, 3131.
6) Y. Kawase and S. Kondô, This Bulletin, **43**, 3268 (1970).
7) Y. Kawase and M. Takashima, *ibid.*, **40**, 1224 (1967).
8) Y. Kawase, M. Hubert-Habart, J. -P. Buisson and R. Royer, C. R. Acad. Sci., Paris, Ser. A. B (C, D), **258**, 5007 (1964).
9) R. Royer, Y. Kawase, M. Hubert-Habart L. René and A. Cheutin, *Bull. Soc. Chim. Fr.*, **1966**, 211.
10) C. Goldenberg, F. Binon and C. Gillyus, *Chim. Ther.*, **1966**, 221.
11) E. Bisagni, J. -P. Marquet, A. Cheutin and R. Royer, *Bull. Soc. Chim. Fr.*, **1965**, 1466.
12) C. Pène, P. Demerseman, A. Cheutin and R. Royer, *ibid.*, **1966**, 586.
13) Y. Kawase, S. Takata and E. Hikishima, This Bulletin, to be published.
14) Y. Kawase, S. Takata and T. Miwa, *ibid.*, **43**, 1796 (1970).

chloroketone **6** was also unexpectedly obtained from 3-(*p*-acetyl-*m*-chlorophenoxy)butanone (**4**) by cyclization with polyphosphoric acid; this also caused a migration of the acetyl group (see Chart 1).

The acetylation of 5-chloro- and 5-bromo-2,3-dimethylbenzofurans (**11a** and **11b**) afforded the 6-acetyl compounds (**12a** and **12b**), while that of 7-chloro- and 7-bromobenzofurans (**18a** and **18b**) afforded the 4-acetyl compounds (**19a** and **19b**) (see Charts 2 and 3). The positions of the acetyl groups were determined by NMR and UV spectroscopy. In the NMR spectra, **12a** and **12b** have two singlets corresponding to aromatic, two-para protons, while **19a** and **19b** have two doublets of $J=7$ Hz corresponding to aromatic, two-ortho protons. However, the positions of the acetyl groups of **19a** and **19b** were not clear from the NMR data; they might be at the 4- or 6-positions, although they seemed to be at the 4-positions, judging from the patterns of the UV spectra, which were comparable to each other and to that of 4-acetyl-2,3-dimethylbenzofuran[14] (see Table 4). The isomeric 5-acetyl-2,3-dimethyl-7-halobenzofurans (**24a** and **24b**) were also prepared by the cyclization of 3-(*p*-acetyl-*o*-halophenoxy)butanones (**23a** and **23b**), which had been prepared by the action of 3-chlorobutanone on *m*-halo-*p*-hydroxyacetophenones (**22a** and **22b**). In the case of the acetylation of the 7-halobenzofurans (**18a** and **18b**), diacetylation occurred to give 4,6-diacetyl compounds (**21a** and **21b**) when double amounts of the reagents were used, analogously to the case of 7-alkyl compounds.[5,8,9] The diacetyl, compound **21a** was also obtained by the acetylation of the ketone **19a**.

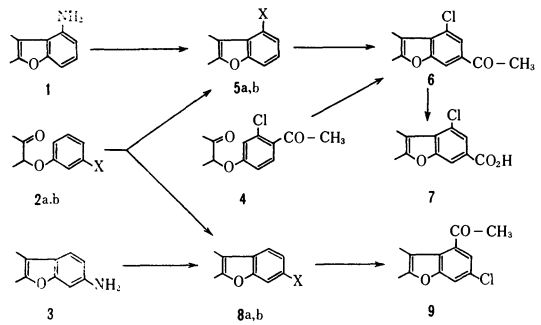

For all chart: a) X=Cl, b) X=Br

Chart 1

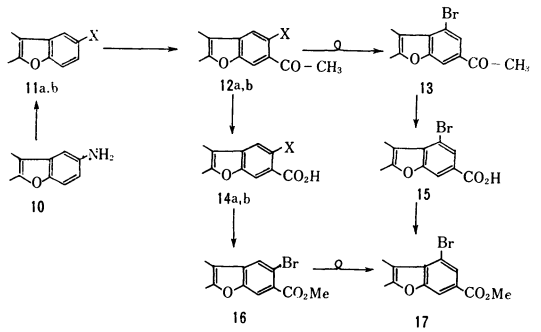

Chart 2

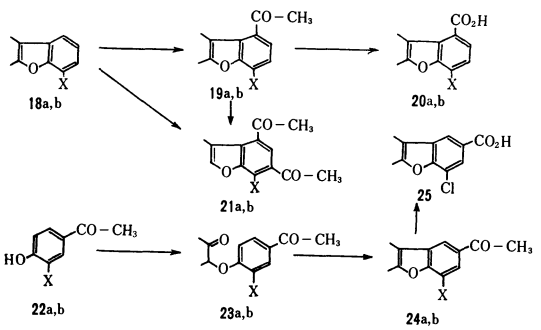

Chart 3

It is found from these results that, in the electrophilic substitution, all the positions on the benzene ring of 2,3-dimethylbenzofuran, especially the 6- and then 4-positions, are activated by the furan ring, and that the acetylation occurs at the 6- or 4-position, regardless of the position of the halogen atom.

The action of aluminum bromide in carbon disulfide at room temperature on the 5-bromoketone (**12b**) thus obtained caused a migration of the bromine atom to the 4-position to give 4-bromoketone (**13**), analogously to the case of 6-acetyl-5-alkyl-2,3-dimethylbenzofurans.[5,8,14] The structure of the migrated compound (**13**) was confirmed by NMR and UV spectroscopy. In the NMR spectra, it has two doublets of $J=2$ Hz corresponding to aromatic, two-meta protons, and the peak corresponding to the 3-methyl protons is in a low field, indicating that the halogen atom is at the 4-position. In the UV spectra, the haloketones (**12a** and **12b**) have two peaks, at around 225 and 290 mμ, while the haloketones (**6** and **13**) have additional peaks at around 240 mμ, such as do 6-acetyl-4- and -5-alkylbenzofurans.[14]

Further, the haloketones (**6**, **12a**, **12b**, **13**, **19a**, **19b**, and **24a**) thus obtained were converted to the corresponding carboxylic acids (**7**, **14a**, **14b**, **15**, **20a**, **20b**, and **25** respectively) by the bromoform reaction. The bromine atom of the methyl ester (**16**) of 5-bromo-6-carboxylic acid (**14b**) also migrated, as a result of the action of aluminum bromide, to the 4-position, to give methyl 4-bromobenzofuran-6-carboxylate (**17**), which was identical with the sample obtained by the esterification of the acid (**15**).

Experimental

All the melting points and boiling points are uncorrected, the UV spectra were measured on a Hitachi

TABLE 1. SUMMARIZED DATA OF REACTIONS

Start	Reagent[a]	Prod	Mp°C (solv.[b]) or bp° C/mmHg n (°C)	Yield %
		Aryloxybutanones		
c)	Cl-butanone	**2a**	136—143/18 1.5200 (26.5)	53
d)	Cl-butanone	**2b**	144—150/20 1.5415 (20)	79
e)	Cl-butanone	**4**	192—195/18 1.5420 (26)	56
22a	Cl-butanone	**23a**	205—209/23 1.5439 (27)	49
22b	Cl-butanone	**23b**	55—57 (Cy)	36
		Halobenzofurans		
2a	H_2SO_4	**5a**+**8a**	135—138/27	75[f]
2a	PPA	**5a**+**8a**	132—135/19	70[f]
2b	H_2SO_4	**5b**+**8b**	140—143/21	79[g]
2b	PPA	**5b**+**8b**	140—143/21	75[h]
1	Sandmeyer	**5a**	120—130/19	35
3	Sandmeyer	**8a**	35— 36 (Pe)	22.5
10	Sandmeyer	**11a**	40— 41 (Pe)[i]	12.5
		Haloketones		
4	PPA	**6**	89.5—90 (Cy)	5
5a	AcCl+$AlCl_3$	**6**	89.5—90 (Cy)	58.5
8a	AcCl+$AlCl_3$	**9**	76—78 (Cy)	50
11a	AcCl+$AlCl_3$	**12a**	36—38 (Cy)	50.5
11b	AcCl+$AlCl_3$	**12b**	59—61 (Cy)	74
12b	$AlBr_3$	**13**	98—99.5 (Cy)	38.5
18a	AcCl+$AlCl_3$	**19a**	105—106 (Cy)[j]	75
18b	AcCl+$AlCl_3$	**19b**	113—115 (Cy)	11.5
18a	AcCl+$AlCl_3$	**21a**	100—101 (Cy)	34
19a	AcCl+$AlCl_3$	**21a**	100—101 (Cy)	75
18b	AcCl+$AlCl_3$	**21b**	119—120.5 (Cy)	11
23a	PPA	**24a**	112—113 (Cy)	11
23b	PPA	**24b**	127—128 (Cy)	6
		Haloacids		
6	NaOBr	**7**	220—221 (Me)	63
12a	NaOBr	**14a**	237.5—239 (Me)	66
12b	NaOBr	**14b**	233—235 (Me)	84
13	NaOBr	**15**	255—256 (Me)	75
19a	NaOBr	**20a**	203—205 (Me)	80
19b	NaOBr	**20b**	199.5—200.5 (Me)	40
24a	NaOBr	**25**	246—247 (Me)	63
		Haloesters		
14b	Me_2SO_4	**16**	96—98 (Cy)	84
15	Me_2SO_4	**17**	119—120 (Cy)	60
16	$AlBr_3$	**17**	119—120 (Cy)	20

a) PPA: polyphosphoric acid. b) Cy: cyclohexane, Pe: petroleum ether, Me: methanol. c) *m*-Chlorophenol. d) *m*-Bromophenol. e) *o*-Chloro-*p*-hydroxyacetophenone. f) A mixture of 67% of **5a** and 33% of **8a**. g) A mixture of 46% of **5b** and 54% of **8b**. h) A mixture of 58% of **5b** and 42% of **8b**. i) Lit mp 42°C (Ref. 11). j) Lit mp 102°C (Ref. 10).

139 spectrophotometer, and the NMR spectra were measured on a JEOL JNM-C-60H (60 MHz) spectrometer. Detailed data are summarized in Tables 1—4.

Aryloxybutanones (2a, 2b, 4, 23a, and 23b). Potassium carbonate (80 g) was added to a solution of *m*-chlorophenol (25 g) and 3-chlorobutanone (22.7 g) in acetone (200 m*l*), and the mixture was refluxed for 8 hr. Most of the acetone was distilled off, and the residue was treated with water and then extracted with ether. The ethereal solution was washed with an aqueous sodium hydroxide solution, and the residual product from the ether solution was distilled to give 3-(*m*-chlorophenoxy)butanone (**2a**), bp 136—143°C/18 mmHg, 20.5 g (53%). Similarly, 3-(*m*-bromophenoxy)butanone (**2b**), 3-(*p*-acetyl-*m*-chlorophenoxy)butanone (**4**), and 3-(*p*-acetyl-*o*-chloro- and -bromophenoxy)butanones (**23a** and **23b**) were also prepared by this procedure.

Cyclization of the Aryloxybutanones. *a) By Sulfuric Acid.* Concentrated sulfuric acid (10 g) was stirred into **2a** (10 g) with cooling below 30°C, and the mixture was kept at 30°C for 1 hr. The cooled mixture was then poured into ice water and extracted with ether, and the residual product from the

Table 2. Analyses of the new compounds

Compd	Formula	Found C%	Found H%	Calcd C%	Calcd H%
	Aryloxybutanones				
2a	$C_{10}H_{11}O_2Cl$	60.49	5.64	60.48	5.58
2b	$C_{10}H_{11}O_2Br$	49.69	4.50	49.40	4.56
4	$C_{12}H_{13}O_3Cl$	60.15	5.72	59.88	5.45
23a	$C_{12}H_{13}O_3Cl$	60.51	5.65	59.88	5.45
23b	$C_{12}H_{13}O_3Br$	50.67	4.60	50.54	4.60
	Halobenzofurans				
5a	$C_{10}H_9OCl$	66.74	5.11	66.51	5.02
8a	$C_{10}H_9OCl$	66.41	4.92	66.51	5.02
	Haloketones				
6	$C_{12}H_{12}O_2Cl$	64.71	4.91	64.73	4.98
9	$C_{12}H_{12}O_2Cl$	64.49	4.74	64.73	4.98
12a	$C_{12}H_{12}O_2Cl$	64.79	5.10	64.73	4.98
12b	$C_{12}H_{12}O_2Br$	53.79	4.05	53.95	4.15
13	$C_{12}H_{12}O_2Br$	54.22	3.93	53.95	4.15
19b	$C_{12}H_{12}O_2Br$	54.11	4.11	53.95	4.15
21a	$C_{12}H_7O_2Cl_2$	63.36	4.94	63.52	4.95
21b	$C_{12}H_7O_2Br_2$	54.53	4.38	54.39	4.24
24a	$C_{12}H_{12}O_2Cl$	64.73	4.95	64.73	4.98
24b	$C_{12}H_{12}O_2Br$	53.88	3.88	53.95	4.15
	Haloacids				
7	$C_{11}H_9O_3Cl$	58.61	4.15	58.81	4.04
14a	$C_{11}H_9O_3Cl$	58.62	4.09	58.81	4.04
14b	$C_{11}H_9O_3Br$	49.04	3.25	49.09	3.37
15	$C_{11}H_9O_3Br$	49.33	3.22	49.09	3.37
20a	$C_{11}H_9O_3Cl$	58.57	4.00	58.81	4.04
20b	$C_{11}H_9O_3Br$	48.99	3.53	49.09	3.37
25	$C_{11}H_9O_3Cl$	59.03	3.81	58.81	4.04
	Haloesters				
16	$C_{12}H_{11}O_3Br$	51.17	3.80	50.90	3.92
17	$C_{12}H_{11}O_3Br$	50.64	3.72	50.90	3.92

Table 3. The NMR spectra[a)]

Compd	Ph-H[b)]	-COMe	2-Me	3-Me
	Halobenzofurans			
5a			2.35	2.35
8a			2.25	2.02
11a			2.28	2.01
11b			2.29	2.03
18a			2.31	2.04
18b			2.32	2.03
	Haloketones			
6	7.55(d) 7.60(d) J=1 Hz	2.51	2.36	2.33
9	7.36(d) J=3 Hz	2.55	2.34	2.09
12a	7.43 7.22	2.54	2.31	2.04
12b	7.48 7.41	2.57	2.34	2.07
13	7.67(d) 7.75(d) J=2 Hz	2.48	2.31	2.27
19a	7.04(d) 7.33(d) J=7 Hz	2.50	2.38	2.10
19b	7.24(d) J=7 Hz	2.54	2.42	2.12
21a	7.84	2.69, 2.62	2.47	2.16
21b[b)]	7.75	2.74, 2.66	2.46	2.17
24a	7.92(d) J=1 Hz	2.62	2.50	2.24
24b[c)]	8.03(d) 7.99(d) J=1 Hz	2.63	2.44	2.18

a) δ(ppm) values in CCl_4 solution (about 5%), with TMS as the internal standard. b) d: Doublet. c) In $CDCl_3$.

Table 4. The UV spectra

Compd.	λ_{max}^{EtOH} mμ[a)] (log ε)
	Halobenzofurans
5a	218(4.37), 260(4.07), 288(3.34)
8a	220(4.35), 256(4.13), 261(4.12), 286(3.66), 294(3.56)
11a	215(4.55), 257(4.06), 287(3.63), 295(3.62)
11b	216(4.44), 258(4.06), 287(3.65), 295(3.65)
18a	217(4.30), 256(4.07), 287(3.30)
18b	219(4.30), 257(4.01), 286(3.25)
	Haloketones
6	211.5(4.23), 237(4.18), 292.5(4.17)
12a	225(4.28), 291(4.11)
12b	224(4.27), 290(4.07)
13	217.5(4.27), 241(4.25), 294(4.24)
19a	237.5(4.37), 285(3.98), 315[s](3.76)
19b	239(4.34), 285.5 (4.00), 314[s](3.75)

a) s: Shoulder.

ether solution was distilled to give a crude product, bp 135—138°C/27 mmHg, 6.8 g (75%), which was found by the NMR spectrum to be a mixture of 4- and 6-chlorobenzofurans (**5a** and **8a**). Analogously, the product from **2b** was also a mixture of 4- and 6-bromo compounds (**5b** and **8b**).

b) By Polyphosphoric Acid. A mixture of **2a** (10 g) and polyphosphoric acid (n=2.5, 200 g) was heated at 100°C for 1.5 hr. The cooled mixture was poured into ice water and extracted with ether, and the residual product from the ether solution was distilled to give a mixture of the 4- and 6-chloro compounds (**5a** and **8a**), bp 132—135°C/19 mmHg, 6.4 g (70%). Analogously, a mixture of **5b** and **8b** was also obtained from **2b**. 6-Acetyl-2,3-dimethyl-7-halobenzofurans (**24a** and **24b**) were obtained from **23a** and **23b** by the same procedure; in the case of the aryloxybutanone (**4**), there was also a migration of the acetyl group to give 6-acetyl-4-chloro-2,3-dimethylbenzofuran (**6**).

Chlorobenzofurans (5a, 8a, and 11a) by the Sandmeyer Reaction. 4-Amino-2,3-dimethylbenzofuran[13] (**1**) (3 g) was diazotized and then treated with cuprous chloride in the usual manner[15] to give **5a**, bp 120—130°C/20 mmHg, 1.2 g (35%). Similarly, 5- and 6-chloro-2,3-dimethylbenzofurans (**11a** and **8a**) were also prepared from amines (**10** and **3**).

Acetylation of Halobenzofurans (5a, 8a, 11a, 11b, 18a, and 18b) and Chloroketone (19a). Anhydrous aluminum chloride (1 g) was stirred, with cooling, into a solution of **5a** (1 g) and acetyl chloride (0.5 g) in carbon disulfide (50 m*l*); after the mixture had then been stirred at room temperature for 4 hr, it was poured into ice water. The resulting mixture was extracted with chloroform, and the chloroform solution was washed with an aqueous sodium hydroxide solution. The residual product from the chloroform solution was distilled and then crystallized from cyclohexane to give 6-acetyl-4-chloro-2,3-dimethylbenzofuran (**6**), mp 89.5—90°C, 0.7 g (58%). Similarly, 4-acetyl-6-chloro-, -7-chloro-, and -7-bromo-2,3-dimethylbenzofurans (**9**, **19a**, and **19b**), and 6-acetyl-5-chloro- and -5-bromo-2,3-dimethylbenzofurans (**12a** and **12b**) were also obtained. The acetylation of 7-chloro- and 7-bromobenzofurans (**18a** and **18b**) by double amounts of reagents afforded 7-chloro- and 7-bromo-4,6-diacetyl-2,3-dimethylbenzofurans (**21a** and **21b**); **21a** was also obtained by the acetylation of the haloketone **19a**.

Migration of the Bromine Atom of Bromoketone (12b) and Bromoester (16). Anhydrous aluminum bromide (10.4 g) was stirred into a solution of **12b** (5.2 g) in carbon disulfide (70 m*l*); after the mixture had been stirred for 4 hr, it was then treated such as has been described for the acetylation. The product was distilled and crystallized from cyclohexane to give 6-acetyl-4-bromo-2,3-dimethylbenzofuran (**13**), mp 98—99.5°C. 2 g (38.5%). Similarly, methyl 4-bromo-2,3-dimethylbenzofuran-6-carboxylate (**17**) was obtained from **16**.

Haloacids (7, 14a, 14b, 15, 20a, 20b, and 25) by the Bromoform Reaction. A solution of the chloroketone **6** (1 g) in dioxane (20 m*l*) was stirred, with cooling, into an aqueous sodium hypobromite solution, prepared by the addition of bromine (3.4 g) to a cold mixture of sodium hydroxide (2 g), water (6 m*l*), and ice (6 g); the mixture was stirred for 30 min at 15°C and then for 1.5 hr at 45°C. The cooled solution was extracted with ether, and the aqueous layer was acidified after the addition of a small amount of sodium sulfite. The precipitates thus formed were crystallized from methanol to give 4-chloro-2,3-dimethylbenzofuran-6-carboxylic acid (**7**), mp 220—221°C, 0.7 g (63%). Similarly, 4-bromo-, 5-chloro-, 5-bromo-, and 7-chloro-2,3-dimethylbenzofuran-6-carboxylic acids (**15**, **14a**, **14b**, **and 25**) and 7-chloro- and 7-bromo-2,3-dimethylbenzofuran-4-carboxylic acids (**20a** and **20b**) were also prepared.

Esterification of the Acids (14b and 15). The acids were esterified by refluxing them for 8 hr with methyl sulfate and sodium carbonate in acetone; the product was crystallized from cyclohexane to give two esters (**16** and **17**).

The authors are grateful to the members of the Laboratory of Analysis, Faculty of Pharmacology, Toyama University, for doing the microanalyses and NMR spectroscopy.

15) Cf. W. W. Hartman and M. R. Brethen, "Org. Synth.," Coll. Vol. 1, p. 162 (1956).

BULLETIN OF THE CHEMICAL SOCIETY OF JAPAN VOL. 43 3501—3504 (1970)

Liquid Phase Chlorination of Olefins with Cupric Chloride. II. Stereochemistry of the Reactions of 2-Butenes and Cyclohexene

Takashi KOYANO

Central Research Laboratory, Toa Nenryo Kogyo Co., Oi-machi, Iruma-gun, Saitama

(Received April 13, 1970)

Chlorination of *cis*-and *trans*-2-butenes with cupric chloride yields a mixture of *meso*- and *dl*-2,3-dichlorobutanes with *meso*/*dl* ratio of about 60/40, which is almost independent of the starting olefin configuration. For cyclohexene, *trans*-1,2-dichlorocyclohexane is accompanied with the *cis*-dichloride, the amount of which depends upon the solvent polarities. In all cases the starting olefins and the product dichlorides are sufficiently stable under the reaction conditions. The results indicate that open ionic intermediates are involved in the chlorination of simple olefins in liquid phase reaction.

The stereochemical sequence of addition of molecular chlorine to olefins in polar media varies with the structure of the substrate. Stereospecific *trans* addition has been observed for the reactions with 2-butenes in acetic acid,[1] di-*t*-butylethylenes in methanol,[2] and 2-pentenes in various polar solvents including acetic acid and methanol.[3] Chlorination of 1-phenylpropenes in acetic acid and in methanol,[1] and phenanthrene[4] or methyl *trans*-cinnamate[5] in acetic acid leads to mixtures of stereoisomeric dichlorides. It is generally accepted that the chlorination of simple alkenes proceeds *via* a chloronium ion intermediate, while that of conjugated olefins occurs *via* an open carbonium ion. The same conclusion has been drawn for non-polar chlorination, evidenced by reactions with 2-butenes,[6] cyclohexene,[7] and *trans*-stilbene.[8]

Similarly, chlorination of 2-butenes with cupric chloride is highly stereoselective in vapor phase reaction.[9] The formation of *cis*-addition products has been attributed to olefin isomerization and interconversion of 2,3-dichlorobutane diastereomers.[10] The chlorination product of cyclohexene with cupric chloride in acetic acid has been reported to be *trans*-dichloride practically with no *cis*-isomer,[11,12] and a bridged type intermediate has been proposed.[13]

However, when 2-butenes were treated with cupric chloride in methanol, isomeric dichlorides were formed where the product composition is almost the same regardless of the starting olefin configuration.[14] The present studies were undertaken in order to obtain further evidence on the stereochemistry of the cupric chloride chlorination in liquid phase. The results with 2-butenes and cyclohexene give a clue to solve the nature of the reaction intermediate.

Results

Chlorination of either *cis*- or *trans*-2-butene with cupric chloride was carried out in several polar solvents at 100—150°C. The principal products were *dl*- and *meso*-2,3-dichlorobutanes with a small amount of 2-chloro-3-methoxybutanes.[14] The compositions of the dichlorides are shown in Table 1.

Comparing results from the same reaction conditions, we see that the ratios of *meso* to *dl* dichlorides are very similar for both 2-butenes, although slightly larger for *trans*-2-butene. The extent of 2-butene isomerization was too small to account for. Isomerization between the dichlorides was not observed in methanol under the reaction conditions,[14] and no significant variation in the dichloride com-

1) R. C. Fahey and C. Schubert, *J. Amer. Chem. Soc.*, **87**, 5172 (1965)
2) R. C. Fahey, *ibid.*, **88**, 4681 (1966).
3) M. L. Poutsma and J. L. Kartch, *ibid.*, **89**, 6595 (1967).
4) P. B. D. de la Mare and R. Koenigsberger, *J. Chem., Soc.*, **1964**, 5327.
5) M. C. Cabaleiro and M. D. Johnson, *ibid.*, *B*, **1967**, 565.
6) M. L. Poutsma, *J. Amer. Chem. Soc.*, **87**, 2172 (1965).
7) M. L. Poutsma, *ibid.*, **87**, 2161 (1965).
8) S. J. Cristol and R. S. Bly, Jr., *ibid.*, **82**, 142 (1960).
9) R. P. Arganbright and W. F. Yates, *J. Org. Chem.*, **27**, 1205 (1962).
10) P. P. Nicholas and R. T. Carroll, *ibid.*, **33**, 2345 (1968).
11) K. Ichikawa, S. Uemura, T. Hiramoto and Y. Takagaki, *Kogyo Kagaku Zasshi*, **71**, 1657. (1968).
12) S. Uemura, T. Hiramoto, Y. Takagaki and K. Ichikawa, *ibid.*, **72**, 2390 (1969).
13) S. Uemura, Y. Takagaki and K. Ichikawa, *ibid.*, **72**, 2577 (1969).
14) T. Koyano, This Bulletin, **43**, 1439 (1970).

Table 1. Chlorination of 2-butenes

Solvent	Dielectric constant[15]	Additive	Temp. (°C)	Time (hr)	Dichloride (%) from *cis* *meso*	from *cis* *dl*	from *trans* *meso*	from *trans* *dl*
Acetic acid	6.2 (20°)		150	2	58.2	41.8	63.8	36.2
1-Octanol	10.3 (20°)		150	2	53.5	46.5	54.8	45.2
1-Butanol	17.1 (25°)		150	2	57.7	42.3	62.9	37.1
Methanol	32.6 (25°)		150	2	61.0	39.0	65.7	34.3
		H_2O (10%)	150	2	61.4	38.6	—	—
		H_2O (20%)	150	2	63.3	36.7	—	—
		LiCl*	150	2	63.7	36.3	—	—
			120	2	63.4	36.6	—	—
			120	5	63.7	36.3	—	—
			100	5	66.5	33.6	—	—
Nitromethane	35.9 (30°)		150	2	58.3	41.7	64.1	35.9

500 m*l* glass-lined autoclave, 2-butene 0.30 mol, $CuCl_2$ 0.045 mol, solvent 150 m*l*
* 0.045 mol

Table 2. Chlorination of cyclohexene

Solvent	Dielectric constant[15]	Additive	Dichloride (%) *trans*	*cis*
Acetic acid	6.2 (20°)		87.6	12.4
1-Butanol	17.1 (25°)		91.0	9.0
Ethanol	24.3 (25°)		95.6	5.4
Methanol	32.6 (25°)		96.0	4.0
		H_2O (10%)	96.6	3.4
		H_2O (20%)	100	trace
Nitromethane	35.9 (30°)		96.1	3.9

50 m*l* glass sealed tube, cyclohexene 0.01 mol, $CuCl_2$ 0.01 mol, solvent 30 m*l*, 150°C, 2 hr

position with the reaction time was observed, *e.g.*, in the case of *cis*-2-butene at 120°C. It appears that the results reflect the kinetically controlled product composition.

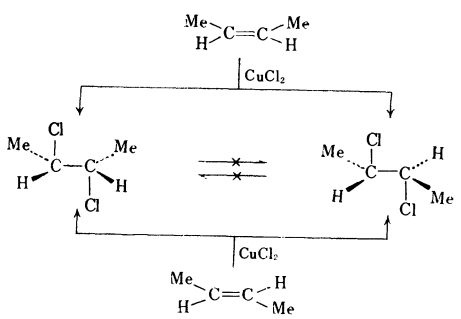

The stereochemistry of chlorination of cyclohexene with cupric chloride was also studied at 150°C (Table 2). The reaction products were mainly dichlorides with small quantities of by-products which were not analyzed. The composition of dichlorides was determined by means of gas chromatography. The results with two different columns (C and D) coincided well with each other (within a variation of 0.5%), proving the identity of *cis*-dichloride. The portion of *cis* compound increases with decrease in polarity of the solvent. In this case also no isomerization occurred between two isomeric dichlorides at 150°C in the presence of cupric chloride, so that the *cis* dichloride must have been formed directly from the starting olefin.

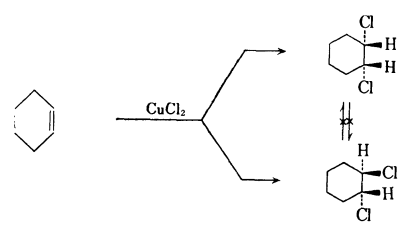

15) N. A. Lange, "Handbook of Chemistry," 10th Ed., McGraw-Hill Book Co., New York, N. Y. (1967), p. 1234.

Discussion

The lack of stereospecificity in the results cannot be ascribed to prior isomerization of the olefin or to secondary isomerization of the product dichlorides, since the olefins and the dichlorides have been shown to be stable under the reaction conditions. The results of the 2-butene chlorination are most reasonably interpreted by an assumption that the intermediate consists of two convertible isomeric species, one being the precursor to the *meso* dichloride and the other to the *dl* compound, the composition of which is the same for both starting *cis*- and *trans*-olefins. This can only be attained by rotation along the central C=C bond of the substrate. Therefore, the intermediate complex resembles an open type cation, in which the rotation is faster than the attack of second chlorine to establish an equilibrium, rather than a bridged chloronium ion. Radical mechanisms are improbable in such polar solvent reactions in the presence of oxygen and in the dark.

There is a tendency that *dl* formation is comparatively favored in less polar solvents, obviously in the hydroxylic series. The reason for the slight discrepancy in acetic acid and nitromethane is not clear, but it is probably due to their somewhat different solvent characters.*1

The chlorine species in the reaction intermediate should not be a free cationic chlorine as is suggested in the addition of a chlorine molecule to simple alkenes[1-3] where a strong chlorine bridging is characteristic. Thus, when chlorine of cupric chloride attacks olefin in an electrophilic manner, a fairly large interaction can be expected between the attacking chlorine and the remaining CuCl group. Then, because of some electron cloud localization on Cl–CuCl bond, polarizability of the chlorine is decreased, which is reflected in almost no bridging interaction to the cationic center and leaves the intermediate open enough for free rotation. However, a faint bridging might still exist in view of the slight preference for *trans* addition, which appears in the slightly larger *meso*/*dl* ratio for *trans*-2-butene than for *cis*-2-butene reaction.

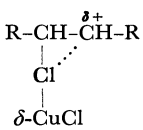

Among six possible relative configurations of the intermediate complexes of free rotation, III and IV are assumed to be the most stable rotamers as the *dl* and the *meso* precursors, respectively, since they are less crowded and suffer less interference between the substituents than the other four. The less polar the solvents, the larger the interaction between Cl and CuCl in attacking $CuCl_2$ should be, due to disadvantage in charge separation. Therefore, in such cases, the bulkiness of the first attacking group increases, so that IV would have a tendency to shift toward III owing to increasing steric repulsion between Cl–CuCl group and methyl group on the adjacent carbon. Thus, the *meso* dichloride formation becomes less favorable in less polar solvents.

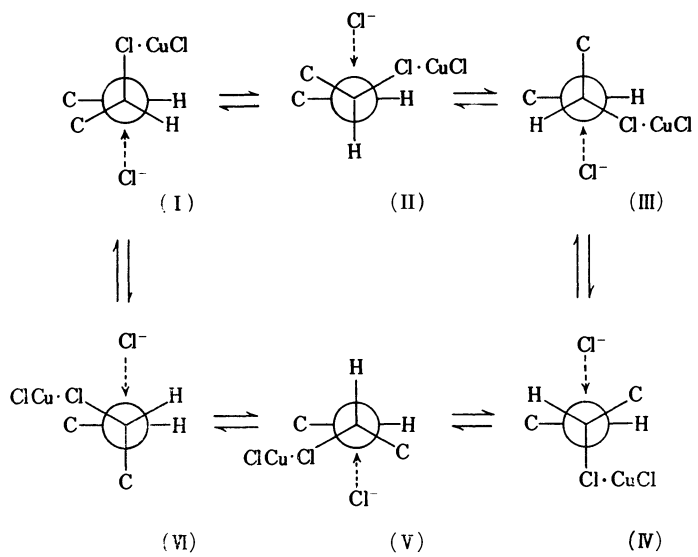

*1 In acetic acid, there is some evidence that it reacts on cupric chloride to form copper(II) acetate by releasing hydrogen chloride.[12] On the other hand, methanolysis of cupric chloride is improbable and no green solid (Cu(OMe)Cl)[16] or blue solid $(Cu(OMe)_2)$[16,17] was detected in the reaction mixture.

16) C. H. Brubaker, Jr., and M. Wicholas, *J. Inorg. Nucl. Chem.*, **27**, 59 (1965).

17) G. Costa, A. Camus and N. Marsich, *ibid.*, **27**, 281 (1965).

The formation of some *cis*-1,2-dichlorocyclohexane from cyclohexene strongly suggests that the intermediate complex is also of an open type. By analogy with photochlorination of chlorocyclohexane,*2 the intermediate may assume an *axial* conformation (VII) rather than an *equatorial* one (VIII). The latter is unfavoravle because

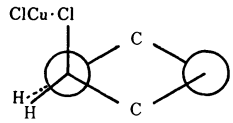

(VII)

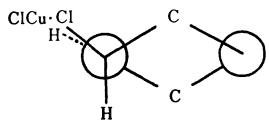

(VIII)

of repulsion between eclipsing Cl–CuCl group and hydrogen. Thus, chloride ion*3 attacks VII preferentially from the *axial* side to yield the *trans* product, since the two incoming chlorine species are farther apart in transition state than in the case of an *equatorial* attack. However, in less polar solvents, increasing tightness of Cl–CuCl bond causes the first attacking group to be more bulky. As a result of greater repulsion between Cl–CuCl group and *axial* hydrogens on the ring, some inversion (or distortion) toward the *equatorial* conformation (VIII) would occur. In VIII, the difference in steric requirements between *axial* attack and *equatorial* attack is not pronounced and *cis* compound would result from the *axial* attack.

Experimental

Materials. *cis*- and *trans*-2-Butenes (pure grade, Takachiho Chemical Industrial Co.) were used. Cyclohexene (Koso Chemical Co.) was distilled under N_2 after drying over Na_2SO_4, which was gas chromatographically pure. Cupric chloride was of anhydrous GR grade (Koso). Methanol (GR, Koso) was distilled from $Mg(OMe)_2$, and acetic acid (GR, Koso) from $B(OAc)_3$[19] under N_2. The other solvents were commercially available purest reagents, distilled prior to use. Authentic *meso*- and *dl*-2,3-dichlorobutanes were synthesized by addition of chlorine to *trans*- and *cis*-2-butenes.[20] *trans*-1,2-Dichlorocyclohexane was prepared by chlorine addition to cyclohexene,[21] and *cis*-dichloride was prepared by chlorination of *trans*-2-chlorocyclohexanol[22] with $SOCl_2$[21].

Analytical Methods. The reaction products were analyzed by gas chromatography with He as a carrier gas. The apparatus, column and temperature were as follows. For dichlorobutanes: (A) Shimadzu GC-2C, dioctyl sebacate (plus sebacic acid) on Chromosorb W, 120°C; (B) Shimadzu GC-4APT, Igepal CO-990 on Diasolid L, 100°C. For dichlorocyclohexanes: (C) the same as B, 180°C; (D) Shimadzu GC-4APT, Ucon -50-HB5100 on Chromosorb P, 160°C. For analysis of 2-butenes: (E) Shimadzu GC-3AH, propylene carbonate plus glutaronitrile on Chromosorb W, room temp.

Reaction of 2-Butenes. In a 500 m*l* glass-lined autoclave (with a glass-coated thermo-well and an agitator made of Ta metal) were placed cupric chloride (6.05 g, 0.045 mol) and solvent (150 m*l*), and after slight evacuation on cooling 2-butene (*ca.* 17 g, 0.30 mol) was introduced from a pressure bottle. The autoclave was heated in an oil bath (+1.0°C) with stirring. After the reaction, the autoclave was cooled to room temperature and the reaction solution was immediately subjected to gas chromatographic analysis. The results were shown in Table 1.

When *cis*-2-butene (containing 0.4% *trans*) was reacted with cupric chloride in methanol at 150°C for 2 hr, the waste gas consisted of 97.1% *cis* and 2.9% *trans*. For *trans*-2-butene (100% *trans*) under the same reaction conditions, the composition of the waste gas was 99.0% *trans* and 1.0% *cis*.

Reaction of Cyclohexene. Cyclohexene (0.82 g, 0.01 mol), cupric chloride (1.34 g, 0.01 mol) and solvent (30 m*l*) were sealed in a 50 m*l* glass tube, which was then placed in a 500 m*l* autoclave. The autoclave was heated at 150°C (±1.0°C) with an oven for 2 hr with shaking (75/min). The reaction solution was taken out and analyzed by gas chromatography. The results are summarized in Table 2.

Stability of Dichlorocyclohexane. *trans*-1,2-Dichlorocyclohexane (1.53 g, 0.01 mol) was treated with cupric chloride (1.34 g, 0.01 mol) in methanol or acetic acid (30 m*l*), being placed in a 50 m*l* glass sealed tube, at 150°C for 2 hr with shaking. No *cis*-1,2-dichlorocyclohexane was detected in the reaction mixture by gas chromatography. Similarly, when a mixture (*cis* 47.1%, *trans* 52.9%) of dichlorides (0.51 g, 3.3 mmol) in methanol (10 m*l*) was heated with cupric chloride (0.45 g, 3.3 mmol) or cuprous chloride (0.33 g, 3.3 mmol) in a 15 m*l* glass sealed tube at 150°C for 8 hr, no fluctuation of the composition of dichlorides was observed.

The author is indebted to Professor Naoki Inamoto for valuable discussions and also to Dr. Shozo Wada for encouragement in this work.

*2 2-Chlorocyclohexyl radicals were discussed in literature.[18] The present intermediate should resemble this radical closely because of its open chain character.

18) G. A. Russell, A. Ito and R. Konaka, *J. Amer. Chem. Soc.*, **85**, 2988 (1963).

*3 From analysis of the kinetic data, the second chlorinating species is very likely chloride ion (unpublished result).

19) L. F. Fieser, "Experiments in Organic Chemistry," 3rd Ed., D. C. Heath Co., Boston (1955), p. 281.

20) H. J. Lucas and C. W. Gould, Jr., *J. Amer. Chem. Soc.*, **63**, 2541 (1941).

21) B. Carroll, D. G. Kubler, H. W. Davis and A. M. Whaley, *ibid.*, **73**, 5382 (1951).

22) M. S. Newman and C. A. VanderWerf, *ibid.*, **67**, 233 (1945).

BULLETIN OF THE CHEMICAL SOCIETY OF JAPAN VOL. 43 3505—3510 (1970)

A Study on the Photochemistry of α,β-Unsaturated γ-Lactones. I. The Structures of the Photodimers of 4-Hydroxycrotonic Acid γ-Lactone*1

Kazuya OHGA and Taku MATSUO

Department of Organic Synthesis, Faculty of Engineering, Kyushu University, Hakozaki, Fukuoka

(Received April 27, 1970)

The structures of the photodimers obtained from 4-hydroxycrotonic acid γ-lactone under several conditions were determined. The products of irradiations in the solution were a pair of *anti* dimers: one is a *head-to-head* cyclo-adduct, and the other a *head-to-tail* adduct. The corresponding product in the solid state, on the other hand, was a *head-to-head* cyclo-adduct in the *syn* form.

Irradiation of 2-cyclopentenone and 2-cyclohexenone has been well known to afford the photodimers only in the *anti* forms.[1] In the case of coumarine, however, a photodimer in the *syn* form was obtained provided that the reaction was carried out in polar solvents.[2] The stereo-specificities of these photo-dimerizations are very important both from theoretical and from practical points of view. In this connection, we studied the photochemical reactions of 4-hydroxycrotonic acid γ-lactone (I), the most simple α,β-unsaturated γ-lactone, in the liquid phase*2 and also in the solid state. Three photodimers with a cyclobutane ring were obtained: two from the liquid phase and one from the solid state irradiations. The molecular structures of these photodimers were determined as described in the present paper.

Results and Discussion

Irradiation of I in polar solvents with a low-pressure mercury lamp yielded white, crystalline materials (yields calculated as the dimers, 20—30%). The solid material was later confirmed to consist of two components, Ia and Ib. At first, Ia was separated by recrystallizations. Several chemical treatments on the remaining fraction eventually yielded Ib″, which was identified with Ib as described in the experimental section. Irradiation of I in the solid state at low temperature (−78°C) with the same low-pressure mercury lamp yielded Ic (yield calculated as the dimer, 26%). The molecular weights, the results of elementary analyses, and the characteristic IR absorption bands indicate that Ia, Ib″(Ib), and Ic are isomeric dimers of I as shown in Table 1.

On the basis of the results of treating Ia, Ib″ and Ic with alkaline and then with acidic reagents, each of the above isomeric dimers is suggested to possess a lactone ring in the molecular structure. The NMR spectra also are in agreement with the proposed structure with a cyclobutane ring for each isomer as shown in Fig. 1. All of the conceivable structures of the dimers are listed in Fig. 2.

In order to distinguish the above stereo-isomers, the isolated products were oxidized at first. Ia was oxidized with potassium permanganate in acidic media, and then esterified with diazomethane. The product (overall yield, 54%) was identified with the authentic sample of 1,2,3,4-*cis, trans, cis*-tetramethoxycarbonyl cyclobutane (abbreviated to *cis, trans, cis*-TMCCB, hereafter), as prepared according to the method of Griffin *et al.*[3] by the NMR and IR spectra and the mixed melting-point measurements. *cis, trans, cis*-TMCCB was also obtained (yield, 69%) by the esterification of the oxidation products of Ib′, which was a dimer of 4-hydroxycrotonic acid obtained by the

*1 Contribution No. 207 from the Department of Organic Synthesis, Faculty of Engineering, Kyushu University.

*2 Photodimerization of the same compound was reported also by Odaira and his associates at the Discussion Meeting on the Photochemistry (Tokyo, November, 1967), where the present authors partially presented their results reported here.

1) P. J. Wagner and D. J. Bucheck, *J. Amer. Chem. Soc.*, **91**, 5090 (1969); J. L. Ruhlen and P. A. Leermakers, *ibid.*, **89**, 4944 (1967); *ibid.*, **88**, 5671 (1969); P. E. Eaton and W. S. Hurt, *ibid.*, **88**, 5038 (1966); P. E. Eaton, *ibid.*, **84**, 2344 (1962); *ibid.*, **84**, 2454 (1962); E. Y. Y. Lam, D. Valentine and G. S. Hammond, *ibid.*, **89**, 3482 (1967); D. Valentine, N. J. Turro, Jr., and G. S. Hammond, *ibid.*, **86**, 5202 (1964).

2) H. Morrison and R. Hoffmann, *Chem. Commun.*, **1968**, 1453; H. Morrison, H. Curtis and T. McDowell, *J. Amer. Chem. Soc.*, **88**, 5415 (1966); C. H. Kranch, S. Farid and G. O. Schenck, *Chem. Ber.*, **99**, 625 (1966).

3) G. W. Griffin, A. F. Vellturo and K. Furukawa, *J. Amer. Chem. Soc.*, **83**, 2725 (1961).

Table 1. Characteristics of photodimers

Isomer	Molecular* weight	Elementary analyses† C%	H%	Characteristic ν(C=O)	IR Bands ν(C-O-C)
Ia	168	56.93	4.77	1760	1168 cm^{-1}
Ib''(Ib)	168	57.20	4.86	1775	1160
Ic	168	57.11	5.02	1780	1174

* Obtained from *m/e* value for the parent peak of the mass spectra.
† Calculated values for $C_8H_8O_4$: C, 57.14; H, 4.80%.

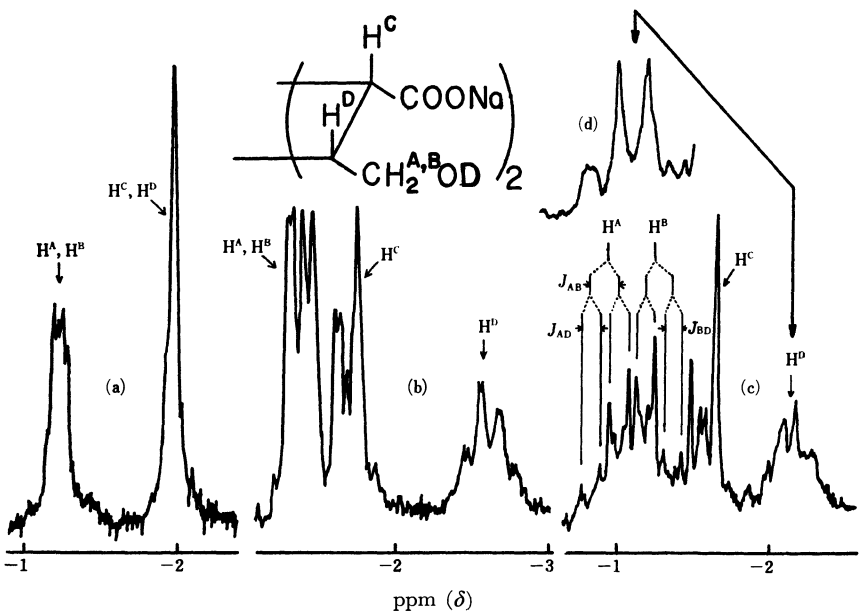

Fig. 1. NMR spectra of photodimers in 4 N NaOD/D_2O solution.
(a): Ia, (b): Ib'', (c): Ic (ν_{AB}=18, J_{AB}=11, J_{AD}=8, and J_{BD}=7 Hz), and (d): the methylene proton signals of Ic when H^D protons were decoupled (difference frequency, +65 Hz). The chemical shifts were measured from the internal H_2O signal.

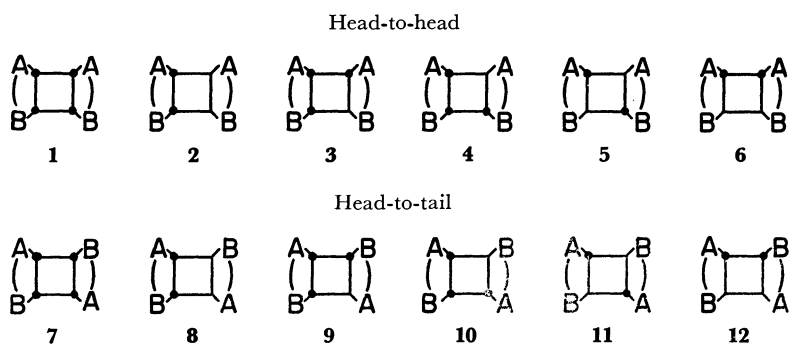

Fig. 2. Conceivable geometrical isomers of the photodimers.
The symbols A and B stand for C=O and CH_2O groups, respectively.

hydrolysis of Ib as described in the experimental section. As to TMCCB, it has been established that the most stable isomer is the one with the four methoxycarbonyl groups in all *trans* form.[3] Among the twelve isomers in Fig. 2, the isomers 5 and 11 are surely expected then to give *trans, trans*-TMCCB. Four other isomers (**3**, **4**, **9** and **10**) will end up with either *cis, cis, trans*- or *trans, trans, trans*-TMCCB. Thus, the experimental results of oxidations are taken to indicate that neither Ia nor Ib could be one of the above six stereo-isomers (**3**, **4**, **5**, **9**, **10** and **11**). Since the

yield of *cis, trans, cis*-TMCCB is fairly high, the isomers **1** and **7** should be also eliminated from the list of the possible isomers.

At this point, one should notice that among the remaining four isomers (**2, 6, 8** and **12**), the isomer **2** alone does not have any symmetry element. In other words, one can expect that the isomer **2** exists as a racemate. This expectation was verified by resolving Ib′ into a pair of optically active isomers as described in the experimental section. The optical activities still remained even after the lactone ring was formed again (Fig. 3). Therefore, Ib (Ib″) is uniquely assigned to a racemate corresponding to the structure **2** in Fig. 2.

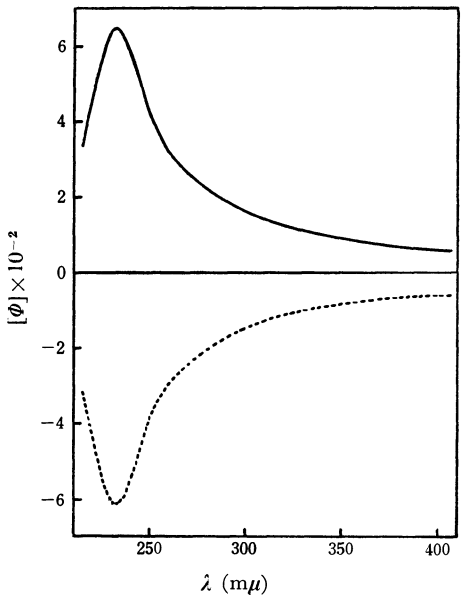

Fig. 3. ORD curves of Ib″(Ib) in acetonitrile at 24°C. The solid line represents (+)-enantiomer, and dotted line represents (−)-enantiomer.

For the rest, the isomers **6** and **12** are *trans* adducts, where the presence of extremely high steric strain is expected of the *trans*-fused lactone ring. Once such highly-strained lactone ring is opened, it will be quite difficult to be restored. Since **Ia** can be recovered from the alkaline solution, however, more easily than Ib, Ia can not be one of those *trans* adducts. Consequently, Ia may be assigned to the remaining *anti* dimer as represented by the structure **8** in Fig. 2.

On the other hand, Ic was converted into *cis, cis, cis*-TMCCB by the oxidation followed by the esterification (yield, 10%). From thermodynamicals points of view, *cis, cis, cis*-TMCCB is the most unstable among the stereo-isomers under discussion. Hence, Ic is suggested to be one of the two *syn* dimers (**1** and **7**) in Fig. 2, which will afford *cis, cis, cis*-TMCCB without any epimerization.

The structure of Ic may be further elucidated by the investigation of the NMR spectra. The methylene proton signals of Ic are much more complicated than those of Ia and Ib (Fig. 1). Then, the geminal protons of the methylene group in Ic are suspected to be in magnetically non-equivalent environments. In agreement with this suggestion, the methylene proton signals of Ic appear as a pattern close to AB type when H^A and H^B protons are decoupled from H^D (Fig. 1). The NMR parameters (J_{AB}=11 Hz. ν_{AB}=18 Hz), thus obtained, are successfully applied to analyze the original signals of the methylene protons of Ic. In the case of the isomer **1** in Fig. 2, the geminal protons are certainly in magnetically non-equivalent environments. This is not true in the case of the isomer **7**, however, because there is a plane of symmetry which contains the carbon atom of the methylene group under consideration. Therefore, Ic is assigned to the isomer **1** in conclusion.

In short, the photodimerization of I in solution was found to afford a pair of *anti* dimers. One of them was a *head-to-tail* dimer (Ia), and the other was a *head-to-head* dimer (Ib). The scheme for the chemical separation and the structures of the dimers, thus determined, are summarized in Fig. 4. Because of the extremely low solubilities of the photodimers, the IR spectra could not be used in order to determine the isomer ratio. On the same reason, it could not be possible either to convert the dimers into more soluble derivatives suited to quantitative analysis. Then, the NMR spectra obtained in NaOD solutions were used to estimate the relative yield of the isomers. Even in this case, however, accurate data could not be obtained either because the signals of the two isomers overlapped each other. On the basis of the NMR spectra, anyhow, the relative yield of Ia was approximately the same as that of Ib, when the aqueous solution of I (0.2 M) was irradiated with a low-pressure mercury lamp. The relative yield of Ia with respect to Ib increased as the solvent was changed from water to acetonitrile and then to acetic acid.

The effect of internal irradiations with a high-pressure mercury lamp was also investigated. The same photodimers as above were obtained from the benzene or formic acid solutions of 4-hydroxycrotonic acid γ-lactone, provided that acetone was present in the solution. The relative yield of Ib with respect to Ia was higher in formic acid than that in benzene. Since the water jacket surrounding the lamp was made of pyrex glass, the most of the light should have been absorbed by acetone in these cases. In other words, the dimerization of I could be sensitized by acetone.

Although more quantitative data are required to clarify the mechanistic details of the present

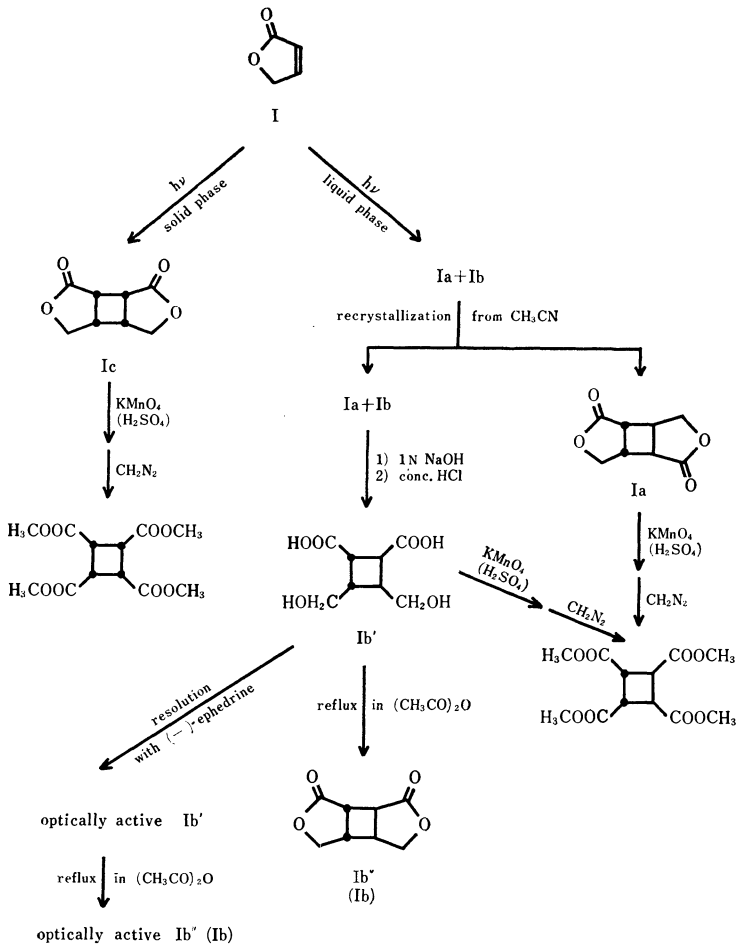

Fig. 4. The scheme for the chemical separation and the structure determination of the photodimers.

reaction, one may conclude now that at least a part of the reaction proceed *via* a triplet state. It is not clear, however, whether the photodimerization induced by the direct excitation of 4-hydroxycrotonic acid γ-lactone also proceeds *via* a triplet state or not. In any case, it should be noticed that the products of the present reactions are *anti* dimers just as in the cases of 2-cyclopentenone and 2-cyclohexenone. The solvent dependence of the isomer ratio is also interesting enough to be investigated. The investigation of this kind, however, should be waited until some reliable means for quantitative analysis are established in future.

Irradiation of I in the solid state with the low-pressure mercury lamp, on the other hand, yielded a *head-to-head, syn* dimer (Ic). The structure of the molecular crystal may be responsible for the unique mode of dimerization.

Experimental

Instrumental Analysis. The IR spectra were obtained with KBr disk on a JASCO Model DS-301 IR spectrophotometer. The NMR spectra were measured with a Varian Model A-60 analytical NMR spectrometer combined with a Varian Model V-5068A spin decoupler. The photodimers were dissolved in 4N deuterated alkali metal hydroxide solutions and the water signal was used as the internal standard. 1,2,3,4-Tetramethoxycarbonylcyclobutanes were measured as the deuteriochloroform solution with tetramethylsilane as the internal standard. The mass spectrum of Ia was recorded on a Hitachi Model RMU mass spectrometer, and the rest on a JEOL Model JMS-01SG spectrometer. The optical rotatory dispersion curves were measured with a JASCO Model ORD/UV-5 optical rotatory dispersion recorder by the use of a 1 dm cell. The melting points were measured on a Yanagimoto micro melting-point measurement apparatus and are uncorrected.

Preparation of 4-Hydroxycrotonic Acid γ-Lactone (I). The preparation of I was carried out, according to the method of a literature,[4] through hydrolysis of glycerol-α-cyanohydrin and purification with

4) J. W. E. Glattfeld, G. Leavell G. E. Spieth and D. Hutton, *ibid.*, **53**, 3164 (1931).

aqueous silver nitrate solution, followed by distillation under reduced pressure (bp 90.0°C/13 mmHg). The distillate showed a single peak on inspection by the gas chromatography (25% Silicon DC200 on Shimalite, 2.25 m×3 mm). The NMR spectra were also in good agreement with that reported by Freeman.[5] UV absorptions: ε, 8.0×10^3 (at 206 mμ, the absorption maximum), 1.6×10^1 (at 254 mμ) in water; ε, 3.4×10^3 (at 216 mμ), 2.5×10^1 (at 254 mμ) in *n*-hexane.

Irradiation of the Solution with a Low-Pressure Mercury Lamp. In the experiments with various solvent such as acetic acid, acetonitrile, and water, the solution (0.2—0.6 M) was internally irradiated with a 30 W low-pressure mercury lamp (Riko-Sha UVL 303 Q) equipped with a quartz jacket. The reactions were carried out at temperatures between 20 and 30°C in nitrogen atmosphere. White crystals had separated out of the solution during the irradiation which continued for the period of 20—30 hr.

Irradiation of the Solution with a High-Pressure Mercury Lamp. Either benzene solution (0.6 M) or formic acid solution (0.4 M) of I was internally irradiated with a high-pressure mercury lamp (Riko-Sha UVL-700P) equipped with a pyrex water-jacket for the period between 40 and 50 hours at 20°C. Acetone was added as the sensitizer: 0.7 M for the benzene solution and 0.1 M for the formic acid solution, respectively.

Irradiation of I in the Solid State. The reaction vessel containing neat liquid of I was held so that one side could be dipped into a dry ice-methanol mixture. The vessel was rotated slowly. After a short period of time, the wall was coated with a thin film of I. Then the vessel was held in the dry ice-methanol mixture, and was internally irradiated with the above-mentioned low-pressure mercury lamp under nitrogen flow.

Isolation of the Isomers. After the irradiation of the solution, the solvent and the raw material were removed by distillation under reduced pressure to leave white crystalline materials. Recrystallization of the crystalline materials from acetonitrile afforded pure samples of Ia (mp 292—293°C). The filtrate was dissolved into 1 N sodium hydroxide solution, and the pH of the solution was adjusted with concentrated hydrochloric acid to a value between 2 and 4. At this point, Ib′ separated out as white crystals. The presence of both hydroxyl and carbonyl groups was indicated by the IR spectra (KBr disk, 3360 (broad); 3260; 3100—2400 (broad); 1722 and 1700 cm^{-1}). Since the same treatments on Ia could only reproduce Ia, the origin of Ib′ must be a compound Ib but not Ia. Ib′ was quantitatively converted into a lactone Ib″ (mp 280—281°C, as recrystallized from acetonitrile) by refluxing the acetic anhydride solution for 3 hr. Ib′ was also converted into Ib″ during the measurement of the melting point. On the basis of the above behaviors, Ib′ was suggested to be a dimer of 4-hydroxycrotonic acid obtained by the hydrolysis of Ib. In agreement with this suggestion, the mass spectra of Ib′ showed a peak (m/e= 168) which corresponded to a fragmention formed on the release of two water molecules from the molecular ion. Furthermore, Ib′ was resolved into a pair of optically active isomers as described later. The results of elementary analyses of the isomers were also in good agreement with the values calculated from the dimer of 4-hydroxycrotonic acid.

On the treatment with alkaline and then with acid solutions, Ib″ afforded Ib′. Hence Ib″ was identified with Ib, the counterpart of Ia in the original mixture. This suggestion was verified by comparing the IR, far IR, and NMR spectra of the concerning materials.

Ic was easily separated from I, after the irradiation, by the same procedure as described in the cases of the irradiation of the solution. The obtained solid material was purified by recrystallization from acetone (mp 235—236°C). Ic was recovered again when the sample was dissolved into sodium hydroxide solution, and then acidified with hydrochloric acid.

Oxidation and Esterification of Ia. Ia (168 mg) was suspended in 15 m*l* of 0.7 N sulfuric acid, and aqueous solution (20 m*l*) of potassium permanganate (520 mg) was added dropwise into it under vigorous stirring. The reaction temperature was kept to 60°C by the use of a water bath. After 2 hr, sodium hydrogensulfite was added to the solution, and then 2 N sodium hydroxide solution was added until the solution became basic to litmus. The solution was acidified with concentrated hydrochloric acid. The acidic solution was evaporated to dryness and the residue was extracted with 100 m*l* of dry acetone by the use of a Soxlet extractor. Diazomethane in ether was added to the extracts dissolved in methanol at 0°C. The solution was evaporated to dryness. The residue was purified by the column chromatography on a silica gel column with benzene-ethyl acetate (20 : 1) as the eluting solvent, and then recrystallized from benzene. Yield, 154 mg (54%); mp 149.0—150.5°C; Found: C, 50.08; H, 5.64%. Calcd for $C_{12}H_{16}O_8$: C, 50.00; H, 5.60%. The product was identified with *cis*, *trans*, *cis*-TMCCB by means of the mixed melting point measurements and comparison of the NMR and IR spectra with those of the authentic sample, prepared by the method of Griffin *et al.*[3]

Oxidation and Essterification of Ib′. Ib′ (77 mg) was oxidized at 70°C by the similar procedure applied to Ia (1.6 N sulfuric acid, 240 mg $KMnO_4$/5 m*l* H_2O). After the reaction was completed, methanol was added to the solution, which was succeedingly made basic to litmus with 2 N sodium hydroxide solution. Manganese dioxide was filtered off and the filtrate was acidified with concentrated hydrochloric acid, and thne evaporated to dryness. The residue was extracted, treated with diazomethane as described in the case of Ia. The product was also purified as above, and was identified with *cis*, *trans*, *cis*-TMCCB. Yield, 77 mg (69%); mp 148—150°C; Found: C, 50.07; H, 5.66%. Calcd for $C_{12}H_{16}O_8$: C, 50.00; H, 5.60%.

Oxidation and Esterification of Ic. Ic (163 mg) was oxidized and esterified by the same procedure as applied to Ia. The product was purified by the column chromatography on a silica gel column with ethyl acetate as the eluting solvent and then recrystallized from methanol. Yield, 29 mg (10%); mp 222—223°C; Found: C, 49.97; H, 5.57%. Calcd for $C_{12}H_{16}O_8$: C, 50.00; H, 5.60%. The IR spectra (KBr) presented the same characteristic absorption bands as those of *cis*, *cis*, *cis*-TMCCB[6] at 2990 (m), 2940 (m), 2845 (w),

5) R. Freeman *Mol. Phys.*, **5**, 499 (1962).

6) M. Avram, I. G. Dinulescu, E. Marica, G. Mateescu, E. Slaim and C. D. Nenitzescu, *Chem. Ber.*, **97**, 382 (1964); G. W. Griffin and D. Veber, *J. Amer. Chem. Soc.*, **82**, 6417 (1960).

1743 (vs), 1452 (m), 1437 (m), 1350 (s), 1220 (s), 1195 (vs), 1175 (vs), 1115 (m), 1072 (m), 955 (m), 830 (m), 770 (m) cm^{-1} (w: weak, m: medium, s: strong, vs: very strong). The NMR spectrum ($CDCl_3$ solution) consisted of two singlet peaks at 3.64 and 3.73 ppm (the ratio of the area under the peak, 1 : 3). The mass spectrum gave the base peak at *m/e* 257, which corresponds to the loss of a methoxyl group from the molecular ion. On the basis of these data, the product is identfied with *cis, cis, cis*-TMCCB.

Resolution of Ib′. Ib′ (342 mg) was dissolved into 30 m*l* of methanol containing 508 mg of (−)-ephedrine. The solution was concentrated to 2 m*l* and then 15 m*l* of acetonitrile was added to it. After the solution was allowed to stand overnight, the salt crystallized out (334 mg, mp 130—136°C). Recrystallization was repeated twice by the similar procedure (yield, 193 mg; mp 134.5—135.5°C). The purified salt was decomposed with dilute hydrochloric acid. The separated white needles were filtered off and washed with water and methanol. Yield, 68 mg; Found: C, 46.40; H, 6.14%. Calcd for $C_8H_{12}O_6$: C, 47.06; H, 5.92%. The characteristic IR absorption bands (KBr disk) were found at 3400 (broad), 3320, 3100—2400 (broad), 1715 and 1693 cm^{-1}. This compound, (+)-Ib′, exhibited a positive Cotton effect curve in 0.2 N sodium hydroxide solution (C, 0.600) at 24°C: $[\Phi]_{690}$ +20°, $[\Phi]_{589}$ +28°, $[\Phi]_{235}$ +311° (infl.), $[\Phi]_{218}$ +492°. The filtrate, which contained the fraction of more soluble ephedrine salt of Ib′, was treated with dilute hydrochloric acid as above. The isolated acid was purified by the treatment with aqueous sodium hydroxide solution and then with concentrated hydrochloric acid. Yield, 59 mg. Found: C, 46.62; H, 6.13%. Calcd for $C_8H_{12}O_6$: C, 47.06; H, 5.92%. The IR spectrum was similar to that of (+)-Ib′. This compound, (−)-Ib′, exhibited a negative Cotton effect curve in 0.2 N sodium hydroxide (C, 0.695) at 24°C: $[\Phi]_{690}$ −23°, $[\Phi]_{589}$ −32°, $[\Phi]_{235}$ −327° (infl.), $[\Phi]_{218}$ −522°.

Preparation of Optically Active Ib. Dehydration of (+)-Ib′ with acetic anhydride gave optically active Ib which exhibited a negative Cotton effect curve in acetonitrile. Repeated recrystallization from acetonitrile afforded a pure sample (mp 288—289°C). In the same way, (−)-Ib′ was dehydrated to give the other enantiomer which exhibited a positive Cotton effect curve in acetonitrile (mp 290.0—290.5°C). These enantiomers showed characteristic IR absorption bands at 1778, 1755, 1179 and 1160 cm^{-1}. The ORD curves of the same compounds (Fig. 3) in acetonitrile at 24°C are as the following: (a) the (+)-enantiomer (C, 0.250): $[\Phi]_{690}$ +20°, $[\Phi]_{589}$ +23°, $[\Phi]_{232}$ +646° (peak), $[\Phi]_{214}$ +332°, and (b) the (−)-enantiomer (C, 0.642): $[\Phi]_{690}$ −19°, $[\Phi]_{589}$ −22°, $[\Phi]_{232}$ −614° (trough), $[\Phi]_{214}$ −317°.

The authors are grateful to Dr. H. Kobayashi and Mr. H. Saito at the Department of Organic Synthesis of Kyushu University, for their helpful suggestions in the resolution of the optical isomers. Thanks are also due to Dr. I. Aiga and T. Matsui. at the Biotron Institute of the same university, and Miss. Y. Inatsu at the Faculty of Medicine, for their helps in the measurements of ORD and mass spectra, respectively. The authors are also indebted to Hitachi Manufacturing Co., Ltd., and Japan Electron Optics Laboratory Co., Ltd. for the measurements of mass spectra.

BULLETIN OF THE CHEMICAL SOCIETY OF JAPAN VOL. 43 3511—3514 (1970)

Synthesis of Poly-malonylpolymethylenes*1

Kiyotada MATSUI, Sadaichi MUROTANI,*2 Tetsuro NOJIRI and Masatoshi MOTOI

Department of Industrial Chemistry, Faculty of Technology, Kanazawa University, Kodatsuno, Kanazawa

(Received May 4, 1970)

Treatment of acetic anhydride with aliphatic dibasic acid chloride in the presence of 3 equivalents of aluminum chloride in nitrobenzene at 50°C afforded a polymer with the structure assigned to poly-malonylpolymethylene, R–[$(CH_2)_m$–$COCH_2CO]_n$–$(CH_2)_m$–R, (R=–COOH and/or $-COCH_3$, n=8—16). Polymalonyl-heptamethylene, -hexamethylene and -pentamethylene were prepared and their properties were recorded. The product obtained by the reaction of acetic anhydride with adipoyl chloride seems to have a few cross-linkings in its structure.

In a previous report[1] it was suggested that polymalonylphenylene could be synthesized by the reaction of ethyl acetoacetate with terephthaloyl chloride in the presence of aluminum chloride according to the following reaction:

$$CH_3COCH_2COOC_2H_5 + C_6H_5COCl \xrightarrow[-CH_3COCl,\ -CO_2,\ -C_2H_5Cl]{AlCl_3} (C_6H_5CO)_2CH_2$$

However, a polymer was obtained which might be considered to be an aluminum chelate polymer consisting of phenylene and malonyl groups, some of which have a carbethoxy group. The polymer insoluble in ordinary organic solvents could not be freed from aluminum, and therefore was supposed to have three-dimensional structure containing some methine carbon atoms as in tribenzoylmethane, a minor product in the above reaction.

This paper deals with the synthesis of polymalonylpolymethylene with a linear structure. In order to exclude reactions favorable for cross-linking formation as much as possible, several comparative and preliminary experiments using azelaoyl chloride in the presence of aluminum chloride were carried out with ethyl acetoacetate, acetyl chloride or acetic anhydride. The product was separated into a benzene-soluble and a benzene-insoluble fraction, from which an acetone-insoluble substance (if present) was removed, then the molecular weights of the fractions were determined. The reaction conditions and results are summarized in Table 1.

Treatment of ethyl acetoacetate with an equimolar quantity of azelaoyl chloride in the presence of aluminum chloride in nitrobenzene gave only a benzene-soluble product of low molecular weight at 50°C. Use of acetyl chloride in place of ethyl acetoacetate afforded a benzene-insoluble product contaminated with an acetone-insoluble substance, which increased with incease of acetyl chloride. In the case of acetic anhydride the benzene-insoluble product of relatively high molecular weight, obtained in a slightly lower yield, increased slightly with the increase of aluminum chloride. When the amount of azelaoyl chloride increased from 0.2 to 1 molar excess, an acetone-insoluble substance was formed and obtained as a single product in a high yield. The acetone-insoluble substance, from which aluminum could not be removed by the usual procedure, seems to have a three-dimensional structure owing to the acylation caused by the excess of acid chloride. For preparation of the required linear polymer, use of acetic anhydride is found to be most suitable.

Other than polymalonylheptamethylene, polymalonyl-hexamethylene and -pentamethylene were also prepared in a similar manner from acetic anhydride using suberoyl and pimeloyl chloride, respectively. Treatment with adipoyl chloride gave a benzene-insoluble product containing a small amount of an acetone-insoluble substance. The details and properties of the polymers are given in Table 2.

From the fact that dibenzoylmethane is obtained by the reaction[2] of acetic anhydride or acetyl chloride with benzoyl chloride under a similar reaction condition, it seems that the polymer consists of malonyl and polymethylene groups. This is also supported by the formation of either its alkali salt insoluble in water only in the case of a polymer of higher molecular weight, or its copper complex (*e.g.*, copper content of the polymalonyl-

*1 Presented at the 22nd Annual Meeting of the Chemical Society of Japan, Tokyo, April, 1969.

*2 Present address: Idemitsu Petrochemical Co., Tokuyama, Yamaguchi.

1) K. Matsui, M. Motoi, T. Nojiri and K. Wakabayashi, This Bulletin, **41**, 1151 (1968).

2) T. Nojiri, H. Kataoka, O. Murata, T. Murai and K. Matsui presented at the 16th Annual Meeting of the Chemical Society of Japan, Tokyo, April, 1963.

Table 1. Reactions of ethyl acetoacetate, acetyl chloride, and acetic anhydride with azelaoyl chloride

Reactant: $ClOC(CH_2)_7COCl$ 2.3 g (0.01 mol), a) 2.7 g (0.012 mol); b) 4.5 g (0.02 mol)
Solvent: Nitrobenzene 10 ml
Reaction temp: 50°C, c) 45°C

Substrate		$AlCl_3$ mole ratio	Reaction time day	Yield and mol. weight			
				BS g	MW	BI g	MW
$CH_3COCH_2COOC_2H_5$	1.3 g (0.01 mol)	4.0 3	6	2.20	640		
CH_3COCl	0.8 g (0.01 mol)	2.7 2	2[c]	0.62	450	1.04	1000
	1.6 g (0.02 mol)	2.7 2	6[c]	0.67	540	1.35*1	2300
		4.0 3	6	0.77	610	1.36*1	2000
$(CH_3CO)_2O$	1.0 g (0.01 mol)	1.3 1	6	1.15	500	0.28	910
		2.7 2	2	1.98	700	—	
		2.7 2	5	1.64	800	0.36	3000
		4.0 3	6	1.16	600	0.68	2060
		a) 2.7 2	6	1.06	770	1.10*1	2100
		b) 2.7 2	6	—		2.3*2	

BS: Benzene-soluble polymalonylheptamethylene
BI: Benzene-insoluble polymalonylheptamethylene
MW: Molecular weight
*1 This fraction was contaminated with an acetone-insoluble substance. The molecular weight was determined after removal of the contaminant.
*2 An acetone-insoluble substance

Table 2. Reaction of acetic anhydride with dibasic acid chlorides

Substrate: $(CH_3CO)_2O$ 1.0 g (0.01 mol)
Condensing agent: $AlCl_3$ 4.0 g (0.03 mol)
Solvent: Nitrobenzene 10 ml
Reaction temp: 50°C
Reaction time: 6 days

Reactant (0.01 mol) $ClOC(CH_2)_mCOCl$		Yield, mol weight and property			
m	g	g	MW	State	Softening temp. °C
7	2.3	BS 1.16	600	brown paste	oily at 40
		BI 0.68	2060	brown flex. solid	50
6	2.2	BS 1.35	550	brown paste	oily at 40
		BI 0.29	1460	brown flex. solid	50
5	2.0	BS 1.03	450	brown paste	oily at 40
		BI 0.12	1450	dark brown rigid solid	80
4	1.9	BS 0.42	350	dark brown paste	oily at 40
		BI 0.13*	900	dark brown rigid solid	120

BS: Benzene-soluble polymer
BI: Benzene-insoluble polymer
MW: Molecular weight
* This fraction was contaminated with an acetone-insoluble substance. The molecular weight was determined after removal of the contaminant.

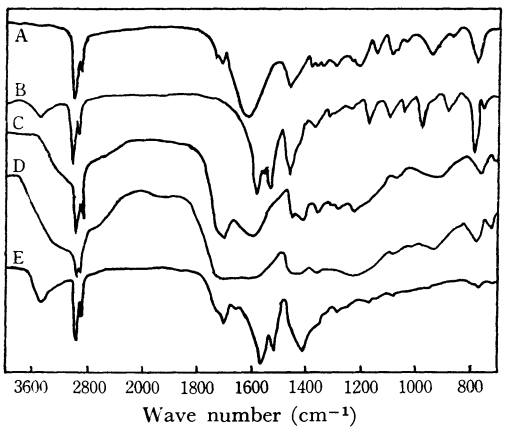

Fig. 1. Infrared spectrum of di-*n*-butyrylmethane (NaCl plate)(A); its copper chelate(KBr disk)(B); benzene-soluble polymalonylheptamethylene (NaCl plate)(C); benzene-insoluble polymalonylheptamethylene(NaCl plate)(D); and its copper chelate(KBr disk)(E).

heptamethylene complex was 11—15%; calculated for $Cu(C_8H_{15}C_2O_2)_2$: about 16%).

General aspects of the IR spectra of the benzene-soluble and -insoluble polymalonylheptamethylene resemble each other, except that absorptions at 1728 (sh), 1710 (m) and 1613 (br) cm^{-1} for the former are replaced by a broad band in the region 1742—1548 cm^{-1} for the latter. The spectrum of the former corresponds to that of di-*n*-butyrylmethane which exhibits absorptions at 1730 (w), 1708 (w) and 1616 (br) cm^{-1}. However, the spectrum of each polymer differs from that of di-*n*-butyrylmethane in having a broad band in 3500—3100 cm^{-1} region due to a hydroxy and a carboxyl group. The spectrum of the copper chelate of the benzene-insoluble polymer, though having the same absorption peaks at 1573 and 1522 cm^{-1} as those for the copper chelate of di-*n*-butyrylmethane, shows two additional absorptions. One is observed at 1710 cm^{-1}, which seems to be due to a carbonyl group not complexed with copper and to acetyl end group from the decarboxylation of *β*-ketonic acid group, and the other is a broad band centered at 3440 cm^{-1} attributed to hydroxy group, without an absorption due to carboxyl group. The NMR spectrum of the benzene-insoluble polymalonylheptamethylene shows two broad singlets at 6.40 τ ($COCH_2CO$), and 4.53 τ (vinyl proton on COCH=C(OH)), a sharp singlet at 7.95 τ ($COCH_3$ as end group). A similar spectral evidence was also observed generally from the IR and NMR spectra of the other polymers. On being burnt, all acetone-soluble polymers give ash, which is considered to be alumina derived from a small amount of the condensing agent (*e.g.*, less than 0.5% in the case of the benzene-insoluble polymalonylheptamethylene). However, no NMR signals were observed due to a methine group. Thus, the structure of the benzene-insoluble polymer can be assigned to poly-malonylpolymethylene:

$$R\text{-}[\text{-}(CH_2)_m\text{-}COCH_2CO\text{-}]_n\text{-}(CH_2)_m\text{-}R$$

$R = -COOH$ and/or $-COCH_3$; $m = 5, 6, 7$; $n = 8-16$.

In the case of a polymer from adipoyl chloride which becomes easily dark brown in the presence of aluminum chloride, a small singlet at 7.14 τ attributed to a methine group appears even after removal of the acetone-insoluble substance. This suggests the presence of a few cross-linkings.

Experimental

Materials. Ethyl acetoacetate, acetyl chloride and acetic anhydride, commercial materials, were distilled and each stored in an ampul. Their bp were 75—77°C/15 mmHg, 52°C and 139°C, respectively. Commercial dibasic acids, azelaic, suberic and adipic acid, were converted into methyl esters, which were rectified *in vacuo* to give their glc charts showing sufficient purities, and were hydrolyzed to the original dibasic acids. Pimelic acid was prepared according to literature[3] and purified similarly. Acid chlorides of these acids were prepared by a modification of the methods in literature,[4] then rectified twice and stored separately in an ampul, bp 125—126°C/5 mmHg for azelaoyl chloride, by 126—127°C/6 mmHg suberoyl chloride, bp 106—107°C/4 mmHg pimeloyl chloride and bp 103—105°C/7 mmHg adipoyl chloride. Di-*n*-butyrylmethane was prepared according to literature,[5] bp 82—84°C/11 mmHg.

Measurements. The melting and softening points were determined on a Yanagimoto micro-melting point apparatus model MP-S 1 and uncorrected. The molecular weight was determined with a Hitachi model-115 vapor pressure osmometer in a 0.10—0.15/25 m*l* acetone solution at 35°C. The IR spectra (KBr for copper chelates, NaCl plate for polymers) were obtained on a Nihon Bunko model DS-301 infra-red spectrometer. The NMR spectra were measured on a Nihon Denshi-JEOL model C-60 H spectrometer operating at 60 MHz in 10—20 wt/vol% deuteriochloroform solutions with tetramethylsilane as internal standard.

Procedure. To a cold solution of aluminum chloride and substrate in dry nitrobenzene, which was placed a 50 m*l* flask equipped with a calcium chloride tube, dibasic acid chloride was added, and the mixture was kept in a thermostat at 50°C. The reddish brown gelatinous reaction mixture was stirred into a mixture of hydrochloric acid and crushed ice and then allowed to stand for 0.5 hr. The mixture was shaken with chloroform on a mechanical shaker for 1 hr. The

3) J. M. Straley and A. C. Adams, "Organic Syntheses," Coll. Vol. II, p. 531 (1963).

4) C. H. Gerhart and L. Chiozza, *Ann. Chem.*, **87**, 293, (1853); D. Vorländer, *ibid.*, **280**, 183 (1884).

5) G. T. Morgan and R. W. Thomason, *J. Chem. Soc.*, **125**, 754 (1924).

organic layer separated was washed repeatedly by shaking with fresh 6 N hydrochloric acid for 15 min until the aqueous layer gave no detectable amount of aluminum compound, then was steam-distilled *in vacuo* to remove organic solvent. The residue dissolved in a small amount of chloroform was washed repeatedly with warm water to remove the dibasic acid and then was shaken with hot benzene to separate into a benzene-soluble and a benzene-insoluble fraction. The former, after partial evaporation, afforded an oil on addition of petroleum ether. From the latter an acetone-insoluble substance (if present) was separated by treatment with acetone followed by filtration. Evaporation of the filtrate gave an oil. Each oil obtained was dried *in vacuo* to a constant weight at 50°C.

The present authors wish to express their thanks to Prof. Katsumasa Kaneko and Assistant Prof. Shin-ichiro Ishida of this Faculty for their help in molecular weight measurements and to Mr. Yoshitaka Itatani of the Faculty of Pharmacy, Kanazawa University carrying out NMR measurements.

BULLETIN OF THE CHEMICAL SOCIETY OF JAPAN VOL. 43 3514—3521 (1970)

Studies of Acenaphthene Derivatives. XX.[1] The Reactions of Benzylideneacenaphthenones with Sulfonium Ylides

Otohiko Tsuge and Ichiro Shinkai

Research Institute of Industrial Science, Kyushu University Hakozaki, Fukuoka

(Received May 9, 1970)

The reactions of benzylideneacenaphthenones with sulfonium ylides were studied extensively. Although the reactions of benzylidene- and *p*-methylbenzylideneacenaphthenone with dimethylsulfonium methylide gave only resinous materials, the *p*-chlorobenzylidene derivative condensed with the ylide to afford the corresponding spiroxirane compound in a good yield. In the reactions with dimethyloxosulfonium methylide and carbonyl-stabilized sulfonium ylides such as ethyl (dimethylsulfuranilidene)acetate and dimethylsulfonium phenacylide, benzylideneacenaphthenones gave the corresponding spirocyclopropyl ketones in good yields. The products obtained in the latter reactions were established to be *cis*-cyclopropyl compounds on the basis of NMR spectral studies. On the other hand, ethoxycarbonylmethyleneacenaphthenone condensed with carbonyl-stabilized sulfonium ylides to give *trans*-cyclopropyl ketones. On the basis of these results, the reaction mechanism was discussed. Also, bis-2,2′-methyleneacenaphthenone reacted with ethyl (dimethylsulfuranilidene)acetate to give the bis-spirocyclopropyl ketone.

From the study of the reactions of benzylideneacenaphthenones (I)[2] with hydrazines[3] and Grignard reagents,[1,4] it has been established that I behaves differently from ordinary α,β-unsaturated ketones such as chalcones, and that the β-carbon atom in I acts as a strong Michael acceptor toward the above reagents. In connection with our current studies of the reactivity of I, we wish to obtain further information concerning the ability of the conjugate addition of I, which are cyclic α,β-unsaturated ketones possessing a cisoid arrangement of the conjugated double bond with the carbonyl group.

Recently, it has been reported that reactive dimethylsulfonium methylide (II) interacts with chalcones to afford oxiranes, while less reactive dimethyloxosulfonium methylide (III) and carbonyl-stabilized sulfonium ylides (IV) such as dimethylsulfonium phenacylide react to give cyclopropyl ketones exclusively.[5-7] However, there have been few investigations of the reactions of cyclic α,β-unsaturated ketones with sulfonium ylides.

In the present work, the reactions of I with sulfonium ylides II—IV were studied in order to prepare spiroxiranes and spirocyclopropanes, and

1) Part XIX: O. Tsuge, I. Shinkai and M. Tashiro, *Kogyo Kagaku Zasshi*, **72**, 1680 (1969).

2) O. Tsuge, M. Tashiro and I. Shinkai, This Bulletin, **42**, 181 (1969).

3) O. Tsuge, I. Shinkai and M. Tashiro, *ibid.*, **42**, 185 (1969).

4) O. Tsuge, I. Shinkai and M. Tashiro, *Tetrahedron Lett.*, **1968**, 3631.

5) E. J. Corey and M. Chaykovsky, *J. Amer. Chem. Soc.*, **87**, 1353 (1965).

6) H. König, H. Metzger and K. Seelert, *Chem. Ber.*, **98**, 3712 (1965).

7) H. Nozaki, D. Tunemoto, S. Matubara and K. Kondo, *Tetrahedron*, **23**, 545 (1967).

the stereochemistry of the products were investigated on the basis of NMR spectral studies. In addition, the reactions of ethoxycarbonylmethylenacenaphthenone (V) and bis-2,2′-methyleneacenaphthenone (VI) with sulfonium ylides were studied.

Results and Discussion

Although the reactions of benzylidene- (Ia) and *p*-methylbenzylideneacenaphthenone (Ib) with II which had been generated *in situ* by the treatment of trimethylsulfonium iodide with potassium *t*-butoxide in dimethylsulfoxide (DMSO) gave only resinous materials, the *p*-chlorobenzylidene analogue (Ic) condensed with II under similar conditions to give the expected spiroxirane (VII), mp 113—114°C (decomp), in an 85% yield. The structure of VII was confirmed by a study of the mass (M^+ *m/e* 304), infrared, and NMR spectra as well as by elemental analysis. The infrared spectrum did not show any bands due to the carbonyl group, while the NMR spectrum in deuterochloroform ($CDCl_3$) exhibited signals at τ 7.60 (2H, methylene-protons, singlet), 3.26 (1H, olefinic proton, singlet), and 2.0—2.9 (10H, aromatic protons, multiplet).

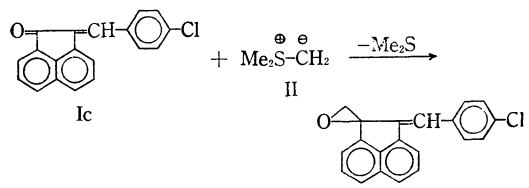

The compound VII was relatively unstable and decomposed on standing at room temperature for a few days. Although it is well known that epoxides rearrange to the corresponding aldehydes upon treatment with boron trifluoride, VII did not give the aldehyde, but only resinous materials.

When Ia was allowed to react in tetrahydrofuran (THF) at room temperature with III which had been generated *in situ* from trimethyloxosulfonium chloride and sodium hydride, the expected spirocyclopropyl ketone (VIIIa), mp 118—119°C, was obtained in a 74% yield. Its structure was established by a study of the mass (M^+ *m/e* 270), infrared, and NMR spectra as well as by elemental analysis. The infrared spectrum showed the band ascribed to the carbonyl group at 1705 cm^{-1}, while the NMR spectrum in $CDCl_3$ did not reveal any signals for olefinic protons, but did show a typical ABX pattern for cyclopropyl-protons: double-doublets appeared at τ 6.65 (1H, H_X), 7.70 (1H, H_A) and 7.90 (1H, H_B) with J_{AX} (*cis*)=9.0, J_{BX} (*trans*)=8.7 and J_{AB} (*gem*)=3.3 Hz, and a multiplet at τ 1.8—2.9 (11H, aromatic protons).[8]

A similar reaction of Ic with III gave the spirocyclopropyl analogue (VIIIb), mp 141—142°C, in a 93% yield. Its infrared spectrum showed the carbonyl band at 1691 cm^{-1}, and the NMR spectrum in $CDCl_3$ exhibited double-doublets at τ 6.60 (1H, H_X), 7.71 (1H, H_A) and 7.93 (1H, H_B) with J_{AX} (*cis*)=9.0, J_{BX} (*trans*)=8.4 and J_{AB} (*gem*)=3.5 Hz, and a multiplet at τ 1.8—2.9 (10H, aromatic protons).[8]

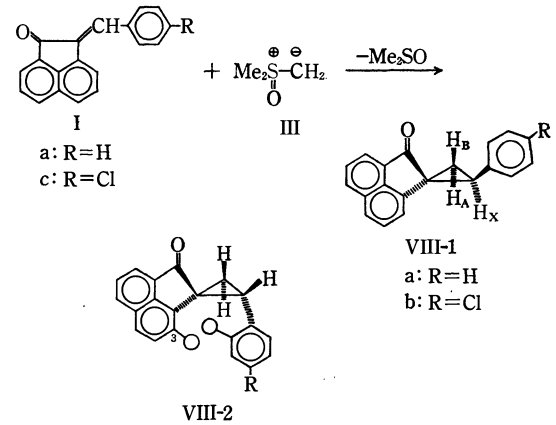

Two geometrical isomers resulting from the conformation of the spiro-carbon atom are, then, possible for the structure of VIII: one (VIII-1) in which the phenyl group overlooks the carbonyl group, and the other (VIII-2) in which it sees the acenaphthenone ring.

An inspection of Dreiding models for VIII indicates that the hydrogen atom on the *ortho* position of the phenyl ring interacts with that on the 3-position of the acenaphthenone ring in VIII-2, but does not interact in VIII-1. Consequently,

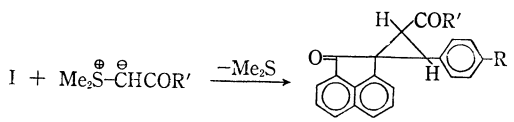

IV

a: R=H
b: R=Me
c: R=Cl

a: R′=OEt
b: R′=Ph
c: R′=*p*-BrC_6H_4

IX

a: R=H, R′=OEt
b: R=Me, R′=OEt
c: R=Cl, R′=OEt
d: R=H, R′=Ph
e: R=H, R′=*p*-BrC_6H_4
f: R=Cl, R′=Ph

8) J. D. Graham *et al.* observed that the values of $J_{cis}+J_{trans}+J_{gem}$ in 1,1,2-trisubstituted cyclopropanes are virtually constant (about 21 Hz), regardless of the nature of the substituents.[9] The values of $J_{cis}+J_{trans}+J_{gem}$ are 21 and 20.9 Hz in VIIIa and VIIIb respectively. These observations are also in agreement with the structures of 1,1,2-trisubstituted cyclopropane derivatives proposed for VIIIa and VIIIb.

9) J. D. Graham and M. T. Rogers, *ibid.*, **84**, 2249 (1962).

Table 1. *cis*-Spirocyclopropyl ketones (IX)

IX	R	R'	Yield (%)	Appearance[1]	Mp (°C)	Formula	Analysis (%) Found (Calcd) C	H	Mol wt (*m/e*)
a	H	OEt	77	colorless needles	150—151	$C_{23}H_{18}O_3$	80.87 (80.68)	5.15 (5.30)	342
b	Me	OEt	62	colorless prisms	140.5	$C_{24}H_{20}O_3$	81.08 (80.88)	5.29 (5.66)	356
c	Cl	OEt	57	colorless prisms	144—145	$C_{23}H_{17}O_3Cl$	73.57 (73.40)	4.26 (4.52)	376
d	H	Ph	82	colorless needles	168—169	$C_{27}H_{18}O_2$	86.81 (86.61)	4.71 (4.85)	374
e	H	*p*-BrC_6H_4	81	colorless grains	155—156	$C_{27}H_{17}O_2Br$	71.62 (71.52)	3.37 (3.75)	453
f	Cl	Ph	55	colorless prisms	157—158	$C_{27}H_{17}O_2Cl$	79.37 (79.41)	4.07 (4.12)	408

1) Recrystallized from methanol.

it may be deduced that VIII-1 is a more favorable configuration than that of VIII-2.

The treatment of Ia with ethyl (dimethylsulfuranilidene)acetate (IVa) which had been generated *in situ* from the corresponding sulfonium bromide and sodium hydride in THF gave the spirocyclopropyl ketone (IXa). Similar reactions of I with carbonyl-stabilized sulfonium ylides (IVa—IVc) gave the corresponding spirocyclopropyl ketones (IXb—IXf).

The yields, physical properties, elemental analyses, and spectral data are summarized in Tables 1 and 2.

Table 2. Infrared and NMR data of IX[1]

IX	H_A (τ)	H_B (τ)	J_{AB} (Hz)	$\nu_{C=O}$ (cm^{-1})	
a	6.43	5.99	9.0	1712	1732
b	6.50	6.16	8.9	1705	1728
c	6.05	5.76	9.0	1715	1729
d	5.65	5.44	8.7	1675	1712
e	5.71	5.54	9.0	1675	1710
f	5.75	5.53	8.4	1670	1712

1) NMR spectra were measured in $CDCl_3$.

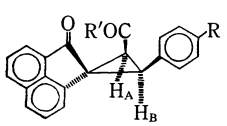

IX-1 (*cis*)

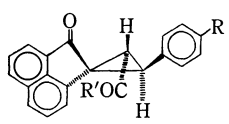

IX-2 (*trans*)

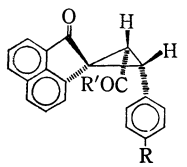

IX-3 (*cis*)

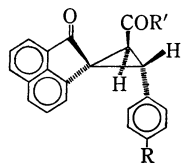

IX-4 (*trans*)

As a result of the conformation of the spiro-carbon atom and the *cis-trans* configuration of hydrogens in the cyclopropyl ring of IX, the following four isomers (IX-1—IX-4) are possible for the structure of IX.

As is illustrated in Fig. 1, the NMR spectrum of IXa in $CDCl_3$ exhibits peaks at τ 8.76 (3H, methyl-protons, triplet) 6.43 (1H, H_A, doublet), 5.99 (1H, H_B, doublet) (J_{AB}=9.0 Hz), and 5.75 (2H, methylene-protons, quartet), besides aromatic protons.

It is well known that *cis*-cyclopropanes exhibit higher coupling constants (8—10,[10] 7.9—9.3 Hz[9]) than those (4—7,[10] 5.3—6.6 Hz[9]) of the corresponding *trans* isomers.

As is shown in Table 2, the vicinal coupling constants (J_{AB}=8.4—9.0 Hz) of IX correspond to those of *cis*-cyclopropanes. In addition, the configurations, IX-3 and IX-4, in which the phenyl group sees the acenaphthenone ring may be disregarded as unreasonable because of the steric hindrance mentioned in the case of VIII-2.

Consequently, it may be deduced that the most reasonable structure for IX is the configuration IX-1, in which H_A and H_B are situated *cis*, and in which the phenyl group overlooks the carbonyl group in acenaphthenone. As will be described below, this conclusion is also supported by the fact that the shielding effect of the acenaphthenone ring does not exert any effect on the methyl resonance of the ethoxycarbonyl group in the respective NMR spectrum of IXa, IXb, or IXc.

The fragmentation on electron impact was compatible with the proposed structure for IX. For example, the mass spectrum of IXa shows peaks at *m/e* 342 (M^+), 298 ([M–MeCHO]$^+$), 270

10) K. B. Wiberg and B. J. Nist, *J. Amer. Chem. Soc.*, **85**, 2788 (1963).
11) B. M. Trost, *ibid.*, **89**, 138 (1967).
12) G. B. Payne, *J. Org. Chem.*, **32**, 3351 (1967).

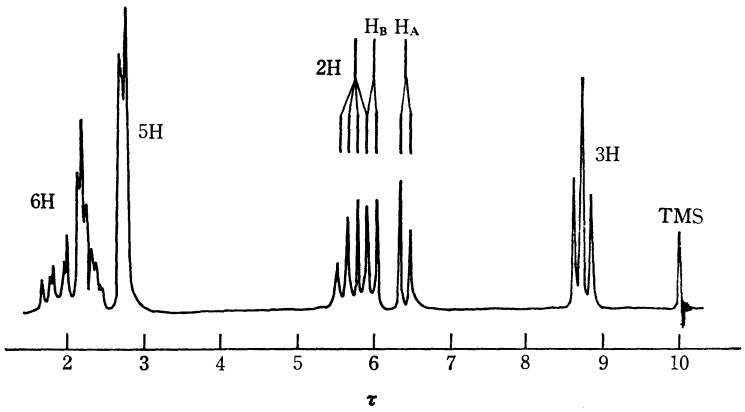

Fig. 1. NMR spectrum of IXa in $CDCl_3$.

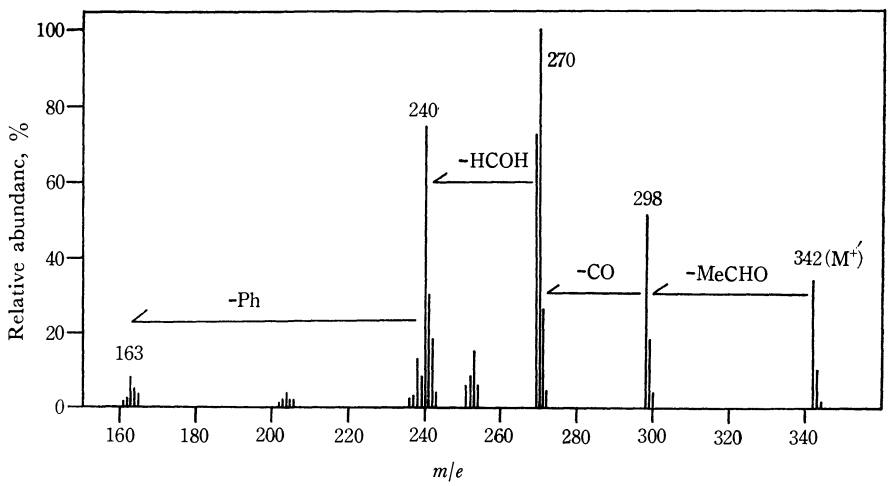

Fig. 2. Mass spectrum of IXa.

([298-CO]$^+$), 240 ([270-CH_2O]$^+$), and 163 ([240-Ph]$^+$), as is shown in Fig. 2.

It has been reported that dimethylsulfonium phenacylide (IVb) condensed with chalcone to afford a mixture of *cis*- and *trans*-cyclopropane in the ratio of 1 : 2.[11] Also, Payne[12] found that the corresponding *trans*-cyclopropanes were obtained predominantly in the reactions of IVa with α,β-unsaturated carbonyl compounds, such as acrolein and mesityl oxide.

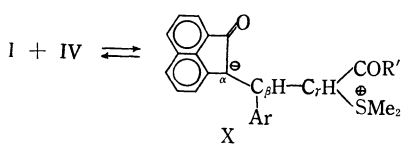

(1)

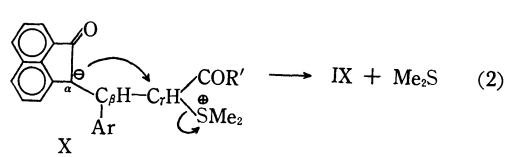

(2)

Although the exact course of the reaction of I with IV is not clear, it is thought to consist of step 1, a reversible nucleophilic attack by the ylide carbanion on the β-carbon atom in I to form a betain intermediate X, followed by step 2, an irreversible intramolecular ring closure with the *trans*-elimination of dimethyl sulfide.

As is shown in Table 1, all the reactions of I with IV gave the corresponding *cis*-cyclopropyl ketones exclusively. The relative amounts of *cis*-(IX-1) and *trans*-cyclopropyl ketone (IX-2) must be reflected by the relative energies of the *threo*-precursor (Xa) of IX-1 and the *erythro*-precursor (Xb) of IX-2; the betains which are precursors of IX-3 and IX-4 are excluded from our discussion.[13]

The Newman projections clearly indicate that Xa is a more unfavorable conformation than Xb, because the four bulky groups in Xa are in a *gauche* position relative to each other.

13) In this paper, the prefixes of *threo* and *erythro* are used assuming that the substituent COR′ is larger than SMe_2.

However, an inspection of the Dreiding models indicates that the free rotation of the C_α-C_β bond in Xb to form Xb′ is hindered by the steric interaction between the acenaphthenone ring and the phenyl group, and that, in an intramolecular ring closure with a backside attack of the carbanion on the γ-carbon atom (step 2), there is a significant repulsion between the substituent COR′ and the acenaphthenone ring in Xb.

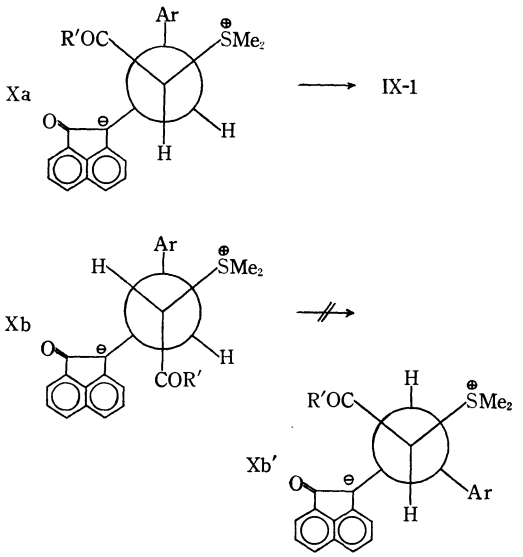

Accordingly, it will be very difficult for the ring-closure reaction of Xb to IX-2 to take place and Xb will return to the starting materials, I and IV. These situations result in the stereoselective formation of the *cis*-cyclopropyl ketone IX-1 from the precursor Xa.

If the free rotation of the C_α-C_β bond in a betain were possible, one might expect the formation of the *trans*-cyclopropyl ketone from the *erythro*-betain in a lower energy. In order to make this point clear, the reactions of two isomeric ethoxycarbonylmethyleneacenaphthenone, V[2] and V′[2], which have an ethoxycarbonyl group in place of a phenyl group in I, with sulfonium ylides were investigated.

The reaction of V, whose ethoxycarbonyl group overlooks the carbonyl group in acenaphthenone, with IVa afforded the expected *trans*-spirocyclopropyl ketone (XI), mp 110—111°C, in a good yield. In order to confirm whether or not the conformation of the ethoxycarbonyl group in V is maintained in XI, the reaction of the isomer V′, in which the ethoxycarbonyl group sees the acenaphthenone ring, with IVa was carried out; the same product, XI, was thus obtained in an excellent yield. This shows that the free rotation of the C_α-C_β bond in a betain takes place, as was expected.

The structure of XI was confirmed by the infrared, mass, and NMR spectra as well as by the results of the elemental analyses.

As is shown in Fig. 3, the NMR spectrum of XI in $CDCl_3$ exhibits signals at τ 8.82, 8.75 (each 3H, methyl-protons, triplet, J=4.2 Hz), 6.56 (2H, methine-protons H_A and H_B), 5.84, 5.77 (each 2H, methylene-protons, quartet, J=4.2 Hz), 1.8—2.5 (6H, aromatic protons). The vicinal coupling constant is very small ($J \fallingdotseq 0$); this indicates that H_A and H_B are situated *trans*. Furthermore, it is clear that the two ethoxycarbonyl groups in XI are in an unequivalent situation. This phenomenon can be understood in terms of the shielding effect of the acenaphthenone ring in

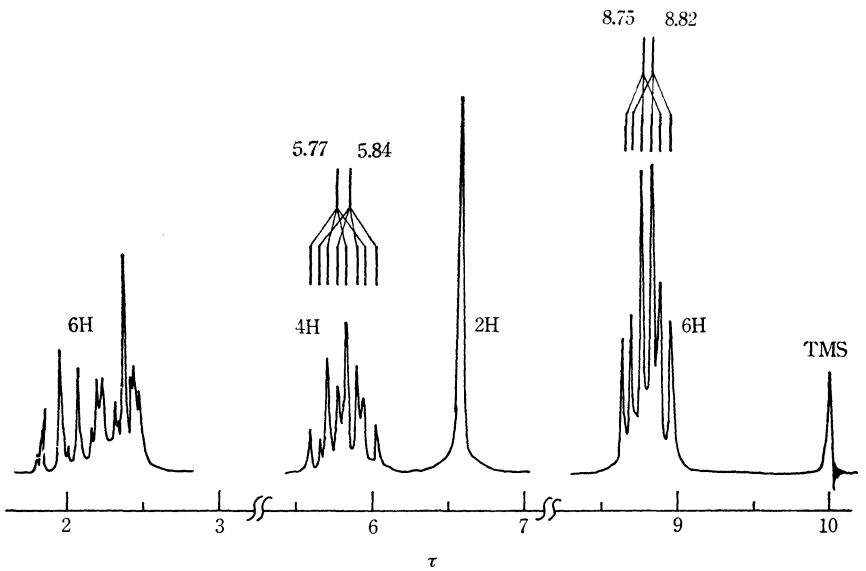

Fig. 3. NMR spectrum of XI in $CDCl_3$.

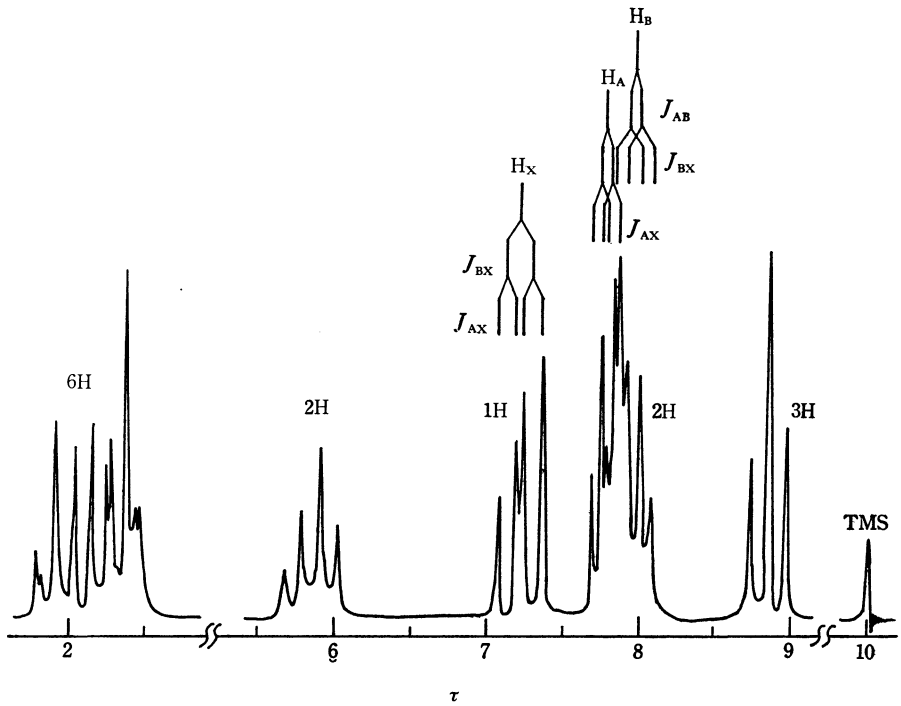

Fig. 4. NMR spectrum of XII in $CDCl_3$.

XI: one (methyl at τ 8.82) sees the acenaphthenone ring, and the other (methyl at τ 8.75) overlooks the carbonyl group in acenaphthenone.

Similar reactions of V with III and dimethylsulfonium *p*-chlorophenacylide (IVd) afforded spirocyclopropyl ketones, XII (mp 74—75°C) and XIII (mp 147—148°C) respectively. The structures for XII and XIII were established by spectral studies as well as by elemental analyses.

The NMR spectrum of XII in $CDCl_3$ is illustrated in Fig. 4. Signals appear at τ 8.82 (3H, methyl-protons, triplet), 5.86 (2H, methylene-protons, quartet), and 1.8—2.5 (6H, aromatic protons), besides a typical ABX pattern for cyclopropylprotons at τ 7.25 (1H, H_X), 7.75 (1H, H_A), and 7.95 (1H, H_B) with J_{AX} (*trans*)=6.5, J_{BX} (*cis*)=9.9 and J_{AB} (*gem*)=4.5 Hz. On the basis of the above observations, XII can be said to be consistent with the cyclopropyl ketone, in which the ethoxycarbonyl group sees acenaphthenone ring.[14]

On the other hand, the NMR spectrum of XIII in $CDCl_3$ showed signals at τ 8.81 (3H, methyl-protons, triplet), 6.25 and 6.17 (each 1H, methine-proton, doublet, J=5.8 Hz), 5.84 (2H, methylene-protons, quartet) and a lower field (10H, aromatic protons); XIII is compatible with the *trans*-cyclopropyl ketone, in which the ethoxycarbonyl group sees the acenaphthenone ring.

The original conformation of the ethoxycarbonyl group in V is not maintained in either XII or XIII.

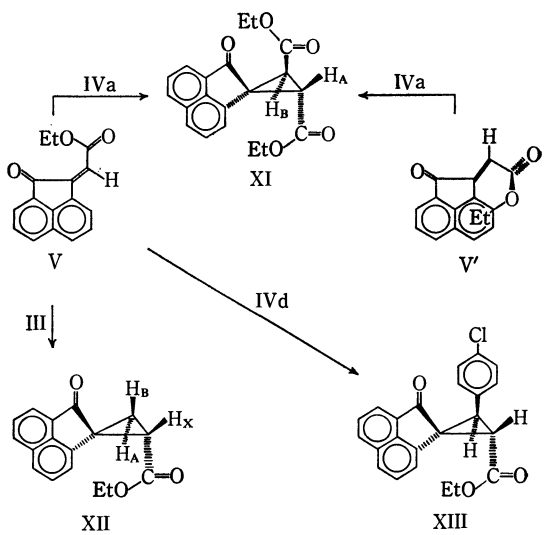

The methyl-protons signals of ethoxycarbonyl groups in IXa, IXb, and IXc appeared at τ 8.76, 8.75 and 8.77 respectively in the NMR spectra.

14) The value of $J_{cis}+J_{trans}+J_{gem}$ is 20.9 Hz.[8] In the reaction of diazoacenaphthenone with ethyl acrylate in refluxing benzene, XII and the isomeric spirocyclopropyl ketone in which the ethoxycarbonyl group overlooks the carbonyl group in acenaphthenone were obtained; these results will be reported shortly in more detail.

No ethoxycarbonyl group in IX is affected by the shielding effect of the acenaphthenone ring, but each overlooks the carbonyl group in acenaphthenone. This fact indicates that IX is compatible with the proposed structure, IX-1.

The formation of the *trans*-cyclopropyl ketone in the reaction of V with IV can, then, be understood in terms of the following considerations.

As has been pointed out in the discussion of the formation of IX, it must be determined by the relative energies of *erythro*- (XIV) and *threo*-betain (XV) which isomer, the *trans* or the *cis*, is formed predominantly in the reaction of V with IV.[13] The Newman projections indicate that the precursor, XIV, of the *trans*-isomer is a more favorable conformation than the precursor, XV, of the *cis*-isomer.

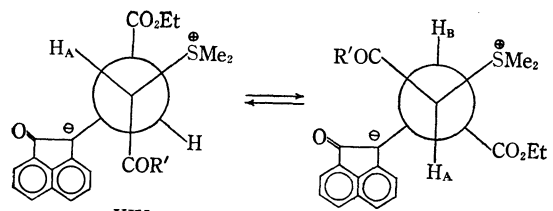

XIV XIV'

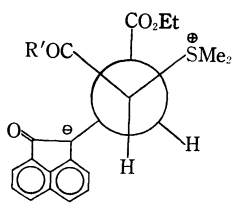

XV

The exclusive formation of the *cis*-cyclopropyl ketone IX-1 in the reaction of I with IV may be attributed to the fact that the transformation of *erythro*-betain Xb to the *trans*-isomer IX-2 can not occur because of the steric repulsion between the acenaphthenone ring and COR′ at the step 2, but Xb reverts to the starting materials.

Contrary to the case of Xb, it becomes feasible of the C_α- C_β bond in XIV to rotate, as is shown by the fact that the reactions of both V and V′ with IVa gave the same product, XI. That is, XIV can convert to XIV′, in which the steric repulsion between the acenaphthenone ring and COR′ is absent in the ring-closure reaction.

Thus, the above situation leads to the formation of the *trans*-cyclopropyl ketone, whose ethoxycarbonyl group does not retain the original conformation in V, from the preferred betain, XIV′.

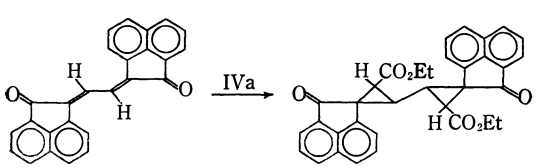

VI XVI

The reaction of bis-2,2′-methyleneacenaphthenone (VI)[2] with IVa afforded the bis-spirocyclopropyl ketone (XVI), mp 225°C (decomp), in a 57% yield. However, the stereochemistry of XVI is not yet clear.

Experimental

All the melting points are uncorrected. The infrared spectra were measured in KBr disks, while the NMR spectra were recorded on a 60 MHz Hitachi R-20 NMR spectrometer, using TMS as an internal reference. The mass spectra were obtained on a Hitachi RMS-4 mass spectrometer, using a direct inlet and an ionization energy of 70 eV.

Benzylideneacenaphthenones (I), ethoxycarbonylmethyleneacenaphthenone (V), and bis-2,2′-methyleneacenaphthenone (VI) were prepared by a previously-reported method.[2]

Trimethylsulfonium iodide,[5] trimethyloxosulfonium chloride[5] dimethylethoxycarbonylmethyl-,[15] dimethylphenacyl-[15], dimethyl-*p*-bromo-,[15] and -*p*-chlorophenacylsulfonium bromides[16] were prepared by methods described in the literature.

The Reaction of *p*-Chlorobenzylideneacenaphthenone (Ic) with Dimethylsulfonium Methylide (II). A solution of the ylide II was prepared by stirring a mixture of trimethylsulfonium iodide (1.0 g), potassium *t*-butoxide (0.56 g), and DMSO (20 m*l*) for 25 min under a nitrogen atmosphere. A solution of Ic (350 mg) in DMSO (10 m*l*) was then slowly added, drop by drop, to the solution of II, and the reaction mixture was stirred at room temperature for 1 hr. After the mixture had been poured into 15 m*l* of cold water, yellow crystals were collected by filtration, washed with water, and dried. Yield, 310 mg (85%). Recrystallization from petroleum benzine (bp 40—65°C) gave spiroxirane (VII), mp 113—114°C (decomp), as yellow needles.

Found: C, 78.60; H, 4.00%. Calcd for $C_{20}H_{13}OCl$: C, 78.95; H, 4.28%.

Similar reactions of benzylidene- (Ia) and *p*-methylbenzylideneacenaphthenone (Ib) with the ylide II gave only resinous materials.

The Reaction of Ic with Dimethyloxosulfonium Methylide (III). A solution of the ylide III was prepared by refluxing a mixture of trimethyloxosulfonium chloride (450 mg), sodium hydride (200 mg) as a 50% mineral oil dispersion, and THF (20 m*l*) for 3.5 hr under a nitrogen atmosphere. To a stirred solution of Ic (1.0 g) in THF (15 m*l*) was then slowly added, drop by drop, the solution of the ylide III at 0°C, after which the reaction mixture was stirred at room temperature for 2 hr. After the mixture had been concentrated *in vacuo*, methanol (10 m*l*) was added to the residue and the mixture was allowed to stand at room temperature for several hours, thus giving 974 mg (93%) of colorless crystals. Recrystallization from methanol gave the spirocyclopropyl ketone (VIIIb), mp 141—142°C, as colorless needles.

Found: C, 78.80; H, 4.19%. Calcd for $C_{20}H_{13}$-

15) K. W. Ratts and A. N. Yao, *J. Org. Chem.*, **31**, 1185 (1966).
16) K. W. Ratts and A. N. Yao, *ibid.*, **33**, 70 (1968).

OCl: C, 78.95; H, 4.28%. M^+: *m/e* 304.

A similar reaction of Ia with III afforded the spirocyclopropyl ketone (VIIIa), mp 118—119°C, as colorless prisms (from methanol). Yield, 74%.

Found: C, 88.55; H, 5.06%. Calcd for $C_{20}H_{14}O$: C, 88.86; H, 5.22%.

The Reaction of I with the Carbonyl-stabilized Sulfonium Ylide (IV). The procedure used is illustrated with the reaction of Ia with ethyl (dimethylsulfuranilidene)acetate (IVa).

A solution of the ylide IVa was prepared by the following procedure. To a stirred suspension of dimethylethoxy-carbonylmethylsulfonium bromide (1.2 g) in THF (10 m*l*), sodium hydride (0.3 g) was added as a 50% mineral oil dispersion in one portion. After the mixture had then been stirred at room temperature for 3 hr, it was filtered to remove the sodium bromide, thus giving a yellow solution of IVa.

After the solution of IVa had been added to a solution of Ia (1.2 g) in THF (10 m*l*) at 0°C, the reaction mixture was stirred at room temperature for 12 hr and then at 70—80°C for 30 min. The mixture was concentrated *in vacuo*, and methanol (10 m*l*) was added to the residue. It was then allowed to stand at room temperature for several hours, giving 1.23 g (77%) of colorless crystals, mp 148—150°C. Recrystallization from methanol afforded the *cis*-spirocyclopropyl ketone (IXa) as colorless needles.

Similar reactions of Ia Ib, and Ic with IVa, dimethylsulfonium phenacylide (IVb), and dimethylsulfonium *p*-bromophenacylide (IVc) gave the corresponding *cis*-spirocyclopropyl ketones (IX-IXf).

The yields, physical properties, spectral data, and elemental analyses are summarized in Tables 1 and 2.

The Reaction of Ethoxycarbonylmethyleneacenaphthenone (V) with the Ylide IVa. A solution of the ylide IVa, prepared from the corresponding sulfonium bromide (250 mg) and sodium hydride (65 mg) as a 50% mineral oil dispersion in THF (15 m*l*), was slowly added to a solution of V (250 mg) in THF (10 m*l*) at 0°C, and then the reaction mixture was stirred at room temperature for 3.5 hr. After the mixture had been concentrated *in vacuo* to leave a residue, the addition of methanol (10 m*l*) to the residue gave 290 mg (88%) of colorless crystals. Recrystallization from methanol gave the *trans*-spirocyclopropyl ketone (XI), mp 110—111°C, as colorless prisms.

Found: C, 71.29; H, 5.27%. Calcd for $C_{20}H_{18}O_5$: C, 70.99; H, 5.36%. M^+: *m/e* 338. IR: $\nu_{C=O}$ 1735, 1724 and 1712 cm^{-1}.

The same spirocyclopropyl ketone, XI, was obtained in a 90% yield from a similar reaction of isomeric ethoxycarbonylmethyleneacenaphthenone (V′) with the ylide IVa.

The Reaction of V with the Ylide III. To a solution of V (250 mg) in THF (5 m*l*) added a solution of the ylide III, prepared from the corresponding sulfonium chloride (250 mg) and sodium hydride (90 mg) as a 50% mineral oil dispersion in THF (10 m*l*); the reaction mixture was then stirred at room temperature for 20 hr, and then at 70—80°C for 10 min. After the mixture had been concentrated *in vacuo*, petroleum ether (10 m*l*) was added to the residue, giving 145 mg (54%) of colorless crystals. Recrystallization from petroleum ether gave the spirocyclopropyl ketone (XII), mp 74—75°C, as colorless prisms.

Found: C, 76.78; H, 5.04%. Calcd for $C_{17}H_{14}O_3$: C, 76.67; H, 5.30%. M^+: *m/e* 266. IR: $\nu_{C=O}$ 1708 cm^{-1}.

The Reaction of V with Dimethylsulfonium *p*-Chlorophenacylide (IVd). A solution of the ylide IVd, prepared from the corresponding sulfonium bromide (310 mg) and sodium hydride (60 mg) as a 50% mineral oil dispersion in THF (15 m*l*), was added to a solution of V (250 mg) in THF (10 m*l*) at 0°C. After the reaction mixture had been stirred at room temperature for 3 hr and then at 70—80°C for 30 min, the mixture was concentrated *in vacuo* to leave a residue. To the residue then added methanol (10 m*l*), giving 230 mg (57%) of colorless crystals. Recrystallization from methanol afforded the *trans*-spirocyclopropyl ketone (XIII), mp 147—148°C, as colorless prisms.

Found: C, 71.43; H, 3.79%. Calcd for $C_{24}H_{17}O_4Cl$: C, 71.29; H, 4.21%. M^+: *m/e* 404. IR: $\nu_{C=O}$ 1730, 1710 and 1675 cm^{-1}.

The Reaction of Bis-2,2′-methyleneacenaphthenone (VI) with the Ylide IVa. After a solution of the ylide IVa, prepared from the corresponding sulfonium bromide (300 mg) and sodium hydride (75 mg) as a 50% mineral oil dispersion in THF (15 m*l*), was added to a solution of VI (180 mg) in THF (10 m*l*), the reaction mixture was stirred at room temperature for 3 hr and then at 70—80°C for an additional hour. The mixture was concentrated *in vacuo* to give a residue, to which methanol was then added, giving 150 mg (57%) of colorless crystals. Recrystallization from petroleum benzine afforded the *bis*-spirocyclopropyl ketone (XVI), mp 225°C (decomp), as colorless prisms.

Found: C, 76.99; H, 5.01%. Calcd for $C_{34}H_{26}O_6$: C, 76.97; H, 4.94%. M^+: *m/e* 530. IR: $\nu_{C=O}$ 1730 and 1710 cm^{-1}.

BULLETIN OF THE CHEMICAL SOCIETY OF JAPAN VOL. 43 3522—3527 (1970)

Reactions of Ferrocenylcarbene. III. The Addition Reactions of Some α-Ferrocenylcarbenes to 1,1-Diphenylethylene*1

Akio SONODA and Ichiro MORITANI

Department of Chemistry, Faculty of Engineering Science, Osaka University, Machikaneyama, Toyonaka, Osaka

(Received May 11, 1970)

The addition reactions of α-ferrocenylcarbenes (ferrocenyl, ferrocenylmethyl, and ferrocenylphenyl carbene) to 1,1-diphenylethylene have been examined by means of the thermal decomposition of the corresponding acylferrocene tosylhydrazone sodium salts. Then, the reactivities of the ferrocenylcarbenes have been compared with those of the corresponding phenyl and *p*-anisylcarbenes. It has been found that, of the carbenes investigated, the ferrocenylcarbenes show the lowest reactivity in addition reactions to the olefin. It has been established by a study of the NMR spectra that, in the ferrocenylcyclopropanes only, there is a restricted rotation about the bond between ferrocenyl and cyclopropyl groups. On this basis, the reactivity of the ferrocenylcarbenes has been discussed in terms of the steric hindrance of the bulky ferrocenyl group.

In previous papers[1] on the reactions of ferrocenylcarbenes, we have reported that the α-ferrocenylcarbenes (Ia, Ib, and Ic) are all triplets. Thus, it has been revealed that these ferrocenylcarbenes abstract hydrogen atoms or halogen atoms from solvents and easily react with oxygen to form the corresponding carbonyl compounds. Further, they add to particular olefins bearing effective radical-stabilizing group(s), such as phenyl or ferrocenyl, to form ferrocenylcyclopropane derivatives.

It is known that a triplet carbene adds to 1,1-diphenylethylene, yielding a cyclopropane derivatives.[2] This carbene trapping ability of the olefin is probably due to the intermediary formation of a stable diphenylmethylradical. In order to elucidate the reactivity of ferrocenylcarbenes, the addition reactions of these carbenes to 1,1-diphenylethylene has been investigated and compared with those of phenyl and *p*-anisylcarbenes.[3]

Results and Discussion

When the thermal decompositions of acylferrocene tosylhydrazone sodium salts[4] were carried out in a mixed solution of dry pyridine and about a tenfold excess of 1,1-diphenylethylene, as addition products 1,1-diphenyl-2-ferrocenylcyclopropane derivatives were obtained, plus a small amount of azine derivatives.

The yields of ferrocenylcyclopropane derivatives might directly reflect the addition reactivity of ferrocenylcarbenes formed in the thermal decomposition of the tosylhydrazone salts. Therefore, the reactions of the corresponding phenyl and *p*-anisylcarbenes with 1,1-diphenylethylene were investigated under similar conditions in order to estimate the effect of the ferrocenyl group on the reaction of an adjacent divalent carbon by comparing it with phenyl and *p*-anisyl groups. The yields of the cyclopropane derivatives are listed in Table 1.

TABLE 1. THE YIELDS OF CYCLOPROPANE DERIVATIVES FORMED BY THE THERMAL DECOMPOSITION OF SODIUM SALTS OF I IN 1,1-DIPHENYLETHYLENE

R′	R-		
	Ferrocenyl	Phenyl	*p*-Anisyl
H	13%	6%	35%
CH_3	41	59	75
C_6H_5	14	23	27

It appears from Table 1 that the reactivity of carbenes increases in the following sequence; ferrocenyl<phenyl<*p*-anisyl. Thus, when R′ is methyl or phenyl, the yield of ferrocenylcyclopropane was found to be the lowest. It should be

*1 Presented at the 21st Annual Meeting of the Chemical Society of Japan, Osaka, April, 1968.

1) A. Sonoda, I. Moritani, T. Saraie and T. Wada, *Tetrahedron Lett.*, **1969**, 2943; b) A. Sonoda, I. Moritani, S. Yasuda and T. Wada, *Tetrahedron*, **26**, 3075 (1970).

2) a) R. M. Etter, H. S. Skovronek and P. S. Skell, *J. Amer. Chem. Soc.*, **81**, 1008 (1959); b) J. E. Hodgikins and M. P. Hughes, *J. Org. Chem.*, **27**, 4187 (1962).

3) It is well known that arylcarbenes are triplet: W. Kirmse "Carbene Chemistry," Academic Press, New York, N. Y. (1964), Chapter 5.

4) W. R. Bamford and T. S. Stevens, *J. Chem. Soc.*, **1952**, 4735.

Reaction scheme

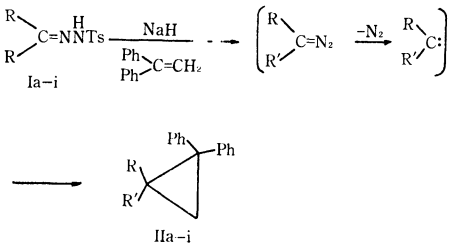

Ia–i

IIa–i

	R	R′
a:	$C_{10}H_9Fe$	H
b:	$C_{10}H_9Fe$	CH_3
c:	$C_{10}H_9Fe$	C_6H_5
d:	C_6H_5	H
e:	C_6H_5	CH_3
f:	C_6H_5	C_6H_5
g:	$CH_3OC_6H_4$	H
h:	$CH_3OC_6H_4$	CH_3
i:	$CH_3OC_6H_4$	C_6H_5

noted that the reactivity of the ferrocenylcarbenes is the lowest. This fact is of interest, since the radical stabilizing effect of the ferrocenyl group may be considered to be not less than that of the *p*-anisyl group, as deduced from their resonance stabilizing effect on the α-carbonium ions.[5] Table 1 also shows that the effecs of R′ on the reactivity increases in the order of: $H \ll Ph < CH_3$. This result indicates that a steric factor palys an important role, since the expected order of the radical-stabilizing effect between phenyl and methyl groups appears to be reversed.

The structural elucidation of the addition products suggests that there is a significant steric crowding in the 1,1-diphenyl-2-ferrocenyl cyclopropane derivatives. Thus, in the NMR spectra of IIa—c, it was found that the signal of one *ortho* (adjacent to the cyclopropyl group) proton of the ferrocenyl ring shifted unusually to a higher field.[6] This phenomenon can reasonably be explained in terms of an anisotropic effect of a spacially-fixed phenyl ring attached to the cyclopropane ring in *cis* configuration to the ferrocenyl group.[7]

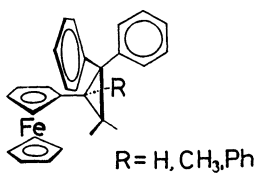

Fig. 1.

For example, in the NMR spectrum of 1,1-diphenyl-2-ferrocenylcyclopropane (IIa), ferrocenyl ring proton signals were observed at τ 5.97, 6.19,

IIb in diphenylether. (HMDS internal standard)

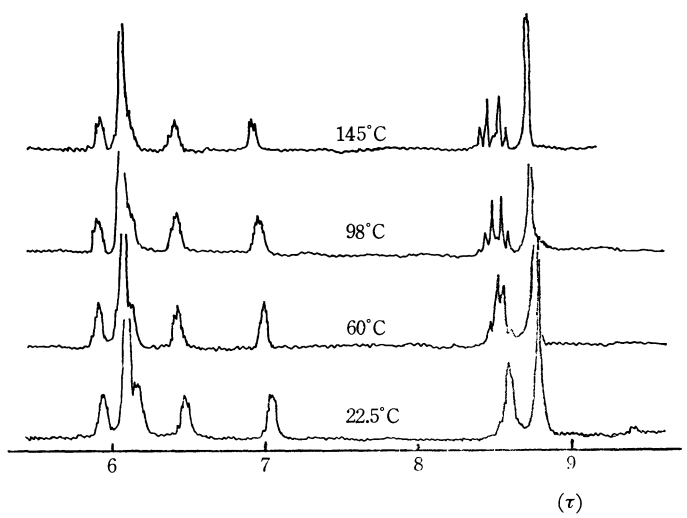

Fig. 2. Temperature dependence of NMR spectra of IIb (100 MHz).

5) T. G. Traylor and J. C. Ware, *J. Amer. Chem. Soc.*, **89**, 2304 (1967).

6) It is known that in ferrocene system, electron donating groups such as alkyl substituents exert an effect of some higher field shifts on the ferrocenyl ring protons: M. Rosenblum, "Chemistry of the Iron Group Metallocenes," Interscience Publishers, New York, N. Y. (1965), p44. But, such an extraordinary high field signal of ferrocenyl ring proton as appeared in this ferrocenylcyclopropane system has not been reported.

7) In *o*-ferrocenyl-biphenyl derivatives, the ferrocenyl ring protons of 2 and 5 position are known to be considerably shielded by a phenyl ring current: Ref. 6, p. 217. This situation resemble to our case. On the other hand, the shilding by cyclopropane ring might be estimated to be less extensive in five membered ring system than that in phenylcyclopropane.

6.41 (each one proton), τ 6.09 (five protons), and τ 6.88 (one proton). The methylene and methine protons of the cyclopropane ring gave signals of an ABX pattern at a high field. This great upfield shift of a proton signal of the ferrocenyl ring can also be observed in two other ferrocenylcyclopropanes; in both IIb and IIc the signal appears at τ 7.05. These NMR data are listed in Table 3.

By the examination of molecular models, it is found that the rotation of the bond between the ferrocenyl group and the cyclopropane ring is greatly restricted by the conflict of the *cis* phenyl group with the unsubstituted cyclopentadienyl ring.

When the temperature dependence of the NMR spectrum of 1,1-diphenyl-2-ferrocenyl-2-methylcyclopropane (IIb) was investigated in a diphenyl ether solution, using HMDS as the internal standard and at 22.5, 60, 98, and 145°C, it was observed that the higher-field one-proton signal tended to move slightly down field with an increase in the temperature, while the other signals, with the exception of the methylene signal, remained almost unchanged. The results are shown in Fig. 2.

It should be noticed here that the methylene protons of the cyclopropane in IIb, which unexpectedly give a singlet peak at τ 8.51 in CS_2 at room temperature (Table 3), split into an AB pattern with an increase in the temperature in diphenyl ether. This interesting NMR behavior the methylene signal might be reasonably interpreted as follows; at room temperature the chemical shifts of the two proton signals under the most favorable conformation of IIb become, by chance, coincident, resulting in a singlet peak, while at an elevated temperature they are split by thermal perturbation.

These observations obviously indicate that the rotation of the bond between ferrocenyl and cyclopropyl groups is highly hindered and that even at elevated temperatures, the rotation is completely restricted.

On the other hand, in the NMR spectra of 1,1-diphenyl-2-(*p*-anisyl)cyclopropanes (IIg—i), and 1,1,2-triphenylcyclopropanes (IId—e), no such anisotropy was observed. In these NMR spectra of IIg—i, the ring protons of the *p*-anisyl group showed the usual AB splitting pattern. It may safely be said that the anisyl and phenyl groups are freely rotating.

After these discussions, it can be concluded that, among these reaction products (IIa—i), there exists strongly restricted rotation only in 1,1-diphenyl-2-ferrocenylcyclopropanes, and that the addition of ferrocenylcarbenes to 1,1-diphenylethylene, producing these ferrocenylcyclopropanes, must overcome a much greater steric hindrance than those of phenyl and *p*-anisylcarbenes. Accordingly, the low reactivity of the ferrocenylcarbenes can be attributed to the steric hindrance of a bulky ferrocenyl group.

Experimental

The infrared spectra were recorded on a Hitachi EPI-S2 spectrophotometer, the visible and ultra violet spectra, on a Hitachi EPS-2U, and the NMR spectra, on a JEOLCO JNM-4H-100 at 100 MHz. All the reactions were carried out under an atmosphere of high-purity nitrogen gas or argon gas. All the temperatures are uncorrected.

Materials. The 1,1-diphenylethylene was prepared by the usual Grignard reaction of phenylmag-

TABLE 2. THE PHYSICAL CONSTANTS AND ANALYTICAL DATA OF TOSYLHYDRAZONES I

Tosylhydrazone (Recrystallization solvent)	Mp °C (lit.)	Analysis (calcd) C%	H%	N%
Ia (benzene)	154—156*	56.62 (56.56)	5.07 (4.77)	7.29 (7.33)
Ib (benzene)	186--187*	57.59 (57.58)	5.16 (5.09)	7.05 (7.07)
Ic (EtOH)	167—169*	63.14 (62.88)	4.87 (4.80)	6.34 (6.11)
Id (benzene)	125—126 (128)[a]	61.40 (61.29)	5.15 (5.14)	10.26 (10.21)
Ie (benzene)	146—147 (148)[a]	62.29 (62.47)	5.68 (5.60)	9.88 (9.71)
If (benzene)	181—182 (184)[a]	68.33 (68.51)	5.19 (5.18)	7.89 (7.99)
Ig (MeOH)	121—122 (112—114)[b]	59.29 (59.19)	5.37 (5.30)	9.24 (9.24)
Ih (AcOEt)	175—176	60.44 (60.36)	5.85 (5.70)	8.83 (8.80)
Ii (MeOH)	156—158	66.24 (66.30)	5.21 (5.30)	7.33 (7.36)

* With decomp. a) Ref. 4. b) Ref. 18.

8) D. G. Farnum, *J. Org. Chem.*, **28**, 870 (1963).

Table 3. The NMR spectral of II (τ-Value in CS_2, (Intensity, signal pattern)[a])

Compounds	Benzene ring protons		Cyclopentadienyl ring protons (unsubst.)	(subst.)		Cyclopropyl		Other
IIa	3.02(5H,s)	3.07(5H,s)	6.09(5H,s)	5.97(1H,m)	6.19(1H,m)	7.64(1H,q)	8.48(2H,m)	
				6.41(1H,m)	6.88(1H,m)			
IIb	2.42(5H,m)	3.12(5H,s)	6.08(5H,s)	5.90(1H,m)	6.09(1H,m)		8.51(2H,s)	8.75(3H,s)[b]
				6.43(1H,m)	7.05(1H,m)			
IIc	2.91(5H,m)	3.02(5H,s)	6.26(5H,s)	6.28(1H,m)	6.40(2H,m)	7.50(1H,d)[d]	8.18(1H,d)[d]	
	3.29(5H,s)			7.05(1H,m)				
IId	2.8–3.3(15H,c)					7.22(1H,q)	8.21(2H,m)	
IIe	2.4–3.2(15H,c)					7.85(1H,d)[e]	8.51(1H,d)[e]	8.65(3H,s)[b]
IIf	3.14(20H,s)					7.64(2H,s)		
			Anisyl ring protons					
IIg	2.96(5H,s)	3.09(5H,s)	3.41(2H,d)[f]	3.61(2H,d)		7.38(1H,q)	8.36(1H,m)	6.46(3H,s)[c]
IIh	2.6–3.3(10H,c)		3.12(2H,d)[g]	3.53(2H,d)[g]		8.03(1H,d)[i]	8.63(1H,d)[i]	8.79(3H,s)[b]
								6.46(3H,s)[c]
IIi	3.11(5H,s)	3.13(5H,s)	3.21(2H,d)[h]	3.61(2H,d)[h]		7.68(2H,s)		6.46(3H,s)[c]

a) s: singlet, d: doublet, q: quartet, m: multiplet, c: complex. b) methyl protons. c) methoxy protons. d) J=6Hz. e) J=5Hz. f) J=8Hz. g) J=8Hz. h) J=8Hz. i) J=5Hz.

Table 4. The ultraviolet spectral data and analytical data of II

	Mp (Bp) °C	UV. λ_{max} in nm (log ε) in *n*-hexane	Analysis and M.W* (calcd) C%	H%	M.W.
IIa	120—120.5	250 (3.94 sh) 442 (2.21)	79.13 (79.37)	5.85 (5.86)	389 (378.3)
IIb	127—128	253 (3.85 sh) 444 (2.15)	79.51 (79.60)	6.24 (6.12)	396 (392.3)
IIc	175—176	250 (4.03 sh) 447 (2.27)	81.80 (81.79)	5.72 (5.98)	456 (455.4)
IId	(150—155/1.5 mmHg)	227 (4.23) 269 (3.27) 277 (2.99)	93.19 (93.29)	6.81 (6.71)	266 (270.4)
IIe	67—68 (161—162/2 mmHg)	214 (4.64) 254 (3.22) 261 (3.11)	92.97 (92.91)	7.06 (7.09)	278 (284.9)
IIf	165—166	212 (4.53) 241 (4.29) 270 (3.42) 278 (3.12)	93.78 (93.60)	6.51 (6.40)	357 (346.5)
IIg	111—112	225 (4.43) 236 (4.40) 272 (3.78) 278 (3.56) 292 (3.32)	88.06 (87.96)	6.63 (6.71)	280 (300.4)
IIh	82—83	227 (4.60) 279 (3.13) 285 (3.06)	88.12 (87.86)	7.17 (7.05)	308 (314.4)
IIi	142.5—143.5	240 (4.34) 277 (3.60) 286 (3.48) 291 (3.30 sh)	89.18 (89.32)	6.42 (6.43)	374 (376.5)

* VPO in benzene.

nesium bromide with acetophenone in ether, followed by dehydration with dil. sulfuric acid. The resulting crude substance was distilled twice through a short column under reduced pressure. Bp 114—115°C/3 mmHg, (lit,[9] 113°C/2 mmHg).

All the tosylhydrazones used in this study were prepared by the reactions of the corresponding ketones or aldehydes with a slight excess of tosylhydrazine in boiling ethanol. Among the starting materials, formylferrocene,[10] acetylferrocene,[10] benzoylferrocene,[11] *p*-methoxyacetophenone,[12] and *p*-methoxybenzophenone,[12] were prepared by known synthetic routes. The others were obtained from a commercial source.

The melting points and analytical data of these tosylhydrazones are summarized in Table 2.

Thermal Decomposition of Ia-i in a Pyridine-1,1-diphenlethyleyne Mixture. The physical properties, analytical data, and spectral data of the reaction products, IIa-i, are summarized in Tables 3 and 4.

Reaction of Ia. To a solution of Ia (7.65 g, 0.02 mol) in 50 m*l* of dry pyridine (over BaO), sodium hydride (1.38 g, 50% in oil) was added in one portion. Then the solution was mixed with mechanical stirring. After the rapid hydrogen gas evolution had been completed, 35 g (0.2 mol) of 1,1-diphenylethylene was added to the mixture. After the reaction system had then been flushed with Ar gas, the mixture was stirred vigorously at 90—98°C until the nitrogen gas evolution ceased (2 hr). The resulting mixture was cooled to room temperature, and then decomposed by adding 30 m*l* of water. The resulting solution was extracted with 300 m*l* of ether. The organic phase was separated and combined with extracts of the aqueous phase. The ether solution was washed with 100-m*l* portions of water seven times and dried over sodium sulfate. After the ether had then been evaporated, the residual oil was distilled under reduced pressure. The unreacted 1,1-diphenylethylene was recovered at 105—110°C/3 mmHg (31 g). The dark brown residual oil (8.5 g) was subjected to alumina-column elution chromatography (100 g of Al_2O_3). IIa was eluted with pentane as yellow needles; 0.93 g (12.5%); mp 114—118°C. Recrystallization from hexane afforded yellow needles; mp 120—120.5°C. IR spectrum (Nujol): 1603, 1496, 1102, 1073, 1050, 1030, 1015, 998, 961, 825, 810, 755, and 698 cm^{-1}.

Benzene-hexane (1 : 1) eluted orange-red crystals of formylferrocene azine; mp 267—268°C (lit,[10] 245°C). Found: C, 62.11; H, 4.92; N, 6.40%. Calcd for $C_{22}H_{20}N_2Fe$: C, 62.31; H, 4.75; N, 6.61%. IR spectrum (Nujol): 1635 (C=N), 1410, 1105, 1000, and 830 cm^{-1}. This azine was identified by means of comparing its mp with that of an authetic sample synthesized from the reaction of formylferrocene with hydrazine hydrate in boiling ethanol. The elution with methanol afforded a black polymeric material which was unidentified (ca. 3 g).

Reaction of Ib. The reaction of Ib was performed with 15.2 g (0.038 mol) of the tosylhydrazone in 95 m*l* of dry pyridine and 65 g (0.36 mol) of diphenylethylene under conditions similar to those above. An alumina chromatography of reaction mixture afforded 6.03 g (40.5%) of IIb, (mp 127—128°C), from hexane. IR spectrum (Nujol): 1598, 1492, 1178, 1135, 1102, 1042, 1030, 1015, 1000, 981, 943, 913, 860, 822, 808, 766, 751, and 702 cm^{-1}.

9) C. F. H. Allen and S. Converse, "Organic Syntheties," Coll. Vol. I, p. 226 (1956).

10) P. J. Graham, R. V. Rindsey, G. W. Parshall, M. L. Peterson and G. M. Whiteman, *J. Amer. Chem. Soc.*, **79**, 3416 (1957).

11) N. Weliky and E. S. Gould, *ibid.*, **79**, 2742 (1957).

12) R. Adams and C. R. Noller, "Organic Syntheses," Coll. Vol. I, p. 111 (1956).

From the benzene-hexane eluate, small amounts of two crystalline materials (mp 149—150°C, M.W. 880, and mp 147—148°C, M.W. 392) were isolated, besides a trace amount of azine. These structures have not yet been elucidated.

Reaction of Ic. Ic, 9.15 g (0.02 mol) were reacted in 50 m*l* of pyridine and 36 g of diphenylethylene under similar conditions. This reaction afforded IIc: 1.22 g; mp 175—176°C, (13.5%). IR spectrum (Nujol): 1601, 1495, 1103, 1072, 1035, 1026, 1000, 975, 900, 813, 800, 771, 750, 712, 700, and 690 cm^{-1}. Benzene-hexane eluted benzoylferrocene azine, 1.9 g, mp 155—157°C, which was identified by comparison with an authentic specimen (mixed mp and IR).

Reactions of Id-f. Each of the tosylhydrazones, Id, Ie, and If, (0.038 mol) was reacted in the usual manner. IId was obtained as a colorless liquid; 0.580 g (5.7%); 150—155°C/1.5 mmHg. IR spectrum (liquid film): 3120, 3080, 1605, 1500, 1450, 1072, 1030, 963, 772, 760, 733, and 695 cm^{-1}. IIe was obtained as colorless crystals; 6.35 g (58.7%); mp 161—162°C. IR spectrum (liquid film): 1598, 1490, 1440, 1075, 1064, 1011, 770, 746, and 700 cm^{-1}. IIf was obtained as colorless crystals; 3.08 g (23.4%); mp 165—166°C, (lit[2b] 165—165.5°C). IR spectrum (Nujol): 1600, 1495, 1072, 1031, 1006, 907, 795, 755, 717, and 695 cm^{-1}.

Reactions of Ig-i. Ig, Ih, and Ii (0.040 mol) were all reacted as usual. However in the reactions of Ih and Ii the temperature was raised to 120°C in order to smooth the decomposition of the salts. IIg was obtained as colorless crystals; 4.20 g (35.0%); mp 111—112°C. IR spectrum (Nujol): 1610, 1600, 1514, 1495, 1300, 1245, 1185, 1030, 967, 835, 812, 766, 757, 733, and 700 cm^{-1}. IIh (9.43 g, 75%) was obtained. Mp 82—83°C. IR spectrum (liquid film): 3100, 3070, 2960, 1612, 1603, 1512, 1495, 1450, 1380, 1245, 1180, 1030, 829, 770, 750, 706, and 695 cm^{-1}. IIi (4.10 g 27%) was obtained. Mp 142.5—143.5°C. IR spectrum (Nujol): 1612, 1602, 1510, 1495, 1245, 1173, 1106, 1029, 782, 750, 730, and 699 cm^{-1}.

The authors wish to thank Mr. Katsuhiko Maruo for his technical assistance and Dr. Koji Yamamoto for his helpful discussions.

BULLETIN OF THE CHEMICAL SOCIETY OF JAPAN VOL. 43 3528—3534 (1970)

Tri(hetero)substituted Carbonium Ions. IV. Reactions of *N,N*-Dimethyl-*S,S'*-dimethyldithiocarbamidium Ion with Various Nucleophiles*

Takeshi NAKAI and Makoto OKAWARA

Research Laboratory of Resources Utilization, Tokyo Institute of Technology, Ookayama, Meguro-ku, Tokyo

(Received May 13, 1970)

A wide spectrum of electrophilic reactivity has been shown by *N,N*-dimethyl-*S,S'*-dimethyldithiocarbamidium perchlorate (II). Results obtained reveal that II behaves toward nucleophiles as an ambident electrophile with two reactive sites, a centered electron-definicent carbon and *S*-methyl carbon atom. The electrophilic behavior of II has been compared with that of a cyclic analog, 2-dimethylamino-1,3-dithiolanylium ion, and of a sulfur analog, tris(methylthio)-carbonium ion. Attempts to utilize II for synthetic reactions were made. Reactions of II with active methylene compounds gave ketone *N,S*-acetals which are of great interest from the standpoint of structural chemistry. *o*-Phenylenediamine and *o*-aminophenol reacted with II to give 2-dimethylamino-benzimidazole and -benzoxazole, respectively, in good yields. The reactions may provide a new method of introducing 2-dialkylamino groups into these heterocycles. Reactions of II with two equivalents of primary amines afforded tetrasubstituted guanidines. Reactions of II with *p*-toluenesulfonylhydrazine and an enamine were also studied.

In our previous papers[1-3] information on the characterization and electrophilic reactivity, of 2-dialkylamino-1,3-dithiolanylium ions (I) was given. The stable carbonium ions behave toward nucleophiles as an ambident electrophile with two reactive sites. *a* and *b* in formula (I) and the reaction course are greatly affected by the nucleophilicity of the reagent used.

In the present work the electrophilic behavior of an open-chain analog of I, *N,N*-dimethyl-*S,S'*-dimethyldithiocarbamidium ion (II),[4] has been investigated in detail. Our previous studies on I lead us to expect a similar ambident behavior of II. The reactions of a sulfur analog of II, tris-(methylthio)carbonium ion (III) with nucelophiles have been reported.[5]

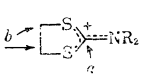

I

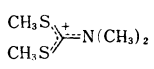

II

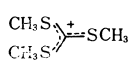

III

The purpose of this work is to clarify differences in the electrophilic behavior between open-chain cation II and cyclic I or sulfur analog III, and to utilize II for synthetic reactions.

Results and Discussion

N,N-Dimethyl-*S,S'*-dimethyldithiocarbamidium perchlorate (IIa) was obtained in 78% yield by methylation of methyl *N,N*-dimethyldithiocarbamate with dimethyl sulfate[6] followed by treatment with sodium perchlorate. The white crystals melted at 84—86°C and its NMR spectrum showed two singlet signals at δ 2.85 (SCH_3) and 3.70 ppm (NCH_3).

Reactions with Simple Nucleophiles. In order to demonstrate the spectrum of reactivity of II, the reactions of IIa with a variety of nucleophiles including hydroxide, alkoxides, mercaptides, cyanide and dimethyldithiocarbamate ions were investigated. Scheme 1 indicates products obtained and the possible reaction sequences. Characterization of products isolated includes comparisons of their IR and NMR spectra, boiling and melting points, and refractive indexes with those of authentic compounds.

After our preliminary communication ap-

*1 Presented in part at the 20th Annual Meeting of the Chemical Society of Japan, Tokyo, 1967.

1) T. Nakai, Y. Ueno and M. Okawara, *Tetrahedron Lett.*, **1967**, 3831; This Bulletin, **43**, 156 (1970).

2) T. Nakai and M. Okawara, *Tetrahedron Lett.*, **1967**, 3835; This Bulletin, submitted.

3) T. Nakai, Y. Ueno and M. Okawara, Abstracts of papers presented at the 18th Symposium on Organic Reaction Mechanisms, Kyoto, 1967, p. 77.

4) This cation may be also termed bis(methylthio)-dimethylaminocarbonium ion.[3]

5) W. P. Tucker and G. L. Roof, *Tetrahedron Lett.*, **1967**, 2747,

6) Rinteln and Riester have reported the formation of several methyl sulfate of dithiocarbamidium ions, but no physical properties are available: H. v. Rinteln and O. Riester, *Mitt. Forschungslab. Agfa Leverkussen-München*, **1**, 65 (1955); *Chem. Abst.*, **51**, 7013 (1957).

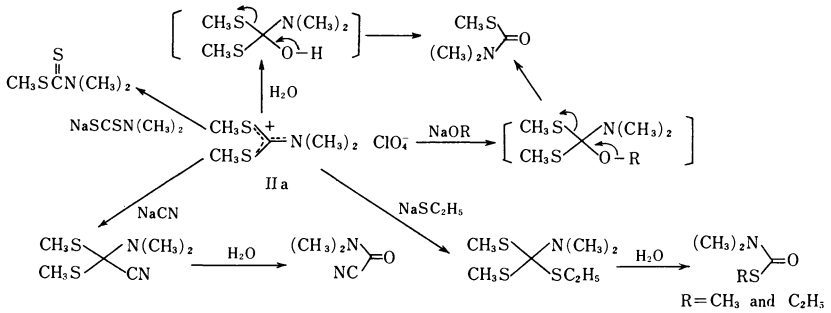

Scheme 1. Reaction Sequences.

Table 1. The attacking site of nucleophiles

Nucleophile	CH_3S, CH_3S $\overset{+}{C}$ $N(CH_3)_2$ *1 (II)	S, S $\overset{+}{C}$ $N(CH_3)_2$ *2 (I)	CH_3S, CH_3S $\overset{+}{C}$ SCH_3 *3 (III)
$^-$OH, $^-$OR	*a*	*a*	*a*
$^-$CN	*a*	*a*	*a*
$^-$SR	*a*	*b*	*a*
$^-SCSNR_2$	*b*	*b*	*b**4
RNH_2	*a**5	*a*	*a**4
R_3N	*b**6	*7	*b*
R_2S	*b**6		

*1 Unless otherwise indicated, this work.
*2 Ref. 2.
*3 Unless otherwise indicated, ref. 5.
*4 Our unpublished results.
*5 The results are described below.
*6 Ref. 7.
*7 *S*-Vinyl *N,N*-dimethyldithiocarbamate was obtained; Ref. 2.

peared,*1 Tarbell and co-workers briefly reported on reactions of the iodide of II with triethylamine and dimethyl sulfide[7]; II reacts with these nucleophiles to produce the methylated compounds of the nucleophiles and methyl *N,N*-dimethyldithiocarbamate. The behavior of II toward nucleophiles are summarized in Table 1 together with those of I and III.

Table 1 shows that, as expected, carbonium ion II is an ambident electrophile with two reactive sites, the centered carbon (*a*) and *S*-methyl carbon atom (*b*) and that, on the whole, II directs the attack of nucleophiles in the same manner as I and III. However, some significant differences between II and I or III were observed; (i) II directs the attack of $^-$SEt to position *a*, while I reacts with the anion at position *b*; (ii) under the given conditions II resists reacting with $^-SC_6H_4$-CH_3-*p* (see Experimental), but I readily reacts with the anion at position *b*; (iii) II reacts with $^-$CN at *a*, while III directs the attack of the anion to *b*; (iv) II directs the attack of NEt_3 to *b*, while I reacts with the amine to afford *S*-vinyl dithiocarbamates *via* hydrogen abstraction reactions. Difference (i) is the first example that the reaction course undergoes with a change in the structure of carbonium ion having the same three α-hetero atoms.

These differences cannot be reasonably explained in the present stage. In the case of the reaction with $^-$SEt, however, the difference in reaction course between I and II might be interpreted in terms of the stability of the two carbonium ions described below.

According to our classification of reactions, the reaction at site *a* is mode A and the reaction at *b* is mode B, and the former is controlled kinetically and the latter thermodynamically.[2,3] In consequence, the free activation energy for mode A always much less than that for mode B since mode A corresponds to a simple association between the cation and the anion. It might be assumed that the position of equilibrium between the cation and the adduct in mode A should depend upon the difference in free energy (ΔF_A). On the other hand, the fact that II is greatly less stable than I has been confirmed not only by the kinetic observation that the rate of reaction of II with $^-$OH is about 10^4 times larger than that of I,[3] but also by the spectral observation that the absorption maximum of II appears at a longer wavelength (276 mμ) than

7) J. L. Richard, D. S. Tarbell and E. H. Hoffmeister, *Tetrahedron*, **24**, 6485 (1968).

that of I (249 mμ).[8] It may be further expected that adduct IV from II and $^-$SEt is comparable to or slightly less stable than adduct V from I and the anion. Accordingly, it may be said that the difference in free energy between II and IV is larger than that between I and V, *i.e.*, $\Delta F_A(II) > \Delta F_A(I)$. Alternatively, the position of equilibrium in Eq. 1 is shifted to the right leading to the formation of IV, while the position in Eq. 2 is shifted to the left, which, in turn, results in the formation of β-(ethylthio)ethyl dithiocarbamate (VI) *via* mode B, as found experimentally. These considerations confirm the postulate previously proposed that the major factor deciding the reaction course is the relative position of kinetically controlled product such as IV and V in the energy diagram.

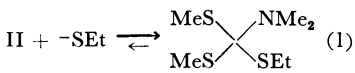

(1)

IV

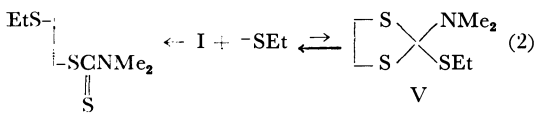

(2)

V

VI

Furthermore, it is interesting to note that as exemplified in the reaction of II with hydroxide ion, II may be expected to react with nucleophiles bearing an active hydrogen atom ($^-$NuH) to afford compounds of a type of ketene *N,S*-acetal (VII), which are of some use from the preparative point of view.

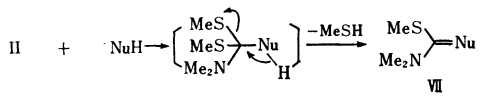

VII

Thus, the reactions of IIa with active methylene compounds, primary amines and an enamine were studied and the results are described below.

Reactions with Active Methylene Compounds. A suspension of IIa and the sodium enolate of active methylene compound in dioxane was stirred at 80°C to afford ketene *N,S*-acetal (VIII) accompanied by evolution of methylmercaptan. These products were identified by IR and NMR spectra. Yields and physical properties of VIII are shown in Table 2.

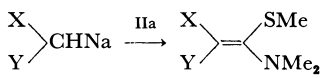

VIII

These ketene *N,S*-acetals are of special interest from the standpoint of structural chemistry because observations of unusually low barriers to internal rotation around the carbon-carbon double bond may be anticipated.[9] Table 3 shows the

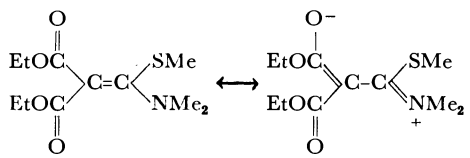

VIII VIIIa′

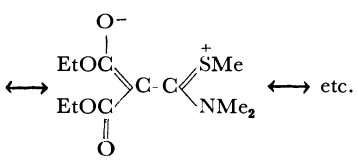

VIIIa″

Table 2. Yields and physical properties of VIII

Compd.	X	Y	Yield %	Bp/mmHg °C	Mp °C	N, % Found	N, % Calcd
VIIIa	$COOC_2H_5$	$COOC_2H_5$	52	139—141/0.4	---	4.99	5.36
b*1	$COOC_2H_5$	$COCH_3$	28	144—146/0.4	62—65*2	6.10	6.06
c*1	$COOC_2H_5$	CN	68	160—162/0.4	92—93*3	12.95	13.08
d	$COCH_3$	$COCH_3$	41	150—151/0.4	solid*4	6.75	6.96
e	CN	CN	62	—	76—77*3	24.86	25.14

*1 No attempt was made to determine the geometric configration (see text).
*2 Recrystallized from hexane.
*3 Recrystallized from cyclohexane.
*4 Very hygroscopic.

8) For the α-hetero atom effects on electronic spectra of tri(hetero)substituted carbonium ions, a definite trend has been observed. As SCH_3 in tris(methylthio)-carbonium ion (III) is progressively replaced by the more electron-donating $N(CH_3)_2$, there is a strong shift of absorption maxima to short wavelengths (high energies). This trend suggests that as the carbonium ion becomes more stabilized, the absorption maximum appears at shorter wavelength. The conclusion has been confirmed by simple Hückel molecular orbital calculations: T. Nakai, K. Hiratani and M. Okawara, unpublished results.

9) Recently Sandström and co-workers have reported on the observations of low barriers to internal rotation around the C=C bonds in ketene mercaptals and the aminals: G. Isakson, J. Sandström and I. Wennerbeck, *Tetrahedron Lett.*, **1967**, 2233.

Table 3. Spectral data of VIII

Compd.	IR,*1 cm^{-1}			NMR,*2 δ ppm		
	$\nu_{C=\overset{+}{N}<}$	$\nu_{C=O}$ ($\nu_{C=N}$)	$\Delta\nu_{C=O}$ ($\Delta\nu_{C=N}$)*3	CH_3S	CH_3N	Others
VIIIa	1550	1690	40	2.30 (s)	3.08 (s)	$C\underline{H}_3CH_2$ 1.24 (t)*4 $CH_3C\underline{H}_2$ 4.07 (q)*4
VIIIb	1532	1665 (ester) 1575 (ketone)	80 145	2.40 (s)	3.34 (s)	$C\underline{H}_3CH_2$ 1.24 (t)*4 $CH_3C\underline{H}_2$ 4.08 (t)*4 CH_3CO 2.25 (s)
VIIIc	1545	1670 (2210)	70 (~90)	2.62 (s)	3.25 (s)	$C\underline{H}_3CH_2$ 1.24 (t)*4 $CH_3C\underline{H}_2$ 4.17 (q)*4
VIIId	1525	1575	135			
VIIIe	1545	(2220)				

*1 Spectra were recorded on KBr disks except for VIIIa (in liquid film).
*2 Spectra were obtained in CCl_4 (VIIIa, b) and in $CDCl_3$ (VIIIc).
*3 The difference in wave number between ketene *N,S*-acetal and the parent methylene compound.
*4 J=8.0 Hz.

Table 4. Reactions of IIa with primary amines

Amine	Product	Yield %	Mp °C	C, %		H, %		N, %	
				Calcd	Found	Calcd	Found	Calcd	Found
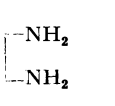	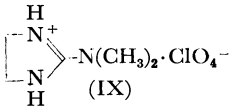 (IX)	56	159—160	28.10	28.10	5.65	5.77	19.67	19.38
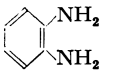	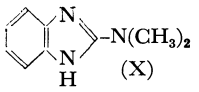 (X)	90	297—301*1	(41.31	41.34	4.62	4.72	16.06	15.91)*2
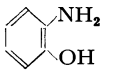	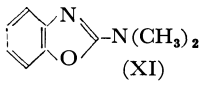 (XI)	78	83—85	66.65	66.86	6.22	6.08	17.27	16.79

*1 Reported mp 301°C: ref. 11.
*2 For benzimidazolium perchlorate (mp>310°C).

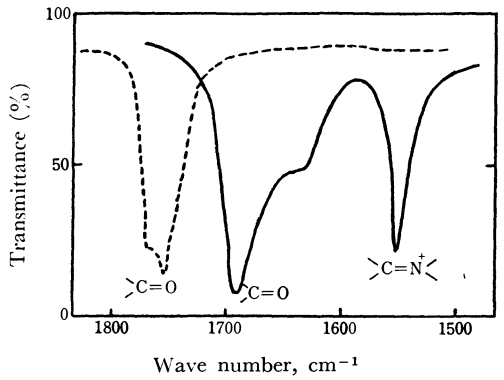

Fig. 1. IR spectra.
——: Diethyl malonate (neat).
- - -: VIIIa (neat).

spectral data of VIII. It is interesting to note that the IR spectra of compounds (VIIIa, b, c and d) showed the carbonyl stretching band ($\nu_{C=O}$) at lower wave numbers than those of the parent methylene compounds. A typical example is shown in Fig. 1. This spectral trend suggests that the polar structures such as VIIIa′ and VIIIa″ significantly contribute to the ground state.

Recently Sandström has reported on unusually low barriers to internal rotation around the C=C bonds in ketene *N,S*-acetals by means of temperature variable NMR spectroscopy.[10] The significant contribution of the polar structures would be responsible for the unusually low barriers to internal rotation. In consequence, it seems to be impossible to determine the geometric configuration of VIIIb and VIIIc at room temperature since a fast interconversion between the *cis* and *trans* isomers occurs.

Reactions with Primary Amines. Carbonium salt IIa reacted with ethylenediamine at 50°C to give an imidazolium salt (IX) in 50% yield. Similarly, carbonium salt IIa reacted with *o*-phenylenediamine and *o*-aminophenol followed by treatment with base to afford 2-dimethylaminobenzimidazole (X) and the benzoxazole derivative (XI), respectively. The formation of these heterocyclic compounds may be explained by the following scheme which involves an intramolecular reaction of intermediate XII of type of VII. Table 4 shows yields and physical properties of these products.

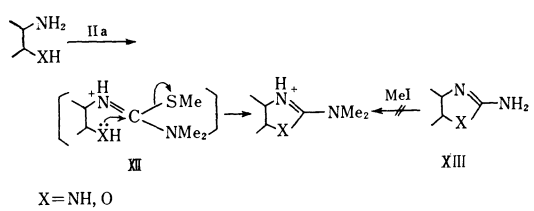

These reactions are of some avail since they provide a new method for introducing dialkylamino groups into the 2 position of these heterocyclic systems; 2-dialkylamino-benzimidazoles and the benzoxazole analogs cannot be prepared by alkylation of easily obtainable 2-amino derivatives owing to the basic properties of the nitrogen atom in the rings. Recently Eilingsfeld and Möbius have reported that compound X was obtained in 57% yield from *N,N*-dimethyl-(2-methoxycarbonylethylmercapto)-formamide chloride and *o*-phenylenediamine.[11]

It was found that IIa reacted with two equivalents of primary amines (cyclohexylamine and aniline) to afford tetrasubstituted guanidium salts (XIV) *via* an intermolecular reaction of the intermediate of a VII type with the amine. These salts were hydrolyzed to produce disubstituted ureas (XV). The formation of the guanidium salts is of some interest since there is the possibility that guanidine obtained by treatment of XIV with an appropriate base thermally decomposes to give carbodiimides (XVI) accompanied by elimination of dimethylamine[12] (see Experimental).

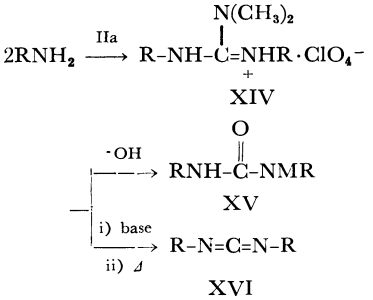

In contrast to these primary amines, *p*-toluenesulfonylhydrazine reacted with IIa to give hydrazone XVII accompanied by elimination of dimethylammonium salt. Hydrazone XVII has been employed as a precursor of bis(methylthio)-carbene.[13]

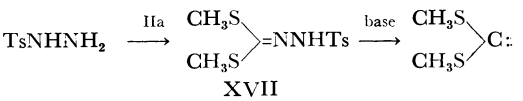

Reaction with An Enamine. Carbonium salt IIa reacted with 1-*N*-morpholino-1-cyclo-

10) For ketene *N,S*-acetal VIIIc, the following data was available: coalescene temperature (Tc) is −67.5°C and free activation energy for internal rotation (ΔG^*) is 10.4 kcal/mol: J. Sandström, private communication.

11) E. Eilingsfeld and L. Möbius, *Chem. Ber.*, **98**, 1293 (1965).

12) W. Weith [*Ber.*, **7**, 1303 (1874)] prepared diphenylcarbodiimide by thermal decomposition of *sym*-triphenylguanidine.

13) D. M. Lemal and E. H. Banitt, *Tetrahedron Lett.*, **1964**, 245; U. Schöllkopf and E. Wiskott, *Ann.*, **694**, 44 (1966).

hexene to give iminium salt XVIII, a compound of type of VII, which was isolated as tetraphenylborate in 43% yield. Hydrolysis of the salt gave α-(*N,N*-dimethylcarbamoyl)cyclohexanone (XIX), which was identified by IR spectrum and by conversion to the 2,4-dinitrophenylhydrazone. The reaction sequences are shown below.

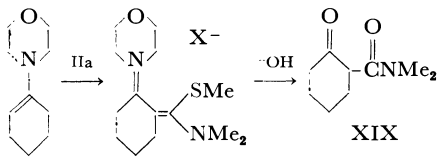

XVIII, X = ClO_4, BPh_4 XIX

Experimental

General. All melting and boiling points are uncorrected. Infrared and ultraviolet spectra were recorded on Hitachi EPI-S2 and EPS-2 spectrometers, respectively. NMR spectra were obtained with a Japan Electron Optics C-60 spectrometer. Chemical shifts are given in parts per million (ppm) from tetramethylsilane as an internal standard. Multiplicity of signals is indicated as follows; s=singlet, t=triplet, q=quartet and m=multiplet.

N,N-Dimethyl-S,S′-dimethyldithiocarbamidium Perchlorate (IIa). Methyl *N,N*-dimethyldithiocarbamate (13.5 g, 0.10 mol) was dissolved in 12.5 g (0.10 mol) of dimethyl sulfate. When the mixture was heated to 60°C, a vigorous exothermic reaction occurred. The reaction temperature was kept below 100°C. After the exothermic reaction stopped the mixture was stirred at 90°C for an additional 30 min. The mixture was poured into 100 m*l* of a saturated aqueous solution of sodium perchlorate giving 19.0 g (76%) of pale yellowish precipitate. The precipitate was washed with ether and recrystallized from methanol giving white crystals: mp 84—86°C.

Found: C, 23.73; H, 4.68; N, 5.13%. Calcd for $C_5H_{12}ClNO_4S_2$: C, 24.05; H, 4.85; N, 5.61%.

Hydrolysis of IIa. Carbonium salt IIa (12.5 g, 0.05 mol) was added to a solution of water (1.0 g, 0.05 mol) and triethylamine (5.0 g, 0.05 mol) in 50 m*l* of dioxane. The mixture was stirred at 80°C for 6 hr, then poured into water. The ethereal extract was dried over anhydrous sodium sulfate and the solvent evaporated *in vacuo*. Distillation of the residue gave 3.7 g (62%) of methyl *N,N*-dimethylthiolcarbamate; bp 91—92°C/31 mmHg; n_D(21°C) 1.4964 (lit, [11] bp 115—116°C/89 mmHg; n_D(30°C) 1.4932); IR (neat) 1650 cm^{-1} (C=O); NMR (CCl_4): δ 2.26 (s, SCH_3) and 3.00 ppm (s, NCH_3). The infrared spectrum of this distillate was in agreement with that of the authentic sample.

Reactions with Sodium Alkoxides. A suspension of IIa (0.05 mol) and sodium methoxide (8.0 g, 0.15 mol) in 70 m*l* of dioxane was stirred at 70°C for 2 hr. Work-up gave methyl *N,N*-dimethylthiolcarbamate in 69% yield.

The reaction of IIa with sodium ethoxide carried out as in the case of sodium methoxide gave the same product in 60% yield.

Reaction with Sodium Cyanide. Carbonium salt IIa (0.05 mol) and sodium cyanide (7.5 g, 0.15 mol) were dissolved in 50 m*l* of dimethylformamide (DMF). The mixture was stirred at 60°C for 5 hr, then poured into an aqueous solution of sodium carbonate. After being put to stand overnight, the mixture was extracted with ether. The ethereal solution was dried over anhydrous sodium sulfate and the solvent evaporated *in vacuo*. Distillation of the residue gave 4.4 g (90%) of *N,N*-dimethylcarbamoyl cyanide; bp 39—41°C/1.0 mmHg (lit,[15] 202—203°C); n_D(22°C) 1.4873; IR (neat): 2270 (C≡N) and 1670 cm^{-1} (C=O).

Attempts made to isolate the initial adduct, bis(methylthio)-*N,N*-dimethylaminocarbinyl cyanide, failed.

Reaction with Sodium N,N-Dimethyldithiocarbamate. Carbonium salt IIa (0.01 mol) and sodium *N,N*-dimethyldithiocarbamate (1.8 g, 0.01 mol) were dissolved in 20 m*l* of DMF. The mixture was stirred at 70°C for 3 hr, then poured into cold water giving 1.1 g (41%) of white precipitate of methyl *N,N*-dimethyldithiocarbamate: mp 44—46°C. The IR spectrum of the product was in agreement with that of the authentic sample. The low yield might be due to dissolution of the product in the solvents.

Reactions with Sodium Mercaptides. A suspension of carbonium salt IIa (20.0 g, 0.08 mol) and sodium ethylmercaptide (5.0 g, 0.05 mol) in 50 m*l* of dioxane was stirred at 80°C for 5 hr under a nitrogen atmosphere. The reaction mixture was poured into water, then extracted with ether. The ethereal extract was dried over anhydrous sodium sulfate and the solvent evaporated *in vacuo*. Distillation of the oily residue gave two distillates: bp 55—57°C/51 mmHg (4.7 g) and bp 125—140°C/39 mmHg (1.6 g).

The IR spectrum of the former product showed a strong absorption band at 1650 cm^{-1} (C=O) and the NMR spectrum showed proton signals at δ 2.25 (s, SCH_3), 3.00 (s, NCH_3), 1.25 (t, $C\underline{H}_3CH_2S$) and 4.65 ppm (q, $CH_3C\underline{H}_2S$). Results indicate that the former product is a mixture of *S*-methyl *N,N*-dimethylthiolcarbamate and its *S*-ethyl analog.

On the other hand, the IR spectrum of the latter product exhibited no absorption band due to carbonyl groups and the NMR spectrum showed proton signals at δ 1.25 (t, $C\underline{H}_3CH_2S$), 2.06 (s, SCH_3), 2.33 (s, NCH_3) and 4.65 ppm (q, $CH_3C\underline{H}_2S$). The data indicate that the latter prodact seems to be $(MeS)_2(EtS)C(NMe_2)_2$.

The reaction of IIa with sodium *p*-tolylmercaptide carried out as in the case of sodium ethylmercaptide gave no organic products.

Reactions with Active Methylene Compounds. Sodium (1.2 g, 0.050 mol) was added to a solution of an active methylene compound (0.055 mol) in 75 m*l* dioxane. The mixture was heated at 50°C giving a precipitate of sodium enolate accompanied by evolution of hydrogen gas. Carbonium salt IIa (0.050 mol) was then added to the suspension and the mixture was stirred at 80°C for 2 hr under a nitrogen atmosphere. Sodium perchlorate formed on cooling was filtered off. Distillation of the filtrate under reduced pressure gave ketene *N,S*-acetal (VIII). In the case of malononitrile, the solvent was removed from the filtrate giving a solidified residue. The residue was recrystallized

14) H. Tilles, *J. Amer. Chem. Soc.*, **81**, 714 (1959).

15) F. K. Beilstein, "Handbuch der Organischen Chemie," Vol. 5, Suppl. II, p. 330 (1943).

from acetonitrile.

Yields and physical properties of VIII are shown in Tables 2 and 3.

Reaction with Ethylenediamine. Carbonium salt IIa (5.0 g, 0.02 mol) and ethylenediamine (1.2 g, 0.02 mol) were dissolved in 40 m*l* of ethanol. The mixture was refluxed for 5 hr, and the solvent was evaporated *in vacuo* to give precipitates of IX: mp 159—160°C (ethanol).

Reaction with *o*-Phenylenediamine. The reaction of IIa (0.02 mol) and *o*-phenylenediamine (2.0 g, 0.02 mol) carried out as in the case of the reaction with ethylenediamine gave benzimidazolium perchlorate (Xa); mp>310°C (ethanol). Treatment of Xa with an ethanolic solution of sodium methoxide gave 2-dimethylamino-benzimidazole (X).

Reaction with *o*-Aminophenol. The reaction of IIa (0.02 mol) with *o*-aminophenol (2.0 g, 0.02 mol) carried out as in the case of the reaction with *o*-phenylenediamine gave 2-diaethylamino-benzoxazole (XI) (recrystallized from ethanol).

Yields and physical properties of products from reactions with the three amines are shown in Table 4.

Reactions with Primary Amines. *With Cyclohexylamine.* A solution of IIa (0.02 mol) and cyclohexylamine (4.0 g, 0.04 mol) in 50 m*l* of ethanol was heated at 50°C for 5 hr. The solvent was removed *in vacuo* giving a viscous residue. An aqueous solution of $NaBPh_4$ was added to the residue giving a white precipitate of guanidinium salt (XIV; R=C_6H_{11}, X=BPh). However, the precipitate did not give satisfactory data of elementary analysis. On the other hand, an aqueous solution of sodium carbonate was added to the viscous residue (XIV, X=ClO_4) giving a white precipitate accompanied by evolution of dimethylamine. Recrystallization of the precipitates from ethanol gave colorless needles of *N,N'*-dicyclohexylurea: mp 227—228°C. The IR spectrum of the precipitate was in agreement with that of the authentic sample.

Some attempts were made to prepare carbodiimide from guanidinium salt; a solution of potassium *t*-buthoxide in *t*-buthanol was added to the viscous residue (XIV, X=ClO_4) and anhydrous ether was then added to the resulting mixture giving a precipitate of potassium perchlorate. The precipitate was filtered off and the solvents were evaporated from the filtrate giving an oily residue. The residue was heated at 150°C for 2 hr under reduced pressure (30 mmHg). The IR spectrum of the resulting residue showed a strong band at 2200 cm^{-1} presumably due to the –N=C=N– group. However, isolation of dicyclohexylcarbodiimide in pure form was unsuccessful.

With Aniline. The reaction of IIa (0.02 mol) with aniline (3.6 g, 0.04 mol) carried out as in the case of cyclohexylamine gave a viscous residue of guanidinium salt (XIV; R=Ph, X=ClO_4). Addition of a solution of $NaBPh_4$ to the residue gave a precipitate of tetraphenylborate: mp 130—132.5°C (from ethanol). However, the data of elementary analysis were unsatisfactory. Treatment of the viscous residue with an aqueous solution of sodium carbonate gave a precipitate of *N,N'*-diphenylurea: mp 233—235°C. The IR spectrum of the precipitate was in agreement with that of the authentic sample.

Reaction with Tosylhydrazine. Tosylhydrazine (3.7 g, 0.02 mol) was suspended in a solution of IIa (0.02 mol) in 40 m*l* of ethanol. The suspension was heated with stirring at 55—60°C for 4 hr. The resulting clear solution was cooled in an ice box giving 2.7 g (61%) of precipitates of XVII. Recrylstallization from ethanol gave colorless needles: mp 149—150°C (lit,[13] 150.5—151.5°C).

Found: C, 41.27; H, 4.92; N, 9.87%. Calcd for $C_{10}H_{14}N_2O_2S_3$: C, 41.38; H, 4.86; N, 9.65%.

Reaction with An Enamine. Carbonium salt IIa (0.02 mol) was added to a solution of 1-*N*-morpholino-1-cyclohexene (0.02 mol) in 30 m*l* of dioxane. The suspension was heated with stirring at 50—60°C for 30 min. The solvent was then evaporated *in vacuo* producing a viscous residue containing iminium salt (XVIII; X=ClO_4). An aqueous solution of $NaBPh_4$ was added to the residue giving a precipitate (43%) of iminium salt XVIII (X=BPh_4): mp 187—189°C; IR (KBr): 1565 cm^{-1} (C=N).

Found: N, 4.42%. Calcd for $C_{38}N_{45}BN_2OS$: N, 4.76%.

The viscous residue was treated with a dilute aqueous solution of sodium hydroxide and the mixture was extracted with ether. The ethereal layer was dried over anhydrous sodium sulfate. The solvent was then evaporated *in vacuo* affording an oily residue, 2-*N,N*-dimethylcarbamoylcyclohexanone (XIX); IR (neat): 1695 (ketone) and 1645 cm^{-1} (amide). Treatment of the oily residue with 2,4-dinitrophenylhydrazine gave a precipitate of the corresponding hydrazone; mp 83—85°C (ethanol).

Found: C, 51.84; H, 5.30%. Calcd for $C_{13}H_{18}N_5O_5$: C, 51.57; H, 5.48%.

The authors are grateful to Dr. J. Sandström, University of Lund, Sweden, for disclosing the results of his work on internal rotation prior to publication, and to Mr. Y. Ueno for his technical assistance.

BULLETIN OF THE CHEMICAL SOCIETY OF JAPAN VOL. 43 3535—3539 (1970)

The Preparation, Lithium Aluminum Hydride Reduction, and Electronic Spectra of Halogen-substituted 3,4-Bis(diphenylmethylene)-cyclobutenes and -cyclobutanes

Fumio TODA, Kunihiro KUMADA, Nobuo ISHIGURO and Katsuhiko AKAGI

Department of Industrial Chemistry, Faculty of Engineering, Ehime University, Matsuyama

(Received May 20, 1970)

The title compounds were prepared, and their physical and chemical properties were investigated. The reduction of the cyclobutenes with lithium aluminum hydride afforded halogen-free cyclobutane. The mechanism of the reduction is discussed. The cyclobutenes showed their K-bands in a wavelength region *ca.* 100 nm shorter than in the cases of the corresponding cyclobutanes. Furthermore, the K-band of the cyclobutenes is comparable to that of 1-phenylbuta-1,3-diene. On the basis of the electronic spectral data, a puckered structure was postulated for the cyclobutenes.

Molecular orbital calculations have indicated that dimethylenecyclobutene has a delocalization energy of 1.21 β, which is almost equal to that of cyclobutenedione, 1.24 β.[1-3] Those calculated values, however, might not always show the stability or aromaticity of such a small-ring system, since calculations are carried out without consideration of any ring-strain factor.

Some anomalous ultraviolet spectral data of dimethylenecyclobutenes have been discussed. Since the two strong absorption bands of dimethylenecyclobutenes having no conjugated substituents, 209—213 and 245—249 nm, are comparable to those of 1,2-dimethylenecyclobutane, 237, 246, and 255 (sh) nm, it has been suggested that dimethylenecyclobutene is better viewed as a cross-conjugated diene rather than as a conjugated triene.[3-5] On the other hand, the absorption bands of 1,2-diphenyldimethylenecyclobutene, 237, 262, and 328 nm, are not derivable by the simple overlap of the spectra of dimethylenecyclobutane and *cis*-stilbene, 285 nm.[3,6,7]

The discrepancy of the calculated delocalization energy and the spectral data of dimethylenecyclobutene probable arises because of the *endo*-double bond's causing ring strain. In order to clarify the nature of such *endo*-double bonds, we have studied the electronic spectra and lithium aluminum hydride (LAH) reduction of the title compounds (III—X). Electronic spectral studies of those compounds have shown that bis(diphenylmethylene)cyclobutanes (IV, V, VII, IX and XII) absorbed at a much longer wavelength region, *ca.* 390 nm, than did bis(diphenylmethylene)-cyclobutenes (III, VIII and X) (*ca.* 290 nm). The reduction of the compounds of both series by LAH afforded bis(diphenylmethylene)cyclobutane (XII). Studies of the reduction mechanism, disclosed that the reduction of the *endo*-double bond of III and X to afford XII proceeds by way of competing addition and elimination processes.

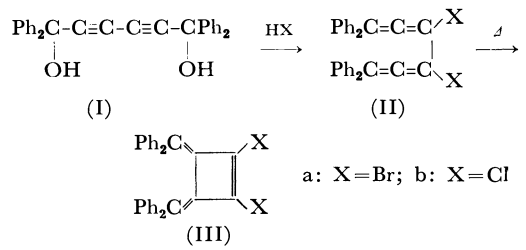

Scheme 1

Preparation of Compounds. The treatment of 1,1,6,6-tetraphenylhexa-2,4-diyne-1,6-diol (I) with hydrohalogeno acid in acetic acid at about 0°C afforded 3,4-dihalo-1,1,6,6-tetraphenylhexa-1,2,4,5-tetraene (II).*1 By heating a benzene solu-

1) J. D. Roberts, A. Streitwieser, Jr., and C. M. Regan, *J. Amer. Chem. Soc.*, **74**, 4579 (1952).

2) S. L. Manatt and J. D. Roberts, *J. Org. Chem.*, **34**, 1336 (1959).

3) M. P. Cava and M. J. Mitchell, "Cyclobutadiene and Related Compounds," Academic Press, New York and London (1967), pp. 157—179.

4) A. T. Blomquist and P. M. Maitlis, *Proc. Chem. Soc.*, **1961**, 332.

5) A. T. Blomquist and J. A. Verdol. *J. Amer. Chem. Soc.*, **77**, 1806 (1955).

6) A. T. Blomquist and Y. C. Meinwald, *ibid.*, **81**, 667 (1959).

7) A. T. Blomqist and Y. C. Meinwald, *ibid.*, **79**, 5317 (1957).

*1 The preparation of IIa and its transformation to 2,5,6,6-tetraphenyl-3-bromofulvene by protonation, accompanied by the cyclization and migration of phenyl, have been reported in a preliminary communication: M. Higashi, F. Toda and K. Akagi, *Chem. Ind.* (London), **1969**, 491.

tion of II under reflux for 1 hr in a nitrogen atmosphere, a cyclization product, 1,2-dihalo-3,4-bis(diphenylmethylene)cyclobutene (III), was obtained in a quantitative yield. The IIIa and IIIb thus obtained showed the medium band of the *endo*-double bond at 1510 and 1530 cm^{-1} respectively, in addition to the weak band of the *exo*-double bond at 1660 cm^{-1}. The method of preparing III from II is comparable to that used for preparing dimethylenecyclobutene from 1,5-hexadiyne by pyrolysis at 350°C.[8] The reaction is believed to proceed through an intermediate diallene.[8]

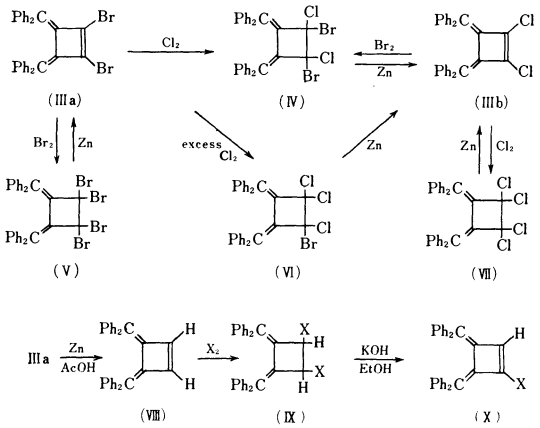

a: X=Br; b: X=Cl

Scheme 2

The addition of bromine to IIIa and that of chlorine to IIIb in chloroform afforded tetrabromide (V) and tetrachloride (VII) respectively, in almost quantitative yields. Heating the tetrahalides with zinc powder in ethanol gave the corresponding dihalides (III) quantitatively. The action of chlorine on IIIa, which affords mainly monobromotrichloride (VI) (71%), is in contrast to that of bromine on IIIb, which gives dibromodichloride (IV). The addition of chlorine, however, under carefully-controlled conditions afforded mainly IV. Both IV and VI afforded IIIb when treated with zinc powder in boiling ethanol. Since the cross-addition reactions of IIIa and IIIb afforded the same product, IV, it is clear that the addition occurs on the *endo*-double bond. Furthermore, the structures of the tetrahalides (IV, V, VI, and VII) were determined on the basis of the electronic spectral data: those data showed that all the tetrahalides absorbed at nearly the same region, 400—388 nm (Table 2).

It has been reported[3,9] that the reduction with zinc powder of the tetrachloride (VII, mp 202°C) prepared by the thermal dimerization of 1,1-diphenyl-3,3-dichloropropadiene afforded benzophenone, but not cyclobutene (IIIb). This finding differs widely from the present observation that VII (mp 210—211°C) was easily dehalogenated with zinc powder to IIIb.

Bis(diphenylmethylene)cyclobutene (VIII), 3,4-dihalo-bis(diphenylmethylene)cyclobutane (IX), and 1-bromo-3,4-bis(diphenylmethylene)cyclobutene (X) were successively prepared from IIIa by the manner shown in Scheme 2. Adding an equimolar amount of bromine to a chloroform solution of VIII at room temperature afforded IXa in an 82% yield. The reaction of VIII with an excess of chlorine afforded IXb in a 36% yield, together with the tetrachloride (VII) and an unidentified tetrachloride (mp 183—184.5°C) in 18 and 26% yields respectively. The tetrachloride (VII) must be produced by the chlorine substitution on the IXb initially formed, since the same treatment of IXb with chlorine yielded VII.

The structure of IX was determined by comparing its NMR spectral data with those reported for the same compound which had been prepared by the dimerization of 1,1-diphenyl-3-halopropadiene.[10,11] The τ-values of the methyne proton signal of IXa (mp 145—146°C), 4.85, and of IXb (mp 189—190°C), 4.96, were almost the same as the reported values for IXa (mp 143—144°C), 4.87[10], and for the *cis*-isomer of IXb (mp 191—192°C), 4.98.[11] Since the *cis*-addition of halogen to olefin is unlikely, dihalide (IX) must have a *trans*-geometry. Therefore, the reported *cis*-geometry of the dichloride (IXb)[11] is doubtful. After our work had been finished, the fact that the *cis*-geometry of IXb is erroneous was reported.[12] Therefore, the reaction of IX with base to afford X proceeds by means of *cis*-elimination.

Few additions of halogen to the *endo*-double bond of dimethylenecyclobutene have been known. It has, however, been reported[13] that the addition of chlorine to 1,2-dichloro-3,4-bis(dichloromethylene)cyclobutene to afford perchloromethylenecyclopentene probably proceeds *via* the intermediate 1,1,2,2-tetrachloro-3,4-bis(dichloromethylene)-cyclobutane initially produced by the addition of chlorine to the *endo*-double bond.

Reduction by Lithium Aluminum Hydride. Heating a mixture of IIIa, IIIb or Xa, and LAH

8) W. D. Huntsman and H. J. Wristers, *ibid.*, **85**, 3307 (1963).

9) A. Roedig and H. Niedenbruck, *Chem. Ber.*, **90**, 673 (1957).

10) P. Martinet and H. Doupeux, *C. R. Acad. Sci., Paris, Ser. C*, **261**, 2498 (1965).

11) P. D. Landor and S. R. Landor, *J. Chem. Soc.*, **1963**, 2707.

12) E. V. Dehmlow, *Tetrahedron Lett.*, **1969**, 4283; T. L. Jacobs, J. R. McClenon and O. J. Muscio, Jr., *J. Amer. Chem. Soc.*, **91**, 6038 (1969).

13) A. Roedig, F. Bischoff, B. Heinrich and G. Markl, *Ann. Chem.*, **670**, 8 (1963).

THF-ether under reflux for 2 hr afforded 1,2-bis-(diphenylmethylene)cyclobutane (XII) and 2,3-bis(diphenylmethylene)-1,4-butanedial (XVIII) in the yields summarized in Table 1. In order to clarify the reaction mechanism, V, VII, and IXa were also treated with LAH under the same conditions as above, but this yielded XII, not XVIII. By the same treatment, however, VIII afforded XVIII quantitatively. Those results are also shown in Table 1.

Table 1. Yields (%) of the reduction products

Product	Reactant						
	IIIa	IIIb	Xa	VIII	V	VII	IXa
XII	33	41	30	—	71	67	78
XVIII	8	9	15	100	—	—	—

The transformation of V, VII, and IX into XII may be due to direct and/or successive substitution, as is shown in Scheme 3, since it has been well established[14,15] that halogen at an allylic position is easily reduced by LAH. On the other hand,

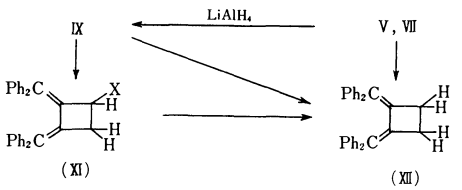

Scheme 3

the reduction of III and X to afford XII and XVIII must proceed by the following two competing paths. One consists of addition followed by substitution, such as III→XIII→XII and X→XIV (and/or XV)→XII. The other one consists of substitution, III→X→VIII, finally yielding the photooxidation product XVIII, probably *via* the cyclic intermediate (XVII). It is clear that the VIII formed initially by the substitution is converted to XVIII during the procedure of isolation, since it has been reported that VIII is easily photooxidized into XVIII even in the course of recrystallization from a usual organic solvent,[16] and since the same treatment of VIII with LAH afforded XVIII quantitatively. The above speculation on the two competing paths is further supported by the observation that the reduction of X afforded XVIII in a yield about twice that of the XVIII obtained from III, Table 1.

Since no LAH reduction of carbon-carbon double bonds has yet been reported, except where the double bond is conjugated with an electronegative group, such as carbonyl, nitro, or cyano, the present results show an anomalous reactivity of the strained *endo*-double bond of III and X. However, the results of LAH reduction differ from those of the sodium borohydride reduction[16] of IIIa in ethanol to Xa by the addition-elimination process.

Electronic Spectra. The K-bands of the electronic spectra are summarized in Table 2. Those data show distinct difference in the absorption maxima between cyclobutene (III, VIII, or X) and cyclobutane (IV, V, VI, VII, IX, or XII). The former, formally conjugated triene. absorbs at a wavelength region shorter by about 100 nm than the latter, conjugated diene. It is

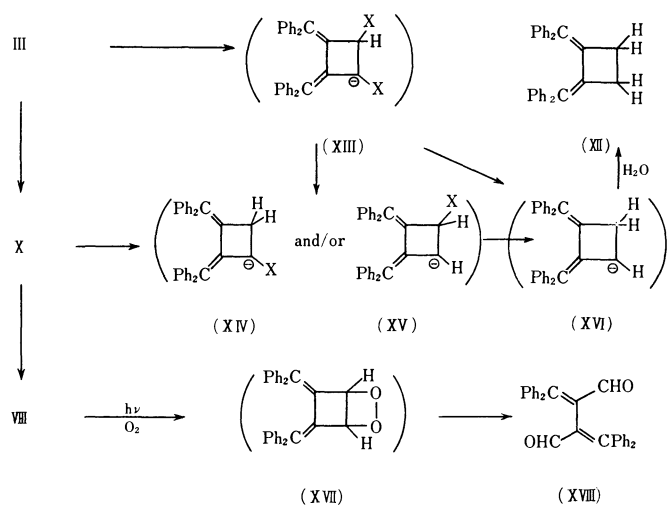

Scheme 4

14) R. F. Nystrom and W. G. Brown, *J. Amer. Chem. Soc.*, **70**, 3738 (1948).
15) L. F. Hatch and R. H. Perry, *ibid.*, **71**, 3262 (1949).
16) F. Toda, M. Higashi and K. Akagi, *Chem. Commun.*, **1969**, 1219.

Table 2. K-Bands of 3,4-bis(diphenylmethylene)-cyclobutenes and -cyclobutanes in chloroform

K-Band	Cyclobutenes				Cyclobutanes					
	IIIa	IIIb	Xa	VIII	V	IV	VI	VII	IXa	XII
λ_{max} (nm)	290	285	285	280	400	395	390	388	378	357
$\varepsilon_{max} \times 10^{-2}$	364	364	306	287	162	140	159	159	145	209

very clear that the cyclobutene is not to be viewed as a conjugated triene, since the K-band of the cyclobutene differs widely from those of such conjugated trienes as *trans*-1,6-diphenyl-[17] and *trans*-1,1,6,6-tetraphenyl-hexa-1,3,5-triene.[18] 358 and 370 nm respectively.

Since the K-band of the cyclobutane, 357—400 nm, is comparable to those of 1,4-diphenyl-[19] and 1,1,4,4-tetraphenyl-buta-1,3-diene,[20] 328 and 342 nm, respectively, the cyclobutane can be considered as a conjugated diene. On the other hand, the K-band of cyclobutene, 284—290 nm, is comparable to that of 1-phenylbuta-1,3-diene,[21] 283 and 308 nm, rather than to those of 1,4-diphenyl- and 1,1,4,4-tetraphenyl-buta-1,3-diene.

The above data of cyclobutene can reasonably be interpreted by assuming the puckered structure shown in Fig. 1, in which one diphenylmethylene group is out of the plane containing the other diphenylmethylene and the *endo*-double bond. It is not unreasonable to assume that the four-membered ring with the large ring strain, which is due to the combination of the *endo*-double bond and to steric crowding among the four phenyl rings, is stabilized, with relaxation from the steric crowding among the four phenyl rings by means of the puckering. Recently, a similar puckered structure of a cyclobutenone derivative has been reported.[22]

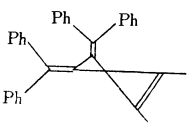

Fig. 1. Puckered structure of 3,4-bis(diphenylmethylene)cyclobutenes.

Experimental

All the melting points were uncorrected. The electronic spectra were measured in chloroform on a Hitachi spectrophotometer, model 124. The infrared spectra were recorded on a grating spectrophotometer, IR-G, of the Japan Spectroscopic Co. The NMR spectra were recorded in deuterochloroform on a Japan Electron Optics Laboratory H-100 spectrometer, TMS being used as the internal standard.

Thermal Isomerization of II into 1,2-Dihalo-3,4-bis(diphenylmethylene)cyclobutene (III). A solution of IIa* in benzene was heated under reflux in a nitrogen atmosphere for 1 hr. The crude crystals obtained by the subsequent evaporation of the solvent were recrystallized from ethyl acetate to afford IIIa as colorless needles in a practically quantitative yield; mp 190—191°C. IR ($CHCl_3$), 1510 cm^{-1} (C=C); the NMR spectrum showed only aromatic protons.

Found: C, 66.97; H, 3.49; Br, 29.41%; mol wt (benzene), 551. Calcd for $C_{30}H_{20}Br_2$: C, 66.67; H, 3.70; Br, 29.58%; mol wt, 540.

The chloro-analog (IIb) afforded IIIb quantitatively when treated like IIa; mp 195°C. IR ($CHCl_3$), 1530 cm^{-1} (C=C).

Found: C, 80.01; H, 4.25; Cl, 15.99%; mol wt (benzene), 455. Calcd for $C_{30}H_{20}Cl_2$: C, 79.84; H, 4.44; Cl, 15.72%; mol wt, 450.9.

Addition of Halogen to III. An equimolar amount of bromine was added to, or an equimolar amount of chlorine was bubbled through a stirred solution of III in chloroform at room temperature. After the subsequent evaporation of the solvent, curde crystals were recrystallized from ethyl acetate, affording the corresponding tetrahalide (IV, V or VII) almost quantitatively in all cases. All the tetrahalides are orange yellow prisms. The melting points and analytical data of those tetrahalides were as follows: IV, mp 208—209°C (dec).

Found: C, 58.86; H, 3.21%. Calcd for $C_{30}H_{20}Br_2Cl_2$: C, 58.92; H, 3.27%. V, mp 203—204°C (dec).

Found: C, 51.18; H, 2.73%. Calcd for $C_{30}H_{20}Br_4$: C, 51.43; H, 2.85%. VII, mp 210—211°C (lit[9], mp 202°C).

Found: C, 69.29; H, 3.60%. Calcd for $C_{30}H_{20}Cl_4$: C, 68.98; H, 3.87%. When IIIa was treated with an excess of chlorine, monobromotrichloride (VI) was obtained as the main product. An excess of chlorine was bubbled through a solution of IIIa (1.0 g, 1.85 mmol) in chloroform (10 *ml*) at room temperature. The residue obtained on evaporation was recrystallized from ethyl acetate to afford VI; 0.88 g (71%); mp 179—181°C.

Found: C, 63.51; H, 3.43%. Calcd for $C_{30}H_{20}BrCl_3$: C, 63.77; H, 3.54%.

The treatment of V and VII with zinc powder in boiling ethanol for 5 min afforded IIIa and IIIb respectively. By a similar treatment, both IV and VI afforded IIIb.

Preparation of 3,4-Bis(diphenylmethylene)-cyclobutene (VIII). A mixture of IIIa (1.08 g, 2 mmol), zinc powder (1 g), and glacial acetic acid (30 ml) was heated under reflux for 30 min. An insoluble

17) K. W. Hausser, R. Kuhn and A. Smakula, *Z. phys. Chem.*, **B29**, 384 (1935).

18) F. Toda and H. Tani, This Bulletin, **37**, 915 (1964).

19) R. E. Lutz and P. S. Bailey, *J. Amer. Chem. Soc.*, **67**, 2229 (1945).

20) G. Lortum and G. Dreesen, *Chem. Ber.*, **84**, 182 (1951).

21) Y. Hirshberg, E. Bergmann and F. Bergmann, *J. Amer. Chem. Soc.*, **72**, 5120 (1950).

22) S. M. Krueger, J. A. Kapecki, I. C. Prul and J. E. Baldwin. *J. Chem. Soc., B*, **1969**, 796.

solid was then removed by decantation. After the organic layer had been cooled, colorless needles which spearated out were collected by filtration, washed with water, and dried to give VIII; 0.61 g (80%); mp 182°C. NMR, 2.68 (m, Ph, 10H), 2.94 (s, =CH, 2H) and 3.16τ (m, Ph, 10H). The analytical sample was made by recrystallization from ethyl acetate in the dark, since VIII was easily photooxidized in daylight during the course of the recrystallization into the dialdehyde (X-VIII). Upon the recrystallization, however, its mp did not change.

Found: C, 93.60; H, 5.68%. Calcd for $C_{30}H_{22}$: C, 94.20; H, 5.80%.

Photooxidation of VIII into 2,3-Bis(diphenylmethylene)-1,4-butanedial (XVIII). A solution of VIII (0.382 g, 1 mmol) in ethyl acetate (20 m*l*) was irradiated using a high-pressure Hg-lamp under oxygen for 1 hr. The curde product obtained on the evaporation of the solvent was recrystallized from ethyl acetate to yield XVIII, 0.29 g (70%), as pale yellow rhombs; mp 208.5°C. λ_{max}, 300 (16100) and 335 sh nm (ε, 11600); IR ($CHCl_3$), 2870 and 2750 (CHO), 1670 and 1655 (CO), and 1580 and 1555 cm^{-1} (C=C); NMR, 0.45 (s, CHO, 2H) and 2.90τ (m, Ph, 20H).

Found: C, 86.65; H, 5.39%. Calcd for $C_{30}H_{22}O_2$: C, 86.93; H, 5.35%.

Addition of Halogen to VIII. An equimolar amount of bromine (0.38 g) was added to a solution of VIII (0.8 g. 2.1 mmol) in chloroform (15 m*l*) at room temperature. After the subsequent removal of the solvent by distillation, the crude crystals which remained were recrystallized from ethanol to afford IXa, 0.95 g (82%), as yellow rhombs; mp 145—146°C (lit,[10] mp 143—144°C). NMR, 2.64 (s, Ph, 10H), 3.12 (s, Ph, 10H) and 4.85τ (s, CH, 2H).

Found: C, 66.73; H, 4.15%. Calcd for $C_{30}H_{22}Br_2$: C, 66.42; H, 4.06%.

Through a solution of VIII (0.5 g, 1.3 mmol) in chloroform (30 m*l*) an excess of chlorine was bubbled at room temperature. The residue obtained by the evaporation of the solvent was fractionated into three components by means of fractional recrystallization from acetone. The orange-yellow crystals which separated out initially were collected by filtration and recrystallized from acetone. The product was VIIb, 0.12 g (18%), the structure of which was identified by a comparison of its spectral data with those of an authentic sample prepared by the addition of chlorine to IIIb. The second crop obtained from the above filtrate was recrystallized from acetone to afford IXb as pale yellow needles; 0.21 g (36%); mp 189—190°C (lit,[11] mp 191—192°C): NMR, 2.72 (s, Ph, 10H), 3.22 (s, Ph, 10H) and 4.90τ (s, CH, 2H).

The acetone mother liquor which remained after the removal of VIIb and IXb was concentrated to dryness, and the residue was recrystallized from ethyl acetate to give an unidentified tetrachloride ($C_{30}H_{20}Cl_4$) as pale yellow needles; 0.18 g (26%); mp 183—184.5°C. λ_{max}, 245 (25000) and 288 nm (ε, 28800).

Found: C, 68.42; H, 3.60%. Calcd for $C_{30}H_{20}Cl_4$: C, 68.97; H, 3.83%.

Preparation of 1-Bromo-3,4-bis(diphenylmethylene)cyclobutene (Xa). A mixture of IXa (0.54 g, 1 mmol), potassium hydroxide (0.3 g), and ethanol (20 m*l*) was heated under reflux for 10 min. After cooling, the reaction mixture was decomposed with water, and the solid formed was filtered and washed with water. The dried solid was recrystallized from ethyl acetate-ethanol to afford Xa as colorless needles; 0.45 g (97%), mp 172—173°C (lit,[16] mp 172—173°C). NMR, 2.67 (m, ph, 10H), 2.80 (s, =CH, 1H) and 3.15τ (m, Ph, 10H). The UV (Table 1) and NMR spectral data were identical with those of an authentic sample prepared by the sodium borohydride reduction of IIIa according to the reported method.[16]

LAH Reduction of Halogen-substiuted 3,4-Bis(diphenylmethylene)cyclobutanes (V, VII, and IXa). To a solution of LAH (0.11 g, 3 mmol) in ether (15 m*l*) under nitrogen, a solution of V (0.62 g, 1 mmol) in tetrahydrofuran (10 m*l*) was added, drop by drop, over a period of 1 hr. Then, the mixture was boiled under reflux for 2 hr in a nitrogen atmosphere. After cooling, the reaction mixture was decomposed with water and then with hydrochloric acid, and diluted with ether. The organic layer was repeatedly washed with water and dried over sodium sulfate. The crude product obtained on the evaporation of the solvent was recrystallized from acetone to give XII; 0.27 g (71%): mp 179.5—180°C. NMR, 2.89 (s, Ph, 10H), 3.30 (s, Ph, 10H) and 7.16τ (s, CH_2, 4H).

Found: C, 93.29; H, 6.36%. Calcd for $C_{30}H_{24}$: C, 93.71; H, 6.29%.

Upon similar treatment, VII and IXa also afforded XII; the yields are shown in Table 1.

LAH Reduction of Halogen-substituted 3,4-Bis(diphenylmethyene)cyclobutenes (IIIa, IIIb, and Xa). A solution of IIIb (1.0 g, 2.22 mmol) in tetrahydrofuran (20 m*l*) was treated with a solution of LAH (0.25 g, 6.66 mmol) in ether (30 m*l*) by the same procedure as that employed for V. After decomposition with water and then with hydrochloric acid, the product was taken up in ether. The ether layer was repeatedly washed with water and dried over sodium sulfate. The residue obtained on the evaporation of the solvent was fractionated into two compounds by fractional recrystallization from acetone. The yellow prisms which crystallized initially were recrystallized from acetone to afford XVIII; 0.74 g (8%); mp 208.5°C. The structure was determined by a comparison of its spectral data with those of an authentic sample prepared by the photooxidation of VIII. The pale yellow crystals obtained by the concentration of the acetone mother liquor remaining after the isolation of XVIII were recrystallized from acetone to give XII; 0.28 g (33%); mp 179.5—180°C. The structure was determined by a comparison of its spectral data with those of an authentic specimen.

Upon similar treatment, IIIa and Xa afforded XII and XVIII in the yields shown in Table 1.

LAH Reduction of 3,4-Bis(diphenylmethylene) cyclobutene (VIII). The treatment of a solution of VIII (0.9 g, 2.36 mmol) in tetrahydrofuran (20 m*l*) with a solution of LAH (0.27 g, 7.0 mmol) in ether (20 m*l*) under the conditions employed for V and IIIb afforded XVIII; 0.98 g (100%).

The authors wish to express their thanks to Mr. Shoichi Kato for his elemental analyses and to Miss Toshiko Matsutomo for the measurement of the electronic spectra and molecular weights.

BULLETIN OF THE CHEMICAL SOCIETY OF JAPAN VOL. 43 3540—3542 (1970)

The Synthesis of 1-Methyl-2-pyridones from 2-Chloromethylpyridines

Eizo MATSUMURA, Takeo NASHIMA and Fumihide ISHIBASHI

Department of Chemistry, Osaka Kyoiku University, Tennoji-ku, Osaka

(Received May 20, 1970)

The reaction of 2-chloromethylpyridine (Ia) and its homologs, 5-ethyl- (Ib), 6-methyl- (Ic), and 4-methyl-2-chloromethylpyridine (Id), with pyridine gave the corresponding 1-(2′-pyridylmethyl)-pyridinium chlorides (II), from which, on heating with dimethyl sulfate, 1-methyl-2-(pyridiniomethyl)-pyridinium salts (III) were obtained. The pyridinium salts were treated with aqueous alkali at a low temperature to yield 1-methyl- (IVa), 5-ethyl-1-methyl- (IVb), 1,6-dimethyl- (IVc), and 1,4-dimethyl-2-pyridone (IVd). The reaction sequence, in combination with the 1-oxidation of 2-picolines and followed by the reaction of the 1-oxides with tosyl chloride to yield 2-chloromethylpyridines, is recommended as a convenient route for the synthesis of 1-methyl-2-pyridones starting with 2-picolines.

There have been reported a variety of methods for the synthesis of 1-methyl-2-pyridones, of which the following procedures are typical. The method of Decker for the synthesis of 1-methylpyridones consists, as is well known, of the treatment of pyridines with dimethyl sulfate, followed by oxidation with ferricyanide. Berson and Cohen[1] obtained 1-methyl-2-pyridone by heating a mixture of 2-picoline methiodide and iodine in a pyridine solution and by treating the resultant dipyridinium salt with aqueous alkali. The 1-methylation of 2-pyridones has also been reported.[2,3]

In previous papers,[4,5] we reported that the reaction of the 1-oxides of pyridine and thiazole derivatives bearing a methyl group at the 2-position with tosyl chloride gave 2-chloromethyl derivatives in a good yield, and suggested that the 2-chloromethylpyridines thus obtained might be used to synthesize a variety of pyridine derivatives.

In the present paper, a study of the conversion of 2-chloromethylpyridines into the corresponding 1-methyl-2-pyridones will be reported.

Results and Discussion

2-Chloromethylpyridine (Ia) and its homologs, 5-ethyl- (Ib) and 6-methyl-2-chloromethylpyridine (Ic), were prepared from the 1-oxides of the corresponding parent bases, that is, 2-picoline, 5-ethyl-2-picoline, and 2,6-lutidine respectively, by a reaction with tosyl chloride. 4-Methyl-2-chloromethylpyridine (Id) was also prepared by the same method from 2,4-lutidine 1-oxide. The identification of Id was not carried out with the free base, because of its facile decomposition during fractionation. The results of the elemental analysis of the picrate obtained from Id agreed with the calculated value required for the methyl-chloromethylpyridinium picrate. The position attacked by the chloride anion was not confirmed directly, but on the bases of the results of a series of reactions described below it was found that the 2-methyl group rather than the 4-methyl group was chlorinated.

The reaction of Ia—d with pyridine proceeded readily upon warming. The removal of the excess pyridine from the reaction mixture *in vacuo* gave a hygroscopic residue which consisted mainly of 1-(2′-pyridylmethyl)-pyridinium chlorides (IIa—d). Thus, on the addition of a silver nitrate solution to an aqueous solution of the residue, silver chloride was deposited immediately, and the dipicrates were subsequently obtained from the alcoholic solution of the residue.

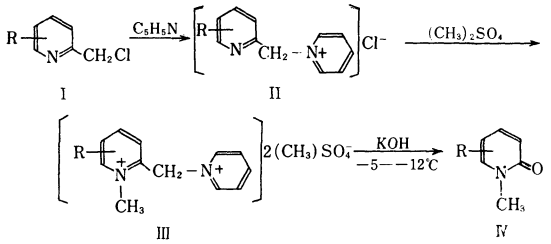

Ia, IIa, IIIa, and IVa, R=H
Ib, IIb, IIIb, and IVb, R=5-C_2H_5
Ic, IIc, IIIc, and IVc, R=6-CH_3
Id, IId, IIId, and IVd, R=4-CH_3

1) J. A. Berson and T. Cohen, *J. Amer. Chem. Soc.*, **78**, 416 (1956).
2) R. Adams and A. W. Schrecker, *ibid.*, **71**, 1186 (1949).
3) D. J. Cook, R. E. Bowen, P. Sorter and E. Daniels, *J. Org. Chem.*, **26**, 4949 (1961).
4) E. Matsumura, *Nippon Kagaku Zasshi*, **74**, 363 (1953).
5) E. Matsumura, T. Hirooka and K. Imagawa, *ibid.*, **82**, 616 (1961).

A gentle heating of the mixture of crude IIa—d and dimethyl sulfate gave, with the liberation of methyl chloride, a hygroscopic residue of crude 1-methyl-2-(pyridiniomethyl)-pyridinium salts (IIIa—d). The formation of the cation of III was confirmed by an elemental analysis of the dipicrate formed from an ethanolic solution of the residue.

On the treatment of crude IIIa—d with an aqueous potassium hydroxide solution at a low temperature, 1-methyl-2-pyridones (IVa—d) were obtained.

In the cation of III, *i.e.*, the 1-methyl-2-(pyridiniomethyl)-pyridinium ion, the 2-position is greatly activated to be attacked by a nucleophilic reagent due to the quaternization of the nitrogen atoms of both the pyridine rings. Therefore, the attack by a hydroxide ion under mild conditions at that site, resulting in the cleavage of the C_2-methylene linkage and eventually in the formation of 1-methyl-2-pyridones, proceeds through the course depicted in Scheme 1. This step in the reaction sequence is essentially the same as that proposed by Berson and Cohen.[1]

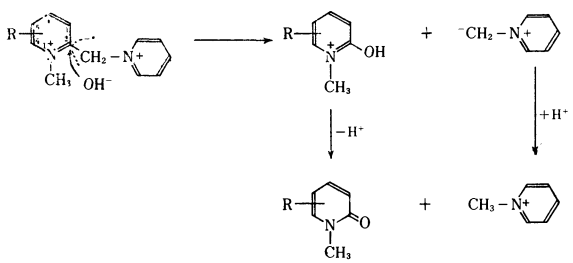

IV

Scheme 1

IVa, IVc and IVd were identified as the corresponding picrates by a mixed-melting-point determination with authentic samples.[3,6] The fact that VId was obtained from Id confirmed that the chloromethyl and methyl groups in Id were, as expected, attached to the 2- and 4-positions respectively. In the case of the reaction sequence starting with Ib, the structure of the resulting IVb was established by the following observations. The elemental analysis of the IVb supported the required molecular formula, the melting point of the picrate agreed with that reported by Sugasawa and Kirisawa,[7] and the IR spectrum of IVb showed its absorption maximum at 1660 cm^{-1}, suggesting the presence of a carbonyl group. Sugasawa and Kirisawa[7] reported that the oxidation of 3-ethylpyridine by the method of Decker afforded a mixture in which 1-methyl-3-ethyl-2-pyridone greatly predominated over the 5-ethyl isomer (IVb). Therefore, they synthesized IVb by a tedious method which involved the conversion of 3-ethylpyridine into 3-acetylpyridine, subsequent Decker's oxidation to 1-methyl-5-acetyl-2-pyridone, and the reconversion of the acetyl into the ethyl group. Also, IVc and IVd, which could not be prepared by the direct Decker method and which were, therefore, prepared by the same tedious procedure, were easily obtained by the present method.

This method is thus recommended as a convenient route for the synthesis of 1-methyl-2-pyridones starting with 2-picolines, since 2-chloromethylpyridines can readily be obtained by the reaction of 2-picoline 1-oxides with tosyl chloride.

Experimental

2-Chloromethyl-4-methylpyridine (Id). A solution of 2,4-lutidine 1-oxide (12.0 g) and tosyl chloride (24.1 g) in dry benzene (70 m*l*) was allowed to stand at room temperature for 15 min. After the subsequent removal of the solvent, the residue was heated at 70°C for 2 hr, and then at 100°C for 1 hr. Water was added to the cooled reaction mixture, the excess tosyl chloride was removed by filtration, and the filtrate, after the adjustment of the pH to 6.0 with sodium carbonate, was steam-distilled. The distillate was extracted with ether, the extract was dried over sodium sulfate, and the solvent was removed *in vacuo* to give crude Id as a stimulative oil (9.8 g, 68.0%); this oil was used for the next step without purification. Picrate: mp 138—139°C.

Found: C, 42.37; H, 3.03; N, 15.22%. Calcd for $C_{13}H_{11}O_7N_4Cl$: C, 42.10; H, 3.00; N, 15.11%.

1-Methyl-2-pyridone (IVa). A mixture of dry pyridine (10.0 g) and Ia (8.0 g) was heated at 80°C for 5 hr. At the end of the reaction time, a dark red, oily material separated at the bottom of the reaction vessel. The removal of the excess pyridine *in vacuo* and the washing of the residue with ether gave crude IIa as a hygroscopic syrup. Dipicrate: mp 168—169°C.

Found: C, 43.84; H, 2.51; N, 17.96%. Calcd for $C_{23}H_{16}O_{14}N_8$: C, 43.96; H, 2.57; N, 17.83%.

A mixture of dimethyl sulfate (23.8 g) with the crude IIa was kept for 20 min at room temperature and then heated at 80°C for 3 hr until a homogeneous solution was formed; this gave a hygroscopic syrup consisting mainly of IIIa. Dipicrate: mp 192—193°C.

Found: C, 44.75; H, 2.91; N, 17.15%. Calcd for $C_{24}H_{18}O_{14}N_8$: C, 44.87; H, 2.83; N, 17.44%.

A solution of potassium hydroxide (17.1 g) in water (150 m*l*) was stirred, drop by drop, into a solution of crude IIIa in water (76 m*l*) over a period of 3 hr at 2—5°C; the stirring was then continued for another 2 hr at the same temperature. The mixture was extracted with ether using a continuous extractor, the extract was evaporated, and the residue was distilled *in vacuo* to yield IVa as a yellow oil (4.5 g, 65.0%) boiling at 117°C/10 mmHg. The melting point of the picrate of IVa (142—143°C) was undepressed in a mixed-melting-point determination with an authentic sample.

1-Methyl-5-ethyl-2-pyridone (IVb). A solution of dry pyridine (9.5 g) and Ib (15.5 g) in ether (106

6) E. A. Prill and S. M. McElvain, "Organic Syntheses", Coll. Vol. II, p. 487.

7) S. Sugasawa and M. Kirisawa, *Chem. Pharm. Bull.* (Tokyo), **4**, 139 (1956).

ml) was allowed to stand at room temperature for 30 min. After the removal of the solvent, the residue was heated at 50°C for 6 hr, and then at 80°C for 3 hr. The same treatment as with IIa gave a hygroscopic oil of IIb. Dipicrate: mp 155°C.

Found: C, 45.48; H, 3.06; N, 17.17%. Calcd for $C_{25}H_{20}O_{14}N_8$: C, 45.74; H, 3.07; N, 17.07%.

A mixture of dimethyl sulfate (36.8 g) and the crude IIb was heated at 80°C for 3 hr to give a hygroscopic syrup consisting mainly of IIIb. Dipicrate: mp 163°C.

Found: C, 46.39; H, 3.34; N, 16.58%. Calcd for $C_{26}H_{22}O_{14}N_8$: C, 46.57; H, 3.31; N, 16.71%.

A solution of potassium hydroxide (20.7 g) in water (186 ml) was stirred, drop by drop, into a solution of crude IIIb in water (392 ml) over a period of 2 hr at −7—−10°C; the stirring was then continued for another 2 hr at the same temperature. Subsequent treatment similar to that used with IVa gave IVb as a yellow oil (8.4 g, 64.0%) boiling at 114—115°C/3 mmHg. The product showed its absorption maximum at 1660 cm^{-1} in the IR spectrum, and the picrate recrystallized from ethanol melted at 122—123°C.[7] Picrate: mp 122—123°C.

Found: C, 45.90; H, 3.85; N, 15.30%. Calcd for $C_{14}H_{14}O_8N_4$: C, 46.00; H, 3.94; N, 15.31%.

1,6-Dimethyl-2-pyridone (IVc). A mixture of dry pyridine (23.3 g) and Ic (13.8 g) was allowed to stand at room temperature for 30 min, and then heated at 60°C for 3 hr and subsequently at 70°C for 2 hr. The removal of the excess pyridine *in vacuo* gave hygroscopic crystals of IIc. Dipicrate: mp 179°C.

Found: C, 44.83; H, 2.98; N, 17.48%. Calcd for $C_{24}H_{18}O_{14}N_8$: C, 44.87; H, 2.83; N, 17.44%.

A mixture of dimethyl sulfate (27.6 g) and crude IIc was heated at 80°C for 3 hr, subsequent treatment like that of IIIa gave IIIc as hygroscopic crystals. Dipicrate: mp 186°C.

Found: C, 45.52; H, 3.03; N, 17.12%. Calcd for $C_{25}H_{20}O_{14}N_8$: C, 45.72; H, 3.07; N, 17.07%.

A solution of potassium hydroxide (24.2 g) in water (217.8 ml) was stirred, drop by drop, into a solution of crude IIIc in water (278 ml) over a period of 2 hr at −10—−12°C. The stirring was then continued for another 4 hr at the same temperature. Subsequent treatment similar to that of IVa gave IVc as hygroscopic crystals (7.5 g, 62.8%) boiling at 116—117°C/3 mmHg.

Found: C, 68.27; H, 7.36; N, 11.37%. Calcd for C_7H_9ON: C, 68.27; H, 7.36; N, 11.68%.

The IR spectrum of IVc agreed with that of the authentic sample,[2] and the melting point of the picrate of IVc (133—134°C) was undepressed upon a mixed-melting-point determination with an authentic sample.

1,4-Dimethyl-2-pyridone (IVd). A mixture of dry pyridine (11.7 g) and Id (15.0 g) was heated at 80°C for 5 hr. Subsequent treatment similar to that of IIa gave IId as a hygroscopic oil. Dipicrate: mp 185.5—186.5°C.

Found: C, 45.01; H, 2.92; N, 17.55%. Calcd for $C_{24}H_{18}O_{14}N_8$: C, 44.87; H, 2.83; N, 17.44%.

A mixture of dimethyl sulfate (37.8 g) and IId in water (295 ml) was heated at 80°C for 3 hr. When it was then treated as IIIa had been, a hygroscopic syrup of IIId was obtained. Dipicrate: mp 202.5°C.

Found: C, 45.41; H, 3.17; N, 17.30%. Calcd for $C_{25}H_{20}O_{14}N_8$: C, 45.74; H, 3.07; N, 17.07%.

A solution of potassium hydroxide (26.6 g) in water (234 ml) was stirred, drop by drop, into a solution of IIId over a period of 2 hr at −7—−10°C, after which the stirring was continued for 3 hr. Subsequent treatment of the mixture much like that of IVa gave IVd of hygroscopic crystals (6.9 g, 53.6%) boiling at 110—111°C/3 mmHg. The IR spectrum of IVd was identical with that of the authentic sample,[2] and the melting point of the picrate of IVd was undepressed by a mixed-melting-point determination with an authentic sample. Picrate: mp 163—164°C.

Found: C, 44.32; H, 3.36; N, 15.62%. Calcd for $C_{13}H_{12}O_4N_8$: C, 44.32; H, 3.43; N, 15.91%.

BULLETIN OF THE CHEMICAL SOCIETY OF JAPAN VOL. 43 3543—3549 (1970)

The Cycloaddition Reactions of Benzoylsulfene with Anils

Otohiko TSUGE and Sumio IWANAMI

Research Institute of Industrial Science, Kyushu University, Hakozaki, Fukuoka

(Received May 30, 1970)

The reactions of benzoylmethanesulfonyl chloride with various anils (Ar–CH=N–R) in the presence of triethylamine have been studied. It has been found that the corresponding (4+2) and/or (2+2) cycloadducts of benzoylsulfene and the anil were obtained, depending on the nature of the substituents, R, in the anils. The reaction of the chloride with benzylidene-*n*-propylamine in the absence of triethylamine gave only the (2+2) cycloadduct, while the (4+2) cycloadduct was exclusively obtained in the presence of triethylamine. The chloride reacted with dibenzylidenethylenediamine in the presence of triethylamine to give the corresponding bis(4+2) cycloadduct.

Recently, Fusco and his co-workers[1] found that the treatment of benzoylmethanesulfonyl chloride (I) with triethylamine (NEt_3) afforded the 1,2,4-oxadithin tetroxide. Later, it has been shown in a review[2] that, in the presence of NEt_3, I reacted with isobutenyl ether to give the 1,4-oxathin dioxide, while it reacted with 2-methyl-1-pyrrolidino-1-propene to give the thiethane dioxide (Scheme 1). These reactions can be formulated as below, assuming a benzoylsulfene ($PhCOCH{=}SO_2$) intermediate.

The above observations indicate that, in the cycloaddition reaction with unsaturated substances benzoylsulfene behaves as a 1,2- and/or 1,4-dipole, depending on the nature of the unsaturated substances.

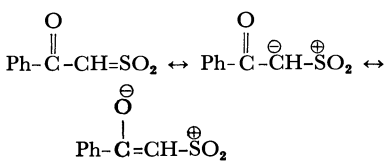

The reactions of sulfenes ($RCH{=}SO_2$), generated *in situ* from alkanesulfonyl chlorides and NEt_3, with electron-rich olefins, such as enamines or ketene acetals, have been extensively investigated. However, the study of the cycloaddition of sulfene to the C=N bond has not been extended beyond of Staudinger and Pfenninger,[3] who reported that the reaction of diphenylsulfene, generated from diphenyldiazomethane and sulfur dioxide, with benzylidenaniline gave the four-membered cyclic compound.

New heterocyclic compounds may be formed by the cycloaddition of benzoylsulfene to the C=N bond, because the electron-attracting benzoyl group will make benzoylsulfene more reactive than sulfenes ($RCH{=}SO_2$).

In the present paper we wish to report on the formation of (2+2) and (4+2) cycloadducts *via* the reactions of benzoylsulfene with various benzylidenamines. In this cycloaddition reaction, for the first time, a sulfene, generated from sulfonyl chloride and a base, reacted with a C=N bond

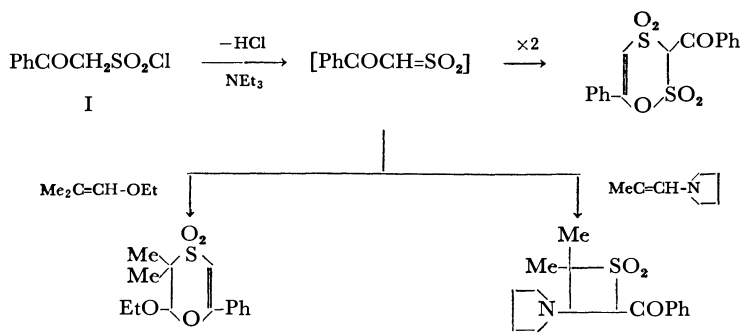

Scheme 1

1) R. Fusco, S. Rossi, S. Maiorana and G. Pagani, *Gazz. Chim. Ital.*, **95**, 774 (1965).

2) Opitz, *Angew. Chem.*, **79**, 162 (1967).

3) H. Staudinger and E. Pfenninger, *Ber.*, **49**, 1941 (1916).

to give a cycloadduct.

Results and Discussion

The reaction of I with equimolar benzylidene-*n*-propylamine (IIa) and NEt_3 in dioxane at room temperature for 15 hr gave a crystalline compound IIIa, mp 123°C (decomp.), in a 57% yield, besides triethylammonium chloride in a quantitative yield. The results of elemental analysis and the molecular weight (M^+ *m/e* 329) of IIIa were consistent with those of the expected 1 : 1 adduct of benzoylsulfene and IIa.

On the other hand, I reacted with two molar quantities of IIa in the absence of NEt_3 at room temperature for 3 hr, thus affording IIIa and its isomeric 1 : 1 adduct, IVa, mp 148°C, in 57 and 13% yields respectively, together with benzylidene-*n*-propylamine hydrochloride.

The infrared spectrum of IIIa showed characteristic bands at 1575 ($\nu_{C=C}$), 1150, and 1335 cm^{-1} (ν_{SO_2}), while the NMR spectrum in deuteriochloroform ($CDCl_3$) exhibited singlets at τ 3.56 (1H, methine proton) and 3.00 (1H, olefinic proton), besides signals of *n*-propyl and aromatic protons. These observations indicate that IIIa is the (4+2) cycloadduct of benzoylsulfene, and IIa, 2,6-diphenyl-3-*n*-propyl-1,4,3-oxathiazine 4,4-dioxide. The mass spectrum was also in harmony with the proposed structure: peaks appeared at *m/e* 329 (M^+), 300 (M^+-29[Et]), 288 (M^+-41[CH_2=CH-CH_2]), and 265 (M^+-64[SO_2]) in the spectrum. Furthermore, IIIa was reduced with sodium borohydride in methanol at 30°C for 20 min to *N*-benzyl-*N*-*n*-propyl-2-hydroxy-2-phenylethane-1-sulfonamide (V) in a 73% yield (Scheme 2). The structure for IIIa is also supported by this fact.

On the other hand, IVa was confirmed to be the (2+2) cycloadduct, 4-benzoyl-3-phenyl-2-*n*-propyl-1,2-thiazetidine 1,1-dioxide, by the spectral studies as well as by the chemical transformation. The infrared spectrum showed strong bands at 1690 ($\nu_{C=O}$), 1165, and 1315 cm^{-1} (ν_{SO_2}), and the NMR spectrum in deuterionitromethane (CD_3NO_2) revealed two pairs of doublets, at τ 5.07 and 4.42 (each 1H, J=6 Hz), besides the peaks of the *n*-propyl and aromatic protons. Although the molecular ion peak was not observed, the peak of *m/e* 265 (M^+-64[SO_2]) appeared in the mass spectrum of IVa.

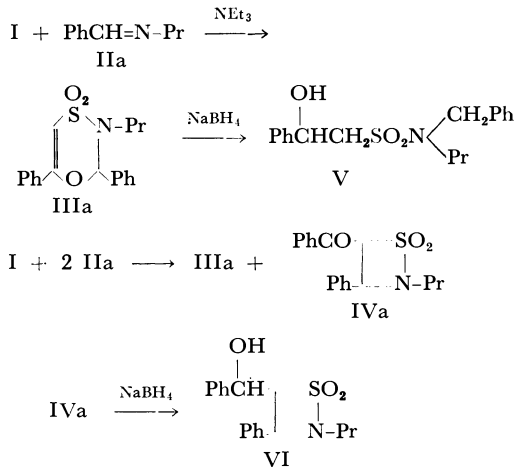

Scheme 2

When IVa was treated with sodium borohydride under the same conditions as were used for IIIa, a ring cleavage did not take place, but IVa was reduced to the 4-(α-hydroxybenzyl)thiazetidine VI in an 84% yield (Scheme 2).

In order to make it clear whether or not IVa is virtually formed in the reaction under the influence of NEt_3, the amounts of products and reactants in the reaction system were estimated by NMR spectroscopy. As is shown in Table 1, in the presence of NEt_3 only IIIa was formed.

The effect of the amount of IIa on the yields of IIIa and IVa was investigated in the absence of NEt_3; the results are also shown in Table 1. It is shown that IIIa and IVa were formed even when I was caused to react with an equimolar amount of IIa. As the adduct IIIa proved rather unstable and decomposed during purification, however, the yield isolated was lower than that estimated by NMR spectroscopy.

The interconversion of IIIa and IVa was not observed under these reaction conditions. The reason why benzoylsulfene behaves differently depending on the nature of the dehydrochlorinating agents is not clear.

In the reaction of I with benzylidenaniline (IIb) under the influence of NEt_3 for 1 hr, the (4+2) cycloadduct, 2,3,6-triphenyl-1,4,3-oxathiazine 4,4-dioxide (IIIb), was exclusively formed, but it

Table 1. Reaction of I with IIa in the presence or absence of NEt_3 in dioxane at room temperature for 3 hr

I	IIa	NEt_3	Products (%)		Unreacted reactants (%)	
	(molar ratio)		IIIa	IVa	I	IIa
1	1	1	82	0	0	9
1	1	0	36	6	40	0
1	2	0	82	13	0	0
1	3	0	84	14	0	33

could not be isolated in a pure form because of its instability. On the other hand, a similar reaction for 24 hr gave the (2+2) cycloadduct, 4-benzoyl-2,3-diphenyl-1,2-thiazetidine 1,1-dioxide (IVb), in a 22% yield, but here the formation of IIIb was not observed.

The structures for IIIb and IVb were confirmed by the spectral studies as well as by the chemical transformations. The infrared spectrum of a relatively pure IIIb showed bands at 1570 ($\nu_{C=C}$), 1150, and 1335 cm^{-1} (ν_{SO_2}), while the NMR spectrum in dioxane revealed a singlet at τ 3.05 (1H, methine proton) and a vinyl proton signal in a region of aromatic protons. When IIIb was refluxed in methanol for several minutes, a ring cleavage took place to give the sulfonamide VII in a 64% yield (Scheme 3).

On the other hand, the infrared spectrum of IVb showed strong bands at 1685 ($\nu_{C=O}$), 1151, and 1324 cm^{-1} (ν_{SO_2}), while the NMR spectrum in CD_3NO_2 revealed two pairs of doublets, at τ 3.85 and 4.19 (each 1H, $J=6$ Hz). The structure for IVb was also supported by the mass spectrum: peaks of *m/e* 363 (M^+) and 299 (M^+-64[SO_2]) appeared in the spectrum.

The treatment of IVb with methanolic sodium hydroxide gave β-benzoyl-β-phenylsulfamoylstyrene (VIII), which was identical with the authentic sample prepared from benzoyl methanesulfonanilide and benzaldehyde. Furthermore, IVb was reduced with sodium borohydride to give the 4-(α-hydroxybenzyl)thiazetidine compound, IX (Scheme 3).

The effect of the reaction time on the yields of IIIb and IVb was investigated by the quantitative estimation of IIIb and IVb, using NMR spectroscopy. The results are shown in Table 2.

The data in Table 2 indicate that, when the reaction is carried out under the same conditions, the quantity of unreacted IIb is essentially independent of the reaction time, and that the quantity of IIIb decreases, and that of IVb increases with an increase in the reaction time.

The reactions of I with various benzylidenamines (II) were investigated in the presence of NEt_3; the results are summarized in Table 3.

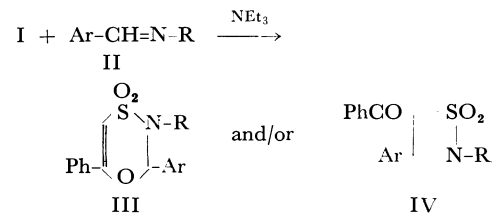

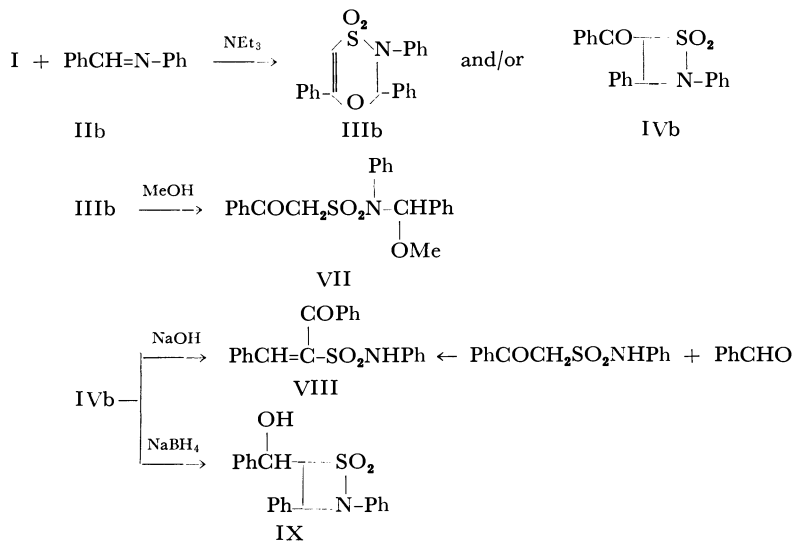

Scheme 3

TABLE 2. REACTION OF I WITH IIb IN THE PRESENCE OF NEt_3 IN DIOXANE AT ROOM TEMPERATURE

I	IIb (molar ratio)	NEt_3	Time (hr)	Products (%) IIIb	Products (%) IVb	Unreacted IIb (%)
1	1	1	1	38	0	59
1	1	1	12	ca. 14	20	56
1	1	1	24	0	30	56
2	1	2	1	66	0	34
2	1	2	24	0	44	30

Table 3. Reaction of I with II in the presence of NEt_3 in dioxane at room temperature

II	Ar	R	Reaction time (hr)	Products (%) III	Products (%) IV
a	Ph	*n*-Pr	15	57	0
b	Ph	Ph	25	0	22
c	Ph	*p*-MeC_6H_4	100	0	24
d	Ph	*p*-$MeOC_6H_4$	50	0	10*
e	*p*-$NO_2C_6H_4$	Ph	15	0	0*
f	Ph	$PhCH_2$	100	32	5
g	Ph	Cyclohexyl	15	27	0

* Unreacted IId and IIe were recovered in 25 and 10% yields respectively.

The structures of the products were established by the spectral studies as well as by the elemental analyses (Table 4).

When the substituent, R, in II is aliphatic, such as *n*-propyl and cyclohexyl, only the (4+2) cycloadduct III was obtained in the presence of NEt_3. On the other hand, the reaction with II when R is aromatic, such as phenyl and *p*-tolyl, for a long time gave the (2+2) cycloadduct IV exclusively; this can presumably be attributed to the fact that the 3-aryl-1,4,3-oxathiazine compound is unstable compared with the corresponding 3-alkyl compound. On the other hand, benzylidenebenzylamine (IIf) exhibited an intermediate character to give both the (4+2) and (2+2) cycloadducts. A similar reaction of I with diphenylmethylenaniline for 25 hr did not give the expected cycloadduct of benzoylsulfene and the anil, but rather the dimer of benzoylsulfene, 3-benzoyl-6-phenyl-1,2,4-oxadithin tetroxide,[1] in a 55% yield.

It may be assumed that benzoylsulfene reacts with a compound with two C=N bonds, thus leading to the formation of a mono-, bis(2+2), bis(4+2), or mixed biscycloadduct.

When dibenzylidenethylenediamine (X) was caused to react with two molar quantities of I in the presence of NEt_3, the expected 2 : 1 adduct of benzoylsulfene and X was obtained in a 52% yield, together with a small amount of an unidentified substance. Although the NMR spectrum of XI could not be measured because of its poor solubility, the infrared spectrum was very similar to that of IIIa and did not show any carbonyl bands except the band ascribed to the C=C bond at 1572 cm^{-1}. This fact indicates that XI is a bis-oxathiazine.

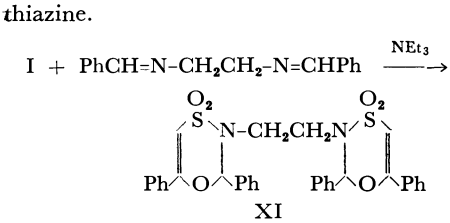

XI

The mass spectrum was in harmony with the proposed structure: the molecular ion peak was not observed, but peaks of *m/e* 418 (M^+-182[PhCOCH=SO_2]), 354 (418$^+$-64[SO_2]), and 250 (354$^+$-104[PhCNH]) appeared in the spectrum.

Experimental

All the melting and boiling points are uncorrected. The infrared spectra were measured in KBr disks, and the NMR spectra were determined at 60 MHz with a Hitachi R-20 NMR spectrometer, using TMS as an internal reference. The mass spectra were obtained on a Hitachi RMS-4 mass spectrometer, using a direct inlet and an ionization energy of 70 eV.

Materials. Benzoylmethanesulfonyl chloride (I), mp 88°C (lit,[4] mp 87.5—88.2°C), was prepared according to the method of Truce and Vriesen.[4] Benzylidenamines (II) and dibenzylidenethylenediamine (X) were prepared from the corresponding aldehyde and amine. Benzylidene-*n*-propylamine (IIa), bp 101—102°C/15 mmHg (lit,[5] bp 208—210°C/744 mmHg); -aniline (IIb) mp 54°C (lit,[6] mp 53.5°C); -*p*-toluidine (IIc), bp 176—177°C/10 mmHg (lit,[7] bp 178°C/10 mmHg); -*p*-anisidine (IId), mp 73—74°C (lit,[8] mp 72°C); -benzylamine (IIf), bp 200—201°C/18 mmHg (lit,[9] bp 205°C/20 mmHg); -cyclohexylamine (IIg), bp 154°C/18 mmHg (lit,[10] bp 136°C/16 mmHg); *p*-nitrobenzylidenaniline (IIe), mp 93°C (lit,[11] mp 93°C); dibenzylidenethylenediamine (X), mp 54°C (lit,[12] mp 53—54°C). Diphenylmethylenaniline was prepared from benzophenone dichloride and aniline; mp 116—117°C (lit,[13] mp 116°C).

General Procedure for the Reaction of I with II in the Presence of NEt_3. To a vigorously stirred solution of 0.01 mol of II and 1.0 g (0.01 mol) of NEt_3 in 10 m*l* of dioxane, a solution of 2.2 g (0.01 mol) of I in 40 m*l* of dioxane was added, drop by drop, at room

4) W. E. Truce and C. W. Vriesen, *J. Amer. Chem. Soc.*, **75**, 2525 (1953).
5) H. Zaunschirm, *Ann. Chem.*, **245**, 282 (1888).
6) G. Pyl, *Ber.*, **60**, 288 (1927).
7) A. Pictet, *ibid.*, **19**, 1063 (1886).
8) F. G. Pope and R. Fleming, *J. Chem. Soc.*, **93**, 1915 (1908).
9) A. T. Mason and G. R. Winder, *ibid.*, **65**, 191 (1894).
10) A. Skita and C. Wulff, *Ber.*, **59**, 2691 (1926).
11) O. Fischer, *ibid.*, **14**, 2525 (1881).
12) A. T. Mason, *ibid.*, **20**, 270 (1887).
13) M. Pauly, *Ann. Chem.*, **187**, 198 (1877).

Table 4. Physical properties and elemental analyses of III and IV

3-Substituted 2,6-diphenyl-1,4,3-oxathiazine 4,4-dioxide

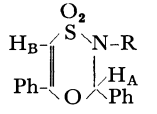

III

III	R	Mp (°C)	Appearance	IR (cm^{-1}) $\nu_{C=C}$	IR (cm^{-1}) ν_{SO_2}		NMR $H_A(\tau)$	NMR $H_B(\tau)$	NMR Solvent	Analysis (%) Found (Calcd) C	H	N	M+ (m/e)
a	*n*-Pr	123 (decomp.)	colorless prisms	1575	1335	1150	3.26 3.56	2.93 3.00	dioxane $CDCl_3$	65.86 (65.64)	5.67 (5.82)	4.07 (4.25)	329
f	$PhCH_2$	158 (decomp.)	colorless prisms	1573	1340	1160	3.24	*	$CDCl_3$	70.30 (70.02)	5.23 (5.07)	3.53 (3.71)	377
g	Cyclohexyl	153 (decomp.)	colorless prisms	1570	1318	1145	3.47	2.90	$CDCl_3$	68.34 (68.28)	6.30 (6.28)	3.79 (3.79)	369

2-Substituted 4-benzoyl-3-phenyl-1,2-thiazetidine 1,1-dioxide

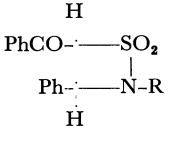

IV

IV	R	Mp (°C)	Appearance	IR (cm^{-1}) $\nu_{C=O}$	IR (cm^{-1}) ν_{SO_2}		NMR >CH(τ)	NMR J(Hz)	NMR Solvent	Analysis (%) Found (Calcd) C	H	N	M+ (m/e)
b	Ph	164—165	colorless needles	1685	1324	1151	3.85 3.88	4.19 4.23	6 6	CD_3NO_2 dioxane	69.63 (69.41)	4.56 (4.72)	3.82 (3.82)	363
c	*p*-MeC_6H_4	163	colorless prisms	1690	1339	1160	3.85	4.23	6	CD_3NO_2	70.25 (70.02)	4.95 (5.07)	3.69 (3.71)	377
d	*p*-$MeOC_6H_4$	138	colorless needles	1698	1337	1165	3.90	4.32	6	dioxane	67.20 (67.17)	4.78 (4.87)	3.52 (3.71)	393
f	$PhCH_2$	143	colorless needles	1680	1335	1165	4.05 4.43	4.98 5.03	7 6	dioxane $CDCl_3$	69.70 (70.02)	5.17 (5.07)	3.75 (3.71)	**

* The H_B signal appeared in a region of phenyl protons.

** A molecular ion peak was not observed but [M^+-SO_2] peak appeared at *m/e* 313 in the mass spectrum.

temperature over a period of 30 min. After the reaction mixture had been stirred at the same temperature for a long while, triethylammonium chloride was removed by filtration. The filtrate was evaporated *in vacuo* to leave an oily substance, which was then crystallized on trituration with methanol or petroleum benzine (bp 45—60°C).

The reaction conditions, yields, physical properties, and elemental analyses of adducts are summarized in Tables 3 and 4.

Reaction of I with IIa in the Absence of NEt_3. To a solution of 3.0 g (0.02 mol) of IIa in 10 m*l* of dioxane, was added, drop by drop, a solution of 2.2 g (0.01 mol) of I in 40 m*l* of dioxane. After the mixture had then been stirred at room temperature for 2.5 hr, the precipitated benzylidene-*n*-propylamine hydrochloride was removed by filtration. The filtrate was evaporated *in vacuo* to give 3.4 g of a viscous oily substance, found to be a mixture of IIIa (85%) and IVa (15%) by NMR spectroscopy. Although IIIa could not be isolated in a pure state because of its instability, the recrystallization of the mixture from methanol gave IVa, mp 148°C, as colorless prisms.

Found: C, 65.85; H, 6.22; N, 4.24%. Calcd for $C_{18}H_{19}O_3NS$: C, 65.64; H, 5.82; N, 4.25%.

Reduction of IIIa with Sodium Borohydride. A mixture of 0.45 g of IIIa and 0.5 g of sodium borohydride in 20 m*l* of methanol was stirred at 30°C for 20 min. To the mixture was added 50 m*l* of water, and then the mixture was extracted with benzene. The benzene-extract was washed twice with water, dried over sodium sulfate, and then evaporated *in vacuo* to give a colorless, viscous oil (0.3 g, 73%), which crystallized on standing for a long while. Recrystallization from petroleum benzine (bp 45—60°C) gave *N*-benzyl-*N*-*n*-propyl-2-hydroxy-2-phenylethane-1-sulfonamide (V), mp 48—49°C, as colorless needles.

Found: C, 64.68; H, 6.82; N, 4.25%. Calcd for $C_{18}H_{23}O_3NS$: C, 64.85; H, 6.95; N, 4.20%.

IR: 3520 (ν_{OH}), 1325, 1137 cm^{-1} (ν_{SO_2}). NMR ($CDCl_3$): τ 2.67 (10H, singlet, aromatic protons), 4.76 (1H, quartet, $\geqslant$CH), 5.63 (2H, singlet, $-C\underline{H}_2Ph$), 6.17 (1H, broad signal, OH, exchanged with D_2O), 6.5—7.1 (4H, multiplet, $-C\underline{H}_2SO_2-$ and $-\underline{N}-C\underline{H}_2-$), 8.3—8.9 (2H, quintet, $-CH_2-C\underline{H}_2-Me$), 9.13 (3H, triplet, CH_3).

The mass spectrum gave a parent peak at *m/e* 333 (M^+) and other peaks at *m/e* 316 (M^+-OH), 304 (M^+-Et), and 242 ($M^+-C_7H_7$).

Reduction of IVa with Sodium Borohydride. A mixture of 0.12 g of IVa and 0.15 g of sodium borohydride in 10 m*l* of methanol was stirred at 30°C for 20 min. Fifty m*l* of water were then added to the mixture, affording 0.1 g (84%) of colorless crystals. Recrystallization from a mixture of benzene-petroleum benzine gave 4-(α-hydroxybenzyl)-3-phenyl-2-*n*-propylthiazetidine 1,1-dioxide (VI), mp 103—104°C, as colorless needles.

Found: C, 65.46; H, 6.47; N, 4.22%. Calcd for $C_{18}H_{21}O_3NS$: C, 65.24; H, 6.39; N, 4.23%.

IR: 3480 (ν_{OH}), 1300, 1147 cm^{-1} (ν_{SO_2}). NMR ($CDCl_3$): τ 2.6—3.1 (10H, multiplet, aromatic protons), 4.76 (1H, doublet, $Ph\underline{C}H-N\langle$), 5.58 (1H, quartet, $\rangle CH-SO_2-$), 6.14 (1H, doublet, OH, exchanged with D_2O), 6.6—7.5 (3H, multiplet, $-CH_2-\underline{N}-$ and $PhC\underline{H}-$(OH)-), 8.2—8.8 (2H, quintet, $-CH_2-CH_2-Me$), 9.10 (3H, triplet, CH_3).

The mass spectrum showed a parent peak at *m/e* 331 (M^+) and other peaks at *m/e* 313 (M^+-H_2O), 301 ($M^+-C_2H_4$), and 267 (M^+-SO_2).

A similar reduction of IVb with sodium borohydride gave the corresponding 4-(α-hydroxybenzyl)thiazetidine IX, mp 195°C (decomp.), as colorless prisms (from acetonitrile). Yield, 83%.

Found: C, 68.76; H, 5.45: N, 3.58%. Calcd for $C_{21}H_{19}O_3NS$: C, 69.03; H, 5.24; N, 3.83%.

IR: 3550 (ν_{OH}), 1315, 1170 cm^{-1} (ν_{SO_2}). NMR (CD_3CN): τ 2.4—3.3 (15H, multiplet, aromatic protons), 4.65 (1H, quartet, $ph\underline{C}H(OH)-$), 5.2—5.5 (2H, multiplet, $-\underline{C}H-SO_2-$ and $PhC\underline{H}-\underline{N}-$), 5.86 (1H, doublet, OH, exchanged with D_2O).

Methanolysis of IIIb. A solution of 0.5 g of IIIb in 50 m*l* of methanol was refluxed for several minutes and then cooled to give the sulfonamide VII, mp 120—121°C, as colorless needles. Yield, 0.35 g (64%).

Found: C, 66.60; H, 5.28; N, 3.40%. Calcd for $C_{22}H_{21}O_4NS$: C, 66.82; H, 5.35; N, 3.54%.

IR: 1680 (ν_{CO}), 1250, 1150 cm^{-1} (ν_{SO_2}). NMR ($CDCl_3$): τ 1.9—3.0 (15H, multiplet, aromatic protons), 3.6 (1H, singlet, $\geqslant$CH), 5.25 (2H, double doublet, J=14 Hz, $-CH_2-$), 6.36 (3H, singlet, OCH_3).

The mass spectrum showed peaks at *m/e* 395 (M^+), 364 (M^+-OMe), 275 (364^+-PhC), 182 (275^+-PhNH_2), and 105 ($PhCO^+$).

***β*-Benzyl-*β*-phenylsulfamoylstyrene (VIII).** *i*) After a solution of 0.4 g of IVb and 0.1 g of sodium hydroxide in aqueous methanol (methanol 20 m*l* and water 5 m*l*) had been refluxed for 20 min, the mixture was extracted with benzene. The benzene-extract was evaporated *in vacuo*, affording 52 mg (13%) of colorless crystals. Recrystallization from petroleum benzine (bp 45—60°C) gave VIII, mp 188—189°C, as colorless needles.

Found: C, 69.54; H, 4.68; N, 3.77%. Calcd for $C_{21}H_{17}O_3NS$: C, 69.41; H, 4.72; N, 3.86%.

IR: 3230 (ν_{NH}), 1635 (ν_{CO}), 1615 ($\nu_{C=C}$), 1340, 1150 cm^{-1} (ν_{SO_2}). The mass spectrum showed peaks at *m/e* 363 (M^+), 299 (M^+-SO_2), 271 (M^+-PhNH), and 105 ($PhCO^+$).

ii) A solution of 1.0 g of benzoylmethanesulfonanilide, 0.5 g of benzaldehyde, and 2 m of 1 N sodium hydroxide aqueous solution in 50 m*l* of ethanol was fluxed for 2 hr and then evaporated *in vacuo* to give an oily substance. A benzene solution of it was chromatographed over alumina, affording colorless crystals which were proved, by a study of their infrared spectrum, to be identical with VIII. Yield, 0.1 g (8%). The other products were not examined.

Spectroscopic Determination. After the reac-

TABLE 5. KEY SIGNALS FOR I, II AND III

Compound	Key signal
I	4.31 (singlet, $-CH_2-$)
IIa	1.82 (singlet, $-CH=N-$)
IIb	1.50 (singlet, $-CH=N-$)
IIIa	3.26 (singlet, $\geqslant$CH)
IIIb	3.05 (singlet, $\geqslant$CH)
IVa	4.43 (doublet, $\geqslant$CH)
IVb	3.88 (doublet, $\geqslant$CH)

tion of I with IIa or IIb in the presence or absence of NEt_3 had been carried out in dioxane for a definite time, 1-m*l* aliquots of the mixture were withdrawn by means of a pipet and triethylammonium chloride or benzylidene-*n*-propylamine hydrochloride was removed by filtration. The quantitative estimation of the reactants and products in the filtrate was done by means of NMR spectroscopy. The key signals for the reactants and products are shown in Table 5, while the results are summarized in Tables 1 and 2.

Reaction of I with X. To a stirred solution of 1.6 g (6.8 mmol) of X and 1.4 g (13.8 mmol) of NEt_3 in 10 m*l* of dioxane, a solution of 3.0 g (13.8 mmol) of I in 40 m*l* of dioxane was added, drop by drop, at room temperature over a period of 30 min. After the reaction mixture had then been stirred at room temperature for 14.5 hr, colorless crystals were collected by filtration and washed three times with 10 m*l* of methanol to leave 2.1 g (52%) of the bis(4+2) cycloadduct XI, mp 153°C (decomp.).

Found: C, 63.83; H, 4.88; N, 4.74%. Calcd for $C_{32}H_{28}O_6N_2S_2$: C, 63.99; H, 4.70; N, 4.66%.

Triethylammonium chloride was obtained from the methanol washings; yield, 1.9 g (quantitative). On the other hand, the dioxane filtrate was after the reaction, evaporated *in vacuo* to give an oily substance which solidified on treatment with methanol. Recrystallization from methanol gave colorless prisms, mp 139°C. Yield, 0.4 g. This compound could not be identified (Found: C, 60.97; H, 5.58; N, 4.27%).

BULLETIN OF THE CHEMICAL SOCIETY OF JAPAN VOL. 43 3549—3552 (1970)

Structure and Reactivity of α,β-Unsaturated Ethers. XI. Cationic Copolymerization and Acetal Addition of *cis*- and *trans*-Styryl Ethyl Ethers

Tadashi OKUYAMA, Nobuhiro ASAMI and Takayuki FUENO

Faculty of Engineering Science, Osaka University, Toyonaka, Osaka

(Received June 1, 1970)

The cationic copolymerization between *cis*- and *trans*-styryl ethyl ethers in methylene chloride was investigated in the temperature range from −70 to 0°C with boron trifluoride etherate as catalyst. It was found that at lower temperatures the *trans* ether is more reactive than its *cis* isomer, although the relative reactivities are reversed at 0°C. Addition reactions of various acetals to *cis*- and *trans*-styryl ethyl ethers were carried out at 0°C with the same Lewis acid as catalyst. The relative *cis-trans* reactivities are largely dependent on the bulkiness of an attacking oxycarbonium ion. It was concluded that the *cis* isomer, which is electronically more reactive toward cations, is liable to suffer adverse steric effect, especially when the attacking carbonium ion is bulky.

β-Substituted vinyl ethers are known to be easily polymerized by cationic mechanism. Previous investigations dealt mostly with alkenyl[1-4] and β-chlorovinyl[5] alkyl ethers. In all these cases, *cis* isomers were found to be more reactive than the corresponding *trans* isomers. In the case of β-methylstyrene, however, the *trans* isomer proved to be more reactive.[6,7] The relative *cis-trans* reactivities of α,β-disubstituted olefins in cationic polymerization are apparently not simple and the origin remains to be clarified.

In terms of chemical constitution, styryl alkyl ethers may be regarded as derivatives of either vinyl ether or styrene. Mizote *et al.* reported that the *cis* ether can readily be polymerized by cationic agents.[8] Our interest in the relative reactivities of geometrical isomer pairs of α,β-unsaturated ethers led us to compare the cationic polymerizabilities of *cis*- and *trans*-styryl ethyl ethers.

In the present study, we first investigated the mutual copolymerization between *cis*- and *trans*-styryl ethyl ethers (SEE) at various temperatures. Next, addition reactions of various acetals[4,9]

1) T. Okuyama, T. Fueno and J. Furukawa, *J. Polym. Sci. A*-1, **6**, 993 (1968).

2) T. Okuyama, T. Fueno, J. Furukawa and K. Uyeo, *ibid.*, **6**, 1001 (1968); and references cited therein.

3) T. Higashimura, S. Kusudo and S. Okamura, *Kobunshi Kagaku*, **25**, 698 (1968); and their previous papers.

4) T. Okuyama, T. Fueno and J. Furukawa, *J. Polym. Sic. A*-1, **7**, 3045 (1969).

5) T. Okuyama, T. Fueno and J. Furukawa, *ibid.*, **7**, 2433 (1969); and references cited therein.

6) C. G. Overberger, D. Tanner and E. M. Pearce, *J. Amer. Chem. Soc.*, **80**, 4566 (1958).

7) A. Mizote, T. Higashimura and S. Okamura, *J. Polym. Sci. A*-1, **6**, 1825 (1968).

8) A. Mizote, T. Higashimura and S. Okamura, *J. Macromol. Sci. (Chem.)*, **A2**, 717 (1968).

9) R. I. Hoaglin and D. H. Hirsh, *J. Amer. Chem. Soc.*, **71**, 3468 (1949).

toward *cis*- and *trans*-SEE's were studied kinetically in order to obtain information on the steric effect of attacking carbonium ions on the reactivities of SEE.

$$RCH(OC_2H_5)_2 + BF_3 \rightarrow RCH(OC_2H_5)^+ + BF_3\cdot C_2H_5O^-$$

$$C_6H_5CH{=}CH(OC_2H_5) \xrightarrow{+RCH(OC_2H_5)^+}$$

$$RCH(OC_2H_5)-CH(C_6H_5)-CH(OC_2H_5)^+ \xrightarrow[-BF_3]{+BF_3\cdot C_2H_5O^-}$$

$$RCH(OC_2H_5)-CH(C_6H_5)-CH(OC_2H_5)_2$$

From the results obtained, the factors influencing the *cis-trans* reactivities have been discussed.

Experimental

Materials. SEE was obtained as described previously[10] and distilled from calcium hydride under dry nitrogen immediately before use.

1,1-Diethoxyethane and 1,1-diethoxypropane were prepared by the method described previously.[4] 1,1-Diethoxybutane and 1,1-diethoxy-2-methylpropane were prepared from appropriate aldehydes and ethanol.[4,11] The boiling points were 144—146°C and 136—137°C, respectively. All the acetals were purified by distillation from metallic sodium.

Methylene chloride, tetralin, *o*-dichlorobenzene and boron trifluoride etherate ($BF_3\cdot OEt_2$) were purified as described previously.[1,12]

Cationic Polymerization. Polymerization technique was essentially the same as that described previously.[1]

Polymerization temperature (−70 to −20°C) was controlled to within ±0.5°C with a bath filled with dry ice-cold methanol. Monomer concentrations were determined by means of a Shimadzu gas chromatograph Model 4APT. A 3-m column packed with Apiezon Grease L was operated at *ca.* 130°C with hydrogen as a carrier gas. The internal standard method with half-height width evaluation of peak areas was applied for determining the monomer concentrations. Tetralin or dichlorobenzene was used as internal standard.

For experiments conducted at −70°C, the monomer reactivity ratios were evaluated with the aid of the integral form of the Mayo-Lewis copolymerization equation.[1] In all other cases, the monomer reactivities were evaluated from the slopes of the linear plots of the logarithms of instantaneous concentrations of *cis*-SEE *vs.* those of the *trans*-SEE isomer.

Acetal Addition. The method of the reaction was the same as that described previously.[4] The reaction was allowed to take place in excess acetal at 0°C with $BF_3\cdot OEt_2$ as catalyst. The residual ethers were determined by gas chromatography as in cationic polymerization.

Results

Cationic Copolymerization. A nearly equimolar mixture of *cis*- and *trans*-SEE's was copolymerized in methylene chloride at temperatures between 0 and −70°C. Concentration of each comonomer decreased with the progress of reaction in such a way that a linear relationship held between log[*cis*-SEE] and log[*trans*-SEE] down to at least 80% conversion of the *trans* isomer. The linear relationships at various temperatures are shown in Fig. 1. These results evidently indicate that no geometrical isomerization accompanies the polymerization reaction in the temperature range we studied. The slopes of these linear relationships may then be taken as indicating the relative reactivity *r* of *cis*- to *trans*-SEE at the given temperatures:

$$r = \frac{\log [cis\text{-SEE}]/[cis\text{-SEE}]_0}{\log [trans\text{-SEE}]/[trans\text{-SEE}]_0} \quad (1)$$

where the subscript 0 indicates initial concentrations.

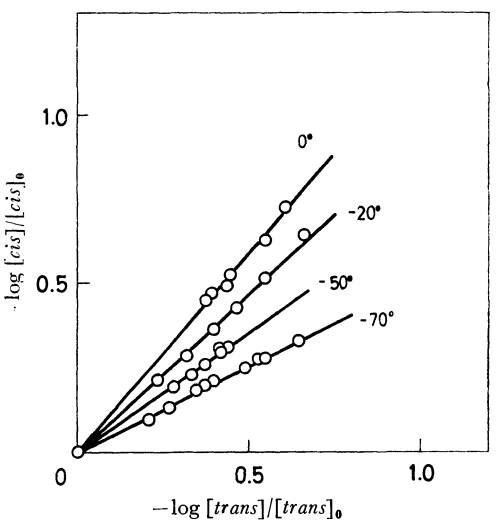

Fig. 1. Variations of monomer concentrations in the mutual copolymerization between *cis*- and *trans*-styryl ethyl ethers at various temperatures. Solvent, methylene chloride. Initial monomer concentration, 7 vol%, in which $[cis\text{-SEE}]_0/[trans\text{-SEE}]_0 = 1.08—1.34$. Catalyst, $BF_3\cdot OEt_2$.

In principle, the above treatment is based on the assumption that the monomer selection in the chain growth is governed by the statistics of the Bernoullian type:

$$r_{cis}r_{trans} = 1 \quad (2)$$

Strictly, it is only when Eq. (2) is satisfied that the

10) T. Okuyama, T. Fueno and J. Furukawa, This Bulletin, **43**, 3256 (1970). Part X of this series.

11) H. Adkins and B. H. Nissen, "Organic Syntheses," Coll. Vol. 1, p. 1 (1932).

12) T. Fueno, T. Okuyama, I. Matsumura and J. Furukawa, *J. Polym. Sci. A*-1, **7**, 1447 (1969).

customary equation for binary copolymerization can be replaced by an expression of the type of Eq. (1).

In order to examine whether the relative reactivity as determined from Eq. (1) really makes sense, we have undertaken the usual copolymerization experiments between *cis*- and *trans*-SEE's of varying isomeric ratios at −70°C. The least-squares treatment[12] (Fig. 2) of the data with the aid of the integral form of the Mayo-Lewis copolymerization equation gave $r_{cis}=0.46\pm0.08$ and $r_{trans}=1.42\pm0.25$. The monomer reactivity ratios thus obtained lead to the $r_{cis}r_{trans}$ product value amounting only to 0.65 ± 0.26, which clearly violates the requirement (2). In such a case, the relative reactivity may best be estimated[1,2] from the value of $(r_{cis}/r_{trans})^{1/2}$. The relative reactivity thus evaluated turned out to be 0.57, which is in perfect agreement with the value 0.58 obtained from Eq. (1) at the same temperature. Thus, the convenient log—log method for evaluating the relative reactivity seems to be useful for copolymerization systems including the cases where the condition (1) is not rigorously satisfied.

The relative reactivity data evaluated from the plots in Fig. 1 are listed in Table 1. At lower temperatures, *cis*-SEE is less reactive than *trans*-SEE. However, the relative reactivity of the former isomer tends to increase with the rise in temperature and exceeds that of the latter at 0°C.

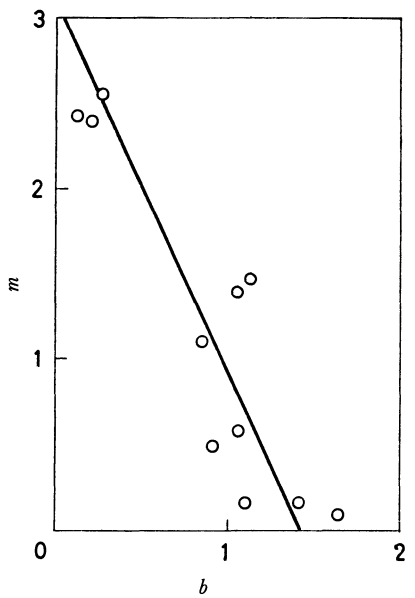

Fig. 2. An *m*-*b* plot for copolymerization between *cis*- and *trans*-styryl ethyl ethers at −70°C.
Quantities *m* and *b* were determined experimentally with the aid of the integral form of the Lewis-Mayo copolymerization equation and are related with the monomer reactivity ratios by $b=-r_{cis}m+r_{trans}$.[12]
Solvent, methylene chloride. Initial monomer concentration, 7 vol%. Catalyst, $BF_3\cdot OEt_2$ (0.024 M).

Table 1. Relative cationic polymerizabilities of *cis*- to *trans*-styryl ethyl ether

Temp., °C	Rel. polym. *cis*/*trans*
−70	0.58
−50	0.71
−20	0.94
0	1.16

Acetal Additions. Additions of various acetals to SEE have been carried out at 0°C with the use of $BF_3\cdot OEt_2$ as catalyst in excess of acetals themselves. An example of the kinetic courses is shown in Fig. 3. From such kinetic courses which are first-order in SEE (for *cis* and *trans* separately), relative reactivities of geometrical isomers have been evaluated and given in Table 2. The relative reactivities are largely dependent on the attacking acetals. For acetals of normal aldehydes, the *cis* isomer is more reactive, while, for the acetals of

Table 2. Relative reactivities of *cis*- to *trans*-styryl ethyl ether toward various alkoxycarbonium ions, $RCH(OC_2H_5)^+$

R	E_s	Rel. react. *cis*/*trans*
CH_3	0	4.26
C_2H_5	−0.07	2.26
n-C_3H_7	−0.36	1.47
i-C_3H_7	−0.47	0.61

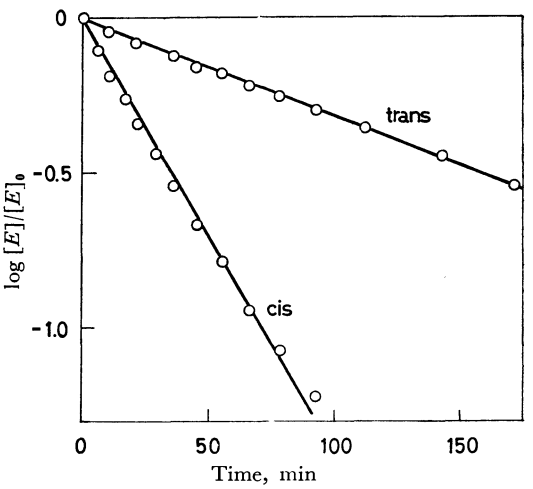

Fig. 3. First-order plots for the reaction of 1,1-diethoxyethane with *cis*- and *trans*-styryl ethyl ethers at 0°C.
Initial concentration, 9 vol%, in which $[cis\text{-SEE}]_0/[trans\text{-SEE}]_0=1.10$. Catalyst, $BF_3\cdot OEt_2$ (8×10^{-3} M).

branched aldehydes, the *trans* isomer is more reactive.

Discussion

Orientation in Polymerization. The head-to-tail orientation of SEE in cationic polymerization might not be intuitively obvious. Mizote *et al.*[8] concluded from the studies on polymerization kinetics that styryl alkyl ethers polymerize through the β-addition of a polymer chain end.

$$C_6H_5CH{=}CHOR \xrightarrow{-C^+} C_6H_5\overset{H}{\underset{}{\diagdown}}\overset{\vdots}{C}\overset{+}{-}\overset{H}{\underset{OR}{\diagup}} \qquad (3)$$

The conclusion seems to be reasonable from the stability of an intermediate carbonium ion. An alkoxycarbonium ion is recognized to be more stable than benzyl-type cations.[13] The previous investigation[10] on the acid-catalyzed hydrolysis ascertained that the protonation of SEE takes place at the β-carbon atom:

$$C_6H_5CH{=}CHOC_2H_5 \xrightarrow{+H^+} C_6H_5\overset{+}{C}H_2CHOC_2H_5$$
$$\xrightarrow{+H_2O} C_6H_5CH_2CHO + C_2H_5OH \qquad (4)$$

a fact which lends support to the reaction mode as represented by (3).

***cis-trans* Polymerizability.** At lower temperatures, *cis*-SEE is less reactive than *trans*-SEE. However, the relative reactivity is considerably dependent on temperature as is seen in Table 1. From the Arrhenius-type plots of the data, the differences in activation parameters have been evaluated to be $\delta\Delta H^{\neq} = 1.4$ kcal/mol and $\delta\Delta S^{\neq} = 5.6$ e.u. That is, the *trans* isomer is energetically more reactive by 1.4 kcal/mol. This is contradictory to the expectationfrom the ground-state stability[16] and seems to be ascribable to the structural difference between the geometrical isomers; *cis*-SEE is non-planar whereas *trans*-SEE is planar as has been concluded previously.[10,17]

One possible interpretation is that the twisted phenyl group in *cis*-SEE hinders an attacking carbonium ion from approaching the olefinic bond, thus rendering the transition state of polymerization far less stable for *cis*-SEE than for *trnas*-SEE. The looser activated complex for the *cis* isomer might be rationalized from its greater entropy of activation as compared with that for the *trans* isomer. The situation seems to be similar to that in the acid-catalyzed hydrolysis.[10]

A greater reactivity of *trans* isomer has been noted or the cationic polymerization of β-methylstyrene and a similar reasoning has been presented.[6,7] In the investigation of the cationic oligomerization of stilbene, Brackman and Plesch[18] estimated that the rate of reaction of a stilbene ion with *trans*-stilbene is at least one hundred times as great as that of its reaction with *cis*-stilbene. The large difference in reactivity was likewise ascribed to steric reasons.

Acetal Additions. The addition reaction of an acetal to α,β-unsaturated ethers is essentially an addition of the alkoxycarbonium ion formed from the acetal to the double bond of ethers.[4,9] Thus, the primary reaction is the same as that of the propagation step of the cationic polymerization of ethers.[4]

The data given in Table 2 indicate that the relative reactivities of *cis*- and *trans*-SEE's are largely dependent on the attacking carbonium ions, $RCH(OC_2H_5)^+$. The magnitude of reactivity seems to be influenced primarily by the bulkiness of carbonium ion. Reactivity of the *cis* isomer relative to the *trans* isomer tends to decrease with the increasing bulkiness (Taft's steric substituent constants E_s[19]) of group R.

The present observation is consistent with the conclusion that the greater reactivity of the *trans* isomer in the cationic polymerization of SEE is due to steric reasons. The steric hindrance in the reaction becomes greater as the attacking species becomes bulkier, and thus the *cis* isomer becomes less reactive with the increasing bulkiness of R in acetals.

In terms of the electronic factor, on the other hand, *cis*-SEE may be considered to be more reactive than *trans*-SEE, as has been observed with a simple acetal. This seems to be related with the observation[1,2,5] that all the β-substituted vinyl ethers studied so far are more reactive in the *cis* form in cationic polymerization, irrespective of the relative thermochemical stabilities of geometrical isomer pairs. The coincidence is reasonable, since from the viewpoint of reaction mode SEE can be considered as a vinyl ether derivative rather than a styrene derivative.

13) The appearance potential of $CH_3OCH_2^+$ is lower than that of $C_6H_5CH_2^+$,[14] and α-chloromethyl ethers are easily solvolyzed as compared with benzyl chloride.[15]

14) R. W. Taft, R. H. Martin and F. W. Lampe, *J. Amer. Chem. Soc.*, **87**, 2490 (1956).

15) H. Böhme, *Ber.*, **74**, 248 (1941).

16) *trans*-SEE is thermochemically more stable than the *cis* isomer.[17]

17) T. Okuyama, T. Fueno and J. Furukawa, *Tetrahedron*, **25**, 5409 (1969).

18) D. S. Brackman and P. H. Plesch, *J. Chem. Soc.*, **1958**, 3563.

19) R. W. Taft, Jr., "Steric Effects in Organic Chemistry," ed. by M. S. Newman, John Wiley & Sons, Inc., New York, N.Y. (1956), Chapter 13.

BULLETIN OF THE CHEMICAL SOCIETY OF JAPAN VOL. 43 3553—3556 (1970)

Structure and Reactivity of α,β-Unsaturated Ethers. XII. Cationic Copolymerization of Ring-Substituted Styryl Ethyl Ethers

Tadashi OKUYAMA, Nobuhiro ASAMI and Takayuki FUENO

Faculty of Engineering Science, Osaka University, Toyonaka, Osaka

(Received June 1, 1970)

Several ring-substituted derivatives of *cis*- and *trans*-styryl ethyl ethers were copolymerized with the unsubstituted *trans* ether in methylene chloride at −70°C with the use of boron trifluoride etherate as a catalyst. The ring substituents investigated include *p*-CH_3O, *p*-CH_3, *m*-CH_3, *p*-Cl, and *m*-Cl. It was found that the effects of substituents on the polymerizability obey the Hammett $\rho\sigma$ relationship with reaction constants $\rho=-2.4$ and -2.0 for *cis* and *trans* isomers, respectively. The structure of the transition state of the cationic polymeization was discussed.

There are many reports concerning the effects of ring substituents on various types of side-chain reactions of benzene derivatives.[1,2] In polymer chemistry, styrene and its derivatives are a typical class of compound which can be subjected to investigation. Thus, the effects of ring substituents on the polymerizability of styrene have been studied under various polymerization conditions.[3-6] Studies have recently been extended to the cationic copolymerization of phenyl vinyl ethers.[7]

We reported the cationic polymerization of styryl ethyl ether (SEE) with particular attention to the relative reactivities of its geometrical isomers.[8] Cationic polymerization of SEE takes place through the addition of a polymer chain-end on the carbon *alpha*[9] to the phenyl group.

$$C_6H_5CH{=}CHOC_2H_5 \longrightarrow \cdots C^+ \quad \begin{matrix} C_6H_5 \\ | \\ H \end{matrix} \!\!>\!\! C \!-\! C \!<\!\! \begin{matrix} H \\ | \\ OC_2H_5 \end{matrix} \quad (1)$$

This presents a striking contrast to the cationic polymerization of styrene, in which a chain-end addition occurs on the *beta*-carbon.[9]

$$C_6H_5CH{=}CH_2 \longrightarrow \cdots CH_2{-}C^+ \!<\!\! \begin{matrix} H \\ | \\ C_6H_5 \end{matrix} \quad (2)$$

Thus, it seems interesting to compare the effects of ring substituents on the cationic polymerizability of SEE with those of styrene.

In the present investigation, *trans*-SEE has been copolymerized with several of its own ring-substituted derivatives as well as various *cis*-SEE derivatives in methylene chloride at −70°C, using $BF_3\cdot OEt_2$ as a catalyst. The results have been examined in comparison with those of related reactions. From the magnitude of the reaction constants, it has been suggested that the cationic polymerization of SEE as well as that of styrene takes place through a cyclic intermediate.

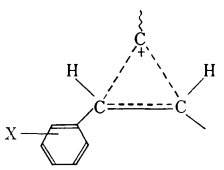

Experimental

Materials. SEE and its ring-substituted derivatives were obtained as described previously[10] and distilled from calcium hydride under nitrogen atmosphere immediately before use.

Methylene chloride, tetralin and boron trifluoride etherate ($BF_3\cdot OEt_2$) were purified as before.[7,11]

Procedure. Polymerization technique was the same as that described previously.[11] The relative reactivities were evaluated by the method of log-log plots.[8]

1) L. P. Hammett, "Physical Organic Chemistry," McGraw-Hill, New York, N. Y. (1940), Chapter 7.
2) H. H. Jaffé, *Chem. Rev.*, **53**, 191 (1953).
3) C. Walling, E. R. Briggs, K. B. Wolfstirn and F. R. Mayo, *J. Amer. Chem. Soc.*, **70**, 1537 (1948).
4) J. P. Kennedy, "Copolymerization," ed. by G. E. Ham, Interscience, New York, N. Y. (1964), p. 308.
5) M. Shima, D. N. Bhattacharyya and M. Szwarc, *J. Amer. Chem. Soc.*, **85**, 1306 (1963).
6) G. Natta, F. Dannuso and D. Sianesi, *Makromol. Chem.*, **30**, 238 (1959).
7) T. Fueno, T. Okuyama, I. Matsumura and J. Furukawa, *J. Polym. Sci., A-1*, **7**, 1447 (1969).
8) T. Okuyama, N. Asami and T. Fueno, This Bulletin, **43**, 3549 (1970).
9) We use the words *alpha* and *beta* in reference to the olefinic carbon atoms located in the α- and β-positions, respectively, with respect to the phenyl ring. For this convention, see Ref. 10, Footnote 15.
10) T. Okuyama, T. Fueno and J. Furukawa, This Bulletin, **43**, 3256 (1970).
11) T. Okuyama, T. Fueno and J. Furukawa, *J. Polym. Sci., A-1*, **6**, 993 (1968).

Results

Polymerization was carried out in methylene chloride at the dry ice-methanol temperature (*ca.* −70°C) with the use of $BF_3 \cdot OEt_2$ as a catalyst. *trans*-SEE was used as a reference monomer for all runs of copolymerization.

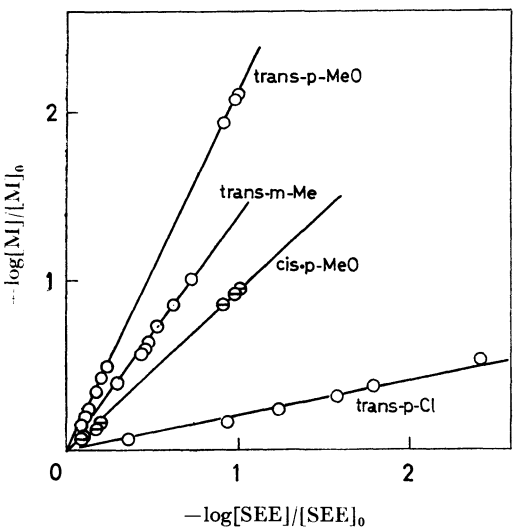

Fig. 1. Variations of monomer concentrations in the copolymerization of various ring-substituted SEE's with *trans*-SEE at −70°C: Solvent, methylene chloride; Catalyst, $BF_3 \cdot OEt_2$.

Examples of the courses of copolymerization between substituted SEE's and *trans*-SEE are shown in Fig. 1. Slopes of the linear relationships provide the relative reactivities[8] of the relevant SEE derivatives. The reactivity data thus obtained are summarized in Table 1.

Table 1. Relative polymerizabilities of ring-substituted styryl ethyl ethers at −70°C

Substituent	Relative polymerizability	
	cis	*trans*
p-CH_3O	0.92	2.11
p-CH_3	0.65	1.98
m-CH_3	—	1.41
H	0.57	1.00
p-Cl	0.17	0.22
m-Cl	0.06	0.09

The reactivity of *trans*-*m*-CH_3-SEE (M_2) relative to *trans*-SEE (M_1) was also evaluated by the usual copolymerization experiments, in which variations of the comonomer composition were analyzed by the aid of the Mayo-Lewis copolymerization equation in an integral form. The *m*-*b* plot[7,8] pertinent to this analysis is shown in Fig. 2. The monomer reactivity ratios obtained were $r_1 = 0.62 \pm 0.01$ and

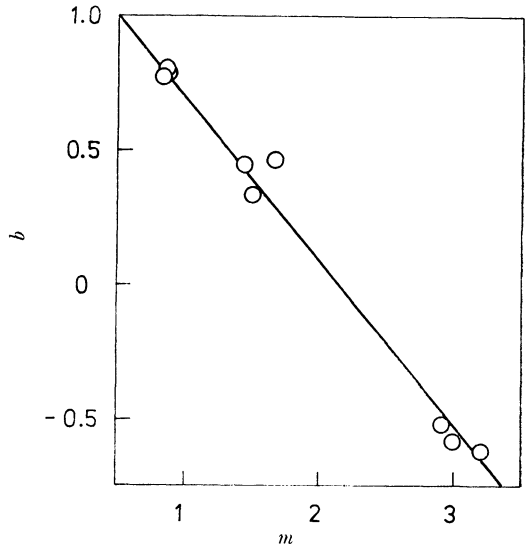

Fig. 2. The *m*–*b* plots for the copolymerization of *trans*-SEE (M_1) and *trans*-*m*-CH_3-SEE (M_2) at −70°C: Solvent, methylene chloride; Initial monomer concentration=8 vol%; Catalyst, $BF_3 \cdot OEt_2$ (0.024M).

$r_2 = 1.32 \pm 0.01$, which lead to the relative reactivity $(r_2/r_1)^{1/2} = 1.45$, in essential agreement with the value, 1.41, listed in Table 1.

At the present polymerization temperature, the *trans* isomers are more reactive than the corresponding *cis* isomers. The polymerizability of SEE derivatives is clearly enhanced with the increase in the electron-releasing character of the ring substituents.

Discussion

Effects of Substituents. Figure 3 shows the Hammett plots of the observed polymerizabilities.

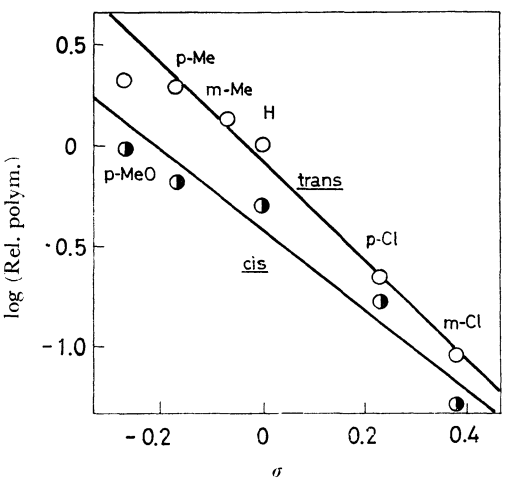

Fig. 3. The Hammett plots of cationic polymerizability of SEE derivatives.

Table 2. Reaction constants for various electrophilic reactions of styryl compounds, XC_6H_4-CH=CH-Y

No.	Compound	Y	Reaction	ρ	Intermediate[a]	Product orientation[b]	Ref.
1	*cis*-Cinnamic acid	COOH	Isomerization	−4.3	I	—	12
2[c]	Styrene	H	Bromination	−4.3	I	*beta*	13
3	Cinnamic acid	COOH	Chlorination	−4.01	I	*beta*	14
4	Styrene	H	Hydration	−3.43	I	*beta*	15
5	*cis*-Stilbene	C_6H_5	Isomerization	−3.30	I	—	16
6	Styrene	H	ArSCl addition	−2.41——2.29	III	*beta*	17
7[d]	Styrene	H	Bromination	−2.24——1.93	III	*beta*	18
8	Styrene	H	Cationic polymn	−2.03	?	*beta*	4
9	SEE	OC_2H_5	Cationic polymn	−2.4, −2.0	?	*alpha*	Present work
10	SEE	OC_2H_5	Hydrolysis	−1.1, −0.7	II	*alpha*	10
11	*cis*-Stilbene	C_6H_5	Isomerization	−0.96	II	—	16

a) See text.
b) Position of the addition of an electrophile in the product.
c) Substituents studied include *p*-CH_3O, *p*-CH_3, *m*-CH_3, and *p*-F.
d) Substituents studied include *m*-F, *m*-Cl, *m*-Br, *m*-NO_2, *p*-NO_2, and *p*, *m*-dichloro.

Although the substituents adopted for the plots are few in number, they still suffice to show a general trend. It appears that linear relationships hold for both *cis* and *trans* isomers. The reaction constants, ρ, are roughly −2.0 and −2.6 for *cis* and *trans* isomers, respectively.

These ρ values are comparable in magnitude with the value (−2.03) for the cationic polymerization of styrenes,[4] even though the reaction sites of SEE and styrene are different; the former polymerizes through the addition of polymer chain end on the carbon *alpha* to the phenyl group while the latter polymerizes through the addition on the *beta*-carbon. Therefore, it seems interesting to further examine the magnitudes of substituent effects in these reactions.

Magnitude of the ρ Values. The reaction constants of the Hammett $\rho\sigma$ relations for various electrophilic reactions of styryl compounds related to the present reaction range from −4.3 to −0.7, depending on the type of reaction. Examples in the literature are compared in Table 2.

The reactions listed in Table 2 can be classified by the magnitude of the ρ values into three groups; $\rho = -3.8 \pm 0.5$ (Nos. 1—5), *ca.* −2 (Nos. 6—9) and *ca.* −1 (Nos. 10 and 11).

The first group undoubtedly consists of reactions involving an *alpha*-carbonium ion intermediate (I), which is produced by the electrophilic attack of reagents on the *beta*-carbon (with respect to the phenyl group).

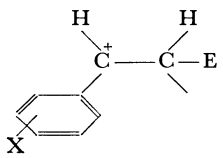

I. *alpha*-Carbonium ion

The ρ values around −4 for the reactions involving the rate-determining formation of the *alpha*-carbonium ions (I) are also known for the solvolyses (S_N1) of benzyl-type compounds, $C_6H_5C(CH_3)_2Cl$ and $C_6H_5CH(CH_3)Cl$.[19] In this type of intermediate, charge delocalization into the phenyl group is very important and the effect of substituents on the charge delocalization should be great.

The last group of reactions with $\rho \simeq -1$ include those taking place with the attack of an electrophile on the carbon attached by the phenyl group, thus forming a *beta*-carbonium ion intermediate like II.

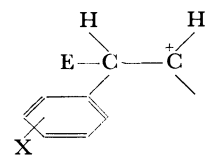

II. *beta*-Carbonium ion

This type of reaction has hitherto been known only in a very limited number; there are only two examples reported so far.[10,16] The smaller effects

12) D. S. Noyce, and H. S. Avarbock *J. Amer. Chem. Soc.*, **84**, 1644 (1968).
13) J. E. Dubois and A. Schwarcz, *Tetrahedron Lett.*, **1964**, 2167.
14) H. P. Rothbaum. I. Ting and P. W. Robertson, *J. Chem. Soc.*, **1948**, 980.
15) W. H. Schubert, B. Lamm and J. R. Keefe, *J. Amer. Chem. Soc.*, **86**, 4272 (1964).
16) D. S. Noyce, D. R. Hatter and F. B. Miles, *ibid.*, **90**, 4633 (1968).
17) W. L. Orr and N. Kharasch, *ibid.*, **78**, 1201 (1956).
18) K. Yates and W. V. Wright, *Can. J. Chem.*, **45**, 167 (1967).
19) *E. g.*, H. C. Brown and Y. Okamoto, *J. Amer. Chem. Soc.*, **79**, 1913 (1957).

of substituents are easily understandable since the carbonium-ion center is insulated from the ring by an intervening methylene group.

The second group, which have ρ values intermediate in magnitude (*ca.* -2), include the reactions of some intermediate character. In these reactions, addition of sulfenyl chlorides to olefins (No. 6) is well established to take place through cyclic episulfonium ions.[17,20] Bromination of styrenes (No. 7) carrying an electron-attracting substituent has been confirmed to occur with the formation of cyclic bromonium ions like III.[21]

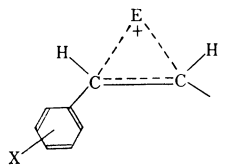

III. α,β-Intermediate

Thus, the reactions seem to take place with simultaneous attack of an electrophile on both the α- and β-carbons forming an intermediate like III. Cationic polymerization of both styrenes and SEE's apparently belongs to this category and should involve the cyclic α,β-intermediate III.[22]

Styrene and SEE differ from each other in product orientation. The identical magnitudes of the ρ values for these two reactions may be reconciled if we assume a common mechanism involving the formation of a cyclic α,β-intermediate of type III. The cationic polymerization of vinyl ethers proceeds through the cyclic α,β-intermediate, which agrees with our previous conclusion obtained from the results of calculations of the transition state stability.[23] An experimental investigation[7] of the ring-substituent effects on the phenyl vinyl ether polymerizability also supports the low carbonium-ion character of the transition state. Our recent results on the cationic polymerizations of benzofuran derivatives lend further support to the validity of the α,β-intermediate mechanism.[24]

20) W. H. Mueller and P. E. Butler, *ibid.*, **90**, 2075 (1968); and references cited therein.

21) The conclusion was based on a comparison of the ρ-values of the first and second groups of reactions.[18]

22) This intermediate does not necessarily mean a symmetrical one with respect to the strength of the bonds which an electrophile formed with the α- and the β-carbons. Rather, some asymmetry must be present in view of the definite product orientation.

23) T. Fueno, T. Okuyama and J. Furukawa, *J. Polym. Sci., A-1*, **7**, 3219 (1969).

24) T. Okuyama, K. Kunugiza and T. Fueno, to be published.

BULLETIN OF THE CHEMICAL SOCIETY OF JAPAN VOL. 43 3556—3560 (1970)

The Syntheses of 2-Phenethyl-2,3-dihydro-4(1*H*)-pyridones

Noboru SUGIYAMA, Makoto YAMAMOTO and Choji KASHIMA

Department of Chemistry, Tokyo Kyoiku University, Otsuka, Tokyo

(Received June 15, 1970)

In the presence of three moles of potassium amide in liquid ammonia, the reactions of β-diketones with cinnamylidenaniline gave derivatives of 1-phenyl-2-styryl-2,3-dihydro-4-pyridone. By the catalytic hydrogenation of 6-methyl-1-phenyl-2-styryl-2,3-dihydro-4-pyridone, 6-methyl-2-phenethyl-1-phenyl-2,3-dihydro-4-pyridone was obtained. When β-diketones were treated with cinnamaldehyde azine, instead of cinnamylidenaniline, 1-cinnamylidenamino-2-styryl-2,3-dihydro-4-pyridones were produced; these were then catalytically hydrogenated to the corresponding 2-phenethyl-2,3-dihydro-4(1*H*)-pyridones, accompanied with 2-phenethyl-1-(3-phenylpropylamino)-2,3-dihydro-4-pyridones.

In the presence of three moles of potassium amide in liquid ammonia, dihydropyridone derivatives (A) which contain two phenyl groups at the 1- and 2-positions have been synthesized from β-diketones and benzylidenaniline.[1] The reactions of acetylacetone (**1**) with ethylidenaniline or benzylidenemethylamine, instead of benzylidenaniline, did not give the corresponding 1-phenyl- or 2-phenyldihydropyridone.[1]

The condensation of β-diketones with benzaldazine yielded 1-benzylidenamino-2,3-dihydro-4-pyridones,[2] which were then catalytically hydro-

1) N. Sugiyama, M. Yamamoto and C. Kashima, This Bulletin, **42**, 1357 (1969).

2) N. Sugiyama, M. Yamamoto and C. Kashima, *ibid.*, **43**, 901 (1970).

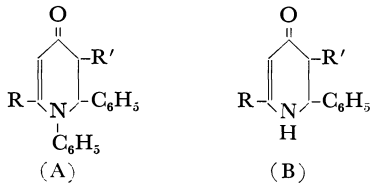

(A) (B)

Fig. 1.

genolyzed to the corresponding 2,3-dihydro-4(1*H*)-pyridones (B). According to this procedure, dihydropyridone with a phenyl group at the 2-position was obtained.

The condensation of *β*-diketones with cinnamylidenaniline gave 2-styryl-dihydropyridones, which were then catalytically hydrogenated to the dihydropyridones with the phenethyl group at the 2-position.

Results and Discussion

In an attempt to synthesize dihydropyridones with aliphatic substituents, 1-phenyl-dihydropyridones with an aliphatic substituent at the C-2 position was synthesized first.

The reaction of acetylacetone (**1**) with cinnamylidenaniline (**4**) in the presence of sodium or potassium amide in liquid ammonia produced 6-methyl-1-phenyl-2-styryl-2,3-dihydro-4-pyridone (**5**). When three moles of sodium amide and one mole of **4** to **1** were used, the yield of **5** was 4.5%. When two moles of potassium amide were used, the yield of **5** was 5.8%. The mole ratio of 1 : 1 : 3 for **1**, **4** and potassium amide is the best condition for this reaction; this yield was 13.1%.

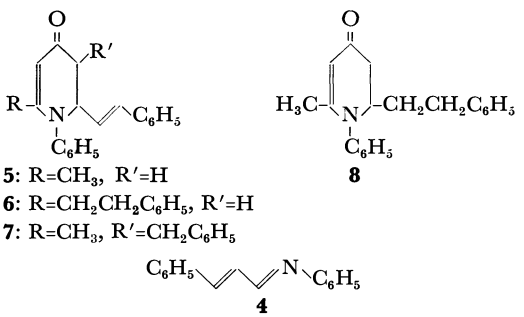

5: R=CH_3, R′=H
6: R=$CH_2CH_2C_6H_5$, R′=H
7: R=CH_3, R′=$CH_2C_6H_5$

8

4

Fig. 2.

The structure of **5** was determined by studying the spectral data and by elemental analyses.

The condensation of 6-phenyl-2,4-hexanedione (**2**) with **4** gave 6-phenethyl-1-phenyl-2-styryl-2,3-dihydro-4-pyridone (**6**) and its isomer, 3-benzyl-6-methyl-1-phenyl-2-styryl-2,3-dihydro-4-pyridone (**7**) in 13.5 and 4.5% yields respectively. Thus, in the reaction of **2** with benzylidenaniline, C-1 methyl was more reactive than the C-5 methylene of **2**.[1]

It was shown that the dihydropyridone ring is not changed in ethanol during catalytic reduction with a palladium charcoal or a platinum oxide catalyst,[3] but in acetic acid it is hydrogenated by a platinum oxide catalyst to piperidone or piperidinol.[4] These results suggested that when dihydropyridones with a styryl group at the C-2 position are treated with platinum oxide in ethanol, dihydropyridones with a phenethyl group at C-2 may be produced.

The catalytic hydrogenation of **5** gave the expected product, 6-methyl-2-phenethyl-1-phenyl-2,3-dihydro-4-pyridone (**8**) in a poor yield. The ultraviolet spectrum of **8** showed an absorption maximum at 324 m*μ* which is attributable to the *α*,*β*-unsaturated *β*-aminoketone chromophore, but the absorption at 254 m*μ*, corresponding to that of the cinnamyl group, disappeared. This proved the formation of **8**.

On the basis of these results and those described in a previous paper,[4] the condensation products of *β*-diketones with cinnamaldehyde azine (**9**) can be said to be, in fact, catalytically hydrogenated to 2-phenethyl-dihydropyridones.

The condensation of one mole of **1** with a half mole of **9** in the presence of three moles of potassium amide in liquid ammonia gave 1-cinnamylidenamino-6-methyl-2-styryl-2,3-dihydro-4-pyridone(**10**) in a 14.0% yield. Under the same conditions, from benzoylacetone (**3**) and **9**, 1-cinnamylidenamino-6-phenyl-2-styryl-2,3-dihydro-4-pyridone(**11**) was obtained in a poor yield. Similarly, **2** condensed

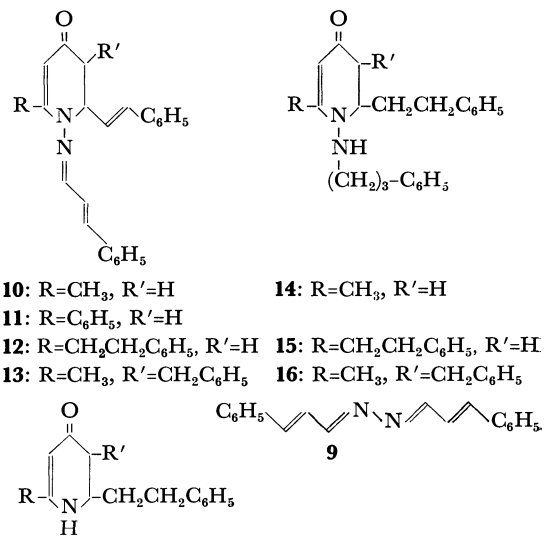

10: R=CH_3, R′=H
11: R=C_6H_5, R′=H
12: R=$CH_2CH_2C_6H_5$, R′=H
13: R=CH_3, R′=$CH_2C_6H_5$

14: R=CH_3, R′=H
15: R=$CH_2CH_2C_6H_5$, R′=H
16: R=CH_3, R′=$CH_2C_6H_5$

9

17: R=CH_3, R′=H
21: R=$CH_2CH_2C_6H_5$, R′=H
22: R=CH_3, R′=$CH_2C_6H_5$

Fig. 3.

3) N. Sugiyama, M. Yamamoto and C. Kashima, unpublished data.

4) C. Kashima, M. Yamamoto and N. Sugiyama, This Bulletin, **42**, 2690 (1969).

with **9** to give 1-cinnamylidenamino-6-phenethyl-2-styryl-2,3-dihydro-4-pyridone (**12**) and its isomer, 3-benzyl-1-cinnamylidenamino-6-methyl-2-styryl-2,3-dihydro-4-pyridone (**13**) in 15.7 and 5.0% yields respectively. In this reaction of **9**, C-1 is more reactive than the C-5 of **2**.

The structures of **10** and **12** were confirmed by a study of their spectral data and by elemental analyses, but those of both **11** and **13** had to be assigned only from the spectral data.

Compounds **10**, **12**, and **13** were hydrogenated with platinum oxide in ethanol. The hydrogenation of **10** gave 6-methyl-2-phenethyl-1-(3-phenylpropylamino)-2,3-dihydro-4-pyridone (**14**) and 6-methyl-2-phenethyl-2,3-dihydro-4(1*H*)-pyridone (**17**) in 19 and 52% yields respectively. The structures of **14** and **17** were confirmed by studying their spectral data.

In the hydrogenation of **10**, many intermediate products were expected to be obtained, as is illustrated in Scheme 1. The hydrogenation of **10** was interrupted after about 1.7 mol of hydrogen to **10** had been absorbed. From this reaction mixture, 1-cinnamylidenamino-6-methyl-2-phenethyl-2,3-dihydro-4-pyridone (**18**) and **14** were obtained, both in 29% yields, accompanied by a trace of **17**, but neither **19** nor **20** was detected. The further hydrogenation of **18** with platinum oxide in ethanol gave **14** and **17**, while the same treatment of **14** gave only **17**. These results suggest that the hydrogenation proceeds through the route **10**→**18**→**14**→**17**.

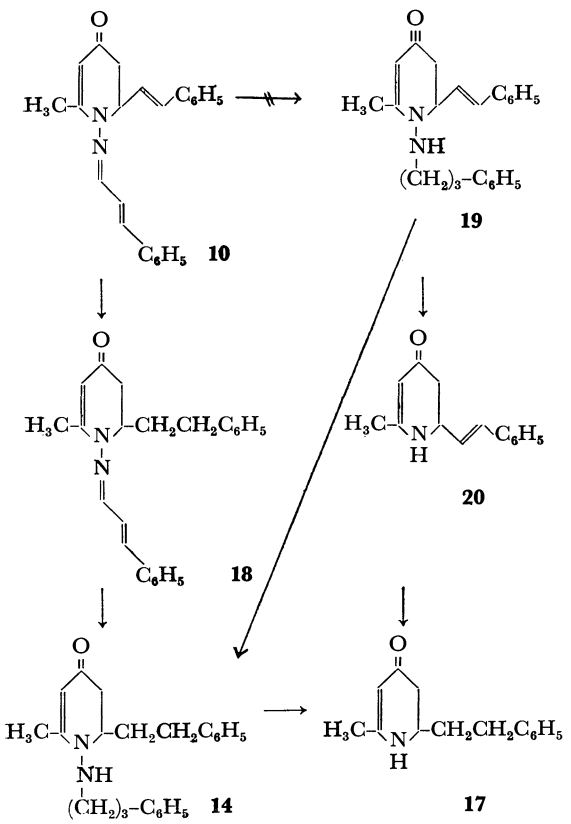

Scheme 1.
Intermediates of the Hydrogenation of **10** to **17**

The hydrogenation of **12** gave **15** and **21**, and that of **13** gave **16** and **22**. The structures of **15**, **16**, **21**, and **22** were confirmed by a study of their spectral data,[5,6] and, in the case of **21**, by elemental analyses.

By the use of the procedure described above, dihydropyridones with aliphatic substituents can be synthesized. This procedure consists of simple reaction steps, so that it can be a general method of dihydropyridone synthesis.

Experimental

The Condensation Reaction in Liquid Ammonia. General Procedure. In a 500-m*l*, three necked flask, about 300 m*l* liquid ammonia was placed. A small amount of sodium or potassium was added and dissolved completely. Into the resulting blue solution a catalytic amount of ferric chloride was stirred, and then 0.09 g atom of sodium or potassium in small portions. The color of the solution changed from blue to dark gray within 60—90 min. To this solution 0.03 mol of β-diketone in 30 m*l* of anhydrous ether was added in small portions. After stirring for an hour, 0.03 mol of cinnamylidenaniline (**4**) or cinnamaldehyde azine (**9**) in 50 m*l* of anhydrous ether was added in small portions. After stirring for four hours at −33°C, the reaction mixture was neutralized with solid ammonium chloride (8.0 g). The liquid ammonia was evaporated rapidly on a water bath, and 100 m*l* of ether was added gradually to the residue. The ethereal layer was separated. The ether-insoluble layer was dissolved in 150 m*l* of dilute hydrochloric acid, and then extracted with chloroform. The ether and chloroform layers were washed with water and dried over anhydrous sodium sulfate. The ether and chloroform were evaporated to give the same condensation product.

6-Methyl-1-phenyl-2-styryl-2,3-dihydro-4-pyridone (5). According to the general procedure, 0.03 mol of **1** and 0.03 mol of **4** were allowed to react in the presence of 0.09 mol of sodium amide. The reaction mixture was chromatographed on a silica gel (Merck 7734, 0.05—0.2 mm) column with a benzene - ethyl acetate (2 : 1 v/v) mixture. A fraction that showed a brownish green ferric chloride test was collected, worked up as usual, and recrystallized from benzene to give 0.39 g (4.5%) of **5** as pale yellow prisms; mp 62—63°C.

Found: C, 83.05; H, 6.80; N, 4.87%. Calcd for $C_{20}H_{19}NO$: C, 83.01; H, 6.62; N, 4.84%.

IR(KBr): 1630 (ν C=O), 1550 cm^{-1} (ν C=C).

UV: λ_{max}^{EtOH} mμ(ε): 254 (16900), 286 (5400), 295 (6750) and 325 (17100).

NMR(in $CDCl_3$)(τ): 8.18 (singlet, 3H, C-6 methyl protons), 7.67—6.78 (multiplet, 2H, C-3 methylene

5) H. E. A. Kramer, *Ann. Chem.*, **696**, 15 (1966).
6) C. Kashima, M. Yamamoto and N. Sugiyama, *J. Chem. Soc., C.* **1970**, 111.

protons), 5.60—5.30 (multiplet, 1H, C-2 methine proton), 4.81 (singlet, 1H, C-5 olefin proton), 3.63 (doublet, 1H, β-olefin proton of C-2 styryl group), and 2.77—2.50 (11H, multiplet, aromatic and α-olefin proton of C-2 styryl group).

The reaction of 0.015 mol of **1** with equimolar **4** was carried out in the presence of 0.03 mol of potassium amide by the general procedure. The purification of the reaction product by column chromatography gave 0.25 g (5.8%) of **5**. The reaction of 0.04 mol of **1**, 0.04 mol of **4**, and 0.12 mol of potassium amide yielded 1.52 g (13.1%) of **5**.

6-Phenethyl-1-phenyl-2-styryl-2,3-dihydro-4-pyridone (6). The reaction of 0.015 mol of **2** with an equimolar amount of **4** was carried out in the presence of 0.045 mol of potassium amide by the general procedure. By the chromatography of the reaction product on a silica-gel (Merck 7734) column with a benzene - ethyl acetate (2 : 1 v/v) mixture, a fraction with the R_f-value of 0.27 (on the thin-layer chromatography of silica-gel (Wako gel B-5) with benzene - ethyl acetate (2 : 1 v/v)) was collected. When this fraction was worked up by the usual procedure and recrystallized from benzene, 764 mg (13.5%) of **6** were afforded as colorless plates; mp 174—176°C.

Found: C, 85.64; H, 6.73; N, 3.75%. Calcd for $C_{27}H_{25}NO$: C, 85.45; H, 6.64; N, 3.69%.

IR(KBr): 1630 (ν C=O), 1550 (ν C=C), and 700 cm^{-1} (phenyl).

UV: λ_{max}^{EtOH} mμ(ε): 254 (19800), 285 (4900), 295 (5000) and 331 (17700).

NMR(in $CDCl_3$)(τ): 7.64—7.16 (multiplet, 4H, ethylene protons of the C-6 phenethyl group), 7.78—6.76 (multiplet, 2H, C-3 methylene protons), 5.73—5.45 (multiplet, 1H, C-2 methine proton), 4.70 (singlet, 1H, C-5 olefin proton), 3.60 (doublet, 1H, β-olefin proton of the C-2 styryl group), and 3.20—2.57 (multiplet, 16H, aromatic protons and α-olefin proton of the C-2 styryl group).

3-Benzyl-6-methyl-1-phenyl-2-styryl-2,3-dihydro-4-pyridone (7). Compound **7** was obtained from the same reaction mixture as **6**. By column chromatography with benzene - ethyl acetate (2 : 1 v/v), **7** was eluted ahead of **6**. On silica-gel (Wako gel B-5) thin-layer chromatography with benzene - ethyl acetate (2 : 1 v/v), **7** showed an R_f-value of 0.35, while that of **6** was 0.27. The fraction containing **7** was concentrated and recrystallized from ethyl acetate to give 255 mg (4.5%) of **7** as pale yellow prisms; mp 155—156°C.

Found: C, 85.49; H, 6.66; N, 3.79%. Calcd for $C_{27}H_{25}NO$: C, 85.45; H, 6.64; N, 3.69%.

IR(KBr): 1635 (ν C=O), 1560 (ν C=C) and 705 cm^{-1} (phenyl).

UV: λ_{max}^{EtOH} mμ(ε): 253 (18300), 285 (4950), 294 (5460) and 328 (17900).

NMR(in $CDCl_3$)(τ): 8.10 (singlet, 3H, C-6 methyl protons), 7.60—6.64 (multiplet, 3H, C-3 methine and methylene protons of the C-3 benzyl group), 5.94 (quartet, 1H, C-2 methine proton), 4.80 (singlet, 1H, C-5 olefin proton), 3.98—3.31 (multiplet, 1H, β-olefin proton of the C-2 styryl group), and 2.85—2.55 (multiplet, 16H, α-olefin proton of the C-2 styryl group, and aromatic protons).

6-Methyl-2-phenethyl-1-phenyl-2,3-dihydro-4-pyridone (8). A mixture of 30 ml of ethanol, 150 mg of **5**, and 100 mg of platinum oxide was stirred under the atmospheric pressure of hydrogen. After absorbing 49 ml of hydrogen, the reaction mixture was treated in the usual manner and then purified by chromatography on a silica-gel (Merck 7729, 0.08 mm) column, using a benzene - ethyl acetate (2 : 1 v/v) mixture. A fraction with an R_f-value of 0.25 was collected on silica-gel (Wako gel B-5) thin-layer chromatography, using a benzene - ethyl acetate (2 : 1 v/v) mixture; this value was different from that of **5**, 0.16. However, this fraction was proved to contain a trace of **8** and 111 mg (74%) of recovered **5**.

Syntheses of 1-Cinnamylidenamino-2,3-dihydro-4-pyridones. According to the general procedure, 1-cinnamylidenamino-2,3-dihydro-4-pyridones were prepared from 0.015 mol of β-diketone and 0.015 mol of cinnamaldehyde azine (**9**). The crude product was chromatographed on a silica-gel (Merck 7734) column, using a benzene - ethyl acetate (4 : 1 v/v) mixture. A fraction which showed a green color with ferric chloride was collected and then again chromatographed on a silica-gel (Merck 7729) column, using a benzene - ethyl acetate (2 : 1 v/v) mixture. A fraction which showed a green color with ferric chloride was collected, concentrated, and recrystallized from the appropriate solvent to yield pure dihydropyridones, **10**, **11**, **12** and **13**.

1-Cinnamylidenamino-6-methyl-2-styryl-2,3-dihydro-4-pyridone (10). Compound **10** was prepared from 0.015 mol of **1** and 0.015 mol of **9**. Yield, 0.70 g (14.0%); yellow prisms (recrystallized from benzene); mp 185—186°C.

Found: C, 80.57; H, 6.61; N, 8.08%. Calcd for $C_{23}H_{22}N_2O$: C, 80.67; H, 6.48; N, 8.10%.

IR(KBr): 1640 (ν C=O), 1590 (ν C=N) and 1555 cm^{-1} (ν C=C).

UV: λ_{max}^{EtOH} mμ(ε): 238 (18700), 246 (21500), 256 (22000), 286 (16000), 372 (40400) and 382 (40400).

NMR(in $CDCl_3$)(τ): 7.70 (singlet, 3H, C-6 methyl protons), 7.42 (quartet, 1H, C-3 methylene proton, ABX type), 6.85 (quartet, 1H, C-3 methylene proton, ABX type), 4.95 (multiplet, 1H, C-2 methine proton, ABX type), 4.85 (singlet, 1H, C-5 olefin proton), 4.04 (quartet, 1H, α-olefin proton of the C-2 styryl group), 3.67(doublet, 1H, β-olefin proton of the C-2 styryl group), 3.15 (multiplet, 2H, β′-, γ′-olefin protons of the 1-cinnamylidenamino group), and 2.76—2.30 (multiplet, 11H, α′-olefin proton of the 1-cinnamylidenamino group and aromatic protons).

1-Cinnamylidenamino-6-phenyl-2-styryl-2,3-dihydro-4-pyridone (11). Compound **11** was prepared from 0.015 mol of **3** and an equimolar amount of **9** in a poor yield (yellow solid). UV spectrum of **11**: λ_{max}^{EtOH} 251, 295 and 378 mμ.

1-Cinnamylidenamino-6-phenethyl-2-styryl-2,3-dihydro-4-pyridone (12). From 0.015 mol of **2** and an equimolar amount of **9**, 1.02 g (15.7%) of **12** were prepared. Yellow prisms; mp 131—134°C (recrystallized from ethanol).

Found: C, 83.11; H, 6.65; N, 6.43%. Calcd for $C_{30}H_{28}N_2O$: C, 83.30; H, 6.53; N, 6.48%.

IR(KBr): 1635 (ν C=O), 1580 (ν C=N) and 1550 cm^{-1} (ν C=C).

UV: λ_{max}^{EtOH} mμ(ε): 247 (23100), 256 (22400), 286 (15700), 293 (14400), 373 (42300) and 385 (42500).

NMR(in $CDCl_3$)(τ): 7.00 (singlet, 3H, ethylene protons of the C-6 phenethyl group), 6.64—7.58 (ABX type double quartet, 2H, C-3 methylene protons, J_{AB}=16.5, J_{AX}=7.2 and J_{BX}=1.5 Hz), 4.85 (multiplet, 1H, C-2

methine proton), 4.83 (singlet, 1H, C-5 olefin proton), 4.00 (quartet, 1H, α-olefin proton, $J_{\alpha X}$=4.5 Hz), 3.58 (doublet, 1H, β-olefin proton, $J_{\alpha\beta}$=15.7 Hz), 3.10 (multiplet, 2H, β′- and γ′-olefin protons of the 1-cinnamylidenamino group), and 2.75—2.30 (multiplet, 16H, α′-olefin proton of the 1-cinnamylidenamino group and aromatic protons).

3-Benzyl-1-cinnamylidenamino-6-methyl-2-styryl-2,3-dihydro-4-pyridone (13). Compound **13** was obtained from the same reaction mixture as **12**. The fraction which was eluted first showed an R_f-value of 0.21 on silica-gel (Wako gel B-5) thin-layer chromatography with a benzene - ethyl acetate (10 : 1 v/v) mixture. However, **12** showed an R_f-value of 0.10. When it was worked up as usual, 0.32 g (5.0%) of **13** was yielded as a viscous yellow oil.

IR(liquid film): 1630 (ν C=O), 1585 (ν C=N) and 1550 cm^{-1} (ν C=C).

Catalytic Hydrogenation of 10. A solution of 390 mg of **10** in 50 m*l* of ethanol was hydrogenated with 100 mg of platinum oxide at room temperature and under an atmospheric pressure. After absorbing about 105 m*l* of hydrogen (calculated 111 m*l*), the absorption of hydrogen almost ceased. After the catalyst had then been filtered off, the ethanol solution was worked up as usual. It was chromatographed on a silica-gel (Merck 7729) column with a benzene - ethyl acetate (1 : 1 v/v) mixture. Two fractions which showed brown and green colors with ferric chloride were collected. The brown-colored fraction was again chromatographed on a silica-gel (Merck 7729) column with a benzene - ethyl acetate (2 : 1 v/v) mixture to give 76 mg (19%) of 6-methyl-2-phenethyl-1-(3-phenylpropylamino)-2,3-dihydro-4-pyridone (**14**) as a yellow oil.

NMR(in $CDCl_3$)(τ): 8.00 (singlet, 3H, methyl protons), 8.43—7.00 (multiplet, 12H, C-3 methylene protons and ethylene protons of the C-2 phenethyl group and trimethylene protons of the 1-(3-phenylpropylamino-group), 6.54—6.20 (multiplet, 1H, C-2 methine proton), 6.05 (broad singlet, 1H, NH; this signal disappeared upon treatment with D_2O[2]), 5.17 (singlet, 1H, C-5 olefin proton), and 2.89—2.55 (multiplet, 10H, aromatic protons).

The fraction which showed a green color with ferric chloride was again chromatographed on a silica-gel (Merck 7729) column with a benzene - ethyl acetate (1 : 2 v/v) mixture to give 128 mg (52%) of 6-methyl-2-phenethyl-2,3-dihydro-4(1*H*)-pyridone (**17**) as colorless needles; mp 143—145°C.

Found: C, 77.93; H, 8.08; N, 6.45%. Calcd for $C_{13}H_{17}NO$: C, 78.10; H, 7.96; N, 6.51%.

IR(KBr): 3220 (ν NH), 1600 (ν C=O) and 1575 cm^{-1} (ν C=C).

UV: λ_{max}^{EtOH} mμ(ε): 314 (15400) and $\lambda_{max}^{HCl/EtOH}$ 307 (10300).

NMR(in $CDCl_3$)(τ): 8.10 (singlet, 3H, C-6 methyl protons), 8.02—7.12 (multiplet, 6H, C-3 methylene protons and ethylene protons of the C-2 phenethyl group), 6.50—6.20 (multiplet, 1H, C-2 methine proton), 5.10 (singlet, 1H, C-5 olefin proton), 4.73 (broad singlet, 1H, NH), and 2.85—2.70 (multiplet, 5H, aromatic protons).

According to the same procedure, from the compound **12**, **15** and **21** were obtained, and from the compound **13**, **16** and **22** were prepared. The compounds **15**, **16** and **22** could not be purified well, so the structures of these compounds were confirmed only by the spectral data.

2,6-Diphenethyl-1-(3-phenylpropylamino)-2,3-dihydro-4-pyridone (15). From 1.40 g of **12**, 380 mg (26.8%) of **15** and 264 mg (26.7%) of **21** were obtained.

IR of **15** (liquid film): 3250 (ν NH), 1610 (ν C=O) and 1540 cm^{-1} (ν C=C).

UV: λ_{max}^{EtOH} 329 mμ, $\lambda_{max}^{HCl/EtOH}$ 325 mμ.

NMR(in $CDCl_3$)(τ): 8.45—6.95 (multiplet, 16H), 6.96—6.69 (broad singlet, 1H, NH), 6.50—6.18 (multiplet, 1H, C-2 methine proton), 5.10 (singlet, 1H, C-5 olefin proton), 2.79, 2.80, 2.82 (singlets, 15H, aromatic protons).

2,6-Diphenethyl-2,3-dihydro-4(1*H*)-pyridone (21). Mp 144—146°C; colorless needles.

Found: C, 82.46; H, 7.55; N, 4.54%. Calcd for $C_{21}H_{23}NO$: C, 82.58; H, 7.59; N, 4.59%.

IR(KBr): 3250 (ν NH), 1605 (ν C=O) and 1570 cm^{-1} (ν C=C).

UV: λ_{max}^{EtOH} mμ(ε): 316 (15000), $\lambda_{max}^{HCl/EtOH}$ 310 (10200).

3-Benzyl-6-methyl-2-phenethyl-1-(3-phenylpropylamino)-2,3-dihydro-4-pyridone (16). From 400 mg of **13**, 158 mg of **16** were obtained. $FeCl_3$ test: brown.

IR(liquid film): 3250 (ν NH), 1615 (ν C=O), and 1555 cm^{-1} (ν C=C).

From the above reaction mixture, a trace of 3-benzyl-6-methyl-2-phenethyl-2,3-dihydro-4(1*H*)-pyridone (**22**) was obtained. $FeCl_3$ test: green.

UV: λ_{max}^{EtOH} 318 mμ, $\lambda_{max}^{HCl/EtOH}$ 310 mμ.

1-Cinnamylidenamino-6-methyl-2-phenethyl-2,3-dihydro-4-pyridone (18). A solution of 2.0 g of **10** in 50 m*l* of ethanol was hydrogenated with 150 mg of platinum oxide. After the mixture had absorbed about 24 m*l* (calculated 56 m*l*) of hydrogen, absorption was stopped. After the catalyst had been filtered off and the ethanol solution worked up as usual, the reaction product was purified by a column chromatography similar to that described above to afford 575 mg (29%) of **18** as a viscous orange oil.

UV: λ_{max}^{EtOH} 244, 249, and 340 mμ.

NMR(in $CDCl_3$)(τ): 7.91 (singlet, 3H, C-6 methyl protons), 7.78—7.00 (multiplet, 6H, ethylene protons of the phenethyl group and C-3 methylene protons), 6.15—5.75 (multiplet, 1H, C-2 methine proton), 5.01 (singlet, 1H, C-5 olefin proton), 3.52 (triplet, 1H, β′-olefin proton of the 1-cinnamylidenamino group) and 2.90—2.60 (multiplet, 12H, α′-, γ′-olefin protons of the 1-cinnamylidenamino group and aromatic protons).

As well as **18**, 460 mg (29%) of **14** and a trace of **17** were afforded.

Hydrogenation of 18. Compound **18** (120 mg) was hydrogenated with 50 mg of platinum oxide in 30 m*l* of ethanol. After about 20 m*l* of hydrogen had been absorbed, the absorption of hydrogen was stopped. The reaction mixture was then treated as usual; we thus obtained **14** and **17** which were identified with authentic samples by means of thin-layer chromatography.

Hydrogenation of 14 to 17. In the presence of 100 mg of platinum oxide in 50 m*l* of ethanol, 400 mg of **14** were hydrogenated. After about 50 m*l* of hydrogen had been absorbed, the absorption of hydrogen almost ceased. When the reaction mixture was worked up as usual it gave **17**, which was identified with an authentic sample by means of thin-layer chromatography.

BULLETIN OF THE CHEMICAL SOCIETY OF JAPAN VOL. 43 3561—3566 (1970)

Linear Conjugated Systems Bearing Aromatic Terminal Groups. II. The Synthesis and the Electronic Spectra of 9,9′-Dianthrylpoly-ynes

Shuzo AKIYAMA and Masazumi NAKAGAWA

Department of Chemistry, Faculty of Science, Osaka University, Toyonaka, Osaka

(Received June 15, 1970)

A series of 9,9′-dianthrylpoly-ynes (II_1–II_6) were prepared, and their electronic spectra were measured. It was found that the novel linear relation between λ_{max} and the square of the number of the triple bond (n^2) which has been found in the spectra of 1,1′-dianthrylpoly-ynes (I_1–I_6) also held in the 9,9′-series.

The present authors have pointed out in previous papers that the plot of the λ_{max} of the electronic spectra of 1,1′-dianthrylpoly-ynes (I_n) against the square of the number of the triple bond (n^2) gave a straight-line relationship;[1] this novel relationship has been explained in terms of HMO, applying a modified bond-alternation approximation.[2]

This interesting spectral behavior prompted the authors to the synthesis of 9,9′-dianthrylpoly-ynes (II_1–II_6) in order to get further information on

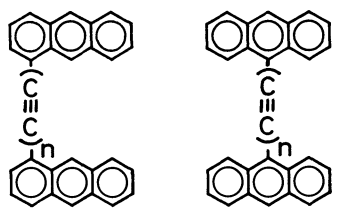

I_n II_n

n=1, 2, 3, 4, 5, 6

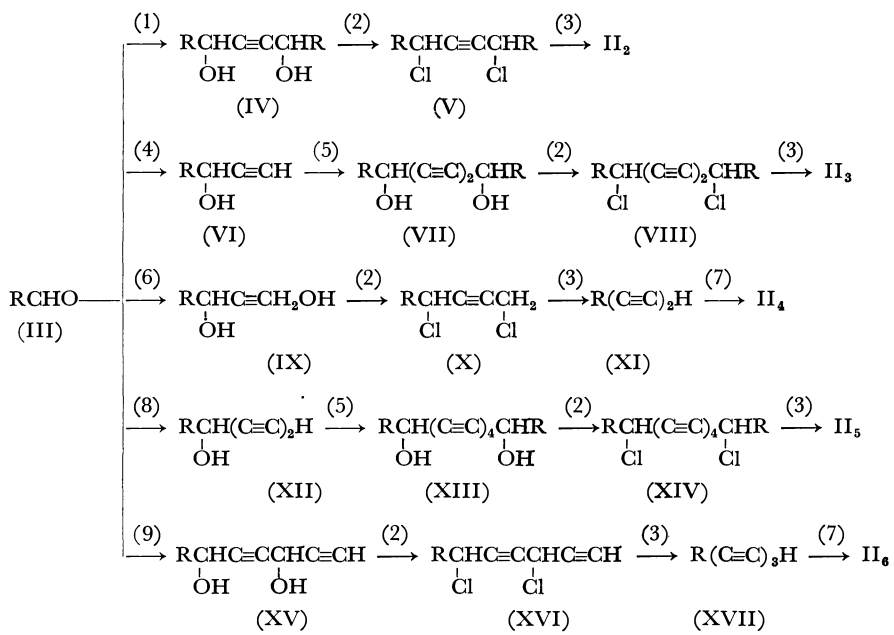

Scheme 1. Synthesis of 9,9′-Dianthrylpoly-ynes (II_2–II_6)

R=9-Anthryl. (1) BrMgC≡CMgBr in benzene-THF; (2) $SOCl_2$-pyridine in THF; (3) $NaNH_2$ in liq. NH_3; (4) LiC≡CH in liq. NH_3; (5) CuCl-NH_4Cl-O_2 in CH_3OH; (6) $BrMgC{\equiv}CCH_2OMgBr$ in THF; (7) $Cu(OAc)_2$ in pyridine; (8) $Li(C{\equiv}C)_2H$ in liq. NH_3; (9) BrMgC≡CCH(OMgBr)C≡CH in THF. THF=tetrahydrofuran.

1) S. Akiyama and M. Nakagawa, This Bulletin, **40**, 340 (1967). The paper is to be regarded as Part I of this series. For a preliminary report, see *Tetrahedron Lett.*, **1968**, 1121.

2) K. Nishimoto, S. Akiyama, M. Nakagawa and R. Fujishiro, This Bulletin, **39**, 2320 (1966).

Table 1. The colors and the melting points of II_n and I_n

n	II_n		I_n	
	Color	Mp (°C)	Color	Mp (°C)
1	orange	*ca.* 310 (dec.)	yellow	272—273
2	orange	290—292 (dec.)	bright yellow	289—291 (dec.)
3	deep orange	*ca.* 295 (dec.)	deep yellow	*ca.* 270 (dec.)
4	orange red	*ca.* 265 (dec.)	golden yellow	*ca.* 245 (dec.)
5	red	*ca.* 250 (dec.)	orange	*ca.* 220 (dec.)
6	dark red	*ca.* 200 (dec.)	red	*ca.* 210 (dec.)

the role of the terminal groups on the electronic spectra of diarylpoly-yne compounds.

Synthesis. The synthesis of 9,9′-dianthrylacetylene (II_1) by means of an intramolecular Wittig reaction will be reported in the following paper, together with the synthesis of other diarylacetylenes. The higher members (II_2–II_6) have been synthesized according to the sequence depicted in the following scheme, starting from the common precursor, 9-formylanthracene (III).[3]

The color of the crystals and the melting points of 9,9′-dianthrylpoly-ynes (II_1–II_6) are compared with those of 1,1′-analogs in Table 1.

Infrared Spectra. Just as in the case of the 1,1′-series,[1] a remarkable intensification of the absorption ($A=1-I/I_0$) due to $\nu_{C\equiv C}$ with an increase in the number of n was also observed in the case of II_n, as is illustrated in Fig. 1. The absorption intensity of the $\nu_{C\equiv C}$-band relative to the intensity of the 880 cm^{-1}-band (ν_{C-H} of the isolated hydrogen atom in the anthryl groups) and to the 730 cm^{-1}-band (ν_{C-H} of the adjacent four hydrogen atoms in the terminal groups) is summarized in Table 2. It seems to be noteworthy that the $\nu_{C\equiv C}$-band of the tetraacetylene (II_4) exhibited the highest wavenumber, as in the cases of diphenyl-, dimethyl-,[4] and 1,1′-dianthrylpoly-ynes.[1]

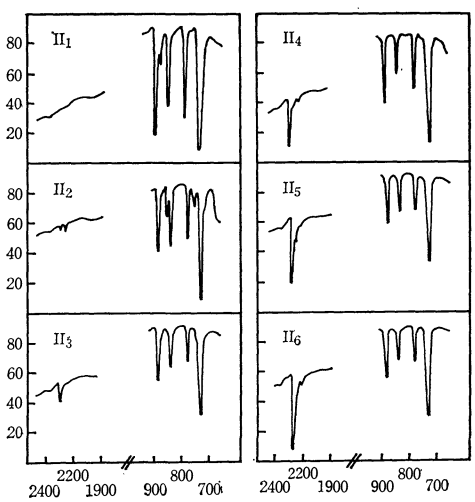

Fig. 1. Infrared spectra of 9,9′-dianthrylpoly-ynes (II_1–II_6) in the 1900—2400 cm^{-1} and 700—900 cm^{-1} region.

Table 2. The wave numbers and the relative absorption intensities of $\nu_{C\equiv C}$ -band of II_n (KBr-disk)

II_n	$\nu_{C\equiv C}$-band	Relative absorption intensities	
		Ratio to the 880 cm^{-1} -band	Ratio to the 730 cm^{-1} -band
II_1	—	—	—
II_2	2180†, 2115	0.07	0.04
II_3	2185†, 2150*	0.52	0.32
II_4	2200†, 2060	1.26	0.76
II_5	2150†, 2100, 2040*	1.95	1.09
II_6	2120†, 2010	2.30	1.29

The daggers indicate the absorption bands used in the calculation.
The asterisks denote the shoulders.

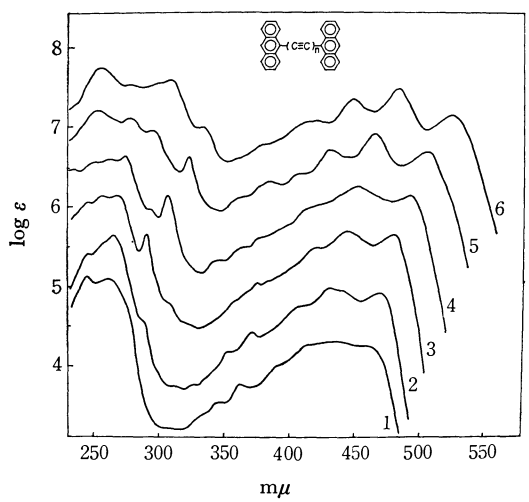

Fig. 2. The absorption curves of 9,9′-dianthrylpoly-ynes (II_1–II_6) . The curves, with the exception of the monoacetylene at the bottom, have been displaced upward on the ordinate axis by 0.5 log ε unit increments from the curve immediately below (in tetrahydrofuran).

3) E. Campaigne and W. L. Archer, *J. Amer. Chem. Soc.*, **75**, 989 (1953).

4) C. L. Cook, E. R. H. Jones and M. C. Whiting, *J. Chem. Soc.*, **1952**, 2883.

Table 3. The spectral data of 9,9′-dianthrylpoly-ynes (II_1–II_6)

n	λ_{max} in mμ and log ε (in parentheses) in tetrahydrofuran									
1	245.5 (5.14)	262 (5.10)	346 (3.59)	362 (3.81)	416* (4.30)	436 (4.34)	457* (4.27)			
2	224.5 (4.60)	246.5 (4.94)	265.5 (5.18)	287* (4.14)	345 (3.76)	372 (4.00)	410 (4.33)	431 (4.55)	470 (4.50)	
3	246 (5.06)	256 (5.14)	269 (5.15)	290 (4.66)	308* (3.78)	356* (3.81)	374 (4.04)	422* (4.51)	443 (4.69)	479 (4.66)
4	235 (5.00)	262 (5.12)	273.5 (5.15)	294 (4.47)	306 (4.65)	366* (4.00)	376* (4.12)	451 (4.77)	491 (4.65)	
5	254.5 (5.20)	277 (5.11)		294.5 (4.96)	322.5 (4.63)	386 (4.32)	412 (4.45)	431 (4.73)	466 (4.93)	505 (4.71)
6	256.5 (5.19)	278.5 (4.98)		308.5 (5.06)	333 (4.50)	376* (4.28)	417 (4.57)	447 (4.84)	482 (4.95)	523 (4.65)

The asterisks indicate the shoulders.

Electronic Spectra. The absorption curves and the numerical data of the electronic spectra of II_n are shown in Fig. 2 and Table 3. Similarly to the case of 1,1′-dianthrylpoly-ynes (I_n),[1] the electronic spectra of II_n could be divided into three groups, *i. e.*, the short-wavelength band (240—280 mμ), the medium-wavelength band (280—330 mμ), and the long-wavelength band (330—500 mμ). The appearance of the medium-wavelength band and the distinct vibrational fine structure of the long-wavelength maxima are characteristics of the spectra of the poly-ynes (I_n and II_n). However, the long-wavelength band of II_1 was found to be rather broad, and the peak corresponding to the longest-wavelength sub-bands in II_2–II_6 could not be observed. The bathochromic shift of the longest-wavelength maximum (λ_L) caused by the addition of an acetylenic linkage becomes progressively greater as the length of the polyacetylenic chain is increased. The shifts were found to be 9, 12, 14, and 18 mμ respectively in the II_2–II_6 series. Just as in the case of I_n, the ratios of λ_L to the wavelength of the medium-wavelength maxima (λ_M) were found to be almost constant, regardless of the length of the poly-yne chain (n) and the nature of the solvent (Table 4).

A good correlation between the λ_L of II_2–II_6 and the square of the number of the acetylenic bond (n^2) has also been observed. A plot of this relation is shown in Fig. 3, together with that of the I_n-series.*1 The linear relationship could be expressed by the following empirical formulae, which shows excellent agreement with the observed values, as is summarized in Table 5. As is clearly shown in Fig. 3, II_n absorbs at a longer wavelength

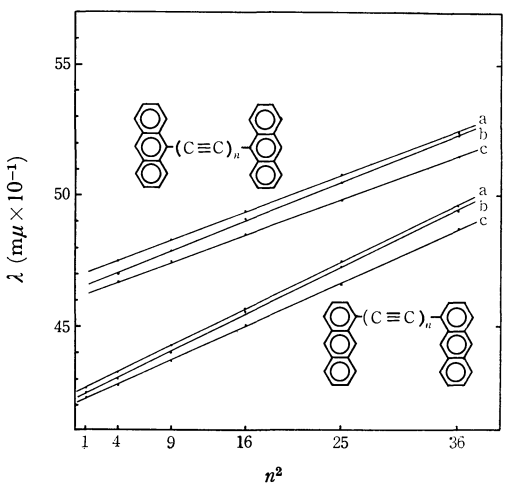

Fig. 3. Plot of λ_{max} *versus* n^2 for 9,9′-dianthrylpoly-ynes (II_1–II_6) and 1,1′-dianthrylpoly-ynes (I_1–I_6).
a: benzene; b: tetrahydrofuran; c: cyclohexane

Table 4. The ratios of the wavelength of the absorption maxima

II_n	λ_M			λ_L			λ_L/λ_M		
	a	b	c	a	b	c	a	b	c
II_2	287*	287*	289*	467	470	475	1.63	1.64	1.65
II_3	289	290	292	475	479	483	1.64	1.65	1.65
II_4	305	306	309	485	491	494	1.59	1.61	1.60
II_5	320	322.5	324	498	505	508	1.56	1.57	1.58
II_6	332	333	336	515	523	524	1.55	1.58	1.56

a: cyclohexane; b: tetrahydrofuran; c: benzene.
The asterisks indicate the shoulders.

*1 The synthesis of 1,1′-dianthrylacetylene (I_1) will be reported in the following paper.

Table 5. The longest wavelength absorption maxima (mμ)

II_n	Benzene		Tetrahydrofuran		Cyclohexane	
	Obsd	Calcd	Obsd	Calcd	Obsd	Calcd
II_2	475	475	470	471	467	467
II_3	483	483	479	479	475	475
II_4	494	494	491	490	485	485
II_5	508	508	505	505	498	499
II_6	524	525	523	523	515	515

$\lambda_{max} = 1.50\,n^2 + 461$ mμ (cyclohexane)

$\lambda_{max} = 1.65\,n^2 + 464$ mμ (tetrahydrofuran)

$\lambda_{max} = 1.55\,n^2 + 469$ mμ (benzene)

than the corresponding I_n. However, the slopes of the straight lines of the 1,1′-series (I_n) are steeper than those of the 9,9′-series (II_n). Accordingly, the difference in the wavelength between the corresponding members of these two series diminishes with the increase in the length of the poly-yne chain (n=2, 42; n=3, 40; n=4, 37; n=5, 30 and n=6, 28 mμ) in tetrahydrofuran. The solvent effect is found to be more pronounced in the case of II_n, even in the lower members.

It seems to be important to obtain the knowledge regarding electronic spectra of 2,2′-dianthrylpoly-ynes, as the polyacetylenic chromophore extends in the direction of the polarization of the ^1B_b-band of the anthracene nucleus, whereas in the cases of 1,1′- and 9,9′-dianthrylpoly-ynes (I_n and II_n) the direction of the polyacetylenic chromophore is parallel with the direction of the polarization of the ^1L_a-band of the aromatic nucleus.[5] Unfortunately, all attempts to prepare 2,2′-dianthrylpoly-ynes impeded by the extremely poor solubilities of the 2-substituted anthracene derivatives.

The studies of the synthesis and the spectral properties of dinaphthylpoly-ynes will be reported in the following paper.

Experimental

All the melting points are uncorrected. The electronic spectra were obtained on a Hitachi EPS-3T spectrophotometer at room temperature using a well-matched pair of 1-cm cells. A Hitachi EPI-2 spectrophotometer was used for the infrared spectroscopy.

1,4-Di(9-anthryl)-1,4-dihydroxy-2-butyne (IV). 9-Anthraldehyde (III[3], 6.18 g, 0.03 mol) in tetrahydrofuran (100 m*l*) was added to an ice-cooled solution of acetylene dimagnesium bromide [from excess acetylene, magnesium (1.75 g, 0.073 g atom), and ethyl bromide (9.70 g, 0.088 mol)] in benzene - tetrahydrofuran (50m*l*). The mixture was stirred overnight at room temperature, and then the strongly cooled mixture (ice-salt bath) was treated with a saturated aqueous solution of ammonium chloride. After the separation of the organic layer, the aqueous layer was extracted with benzene. The combined organic layer was dried (magnesium sulfate). The orange-red viscous liquid obtained by evaporating the solvent under reduced pressure was dissolved in benzene (40 m*l*). The solution was filtered through a short column of alumina (8 g). The filtrate was concentrated under reduced pressure, and a small amount of benzene - cyclohexane (1 : 1) was added to the residue. The mixture was warmed on a water bath, resulting in crystallization (4.7 g, 71%). The crystals were recrystallized twice from benzene, yielding IV, mp 204—207°C (dec.), as pale yellow needles.

Found: C, 88.06; H, 5.32%. Calcd for $C_{17}H_{12}O$: C, 87.64; H, 5.06%. IR (KBr-disk): 3400 (O–H), 1040 (C–O) cm^{-1}. *Cf.* IRDC Cards No. 3642.

9,9′-Dianthryldiacetylene (II_2). *The Preparation of the Dichloride (V).* A mixture of thionyl chloride (0.36 g, 3 mmol), pyridine (0.24 g, 3 mmol), and ether (5 m*l*) was added, drop by drop over a 30-min period to a cooled solution (−20°C) of IV (0.440 g, 1 mmol) in tetrahydrofuran (10 m*l*) under vigorous shaking. The immediate deposition of a yellow crystalline solid was observed. Shaking was then continued for an additional hour.

The Dehydrochlorination of V. The above-mentioned reaction mixture was added, in one portion, to a stirred suspension of sodium amide [from sodium 0.40 g (0.017 g atom)] in liquid ammonia (50 m*l*) at −70°C. After 1 hr, ammonium chloride (2.0 g) was added to the mixture and the ammonia was allowed to evaporate. The residue, after the organic solvent had been removed under reduced pressure, was mixed with water. The insoluble material was washed with small amounts of ethanol and benzene successively, resulting in a yellowish brown powder. This was dissolved in benzene (100 m*l*) and passed through a short column of alumina (8 g). Yellowish brown crystals obtained by evaporating the filtrate were recrystallized from benzene, yielding II_2, as orange cubes; 0.160 g (40%). An analytical specimen was obtained by recrystallizing the crystals twice from benzene; mp 290—292°C (dec.).

Found: C, 95.64; H, 4.58%. Calcd for $C_{32}H_{18}$: C, 95.49; H, 4.51%. IR: *Cf.* IRDC Cards No. 3717.

9-Anthryl-2-propyn-1-ol (VI). A solution of 9-anthraldehyde (III, 16.0 g, 0.078 mol) in tetrahydrofuran (300 m*l*) was added to a suspension of lithium acetylide [from lithium 1.6 g (0.24 g atom)] at −70°C over a 1-hr period. The mixture was stirred a further 5.5 hr at −50°C, and then ammonium chloride (8.0 g) was added. After the evaporation of the ammonia, a saturated aqueous solution of ammonium chloride was added to the residue. The aqueous layer was extracted with benzene and combined with the organic layer. The combined organic layer was dried (magnesium sulfate) and concentrated under reduced pressure. The residue was dissolved in hot benzene (40 m*l*) to yield crude crystals of VI (14.4 g, 72%). The second crop of VI (1.3 g, 7%) was obtained from the mother liquor. Recrystallization of the crude material from tetrahydrofuran-benzene yielded pure VI as pale yellow plates; mp 124—125°C.

Found: C, 87.73; H, 5.30%. Calcd for $C_{17}H_{12}O$: C, 87.90; H, 5.21%. IR (KBr-disk): 3570 (O–H), 1022, 1013 (C–O), 3280 (≡CH) and 2130 (C≡C) cm^{-1}. *Cf.* IRDC Cards, No. 4161.

1,6-Di(9-anthryl)-1,6-dihydroxy-2,4-hexadiyne

5) *Cf.* R. N. Jones, *Chem. Rev.*, **41**, 365 (1947).

(VII). A mixture of the anthrylpropynol (VI, 2.32 g, 0.01 mol), cuprous chloride (0.10 g, 1 mmol), ammonium chloride (0.07 g), and methanol (40 m*l*) was vigorously stirred at room temperature under an atmosphere of oxygen at a slight elevated pressure. After 30 min, a minor amount of the cuprous acetylide which deposited was dissolved, two drops of concentrated hydrochloric acid were added, and the stirring was continued overnight. The coupling product thus deposited was collected by filtration, washed with methanol, and dissolved in acetone (40 m*l*) to remove any inorganic material. The oily residue obtained by concentrating the acetone solution was triturated with hot benzene, resulting in crystallization (1.79 g, 78%; mp *ca.* 220°C (dec.)). This was recrystallized three times from acetone - benzene to yield pure VII as pale yellow cubes; mp *ca.* 220°C (dec.).

Found: C, 88.40; H, 4.93%. Calcd for $C_{34}H_{22}O_2$: C, 88.29; H, 4.79%. IR (Nujol): 3350 (OH), 1009 (C–O), 2130 (C≡C) cm^{-1}. *Cf.* IRDC Cards, No. 3270.

9.9′-Dianthryltriacetylene (II_3). *The Preparation of the Dichloride (VIII).* A mixture of thionyl chloride (0.24 g, 2 mmol), and pyridine (0.16 g, 2 mmol) in ether (5 m*l*) was added, drop by drop, a cooled solution (−20°C) of the glycol (VII, 0.308 g, 0.67 mmol) in tetrahydrofuran (15 m*l*) over a 15 min-period, and then the mixture was shaken for an additional hour. The orange-yellow reaction mixture containing a yellow precipitate was directly subjected to the following dehydrochlorination reaction.

Dehydrochlorination of VIII. To a vigorously-stirred suspension of sodium amide [from sodium 0.35 g (0.016 g atom)] in liquid ammonia (60 m*l*) the above-mentioned solution of the dichloride (VIII) was added in one portion at −70°C. After 1 hr, ammonium chloride (2.0 g) was added and the ammonia was allowed to evaporate. The organic solvent which remained was removed under reduced pressure. The residue was mixed with water, and the resulting insoluble material was washed with a small amount of methanol and benzene, affording a yellowish brown, crystalline mass (0.255 g, 90%; mp *ca.* 280°C (dec.)). The crude material was recrystallized from toluene to give pure II_3, as deep orange needles; mp 295°C (dec.); 0.203 g (71%).

Found: C, 95.72; H, 4.17%. Calcd for $C_{34}H_{18}$: C, 95.75; H, 4.25%. IR: *Cf.* IRDC Cards, No. 3719.

1-(9-Anthryl)-2-butyne-1,4-diol (IX). To a stirred and ice-cooled solution of the Grignard derivative of propargyl alcohol in tetrahydrofuran (170 m*l*), which had been prepared from magnesium (8.65 g (0.36 g atom)), ethyl bromide (32.2 g (0.36 mol)), and propargyl alcohol (10.1 g (0.18 mol)), there was added a solution of 9-anthraldehyde (III, 12.4 g, 0.06 mol) in tetrahydrofuran (180 m*l*) over a 30 min-period. The mixture was stirred a further 30 min, refluxed for 3 hr, and allowed to stand overnight. A saturated aqueous solution of ammonium chloride was added to the reaction mixture, and the organic layer was separated. The aqueous layer was extracted 4 times with tetrahydrofuran - benzene (total 400 m*l*). The combined organic layer was dried (magnesium sulfate) and concentrated under reduced pressure. The residue was treated with hot benzene (10 m*l*), affording fine, pale yellow crystals; 6.9 g (44%); mp 224—228°C (dec.). A second crop of crystals (1.1 g (7%)) was obtained from the mother liquor. The crystals were recrystallized from tetrahydrofuran to yield pure IX as tiny, pale yellow cubes; mp 227—229°C (dec.).

Found: C, 82.27; H, 5.41%. Calcd for $C_{18}H_{14}O_2$: C, 82.42; H, 5.38%. IR (KBr-disk): 3220 (OH), 1019 (C–O) cm^{-1}. *Cf.* IRDC Cards, No. 3640.

9-Butadiynylanthracene (XI). *The Preparation of the Dichloride (X).* A solution of thionyl chloride (6.0 g, 0.05 mol) in tetrahydrofuran (10 m*l*) was added to a stirred and ice-cooled solution of the anthrylbutyne diol (IX, 2.60 g, 0.01 mol), and pyridine (3.0 g, 0.04 mol) in tetrahydrofuran (20 m*l*) over a period of 50 min. The stirring was continued for 30 min at room temperature, and then the mixture was gradually heated to the boiling point. After refluxing for 1 hr, cracked ice was added to the chilled reaction mixture (ice-salt bath) and it was extracted with benzene (70 m*l*). The extract was washed with water, a sodium hydrogen carbonate solution, and water successively, dried (sodium sulfate), and concentrated under reduced pressure. The resulting dark red oil (crude X) was subjected to the subsequent reaction without further purification.

The Dehydrochlorination of X. The above-mentioned crude X in tetrahydrofuran (25 m*l*) was added to a stirred suspension of sodamide [from sodium (4.6 g (0.2 g atom))] in liquid ammonia (150 m*l*) at −70°C over a 30-min period and then stirred for 1.5 hr. Ammonium chloride (10 g) was added to the mixture, and the ammonia was allowed to evaporate. The residue was repeatedly digested with *n*-hexane (total, 1000 m*l*). The hexane solution was concentrated to 350 m*l* and percolated through a short column of alumina (13 g). The resulting pale yellow solution, with a strong lavender fluorescence, was concentrated under reduced pressure thus affording XI as yellow cubes (0.36 g (16% based on the glycol, IX)). The diacetylene, XI, was found to be a fairly unstable substance, and an explosive decomposition at *ca.* 130°C was observed. Also, the crystals rapidly turned black at room temperature.

Found: C, 95.32; H, 4.54%. Calcd for $C_{18}H_{10}$: C, 95.54; H, 4.46%. IR (KBr-disk): 3280 (≡CH), 2190 (C≡C) cm^{-1}. UV (in *n*-hexane): λ_{max} (mμ) (log ε): 226 (3.47), 260.5 (5.11), 283 (4.09), 355 (3.70), 371 (4.04), 392 (4.28), 414.5 (4.29).

9,9′-Dianthryltetraacetylene (II_4). Cupric acetate monohydrate (5.3 g) was added to a stirred solution of the diacetylene (XI, 0.27 g, 0.013 mol) in pyridine (35 ml);[6] the mixture was then stirred for 45 min at 23°C, and for 2 hr at 40°C. Further stirring was continued overnight at room temperature, after which insoluble material was collected by filtration, and washed with water. This yielded fine, orange-brown crystals; 0.23 g (79%); mp 255°C (dec.). The mother liquor was concentrated under reduced pressure and mixed with water to afford crude II_4 (0.05 g, 17%). The combined crystals were recrystallized from benzene and toluene successively to give pure II_4, as orange-red needles; mp 265°C (dec.).

Found: C, 95.86; H, 4.00%. Calcd for $C_{36}H_{18}$: C, 95.97; H, 4.03%. IR: *Cf.* IRDC Cards, No. 4164.

9,9′-Dianthrylpentaacetylene (II_5). *The Preparation of 9-Anthrylbutadiynyl Carbinol (XII).* 9-Anthraldehyde (III, 3.05 g, 0.015 mol) in tetrahydrofuran (50 m*l*) was added to a suspension of lithium diacetylide in liquid ammonia at −70°C, which was prepared by the reaction

6) G. Eglinton and A. R. Galbraith, *J. Chem. Soc.*, **1959**, 889.

of 1,4-dichloro-2-butyne (2.40 g, 0.059 mol) in ether (5 ml) with lithium amide [from lithium 1.24 g (0.177 g atom)] in liquid ammonia (80 ml). The temperature of the reaction mixture was raised to −45°C, and the mixture was stirred for a further 2 hr at the temperature. Ammonium chloride (2 g) was then added, and the ammonia was allowed to evaporate. The residue was digested with benzene (50 ml). The extract was washed with water and dried (magnesium sulfate). The solvent was removed under reduced pressure, resulting in an unstable, viscous, light brown oil. The absence of carbonyl and the presence of hydroxyl and ethynyl groups were revealed by the IR sepectroscopy of the crude material (XII). This was used without further purification in the subsequent oxidative coupling.

The Oxidative Coupling of XII. A mixture of the above-mentioned crude XII, cuprous chloride (0.30 g), ammonium chloride (0.20 g), and methanol (50 ml) was vigorously stirred in an atmosphere of oxygen at room temperature. Two drops of concentrated hydrochloric acid was added to prevent the precipitation of the cuprous acetylide, and then the stirring was continued overnight. The crystalline material thus deposited was collected by filtration, washed with a small amount of methanol, and dissolved in tetrahydrofuran (15 ml). The insoluble material was removed by filtration. The filtrate was passed through a short column of alumina (5 g) and concentrated under reduced pressure. The tarry residue was triturated with benzene, resulting in light brown needles; 1.37 g (36%); mp *ca.* 160°C (dec.). A second crop of the crystals (0.22 g (6%)) was obtained from the mother liquor. The tetraacetylene glycol (XIII) thus obtained was found to be a rather unstable substance, and repeated recrystallizations from acetone - benzene gave only a somewhat impure material whose IR spectrum was in accord with that expected for XIII.

The Preparation of the Dichloride (XIV). To a stirred solution of the crude glycol (XIII, 0.130 g, 0.23 mol) in tetrahydrofuran (20 ml), there was added a mixture of thionyl chloride (0.090 g, 0.76 mmol), pyridine (0.055 g, 0.76 mmol), and ether (5 ml) over a period of 30 min at −20°C. The mixture was stirred for a further 2 hr and then directly subjected to the subsequent reaction.

The Dehydrochlorination of XIV. The above-mentioned solution of XIV was added in one portion to a vigorously-stirred suspension of sodium amide [from sodium (0.10 g) 4.4 mg atom) in liquid ammonia (80 ml)] at −70°C. After 2 hr, ammonium chloride (0.5 g) was introduced into the reaction mixture and the ammonia was allowed to evaporate. The organic solvent was removed under reduced pressure. The residue was mixed with water, and the insoluble material was collected by filtration and washed with small amounts of methanol and benzene. Recrystallization from toluene (400 ml) yielded fine, red needles; 0.046 g (38%); mp *ca.* 245°C (dec.). The second crop [0.33 g (27%); mp 245°C (dec.)] was obtained from the mother liquor. Recrystallization from the same solvent afforded the pure pentaacetylene, II_5, as fine, red needles; mp *ca.* 250°C (dec.).

Found: C, 96.21; H, 3.88%. Calcd for $C_{38}H_{18}$: C, 96.18; H, 3.82%.

1-(9-Anthryl)-2,5-hexadiyn-1,4-diol (XV). A solution of 9-anthraldehyde (III, 6.10 g, 0.03 mol) in tetrahydrofuran (120 ml) was added to a stirred and ice-cooled solution of the Grignard derivative of 2,4-pentadiyn-3-ol, which had been prepared from 2.64 g (0.033 mol) of the alcohol according to a previously-reported method.[1] The mixture was stirred overnight at 17—18°C, and then a saturated aqueous solution of ammonium chloride was added. The organic layer was separated, and the aqueous layer was extracted with ether. The combined organic layer was dried (sodium sulfate) and evaporated under reduced pressure; this yielded a dark red oil. This crystallized on standing; after treatment with hot benzene (20 ml), it was filtered and washed with benzene to afford a pale yellow crystalline powder; 3.60 g (45%); mp *ca.* 150°C (dec.). The crude material was recrystallized four times from benzene to give pure XV, as pale yellow leaflets; mp 195—198°C (dec.).

Found: C, 83.62; H, 4.88%. Calcd for $C_{20}H_{14}O_2$: C, 83.90; H, 4.93%. IR (Nujol): 3300 (O–H, C≡CH), 2110 (C≡C), 1050, 1015, 1001 (C–O) cm^{-1}. *Cf.* IRDC Cards, No. 3715.

9-Anthryltriacetylene (XVII). *The Chlorination of XV.* A mixture of thionyl chloride (1.43 g, 0.012 mol), pyridine (0.95 g, 0.012 mol), and ether (7 ml) was added, over a period of 30 min, to a solution of the glycol (XV, 0.860 g, 3 mmol) in tetrahydrofuran (15 ml) at −15°C. The mixture was stirred for a further 30 min and then subjected to the dehydrochlorination reaction without the isolation of the dichloride (XVI).

The Dehydrochlorination of XVI. To a vigorously-stirred suspension of sodium amide [from sodium (0.30 g) (0.013 mol)] in liquid ammonia held at −70°C, there was added the above-mentioned solution of XVI in one portion. Stirring was continued for one more hour, and then ammonium chloride (2 g) was added. After the evaporation of the ammonia, the organic solvent was removed under reduced pressure. The residue was repeatedly digested with petroleum ether (bp 40—60°C; total 150 ml). The orange yellow solution was percolated through a short alumina column (5 g). The concentration of a small portion of the filtrate under reduced pressure gave XVII as yellow needles; this substance was found to extremely unstable, and the color of the crystals rapidly changed from green to a brownish grey, forming an entirely insoluble decomposition product. The petroleum ether solution was used directly for the subsequent reaction. The triacetylene (XVII) gave red cuprous and yellow silver acetylides. UV (petroleum ether): the longest wavelength absorption maximum, 429 mμ.

9,9′-Dianthrylhexaacetylene (II_6). A mixture of the above-mentioned solution of the triacetylene (XVII), cupric acetate monohydrate (2.0 g), and pyridine (15 ml) was concentrated to *ca.* 15 ml under reduced pressure. The concentrated solution was then stirred overnight at room temperature. After the addition of a small amount of water to the mixture, the insoluble material was collected and washed with water, acetone, and benzene successively, yielding a dark red powder (68 mg) [9% based on the glycol (XV)]. This was recrystallized twice from toluene to give the pure hexaacetylene (II_6), as fine, dark red needles; mp *ca.* 200°C (dec.). II_6 was found to have a poor solubility in common organic solvents.

Found: C, 96.19; H, 3.84%. Calcd for $C_{40}H_{18}$: C, 96.36; H, 3.64%.

BULLETIN OF THE CHEMICAL SOCIETY OF JAPAN VOL. 43 3567—3576 (1970)

Linear Conjugated Systems Bearing Aromatic Terminal Groups. III. The Synthesis and the Electronic Spectra of 1,1′-Dinaphthyl- and 2,2′-Dinaphthylpoly-ynes

Kazuhiro NAKASUJI, Shuzo AKIYAMA, Kazuko AKASHI and Masazumi NAKAGAWA

Department of Chemistry, Faculty of Science, Osaka University, Toyonaka, Osaka

(Received June 15, 1970)

1,1′-Dinaphthylpoly-ynes (I_n, $n=1$—6) and 2,2′-dinaphthylpoly-ynes (II_n, $n=1$—6) were synthesized, and their electronic spectra were measured. The I_n-series gave an excellent agreement with the $\lambda_{max} \propto n^{1.5}$ relationship, and the II_n-series followed a straight line, $\lambda_{max} \propto n^{1.3}$. These relationships are different from those of 1,1′-dianthryl- and 9,9′-dianthrylpoly-ynes, in which the plots of λ_{max} *versus* n^2 give excellent straight lines (*Bull. Chem. Soc. Jap.*, **39**, 2320 (1966); **40**, 340 (1967)). The new linear relationships found in the dinaphthyl-series offer further evidence of the prominent effect of the terminal groups upon the electronic spectral properties of the conjugated poly-yne system.

In previous papers,[1,2] two of the present authors (S. A and M. N.) have reported the novel electronic spectral properties of 1,1′-dianthryl- and 9,9′-dianthrylpoly-ynes. In the two series of dianthrylpoly-ynes, the variation in λ_{max} with an increase in the number of acetylenic bonds (n) is expressed by the linear relation: $\lambda_{max}=An^2+B$.

We now hoped to synthesize the poly-ynes bearing different types of aromatic terminal groups in order to clarify the role of terminal groups on the electronic spectral regularity of the poly-yne system.

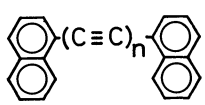

I_n

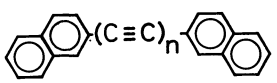

II_n

$n=1, 2, 3, 4, 5, 6$

Synthesis. The synthesis of the mono-, di-, tri-, and tetra-acetylenes (I_{1-4} and II_{1-4}) has been carried out according to the reaction sequence outlined in Scheme 1. The dinaphthylacetylenes (I_1 and II_1) were prepared according to the method of Curtius.[3] The dinaphthyldi-, tri-, and tetra-acetylenes (I_{2-4} and II_{2-4}) were synthesized employing 1- and 2-naphthaldehydes as the starting materials. As is shown in Scheme 2, the naphthylpropargylaldehydes (XVII and XVII′), which had been derived from the acetylnaphthalenes (XV and XV′), were used as the starting materials for the synthesis of the penta- and the hexa-acetylenes (I_5, I_6 and II_5 and II_6). It was found that the replacement reaction of the hydroxyl group in the acetylenic alcohol or glycol by the chlorine atom by means of the action of thionyl chloride and pyridine in tetrahydrofuran was rather sensitive to the reaction conditions, a good result was obtained only under limited reaction conditions (see, the Experimental section).

The colors, the melting points, and the wave-numbers of the IR absorptions due to $\nu_{C\equiv C}$ are summarized in Tables 1 and 2.

Table 1. Physical properties of 1,1′-dinaphthylpoly-ynes (I_n)

n	Color of crystals	Mp (°C)	$\nu_{C\equiv C}$(cm^{-1})
1	colorless	129	—
2	light yellow	175—177	2130
3	yellow	192—193	2190
4	deep yellow	205—207	2205
5	orange yellow	*ca.* 195 (dec.)	2180
6	orange	*ca.* 175 (dec.)	2155

Table 2. Physical properties of 2,2′-dinaphthylpoly-ynes (II_n)

n	Color of crystals	Mp (°C)	$\nu_{C\equiv C}$(cm^{-1})
1	colorless	228—229	—
2	colorless	202—203	—
3	faint yellow	173—174	2190
4	light yellow	*ca.* 172 (dec.)	2185
5	yellow	*ca.* 180 (dec.)	2170
6	orange yellow	*ca.* 200 (dec.)	2140

1) S. Akiyama and M. Nakagawa, This Bulletin, **40**, 340 (1967); K. Nishimoto, S. Akiyama, M. Nakagawa and R. Fujishiro, *ibid.*, **39**, 2320 (1966).

2) The preceding paper.

3) Th. Curtius and K. Thun, *J. Prakt. Chem.*, [2] **44**, 171 (1891).

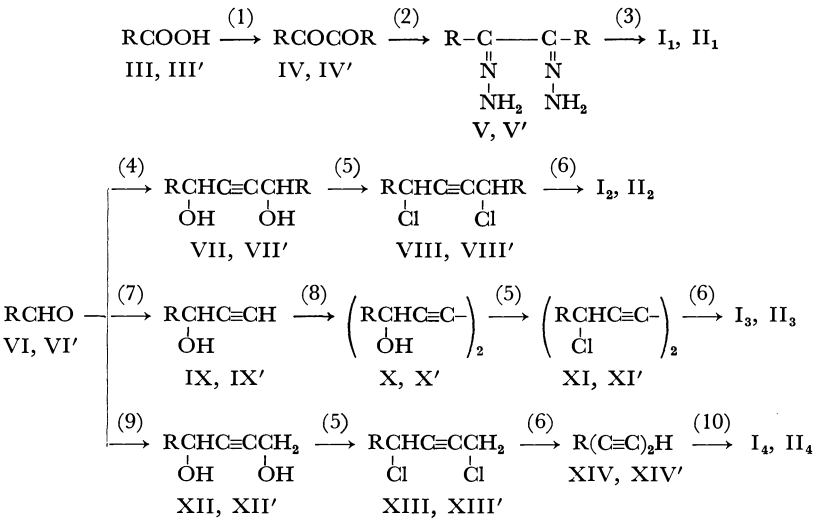

Scheme 1. Synthesis of Dinaphthylpoly-ynes (I_{1-4}, II_{1-4})

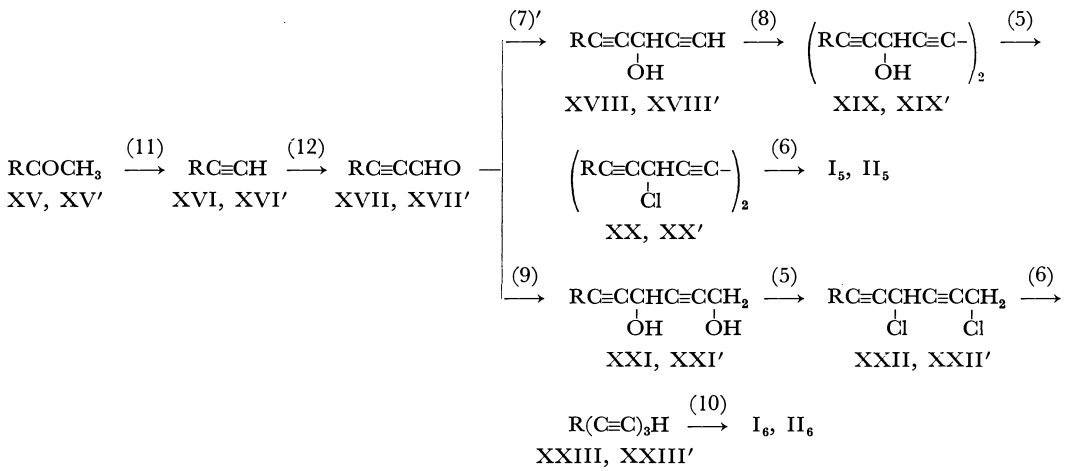

Scheme 2. Synthesis of Dinaphthylpenta- and hexa-acetylenes

R means a 1- or 2-naphthyl group, and the prime on the Roman figure indicates that R is a 2-naphthyl group.

(1) i. Mg-MgI_2, ii. $Cu(OAc)_2$, NH_4NO_3; (2) $H_2NNH_2 \cdot H_2O$/*n*-PrOH; (3) HgO; (4) BrMgC≡CMgBr/THF; (5) $SOCl_2$-Pyridine/THF; (6) $NaNH_2$/liq.NH_3; (7) HC≡CLi/liq.NH_3; (7)′ HC≡CMgBr/THF; (8) CuCl-NH_4Cl-O_2/MeOH or Hay's method[4]; (9) $BrMgC{\equiv}CCH_2OMgBr$/THF; (10) Cu $(OAc)_2$/pyridine; (11) i. PCl_5, ii. $NaNH_2$/liq.NH_3; (12) i. C_2H_5MgBr/THF, ii. dimethylformamide/THF, iii, dil.H_2SO_4. THF=tetrahydrofuran.

Electronic Spectra. The absorption curves and the numerical data of the electronic spectra of the two series of dinaphthylpoly-ynes (I_n and II_n) are shown in Figs. 1 and 2 and in Tables 3 and 4. In both series, the spectra can be regarded as consisting of two groups of absorption bands, *i. e.*, the short-wavelength absorption bands and the long-wavelength absorption bands. The most characteristic feature of the spectra of I_n and II_n is found in the pronounced vibrational structure in the long-wavelength band, which is more distinct than that of the dianthrylpoly-ynes.[1,2]

The long-wavelength band can reasonably be attributed to the interaction of the polyacetylenic chromophore with the ^1L_a-band of the naphthalene nucleus. As the direction of the polarization of the ^1L_a-band is parallel to the short axis of the naphthalene nucleus, the red shift of the long-wavelength bands in the 1,1′-dinaphthyl-series (I_n) as compared with that in the 2,2′-series (II_n) can be ascribed to the more effective extension of conjugation by the polyacetylenic substituent in the 1,1′-series, which extends parallel to the short axis of the nucleus. The difference in wavelength of

4) A. S. Hay, *J. Org. Chem.*, **27**, 3320 (1962).

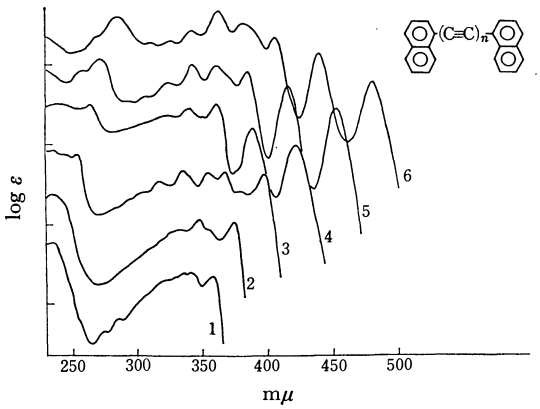

Fig. 1. The absorption curves of 1,1′-dinaphthylpoly-ynes (I_1–I_6). The curves, with the exception of the monoacetylene at the bottom, have been displaced upward on the ordinate axis by 0.5 log ε unit increments from the curve immediately below (in tetrahydrofuran).

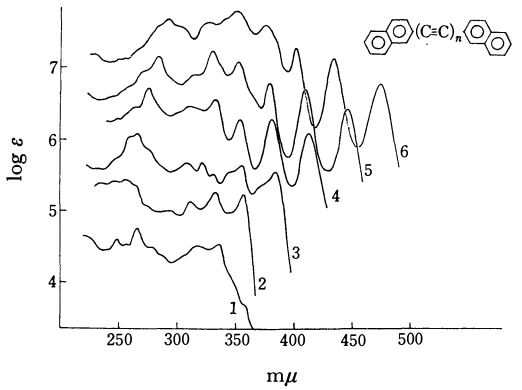

Fig. 2. The absorption curves of 2,2′-dinaphthylpoly-ynes (II_1–II_6). The curves, with the exception of the monoacetylene at the bottom, have been displaced upward on the ordinate axis by 0.5 log ε unit increments from the curve immediately below (in tetrahydrofuran).

Table 3. The electronic spectral data of 1,1′-dinaphthylpoly-ynes (I_n)

n	λ_{max} in mμ and log ε (in parentheses) in tetrahydrofuran										
1	235.5 (4.83)	273.5 (3.65)	284.5 (3.81)	322* (4.31)	336 (4.40)	342 (4.41)	359 (4.36)				
2	234 (4.89)	326* (4.42)	333 (4.44)	348 (4.57)	375 (4.54)						
3	235 (4.92)	244 (4.87)	255.5 (4.87)	285* (3.17)	307* (3.10)	317 (3.12)	336 (4.71)	355 (4.63)	367 (4.64)	378 (3.37)	397 (4.60)
4	238.5 (4.90)	265 (4.86)	286* (4.28)	324 (4.64)	340 (4.80)	361 (4.86)	389 (4.70)	422 (4.49)			
5	259.5 (4.95)	272.5 (5.09)	310 (4.61)	325 (4.74)	343 (4.96)	362 (4.94)	385 (4.85)	415 (4.69)	452 (4.42)		
6	285.5 (5.11)	301 (4.79)	326 (4.80)	343 (4.93)	363 (5.16)	382 (5.00)	407 (4.83)	440 (4.62)	479 (4.27)		

The asterisks indicate shoulders.

Table 4. The electronic spectral data of 2,2′-dinapthylpoly-ynes (II_n)

n	λ_{max} in mμ and log ε (in parentheses) in tetrahydrofuran						
1	257 (4.54)	267 (4.77)	317 (4.56)	336 (4.59)	358* (3.89)		
2	236 (4.81)	248 (4.83)	257 (4.85)	294.5 (4.44)	312 (4.56)	333 (4.70)	357 (4.66)
3	261 (5.06)	267 (5.09)	308 (4.67)	322 (4.69)	332 (4.53)	356 (4.64)	384 (4.57)
4	264.5 (4.90)	276 (5.16)	311 (4.91)	332 (4.99)	354 (4.72)	381 (4.74)	413 (4.54)
5	284.5 (5.18)	330 (5.24)	353 (5.08)	379 (4.80)	409 (4.71)	445 (4.43)	
6	292 (5.00)	327.5 (4.97)	350 (5.12)	374 (4.91)	401 (4.68)	434 (4.54)	473 (4.21)

The asterisk indicates the shoulder.

the longest-wavelength maxima between I_n and II_n was found to decrease with an increase in the number of n (Table 5). This fact seems to indicate a diminishing contribution of the terminal groups with an increase in the length of the polyacetylenic chain. The intensities of the strongest sub-bands in the long-wavelength absorption increase with an

Table 5. The bathochromic shift of thf longest-wavelength maxima in I_n (mμ)

n	1	2	3	4	5	6
I_n	359	375	397	422	452	479
II_n	336	357	384	413	445	473
$\Delta\lambda$	23	18	13	9	7	6

increase in the number of n. However, the intensities of the longest-wavelength sub-bands reach their maxima at $n=3$ in the 1,1′-series (I_n) and at $n=2$ in the 2,2′-series (II_n), and then decrease monotonously with an increase in the number of n. As is summarized in Table 6, the spacing between the longest-wavelength sub-band and the second-longest-wavelength sub-band diminishes with an increase in the number of n. This tendency seems to reflect the decrease in the triple-bond character, *i.e.*, the increasing contribution of a cumulene-type structure in the excited state with an increase in the length of the poly-yne chain. The short wavelength bands in I_n and II_n clearly relate to the ^1B_b-band of naphthalene. The direction of the polarization of the ^1B_b-band has been known to be parallel to the long axis of the naphthalene nucleus. Therefore, the introduction of a poly-acetylene chain at the 2-position, thus extending the conjugation of the naphthalene nucleus, should exert a more prominent effect than such an introduction at the 1-position. In fact, as is summarized in Table 7, we observed a remarkable bathochromic shift of the absorption maximum in the short-wavelength band in II_n as compared with that in I_n. Just as in the case of the ^1L_a-band, the extent of the bathochromic shift decreases with an increase in the number of the acetylenic linkage, suggesting a diminishing contribution of the terminal groups.

Table 6. Spacing of the vibrational sub-band (cm^{-1})

n	2	3	4	5	6
I_n	2070	2060	2010	1980	1850
II_n	2020	2040	2010	1980	1900

Table 7. The bathochromic shift of the maxima in the short-wavelength band in II_n (mμ)

n	1	2	3	4	5	6
II_n	267	264	267	276	285	292
I_n	236	234	256	265	273	286
$\Delta\lambda$	31	30	11	11	12	6

In the previous series of this series,[1,2] it was pointed out that the plots of λ_{max} against the square of the number of the acetylenic bond (n^2) gave an excellent straight line in the cases of 1,1′-dianthryl- and 9,9′-dianthrylpoly-ynes. In the case of 1,1′-dinaphthylpoly-ynes (I_n), it was found that the variation in the wavelength of the longest-wavelength maximum (λ_{max}) with an increase in the number of the acetylenic bond (n) can be expressed by the linear relation:

$$\lambda_{max} = 9\, n^{1.5} + 350 \text{ (tetrahydrofuran)}$$

The plots of λ_{max} *versus* $n^{1.5}$ are illustrated in Fig. 3. The observed and the calculated values of λ_{max} are compared in Table 8.

Table 8. The longest-wavelength maxima of I_n (mμ)

n	1	2	3	4	5	6
Calcd.	359	375	397	422	452	479
Obs.	359	375	397	422	451	482
$\Delta\lambda$	0	0	0	0	−1	3

A good correlation between the wavelength of the longest-wavelength maxima (λ_{max}) and $n^{1.3}$ was observed in the case of 2,2′-dinaphthylpoly-ynes (II_n). The linear relation is well expressed by the empirical formula:

$$\lambda_{max} = 15.5\, n^{1.3} + 319 \text{ (tetrahydrofuran)}$$

The observed and the calculated values of λ_{max} are listed in Table 9, while the plots of λ_{max} against $n^{1.3}$ are shown in Fig. 4. As is shown by the B lines in Figs. 3 and 4, the second-longest-wavelength peaks of I_n and II_n also gave straight lines when plotted against $n^{1.5}$ and $n^{1.3}$ respectively.

Table 9. The longest-wavelength maxima of II_n (mμ)

n	1	2	3	4	5	6
Calcd.	335	357	384	413	445	478
Obs.	336	357	384	413	445	473
$\Delta\lambda$	−1	0	0	0	0	5

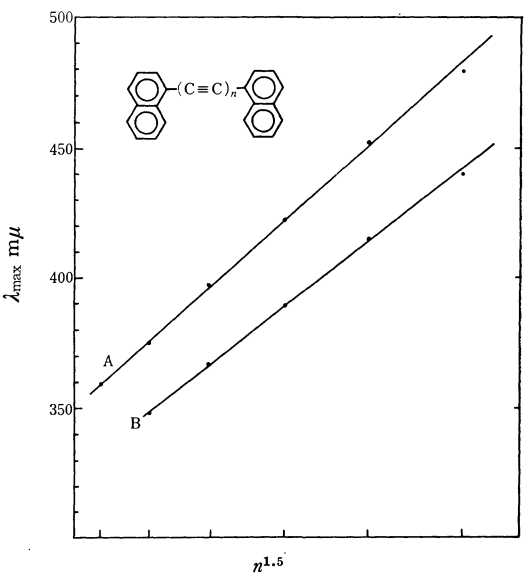

Fig. 3. Plot of λ_{max} *vs.* $n^{1.5}$ for 1,1′-dinaphthylpoly-ynes (I_1–I_6).
A: longest-wavelength maxima
B: second-longest-wavelength maxima

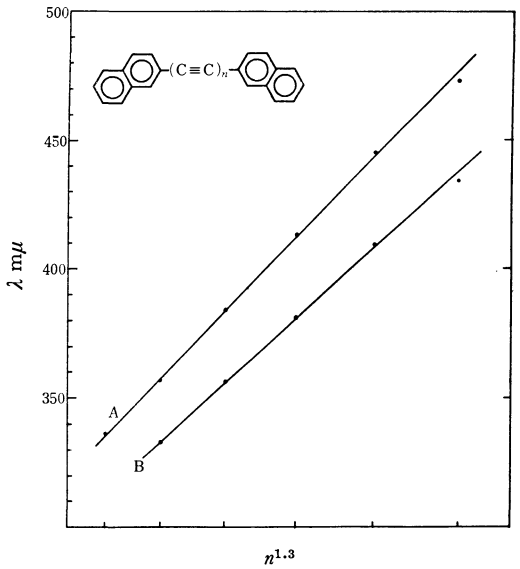

Fig. 4. Plot of λ_{max} *vs.* $n^{1.3}$ for 2,2′-dinaphthylpoly-ynes (II_1–II_6).
A: longest-wavelength maxima
B: second-longest-wavelength maxima

In both series, the deviation from the straight line is distinct in the case of $n=6$. This fact seems to indicate that the diminishing contribution of the terminal groups to the electronic excitation as the number of n increases causes a gradual change in the spectral properties of these diarylpoly-ynes. If the length of the poly-yne chains in these diarylpoly-ynes is large enough, the spectral shift might be similar to that of simple poly-yne or dialkylpoly-yne. However, it is evident that the regularities in the relationship between λ_{max} and the length of the conjugated polyacetylene chain (n) are markedly influenced by the nature of the aromatic terminal groups, at least in the range of a small number of n. Further studies along this line are now in progress.

Experimental

All the melting points are uncorrected. The electronic spectra were obtained on a Hitachi EPS-3T Spectrophotometer at room temperature using a well-matched pair of 1-cm cells. The infrared spectra were determined with a Hitachi EPI-2 Infrared Spectrophotometer.

1,1′-Naphthil Dihydrazone (V). A mixture of 1,1′-naphthil[5] (IV, 3.10 g, 0.01 mol), 80% hydrazine hydrate (3.10 g, 0.05 mol), and *n*-propanol (80 m*l*) was refluxed for 43.5 hr. The mixture was then cooled in an ice-bath. The crystalline solid which was thus separated was collected by filtration and washed with a small amount of methanol to yield V as fine colorless crystals; 1.15 g; mp 270—275°C (dec.). The mother liquor was refluxed for a further 48 hr to afford additional V; 0.5 g (total yield, 49%).

Found: C, 78.25; H, 5.31; N, 16.14%. Calcd for $C_{22}H_{18}N_4$: C, 78.08; H, 5.36; N, 16.56%.

1,1′-Naphthil Monohydrazone (colorless cubes; 0.35 g; 11%; mp 173—175°C) was obtained by concentrating the filtrate.

Found: C, 81.12; H, 5.06; N, 8.69%. Calcd for $C_{22}H_{16}N_2O$: C, 81.46; H, 4.97; N, 8.64%.

1,1′-Dinaphthylacetylene (I). A mixture of the dihydrazone (V, 1.52 g, 4.5 mmol), yellow mercuric oxide (4.0 g, 0.018 mol), sodium sulfate (0.9 g), powdered potassium hydroxide (0.8 g), and toluene (200 m*l*) was refluxed for 3.5 hr and then filtered. The concentration of the filtrate under a reduced pressure yielded light brown needles; 1.03 g (82%); mp 120—126°C. The crystals were dissolved in benzene and percolated through a small column of alumina (10 g). The filtrate was then concentrated to yield colorless needles; 0.99 g (79%); mp 127—128°C. The crystals were recrystallized twice from methanol to give pure I; mp 129°C*1.

Found: C, 95.00; H, 5.04%. Calcd for $C_{22}H_{14}$; C, 94.93; H, 5.07%.

1,4-Di(1-naphthyl)-1,4-dihydroxy-2-butyne (VII). A solution of 1-naphthaldehyde (VI, 6.20 g, 0.04 mol) in tetrahydrofuran (30 m*l*) was added to a stirred and ice-cooled solution of acetylene dimagnesium bromide [from magnesium 1.92 g, 0.08 g atom and ethyl bromide 8.72 g, 0.08 mol] in benzene - tetrahydrofuran (60 m*l*) over a period of 15 min. After this mixture had been stirred overnight at room temperature, a saturated aqueous solution of ammonium chloride was added under cooling with an ice-salt bath. The aqueous layer was removed and extracted with ether. The extract was combined with the organic layer and dried (magnesium sulfate). It was concentrated under reduced pressure to yield an oily material which crystallized on standing. The crude material was treated with a small amount of benzene to give colorless crystals; 4.80 g (71%). Two recrystallizations of the crystals from benzene gave pure VII; mp 186.5—187.5°C.

Found: C, 85.61; H, 5.38%. Calcd for $C_{24}H_{18}O_2$: C, 85.18; H, 5.36%. IR (in Nujol): 3300—3400 (O–H), 1010 (C–O) cm^{-1}.

1,1′-Dinaphthyldiacetylene (I_2). *The Preparation of the Dichloride (VIII).* To an ice-cooled and stirred mixture of the glycol (VII, 1.01 g, 3 mmol), pyridine (0.95 g, 0.012 mol), and tetrahydrofuran (10 m*l*), there was added a solution of thionyl chloride (1.40 g, 0.012 mol) in tetrahydrofuran (3 m*l*) over a period of 30 min, then the mixture was warmed to 40°C over a period of 1 hr, after which it was stirred an additional hour at that temperature. Cracked ice was added to the reaction mixture, and it was extracted with benzene. The extract was washed with water and aqueous sodium hydrogen carbonate successively, and then dried (magnesium sulfate). The crude dichloride (VIII, 1.00 g, 90%) which was obtained as a yellowish-brown mass by evaporating the solvent *in vacuo* was used in the following reaction without purification.

The Dehydrochlorination of VIII. A solution of the above-mentioned crude chloride (VIII) in tetrahydro-

5) M. Gomberg and W. E. Bachmann, *J. Amer. Chem. Soc.*, **50**, 2762 (1928).

*1 It should be noted that the description of 1,1′-dinaphthylacetylene in Beilstein, Bd. V, p. 735, is erroneous. It concerns the 2,2′-isomer.

furan (7 ml) was added over a period of 5 min to a stirred suspension of sodium amide [from sodium 0.7 g, 0.03 g atom] in liquid ammonia (50 ml) at −70°C. After 4 hr, ammonium chloride (2.5 g) was added to the reaction mixture, and the ammonia was allowed to evaporate. The residue was repeatedly digested with benzene (total 250 ml), and the benzene solution was concentrated to 50 ml and passed through a short column of alumina (15 g). The yellow crystals [0.28 g, (31% based on VII), mp 171—175°C] which were obtained by concentrating the filtrate under a reduced pressure were recrystallized twice from benzene to give pure I_2; mp 175—177°C. [lit. value, mp 171°C[6]].

Found: C, 95.32; H, 4.69%. Calcd for $C_{24}H_{14}$: C, 95.33; H, 4.67%.

The Oxidative Coupling of 1-Ethynylnaphthalene (XVI). The diacetylene (I_2) was obtained in a quantitative yield by stirring a mixture of 1-ethynylnaphthalene (XVI, 0.86 g, 5.7 mmol), cupric acetate monohydrate (3.0 g), pyridine (8 ml), and methanol (0.5 ml) at 30°C overnight. The crystals thus obtained were recrystallized 3 times from benzene and once from acetone to give pure I_2; mp 175—177°C.

Found: C, 95.42; H, 4.79%. Calcd for $C_{24}H_{14}$: C, 95.33; H, 4.67%.

1-(1-Naphthyl)-2-propyn-1-ol (IX). A solution of 1-naphthaldehyde (VI, 56 g, 0.36 mol) in tetrahydrofuran (300 ml) was added to a stirred solution of lithium acetylide [from lithium 7.45 g (1.08 g atom)] in liquid ammonia (1.2 l) at −70°C over a period of 30 min. Stirring was then continued for 28 hr at −60——65°C. After the addition of ammonium chloride (36 g), the ammonia was allowed to evaporate. The organic layer was separated, and the residue was digested with benzene. The combined organic layer was evaporated *in vacuo*, resulting in a viscous red oil which crystallized on standing. The crude material was treated with benzene - cyclohexane (2 : 5), filtered, and washed with the same solvent to yield a light brown, crystalline powder; 45.4 g (69%). This was recrystallized 5 times from the same solvent to give pure IX as colorless needles; mp 61—63°C.

Found: C, 85.68; H, 5.37%. Calcd for $C_{13}H_{10}O$: C, 85.69; H, 5.53%. IR (Nujol): 3200—3300 (OH), 3300 (≡CH), 2100 (C≡C), 1060 (C–O) cm^{-1}.

1,6-Di(1-naphthyl)-1,6-dihydroxy-2,4-hexadiyne (X). A mixture of the ethynyl carbinol (IX, 6.90 g, 0.038 mol), *N,N,N',N'*-tetramethylethylenediamine (0.22 g, 0.002 mol), cuprous chloride (0.19 g, 0.002 mol), and acetone (50 ml) was vigorously stirred in an atmosphere of oxygen for 2 hr at room temperature and then for 4 hr at 40°C.[4] The oily material which was obtained by evaporating the solvent was dissolved in tetrahydrofuran (100 ml). Benzene (25 ml) was added to the solution, and it was washed with a saturated aqueous solution of sodium chloride, diluted sulfuric acid, a sodium chloride solution and an aqueous sodium hydrogen carbonate solution successively, and then dried (magnesium sulfate). The residue obtained by evaporating the solvent *in vacuo* was mixed with benzene (30 ml), resulting in crude brown crystals; 5.76 g(80%). Five recrystallizations from benzene and two from ethanol - benzene yielded pure X as fine colorless needles; mp 156—176°C.[7]

Found: C, 85.89; H, 4.97%. Calcd for $C_{26}H_{18}O_2$: C, 86.16; H, 5.01%. IR (Nujol): 3200—3300 (OH), 1065 (C–O) cm^{-1}.

1,1'-Dinaphthyltriacetylene (I_3). *The Preparation of the Dichloride (XI).* To a stirred mixture of the glycol (X, 1.09 g, 3 mmol), pyridine (0.71 g, 9 mmol), and tetrahydrofuran (10 ml), there was added a solution of thionyl chloride (1.07 g, 9 mmol) in tetrahydrofuran (3 ml) over a period of 30 min at 0°C. After further stirring for 1 hr at room temperature and then 30 min at 40°C, cracked ice was added to the reaction mixture and it was extracted with benzene. The extract was washed with water, a sodium hydrogen carbonate solution, and water successively, and then dried (magnesium sulfate). The crude dichloride (XI), which was obtained as a deep brown oil by evaporating the solvent *in vacuo*, was subjected to the subsequent reaction without purification.

The Dehydrochlorination of XI. A solution of the crude dichloride (XI) in tetrahydrofuran (10 ml) was added, over a period of 5 min, to a suspension of sodium amide [from sodium 0.41 g, 0.018 g atom] in liquid ammonia (50 ml) at −70°C. After 1 hr, ammonium chloride (2 g) was added to the mixture, and the ammonia was allowed to evaporate. The residue was repeatedly digested with petroleum benzine (total 300 ml). The extract was concentrated under reduced pressure to yield crude I_3, as yellow crystals; 0.26 g (27% based on X). This was dissolved in benzene and percolated through a short column of alumina. The crystals obtained by concentrating the filtrate *in vacuo* were recrystallized twice from acetone to afford pure I_3 as yellow needles; mp 192—193°C.

Found: C, 95.56; H, 4.30%. Calcd for $C_{26}H_{14}$: C, 95.68; H, 4.32%.

1-(1-Naphthyl)-2-butyne-1,4-diol (XII). A solution of propargyl alcohol (11.20 g, 0.2 mol) in tetrahydrofuran (30 ml) was added, over a period of 30 min, to a stirred and water-cooled solution of ethylmagnesium bromide [from magnesium 9.60 g (0.40 g atom) and ethyl bromide 43.9 g (0.40 mol)] in the same solvent (150 ml). After it had refluxed for 1 hr, the mixture was cooled in an ice-bath. 1-Naphthaldehyde (VI, 15.60 g, 0.1 mol) in the same solvent (80 ml) was introduced to the cooled mixture, and it was stirred overnight at 20°C. After refluxing for 1.5 hr, the reaction mixture was then mixed with 4N sulfuric acid (100 ml) and extracted with ether. The extract was washed successively with a saturated solution of sodium chloride and a sodium hydrogen carbonate solution, and then dried (magnesium sulfate). The removal of the solvent *in vacuo* resulted in a dark red oil which crystallized on standing. The crude crystals were treated with a small amount of benzine - cyclohexane (1 : 1), collected by filtration, and washed with the same mixed solvent to yield fine pale yellow cubes; mp 120—123°C; 14.20 g (67%). The crystals were recrystallized 4 times from benzene to give pure XII as colorless needles; mp 125—126°C.

Found: C, 78.97; H, 5.70%. Calcd for $C_{14}H_{12}O_2$: C, 79.22; H, 5.70%. IR (KBr-disk): 3200—3300 (OH), 1020 (C–O) cm^{-1}.

1-Butadiynylnaphthalene (XIV). *The Preparation*

6) V. Grignard and H. Perrichon, *Ann. Chim. et Phys.*, **5**, 5 (1926).

7) This is a mixture of meso- and rac-isomers of X. *Cf.* I. Iwai and T. Konotsune, *Yakugaku Zasshi*, **78**, 505 (1958).

of the Dichloride (XIII). To an ice-cooled mixture of the glycol (XII, 4.24 g, 0.02 mol), pyridine (4.80 g, 0.06 mol), and tetrahydrofuran (50 m*l*), we added, drop by drop, a solution of thionyl chloride (7.20 g, 0.06 mol) in tetrahydrofuran (10 m*l*) over a period of 30 min. The temperature of the reaction mixture was gradually raised to 40°C in 60 min. After stirring for 30 min at that temperature, crushed ice was added to the ice-cooled reaction mixture. The reaction product was extracted with ether. The extract was washed with water, and aqueous sodium hydrogen carbonate successively, and then dried (magnesium sulfate). The crude dichloride (XIII) obtained by evaporating the solvent *in vacuo* was subjected to the following dehydrochlorination without further purification.

The Dehydrochlorination of XIII. A solution of the above-mentioned crude dichloride (XIII) in tetrahydrofuran (10 m*l*) was added, over a 5-min period to a suspension of sodium amide [from sodium 3.5 g, 0.152 g atom] in liquid ammonia (150 m*l*) at −70°C. The mixture was stirred for 1.5 hr, and then the ammonia was allowed to evaporate after the addition of ammonium chloride (9.0 g). The organic solvent was removed under reduced pressure. The residue was extracted with petroleum ether (400 m*l*). The concentrated extract (*ca.* 150 m*l*) was passed through a short column of alumina (5 g). The light yellow filtrate was concentrated under reduced pressure to yield crude XIV as yellow leaflets; 1.39 g (40%); mp *ca.* 40°C. The crude XIV was dissolved in petroleum ether and passed through a thin-layer of alumina (4 g). The filtrate was chilled in a dry ice-ethanol-bath to yield analytically pure XIV as pale yellow leaflets; mp 44—45°C. XIV gave orange yellow cuprous and pale yellow silver acetylide. XIV was found to be a fairly unstable substance. The crystals rapidly changed to an insoluble brown substance.

Found: C, 95.11; H, 4.55%. Calcd for $C_{14}H_8$: C, 95.42; H, 4.58%. IR (Nujol): 3270 (≡CH), 2190, 2205 (C≡C) cm^{-1}.

1,1′-Dinaphthyltetraacetylene (I_4). Cupric acetate monohydrate (4.0 g) was added to a solution of the diacetylene (XIV, 0.50 g, 2.8 mmol) in pyridine (20 m*l*), after which the mixture was stirred for 1 hr at 45°C.[8] The stirring was continued overnight at room temperature. The reaction mixture was then chilled in an ice-bath, and the insoluble material was collected by filtration, and washed successively with a small amount of methanol and with water, thus affording crude I_4 as fine greenish-yellow needles; 0.37 g (77%); mp *ca.* 200°C (dec.). A second crop of I_4 (0.07 g) was obtained from the filtrate. A benzene solution of the crude I_4 was passed through a short column of alumina. The crystals obtained by concentrating the filtrate were recrystallized twice from acetone to yield pure I_4 as yellow needles; mp 205—206°C (dec.).

Found: C, 95.70; H, 4.04%. Calcd for $C_{28}H_{14}$: C, 95.97; H, 4.03%.

1-Ethynylnaphthalene (XVI). Phosphorus pentachloride (168 g, 0.81 mol) was added to a solution of 1-acetylnaphthalene (134 g, 0.79 mol) in dry benzene (250 m*l*). After the vigorous reaction had subsided, the mixture was gradually heated and refluxed for 1.5 hr. The reaction mixture was poured onto ice water, and the organic layer was separated. The aqueous layer was extracted with benzene. The combined benzene layer was washed successively with water and with aqueous sodium hydroxide, and then dried (sodium sulfate). After the solvent had been removed under reduced pressure, the residue was distilled *in vacuo* to yield 1-(α-chlorovinyl)-naphthalene; 141.3 g (95%); bp 113—114°C/3 mmHg.

Found: C, 76.33; H, 4.79; Cl, 19.02%. Calcd for $C_{12}H_9Cl$: C, 76.40; H, 4.81; Cl, 18.79%.

The chloride thus obtained (75.5 g, 0.40 mol) was dissolved in ether (100 m*l*), and the solution was added, drop by drop, to a suspension of sodium amide [from sodium 33 g, 1.44 g atom] in liquid ammonia (1.2 *l*) at −70°C over a period of 1 hr. After stirring for a further 2.5 hr, the ammonia was allowed to evaporate. Petroleum benzine (350 m*l*) and then a saturated solution of ammonium chloride were added to the residue at −40°C. The organic layer was separated, and the aqueous layer was extracted with the same solvent. The combined benzine solution was dried (sodium sulfate), and the solvent was removed under reduced pressure. The residue was distilled *in vacuo* to yield XVI; 56.3 g (92%); bp 76—77°C/0.1 mmHg [lit. values: bp 143°C/25 mmHg;[9] bp 45°C/0.25 mmHg;[10] bp 92°C/4 mmHg[11]].

Found: C, 94.78; H, 5.30%. Calcd for $C_{12}H_9$: C, 94.70; H, 5.30%.

3-(1-Naphthyl)-prop-2-ynal (XVII). Into an ice-cooled solution of ethylmagnesium bromide [from magnesium (10.8 g, 0.44 g atom) and ethyl bromide (57.8 g, 0.53 mol)] in tetrahydrofuran (300 m*l*), there was added, drop by drop, a solution of XVI (56 g, 0.37 mol) in tetrahydrofuran (100 m*l*) under stirring, the mixture was then refluxed for 1 hr. *N,N*-Dimethylformamide (84 m*l*) in the same solvent (100 m*l*) was added in one portion to the mixture chilled in an ice-salt-bath. After 30 min stirring, the cooling bath was removed and the stirring was continued for a further 2 hr at 30°C. The reaction mixture was then mixed with 5% sulfuric acid (2 *l*) under vigorous agitation, after which the stirring was continued overnight. The mixture was then extracted with benzene. The extract was washed with water and aqueous alkali, and dried. The viscous liquid obtained by evaporating the solvent under reduced pressure was mixed with cyclohexane - ether (2 : 1). The solution was then cooled, yielding crude XVII, 35 g (52%). This was recrystallized twice from the same solvent to afford pure XVII; mp 20.5—21.5°C; colorless needles.

Found: C, 86.22; H, 4.37%. Calcd for $C_{13}H_8O$: C, 86.65; H, 4.48%. [lit. value: bp 85—86°C/0.5 mmHg[10]].

1-(1-Naphthyl)-1,4-pentadiyne-3-ol (XVIII). A solution of the aldehyde (XVII, 4.68 g, 0.026 mol) in tetrahydrofuran (30 m*l*) was added to a stirred and ice-cooled solution of ethynylmagnesium bromide[12] [from magnesium (1.37 g, 0.057 g atom) and ethyl

8) G. Eglinton and A. R. Galbraith, *J. Chem. Soc.*, **1959**, 889.

9) R. E. Atkinson, R. E. Curtis, D. M. Jones and J. A. Taylor, *Chem. Commun.*, **1967**, 718.

10) Idem., *J. Chem. Soc., C.*, **1969**, 2173.

11) D. Bertin, *Ann. Chim. (Paris)*, **8**, 296 (1953).

12) E. R. H. Jones, L. L. Skattebøl and M. C. Whiting, *J. Chem. Soc.*, **1956**, 4765; "*Org. Synth.*" Vol. 39, p. 56 (1959).

bromide (6.6 g, 0.06 mol)] in tetrahydrofuran (100 ml), after which the mixture was stirred for a further hour at the same temperature. Then the cooling-bath was removed and the mixture was stirred overnight at room temperature. The ice-cooled reaction mixture was then treated with a saturated aqueous solution of ammonium chloride and extracted with benzene. The extract was dried (magnesium sulfate), and the solvent was removed *in vacuo*, resulting in crude crystals. A benzene solution of the crude material was percolated through a short column of alumina (10 g). The filtrate was concentrated under reduced pressure, and the residue was treated with charcoal in methanol. Recrystallization from benzene - petroleum ether (1 : 3) gave XVIII; 3 g (56%). An analytical specimen was obtained by recrystallizing the crystals 3 times from the same solvent; mp 86—87°C.

Found: C, 87.09; H, 4.85%. Calcd for $C_{15}H_{10}O$: C, 87.35; H, 4.89%. IR (KBr-disk): 3280 (≡CH), 2100 2220 (C≡C), 1015 (C–O) cm^{-1}.

1,10-Di(1-naphthyl)-1,4,6,9-decatetrayne-3,8-diol (XIX). A solution of the diyne-ol (XVIII, 1.03 g, 0.005 mol) in methanol (15 ml) was mixed with cuprous chloride (0.1 g, 0.001 mol) and ammonium chloride (0.075 g, 0.0014 mol); then one drop of concentrated hydrochloric acid was added. The mixture was vigorously stirred at 32°C in an atmosphere of oxygen under a slightly elevated pressure until the uptake of oxygen ceased (4 hr). The inorganic material was removed by filtration, and the filtrate was concentrated under reduced pressure. The residue was mixed with ether and treated with 2N hydrochloric acid. The organic layer was washed successively with water, aqueous sodium hydrogen carbonate, and water, and then dried (magnesium sulfate). The crude crystals obtained by evaporating the solvent under reduced pressure were recrystallized from benzene, resulting in XIX; 0.80 g (80%). This was recrystallized 3 times from the same solvent to yield pure XIX; mp 165°C (dec.).

Found: C, 87.34; H, 4.42%. Calcd for $C_{30}H_{18}O_2$: C, 87.78; H, 4.42%. IR (KBr-disk): 3100—3300 (≡CH, OH), 2220 (C≡C), 1005 (C–O) cm^{-1}.

1,1′-Dinaphthylpentaacetylene (I_5). *The Preparation of the Dichloride (XX).* To a cooled (ice-salt-bath) mixture of the tetraacetylene glycol (XIX, 0.62 g, 0.0015 mol), pyridine (0.36 g, 0.0045 mol), and tetrahydrofuran (10 ml), there was added, over a period of 20 min, a solution of thionyl chloride (0.54 g, 0.0045 mol) in tetrahydrofuran (10 ml). After stirring for an additional hour at the same temperature, crushed ice was added to the reaction mixture. The organic layer was washed successively with water and with aqueous sodium carbonate, and then dried. The organic layer was concentrated *in vacuo* to *ca.* 10 ml. The solution of XX thus obtained was used immediately for the following reaction.

The Dehydrochlorination of XX. The above-mentioned solution of XX was added, drop by drop and over a 5-min period, into a suspension of sodium amide [from sodium 0.20 g (0.0087 g atom)] in liquid ammonia (30 ml) at −70°C. After stirring for 1 hr at that temperature, ammonium chloride (1.0 g) was added to the reaction mixture; then the ammonia was allowed to evaporate. The residue was repeatedly digested with petroleum benzine. The crude crystals obtained by removing the solvent under reduced pressure were dissolved in benzene. The benzene solution was passed twice through a thin-layer of alumina (each 6 g). The filtrate was then concentrated, yielding I_5 as orange yellow crystals; 114 mg (20% based on XIX). This was recrystallized twice from benzene to give pure I_5; mp *ca.* 195°C (dec.).

Found: C, 96.14; H, 3.81%. Calcd for $C_{30}H_{14}$: C, 96.23; H, 3.77%.

1-(1-Naphthyl)-1,4-hexadiyne-3,6-diol (XXI). Propargyl alcohol (11.20 g, 0.2 mol) in tetrahydrofuran (30 ml) was added, over a period of 30 min, into a stirred solution of ethylmagnesium bromide [from magnesium (9.60 g, 0.40 g atom) and ethyl bromide (43.9 g, 0.40 mol)] in tetrahydrofuran (150 ml) at a temperature lower than 30°C. The mixture was refluxed for 1 hr, and then greatly cooled in an ice-salt-bath. A solution of the aldehyde (XVII, 18 g, 0.1 mol) in tetrahydrofuran (80 ml) was then added, drop by drop, to the cooled mixture. The cooling bath was removed, and the reaction mixture was stirred overnight. A saturated aqueous solution of ammonium chloride was added to the ice-cooled reaction mixture. The organic layer was separated, and the aqueous layer was repeatedly extracted with benzene. The combined organic layer was dried (magnesium sulfate). The crystals obtained by evaporating the solvent *in vacuo* were recrystallized from benzene to yield XXI; 15.6 g (66%). The crude material was recrystallized 3 times from benzene, thus affording pure XXI; mp 113—114°C.

Found: C, 80.93; H, 5.14%. Calcd for $C_{16}H_{12}O_2$: C, 81.34; H, 5.12.% IR (KBr-disk): 3100—3400 (OH), 2220 (C≡C), 1025 (C–O) cm^{-1}.

1,1′-Dinaphthylhexaacetylene (I_6). *The Preparation of the Dichloride (XXII).* A solution of thionyl chloride (3.1 g, 0.026 mol) in tetrahydrofuran (10 ml) was added, drop by drop and over a 30-min period, into a cooled (in an ice-salt-bath) and stirred mixture of the diacetylenic glycol (XXI, 2.04 g, 0.0086 mol), pyridine (2.06 g, 0.026 mol), and tetrahydrofuran (25 ml). The temperature of the reaction mixture was gradually raised to room temperature, and then the mixture was stirred at 40°C for 30 min. Cracked ice was added to the ice-cooled reaction mixture, and the product was extracted with benzene. The extract was washed successively with water and with aqueous sodium hydrogen carbonate, and then dried (magnesium sulfate). The extract was concentrated to *ca.* 10 ml under reduced pressure and immediately subjected to the following reaction.

The Preparation of 1-Naphthyltriacetylene (XXIII). To a suspension of sodium amide [from sodium 1.2 g (0.052 g atom)] in liquid ammonia (50 ml), there was added the above-mentioned solution of XXII over a period of 5 min at −70°C. After the mixture had been stirred for 1.5 hr at the same temperature, ammonium chloride (3.6 g) and petroleum benzine (120 ml) were added and the ammonia was allowed to evaporate. The organic layer was then separated, and the residue was digested with petroleum benzine. The orange-yellow organic layer was concentrated to *ca.* 200 ml under reduced pressure and passed through a short column of alumina (3.5 g), thus yielding a colorless filtrate. As the triacetylene was found to be a fairly unstable substance, the colorless filtrate was used in the subsequent reaction without isolation. UV (measured with an uncertain concentration in petroleum benzine): λ_{max} 350, 329, 308 and 296 mμ.

The Oxidation Coupling of XXIII. To a stirred solution of cupric acetate monohydrate (3.0 g) in pyridine (15 m*l*), there was added a 30 m*l* portion of the above-mentioned solution of the triacetylene (XXIII), and then the petroleum benzine was removed under reduced pressure at room temperature; the second portion (30 m*l*) of the solution was then added, and the benzine was removed again *in vacuo*. The entire benzine solution was added, portion by portion to the oxidizing reagent, repeating the above procedure. After the addition of the solution and the removal of the benzine had been completed, the mixture was stirred for 1.5 hr at 40°C. The reaction mixture was greatly chilled in an ice-salt-bath, and the precipitated solid was collected by filtration and washed with a small amount of cold pyridine. The brown crystals which were obtained by washing the solid thoroughly with water were dissolved in benzene and percolated through a short column of alumina (8 g). The filtrate was concentrated *in vacuo*, thus yielding orange crystals; 118 mg (14% based on XXI). They were recrystallized from benzene to give pure I_6; mp 175°C (dec.).

Found: C, 96.15; H, 3.54%. Calcd for $C_{32}H_{14}$: C, 96.46; H, 3.54%.

2,2′-Naphthil (IV′). The compound IV′ was prepared according to the method used in the case of the 1,1′-isomer (IV).

2,2′-Naphthil Dihydrazone (V′). The method used in the preparation of the 1,1′-isomer (V) was applied successfully in this case. mp 187—188°C. Yield, 83%.

Found: C, 77.86; H, 5.46; N, 16.51%. Calcd for $C_{22}H_{18}N_4$: C, 78.08; H, 5.36; N, 16.56%.

2,2′-Dinaphthylacetylene (II_1). Exactly the same procedure used in the preparation of I_1 was followed, yielding 0.95 g (77%) of crude light yellow II_1. This crude material was recrystallized successively from benzene - ethanol and from benzene, thus yielding pure II_1; colorless needles; mp 228—229°C. [lit. value: mp 225°C[13]].

Found: C, 94.55; H, 5.30%. Calcd for $C_{22}H_{14}$: C, 94.93; H, 5.37%.

1,4-Di(2-naphthyl)-1,4-dihydroxy-2-butyne (VII′). 2-Naphthaldehyde (VI′, 6.20 g, 0.04 mol) gave 5.3 g (85%) of slightly crude VII′ when treated by the method described in the case of the 1-naphthyl isomer. The crude material was recrystallized 3 times from benzene-ethanol to give pure VII′ as fine colorless crystals; mp 159—160°C.

Found: C, 85.33; H, 5.41%. Calcd for $C_{24}H_{18}O_2$: C, 85.18; H, 5.36%. IR (KBr-disk): 3100—3400 (OH), 1000 (C–O) cm^{-1}.

2,2′-Dinaphthyldiacetylene (II_2). The acetylene glycol (VII′, 1.0 g, 3 mmol) was treated according to the procedure used in the case of VII, thus yielding crude II_2; 297 mg (33%). A benzene solution of the crude material was passed through a thin-layer of alumina. The crystals obtained from the filtrate were recrystallized twice from benzene, thus affording pure II_2 as colorless fine leaflets; mp 202—203°C.

Found: C, 95.44; H, 4.75%. Calcd for $C_{24}H_{14}$: C, 95.33; H, 4.67%.

1-(2-Naphthyl)-2-propyn-1-ol (IX′). 2-Naphthaldehyde (VI′, 12.5 g, 0.08 mol) was treated with lithium acetylide in liquid ammonia according to the procedure described in the case of IX; this afforded slightly impure IX′; 7.7 g (52%); mp 58—62°C.

IR (KBr-disk): 3300—3400 (OH), 3290 (≡CH), 2110 (C≡C), 1015 (C–O) cm^{-1}.

1,6-Di(2-naphthyl)-1,6-dihydroxy-2,4-hexadiyne (X′). A mixture of the ethynyl carbinol (IX′, 4.6 g, 0.025 mol), cuprous chloride (0.5 g, 0.005 mol), ammonium chloride (0.375 g, 0.007 mol), and methanol (75 m*l*) containing 3 drops of concentrated hydrochloric acid was vigorously stirred at room temperature under an oxygen atmosphere at a slightly elevated pressure for 9 hr. An inorganic material was then removed by filtration and washed with a small amount of methanol. The combined filtrate and washings were concentrated *in vacuo*. The residue was dissolved in ether containing a small amount of tetrahydrofuran and treated with 2N hydrochloric acid to remove the inorganic material. The organic layer was washed with water and dried. The crystals, 4.1 g (90%) obtained by evaporating the solvent under reduced pressure were recrystallized 3 times from benzene - methanol to afford pure X′ as colorless cubes; mp 170°C (dec.).

Found: C, 86.28; H, 5.20%. Calcd for $C_{26}H_{18}O_2$: C, 86.16; H, 5.01%. IR (KBr-disk): 3200—3400 (OH), 1010 (C–O) cm^{-1}.

2,2′-Dinaphthyltriacetylene (II_3). *The Preparation of the Dichloride (XI′).* Thionyl chloride (1.07 g, 0.009 mol) in tetrahydrofuran (5 m*l*) was added, drop by drop, into a cooled (in an ice-salt-bath) and stirred mixture of the diacetylene glycol (X′, 1.09 g, 0.003 mol), pyridine (0.71 g, 0.009 mol), and tetrahydrofuran (15 m*l*). After 1 hr, the cooling bath was removed, after which the stirring was continued for an additional hour at room temperature. Then the ice-cooled reaction mixture was mixed with cracked ice and extracted with benzene. The extract was washed successively with water and sodium carbonate, and dried. The crude dichloride (XI′, a deep-brown liquid) obtained by evaporating the solvent *in vacuo* was immediately subjected to the following reaction without purification.

The Dehydrochlorination of XI′. The above-mentioned crude XI′ was treated according to the procedure used in the case of XI, thus affording crude II_3; 246 mg (25% based on X′). The crude material was recrystallized 4 times from acetone to give pure II_3; pale yellow needles; mp 173—174°C.

Found: C, 95.40; H, 4.42%. Calcd for $C_{26}H_{14}$: C, 95.68; H, 4.32%.

1-(2-Naphthyl)-2-butyne-1,4-diol (XII′). The procedure used in the synthesis of XII was employed. 2-Naphthaldehyde (VI′, 10 g, 0.064 mol) gave 9.7 g (71%) of XII′. Three recrystallizations of the crystals from benzene gave pure XII′ as colorless leaflets; mp 74—75°C.

Found: C, 78.91; H, 5.68%. Calcd for $C_{14}H_{12}O_2$: C, 79.22; H, 5.70%. IR (KBr-disk): 3100—3300 (OH), 1005 (C–O) cm^{-1}.

2-Butadiynylnaphthalene (XIV′). The acetylene glycol (XII′, 8.0 g, 0.038 mol) gave 2.4 g (36%) of XIV′ according to the method used in the preparation of the 1-isomer (XIV). This was recrystallized from petroleum ether to give pure XIV′ as colorless needles; mp 58—60°C (dec.).

Found: C, 95.20; H, 4.70%. Calcd for $C_{14}H_8$: C, 95.42; H, 4.58%. IR (KBr-disk): 3270 (≡CH), 2200 (C≡C) cm^{-1}.

13) J. Grabowsky, *Ber.*, **11**, 298 (1878).

2,2'-Dinaphthyltetraacetylene (II_4). The oxidative coupling of 2-butadiynylnaphthalene (XIV', 1.3 g, 7.4 mmol) according to the method used for the 1-isomer (I_4) afforded crude II_4; 680 mg (53%). The crude material was recrystallized twice from acetone - benzene to yield pure II_4 as fine pale yellow crystals; mp 172°C (dec.).

Found: C, 95.90; H, 4.07%. Calcd for $C_{28}H_{14}$: C, 95.97; H, 4.03%.

2-Acetylnaphthalene (XV'). A solution of 2-naphthoic acid chloride (190 g, 1 mol) in benzene (500 m*l*) was added, drop by drop, to a solution of ethoxymagnesiomalonate [prepared from magnesium (44.3 g, 1.7 g atom), diethyl malonate (315.4 g, 1.7 mol), dry ethanol (156.4 g, 3.4 mol) and dry benzene (500 m*l*). The excess of the ethanol was removed by azeotropic distillation with benzene] in benzene (500 m*l*) at 20°C, and then the mixture was refluxed for 3.5 hr. Aqueous sulfuric acid (concentrated sulfuric acid 50 m*l*, water 350 m*l*) was added, drop by drop, to the mixture under cooling. The organic layer separated was washed with water and dried (magnesium sulfate). The crude keto-malonate obtained by evaporating the solvent *in vacuo* was mixed with propionic acid (500 m*l*) and concentrated sulfuric acid (5 m*l*), and the mixture was gradually heated. After 2 hr refluxing, 4N sulfuric acid (500 m*l*) was added and the mixture was refluxed for a further 6 hr. The organic layer was separated after the addition of water, and the aqueous layer was extracted with benzene. The combined benzene layer was washed successively with aqueous sodium hydroxide and with water, and then dried. The residue obtained by removing the solvent under reduced pressure was distilled *in vacuo*, thus affording XV'; 128 g (75%); bp 120—123°C/3 mmHg, mp 52—54°C. [lit. value: mp 53°C[14]].

2-Ethynylnaphthalene (XVI'). The methyl ketone (XV', 68 g, 0.4 mol) was converted to XVI' (32 g (52%), mp 40.5—41.5°C) according to the method used in the preparation of XVI.

Found: C, 94.82; H, 5.41%. Calcd for $C_{12}H_8$: C, 94.70; H, 5.30%.

3-(2-Naphthyl)-prop-2-ynal (XVII'). According to the procedure used in the synthesis of XVII, the 2-ethynyl compound (XVI', 30 g, 0.198 mol) gave XVII' (25 g (70%)). Recrystallization from cyclohexane - ether (2 : 1) afforded pure XVII' as colorless leaflets; mp 52—53°C.

Found: C, 86.77; H, 4.50%. Calcd for $C_{13}H_8O$: C, 86.65; H, 4.48%.

1-(2-Naphthyl)-1,4-pentadiyne-3-ol (XVIII'). The procedure used in the case of XVIII was followed. XVII' (9.4 g, 0.052 mol) gave XVIII' (7.0 g (65%)). This was then recrystallized from cyclohexane - benzene (1 : 1) to give pure XVIII'; mp 91—92°C.

Found: C, 87.25; H, 4.93%. Calcd for $C_{15}H_{10}O$: C, 87.35; H, 4.89%. IR (KBr-disk): 3290 (≡CH), 2110, 2230 (C≡C), 1000—1040 (C–O) cm^{-1}.

1,10-Di(2-naphthyl)-1,4,6,9-decatetrayne-3,8-diol (XIX'). The oxidative coupling used in the synthesis of XIX was applied to XVIII' (3.1 g, 0.015 mol), thus yielding XIX', 1.4 g (45%). An analytical specimen was obtained by recrystallizing the crystals 3 times from benzene; fine needles; mp 150°C (dec.).

Found: C, 87.91; H, 4.60%. Calcd for $C_{30}H_{18}O_2$: C, 87.78; H, 4.42%. IR (KBr-disk): 3200—3300 (OH), 2220 (C≡C), 1000—1030 (C–O) cm^{-1}.

2,2'-Dinaphthylpentaacetylene (II_5). The same reaction sequence under the same reaction conditions as were used in the synthesis of I_5 from XIX were employed. The tetraacetylene glycol (XIX', 0.5 g, 1.2 mmol) gave 110 mg of II_5 (22% based on XIX'). Pure II_5, mp 180°C (dec.). Yellow needles were obtained by recrystallizing the crystals twice from benzene.

Found: C, 96.27; H, 3.82%. Calcd for $C_{30}H_{14}$: C, 96.23; H, 3.77%.

1-(2-Naphthyl)-1,4-hexadiyne-3,6-diol (XXI'). The reaction of the Grignard derivative of propargyl alcohol with the aldehyde (XVII', 8.0 g, 0.044 mol) according to the method used in the preparation of XXI afforded XXI'; 6.0 g (58%). This was recrystallized from benzene - ethanol to yield pure XXI'; mp 126—127°C; fine needles.

Found: C, 81.45; H, 5.15%. Calcd for $C_{16}H_{12}O_2$: C, 81.34; H, 5.12%. IR (KBr-disk): 3200—3400 (OH, ≡CH), 2200 (C–C), 1010—1035 (C≡O) cm^{-1}.

2,2'-Dinaphthylhexaacetylene (II_6). *The Preparation of 1-(2-Naphthyl)-1,3,5-hexatriyne (XXIII').* According to the procedure described in the case of XXIII, the diacetylenic glycol (XXI', 2.7 g, 0.0113 mol) was converted to the dichloride (XXII') and dehydrochlorinated to yield the triacetylene (XXIII'). Because of the unstable nature of XXIII', the petroleum benzine solution of the crude XXIII' was immediately used in the following reaction. UV (measured with an uncertain concentration in petroleum benzine): λ_{max} 339, 318, 296 and 285 mμ.

The Oxidative Coupling of XXIII'. The oxidative coupling of the above-mentioned crude XXIII' according to the procedure used in the synthesis of I_6 gave 120 mg of II_6 (11% based on XXI'). This was recrystallized 3 times from benzene to give pure II_6 as orange yellow needles; mp 200°C (dec.).

Found: C, 96.25; H, 3.51%. Calcd for $C_{32}H_{14}$: C, 95.46; H, 3.54%.

14) T. Immediata and A. R. Day, *J. Org. Chem.*, **5**, 516 (1940).

BULLETIN OF THE CHEMICAL SOCIETY OF JAPAN VOL. 43 3577—3581 (1970)

Aminocyclitols. XXIV. Synthesis of Inosamines from Bromodeoxyinositols

Tetsuo SUAMI, Seiichiro OGAWA and Masaru UCHIDA

Department of Applied Chemistry, Faculty of Engineering, Keio University, Koganei-shi, Tokyo

(Received June 16, 1970)

Seven inosamines (*scyllo*, *chiro*-1, *myo*-2, *myo*-4, *allo*-5, *neo*-1 and *chiro*-3) have been prepared from four bromodeoxyinositols (*scyllo*, *chiro*-1, *allo*-5 and *neo*-1). When bromodeoxyinositols were treated with sodium azide in boiling aqueous 2-methoxyethanol or dimethylformamide, followed by acetylation, pentaacetyl azidodeoxyinositols were obtained in 60—80% yield. On catalytic hydrogenation using Adams' platinum oxide, the azido compounds yielded hexaacetyl inosamines in good yields. Proton magnetic resonance (PMR) spectra of acetyl azidodeoxyinositols have been studied.

In the course of synthetic studies on aminocyclitols derivatives,[1] it has been recognized that some derivatives showed remarkable biological activities against certain bacteria and Hela cells. Therefore, these findings led us to further investigations of a convenient synthesis of inosamines from a readily accessible material.

Wolfrom and his co-workers[2] have first succeeded

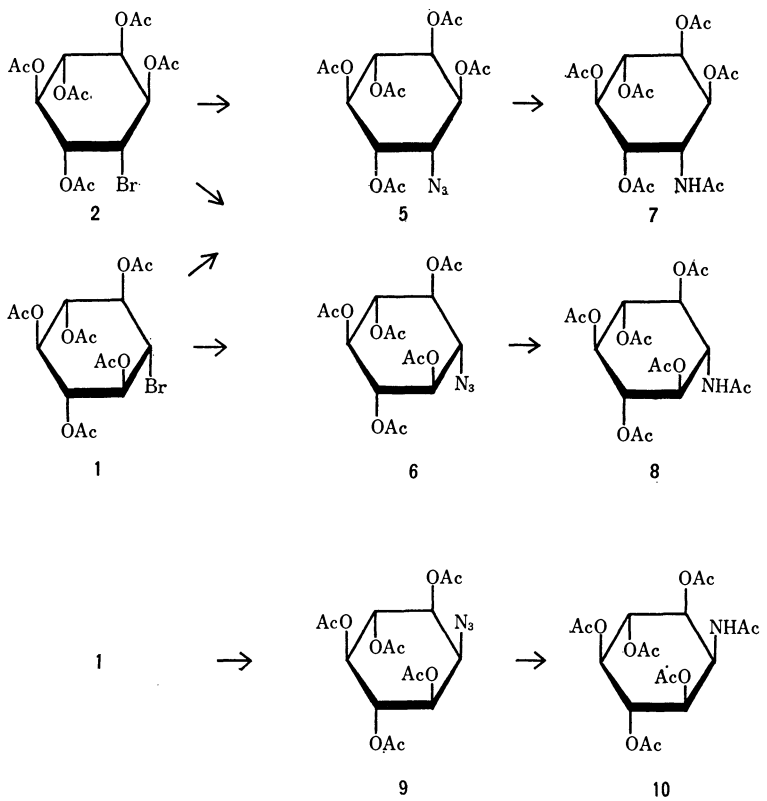

Fig. 1.

1) T. Suami, Y. Sato, Y. Fukai and Y. Sakota, *J. Heterocycl. Chem.*, **6**, 663 (1969); T. Suami and T. Machinami, This Bulletin, **43**, 2953 (1970).

2) M. L. Wolfrom, J. Radell, R. M. Husband and G. E. McCasland, *J. Amer. Chem. Soc.*, **79**, 160 (1957).

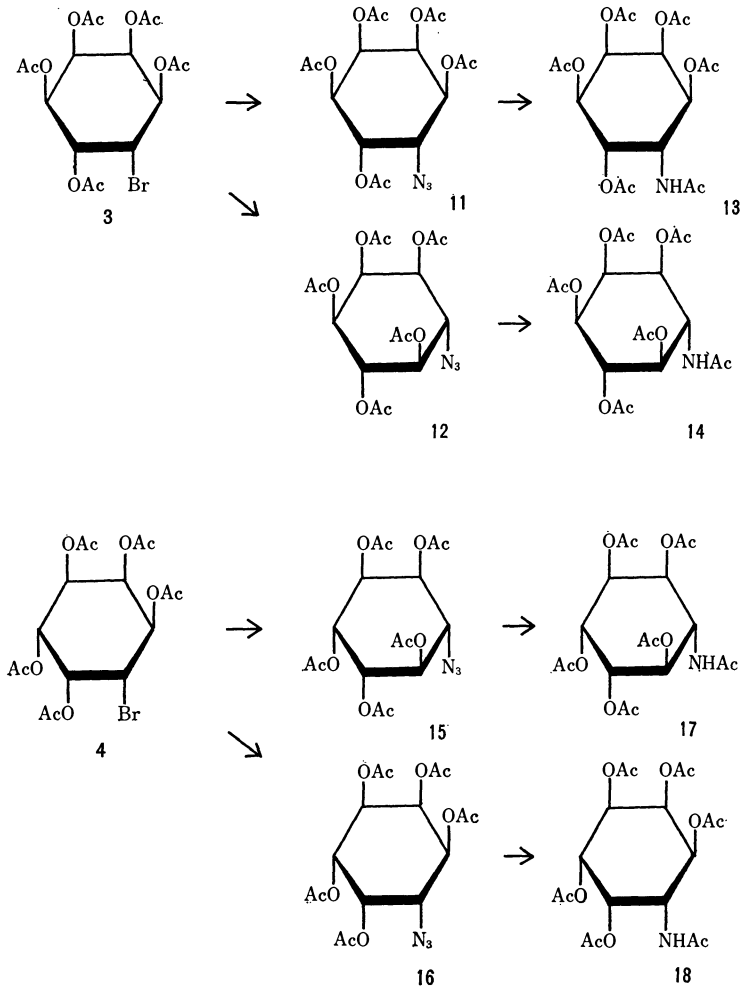

Fig. 2

in converting bromodeoxyinositols to aminodeoxyinositols (inosamines) by heating with ammonia in a sealed tube. By such treatment of crude pentaacetyl 1-bromo-1-deoxy-*scyllo*-inositol (**1**), though in a small yield, two inosamines could be isolated and the structures were proposed by the reaction sequence.

Later, we have reported that 2,4-dibromo-2,4-dideoxy-*chiro*-inosamine-3, on treatment with sodium azide, followed by hydrogenation, gave rise to two inosadiamines in a comparatively good yield.[3] Also, Nakajima and his co-workers[4] have described the synthesis of streptamine from dibromodideoxyinositol by the similar procedure.

The present article reports a facile synthesis of inosamines from readily available bromodeoxyinositols.

According to a modified method of McCasland,[5] two bromodeoxyinositols: **1** and pentaacetyl 1-bromo-1-deoxy-*chiro*-inositol (**2**) were prepared by drastic bromination of *myo*-inositol with acetyl bromide and acetic anhydride at 130—140°C. Analogously, pentaacetyl 5-bromo-5-deoxy-*allo*-inositol (**3**) and 1-bromo-1-deoxy-*neo*-inositol (**4**) were obtained from *epi*-inositol.[6,7]

When **1** was refluxed with an excess amount of sodium azide in 90% aqueous 2-methoxyethanol for 50 hr and subsequently acetylated, an unknown pentaacetyl azidodeoxyinositol (**5**) was obtained together with pentaacetyl 1-azido-1-deoxy-*scyllo*-inositol (**6**)[8] in 64 and 12% yield, respectively.

3) T. Suami, S. Ogawa, Y. Nakashima and H. Sano, This Bulletin, **40**, 2958 (1967).

4) N. Kurihara, T. Kurokawa and M. Nakajima, *Agr. Biol. Chem.* (Tokyo), **31**, 1162 (1967).

5) G. E. McCasland and E. C. Horswill, *J. Amer. Chem. Soc.*, **75**, 4020 (1953).

6) G. E. McCasland and J. M. Reeves, *ibid.*, **77**, 1812 (1955).

7) T. Suami, A. Suzuki, M. Uchida and S. Yanagida, This Bulletin, **42**, 2672 (1969).

8) T. Suami, F. W. Lichtenthaler and S. Ogawa, *ibid.*, **39**, 170 (1966).

Also, on a similar treatment with sodium azide, **2** gave **5** and **6** in 67 and 6% yield, respectively.

The assignment of the structures of azidodeoxyinositols so obtained was carried out by a conversion to known inosamines, along with PMR spectra.

Hydrogenation of **5** using Adams' platinum oxide afforded hexaacetyl *chiro*-inosamine-1 (**7**)[2,9] in 76% yield. Then **5** could be assigned to be pentaacetyl 1-azido-1-deoxy-*chiro*-inositol. These result showed that the azidation reaction of **1** and **2** proceeded through a formation of a same acetoxonium ion intermediate and its preferential diaxial opening by an azide ion.

On the other hand, according to the preferred all equatorial conformation of **1**, it might be proposed that, if dipolar aprotic solvent was used as a reaction solvent, a direct S_N2 attack of azide ion would be possible. Analogous result had been observed in the case of the reaction of 1,3-di-*O*-acetyl-2-*O*-methanesulfonyl-1,2,3-cyclohexanetriol and sodium azide.[10]

Then the reaction of **1** and sodium azide was carried out in boiling aqueous dimethylformamide, instead of 2-methoxyethanol, and a successive acetylation of the reaction product yielded hitherto unknown pentaacetyl azidodeoxyinositol (**9**) in 61% yield. Hydrogenation of **9** gave hexaacetyl *myo*-inosamine-2 (**10**)[11] in 70% yield. Therefore, **9** could be assigned as pentaacetyl 2-azido-2-deoxy *myo*-inositol.

Compound **3**, by a similar treatment with sodium azide, gave pentaacetyl 5-azido-5-deoxy-*allo*-inositol (**11**) and pentaacetyl 4-azido-4-deoxy-*myo*-inositol (**12**) in 46 and 11% yield, respectively. On hydrogenation, **11** and **12** afforded corresponding hexaacetyl *allo*-inosamine-5 (**13**)[12] and hexaacetyl *myo*-inosamine-4 (**14**)[9,13] in 82 and 91% yield, respectively.

From **4**, pentaacetyl 3-azido-3-deoxy-*chiro*-inositol (**15**) and pentaacetyl 1-azido-1-deoxy-*neo*-inositol (**16**) were obtained by the analogous procedure in 68 and 10% yield, respectively. On hydrogenation, **15** and **16** gave corresponding hexaacetyl *chiro*-inosamine-3 (**17**)[9] and hexaacetyl *neo*-inosamine-1 (**18**)[12] in 78 and 68% yield, respectively.

Considering from the products obtained, the azidation reaction of **3** and **4** also proceeded through a formation of an acetoxonium ion intermediate.

PMR data for the pentaacetyl azidodeoxyinositols are given in Table 1. The signals of the equatorial

Table 1. PMR data of pentaacetyl azidodeoxyinositol[a]

Compound		>CHN$_3$	−OAc	
			axial	equatorial
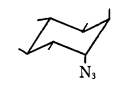	**5**	5.92 (m)[b]	7.83 (6)	7.90 (3) 7.96 (3) 8.00 (3) 8.03 (3)
	6	6.27[c]		7.92 (6) 8.02 (9)
	9	5.70 (t) J=3.0 Hz		7.91 (6) 8.01 (9)
	11[d]	5.87 (q) J=8.0 Hz 3.0 Hz	7.87 (3) 7.94 (6)	7.94 (3) 7.99 (3)
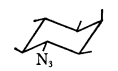	**12**	6.06 (t) J=10.0 Hz	7.82 (3)	7.90 (3) 7.94 (3) 8.00 (3) 8.02 (3)
	15	6.12 (t) J=10.5 Hz	7.84 (6)	7.90 (3) 7.95 (3) 8.02 (3)
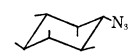	**16**	6.18 (q) J=11.0 Hz 3.0 Hz	7.87 (6)	7.96 (3) 8.04 (6)

—=—OAc

Table 2. PMR data of tetraacetyl diazidodideoxyinositol[a]

Compound		>CHN$_3$	-OAc	
			axial	equatorial
	19	6.36 (t)[b] J=9.5 Hz		7.80 (3) 7.90 (6) 7.99 (3)
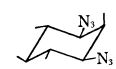	**20**	6.23 (q) J=9.0 Hz 3.0 Hz	7.81 (3)	7.93 (6) 7.98 (3)
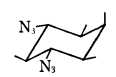	**21**[e]	6.16 (t) J=10.5 Hz	7.80 (3)	7.80 (3) 7.94 (6)

a) Chemical shifts are expressed in τ-values. Values in parenthesis show number of protons. First order coupling constants are expressed.

b) Abbreviations: m, multiplet; t, triplet; q, quartet.

c) Measurement is difficult, because of the poor solubility of **6** in $CDCl_3$.

d) It might be considered that, owing to the distortion of chair conformation, signals of the axial acetoxy groups are somewhat up-shifted and have the same chemical shifts as that of equatorial one does.

e) The PMR spectrum of hexaacetyl *myo*-inosadiamine-4,6, which was obtained by hydrogenation of **21**, showed four peaks at τ 8 region: τ 7.81 (3), 7.94 (3), 8.00 (6) and 8.10 (6). Therefore it is apparent that, in the PMR spectrum of **21**, the signal of equatorial acetoxy group on C-5 and that of axial one on C-2 overlap, because of the down-shift of the former.

9) M. Nakajima, N. Kurihara and A. Hasegawa, *Chem. Ber.*, **95**, 141 (1962).

10) T. Suami, F. W. Lichtenthaler and S. Ogawa, This Bulletin, **38**, 754 (1965).

11) H. E. Carter, R. K. Clark, Jr., B. Lytle and G. E. McCasland, *J. Biol. Chem.* (Tokyo), **175**, 683 (1948).

12) M. Nakajima, A. Hasegawa and N. Kurihara, *Chem. Ber.*, **95**, 2708 (1962).

13) H. Straube-Rieke, H. A. Lardy and L. Anderson, *J. Amer. Chem. Soc.*, **75**, 649 (1953).

acetoxy methyl groups adjacent to azido groups, which are either in an equatorial or an axial conformation, appeared at a region of τ 7.90—7.95 and whose chemical shifts are substantially in a down field (0.05—0.07 ppm in all cases studied) from those of equatorial ones which are adjacent to acetoxy or acetamide groups (τ 7.93—8.03[14]). This phenomenon is readily explained by a strong local magnetic field exerted by an azido group. In the case of tetraacetyl diazidodideoxyinositols listed in Table 2, the similar effect of azido groups on the chemical shifts of vicinal acetoxy groups is recognized. The signal of acetoxy methyl protons on C-5 in tetraacetyl 1,3-diazido-1,3-dideoxy-*scyllo*-inositol (**19**)[15] appears at τ 7.99, but those on C-4 and C-6 are down-shifted by 0.09 ppm (τ 7.90) and a signal of that on C-2 which are surrounded by two azido groups is considerably downshifted (τ 7.80). Similar results are also obtained in tetraacetyl 1,3-diazido-1,3-dideoxy-*myo*-inositol (**20**)[15] and tetraacetyl 4,6-diazido-4,6-dideoxy-*myo*-inositol (**21**).[16]

While, the signals of protons on carbon atoms bearing azido groups appeared at τ 6.06—6.36 (axial) and τ 5.70—5.90 (equatorial). Therefore, it may be possible to distinguish axial protons from equatorial ones by the differences of about 0.40 ppm. But the considerable down-shift effects on chemical shift of the axial proton are observed in the case of **11** by the possibility of serious distortion of the chair conformation or a long range deshielding effect of 1,3-diaxial acetoxy groups.

Experimental

The melting points were determined on a Mitamura Riken micro hot stage and are uncorrected. The PMR spectra were determined with a Japan Electron Optics Laboratory JNM-C-60 spectrometer or a Varian Associates A-60D spectrometer at the frequency of 60 MHz in deuteriochloroform with tetramethylsilane as an internal standard. Evaporations were accomplished under reduced pressure at 40—50°C with a Tokyo Rikakikai rotary evaporator.

Pentaacetyl 1-Bromo-1-deoxy-*scyllo*-inositol (1) and Pentaacetyl 1-Bromo-1-deoxy-*chiro*-inositol (2). These compounds were prepared from *myo*-inositol following a modified method of McCasland.[5]

Throughly dried *myo*-inositol (2.5 g) was treated with acetyl bromide (2.2 m*l*) and acetic anhydride (7.8 m*l*) in a sealed tube at 130—140°C for 8 hr. Then the reaction mixture was poured into ethanol (10 m*l*) and resulting precipitates were collected by filtration. Ten sealed tubes gave 37.5 g of crude **1**, mp 220—235°C. Two recrystallizations from ethylacetate and acetone afforded pure crystals of **1** (36.5 g), mp 238—240°C (lit,[5] mp 241—241.5°C). The yield was 29%. Then the mother liquor of **1** yielded crude **2** (39.0 g), mp 96—103°C, after allowing to stand at room temperature for several weeks. Three recrystallizations from ethanol gave practically pure **2** (31.4 g, 24.8%), mp 114—116°C (lit,[5] mp 124—125°C). (Found: C, 42.30; H, 4.79; Br, 17.79%).

Pentaacetyl 5-Bromo-5-deoxy-*allo*-inositol (3) and 1-Bromo-1-deoxy-*neo*-inositol (4). These compounds were prepared from *epi*-inositol following a modified method of McCasland.[6,7]

Pentaacetyl 1-Azido-1-deoxy-*chiro*-inositol (5) and Pentaacetyl 1-Azido-1-deoxy-*scyllo*-inositol (6). a) A mixture of **2** (2.0 g), sodium azide (1.5 g) and 90% aqueous 2-methoxyethanol (80 m*l*) was refluxed for 50 hr. Then the reaction mixture was evaporated to dryness and the residue was treated with a mixture of pyridine (20 m*l*) and acetic anhydride (20 m*l*) at room temperature overnight. An insoluble material was filtered off and the filtrate was evaporated to give a solid residue. The crude compound was recrystallized from ethanol to afford needles (110 mg, 6.3%), mp 206—207°C, which was identified with an authentic sample of **6** (lit,[8] mp 205—205.5°C) by mixed melting point and comparing with IR spectra. The second and third crops obtained from the mother liquor of **6** were combined and recrystallized from ethanol to give crystals (1.5 g, 66.8%) of **5**, mp 111—113°C. Analytical sample was obtained by recrystallization from methanol, mp 115.5—117°C.

Found: C, 46.18; H, 5.25; N, 10.33%. Calcd for $C_{16}H_{21}N_3O_{10}$: C, 46.26; H, 5.10; N, 10.12%.

b) A mixture of **1** (1.2 g), sodium azide (1.8 g) and 90% aqueous 2-methoxyethanol (30 m*l*) was refluxed for 64 hr. An insoluble material was filtered off and the filtrate was evaporated to dryness. The residue was dried by codistillation with toluene and then treated with a mixture of acetic anhydride (10 m*l*) and pyridine (10 m*l*) at 80°C for 2 hr. A filtered reaction mixture was poured into ice and water. An oily precipitate solidified gradually to give a white solid, which was collected by filtration. The crude product was fractionally crystallized from ethanol to yield **6** (0.12 g, 12%), mp 200—205°C. On evaporation, followed by trituration with methanol, the mother liquor afforded **5** (0.68 g, 64%), mp 110—113°C.

When **1** was treated with sodium azide similarly as described in (a), **5** was obtained only in 17% yield and **1** was recovered in 50% yield.

Hexaacetyl *chiro*-Inosamine-1 (7). A solution of **5** (270 mg) in ethanol (40 m*l*) was hydrogenated in the presence of Adams' platinum oxide (20 mg) in a Parr shaker type apparatus for 20 hr (at the initial hydrogen pressure of 3.4 kg/cm^2). The catalyst was filtered off and the filtrate was evaporated to dryness. The residue was treated with a mixture of acetic anhydride (5 m*l*) and pyridine (5 m*l*) at room temperature overnight. The reaction mixture was evaporated to give a solid residue, which was crystallized from ethyl acetate yielding 210 mg (76.2%) of **7**, mp 157—159°C (lit,[9] mp 156—157°C). **7** was identified with an authentic sample[9] by mixed melting point and IR spectra. (Found: C, 50.42; H, 6.17; N, 3.00%).

Hexaacetyl *scyllo*-Inosamine (8). A 67 mg portion of **6** was hydrogenated in a mixture of ethanol (30 m*l*) and dimethylformamide (10 m*l*) in the presence of

14) F. W. Lichtenthaler and P. Emig, *Carbohyd. Res.*, **7**, 121 (1968).

15) S. Ogawa, T. Abe, H. Sano, K. Kotera and T. Suami, This Bulletin, **40**, 2405 (1967).

16) T. Suami and S. Ogawa, *ibid.*, **38**, 2026 (1965).

Adams' platinum oxide (15 mg) for 20 hr. Filtering off the catalyst, the filtrate was evaporated to dryness and the residue was acetylated to give crude **8**, which was recrystallized from ethanol to afford needles (45 mg, 80.0%), mp 272—283°C with decomposition (lit,[2,11] mp 275—280°C). The product was identified with an authentic sample by mixed melting point and IR spectra.

Pentaacetyl 2-Azido-2-deoxy-*myo*-inositol (9). A mixture of **1** (2.0 g), sodium azide (1.5 g) and 90% aqueous dimethylformamide (80 m*l*) was refluxed for 25 hr. The reaction mixture was treated similarly as described in the preparation of **5** and **6**. The crude product was acetylated to give crude **9** (1.1 g), mp 200—210°C. Recrystallization from ethanol afforded needles (0.85 g, 61%), mp 207.5—209°C.

Found: C, 46.10; H, 5.26; N, 9.93%. Calcd for $C_{16}H_{21}N_3O_{10}$: C, 46.26; H, 5.10; N, 10.12%.

Hexaacetyl *myo*-Inosamine-2 (10). A solution of **9** (1.0 g) in 2-methoxyethanol (80 m*l*) was hydrogenated in the presence of Adams' platinum oxide (50 mg) for 20 hr. The hydrogenated product was acetylated to give crude **10** (0.81 g), mp 240—245°C. Recrystallization from ethanol afforded needles (0.76 g, 70%), mp 248—250°C (lit.[11] mp 242°C). (Found: C, 50.08; H, 6.06; N, 3.17%).

Pentaacetyl 5-Azido-5-deoxy-*allo*-inositol (11) and Pentaacetyl 4-Azido-4-deoxy-*myo*-inositol (12). A mixture of **3** (2.0 g), sodium azide (1.5 g) and 90% aqueous 2-methoxyethanol (60 m*l*) was refluxed for 20 hr. The reaction mixture was treated similarly as described in the preparation of **5** and **6**. The crude crystalline product was fractionally crystallized from ethanol to afford **11** (0.64 g, 46%), mp 129—130°C, and **12** (0.16 g, 11%), mp 147—150°C. Recrystallization of **11** from ethanol or methanol did not raise its melting point. Analytically pure **12** was obtained by recrystallization from methanol, mp 149—151°C.

11: Found: C, 46.40; H, 5.33; N, 9.80%.

12: Found: C, 46.30; H, 5.30; N, 10.03%.

Calcd for $C_{16}H_{21}N_3O_{10}$: C, 46.26; H, 5.10; N, 10.12%.

Hexaacetyl *allo*-Inosamine-5 (13). A 0.42 g portion of **11** was hydrogenated in the presence of Adams' platinum oxide (20 mg) in ethanol (50 m*l*) for 20 hr. The hydrogenated product was treated with acetic anhydride and pyridine at room temperature overnight. The crude product was crystallized from ethanol and ether to yield crude **13**, mp 180—196°C. Recrystallization from ethanol gave pure crystals (0.36 g, 82%), mp 195—196°C (lit,[12] mp 195°C). (Found: C, 50.50; H, 5.94; N, 3.47%).

Hexaacetyl *myo*-Inosamine-4 (14). A 0.10 g portion of **12** was hydrogenated in ethanol (50 m*l*) in the presence of Adams' platinum oxide (20 mg) for 12 hr. The hydrogenated product was treated with acetic anhydride and pyridine at room temperature overnight. The crude product was crystallized from ethanol to give **14** (95 mg, 91%), mp 228—236°C. Recrystallization from ethanol gave pure sample, mp 234—236°C (lit,[9] mp 236°C). The compound was identified with an authentic sample[9] by mixed melting point and IR spectra.

Pentaacetyl 3-Azido-3-deoxy-*chiro*-inositol (15) and Pentaacetyl 1-Azido-1-deoxy-*neo*-inositol (16). A mixture of **4** (1.0 g), sodium azide (1.0 g) and 90% aqueous 2-methoxyethanol (50 m*l*) was refluxed for 40 hr. The reaction mixture was treated similarly as described in the preparation of **5** and **6**. The crude crystals were fractionally crystallized from ethanol to afford **15** (1.2 g, 68%), mp 153—156°C, and **16** (0.17 g, 10%), mp 185—187°C.

15: Found: C, 46.66; H, 5.39; N, 10.37%.

16: Found: C, 46.85; H, 5.48; N, 10.11%.

Calcd for $C_{16}H_{21}N_3O_{10}$: C, 46.26; H, 5.10; N, 10.12%.

Hexaacetyl *chiro*-Inosamine-3 (17). A 0.55 g portion of **15** was hydrogenated in ethanol (50 m*l*) in the presence of Adams' platinum oxide (20 mg) for 5 hr. The hydrogenated product was acetylated to give crude **17**, which was crystallized from ethanol and ether to afford crystals (0.39 g, 78%), mp 184—187°C. Recrystallization from the same solvent gave a pure sample, mp 186—188°C (lit,[9] mp 189—191°C). (Found: C, 50.35; H, 5.70; N, 3.40%).

Hexaacetyl *neo*-Inosamine-1 (18). A 0.10 g portion of **16** was hydrogenated in ethanol (50 m*l*) in the presence of Adams' platinum oxide (20 mg) for 5 hr. The hydrogenated product was acetylated and crystallized from ethanol to give **18** (70 mg, 68%), mp 237—240°C (lit,[12] mp 240°C). (Found: C, 49.83; H, 5.87; N, 3.21%).

The authors wish to thank Professor Sumio Umezawa for his helpful advices and Mr. Saburo Nakada for his elementary analyses. This research has been financially supported by a grant of the Japanese Ministry of Education.

BULLETIN OF THE CHEMICAL SOCIETY OF JAPAN VOL. 43 3582—3587 (1970)

Quantum Yield of Photo-rearrangement of Nitrones

Kinko KOYANO and Hiroshi SUZUKI[1)]

Department of Chemistry, College of General Education, The University of Tokyo, Komaba, Meguro-ku, Tokyo

and Yuji MORI and Ikuzo TANAKA

Department of Chemistry, Tokyo Institute of Technology, Ohokayama, Meguro-ku, Tokyo

(Received July 1, 1970)

Fifteen nitrones, *N*-butylidenecyclohexylamine *N*-oxide, *N*-benzylidenemethylamine *N*-oxide, *N*-diphenylmethylenemethylamine *N*-oxide, *N*-benzylidenaniline *N*-oxide, and its derivatives, were irradiated with light in solution, each at its longest-wavelength absorption band. Each nitrone isomerized to the corresponding oxazirane. The quantum yield of this photo-rearrangement, Φ, was measured. For each nitrone, the value of Φ is larger in cyclohexane solution than in ethanol solution. In the series of *N*-benzylidenaniline *N*-oxide and its *para*-substituted derivatives, the substituent lowers Φ, and the more electron-donating or the more electron-withdrawing the substituent is, the smaller is Φ. These facts are explained on the basis of a hypothesis that Φ should increase with the change in the π-bond order between the carbon and oxygen atoms of the nitrone group upon the lowest-energy electron excitation, $\Delta P_{C,O}$, calculated by the simple MO method.

It has been reported that nitrones isomerize to oxaziranes by light absorption,[2-7)] while photosensitization by dye molecules results in the geometrical isomerization about the C=N bond.[7)]

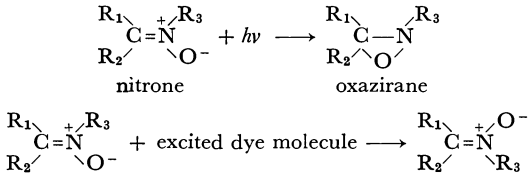

We have concluded previously that nitrone molecules in the lowest excited singlet state isomerize to the corresponding oxaziranes by oxygen atom rearrangement and that nitrone molecules excited to a triplet state as a result of energy transfer from triplet dye molecules undergo the *cis-trans* isomerization.[6,7)]

In the present paper it is elucidated how the groups R affect the quantum yield of the photochemical nitrone→oxazirane rearrangement.

Experimental

The nitrones used in this work are as follows: *N*-butylidenecyclohexylamine *N*-oxide (I), *N*-benzylidenemethylamine *N*-oxide (II), *N*-diphenylmethylenemethylamine *N*-oxide (α-phenyl-II), *N*-benzylidenaniline *N*-oxide (α,*N*-diphenylnitrone, III; see Fig. 1), and its

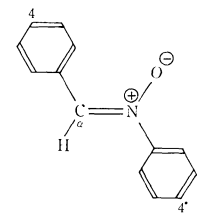

Fig. 1. α,*N*-Diphenylnitrone (*N*-benzylidenaniline *N*-oxide).

derivatives, which are listed in Table 1 and are hereafter referred to with the entry numbers in this table. The synthesis and some physical properties of the nitrones except 1, 3, 5, and 15[8)] were described in previous papers.[9,10)]

1) To whom any correspondence should be addressed.

2) M. J. Kamlet and L. A. Kaplan, *J. Org. Chem.*, **22**, 576 (1957).

3) J. Splitter and M. Calvin, *ibid.*, **23**, 651 (1958).

4) R. Bonnett, V. M. Clark and A. Todd, *J. Chem. Soc.*, **1959**, 2102.

5) L. S. Kaminsky and M. Lamchen, *Chem. Commun.*, **1965**, 130; *J. Chem. Soc., C*, **1966**, 2295; M. Lamchen and T. W. Mittag, *ibid.*, **1968**, 1917.

6) K. Shinzawa and I. Tanaka, *J. Phys. Chem.*, **68**, 1205 (1964).

7) K. Koyano and I. Tanaka, *ibid.*, **69**, 2545 (1965).

8) The authors are indebted to Dr. T. Kubota of Shionogi Research Laboratory, Shionogi and Co., Ltd. for kindly supplying the specimens of nitrons 3 (mp 106.5—108°C) and 5 (mp 221—222°C). Nitrone 1 (mp 34°C) was synthesized by the usual method,[10)] and nitrone 15 (mp 216—217°C) was prepared by following the procedure described by F. Barrow and E. D. Griffiths (*J. Chem. Soc.*, **119**, 212 (1921)).

9) K. Koyano and H. Suzuki, *Tetrahedron Lett.*, **1968**, 1859.

10) K. Koyano and H. Suzuki, This Bulletin, **42**, 3306 (1969).

Ultraviolet absorption spectra were measured with a Hitachi Spectrophotometer EPS2U at room temperature. Cyclohexane and ethanol were used as solvents. Cyclohexane was purified by being passed through silica gel and distilled. Ethanol of guaranteed reagent grade was used without further purification.

The procedure of the irradiation experiment is quite similar to that described in a previous paper.[6] Three different light sources were used: (a) a 253.7 nm light source, a low pressure mercury lamp without filter; (b) a 313.0 nm light source, a high pressure mercury lamp with a combination of filters of cobalt - nickel sulfate solution and a glass which completely absorbs light below 300 nm; (c) a 365.0 nm light source, a high pressure mercury lamp with a combination of filters of Toshiba UVD1 and a glass. For each nitrone the light source was selected so that the light was absorbed by the nitrone at its longest-wavelength absorption band. The irradiation was carried out at room temperature. The intensity of the incident light was measured by potassium ferrioxalate actinometry.[11] The ratio of the decrease in the number of nitrone molecules to the number of photons absorbed was taken as the quantum yield of the photo-rearrangement.

Results and Discussion

Absorption Spectra and the Quantum Yield. The ultraviolet absorption spectra of the nitrones in solution changed markedly on irradiation, as exemplified by Fig. 2. The products are considered to be oxaziranes since their absorption bands appear at much shorter wavelength than those of the nitrones, indicating the break of the π bond between the α-carbon and the nitrogen atom. The formation of oxaziranes from nitrones 2, 3, 4, and 5 was confirmed by the fact that the products liberated iodine from acid solution of potassium iodide.[12,13]

In Table 1 are listed the values of the wavenumber (ν_{max}) and molar extinction coefficient (ε_{max}) at the peak of the longest-wavelength absorption bands of the nitrones, the quantum yield of the photo-rearrangement (Φ), and the wavelength at the peak of the absorption bands of the products (λ_{max}). There are some correlations between ν_{max} and Φ as follows.

(i) The values of Φ for the nitrones except 11 are larger in cyclohexane solution than in ethanol solution, and the values of ν_{max} for most of the nitrones are smaller in cyclohexane solution than in ethanol solution.

(ii) The values of Φ and ν_{max} for nitrone 1 are larger than the corresponding values for the other nitrones. In each solvent, a nitrone having a higher ν_{max} value has a larger Φ value than does a nitrone having a lower ν_{max} value. There seems to be no clear relation between ε_{max} and Φ. The introduction of the second phenyl group to the α-carbon atom decreases the value of ε_{max} to about a half, but

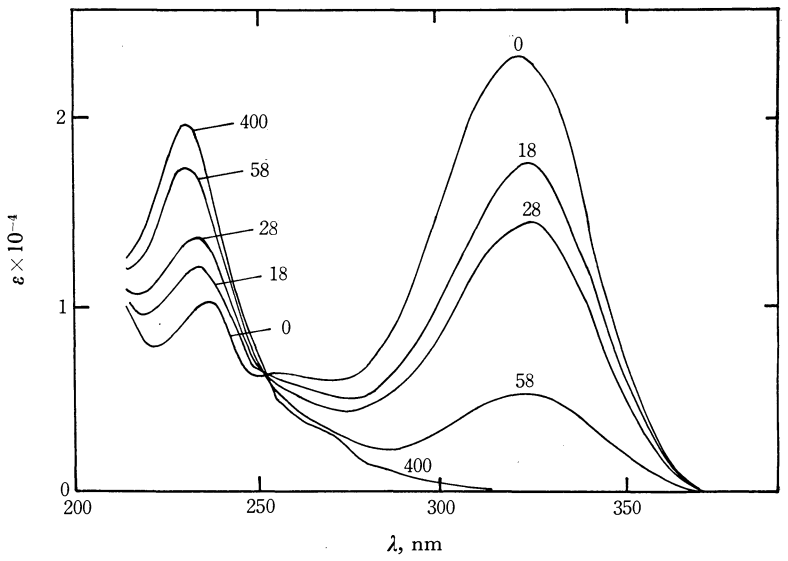

Fig. 2. The electronic absorption spectrum of *N*-(*p*-chlorobenzylidene)-aniline *N*-oxide (nitrone 7) in ethanol at room temperature and its change caused by irradiation with 313 nm light. The numbers represent the irradiation time in seconds.

11) C. A. Parker, *Proc. Roy. Soc.* (London), **220A**, 104 (1953).

12) The oxaziranes were so unstable that they could not be isolated.

13) S. Siggia, "Quantitative Organic Analysis *via* Functional Groups," John Wiley and Sons, Inc., New York (1949), p. 100.

TABLE 1. THE FIRST ABSORPTION MAXIMA OF NITRONES, THE QUANTUM YIELDS OF THE PHOTO-REARRANGEMENT OF THE NITRONES, AND THE ABSORPTION MAXIMA OF THE PRODUCTS

No.	Nitrone[a]	Absorption maximum				Quantum yield		Product	
		In Cy[b]		In Et[b]		In Cy[b]	In Et[b]	In Cy[b]	In Et[b]
		ν_{max} kK	ε_{max} $\times 10^{-4}$	ν_{max} kK	ε_{max} $\times 10^{-4}$			λ_{max} nm	λ_{max} nm
1	I	40.5	0.81	42.5	0.87	0.49[c]	0.42[c]	<210	<210
2	II	33.4	1.90	34.3	1.89	0.49[d]	0.36[d]	<210	<210
3	α-Phenyl-II	32.7	0.72	34.1	0.67	0.48[d]	0.33[d]	<210	<210
4	III	31.3	1.86	31.8	2.07	0.52[d]	0.36[d]	<220	<220
5	α-Phenyl-III	31.3	1.17	32.1	1.13	0.40[d]	0.24[d]	<210	<210
6	4-Methyl-III	30.6	2.10	31.4	2.35	0.43[d]	0.35[d]	229	229
7	4-Chloro-III	30.6	2.22	31.2	2.34	0.23[d]	0.24[d]	232.5	231
8	4-Bromo-III	30.4	2.32	31.0	2.44	0.25[d]	0.22[d]	237	236
9	4-Hydroxy-III	30.0[f]	2.00[f]	29.9	2.49		0.03[e]		241
10	4-Methoxy-III	29.9	2.11	30.2	2.41	0.16[e]	0.11[e]	240	239
11	4-Dimethylamino-III	26.9	2.40	26.0	3.21	0.13[e]	0.16[e]	274	269
12	4-Cyano-III	29.7	2.73	30.2	2.68	0.50[d]	0.34[d]	236.7	236.5
13	4-Methoxycarbonyl-III	29.5	2.62	30.2	2.75	0.39[d]	0.28[d]	240	240
14	4-Nitro-III	27.6	1.76	28.1	1.95	0.19[e]	0.09[e]	261	265
15	4-Nitro-4′-dimethylamino-III			23.5	2.12		0.01[e]		261

a) I, α-propyl-*N*-cyclohexylnitrone (*N*-butylidenecyclohexylamine *N*-oxide); II, α-phenyl-*N*-methylnitrone (*N*-benzylidenemethylamine *N*-oxide); III, α,*N*-diphenylnitrone (*N*-benzylidenaniline *N*-oxide).
b) Cy, cyclohexane; Et, ethanol.
c) Irradiated with 253.7 nm light.
d) Irradiated with 313.0 nm light.
e) Irradiated with 365.0 nm light.
f) In benzene.

does the values of Φ only slightly. (Compare nitrones 3 and 5 with 2 and 4, respectively.)

(iii) The value of Φ and ν_{max} for α,*N*-diphenylnitrone (nitrone 4) are larger than those for the 4-substituted derivatives (nitrones 6—15). In the case where the substituent is electron-donating, the more electron-donating the substituent is, the smaller are the values of Φ and ν_{max}. Thus, the decreasing order of Φ and ν_{max} is $CH_3 > Cl \approx Br > CH_3O > (CH_3)_2N$, and this is in accordance with the increasing order of the absolute value of the Hammett σ constant. In the case where the substituent is electron-withdrawing, the values of Φ and ν_{max} decrease in the order $CN > CH_3COO > NO_2$. This order is the increasing order of the electron-withdrawing property of the substituent, that is, the increasing order of the Hammett σ constant. The values of Φ and ν_{max} for nitrone 15 are the lowest of all. The relation between Φ and ν_{max} is shown in Fig. 3. From the fact that both the electron-donating and the electron-withdrawing substituents decrease Φ, it is evident that the reactivity of the nitrone group ($C{=}N^+{-}O^-$) can not be interpreted in terms of the polarity of the group or the electron density of the atoms involved.

Simple MO Calculation. The reactivity of nitrones can be elucidated in terms of simple molecular orbitals. The molecular orbitals of the nitrone group were calculated by the use of parameters $\alpha_C = \alpha + 0.5\beta$, $\alpha_N = \alpha + 1.6\beta$, $\alpha_O = \alpha + 1.2\beta$, and $\beta_{CN} = \beta_{NO} = \beta$. These parameter values are the values used by Kubota and Yamakawa in simple MO calculation on the π electron system of *N*-benzylidenalkylamine *N*-oxides, that is, the α-phenylnitrone π electron system.[14] The results are given in Table 2. In the ground state MO's ϕ_1 and

TABLE 2. THE SIMPLE MOLECULAR ORBITALS OF THE NITRONE GROUP ($C{=}\overset{+}{N}{-}\overset{-}{O}$)*

MO	Energy	Coefficients of AO's		
		C	N	O
ϕ_1	$\alpha + 2.7129\beta$	0.3527	0.7806	0.5159
ϕ_2	$\alpha + 0.8927\beta$	−0.5990	−0.2352	0.7654
ϕ_3	$\alpha - 0.3056\beta$	0.7188	−0.5791	0.3846

* The parameter values used: $\alpha_C = \alpha + 0.5\beta$, $\alpha_N = \alpha + 1.6\beta$, $\alpha_O = \alpha + 1.2\beta$, and $\beta_{CN} = \beta_{NO} = \beta$.

14) T. Kubota and M. Yamakawa, This Bulletin, **36**, 1564 (1963).

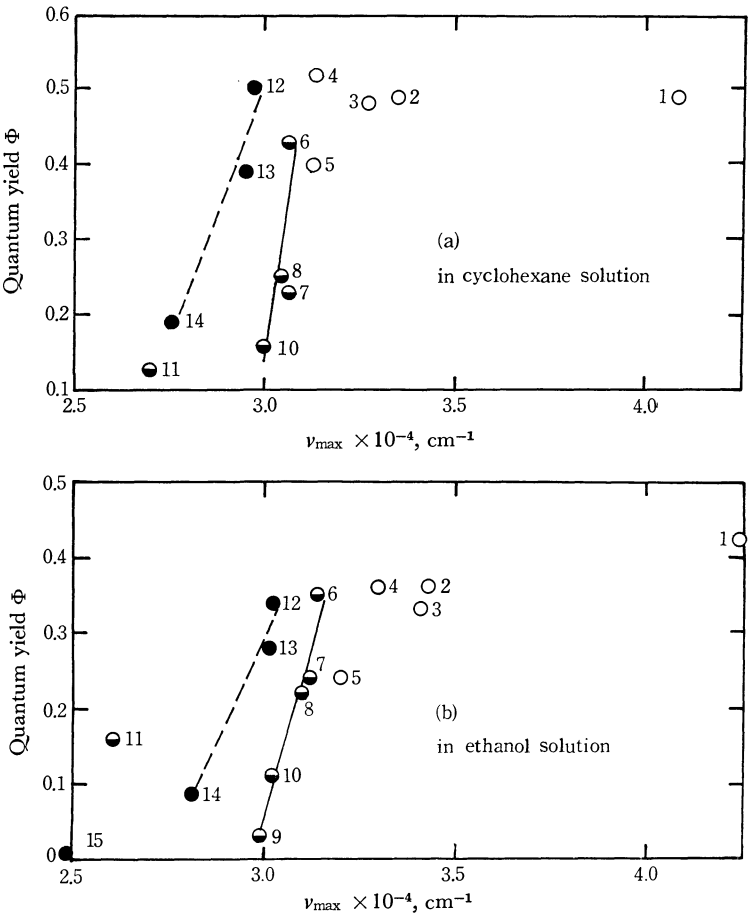

Fig. 3. The relation between Φ and ν_{max}: (a) in cyclohexane; (b) in ethanol. ◒, for 4-X-α,*N*-diphenylnitrones in which X is an electron-donating substituent; ●, for those in which X is an electron-withdrawing substituent; ○, for the other nitrones. The numbers are the entry numbers of the nitrones in Table 1.

ϕ_2 are filled with electrons.

The π-bond order of the C=N bond, P_{CN}, is calculated to be 0.832 in the ground state and 0.275 in the excited state where one electron has been excited from ϕ_2 to ϕ_3. The π-bond order of the N–O bond, P_{NO}, is 0.445 in the ground state and 0.403 in the excited state. The π-bond order of the hypothetical bond between the chemically non-bonded carbon and oxygen atoms, $P_{C,O}$, is −0.553 in the ground state and 0.182 in the excited state. Thus, on the excitation, P_{CN} decreases largely, P_{NO} decreases slightly, and $P_{C,O}$ increases largely. This tendency remains unchanged when the values of parameters α_N and α_O are changed in the ranges between $\alpha+1.5\beta$ and $\alpha+3.0\beta$ and between $\alpha+1.0\beta$ and $\alpha+2.0\beta$, respectively. The photo-rearrangement of nitrones to oxaziranes is safely interpreted as the result of the decrease in bonding character of the C=N bond and the large increase in bonding character of the hypothetical C···O bond caused by light absorption.

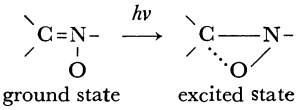

Correlation of the Quantum Yield with the Change in the π-Bond Order. The longest-wavelength absorption bands of the nitrones are attributed approximately to the one-electron excitation from the highest occupied π orbital to the lowest vacant one. The energy of this excitation is denoted by ΔE, and the changes in the π-bond orders associated with this excitation are denoted by ΔP. The effects of solvent and substituent on Φ can be interpreted in terms of the change in the $\Delta P_{C,O}$ value, and those on ν_{max} can be interpreted in terms of the change in the ΔE value.

(a) As the value of α_O becomes negatively arger, the value of $\Delta P_{C,O}$ decreases and the value

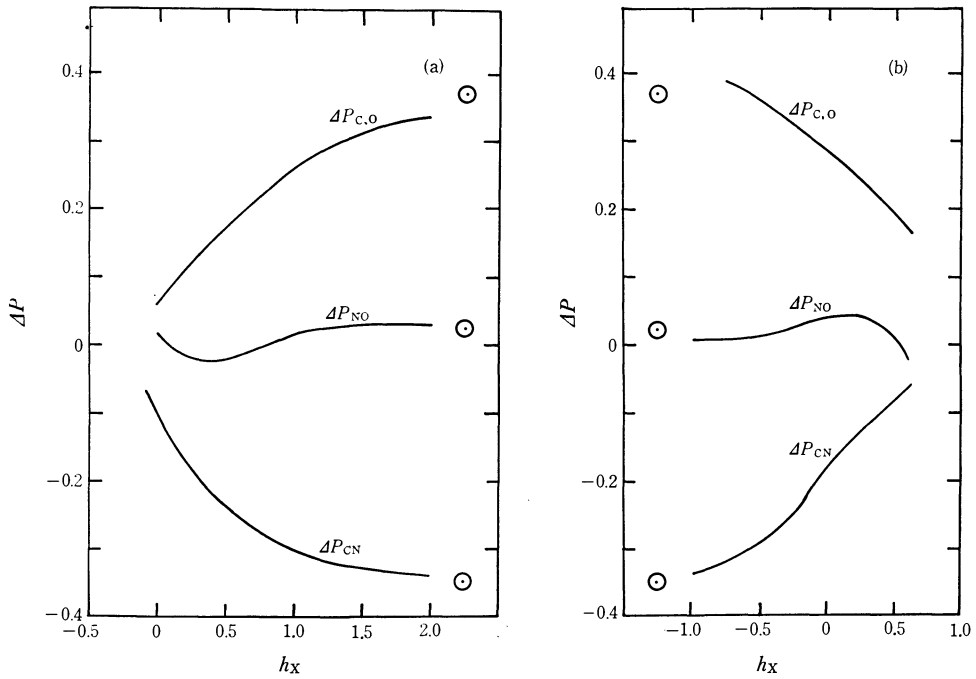

Fig. 4. The relations between ΔP's and h_X in the 4-X-α,N-diphenylnitrone π electron system: (a) in the case where X is an electron-donating substituent; (b) in the case where X is an electron-withdrawing substituent. The marks ⊙ represent ΔP's for the unperturbed α,N-diphenylnitrone π electron system.

of ΔE increases. The formation of a hydrogen bond has been found between the solvent alcohol and nitrone molecules, the oxygen atom of the nitrone group acting as a proton acceptor.[15] The value of the Coulomb integral for a hydrogen-bonding oxygen atom should be larger than that for a non-hydrogen-bonding oxygen atom. This can interpret well the solvent effects on Φ and ν_{max}.

The possible increase in the energy dissipation rate due to hydrogen bond formation in ethanol solution may also decrease the quantum yield.

(b) The simple molecular orbitals were calculated for the 4-X-α,N-diphenylnitrone π electron system by using various values for parameter h_x in the Coulomb integral of the substituent X, $\alpha_x = \alpha + h_x\beta$. In the case where X is an electron-donating substituent, 18 electrons participate in the π electron system, and the lowest-energy-electron excitation takes place from the 9th to the 10th orbital. In this case a smaller value of h_x correponds to a stronger electron-donating power of X. On the other hand, in the case where X is electron-withdrawing, it is assumed that 16 electrons participate in the π electron system. In this case, the lowest-energy electron excitation takes place from the 8th to the 9th orbital, and a larger value of h_x cor-

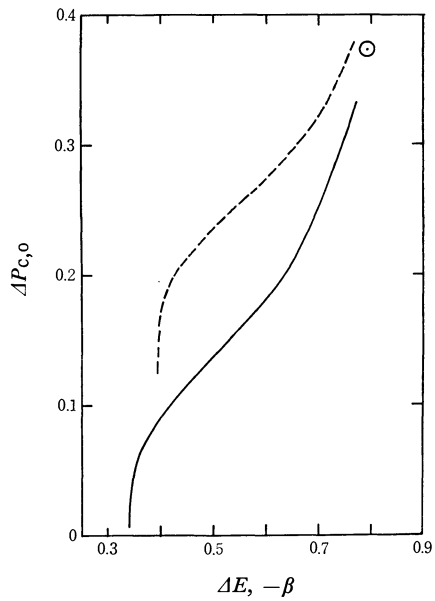

Fig. 5. The relation between $\Delta P_{C,O}$ and ΔE in the 4-X-α,N-diphenylnitrone π electron system. The solid line represents the relation in the case where X is electron-donating, and the broken line represents the relation in the case where X is electron-withdrawing. The mark ⊙ is for the case where X is absent.

15) T. Kubota, M. Yamakawa and Y. Mori, This Bulletin, **36**, 1552 (1963).

responds to a stronger electron-withdrawing power of X.

The relations between ΔP's and h_x are shown in Fig. 4.[16] As is seen in this figure, the value of $\Delta P_{C,O}$, which is positive in the range shown in the figure, is almost at its maximum when X is absent, and decreases as the effect of X increases, whether it is electron-donating or electron-withdrawing. This explains well the effect of X on Φ.

The value of ΔE decreases as the value of h_x decreases when X is electron-donating, and as the value of h_x increases when X is electron-withdrawing. This means that the first absorption band should shift to longer wavelength as the 4-substituent becomes more electron-donating or more electron-withdrawing, in accordance with the observation. The relation between $\Delta P_{C,O}$ and ΔE is shown in Fig. 5. This relation corresponds to the relation between Φ and ν_{max} shown in Fig. 3.

In nitrone 15, which has an electron-donating substituent at the 4-position and an electron-withdrawing substituent at the 4′-position, both the values of $\Delta P_{C,O}$ and ΔE must be small.

(c) The variation in the value of Φ in the series of α,*N*-diphenylnitrone and its 4-substituted derivatives has so far been explained well by saying that the value of Φ decreases as the value of $\Delta P_{C,O}$ decreases. The values of $\Delta P_{C,O}$ for the α,*N*-diphenylnitrone, α-phenylnitrone, and nitrone group π electron systems are 0.370, 0.508, and 0.735, respectively. Therefore, the value of Φ would be expected to increase rapidly in this sequence. In fact, however, the values of Φ for nitrones 1 and 2 are not much different from the values for nitrone 4. Thus, in this series of nitrones, it appears that the value of Φ does not monotonously increase with the value of $\Delta P_{C,O}$, but approaches a limiting value of about 0.5. There seem to be some fast processes which deactivate excited nitrone molecules and thereby depress Φ.

16) The energies of the lowest vacant and highest occupied orbitals of α,*N*-diphenylnitrone are calculated to be $\alpha-0.1830\beta$ and $\alpha+0.6103\beta$, respectively. In Fig. 4, in the case where X is electron-donating (case a) values larger than -0.1830 were taken for h_x, and in the case where X is electron-withdrawing (case b) values smaller than 0.6103 were taken for h_x. The case a where the value of h_x is sufficiently large and the case b where the value of h_x is sufficiently small correspond to the case where the α,*N*-diphenylnitrone π electron system is not perturbed by the substituent X.

BULLETIN OF THE CHEMICAL SOCIETY OF JAPAN VOL. 43 3587—3590 (1970)

2*H*,5*H*-Triazolo[4,5-*d*]triazoles. A New Heteroaromatic System

Masayuki YOSHIDA, Akira MATSUMOTO and Osamu SIMAMURA

Department of Chemistry, Faculty of Science, Tokyo University, Hongo, Tokyo

(Received July 8, 1970)

2-Aryl-5-phenyltriazolo[4,5-*d*]triazoles and related compounds, a new heteroaromatic system, have been prepared from 4,5-diamino-2-phenyl-1,2,3-triazole. The meso-ionic character of the new ring system is discussed on the basis of proton NMR shifts.

Syntheses of 2,3,5,6-tetraaryl-1,2,4,5-tetraazapentalenes (I), meso-ionic heteroaromatics, have recently been described.[1] A further replacement of the ring carbon atoms by nitrogen may yield another stable azapentalene. This paper presents the synthesis of 2-aryl-5-phenyl-1,2,3,4,5,6-hexaazapentalenes (2-aryl-5-phenyltriazolo[4,5-*d*]triazoles, II: $R^1=C_6H_5$, $R^2=Ar$) and related compounds.

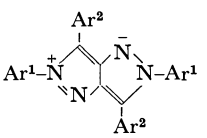

I

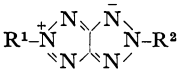

II: $R^1=C_6H_5$, $R^2=Ar$
XI: $R^1=C_6H_5$, $R^2=CH_3$
XII: $R^1=C_6H_5$, $R^2=$cyclo-C_6H_{11}
XIII: $R^1=R^2=$cyclo-C_6H_{11}

Condensation of 4,5-diamino-2-phenyl-1,2,3-triazole[2] (III) with nitrosobenzene in aqueous potassium hydroxide yielded 4-amino-2-phenyl-5-phenylazo-1,2,3-triazole, $C_{14}H_{12}N_6$ (IV, 72%), mp 206—208°C. Diazotization of the aminotriazole (IV) by means of sodium nitrite and hydrochloric acid followed by treatment with aqueous sodium azide precipitated 4-azido-2-phenyl-5-phenylazo-1,2,3-tri-

1) J. H. Lee, A. Matsumoto, O. Simamura and M. Yoshida, *Chem. Commun.*, **1969**, 1393.

2) J. Thiele and K. Schleussner, *Ann. Chem.*, **295**, 129 (1897).

azole, yellow needles, $C_{14}H_{10}N_8$ (V, 76%), which did not show any definite melting point owing to gradual decomposition on heating, the structure being confirmed on the basis of its IR spectrum (ν_{N_3} 2120 cm^{-1}) and analytical data. On being heated gently in decahydronaphthalene until nitrogen evolution ceased, it gave an almost quantitative yield of colorless leaflets, $C_{14}H_{10}N_6$, mp 249°C, sparingly soluble in ordinary organic solvents. This compound shows ultraviolet absorption maxima at 231 and 342 nm (log ε 4.1 and 4.6, respectively) in ethanol. The mass spectrum shows a molecular ion at 262, which was 53% of the base peak at 77. Thus, the compound was assigned the structure of 2,5-diphenyltriazolo[4,5-*d*]triazole (II: Ar=C_6H_5) on the ground of its mode of formation and of its spectral and analytical data.

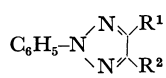

III: $R^1=R^2=NH_2$
IV: $R^1=C_6H_5N_2$, $R^2=NH_2$
V: $R^1=C_6H_5N_2$, $R^2=N_3$

The following triazolo[4,5-*d*]triazoles have been prepared in a similar way: II (Ar=*p*-$CH_3\cdot C_6H_4$), mp 233—234°C; II (Ar=*p*-$Cl\cdot C_6H_4$), mp 265.5—266.0°C; II (Ar=*p*-$(CH_3)_2N\cdot C_6H_4$), mp 285—286°C.

The parent structure underlying these compounds, 2*H*,5*H*-triazolo[4,5-*d*]triazole, comprises ten π-electrons distributed over the two rings and is satisfactorily represented only by the resonance of several charge-separated structures such as VI and VII, while its isomer, 1*H*,5*H*-triazolo[4,5-*d*]triazole, is represented by structure VIII without any charge-separation in the ground state. The effect of positive charge situated on positions 2 and 5 in derivatives of 2*H*,5*H*-isomer should be reflected in low field shift of proton NMR signals of substituents at positions 2 and 5. The following observations substantiate this view.

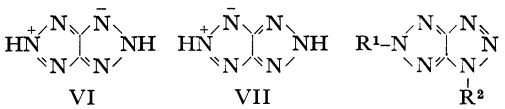

VI VII

VIII: $R^1=R^2=H$
IX: $R^1=C_6H_5$, $R^2=H$
X: $R^1=C_6H_5$, $R^2=CH_3$

Treatment of the silver salt of 5-phenyl-1*H*-triazolo[4,5-*d*]triazole[2] (IX) with excess of methyl iodide in boiling benzene afforded two mono-methylated products, $C_9H_8N_6$ (X, 51%), mp 139.2—139.8°C and $C_9H_8N_6$ (XI, 27%), mp 149.0—149.8°C. The NMR spectrum of X shows a sharp singlet at τ 5.72 (3H) and two multiplets centered at τ 2.54 (3H) and 1.87 (2H) corresponding to methyl and phenyl protons, respectively. The NMR spectrum of XI exhibits three signals at τ 5.47, 2.48 and 1.69 quite similar in appearance to those of X. The fact that the signals from XI are all shifted to lower field regions relative to the corresponding ones of X leads to the assignment of the structure of 2-methyl-5-phenyltriazolo[4,5-*d*]triazole to XI and that of 1-methyl-5-phenyltriazolo[4,5-*d*]triazole to X, because the low field shift is attributable to positive charges at positions 2 and 5 due to the meso-ionic structure of XI causing deshielding of the relevant protons, while such a charge is absent from structure VIII. Analogous deshielding of protons due to positive nature of nuclear positions is found in the methyl protons (τ 5.99) of 1,3-dimethylimidazolium iodide[3] in comparison with those (τ 6.33) of 1-methylimidazole.[4]

Catalytic hydrogenation of II (Ar=C_6H_5) with platinum oxide in acetic acid at room temperature gave two products without ring-opening, $C_{14}H_{16}N_6$ (XII, 30%), mp 128.5—129.5°C, and $C_{14}H_{22}N_6$ (XIII, 15%), mp 171.0—171.2°C. XII was assigned the structure of 2-cyclohexyl-5-phenyltriazolo-[4,5-*d*]triazole, and XIII, that of 2,5-dicyclohexyltriazolo[4,5-*d*]triazole on the basis of spectral and analytical data. The NMR shifts of these compounds are recorded in Experimental part; the phenyl protons and the methine protons in a cyclohexyl group are found shifted more or less to lower field regions than the usual positions, obviously because of the deshielding effect of the positively charged nitrogen at positions 2 and 5.

Experimental

4-Amino-2-phenyl-5-phenylazo-1,2,3-triazole (IV). To a suspension of 4,5-diamino-2-phenyl-1,2,3-triazole[2] (8.5 g) in a mixture of 5 m*l* of benzene and 85 m*l* of 50% sodium hydroxide solution heated at 60°C was added nitrosobenzene (5.1 g) in small portions over a period of 10 minutes. The mixture was stirred for a further 10 minutes at 60°C. On pouring it into 900 m*l* of water it gave 4-amino-2-phenyl-5-phenylazo-1,2,3-triazole as brownish red precipitate (9.5 g, 72%), mp 206—208°C (from benzene).

Found: C, 63.64; H, 4.34; N, 31.96%. Calcd for $C_{14}H_{12}N_6$: C, 63.62; H, 4.58; N, 31.80%.

4-Azido-2-phenyl-5-phenylazo-1,2,3-triazole (V). 4-Amino-2-phenyl-5-phenylazo-1,2,3-triazole (4.3 g) was dissolved by heating in 70 m*l* of concentrated hydrochloric acid. A slurry of the amine hydrochloride formed upon cooling was diluted with 14 m*l* of water and diazotized by addition of a solution of sodium nitrite (1.2 g) in 15 m*l* of water over a period of 30 min at 0—5°C. The mixture was stirred for an additional hour to complete the reaction at 0—5°C. The resulting diazonium solution was filtered to remove a small amount of insoluble material. A solution of sodium azide (1.5 g) in 20 m*l* of water was added to the filtrate over a period

3) C. G. Overberger, J. C. Salamone and S. Yaroslavsky, *J. Org. Chem.*, **30**, 3580 (1965).

4) G. S. Reddy, R. T. Hobgood, Jr., and J. H. Goldstein, *J. Amer. Chem. Soc.*, **84**, 336 (1962).

of 30 min at 0—5°C, during which violent nitrogen evolution was observed. Stirring was continued for 10 min to complete the reaction at 0—5°C. The yellow solid deposited was collected to yield 3.6 g of 4-azido-2-phenyl-5-phenylazo-1,2,3-triazole (76%). This crude material was carefully recrystallized from methanol to give yellow needles, which softened at 159—161°C, but changed to infusible white crystals at elevated temperatures.

Found: C, 58.05; H, 3.20; N, 38.47%. Calcd for $C_{14}H_{10}N_8$: C, 57.93; H, 3.47; N, 38.60%.

2,5-Diphenyltriazolo[4,5-*d*]triazole (II: Ar=C_6H_5). 4-Azido-2-phenyl-5-phenylazo-1,2,3-triazole (2.5 g) in 300 m*l* of decahydronaphthalene was heated gently at 105—115°C with stirring. After vigorous evolution of nitrogen had ceased, the temperature was raised to 160°C to complete the decomposition. The reaction mixture, upon cooling to room temperature, deposited crystals of 2,5-diphenyltriazolo[4,5-*d*]triazole, which were filtered off, and the filtrate was concentrated to 20 m*l* under reduced pressure to give a second crop. The total yield of the crude products was almost quantitative. The combined products were recrystallized three times from benzene (with active charcoal) to give 1.74 g of colorless leaflets, mp 249°C.

Found: C, 64.39; H, 3.84; N, 32.14%. Calcd for $C_{14}H_{10}N_6$: C, 64.11; H, 3.84; N, 32.05%.

2-Phenyl-5-*p*-tolyltriazolo[4,5-*d*]triazole (II: Ar=*p*-$CH_3\cdot C_6H_4$). This compound (Found: C, 65.04; H, 4.41; N, 30.50%. Calcd for $C_{15}H_{12}N_6$: C, 65.20; H, 4.38: N, 30.42%.), mp 233—234°C (from ligroin and benzene), was prepared from 4,5-diamino-2-phenyl-1,2,3-triazole and *p*-methylnitrosobenzene through 4-amino-2-phenyl-5-*p*-tolylazo-1,2,3-triazole, mp 208°C (Found: C, 64.88; H, 4.99; N, 30.26%. Calcd for $C_{15}H_{14}N_6$: C, 64.73; H, 5.03; N, 30.20%.), and 4-azido-2-phenyl-5-*p*-tolylazo-1,2,3-triazole, mp 115°C (dec.), in a way similar to the above.

5-*p*-Chlorophenyl-2-phenyltriazolo[4,5-*d*]triazole (II: Ar=*p*-Cl$\cdot C_6H_4$). This compound (Found: C, 56.90; H, 3.48; N, 29.12%. Calcd for $C_{14}H_9N_6Cl$: C, 56.67; H, 3.06; N, 28.32%.), mp 265.5—266.0°C (from benzene), was prepared from 4,5-diamino-2-phenyl-1,2,3-triazole and *p*-chloronitrosobenzene, through 4-amino-5-*p*-chlorophenylazo-2-phenyl-1,2,3-triazole, mp 239°C (Found: C, 56.21; H, 4.03; Cl, 11.18%. Calcd for $C_{14}H_{11}N_6Cl$: C, 56.28; H, 3.71; Cl, 11.53%.), and 4-azido-5-*p*-chlorophenylazo-2-phenyl-1,2,3-triazole, in a way similar to the above except for the preparation of the azidoazotriazole.

This azidoazotriazole was prepared as follows: 4-Amino-5-*p*-chlorophenylazo-2-phenyl-1,2,3-triazole (0.71 g) in 15 m*l* of concentrated sulphuric acid was added to a solution of sodium nitrite (0.195 g) in 10 m*l* of concentrated sulphuric acid over a period of 10 min at room temperature. The mixture was stirred for 20 min at room temperature and poured into a large amount of ice water. It was treated with sodium azide (0.20 g) and left at room temperature with stirring for an hour. 4-Azido-5-*p*-chlorophenylazo-2-phenyl-1,2,3-triazole was obtained as yellow precipitate (0.70 g, 91%), which did not show any definite melting point owing to gradual decomposition on heating. The infrared spectrum showed a peak at 2130 cm^{-1} corresponding to the azido stretching vibration.

5-Dimethylaminophenyl-2-phenyltriazolo[4,5-*d*]-triazole (II: Ar=*p*-$(CH_3)_2N\cdot C_6H_4$). 4-Amino-5-*p*-dimethylaminophenylazo-2-phenyl-1,2,3-triazole[2] was converted, as described for the preparation of II (Ar=C_6H_5), into 5-dimethylaminophenyl-2-phenyltriazolo-[4,5-*d*]triazole (Found: C, 62.88; H, 4.72; N, 32.29%. Calcd for $C_{16}H_{15}N_7$: C, 62.94; H, 4.95; N, 32.11%.), mp 285—286°C (from benzene and dioxane).

1-Methyl- and 2-Methyl-5-phenyltriazolo[4,5-*d*]-triazole (X and XI). 5-Phenyl-1*H*-triazolo[4,5-*d*]-triazole[2] (0.50 g) was dissolved in 10 m*l* of concentrated ammonium hydroxide and treated with a solution of silver nitrate (0.60 g) in 5 m*l* of concentrated ammonium hydroxide. The mixture was stirred for 10 min at room temperature and the pale yellow precipitate was collected and washed with water to yield 0.79 g of the silver salt of 5-phenyl-1*H*-triazolo[4,5-*d*]triazole (92%). The silver salt (0.77 g) was heated in a mixture of benzene (15 m*l*) and methyl iodide (1.5 m*l*) under reflux for 3 hr. On cooling, the supernatant solution was separated from precipitate by decantation and the residue was treated with benzene—methyl iodide solution twice more as above. Then, the precipitate was separated by filtration and washed with benzene. The combined benzene solutions gave 0.495 g of a light yellowish brown solid on evaporation of the solvent under reduced pressure. The crude material (0.20 g) was subjected to purification by preparative thin-layer chromatography on silica gel. After development with dichloromethane, the bands having R_f values of 0.24—0.36 and 0.37—0.44 were scraped off the plates and eluted with ethanol. Evaporation of the eluants gave 0.118 g of X (51%) and 0.064 g of XI (27%).

1-Methyl-5-phenyltriazolo[4,5-*d*]triazole (Found: C, 53.92; H, 3.78; N, 42.05%. Calcd for $C_9H_8N_6$: C, 53.99; H, 4.03; N, 41.98%.), X: mp 139.2—139.8°C (from ethanol); UV max. (ethanol) 299, 223 nm (log ε=4.33, 3.86, respectively).

2-Methyl-5-phenyltriazolo[4,5-*d*]triazole (Found: C, 54.11; H, 4.11; N, 41.89%. Calcd for $C_9H_8N_6$: C, 53.99; H, 4.03; N, 41.98%.), XI: mp 149.0—149.8°C (from ethanol); UV max. (ethanol) 301, 226 nm (log ε=4.40, 3.79, respectively).

Catalytic Hydrogenation of 2,5-Diphenyltriazolo-[4,5-*d*]triazole. 2,5-Diphenyltriazolo[4,5-*d*]triazole (0.99 g) in 250 m*l* of acetic acid was hydrogenated over platinum oxide (0.206 g) for 58 hr at room temperature. Insoluble starting material (0.125 g) was recovered by filtration. The filtrate was concentrated to 20 m*l* and poured into a large volume of water. The precipitate formed was filtered off to yield 0.615 g of colourless material. The crude material (0.13 g) was subjected to purification by preparative thin-layer chromatography on silica gel. After development with benzene, the bands having R_f values of 0.08—0.16, 0.18—0.32 and 0.35—0.52 were scraped off the plates and eluted with ethanol and chloroform and gave, on evaporation of the eluant, 0.022 g of 2,5-dicyclohexyltriazolo[4,5-*d*]triazole (XIII, 15%), 0.044 g of 2-cyclohexyl-5-phenyltriazolo[4,5-*d*]-triazole (XII, 30%) and 0.036 g of the starting material, respectively.

2-Cyclohexyl-5-phenyltriazolo[4,5-*d*]triazole (Found: C, 62.94; H, 5.95; N, 28.77%. Calcd for $C_{14}H_{16}N_6$: C, 62.67; H, 6.01; N, 31.32%.), XII: mp 128.5—129.5°C (from ethanol); UV max. (ethanol) 304, 216 nm (log ε=4.52, 3.93, respectively); NMR ($CDCl_3$) τ 8.27 (m, 10H, cyclohexyl *H*), 5.22 (broad s, 1H, methine *H*),

2.55 (m, 3H, phenyl *H*), 1.74 (m, 2H, phenyl *H*).

2,5-Dicyclohexyltriazolo[4,5-*d*]triazole (Found: C, 61.07; H, 8.33; N, 30.33%. Calcd for $C_{14}H_{22}N_6$: C, 61.29; H, 8.08; N, 30.63%.), XIII: mp 171.0—171.2°C (from ethanol); UV max. (ethanol) 258 nm (log ε=4.43); NMR ($CDCl_3$) τ 8.2 (m, 10H, cyclohexyl *H*), 5.4 (broad s, 1H, methine *H*).

BULLETIN OF THE CHEMICAL SOCIETY OF JAPAN VOL. 43 3590—3593 (1970)

Homolytic Aromatic Isopropyloxycarbonyloxylation Induced by Oxygen*1

Toshio NAKATA, Katsumi TOKUMARU and Osamu SIMAMURA

Department of Chemistry, Faculty of Science, The University of Tokyo, Hongo, Tokyo

(Received July 20, 1970)

Thermal decomposition of diisopropyl peroxydicarbonate in benzene was carried out at several temperatures ranging from 40 to 70°C under an atmosphere of nitrogen, air or oxygen; the presence of oxygen caused the production of isopropyl phenyl carbonate. For this aromatic isopropyloxycarbonyloxylation induced by oxygen, a mechanism is proposed, which involves reversible addition of an isopropyloxycarbonyloxy radical to an aromatic nucleus to give a cyclohexadienyl intermediate, followed by oxidation with oxygen to produce the carbonate ester. The reaction in a mixture of benzene and hexadeuteriobenzene showed isotope effects for the formation of the ester, $k_H/k_D=2.1$—2.3, thus supporting the reversibility of the addition step of the isopropyloxycarbonyloxy radical to benzene.

In a previous communication[1] we reported that the decomposition of benzoyl peroxide in aromatic solvents under oxygen resulted in the aromatic benzoyloxylation and proposed a mechanism, in which the reversible addition of a benzoyloxy radical to an aromatic nucleus takes place to give a benzoyloxycyclohexadienyl radical, followed by oxidation with molecular oxygen to afford aryl benzoate.

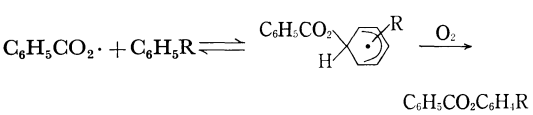

In order to obtain further evidence for this mechanism we have extended the study to other aromatic acyloxylation. Thermal decomposition of diisopropyl peroxydicarbonate in benzene under an atmosphere of nitrogen, oxygen or air was carried out, and the effect of temperature and the isotope effect, utilizing hexadeuteriobenzene, in the aromatic isopropyloxycarbonyloxylation induced by oxygen was examined.

Experimental

Materials. Commercial diisopropyl peroxydicarbonate (purchased from Nippon Oils and Fats Co., Ltd.; purity as determined by iodometric titration, 100%) was used without further purification. Thiophene-free benzene was dried over calcium chloride and fractionated through a Vigreux column. Hexadeuteriobenzene (supplied by Showa Denko Co., Ltd.) was used without further purification.

Gas Chromatography. Gas chromatographic analysis was carried out with a Perkin-Elmer 154D Vapour Fractometer. Isopropyl phenyl carbonate was determined with the use of a 2 m-column of 10% Apiezon M grease on Diasolid H (40 mesh) at 170°C or a 2 m-column of 10% HV DC Silicone grease on Diasolid H at 167°C with *p*-chloroanisole as an internal standard. A mixture of phenyl and phenyl-d_5 isopropyl carbonates was collected from reaction mixtures using the above-mentioned column of Silicone grease at 132°C, and subjected to mass spectrometric analysis.

Decomposition of Diisopropyl Peroxydicarbonate in Benzene. A solution of diisopropyl peroxydicarbonate (8 mmol) in benzene (300 m*l*) was placed in a three-necked flask, fitted with a stirrer, a thermometer, a gas inlet tube and a condenser. An appropriate gas (nitrogen, oxygen or air) after purification was bubbled through the solution to produce the desired atmosphere and the bubbling was continued during the whole reaction time. The flask was immersed in an oil bath maintained at a constant temperature (40—70±1°C). The peroxide was allowed to decompose completely and the reaction mixture was concentrated to 5—10 m*l* by distillation of benzene through a Vigreux

*1 Most part of this article was presented at the 21st (April, 1968, Osaka) and the 22nd (April, 1969, Tokyo) Annual Meetings of the Chemical Society of Japan.

1) T. Nakata, K. Tokumaru and O. Simamura, *Tetrahedron Lett.*, **1967**, 3303.

Table 1. Yield of isopropyl phenyl carbonate and carbon dioxide from decomposition of diisopropyl peroxydicarbonate in benzene[a] (In mol% of the peroxide)

Exp. No.	1	2[b]	3[b]	4	5	6	7	8	9
Reaction temp. (°C)	60	60	60	40	40	50	50	70	70
Atmosphere	N_2	O_2	Air	N_2	O_2	N_2	O_2	N_2	O_2
Reaction time (hr)	22	22	24	96	144	43	46	6.5	8
CO_2	183	136	—	185	65	186	111	184	181
i-PrOCOOPh	1	57	15	0.7	123	0.6	95	0.8	15
CO_2 group accounted for	184	193	—	186	188	187	206	185	196

a) Diisopropyl peroxydicarbonate (1.6 g) was allowed to decompose in benzene (300 m*l*).
b) Biphenyl (about 3%) was detected by VPC.

column on a water bath. The concentrated solution was subjected to gas chromatographic analysis to determine isopropyl phenyl carbonate. Determination of carbon dioxide was carried out by passing the exist gas from the top of a condenser attached to the reaction flask successively through a trap cooled with dry ice-ethanol, a tube with anhydrous calcium chloride and one with Ascarite, which was finally weighed.

Decomposition of Diisopropyl Peroxydicarbonate in a Mixture of Benzene and Hexadeuteriobenzene. Diisopropyl peroxydicarbonate (*ca.* 2 mmol) was dissolved in an equimolar mixture (25 m*l*) of benzene and hexadeuteriobenzene and allowed to decompose completely at 60°C under an atmosphere of oxygen or air. The reaction mixture was concentrated carefully to a volume of 1—2 m*l* by using a spinning band distillation column. From a portion of the concentrated solution a mixture of phenyl and phenyl-d_5 isopropyl carbonate was collected by gas chromatography. Both the concentrated solution and the collected ester-mixture were analyzed by using a Hitachi mass spectrometer RMU-E6 with ionizing beam of 70 eV to determine the ratio of phenyl to phenyl-d_5 isopropyl carbonates by comparison of the relative intensities of the following pairs of ion peaks:[2] *i*-$PrOCOOC_6H_5^+$ at *m/e* 180 and *i*-$PrOCOOC_6D_5^+$ at *m/e* 185; $C_6H_5OCO^+$ and $C_6H_5OCHCH_3^+$ at *m/e* 121 and $C_6D_5OCO^+$ and $C_6D_5OCHCH_3^+$ at *m/e* 126; $C_6H_5OH^+$ at *m/e* 94 and $C_6D_5OH^+$ at *m/e* 99.

Results and Discussion

The results of the decomposition of diisopropyl peroxydicarbonate in benzene at several temperatures (40—70°C) under nitrogen, oxygen or air are summarized in Table 1 and Fig. 1.

While decomposition of diisopropyl peroxydicarbonate in benzene at 60°C under nitrogen gave carbon dioxide and isopropyl phenyl carbonate in 183 and 1%, respectively, passage of oxygen through the reaction mixture under otherwise the same reaction conditions caused a remarkable increase in the yield of isopropyl phenyl carbonate (57%) with the corresponding decrease of carbon dioxide (136%). The balance of the CO_2 group originally contained in the peroxide was accounted

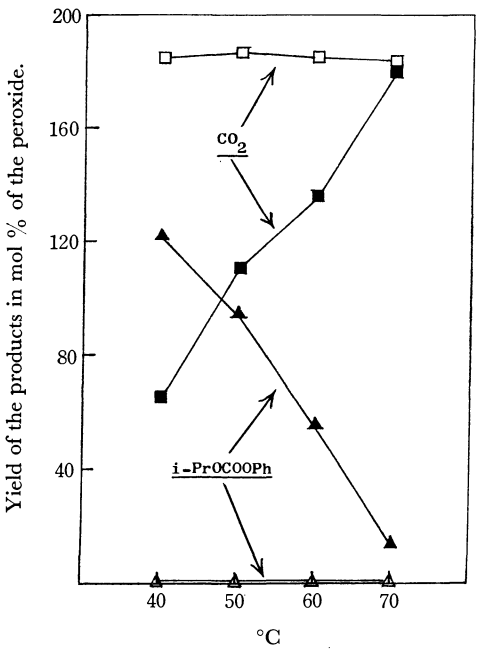

Fig. 1. Thermal decomposition of diisopropyl peroxydicarbonate (1.6 g) in benzene (300 m*l*): □, CO_2 under N_2; ■, CO_2 under O_2; △, *i*-PrOCOOPh under N_2; ▲, *i*-PrOCOOPh under O_2.

for nearly quantitatively under nitrogen and oxygen (92 and 97%, respectively). These results are satisfactorily explained by a mechanism similar to that proposed for the aromatic benzoyloxylation induced by oxygen[1]

$$(i\text{-PrOCOO})_2 \xrightarrow{k_1} 2\,i\text{-PrOCOO}\cdot \quad (1)$$

$$i\text{-PrOCOO}\cdot \xrightarrow{k_2} i\text{-PrO}\cdot + CO_2 \quad (2)$$

$$i\text{-PrOCOO}\cdot + C_6H_6 \underset{k_{-3}}{\overset{k_3}{\rightleftharpoons}} i\text{-PrOCOO}\text{-}C_6H_6\cdot \quad (\mathrm{I}) \quad (3)$$

$$(\mathrm{I}) + O_2 \xrightarrow{k_4} i\text{-PrOCOOC}_6H_5 + HO_2\cdot \quad (4)$$

The formation of isopropyl phenyl carbonate, aromatic isopropyloxycarbonyloxylation, consists of two steps, the reversible addition of an isopropyloxycarbonyloxy radical to an aromatic nucleus

2) P. Brown and C. Djerassi, *J. Amer. Chem. Soc.*, **88**, 2469 (1966).

to give an isopropyloxycarbonyloxycyclohexadienyl radical (reaction (3)), which proceeds competitively with decarboxylation (reaction (2)), and its subsequent oxidation by oxygen to afford isopropyl phenyl carbonate (reaction (4)). The proposal of a reversible addition step (reaction (3)) is based on the following reasons. If the addition were not reversible, in the first place, the decomposition, irrespective of the nature of the atmosphere, would give rise to carbon dioxide in approximately constant yield at a given temperature; and secondly, the decomposition under nitrogen might afford the carbonate ester in fairly good yield, by way of, for example, the disproportionation between isopropyloxycarbonyloxycyclohexadienyl radicals (I), similarly to that between phenylcyclohexadienyl radicals to yield biphenyl and dihydrobiphenyl.[3] The fact that the yield of the ester was dependent on the concentration of oxygen dissolved in the reaction mixture as shown (by the result under air) in Table 1 clearly indicates that the oxidation of the isopropyloxycarbonyloxycyclohexadienyl radical by molecular oxygen competes with its reversible dissociation to an isopropyloxycarbonyloxy radical and benzene.

The above mechanism is further supported by the study of the effect of temperature on the yield of the products under nitrogen or oxygen; the results are shown in Fig. 1. Under oxygen, the yield of isopropyl phenyl carbonate increased with lowering the reaction temperature, being 15 and 123% at 70 and 40°C, respectively, whereas the yield under nitrogen was invariably very low (less than 1%). With lowering the temperature, the yield of carbon dioxide did not change under nitrogen (about 185%), but decreased under oxygen with the corresponding increase of the carbonate ester. The effect of temperature on the yield of the ester under oxygen is certainly due to increase in the concentration of oxygen dissolved in the reaction mixture as well as decrease in the rate of decarboxylation from the isopropyloxycarbonyloxy radical with decrease in the reaction temperature.

In order to obtain further evidence for the reversibility of the addition of isopropyloxycarbonyloxy radicals to benzene, decomposition of diisopropyl peroxydicarbonate in large excess of an equimolar mixture of benzene and hexadeuteriobenzene was carried out at 60°C under oxygen and air, the apparent isotope effect for the formation of isopropyl phenyl carbonate being determined. The apparent isotope effect k_H/k_D is defined by

$$\frac{k_H}{k_D} = \frac{(\text{yield of } i\text{-PrOCOOC}_6H_5)}{(\text{yield of } i\text{-PrOCOOC}_6D_5)} \times \frac{[C_6D_6]}{[C_6H_6]} \quad (5)$$

According to the reaction sequence (reactions (3) and (4)) shown above, the ratio between the isotopic esters formed is given by

$$\frac{(\text{yield of } i\text{-PrOCOOC}_6H_5)}{(\text{yield of } i\text{-PrOCOOC}_6D_5)} = \frac{k_4^H}{k_4^D} \times \frac{[C_6H_6]}{[C_6D_6]} \times K_{H/D} \times \frac{(1+k_4^D[O_2]/k_{-3}^D)}{(1+k_4^H[O_2]/k_{-3}^H)} \quad (6)$$

where $K_{H/D}=\frac{k_3^H/k_{-3}^H}{k_3^D/k_{-3}^D}$ and superscripts H and D refer to the reactions involving ordinary benzene and deuterated benzene, respectively.

TABLE 2. ISOTOPE EFFECTS IN AROMATIC ISOPROPYLOXYCARBONYLOXYLATION[a] (60°C)

Exp. No.	Atmosphere	Reactant benzene[b),d)] I_{78}/I_{84}	Isopropyl phenyl carbonate[d)] Sample analysed[c)]	I_{94}/I_{99}	I_{121}/I_{126}	I_{180}/I_{185}	Apparent isotope effect
1	O_2	0.996	A	2.29	2.10	2.30	2.1—2.3
			B	2.23	2.10	2.34	
2	O_2	0.996	A	2.27	2.10	2.34	2.1—2.3
			B	2.22	2.08	2.36	
3	Air	1.06_2	A	1.91	1.75	1.90	1.6—1.8
			B	1.87	1.68	1.91	
4	Air	1.00_3	A	1.64	1.50	1.60	1.5—1.7
			B	1.67	1.38	1.75	

a) Diisopropyl peroxydicarbonate was allowed to decompose at 60°C in an equimolar mixture of benzene and hexadeuteriobenzene under a specified atmosphere. The initial peroxide concentration was 0.07—0.1 mol/*l*.

b) The hexadeuteriobenzene used was found to contain less than 3.3% of pentadeuteriobenzene, by mass spectrometric analysis with ionizing beam of 15 eV.

c) A denotes the carbonate collected from concentrated reaction mixtures by VPC; B, concentrated reaction mixtures.

d) Average of three measurements. I is the intensity of a mass spectrometric peak at *m/e* indicated as subscript of I.

3) D. F. DeTar and R. A. J. Long, *J. Amer. Chem. Soc.*, **80**, 4742 (1958).

Table 2 contains values, as determined by mass spectrometry, for the ratio of the resulting isotopic esters, which is equal to the apparent isotope effect because of the use of equimolar amounts of benzene and hexadeuteriobenzene. Fairly large isotope effects, 2.1—2.3 under oxygen and 1.5—1.8 under air, were observed. If the rate of dissociation of the isopropyloxycarbonyloxycyclohexadienyl radical (I) is much lower than that of the reaction with oxygen, *i.e.*, $k_4[O_2] \gg k_{-3}$, the apparent isotope effect would be expressed by $k_H/k_D = k_3^H/k_3^D$. Numerical estimation of this ratio is difficult, since there has hitherto been no experimental results concerning the secondary isotope effect in the homolytic aromatic substitution. Small reverse secondary isotope effects have been noticed for the radical addition to deuterio-olefins,[4] however; it would therefore seem reasonable to assume that k_3^H/k_3^D is unity or slightly less than unity. The observed apparent isotope effects are distinctly greater than this estimate. On the other hand, if $k_{-3} \gg k_4$ $[O_2]$, Eq. (6) reduces to

$$\frac{(\text{yield of } i\text{-PrOCOOC}_6H_5)}{(\text{yield of } i\text{-PrOCOOC}_6D_5)} = \frac{k_4^H}{k_4^D} \times K_{H/D} \times \frac{[C_6H_6]}{[C_6D_6]}$$

and $$k_H/k_D = (k_4^H/k_4^D) \times K_{H/D}$$

so that a fairly large apparent isotope effect is to be observed owing to the primary isotope effect for the oxidation step (reaction (4)), $K_{H/D}$ being not appreciably different from unity as mentioned above. Whether or not the actual situation corresponds to this extreme condition is not certain, but the observed isotope effects as a whole clearly indicate that the dissociation step competes favorably with the reaction with oxygen to give isopropyl phenyl carbonate, thus corroborating the reversibility of the addition step of the isopropyloxycarbonyloxy radical to an aromatic nucleus.*2

It is worth noting that the present results of isotope effect measurements for the production of the carbonate ester in the presence of oxygen, contrast with the observation of no apparent isotope effect in the presence of cupric chloride as an oxidant in place of oxygen reported by Kurz, Kovacic, Bose and Kugajevsky.[5] In the presence of cupric chloride, isopropyl phenyl carbonate has been proposed to arise by the following oxidative reaction:

$$i\text{-PrOCOOC}_6H_6\cdot + CuCl_2 \xrightarrow{k_4'} i\text{-PrOCOOC}_6H_5 + CuCl + HCl$$

The absence of apparent isotope effect leads to the conclusion that $k_4' \cdot [CuCl_2]$ is much larger than k_{-3}, in contrast with the present result that $k_4 \cdot [O_2]$ is smaller than k_{-3}. The fact that $k_4 \cdot [O_2]$ is, thus, much smaller than $k_4' \cdot [CuCl_2]$ is probably attributable both to higher efficiency (k_4') of cupric chloride than oxygen ($k_4' > k_4$) in oxidizing the cyclohexadienyl intermediate and to the higher concentration of cupric chloride used than that of oxygen dissolved in benzene.*3

Finally, it must be pointed out that the present observation of the isotope effect is in keeping with Denney and Klemchuk's finding of isotope effect, $k_H/k_D = 1.32$, for the intramolecular formation of 3,4-benzocumarin from 2-(2-deuteriophenyl)benzoyl peroxide, which led to the postulation of the intramolecular reversible cyclization of the *o*-phenylbenzoyloxy radical to give a cyclohexadienyl intermediate, followed by oxidation to the benzocumarin, without mention of the nature of the oxidant.[6]

The authors wish to thank Drs. M. Fukuyama and M. Anbe of Sagami Research Center for mass spectrometric measurements.

4) M. Feld, A. P. Stefani and M. Szwarc, *J. Amer. Chem. Soc.*, **84**, 4451 (1962); M. Takahasi and R. J. Cvetanović, *Can. J. Chem.*, **40**, 1037 (1962).

*2 The observation of somewhat smaller isotope effects for the reaction under air than under oxygen was contrary to the prediction from Eq. (6). The cause for this is unknown.

5) M. E. Kurz, P. Kovacic, A. K. Bose and I. Kugajevsky, *J. Amer. Chem. Soc.*, **90**, 1818 (1968).

*3 In connection with the aromatic isopropyloxycarbonyloxylation caused by cupric chloride, Kurz and Kovacic examined the effect of several non-metallic oxidants in the reaction of diisopropyl peroxydicarbonate with toluene in acetonitrile at 60°C, and stated that oxygen brought about a small, but real, increase in isopropyl tolyl carbonate (in 6.6% yield), whereas, without any oxidant, the yield was very low (0.7%) (M. E. Kurz and P. Kovacic, *J. Org. Chem.*, **33**, 266 (1968)). In a preliminary experiment carried out during the present investigation, the presence of oxygen in the decomposition of diisopropyl peroxydicarbonate in toluene at 60°C caused a remarkable increase of isopropyl tolyl carbonate (in about 20% yield).

6) D. B. Denney and P. P. Klemchuk, *J. Amer. Chem. Soc.*, **80**, 3289 (1958).

BULLETIN OF THE CHEMICAL SOCIETY OF JAPAN VOL. 43 3594—3596 (1970)

The Constituents of Hops. V.[1] The Volatile Composition of *Humulus japonicus* Sieb. et Zucc.

Yoko NAYA and Munio KOTAKE

The Institute of Food Chemistry, Dojimanaka, Kita-ku, Osaka

(Received July 13, 1970)

The steam-volatile constituents of *Humulus japonicus* Sieb. et Zucc. have been studied, and 50 compounds of the oil have been identified mainly by means of the temperature-programmed capillary GLC mass-spectra method. Beside the previously-reported principal components of hops (α-humulene, caryophyllene, α-copaene, α- and β-selinenes, γ-cadinene, caryophyllene-oxide, and humulene-epoxide-II), benzyl alcohol and phenethyl alcohol were found in high concentrations, whereas the myrcene was negligible. The proportion of the main compound, humulene, to the next highest one, caryophyllene, was approximately in the ratio of two to one, as in the essential oil of *H. lupulus*. As far as the chemical composition of the essential oils is concerned, *H. japonicus* seems to be related rather more closely to *H. lupulus* than to *H. cordifolius*.

The genus *Humulus* is represented by two species, the common hop, *Humulus lupulus* L., and the annual climbing plant from Japan, *H. joponicus* Sieb. et Zucc., which is synonymous with *H. scandens* Merr. and which belongs to the natural family *Cannabiaceae*. The wild hops of North America, *H. americanus* and *H. neomexicanus*, and the Asian *H. cordifolius*, the chemical composition of which was recently reported,[1] are generally considered to be varieties of *H. lupulus*. In this paper, the identification of the volatile constituents contained in the above-ground parts with the cones of *H. japonicus* is reported for the first time, and the chemical similarities between the above-mentioned species are discussed.

Experimental

Separation. The above-ground parts with the cones of *H. japonicus* (18 kg) gathered in the suburbs of Osaka at the beginning of October, 1969, were extracted with

TABLE 1. THE CONSTITUENTS OF HYDROCARBONS

Peak No. in Fig. 1	Identity of Constituent	Peak No. in Fig. 1	Identity of Constituent
1	α-Pinene	37	β-Selinene
2	β-Pinene	38	α-Selinene
3	Myrcene	38	α-Muurolene
4	*n*-Undecane	39	β-Bisabolene
8	*n*-Dodecane	40	α-Curcumene
15	*n*-Tridecane	41	γ-Cadinene
20-1	*n*-Tetradecane	41	δ-Cadinene
22	α-Ylangene	43	β-Sesquiphellandrene
23	α-Copaene	47	Calamenene
25	β-Bourbonene	50	γ-Calacorene
27	*n*-Pentadecane	51	α-Calacorene
27	β-Elemene	62	Cadalene
27	*trans*-α-Bergamotene		* $C_{12}H_{24}$ 168 (43)
28	Caryophyllene		* $C_{13}H_{26}$ 182 (43)
32	α-Humulene		* $C_{14}H_{28}$ 196 (43)
33	β-Farnesene		* $C_{15}H_{30}$ 210 (43)
34	γ-Muurolene		* $C_{16}H_{32}$ 224 (43)
35	*n*-Hexadecane		iso $C_{13}H_{28}$ 184 (57)
35	α-Amorphene		iso $C_{14}H_{30}$ 198 (57)

1) Previous paper of this series: Y. Naya and M. Kotake, This Bulletin, **43**, 2956 (1970).

Table 2. The constituents of oxygenated compounds

Peak No.	Identity of Constituent	Peak No.	Identity of Constituent
6	Hexanol	35	Phenethyl alcohol
8	*trans*-3-Hexenol-1	39	Geraniol
9	*cis*-2-Hexenol-1	52	Caryophyllene-oxide
13	1-Octene-3-ol	54	Humulene-epoxide-I
18	Linalool	55	Humulene-epoxide-II
20	* M^+, *m/e* 124 (109)	59	Humulol
24	* M^+, *m/e* 124 (82)	60	T-Cadinol
26	* M^+, *m/e* 138 (95)	64	Humulenol-II
26-1	α-Terpineol	66	Humulene-dioxide
29	* M^+, *m/e* 138 (82)	67	α-Cyperone
31	Benzyl alcohol		

* Unknown compound together with molecular weight and base peak on MS spectrum.

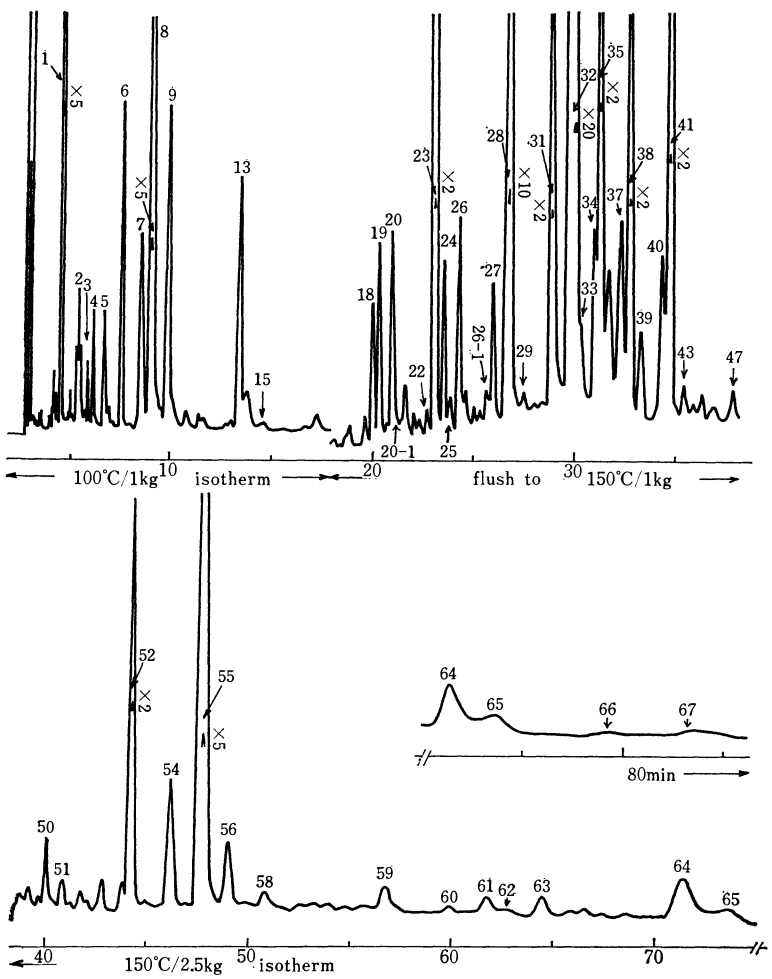

Fig. 1. A capillary gas chromatogram obtained for *H. japonicus* "kanamugura." Column 45 m × 0.25 mm coated with HB 2000.

ether. The extract was steam-distilled to obtain the essential oil (1.8 g). This oil was subjected to selective adsorption chromatography on neutral alumina to separate it into hydrocarbon (0.8 g) and oxygenated constituents (0.6 g). Each fraction was divided into several parts by programmed preparative gas-liquid chromatography (Carbowax 20 M), and then examined by means of the temperature-programmed capillary GLC mass spectra method. In addition, the major constituents were isolated by a combination of adsorption chromatography and preparative gas-liquid chromatography (Carbowax 20 M) and were identified by comparing their IR spectra with those of authentic samples.

Apparatus. The mass spectrometer employed was a Hitachi Model RMU-6 instrument; the operating conditions were as follows: ionization energy, 80 eV; accelerating voltage, 2000 V; ionization chamber, 150°C.

For the GLC, a Hitachi Model K-53 was used. The capillary column used for the analysis was 45 m long by 0.25 mm in I.D., made of stainless steel and coated with HB 2000; the column temperature was programmed non-linearly from 100 to 150°C. The helium-carrier gas-inlet pressure was set at 1.5 kg/cm^2 for initiation and 2.5 kg/cm^2 at the end.

For preparative gas-chromatography, a model 90-P Varian Aerograph equipped with a thermal conductivity detector was employed. A 10-ft.$\times$3/8 in. aluminum column packed with 20% Carbowax 20 M on Chromosorb W (60—80 mesh) was used. Helium was used as the carrier gas, and the column temperature was set at 100—220°C.

Results and Discussion

The compounds identified from the oil of *H. japonicus* are listed in Table 1 and 2, together with the peak number on the programmed GLC (Fig. 1). The authentic compounds used for identification were obtained from reliable sources and were purified by GLC separation before use. α-Humulene and the related oxides, together with humulol and humulenol-II, were found in great abundance. α-Copaene, caryophyllene and its oxide, α- and β-selinenes, and γ-cadinene have been found to be the common major components of the "Shinshu-wase" (*H. lupulus*).[2,3] It is significant, compared with the composition of "Shinshu-wase," that myrcene is here found to be negligible, whereas benzyl alcohol and phenethyl alcohol are detected in abnormally high concentrations. Mention has been made previously of the botanical relationship among the *H. lupulus*, *H. cordifolius*, and *H. japonicus*. It is interesting that the similarities in the essential oil of *H. lupulus* and *H. japonicus*, are however, distinct from that of *H. cordifolius* to some extent; this seems to be in disagreement with the botanical relationship of the three concerned plants. That is, the former two are humulene-rich, and the later is caryophyllene-rich, in the ratio of approximately two to one. The proportion of humulene-epoxide-II to caryophyllene-oxide corresponds with that in the corresponding hydrocarbons. In addition, in *H. cordifolius*, bisabolene-type sesquiterpenes (zingiberene and α-curcumene, together with β-bisabolene and β-sesquiphellandrene), selina-3,7(11)-diene, and selina-4(14), 7(11)-diene were found in abnormally high concentrations, as has previously been reported.[1]

2) Y. Naya and M. Kotake, *Nippon Kagaku Zasshi*, **88**, 1307 (1967); **89**, 1113 (1968); **91**, 275 (1970).

3) R. G. Buttery and L. C. Ling, *Brewers Digest*, **1966**, 71.

BULLETIN OF THE CHEMICAL SOCIETY OF JAPAN VOL. 43 3597—3601 (1970)

High Resolution NMR Study of Vinyl Chloride-Ethylene Copolymers

Akira MISONO and Yasuzo UCHIDA

Department of Industrial Chemistry, Faculty of Engineering, The University of Tokyo, Hongo, Tokyo

and Kunikazu YAMADA

Research Laboratory, Sekisui Chemical Co., Shimamoto-cho, Mishima-gun, Osaka

(Received May 14, 1970)

The high resolution NMR spectra of vinyl chloride-ethylene copolymers obtained by trialkylboron catalyst have been analyzed. The copolymer composition could be determined from the resonance peak area, and the monomer reactivity ratios thus obtained were in good consistency with those determined from the results of elementary analysis. The fine structure of the copolymers have been elucidated in terms of the run number concept, and the distribution of dyads as well as the average sequence lengths of the monomer unit have been determined. It was found that the observed values fitted theoretical values, indicating that a terminal model holds in this copolymerization.

High resolution NMR spectroscopy has been proved to be a superior method in investigation of fine structures of copolymers, and many copolymer systems have been analyzed thus for the purpose of obtaining precise information concerning the nature of copolymerization.[1-12] Vinyl chloride copolymers have been prepared and consumed on an industrial scale since long ago. However, they have not been studied by high resolution NMR spectroscopy probably because of complexities of the spectra. Vinyl chloride - ethylene copolymer, in which the ethylene unit has no substituent group, gives a more simple NMR spectrum than the vinyl copolymers with substituted ethylenic comonomers. We have presented a qualitative interpretation of the spectra.[13-15] Schaefer[16] as well as Wilkes and coworkers[17] have also reported on the NMR studies of vinyl chloride - ethylene copolymers. In this paper, we wish to report results of our high resolution NMR study of the copolymer concerning the determination of the monomer reactivity ratios as well as the elucidation of the fine structure of the copolymer obtained by the tri-*n*-butylboron/*t*-butyl hydroperoxide catalyst system.

Experimental

The samples were prepared by using a catalyst system consisting of tri-*n*-butylboron and *t*-butyl hydroperoxide in a water-methanol mixture (1 : 1 by volume) at 0°C.[13] Most of the copolymer samples were obtained in conversions lower than 10%. However, a few samples were obtained in conversions between 10 and 13%. The composition of the copolymer was determined from the results of elementary analysis of C and Cl. The NMR spectrum of the copolymer was measured with a Japan Electron Optics high resolution NMR spectrometer, model, JNM-C-60, in a 10wt/vol% monochlorobenzene solution of the sample at 60 MHz and 110°C using tetramethylsilane as an internal standard. The NMR spectrum was copied and each peak was separated by cutting, and then weighed for the determination of relative peak area.

1) F. A. Bovey, *J. Polym. Sci.*, **62**, 197 (1962).
2) A. Nishioka, Y. Kato and N. Ashikari, *ibid.*, **62**, S10 (1962).
3) R. Chujo, S. Sato and E. Nagai, *ibid.*, **A2**, 895 (1964).
4) Y. Kato, N. Ashikari and A. Nishioka, This Bulletin, **37**, 1630 (1964).
5) J. L. McClanahan and S. A. Previtera, *J. Polym. Sci.*, **A3**, 3919 (1965).
6) K. Ito and Y. Yamashita, *ibid.*, **B3**, 625, 637 (1965).
7) T. Harada and N. Ueda, *Kobunshi Kagaku*, **22**, 685 (1965).
8) U. Johnsen, *Ber. Bunsenges.*, **70**, 320 (1966).
9) T. Fischer, J. B. Kinsinger and C. W. Wilson, *J. Polym. Sci.*, **B4**, 379 (1966).
10) K. Ito and Y. Yamashita, *ibid.*, **A4**, 631 (1966).
11) J. B. Kinsinger, T. Fischer and C. W. Wilson, *ibid.*, **B5**, 285 (1967).
12) R. Yamadera and M. Murano, *ibid.*, **A5** 2259 (1967).
13) A. Misono, Y. Uchida and K. Yamada, This Bulletin, **39**, 2458 (1966).
14) A. Misono, Y. Uchida and K. Yamada, *ibid.*, **40**, 2366 (1967).
15) A. Misono, Y. Uchida, K. Yamada and T. Saeki, *ibid.*, **41**, 2995 (1968).
16) J. Schaefer, *J. Phys. Chem.*, **70**, 1975 (1966).
17) C. E. Wilkes, J. C. Westfahl and R. H. Backderf, *Amer. Chem. Soc. Polymer Preprints*, **8(1)**, 386 (1967).

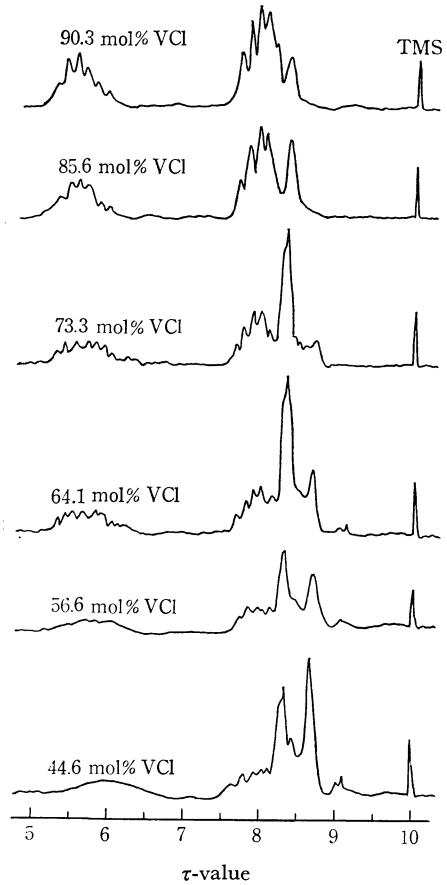

Fig. 1. NMR spectra of copolymers.

Results and Discussion

Peak Assignment. In Fig. 1 are shown the NMR spectra of several copolymers. A multiplet observed between 5.5 and 6.0 τ can be assigned to the methylene proton of vinyl chloride sequence based on the results of other workers.[18-21] The multiplet shifts to higher magnetic fields and becomes weaker in intensity as the vinyl chloride content of copolymer decreases. Since no methine proton absorption is observed at lower fields than those observed for pure polyvinyl chloride, and the infrared spectrum of the copolymer shows no absorption due to the $-(CH_2)_2-$ and the $-(CH_2)_4-$ sequences,[22] occurrence of the head-to-head or tail-to-tail linkage of vinyl chloride units can be ruled out.

In the region of methylene proton resonance, three groups of peaks can be observed in the spectrum of the copolymer; a multiplet centered at 7.85 τ, a singlet at 8.35 τ and a singlet at 8.65 τ. An additional peak is observed at 8.55 τ in the spectrum of the copolymer with a higher ethylene content. Hereafter, the methylene peaks are denoted by A, B and C, respectively, for the sake of convenience. The position of these methylene peaks does not seem to shift with change in copolymer composition.

The NMR spectra of polyvinyl chloride and polyethylene are shown in Fig. 2 and those of 2,6-di-

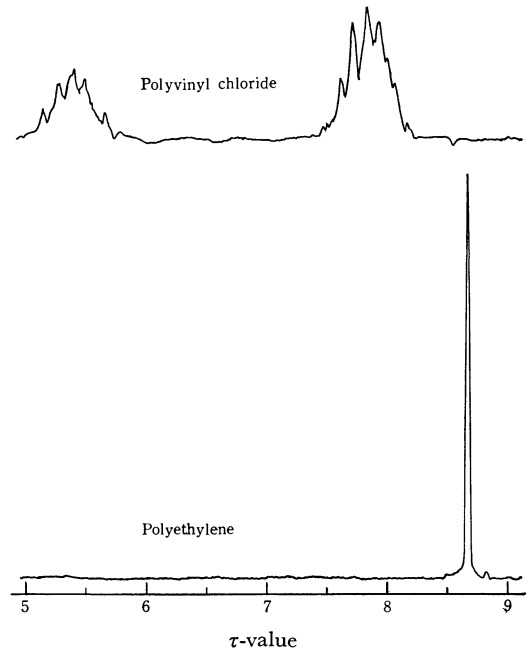

Fig. 2. NMR spectra of polyvinyl chloride and polyethylene.

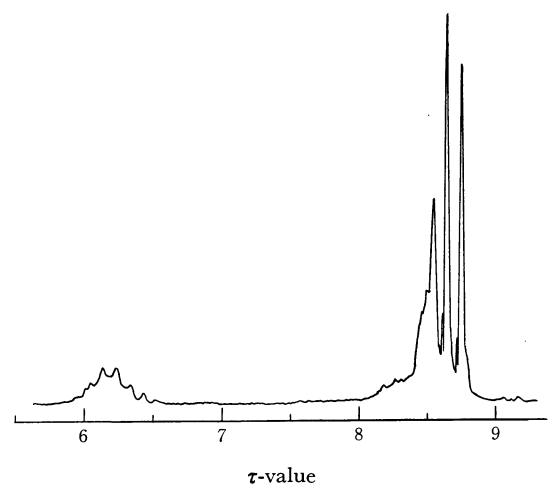

Fig. 3. NMR spectrum of 2,6-dichloroheptane.

18) U. Johnsen, *J. Polym. Sci.*, **54**, S6 (1961).
19) W. C. Tincher, *ibid.*, **62**, S148 (1962).
20) R. Chujo, S. Sato, T. Ozeki and F. Nagai, *ibid.*, **61** S12 (1962).
21) F. A. Bovey and G. V. D. Tiers, *Chem. & Ind.*, **1962**, 1826.
22) A. Misono, Y. Uchida and K. Yamada, This Bulletin, **40**, 2696 (1967).

chloroheptane in Fig. 3. Peaks A and C are also observed in the spectrum of polyvinyl chloride and polyethylene, respectively, and thus can be assigned to the methylene proton absorption of $(CH_2\text{–}CHCl)_m$ and $(CH_2\text{–}CH_2)_n$ sequence, respectively, where m and n are greater than two. The observations of the NMR spectrum of the copolymer enable us to deduce that peak B can be assigned to the methylene group of a boundary structure located at a junction point of vinyl chloride unit and ethylene unit. In the spectrum of 2,6-dichloroheptane, a resonance peak is observed at 8.55 τ which can be assigned to a methylene group having two methylene groups in both nearest neighbors. Accordingly, the methylene peak mentioned previously appearing in the copolymer richer in ethylene may arise from the structure CHCl–CH_2–CH_2*–CH_2–CHCl. Thus, it seems reasonable to assign peak B to the methylene group having a methine and a methylene group in the nearest neighbors, namely CHCl–CH_2*–CH_2.

Table 1. Assignment of dyads

Dyad	Chemical shift (τ)	Structure
V–V	7.85	CH_2–CHCl–CH_2*–CHCl
V–E	8.35	CH_2–CHCl–CH_2*–CH_2
E–V	8.35	CH_2–CH_2–CH_2*–CHCl
E–E	8.65	CH_2–CH_2*–CH_2*–CH_2

If one describes the fine structure of the copolymer in terms of dyads, the above mentioned relationship can be summarized as shown in Table 1. Since each vinyl chloride unit contains one methylene group and each ethylene unit contains two, the mole fraction of each dyad can be easily calculated by using the following relationships taking into account the double counting of methylene group belonging to the E–E dyad, a part of which consists of the V–E or the E–V dyad.

$$f(\mathrm{V-V}) = 2a/\{2a+2b+(c-b/2)\} \quad (1)$$

$$2f(\mathrm{V-E}) = 2b/\{2a+2b+(c-b/2)\} \quad (2)$$

$$f(\mathrm{E-E}) = (c-b/2)/\{2a+2b+(c-b/2)\} \quad (3)$$

$$f(\mathrm{V-V}) + 2f(\mathrm{V-E}) + f(\mathrm{E-E}) = 1 \quad (4)$$

where a, b and c denote the relative peak areas of peaks A, B and C, respectively.

Determination of Monomer Reactivity Ratios. In Table 2 are shown the copolymer composition and the percentage of the methylene peak areas a, b and c. The vinyl chloride or ethylene mole fraction of the copolymer can be readily calculated by using the following equations derived from the above relationships of dyad distribution, where $F(\mathrm{V})$ and $F(\mathrm{E})$ denote the mole fraction of vinyl chloride and ethylene in the copolymer, respectively.

Table 2. Relative peak of methylene resonance

Copolymer composition (VCl mol%)	f_A	f_B	f_C
44.6	12.5	33.5	53.9
56.6	20.5	39.2	40.4
64.1	28.7	36.6	34.8
73.3	39.0	40.7	20.3
78.8	52.6	32.3	15.1
81.0	53.3	32.4	14.3
85.6	69.3	21.7	9.0
90.3	79.5	15.0	5.5
99.0	94.5	5.5	0

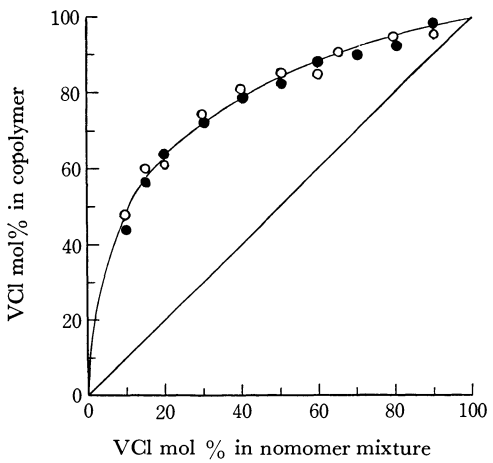

Fig. 4. Determination of copolymer composition.
open circle: from NMR peak area
closed circle: from C analysis

$$F(\mathrm{V}) = f(\mathrm{V-V}) + 2f(\mathrm{V-E})/2 = (a+b)/(2a+3b/2+c) \quad (5)$$

$$F(\mathrm{E}) = f(\mathrm{E-E}) + 2f(\mathrm{V-E})/2 = (b/2+c)/(2a+3b/2+c) \quad (6)$$

In Fig. 4 are compared the copolymer composition calculated from the results of elementary analysis and those obtained from NMR peak areas. Coincidence between the results from the two methods is obvious. Figure 5 shows the result of the determination of the monomer reactivity ratios using the fraction of the V–E dyad with the relationship given by Kinsinger and Colton.[23]

$$F_0\{1-2f(\mathrm{V-E})\}/f(\mathrm{V-E}) = r_2 + r_1F_0^2 \quad (7)$$

where F_0 denotes the monomer feed ratio, namely vinyl chloride/ethylene molar ratio in initial monomer mixture. The monomer reactivity ratios determined by means of the two methods are good agreement with each other:

23) J. B. Kinsinger and D. Colton, *J. Polym. Sci.*, **B3**, 797 (1965).

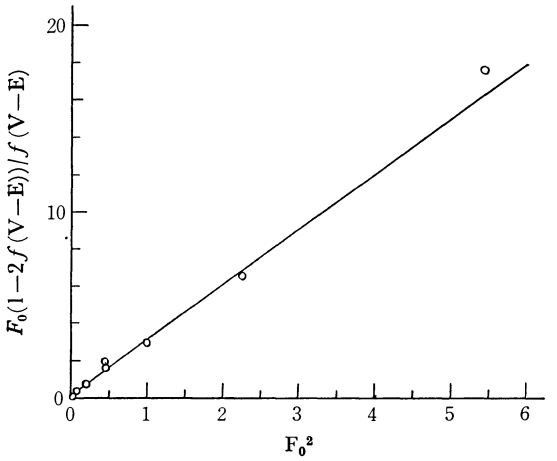

Fig. 5. Determination of monomer reactivity ratios by Kinsinger-Colton relationship

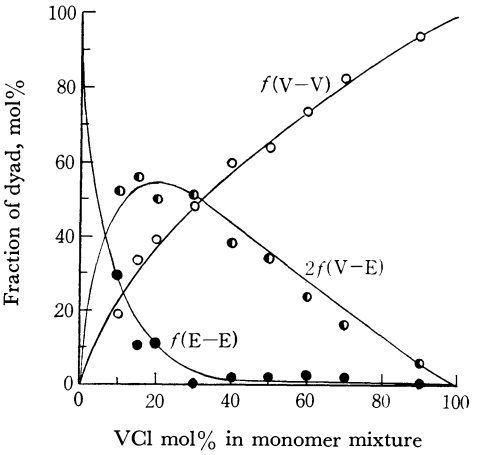

Fig. 6. Change in fraction of dyad as a function of monomer composition.

From elementary analysis,

$$r_1\,(\mathrm{V}) = 3.39 \text{ and } r_2\,(\mathrm{E}) = 0.20$$

From NMR peak area,

$$r_1\,(\mathrm{V}) = 2.96 \text{ and } r_2\,(\mathrm{E}) = 0.20$$

Elucidation of Fine Structure. Fine structures of copolymers have been nicely characterized by means of the run number (R) concept proposed by Harwood.[24] R has been defined as the average number of monomer sequences (runs) occurring in the copolymer per 100 monomer units. According to the definition, R can be easily calculated by means of Eq. (2) because R equals the mole fraction of the V–E and E–V dyads. Hence

$$R_{\mathrm{obs}} = 2f(\mathrm{V-E}) = 2b/(2a+3b/2+c) \qquad (8)$$

In an ideally random copolymerization in the sense of Mayo-Lewis statistics of copolymerization, R should be expressed by the relationship[24]

$$R_{\mathrm{calc}} = 200/(r_1x+r_2/x+2) \qquad (9)$$

where x represents the monomer feed ratio. If R_{obs} is greater than R_{calc} the monomer units tend to alternate in the copolymer, and if R_{obs} is smaller than R_{calc} the monomer units tend to cluster in blocks of like units.

The mole fractions of the V–V and E–E dyads can be calculated by using the theoretical run number with the following equations.

$$f(\mathrm{V-V})_{\mathrm{calc}} = F(\mathrm{V}) - R_{\mathrm{calc}}/2 \qquad (10)$$

$$f(\mathrm{E-E})_{\mathrm{calc}} = F(\mathrm{E}) - R_{\mathrm{calc}}/2 \qquad (11)$$

In Fig. 6 are compared the observed and calculated mole fractions of the three dyads as a function of the monomer feed ratio. We see that the observed points fit well the calculated lines over the whole range of the monomer feed ratio. This indicates that the copolymerization initiated by the trialkylboron catalyst should be described as a random or zeroth-order Markoffian process.[25] This means that the rates of four propagation processes involved in the copolymerization depend only on the kind of terminal monomer unit (terminal model), and is in agreement with what has been found in most cases of radical copolymerization, though an exceptional case has been reported.[9]

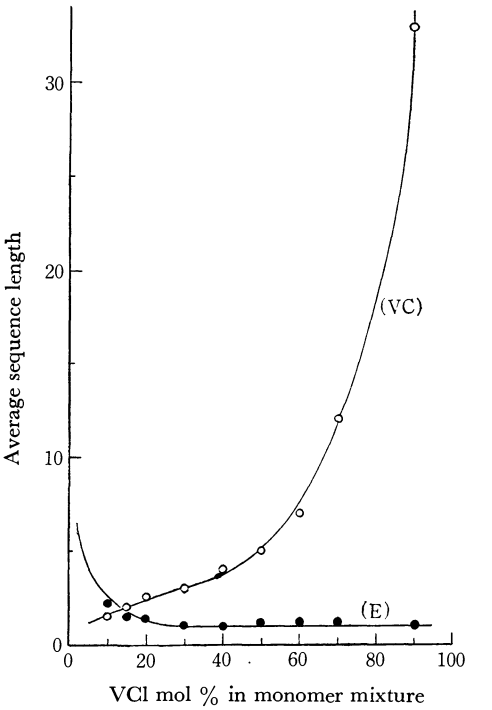

Fig. 7. Change in average sequence length as a function of monomer composition.

24) H. J. Harwood and W. M. Ritchey, *J. Polym. Sci.*, **B2**, 610 (1964).

25) F. P. Price, *J. Chem. Phys.*, **36**, 209 (1962).

Recently, the occurrence of the complexed radical propagation mechanism has been proposed by Arimoto[26] in order to elucidate the ineffectiveness of radical inhibitors on vinyl polymerization initiated by trialkylboron. Hydroquinone did not inhibit the reaction at all in our case of copolymerization either. In spite of this appreciable existence of complexed radical propagation, it might have only a little, if any, significance on the monomer reactivity ratios and the fine structure of the copolymer.

Figure 7 shows the observed and calculated average monomer sequence lengths as a function of the monomer feed ratio. The following relationships were used for the calculation.

$$\text{av. sequence length of } V = F(\mathrm{V})/R/2 \tag{12}$$

$$\text{av. sequence length of } E = F(\mathrm{E})/R/2 \tag{13}$$

where R is the observed or calculated run number.

The average sequence length of vinyl chloride unit decreases rapidly as the vinyl chloride fraction in the monomer feed decreases, whereas that of ethylene unit increases only slowly from unity according to the increase in ethylene fraction in the monomer feed. It seems interesting to note that the average sequence lengths of both monomer units reach *ca.* 2 when the copolymer composition approaches 50 : 50 molar ratio. As in the dyad distribution the observed average sequence lengths fit the calculated values.

26) F. S. Arimoto, *J. Polym. Sci.*, **A4**, 275 (1966).

NOTES

BULLETIN OF THE CHEMICAL SOCIETY OF JAPAN VOL. 43 3602—3603 (1970)

Studies of the *N*-Oxides of *N,N*-Dialkylamino Acids. III. The Syntheses of *N,N*-Dimethyl Acidic Amino Acids and Related Compounds

Yoshikazu IKUTANI

Department of Chemistry, Osaka Kyoiku University, Tennoji-ku, Osaka

(Received December 30, 1969)

In the previous papers of this series, the preparations of *N,N*-dimethyl neutral amino acid *N*-oxides,[1] and *N,N*-dialkylglycine *N*-oxides[2] were investigated. In the present studies, the preparations of *N,N*-dimethyl acidic amino acid *N*-oxides have been investigated. The *N,N*-dimethylations of acidic amino acids by catalytic reductive condensation with formaldehyde were performed by means of a procedure similar to that reported in the previous papers. The results obtained are summarized in Table 1.

The oxidations of *N,N*-dimethyl L- and DL-glutamic acid with a mixture of aqueous hydrogen peroxide and acetic acid gave the corresponding *N*-oxides in good yields after treatment as described in the previous paper. However, in the similar reaction of *N,N*-dimethyl-L-aspartic acid, the expected *N*-oxide could not be obtained with a similar treatment, rather, fumaric acid, the decomposition product of the corresponding *N*-oxide, was obtained in an almost pure state in a good yield. This type of decomposition is well-known as "Cope elimination".[3] Unfortunately, all attempts to obtain the corresponding *N*-oxide in the pure state were unsuccessful. The results obtained are summarized in Table 2.

When water was used instead of aqueous hydrogen peroxide in the above reaction, no reaction occurred under the same reaction conditions and the unchanged starting material was recovered.

TABLE 1. *N,N*-DIMETHYL ACIDIC AMINO ACIDS

Parent amino acid	Reduction period (50°C)	Yield (%)	Mp (°C)	R_f Value[a]	C%		H%		N%	
					Found	Calcd	Found	Calcd	Found	Calcd
L-Asp	7 hr	88	198	0.27	44.57	44.71	6.74	6.88	8.63	8.69
DL-Asp	7	89	195	—	44.74	44.71	6.84	6.88	8.68	8.69
L-Glu	6	89	196	0.36	47.87	47.99	7.56	7.48	7.84	8.00
DL-Glu	6	90	199	—	47.94	47.99	7.45	7.48	8.02	8.00

a) A 1-butanol-acetic acid-water (60:15:25) solvent system was used. The location of the paper chromatogram was detected by spraying 50% aqueous ethanol solution of bromophenol blue.

TABLE 2. OXIDATION PRODUCT OF *N,N*-DIMETHYL ACIDIC AMINO ACIDS

Starting amino acid	Oxidation period (60°C)	Yield of product (%)	Mp (dec.) (°C)	R_f Value[a]	C%		H%		N%		ν_{N-O} cm^{-1}
					Found	Calcd	Found	Calcd	Found	Calcd	
L-Asp	7 hr	72[b]	—	0.81[c]	41.73	41.39	3.47	3.47	—	—	—
L-Glu	8	87	163	0.49	43.98	43.97	6.85	6.85	7.36	7.33	971
DL-Glu	8	89	160	—	44.20	43.97	6.84	6.85	7.06	7.33	970

a) The same procedure was used as described in Table 1.
b) This is yield of fumaric acid. c) This vlaue is that of fumaric acid.

1) Y. Ikutani, This Bulletin, **41**, 1679 (1968).
2) Y. Ikutani, *ibid.*, **42**, 2330 (1969).
3) A. C. Cope and E. R. Trumbull, "Organic Reactions," Vol. 11, Chap. 5 (1960).

However, on prolonged heating at an elevated temperature, deamination occurred to afford dimethylammonium hydrogen fumarate.

A similar reaction partially occurred in the aqueous solution of *N,N*-dimethyl-L-aspartic acid, and dimethylammonium hydrogen fumarate and *N,N*-dimethyl-DL-aspartic acid were thus obtained in 42 and 40% yields respectively. *N,N*-Dimethyl-L-glutamic acid was not decomposed under similar conditions, but a complete racemization occurred.

Experimental

***N,N*-Dimethyl-L-glutamic Acid.** A mixture of 15 g of L-glutamic acid, 1.5 g of a silk-palladium catalyst, 50 m*l* of 37% aqueous formaldehyde, and 150 m*l* of water was shaken in an autoclave at 50—55°C for 6 hr. The catalyst was then removed by filtration, and the filtrate was evaporated to dryness under reduced pressure. A small amount of paraformaldehyde was present in the product; it was removed by re-evaporation with water. The resulting solid was crude *N,N*-dimethyl-L-glutamic acid. It was collected, washed with acetone several times, and dried. The crude product was dissolved in a minimum volume of hot 50% aqueous ethanol, decolorized with a small amount of charcoal, and filtered. About the same volume of acetone was then added in small portions, and the mixture was stored in a refrigerator overnight. Fine crystals of *N,N*-dimethyl-L-glutamic acid were collected by filtration, washed with acetone, and dried under reduced pressure. The yield was 15.5 g (89%).

***N,N*-Dimethyl-L-glutamic Acid *N*-Oxide.** A mixture of 4.0 g of *N,N*-dimethyl-L-glutamic acid, 20 m*l* of 30% aqueous hydrogen peroxide, and 40 m*l* of acetic acid was warmed at 60°C for 8 hr. To the reaction mixture, about 50 m*l* of water was then added, after which the mixture was concentrated to about a half volume under reduced pressure while being gently warmed below 40°C. After this procedure had been repeated until the distillate gave a negative reaction to a potassium iodide starch test, the solution was evaporated to dryness under reduced pressure. The crude products were collected by filtration with a small amount of acetone, washed with acetone, and dried under reduced pressure. The crude *N,N*-dimethyl-L-glutamic acid *N*-oxide thus obtained was dissolved in a minimum volume of hot water, decolorized with a small amount of charcoal, and filtered. About the same volume of acetone was then added in small portions, and the mixture was stored in a refrigerator overnight. Fine crystals were then collected by filtration, washed with acetone, and dried under reduced pressure. The yield was 4.0 g (87%).

The Oxidation of *N,N*-Dimethyl-L-aspartic Acid. A mixture of 4.0 g of *N,N*-dimethyl-L-aspartic acid, 20 m*l* of 30% aqueous hydrogen peroxide, and 40 m*l* of acetic acid was warmed at 60°C for 7 hr. The reaction product was then treated in a manner similar to that in the experiment described in the case of *N,N*-dimethyl-L-glutamic acid. The residue thus obtained was fumaric acid in an almost pure state; it was collected by filtration with a small amount of cold water. The yield was 2.1 g (72%). (Found: C, 41.73; H, 3.47%.)

The Decomposition of *N,N*-Dimethyl-L-aspartic Acid with Aqueous Acetic Acid. A mixture of 4.0 g of *N,N*-dimethyl-L-aspartic acid, 20 m*l* of water, and 40 m*l* of acetic acid was heated on a boiling water bath for 24 hr. The residual solution was then dried up under reduced pressure. The residual syrup was dissolved in a small volume of water, and the solution was dried up under reduced pressure. This procedure was repeated twice; the residue was then solidified, collected by filtration with a small amount of acetone, and dried under reduced pressure. This substance was identified as dimethylammonium hydrogen fumarate by a comparison with an authentic sample prepared from equimolar fumaric acid and dimethylamine. The yield was 3.3 g (83%). (Found: C, 44.43; H, 6.82; N, 8.81%.)

The Decomposition and Racemization of *N,N*-Dimethyl-L-aspartic Acid in an Aqueous Solution. A solution of 5.0 g of *N,N*-dimethyl-L-aspartic acid in 100 m*l* of water was heated on a boiling water bath for 24 hr. The residual solution was then evaporated to dryness under reduced pressure. The residue was suspended in a small volume of ethanol, and the suspension was dried up under reduced pressure to remove a trace of water. This procedure was repeated twice; then the residue was collected by filtration with a small amount of acetone, washed with acetone, and dried under reduced pressure. The residue was extracted with a small amount of hot ethanol several times; *N,N*-dimethyl-DL-aspartic acid was thus separated as precipitates from the mixture because of its insolubility. The yield was 2.0 g (40%). (Found: C, 44.74; H, 6.84; N, 8.68%.) The extract was dried up under reduced pressure; 2.1 g (42%) of dimethylammonium hydrogen fumarate were thus obtained.

The Racemization of *N,N*-Dimethyl-L-glutamic Acid. A mixture of 4.0 g of *N,N*-dimethyl-L-glutamic acid, 20 m*l* of water, and 40 m*l* of acetic acid was heated on a boiling water bath for 20 hr. The residual solution was then treated in a manner similar to that used in the experiment described in the case of *N,N*-dimethyl-L-aspartic acid, The product thus obtained was *N,N*-dimethyl-DL-glutamic acid, weighing 3.8 g (95%). (Found: C, 47.87; H, 7.58; N, 8.10%).

The author is indebted to Professor Eizo Matsumura for his constant guidance in the course of the work, and to Professor Yoshiharu Izumi of Osaka University for his valuable advice and encouragement.

BULLETIN OF THE CHEMICAL SOCIETY OF JAPAN VOL. 43 3604—3607 (1970)

Cobalt(II) Complexes Containing Diacetylacetone and Its Thio Derivative

Akiko FURUHASHI

Department of Chemistry, College of Science and Engineering, Aoyama Gakuin University, Megurisawa, Setagaya-ku, Tokyo

(Received March 27, 1970)

The complex compounds of many metal ions containing β-diketones have already been synthesized and studied.[1,2] The metal complexes of thio-derivatives of β-diketones were reported first by Martin and Stewart.[3]

These thio-β-diketonates were obtained by passing hydrogen chloride and hydrogen sulfide through ethanol solutions containing acetylacetone and metal halide because of the difficulty of the isolation of dithioacetylacetone, which has a tendency to dimerize.

Diacetylacetone is also expected to form metal complexes as β-diketones. Moreover as it has three carbonyl groups in each molecule, it probably acts as both a bidentate and a tridentate ligand.

Sagara and his co-workers[4] reported on Cu(II) and Ni(II) chelates containing bidentate or tridentate diacetylacetone. It has also been reported that trithiodiacetylacetone can be synthesized and isolated by the reaction of diacetylacetone and phosphorus pentasulfide.[5] The present author has previously synthesized the Rh(III) and Pt(II) trithiodiacetylacetone complexes[6] from the metal salts and the ligand. As an extension of this work, although the attempts at the synthesis of the cobalt complexes of trithiodiacetylacetone have not yet been successful, the monothiodiacetonates were obtained.

In this paper the synthesis and properties of Co(II) complexes of $C_7H_{10}SO_2$ as well as of $C_7H_{10}O_3$ will be described.

Experimental

Starting Materials. The cobalt(II) chloride hexahydrate ($CoCl_2 \cdot 6H_2O$) and cobalt(II) bromide hexahydrate ($CoBr_2 \cdot 6H_2O$) of a G. R. Grade were used without further purification. The diacetylacetone (DAA) was synthesized from dehydroacetic acid by the method of Bethell and Maitland.[7] The trithiodiacetylacetone (TTDAA) was obtained by the method of Arndt[5] from DAA and phosphorus pentasulfide.

Syntheses of the Complexes. $Co(C_7H_{10}SO_2)_2X_2$: Powdered Co(II) halide hexahydrate and TTDAA were mixed (1 : 2 mole ratio) for 1 hr in an agate motor. During the procedure, the mixture turned green. The unreacted TTDAA was removed by washing with hot benzene. The crude product thus obtained was dissolved into chloroform, and the insoluble, unreacted cobalt halide was filtered off. The filtrate was concentrated using a rotary evaporator at about 50°C, and from the solution a green product was precipitated by adding

TABLE 1. ANALYSIS AND MAGNETIC MOMENTS OF COMPLEXES
(Analytical data are given in % and magnetic moments are given in B.M.)

		C	H	S	X	M	O*	B.M
$Co(II)(C_7H_{10}SO_2)_2Cl_2$	Calcd	37.68	4.53	14.37	15.89	13.20	14.33	4.46
	Found	37.80	4.10	15.30	15.00	13.40	14.41	
$Co(II)(C_7H_{10}O_3)_2Cl_2$	Calcd	40.60	4.88		17.12	14.23	23.17	4.77
	Found	41.55	4.62		17.56	14.50	23.53	
$Co(II)(C_7H_{10}SO_2)_2Br_2$	Calcd	31.42	3.77	11.98	29.86	11.01	11.96	4.77
	Found	32.00	3.21	11.90	30.90	10.90	11.31	
$Co(II)(C_7H_{10}O_3)_2Br_2$	Calcd	33.42	4.02		31.77	11.71	19.08	4.55
	Found	33.90	4.04		32.00	12.00	18.66	

* Obtained by substraction of the sum of the analyses of other elements from 100%

1) A. E. Martell and M. Calvin, "The Chemistry of Metal Chelate Compounds," Prentice-Hall, INC. Engelewood Cliffs, N. J. (1952).

2) W. C. Fernelius, B. E. Bryant, *Inorg. Synthesis*, **5**, 105 (1957).

3) R. L. Martin and I. M. Stewart, *Nature*, **210**, 522 (1966).

4) F. Sagara, H. Kobayashi and K. Ueno, This Bulletin, **41**, 266 (1968).

5) F. Arndt, P. Nacktwey and J. Pusch, *Ber.*, **58**, 1633 (1925).

6) A. Furuhashi, Y. Hayakawa and A. Ouchi, Symposium on Coordination Chemistry, Sendai, Sept. 1969.

7) J. R. Bethell and P. Maitland, *J. Chem. Soc.*, **1962**, 3751.

TABLE 2. INFRARED SPECTRA OF COMPLEXES (Figures are given in cm^{-1}.)

$C_7H_{10}O_3$	$C_7H_8S_3$	$Co(C_7H_8O_3)_2Cl_2$	$Co(C_7H_8O_3)_2Br_2$	$Co(C_7H_8O_2S)_2Cl_2$	$Co(C_7H_8O_2S)_2Br_2$	Tentative assignments
1635 (br. v.s)	1640 (br. v.s)	1650 (v.s)	1650 (v.s)			
				1620 (s)	1625 (s)	C=C stretch
		1573 (m)	1573 (m)	1568 (w)	1568 (w)	
		1550	1550	1540 (m)	1540 (s)	
1540 (m)		1535 (s)	1535 (s)			
	1490 (s)	1488 (w)	1488 (w)			or C=O stretch
	1430 (w)	1450 (w)	1450 (w)	1440 (m)	1445 (m)	
		1418 (m)	1418 (m)		1400 (w)	CH_3 deform.
1395 (s)	1372 (s)	1380 (w)	1380 (w)	1375 (w)	1375 (w)	
1355 (s)		1350 (s)	1350 (s)		1350 (w)	
	1295 (s)			1285 (s)	1285 (s)	
1240 (s)	1250 (s)					
	1210 (s)	1202 (s)	1202 (s)			
1180 (s)		1170 (m)	1170 (m)	1170 (w)	1170 (w)	C–CH_3 stretch
1140 (s)						
	1120 (s)			1100 (s)	1102 (s)	
1035 (s)		1045 (m)	1045 (m)	1040 (w)	1030 (w)	
	1020 (w)			1007 (s)	1007 (s)	CH_3 rocking mode
978 (w)		960 (m)	961 (m)	950 (w)	950 (w)	CH deform.
945 (m)		909 (s)	909 (s)	940 (m)	942 (m)	(out of plane)
					910 (w)	
895 (s)		890 (m)	890 (m)	899 (v.w)	889 (w)	
		879 (m)	897 (m)	872 (w)		
	850 (v.s)			855 (s)	855 (s)	C–H out of plane bend
820 (v.s)						
750 (m)	740 (w)					
735 (s)	698 (s)			689 (m)	698 (m)	C=S stretch
	665 (m)					
		627 (m)	630 (m)			
	600 (m)					
555 (s)	595 (m)	555 (m)	557 (m)	570 (m)	570 (m)	C–CH_3 deform.
		525 (m.w)	528 (m.w)			
488 (s)	471 (m)	457 (v.w)	460 (v.w)	470 (v.w)	470 (w)	

v.s: very strong, s: strong, m: medium, w: weak, v.w: very weak, br: broad

an equivolume of petroleum ether.

$Co(C_7H_{10}O_3)_2X_2$: $Co(C_7H_{10}O_3)_2X_2$ was similarly synthesized using cobalt halide hexahydrate and DAA. The product was blue.

Instruments. The magnetic moments of the compounds were measured by Gouy's method at room temperature (25°C). The infrared spectra were obtained on a KBr disk sample by using a Model IR-G infrared spectrophotometer of the Japan Spectroscopic Co., Ltd. The electronic spectra were obtained with a Shimadzu MPS-50-type automatic recording spectrophotometer. The NMR spectra were obtained with a Hitachi Perkin-Elmer Model-R-20 NMR spectrometer.

Results and Discussion

The analytical data and magnetic moments are summarized in Table 1.

The magnetic data show that these compounds have magnetic moments of 4.5—4.8 B.M. In the case of cobalt(II) complexes, the magnetic moment of the tetrahedral form is found mostly in the 4.4—4.7 B.M. range, that of the octahedral form in the 4.7—5.2 B.M. range and that of the square-planar form in the 2.4—2.8 B.M. range, because of the orbital angular momentum contribution. In view of these facts, it is reasonable to conclude that the compounds are tetrahedral.

The infrared spectra data of the compounds are summarized in Table 2.

As there are almost no differences between the spectra of chloro and bromo complexes, the chlorine or bromine can be said not to have any serious effect on the vibrational frequencies in the complexes. Two strong characteristic bands which seem to be ν (C=O) appear near the 1962—1650 cm^{-1} range.

It is rather difficult to assign the ν (C=S) bands of these compounds. Barraclough[8] has reported that the ν (C=S) bands appear near 660—750 cm^{-1}; he based the conclusion on the results of the coordination analyses as well as on the experimental data of the metal dithioacetylacetonato complexes. As the 698 cm^{-1} band of the $Co(C_7H_{10}SO_2)_2X_2$ seems to correspond to the 740, 698 and 665 cm^{-1} bands of $C_7H_8S_3$, it is probably the ν (C=S) band or at least one containing ν (C=S), although the intensity of the band of the metal complexes was not so strong as that of the bands of $C_7H_8S_3$. This fact seems to indicate that the $Co(C_7H_{10}SO_2)_2X_2$ has only one C=S bond, as is also shown by the analytical data. As the shift of the ν(C=S) band by the formation of the coordination bond with the central metal is not extensive, the bond between sulfur and the metal atom in the complex seems not to be strong.

The findings regarding the NMR spectra also support the above conclusion. The NMR spectra of TTDAA in $CDCl_3$ (standard : TMS) shows four peaks, at 7.45, 6.84, 2.60, and 2.18 ppm; the ratio of the areas of the peaks was 1 : 1 : 3 : 3. This can probably be explained by the fact that TTDAA has a five-membered ring containing as S–S bond and a free C=S bond, as is shown by Fig. 1.

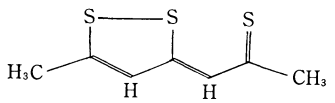

Fig. 1. Structure of TTDAA.

Therefore, both the methyl groups and the hydrogen atoms combined with 3rd and 5th carbon atoms are indifferent. The NMR spectra of both $Co(C_7H_{10}SO_2)_2X_2$ and $Co(C_7H_{10}O_3)_2X_2$ show only one peak, at about 2.58 ppm. Therefore, the two methyl groups of the ligand of the cobalt(II) compounds are symmetric; however, as these compounds are hardly soluble into $CDCl_3$, the peaks due to the hydrogen atoms bonding to the 3rd and 5th carbon atoms can not be deserved. The peaks of the latter hydrogen atoms were, however, found in the case of the DMF solution, 6.74 ppm for $Co(C_7H_{10}SO_2)_2X_2$ and 5.75 ppm for $Co(C_7H_{10}O_3)_2X_2$, although the effect of the solvent on the species may be a little different in this case. Consequently, in the case of $Co(C_7H_{10}O_3)_2X_2$, the central oxygen atoms of the ligand seem to bond with the cobalt atom, and in the case of $Co(C_7H_{10}SO_2)_2X_2$ the sulfur atom, which replaces the central oxygen atom of the $C_7H_{10}O_3$ ligand, is probably combined with the cobalt atom.

The electronic spectra of these compounds of a chloroform solution are summarized in Table 3.

The bands at about 38000—40000 cm^{-1} seem to be the π–π bands of the ligands. Trithiodiacetylacetonates of Cu(I) and Pt(II)[5] also show the band at 38000 cm^{-1}. Therefore, the band due to ligands moves to the lower wave number side as the number

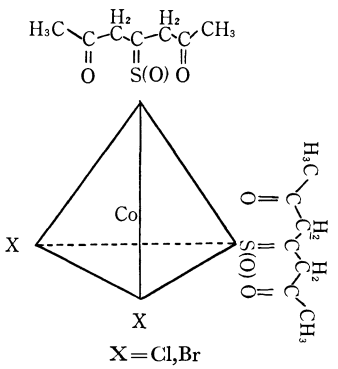

Fig. 2. Structure of Co(II) complex.

Table 3. Electronic spectra of complexes

(Figures are given in cm^{-1} for wave numbers and log ε for intensities (in parentheses).)

$C_7H_{10}O_3$	$C_7H_8S_3$	$Co(C_7H_{10}O_3)_2Cl_2$	$Co(C_7H_{10}O_3)_2Br_2$	$Co(C_7H_{10}SO_2)_2Cl_2$	$Co(C_7H_{10}SO_2)_2Br_2$
		40240 (4.10)			
39540 (3.62)	38020 (4.82)		39920 (4.24)	39370 (4.22)	39370 (4.31)
38020 (3.61)					
31250 (4.27)		30670 (sh) (2.49)	30670 (sh) (2.57)		
				28820 (4.60)	28820 (4.59)
	28090 (sh) (2.70)	26320 (sh) (1.99)	26600 (sh) (1.86)		
				24270 (sh) (3.21)	24270 (sh) (3.16)
		22220 (1.83)	22220 (1.00)		
	21140 (3.92)				

8) C. G. Barraclough, R. L. Martin and I. M. Stewart, *Aust. J. Chem.*, **22**, 891 (1969).

of sulfur atoms in a ligand molecule increases.

The bands at about 22000—26000 cm^{-1} seem to be mixtures of d–d and d-π bands. Generally, tetrahedral cobalt(II) complexes have an intense band at about 15000 cm^{-1}. Although the solid compounds have an intense color, the solution of these compounds lost its intense color and turned pink rapidly. This is probably because the complexes decompose and change into octahedral complexes in such a dilute solution.

The results suggest that these compounds have a tetrahedral configuration and that the ligand works as a zero-valent monodentate in it. The structure shown in Fig. 2 is proposed for these compounds.

The author wishes to express her gratitude to Dr. A. Ouchi of The University of Tokyo for his frequent, stimulating, and helpful discussions. The author is also indebted to Mr. N. Tashiro for his assistance and to Professor Yasumasa Hayakawa and the staff of the Department of Chemistry of Aoyama Gakuin University for their encouragement.

BULLETIN OF THE CHEMICAL SOCIETY OF JAPAN VOL. 43 3607—3608 (1970)

2-Hydroxy-3-oxo-2,3-dihydrofuran-2-carboxylic Ester: The Oxidation Product of 3-Hydroxyfuran-2-carboxylic Ester

Hisashi TAKEI and Teruaki MUKAIYAMA

Laboratory of Organic Chemistry, Tokyo Institute of Technology, Ookayama, Meguro-ku, Tokyo

(Received April 1, 1970)

In a preceding communication,[1] it was shown that carbonyl-stabilized sulfonium ylides reacted with ketene dimer to give 2-acyl-3-hydroxy-5-methylfurans in good yields. For example, the reaction of ethyl dimethylsulfuranilideneacetate with ketene dimer in THF in an atmosphere of nitrogen afforded ethyl 3-hydroxy-5-methylfuran-2-carboxylate (Ia), mp 49—50°C, in a 60% yield. In this case, the furan was purified by distillation and analytical sample was obtained by subsequent sublimation.

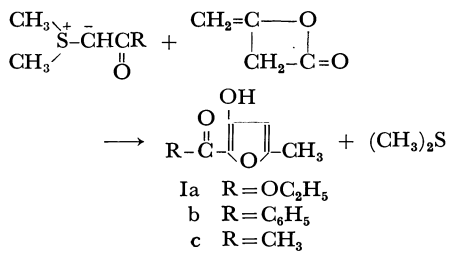

Ia R=OC_2H_5
b R=C_6H_5
c R=CH_3

It was found by the present experiment that when the reaction mixture was chromatographed over silica gel, colorless needles (IIa), mp 102—103°C, were isolated instead of Ia. Elemental analyses showed that IIa might be an oxidized product of Ia. Therefore, it is suggested that Ia was oxidized in the course of process for purification. Indeed, it was also found that the repetition of recrystallization from petroleum ether or the exposure of crystalline Ia to air for a long time resulted in the formation of IIa by air oxidation.

The structure of IIa was assigned to be ethyl 2-hydroxy-5-methyl-3-oxo-2,3-dihydrofuran-2-carboxylate, which is thought to be a cyclic hemiketal of III, on the basis of UV, NMR and IR spectra.

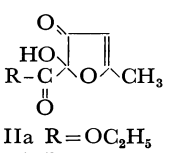

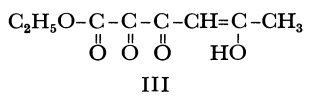

III

IIa R=OC_2H_5
b R=C_6H_5
c R=CH_3

The UV spectrum of Ia in methanol showed a single peak at 265 mμ with εm 18000. Whereas, that of IIa in methanol gave εm 9200 at 269 mμ. This peak coincides with that reported[2] for 5-alkyl-3-oxo-2,3-dihydrofurans at 260—265 mμ with εm 8750—12200. The NMR spectrum has a singlet at 7.68 τ (3H, methyl), a triplet at 8.70 τ and a quartet at 5.65 τ (3H and 2H, ethyl ester) and a singlet at 4.43 τ (2H, furan nuclear proton and hydroxy proton). The last signal may be inadvertently superposed upon each other. The IR spectrum in KBr showed a band at 3170 cm^{-1} which suggested the presence of hydrogen bonding hydroxyl and three bands in carbonyl region at 1760, 1700 and 1600 cm^{-1} due to the carbonyl of five membered ring, hydrogen bonded ester carbonyl

1) H. Takei, M. Higo, K. Saito and T. Mukaiyama, This Bulletin, **41**, 1738 (1968).

2) R. E. Rosenkranz, K. Allner, R. Good, W. V. Philisborn and C. H. Eugster, *Helv. Chim. Acta*, **46**, 1259 (1963).

and carbon–carbon double bond, respectively. Whereas IIa in methylene chloride solution gave three peaks in carbonyl region at 1740, 1720 and 1600 cm^{-1} attributable to hydrogen bonded carbonyl, ester carbonyl and carbon–carbon double bond, respectively. These facts suggest that the IIa may exist as IIa′ in crystalline, whereas IIa″ in solution.

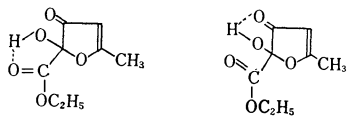

IIa′ IIa″

On the other hand, it was found that analogous furans such as Ib, the methyl ether of Ib, and Ic were stable towards air oxidation. Then these furans were treated with various oxidizing agents in order to obtain IIb and IIc. But, all attempts were unsuccessful and in the cases of Ib and of its methyl ether, benzoic acid was obtained as a main product.

Finally the reaction of IIa was tried with the expectation that it would be used as a useful intermediate in the field of synthetic chemistry. When IIa was allowed to react with *o*-phenylenediamine, ethyl 3-(2-oxopropyl) quinoxaline-2-carboxylate (IV) was obtained in a 69% yield.[3]

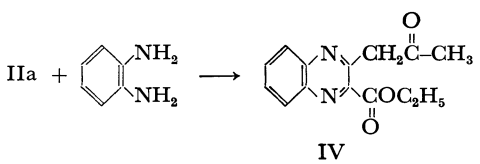

IV

3) In this connection, Lutz *et al.* have reported that 2-hydroxy-3-oxo-2,3-dihydrofuran, hemiketal of enol form of 1,2,4-triketone, reacts with *o*-phenylenediamine to give quinoxaline derivative. R. E. Lutz and A. H. Stuart, *J. Amer. Chem. Soc.*, **58**, 1885 (1936), and references cited therein, See, also J. C. E. Simpson, "The Chemistry of Heterocyclic Compounds. Condensed Pyridazine and Pyrazine Rings," Interscience Publishers Inc., New York (1953), p. 293.

Experimental

Reaction of Ethyl Dimethylsulfuranilideneacetate with Ketene Dimer. a) To a solution of ethyl dimethylsulfuranilideneacetate (1.48 g, 0.01 mol) in THF, ketene dimer (0.84 g, 0.01 mol) in the same solvent was added dropwise under ice cooling in an atmosphere of nitrogen. The reaction mixture was allowed to stand at room temperature for an hour and then was refluxed for 20 min. After removal of the solvent, the resulting dark brown syrup was distilled to give crude Ia (1.00 g, 60%), bp 80—90°C/2 mmHg, which solidified immediately. The analytical sample was obtained by the subsequent sublimation under reduced pressure, mp 49—50°C.

Found: C, 56.59; H, 5.93%. Cacld for $C_8H_{10}O_4$: C, 56.46; H, 5.92%.

b) When the dark brown syrup in the above experiment was submitted to silica gel column chromatography, semi-crystalline material was eluted by benzene-methylene chloride. The crystals were collected and recrystallized twice from cyclohexane with small amount of benzene to give colorless needles, IIa, (0.62 g, 33%) mp 100—103°C.

Found: C, 51.72; H, 5.25%. Calcd for $C_8H_{10}O_5$: C, 51.61; H, 5.41%.

Reaction of IIa with *o*-Phenylenediamine. A mixture of IIa (0.19 g, 0.001 mol), *o*-phenylenediamine (0.11 g, 0.001 mol) and two drops of acetic acid in ethanol was kept at room temperature for 2 days. After evaporation of the solvent, the residue was submitted to preparative thinlayer chromatography. When it was developed by ethyl acetate, pale orange crystals, IV, were obtained from the part of R_f value about 0.7—0.85, which were recrystallized from dilute alcohol, mp 86—87.5°C (0.18 g, 69%). The infrared spectrum (KBr) showed strong absorptions at 1740 (ester carbonyl) and at 1720 cm^{-1} (ketone).

Found: C, 64.87; H, 5.46; N, 10.92%. Calcd for $C_{14}H_{14}N_2O_3$: C, 65.10; H, 5.46; N, 10.85%.

BULLETIN OF THE CHEMICAL SOCIETY OF JAPAN VOL. 43 3609—3611 (1970)

An Acyl Migration with Oxalic Acid

Hideki KINOSHITA and Hiroshi KOTAKE

Faculty of Science, Kanazawa University, Kanazawa

(Received April 17, 1970)

In the past few years, the structures of a number of new antibiotics have been reported in the literature; all have had the common feature of a lactone that is formed from the carboxyl function of an amino acid and the hydroxyl group of a hydroxy-amino acid.

For the synthesis of these peptide lactone antibiotics, it is necessary to synthesize a chain that will include the desired ester bond. As a preliminary investigation for this purpose, we have first prepared an ester chain, namely, *O*-(*t*-butyloxycarbonyl-L-phenylglycyl)-*N*-benzyloxycarbonyl-L-threonine (I), which has already been reported by Ondetti and Thomas.[1)]

The coupling of *t*-butyloxycarbonyl-L-phenylglycine and *N*-benzyloxycarbonyl-L-threonine was carried out by the method reported by Ondetti and Thomas; then the reaction mixture was separated by Sephadex LH-20, using chloroform as the elution solvent. By this separation method, we easily obtained the desired ester chain as an oily substance, which was then crystallized as dicyclohexylammonium salt (II) by treatment with dicyclohexylamine in an acetone - hexane solution.

The values of the physical constant and the spectroscopic data of this dicyclohexylammonium salt (II) were identical with those of the dicyclohexylammonium salt of I reported in the literature.[1)] From this finding, it is obvious that the substance containing the ester bond obtained here was the compound I. For the purification of this salt, II, it was dissolved in acetone while being heated and then allowed to stand for several hours at room temperature; this gave crystals which melted at 154—155°C, but its IR spectrum showed that this product was not the ester-bond compound, but a compound resulting from the *O*,*N* acyl migration. This migration has also been seen when II was dissolved in chloroform or benzene without heating and allowed to stand at room temperature. We have assumed that this *O*,*N* acyl migration product was *t*-butyloxycarbonyl-L-phenylglycyl-*N*-benzyloxycarbonyl-L-threonine (III), which was obtained in this case as its dicyclohexylammonium salt (IV); this structure was confirmed by synthesis, as is shown in Fig. 3.

The salt IV was treated with equal moles of oxalic acid in acetone, and then the deposited ammonium salt of oxalic acid was filtered and the acetone was removed; this left an oily substance which was crystallized as its salt in a 96% yield by the addition of dicyclohexylamine. Since the

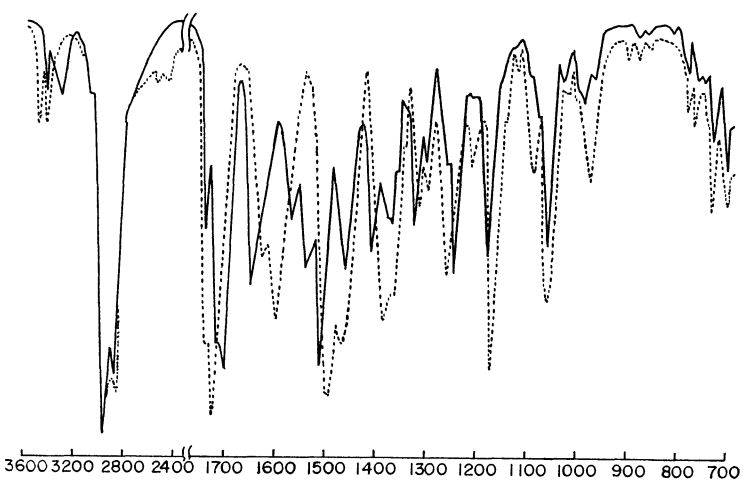

Fig. 1. Infrared spectra.
—— (II) ------ (IV)

1) M. A. Ondetti and P. L. Thomas, *J. Amer. Chem. Soc.*, **87**, 4373 (1965).

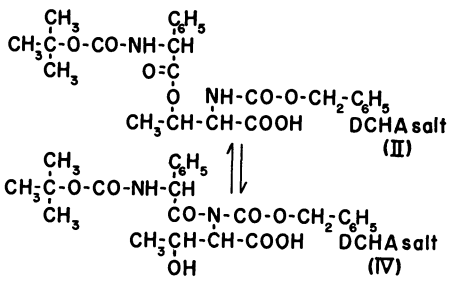

Fig. 2

IR spectrum of this salt was identical with that of the salt II, it is clear that the *N,O* acyl migration had occurred upon the treatment of the oxalic acid. Though the melting point and the specific rotation value of the salt obtained by the *N,O* acyl migration are higher than the values of the salt II, it is possible, in view of the value of specific rotation, that the purity of the former compound is slightly higher.

In the present case it was also found that the *N,O* acyl migration with oxalic acid did not affect the *N*-protecting *t*-butyloxycarbonyl- and benzyloxycarbonyl- groups and that no racemization occurred.

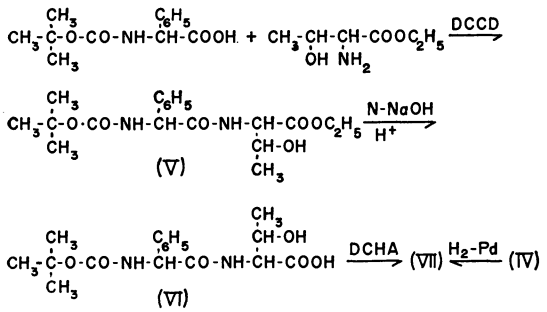

Fig. 3

t-Butyloxycarbonyl-L-phenylglycyl-L-theronine (VI) was prepared in the following way. *t*-Butyloxycarbonyl-L-phenylglycyl-L-threonine ethyl ester (V), obtained by the coupling of *t*-butyloxycarbonyl-L-phenylglycine and L-threonine ethyl ester in the presence of dicyclohexylcarbodiimide in acetonitrile, was hydrolyzed by 1N sodium hydroxide at room temperature to give VI. The dicyclohexylammonium salt of VI was found to be identical with the debenzyloxycarbonylation product of IV in melting point, IR spectra, and specific rotation value.

Experimental

***O*-(*t*-Butyloxycarbonyl-L-phenylglycyl)-*N*-benzyloxycarbonyl-L-threonine Dicyclohexylammonium Salt (II).** *t*-Butyloxycarbonyl-L-phenylglycine (920 mg, 3.5 mmol) and *N*-benzyloxycarbonyl-L-threonine (1.75 g, 3.5 mmol) and *N*-benzyloxycarbonyl-L-threonine (1.75 g, 7 mmol) were treated by the method reported in the literature.[1] The crude reaction product thus obtained showed two spots (R_f 0.79 and 0.41) on thin-layer chromatography. This mixture was separated by Sephadex LH-20, using chloroform as the elution solvent. The compound, with an R_f value of 0.41, which was shown to be the desired product, was isolated from acetone - hexane in the form of a crystalline dicyclohexylammonium salt. Yield, 640 mg (38%); mp 146.5—149°C; $[\alpha]_D^{21}$ +34.0° (*c* 0.838, DMF) (lit. mp 145—147°C; $[\alpha]_D^{28}$ +35.1°).

Found: C, 66.48; H, 8.08; N, 6.38%. Calcd for $C_{37}H_{53}O_8N_3$: C, 66.57; H, 7.95; N, 6.30%.

***t*-Butyloxycarbonyl-L-phenylglycyl-*N*-benzyloxycarbonyl-L-threonine Dicyclohexylammonium Salt (IV).** The salt II (76.8 mg, 0.114 mmol) was dissolved in hot acetone (1 m*l*) and then allowed to stand for several hours at room temperature. By the addition of hexane to this solution, crystals of IV were precipitated. Yield, 69.5 mg (90%); mp 154—155°C; $[\alpha]_D^{25}$ +41.1° (*c* 0.953, DMF).

Found: C, 66.22; H, 8.26; N, 6.51%. Calcd for $C_{37}H_{53}O_8N_3$: C, 66.57; H, 7.95; N, 6.30%.

Migration of IV to II with Oxalic Acid. To a solution of IV (188 mg, 0.282 mmol) in hot acetone (1 m*l*), we added oxalic acid-$2H_2O$ (35.5 mg, 0.282 mmol); the solution was then refluxed for 5 min and subsequently left standing for 2 hr at room temperature. A dicyclohexylammonium salt of oxalic acid thus deposited was filtered off, the mother liquor was removed *in vacuo*, and the residue was dissolved in ethyl acetate. After the filtration of an insoluble oxalic acid, the solvent was removed and the residual oil was again dissolved in 0.5 m*l* of acetone. To this solution dicyclohexylamine (0.05 m*l*) in hexane was then added. After a short time, crystalline salts were obtained. Yield, 181 mg (96.2%); mp 154—155°C; $[\alpha]_D^{25}$ +40.1° (*c* 0.983, DMF). The IR spectrum of this salt was identical with that of II, and a mixed-melting-point determination with IV was depressed to 151—152°C.

***t*-Butyloxycarbonyl-L-phenylglycyl-L-threonine Ethyl Ester (V).** *t*-Butyloxycarbonyl-L-phenylglycine (200 mg, 0.8 mmol) and L-threonine ethyl ester (117 mg, 0.8 mmol) were dissolved in acetonitrile (4 m*l*) and cooled at −3°C. A solution of dicyclohexylcarbodiimide (165 mg, 0.8 mmol) in acetonitrile (2 m*l*) was added, with stirring and cooling below −1°C; stirring was continued for 3 hr at −1°C and then for 7 hr at room temperature. The precipitate of dicyclohexylurea was filtered, and the filtrate was concentrated to dryness *in vacuo*. The oily product was dissolved in ethyl acetate; then the solution was washed with 3% hydrochloric acid, 3% sodium bicarbonate, and then with water, and dried over anhydrous sodium sulfate. The concentration of the solution *in vacuo* left a crystalline product which was recrystallized twice from ethyl acetate - petroleum ether. Yield, 170 mg (68%); mp 107—108.5°C; $[\alpha]_D^{20}$ +48.0° (*c* 1.03, abs. ethanol).

Found: C, 59.87; H, 7.45; N, 7.41%. Calcd for $C_{19}H_{28}O_6N_2$: C, 59.98; H, 7.42; N, 7.36%.

***t*-Butyloxycarbonyl-L-phenylglycyl-L-threonine (VI).** Into a solution of V (150 mg, 0.4 mmol) in ethanol (3 m*l*), 1N aqueous sodium hydroxide (0.4 m*l*, 0.4 mmol) was added with stirring. After the solution had stood at room temperature for 1.5 hr, 2 m*l* of water as

added to the reaction mixture and ethanol was removed *in vacuo*. The aqueous residue was treated with ethyl acetate, and the aqueous layer was adjusted to pH 3 to give an oily product. This product was extracted with ethyl acetate, and the solution was washed with water and dried over anhydrous sodium sulfate. The concentration of the solution *in vacuo* left a crystalline product (112 mg, 80%), which was subsequently recrystallized from ethyl acetate - petroleum ether. Yield, 98 mg (70%); mp 150—151°C; $[\alpha]_D^{26}$ +60.9° (*c* 1.04, abs. ethanol).

Found: C, 57.61; H, 6.77; N, 7.99%. Calcd for $C_{17}H_{24}O_6N_2$: C, 57.94; H, 6.87; N, 7.95%.

The dicyclohexylammonium salt (VII) of this compound (VI) was prepared in the usual way; mp 145—146°C; $[\alpha]_D^{25}$ +45.3° (*c* 1.03, DMF). No depression of the melting point was observed on admixture with the debenzyloxycarbonylation product of IV.

BULLETIN OF THE CHEMICAL SOCIETY OF JAPAN VOL. 43 3611—3613 (1970)

Nuclear Magnetic Resonance for the Pathway of the Reaction of *N*-Sulfinylanilines with Ethylene Oxide

Fukiko YAMADA, Tomihiro NISHIYAMA, Motokazu KINUGASA and Masayoshi NAKATANI

Department of Applied Chemistry, Faculty of Engineering, Kansai University, Senriyama, Suita, Osaka

(Received May 14, 1970)

The reaction of *N*-sulfinylanilines (I) with either ethylene carbonate or alkene oxides have been well studied in recent years. For example, Tsuge and his co-workers[1] reported that, in the presence of catalytic amounts of lithium halide, I reacted with ethylene carbonate at temperatures above 140°C to form the corresponding *N,N'*-diarylpiperazines (V). Etlis *et al.*[2] confirmed that, in the presence of NEt_4-Br, I reacted with alkene oxide at 95—100°C in sealed ampules to give 2-oxo-3-aryl-1,2,3-oxathiazolidines (III). Recently Deyrup and Moyer[3] have prepared several derivatives of III by reactions of β-amino alcohol with thionyl chloride in the presence of a base; the general structure of these compounds was determined by means of their NMR spectra. In these circumstances, we thought it desirable to study how the reaction of I with ethylene oxide (II) takes place in the absence of a catalyst and at a low temperature. In this paper, the reaction of I with II and the NMR data of the resulting products will be reported. The reaction scheme will also be discussed.

Experimental

The NMR spectra were obtained at 60 MHz with a Japan Electron Optics, Model JNM 3H-60, spectrometer. The chemical shifts were described in ppm downfield from the internal TMS (δ). The IR spectra were recorded on a Hitachi, Model EPI-2, grating spectrophotometer. The molecular-weight determination was made by a vapor-pressure osmometer, Hewlett Packard 302.

Materials. *N*-Sulfinylaniline (Ia), *N*-sulfinyl-*p*-toluidine (Ib), and *N*-sulfinyl-*p*-chloroaniline (Ic) were prepared and purified by the reported method.[4] II was of a commercially-available, pure grade and was dried by using a potassium hydroxide tube just before use. All the reagents used were of an analytical grade.

The Reaction of I with II. In a three-necked, 100-m*l* flask, 30 g of I was placed, the flask was then kept at a constant temperature. A constant flow of II (4.5 *l*/hr) was introduced into the reaction mixture throughout the reaction. The progress of the reaction was periodically checked by measuring the NMR spectrum of the reaction mixture. After the reaction had been completed and the excess II had been evaporated, a red-brown sirup remained. For the isolation of pure compounds from the mixture, the following two procedures were employed.

Procedure A. Fractionation of the Products. The above mixture (10—20 g) was chromatographed on 100 g of silica gel, using methylene chloride and methanol as eluents. Each eluate was examined by means of its NMR spectrum. The eluates which showed the same NMR spectra were combined and then evaporated *in vacuo*. The combined solutions (1, 2, and 3) were classified as follows: the initial eluate (1) was almost entirely composed of compound III, the middle one (2) contained mainly a resinous compound, IV, and the third one (3) gave small amounts of *N*-(2-hydroxyethyl)anilines (1—2 wt%). 2-Oxo-3-phenyl-1,2,3-oxathiazolidine (IIIa, 12 wt% yield) or 2-oxo-3-*p*-tolyl-1,2,3-oxathiazolidine (IIIb, 12 wt% yield) was obtained from the reaction of II with Ia or Ib. 2-Oxo-3-*p*-chloro-

1) O. Tsuge, S. Mataka, N. Tashiro and F. Mashiba, This Bulletin, **40**, 2709 (1967).

2) V. S. Etlis, A. P. Sineokov and M. E. Sergeeva, *Khim. Geterotskil. Soedin*, 682 (1966).

3) J. A. Deyrup and C. L. Moyer, *J. Org. Chem.*, **34**, 175 (1969).

4) A. Michaelis and R. Herz, *Ber.*, **23**, 3480 (1890).

phenyl-1,2,3-oxathiazolidine (IIIc) was not isolated from the reaction of Ic. IIIa and IIIb were purified by recrystallization from methylene chloride and *n*-hexane. The analytical results and melting points of IIIa and IIIb coincided with those of the compounds previously reported.[2] The resinous compounds, IVa, IVb, and IVc, were purified by rechromatography on silica gel. IVa: 78 wt% yield, mol wt 579, Found: C, 55.83; H, 6.26; N, 6.79; S, 11.01%. IVb: 71 wt% yield, mol wt 403, Found: S, 13.41%. IVc: 85 wt% yield, mol wt 485, Found: S, 12.31%.

Precedure B. Thermal Decomposition. The mixture described above was maintained at 160°C for about 1 hr under reduced pressure, and then it was extracted with benzene. The benzene extract was evaporated to give V as a solid. This was recrystallized from benzene to give colorless needles. *N,N'*-Diphenylpiperazine (Va, 73 wt% yield), *N,N'*-di-*p*-tolylpiperazine (Vb, 56 wt% yield), and *N,N'*-di-*p*-chlorophenylpiperazine (Vc, 78 wt% yield) were obtained from the corresponding reaction mixture by Procedure B. The analytical results and melting points of Va, Vb, and Vc coincide with those of the compounds previously reported.[1]

Results and Discussion

The Reaction Process. In the case of the reaction of Ia with II, the changes in the NMR spectra with the reaction time are shown in Fig. 1. The two-proton and three-proton multiplets due to the ring protons of Ia appear in the regions of 8.0—8.2 and 7.6—7.7 ppm respectively. These signals changed with the reaction time. Of these signals, the three-proton signal changed most remarkably as a result of the overlapping of the ring-proton signal of the reaction product. The two-proton signal gradually decreased, and it disappeared when the reaction was over. However, the two-proton signal does not overlap with any other signal. Therefore, the conversion of Ia can be determined by means of the data of the integrated two-proton

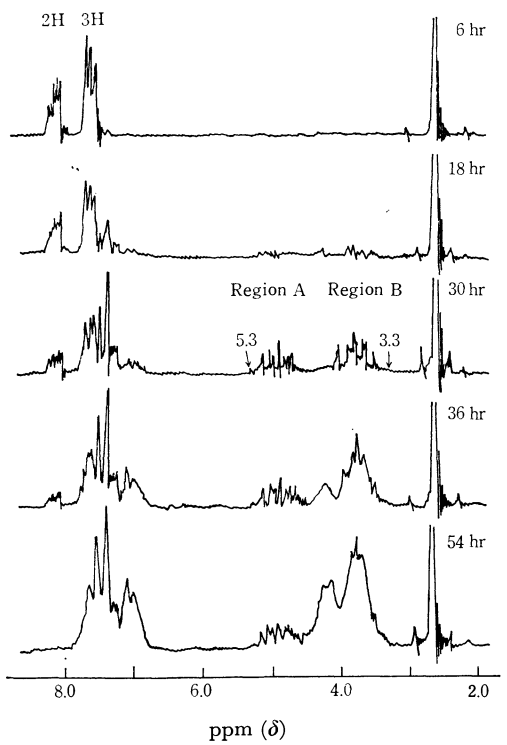

Fig. 1. Changes of the NMR spectra with reaction time at 25°C.

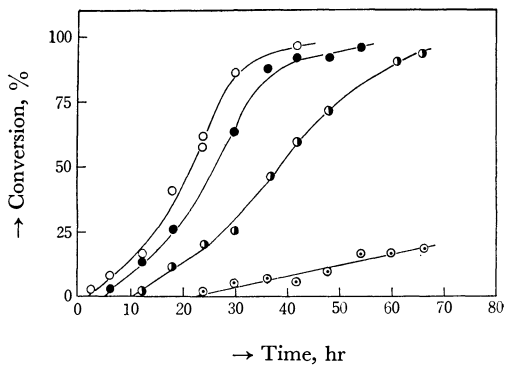

Fig. 2. Time-conversion curves at various temperatures in the reaction of Ia with II.
—○—: the reaction at 15°C
—●—: the reaction at 25°C
—◑—: the reaction at 40°C
—⊙—: the reaction at 65°C

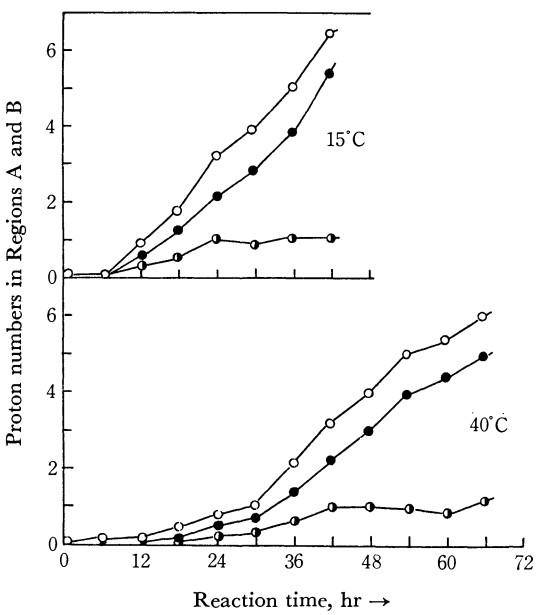

Fig. 3. Plots of the proton numbers in Regions A and B *vs.* reaction time in the reaction of Ia with II.
◑: Proton numbers in Region A; ●: Proton numbers in Region B; ○: Total proton numbers in Region (A+B).

Table 1. Spectral properties of III and IV

Compound No.	IR (S=O) cm^{-1}	NMR data, δ, ppm in CH_2Cl_2			
		methylene		aromatic ring	CH_3
		$-\overset{|}{N}-CH_2-$	$-O-CH_2-$		
IIIa	1172	m 3.3—4.1	m 4.3—5.2	m 6.9—7.6	
IIIb	1169	m 3.4—4.1	m 4.4—5.1	q 7.1	s 2.4
IVa	1195	m 3.2—4.5 (6.6H)*		m 6.7—7.7	
IVb	1190	m 3.3—4.5 (8.5H)*		m 6.6—7.5	s 2.4
IVc	1133	m 3.0—4.8 (9.3H)*		m 6.5—7.8	

( )*: proton numbers

spectrum. The methylene-proton signal of II exhibits a singlet peak at 2.68 ppm. In the earlier stage of the reaction, new signals were observed in the region of 3.3—5.3 ppm and gradually increased with the reaction time. These signals consist of two parts; one (Region A) is in the region of 4.6—5.3 ppm, and the other (Region B) in the region of 3.3—4.3 ppm. The proton numbers of the signal in the A or B region can be evaluated by comparing the data of the integrated signal with those of the signals due to the phenyl protons, which are unchanged by the reaction. Plots of the conversion *versus* the reaction time and of the proton numbers in the A or B region against the time are shown in Figs. 2 and 3 respectively. The NMR data of III and IV are shown in Table 1, and the chemical shifts in the A and B regions are shown in Table 2.

Table 2. NMR data (δ) of the regions A and B

Reaction of II with	Region A	Region B
Ia	4.6—5.3	3.3—4.3
Ib	4.5—5.4	3.2—4.5
Ic	4.7—5.4	3.3—4.7

By comparing the NMR data of IIIa and IVa with those in the A and B regions, the signals in the regions can be assigned to the methylene groups of the oxathiazolidine ring produced by the reaction. The methylene proton numbers in the B region increased with the reaction time up to about 7 (Fig. 3). These facts may indicate, therefore, that the expansion of the oxathiazolidine ring is caused by the insertion of either II or IIIa into the ring.

Probable Mechanism. On the basis of the results presented above, the probable reaction pathway is that shown in Chart 1. The reaction proceeds gradually after an induction period (Figs. 2 and 3). The intermediate A may be expected to be formed in this induction period.

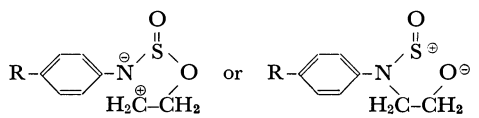

Intermediate A

The authors wish to thank Miss H. Nishikawa, the micro analytical laboratory of this department and the staff of the Research Laboratories, Fujisawa Pharmaceutical Co., Ltd. for the elementary analyses.

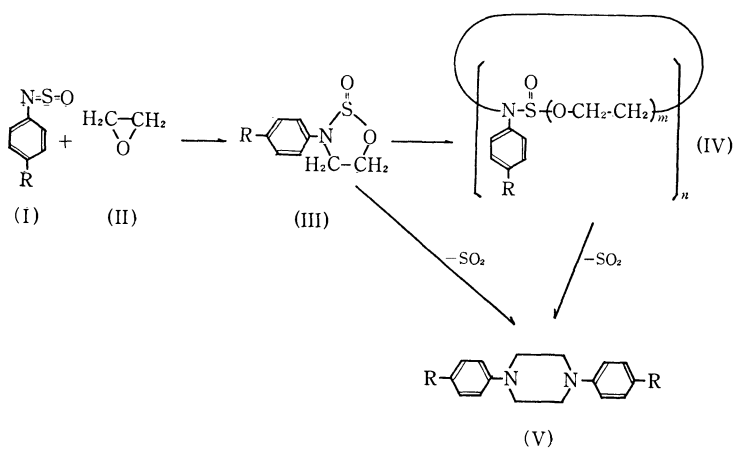

Chart 1

Ia, IIIa, IVa and Va; R=H
Ib, IIIb, IVb and Vb; R=CH_3
Ic, IIIc, IVc and Vc; R=Cl

BULLETIN OF THE CHEMICAL SOCIETY OF JAPAN VOL. 43 3614—3615 (1970)

The Reaction of Nitric Oxide with Rhodium Complexes

Jitsuo KIJI, Susumu YOSHIKAWA and Junji FURUKAWA

Department of Synthetic Chemistry, Kyoto University, Sakyo-ku, Kyoto

(Received June 8, 1970)

There has been considerable interest in recent years in the preparation of d^8 complexes because of their significance in oxidative addition and their potentiality in catalysis. The formation and properties of the carbonyl complexes of rhodium have been studied extensively.[1] On the other hand, there have been few reports on the reaction of nitric oxide. Nitric oxide is unique among ligands in that it contains an unpaired electron. The present work stems from our interest in expanding the scope of rhodium complexes by reaction with nitric oxide. Recently Hughes has reported a reaction between nitric oxide and square-planar rhodium complexes of the $RhClL_3$ type to produce nitrosyl-nitro derivatives, $RhCl(NO)(NO_2)L_2$.[2] Both triphenylphosphine and triphenylarsine derivatives exhibit two infrared absorption bands in the N–O stretching region; this splitting is attributed to the presence of isomers.[2] This report prompted us to reveal the results of our own investigation.

This paper deals with the isolation of two nitrosyl complexes. We conclude that the lower band in the N–O stretching region can be assigned to a polymeric nitrosyl complex. Furthermore, we report here about the replacement of the nitrosyl group by carbon monoxide and about the reaction of a diphosphine complex with nitric oxide.

Experimental

Reaction of Nitric Oxide with $RhCl(PPh_3)_3$. Nitric oxide was introduced into 20 m*l* of a benzene solution containing 200 mg of $RhCl(PPh_3)_3$ and 500 mg of triphenylphosphine at room temperature over a 20-min period. The color of the solution thus changed from brown to green. The evaporation of the benzene and subsequent washing with ether gave 123 mg of $RhCl(NO)(NO_2)(PPh_3)_2$. IR: 818, 1310, 1415 (due to NO_2 group), and 1660 cm^{-1} (ν_{NO}).

Found: C, 59.27; H, 4.65; N, 2.95%; mol wt, 718. Calcd for $RhC_{36}H_{30}N_2O_3P_2Cl$: C, 58.52; H, 4.09; N, 3.78%; mol wt, 738.9.

Attempted Isolation of Complex I. A green solution, prepared by the method which has been described above except that triphenylphosphine was added, gradually formed a brown precipitate in a low yield. It was sparingly soluble in organic solvents. IR: 1635 cm^{-1} (ν_{NO}). The average values obtained from two sets of analyses are as follows: C, 56.74; H, 4.48; N, 4.02%.

Reaction of Carbon Monoxide with $RhCl(NO)(NO_2)(PPh_3)_2$. Into 20 m*l* of a benzene solution containing $RhCl(NO)(NO_2)(PPh_3)_2$, prepared from 200 mg of $RhCl(PPh_3)_3$ and 500 mg of triphenylphosphine as has been described above, carbon monoxide was introduced at room temperature over a 60-min period. The addition of ether to the concentrated solution gave 110 mg of a yellow solid, which was identified with $RhCl(CO)(PPh_3)_2$ on the basis of its mp and IR spectrum.

Reaction of Nitric Oxide with $RhCl(CO)(Ph_2PCH_2CH_2PPh_2)$. The treatment of 10 m*l* of a benzene solution containing 77 mg of $Rh_2Cl_2(CO)_4$ with 157 mg of bis(diphenylphosphino)ethane at room temperature for 3 hr gave 195 mg of $RhCl(CO)(Ph_2PCH_2CH_2PPh_2)$,*1 which had an IR absorption band due to ν_{CO} at 2000 cm^{-1}. Nitric oxide was introduced into 5 m*l* of a benzene solution containing 30 mg of the complex at room temperature. Yellow-green $RhCl(NO)(NO_2)(Ph_2PCH_2CH_2PPh_2)$ (25 mg) was thus precipitated from the solution. IR: 825, 1315, 1385 (due to NO_2 group) and 1655 cm^{-1} (ν_{NO}).

Found: C, 50.18; H, 4.49; N, 3.93%. Calcd for $RhC_{26}H_{24}N_2O_3P_2Cl$: C, 50.96; H, 3.94; N, 4.56%.

Results and Discussion

The reaction of $RhCl(PPh_3)_3$ or $RhCl(CO)(PPh_3)_2$ with nitric oxide proceeded smoothly at room temperature. When the benzene solution of $RhCl(PPh_3)_3$ or $RhCl(CO)(PPh_3)_2$ was treated with nitric oxide, a green solution was obtained. The evaporation of the benzene gave a green solid with infrared absorption bands at 1660 and 1635 cm^{-1}*2 ascribed to ν_{NO}. When the benzene solution was allowed to stand at room temperature under a nitrogen atmosphere, a dark brown complex (1) involving a band at 1635 cm^{-1} due to

1) J. A. Osborn, F. H. Jardine, J. F. Young and G. Wilkinson, *J. Chem. Soc., A*, **1966**, 1711.

2) W. B. Hughes, *Chem. Commun.*, **1969**, 1126.

*1 When the diphosphine complex (obtained from 55 mg of $Rh_2Cl_2(CO)_4$ and 110 mg of bis(diphenylphosphino)ethane) was allowed to stand in benzene at room temperature for 2 weeks, a yellow solid (30 mg) was separated out; this was identified with $[Rh(Ph_2PCH_2CH_2PPh_2)_2]Cl$. The evaporation of the benzene from the filtrate gave orange needles, which were identical with $Rh_2Cl_2(CO)_4$. These data suggest that the following reaction occurs:

$$2\,RhCl(CO)(Ph_2PCH_2CH_2PPh_2) \rightarrow [Rh(Ph_2PCH_2CH_2PPh_2)_2]Cl + 1/2\,Rh_2Cl_2(CO)_4$$

*2 W. D. Hughes has reported 1666 and 1640 cm^{-1} for ν_{NO}.

ν_{NO} gradually precipitated. No reliable information could be obtained on this complex because of the difficulty of purifying it. A reasonable formulation for I is, however, as a dimeric or polymeric nitrosyl complex involving bridging chlorine. We base this on the following facts: (1) I is sparingly soluble in organic solvents, (2) its formation is suppressed by the presence of an excess of triphenylphosphine (see below), and (3) there is no band due to the nitro group.

The reaction of nitric oxide with $RhCl(PPh_3)_3$ in the presence of an excess of triphenylphosphine led to a green, air-stable complex (II). The infrared absorption spectrum (KBr) showed a single nitrosyl band at 1660 cm^{-1} and the band assignable to the nitro group. Elemental analysis and molecular-weight measurement support the $RhCl(NO)(NO_2)(PPh_3)_2$ formula. Thus, an excess of triphenylphosphine can be used to prevent the formation of the polymeric nitrosyl complex (I) with the N–O stretching band at 1635 cm^{-1} and a nitrosylnitro complex (II) free from I can be obtained.

On treating a solution of a mixture of I and II with carbon monoxide, the nitrosyl (ν_{NO} at 1660 cm^{-1}) and the nitro groups were replaced by carbon monoxide than that in I. The displacement of the nitrosyl group in I by carbon monoxide was only possible when I was treated under pressure. A carbonyl complex formed from I had, however, an infrared absorption band due to ν_{CO} at 1985 cm^{-1} (KBr).

An attempt to reduce the coordinated nitrosyl group in I or II with molecular hydrogen was unsuccessful.

The reaction of nitric oxide with the diphosphine complex proceeded similarly at room temperature. The following formulation of $RhCl(CO)(Ph_2PCH_2CH_2PPh_2)$ is envisaged:

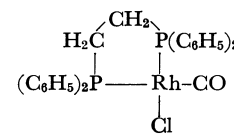

since the carbonyl group absorbs at 2000 cm^{-1}.[3-5] The treatment of the solution of $RhCl(CO)(Ph_2PCH_2CH_2PPh_2)$ in benzene with nitric oxide gave a yellow-green complex. The infrared spectrum showed a band at 1655 due to ν_{NO} and nitro-group bands at 1385, 1315, and 825 cm^{-1}. On the basis of the infrared spectrum and the elemental analysis, the complex may be formulated as $[RhCl(NO)(NO_2)(Ph_2PCH_2CH_2PPh_2)]_n$. The insolubility of this complex supported a dimeric or polymeric formulation involving a bridging diphosphine molecule. In contrast to the triphenylphosphine derivative, the diphosphine derivative exhibits only one band in the N–O stretching region.

3) W. Hieber and R. Kummer, *Chem. Ber.*, **100,** 148 (1967).

4) A. Sacco and R. Ugo, *J. Chem. Soc.*, **1964**, 3274.

5) J. T. Mague and J. P. Mitchener, *Inorg. Chem.*, **8**, 119 (1969).

BULLETIN OF THE CHEMICAL SOCIETY OF JAPAN VOL. 43 3615—3617 (1970)

The Influence of the Number of Sulfur Atoms on the PMR Chemical Shifts in Aryl Polysulfides

Tamotsu FUJISAWA and Gen-ichi TSUCHIHASHI

Sagami Chemical Research Center, Ohnuma, Sagamihara-shi, Kanagawa

(Received June 15, 1970)

The proton magnetic resonance for sulfur compounds has received major study.[1] But limited information for aromatic proton signals has been offered among aromatic sulfur derivatives because the aromatic signals were generally complex.[2] A number of aromatic sulfur compounds have been synthesized in our laboratory on the study of iron-catalyzed aromatic sulfuration.[3] During the course of the study, the aromatic proton signals are found to be influenced by increasing the sulfur chain length in the compounds. In this paper, the results of such observation and discussion for them are reported.

The ortho protons to sulfur atoms of aryl poly-

1) S. R. Heller, "NMR Spectra of Sulfur Compounds," Intra-Science Chemistry Reports, Vol. 2, No. 4, Intra-Science Research Foundation, California (1968).

2) C. Brown and D. R. Hogg, *J. Chem. Soc., B*, **1968**, 1315.

3) T. Fujisawa, N. Ohtsuka, T. Kobori and G. Tsuchihashi, *Tetrahedron Lett.*, **1968**, 4533, 5071; *ibid.*, **1969**, 4291; T. Fujisawa and M. Kakutani, *J. Polym. Sci., B*, **8**, 19 (1970); T. Fujisawa, N. Ohtsuka and G. Tsuchihashi, This Bulletin, **43**, 1189 (1970).

Table 1. Chemical shifts of

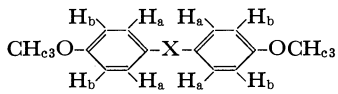

(δ in CCl_4)

X	H_a(d)	H_b(d)	H_c(s)	J_{ab}(Hz)
-S-	7.17	6.71	3.73	8.4
-SS-	7.30	6.71	3.74	8.4
-SSS-	7.39	6.71	3.76	8.5
-SO-	7.43	6.85	3.79	8.8
$-SO_2-$	7.80	6.89	3.79	9.0 ($CDCl_3$)

Abbreviations used: s, singlet; d, doublet.

Table 2. Chemical shifts of

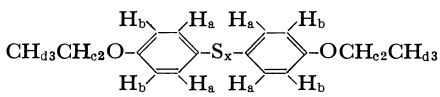

(δ in CCl_4)

X	H_a(d)	H_b(d)	H_c(q)	H_d(t)	J_{ab}	J_{cd}(Hz)
1	7.15	6.66	3.89	1.37	8.8	6.8
2	7.28	6.69	3.93	1.39	9.2	7.0
3	7.37	6.68	3.95	1.41	9.2	7.0

Abbreviations used: d, doublet; t, triplet; q, quartet.

sulfides vary their PMR chemical shifts to lower field with increase of the number of the sulfur atoms. As shown in Tables 1 and 2, the number of the sulfur atoms exerts a considerable effect on the chemical shifts of H_a protons of anisole and phenetole derivatives in contrast with that of H_b. The slight shift of alkoxyl protons toward lower field was also observed. The similar effect of polysulfide linkage has already been reported in aliphatic series by Van Warzer and Grant,[4] although their data fit to an approximation based on the theory for the "neighbor anisotropy effect". The observation of the same tendency between aromatic and aliphatic protons is interesting because they often exist in different electronic circumstances. For example, in *p*-methoxyphenyl methyl sulfide, the signal for S-methyl protons (δ=2.36) appears at higher field than that for O-methyl protons (δ=3.70), but the situation is reverse in the chemical shift of ortho ring protons to oxygen (δ=6.69) and that to sulfur (δ=7.14). This is reasonably explained by inductive effect in aliphatics and by mobile π-electron system in aromatics. The chemical shift of the O-ortho protons moves considerably to higher field than that of benzene by electron releasing resonance by oxygen, whereas the signal of the S-ortho protons appears at about the same position of that of benzene because the conjugation between the ring and sulfur is suggested to be relatively small. In general, chemical shifts of ortho protons of substituted benzene ring are known to shift by influence of π-electron density and of anisotropy and/or inductive effect of the substituents.[5]

Signals for neighboring protons to electron-withdrawing group shift to lower field with the inductive order as shown in sulfide-sulfoxide-sulfone series (Table 1 and Ref. 6). Accordingly, it is reasonably assumed that as number of sulfur atoms in the polysulfide series increases, the strength of inductive effect becomes more intense. It is noteworthy that the same tendency has been also observed in the ultraviolet absorption spectra of di-*p*-tolyl polysulfides, in which as number of sulfur atoms increases, the shift toward the shorter wavelength occurs in primary band attributable to benzene ring and the absorbance becomes more intense.[7] This phenomenon suggests that the electron density of the benzene ring decreases by the localization of the electron to the center of polysulfide linkage with increasing chain length of sulfur atoms, coupled with the fact that the shift toward the longer wavelength occurs in secondary band attributable to linear sulfur–sulfur linkage. In other words, this is due to the electron-withdrawing effect of polysulfide linkage and strongly supports above inductive effect by polysulfide group.

A remarkable example of this tendency is found in the chemical shifts of thiobis(2,6-di-*t*-butylphenol) series as shown in Table 3. These chemical shifts of the ortho ring protons are particularly suited for the quantitative analyses of the mixture of the polysulfides with their integration ratio because independent singlet peaks for these absorptions can be assigned clearly.

As shown above, the data of the chemical shifts for polysulfides can be explained in terms of the inductive effect of polysulfide linkage, but a system illustrative of anisotropy effect was also observed. The chemical shifts of ortho protons of various

Table 3. Chemical shifts of

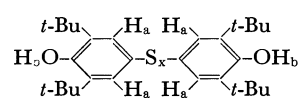

(δ in CCl_4)

X	H_a(s)	H_b(s)	*t*-Bu(s)
1	7.02	4.98	1.40
2	7.21	5.06	1.41
3	7.31	5.13	1.42
4	7.38	5.22	1.46

Abbreviation used: s, singlet.

4) J. R. Van Warzer and D. Grant, *J. Amer. Chem. Soc.*, **86**, 1450, 3021 (1964). For methyl polysulfide: G. R. Pettit, I. B. Douglass, and R. A. Hill, *Can. J. Chem.*, **42**, 2357 (1964).

5) H. Spiesecke and W. G. Schneider, *J. Chem. Phys.*, **35**, 731 (1961).

6) J. B. Hyne and J. W. Greidanus, *Can. J. Chem.*, **47**, 803 (1969).

7) Y. Minoura, *Nippon Kagaku Zasshi*, **73**, 244 (1952).

Table 4. Chemical shifts of S-ortho ring protons of aromatic sulfur compounds (δ in CCl_4)

Ar	ArSH	ArSAr	ArSSAr	ArSCl	ArSSCl
2,4-$(NO_2)_2C_6H_3$-	7.64 (d)*		8.45 (d)**	8.21 (d)	8.50 (d)
2-$NO_2C_6H_4$-	7.35 (m)		7.85 (q)*	8.00 (q)	8.31 (q)
4-$NO_2C_6H_4$-	7.32 (d)*		7.67 (d)	7.58 (d)	7.80 (d)
2-ClC_6H_4-	7.20 (m)		7.30 (m)	7.49 (q)	7.84 (q)
4-ClC_6H_4-	7.13 (s)	7.23 (s)	7.34 (d)	7.52 (d)	7.48 (d)
C_6H_5-	7.16 (m)	7.22 (m)	7.40 (m)	7.59 (m)	7.54 (m)
2-$CH_3C_6H_4$-	7.16 (m)	7.09 (m)	7.40 (m)	7.63 (d)	7.72 (t)
4-$CH_3C_6H_4$-	7.10 (d)	7.15 (d)	7.29 (d)	7.51 (d)	7.45 (d)
4-$CH_3OC_6H_4$-	7.17 (d)	7.17 (d)	7.30 (d)	7.63 (d)	

Abbreviations used: s, singlet; d, doublet; t, triplet; q, quartet; m, multiplet.
* in chloroform ** in tris(dimethylamino)phosphine oxide.

aromatic sulfur compounds are shown in Table 4. Of particular interest in the Table is sulfenyl chloride-thiosulfenyl chloride series. The chemical shifts in phenyl, *p*-tolyl and *p*-chlorophenyl derivatives move toward higher field as the number of sulfur atoms increases, which makes a marked contrast to the lower-field shift in polysulfide series. This tendency has been reported in methanesulfenyl chloride series.[4] This can be also explained in terms of the inductive effect attributable to the polarization of sulfur-chlorine bond as shown by $\overset{\delta+}{S}—\overset{\delta-}{Cl}$. On the other hand, the lower field shift was observed in ortho substituted benzenesulfenyl chloride series, which is accounted for by the anisotropy effect of sulfur-chlorine atoms because distance between the ortho ring proton and chlorodithio group becomes more close by the buttressing effect of ortho substituents. However, the chemical shifts in *p*-nitrophenyl derivatives move toward lower field with increasing chain length of sulfur atoms. This fact does not fit above explanation. The reason may be as follows: the ring protons may be affected mainly by anisotropy effect of chlorodithio group rather than by the inductive effect of chlorodithio group because strong electron-withdrawing effect of nitro group overshadows the inductive effect.

In summary, the above mentioned dependence of the chemical shifts of the aromatic protons on the chain length of polysulfide linkage, gives important informations for the qualitative and quantitative analyses of aromatic sulfur compounds by NMR.

Experimental

Materials. All known sulfur compounds used in this experiment were prepared by known methods or simple modifications thereof. 4,4′-Tetrathiobis(2,6-di-*t*-butylphenol) was prepared from the corresponding thiophenol and sulfur chloride, mp 106—107°C; found S, 23.52%, calcd S, 23.76%. Substituted benzenethiosulfenyl chlorides were prepared from corresponding thiophenols and sulfur dichloride. Bp (mp) and elementary analyses of sulfur (calcd.) of new thiosulfenyl chlorides are: 2,4-di-NO_2, (73—75°C), 23.66% (24.02%); 4-NO_2, (35—37°C), 29.03% (28.96%); 2-Cl, 77—79°C/0.2 mmHg, 29.97% (30.33%); 4-Cl, 73—74°C/0.08 mmHg, 30.12% (30.33%); 2-CH_3, 76—77°C/0.2 mmHg, 33.23% (33.60%); 4-CH_3, 67—68°C/0.1 mmHg, 34.07% (33.60%).

Measurement of the NMR. The PMR spectra were determined with a Varian HA-100 instrument. All the spectra without note were measured in carbon tetrachloride at a concentration of 10% (w/v) at room temperature with tetramethylsilane as an internal standard and the peak positions were expressed in δ-values.

The authors are grateful to Mr. Ken-ichi Sato for the measurement of the NMR spectra. Acknowledgement is made to Messrs. Mizuo Yamamoto and Takeo Kobori, and to Mrs. Noriko Ohtsuka for their assistances in the preparation of the samples.

BULLETIN OF THE CHEMICAL SOCIETY OF JAPAN VOL. 43 3618—3619 (1970)

The Magnetic Susceptibility of the 1,3-Bis-(4-methylphenyl)-5-phenyl-verdazyl Radical from 1.55 to 300°K

Kazuo MUKAI, Nagao AZUMA and Kazuhiko ISHIZU

Department of Chemistry, Faculty of Science, Ehime University, Matsuyama

(Received June 20, 1970)

Recently, the magnetic properties of several species of stable crystalline neutral radicals, including hydrazyl,[1] nitroxide,[2] and phenoxyl[3] radicals, were reported. On the other hand, the verdazyls, a series of very stable neutral radicals containing four nitrogen nuclei, were previously studied by Kuhn, Neugebauer, and Trischmann.[4,5] However, the magnetic properties of the verdazyls have never been studied except for the preliminary susceptibility measurements, which showed the presence of one unpaired electron per molecule. We wish to describe here the magnetic susceptibility of a verdazyl radical in the temperature range from 1.55 to 300°K; this radical has the structure shown in Fig. 1.

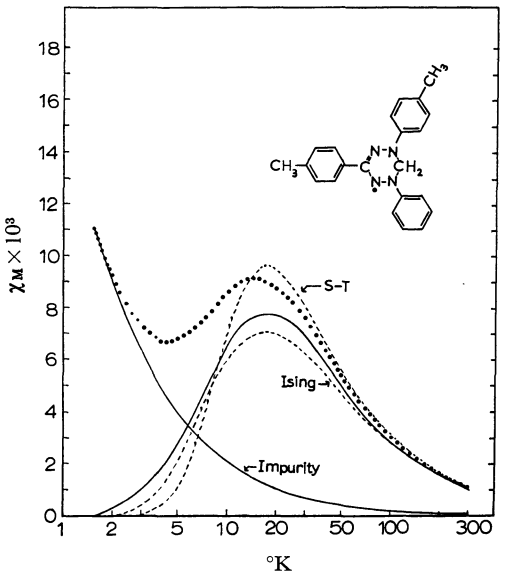

Fig. 1. Paramagnetic molar susceptibility of 1,3-Bis(4-methylphenyl)-5-phenyl-verdazyl radical. The "full circle" curve is the experimental curve. The "impurity" curve is an extrapolation of the low-temperature Curie-Weiss data. The solid line curve is the difference between experimental and impurity curves. The dashed curves are theoretical fits as explained in the text.

Experimental

1,3-Bis-(4-methylphenyl)-5-phenyl-verdazyl was prepared from the corresponding formazan by ring formation with formaldehyde, following the same process as that of Kuhn *et al.* After recrystallizing two times from methanol, a deep green crystalline compound, mp 116.0—116.3°C, was obtained.

The susceptibility measurements were carried out in the continuous temperature range between 1.55°K and 300°K, using a magnetic torsion balance on powder samples of about 100 mg in a heterogeneous magnetic field up to about 10 koe.[6]

Results and Discussion

The measured molar paramagnetic susceptibility, χ_p, shown in Fig. 1 as a function of the temperature, has been corrected for the diamagnetic contribution of $\chi_{dia} = -0.200 \times 10^{-3}$ emu/mol calculated by Pascal's method. Between 30°K and room temperature χ_p follows the Curie-Weiss law, with a Weiss constant of $\theta = -14.6 \pm 0.4$°K and a spin concentration of 93.9%. When the temperature is lowered from 30°K, the $\chi_p - T$ curve gradually deviates from the Curie-Weiss law and reaches a broad maximum at 14.2 ± 0.5°K. After passing through the maximum, χ_p falls off slowly till 4°K. However, below 4°K the susceptibility increases again as the temperature is lowered. In the region from 1.55°—1.8°K, the Curie-Weiss law was observed, corresponding to a spin concentration of 5.8% and a Weiss constant of -0.4 ± 0.1°K. When this low-temperature paramagnetic impurity curve

1) a) A. S. Edelstein, *J. Chem. Phys.*, **40**, 488 (1964). b) W. Duffy, Jr., and D. L. Strandburg, *ibid.*, **46**, 456 (1967).

2) a) J. Yamauchi, T. Fujito, E. Ando, H. Nishiguchi and Y. Deguchi, *J. Phys. Soc. Jap.*, **25**, 1558 (1968). b) Yu. S. Karimov, *ZhETF. Pis. Red.*, **8**, 239 (1968). c) W. Duffy, Jr., D. L. Strandburg and J. F. Deck, *Phys. Rev.*, **183**, 567 (1969).

3) a) K. Mukai, This Bulletin, **42**, 40 (1969). b) K. Mukai, K. Ishizu and Y. Deguchi, *J. Phys. Soc. Jap.*, **27**, 783 (1969).

4) R. Kuhn and H. Trischmann, *Angew. Chem.*, **75**, 294 (1963); *Monatsh. Chem.*, **95**, 457 (1964).

5) R. Kuhn, F. A. Neugebauer and H. Trischmann, *Angew. Chem.*, **76**, 691 (1964); *Monatsh. Chem.*, **97**, 525 (1966).

6) M. Mekata, *J. Phys. Soc. Jap.*, **17**, 796 (1962).

is extrapolated to higher temperatures and substracted from the experimental curve observed there, the corrected curve shown in Fig. 1 is obtained. The experimental curve has a general appearance very similar to that found in many organic free radical and radical salts; thus, the unpaired electrons on the verdazyl molecules also appear to be paired up by an negative exchange interaction.

In order to account for the experimental data on the verdazyl radical, we shall examine two typical models, that is, the singlet-triplet model[7] and the linear Ising model.[8]

In the singlet-triplet model (Case I), the susceptibility is given by:

$$\chi_p = \frac{N_0 g^2 \beta^2}{kT} \cdot \frac{1}{3+e^{\delta/kT}}$$

where δ is the singlet-triplet energy separation and equals to $2|J|$, and where N_0 is Avogadro's number. The other subscripts have the usual meanings.

In the linear Ising model (Case II), the susceptibility is expressed by:

$$\chi_p = \frac{N_0 g^2 \beta^2}{4kT} e^{J/kT}$$

The values of the exchange energy, J, in both models are determined from the temperature, T_{max}, at which the corrected susceptibility shows a maximum, by using the relations $J=-0.81kT_{max}$ for case I and $J=-kT_{max}$ for case II. Taking this temperature as 17.0°K, the values of J are estimated to be 9.5 cm^{-1} (Case I) and 11.8 cm^{-1} (Case II) respectively. The theoretical curves require multiplication by a constant p if they are to be compared with the experimental data. Thus, with $p=0.881$, the two theoretical curves can be fitted to the experimental data.

Figure 1 indicates that the linear Ising model gives rather a better fit with the observed susceptibility of the verdazyl. A good agreement may be obtained if Soos's alternating parameter is taken into account.[9]

The authors are much obliged to Professors H. Takaki and Y. Deguchi, and Drs. M. Mekata and H. Nishiguchi of Kyoto University for magnetic susceptibility measurements.

7) B. Bleaney and K. D. Bowers, *Proc. Roy. Soc.*, **A 214**, 451 (1952).

8) J. W. Stout and R. C. Chisholm, *J. Chem. Phys.*, **36**, 979 (1962).

9) Z. G. Soos, *ibid.*, **43**, 1121 (1965).

BULLETIN OF THE CHEMICAL SOCIETY OF JAPAN VOL. 43 3619—3620 (1970)

A Convenient Method for the Synthesis of Nucleoside Phosphorothioates

Tsujiaki HATA and Iwao NAKAGAWA

Department of Chemistry, Tokyo Institute of Technology, Ookayama, Meguro-ku, Tokyo, Japan

(Received July 4, 1970)

Recently, interest in polymers of nucleoside phosphorothioates was caused by strong induction effect of interferon[1] production. Eckstein[2] first prepared thymidine- and uridine-phosphorothioates by way of thiophosphorylation using tri-imidazoyl-1-phosphinesulfide and reported the enzymatic activities of dinucleoside phosphorothioates. Murray and Atkinson[3] synthesized adenosine 5′-phosphorothioate and tested the activity for some enzymes as a nucleotide analog.

In the present experiment, a general synthetic procedure for the preparation of nucleoside 5′-phosphorothioates starting from nucleoside and thiophosphoryl chloride, which is a readily available and inexpensive starting material, was investigated. For example, one equivalent of 2′,3′-*O*-isopropylidene uridine was allowed to react with two equivalent of thiophosphoryl chloride in dry pyridine at 0°C for 30 min. After hydrolysis of the resulting mixture under cooling, 2′,3′-*O*-isopropylidene uridine 5′-phosphorothioate was obtained in 85% yield. The structure was confirmed by elemental analysis, paper electrophoresis and UV spectrum.

In a similar manner, various nucleoside 5′-phosphorothioates were prepared in high yields as shown in Table 1.

It was found that phosphorothioate group was detected sensitively on paper chromatogram as a

1) S. Baron and B. Levy, "Annual Review of Microbiology," Vol. 20, Annual Reviews, Inc., Palo Alto, California, U.S.A. (1966), p. 291.

2) F. Eckstein, *J. Amer. Chem. Soc.*, **88**, 4292 (1966); *Tetrahedron Lett.*, **1967**, 1157, 3495.

3) A. W. Murray and M. R. Atkinson, *Biochemistry*, **7**, 4023 (1968).

Table 1. Preparation of protected nucleoside 5′-phosphorothioates

Nucleoside		Product	
	(g)	Yield (%)	R_f value*
2,′3′-*O*-isopropylidene adenosine	1.54	81	0.23
2′,3,-*O*-isopropylidene guanosine	1.64	89	0.10
2′,3′-*O*-isopropylidene inosine	1.54	85	0.11
2′,3′-*O*-isopropylidene uridine	1.42	85	0.22
2′,3′-di-*O*-benzoyl uridine	2.26	73**	0.10***
3′-*O*-acetyl thymidine	1.42	83	0.18***

* Paper chromatography was carried out by descending technique using Toyo Roshi No. 51 paper. Solvent system used was: isopropyl alcohol-concentrated ammonium hydroxide-water (7 : 1 : 2 *v/v*).
** The reaction time was 1 hr.
*** The R_f value shows that after removal of protecting group.

brownish spot by spraying 10% aqueous copper(II) sulfate solution. It was further detected by Isherwood Reagent.[4]

In the above reactions, it was found that the yields of nucleoside 5′-phosphorothioates considerably decreased when just one equivalent of thiophosphoryl chloride was used, or when the reaction was carried out without ice-cooling.

In conclusion, it is noted that this procedure has two advantageous points over the previous method, namely, (1) satisfactory yields are obtained with respect to various nucleosides, (2) products can be handled by conventional organic technique on a relatively large scale without using column chromatography as described in the experimental part.

Experimental

Materials. 2′,3′-*O*-Isopropylidene adenosine,[5] 2′,3′-*O*-isopropylidene inosine,[6] 2′,3′-*O*-isopropylidene guanosine,[7] 2′,3′-*O*-isopropylidene uridine,[8] 2′,3′-di-*O*-benzoyl uridine[9] and 3′-*O*-acetyl thymidine[10] were prepared by literature procedures.

Preparation of Protected Nucleoside 5′-Phosphorothioate. *(A general procedure).* To a solution of freshly distilled thiophosphoryl chloride (1 m*l*, 10 mmol) in 25 m*l* of dry pyridine was added, portionwise, a protected nucleoside (5 mmol) (see Table 1) with stirring at 0°C. The stirring was continued for 30 min under cooling. Then, the reaction mixture was poured with stirring into 50 m*l* of ice water. After the addition of 5 m*l* of triethylamine (*ca.* 92 mmol), the resulting aqueous solution was concentrated under reduced pressure at a temperature below 30°C until white crystals appeared. The crystals, triethylammonium chloride, was filtered off by using Toyo Roshi No. 131 paper (for fine precipitates) and the filtrate was concentrated to dryness. The residual oil was still contaminated by triethylammonium chloride and then it was diluted with dry pyridine. The precipitate was filtered off by the No. 131 paper, and the filtrate was concentrated to dryness. The corresponding nucleoside phosphorothioate was isolated as triethylammonium salt by means of either method A or method B. Uridine- and thymidine-phosphorothioates were obtained according to method A and the other nucleoside phosphorothioates, such as adenosine, guanosine and inosine derivatives were isolated by method B.

Method A. The syrup was dissolved in 100 m*l* of dry chloroform and it was allowed to stand overnight in a refrigerator. Triethylammonium salt of inorganic thiophosphate was successively precipitated. After removal of the salt by centrifuge, (if the resulting supernant was a slightly cloudy solution, it should be again filtered by the No. 131 paper) the chloroform was removed by evaporation. Mono-triethylammonium salt of 2′,3′-*O*-isopropylidene uridine 5′-phosphorothioate (2.05 g, 4.26 mmol) was obtained in 85% yield (based on 2′,3′-*O*-isopropylidene uridine) as white powder.

Found: C, 44.43; H, 5.80; N, 8.48; S, 6.98%. Calcd for $C_{18}H_{32}N_3O_8PS$: C, 44.87; H, 6.65; N, 8.72; S, 6.65%. Ratio uridine : phosphorus, Found: 1.00 : 0.93. Required: 1 : 1.

Method B. The syrup was dissolved in 100 m*l* of isopropyl alcohol. A white precipitate soon appeared in the solution. The precipitate was collected by filtration. Mono-triethylammonium salt of 2′,3′-*O*-isopropylidene guanosine phosphorothioate (2.31 g, 4.44 mmol) was obtained in 89% yield (based on 2′,3′-*O*-isopropylidene guanosine) as white powder. Repeated reprecipitations by means of isopropyl alcohol and a small amount of methanol afforded white powder for analytical sample.

Found: C, 41.90; H, 5.90; N, 16.29; S, 6.25%. Calcd for $C_{19}H_{33}N_6O_7PS$: C, 43.85; H, 6.35; N, 16.15; S, 6.14%. Ratio guanosine : phosphorus, Found: 1.00 : 0.99. Required: 1 : 1.

We heartily thank Professor Dr. Teruaki Mukaiyama for his encouragement and discussion throughout the investigation. We also wish to thank Mr. Masaru Koezuka for his help with elemental analysis.

4) C. A. Hanes and F. A. Isherwood, *Nature*, **164**, 1107 (1949).
5) E. C. Taylor and W. A. Ehrhart, *J. Amer. Chem. Soc.*, **82**, 3138 (1960).
6) N. Nagasawa, I. Kumashiro and T. Takenishi, *J. Org. Chem.*, **31**, 2685 (1966).
7) A. Hampton, *J. Amer. Chem. Soc.*, **83**, 3640 (1961).
8) N. C. Yung and J. J. Fox, *ibid.*, **83**, 3060 (1961).
9) R. Lohrmann and H. G. Khorana, *ibid.*, **86**, 4188 (1964).
10) A. M. Michelson and A. R. Todd, *J. Chem. Soc.*, **1953**, 954.

BULLETIN OF THE CHEMICAL SOCIETY OF JAPAN VOL. 43 3621—3622 (1970)

Photolysis of Acetylene at 1849 Å

Masao TSUKADA and Shoji SHIDA

Laboratory of Physical Chemistry, Tokyo Institute of Technology, Meguro-ku, Tokyo

(Received July 17, 1970)

The direct photolysis of acetylene produces mainly diacetylene, benzene, and solid polymers. For the formation of benzene, Zelikoff and Aschenbrand[1] suggested an excited-molecule mechanism. Meanwhile, for the mercury photosensitization both the the free radical mechanism[2,3] and the modified excited-molecule mechanism[4] were proposed and final agreement has not yet been attained. The present work was undertaken as a re-examination of the reaction mechanism of the direct photolysis.

Experimental

Preparation, purification and purity of acetylene, acetylene-d_2, and nitric oxide were similar to those described before.[5] The light source was a low-pressure mercury resonance lamp. The reactant was circulated through a closed loop system (volume=680 m*l*). Total pressure change was measured with a Bourdon gauge. Special precaution was taken to keep the vacuum line free of mercury. The products were analyzed by gas chromatography (dioctyl phthalate column at 80°C). The analytical method of isotopically substituted benzenes was the same as that used before.[5]

Results and Discussion

Figure 1 shows the pressure dependence of the rates of the major products. The distinct differences between the mercury-photosensitized reaction[5] and the direct photolysis are that diacetylene is one of the major products and that the pressure dependence curves of benzene and of polymer have no maximum in the direct photolysis.

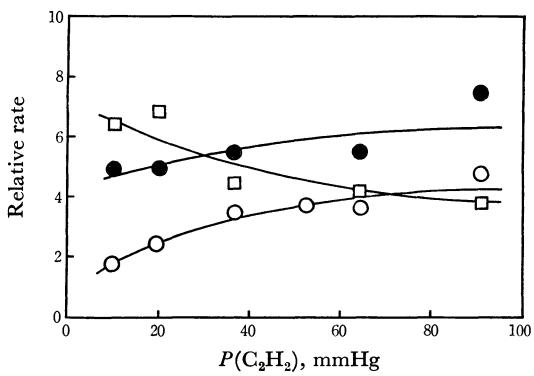

Fig. 1. Relative rate of product formation in the photolysis at 1849 Å against the acetylene pressure.
—○— C_6H_6 (10^{-8} mol/min)
—□— C_4H_2 (10^{-8} mol/min)
—●— Pressure decrease (10^{-2} mmHg/min)

Table 1 shows the distribution of isotopically substituted benzenes formed in equimolar C_2H_2–C_2D_2 mixtures. It can be seen that the yields of benzenes containing an odd number of H or D

Table 1. The distribution of isotopic benzenes formed in the photolysis of equimolar C_2H_2-C_2D_2 mixtures at 1849 Å

Acetylene initial pres. mmHg	6.0	9.5	13.8	19.5	27.7	39.7	71.3	100.7	Av.[a]	Calc.[b]
C_6H_6	6.7%	8.0%	7.6%	8.9%	9.7%	8.9%	9.1%	9.7%	9.4%	9.4%
C_6H_5D	8.6	7.3	7.5	6.8	7.0	6.6	6.6	5.7	6.5	6.25
$C_6H_4D_2$	22.0	23.6	24.5	24.8	24.8	27.0	26.9	27.5	26.6	28.2
$C_6H_3D_3$	17.7	16.3	15.1	14.0	13.2	12.5	12.2	10.9	12.2	12.5
$C_6H_2D_4$	26.0	26.5	27.7	27.6	27.5	28.5	28.4	29.1	28.4	28.2
C_6HD_5	9.2	9.2	8.0	7.3	7.0	6.7	7.0	6.3	6.8	6.25
C_6D_6	9.8	9.1	9.6	10.6	10.7	9.8	9.8	10.8	10.3	9.4

a) Average distribution (of column 6, 7, 8, and 9).
b) Calculated from molecular mechanism, (1), (2), (3), and (5).

1) M. Zelikoff and L. M. Aschenbrand, *J. Chem. Phys.*, **24**, 1034 (1956).
2) D. J. LeRoy and E. W. R. Steacie, *ibid.*, **12**, 117 (1944).
3) D. J. LeRoy, *ibid.*, **45**, 3482 (1966).
4) S. Shida, M. Tsukada, and T. Oka, *ibid.*, **45**, 3483 (1966).
5) S. Shida and M. Tsukada, This Bulletin, **43**, 2740 (1970).

atoms are relatively large from the view-point of simple molecular mechanism and that the distribution is almost constant at higher pressures.

The distribution observed here may be quantitatively explained by the free radical mechanism initiated by hydrogen atom as suggested for the mercury photosensitization by LeRoy,[3] but it can be accounted for as well by the modified excited-molecule mechanism[4,5]; the isotopic distribution predicted on the basis of either mechanism is quite the same (Table 1, the last column).

In low pressure region, however, the observed distribution depends on the acetylene pressure (Table 1) and the yields of benzenes containing an odd number of H or D atoms tend to increase with decreasing acetylene pressure in the same manner as in the mercury photosensitization.[5] The free radical mechanism could not explain the change of the distribution at low pressures, because the distribution expected from the mechanism should be independent of the acetylene pressure.

If an excited acetylene dimer molecule is assumed to repeat dissociation and regeneration to form an excited acetylene molecule at low pressures as follows,

$$C_2H_2^* + C_2H_2 \rightarrow C_4H_4^* \quad (1)$$

$$C_4H_4^* \rightarrow C_2H_2^{**} + C_2H_2 \quad (2)$$

$$C_2H_2^{**} + C_2H_2 \rightarrow C_4H_4^{**} \quad (3)$$

$$C_4H_4^{**} \rightarrow C_2H_2^{**} + C_2H_2 \quad (4)$$

$$C_4H_4^{**} + C_2H_2 \rightarrow C_6H_6 \quad (5)$$

where $C_2H_2^{**}$ and $C_4H_4^{**}$ mean lower excited molecules, the yields of benzenes containing an odd number of H or D atoms should increase.

Figure 2 shows the effects of the addition of nitric oxide on the rate of pressure decrease and of product formation. Nitric oxide markedly suppresses the benzene formation. But this effect of nitric oxide on the benzene formation does not necessarily indicate the radical mechanism. It would be considered that the excited singlet acetylene is converted into the triplet state and the latter

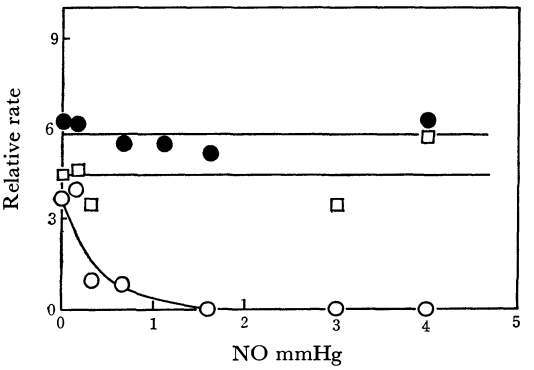

Fig. 2. Effect of nitric oxide on the relative rate of product formation. Acetylene initial pressure 37 mmHg.
—○— C_6H_6 (10^{-8} mol/min)
—□— C_4H_2 (10^{-8} mol/min)
—●— Pressure decrease (10^{-2} mmHg/min)

initiates the benzene formation. If it is the case, nitric oxide could quench the triplet acetylene.[6]

The diacetylene formation is not influenced practically by nitric oxide, but it has been found that ethynyl radicals do not react with NO.[7] Thus, it can be considered that diacetylene is produced by the radical reaction of ethynyl radicals.

Summarizing the above results, a possible reaction mechanism is depicted as follows.

$$C_2H_2 + h\nu \rightarrow C_2H_2^*$$

$$C_2H_2^* \rightarrow C_2H + H$$

$$C_2H_2^* \longrightarrow C_6H_6 + 2C_2H_2$$

$$C_2H + C_2H \rightarrow C_4H_2$$

$$H + nC_2H_2 \rightarrow \text{Polymer}$$

$$C_2H + nC_2H_2 \rightarrow \text{Polymer}$$

6) For example, G. Porter and M. R. Write, *Discuss. Faraday Soc.*, **27**, 18 (1959).

7) A. G. Sherwood and H. E. Gunning, *J. Phys. Chem.*, **69**, 1732 (1965).

BULLETIN OF THE CHEMICAL SOCIETY OF JAPAN VOL. 43 3623—3624 (1970)

Multi-channel Possibility of Electron Transfer Reaction in the Excited State

Noboru MATAGA

Faculty of Engineering Science, Osaka University, Toyonaka, Osaka

(Received July 18, 1970)

Recently, we have studied the quenching of pyrene fluorescence by several electron acceptors and donors in polar solvents.[1] We have observed extraordinary strong quenching in the case of pyrene-TCNE-acetonitrile system, where the value of δ in the equation of relative fluorescence yield, $\eta'/\eta=\delta/(1+k_q\tau[\mathrm{B}])$, is remarkably smaller than unity. We have further confirmed that k_q is not simply proportional to the diffusion coefficient, D, at low temperatures, *i. e.*, $k_q \propto D^m$ ($m<1$) in contrast to other systems where $k_q \propto D$. These facts for pyrene-TCNE system have been given a tentative interpretation that somewhat long range electron transfer process in a quite loose encounter pair is involved in the reaction.[1]

As we have pointed out previously,[2] the mechanism of fluorescence quenching reaction due to the electron transfer process in a polar solvent may be discussed on the basis of Marcus' theory of electron transfer.[3] According to Marcus,[3a] the reaction scheme may be written as,

$$\mathrm{A}^* + \mathrm{B} \underset{k_{-1}}{\overset{k_1}{\rightleftarrows}} \mathrm{A}^*\cdots\mathrm{B} \underset{k_{-2}}{\overset{k_2}{\rightleftarrows}} \mathrm{A}^{\pm}\cdots\mathrm{B}^{\mp} \xrightarrow{k_3} \quad (1)$$
$$\swarrow 1/\tau$$

Then, we have,

$$\begin{aligned} k_q &= k_1/[1+(k_{-1}/k_2)+(k_{-1}k_{-2}/k_2k_3)] \\ &= k_1/[1+(k_{-1}/k_2^0)\exp(\Delta F^*/RT) \\ &\quad +(k_{-1}/k_3)\exp(\Delta F^0/RT)] \end{aligned} \quad (2)$$

where $k_2=k_2^0\exp(-\Delta F^*/RT)$, $k_2/k_{-2}=\exp(-\Delta F^0/RT)$, ΔF^* and ΔF^0 are respectively the free energy of activation and the standard free energy for the electron transfer process. Rehm and Weller[4] have shown by measuring k_q for many systems that k_q is nearly constant and equal to $1.6\times10^{10}\mathrm{M}^{-1}\mathrm{sec}^{-1}$ for $\Delta F^0 \lesssim -10$ kcal/mol while it becomes much smaller for $\Delta F^0 > -10$ kcal/mol. They have derived also numerical values for rate constants of Eq. (2) and equations for ΔF^* in terms of ΔF^0, which reproduce satisfactorily the observed k_q values. ΔF^0 value can be estimated by Eq. (3),

$$\Delta F^0 = E^{(+)}(\mathrm{B}) - E^{(-)}(\mathrm{A}) - C - \Delta E(\mathrm{A}^*)$$
or (3)
$$\Delta F^0 = E^{(+)}(\mathrm{A}) - E^{(-)}(\mathrm{B}) - C - \Delta E(\mathrm{A}^*)$$

where $E^{(+)}$ and $E^{(-)}$ are oxidation and reduction potentials of electron donor and acceptor, respectively, ΔE is the excitation energy of A to the luminescent state and C is the coulomb interaction energy in $\mathrm{A}^{\pm}\cdots\mathrm{B}^{\mp}$. C is approximately given by $C\approx e^2/\varepsilon R_{ab}$, where R_{ab} is the inter-ionic distance and ε is the dielectric constant of solvent.

For several pyrene-quencher systems in acetonitrile, we have evaluated ΔF^0 as follows. $E^{(+)}$ and $E^{(-)}$ values in acetonitrile solution were taken from literature.[5] R_{ab} was assumed to be 7 Å. (Even if we take somewhat smaller or larger value for R_{ab}, our conclusion in this report remains unchanged.) Then, ΔF^0 values are -2.5 eV, -1.5 eV, -0.45 eV and -0.55 eV for the quenchers TCNE, TCNB (tetracyanobenzene), *p*-DCNB (*p*-dicyanobenzene) and DMA (*N,N*-dimethylaniline), respectively. TCNE, TCNB and *p*-DCNB work as electron acceptors while DMA works as a donor.

If the $|\Delta F^0|$ value is very large just as in the case of pyrene-TCNE system, it might be possible that the electron transfer reaction occurs not only to the ground state of $\mathrm{A}^{\pm}\cdots\mathrm{B}^{\mp}$ but also to its various excited states when the ion radicals have low energy excited levels. The pyrene cation and anion radicals have presumably three excited levels in the range of excitation energies of 1.5—2.0 eV and 1.3—2.0 eV, respectively.[6] Accordingly, the standard free energies of the electron transfer processes leading to the

1) T. Okada, H. Oohari and N. Mataga, This Bulletin, **43**, 2750 (1970).

2) N. Mataga, T. Okada and N. Yamamoto, *Chem. Phys. Lett.*, **1**, 119 (1967).

3) R. A. Marcus, a) *J. Chem. Phys.*, **24**, 966 (1956); b) *Ibid.*, **26**, 867 (1957); c) *Ibid.*, **26**, 872 (1957); d) *Ibid.*, **43**, 679 (1965); e) *Ann. Rev. Phys. Chem.*, **15**, 155 (1964).

4) D. Rehm and A. Weller, *Ber. Bunsenges. Phys. Chem.*, **73**, 834 (1969).

5) M. E. Peover, *Trans. Faraday Soc.*, **58**, 2370 (1962); E. S. Pysh and N. C. Yang, *J. Amer. Chem. Soc.*, **85**, 2124 (1963); H. Beens and A. Weller, *Acta Phys. Polon.*, **34**, 593 (1968). The $E^{(+)}$ value of DMA in acetonitrile has been measured kindly by T. Kubota and H. Miyazaki at Shionogi Research Laboratory, to whom the author expresses his sincere gratitude.

6) T. Shida and W. H. Hamill, *J. Chem. Phys.*, **44**, 4372 (1966); R. Zahradnik and P. Cársky, *J. Phys. Chem.*, **74**, 1240 (1970).

excited states of $A^{\pm}\cdots B^{\mp}$, are all lower than -0.5 eV, in the case of pyrene-TCNE system. Thus, there are presumably four reaction paths of electron transfer, all of which have the rate constant of 10^{10}M^{-1} sec.$^{-1}$. On the other hand, only the electron transfer process to the ground state of $A^{\pm}\cdots B^{\mp}$ is possible when TCNB, p-DCNB and DMA are used as the quenchers. In these cases, the rate constant of the reaction to the excited states of $A^{\pm}\cdots B^{\mp}$ is much smaller than $10^{10}\text{M}^{-1}\,\text{sec}^{-1}$ according to the treatment of Marcus.[3]

From the reasoning described above, the reaction in the case of pyrene-TCNE system may be a multi-channel process, the rate constant of which is the sum of four rate constants, $k_q=\sum_i k_{qi}$. Accordingly, it may be possible for the electron transfer process from the excited pyrene to TCNE to occur at much larger intermolecular distance compared to the case of the other single channel systems.

BULLETIN OF THE CHEMICAL SOCIETY OF JAPAN VOL. 43 3624—3625 (1970)

Crystal Structure of *p*-Bromobenzylideneacetone

Kunio SUGIYAMA, Hirotaka SHIMANOUCHI and Yoshio SASADA

Laboratory of Chemistry for Natural Products, Faculty of Science, Tokyo Institute of Technology, Ookayama, Meguro-ku, Tokyo

(Received July 22, 1970)

The topochemical studies on the solid-state photodimerization of *trans*-cinnamic acid and its derivatives by Schmidt *et al.* have disclosed a correlation between crystal structure and photochemical behavior;[1] the dimerization takes place to form a cyclobutane ring between the carbon–carbon double bonds separated by no more than 4.1 Å, while no photoreaction occurs if the separation is more than 4.7 Å.

We found that benzylideneacetone, one of acyclic α,β-unsaturated ketones, readily yielded a photodimer in a solid state.[2] It may be interesting to see whether Schmidt's conclusion is also valid in this case. For convenience of X-ray anaylsis the *p*-bromo derivative was prepared, and examined for the photodimerization. The present paper will deal with the crystal structure of *p*-bromo-*trans*-benzylideneacetone in relation with photochemical reaction.

Experimental

p-Bromo-*trans*-benzylideneacetone was prepared by condensation of *p*-bromobenzaldehyde with acetone. Colorless tabular crystals, with well-developed (100), were obtained by recrystallization from acetone.

Photochemical Reaction. The solid-state ultraviolet irradiation (with a 125w high pressure mercury lamp) of the *p*-bromobenzylideneacetone for 12 days gave a dimer as a main product (48% yield, estimated from NMR data) and *cis*-benzylideneacetone (20%). The analytical and spectrometric data of the dimer are shown below; Found: C, 53.13; H, 4.03%, Calcd for $C_{20}H_{18}O_2Br_2$: C, 53.35; H, 4.02%. IR: ν_{max} 1707 cm^{-1} (C=O), UV: λ_{max} 261 nm (ε 540), NMR (100MHz): δ^{CDCl_3} 1.67 (s, 6H), 3.85 (q, J=11.0, 7.4 Hz, 2H), 4.56 (q, J=11.0, 7.4 Hz, 2H) and 7.37 (m, 8H). The mass spectrum showed a parent peak at *m/e* 448 and very strong peaks at 224 ($M^+/2$) and 209 ($M^+/2$—Me). These spectroscopic data well correspond to those of non-substituted benzylideneacetone. Therefore, the same conclusion can be drawn that the dimer is a centrosymmetric cyclobutane derivative.[2]

Crystallographic Data. Preliminary photographs taken with Cu$K\alpha$ radiation gave the crystallographic data as below: *p*-Bromobenzylideneacetone, $C_{10}H_9OBr$, M.W.: 225, mp 84°C, monoclinic: a=10.79, b=14.18, c=6.2 Å, β=91.2°, U=947.7 Å^3, Dm=1.59 g·cm^{-3}, Dx=1.59 g·cm^{-3}, Z=4. μ (Cu$K\alpha$)=61.4 cm^{-1}. Absent spectra: ($h0l$) when l is odd, ($0k0$) when k is odd, Space group is $P2_1/c$.

Three-dimensional intensity data were collected on multiple-film equi-inclination Weissenberg photographs taken with Cu$K\alpha$ radiation. Layer lines of zero to ten around the b axis and zero to four around the c axis were recorded. Measurement of the intensities was made by visual comparison with the standard intensity scale. Lorentz and polarization corrections were applied in the usual way and the structure factors obtained were put on a common scale by comparing those of the equivalent reflections appearing on different layers.

Structure Determination

The crystal structure was determined by the heavy atom method. Approximate coordinates of the bromine atom were derived from three-dimen-

1) M. D. Cohen and G. M. J. Schmidt, *J. Chem. Soc.*, **1964**, 1966.

2) N. Sugiyama, K. Yamada, K. Sugiyama and H. Kataoka, *Nippon Kagaku Zasshi*, **88**, 769 (1967).

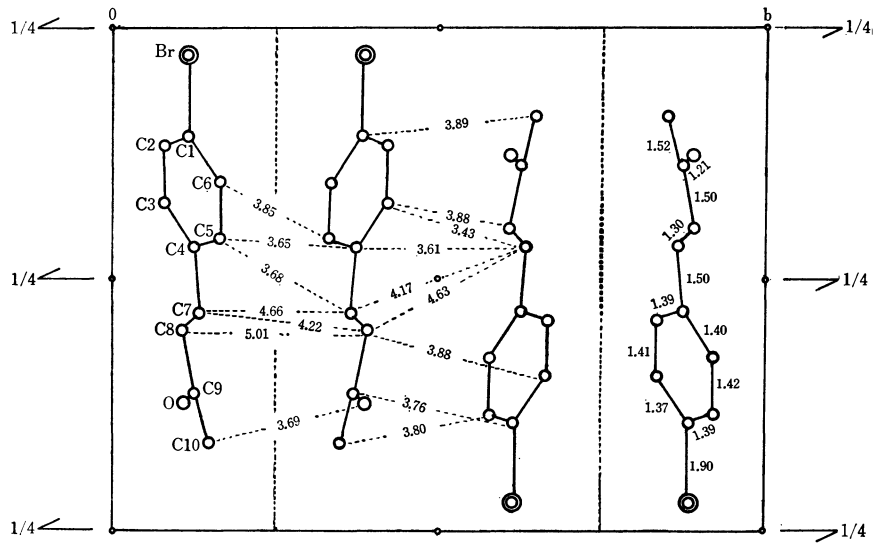

Fig. 1. Arrangement of molecules projected along [001].

Table 1. Final atomic coordinates and temperature factors

The anisotropic temperature factors are in the form: $\exp[-(B_{11}h^2+B_{22}k^2+B_{33}l^2+B_{12}hk+B_{13}hl+B_{23}kl)]$.

Atom	x/a	y/b	z/c	B(Å^2)
Br	0.0496	0.1158	1.2657	*
O	0.7502	0.1074	0.4248	5.83
C(1)	0.2108	0.1177	1.1492	3.68
C(2)	0.2280	0.0793	0.9455	3.26
C(3)	0.3476	0.0797	0.8529	3.58
C(4)	0.4446	0.1202	0.9759	3.14
C(5)	0.4241	0.1581	1.1780	3.41
C(6)	0.3054	0.1572	1.2676	3.40
C(7)	0.5736	0.1274	0.8935	3.33
C(8)	0.6049	0.1075	0.6977	4.03
C(9)	0.7325	0.1229	0.6133	4.13
C(10)	0.8376	0.1514	0.7659	4.76

* $B_{11}=0.00765$, $B_{22}=0.00826$, $B_{33}=0.04249$, $B_{12}=0.00168$, $B_{13}=0.00635$, $B_{23}=-0.00204$.

sional sharpened Patterson function without ambiguity. The three-dimensional Fourier synthesis, with the phases of bromine atom only, revealed all the non-hydrogen atoms. At this stage, $R=0.21$. The refinement of the structural parameters was carried out by the method of least-squares, using all the 1956 observed reflections. Three cycles of block-diagonal matrix refinement reduced the R to 0.148, only the bromine atom being treated as anisotropic. The final atomic coordinates and temperature factors are listed in Table 1.

Discussion

The bond lengths, angles and intermolecular contacts obtained show no unusual value in view of e. s. d. 's. The nearest carbon–carbon double bonds are those related by center of symmetry, at a center-to-center distance of 4.63 Å, and those by glide-plane at a center-to-center distance of 4.84 Å. In the latter pair, the molecules are somewhat farther and not parallel with each other. Therefore, dimerization of the latter pair may be less probable, according to the least motion principle,[3] which describes that the most favorable elementary reactions should be those involving the least change in atomic position and electronic configuration. On the other hand, the dimerization between the former pair might be more favorable and this is compatible with the conclusion that the main product of the solid-state photochemical reaction of *p*-bromobenzylideneacetone is a centrosymmetric dimer.[2]

We thank Professor Noboru Sugiyama, Tokyo University of Education, and Assistant Professor Kazutoshi Yamada, Chiba University, for helpful advice on the photochemical reaction.

3) F. O. Rice and E. Teller, *J. Chem. Phys.*, **6**, 489 (1938); **7**, 199 (1939).

BULLETIN OF THE CHEMICAL SOCIETY OF JAPAN VOL. 43 3626—3627 (1970)

Polarized Absorption Spectra of the TCNQ Crystal

Shoji HIROMA,*1 Haruo KURODA and Hideo AKAMATU

Department of Chemistry, Faculty of Science, The University of Tokyo, Hongo, Tokyo

(Received July 23, 1970)

Tetracyano-*p*-quinodimethane (TCNQ) is known to be one of the strongest electron acceptor. A number of radical salts have been prepared from the reaction between TCNQ and an electron donor. Such salts are often organic semiconductors of high conductivity. Although extensive investigations have been carried out on the electrical properties of these salts,[1,2] little has been known on the electronic properties of the crystal of TCNQ itself. Recently we have noticed that the TCNQ crystal exhibits a photoconduction with a relatively high sensitivity in the visible region.*2 In connection with such phenomenon, we have examined the polarized absorption spectra of the single crystal.

Experimental

TCNQ was synthesized by the method described by Acker and Hartler,[3] and purified by recrystallization followed by twice sublimation *in vacuo*. Single crystals of microscopic size, for the measurement of absorption spectra, were prepared from such purified sample by vacuum sublimation onto cotton wool or by crystallization from acetone solution. The crystal spectra were measured with a microspectrophotometer which we have described elsewhere.[4]

Results and Discussions

According to Long *et al.*,[5] the TCNQ crystal is monoclinic, $C2/c$ with the lattice constants, $a=8.906$ Å, $b=7.060$ Å, $c=16.395$ Å, and $\beta=98.54°$, four molecules being contained in the unit cell. We obtained diamond-shaped crystals bounded with{110} with the developed face of (001).

The *a*-axis and *b*-axis polarized spectra were observed from the direction nomal to the (001) plane. The results are given in Fig. 1, and the wavenumbers and polarization ratios are listed in Table 1.

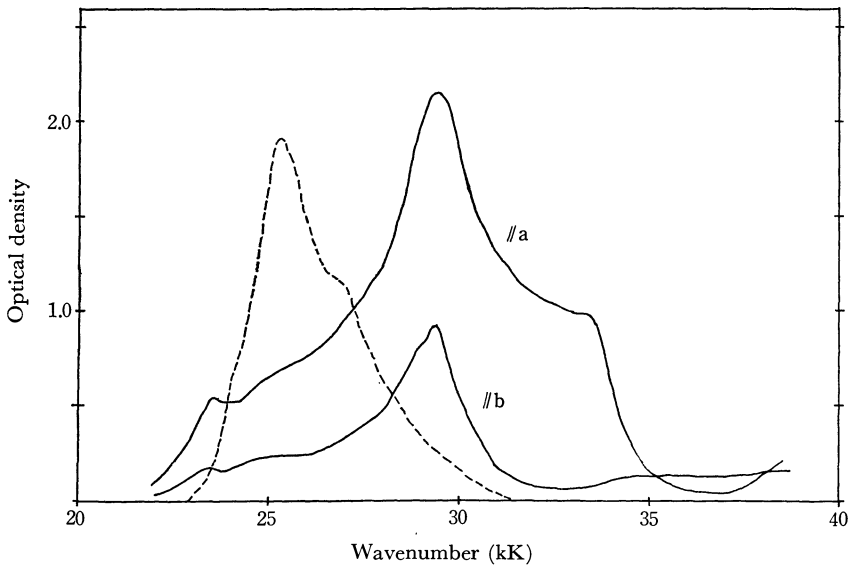

Fig. 1. The polarized absorptions spectra of TCNQ crystal.
(------ solution spectrum)

*1 Present adress: Hitachi Reserch Laboratory, Hitachi, Ltd., Hitachi, Ibaragi.

1) W. J. Siermons, P. E. Bierstedt and R. G. Kepler, *J. Chem. Phys.*, **39**, 3523 (1963).

2) N. N. Usov and V. A. Bendershkii, *Phys. Stat. Sol.*, **37**, 535 (1970).

*2 Photo-conductive properties of TCNQ crystal will be reported separately.

3) D. S. Acker and W. R. Hartler, *J. Amer. Chem. Soc.*, **84**, 3370 (1962).

4) H. Kuroda, T. Kunii, S. Hiroma and H. Akamatu, *J. Mol. Spectry.*, **22**, 60 (1967).

5) R. E. Long, R. A. Sparks and K. N. Trueblood, *Acta. Crystallogr*, **18**, 932 (1965).

Table 1. Wavenumbers and polarization ratios of absorption peaks (in kK)

$\tilde{\nu}_a$	$\tilde{\nu}_b$	I_a/I_b
23.6	23.6	3.1
24.9	24.9	2.8
29.4	29.4	2.4
33.0	~34	

In the near-ultraviolet region of the solution spectrum, TCNQ exhibits only one strong absorption band at 25.4 kK (f=0.94). By using oriented gas model, the polarization ratio, I_a/I_b, of the absorption band due to this transition ($^1B_{1u}\leftarrow{}^1A_g$) is estimated as 5.9. As we compare the crystal spectra with the solution spectra, we notice, first that the band is markedly broadened in the crystal state, and, second that its shape is quite asymmetric.

From the symmetry of the crystal lattice, we can predict that each intramolecular transition would give two optically-allowed factor group components, namely, A_u and B_u, which give the transitions polarized respectively in the b-axis and a-axis direction. We have carried out a theoretical estimation of the crystal shift and splitting on the 25.4 kK ($^1B_{1u}\leftarrow{}^1A_g$) and 43.9 kK ($^1B_{2u}\leftarrow{}^1A_g$) transitions of TCNQ molecule.*3 The energy levels of exciton states thus estimated are given in Table 2.

Table 2. Estimated energies of optically allowed exciton levels of TCNQ (in kK)

	Molecular transition	
	$^1B_{1u}$ (25.4 kK)*	$^1B_{2u}$ (43.9 kK)*
A_u (b-polarized)	32.3	43.8
B_u (a-polarized)	28.9	44.1
$\Delta\nu$**	3.36	−0.28

* Observed energy for solution spectrum.
** Splitting between the A_u and B_u components.

We could attribute the highest peak at 29.4 kK found in the a-axis spectrum to the B_u component of $^1B_{1u}$ transition. However, a corresponding peak is observed also in the b-axis spectrum. Situation is again puzzling as regards the A_u component, namely, although we can find a peak in the b-axis spectrum at about 34 kK as predicted by the calculation, the corresponding band appears also in the a-axis spectrum. Thus the observed polarization is difficult to be explained on the basis of the above treatment.

The observed spectra suggests the presence of another band in 23—27 kK region. The energy of the charge transfer from a TCNQ molecule to the neighboring one, is estimated as 20.5 kK, if we assume the electron affinity of TCNQ molecule as 2.88 eV and the ionization potential as 7.83 eV.*4 Thus it is likely that the absorption in the 23—27 kK region is associated with the intermolecular charge transfer. This assignment seems to be consistent with the polarization of the absorption in this region, although the observed polarization ratio is appreciably larger than the oriented gas value, 1.6.

Since the interaction between the neighboring molecules is expected to be the most important factor in the case of the TCNQ crystal, we have examined this from another point of view, by calculating the electronic structure of the molecular pair where the two molecules are taking the mutual orientation exactly the same as found for the two molecules closely contacting to each other in the TCNQ crystal. We have applied here a semiempirical SCF·MO·CI method treating the molecular pair as a single π-conjugated system.[5] The results of this calculation are shown in Table 3. It should

Table 3. Transitions predicted by the SCF·MO·CI calculation on the TCNQ molecule and the molecular pair (in eV)

	Monomer		Molecular pair	
	ΔE	f	ΔE	f
(CT)			2.68	0.02
$^1B_{1u}\leftarrow{}^1A_g$	2.68	1.99	3.06	4.65
$^1B_{2u}\leftarrow{}^1A_g$	4.21	0.60	4.36	0.89

be noted that the lowest transition of TCNQ molecule, ($^1B_{1u}\leftarrow A_{1g}$), is predicted to be shifted to higher energy by 3.5 kK in the molecular pair, and that a transition associated with intermolecular charge-transfer interaction is predicted at a lower energy. These results again support our tentative interpretation of the crystal spectra of TCNQ.

The authors are indebted to Mr. T. Ohta in this laboratory for his assistance in the computations presented here.

*3 Since the oscillator strength of this band is large, we treated the problem as a strong coupling case. We have taken the dipole-dipole approximation for the molecular pair separated larger than 30 Å, but estimated the interaction terms directly by use of the molecular wave-function assuming the point-charge model, for the molecular pair within 30 Å.

*4 Excitation energy was estimated by the equation, $\Delta E=I-A-C$, where I was estimated by using the highest occupied SCF MO, A is of electron capture measurement (A. L. Farragher and F. M. Page, *Trans. Faraday. Soc.*, **63**, 2369 (1967)], and the Coulomb attraction energy, C, was estimated by the point charge model.

*5 The details of the method are reported elsewhere (T. Ohta, T. L. Kunii and H. Kuroda, *Theor. Chim. Acta*, to be published).

SHORT COMMUNICATIONS

Red and Green Forms of Bis(*N*-isopropyl-3-methoxysalicylideneiminato) copper(II)

Akira TAKEUCHI and Shoichiro YAMADA

Institute of Chemistry, College of General Education, Osaka University, Toyonaka, Osaka

(Received July 9, 1970)

The structural versatility of bis(*N*-alkylsalicylideneiminato)copper(II) complexes*1 now seems to be fairly well known,[1] and their geometries may be expected to become even more complicated, when the *N*-substituent R denotes an α-branched alkyl. For example, because of the steric effect caused by considerably bulky isopropyl groups, the complexes of the type Cu(X–SAL·*iso*–C_3H_7)$_2$ take either a tetrahedral or a planar configuration, depending upon the nature of X.[2,3] Only one of them, however, is usually obtained as crystals, and two forms of crystals consisting of complexes with different configurations have never been isolated for a set of X and R. The present communication deals with successful isolation of two forms of Cu(3-CH_3O-SAL·*iso*-C_3H_7)$_2$.

The compound Cu(3-CH_3O-SAL·*iso*-C_3H_7)$_2$ was obtained in two forms, one being olive-green (Form I) and the other red-brown (Form II). The crude product was prepared by the reaction between bis(3-methoxysalicylaldehydato)copper(II) (0.02 mol) and isopropylamine (0.045 mol) in 90% methanol (75 m*l*) at about 40°C for a few hours. Evaporation at about 30°C of a concentrated solution of the crude product in methanol, ethyl ether, chloroform or dioxane yielded pure red-brown crystals (Form II) of the required complex. Olive-green crystals (Form I) of the same complex were obtained by spontaneous evaporation of a concentrated methanolic solution of the crude product at 5—10°C.

Elementary analyses of both the red-brown and the olive-green forms agree with the formula Cu(3-CH_3O-SAL·*iso*-C_3H_7)$_2$. Found: C, 58.84; H, 6.08; N, 6.14% (for the red-brown form). C, 59.00; H, 6.46; N, 6.14% (for the olive-green form). Calcd for $C_{22}H_{28}N_2O_4Cu$: C, 58.98; H, 6.30; N, 6.25%. Both forms, when dissolved in chloroform, benzene or ethanol, show the same electronic absorption spectra.

The solid spectrum of Form II is almost the same as that of its solution in non-donor solvents, having absorption bands at about 9.0, 14.5 and 21.5 kK. This is also similar to that of Cu(H-SAL·*iso*-C_3H_7)$_2$, which was previously concluded to have a distorted tetrahedral configuration.[2–4]

On the contrary, the *d–d* absorption band of Form I in the solid state, which appears at about 13.5 kK with a shoulder at about 11.0 kK, is shifted toward a much lower frequency, as compared with the spectra of the planar copper(II) complexes such as Cu(H-SAL·*n*-C_4H_9)$_2$[5] and Cu(3-CH_3O-SAL·*n*-C_3H_7)$_2$. The solid spectrum of Form I is remarkably similar to the spectrum of the binuclear Cu_2(H-SAL·CH_3)$_4$ containing copper(II) ions with a bipyramidal five-coordination,[6] suggesting this geometry for Form I.

Form II melts at 121—122°C, while with the rise of temperature Form I is transformed into Form II (red-brown) at 101°C, whose X-ray powder diagram and solid spectrum agree with those of the red-brown crystals (Form II) obtained by evaporation at about 30°C of the solution.

In the case of the corresponding nickel(II) complex Ni(3-CH_3O-SAL·*iso*-C_3H_7)$_2$, there are brown tetrahedral (Form I) and green planar (Form II) forms, and with the rise of temperature the planar form is transformed into a tetrahedral one at 157—158°C.[7] Comparison seems to indicate that the bis(*N*-substituted salicylideneiminato)nickel(II)complexes have a greater tendency to assume a planar structure than the corresponding copper(II) complexes, in agreement with a previous result.[2]

*1 The complexes of this series are abbreviated as Cu(X-SAL·R)$_2$, where R and X denote an alkyl group on the nitrogen atom and a substituent on the benzene ring, respectively.

1) D. Hall, S. V. Sheat and T. N. Waters, *Chem. Commun.*, **1966**, 436.

2) L. Sacconi, "Essays in Coordination Chemistry," ed. by W. Schneider, G. Anderegg and R. Gut, Birkhäuser Verlag, Basel (1964), p. 148.

3) S. Yamada and H. Nishikawa, This Bulletin, **36**, 755 (1963).

4) P. L. Orioli and L. Sacconi, *J. Amer. Chem. Soc.*, **88**, 277 (1966).

5) D. Hall, R. H. Sumner and T. N. Waters, *J. Chem. Soc., A*, **1969**, 420.

6) L. Sacconi, M. Ciampolini and G. P. Speroni, *J. Amer. Chem. Soc.*, **87**, 3102 (1965).

7) A. Takeuchi and S. Yamada, This Bulletin, **42**, 3046 (1969).

Isomerism and Configurational Change by Adduct Formation in Bis(*N*-cyclohexyl-3-methoxysalicylideneiminato)copper(II)

Akira TAKEUCHI and Shoichiro YAMADA

Institute of Chemistry, College of General Education, Osaka University, Toyonaka, Osaka

(Received August 1, 1970)

In a previous communication,[1] we reported on the isolation of two forms having different configurations for bis(*N*-isopropyl-3-methoxysalicylideneiminato)copper(II) (abbreviated as Cu(3-CH_3O-isopropyl)$_2$). The steric effect arising from the isopropyl group is remarkable in that the complexes of the type Cu(X-SAL·*iso*-C_3H_7)$_2$ take either a tetrahedral or a planar configuration, depending upon the nature of X.[2,3] Since the cyclohexyl group is somewhat similar to the isopropyl group with respect to the steric effect in the complexes of this series,[2] we found it desirable to extend our study to the corresponding cyclohexyl complexes. This resulted in the successful isolation of green (Form I) and red forms (Form II) of Cu(3-CH_3O-SAL·Ch)$_2$, where the notation Ch denotes a cyclohexyl group. Moreover, it has been found that the green form absorbs chloroform and bromoform to yield red-brown adducts.

Form I was obtained as olive-green crystals by recrystallizing from methanol-chloroform or benzene the crude product, which had been prepared by a reaction of bis(3-methoxysalicylaldehydato)-copper(II) with cyclohexyl amine in methanol.

With the rise of temperature, Form I was converted into a red-brown substance (Form II) at about 180°C, the change being reversible. Elementary analysis of Form II agrees with that of Form I, both forms being represented by Cu(3-CH_3O-SAL·Ch)$_2$.

Electronic absorption spectra for many copper(II) complexes of this series have so far been reported, and it now seems to be possible to determine the configuration of a copper(II) complex on the basis of its spectra in many cases.[1-4] Examination of the solid spectra reveals that Forms I and II consist of planar and tetrahedral complexes, respectively. They show identical spectra in solution, and spectra typical of the distorted tetrahedral complex in non-donor solvents.

Red-brown crystals (Form III) were obtained by evaporating a solution of Form I in chloroform, or by exposing Form I to the vapour of chloroform in a desiccator for a few days. Elementary analysis shows that Form III is represented by Cu(3-CH_3O-SAL·Ch)$_2$·2$CHCl_3$. The crystals of Form III may be kept in a tightly closed sample-tube without decomposition for at least a few weeks. When allowed to stand in the atmosphere, Form III is transformed into Form I, losing two molecules of chloroform, as confirmed by the weight-loss measurement.

The remarkable colour change on the adduct formation apparently indicates that some configurational change takes place in this process, and that Form III does not contain the planar copper(II) complex of the starting compound. Combination of the chloroform molecule with the copper(II) ion to form complexes with coordination number five or six seems to be unlikely, in view of the finding that the electronic absorption spectrum of Form III as well as that of Form I in chloroform are similar to those of their ethanol solutions, and also to the solid spectrum of Form II; all of them are typical of the distorted tetrahedral complexes. It may thus be presumed that Form III in the solid state consists of the distorted tetrahedral complex, and that the chloroform molecule is not involved in the bonding with the copper(II) ion. It may be remembered that the chloroform molecule was previously reported to function in a similar way in its adduct with *N*,*N*′-ethylenebis(salicylideneiminato)-copper(II).[5]

When bromoform was employed instead of chloroform, an adduct represented by Cu(3-CH_3O-SAL·Ch)$_2$·2$CHBr_3$ was obtained as red-brown crystals. Its properties are similar to the chloroform adduct, and it is considered to consist of the copper(II) complexes with a similar configuration.

1) A. Takeuchi and S. Yamada, This Bulletin, **43**, 3628(1970).

2) S. Yamada and H. Nishikawa, *ibid.*, **36**, 755 (1963).

3) L. Sacconi, "Essays in Coordination Chemistry," ed. by W. Schneider, G. Anderegg and R. Gut, Birkhäuser Verlag, Basel, (1964), p. 148.

4) L. Sacconi, M. Ciampolini and G. P. Speroni, *J. Amer. Chem. Soc.*, **87**, 3102 (1965).

5) E. N. Baker, D. Hall, A. J. McKinnon and T. N. Waters, *Chem. Commun.*, **1967**, 134.

Dimerization of Ethylene Catalyzed by σ-Arylnickel(II) Compounds

Ken-ichi MARUYA, Tsutomu MIZOROKI and Atsumu OZAKI

Research Laboratory of Resources Utilization, Tokyo Institute of Technology, Ohokayama, Meguro-ku, Tokyo

(Received July 31, 1970)

In a previous paper,[1] it was reported that an isotopic exchange between C_2H_4 and C_2D_4 is effectively catalyzed by bis(triphenylphosphine)nickel(II) halide in an aprotic solvent in the presence of molecular hydrogen without accompaning any hydrogenation or dimerization. The complex shows some catalytic activity for the ethylene dimerization when it is used together with boron trifluoride etherate. During the course of study dealing with the effect of ligand coordinated to nickel(II) atom, it has been found that the activity of the nickel(II) complex for the ethylene dimerization is highly increased by substituting one of the halogen ligands by a σ-aryl ligand such as 1-naphthyl, *o*-tolyl, *etc.* This communication reports a highly selective dimerization of ethylene catalyzed by bis(triphenylphosphine)σ-aryl nickel(II) bromide[2] in the presence of boron trifluoride etherate in benzene or methylene chloride.

Ethylene dimerization with this catalyst system took place almost quantitatively(95%) without any induction period at room temperature under atmospheric pressure. Only a trace amount of hexene was detected in the product. Co-dimerization of ethylene with propylene occurred to some extent, but no dimer of propylene was detected under these mild reaction conditions. Butadiene as well as triphenylphosphine strongly inhibited the ethylene dimerization. 1-Naphthyl ligand and triphenylphosphine seem to remain in the nickel complex during the reaction, because only small amounts of decomposed products of the complex such as naphthalene, 1,1′-dinaphthyl and triphenylphosphine were detected in the solution after the reaction. Bis(triphenylphosphine) *o*-tolyl nickel(II) bromide is more effective than the corresponding 1-naphthyl complex. The treatment of bis(triphenylphosphine) 1-naphthyl nickel(II) bromide with sodium tetraphenylborate ($1\text{-}C_{10}H_7Ni(P\phi_3)_2Br + NaB\phi_4 + s \rightarrow [1\text{-}C_{10}H_7Ni(P\phi_3)_2(s)]^+[B\phi_4]^- + NaBr$, $\phi = C_6H_5$, s=solvent)[3] results in a considerable decrease in catalytic activity for ethylene dimerization. This suggests that halogen ligand is important for the catalytic activity.

The experimental procedure is illustrated by the following ethylene dimerization. To a solution of bis(triphenylphosphine) 1-naphthyl nickel(II) bromide (1 mmol, 0.79 g) in dry methylene chloride (20 m*l*) under nitrogen in a 50 m*l*-flask was added boron trifluoride etherate (1 mmol, 0.125 g). The nitrogen gas in the flask had been evacuated before ethylene gas (64.5 m*l* at STP) was introduced at the temperature of liquid nitrogen. The flask was warmed up to 0°C and kept at that temperature for 1 hr with vigorous stirring. Subsequently all volatile materials (C_2H_4, C_4H_8 and solvent) were transferred into another 50 m*l*-flask by means of a liquid nitrogen trap. Their amounts were determined by gas chromatography. From the residual materials only trace amounts of naphthalene, 1,1′-dinaphthyl and triphenylphosphine were extracted by *n*-hexane. The results are shown in Table 1.

TABLE 1. DIMERIZATION OF ETHYLENE CATALYZED BY σ-ARYL NICKEL(II) COMPOUNDS

Catalyst (mmol)		Olefin introduced (m*l* STP) and solvent(m*l*)	Reaction time and temperature	Products (m*l* STP)
$(1\text{-}C_{10}H_7)Ni(P\phi_3)_2Br$,	1.0	C_2H_4(64.5)	1 hr	C_4H_8(30.8)
$BF_3\cdot O(C_2H_5)_2$,	1.0	CH_2Cl_2(20)	0 °C	C_2H_4(2.5)
$(o\text{-tolyl})Ni(P\phi_3)_2Br$,	0.1	C_2H_4(99.1)	5 min	C_4H_8(44.0)
$BF_3\cdot O(C_2H_5)_2$,	1.0	CH_2Cl_2(5.0)	0 °C	C_6H_{12}(0.90)
				C_2H_4(6.2)
$(1\text{-}C_{10}H_7)Ni(P\phi_3)_2Br$	1.0	C_2H_4(59.7)	15 hr	C_4H_8(26.3)
$BF_3\cdot O(C_2H_5)_2$,	5.0	C_3H_6(60.4)	34°C	C_5H_{10}(7.0)
		C_6H_6(50)*		C_2H_4(tr.)
				C_3H_6(48.1)

* The reaction was carried out in a 100 m*l*-flask.

1) N. Ando, K. Maruya, T. Mizoroki and A. Ozaki, *J. Catalysis*, in press.
2) J. Chatt and B. L. Show, *J. Chem. Soc.*, **1960**, 1718.
3) H. C. Clark and K. R. Dixon, *J. Amer. Chem. Soc.*, **91**, 596 (1969).

Structures of Lignans of *Magnolia fargesii*

Hiroshi KAKISAWA, Takenori KUSUMI,* Hong-Yen HSŪ and Yuh Pan CHEN**

* *Department of Chemistry, Tokyo Kyoiku University, Otsuka, Tokyo*
** *Bristol Research Institute of Taiwan, Taipei, Taiwan*

(Received August 7, 1970)

Alcoholic extract of flower buds of *Magnolia fargesii* afforded four kinds of lignans besides some alkaloids. Two of the neutral compounds were known lignans, eudesmin (**1**), $C_{22}H_{26}O_6$, and lirioresinol-B dimethyl ether (**2**), $C_{24}H_{30}O_8$, while the remaining two were new lignans designated as magnolin and fargesin.

Magnolin, $C_{23}H_{28}O_7$, mp 97°C, ν^{KBr} 1590, 1520 cm^{-1}, $[\alpha]_D$ +55.7°, λ_{max} 231, 279 mμ, and fargesin, $C_{21}H_{22}O_6$, mp 139°C, ν^{KBr} 1605, 1590, 1505 cm^{-1}, λ_{max} 233, 284 mμ, have all their oxygen atoms in ether linkages because the IR spectra of both compounds did not show hydroxyl or carbonyl absorption. The NMR spectra (Table 1.) of both compounds are best interpreted on the basis of the skeleton of 2,6-diphenyl-3,7-dioxabicyclo[3.3.0]octane, and the structures (**3**) and (**4**) were assigned for magnolin and fargesin, respectively. These structures were supported by mass spectra.[1] The mass spectrum of magnolin (**3**) is composed of two series of fragmentation, one of which is the same as the spectrum of eudesmin (**1**), and the other lirioresinol-B dimethyl ether (**2**). Simple addition of the mass spectra of **1** and **2** led to a composite almost identical with the spectrum of magnolin. The mass spectrum of fargesin (**4**) was in a similar situation and in good agreement with the composite of the spectra of **1** and sesamin.

All six aliphatic protons attached to carbon atoms bearing the ethereal oxygens in the hydrofuran rings of magnolin appear at a lower field than δ 3.8 ppm in the NMR spectrum. Birch *et al.*[2] reported that *endo* aryl group bonded at C-2 of 3,7-dioxabicyclo[3.3.0]octane system is held very close to the *endo* hydrogen atom (8-H) on the opposite ring, which causes a high field shift (δ 3.1—3.5 ppm) of the hydrogen from the normal position (δ 3.8—4.0 ppm) by the anisotropic effect of the aryl group. These NMR features show that two aryl groups of magnolin are in the *exo* positions, and thus their stereochemistry is assigned to **3**. In contrast with magnolin, all aliphatic protons attached to the hydrofuran skelton of fargesin appeared in different positions and one of C_4-methylene protons is found at upfield (δ 3.25—3.45 ppm). Thus *endo*-C_4-hydrogen is within a shielding cone of the aryl group, which must be held at *endo* position of the opposite ring. These NMR properties are very similar to those of epieudesmin as shown in the table, and the stereochemistry of fargesin is assigned to **4**.

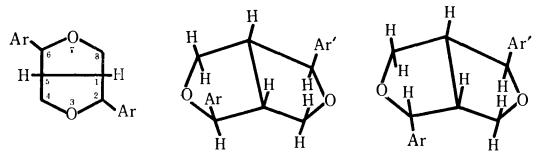

(**1**), (**2**) (**3**) (**4**)

(**1**) Ar=3,4-dimethoxyphenyl
(**2**) Ar=3,4,5-Trimethoxyphenyl
(**3**) Ar=3,4-dimethoxyphenyl
Ar′=3,4,5-trimethoxyphenyl
(**4**) Ar,Ar′=3,4-dimethoxyphenyl, 3,4-methylenedioxyphenyl

TABLE 1. NMR SPECTRA OF MAGNOLIN, FARGESIN, EUDESMIN AND EPIEUDESMIN

Protons	Magnolin (**3**)	Fargesin (**4**)	Eudesmin (**1**)	Epieudesmin
1-H	3.15 m	2.9 m	3.15 m	2.9 m
5-H		3.35 m		3.3 m
2-H	4.8 d(4)	4.88 d(5)	4.75 d(4)	4.85 d(5.5)
6-H		4.45 d(7)		4.45 d(7)
4-H	4.2—4.5 m (2H)	3.25—3.45 m	3.8—4.0 m (2H)	3.25—3.45 m
		3.7—4.0 m (2H)		3.7—3.9 m (2H)
8-H	3.8—4.0 m (2H)	4.1—4.25 m	4.2—4.4 m (2H)	4.1—4.4 m
OCH_3	3.85, 3.90	3.90	3.86, 3.88	3.87, 3.90
$-OCH_2O-$		5.95		
Aromatic	6.61, 6.90	6.8—6.95	6.8—7.0	6.9—7.1

1) A. Pelter, *J. Chem. Soc., C*, **1967**, 1376.

2) A. J. Birch, P. L. Macdonald and A. Pelter, *ibid.*, **1967**, 1968.

[2.1.1]Metacyclophane[1)]

Takeo SATO, Meiko WAKABAYASHI and Kazuo HATA

Department of Chemistry, Faculty of Science, Tokyo Metropolitan University, Setagaya-ku, Tokyo

(Received August 10, 1970)

Recently interest has been shown in the chemistry of multi-benzene cyclophanes.[2)] We wish to report the preparation and conformational studies of [2.1.1]metacyclophane. The compound was obtained *via* new cycloalkylation, in which a benzene molecule was incorporated in the cyclic system as a *m*-phenylene unit.

Slow addition of a benzene solution containing 3,3′-bis(hydroxymethyl)bibenzyl[3)] to concentrated sulfuric acid at room temperature in course of 20 hr produced a mixture of hydrocarbons from which 22.8% of bis-phenylation product, 3,3′-dibenzylbibenzyl, and a crystalline material having a formula $C_{22}H_{20}$ was isolated by column chromatography on Florisil (eluted by *n*-hexane-benzene).

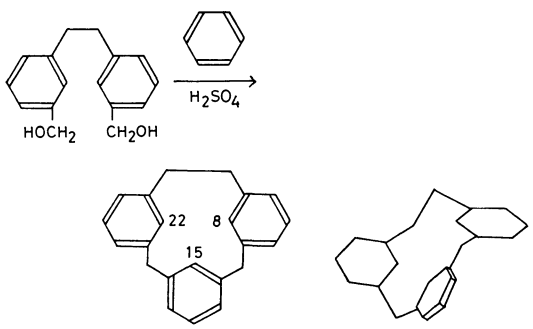

I Ia

The C_{22} hydrocarbon was obtained as colorless needles, mp 130—132°C, in 17% yield. Found: C, 92.74; H, 7.14%. Calcd for $C_{22}H_{20}$: C, 92.21; H, 7.09%. Spectral data suggested a cyclic structure in which benzene was cycloalkylated by diol. It showed a parent peak at *m/e* 284 together with abundant $P-91$, $P-106$ and $P-119$ peaks. Convincing evidence for the suggested structure was obtained by NMR spectra, which showed singlets at δ 2.78 (ethylene) and 3.60 (methylene) and three groups of absorption for the arylprotons at δ 6.27 (2H), 6.49 (1H), and 6.90 (9H). The upfield shift of two-proton and one-proton aryl signals which can be assigned to $C_{8,22}$ and C_{15} protons, respectively, suggests a metacyclophane structure. They appeared as triplets with $J=1.74$ Hz (*m*-coupling) by irradiating the benzyl methylene signal at 3.60.

The upfield shift of inner aryl protons favors the stepped conformation Ia (C_2 symmetry) over a folded one (C_s symmetry), in which two benzene rings take an overlapping arrangement. This was also supported by the UV spectrum determined in *n*-hexane, which showed benzenoid bands at 250 (ε 726), 265 (787), 270 (626) and 274 mμ (537). The absorption curve is quite similar to the overlapping spectra of *m*-xylene and diphenylmethane.

Comparison of the UV spectrum of I with that of [2.2]metacyclophane[4)] reveals that anomalies associated with bent benzene structure and transannular electron interaction found in the latter compound no longer prevail, suggesting that the 13-membered ring would be quite free to undergo conformational changes. This was further confirmed by low temperature NMR spectroscopy, which showed that both the methylene and ethylene signals stayed singlets over a wide range of temperature. They showed slight broadening only at low temperatures, the half-height width being doubled at −100°C.

Attempts to obtain [1.1.1]metacyclophane by a similar reaction of bis(3-hydroxymethylphenyl)methane failed and gave only bis-phenylation product in 60% yield. Similarly the treatment of 1,2-bis(hydroxymethyl)benzene under the same conditions gave *o*-dibenzylbenzene in 64% yield.

1) Medium-Sized Cyclophanes. XI. Part X: T. Sato, T. Akima, S. Akabori, H. Ochi, and K. Hata, *Tetrahedron Lett.*, **1969**, 1767.

2) For recent advances see the following papers. [2.0.0.]system: F. Vögtle, *Chem. Ber.*, **102**, 1449 (1969); [3.0.0]: F. Vögtle and Schunder, *Ann. Chem.*, **721**, 129 (1969); [2.2.0] and [2.0.2.0.]: F. Vögtle, *ibid.*, **728**, 17 (1969); [2.2.2]: W. Baker, J. F. W. McOmie, and J. M. Norton, *J. Chem. Soc.*, **1951**, 1114; [1.1.1.1] and [1.0.1.0]: N. Sommer, and H. A. Staab, *Tetrahedron Lett.*, **1966**, 2837; [2.1.1.1.1]: T. Inazu and T. Yoshino, This Bulletin, **41**, 647 (1968); [2.*n*]: K. Burri, and W. Jenny, *Helv. Chim. Acta*, **50**, 1978 (1967); R. Flammang, H. P. Figeys, and R. H. Martin, *Tetrahedron*, **24**, 1171 (1968).

3) T. Sato, M. Wakabayashi, M. Kainosho, and K. Hata, *Tetrahedron Lett.*, **1968**, 4185.

4) N. L. Allinger, M. A. DaRooge and R. B. Hermann, *J. Amer. Chem. Soc.*, **83**, 1974 (1961).

Structure of Cobalt(III) Complexes of *d*-, *l*-, and *meso*-2,4-Pentanediaminetetraacetate

Fujio MIZUKAMI, Haruko ITO, Junnosuke FUJITA and Kazuo SAITO

Department of Chemistry, Faculty of Science, Tohoku University, Sendai

(Received August 21, 1970)

The conformation of a six-membered chelate ring of the tristrimethylenediaminecobalt(III) complex was first determined to be of chair form by X-ray diffraction by Y. Saito *et al.*[1] van Saun and Douglas, and Ogino *et al.*[2] synthesized cobalt(III) complex of trimethylenediaminetetraacetate ($trdta^{4-}$) and suggested that the six-membered chelate should have a twist form. We examined the influence of the methyl group on α-carbon atom of the trimethylene part upon the chelate structure, and found a stereospecific formation of 2,4-pentanediaminetetraacetatocobaltate(III) complex depending on the optical isomerism of 2,4-pentanediamine.

2,4-Pentanediamine was synthesized by the known method[3] and the racemic and meso forms were separated by utilizing the difference in solubility of their dihydrochlorides in 95% ethanol.*1 The amine was converted into 2,4-pentanediaminetetraacetic acid ($ptntaH_4$) by Weyh and Hamm's method.[4] A violet complex was formed by heating $Na_3[Co(NO_2)_6]$ and racemic $ptntaH_4$ in water at 60—70°C for 15 hr. The product was converted into diastereomers of d-$[Co(NO_2)_2en_2]^+$ salt (en= ethylenediamine) with $[\alpha]_D$ +887° and −696°. They were treated with potassium iodide to give $K[Co(ptnta)]\cdot H_2O$. Found: $(+)_D$ isomer, C, 34.40; H, 4.55; N, 6.31: $(-)_D$ isomer, C, 34.61; H, 4.53; N, 6.27%. Calcd for $C_{13}H_{20}CoKN_2O_9$: C, 34.98; H, 4.55; N, 6.28%. When *meso*-$ptntaH_4$ was used in place of racemic $ptntaH_4$ the violet complex was not formed, and only a blue complex H[CoCl(ptntaH)] was isolated crystalline on treatment with dilute hydrochloric acid. Found: C, 36.35; H, 5.58; N, 6.55%. Calcd for $C_{13}H_{20}ClCoN_2O_8$: C, 36.59; H, 4.72; N, 6.57%.

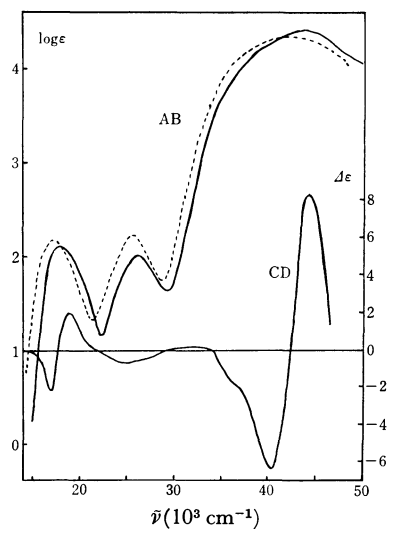

Fig. 1. AB and CD spectra of $(+)_D$-K[Co(RR-ptnta)]·H_2O in H_2O (——) and AB spectrum of H[CoCl(*meso*-ptntaH)] in dil. HCl (------).

The violet complex gives an absorption spectrum (AB) in water very similar to that of $[Co(trdta)]^-$ or $[Co(edta)]^-$. Its infrared spectrum shows no absorption of free carboxylate. Its PMR spectrum in D_2O gives only one methyl signal and two kinds of acetate methylene signal. The $(+)_D$ complex is assigned to be Δ, from comparison of its circular dichroism (CD) with that of Δ-$[Co(trdta)]^-$.[2] It is thus clear that the complex contains sexadentate $ptnta^{4-}$ ligand and the trimethylenediamine chelate takes a twist form. Since methyl groups should take an equatorial position in the chelate, the $ptnta^{4-}$ in the $(+)_D$ complex should have RR configuration.

The blue complex gives an absorption pattern similar to that of $[CoCl(edta)]^{2-}$ and the infrared absorption gives the peak of free carboxylate. The PMR spectrum gives two kinds of methyl signal, and the signals of acetate methylene are much more complicated than those of the violet complex. We consider that the ligand is quinquedentate in this blue complex. So far as the methyl groups orientate equatorially to the chelate ring, the trimethylenediamine ring should take the chair form and only three out of four acetate branches seem to be allowed to coordinate to cobalt(III).

Such a stereospecific formation of sexa- and quinquedentate complex from racemic and meso $ptnta^{4-}$ indicates that the steric regulation coming from the methyl group on the α-carbon atom is very strong in six-membered as well as in five-membered rings.

1) Y. Saito, T. Nomura and F. Marumo, This Bulletin, **41**, 530 (1968).

2) C. W. van Saun and B. E. Douglas, *Inorg. Chem.*, **8**, 1145 (1969); H. Ogino, M. Takahashi and N. Tanaka, This Bulletin, **43**, 424 (1970).

3) C. Harries and T. Haga, *Ber*, **32**, 1191 (1899); C. J. Dippel, *Rec. Trav. Chim. Pays-Bas*, **50**, 525 (1931).

*1 Dippel seems to have given a wrong identification; his *meso* was racemic and his racemic was *meso*. When $(+)_D$ violet complex was decomposed, the free ligand gave (+) normal dispersion.

4) J. A. Weyh and R. E. Hamm, *Inorg. Chem.*, **7**, 2431 (1968).

Five Co-ordination in Isocyanide Insertion Complexes of Pd(II)

Yasuhiro YAMAMOTO and Hiroshi YAMAZAKI

The Institute of Physical and Chemical Research, Yamatomachi, Saitama

(Received August 29, 1970)

We have already reported that the reaction of cyclohexyl isocyanide (**1**) with *trans*-Pd(PPh_3)$_2$I(CH_3) underwent the insertion of isocyanide molecules into a methyl-palladium σ-bond, affording imidoyl complexes.[1]

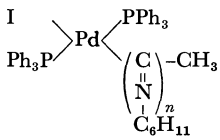

n=1 or 2

In our further studies of the insertion reaction of isocyanide,[2-4] we concluded that it had a five co-ordinate structure complexes to palladium through the lone-pair electrons of imino nitrogen atom; our conclusion was based on the NMR spectra of these types of complexes with dimethylphenylphosphine. We wish now to report on this subject.

The treatment of **1** with *trans*-Pd($PPhMe_2$)$_2$I(CH_3) in a 1 :1 or 2 : 1 molar ratio in benzene at 0°C underwent the single or double insertion of isocyanide into a methyl-palladium σ-bond, producing *trans*-Pd($PPhMe_2$)$_2$I[C(CH_3)=NC_6H_{11}] (**2**)[5] (as very pale yellow crystals, 59%, mp 169—172°C dec., $\nu_{C=N}$(KBr) 1627 cm^{-1}) and *trans*-Pd($PPhMe_2$)$_2$-I[CH_3(C=NC_6H_{11})$_2$] (**3**)[5] (as yellow crystals, 54%, mp 223—227°C dec., $\nu_{C=N}$(KBr) 1632 and 1583 cm^{-1}) respectively. The complex **3** was more stable than **2**.

In the NMR spectrum of **2** in C_6D_6 at 23°C, the methyl resonances of dimethylphenylphosphine ligands showed a well-defined 1 : 2 : 2 : 2 : 1 pattern. This may be considered to arise from two overlapping 1 : 2 : 1 patterns (8.47 and 8.35 τ), separated by 7.2 Hz, in which the triplet resonance suggests that the two phosphorus ligands were co-ordinated to a metal in mutual *trans*-positions.

The presence of two triplet signals indicates that the two methyl groups on the same phosphorus atom are magnetically nonequivalent, for there is no plane of symmetry resulting from the co-ordination of the imino nitrogen to the palladium atom.[6]

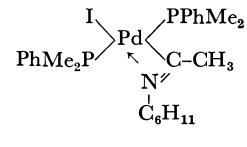

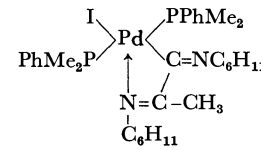

An elevation of the temperature might be expected to give the four co-ordinate complex by releasing the imino nitrogen. This would cause the two methyl proton resonances to be magnetically equivalent.

The P–CH_3 protons of **2** at 42°C appeared as two triplets (with the same coupling constant, $|^2J_{P,H}+{}^4J_{P,H}|$=6 Hz), and separated by 4.6 Hz. At 63°C and 81°C, the spectra showed 1 : 3 : 3 : 1 and 1 : 1 : 2 : 2 : 1 : 1 patterns, separated by 3 and 1 Hz, respectively, indicating two overlapping 1 : 2 : 1 patterns. At 85°C, the two P–CH_3 resonances converged to a triplet peak, indicating the absence of magnetic nonequivalence.

Analogous NMR behavior was observed in the complex **3**. In the spectrum of **3** in C_6D_6 at 23°C, the methyl proton resonances of the phosphorus ligands showed two triplets at 8.45 ($|^2J_{P,H}+{}^4J_{P,H}|$= 6.5 Hz) and 8.22 τ ($|^2J_{P,H}+{}^4J_{P,H}|$=6.5 Hz), indicating also the presence of magnetic nonequivalence. The magnitude of the chemical-shift difference of the two triplets due to the P–CH_3 resonances decreased with a rise in the temperature without changing their forms. The convergence of the two triplets to a triplet peak was ultimately observed at *ca.* 130°C, indicating that the co-ordination strength of **3** is higher than that of **2**. This indicates a parallel between the co-ordination strength and the difference in stability of the two iminoacyl complexes. Detailed studies are in progress.

1) Y. Yamamoto and H. Yamazaki, This Bulletin, **43**, 2653 (1970).

2) Y. Yamamoto, H. Yamazaki and N. Hagihara, *ibid.*, **41**, 532 (1968); *J. Organometal. Chem.*, **18**, 189 (1969).

3) Y. Yamamoto and H. Yamazaki, This Bulletin **43**, 143 (1970).

4) Y. Yamamoto and H. Yamazaki, *J. Organometal. Chem.*, **24**, 717 (1970).

5) Both complexes gave satisfactory results in elementary analysis and molecular-weight determinations.

6) The triple-inserted complex, Pd(PPh_2Me)I[CH_3-(C=NC_6H_{11})$_3$], obtained from the reaction of *trans*-Pd-(PPh_2Me)$_2$I(CH_3) with **1** in a 1 : 3 molar ratio had a four-co-ordinated structure containimg the five-membered chelate co-ordinated to palladium through the terminal imino nitrogen atom; see Ref. 1. An analogous structure was noted in the nickel complexes; see S. Otsuka, A. Nakamura and K. Yoshida, *J. Amer. Chem. Soc.*, **91**, 7196 (1969).

Structure Analysis of *p*-Bromobenzoate of Sterigmatocystin by X-ray Diffraction Method

Nobuo TANAKA,[*1] Yukiteru KATSUBE, Yuichi HATSUDA,[*2] Takashi HAMASAKI[*2] and Masayoshi ISHIDA[*2]

Faculty of Engineering, Tottori University, 1-1, *Koyama-cho, Tottori*

(Received July 16, 1970)

Sterigmatocystin, a metabolite of Aspergillus versicolor (Vuillemin) Tiraboshi, is a natural product containing the dihydrofurobenzofuran system. The structure was postulated by means of spectrometry and various chemical methods.[1,2] In order to establish the structure, *p*-bromobenzoate of sterigmatocystin was investigated by X-ray diffraction method.

TABLE 1. CRYSTAL AND PHYSICAL DATA

Molecular weight:	$C_{25}H_{15}O_7Br$ 507.31
Melting point :	260°C
Monoclinic :	$a=13.01\pm0.04$ Å
	$b=9.03\pm0.03$ Å
	$c=8.93\pm0.03$ Å
	$\beta=102.5\pm0.5°$
Space group :	$P2_1$
Density (by flotation) :	1.640 g/cm³
Density (calculation) :	1.645 g/cm³
Two molecules per unit cell.	
Volume of the unit cell :	1023.8 Å³

The compound was obtained by the reaction between sterigmatocystin and *p*-bromobenzoylchloride. The crystal grown from acetone solution was light brown needles elongated along the *b* axis. The unit cell dimensions shown in Table 1 were obtained from NaCl-calibrated Weissenberg and rotation photographs about the *b* and c axes. Intensities of 1545 independent reflections were measured visually from equi-inclination Weissenberg photographs of 0—6 layers around the *b* axis.

The bromine atom was easily located as $x=-0.06$, $y=0.25$(arbitrary chosen) and $z=0.16$ from the Harker peak of a sharpened three-dimensional Patterson function. The nine atoms were assigned in the benzoyl group near the bromine atom, though the first Fourier map based on the bromine atom alone was confused by false symmetry. The whole structure of the molecule was revealed after five successive structure factor and Fourier synthesis calculations.

Refinement of the structural parameters was carried out by the block-diagonal least-squares method. The discrepancy factor was reduced to 0.168 after six cycles of the refinement with the isotropic thermal parameters. The average standard deviation of the bond length is 0.041 Å. The current three-dimensional electron density distribution viewed along the *b* axis is shown in Fig. 1. The structure of sterigmatocystin in this molecule is in agreement with that proposed by Bullock *et al.*[2]

Further refinement of the structure and determination of the absolute configuration will be published later.

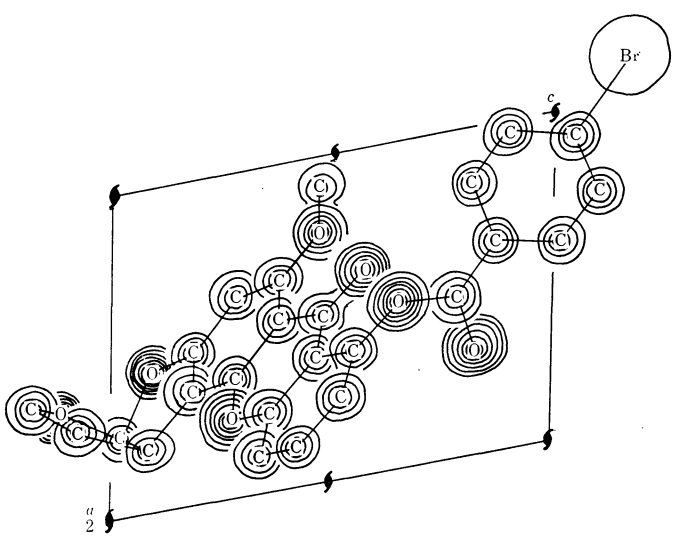

Fig. 1. Electron density distribution viewed along the *b* axis

*1 Present address; Faculty of Engineering Science, Osaka University.

*2 Faculty of Agriculture, Tottori University.

1) Y. Hatsuda and S. Kuyama, *J. Agr. Chem. Soc. Jap.*, **28**, 989 (1954).

2) E. Bullock, J.C. Roberts and J.G. Underwood, *J. Chem. Soc.*, **1962**, 4179.

A New Observation on the Polarized Absorption Spectra of TCNNQ Molecular Complexes

Yasumasa J. I'HAYA, Toru YUNOKI and Noboru SUZUKI

Department of Materials Science, The University of Electrocommunications, Chofu-shi, Tokyo

(Received July 22, 1970)

A current explanation for the origin of a second charge-transfer (CT) band which appears in some CT molecular complexes is that the second CT band is mainly associated with a charge transfer from the second highest occupied molecular orbital (HOMO) of a donor molecule to the lowest vacant molecular orbital (LVMO) of an acceptor molecule[1]. In this communication, we show a possibility of the charge transfer from the HOMO of donor to the *second* LVMO of acceptor in some TCNNQ (11, 11, 12, 12,-tetracyano-1,4,-naphthaquinodimethane)-polycyclic aromatic hydrocarbon complexes. A similar interpretation was first given by Iwata, Tanaka and Nagakura for the 1,2,4,5- tetracyanobenzene complexes[2].

We measured the polarized absorption spectra in the visible and ultraviolet regions at room temperature and 80°K for the molecular complexes which involve TCNNQ as an acceptor and anthracene (An), pyrene (Py), phenanthrene (Ph), 1,2-benzanthracene (Ba), chrysene (Ch), and triphenylene (Tp) as donors. The mole ratio of donor and acceptor was found to be 2:1 for TCNNQ-An, -Py, -Ph complexes (Group 1), while that for TCNNQ-Ba, -Ch, and -Tp complexes (Group 2) was 1:1. Two broad bands were observed in each polarized absorption spectrum of these complexes. In Group 1 complexes, the longer wavelength bands (14-19kK) are clearly polarized along the crystal elongated axes, and the shorter wavelength bands (19-23kK) are perpendicular to them. The two bands of Group 2 complexses, however, both have polarization components, though the dichroic ratios of the longer wavelength bands are two to five times larger than those of the shorter wavelength bands. These two bands are not local excitation bands but can be assigned to be the first and second CT bands, since the lowest transition of TCNNQ has an absorption maximum at 25kK and those of the donors appear at much shorter wavelength regions.

The wave numbers of the absorption maxima ($h\nu_{CT1}$ and $h\nu_{CT2}$) are plotted in Fig. 1 against the HOMO energy of donor. For the first CT bands, a straight line is obtained (Line I) as usual, so that

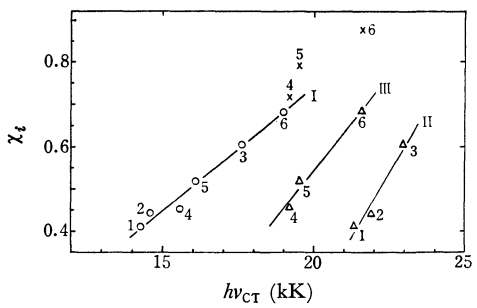

Fig. 1. Charge-transfer transition energies *vs* the Hueckel molecular orbital coefficients, χ_i, of the polycyclic aromatic donors. ○: 1st CT band, △: 2nd CT band; 1:An, 2:Py, 3:Ph, 4:Ba, 5:Ch, 6:Tp. Values of χ_i are taken from C. A. Coulson and A. Stereitwieser, Jr., Dictionary of π-Electron Calculations, W. H. Freeman and Co., San Francisco (1965).

these bands are undoubtedly associated with the charge transfer from the HOMO of donor to the LVMO of acceptor.

A plot of $h\nu_{CT2}$ *versus* the HOMO energy of donor produces two linear relationships, one for Group 1 complexes (Line II) and the other for Group 2 complexes (Line III). The charge transfer mechanism for the second CT bands may, therefore, be divided into two classes depending on the mole ratio of donor and acceptor. If we assume a charge transfer from the second HOMO of donor in Group 1 complexes, the magnitude of $h\nu_{CT2}$ should be in the order An>Py>Ph, which is inconsistent with the present observation. Thus it should be tentatively concluded, that the second CT bands of Group 1 complexes are associated mainly with the charge transfer from the HOMO of donor to the second LVMO of acceptor.

On the other hand, if we plot $h\nu_{CT2}$ of Group 2 complexes against the second HOMO energy of donor, we obtain the crosses in Fig. 1. Although the data deviate considerably from linearity, some relationship between $h\nu_{CT2}$ and the second HOMO energy of donor can be recognized. Therefore, we tentatively conclude that the second CT bands of Group 2 complexes are due to a mixed charge transfer mechanism, one from the HOMO of donor to the second LVMO of acceptor and the other from the second HOMO of donor to the LVMO of acceptor.

1) H. Kuroda, I. Ikemoto and H. Akamatu, This Bulletin, **39**, 1842 (1966), and the references cited therein.

2) S. Iwata, J. Tanaka and S. Nagakura, *J. Amer. Chem. Soc.*, **88**, 894 (1966).

Photochemical Reactions of Nicotinic Acid in Aqueous and Ethanol Solutions

Fumikatsu TAKEUCHI, Takako FUJIMORI and Akira SUGIMORI

Department of Chemistry, Faculty of Science and Technology, Sophia University, Kioi-cho, Chiyoda-ku, Tokyo

(Received August 4, 1970)

In a previous paper, photodecarboxylation of pyridinecarboxylic acids was reported.[1] The present paper deals with pH dependence of the photoreaction of nicotinic acid in aqueous and ethanol solutions.

Nicotinic acid was irradiated with a low pressure mercury lamp at room temperature in 5×10^{-4}M solution. The acidity of the solution was adjusted with acetate or phosphate buffer. Before irradiation nitrogen was bubbled to eliminate oxygen in the solution. Photo-products were separated by anion exchange chromatography (column; Dowex-1 formate, eluent; formic acid) and identified by elementary analysis, IR, NMR and comparison with authentic specimens synthesized.

Nicotinic acid shows manifold photoreactivity depending on solvent and acidity. In Scheme 1 are summarized photoreactions of nicotinic acid. In Fig. 1 is shown pH dependence of the photoreaction in aqueous solutions, together with pH dependence of λ_{max} of UV spectra of nicotinic acid.

The cationic form of nicotinic acid undergoes photo-hydroxylation at 2-position.[2] The anionic form is photoreactive in lower pH region to give 2-(3-pyridyl-)pyridine-5-carboxylic acid (decarboxylative bipyridyl formation), while this form is stable in alkaline solution.

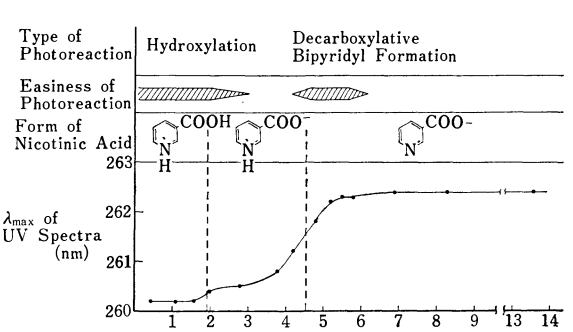

Fig. 1. pH dependence of the photoreaction and λ_{max} of nicotinic acid in aqueous solutions.

The photoreactivity of nicotinic acid in ethanol solutions differs from that in aqueous solutions. Nicotinic acid in ethanol undergoes photo-ethylation in acidic media and photo-decarboxylation in alkaline media. Since the photoreactions in ethanol were not affected by the addition of 1,3-pentadiene, the photoreactions in ethanol would proceed from excited singlet state.

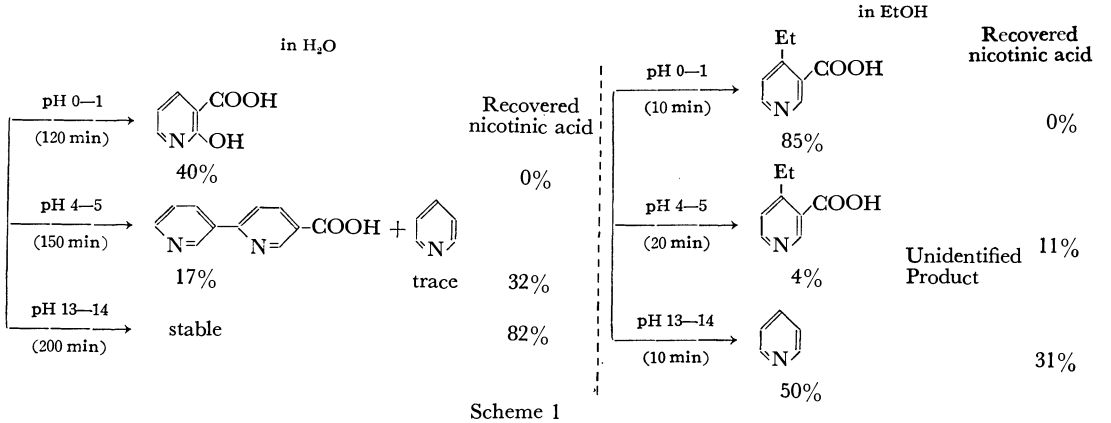

Scheme 1

1) C. Azuma and A. Sugimori, *Kogyo Kagaku Zasshi*, **72**, 239 (1969).

2) Photo-induced hydroxylation of pyridine nucleus was reported with *N*-methylnicotinamide, but the reaction was not observed with *N*-methylnicotinic acid. S. Y. Wang, *Biochemistry*, **7**, 3740 (1968).

3) Photo-induced alkylation of *N*-heteroaromatic compounds in alcoholic solutions was reported with quinoline, phenanthridine, pyrimidine and pyridine. F. R. Stermitz, C. C. Wei and W. H. Huang, *Chem. Commun.*, **1968**, 482; F. R. Stermitz, C. C. Wei and C. M. O'Donnel, *J. Amer. Chem. Soc.*, **92**, 2745 (1970); F. R. Stermitz, R. R. Seiber and D. E. Nicodem, *J. Org. Chem.*, **33**, 1395 (1968); M. Ochiai, E. Mizuta, Y. Asahi and K. Morita, *Tetrahedron*, **24**, 5861 (1968); E. F. Travecedo and V. I. Sternberg, *Chem. Commun.*, **1970**, 609.

Chemically Induced Nuclear Polarization in the Hydroxylamine Derivatives Obtained by Addition of 1-Cyano-1-methylethyl Radicals

Hiizu IWAMURA, Michiko IWAMURA, Masako TAMURA and Kengo SHIOMI

Department of Chemistry, Faculty of Science, The University of Tokyo, Bunkyo-ku, Tokyo
and
Department of Chemistry, Faculty of Science, Toho University, Narashino-shi, Chiba

(Received July 21, 1970)

We would like to report the observation of polarized NMR in the adducts I and II of 1-cyano-1-methylethyl radicals. When a solution of α,α'-azobisisobutyronitrile (AIBN) and excess nitrosobenzene in 1,1,2,2-tetrachloroethane/*o*-dichlorobenzene (1 : 1 v/v) was placed in an NMR probe which had been heated at 110°, AIBN decomposed with an approximate half-life of 89 sec as judged by exponential decay of its NMR absorption at 1.61 ppm.[1] At the same time an intense emission line was observed at 1.44 ppm. The amplitude reached its maximum in a negative sense at 40 sec after insertion of the sample tube, and decayed to the apparent zero in 80 sec.[2] By comparison with the authentic sample[3] it was found that the emission originated from one of the methyl signals of adduct I. Intensity of

$$\mathrm{Ph\text{-}N{=}O \xrightarrow{\cdot CMe_2CN} Ph\text{-}N(CMe_2CN)\text{-}O\cdot \xrightarrow{\cdot CMe_2CN} Ph\text{-}N(CMe_2CN)\text{-}O\text{-}CMe_2CN}$$

III I

the remaining methyl signal at 1.51 ppm, on the other hand, increased exponentially as expected for a normal growth of the chemical species as the reaction proceeds.

AIBN was similarly decomposed thermally in the presence of α,N-diphenylnitrone.[4] Adduct II shows four separate

$$\mathrm{Ph\text{-}CH{=}N(\rightarrow O)\text{-}Ph \xrightarrow{\cdot CMe_2CN} Ph\text{-}CH(CMe_2CN)\text{-}N(\text{-}O\cdot)\text{-}Ph} \quad \text{(IV)}$$

$$\mathrm{\xrightarrow{\cdot CMe_2CN} Ph\text{-}CH(CMe_2CN)\text{-}N(\text{-}OCMe_2CM)\text{-}Ph}$$

(II)

peaks (δ 1.19, 1.41, 1.70 and 1.88 ppm) of the methyl protons due to the presence of the asymmetric carbon atom in the molecule. Out of these four only a pair at 1.41 and 1.70 gave emission signals.[2]

It is reasonably assumed that the first addition of a 1-cyano-1-methylethyl radical would lead to more or less stable nitroxide radicals III and IV.[4,5] Thus the present findings that only half of the methyl groups in I and II showed emission can be considered to indicate that nuclear polarization which is developed by dipolar cross relaxation during the second step of the free radical addition is observable as emission signals.[6] It then follows that the methyl signals which appeared as emission should be assigned to the *O*-CMe_2CN of the hydroxylamine derivatives I and II.

This is the first example in which the polarized NMR signals have been applied to the assignment of the spectra. Conversely the method will find application for discussing the chronology of free radical addition when the assignment of the spectra is unambiguously available.

1) NMR measurements were carried out on a Japan Electron Optics 4H-100 spectrometer. The proton signal of the solvent tetrachloroethane was used as the lock signal and the chemical shifts are expressed relative to the internal TMS.

2) In addition to this emission two pairs of polarized NMR were always observed in the *C*-methyl region of the spectra due to isobutyronitrile and methacrylonitrile formed by disproportionation of the 1-cyano-1-methylethyl radicals. See H. Fischer and J. Bargon, *Accounts Chem. Res.*, **2**, 110 (1969), and H. Iwamura and M. Iwamura, *Tetrahedron Lett.*, **1970**, 3723.

3) B. A. Gingras and W. A. Waters, *J. Chem. Soc.*, **1954**, 1920.

4) M. Iwamura and N. Inamoto, This Bulletin, **40**, 702, 703 (1967); **43**, 856, 860 (1970).

5) A. Mackor, Th. A. J. W. Wajer, Th. J. de Boer and J. D. W. van Voorst, *Tetrahedron Lett.*, **1966**, 2115.

6) The spin-lattice relaxation time was found to be 2.5 sec for all the four methyl signals of II.

BULLETIN OF THE CHEMICAL SOCIETY OF JAPAN VOL. 43 3639—3643 (1970)

Redox Reactions on α-Ferric Oxide Electrode

Hiroshi YONEYAMA, Shiñichi HAMAMATSU and Hideo TAMURA

Department of Applied Chemistry,[*1] *Faculty of Engineering, Osaka University, Yamadakami, Suita, Osaka*

(Received August 18, 1969)

The redox reactions of $Fe(CN)_6^{4-}/Fe(CN)_6^{3-}$, Fe^{2+}/Fe^{3+}, and Ce^{3+}/Ce^{4+} systems on α-Fe_2O_3 electrodes containing different amounts of titanium were studied. The anodic current showed a tendency to be saturated in the $Fe(CN)_6^{4-}/Fe(CN)_6^{3-}$ and Fe^{2+}/Fe^{3+} systems. The forward direction of the current flow in these systems was the reverse of the case with the lithiated NiO electrode. On the other hand, the cathodic current flow was negligible and the redox potential was not observed for the Ce^{3+}/Ce^{4+} system. It was concluded that the reaction proceeds through electron transfer and that *I–V* curves are determined by the influence of the potential barrier formed on the electrode surface over which an electron transfers from the electrode into the electrolyte or in the reverse direction.

In a previous paper,[1] it was reported that redox reactions in the $Fe(CN)_6^{4-}/Fe(CN)_6^{3-}$, Fe^{2+}/Fe^{3+}, and Ce^{3+}/Ce^{4+} systems on a lithiated NiO electrode which had a P-type conduction were affected by the electrical properties of the electrode and the electrode potential of the redox system. The *I-V* characteristics of these redox systems show directly how charge carriers in the electrode relate with the reaction system, for at least the reactions of the Fe^{2+}/Fe^{3+} and Ce^{3+}/Ce^{4+} systems proceed *via* only a solvent-reorganization process[2] without any formation of the adsorbed intermediate to cause a change in the surface property of the electrode. In this paper, we will study the redox reactions of these systems on a Ti-doped α-Fe_2O_3 electrode in order to clarify the relation between the charge carrier in the N-type 3*d* transition metal oxide electrode and the reaction systems. These studies will provide some information on the role of the oxide film on the electrode reaction; this film is often formed on the electrode during electrolysis.

Experimental

Electrode. The electrode was prepared and the effective area of the electrode was estimated by a method described previously.[3] The material in contact with α-Fe_2O_3 was platinum, for this material act as an ohmic contact and platinum is electrochemically inert even if the electrolyte penetrates into the electrode. The α-Fe_2O_3's used as electrodes had specific resistivities of 15, 30, 280, and 7500 Ω-cm.

Cell Equipment and Chemicals. The cell equipment and chemicals were the same as those reported previously.[1] The redox systems used in this study are also the same; they are shown in Table 1. All of the measurements were carried out at 25±1°C.

Table 1. Redox system studied

System	Medium
10 mM Ce^{3+} 10 mM Ce^{4+}	1N H_2SO_4
5 mM Fe^{2+}, 5 mM Fe^{3+}	0.1N H_2SO_4
5 mM $Fe(CN)_6^{4-}$, 5 mM $Fe(CN)_6^{3-}$	0.1N H_2SO_4

Results

The polarization curves of the α-Fe_2O_3 electrode in electrolytes containing the redox systems are

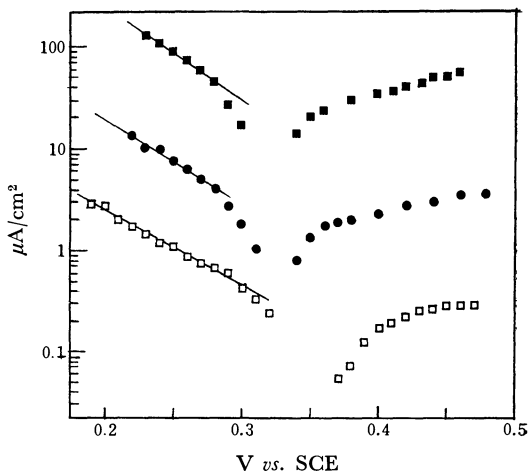

Fig. 1. *I-V* curves of $Fe(CN)_6^{4-}/Fe(CN)_6^{3-}$ on α-Fe_2O_3 electrodes.
—■— 15 Ω-cm, —●— 280 Ω-cm,
—□— 7500 Ω-cm

*1 Previous name: Chemical Technology.

1) H. Yoneyama and H. Tamura, This Bulletin, **43**, 1603 (1970).

2) E. Sacher and K. J. Laidler, "Modern Aspects of Electrochemistry," Vol. 3, ed. by J.O'M. Bockris and B. E. Conway, Butterworth, London (1964), p. 7.

3) H. Yoneyama and H. Tamura, This Bulletin, **43**, 350 (1970).

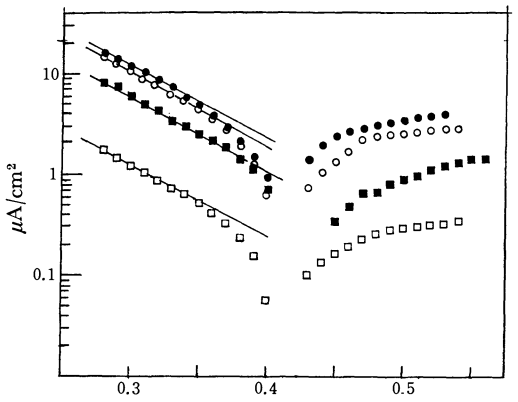

Fig. 2. *I-V* curves of Fe^{2+}/Fe^{3+} system on α-Fe_2O_3 electrodes.
—■— 15 Ω-cm, —○— 30 Ω-cm,
—●— 280 Ω-cm, —□— 7500 Ω-cm

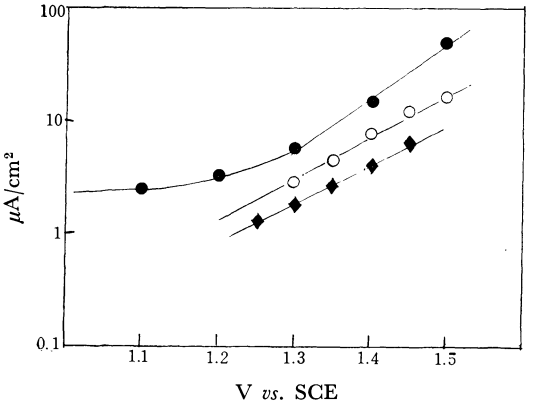

Fig. 3. *I-V* curves of α-Fe_2O_3 electrode in 0.01M Ce^{3+}/Ce^{4+} system.
—●— 15 Ω-cm, —○— 30 Ω-cm,
—◆— 280 Ω-cm

presented in Figs. 1, 2, and 3 for the $Fe(CN)_6^{4-}/Fe(CN)_6^{3-}$, Fe^{2+}/Fe^{3+}, and Ce^{3+}/Ce^{4+} systems respectively. The cathodic reaction seems to proceed under an "activation controlled condition" in the former two redox systems, which have relatively low redox potentials,[4] while in the Ce^{3+}/Ce^{4+} system, which has a higher redox potential, a distinct reaction seems to occur in the case of the anodic polarization and the measured open circuit potential was below 0.6V *vs.* SCE.

To clarify the nature of the anodic current hindrance in the Fe^{2+}/Fe^{3+} system, the dependence of the concentration of Fe^{2+} on the anodic portion of the current was measured. An approximate proportionality was observed between the concentration of Fe^{2+} and its oxidation current, as Fig. 4 shows. Likewise, the effect of the concentrations of Ce^{3+}

4) W. M. Latimer, "Oxidation Potential," 2nd ed. Prentice-Hall, Englewood Cliffs, N. J. (1961), p. 340.

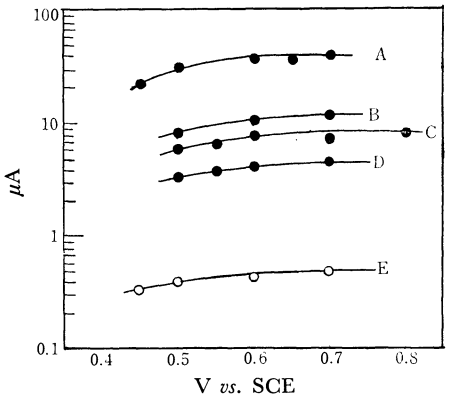

Fig. 4. *I-V* curves of α-Fe_2O_3 electrode in 1N H_2SO_4 solution containing different amount of Fe^{2+}.
A: 1M B: 0.2M C: 0.1M D: 0.05M E: 0M
Electrode area 0.2 cm^2.

and Ce^{4+} on the anodic current was investigated. The *I-V* curves of the α-Fe_2O_3 obtained in 1N H_2SO_4 were not changed by the addition of these ions, as Fig. 5 shows. This result caused us to doubt whether the anodic current shown in Fig. 3 directly showed the reaction current of the redox system itself. In order to elucidate this question, the quantity of Fe which had been produced by the anodic dissolution of the α-Fe_2O_3 electrode into the electrolyte during polarization for a known period and at fixed potential was analytically determined for the

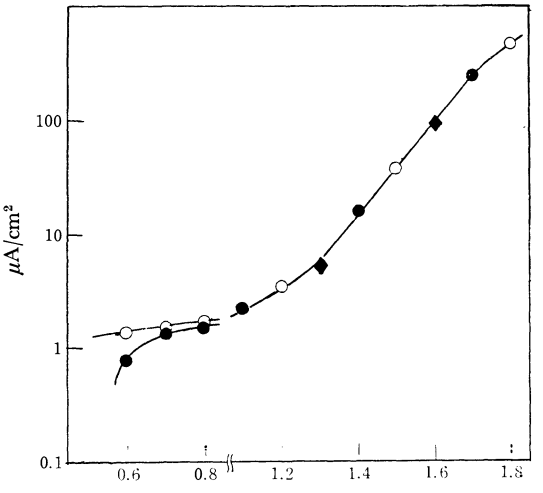

Fig. 5. *I-V* curves of α-Fe_2O_3 electrode in 1N H_2SO_4, 0.01M Ce^{3+}/1N H_2SO_4 and 0.01M Ce^{4+}/1N H_2SO_4. Data was obtained with 0.1 v step in each electrolyte, but only some of them are plotted in this figure. Noticeable difference was not detected for the above three electrolytes except for especially figured.
—○— 1N H_2SO_4, —◆— 0.01M Ce^{3+}/1N H_2SO_4,
—●— 0.01M Ce^{4+}/1N H_2SO_4

Table 2. Quantity of Fe in the electrolyte after polarization of electrode

Electrolyte	Potential V	Time of electrolysis hr	Quantity of electricity Q (coulomb)	Quantity of Fe g	Fe produced per unit coulomb g/Q
1N H_2SO_4	1.3	3	2.7×10^{-3}	4.5×10^{-4}	1.7×10^{-1}
	1.3	8.2	1.1×10^{-2}	2.2×10^{-4}	2.0×10^{-2}
5 mM Ce^{3+}, 5 mM	1.5	25.1	3.2×10^{-1}	9.3×10^{-5}	2.9×10^{-4}
Ce^{4+}/1N H_2SO_4	1.5	25.8	1.2×10^{-1}	19.7×10^{-4}	1.6×10^{-4}

case of 1N H_2SO_4 containing Ce^{3+}/Ce^{4+} and of 1N H_2SO_4 only. Table 2 indicates that the dissolution of the electrode was distinctly suppressed when the Ce^{3+}/Ce^{4+} was present. The current in Fig. 3, therefore, exhibits the reaction current of the redox system itself.

The apparent exchange current density, i_0, was obtained from the extrapolation of the Tafel region of the *I-V* curves on various electrodes to an open-circuit potential of each redox system, as measured with a Pt electrode, and was plotted against the conductivity of the electrodes for the $Fe(CN)_6^{4-}$/

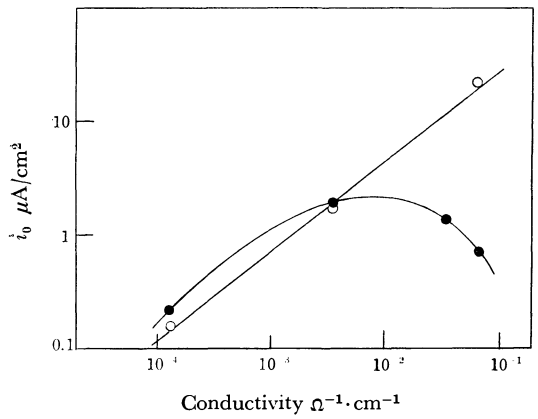

Fig. 6. Exchange current densities of $Fe(CN)_6^{4-}$/$Fe(CN)_6^{3-}$ and Fe^{2+}/Fe^{3+} systems as a function of the electrical conductivity of the electrodes.
—○— $Fe(CN)_6^{4-}/Fe(CN)_6^{3-}$, —●— Fe^{2+}/Fe^{3+}

$Fe(CN)_6^{3-}$ and Fe^{2+}/Fe^{3+} systems. Figure 6 shows a linear relationship between i_0 and the conductivity of the electrode for the $Fe(CN)_6^{4-}/Fe(CN)_6^{3-}$. Such a relation has already been observed with the redox reactions on the lithiated NiO electrode,[2] though i_0 had its maximum value at the specified conductivity of the α-Fe_2O_3 electrode in the Fe^{2+}/Fe^{3+} system.

Discussion

The *I-V* curves of the $Fe(CN)_6^{4-}/Fe(CN)_6^{3-}$ and Fe^{2+}/Fe^{3+} systems were quite different from those on the lithiated NiO electrode,[1] where the cathodic current flow was hindered and where the anodic reaction proceeded under activation-controlled conditions. The suppression of the anodic current flow in these systems must occur as a result of either the delay of the supply of the charge carrier in the electrode[5-7] or the hindrance of the flow of the change carriers by the rectifying portion present in the electrolytic system. The former possibility is, however, obviated by the fact that the anodic current was proportional to the concentration of Fe^{2+}, as Fig. 4 shows. Therefore, the anodic current must be suppressed by the potential barrier.

The role of the potential barrier which might

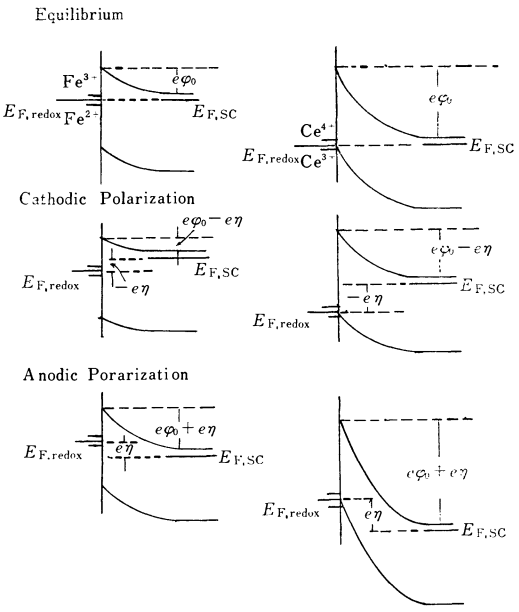

(a) Fe^{2+}/Fe^{3+} system (b) Ce^{3+}/Ce^{4+} system

Fig. 7. Schematic energy level diagram of α-Fe_2O_3/redox electrolyte interface. (a) Fe^{2+}/Fe^{3+} system-electrode, (b) Ce^{3+}/Ce^{4+}-electrode. Each energy state in this diagram means the state of the maximum distribution probability of each species

5) D.R. Turner, *J. Electrochem. Soc.*, **103**, 252 (1956).
6) R. Greth and M. E. Cowler, *J. Electrochem. Soc.*, **115**, 645 (1968).
7) H. Gerischer, *Z. Elektrochem.*, **63**, 500 (1959).

exists at the Pt-α-Fe_2O_3 interface can be ignored, as was discussed previously.[3] Another possible potential barrier is the one formed on the electrode surface.[8] The electron density on the surface of the electrode must be poor in the potential shown in Fig. 4, since the flat-band potential is by far the lower.[3] Thus, the energy profile of the electrode/electrolyte interface can be pictured as is shown in Fig. 7(a), although the application of the band model to the energy structure of the 3*d* transition metal oxide may not necessarily be adequate.[9] In Fig. 7, the energy state of the redox electrolyte is also presented using a concept of the electron state which is fully anologous to that of the solid state.[10] In this figure, $E_{F,redox}$ and $E_{E,sc}$ represent the Fermi level of the redox electrolyte[10] and that of the semiconductor respectively. ϕ_0 is the potential drop in the space-charge layer formed on the semiconductor electrode when it is in equilibrium with the redox electrolyte, and η is the overpotential.

According to Fig. 7(a), no potential barrier exists to the hole transfer from the electrode into the electrolyte. The hole transfer in this direction is equivalent to the anodic current. Therefore, if the positive holes were abundant in the electrode, the anodic current would not be saturated at such a small value as 10—100 μA/cm^2. By combining this fact with the fact that there is no possibility of a delay in the supply of a charge carrier in the electrode, the possibility of the hole transfer mechanism in these reactions can be denied.

On the other hand, there will be a potential barrier for electron transfer in the electrode/electrolyte interface, as Fig. 7(a) shows. However, the height of the potential barrier for the electron transfer from the electrode into the electrolyte will decrease in proportion to the cathodic polarization, because much of the polarization potential will be applied to the surface of the electrode. Thus, the cathodic current resulting from the electron transfer from the electrode into the electrolyte will not be suffered to pass through this potential barrier. In the case of the reverse direction of the current flow, the electron must flow from the electrolyte into the electrode, and during this process the electron should jump over the potential barrier. The height of the potential barrier in this case would not be changed distinctly with the polarization[11] if the polarization voltage is almost entirely applied in the electrode surface region. Then the situation could resemble the rectifying junction formed on the metal *N*-type semiconductor interface. The anodic current would, therefore, be saturated with the anodic polarization.[12] Almost the same interpretations is applicable to the reaction of the $Fe(CN)_6^{4-}$/$Fe(CN)_6^{3-}$ system, because the redox potential of this system is near to that of the Fe^{2+}/Fe^{3+} system and the *I-V* curves of these two system resemble each other.

The situation is quite different in the Ce^{3+}/Ce^{4+} system (Fig. 7(b)). The charge carriers in the redox electrolyte will have a chance to come in contact with the unoccupied state of the electrode because of their high redox potentials. If the electron-transfer mechanism is also acceptable under these circumstances, the electron should jump over by far the higher potential barrier in the electrode surface and then flow into the electrolyte, although the height of this potential barrier decreases with an increase in the cathodic polarization.

Therefore, the reduction current necessarily decreases in this system compared with those in the Fe^{2+}/Fe^{3+} or the $Fe(CN)_6^{4-}$/$Fe(CN)_6^{3-}$ systems. The distinct reduction current which was observed below 0.6V may indicate that a distinct electron transfer over this barrier is possible below 0.6V (see Fig. 5). On the contrary, a distinct cathodic current would have been observed if the hole density had been rich enough in the electrodes. The almost negligible reduction current in the potential near the redox potential, that is, 1.3 $-$1.0V *vs.* SCE, suggests, however, that positive hole were scarce, if any existed at all. As has already been described, the distinct anodic current above 1.2V was not affected by the addition of Ce^{4+} or Ce^{3+}, although the dissolution of the electrode was suppressed by these ions. This finding suggests that

8) H. Gerischer, "Advances in Electrochemistry and Electrochemical Engineering," Vol. 1, ed. by P. Delahey and C. W. Tobias, Interscience Publishers, New York, N.Y. (1961), p. 151.

9) F. J. Morin, *Phys. Rev.*, **93**, 1195 (1954).

10) H. Gerischer, *Z. Physik. Chem. N.F.*, **26**, 223 (1960).

11) In the energy profile for the lithiated NiO/redox electrolyte interface presented previously (Ref. 1), a bending of the energy band of the electrode surface with the polarization was shown, but the energy difference between the electrode and the redox electrolyte during a steady-state polarization was not taken into consideration. However, an energy difference equivalent to the overvoltage will eventually exist between the redox electrolyte and the electrode. In this respect, the energy profile represented in the previous paper should be modified in such a manner that the Fermi level of the electrode is different from that of the redox electrolyte by an energy equivalent to the overvoltage. Accordingly, it should be possible to understand similarly the cathodic current of the redox system on the lithiated NiO electrode, presented previously, assuming that an almost constant potential difference is preserved between the redox electrolyte and the upper, or the lower energy state at the band edge of the electrode whether the electrode is polarized or not.

12) According to the Mott-Schottoky theory, the current, J, is related to applied voltage, V, as in the following formula when there is a rectifying junction between a metal and a semiconductor:

$$J=J_0[\exp(eV/kT)-1]$$

the current was restricted by a factor other than the concentration of ions in the electrolyte.

The hole transfer mechanism may, then be considered to be inadequate. Therefore, an electron transfer mechanism should be considered. The distinct current increase above 1.2V might be brought by the electron tunneling[13] through the barrier layer. Under a high anodic polarization, the redox electrolyte will meet the electron in the electrode through the narrower part of the potential barrier, though the width of the potential barrier increases with an increase in the potential.[14] Thus, the electron tunneling through the narrower part of the potential barrier becomes possible. The width of the barrier layer at the same polarization potential is narrower for a electrode with a low resistivity.[14] Therefore, the probability of the electron tunneling is larger for the electrode with a low resistivity at the same polarization potential.

According to the above discussion, i_0 is determined by the numbers of the charge carriers which jump over the potential barrier. Therefore, i_0 may be expected to be larger for the electrode with the lower resistivity. Nevertheless, the highest i_0 was observed in the Fe^{2+}/Fe^{3+} system. The Fe^{2+}/Fe^{3+} system is the simpler redox system and are not usually form the adsorbed intermediate. However, either the ferric of the ferrous ion, or the both, in the electrolyte might adsorb on the electrode surface, which has unshared electrons pointing into the electrolyte, since ferric and ferrous ions were also constituent ions of the electrode. The energy-barrier height formed in the electrode surface region is conceivably determined by the quantity of the adsorbed ions and the polarization potential. The electrode with a large Ti content is rich in nonstoichiometry. Therefore, if it is assumed that the adsorption of the ions in the electrolyte occurs most effectively on the nontoichiometric parts of the electrode surface,[15] the quantity of adsorbant will be large for the electrode with a large Ti content; then, the potential barrier height of this electrode will be changed distinctly. The i_0 in the Fe^{2+}/Fe^{3+} system was possibly determined by this effect as well as by the concentration of the charge carriers in the bulk of the electrode.

Among 3*d*-transition metal oxides, Ti-doped α-Fe_2O_3 and Li-doped NiO are usually accepted as typical "hopping-type" semiconductors, while TiO_2 shows a typical "drift-type" conduction. In the drift-type semiconductor electrodes, such as Ge, ZnO, and TiO_2, the electrochemical reaction is occasionally controlled by the behavior of the minority carriers.[16] As has been discussed above, however, it seems that only the majority carrier is conceivably concerned in the electrochemical reaction on the α-Fe_2O_3 electrode. This is also suggested in the case of the lithiated NiO electrode.[1] In this sense, the electrode of a hopping-type semiconductor may play a different role in the electrochemical reaction from a drift-type semiconductor.

13) R. Stratton, *J. Phys. Chem. Solid*, **23**, 1177 (1962).

14) A. R. Plummer, "The Electrochemistry of Semiconductors," ed. by P. J. Holmes, Academic Press, New York (1962), p. 162.

15) H. Yoneyama and H. Tamura, *Denki Kagaku*, **38**, 644 (1970).

16) For example, F. Beck and H. Gerischer, *Z. Elektrochem.*, **63**, 943 (1959); W. P. Gomes, T. Freund and S. R. Morrison, *J. Electrochem. Soc.*, **115**, 818 (1968); A. Fujishima, K. Honda and S. Kikuchi, *Kogyo Kagaku Zasshi*, **72**, 108 (1969).

BULLETIN OF THE CHEMICAL SOCIETY OF JAPAN VOL. 43 3644—3650 (1970)

Studies on the Effect of Some Anionic Detergents on the Stability of Emulsions Stabilised by Partially Flocculated Sols

S. P. JAIN and S. N. SRIVASTAVA

Chemical Laboratories, Agra College, Agra, India

(Received October 30, 1969)

A partially flocculated $Fe(OH)_3$ sol has been used as an emulsifying agent to stabilize toluene/water system. The electrophoretic mobilities of the emulsion thus obtained in the presence of different anionic detergents have been measured microelectrophoretically and from these values the zeta potentials have been calculated. At the charge reversal concentrations the adsorption and free energy constants were calculated. From the surface potential values the repulsion and attraction energies were evaluated which clearly showed that the flocculation occurrs in the secondary minima. The operating van der Waals constant A has been estimated by correlating the results of degree of aggregation obtained haemocytometrically with the theoretical values. It was found to be 1.05×10^{-12} erg. The values of interfacial tension have been reduced by the addition of these detergents which are directly connected with the chain length of the detergent and adsorption characteristics.

Adoorption and its relation with electrokinetic potential for various detergents has been studied by some workers.[1-6] Haydon[7] also studied the relationship between the electrokinetic potential and surface charge density for long chain alkyl sulphates. Levich and Kuzhetsov[8] observed the retardation effect of surface active agent on the movement of the drop in a liquid between the regions of high and low interfacial tensions. The coagulation kinetics of rutile in hydrocarbon solutions of Aerosol OT reported by McGown and Parfit[9] showed an excellent agreement with the DLVO theory over a wide range of zeta potential.

A study of literature reveals that detergents influence the stability of colloidal systems, as they get ionized and affect zeta potentials. In the case of emulsions stabilized by solid substances and specially by metal hydroxides, practically no quantitative measurement has been done on the stability in the presence of detergents. In the present work an attempt has been made to study quantitatively the stability of emulsions in the presence of anionic detergent especially in the light of DLVO[10-12] theory. Electrokinetic measurements have been used for the interaction between the droplets and haemocytometric device for flocculation studies.

Theoretical

According to Derjaguin and Kussakov,[13] the repulsion energy V_R between the two spherical particles for the system having $\kappa a \gg 1$ is given by

$$V_R = \frac{\varepsilon a \psi_0^2}{2} \ln (1+\exp(-\kappa H)) \qquad (1)$$

where ψ_0 is the surface potential (approximately equal to zeta potential for the present system), H is the distance of separation of the droplets and κ is the Debye-Hückel parameter equal to the reciprocal thickness of the double layer

1) A. Fava and H. Eyring, *J. Phys. Chem.*, **60**, 390 (1956).
2) P. J. Anderson, *Trans. Faraday Soc.*, **54**, 130 (1958).
3) J. Powney and L. Wood, *Trans. Faraday Soc.*, **37**, 152 (1941).
4) B. D. Powell and A. E. Alexander, *Can. J. Chem.*, **30**, 1044 (1952).
5) Marcinez, J. M. Moreno, F. Cataline and G. Herrena, C. Fette-Seife, *Anstrichmittel*, **63**, 915 (1961).
6) D. A. Haydon and F. H. Taylor, III Intern. Congr. Surface Activity, Cologne Vol. 2 (1960).
7) D. A. Haydon, *Proc. Roy. Soc.*, **A 258**, 319 (1960).
8) V. G. Levich and A. M. Kuzhetsov, *Dokl. Alad. Nauk. SSSR*, **146**, 145 (1962).
9) D. N. L. McGown and G. D. Parfitt, *Discuss. Faraday Soc.*, **42**, 225 (1966); *Kolloid-Z.*, **56**, 220 (1967).
10) B. Derjaguin, *J. Expt. Thur. Phys., USSR*, **11**, 802 (1941).
11) B. Derjaguin and L. D. Landau, *Acta Phys. Chim.*, **14**, 633 (1941).
12) E. J. W. Verwey and J. Th. G. Overbeek, "Theory of stability of lyophobic colloids," Elsevier, Amsterdam (1948).
13) B. Derjaguin and M. Kussakov, *Acta Phys. Chim., URSS*, **10**, 24, 155 (1939).

$$\kappa = \frac{1}{d} = \left[\frac{4\pi e^2 \sum n_i z_i^2}{\varepsilon k T}\right]^{1/2} \quad (2)$$

where z is the valency of the ions of ith kind and n_i is the number of ions per m*l*.

The attraction energy V_A at intermediate distances where the force is partially retarded is given by Schenkel and Kitchener[14] as follows.

For $H > 150$ Å,

$$V_A = -\frac{Aa}{\pi}\left(\frac{2.45\lambda}{120H^2} - \frac{\lambda^2}{1045H^3} + \frac{\lambda^3}{5.62\times10^4 H^4}\right) \quad (3)$$

For $H > 150$ Å

$$V_A = -\frac{Aa}{12H}\left(\frac{\lambda}{\lambda+3.54\pi H}\right) \quad (4)$$

where λ, the wavelength of the intrinsic electronic oscillations of the atoms, is taken to be equal to 1000 Å.

The change in charge density caused by the addition of a small quantity of foreign ions which are adsorbed on emulsion particles will be given by the Stern equation[15,16]

$$\sigma_C = \frac{N_1 ze}{1 + \frac{55.6}{C}\exp\left(\frac{\Delta G}{kT}\right)} \quad (5)$$

where C is the molar concentration of the added detergent, N_1 the number of binding sites available per cm^2 and ΔG is the electrochemical free energy of adsorption per molecule. This can also be put in the form[17-19]

$$\Delta\sigma_C = \frac{K_1 C}{1+K_2 C} \quad (6)$$

which is similar to Langmuir adsorption isotherm.[20] K_1 and K_2 are called adsorption constants.

The relation between log C, ψ_δ (here $\psi_\delta = \xi$) and N_1 at the isoelectric points where $\kappa a \gg 1$ is given by the equations

$$\frac{1}{C} = K_2\left\{\left[\frac{4\pi e N_1 Z}{\xi'\varepsilon\kappa}\right] - 1\right\} \quad (7)$$

where C is the concentration of detergents at ($\xi = 0$) zero point of charge and ξ' is the initial zeta potential taken instead of ψ_δ, and assuming that only a single adsorbed layer was formed upto $\xi = 0$.

$$\left(\frac{d\xi}{d\log C}\right)_{\xi=0} = 2.303\xi'\left(\frac{\xi'\varepsilon\kappa}{4\pi e z N_1} - 1\right) \quad (8)$$

The chemical free energy of adsorption ΔG has been calculated by the equation[21]

$$-\Delta G = kT(\ln K_2 + \ln 55.6) \quad (9)$$

The degree of aggregation, *viz.*, the total number of particles associated with a given central particle can be determined with knowledge of the depth of the secondary minima by solving the following equation where the integration has been carried out graphically.

$$D = 4\pi a^3 n_0 \int s^2 \exp(-V/kT)\,ds \quad (10)$$

Experimental

A positively charged ferric hydroxide sol was prepared, dialyzed and partially flocculated by the addition of 0.15 mmol of potassium oxalate. To this sol toluene (5%, weight) was dispersed by shaking by hand and the emulsion was then well homogenized using a stainless steel homogenizer (C. W. Logemann Co. U.S.A.). After half an hour the creamed layer was removed and same emulsion was prepared under the same conditions.

In order to study the effect on stability the following detergents have been used: dibutyl ester of sodium sulphosuccinic acid, dioctyl ester of sodium sulphosuccinic acid, sodium salt of secondary alkyl sulphate containing 17 carbon atoms and sodium lauryl sulphate. All the detergents were obtained from BDH and used as they are. For the sake of convenience they have been represented by the BSS, OSS, SAS and SLS. The other chemicals and reagents used were of Analar grade.

Electrokinetic measurements were carried out by micro electrophoresis apparatus using a Northrup-Kunitz rectangular type cell in which the direct movement of the emulsion droplets was observed with a microscope for a definite distance under a suitable electric voltage which was measured by the VTVM across the two ends of the cell. An equiconducting solution of KCl was used in electrode vessels and the zeta potentials were calculated by means of the relation

$$z = \frac{4\pi n u}{\varepsilon} \quad (11)$$

the relaxation correction being neglected because of the large sized particle (radius 1.12 μ) (Fig. 1 and Fig. 2).

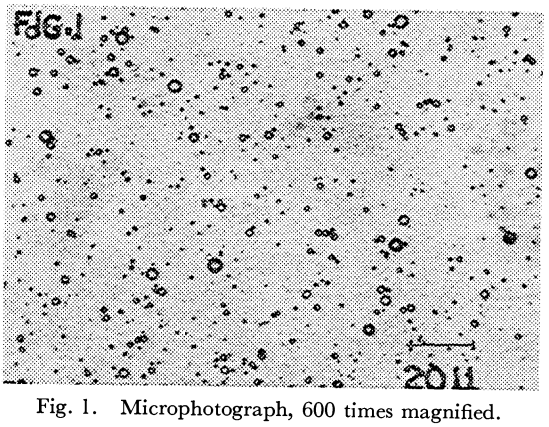

Fig. 1. Microphotograph, 600 times magnified.

14) J. N. Schenkel and J. A. Kitchener, *Trans. Faraday Soc.*, **56**, 161 (1960).
15) K. H. Stern, *Z. Electrochem.*, **30**, 568 (1924).
16) D. S. Persons, in Bockris, "Modern Aspects of Electrochemistry."
17) R. H. Ottewill, N. C. Rastogi and A. Watanabe, *Trans. Faraday Soc.*, **56**, 854 (1960).
18) Wilkins *et al.*, *J. Theoret. Biol.*, **2**, 173, 186 (1962).
19) S. N. Srivastava, *J. Ind. Chem. Soc.*, **41**, 203 (1964).
20) Langmuir, *J. Amer. Chem. Soc.*, **40**, 1361 (1918).
21) R. H. Ottewill and A. Watanabe, *Kolloid-Z.*, **170**, 38, 132 (1960); **171**, 33 (1960).

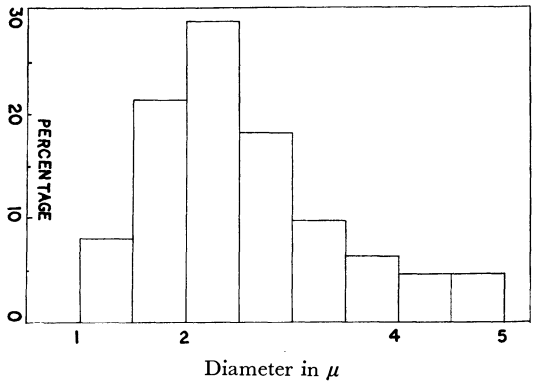

Fig. 2. Size-distribution curve of the emulsion globules, radius 1.12 μ.

Results and Discussion

Effect of Anionic Surface Active Agents on Zeta Potential. The zeta potentials of the emulsions in the presence of different concentrations of surface active agents have been plotted against log molar concentrations in Fig. 3. In general, as the

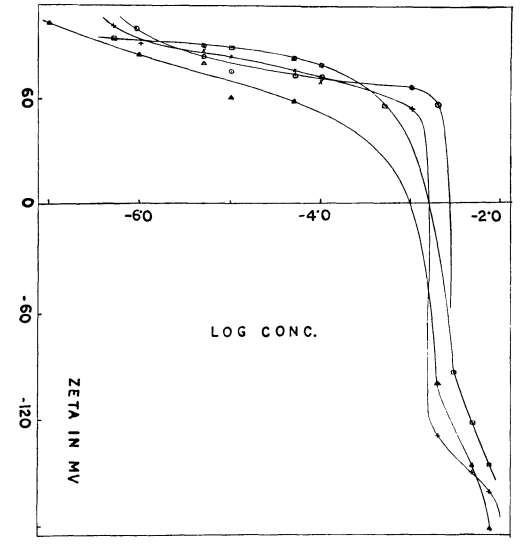

Fig. 3. Curves showing the variation of zeta with concentration for △ SLS, × OSS, ⊡ SAS and ⊙ BSS.

concentration of these detergents is increased in a low range the zeta potential decreases very slowly until a certain concentration is reached after which it gradually decreases to a certain fixed value of nearly 50 mV, with increasing gradient. Further increase in concentration gave visible flocculation where the measurements were not feasible because of agglomeration of a large number of solid particles on oil globules on account of small zeta value. On a further increase of concentration, reversal of charge took place and the zeta became increasingly negative.

Increase in zeta value in this range of concentration is very sharp. With a small change in concentration an appreciable increase in zeta took place which increases upto critical micelle concentration. Over this CMC there should be no further change theoretically. However, a decrease was observed only in one case with SLS. The decrease in zeta after CMC can be explained as follows. It is likely that during the mixing of concentrated solution of detergent to the system, conditions could occur in which the miceller solution of the detergent becomes submiceller. The breakdown of micelles to submicelles is a very fast reaction.[22] The time required during mixing of the detergent in to the system is of the same order as required for breaking down of the micelles, and mutual coagulation would have occurred between the micelles and the stabilized emulsion droplets resulting in an artificial decrease of stability.

The flocculating concentration at which zeta potential becomes zero was obtained from zeta-log C curves. From them the efficiency of reversing the charge or the extent of adsorption is in the order SLS>OSS>SAS>BSS, and their CMC are to be expected in the increasing order. Thus a higher concentration of SAS is required to reverse the charge than SLS. The charge reversal was not obtained with BSS though relatively high concentration of the order of 2.0×10^{-3} mol/l has been reached. This is presumably on account of a comparatively smaller chain length of the detergent. This order of their efficiencies is also confirmed by their structural formulae; SLS possesses a long chain of 12 carbon atoms, OSS and SAS possess of only eight carbon atoms while BSS has only 4 carbon atoms in its chain. Thus their efficiencies increase as carbon chain increases. The distinction between SAS and OSS is on the basis that OSS possesses a bigger head group than SAS.

Charge Density and Binding Parameters. The number of binding sites available per cm^2,

TABLE 1. BINDING PARAMETERS AND NUMBER OF BINDING SITES FOR DIFFERENT DETERGENTS

Detergent	K_1 Coulomb l/cm^2 mol.	K_2 l/mol	$\frac{K_1}{K_2}\times10^7$ Coulomb/cm^2	Binding sites N_1 group/cm^2
SLS	1.55×10^{-3}	2.1×10^3	7.37	4.6×10^{12}
OSS	4.26×10^{-5}	6.6×10^2	0.65	0.4×10^{12}
SAS	0.72×10^{-5}	1.0×10^3	6.84	4.3×10^{12}
BSS	9.23×10^{-5}	4.5×10^2	2.05	1.3×10^{12}

22) R. H. Ottewill and M. C. Rastogi, *Trans. Faraday Soc.*, **56**, 866, 880 (1960).

Table 2. Free energy and surface charge of stern layer for different detergents

Detergent	σ_s Coulomb/mol	$-\Delta G$ kcal/mol	Area/mol Sq. Å
SLS	1.5×10^{3}	2.95	2174
OSS	1.0×10^{2}	2.66	25000
SAS	1.3×10^{3}	2.78	2326
BSS	3.2×10^{2}	2.32	9793

N_1, binding parameters and charge density have been calculated with the help of the slope of zeta-log C curves and the concentration at which $\zeta=0$, and are represented in Table 1. The area occupied by each anionic surface active agent when all the sites are covered is also calculated. The value of free energy of adsorption ΔG which determines the strength of binding of these surface active ions are shown in Table 2.

From the table we see that the values of K_2 are in the order SLS>OSS>SAS>BSS, which gives the order of adsorption. This can also be seen from zeta-log$C$ curves, where the slope of the curves are found to increase with increasing chain length of the surface active agents, and a shift of the zero point of charge to higher concentration for a smaller chain length is also observed.

The nature of adsorption of these anionic surface active ions can be explained on the basis of the binding parameters. At a smaller concentration the surface active ions go to the positively charged surface of oil globule, probably the surface occupied by potential determining ions. The surface sites are essentially the same for different surface active agents, because the values of N_1 obtained for each detergent are reasonably consistent. However, it is clear that the maximum number of sites is greater than the surface excess of ferric ions since the sign of zeta is reversed. Thus, it seems reasonable to assume that at a certain concentration nearly 5×10^{-4} mol/l, the surface active ion may be adsorbed directly on the surface at the sites other than those occupied by potential determining ions. Uncertainty may arise due to a slight differences in the values of N_1.

The adsorption can also be explained by the consideration that the oil phase is in reversible equilibrium with the ions in the solution. When surface active agents are added, one particle of it is adsorbed on one potential determining ion site, and an additional potential determining ion is adsorbed and this process will continue until the system becomes irreversible. In this process with the adsorption of detergent on potential determining ions, the adsorption directly on the oil surface also occurs.

Interaction Energy Curves and Secondary Minimum Flocculation. The interaction energies of the double layer around the particles at the different concentrations of the detergents SLS, OSS, SAS and BSS have been calculated with respective values of the zeta potentials, and are tabulated in Table 3. The corresponding curves for the interaction energy *vs.* the distance between the two particles are plotted, the only representative figure

Table 3. Zeta potentials, maximum energy and depth of secondary minima for different detergents

Concentration mol/l	κa	Zeta potential in mV	Maximum energy in kT	Distance at $V=0$. Å	Depth of sec. minima
SLS					
2.0×10^{-8}	141.2	106.3	6834	665	−2.08
1.0×10^{-7}	141.2	101.9	6203	650	−2.08
5.0×10^{-7}	141.2	93.1	5029	635	−2.15
1.0×10^{-6}	141.3	86.2	4063	620	−2.18
5.0×10^{-6}	141.5	79.5	3416	610	−2.24
1.0×10^{-5}	141.7	60.5	1717	540	−2.49
5.0×10^{-5}	143.6	57.5	1481	520	−2.90
Reversal					
2.0×10^{-3}	217.4	−101.3	5416	360	−5.57
5.0×10^{-3}	297.2	−147.3	12719	290	−9.87
7.5×10^{-3}	350.1	−182.0	19901	240	−12.86
OSS					
5.0×10^{-7}	141.2	101.5	6146	655	−2.10
1.0×10^{-6}	141.3	91.9	4866	635	−2.05
5.0×10^{-6}	141.5	86.3	4191	620	−2.06
1.0×10^{-5}	141.7	82.5	3744	610	−2.14
5.0×10^{-5}	143.6	74.6	2904	590	−2.28
1.0×10^{-4}	146.0	68.4	2330	560	−2.53
1.0×10^{-3}	183.2	54.5	1131	340	−5.28
Reversal					
2.0×10^{-3}	217.4	−103.3	10139	410	−4.99
5.0×10^{-3}	297.2	−150.7	13400	290	−9.59
7.5×10^{-3}	250.1	−162.1	15189	230	−13.69
SAS					
5.0×10^{-8}	141.2	103.4	6415	660	−2.08
5.0×10^{-7}	141.2	94.2	5162	640	−2.08
5.0×10^{-6}	141.5	89.2	4533	625	−2.14
1.0×10^{-5}	141.7	88.5	4447	620	−2.15
5.0×10^{-5}	143.6	80.8	3541	590	−2.26
1.0×10^{-4}	163.6	55.8	1281	420	−3.96
Reversal					
3.0×10^{-3}	246.9	− 94.6	4386	290	−7.90
5.0×10^{-3}	297.2	−123.4	8309	270	−10.80
7.5×10^{-3}	350.1	−146.0	11939	222	−14.29
BSS					
5.0×10^{-8}	141.2	108.1	7100	665	−2.08
5.0×10^{-7}	141.2	99.2	5837	650	−2.15
5.0×10^{-6}	141.5	83.3	3835	610	−2.20
1.0×10^{-5}	141.7	74.8	2917	590	−2.28
1.0×10^{-4}	146.0	71.0	2563	565	−2.46
1.0×10^{-3}	183.2	65.9	1915	380	−4.80
2.0×10^{-3}	217.4	56.5	1124	270	−7.95

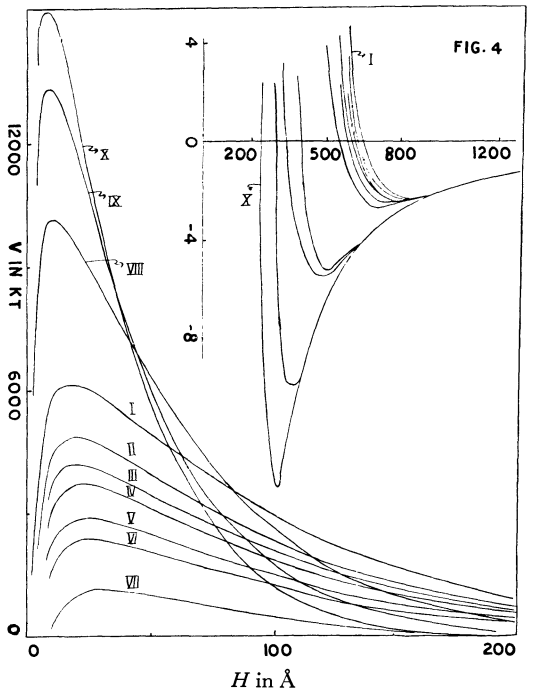

Fig. 4. Potential energy profiles and elaborated secondary minima for OSS at I, 5×10^{-7}, II 1×10^{-6}, III 5×10^{-6}, IV 1×10^{-5}, V 5×10^{-5}, VI 1×10^{-4}, VII 1×10^{-3}, VIII 2×10^{-3}, IX 5×10^{-3} and X 7.5×10^{-3} mol/*l*.

is shown in Fig. 4. The value of *A i. e.* van der Waals constant has been taken to be equal to 1.0×10^{-12} erg.

From the equations of interaction energies it can be seen that the value of V depends mainly on the factors ψ_δ, κ and a which change with concentrations of the detergent. The κa values remain almost the same nearly upto the concentration 1×10^{-4} mol/*l* in case of all the detergents, *i. e.* the ionic strength will not change much and hence practically no change in the value of interaction energies will be observed. Addition of the surfactants has an effect on ψ_δ or ξ. However, at higher concentrations both the factors κ a and ξ change and affect the value of V.

At smaller distances the values of interaction energies obtained are considerably high in all cases while at larger distances attraction prevails and secondary minima are obtained in which particles aggregate reversibly. The depth of secondary minima is nearly constant in the low range of concentrations and is equal to $2.5kT$ for all detergents. This is too shallow to trap the particles but at higher concentrations the depth increases upto 10—15kT which is reasonable for the occurrence of flocculation. These high energy values and the occurrence of the secondary minima may be due to large particle radius ($a=1.1$ μ).

The relation between the interparticle distance H_m at which the minimum energy occurs and Debye-Hückel parameter κ can be represented by the equation

$$H_m{}^2e^{-\kappa H_m} = 1.80\times10^{-9}\frac{v^2}{\kappa V^2}$$

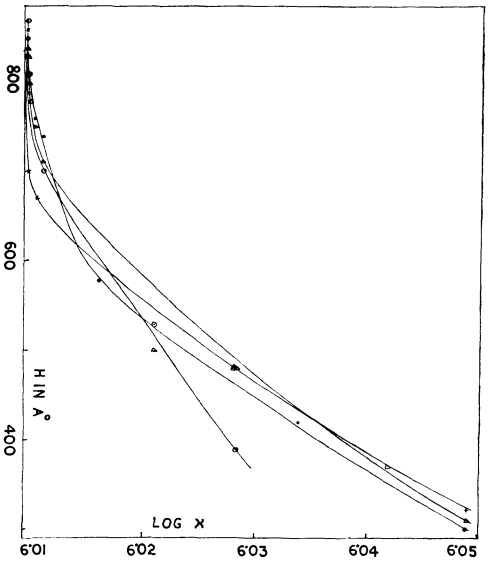

Fig. 5. Curves showing the depencence of κ Debye-Hückel parameter to H_m for × SLS, △ OSS, ● SAS and ⊙ BSS.

The effect of κ upon H_m separation of particles when they are reversibly flocculated in secondary minima is shown in Fig. 5. The distance H_m decreases with the increase in concentration of the detergents. This H_m distance is also directly proportional to the valency of the added ions which are uni valent. Thus the value of H_m is nearly the same at low range of concentration and is just linear, but it varies with κ at higher concentrations. The depth of the secondary minima also depends

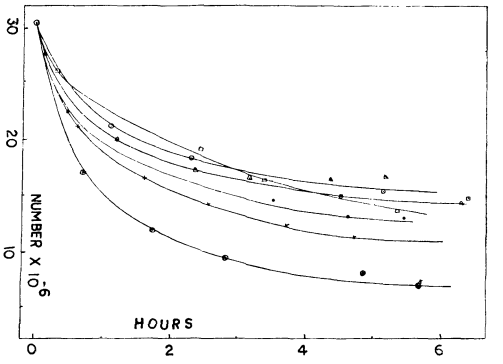

Fig. 6. Curves showing the change in number of monomers with time for SAS at ⊙ 5×10^{-8}, △ 5×10^{-7}, ⊡ 5×10^{-6}, ● 5×10^{-5}, × 1×10^{-4} and ⊗ 5×10^{-4}M.

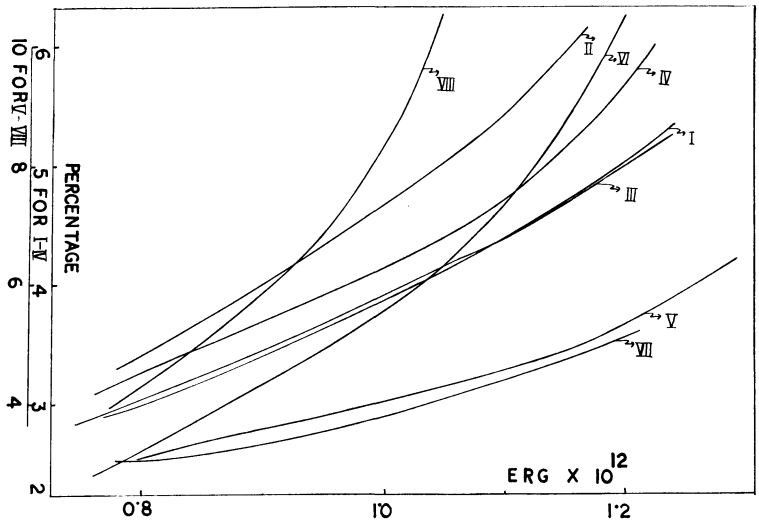

Fig. 7. Curves showing the variation in degree of aggregation D with van der Waals constant A at, I 1×10^{-7}, II 5×10^{-5}, mol of SLS, III 5×10^{-7}, IV 5×10^{-6} mol of OSS, V 1×10^{-4}, VI 5×10^{-4} mol of SAS, VII 5×10^{-7} and VIII 1×10^{-3} mol of BSS.

on the value of the van der Waals constant A.

Concerning flocculation, the singlets and doublets as obtained haemocytometrically were plotted with respect to time at different concentrations of detergents, the representative plot being shown in Fig. 6. They are levelled off after certain time because of attainment of a temporary equilibrium between singlets and doublets. This confirms the occurrence of secondary minimum flocculation in the emulsion of large particles.

Determination of the van der Waals Attraction Constant. In order to determine the van der Waals constant, the value of degree of aggregation D is required which has been calculated by Eq. (10) with the help of depth of secondary minima at different values of the van der Waals constant. These values of D are plotted for the different values of A as shown in Fig. 7. The observed value of D has been determined haemocytometrically with the help of the equation

$$D = \frac{\text{number of singlets}}{\text{number of singlets} + \text{number of doublets}} \qquad (12)$$

The value of A corresponding to these values has been deduced from the graphs and given in Table 4. The mean value of A was found to be 1.0×10^{-12} erg which is reasonable for oil droplets coated by solid particles and agrees with the theoretical value calculated by physico optical data.[23]

Effect of Anionic Detergents on Interfacial Tension. The interfacial tension between oil phase and continuous phase were measured by an Agla micrometer syringe. The volume of a drop falling in oil phase was noted and the interfacial tension was calculated by the density difference of the two phases by equation

$$\nu = \frac{(d_2-d_1)v}{gr}f \qquad (13)$$

The interfacial tensions in presence of different

Table 4. Values of the van der Waals constant in different detergents

Detergent	Concentration mol/l	Degree of aggregation D in %	van der Waals constant $A\times10^{12}$ in erg.
SLS	1.0×10^{-7}	3.5	0.91
	5.0×10^{-7}	3.2	0.83
	1.0×10^{-6}	4.2	1.02
	5.0×10^{-5}	6.1	1.16
OSS	5.0×10^{-7}	4.2	1.06
	5.0×10^{-6}	3.8	0.96
	5.0×10^{-5}	5.5	1.18
	1.0×10^{-4}	5.6	1.18
SAS	5.0×10^{-8}	3.3	0.86
	5.0×10^{-6}	5.0	1.16
	1.0×10^{-4}	6.4	1.28
	5.0×10^{-4}	7.7	1.14
BSS	5.0×10^{-7}	3.5	9.93
	5.0×10^{-6}	4.0	0.98
	5.0×10^{-5}	5.3	1.16
	1.0×10^{-3}	8.9	1.01

23) S. P. Jain and S. N. Srivastava, *Kolloid-Z. Z. Polym.*, **235**, 1230 (1969).

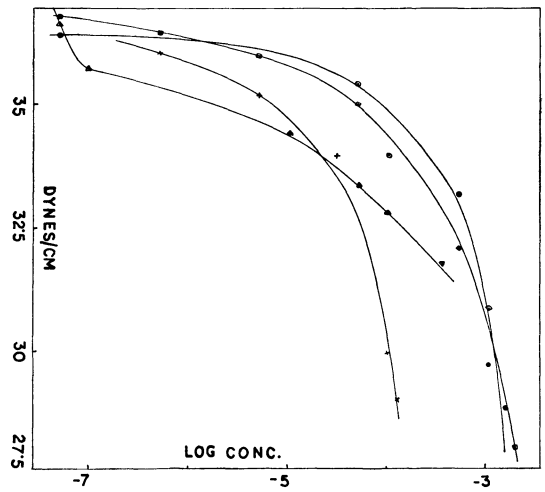

Fig. 8. Curves showing the change in interfacial tension with log molar concentration for △SLS, × OSS, ⊙ SAS and ⊡ BSS.

amounts of anionic detergents have been measured and the curves between interfacial tension and log molar concentration are given in Fig. 8. Th change in interfacial tension and the volume of each drop are reported for all the detergents in Table 5. The value of interfacial tension decreases which implies a positive adsorption as suggested by Gibbs adsorption equation. These anionic surface active ions are adsorbed at the surface of positively charged oil particles and cause instability with increase in concentration of the detergents. The decrease in interfacial tension is greater in the cases of SLS and OSS than in cases of SAS and BSS which indicates that the effect depends on the chain lengths of the detergents. This is also in accordance with electrokinetic results.

TABLE 5. EFFECT OF ANIONIC SURFACE ACTIVE AGENTS ON INTERFACIAL TENSION

Detergent	Concentration mol/l	Volume of one drop in ml	Interfacial tension in dynes/cm
SLS	5.0×10^{-8}	0.2472	36.37
	1.0×10^{-7}	0.2430	35.75
	1.0×10^{-5}	0.2336	34.43
	5.0×10^{-5}	0.2258	33.39
	1.0×10^{-4}	0.2218	32.82
	3.5×10^{-4}	0.2145	31.78
OSS	5.0×10^{-7}	0.2452	36.08
	5.0×10^{-6}	0.2392	35.21
	3.0×10^{-5}	0.2304	33.98
	8.0×10^{-5}	0.2115	31.34
	1.0×10^{-4}	0.2014	29.85
	2.5×10^{-4}	0.1973	29.39
SAS	5.0×10^{-8}	0.2478	36.45
	5.0×10^{-5}	0.2414	35.50
	1.0×10^{-4}	0.2308	34.05
	5.0×10^{-4}	0.2146	33.22
	1.0×10^{-3}	0.1996	29.70
	1.5×10^{-3}	0.1932	28.82
BSS	5.0×10^{-8}	0.2503	36.84
	5.0×10^{-7}	0.2482	36.51
	5.0×10^{-6}	0.2450	36.04
	5.0×10^{-5}	0.2380	25.04
	5.0×10^{-4}	0.2166	32.10
	1.0×10^{-3}	0.2080	30.89
	2.0×10^{-3}	0.1876	28.06

BULLETIN OF THE CHEMICAL SOCIETY OF JAPAN VOL. 43 3651—3652 (1970)

Thermal Decarboxylation of Nitrobenzoic Acids. I

D. S. MANIKYAM and E. V. SUNDARAM

Chemistry Department, Osmania University, Hyderabad, India

(Received November 12, 1969)

Thermal decarboxylation of *o*-, *m*- and *p*-nitro benzoic acids was studied in glycerol in the temperature range 210—250°C *m*- and *p*-Nitrobenzoic acids exhibited first order rate constants and in support of the proposed S_E1 mechanism, the isomers were also studied in aniline at 110—140°C. Pseudo-first order rate constants of the ortho isomer in glycerol suggested a change in mechanism from S_E1 to S_E2. The rate constants were influenced by boric acid or aniline added to glycerol as the result of a change in pH and confirmed thus the proposed S_E1 or S_E2 mechanisms. Activation energies, enthalpies and entropies of activation were obtained for the three isomers.

A survey of literature of several organic acids reveals that decarboxylation occurs either by unimolecular or bimolecular electrophilic substitutions, S_E1 or S_E2.[1] The S_E1 mechanism requires the loosening of R–C bond, and the substituents which diminish the electron density on the α-carbon atom facilitate this mechanism as in the cases of nitro acetic, nitro-isobutyric,[2] trihaloacetic[3] and cyano-acetic acids.[4]

The view that decarboxylation by S_E2 mechanism involves the attack of a proton or a protonated solvent on the α-carbon atom of the carboxyl group is supported by Schenkel and Schenkel-Rudin,[5] Hammick and coworkers[6] and Muhammad and Siddiqui.[7] A polyhydric alcohol glycerol was used as a solvent in the studies of decarboxylation of hydroxy benzoic and chlorobenzoic acids and 1-hydroxy-2-naphthoic acid.[8]

In view of the above studies, the decarboxylation of *o*-, *m*- and *p*-nitrobenzoic acids was carried out in the solvents glycerol and aniline in order to study their mechanisms.

Results and Discussion

***m*- and *p*-Nitrobenzoic Acids.** Decarboxylation of the *m*- and *p*-nitrobenzoic acids in the solvents glycerol and aniline is kinetically first order. The rates, being faster in the basic solvent aniline than in glycerol, suggest that these isomers follow the unimolecular S_E1 mechanism. The rate constants and the other thermodynamic parameters are shown in Table 1.

Substances such as aniline and boric acid added to glycerol alter the acidity of the medium and the rate constants, as in Table 2 (a) and (b), also exhibit a marked increase and decrease for the meta and para isomers respectively in support of the S_E1 mechanism. The stability of the two isomers in the acidic solvent, resorcinol is an additional support for the proposed mechanism.

The presence of a nitro group either in the meta or para position in benzoic acid, by withdrawing electrons, deactivates the ring and facilitates the C–C bond cleavage. Glycerol being a polyhydric alcohol ionizes the acids to a less extent than aniline.

A comparison of the rates, enthalpies and entropies of activation reveals that a more basic solvent aniline favours the S_E1 mechanism rather than a neutral solvent glycerol, and is in good agreement with the observation of Clark.[9a] In these solvents it has been visualised that the electrophilic carbon

TABLE 1. THERMODYNAMIC PARAMETERS FOR DECARBOXYLATION IN GLYCEROL AND ANILINE

Acid	pK_a	Solvent: Glycerol, Temp.: 200—250°C $k\times10^4$ 230° sec^{-1}	$\Delta E^{\ddagger}$ kcal·mol^{-1}	$\Delta H^{\ddagger}$ kcal·mol^{-1}	$\Delta S^{\ddagger}$ e.u.	Solvent: Aniline, Temp.: 100—150°C $k\times10^3$ 130° sec^{-1}	$\Delta E^{\ddagger}$ kcal·mol^{-1}	$\Delta H^{\ddagger}$ kcal·mol^{-1}	$\Delta S^{\ddagger}$ e.u.
o-NO_2	2.17	6.26	35.10	34.10	− 6.04	—	—	—	—
m-NO_2	3.46	11.66	17.31	16.31	−40.95	1.25	26.15	25.22	−9.59
p-NO_2	3.43	11.39	17.30	16.30	−41.02	2.33	30.52	29.59	+2.43

1) B. R. Brown, *Quart. Rev.* (London), **5**, 131 (1951).
2) Pedersen, *J. Phys. Chem.*, Ithaca, **38**, 559 (1934).
3) Verhock, *J. Amer. Chem. Soc.*, **61**, 186 (1939)
4) J. W. Wilt, *J. Org. Chem.*, **21**, 920 (1956).
5) H. Schenkel and M. Schenkel-Rudin, *Helv. Chim. Acta*, **31**, 514 (1948).
6) B. R. Brown, D. U. Hamick and A. J. B. Scholefield, *J. Chem. Soc.*, **1950**, 778.
7) Aziz Mirza, Ph. D., Thesis approved by the Osmania University (1957), pp. 199—106.
8) S. S. Muhammad, J. Lalitha and E. V. Sundaram, *Acta Chem. Hangarica*, **22**, 455 (1960).

TABLE 2. EFFECT OF ADDED SUBSTANCES ON DECARBOXYLATION IN GLYCEROL

a) *m*-Nitrobenzoic acid at temp. 214°C		b) *p*-Nitrobenzoic acid at temp. 230°C	
Amount of aniline added	$k \times 10^4$ sec^{-1}	Amount of Boric acid added	$k \times 10^4$ sec^{-1}
0%	7.35	0%	12.01
0.4%	13.96	1%	10.75
0.8%	16.58	2%	7.60
1.4%	18.32	8%	2.63

TABLE 3. EFFECT OF ADDED BORIC ACID IN THE DECARBOXYLATION OF *o*-NITROBENZOIC ACID IN SOLVENT GLYCEROL AT TEMPERATURE 235°C

Amount of boric acid added	pH	$k \times 10^4$ sec^{-1}
0%	7.20	8.90
0.5%	3.07	11.89
1.0%	3.02	15.26
1.5%	2.97	18.01
2.0%	2.94	21.95

atom of an undissociated acid apparently co-ordinates with an unshared pair of electrons on a nucleophilic atom of the polar solvent favouring the subsequent cleavage of the molecule into the products.[9b]

Since the rate determining step involves the decomposition of the transition state, the extent of formation of this state depends on the polarizability of the carboxyl carbon atom as well as on the nucelophilicity of the solvent. Therefore, it can be suggested that the greater the availability of the electrons on the neucleophilic atom of the solvent, the greater would be the probability of the formation of the activated state. Hence, in the activated state, the nucleophilic aniline interacts more readily than glycerol with the carbon atom of the carboxyl group resulting in high enthalpies and entropies of activation. However, as the accepting ability of the carbon atom of the carboxyl group does not change much in the two isomers, it is the basicity of the solvent that plays an important role in the formation of the transition stage. The rate constants, activation energies and other thermodynamic parameters are nearly the same in the weakly basic solvent glycerol comparable to their pK_a value. But in the highly basic solvent aniline, the effective electrophilicity developed on the α-carbon atom of the carboxyl group in the two isomers also plays a role and shows an increase in the thermodynamic parameters, similar to the change from glycerol to aniline.

o-Nitrobenzoic Acid. The kinetics of decarboxylation of *o*-nitrobenzoic acid in glycerol follows a different pattern from that of the other two isomers. The rate of ortho acid (Table 1) is small compared to its meta and para isomers and exhibit pseudo-first order rate constants. The rate constants also show an increase with added boric acid to glycerol as the result of a change in pH (Table 3).

It was also observed that the ortho isomer decarboxylates more easily in acidic solvent, resorcinol, and is stable in basic solvent, aniline, unlike the meta and para isomers. This exhibits a change in mechanism from S_E1 to S_E2 since the latter are acid-catalyzed.

It has been suggested that the geometry of the ortho-transition state of *o*-nitrobenzoate ion exhibits a dipolar interaction of the type as in Fig. 1, the stereochemistry of the transition state being suitable for the electrophilic substitution. This type of internal chelation[10] is mainly responsible for a change in mechanism and the decarboxylation proceeds in the anionic form.

$$k = [RCOO^-][H^+]$$

Fig. 1

Besides the chelation in the case of ortho isomer, deactivating influence of nitro group in ortho position will be less. This is due to the fact that the nitro group, which is in the same plane as the benzene in para isomer, deactivates the carbon atom mostly due to resonance interaction. However, in ortho position, because of steric effect, the nitro group is twisted out of the plane of benzene ring. Hence, the resonance inter-action will become less, and deactivating influence will be diminished compared to its para or meta isomer.

Experimental

The experimental procedure and the calculation of the rate constants were similar to the one adopted in 1-hydroxy-2-naphthoic acid.[8] The experiments were carried out with B.D.H. and analar samples of ortho, meta and para nitrobenzoic acids and the solvents glycerol and aniline were of pure quality, which did not emit any carbon dioxide when heated alone. In all the experiments, the final volume of carbon dioxide was calculated theoretically. The kinetics were followed in all cases, till 25—30% of acid was decarboxylated. The reactions were studied in the temperature range 200—250°C in glycerol and 110—135°C in anilline.

The authors wish to thank Professor N.V. Subbarao for his keen interest and one of the authors (D.S.) is grateful to the Government of India for the Award of a Research Training Scholarship.

9) a) L. W. Clark, Ithaca, *J. Phys. Chem.*, **62**, 79 (1958). b) Gopalan and I. M. Malhai, *Proc. Ind. Acad. Sci.*, **11**, 92 (1969).

10) J. D. Roberts and M. C. Caserio, "Basic Principles of Organic Chemistry," W. A. Benjamin, Inc., New York, Amsterdam (1965), p. 961.

BULLETIN OF THE CHEMICAL SOCIETY OF JAPAN VOL. 43 3653—3657 (1970)

Mechanism of Hydrogenolysis. I. Effect of Methyl Substituent on the Demethylation Rate of Polymethylbenzenes

Akira AMANO, Masao UCHIYAMA and Yoshiki SATO

Department of Applied Chemistry, Faculty of Engineering, Tohoku University, Aoba-Aramaki, Sendai

and Hiroo TOMINAGA, Hiromichi ARAI and Taiseki KUNUGI

Department of Synthetic Chemistry, Faculty of Engineering, the University of Tokyo, Hongo, Bunkyo-ku, Tokyo

(Received January 31, 1970)

Rates of demethylation of six different polymethylbenzenes have been measured, at 702°C and residence times ranging from 0.5 to 6.0 sec in the presence of five-fold in excess hydrogen, by using toluene as an internal reference. The rates per one equivalent methyl group were: 1.08 for *p*-xylene, 1.73 for *o*-xylene, 1.26 for 4-position of 1,2,4-trimethylbenzene, 1.87 for 2-position of 1,2,4-trimethylbenzene, 1.85 for 1-position of 1,2,4-trimethylbenzene, 1.20 for 1,3,5-trimethylbenzene, 2.22 for 1-position of 1,2,3-trimethylbenzene, 3.25 for 2-position of 1,2,3-trimethylbenzene, 1.5 for 5-position of 1,2,3,5-tetramethylbenzene, 2.1 for 1-position of 1,2,3,5-tetramethylbenzene, and 2.8 for 2-position of 1,2,3,5-tetramethylabenzene, all the figures being expressed against the standard value of 1.00 for toluene. The observed accelerating effect of neighboring methyl groups on the demethylation rates of crowded reactant molecules has been correlated with modified superdelocalizability in z direction for radical aromatic substitution. The latter values calculated by the extended Hückel molecular orbital method were: 0.4070, 0.4116, 0.4908, 0.4169, 0.4124, 0.4116, 0.4131, 0.4133, 0.4148, 0.4204, 0.4120, and 0.4029 (toluene) in the order given above. The general parallelism between the observed and the theoretical values may be taken as a support not only of the extention of the concept of superdelocalizability to radical aromatic substitution, but also of our mechanistic interpretation on the key reaction of hydrogenolyses.

Considerable number of kinetic investigations were reported on the thermal hydrogenolytic demethylation of toluene.[1] Observed rates of the hydrogenolysis, $C_6H_5CH_3+H_2\rightarrow C_6H_6+CH_4$, can best be summarized within the specified deviations by $-d(C_6H_5CH_3)/dt=10^{(11.0\pm1.0)-(55\pm5)/\theta}\ (C_6H_5CH_3)\cdot(H_2)^{0.5}$ mol/l·sec over strikingly wide ranges of both temperature and pressure. The following chain mechanism initially proposed by us[2] and later supported by Benson and Shaw,[3] gives reasonable accounts for the observed overall three-halves reaction order as well as the values of Arrhenius kinetic parameters.

$$C_6H_5CH_3 \rightleftarrows C_6H_5CH_2 + H$$

$$H + C_6H_5CH_3 \rightleftarrows H_2 + C_6H_5CH_2$$

$$H + C_6H_5CH_3 \xrightarrow{(a)} C_6H_6 + CH_3$$

$$CH_3 + C_6H_5CH_3 \rightleftarrows CH_4 + C_6H_5CH_2$$

In the above chain scheme, the propagation rate is effectively controlled by reaction (*a*). This reaction can be pictured as a perpendicular approach of hydrogen atom to ring carbon atom to which methyl group is attached. This is followed by elimination of methyl group to complete the reaction. Energetics of the concerted process, quoted by Benson and Shaw as abstraction-elimination reaction,[3] has been successfully treated in our following communication[4] in terms of total electron energies of postulated transition structures using extended Hückel molecular orbital calculations.

The rate measurements were also reported for

1) a) H. Matsui, A. Amano and H. Tokuhisa, *Bull. Japan Petrol. Inst.*, **1**, 67 (1959); A. Tsuchiya, A. Hashimoto, H. Tominaga and S. Masamune, *ibid.*, **1**, 73 (1959); S. Masamune, A. Amano and H. Tokuhisa, *Tech. Reports Tohoku Univ.* (Japan), **25(1)**, 27 (1960); J.G. Burr, R.A. Meyer and J.D. Strong, *J. Amer. Chem. Soc.*, **86**, 3846 (1964). b) R. I. Silsby and E. W. Sawyer, *J. Appl. Chem.*, **6**, 347 (1956); W. D. Betts, F. Popper and R. I. Silsby, *ibid.*, **7**, 497 (1957); H. Morii, A. Hashimoto and H. Tominaga, *World Petrol. Congr. Proc. 6th*, Frankfurt, Germany 1963, 131.

2) A. Amano, H. Tominaga, and H. Tokuhisa, *Bull. Japan Petrol. Inst.*, **7**, 59 (1965).

3) S. W. Benson and R. Shaw, *J. Chem. Phys.*, **47**, 4052 (1967).

4) H. Tominaga, H. Arai, T. Kunugi, A. Amano, M. Uchiyama and Y. Sato, This Bulletin, **43**, 3658 (1970).

xylenes,[1b,5,6] 1,3,5-trimethylbenzene,[6] and 1,2,4-trimethylbenzene.[7] The reaction order was again found to be three-halves, indicating the validity of the same chain scheme proposed for toluene.[3] There is certain evidence,[5,7] however, that the specific rate of demethylation is affected by both number and position of methyl substituents of the reactant molecule. Thus, demethylation of the first methyl group of xylene and trimethylbenzenes was quite definitely easier than that of toluene. Unequal amounts of *o*-, *m*-, and *p*-xylenes were formed from 1,2,4-trimethylbenzene.

In the first part of the present work, effort has been made to evaluate quantitatively the ease with which any particular methyl group is substituted. Experiments are carried out for six different polymethylbenzenes at a fixed temperature of 702.1°C by an internal competitive reaction system. The latter technique assures a fair comparison of the demethylation rates. The value of demethylation rate constant for any given methyl group relative to that of toluene is then correlated with the relevant reactivity index for radical substitution.

Experimental

Commercial reagent grade polymethylbenzenes were used as received. Purities of the reagents as analyzed by gaschromatography were: benzene, >99.9 mol%; toluene, >99.9 mol%; *o*-xylene, 94.2 mol%; *m*-xylene, 97.3 mol%; *p*-xylene, >99.9 mol%; 1,2,3-trimethylbenzene, >99mol%; 1,2,4-trimethylbenzene, 99.7mol%; 1,3,5-trimethylbenzene, 99.8 mol%; 1,2,3,5-tetramethylbenzene, 96.6 mol%. Balancing impurities were consisted of hydrocarbons in the neighboring boiling ranges. Cylinder hydrogen of not less than 99.9 mol% purity was used after a conventional purification.

An all-glass flow apparatus was operated under an atmospheric pressure. Reactant polymethylbenzene was mixed with an adequate amount of toluene, and the mixture was introduced into the apparatus by using a glass syringe. The polymethylbenzene-toluene vapor was then carried into a reaction vessel along with a stream of hydrogen dried over magnesium perchlorate. Rate of hydrogenolysis of any given polymethylbenzene was thus evaluated in relation with that of toluene admixed as a standard reference. The use of the internal competitive reaction technique could afford a sufficiently reliable measure as to the reactivity ratios. In a few runs, where toluene was not a convenient reference because of an interference in the product analyses, 1,3,5-trimethylbenzene was used as a reference material.

The reaction vessel was made of a quartz tubing, 23 mm in inside diameter and 90 mm in length, and was equipped with a thermo-sheath placed along its central axis. The vessel was fitted in an electrically heated aluminum-bronze block furnace, the temperature of which was controlled electronically within ±0.5°C. Temperature profiles of the reaction vessel were determined, during each run while the reaction was taking place, by a movable Pt-Pt·Rh thermocouple in the sheath. Annular space of the vessel was filled with quartz tips, resulting in a free volume of about 10 ml. Reaction temperature and residence time were defined by the method described elsewhere.[8] The reaction was carried out at a fixed temperature of 702.1°C, hydrogen-hydrocarbon mole ratio of 5, and residence times ranging from 0.5 to 6.0 sec.

Condensable components of the products were collected in a train of cold traps immersed in liquid nitrogen, and were subjected to the conventional gaschromatographic analysis using dinonylphthalate (3 m) and polyethyleneglycol (3 m) packed columns.

Results

The gaseous products consisted mainly of methane and unreacted hydrogen with trace amounts of ethane, propane, propene, *etc.* The liquid products were compared of lower homologues of reactant polymethylbenzenes. Distributions of the products were in accord with those already reported for trimethylbenzenes.[6,7] The hydrogenolyses of polymethylbenzenes should therefore follow the general consecutive scheme: $C_6H_{6-n}(CH_3)_n+H_2\rightarrow C_6H_{7-n}(CH_3)_{n-1}+CH_4$. The relative rate of demethylation per one equivalent methyl group of polymethylbenzenes could thus be obtained directly from the composition of liquid products. The procedure assumes that the first order reaction with respect to polymethylbenzene takes place in an ideal plug flow reactor. It should be noted, however, that the deviations from the ideality do not produce substantial error in the values of reactivity ratio.

Demethylation rates of *o*-xylene and *p*-xylene were measured in relation with that of 1,3,5-trimethyl-

Table 1. Relative demethylation rate, *o*-xylene *vs.* 1,3,5-trimethylbenzene

Conversions (mol%)		Relative rates
o-Xylene	1,3,5-Trimethylbenzene	
2.28	2.39	0.95
4.17	4.47	0.94
7.46	8.05	0.93
11.73	11.62	1.01
		(Av. 0.96)

5) S. Masamune, M. Uchiyama, and H. Tokuhisa, *Tech. Reports Tohoku Univ.* (Japan), **25**(**1**), 39 (1960); A. Tsuchiya, A. Hashimoto, H. Tominaga and S. Masamune, *Bull. Japan Petrol. Inst.*, **2**, 85 (1960); J. G. Burr and J. D. Strong, *J. Am. Chem. Soc.*, **86**, 5065 (1964).

6) S. E. Shull and A. N. Hixon, *Ind. Eng. Chem., Process Design and Develop.*,**5**, 146 (1966),

7) H. Tominaga, K. Takagi, K. A. Moghul and T. Kunugi, *Kogyo Kagaku Zasshi*, **71**, 48 (1968); H. Tokuhisa, A. Amano, M. Uchiyama and Y. Sato, Preprints for the 21st Annual Meeting of Japan Chem. Soc., Tokyo (1968).

8) A. Amano and M. Uchiyama, *J. Phys. Chem.*, **67**, 1242 (1963).

Table 2. Relative demethylation rate, *p*-xylene *vs.* 1,3,5-trimethylbenzene

Conversions (mol%)		Relative rates
p-Xylene	1,3,5-Trimethylbenzene	
2.02	3.61	0.55
3.76	5.81	0.64
		(Av. 0.60)

benzene by analyzing for toluene and *m*-xylene produced. The results obtained under varying conversion levels are listed in Table 1 and 2. In excellent agreement with previously reported values,[1b,5] *o*-Xylene is shown 1.6 times as reactive as *p*-xylene.

Demethylation rates of other polymethylbenzenes were measured using toluene as internal referance. The results are listed in Tables 3, 4 and 5. In these instances, either two or three structural isomers were initially formed depending on the number of unequivalent methyl groups in the reactant molecule. Thus, the liquid product from 1,2,4-trimethylbenzene at a conversion level of 2.73 mol% was composed of *o*-xylene (0.64 mol%), *m*-xylene (0.98 mol%), *p*-xylene (1.01 mol%), and toluene (0.10 mol%). The amount of toluene produced from the three xylene isomers by secondary reaction was then corrected based on the reported relative reactivity among these isomers, resulting in the initial isomer distribution of *o*-xylene (21.1 mol%), *m*-xylene (38.7 mol%), and *p*-xylene (40.2 mol%). The values of the initial distribution corrected by the method described above are listed in the second column of Tables 3, 4 and 5. Relative rate to produce any particular isomer was deduced from the overall relative rate and the initial distribution, giving proper consideration of statistical factor if necessary. Thus, for example, relative rate to produce *o*-xylene from 1,2,3-trimethylbenzene was obtained by dividing analytical value by statistical factor of two. The final values of the relative rate are listed in the last column of the tables. A check of the data can be made, for example, by comparing the overall relative rate of 4.98 given in Table 3 with the reported value of 5.0.[7]

Table 6 lists the results obtained for a mixed feed of toluene and 1,3,5-trimethylbenzene. Summarized in Table 7 are the relative rates of demethylation per one equivalent methyl group based on the averaged value of 3.59 given in Table 6. It should be emphasized at this point that the values of relative rates listed in Table 7 are essentially those for (*a*), and are free from other elementary reactions included in our mechanism.[2] This is, in fact, one of the advantages of the present experimental method.

Table 3. Relative demethylation rate, 1,2,4-trimethylbenzene *vs.* toluene

Conversions (mol%)			Relative rates	
1,2,4-Trimethylbenzene		Toluene		
2.73	*m*-Xylene 38.7%	0.53	5.20	*m*-Xylene 2.01
	p-Xylene 40.2%			*p*-Xylene 2.09
	o-Xylene 21.1%			*o*-Xylene 1.10
4.66	*m*-Xylene 36.7%	0.93	5.10	*m*-Xylene 1.88
	p-Xylene 37.9%			*p*-Xylene 1.93
	o-Xylene 25.4%			*o*-Xylene 1.29
7.69	*m*-Xylene 35.6%	1.63	4.72	*m*-Xylene 1.68
	p-Xylene 37.1%			*p*-Xylene 1.76
	o-Xylene 27.3%			*o*-Xylene 1.28
12.65	*m*-Xylene 37.1%	2.72	4.90	*m*-Xylene 1.82
	p-Xylene 36.3%			*p*-Xylene 1.78
	o-Xylene 26.6%			*o*-Xylene 1.30
18.14	*m*-Xylene 37.3%	3.96	4.95	*m*-Xylene 1.84
	p-Xylene 36.0%			*p*-Xylene 1.78
	o-Xylene 26.7%			*o*-Xylene 1.35
			Av. 4.98	*m*-Xylene 1.85
				p-Xylene 1.87
				o-Xylene 1.26

Table 4. Relative demethylation rate, 1,2,3-trimethylbenzene *vs.* toluene

Conversions (mol%)			Relative rates	
1,2,3-Trimethylbenzene		Toluene		
12.72	*o*-Xylene 57.8%	1.60	8.44	*o*-Xylene 2.44
	m-Xylene 42.2%			*m*-Xylene 3.56
16.19	*o*-Xylene 57.4%	2.24	7.79	*o*-Xylene 2.24
	m-Xylene 42.6%			*m*-Xylene 3.31
20.08	*o*-Xylene 58.1%	3.02	7.31	*o*-Xylene 2.12
	m-Xylene 41.9%			*m*-Xylene 3.07
26.27	*o*-Xylene 57.2%	4.14	7.21	*o*-Xylene 2.06
	m-Xylene 42.8%			*m*-Xylene 3.09
			Av. 7.69	*o*-Xylene 2.22
				m-Xylene 3.25

Table 5. Relative demethylation rate, 1,2,3,5-tetramethylbenzene *vs.* toluene

Conversions (mol%)			Relative rates	
1,2,3,5-Tetramethylbenzene		Toluene		
22.01	1,3,5-TriMB 34.0%	2.93	8.4	1,3,5-TriMB 2.8
	1,2,4-TriMB 46.1%			1,2,4-TriMB 2.0
	1,2,3-TriMB 19.9%			1,2,3-TriMB 1.6
13.15	1,3,5-TriMB 33.0%	1.62	8.7	1,3,5-TriMB 2.8
	1,2,4-TriMB 49.9%			1,2,4-TriMB 2.2
	1,2,3-TriMB 17.1%			1,2,3-TriMB 1.5
			Av. 8.6	1,3,5-TriMB 2.8
				1,2,4-TriMB 2.1
				1,2,3-TriMB 1.6

TABLE 6. RELATIVE DEMETHYLATION RATE, 1,3,5-TRIMETHYLBENZENE *vs.* TOLUENE

Conversion (mol%)		Relative rates
1,3,5-Trimethylbenzene	Toluene	
1.23	0.305	3.98
2.50	0.708	3.56
5.02	1.44	3.55
5.25	1.49	3.56
6.24	1.78	3.59
9.25	2.92	3.28
7.45	2.73	3.60
13.65	4.03	3.57
		(Av. 3.59)

TABLE 7. RELATIVE RATES OF DEMETHYLATION PER ONE EQUIVALENT METHYL GROUP

Compound	Position of methyl group	Relative reactivity
Toluene	—	1.00 (reference)
o-Xylene	1, 2	1.72
p-Xylene	1, 4	1.08
1,2,4-Trimethylbenzene	1	1.85
1,2,4-Trimethylbenzene	2	1.87
1,2,4-Trimethylbenzene	4	1.26
1,3,5-Trimethylbenzene	1, 3, 5	1.20
1,2,3-Trimethylbenzene	1, 3	2.22
1,2,3-Trimethylbenzene	2	3.25
1,2,3,5-Tetramethylbenzene	1, 3	2.1
1,2,3,5-Tetramethylbenzene	2	2.8
1,2,3,5-Tetramethylbenzene	5	1.5

Discussion

As has been shown by the foregoing experimental results, the rate of reaction *a* is affected by both number and position of methyl substituents in any given reactant molecule. In the word of classical organic chemistry, this is due obviously to a cummulative result of inductive and resonance effects. Such effects should modify electronically the reactivity of methylated carbon atoms in benzene ring toward hydrogen atom attack, reaction (*a*), which in turn controls the rate of the overall hydrogenolysis. Fukui, Yonezawa, and Nagata have successfully introduced an index termed superdelocalizability,[9] in their work calculated by the simple Hückel method, as a measure of the reactivity of aromatic compounds for substitution reactions.

We adopt in the present paper the concept put forward by Fukui *et al.* but using the extended Hückel method. The use of the latter method should be preferred in elucidating the electronic structures of polymethylbenzenes, since *sigma* and *pi* electrons can be treated without arbitrary parametrizations. The modified superdelocalizability radical substitution, $S_p(\mathrm{R})$, defined by the following equation is thus taken as reactivity index.

$$S_p(\mathrm{R}) = \sum_{i}^{\mathrm{occ}} \{(c_{p_i})^2/\lambda_i\} + \sum_{j}^{\mathrm{unocc}} \{(c_{p_j})^2/-\lambda_j\}$$

where $\lambda_i = -\varepsilon_i + \alpha_0$, and $\alpha_0 \fallingdotseq (\varepsilon_{\mathrm{ho}} + \varepsilon_{\mathrm{lv}})/2$. ε_i and c_{p_i} are eigen value and eigen vector of the *i*th molecular orbital, respectively. The validity of the approximation in estimating the value of α_0 can be tested for the case of toluene hydrogenolysis where the energy level of half-filled orbital of the activated complex was estimated as being −10.439 eV in our follwing paper.[4] This should be compared with −10.426 eV deduced from the energy level of the highest occupied orbital, $\varepsilon_{\mathrm{ho}}$, of −12.491 eV and that of the lowest unoccupied orbital, $\varepsilon_{\mathrm{lv}}$, of −8.361 eV for toluene both listed in Table 8.

Detail of the molecular orbital calculations by the extended Hückel method have been described.[4] The calculations are carried out for ten different polymethylbenzenes based on the following molecular geometries: coplanar skeletal structure;[10] C-(ring)-C(ring) distance, 1.40 Å; C(ring)-C(methyl) distance, 1.51 Å; C(ring)-H distance, 1.09 Å; C-(methyl)-H distance, 1.09 Å. It is further assumed

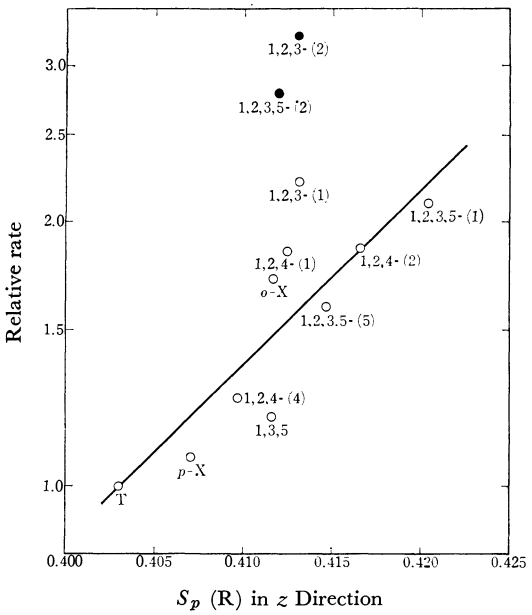

Fig. 1. Correlation between observed relative reactivity and modified superdelocalizability.

9) K. Fukui, T. Yonezawa, and C. Nagata, This Bulletin, **27**, 423 (1954); *J. Chem. Phys.*, **27**, 1247 (1957).

10) G. Furguson and J. M. Robertson, "Advances in Physical Organic Chemistry," Vol. 1, Academic Press, New York (1963), p. 202.

TABLE 8. REACTIVITY INDICES BY EXTENDED HÜCKEL METHOD

Compound	Energy levels (eV)		Position	Modified superdelocalizability in z direction			Atomic bond population
	ε_{ho}	ε_{lv}		$S_p(R)$	$S_p(E)$	$S_p(N)$	
Toluene	−12.4906	−8.3615	1	0.4029	0.2749	0.5309	0.7744
o-Xylene	−12.3253	−8.2432	1,2	0.4116	0.2987	0.5245	0.7748
m-Xylene	−12.3794	−8.2510	1,3	0.4063	0.2609	0.5517	0.7745
p-Xylene	−12.2094	−8.3625	1,4	0.4070	0.2998	0.5142	0.7712
1,3,5-Trimethylbenzene	−12.3777	−8.0057	1,3,5	0.4116	0.2468	0.5765	0.7746
1,2,3-Trimethylbenzene	−12.3021	−8.0287	1,3	0.4131	0.2828	0.5434	0.7750
1,2,3-Trimethylbenzene	—	—	2	0.4133	0.3208	0.5058	0.7750
1,2,4-Trimethylbenzene	−12.1232	−8.2170	1	0.4124	0.3235	0.5013	0.7716
1,2,4-Trimethylbenzene	—	—	2	0.4169	0.2846	0.5493	0.7750
1,2,4-Trimethylbenzene	—	—	4	0.4098	0.2839	0.5357	0.7713
1,2,4,5-Tetramethylbenzene	−11.9715	−8.1369	1,2,4,5	0.4168	0.3089	0.5248	0.7718
1,2,3,4-Tetramethylbenzene	−12.0974	−8.0212	1,4	0.4126	0.3067	0.5184	0.7719
1,2,3,4-Tetramethylbenzene	—	—	2,3	0.4158	0.3058	0.5257	0.7754
1,2,3,5-Tetramethylbenzene	−12.0826	−8.0031	1,3	0.4204	0.2691	0.5717	0.7752
1,2,3,5-Tetramethylbenzene	—	—	2	0.4120	0.3417	0.4823	0.7719
1,2,3,5-Tetramethylbenzene	—	—	5	0.4148	0.2682	0.5613	0.7714

that the conformation of neighboring methyl groups is such that the separation between two hydrogen atoms should be maximum. Summarized in Table 8 are the values of the modified superdelocalizability in z-direction, namely perpendicular to ring plane, of ring carbons for radical substitution together with eigen values of the highest occupied and the lowest unoccupied orbitals. The values of the modified superdelocalizability for electrophilic and nucleophilic substitutions are also included in Table 8 for comparison.

The observed rates of demethylation per one equivalent methyl group of polymethylbenzenes relative to that of toluene have already been listed in Table 7. These values are plotted in Fig. 1 against the relevent values of modified superdelocalizability. Since the latter quantity should relate primary with the energetics of the critical reaction path, the observed relative rates are expressed by logarithmic scale in Fig. 1.

The linearity shown by empty circles in Fig. 1 serves as an evidence for the extension of Fukui's concept of superdelocalizability which has been largely confined within ionic substitutions.[9] Conversely, if it is assumed that the aromatic reactivity for radical substitution can be properly described by the value of $S_p(R)$, the linearity may be taken as a support of our mechanistic interpretation on the hydrogenolyses and hence the role of reaction (*a*) in the chain scheme.[2,4]

11) R. S. Mulliken, *J. Chem. Phys.*, **23**, 1833, 1841, 2338, 2343 (1955).

The values of atomic bond population[11] M[C(ring)-C(methyl)] have also been calculated by the extended Hückel method, and are listed in the last column of Table 8.

$$M[\mathrm{C(ring)-C(methyl)}] = \sum_p \sum_q N_{pq}$$

$$N_{pq} = 4 \sum C_{p_i} C_{q_i} S_{pq}$$

They exhibit no radical correlation what so ever with the observed reactivity ratios. This indicates that the reactivity for aromatic substitution is determined by the dynamic property of the ring carbon atom at whicn the substitution takes place, and not by the static property such as atomic bond population at the bond which is to be broken. The conclusion drawn here is in conformity with our following computational analysis[4] in which hydrogen atom attack has been reckoned as rate-determing step of reaction (*a*).

Deviation from the theory is, however, beyond any conceivable uncertainty for cases marked by filled circles in Fig. 1. They include 2-positions of 1,2,3-trimethylbenzene and 1,2,3,5-tetramethylbenzene where neighboring methyl groups have an effect toward higher reactivity than can be predicted by the theory. The following may possibly be the reasons for the present discrepancy. (1) Slight alternations in the planar conformation of these highly crowded homologues may lead to a significant effect on the values of $S_p(R)$. (2) Structure of transition-state for the hydrogen atom attack toward the 2-positions may be influenced by the presence of neighboring methyl groups.

BULLETIN OF THE CHEMICAL SOCIETY OF JAPAN VOL. 43 3658—3662 (1970)

Mechanism of Hydrogenolysis. II. A Molecular Orbitals Study of Hydrogenolysis of Toluene

Hiroo TOMINAGA, Hiromichi ARAI and Taiseki KUNUGI

Department of Synthetic Chemistry, Faculty of Engineering, University of Tokyo, Hongo, Bunkyo-ku, Tokyo

and Akira AMANO, Masao UCHIYAMA and Yoshiki SATO

Department of Applied Chemistry, Faculty of Engineering, Tohoku University, Aoba-Aramaki, Sendai

(Received January 31, 1970)

In hydrogenolysis of toluene to produce benzene and methane, atomic cracking process $H+C_6H_5CH_3 \rightarrow C_6H_6CH_3$ (*a*) or $H+C_6H_5CH_3 \rightarrow C_6H_5+CH_4$ (*b*) has been presumed as rate controlling in chain propagation step of the radical chain mechanism. These two alternative processes are compared on the energetics calculated by the extended Hückel M.O. method. The reaction (*a*), an addition of the attacking hydrogen atom to phenyl carbon atom adjacent to methyl group followed by an elimination of methyl radical in a concerted manner, is found to be the most likely pathway.

In the last decade a considerable number of kinetic investigations have been reported on the thermal hydrogenolytic demethylation of toluene.[1] The reaction can be expressed by the stoichiometry,

$$C_6H_5CH_3 + H_2 \longrightarrow C_6H_6 + CH_4,$$

and is sufficiently clean for rate measurements. The observed rates can be described within the specified deviations by

$$-d[C_6H_5CH_3]/dt = k[C_6H_5CH_3][H_2]^{1/2} \text{ mol}\cdot l^{-1}\cdot\text{sec}^{-1},$$
$$k = 10^{(11\pm1)-(55\pm5)/\theta},$$

where θ being $(2.303\,RT)$ in kcal mol^{-1}.

The values of Arrhenius kinetic parameters and the overall three-halves order were interpreted by these authors in terms of a free radical chain mechanism, which was subsequently supported by Benson and Shaw.[2b] The chain propagation step was controlled by the following *atomic cracking* process:[2a]

$$H + C_6H_5CH_3 \xrightarrow{(a)} C_6H_6 + CH_3, \text{ or}$$
$$H + C_6H_5CH_3 \xrightarrow{(b)} C_6H_5 + CH_4$$

The latter alternative was suggested by Silsby and Sawyer,[1a] and also by Burr, Meyer and Strong.[1c] However, exact mechanistic natures of the reactions have not hitherto been discussed in any detail. In the present paper a comparison will be made on the energetics between the two reactions; perpendicular approach of hydrogen atom to phenyl carbon atom to which methyl group is attached (reaction (*a*)) on one hand, and direct Walden inversion type hydrogen attack to methyl carbon atom (reaction (*b*)) on the other. The comparison is to be based on the total electron energy calculations of the postulated transition structures using the extended Hückel M.O. method. As will be discussed in the present paper, reaction (*a*) is the most likely pathway in hydrogenolytic demethylation. The *atomic cracking* is, therefore, an addition of hydrogen atom to phenyl carbon followed by an elimination of methyl radical in a concerted manner.

Molecular Orbitals Calculation

To investigate which one of the two alternative reaction mechanisms is operative, the changes in total electron energies of the transition structures along presumed reaction coordinates are calculated. An empirical molecular orbitals theory developed by Hoffmann,[3] that is, extended Hückel method is employed which has proved useful in discussing the hydrocarbon conformational problems such as barriers to internal rotation, geometric iso-

1) a) R. I. Silsby and E. W. Sawyer, *J. Appl. Chem.*, **6**, 347 (1956); W. D. Betts, F. Popper and R. I. Silsby, *ibid.*, **7**, 497 (1957). b) H. Matsui, A. Amano and H. Tokuhisa, *Bull. Japan Petrol. Inst.*, **1**, 67 (1959); A. Tsuchiya, A. Hashimoto, H. Tominaga and S. Masamune, *ibid.*, **1**, 73 (1959); S. Masamune, A. Amano and H. Tokuhisa, *Tech. Reports Tohoku Univ.* (Japan), **25**(**1**), 27 (1960); H. Morii, A. Hashimoto and H. Tominaga, World Petrol. Congr. 6th, Frankfurt, Germany (1963). c) J. G. Burr, R. A. Meyer and J. D. Strong, *J. Amer. Chem. Soc.*, **86**, 3846 (1964).

2) a) A. Amano, H. Tominaga and H. Tokuhisa, *Bull. Japan Petrol. Inst.*, **7**, 59 (1965). b) S. W. Benson and R. Shaw, *J. Chem. Phys.*, **47**, 4052 (1967).

merism,[3] as well as electronic structure of transient species.[4]

The secular determinant, with the order of $(4n+m)$ for a molecule C_nH_m, of which atomic orbitals are $2s$, $2p_x$, $2p_y$, $2p_z$ for carbon and $1s$ for hydrogen, is solved using an electronic computor HITAC 5020 for eigen values ε_i and eigen vectors C_{pi} of the molecular orbitals. The complete secular determinant is treated, namely, all overlap integrals computed, and off diagonal E's retained. The Coulomb integrals H_{pp} are chosen as valence state ionization potentials of Pritchard and Skinner.[5] The reasonance integrals H_{pq} are approximated as

$$H_{pq} = 0.5K(H_{pp}+H_{qq})S_{pq},$$

where

$$K = 1.75,$$

after the original proposal by Hoffmann.[3] The effective nuclear charges of Slater orbitals are employed.[6] The ovelap integrals S_{pq} are calculated by Mulliken's procedure.[7] For radicals and transient species with odd number of electrons, the highest orbital is assumed to be half-occupied.

Reaction Co-ordinate and Conformation

The configuration of toluene molecule is presented in Fig. 1, where large open circles indicate carbon atom and small full circles hydrogen atom. The bond lengths and angles are found in chemical dictionary.

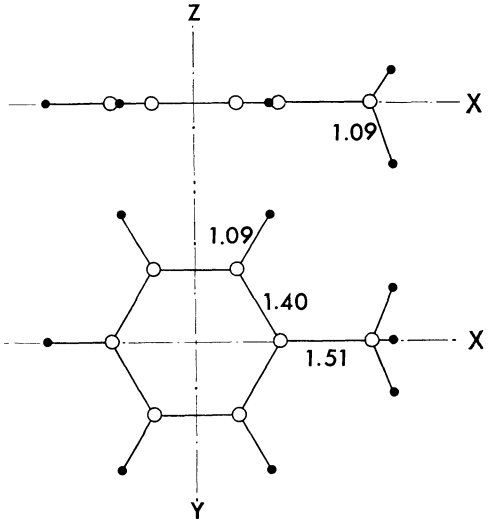

Fig. 1. Conformation of toluene.

Reactions (*a*) and (*b*) are considered to proceed through the following transition states, respectively;

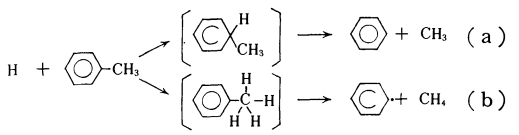

The former route denotes the approach of hydrogen atom to the phenyl carbon atom adjacent to methyl group in perpendicular direction to toluene ring plane. This forms the σ-complex with pseudo sp^3 hybrid structure, ending with the elimination of methyl radical to form benzene. While the latter signifies the approach of hydrogen atom to the methyl carbon atom in the horizontal direction along methyl - ring (C7-C1) axis. Through penta - valent carbon complex, this results in Walden type inversion to form phenyl radical and methane.

Perspective sketched for the two transient species are illustrated in Figs. 2 and 3, where H16 stands

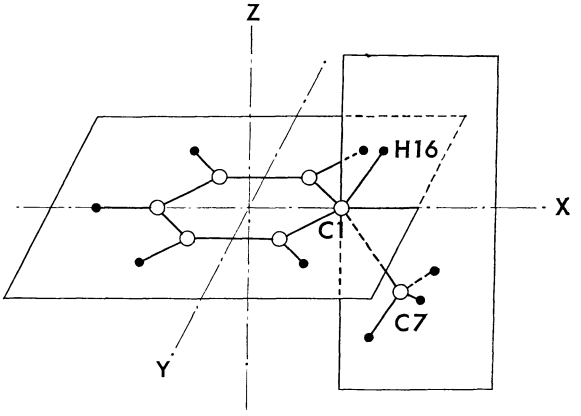

Fig. 2. Perspective view of transition state for reaction (a).

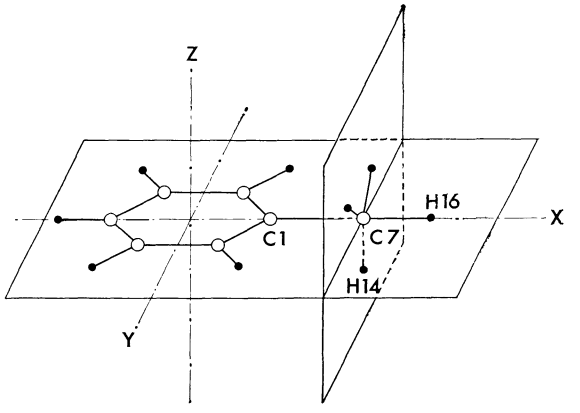

Fig. 3. Perspective view of transition state for reaction (b).

3) R. Hoffmann, *J. Chem. Phys.*, **39**, 1397 (1963).
4) H. Kato, K. Morokuma, T. Yonezawa and K. Fukui, This Bulletin, **38**, 1749 (1965).
5) H. O. Pritchard and H. A. Skinner, *Trans. Faraday Soc.*, **49**, 1254 (1953).
6) J. C. Slater, *Phys. Rev.*, **36**, 57 (1930).
7) R. S. Mulliken, C. A. Ricke and D. Orloff, *J. Chem. Phys.*, **17**, 1248 (1949).

Table 1. Change of total electron energy with approach of attacking hydrogen atom along vertical (z) axis

No.	Bond length, Å		Bond angle		Conformation	Total electron energy, eV.	Energy level of half-filled orbital, eV
	Cl-H16	C1-C7	∠H16-C1-x	∠C7-C1-x			
I[a]	5.0	1.51	90°	0°	Toluene	−645.79	—
II	3.0	1.51	90°	0°	Toluene	−645.75	—
III	2.0	1.52	80°	25°	Toluene	−645.53	—
IV	1.5	1.53	70°	35°	Toluene	−645.67	−10.750
V	1.5	1.53	70°	35°	Cyclohexadienyl	−646.04	−10.432
	1.22	1.53	60°	60°	Cyclohexadienyl	−646.81	—
	1.22	1.68	60°	60°	Cyclohexadienyl	−647.50	—
VI[b]	1.11	1.54	55°	55°	Cyclohexadienyl	−647.21	−10.439
	1.11	1.68	60°	60°	Cyclohexadienyl	−647.62	—
VII[c]	1.10	2.00	25°	80°	Benzene and methyl	−647.24	—
VIII	1.09	3.0	0°	90°	Benzene and methyl	−649.28	—
IX	1.09	5.0	0°	90°	Benzene and methyl	−649.42	—

Remarks
a) Refer to Fig. 1 for the conformation of toluene.
b) Refer to Fig. 4. The conformation of cyclohexadienyl is proposed by Russel S. Drago and Harold Peterson, Jr.
c) CH_3 in the ground state, $2A_2''$, is taken as planar with a CH distance of 1.08 Å after G. Herzberg.

Table 2. Change of total electron energy with approach of attacking hydrogen atom along horizontal C1-C7 (x) axis

No.	Bond length, Å		Bond angle	Confromation		Total electron energy, eV
	C7-H16	C1-C7	∠H14-C7-C1	Phenyl	Methyl	
I′	5.0	1.51	109°28′	Toluene		−645.79
II′	3.0	1.51	109°28′	Toluene		−645.71
III′	2.0	1.51	100°	Toluene		−644.32
IV′	1.5	1.60	95°	Benzene	Shallow pyramid	−643.18
V′	1.3	1.66	90°	Benzene	Planar	−643.55
	1.3	1.81	90°	Benzene	Planar	−644.11
	1.3	1.90	90°	Benzene	Planar	−644.33
VI′	1.2	1.81	90°	Benzene	Planar	−644.19
	1.3	1.66	90°	Benzene	Planar	−643.66
VII′	1.15	2.0	85°	Benzene	Shallow pyramid	−644.71
VIII′[a]	1.09	3.0	70°32′	Benzene	Methane	−648.23
IX′[b]	1.09	5.0	70°32′	Benzene	Methane	−648.44

Remarks
a) Conformation of phenyl radical is taken as the same with that of benzene except one ring hydrogen lost. Refer to G. Porter and B. Ward.
b) Conformation of methane; CH bond length 1.09 Å with bond angle ∠HCH 109°28′.

for the attacking hydrogen atom, Cl the phenyl carbon atom adjacent to the methyl group, and C7 the carbon atom of the methyl group to be removed. The total electron energies of 24 transient species are calculated based on the conformational parameters listed in Tables 1 and 2. The distance between Cl and H16, or C7 and H16, is arbitrarily chosen as reaction co-ordinate. The calculation covers the range from 5 Å to 1.09 Å that is equivalent to the normal C–H bond length for benzene or methane. With the approach of H16, the bond length Cl-C7 correspondingly increases from the original 1.51 Å to 5 Å and the bond angles also change as are shown in the tables. In this course the C–H bond length of methyl group is assumed to remain constant at 1.09 Å with a sole exception of 1.08 Å for methyl radical.

The conformation of σ-complex, VI in Table 1, is presumed as is shown in Fig. 4 based on that of cyclohexadienyl radical proposed by Drago and

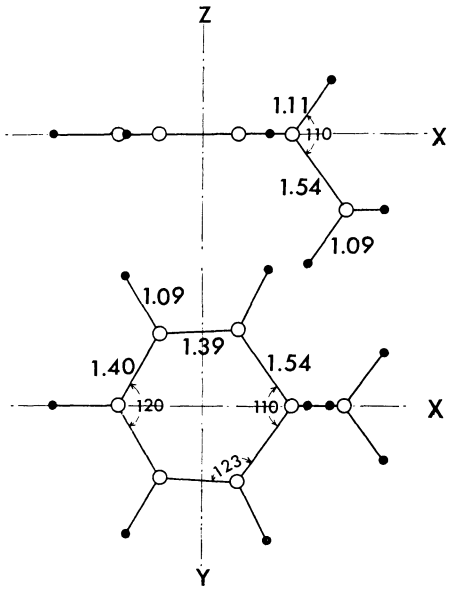

METHYL CYCLOHEXADIENYL RADICAL

Fig. 4. Conformation of methyl cyclohexadienyl radical.

Peterson.[8] As for the penta-valent carbon complexes, V′ and VI′ in Table 2, the bond distance C7-H16 (or C1-C7) is taken as 20% (or 10%) longer than that of methane (or of toluene) for V′, and *vice versa* for VI′. The conformation of methyl radical is taken as planar with C–H distances of 1.08 Å as is presented by Herzberg.[9] Phenyl radical is supposed to have the same conformation with that of benzene except that one hydrogen atom is lost. This is suggested by Porter and Ward.[10]

At a given reaction co-ordinate, namely at a given approach of the attacking hydrogen atom to carbon atom C1 or C7, effects of some changes in C1-C7 bond distance or bond angle are evaluated. Indicated are the lower total electron energies for the transient species with the longer bond distances between departing carbon atoms. The formation of these transient species with the lower energies, however, seems less favoured due to the less chance of hydrogen atom attack on one of the carbon atoms with the C1-C7 bond which is longer than in equilibrium and in vibration.

Results and Discussion

Indicated in Fig. 5 are the changes in total electron energies of the reacting systems with the two different ways of approach of attacking hydrogen

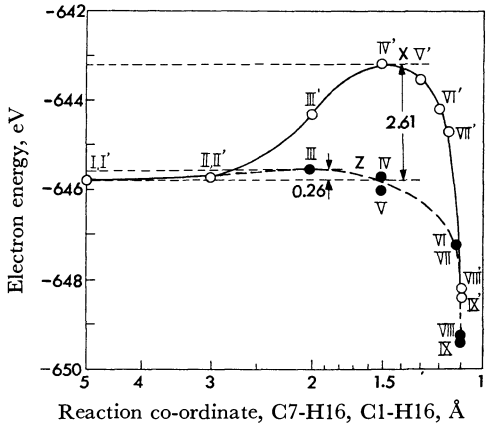

Fig. 5. Reaction co-ordinate energy diagram for reactions (a) and (b).

atom. It is clearly demonstrated that the approach to C1, the phenyl carbon atom, in parallel with z axis requires much less energy than the approach to C7, the methyl carbon atom, along x axis does. The energy barrier of the former reaction route, E_z, is calculated as 0.26 eV (*ca.* 6 kcal mol^{-1}) while that of the latter, E_x, is approximated as 2.61 eV (*ca.* 60 kcal mol^{-1}), 10 times larger than E_z. The value E_x=60 kcal mol^{-1} does not seem exceedingly large in view of the high activation energies that are generally associated with ionic Walden inversion reactions.

The value E_z=6 kcal mol^{-1}, on the other hand, is in surprisingly good agreement with the value of 5 kcal mol^{-1} predicted by these authors.[2a] They have evaluated the kinetic parameters of a number of possible elementary reactions involved in the thermal hydrogenolysis of toluene based on the bulk of kinetic and thermodynamic informations. More important elementary reactions are thus selected, and the following formulation is obtained to describe the main scheme of the hydrogenolysis:

$$C_6H_5CH_3 \underset{2}{\overset{1}{\rightleftharpoons}} C_6H_5CH_2 + H$$

$$H + C_6H_5CH_3 \underset{4}{\overset{3}{\rightleftharpoons}} H_2 + C_6H_5CH_2$$

$$H + C_6H_5CH_3 \xrightarrow{(a)} C_6H_6 + CH_3$$

$$CH_3 + H_2 \underset{6}{\overset{5}{\rightleftharpoons}} CH_4 + H$$

$$CH_3 + C_6H_5CH_3 \underset{8}{\overset{7}{\rightleftharpoons}} CH_4 + C_6H_5CH_2$$

The proposed mechanism is shown to be in conformity with hitherto observed kinetic behaviours of the reaction. Assuming steady-state approximation, the overall rate equation is given by the equation:

$$-d[C_6H_5CH_3]/dt \fallingdotseq k_a\left(\frac{k_1 \cdot k_4}{k_2 \cdot k_3}\right)^{1/2}[C_6H_5CH_3][H_2]^{1/2}$$

8) R. S. Drago and H. Peterson, Jr., *J. Amer. Chem. Soc.*, **89**, 3978 (1967).
9) G. Herzberg, *Proc. Roy. Soc.*, **262A**, 291 (1961).
10) G. Porter and B. Ward, *Proc. Chem. Soc.*, **1964**, 288.

Therefore the overall values of A-factor and activation energy can be expressed in terms of individual kinetic parameters by the following equations:

$$A \text{ overall} = A_a(A_1A_4/A_2A_3)^{1/2}$$
$$= A_a \cdot 10^{3.06}\ l^{1/2} \cdot \text{mol}^{-1/2} \cdot \text{sec}^{-1}$$
$$E \text{ overall} = E_a + \frac{1}{2}(E_1 - E_2 - E_3 + E_4)$$
$$= E_a + 51.6 \text{ kcal} \cdot \text{mol}^{-1}$$

The comparison of these theoretical values with the experimental ones would thus place the values of A_a and E_a as approximately 10^8 l mol^{-1} sec^{-1} and 5 kcal mol^{-1}, respectively. The value E_a coincides fairly well with the value E_z obtained in the present paper.

The calculated values of E_z=6 kcal mol^{-1} is also supported by some experiments. In the gamma radiolysis of propane, Kan Yang[11] observed the rate of formation of hydrogen is reduced by the presence of olefins or benzene. The effect of temperature on this inhibition indicates that it results from the hydrogen atom addition to olefins or benzene. The activation energy of 3.5 kcal mol^{-1} is obtained for benzene and can be compared to the value E_z=6 kcal mol^{-1}. Myran C. Sauer, Jr. and Barry Ward used the technique of pulsed radiolysis obtaining the rate constants at 25°C for the gas phase reaction of hydrogen atoms with benzene and toluene as 0.37×10^8 and 1.0×10^8 l mol^{-1} sec^{-1}, respectively.[12] The activation energy in the case of benzene is about 3 kcal mol^{-1}. Benzene and toluene was found to yield the cyclohexadienyl and methylcyclohexadienyl radicals, respectively, with absorption maxima at 302 and 307 mμ, respectively, in the gas phase. These experimental data are also in excellent agreement with the calculated kinetic parameters aforementioned.

This agreement might be rather fortuitous, because neither nuclear nor electronic repulsion is explicitly considered in the extended Hückel molecular orbitals calculation. Development of a more advanced molecular orbitals treatment and its application to this study is now in progress in this laboratory.

Conclusion

These considerations lead to the conclusion that the atomic cracking of toluene by hydrogen atom is a radical substitution proceeding through a methylcyclohexadienyl radical type σ-complex, to give benzene and methyl radical in a concerted manner. The validity of this conclusion may be further supported by the previous study[13] where the effect of methyl substitution on the hydrogenolytic demethylation of polymethylbenzenes has been discussed in terms of reactivity index deduced from molecular orbitals theory.

11) Kan Yang, *J. Amer. Chem. Soc.*, **84**, 3795 (1962).

12) Myran C. Sauer, Jr., and Barry Ward, *J. Phys. Chem.*, **71**, 3971 (1967).

13) A. Amano, M. Uchiyama, Y. Sato, H. Tominaga, H. Arai and T. Kunugi, This Bulletin, **43**, 3653 (1970).

BULLETIN OF THE CHEMICAL SOCIETY OF JAPAN VOL. 43 3663—3666 (1970)

The Effect of Solvents on the Optical Rotation of Poly(propylene Oxide)

Yoshiyuki KUMATA, JUNJI FURUKAWA and Takayuki FUENO*1

Department of Synthetic Chemistry, Kyoto University, Sakyo-ku, Kyoto

(Received March 28, 1970)

The change in the rotatory direction of optically active poly(propylene oxide) in different solvents has been discussed from the viewpoint of dielectric theory of solution. It has been pointed out that, in general, the shapes of the optical rotatory dispersion curves of polymers cannot directly be related to their conformation.

Price and Osgan[1] first noted that the optical rotation of poly(propylene oxide) measured at 589 mμ in chloroform and in benzene are of opposite sign. Tsunetsugu *et al.*[2] have suspected that this phenomenon might be due to a change in local polarizability of the asymmetric center effected by some weak complexation of polymer with solvent. Alternatively, Hirano *et al.*,[3] have interpreted this phenomenon as resulting from the formation of some helical component (gauche conformation) in chloroform solution.

According to the usual interpretation of optical rotatory dispersion, an optically active polymer having a helical conformation should exhibit an "anomalous" dispersion curve.[4] However, we have observed that the dispersion curves of poly(propylene oxide) prepared from optically active monomer are plain for all the solvents examined. In the present paper, we will reconsider the physical meaning of the anomalous dispersion, and show that the effect of solvents on the optical rotatory dispersion of poly(propylene oxide) might also be interpreted from a factor other than the conformational change of the polymer in different solvents.

Experimental

Optically active propylene oxide was polymerized by potassium hydroxide as a catalyst. The benzene solution of polymer was washed successively with dilute hydrochloric acid and water, and then freeze-dried. The molecular weight of the polymer obtained was determined by osmometry to be *ca.* 3200.

Measurements of the optical rotation of this polymer in various solvents were carried out at ambient temperature using a JASCO polarimeter Model ORD, UV-5. The concentration of polymer was fixed at 2.5 g/100 m*l*.

Results and Discussion

The specific rotation of poly(propylene oxide) at 589 mμ measured in various solvents is listed in Table 1. In any solvent used, the sample polymer gave a plain dispersion curve. Some typical curves are compared in Fig. 1, and the corresponding Moffitt-type plots (Eq. (1)) are shown in Fig. 2.

$$\frac{[M](\lambda^2-\lambda_0^2)}{\lambda_0^2} = a + \frac{b\lambda_0^2}{(\lambda^2-\lambda_0^2)} \qquad (1)$$

It may be seen in Fig. 2 that in all cases the values of $[M](\lambda^2-\lambda_0^2)/\lambda_0^2$ linearly decrease with increasing magnitudes of $\lambda_0^2/(\lambda^2-\lambda_0^2)$ and that no line crosses the zero line of $[M](\lambda^2-\lambda_0^2)/\lambda_0^2$ in the wavelength region of observation. This latter feature is in contrast to that encountered in the case of propylene oxide monomer, in which the quantity $[M](\lambda^2-\lambda_0^2)/\lambda_0^2$ becomes zero for some solvents (Fig. 3). In both Figs. 2 and 3, the values of λ_0 were chosen by the trial-and-error method so as to allow the best fit of observation to the Moffitt equation (1). The λ_0 values thus chosen are listed in Table 2.

It should be noted that the Moffitt equation (1) has proved to hold even in propylene oxide which has a rigid ring structure. Equation (1) was originally introduced as an approximation of Drude's two-term equation (2).[5]

$$[\alpha] = \frac{A}{\lambda^2-\lambda_1^2} - \frac{B}{\lambda^2-\lambda_2^2} \qquad (2)$$

The two-term equation of Drude has hitherto customarily been interpreted as equivalent to a summation of partial rotations originating from different

*1 Present address: Faculty of Engineering Science, Osaka University, Toyonaka, Osaka.

1) C. C. Price and M. Osgan, *J. Amer. Chem. Soc.*, **78**, 4787 (1956).

2) T. Tsunetsugu, J. Furukawa and T. Fueno, Preprint of 16th Symposium of Polymer Chemistry, Japan (1967), p. 402.

3) T. Hirano, S. Akutsu and T. Tsuruta, Preprint of 17th Symposium of Polymer Chemistry, Japan (1968), p. 1121; *J. Makromol. Sci.*, **A3**, 315 (1969).

4) M. Goodmann and M. Fried, *J. Amer. Chem. Soc.*, **89**, 1264 (1967).

5) J. Y. Cassim and E. Taylor, *Biophys. J.*, **5**, 553 (1965).

TABLE 1. OPTICAL ROTATIONS OF POLY(PROPYLENE OXIDE) IN VARIOUS SOLVENTS

Solvent	$[\alpha]_D$	$\frac{3[\alpha]_D}{n_D^2+2}$	Solvent	$[\alpha]_D$	$\frac{3[\alpha]_D}{n_D^2+2}$
A Benzene	−25.0	−17.6	R Tetrahydrofuran	+18.2	+13.7
B *N,N*-Dimethylaniline	−25.0	−16.9	S Ethylacetate	+13.6	+10.5
C Anisole	−25.5	−17.8	T *N,N*-Dimethylformamide	x	x
D Tetrachloroethylene	−9.3	−6.5	U Dimethylsulfoxide	x	x
E Carbon disulfide	−49.3	−31.8	V Cyclohexane	x	x
F Chlorobenzene	−24.0	−16.6	W Aniline	−15.4	−10.3
G Carbon tetrachloride	−7.4	−5.3	X Benzonitrile	−18.9	−13.1
H Hexamethylphosphoric triamide	+14.8	+10.8	Y Chloroform	+18.0	+13.2
I Pyridine	−19.8	−13.9	Z Acetone	x	x
J *p*-Dioxane	+9.6	+7.2	a Ethanol	x	x
K *o*-Nitroanisole	—	—	b Cyclohexanone	+15.3	+11.2
L Diethyl ether	x	x	d Methanol	x	x
M Triethylamine	x	x	e Acetonitrile	x	x
N Nitrobenzene	−18.8	−12.8	f 1,2-Dichloroethane	+4.8	+3.5
O Methylene iodide	—	—	g Methylene chloride	+6.0	+4.5
P *n*-Pentane	x	x	h Nitromethane	x	x
Q *N*-Methylacetamide	—	—	i Acetic acid	—	—
			j Water	x	x

——: Not determined.
x: Insoluble.

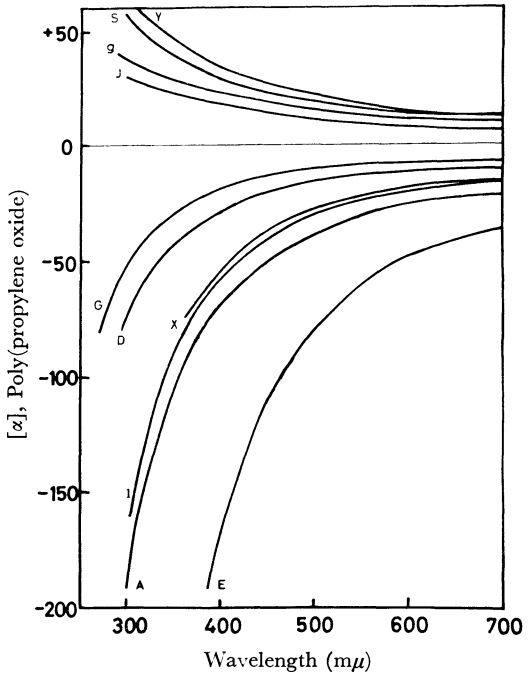

Fig. 1. The optical rotatory dispersion curves of poly(propylene oxide) in various solvents. The symbols appended to the curves indicate the solvents listed in Table 1.

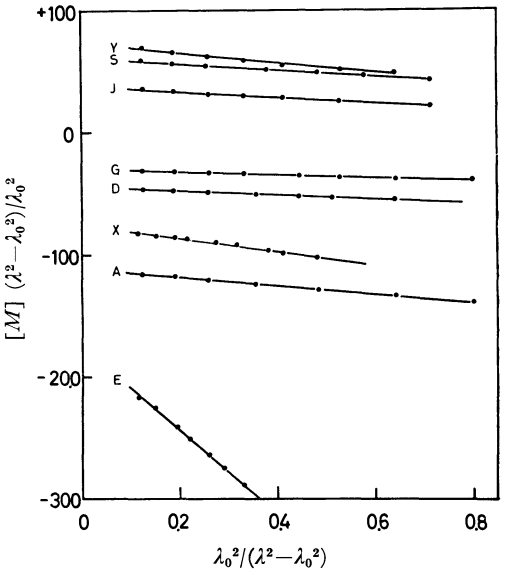

Fig. 2. Moffitt-type plots of the dispersion curves of Fig. 1. The symbols appended to the curves indicate the solvents listed in Table 1.

optical asymmetries of molecules. However, it is known that even the optical dispersions of several amino acids, which have only one asymmetric carbon, fit the two-term equation.[6] We thus feel it necessary to reconsider physical meanings underlying equations (1) and (2).

Let us briefly outline the fundamental logic necessary for understanding optical rotatory dis-

6) L. I. Katzin and E. Gulyas, *J. Amer. Chem. Soc.*, **86**, 1655 (1964).

Table 2. The best fitted λ_0 values for figs. 2 and 3

Solute		Solvent	λ_0 (mμ)
Poly(propylene oxide)	Y	Chloroform	150
	S	Ethyl acetate	200
	J	Dioxane	130
	G	Carbon tetrachloride	160
	D	Tetrachloroethylene	200
	X	Benzonitrile	230
	A	Benzene	210
	E	Carbon disulfide	150
Propylene oxide	A	Benzene	180
	J	Dioxane	160
	V	Cyclohexane	180
	d	Methanol	165
	j	Water	155

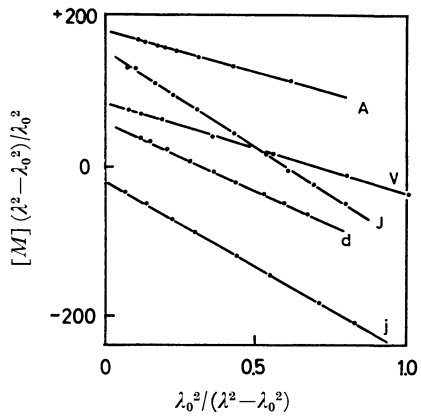

Fig. 3. Moffitt-type plots of optically active propylene oxide in various solvents. The symbols appended to the curves indicate the solvents listed in Table 1.

persion. Theoretical interpretation of the optical rotation owes much to Fresnel's equation

$$\alpha = \frac{\pi}{\lambda} x(n_R - n_L) \tag{3}$$

where α is the optical rotation expressed in the radian scale, x is the optical path length, and n_R and n_L are the refractive indexes of the right- and left-handed circular polarized lights, respectively. It is known that the refractive indexes themselves are subject to dispersion, as may be represented, for example, by the Ketteler-Helmholtz equation (4) or the Sellmeier equation (5).[7]

$$n^2 = a + \sum_m \frac{b_m}{\lambda^2 - \lambda_m^2} \tag{4}$$

$$n^2 = 1 + \sum_i \frac{A_i}{\lambda^2 - \lambda_i^2} \tag{5}$$

Quantum-mechanical treatments[8] of the refraction support the form of Eq. (4).

From Eqs. (3) and (5), coupled with suitable approximations, we may derive Drude's many-term equation[7]

$$[\alpha] = \sum_i \left(\frac{A_{iR}}{\lambda^2 - \lambda_{iR}^2} - \frac{A_{iL}}{\lambda^2 - \lambda_{iL}^2} \right) \tag{6}$$

In short, the optical rotatory dispersion can be interpreted as a difference in the refractive dispersions of the two polarized light beams. Hence, an "anomalous" dispersion that does not conform to Drude's one-term equation does not suggest that there exist more than one type of asymmetric center in the system under examination. This conclusion finds strong support in our previous demonstration that even monomeric R-propylene oxide, which has only asymmetric center, exhibits an anomalous dispersion.[9]

We now inquire why each term of Drude's equation should depend on solvent. According to the dielectric theory,[10] it is considered that, in a non-spherical cavity field which is surrounded by partially oriented solvent, both polarization and polarizability tensor of solute are transformed by change of solvent. This in turn will effect a change in the difference between the refractive indexes of the right- and left-handed circular polarized lights. The change will usually be very small but large enough to influence the optical rotation which may be calculated from equation (3). In the case of quartz,[7] for example, the difference in refractive indexes at 589 mμ is calculated from its optical

7) P. Drude, "The Theory of Optics," translated edition, Longmans Green and Co. (1920), Chapter 6.

8) J. H. Van Vleck, "The Theory of Electronic and Magnetic Susceptibilities," Oxford University Press, Oxford (1932), Chapter 8.

9) Y. Kumata, J. Furukawa and T. Fueno, This Bulletin, **43**, 3920 (1970).

10) a) K. Higashi, *Bull. Inst. Phys. Chem. Res.*, **14**, 146 (1935). b) H. Frölich, "Theory of Dielectrics," Oxford at the Clarendon Press (1949), Chapters 2 and 3.

rotation ($[\alpha]_D=2170°$) to be 0.000071, so that the variation in the refractive index difference by 0.00001 should lead to a variation in $[\alpha]_D$ amounting to *ca.* 310°. In some cases, the influence of solvent on polarization and polarizability of solute may become complicated to cause a change even in the direction of optical rotation.

It is difficult to express the shape of cavity and the degree of orientation by numeral parameters. Thus we will examine the effects of solvent on the optical rotation only qualitatively in terms of some empirical polarity parameter of solvents.

In Fig. 4 are shown the relations of the rotivities of propylene oxide and poly(propylene oxide) with the solubility parameter of solvents. Here, a rotivity is described by the equation[11]

$$\text{rotivity} = \frac{[\alpha]_D}{n_D^2+2} \qquad (7)$$

According to Herbandson *et al.*, the solubility parameter is a kind of polarity parameter of solvents.[12]

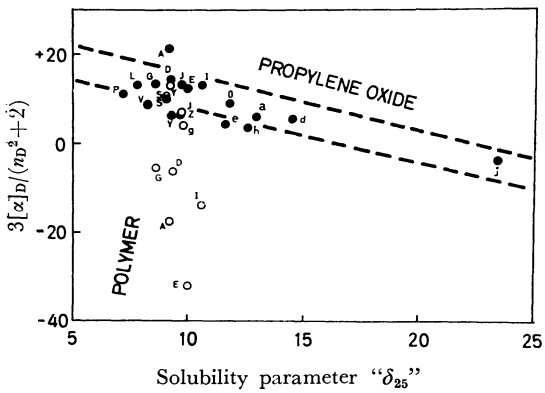

Fig. 4. Plots of the optical rotations of R-propylene oxide and its polymer measured in various solvents against the solubility parameter of the solvents. The symbols attached to the plots indicate the solvents listed in Table 1.

It may be seen in Fig. 4 that the rotivity of the monomer is dependent on the solubility parameter of solvents just in the same manner as it depended on various solvent polarity parameters.[9]

The rotivity of the polymer, on the other hand, appears not to be related with the solubility parameter in any simple manner. However, because the rotivities themselves of the monomer and polymer observed in various solvents are roughly correlated with each other as may be seen in Fig. 5. The polymer rotivity might increase with increasing solubility parameter of solvents, in contrast to the monomer rotivity.

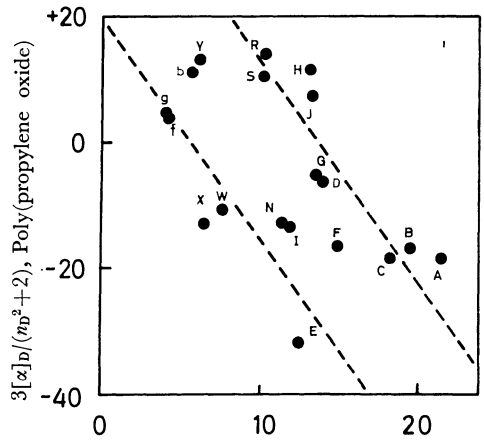

Fig. 5. The rotivity of polypropylene oxide *vs.* that of propylene oxide. The symbols attached to the plots indicate the solvents listed in Table 1.

In a solvent having a large solubility parameter, our polymer is hardly soluble and is aggregated. However, the variation of rotatory direction would not be due to the aggregated conformation, because even propylene oxide which has a rigid skeltal structure is apparently subject to variation in rotatory power in varying solvents. A similar situation is reported in isofenchon,[13] conformation of which is also difficult to change because of its rigid bicyclic ring structure.

Moreover, we found a poly(propylene oxide) film casted from the polymer melt to have a large negative rotation; the α_D value observed for a polymer film of 0.04 mm in thickness being $-1.5°$, a value which leads to a specific rotation of *ca.* $-2000°$. The specific rotation observed is far greater in magnitude than that reported by Hirano *et al.* for a film casted from solution. The different results are probably because our film was formed with polymer molecules highly oriented as in a liquid crystal.

In conclusion, the variation in the rotatory dispersion of poly(propylene oxide) with solvent can be interpreted, at least partially, as a result of the different variations of the refractive indexes toward the right- and left-handed circular polarized lights. The dispersions of the refractive indexes toward the two polarized light beams probably are influenced in a different way by the so-called cavity field which is induced by partially oriented polar solvents.

The authors are grateful to Mr. Ikuo Morino for assistance in the numerical analysis of the dispersion curves.

11) R. Gans, *Z. Phys.*, **27**, 164 (1924); *Ann. Phys. Leipzig*, (4), **79**, 547 (1926).

12) H. F. Herbrandson and F. R. Neufeld, *J. Org. Chem.*, **31**, 1140 (1966).

13) H. P. Gervais and A. Rassat, *Bull. Soc. Chim. Fr.*, **1961**, 743.

BULLETIN OF THE CHEMICAL SOCIETY OF JAPAN VOL. 43 3667—3671 (1970)

Surface Activities of Nonionic Polymeric Surfactants

Masao NAKAMURA*1 and Tsunetaka SASAKI

Department of Chemistry, Faculty of Science, Tokyo Metropolitan University, Setagaya, Tokyo

(Received April 6, 1970)

The relationship between surface activity and molecular structure has been studied for the nonionic polymeric surfactants which have 2,3,4 or 6 branches of polypropylene glycol-polyethylene glycol (PPG-PEG) chain in their molecules. A linear relation, $1/\Delta\gamma = A + B \cdot x/y$ has been found to hold for each series, where $\Delta\gamma$ is the surface tension depression of surfactant solution of a given concentration from that of water, x/y is the molecular structure index, in which x is the weight percent of PEG group in a molecule and y is the molar weight of PPG part, and A and B are constatns. Constant A, being equal to 0.025 cm/dyn, is independent of the concentration and the number of PPG-PEG branches and corresponds to the reciprocal of surface tension lowering of an aqueous solution of infinitely large PPG polymer. Constant B decreases linearly with the logarithm of molar concentration, and increases with the number of branches. It also depends on the hydrophilic nature of the central group of molecule.

Recently, numerous nonionic surfactants have been prepared for various practical purposes, and the selection of surfactant has become much simpler by application of the HLB system proposed by Griffin.[1] Studies have been made on the relation between the HLB value and the molecular constitution of nonionic surfactants.[2] However, the relation between molecular structure and surface activity is not yet clear.

As regards nonionic surfactants, block copolymer (PPG-PEG) composed of polypropylene glycol (PPG) and polyethylene glycol (PEG) has recently attracted attention in relation to theoretical and practical problems. These surfactants are favorable for studying the relation between molecular structure and surface activity, because a slight difference in nature of the hydrophobic propylene glycol unit (PG) of the PPG group and the hydrophilic ethylene glycol unit (EG) of the PEG group makes a delicate control of surface activity possible by the change of degree of polymerization of PG and EG. In the present study we tried to obtain systematic information on the relation between surface activity and molecular structure for this type of polymer surfactants, from the study of surface tension lowering of the solution.

Experimental

Materials. PPG-PEG type of surfactants employed in the present study are of the following molecular structure:

"Pluronic" m, n (2-branch series)

$$HO(CH_2CH_2O)_{n/2}(\overset{\displaystyle CH_3}{\overset{|}{C}}HCH_2O)_m(CH_2CH_2O)_{n/2}H$$

"Trinic" m, n (3-branch series)

$$N{\equiv}[CH_2CH_2O(\overset{\displaystyle CH_3}{\overset{|}{C}}HCH_2O)_{m/3}(CH_2CH_2O)_{n/3}H]_3$$

"Tetronic" m, n (4-branch series)

$$\begin{array}{l}[H(OCH_2CH_2)_{n/4}(OCH_2\overset{\displaystyle CH_3}{\overset{|}{C}}H)_{m/4}]_2{=}NCH_2\\ \qquad\qquad\qquad\qquad\qquad\qquad\quad |\\ [H(OCH_2CH_2)_{n/4}(OCH_2\overset{\displaystyle CH_3}{\overset{|}{C}}H)_{m/4}]_2{=}NCH_2\end{array}$$

"Hexonic" m, n (6-branch series)

$$C_6H_8O_6[(\overset{\displaystyle CH_3}{\overset{|}{C}}HCH_2O)_{m/6}(CH_2CH_2O)_{n/6}H]_6$$

in which m and n are the average degrees of polymerization of PG and EG, respectively. The Pluronic and Tetronic series were obtained from Asahi Denka Industry Co., and the rest from Nihon Surfactant Industry Co. The Trinic, Tetronic and Hexonic series may be regarded as having 3, 4 and 6 branches of PPG-PEG chains of equal average length in respective molecules and the Pluronic series is conventionally seen to have two branches. The Hexonic series is the ether derivative of sorbitol. The surfactants investigated are listed in Table 1.

Polypropylene glycols, glycerine polyoxypropylene ethers and trimethylolpropane polyoxypropylene ethers of molecular weights ranging from 260 to 2500 were used as samples having no hydrophilic PEG group.

*1 Present address: Department of Chemistry, Faculty of Science, Tokai University, Hiratsuka, Kanagawa.

1) W. C. Griffin, *J. Soc. Cosmet. Chem.*, **1**, 311 (1949).

2) W. C. Griffin, *Soap, Sanit. Chem.*, **27**, No. 11, 128 (1951); *Amer. Perfumer*, **65**, No. 5, 26 (1955). J. T. Davies, *Proc. 2nd Intern. Congr. Surface Activity*, **1**, 426 (1957).

TABLE 1. THE POLYPROPYLENE GLYCOL-POLYETHYLENE GLYCOL (PPG-PEG) BLOCK COPOLYMER SURFACTANTS, THEIR MOLECULAR STRUCTURE INDICES (x/y) AND EQUILIBRIUM SURFACE TENSIONS (γ_∞) OF AQUEOUS SOLUTIONS AT 25.8°C

Series	Trade No.	m	n	x/y	γ_∞ (dyn/cm)		
					1×10^{-4} (mol/l)	1×10^{-5} (mol/l)	1×10^{-6} (mol/l)
Pluronic (2-branch)	F-88	40	300	0.0366		47.4	49.1
	F-68	28	210	0.0523	46.7	47.3	50.1
	F-38	16	120	0.0916	51.8	55.8	59.7
	L-64	28	31	0.0164	36.0	39.0	41.0
	L-62	28	13	0.0283	39.3	42.1	47.5
Trinic (3-branch)	20.30	20	30	0.0384	46.0	50.6	54.5
	20.50	20	50	0.0479	46.6	51.4	57.3
	20.100	20	100	0.0589		53.9	51.1
	20.150	20	150	0.0638	49.4	54.6	56.2
	20.190	20	190	0.0661		54.1	59.2
	33.100	33	100	0.0330	45.4	48.0	
	33.150	33	150	0.0369	45.3	49.4	51.5
	50.30	50	30	0.0100	36.1	37.8	41.0
	50.100	50	100	0.0194	40.2	42.9	46.3
	50.150	50	150	0.0224	43.3	45.3	48.1
	50.200	50	200	0.0243	44.3	46.3	49.4
	50.300	50	300	0.0266	46.6	48.9	51.3
Tetronic (4-branch)	304	12	14	0.0641	48.5	50.2	54.1
	501	29	7	0.0086	37.5	39.0	42.3
	504	29	32	0.0263	42.4	44.4	47.0
	508	29	217	0.0498	50.5	52.5	54.0
	701	46	11	0.0054	33.2	34.9	37.3
	702	46	20	0.0091	34.6	36.6	37.9
	707	46	182	0.0277	46.5	48.7	51.1
	904	69	74	0.0111	35.5	36.5	39.3
	908	69	501	0.0211	40.7	46.0	53.0
Hexonic (6-branch)	6000.30	91	30	0.0030			33.6
	6000.60	91	60	0.0051		33.2	34.8
	6000.120	91	120	0.0078	33.3	33.6	36.8

These samples were also obtained from Asahi Denka Industry Co.

In order to remove water and impurities having low boiling points, all the samples had been vacuum dried for about 48 hr until their weights became constant at room temperature. Solutions were prepared immediately after purification.

Aqueous solutions of 1×10^{-4}, 1×10^{-5} and 1×10^{-6} mol/l were made by dissolving the substances in water which had been obtained by refluxing a solution of $KMnO_4$ and NaOH in ion-exchanged water for about 15 hr in a borosilicate glass apparatus and then distilling.

Method. The equilibrium surface tension lowering from pure water was measured and taken as a parameter of surface activity. Since the surface tension of an aqueous surfactant solution of a concentration below the critical micelle concentration usually changes gradually over a long period after the surface is freshly formed,[3] a method should be adopted which allows a continuous measurement over a long period with minimum disturbance of the system under examination. For this purpose, a modified Wilhelmy plate method was used.[4]

The vessel containing the solution was a Petri-dish of 6.5 cm in diameter and 1.5 cm in depth, the edge of which was coated smoothly with paraffin for the purpose of bringing an aqueous surface level higher than the rim of the vessel and for avoiding contamination creeping in from the outer wall.

The solution was introduced into the vessel immediately after preparation. After about 1 hr a fresh surface was formed by sweeping off the surface of the solution in the vessel with a paraffin-coated glass barrier in order to keep the bulk aging effects constant. Surface tension was measured with time about 1 min after the sweep of the aqueous surface. Throughout the measurement, the temperature was controlled to 25.8 ± 0.2°C in an air thermostat, which also served to prevent evaporation.

3) G. C. Nutting, F. A. Long and W. D. Harkins, *J. Amer. Chem. Soc.*, **62**, 1496 (1940). K. L. Sutherland, *Aust. J. Chem.*, **12**, 1 (1959).

4) M. Nakamura and T. Sasaki, *J. Sci. Instrum.*, **44**, 855 (1967).

Results and Discussion

It was confirmed that for all surfactant solutions the surface tension generally decreases with time and does not attain an equilibrium value even 120 min after the formation of a fresh surface, as illustrated by Tetronic 46, 20 in Fig. 1. Concerning

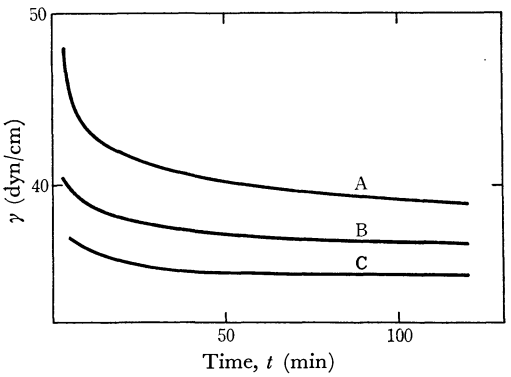

Fig. 1. Surface tension (γ) of the aqueous solutions of Tetronic 46, 20.
Concentration: A, 1×10^{-6}; B, 1×10^{-5}; C, 1×10^{-4} mol/l

the time dependence of surface tension of surfactant solution, some empirical relations have been reported: Lange[5] used the equation

$$\gamma = \gamma_0 - (\gamma_0-\gamma_\infty)/(b/t^{1/2}-1) \quad (1)$$

and Boutaric and Berthier[6]

$$\gamma = \gamma_\infty + (\gamma_0-\gamma_\infty)e^{-\alpha t}. \quad (2)$$

The present authors propose another equation of the following type

$$\gamma = \gamma_\infty + a/t - b/t^2. \quad (3)$$

In the above three equations, γ and γ_∞ are the surface tension of a solution at time t and at equilibrium respectively, γ_0 that of the solvent, and a, b and α are constants. To evaluate γ_∞, Eq. (3) is transformed into

$$t\cdot\frac{d\gamma}{dt} + 2\gamma = 2\gamma_\infty + a/t \quad (4)$$

and $t\cdot d\gamma/dt+2\gamma$ is plotted against $1/t$, $t\cdot d\gamma/dt$ being graphically obtained from the $\gamma-t$ plot. The extrapolated value of $t\cdot d\gamma/dt+2\gamma$ at $1/t=0$ gives $2\gamma_\infty$ as Fig. 2 shows. Table 1 shows γ_∞, the values thus obtained for the surfactants studied. The value $\Delta\gamma=\gamma_0-\gamma_\infty$ is taken as a measure of surface activity, where $\gamma_0=71.8$ dyn/cm is the surface tension of water at 25.8°C. A linear relationship is found to hold between the reciprocal of $\Delta\gamma$ for each concentration and the molecular structure index x/y, as

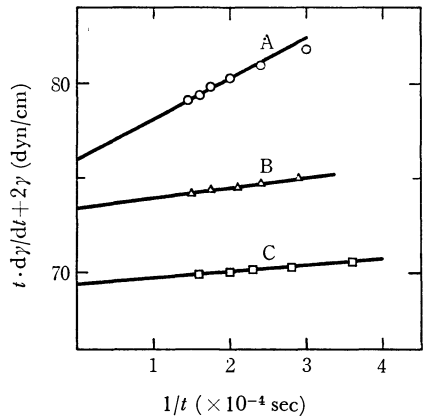

Fig. 2. $t\cdot d\gamma/dt+2\gamma$ *vs.* $1/t$ plot for Tetronic 46, 20.
Concentration: A, 1×10^{-6}; B, 1×10^{-5}; C, 1×10^{-4} mol/l

shown in Fig. 3, where x is the weight percent of hydrophilic PEG group in the molecule and y is the molar weight of PPG part. This plot is well expressed by

$$1/\Delta\gamma = A + B\cdot x/y, \quad (5)$$

where A and B are constants. In Fig. 3, plots scatter in the region of large values of $1/\Delta\gamma$ due to the small values of $\Delta\gamma$ observed. Constant A which is equal to 0.025 cm/dyn turned out to be independent of the concentration and the number of PPG-PEG branches. It depends only on the nature of hydrophobic group in a polymer chain, in this case PPG, as will be mentioned later. The value B was found to depend on both the concentration and the number of PPG-PEG branches.

Constant B, when compared at the same concentration, is indistinguishable with respect to 3- and 4-branch series, while the value for 2-branch series is slightly smaller than the value for 3- and 4-branch series. Further it was found that B decreases linearly with the logarithm of concentration C for 2-, 3- and 4-branch series as shown in Fig. 4. Thus we obtain the relations

$$B = -1.1\log C - 0.41 \quad (6)$$

for 2-branch series and

$$B = -1.3\log C - 0.45 \quad (7)$$

for 3- and 4-branch series, where C is expressed in mol/l. By substituting Eqs. (6) and (7) into Eq. (5), the surface tension lowering $\Delta\gamma$ can be expressed as a function of the structure index x/y and the concentration C for these series: The relation for 2-branch series is

$$1/\Delta\gamma = 0.025 - (1.1\log C + 0.41)x/y \quad (8)$$

and that for 3- and 4-branch series is

$$1/\Delta\gamma = 0.025 - (1.3\log C + 0.45)x/y \quad (9)$$

In these equations $\Delta\gamma$ can be taken as the measure of surface activity, at a given concentration C.

5) H. Lange, *Proc. 3rd Intern. Congr. Surface Activity*, **1**, 279 (1960).
6) A. Boutaric and P. Berthier, *J. Chim. Phys.*, **36**, 1 (1939).

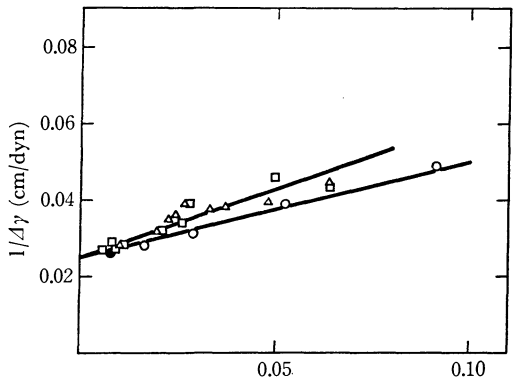

Fig. 3(a)

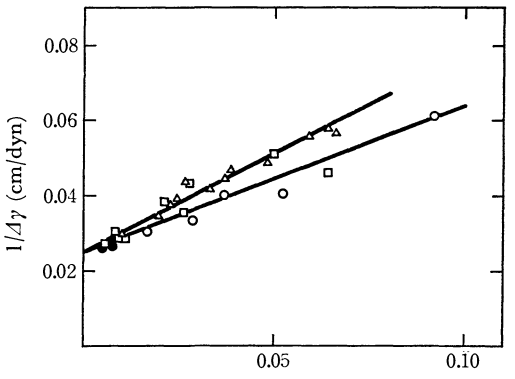

Fig. 3(b)

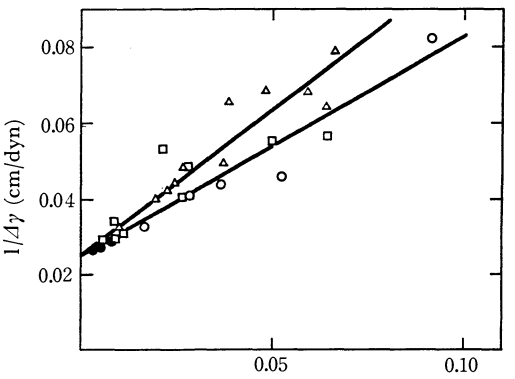

Fig. 3(c)

Fig. 3. Surface tension lowering ($\Delta\gamma$) *vs.* molecular structure index (x/y) plot for Pluronic (○), Trinic (△), Tetronic (□) and Hexonic (●) (2-, 3-, 4- and 6-branch) series.
Concentration: (a), 1×10^{-4}; (b), 1×10^{-5}; (c), 1×10^{-6} mol/l

As to 6-branch series, since all samples employed are those of small values of the molecular structure index x/y, it is difficult to confirm the applicability of Eq. (5) and to obtain the exact values of constant B. But the value $1/\Delta\gamma$ is seen to approach 0.025 cm/dyn, the value of constant A in Eq. (5),with the decrease of x/y for the substance of this series.

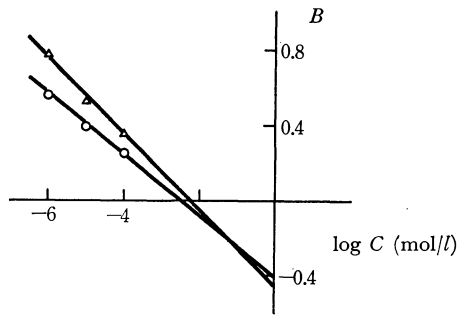

Fig. 4. Constant B *vs.* concentration C plot for Tetronic (4-branch), Trinic (3-branch) (both △) and Pluronic (2-branch) (○) series.

Constant A should correspond to $1/\Delta\gamma$ for a polymer having no hydrophilic PEG group or having PEG groups with hydrophobic PPG groups of infinitely high molecular weight. The surface activity of PPG is considered to depend on molecular weight, since the surface tension of aqueous PPG solution has been reported to depend on the molecular weight.[7] To study further details of the constants A and B, the surface tensions of polypropylene glycol (PPG) series, glycerine polyoxypropylene ether (GP) series, and trimethylolpropane polyoxypropylene ether (TP) series, as the samples having no PEG groups, were measured under the same conditions as for the above surfactants. The relation between the surface tension lowering $\Delta\gamma$ thus obtained and the molar weight y of PPG or PPG part of the molecule for each series is shown in Fig. 5. No distinction is seen between the surface activity of PPG

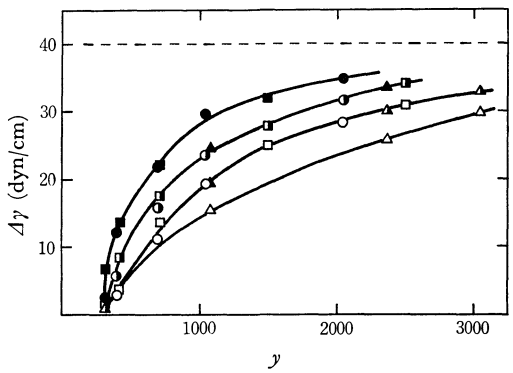

Fig. 5. Surface tension lowering ($\Delta\gamma$) *vs.* molar weight (y) plot.

	1×10^{-4}	1×10^{-5}	1×10^{-6} mol/l
PPG	●	◑	○
GP	▲	◭	△
TP	■	◨	□

7) Y. Nemoto, H. Funahashi, K. Kunugi and M. Kashima, *Yukagaku*, **14**, 246 (1965).

and TP series and the less surface activity of GP series, where the surface tension of GP is equal to that of the PPG or TP solution of the concentration, being about one tenth of the GP solution.

The fact that the GP series is less surface active than the TP series shows some other factors than those mentioned above affecting surface activity. It is evident that these two series differ only in the central group of their molecules. Therefore it may be presumed that the surface activity of polymeric surfactant is also affected by the nature of its central group to which polymer branches are attached. It is conceivable that glycerine is more hydrophilic than trimethylolpropane so that GP is less surface active then TP. The fact that the plots of PPG and TP series, differing in the number of branches, fall on the same curve suggests the effect of central groups on the surface activity. Thus, it may be concluded that the surface activity decreases with either the increase of branching or the degree of hydrophile of the central group.

It is seen in Fig. 5 that when the molecular weight increases towards infinity, the surface tension lowering is seen to approach a constant value (broken line in Fig. 5), 40 dyn/cm, for each curve; the value taken to be equal to $1/A$ in Eq. (5). This may indicate the constant A being independent of the value of x under the condition of $y=\infty$, and it can naturally be concluded that Eq. (5) can not be applied exactly if the value y is too small; a small value of y might give a larger value of A, as presumed from Fig. 5.

From the results of the above PPG polymers and their ethers it may be quite reasonable to consider that the difference of B in Eqs. (6) and (7) depends not only on the number of branches as was mentioned in the earlier section but also on the nature of the central groups. The fact that both the molecules of 3- and 4-branch series tend to ionize to a certain extent, while 2-branch series has no such ionizing nitrogen atom, can be taken at least as the cause of the difference in surface activity. The fact that 3- and 4-branch series show a similar surface activity (Eq. (9)) in spite of the difference in branching suggests a more hydrophobic nature of the central group of the latter series, since the increase in number of branches from 3 to 4 should be balanced with the stronger hydrophobic nature of the central group of the latter in order to keep the same surface activity.

In conclusion, the surface activities of the nonionic polymeric surfactants of PPG-PEG derivatives type depend upon the ratios of the amount of PPG to that of PEG groups, the molecular weights, the number of branches, and the nature of central group. Constant A in Eq. (5) depends only on the nature of hydrophobic group in polymer chain. In the present case it is the reciprocal of the surface tension lowering of the PPG polymer having a sufficiently large molecular weight. Constant B is in linear relationship with the logarithm of the surfactant concentration; it also depends upon the molecular structure of the surfactant, particularly the number of PPG-PEG branches and the hydrophilic nature of the central group to which they are attached.

BULLETIN OF THE CHEMICAL SOCIETY OF JAPAN VOL. 43 3672—3679 (1970)

The Mechanism of the Reaction between Molecular Hydrogen and the Electron Donor-Acceptor Complexes (1:1 and 1:2) of Various Aromatic Hydrocarbons with Sodium*1

Masaru ICHIKAWA, Mitsuyuki SOMA, Takaharu ONISHI and Kenzi TAMARU

Department of Chemistry, The University of Tokyo, Hongo, Bunkyo-ku, Tokyo

(Received May 16, 1970)

The mechanism of the reaction between molecular hydrogen and the electron donor-acceptor complexes (A^-Na^+ and $A^{=}2Na^+$) of various aromatic hydrocarbons (A) with sodium were studied kinetically and spectroscopically. The relative activity of each electron donor-acceptor (EDA) complex for the hydrogen uptake was associated with its electronic properties, especially with the reduction potential of its anion. It was found that the hydrogen molecule reacts more readily with stronger electron-donating EDA complexes, whose anions have higher reduction potentials. It was also suggested that, on the hydrogen adsorption over the A^-Na^+ and $A^{=}2Na^+$ films (or in their solutions), the corresponding monohydroanion complexes (AH^-Na^+) and NaH were produced as follows:

$$2A^-Na^+ + H_2 = AH^-Na^+NaH + A$$
$$A^{=}2Na^+ + H_2 = AH^-Na^+ + NaH$$

The behavior of AH^-Na^+ was closely correlated with the localization energies of electrons in the anions of the aromatic hydrocarbons.

As has been demonstrated in previous papers, some catalytic reactions, such as the hydrogen exchange reaction of molecular hydrogen[1a] (or acetylene[1b]), the selective hydrogenation of unsaturated hydrocarbons[1c], and the isomerization of butenes[1d], take place readily at room temperature over the electron donor-acceptor (EDA) complexes of some aromatic compounds with strong donors, such as alkali metals, metallocenes, and phenothiazine.

The results obtained by electronic spectroscopy and ESR measurements suggest[2] that these EDA complexes studied are, in general, characterized by having their ionic salt between the anion radical or poly-valent anions of aromatic compounds (A) and the cation radical or cations of donor atoms or molecules (D), which are formed by the charge-transfer as follows:

$$mA + nD = mA^{n-} + nD^{m+} \quad (1)$$
$$n, m = 1 - 4.$$

In the solid state of the EDA complexes, their ion pairs come close to each other, resulting in strong electrostatic interactions.

Such stoichiometric EDA complexes are easily prepared, and various catalytic reactions proceed over their complex films[3a] or in solutions, for instance, for the 1 : 1 and 1 : 2 anthracene-sodium complexes.[3b]

In this investigation the stoichiometric EDA complexes of various aromatic hydrocarbons with sodium were prepared and the kinetics of the uptake of hydrogen was measured on their complex films and in their solutions. The behavior of the hydrogen

*1 A preliminary communication of this paper has been published in *J. Amer. Chem. Soc.*, **91**, 6050 (1969).

1) a) M. Ichikawa, M. Soma, T. Onishi and K. Tamaru, *J. Catal.*, **6**, 336 (1966); *Trans. Faraday Soc.*, **63**, 997, 1215, 2528 (1967); This Bulletin, **40**, 1015, 1294 (1967). b) M. Ichikawa, M. Soma, T. Onishi and K. Tamaru, *J. Phys. Chem.*, **70**, 2069, 3020 (1966), *Tetrahedron Lett.*, **47**, **1966**, 5841, *Trans. Faraday Soc.*, **63**, 997, 1215 (1967). c) M. Ichikawa, M. Soma, T. Onishi and K. Tamaru, *J. Catal.*, **9**, 418 (1968); M. Sudo, M. Ichikawa, M. Soma, T. Onishi and K. Tamaru, *J. Phys. Chem.*, **73**, 1174 (1969); M. Ichikawa, M. Sudo, M. Soma, T. Onishi and K. Tamaru, *J. Amer. Chem. Soc.*, **91**, 1538 (1969). d) M. Ichikawa, M. Soma, T. Onishi and K. Tamaru, *Trans. Faraday Soc.*, **63**, 2012 (1967).

2) M. Szwarc, *Progr. Phys. Org. Chem.*, **6**, 323 (1968); R. Taube, *Z. Chem.*, **6**, 8 (1966); G. J. Hoijtink and P. J. Zandstra, *Mol. Phys.*, **3**, 371 (1960); P. H. Rieger, I. Bernal, W. H. Reinmuth and G. K. Fraenkel, *J. Amer. Chem. Soc.*, **85**, 683 (1963); N. Hirota, *J. Amer. Chem. Soc.*, **90**, 3603 (1968).

3) a) M. Ichikawa, M. Soma, T. Onishi and K. Tamaru, This Bulletin, **41**, 1739 (1968); *Z. Phys. Chem., N. F.*, **68**, 309 (1969); N. Wakayama and H. Inokuchi, *J. Catal.*, **11**, 143 (1968); **15**, 417 (1969); N. Wakayama, Y. Mori and H. Inokuchi, *J. Catal.*, **12**, 15 (1968). b) S. Tanaka, M. Ichikawa, S. Naito, M. Soma, T. Onishi and K. Tamaru, This Bulletin, **41**, 1739 (1968); M. Ichikawa, S. Tanaka, S. Naito, M. Soma, T. Onishi and K. Tamaru, *Trans. Faraday Soc.*, in press.

absorbed by the EDA complexes was also studied by means of UV, NMR, and ESR spectrometries.

Experimental

The stoichiometric EDA (1 : 1 and 1 : 2) complexes of aromatic hydrocarbons with sodium were prepared in a manner similar to that described previously.[3a,3b]

A dry tetrahydrofuran (THF) or dimethoxyethane (DME) was allowed to run into a reaction vessel, in which purified aromatic hydrocarbon (*ca.* 3×10^{-3} mol) and distilled sodium (in excess) had previously been placed. After the reaction vessel had then been shaken at room temperature for a long time, a deep-colored complex solution was obtained. The 1 : 1 complexes of anthracene, pyrene, perylene, tetracene, and 1,2-benzanthracene were prepared by controlling the reaction between each aromatic hydrocarbon and sodium. After the identification of their compositions by means of their electronic absorption spectra,[2] the complex solutions were introduced into the reaction cell through a glass filter.*2 The reaction-cell was equipped with a closed circulating system (the dead space of the reaction system was *ca.* 170 m*l*). The complex films were deposited on the glass wall or on silica wool by evaporating the solvent.

The complex films were evacuated further for a day at 90°C prior to the experiments. The complexes of weaker acceptors, such as biphenyl and naphthalene, were partly decomposed into their components by evacuation at 90°C, but other complex films of aromatic hydrocarbons with sodium were comparatively stable at higher temperatures, such as 120°C.

The uptake of hydrogen over the complex films and in solutions was determined by PVT measurements at a constant pressure or a constant volume.

The properties of the EDA complexes which adsorbed hydrogen were studied by the UV (HITACHI-spectrophotometer (EPS-2)), esr- (Varian Associates epr spectrometer), and NMR- (100 MHz high-resolution nmr-spectrometer (JEOL-JNR-4H100)) techniques.

Similar experiments were carried out for their complex solutions in THF or DME by introducing hydrogen.

Results and Discussion

I. The Kinetics of Hydrogen Adsorption over A^-Na^+ and $A^=2Na^+$ Films of Various Aromatic Hydrocarbons with Sodium. When hydrogen (10—35 cmHg) was applied to such complex films as biphenyl, naphthalene, pyrene, and phenanthrene with sodium (1 : 1) in the temperature range between 20 and 90°C, a small amount of hydrogen was adsorbed readily in the initial stage of the adsorption; further adsorption then proceeded slowly for several days, as is shown in Fig. 1, where the kinetics of hydrogen adsorption over the phenanthrene$^-$Na$^+$ complex film is presented. At temperatures higher than 60°C, a small amount of neutral acceptor molecules was separated from each

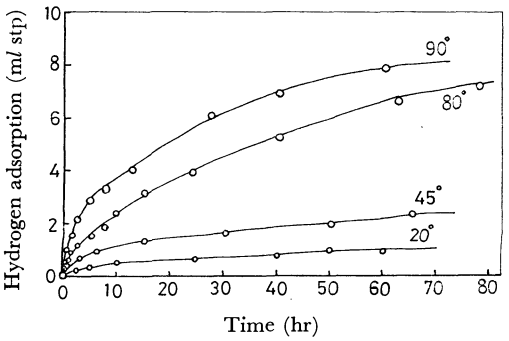

Fig. 1. The kinetics of the hydrogen adsorption over the phenanthrene$^-$Na$^+$ film (3×10^{-3} mol) at P_{H_2}=20 cmHg at the temperatures between 20 and 90°C.

complex film of these 1 : 1 complexes with the progress of the hydrogen adsorption in a manner similar to the case with anthracene$^-$Na$^+$.[4]

The slow adsorption of hydrogen in the later stage continued at higher temperatures and reached the saturation point. Judging from the total amount of hydrogen adsorbed at the saturation point, it may be suggested that the hydrogen uptake took place homogeneously throughout the A^-Na^+ films.

The desorption of hydrogen was very slow, even at higher temperatures such as 90°C; the complexes were partly restored by evacuation at 100°C for 20 hr, and a trace of a neutral molecule was also separated from the reaction systems.

When the phenanthrene$^-$Na$^+$ (3×10^{-3} mol) was deposited over a silica gel,*3 the surface area of which was estimated to be 60 m^2 by the BET method using nitrogen, the hydrogen uptake at the initial stage for the same amount of the complex increased

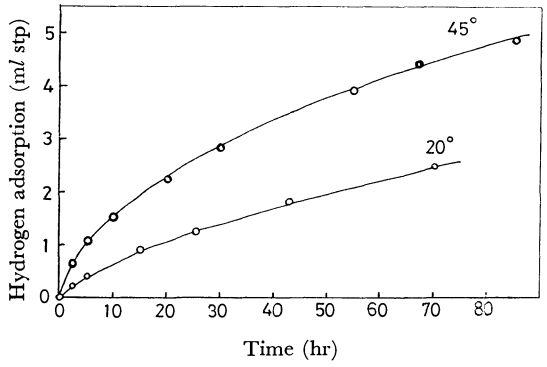

Fig. 2. The kinetics of the hydrogen adsorption on the THF solution of phenanthrene$^-$Na$^+$ (8×10^{-3} mol/50 m*l* of THF) at P_{H_2}=20 cmHg.

*2 The separation of the residual sodium metal was achieved by taking special cape.

4) S. Tanaka, S. Naito, M. Ichikawa, M. Soma, T. Onishi and K. Tamaru, *Trans. Faraday Soc.*, **66**, 976 (1970).

*3 The silica gel was evacuated at 400°C for 20 hr prior to use.

to several times that on the complex film deposited on the glass wall (the surface area was less than 1 m^2) under similar reaction conditions: $P_{H_2}=20$ cmHg, 65°C.

It was demonstrated that the uptake of hydrogen also occurred uniformly on a THF solution of the phenanthrene$^-$Na$^+$ complex, as is shown in Fig. 2, with simple first-order kinetics in the temperature range between 20 and 60°C.

It may, accordingly, be suggested that the slow adsorption in the later stage over the complex films is to be attributed to that hydrogen gas diffused with difficulty into the bulk from the surface of the complex films.

For the 1 : 2 complex films of anthracene,[4] pyrene, perylene, 1,2-benzanthracene, and tetracene with sodium, hydrogen was adsorbed at temperatures of 20 to 140°C with similar kinetics. Hydrogen was readily taken up in the initial stage, but thereafter was adsorbed rather slowly until saturation was reached. The hydrogen desorption from these 1 : 2 complex films took place slowly, but the complexes were restored completely by evacuation at 100°C for 20 hr without any appreciable decomposition of the complexes. It should be noted that only negligible amounts of the neutral molecules or other products were separated from these 1 : 2 complex films throughout the hydrogen adsorption.

The activation energies for the rate of the hydrogen uptake were measured over fresh 1 : 1 and 1 : 2 complex films of various aromatic hydrocarbons; the results are summarized in Table 1. The rates of hydrogen adsorption (V: m*l*/mol hr) listed were observed in the initial stage of the adsorption. The surface areas of all the complex films were found to be almost equal (less than 1 m^2) when the complexes were deposited on the glass wall of the vessel.

Table 1

Compelxes*	Amount of the complexes (mol)	V_{ads} (m*l*/mol hr) $P_{H_2}=20$ cmHg, 80°C	E** (kcal/mol)
Biphenyl$^-$Na$^+$	1.1×10^{-3}	1.8×10^{2}	10
Naphthalene$^-$Na$^+$	3×10^{-3}	3.2×10^{2}	10
Phenanthrene$^-$Na$^+$	3×10^{-3}	6.5×10^{2}	11
Anthracene$^-$Na$^+$	3.8×10^{-3}	1.0×10^{2}	15
Pyrene$^-$Na$^+$	4×10^{-3}	0.43×10^{2}	14
Anthracene$^=$2Na$^+$	5×10^{-3}	12×10^{2}	13
Pyrene$^=$2Na$^+$	4×10^{-3}	3.3×10^{2}	10
Perylene$^=$2Na$^+$	2×10^{-3}	0.38×10^{2}	14
Tetracene$^=$2Na$^+$	2×10^{-3}	0.14×10^{2}	17
Na	3×10^{-2}	negligible	—

* Each complex was deposited over the glass-wall of the reaction vessel (the surface area was less than 1 m^2). The complex formation was almost complete in a film at reaction conditions except the biphenyl$^-$Na$^+$, which exists less than 40%[2] of a given amount of biphenyl at an equilibruium in solution or in a film. The amount of the active biphenyl$^-$Na$^+$ complex was estimated from these consideration.

** The activation energies for the hydrogen adsorption were obtained from the Arrhenius' plots of the inititial rates of hydrogen adsorption (V_{ads}) at the temperatures between 20 and 90°C.

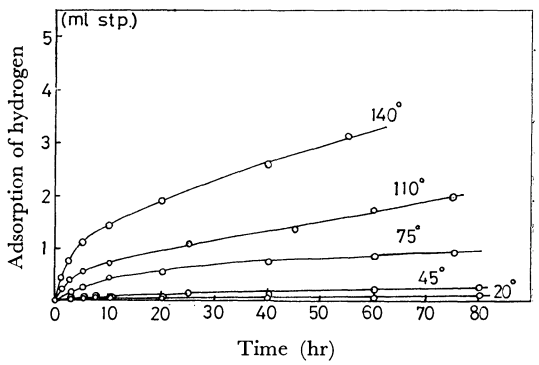

Fig. 3. The kinetics of hydrogen adsorption over the perylene$^=$2Na$^+$ film (1.0×10^{-3} mol, deposited on a silica gel (the surface area was *ca.* 46 m^2)) at $P_{H_2}=27$ cmHg. The dead volume of the reaction system was 168 m*l*.

II. Reactivities of Various EDA Complexes (A$^-$Na$^+$ and A$^=$2Na$^+$) for the Hydrogen Adsorption, and Their Electronic Properties. The rates of the hydrogen uptake were measured over the A$^-$Na$^+$ and A$^=$2Na$^+$ films (*ca.* 3×10^{-3} mol) of each of various aromatic hydrocarbons with sodium, which were deposited over silica gel (the surface area of which was *ca.* 60 m^2) by introducing hydrogen (26cmHg) at temperatures from 20 to 90°C. When the rates of hydrogen adsorption (V: m*l*/mol hr) were plotted against the reduction potentials of the mono- and di-anions of the corresponding aromatic hydrocarbons, a volcano-shape curve was obtained, as is shown in Fig. 4. Their reduction potentials ($-E'$ volt) have been obtained from the potentiometric measurements of Hoijtink and his coworkers'.[5]

5) J. Hoijtink, E. de Boer, P. H. van der Meij and W. P. Weijland, *Rec. Trav. Chim. Pays-Bas.*, **75**, 487 (1956).

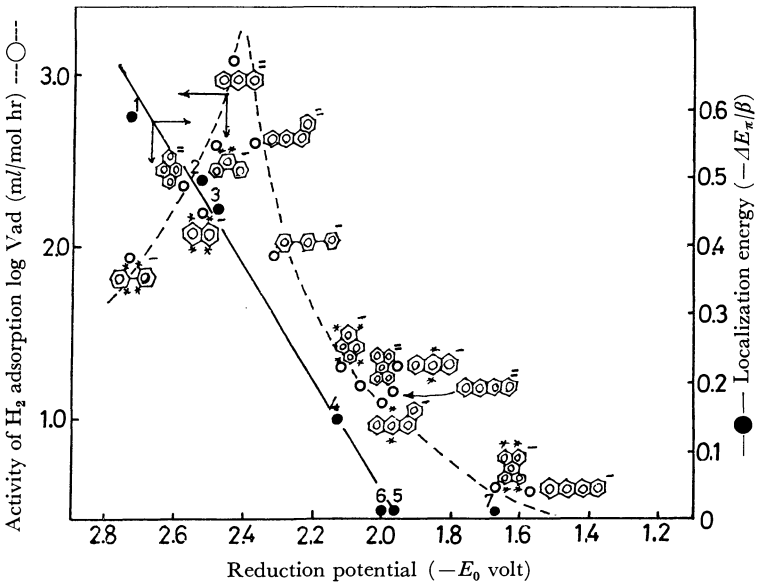

Fig. 4. The plots of the activities of hydrogen adsorption over various mono- and di-anion complex films with sodium against their reduction potentials ($-E_0$ volt), ---○---, and the plot of the localization energies of each acceptor molecules against the reduction potential of their mono-anions, —●—: 1) biphenyl 2) naphthalene 3) phenanthrene 4) pyrene 5) anthracene 6) 1,2-benzanthracene 7) perylene.
The asterisk (*) shows the position of the minimum localization energy in each of the anions of the corresponding aromatic hydrocarbons.

$$A + e \longrightarrow A^- \quad -E_1'$$
$$A^- + e \longrightarrow A^= \quad -E_2'$$

From these results it may be suggested that generally such EDA complexes which contain electron-donating anions with higher reduction potentials react readily with molecular hydrogen to cause a dissociative adsorption of hydrogen.

For the 1 : 1 and 1 : 2 complexes of pyrene, anthracene, 1,2-benzanthracene, perylene, and tetracene with sodium, each of these 1 : 2 complexes was about ten times as active as the corresponding 1 : 1 complex in the uptake of hydrogen. This can be reasonably understood in terms of the higher electron-donating properties of their di-negative ions than those of mono-anions.

It is also interesting to note in Fig. 4 that the activities of the EDA complexes with comparatively weak acceptors such as biphenyl, naphthalene, and phenanthrene, were lower in the hydrogen uptake that were expected from their reduction potentials. These acceptors have characteristically larger localization energies, as is presented in Fig. 4 to the right ordinate, where each localization energy has been calculated by the SCF MO method.[6] Accordingly, their lower activities for the hydrogen adsorption might be due to their difficulty in localizing an unpaired electron at the active position in the anions, in spite of their strong electron-donating properties.

A similar correlation was observed for the relative activities of the solutions of various complexes in connection with the reduction potentials of those anions. When hydrogen (10—45 cmHg) was introduced onto the 1:1 and 1:2 complex solutions (*ca.* 3

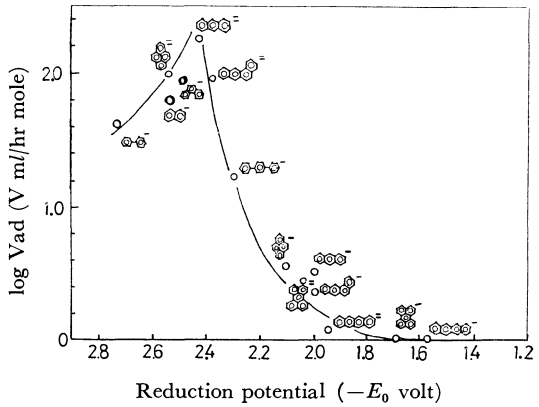

Fig. 5. The plot of the activities of the hydrogen-uptake onto the THF solution of various 1:1 and 1:2 complexes (*ca.* 3×10^{-3} mol/50 m*l* of THF) at 20°C and P_{H_2}=20 cm Hg against the reduction potentials of these anions.

6) G. Dallinga, A. A. V. Stuart, P. J. Smit and E. L. Mackor, *Z. Elektrochem.*, **61**, 1019 (1957).

$\times 10^{-3}$ mol) of biphenyl, naphthalene, phenanthrene, anthracene, 1,2-benzoanthracene, pyrene, perylene, and tetracene with sodium in THF or DME, a considerable amount of hydrogen was adsorbed in the temperature range between 20 and 45°C over 20-hr period. The relative amount of hydrogen uptake by each complex solution in THF at 20°C in 20 hr*4 is plotted in Fig. 5.

For the 1 : 1 complexes of biphenyl, naphthalene and phenanthrene with sodium, these THF solutions were gradually decolorized with the progress hydrogen adsorption, and a considerable amount of NaH was precipitated and almost completely converted in several days to a neutral molecule and dihydro-species.*5

III. The Behavior of Adsorbed Hydrogen over A^-Na^+ and $A^=2Na^+$ Films or Solutions. In order to study the change in the electronic properties of the EDA complexes in reactions with hydrogen, each of the A^-Na^+ and $A^=2Na^+$ films of various aromatic hydrocarbons with sodium was deposited*6 from their THF solutions onto the wall of a quartz cell by evaporating the solvent; hydrogen was then admitted onto their films at the reaction temperatures.

As is shown in Fig. 6a, when hydrogen (10—40 cmHg) was admitted onto the phenanthrene$^-Na^+$ complex films at temperatures from 20 to 90°C, the absorption peak at 620 mμ gradually decreased at 60°C for several hours and new, broad adsorption peaks appeared at 440 and 580 mμ. When the temperature was raised to 90°C, the new peak increased in intensity, while a small amount of neutral phenanthrene was separated. On the other hand, the phenanthrene$^-Na^+$ film, which adsorbed hydrogen sufficiently, was dissolved in THF in an NMR tube. An intense peak appeared at $t=8.73$ ppm in the NMR spectra; it was attributed to that of sodium hydride much as has previously been described.[4]

In addition, when hydrogen was admitted onto the phenanthrene$^-Na^+$ deposited on an ESR tube, the spin concentration of the complex film ($g=2.0036$) decreased markedly and became almost diamagnetic upon hydrogen adsorption at 60°C for several days.

It was also found that, by introducing hydrogen into the phenanthrene$^-Na^+$ solution of THF, a similar absorption spectra newly appeared in the temperature range between 20 and 45°C for several hours, as is shown in Fig. 6b. It should intensity gradually and that a small amount of sodium hydride was precipitated in the solution.

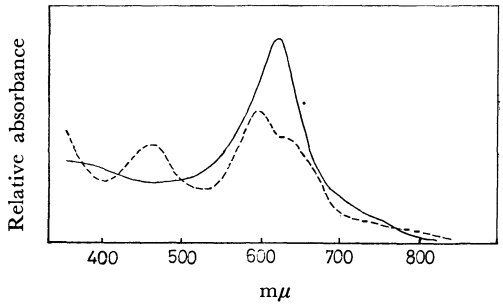

Fig. 6a. The change of the electronic spectra of the phenanthrene$^-Na^+$ film by the hydrogen adsorption. The solid line= that of the phenanthrene$^-Na^+$ film, and the dotted line= that after the hydrogen adsorption on the complex film at 60°C in 20 hr.

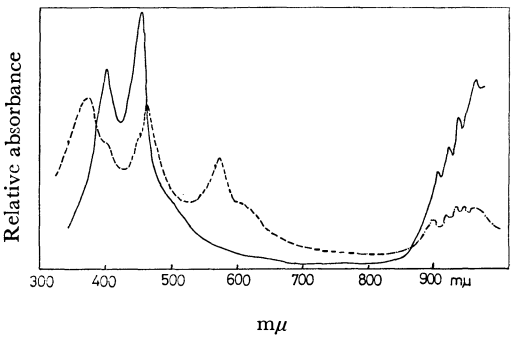

Fig. 6b. The electronic spectra of the THF solution of phenanthrene$^-Na^+$ (———) and after the uptake of the hydrogen at 20°C for 20 hr (--------).

The peaks which newly appeared upon hydrogen adsorption were attributed to the 9-monohydrophenanthrenium anion complex by means of a comparison with those of the 9-monohydrophenanthrenium cation,[7b] as in the case of the 1 : 1 and 1 : 2 anthracene-sodium complexes.[4] These results suggest that hydrogen adsorption proceeded on the phenanthrene$^-Na^+$ film as well as in its solution as follows:

*4 The hydrogen adsorption proceeded in almost first-order kinetics in the initial stage, as is shown in Fig. 2.

*5 After a complete reaction with hydrogen, the THF solutions of these complexes were examined by NMR spectrometry at 20°C.

*6 The electronic absorption spectra of the complex films were comparatively broad and were considerably different from those of the corresponding complex solutions in THF or DME. This change in the spectra occurred reversibly; it is seemingly to be attributed to the formation of the anion dimer in a solid or condensed phase.

7) a) G. Dallinga, E. L. Mackor and A. A. V. Stuart, *Mol. Phys.*, **1**, 123 (1958); E. L. Mackor, G. Dallinga, J. H. Kruizinga and A. Hofstra, *Rec. Trav. Chim. Pays-Bas*, **75**, 836 (1956). b) N. H. Velthorst and G. J. Hoijtink, *J. Amer. Chem. Soc.*, **87**, 4529 (1965).

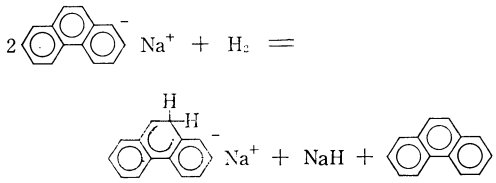

For the 1 : 1 and 1 : 2 complexes of other aromatic hydrocarbons, such as biphenyl, naphthalene, pyrene, anthracene, perylene, 1,2-benzanthracene, and tetracene with sodium, it was found similarly, in the UV, NMR and ESR measurements, that new and characteristic absorption spectra were observed after introducing hydrogen gas onto each of the complex films or THF solutions at temperatures of 20 and 90°C. The results are summarized in Table 2a for the hydrogen adsorption on the complex films and in Table 2b for that on the complex solutions. In Table 2a the positions of the absorption peaks newly appearing upon the hydrogen adsorption, the detection of sodium hydride, and the structures of the monohydroanion complexes (AH^-Na^+)*[7] in the hydrogen-adsorbed species are also presented. In Table 2b there are also the absorption peaks of the carbonium cations (AH^+) and the localization energies (L.E. $= -\Delta E\pi/\beta$) at each carbon atom in a given anion of aromatic hydrocarbons.

These results confirm that the adsorbed hydrogen was combined with the carbon atom of the mono- or di-anion at the position which has the lowest localization energy to form the corresponding monohydroanion complexes (AH^-Na^+), and that NaH was also formed simultaneously with the hydrogen adsorption.

Table 2a (film)

A⁻Na⁺, A2Na⁺	The characteristic absorption peaks (complex films)	(on H_2-ads.)*	The probable structures of AH^-Na^+**	NaH***
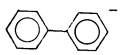	380 mμ	—	—	##
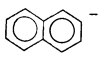	380	450 mμ	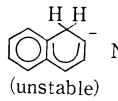 (unstable)	##
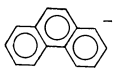	620	{440 {580	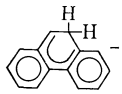	##
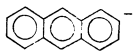	720	420	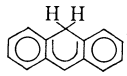	+
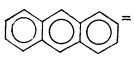	620			##
	500	{430 {520	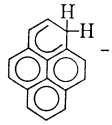	+
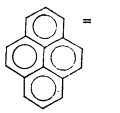	610			##
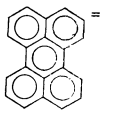	530	470	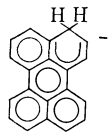	+

* New absorption peaks appeared by the H_2-adsorption on each of these complex films.

** The structures of the AH^-Na^+ in the H_2-adsorbed species were predicted from their characteristic new absorption peaks in comparison with those of the corresponding carbonium ions.[7a,7b]

*** The relative amount of NaH in the H_2-adsorbed species, which was detected by the NMR-spectra at 8.73 ppm: ## very large # large + detectable

*[7] The structures of several monohydroanions have been discussed in comparison with those of the corresponding carbonium ions; *e.g.*, see Ref. 7b.

Table 2b (solution)

A^-Na^+, $A^{=}2Na^+$	new peaks by H_2 ads. (mμ)	AH^-Na^+	$AH^+BF_4^-$*	L.E.** ($-\Delta E/\beta$)
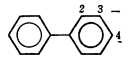 Na^+	425 (s)	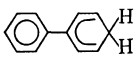 Na^+	380 (s)	2 0.59
				3 0.88
	500 (s)	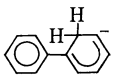 Na^+	445 (s)	4 0.61
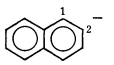 Na^+	435 (s) 465 (w)	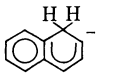 Na^+	390 (s) 280 (w)	1 0.50 2 0.73
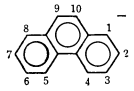 Na^+	360 (s) 450 (s) 580 (w)	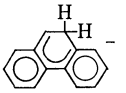 Na^+	280 (s) 410 (s) 520 (s)	4 0.54 3 0.58 2 0.67 1 0.45 9 0.45
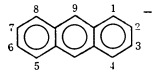 Na^+	432 (vs)	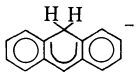 Na^+	408 (vs)	1 0.31
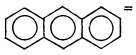 $2Na^+$				2 0.57 9 0.01
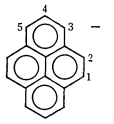 Na^+	430 (vs)	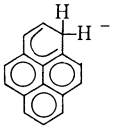 Na^+	385 (s)	3 0.15
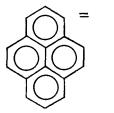 $2Na^+$	540 (s)		460 (s)	1 0.37
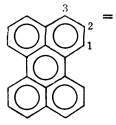 $2Na^+$	460 (s)	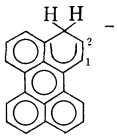 Na^+	410 (s) 600 (s)	3 0.03 1 0.13

* The absorption peaks of the carbonium ions (AH^+) were obtained from the mixed solutions of a given aromatic hydrocarbon(A) and $HF+BF_4$ solution.[7a]

** Localization energy used has been calculated for the corresponding carbonium ions (AH^+): see Ref. 6.

It should be noted here that biphenyl$^-Na^+$ complex in the THF solution slowly changed to monohydro-anion by abstracting hydrogen from the solvent even in the absence of hydrogen gas.

In addition, AH^-Na^+ was also prepared independently by the following reactions in THF and the similar absorption peaks (AH^-Na^+) were observed in the resultant solutions.

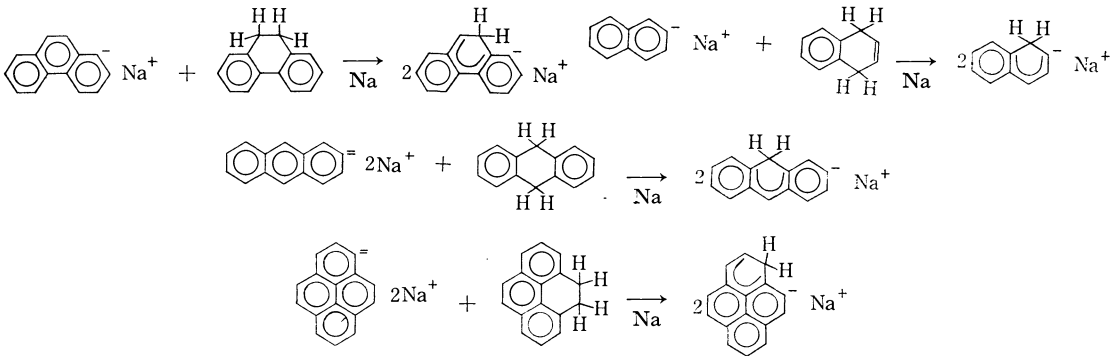

It may also be suggested that the same monohydro-anion complex was produced in the hydrogen adsorption over the A^-Na^+ and $A^=2Na^+$ films and the solutions of pyrene, anthracene,[4] perylene, and 1,2-benzathracene with sodium.

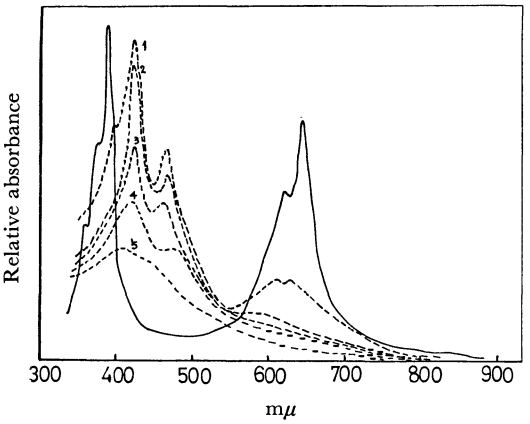

Fig. 7. The change of the electronic spectra of the biphenyl$^-Na^+$ solution in THF (———) after introducing H_2 at 20°C: (---------).
1) 10 min after 2) 20 min 3) 40 min 5) 200 min

For the biphenyl$^-Na^+$, it was found that no absorption peaks were newly observed upon introducing hydrogen on the complex film, even at higher temperatures. However, as is shown in Fig. 7, when hydrogen was admitted onto the THF solution at 20°C for several hrs, two new peaks appeared, at 425 and 490 mμ; these peaks may be attributed to the para- and ortho-monohydro-biphenyl anion respectively. These peaks decreased, however, at a considerable rate, and disappeared completely within several hrs, probably because to their decomposition, as follows:

$$AH^-Na^+ \longrightarrow A + NaH$$
$$2AH^-Na^+ \longrightarrow A + AH_2$$

For the tetracene$^=2Na^+$ complex, we found neither any appreciable change in the absorption spectra of the tetracene dianion nor the formation of sodium hydride upon the introduction of hydrogen in the temperature range between 20 and 120°C for several days. It was, however, demonstrated that a small and broad peak could be detected at 490 mμ*[8] after hydrogen treatment at 140°C for 10 days. It has previously been reported[8] that the proton complex of tetracene ($AH^+BF_4^-$) has an absorption peak at 448 mμ. The same absorption peak at 490 mμ could be observed in the slow reaction between tetracene$^=2Na^+$ and 9,10-dihydrotetracene at room temperature; this suggests that the new peak at 490 mμ can be attributed to the formation of the 9-monohydrotetracenium anion complex.

Therefore, these results suggest that a possible mechanism for the hydrogen activation by the A^-Na^+ and $A^=2Na^+$ is an electron transfer from mono- or di-anions to molecular hydrogen to form hydride and a hydrogen atom, which is then combined with each anion (A^-) to form the corresponding monohydro anion complexes (AH^-Na^+) as follows:

$$A^=2Na^+ + H_2 = A^-Na^+ + NaH + H$$
$$A^-Na^+ + H = AH^-Na^+ \qquad (1')$$
$$A^-Na^+ + H_2 = A + NaH + H$$
$$A^-Na^+ + H = AH^-Na^+ \qquad (2')$$

For the naphthalene$^-Na^+$ complex in the solution, a mechanism similar to (2′) has been proposed by Bank and his coworkers.[9] There has, however, been no crucial evidence to indicate a hydrogen atom in these reaction systems, probably because its life is too short for it to combine with radical anions (A^-).

*[8] When the film adsorbed hydrogen was dissolved in THF, a comparatively strong absorption peak appeared at 498 mμ.

8) A. A. V. Stuart and E. L. Mackor, *J. Chem. Phys.*, **26**, 826 (1958).

9) S. Bank, T. A. Lois, and M. C. Priolopski, *J. Amer. Chem. Soc.*, **91**, 5407 (1969).

BULLETIN OF THE CHEMICAL SOCIETY OF JAPAN VOL. 43 3680—3684 (1970)

Evaluation of Softness from the Stability Constants of Metal-ion Complexes*1

Makoto Misono and Yasukazu Saito

Department of Synthetic Chemistry, Faculty of Engineering, The University of Tokyo, Hongo, Bunkyo-ku, Tokyo

(Received May 23, 1970)

Utilizing the dual parameter equation we derived previously, we have evaluated quantitatively softness or class (b) character of metal ions on the basis of the original criteria of soft-hard classification, *viz.*, the stability of metal-ion complexes. Various softness parameters proposed so forth have been proved insufficient to describe softness quantitatively, although they are useful for a rough classification of metal ions into soft and hard acids. Discussion is also given concerning origin of softness, especially from the viewpoint of its closs correlation with the solvation effect.

The general idea of classifying acids and bases into class (a) and (b) (hard and soft) acids and bases has been proposed,[2] according to which hard acids prefer to coordinate with hard bases and soft acids with soft bases. This concept is based on the general trend in inorganic stability constants, that is, some acids (hard) form stable complexes in the sequence F>Cl>Br>I, while others in I>Br>Cl>F. This classification has been shown to be useful even in organic chemistry, although prediction remains qualitative, owing to the lack of quantitative scales for the acid or base strength.

Attempts were made to calculate the softness quantitatively from the fundamental properties of elements such as ionization potentials and ionic radii.[3-7] It has been claimed that a certain dual parameter scale is inevitably required in order to express the acid or base strength completely.[8,9]

The purpose of the present work is to determine the softness of metal ion on the basis of the original criteria for the soft-hard classification, utilizing the dual scale equation proposed before.[4] The most commonly used criterion for the soft-hard classification is the stability constants of halogeno-complexes. The concept of softness recently seems to be more or less subjective. The present attempt would make objective evaluation possible.

The dual parameter scale proposed by the authors is as follows.[4] One parameter X is closely related to "hardness" or the electronegativity, and another parameter Y to "softness." With these parameters, the log of stability constants of metal-ion complexes, log K,*2 is expressed well for hard-hard complexes and, to a lesser extent, for soft-soft complexes by the equation

$$\log K = \alpha X + \beta Y + \gamma \qquad (1)$$

where α and β are the dual basicity parameters of a ligand corresponding to X and Y, respectively, and γ is a constant determined for each ligand. The instability constants of hard-hard complexes are mainly determined by αX term and there is a good linear correlation between X and log K.[4] However, the correlation between Y and log K of soft-soft complexes was less satisfactory. It was, therefore, suggested that if one can adjust Y values, Eq. (1) will be much improved for stability constants.[4] Thus, we attempted to improve Y values using the dual parameter equation of the form of Eq. (1) and the regularities found among log K of halogeno-complexes of metal ions.

Results

Procedure for the Derivation of Softness Parameters, Y'. The stability constants of metal-

*1 A part of this work has been referred elsewhere.[1]

1) M. Misono, *Shokubai (Catalyst)*, **9**, 252 (1967).

2) a) R. G. Pearson, *J. Amer. Chem. Soc.*, **85**, 3533 (1963). b) S. Ahrland, J. Chatt and N. R. Davies, *Quart. Rev.*, **12**, 265 (1958).

3) R. S. Nyholm, Proceeding of the Third International Congress on Catalysis, Amsterdam, 1964, p. 25, North-Holland, Amsterdam (1965).

4) M. Misono, E. Ochiai, Y. Saito and Y. Yoneda, *J. Inorg. Nucl. Chem.*, **29**, 2685 (1967).

5) R. J. P. Williams and J.D. Hale, *Structure and Bonding*, **1**, 249 (1966).

6) G. Klopman, *J. Amer. Chem. Soc.*, **90**, 223 (1968).

7) A. Yingst and D. H. McDaniel, *Inorg. Chem.*, **6**, 1067 (1967).

8) J. O. Edwards, *J. Amer. Chem. Soc.*, **76**, 1540 (1954); **78**, 1819 (1956).

9) R. S. Drago and B. B. Wayland, *ibid.*, **87**, 3571 (1965).

*2 The stability constant, K, is the equilibrium constant of $M^{n+}+mL \rightarrow ML_m^{n+}$. In the previous paper,[4] K was the equilibrium constant of the reverse reaction, that is, the instability constant. Therefore, log K in the present paper is equal to pK in the previous paper.

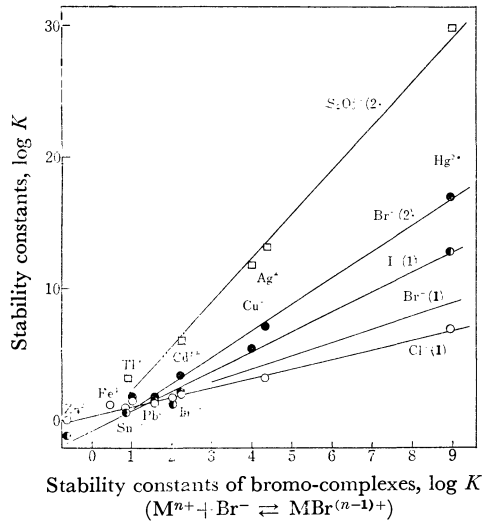

Fig. 1. Regularity among the stabilities of soft-soft complexes.
Log of stability constants of several soft ligand complexes are plotted against those of bromo-complexes. Numbers in parentheses indicate coordination numbers.

ion complexes with various soft ligands, log K, are plotted against those of bromo-complexes for several metal ions in Fig. 1. A fairly good regularity is found among these stability constants. In this figure two apparent trends should be noted: (i) soft metal ions have large log K values ($Hg^{2+}>Cd^{2+}>Zn^{2+}$), and (ii) soft ligands have steep slopes ($I^->Br^->Cl^-$). The trends are well interpreted with the softness sequences and are also expected from the βY term of Eq. (1), suggesting that this type of equation holds among these complexes.

Usefulness of a dual scale equation like Eq. (1) and the regularity in Fig. 1 demonstrated for these complexes prompted us to estimate the softness upon these bases. X values have already been proved to be satisfactory as the hardness parameter in Eq. (1). Thus, if one can choose such Y values that the equation gives satisfactorily the observed log K values, they may be considered to be good softness parameters. In order to avoid confusion, Y', α', β' and γ' will be used hereafter for the new parameters. Then the equation is written as

$$\log K = \alpha' X + \beta' Y' + \gamma' \qquad (2)$$

where X values are common to Eq. (1). From $\beta' Y'$ term which is obtained by the substraction of $\alpha' X + \gamma'$ from log K value, the softness of each metal ion can be estimated with the following procedure.

1) The log K of chloro-complexes is taken, to a first approximation, as Y' value respectively as follows: Hg^{2+}(7.2), Tl^{3+}(6.5), Ag^+(3.8), Cu^+(3.5), Cd^{2+}(2.1), In^{3+}(1.9), Fe^{3+}(1.6), Pb^{2+}(1.6), Sn^{2+}(1.6), Tl^+(1.2) and Zn^{2+}(1.0). Since there are linear correlations among the stability constants of halogeno-complexes (Fig. 1), the stability constants of any halogeno-complexes may be used as the basis for Y' values. Here, chloro-complexes are chosen, simply because a good number of reliable stability constants are available and they give Y' values whose magnitude is better to handle. When there is no experimental log K value of chloro-complex, estimation is made from log K of other halogeno-complexes, considering the regularity in Fig. 1.

2) By the method of least squares, α', β', and γ' are then calculated by Eq. (2) for several soft ligands, including different coordination numbers.

3) Improved Y' values are tentatively obtained from the slopes in log $K-\alpha' X-\gamma'$ *vs.* β' plots (Fig. 2).

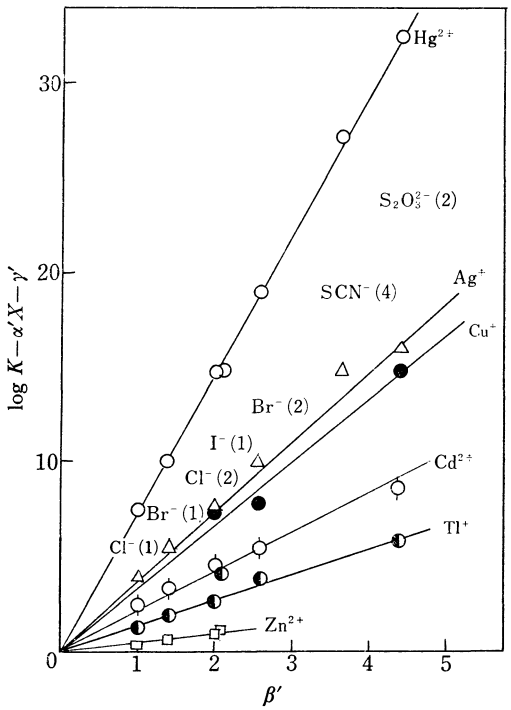

Fig. 2. log $K-\alpha' X-\gamma'$ *vs.* β' plot.

Repeating the above procedure one can get the most reasonable value of Y' for each metal ion. Iteration was not actually continued, since the agreement of the second Y' with the first ones was good enough. The final Y' values are Hg^{2+} (7.3), Tl^{3+} (6.0), Ag^+ (3.8), Cu^+ (3.3), Cd^{2+} (2.0), In^{3+} (1.8), Sn^{2+} (1.8), Pb^{2+} (1.6), Fe^{3+} (1.4), Tl^+ (1.3), and Zn^{2+} (0.7). Linearity of the plots in Fig. 2 is significantly improved compared to that in Fig. 1, which provides a good support for Y' as a good softness parameter which is based on the original criteria for the soft-hard classification. Additional Y' values are determined in a similar manner, using only log K of halogeno-complexes, as follows: Au^+ (10.9), Au^{3+} (9.4), Pt^{2+} (6.9), Pd^{2+} (5.6), Co^{2+} (1.2) Fe^{2+} (0.3) and Mn^{2+} (0.0). Although these values might be less reliable because of the limited number

Table 1. Calculated and observed stability constants of metal-ion complexes

	Y'[b]	OH^-		Stability Constants, log K[a] NH_3		pyridine		Br^-		I^-		$S_2O_3^{2-}$	
		calcd	obsd										
Na^+	0	−1.3	−0.5										
Ag^+	3.8	2.7	2.3	2.9	3.2	1.9	2.0	4.3	4.3			13.7	13.0
Cu^+	3.3											11.5	11.7
Tl^+	1.3							0.8	0.9	0.9	0.7	2.6	3.1
Mg^{2+}	0	2.5	2.6	0.6	0.2								
Ca^{2+}	0	1.4	1.3	0.0	−0.2								
Fe^{2+}	0.3	4.1	3.9	1.8	1.4	0.7	0.7						
Ni^{2+}	1.7	5.4	4.6	3.3	2.8	1.7	1.8					3.7	1.0
Cu^{2+}	1.9	6.0	6.5	3.8	4.2	1.9	2.5	1.5	~0				
Zn^{2+}	0.7	4.5	4.4	2.2	2.4	1.0	1.0	−0.1	−0.6	−0.7	−1.3	2.6	3.1
Cd^{2+}	2.0	5.3	2.3?	3.4	2.7	1.8	1.3	1.8	2.2	2.0	2.3	6.1	5.8
Hg^{2+}	7.3	9.4	10.3	8.8	8.8	5.3	5.1	9.1	9.0	12.9	12.8	29.5	29.7
Fe^{3+}	1.4	11.1	11.8					0.9	0.5				
In^{3+}	1.8	9.8	10.3					1.4	2.0	1.2	1.2		
Number of log K data used for calculation		17		13		8		9		6		7	
α'		1.50		0.89		0.41		−0.01		−0.12		0.12	
β'		0.59		0.90		0.60		1.40		2.08		4.40	
γ'		−2.79		−2.50		−1.29		−0.97		−1.63		−3.31	

a) The values on the left part of each row are those calculated by $\log K=\alpha' X+\beta' Y'+\gamma'$ and those on the right are the observed ones, which are the same as in the previous paper[4] except for some revision and supplements using data in Ref. 14. The values for $S_2O_3^{2-}$ are the overall instability constants of $M(S_2O_3)_2^{(n-4)+}$. Other values are of mono-coordinated complexes.

b) Since very few log K values have been reported for the complexes of less soft metal ions, such as Fe^{2+}, Co^{2+} and Cu^{2+}, Y' was estimated from $Y'=2.8Y-6.2$ which is found to hold approximately between Y and Y'. Y' was put to zero when $2.8Y-6.2$ became negative. This estimation seems sufficient for log K calculation, becuase $\beta' Y'$ term in Eq. (2) contributes little in these cases.

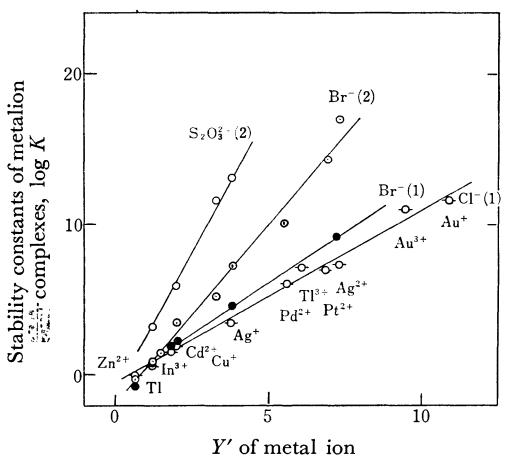

Fig. 3. Stability of metal-ion complex as a function of softness parameter, Y'.
Numbers in parentheses are the same as in Fig. 1.

of reported log K, satisfactory linear correlation of new parameters, Y', with log K values of soft-soft complexes is obtained as demonstrated in Fig. 3. This good correlation is comparable with that of X with log K of hard-hard complexes.[4] A part of the deviation from the straight line found in Fig. 3 may be due to the minor contribution from $\alpha' X$ term in Eq. (2). Some of the calculated log K values by Eq. (2) are given in Table 1 for several metal-ion complexes. The results for the complexes of ligands with considerable softness are given in this table. For hard ligand complexes, the agreement between the calculated and the observed log K values[4] was as good as the present one. Agreements between the calculated and the measured log K in this table are excellent as a whole. Remarkable improvements in agreement are observed especially for I^- and $S_2O_3^{2-}$($\beta'>1$). As for the magnitude of β there is little change; both β and β' follow the softness sequence and are linearly correlated with $n_{P.}$, the reactivity index of a nucleophile for the displacement reaction of Pt^{2+}-complex.[10]

10) U. Belluco, L. Cattalini, F. Basolo, R. G. Pearson and A. Turco, *J. Amer. Chem. Soc.*, **87**, 241 (1965).

Discussion

Comparison of Y′ with Other Softness Parameters. The proposed parameter Y' thus obtained semi-empirically on the basis of the original criteria for the soft-hard classification, may reasonably be considered as a quantitative expression of softness (see Figs. 1 and 2). It seems of interest to compare such various parameters proposed for the quantitative expression of softness of metal ion, as R(N),[3] R(W),[5] Y,[4] α/β[7] and $E_n^=$,[6] with the present parameter Y' and look into the physical meaning of softness. All of these parameters are useful as rough criteria for the soft-hard classification of metal ions, although a few exceptions are always inevitable.

However, it is apparent that the correlations are only qualitative. If one plots these parameters against Y', only fair correlations are obtained for $E_n^=$ and Y, and rather poor ones for R(N), R(W) and α/β. This means that the approximation used for the derivation of the parameters previously proposed are too simple for quantitative use.

Origin of Softness. The soft-hard classification is based on the fact that, reviewing inorganic stability constants in *aqueous* solution, metal ions fall into two distinct groups: those which form halogeno-complexes whose stability order is (i) F>Cl>Br>I, and (ii) I>Br>Cl>F. This situation, however, contrasts with that observed in the gas phase, where the sequence of molecular stability is always found to be MF_2>MCl_2>MBr_2>MI_2. This obviously demonstrates the importance of solvent effect, that is, the change in solvation state during the complex formation. Klopman[6] has recently derived his softness parameter as the difference between the bond energy and the desolvation energy accompanying complex formation. The bond energy consists of electrostatic and charge-transfer interaction energies. In his treatment, the extent of softness of metal ion depends on how much the bond energy overcomes the energy loss due to desolvation. We have previously discussed the bond energy of coordination and the soft-hard properties, dividing the total bond energy into electrostatic, σ-bond and π-bond energies.[4] In this treatment the heat of solvation was assumed to be proportional to the electronegativity X, since the bond energy of metal ion to aquo ligand is mainly correlated to the αX term.

The heat of complex formation, $M^{n+}+mL^- \rightarrow ML_m^{(n-m)+}$(L=F, Cl, Br and I) is equal to the difference between the heat of M-L bond formation and the desolvation energy. Since the latter is roughly equal, with opposite sign, to the solvation energies of M^{n+} and L^-, the stability sequence for a given metal ion, either F>Cl>Br>I or F<Cl<Br<I, may be determined by the change in M-L bond energy relative to that in solvation energy of L^- from F to I.

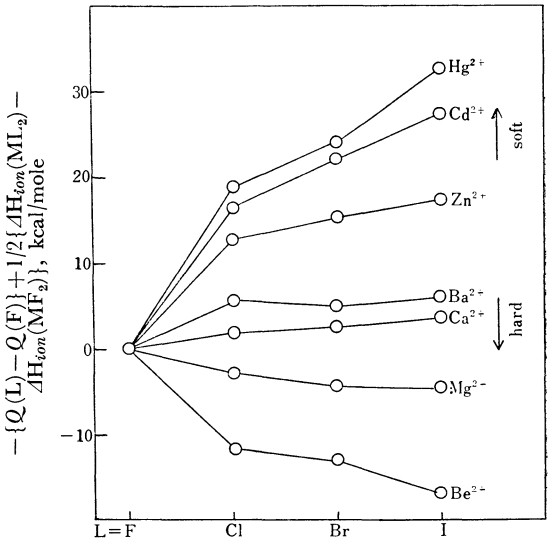

Fig. 4. The change in metal-halogen bond energy from F to I relative to the change in the heat of hydration of halide ion.
Q(L): Heat of hydration of halide ion (L^-).
Q(F): Heat of hydration of fluoride ion.
$\Delta H_{ion}(ML_2)$: Heat of reaction of M^{2+}(gas)+$2L^-$(gas)→ML_2(gas).

In Fig. 4, this situation is demonstrated for some metal ions. The coordinate represents the difference between the changes among halogens from F to I in M-L bond energies and those in solvation energies of L^- by refering to fluoride ion in both cases. In contrast to the M-L bond energy which is approximated by half of the heat of the reaction of $M^{2+}+2L^- \rightarrow ML_2$ in the gas phase, F>Cl>Br>I, the desolvation energy of L^- suggests a favorable order for the stable complex formation (F<Cl<Br<I). It may be stated, therefore, that the main factor to determine the stability sequence of metal-halogeno complexes is how much the decrease in M-L bond energy in F, Cl, Br, I series is compensated by the decrease in desolvation energy in the same series. Thus Hg^{2+} and Cd^{2+} are soft, because their M-L bond energies decrease more moderately than those of metal ions such as Be^{2+} and Ca^{2+}.

Roughly speaking, both the solvation energy and

Table 2. Calculated stability constants of the complexes of methylmercuric ion, CH_3Hg^+ by Eq. (2) and the observed values

	OH^-	Ac^-	NH_3	pyridine	Cl^-	Br^-	I^-
calcd[a]	12.9	4.0	10.6	5.9	5.9	7.4	10.4
obsd[b]	12.8	4.4	10.5	6.1	5.9	7.6	10.3

a) Calculated using X=6.52 and Y'=5.35 together with α', β' and γ' in Table 1.
b) Taken from Ref. 15.

Table 3. Calculated reactivity indices by Eqs. (3), (4) and (5) and reported values

		Ac^-	pyridine	Cl^-	Br^-	OH^-	NH_3	I^-	$S_2O_3^{2-}$ [a]
n	calcd	1.48	2.51	2.79	3.63	5.00	4.40	5.15	6.67
	reported[b]	2.72	3.6	3.04	3.89	4.20	—	5.04	6.36
E_n	calcd	0.57	0.98	1.12	1.45	1.92	1.71	2.06	2.65
	reported[c]	0.95	1.20	1.24	1.51	1.65	1.84	2.06	2.52
H	calcd	6.86	4.56	−0.5	−2.1	20.0	10.5	−4.6	−2.8
	reported[c]	6.46	7.04	−3.0	−6.0	17.5	11.2	−9.0	3.6

a) The values of α', β' of $S_2O_3^{2-}$ are estimated as $\alpha'=0.06$ and $\beta'=2.50$ for mono-coordinated complexes, from those of dicoordinated ones considering the dependency of α' and β' of other ligands on the changes in the coordination number.
b) Taken from Ref. 11.
c) Taken from Ref. 8.

the σ-bond energy linearly depend on X,[4] probably the latter, to a lesser degree. As shown in Fig. 4, the more ionic the M-L bond, the more strongly the bond energy depends on X, resulting in a more negative slope in Fig. 4. In other words, an increase in covalency increases softness. The ability of π-bond formation (back donation) strongly favors the sequence I>Br>Cl>F. The reason why $E_n^{\neq}$ of Pd^{2+}, Pt^{2+} and Au^+ are lower than those expected from Y' may be explained by the fact that π-bonding was neglected in $E_n^{\neq}$ calculation. Thus, if the decrease in M-L bond energy from F to I of a certain metal ion becomes moderate, by the enhancement of covalency, especially of π-bonding in M-L bond, class (b) character or softness, increases.

Changes in softness may also occur by the solvent effect in the way pointed out by Williams and Hale.[5] Reduction of dielectric constant of solvent decreases the change in the solvation energy from F to I, so that the solvation becomes less important. As a consequence all cations revert to class (a) character as dielectric constants approach unity, that is, for example, in the gas phase.

Some Examples of Applications. The values of softness and hardness, (X, Y'), of CH_3Hg^+, CF_3Hg^+ and $C_3F_7Hg^+$ are calculated by Eq. (2) as (X=6.52, Y'=5.35), (6.79, 5.80) and (6.54, 5.89), respectively. These calculated log K values agree well with the reported ones (Table 2). Y' are large as expected, but it is to be noted that X values are also large. Belluco *et al.*[10] reported poor correlation of the log K of CH_3Hg^+ complexes with n_{Pt}. However, n_{Pt} correlates well with β[4] or β'. This discrepancy is understandable, if one takes into account the considerable hardness of CH_3Hg^+; n_{Pt} and β are determined by softness[4] while log K of CH_3Hg^+ complexes depends on both softness and hardness. The ability of mercuric ion to form strong σ-bond may partly account for the hardness, as σ-bond energy depends on X.[4]

The reactivity indices of a nucleophile in various displacement reactions on carbon, such as n,[11] E_n and H,[8] have been related to the present α' and β' by the formulas

$$n = 2.3\alpha' + 2.6\beta' \quad (3)$$

$$E_n = 0.9\alpha' + 1.0\beta' \quad (4)$$

$$H = 13.2\alpha' - 1.4\beta' \quad (5)$$

n and E_n are the nucleophilic constants (approximately, $n \propto E_n$) and H the basicity of a nucleophile (oxibase scale[12]). The values calculated by the above equations are in fair agreement with the reported values of n and E_n, but not with H (Table 3). Poor argeement for H may not be serious, because H is usually of little importance in the reactivity which depends mostly on n (or E_n). Equations (3) and (4) demonstrate that the reactivity of a nucleophile depends almost equally on hardness α' and softness β'. The ratio of these two coefficients, which gives the relative dependency of the reactivity on hardness to that on softness, is expected to vary from one type of reaction to another. In fact, in the case of the ligand displacement of Pt^{2+} complexes, the reactivity n_{Pt} is mainly controlled by softness.[4] The reactivities for the displacement reactions of CH_3I and CH_3Br by a nucleophile, n_{CH_3I} and n_{CH_3Br}, are determined by both hardness and softness, since they are proportional to E_n.[13]

The authors are indebted to Professor Y. Yoneda for his helpful discussions.

11) C. G. Swain and C. B. Scott, *J. Amer. Chem. Soc.*, **75**, 141 (1953).
12) R. E. Davis, *ibid.*, **87**, 3010 (1965).
13) R. G. Pearson, H. Sobel and J. Songstad, *ibid.*, **90**, 319 (1968).
14) Chem. Soc. Special Publication, No. 17, Stability Constants of Metal-ion Complexes, London (1964).
15) R. S. Tobias, *Organometal. Chem. Rev.*, **1**, 93 (1966).

BULLETIN OF THE CHEMICAL SOCIETY OF JAPAN VOL. 43 3685—3688 (1970)

The Phase Transitions of the Anion Radical Salts Containing Mixed Cations; $[(C_6H_5)_3PCH_3]_{1-x}^{+}[(C_6H_5)_3AsCH_3]_x^{+}(TCNQ)_2^{-}$, $(0 \leq x \leq 1)$

Yôichi IIDA

Department of Chemistry, Faculty of Science, Hokkaido University, Sapporo

(Received May 27, 1970)

The phase transitions of the anion radical salts containing mixed cations represented by $[(C_6H_5)_3PCH_3]_{1-x}^{+}[(C_6H_5)_3AsCH_3]_x^{+}(TCNQ)_2^{-}$, $(0 \leq x \leq 1)$ were investigated. The transition temperature, T_c, and the magnitude of the heat, ΔH, of the transition were determined as a function of the composition parameter, x, by means of a differential scanning calorimeter. It was found that T_c increases, and ΔH decreases, monotonously with an increase in the value of x, and that the phase transition disappears with $x=1.00$. The mechanism of the phase transitions was discussed on the basis of the theory of triplet exciton-exciton interaction proposed by Chesnut. The theoretical values of the entropy changes of the transitions were found to be much less than those observed. In view of these results, it was concluded that the anomalies in the magnetic susceptibilities of these salts were induced by the change in the crystal structure.

There are a few ion-radical salts that are known to undergo phase transitions.[1-7] The phase transitions of such ion-radical salts are particularly interesting, because the anomalies in the magnetic susceptibilities are associated with the phase transitions.[1-6]

Much attention has been paid to the solid anion-radical salts of 7,7,8,8-tetracyanoquinodimethane (TCNQ).[5,6,8-10] In the course of our study of these salts, we found that the ESR absorption intensity, which is proportional to the paramagnetic susceptibility, of the salt of methyltriphenylphosphonium, $[(C_6H_5)_3PCH_3]^{+}(TCNQ)_2^{-}$, increases abruptly at 40°C when the temperature is raised.[6] This discontinuity was also found in the electrical conductivity at that temperature.[6] This anomaly was ascribed to the phase transition of the crystal, as evidenced by the differential thermal analysis.[11] The methyltriphenylarsonium salt, $[(C_6H_5)_3AsCH_3]^{+}(TCNQ)_2^{-}$, exhibits electronic properties almost identical with those of the phosphonium salt; on the other hand, the arsonium salt is known to have no such anomaly. One can prepare the salts containing mixed cations, which may be expressed as $[(C_6H_5)_3PCH_3]_{1-x}^{+}[(C_6H_5)_3AsCH_3]_x^{+}(TCNQ)_2^{-}$, $(0 \leq x \leq 1)$.[5,8] Therefore, it seemed that it would be interesting to investigate the effect of the compositon upon the phase-transition phenomenon. The present investigation was performed by means of a differential scanning calorimeter (DSC).

An attempt has previously been made to explain the mechanism of the phase transitions of ion-radical salts in terms of the cooperative spin-exchange interaction.[12] Hence, the experimental results of our DSC measurements will be discussed in terms of such a theoretical consideration. In other words, we shall examine to what extent the spin-exchange interaction of these TCNQ anion radical salts contributes to the phase transition mechanism. Knowledge as to the effect of the chemical composition upon the phase transition is useful for this purpose.

The present study has already been reported in part in a short communication.[13]

Experimental

Materials. The preparation of TCNQ has been described by Acker and Hertler.[14] It was purified by recrystallization from acetonitrile. The anion-radical salts containing the mixed cations, $[(C_6H_5)_3PCH_3]_{1-x}^{+}[(C_6H_5)_3AsCH_3]_x^{+}(TCNQ)_2^{-}$, $(0 \leq x \leq 1)$, were synthesized according to the method of Melby *et al.*[8] The six salts were prepared with compositions of $x=0.00$,

1) N. Elliot and M. Wolfsberg, *Phys. Rev.*, **91**, 435 (1953).
2) W. Duffy, Jr., *J. Chem. Phys.*, **36**, 490 (1962).
3) K. Okumura, *J. Phys. Soc. Jap.*, **18**, 69 (1963).
4) D. D. Thomas, H. Keller and H. M. McConnell, *J. Chem. Phys.*, **39**, 2321 (1963).
5) R. G. Kepler, *ibid.*, **39**, 3528 (1963).
6) Y. Iida, M. Kinoshita, M. Sano and H. Akamatu, This Bulletin, **37**, 428 (1964).
7) H. Chihara, M. Nakamura and S. Seki, *ibid.*, **38**, 1776 (1965).
8) L. R. Melby, R. J. Harder, W. R. Hertler, W. Mahler, R. E. Benson and W. E. Mochel, *J. Amer. Chem. Soc.*, **84**, 3374 (1962).
9) W. J. Siemons, P. E. Bierstedt and R. G. Kepler, *J. Chem. Phys.*, **39**, 3523 (1963).
10) Y. Iida, This Bulletin, **42**, 71, 637 (1969).
11) Y. Iida, M. Kinoshita, A. Kawamori and K. Suzuki, *ibid.*, **37**, 764 (1964).
12) D. B. Chesnut, *J. Chem. Phys.*, **40**, 405 (1964).
13) Y. Iida, This Bulletin, **43**, 578 (1970).
14) D. S. Acker and W. R. Hertler, *J. Amer. Chem. Soc.*, **84**, 3370 (1962).

0.20, 0.40, 0.60, 0.80, and 1.00.

Hexachloroethane (Wako Pure Chemical Industries, Ltd., GR grade) was used without further purification. Hexamethylbenzene (Eastman Kodak Co., white-label grade) was purified by recrystallization from ethanol.

Measurements. The DSC measurements were performed by means of a Rigakudenki Thermoflex apparatus. The rate of raising the temperature was 3.0°C/min. As a reference, powdered α-alumina was employed. The sample and the reference were packed and sealed, respectively, into aluminium vessels in order to prevent weight loss due to the sublimation. In DSC measurements, the peak area of the signal line should be proportional to the magnitude of the heat, ΔH, associated with the phase transition. Therefore, in order to determine the heat of transition, the integrated area of the peak of $[(C_6H_5)_3PCH_3]_{1-x}^+[(C_6H_5)_3AsCH_3]_x^+(TCNQ)_2^-$ was compared with that of hexachloroethane or hexamethylbenzene. The phase transition of hexachloroethane is known to take place at 318.1°K with ΔH=0.613 kcal/mol and at 344.4°K with ΔH=1.965 kcal/mol,*1 and that of hexamethylbenzene, at 384.1°K with ΔH=0.42 kcal/mol.[15] In this technique, it was necessary to employ standard materials whose transition temperatures were close to those under investigation.

Results

In $[(C_6H_5)_3PCH_3]_{1-x}^+[(C_6H_5)_3AsCH_3]_x^+(TCNQ)_2^-$, where $0 \leq x \leq 1$, all the salts except for that with x=1.00 were found to show phase transitions. For instance, one of the DSC thermograms for $[(C_6H_5)_3PCH_3]_{0.80}^+[(C_6H_5)_3AsCH_3]_{0.20}^+(TCNQ)_2^-$ is reproduced in Fig. 1. These phase transitions were endothermic when the temperature was raised, and reversible when the temperature was lowered. The transition temperature, T_c, and the magnitude

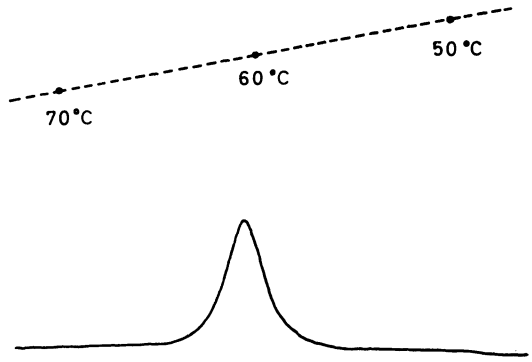

Fig. 1. One of the DSC thermograms for $[(C_6H_5)_3PCH_3]_{0.80}^+[(C_6H_5)_3AsCH_3]_{0.20}^+(TCNQ)_2^-$. The rate of raising temperature was 3.0°C/min.

of the heat, ΔH, associated with the phase transitions of these salts are listed in Table 1, together with the molecular weight, the sample weight used for this experiment, and the heat of transition of the specimen. On the basis of these results, the relations of T_c and of ΔH to the composition parameter, x, are illustrated in Fig. 2.

In the salt of $[(C_6H_5)_3PCH_3]^+(TCNQ)_2^-$, where x=0.00, the values of T_c=41.5°C and $\Delta H=4.5\times10^2$ cal/mol were obtained from these DSC measurements. These values were in agreement with the values, T_c=315.7°K and ΔH=487 cal/mol respectively, which were obtained from the heat-capacity measurement by Kosaki *et al.*[16]

As is shown in Fig. 2, it was found that, in the salts where $0<x<1$, T_c increases and the value of ΔH decreases, monotonously with an increase in the value of x, and that the phase transition

Table 1. The data on the transition temperature, T_c, and the heat, ΔH, associated with the phase transition in $[(C_6H_5)_3PCH_3]_{1-x}^+[(C_6H_5)_3AsCH_3]_x^+(TCNQ)_2^-$, $(0 \leq x \leq 1)$*

Composition parameter x	Molecular weight	Sample weight (mg)	T_c (°C)	ΔH** (cal/s.w.)	ΔH (cal/mol)
0.00	685.70	26.6	41.5	1.7×10^{-2}	4.5×10^2
0.20	694.49	29.8	59.0	1.9×10^{-2}	4.4×10^2
0.40	703.28	32.0	76.3	1.6×10^{-2}	3.5×10^2
0.60	721.07	26.2	103.0	9.2×10^{-3}	2.5×10^2
0.80	720.86	29.2	124.3	4.3×10^{-3}	1.1×10^2
1.00	729.65	24.9	—	0	0

* The data on the molecular weight, the sample weight used for this DSC measurement and the heat of transition per the sample weight are also given.

** The value of the heat of transition per the sample weight.

*1 We should keep in mind that hexachloroethane is somewhat volatile. However, although this material, when packed and sealed into the aluminium vessel, was heated up to about 350°K at the rate of 3.0°C/min, the weight loss due to the sublimation was found to be less than 0.5%.

15) Landort-Börnstein, "Zahlenwerte und Funktionen aus Physik, Chemie, Astronomie, Geophysik, Technik," II Band, 4 Teil, 6 Auflage, Springer-Verlag, Berlin (1961); Nippon Kagakukai, "Kagaku Binran," Maruzen, Tokyo (1966).

16) A. Kosaki, Y. Iida, M. Sorai, H. Suga and S. Seki, Preprint of the 5th Japanese Calorimetry Conference, B211 (1969).

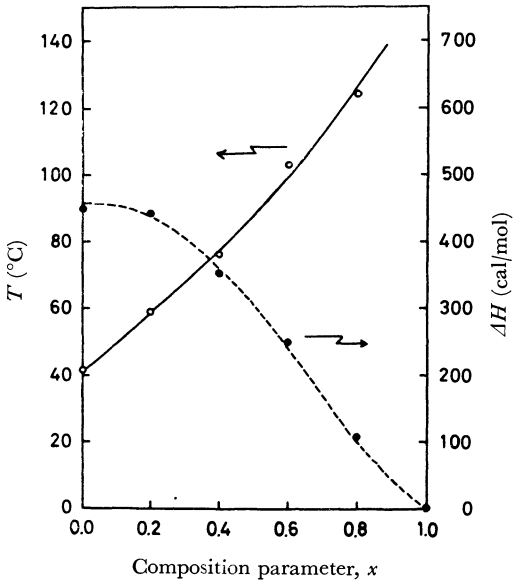

Fig. 2. The relations of the transition temperature, T_c, and of the magnitude of the heat, ΔH, associated with the phase transition, to the composition parameter, x, in $[(C_6H_5)_3PCH_3]_{1-x}^+[(C_6H_5)_3AsCH_3]_x^+$ $(TCNQ)_2^-$, $(0 \leq x \leq 1)$.

disappears at $x=1.00$. We can see that T_c is raised almost linearly as the value of x increases. On the other hand, the value of ΔH decreases slowly as the value of x increases in the region where $0 \leq x \leq 0.4$, while it decreases almost linearly as the value of x increases in the region where $0.4 \leq x \leq 1.0$. When $x \approx 1.00$, T_c may be extrapolated to about 160°C, although the value of ΔH tends towards zero.

Discussion

Triplet Exciton Interaction. These TCNQ anion-radical salts are composed of diamagnetic cations, TCNQ anion-radicals, and formally neutral TCNQ molecules. If the spins associated with the TCNQ anion-radicals did not interact, the magnetic susceptibility of these compounds would follow the Curie law. However, the magnetic susceptibility measurements have shown that this is not the case.[5] The extra electrons on the TCNQ molecules appear to be paired by an exchange interaction. These systems are known to contain a singlet ground state and a triplet exciton state. The TCNQ molecules are believed to be arranged in plate-like fashion in a unique crystal direction.[5,9]

In order to account for the occurrence of the phase transitions of these anion-radical salts, a simple phenomenological model has been proposed by Chesnut.[12] He showed that a certain type of order-disorder transition with respect to triplet excitation density does occur if one includes in the interaction a term which is quadratic in the triplet excitation density, ρ. In this case, the free energy, A, and the entropy, S, of the system for the N anions are represented by:

$$A = \frac{1}{2}N\left[\varepsilon_0\rho + \frac{1}{2}\varepsilon_1\rho^2 - kT\left\{\rho \ln g - \rho \ln \rho - (1-\rho)\ln(1-\rho)\right\}\right], \quad (1)$$

$$S = \frac{1}{2}Nk\left\{\rho \ln g - \rho \ln \rho - (1-\rho)\ln(1-\rho)\right\}, \quad (2)$$

where g is the multiplicity ($g=3$ for the triplet state), where ε_0 is the singlet-triplet energy separation, and where ε_1 is the interaction energy due to triplet exciton-exciton interaction.

The equilibrium value of ρ may be found by minimizing A with respect to ρ. The phase transition will take place at the temperature where two equally stable minima occur. In this case, the transition is of the first order. The spin entropy change will be:

$$\Delta S_{\text{spin}} = \frac{1}{2}R\Delta\rho \ln g, \quad (3)$$

where $\Delta\rho$ is the change in the triplet excitation density at the transition. $\Delta\rho$ can be calculated from the magnetic susceptibility data, since an abrupt change in the paramagnetic susceptibility at the transition temperature is due to the change in the triplet exciton population, $\Delta\rho$. Therefore, one can evaluate the magnitude of the spin entropy change by means of Eq. (3).

Comparison with Experimental Results. Kepler found a sharp discontinuity in the temperature variation of magnetic susceptibility in the crystals of $[(C_6H_5)_3PCH_3]_{1-x}^+$ $[(C_6H_5)_3AsCH_3]_x^+$ $(TCNQ)_2^-$, except for the salt with $x=1.00$.[5] At the temperature where the discontinuity occurred, there was an abrupt increase in the magnetic susceptibility in the higher temperature range. This critical temperature shifts to higher temperatures as the value of x increases. This relation is in good accordance with that obtained from the DSC measurements.

The values of $\Delta\rho$ were calculated from Kepler's susceptibility data. For example, in $[(C_6H_5)_3PCH_3]^+(TCNQ)_2^-$, where $x=0.00$, $\Delta\rho=0.12$ is centered about the point where $\rho=0.37$. This leads, by Eq. (3), to; $\Delta S_{\text{spin}}=0.13$ cal/deg·mol. Similar calculations were made for the mixed crystals. Thus, the relation of ΔS_{spin} to x was found to be as shown in Fig. 3.

On the other hand, the observed entropy changes, ΔS_{obs}, at the transition were evaluated from the observed values of T_c and ΔH. The relation of ΔS_{obs} to x is also illustrated in Fig. 3.

As is shown in Fig. 3, it was found that the values of ΔS_{spin} were much less than those of ΔS_{obs} for all of the compounds. For example, in $[(C_6H_5)_3$-

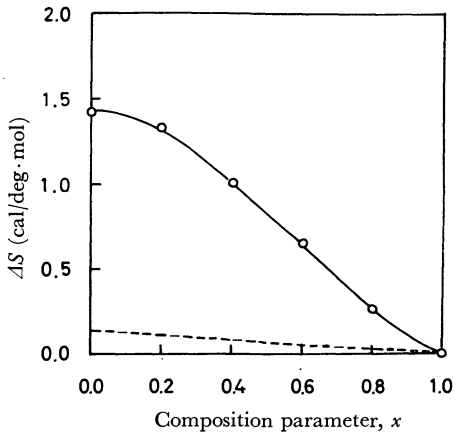

Fig. 3. The relation of the entropy change at the phase transition to the composition parameter, x, in $[(C_6H_5)_3PCH_3]_{1-x}^+[(C_6H_5)_3AsCH_3]_x^+(TCNQ)_2^-$, $(0 \leq x \leq 1)$. ΔS_{obs} (the solid line) represents the total entropy change estimated from the observed values of ΔH and T_c in Fig. 2. ΔS_{spin} (the dotted line) represents the spin entropy change calculated from the Chesnut's theory by Eq. (3).

$PCH_3]^+(TCNQ)_2^-$, $\Delta S_{spin}=0.13$ cal/deg·mol, while $\Delta S_{obs}=1.4$ cal/deg·mol. Therefore, the value of ΔS_{spin} is as small as 9.1% of that of ΔS_{obs}. Although the values of both ΔS_{spin} and ΔS_{obs} decrease with an increase in x, the ratio of ΔS_{spin} to ΔS_{obs} remains nearly constant in the mixed crystals.

Conclusion

The above-mentioned results clearly indicate that the total entropy change can not be understood solely by the spin-entropy change calculated from Chesnut's theory. This means that it is hopeless to consider only the spin system as the source of entropy creation at the transition. Therefore, one must also take into consideration the entropy change due to the change in the crystal structure. In this case, the magnitude of this entropy change reaches about 90% of the observed total entropy change. This kind of entropy change decreases as the percentage of the methyltriphenylarsonium cation of the salt increases. Since, in these TCNQ anion-radical salts, the crystal structure above the transition temperature is expected to be appreciably different from that below the transition temperature, it is desirable to study the difference in these crystal structures by X-ray analysis.*2 The anomalies in the magnetic susceptibilities of these anion-radical salts are probably induced by the change in the crystal structures.

*2 There are some other ion-radical salts that undergo phase transitions. It is well known that the phase transition of *N,N,N',N'*-tetramethyl-*p*-phenylenediamine (Würster's Blue) perchlorate, one of the stable cation-radical salts, takes place at 189°K. Elliot and Wolfsberg,[1] Duffy,[2] and Okumura[3] found a sharp decrease in the paramagnetic susceptibility below this transition temperature, where Würster's Blue cations are known to pair up to form dimers with a ground singlet state and an excited triplet state.[4] If Chesnut's theory is applied to this transition, Okumura's susceptibility data indicate that $\Delta\rho=0.087$ symmetrically about $\rho=0.643$. This leads by Eq. (3) to: $\Delta S_{spin}=0.095$ cal/deg·mol. This value is much less than the value, $\Delta S_{obs}=2.19\pm0.02$ cal/deg·mol, which was obtained from the heat-capacity measurements by Chihara *et al.*[7] They said that it was difficult to consider only the spin system as the source of entropy creation at the transition.[7] Again, in this salt, the rest of the entropy must then come from some structural changes. In fact, X-ray diffraction studies, cited by McConnell,[4] show that the transition is accompanied by a small structural change from the room-temperature orthorhombic phase to the low-temperature monoclinic phase. These results seem to be, in some respects, very similar to those for the present TCNQ anion-radical salts.

BULLETIN OF THE CHEMICAL SOCIETY OF JAPAN VOL. 43 3689—3694 (1970)

An Electron Spin Resonance Study of the 5,12-Dihydrotetracene Radical Anion and Its Ion Pairs with Alkali Metal Cations

Masamoto IWAIZUMI and Taro ISOBE

Chemical Research Institute of Non-Aqueous Solutions, Tohoku University, Katahira-nichome, Sendai

(Received May 27, 1970)

The 5,12-dihydrotetracene radical anion and its ion pairs with alkali-metal cations have been investigated by electron spin resonance (ESR). It has been found that the frequency of the inversion of the radical molecule is $\gg 10^8$ Hz and that the unpaired electron is distributed between the benzene and naphthalene rings. Such a distribution of the unpaired electron between the two conjugated systems is assumed to occur *via* a hyperconjugation mechanism. On the other hand, it was observed that the proton hyperfine splittings of the radical anion are appreciably affected by the association of an alkali-metal cation. In the case of the 5,12-dihydrotetracene-potassium ion-pair in THF, the hyperfine components of the methylene protons show an alternating line-width effect. On the basis of the observed effects of the alkali metal cations, a model of the ion-pair structure is proposed, and the alternating line-width effect is explained in terms of an intramolecular migration of the potassium ion from one side of the molecular plane to the other. The activation energy of this motion of the potassium ion has been estimated to be 3.1 ± 0.2 kcal.

In this paper we wish to report the results of an investigation of the 5,12-dihydrotetracene radical anion and of the ion pair formed between the 5,12-dihydrotetracene radical anion and alkali-metal cations. It is well known that the ESR technique provides us with interesting and important information on the spin distribution in free radicals.[1,2] It is also useful in providing information on the conformation of the molecules of free radicals, and some times allows measurements of the dynamic motions of the molecule, such as the conformational interconversion and the *cis-trans* conversion.[3-6] The 5,12-dihydrotetracene (I) treated here is an interesting molecule in that it can be considered as consisting of two conjugated systems, benzene and naphthalene rings, weakly coupled through two methylene bridges. By analogy with the 9,10-dihydroanthracene molecule, which is in a non-planar conformation,[7] it can also be considered that the conformation of the 5,12-dihydrotetracene radical anion is non-planar, which may therefore lead to an inversion process. It seemed interesting to investigate the spin distribution and the inversion process of such a molecule. In this paper we will show that the unpaired electron is distributed between the benzene and naphthalene rings by a weak coupling between the two rings, although a large portion of the spin densities exist on the naphthalene ring; the transfer of the unpaired electron between the two conjugated systems may be explained by the hyperconjugation effect of the methylene bridges. We will also show that the rate of inversion must be: $\gg 10^8$ Hz.

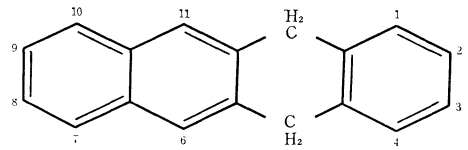

I

On the other hand, it has been observed that the proton hyperfine splitting constants of the 5,12-dihydrotetracene radical anion change appreciably upon the formation of the ion pair with an alkali-metal cation. For the case of the ion pair with the potassium ion in THF, the hyperfine splitting due to the methylene protons changes markedly with the temperature, and it shows an alternating line-width effect at high temperatures. It is shown that the observed effects of the cations can be explained by an ion-pair model where the alkali ion favors a situation above the naphthalene skeleton, and that

1) P. B. Ayscough, "Electron Spin Resonance in Chemistry," Methuen, London (1967), p. 239.
2) J. R. Bolton, "Radical Ions," ed. by E. T. Kaiser and L. Kevan, Interscience Publishers, New York, N. Y. (1968), p. 1.
3) G. K. Fraenkel, *J. Phys. Chem.*, **71**, 139 (1967).
4) A. Hudson and G. R. Luckhurst, *Chem. Rev.*, **69**, 191 (1969).
5) D. H. Geske, *Progr. Phys. Org. Chem.*, **4**, 125 (1967).
6) P. D. Sullivan and J. R. Bolton, "Advances in Magnetic Resonance," Vol. 4, ed. by J. S. Waugh, Academic Press, New York, N. Y. (1970), p. 39.
7) I. G. M. Campbell, C. G. LeFevre, R. J. W. LeFevre and E. E. Turner, *J. Chem. Soc.*, **1938**, 404.

the alternating line-width effect may be attributed to the migration of the potassium ion form one side of the naphthalene ring to the other. Previously, de Boer *et al.*[8] proposed an ion-pair model for the pyracene-alkali metal ion-pair, which gave us the impression that the alkyl groups have a strong affinity to the alkali ion. However, in our studies of the ion-pairs of acenaphthene[9] and 9,10-dihydroanthracene radical anions[10] with alkali ions we pointed out that an electrostatic interaction model, which predicts the ion-pair structure where an alkali ion is situated at the position of the highest negative charge, is more reliable than de Boer's model. The present result supports our prediction. This is also one of the rare sources of information about the migration of the alkali ion form one side of a molecular plane to the other.

Experimental

The anion radical of the 5,12-dihydrotetracene was prepared by reduction with lithium, sodium, and potassium. The solvents used were 1,2-dimethoxyethane (DME), tetrahydrofuran (THF), and tetrahydropyran (THP). In DME and THF, three kinds of alkali metals were used as reducing agents, while in THP only potassium was used. The 5,12-dihydrotetracene used was obtained commercially (Tokyo Kasei, G. R.) and was purified by recrystallization from benzine. The ESR spectra were measured by a Hitachi X-band ESR spectrometer, model MES 4001, employing field modulation at 100 kHz. As the radical anion was unstable above room temperature, the radical anion was prepared and the ESR spectra were measured below room temperature. Low temperatures were obtained by letting cool nitrogen gas flow through a Dewar jacket leading through the sample cavity. The temperature was controlled by adjusting the flow rate of the cool nitrogen gas, and was checked with a copper constantan thermocouple placed just below the sample. The magnetic field was calibrated by a Hitachi field marker.

Results

Representative spectra obtained in the present experiment are shown in Figs. 1 to 4. The proton

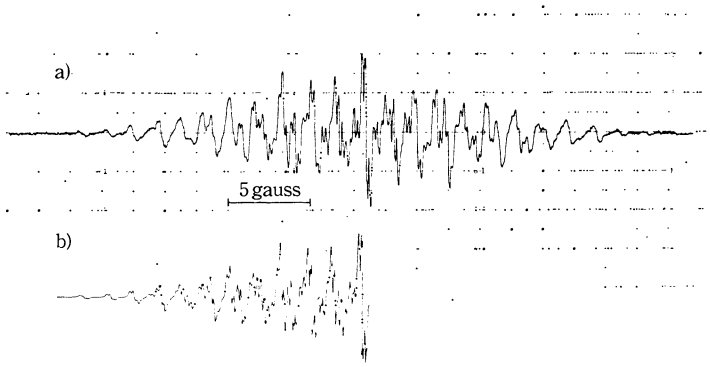

Fig. 1. ESR spectra of the 5,12-dihydrotetracene radical anion in DME with potassium as a counter ion.
a) observed spectrum at −72°C.
b) computer simulated spectrum using the hyperfine splitting constants given in Table 1.*1
The magnetic field increases from right to left.

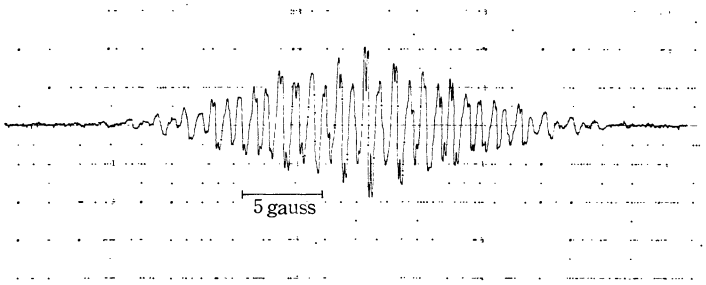

Fig. 2. ESR spectrum observed at −92°C (for) the lithium-5,12-dihydrotetracene radical - THF system.

8) a) E. de Boer and E. L. Mackor, *J. Amer. Chem. Soc.*, **86**, 1513 (1964). b) E. de Boer, *Rec. Trav. Chim. Pays-Bas*, **84**, 609 (1965).

9) M. Iwaizumi, M. Suzuki, T. Isobe and H. Azumi, This Bulletin, **40**, 2754 (1967).

10) M. Iwaizumi and J. R. Bolton, *J. Mag. Resonance*, **2**, 278 (1970).

*1 The line-widths at the central part of the spectra differ from those at the wings in the observed spectra. Such an effect was not taken into account in the computation of the spectrum.

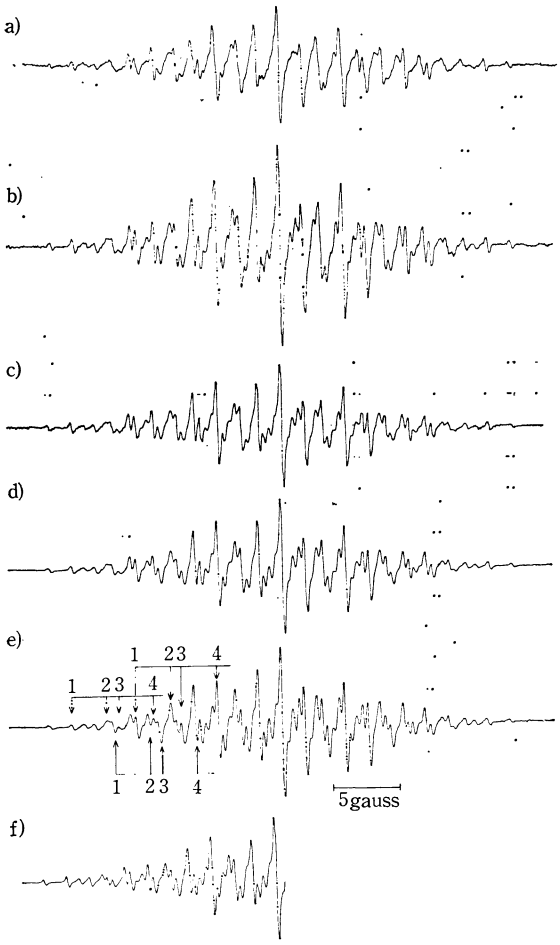

Fig. 3. ESR spectra obtained for the potassium-5,12-dihydrotetracene radical - THF system a) at −30°C, b) at −56°C, c) at −66°C, d) at −78°C and e) at −99°C. Spectrum f) is a computer simulated spectrum for d) obtained using the Bloch's two jump model with $\tau = 1.7 \times 10^{-6}$ sec.*1 The magnetic field increases from right to left.

hyperfine splitting constants are listed in Table 1. For purposes of comparison, the hyperfine splitting constants of the *o*-xylene[11] and 2,3-dimethylnaphthalene[12] radical anions are collected, along with those of the 5,12-dihydrotetracene radical anion. All the splitting constants of the 5,12-dihydrotetracene radical anion were assigned on the basis of the Hückel molecular-orbital calculation, which is shown in Table 2, and by comparison with the hyperfine splitting constants of the *o*-xylene and 2,3-dimethylnaphthalene radical anions. In the molecular-orbital calculation, the hyperconjugation effect of the methylene bridges is included. The parameters used were as follows:

$$\delta\alpha_1 = -0.5\beta \quad \delta\alpha_2 = -0.1\beta \quad \delta\alpha_3 = -0.1\beta$$
$$\beta_{12} = 2.0\beta \quad \beta_{23} = 0.8\beta \quad \beta_{13} = 0.3\beta$$

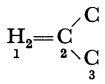

Here, β_{13} was introduced since the methylene protons at the axial positions must be situated in close proximity to the π-orbital in the benzene and naphthalene rings if the molecule is non-planar. The inclusion of this parameter improved the agreement between the observed hyperfine splitting constants and the calculated ones. Table 2 also lists such results of the electrostatic perturbation calculation[13,14] on the effect of the alkali ion on the proton hyperfine splittings as relate to the following discussion.

The ESR spectra observed in DME with lithium, sodium, and potassium ions as counter ions show the same hyperfine structure, and no appreciable change with the alkali ions is observed (see Table 1). Although the line width broaden and the resolution of the spectra becomes worse with an increase in the temperature, there seems to be no large change in the hyperfine splitting constants with the temperature. It may be considered, therefore, that in DME the radical anion exists as a free anion or as an ion pair bound very loosely, for there is no marked effect of the cations on the ESR spectra. It may be noted here that, in these systems, the four methylene protons show a normal quintet splitting, although they must exist as axial and equatorial protons.

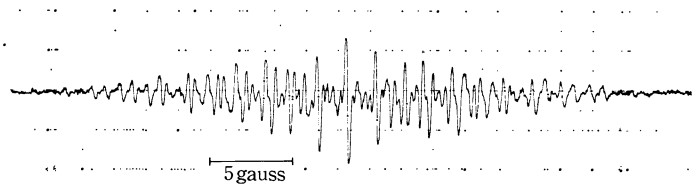

Fig. 4. ESR spectrum obtained for the potassium-5,12-dihydrotetracene radical - THP system at −50°C.

11) J. R. Bolton, *J. Chem. Phys.*, **41**, 2455 (1964).
12) F. Gerson, B. Weidmann and E. Heilbronner, *Helv. Chim. Acta*, **47**, 1951 (1964).
13) B. J. McClelland, *Trans. Faraday Soc.*, **57**, 1458 (1961).
14) M. Iwaizumi, M. Suzuki, T. Isobe and H. Azumi, This Bulletin, **40**, 1325 (1967).

Table 1. Observed hyperfine splitting constants of the 5,12-dihydrotetracene, 2,3-dimethylnaphthalene and *o*-xylene radical anions (gauss)

a) 5,12-Dihydrotetracene radical anion

Solvent and Cation	Temperature	Position (1,4)	(2,3)	(6,11)	(7,10)	(8,9)	CH_2	Alkali-metal
DME-Li	−72°C	0.194	0.080	4.359	5.038	1.693	3.133	···
DME-Na	−72°C	0.194	0.080	4.359	5.038	1.693	3.133	···
DME-K	−72°C	0.194	0.080	4.359	5.038	1.693	3.133	···
THF-Li	−92°C	0.198	0.081	4.308	5.034	1.726	3.356	···
THF-Na	−88°C	0.196	0.080	4.022	5.082	1.636	3.448	0.868(−27°C)*1 1.168(+11°C)
THF-K	−99°C	<0.09	···	4.659	4.820	1.737	3.412, 2.651	···
THP-K	−50°C	<0.07	···	4.635	4.845	1.754	3.509, 2.495	···

b) 2,3-Dimethylnaphthalene radical anion*2

Solvent and Cation	Temperature	Position α	α′	β	CH_3	Alkali-metal
DME-Na	−70°C	4.93	4.67	1.76	1.69	···

c) *o*-Xylene radical anion*3

Solvent and Cation	Temperature	Position (3,6)	(4,5)	CH_3	Alkali-metal
DME-K	−80°C	6.93_5	1.81_5	2.00_6	···

*1 Sodium hyperfine splitting was not observed at −88°C.
*2 cited from Ref. 12.
*3 cited from Ref. 11.

Table 2. Calculated ring proton hyperfine splitting constants*1 of 5,12-dihydrotetracene radical anion (gauss)

		Position (1,4)	(2,3)	(6,11)	(7,10)	(8,9)
Free-anion		0.110	0.040	4.018	5.018	1.812
Ion-pair*2	model A	0.049	0.040	3.577	5.027	1.923
	model B	8.160	1.944	0.302	0.119	0.071

*1 The splitting constants of the ring protons were calculated by $a_i = Q^H_{CH}\,\rho_i$ with $Q^H_{CH} = 27$ gauss.
*2 The calculations were carried out using McClelland method[13,14] with the alkali metal placed 4.0 Å above the center of the naphthalene ring (model A) and with that placed 4.0 Å above the center of the benzene ring (model B).

When THF or THP was used as a solvent, appreciable effects of the cation were observed on the hyperfine structure of the ESR spectra. The proton hyperfine splitting constants change with the cations, and when sodium is used as a reducing agent, an additional splitting arising from the sodium nucleus is observed. In THF, this sodium hyperfine splitting has a positive temperature coefficient and disappears below a temperature of about −50°C.

The effect of the cation on the proton hyperfine splittings is especially remarkable when the cation is a potassium ion in THF and in THP. The hyperfine splittings due to the protons at 1,4 and 2,3 positions are much smaller than those in the other systems, and that of the methylene protons splits into two sets of triplets. Moreover, in THF the methylene proton hyperfine splitting changes markedly with the temperature and the two sets of triplet splittings coalesce to a quintet splitting at a higher temperature, showing the effect of the alternating line width. In Fig. 3, four of the hyperfine lines with spin states, (1,1), (1,0), (0,1), and (0,0), are numbered from 1 to 4 respectively. Here the numbers in parentheses are the magnetic index numbers[15] for the two sets of methylene protons. One can see from the figure that, as the temperature increases, the 2 and 3 lines become broad and tend to coalesce to form the quintet splitting as a result of hyperfine interaction with the methylene protons.

Discussion

Spin Distribution and Inversional Motion of the 5,12-Dihydrotetracene Radical Anion. As Table 1 shows, the unpaired electron is dis-

15) J. H. Freed and G. K. Fraenkel, *J. Chem. Phys.*, **40**, 1815 (1964).

tributed between the naphthalene and benzene conjugated systems in the radical anion molecule. The distributions of the spin densities in the benzene and naphthalene rings are quite similar to those in the *o*-xylene and 2,3-dimethylnaphthalene radical anions respectively, although a large portion of the spin densities exist on the naphthalene ring. This implies that this molecule can be considered in terms of two weakly-coupled benzene and naphthalene rings. The coupling mechanism is presumably due to a hyperconjugation effect of the methylene bridges, as has also been suggested for the case of the 9,10-dihydroanthracene radical anion.[16] The molecular-orbital calculation for the hyperfine splitting constants including the hyperconjugation effect of the methylene bridges, given in Table 2, well predicts the observed spin distribution.

On the other hand, as was mentioned in the preceeding section, the methylene protons show the normal quintet splitting except when there is a strong perturbation due to the alkali metal cation, as in the case of the ion-pairs with a potassium ion in THF and in THP. From the fact that the conformation of the 9,10-dihydroanthracene is non-planar,[7] it seems reasonable to consider that the 5,12-dihydrotetracene also has a non-planar conformation, which would lead to an inversion process. The methylene protons which are in axial and equatorial positions can thus be expected to exchange their positions in the inversional process with each other. The equivalence of the methylene protons in the ESR spectrum implies that the rate of the inversional motion is $\gg 10^8$ Hz.

Ion-pair Formation and Structure of the Ion Pair. As was mentioned in the previous section, the hyperfine splitting constants change with the association of the alkali ion. The effect of the potassium ion observed in THF and in THP is especially remarkable. Such cation effects provide us with very useful information about the structure of the ion pair. In such a system as two-conjugated systems weakly coupled, the spin distribution between the two conjugated systems is considered to be sensitive to the association of a cation on either of the conjugated systems.[10] In the present case, it was observed that the association of the cation causes a migration of the unpaired electron density from the benzene ring to the naphthalene ring. This effect implies that the potassium ion may associate with the radical anion on the side of the naphthalene ring. The electrostatic perturbation calculations[13,14] were carried out in order to establish the effect of the cation. The results given in Table 2 are for two ion-pair models, one where the cation is placed 4.0 Å above the center of the naphthalene ring (model A) and the other where the cation is placed 4.0 Å above the center of the benzene ring (model B). As may be seen from Table 2, Model A well explains the observed effect of the migration of the unpaired electron density from the benzene ring to the naphthalene ring. It is also consistent with the electrostatic interaction model, since the electron density and, hence, the negative-charge density are at maxima on the naphthalene ring.

In this ion-pair model, the two different hyperfine splittings observed for the methylene protons are attributed to the hyperfine interaction with the methylene protons on the same side of the molecular plane as the potassium ion and with those at the reverse side. Therefore, the alternating line-width effect observed in the potassium-5,12-dihydrotetracenide ion-pair in THF can be explained by the exchange of the potassium ion between the two preferred positions, above and below the molecular plane.*2

The exchange reaction mentioned above can proceed by both *inter*- and *intra*-molecular processes, (1) and (2);

$$K^+ + A^-K^{*+} \rightleftarrows K^+A^- + K^{*+} \quad (1)$$

$$A^-K^+ \rightleftarrows K^+A^- \quad (2)$$

where A^- stands for the radical anion. In some cases of ESR studies of ion pairs, additional alkali-metal hyperfine splittings were very useful in getting information on the life time of the ion pairs and in deducing whether exchange reactions were *inter*-molecular or *intra*-molecular in nature.[8-10,17]

16) M. Iwaizumi, T. Isobe and J. R. Bolton, to be published.

*2 The alternating line width effect can be caused also by the inversional motion of the molecule. However in the present case we do not prefer a hypothesis that the observed alternating line width effect is related to the inversional motion of the molecule. If the ratio of axial to equatorial splitting constants follows from the angular dependence of the β proton splitting constants, $a_\beta^H = B\cos^2\theta$, it must be about 4.0.[6] However the observed ratios of the methylene proton splitting constants change with strength of association of the cation and have the values 1.287 for the potassium-5,12-dihydrotetracenide ion-pair in THF and 1.406 for that in THP. These ratios are rather close to the value observed in the methylene protons for the potassium-acenaphthenide ion-pair, 1.05. In the acenaphthene ion-pair system, two hyperfine splitting constants coming from the methylene protons were explained by the effect of the electrostatic force of the associated cation. In view of these facts it seems reasonable to attribute the present observation to the electrostatic effect of the associated cation on the proton splitting constants. It is considered that the rapid inversion process of the molecule still occur.

17) a) N. M. Atherton and A. E. Goggins, *Mol. Phys.*, **8**, 99 (1964). b) E. E. Gough and M. C. R. Symons, *Trans. Faraday Soc.*, **62**, 269 (1966). c) T. A. Claxton, W. M. Fox and M. C. R. Symons, *ibid.*, **63**, 2570 (1967). d) D. H. Chen, E. Warhurst and A. M. Wilde, *ibid.*, **63**, 2561 (1967). e) P. S. Gill and T. E. Gough, *Can. J. Chem.*, **45**, 2112 (1967). f) J. Gendell, *J. Chem. Phys.*, **46**, 4152 (1967). g) K. Nakamura, This Bulletin, **40**, 1019 (1967).

In the present system, however, the hyperfine splitting due to the cation was not observed. It is possible that the alkali metal hyperfine splitting is averaged to zero by a rapid *inter*-molecular exchange reactoin of the alkali ion, and in some cases rapid *inter*-molecular equilibria have been concluded from the absence of cation splittings in the ESR spectra of the ion-pair systems.[18] We consider, however, that the observed reaction is the *intra*-molecular process for the following reasons.

(1) No potassium hyperfine splitting was observed, even under slow exchange conditions, such as in the potassium-5,12-dihydrotetracenide in THP, where the methylene protons showed two definite sets of triplet splittings. This implies that the potassium splitting constants are essentially too small to be resolved and that the absence of the metal splitting constant is not due to the rapid *inter*-molecular exchange of the cation. Previously, Dodson and Reddoch[19] showed that, in the naphthalene-alkali metal ion-pair system, potassium hyperfine splittings are very small, or are not observed at all, because the contributions of the hyperfine interaction with the positive and negative signs cancel each other out, although stable ion pairs are formed. It is considered that the alkali metal couplings in the present system are in a situation similar to that of the naphthalene ion-pair system.

(2) The sodium 5,12-dihydrotetracenide ion pair in THF shows a well-resolved sodium hyperfine splitting above $-30°C$, from which the lifetime of the ion pair can be estimated to be $\gg 10^{-6}$ sec. In view of the fact that the potassium ion generally has a greater tendency to associate with anion radicals than does the sodium ion,[14,18,20,21] the lifetime of the potassium-5,12-dihydrotetracenide ion pair in THF may be considered to be $\gg 10^{-6}$ sec. On the other hand, the lifetime of the static conformation of the ion pair is estimated to be about 6×10^{-7} sec from the observed alternating line-width effect in the same temperature range.

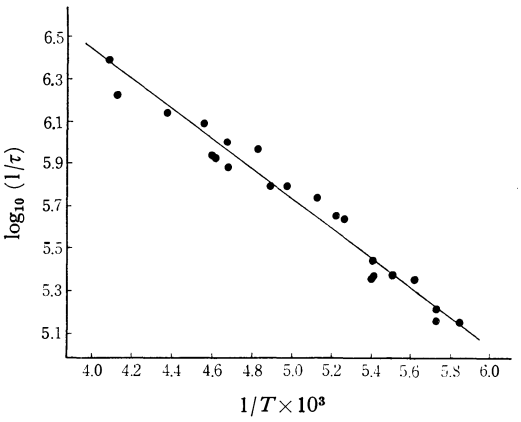

Fig. 5. Plot of $\log_{10} 1/\tau$ against $1/T\times 10^3$.

It may be concluded from these facts that the observed exchange reaction proceeds by the *intra*-molecular process. We computed spectra for different values of the lifetime of the ion-pair conformation, τ. Figure 5 shows the plot of the $\log_{10}(1/\tau)$ $(=\log_{10} k)$ thus estimated against $1/T$. Here k is the rate of the exchange reaction. As is expected from the Arrhenius equation,

$$k = 1/\tau = k_0 \exp(-E_A/RT) \qquad (3)$$

it shows a straight line. This gives a potential barrier to the migration of the potassium ion from one side of the molecular plane to the other; $E_A = 3.1\pm 0.2$ kcal/mol, and the frequency factor, $k_0, = 1.4\pm 0.5\times 10^9$ sec^{-1}.

On the other hand, one can see from Table 1 that effects of the cations on the proton hyperfine splittings vary with the cations. This implies that there may be slight differences in the equilibrium positions of the cations, but the ion-pair structure is not discussed in detail here. It may also be seen from the table that, in the case of the lithium or sodium-5,12-dihydrotetracenide in THF, the effects of the cations are smaller than in the case of the potassium-5,12-dihydrotetracenide in THF or in THP, suggesting that, in the former cases, the radical anion is in a more loosely bound ion-pair state.

The numerical calculations were carried out on the NEAC 2200 Model 500 computer at the Computer Center, Tohoku University.

18) A. H. Reddoch, *J. Chem. Phys.*, **43**, 225 (1965).
19) C. L. Dodson and A. H. Reddoch, *ibid.*, **48**, 3226 (1968).
20) A. C. Aten, J. Dieleman and G. J. Hoijtink, *Discuss. Faraday Soc.*, **29**, 182 (1960).
21) N. Hirota, R. Carraway and W. Schook, *J. Amer. Chem. Soc.*, **90**, 3611 (1968).

BULLETIN OF THE CHEMICAL SOCIETY OF JAPAN VOL. 43 3695—3698 (1970)

Microwave Spectra of Vinylacetylene and Monodeutero Vinylacetylene in Ground and Excited Vibrational States

Chiaki HIROSE

Laboratory of Molecular Spectroscopy, Tokyo Institute of Technology, Ookayama, Meguro-ku, Tokyo

(Received May 22, 1970)

The microwave spectra of vinylacetylene, CH_2CHCCH, and monodeutero-vinylacetylene, CH_2CHCCD, have been observed in the ground state and several vibrational excited states. The vibration-rotation constants $\alpha_1^{(a)}$, $\alpha_1^{(b)}$, $\alpha_1^{(c)}$, $\alpha_2^{(a)}$, $\alpha_2^{(b)}$, and $\alpha_2^{(c)}$, have been obtained as 1 370, −18.32, −7.73, −907, −2.78, and −8.97 MHz for CH_2CHCCH, and 2 010, −16.66, −7.05, −1 640, −2.18 and −7.84 MHz for CH_2CHCCD, respectively, the error limits being ±50 MHz for $\alpha^{(a)}$'s and ±0.03 MHz for $\alpha^{(b)}$'s and $\alpha^{(c)}$'s. Electric dipole moments obtained are 0.223± 0.020 and 0.206±0.008 Debye for CH_2CHCCH and CH_2CHCCD, respectively, which are quite different from the values reported previously.

The present study was begun with the purpose of getting the rotational constants of normal- and monodeutero-vinylacetylene. The values obtained have been used by Fukuyama *et al.* in their research on the structure of a series of molecules with conjugated carbon-carbon multiple bonds.[1]

The study of vibration-rotation interactions of the molecule presents another interesting theme, since infrared spectroscopy gives relatively poor information, especially below 550 cm^{-1}, where three or five fundamentals, one overtone, and one combination-tone are known to exist,[2] and some perturbations on the energy levels are supposed to exist. The data on vibrational frequencies are listed in Table 1.*1 The author has investigated the rotational spectra in the above-mentioned vibrational states and found that strong resonances among the levels take place.

Table 1. Low-lying vibrational levels[a] (in cm^{-1})

Mode of vibration		CH_2C-HCCH	CH_2C-HCCD
ν_1 (A')	C≡C-C in plane deformation	225	212
ν_2 (A'')	C≡C-C out of plane deform.	307	287
ν_3 (A')	C=C-C bending	539	541
ν_4 (A'')	C≡C-H out of plane deform.	624	489
ν_5 (A')	C≡C-H in plane bending	667	494
ν_6 (A'')	CH_2 twisting	673[b]	676
$2\nu_1$ (A')[c]		450	424
$\nu_1+\nu_2$ (A'')[c]		532	499
$3\nu_1$ (A')[c]		675	636

a) Observed and assigned by Abe.[2]
b) Calculated by Abe.[2]
c) Sum of the corresponding fundamentals.

The electric dipole moment of the molecule has been reported by Sobolev *et al.* to be 0.43 Debye, which is obtained by analyzing the Stark effect of the transition $1_{0,1}\leftarrow 0_{0,0}$ on the assumption that $\mu_b=0$.[3] The author has tried to obtain the electric dipole moment without this assumption by analyzing transitions $J=1\leftarrow 0$ and $J=2\leftarrow 1$.

Experimental

Normal vinylacetylene, CH_2CHCCH, was supplied by Denki Kagaku Co. and was used without further purification. Impurities were checked using infrared and microwave spectra and believed to be less than 10%. Monodeutero-vinylacetylene, CH_2CHCCD, synthesized by reacting the normal species with D_2O, was contaminated with a few percent of normal vinylacetylene but was used without purification.

The rotational spectra were observed using a conventional microwave spectrometer with 110 kHz Stark modulation. Most lines were observed by cooling the waveguide cell with dry ice. The rotational transitions were assigned from the Stark effects of the lines. The relative intensities of the lines which had nearly the same Stark effect were the principal means for vibrational assignments.

1) T. Fukuyama, K. Kuchitsu and Y. Morino, This Bulletin, **42**, 379 (1969).

2) K. Abe and T. Shimanouchi, *Spectrochim. Acta*, to be published.

*1 For the sake of simplicity, subscripts for the vibrational modes start from the lowest frequency ignoring the symmetry properties.

3) G. A. Sobolev, A. M. Scherbakov and P. A. Akishin, *Optics and Spectry.*, **12**, 78 (1962).

TABLE 2. OBSERED TRANSITIONS FOR GROUND AND LOW-LYING VIBRATIONAL STATES (in MHz)

CH_2CHCCH Transition	G. S. Obsd	ν_1 Obsd	ν_2 Obsd
$0_{0,0}\rightarrow 1_{0,1}$	9 074.74±0.02	9 100.73±0.02	9 086.3 ±0.02
$1_{0,1}\rightarrow 2_{0,2}$	18 146.58±0.02	18 198.58±0.02	18 169.97±0.02
$1_{1,1}\rightarrow 2_{1,2}$	17 734.53±0.02	17 776.05±0.02	17 763.05±0.02
$1_{1,0}\rightarrow 2_{1,1}$	18 564.91±0.02	18 627.64±0.02	18 582.16±0.02
$2_{0,2}\rightarrow 3_{0,3}$	27 212.62±0.02	27 290.06±0.02	27 248.22±0.02
$2_{1,2}\rightarrow 3_{1,3}$	26 599.93±0.02	26 662.18±0.02	26 644.19±0.02
$2_{1,1}\rightarrow 3_{1,2}$	27 845.38±0.02	27 939.32±0.02	27 871.38±0.02
$2_{2,1}\rightarrow 3_{2,2}$	27 225.99±0.02	27 303.86±0.02	27 261.07±0.02
$2_{2,0}\rightarrow 3_{2,1}$	27 237.27±0.02	27 316.07±0.02	27 271.76±0.03
CH_2CHCCH Transition	$\nu_1+\nu_2$ Obsd	$2\nu_1$ Obsd	$2\nu_2$ Obsd.
$0_{0,0}\rightarrow 1_{0,1}$	9 113.0 ±0.1	9 127.5 ±0.1	
$1_{0,1}\rightarrow 2_{0,2}$	18 221.1 ±0.1	18 429.1 ±0.1	
$1_{1,1}\rightarrow 2_{1,2}$	17 806.5 ±0.1	17 816.5 ±0.1	17 794.0 ±0.3
$1_{1,0}\rightarrow 2_{1,1}$	18 643.0 ±0.2	18 689.3 ±0.1	18 600.3 ±0.3
$2_{0,2}\rightarrow 3_{0,3}$		27 365.77±0.05	
$2_{1,2}\rightarrow 3_{1,3}$	26 707.0 ±0.1	26 723.00±0.05	26 688.0 ±0.3
$2_{1,1}\rightarrow 3_{1,2}$	27 961.70±0.05	28 031.60±0.05	27 898.0 ±0.3
$2_{2,1}\rightarrow 3_{2,2}$		27 380.29±0.05	
$2_{2,0}\rightarrow 3_{2,1}$		27 392.95±0.05	
CH_2CHCCD Transition	G. S. Obsd	ν_1 Obsd	ν_2 Obsd
$0_{0,0}\rightarrow 1_{0,1}$	8 441.80±0.01	8 465.51±0.01	8 451.79±0.02
$1_{0,1}\rightarrow 2_{0,2}$	16 881.20±0.02	16 928.58±0.02	16 901.31±0.03
$1_{1,1}\rightarrow 2_{1,2}$	16 517.60±0.02	16 555.46±0.02	16 543.22±0.03
$1_{1,0}\rightarrow 2_{1,1}$	17 249.87±0.02	17 307.00±0.02	17 264.30±0.03
$2_{0,2}\rightarrow 3_{0,3}$	25 316.27±0.01	25 386.83±0.02	25 346.73±0.03
$2_{1,2}\rightarrow 3_{1,3}$	24 774.82±0.01	24 831.33±0.02	24 813.36±0.03
$2_{1,1}\rightarrow 3_{1,2}$	25 873.50±0.01	25 958.95±0.02	25 895.14±0.03
$2_{2,1}\rightarrow 3_{2,2}$	25 326.13±0.01	25 397.10±0.02	25 357.46±0.03
$2_{2,0}\rightarrow 3_{2,1}$	25 334.49±0.01	25 406.26±0.02	25 365.29±0.03
$3_{0,3}\rightarrow 4_{0,4}$	33 745.50±0.01		33 776.6 ±0.1
$3_{1,3}\rightarrow 4_{1,4}$	33 030.31±0.01	33 105.75±0.01	33 082.04±0.02
$3_{1,3}\rightarrow 4_{1,3}$	34 495.38±0.01	34 609.02±0.01	34 524.30±0.02
$3_{2,2}\rightarrow 4_{2,3}$	33 767.46±0.01	33 862.11±0.01	33 800.70±0.02
$3_{2,1}\rightarrow 4_{2,2}$	33 789.54±0.01	33 885.69±0.01	33 821.56±0.02
$3_{3,1}\rightarrow 4_{3,2}$ $3_{3,0}\rightarrow 4_{3,1}$	33 776.76±0.05	33 870.98±0.07	33 812.07±0.08
CH_2CHCCD Transition	$2\nu_1$ Obsd	$3\nu_1$ Obsd	$2\nu_2$ Obsd
$0_{0,0}\rightarrow 1_{0,1}$	8 489.0 ±0.1	8 512.0 ±0.1	
$1_{0,1}\rightarrow 2_{0,2}$	16 975.5 ±0.2	17 019.5 ±0.2	16 922.0 ±0.3
$1_{1,1}\rightarrow 2_{1,2}$	16 592.5 ±0.2		16 569.0 ±0.3
$1_{1,0}\rightarrow 2_{1,1}$	17 362.3 ±0.3	17 418.7 ±0.3	17 279.5 ±0.3
$2_{0,2}\rightarrow 3_{0,3}$			
$2_{1,2}\rightarrow 3_{1,3}$	24 886.5 ±0.3	24 942.1 ±0.3	24 853.1 ±0.3
$2_{1,1}\rightarrow 3_{1,2}$	26 043.3 ±0.3	26 125.3 ±0.5	25 918.3 ±0.3
$2_{2,1}\rightarrow 3_{2,2}$	25 468.3 ±0.5	25 536.8 ±0.5	
$2_{2,0}\rightarrow 3_{2,1}$	25 476.5 ±0.5	25 546.0 ±0.5	
$3_{0,3}\rightarrow 4_{0,4}$			
$3_{1,3}\rightarrow 4_{1,4}$	33 179.8 ±0.3	33 251.7 ±0.3	
$3_{1,2}\rightarrow 4_{1,3}$	34 720.0 ±0.3	34 831.0 ±0.3	34 554.0 ±0.3
$3_{2,2}\rightarrow 4_{2,3}$	33 955.0 ±0.5		
$3_{2,1}\rightarrow 4_{2,2}$	33 980.3 ±0.5		
$3_{3,1}\rightarrow 4_{3,2}$	33 964.0 ±0.5		
$3_{3,0}\rightarrow 4_{3,1}$	33 964.0 ±0.5		

Results

The transitions assigned are listed in Table 2. No b-type transition was observed in spite of a careful search. Because of this and a slight asymmetry of the molecule, it was impossible to obtain the exact value of the rotational constant A. Table 3 lists the derived constants B_0 and C_0 for the ground vibrational state and vibration-rotation constants $\alpha_i^{(b)}$ and $\alpha_i^{(c)}$ for ν_1 and ν_2 states. When the perturbation method is used, the value of A can be obtained from the deviation of the observed lines from the symmetric-top pattern through the value of $(B-C)^2/(A-(B+C)/2)$. The values of A_0, $\alpha_1^{(a)}$, and $\alpha_2^{(a)}$ thus obtained are listed also in Table 3.

Table 3. Derived molecular constants (in MHz)

	CH_2CHCCH	CH_2CHCCD
A_0	49 900 ±750	48 900 ±1600
B_0	4 744.66± 0.03	4 403.82± 0.08
C_0	4 329.68± 0.03	4 037.58± 0.08
$\alpha_1^{(a)}$	1 370 ± 50	2 010 ± 70
$\alpha_1^{(b)}$	−18.32± 0.03	−16.66± 0.05
$\alpha_1^{(c)}$	− 7.73± 0.03	− 7.05± 0.05
$\alpha_2^{(a)}$	−907 ± 50	−1 640 ± 50
$\alpha_2^{(b)}$	− 2.78± 0.03	− 2.18± 0.03
$\alpha_2^{(c)}$	− 8.97± 0.03	− 7.84± 0.03

Assignment of the rotational transitions in ν_3, ν_4, and ν_5 states was unsuccessful, because the Coriolis coupling between the states disturbs the spectra strongly in both CH_2CHCCH and CH_2CHCCD, and the $\nu_1+\nu_2$ state of the latter interacts with ν_4 and ν_5 through Fermi resonance. Further analysis and discussion on the problem will be given in a separate paper.

The Stark effects of the transitions $J=1\leftarrow0$ and $J=2\leftarrow1$ in the ground vibrational state were measured. From the results (Table 4), the electric dipole moments μ_a of the molecule were derived to be 0.223 ± 0.020 and 0.206 ± 0.008 Debye for normal and monodeutero-vinylacetylene, respectively. Analysis of the Stark effect revealed that μ_b is very small. Its value can not be determined accurately in spite of the fact that some of the transitions such as $3_{1,3}\leftarrow2_{1,2}$ $(M=0)$ have an appreciable dependence on μ_b^2.

As suggested by Morgan and Goldstein,[4] who observed five lines of the transitions $J=3\leftarrow2$ in the ground vibrational state of CH_2CHCCH, the effect of the centrifugal distortion is not negligible, and centrifugal distortion shifts of a few MHz is observed even in $J=3\leftarrow2$ transitions. However, because of the smallness of the molecular asymmetry and the failure to observe b-type transitions, it was not possible to determine the centrifugal distortion constants.

Discussion

Molecular Structure. The rotational constants observed in the present study were used by Fukuyama *et al.*[1] in combination with their electron-differaction data to determine the structure of the molecule.

Vibration-Rotation Constants. The rotational energy levels in an excited vibrational state are known to approximate a rigid rotor model when no vibrational state perturb the state,[5] and the rotational constants in the state v are expressed as B_v, which can be written in terms of α_v constants as

$$B_v^{(x)} = B_0^{(x)} - \alpha_v^{(x)} \qquad (1)$$

The $\alpha_v^{(x)}$ constants are the sum of two terms, one determined by the harmonic terms in the internal

Table 4. Stark effects of absorption lines (in 10^{-5} MHz(V/cm)^2) and electric dipole moment of the molecule (in Debye)

Transition		CH_2CHCCH Obsd	CH_2CHCCH Calcd	CH_2CHCCD Obsd	CH_2CHCCD Calcd
$0_{0,0}\rightarrow1_{0,1}$	$M=0$	0.290 ±0.003	0.293	0.256 ±0.006	0.269
$1_{0,1}\rightarrow2_{0,2}$	$M=0$	−0.0887±0.0005	−0.0836	−0.0772±0.0006	−0.0771
	$M=1$	0.0730±0.0008	0.680	0.0619±0.0006	0.0620
$1_{1,1}\rightarrow2_{1,2}$	$M=0$	0.0745±0.0006	0.0696	0.0658±0.0008	0.0635
	$M=1$	2.873 ±0.07	2.930		
$1_{1,0}\rightarrow2_{1,1}$	$M=0$	0.0617±0.0007	0.0665	0.0614±0.0008	0.0608
	$M=1$	−2.554 ±0.06	−2.840		
	μa	0.223 ±0.020		0.206 ±0.008	
	μb	0.02		0.02	

4) H. W. Morgan and J. H. Goldstein, *J. Chem. Phys.*, **20**, 1981 (1952).

5) H. H. Nielsen, *Phys. Rev.*, **75**, 1961 (1949); T. Oka and Y. Morino, *J. Mol. Spectry.*, **6**, 472 (1961); T. Oka, *J. Chem. Phys.*, **47**, 5410 (1967).

6) Y. Morino and C. Hirose, *J. Mol. Spectry.*, **22**, 99 (1967).

7) Y. Morino and C. Hirose, *ibid.*, **24**, 204 (1967).

Table 5. The values of $\alpha v^{(x)}/(B_0^{(x)})^2$

	$\alpha_1^{(b)}/B_0^2$	$\alpha_1^{(c)}/C_0^2$	$\alpha_2^{(b)}/B_0^2$	$\alpha_2^{(c)}/C_0^2$	
C_4H_4	−8.14	−4.12	−1.23	−4.76	10^{-7}MHz^{-1}
C_4H_3D	−8.59	−4.32	−1.12	−4.81	

potential field and the other which depends on the anharmonic potential field; both are proportional to the square of the rotational constants.[5] The values of $\alpha_v^{(x)}/B_0^{(x)2}$ derived from the constants given in Table 3 are listed in Table 5. The values for C_4H_4 and C_4H_3D show a good correspondence with each other.

The author is indebted to Professor Kunio Kozima of Tokyo Institute of Technology for his support and encouragement throughout this work. He also expresses his thanks to Dr. Koichi Abe of the University of Tokyo for his information on vibrational spectra before publication and for his offer of the sample of C_4H_3D, to Professor Kozo Kuchitsu and Mr. Tsutomu Fukuyama of the University of Tokyo, and to Professor Robert F. Curl and Dr. Harold Jones of Rice University, who read through the manuscript and gave important suggestions.

BULLETIN OF THE CHEMICAL SOCIETY OF JAPAN VOL. 43 3698—3705 (1970)

An ESR Study of an Al_2O_3-MoO_3-CoO Catalyst in a System with H_2 and Thio-β-naphthol

Hisashi UEDA and Naoyuki TODO

Government Chemical Industrial Research Institute, Tokyo, Mita, Meguro-ku, Tokyo

(Received June 3, 1970)

This work was planned in order to determine the reaction mechanism of the catalytic, direct desulfurization of organic sulfur compounds on the surface of Al_2O_3-MoO_3-CoO particles. The experimental method consists of quantitative ESR measurements, by means of which the paramagnetic species on the surface of Al_2O_3, Al_2O_3-MoO_3, and Al_2O_3-MoO_3-CoO in the presence and in the absence of H_2 and thio-β-naphthol were studied. As it is expected that, in an ideal and fast-reacting catalytic reaction system, no reaction intermediate can be found because it will be immediately converted to the final product, several artificial reaction systems were investigated in which either one of the reactants, catalyst components, or reaction conditions (*e. g.*, temperature) was deficient. In such deficient systems, the reaction cycle is cut off and some intermediates are expected to accumulate. The paramagnetic species observed were Co^{3+}, Mo^{5+}, thio-β-naphthol$^+$–O^{*2-} or RS^+H–O^{*2-}, and some species formed on the surface of Al_2O_3, in the temperature region of 20°C—200°C. Mo^{6+} is concluded to be the electron trap to facilitate the formation of RS^+H–O^{*2-}, Co^{3+} is concluded to oxidize the Mo^{5+} thus formed to Mo^{6+}, and Co^{2+} is concluded to reduce the R–S^+H_2–O^{*2-} species. The latter then decomposes to H_2S and R·.

The catalytic desulfurization of organic sulfur compounds contained in residual oil using an Al_2O_3-MoO_3-CoO catalyst (to be abbreviated as "AMC catalyst") has been considered to be one of the most promising techniques for lessening the atmospheric pollution. Though several works have been done on the mechanism of the catalysis,[1-4] most of the results obtained are not conclusive. There has been, for example, no clear-cut explanation of the role of each component of the catalyst. One of the present authors previously obtained some information on the nature of the paramagnetic species formed on the surface of various oxides by the ESR method;[5] he found that the results obtained in that work would be useful in analysing the desulfurization reaction with an AMC catalyst.

As organic compounds are processed with the catalyst, the organic reaction intermediates as well as the inorganic reaction intermediates must be determined. Since it is said that a considerable portion of the sulfur compounds in petroleum are

1) J.T. Richardson, *Ind. Eng. Chem. Fundam.*, **3**, 154 (1964).

2) J. H. Ashley and P. C. H. Mitchel, *J. Chem. Soc., A*, **1968**, 2861.

3) J. M. Lipsch and G. C. A. Schuit, *J. Catal.*, **15**, 163 (1969).

4) S. Namba, T. Aonuma and T. Shiba, *Kogyo Kagaku Zasshi*, **73**, 38 (1970).

5) H. Ueda, This Bulletin, **43**, 319 (1970).

in the form of thiophenols and thioethers,[6] thio-β-naphthol (to be abbreviated as "TN") was chosen as the model compound to be added to the catalyst. The analysis of the catalytic reaction system consisting of TN, H_2, and the AMC catalyst has been carried out in the present work by a procedure based upon the results obtained in the previous paper.

The actual desulfurization reaction currently being engineered is at 400°C and at a hydrogen pressure of 200 atm. Industrial operation demands such conditions in order to get a reasonably fast reaction rate, thus securing a quick processing of the oil, mainly for economic reasons. In the present work, however, as the first and easiest possible approach to observe the actual reaction intermediates of the desulfurization reaction, a hydrogen pressure of lower than 1 atm and the highest observation temperature attainable with the attachment to our ESR equipment, 210°C, were used.

Experimental

The oxides and mixed oxides used in this study were all in the form of fine powder. Two different γ-alumina were used. One of them was prepared from aluminum isopropoxide (to be abbreviated as "Ai"), while the other was commercially-available (Shokubai Kasei Co., to be referred to as "Ac"). Al_2O_3-MoO_3 (the content of the latter being 5.44%; to be abbreviated as "AM") was prepared by precipitating ammonium molybdate on the surface of Ac, which was then oxidized in air. The AMC catalyst, consisting 91.38% of Al_2O_3, 5.44% of MoO_3, and 3.18% of CoO, was prepared by precipitating cobalt nitrate on the surface of AM, which was then oxidized in air. All of them were calcined at 500°C for one hour prior to use. The thio-β-naphthol was used after recrystallization. The H_2 used was 99.999% pure (Takachiho Co.) and was used at a pressure above 430 mmHg and at 20°C. Measurements of the ESR were made in the same way as in the previous paper,[5] except for the temperature of the measurements, which were here carried out in the temperature region between 20°C and 200°C. As quantitative ESR measurements are an essential part of this work, particular care had to be taken with them. Quartz tubes which gave almost no ESR signal in the D.C. magnetic field region of 300—5000 gauss and at *x*-band microwave frequencies, and which had almost identical dimensions, were used. As has been reported by Setaka *et al.*,[7] non-resonant microwave absorption by the specimen can affect the magnitude of the output of the microwave detector, which is due to the resonance absorption, even when the input power to the specimen is kept always constant. In the present specimens, all the samples have almost identical non-resonant absorptions, since all of them consist mostly of alumina (more than 90%). The resonant absorption is mostly due to the minor part of the sample components (less than 10%) existing on the surface. Therefore, the consideration of the non-resonant microwave absorption has been almost unnecessary in the present measurements. However, each of the intensities observed in the present work was calibrated by using the intensity of one of the lines from a Mn^{2+} (g=2.1401) sample which was placed inside the cavity, but not inside the sample section, which is inside a Dewar system. As this absorption line has a ralatively narrow line width compared to those of the absorption lines observed from the present specimens, a relatively slow sweeping rate of the magnetic field (0.16 gauss/sec) was necessary in order to record the intensity of this line accurately. The temperature variation of the sample also changes the non-resonant absorption of microwave. This, however, was the same value at 20°C and at 200°C under the present measuring conditions. The warming up of the 100 kHz lock-in amplifier was necessary to get a constant and stable amplification of the signal.

Results

As it is extremely difficult to measure ESR absorption under conditions identical with those actually employed in an engineering desulfurization reaction, it might be wise to start the research by examining the catalyst by conventional measurements. As will be discussed later, the quality of information obtained by conventional (meaning, at room temperature, and either in a vacuum or in atmospheric air) measurements are not as straightforward as might be expected. Figures 1a—1c illustrate the effects of the temperature of measurements, t_m, on the ESR intensities. In Fig. 1a, the intensity of the ESR line with g=1.9328 (for Mo^{5+}) of the sample consisting of AM and TN in a vacuum is shown. The sample which had not been subjected to any

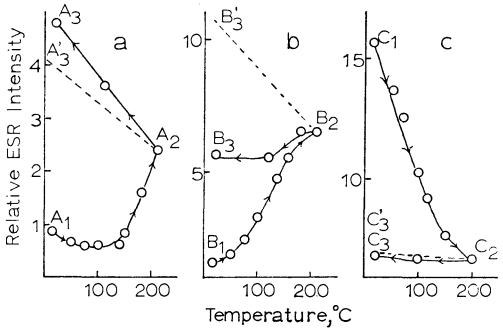

Fig. 1. Relative (the relative scale is not the same as that for the tables) ESR absorption intensities of Mo^{5+} and thio-β-naphthol$^+$-O^{2-} during a heating cycle. The temperature means t_m or the temperature at which measurements were made. a, Mo^{5+} in Al_2O_3-MoO_3 with thionaphthol and in vacuum. g=1.9328. b, thionaphthol$^+$-O^{2-} in the specimen same as a. g=2.0036. c, thionaphthol$^+$-O^{2-} in Al_2O_3-MoO_3-CoO with thionaphthol and in H_2, g=2.0036.

6) B. T. Brooks in "The Chemistry of Petroleum Hydrocarbons," B. T. Brooks, C. E. Boord, S. S. Kartz, Jr., and L. Schmerling, eds., Vol. 1, Reinhold Publ. Co., New York, N. Y. (1954), p. 79.

7) M. Setaka, K. M. Sancier and T. Kwan, *J. Catal.*, **16**, 44 (1970).

thermal treatment before was measured at 20°C (point A_1), and then the t_m was elevated to as high as to 210°C (point A_2), after which the t_m was decreased to as much as to 20°C (point A_3). The A_3' point shows the value which is expected from the value for A_2 point by Curie's law. Figure 1b indicates the temperature variation in the intensity of the ESR line with $g=2.0036$ (for $TN^{+}-O^{*2-}$), for the specimen identical with that for Fig. 1a during one heating cycle. The B_1, B_2, B_3, and B_3' points correspond to A_1—A_3' in Fig. 1a. Figure 1c indicates the same quantity as does Fig. 1b for the specimen consisting of AMC, TN, and H_2. The C_1, C_2, C_3, and C_3' correspond to A_1—A_3' in Fig. 1a. These results indicate that the thermal history of the specimen, as well as the t_m value, strongly affects the concentration of these species on the surfaces of catalyst particles. In Fig. 2, the ESR spectra of

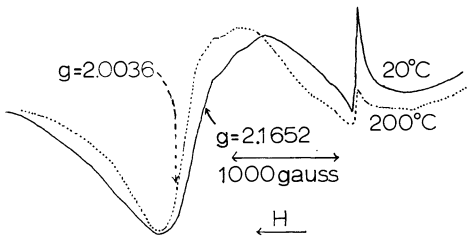

Fig. 2. ESR spectra of γ-alumina prepared from aluminum isopropoxide. Measurements were made at 20°C and at 200°C. Sample in vacuum.

alumina powder, Ai, are shown. The figure indicates that some unexplained paramagnetic species exist on the surface of the alumina specimen, which was supposed to be highly pure except for a small amount of organic contamination left when it was prepared from aluminum isopropoxide by decomposition. It is also shown that some new paramagnetic species are formed at higher temperatures, and that these species disappear when cooled to 20°C again. In Fig. 3, the ESR spectra of AM powder are shown. It will be seen that a new absorption appears at $g=2.1$ if the sample is observed at 200°C. In Fig. 4 the ESR spectra of AMC powder at 20°C are shown. In the spectra the broad absorption

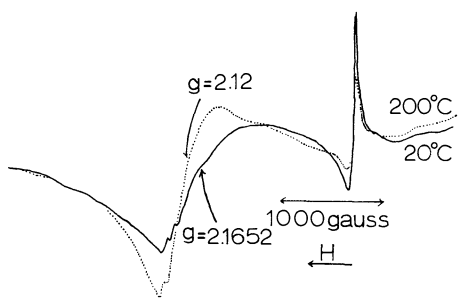

Fig. 3. ESR spectra of Al_2O_3-MoO_3. Measurements identical to Fig. 2.

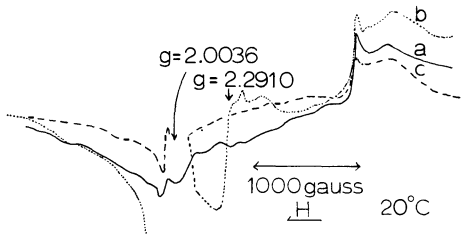

Fig. 4. ESR spectra of Al_2O_3-MoO_3-CoO with and without thio-β-naphthol at 20°C. a, with neither thionaphthol nor H_2. b, with thionaphtol and in vacuum. c, with thionaphthol in H_2.

with $g=2.1$—2.2 which was found in Ai and AM at 20°C, is not found at all, or it is relatively very weak. In Fig. 4b and 4c, the part of the spectra where the absorption of $R^{+}O^{*2-}$ is to be seen is not shown because the absorption in these parts is too strong to be shown together with the entire spectrum. It will be seen that the absorption with $g=2.2910$ appears if TN is added to the AMC powder in a vacuum, and that this species disappears when H_2 is introduced into the sample tube. In Fig. 5, the

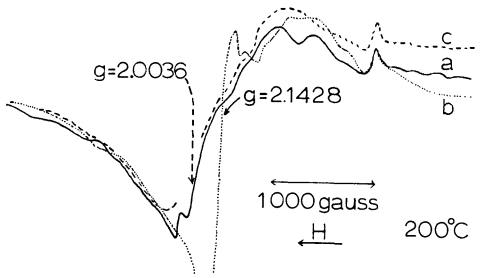

Fig. 5. ESR spectra of Al_2O_3-MoO_3-CoO with and without thio-β-naphthol at 200°C. a, b, and c are corresponding to those in Fig. 4.

ESR spectra of AMC powder at 200°C are shown. a, b, and c correspond to those values in Fig. 4. The broad absorption with $g=2.1$—2.2, which was found in Fig. 2 and Fig. 3, but which was not found in Fig. 4, again appears in this figure. The absorption with $g=2.2910$, previously found only in Fig. 4b, is again found in Fig. 5b with a somehow decreased g-factor of 2.1428. The temperature dependence of the g-factor for this line is shown in Fig. 6. In Fig. 7, the effects of N_2O and NH_3 on the intensities of the line, the g-factor of which is shown in Fig. 6, are shown. The solid curves indicate those in N_2O, while the dotted curves indicate those in NH_3. It will be seen that N_2O intensifies this line at higher temperatures, while NH_3 cancels it. The amplitudes of the curves have been calibrated with one of the Mn^{2+} absorption lines. In Tables 1—4, the relative ESR intensities of the lines with $g=$ 2.0036 and $g=1.9328$, observed with the catalyst components of x, y, and z at 20°C and at 200°C, are shown. The relative intensities for the line with

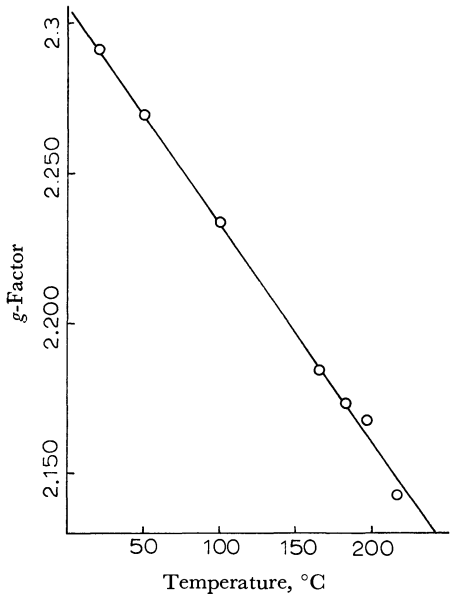

Fig. 6. The temperature dependence of the g-factor of the ESR absorption from Co^{3+} on the surface of a catalyst particle.

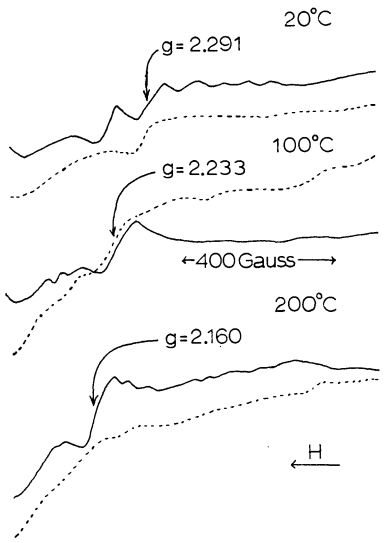

Fig. 7. ESR absorption from the sample consisting of AMC-TN in the region for $g=2.0$ to 3.0. The temperatures indicated are those of the measurements. The dotted curves are those in NH_3 while the solid curves are those in N_2O, both at 400 mmHg/20°C.

Table 1. Relative ESR Intensities[a] of thionaphthol$^+$ $-O^{2-}$ at 20°C.[b]

Oxide components x	y	z	Additive	Gas	Intensity	Data number
Al_2O_3			Thio-β-naphthol		11700	1
Al_2O_3			Thio-β-naphthol	H_2	8900	2
Al_2O_3	MoO_3		Thio-β-naphthol		1500	3
Al_2O_3	MoO_3		Thio-β-naphthol	H_2	1183	4
Al_2O_3	MoO_3	CoO	Thio-β-naphthol		22500	5
Al_2O_3	MoO_3	CoO	Thio-β-naphthol	H_2	16766	6

Table 2. Relative ESR Intensities of thionaphthol$^+$ $-O^{2-}$ at 200°C.

Oxide components x	y	z	Additive	Gas	Intensity	Data number
Al_2O_3			Thio-β-naphthol		5500	7
Al_2O_3			Thio-β-naphthol	H_2	5246	8
Al_2O_3	MoO_3		Thio-β-naphthol		6610	9
Al_2O_3	MoO_3		Thio-β-naphthol	H_2	5316	10
Al_2O_3	MoO_3	CoO	Thio-β-naphthol		2800	11
Al_2O_3	MoO_3	CoO	Thio-β-naphthol	H_2	6800	12

a) The relative scale used in the tables 1,2,3, and 4 is exactly the same and is consistent between Table 1 and Table 2, and between Table 3 and Table 4. It is also possible, if desired, to compare the values in Table 1 and Table 2 with the values in Table 3 and Table 4 provided that the line width difference is taken into account.

b) The values in Table 1 and Table 3 correspond to A_1, B_1, and C_1 in Fig. 1 and not to A_3, B_3, and C_3 in Fig. 1.

Table 3. Relative ESR Intensities of Mo^{5+} at 20°C.

Oxide components x	y	z	Additive	Gas	Intensity	Data number
Al_2O_3	MoO_3				160	13
Al_2O_3	MoO_3			H_2	80	14
Al_2O_3	MoO_3		Thio-β-naphthol		9000	15
Al_2O_3	MoO_3		Thio-β-naphthol	H_2	17900	16
Al_2O_3	MoO_3	CoO			80	17
Al_2O_3	MoO_3	CoO		H_2	30	18
Al_2O_3	MoO_3	CoO	Thio-β-naphthol		570	19
Al_2O_3	MoO_3	CoO	Thio-β-naphthol	H_2	433	20

Table 4. Relative ESR intensities of Mo^{5+} at 200°C.

Oxide components x	y	z	Additive	Gas	Intensity	Data number
Al_2O_3	MoO_3				240	21
Al_2O_3	MoO_3		Thio-β-naphthol		10956	22
Al_2O_3	MoO_3		Thio-β-naphthol	H_2	13349	23
Al_2O_3	MoO_3	CoO			240	24
Al_2O_3	MoO_3	CoO	Thio-β-naphthol		10000	25
Al_2O_3	MoO_3	CoO	Thio-β-naphthol	H_2	6400	26

temperature-dependent g-factor have not been listed in the tables because of the irregular and temperature-dependent line shape.

Discussion

In the previous paper it was concluded that the species giving rise to the ESR absorption with $g=2.002$—2.004 was most properly written as R^+O^{*2-}, where R signifies the additive with a π-electron orbital and where O^{*2-} signifies some active surface oxygen anion at which the chemisorption of R takes place. The species for the ESR line with $g=1.9328$ has been concluded to be Mo^{5+}. The species for the ESR line, with a temperature-dependent g-factor as is shown in Fig. 6, has appeared in this study for the first time. It is most likely described to be Co^{3+} for the following reasons: (a) It is observed only in the specimen which has CoO as an oxide component. The unpaired electron may, therefore, be supposed to belong to the cobalt atom. (b) It is observed only when TN is added to the AMC powder. As TN forms TN^+–O^{*2-}, it may be concluded that the unknown species is a product of this reaction: $Co^{2+}+TN^+-O^{*2-}\rightarrow Co^{3+}+TN-O^{*2-}$. (c) It disappears if H_2 is introduced. (d) It disappears if NH_3 is introduced and the specimen is heated to above 100°C, but it is intensified if N_2O is added and the specimen is heated at above 100°C, as is shown in Fig. 7. As has previously been shown by one of the present authors,[5,8] NH_3 destroys a hole or an oxidized state, while N_2O eats a captured or solvated electron or an anion. The reactivity of this unknown species, as has been indicated above, is just like a hole. A hole formed in Co^{2+} should be a Co^{3+}. It can not be a free Co^{3+}; it would more properly be shown as $(Co-O_n)^{-(2n-3)}$ and so on, but in the present work the covalent bonds or molecular orbitals among the surface ions are neglected or are not discussed. For this reason, the "hole" found in some species which include at least a Co^{2+} ion is conveniently written as Co^{3+} in this paper. Therefore, it must be noted that the Co^{3+} postulated in this paper has not been obtained by the analysis of a single crystal spectrum, but has been concluded from the reactivity only; therefore, it must not be understood as having validity beyond the fact that it is a convenient nomenclature for a hole in a Co^{2+}. However, the fact that a surface species cannot be studied with a single crystal, or in an oriented state, and the fact that these surface species exhibit considerable anisotropy in their ESR spectra, both lead to the conclusion that an exact determination of the structures of these surface species by an analysis of the ESR spectra is impossible; therefore, the method employed in this report, reaching a conclusion after examining the reactivities of the species under investigation, is the only possible way to proceed.

Co^{3+}, $(3d)^6$, in an octahedral crystal field can be either paramagnetic or diamagnetic, depending on

8) H. Ueda, This Bulletin, **41**, 2578 (1968).

the strength of the field.[9,10] In the present AMC specimen, "Co^{3+}" must be formed from the Co^{2+} which is deposited on the surface of an Al_2O_3 particle, together with MoO_3; therefore, the crystal field surrounding "Co^{3+}" will not be a strong octahedral field, and will probably be of a C_{4v} or of C_{4d} symmetry. For this reason, paramagnetism can well be expected from the "Co^{3+}" in the present specimen. The temperature dependence of the g-factor in Fig. 6 would indicate a labile crystal field around this species; therefore, it is good evidence for rejecting the existence of a strong octahedral crystal field surrounding "Co^{3+}". A g-factor larger than 2.0 is to be expected from the $(3d)^6$ configuration. Generally speaking, the ESR spectrum from a d^6 ion in a symmetric crystal field is broadened or easily saturated, and is observed only at low temperatures and with a low microwave power. Only a few spectra, *e.g.*, that of Fe^{2+}, has been recorded. However, the effect of an asymmetric crystal field, such as that on a surface, on the ESR spectra of d^n metal ions has not been explored much; therefore, the experimental results obtained for "the ions in a symmetric crystal field or in a bulk state" are not always useful for analysing the spectra on the basis of the species on a surface.

It seems that cobalt affects the nature of the catalyst surface greatly. Evidence for this is the spectra in Fig. 4. The ESR absorption found in Fig. 2 and Fig. 3, which is due to some species on the alumina surface, has been almost totally cancelled by cobalt ions. The chemisorption of TN is greatly enhanced by cobalt ions. The datum No. 5, when compared to No. 3 in Table 1, shows that the ESR intensity at 20°C due to TN^+–O^{2-} is increased 15 times if cobalt ions are added to the surface of AM. These tendencies are not observed at 200°C; see the data No. 11 and No. 9, in Table 2, and B_1 and C_1 in the b and c of Fig. 1. These facts indicate that the cobalt ions are located on the catalyst surface so as to make it easy for foreign ligands to coordinate with them or to escape from them.

In the previous paper it has been established that Mo^{6+} ions act as electron acceptors on the surface, themselves being reduced to Mo^{5+}. By definition, the word "catalyst" signifies that, though it promotes a chemical reaction, there can be no overall change in the amount and structure of the catalyst itself during and after the reaction, if the circumstances are ideal. If so, it is quite hopeless to observe any reaction intermediate, at least on the side of the catalyst, if the catalytic reaction is proceeding in an ideal manner, except in a case where the catalyst itself is the intermediate. The accumulation of the intermediate is, then, to be expected only when some of the reaction components or some of the reaction conditions are lacking. The intensity of the ESR absorption is determined by the following formula:

$$\text{ESR intensity of a sample} = (x, y, z \text{ R and G})_{g,\, t_m}$$

if we ignore the history of the specimen. In this formula, x, y, and z are the oxide components (see Tables 1 to 4), R is an added compound such as TN, G is the gas added to the sample tube, and g is the g-factor of the line being measured. A sample have many absorption lines with varied g-factors and with different intensities. The effect of one of the variables, say, z_0, can be judged by comparing $(x, y, z=z_0, \text{R and G})_{g,\, t_m}$ with $(x, y, z=\text{O, R and G})_{g,\, t_m}$. For example, the datum No. 26 in Table 3 is for $x=91.38\%$ Al_2O_3, $y=5.44\%$ MoO_3, $z=3.18\%$ CoO, R=TN at the concentration of 0.2 mM/g of oxide, G=H_2 at 450 mmHg/20°C, $g=1.9328$ (the absorption by Mo^{5+}), and $t_m=200$°C, while the datum No. 23 is for the variables almost identical with those for the datum No. 26 except that no CoO was added to the system (accordingly, the value of $x=94.54\%$); in other words, $z=0$. The ratio of these two data, 6400/13349=0.48, can be accepted as indicating that Co^{2+} reduces the amount of Mo^{5+} at 200°C in the presence of H_2.

By similar arguments, it is possible to write the reaction cycle shown in Fig. 8. The equilibrium between charged species on the surface of oxide particles has been discussed in previous papers.[5,11] The process (1) in Fig. 8 has already been used to describe how "Mo^{6+} behaves as an electron trap in the formation of R^+O^{*2-} from RO^{*2-}." The process (2) is the reduction of Mo^{6+} by H_2, which is confirmed by comparing the datum No. 23, Table 4, with the datum No. 22. The process (3) can, in other words, be written as $Mo^{5+}+Co^{3+}\rightarrow Co^{2+}+Mo^{6+}$. Comparisons of the datum No. 25 with the datum No. 22, Table 4, and especially No. 19 with No. 15, Table 3, and No. 20 with No. 16, indicate that added cobalt oxide reduces the amount of Mo^{5+}. Such an effect of cobalt oxide can be explained only by the action of the Co^{3+} formed. Co^{3+} was observed only when TN was added in the absence of H_2 (see Fig. 4 and Fig. 5). Without H_2, the $H_2+Co^{3+}\rightarrow H^+ + H + Co^{2+}$ process does not occur, and so an observable amount of Co^{3+} is accumulated. It is also possible that, in a vacuum, the $Mo^{6+}+Co^{2+}\rightarrow Mo^{5+}+Co^{3+}$ equilibrium moves to the right, No. 25 and No. 26. The overall flow of electrons by the processes (1) and (3) can be seen in Table 1 and Table 3. The AM–TN system in a vacuum give the ESR intensity of 1500 at 20°C and for $g=2.0036$, the datum No. 3, which is increased to 22500 by the addition of cobalt to the above system, the datum No. 5. On the contrary, the AM–TN

9) J. S. Griffith and L. E. Orgel, *Trans. Faraday Soc.*, **53**, 601 (1957).

10) C. J. Ballhausen, "Introduction to Ligand Field Theory," McGraw-Hill Book Co., New York, N. Y. (1962), p. 274.

11) H. Ueda, *Can. J. Chem.*, **64**, 891 (1968).

system in a vacuum gives the ESR intensity of 9000 at 20°C and for $g=1.9328$, the datum No. 15, which is decreased to 570 by the addition of cobalt to the above system, the datum No. 19. The fact that, at lower temperatures, where the reactions of cobalt ions with H_2 and $RS^+O^{*2-}H$ are relatively slower, cobalt ions decrease the amount of Mo^{5+} and simultaneously increase the amount of TN^+–O^{*2-}, fits very well with the scheme. Though the electron-transfer reaction (5) can be postulated for the reason stated above, the products of the reaction (6) cannot be determined by the present results. As the species RS^+H–O^{*2-} has an unpaired electron, it is very likely that it will react with a hydrogen atom to yield RS^+H_2–O^{*2-}, which is then neutralized by the step (5) and decomposes to H_2S and R·. The R·, which may be $C_{10}H_7$· in the present case, will subsequently react with H_2 and/or with another R· to form some hydrocarbons.

The vast difference between the present conditions of ESR measurements, 200°C and 0.6 atm pressure of H_2, and the engineering conditions of the desulfurization reaction, 400°C and a 200 atm pressure of H_2, would lead one to suspect the suitability of the present ESR experiments for analyzing the reaction scheme in the engineering desulfurization. However, there is actually no reason to conclude that the reactions occurring under these two sets of conditions are contrary in nature, though the rates of reaction are enormously different. The present authors are planning to fill this gap by further studying this subject; the effect of the pre-treatments with H_2 and H_2S on ESR spectra is particularly interested.

In the engineering desulfurization, the oxide is pre-sulfurized. The actual desulfurization is, therefore, carried out by the sulfide catalyst. As the present ESR measurements are made with oxide powders, this difference must be considered. Since oxygen and sulfur belong to the same group in the periodic table of elements, the VIb group, and since both have the same number of *p*-electrons in the outermost shell, the species R^+O^{*2-} should have its sulfide version, R^+S^{*2-}, on the sulfide particles. Therefore, it is not likely that the difference between S^{2-} and O^{2-} essentially alters the reaction scheme on the surface of these particles. The fact, that, in the engineering operation, the pre-sulfurization is made with H_2 and the residual oil diluted with kerosene shows that desulfurization is actually going on with the oxide catalyst.

It may often happen that an intermediate or an intermediate-like species which is detected only after a lot of time and labor proves to be not the essential component of the reaction system under investigation, but one of the by-product of the reaction. The reaction cycle found, Fig. 8, might be one such off-route phenomenon. The first step of the reaction, the formation of the cation-like species, might be untrue; instead the formation of

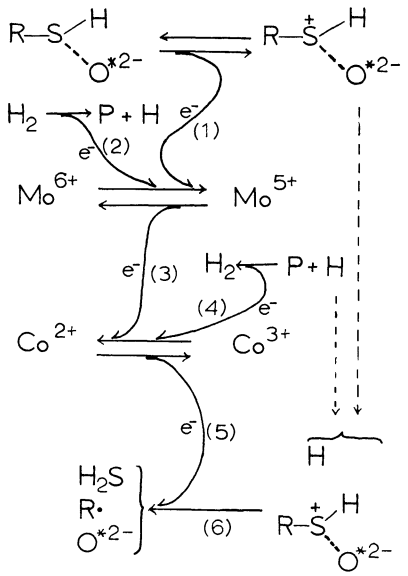

Fig. 8. The catalysis cycle of the desulfurization reaction of thio-β-naphthol with H_2 on the Al_2O_3-MoO_3-CoO catalyst particles. R signifies $C_{10}H_7$– group. S-O*2- signifies the chemisorbed state. About O*2-, see text and Ref. (5). P signifies a proton.

an anion might be the real first step. The discussion in the previous paper led to the conclusion that the formation of an anion is not likely on an oxide surface. The evidence of the succeding steps has already been discussed.

Another species which it might be necessary to consider as a component in the desulfurization cycle shown is Mo^{4+}. As Mo has the electronic configuration of (Krypton shell)$(4d)^5(5s)^1$, it can have four oxidation states, 3+, 4+, 5+, and 6+. Actually, MoS_2 is accumulated on the catalyst surface during desulfurization. Therefore, Mo^{5+}–Mo^{4+} might play some important role in the desulfurization cycle instead of Mo^{6+}–Mo^{5+}. The Mo^{4+} ion is paramagnetic in an octahedral crystal field, and it may or may not have paramagnetism in a field of lower symmetry.[10] In the present work, no ESR evidence for Mo^{4+} was found. This fact indicates that either the absence of the Mo^{4+} ions or the presence of the crystal field surrounding the Mo^{4+} ion, which makes the Mo^{4+} ion diamagnetic. However, the conclusions in the previous paper indicated the importance of Mo^{6+} as an electron trap on the surface of oxides. For this reason, it is unlikely that Mo^{4+} is an essential component of the catalysis cycle. If this is true, then it follows that the deactivation of the catalyst is due to the accumulation of Mo^{4+} on the catalyst surface.

Among the ingredients of the catalyst, the most important ingredient is alumina. The activity and the life of a catalyst is actually decided with it. In the reaction scheme (Fig. 8), this important role of

alumina appears in the form of O^{*2-}, indicating the active oxygen anion where the chemisorption occurs. The difference between a good alumina and a bad one lies not in the quality of their properties, but in the quantity of their properties; some quantitative measurement of the ESR absorption by the alumina surface might, therefore, be helpful in explaining the difference between good and bad carriers.

The authors thank Dr. K. Muramatsu for his cooperation in the preparation of the mixed-oxide catalysts. They also thank Dr. Y. Kotera for his encouragement in this work.

BULLETIN OF THE CHEMICAL SOCIETY OF JAPAN VOL. 43 3705—3710 (1970)

Phosphorus Nuclear Magnetic Resonance in Polyphosphates and Determination of Their Hydrolysis Rate Constants

Makoto KAWABE, Osamu OHASHI and Ichiro YAMAGUCHI

Department of Chemistry, Faculty of Science and Engineering, Sophia University, Tokyo

(Received June 4, 1970)

The phosphorus nuclear magnetic resonance spectra of several condensed phosphates (polyphosphates) were measured in aqueous solutions. The NMR spectra generally consist of three peaks which correspond to the phosphorus atoms at the end and middle of the molecular chain and in orthophosphoric acid which is the final product of the hydrolysis. The chemical shift and, for some phosphates, spin-spin coupling constants were obtained. Both depend on pH of the solution. The chemical shifts for the end and middle phosphorus atoms depend also on the chain length of the molecule. The hydrolysis process of the phosphates can be traced by the observation of the time dependence of spectral line intensities. From this observation the rate constant of the hydrolysis is obtained for several phosphates. The values are comparable with those obtained by other methods.

The chain of –P–O–P– in polyphosphoric acid or polyphosphates molecule has been known to degrade by hydrolysis in aqueous solutions.[1-11] The degradation results in shorter chain molecules and finally in orthophosphoric acid. The rate of the hydrolysis is very slow at ordinary temperature and in neutral aqueous solution. Some of the polyphosphates have long half-life up to several years under such conditions.[8,9]

Phosphorus nuclear magnetic resonance is a useful method for the study of phosphates and related compounds. Several papers on this subject appeared in the past decade.[11-16] The reported studies so far, however, concern with the phosphorus compounds in their "static" state. This work deals with the "dynamical" process of the phosphorus compounds by nuclear magnetic resonance, that is, the hydrolysis process of polyphosphoric acids and polyphosphates.

The slow rate process of hydrolysis of the compounds enables us to study it by observing the

1) G. A. Abott, *J. Amer. Chem. Soc.*, **31**, 763 (1909).
2) S. J. Kiehl and E. Claussen, Jr., *ibid.*, **57**, 2284 (1935).
3) D. O. Campbell and M. L. Kilpatrick, *ibid.*, **76**, 893 (1954).
4) J. P. Crother and A. E. R. Westman, *Can. J. Chem.*, **32**, 42 (1954).
5) J. R. Van Wazer, E. J. Griffith and J. F. McCullough, *J. Amer. Chem. Soc.*, **77**, 287 (1955).
6) J. R. Van Wazer and E. J. Griffith, *ibid.*, **74**, 4977 (1952); *Anal. Chem.*, **26**, 1755 (1954).
7) E. Thilo and W. Wieker, *Z. Anorg. Allg. Chem.*, **291**, 164 (1957).
8) J. R. Van Wazer, "Phosphorus and its Compounds," Vol. 1, Interscience Publishers, New York, N. Y. (1964).
9) T. Otani, M. Miura and T. Doi, *Kogyo Kagaku Zasshi*, **66**, 593 (1963).
10) R. E. Mesmer and R. L. Caroll, *J. Amer. Chem. Soc.*, **88**, 1381 (1966).
11) J. R. Van Wazer, C. F. Callis and J. N. Shoolery, *ibid.*, **77**, 4945 (1955).
12) E. J. Griffith and R. L. Burton, *Inorg. Chem.*, **4**, 549 (1965).
13) M. M. Crutchfield, C. F. Callis, R. R. Irani and G. C. Roth, *ibid.*, **1**, 813 (1962).
14) J. R. Van Wazer, C. F. Callis, J. N. Shoolery and R. C. Jones, *J. Amer. Chem. Soc.*, **78**, 5715 (1956).
15) C. F. Callis, J. R. Van Wazer, J. N. Shoolery and W. A. Anderson, *ibid.*, **79**, 2719 (1957).
16) J. C. Guffy and G. R. Miller, *Anal. Chem.*, **31**, 1895 (1959).

increase or decrease of the intensity of phosphorus nuclear magnetic resonance signals as the hydrolysis process is going on. Rate constants were determined for several compounds from the data of the time dependence of the intensity, and assignment of the signals was made. The chemical shift and, in some cases, the magnitude of the spin-spin coupling constants were obtained.

Experimental

The compounds studied are shown in Table 1, with their structural formulas. Compounds Nos. 1,2,3,7,11 and 12 were commercial products, and Nos. 4,5,6,8,9 and 10 were synthesized.

Samples were dissolved in hydrochloric acid (0.5, 1, 3 and 6N), water, calcium chloride (3N) and sodium hydroxide (0.5, 1 and 12N). Concentration of the compounds was small because of their poor solubility. Saturated solutions (2—3 g in 10 ml) were used in most cases. The pH of solutions was measured with a pH meter.

Some compounds evolve a large amount of heat when dissolved and the temperature of the solutions is 90—110°C immediately after the dissolution. The temperature, however, decreases in several minutes to around 60°C. The effect of the heat evolution was taken into account for the analysis of data.

The NMR spectrometers used were Varian DP-60 and HR-60 operated at 15.1 MHz. The sample tube was 15 mm in outer diameter. The external reference for the chemical shift measurements was 85% orthophosphoric acid sealed in a glass tube 5 mm in outer diameter. The value of the chemical shift with respect to the orthophosphoric acid was determined by the usual sideband method. For the sample with fast rate of hydrolysis, the reference was the signal of orthophosphoric acid produced in the sample itself.

The relative amount of phosphorus atoms with different chemical environments in the course of hydrolysis was determined by measuring the height of the signals. Assignment of the signals to the phosphorus chemical species involved was made according to the fact that the phosphorus NMR signals of polyphosphates are classified into three groups.[11,13] They are signals M,E and O, and are the resonance lines of phosphorus atoms at the middle and end of -P-O-P- chain in a molecule and of the atom in orthophosphoric acid, respectively. In the spectrum, signal M appears at the highest field, signal E next and signal O at the lowest. The behavior of the signal intensity was in line with generally accepted hydrolysis process.[6-10] The spin-spin interaction splitting of the signal also supported the assignment.

Table 1. PHOSPHORUS COMPOUNDS STUDIED

1.	Pyrophosphoric acid	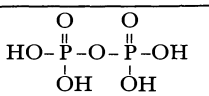
2.	Na-Pyrophosphate	$Na_4P_2O_7$
3.	Na-Tripolyphosphate	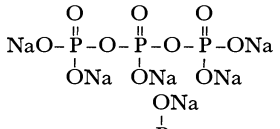
4.	Na-Trimetaphosphate	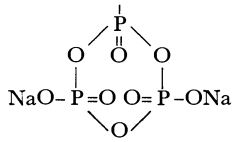
5.	Na-Tetrametaphosphate	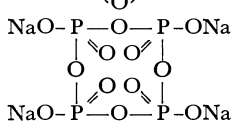
6.	Na-Hexapolyphosphate	$Na_8P_6O_{19}$
7.	Na-Hexametaphosphate[a]	$(NaPO_3)_n$, $n=20$?
8.	Na-Icosapolyphosphate	$Na_{22}P_{20}O_{61}$
9.	Na-Polyphosphate ($\bar{n}=40$)[b]	$Na_{\bar{n}+2}P_{\bar{n}}O_{3\bar{n}+1}$
10.	Na-Polyphosphate ($\bar{n}=80$)[b]	$Na_{\bar{n}+2}P_{\bar{n}}O_{3\bar{n}+1}$
11.	Polyphosphoric acid	Mixture, linear.
12.	Na-Metaphosphate	$(NaPO_3)_n$

a) Commercial name.
b) $\bar{n}$ is the average chain length for the mixture of linear molecules with various chain lengths, counted by the number of phosphorus atoms in the chain.

Results and Discussion

NMR Spectrum. Polyphosphates in aqueous solution generally give three peaks which can be assigned to signals M (middle), E (end) and O

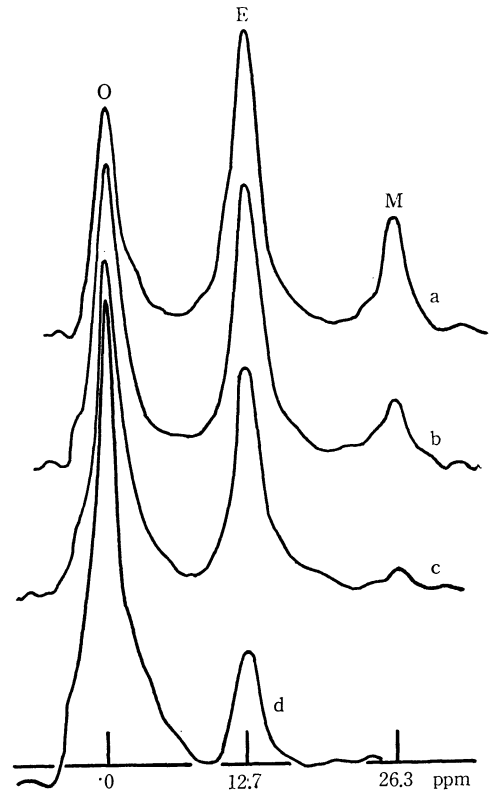

Fig. 1. NMR spectra of polyphosphoric acid in aqueous solution at different times after the dissolution of compounds. Spectra a, b, c and d correspond to 3, 9, 25 and 89 min, respectively.

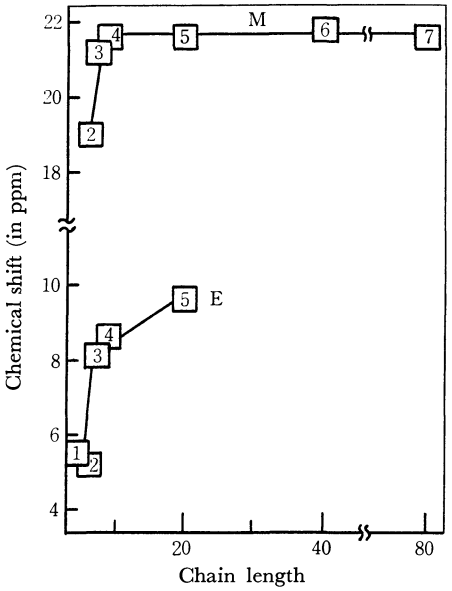

Fig. 2. Chemical shifts of M and E phosphorus atoms of the Na-phosphates with different chain length, refer to the phosphorus resonance in orthophosphoric acid. 1. Na-pyro-; 2. Na-tripoly-; 3. Na-tetrapoly-; 4. Na-hexapoly-; 5. Na-icosapoly; 6. Na-poly- ($\bar{n}$=40), 7. Na-poly- ($\bar{n}$=80), phosphates.

(ortho). A spectrum of polyphosphoric acid in aqueous solution is shown in Fig. 1 as a typical example. The time after dissolution is indicated. The heights of the signals vary with time. Each signal can be assigned unequivocally to M, E or O species. The chemical shifts for these species were measured.

Chemical Shift. The chemical shift of peaks M and E varies with the increase of the chain length of molecule as shown in Fig. 2. (The chemical shift of peak O referring to the external reference seems to be very small and can not be measured due to relatively poor resolution of the spectra.) The chemical shifts of species M and E increase for the compounds of short chain lengths up to n=6, where n is the number of phosphorus atoms in a chain of a molecule. In this range the chemical shift clearly depends on the chain length. However, the shifts for $n>6$ are almost constant. This suggests that in a long chain molecule most phosphorus nuclei are not much affected by their position in the molecule. The phosphorus nucleus at the boundary position between normal E and M species is expected to be sensitive to the change of position in a chain. However, for a long chain molecule the contribution of this kind of species to the whole signal intensity is very small, and its signal seems to lie at the skirt of signal M with very weak intensity and is not observed separately.

The chemical shift for compounds studied also depends on pH of the solution as shown in Fig. 3.

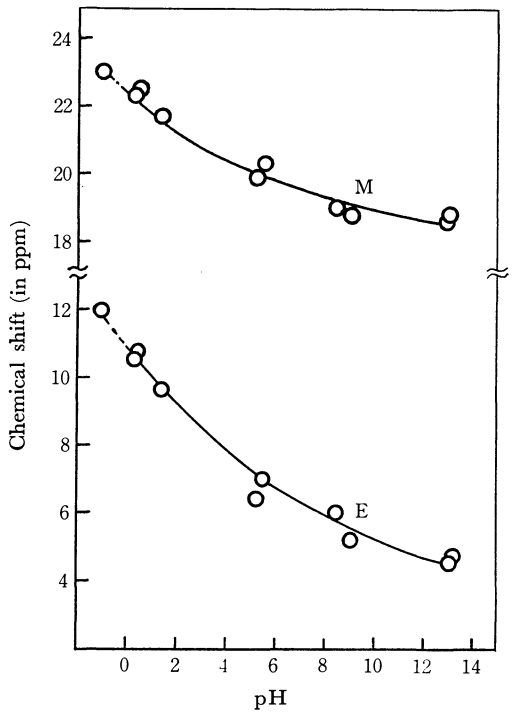

Fig. 3. pH Dependence of the chemical shift of Na-tripolyphosphate.

The signals do not cross (in the chemical shift scale) in the pH range observed. This shows that at any pH unique assignment of the signals can be made in the order of the field strength.

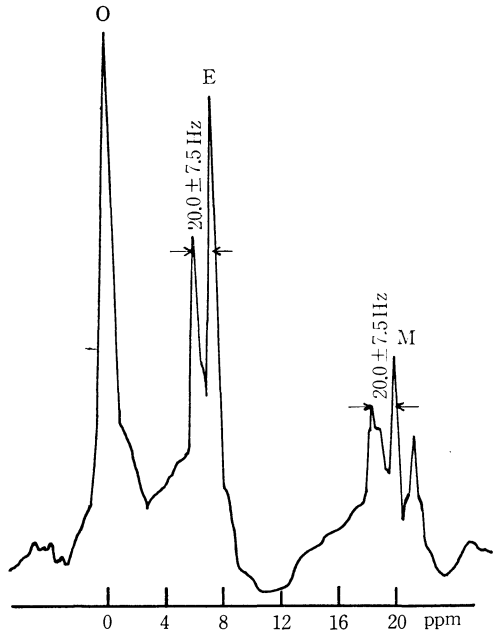

Fig. 4. Phosphorus NMR spectrum of Na-tripolyphosphate in 1N HCl solution.

Spin-spin Coupling. Sodium tripolyphosphate in solutions with pH 5, 9 and 13 gives spectra with splittings due to spin-spin coupling. This is the only case in which the spin-spin interaction splitting was observed. The splitting of the peaks are doublet and triplet as shown in Fig. 4. The magnitude of the splitting is around 20 Hz. This indicates that the coupling is between neighboring phosphorus atoms in the molecular chain.[13-15] The splitting gives a concrete assignment of the signals; the doublet at the low field side is due to species E and the triplet at the high field is due to species M.

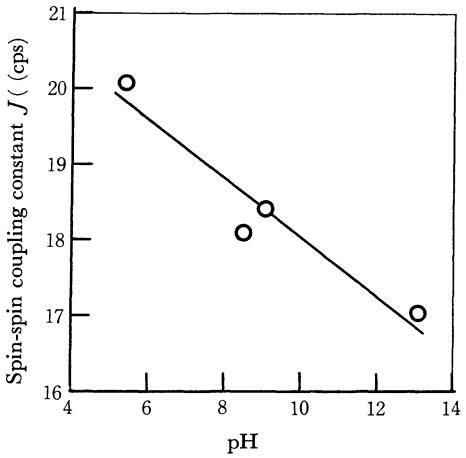

Fig. 5. pH Dependence of the spin-spin coupling constant of Na-tripolyphosphate.

The pH dependence of the coupling constant is evident for this compound as shown in Fig. 5. The coupling constant decreases from 20 to 17 Hz as pH increases from 4 to 13. This is in contrast to that by Crutchfield *et al.*[13]

Analysis of Hydrolysis. The time variation of the NMR signal height is plotted in Figs. 6 and 7. Apparent variations of the spectra are summarized in Table 2.

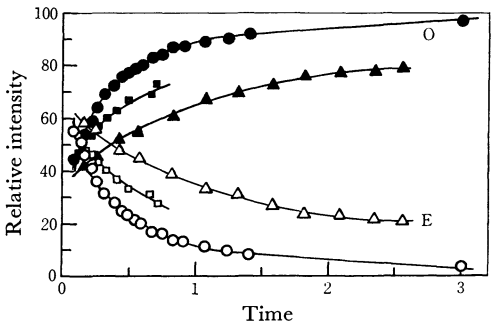

Fig. 6. Variation of the peak height (normalized to 100%) of phosphorus NMR spectral lines for species E and O in pyrophosphate molecules.
○, ●: 6N HCl solution; □, ■: aqueous solution; △, ▲: 3N $CaCl_2$ solution.

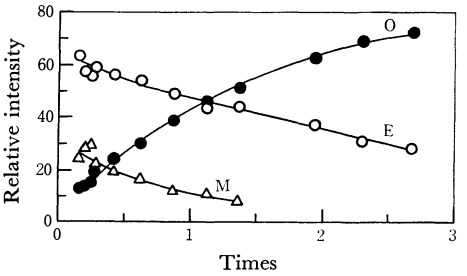

Fig. 7. Variation of the peak height (normalized to 100%) of phosphorus NMR spectral lines for species E, M and O in tripolyphosphate molecule (6N HCl solution).

TABLE 2. APPARENT BEHAVIORS OF THE NMR SPECTRUM

Compound in soln.	Obsd. period	Variation of peaks O E M	% of O at final obs.
Pyrophosphoric acid			
6N HCl	3 hr	I. D. —	96%
aq.	1 hr	I. D. —	80%
3N $CaCl_2$	4 hr	I. D. —	83%
6N NaOH	96 hr	I. D. —	96%
Na-Tripolyphosphate			
6N HCl	3 hr	I. D. D.	72%
aq. (pH 8.5)	24 hr	slightly	9%
Polyphosphoric acid			
6N HCl	2.5 hr	I. D. D.[a]	94%
aq.	1.5 hr	I. D. D.[b]	84%
6N NaOH	4 hr[c]	I. D. D.	65%
Na-Tetrametaphosphate			
aq. (pH 6.0)	9 day	almost no	9%
Na-Metaphosphate			
6N HCl	2 hr	I.I-D.[d]D.	80%
aq. (pH 5.7)	9 day	almost no	5%

I.: Intensity increasing; D.:Intensity decreasing.
a) disappeared in 15 min.
b) disappeared in 1 hr.
c) reached equilibrium in 1 hr.
d) initially increased then decreased.

Basic assumptions for the treatment of the time dependence of the NMR signal intensity are as follows:

i) Hydrolysis of polyphosphoric acid or polyphosphate produces shorter chain compounds. The final product in the process is orthophosphoric acid.

ii) The phosphorus NMR spectra of original compounds and intermediates of the hydrolysis process consist of three peaks due to species M, E and O.

iii) In the course of hydrolysis, the chain degradation proceeds as a first order reaction process[2-9], and the rate equation is

$$-\frac{d[\text{polyphosphate}]}{dt} = k[\text{polyphosphate}]$$

where k is the first order reaction rate constant.

iv) The peak height of the NMR signal is proportional to the amount of the phosphorus atoms in question.

Three unit degradation processes can be considered:

Process-1; the scission of E and M,

$$\text{-M-E} \longrightarrow \text{-E} + \text{O}.$$

Process-2; the scission of two M's,

$$\text{-M-M-} \longrightarrow \text{-E} + \text{-E}.$$

Process-3; the scission of two E's,

$$\text{E-E} \longrightarrow \text{O} + \text{O}.$$

If the original molecule is a linear chain, the initial numbers of the phosphorus species in a molecule are $(n-2)$ and 2 for M and E respectively, and if the molecule is in a ring form the number is n for M, where n is the number of phosphorus atoms in the original molecule. In the final stage of hydrolysis, the numbers of the species corresponding to one original molecule should be n for O and 0 for M and E when hydrolysis is completed. In principle, the relative amount of each species may be estimated at any intermediate stage of the degradation through processes 1, 2 and 3. For long chain molecules, however, there are many possibilities for the position of the chain scission in the degradation process. It is almost impossible to determine the relative amount of each species without knowing the rate of each degradation process. Thus, significant rate constants are obtained only for relatively simple systems such as pyrophosphate and tripolyphosphate.

Determination of the Rate Constant of Hydrolysis. *Pyrophosphoric Acid.* Pyrophosphoric acid has the simplest structure of the compounds studied. It undergoes hydrolysis to give orthophosphoric acid in one step by Process-3 as follows.

$$\text{P-O-P} \xrightarrow{k_3} 2\text{P}$$

Let us assume a first order reaction for the degradation. Then the rate of the hydrolysis is determined by the equation

$$\frac{dx}{dt} = k_3(a-x), \text{ or } \ln\frac{(a-x_1)}{(a-x_2)} = k_3(t_2-t_1),$$

where a is the initial quantity of the pyrophosphoric acid or the peak height of the NMR signal (species E). Therefore $(a-x_1)$ is the quantity at $t=t_1$ and k_3 is the rate constant (for Process-3).

Figure 8 shows the plot of $\ln[(a-x_1)/(a-x_2)]$ *vs.* (t_2-t_1) for pyrophosphoric acid. The plot gives a fairly straight line for a certain interval of time, and shows that the reaction is almost of the first order in the interval. The plot consists of two parts of straight lines. This is interpreted as follows: Phosphoric acid evolves a large amount of heat when dissolved in water. It is reasonable to consider that the heat accelerates the reaction and gives rise to a steeper slope at the first part of the plot leading to a large rate constant. After the lapse of ten to twenty minutes the temperature is lowered to room temperature, and the hydrolysis retarded. The straight line after a break can be assigned to the hydrolysis process at room temperature. Thus, the rate constant for the hydrolysis at room temperature, k_3, is obtained from the slope after the break point. (k_3' denotes the rate constant for the system immediately after dissolution.)

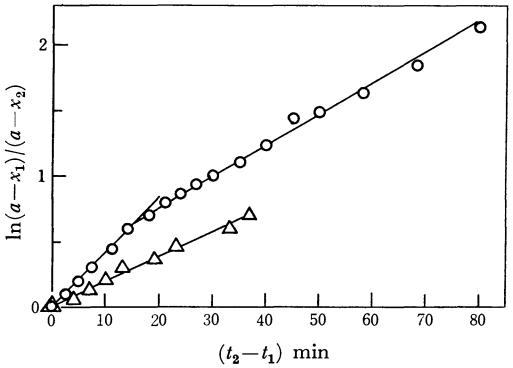

Fig. 8. Plot for the determination of the hydrolysis rate constant of pyrophosphoric acid.
○: 6N HCl solution; △: aqueous solution.

The obtained rate constants are shown in Table 3. The constant depends upon pH and ion concentration of the solution; k_3(6N HCl)$>k_3$(aq. soln.)$>k_3$(3N $CaCl_2$)$>k_3$(6N NaOH). This means that the hydrolysis process is accelerated by the H^+ ion. This is in line with results of several authors.[4-6,8-10] In $CaCl_2$ solution the rate constant is smaller than in aqueous solution. It seems that Ca^{2+} ion as well as pH of this solution affects the hydrolysis rate.[8-10,17]

Sodium Tripolyphosphate. Tripolyphosphate gives a spectrum with three peaks. Peaks M and E decreases their intensity with time, whereas peak O increases. This is shown in Fig. 7. Peak M diminishes in an hour in hydrochloric acid solution. Hydrolysis seems to reach equilibrium two hours after dissolution.

The hydrolysis of tripolyphosphate proceeds in the following pattern.

$$\text{P-O-P-O-P (tripoly-)} \xrightarrow{k_1} \text{P-O-P (pyro-)} + \text{P},$$
$$\xrightarrow{k_3} \text{P}.$$

The rate equations are as follows.

$$dx/dt = -k_1x \text{ or } x_2 = x_1\exp[-k_1(t_2-t_1)],$$

and $$dy/dt = -k_3y + k_1x \text{ or}$$

17) W. Wieker and E. Thilo, *Z. Anorg. Allg. Chem.*, **306**, 48 (1960).

$$y_2 = \frac{k_1 x_1}{k_1 - k_2}\{\exp[-k_3(t_2-t_1)] - \exp[-k_1(t_2-t_1)]\},$$

where x is the concentration of polyphosphate and y pyrophosphate, and their values are given by the peak heights as M and E−2M, respectively. The obtained results for the hydrochloric acid solution were $k_1=1.7\times10^{-2}$ min^{-1} and $k_3=0.8\times10^{-2}$ min^{-1}, and $k_1>k_3$. This relation of magnitudes of k's means that the amount of the primary product, pyrophosphate, in the solution increases at first because of slow rate of the second step degradation.

In aqueous solution of sodium tripolyphosphate, hydrolysis is very slow and the rate constant could not be determined although the observation was carried out for 24 hr. Hydrolysis is considerably slowed down in a solution with high pH value.

Polyphosphoric Acid. Both the structure of this compound and the mechanism of hydrolysis are not clear. It is difficult to determine the rate constant for the whole hydrolysis process. However, acceleration of the reaction due to the existence of H^+ ion is evident from comparison of the variation of the peak intensity for 6N HCl and aqueous solutions. Peak M disappeared within ten to several tens of minutes.

After the disappearence of peak M, only peak E can be traced. Analysis of the intensity of peak E for 6N HCl solution gives the rate constants $k_3'=5.36\times10^{-2}$ min^{-1} and $k_3=1.04\times10^{-2}$ min^{-1}. For aqueous solution there was no remarkable heat evolution and the rate constant $k_3=9.80\times10^{-3}$ min^{-1} was obtained. The values also show acceleration of the hydrolysis by H^+ ion.

Other Phosphates and Phosphoric Acids. Sodium metaphosphate and sodium pyrophosphate undergo hydrolysis in aqueous solution very slowly, but in 6N HCl solution they change to orthophosphoric acid in a day. It is concluded that the H^+ ion accelerates hydrolysis for the compounds studies.

The rate constants are summarized in Table 3. They are compared with those obtained by methods other than NMR.[1,7,9,18]

Table 3. Hydrolysis reaction rate constants (in min^{-1})

Compound	Solution	Rate constant
Pyrophosphoric acid	6N HCl	$k_3'=4.39\times10^{-2}$
		$k_3=2.50\times10^{-2}$
	aq.	$k_3=1.18\times10^{-2}$
	3N $CaCl_2$	$k_3'=9.80\times10^{-3}$
		$k_3=3.68\times10^{-3}$
	6N NaOH	$k_3'=1.65\times10^{-3}$
		$k_3=1.74\times10^{-4}$
Na-Tripolyphosphate	6N HCl	$k_1=1.7\times10^{-2}$
		$k_3=0.8\times10^{-2}$
Polyphosphoric acid	6N HCl	$k_3'=5.36\times10^{-2}$
		$k_3=1.04\times10^{-2}$
	aq.	$k_3=9.80\times10^{-3}$

k_1 : 1-st order rate constant for Process-1 at room temperature.
k_3 : 1-st order rate constant for Process-3 at room temperature.
k_3': 1-st order rate constant for Process-3 at the temperature of solution immediately after dissolution.

Conclusion

The chemical shifts of phosphorus NMR observed for polyphosphates appear to change with the chain length (so far it is short), the pH as well as the cation of the solution. The spin-spin coupling constant between phosphorus nuclei also depends on the pH of the solution.

The hydrolysis process of various kinds of phosphates was studied by NMR. The NMR gives clear information on the hydrolysis process from the observation of the signal intensities for the phosphorus species in molecules. For simple systems, this information gives the concentration of various molecular species in the course of the hydrolysis.

Analysis of the hydrolysis process with the intensity variation of the NMR signal is relatively simple when the structure of the molecule is known. The obtained values of the rate constant for the hydrolysis can be compared with those obtained by various methods other than NMR and thus the NMR method appears to be very useful.

The authors are greatly indebted to Professor M. Amagasa for the gift of samples. They also wish to thank Dr. O. Yamamoto, Government Research Institute; and Mr. N. Hayakawa, Japan Atomic Energy Research Institute, for use of their NMR instruments.

18) W. Wieker, *Z. Elektrochem.*, **64**, 1047 (1960).

BULLETIN OF THE CHEMICAL SOCIETY OF JAPAN VOL. 43 3711—3715 (1970)

The Radiolysis of Liquid Nitrogen Containing Hydrocarbons. II. Acetonitrile Formation from the Solution of Ethylene

Takefumi Oka and Shin Sato

Department of Applied Physics, Tokyo Institute of Technology, Ookayama, Meguro-ku, Tokyo

(Received June 4, 1970)

The ^{60}Co γ-radiolysis of liquid nitrogen containing ethylene has been reinvestigated in order to elucidate the mechanism of the formation of nitrogenous products. When the conversion of ethylene was 10%, the G-values of hydrogen cyanide and acetonitrile were 0.21 ± 0.03 and 0.05 ± 0.01 respectively. The isotopic distributions in acetonitrile, *n*-butane, and acetylene were examined by using an equimolar mixture of C_2H_4 and C_2D_4 as the solute. From the analysis of these distributions, it has been concluded that acetonitrile is produced mainly from the reaction between nitrogen atoms and ethyl radicals.

Recently we have reported on our study of the radiolysis of liquid nitrogen containing small amounts of ethylene and propylene.[1] In the case of propylene, the only nitrogenous product observed was acetonitrile, most of which could be explained as resulting from the reaction between nitrogen atoms and propylene molecules. In the system of ethylene, however, the mechanism of the formation of the nitrogenous products, hydrogen cyanide and acetonitrile, could not be ascertained in the previous experiment. We have, therefore, reinvestigated the liquid nitrogen-ethylene system more thoroughly and have now been able to elucidate the mechanism of the formation of acetonitrile in some detail.

Experimental

Nitrogen gas of a high purity was purchased from the Nippon Sanso Co. Fully-deuterated ethylene C_2D_4 was synthesized from C_2D_2,[2] which had been synthesized from CaC_2 and D_2O. The nitric oxide, carbonyl sulfide, and ordinary ethylene were purchased from the Takachiho Chemical Industrial Co.

The samples were prepared and irradiated in the same manner as has been previously described.[1] For the determination of isotopic species, a mass-spectrometric analysis was made at a voltage near the appearance potential of the respective parent ions after separating the products with a gas chromatograph (a dioctyl phthalate column for acetonitrile and benzyl ether for acetylene and butane).

The rest of the procedure was similar to that previously described.[1]

Results

To assure the homogeneity of the reaction, the yields of hydrogen cyanide and acetonitrile were measured with various amounts of liquid nitrogen. The results are shown in Fig. 1. Obviously the yields are directly proportional to the amount of liquid nitrogen. This supports the assumption that the reactions take place in the bulk. In order to examine the effect of any impurity in liquid nitrogen, several experiments were carried out by using liquid nitrogen preirradiated in the presence of ethylene, but such treatment did not affect the G-values of the nitrogenous products.

Figure 2 shows the G-values of the main products

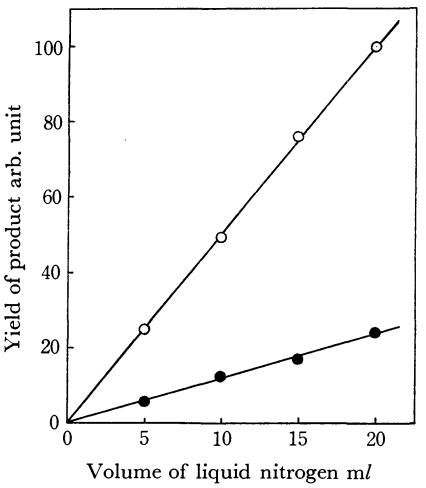

Fig. 1. Relative yields of hydrogen cyanide (○) and acetonitrile (●) as a function of the volume of liquid nitrogen. Ethylene concentration is 4×10^{-4} in mole fraction. Irradiation time is one hour.

1) T. Oka, Y. Suda and S. Sato, This Bulletin, **42**, 3083 (1969).

2) Y. Hatano, S. Shida and S. Sato, *ibid.*, **41**, 1120 (1968).

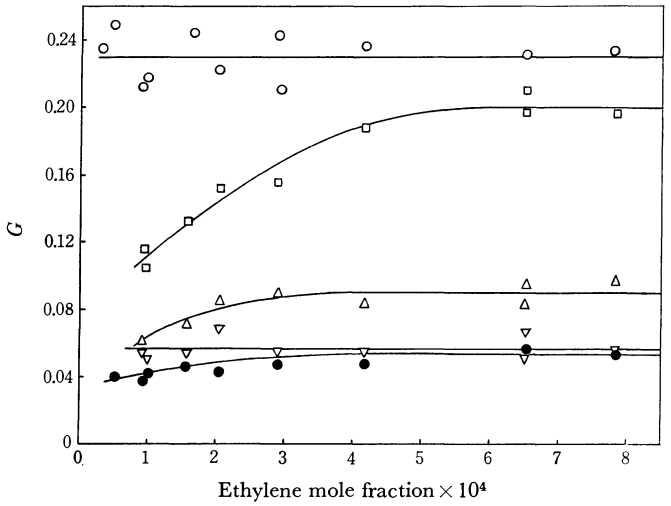

Fig. 2. *G*-values of hydrogen cyanide (○), ethane (□), acetylene × 1/10 (△), propane (▽) and acetonitrile (●) as a function of the concentration of ethylene. Volume of liquid nitrogen is 10 m*l* and irradiation time is one hour.

as a function of the concentration of ethylene. The products other than those shown in Fig. 2 were *n*-butene, 1-butane, and hexenes. A small amount of a paste-like material which may consist of more than two compounds was also formed. A part of it at least was yellow-colored and was soluble in methanol.

The *G*-values of ethane and acetylene decreased with a decrease in the concentration of ethylene. The *G*-value of acetonitrile also decreased slightly at the lower concentration. On the other hand, the *G*-values of hydrogen cyanide and propane were independent of the reactant concentration. The *G*-value of hydrogen cyanide was 0.21 ± 0.03.

In order to check whether the decrease in the *G*-values of ethane and acetylene at lower concentrations of ethylene is due to the high conversion or to the consumption of the primary products by the secondary reactions, the irradiation time dependence of the yields of the products was measured at two concentrations, 1×10^{-4} and 6.5×10^{-4} in mole fraction. The results are shown in Figs. 3, 4, and 5. At lower concentrations, the yields of acetylene, ethane, and propane deviated from a linear relationship at one hour and the reactant

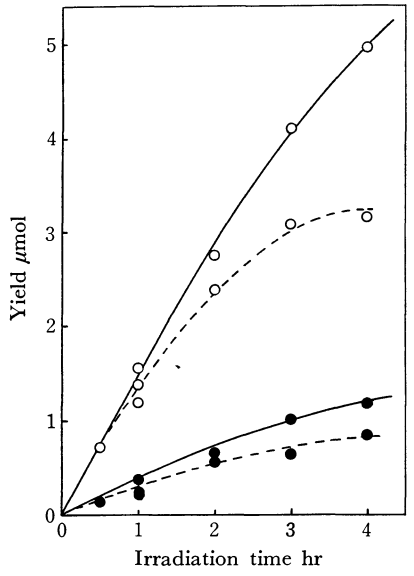

Fig. 3. Irradiation time dependence of the yields of hydrogen cyanide (○) and acetonitrile (●).
——, ethylene concentration is 6.5×10^{-4} in mole fraction.
------, 1.0×10^{-4} in mole fraction.

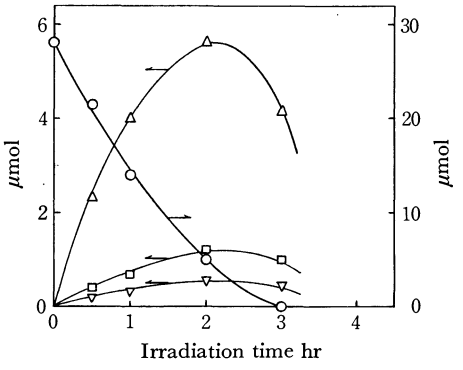

Fig. 4. Irradiation time dependence of the yields of acetylene (△), ethane (□) and propane (▽), and the amount of ethylene recovered (○). Initial ethylene concentration is 1.0×10^{-4} in mole fraction.

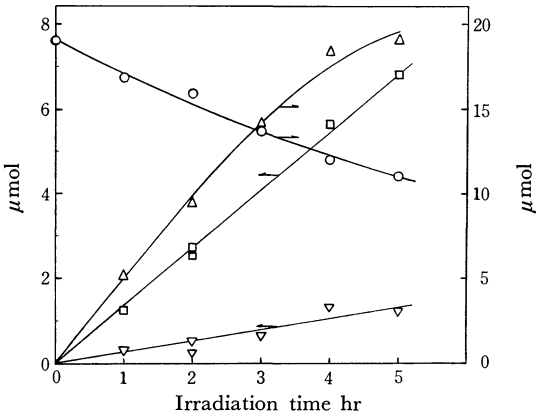

Fig. 5. Irradiation time dependence of the yields of acetylene (△), ethane (□) and propane (▽), and the amount of recovered ethylene × 1/10 (○). Initial ethylene concentration is 6.5×10^{-4} in mole fraction.

ethylene was almost completely consumed in three hours. At higher concentrations, the yields of all the products increased linearly up to about three hours and the conversion of ethylene in one hour was 10%. From these results, it may be concluded that the decrease in the *G*-values of ethane and acetylene at the lower concentrations of ethylene in Fig. 2 is not due to the high conversion.

Tables 1 and 2 show the isotopic distributions of acetonitrile, *n*-butane, and acetylene obtained when an equimolar mixture of C_2H_4 and C_2D_4, and pure C_2D_4 were used as the solutes. The isotopic distribution of hydrogen cyanide could not be obtained, because the H–D exchange reaction took place during the gas-chromatographic analysis. For example, the hydrogen cyanide obtained in Run No. 4 in Table 1 should be DCN, but the mass-spectrometric analysis showed HCN only.

For acetonitrile such an exchange occurred to only a negligible extent, as is shown in Table 1. In spite of the possibility of experimental error, it may be said that the *G*-value of DCN from the C_2D_4 solution is lower than that of HCN from the C_2H_4 solution. The isotopic distributions of *n*-butane and acetylene shown in Table 2 are averages of three measurements. These values will be discussed in detail later.

Table 1. Hydrogen cyanide and acetonitrile from the radiolysis of liquid nitrogen containing equimolar mixture of C_2H_4 and C_2D_4

Run	*G*		Acetonitrile			
	Hydrogen cyanide	Aceto-nitrile	d_0	d_1	d_2	d_3
1 mix.	0.18_4	0.04_3	100	36	54	78
2 mix.	0.14	0.03_5	100	35	55	83
3 mix.	0.15_3	0.03_5	100	37	59	80
		mean	100	36±1	56±3	80±3
4 C_2D_4	0.09_3	0.04_9	1.9	2.9	2.9	100

Table 2. *n*-Butane and acetylene from the radiolysis of liquid nitrogen containing equimolar mixture of C_2H_4 and C_2D_4

n-Butane		Acetylene	
d_0	44±3	d_0	100
d_1	49±1	d_1	0
d_2	21±3	d_2	90±1
d_3	(0)		
d_4	74±2		
d_5	100		
d_6	37		
d_7	(0)		
d_8	32±2		
d_9	56±5		
d_{10}	23±4		

Table 3. The effects of additives

Additive*	*G*					
	HCN	CH_3CN	C_2H_6	C_3H_8	*n*-C_4H_{10}	C_2H_2
none	0.19_4	0.04_2	0.18_7	0.06_8	0.06_8	0.79_8
8% NO	0.16	0.01_8	0.15_4	0.01	0.00_5	0.70
18% NO	0.10	0.01_5	0	0	0	0.65_6
14% COS	0.21	0.05_1	0.15_2	0.06_3	0.05_8	0.76_2
17% COS	0.21	0.04_7	0.17_3	0.03_8	0.03	0.77_7

* Per cent for ethylene of 6.5×10^{-4} m.f.

In Table 3, the effects of additives are summarized. Nitric oxide reduced the yields of all hydrocarbons except for acetylene to a large extent, and those of nitrogenous products to a certain extent. Carbonyl sulfide, which is now known as an electron scavenger in the condensed-phase radiolysis,[3] slightly reduced the yields of propane and *n*-butane.

Discussion

In a previous paper,[1] we have tentatively discussed the mechanism of the formation of nitrogenous products in the radiolysis of liquid nitrogen containing ethylene. We there suggested that the reaction between nitrogen atoms and ethyl radicals might be the only source of acetonitrile. Since the *n*-butane obtained in the present system is believed to be formed by the combination reaction of two ethyl radicals,[1] the isotopic distributions of *n*-butane and acetonitrile from solutions containing equimolar mixtures of C_2H_4 and C_2D_4 should have a certain relationship if the acetonitrile is

3) S. Hirokami, S. Shishido and S. Sato, *ibid.*, **43**, 973 (1970).

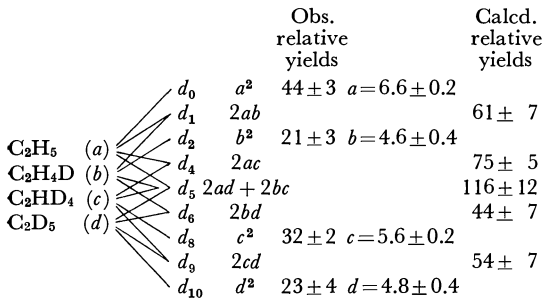

Scheme 1

produced by the reaction between nitrogen atoms and ethyl radicals.

The ethyl radicals formed by γ-irradiation in liquid nitrogen containing a mixture of C_2H_4 and C_2D_4 may be expected to be of four kinds, shown in the first column in the scheme 1 of calculation. Here, the *a*, *b*, *c*, and *d* in parentheses denote the relative concentrations. The relative amounts of isotopic *n*-butanes formed on the combination of ethyl radicals are those in the fourth column. Butane-d_3 and -d_7 are probably not formed; this is in agreement with the experimental data. Now, let us introduce from Table 2 the experimental values for a^2, b^2, c^2, and d^2; then we can calculate the relative yields of the isotopic ethyl radicals, *a*, *b*, *c*, and *d*. The results are shown in the sixth column. By using these values, we can calculate the relative yields of butane-d_1, -d_4, -d_5, -d_6, and -d_9. The calculated values can then be compared with those shown in Table 2. The agreement is satisfactory.

If acetonitrile is formed by the following reaction; Ethyl radical+N→Acetonitrile+2 Hydrogen atoms (1) the isotopic distribution of acetonitrile can be calculated by using the values for *a*, *b*, *c*, and *d*. However, in this calculation we need another assumption regarding the detachment of two hydrogen atoms in the reaction (1). We have calculated for two types of detachment:

1) Every hydrogen atom in an ethyl radical has an equal probability of detachment. On the basis of this assumption, the relative yields obtained for the isotopic distribution of acetonitrile are as follows:

d_0	d_1	d_2	d_3
100	33±5	40±4	83±11

These values are in good agreement with those shown in Table 1.

2) Two hydrogen atoms at the α position in ethyl radical preferentially detach in the reaction (1). In this case, the calculated results are as follows, far from the experimental data:

d_0	d_1	d_2	d_3
100	70±6	83±3	73±6

However, if a part of the acetonitrile is produced by such reactions as;

$$\text{Ethylene} + \text{N} \longrightarrow \text{Acetonitrile} + \text{Hydrogen atom} \quad (2)$$

and;

$$\text{Vinyl radical} + \text{N} \longrightarrow \text{Acetonitrile} \quad (3)$$

the relative yields of acetonitrile-d_0 and -d_3 will be increased and the isotopic distribution calculated will become consistent with the experimental data. The best-fit distribution was obtained by assuming that 65% of the acetonitrile is produced by the reaction (1) and the rest by the reaction (2) or (3) with the ratio of the isotope effect in the reaction (2) or (3) being 1 : 0.87 for $d_0 : d_3$. The obtained distribution is as follows:

d_0	d_1	d_2	d_3
100	36±3	44±2	80±3

Obviously, even when two α-positioned hydrogen atoms are detached in the reaction (1), it can be concluded the formation of acetonitrile is mainly due to the reaction (1), *i. e.*, the reaction of ethyl radicals and nitrogen atoms.

As is shown in Table 3, nitric oxide efficiently reduces the yields of ethane, propane, and *n*-butane. Since these hydrocarbon products are believed to be formed by the radical reactions, the above result indicated that nitric oxide is a radical scavenger, even at the temperature of liquid nitrogen. In the gas phase, nitric oxide is known as an effective scavenger for nitrogen atoms;[4]

$$\text{N} + \text{NO} \longrightarrow \text{N}_2 + \text{O} \quad (4)$$

The decrease in hydrogen cyanide and acetonitrile by the presence of nitric oxide is probably due to this reaction. However, if acetonitrile is formed solely by the reaction between nitrogen atoms and ethyl radicals, the presence of nitric oxide should reduce the yields of acetonitrile as much as that of *n*-butane, but acetonitrile was observed to the extent of G=0.015 even at the nitric oxide concentration, whereas the formation of *n*-butane was almost completely suppressed. This suggests that a part of the acetonitrile is produced by a process other than the reaction (1). In the preceding section, we have discussed two types of ethyl radical reactions producing acetonitrile; in the first, the hydrogen atom-detachment was indiscriminative, while in the second α-positioned hydrogen atoms were predominant in the detachment. Moreover, in the latter case a part of the acetonitrile formation has to be attributed to a process other than the reaction (1). If this is the reaction (2), the effect of nitric oxide on the formation of acetonitrile can be ex-

4) P. Harteck, R. R. Reeves and G. Mannella, *J. Chem. Phys.*, **29**, 608 (1958).

plained consistently.*1 A similar explanation may serve to explain the effect of nitric oxide on the formation of hydrogen cyanide; this product is formed by two processes, the one containing ethylene as the reactant, and the other containing methyl radicals, which are subject to the radical scavenging of nitric oxide:

$$C_2H_4 + N \longrightarrow HCN + CH_3 \quad (5)$$

$$CH_3 + N \longrightarrow HCN + 2H \quad (6)$$

Although the effect was small, the addition of COS reduced the yields of hydrocarbon products. Since COS is known to be an electron scavenger, even at the temperature of liquid nitrogen,[6] the participation of ionic species in the formation of propane and *n*-butane cannot be completely ruled out. However, the contribution of this type of reaction is obviously minor.

In the study of the argon-sensitized radiolysis of ethylene, Klassen found that $G(C_2H_2) \simeq G(C_2H_6) + G(n\text{-}C_4H_{10})$ and that $G(C_3H_8)$ is much smaller than $G(n\text{-}C_4H_{10})$.[7] The present system is similar to that of Klassen, the only difference being in the solvent, but the relative yields of the hydrocarbon products are quite different. For example, $G(C_2H_6)$ is much larger than $G(n\text{-}C_4H_{10})$ and $G(C_3H_8)$ is nearly equal to $G(n\text{-}C_4H_{10})$. These discrepancies may be explained by the reactions of radicals produced by the reactions (1), (2) and (5); that is, the following reactions become important in the present system:

$$H + C_2H_5 \longrightarrow C_2H_6$$

$$CH_3 + C_2H_5 \longrightarrow C_3H_8$$

$G(C_2H_2)$ is not affected by the presence of nitric oxide. The formation, therefore, can be explained by this reaction;

$$N_2^* + C_2H_4 \longrightarrow N_2 + C_2H_2 + H_2(\text{or } 2H),$$

which has already been discussed.[1]

*1 In the presence of nitric oxide, another source of acetonitrile is possible:[5] $C_2H_5 + NO \rightarrow C_2H_5NO \rightarrow CH_3CN + H_2O$. However, if this reaction should occur, the *G*-value of acetonitrile should be much larger than that observed.

5) G. L. Pratt and J. H. Purnell, *Trans. Faraday Soc.*, **60**, 371 (1964).

6) S. Mizutani and S. Sato, to be published.

7) N. V. Klassen, *J. Phys. Chem.*, **71**, 2409 (1967).

BULLETIN OF THE CHEMICAL SOCIETY OF JAPAN VOL. 43 3716—3722 (1970)

An Infrared Spectroscopic Study of Hydrogen Bonding Interaction. Structural Studies of Proton-donating and -accepting Powers

Tsutomu KAGIYA, Yūzō SUMIDA and Toshihiro TACHI

Faculty of Engineering, Kyoto University, Sakyo-ku, Kyoto

(Received June 19, 1970)

The relationship between the proton-donating and proton-accepting powers and the structures of various proton donors and acceptors was studied in the liquid phase by means of an infrared spectrophotometer. The proton-donating powers of the donors were evaluated by means of the ratios of the O–H shifts of the donors (RO–H) to those of methanol in various proton acceptor solutions. The proton-accepting powers of the acceptors were evaluated by means of the division of the O–H shifts by the proton-donating powers of the donors used. The proton-donating powers increased with the decrease in the pK_a or the ionic RO–H bond dissociation energies and with the increase in the electron affinities of RO radicals, *i. e.*, *t*-butanol$<$methanol$\ll$trimethylsilanol$<$phenol$<$*p*-nitrophenol. In a homologous series, the proton-accepting powers increased with the decrease in the ionization potentials. In the case of the aromatic ethers with two proton accepting sites, two characteristic O–H vibrational bands were observed. The difference in the proton-accepting powers of the vinyl and ethyl compounds with the same substituent was observed, and the π-electron-mobility index, which was considered to be a measure of the energy level of the π-electrons of the vinyl group, was defined and discussed.

Since the hydrogen bond was first recognized, great attention has been paid to the physicochemical behavior of many types of polar compounds.[1] Enormous studies dealing with the intra- and intermolecular hydrogen bond have been made by many researchers from the theoretical and the experimental aspects; they were summarized by Pimentel *et al.*[2,3] However, the main studies in this field have been focused on the physical properties of liquid and crystal states, except for the gaseous adsorption on a solid.[4,5]

In our previous papers,[6–8] we have concluded that the shifts of the O–D or the C=O vibrational bands of monodeuteromethanol as a proton donor, or of acetophenone as a proton acceptor, in various liquid organic compounds can be regarded as a measure of the electron-donating powers, or of the electron-accepting powers, of compounds respectively.

The objective of the present spectroscopic work is to discuss quantitatively the relationship between the proton-donating and proton-accepting powers and the structures or the electronic natures of various proton donors and acceptors. Moreover, on the basis of the experimental results of the proton-accepting powers of the vinyl and ethyl compounds with the same substituent, the π-electron-mobility index, as a measure of the energy level of the π-electrons of the vinyl group, will be defined and discussed.

Experimental

Materials. Methanol, monodeuteromethanol, *t*-butanol, phenol, *p*-nitrophenol, and trimethylsilanol were used as the proton donors. All the compounds but trimethylsilanol were obtained commercially and were purified by distillation or recrystallization. The trimethylsilanol was synthesized by the method of Sommer.[9]

Apparatus and Method. A small quantity (0.03—0.08 mol/*l*) of the proton donor was added to 1.0 m*l* of the proton acceptor in a weighing bottle. After the

1) W. Gordy and S. C. Stanford, *J. Chem. Phys.*, **9**, 204 (1941).

2) E. R. Lippincott and R. Schroeder, *ibid.*, **23**, 1099 (1955). N. D. Coggeshall, *ibid.*, **18**, 978 (1950); Z. Yoshida and E. Osawa, *J. Amer. Chem. Soc.*, **87**, 1467 (1965); A. Allerhand and P. von R. Schleyer, *ibid.*, **85**, 371 (1963).

3) G. C. Pimentel and A. L. McClellan, "The Hydrogen Bond," W. H. Freeman and Company, San Francisco and London, 1960.

4) J. Donohue, *J. Phys. Chem.*, **56**, 502 (1952).

5) A. V. Kiselev and V. I. Lygin, "Infrared Spectra of Adsorbed Species," ed. by L. H. Little, Academic Press, London and New York (1966), p. 274.

6) T. Kagiya, Y. Sumida and T. Inoue, This Bulletin, **41**, 767 (1968).

7) T. Kagiya, Y. Sumida and T. Inoue, *ibid.*, **41**, 773 (1968).

8) T. Kagiya, Y. Sumida and T. Inoue, *ibid.*, **41**, 779 (1968).

9) L. H. Sommer, E. Pietrusza and F. C. Whitmore, *J. Amer. Chem. Soc.*, **68**, 2282 (1946).

Table 1. Frequency shifts of O–H vibrational bands of various proton donors in proton acceptor solutions (cm^{-1})

	t-Butanol		Methanol		Trimethylsilanol		Phenol		*p*-Nitrophenol		Monodeuteromethanol[a]	
	ν	$\Delta\nu$	ν	$\Delta\nu$	ν	$\Delta\nu$	ν	$\Delta\nu$	ν	$\Delta\nu$	ν	$\Delta\nu$
Chloroform	3605	−15	3642	−19	3668	−26	3608	−40	3594	−59	2679	−11
Benzene	3590	0	3623	0	3642	0	3568	0	3535	0	2668	0
Ethyl acetate	3541	49	3561	62	3540	102	3434	134	3356	179	2628	40
Acetonitrile	3533	57	3551	72	3524	118	3411	157	3321	214	2613	55
Diethyl ether	3506	84	3516	107	3464	178	3341	227	3218	317	2589	79
1,4-Dioxane	3503	87	3515	108	3466	176	3340	228	3219	316	2593	75
Tetrahydrofuran	3492	98	3495	128	3430	212	3300	268	3180	355	2578	90

a) See Ref. 6.

bottle had then been shaken for 10 min at room temperature (20±3°C), the mixture was used for the measurement of the infrared spectrum. All the spectral measurements were made in the O–H (or O–D) fundamental region, using a Japan Spectroscopic Co. Model DS-402G or DS-403G infrared spectrophotometer. The thickness of the KBr fixed cell used was 0.010 cm. The dependence of the concentration of the proton donor on the shift of the O–H (or O–D) band was negligible in this concentration range. The experimental error in the measured shifts of the O–H (or O–D) bands was not more than ±1.0 cm^{-1}.

Results and Discussion

Proton-donating Powers and Proton-accepting Powers. The positions of the unassociated hydroxyl fundamental vibrational bands of various proton donors involved in several proton acceptor solutions are summarized in Table 1. According to the definition of the electron-donating powers of compounds presented in a previous paper,[6] the relative differences in the O–H frequency shifts of the proton donors (RO–H) observed in the proton acceptor solutions from that in benzene were calculated:

$$\Delta\nu_{RO-H}(\text{proton acceptor}) = \nu_{RO-H}(\text{benzene}) - \nu_{RO-H}(\text{proton acceptor}) \quad (1)$$

Obviously, the magnitudes of the O–H frequency shifts are due to the relative strengths of the intermolecular interaction between the proton donors and the proton acceptors, *i. e.*, the proton-donating powers and the proton-accepting powers.

In order to evaluate quantitatively the proton-donating powers of proton donors with the use of the definition expressed by Eq. (1), the O–H frequency shifts of the proton donors in several acceptor solutions were plotted against those of methanol in the same solution. As is shown in Fig. 1, linear relations with different slopes were found between them. The slopes are obviously the characteristic values, depending only on the structures of the proton donors, not on those of the proton acceptors.

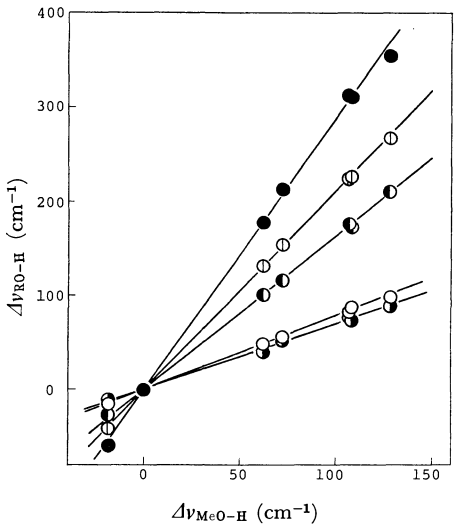

Fig. 1. O–H Frequency shifts of the proton donors in the typical proton acceptor solutions and O–H frequency shifts of methanol in the same solutions.
Proton donor: ◑, Monodeuteromethanol; ○, *t*-Butanol; ◐, Trimethylsilanol; ①, Phenol; ●, *p*-Nitrophenol

Therefore, we believe that the values of the (Φ_D) slopes, which represent the magnitudes of the O–H shifts of the proton donors relative to that of methanol as a standard proton donor, indicate a quantitative measure of the proton-donating powers:

$$\Phi_D = \frac{\Delta\nu_{RO-H}}{\Delta\nu_{MeO-H}} \quad (2)$$

On the basis of the same consideration, we defined the proton-accepting powers of proton acceptors (Φ_A), independent of the kind of proton donors, as the division of the O–H shifts of a certain proton donor in the proton-acceptor solutions by the Φ_D of the proton donor, as follows:

$$\Phi_A = \frac{\Delta\nu_{RO-H}(\text{proton acceptor})}{\Phi_D} \quad (3)$$

TABLE 2. COMPARISON OF PROTON-DONATING POWERS OF PROTON DONORS RO–H WITH RADICAL- AND IONIC-DISSOCIATION ENERGIES OF RO–H BONDS AND ELECTRON AFFINITIES OF RO RADICALS

Proton Donor RO–H	Φ_D	pK_a	D(RO–H) (kcal/mol)	D(RO$^-$–H$^+$)[a] (kcal/mol)	EA(RO)[b] (kcal/mol)
t-Butanol	0.79	19	105	325	56
Methanol	1.00	16	100	315	61
Trimethylsilanol	1.65	11	88[c]	295[c]	69
Phenol	2.13	10	84	290	70
p-Nitrophenol	2.92	7.1	75[c]	276[c]	75
Monodeuteromethanol	0.71	—	102	—	61

a) Values estimated by using $D(RO^-–H^+)=D(RO–H)+IP(H)-EA(RO)$.
b) Values estimated from the pK_a values. See Ref. 11.
c) Approximate values.

It is obvious from this definition (3) that the proton-accepting powers should be equal to the O–H frequency shifts of methanol as a standard proton donor.

Proton-donating Powers and the Structures of Proton Donors. The acid-dissociation constant (pK_a) of the proton donor in an aqueous solution corresponds to the free-energy change of the equilibrium reaction to form the hydrated proton and corresponding anion; therefore, the pK_a is a thermodynamic measure of the proton-donating powers. As Fig. 2 shows, the Φ_D increases with the decrease in the pK_a.[3,10] By using the pK_a values of the proton donors, the Φ_D value and then the O–H frequency shifts can be approximately predicted. The unknown values of pK_a can also be estimated from the frequency shifts.

In Table 2, the dissociation energies, D(RO–H), the ionic-dissociation energies, D(RO$^-$–H$^+$), of the RO–H bonds of the proton donors, and the electron affinities, EA(RO), of the RO radicals are listed. A correlation between the Φ_D and the ionic-dissociation energies of the RO–H bonds is illustrated in Fig. 3; the Φ_D becomes larger as the ionic-dissociation energy decreases. It can also be seen that, for the proton donors employed, the Φ_D increases with the increase in the electron affinity of the RO radical and the decrease in the dissociation energy of the

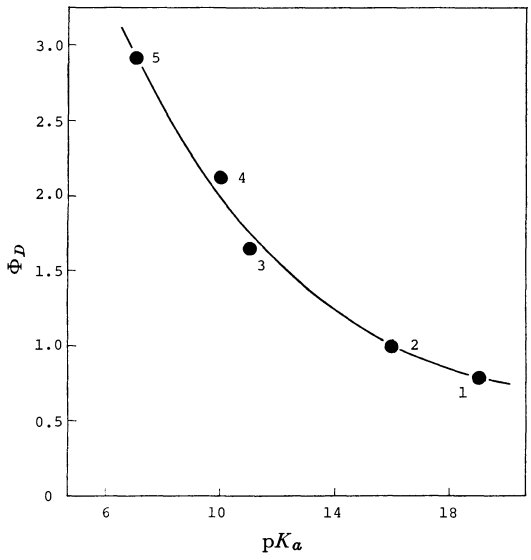

Fig. 2. Relation between the proton-donating powers Φ_D and the acid dissociation constants pK_a of proton donors.
Proton donor: 1, *t*-Butanol; 2, Methanol; 3, Trimethylsilanol; 4, Phenol; 5, *p*-Nitrophenol

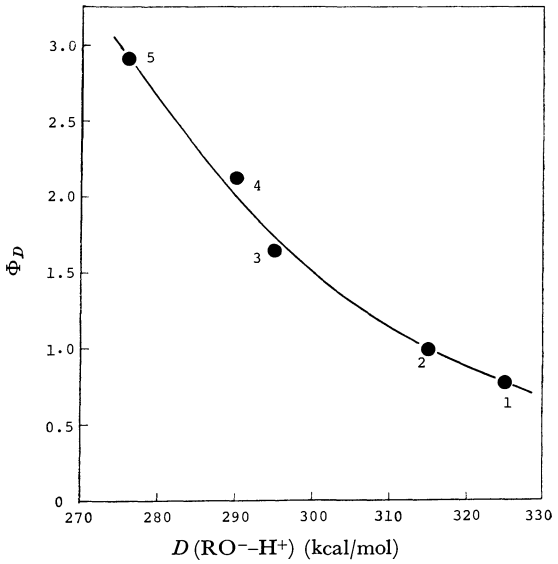

Fig. 3. Relation between the proton-donating powers Φ_D and the ionic-dissociation energies D(RO$^-$–H$^+$) of proton donors RO–H.
Proton donor: 1, *t*-Butanol; 2, Methanol; 3, Trimethylsilanol; 4, Phenol; 5, *p*-Nitrophenol

10) C. M. Huggins and G. C. Pimentel, *J. Phys. Chem.*, **60**, 1615 (1956).

RO–H bond. However, although the dissociation energies of the C–H bonds are slightly smaller than those of the RO–H bonds, the hydrocarbons have little proton-donating properties. This is due to the smaller electron affinities (12~25 kcal/mol) of the hydrocarbon radicals, compared with those (55~75 kcal/mol) of the RO radicals. It may be concluded from these considerations that the proton-donating powers, Φ_D, are mainly affected by the electron affinities of the RO radicals rather than by the dissociation energies of the RO–H bonds.

Moreover, in order to examine the isotope effect on the proton-donating powers, we compared the shifts of methanol and monodeuteromethanol. As is shown in Table 2, the values of Φ_D should fall to about 0.7 times by deuteration; this agreed well with the theoretical prediction proposed by Coggeshall.[2)]

Proton-accepting Powers and the Structures of Proton Acceptors. When trimethylsilanol was used as a proton donor, the O–H vibrational bands were sharp and symmetrical in all of the proton

TABLE 3. FREQUENCY SHIFTS OF O–H VIBRATIONAL BANDS OF TRIMETHYLSILANOL IN VARIOUS PROTON ACCEPTOR SOLUTIONS AND PROTON-ACCEPTING POWERS OF PROTON ACCEPTORS

Proton acceptor	ν_{RO-H} (cm^{-1})	$\Delta\nu_{RO-H}$ (cm^{-1})	$\Delta\nu_{MeO-D}$[a)] (cm^{-1})	Φ_A[b)] (cm^{-1})
Aliphatic Hydrocarbons and Derivatives				
Chloroform	3668	−26	−11	−16.8
Aromatic Hydrocarbons and Derivatives				
Benzene	3642	0	0	0
Toluene	3636	6	2	3.2
Ethylbenzene	3631	11	4	6.2
m-Xylene	3630	12	7	8.6
Chlorobenzene	3662	−20	−8	−11.7
Anisole	3620, 3533[c)]	22, 109[c)]	—	13.3, 66.1[c)]
Phenetole	3621, 3542[c)]	21, 100[c)]	—	12.7, 60.6[c)]
Styrene oxide	3615, 3528[c)]	27, 114[c)]	—	16.4, 69.1[c)]
Esters				
Ethyl acetate	3540	102	40	59.2
Methyl propionate	3549	93	33	51.5
Vinyl acetate	3576	66	25	37.7
Methyl acrylate	3551	91	30	48.8
Nitriles				
Acetonitrile	3524	118	55	73.7
Propionitrile	3526	116	52	71.9
Acrylonitrile	3545	97	38	56.3
Ketones				
Acetone	3532	110	64	78.5
Methyl ethyl ketone	3534	108	57	73.0
Methyl vinyl ketone	3480	162	89	112.0
Ethers				
Diethyl ether	3464	178	79	108.8
Di-*n*-propyl ether	3459	183	73	107.0
n-Butyl ethyl ether	3456	186	77	110.8
1,2-Dimethoxyethane	3470	172	71	102.3
Ethyl vinyl ether	3553	89	35	51.7
n-Butyl vinyl ether	3554	88	33	50.0
Diallyl ether	3475	167	66	97.3
Propylene oxide	3508	134	59	82.3
Epichlorohydrin	3539	103	49	65.8
Tetrahydrofuran	3430	212	90	127.9
1,4-Dioxane	3466	176	75	106.9
Furan	3638	4	2	2.6

a) Data in Ref. 6 and the remeasured values.
b) Average values of Φ_A obtained from the different proton donors.
c) the OH vibrational band with the higher intensity.

acceptor solutions except in case of the aromatic ether solutions. The experimental data are summarized in Table 3.

In the aromatic hydrocarbons, it is observed that the introduction of electron-withdrawing groups or of electron-relieving groups to the benzene rings results in a decrease or an increase in the proton-accepting powers. For the aromatic ethers, represented by anisole, two unassociated O–H vibrational bands were observed. It is known that one showing the larger shift and intensity is to be assigned to the hydrogen bond formed by the lone-pair electrons of ether oxygen, while the other, showing the smaller shift and intensity, is to be assigned to the bond formed by the benzene ring.*1

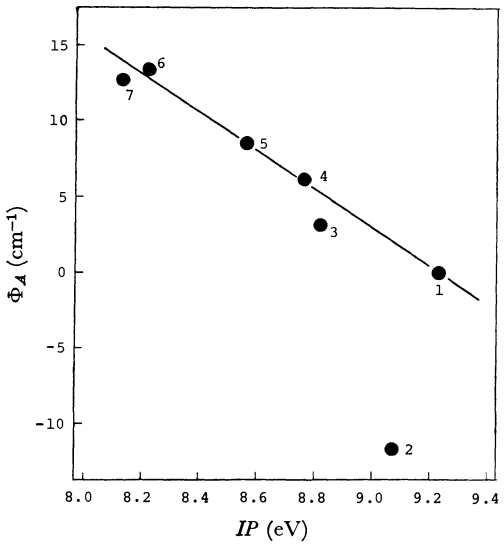

Fig. 4. Relation between the proton-accepting powers Φ_A and the ionization potentials of benzene derivatives.
Benzene derivative: 1, Benzene; 2, Chlorobenzene; 3, Toluene; 4, Ethylbenzene; 5, *m*-Xylene; 6, Anisole; 7, Phenetole

In order to determine a correlation between the proton-accepting powers, Φ_A, and the electronic natures of benzene derivatives, the Φ_A was plotted against the ionization potential. As is shown in Fig. 4, a linear relationship with a negative slope was observed between them. If the first ionization of the benzene derivatives is caused by the benzene ring, the results in Fig. 4 should indicate the intermolecular interaction between the silanol proton and the π-electrons on the benzene ring. Similarly, a straight line with a negative slope was also drawn between the Φ_A and the Hammett substituent constants (Fig. 5). This fact also supports the above consideration.

*1 Detailed descriptions on this phenomenon will be given in a subsequent paper.

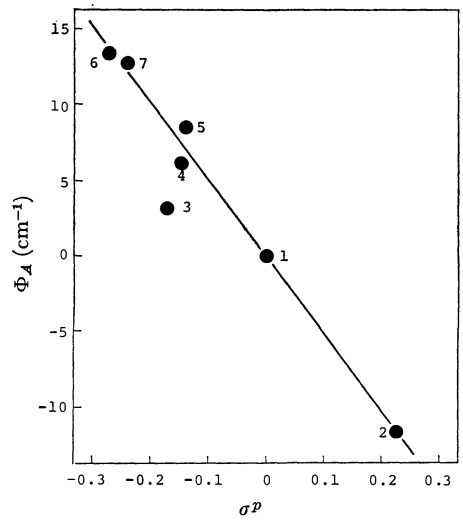

Fig. 5. Relation between the proton-accepting powers Φ_A and the Hammett substituent constants σ^p of benzene derivatives.
Benzene derivative: 1, Benzene; 2, Chlorobenzene; 3, Toluene; 4, Ethylbenzene; 5, *m*-Xylene; 6, Anisole; 7, Phenetole

On the other hand, it is of interest to ascertain information on the electronic state of the π-electrons, not only on the benzene ring, but also on the vinyl groups of vinyl compounds. From this point of view, the Φ_A values of a pair of the proton acceptors (CH_2=CHY and CH_3CH_2Y) with analogous chemical structures were compared as an example, methyl

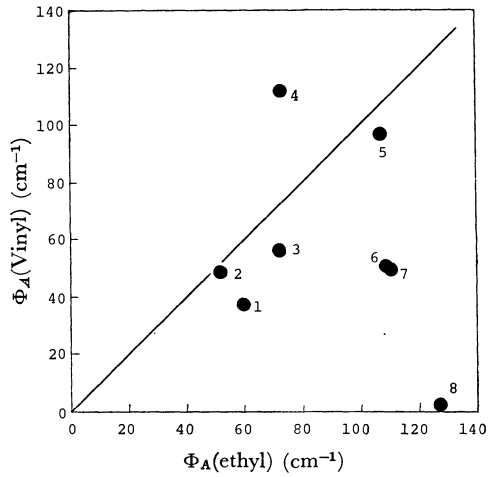

Fig. 6. Plots of the proton-accepting powers Φ_A (vinyl) of vinyl compounds *versus* the proton-accepting powers Φ_A(ethyl) of ethyl compounds.
Vinyl compound–Ethyl compound: 1, Vinyl acetate–Ethyl acetate; 2, Methyl acrylate–Methyl propionate; 3, Acrylonitrile–Propionitrile; 4, Methyl vinyl ketone–Methyl ethyl ketone; 5, Diallyl ether–Di-*n*-propyl ether; 6, Ethyl vinyl ether–Diethyl ether; 7, *n*-Butyl vinyl ether–*n*-Butyl ethyl ether; 8, Tetrahydrofuran–Furan.

TABLE 4. π-ELECTRON-MOBILITY INDEXES AND ELECTRONIC PROPERTIES OF VINYL COMPOUNDS

No.	Vinyl compound	I_{em}	λ_{ho}[a] (β)	η_{lv}[a] (β)	q_α[b]	q_β[b]	$\frac{q_\alpha+q_\beta}{2}$[b]	D_π[c] (kcal/mol)	σ_R^p
1	Furan	0.98	—	—	—	—	—	—	—
2	*n*-Butyl vinyl ether	0.55	—	—	—	—	—	—	−0.58
3	Ethyl vinyl ether	0.53	0.354	1.118	—	—	—	—	−0.50
4	Vinyl acetate	0.36	0.850	0.958	1.033	0.931	0.982	58.2	−0.08
5	Acrylonitrile	0.22	0.855	0.407	1.019	0.849	0.934	46.2	0.08
6	Diallyl ether	0.092	—	—	—	—	—	—	—
7	Methyl acrylate	0.053	1.077	0.453	1.037	0.804	0.921	49.3	0.13
8	Ethyl acrylate	−0.03	—	—	—	—	—	—	0.13
9	4-Vinylpyridine	−0.08	—	—	—	—	—	—	—
10	Methyl methacrylate	−0.16	0.845	0.487	—	—	—	40.3	—
11	Acrolein	−0.44	1.161	0.315	1.087	0.685	0.886	48.7	0.15
12	Methyl vinyl ketone	−0.53	1.137	0.448	1.052	0.769	0.910	50.9	0.22

a) λ_{ho} and η_{lv} are the coefficients of the energies of the highest occupied π-level ($\varepsilon_{ho}=\alpha+\lambda_{ho}\beta$) and of the lowest vacant π-level ($\varepsilon_{lv}=\alpha-\eta_{lv}\beta$), respectively. Data in Ref. 11.

b) q_α and q_β are the π-electron densities of α-carbon and β-carbon in the vinyl compound ($\overset{\beta}{C}H_2=\overset{\alpha}{C}HY$).

c) Data in Ref. 12.

vinyl ketone and methyl ethyl ketone. It may be noted from this comparison that the Φ_A is markedly affected by the substitution of vinyl group for ethyl group bonding with the substituent group Y. In order to clarify the phenomena, we plotted the Φ_A of the vinyl compounds against that of the ethyl compounds, as is shown in Fig. 6; for convenience, we classified them into the following three types: (i) Φ_A(vinyl)$>\Phi_A$(ethyl), (ii) Φ_A(vinyl)$\simeq\Phi_A$(ethyl), and (iii) Φ_A(vinyl)$<\Phi_A$(ethyl). Since the introduction of a hetero atom to the proton-accepting molecule as an unsaturated hydrocarbon molecule results in an enhanced Φ_A, the hydrogen atom in a silanol molecule is considered to form a hydrogen bond more preferentially with the hetero atom than with the vinyl group. Therefore, the difference in the Φ_A values of the vinyl and ethyl compounds with the same substituent should indicate directly the difference in the electronic natures of the hetero atoms in the substituents. In other words, it can be said that the difference in the Φ_A indicated the π-electron drift between the vinyl group and the neighboring hetero atom.

Typical pairs of compounds belonging to the (i) and (iii) types are methyl vinyl ketone–methylethyl ketone and ethyl vinyl ether–diethyl ether respectively:

Methyl vinyl ketone
Φ_A(vinyl) = 112.0 cm^{-1}
Φ_A(ethyl) = 73.0 cm^{-1}

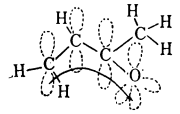

Ethyl vinyl ether
Φ_A(vinyl) = 51.7 cm^{-1}
Φ_A(ethyl) = 108.8 cm^{-1}

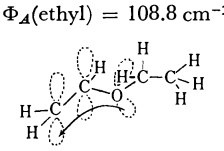

In methyl vinyl ketone, it can be considered that the π-electrons of the vinyl group migrate from the vinyl group to the carbonyl oxygen whose lone-pair electrons associate with the hydrogen atom in a silanol molecule, resulting in a lowering of the π-electron density of the vinyl group or in a lowering of the energy level of the π-electrons of the vinyl group. In the case of ethyl vinyl ether, it can be considered that the lone-pair electrons of an oxygen atom which have some π-characteristics transfer to the vinyl group and enhance the energy level of π-electrons of the vinyl group.

On the basis of the above qualitative consideration, we may defined the π-electron-mobility index (I_{em}), which represents the degree of the mobility of π-electrons of the vinyl group, as follows:

$$I_{em}=\frac{\Phi_A(\text{ethyl})-\Phi_A(\text{vinyl})}{\Phi_A(\text{ethyl})} \quad (4)$$

The I_{em} values are listed in Table 4.

In order to confirm this definition, we examined the relationships between the I_{em} and the other measures representing the energy level of π-electrons of the vinyl group (Table 4). It is obvious from Table 4 that the I_{em} values are in relation to the coefficients (λ_{ho}) of the highest occupied π-levels ($\varepsilon_{ho}=\alpha+\lambda_{ho}\beta$) rather than to those ($\eta_{lv}$) of the lowest vacant π-levels ($\varepsilon_{lv}=\alpha-\eta_{lv}\beta$) of vinyl compounds, as calculated by the method of the simple Hückel MO.[11]

It may also be seen in Table 4 that the I_{em} values are correlated with the average π-electron densities

11) T. Kagiya, Y. Sumida and T. Nakata, This Bulletin, **41**, 2239, 2247 (1968).

$(q_\alpha+q_\beta)/2$ of the vinyl groups, where q_α and q_β are, respectively, the π-electron densities of α-carbon and β-carbon; the larger the values of $(q_\alpha+q_\beta)/2$, the larger the I_{em} values. It may be concluded from these results that the I_{em} is a measure not only of the energy level of the highest occupied π-orbital of vinyl compound, but also of the average π-electron density of the vinyl group.

There is, however, no relationship between the I_{em} and the π-bond dissociation energies of the vinyl compounds, which depend upon the electronic nature of the vinyl group.[11,12] This means that the I_{em} indicates the degree of π-electron drift in the molecule, but not essentially the strength of the π-bond.

Moreover, in order to elucidate the resonance effect on the I_{em} values, we then plotted the I_{em} against the substituent constants, $(\sigma_R{}^p)$, due to the resonance effect. As is shown in Fig. 7, there exists a good correlation — the I_{em} becomes larger as the $\sigma_R{}^p$ decreases.

It seems reasonable to conclude from the above correlations that the I_{em} is a semi-quantitative measure of the various electronic properties of π-electrons of the vinyl groups.

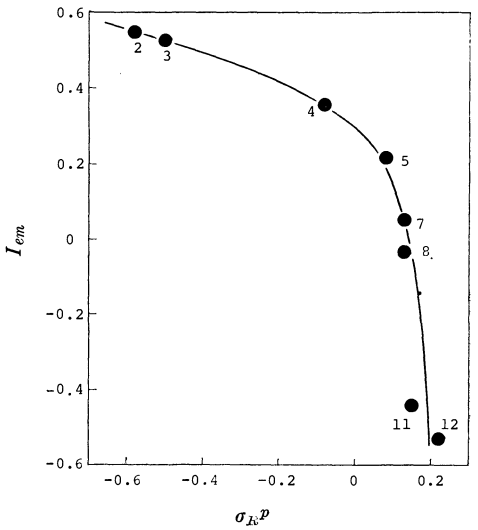

Fig. 7. Relation between the π-electron-mobility indexes I_{em} and the resonance substituent constants $\sigma_R{}^p$. The number of a point represents the number in Table 4.

The authors would like to express their gratitude to Mr. Takeshi Watanabe for his technical assistance.

12) T. Kagiya and Y. Sumida, *Polymer J.*, **1**, 137 (1970).

BULLETIN OF THE CHEMICAL SOCIETY OF JAPAN VOL. 43 3722—3728 (1970)

Sound Velocity in Polyoxyethylene(6)laurylether Aqueous Solution

Otohiko NOMOTO*,** and Harumi ENDO*

* *Department of Applied Physics, Defense Academy, Yokosuka*
** *Kobayasi Institute of Physical Research, Kokubunji, Tokyo*

(Received June 20, 1970)

The sound velocity and density of polyoxyethylene(6)lauryether and its aqueous solutions are measured, and the adiabatic compressibility is computed from these results. The virtual sound velocity was calculated in ideal mixtures by using Kudriavtsev's formula, and above 33°C for ideal suspensions by the use of the equation of Urick and Ament for dispersed systems. Some deviations in the experimental velocity from the calculated value are ascribed to the interaction energy of mixing. This energy, or the heat of the hydration of a nonionic surfactant, is obtained as a function of the temperature. The diagrams of the density, sound velocity, and adiabatic compressibility *vs.* the temperature at various concentrations always exhibit a common crossing point, nearly at the cloud point. It may thus be concluded that the measurements of the sound velocity and density give a new method for determining the cloud point.

The dissolved state and the properties of ionic surfactants in aqueous solutions have been studied with ultrasonics by Yasunaga *et al.*[1,2] and by Shigehara,[3-5] but so far no study of the dissolved state and properties of nonionic surfactants in aqueous

1) T. Yasunaga, H. Oguri and M. Miura, *J. Colloid Interfac. Sci.*, **23**, 352 (1967).
2) T. Yasunaga, S. Fujii and M. Miura, *6th Inter. Congr. Acoust.*, **V**, J-61 (1968).
3) K. Shigehara, This Bulletin, **38**, 1700 (1965).
4) K. Shigehara, *ibid.*, **39**, 2332 (1966).
5) K. Shigehara, *ibid.*, **39**, 2643 (1966).

solutions using ultrasonics has been reported.

In the present study, we adopted polyoxyethlene-(6)laurylether as the nonionic surfactant and measured its sound velocity in aqueous solutions.

The experimental data were compared with the results of the thermodynamical calculation of sound velocity using the Lennard-Jones potential. The heat of the hydration of the nonionic surfactant was estimated from deviation of the sound velocity from that of an ideal solution.

It is known that a nonionic surfactant in an aqueous solution suddenly turns cloudy white at a specified temperature called the cloud point (in our specimen, at 33°C). The curve of the difference in sound velocity between solvent and solution plotted against the temperature shows a sharp turn at nearly this temperature.

Solutions of a surfactant with a distribution of molecular weight exhibit a second transition temperature, the double cloud point (at 42°C for our specimen), above which two separated phases appear.

In the temperature range below 33°C, we computed the heat of hydration from the deviation of the experimental sound velocity from the ideal-solution sound velocity, as obtained by Kudriavtsev's formula.[6] In the 33—42°C temperature range, the present system becomes a dispersive system, or an emulsion. The sound velocity for emulsion or suspension is different from that of an ideal solution of the same composition, also in the absence of the heat of hydration. The ideal value of the sound velocity in this temperature range (33—42°C) was computed by Urick and Ament's formula;[7] we obtained the heat of hydration from the deviation of the experimental velocity from this ideal suspension value.

Experimental

Material. Polyoxyethylene(6)laurylether. The $C_{12}H_{25}O(C_2H_4O)_6H$ sample is a commercial product*1 and is used without further purification. The surfactant has its cloud point and double cloud point at 33°C and 42°C respectively.

Apparatus. The sound velocity is measured with a variable-path ultrasonic interferometer with a 1/1000 mm reading and a frequency of 5 MHz. The density measurements are made by means of an Ostwald-type pycnometer to an accuracy higher than 1 part in 10^4. The temperature-regulated water in a thermostat of ± 0.05°C is circulated in the mantle surrounding the cell by means of a circulation pump. The overall accuracy of velocity measurement is ± 0.3 m/sec.

6) B. Kudriavtsev, *Soviet Physics Acoustics*, **2**, 36 (1956).

7) R. Urick and W. Ament, *J. Acoust. Soc. Amer.*, **21**, 115 (1948).

*1 Products of Nippon Surfactant Industr. Inc., Tokyo.

Theoretical

The sound velocity in binary liquid mixtures has been thermodynamically calculated by Kudriavtsev.[6] It is assumed that, in an ideal mixture, the internal energy, E, and the volume, V, are additive;

$$E = x_1E_1 + (1-x_1)E_2 \tag{1}$$

$$V = x_1V_1 + (1-x_1)V_2 \tag{2}$$

where the suffixes 1 and 2 refer to the first and second components of the mixture respectively, and where x_1 is the mole fraction of the first component. By differentiating Eq. (1) twice with respect to the volume at a constant entropy, S, and noting that

$$\left(\frac{\partial^2 E}{\partial V^2}\right)_S = \frac{MC^2}{V^2} \tag{3}$$

where C is the sound velocity, and M, the molecular weight, we obtain this expression for the sound velocity in the mixture:

$$C^2 = x_1\frac{M_1}{\bar{M}}C_1^2 + (1-x_1)\frac{M_2}{\bar{M}}C_2^2 \tag{4}$$

Here, C_1 and C_2 are, respectively, the sound velocities in the first and second components, M_1 and M_2 are the molecular weights of the two components, and $\bar{M}$ is the average molecular weight:

$$\bar{M} = x_1M_1 + (1-x_1)M_2 \tag{5}$$

The Eq. (4) obtained by Kudriavtsev is only approximate, because the thermodynamic relation (3) gives the result more exactly:

$$MC^2 = \frac{E}{\chi'} \tag{6}$$

χ' is dependent on each liquid (and also somewhat on the temperature), as obtained by Nomoto,[8] though the range of χ' for various liquids is not very wide ($\chi' \fallingdotseq 0.2-0.3$). Therefore, we have, in place of Eq. (4), more exactly:

$$C^2 = x_1\frac{M_1}{\bar{M}}\frac{\chi}{\chi_1}C_1^2 + (1-x_1)\frac{M_2}{\bar{M}}\frac{\chi}{\chi_2}C_2^2 \tag{7}$$

Experimentally, however, Kudriavtsev's relation (4) is known to be quite valid for many liquid mixtures, and we use it below to represent the sound velocity in ideal mixtures.

Assuming the Lennard-Jones potential for the intermolecular potential of the liquids, we obtain:

$$\Phi(r) = \frac{A}{r^{12}} - \frac{B}{r^6} \tag{8}$$

Here, r is the intermolecular distance. The A and B quantities are functions of the temperature, but at a constant temperature they are constants

8) O. Nomoto, *J. Phys. Soc. Jap.*, **18**, 1526 (1963).

characteristic of the specified liquid. We can also write Eq. (8) in terms of the molar volume, V, as:

$$\Phi(V) = \frac{A_0}{V^4} - \frac{B_0}{V^2} \quad (9)$$

The deviation from ideal behavior expressed in Eq. (1) may be accounted for by taking into account the interaction energy of mixing ΔE_{12}:

$$E = x_1E_1 + (1-x_1)E_2 + \Delta E_{12} \quad (10)$$

If we assume that the internal energy of molecular interaction between the components of the mixture also obeys Eq. (9), then from Eq. (10) we can find:

$$C^2 = x_1\frac{M_1}{\bar{M}}C_1^2 + (1-x_1)\frac{M_2}{\bar{M}}C_2^2 + 2 \times 4\gamma\Delta E_0 \quad (11)$$

where γ is the ratio of the specific heats. If we use for ΔE_0 the heat of hydration, L (cal/solution 1 g), then we have, as the sound velocity in mixtures, the expression:

$$C^2 = x_1\frac{M_1}{\bar{M}}C_1^2 + (1-x_1)\frac{M_2}{\bar{M}}C_2^2 + 3.35 \times 10^8L \quad (12)$$

In the temperature range from the cloud point to the double cloud point, we have emulsions. Urick and Ament[7] obtained the propagation constant in a medium containing numerous small spherical particles. In our notations, their expression takes the form:

$$\left(\frac{C_2}{C_s}\right)^2 = \{1+\alpha(\beta_1-\beta_2)/\beta_2\}\{1+3\alpha\sigma/(2\sigma+3)\} \quad (13)$$

Here, C_2 and C_s are the sound velocities in the solvent water and in the dispersive system respectively. β_1 and β_2 are the adiabatic compressibilities of the surfactant and the solvent respectively, and $\sigma=(\rho_1-\rho_2)/\rho_2$, with ρ_1 and ρ_2 the densities of the surfactant and the solvent, and α, the volume fraction of the surfactant. We use Eq. (13) in place of Eq. (4) and use:

$$C^2 = C_s^2 + 3.35 \times 10^8L \quad (14)$$

to represent the deviation from an ideal emulsion in this temperature range.

Results and Discussion

We studied the behavior of sound velocity in dilute aqueous solutions of polyoxyethylene(6)-laurylether (a commercial product). The phase diagram of this purified surfactant + water system was previously studied by Balmbra *et al.*[9]

Figures 1—4 show the sound velocity as functions of the temperature for solutions with various concentrations of the nonionic surfactant. The experimental values and computations for ideal solutions by Eq. (4) and for an ideal emulsion by Eq. (12) are shown. The difference between the observed sound velocity and the ideal-solution (or -emulsion) velocity increases with an increase in the concentration. The emulsion velocity (C_s) is somewhat lower than the ideal solution velocity, though the difference is rather small.

As L represents the heat of hydration per gram of solution (p wt%), the heat of mixing L_M per mole of the solute becomes:

$$L_M = \frac{ML}{1000\left(\frac{p}{100}\right)} \text{ (kcal/mol)} \quad (15)$$

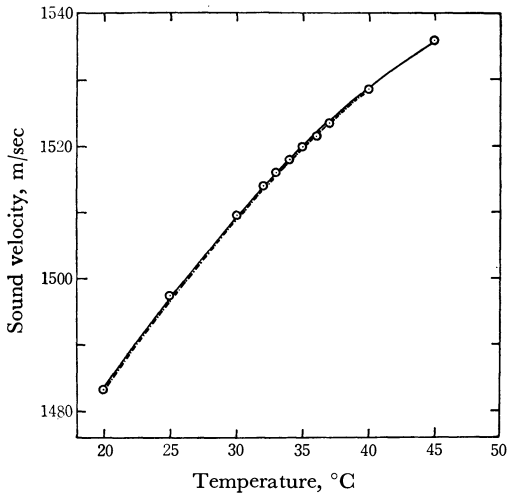

Fig. 1. Sound velocity as function of temperature for 0.5 g/100 cm³ water-solution.
—·—· computation with Eq. (4)
-------- computation with Eq. (12)
—⊙— observed values

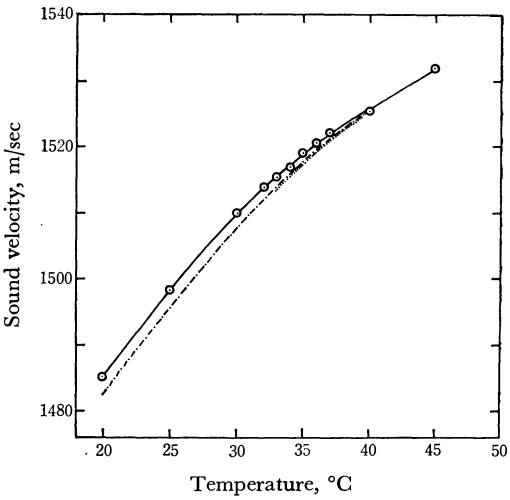

Fig. 2. Sound velocity as function of temperature for 3 g/100 cm³ water-solution.
—·—· computation with Eq. (4)
-------- computation with Eq. (12)
—⊙— observed values

9) R. Balmbra, J. Clunie, J. Cokill and J. Goodman, *Trans. Faraday Soc.*, **58**, 1661 (1962).

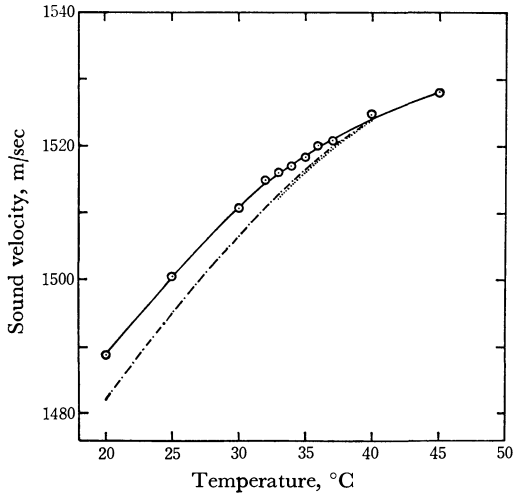

Fig. 2. Sound velocity as function of temperature for 5 g/100 cm³ water-solution.
—·—· computation with Eq. (4)
-------- computation with Eq. (12)
—⊙— observed values

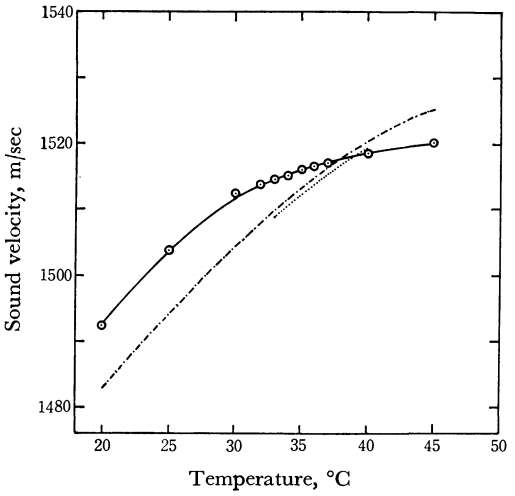

Fig. 4. Sound velocity as function of temperature for 10 g/100 cm³ water-solution.
—·—· computation with Eq. (4)
-------- computation with Eq. (12)
—⊙— observed values

In the temperature range betweem the two cloud points, both the values of L_M, these calculated by using $C_{cal}=C_{ideal}$ and $=C_s$, are as shown in Table 1. Each datum is the average of four determinations. It may be seen in Table 1 that the calculated energies from an ideal solution and from a dispersive solution are nearly equal. As is also to be seen from Table 1, the mixing is exothermic at lower temperatures, but it becomes endothermic at higher temperatures. As regards the sound velocity, we can see from Figs. 1—4 that C_{exp} is higher than C_{ideal} in the lower temperature range, while $C_{exp}<C_{cal}$ in the higher temperature range. From Table 1, it is also to be seen that the value of energy found is comparable to the energy for the breakdown of the hydrogen bond (3.4 kcal/mol[10]) between water molecules. According to Chwala and Martina,[11] in an aqueous solution of ethylene oxide derivatives a hydrogen bridge is formed between the ether-like combined oxygen atom and the water molecule as is illustrated below:

$$-CH_2-O-CH_2-$$
$$\updownarrow$$
$$H-O-H$$

Table 1

Temperature °C	From Eq. (12) L_M kcal/mol	From Eq. (14) L_M kcal/mol	From Eq. (16) L_M kcal/mol
45	−1.77		
40	−0.29	+0.98	
37	0.66	1.20	
36	0.55	1.13	
35	1.30	2.19	
34	1.44	2.18	
33	2.23	2.56	
32	3.02		
25	4.09		
20	5.03		2.30

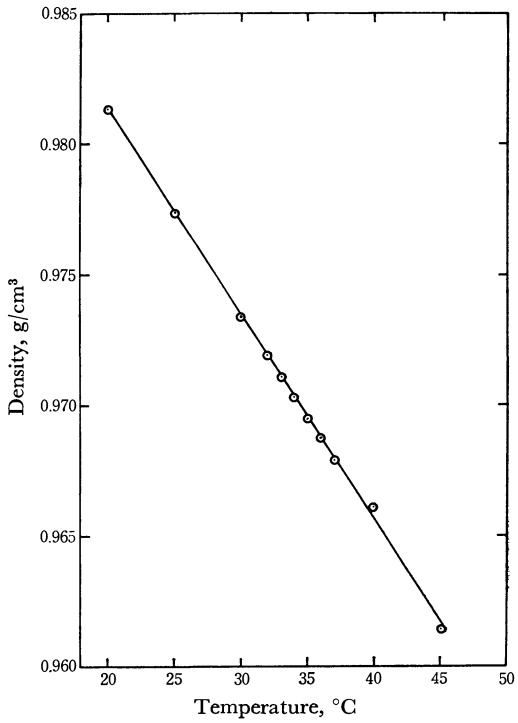

Fig. 5. Temperature dependence of density for surfactant.

10) G. Pimentel and A. McClellan, "The Hydrogen Bond," Reinhold Publishing Corp., New York (1960), p. 363.

11) A. Chwala and A. Martina, *Melliand Textilber.*, **18**, 992 (1937).

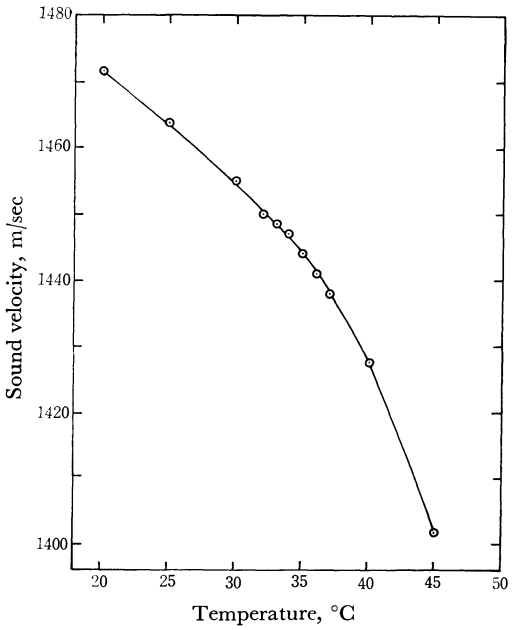

Fig. 6. Temperature dependence of sound velocity for surfactant.

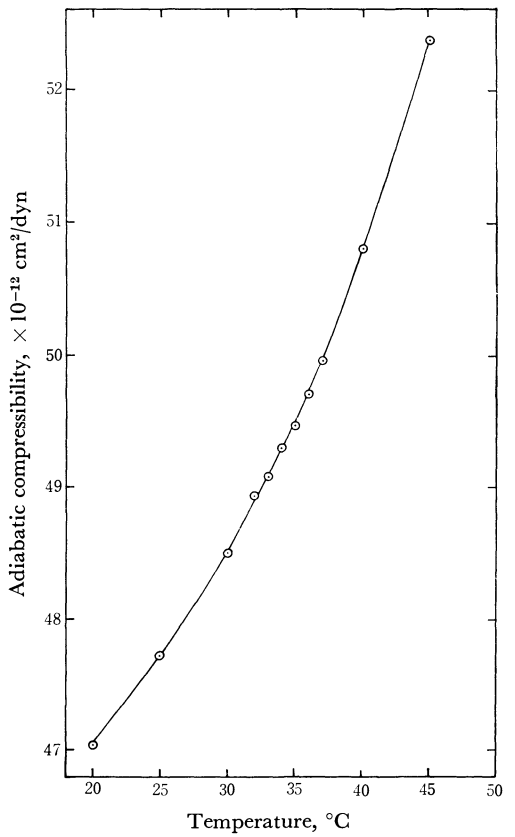

Fig. 7. Temperature dependence of adiabatic compressibility for surfactant.

At temperatures above the cloud point, dehydration phenomena of the nonionic surfactant may be expected in forming the emulsions.

As the value of the heat of hydration decreases with an increase in the temperature, it may be inferred that the cloud point phenomenon does not take place abruptly at a specified temperature, but that the phase separation takes place gradually in the temperature range slightly below the cloud point. Our sample being a high polymer, it may have a distribution of molecular weights, and the gradual-phase separation may thus be attributed to the distribution of molecular weights. This makes it difficult to analyse the dissolved state and the properties of the solution. If we can get a substance with a narrow distribution of molecular weight by the method of solvent extraction, molecular distillation or particular synthesis, we may be able to clarify the relationship between the heat of hydration and the phase separation.

The energy set free in the form of heat is measurable by the calorimetric method, but we obtained the heat of hydration from the deviation of the sound velocity from that of an ideal mixture instead of by calorimetric study. From their calorimetric measurements, Racz and Orban[12] give an empirical

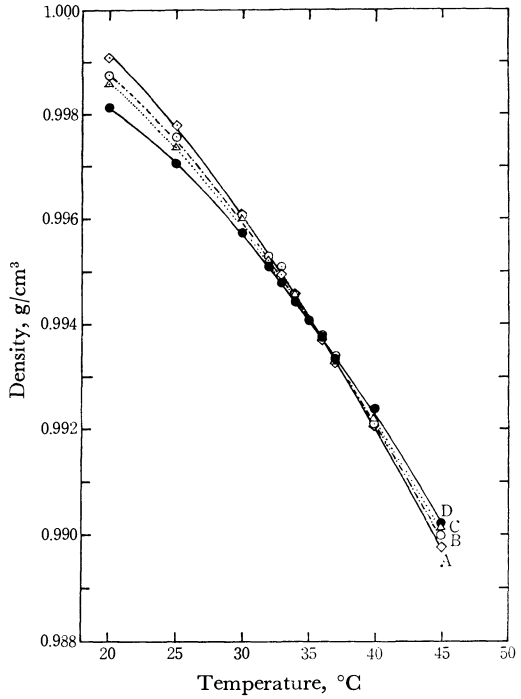

Fig. 8. Density as functions of temperature for various concentrations.
(A) 10g/100cm³ water
(B) 5g/100cm³ water
(C) 3g/100cm³ water
(D) 0.5g/100cm³ water

12) I. Racz and E. Orban, *J. Colloid Sci.*, **20**, 99 (1965).

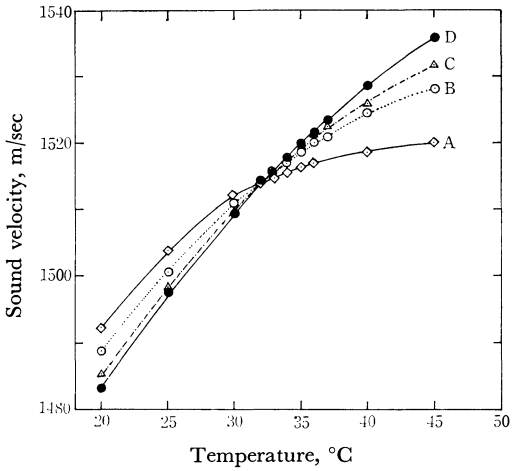

Fig. 9. Sound velocity as function of temperature for various concentrations.
(A) 10g/100cm³ water
(B) 5g/100cm³ water
(C) 3g/100cm³ water
(D) 0.5g/100cm³ water

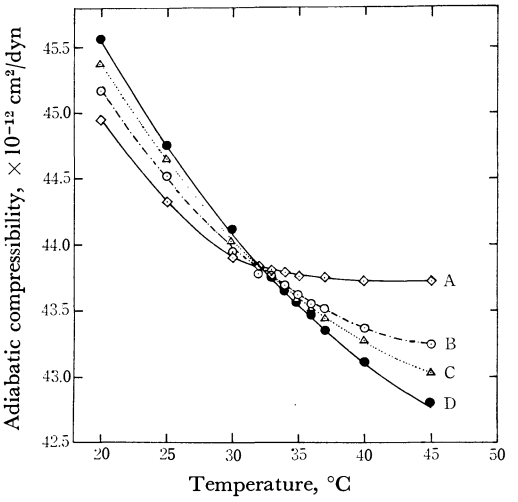

Fig. 10. Adiabatic compressibility as function of temperature for various concentrations.
(A) 10g/100cm³ water
(B) 5g/100cm³ water
(C) 3g/100cm³ water
(D) 0.5g/100cm³ water

relation between the hydrophile lipophile balance (*HLB*) of a liquid nonionic surfactant and the heat of hydration (at the temperature of 20°C):

$$HLB = 0.42Q + 7.5 \qquad (16)$$

where Q=heat of hydration in cal/g surfactant. Using Eq. (16) for our specimen with HLB=9.6,[13] we obtain the energy of hydration, L_M, as 2.3 kcal/mol. Though the value of *HLB* in our specimen is in nearly the same range as that investigated by Racz and Orban, the samples are somewhat different in the two cases. The samples of Racz and Orban were Tweens.*2 Therefore it is not certain

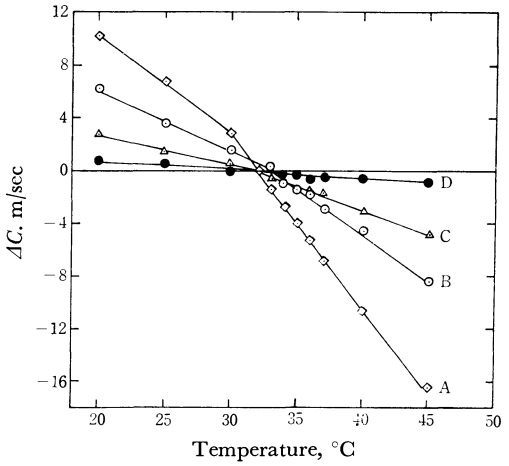

Fig. 11. The difference of sound velocity (ΔC) between solution and solvent as function of temperature in solutions of various concentrations.
(A) 10g/100cm³ water
(B) 5g/100cm³ water
(C) 3g/100cm³ water
(D) 0.5g/100cm³ water

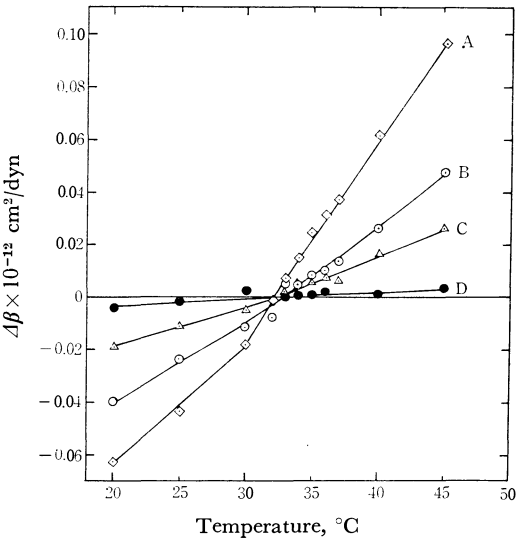

Fig. 12. The difference of adiabatic compressibility ($\Delta\beta$) between solution and solvent as function of temperature in solutions of various concentrations.
(A) 10g/100cm³ water
(B) 5g/100cm³ water
(C) 3g/100cm³ water
(D) 0.5g/100cm³ water

13) *Nikkol*, (1966), p. 23, Nippon Surfactant Industr. Inc., Tokyo.

*2 Products of Atlas Chemical Industr. Inc., Wilmington Delaware.

whether this value of $L_M=2.3$ kcal/mol is sufficiently accurate. We may thus conclude that the acoustically-determined energy of hydration for the nonionic surfactant is nearly in agreement with the calorimetric measurements.

Figures 5—7 show the temperature dependence of the sound velocity(C), density(ρ), and the adiabatic compressibility(β), respectively, for polyoxyethylene(6)laurylether. As is to be seen in Fig. 5, ρ plotted against T becomes a straight line, while we see from Figs. 6 and 7 that the curves of $C(T)$ and $\beta(T)$ have somewhat different slopes in different temperature ranges.

Figures 8—10 show the values of ρ, c, and β as functions of T for various concentrations. It may be seen that all of these curves intersect at one temperature, independent of the concentration. This temperature is about 32°C and is to be identified as the cloud point.

It is to be noticed that the sound velocity, the density, and the adiabatic compressibility are all independent of the concentration at the cloud point. We obtain the "acoustical cloud point" 32—33°C from Fig. 9; it coincides with the visual cloud point (33°C) within the range of experimental error.

Figures 11 and 12 show the difference in sound velocity (ΔC) and adiabatic compressibility ($\Delta\beta$) between the solution and the solvent as functions of the temperature in solutions of various concentrations. Each curve consists of two linear segments, with a turn at nearly 32—33°C. This break point, independent of the concentration of the surfactant, may reasonably be ascribed to the cloud point. The slopes per unit of concentration of ΔC–T curves and $\Delta\beta$–T curves are nearly constant above and below the cloud point respectively.

Mr. Noriaki Ohba of Nippon Surfactant Industr. Inc. has kindly supplied the surfactant sample for us. We express our sincere thanks to him in this place.

BULLETIN OF THE CHEMICAL SOCIETY OF JAPAN VOL. 43 3728—3740 (1970)

The γ-Radiolysis of Liquid *n*-Hexane. The Effects of Radical, Electron, and Positive-ion Scavengers

Kyoji SHINSAKA and Shoji SHIDA

Laboratory of Physical Chemistry, Tokyo Institute of Technology, Meguro-ku, Tokyo

(Received June 23, 1970)

The effects of various additives, SF_6, NH_3, C_2H_5OH, N_2O, NO, SO_2, and C_2H_4, on the product yields in the γ-radiolysis of liquid *n*-hexane at room temperature have been investigated. The following conclusions have been drawn: (i) The added SO_2 acts mainly as a radical scavenger. (ii) The added NO shows not only the effect of radical scavenging, but also other effects. Therefore, it is inadequate to use NO as a simple radical scavenger. (iii) The C_7-C_{12} products are formed from a combination reaction of alkyl radicals, but not from an ion-molecule reaction. (iv) The formation of $C_6H_{13}^+$ ions by the direct action of radiation is suggested. (v) The *G*-value of ionization is evaluated to be 4.0. A brief discussion concerning the formation of N_2 in the presence of N_2O is also given.

One of the methods of investigating the radiation chemistry of liquid hydrocarbons is the scavenger technique. This method aims at elucidating the mechanism of radiolysis from the effect of additives, which react selectively with radicals or charged species produced by irradiation, on the yields of the radiolytic products. Product analysis, however, has usually been carried out on fragment products. Thus, in the case of alkane radiolysis, there have been only a few works in which the effects of scavengers for charged species on the product yields, including those of olefins and of dimeric paraffins, have been investigated. Consequently, there remain several unsolved problems even in the radiolysis of *n*-hexane, which has been widely investigated by many researchers[1-7] as a typical liquid paraffin. For

1) L. Kevan and W. F. Libby, *J. Chem. Phys.*, **39**, 1288 (1963).
2) H. A. Dewhurst, *J. Phys. Chem.*, **62**, 15 (1958).
3) H. Widmer and T. Gäumann, *Helv. Chim. Acta*, **46**, 2766 (1963).
4) T. J. Hardwick, *J. Phys. Chem.*, **64**, 1623 (1960).
5) T. Gäumann and B. Reipso, *Advan. Chem. Series*, **82**, 441 (1968).
6) A. Menger and T. Gäumann, *Helv. Chim. Acta*, **52**, 2129 (1969).
7) A. Menger and T. Gäumann, *ibid.*, **52**, 2477 (1969).

example, there are two views concerning the mechanism of the formation of dodecanes; one[1] attaches importance to the ion-molecule reaction, and the other,[4] to the combination reaction of hexyl radicals.

In order to clarify the problems, it appears suitable to investigate the effect of additives on the yields of products, including hexenes and dodecanes. The additive should be carefully selected in such a way that it scavenges selectively one reactive species. Thus, SF_6,[8] which is often used as an electron scavenger, and NH_3[9] and C_2H_5OH,[10] which are often used as proton scavengers, appear to be suitable in view of their physical and chemical properties. In order to investigate the radical processes, a pertinent radical scavenger is necessary. For this purpose, SO_2 is tentatively chosen in view of its physical and chemical properties, although there is a possibility that SO_2 scavenges an electron due to its electron affinity ($EA(SO_2)=ca.$ 1 eV[11]). SO_2 shows a much higher reactivity to alkyl radicals (the rate constant of addition to methyl radicals is $5.0\times10^6 M^{-1}$ sec^{-1} at 25°C[12]) than that of ethylene, which is known as an effective hydrogen atom scavenger,[13] a higher ionization potential (IP (SO_2)=12.34 eV[14]) than that of n-hexane (IP(n-hexane)=10.17 eV[15]), and a much higher solubility in n-hexane than that of oxygen, which has been often used as an effective radical scavenger. There are few cases, at most, in which SO_2 has been used as a radical scavenger; to the authors' knowledge, the only example seems to be the work by Henglein *et al.*[16] They regarded SO_2 as a radical scavenger on the basis of the fact that the G-values of the SO_2 absorbed in the radiolysis of various liquid hydrocarbons were nearly equal to the radical yields determined with DPPH or I_2.

In a previous work,[17] the present authors used N_2O and NO as an electron scavenger and a radical scavenger respectively. With regard to NO, however, it has been pointed out that this is apt to undergo a charge-transfer reaction[18] due to its ionization potential (IP(NO)=9.25 eV[14]) being lower than that of n-hexane, and that it is also apt to form ionic addition products.[19] As for N_2O, the relation of the N_2 yield to that of the electron is still unclear. Therefore, N_2O and NO are again used in order to obtain more information on their effects.

Experimental

Materials. Research-grade n-hexane obtained from the Phillips Petroleum Co. was purified for the analysis of the C_7–C_{12} products by passing it through silica-gel, soda-asbestos, and magnesium perchlorate columns, besides the usual purification of freeze-pump-thaw cycles, as has been described in a previous paper;[17] it was purified for the analysis of H_2 and C_1–C_6 products, and N_2 in the presence of N_2O, by only the usual freeze-pump-thaw cycles, for the H_2 yield from the radiolysis of n-hexane purified by the latter, more convenient way was the same as the result of the former purification. The purity of n-hexane was determined to be more than 99.98% by gas chromatography. The additives were all commercially obtained. SF_6 (minimum purity: 98.0%) obtained from the Matheson Co.; N_2O(99.9%), NH_3(99.5%), SO_2(98.0%), NO(99.9%), and C_2H_4-(99.8%) obtained from the Takachiho-shoji Co., and C_2H_5OH(99.5%) obtained from the Wako-junyaku-kogyo Co. were used after the usual degassing by freeze-pump-thaw cycles. For C_2H_5OH, a further purification to remove a trace of dissolved water was carried out by mixing the ethanol with powder cupric sulfate which was degassed and thoroughly dehydrated.

Sample Preparation and Irradiation. The samples were prepared in the way which has been described before[17] except that the amount of n-hexane used for the analysis of H_2, the C_1–C_6 products, and N_2 was 5 cc; it was measured by a pipet, degassed by the usual freeze-pump-thaw cycles, and led into a glass ampoule fitted with a break-off seal. The samples were irradiated at room temperature by a ^{60}Co γ-source either at a dose rate of 6.67×10^{19} eV/g·h to a total dose of 8.0×10^{20} eV/g for the analysis of the C_7–C_{12} products, or at a dose rate of 5.85×10^{19} eV/g·h to a total dose of 5.85×10^{19} eV/g for the analysis of the H_2 and C_1–C_6 products, and of N_2 in the presence of N_2O, unless otherwise specified. In estimating the dose rates, a $G(Fe^{3+})$ value of 8.2 in the Fricke dosimeter saturated with nitrogen was used with the electron-density correction.

Analysis. The analysis of noncondensable gases at −196°C was carried out in the same way as has been described in the previous paper.[17] The C_2–C_{12} products were analyzed gas chromatographically. For the analysis of the C_2–C_6 products, the residual liquid after the analysis of noncondensable gases was sealed in a new glass ampoule under a vacuum at −196°C. Immediately after breaking the seal of the ampoule, a fixed volume of the contents was injected, by means of a micro-syringe, into a gas chromatograph equipped with a flame ioniza-

8) G. Sholes and M. Simic, *Nature*, **202**, 895 (1964).
9) W. R. Busler, D. H. Martin and F. Williams, *Discuss. Faraday Soc.*, **36**, 102 (1963).
10) J. W. Buchanan and F. Williams, *J. Chem. Phys.*, **44**, 4377 (1966).
11) K. Kraus, W. M. -Duysing and H. Neuert, *Z. Naturforsch.*, **16a**, 1385 (1961).
12) A. Good and J. C. J. Thynne, *Trans. Faraday Soc.*, **63**, 2708 (1967).
13) R. A. Holroyd, *J. Phys. Chem.*, **70**, 1341 (1966).
14) K. Watanabe, *J. Chem. Phys.*, **26**, 542 (1957).
15) W. C. Price, R. Bralsford, P. V. Harris and R. Ridley, *Spectrochim. Acta*, **14**, 45 (1959).
16) A. Henglein, K. Heine, W. Hoffmeister, W. Schnabel, C. Schneider and H. Url, *Proc. Second Intern. Conf. Peaceful Uses Atomic Energy, United Nations, Geneva*, **29**, 206 (1958).
17) K. Shinsaka and S. Shida, This Bulletin, **40**, 2796 (1967).
18) G. G. Meisels, *J. Chem. Phys.*, **42**, 3237 (1965).
19) P. Kebarle, R. M. Haynes and S. Searles, "Ion-Molecule Reactions in the Gas Phase," Amer. Chem. Soc. Pub., Washington, D. C. (1966) p. 210.

tion detector. An 11-m column with 20% dimethylsulfolane on 60/80 mesh Neosorb NP was used at room temperature (*ca.* 20°C). This column could not resolve *trans*-2-hexene and *cis*-3-hexene so as to allow separate values to be quoted for their yields; therefore, the total yield of these products was determined. After the gas chromatogram of an irradiated sample had been obtained, the same operation was repeated with a reference sample which contained a known quantity of each product component in a fixed quantity of *n*-hexane (nearly as much as in the irradiated sample). The product yields were determined by comparing the peak area of a gas chromatogram of the irradiated sample with that of the reference sample. In this method there was a possibility that a part of the low-molecular-weight products, such as ethane, ethylene, propane, and propylene, escaped into the air during the period from the break of the ampoule to the injection of the sample into the gas chromatograph. This fear could, however, be excluded because the dose dependence of the yields of the fragment products obtained by this method was reasonable; that is, the yields of ethane and propane showed no dose dependence, while the yields of ethylene and propylene indicated the dose dependence that these yields decreased with an increase in the dose. In the presence of a large quantity of an additive which does not dissolve so much in *n*-hexane, the low-molecular-weight product yields obtained by the above method may be somewhat inferior in accuracy to the case without additives, because the time required from the break of the ampoule to the injection of the sample into a gas chromatograph is a little longer than in the case without additives. The C_7–C_{12} products were analyzed in almost the same manner as were the C_2–C_6 products after the irradiated ampoule, without having been submitted to the analysis of noncondensable gases, had been broken open. A 5-m column with 25% Silicone DC 550 on 60/80 mesh Shimalite was used at 130°C. Under these conditions, *iso*-peaks were normally obtained for each hydrocarbon product, one corresponding to the *n*-isomer, and the other, to branched-chain isomers. The *iso*-C_7 peak was not resolved from the tail of the *n*-hexane peak; therefore, the yield of *iso*-C_7 has not been included in the results. Similarly, the *n*-C_{11} peak was not resolved from the *iso*-C_{12} peak and the *iso*-C_{11} peak was not determined quantitatively because the *iso*-C_{11} peak overlapped with that of an impurity peak. These product yields, however, contribute little to the C_7–C_{12} product yields. The C_7–C_{12} products were identified by using authentic samples and by comparison with the results of Widmer *et al.*[3]

Additive Concentration. There seem to be no data showing the solubility of SF_6, N_2O, and NO in *n*-hexane. However, on the assumption that the solubilities of SF_6 and N_2O in *n*-hexane are similar to the case of *n*-heptane,[20,21] in which the solubilities of SF_6 and N_2O have been reported, more than 95% of the amount of added SF_6 and more than 97% of the amount of added N_2O, respectively, were calculated to dissolve in the liquid phase of *n*-hexane in view of the fact that the volume of the gas phase in an irradiated ampoule was less than one-tenth of the total inner volume. On the other hand, it was confirmed that it was easy to dissolve C_2H_5OH in *n*-hexane, and it has been shown that SO_2[22] dissolves very much in *n*-hexane and that C_2H_4[23] dissolves also to about the same degree of N_2O in *n*-heptane. All the concentrations of the additives were estimated by assuming that the additives dissolved completely in the liquid phase of *n*-hexane, for the solubilities of the additives in *n*-hexane would not differ very much from those in *n*-heptane. This assumption is adequate except for the case of the addition of NO, whose concentration in *n*-hexane was estimated to be a few tens of percent less than the value calculated from the assumption of complete dissolution in view of the solubility of NO[21] in cyclohexane.

Results

The results obtained regarding the dose dependence of the C_6–C_{12} product yields from the radiolysis of *n*-hexane are as follows. The hexene yields decrease with an increase in the dose, the degree of the decrease depending on the type of hexene isomer. The dose dependence of hexene yields is very conspicuous in 1-hexene and *trans*-2-hexene+*cis*-3-hexene,*1 and weak in *cis*-2-hexene and *trans*-3-hexene. The yields of the C_7–C_{12} products, however, show no dose dependence within doses up to 8.0×10^{20} eV/g. The difference between the dose dependence of the hexene yields and that of the C_7–C_{12} product yields will be briefly discussed later. The *G*-values of the products obtained at the total dose of 5.85×10^{19} eV/g and at room temperature are shown in Tables 1 and 2, along with the results of other previous investigations.[1,3,4] The *G*-values in this work, shown in these tables, may be regarded as almost the initial values in view of the dose dependence of the hexene yields; they agree well with the results given by Widmer *et al.*[3] except for somewhat larger differences in the cases of ethane, ethylene, and propane. The ratio of the total number of carbon atoms to that of the hydrogen atoms calculated, respectively, from the *G*-values in Tables 1 and 2 is 0.420; this agrees well with the ratio in an *n*-hexane molecule, *i. e.*, 0.429. The

20) L. C. Yen and J. J. Mcketta, Jr., *J. Chem. Eng. Data*, **7**, 288 (1962).

21) G. Archer and J. H. Hildebrand, *J. Phys. Chem.*, **67**, 1830 (1963).

22) "Solubilities of Inorganic and Organic Compounds," Vol. 1, ed. by H. Stephen and T. Stephen, Pergamon Press, London (1963) p. 970.

23) *Ibid.*, p. 1179.

24) *Ibid.*, p. 921.

*1 Since the seperate values of *trans*-2-hexene yield and *cis*-3-hexene yield could not be obtained, the total value of these product yields was represented using the plus sign, +. The *cis*-3-hexene yield was calculated to be 0.076—0.17 by using the ratio, $trans/cis=4\pm1.5$ given by Hardwick[4] in regard to 3-hexene, and by using the *trans*-3-hexene yield obtained in this work. Therefore, the total yield of *trans*-2-hexene and *cis*-3-hexene may be regarded almost as the yield of *trans*-2-hexene and the total yield is approximately represented as the *trans*-2-hexene yield in Table 1.

Table 1. The *G*-values of hydrogen, fragment products and hexenes from the radiolysis of liquid *n*-hexane

Product	a	b	c	d
H_2	5.01	5.25	5.28	5.09
CH_4	0.18_0	0.15	0.10	
C_2H_6	0.42_3	0.22	0.21	0.50
C_2H_4	0.24_5	0.14	0.23	
C_3H_8	0.41_0	0.31	0.13	0.26
C_3H_6	0.19_3	0.18	0.07	0.07
iso-C_4H_{10}	0			0.02
n-C_4H_{10}	0.35_4	0.36	0.05	0.46
iso-C_4H_8	0			0.02
1-C_4H_8	0.14_0	0.12		0.08
trans-2-C_4H_8	0.01_3	0.01		0.02
iso-C_5H_{12}	0			0.05
n-C_5H_{12}	0.10_1	0.09	0.02	0.12
1-C_5H_{10}	0.03_6	0.04		
trans-2-C_5H_{10}	0.02_1	0.02		
1-C_6H_{12}	0.86	0.64±0.05	0.73	0.46
trans-2-C_6H_{12}	1.23[e]	11.3±0.07	1.82	1.15
cis-2-C_6H_{12}	0.55	0.43±0.10		0.46
trans-3-C_6H_{12}	0.42	0.34±0.05	0.55	0.13
cis-3-C_6H_{12}				0.04
Total hexane	3.06	2.54	3.10	2.24

a) Obtained in this work. Irradiation with ^{60}Co γ-rays at 5.85×10^{19} eV/g at room temperature.
b) Obtained by Widmer *et al.*[3] Initial values. Irradiation with ^{60}Co γ-rays at 25°C.
c) Obtained by Hardwick.[4] $G(H_2)$, $G(C_6H_{12})$: initial values. The dose for other products is not clear. Electron irradiation at 25°C.
d) Obtained by Kevan *et al.*[1] $G(H_2)$ obtained at 1.24×10^{19} eV/g. *G*-values of the fragment products obtained at 16.2×10^{20} eV/g. $G(C_6H_{12})$ obtained at 10.2×10^{20} eV/g. Irradiation with ^{60}Co γ-rays at 20°C.
e) This value shows more exactly the total yield of *trans*-2-hexene and *cis*-3-hexene. See the text.

G-value of a net decomposition of *n*-hexane is defined by the following equations:

$$G_{no}(-n\text{-}C_6H_{14}) = \sum_{i=1}^{12} iG(C_i)/6 \qquad (A)$$

or

$$G_{no}(-n\text{-}C_6H_{14}) = \sum_{i=1}^{13} 2iG(H_{2i})/14 \qquad (B)$$

where $G_{no}(-n\text{-}C_6H_{14})$ indicates the *G*-value of the net decomposition of *n*-hexane, and where $G(C_i)$ and $G(H_{2i})$ indicate the *G*-values of the products, whose numbers of carbon atoms and hydrogen atoms are i and $2\times i$ respectively. The average, $G_{no}(-n\text{-}C_6H_{14})$, of the two values obtained by the use of Eq. (A) and Eq. (B) is calculated to be 7.30. The percentage of the decomposition of *n*-hexane is calculated to be 0.061% at the dose of 5.85×10^{19}

Table 2. The *G*-values of the C_7-C_{12} products from the radiolysis of liquid *n*-hexane

Product	a	b	c	d
$2MeC_6$		0.014	0.06	
$3MeC_6$		0.011		
n-C_7H_{16}	0.01_6	0.021		
$3EtC_6$	0.13	0.12	0.26	
$3MeC_7$				
n-C_8H_{18}	0.02_8	0.032		
$4EtC_7$	0.09_6	0.036	0.23	0.61
$4MeC_8$		0.048		
n-C_9H_{20}	0.01_9	0.025		
4-EtC_8	0.08_7	0.041	0.27	
5-MeC_9		0.050		
n-$C_{10}H_{22}$	0.01_6	0.023		
$4EtC_9$		0.017	0.02	
$5MeC_{10}$				
n-$C_{11}H_{24}$				
$4,5Et_2C_8$	0.21_5	0.17	1.70	0.20
$4Et5MeC_9$	0.51_0	0.49		0.39
$5,6Me_2C_{10}$	0.31_4	0.32		0.24
$4EtC_{10}$	0.10_2	0.11		0
$5MeC_{11}$	0.13_0	0.14		0.21
n-$C_{12}H_{26}$	0.02_3	0.029		0.025
Total dodecane	1.29	1.26	1.70	1.06

a) Obtained in this work. Irradiation with ^{60}Co γ-rays at room temperature.
b) Obtained by Widmer *et al.*[3] Initial values. Irradiation with ^{60}Co γ-rays at 25°C.
c) Obtained by Hardwick.[4] The dose is not clear. Electron irradiation at 25°C.
d) Obtained by Kevan *et al.*[1] *G*-values of the C_7-C_{11} products obtained at 16.2×10^{20} eV/g. $G(C_{12}H_{26})$ obtained at 3.38×10^{20} eV/g. Irradiation with ^{60}Co γ-rays at 20°C.

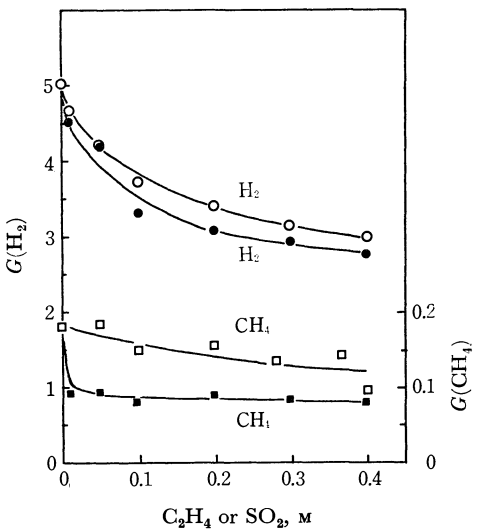

Fig. 1. Yields of H_2 and CH_4 as functions of SO_2 or C_2H_4 concentration.
○, □; C_2H_4 ●, ■; SO_2

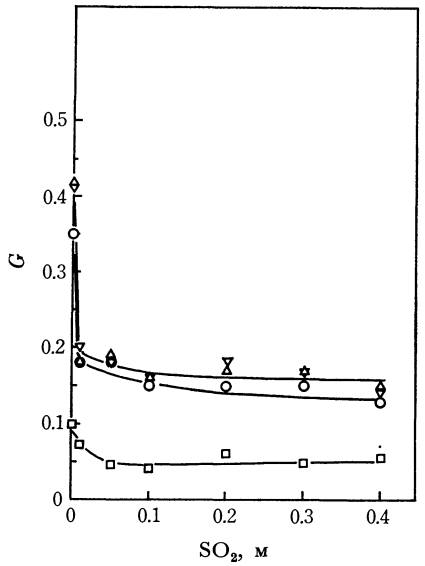

Fig. 2(a). Yields of fragment paraffin products as functions of SO_2 concentration.
Dose: *ca.* 6×10^{19} eV/g
△, C_2H_6 ▽, C_3H_8 ○, *n*-C_4H_{10} □, *n*-C_5H_{12}

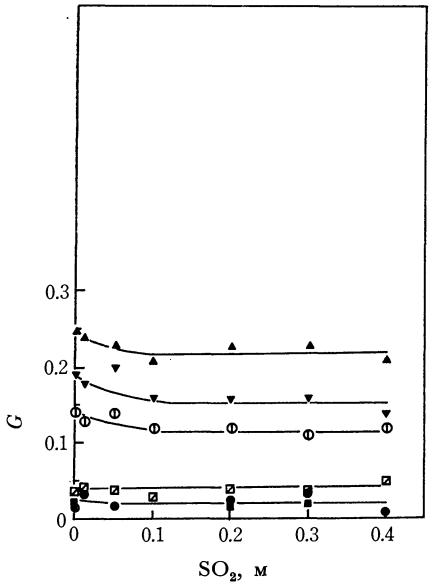

Fig. 2(b). Yields of fragment olefin products as functions of SO_2 concentration.
Dose: *ca.* 6×10^{19} eV/g
▲, C_2H_4 ▼, C_3H_6 ⓘ, 1-C_4H_8 ▨, 1-C_5H_{10}
■, *trans*-2-C_5H_{10} ●, *trans*-2-C_4H_8

eV/g and 0.84% at the dose of 8×10^{20} eV/g by using this value, 7.30.

The effects of additives on the C_7–C_{12} products were investigated with samples irradiated up to a dose of 8×10^{20} eV/g. This dose is permissible in view of the finding that the C_7–C_{12} product yields showed no dose dependence in the absence of additives and that the C_{12} product yields also showed no dose dependence in the presence of 0.55M N_2O. Figure 1 shows the changes in the *G*-values of hydrogen and methane upon the addition of SO_2, togeth-

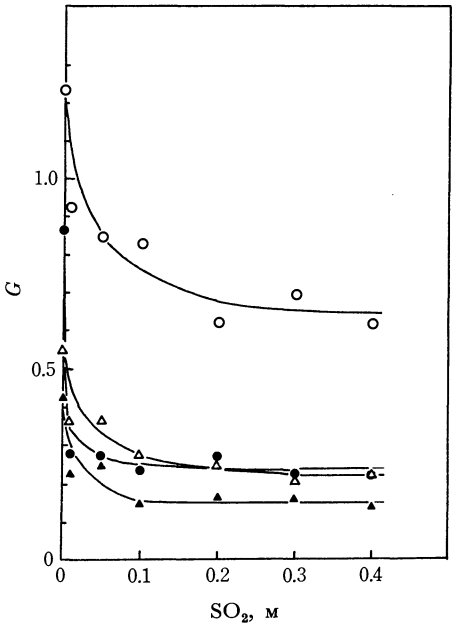

Fig. 2(c). Yields of hexenes as functions of SO_2 concentration.
Dose: *ca.* 6×10^{19} eV/g
○: *trans*-2-C_6H_{12}+*cis*-3-C_6H_{12}, ●: 1-C_6H_{12},
△: *cis*-2-C_6H_{12}, ▲: *trans*-3-C_6H_{12}

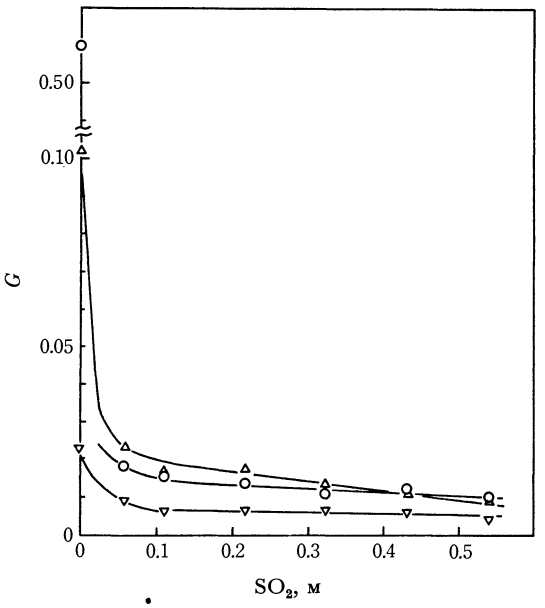

Fig. 2(d). Yields of 4-ethyldecane, 4-ethyl-5-methylnonane and *n*-dodecane as functions of SO_2 concentration.
△, $4EtC_{10}$ ○, 4Et5MeC_9 ▽, *n*-C_{12}

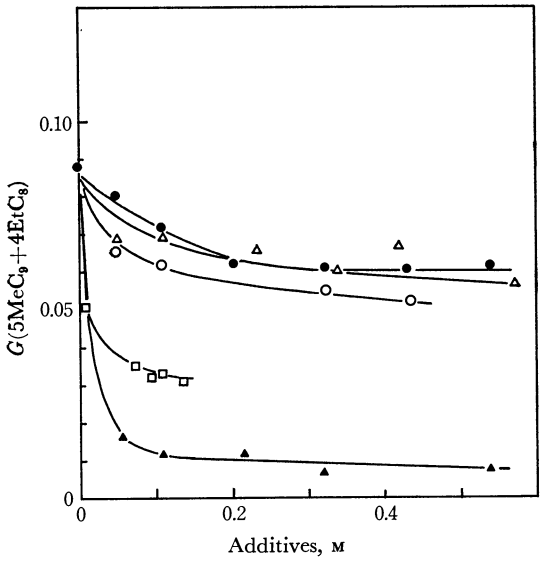

Fig. 3. Yields of 5-methylnonane+4-ethyloctane as functions of concentration of various additives.
●, NH_3 △, C_2H_5OH ○, N_2O □, SF_6 ▲, SO_2

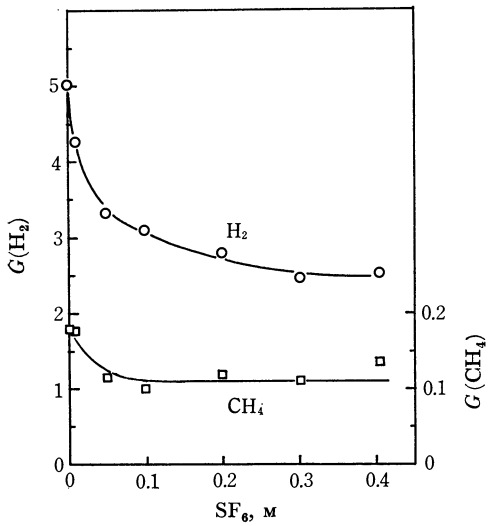

Fig. 4(a). Yields of H_2 and CH_4 as functions of SF_6 concentration.

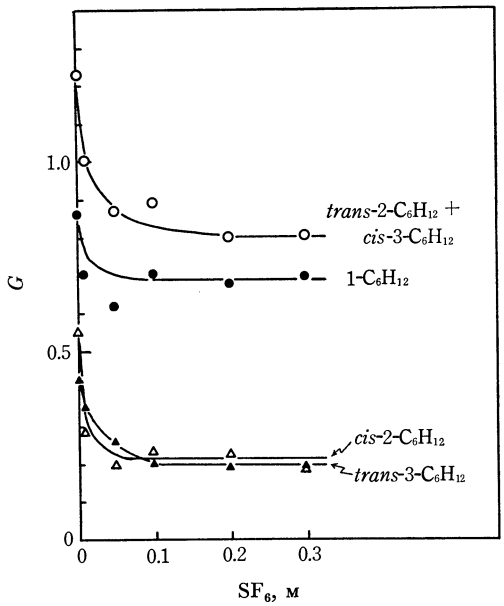

Fig. 4(b). Yields of hexenes as functions of SF_6 concentration.
Dose: *ca.* 6×10^{19} eV/g

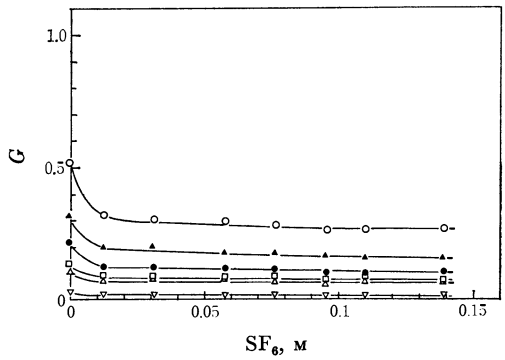

Fig. 4(c). Yields of dodecanes as functions of SF_6 concentration.
○, 4Et5MeC$_9$ ▲, 5,6Me$_2$C$_{10}$ ●, 4,5Et$_2$C$_8$
□, 5MeC$_{11}$ △, 4EtC$_{10}$ ▽, *n*-C$_{12}$

er with those in the case of the addition of C_2H_4. The change in the *G*-value of hydrogen in the presence of SO_2 is very similar to that obtained in the presence of C_2H_4. The changes in the *G*-value of methane are, however, very different for SO_2 and C_2H_4. The *G*-value of methane decreases drastically to about a half of the initial value at a low concentration of SO_2, and afterward comes to show almost no change. On the other hand, with the concentration of C_2H_4 the *G*-value of methane gradually decreases.

Figures 2(a) and 2(b) show the changes in the *G*-values of the other fragment products upon the addition of SO_2. The *G*-values of the saturated fragment products decrease to about a half of the initial value, or more, upon the addition of SO_2. The *G*-values of the unsaturated fragment products, however, show only a small decrease. Figure 2(c) shows the changes in the *G*-values of hexenes upon the addition of SO_2. The *G*-values of hexenes decrease to about a half of the initial value, or more. Figure 2(d) shows the changes in three kinds of C_{12} products as examples of the effect of the addition of SO_2; the *G*-values of all the C_{12} products decrease drastically, *e. g.*, to a value less than one-fiftieth of the initial value in 4-ethyl-5-methylnonane (4Et5MeC$_9$ for brevity), which shows the most conspicuous decrease, and to a value less than one-fourth of the

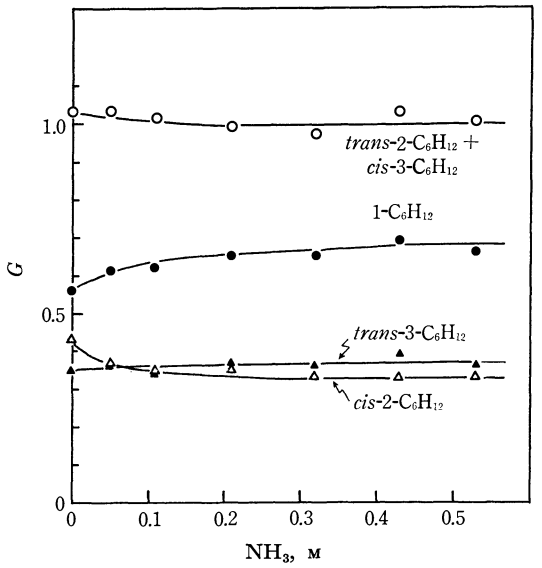

Fig. 5(a). Yields of hexenes as functions of NH_3 concentration.
Dose: 8.0×10^{20} eV/g

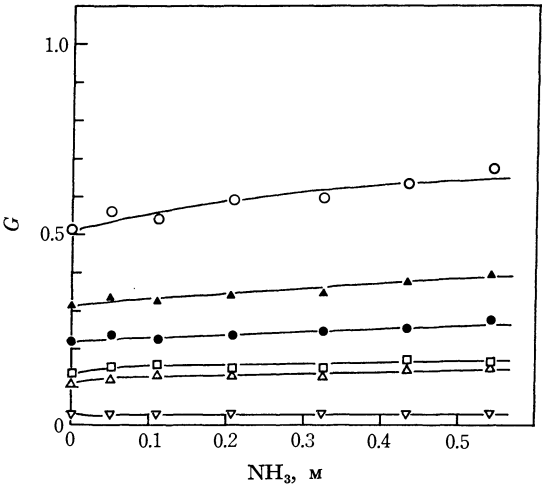

Fig. 5(b). Yields of dodecanes as functions of NH_3 concentration.
○: $4Et5MeC_9$, ▲: $5,6Me_2C_{10}$, ●: $4,5Et_2C_8$, □: $5MeC_{11}$, △: $4EtC_{10}$, ▽: n-C_{12}

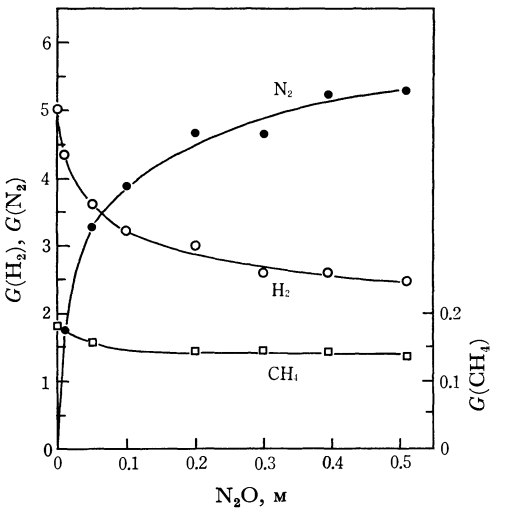

Fig. 6. Yields of H_2, CH_4 and N_2 as functions of N_2O concentration.

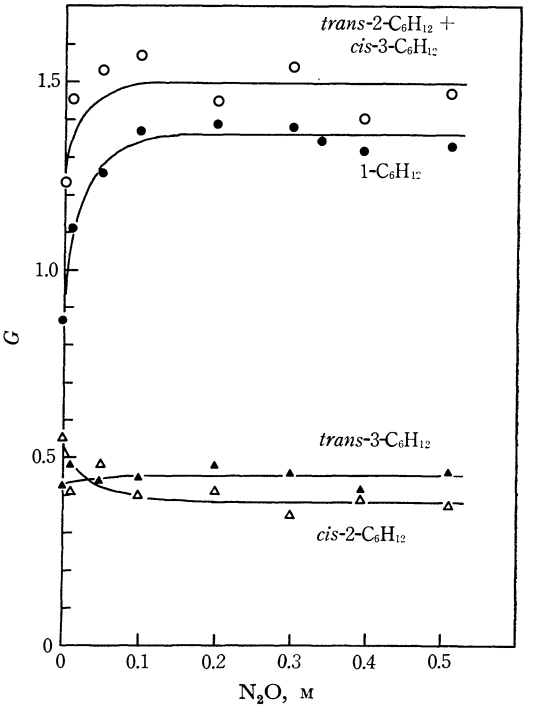

Fig. 7(a). Yields of hexenes as functions of N_2O concentration.

initial value even in n-dodecane (n-C_{12} for brevity), which shows the smallest decrease. Figure 3 shows the changes in the G-value of 5-methylnonane+4-ethyloctane ($5MeC_9+4EtC_8$ for brevity) as a typical example of the C_7–C_{10} products affected by the addition of SO_2, together with the results of other additives.

Upon the addition of SO_2, the G-values of all the C_7–C_{10} products decrease drastically, *i. e.*, to a value less than one-tenth of the initial value in the most conspicuous decrease and to a value less than one-fourth of the initial value even in the smallest decrease, except for the case of n-heptane, whose G-value is poorer in accuracy due to its inclusion in the tail of n-hexane. Furthermore, the G-values of all the C_7–C_{12} products continue to decrease gradually with an increase in the concentration of SO_2 after the initial sharp decrease. Figure 4(a) shows the changes in the G-values of H_2 and CH_4 upon the addition of SF_6. Figures 4(b) and 4(c) show the changes in the G-values of hexenes and do-

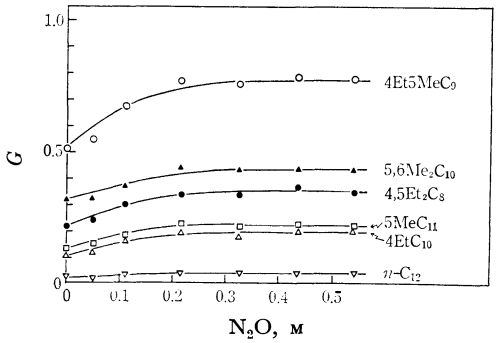

Fig. 7(b). Yields of dodecanes as functions of N_2O concentration.

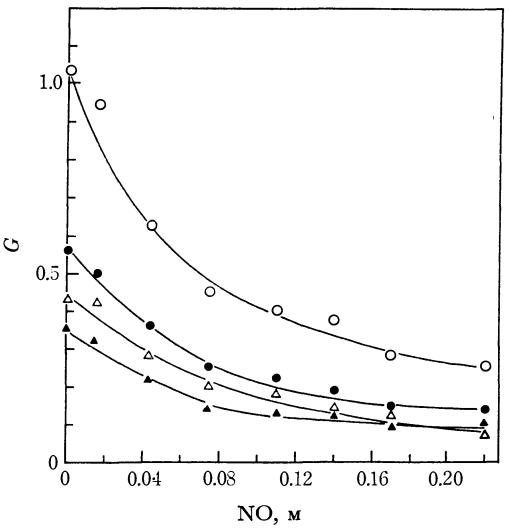

Fig. 8. Yields of hexenes as functions of NO concentration.
Dose: 8.0×10^{20} eV/g
○: *trans*-2-C_6H_{12}+*cis*-3-C_6H_{12}, ●: 1-C_6H_{12},
△: *cis*-2-C_6H_{12}, ▲: *trans*-3-C_6H_{12}

decanes respectively upon the addition of SF_6. As is shown in Figs. 3, 4(a), 4(b), and 4(c), the *G*-values of all the products decrease to about a half of the initial values, or less, upon the addition of SF_6 and come to show little change at higher concentrations of SF_6.

Figures 5(a) and 5(b) show the changes in the *G*-values of hexenes and dodecanes upon the addition of NH_3. Though the changes in the *G*-values of hexenes depend on the kind of hexene, the total *G*-value of hexenes in the presence of NH_3 is almost equal to that obtained in the absence of the additive. The *G*-values of the dodecanes increase more or less with the concentration of NH_3. A tendency similar to the changes in the product yields obtained upon the addition of NH_3 is also observed upon the addition of C_2H_5OH. Figure 6 shows the changes in the *G*-values of H_2, CH_4, and N_2 upon the addition of N_2O. Figures 7(a) and 7(b) show the

Table 3. Effects of additives on the *G*-values of hydrogen, fragment products and hexenes
Dose: 5.85×10^{19} eV/g

Product	Additive					
	None	SF_6	NH_3	SF_6+NH_3	SO_2	N_2O
H_2	5.01	2.50	5.53	2.72	2.80	2.45
CH_4	0.18_0	0.11_0	0.14_1	0.15_4	0.08_5	0.14_0
C_2H_6	0.42_3	0.20_0	0.16_0	0.08_2	0.16_0	0.26_0
C_2H_4	0.24_5	0.10_0	0.09_1	0.04_7	0.22_0	0.16_0
C_3H_8	0.41_0	0.26_0	0.24_0	0.13_4	0.16_0	0.28_0
C_3H_6	0.19_3	0.08_5	0.11_0	0.06_6	0.15_5	0.12_0
n-C_4H_{10}	0.35_4	0.25_0	0.22_0	0.15_3	0.14_0	0.24_0
1-C_4H_8	0.14_0	0.07_5	0.11_0	0.07_4	0.11_5	0.09_0
trans-2-C_4H_8	0.01_3	0.01_5			0.02_0	0.01_5
n-C_5H_{12}	0.10_1	0.07_5	0.06_0	0.04_0	0.05_0	0.08_0
1-C_5H_{10}	0.03_6	0.02_5	0.02_8	0.02_8	0.04_0	0.02_5
trans-2-C_5H_{10}	0.02_1	0.04_0			0.02_0	
1-C_6H_{12}	0.86	0.69	0.98	1.14	0.24	1.36
trans-3-C_6H_{12}	0.42	0.20	0.37	0.45	0.15	0.45
trans-2-C_6H_{12}+*cis*-3-C_6H_{12}	1.23	0.80	1.27	1.38	0.65	1.50
cis-2-C_6H_{12}	0.55	0.22	0.36	0.38	0.22	0.38
Total hexene	3.06	1.91	2.98	3.35	1.26	3.69

Table 4. Effects of additives on the *G*-values of the C_7-C_{12} products
Dose: 8.0×10^{20} eV/g

Product	Additive					
	None	SF_6	NH_3	SF_6+NH_3	SO_2	N_2O
n-C_7H_{16}	0.01_6	0.01_1	0.01_8		0.01_0	0.01_6
$3EtC_6+3MeC_7$	0.13_4	0.06_2	0.09_9	0.03_6	0.01_1	0.10_0
n-C_8H_{18}	0.02_8	0.01_6	0.02_0	0.01_3	0.00_6	0.02_0
$4EtC_7+4MeC_8$	0.09_6	0.04_0	0.07_5	0.03_3	0.00_9	0.06_4
n-C_9H_{20}	0.01_9	0.00_9	0.01_4	0.01_9	0.00_5	0.01_4
$4EtC_8+5MeC_9$	0.08_7	0.03_2	0.06_0	0.02_5	0.00_7	0.05_2
n-$C_{10}H_{22}$	0.01_6	0.00_9	0.01_3	0.00_9	0.00_3	0.01_0
$4,5Et_2C_8$	0.21_5	0.10_4	0.27_0	0.09_0	0.00_5	0.34_9
$4Et5MeC_9$	0.51_0	0.26_4	0.65_0	0.20_0	0.01_0	0.77_9
$5,6Me_2C_{10}$	0.31_4	0.15_8	0.39_0	0.11_7	0.00_6	0.43_4
$4EtC_{10}$	0.10_2	0.06_4	0.14_7	0.07_3	0.00_9	0.19_6
$5MeC_{11}$	0.13_0	0.07_2	0.16_5	0.07_5	0.01_1	0.22_0
n-$C_{12}H_{26}$	0.02_2	0.01_5	0.02_6	0.02_1	0.00_5	0.03_8
Total dodecane	1.29	0.67	1.66	0.58	0.05	2.02

Table 5. Effects of added NO and C_2H_5OH in comparison with added SO_2 and NH_3 on the *G*-values of hexenes and dodecanes
Dose: 8.0×10^{20} eV/g

Product	Additive				
	None	SO_2	NO	NH_3	C_2H_5OH
1-C_6H_{12}	0.56	0.25	0.14	0.68	0.59
trans-3-C_6H_{12}	0.35	0.20	0.10	0.37	0.34
trans-2-C_6H_{12}+ *cis*-3-C_6H_{12}	1.03	0.51	0.25	1.00	0.92
cis-2-C_6H_{12}	0.43	0.16	0.08	0.33	0.33
Total hexene	2.37	1.22	0.57	2.38	2.18
$4,5Et_2C_8$	0.21_5			0.27_0	0.24_7
$4Et5MeC_9$	0.51_0			0.65_0	0.55_5
$5,6Me_2C_{10}$	0.31_4			0.39_0	0.35_1
$4EtC_{10}$	0.10_2			0.14_7	0.12_0
$5MeC_{11}$	0.13_0			0.16_5	0.14_1
n-C_{12}	0.02_3			0.02_6	0.02_0
Total dodecane	1.29			1.66	1.43

changes in the *G*-values of hexenes and dodecanes respectively upon the addition of N_2O. Though the changes in the *G*-values of hexenes are different, depending on the kind of hexene, the total yield of hexenes increases markedly with the concentration of N_2O. Figure 8 shows the changes in the *G*-values of hexenes upon the addition of NO. As has been stated before, the actual concentration of NO is estimated to be less than the value indicated in Fig. 8 because of the small solubility of NO. The decrease in hexene yields upon the addition of NO is much larger than that upon the addition of SO_2.

As is shown in the figures given above, the *G*-values of the products, with some exceptions, generally come to show little change at higher concentrations of the additives. The *G*-values obtained at sufficiently high concentrations of the additives are tabulated in Tables 3, 4, and 5, together with the data which have not been shown before.

Discussion

i) Effects of SF_6, NH_3, and SO_2. SF_6 is known to scavenge efficiently thermal electrons such as reaction (1):[25]

$$e^- + SF_6 \longrightarrow SF_6^- \quad (1)$$

On the other hand, SF_6 does not react with a methyl radical, even up to the temperature of 350°C.[26] Consequently, SF_6 added to *n*-hexane may safely be assumed to act as an electron scavenger, but not to react with radicals. Further, the possibility of a charge-transfer reaction from a parent *n*-hexane ion to SF_6 can be excluded because the ionization potential of SF_6 (IP=16.15 eV)[27] is much higher than that of *n*-hexane. SF_6^- can be assumed subsequently to undergo a neutralization reaction with a hydrocarbon ion; this reaction can also be assumed to be such a moderate reaction that it does not cause the decomposition of either ion because of a comparatively high electron affinity of SF_6 (EA=1.49 eV).[28] The major neutralization reaction is shown by reacion (2):

$$SF_6^- + n\text{-}C_6H_{14}^+ \longrightarrow SF_6 + n\text{-}C_6H_{14} \quad (2)$$

As for the effect of added NH_3, the proton-transfer reaction shown by reaction (3) and the subsequent neutralization reaction, (4), can be assumed for the following reasons.

$$n\text{-}C_6H_{14}^+ + NH_3 \longrightarrow C_6H_{13} + NH_4^+ \quad (3)$$

$$NH_4^+ + e^- \longrightarrow NH_3 + H \quad (4)$$

NH_3 has a high proton affinity (PA=8.78 eV).[29] On the other hand, the possibility of the reaction of NH_3 with a hydrogen atom can be excluded because the reaction is very slow ($H+NH_3 \xrightarrow{k} H_2+NH_2$; $k=2.2\times10^2 M^{-1}\,sec^{-1}$, 25°C).[30] Furthermore, the possibility of a charge-transfer reaction from a hydrocarbon ion to NH_3 may be also excluded because the ionization potential of NH_3 (IP=10.15 eV)[31] is almost equal to that of *n*-hexane (IP=10.17 eV)[15] and because the concentration of NH_3 is 9 mol% at most. The above assumptions concerning the effects of SF_6 and NH_3 are the same as those adopted in other works.[9,32-35]

As was stated in the introduction to this paper, the most likely effect of the added SO_2 is radical scavenging, although there is a possibility that SO_2 also scavenges an electron, as has been shown by Guarino *et al.*[36] They reported that the electron-scavenging efficiency of SO_2 was relatively high in the irradiated matrix of MTHF at −196°C. Their results, however, were obtained very different conditions from this work, so it is inappropriate to use

25) D. C. Frost and C. A. McDowell, *J. Chem. Phys.*, **29**, 503 (1958).
26) H. F. Lefevre, J. D. Kale and R. B. Timmons, *J. Phys. Chem.*, **73**, 1614 (1969).
27) E. D. Nostrand and A. B. F. Duncan, *J. Amer. Chem. Soc.*, **76**, 3377 (1954).
28) J. Kay and F. M. Page, *Trans. Faraday Soc.*, **60**, 1042 (1964).
29) A. P. Altschuller, *J. Amer. Chem. Soc.*, **77**, 3480 (1955).
30) C. Willis, A. Boyd and O. A. Miller, *Can. J. Chem.*, **47**, 3007 (1969).
31) K. Watanabe and J. R. Mottl, *J. Chem. Phys.*, **26**, 1773 (1957).
32) K. Tanno, T. Miyazaki, K. Shinsaka and S. Shida, *J. Phys. Chem.*, **71**, 4290 (1967).
33) K. Tanno, S. Shida and T. Miyazaki, *ibid.*, **72**, 3496 (1968).
34) T. Miyazaki and S. Shida, This Bulletin, **38**, 2114 (1965).
35) T. Miyazaki and S. Shida, *ibid.*, **39**, 2344 (1966).
36) J. P. Guarino, M. R. Ronayne and W. H. Hamill, *Radiation Res.*, **17**, 379 (1962).

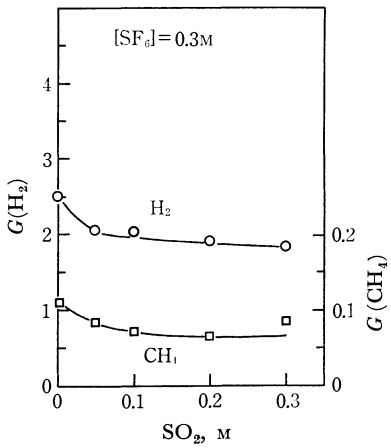

Fig. 9. Yields of H_2 and CH_4 as functions of SO_2 concentration in the presence of 0.3M of SF_6.

their results in the interpretation of the results of this work.

In order to estimate the effect of electron scavenging, the G-values of H_2 and CH_4 from the radiolysis of *n*-hexane in the presence of SO_2 were compared with those obtained in the coexistence of SO_2 and SF_6. The changes in the G-values of H_2 and CH_4 in the presence of 0.3M of SF_6 with the concentration of SO_2 are shown in Fig. 9. The G-value of H_2 at a sufficiently high concentration of SO_2 in Fig. 9 is 1.85, which is about one unit less than the case in which only SO_2 is added. The difference of one unit can not be explained if SO_2 also acts as an electron scavenger. On the other hand, in the coexistence of 0.3M SO_2 and 0.3M N_2O, the $G(N_2)$ value was determined to be 4.3, while in the presence of 0.3M N_2O only, $G(N_2)$ was 4.9. This small decrease in $G(N_2)$ due to the added SO_2 appears to indicate that the electron-scavenging effect of SO_2 is minor. The similarity in the changes in $G(H_2)$ between the addition of SO_2 and that of C_2H_4 supports the effect of radical scavenging of SO_2, because C_2H_4 in *n*-hexane can be regarded as an effective hydrogen-atom scavenger.[13] Consequently, the SO_2 added to *n*-hexane can be regarded mainly as a radical scavenger, and the decreases in the products upon the addition of SO_2 shown in the results may be considered to be brought about by the radical scavenging of SO_2. The sharp decrease in $G(CH_4)$ upon the addition of SO_2 in contrast with the result of the addition of C_2H_4 in Fig. 1 is considered to show that SO_2 is much more effective as a radical scavenger to the methyl radical than is C_2H_4. The C_7–C_{12} products appear to be almost exclusively formed from the combination reaction of alkyl radicals in view of the fact that the addition of SO_2 to *n*-hexane remarkably decreases the G-values of the C_7–C_{12} products to values ranging from one-fourth to one-fiftieth of the values obtained in the absence of the additives, as is shown in Tables 3 and 4.

The results shown in Tables 3 and 4, which were obtained when SF_6, NH_3 or SO_2 was separately added, can be explained qualitatively in terms of the effects of these additives, as has been mentioned before, assuming the following mechanism of *n*-hexane radiolysis:

$$n\text{-}C_6H_{14} \rightsquigarrow n\text{-}C_6H_{14}^+ + e^- \quad (5)$$

$$n\text{-}C_6H_{14} \rightsquigarrow n\text{-}C_6H_{14}^* \quad (6)$$

$$n\text{-}C_6H_{14}^+ + e^- \longrightarrow \begin{cases} C_6H_{13} + H & (7) \\ C_6H_{12} + H_2 & (8) \\ R_1H + R_2H & (9) \end{cases}$$

$$n\text{-}C_6H_{14}^* \longrightarrow \begin{cases} C_6H_{13} + H & (10) \\ C_6H_{12} + H_2 & (11) \\ R_1H + R_2H & (12) \end{cases}$$

$$H + n\text{-}C_6H_{14} \longrightarrow H_2 + C_6H_{13} \quad (13)$$

$$R_1H + R_2H \longrightarrow \begin{cases} R_1HH + R_2 & (14) \\ R_1 + R_2HH & (15) \\ R_1HHR_2 & (16) \end{cases}$$

$$R_1H + C_6H_{13} \longrightarrow \begin{cases} R_1HH + C_6H_{12} & (17) \\ R_1 + n\text{-}C_6H_{14} & (18) \\ R_1HC_6H_{13} & (19) \end{cases}$$

$$C_6H_{13} + C_6H_{13} \longrightarrow \begin{cases} C_6H_{12} + n\text{-}C_6H_{14} & (20) \\ C_{12}H_{26} & (21) \end{cases}$$

where reactions (5) and (6) are the ionization process and the direct-excitation process respectively, and where R_1H and R_2H represent fragment alkyl radicals other than hexyl radicals. Reactions (1) and (2) probably occur instead of reactions (7), (8) and (9) in the presence of SF_6 and cause the decreases in the product yields shown in Tables 3 and 4. On the other hand, reactions (3) and (4) probably occur instead of reactions (7), (8) and (9) in the presence of NH_3.

The results obtained upon the addition of NH_3 can be explained as follows. (i) The small increase in $G(H_2)$ from the value obtained without additives may correspond to the yield by which NH_3 replaces reaction (9) by reactions (3), (4) and (13). (ii) The result that the G-values of the fragment products (from C_1 to C_5) are nearly equal to the values obtained upon the addition of SF_6 may be because reaction (9) is interfered with, as in the case of SF_6. (iii) The result that the total G-value of hexenes is nearly equal to the value obtained in the absence of additives may be explained on the assumption that the decrease in the molecular yield of hexene by reaction (8) is nearly equal to the increase in the hexene yield by the disproportionation reaction (20). (iv) The results that the G-values of the C_7–C_{10} products are somewhat larger than those with SF_6, and that the G-values of dodecanes are somewhat larger than the values obtained in the absence of additives, may be because the increase of hexyl radicals in the presence of

NH_3 twice the yield by which the added NH_3 interferes with reactions (8) and (9).

ii) Dose Dependence of the Product Yields. The difference in the dose dependence between the yields of the hexenes and those of the dodecanes can be explained in the same way as Dewhurst[37] did in the case of cyclohexane. That is, when a hydrogen atom is added to a hexene molecule, as in reaction (22), the hexene yield decreases and the hexene scavenging the hydrogen atom becomes a hexyl radical:

$$C_6H_{12} + H \longrightarrow C_6H_{13} \quad (22)$$

Consequently, the yield of hexyl radicals would not change whether reaction (13) or reaction (22) occurs. On the other hand, the dodecanes are probably produced only by reaction (21). Therefore, the dodecane yields do not change with an increase in the dose, while the hexene yields decrease with such an increase.

iii) Effects of C_2H_5OH and NO. As is shown in Fig. 3 and Table 5, the *G*-values of the radiolysis products in the presence of C_2H_5OH are similar to the case of NH_3. Since the ionization potential of C_2H_5OH (IP=10.50 eV)[14] is a little higher than that of *n*-hexane (IP=10.17 eV),[15] the charge-transfer reaction, if any, from a parent *n*-hexane ion to C_2H_5OH can be ignored. As C_2H_5OH has a comparatively high proton affinity (PA=8.39 eV),[38] the proton-transfer reaction from a parent *n*-hexane ion to C_2H_5OH is most probable. On the other hand, the reaction of C_2H_5OH with electrons and radicals is probably unimportant under the present conditions in view of the reactivity of these reactive species and the concentration of C_2H_5OH. Therefore, the proton-scavenging effect of C_2H_5OH shown by Buchanan *et al.*[10] in the case of cyclohexane appears to have an effect similar to that of the addition of NH_3. The proton-scavenging reaction and the subsequent neutralization reaction are shown by the following schemes:

$$n\text{-}C_6H_{14}^+ + C_2H_5OH \longrightarrow C_6H_{13} + C_2H_5OH_2^+ \quad (23)$$

$$C_2H_5OH_2^+ + e^- \longrightarrow C_2H_5OH + H \quad (24)$$

The results with added NO are shown in Fig. 8 and Table 5. Since the *G*-values of hexenes in the presence of NO are much less than those with added SO_2, whose main effect is concluded to be radical scavenging, the added NO apparently undergoes reactions other than radical scavenging. Though the details of the effect other than radical scavenging can not be clarified in this work, it may be concluded that NO can not be used as a simple radical scavenger.

iv) Formation of the $C_6H_{13}^+$ Ion. The results obtained in the coexistence of SF_6 and NH_3 are shown in Tables 3 and 4. Since the results are somewhat singular, a re-examination of the radiolysis mechanism described in the previous section is necessary. The results show that, when SF_6 and NH_3 are both present, the total *G*-value of the hexenes increases more than one unit from the value obtained in the presence of SF_6 only, but that the other product yields are nearly equal to the values obtained in the presence of SF_6 only. In the coexistence of SF_6 and NH_3, it can be assumed that reactions (1) and (3) and the subsequent neutralization reaction (25) occur:

$$NH_4^+ + SF_6^- \longrightarrow NH_4F + SF_5 \quad (25)$$

The evidence for reaction (25) is as follows. The reaction (25) is calculated to be exothermic by *ca.* 7 eV. In the coexistence of SF_6 and NH_3, an insoluble product was found in *n*-hexane. The product dissolved easily in water, and the resultant aqueous solution showed the existence of F^- and NH_4^+ ions when alizarin complexone[39] and Nessler's reagent were used respectively. If, in the radiolysis mechanism of *n*-hexane assumed before, the SF_5 produced from reaction (25) caused the *G*-value of the total hexene to increase by 1.44, as is shown in Table 3, and if it simultaneously made the *G*-values of other products to remain almost at the values obtained by the addition of SF_6 only, the following two reactions, (26) and (27) would have also to be assumed and, further, all the hexyl radicals produced from reaction (3) would have to carry out these reactions:

$$SF_5 + C_6H_{13} \begin{cases} \nearrow SF_5H + C_6H_{12} & (26) \\ \searrow SF_5C_6H_{13} & (27) \end{cases}$$

However, it is unreasonable to consider that all the hexyl radicals produced from reaction (3) undergo only reaction (26) and (27), for reactions (20), (21), and (28) could also be considered.

$$SF_5 + SF_5 \longrightarrow S_2F_{10} \quad (28)$$

Consequently, the formation of the $C_6H_{13}^+$ ion during irradiation could be suggested as explaining the results obtained in the coexistence of NH_3 and SF_6. If the fragment ions had been produced according to the pattern of the mass-spectra of *n*-hexane[40] in such a large yield as to correspond to the required yield of $C_6H_{13}^+$ ions, the yield of fragment paraffin products would have been larger than that of the congruent fragment olefin products; *e. g.*, the yield of C_3H_8 would have been larger than that of C_3H_6 in the presence of a radical scavenger because of an H^--transfer reaction from *n*-hexane to a fragment ion. However, such a result could not be obtained, as is shown in Table 3 (column: SO_2). Therefore, H^--transfer reaction from *n*-

37) H. A. Dewhurst, *J. Phys. Chem.*, **63**, 813 (1959).
38) V. L. Tal'rose and E. L. Frankevitch, *J. Amer. Chem. Soc.*, **80**, 2344 (1958).
39) H. Hashitani, H. Yoshida and H. Muto, *Bunseki Kagaku*, **16**, 44 (1967).
40) L. Friedman, F. A. Long and M. Wolfsberg, *J. Chem. Phys.*, **30**, 1605 (1959).

hexane to fragment ions, *e. g.*, the $C_3H_7^+$ ion, does not appear to play an important role in the formation of the $C_6H_{13}^+$ ion; the $C_6H_{13}^+$ ion can be thus tentatively assumed to be produced by the direct excitation shown by reaction (29):

$$n\text{-}C_6H_{14} \longrightarrow C_6H_{13}^+ + H + e^- \quad (29)$$

In the case of the addition of SF_6, an additional reaction, (30), may be assumed to occur besides reactions (1) and (2), and in the case of addition of NH_3, an additional reaction, (31), may be assumed to occur besides reactions (3) and (4). The SF_5 produced by reaction (25) probably undergoes reactions (26), (27) and (28).

$$C_6H_{13}^+ + SF_6^- \longrightarrow C_6H_{13} + SF_6 \quad (30)$$

$$C_6H_{13}^+ + NH_3 \longrightarrow C_6H_{12} + NH_4^+ \quad (31)$$

Assuming such a radiolysis mechanism including the existence of the $C_6H_{13}^+$ ion as has been described above, the increase in the hexene yield in the presence of both SF_6 and NH_3 from the value obtained in the presence of SF_6 only would be due to reactions (26) and (31), and the result that the *G*-values of all the products except for hexenes in the presence of both SF_6 and NH_3 are almost the same as in the case of the addition of SF_6 only is qualitatively explicable by the inferences that a part of the hexyl radicals produced by reaction (3) escapes reactions (26) and (27), and that the escaping amount is almost equal to the amount produced by reaction (30) in the presence of SF_6 only. As there seem to be no data on the reactivity of SF_5 except that Ingen *et al.*[41] have recently suggested that SF_5 does not abstract an H atom from cyclohexane, the *G*-value of the $C_6H_{13}^+$ ion can not be accurately estimated. However, it must be less than 1.26, which is the total hexene yield obtained in the presence of SO_2. Further investigation is necessary to confirm that the assumption of the existence of the $C_6H_{13}^+$ ion in the liquid phase is appropriate, for it seems to difficult for such a direct fragmentation as is shown by reaction (29) to occur in the gas phase.[40]

v) The *G*-value of Ionization. Considering the radiolysis mechanism and the effect of added SF_6 described before, the decrease in the *G*-value of the decomposition of *n*-hexane upon the addition of SF_6 from that obtained without additives can be approximately regarded as the *G*-value of the ionization of *n*-hexane in the liquid phase. The *G*-value of the decomposition of *n*-hexane can be obtained by adding the *G*-value of hexyl radicals which react with other radicals to give a *n*-hexane molecule by disproportionation to the *G*-value of the net decomposition of *n*-hexane. The *G*-value of net decomposition in the presence of SF_6 is obtained in the same manner, as is shown by Eqs. (A) and (B), except that the *G*-value obtained in the presence of SF_6 is used instead of that obtained without additives; this value was calculated to be 4.16 from Tables 3 and 4. The *G*-value of hexyl radicals which react with other radicals to give a *n*-hexane molecule by disproportionation is not included in the above *G*-value of the net decomposition; it can be approximately calculated by using the *G*-value of the total dodecanes and the ratio of k_d to k_c, k_d/k_c, where k_d and k_c indicate the average rate constants of the disproportionation reaction and the combination reaction between hexyl radicals respectively. To be exact, there are three kinds of hexyl radicals produced by irradiation, and the ratio of the rate constants of the disproportionation reaction to that of the combination reaction between these radicals seems to be dependent on the combination of these three kinds of radicals. In this work, however, the average rate constants, k_d and k_c, were used as approximate values. Considering the radiolysis mechanism and the effect of added SO_2 described above, the k_d/k_c ratio can be approximately expressed by the following equation, (C):

$$k_d/k_c = \{G_o(C_6H_{12}) - G_1(C_6H_{12}) - \Delta G\}/G_o(C_{12}H_{26}) \quad (C)$$

where $G_0(C_6H_{12})$ and $G_0(C_{12}H_{26})$ indicate the total hexene yield and the total dodecane yield in the absence of additives respectively, where $G_1(C_6H_{12})$ indicates the total hexene yield in the presence of SO_2, and where ΔG indicates the hexene yield formed by reaction (17) in the absence of additives. ΔG was calculated by using the radical yields obtained by Holroyd[42] and the *G*-values of the C_7-C_{10} products shown in Table 2 on the assumptions that the ratio of the rate constants of the disproportionation reactions, (17) and (18), to the combination reaction, (19), is 0.25 and that the rate constant of reaction (17) is equal to that of reaction (18). Thus, ΔG was calculated to be about 0.09. By substituting the values of $G_0(C_6H_{12})$, $G_0(C_{12}H_{26})$, and $G_1(C_6H_{12})$ shown in Tables 3 and 4, and ΔG for Eq. (C), k_d/k_c was estimated to be 1.33. Consequently, the decomposition yield in the presence of SF_6 was calculated to be 5.05 by adding the *G*-value of the disproportionation reaction of the hexyl radical, 0.89, to the *G*-value of the net decomposition, 4.16. On the other hand, the decomposition yield in the absence of additives was calculated to be 9.02 in the same manner. The difference, 3.97, can be regarded as the *G*-value by which the decomposition of *n*-hexane is suppressed by the added SF_6; it may also be regarded as approximately the *G*-value of the ionization of *n*-hexane in the liquid phase. This value is a little smaller than the value, 4.27, obtained by using the

41) J. W. F. van Ingen and W. A. Cramer, *J. Phys. Chem.*, **74**, 1134 (1970).

42) R. A. Holroyd, "Aspects of Hydrocarbon Radiolysis," ed. by T. Gäumann and J. Hoigné, Academic Press, New York, N. Y. (1968), p. 13.

W-value[43] of n-hexane in the gas phase, but it is close to the corresponding value, 3.9, obtained for liquid cyclohexane by Warman *et al.*[44]

vi) $G(N_2)$ in the Presence of N_2O. In the presence of N_2O, the following reaction, (32), which shows the electron - scavenging effect of N_2O, is well known[8,45,46] as one of the processes which bring about nitrogen:

$$e^- + N_2O \longrightarrow N_2 + O^- \qquad (32)$$

Though reaction (33) also produces nitrogen, this reaction may be ruled out because the rate constant of this reaction is relatively small, *i.e.*, $k = 1.2 \times 10^4 M^{-1}\ sec^{-1}$ at 150°C.[47]

$$H + N_2O \xrightarrow{k} HO + N_2 \qquad (33)$$

As another reaction producing nitrogen, Holroyd[48] has suggested the following reaction, (34), which includes the decomposition of N_2O by excitation transfer from the excited n-hexane to N_2O:

$$n\text{-}C_6H_{14}^* + N_2O \longrightarrow n\text{-}C_6H_{14} + N_2 + O \qquad (34)$$

Though the formation of nitrogen as a result of a subsequent reaction of O^- ion with N_2O can not be excluded completely, such a reaction to form nitrogen may tentatively be assumed to be negligible compared with the reaction of the O^- ion with n-hexane because the latter reaction seems to be quite fast (the rate constant of hydrogen - atom abstraction reaction from n-C_4H_{10} by the O^- ion has been reported to be $7.2 \times 10^{11} M^{-1}\ sec^{-1}$ in the gas phase).[49] By using the G-value of ionization obtained in the previous section, the $G(N_2)$ evolving from reaction (32) may be 3.97 at most. On the other hand, as may be seen in Fig. 6, $G(N_2)$ in the presence of N_2O shows little increase at a concentration of about 0.5M and the G-value at 0.5M of N_2O was 5.29. At least, the difference in these G-values, 1.32, may be attributed to a reaction other than reaction (32). Assuming that reaction (34) is responsible for this difference, and that the O^- ion and the oxygen atom produced by reactions (32) and (34) respectively subsequently undergo the following reactions, (35) to (39), water should be observed at the same G-value as that of nitrogen, and the decomposition yield of n-hexane in the presence of N_2O should increase by at least the G-value, 2.64, which is calculated to be twice as much as the G-value of reaction (34):

$$O^- + n\text{-}C_6H_{14} \longrightarrow OH^- + C_6H_{13} \qquad (35)$$

$$OH^- + n\text{-}C_6H_{14}^+ \longrightarrow H_2O + C_6H_{13} \qquad (36)$$

$$OH^- + C_6H_{13}^+ \longrightarrow H_2O + C_6H_{12} \qquad (37)$$

$$O + n\text{-}C_6H_{14} \longrightarrow OH + C_6H_{13} \qquad (38)$$

$$OH + n\text{-}C_6H_{14} \longrightarrow H_2O + C_6H_{13} \qquad (39)$$

Gäumann *et al.*[5,7] have reported that, in the same system as was studied in this work, *i.e.*, an n-hexane solution of N_2O, hexanol could not be observed as a product, but that water was observed in yield of 3.2 ± 0.8 at the N_2O concentration of 0.06M. This G-value of water is approximately equal to the G-value of nitrogen, 3.35, as may be seen in Fig. 6. This is not inconsistent with the reaction mechanism discussed above in terms of the yield of nitrogen. On the other hand, the decomposition yield of n-hexane in the presence of N_2O was calculated to be 11.28 by using the product yields shown in Tables 3 and 4 and the value of k_d/k_c in the manner described earlier. Since the decomposition yield of n-hexane in the absence of additives is 9.02, the difference in these values, 2.26, may be regarded as the G-value by which the decomposition of n-hexane is promoted by the addition of N_2O. This value is close to the value, 2.64, mentioned earlier. This result seems to support the reaction mechanism supposed earlier in regard to the yield of nitrogen. For the purpose of clarifying further the mechanism for producing nitrogen, however, it is necessary to measure more accurately the yields of water and other oxygenated products.

The authors wish to express their thanks to Dr. S. Sato, Dr. H. Yamazaki and Dr. Y. Hatano of this institute and Dr. T. Miyazaki of Nagoya University for their helpful suggestions. They also wish to thank Miss H. Yamaguchi for assistance in preparing the manuscript.

43) P. Adler and H. K. Bothe, *Z. Naturforsch.*, **20a**, 1700 (1965).
44) J. M. Warman, K.-D. Asmus and R. H. Schuler, *J. Phys. Chem.*, **73**, 931 (1969).
45) S. Sato, R. Yugeta, K. Shinsaka and T. Terao, This Bulletin, **39**, 156 (1966).
46) G. J. Schulz, *J. Chem. Phys.*, **34**, 1788 (1961).
47) M. Schiavello and G. G. Volpi, *ibid.*, **37**, 1510 (1962).
48) R. A. Holroyd, *J. Phys. Chem.*, **72**, 759 (1968).
49) D. K. Bohme and F. C. Fehsenfeld, *Can. J. Chem.* **47**, 2717 (1969).

BULLETIN OF THE CHEMICAL SOCIETY OF JAPAN VOL. 43 3741—3745 (1970)

The Temperature Dependence of Hole Injection into Anthracene Crystals

Akihiko YAMAGISHI*1 and Mitsuyuki SOMA

Department of Chemistry, Faculty of Science, The University of Tokyo, Hongo, Bunkyo-ku, Tokyo

(Received June 29, 1970)

The temperature dependence of dark- and photo-currents was studied for the hole injection into anthracene crystals between 0 and 30°C. It was observed that the photocurrent or, as has been previously established, the electron-transfer rate from an excited anthracene crystal to an acceptor had a small temperature dependence, while the dark current or the electron-transfer rate from the crystal in its ground state to an acceptor had a definite value of activation energy. The observed small activation entropy for the dark reaction was interpreted in terms of Marcus' theory, and the small polarizability of the organic crystal was, accordingly, suggested to increase the probability of the electron transfer.

During the past few years, a considerable number of studies have been concerned with the electron-transfer reactions involving organic molecules. The hole injection into an organic crystal from electrodes is regarded as a reaction of this type. The saturation current which appears in a sufficiently high voltage region is associated with the rate of the electron-transfer process between the organic molecule (Ar) on the crystal surface and an organic or inorganic acceptor (M) in an electrode;

$$Ar + M \longrightarrow Ar^+ + M^- \qquad (1)$$

Although some pieces of evidence indicate that a qualitative interpretation of this reaction is possible on the basis of the "outersphere" type of reaction mechanism, no direct measurement has yet been performed to show that this process has an activation free energy such as is predicted by the theory.

This work is concerned with the temperature dependence of the saturation current and, for the most part, deals qualitatively with the factors influencing the rate of this process.*2

Several previous theoretical discussions have been presented, notably by Mehr.[1] Applying Marcus' theory,[2] he attempted to calculate the probability of the electron transfer from an organic crystal to an electron acceptor. His results demonstrated a qualitative agreement with the experimental results. It is, however, still open to question whether or not the theory is consistent with the temperature dependence and other features of the process.

In the present work, an attempt has been made to estimate the activation free energy and to examine the applicability of the Marcus theory.

Experimental

Single crystal platelets of zone-refined anthracene about 50 μ-thick were obtained by the sublimation technique. They were mounted with paraffin wax on the glass cell which is shown in Fig. 1. The back side of the cell, on which the negative potential was applied, contained an aqueous solution of the injecting species. The surface area of the anthracene crystal in contact with the solution was about 0.01 cm^2.

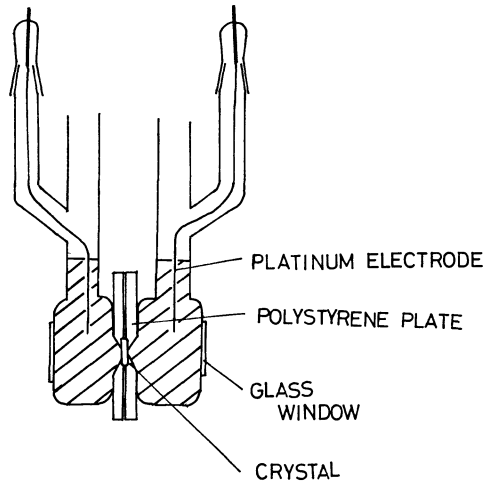

Fig. 1. Measuring cell.

*1 Present address: Department of Chemistry, Faculty of Science, Hokkaido University, Sapporo, Hokkaido.

*2 Recently Sworakowski reported the temperature dependence of the hole injection into anthracene crystals from an electrode containing inorganic oxidants. J. Sworakowski, *Acta Phys. Pol.*, **35**, 33 (1969).

1) W. Mehl and T. M. Hale, *Discuss. Faraday Soc.*, **45**, 30 (1968).

2) R. A. Marcus, *J. Chem. Phys.*, **24**, 966 (1956); **38**, 1858 (1963).

When the dc photocurrent in the above arrangement was measured, the front side was illuminated by a tungsten lamp with a filter which had a maximum transmission at 401 nm and a half width of 11 nm.

The current was measured with a Kawaguchi-type, direct coupled ammeter, Model NA-12E.

The crystals of the other organic molecules were obtained in the following ways:

a) Tetracene was purified by repeated sublimation and was sublimed in a sealed tube under N_2 atmosphere to form single crystals.

b) Phenanthrene and *p*-terphenyl were zone-refined, and single crystals of them were obtained by the sublimation method.

The temperature of the cell was controlled by immersing it in a thermostated water bath.

Results

A. Photocurrents. Ethanol acted as a hole-injecting electrode for the illuminated anthracene crystal, and the various electron acceptors in the electrode were shown to enhance the hole-photocurrent.[3] Phthalonitrile (PN) dissolved in the ethanol electrode was found to enhance the photocurrent, as is shown in Fig. 2. It had previously been observed that tetrachlorophthalonitrile (TCPN) had a similar, but stronger, effect.[3] The increase in the current was proportional to the concentration of the acceptor in both cases. No absorption of light in this wavelength region was found by PN or TCPN. Therefore, the increase in the current is due to the reaction:

$$Ar^* + PN(\text{or TCPN}) \longrightarrow Ar^+ + PN^-(\text{or TCPN}^-)$$

where Ar* is an electronically-excited anthracene and where Ar^+ is an anthracene cation.

The temperature dependence of the photocurrents for the anthracene crystal with the ethanol electrode containing PN or TCPN was measured. The results are shown in Fig. 3 and Table 1. Table 1 gives the apparent activation energy and the magnitude of the saturation currents at room temperature. The difference in the apparent activation energy between PN and TCPN determined experimentally is 1.8 kcal/mol. On the other hand, from the value of the saturation current at room temperature, PN is calculated to have an activation energy about 2.1 kcal/mol larger than TCPN, assuming that they have the same activation entropy.

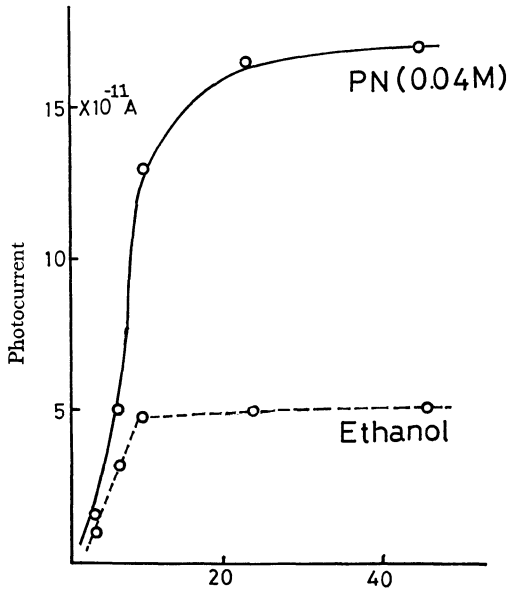

Fig. 2. Voltage dependence of photocurrents in anthracene crystal.
Electrode arrangement: Water|Anthracene| Ethanol or Phthalonitrile in Ethanol

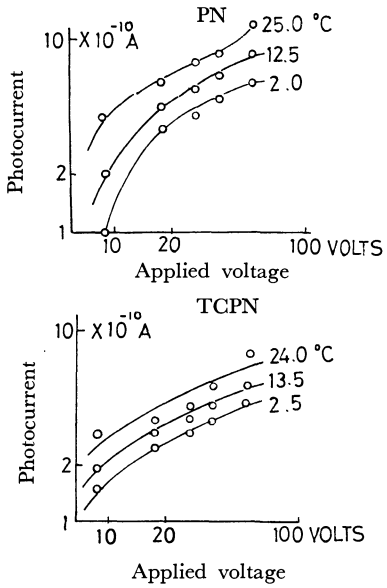

Fig. 3. Temperature dependence of photocurrents in anthracene crystal.
Electrode arrangement: Water|Anthracene| Phthalonitrile or Tetrachlorophthalonitrile in Ethanol

TABLE 1. THE TEMPERATURE DEPENDENCE OF THE SATURATION PHOTO-CURRENT DUE TO THE HOLE INJECTION FROM THE ETHANOL ELECTRODE CONTAINING ORGANIC ELECTRON ACCEPTORS

Electrode	Saturation current at room temperature Amp/cm²	Apparent activation energy, kcal/mol
Ethanol	4×10^{-11}	0.5
TCPN(10^{-3}M)	2600	2.3
PN(10^{-3}M)	70	4.1

3) M. Soma, *J. Amer. Chem. Soc.*, **92**, 3289 (1970).

B. Dark Current. Most of the dark-injecting ions corroded the crystal surface because of their strong oxidizing power. Accordingly, the dark currents more or less decreased with the time.

$K_2Cr_2O_7$ in aqueous H_2SO_4 provided a rather stable dark current, which was kept constant for almost two hours. The results of the temperature dependence measurements of the saturation dark current for the electrode containing $K_2Cr_2O_7$ are shown in Table 2. It definitely confirms that

Table 2. The temperature dependence of the saturation current due to the hole injection by $K_2Cr_2O_7$ (3×10^{-3}M in 1.1NH_2SO_4) into anthracene crystal

Temperature, °C	Saturation current Amp/cm²	Apparent activation energy, kcal/mol
0.5	1.2×10^{-7}	11
12.2	2.4	11
22.0	4.7	12
33.0	9.4	—

the dark current has a constant activation energy over the measured temperature range, which was not necessarily the case for the photocurrent. An additional experiment, which examined the dependence of the saturation dark current on the concentration of $K_2Cr_2O_7$ and the proton, indicated that the saturation dark current follows the expression $i_d=k[HCrO_4^-][H^+]^2$, where k is a constant value and where $[HCrO_4^-]$ and $[H^+]$ are the concentrations of the $HCrO_4^-$ ion and the proton respectively.

In addition, when sulfuric acid was replaced by deuterated sulfuric acid, and the solvent, by heavy water, the current was found to increase by a factor of 3.3 or the kinetic isotope effect was $i_H/i_D=1/3.3$. These facts suggest that protons are involved in this electron-transfer reaction.

In the case of an aqueous solution of the Ce^{4+} ion, the dark current decreased rather rapidly with the time. The reproducible initial values, however, were obtained by washing the crystal surface with ethanol. The temperature dependence was obtained by this technique; the results are given in Fig. 4.

Since the current was proportional to the concentration of the Ce^{4+} ion and was almost independent of the concentration of H_2SO_4 in the range of 0.1—1.0M, it may be concluded that a one-step electron-transfer reaction takes place from the molecule at the crystal surface to the Ce^{4+} ion or, specifically, the $Ce(SO_4)_3^{2-}$ complex ion.[4]

Taking the collision frequency as 2×10^{24} cm^{-2} $sec^{-1}mol^{-1}$, the activation entropy and free energy

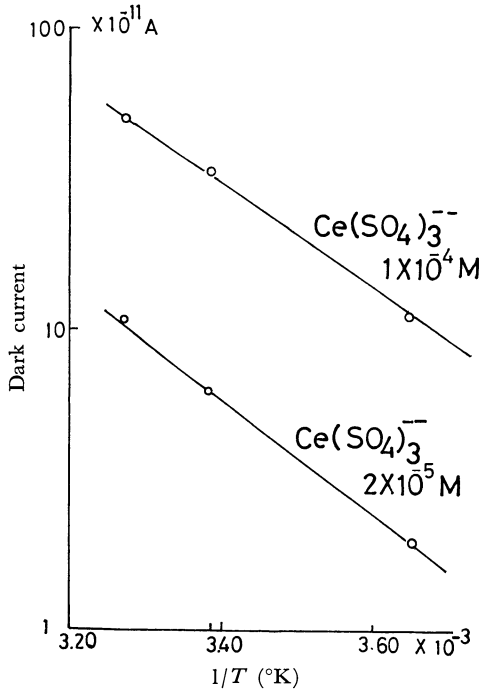

Fig. 4. Temperature dependence of dark currents in anthracene crystal.
Electrode arrangement: Water|Anthracene|Ce^{4+} in aqueous H_2SO_4

were calculated to be as shown in Table 3, in which the thermodynamic data for the isotopic exchange reaction of cerium ions[5] are given for comparison. It is demonstrasted that the activation entropy for the present reaction is considerably smaller than that for the homogeneous reaction. This feature will be discussed in the following section in terms of the Marcus theory.

The dark currents due to the hole injection by Ce^{4+} into various organic crystals were measured at room temperature. As is shown in Fig. 5, all the crystals exhibited current-voltage characteristics similar to those of anthracene. In Table 4, the saturation currents and the activation free

Table 3. Thermodynamic parameters for the electron transfer reaction in the system $Ce(SO_4)_3^{2-}$/anthracene crystal and Ce^{4+}/Ce^{3+} in aqueous solution[5]

System	Activation enthalpy kcal/mol	Activation entropy e.u.	Activation free energy kcal/mol
$Ce(SO_4)_3^{2-}$/ Anthracene	8.7	−3.5	10.7
Ce^{4+}/Ce^{3+}	7.7	−40	19.3

4) T. J. Hardwick and E. Robertson, *Can. J. Chem.*, **29**, 818 (1951).

5) J. W. Gryder and R. W. Dodson, *J. Amer. Chem. Soc.*, **73**, 2890 (1951).

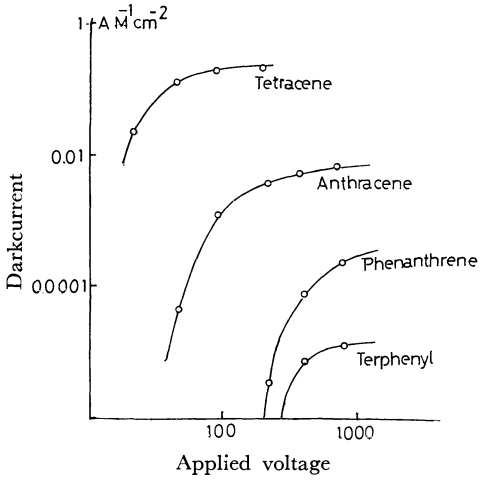

Fig. 5. Voltage dependence of dark currents in various organic crystals.
Electrode arrangement: Water|Crystal|Ce^{4+} in aqueous H_2SO_4

TABLE 4. HOLE INJECTION INTO ORGANIC CRYSTALS FROM CERIC ELECTRODE

Crystal (ionization energy, eV)	Saturation dark current Amp/cm²M	$\Delta F^{\ddagger}$ (obs.) kcal/mol	ΔF° kcal/mol	$\Delta F^{\ddagger}$ (calcd)[a] kcal/mol
Tetracene (5.32)	13000×10^{-5}	9.0	−16.8	7.5
Anthracene (5.65)	7500	10.7	−9.2	10.7
Phenanthrene (6.45)	250	12.8	6.9	20.8
Terphenyl[b] (6.71)	11	14.6	15.2	23.8

a) Calculated by assuming λ is 59 kcal/mol
b) Estimated from the charge transfer band of the tetracyanoethylene complex in CH_2Cl_2,[6] setting the polarization energy equal to that of naphthalene crystal.[7]

energies are given; the latter were calculated by assuming that the activation entropy is equal to that for anthracene.

Discussion

A. Activation Free Energy. By applying the Marcus theory to the present system, the free energy of activation for the electron-transfer reaction (1) at the surface of organic crystals is expressed as follows:

$$\Delta F^{\ddagger} = \frac{\lambda}{4}\left(1 + \frac{\Delta F^{0}}{\lambda}\right)^{2} \qquad (2)$$

where ΔF° denotes the standard free energy change in the reaction (1) and λ is the energy parameter relating to the orientation of solvent molecules in an activated state. When the reactants are approximated by charged conducting spheres, λ is expressed as:

$$\lambda = \frac{1}{2a_1}\left(\frac{1}{D_{op_1}} - \frac{1}{D_{s_1}}\right) + \frac{1}{2a_2}\left(\frac{1}{D_{op_2}} - \frac{1}{D_{s_2}}\right) - \frac{2}{r_1 + r_2}\left(\frac{1}{D_{op_1} + D_{op_2}} - \frac{1}{D_{s_1} + D_{s_2}}\right) + \frac{1}{4r_1}\left\{\frac{D_{op_1} - D_{op_2}}{D_{op_1}(D_{op_1} + D_{op_2})} - \frac{D_{s_1} - D_{s_2}}{D_{s_1}(D_{s_1} + D_{s_2})}\right\} + \frac{1}{4r_2}\left\{\frac{D_{op_2} - D_{op_1}}{D_{op_2}(D_{op_1} + D_{op_2})} - \frac{D_{s_2} - D_{s_1}}{D_{s_2}(D_{s_1} + D_{s_2})}\right\} \qquad (3)$$

where the 1 and 2 indices refer to the crystal and the electrode medium respectively; where D_{OP} and D_s are the optical and static dielectric constants; r, the distance between the center of a change and the boundary of the two phases, and a, the radius of a charged sphere. The last two terms in (3) arise from the interaction between a real charge and an image charge induced in each medium. It is evident that Eq. (3) gives the known formula for the electron-transfer reaction in the homogeneous phase when $D_1 = D_2$, and for the electrochemical case at metal electrodes when D_1 is infinite.

B. Photocurrent. In a previous paper,[3] it was concluded that the electron-transfer reaction from an excited anthracene at the surface of the crystal to TCPN is almost diffusion-controlled. The present low value of the activation energy for TCPN confirms this; it may be attributed to the diffusion process. The relatively large activation energy for PN may arise from the lower electron affinity. Table 5 gives a rough estimation of ΔF°, the free-energy change of the reaction for each acceptor. It shows that a change of about 0.5 eV in ΔF° caused a change of about 0.09 eV (Table 1) in the activation free energy. As this difference

TABLE 5. THE ESTIMATION OF THE FREE ENERGY CHANGE ΔF° FOR THE PHOTO HOLE INJECTION

Acceptor	Electron affinity (eV)	Solvation energy (eV)	ΔF°[a] (eV)
PN	1.1[b]	2.2[c]	−0.7
TCPN	1.6[d]	2.2[e]	−1.2

a) ΔF° = (ionization energy of anthracene crystal, 5.7 eV) − (electron affinity of acceptor + solvation energy + photon energy, 3.1 eV).
b) Ref. 8.
c) Calculated from the difference between the reduction potential in polar organic solvent and the gaseous electron affinity.[8]
d) Estimated from the charge transfer band of pyrene-complex in $CHCl_3$.
e) Assumed to be the same with PN.

6) R. E. Merrifield and W. D. Phillips, *J. Amer. Chem. Soc.*, **80**, 2778 (1958).

may be attributed to the difference in ΔF^{*} expressed by Eq. (2), the required value of λ is about 1.4 eV. On the other hand, the theoretical estimate gives λ to be about 0.5 eV using Eq. (3), where the radius, a, for the acceptor is assumed to be 3.3 Å and that for anthracene to be 3.0 Å, those values being consistent with the experimental solvation energy in polar solvents[8] and with the polarization energy in the crystal[7] respectively. The experimental value of λ is considerably larger than the theoretical one. As the electron-transfer reaction can reasonably be described as an "outer-sphere" type,[9] this discrepancy cannot be attributed to the contribution of the reorganization in "inner-sphere" to λ, but must be attributed to some flaws in estimating ΔF° and λ, or in the theory itself.

C. Dark Current. According to the Marcus theory, the greater part of the free energy of activation in the electron-transfer process is to be attributed to the reorientation of solvent molecules in the activated state, in which they are not electrostatically in equilibrium. This brings about a largely negative activation entropy, since the solvent molecules lose many degrees of freedom in such a state.

The present system is considered to have half of its medium replaced by an anthracene crystal. Since anthracene crystals have a negligible orientational polarizability as compared with water, the observed low value of the activation entropy supports this prediction.

In order to put this interpretation into more quantitative form, we will below calculate for various cases, since λ determines the main part of the free energy of activation and, moreover, includes the contribution of the solvent molecules described above in terms of polarizability. The λ's were calculated in three cases: 1. the present system (Ce^{4+}/anthracene crystal), 2. the electron-transfer reaction from an anthracene molecule to Ce^{4+} in a water solvent, 3. the homogeneous reaction between Ce^{4+} and Ce^{3+}. The resulting λ's were 0.35 eV, 1.35 eV, and 0.66 eV respectively. These values are calculated from Eqs. (2) and (3), assuming that a_1 of an anthracene molecule is 3.5 Å, and the a_2 values of Ce^{4+} and Ce^{3+} ions, 6 Å. The assumed value of a_1 is obtained as the mean value of the required radius for the ion in polar solvents and in the crystal, while that of a_2 is obtained as a sum of the bond lengths and the van der Waals radius of an oxygen ion. The above results show that value for the (1) reaction is the smallest, or the presence of anthracene crystals lowers the ΔF^{*} because of its low polarizability; this finding is in qualitative agreement with the experimental observations shown in Table 3.

The results given in Table 4 show that the saturation current or electron-transfer rate increases as the ionization potential decreases. It should, however, be noted that the change in the activation free energy with the ionization energy is much smaller than that predicted by Eq. (2). In making this discrepancy clear, we calculated the activation free energy from Eq. (2), assuming each crystal have the same value λ (59 kcal/mol) as anthracene.

Mehr noticed[10] that, in the case of naphthalene crystals, the dark current for Ce^{4+} is much larger than predicted by Eq. (2). He attributed this to the formation of a charge-transfer complex between the naphthalene molecule and the Ce^{4+} ion. However, the present results suggest that the small dependence of the current on the ionization potential is not limited to naphthalene but is, rather, common to all crystals. This fact makes us doubt the applicability of Eq. (2). The real situation may be that, although λ determines the greater part of the activation free energy, ΔF^{*} dose not depend on λ and ΔF° in the way expressed by Eq. (2).

The authors are grateful to Professor Kenzi Tamaru for his constant encouragement and helpful discussions throughout this work.

7) L. E. Lyons and G. C. Morris, *J. Chem. Soc.*, **1960**, 5192.

8) A. L. Farragher and F. M. Page, *Trans. Faraday Soc.*, **63**, 2369 (1967).

9) D. Rehm and A. Weller, *Ber. Bunsenges. Phys. Chem.*, **73**, 834 (1969).

10) F. Lohmann and W. Mehl, *J. Chem. Phys.*, **50**, 500 (1969).

BULLETIN OF THE CHEMICAL SOCIETY OF JAPAN VOL. 43 3746—3750 (1970)

The Relation between the Amounts of Chemisorbed and Physisorbed Water on Zinc Oxide

Tetsuo MORIMOTO and Mahiko NAGAO

Department of Chemistry, Faculty of Science, Okayama University, Tsushima, Okayama

(Received July 1, 1970)

In the system ZnO-H_2O, in which a jump appears in the adsorption isotherm, the relation between the amounts of chemisorbed and physisorbed water has been investigated, on the basis of the measurements of the water adsorption isotherms and the water content. The first adsorption isotherm of water was measured at 18°C on a sample degassed at 450°C. After degassing the sample again at 30°C, the second adsorption isotherm was obtained at the same temperature as before. The water content (V_h) on the surface of the sample was determined by the successive ignition-loss method. In the present system, the amount of water physisorbed in the first layer is composed of two parts: one (V_{p1}) is the amount adsorbed at lower vapor pressures, up to the beginning of the jump in the isotherm, and the other (V_{p2}), the amount adsorbed during the jump. The amount of water chemisorbed (V_c) during the adsorption process could be estimated as the difference between the monolayer capacities of the first and second isotherms, the total amount of chemisorbed water being the sum of V_h and V_c. The ratio of the total amount of physisorbed water ($V_{p1}+V_{p2}=V_p$), expressed in the number of water molecules per unit of area, to that of chemisorbed water (V_c+V_h), expressed in the number of hydroxyl groups per unit of area, was found to be about 1 : 1 in the first physisorption layer for all the samples tested, irrespective of their origin, while the ratio of V_{p1} to V_{p2} varied extensively with the origin of the samples.

The surface of most metal oxides adsorbs water molecules physically and chemically. In a previous paper,[1] it has been found in TiO_2 (rutile) and two kinds of α-Fe_2O_3 (hematite) that the ratio of the number of physisorbed water molecules in the monolayer to the number of surface hydroxyl groups (chemisorbed water) is about 1 : 2. The type of the water adsorption isotherms on these oxides was that of the polymolecular adsorption isotherm, whereas on zinc oxide the type of the isotherm has been found to be quite different from that on the other metal oxides:[2,3] the amount of water adsorbed increases remarkably in the relative pressure range of 0.2—0.3. No such phenomenon has been found in the other oxide-water systems; it was called the "hump" of the adsorption isotherm in previous papers.[2,3] The purpose of the present work is to ascertain the relation between the amounts of water physisorbed and chemisorbed on zinc oxide by analysing the adsorption isotherms, and to investigate the structure of the adsorption layer in this system.

Experimental

Materials. Three kinds of zinc oxide samples were used in the present work. One of them was the same sample as had been studied previously;[2-4] it was presented from Sakai Kagaku Co., being prepared by burning zinc metal in air (sample A). The second sample was made by the pyrolysis of zinc hydroxide in air, the latter being precipitated by mixing 0.37M ammonia water with a 0.34M zinc-nitrate solution. In the present procedure, the precipitate of zinc hydroxide was first washed sufficiently with distilled water, dried at 100°C, and then calcined at 500°C for 4 hr (sample B). The last sample was prepared from zinc oxalate precipitated by mixing 0.20M zinc-nitrate and 0.22M oxalic-acid solutions. This precipitate was treated in the same way as sample B, and was finally calcined at 500°C for 4 hr (sample C). From X-ray analysis, the sample B and C were found to be only pure zinc oxide, their crystallinity being to the same extent as that of the sample A.

Surface-area Measurement. The specific surface area of the ZnO samples was determined by applying the BET theory to the nitrogen adsorption data which had been obtained at the temperature of liquid nitrogen; the cross-sectional area of a nitrogen molecule was assumed to be 16.2 Å^2.

Water-adsorption Isotherm. The adsorption isotherms of water on the surfaces of ZnO samples were

1) T. Morimoto, M. Nagao and F. Tokuda, *J. Phys. Chem.*, **73**, 243 (1969).

2) T. Morimoto, M. Nagao and F. Tokuda, This Bulletin, **41**, 1533 (1968).

3) M. Nagao and T. Morimoto, *J. Phys. Chem.*, **73**, 3809 (1969).

4) T. Morimoto, M. Nagao and M. Hirata, *Kolloid-Z. Z. Polym.*, **225**, 29 (1968).

determined volumetrically by using a usual adsorption apparatus equipped with an oil manometer. About a 10-m^2 sample was used in each measurement. Initially, the sample was degassed at 450°C under a reduced pressure of 10^{-5} Torr for 4 hr, and then the adsorption isotherm of water was measured at 18°C. After the first adsorption isotherm had been obtained, the sample was degassed at 30°C in order to remove only the physisorbed water;[2,5-8] the measurement of the second adsorption isotherm was then carried out at the same temperature as before. The adsorption equilibrium was attained within 30 min after each dose of water vapor. A preliminary experiment of desorption was done on each sample; it revealed no hysteresis, indicating that the samples used were nonporous.

Water-content Measurement. It has become clear that the surfaces of metal oxides placed in an atmosphere have water molecules adsorbed both physically and chemically. The physisorbed water can be removed *in vacuo* at relatively low temperatures, *i. e.*, even at room temperature, whereas the surface hydroxyl groups (chemisorbed water) can be removed only gradually at higher temperatures. The temperature at which the removal of the surface hydroxyl groups starts has been found to vary with the nature of the metal oxides, and to be about 200°C in the case of ZnO.[2] The amount of chemisorbed water, that is, the water content (V_h), on the surfaces of ZnO samples was determined by the successive ignition-loss method[1,9] using the same apparatus as that used for the water-adsorption measurement: the sample was heated at various temperatures *in vacuo*, and the gas evolved at every stage of the treatment was measured volumetrically.

When the ZnO sample was treated *in vacuo* at elevated temperatures, a small amount of a gas other than water vapor was found. The gas expelled was condensed in a vessel kept in liquid nitrogen, and was determined volumetrically in the measuring system after having been re-evaporated at room temperature. Next, when the gas was allowed to condense again at −72°C, a small part of the gas was found to remain uncondensed. When only the water vapor was present in the gas, however, this procedure did not leave a uncondensed gas phase. Mass spectroscopy showed that this uncondensed gas was, for the most part, composed of carbon dioxide. The values (V_h) given in Table 1 are the true water content; they do not include the amount of gas uncondensed at −72°C.

Results and Discussion

The first and second adsorption isotherms of water on ZnO at 18°C are given in Figs. 1, 2, and 3. The sample A shows a remarkable jump in its adsorption isotherm in the relative pressure range of 0.2—0.3, as has been observed in the previous works.[2,3] From Figs. 2 and 3 it is clear that, in the cases of the samples B and C, the jumps are considerably smaller than that of the sample A, though they all appear in the same pressure region. These results present important problems yet to be solved concerning the adsorption properties of the

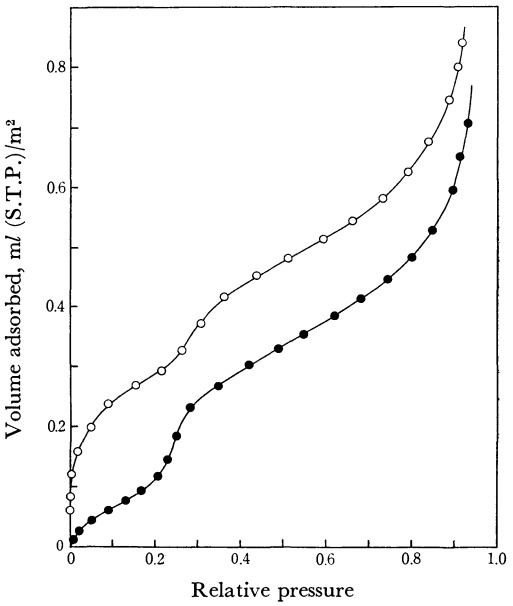

Fig. 1. Adsorption isotherms of water at 18°C on sample A: ○, first adsorption; ●, second adsorption.

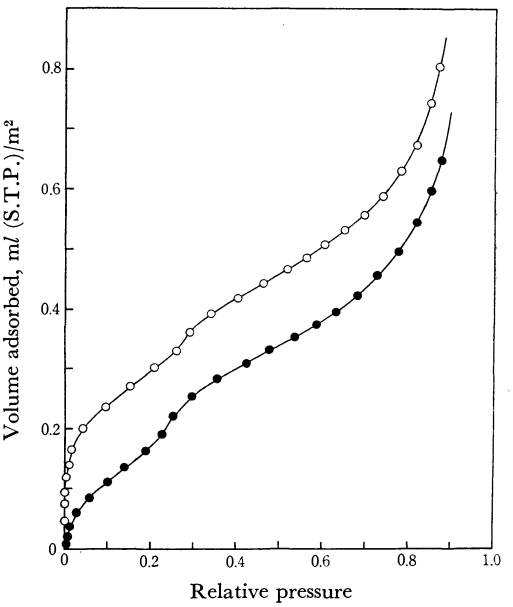

Fig. 2. Adsorption isotherms of water at 18°C on sample B: ○, first adsorption; ●, second adsorption.

5) F. H. Healey, J. J. Chessick and A. V. Fraioli, *J. Phys. Chem.*, **60**, 1001 (1956).
6) G. Srinivasan, J. J. Chessick and A. C. Zettlemoyer, *ibid.*, **66**, 1819 (1962).
7) J. J. Jurinak, *J. Colloid Sci.*, **19**, 477 (1964).
8) V. Pravdic, E. McCaffery and A. C. Zettlemoyer, *Surface Sci.*, **7**, 380 (1967).
9) T. Morimoto, K. Shiomi and H. Tanaka, This Bulletin, **37**, 392 (1964).

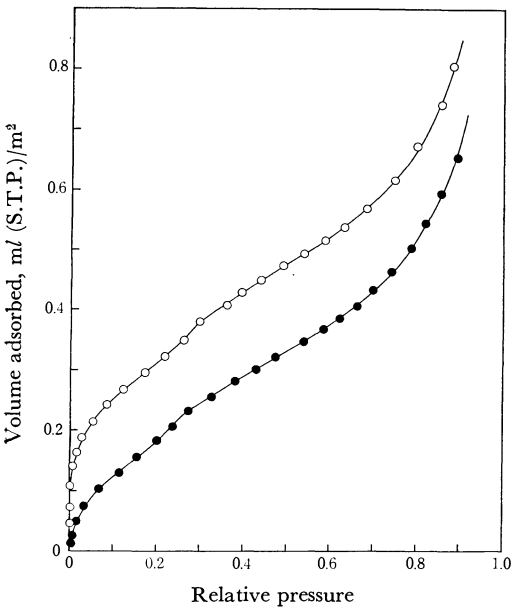

Fig. 3. Adsorption isotherms of water at 18°C on sample C: ○, first adsorption; ●, second adsorption.

system ZnO–H_2O: (1) a jump appears on the adsorption isotherm at relative pressures of 0.2—0.3, (2) the height of the jump depends on the origin of the samples, and (3) the relation between the amounts of physisorbed and chemisorbed water is unclear. The former two problems will be discussed in detail in subsequent papers. Here, mainly the last problem will be dealt with, using, for comparison, the data on the other oxides reported previously.[1]

As was reported in the previous paper, the amount of adsorbed water on metal oxide evacuated at an elevated temperature increases with a rise in the pretreatment temperature. Furthermore, it was found that the adsorption isotherms can be treated by the BET method; the plot of the resulting V_m values against the pretreatment temperature suggests the temperature at which the removal of the chemisorbed water starts.[2] In other words, on the surfaces of metal oxides degassed at elevated temperatures, the chemisorption and physisorption of water occur simultaneously, whereas only the physisorption occurs on the surfaces treated at room temperature.[2,5–8] A conventional application of the BET theory to the first adsorption isotherms of water on various kinds of metal oxides, including both physisorbed and chemisorbed water, has given the monolayer capacity.[5–8] Also, in the present system we can apply the BET theory to the initial part of the isotherms and thus obtain the monolayer capacity. Thus, the V_m value in Table 1 is the monolayer capacity calculated from the first adsorption isotherm, and the V_{p_1}, that calculated from the second one. As has been described above, the former should include the physisorbed and chemisorbed water, whereas the latter, only the physisorbed water. The difference between the values V_m and V_{p_1}, therefore, will indicate the amount of water chemisorbed during the adsorption process. V_c in Table 1 is this amount of chemisorbed water expressed in terms of the number of hydroxyl groups per 100 Å² of the surface, by taking into account the fact that one water molecule forms two hydroxyl groups. V_h is the surface water content, being the amount of the water chemisorbed on the surface just before the adsorption process. The sum of V_c and V_h is, therefore, the total amount of water chemisorbed after the adsorption process; this water may act as the sites for the physisorption of water molecules.

On the other hand, by applying the B-point method to the second adsorption isotherm, we can obtain the overall monolayer capacity of physisorption. This value is listed in the V_p column in Table 1. The V_p value may be considered to be composed of two parts: one is the initial part of the adsorption isotherm (V_{p_1}), as has been calculated above, while the other is the part of the jump, the latter being obtained by subtracting V_{p_1} from V_p. Thus, V_{p_2} is the second part of physisorption. In conclusion, the chemisorbed water layer is present as a substrate on which the water molecules are adsorbed physically. Here, we can estimate the relation between the numbers of the molecules present in the two layers up to the attainment of the B point.

This ratio is given in the last column of Table 1, in which the total amount of physisorbed water is

Table 1. The relation between the amounts of chemisorbed and physisorbed water on ZnO

Sample	Calcn. temp. (°C)	Surface area (m^2/g)	V_m (ml(S.T.P.)/m^2)	Physisorbed amount (H_2O molecules/100Å²)			Chemisorbed amount (OH groups/100Å²)			$V_p/(V_c+V_h)$ (H_2O/OH)
				V_{p_1}	V_{p_2}	V_p	V_c	V_h	V_c+V_h	
A	—	4.79	0.247	3.47	4.52	7.99	6.27	1.10	7.37	1.08
B	500	1.97	0.308	5.70	1.16	6.86	5.17	3.20	8.37	0.82
C	500	11.3	0.290	5.25	2.15	7.40	5.11	2.48	7.59	0.97
A	—	4.79	0.247	—	—	4.92	6.27	1.10	7.37	0.67

expressed in H_2O molecules/100 Å^2, and that of the underlying chemisorbed water, in OH groups/100Å^2. It may be seen from Table 1 that the ratio is about 1 : 1 for every sample tested.

It is well known that the crystal of ZnO is of the same type as wurtzite. The numbers of the zinc atom on the (0001) and (10$\bar{1}$0) planes, both of which are known to have excellent cleavage,[10,11] can be estimated crystallographically to be 11 and 6/100 Å^2 respectively. If we assume that these two kinds of planes are equally present on the actual surfaces, and that a surface hydroxyl group is bonded to a zinc atom, the total amount of chemisorbed water will become to about 8.5 OH groups/100 Å^2; this figure agrees fairly well with the results in Table 1. Furthermore, the experimental results show that the water molecules are adsorbed on these surface hydroxyl groups in the ratio of 1:1. If the molecular area of water is assumed to be 10.8 Å^2, as usual, it is found that the number of water molecules of 7—8/100 Å^2 is suitable to be adsorbed as a monolayer. When we calculate the ratio of each physisorbed amount, V_{p_1} or V_{p_2}, to the total amount of chemisorbed water, they are very different from each other, depending on the origin of the samples. With the sample A, V_{p_1} is smaller than V_{p_2}, whereas the situation is quite the reverse with the samples B and C; the value of V_{p_2} is only 20% of the value of V_{p_1} in the case of the sample B and only 41% in the case of the sample C respectively, corresponding to the smaller jump in the isotherms with the two samples than with the sample A. Here it is noticeable that the larger the V_{p_1} value, the smaller the V_{p_2} value.

In the cases of α-Fe_2O_3 (hematite) and TiO_2 (rutile), which give the polymolecular adsorption isotherm of water, the ratio of the amounts of physisorbed to chemisorbed water has been found to be nearly 1 : 2, as has been reported previously.[1] In the present work, we could not prepare the sample of ZnO, which gives a usual polymolecular adsorption isotherm of water, though Egorov *et al.*[11] obtained a sample of ZnO in which the jump was not observed in the water adsorption isotherm. It can be seen from Fig. 4 that the second adsorption isotherms of the three samples agree fairly well with one another in the range of relative pressures higher than 0.3 (*i. e.*, above the "B-point"), but at lower relative pressures they are quite different, depending on the origin of the samples. The results show that V_{p_2} decreases when V_{p_1} increases, the sum of V_{p_1} and V_{p_2} keeping almost constant. From the features of the adsorption isotherms observed here, we can

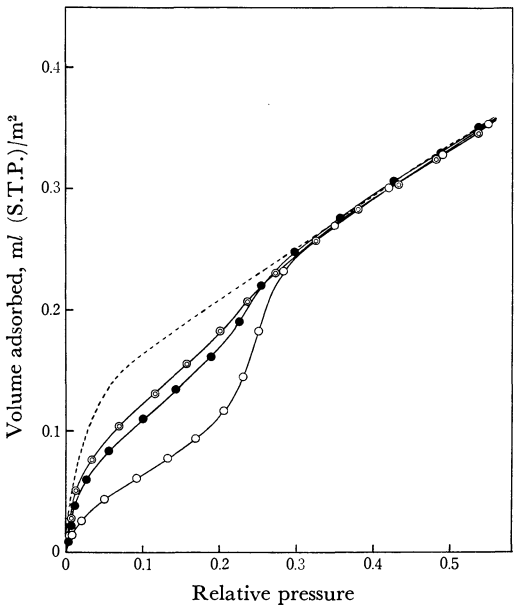

Fig. 4. Second adsorption isotherms of water at 18°C on ZnO samples: ○, sample A; ◎, sample B; ●, sample C; dotted line represents a hypothetical isotherm.

expect, as the limiting case, an adsorption isotherm in which the jump does not appear. The curve expressed by the dotted line in Fig. 4 shows this hypothetical isotherm, which is obtained by extrapolating the upper part of the real isotherms to the lower pressures. By applying the BET theory to this hypothetical isotherm, we can obtain the V_m value and calculate the other quantities as being similar to those obtained in the preceding paper.[1] The values thus obtained are given in the bottom row of Table 1. As a matter of fact, when the initial adsorption amount increases, the slope of the linear part of the adsorption isotherm after the attainment of the monolayer coverage often tends to fall. Therefore, the hypothetical isotherm may scarcely be realized unless all the features of the isotherm are changed. However, there is a great indication in Table 1 that if we prepare a sample of ZnO which does not reveal the jump in the water adsorption isotherm, we can expect the ratio of H_2O : OH to rise to 1 : 2.

Fisher and McMillan[12] and Ross *et al.*[13–17] studi-

10) S. Dana and W. E. Ford, "A Textbook of Mineralogy," John Wiley, New York, N. Y. (1960), p. 480.

11) M. M. Egorov, N. N. Dobrovol'skii, V. F. Kiselev, G. Furman and S. V. Khrustaleva, *Zh. Fiz. Khim.*, **39**, 3070 (1965).

12) B. B. Fisher and W. G. McMillan, *J. Amer. Chem. Soc.*, **79**, 2969 (1957).

13) S. Ross and W. Winkler, *ibid.*, **76**, 2637 (1954).

14) S. Ross and H. Clark, *ibid.*, **76**, 4291, 4297 (1954).

15) S. Ross, J. P. Olivier and J. J. Hinchen, *Advan. Chem. Ser.*, **33**, 317 (1961).

16) J. P. Olivier and S. Ross, *Proc. Roy. Soc.* (London), *Ser. A*, **265**, 447 (1962).

17) W. D. Machin and S. Ross, *ibid.*, *Ser. A*, **265**, 455 (1962).

ed the adsorption isotherms on systems containing a nonpolar adsorbent with homotattic surfaces and found that the nonpolar molecules adsorbed on such surfaces behave like a mobile film according to the two-dimensional van der Waals equation. Furthermore, when the pressure exceeds a limiting value, the film give rise to a two-dimensional phase transition, resulting in a sudden change to a close-packed state of the adsorbed molecules. Also, in the present system a similar circumstance may hold between the surfaces of the ZnO and the water molecules: the amount of water physisorbed on the homotattic layer of surface hydroxyl groups on ZnO is depressed initially, but increases steeply to the adsorption ratio of 1 : 1 (H_2O : OH) when the vapor pressure exceeds a certain value.

Usually, the surfaces of most metal oxides are considered to be inhomogeneous, and it has been reported that, on such surfaces, the adsorption of molecules first occurs on the highest energy sites and later on successively lower energy sites. Moreover, on such surfaces no jump in the adsorption isotherm appears and the stable ratio of H_2O : OH is 1 : 2 in the first layer of adsorption.[1] On the contrary, the present system shows depressed adsorption at lower pressures and a stable ratio of 1 : 1 (H_2O : OH). Also, this comparison makes it possible to predict that the surfaces of ZnO may be homotattic for the physisorption of water molecules. Further investigations will appear in the next paper.

BULLETIN OF THE CHEMICAL SOCIETY OF JAPAN VOL. 43 3750—3754 (1970)

Dielectric Absorption in Crystalline Pentachloronitrobenzene

Ariyuki AIHARA, Chikazu KITAZAWA and Akira NOHARA

Department of Materials Science, Denki-Tsushin University, Chofu, Tokyo

(Received July 2, 1970)

Dielectric measurements have been performed with pentachloronitrobenzene in polycrystalline state using a trans-former bridge, between 30 Hz and 1 MHz and in the temperature range 20—99°C. The substance shows distinct dielectric absorption in the frequency and temperature ranges, presumably due to molecular rotation in the solid state similar to that of pentachlorotoluene and 1,2,4-trimethyl-3,5,6-trichlorobenzene as has been found by Turney. The frequency factor and the energy of the barrier for the rotation are $\log A = 15.2$ (A in sec^{-1}) and $\Delta H = 16.1$ kcal/mol. A possible mechanism for the rotational transition of the molecule in the crystalline lattice has been discussed. The dipole moment of this substance in benzene solution has been measured, the result being $\mu = 2.33$ Debye.

Despite the fact that both pentachlorotoluene and 1,2,4-trimethyl-3,5,6-trichlorobenzene in crystalline state show anomalous dielectric dispersion at radio frequencies, without undergoing any phase transitions,[1] hexasubstituted benzenes with the nitro group as one of the substituents have been thought to show no molecular rotation in the solid state.[2] Of six hexasubstituted benzenes with one or two nitro groups among the substituents, only 1,2,3,4-tetramethyl-5,6-dinitrobenzene has been referred to by White, Biggs and Morgan[3] as a substance showing molecular rotation in the solid state.

1) A. Turney, *Proc. Instn. Elect. Engrs.*, IIA, **100**, 46 (1953).

2) C. P. Smyth, "Physics and Chemistry of the Organic Solid State," ed. by D. Fox, M. M. Labes and A. Weissberger, Interscience, New York, 1963, p. 723.

3) A. H. White, B. S. Biggs and S. O. Morgan, *J. Amer. Chem. Soc.*, **62**, 16 (1940).

Pentachloronitrobenzene, whose molecular shape and symmetry might be regarded as similar to that of pentachlorotoluene, is a substance left so far uninvestigated in relation to this problem. Thus, with a view that this substance may also exhibit molecular rotation in the crystalline state, a dielectric investigation on pentachloronitrobenzene has been performed. The result seems to confirm our view that the dielectric absorption should be due to rotational movement of the molecule.

In connection with this, the dipole moment of this molecule, too, has been measured in benzene solutions.

Experimental

Material. Commercial product was first recrystallized from ethanol several times and then purified by means of zone-refining. The sample was subjected to dielectric measurements as a disc of 4 cm in diameter

and 1.08 mm in thickness, which was shaped under the pressure of 3 ton/cm^2.

Apparatus. Measurements of dielectric permittivity and loss in the solid phase were performed with a transformer bridge*1 over the frequency range of 30 Hz to 1 MHz and at temperatures 20—99°C. The measuring cell consists of two circular plate electrodes and a guard ring, the diameters of the main electrode being 37 mm. The separation of the two electrodes can be adjusted so as to make close contact with the surface of samples.

The dipole moment of the substance in benzene solution was measured with a heterodyne double-beat permittivity measuring equipment (1 MHz).[4]

Results and Discussion

In view of the possible effect of cold working on dielectric loss factors, the sample was kept at a temperature some degrees below the melting point 151.0°C for several hours prior to the measurement. After repeating runs three times, observed values of ε' and ε'' were found to remain almost invariant.

The plot of ε' and ε'' as a function of frequency at several temperatures are shown in Fig. 1. We see that pentachloronitrobenzene exhibits distinct anomalous dispersions in the frequency and temperature ranges investigated, region of the dispersion making a gradual shift toward the higher frequency range with the rise of temperature.

The absorption curves are somewhat broader than the normal Debye absorption due presumably to the distribution of relaxation times, while the heights of the absorption curves, that is the intensity of maximum absorption, ε''_{max}, show a slight tendency to decrease with the rise of temperatures.

The Cole-Cole plots of ε' versus ε'' (Fig. 2) form arcs, the values of distribution parameters decreasing from $\beta=0.21$ at 20.0°C to 0.05 at 99.1°C. It is obvious that the absorption will become a real Debye type at higher temperatures. The values of static and optical permittivities, ε_0' and ε'_∞, have been determined from these diagrams as listed in Table 1.

Table 1. Experimental values of static permittivities (ε_0'), optical permittivities (ε'_∞), maximum loss factors (ε''_{max}), and distribution parameters (β)

Temp. °K	ε_0'	ε'_∞	$(\varepsilon_0'-\varepsilon'_\infty)$	$2\varepsilon''_{max}$	β
293.2	4.09	2.58	1.51	1.16	0.21
313.6	4.00	2.55	1.45	1.12	0.15
333.2	3.87	2.52	1.35	1.10	0.14
353.9	3.74	2.49	1.25	1.08	0.08
373.2	3.65	2.46	1.19	1.06	0.05

The dielectric dispersion $(\varepsilon_0'-\varepsilon'_\infty)$ which should be equal to $2\,\varepsilon''_{max}$ if the absorption follows the Debye mechanism, increases almost linearly with $1/T$, T being the temperature expressed in °K. A comparison of $(\varepsilon_0'-\varepsilon'_\infty)$ with $2\,\varepsilon''_{max}$ (experimental) is also shown in the table. Considering the rather broad feature of these absorptions, $(\varepsilon_0'-\varepsilon'_\infty)/2$ should be

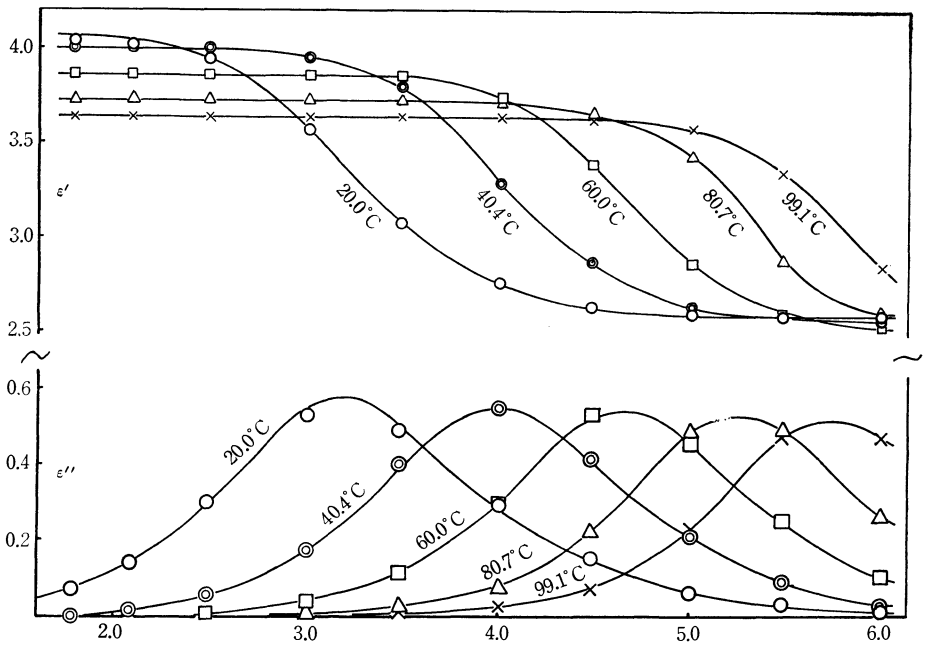

Fig. 1. Dielectric dispersion and absorption of pentachloronitrobenzene crystal.

4) C. Kitazawa and A. Aihara, *Nippon Kagaku Zasshi*, **90**, 365 (1969).

*1 Ando Electric Co. TRS-1B.

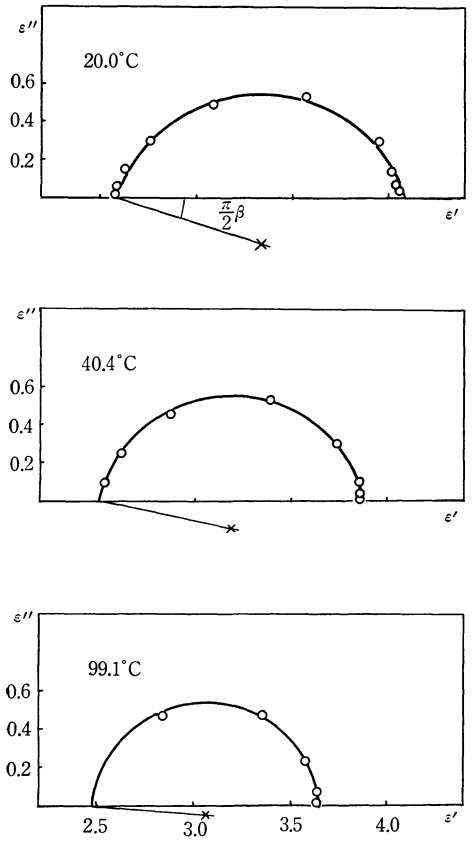

Fig. 2. Cole-Cole arc plots of ε'' versus ε'.

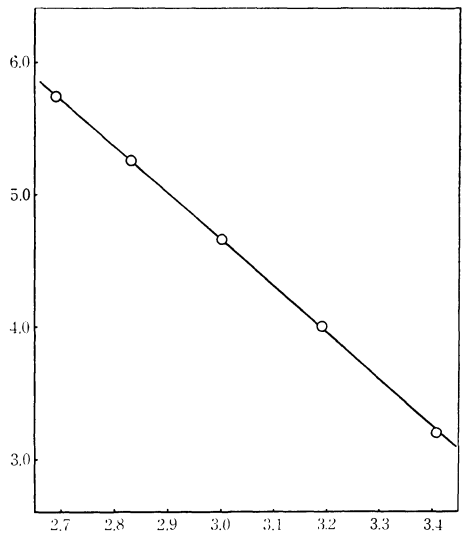

Fig. 3. Relation between $\log f_{max}$ and $1/T$.

TABLE 2. COMPARISON OF FREQUENCY FACTORS, ENERGY BARRIERS, AND OTHER ENERGY DATA

Substances	$\log A$ (A in sec^{-1})	ΔH kcal/mol	ΔS e.u.	$\Delta F^{20°}$ kcal/mol	ΔE_0 kcal/mol
$C_6Cl_5NO_2$	15.2	16.1	12.8	12.4	0
$C_6Cl_5CH_3$[1]	14.1	11.6	9.3	8.9	0
$C_6(CH_3)_3Cl_3$[1]	14.7	10.3	12.3	6.7	0

taken to stand for the intensity of maximum dielectric absorption.

The enthalpy of activation for the molecular rotation in the solid state ΔH as well as the frequency factor A have been calculated with the use of the equation[5,6]

$$f_{max} = A \exp(-\Delta H/\boldsymbol{R}T), \quad (1)$$

where f_{max} means the frequency at which the absorption becomes of maximum value, $\boldsymbol{R}$ is the gas constant and T is the absolute temperature;

$$\Delta H = 16.1 \text{ kcal/mol},$$
$$\log A = 15.2 \ (A \text{ in } sec^{-1}).$$

These values can be compared with those of pentachlorotoluene and 1,2,4-trimethyl-3,5,6-trichlorobenzene obtained by Turney[1] as shown in Table 2.

ΔE_0, the difference of energy in equilibrium positions between which the rotational transitions of the dipole might occur in the crystalline lattice, can be calculated according to the equation[6]

$$\varepsilon_0' - \varepsilon_\infty' = C/T\{1 + \cosh(\Delta E_0/\boldsymbol{R}T)\}, \quad (2)$$

where C is a constant. This expression approximates to

$$\varepsilon_0' - \varepsilon_\infty' = B \exp(-\Delta E_0/\boldsymbol{R}T)/T \quad (3)$$

when $\Delta E_0 \gg \boldsymbol{R}T$, B being a constant. If $\Delta E_0 \doteqdot 0$, we get a simple relation

$$\varepsilon_0' - \varepsilon_\infty' = C/2T, \quad (4)$$

that is, the magnitude of dielectric dispersion is inversely proportional to temperature. Conversely, we may safely conclude that the energy difference ΔE_0 must be almost zero when $(\varepsilon_0' - \varepsilon_\infty')$ increases with 1/T, as is the case with pentachloronitrobenzene.

An inspection of Table 2 leads to an interesting conclusion that despite a bulky substituent, $-NO_2$, instead of $-CH_3$, the molecule of pentachloronitrobenzene can perform a rotational transition in the solid state probably about an axis perpendicular to the molecular plane, as has been found with pentachlorotoluene by Turney,[1] but with a larger potential barrier as well as a larger entropy change for rotation. The difference of entropy between the stationary and transitional positions, ΔS, was calculated assuming $f_0/\pi = 10^{12}$ sec^{-1} [6] in the following relation between A and ΔS.

5) H. Fröhlich, "Theory of Dielectrics," Oxford Univ. Press, Oxford (1949), Section 11.

6) J. S. Dryden and R. J. Meakins, *Rev. Pure Appl. Chem.*, **7**, 15 (1957); R. J. Meakins, *Progress in Dielectrics*, **3**, 150 (1961).

$$A = f_0/\pi \cdot \exp(\Delta S/R), \quad (5)$$

where f_0 is the frequency of oscillation of the dipole about the equilibrium position. Due to this rather unfavorable assumption, no serious conclusion should be drawn from the larger value of ΔS, 12.8 cal/deg. mol, for pentachloronitrobenz enecompared with that of pentachlorotoluene, 9.3 cal/deg. mol,[1] although the difference suggests the more regular arrangement of molecules in the crystalline lattice in the case of pentachloronitrobenzene.

In relation to the mode of aggregation of molecules in crystalline state, Fröhlich's $B(T)$ function has also been examined.

$$B(T) = 4\pi N_0 \overline{\mathbf{mm}^*}/3k = (\varepsilon_0 - \varepsilon_\infty)(2\varepsilon_0 + \varepsilon_\infty)T/3\varepsilon_\infty \quad (6)$$

where $\overline{\mathbf{mm}^*}$ is the average value of the product $\mathbf{mm}^*$, $\mathbf{m}$ and $\mathbf{m}^*$ being a dipole moment and a moment polarized by the former, respectively, k is Boltzmann's constant and N_0 is the number of dipoles per unit volume. According to Fröhlich,[7] $B(T)$ should be constant independent of temperature, "if Onsager's equation holds, *i. e.*, if the dipole moment of a molecule can be considered as a constant, and if there are no short-range forces leading to mutual orientation of dipole." Actually the calculated values of $B(T)$ with pentachloronitrobenzene remain almost constant independent of the rise of temperature as shown in Table 3, suggesting that there is no particular preferential interaction between neighboring molecules, such as a pair formation. In Table 3 are also shown the values of dipole moment in the solid state calculated tentatively with the use of Onsager's equation which has been derived for the pure dipolar liquid:[8]

$$\varepsilon_0 - \varepsilon_\infty = 4\pi N_0 \mu^2 \varepsilon_0 (\varepsilon_\infty + 2)^2 / 9kT(2\varepsilon_0 + \varepsilon_\infty) \quad (7)$$

where ε_0, ε_∞, N_0, k and T have the same meanings as in (6), and μ is the dipole moment.

Table 3. Fröhlich's $B(T)$ function and the dipole moment in solid state

Temp. °C	$B(T)\times 10^{-2}$ deg.	μ Debye (solid phase)
20.0	3.88	1.18
40.4	4.01	1.19
60.0	3.98	1.20
80.7	3.94	1.21
99.1	3.95	—[a]

a) The μ value at 99.1°C was not calculated because of the lack of the density value: μ values at other temperatures were calculated using the density values, 1.959 (20.3°C), 1.954 (40.4°C), 1.949 (60.0°C), 1.944 (80.7°C), g/cc, measured with a pycnometer.

The dipole moment values in Table 3 are definitely lower than those in benzene solutions, 2.33 and 2.32 Debyes (28.8°C), obtained by following the usual Halverstadt-Kumler procedure and that of Guggenheim-Smith, respectively.

Experimental details of the measurement of dipole moment in benzene solutions are to be published elsewhere,[9] but some of the data are shown in Table 4.

The fact that the moment values, estimated for a molecule in the solid state, applying Onsager's equation, are far smaller than the actual value of the dipole moment in benzene solutions, offers clear evidence that the equilibrium positions for the dipole to perform rotational transitions in the crystalline lattice should be less than 180° apart instead of being located in completely opposite directions, *i. e.*, 180° separation.

Thus, the molecule of pentachloronitrobenzene in the crystalline state is supposed to perform rotational transitions between several equilibrium posi-

Table 4. Experimental data on the dipole moment measurement in benzene solution (28.8°C)

$W_2\times 10^2$	ε_{12}	d_{12}	n_{12}	H-K	G-S
0.000	2.2650	0.8685	1.4956	P_2=164.1 (cc)	
0.867	2.2832	0.8725	1.4961		
1.213	2.2887	0.8741	1.4963	MR=54.7 (cc)	
2.220	2.3088	0.8789	1.4970		
3.244	2.3300	0.8837	1.4975	P_0=110.4 (cc)	P_0=108.3 (cc)
6.753	2.4068	0.9002	1.4995		
	α=2.10	β=0.47	γ=0.17	μ =2.33D	μ =2.32D

W_2=weight fraction of the solute; ε_{12}=dielectric permittivity of the solution; d_{12}=density of the solution; n_{12}=refractive index of the solution (D line); α, β, γ are the rates of increase of ε_{12}, d_{12} and n_{12} with concentration, respectively; H-K and G-S stand for Halverstadt-Kumler' and Guggenheim-Smith' procedures, respectively; P_2=total polarization of the solute; P_0=orientation polarization of the solute; MR=molar refraction of the solute; μ=dipole moment of the solute. Atomic polarization is assumed to be negligible.

7) H. Fröhlich, *loc. cit.*, pp. 136—138.
8) L. Onsager, *J. Amer. Chem. Soc.*, **58**, 1486 (1936).
9) C. Kitazawa and A. Aihara, *J. Denki-Tsushin Univ.*, **28**, 105 (1970).

tions, equal in energy but separated from each other by potential barriers of different magnitude, which are most likely to become identical at temperatures higher than 100°C leading to a single relaxation time.

No mention has been made so far of the molecular structure of pentachloronitrobenzene. Problems to be solved in this connection are whether the molecule is distorted or not with respect to the C–Cl bonding, on the one hand, and how far twisted the nitro group is about the C–N bond, on the other.

This twisting of the nitro group may be inevitable for reducing the steric repulsion between oxygen and chlorine atoms on both ortho positions to the nitro group,[10] which in turn produces a possibility of the molecule existing as two isomeric conformations, with a nitro group twisted clockwise and with a group twisted anti-clockwise, and consequently, interconversion between the two isomers may happen through a potential barrier separating the two equilibrium orientations of the nitro group. It is probable, therefore, that the nitro group will acquire, on the average, almost axial symmetry around the C–N bond and hindrance against rotation of the molecule as a whole, in the crystalline lattice, will be fairly reduced.

In order to discuss the mechanism of dielectric absorption more precisely, details of molecular as well as crystal structure of this substance are necessary. A three-dimensional X-ray crystal structure analysis with pentachloronitrobenzene is now in progress.

10) J. R. Holden and C. Dickinson, *J. Phys. Chem.*, **73**, 1199 (1969).

BULLETIN OF THE CHEMICAL SOCIETY OF JAPAN VOL. 43 3754—3761 (1970)

Electronic Structure of Lone Pairs. V.*1 Thiothiophthene and 2,5-Dimethyl-dithiofurophthene

Hiroko YAMABE, Hiroshi KATO*2 and Teijiro YONEZAWA

Department of Hydrocarbon Chemistry, Faculty of Engineering, Kyoto University, Sakyo-ku, Kyoto

(Received July 4, 1970)

The electronic structure and the electronic transition of thiothiophthene(I) and 2,5-dimethyl-dithiofurophthene(II) are calculated by the semi-empirical ASMO SCF method. The E_{AB} value, used instead of the bond order of the S···S bond of Compound I, and those of the S···S bond and the S···O interaction of Compound II are found to be −6.125 eV, −12.957 eV, and −0.740 eV respectively. These E_{AB} values are compared with that of the previously-obtained transannular interaction and the hydrogen bond of water dimers calculated by the same method. The properties of the electronic transition of these compounds are discussed. No separability of the π–$\pi^*(B_2)$-type and σ-$\sigma^*(B_2)$-type transitions of the Compound I is indicated. The orbital energy of the highest occupied MO of the Compound I is remarkably high, which corresponds well with the very small I_p value.

Once the structures of thiothiophthene (I of Fig. 1) and 2,5-dimethyl-dithiofurophthene (II of Fig. 1) had been determined correctly, using X-ray diffraction, and once the concept of the 'no-bond' resonance of thiothiophthene had been presented by Bezzi *et al.*[1–3] in 1958, various investigations of their properties were performed. Thiothiophthene has been prepared by different routes, and many derivatives*3 have been prepared, employing

*1 Supported in part by a Fellowship from the Japan Society for the Promotion of Science, from October, 1968, to March, 1969.

*2 Present address: Department of General Education, Nagoya University, Chikusa-ku, Nagoya.

1) S. Bezzi, M. Mammi and C. Garbuglio, *Nature*, **182**, 247 (1958); M. Mammi, R. Bardi, C. Garbuglio and S. Bezzi, *Acta Cryst.*, **13**, 1048 (1960).

2) M. Mammi, R. Bardi, G. Traverso and S. Bezzi, *Nature*, **182**, 247 (1958).

3) A. A. Bothner-By and G. Traverso, *Chem. Ber.*, **90**, 453 (1957).

*3 The non-benzonoid aromatic hydrocarbon pentalene, 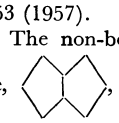 , has not been prepared, in spite of the large resonance energies predicted (D. P. Craig and A. Maccoll, *J. Chem. Soc.*, **1949**, 964.

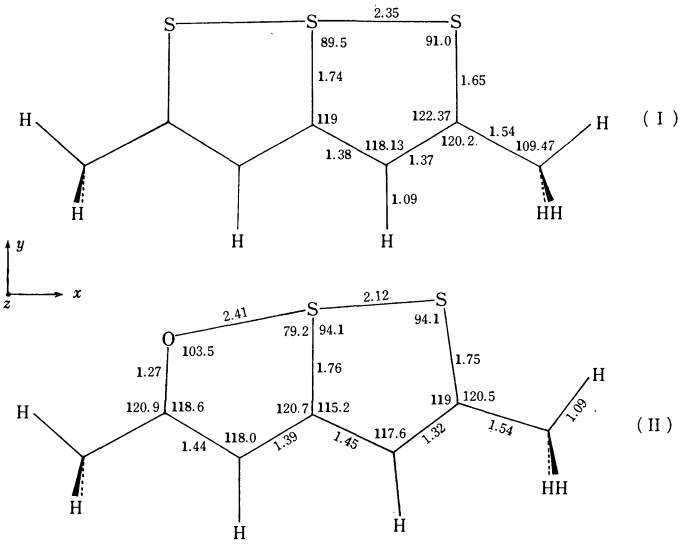

Fig. 1. Bond angles (in degree), bond lengths (in Å) employed and coordinate axis of Thiothiophthene (I) and 2,5-dimethyl-dithiofurophthene (II).

the UV, IR, and NMR techniques.[4-12] Some reviews[13] of these compounds have been presented. According to Bezzi *et al.*[1-3] the two end sulfur atoms of thiothiophthene are equivalent, judging from the results of X-ray analysis.*4 The S–S bond length is 2.36 Å, greater than that of 2.00—2.10 Å in disulfides, but less than the sum of the van der Waals radii of 3.07 Å between two sulfur atoms.[13] The C–C bonds are all in the 1.37—1.38 Å range, the bond length of aromatic double bonds. This compound was considered to exhibit a 'no-bond' resonance,[1] which confers an aromatic character on the rings, this is in agreement with the properties of the substance[3] (see Fig. 2).

In Compound II[2,13], the S–S distance of 2.12 Å is the normal bond length, suggesting a contribution by structure IIa of Fig. 2. However, the S–O distance*5 of 2.41 Å is halfway between the normal S–O single bond length and the sum of the van der Waals radii of the sulfur and oxygen atoms.[13] This compound shows no lines of anormal shift for CO-CH_3 protons in its NMR[4,5] spectrum, and it lacks infrared carbonyl absorption.[6,12] The absence of a ketonic character can be accounted for by the polarized structure of IIb. Bezzi *et al.* established that the essential features characterizing thiothiophthene were present in Compound II, but to a small extent; therefore, the actual electronic distribution is best represented by the formula IIa in Fig. 2.

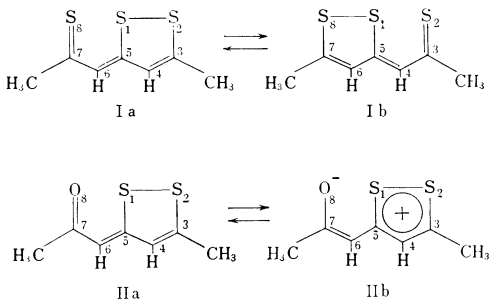

Fig. 2

As for the theoretical investigation of these molecules, a simple LCAO MO calculation of the electronic structure, including only the *p* orbitals, was carried out by Giacometti;[14] they mentioned that

4) H. G. Hertz, G. Traverso and W. Walter, *Ann. Chem.*, **625**, 43 (1959).

5) G. Pfisfer-Gillouso and N. Lozach, *Bull. Soc. Chim. Fr.* **1964**, 3254.

6) E. Klingsberg, *J. Org. Chem.*, **31**, 3489 (1966).

7) H. Behringer, M. Ruff and R. Wiedenmenn, *Chem. Ber.*, **97**, 1732 (1964).

8) H. Behringer and D. Weber, *ibid.*, **97**, 2567 (1964).

9) H. Behringer and R. Wiedenmann, *Tetrahedron Lett.*, **1965**, 3705.

10) E. Klingsberg, *J. Org. Chem.*, **31**, 3489 (1966).

11) R. J. S. Beer, D. Cartwright and D. Harris, *Tetrahedron Lett.*, **1967**, 953.

12) G. Claeson and J. Pedersen, *ibid.*, **1967**, 3283.

13) a) W. G. Salmond, *Quart. Rev.*, **22**, 253 (1968); b) H. A. Bent, *Chem. Rev.*, **68**, 587 (1968); c) E. Klingsberg, *Quart. Rev.*, **23**, 537 (1969).

*4 Recently there have been several discussions of the question of whether or not the S–S spacing is equal (Ref. 13(c)).

*5 A heterocycle with a very short (2.034 Å) S...O intermolecular distance has been reported (P. L. Johnson and I. C. Paul, *J. Amer. Chem. Soc.*, **91**, 781 (1969)).

14) G. Giacometti and G. Rigatti, *J. Chem. Phys.*, **30**, 1633 (1959).

the abnormal bond lengths can be interpreted. Later Maeda[13,15] reported that the S–S–C bond angles and the S–S bond lengths of Compound I can be understood by considering the system to be bicyclic and the central sulfur atom to be quadrivalent, judging from the *p–d* hybridization. Gleiter and Hoffmann[16] regarded the bonding in Compound I as an electron-rich, three-centered bond.[6] Very recently theoretical work on Compound I and its analogues has been reported by Johnstone *et al.*[17] They observed the I_p and UV spectra and made a semi-empirical SCF LCAO calculation of the π electron system. However, no MO calculation including all the valence σ and π electrons has yet been made, as far as we know.

Previously we investigated the electronic structure and the interaction of the lone pair of the sulfur atom of trimethylene disulfide, $(CH_2)_3S_2$,[18] which is a five-membered cyclic disulfide. It seemed that it would be interesting to know the interaction of the lone pair of the S···S···S system of Compound I and to compare it with the S–S system of trimethylene disulfide. Futhermore, compound I has a fused form of five-membered cyclic disulfides, and its electronic structure has been calculated before.[18] On the other hand, the S···S interaction of compound I and the S···O interaction of Compound II have the character of a transannular interaction. It seemed that there would be some value in obtaining the amount of such an interaction in terms of the bond order and in comparing it with the value obtained previously in our MO calculation of the transannular interaction.[19] This S···S···S interaction of Compound I is also interesting as a form of reaction intermediate.[20] Though the UV spectra of Compound I[7] and its analogues[8,9] have been observed, an interpretation of them based on MO calculations has been tried for only an electron system.[17]

Under these circumstances, we calculated the electronic structures of Compounds I and II by the semi-empirical ASMO SCF method,[21],*6 taking into account all the valence and electrons, but excluding the contribution of the *d* orbitals of the sulfur. The bond lengths and bond angles exployed here are shown in Fig. 1; they were taken from the work by Bezzi *et al.*,[1] but slightly modified.

Results and Discussion

Population Analysis of Thiothiophthene. In the present treatment, the following E_{AB} value[21] is used instead of the bond order:

$$E_{AB} = \sum_{r}^{\text{on A}} \sum_{s}^{\text{on B}} P_{rs}(H_{rs}+F_{rs})$$

where H_{rs} is the core resonance integral,[21] where F_{rs} is the Fock's operator, and where $\sum_{r}^{\text{on A}}$ denotes

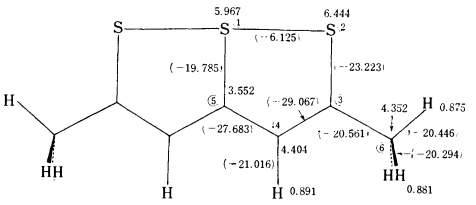

Fig. 3. Atomic density and E_{AB} value (eV) of thiothiophthene (I).

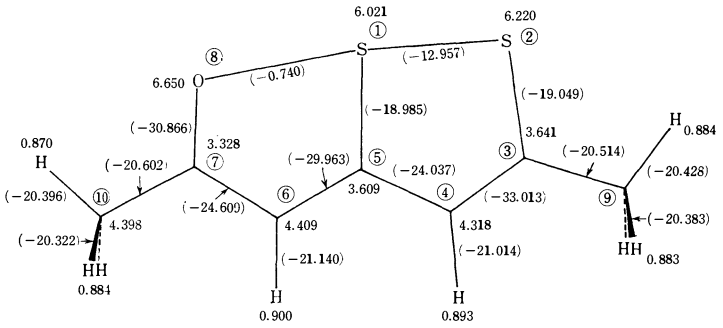

Fig. 4. Atomic density and E_{AB} value (eV) of 2,5-dimethyl-dithiofurophthene (II).

15) K. Maeda, This Bulletin, **33**, 1466 (1960).
16) R. Gleiter and R. Hoffmann, *Tetrahedron*, **24**, 5899 (1968).
17) A. W. Johnstone and S. D. Ward, *Theor. Chim. Acta* (Berl), **14**, 420 (1969).
18) H. Yamabe, H. Kato and T. Yonezawa, "Electronic Structure of Lone Pairs. II. Disulfides and Acylthiol" (to be published in This Bulletin).
19) H. Yamabe, H. Kato and T. Yonezawa, "Electronic Structure of Lone Pairs. IV. Transannular interaction of Some Mesocycles" (to be published in This Bulletin).
20) A. Fava, A. Iliceto and E. Camera, *J. Amer. Chem. Soc.*, **79**, 833 (1956).
21) T. Yonezawa, H. Konishi and H. Kato, This Bulletin, **42**, 933 (1969); Symposium on the electronic structure of molecules, Hokkaido, October, 1967.
*6 In the previous calculation of the cyclic disulfides (Ref. 18), the value of the orbital exponents was evaluated by Slater's rule. In the present work, the exponents by Clementi *et al.* are adopted (Ref. 21).

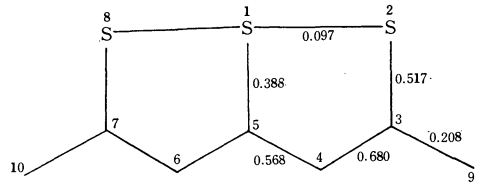

Fig. 5. π Bond orders of thiothiophthene (I).

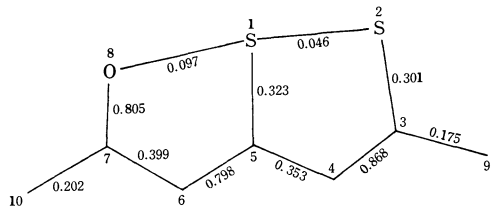

Fig. 6. π Bond orders of 2,5-dimethyl-dithiofurophthene (II).

Table 1. Atomic orbital density of thiothiophthene

S_1s	1.838	C_3s	1.116	C_5s	1.109
x	0.914	x	0.900	x	0.942
y	1.350	y	0.838	y	0.785
z	1.866	z	0.659	z	0.716
S_2s	1.773	C_4s	1.091	C_6s	1.008
x	1.588	x	0.968	x	1.074
y	1.295	y	1.035	y	1.136
z	1.789	z	1.310	z	1.135

Table 2. Atomic orbital density of 2,5-dimethyl-dithiofurophthene

S_1s	1.771	C_5s	1.125	C_8s	1.814
x	1.022	x	0.915	x	1.928
y	1.322	y	0.782	y	1.423
z	1.905	z	0.787	z	1.484
S_2s	1.755	C_6s	1.108	C_9s	1.001
x	1.190	x	0.994	x	1.052
y	1.355	y	1.030	y	1.131
z	1.920	z	1.276	z	1.140
C_3s	1.123	C_7s	1.106	$C_{10}s$	1.008
x	0.916	x	0.837	x	1.119
y	0.787	y	0.710	y	1.141
z	0.815	z	0.675	z	1.131
C_4s	1.095				
x	0.979				
y	1.026				
z	1.218				

the summation over all the valence AO's belonging to the A atom. The atomic density and the E_{AB} value of Compound I are shown in Fig. 3, and those of Compound II, in Fig. 4. The π bond orders of Compounds I and II are shown in Figs. 5 and 6 respectively. The atomic orbital (AO) density of Compound I is given in Table 1, and that of Compound II, in Table 2.

First we will discuss the electron density of thiothiophthene. From the value of the atomic density of Fig. 3, three sulfur atoms of Compound I polarize $\bar{S}$–$\bar{S}$–$\overset{+}{S}$. The AO densities of the p_z orbital of the S_1 and S_2 atoms, which constitute a MO of the π type with the p_z orbitals of the carbon atoms, are 1.866 and 1.789.*[7] In the limiting structure of Ia in Fig. 2, 5 electrons are offered formally to the π orbital from three sulfur atoms, namely, two lone pairs from the central sulfur S_1 atom and the S_2 atom, and a p_z electron from the S_8 atom. If this contribution of the S_2 and S_8 atoms is replaced mutually, a similar relation is seen in the structure I_b. The summation of the AO densities of the p_z AO of the three sulfur atoms, 5.444, nearly equals the above-mentioned value of 5. The excess electrons of 0.444 are drawn mainly from the electron of the carbon (see Table 1). Four electrons from the three sulfuratoms contribute formally to the S···S···S p_σ bond of I_a, namely two p_x electrons from the S_1 and S_2 atoms, and a lone pair (p_x) from the S_8 atom. The summation of the AO densities of the p_x AO's is 4.090; it agrees with the above value, 4.0. The AO densities of the p_x AO of the S_2 and S_8 atoms are both 1.588. This value is reasonable, because the offered electrons from the S_2 atom and S_8 atoms are formally 3.0. As the electron density of the p_y AO of the S_1 and S_2 atoms is considerably larger than 1.0, and as that of the C_3 or C_5 atom is smaller than 1.0, the electrons of the S–C p_σ bond can be said to depend much on the sulfur atom. Judging from the E_{AB} value between the S_1 and the S_2 atoms (−6.125 eV), the S···S bond is considerably weaker than the other bonds, while it should be much stronger than the usual transannular interaction.*[7] However, this interaction may be considered to be a sort of transannular interaction, in an extended sense, between the p_x orbital (a pseudo lone-pair orbital) of the S_2 atom and the central atom S_1. Otherwise, it can be regarded as a sort of intramolecular nucleophilic interaction of the p_x orbital of the S_2 to the S_1–S_8 bond. As will be shown later, in Table 5, the MO coefficient of $S_2(x)$ in HO and those of $S_1(x)$ and $S_8(x)$ in LV are large. On the other hand, in our previous calculation of trimethylene disulfide(five-membered ring), we found that the nucleophilic interaction takes place in the direction of the S–S bond. This type of interaction should play an important role in the formation of a nucleophilic intermediate,[20] such as RS–S–SR. The symmetric property of a molecule, such as compound I and RS–S–SR about the central S–C bond will stabilize this interaction to a great extent.

Population Analysis of 2,5-Dimethyl-dithiofurophthene. Next let us discuss the electron den-

sity of compound II, in which the symmetry of the S···S···S bond of the compound I is disturbed. Some electronic properties of the compound II which are different from those of I are observed in our calculation, but there are similarities as well. In view of the atomic density shown in Fig. 4, the O_8, S_1 and S_2 atoms can all be said to be electronegative, but the central sulfuratom, S_1 is most electron-poor, much like compound I. The AO densities of the p_z AO of the S_1 and the S_2 atoms are 1.905 and 1.920, which form a lone pair of the p type and which constitute a π MO with the other

TABLE 3. TRANSITION ENERGIES (eV) AND TRANSITION MOMENTS OF THIOTHIOPHTHENE

Transition	Type of transition	Transition energies			Transition moment M and its components			
		Calcd	Obsd[8]	Obsd (der)[8]	m	$m(x)$	$m(y)$	$m(z)$
2→2*	π-$\pi^*(B_2)$[a]	3.84	~2.38	~2.92	1.483	1.483	0.000	0.000
1→1*	σ-$\sigma^*(B_2)$[a]	4.26	~4.55	~6.02	2.069	2.069	0.000	0.000
3→2*	π-$\pi^*(A_1)$	5.40	—	—	0.936	0.000	0.936	0.000

Obsd(der): The observed value of phenyl derivative, which is estimated from the absorption spectra of Fig. 7 (Ref. 8).

a) The matrix element between these two transitions, π-$\pi^*(B_2)$ and σ-$\sigma^*(B_2)$, is large(−1.197 eV). This indicates a possibility of large mixing and no separability of the transitions of the two types. Including 2 excitations for B_2, 4 excitations for A_1 and 3 excitations for B_1, the CI calculation does not give better results. The exctitations with higher energies being included, the better results will be expected.

TABLE 4. TRANSITION ENERGIES (eV) AND TRANSITION MOMENTS OF 2,5-DIMETHYL-DITHIOFUROPHTHENE

Transition	Type of transition	Transition energies		Transition moment M and its components			
		Calcd	Obsd(der)[8]	m	$m(x)$	$m(y)$	$m(z)$
1→2*	π-$\pi^*(A')$[a]	4.15	~3.27	1.305	1.223	0.456	0.000
2→1*	σ-$\sigma^*(A')$[a]	4.88	~5.04	0.759	0.726	0.222	0.000
3→2*	π-$\pi^*(A')$	5.77	—	0.794	0.457	−0.649	0.000

Obsd(der): The observed value of phenyl derivative, which is estimated from the absorption spectra of Fig. 7 (Ref. 8).

a) The matrix element between these two transition, π-π^*(A′) and σ-σ^*(A′) is not so large (0.476 eV). After the CI calculations including seven (A′) excitations, the transition energies and transition moments of π-π^*(A′) and σ-σ^*(A′) transitions become as follows:

π-π^* 3.83 eV: m=0.778, $m(x)$=0.74782, $m(y)$=0.21326, $m(z)$=0.00000

σ-σ^* 5.02 eV: m=1.123, $m(x)$=0.93344, $m(y)$=0.44116, $m(z)$=0.00000

Transition energies considerably approach to the observed values, but the relative intensity become inverse to the observation in Fig. 7.

TABLE 5. ENERGY LEVELS (eV) CONCERNING TO THE TRANSITIONS OF TABLE 3 AND ORBITAL COEFFICIENTS[a] OF THIOTHIOPHTHENE

No of level	$3(b_1)$	$2(a_2)$	$1(a_1)$	$1^*(b_2)$	$2^*(b_1)$
Energy (eV)	−11.178	−9.727	−8.926	−1.576	−1.418
Type	π	π	σ	σ^*	π^*
MO Coefficient	$S_1(z)$ 0.647		$S_1(s)$ −0.265	$S_1(x)$ 0.731	$S_1(z)$ 0.238
			$S_1(y)$ −0.157		
	$S_2(z)$ −0.434	$S_2(z)$ −0.442	$S_2(x)$ −0.626	$S_2(s)$ −0.123	$S_2(z)$ −0.245
				$S_2(x)$ 0.440	
	$C_3(z)$ −0.230	$C_3(z)$ 0.174			$C_3(z)$ 0.482
		$C_4(z)$ 0.516		$C_4(x)$ 0.100	
	$C_5(z)$ 0.172				$C_5(z)$ −0.572

a) The orbital coefficients larger than 0.1 are shown in this table.

Table 6. Energy levels (eV) concerning to the transitions of table 4 and main orbital coefficients[a] of 2,5-dimethyl-dithiofurophthene

No of level	3(a″)	2(a′)	1(a″)	1*(a′)	2*(a″)
Energy (eV)	−11.140	−9.692	−9.460	−0.915	−0.786
Type	π	σ	π	σ*	π*
MO Coefficient	$S_1(z)$ −0.625	$S_1(s)$ 0.111	$S_1(z)$ 0.375	$S_1(s)$ 0.192	$S_1(z)$ 0.192
				$S_1(x)$ 0.692	
	$S_2(z)$ 0.347	$S_2(x)$ 0.217	$S_2(z)$ −0.403	$S_2(s)$ −0.206	$S_2(z)$ −0.168
				$S_2(x)$ 0.621	
	$C_3(z)$ 0.259		$C_3(z)$ 0.222		$C_3(z)$ 0.541
	$C_4(z)$ 0.170	$C_4(x)$ 0.126	$C_4(z)$ 0.349		$C_4(z)$ −0.216
	$C_5(z)$ −0.204		$C_5(z)$ −0.203		$C_5(z)$ −0.546
		$C_6(x)$ −0.294	$C_6(z)$ −0.571		$C_6(z)$ 0.347
		$C_6(y)$ 0.111			
	$C_7(z)$ 0.257	$C_7(x)$ 0.240			$C_7(z)$ 0.289
	$O_8(z)$ 0.474	$O_8(x)$ −0.752	$O_8(z)$ 0.384		$O_8(z)$ −0.270
	$C_9(z)$ −0.123				
	$C_{10}(z)$ −0.121	$C_{10}(s)$ −0.111			
		$C_{10}(x)$ −0.312			
		$C_{10}(y)$ −0.155			

a) The orbital coefficients larger than 0.1 are shown in this table.

p_z AO's of the C atom and the O atom. From the value of the AO density, the p_x AO of the O atom can be considered to be a lone-pair orbital. The AO densities of the p_x AO's of the S_1 and S_2 atoms are approximately 1.0. This is different from the case of compound I (see Table 1). That is, the resonance between five-membered rings, as in compound I, can not be expected; rather, a nucleophilic interaction (a transannular interaction) between the lone pair of the O_8 atom and the S_1–S_2 bond of the five-membered cyclic disulfide is observed. The E_{AB} value between the S_1 and O_8 atoms in Fig. 4 confirms this. That is, the E_{AB} values of the $O_8\cdots S_1$ and $S_1\cdots S_2$ bonds are −0.740 eV and −12.957 eV respectively. The order of the $O_8\cdots S_1$ interaction seems to be that of a usual transannular interaction*[8,19]; it is ten times as small as the S···S interaction of compound I (Fig. 3). The S–S bond of Compound II is about two times as strong as the S···S interaction of Compound I and about one half as weak as a usual σ bond.

For comparison, an example of the hydrogen bond has been calculated by the same semi-empirical ASMO SCF method,[21] though only the relative value of the E_{AB} value will be discussed. The E_{AB} value corresponding to the hydrogen bond between the oxygen atom, O_I and the hydrogen atom, H_{II}, of the water dimer is found to be −1.493 eV.*[8] From these calculations, the S···O interaction of compound II seems to be weaker than, or approximately equal to, the hydrogen bond.*[9,10] This type and this order of interaction will be important in a catalytic interaction of a biochemical substance, as has been discussed in a previous paper.[19] Some examples may be seen in the literature.[22]

*[7] In the calculation of $(CH_2)_3S_2$, the atomic density of the lone-pair AO of the sulfur atom was almost 2.00 at the various dihedral angles (Ref. 18).

*[8] In our previous calculation of the electronic structure of several mesocycles with transannular interactions, this interaction was found to be −0.5 eV—−1.2 eV in terms of the E_{AB} value. In the extreme conformation, its value was −7.6 eV. However, this value is too large, for the conformation has been revealed as too extreme (Ref. 19).

*[9] The ∠HOH angle is taken as 105°, and a planar configuration of the dimers is adopted. The O–H bond length and the O···O distance are taken to be 0.96 Å and 2.76 Å respectively. The atomic densities and the E_{AB} values, denoted by the parentheses, are calculated to be as follows:

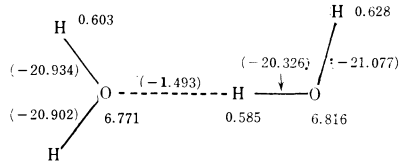

The E_{AB} value, −1.493 eV, of the hydrogen bond is slightly larger than that of the transannular interaction (*7); this is in accordance with the experimental trend. That is, the frequenncy shift of IR caused by the hydrogen bond is about 10 cm^{-1} several hundred cm^{-1}, while that of the transannular interaction reported is about 10 cm^{-1}~20 cm^{-1} (Ref. 19).

*[10] The E_{AB} value of the hydrogen bond varies over some range of values, depending on the kind of hydrogen bond, although only are example of a water dimer is calculated in the present work.

22) "Organic Sulfur Compounds," ed. by N. Kharasch, Pergamon Press (1961), Chap., 9 35, *etc.*; T. C. Bruice, *J. Amer. Chem. Soc.*, **81**, 5444 (1959); T. C. Bruice and B. Holmquist, *ibid.*, **89**, 4028 (1967).

π-Bond Orders. The main bond densities among the p_z orbitals (the π-bond orders) of compounds I and II are shown in Fig. 5 and 6. The π-bond order of the S···S bond of the compound I and those of the S–S bond and the S···O bond of the compound II are not very different. The π character of the C–O bond of Compound II, and conjugation with a π electron system from the C_7 atom to the C_9 atom, hexene, are seen. The S–C bond of the compound I has something of the nature of the single bond. The alternating π-bond order of the hexene is more flattened in the compound I, and the π-bond orders in the ring are averaged out, compared to the compound II.

Electronic Transitions. The calculated transition energies and transition moments are listed in Tables 3 and 4. The energy levels connected with these transitions and the main orbital coefficients are shown in Tables 5 and 6. The levels are numbered from the highest occupied level to the lower levels, and from the lowest unoccupied level, denoted by *, to the higher levels. In Table 6, the highest occupied MO and the next highest occupied MO of the compound II are, approximately, degenerated π and σ orbitals. The contribution of the p_x AO of the oxygen atom (denoted by $O(x)$), which is a lone-pair AO of the oxygen atom to this σ orbital is large. That is, this σ MO has the character of the lone-pair MO. In the π MO's and the π MO's of Table 5 and 6, the coefficients of the $S(z)$ AO's, which are lone-pair-type AO's of the sulfur atom, are comparatively large.

The highest occupied σ orbital of the compound I has a remarkably high energy (-8.926 eV).*11 Though there is a possibility that the inclusion of the $3d$ orbital of the sulfur atom stabilizes the S···S···S interaction, more or less, and lowers the enregy of this σ MO, the highest occupied MO of this compound seems to be higher than that of an ordinary molecule with lone pairs. This may correspond to the very small I_p (7.47 eV) of the Compound I.[17] In Table 5, the main contributions to this σ orbital of the Compound I are shown to be made by $S_1(s)$ AO and $S_2(s)$ AO, which is a pseudo lone-pair AO of the S_2 atom. That is, this orbital has the character of a lone-pair MO and of a S···S···S p_σ bond. Perhaps the reaction in termediate,[20] RS–S–SR, also
R
has such a high energy and becomes very reactive.

The UV spectrum of the Compound I (in cyclohexane and/or dioxane) has been reported,[7] but there is no data on the Compound II in the same solvent. In these calculations, there is an unexpected agreement of the absolute values of the calculated and the observed transition energies, as may be seen in Table 3. Therefore, as the experimental values of the UV spectrum, those of the phenyl derivatives in the same solvent (in acetic acid.[8]) are adopted in making a comparison of the electronic transitions of the Compounds I and II.

The spectra of these derivatives are shown in Fig. 7(Ic[8] and IIc),[8] together with that of the Compound I.[7] In Fig. 7, the spectra of I and Ic show typical electronic absorptions, with a strong peak in the ultraviolet region and a weaker peak in the visual region. That is, the strong peak of the Compound Ic at $\sim$210 mμ[8] and that of Compound I at 273 mμ[7] are characteristic of the S···S···S bond of the series[10] and are shifted, more or less, among them. Another property of these spectra[7,8,10] is that the oxygen compound, IIc, absorbs much more weakly in the ultraviolet region about 250 mμ, and more strongly in the visual region, but at a lower wave length than I and Ic. This feature is also seen in the UV spectra of other derivatives.[10] That is, the spectra of Fig. 7 conform closely to the pattern that is evidently characteristic of the series.[7,8,10]

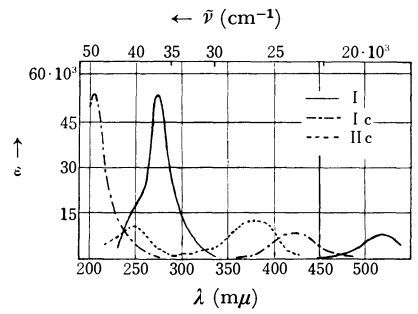

Fig. 7. UV spectra of 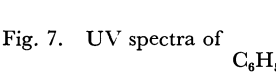 (Ic) (Ref. 8), 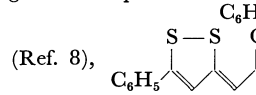 (IIc) (Ref. 8) and 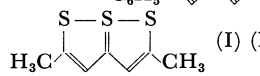 (I) (Ref. 7).

In view of the calculated transition moment, the observed longer wavelength absorption of the Compound I (C_{2v}) may be said to correspond to π–π^* (B_2, 2→2*)-type transition, and the shorter one may be said to be a σ–σ^*(B_2, 1→1*)-type transition, as primary results. However, the matrix element between these π–π^* and σ–σ^* excitations is calculated to be large, -1.197 eV. This indicates the possibility of a large mixing and no separability of the transitions of the two types after the configuration interaction is calculated. Furthermore, the longer wavelength absorption of Compound II (C_{1h}) may correspond to the π–π^*(A', 1→2*)-type transition, and the shorter one may correspond to the σ–σ^*(A', 2→1*) type.*12 The agreement between

*11 No such high energy, higher than -9 eV, of the highest occupied level has ever before been found in our ASMO SCF calculations.

*12 Johnston *et al.* ascribed the absorption to the π–π^* transition only in their semi-empirical SCF LCAO calculation of the π electron system (Ref. 17).

the observed[8] and the calculated transition energies is not very good, but a relatively high intensity of the absorption in the 270(210)mμ region of the Compound I can be obtained in our calculations. This high intensity is caused mainly by the delocalized S···S···S interaction (σ bond character) of the Compound I, as has previously been mentioned. The relative position of the absorption in the visual region of I (Ic) and IIc (that is the fact that IIc absorbs at a lower wavelength), is correctly predicted in these calculations.

The previous semi-empirical ASMO SCF calculation[21] of the electron structure of the cyclic disulfides,[18] neglecting the contribution of *d* orbitals, predicted the main absorption maximum in the UV spectra well. In the present case, however, for quantitative discussions a consideration of the *d* orbitals and of the configuration interaction seems to be necessary.

The calculations were carried out on an HITAC 5020 computer at the Computation Center of the University of Tokyo.

BULLETIN OF THE CHEMICAL SOCIETY OF JAPAN VOL. 43 3761—3765 (1970)

An ESR Study of Intermediates in γ-Irradiated Methylcyclohexane and Isobutane Containing Benzene

Terunobu WAKAYAMA, Tetsuo MIYAZAKI, Kenji FUEKI and Zen-ichiro KURI

Department of Synthetic Chemistry, Faculty of Engineering, Nagoya University, Chikusa-ku, Nagoya

(Received July 6, 1970)

The present work was undertaken in order to examine intermediates from benzene and toluene in γ-irradiated glassy methylcyclohexane (MCH) and polycrystalline isobutane matrices at 77°K. The γ-irradiation of MCH containing low concentrations of benzene gave an ESR spectrum with a good hyperfine resolution, which can be ascribed to the benzene anion, while at higher concentrations of benzene it gave an ESR spectrum with a poor resolution, which is attributable to the benzene monomer and dimer anions. On the contrary, the γ-irradiation of polycrystalline isobutane containing benzene did not yield an ESR spectrum which can be attributed to the benzene anion. However, the γ-irradiation of a mixed glass of isobutane and 4 mol% MCH containing benzene gave an ESR spectrum which is attributable to the benzene anion. The yield of trapped electrons in this system was three times as large as that in pure γ-irradiated MCH. Such a difference in the results between glassy MCH and polycrystalline isobutane matrices gives evidence of a phase effect on the radiolysis of solid hydrocarbon.

In a previous paper,[1] we reported a study of radiation-induced intermediates from toluene in solid isobutane in which the electron spin resonance technique was used. The ESR spectrum observed consisted of five lines, with a splitting constant of 4.2 G; it was ascribed to the toluene anion. These results indicated that toluene has some electron scavenging ability in a hydrocarbon matrix at 77°K. However, γ-irradiated polycrystalline isobutane containing benzene did not give an ESR spectrum which is attributable to the benzene anion. Recently, it was found by optical absorption spectroscopy that a γ-irradiated glassy matrix of 3MP containing low concentrations of benzene yielded the benzene anion and cation, while at higher concentrations of benzene it yielded the dimer anion and cation.[2] We have investigated, by the ESR method, radiation-induced intermediates from benzene in glassy matrices of MCH and of isobutane- 4 mol% MCH, independently of the optical study referred to above. In this paper, we will report the ESR results on the reaction intermediates and will attempt to compare these results with the optical results.

Experimental

The isobutane, methylcyclohexane (MCH), and 3-methylpentane (3MP) were more than 99.9% pure. The gas-chromatographic analysis did not show any detectable impurities. These materials were used after degassing and distillation on a vacuum line. The

1) T. Wakayama, T. Kimura, T. Miyazaki, K. Fueki and Z. Kuri, This Bulletin, **43**, 1017 (1970).

2) A. Ekstrom, *J. Phys. Chem.*, **74**, 1705 (1970).

benzene and toluene (99.9%) were used after vacuum distillation. The nitrous oxide and sulfur hexafluoride were of a high purity, while the cyclohexene was 99.9% pure and was used after vacuum distillation.

The samples were irradiated with γ-rays from Co-60 at a dose rate of 4.2×10^5 rad/hr. The photobleaching of γ-irradiated samples was carried out at 77°K with light from an infrared or tungsten lamp.

The ESR measurements were made on a JES-3BX ESR spectrometer. The G-value of the benzene anions was determined by assuming G(radical)$=1.6$ for radicals produced in γ-irradiated 3MP at 77°K.[3]

Results and Discussion

A) Intermediates Produced at Lower Concentrations of Benzene.

When 0.05 mol% benzene in MCH glass is γ-irradiated at 77°K, a species is formed which displays an ESR spectrum with a good hyperfine resolution. This ESR spectrum consists of five lines whose splitting constant is 3.8 G, and it can be bleached by exposure to infrared light for a few minutes (Fig. 1(A)).

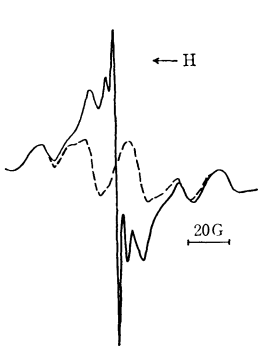

Fig. 1. A

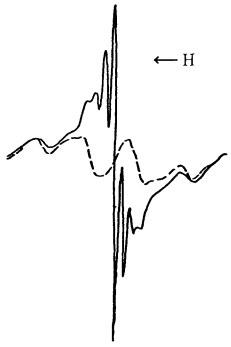

Fig. 1. B

A) ESR spectrum of γ-irradiated MCH containing 0.05 mol% benzene at 77°K.
——, after γ-irradiation.
------, after 5 min illumination with infrared light.
Dose, 1.7×10^5 rad.
B) ESR spectrum of γ-irradiated MCH containing 0.05 mol% benzene and 1.0 mol% cyclohexene at 77°K.
——, after γ-irradiation.
------, after 5 min illumination with infrared light.
Dose, 1.7×10^5 rad.

As the benzene concentration in MCH matrix is increased, the intensity of the five-line spectrum at first increases, and then reaches a plateau at 0.05 mol% benzene concentration (Fig. 2).

In order to determine whether the species produced in γ-irradiated MCH containing benzene is the benzene anion or the benzene cation, we used SF_6 and N_2O as electron scavengers, and cyclohexene as a cation scavenger. Since the hyperfine splitting constants for the benzene anion and cation have been reported to be 3.75[4] and 4.2 G[5] respectively, it is difficult to distinguish between the anion and the cation by their ESR spectra under our experimental conditions.

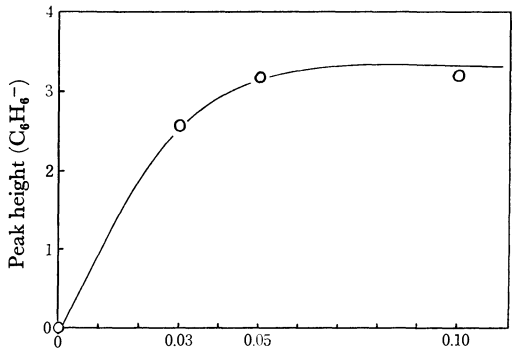

Fig. 2. Effect of benzene concentration in MCH glass on the yield of the benzene anion at 77°K.
Dose, 1.7×10^5 rad.

It is known that when olefin is added to hydrocarbon matrices, the yield of trapped electrons in γ-irradiated hydrocarbons increases.[6] Such a result was obtained for γ-irradiated MCH containing cyclohexene in the present study (Fig. 3). Cyclohexene may stabilize trapped electrons, since a charge transfer from MCH to cyclohexene would suppress cation-electron recombination by trapping the positive charge.

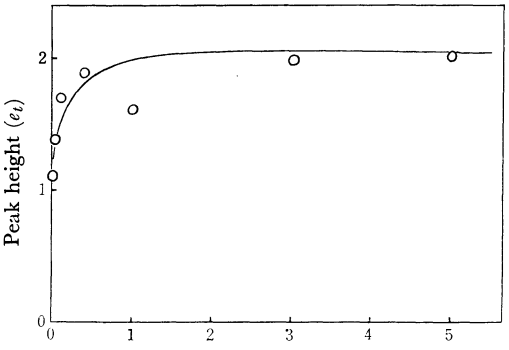

Fig. 3. Effect of cyclohexene concentration in MCH glass on the yield of the trapped electron at 77°K.
Dose, 1.7×10^5 rad.

3) M. Shirom and J. E. Willard, *J. Phys. Chem.*, **72**, 1702 (1968).

4) S. P. Solodovnikov, *Zh. Strukt. Khim.*, **2**, 282 (1961).

5) J. R. Bolton, A. Forman and L. E. Orgel, *Mol. Phys.*, **5**, 43 (1962).

6) M. Irie, K. Hayashi, S. Okamura and H. Yoshida, *J. Chem. Phys.*, **48**, 922 (1968).

$$MCH \rightsquigarrow MCH^+ + e^- \quad (1)$$

$$MCH^+ + C_6H_{10} \longrightarrow MCH + C_6H_{10}^+ \quad (2)$$

When 0.05 mol% benzene in MCH glass containing 1.0 mol% cyclohexene as a cation scavenger is γ-irradiated at 77°K, a species is formed which displays an ESR spectrum with a good resolution (Fig. 1(B)). This spectrum consists of seven lines, and its splitting constant is 3.8 G. It can be bleached by exposure to infrared light for a few minutes.

γ-Irradiated MCH containing 0.07 mol% benzene and 0.07 mol% SF_6 displays a very different ESR spectrum from that of γ-irradiated MCH containing 0.07 mol% benzene and 0.4 mol% SF_6 (Fig. 4(A)). The former spectrum has a seven-line component with a hyperfine splitting constant of 3.8 G and is attributed to the benzene anion, while the latter does not have a seven-line component and indicates only MCH radicals. This result can be interpreted in terms of the following competitive reactions:

$$e^- + C_6H_6 \longrightarrow C_6H_6^- \quad (3)$$

$$e^- + SF_6 \longrightarrow SF_6^- \quad (4)$$

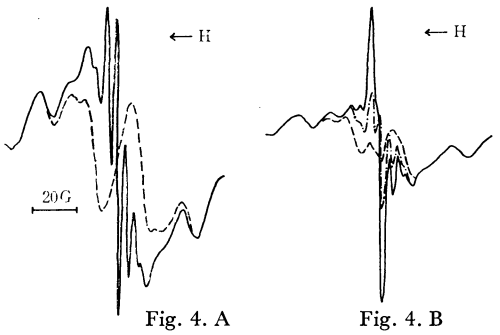

Fig. 4. A Fig. 4. B

A) ESR spectrum of γ-irradiated MCH containing 0.07 mol% benzene in the presence of SF_6 at 77°K.
——, 0.07 mol% SF_6.
------, 0.4 mol% SF_6.
B) ESR spectrum of γ-irradiated MCH containing 0.07 mol% benzene and 0.07 mol% N_2O at 77°K.
——, after γ-irradiation.
-·-·-, after 1 sec illumination with infrared light.
------, after 40 sec illumination with infrared light.
Dose, 1.7×10^5 rad.

Figure 4(B) shows the ESR spectrum, obtained after γ-irradiation, of MCH, containing 0.07 mol% benzene and 0.07 mol% N_2O, as an electron scavenger. The center line in the spectrum may be ascribed to the electron trapped near the N_2O superimposed on the spectrum of the benzene anion and the solvent radical. The narrow side lines are due to the benzene anion. The center line does not saturate so easily upon an increase in the microwave power as does the trapped electron in pure MCH. A similar result is obtained upon microwave saturation and the photobleaching of the trapped electron (ESR singlet with $\Delta H_{ms1}=4.1$ G) produced in MCH containing N_2O.[7] The ESR spectra obtained by illuminating the preceding sample with infrared light for 1 sec and for 40 sec are shown in Fig. 4(B). As can be seen in Fig. (4B), the spectrum of the trapped electron decreases remarkably in intensity upon illumination, while that of the benzene anion does not change very much. This result indicates that the trapped electron can be photobleached more efficiently than the benzene anion.

Thus, the seven-line spectrum may be attributed to the benzene anion, and the *G*-value of the benzene anion in MCH containing 0.05 mol% benzene and 1.0 mol% cyclohexene is 1.3. This value is in accordance with the *G*-value of the biphenyl anion in a γ-irradiated hydrocarbon containing biphenyl.[8] The results presented above indicate that benzene has some electron scavenging ability at low concentrations.

B) Intermediates Produced at Higher Concentrations of Benzene.

When 3MP glass, MCH glass, or isobutane-4 mol% MCH glass containing 5 mol% benzene is γ-irradiated at 77°K, a species is formed which displays an ESR spectrum with a poor resolution. This ESR spectrum has a hyperfine splitting constant of 3.8 G, and it can be bleached by exposure to infrared light for a few minutes (Fig. 5(A)). The formation of this species is suppressed by the presence of N_2O as an electron scavenger in 3MP. On the contrary, the species produced in MCH is not suppressed by the presence of 1 mol% N_2O or SF_6, and in this case the ESR spectrum can not be

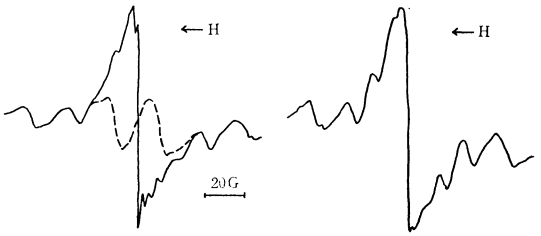

Fig. 5. A Fig. 5. B

A) ESR spectrum of γ-irradiated MCH containing 5 mol% benzene at 77°K.
——, after γ-irradiation.
------, after 5 min illumination with infrared light.
B) ESR spectrum of γ-irradiated MCH containing 5 mol% benzene and 1 mol% N_2O at 77°K.
Dose, 1.7×10^5 rad.

7) A similar effect of N_2O on the trapped electron in 3-methylhexane was reported by Yamazaki *et al.* at the 22nd Annual Meeting of the Chemical Society of Japan, 1969, Tokyo, Japan.

8) J. Lin, K. Tsuji and F. Williams, *J. Amer. Chem. Soc.*, **90**, 2766 (1968).

bleached by exposure to a tungsten light (Fig. 5(B)).

These results suggest that an anion is produced in γ-irradiated 3MP, MCH, and isobutane- 4 mol% MCH containing 5 mol% benzene, while the species produced in γ-irradiated MCH containing 5 mol% benzene and 1 mol% N_2O or SF_6, is a cation. Recently Ekstrom suggested, in an optical absorption study, that the species produced in γ-irradiated 3MP could be attributed to the benzene monomer anion and cation, or to the benzene dimer anion and cation, depending on the benzene concentration. We would also like to suggest that the ESR spectra obtained at higher concentrations of benzene in the hydrocarbons may be ascribed to the benzene monomer and dimer anions, while the species produced in γ-irradiated MCH containing 5 mol% benzene and 1 mol% electron scavengers may be ascribed to the benzene monomer and dimer cations. Our results indicate that the dimer anion is formed at benzene concentrations above about 1 mol%, a value which is in good agreement with the optical values.[2)]

TABLE 1. EFFECTS OF THE HYDROCARBON MATRIX ON THE FORMATION OF BENZENE AND TOLUENE ANIONS

	Benzene	Toluene
MCH	Benzene anion	No
Isobutane	No	Toluene anion
Isobutane- 4 mol% MCH	Benzene anion	Toluene anion

C) Effects of the Hydrocarbon Matrix on the Formation of Benzene and Toluene Anions.

Table 1 shows the anionic species produced in γ-irradiated hydrocarbon matrices (MCH, isobutane, and isobutane- 4 mol% MCH) containing 3 mol% benzeene or toluene at 77°K. The benzene anion is produced in a MCH matrix, but not in an isobutane matrix. On the contrary, the toluene anion is produced in an isobutane matrix, but in a MCH matrix. Both the benzene and toluene anions, however, can be produced in a mixture of isobutane- 4 mol% MCH.

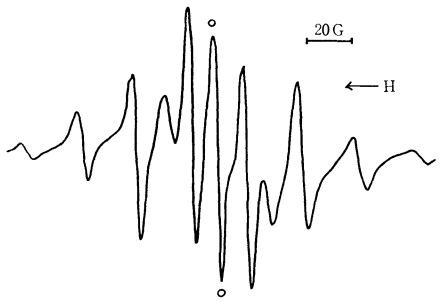

Fig. 6. ESR spectrum of γ-irradiated isobutane- 4 mol% MCH at 77°K. ○ represents a signal of the trapped electron.
Dose, 0.7×10^5 rad.

It is found by ESR measurements that the species produced in γ-irradiated pure isobutane, which is polycrystalline at 77°K, is the isobutyl radical, while the species produced in a γ-irradiated mixture of isobutane- 4 mol% MCH, which is glassy at 77°K, consists of the isobutyl and t-butyl radicals and trapped electrons (Fig. 6). The yield of t-butyl radicals in this system is much greater than that of isobutyl radicals, and the yield of trapped electrons in a γ-irradiated mixture matrix is three times as large as that in γ-irradiated pure MCH.

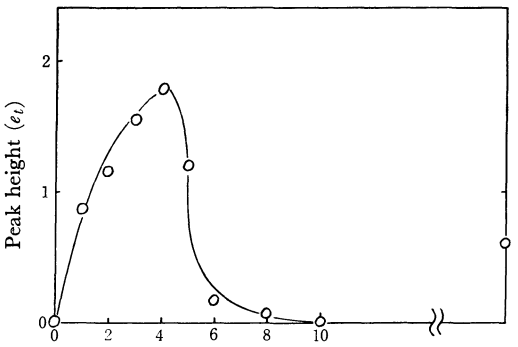

Fig. 7. Effect of MCH concentration in isobutane on the yield of the trapped electron at 77°K.
Dose, 0.7×10^5 rad.

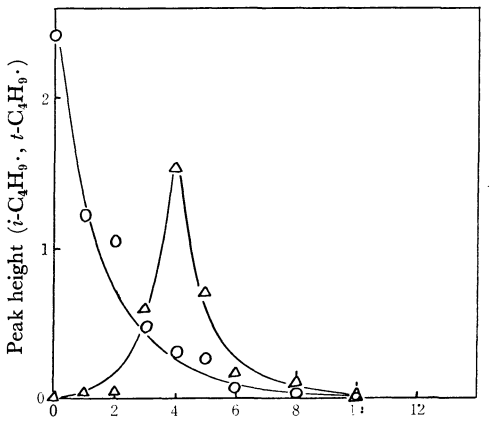

Fig. 8. Effect of MCH concentration in isobutane on the yields of the i-butyl radical and of the t-butyl radical at 77°K.
○, isobutyl radical. △, t-butyl radical.
Dose, 0.7×10^5 rad.

Figures 7 and 8 show the dependence of the yields of trapped radicals and electrons on the concentration of MCH. As the concentration of MCH in isobutane is increased, the yields of both t-butyl radicals and trapped electrons increase, while the yield of isobutyl radicals decreases. The yields of t-butyl radicals and trapped electrons decrease in the range of MCH concentrations above

4 mol%, where the matrix becomes so soft that the radicals and electrons are not trapped in the matrix. As the concentration of MCH increases, the matrix becomes glassy, so benzene and toluene dissolve easily in the matrix; both the benzene and toluene anions may be trapped in an isobutane-4 mol% MCH mixture.

Accordingly, the results presented above indicate that the viscosity of a matirx has an important influence upon the formation of trapped anions, cations, electrons, and radicals in the matrix.

BULLETIN OF THE CHEMICAL SOCIETY OF JAPAN VOL. 43 3765—3773 (1970)

The Interaction of Oxygen with Organic Molecules. III.[1] Electron Transfer between Oxygen and Aromatic Amines Studied by Flash Technique

Mitsufusa HORI,[2] Hiroyasu ITOI and Hiroshi TSUBOMURA

Department of Chemistry, Faculty of Engineering Science, Osaka University, Toyonaka, Osaka

(Received July 6, 1970)

Flash photolysis of aniline derivatives in various solutions has been studied in oxygenated and deoxygenated conditions. Absorption spectra of the triplet states appeared in deoxygenated liquid paraffin solutions, but no transient absorption was observed in the oxygenated liquid paraffin solutions. Transient spectra, due to the cations of the anilines, were observed in deoxygenated ethanol solutions, but none in oxygenated ethanol. In highly polar solvents — acetonitrile, water, and formamide — either deoxygenated or oxygenated, the cation was observed. In the case of oxygenated solutions, the initial yield of the cation was found to be proportional to the intensity of the flash light, indicating that the ionization is a one-photon process. These results, together with the previous findings that the photo-ionization of organic molecules in solutions are caused by the two-step, biphotonic excitation processes strongly suggest that the charge transfer states are formed between the aromatics and the oxygen molecule, either by direct excitation or *via* the interaction of excited anilines and the ground state of oxygen, and the charge transfer states then lead to the solvated cations and anions in highly polar solvents. The decay of the ions have been found to follow the second order kinetics.

Oxygen molecule is known for its various special actions on the photochemical behaviors of organic molecules, such as quenching of phosphorescence and fluorescence, photo-oxidation, and enhancement of T←G transition (transition from the ground state to the lowest triplet state). It is also known that oxygen induces absorption spectra in ultraviolet or visible regions when dissolved in various organic solvents. The absorption has been attributed to a type of contact charge transfer absorption by Evans,[3] and Tsubomura and Mulliken.[4] This theory assumes the existence of charge transfer (CT) excited states between oxygen and organic molecules, where oxygen acts as the electron acceptor. Tsubomura and Mulliken explained the mechanism of enhanced intercombination between singlet and triplet states using this concept of CT states.

Although the assumption of these CT states is consistent with all known experimental observations, more evidence to verify the CT nature of the excited states is desirable. Measurement of the dipole moments of the excited states and other experiments to show the highly polar nature of the excited states are, however, very difficult in this case, because of the non-fluorescent nature of the CT states.

Some years ago, Leonhardt and Weller[5] showed that flash excitation of a solution of perylene and *N,N*-dimethylaniline in a polar solvent leads to the transient formation of perylene anion. They proposed that the perylene anion and the aniline cation were formed from a CT excited state where perylene acts as an acceptor and aniline a donor. We have

1) Part II. of this series: E. Ishida, H. Takahashi and H. Tsubomura, This Bulletin, **43**, 3130 (1970).

2) Central Research Laboratory, Fuji Electric Co., Ltd., Nagasaka, Yokosuka.

3) D. F. Evans, *J. Chem. Soc.*, **1961**, 1987, and other papers preceding it.

4) H. Tsubomura and R. S. Mulliiken, *J. Amer. Chem. Soc.*, **82**, 5966 (1960).

5) H. Leonhardt and A. Weller, *Z. Phys. Chem. N. F.*, **29**, 277 (1961); *Ber. Bunsenges. Phys. Chem.*, **67**, 791 (1963).

obtained similar results for other organic donor-acceptor systems and shown that such transient formation of ionic species after the CT interaction is a general phenomena.[6,7]

It should be pointed out here that the formation of a CT state may not be a prerequisite for the appearance of ionic species in polar solutions, because ionic species may be formed either by spontaneous ionization from a charge transfer state or by photo-ejection of electrons (which will be discussed later in this article) followed by capture of the electron by electron acceptors. We thought that it was important to study the photochemical behavior of oxygen and organic substances under flash illumination, and to find more detailed mechanism of the formation of transient ionic species.

In order to clarify the role of oxygen in photo-ionization processes involving aromatic donor molecules, it was necessary to study whether photo-ionization could occur in solutions containing only aromatic compounds and no oxygen. It has been well established that many aromatic hydrocarbons and amines are photo-ionized in solutions. In cases where the exciting radiation contains only near-ultraviolet or visible light, the photo-ionization in low temperature matrix occurs by the two-step excitation, *via* the lowest triplet states of the aromatics.[8] We have found that the two-step ionization takes place not only in non-polar matrix at low temperature but in fairly polar solutions like ethanol[7] at room temperature. The ionic species formed are no doubt stabilized to a great extent in polar solutions. However, we found the photon energy necessary for an effective production of ions to be only a few tenth electron volt smaller than the gas-phase ionization potential of the donor.

In the present work, particular emphasis was laid on the study of the difference in the photochemical behaviors of aromatics in oxygenated and deoxygenated polar solutions.

Potashnik *et al.* reported independently that a spontaneous ionization may occur from a charge transfer triplet state of an electron-donor-acceptor pair in a polar matrix.[9] They also studied the photo-ionization of *N,N,N',N'*,-tetramethyl-*p*-phenylenediamine (TMPD) at various oxygen concentrations[10] using a flash technique. Their main conclusion is that the photo-ionization in polar solutions is mainly a bi-photonic process *via* an intermediate whose nature is still not thoroughly understood, and the photo-ionization in less polar solutions is mostly a mono-photonic process due to the interaction of the triplet TMPD and oxidizing impurities.

Experimental

Materials. *N,N*-Dimethyl-*p*-anisidine was recrystallized from 60% ethanol and sublimed in a vacuum. *n*-Hexane was purified by passing through a silica-gel column. Acetonitrile was twice refluxed with phosphorous pentoxide for several hours, followed in each case by fractional distillation. Formamide was kept overnight with anhydrous sodium sulfate and distilled under 30 Torr at *ca.* 130°C. Water was passed through activated charcoal and ion-exchange resin columns. (Specific resistance: 10^6 ohm/cm). Liquid paraffin was purified by passing through a silica-gel column. All other materials used were purified by methods similar to those described in previous papers.

Methods. The concentrations of most of the solutions of aniline derivatives studied were made 0.3—0.5 $\times 10^{-3}$ mol/*l* so as to give optical densities of *ca.* 1 cm^{-1}. The solutions saturated with either one atmosphere oxygen or nitrogen were placed in a cylindrical silica cell, 1.4 cm in diameter and 20 cm in length. The apparatus used for the flash-spectroscopic measurements is mostly the same as that described in our earlier paper.[11] The light of the exciting flash lamps was filtered by an aqueous solution of cobaltous chloride (0.5 gr/c.c.) using a double-wall sample cell, and only the light in the range from 2800 to 3800 Å was passed in order to minimize the effect of scattered light from the exciting flash lamps.

Results

Oxygen-Saturated Solutions. The transient absorption spectra obtained by flash illumination of *N,N*-dimethylaniline (DMA) in acetonitrile solutions saturated with oxygen is shown in Fig. 1. Similar spectra were obtained for aqueous and formamide solutions. In the case of *n*-hexane, liquid paraffin, and ethanol as solvents, no transient spectra were obtained. In a previous paper, it was reported that the photolysis of DMA in low temperature matrices yields the DMA cation and the neutral radical, and a part of the visible spectrum was assigned as the absorption spectrum of the cation.[12] The transient spectra obtained in the present results agree well with this and the species formed is therefore identified to the DMA cation. This conclusion is supported by the fact that this transient spectrum is not found in solvents having relatively low dielectric constants, because unstable

6) K. Kawai, N. Yamamoto and H. Tsubomura, This Bulletin, **42**, 369 (1969).

7) Y. Nakato, N. Yamamoto and H. Tsubomura, This Bulletin, **40**, 2480 (1967), and previous papers cited there.

8) J. Joussot-Dubien and R. Lesclaux, *Compt. Rend*, **258**, 4260 (1964); W. A. Gibbons, G. Porter and M. I. Savadatti, *Nature*, **206**, 1355 (1965); K. D. Cadogan and A. C. Albreacht, *J. Chem. Phys.*, **43**, 2550 (1965).

9) R. Potashnik, C. R. Goldschmidt and M. Ottolenghi, *J. Phys. Chem.*, **73**, 3170 (1969).

10) R. Potashnik, M. Ottolenghi and R. Bensasson, *J. Phys. Chem.*, **73**, 1912 (1969).

11) N. Yamamoto, Y. Nakato and H. Tsubomura, This Bulletin, **39**, 2603 (1966).

12) S. Arimitsu, K. Kimura and H. Tsubomura, This Bulletin, **42**, 1858 (1969).

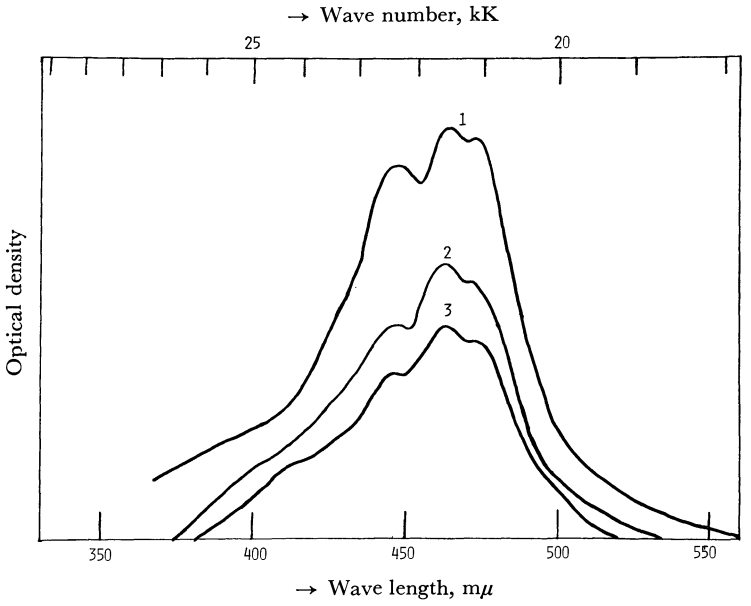

Fig. 1. Transient absorption spectra obtained by flash illumination of *N,N*-dimethylaniline in acetonitrile saturated with oxygen.
Delay time: 1) 8 μsec, 2) 140 μsec, 3) 300 μsec

ionic species like these are only sufficiently stabilized in very polar solvents such as acetonitrile (dielectric constant ε: 37.5), water (ε: 81), and formamide (ε: 109.5), and not in nonpolar solutions or even in ethanol (ε: 24.3). As a further evidence for the formation of DMA cation, we found that a momentary photoconductivity appeared by flash illumination of DMA in these highly polar solutions saturated with oxygen.[13] We also found a weak ESR signal by steady illumination of DMA in acetonitrile

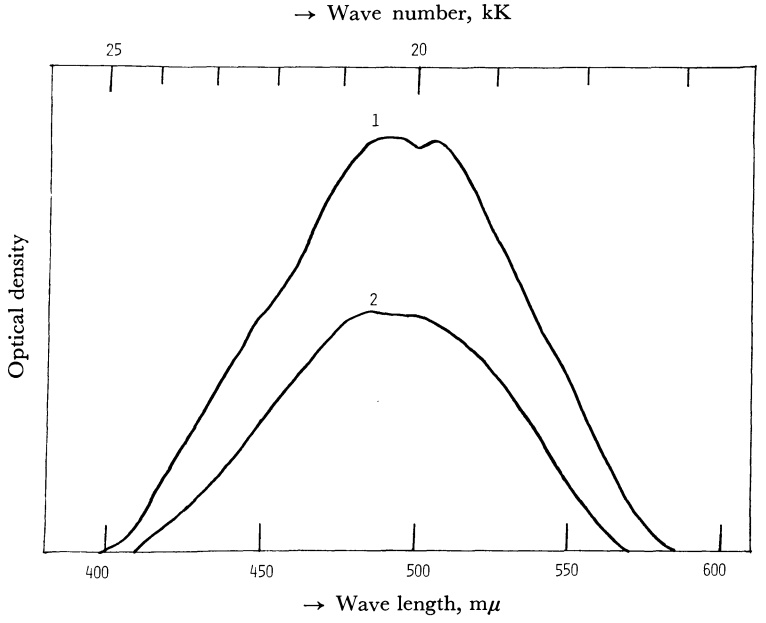

Fig. 2. Transient absorption spectra obtained by flash illumination of *N,N*-dimethyl-*p*-anisidine in acetonitrile saturated with oxygen.
Delay time: 1) 10 μsec, 2) 190 μsec

13) T. Imura, N. Yamamoto and H. Tsubomura, This Bulletin, **43**, 1670 (1970).

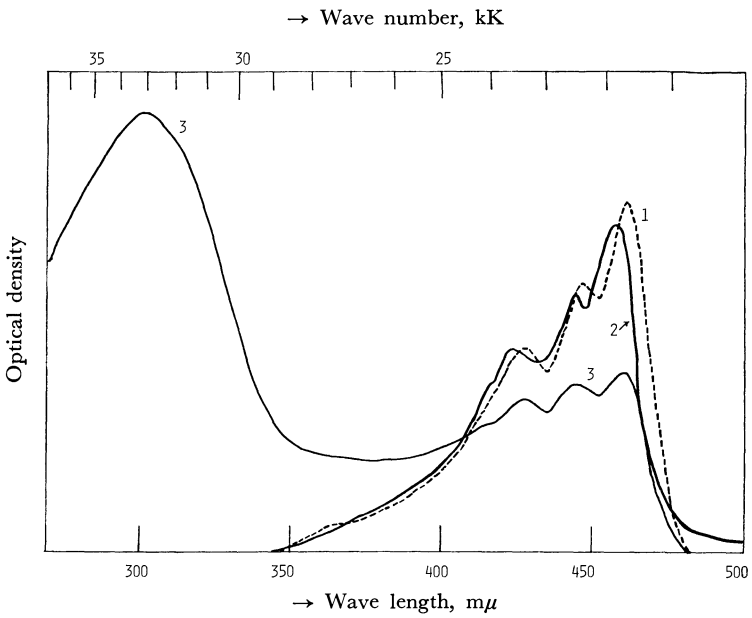

Fig. 3. Transient absorption spectra obtained by flash illumination of benzidine in solutions saturated with oxygen.
1) In ethanol. Delay time: 850 μsec, 2) In acetonitrile. Delay time: 85 μsec. 3) A spectrum obtained by ultraviolet irradiation of benzidine in a (1 : 1) ethanol - ether matrix at 77°K with a 500 W high pressure mercury lamp.

saturated with 1 atmosphere oxygen. It is very interesting that we could not find the absorption spectrum of DMA cation by flash illumination of acetonitrile solutions of DMA saturated with oxygen at 8 Torr and at 20 Torr, discussion on which will be made later in this paper.

In the case of *N*,*N*-dimethyl-*p*-anisidine (DMAN), transient spectra have been observed in acetonitrile, water, and formamide, and not in liquid paraffin or ethanol. As an example, Fig. 2 shows the transient absorption spectrum obtained for the acetonitrile solution. It agrees with that obtained in our laboratory as a result of ultraviolet irradiation of DMAN in the low temperature matrix,[14] and is attributable to that of the cation of DMAN.

In an aqueous solution of DMA or DMAN, a transient band was obtained at 3400 or 4500 Å, respectively, which decayed much faster than the cation spectra. These bands might be assigned to *N*-methylaniline cation and *N*-methyl-*p*-methoxyaniline cation, respectively.

In the case of benzidine, transient absorption spectrum was obtained by flash illumination in ethanol, acetonitrile, water and formamide, and not in liquid paraffin. Absorption spectrum obtained for the case of an ethanol solution is shown in Fig. 3 together with that obtained by the photolysis of benzidine in a low temperature matrix. That the

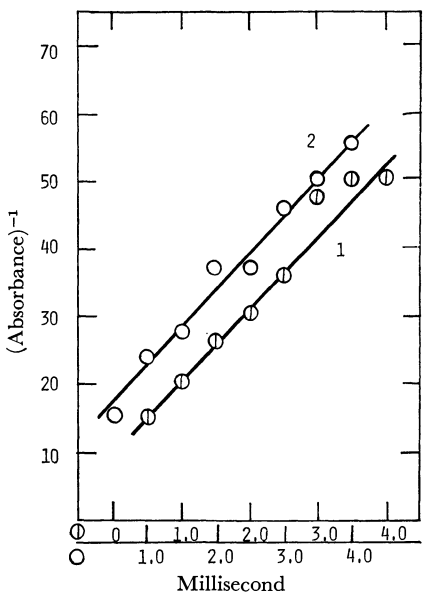

Fig. 4. Plot of reciplocal of absorbance of the cation formed by flash illumination of *N*,*N*-dimethylaniline in oxygenated acetonitrile against time.
1) At a flash with capacitors charged at 11.5 kV.
2) At a flash with capacitors charged at 11.0 kV.

14) K. Kimura, K. Yoshinaga and H. Tsubomura, *J. Phys. Chem.*, **71**, 4485 (1967).

spectrum appearing in the latter is due to the benzidine cation is concluded from the following: 1) The spectrum does not appear by irradiation in a nonpolar matrix. 2) When biphenyl is added in the matrix to be irradiated, the spectrum of biphenyl anion was observed. 3) Thermoluminescence was observed from the irradiated matrix. Agreement between the two spectra clearly shows that benzidine cation was produced by flash illumination of oxygenated benzidine solutions. The result that the cation is formed even in ethanol, contrary to results for DMA and DMAN, is probably related with the lower ionization potential of benzidine compared with the other two.

In the cases of DMA and DMAN in acetonitrile, water and formamide, the decay of the absorption due to the cation formed by flash illumination was found to be second order with respect to the concentration of the cation. As an example, the reciprocal of the absorbance of the cation produced from DMA plotted against time is shown in Fig. 4. By taking the molecular extinction coefficient of the cation at 4600 Å to be 1200,[12] the rate constant of the second order reaction is determined to be as shown in Table 1.

Table 1. Second order decay constants of the cations in various solvents, together with relative viscosities and dielectric constants of the solvents at room temperature

Solvent	Acetonitrile	Water	Formamide
Relative viscosity, centi-poise	0.345	1.00	3.764
Dielectric constant	37.5	80.0	109.0
The second-order decay constant, $10^8 M^{-1}\cdot sec^{-1}$, for *N,N*-dimethylaniline	2.4	0.2	0.7
The same for *N,N*-dimethyl-*p*-anisidine	6.8	7.4	3.0

By extrapolation to zero time, we could obtain the initial cation concentration produced by the flash. Intensity of the flash light can be changed by controlling the voltage applied to the condenser. It was confirmed that the profile of the flash light is fairly constant at all firings of the flash and, therefore, not only the integrated intensity but also the intensity at any stage of a flash is almost exactly proportional to the square of the voltage. Based on these results, the initial concentration of the cation produced was plotted against the flash light intensity. The results for DMA and DMAN are given in Fig. 5. As seen from the figure, the initial concentrations of the cations are proportional to the light intensity for both compounds. For aqueous and formamide solutions, the kinetic data are a little complicated by the formation of other species.

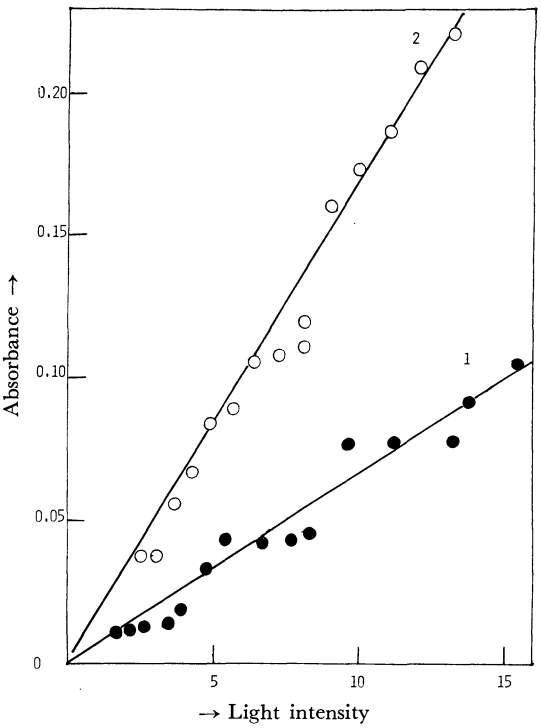

Fig. 5. Plot of initial concentration of the transient cation, in units of absorbance, formed in acetonitrile solutions saturated with oxygen against flash intensity.
1) *N,N*-dimethylaniline, 2) *N,N*-dimethyl-*p*-anisidine.

However, the results obtained show that the decay of the cation in these cases is of the second order and the initial concentration is proportional to the light intensity of the flash.

Deoxygenated Solutions. Flash photolyses of DMA and DMAN have been studied in carefully deoxygenated solutions.

The flash photolysis of DMA in deoxygenated liquid paraffin was studied by Land and Porter,[15] who assigned the spectrum with maxima at 3140 and 4000 Å tentatively to *N,N*-dimethylanilino radical. Kimura *et al.*[16] obtained a similar spectrum with maxima at 3400 and 4800 Å and a life time of the order of 100 μsec, and assigned it to the *T–T* transition. Later, the same authors found that the ultraviolet spectrum consists of two components: one probably due to *T–T* transition and another decaying much more slowly, We studied the flash photolysis of DMA and DMAN in carefully deoxygenated liquid paraffin again. The resulting spectra for DMA are shown in Fig. 6. The visible

15) E. J. Land and G. Porter, *Trans. Faraday Soc.*, **59**, 2027 (1963).
16) K. Kimura, S. Arimitsu, N. Yamamoto and H. Tsubomura, This Bulletin, **41**, 1274 (1968).

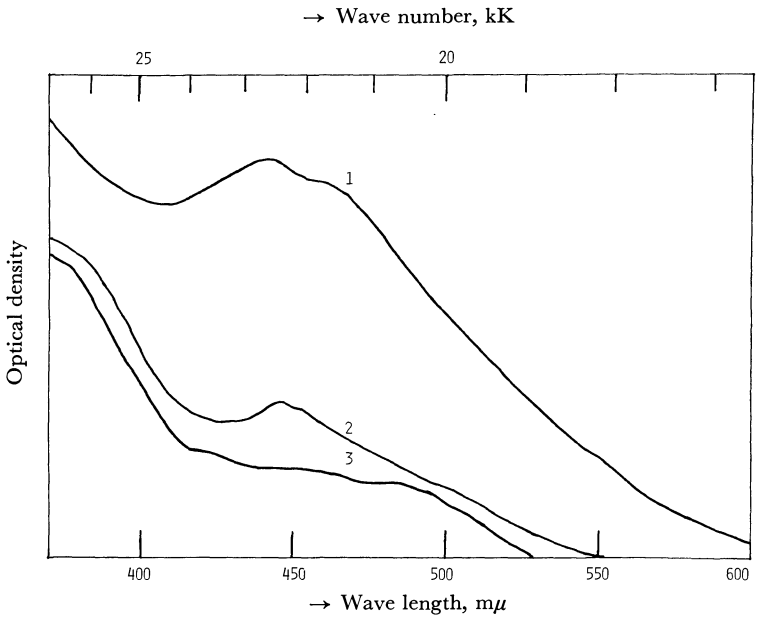

Fig. 6. Transient spectra obtained by flash illumination of *N,N*-dimethyl-aniline in deoxygenated liquid paraffin.
Delay time: 1) 8 μsec, 2) 80 μsec, 3) 270 μsec

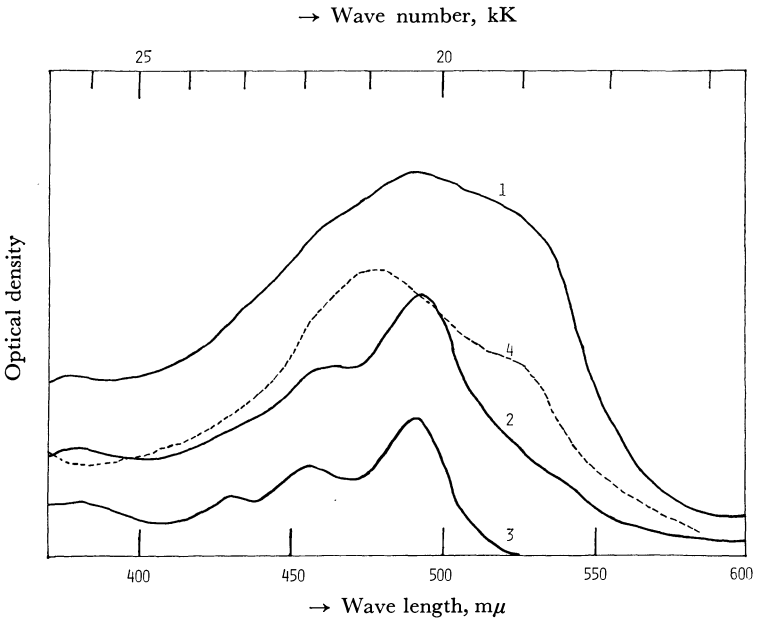

Fig. 7. Transient spectra obtained by flash illumination of *N,N*-dimethyl-*p*-anisidine in deoxygenated liquid paraffin.
Delay time: 1) 20 μsec, 2) 180 μsec, 3) 500 μsec, 4) *T-T* absorption spectrum measured in liquid paraffin at 77°K.

part of the spectrum decays exponentially with a life time of the order of 80 μsec, while most of the ultraviolet part remained after 80 μsec. These results confirm those obtained by Kimura *et al.* and show that the visible spectrum is the *T–T* absorption and most of the ultraviolet spectrum is probably due to *N*-methyl-anilino radical.

The spectra for DMAN also show that there are two components (Fig. 7): one, lying between 4500 and 5500 Å, decayed exponentially with a life time of 1.2 msec. and another, with peaks at 4290, 4500, and 4900 Å, remained for a long time. The yield

of the short-life component was found to be proportional to the flash light intensity, while that for the long-life component, although more difficult to analyse, is roughly proportional to the square of the light intensity. All these results are consistent with the assignment of the short-life component as a T–T band. That of the long-life component is uncertain. It does not agree in positions of the maxima with those of the DMAN cation nor those of *N,N*-dimethylamino-phenoxyl radical. One possible assignment is to *p*-methoxy-*N*-methylanilino radical.

The T–T spectrum of DMAN was also measured in an ethanol matrix and in a liquid paraffin matrix at 77°K using an apparatus constructed in our laboratory.[17] The result in Fig. 7 shows that the T–T spectrum lies in the same region as that of the fast decaying component of the transient spectrum.

The transient spectra obtained for various polar solutions of DMA and DMAN show complicated aspects. In ethanol and acetonitrile, transient spectra quite similar to those of the DMA and DMAN cations were obtained. The decay curves, however, showed in most cases that there are two components with different life times. The decay kinetics and the dependence of the yield of the transient species on the flash light intensity were difficult to determine exactly.

For aqueous solutions of DMAN, the transient spectrum obtained looks like that of the T–T transition. The spectrum, however, is found to have two components: the long-life component decays exponentially, with a life time of 23 min, and the short-life component also decays approximately in the first order with a life time of *ca.* 1 msec., and may be assigned to the T–T band. The long-life component is probably the cation band. Its initial absorbance, extrapolated to zero time, increases approximately proportional to the square of the flash light intensity. For the aqueous solution of DMA, the transient spectra can also be divided into T–T and cation components with life times of 80 μsec and 87 sec, respectively.

Flash photolysis of DMA and DMAN in formamide also showed transient spectra similar to those of the corresponding cations. The decay curves followed the second order kinetics, and the initial yields of the cations were found to be proportional to $I^{1.2}$—$I^{1.3}$.

Discussion

The transient species detected by the flash method are summarized in Table 2. It has been established that the anilines form their cations when flash-photolysed in highly polar solutions, irrespective of whether the solution is saturated with 1 atmosphere oxygen or deoxygenated. This is consistent with the result of our previous work that *N,N,N'N'*-tetramethyl-*p*-phenylenediamine (TMPD) forms its cation when flash-illuminated in deoxygenated ethanol.[7] As has been described earlier, it has been well established that TMPD ionizes from a higher triplet state by the two-step, biphotonic excitation.[7] The photolysis of aniline derivatives in organic matrices at 77°K were studied also in our laboratory.[12] It was concluded that they form the cation and the anilino-radical and the former yields more in polar matrices. The present results of flash photolysis in deoxygenated solutions seem

Table 2.* Transient species formed by flash excitation of aniline derivatives in solutions at room temperature

Solvent	*N,N*-Dimethylaniline		*N,N*-Dimethyl-*p*-anisidine	
	no O_2	O_2	no O_2	O_2
Liquid Paraffin	triplet DMA, 80 μsec radical $\gg$200 μsec	no transient	triplet DMA, 1.2 msec raidcal >400 msec	no transient
Ethanol	cation	no transient	cation, 6 msec long life species	no transient
Acetonitrile	cation, 1 msec long life species (radical?)	cation, decays in 2nd order	cation, 1.5 msec long life species	cation, decays in 2nd order
Water	triplet DMA, 80 μsec cation, increases until 1—2 msec, and decays, 87 sec	short-life species cation, decays in 2nd order	triplet DMAN, 1 msec cation, 23 min	short-life species cation, decays in 2nd order
Formamide	cation K_2, 1.6×10^8 M$^{-1}\cdot$sec^{-1}	cation K_2, 0.8×10^8 M$^{-1}\cdot$sec^{-1}	cation K_2, 2.0×10^8 M$^{-1}\cdot$sec^{-1}	cation K_2, 3.0×10^8 M$^{-1}\cdot$sec^{-1}

* O_2 means that the solution is saturated with oxygen at 1 atm. The species with life times indicated after them are found to decay in the first order. K_2 indicates the second order rate constant.

17) The details will be reported in a later paper.

to be consistent with the two-step photo-ionization mechanism, although quantitative analysis in the deoxygenated solutions is complicated by the formation of more than one species.

In previous papers,[7] we stated that TMPD is photoionized by flash photolysis in deoxygenated ethanol, but the presence of dissolved oxygen retards it to a great extent. In accordance with these findings, it has been found in the present work that DMA and DMAN do not form cations in oxygenated ethanol. The cation of DMA has been found to form in both deoxygenated and oxygenated acetonitrile, but not in acetonitrile saturated with oxygen at 8—20 Torr, as stated previously. This shows that the photo-ionization is retarded by a small amount of oxygen; this may be explained by taking into account the fact that oxygen quenches the lowest triplet states of the donor molecules very efficiently, so that the second step of the excitation hardly takes place.

The most important results obtained in the present work are that the aniline analogues form their cations in highly polar solutions saturated with 1 atmosphere oxygen, and the yields of the cations are proportional to the flash-light intensity. These results indicate that the cations are formed by the single-photon excitation from the ground states. The most plausible interpretation for this is that these cations are formed from the CT states, $D^+\cdots O_2^-$ by the interaction of the highly polar solvents.

$$D^+ \cdots O_2^- \longrightarrow D^+_{solv} + O_{2\,solv}^-$$

The CT states may be formed either by direct excitation from the ground states through the CT absorption, or by the interaction of the singlet excited states of the donor with oxygen in the ground state as follows:

$$^1D^* + O_2 \longrightarrow D^+ \cdots O_2^- \longrightarrow D^+_{solv} + O_{2\,solv}^-$$

As mentioned before, the cations are not detected in the acetonitrile solution of DMA containing a very small amount of oxygen, and this indicates that the excited triplet DMA is quenched by a very small amount of oxygen, because of its long lifetime. Consequently, it is concluded that the encounter of the triplet DMA in its lowest vibrational level and the oxygen molecule in the ground state does not lead to DMA cation even in highly polar solvents. The CT absorption of DMA$\cdots O_2$ extends far beyond the (0–0) band of phosphorescence spectrum (27 kK) of DMA, indicating that the triplet state (v=0) of DMA is higher in energy than the CT (v=0) level. The above result, therefore, seems to be explained by assuming that the process

$$D^+ \cdots A^- \rightsquigarrow D^+_{solv} + A^-_{solv}$$

should have an energy barrier as indicated in Fig. 8. In a highly polar solution, the charge transfer $D^+\cdots A^-$ state is thought to be stabilized by the solvation effect. The stabilization is the greater as the distance R_{DA} gets larger, possibly causing an energy maximum as indicated by the broken curve. In such a solution, the ground state D···A pair is excited to the charge transfer $D^+\cdots A^-$ state, not to the $D^+_{solv}\cdots A^-_{solv}$ state, in accordance with the Franck-Condon principle. It is conceivable, then, that only the excited DA pair, having energy higher than the maximum of the barrier, and accordingly larger intermolecular distance, will transfer to the $D^+_{solv}\cdots A^-_{solv}$ state.

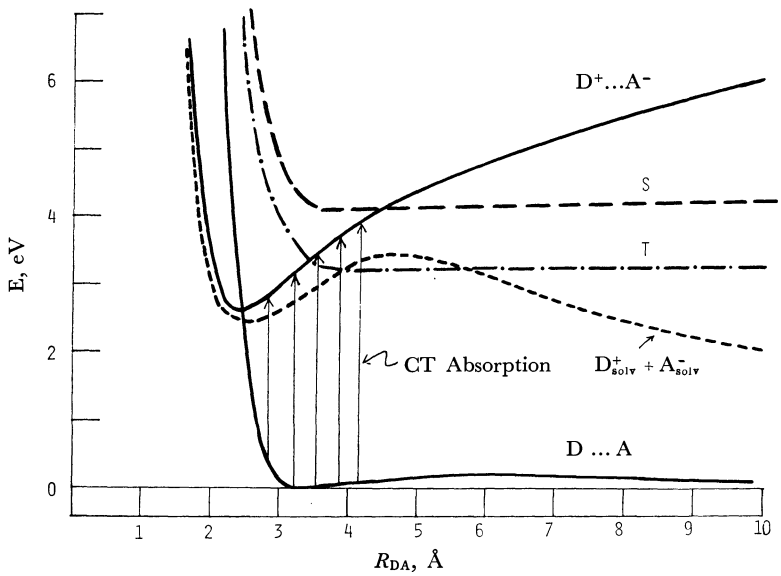

Fig. 8. Schematic diagram of the energy curves for the ground and various excited states of a donor-acceptor system.

Another mechanism, in which collison of oxygen with the donor in the singlet excited state leads to D^+_{solv} and $O_2^-{}_{solv}$ seems rather unlikely, because the short lifetime of the singlet excited donor and relatively low concentration of oxygen in the solution ($\sim$0.01 M) suggest that such a process is of minor importance.

The above interpretation of the experimental results assumes the formation of oxygen anion. In aqueous solutions it has been proved by pulse radiolysis of H_2O–O_2 system.[18] According to this and also to spectroscopic studies of the oxygen-doped alkali-halide crystals,[19] the oxygen anion has absorption spectrum lying in the region around 2400 Å. In our experimental conditions, therefore, it was impossible to detect the spectrum of oxygen anion even if it exists for a certain length of time. It is also very likely that the O_2^- anion reacts with the solvent rapidly, forming other types of anions.

18) G. Czapski and L. M. Dorfman, *J. Phys. Chem.*, **68**, 1169 (1964).

19) J. Rolfe, F. R. Lipsett and W. J. King, *Phys. Rev.*, **123**, 447 (1961).

BULLETIN OF THE CHEMICAL SOCIETY OF JAPAN VOL. 43 3773—3779 (1970)

Electron Spin-Spin Interaction and Methylene Bond Angles in the Quintet Ground State of *m*-Phenylene-dimethylene Radicals

Jiro HIGUCHI

Department of Chemistry, Faculty of Engineering, Yokohama National University, Minami-ku, Yokohama

(Received July 21, 1970)

The effect of the methylene bond angles on the electron spin-spin interaction has been semi-empirically investigated for the quintet ground states of the *m*-phenylene-dimethylene radicals, especially *m*-phenylene-bismethylene and *m*-phenylene-bisphenylmethylene. The D and E values calculated are compared with those observed, and the most probable structure, with a methylene bond angle near 140°, is estimated, as in the phenylmethylene radical.

Previously, the effect of the bond angle in the electron spin-spin interaction was semi-quantitatively investigated for the mono-methylene derivatives, especially the methylene and phenylmethylene radicals.[1] For these radicals, the spin Hamiltonian in the absence of the external magnetic field is expressed as:

$$\mathcal{H} = D\left[S_z^2 - \frac{1}{3}S(S+1)\right] + E[S_x^2 - S_y^2]. \quad (1)$$

In these derivatives, the value of $|E|/|D|$ can be used to determine the angle of the bent methylene carbon (–C–) bond by comparing the observed value with that calculated according to the following formulae:

$$D = \left(\frac{3e^2\hbar^2}{4m^2c^2}\right)\frac{2!(2S-2)!}{(2S)!}\sum_{i,j}\left\langle \phi_i(1)\phi_j(2) - \phi_j(1)\phi_i(2) \times \left| \frac{r_{12}^2 - 3z_{12}^2}{r_{12}^5} \right| \phi_i(1)\phi_j(2) \right\rangle \quad (2)$$

and:

$$E = \left(\frac{3e^2\hbar^2}{4m^2c^2}\right)\frac{2!(2S-2)!}{(2S)!}\sum_{i,j}\left\langle \phi_i(1)\phi_j(2) - \phi_j(1)\phi_i(2) \times \left| \frac{y_{12}^2 - x_{12}^2}{r_{12}^5} \right| \phi_i(1)\phi_j(2) \right\rangle \quad (3)$$

where the ϕ_i's are the unpaired orbitals. This approach is possible because of the facts that the σ-electron spin density is fairly close to unity at the –C– atom and the π-electron spin distribution is insensitive to the change in the –C– bond angle. As a result, the ratio of $|E|/|D|$ is mainly determined by the *s-p* hybridization of the unpaired σ orbital at the –C– atom. In these circumstances, the observed value of $|E|/|D|$ in phenyl derivatives can be explained by a –C– bond angle near 145°.[2]

Recently, electron spin resonance (ESR) absorption by quintet ground states of organic radicals has been reported for *m*-phenylene-bisphenylmethylene [*m*-$C_6H_4(CC_6H_5)_2$] in single crystals of benzophenone by Itoh[3] [$D/\boldsymbol{hc} = \pm 0.07137\ \mathrm{cm}^{-1}$, $E/\boldsymbol{hc} = \pm 0.01963\ \mathrm{cm}^{-1}$],[4] and for *m*-phenylene-bis-

1) J. Higuchi, *J. Chem. Phys.*, **39**, 1339 (1963).

2) J. Higuchi, to be published.

3) K. Itoh, *Chem. Phys. Lett.*, **1**, 235 (1967).

4) K. Itoh, private communications.

methylene [m-$C_6H_4(CH)_2$] [$|D|/hc=0.0844$ cm^{-1}, $|E|/hc=0.0233$cm^{-1}], m-phenylene-bisphenylmethylene [$|D|/hc=0.0701$ cm^{-1}, $|E|/hc=0.020$ cm^{-1}], and m-phenylene-dinitrene [m-$C_6H_4N_2$] [$|D|/hc=0.156$ cm^{-1}, $|E|/hc=0.029$ cm^{-1}] in rigid solvents by Wasserman, Murray, Yager, Trozzolo, and Smolinsky.[5] These reports are the first demonstrations of quintet states in organic radicals. Although the possibility of higher molecular spin multiplets has already been discussed for these molecular species,[6-8] and the D and E values theoretically calculated by assuming the linear –C– bonds,[6,7] the effect of the bent –C– bonds has not yet been treated. In the present work, therefore, such an effect will be discussed for dimethylene derivatives with a quintet ground state, especially for m-$C_6H_4(CH)_2$ and m-$C_6H_4(CC_6H_5)_2$, the observed $|E|/|D|$ values of which are 0.276 and 0.275, respectively.

The treatment adopted here is just the same as in the previous papers.[1,6,7] That is, the one-center integrals were those calculated from the self-consistent field (SCF) atomic orbitals (AO's) of the carbon atom (the ^1D state) expanded by Löwdin.[9] The two-center integrals were approximately evaluated as follows: the $2s$ electron was replaced by a unit point charge at the nucleus, the $2p$ electron was two half-unit point charges located to give the same quadrupole moment, and the atomic dipole effect was added as a positive and a negative charge of

$$\int_0^\infty r^2 dr \int_0^{\pi/2} \sin\theta d\theta \int_0^{2\pi} \chi_{2s}\chi_{2p\sigma} d\phi$$

located to fit the atomic dipole moment. All the methylene bonds were assumed to be coplanar with the central phenylene group. All the C–C distances were taken as 1.393 Å as in the benzene molecule,[10] and the simple LCAO-MO's were used for the π-orbitals. The unpaired σ orbitals were assumed to be hybridized ones located at each –C– atom and directed along the bisector of the –C– bond angle. For the sake of simplicity, configuration interaction was disregarded.

Calculation and Results

In addition to the most important contribution of the n-π (σ-π) type, the spin-spin interaction in the m-phenylene-dimethylene radicals includes the π-π and the n-n types,[7] since the two σ and two π orbitals are occupied by unpaired electrons. As has previously been shown,[7] these two interactions should not be negligibly small compared with the n-π type and should be included in any semi-quantitative discussion of the zero-field splittings of these radicals. In the present paper, therefore, the D and E values [*cf.* Eqs. (2) and (3)] in m-$C_6H_4(CH)_2$ and m-$C_6H_4(CC_6H_5)_2$ radicals were calculated by including all the types of interaction. The coordinate system and the –C– bond angles were taken as shown in Fig. 1.

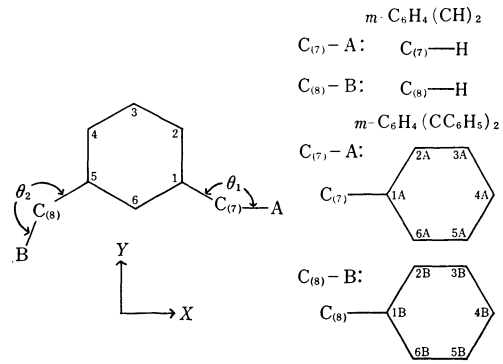

Fig. 1. Coordinate system (right-handed system) and the –C– bond angles in m-$C_6H_4(CX)_2$.

In the first instance, the m-$C_6H_4(CH)_2$ was taken as the simplest example of the ground-state quintet radicals on the assumption of the planar structure. The unpaired orbitals used were as follows:

$$\phi_1 = A_1\left[\chi_{2s7}\cot\frac{\theta_1}{2} + \left(1-\cot^2\frac{\theta_1}{2}\right)^{1/2} \times\left\{\chi_{2px7}\sin\left(\frac{\pi}{3}-\frac{\theta_1}{2}\right) - \chi_{2py7}\cos\left(\frac{\pi}{3}-\frac{\theta_1}{2}\right)\right\}\right] \quad (4)$$

$$\phi_2 = A_2\left[\chi_{2s8}\cot\frac{\theta_2}{2} - \left(1-\cot^2\frac{\theta_2}{2}\right)^{1/2} \times\left\{\chi_{2px8}\sin\left(\frac{\pi}{3}-\frac{\theta_2}{2}\right) + \chi_{2py8}\cos\left(\frac{\pi}{3}-\frac{\theta_2}{2}\right)\right\}\right] \quad (5)$$

$$\phi_3 = (3)^{-1/2}[-\chi_{2pz2}+\chi_{2pz7}+\chi_{2pz8}] \quad (6)$$

$$\phi_4 = (2)^{-1}[\chi_{2pz4}-\chi_{2pz6}+\chi_{2pz7}-\chi_{2pz8}] \quad (7)$$

where

$$A_i = \begin{cases} +1 & \left(\frac{\pi}{2}<\theta_i<\pi\right) \\ -1 & \left(\pi<\theta_i<\frac{3}{2}\pi\right) \end{cases} \quad (i=1,2). \quad (8)$$

The s-p hybridization in the ϕ_1 and ϕ_2 orbitals is determined by the –C– bond angles of θ_1 and θ_2, respectively, on the assumption that each bonding orbital of the –C– atom is equivalent and is directed along each bond. In the case of $\theta_1=\theta_2$, that is, when the radical belongs to the molecular symmetry of C_{2v}, the D and E values shown in Fig. 2 are

5) E. Wasserman, R. W. Murray, W. A. Yager, A. M. Trozzolo and G. Smolinsky, *J. Amer. Chem. Soc.*, **89**, 5076 (1967).
6) J. Higuchi, *J. Chem. Phys.*, **38**, 1237 (1963).
7) J. Higuchi, *ibid.*, **39**, 1847 (1963).
8) A. M. Trozzolo, R. W. Murray, G. Smolinsky, W. A. Yager and E. Wasserman, *J. Amer. Chem. Soc.*, **85**, 2526 (1963).
9) P.-O. Löwdin, *Phys. Rev.*, **90**, 120 (1953).
10) I. L. Karle, *J. Chem. Phys.*, **20**, 65 (1952).

obtained. A similar calculation was carried out on the assumption that $\theta_1+\theta_2=360°$, that is, when the $-C_{(8)}-H_{(8)}$ coincides with the $-C_{(7)}-H_{(7)}$ by the rotation of 120° about the center of the phenylene ring. The results thus obtained are shown in Fig. 3. The other configurations are less probable in view of the equivalence in the methylene bonds. The ratio of E/D thus obtained is shown in Figs. 4 and 5, corresponding to the cases of $\theta_1=\theta_2$ and $\theta_1+\theta_2=360°$, respectively. As the observed value of $|E|/|D|$ is 0.276, one finds eight probable sets of the –C– bond angles, θ_1 and θ_2, where the calculated ratio coincides with the observed ratio, as given in Table 1.

Next, the m-$C_6H_4(CC_6H_5)_2$ radical was treated because it is the only species thus far observed in

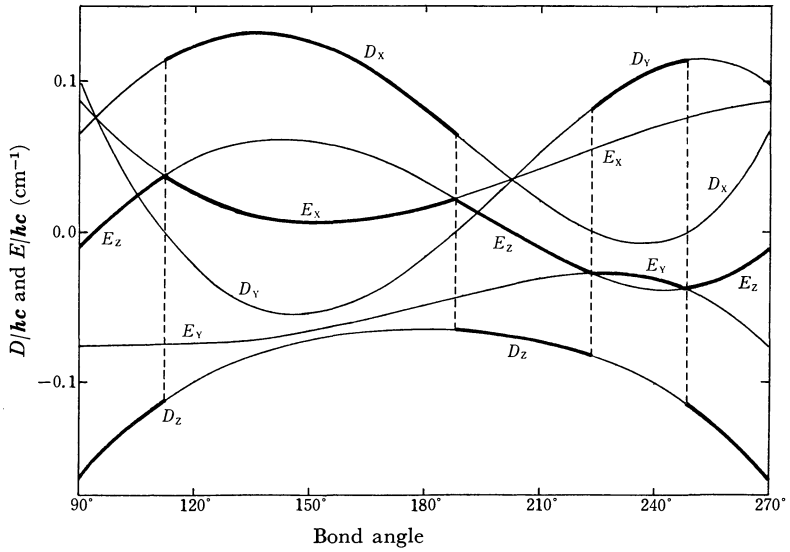

Fig. 2. D and E values of m-$C_6H_4(CH)_2$ in the case of $\theta_1=\theta_2$ (bold lines). The inferior letters, X, Y, and Z, on D and E imply that the set of axes (x, y, z) in Eqs. (2) and (3) should be taken the sets of directions, respectively, (Y, Z, X), (Z, X, Y), and (X, Y, Z) shown in Fig. 1.

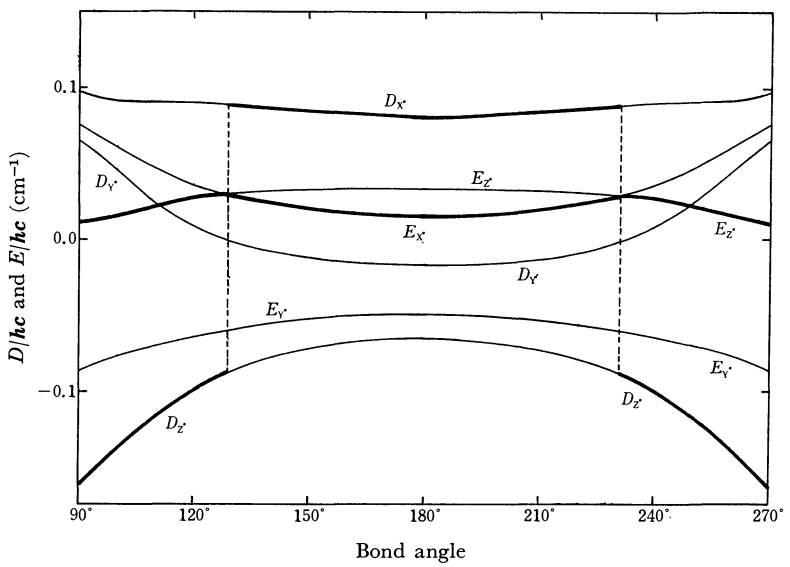

Fig. 3. D and E values of m-$C_6H_4(CH)_2$ in the case of $\theta_1+\theta_2=360°$ (bold lines). The inferior letters, X', Y', and Z', on D and E imply that the set of axes (x, y, z) in Eqs. (2) and (3) are close to the sets of directions, respectively, (Y, Z, X), (Z, X, Y), and (X, Y, Z) shown in Fig. 1. In this case, the deviations of the latter directions from the former axes are seen in the text.

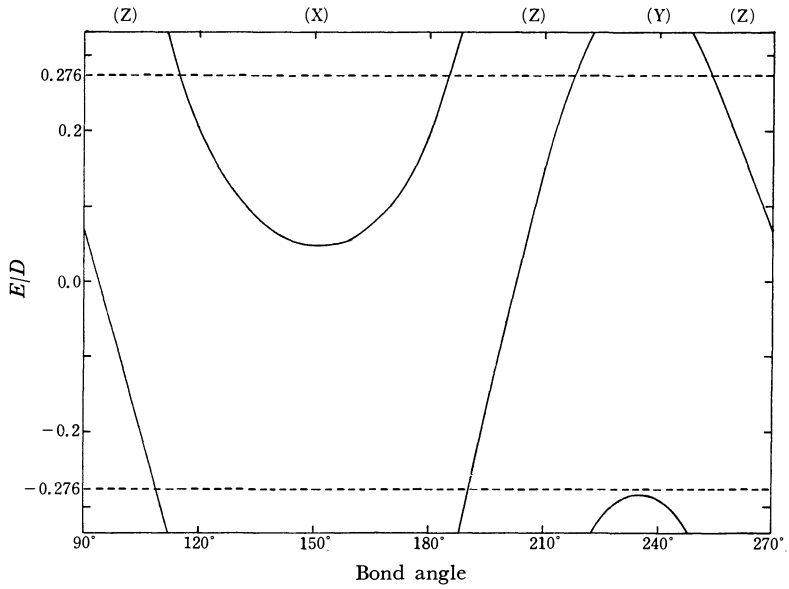

Fig. 4. The ratio of E/D of m-$C_6H_4(CH)_2$ in the case of $\theta_1=\theta_2$. The letters on the top of the figure indicate the directions of the z axis of the fine-structure tensor.

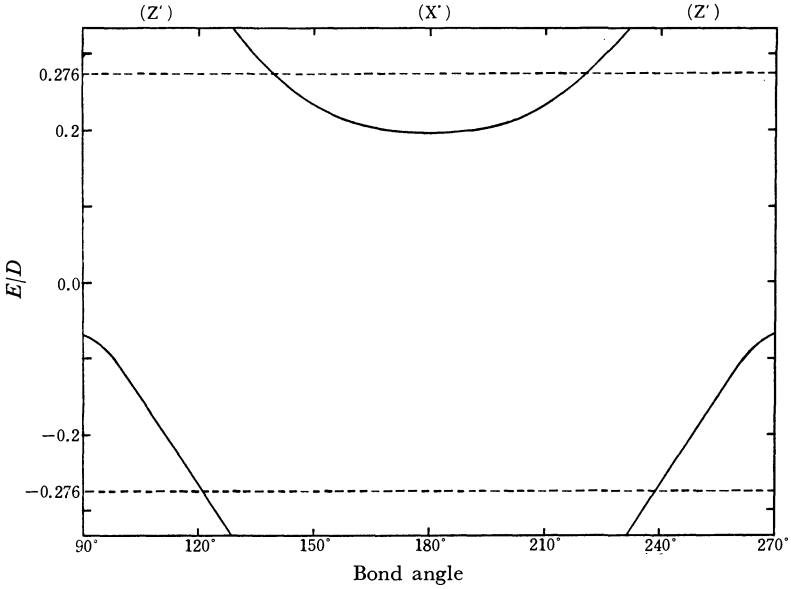

Fig. 5. The ratio of E/D of m-$C_6H_4(CH)_2$ in the case of $\theta_1+\theta_2=360°$. The letters on the top of the figure indicates the approximate directions of the z axis of the fine-structure tensor.

a single crystal. In this case, both the side phenyl groups were assumed to be either coplanar with, or perpendicular to, the central phenylene group. In the coplanar case, the treatment adopted was just the same as in the case of m-$C_6H_4(CH)_2$ except that the π orbitals used were as follows:

$$\phi_3^c = (18)^{-1/2}[-2\chi_{2pz2}+2\chi_{2pz7}+2\chi_{2pz8} -\chi_{2pz2A}+\chi_{2pz4A}-\chi_{2pz6A}-\chi_{2pz2B}+\chi_{2pz4B}-\chi_{2pz6B}] \quad (9)$$

and:

$$\phi_4^c = (22)^{-1/2}[2\chi_{2pz4}-2\chi_{2pz6}+2\chi_{2pz7}-2\chi_{2pz8} -\chi_{2pz2A}+\chi_{2pz4A}-\chi_{2pz6A}+\chi_{2pz2B}-\chi_{2pz4B}+\chi_{2pz6B}]. \quad (10)$$

In the perpendicular case, the following assumption was made: the unpaired orbitals parallel to the phenylene group are given by simple LCAO forms which are constructed from the zero-energy π-orbital

of phenylmethylene and the s-p hybridized orbital of the methylene carbon so as to give the –C– bond angle in question as follows:

$$\phi_3^{\mathrm{p}} = \left(7+\cot^2\frac{\theta_1}{2}\right)^{-1/2}\left[2\left(1+\cot^2\frac{\theta_1}{2}\right)^{1/2}\phi_1 + A_1\left(1-\cot^2\frac{\theta_1}{2}\right)^{1/2}\left\{(\chi_{2px2\mathrm{A}}-\chi_{2px4\mathrm{A}}+\chi_{2px6\mathrm{A}}) \times \sin\left(\frac{5}{6}\pi-\theta_1\right) - (\chi_{2py2\mathrm{A}}-\chi_{2py4\mathrm{A}}+\chi_{2py6\mathrm{A}}) \times \cos\left(\frac{5}{6}\pi-\theta_1\right)\right\}\right] \quad (11)$$

and:

$$\phi_3^{\mathrm{p}} = \left(7+\cot^2\frac{\theta_2}{2}\right)^{-1/2}\left[2\left(1+\cot^2\frac{\theta_2}{2}\right)^{1/2}\phi_2 - A_2\left(1-\cot^2\frac{\theta_2}{2}\right)^{1/2}\left\{(\chi_{2px2\mathrm{B}}-\chi_{2px4\mathrm{B}}+\chi_{2px6\mathrm{B}}) \times \sin\left(\frac{5}{6}\pi-\theta_2\right) + (\chi_{2py2\mathrm{B}}-\chi_{2py4\mathrm{B}}+\chi_{2py6\mathrm{B}}) \times \cos\left(\frac{5}{6}\pi-\theta_2\right)\right\}\right] \quad (12)$$

The calculation was performed in the two cases of the –C– bond angle of $\theta_1=\theta_2$ and $\theta_1+\theta_2=360°$, as in the m-$C_6H_4(CH)_2$ radical. The results thus obtained are quite similar to that obtained in the case of m-$C_6H_4(CH)_2$ shown in Figs. 4 and 5, and no significant differences can be found among these relative relationships. In each case, there are five sets of the –C– bond angles (θ_1 and θ_2), where the $|E|/|D|$ ratio calculated coincides with the observed value of 0.275 at larger –C– bond angles ($120°<\theta_1, \theta_2<240°$), as Table 1 shows.

For a structure with small –C– bond angles ($\theta_1, \theta_2<120°$, or $\theta_1, \theta_2>240°$), the ground state is not a quintet, since the orbitals,[11] $2^{-1/2}(\phi_1-\phi_2)$ and/or $2^{-1/2}(\phi_1+\phi_2)$, are doubly occupied because of the large energy difference between the ϕ_1 (or ϕ_2) and the ϕ_3 (or ϕ_4). As a result, such structures of these radicals, [I], [II], and [VI] in Table 1, are outside the scope of this discussion.

According to the recent experiment on m-C_6H_4-$(CC_6H_5)_2$ by Itoh,[4] the radical was oriented as a substituent for the two nearest neighboring molecules in a single crystal of benzophenone.[12] Taking

Table 1. The –C– bond angles where $|E|/|D|$ coincides with the observed value

		I	II	III	IV	V	VI	VII	VIII
m-$C_6H_4(CH)_2$	θ_1	109°	115°	185°	190°	218°	254°	121°	139°
	θ_2	109°	115°	185°	190°	218°	254°	239°	221°
	Sign of E/D[c]	−	+	+	−	+	+	−	+
	Sign of D	−	+	+	−	−	−	−	+
	z axis of fine-structure tensor	Z	X	X	Z	Z	Z	Z[d]	27.5° from X
m-$C_6H_4(CC_6H_5)_2$ (coplanar)[a]	θ_1			185°	191°	219°		122°	140°
	θ_2			185°	191°	219°		238°	220°
	Sign of E/D[c]			+	−	+		−	+
	Sign of D			+	−	−		−	+
	z axis of fine-structure tensor			X	Z	Z		Z[e]	26.1° from X
m-$C_6H_4(CC_6H_5)_2$ (perpendicular)[b]	θ_1	109°	115°	185°	191°	218°	254°	122°	140°
	θ_2	109°	115°	185°	191°	218°	254°	238°	220°
	Sign of E/D[c]	−	+	+	−	+	+	−	+
	Sign of D	−	+	+	−	−	−	−	+
	z axis of fine-structure tensor	Z	X	X	Z	Z	Z	Z[f]	26.2° from X

a) The planar configuration.
b) The configuration with the two side phenyl groups being prependicular to the central phenylene group.
c) The sign of E/D is not always chosen under the condition of $|D_x|<|D_y|<|D_z|$.
d) The x axis of the fine-structure tensor makes an angle of 38.8° with the X axis in Fig. 1.
e) The x axis of the fine-structure tensor makes an angle of 37.4° with the X axis in Fig. 1.
f) The x axis of the fine-structure tensor makes an angle of 37.7° with the X axis in Fig. 1.

11) The forms of these orbitals are not exactly correct except for the case of $\theta_1=\theta_2$, but may approximately be plausible for the present purpose.

12) The direction cosines of the x, y, z axes of the fine-structure tensor in the benzophenone crystallographic system [E. B. Fleischer, N. Sung and S. Hawkinson, *J. Phys. Chem.*, **72**, 4311 (1968).] are as follows:

Fine-structure axis	Crystal axis		
	a	b	c
x	−0.496	0.110	0.861
y	0.358	−0.878	0.317
z	0.792	0.465	0.396

Table 2. Calculated values of D/hc and E/hc for the permissible structures (cm^{-1})

		[III]		[VIII]		Experimental	
		D/hc	E/hc	D/hc	E/hc	D/hc	E/hc
m-$C_6H_4(CH)_2$		0.0713	0.0196	0.0876	0.0241	0.0844[c]	0.0233[c]
m-$C_6H_4(CC_6H_5)_2$	(coplanar)[a]	0.0440	0.0120	0.0548	0.0151	0.07137[d]	0.01963[d]
	(perpendicular)[b]	0.0348	0.0093	0.0493	0.0136		

a) The planar configuration.
b) The configuration with the two side phenyl groups being perpendicular to the central phenylene group.
c) Ref. 5. d) Ref. 4.

the orientation into consideration, the z axis of the fine-structure tensor does not appear to make a large angle (possibly within 30°) with the line $C_{(8)}$–$C_{(7)}$ (the X axis in Fig. 1). The experimental value of E/D is positive if the principal axes are chosen under the condition of $|D_x|<|D_y|<|D_z|$, as is usually done. These results appear to favor the cases [III] and [VIII] in Table 1. In these cases, the x axis of the fine-structure tensor lies close to the plane of the central phenylene group. It may be noted that these results show that the phenylene group of the radical may be oriented rather perpendicularly to the ab plane in the benzophenone single crystal.

Although the phenyl group is substituted for the hydrogen atom, the electronic property of the methylene bond is not significantly changed, and the relative angular dependence of the D and E is quite similar to that of the phenyl derivatives. As a result of this, one may reasonably assume that the directions of the principal axes of the fine-structure tensor for m-$C_6H_4(CH)_2$ do not much deviate from those of m-$C_6H_4(CC_6H_5)_2$ with respect to the central phenylene group. In that case, the permissible –C– bond angles are also restricted within the cases of [III] and [VIII] in Table 1. For reference, the calculated values of D and E in m-$C_6H_4(CH)_2$ and m-$C_6H_4(CC_6H_5)_2$ with the probably structures, [III] and [VIII], are given in Table 2.

Discussion

The present work includes several approximations, most of which are quite parallel to those of previous papers[1,6,7] and therefore need not be repeated here. As has been discussed already,[1] the approximations of the unpaired orbitals of ϕ_1 and ϕ_2, Eqs. (4) and (5), are not completely satisfactory, but they may be plausible for obtaining the trend of the D and E at larger –C– bond angles.[13] Although the unpaired orbitals of ϕ_1^p and ϕ_2^p, Eqs. (11) and (12), were also obtained so as to give the –C– bond angle in question, the use of these orbitals corresponds to the treatment that disregards the energy difference between the $2p$ and the s-p hybridized orbitals. In this case, the spin density at each –C– atom may be somewhat overestimated. However, the E/D ratio may not be significantly changed because both the D and E values are approximately proportional to the spin density at the –C– atom. Consequently, the approximation of the unpaired orbitals, ϕ_1^p and ϕ_2^p, may also be plausible in discussing the trend of the E/D ratio at larger –C– bond angles.

The contribution of the spin-orbit interaction is important in discussing the exact values of D and E.[14,15] Actually, the energy of this effect is predominatly due to the atomic term, while it is comparatively insensitive to the delocalization of unpaired electrons. In the case of the methylene radical, the E/D ratio is scarcely change if the D and E values of the spin-orbit interaction calculated by Glarum[14] are added to those of the spin-spin interaction.[1,6] In view of these facts, the present results may still be valid in a semi-quantitative sense.

In the case of $\theta_1+\theta_2=360°$ ($\theta_1<\theta_2$), the directions of the principal axes of the fine-structure tensor do not always coincide with those of the coordinate axes shown in Fig. 1. That is, one of the former axes which is perpendicular to the phenylene group (the y axis for $\theta_1 \geqq 129°$, or the

13) As discussed in the previous paper (Ref. 1), the use of the hybridized orbital for the unpaired orbital (*e. g.* ϕ_1 and ϕ_2) is plausible, since the coefficients of the $2s$ and $2p$ orbitals are fairly close to those of the SCF-LCAO-MO of the NH_2 radical [J. Higuchi, *J. Chem. Phys.*, **24**, 535 (1956).] at larger bond angles. Recently, Hoffmann *et al.* [R. Hoffmann, G. D. Zeiss and G. W. Van Dine, *J. Amer. Chem. Soc.*, **90**, 1485 (1968)] showed that the contributions (gross atomic population) of the $2s$ and $2p$ orbitals are somewhat different from those of the extended Hückel orbital of the phenylmethylene radical. However, it may be too hasty to deny the validity of the present approximation from only such a calculation, since the extended Hückel orbitals depend markedly on the selection of the parameters used and are not the best approximation of the SCF-LCAO-MO's.

14) S. H. Glarum, *J. Chem. Phys.*, **39**, 3141 (1963). This is only one calculation of spin-orbit interaction which is available for knowing the effect of methylene bond angle.

15) S. J. Fogel and H. F. Hameka, *J. Chem. Phys.*, **42**, 132 (1965).

z axis for $\theta_1 < 129°$) is actually parallel to the Z axis of the latter system. However, the z axis ($\theta_1 \geq 129°$) or the x axis ($\theta_1 < 129°$) of the fine-structure tensor makes an angle of $90° - \theta_1/2$ counterclockwise with the line $C_{(8)}$–$C_{(7)}$ (the X axis in Fig. 1), if only the n-π interaction at each methylene carbon is taken into account. That is, the angle between the X axis and the z (or x) axis increases with decreasing the –C– bond angle. Actually, such an angle is rather large compared with that of the above one-center approximation, as can be seen in the last column [VIII] in Table 1. Apparently, this is due to the fact that other types of interaction occur in the ground-state quintet radicals.

There are many molecular species which are also expected to yield a multiplet ground state in ESR spectroscopy. Especially for the polyacene dimethylene derivatives, the π-electron distribution is fairly different from that of the present case and the spin densities at the two methylene carbons are not always equivalent. As a result, the angle between the z axis of the fine-structure tensor and the line with the two methylene carbons may be changed somewhat as compared with the cases of the radicals treated here.

It may be noted that, in the case of $\theta_1 \neq \theta_2$ and $\theta_1 + \theta_2 \neq 360°$, there are other possible sets of –C– bond angles where the calculated ratio of E/D coindcies with the observed value and where the z axis of the fine-structure tensor does not make a large angle with the X axis in Fig. 1. Such structures can be seen in configurations with intermediate –C– bond angles between the cases [III] and [VIII], such as $\theta_1 \simeq 160°$ and $\theta_2 \simeq 207°$. However, they may be less important for our present purposes except if a remarkable distortion of the radical in the host crystal were to occur.

The possible structure and the directions of the principal axes of the fine-structure tensor obtained in the present work do not always coincide with those estimated by Wasserman *et al.*[5] However, the details of their work are not clear in their report and comparison may be difficult because of their inclusion of some semi-empirical values.

For the triplet or quintet ground state of the methylene derivatives, the molecular structure has not been conclusively determined, since there seems to be no helpful experimental method except the magnetic resonance technique in the present situation. For the benzophenone molecule, the dihedral angle between the two phenyl groups is 56° in the single crystal.[16] This may suggest that the central phenylene group in m-$C_6H_4(CC_6H_5)_2$ makes some angles with the two planes of methylene bonds [$C_{(1)}$–$C_{(7)}$–$C_{(1A)}$ and $C_{(3)}$–$C_{(8)}$–$C_{(1B)}$] and also the z axis of the fine-structure tensor. The calculation of the diphenylmethylene[2] showed that the E/D value was almost insensitive to the change in the dihedral angle between the two phenyl groups, although it is concerned with only the small contribution of the interatomic spin-spin interaction. If only the n-π interaction at each methylene carbon is taken into account, the E/D ratio in m-$C_6H_4(CC_6H_5)_2$ is changed with an increase in the dihedral angle between the central phenylene and the two planes of the methylene bonds. For the permissible structures given in Table 2, however, the deviation from the planar configuration is small at the above dihedral angles between 0° and 30°.[17] Accordingly, the results obtained for the structures with coplanar –C– bonds may still be useful in discussing the –C– bond angle semi-quantitatively.

If the absolute sign of the D were to be determined by an experiment at a low temperature, one could still not choose between the cases [III] and [VIII] by the present procedure alone, since both the D values calculated are positive. However, it may be possible to obtain some information on the –C– bond angles if the ^{13}C hyperfine splittings of the methylene carbons are obtained. On the other hand, it might also be possible to estimate the probable structure if a detailed calculation of the electronic structure is carried out. Under these circumstances, the following speculation is possible. On the assumption that the –C– bond angles are not very different from the calculated value (146°) of the phenylmethylene,[2] the case [VIII] might be the more probable,[18] although there is still a possibility of the structure [III]. At any rate, the present procedure may, in general, be useful not only for obtaining information on the molecular structures of fairly large radicals with a multiplet ground state, especially their methylene bond angles, but also in estimating their orientation in the host single crystal when that cannot be determined experimentally.

The author wishes to thank Dr. K. Itoh for communicating his experimental results before publication and for his helpful discussion, and Dr. E. Wasserman for communicating his result before publication. Most of the numerical calculation were carried out on the HITAC 5020E at Computer Centre, The University of Tokyo.

16) E. B. Fleischer, N. Sung and S. Hawkinson, *J. Phys. Chem.*, **72**, 4311 (1968).

17) In the benzophenone molecule, the dihedral angle between the plane of carbonyl bond [C–(C=O)–C] and the phenyl group is 30° and the above C–C–C bond angle is 122° (Ref. 16). As a result, the dihedral angle in the methylene derivatives is expected to be rather smaller than 30° because of the –C– bond angle larger than 122°.

18) A preliminary experimental result of 1,3,5-$C_6H_3(CC_6H_5)_3$ radical by Itoh [private communication] is also favorable to the present assumption.

BULLETIN OF THE CHEMICAL SOCIETY OF JAPAN VOL. 43 3780—3789 (1970)

Far Infrared Transmission Spectra and Lattice Vibrations of $RbNiF_3$ and $CsNiF_3$

Kay KOHN*1 and Ichiro NAKAGAWA

Department of Chemistry, Faculty of Science, The University of Tokyo, Hongo, Tokyo

(Received July 21, 1970)

The infrared absorption spectra of $RbNiF_3$ and $CsNiF_3$, both with a perovskite-like structure, have been measured in the region 500—50 cm^{-1} at room temperature and at liquid nitrogen temperature. The observed bands can be classified into three groups, corresponding to the three absorption bands in perovskite. These bands can reasonably be assigned on the basis of the crystal symmetry of the investigated compounds. A normal coordinate analysis of a crystal as a whole has been performed, where the interatomic force constants between the atom pairs within a distance of 3.5 Å are taken into account. It was shown that the normal coordinate treatment of the optically-active vibrations on the basis of a molecular dynamics model is useful for the interpretation of the lattice vibrations in these fluorides. The effects of the structural differences of the lattice vibrations are discussed.

In recent years several investigations of lattice vibrations in perovskite-type fluorides AMF_3 have been made, and the nature of the interatomic forces in these compounds is coming to be clear.[1-5] The observed infrared spectra were well interpreted on the basis of a valence force type potential for MF_6-octahedron and a central force type potential for the other atom pairs, A-F, F-F, and M-A.[5] This means that some covalent character is included in the M-F bond, even in the "ionic" crystal AMF_3.

Various compounds with the composition AMX_3, which have a crystal structure closely related to the perovskite structure, have been discovered, and the stability relations among these structures have been discussed.[6,7] All these compounds are com-

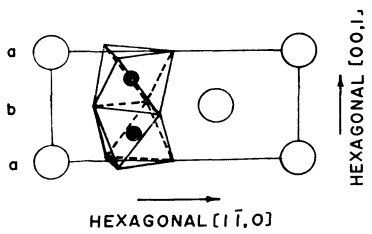

(a)

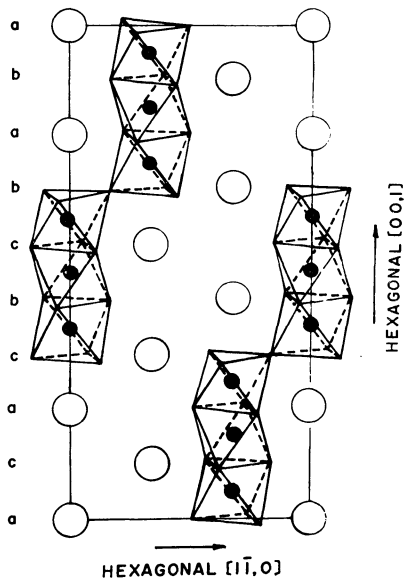

(b)

*1 On leave from the Department of Physics, School of Science and Engineering, Waseda University, Nishi-okubo, Tokyo.

1) G. R. Hunt, C. H. Perry and J. Furguson, *Phys. Rev.*, **134**, A688 (1964).
2) C. H. Perry, *Japanese J. Appl. Phys., Suppl.* 1, **4**, 564 (1965).
3) A. S. Barker, Jr., *Phys. Rev.*, **136**, A1290 (1964).
4) M. Balkanski, P. Moch and G. Parisot, *J. Chem. Phys.*, **44**, 940 (1966).
5) I. Nakagawa, A. Tsuchida and T. Shimanouchi, *ibid.*, **47**, 982 (1967).
6) Y. Syono, S. Akimoto and K. Kohn, *J. Phys. Soc. Jap.*, **26**, 993 (1969).
7) J. M. Longo and J. A. Kafalas, *Solid State Chem.*, **1**, 103 (1969).

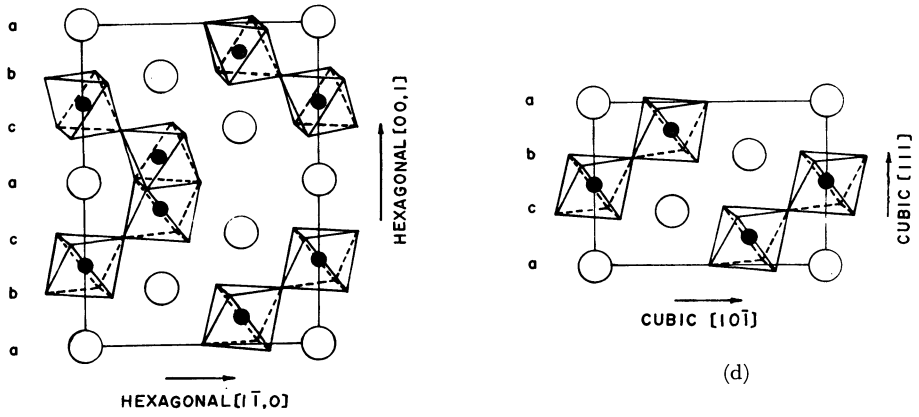

Fig. 1. Crystal structures of $RbNiF_3$ and $CsNiF_3$. All Ni (full circle) and Rb or Cs (open circle) ions on the hexagonal (1.1, 0) plane are illustrated. F ions are located on the octahedra around Ni ions. (a) $CsNiF_3$ 2L, (b) $CsNiF_3$ 9L, (c) $RbNiF_3$ 6L, (d) $RbNiF_3$ cubic.

posed of closely-packed layer lattice of larger cations, A, and anions, X, while smaller cations, M, are located at the octahedral interstices of the AX_3 lattice. The only difference between the several structures is in the stacking order of the closely-packed layers. If we denote the three different phases of such layers in a closely-packed structure as *a*, *b*, and *c*, an ordinary perovskite may be expressed as *abcabc*. The structures with the stacking sequences *ab* (2-layer type: 2L), *abcacb* (6-layer type: 6L), and *ababcbcac* (9-layer type: 9L) appear in fluorides, as is shown in Fig. 1.

The purpose of the present study is to investigate how these structural differences are reflected in the infrared spectra and to clarify the lattice vibrations in these "perovskite-like" compounds. Our aims are to establish the actual forms of vibrations, to test the validity of the pictures used for perovskites in a previous work by one of the present authors (I. N.) on these compounds, and, further, to establish the interrelations between the nature of the bonds and the stabilities of the various structures. For this purpose we have chosen to study two fluorides, $RbNiF_3$ and $CsNiF_3$. $RbNiF_3$ has a 6-layer structure (hexagonal $BaTiO_3$ structure) at ordinary pressure, and it is transformed into a cubic perovskite structure at 10 kbar.[6] $CsNiF_3$ has 2-layer structure at ordinary pressure, and it is transformed into a 9-layer structure at a few kbar.[8,9] Thus, we can compare different structures with the same composition.

We measured the far infrared transmission spectra at room temperature and at liquid nitrogen temperature. We also calculated the lattice vibrations on the same assumptions regarding interatomic forces as in the previous paper. The results show that the picture applied to perovskites is also valid in "perovskite-like" fluorides. The potential constants, which give calculated frequencies in good agreement with the observed, were also determined.

Experimental

Polycrystalline $RbNiF_3$ 6L and $CsNiF_3$ 2L were prepared from an intimate mixture of RbF and NiF_2 or CsF and NiF_2 by reaction at an elevated temperature. The reaction was made in a sealed-off platinum ampoule in order to prevent oxidation and evaporation. The high pressure phases, $RbNiF_3$ cubic and $CsNiF_3$ 9L, were supplied by Dr. Y. Syono of the Institute for Solid State Physics of the University of Tokyo. They were prepared from the corresponding low pressure phases using a tetrahedral anvil type, high pressure apparatus. These samples were dispersed in polyethylene sheets for use in the measurements.

A Hitachi FIS-I vacuum infrared spectrometer (500—50 cm^{-1}) was used. In the low-temperature measurements, samples were placed in direct contact with the metal conductor in the cryostat, and spectral measurements were made according to the procedure described in a previous paper.[5] The observed spectra are reproduced in Fig. 2.

Spectral measurements are limited to the transmittance, and throughout this study we regard the absorption frequencies obtained from the powder samples as ν's (resonance frequencies or minimum transmission frequencies as a thickness $d \to 0$). We checked the difference between the resonance frequencies obtained from the reflection data of a single crystal and those from the transmission data of a powder sample for a closely-related compound, MgF_2, for which both crystal and powder samples are available. This difference was found to be less than 5%, as will be shown in Appendix1.

8) Y. Syono, S. Akimoto and K. Kohn, presented at Colloque International du C.N.R.S. sur les Propriétés Physiques des Solides sous Pression (Grenoble, Sept. 1969).

9) J. M. Longo and J. A. Kafalas, *J. Appl. Phys.*, **40**, 1601 (1969).

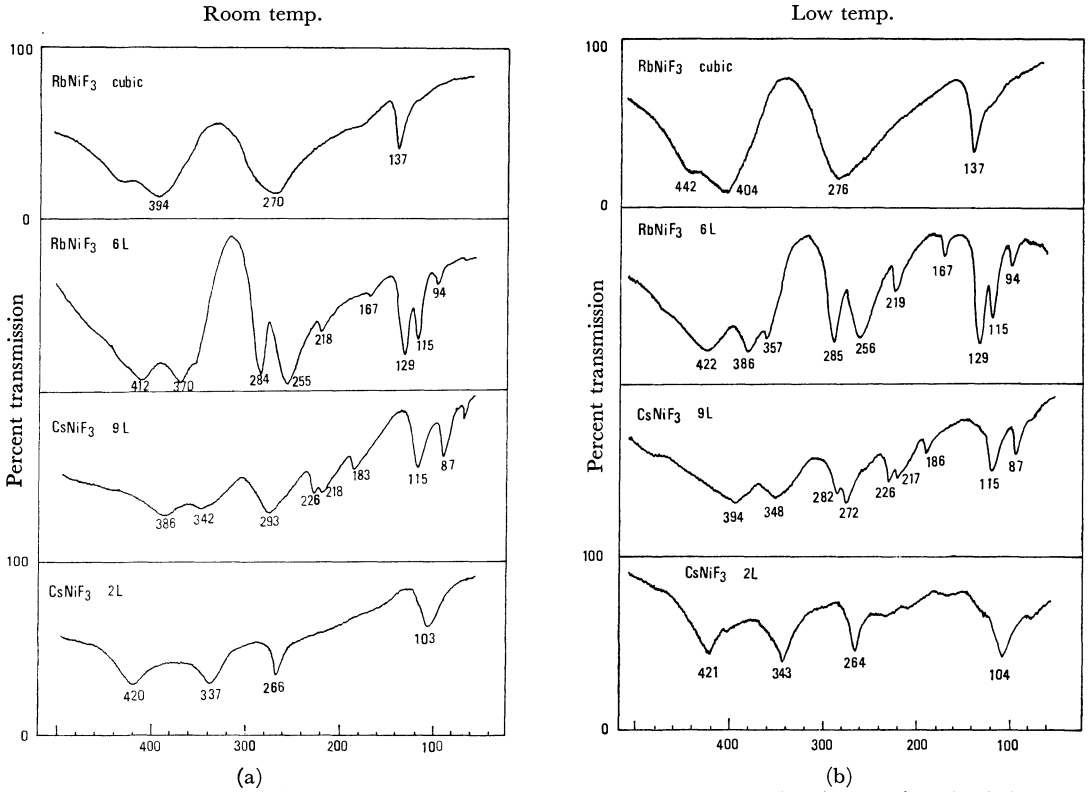

Fig. 2. Infrared absorption spectra of $RbNiF_3$ and $CsNiF_3$. Powdered samples dispersed in polyethylene sheets (*ca.* 1 mg/cm²). (a) spectra of room temperature, (b) spectra of liquid nitrogen temperature.

Observed Spectra

The observed spectrum of $RbNiF_3$ cubic is similar to that of the isomorphous compound $KNiF_3$. It consists of three absorption bands, around 390 cm^{-1}, 270 cm^{-1}, and 140 cm^{-1}. It is clear that they correspond to the Ni-F stretching, F-Ni-F bending, and A-F stretching vibrations respectively. Many more bands appeared in the spectra of $RbNiF_3$ 6L and $CsNiF_3$ 9L. They can also be classified into three groups, the bands in the 350—420 cm^{-1} range, those in the 200—300 cm^{-1} range, and those below 200 cm^{-1}. It can easily be understood that these bands arise from the splitting of the above three bands in more complicated structures. The spectrum of $CsNiF_3$ 2L consists of four bands. The two bands at lower frequencies are considered to arise from the F-Ni-F bending and Cs-F stretching vibrations. However, the two at 420 cm^{-1} and 340 cm^{-1} are either too high or too low to be simply compared with the corresponding band of cubic perovskite.

With a lowering of the temperature almost all the bands become sharp, and a few split into several components. At the same time, they shift to higher frequencies. Among them, the bands around 400 cm^{-1} show the most remarkable shift.

Lattice Vibrations of "Perovskite-like" Fluorides

The crystal structures of $RbNiF_3$ 6L, $RbNiF_3$ cubic, $CsNiF_3$ 2L,[10] and $CsNiF_3$ 9L (Fig. 1) belong to the space groups $D_{6h}^4-P6_3/mmc$, O_h^1-Pm3m, $D_{6h}^4-P6_3/mmc$, and $D_{3d}^5-R\bar{3}m$, and the Bravais primitive cells of these compounds consist of 6, 1, 2, and 3 formula units respectively. The crystallographic data relevant to later discussions are summarized in Table 1. The numbers of optically-active lattice vibrational modes in the different species were determined by factor-group analysis.[11] The results are shown in Table 2.

The optically-active vibrational frequencies and the corresponding vibrational modes were calculated according to the method of Shimanouchi, Tsuboi, and Miyazawa.[12] First, we took a potential function:

$$U = \frac{1}{2}\sum_{i,j}K_i(\Delta r_{\text{Ni-F}}{}^i{}_j)^2 + \frac{1}{2}\sum_{i,j}H_i(\Delta\alpha_{\text{F-Ni-F}}{}^i{}_j)^2 + \frac{1}{2}\sum_{i,j}F_i(\Delta q_{\text{F-F}}{}^i{}_j)^2 + \frac{1}{2}\sum_{i,j}f_i(\Delta q_{\text{A-F}}{}^i{}_j)^2$$

10) D. Babel, *Z. Naturforsch.*, **20a**, 165 (1965).

11) See, for example, S. Bhagavantam and T. Venkatarayudu, "Theory of Groups and Its Applications to Physical Problems," (2nd ed.), Andhra Univ., Waltair, 1951, p. 127.

12) T. Shimanouchi, M. Tsuboi and T. Miyazawa, *J. Chem. Phys.*, **35**, 1597 (1961).

Table 1. Crystal data of $RbNiF_3$ and $CsNiF_3$

Compound	Structure Space group	Lattice Parameters	Ionic positions
$RbNiF_3$ 6L	6 layer $D_{6h}^4-P6_3/mmc$	$a=5.847$Å $c=14.319$Å $Z=6$	Rb 1 in $2(b)$ Rb 2 in $4(f)$ $(z=0.0986)$[a] Ni 1 in $2(a)$ Ni 2 in $4(f)$ $(z=0.8498)$[a] F 1 in $6(h)$ $(x=0.522)$[a] F 2 in $12(k)$ $\begin{pmatrix}x=0.835\\z=0.078\end{pmatrix}$[a]
$RbNiF_3$ cubic	perovskite O_h^1-Pm3m	$a=4.0769$Å $Z=1$	Rb in $1(a)$ Ni in $1(b)$ F in $3(c)$
$CsNiF_3$ 2L	2 layer $D_{6h}^4-P6_3/mmc$	$a=6.255$Å $c=5.237$Å $Z=2$	Cs in $2(c)$ Ni in $2(a)$ F in $6(h)$ $x=-0.1431$[b]
$CsNiF_3$ 9L	9 layer $D_{3d}^5-R\bar{3}m$	$a=6.146$Å $c=22.300$Å $Z=9$ (hexagonal cell)	Cs 1 in $3(a)$ Cs 2 in $6(c)$ $(z=0.2181)$[c] Ni 1 in $3(b)$ Ni 2 in $6(c)$ $(z=0.3819)$[c] F 1 in $9(e)$ F 2 in $18(h)$ $\begin{pmatrix}x=0.156\\z=0.558\end{pmatrix}$[c]

a) see Ref. 13) for $CsMnF_3$
b) see Ref. 10)
c) see Ref. 14) for $BaRuO_3$

Table 2. Result of factor group analysis for optically active lattice vibrations of $RbNiF_3$ and $CsNiF_3$

Space group	Compounds	Number of modes in each species
$D_{6h}^4-P6_3/mmc$	$RbNiF_3$ 6L	$5A_{1g}+1A_{1u}+2A_{2g}+6A_{2u}$ $+6B_{1g}+2B_{1u}+1B_{2g}$ $+6B_{2u}+8E_{1g}+8E_{1u}$ $+6E_{2g}+7E_{2u}$ IR active: A_{2u} and E_{1u} (acoustical modes: $1A_{2u}$ $+1E_u$)
O_h^1-Pm3m	$RbNiF_3$ cubic	$3F_{1u}+1F_{2u}$ IR active: F_{1u} (acoustical modes: $1F_{1u}$)
$D_{6h}^4-P6_3/mmc$	$CsNiF_3$ 2L	$1A_{1g}+1A_{2g}+2A_{2u}+2B_{1g}$ $+1B_{1u}+2B_{2u}+3E_{1g}$ $+3E_{1u}+1E_{2g}+2E_{2u}$ IR active: A_{2u} and E_{1u} (acoustical modes: $1A_{2u}$ $+1E_{1u}$)
D_{3d}^5-R3m	$CsNiF_3$ 9L	$4A_{1g}+2A_{1u}+1A_{2g}+7A_{2u}$ $+5E_g+9E_u$ IR active: A_{2u} and E_u (acoustical modes: $1A_{2u}$ $+1E_u$)

where K_i's and H_i's denote the Ni-F bond-stretching and F-Ni-F angle-bending force constants. The f_i's and F_i's represent the interactions between the A cations (Rb^+ or Cs^+) and the F^- ions, and those between F^- ions, respectively. The sum was taken over all kinds of internal coordinates, i, and all the internal coordinates, j, for each kind of i in a Bravais primitive cell. These potential is a generalization of the potential function described in the previous paper. That is, we assumed a valence force type potential for the NiF_6-octahedron, and a central force type potential for all the atom pairs, for which the nonbonded repulsions or the ionic interactions are expected to be considerable. In the present case, all the interactions between the atom pairs within a distance of 3.5 Å were taken into account.

The internal coordinates, in which the potential function is expressed, are transformed into Cartesian diplacement coordinates, and the potential function is expressed in terms of Cartesian displacement coordinates. The optically-active $\boldsymbol{F}$-matrix (potential energy matrix), $\boldsymbol{F}_{op}$, in terms of the optically-active Cartesian displacement coordinates, is set up; the secular equation,

$$|\boldsymbol{M}^{-1}\boldsymbol{F}_{x\,op}-\boldsymbol{E}\lambda|=0$$

where $\boldsymbol{M}$ is a diagonal mass matrix and $\boldsymbol{E}$ is an unit matrix, gives the eigenvalues and eigenvectors which correspond to the frequencies and the vibrational modes. The normal modes are described on the basis of the Cartesian symmetry coordinates listed in Appendix 2.

In the course of the calculation, the values of the atomic positions and interatomic distances were needed. They were calculated using the lattice parameters given in Table 1. Since precise crystal data were lacking for $RbNiF_3$ 6L and $CsNiF_3$ 9L, we used some parameter values of isomorphous

13) A. Zalkin, K. Lee and D. H. Templeton, *J. Chem. Phys.*, **37**, 697 (1962).
14) P. C. Donohue, L. Katz and R. Ward, *Inorg. Chem.*, **4**, 306 (1965).

compounds, $CsMnF_3$ (6L type) and $BaRuO_3$ (9L type). They are given in parentheses in Table 1. This is justified since the corresponding parameter values in $CsMnF_3$[13] and hexagonal $BaTiO_3$,[15] both of which have a 6L-type structure, are quite the same.

TABLE 3. CALCULATED AND OBSERVED FREQUENCIES OF INFRARED ACTIVE VIBRATIONS IN $RbNiF_3$ AND $CsNiF_3$

$RbNiF_3$ 6L			$RbNiF_3$ cubic	
Calcd. (A_{2u}) cm^{-1}	Calcd. (E_{1u}) cm^{-1}	Obsd. cm^{-1}	Calcd. (F_{1u}) cm^{-1}	Obsd. cm^{-1}
411	411	412	394	394
352		370	273	270
	325	354	129	137
	286	284		
243	253			
	204	218		
183	178	167		
106	112	129 115		
85	82	94		

$CsNiF_3$ 2L			$CsNiF_3$ 9L		
Calcd. (A_{2u}) cm^{-1}	Calcd. (E_{1u}) cm^{-1}	Obsd. cm^{-1}	Calcd. (A_{2u}) cm^{-1}	Calcd. (E_u) cm^{-1}	Obsd. cm^{-1}
		420	370	366	386
350	348	337	347	326	342
	231	266	317		
	81	103			
55			265	289 276	273 (doublet)
				250	226
				205	218
			171		183
			107	129 104	115
			71	69	87

The numerical calculations were carried out with a HITAC 5020E computer at the Computation Center of the University of Tokyo. Programs, AXSM and CART, set up in our laboratory were used.[16] The calculated frequencies of optically-active vibrations are listed in Table 3, together with the observed values. The values of the force constants are given in Table 4. All the force constants were determined in a consistent way, in the sense that the relation between the interatomic distances and force constants was taken as universal for all the fluorides in the present study as well as for perovskite $KNiF_3$ in the previous paper. The following points should be made:

1) The force constants K_i's and F_i's are assumed to be functions of the interatomic distances r_{Ni-F} and r_{F-F}, respectively, regardless of the composition or structure of the compound (see Figs. 3 and 4).

2) The force constants H_i's are taken to have a constant value of 0.30 mdyn·Å in all cases.

3) The force constants f_i's are assumed to be a linear function of the ratio of the actual bond length, r_{A-F}, to the sum of the ionic radii, $r_{A^+}+r_{F^-}$ (see Fig. 5).

TABLE 4(a). FORCE CONSTANTS K_i USED IN THE CALCULATION

Compound	Kind of bond	Bond length (Å)	K_i (mdyn/Å)
$RbNiF_3$ 6L	Ni 2-F 2	1.99	0.70
$RbNiF_3$ 6L	Ni 1-F 2	2.01	0.64
$CsNiF_3$ 2L	Ni 1-F 1	2.03	0.60
$RbNiF_3$ cubic	Ni 1-F 1	2.04	0.58
$RbNiF_3$ 6L	Ni 2-F 1	2.05	0.57
$CsNiF_3$ 9L	Ni 2-F 1	2.09	0.55
$CsNiF_3$ 9L	Ni 1-F 2	2.10	0.54
$CsNiF_3$ 9L	Ni 2-F 2	2.13	0.53

TABLE 4(b). FORCE CONSTANTS f_i USED IN THE CALCULATION

Compound	Kind of bond	Bond length (Å)	f_i (mdyn/Å)
$RbNiF_3$ cubic	Rb 1-F 1	2.88	0.14
$RbNiF_3$ 6L	Rb 2-F 1	2.89	0.14
$RbNiF_3$ 6L	Rb 1-F 1	2.93	0.12
$RbNiF_3$ 6L	Rb 2-F 2	2.94	0.12
$RbNiF_3$ 6L	Rb 1-F 2	2.98	0.10
$RbNiF_3$ 6L	Rb 2-F 2	3.05	0.07
$CsNiF_3$ 9L	Cs 1 -F 1	3.07	0.13
$CsNiF_3$ 9L	Cs 1 -F 2	3.07	0.13
$CsNiF_3$ 9L	Cs 2 -F 2	3.08	0.13
$CsNiF_3$ 9L	Cs 2 -F 2	3.08	0.13
$CsNiF_3$ 9L	Cs 2 -F 1	3.12	0.11
$CsNiF_3$ 2L	Cs 1 -F 1	3.14	0.09
$CsNiF_3$ 2L	Cs 1 -F 1	3.33	0.03

Discussion of Results

The spectrum of $RbNiF_3$ cubic reveals a typical feature characteristic of a regular cubic perovskite structure. The three absorption bands observed correspond to the Ni-F stretching, F-Ni-F angle

15) P. C. Burbank and H. T. Evans, Jr., *Acta Crystallogr.*, **1**, 330 (1948).

16) T. Shimanouchi, "Computer Programs for Normal Coordinate Treatment of Polyatomic Molecules," The University of Tokyo, July 1968.

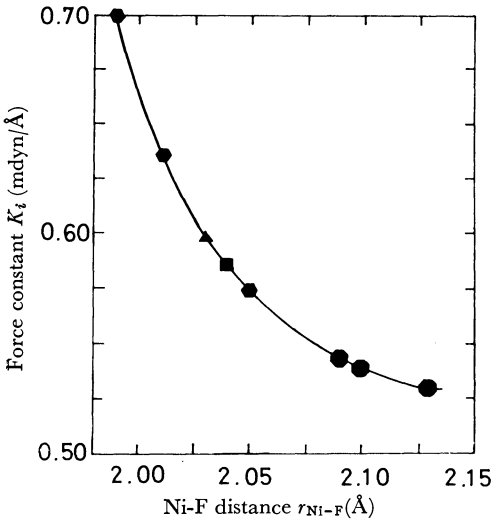

Fig. 3. Dependence of force constants K_i's used in the calculation on interatomic distance r_{Ni-F}. ● $RbNiF_3$ 6L, ■ $RbNiF_3$ cubic, ▲ $CsNiF_3$ 2L ● $CsNiF_3$ 9L

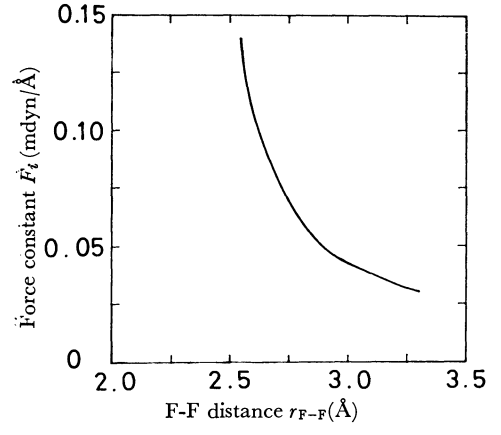

Fig. 4. Dependence of force constants F_i's used in the calculation on interatomic distance r_{F-F}.

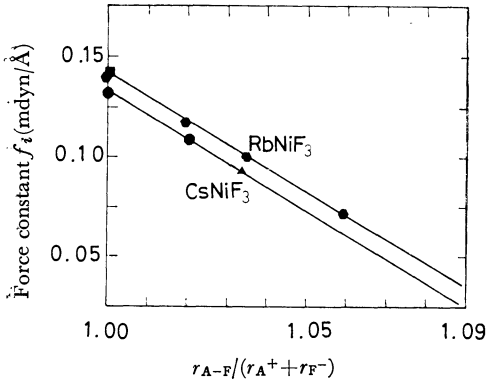

Fig. 5. Dependence of force constants f_i's used in the calculation on the ratio of the actual bond length r_{A-F} to the sum of ionic radii $r_A + r_F$.

bending, and Rb-F stretching modes respectively, all of which belong to the F_{1u} species. In contrast with this simple spectrum, those of $RbNiF_3$ 6L and $CsNiF_3$ 9L are much more complicated. However, they can be explained if we consider that a single band in perovskite splits into several components in more complicated structures. This situation may be clearly seen in the form of the calculated normal modes of vibrations. In Fig.6(a) we show the atomic displacements for the normal modes of the lattice vibrations of $RbNiF_3$ 6L as an example. This is based on the transformation matrix, $\boldsymbol{L}_x$, between the Cartesian coordinates, $\boldsymbol{X}$ and the normal coordinates $\boldsymbol{Q}$, defined as $\boldsymbol{X}=\boldsymbol{L}_x\boldsymbol{Q}$, $\boldsymbol{M}^{-1}\boldsymbol{F}_x\boldsymbol{L}_x=\boldsymbol{L}_x\boldsymbol{\Lambda}$. Here we will examine how the above splittings come about in the Ni-F stretching modes in $RbNiF_3$ 6L. In this phase Ni ions are still surrounded by six F^- ions, as in perovskite-type $RbNiF_3$. However, we can expect that a single band in $RbNiF_3$ cubic will split, since:

1) there are two different sites, (*a*) and (*f*), for Ni ions and the vibrational modes of these NiF_6-octahedra couple together to give two different frequencies;

2) these NiF_6-octahedra are not regular, unlike in perovskite, but are somewhat distorted in different ways (Table 5), and

Table 5. Distortion of NiF_6-octahedra in $RbNiF_3$ and $CsNiF_3$

Compound	Central Ni ion[a)]	Ni-F bond length (Å)	F-Ni-F bond angle
$RbNiF_3$ 6L	Ni 1	2.01	92.1°
	Ni 2	1.99	95.5°
		2.05	76.6°
$RbNiF_3$ cubic	Ni 1	2.04	90°
$CsNiF_3$ 2L	Ni 1	2.10	82.8°
$CsNiF_3$ 9L	Ni 1	2.10	86.2°
	Ni 2	2.08	84.7°
		2.13	95.3°

a) See Table 1.

3) some of the freedom of motion of the F^- ions is inhibited by the symmetry in infrared active vibrations, and the form of the vibrational modes of a single octahedron undergoes some change. It may clearly be seen in Fig. 6 that a simple vibrational mode in perovskite (Fig. 6b) is modified, and that some modes have a feature of the partially angle-bending type. This tendency is essentially the same for all the compounds studied here.

The reasonable agreement between the calculated and the observed frequencies suggests that our model is still applicable to these fluorides. However, we must remark on several points in this connection. First, there are some differences between the values of the force constants K_i's used in this paper and those determined for some perovskite-type fluorides

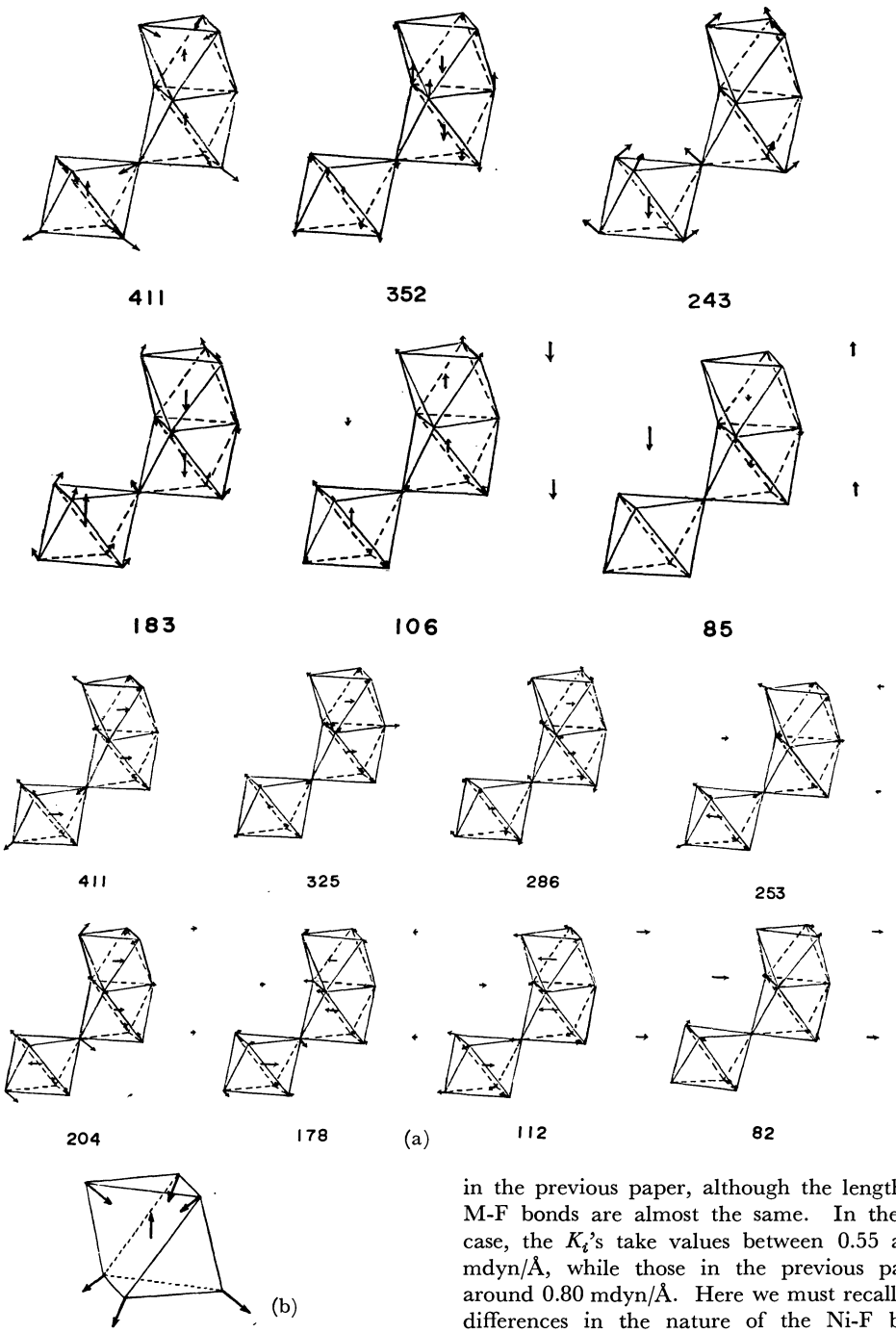

Fig. 6. (a) Displacements of ions for the lattice vibrational modes in $RbNiF_3$ 6L. Only a half of Bravais primitive cell is shown, since the displacements of other ions can be derived by considering inversion symmetry of the modes. The vibrational modes of A_{2u} and E_{1u} species are illustrated in upper and lower halves, respectively. (b) Displacements of ions in MF_6-octahedron for the Ni-F stretching vibrational mode in perovskite type fluoride.

in the previous paper, although the lengths of the M-F bonds are almost the same. In the present case, the K_i's take values between 0.55 and 0.70 mdyn/Å, while those in the previous paper are around 0.80 mdyn/Å. Here we must recall possible differences in the nature of the Ni-F bonds in these two cases. Some of the compounds in this study have a high pressure form, and the atoms are, so to speak, "squeezed together" in them. This will certainly cause a deviation of the force constants from their values in ordinary structures. In addition, there is some change in the covalent character in Ni-F bonds, as is suggested by the distortions of the NiF_6-octahedra. The distortion of NiF_6-octahedra are listed in Table 5. The

covalent character differs from one type of octahedron to another. Such factors are wholly neglected in our calculation, where the K_i's are taken as a function of the bond length only, and where the H_i's are assumed to be constant regardless of the actual bond angles. For instance, in $RbNiF_3$ 6L, the octahedron around the *f*-site Ni ions is much distorted. This suggests some modifications in some force constants, which results in the improvement in some of the calculated frequencies (352, 325, 286, 183, and 178 cm^{-1}). At present, however, we have no sound theoretical ground or empirical information sufficient to guide our estimation of the force constants in such cases. Thus, our simple model serves only as a useful starting point. The force constants, f_i's and F_i's, between nonbonded ions are more satisfactorily used.

As for $CsNiF_3$ 2L, we have some trouble in explaining the Ni-F stretching vibrations, since the calculated frequencies of the A_{2u} and E_{1u} species for this mode are almost the same, while we have two observed bands around 420 cm^{-1} and 340 cm^{-1}. An experimental check for isomorphous compounds is needed. A study about such compounds containing oxides and chlorides is now in progress.

The authors wish to express their thanks to Professor T. Shimanouchi of the University of Tokyo for his kind guidance and valuable discussions. Thanks are also due to Professor S. Akimoto and Dr Y. Syono of the Institute for Solid State Physics of the University of Tokyo for kindly supplying the samples of high pressure phases of $RbNiF_3$ and $CsNiF_3$.

Note Added in Proof.

Recently Dr D. Babel and Dr J. M. Longo have kindly informed us about their crystal data of $RbNiF_3$ 6-layer type (D. Babel: *Z. Anorg. Allgem. Chem.*, **369**, 117 (1969), R. J. Arnott and J. M. Longo: to be published in *J. Solid State Chem.*, **2**, (1970)). Their parameter values of ion sites are very close to those assumed in this paper.

Appendix 1. *Comparison of the Transmission Spectrum of Powdered Samples with the Reflection Spectrum of Single Crystals.*

The results of MgF_2 (uniaxial crystal: D_{4h}^{14}-*Pnnm*) are given in Fig. 7.

A transmission measurement of a MgF_2 powdered sample dispersed in a polyethylene sheet (*ca.* 1 mg/cm^2) was made by using a HITACHI EPI-L spectometer. A reflection measurement of the MgF_2 single crystal was made near a normal incidence on the *c*-plane, using HITACHI EPI-L and FIS-21 spectrometers with reflectance attachments. The optical constants were derived from the measured reflectivity, using the Kramers-Kronig relation.

The reflection spectrum and the real and imaginary parts of the infrared dielectric constant (ε' and ε'') are given in Fig. 7, where they are also compared with the transmission spectrum.

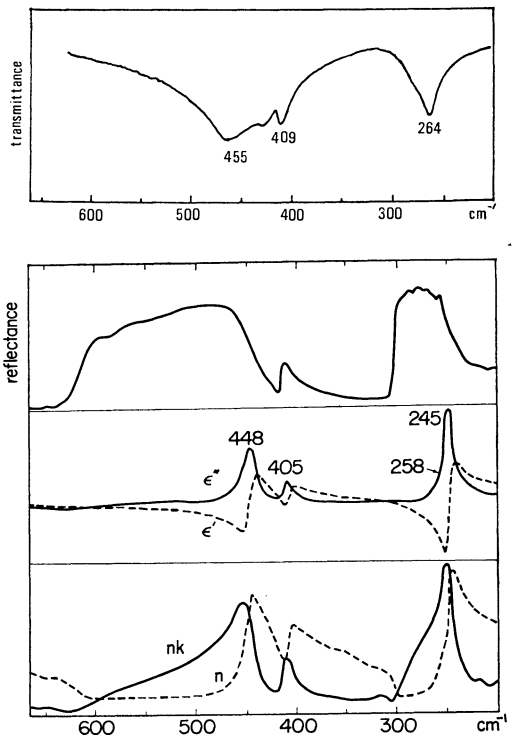

Fig. 7. Comparison of the transmission spectrum of powdered sample with the reflection spectrum of single crystal for MgF_2.

Appendix 2. *Cartesian Symmetry Coordinates of Infrared Active Vibrational Modes in "Perovskite-like" Compounds.*

The Cartesian symmetry coordinates of optically active vibrational modes in 2L, 6L, and 9L structures have been determined. The expressions for the infrared active vibrational modes are as follows:

1) $RbNiF_3$6L: Ions with the Cartesian coordinates given in the parenthesis are indexed as follows:

1 Ni 1; (0, 0, 0),
2 Ni 1; (0, 0, $c/2$),
3 Ni 2; ($-a/\sqrt{3}$, 0, w_1c),
4 Ni 2; ($-a/\sqrt{3}$, 0, $\overline{1/2-w_1c}$),
5 Ni 2; ($a/\sqrt{3}$, 0, $-w_1c$),
6 Ni 2; ($a/\sqrt{3}$, 0, $\overline{-1/2+w_1c}$),
7 F 1; $((\sqrt{3}/2)u_4a, (-3/2)u_4a, c/4)$,
8 F 1; $(-\sqrt{3}u_4a, 0, c/4)$,
9 F 1; $((\sqrt{3}/2)u_4a, (3/2)u_4a, c/4)$,
10 F 1; $(\sqrt{3}u_4a, 0, -c/4)$,
11 F 1; $((-\sqrt{3}/2)u_4a, (3/2)u_4a, -c/4)$,
12 F 1; $((-\sqrt{3}/2)u_4a, (-3/2)u_4a, -c/4)$,
13 F 2; $(-\sqrt{3}u_2a, 0, w_2c)$,
14 F 2; $((\sqrt{3}/2)u_2a, (-3/2)u_2a, w_2c)$,
15 F 2; $((\sqrt{3}/2)u_2a, (3/2)u_2a, w_2c)$,
16 F 2; $(-\sqrt{3}u_2a, 0, \overline{1/2-w_2c})$,
17 F 2; $((\sqrt{3}/2)u_2a, (-3/2)u_2a, \overline{1/2-w_2c})$,

18 F 2; $((\sqrt{3}/2)u_2a, (3/2)u_2a, 1/2-w_2c)$,
19 F 2; $(\sqrt{3}u_2a, 0, -w_2c)$,
20 F 2; $((-\sqrt{3}/2)u_2a, (3/2)u_2a, -w_2c)$,
21 F 2; $((-\sqrt{3}/2)u_2a, (-3/2)u_2a, -w_2c)$,
22 F 2; $(\sqrt{3}u_2a, 0, -1/2+w_2c)$,
23 F 2; $((-\sqrt{3}/2)u_2a, (3/2)u_2a, -1/2+w_2c)$,
24 F 2; $((-\sqrt{3}/2)u_2a, (-3/2)u_2a, -1/2+w_2c)$,
25 Rb 1; $(0, 0, c/4)$,
26 Rb 1; $(0, 0, -c/4)$,
27 Rb 2; $(a/\sqrt{3}, 0, w_3c)$,
28 Rb 2; $(a/\sqrt{3}, 0, 1/2-w_3c)$,
29 Rb 2; $(-a/\sqrt{3}, 0, -w_3c)$,
30 Rb 2; $(-a/\sqrt{3}, 0, -1/2+w_3c)$,

where u_i's and w_i's are parameter values (see Table 1). Then the Cartesian symmetry coordinates of A_{2u} and E_{1u} species are as follows.

(A_{2u})

Ni 1: $s_1=(1/\sqrt{2})\Delta(z_1+z_2)$,
Ni 2: $s_2=(1/\sqrt{4})\Delta(z_3+z_4+z_5+z_6)$,
Rb 1: $s_3=(1/\sqrt{2})\Delta(z_{25}+z_{26})$,
Rb 2: $s_4=(1/\sqrt{4})\Delta(z_{27}+z_{28}+z_{29}+z_{30})$,
F 1: $s_5=(1/\sqrt{6})\Delta(z_7+z_8+z_9+z_{10}+z_{11}+z_{12})$,
F 2: $s_6=(1/\sqrt{12})\Delta(z_{13}+z_{14}+z_{15}+z_{16}+z_{17}+z_{18}+z_{19}+z_{20}+z_{21}+z_{22}+z_{23}+z_{24})$,
F 2: $s_7=(1/\sqrt{12})\Delta\{(x_{13}+(-x_{14}+\sqrt{3}y_{14})/2+(-x_{15}-\sqrt{3}y_{15})/2-x_{16}-(-x_{17}+\sqrt{3}y_{17})/2-(-x_{18}-\sqrt{3}y_{18})/2+x_{19}+(-x_{20}+\sqrt{3}y_{20})/2+(-x_{21}-\sqrt{3}y_{21})/2-x_{22}-(-x_{23}+\sqrt{3}y_{23})/2-(-x_{24}-\sqrt{3}y_{24})/2),\}$

(E_{1u})

Ni 1: $s_1=(1/\sqrt{2})\Delta(x_1+x_2)$,
s_2=the same for y_i,
Ni 2: $s_3=(1/\sqrt{4})\Delta(x_3+x_4+x_5+x_6)$,
s_4=the same for y_i,
Rb 1: $s_5=(1/\sqrt{2})\Delta(x_{25}+x_{26})$,
s_6=the same for y_i,
Rb 2: $s_7=(1/\sqrt{4})\Delta(x_{27}+x_{28}+x_{29}+x_{30})$,
s_8=the same for y_i,
F 1: $s_9=(1/\sqrt{6})\Delta(x_7+x_8+x_9+x_{10}+x_{11}+x_{12})$,
s_{10}=the same for y_i,
F 1: $s_{11}=(1/\sqrt{6})\Delta\{(x_7+(-x_8-\sqrt{3}y_8)/2+(-x_9+\sqrt{3}y_9)/2+x_{10}+(-x_{11}-\sqrt{3}y_{11})/2+(-x_{12}+\sqrt{3}y_{12})/2)\}$,
F 1: $s_{12}=(1/\sqrt{6})\Delta\{(y_7+(\sqrt{3}x_8-y_8)/2+(-\sqrt{3}x_9-y_9)/2+y_{10}+(\sqrt{3}x_{11}-y_{11})/2+(-\sqrt{3}x_{12}-y_{12})/2)\}$,
F 2: $s_{13}=(1/\sqrt{12})(x_{13}+x_{14}+x_{15}+x_{16}+x_{17}+x_{18}+x_{19}+x_{20}+x_{21}+x_{22}+x_{23}+x_{24})$,
s_{14}=the same for y_i,
F 2: $s_{15}=(1/\sqrt{12})\Delta\{(x_{13}+(-x_{14}-\sqrt{3}y_{14})/2+(-x_{15}+\sqrt{3}y_{15})/2+x_{16}+(-x_{17}-\sqrt{3}y_{17})/2+(-x_{18}+\sqrt{3}y_{18})/2+x_{19}+(-x_{20}-\sqrt{3}y_{20})/2+(-x_{21}+\sqrt{3}y_{21})/2+x_{22}+(-x_{23}-\sqrt{3}y_{23})/2+(-x_{24}+\sqrt{3}y_{24})/2)\}$,
F 2: $s_{16}=(1/\sqrt{12})\Delta\{(y_{13}+(\sqrt{3}x_{14}-y_{14})/2+(-\sqrt{3}x_{15}-y_{15})/2+y_{16}+(\sqrt{3}x_{17}-y_{17})/2+(-\sqrt{3}x_{18}-y_{18})/2+y_{19}+(\sqrt{3}x_{20}-y_{20})/2+(-\sqrt{3}x_{21}-y_{21})/2+y_{22}+(\sqrt{3}x_{23}-y_{23})/2+(-\sqrt{3}x_{24}-y_{24})/2)\}$,
F 2: $s_{17}=(1/\sqrt{24})\Delta\{(2z_{13}-z_{14}-z_{15}-2z_{16}+z_{17}+z_{18}+2z_{19}-z_{20}-z_{21}-2z_{22}+z_{23}+z_{24})\}$,
$s_{18}=(1/\sqrt{8})\Delta\{(z_{14}-z_{15}-z_{17}+z_{18}+z_{20}-z_{21}-z_{23}+z_{24})\}$.

2) $CsNiF_3$ 2L: If ions are appropriately indexed, the Cartesian symmetry coordinates has the same expressions as those of $RbNiF_3$ 6L. Then in (A_{2u}), only s_1, s_3, and s_5 in $RbNiF_3$ 6L appear, and in (E_{1u}), only s_1, s_2, s_5, s_6, s_9, s_{10}, s_{11}, and s_{12} in $RbNiF_3$ 6L appear.

3) $CsNiF_3$ 9L: Ions with the Cartesian coordinates given in the parenthesis are indexed as follows:

1 Ni 1; $(0, 0, 0)$
2 Ni 2; $(0, 0, w_1c)$
3 Ni 2; $(0, 0, -w_1c)$
4 F 1; $(-a/2\sqrt{3}, 0, c/6)$
5 F 1; $(a/4\sqrt{3}, -a/4, c/6)$
6 F 1; $(a/4\sqrt{3}, a/4, c/6)$
7 F 2; $(\sqrt{3}u_2a, 0, w_2c)$
8 F 2; $((-\sqrt{3}/2)u_2a, (3/2)u_2a, w_2c)$
9 F 2; $((-\sqrt{3}/2)u_2a, (-3/2)u_2a, w_2c)$
10 F 2; $(-\sqrt{3}u_2a, 0, -w_2c)$
11 F 2; $((\sqrt{3}/2)u_2a, (-3/2)u_2a, -w_2c)$
12 F 2; $((\sqrt{3}/2)u_2a, (3/2)u_2a, -w_2c)$
13 Cs 1; $(\sqrt{3}a, 0, c/6)$
14 Cs 2; $(0, 0, w_3c)$
15 Cs 2; $(0, 0, -w_3c)$,

where u_i's and w_i's are parameter values (Table 1). Then the symmetry coordinates of A_{2u} and E_u species are as follows.

(A_{2u})

Ni 1: $s_1=\Delta z_1$,
Ni 2: $s_2=(1/\sqrt{2})\Delta(z_2+z_3)$,
Cs 1: $s_3=\Delta z_{13}$,
Cs 2: $s_4=(1/\sqrt{2})\Delta(z_{14}+z_{15})$,
F 1: $s_5=(1/\sqrt{3})\Delta(z_4+z_5+z_6)$,
F 1: $s_6=(1/\sqrt{3})\Delta\{(x_4+(-x_5+\sqrt{3}y_5)/2+(-x_6-\sqrt{3}y_6)/2)\}$,
F 2: $s_7=(1/\sqrt{6})\Delta(z_7+z_8+z_9+z_{10}+z_{11}+z_{12})$,
F 2: $s_8=(1/\sqrt{6})\Delta(x_7+(-x_8+\sqrt{3}y_8)/2+(-x_9-\sqrt{3}y_9)/2+x_{10}+(-x_{11}+\sqrt{3}y_{11})/2+(-x_{12}-\sqrt{3}y_{12})/2)$,

(E_u)

Ni 1: $s_1=\Delta x_1$, s_2=the same for y_i,

Ni 2: $s_3=(1/\sqrt{2})\Delta(x_2+x_3)$, $s_4=$the same for y_i,
Cs 1: $s_5=\Delta x_{13}$, $s_6=$the same for y_i,
Cs 2: $s_7=(1/\sqrt{2})\Delta(x_{14}+x_{15})$, $s_8=$the same for y_i,
F 1: $s_9=(1/\sqrt{3})\Delta(x_4+x_5+x_6)$,
$s_{10}=$the same for y_i,
F 1: $s_{11}=(1/\sqrt{3})\Delta\{(x_4+(-x_5-\sqrt{3}y_5)/2+(-x_6+\sqrt{3}y_6)/2)\}$,
F 1: $s_{12}=(1/\sqrt{3})\Delta\{(y_4+(\sqrt{3}x_5-y_5)/2+(-\sqrt{3}x_6-y_6)/2)\}$,
F 1: $s_{13}=(1/\sqrt{6})\Delta(2z_4-z_5-z_6)$,
F 1: $s_{14}=(1/\sqrt{2})\Delta(z_5-z_6)$,
F 2: $s_{15}=(1/\sqrt{6})\Delta(x_7+x_8+x_9+x_{10}+x_{11}+x_{12})$
$s_{16}=$the same for y_i,
F 2: $s_{17}=(1/\sqrt{6})\Delta\{(x_7+(-x_8-\sqrt{3}y_8)/2+(-x_9+\sqrt{3}y_9)/2+x_{10}+(-x_{11}-\sqrt{3}y_{11})/2+(-x_{12}+\sqrt{3}y_{12})/2)\}$,
F 2: $s_{18}=(1/\sqrt{6})\Delta\{(y_7+(\sqrt{3}x_8-y_8)/2+(-\sqrt{3}x_9-y_9)/2+y_{10}+(\sqrt{3}x_{11}-y_{11})/2+(-\sqrt{3}x_{12}-y_{12})/2)\}$,
F 2: $s_{19}=(1/\sqrt{12})\Delta(2z_7-z_8-z_9+2z_{10}-z_{11}-z_{12})$,
F 2: $s_{20}=(1/\sqrt{4})\Delta(z_8-z_9+z_{11}-z_{12})$.

BULLETIN OF THE CHEMICAL SOCIETY OF JAPAN VOL. 43 3789—3793 (1970)

The Preparation of Nitro-Carbonato and -Acetylacetonato Complexes of Cobalt(III) and Their IR and UV Spectra

Hiroyasu Ichikawa and Muraji Shibata

Department of Chemistry, Faculty of Science, Kanazawa University, Kanazawa

(Received March 28, 1970)

Two new nitro complexes of cobalt(III), $K_2[Co(NO_2)_2CO_3acac]\cdot H_2O$ and $K_3[Co(NO_2)_4CO_3]\cdot H_2O$, have been prepared by the reaction of tricarbonatocobaltate(III) and the desired ligand. The 700—200 cm^{-1} region IR spectra for these complexes and the other related dinitro complexes have been measured, and the geometrical structures of these dinitro complexes have been determined as of the *cis*-form on the basis of the IR data. Furthermore, the absorption spectra of these nitro complexes have also been measured, and the stability of these complexes has been related to the spectral data.

We reported, in a previous paper, the preparation of a series of *cis*-dinitro complexes of cobalt(III), namely, $[Co(NO_2)_2(CO_3)_2]^{3-}$, $[Co(NO_2)_2CO_3ox]^{3-}$, and $[Co(NO_2)_2(ox)_2]^{3-}$.[1] In the present paper we will report the preparation of a new dinitro and a new tetranitro complex, namely, $K_2[Co(NO_2)_2CO_3acac]\cdot H_2O$ (acac=acetylacetonato ligand) and $K_3[Co(NO_2)_4CO_3]\cdot H_2O$. It has been found that the above carbonatoacetylacetonato complex is the most unstable of the five nitro complexes, including the previous three complexes. We will also report the 700—200 cm^{-1} region IR spectra for these complexes. On the basis of the data and some elemental knowledge of the group theory, the geometrical structures of the dinitro complexes are determined to be of the *cis*-form.

Furthermore, the frequency values of the nitro specific band of the complexes have been compared in terms of their stability in an aqueous solution.

Experimental

Preparation. 1) *Potassium Dinitrocarbonatoacetylacetonatocobaltate(III) Monohydrate*, $K_2[Co(NO_2)_2CO_3acac]\cdot H_2O$. Into a green solution of tricarbonatocobaltate(III) ($CoCl_2\cdot 6H_2O$ 10 g scale; 0.048 mol) prepared by the usual method,[2] 10 m*l* (0.10 mol) of acetylacetone were added, drop by drop. The mixture was then stirred under an iced condition for half an hour. After filtering the *tris*(acetylacetonato) complex and a residue out, 34 g (0.40 mol) of potassium nitrite were stirred into the filtrate under an iced condition. After a while, red needle-shaped crystals of the desired complex began to appear. The crystals were then washed thoroughly with benzene to remove the *tris*-(acetylacetonato) complex. The yield was about 6 g.

Found: C, 17.79; N, 6.68; H, 2.30%. Calcd for

1) H. Ichikawa and M. Shibata, This Bulletin, **42**, 2873 (1969).

2) M. Shibata, *Nippon Kagaku Zasshi*, **87**, 771 (1966).

$K_2[Co(NO_2)_2CO_3acac]\cdot H_2O$: C, 17.74; N, 6.90; H, 2.24%.

The complex decomposed very rapidly in an aqueous solution, giving a brown residue, but it kept stable in an aqueous solution in which potassium nitrite had been dissolved.

2) *Potassium Tetranitrocarbonatocobaltate(III) Monohydrate*, $K_3[Co(NO_2)_4CO_3]\cdot H_2O$. To a green solution of tricarbonatocobaltate(III) prepared on the same scale as 1), 26 g (0.30 mol) of potassium nitrite were added under cooling. The mixture was then stirred under an iced condition for an hour, after which 30 m*l* of 6N acetic acid were added, drop by drop. The mixed solution was further stirred for 3—4 hr to complete the reaction. Then, the resulting red solution was allowed to stand in a refrigerator overnight. After a small quantity of a precipitated material, $K_3[Co(NO_2)_6]$, had been filtered off, 50 m*l* of ethanol were added to the filtrate; the whole was then kept in a refrigerator for a day to precipitate orange, needleshaped crystals. The yield was about 7 g.

Found: C, 3.04; N, 12.46; H, 0.59%. Calcd for $K_3[Co(NO_2)_4CO_3]\cdot H_2O$: C, 2.74; N, 12.79; H, 0.46%.

When 100 m*l* of ethanol were added to the mother liquor and the mixture was allowed to stand in the cold, a mixture of tetranitrocarbonato- and dinitrodicarbonatocobaltate(III) was obtained.

Measurements. The infrared absorption spectra in the 700—200 cm^{-1} region were measured by the Nujol mull technique using a Hitachi EPI-L grating infrared spectrometer. The IR spectra in the 4000—700 cm^{-1} region and the visible and near-ultraviolet absorption spectra were measured with the same instruments as were used in a previous investigation.[1] In addition, an automatic recording spectrophotometer (JASCO Model UV-5) was used for the rapid measurement of the absorption spectrum of the carbonatoacetylacetonato complex.

Results and Discussion

Preparation and Measurement. As another reaction, we attempted partial replacement of the carbonato ligand in $[Co(NO_2)_2CO_3)_2]^{3-}$ with acetylacetonate, but the reaction gave a mixture of *trans*-$[Co(NO_2)_2(acac)_2]^-$ [3,4] and a brown, unknown material.

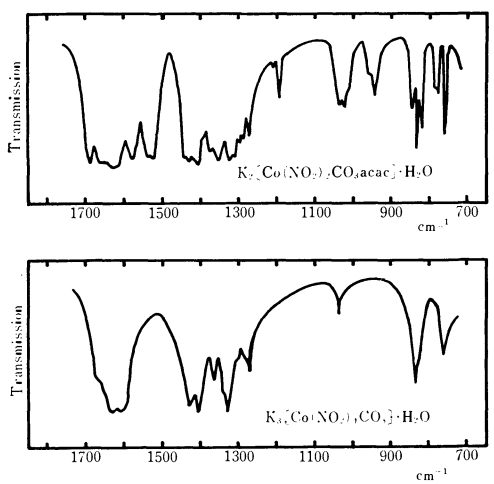

Fig. 1. Infrared absorption spectra of the *cis*-$K_2[Co(NO_2)_2CO_3acac]\cdot H_2O$ and $K_3[Co(NO_2)_4CO_3]\cdot H_2O$.

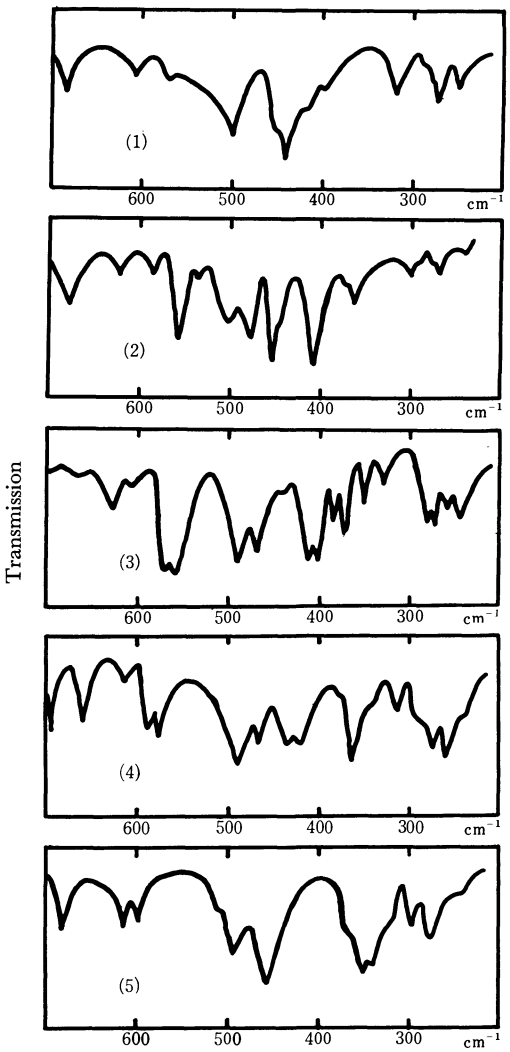

Fig. 2. Far-infrared absorption spectra of the nitro complexes of cobalt(III).
(1) $K_3[Co(NO_2)_2(CO_3)_2]\cdot H_2O$
(2) $K_3[Co(NO_2)_2CO_3ox]$
(3) $K_3[Co(NO_2)_2(ox)_2]\cdot H_2O$
(4) $K_2[Co(NO_2)_2CO_3acac]\cdot H_2O$
(5) $K_3[Co(NO_2)_4CO_3]\cdot H_2O$

The complexes were unstable in an aqueous solution. The measurement, therefore, of the absorption spectrum of the tetranitrocarbonato complex was carried out in a 0.10M potassium bicarbonate aqueous solution. The carbonatoacetylacetonato

3) L. J. Boucher and J. C. Bailar, Jr., *J. Inorg. Nucl. Chem.*, **27**, 1093 (1965).

4) R. O. Archer and B. P. Cotsoradis, *Inorg. Chem.*, **4**, 1584 (1965).

TABLE 1. IR DATA OF THE NITRO COMPLEXES OF COBALT(III) (cm^{-1})

Complex	NO_2^-			CO_3^{2-}				
	asym. ν(NO)	sym. ν(NO)	sym. δ(ONO)	sym. $\nu(C-O_{II})$	asym. $\nu(CO_I)$	sym. $\nu(CO_I)$	out-of-plane $\pi(O_ICO_{II})$	sym. $\delta(O_ICO_I)$
$K_2[Co(NO_2)_2CO_3acac]\cdot H_2O$	1401	1355	840	1683	1291	1025	833	759
		1323	833	1664	1276			
		1310	823	1614				
$K_3[Co(NO_2)_4CO_3]\cdot H_2O$	1436	1366	833	1677sh	1274sh	1031	833	758
	1407	1331sh	830	1641	1267			
		1321		1601				

sh: shoulder

TABLE 2. IR DATA OF THE NITRO AND RELATED COMPLEXES (cm^{-1})

Complex	NO_2^-			CO_3^{2-}			$C_2O_4^{2-}$			
	wagging δ(ONO)	sym. ν(M-N)	rocking δ(ONO)	asym. $\delta(O_ICO_{II})$	asym. $\nu(MO_I)$	sym. $\nu(M-O_I)$	asym. δ(CCO)	asym. ν(MO)	sym. δ(CCO)	
$K_3[Co(NO_2)_6]$	637	418	293							a)
$K_3[Co(NO_2)_2(CO_3)_2]\cdot H_2O$	606	443	295sh	685	503					b)
	576	425	284							
$K_3[Co(NO_2)_2CO_3ox]$	623	443	272	680	502		558	478		b)
	585	407								
$K_3[Co(NO_2)_2(ox)_2]\cdot H_2O$	627	415	280				570	471	444	b)
		405	274				562	490		
$K_2[Co(NO_2)_2CO_3acac]\cdot H_2O$	590	435	274	658	492					b)
	574	423								
$K_3[Co(NO_2)_4CO_3]\cdot H_2O$	613	456		683	493	349				b)
	598					341sh				
$K[Co(NH_3)_2(CO_3)_2]$				673	444	366				c)
					411					
$K_3[Co(ox)_3]\cdot 3H_2O$							559	476	446	d)

a) I. Nakagawa, I. Shimanouchi and K. Yamasaki, *Inorg. Chem.*, **3**, 772 (1964).
b) Present work.
c) J. Fujita, A. Martell and K. Nakamoto, *J. Chem. Phys.*, **36**, 339 (1962).
d) J. Fujita, K. Nakamoto and M. Kobayashi, *J. Phys. Chem.*, **61**, 1014 (1957).

TABLE 3. IR DATA OF THE $K_2[Co(NO_2)_2CO_3acac]\cdot H_2O$ COMPLEX (cm^{-1})

Location			Tentative assignment
1577			sym. ν(CO)
1520			asym. ν(CC)
1440			CH_3 deg. def.
1401			asym. ν(CO)
1374			CH_3 sym. def.
1291	1276		sym. ν(CC)
1196			CH in-plane bend.
1038sh	1033	1025	CH_3 rock.
950sh	942		$\nu(C-CH_3)$
788	785		CH out-of-plane bend.
695			ring def.+ν(M-O)
668sh	658		C-CH_3 bend.+ν(M-O)
467			asym. ν(M-O)
365			ring deformation

complex rapidly changed from red to green in a potassium bicarbonate aqueous solution, but the green solution thus produced rapidly returned to the original red state on the addition of potassium nitrite, and the recovered solution was stable for a few hours at room temperature. This phenomenon seems to arise from the rapid substitution between CO_3^{2-} and NO_2^- ions. Therefore, a potassium nitrite aqueous solution in a high concentration was used as the solvent of the carbonatoacetylacetonato complex. However, because of the absorption of the nitrite ion itself, the absorption spectrum of the complex was measured only in the 700—400 mμ region, with a 0.50M potassium nitrite aqueous solution (Fig. 3, ------). The measurement in the 700—250 mμ region was carried out with a 0.10M aqueous solution (Fig. 3, ——).

IR Spectra. The IR spectra in the 4000—700 cm^{-1} region for the present complexes are shown in Fig. 1, while the numerical data are given in Tables 1 and 3. The 700—200 cm^{-1} region spectra of the present complexes and of related complexes are shown in Fig. 2, and the numerical data are given in Tables 2 and 3.

It is clear that the NO_2^- in the present complexes coordinates to a central atom through the N-atom, because of the absence of a nitrito characteristic band (sym. ν(NO)) at 1050 cm^{-1} [5,6] and a characteristic bridged nitrito band (asym. ν(NO)) near 1520 cm^{-1}.[7]

When we assume that the C_{2v} symmetry of a free nitrite ion is maintained in the complex, the number of infrared active modes becomes 6 for the M–NO_2. These 6 fundamentals were observed for all the complexes except the tetranitro complex in the range of 1450—400 cm^{-1} (Tables 1 and 2). For the tetranitro complex, 5 bands were observed.

In the previous paper,[1] we determined the geometrical structures of the dinitro complexes on the basis of the number of NO_2^- symmetrical stretching and bending vibrations. In this work, we expected that the IR spectra of these complexes in the far-infrared region (below 700 cm^{-1}) would afford more information about the structure, since the Co–NO_2 stretching and the wagging of the nitro group appear in this region. For example, *cis*-$[Co(NO_2)_2(NH_3)_4]^+$ has two bands, at 605 and 587 cm^{-1}, attributable to the NO_2^- wagging vibration, whereas *trans*-$[Co(NO_2)_2(NH_3)_4]^+$ has only one band, at 623 cm^{-1}.[7] In the case of the present complexes, one or two bands attributable to the NO_2^- wagging vibration were observed (Table 2).

From a group theoretical consideration, the *trans* dinitro complex was expected to have one IR active M–NO_2 stretching mode in a D_{4h} or D_{2h} symmetry, and the corresponding *cis* complex, to have two modes in a C_{2v} or C_2. For the present dinitro complexes, two bands attributable to the Co–NO_2 stretching vibration were observed. The assignment was tentatively achieved by the method of Nakagawa *et al.*[8] (Table 2). From this result, it may be concluded that these dinitro complexes belong to the *cis*-form.

The symmetry, D_{3h}, of the free carbonate ion is lowered to C_{2v} by chelation, and the complexed carbonate ion has 9 fundamentals. Among the 9 fundamentals, 7 in-plane modes belong to the A_1 and B_2 representations, and 2 out-of-plane modes belong to B_1. We observed at least 7 bands for the four nitro complexes in the 1700—340 cm^{-1} region. Their locations are shown in Tables 1 and 2.

In our previous paper,[1] we identified a broad and strong band in the 1700—1600 cm^{-1} region as asym. ν(C–O_I) (where O_I represents the oxygen atom coordinated to a central atom), according to the method of Gatehouse.[9] Fujita *et al*,[10] however, have identified the same band as ν(C–O_{II}) (where O_{II} represents the free oxygen atom). Judging from the fact that the C–O_{II} bond has a double-bond character in $[Co(NH_3)_4CO_3]^+$,[11] we will now regard the absorption band (1700—1600 cm^{-1}) as ν(C–O_{II}).

The band near 500 cm^{-1} may be assigned to the M–CO_3 asymmetrical stretching vibration (Table 2). In fact, the corresponding Co–CO_3 mode in the double complex $[Co(NH_3)_6]\cdot[Co(CO_3)_3]$ has been observed at 488 and 465 cm^{-1}.[10] In the case of *trans*-$[Co(NO_2)_2(acac)_2]^-$, no absorption band was observed near 500 cm^{-1}.

When C_{2v} symmetry is assumed for a chelated structure of an oxalate ion, there are 15 fundamentals.[12,13] The number of infrared active modes of M–C_2O_4 is 13 in C_{2v}. Of these fundamentals, 8 bands were observed in the 1750—450 cm^{-1} range. Their locations in the 1750—700 cm^{-1} range were shown previously,[1] while those in the 700—450 cm^{-1} range are shown in Table 2.

The tentative assignment of the complexed acetyl-

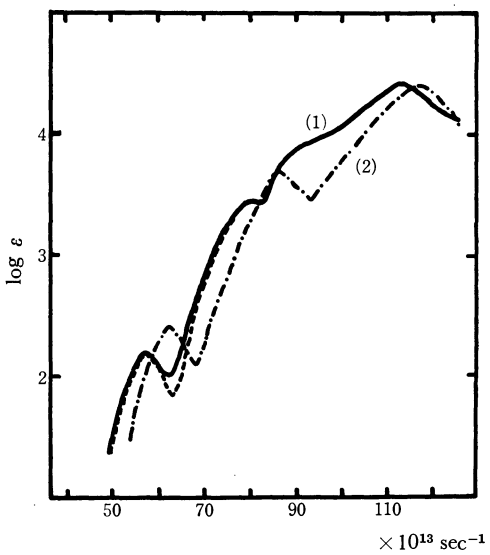

Fig. 3. Absorption spectra of the nitro complexes of cobalt(III).
(1) $K_2[Co(NO_2)_2CO_3acac]\cdot H_2O$ —— in 0.10M KNO_2 and ------ in 0.50M KNO_2
(2) $K_3[Co(NO_2)_4CO_3]\cdot H_2O$ -·-· in 0.10M $KHCO_3$

5) K. Nakamoto, J. Fujita and H. Murata, *J. Chem. Soc.*, **1959**, 4073.
6) R. B. Perland, T. J. Lane and J. V. Quagliano, *J. Amer. Chem. Soc.*, **78**, 883 (1956).
7) K. Nakamoto, J. Fujita and H. Murata, *ibid.*, **80**, 4817 (1958).
8) I. Nakagawa, I. Shimanouchi and K. Yamasaki, *Inorg. Chem.*, **3**, 772 (1964); *ibid.*, **7**, 1332 (1968).
9) B. M. Gatehouse, S. E. Livingstone and R. S. Nyholm, *J. Chem. Soc.*, **1958**, 3137.
10) J. Fujita, A. E. Martell and K. Nakamoto, *J. Chem. Phys.*, **36**, 339 (1962).
11) G. A. Barclay and B. F. Hoskins, *J. Chem. Soc.*, **1962**, 586.
12) K. Nakamoto, J. Fujita, S. Tanaka and M. Kobayashi, *J. Amer. Chem. Soc.*, **79**, 4904 (1957).
13) J. Fujita, A. E. Martell and K. Nakamoto, *J. Chem. Phys.*, **36**, 324 (1962).

Table 4. Absorption data for the new nitro complexes ($\times 10^{13}$sec^{-1})

Complex	ν_1	ν_{sp}	ν_3	$\nu_{sp}-\nu_1$
$K_2[Co(NO_2)_2CO_3acac]\cdot H_2O$	56.10 (2.18)	*ca.* 80.8 (3.39) *ca.* 90.1 (3.75)sh	*ca.* 113.3 (4.36)	*ca.* 24.7
$K_3[Co(NO_2)_4CO_3]\cdot H_2O$	61.56 (2.39)	85.65 (3.69)	114.20 (4.27)	24.09

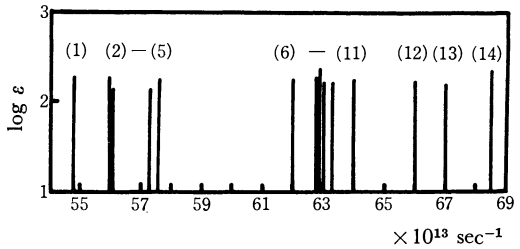

Fig. 4. The position of first absorption band of *cis*-dinitro complexes of cobalt(III).
(1) $[Co(NO_2)_2(CO_3)_2]^{3-}$
(2) $[Co(NO_2)_2CO_3ox]^{3-}$
(3) $[Co(NO_2)_2CO_3acac]^{2-}$
(4) $[Co(NO_2)_2(ox)_2]^{3-}$ (5) $[Co(NO_2)_2(acac)_2]^-$
(6) α-$[Co(NO_2)_2CO_3(NH_3)_2]^-$
(7) $[Co(NO_2)_2CO_3en]^-$ (8) $[Co(NO_2)_6]^{3-}$
(9) α-$[Co(NO_2)_2ox(NH_3)_2]^-$
(10) $[Co(NO_2)_2ox\ en]^-$ (11) $[Co(NO_2)_2(gly)_2]^-$
(12) $[Co(NO_2)_2gly\ en]$
(13) $[Co(NO_2)_2(NH_3)_4]^+$ (14) $[Co(NO_2)_2(en)_2]^+$

acetonate was attempted according to the references.[14-16] The data are given in Table 3.

Absorption Spectra. The absorption spectra in the solution are shown in Fig. 3, while the numerical data are listed in Table 4. The frequency values of the first absorption band for a number of dinitro complexes including the hexanitro complex are diagrammatically represented in Fig. 4. From this figure, it may be seen that the positions of the first absorption band shift according to the spectrochemical series.[17] We therefore calculated the position of the first absorption band of hexanitrocobaltate(III) by the following equation, based on "the rule of average environment"[18];

$$2/3(A) + 1/3(X) = (B)$$
$$(X) = 3(B) - 2(A)$$

where (A) and (B) are the positions of the first band for a $[CoA_6]$-type and a $[Co(NO_2)_2A_4]$-type complex respectively, and where (X) is the frequency value to be estimated. In the case of a $[Co(NO_2)_2$-(aa)(bb)]-type complex, (A) was taken as the mean value of a $[Co(aa)_3]$-type complex and a $[Co(bb)_3]$-type complex. The results are represented in Fig. 5. The positions, estimated from the mixed dinitro complexes with carbonato, oxalato, and acetylacetonato ligands, are at $70—73\times 10^{13}$ sec^{-1}. On the other hand, the positions estimated from the other dinitro-ammine-type complexes are at $75—78\times 10^{13}$ sec^{-1}. From these results, it may be said that the nitro-ligand field of the mixed dinitro complex with the *bis*(bidentate O–O)-type ligand is less weak than that of the mixed-dinitro complex with the ammine-type ligand. In fact, the aqueous solutions of the mixed dinitro complexes with the O–O type ligands are unstable, while the solutions of the dinitro-ammine type complexes are stable.

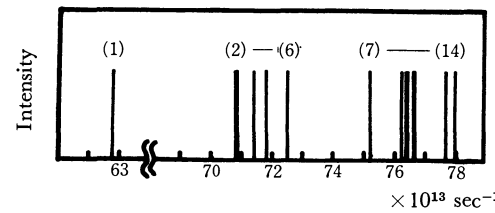

Fig. 5. The estimated position of first absorption band of hexanitrocobaltate(III).
(1) $[Co(NO_2)_6]^{3-}$
(2) $[Co(NO_2)_2(acac)_2]^-$
(3) $[Co(NO_2)_2CO_3acac]^{2-}$
(4) $[Co(NO_2)_2(CO_3)_2]^{3-}$
(5) $[Co(NO_2)_2CO_3ox]^{3-}$
(6) $[Co(NO_2)_2(ox)_2]^{3-}$
(7) $[Co(NO_2)_2(NH_3)_4]^+$
(8) $[Co(NO_2)_2ox\ en]^-$
(9) $[Co(NO_2)_2gly\ en]$
(10) α-$[Co(NO_2)_2ox(NH_3)_2]^-$
(11) $[Co(NO_2)_2(gly)_2]^-$
(12) α-$[Co(NO_2)_2CO_3(NH_3)_2]^-$
(13) $[Co(NO_2)_2en_2]^+$
(14) $[Co(NO_2)_2CO_3en]^-$

The maximum frequency of the nitro specific absorption band was found at *ca.* 80.8×10^{13} sec^{-1} for the carbonatoacetylacetonato complex and at 85.65×10^{13} sec^{-1} for the tetranitrocarbonato complex. The position for the former complex lies in the longest-wavelength side among the dinitro complexes (81.02 for $[Co(NO_2)_2(ox)_2]^{3-}$; 85.85 for $[Co(NO_2)_2CO_3ox]^{3-}$; 87.15 for $[Co(NO_2)_2(CO_3)_2]^{3-}$). It should be noted that the positions for the $[Co(NO_2)_2CO_3acac]^{2-}$, $[Co(NO_2)_2(ox)_2]^{3-}$, and $[Co(NO_2)_6]^{3-}$ complexes, which are unstable in an aqueous solution, are at lower frequencies than that (84.93×10^{13} sec^{-1}) for the free nitrite ion.

14) K. Nakamoto and A. E. Martell, *J. Chem. Phys.*, **32**, 588 (1960).
15) K. Nakamoto, P. J. McCarthy, A. Ruby and A. E. Martell, *J. Amer. Chem. Soc.*, **83**, 1066 (1961).
16) G. T. Behnke and K. Nakamoto, *Inorg. Chem.*, **6**, 433 (1956).
17) Y. Shimura and R. Tsuchida, This Bulletin, **29**, 311 (1956).
18) C. K. Jørgensen, "Absorption Spectra and Chemical Bonding in Complexes," Pergamon Press, New York and London (1961).

BULLETIN OF THE CHEMICAL SOCIETY OF JAPAN VOL. 43 3794—3795 (1970)

An Application of the Oxidation Reaction between Ammonia and Bromate, Permanganate or Dichromate for the Determination of Ammonia Nitrogen in the Kjeldahl Digests without Distillation

M. A. SIDDIQUI and M. K. BHATTY

Pakistan Council of Scientific & Industrial Research Laboratories, Lahore, Pakistan

and Muhammad ASHRAF

Department of Pharmacy, Punjab University, Lahore, Pakistan

(Received March 4, 1970)

Nitrogen in organic compounds, agricultural and animal products is converted into ammonium sulphate by Kjeldahl digestion. The ammonium sulphate is reacted quantitatively with hypobromite produced *in situ* by the addition of an excess of potassium bromate and bromide. The unutilized potassium bromate is determined iodometrically and the amount of ammonia nitrogen can be calculated from the consumed potassium bromate. Accurate results are also obtained when potassium bromate is replaced with potassium permanganate or dichromate for the determination of ammonia nitrogen in Kjeldahl digests. However, the present method is not applicable to the determination of ammonia nitrogen in undigested sample.

It has already been reported by various workers that the distillation step in the Kjeldahl method can be effectively replaced by a bromometric titration. Thus a hypobromite method,[1] employing brominating mixture and potassium tetraborate has been proposed. A similar method in which potassium tetraborate is replaced with an alkali has been applied to the determination of non-protein nitrogen in serum.[2] Recently such a method has been modified and used for the determination of organic nitrogen on both the micro as well as the semi micro scales.[3]

During the present investigations, it has been shown that potassium permanganate and potassium dichromate work as well as potassium bromate in the brominating mixture in this method. In addition, these oxidants have been shown to be successfully applicable to all types and scales of Kjeldahl nitrogen. Both potassium permanganate and potassium dichromate solutions are already employed as analytical reagents whose stability is, at any rate, better than that of hypobromite or even hypochlorite solutions prepared in the laboratory.

Potassium permanganate or dichromate and potassium bromide in the acidic medium generate bromine which on the addition of an alkali, can be coverted into hypobromite *in situ*. Although hypohalite solutions have been previously extensively used for the determination of nitrogen in organic compounds,[4] soil,[5] biological material and agricultural products,[6] yet they are not ordinarily stable. In the matter of stability, hypobromite solutions are hopelessly inferior to hypochlorite solutions.[7] Difficulties encountered in their preparation and application are known too well to be enumerated here. Such difficulties do not arise when bromate, permanganate or dichromate is used as oxidant in the presence of potassium bromide.

Experimental

Apparatus. A 500 m*l* round bottom flask, with B 19 neck fitted with a 15 cm tube attached to B 19 cone, is used for digestion on the macro scale. After digestion the cone is replaced with an *N*-shaped tube[3] having the following dimensions. Tube bore 1.8 cm, the B 19 cone limb 4 cm, the middle limb 16.5 cm, and stoppered (with B 19 joint) limb 14 cm long.

Reagents. Sulphuric acid (d, 1.84), G.R.; Potassium sulphate, G.R.; Mercuric sulphate, G.R.; Glucose, G.R.; Potassium bromate solution, 0.5 N Potassium permanganate solution, 0.5 N; Potassium dichro-

1) F. de A. Bosch and M. C. A. Querol, *Anales real soc. espan. fis. Y quim. Ser. B*, **44**, 737 (1947); *Chem. Abstr.*, **43**, 1285h (1949).

2) M. Krutsay, *Orv. Hetilap*, **108** (2), 72 (1967); *Chem. Abstr.*, **66**, 73168h (1967).

3) M. Ashraf, M. A. Siddiqui and M. K. Bhatty, *Talanta*, **15**, 559 (1968).

4) M. Ashraf, M. K. Bhatty and R. A. Shah, *Pakistan J. Sci. Ind. Res.*, **3**, 1 (1960); *Chem. Abstr.*, **55**, 17357.i (1961).

5) M. Ilyas Qureshi, Naeem Shakir, M. K. Bhatty, Muhammad Ashraf and R. A. Shah, *ibid.*, **5**, 159 (1962).

6) M. Ashraf, M. K. Bhatty and R. A. Shah, *ibid.*, **12**, 103 (1960); *Chem. Abstr.*, **55**, 17358 b (1960).

7) M. A. Siddiqui, M. K. Bhatty and M. Ashraf (Unpublished work).

mate solution, 0.5 N; Sodium hydroxide solution, 60% W/V; Potassium iodide, G.R.; Hydrochloric or sulphuric acid, 10 N; Sodium thiosulphate solution, 0.25 N; Starch solution (aqueous), 1%.

Procedure. Weigh accurately 0.1 to 0.2 g of the organic sample (dried blood=0.1—0.2 g, cereal, tea leaves and meat=1 g, fresh vegetables=2 g, etc) into the flask. Add 5.6 g of the catalyst (5.0 g potassium sulphate and 0.6 g mercuric sulphate) and use 12 m*l* concentrated sulphuric acid for organic compounds and 15 m*l* for commercial materials. Add 1—2 g of glucose and 16 m*l* of sulphuric acid in case of compounds which require reduction prior to digestion. Digest the sample for 1—2 hr. Cool and dilute the digest by rinsing the cone with about 50 m*l* of distilled water. Place the flask in cold water and add 20 m*l* of the potassium bromate, permanganate or dichromate solution. Add 5 g of potassium bromide and immediately fit in the *N* tube containing 35 m*l* of sodium hydroxide solution. In the case of potassium dichromate, add 15 m*l* of sodium hydroxide solution into the *N* tube. Keep the tubes neck open and heat the flask at 70°C. Continue heating for 15 min. Cool the flask and add the remaining 20 m*l* of the sodium hydroxide solution into the tube and stopper it.

Transfer the alkali portion-wise from the *N* tube to the cold contents of the flask by tilting the system slightly. Shake the flask and allow it to stand for 10—15 min. Add 8 g of potassium iodide followed by 25 m*l* of 10 N hydrochloric or sulphuric acid through the *N* tube. Allow to stand for another 5 min, remove the *N* tube and titrate the liberated iodine with sodium thiosulphate solution, using starch solution as an indicator. Carry out a blank determination under similar conditions.

Calculation. 1 m*l* 0.1 N $KBrO_3$ or $KMnO_4$ or $K_2Cr_2O_7$=0.4667 mg. N_2

Discussion and Conclusion

Potassium bromate is a primary standard and advantages realised by its use in nitrogen determination on the micro and semi micro scales have already been listed.[3] Potassium permanganate and dichromate have been used for nitrogen determination for the first time. Their solutions when prepared and stored according to the established practice, can work as well as that of bromate.

The results (Table 1) show that the reagents are applicable to the determination of all those types of organic nitrogen which either as such or after reduction can be digested into ammonium sulphate. It has also been shown (Table 2) that these reagents in general and potassium bromate in particular can be employed with advantage for a variety of nitrogenous commercial materials.

Some difficulties are encountered when nitrogen is determined in the agricultural and animal products by the hypochlorite-arsenite method.[6] For example the neutralized digest in the case of tea leaves becomes reddish brown on the addition of sodium hypochlorite solution with the result that it becomes difficult to mark the end point. Similarly, for larger than 1 g of meat and 0.2 g of blood samples, a yellow precipitate appears after the addition of the hypochlorite. This colour changes to greyish black on the addition of sodium arsenite solution, thus making it difficult to mark the end point.

In the present method, involving the use of potassium bromate, however, the above mentioned difficulties do not arise. The method gives good results even if comparatively large amount of tea leaves, meat and blood samples are used for analysis. It further shows that the present method can also be applied to materials containing metals like iron. It has also been observed that the results are higher when digestion is incomplete. This is due to the fact that some bromine or even acidic potassium permanganate is consumed in the oxidation of the undigested organic matter. Therefore, the present method can not be applied to the determination of ammonia nitrogen in the undigested sample.

Our thanks are due to Mr. M. Aslam, Director, Pakistan Council of Scientific & Industrial Research, Laboratories, Lahore, Pakistan, for providing facilities to carry out this research work.

Table 1. Recovery of nitrogen

Compound	Required %	Found by Bromate %	Permanganate %	Dichromate %
Ammonium sulphate	21.21	21.37, 21.31	21.11, 21.32	21.36, 21.26
DL-Alanine	15.72	15.65, 15.59	15.75, 15.79	15.74, 15.54
Acetanilide	10.36	10.53, 10.35	10.49, 10.54	10.36, 10.42
Diphenylamine	8.28	8.21, 8.04	8.37, 8.21	8.31, 8.19
Phenacetin	7.82	7.95, 7.73	7.75, 7.83	8.01, 7.71
Hippuric acid	7.82	7.97, 7.99	7.84, 7.99	7.71, 7.56
Quinine sulphate	7.16	7.23, 7.16	7.23, 7.10	7.12, 7.33
Atropine	4.84	4.84, 4.93	4.91, 5.00	4.71, 4.90
Phenyl thiourea	18.41	18.35, 18.30	18.21, 18.51	18.32, 18.51
α-Nitroso β-naphthol	8.09	8.16, 8.10	8.00, 8.15	—
p-Nitroaniline	20.29	20.22, 20.09	20.25, 20.29	—
o-Nitrobenzoic acid	8.38	8.49, 8.38	8.32, 8.47	—
Azobenzene	15.38	15.27, 15.29	15.51, 15.37	—

Table 2. Recovery of nitrogen

Commercial materials	Found by Hypochlorite %	Bromate %
Wheat	1.84, 1.83	1.84, 1.90
Rice	1.18, 1.17	1.19, 1.20
Gram (black)	3.49, 3.51	3.61, 3.56
Peas (green)	1.01, 0.98	1.07, 1.05
Milk (Lahore milk plant)	0.49, 0.49	0.50, 0.51
Blood (crude)	11.90, 12.09	11.96, 11.99
Tea leaves (Brook Bond)	4.35, 4.17	4.42, 4.39
Meat (goat)	3.29, 3.14	3.37, 3.34

BULLETIN OF THE CHEMICAL SOCIETY OF JAPAN VOL. 43 3796—3800 (1970)

The Photometric Determination of Minute Amounts of Iodine in Silicate Rocks*1

Norinobu YONEHARA,*2 Minoru YOSHIDA and Iwaji IWASAKI*3

Department of Chemistry, Faculty of Science, Tokyo Institute of Technology, Ookayama, Meguro-ku, Tokyo

(Received June 2, 1970)

A rapid and sensitive method for the determination of minute amounts of iodine in silicate rocks has been developed. A rock was fused with potassium hydroxide, and the cake was treated with water and sulfuric acid. The iodine in the solution was reduced to iodide by sodium sulfite, and was then oxidized to free iodine by sodium nitrite. The free iodine thus obtained was extracted with carbon tetrachloride and then back-extracted with a sodium hydroxide solution. The iodine in this aqueous layer was determined photometrically by a method based on the catalytic effect of iodine on the color-fading of ferric thiocyanate. By the proposed method, amounts of iodine as low as 0.007 μg in a 1-g sample of silicate rocks can be determined. Application to some igneous rock samples gave results with a relative standard deviation of less than 7.2%, except for very low concentrations.

Since von Fellenberg's classical work,[1] there have been almost no data on iodine in rocks. Recent determinations of iodine in meteorites by neutron-activation analysis suggest, however, that the iodine contents of rocks may be much smaller than those reported by von Fellenberg. Therefore, reliable data on iodine in rocks are desirable from the viewpoint of geochemistry. However, the determination of iodine in rocks requires an extremely sensitive method, for the iodine content in rocks is very low, particularly in igneous rocks.

Crouch[2] has developed a spectrophotometric method for determining the iodine in silicate rocks based on the starch-iodine reaction, but this method requires quite a large sample and a time-consuming procedure; there are also some problems still to investigate regarding the treatment of the residue resulting from the dissolution of rocks. The kinetic method,[3] followed by titration, is also not sensitive enough to analyse iodine in igneous rocks. Goles and Anders[4] have determined the iodine contents of some meteorites by neutron-activation analysis. Recently, Tajima and Akaiwa[5] have reported a method of determining the iodine in sedimentary rocks, also by neutron-activation analysis. These methods may be suitable in sensitivity, but their procedures are time-consuming and require considerable manipulation and special equipment.

Yonehara and others[6–8] have previously reported colorimetric methods for the determination of ultramicro amounts of iodine by utilizing its catalytic effect on the color-fading of ferric thiocyanate. According to these methods, 0.005 μg of iodine can be determined colorimetrically. Although the catalytic method is very sensitive, it is supposed that there are some difficulties in the separation of iodine from rocks because of the chemical complexity of silicate rocks and the very low content of iodine. After a rock had been decomposed by fusion, we tried to separate the iodine as follows. As the iodine in the solution obtained by dissolving the cake is presumably in a highly oxidized form, such as the iodate ion, iodate was first reduced to iodide by sodium sulfite. The iodide was then oxidized to free iodine by sodium nitrite. The free iodine was extracted with carbon tetrachloride, and then back-extracted with a sodium hydroxide solution. Finally the iodine in the aqueous layer was determined by the catalytic method.

*1 Presented at the 15th Annual Meeting of the Japan Society for Analytical Chemistry, Fukuoka, Oct., 1966.

*2 Present address: Department of Chemistry, Faculty of Science, Kagoshima University, 201, Kamoike-cho, Kagoshima-shi, Japan.

*3 Present address: Department of Chemistry, Faculty of Science, Tôhô University, Ôkubo, Narashino-shi, Chiba-ken, Japan.

1) Th. von Fellenberg, *Biochim. Z.*, **187**, 1 (1927).

2) W. H. Crouch, Jr., *Anal. Chem.*, **34**, 1698 (1962).

3) L. A. Shneider and A. D. Miller, *Chem. Abstr.*, **62**, 13833b (1965); *Zh. Analit. Khim.*, **20**, 92 (1965).

4) G. G. Goles and E. Anders, *Geochim. et Cosmochim. Acta*, **26**, 723 (1962).

5) E. Tajima and H. Akaiwa, *Radioisotopes*, **17**, 40 (1968).

6) S. Utsumi, M. Shiota, N. Yonehara and I. Iwasaki, *Nippon Kagaku Zasshi*, **85**, 32 (1964).

7) I. Iwasaki, S. Utsumi and N. Yonehara, *ibid.*, **85**, 36 (1964).

8) N. Yonehara, This Bulletin, **37**, 1101 (1964).

According to a previous study,[9] the iodine content in igneous rocks seems to be less than 0.1 μg/g; therefore, a 0.5–1-g sample of silicate rocks is required for the application of the catalytic method to the determination of iodine in rocks. The treatment of the cake obtained by the fusion of a 1-g rock sample requires considerable amounts of water, causing the solution finally obtained to have an extremely low iodine concentration. That the behavior of very small amounts of iodine differs significantly from that of macro amounts of iodine[10,11] suggests the difficulty of achieving the quantitative separation of iodine in low concentrations such as that discussed above.

In the present work, we investigated whether the separation processes involving reduction, oxidation, extraction, and back-extraction could be performed quantitatively at very low concentrations and whether the catalytic method could be applied to the determination of iodine in silicate rocks. In addition, the catalytic method was modified so as to increase the sensitivity by changing the concentration of the reagents and the conditions of the reaction.

Experimental

Apparatus. A Hirama IIB photoelectric-colorimeter with a 460 filter (with maximum transmission at 460 mμ) and 10-mm cells were used to measure the absorbance.

The catalytic reaction was carried out at 60.00± 0.05°C, using a water bath with a Taiyo Thermo Unit.

Reagents. All the chemicals used were of a guaranteed reagent quality.

Redistilled water was used for the reagent preparation and throughout the procedures.

(Treatment of Rocks)

Potassium Hydroxide. The potassium hydroxide used for the fusion of rocks was a special-grade reagent; SV grade, obtained from the Tokyo Ôka Kôgyo Co., Ltd.

Sulfuric Acid Solution (1 : 1).

Sodium Sulfite Solution (about 5%).

Sodium Nitrite Solution (1.0M). Dissolve 6.90 g of sodium nitrite in water and dilute to 100 m*l*.

Sodium Hydroxide Solution (0.1N). Dissolve 2.0 g of sodium hydroxide in water and dilute to 500 m*l*.

(The Catalytic Reaction)

Ferric Ammonium Sulfate-Nitric Acid Solution. Dissolve 6 g of ferric ammonium sulfate in 100 m*l* of a 7.0N nitric acid solution.

Potassium Thiocyanate Solution (0.010M). Diluted from about a 0.1M potassium thiocyanate solution, as standardized by Volhard's method.

Sodium Nitrite Solution (0.014M). Dissolve 0.483 g of sodium nitrite in water and dilute to 500 m*l* in a volumetric flask.

Sodium Chloride Solution (20 g of Chloride per l). Dissolve 32.971 g of sodium chloride in water and dilute to exactly 1*l*.

Standard Iodide Solution. Prepare about a 0.1M potassium iodide solution and standardize by Volhard's method. Prepare the working solutions by diluting this solution adequately.

Standard Iodate Solution. Dissolve 0.847 g of potassium iodate in water and dilute to exactly 500 m*l* to give an iodine concentration of 1000 ppm. Prepare the working solutions by successive dilutions.

Procedure and Calibration Curve. Into a 30-m*l* nickel crucible, add 0.5—1 g of the powdered rock sample and the flux (potassium hydroxide, about six times the weight of the rock sample); heat first over a small flame, gradually raise the temperature to about 500°C, and then heat further for about 30 min. After cooling to room temperature, dissolve the cake with 15—20 m*l* of water and transfer all of the contents to a 50-m*l* centrifuge tube with a glass stopper. Crush the cake with a glass rod and stir the solution to dissolve the soluble material. After the solution has been centrifuged at about 3000 rpm for 5 min, transfer the supernatant liquid to a 50-m*l* glass beaker. Add a 1 : 1 sulfuric acid solution to neutralize the solution, and then add an excess of 1 m*l* of the acid. Then add 0.3 m*l* of a 5% sodium sulfite solution.

Into the centrifuge tube containing the residue, add 10 m*l* of water, 1—2 m*l* of the 1 : 1 sulfuric acid solution, and 0.1 m*l* of the 5% sodium sulfite solution, and shake vigorously to dissolve the residue. It is desirable to use just the amounts of sulfuric acid necessary to dissolve the residue present. Almost all of the precipitate can be dissolved by this procedure. Centrifuge again and pour the supernatant liquid into the same beaker. Wash the remaining residue three times with 2 or 3 m*l* of redistilled water and small portions of the 1 : 1 sulfuric acid, and pour all of the washings into the beaker. Keep the total volume of the 1 : 1 sulfuric acid used in washing at 1 m*l*. Transfer the solution thus obtained into a 100-m*l* separatory funnel and bring the volume of the solution to 60—80 m*l*. Then add 3.0 m*l* of a 1M sodium nitrite solution, mix thoroughly, add 10 m*l* of carbon tetrachloride, and shake the separatory funnel for 1 min. After the layers have

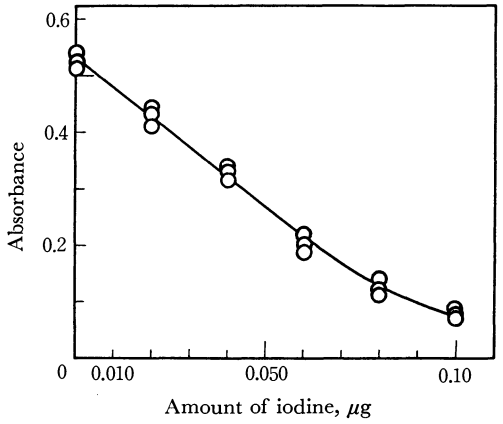

Fig. 1. Calibration curve.

9) M. Yoshida, I. Makino, N. Yonehara and I. Iwasaki, This Bulletin, **38**, 1436 (1965).

10) M. Kahn and A. C. Wahl, *J. Chem. Phys.*, **21**, 1185 (1953).

11) H. M. Eiland and M. Kahn, *J. Phys. Chem.*, **65**, 1317 (1961).

TABLE 1. CONTAMINATION DURING FUSION PROCESS

	Absorbacne				
					Mean
Without fusion*	0.509	0.533	0.539	0.553	0.534
Heated for 1.5 hr**	0.523	0.527	0.542	0.551	0.536
Heated for 3 hr**	0.461	0.526	0.544	0.565	0.519

5 g KOH was used.
* obtained by following the procedure without fusion.
** obtained by the procedure.

been completely separated, transfer the carbon tetrachloride phase into a 50-m*l* separatory funnel.

When a large amount of the residue still remains, dissolve this residue with 60—80 m*l* of water, 2 m*l* of the 1 : 1 sulfuric acid solution, and 0.3 m*l* of the 5% sodium sulfite solution, and then determine the iodine in this solution separately. Add the value obtained to that of the supernatant liquid obtained above.

To the carbon tetrachloride phase thus obtained, add 8.0 m*l* of water, 1.0 m*l* of a 0.1N sodium hydroxide solution, and 1.0 m*l* of a sodium chloride solution (2.0% as chloride), shake the separatory funnel for 1 min, and allow the layers to separate. Then transfer the aqueous layer into a 20-m*l* glass tube with a glass stopper. The iodine in this aqueous phase is then determined by the following catalytic method.

To the solution in the glass tube, add 1.0 m*l* of a 0.014M sodium nitrite solution and 1.0 m*l* of a 0.010M potassium thiocyanate solution, and mix thoroughly. Place the glass tube in a water bath at 60°C for about 10 min. Start the reaction by adding 3.0 m*l* of a nitric acid solution of ferric ammonium sulfate (at the same temperature), and then replace the glass tube in the water bath. Exactly 18 min after the addition of the ferric ammonium sulfate solution, measure the absorbance of the solution at 460 mμ, using water as the reference.

The calibration curve shown in Fig. 1 was prepared by taking 0.0-, 2.0-, 4.0-, 6.0-, 8.0- and 10.0-m*l* aliquot of a 0.010 ppm standard iodate solution and 1—6 g of potassium hydroxide, and by then following the procedure described above without fusion. The variation in sensitivity and in absorbance values resulting from the use of different batches of reagents makes it necessary to check the calibration curve for each set of determinations.

Results and Discussion

The Treatment of Rocks. In order to determine the iodine in rocks, decomposition and separation procedures must be used. In the present work, the fusion with potassium hydroxide was adopted, because this fusion is made at a relatively low temperature and a specially-pure reagent is obtainable. The use of sodium hydroxide gave lower absorbances than those of potassium hydroxide.

When the cake was treated with water, iodine was distributed to both the aqueous phase and the residue. As the iodine in the residue could not be removed to the aqueous phase by washing, it was necessary to dissolve the residue with sulfuric acid and to combine the resultant solution with the aqueous phase obtained above.

Decomposition by hydrofluoric acid was not adaptable because of the volatilization of the iodine during the process.

The Contamination during the Fusion Process. In order to examine the possibility of contamination during a fusion process, absorbances were measured by following the above procedure, after a 5-g portion of potassium hydroxide had been fused in the absence of iodine. The values without fusion were also obtained. As the comparison of these values shows good agreement, as can be seen in Table 1, the contamination during the fusion process was found to be insignificant.

The Reduction of Iodate to Iodide. Several experiments were made to examine the reduction of iodate to iodide by using a 5% sodium sulfite solution. In order to obtain a tolerable reproducibility of the reduction of the minute amounts of iodate,

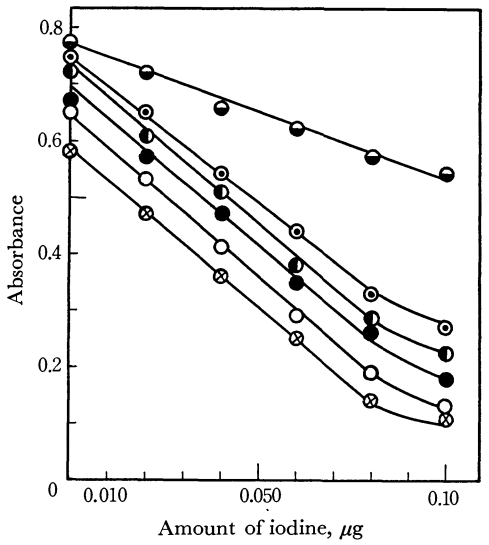

Fig. 2. Effect of amount of nitrite solution. (in the absence of KOH)
1M nitrite solution is used.
—◒— 0.1 m*l* —●— 2.0 m*l*
—⊙— 0.5 m*l* —○— 3.0 m*l*
—◐— 1.0 m*l* —⊗— 4.0 m*l*

less than 0.10 μg as iodine, it was necessary to keep the volume of the solution less than 50 m*l* at the reduction. As the reduction time, more than 15 min was required. No effect was observed on varying the volume of the sodium sulfite solution added.

The Oxidation of Iodide to Free Iodine. In measuring the effect of the amount of sodium nitrite on the oxidation of iodide, several experiments were made using a 1.0M sodium nitrite solution and the procedure featuring the absence of potassium hydroxide. The experimental results are shown in Fig. 2. The effect of the volume of the solution on the oxidation was examined; the same calibration curves were obtained on the volumes of 50, 60, and 80 m*l*.

The Use of Sulfuric Acid. In most cases of rock analysis, the rock samples are treated with hydrochloric acid. However, in this work, reduction, oxidation, extraction and back-extraction were not achieved quantitatively by using hydrochloric acid. Therefore, sulfuric acid was used. As can be seen in Fig. 3, the effect of the amount of sulfuric acid added is quite similar to that of sodium nitrite.

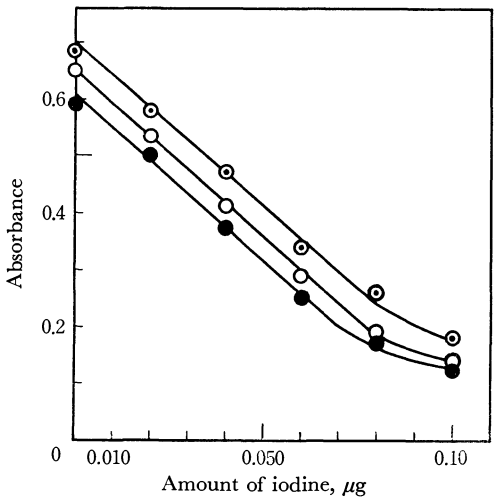

Fig. 3. Effect of amount of sulfuric acid. (in the absence of KOH)
1 : 1 sulfuric acid is used.
—⊙— 1.0 m*l* —○— 2.0 m*l*
—●— 3.0 m*l*

The Extraction and the Back-Extraction. In order to treat the cake obtained by the fusion of a 1-g rock sample, it is desirable to use 200 m*l* of water. The extraction of iodine from 200 m*l* of the solution was first attempted; however, the results obtained were not reproducible enough to determine the iodine. It was necessary to keep the volume of the solution within 80 m*l*. The reproducibility deteriorated slightly when the shaking time was less than 30 sec.

Ten milliliters of a sodium hydroxide solution convenient for the subsequent catalytic method were used. The use of a concentration of 0.005—0.1N gave the same recovery of iodine. The effect of the presence of chloride has been described in previous papers.[7,8]

The Effects of the Amounts of Potassium Hydroxide and Silicate. As considerable amounts of potassium ion and silicate ion are introduced into the solution by the fusion of silicate rocks, the effects of their amounts were examined. The experiments were made using 1–6 g of potassium hydroxide and the procedure without fusion. All of the values obtained fell just on the curve shown in Fig. 1. A 250—700-mg portion of silica was fused with 3 or 6 g of potassium hydroxide and a known amount of iodate was added; the same results were obtained. When the solution contains a considerable amount of the silicate ion, the precipitate of silica appears on neutralization. However, the presence of the precipitate in the solution does not disturb the subsequent procedure.

The Effect of Diverse Ions. To examine the effect of the substances commonly occurring in igneous rocks, several experiments were made in the presence of 0.06 and 0.04 μg of iodate and in its absence. The quantities of these substances studied may be the maximum content present in 1 g of common igneous rocks. There appears to be no significant effect of these substances, as is shown in Table 2.

Table 2. Effect of diverse ions

Ion	Amount added mg	Iodine taken μg	Iodine found μg
Fe^{3+}	100	0.000	0.000
		0.040	0.038
		0.060	0.057
Al^{3+}	130	0.000	0.006
		0.040	0.031
		0.060	0.057
Mg^{2+}	80	0.000	0.000
		0.040	0.039
		0.060	0.058
Ca^{2+}	70	0.000	0.006
		0.040	0.043
		0.060	0.061
Mixture		0.000	0.000
Fe^{3+}	50	0.040	0.043
Al^{3+}	70	0.060	0.056
Ca^{2+}	45		
Silicate ion	535		
KOH	6000		

The Determination of Iodine in Rocks. The iodine in several igneous rocks was determined by the present method; the results are shown in Table 3. The determinations were made by taking 1-g and 0.5-g samples; the results show good agreement

TABLE 3. DETERMINATION OF IODINE IN SILICATE ROCKS

Sample: Name and locality	Sample: Weight g	Iodine found μg/g					Mean μg/g	Std. devn.	Relative std. devn. %
Basalt									
1950—1951 lava	0.500	0.084	0.088	0.084	0.084	0.082	0.082	0.0059	7.2
O-sima, Tokyo, Metr.	1.00	0.075	0.075	0.074	0.085	—			
Andesite									
1946 lava	0.500	0.046	0.040	—	—	—	0.042	0.0027	6.4
Sakura-zima, Kagosima Pref.	1.00	0.044	0.040	0.041	—	—			
Obsidian									
Sirataki, Hokkaido	0.500	0.016	0.016	0.022	—	—	0.020	0.0034	17
	1.00	0.022	0.020	0.024	—	—			

TABLE 4. RECOVERY OF IODINE FROM FUSION PROCESS

	Sample Weight g	Iodine from rock μg	Iodine added μg	Total iodine μg	Iodine found μg	Error %
No. 1	1.00	0.082	0.047	0.129	0.121	−6.6
	0.500	0.041	0.047	0.088	0.086	−2.3
No. 2	1.00	0.042	0.047	0.089	0.095	+6.3
No. 3	1.00	0.020	0.047	0.067	0.066	−1.5

within the limits of experimental error of this method. Table 3 also shows the reproducibility of the method. Samples containing various amounts of iodine were analyzed in replicate by this method. The precision of this method was within 10% except for very low concentrations.

The Recovery of Known Amounts of Iodine. The method was also checked by adding known amounts of iodate to 1.0-g rock samples. The results, presented in Table 4, show the relative errors of the determination to be less than 6.6%. According to these results, it may be concluded that the loss of iodine during the fusion was insignificant and that no major source of interference was present in the rock samples analyzed.

This investigation was supported in part by a grant from the Kawakami Memorial Foundation.

BULLETIN OF THE CHEMICAL SOCIETY OF JAPAN VOL. 43 3801—3804 (1970)

The Crystal Structure of $(+)_{589}$-Dichlorobis(ethylenediamine)-cobalt(III) Chloride Monohydrate

Keiji MATSUMOTO, Shun'ichiro OOI and Hisao KUROYA

Department of Chemistry, Faculty of Science, Osaka City University, Sumiyoshi-ku, Osaka

(Received July 2, 1970)

The crystal structure of *cis*-$(+)_{589}$-$[CoCl_2en_2]Cl \cdot H_2O$ has been determined by the X-ray-diffraction method. The crystal is monoclinic with the cell constants: $a=12.07$, $b=11.52$, $c=8.33$ Å, and $\beta=96.9°$. The space group is $P2_1$, and $Z=4$. There are two crystallographically-independent complexes in the unit cell, but they have the same configuration and almost identical molecular dimensions. The absolute configuration of the complex cation is consistent with that proposed by McCaffery, Mason and Norman and should be denoted as $\Lambda(\delta\delta)$.

Several investigations have been made of the absolute configurations of optically-active *cis*-$[CoX_2en_2]$ or *cis*-$[Co\widehat{XX}en_2]$ complexes, making use of their Cotton effects or chemical interconversions.[1-7] Particularly, McCaffery, Mason and Norman[7] made a detailed study of the CD spectra in the first absorption-band region on the *cis*-series of bisdiamine complexes of cobalt(III) and established a definitive correlation between the major CD bands of these complexes and that of the thoroughly-examined $(+)_{589}$-$[Co\ en_3]^{3+}$;[8] they thus succeeded in making assignment of the absolute configurations to these bisdiamine cobalt(III) complexes.

We have been attempting to determine directly the absolute configurations of several metallic complexes by the X-ray method. We wish here to report on the results obtained for *cis*-$(+)_{589}$-$[CoCl_2en_2]Cl \cdot H_2O$.

Experimental

The racemic "violeo" compound was prepared by the method of Jörgensen and resolved into optical isomers by utilizing its reaction with ammonium (+)-α-bromocamphor-π-sulfonate.[9] The crude chloride obtained from the less soluble diastereoisomer yielded, upon crystallization from a saturated aqueous solution, needle-like, deep violet crystals of $(+)_{589}$-$[CoCl_2en_2]Cl \cdot H_2O$.

The unit cell dimensions were determined by the least-squares refinement of the *hk*0 and *h*0*l* reflection data recorded on Weissenberg photographs. The aluminum powder diffraction lines were superimposed on the films for calibration. The systematic absences were: 0*k*0 for *k*=odd. Hence, the space group could be either $P2_1$ or $P2_1/m$. However, the latter should be excluded, since the crystal contains only one form of the enantiomorphous isomers.

The crystal data are as follows:

monoclinic
space group $P2_1$
$a=12.07$ (0.008)Å
$b=11.52$ (0.007)
$c=8.33$ (0.005)
$\beta=96.9$ (0.2)°
$Z=4$ ($D_m=1.71$, $D_c=1.75$ g·cm^{-3})
$\mu=100.6$ cm^{-1} (for Ni$K\alpha$)

Weissenberg multiple-film photographs were taken for the 0—4 and 0—6 layers about the *c* and [101] axes respectively, with Ni$K\alpha$ radiation ($\lambda=1.6591$ Å). The relative intensities of 1159 independent reflections were measured visually, and the Lorenz, polarization, spot-shape,[10] and absorption corrections were applied. The specimen crystal used was a rod with the approximate dimensions of $0.12 \times 0.07 \times 1.0$ mm.

Determination of the Crystal Structure

Prior to the complete collection of the three-dimensional reflection data, *hk*0 and *h*0*l* data were obtained and the Patterson functions, $P(UV)$ and $P(UW)$, were calculated.*1 Since the unit cell

1) J. P. Mathieu, *Bull. Soc. Chim. Fr.*, **3**, 463, 476 (1936).
2) F. P. Dwyer, T. E. McDermott and A. M. Sargeson, *J. Am. Chem. Soc.*, **85**, 661 (1963).
3) T. Bürer, *Helv. Chim. Acta*, **46**, 242 (1963).
4) T. E. McDermott and A. M. Sargeson, *Aust. J. Chem.*, **16**, 334 (1963).
5) R. D. Gillard and G. Wilkinson, *J. Chem. Soc.*, **1964**, 1368.
6) F. P. Dwyer, A. M. Sargeson and I. K. Reid, *J. Amer. Chem. Soc.*, **85**, 1215 (1963).
7) A. J. McCaffery, S. F. Mason and B. J. Norman, *J. Chem. Soc.*, **1965**, 5094.
8) K. Nakatsu, M. Shiro, Y. Saito and H. Kuroya, This Bulletin, **30**, 158 (1957).
9) S. M. Jörgensen, *J. Prakt. Chem.*, **41**, 448 (1890).
10) D. C. Philips, *Acta Crystallogr.*, **7**, 746 (1954).

*1 At the early stages of the present work, the electronic computer available to us was OKITAC 5090D, with which it is difficult to deal with the three-dimensional data; hence, we started the structure analysis by the two-dimensional method.

TABLE 1. THE FINAL ATOMIC COORDINATES, TEMPERATURE FACTORS AND THELIR e.s.d.

Temperature factors are of the form: $\exp[-(h^2B_{11}+k^2B_{22}+l^2B_{33}+2hkB_{12}+2hlB_{13}+2klB_{23})]$.

Atom	x	y	z	Atom	x	y	z
Co 1	0.2542(5)	0.5000(6)	0.0567(8)	N 4	0.265(2)	0.499(2)	0.298(3)
Co 2	0.1317(5)	0.0877(6)	0.5273(8)	N 5	0.134(2)	0.089(2)	0.286(3)
Cl 1	0.172(1)	0.324(1)	0.050(1)	N 6	0.291(2)	0.052(2)	0.545(4)
Cl 2	0.090(1)	0.595(1)	0.033(1)	N 7	0.097(2)	−0.078(2)	0.532(4)
Cl 3	−0.055(1)	0.122(1)	0.490(1)	N 8	0.135(2)	0.088(3)	0.765(3)
Cl 4	0.173(1)	0.281(1)	0.542(1)	C 1	0.345(3)	0.596(4)	−0.230(5)
Cl 5	0.322(1)	0.781(1)	0.431(1)	C 2	0.310(4)	0.691(4)	−0.117(6)
Cl 6	0.408(1)	0.124(1)	0.911(1)	C 3	0.427(4)	0.323(4)	0.269(6)
O 1	0.050(2)	0.858(2)	0.191(3)	C 4	0.384(4)	0.479(4)	0.370(5)
O 2	0.471(3)	0.349(3)	0.748(4)	C 5	0.251(3)	0.052(3)	0.246(5)
N 1	0.249(2)	0.500(3)	−0.182(3)	C 6	0.337(3)	0.092(3)	0.400(4)
N 2	0.326(2)	0.649(3)	0.054(4)	C 7	0.066(3)	−0.106(3)	0.701(5)
N 3	0.397(3)	0.418(3)	0.084(4)	C 8	0.146(3)	−0.034(3)	0.823(5)

Atom	B_{11}	B_{22}	B_{33}	Atom	B_{12}	B_{13}	B_{23}
Co 1	0.0046(5)	0.0067(5)	0.0062(13)		0.0009(9)	−0.0014(12)	0.0001(14)
Co 2	0.0042(4)	0.0063(5)	0.0073(13)		0.0003(8)	−0.0019(12)	0.0001(14)
Cl 1	0.0063(8)	0.0047(7)	0.0121(22)		−0.0016(12)	−0.0045(19)	−0.0007(19)
Cl 2	0.0036(6)	0.0086(8)	0.0122(21)		0.0023(13)	−0.0035(17)	−0.0030(22)
Cl 3	0.0041(6)	0.0066(8)	0.0134(21)		0.0021(12)	0.0000(18)	0.0021(20)
Cl 4	0.0074(8)	0.0041(6)	0.0104(21)		0.0003(12)	−0.0011(19)	−0.0023(18)
Cl 5	0.0087(9)	0.0072(8)	0.0128(23)		0.0007(15)	0.0026(22)	0.0043(22)
Cl 6	0.0047(7)	0.0115(11)	0.0122(22)		0.0011(15)	−0.0008(19)	0.0022(24)

Atom	B	Atom	B
O 1	4.4(6)	N 8	2.9(6)
O 2	6.8(8)	C 1	5.2(9)
N 1	2.7(5)	C 2	5.1(9)
N 2	3.7(7)	C 3	5.0(9)
N 3	4.9(8)	C 4	4.9(9)
N 4	2.5(5)	C 5	4.2(9)
N 5	2.1(5)	C 6	3.2(7)
N 6	3.4(6)	C 7	3.4(7)
N 7	3.0(6)	C 8	2.8(7)

contains four formula units, there are eight heavy atoms (two cobalt and six chlorine atoms) in the asymmetric unit. $P(UW)$ was difficult to be solved because of the peculiar arrangement of the Patterson peaks. The coordinates of the two Co atoms and one Cl atom were found by an elaborate examination of $P(UV)$. These coordinates were used for a graphical derivation of the minimum function, on which we found seven additional heavy peaks (not including the above three atoms). Of these seven peaks, the five heaviest were assumed to be Cl-atoms. The remaining atoms were found on the electron-density map phased by the eight heavy atoms thus obtained. The z-coordinate of each atom was determined by the use of $P(UV)$ and the Fourier map, $\rho(xz)$. Subsequent refinement by the diagonal least-squares method reduced R to 0.14 for $hk0$ and to 0.19 for $h0l$.

Further refinement of the structure was made by the block-diagonal, least-squares method using the three-dimensional data. The atomic scattering factors were taken from the International Tables for X-ray Crystallography.[11] The real part of the anomalous dispersion correction was taken into account for Co.[12] The function minimized was $\sum w(|F_o|-|F_c|)^2$, and the following weighting scheme was employed:

$w = 0.5$ if $F_0 < F_{\min}$ $(= 5.0)$

$w = 1.0$ if $F_{\min} \leq F_0 \leq F_{\max}$ $(= 44.6)$

11) "International Tables for X-ray Crystallography," Vol. III, Kynoch Press, Birmingham (1962), p. 202.

12) R. W. Games, "The Optical Principles of the Diffraction of X-rays," G. Bell & Sons, London (1948), Appendix, p. 608.

$$w = F_{max}/F_0 \quad \text{if } F_0 > F_{max}$$

Three cycles of the refinement with isotropic thermal parameters reduced R to 0.150. At this stage, anisotropic temperature factors were introduced for the heavy atoms, and three further cycles of the least-squares calculation improved R to 0.109. The atomic parameter shifts in the last cycle of the refinement were less than their standard deviations. The final atomic coordinates, the temperature factors, and their e.s.d.'s are listed in Table 1.

In order to determine the absolute configuration of the complex ion, the $hk1$ and $hk2$ Weissenberg photographs were taken with Cu$K\alpha$ radiation.*2 The inequality relationships which were observed for some Bijvoet pairs of hkl and $h\bar{k}\bar{l}$ are shown in Table 2. In this table, the calculated intensities which were obtained by the use of the atomic coordinates shown in Table 1 are also listed. The values of $\Delta f'_{Co}$ and $\Delta f''_{Co}$ were taken from the International Tables for X-ray Crystallography.[11] A comparison of the observed inequalities with the calculated ones indicates that the atomic coordinates shown in Table 1 can give the absolute structure of the crystal.

Table 2. Calculated and observed intensity

hkl	$F_c^2(hkl)$	obs.	$h\bar{k}\bar{l}$	$F_c^2(hkl)$
$\bar{5}11$	645	<	$\bar{5}\bar{1}1$	1050
$\bar{6}21$	1832	>	$\bar{6}\bar{2}1$	1005
$\bar{7}21$	713	<	$\bar{7}\bar{2}1$	900
$\bar{8}21$	829	<	$\bar{8}\bar{2}1$	1076
$\bar{5}12$	1798	>	$\bar{5}\bar{1}2$	882
$\bar{8}22$	361	<	$\bar{8}\bar{2}2$	1274
$\bar{7}22$	432	>	$\bar{7}\bar{2}2$	196
312	566	<	$3\bar{1}2$	1436
412	4330	>	$4\bar{1}2$	2621
422	1347	<	$4\bar{2}2$	2079

Discussion

The crystal structure viewed along the b and c axes are shown in Figs. 1 and 2 respectively. The crystal is composed of $(+)_{589}$-$[CoCl_2en_2]^+$, Cl^-, and H_2O. Although, as has been stated previously, there are two crystallographically-independent complexes in an asymmetric unit, they have the same configuration and almost identical molecular dimensions, as is shown in Table 3. No significant differences are found in the corresponding bond lengths and angles. The absolute configuration of $(+)_{589}$-$[CoCl_2en_2]^+$ is illustrated in Fig. 3 (together with those of $(+)_{589}$-$[Co(CN)_2en_2]^+$ [13]) and $(+)_{589}$-$[Coen_3]^{3+}$,[8] which are given

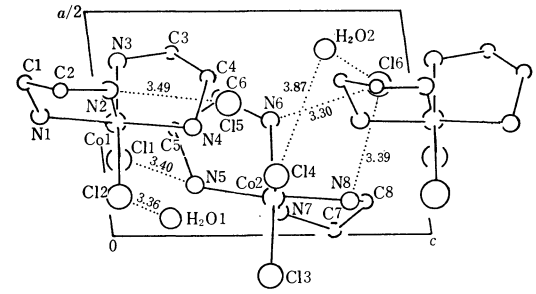

Fig. 1. The structure viewed along the b-axis.

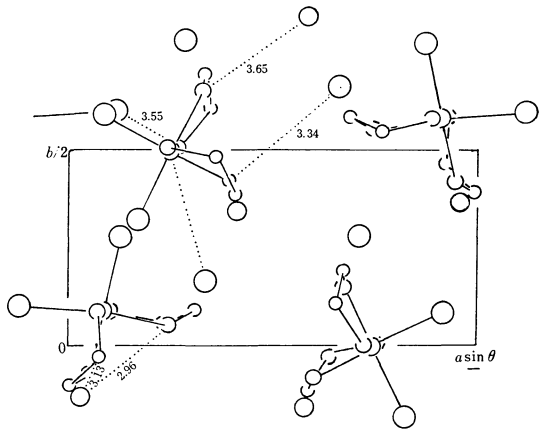

Fig. 2. The projection of the structure on the plane normal to the C-axis.

Table 3. The bond distances and angles in the complex ions

Co1-Cl1	2.26(1)Å	Co2-Cl3	2.27(1)Å
Co1-Cl2	2.25(1)	Co2-Cl4	2.28(1)
Co1-N1	1.98(3)	Co2-N5	2.01(3)
Co1-N2	1.93(3)	Co2-N6	1.95(3)
Co1-N3	1.96(4)	Co2-N7	1.96(3)
Co1-N4	2.00(3)	Co2-N8	1.98(3)
N1-C1	1.52(6)	N5-C5	1.55(5)
N2-C2	1.49(6)	N6-C6	1.46(5)
N3-C3	1.59(6)	N7-C7	1.53(5)
N4-C4	1.50(5)	N8-C8	1.48(5)
C1-C2	1.47(7)	C5-C6	1.61(6)
C3-C4	1.53(6)	C7-C8	1.55(5)
∠Cl1-Co1-Cl2	93(1)°	∠Cl3-Co2-Cl4	92(1)°
∠N1-Co1-N2	87(1)	∠N5-Co2-N6	87(1)
∠N3-Co1-N4	86(1)	∠N7-Co2-N8	87(1)
∠Co1-N1-C1	108(2)	∠Co2-N5-C5	110(2)
∠Co1-N2-C2	107(2)	∠Co2-N6-C6	110(2)
∠Co1-N3-C3	109(3)	∠Co2-N7-C7	107(2)
∠Co1-N4-C4	110(2)	∠Co2-N8-C8	108(2)
∠N1-C1-C2	105(4)	∠N5-C5-C6	105(3)
∠N3-C3-C4	107(3)	∠N7-C7-C8	107(3)
∠N2-C2-C1	111(4)	∠N6-C6-C5	108(3)
∠N4-C4-C3	106(3)	∠N8-C8-C7	106(3)

*2 The right-handed coordinate system was used in the indexing of Weissenberg photographs throughout the present work.

13) K. Matsumoto, Y. Kushi, S. Ooi and H. Kuroya, This Bulletin, **40**, 2988 (1967).

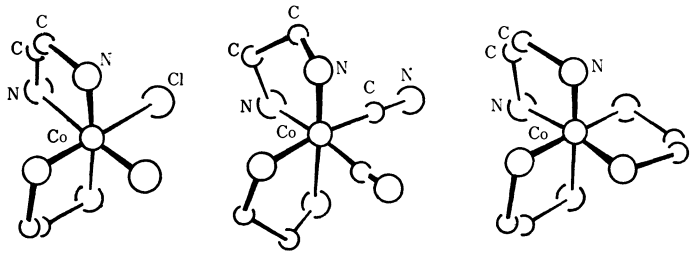

$(+)_{589}$-$[CoCl_2en_2]^+$ $(+)_{589}$-$[Co(CN)_2en_2]^+$ $(+)_{589}$-$[Coen_3]^{3+}$

Fig. 3. The absolute configurations of $(+)_{589}$-$[CoCl_2en_2]^+$, $(+)_{589}$-$[Co(CN)_2en_2]^+$ and $(+)_{589}$-$[Coen_3]^{3+}$.

as references). This configuration is exactly in agreement with that proposed by Mason *et al.* and should be denoted as $\Lambda(\delta\delta)$, following the proposal of the IUPAC Commission.[14]

The conformation of the ethylenediamine molecules is of the "*lel-lel*" form in the present complex, whereas it is of the "*ob-ob*" form in $(+)_{589}$-$[Co(CN)_2en_2]Cl \cdot H_2O$[13] and of the "*ob-lel*" form in $(\pm)$-$[CoCl_2en_2]Cl \cdot H_2O$.[15]

On the basis of a conformational analysis of $[Coen_3]^{3+}$, Corey and Bailar predicted that the difference in the interaction energy between the three chelate rings would be 1.8 kcal/mole, the *lel-lel-lel* form being more stable, and the *ob-ob-ob* form, less stable.[16] This prediction was verified by the equilibrium study of $[Co(l\text{-pn})_3]^{3+}$ by Dwyer *et al.*[17] In the case of *cis*-$[CoX_2en_2]$, however, if the X's are spherical (as in Cl) or cylindrical (as in CN): (1) the potential energy between the X's and each of the chelate rings is indifferent to the arrangement of the en-molecule—*ob* or *lel*—, and (2) the energy between the two chelate rings is one-third of that in the tris-ethylenediamine complex.[15] In short, though the degree of the steric interaction in the complex increases in the order of: *lel-lel*$<$*ob-lel*$<$*ob-ob*, (the *lel-lel* form being accordingly the most stable, and the *ob-ob* form, the least stable), the potential energy differences between these forms are quite small. This enables, on some occasions, the chelate ring to take the less-favored *ob-lel*[15] or *ob-ob*[13] form. The combination of *ob* and *lel* in a complex must, of course, be affected by the surroundings of the cation.

The distances of the notable short contacts are shown in Figs. 1 and 2. The nitrogen atoms of the ethylenediamine molecules form rather weak hydrogen bonds. That is, the cations are not very tightly bound by their environments; this must be the reason why the rings are of the *lel-lel* form in the crystal.[18]

The average value of Co-Cl is 2.26 Å, a value which is comparable to 2.286 Å in $[CoCl(NH_3)_5]Cl_2$[19] and 2.26 Å (average) in $(\pm)$-$[CoCl_2en_2]Cl \cdot H_2O$.[14] $\angle$Cl–Co–Cl is 91.8°, a value in good agreement with the 91.6° found in the racemate.[14] The bond lengths and angles in the ethylenediamine molecules are not accurate enough to be discussed in detail.

A complete list of the observed and calculated structure factors is preserved by the Chemical Society of Japan.*3

The authors wish to express their thanks to Mr. Ken Hirotsu, who adapted the HBLS-IV computer program to the FACOM 270-30 computer at Osaka City University. A part of the cost of this work was defrayed by Scientific Research Grant from the Ministry of Education.

14) IUPAC Information Bull., No. **33**, 68 (1968).

15) K. Matsumoto, S. Ooi and H. Kuroya, *Nippon Kagaku Zasshi*, **89**, 167 (1968).

16) E. J. Corey and J. C. Bailar, Jr., *J. Amer. Chem. Soc.*, **81**, 2620 (1959).

17) F. P. Dwyer, F. L. Garvan and L. Shulman, *ibid.*, **81**, 290 (1959).

18) K. N. Raymond, P. W. R. Corfield and J. A. Ibers, *Inorg. Chem.*, **7**, 1362 (1968); K. N. Raymond and J. A. Ibers, *ibid.*, **7**, 2333 (1968).

19) G. G. Messmer and E. L. Amma, *Acta Crystallogr.*, B**24**, 417 (1968).

*3 The complete data of the F_0—F_c table are kept as Document No. 7008 at the office of the Bulletin of the Chemical Society of Japan. A copy may be secured by citing the document number and by remitting, in advance, ¥600 for photoprints. Pay by check or money order, payable to: The Chemical Society of Japan.

BULLETIN OF THE CHEMICAL SOCIETY OF JAPAN VOL. 43 3805—3813 (1970)

The Ruthenium Complexes Formed by the Reactions of Nitrosylruthenium(III) with Tin(II) in Hydrochloric Acid Solution

Masao MUKAIDA

Department of Chemistry, Faculty of Science and Technology, Sophia University, Kioicho, Chiyoda-ku, Tokyo

(Received July 4, 1970)

The complexes formed by the reactions of nitrosylruthenium(III) in hydrochloric acid solutions with tin(II) chloride were investigated. The following reaction products, $(Me_4N)_2[RuCl_3(SnCl_3)_2NO]$, [1]; $(Me_4N)_4[RuCl_6(SnCl_3)_2(NO)_2]\cdot H_2O$, [2]; $(Me_4N)_4[RuCl(SnCl_3)_5]$, [3] and $K_3[Ru_2Cl_8(H_2O)_2N]$, [4] were isolated as crystals and were characterized. On the basis of chemical and thermal analyses, and on the basis of observations of the magnetic properties, the conductivities, and the infrared spectra, it was concluded that complexes [1], [2], and [3] contain terminal or bridging nitrosyl groups and/or a coordinating $SnCl_3^-$ group, and that complex [4] contains a bridging nitrido group. The presence of the binuclear complex, "$K_3[Ru_2Cl_9(NO)_2]$," which has both the terminal and singly-bridged nitrosyl groups was also suggested. The relations among those complexes were discussed.

The polynuclear metal complexes bridged by carbonyl or nitrosyl groups have recently been studied. Few binuclear ruthenium complexes bridged by nitrosyl groups have been studied. Attention has also recently been focussed on the metal-metal bonds in metal complexes. Complexes of platinum metals with metal-tin bonds have been studied considerably.[1-5] However, nitrosylruthenium complexes with the coordinating $SnCl_3^-$ groups have not yet been reported on. In this study, the binuclear ruthenium complexes bridged by nitrosyl groups and the complexes with ruthenium-tin bonds were prepared by the reactions of nitrosylruthenium(III) with tin(II) in hydrochloric acid solutions. They are $(Me_4N)_2[RuCl_3(SnCl_3)_2(NO)]$ and $(Me_4N)_4[Ru_2Cl_6(SnCl_3)_2(NO)_2]\cdot H_2O$. The complexes will be discussed on the basis of their properties. Two other complexes were also isolated from the reactions of nitrosylruthenium(III) with tin(II). One was $(Me_4N)_4[RuCl(SnCl_3)_5]$, which was identical with the complex prepared from ruthenium (III and IV) and tin(II) in a hydrochloric acid solution.[6] The other was $K_3[Ru_2Cl_8(H_2O)_2N]$, which had been mentioned by Brizard[7] and Charonnat[8] and which has recently been established by Cleare and Griffith[9] and by Ciechanowicz and Skapski.[10]

Nitrosylruthenium(III) is a fairly stable group when exposed to mild chemical reactions. It has been suggested that the reduction of nitrosylruthenium(III) compounds is clearly a field which should be more fully investigated.[11] It was thought that the complexes prepared in this study would give valuable information on the reaction of nitrosylruthenium(III) with tin(II) in hydrochloric acid solutions.

Experimental

Materials. Nitrosylruthenium(III) in a hydrochloric acid solution was prepared by the conventional method.[12] This solution was adjusted to contain 8 mg Ru/ml in 3M hydrochloric acid and was used as the starting solution for the syntheses of the complexes in this study. The ^{15}N-labeled nitrosylruthenium(III) in a hydrochloric acid solution was prepared by the method

1) R. D. Cramer, E. L. Jenner, R. V. Lindsey, Jr., and U. G. Stolberg, *J. Amer. Chem. Soc.*, **85**, 1691 (1963).
2) A. G. Davies, G. Wilkinson and J. F. Young, *ibid.*, **85**, 1692 (1963).
3) J. F. Young, R. D. Gillard and G. Wilkinson, *J. Chem. Soc.*, **1964**, 5176.
4) R. D. Cramer, R. V. Lindsey, Jr., C. T. Prewitt and U. G. Stolberg, *J. Amer. Chem. Soc.*, **87**, 658 (1965).
5) R. V. Lindsey, Jr., G. W. Parshall and U. G. Stolberg, *Inorg. Chem.*, **5**, 109 (1966).
6) H. Okuno, T. Ishimori, K. Mizumachi and H. Ihochi, This Bulletin, submitted for publication.
7) L. Brizard, *Ann. Chim. Phys.*, **21**, 311 (1900).
8) R. Charonnat, "Nouveau Traité de Chimie Minerale," Tome XIX, ed. by P. Pascal, Masson et Cie, Paris (1932), p. 432.
9) M. J. Cleare and W. P. Griffith, *Chem. Commun.*, **1968**, 1302; *J. Chem. Soc.*, A, **1970**, 1117.
10) Maria Ciechanowicz and A. C. Skapski, *Chem. Commun.*, **1969**, 574.
11) W. P. Griffith, "The Chemistry of the Rare Platinum Metals," John Wiley & Sons, London (1968), p. 177.
12) J. M. Fletcher, I. L. Jenkins, F. M. Lever, F. S. Martin, A. R. Powell and R. Todd, *J. Inorg. Nucl. Chem.*, **1**, 378 (1955).

reported by Miki,[13,14] it was used for the syntheses of the ^{15}N-substituted complexes. All the other reagents used were of an analytical grade.

Measurements. The infrared spectra were measured with Leitz 221(4000—400 cm^{-1}), JASCO DS-301 (4000—700 cm^{-1}), Hitachi EPI-L(700—200 cm^{-1}), and Hitachi FIS-1(500—40 cm^{-1}) IR spectrometers. The KBr disk, Nujol mull, HCB mull and polyethylene film techniques were used. The magnetic properties were measured by the Gouy method. An electromagnet was used at the maximum field strength of *ca.* 9 kG. The conductivities of the complexes were measured in nitromethane or distilled water at 30°C with a Yokogawa Universal Bridge, BV-Z-13A. The visible spectra were measured with a Hitachi-Perkin-Elmer 139 spectrometer. The differential thermal analyses were carried out with a Shimadzu DT-2B apparatus. The measurements were made at a heating rate of 10°C/min in an atmosphere. The powder X-ray diffraction data for finely-powdered samples were obtained with a Rigaku-Denki X-ray diffractometer 2001.

The ruthenium in the complexes was determined by the ruthenate method[15] after the samples had been ignited at a rather low temperature. The tin was determined as tin dioxide after tin(IV) cupferrate had been precipitated and had been ignited.[16] The chlorine was determined gravimetrically as silver chloride. The potassium and the tetramethyl ammonium ion were determined by the use of tetraphenyl borate. Elementary analyses were made by the Institute of Physical and Chemical Research, Japan.

Preparations of Complexes. $(Me_4N)_2[RuCl_3(SnCl_3)_2(NO)]$, Complex [1]. The starting solution (1.58 mmol Ru(III)NO in 20 m*l*) was evaporated to dryness on a water bath. The residue was dissolved in 30 m*l* of 4M hydrochloric acid, and then $SnCl_2 \cdot 2H_2O$ (1.5 g, 6.7 mmol) was added gradually. The solution was subsequently vigorously stirred about 20 min at room temperature (20—25°C). After the solution had been filtered, a $(Me_4N)Cl$ solution (500 mg/5 m*l* H_2O) was added to obtain orange needle crystals. The crystals were filtered, washed several times with ethanol and with ether, and dried *in vacuo*, giving 400 mg of the complex. The complex is slightly soluble in both nitromethane and DMF. Found: Ru, 11.87; Sn, 28.13; Cl, 37.91; (Me_4N), 17.92%. Calcd for $(Me_4N)_2[RuCl_3(SnCl_3)_2(NO)]$: Ru, 12.08; Sn, 28.40; Cl, 38.27; (Me_4N), 17.71%.

$(Me_4N)_4[Ru_2Cl_6(SnCl_3)_2(NO)_2] \cdot H_2O$, Complex [2]. The starting solution (1.58 mmol Ru(III)NO in 20 m*l*) was evaporated to dryness on a water bath. The residue was dissolved in 16 m*l* of 3M hydrochloric acid, and $SnCl_2 \cdot 2H_2O$ (1.7 g, 7.6 mmol) was added. The solution was then stirred vigorously about 30 min at room temperature (20—25°C) and subsequently left to stand for 24—30 hr. After the solution had then been filtered, a $(Me_4N)Cl$ solution (0.5 g/10 m*l* H_2O) was added. After this solution had stood for a long period, black or dark brown crystals were separated out. The crystals were filtered, washed several times with water, ethanol, and dried *in vacuo*, giving 200 mg of the complex. The complex is insoluble in most organic solvents.

Found: Ru, 16.27; N, 6.58; Sn, 19.14; Cl, 34.41; (Me_4N), 24.26%. Calcd for $(Me_4N)_4[Ru_2Cl_6(SnCl_3)_2(NO)_2] \cdot H_2O$: Ru, 16.31; N, 6.78; Sn, 19.16; Cl, 34.34; (Me_4N), 23.89%.

$(Me_4N)_4[RuCl(SnCl_3)_5]$, Complex [3]. *Method 1.* To the starting solution (1.58 mmol Ru(III)NO in 20 m*l*), 6M hydrochloric acid (60 m*l*) and $SnCl_2 \cdot 2H_2O$ (1.5 g, 6.7 mmol) were added. The mixed solution was then concentrated to about 20—30 m*l* by boiling it. Again, to the resulting solution, 3M hydrochloric acid (60 m*l*) and $SnCl_2 \cdot 2H_2O$ (0.5 g, 2.2 mmol) were added, and the solution was boiled for 10 min. After this solution had then been filtered, a $(Me_4N)Cl$ solution (1 g/10 m*l* H_2O) was added until crystals appeared. These orange-yellow crystals were separated out. The crystals were washed several times with an ethanol-hydrochloric acid mixture and with ether, and dried *in vacuo*, giving 300 mg of the complex. The complex is slightly soluble in both nitromethane and DMF.

Method 2. An alternative procedure for the preparation of this complex is as follows. The starting solution (1.58 mmol Ru(III)NO in 20 m*l*) was evaporated to dryness on a water bath. The residue was dissolved in 20 m*l* of 6M hydrochloric acid, and $SnCl_2 \cdot 2H_2O$ (1.7 g, 7.6 mmol) was added to the solution. The mixed solution was left to stand overnight at room temperature (20—25°C). After the solution had then been filtered, a $(Me_4N)Cl$ solution (1 g/10 ml H_2O) was added. An orange-yellow complex was thus obtained.

Found: Ru, 6.76; Sn, 38.80; Cl, 36.01; (Me_4N), 18.77%. Calcd for $(Me_4N)_4[RuCl(SnCl_3)_5]$: Ru, 6.48; Sn, 38.08; Cl, 36.45; (Me_4N), 18.99%.

$K_3[Ru_2Cl_8(H_2O)_2N]$, Complex [4]. This complex was prepared by the reduction of nitrosylruthenium(III) with tin(II) or with formaldehyde.

Procedure with Tin(II) Chloride. To the starting solution (1.58 mmol Ru(III)NO in 20 m*l*), potassium chloride (1 g) and $SnCl_2 \cdot 2H_2O$ (2.2 g, 9.8 mmol) were added. The mixture solution was completely evaporated to dryness on a water bath. The product was dissolved with a 3M hydrochloric acid solution (15—20 m*l*) and was then concentrated until crystals appeared. After the solution had then stood overnight, the reddish-brown crystals thus obtained were filtered and washed several times with water-ethanol and ether, and dried *in vacuo*, giving 100—150 mg of a crude product. A mixture of the crude product (250 mg), potassium chloride (0.5 g), and $SnCl_2 \cdot 2H_2O$ (2 g) was dissolved in 6M hydrochloric acid (30 m*l*) by heating, after which the solution was heated vigorously in a flask equipped with a reflux condenser for 2—4 hr. When the resulting solution was concentrated by evaporation, crystals were separated out. The reddish-brown crystals thus obtained were filtered, washed several times with a water-ethanol (1 : 1) mixture and with ether, and dried *in vacuo*, giving 30 mg of the complex. Recrystallization was made from 3M hydrochloric acid containing small amounts of potassium chloride. The complex is slightly soluble in water, but it is not soluble in any organic solvent.

Found: Ru, 30.25; N, 2.27; H, 0.81; Cl, 43.78; K, 17.50% (Ru, 30.18; N, 1.90; H, 0.73; Cl, 42.34;

13) E. Miki, T. Ishimori, H. Yamatera and H. Okuno, *Nippon Kagaku Zasshi*, **87**, 703 (1966).

14) E. Miki, This Bulletin, **41**, 1835 (1968).

15) E. D. Marshall and R. R. Rickard, *Anal. Chem.*, **22**, 795 (1950).

16) W. H. Hillebrand and G. E. F. Lundell, "Applied Inorganic Analysis," Second Ed., John Wiley & Sons, New York (1959), p. 295.

Table 1. The complexes prepared from the reactions of Ru(III)NO with Sn(II) in hydrochloric acid solutions

	Formula	Color in solid state	Absorption maxima (mμ) (ε in parentheses)	
1,	$(Me_4N)_2[RuCl_3(SnCl_3)_2NO]$	orange	440 (9.0×10^2) 326 (1.8×10^4)	*1
2,	$(Me_4N)_4[Ru_2Cl_6(SnCl_3)_2(NO)_2]\cdot H_2O$	black-dark brown	—	
3,	$(Me_4N)_4[RuCl(SnCl_3)_5]$	orange-yellow	444 (1.3×10^3) 293 (2.2×10^4)	*1
4,	$K_3[Ru_2Cl_8(H_2O)_2N]$	reddish brown	440 (1.1×10^2) sh 360 (5.0×10^2) sh	*2
5,	"$K_3[Ru_2Cl_9(NO)_2]$"	brown	—	

*1: in 3M hydrochloric acid solution, *2: in aqueous solution.

K, 17.38% for the crude product). Calcd for $K_3[Ru_2Cl_8(H_2O)_2N]$: Ru, 30.92; N, 2.14; H, 0.61; Cl, 43.47; K, 17.95%. The evaporation of a D_2O solution of the complex gave a deuterium-substituted complex as crystals.

Procedure with Formaldehyde. To the starting solution (1.58 mmol Ru(III)NO in 20 m*l*), enough potassium hydroxide was added to make the pH of the solution higher than 13. After the mixed solution had then been boiled vigorously for about 30 min, the solution gradually turned from brown to pale-violet, and finally to dark red. While a formalin solution (10 m*l*) was poured, drop by drop, into the solution, a gelatinous, brown precipitate was thrown down from the solution. The precipitate thus obtained was centrifuged and then washed several times with water. The precipitate was subsequently dissolved in a hydrochloric acid solution containing 0.3 g of potassium chloride, and the solution was concentrated by evaporation. After the solution had stood overnight, the reddish-brown crystals thus obtained were filtered, washed several times with a water-ethanol (1 : 1) mixture and with ether, and dried *in vacuo*, yielding 50 mg of a crude product.

Found: Ru, 30.31; N, 2.22; H, 0.71; Cl, 41.60; K, 17.58% for the crude product.

Results and Discussion

From the reactions between nitrosylruthenium(III) and tin(II) chloride under the various reaction conditions, two complexes were newly prepared and two complexes which had recently been reported were isolated. The analytical data were in good agreement with the calculated compositions. The complexes are summarized in Table 1, along with the absorption maxima in their visible and UV spectra. All the complexes are fairly stable in an atmosphere. However, exposure to sunlight changes complexes [1] and [3] from the original orange to dark gray. The conditions of preparing complexes [1] and [2] were rigid, and the methods of these preparations were specially examined.

The type of electrolyte in complex [1] was examined by the use of the conductivities in solutions according to the method reported by Feltham and Hayter.[17] The results shown in Table 2 indicate

17) R. D. Feltham and R. G. Hayter, *J. Chem. Soc.*, **1964**, 4587.

Table 2. Type of electrolyte as determined by conductivity measurements

Complex	Solvent	Λ_0 (ohm^{-1})	$\frac{\Lambda_0-\Lambda_e}{\sqrt{C}}$	Type of electrolyte
$(Me_4N)_2[RuCl_3(SnCl_3)_2NO]$	CH_3NO_2	156	660	2:1
$K_3[Ru_2Cl_8(H_2O)_2N]$	H_2O	214	321	3:1

temperature; 30°C, concentration range; 10^{-2}—10^{-3}M. In order to determine the type of electrolyte, the data on $(Me_4N)_2[RuCl_3(SnCl_3)_2NO]$ were compared with those on $[(C_6H_5)_4As]Cl$ and $[Co(phen)_3](ClO_4)_3$, and the data on $K_3(Ru_2Cl_8(H_2O)_2N]$ with those on $[Co(NH_3)_6]Cl_3$.

that complex [1] is an electrolyte of the 2 : 1 type and that no appreciable dissociations of the $SnCl_3^-$ group occur in nitromethane solutions.

On the differential thermal analysis of complex [2], a distinct endothermic peak at 100—130°C was found, accompanied by a relatively small endothermic peak at about 140°C (Fig. 1). A violent decomposition started at 200°C. Infrared spectroscopy suggested that the two endothermic peaks may be based on the dehydration of crystalline water and the structural change in the complex. The gravimetric determination of the crystalline water was impossible.

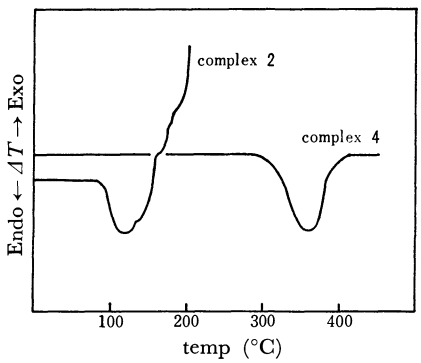

Fig. 1. DTA curves of $(Me_4N)_4[Ru_2Cl_6(SnCl_3)_2(NO)_2]\cdot H_2O$, complex [2] and $K_3[Ru_2Cl_8(H_2O)_2N]$, complex [4].

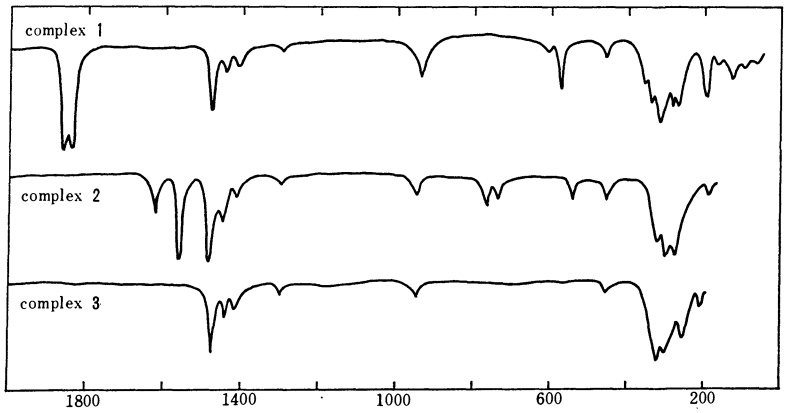

Fig. 2. Infrared spectra of $(Me_4N)_2[RuCl_3(SnCl_3)_2NO]$, complex [1], $(Me_4N)_4[Ru_2Cl_6(SnCl_3)_2(NO)_2]\cdot H_2O$, complex [2] and $(Me_4N)_4[RuCl(SnCl_3)_5]$, complex [3].

Complex [3] was identical with a complex which has previously been prepared by the reaction of ruthenium (III and IV) with the tin(II) in a hydrochloric acid solution.[6]

Complex [4] was prepared by two methods similar to those described by Brizard;[7] the two methods yielded identical complexes. The complex is thought to be the same as that reported by Cleare and Griffith.[9] Complex [4] was shown to be an electrolyte of the 3 : 1 type by the conductivity measurements (Table 2), this supports the formula of complex [4]. A differential thermal analysis was made of complex [4] in order to determine the nature of water in the complex. The DTA curve obtained is shown in Fig. 1. The endothermic peak at about 300—380°C is thought to be caused by the dehydration of the coordinating waters from the complex, because the weight loss (5.66%) at 380°C corresponds to the two molecules of water in the complex and the dehydration temperature observed is considerably higher than the general dehydration temperature for water of crystallization.

The structures of the complexes will be discussed on the basis of the infrared spectra and the diamagnetisms.

Infrared Spectra. As Figs. 2 and 3 and Tables 3 and 4 show, complexes [1], [2], [3] and [4] display quite different spectra, indicating that their structures are also different.

In general, terminal nitrosyl groups in metal complexes are characterized by absorption bands due to the NO stretching vibration. The NO stretching absorptions of complex [1], $(Me_4N)_2[RuCl_3(SnCl_3)_2NO]$, were easily identified, because the NaCl region is free from ligand absorptions except for the absorptions due to the nitrosyl group. Thus, the strong bands at 1865 cm^{-1} and 1842 cm^{-1} can be assigned to the NO stretching frequencies,

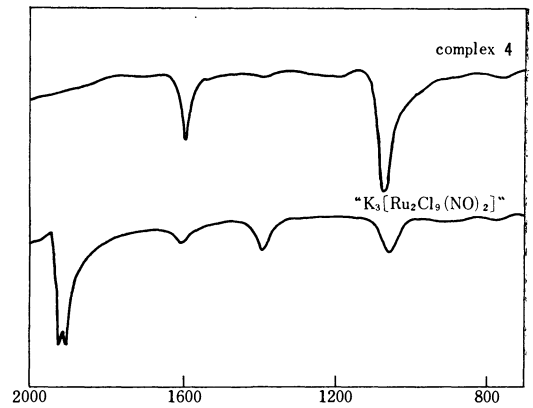

Fig. 3. Typical infrared spectra of $K_3[Ru_2Cl_8(H_2O)_2N]$, complex [4] and "$K_3[Ru_2Cl_9(NO)_2]$."

which are close to those for $K_2[RuCl_5NO]$.[18-20] The remaining two bands in the region about 600—550 cm^{-1} of complex [1] must be attributed to the Ru–NO bending and the Ru–NO stretching frequencies. If a linear Ru–N–O arrangement is assumed, there are three possible isomers of complex [1], one *trans* (C_{2v}) and two *cis* (C_s), with respect to the $SnCl_3^-$ ligands. However, the stereochemistry of complex [1] was not determined by the symmetry treatment and the observation of the infrared absorption bands. Since the NO and the $SnCl_3^-$ ion have strong *trans* effects, so that the *trans* positions of the NO and $SnCl_3^-$ groups may be expected to

18) J. Lewis, R. J. Irving and G. Wilkinson, *J. Inorg. Nucl. Chem.*, **7**, 32 (1958).
19) P. Gans, A. Sabatini and L. Sacconi, *Inorg. Chem.*, **5**, 1877 (1966).
20) M. J. Cleare and W. P. Griffith, *J. Chem. Soc.*, *A*, **1967**, 1144.

TABLE 3. INFRARED SPECTRA OF $(Me_4N)_2[RuCl_3(SnCl_3)_2NO]$, [1], $(Me_4N)_4[Ru_2Cl_6(SnCl_3)_2(NO)_2]\cdot H_2O$, [2], AND $(Me_4N)_4[RuCl(SnCl_3)_5]$, (3)

Complex [1]	Complex [2]	^{15}N-Complex [2]	Complex [3]	Tentative assignments
	3390 m 3370 sh	3390 m 3370 sh		ν OH
1865 vs 1842 vs				ν NO (terminal)
	1625 m	1625 m		δ H_2O
	1566 vs	1538 vs		ν NO (bridging)
	769 s 747 m 543 m	756 m 734 s 527 m		ν Ru-N (bridging) δ RuNO (bridging) in-plane and out-of-plane
606 w				ν Ru-N (terminal)
581 s				δ RuNO (terminal)
360 sh 341 sh 328 vs 293 vs 277 vs	322 sh 303 vs 271 vs	321 sh 320 vs 271 vs	326 vs 310 sh 253 s	ν metal-Cl
200 s	190 w		212 m	ν Ru-Sn
163 w 131 s 87 m				lattice vibration

Absorption bands due to $(Me_4N)^+$ ion are not cited.
Figures are given in cm^{-1}.
Abbreviations: s, strong; m, medium; w, weak; v, very; sh, shoulder; sp, split; br, broad.

TABLE 4. INFRARED SPECTRA OF $K_3[Ru_2Cl_8(H_2O)_2N]$, [4]

Ordinary	^{15}N-Substituted	Deuterated	$K_3[Ru_2Br_8(H_2O)_2N]$	Tentative assignments
3360 s 3210 sh	3360 s 3210 sh	(3360 w)	3350 s	ν OH
		2450 s 2300 sh		ν OD
1611 s	1610 s		1601 s	δ H_2O (scissoring)
	(1403 vw, br)	(1420 vw, br)	(1401 m)	ν NO (bridging) ?
		1190 m		δ D_2O (scissoring)
1082 vs	(1080 w)	1079 vs	1053 vs	ν_{as} Ru-N-Ru
	1047 vs			ν_{as} Ru-^{15}N-Ru
~600 w, br	~600 w, br		~560 w, br	δ H_2O (wagging)
543 w	528 w	551 w	527 w	δ Ru-N-Ru
		~450 w, br		δ D_2O (wagging)

be labile,[21,22] a stable structure of complex [1] can be presumed to be *cis* with respect to any two of the $SnCl_3^-$ and NO groups. However, it has been stated, with regard to the isomerism of the $[PtCl_2(SnCl_3)_2]^{2-}$ ion, that the *cis* isomer is more stable thermodynamically, while the *trans* isomer is favoured kinetically.[3]

The features of the spectra of complex [2], $(Me_4N)_4[Ru_2Cl_6(SnCl_3)_2(NO)_2]\cdot H_2O$, were markedly different from those of complex [1]. No absorption band was observed in the region of 1700—1900 cm^{-1}, where the bands due to the stretching vibrations of the terminal nitrosyl group in nitrosylruthenium complexes had previously been reported. However, a strong absorption band appeared at 1566 cm^{-1}. Since absorption bands due to the stretching vibrations of the bridging nitrosyl group in metal complexes have been found in the region of 1550—1300 cm^{-1},[23-25] the band at 1566

21) O. E. Zvyagintsev, N. M. Sinitsyn and V. N. Pichkov, *Chem. Abstr.*, **67**, 17464k (1967); Proc. 8th Int. Conf. Coord. Chem., Vienna, (1964), pp. 142—145.
22) R. V. Lindsey, Jr., G. W. Parshall and U. G. Stolberg, *J. Amer. Chem. Soc.*, **87**, 658 (1965).
23) T. S. Piper and G. Wilkinson, *J. Inorg. Nucl. Chem.*, **2**, 38 (1956).
24) R. B. King and M. B. Bisnette, *J. Amer. Chem. Soc.*, **85**, 2527 (1963).
25) R. B. King and M. B. Bisnette, *Inorg. Chem.*, **3**, 791 (1964).

cm^{-1} can be assigned to the stretching vibration of the bridging nitrosyl group in complex [2]. The infrared investigation of the bridging nitrosyl groups has not yet dealt with the absorption bands in the lower frequency region. However, three absorption bands were observed, at 769, 747, and 543 cm^{-1}, in complex [2], instead of the two bands due to the skeletal vibrations of the Ru–NO(terminal) group. If the binuclear skeleton shown in Fig. 4, which has a center of symmetry, is assumed for complex [2], there should be three bands, due to Ru–N stretching, RuNO in-plane bending, and RuNO out-of-plane bending vibrations. The three absorption bands observed in the lower region can thus be explained. These three bands and the bands at 1566 cm^{-1} were shifted by the ^{15}N-substitution. The skeletal structure of complex [2] as shown in Fig. 4 is suggested on the basis of its

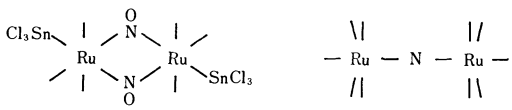

complex [2] complex [4]

Fig. 4. Proposed skeletal structures for $(Me_4N)_4[Ru_2Cl_6(SnCl_3)_2(NO)_2]\cdot H_2O$, complex [2] and $K_3[Ru_2Cl_8(H_2O)_2N]$, complex [4].

infrared absorptions. The dimeric nature thus presumed could not be confirmed by molecular weight and electroconductivity measurements, because of its low solubility with regard to organic solvents. However, when complex [2] was heated at about 150°C, the infrared absorption due to the stretching vibration of the bridging nitrosyl group disappeared and that of the terminal nitrosyl group appeared. This observation suggests a bridge cleavage on the heating of complex [2] and supports its dimer structure.

The infrared spectra of complex [3], $(Me_4N)_4[RuCl(SnCl_3)_5]$, differ greatly from those of complexes [1] and [2]. No absorption bands due to the NO group were found in complex [3]. This confirms that complex [3] does not contain a nitrosyl group.

One of the most interesting investigations was the examination of the Ru–Sn bond in complexes [1], [2] and [3]. The absorption bands due to Ru–Cl stretching and Sn–Cl stretching vibrations have previously been reported.[19, 26–28] A direct comparison of the far infrared spectra of complexes [1], [2] and [3] shows that the bands in the region of 360—250 cm^{-1} must be ascribed to metal-halogen vibrations. In order to make tentative assignments of the remaining bands, it was assumed that the bands observed in the region lower than about 160 cm^{-1} are to be attributed to lattice vibrations in these complexes. Consequently, the strong bands at about 200 cm^{-1} were assigned to the Ru–Sn stretching vibration: 200 cm^{-1} for complex [1], 190 cm^{-1} for complex [2],*1 and 212 cm^{-1} for complex [3]. These assignments are in agreement with those of the absorptions due to metal-tin vibrations in the other metal-tin complexes.[29,30] Thus, it was demonstrated that ruthenium-tin bonds are present in complexes [1], [2], and [3].

Very recently, Cleare and Griffith have reported the preparation of a bridging nitrido complex, $K_3[Ru_2Cl_8(H_2O)_2N]$ (complex [4]), by the Brizard method.[7]

An X-ray diffraction study of this binuclear complex has indicated that the ruthenium atoms, which lie in mirror planes, have a distorted octahedral coordination with water molecules *trans* to the nitrogen.[10] The main features of the infrared spectra of complex [4] in this study were similar to those reported by Cleare and Griffith. Complex [4] displays five absorption bands, at 3360, 1611, 1082, ~600, and 543 cm^{-1}, over the range of 4000—400 cm^{-1}. The band at 1082 cm^{-1} was often accompanied by a shoulder peak at 1045 cm^{-1}. A very weak broad band at about 1410 cm^{-1} was often found. In order to distinguish the bands due to coordinating water from those connected with the nitrogen atom, isotopic substitutions on hydrogen and nitrogen atoms were carried out. The bands at 3360, 1611, and 600 cm^{-1} shifted to at 2450, 1190, and ~450 cm^{-1} respectively in the deuterated complex. Thus, these three bands were assigned to the OH stretching and H_2O bending (scissoring and wagging) vibrations.[28] On ^{15}N-substitution the two remaining bands, at 1082 and 543 cm^{-1}, shifted to the lower-frequency side. It has been reported that a metal complex such as $[Os_2N(NH_3)_8Br_2]Br_3$, which has a bridging nitrido group, is characterized by a strong absorption band in the 1100 cm^{-1} region.[31] On the basis of the structure of complex [4] (Fig. 4), which has been determined by X-ray study,[10] the bands at 1082 and 543 cm^{-1} can be assigned to the asymmetric stretching and bending frequencies respectively of the linear Ru–N–Ru skeleton. On the ^{15}N-isotopic substitution, these bands shifted to 1047 and 528

*1 The author wishes to thank Mr. T. Takakuwa of the Japan Spectroscopic Co., Ltd., for this infrared spectral data.

26) J. Hiraishi, I. Nakagawa and T. Shimanouchi, *Spectrochim. Acta*, **20**, 819 (1964).

27) J. R. Durig, W. A. McAllister, J. N. Willis, Jr., and E. E. Mercer, *ibid.*, **22**, 1091 (1966).

28) J. R. Durig, W. A. McAllister and E. E. Mercer, *J. Inorg. Nucl. Chem.*, **29**, 1441 (1967).

29) D. M. Adams and P. J. Chandler, *Chem. Ind.* (London), **1965**, 269.

30) N. A. D. Carey and H. C. Clark, *Inorg. Chem.*, **7**, 94 (1965).

31) D. J. Hewkin and W. P. Griffith, *J. Chem. Soc.* A, **1966**, 472.

cm^{-1} respectively. These band shifts observed were in good agreement with the calculated ones, 34 and 17 cm^{-1}, which were estimated for the linear three-body model of Ru–N–Ru with the Ru–N distance of 1.718 A.[10] This agreement for the 1082 cm^{-1} band was shown also by Cleare and Griffith.[9]

When the crude product obtained in preparing complex [4] was not heated with Sn(II) in 6M hydrochloric acid, it usually exhibited a broad band at 1409 cm^{-1} with a medium intensity. The repeated recrystallization of the crude product gradually reduced the intensity of the absorption band at 1409 cm^{-1}, but it could not remove the band completely. This absorption band shifted slightly from 1409 to 1403 cm^{-1} on ^{15}N-substitution. The crude product showed identical features in its ^{15}N-substitution for the 1082 and 543 cm^{-1} bands, in its electronic spectra, and in its X-ray powder pattern with that of the purified complex, except that the band at 1409 cm^{-1} was present in the crude product.

It may be suggested that a complex with a singly-bridging nitrosyl group such as $K_3[Ru_2Cl_8(H_2O)_2NO]$ is present in the crude product of complex [4] and that the absorption band at 1409 cm^{-1} is due to the stretching vibration of the singly-bridging nitrosyl group. The disappearance of the absorption band of the crude product of complex [4] on the digestion in 6M hydrochloric acid may be caused by the rupture of the N–O bond in the bridging nitrosyl group and the formation of a bridging nitrido structure. On the other hand, it is also probable that the impurity in the crude product of complex [4] is a material which gives an infrared band only at 1409 cm^{-1}. The present study can not distinguish these possibilities. The impurity in the crude product of complex [4] will be discussed again later in connection with our other findings.

Complex [4] was dehydrated at 400°C under a nitrogen atmosphere, as has been described above. The infrared spectra of the complex heated exhibited two sharp bands at 1592 and 1063 cm^{-1} instead of the three bands at 3360, 1611, and 1082 cm^{-1} usually found in complex [4]. The corresponding two bands were observed at 1594 and 1031 cm^{-1} in the ^{15}N-substituted complex. The recrystallization of the complex dehydrated with a hydrochloric acid solution containing potassium chloride yielded the original complex [4]. These observation suggest a fairly stable skeletal structure of complex [4]. The appearance of the band at 1592 cm^{-1} in the dehydrated complex remained an unsolved problem. A proper assignement of the band at 1592 cm^{-1} was not made, though this infrared region is expected to be that for the stretching vibration of the bridging nitrosyl group. The other band, at 1063 cm^{-1}, is thought to correspond to the band at 1082 cm^{-1} in complex [4]; it may be suggested that the RuNRu skeleton is present in the dehydrated complex.

The preparation of the binuclear complex which has both terminal and singly-bridging nitrosyl groups was attempted. Preparation: to the starting material (0.79 mmol Ru(III)NO in 10 m*l*), 3M hydrochloric acid (20m*l*), potassium chloride (0.5 g), and $SnCl_2 \cdot 2H_2O$ (0.5 g, 2.2 mmol) were added. The mixed solution, in a porcelain dish, was then heated on a water bath for about 30 min. After the solution had subsequently stood for about a week, reddish-brown crystals were obtained. The composition of these crystals compared fairly well with the formula of $K_3[Ru_2Cl_9(NO)_2]$.

Found: Ru, 29.28; N, 3.61; Cl, 44.34; K, 17.38; Sn, 0.15%. Calcd for $K_3[Ru_2Cl_9(NO)_2]$: Ru, 28.91; N, 4.01; Cl, 45.76; K, 16.79%.

The nitrogen content determined was always less than the calculated value. There remains some uncertainty as to the purity of this product. The solubility of this product was much less than that of $K_2[RuCl_5NO]$, but greater than that of complex [4]. However, the recrystallization from hydrochloric acid solutions was not succesful, and it was

Table 5. Infrared spectra of "$K_3[Ru_2Cl_9(NO)_2]$"

^{14}N-Complex	^{15}N-Complex	Tentative assignments
3640 vw	3620 vw	ν NO (terminal) overtone ?
3360 m 3200 w, sh	3360 m 3200 w, sh	ν OH (impurity)
1913 vs 1903 vs	 (1903 m) 1872 vs 1862 vs	ν NO (terminal)
1610 m-w	1610 m-w	δ H_2O (scissoring, impurity)
1405 m-w	1399 m-w	ν NO (bridging)
1082 m	(1082 vw) 1047 s-m	ν_{as} Ru-N-Ru
587 w		δ Ru-NO (terminal)
543 w	528 w	δ Ru-N-Ru

TABLE 6. POWDER X-RAY DIFFRACTION DATA (CuK_α)

$K_2[RuCl_5NO]$		"$K_3[Ru_2Cl_9(NO)_2]$"		$K_3[Ru_2Cl_8(H_2O)_2N]$	
d(Å)	I/I_0	d(Å)	I/I_0	d(Å)	I/I_0
5.7230	0.86	5.7674	1.00	6.9972	1.00
5.5796	1.00	5.6041	0.21	6.4816	0.83
5.2448	0.14	4.9926	0.28	5.4835	0.14
5.1695	0.19	4.7918	0.11	4.2629	0.11
4.7663	0.49	3.5309	0.35	3.9656	0.43
3.9498	0.10	3.1399	0.17	3.8635	0.29
3.5131	0.34	3.0153	0.28	3.5036	0.14
3.3175	0.30	2.8823	0.26	3.4634	0.31
3.0113	0.17	2.8029	0.11	3.4048	0.23
2.9847	0.21	2.7120	0.10	3.2639	0.17
2.8661	0.20	2.5902	0.10	2.8914	0.14
2.7962	0.51	2.4993	0.37	2.8116	0.20
2.7128	0.49	2.3962	0.06	2.7040	0.15
2.5872	0.43	2.2906	0.08	2.6804	0.10
2.3889	0.26	2.2333	0.09	2.5404	0.80
2.0970	0.16	2.0429	0.12	2.1691	0.11
2.0562	0.15	1.9239	0.09	1.9835	0.14
1.8682	0.14	1.7666	0.15	1.7603	0.10

Relative intensities were estimated by comparing the hight of the peak. Less intensity lines are omitted.

observed that the recrystallization brought the decomposition to $[RuCl_5NO]^{2-}$ and/or the crude product of complex [4].

The infrared spectra of this product exhibited its major absorption bands at 3360, 1913, 1903, 1610, 1405, and 1082 cm^{-1} over the 4000—400 cm^{-1} range (Table 5) and are thought to involve absorption bands corresponding to those of complex [4]. The relative intensities of these absorption bands sometimes varied with the samples, and the intensity of the band at 1405 cm^{-1} decreased with an increase in the intensities of the bands at 3360, 1610, and 1082 cm^{-1}. However, the band at 1405 cm^{-1} was a sharp and symmetric band. This band may correspond to the band of the crude product of complex [4] at 1409 cm^{-1}.

The bands at 1913, 1903, and 1082 cm^{-1} are thought to be due to the terminal NO group and the asymmetric stretching vibration of the Ru–N–Ru group respectively. The four bands at 1913, 1903, 1405, and 1082 cm^{-1} shifted on ^{15}N-substitution, as is shown in Table 5. The bands at 3360 and 1610 cm^{-1} may be caused by the coordinating waters of complex [4], an impurity in this product. These observations, along with the chemical properties, indicate that the "$K_3[Ru_2Cl_9(NO)_2]$" complex, with a singly-bridging and a terminal nitrosyl group, may exist and that the sharp absorption bands observed at 1405 cm^{-1} may be due to the stretching vibration of the singly-bridging nitrosyl group in the complex, although the sample used in this infrared study was not pure enough. The X-ray powder patterns of the "$K_3[Ru_2Cl_9(NO)_2]$", $K_2[RuCl_5NO]$ complex and of complex [4] were compared (Table 6); it was thus shown that "$K_3[Ru_2Cl_9(NO)_2]$" is not a mixture of $K_2[RuCl_5NO]$ and complex [4].

When the final filtrate in the preparation of "$K_3[Ru_2Cl_9(NO)_2]$" was allowed to stand for a long time, red crystals were rarely obtained. The infrared spectra of this material exhibited only a strong band at 1408 cm^{-1} in the NaCl region and one at 1400 cm^{-1} for the ^{15}N-substituted material. Though this material is expected to have an interesting structure, the details on this particular crystals have not yet been clarified. However, these findings seem to support the idea that the crude product of complex [4] contains an impurity which gives an infrared band only at 1409 cm^{-1}.

Diamagnetisms. All the complexes prepared were diamagnetic. It is clear that $(Me_4N)_2[RuCl_3(SnCl_3)_2NO]$ (complex [1]) and $(Me_4N)_4[RuCl(SnCl_3)_5]$ (complex [3]) are diamagnetic. The oxidation state of the RuNO group in complex [1] is III, while that of ruthenium in complex [3] is II.

The diamagnetisms of $(Me_4N)_4[Ru_2Cl_6(SnCl_3)_2(NO)_2]\cdot H_2O$ (complex [2]) will be explained on the basis of the skeletal structure, shown in Fig. 4. Complex [2] involves the skeletal group of $Ru_2(NO)_2$, the oxidaton state of which is IV. The formal oxidation states of the ruthenium atoms and nitrosyl groups may be designated as follows: (i) both ruthenium atoms with II, and both bridging nitrosyl groups with zero, or (ii) both ruthenium atoms with III, and both the bridging nitrosyl groups with -1. The diamagnetism of this com-

plex may be satisfactorily understood on the basis of the resonating four-member ring system, which accommodates two electrons of two nitrosyl groups in the case of (i), or those of two ruthenium atoms in the case of (ii), to make the spins of the two electrons paired. The diamagnetism of the binuclear manganese complex has similarly been explained by a four member-ring bridged with two nitrosyl groups.[23] Direct Ru(III)-Ru(III) interaction may also be possible in the case of (ii). Thus, the skeletal structure proposed can explain both the infrared spectra and the diamagnetism of complex [2].

The diamagnetism of $K_3[Ru_2Cl_8(H_2O)_2N]$ has been explained by assuming that the spin-pairing of $4d_{xz}$ and $4d_{yz}$ ruthenium orbitals takes place *via* the $2p_\pi$ nitrogen orbital.[9]

Reactions of Nitrosylruthenium(III) with Tin(II). The reactions of nitrosylruthenium(III) with tin(II) in hydrochloric acid solutions were quite complicated. The isolation of the reaction products is thought to give qualitative information on the reactions, although the isolation depends on the formation of complex ions, the solubilities of the salts of the complex ions formed, and the equilibria which involve the complex ions. The observed relations of these complexes are summarized in Fig. 5. The reactions of nitrosylruthenium(III) in this study may be divided into two broad classes: the coordinations of $SnCl_3^-$ on the ruthenium atom and the changes in the nitrosylruthenium(III) group. The differences in the conditions of preparing complexes [1], [2], and [3] indicate that the donation of $SnCl_3^-$ groups to the ruthenium atom of the nitrosylruthenium(III) group occurs first of all, and that the RuNO group then undergoes dimerization to form a binuclear skeleton bridged doubly by two nitrosyl groups; finally, the elimination of nitrosyl group occurs.

The reaction of $(Me_4N)_4[Ru_2Cl_6(SnCl_3)_2(NO)_2]\cdot H_2O$ with tin(II) chloride in the presence of potassium chloride in a hydrochloric acid solution yields a large amount of $[RuCl(SnCl_3)_5]^{4-}$ and a very small amount of $K_3[Ru_2Cl_8(H_2O)_2N]$ (complex [4]).

A consideration of the conditions for preparing "$K_3[Ru_2Cl_9(NO)_2]$", and $K_3[Ru_2Cl_8(H_2O)_2N]$ suggests that the formation of the skeletal structures becomes easier in the order of: Ru(N)Ru<Ru(NO)Ru<Ru(NO)Ru(NO) (easiest), if $K_3[Ru_2Cl_8(H_2O)_2(NO)]$ is assumed to be present in the crude product of complex [4].

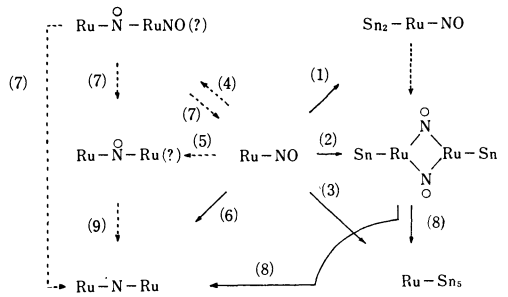

Fig. 5. Reactions of Ru(III)NO with Sn(II). (Only skeletons are cited.) (1)—(6): preparation routes, (7): decomposition of "$K_3[Ru_2Cl_9(NO)_2]$" in hydrochloric acid, (8): reaction of $(Me_4N)_4[Ru_2Cl_6(SnCl_3)_2(NO)_2]\cdot H_2O$ with Sn(II) and (9): reaction of the crude product of $K_3[Ru_2Cl_8(H_2O)_2N]$ with Sn(II).

When nitrosylruthenium(III) and tin(II) (in the mole ratio of 1 : 0.8) were concentrated with potassium chloride under gentle warming, dipotassium pentachloronitrosylruthenate(III) was obtained. On the other hand, nitrosylruthenium(III) can be changed to ruthenium(II) by the method described in the preparation of complex [3].

The author wishes to express his thanks to Professor Hisateru Okuno of St' Paul's(Rikkyo) University for his suggestion that the chemistry of ruthenium would be an interesting subject of study, and to Assistant Professor Ichiro Nakagawa of the Tokyo University, Dr. Eiichi Miki and Dr. Hiroshi Saito of St' Paul's(Rikkyo) University for their valuable suggestions concerning the infrared study. Thanks are also due to Professor Tatsujiro Ishimori of St' Paul's(Rikkyo) University and Assistant Professor Terunosuke Nomura of Sophia University for their continuing interest and encouragement.

BULLETIN OF THE CHEMICAL SOCIETY OF JAPAN VOL. 43 3814—3819 (1970)

A Study of Electronic Spectra of Square Planar Copper(II) and Nickel(II) Complexes by Circular Dichroism*1

Yuzo NISHIDA and Sigeo KIDA

Department of Chemistry, Faculty of Science, Kyushu University, Fukuoka

(Received July 6, 1970)

Using optically active 1,2-propylenediamine we have synthesized several ligands to form square planar Cu(II) and Ni(II) complexes with optical activity. The CD(circular dichroism) and AB (absorption) spectra of these compounds were measured. The broad absorption bands were resolved in the CD spectra into each component due to a *d-d* transition, to which a specific *d-d* transition was assigned. It was found that in these compounds the change in the central atom from Cu(II) to Ni(II) dose not alter the main feature of CD and AB spectra. This seems to be the general rule for the planar Cu(II) and Ni(II) complexes.

The ligand field theory predicts that three spin-allowed *d–d* transitions may be observed in the electronic spectra of square planar copper(II) and nickel(II) complexes. However, the three d–d bands are usually superposed and are observed as one broad band, sometimes with shoulders. Thus our attempt to assign the absorption bands to each electronic transition was accompanied with considerable difficulty.

Recently, Smith[1,2] has developed an elegant approach for the estimation of energy levels of tetragonal copper(II) complexes, making use of Hathaway and his coworkers' detailed experimental data.[3,4] According to Smith, the order of energy levels of $Cu(NH_3)_4X_2$ and Cu en_2X_2, (X=SCN^-, NO_2^-, $CuCl_2^-$, and other various anions) is $d_{x^2-y^2} > d_{z^2} > d_{xy} > d_{xz}$, d_{yz}, but in planar $CuCl_4^{2-}$ the order of d_{xy} and d_{z^2} is reversed. This implies that more detailed studies are necessary for the elucidation of the electronic spectra of copper(II) complexes. As for the electronic spectra of square planar nickel(II) complexes, information is still insufficient.[5]

We have prepared numerous square planar copper(II) and nickel(II) complexes of the $[MN_4]$ and $[MN_2O_2]$ types containing optically active ligands, and tried to obtain more information on the energy states of these complexes by taking advantage of CD spectra which give much more resolved spectra than the AB spectra for superposed bands. In addition, we could obtain some information of the configuration and the conformation of the complexes by CD spectra.

Experimental

The absorption and circular dichroism spectra were obtained by a Jasco ORD-UV/5 optical rotatory dispersion recorder with a CD attachment at room temperature. Optically active (−)D-propylenediamine (abbreviated as (−)pn) was obtained by the method of Dwyer *et al.*[6] These complexes may be classified into the following four types.

A. Complexes with optically active propylenediamine. $[Cu(-)pn_2](ClO_4)_2$, and $[Ni(-)pn_2](ClO_4)_2$ were obtained from metal perchlorate and (−)D-propylenediamine in methanol solution.

B. Complexes with optically active Schiff bases resulted from salicylaldehyde or its derivatives and (−)D-propylenediamine, such as sal(−)pnH_2, naphal(−)pnH_2, 7-mesal(−)pnH_2. (For abbreviation, see Table 2). Each of these complexes was obtained from metal acetate and schiff base, which was obtained from the mixture of salicylaldehyde or its derivatives and (−)D-propylenediamine.

C. Complexes with optically active schiff bases from acetylacetone or benzoylacetone and (−)D-propylenediamine, such as acac(−)pnH_2, bzac(−)pnH_2, (see Table 2). These complexes were obtained from a mixture of metal chloride, schiff base and sodium carbonate in water-methanol mixture.

D. Complexes with the mad(−)pnH_2, oxad(−)-pnH_2, sad(−)pnH_4, which were obtained from the condensation reaction between diethylmalonate, diethyloxalate or methyl salicylate and (−)-propylenediamine. Metal complexes were prepared by a method

*1 Presented in part at the 19th Symposium on Coordination Chemistry, Sendai, September, 1969.

1) D. W. Smith, *J. Chem. Soc., A*, **1969**, 1708.
2) D. W. Smith, *ibid., A*, **1969**, 2529.
3) B. J. Hathaway, D. E. Billing, P. Nicholls and I. M. Procter, *ibid., A*, **1969**, 65, 319.
4) I. M. Procter, B. J. Hathaway and P. Nicholls, *ibid., A*, **1968**, 1678.
5) H. B. Gray, "Transition Metal Chemistry," Vol. 1, ed. by R. L. Carlin, Marcel Dekker, New York (1965), p. 239.
6) F. P. Dwyer, F. L. Garvan and A. Shulman, *J. Amer. Chem. Soc.*, **81**, 290 (1959).

Table 1. Elementary analyses of the complexes

Complex	Formula	Found (%)			Calcd (%)		
		C	H	N	C	H	N
[Cu(−)pn$_2$](ClO$_4$)$_2$H$_2$O	$CuC_6H_{22}O_9N_4Cl_2$	17.35	4.89	13.43	17.14	4.76	13.33
[Ni(−)pn$_2$](ClO$_4$)$_2$	$NiC_6H_{20}O_8N_4Cl_2$	17.88	5.11	13.71	17.73	4.92	13.79
[Cu sal(−)pn]	$CuC_{17}H_{18}O_3N_2$	56.64	5.14	7.70	56.35	4.97	7.71
[Cu 7-mesal(−)pn]	$CuC_{19}H_{20}O_2N_2$	60.81	5.50	7.52	61.20	5.37	7.52
[Ni sal(−)pn]	$NiC_{17}H_{20}O_2N_2$	60.18	4.79	8.21	60.17	4.72	8.26
[Ni naphal(−)pn]*	$NiC_{25}H_{20}O_2N_2$	68.05	4.71	6.25	68.33	4.56	6.37
[Ni 7-mesal(−)pn]*	$NiC_{19}H_{20}O_2N_2$	61.85	5.38	7.82	62.12	5.45	7.63
[Cu acac(−)pn]	$CuC_{13}H_{19}O_2N_2$	52.61	6.89	9.41	52.10	6.68	9.32
[Ni acac(−)pn]	$NiC_{13}H_{19}O_2N_2$	52.77	6.83	9.52	52.88	6.77	9.49
[Ni bzac(−)pn]*	$NiC_{23}H_{24}O_2N_2$	66.02	5.83	6.87	65.60	6.17	6.65
[Cu mad(−)pn]·9H$_2$O*,a)	$CuC_9H_{38}O_{11}N_4$	24.93	7.86	12.98	24.55	8.18	12.98
[Cu mad(−)pn]·3/2H$_2$O*	$CuC_9H_{23}O_{3.5}N_4$	35.24	6.97	18.34	35.61	6.59	18.45
[Cu oxad(−)pn]·3/2H$_2$O*	$CuC_8H_{21}O_{3.5}N_4$	32.90	6.70	18.27	33.02	6.53	18.55
[Ni mad(−)pn]·H$_2$O*	$NiC_9H_{22}O_3N_4$	37.31	6.80	19.14	37.24	6.52	19.31
[Ni oxad(−)pn]·H$_2$O*	$NiC_8H_{20}O_3N_4$	34.46	7.03	19.74	34.77	6.52	19.74
Na$_2$[Cu sad(−)pn]·5.5H$_2$O*,b)	$CuC_{17}H_{25}O_{9.5}N_2Na_2$	39.32	4.22	5.22	39.15	4.70	5.37

* New complex

a) This complex, which is orange, gradually turns violet losing water in the atmosphere.

b) This complex is hygroscopic.

similar to the Ojima's method.[7,8] Since the nickel complex of sad(−)pnH$_4$ did not crystallize, the solution was purified by eluting on alumina and the ion-exchange resin, Amberlite CG 120. The solution thus obtained was immediately used for optical measurements. The obtained spectrum agreed well with that of the ethylenediamine homologue, indicating that [Ni sad(−)pn]$^{2-}$ was formed in the solution.

Results and Discussion

Copper Complexes. It is believed that bis(propylenediamine)copper(II) ion has a nearly tatragonal configuration in methanol solution as in the case of bis(ethylenediamine)copper(II) ion. As is seen in Fig. 3, CD spectrum of Cu(−)pn$_2$(ClO$_4$)$_2$ shows a small band at 15.2 kK. besides the main broad band at 19.7 kK. Gillard[9] assigned the main band to the $d_{xz},d_{yz}\rightarrow d_{x^2-y^2}$ transition and the small bond at 15.2 kK to the $d_{xy}\rightarrow d_{x^2-y^2}$ transition. The band due to the $d_{z^2}\rightarrow d_{x^2-y^2}$ transition was assumed to be located at the region of much lower wave-number (*cf.* Fig. 2). However, from the Gaussian analysis of electronic spectra, measured at room temperature and at the temperature of liquid nitrogen, of the crystals of bis(ethylenediamine)copper(II) salts with different anion, Hathaway *et al.* found three bands in the visible region. They assigned the bands which were found at 20.3—17.9 kK, 18.0—16.2 kK and 16.8—12.2 kK to the transitions $d_{xz},d_{yz}\rightarrow d_{x^2-y^2}$, $d_{xy}\rightarrow d_{x^2-y^2}$, and $d_{z^2}\rightarrow d_{x^2-y^2}$, respectively. The result of Smith's calculation agreed satisfactorily with the experimental values on the same assignment. The band at 15.2 kK of Cu(−)pn$_2^{2+}$ was clearly resolved in our CD measurement, which should correspond to the band of the lowest wave-number in Cu en$_2^{2+}$, and is assigned to the $d_{z^2}\rightarrow d_{x^2-y^2}$ transition. Further support for this assignment will be seen in the following discussion.

In the solvent of stronger donating ability, such as pyridine, the coordination or semi-coordination of the solvent molecule to the copper ion along the

Table 2. Legend for abbreviations of ligands

	Ligand	Abbreviation
I	(−)$_D$-propylenediamine	(−)pn
II	bis(salicylaldehyde)-(−)$_D$-propylenediamine	sal(−)pnH$_2$
III	bis(acetophenone)-(−)$_D$-propylenediamine	7-mesal(−)pnH$_2$
IV	bis(α-naphthol-β-aldehyde)-(−)$_D$-propylenediamine	naphal(−)pnH$_2$
V	bis(acetylacetone)-(−)$_D$-propylenediamine	acac(−)pnH$_2$
VI	bis(benzoylacetone)-(−)$_D$-propylenediamine	bzac(−)pnH$_2$
VII	*N,N'*-bis(2-aminopropyl)-malonamide	mad(−)pnH$_2$
VIII	*N,N'*-bis(2-aminopropyl)-oxalamine	oxad(−)pnH$_2$
IX	*N,N'*-propylene-bis(salicylamide)	sad(−)pnH$_4$

7) H. Ojima and K. Yamada, *Nippon Kagaku Zasshi*, **89**, 490 (1968).

8) H. Ojima, *ibid.*, **88**, 329 (1967).

9) R. D. Gillard, *J. Inorg. Nucl. Chem.*, **26**, 1455 (1964).

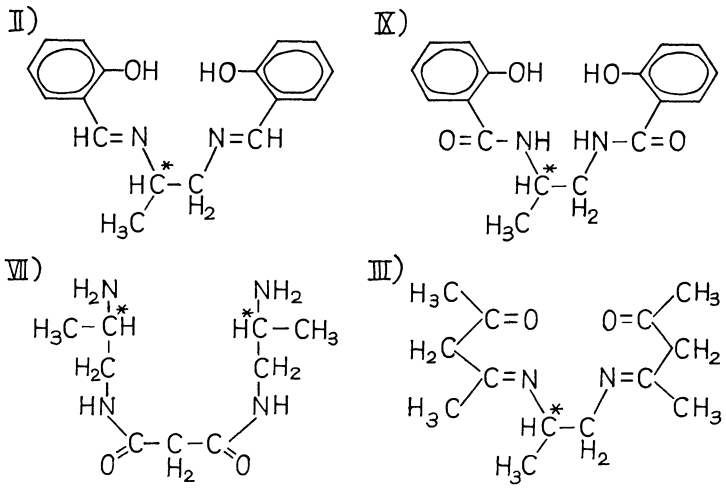

Fig. 1. Structure of ligands (see Table 2).

tetragonal axis would become stronger, and d_{z^2} orbital of the copper ion suffers the most profound effect among the *d*-orbitals (Fig. 2). As a result of this effect, the band due to the $d_{z^2} \rightarrow d_{x^2-y^2}$ transition will show the largest red shift among the *d–d* bands. In fact, as seen in Fig. 3, in the CD and absorption spectra of $Cu(-)pn_2(ClO_4)_2$ in pyridine solution, the red shift of the main peak is only about 1 kK in either AB or CD spectrum compared with that in methanol solution. On the other hand, the CD band, which was observed at 15.2 kK in methanol solution and was assigned to the $d_{z^2} \rightarrow d_{x^2-y^2}$ transition, disappeared in pyridine solution, and a shoulder appeared at 12 kK in the absorption spectrum, suggesting that this band shifted from 15.2 kK to 12 kK.

The CD and AB spectra of [Cu mag(−)pn] are shown in Fig. 4. In this complex two of four coordinated nitrogen atoms are anions of amide nitrogen which has lost a proton. It is accepted that in such a $[CuN_4]$ type complex as involving anion nitrogen in coordination, the coordination bonds in the tetragonal plane is much stronger than those of the complex coordinated by four neutral nitrogen atoms, and the axial coordination becomes very weak.[7,8] As a result of this effect, the d_{z^2} orbital will be stabilized and the $d_{z^2} \rightarrow d_{x^2-y^2}$ band will shift to the higher wave-number. This is the reversal of the spectral change from a methanol solution to a pyridine solution. In fact, only one broad band was observed in either AB or CD spectrum of [Cu mad(−)pn] in the visible region. This is understandable in view of the blue shift of the $d_{z^2} \rightarrow d_{x^2-y^2}$ band to the region of the main band.

The Resemblance of CD Spectra of Planar Cu(II) and Ni(II) complexes. It is readily ob-

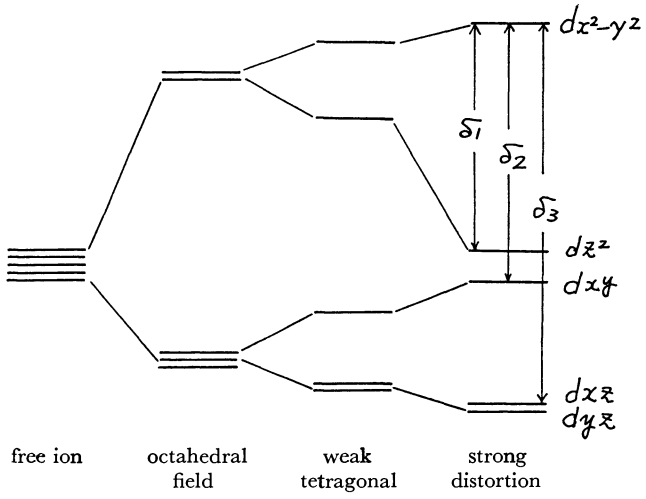

Fig. 2. Assumed scheme of *d*-orbital splitting.

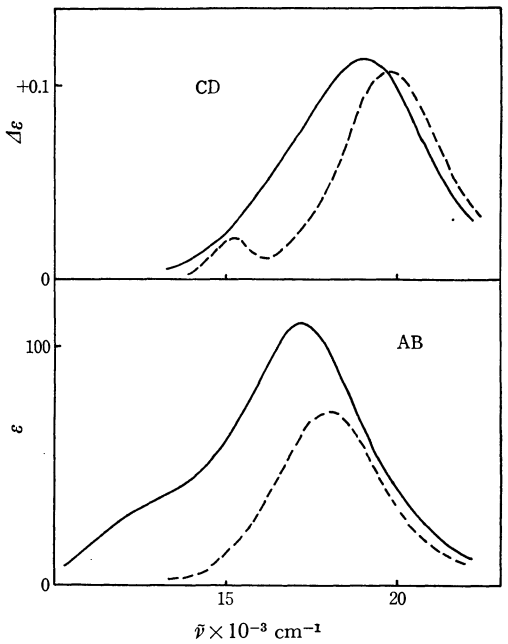

Fig. 3. AB and CD spectra of $[Cu(-)pn_2](ClO_4)_2$.
------ in methanol —— in pyridine

served that the CD and AB spectra of [Cu mad(−)-pn] resemble those of the nickel(II) complex of the same ligand as seen in Fig. 4. In the Cu(II) and Ni(II) complexes of sad(−)pn, which are shown in Fig. 5, the three components of the *d–d* bands are clearly resolved in CD spectra of both complexes. Resemblance of the two spectra is rather surprising, and the three bands may be assigned from the lower wave-number side to $d_{z^2} \rightarrow d_{x^2-y^2}$, $d_{xy} \rightarrow d_{x^2-y^2}$, and $d_{xz}, d_{yz} \rightarrow d_{x^2-y^2}$ in each complex.

The spectra of [Cu acac(−)pn], [Cu sal(−)pn] and [Cu 7-mesal(−)pn] in chloroform are shown in Fig. 6. Judging from the absorption intensity, the bands above 23 kK would not be due to the d–d transition but could be attributed to the origin in the ligand electron. Though the three complexes all belong to the square planar *cis*-$[CuN_2O_2]$ type, the CD spectrum of [Cu sal(−)pn] associated with d–d transision entirely differs from those of the other two complexes, as is obvious from Fig. 6. Downing and Urbach,[10] and the present authors[11] independently reached the same conclusion that this fact may be rationalized in terms of the conformational preference of the central chelate ring resulting from the steric requirements of the ligands.

The nickel(II) complexes of acac(−)pnH_2, sal-(−)pnH_2 and 7-mesal(−)pnH_2 are expected to have a square planar configuration from the electronic spectra and a structure of homologous ethylenediamine derivatives. Each of the CD spectra of the nickel complexes bears a close resemblance to that of the corresponding copper complex, suggesting that the conformations of the bridging propane-1,2 diamine group are similar to each other in the nickel

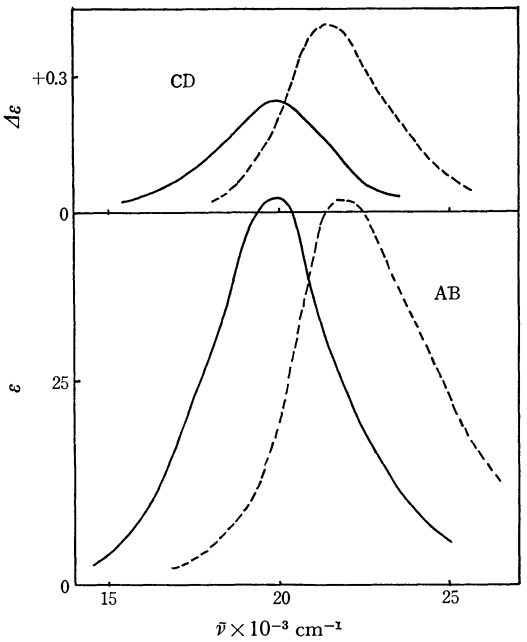

Fig. 4. AB and CD spectra of —— [Cu mad-(−)pn] in methanol ------ [Ni mad(−)pn] in methanol.

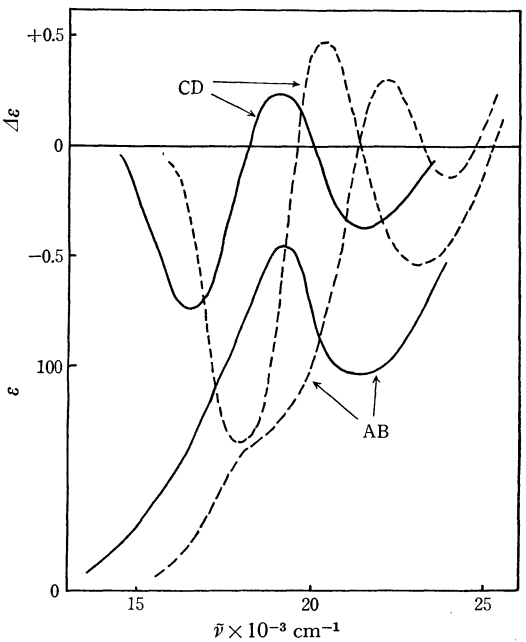

Fig. 5. AB and CD spectra of —— [Cu sad-(−)pn]$^{2-}$ in methanol ------ [Ni sad(−)pn]$^{2-}$ in methanol.

10) R. S. Downing and F. L. Urbach, *J. Amer. Chem. Soc.*, **91**, 5977 (1969).

11) 19th Symposium on Coordination Chemistry, at Tohoku University, September, 1969.

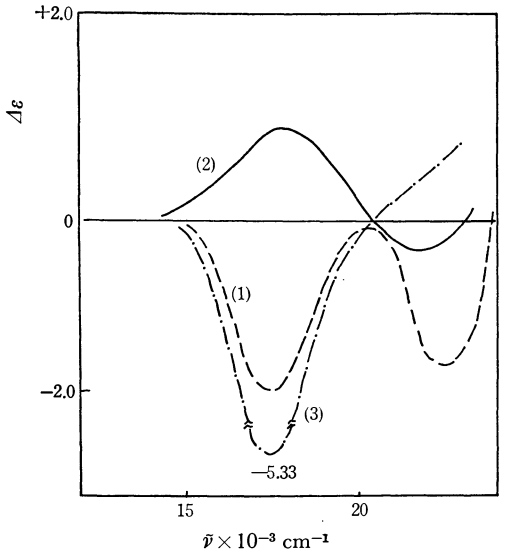

Fig. 6. CD spectra of (1) -------- [Cu acac(−)pn] (2) ——— [Cu sal(−)pn] (3) -·-·- [Cu 7-mesal(−)pn] in chloroform.

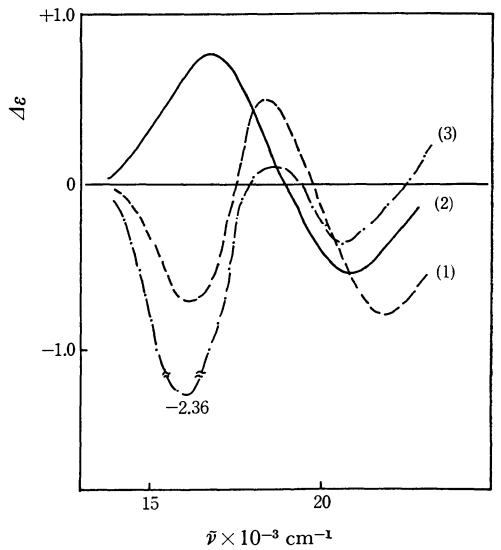

Fig. 7. CD spectra of (1) -------- [Ni acac(−)pn] (2) ——— [Ni sal(−)pn] (3) -·-·- [Ni 7-mesal(−)pn] in chloroform.

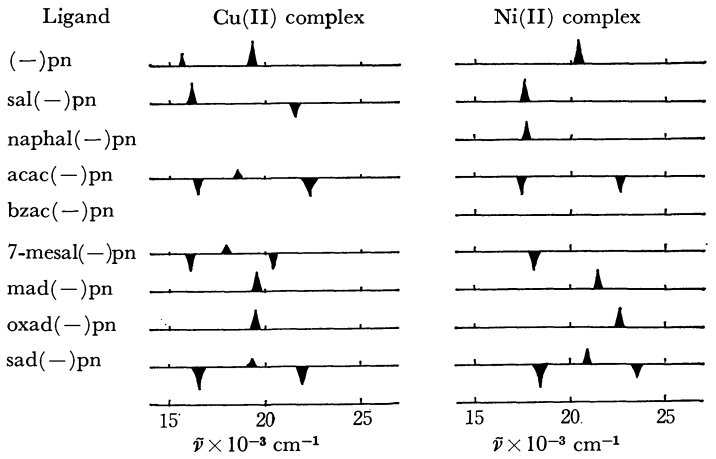

Fig. 8. Simple representation of CD spectra.

and copper complexes of the same ligand (Figs. 6 and 7).

The close resemblance of CD spectra of the planar copper(II) and nickel(II) complexes of the same ligand is too obvious to be considered accidental. In fact, this tendency was observed not only in the above complexes but in the spectra of Ni(II) and Cu(II) complexes of every ligand studied in the present work (Fig. 8). Further, from literature we investigated we have always found such resemblance in CD spectra for each pair of nickel and copper complexes of the same ligand.[12–14] Thus, this appears to be the general rule.

The *d*-orbitals split under the ligand field of square planar coordination as shown in Fig. 2. If interelectronic interaction is neglected, there is no significant difference between planar Cu(II) and Ni(II) complexes. Actually, however, the energy states of nickel(II) complexes are largely dependent on interelectronic repulsion, even if the spin-orbit-coupling is neglected. Accordingly, the energies for some lower singlet states of a planar nickel(II) complex are expressed as

$$^1A_{1g}: E_0 = F_0 + 4F_2 + 36F_4$$
$$^1B_{1g}: E_1 = \delta_1 + F_0 + 21F_4$$
$$^1A_{2g}: E_2 = \delta_2 + F_0 + 4F_2 + F_4$$
$$^1E_g: E_3 = \delta_3 + F_0 + F_2 + 16F_4$$

Following Ballhausen and Liehr,[15] we assume $F_2 = 10F_4 = 1$ kK,

12) T. Komorita, J. Hidaka and Y. Shimura, This Bulletin, **42**, 168 (1969).

13) G. K. Bryce and F. R. N. Gurd, *J. Boil. Chem.*, **241**, 1439 (1969).

14) K. M. Wellman, S. Bogdansky, C. R. Hare and M. Mathiesm, *Inorg. Chem.*, **8**, 1025 (1969).

$$\Delta E_1 = \delta_1 - 4F_2 - 15F_4 = \delta_1 - 5.5\ \text{kK}$$
$$\Delta E_2 = E_2 - E_0 = \delta_2 - 35F_4 = \delta_2 - 3.5\ \text{kK}$$
$$\Delta E_3 = E_3 - E_0 = \delta_3 - 3F_2 - 20F_4 = \delta_3 - 5.0\ \text{kK}$$

and

$$\Delta E_{12} = E_2 - E_1 = \delta_2 - \delta_1 + 4F_2 - 20F_4 = \delta_2 - \delta_1 + 2.0\ \text{kK}$$
$$\Delta E_{23} = E_3 - E_2 = \delta_3 - \delta_2 + 3F_2 + 15F_4 = \delta_3 - \delta_2 - 0.5\ \text{kK}$$

From the above result, the effect due to the interelectronic repulsion is comparable to the observed band separations 2.5—3.0 kK, but is not large enough to change the order of energy levels $E_1 < E_2 < E_3$. Therefore, the same pattern can be expected with the same ligands. However, it is to be noted that the resemblance is close, at least in the examples cited above, and is considered to be more than that expected from the above discussion. An explanation for this tendency is still in question at present.[16]

The reason for the planar Ni(II) and Cu(II) complexes giving similar CD spectra for bands whose origins are the transitions between the same combination of *d*-orbitals is given as follows. According to Condon,[17] the rotational strength R_{ab} associated with the electronic transition from the state, a, to the state, b, is determined by

$$R_{ab} = \text{Im}\langle(a)|\mathbf{P}|(b)\rangle\langle(b)|\mathbf{M}|(a)\rangle$$

where Im denotes the imaginary part of the scalar product of these moments; (a) and (b) stand for the wave functions of the ground and the excited states, and **P** and **M** are the electric and magnetic dipole moment-oparators. In the case of a multi-electron system, (a) and (b) are to be expressed by the Slater determinants. However, since **P** and **M** are one-electron operators, $\langle(a)|\mathbf{P}|(b)\rangle$ and $\langle(b)|\mathbf{M}|(a)\rangle$ are reduced to the simple formulas, $\langle a'|\mathbf{P}|b'\rangle$ and $\langle b'|\mathbf{M}|a'\rangle$, where a' and b' represent the wave functions of simple orbitals between which an electron transfers. Thus, it has been verified that rotational strengths of Ni(II) and Cu(II) complexes of the same ligand may be expressed by the same formula for the transitions between the same combination of *d*-orbitals.

The authors would like to express their thanks to Mr. Masaaki Narimatsu for help in the experiment.

15) C. J. Ballhausen and A. D. Liehr, *J. Amer. Chem. Soc.*, **81**, 538 (1958).

16) The energies due to the interaction with upper $^1A'_{1g}$ and $^1B'_{1g}$ states were found to be less than 0.2 kK which is negligible in the present discussion.

17) E. U. Condon, *Rev. Mod. Phys.*, **9**, 432 (1932).

BULLETIN OF THE CHEMICAL SOCIETY OF JAPAN VOL. 43 3819—3823 (1970)

Stereoselectivity in Mixed Tris-Type Cobalt(III) Complexes with Glycine and L-Aspartic Acid*1

Kiyoshi KAWASAKI, Junko YOSHII and Muraji SHIBATA

Department of Chemistry, Faculty of Science, Kanazawa University, Kanazawa

(Received July 9, 1970)

The reaction of the carbonatobis(glycinato)cobaltate(III) with L-aspartate in the presence of active charcoal led to the stereoselective formation of tris(glycinato-L-aspartato) complexes. By means of ion-exchange chromatography and fractional precipitation, four optically-active complexes, *mer*-Λ- and *fac*-Λ-$[Co(gly)_{3-n}(L\text{-}asp)_n]^{n-}$ ($n=1,2$), have been isolated, and they have been characterized by means of their absorption and circular dichroism spectra. Furthermore, the percent compositions of the geometrical isomers for the complexes ($n=1,2,3$) in the reaction mixture and also of Λ- (or Δ-) isomers for each geometrical isomer have been estimated using the spectral data. A marked stereoselectivity (>90%) has been found in the *fac*-Δ-isomers, while an appreciable selectivity (*ca.* 70%) has been found for the *mer* isomers. These stereoselectivities have been explained in terms of an enhanced stability through hydrogen bonding between the β-carboxylate group in the coodinated L-aspartate and the amino group in the adjacent ligand.

When optically-active ligands are combined with metal ions to make a source of dissymmetry at the central metal, the resulting diastereoisomers are usually unequal in amount. This stereoselectivity has been known for such asymmetric ligands as 1,2-diamines and amino acids. In the case of diamine

*1 Presented at the 19th Symposium on Coordination Chemistry, Sendai, September, 1969.

complexes, the stereoselectivity has been attributed to the interactions of the puckered chelate rings with each other.[1] On the other hand, in the case of aminoacidato complexes two factors have been considered in connection with the selectivity. One factor comes from the presence of bulky substituents in the ligands; the absence of the *mer*-*Λ*-isomer of the tris(L-prolinato)cobalt(III) complex can thus be explained.[2] The other factor is due to the interaction of the polar substituents in the aminoacidato ligand with the other polar site of the adjacent ligand. The stereoselective formation of *Λ*-(+)-$[Co(en)_2(L\text{-glut})]^+$ relative to the *Δ*-isomer, for example, has thus been interpreted.[3],*2 Indeed, an X-ray analysis of the *Λ*-isomer has shown the existence of hydrogen bonding between the *γ*-carboxylate group of the L-glutamate and the amino group of the ethylenediamine chelate.[3,4]

Previously, we reported the preparation of tris-type cobalt(III) complexes with different kinds of amino acids (*i. e.*, glycine, L- or D-alanine, and L-valine).[5] In the present work, the preparation of tris-type mixed complexes with glycinato and L-aspartato ligands was attempted in order to investigate the stereoselective effect of the coordinated L-aspartate ion on the complex formation.

In the course of this study, we succeeded in the spontaneous resolution of the potassium carbonatobis(glycinato)cobaltate(III) which had been used in the above preparation as the starting material.

Experimental

Preparations. Crystals (6.4 g, 0.02 mol) of potassium carbonatobis(glycinato)cobaltate(III) prepared by a previously-described method[5] were dissolved in 100 m*l* of water, and the 5.4 g of L-aspartic acid (0.04 mol) and 2.4 g of potassium hydroxide (0.04 mol) were added to the solution. After adding 2 g of active charcoal, the solution was stirred at 40—50°C for an hour; the color of the solution was thus changed from violet to red-violet. After the removal of the active charcoal and a small amount of a precipitated material by filtration, the solution was adjusted to a pH of about 6 with 6N acetic acid. A portion of this solution was added to an ion-exchange column (diameter, 3.5 cm; height of resin, 30 cm) containing 100—200 mesh Dowex 1×8 resin in chloride form. When the column was swept with water, the *mer* and *fac* isomers of the tris(glycinato) complex were eluted. Then, the column was treated with a 0.1M aqueous solution of calcium chloride at the rate of about 0.3 m*l*/min. After prolonged elution, six bands were separated; they were alternately violet and red in color. Each band was collected in fractions, and the absorption and circular dichroism spectra were measured with each fraction. Strong Cotton-effect peaks were observed, with a negative sign for the red bands and a positive one for the violet bands, in the first absorption-band region. This suggests that the stereoselective formation of either *Λ* or *Δ* isomers has occurred in these complexes. The fractions are conveniently labeled as E-1, E-2, ·····, up to E-6, according to the order of elution. The chromatographic separation was repeated a number of times in order to store up the same fractions. The stored solutions were concentrated to small volumes under reduced pressure. When ethanol was added to the concentrate, the calcium salt of the desired complex was precipitated as a crude material. This was dissolved in a little water, and then the solution was acidified with 6N hydrochloric acid. After a while, the complex precipitated as the hydrogen compound in place of the calcium salt. Recrystallization was performed by dissolving the compound in slightly alkaline water and by then acidifying it with diluted hydrochloric acid. This recrystallization procedure was repeated several times until the resulting complex showed no change in the intensity of its CD peak.

Formation Ratios. Since only one diastereomer could be isolated for each geometrical isomer, we conveniently assumed that the *Λ* and *Δ* isomers of a complex have the same ε and $\Delta\varepsilon$ values, but with the opposite sign, in their first absorption-band region. On the basis of this assumption, the relative concentrations of the six fractions and the formation ratios of the *Λ* and *Δ* isomers were determined spectrophotometrically using the ε and $\Delta\varepsilon$ values of the crystallized complexes. In order to ascertain the effect of the reaction time upon the formation ratios, we employed 5-hour and 10-hour reactions in addition to the usual one-hour reaction.

Spontaneous Resolution. When a supersaturated aqueous solution of potassium carbonatobis(glycinato)-cobaltate(III) was left to stand at room temperature, big crystals (*ca.* 4 mm^2) were separated out. Observing these crystals under a microscope, we were able to select two forms of the crystals which could not be superimposed. The aqueous solution of each piece of these forms gave an $\Delta\varepsilon$ value of the same magnitude, but with the opposite sign (*i. e.*, $\Delta\varepsilon_{max}=\pm 3.2$ in the first band region).

Measurements. The absorption spectra were measured with a Hitachi Perkin-Elmer Model 139 UV-VIS spectrophotometer, while the circular dichroism spectra were recorded on a JASCO Model ORD/UV-5 spectrophotometer with a CD attachment, using 60% perchloric acid as the solvent. The proton magnetic resonance spectra in deuterium oxide were recorded on a JEOL Model C-60H spectrometer, using tetramethylsilane as the internal reference.

Results and Discussion

Preparation. In a previous paper,[5] we reported that the reaction of the carbonatobis(glycinato) complex with L-valine gave the bis(glycinato)L-

1) E. J. Corey and J. C. Bailar, Jr., *J. Amer. Chem. Soc.*, **81**, 2620 (1959).

2) R. G. Denning and T. S. Piper, *Inorg. Chem.*, **5**, 1056 (1966).

3) J. H. Dunlop, R. D. Gillard and N. C. Payne, *J. Chem. Soc., A*, **1967**, 1469.

*2 The representation of the absolute configuration, *Δ* and *Λ* refers to L and D in the original paper.[3]

4) J. H. Dunlop, R. D. Gillard, N. C. Payne and G. B. Robertson, *Chem. Commun.*, **1967**, 874.

5) M. Shibata, H. Nishikawa and Y. Nishida, *Inorg. Chem.*, **7**, 9 (1968).

Table 1. Elemental analyses, absorption spectra and CD spectra of the complexes prepared

Label	Complex		Elemental Anal % N	C	H	Band I ν_{max}	ε_{max}	Band II ν_{max}	ε_{max}	CD ν	$\Delta\varepsilon_{max}$
E-1	*mer*-*Λ*-[Co(gly)$_2$L-aspH]·H_2O	Found	11.72	26.65	3.93	56.1	112	80.4	161	56.7	+3.13
		Calcd	11.77	26.90	4.51					82.4	−0.73
E-2	*fac*-*Δ*-[Co(gly)$_2$L-aspH]·H_2O	Found	11.37	27.19	4.42	57.9	160	80.0	132	56.0	−1.34
		Calcd	11.77	26.90	4.51					82.2	+0.48
E-3	*mer*-*Λ*-[Co gly(L-aspH)$_2$]·2.5H_2O	Found	9.41	27.41	4.43	56.1	151	80.4	171	56.7	+3.00
		Calcd	9.50	27.16	4.79					82.2	−0.50
E-4	*fac*-*Δ*-[Co gly(L-aspH)$_2$]·2H_2O	Found	10.00	27.50	4.29	57.9	171	80.0	142	56.0	−1.41
		Calcd	9.70	27.73	4.16					82.2	+0.45

all ν: 10^{13} sec^{-1}

valinato complex predominantly. In this work, however, the reaction of the bis(glycinato) complex with L-aspartate gave at the same time a series of complexes represented by the general formula of $[Co(gly)_{3-n}(L\text{-}asp)_n]^{n-}$ (n=0,1,2,3). Such a reaction may be the result of the presence of active charcoal in the system.

Characterization of the Complexes. The results of the elemental analyses of the isolated complexes are summarized in Table 1. From the results and the elution order, it is considered that the complexes obtained from the E-1 and E-2 bands are geometrical isomers of bis(glycinato)L-aspartatocobaltate(III), and that the complexes from E-3 and E-4 are those of glycinatobis(L-aspartato)cobaltate(III). Figure 1 shows the absorption spectra of the bis(glycinato) complex from E-1 and E-2. Since the bis(aspartato) complexes have spectra similar to those of the bis(glycinato) complexes, their spectra are omitted. The absorption spectrum of the violet complex obtained from E-1 (and E-3) showed a splitting of the first absorption band, whereas the red complex from E-2 (and E-4) showed no splitting. From these features in the spectra, the geometrical structures of the violet and red complexes could be identified as the *mer* and *fac* forms respectively.[6] The numerical data on the spectra are given in Table 1.

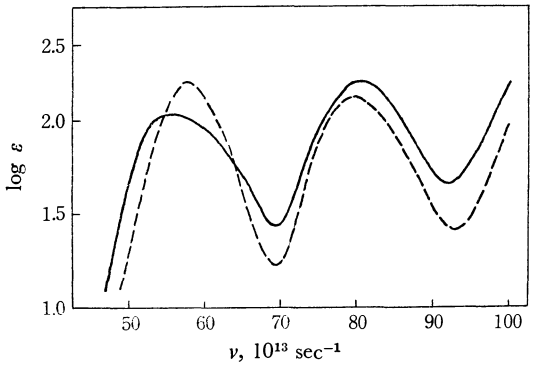

Fig. 1. Absorption spectra of [Co(gly)$_2$ L-aspH]·H_2O.
——: *mer*(from E-1) ------: *fac*(from E-2)

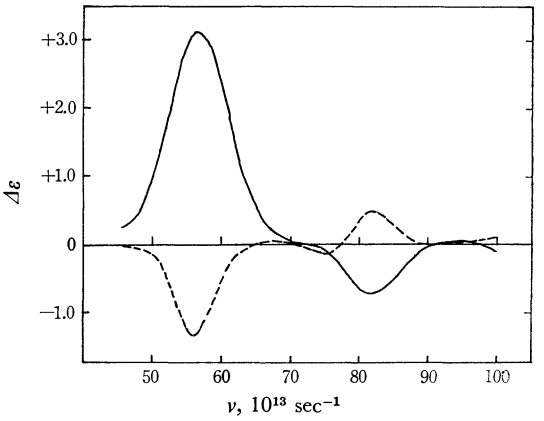

Fig. 2. CD spectra of [Co(gly)$_2$ L-aspH]·H_2O.
——: *mer* ------: *fac*

The CD spectra for the bis(glycinato) complexes are shown in Fig. 2. The spectra are similar in shape to those of the known tris(L-aminoacidato) complexes.[7] It is well known that the absolute configuration for a *fac* isomer of the tris(aminoacidato) complex can be related to that for the tris(ethylenediamine) cobalt(III) complex,[8] whereas the configuration of the corresponding *mer* isomer can be related to that for *mer*-tris(L-alaninato)-cobalt(III).[9] On this basis, the present *fac* isomer, exhibiting a dominant negative peak in the first-absorption-band region, should be identified as the *Δ* isomer, and the *mer* isomer with a dominant positive peak, as the *Λ* isomer.

For the tris-type complex containing two kinds

6) Y. Shimura and R. Tsuchida, This Bulletin, **29**, 311 (1956).

7) B. E. Douglas and S. Yamada, *Inorg. Chem.*, **4**, 1561 (1965); J. H. Dunlop and R. D. Gillard, *J. Chem. Soc.*, **1965**, 6531.

8) K. Nakatsu, M. Shiro, Y. Saito and H. Kuroya, This Bulletin, **30**, 158 (1957).

9) M. G. B. Drew, J. H. Dunlop, R. D. Gillard and D. Rogers, *Chem. Commun.*, **1966**, 42.

of aminoacidato ligands, four geometrical isomers are possible. One of them is the *fac* form, while the other three isomers belong to the *mer* form. It was experimentally found that the eluted solution of the E-3 band contains at least two geometrical-*mer* isomers; when the dominant CD peak was measured for successively-collected fractions of the band, the intensity and sign changed as follows; $+76 \rightarrow +54 \rightarrow +24 \rightarrow +4 \rightarrow -8 \rightarrow +2 \rightarrow +20$ (where the values are given by an arbitrary scale).

For all the complexes isolated, powdered crystals were obtained. On crystallization, the *mer* complexes precipitated as voluminous materials. The Λ isomers of the *mer* form were less soluble than the corresponding Δ isomers, which were not isolated because of their high solubility. On the the other hand, *fac*-Δ complexes precipitated readily, and they were less soluble in the bis(glycinato) complex, and more soluble in the bis(aspartato) complex, than the corresponding Λ isomers, which were not isolated because of their minute quantities.

Stereoselectivity. From the experiments on the formation ratios, we estimated the percent compositions of the *mer* and *fac* isomers and also the percent compositions of the Λ (or Δ) isomer predominantly formed for each geometrical isomer. The results are given in Tables 2 and 3. Since it is assumed that the ε and $|\Delta\varepsilon|$ values for a *mer* or a *fac* complex are the same with both the Λ and Δ isomers, — since, that is, the vicinal effects of the L-aspartate ion are disregarded, the results obtained are not very exact, but they do seem to be useful for estimating the stereoselectivity. For the tris(L-aspartato) complexes, the results were obtained from the data previously reported.[10]

The stereoselective formation of one diastereoisomer was markedly found in the *fac*-Δ isomers of the bis(glycianato), bis(L-aspartato), and tris-(L-aspartato) complexes. That is, the percent compositions of the isomers exceeded 90% in most cases. On the other hand, the selective formation for the *mer* isomers was appreciably found in their Λ isomers; the percent compositions of the Λ isomers ranged from 61% to 77% for a 1-hour reaction.

Table 2. Percent compositions of the reaction mixture

Complex / Reaction time (hr)	$Co(gly)_2asp^-$		$Cogly(asp)_2^{2-}$		$Co(asp)_3^{3-}$	
	mer %	*fac* %	*mer* %	*fac* %	*mer* %	*fac* %
1	17	15	22	30	6	10
5	17	14	23	32	6	8
10	13	10	21	31	8	17

Table 3. Percent compositions of Δ or Λ isomers

Complex / Reaction time (hr)	$Co(gly)_2asp^-$		$Cogly(asp)_2^{2-}$		$Co(asp)_3^{3-}$	
	mer Λ%	*fac* Δ%	*mer* Λ%	*fac* Δ%	*mer* Λ%	*fac* Δ%
1	61	89	73	95	77	95
5	59	83	72	95	78	95
10	57	82	69	95	72	95

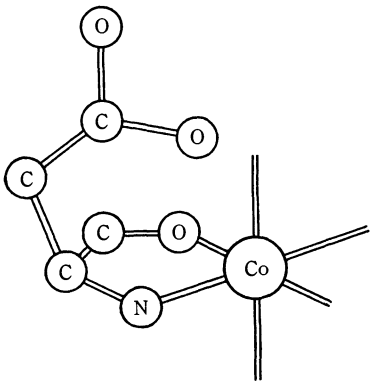

Fig. 3. The molecular model of coordinated L-aspartate.

When the molecular model for the chelation of a L-aspartate ion as a bidentate ligand is constructed, the β-carboxylate group of the aspartato ligand can be directed to the adjacent site of coordination, as is shown in Fig. 3. If the site is occupied by an amino group of the another aminoacidate ion, the β-carboxylate group is likely to interact with the amino group through hydrogen bonding in a manner similar to that found in the Λ(+)-L-glutamatobis(ethylenediamine)cobalt (III) complex.[3,4] If the site is occupied with a carboxylate group of the second ligand, both of the carboxylate groups will repel each other. The *fac*-Δ isomers have the possibility of such hydrogen bonding equal to the number of the chelated aspartato ligand. On the other hand, the *fac*-Λ isomers produce only the repulsion structures. Thus, the highly stereoselective formation of the *fac*-Δ isomers can be attributed to the possibility of such a hydrogen bonding. In the *mer*-bis(aspartato) complexes, the hydrogen bonding is possible for the both the Δ and Λ isomers, but the Λ isomer is favoured in the number of the possible hydrogen bonding. In this way, the preferential formation of the *mer*-Λ complex can be explained.

As may be seen in Table 2, the reaction time has an effect on the amounts of the products; one hour's reaction gives about 32% of the bis(glycinato) complex and about 16% of the tris(aspartato) complex in addition to 52% of the main product, while ten hour's reaction gives about 23% of the bis-(glycinato) and 25% of the tris(aspartato) complex. Such an increase in the tris(aspartato) complex

10) M. Shibata, H. Nishikawa and K. Hosaka, This Bulletin, **40**, 236 (1967).

with the reaction time can also be explained as the stereoselective effect of the L-aspartato ligand through the number of the possible hydrogen bonding.

However, in the bis- or tris(aspartato) complex the reason why the *fac* form is formed in an amount greater than that of the *mer* form cannot be explained by the possible hydrogen bonding, for its number is the same for both forms and, conversely, the *mer* form has more possible isomers than the *fac* form. The reason is suggested by the fact that, in the bis(glycinato) complex, the *mer* form is present in a greater amount than the *fac* form. As is well known, the *mer*-*Λ*-tris(L-prolinato)cobalt(III) isomer cannot exist because of the collision of the substituents with a cyclic structure.[2] Such a collision has also been observed in the *mer*-*Λ*-tris(L-leucinato) complex by means of the PMR spectrum.[2] For similar reasons, the complexes containing more than two aspartate ions appear to be more stable in the *fac*-*Λ* form, where the mutual repulsion in *β*-carboxyl groups is almost negligible. In the *mer* form, this repulsion is fairly large, especially in the *Λ* isomers. In our laboratory, concurrently with this study, the mixed complexes with L-aspartic acid and alanine were investigated. In these complexes, the *fac*/*mer* ratios were larger than in the present case, because of the addition of a methyl group; it must be noted that even in the complex containing one aspartate ion the *fac* form is more stable than the *mer* form.

Spontaneous Resolution. As far as we know, three examples have been reported of the spontaneous resolution of cobalt(III) complexes.[11] They are $K_3[Co(C_2O_4)_3]\cdot 3H_2O$, $[CoC_2O_4(en)_2]Cl\cdot 4H_2O$, and K[Co(trimethylenediaminetetraacetato)]$\cdot 2H_2O$. We are now able to show another example with $K[CoCO_3(gly)_2]\cdot 2H_2O$.*3 For this complex, three geometrical isomers, namely, *trans*(N), C_2-*cis*(N), and C_1-*cis*(N), are possible. However, the circular dichroism spectrum of the complex concerned (Fig. 4) was similar, in shape, to that of the known C_1-*cis*(N)$[CoC_2O_4(gly)_2]^-$;[12] moreover, the PMR spectrum of the present complex showed a pattern similar to that of the C_1-*cis*(N) oxalato complex, namely, two resonance lines due to the CH_2 group at 3.35, 3.51 ppm. Therefore, we can identify the present complex as the C_1-*cis*(N) isomer.[13]

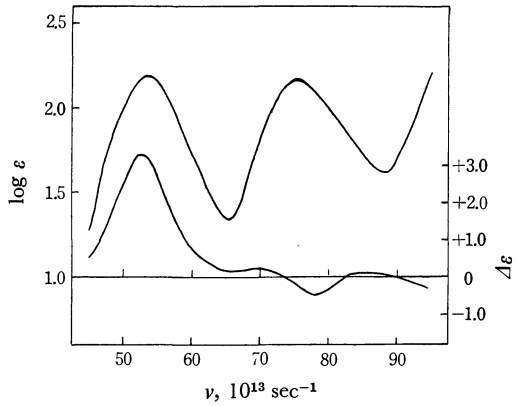

Fig. 4. Absorption and CD specta of $K[CoCO_3(gly)_2]\cdot 2H_2O$.

11) F. M. Jaeger and W. Thomas, *Proc. Acad. Sci. Amsterdam*, **21**, 693 (1919). Y. Igarashi, Y. Yoshikawa and K. Yamazaki, Proceedings of the 21st Annual Meeting of the Chemical Society of Japan, Osaka, April, 1968, p. 1102; H. Ogino, M. Takahashi and N. Tanaka, Proceedings of the 18th Symposium on Coordination Chemistry, Kyoto, October, 1968, p. 9.

*3 In Ref. 5 this complex was reported as mono hydrate.

12) N. Matsuoka, J. Hidaka and Y. Shimura, *Inorg. Chem.*, **9**, 719 (1970).

13) N. Matsuoka, J. Hidaka and Y. Shimura, This Bulletin, **40**, 1863 (1967).

BULLETIN OF THE CHEMICAL SOCIETY OF JAPAN VOL. 43 3824—3829 (1970)

Reactions of Potassium Iron Carbonylate with Olefins and Alkyl Halides*1

Hiromitsu MASADA, Mitsuyuki MIZUNO and Sohei SUGA

Department of Industrial Chemistry, Faculty of Technology, Kanazawa University, Kanazawa

and Yoshihisa WATANABE and Yoshinobu TAKEGAMI

Department of Hydrocarbon Chemistry, Faculty of Engineering, Kyoto University, Kyoto

(Received November 17, 1969)

Potassium iron carbonylate, $KHFe(CO)_4$, reacted with ethyl acrylate, crotonate, 3-butenoate, styrene, and α-olefins at 40—70°C under an atmosphere of carbon monoxide. Methylmalonate was selectively obtained from the acrylate by treatment of the reaction mixture with an alcoholic iodine and hydrogen chloride solutions. Dipotassium iron carbonylate, $K_2Fe(CO)_4$, reacted with β-bromopropionate to give mainly methylmalonate. Isomerization of β-ethoxycarbonylpropionyliron carbonylate to the α-isomer occurred readily in contrast to isomerization of acylcobalt carbonyl. Both crotonate and 3-butenoate gave ethylmalonate as a major product and methylsuccinate and glutarate as minor ones. The results suggest that α-ethoxycarbonylbutyliron carbonylate is more predominant than the corresponding β- and γ-isomers in equilibrium state. This is in striking contrast to the case of acylcobalt carbonyl. Styrene yielded two isomeric aldehydes, α- and β-phenylpropionaldehydes. Ethyl caproate and enanthate were obtained from 1-pentene and 1-hexene, respectively in poor yield.

Some of the present authors demonstrated that cobalt hydrocarbonyl reacted with ethyl acrylate to give, selectively, α-ethoxycarbonylpropionylcobalt carbonyl which readily isomerized to β-isomer.[1] Styrene also reacted similarly with cobalt hydrocarbonyl. In the present work, carbonylation of olefins with iron carbonylate and the isomerization of the intermediate alkyl- or acyliron complexes were investigated in detail. The effect of the functional groups on the isomerization was examined in order to estimate the reaction mechanism. The difference of reactivity between the iron and cobalt complexes was clarified.

Experimental

Preparation of Potassium Iron Carbonylate, $KHFe(CO)_4$ and $K_2Fe(CO)_4$. An alcoholic solution of potassium iron carbonylate was prepared by Krumholz's method.[2] A 200 m*l* three-necked flask, fitted with a 50 m*l* dropping funnel, a gas inlet and a rubber stopple, was connected with a 500 m*l* gas buret and the atmosphere was then replaced with dry carbon monoxide.

A 1N alcoholic potassium hydroxide solution (33 m*l* or 44 m*l*) and iron pentacarbonyl (1.5 m*l*, 11 mmol) were syringed into the flask and then stirred for a few hours at room temperature to give a brown solution of potassium iron carbonylate.

Materials. Ethyl acrylate, ethyl crotonate, styrene, 1-pentene, 1-hexene, ethyl α- and β-bromopropionates, β-phenylpropionate, diethyl methylmalonate, diethyl succinate, ethyl caproate, and ethyl enanthate were commercial reagents. Iron pentacarbonyl was obtained from the Strem Chemicals Inc., bp 102°C. Diethyl ethylmalonate, diethyl methylsuccinate, and diethyl glutarate were prepared by the usual esterification of the corresponding carboxylic acids. Ethyl 3-butenoate was obtained from allyl cyanide[3] (bp 118—119°C, lit, 119°C). α-Phenylpropionaldehyde was obtained from acetophenone.[4] Starting materials were distilled before use and purity was checked by gas chromatography.

Reaction Procedures. To a solution of potassium iron carbonylate prepared as described above, olefin (33 mmol) or alkyl halide (22 mmol) was added with a syringe. The mixture was then stirred vigorously at 25—65°C under an atmosphere of carbon monoxide. After a certain reaction time, a 7N alcoholic hydrogen chloride solution (5—7 m*l*) and 50 m*l* of a saturated benzene solution of iodine were added dropwise into the reacting mixtures at room temperature; stirring was continued until gas evolution ceased. Sodium thiosulfate (5 g) was then applied to remove excess

*1 Presented in part at the 21st Annual Meeting of the Chemical Society of Japan, Osaka, April, 1968.

1) Y. Takegami, C. Yokokawa, Y. Watanabe, H. Masada and Y. Okuda, This Bulletin, **37**, 1190 (1964).

2) P. Krumholz and H. M. Stettiner, *J. Amer. Chem. Soc.*, **71**, 3035 (1949).

3) E. Rietz, "Organic Syntheses," Coll. Vol. III, (1955), p. 851.

4) C. F. H. Allen and J. VanAllen, *ibid.*, Coll. Vol. III, (1955), p. 733.

iodine. After 50 ml of water was added to the solution, the reaction products were extracted three times with 50 ml of benzene and dried over anhydrous magnesium sulfate overnight. The solution was concentrated to about 5% weight by distillation and then subjected to analysis.

Analytical Procedures. The reaction products were gas-chromatographed with a Shimadzu Model GC-3AH on a column, 3 m long, 3 mm in diameter, filled with Apiezon L or Carbowax on cerite at 150—180°C and at the carrier-gas (hydrogen) flow rate of 70 ml/min. Isomeric esters and aldehydes were confirmed and determined by direct comparison with authentic samples. The infrared spectra were measured with a Nippon Bunko Model DS-301 spectrophotometer on NaCl cells.

Results and Discussion

Reaction of $KHFe(CO)_4$ with Ethyl Acrylate. Results are summarized in Table 1. As shown

Table 1. Reaction of ethyl acrylate with potassium iron carbonylate, $KHFe(CO)_4$

Exp. No.	Reaction conditions[a] Temp. (°C)	Time (hr)	CO absorbed[b]	Yield of esters[b]	Distribution of isomers[c] (%) *iso*-Ester	*n*-Ester
1	25	30	0.76	0.14	100	0
2	40	14	1.00	0.16	100	0
3	50	4	1.00	0.59	96	4
4	50	6	1.00	0.22	84	16
5[d]	50	6	1.00	0.30	91	9
6	50	10	1.00	0.26	92	8
7	60	1	0.44	0.88	97	3
8	60	1.5	0.91	0.84	97	3
9	60	3	1.00	0.68	95	5

a) $KHFe(CO)_4$: 11 mmol (EtOH solution), Ethyl acrylate: 33 mmol
b) mol/mol $KHFe(CO)_4$
c) *iso*-Ester: Diethyl methylmalonate, *n*-Ester: Diethyl succinate
d) Methyl acrylate was used instead of ethyl acrylate.

in Scheme 1, ethyl acrylate reacted with potassium iron tetracarbonylate to give two isomeric diesters upon treatment with an alcoholic iodine and hydrogen chloride solutions. These diesters can be derived from the corresponding acyliron complexes, *i. e.*, α- and β-ethoxycarbonylpropionyliron carbonylates (I) and (II), as was proved in the case of acylcobalt carbonyls.[5] Diethyl methylmalonate was afforded as the main product and diethyl succinate as a minor one. Carbonylation of ethyl acrylate took place at temperatures above 25°C and an almost quantitative yield of esters was obtained for 1—1.5 hr at 60°C (Expts. 7 and 8). The consumption of potassium iron carbonylate was estimated by means of carbon monoxide absorption as in the case of cobalt hydrocarbonyl.[1] The absorption volume, however, was not always proportional to the yield of esters. The intermediate acyliron complexes seemed to decompose with a prolonged reaction time. The yield of the derived esters decreased in these cases (Expts. 3—7).

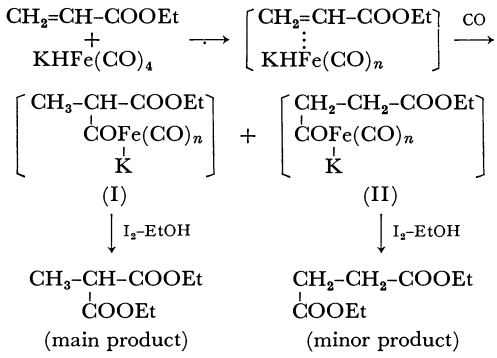

Scheme 1

At 25—40°C methylmalonate only was obtained, while at higher temperatures a small amount of succinate was also obtained (Expts. 3—9). The distribution of the esters was scarcely affected by reaction time and temperature. This implies that the potassium iron carbonylate gives selectively α-ethoxycarbonylpropionyliron carbonyl (I) in the same way as cobalt hydrocarbonyl,[1] but the branched acyliron complex (I) is not converted to the β-isomer (II) so readily as the corresponding acylcobalt complex. From these results, we see that the isomerization of the acyliron complexes is apparently different from that of two acylcobalt complexes between which the equilibrium lies well toward the side of the β-isomer. The following experiments were carried out in order to examine the equilibrium of isomerization.

Reaction of Dipotassium Iron Carbonylate, $K_2Fe(CO)_4$, with Ethyl α- and β-Bromopropionates. Results are shown in Table 2 and Scheme 2. The reaction of α- or β-bromopropionate with dipotassium iron carbonylate was carried out at 30—50°C under an atmosphere of carbon monoxide. The usual treatment resulted in the formation of two isomeric esters, diethyl methylmalonate and diethyl succinate in both reactions.

It is interesting that methylmalonate was predominantly obtained from the reaction of ethyl β-bromopropionate, while the same product was given from ethyl α-bromopropionate at 30—50°C (Expts. 10—17). The percentage of isomerization of the intermediate complexes (I and II) was estimated by the distribution of the derived esters. In the case of α-bromopropionate, the percentage of isomerization to the β-complex (II) was only

5) R. F. Heck and D. S. Breslow, *J. Amer. Chem. Soc.*, **84**, 2499 (1962).

Table 2. Reaction of ethyl α- and β-bromopropionates with dipotassium iron carbonylate, $K_2Fe(CO)_4$

Exp. No.	Substrate	Reaction conditions: Temp. (°C)	Reaction conditions: Time (hr)	CO absorbed[b]	Yield of esters[c]	Isomerization[d] (%)
10[e]	Ethyl α-bromopropionate	30—50	15+2	0.45	0.45	2
11	Ethyl α-bromopropionate	30—50	15+6	0.44	0.52	2
12	Ethyl α-bromopropionate	60	7	0.50	0.34	6
13	Ethyl β-bromopropionate	30—50	15+2	1.00	0.11	94
14	Ethyl β-bromopropionate	30	10	0.31	0.20	81
15	Ethyl β-bromopropionate	30	25	0.77	0.39	95
16	Ethyl β-bromopropionate	40	1.3	0.30	0.30	66
17	Ethyl β-bromopropionate	40	8	1.00	0.20	81

a) $K_2Fe(CO)_4$: 11 mmol (EtOH solution), Ethyl α- and β-bromopropionates: 22 mmol
b) mol/mol $K_2Fe(CO)_4$
c) Diethyl succinate and diethyl methylmalonate, mol/mol $K_2Fe(CO)_4$
d) In the case of α-bromopropionate: Diethyl succinate/Total Esters × 100
In the case of β-bromopropionate: Diethyl methylmalonate/Total Esters × 100
e) The reaction was carried out in two stages, first at 30°C for 15 hr and then at 50°C for 2 hr.

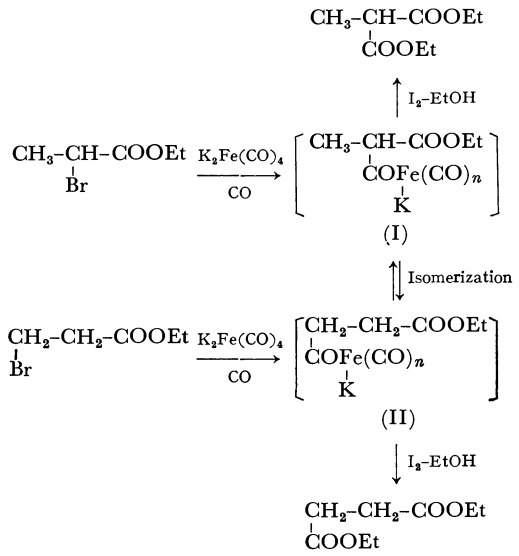

Scheme 2

2—6%, whereas in the case of β-bromopropionate the percentage of isomerization to the α-complex (I) amounted to 95% (Expts. 13—17). Accordingly, isomerization of the straight-chained complex (II) to the branched complex (I), occurs more readily than the reverse isomerization and the equilibrium between these complexes lies far to the side of the branched isomer. Ethyl acrylate was not afforded under the conditions employed and therefore dehydrobromination of α- and β-bromopropionates would not occur in the reaction system.

Reaction of Ethyl Crotonate and Ethyl 3-Butenoate with Potassium Iron Carbonylate, $KHFe(CO)_4$. Results are shown in Table 3. The reactions of ethyl crotonate and its homolog were carried out to confirm a similar isomerization. Ethyl crotonate was carbonylated with potassium iron carbonylate to afford mainly diethyl ethylmalonate (A) and other isomers, diethyl methylsuccinate (B) and diethyl glutarate (C) as by-products (Expts. 18—25). Ethyl 3-butenoate gave the same products as in the case of ethyl crotonate and the distribution of products was similar in both reactions (Expts. 26 and 27). As shown in Scheme 3, isomers (A, B and C) may be derived from the corresponding α-, β- and γ-ethoxycarbonylacyliron carbonylate (III, IV and V), respectively.

The distribution of isomers shown in Table 3 implies that the intermediates, iron complexes (III, IV and V), were isomerized to each other at 60—70°C, and that the equilibrium was favorable to α-isomer (III). The results are consistent with those of the reaction of the ethyl acrylate or the alkyl halides with respect to isomer equilibrium.

Reaction of Potassium Iron Carbonylate with Styrene. Results are summarized in Table 4 and Scheme 4. Styrene reacted with potassium iron carbonylate to give two isomeric aldehydes, α- and β-phenylpropionaldehydes, instead of expected esters, α- and β-phenylpropionates. Tollen's reagent test for the products was positive. The infrared spectra had bands at 1725, 2708, 2800 cm^{-1}, characteristic of aldehydes. They were identified with those of authentic samples. The carbonylation of styrene occurred at 40—65°C, and the yield of aldehydes was not more than 50% in all runs. The poor yield seems to be partly due to instability of the intermediate complexes. These aldehydes may be readily formed with reduction of the α- and β-phenylpropionyliron carbonyls (VI and VII) as shown in Scheme 4. The mechanism is supported by the fact that *n*-propyl iodide reacted with the iron carbonylate to give *n*-butyraldehyde in good

Table 3. Reaction of ethyl crotonate, and ethyl 3-butenoate with potassium iron carbonylate

Exp. No.	Reaction conditions[a] Temp. (°C)	Time (hr)	CO absorbed[b]	Yield of esters[c]	Distribution of esters[d] (A)	(B)	(C)
	Ethyl Crotonate						
18	60	3	0.11	0.02	100	0	0
19	60	5	0.30	0.65	95	5	0
20	60	7	0.45	0.26	93	7	0
21	60	8.5	0.61	0.35	91	9	0
22	60	9.5	1.00	0.23	91	9	0
23	60	10.5	1.00	0.18	86	14	0
24	70	1.5	0.31	0.54	89	7	4
25	70	3.5	1.00	0.19	73	14	13
	Ethyl 3-Butenoate						
26	60	5.5	0.60	0.37	92	5	3
27	60	7	1.00	0.35	80	13	7

a) $KHFe(CO)_4$: 11 mmol (EtOH solution), Ethyl Crotonate or Ethyl 3-Butenoate: 33 mmol
b) mol/mol $KHFe(CO)_4$
c) Diethyl ethylmalonate(A), Diethyl methylsuccinate(B), and Diethyl glutarate(C); mol/mol $KHFe(CO)_4$
d) (A), (B) or (C)/Total Esters × 100

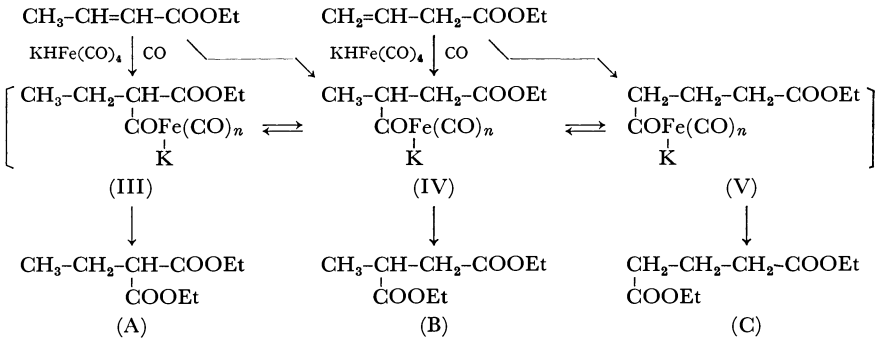

Scheme 3

Table 4. Reaction of styrene with potassium iron carbonylate

Exp. No.	Reaction conditions[a] Temp. (°C)	Time (hr)	CO absorbed[b]	Products[c] Ethylbenzene	Total aldehydes	Distribution of aldehydes[d] (%)
28	40	10	0.32	0.04	0.05	11
29	40	35	1.00	0.09	0.28	11
30	55	5	0.35	0.05	0.07	13
31	55	10	0.76	0.10	0.16	18
32	55	15	1.00	0.18	0.39	21
33	55	20	1.00	0.22	0.50	21
34	65	3	0.66	0.12	0.09	20
35	65	6	1.00	0.10	0.27	26
36	65	10	1.00	0.24	0.24	28

a) $KHFe(CO)_4$: 11 mmol (EtOH solution), Styrene: 33 mmol
b) mol/mol $KHFe(CO)_4$
c) Aldehydes: α- and β-phenylpropionaldehydes, mol/mol $KHFe(CO)_4$
d) β-Phenylpropionaldehyde/Total Aldehydes × 100

yield.[6]

The distribution of β-phenylpropionaldehyde was already attained to 11—13% in the initial stage of the reaction, while in the case of ethyl acrylate or ethyl crotonate, the corresponding β-isomer was not observed initially. The discrepancy may be explained as follows. Potassium iron carbonylate attacked both the α- and β-carbons of styrene, whereas it carbonylated selectively the α-carbon of ethyl acrylate in the early stage.

In general, the distribution of acylmetal carbonyl isomers was affected by the following two factors: (1) the direction of addition of metal carbonylate to a carbon-carbon double bond and (2) the isomerization of intermediate alkyl- or acylmetal carbonyls.[1] The latter factor affected particularly the distribution of products in the case of ethyl acrylate and its homologs.

The reactions of dipotassium iron carbonylate with α- and β-bromoethylbenzenes were carried

6) Y. Takegami, Y. Watanabe, H. Masada and I. Kanaya, This Bulletin, **40**, 1456 (1967).

Table 5. Reaction of α- and β-bromoethylbenzenes with dipotassium iron carbonylate

Exp. No.	Substrate	Conditions[a] Temp. (°C)	Conditions[a] Time (hr)	CO absorbed[b]	Products[c] Ethylbenzene	Products[c] Total aldehydes	Isomerization[d] (%)
37	α-Bromoethylbenzene	40	35	0.77	0.30	0.51	0
38	α-Bromoethylbenzene	65	3	0.30	0.33	0.07	3
39	α-Bromoethylbenzene	65	6	0.33	0.42	0.08	2
40	β-Bromoethylbenzene	40	35	1.00	0.18	0.30	0
41	β-Bromoethylbenzene	65	3	0.72	0.13	0.18	1
42	β-Bromoethylbenzene	65	6	1.00	0.25	0.11	3

a) $K_2Fe(CO)_4$: 11 mmol(EtOH solution), α- and β-Bromoethylbenzenes: 11 mmol
b) mol/mol $K_2Fe(CO)_4$
c) Aldehydes: α- and β-Phenylpropionaldehydes, mol/mol $K_2Fe(CO)_4$
d) In the case of α-bromoethylbenzene: β-Phenylpropionaldehyde/Total Aldehydes × 100
In the case of β-bromoethylbenzene: α-Aldehyde/Total Aldehydes × 100

out to examine the isomerization of α- and β-phenylpropionyliron complexes (VI and VII). The results are summarized in Table 5. Such an isomerization as from VI to VII or from VII to VI was scarcely observed. Thus it seems that the distribution of aldehydes corresponds to the direction of the addition of iron carbonylate to styrene. α-Phenylpropionaldehyde should be derived from α-phenylpropionyliron carbonylate alone as well as in the case of β-phenylpropionaldehyde (Scheme 4).

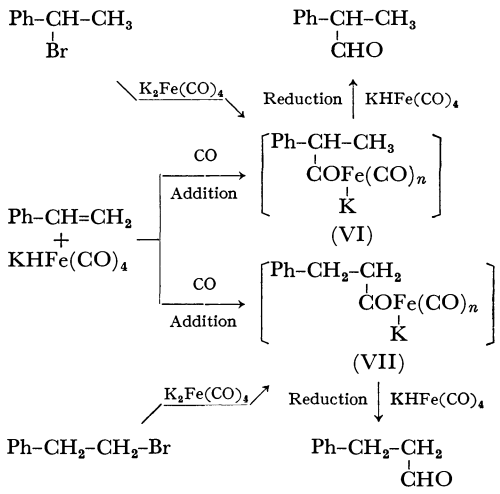

Scheme 4

Reaction of Potassium Iron Carbonylate with 1-Pentene and 1-Hexene. Potassium iron carbonylate reacted with 1-pentene and 1-hexene at 60°C under an atmosphere of carbon monoxide as shown in Table 6. Ethyl enanthate was obtained as a carbonylation product of 1-hexene. The yield of ester was invariably low under various conditions. Most of 1-hexene was readily reduced into *n*-hexane in the reaction system. Similarly 1-pentene was carbonylated with the iron carbonylate to give ethyl caproate in a yield less than 1%, whereas in the case of cobalt hydrocarbonyl, ethly caproate and ethyl α-methylvalerate were obtained in good yield under milder conditions.[7]

At room temperature carbonylation of α-olefin with potassium iron carbonylate could not occur. At higher temperatures, the α-olefin may be readily reduced into *n*-paraffin instead of carbonylation.

Discussion of Acyliron Carbonyls. The reaction of ethyl acrylate was followed by infrared spectra in order to prove the participation of acyliron carbonyls as reaction intermediates. After ethyl acrylate had been carbonylated and the complex formed neutralized with dilute alcoholic hydrogen chloride solution, excess acrylate and solvent were evaporated to dryness at 0°C in a high vacuum. The iron complex was extracted with cold benzene under carbon monoxide atmosphere to give a dark red solution and subjected to analysis immediately. The infrared spectrum in benzene contained coordinated carbonyl bands at 2118(w), 2005(vs) and 1967(s) cm^{-1}, an ester carbonyl band at 1742(s) cm^{-1}, the acyliron carbonyl bands at 1678(m) and 1710(m) cm^{-1}. The sample was then treated with an alcoholic iodine solution. The vapor phase chromatogram showed the presence of 97% of diethyl methylmalonate and 3% of diethyl succinate. Ethyl acrylate and its polymer were not detected by infrared spectra and chromatography. Thus the acyliron carbonyls (I′, II′) are suggested to be intermediate complexes in this reaction.

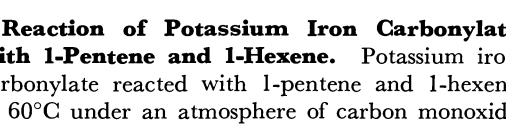

Triphenylphosphine complexes of acyliron carbonylates were scarcely obtained in the usual way on account of the cleavage to iron carbonyl triphenylphosphine, $Fe(CO)_4PPh_3$. Our suggestion of acyl-

7) Y. Takegami, Y. Watanabe, H. Masada and T. Mitsudo, This Bulletin, **42**, 206 (1969).

Table 6. Reaction of potassium iron carbonylate with 1-pentene and 1-hexene

Exp. No.	Substrate	Reaction conditions[a]		CO absorbed[b]	Products	
		Temp. (°C)	Time (hr)		Ester[b] (%)	*n*-Paraffin[c] (%)
43[d]	1-Pentene	25—60	4+20	~0	0.3	—
44	1-Hexene	60	10	~0	0.2	64
45	1-Hexene	60	25	~0	0.2	69
46[e]	1-Hexene	60	10	~0	0.2	50

a) $KHFe(CO)_4$: 11 mmol (EtOH solution), 1-Pentene or 1-Hexene: 33 mmol
b) mol/mol $KHFe(CO)_4 \times 100$; Ester: Ethyl caproate (1-Pentene), Ethyl enanthate (1-Hexene)
c) *n*-Paraffin: *n*-Hexane, mol/mol Hexene × 100
d) The reaction was carried out in two stages, first at 25°C for 4 hr and then at 60°C for 20 hr.
e) Benzene was used as solvent.

iron complexes is strongly supported. Heck and Breslow[8] showed the infrared spectrum of the mixture of α- and β-methoxycarbonylpropionylcobalt tricarbonyl triphenylphosphines, which contained carbonyl bands at 1740(vs) and 1670(m) cm^{-1}. We have elucidated the fact that the α-methoxycarbonylpropionylcobalt complex had bands at 1743(m) and 1706(s) cm^{-1}, while the β-isomer had bands at 1745(s) and 1675(s) cm^{-1} assigned to an ester and acylcobalt carbonyls, respectively. On the other hand, maleyliron tetracarbonyl has a doublet in the 1665 cm^{-1} region due to the absorption of the ketonic groups of the organic ligands.[9] The spectrum of ethoxymalonyliron dicarbonyl(nitrosyl)triphenylphosphine contains acyl and ester bands at 1689 and 1754 cm^{-1}, which are similar to the bands observed in the case of acyliron complex (I').[10]

The results are summarized as follows. Potassium iron carbonylate reacted with unsaturated carboxylic esters and styrene to give carbonylated products under an atmosphere of carbon monoxide at 40—65°C. On the other hand, α-olefin was scarcely carbonylated under these conditions. Cobalt hydrocarbonyl reacted readily with various acrylates and styrene to give the branched-chain complexes mainly at 0°C for several hours.[1]

β-Ethoxycarbonylpropionyliron carbonyl was easily isomerized to the α-isomer and the reverse isomerization hardly occured, whereas α-ethoxycarbonylpropionylcobalt carbonyl completely isomerized to the β-isomer in a few hours at 25°C.[1] It is concluded that the isomeric equilibrium of acyliron complexes lies well towards the side of the α-isomer, in contrast to that of acylcobalt complexes. The isomerization of acyliron complexes was greatly affected by the functional groups in the olefins and alkyl halides. For example, ethoxycarbonylpropionyliron carbonyl was easily isomerized, while phenylpropionyliron carbonyl was scarcely isomerized. The electronic effect of the ethoxycarbonyl group[11] as well as the isomeric equilibrium of acyliron complexes promotes the isomerization of the iron complexes.

8) R. F. Heck and D. S. Breslow, *J. Amer. Chem. Soc.*, **83**, 4026 (1961).
9) W. Hübel, "Organic Syntheses *via* Metal Carbonyls," Vol. I, ed. by I. Wender and P. Pino, Interscience Publishers, New York, N. Y. (1968), p. 325.
10) F. M. Chaudhari, G. R. Knox and P. L. Pauson, *J. Chem. Soc., C*, **1967**, 2255.
11) S. Suga, H. Masada, H. Suda, Y. Takegami and Y. Watanabe, This Bulletin, **42**, 2920 (1969).

BULLETIN OF THE CHEMICAL SOCIETY OF JAPAN VOL. 43 3830—3840 (1970)

Absolute Structure of Acacic Acid*[1]

I. P. VARSHNEY*[2] and K. M. SHAMSUDDIN*[3]

Department of Chemistry, Aligarh Muslim University, Aligarh, India

(Received March 14, 1969)

Acacic acid, a pentacyclic triterpenic acid, is present as a saponin in various members of the family Leguminosae, but the highest yield is obtained from the pods of *Acacia concinna* DC. On the basis of degradative studies, transformations, IR, UV, NMR, mass spectrography, and ORD, and CD studies its absolute stereochemistry and structure have been fixed as 3β, 16β, 21β-trihydroxy-18β-olean-12-en-28-oic acid and that in the acetate the rings E and D are in *boat* and *quasi-boat* forms, respectively, with D/E rings *cis* fused.

Acacia concinna DC. commonly known as 'Shikakai' in Hindi is a member of the family Leguminosae, sub-family Mimosacaea. It is a common bush. It grows in tropical jungles, and especially in the southern part of India. The pods are extensively used as a detergent and are preferred to soap by people taking an oil bath.[1] In India the washing of women's hair with the powder of the pods of Acacia concinna is very prevalent as it is said to increase the length of the hair. It is a rich source of saponin which on hydrolysis yields an acid sapogenin (acacic acid).

No work seems to have been done on the saponin and sapogenin contents of this plant except for some works on the standardization of the conditions for commercial isolation of crude saponin.[2] Recently in these laboratories the seeds of this plant were studied and found to contain a new triterpenic acid, acacic acid,[3] which has been isolated from the seeds and bark of Acacia intsia.[3-5] Acacic acid has also been isolated from the seeds of Albizzia spitulata[6] and Albizzia odoratissima.[7] On preliminary studies the pods of Acacia concinna have been found to contain the saponin of acacic acid. Acacic acid was found to be a trihydroxymonocarboxylic acid belonging either to the α-amyrin group or to the tetracyclic triterpene group.[5,8] Later Varshney[9,10] on biogenetic grounds suggested 3,16, 21-trihydroxyolean-12-en-28-oic acid (I) structure for this acid.

Well powdered pods of *Acacia concinna* DC. obtained from Kerala (South India) were extracted exhaustively with ethanol. Removal of the solvent yielded a dark brown coloured semisolid residue, which was treated in the usual manner[10] to yield a fairly pure sample of the saponin. The saponin was then dissolved in a large amount of water and hydrolyzed with sulphuric acid (10%). All attempts to crystallize the saponin failed, and it was subjected to further purification by potassium salt formation. On acidification with hydrochloric acid the alkaline solution of the potassium salt precipitated the acid genin. It was then acetylated with pyridine and acetic anhydride in the cold. The acetate (II) on cyrstallization from methanol gave fine colourless needles mp 235—36°C. It showed a positive tetranitromethane test for a carbon-carbon double bond. It was found to be identical with acacic acid diacetate lactone by mixed m.p. and superimposable infrared spectra.[3,5] The infrared spectrum of diacetate lactone (Fig. 1) showed bands of acetate and γ-lactone at 8.05 μ and 5.6 μ. The

*1 A resume of some of the findings reported here appeared in an advance short communication in *Tetrahedron Let.*, **1965**, 1187—1197.

*2 Present address: Professor and Head, Department of Chemistry G. S. Institute of Technology and Science, Indore-3, India.

*3 Present address: Department of Applied Science, College of Engineering and Technology, Aligarh Muslim University, Aligarh, (U.P.), India.

1) Wealth of India, C. S. I. R., New Delhi, 1948, Vol. 1, p. 13.

2) M. G. Mohiuddin, *J. Osmania Univ.*, **12**, 19 (1944—46); S. Ranganna, S. Sastry and S. Siddappa, *Indian J. Technol.*, **1**, 97 (1963); Indian 46946; *Chem. Abstr.*, **48**, 1714b (1954).

3) M. O. Farooq, I. P. Varshney and Z. Naim, *Arch. Pharm.*, (Weinheim) **295**, 12, (1962).

4) M. O. Farooq, I. P. Varshney and Z. Naim, *Ann. Pharm. Fr.*, **17**, 442 (1959).

5) M. O. Farooq, I. P. Varshney and Z. Naim, *Arch. Pharm.*, (Weinheim) **294**, 133 (1961).

6) I. P. Varshney, *Proc. Nat. Acad. Sci., India, Sect. A* **XXXV**, 418 (1965).

7) I. P. Varshney and M. S. Y. Khan, *J. Pharm. Sci.*, **50**, 923, (1961); This Bulletin, **38**, 1214 (1965).

8) Z. Naim, Ph. D. thesis, Aligarh Muslim University, 1961.

9) I. P. Varshney, Intern. Sympo. Natural Products, I. U. P. A. C., Bruxelles, 1962, Resume des Communications.

10) I. P. Varshney, *Indian J. Chem.*, **7**, 446 (1969).

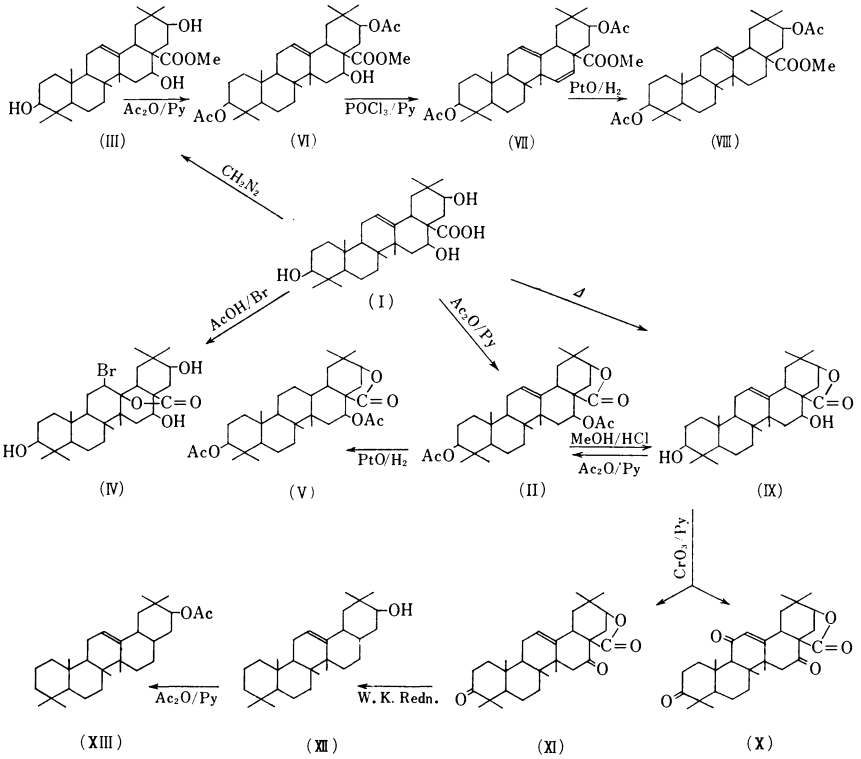
(III)
(VI)
(VII)
(VIII)
(I)
(IV)
(V)
(II)
(IX)
(XIII)
(XII)
(XI)
(X)
Ac2O/Py
POCl3/Py
PtO/H2
CH2N2
AcOH/Br
Δ
MeOH/HCl
W. K. Redn.
CrO3/Py

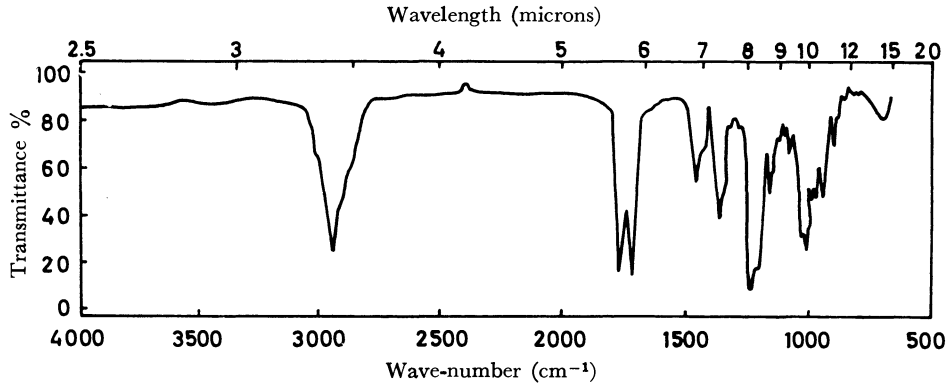
Wavelength (microns)
Transmittance %
Wave-number (cm⁻¹)

Fig. 1

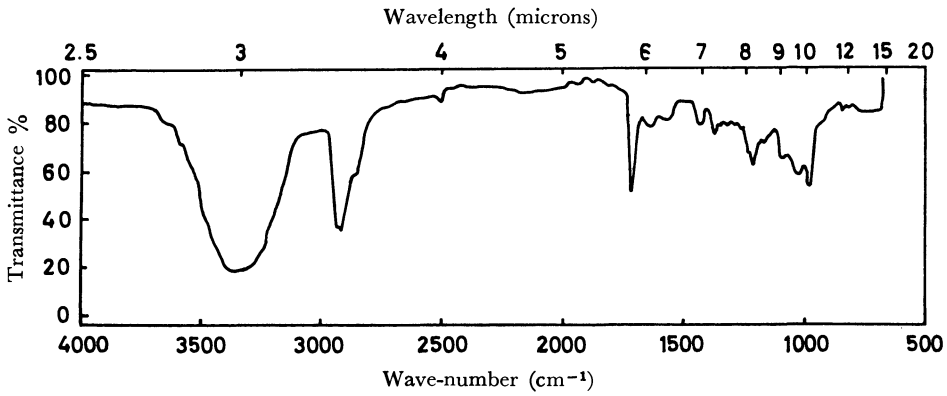
Wavelength (microns)
Transmittance %
Wave-number (cm⁻¹)

Fig. 2

mass spectrum of the compound showed its molecular weight as 554 corresponding to the formula $C_{34}H_{50}O_6$. The general fragmentation pattern was that associated with triterpenes.

The acetate on deacetylation gave colourless needles of the free genin (I) mp 278—282°C. The genin on methylation with diazomethane gave a methyl ester (III) as colourless needles mp 224—225°C. Acetylation of the methyl ester (III) gave diacetate methyl ester (VI) as colourless needles mp 203—205°C. All these compounds gave yellow colour with tetranitromethane. All these evidences and analytical results showed that acacic acid is a trihydroxy-monocarboxylic acid with molecular formula $C_{30}H_{48}O_5$ corresponding to pentacyclic triterpenes.

The relationship of acacic acid to β-amyrin group was fixed by the facile formation of a saturated bromolactone*4(IV) mp 259—262°C, by the action of bromine on acacic acid in acetic acid. Formation of a bromolactone[11] not only indicated an olean type skeleton, but also fixed the position of the carboxyl group at C-28 and the double bond between carbon 12—13.

The infrared spectrum of acacic acid methyl ester in pyridine (Fig. 2), taken under prescribed conditions,[12] through the courtesy of Prof. R. Tschesche, showed only two absorptions at 1380 and 1355 cm^{-1} in region 'A' and three absorptions at 1330, 1300 and 1267 cm^{-1} in region 'B' which clearly indicated its relation to the β-amyrin group.

Furthermore, the relation of acacic acid to the β-amyrin group was fixed by the formation of the (di)acetate methyl ester of the hydrolysis product of sapogenin B of Styphnodendron coriaceum[13] (Proceric acid[14]) (VIII) from acacic acid (I). Acacic acid (I) on methylation with diazomethane gives a methyl ester (III) which on acetylation with acetic anhydride and pyridine in the cold yielded a (di)acetate methyl ester (VI) leaving one of the hydroxyl groups free. This hydroxy acetate methyl ester (VI) on dehydration with phosphorous oxychloride in pyridine gave a diene (VII) (*cf.* Varshney *et al.*,[15] echinocystic acid diene), which gives a very deep colour with tetranitromethane. Diene (VII) on hydrogenation with Adams' platinum yielded a product (VIII) which has been identified as proceric acid (di) acetate methyl ester[14] (diacetate methyl ester of the hydrolysis product of sapogenin B of Styphnodendron coriaceum[13]).

The formation of a diacetate lactone (28→21) (II) by acetylation of acacic acid (I) suggested that one of the hydroxyl groups should be situated at a position γ- to the carboxyl group, *i.e.* at C–15, 19 or 21. The above conversion of acacic acid into a compound of known structure confirmed that the position of the hydroxyl group is 21.

This conversion of acacic acid (I) to a compound of known structure (VIII) established not only the relation of acacic acid to the β-amyrin group but also established that one of the hydroxyl groups in acacic acid (I) is located at C–3, another at C–21, and the carboxyl at C–28.

The formation of the diacetate methyl ester (VI) instead of the expected triacetate on acetylation of the methyl ester paralleling the formation of a monoacetate of methyl echinocystate[15] suggested the possible location of the third hydroxyl group at a position β- to the carboxyl group (*i.e.* on C-16 or C-22), the methylation of which hinders the formation of acetate derivatives.

Methyl ester (III) on periodic oxidation was recovered unchanged, indicating the absence of a 1,2-diol system in the compound. Similarly the methyl ester failed to form an isopropylidene derivative, which while confirming the above observation also indicated the absence of a *cis*-1, 3-diol system (*cf.* Tomentosic acid[16]), thus eliminating the adjacent position (*i.e.* C-22) for the third hydroxyl group, leaving only position C-16 for the third hydroxyl group.

Acacic acid diacetate lactone (II) undergoes hydrogenation at atmospheric pressure in the presence of Adams, catalyst, yielding a saturated compound (V), contrary to the normal behaviour of the members belonging to the β-amyrin group. This abnormal behaviour can only be explained on the basis of some conformational or stereochemical arrangements differing from those accepted. This also suggests the possibility of the location of one hydroxyl group in a γ-position to the carboxyl group (*i.e.* position 21). The diacetate lactone (II) on partial hydrolysis with potassium carbonate in methyl alcohol gave a product mp 307—320°C which could not be characterised. The diacetate lactone (II) on hydrolysis with methanolic hydrochloric acid (10%) gave colourless needles of hydroxy lactone (IX) mp 252—

*4 The purity of the bromolactone (IV) is doubtful but the product obtained does not show any unsaturation with tetranitromethane, indicating that the double bond has been removed by lactone formation.

11) M. Shamma, *Drug Standards*, **27**, 42 (1959).

12) G. Snatzke, F. Lampert and R. Tschesche, *Tetrahedron*, **18**, 1417 (1962).

13) B. Tursch, E. Tursch, I. T. Harrison, Gloria Berenica Chagas Tolentino De Calvalhe Brazao da Silva, H. J. Moterio, B. Gilbert, B. Mors Walter and C. Djerassi, *J. Org. Chem.*, **28**, 2390 (1963).

14) I. P. Varshney and S. Y. Khan, *J. Pharm. Sci.*, **53**, 1532 (1964); I. P. Varshney, *Bull. Chem. of Terpenoids, Natl. Inst. Sci. India, New Delhi*, No. 37, 95—99 (1968).

15) Ch. Sannie, H. Lapin and I. P. Varshney, *Bull. Soc. Chim. Fr.*, **1957**, 1440; I. P. Varshney, Thesis, Dr. es Sc., Univ. Paris, Soutenue le 21 Decembre, 1956.

16) L. R. Row and L. S. R. S. Rao, *Tetrahedron*, **18**, 827 (1962).

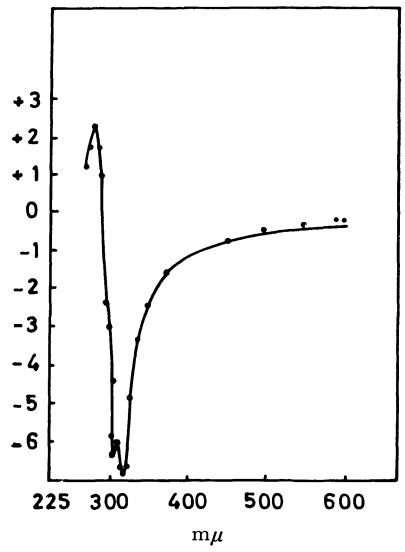

Fig. 3

254°C, which was confirmed by its reacetylation to diacetate lactone (II). Pyrolysis of acacic acid (I) also resulted in the formation of the same dihydroxy lactone (IX). The ORD curve (Fig. 3) of the diketo lactone (XI) formed by the oxidation of dihydroxy lactone (IX) with chromic acid in the cold shows a strong negative multiple Cotton effect, closely resembling that of *nor*-echinocystenolone acetate.[17] This shows that the stereochemical arrangement in acacic acid is iden-

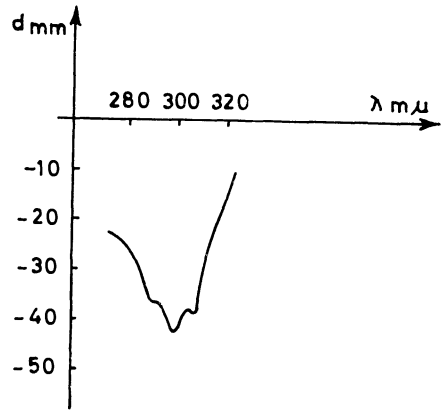

Fig. 4

$\Delta\varepsilon$	309	−2.02
	298	−2.29
	291—292	−1.97

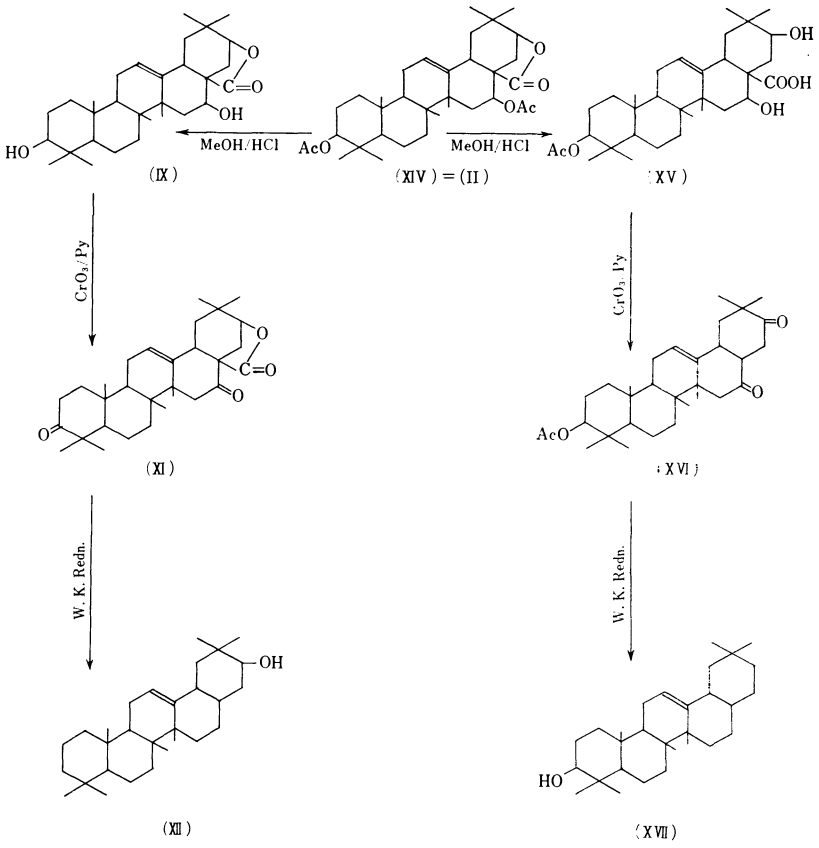

17) C. Djerassi, J. Osiecki and W. Closson, *J. Amer. Chem. Soc.*, **81**, 4587 (1959).

tical with that of *nor*-echiyocystenolone acetate (D-E *cis* fusion). Thus DE *cis* ring junction was assigned to acacic acid. A *trans* fusion should be expected to give a positive Cotton effect. The CD curve (Fig. 4) also supported this finding.

Ketone (XI) on Wolff-Kishner reduction gave colourless needles mp 183—188°C (XII) a *nor*-compound by decarboxylation of the β-keto acid formed under the reaction conditions. This compound on acetylation gave an acetate mp 210—216°C (XIII). The infrared spectrum of compound (XII) showed a strong band in the hydroxyl region. The analytical results correspond to the formula $C_{29}H_{48}O$, and thus this compound should have the structure (XII) on the basis of the scheme outlined.

Earlier, the product (XII) mistakenly thought to be 28 -*nor*-β-amyrin (XVII) according to the scheme shown below (XIV—XVII) as no depression in mp took place when the compound (XII) was mixed with an authentic sample of *nor*-β-amyrin (XVII).[18] But later infrared studies showed that this compound was different from 28-*nor*-β-amyrin. This led to the complete revision of the scheme (XIV—IX—XII). More extensive study of compound (IX) was done through IR, NMR, and mass spectrometry to give structure (IX).

It may be pointed out that compound (XII) and 28-*nor*-β-amyrin (XVII) have given the same R_f values on TLC, and have the same elemental composition. However there is a large difference in the IR spectra of the two compounds.

The formation of *nor*-compound (XII) starting with C-30 ketone (XI) definitely indicated that the ketone was a β-ketolactone, as only this hypothesis can explain the decarboxylation during Wolff-Kishner reduction due to the formation of a β-keto acid under the alkaline conditions of the reaction. All evidences fixed the position of the third hydroxyl group to be C-16. The formation of the acetate methyl ester of the sapogenin B of Styphnodendron coriaceum coupled with other evidences discussed above fixed the structure of acacic acid as 3,16,21-trihydroxyolean-12-en-28-oic acid (I) leaving the question of stereochemistry and conformation undecided.

The NMR spectra of acacic acid diacetate lactone(II) (Fig. 5) showed signals corresponding to the lactonic proton at 4.2 ppm as a doublet. This is quite in agreement with the structure formulated, for the dihedral angle between the hydrogen at C-21 and one of the hydrogens at C-22 is about 90° which leads to a doublet rather than the triplet normally obtained by splitting the vicinal hydrogens. The acetoxyl proton on C-3 appears in the form of quadruplet centered at 4.5 ppm; $J_1=9$ Hz and $J_2=2$ Hz which indicates that the hydrogen is α- and the hydroxyl β-oriented.

The other acetoxyl proton at C-16 appears in the form of a quadruplet centered at 5.0 ppm; $J_1=12$ Hz and $J_2=5$ Hz also indicating a β-orientation for the hydroxyl group at C-16.

The hydroxyl group on C-21, on the basis of lactone formation, can be designated as β. The α-hydroxyl group will not form a lactone with the β-carboxyl group at C-28.

Therefore acacic acid(I) is 3β,16β,21β-trihydroxy-18β-olean-12-en-28-oic acid.

The NMR spectra of compound (IX)(Fig. 6) showed signals corresponding to vinyl proton at 5.38 ppm as a triplet characteristic of the proton of the β-amyrin group. One proton appearing at 4.2 ppm as a doublet should be a lactonic proton (CH–O–C=O). Two hydroxyl protons appeared at 1.53 ppm as singlets.

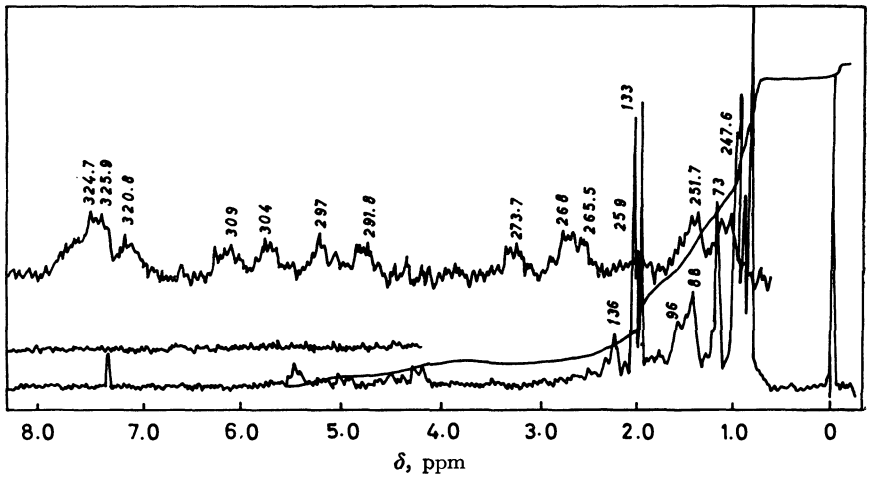

Fig. 5

18) I. P. Varshney and K. M. Shamsuddin, *Tetrahedron Lett.*, **1964**, 2055.

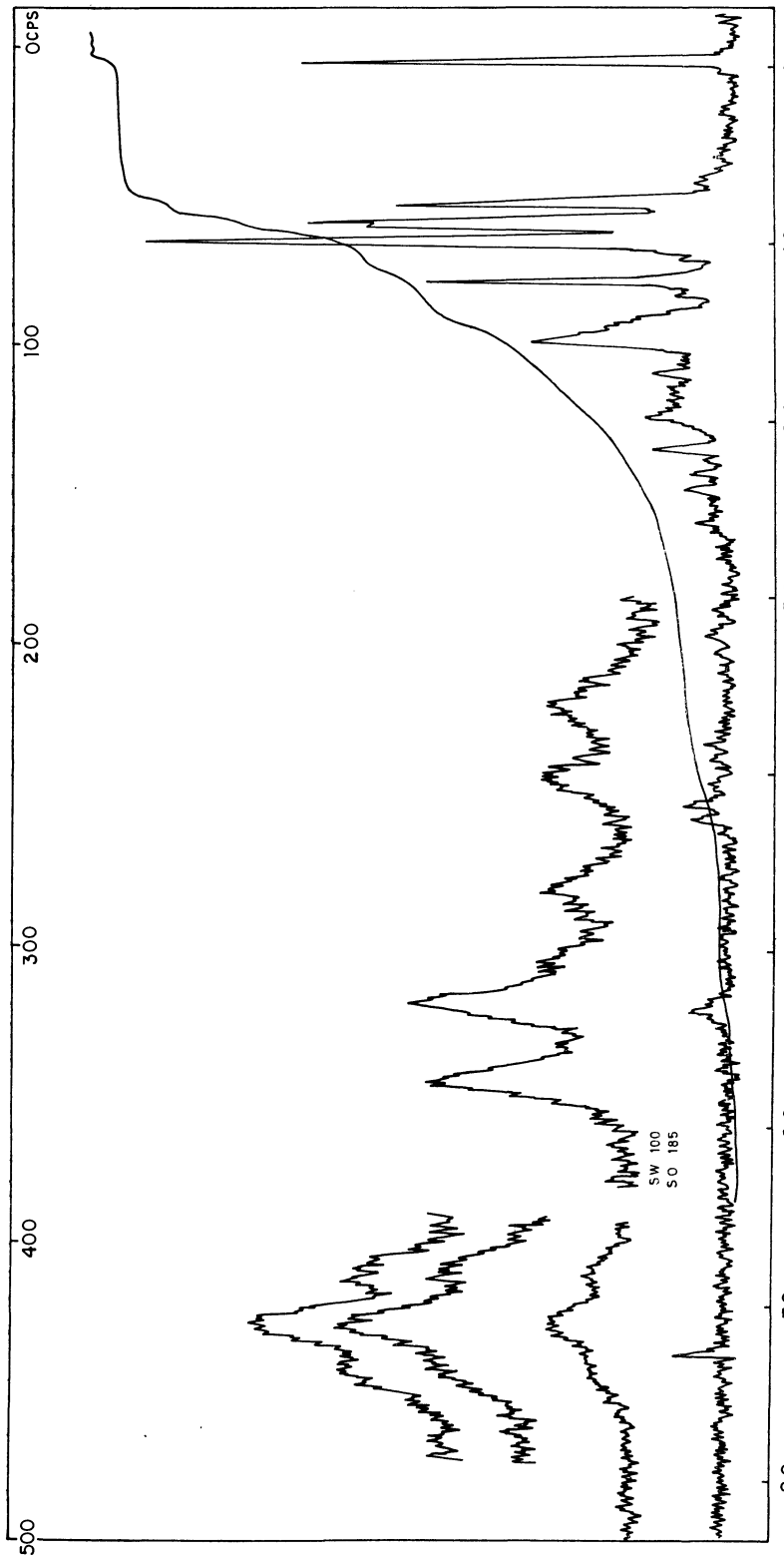

Fig. 6

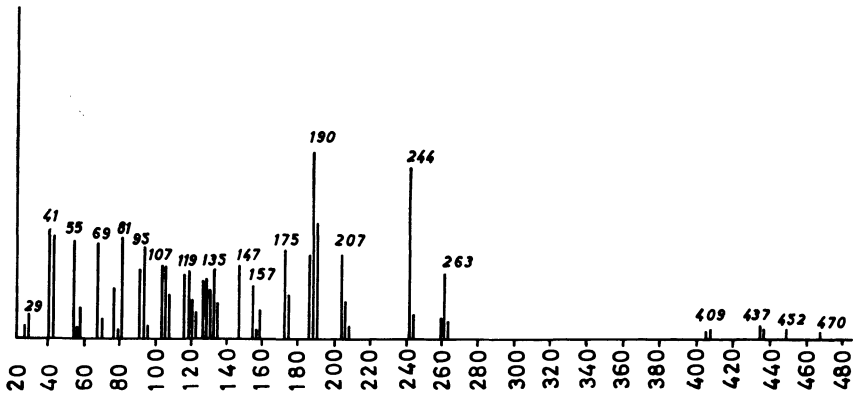

Fig. 7

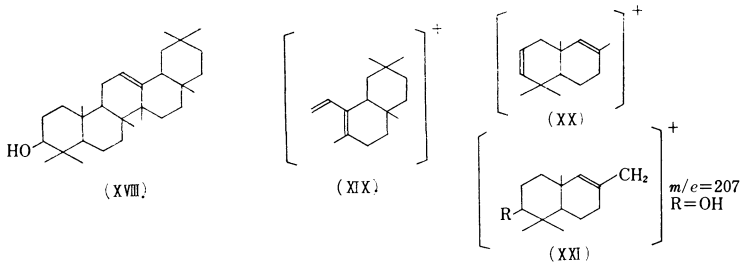

The mass spectrum (Fig. 7) of (IX) had the M^+ peak at 470 which is in definite agreement with the proposed structure, $C_{30}H_{46}O_4$. There is a peak at *m/e* 452 arising out of the loss of one molecule of water. In the triterpenes Δ^{12}-compounds (XVIII) undergo predominantly retro-Diels-Alder reaction leading to fragments (XIX) and (XX) while the rings A and B lead to the fragments (XXI).[19]

Thus the peaks at *m/e* 263 and 244 are due to fragments (XXII) and (XXIII) which correspond to fragment (XIX). The other peak at *m/e* 207 is due to fragment (XXI; R–OH). The peak at *m/e* 175 can be attributed to the *m/e* 190 fragment minus a methyl group.

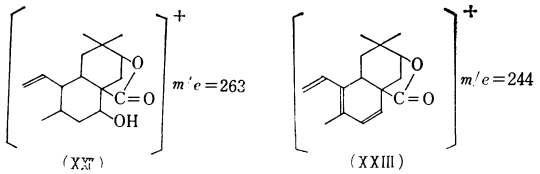

The oxidation of dihydroxy lactone (IX) with pyridine-chromium trioxide complex, gave a product (XI) mp 338—342°C. It gave a yellow colour with tetranitromethane and formed a semicarbazone mp 278—282°C.

The NMR spectrum (Fig. 8) of compound (XI) shows signals of a proton at 4.2 ppm, as a doublet which is due to the lactonic proton as in the case of (IX) (Fig. 6). The spectrum also shows the presence of the vinylic proton at 5.8 ppm.

The mass spectrum (Fig. 9) of this compound also confirms this postulation. It has M^+ peak at 466 which is in entire agreement with the formula $C_{30}H_{42}O_4$ for the diketolactone. The peak at *m/e* 451 should correspond to M-15, due to the loss of a methyl group. The peak at *m/e* 260 is due to the normal fragmentation procedure and corresponds to the 'a' type fragment[13] represented in this case by (XXV), as in the case of sapogenin B of Stryphnodendron coriaceum (XXIV) which has also a lactone function between the carboxyl at C-28 and the hydroxyl at C-21 leading to fragment (XXVII). This compound also gives rise to fragment (XXVI) corresponding to *m/e* 215.

There is a peak at *m/e* 480 which has been assumed to be due to a small quantity of the triketo product (X) formed by allylic oxidation of the dihydroxy lactone (IX) and whose molecular formula is $C_{30}H_{40}O_5$. The presence of traces of the triketo product (X) was detected by thin layer chromatography. A weak peak at *m/e* 315 in the mass spectrum can be attributed to the fragment (XXVIII) arising out of the 11-keto compound (X).

Usually pentacyclic triterpenes of the β-amyrin group have rings A-B, B-C, and C-D *trans* and D-E *cis* fused, with an all chair conformation.

19) H. Budzikiewicz, J. J. M. Wilson and C. Djerassi, *J. Amer. Chem. Soc.*, **85**, 3688 (1963).

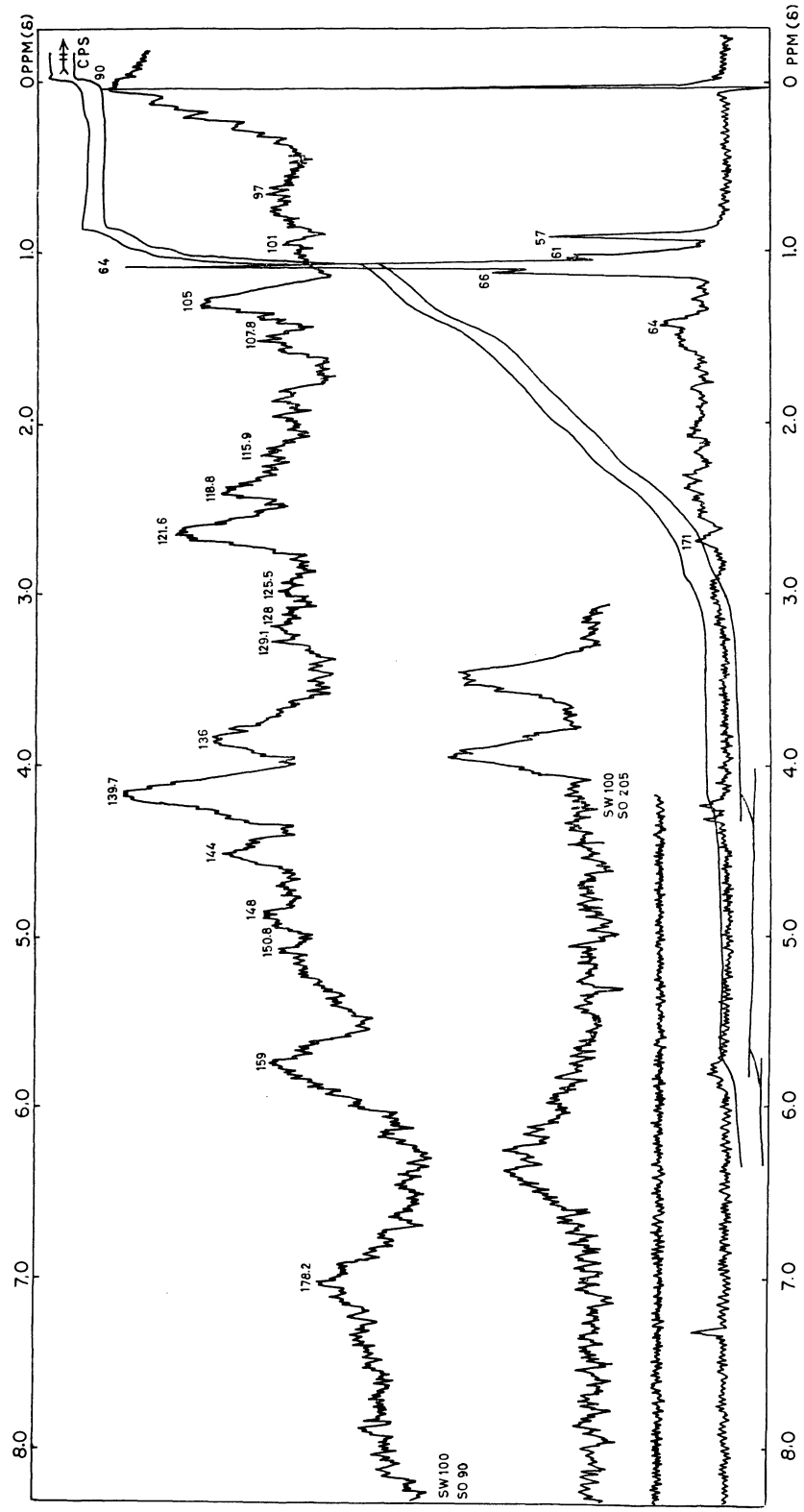
0 PPM (δ)
1.0
2.0
3.0
4.0
5.0
6.0
7.0
8.0
CPS
90
64
97
101
105
107.8
115.9
118.8
121.6
125.5
128
129.1
136
139.7
144
148
150.8
159
178.2
SW 100
SO 90
SW 100
SO 205
57
61
66
64
171

Fig. 8

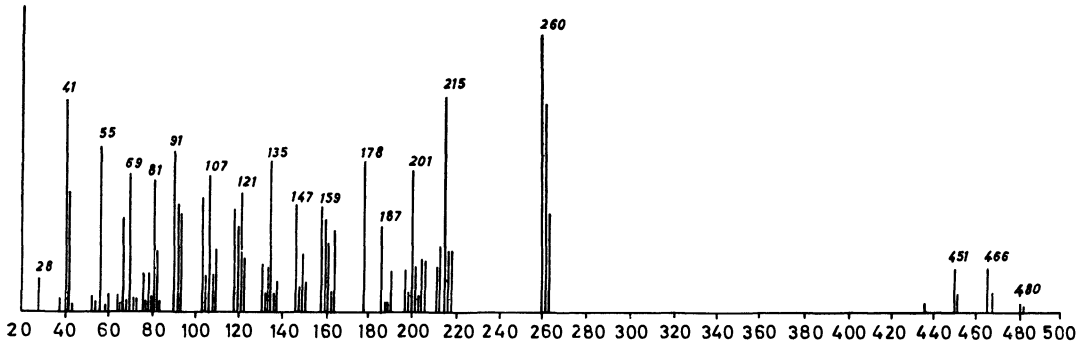

Fig. 9

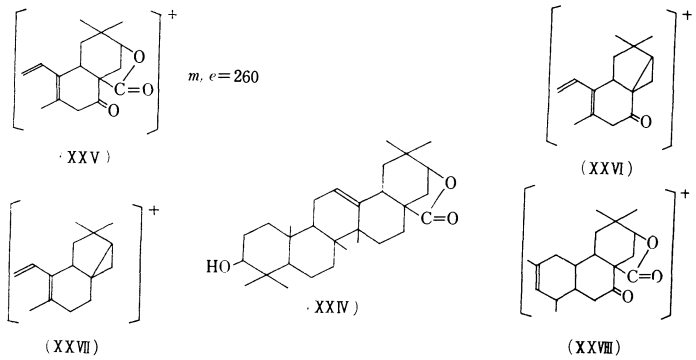

Easy hydrogenation of the diacetate lactone(II) of acacic acid is contrary to the properties of β-amyrin group which cannot be hydrogenated under normal conditions,[11,13] and therefore indicates that some subtle conformational difference exists in this compound. These instances are parallel to the behaviour of sapogenin B of Stryphnodendron coriaceum,[13] and can be explained on the basis that ring E exists in boat form and consequently ring D in a *quasi-boat* form.[13] The proximity of the C-21 hydroxyl and the C-28 carboxyl groups which tends to make the lactonisation easy can be seen by the study of a molecular model of acacic acid. Such a lactonisation could also be possible with a *trans* D-E fusion but this possibility is eliminated on the basis of the ORD (Fig. 3) and circular dichroism (Fig. 4) curves of the diketolactone(XI) which strongly resemble that of *nor*-echinocystenolone acetate.[17] The latter has a ring D-E *cis* fusion, and this resemblance indicates identical stereochemical arrangement around ring D in both the compounds. Thus D-E ring junction is *cis* in case of acacic acid(I). As this assignment made by Djerassi *et al.*[17] is accepted for *nor*-echinocystenolone, acacic acid(I) has an 18β-H configuration, except for the improbable event of an erroneous assignment of configuration to *nor*-echinocystenolone.[17] This would not change the conclusions regarding the stereochemistry except as regards configuration at C-18, in acacic acid.

While acacic acid(I) itself could exist in all chair conformation, this is impossible for the 28—21 lactone(II) of this series. A study of models shows that such a lactone can be easily formed provided ring E is constrained into a boat form. Ring D in the lactone can then adopt several conformations, but one of them, a twist form, appears to minimize all interactions effectively. In this conformation the 16β bond is *quasi*-equatorial and the geometrical relationship between the 16α-H and the 15-CH_2 group is such that the observed coupling constants are explained.

Therefore acacic acid can now be represented as 3β,16β,21β-trihydroxy-18β-olean-12-en-28-oic acid, and in its diacetate lactone (28—21), the rings E and D are in *boat* and *quasi-boat* forms respectively (XXIX).

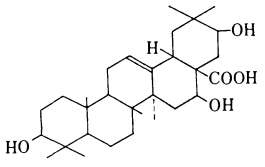

(XXIX)

Experimental*5

Extraction of Saponin. The pods of *Acacia concinna* DC. (900 g) obtained from Kerala (South India) broken into small pieces were exhaustively extracted with ethanol under reflux and solvent recovered. This left a dark brown syrupy residue which was successively treated with ether, petroleum ether, carbon tetrachloride, chloroform, and acetone. The mass left over was dissolved in a small quantity of alcohol, and saponin was precipitated by addition to a large quantity of ether/acetone. This process was repeated several times followed by treatment with activated charcoal to give a fairly pure specimen of saponin (28 g).

Hydrolysis of Saponin. Saponin (10 g) was dissolved in a large volume of water and heated with sulphuric acid (10%) on a water bath for an hour followed by refluxing for another hour. Sapogenin was filtered, and dried (7.5 g).

Purification of Sapogenin. Crude sapogenin (7.5 g) was refluxed with alcoholic potassium hydroxide (10%; 600 cc) for one hour and the volume reduced to half. The solution was then diluted with water (2 *l*) and extracted with ether. The aqueous layer was then acidified with hydrochloric acid and the precipitated acid genin filtered, washed and dried (3.2 g).

Diacetate Lactone (II). Genin (5 g) was acetylated in the usual manner by heating with acetic anhydride and pyridine. The product was crystallized from methanol mp 235—236°C. It gave a positive colour with tetranitromethane. Genin was acetylated by refluxing with acetic anhydride and sodium acetate as well as with acetic anhydride and pyridine in the cold gave the same product mp 235—236°C. It showed no depression in mp when mixed with an authentic sample of acacic acid diacetate lactone obtained from Acacia intsia bark.

Acacic Acid (I). Acetate (II) was refluxed with alcoholic potassium hydroxide (300 cc; 10%) for two hours and the volume reduced to half. The solution was poured into excess of water and acidified with hydrochloric acid which precipitated genin. The precipitated sapogenin was filtered, washed and crystallized from a large volume of methanol mp 278—282°C. It gave yellow colour with tetranitromethane. Mixed mp with authentic sample of acacic acid obtained from Acacia intsia bark showed no depression.

Bromolactone (IV). A suspension of acacic acid (I) (500 mg) in acetic acid (50 cc) containing anhydrous sodium acetate (2 g) was stirred during addition of bromine (1 cc) in acetic acid (25 cc) for an hour and the contents diluted with water. The product was extracted with ether and the water extract washed with sodium thiosulphate, sodium bicarbonate and water. Recovery of ether furnished the bromolactone which was crystallized from methanol, mp 259—262°C (*cf.* *4). It gave no colour with tetranitromethane.

Methyl Ester(III). Acacic acid (I) was treated with an excess of ethereal solution of diazomethane and the reaction mixture was kept overnight at room temperature. The product isolated by the evaporation of ether was crystallized from methanol mp 224—225°C. It gave a yellow colour with tetranitromethane. Mixed mp with an authentic sample was undepressed.

Methyl Ester Diacetate (VI). The methyl ester (1 g) (III) was acetylated with acetic anhydride (100 cc) and pyridine (100 cc) in the cold in the usual manner. It was crystallized from methanol as needles mp 203—205°C. It gave positive colour with tetranitromethane. Mixed mp with authentic sample was undepressed.

Found, C, 71.46, 71.36; H; 9.64, 9.50%. Calcd for $C_{35}H_{54}O_7$: C, 71.64; H, 9.28%.

Periodic Oxidation of Methyl Ester (III). The methyl ester (III) (500 mg) was dissolved in ethanol (95%; 30 cc) and treated with a solution of sodium periodate (150 mg) in sulphuric acid (6 cc). The mixture was kept at room temperature for 18 hours and then poured into excess of water. The precipitate was filtered, washed and crystallized from methanol as colourless needles mp 223—224°C. The mixed mp with the starting material was undepressed.

Isopropylidene Derivative of Methyl Ester. The methyl ester (III) (500 mg) in dry acetone (25 cc) was treated with a drop of concd. hydrochloric acid. It did not give any precipitate. The solvent was then removed and the product left over was crystallized from methanol mp 223—224°C. The mixed mp with the starting material showed no depression.

Dehydration of VI. The diacetate methyl ester (VI) (300 mg) was refluxed with pyridine (10 cc) and phosphorous oxychloride (2 cc) for 5 hr. It was then diluted with ice cold water. The product was extracted with ether, and the ethereal extracts washed with water. Evaporation of ether and crystallization from methanol furnished compound (VII) mp 280—282°C. It gave a deep yellow colour with tetranitromethane.

Found: C, 73.54, 73.78; H, 9.65, 9.19%. Calcd for $C_{35}H_{52}O_6$: C, 73.91; H, 9.22%.

Hydrogenation of VII. The dehydration product (VII) (200 mg) was dissolved in acetic acid (50 cc) and hydrogenated at atmospheric pressure and room temperature in the presence of Adams' catalyst. The product was crystallized from methanol as colourless shining needles mp 266—270°C. It still gave positive reaction with tetranitromethane.

Found: C, 72.88, 72.76; H, 9.24, 9.15%. Calcd for $C_{35}H_{54}O_6$: C, 73.64; H, 9.54%.

Hydrogenation of II. The diacetate lactone (II) (100 mg) was hydrogenated in acetic acid (20 cc) in the presence of Adams' catalyst at room temperature and pressure. It was crystallized from methanol in the form of colourless plates mp 280—285°C (V). It did not give any colour with tetranitromethane.

Found: C, 72.73, 72.50; H, 9.78, 9.90%. Calcd for $C_{34}H_{52}O_6$: C, 73.34; H, 9.41%.

Partial Hydrolysis of II. The diacetate lactone (II) (500 mg) was refluxed with methanol (50 cc) containing hydrochloric acid (10 cc) for two hours and the product worked out in the usual manner. It was crystallized from methanol as colourless crystals mp 252—254°C (IX). It gave a yellow colour with tetra-

*5 All the melting points recorded in this paper have been taken on Koflers hot microscopical melting point apparatus and are corrected. NMR spectra have been taken on varian A-60 and CD on Roussel Jouan Dichrograph. IR spectra have been recorded on Perkin-Elmer models 137, 21, 221 and Beckman IR5A.

nitromethane.

Acetylation of IX. The partial hydrolysis product (IX) (200 mg) was acetylated in the cold with pyridine (10 cc) and acetic anhydride (10 cc) in the usual manner and crystallized from methanol mp 234—236°C. Mixed mp with diacetate lactone (II) showed no depression.

Pyrolysis of I. Acacic acid (I) (150 mg) was taken in a pyrex tube and heated in an oil bath at 290—300°C for 25 min. The melt obtained was extracted and crystallized from methanol 252—254°C. It gave no depression on mixed melting with dihydroxy lactone (IX).

Oxidation of IX. A solution of dihydroxy lactone (IX) (200 mg) in pyridine (5 cc) was added to a suspension of chromium trioxide pyridine complex prepared from chromium trioxide (300 mg) and pyridine (8 cc) and the mixture kept at room temperature for 24 hours after which it was poured into crushed ice. The product worked out in the usual manner was crystallized from methanol-chloroform mixture mp 338—342°C (XI). It gave yellow colour with tetranitromethane. This product formed a semicarbazone mp 278—282°C.

Thin layer chromatography of the ketone using cyclohexane; ethylacetate system showed two spots, one major and one minor, the latter with a faster running rate. The product was purified by preparative thin layer chromatography and the pure ketone (XI) used for NMR measurements. Mass spectrometry was carried out with untreated product which clearly showed the impurity.

Wolff-Kishner Reduction of XI. Ketone (XI) (100 mg) was dissolved in diethylene glycol (20 cc) containing metallic sodium (400 mg) and to it was added hydrazine hydrate (100%). Then the reaction mixture boiled at 180°C. It was refluxed at this temperature for 18 hours after which hydrazine hydrate was evaporated till the solution boiled at 210°C. Refluxing was continued for another 24 hr and the reaction mixture worked out in the usual manner. No acidic product could be isolated, and the neutral product was crystallized from methanol-ethyl acetate mixture; mp 183—188°C (XII). It gave a positive colour with tetranitromethane.

Found: C, 84.20; H, 11.73%. Calcd for $C_{29}H_{48}O$: C, 84.40; H, 11.73%.

Acetylation of XII. The reduction product (XII) (60 mg) was acetylated with pyridine and acetic anhydride in the usual manner. The acetate was crystallized from ethyl acetate methanol mixture; mp 210—216°C (XIII). It gave positive colour with tetranitromethane.

The authors are thankful to Professor R.E. Beyler for the material help given by him during his stay at Strasbourg. Thanks are due to Professor G. Ourisson, Professor R. Tschesche, Professor C. Djerassi, Dr. G. Snatzke, and Dr. A. J. Shannon for their help in IR, NMR, ORD, CD, and mass spectrometry. Thanks are also due to the Council of Scientific and Industrial Research, New Delhi for the award of a Junior Research fellowship to one of the authors (K.M.S.) and to Dr. B. Tursch for comparing our sample with acetate methyl ester of the hydrolysis product of sapogenin B of Stryphnodendron coriaceum.

BULLETIN OF THE CHEMICAL SOCIETY OF JAPAN VOL. 43 3841—3845 (1970)

Kinetics of the Chromic Acid Oxidation of Glycollic and Benzilic Acids

Kalyan K. SENGUPTA, A. K. CHATTERJEE and S. P. MOULIK

Department of Physical Chemistry, Jadavpur University, Calcutta-32, India

(Received December 15, 1969)

The kinetics of chromic acid oxidation of glycollic and benzilic acids have been studied. Catalysis by H^+ ions has been noticed in both cases of oxidation. The results show that the logarithm of the rate constants increases with increase in the proportion of acetic acid in the mixture. Ionic strength decreases the rate of oxidation. Pyridine catalyzes the oxidation of glycollic acid whereas the catalysis in the case of benzilic acid is negligible. The energy of activation and entropy of activation have been calculated. Both kinetics and spectrophotometric results indicate the formation of intermediate chromium(VI)-hydroxycarboxylate complex in each case. The complex finally decomposes to give reaction products. Glycollic acid initially produces glyoxylic acid which subsequently gives formic acid whereas benzilic acid is oxidized to benzophenone.

Oxidation of a variety of organic compounds by chromic acid has been extensively studied. Bakore *et al.* have studied the oxidation of a number of α-hydroxy acids[1] *viz.*, lactic, malic and mandelic acids (all of them having C–H bond in the α-carbon atom) and explained the mechanism on the basis of the Kwart-Francis scheme,[2] which is a minor variation of the well known Westheimer's[3] mechanism. In the previous case[2] proton is removed intramolecularly instead of by an external base. However, no kinetic data for the oxidation of glycollic acid with chromic acid are known which may also be explained in the light of the above mechanisms. On the other hand, for benzilic acid having no C–H linkage in the molecule, the Kwart-Francis mechanism as well as Westheimer[3] type of mechanism (applicable in the case of chromic acid oxidation of isopropyl alcohol) could not be operative. Westheimer[3] considered that the oxidation of alcohols by chromic acid involves reversible formation of a chromate ester which slowly decomposes by a process catalyzed by bases. Presumably, the oxidation of benzilic acid may be explained on the basis of rupture of C–C bond[4] which is the other possible alternative. With this idea, we report in this communication, the chromic acid oxidation of two α-hydroxy acids, *viz.*, glycollic and benzilic acids.

Experimental

Potassium dichromate (G. R., Merck), glycollic acid (Riedel, Germany) and benzilic acid (Pure, E. Merck) were used without further purification. Manganous sulphate used was of 'Anala R' grade. 60% perchloric acid (E. Merck) was used. Sodium perchlorate was prepared by the neutralization of perchloric acid with sodium hydroxide. Neutralized benzilic acid solution was used. All other reagents were chemically pure. Details of kinetic measurements have been described elsewhere.[5] All experiments were carried out at 35°C unless otherwise mentioned. Spectral measurements were carried out with a Beckman DB. model spectrophotometer.

Results

The stoichiometry of the reactions were determined by allowing reaction mixtures, containing a large excess of dichromate ion, to stand for 48 hrs at 30°C. The unreacted oxidant was then estimated by the usual procedure.[5] The reactions may be represented by the following equations.

$$6CH_2(OH)COOH + 4Cr_2O_7^{2-} + 32H^+ \rightarrow 6HCOOH + 8Cr^{3+} + 22H_2O + 6CO_2$$

Found: 0.63 mol of the oxidant per mol of the substrate.

$$3(C_6H_5)_2C(OH)COOH + Cr_2O_7^{2-} + 8H^+ \rightarrow 3(C_6H_5)_2CO + 2Cr^{3+} + 7H_2O + 3CO_2$$

Found: 0.31 mol of the oxidant per mol of the substrate. The products of the reactions were formic acid and benzophenone respectively which were confirmed by the usual tests. Formic acid was tested by the chromotropic acid reaction and benzophenone was tested by the preparation of a 2,4-dinitrophenyl hydrazine derivative.

In both cases of oxidation a 8 min period of

1) G. V. Bakore and S. Narain, *J. Chem. Soc.*, **1963**, 3419.

2) H. Kwart and P. S. Francis, *J. Amer. Chem. Soc.*, **77**, 4097 (1955).

3) F. H. Westheimer, *Chem. Rev.*, **80**, 3022 (1958).

4) Y. W. Chang and F. H. Westheimer, *J. Amer. Chem. Soc.*, **82**, 1401 (1960).

5) K. K. Sen Gupta, This Bulletin, **43**, 590 (1970).

TABLE 1. EFFECT OF OXIDANT ON THE REACTION RATE
(a) [Glycollic Acid]$=3.00\times10^{-2}$ M, $\mu=0.22$, pH$=0.69$
(b) [Benzilic Acid]$=8.3\times10^{-3}$ M, $\mu=0.14$, pH$=0.90$

	a		b	
No.	[Cr(VI)]$\times10^{3}$ M	$k_a\times10^{3}$(sec^{-1})	[Cr(VI)]$\times10^{3}$ M	$k_b\times10^{3}$(sec^{-1})
1	5.0	3.53	1.38	1.34
2	6.6	3.22	2.07	1.21
3	8.3	2.88	2.77	0.89
4	10.0	2.57	3.47	0.63

disturbance was observed. This disturbance is possibly due to some side reactions which progressively slow down as the complex formation approaches completion. A good first order reaction kinetics was found to occur after this period. Table 1 summarizes the values of rate constants at various initial concentrations of chromic acid. It is seen that the rates decreased with the increase of initial concentration of chromic acid.

To study the effect of [α-hydroxy group]$_0$ on k, a series of runs were made holding all the initial parameters constant. Increase in the concentration of α-hydroxy acids increased the rate of oxidation. The data on the effect of α-hydroxy acids on the rate of oxidation is shown in Fig. 1. The plots of $1/k$ against 1/[substrate] cut y-axis indicating the formation of an intermediate compound in both cases of oxidation. The spectrophotometric results also support the contention.

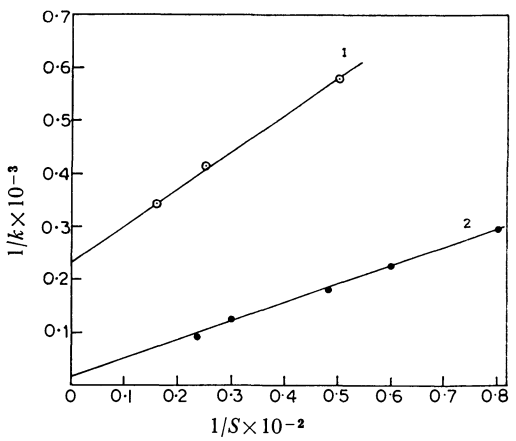

Fig. 1. Influence of substrate on the rate constant.

1. [Cr(VI)]$=3.30\times10^{-3}$ M
2. [Cr(VI)]$=1.38\times10^{-3}$ M

The experimental curves of Fig. 2 are physical evidences for complexation between chromium(VI) and hydroxy acids used. The spectra reported here were all taken after immediate mixing of the components. The strength of the dichromate solution was of the same order as used in the kinetic study. The change in the nature of the optical density/wavelength trend in the region 410—450 mμ of chromium(VI) (Curve 1), when ligands were added (Curves 2 and 3), seems to be due to new compound (complex) formation. A shift in the position of the shoulder towards longer wavelength from glycollate to benzilate was also noticed. The new nature of chromium(VI)-hydroxylate spectra cannot be due to change of pH. The effect of pH on the absorption spectra of dichromate solution is presented in curves 4, 5 and 6. Addition of glycollate and benzilate both changed (increased) the pH of the dechromate solution. The nature of both the curves (2 and 3), though similar to each other, differs from that of dichromate solutions having different acidities (curves 4, 5 and 6). All these observations support the

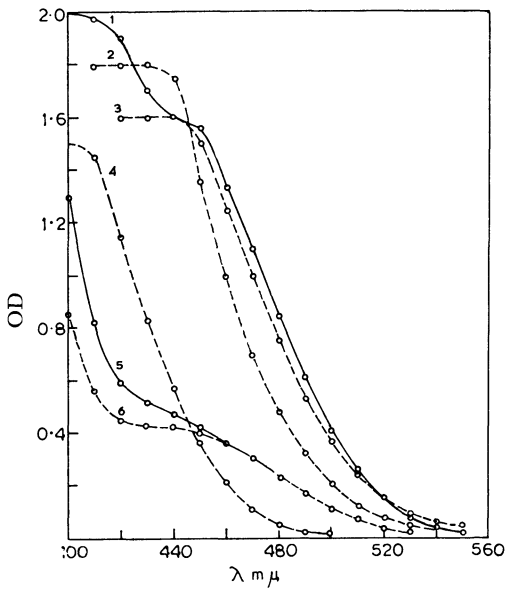

Fig. 2. Absorption spectra of chromium(VI) and its complexes.

1. [Cr(VI)] in water$=3.3\times10^{-3}$ M
2. [Cr(VI)]$=3.3\times10^{-3}$ M, [Na-glycollate]$=0.48$ M
3. [Cr(VI)]$=3.3\times10^{-3}$ M, [Na-benzilate]$=0.48$ M
4. [Cr(VI)] in water$=1\times10^{-3}$ M at pH 12.3
5. [Cr(VI)] in water$=1\times10^{-3}$ M at pH 4.53
6. [Cr(VI)] in water$=1\times10^{-3}$ M at pH 1.70

formation of chromium (VI)-hydroxycarboxylate complex upon immediate mixing.

The rate studies were made at various hydrogen ion concentrations. The acid dependence was studied, in a series of runs at fixed [substrate]$_0$ and [Cr(VI)]$_0$, by varying perchloric acid concentration but keeping the ionic strength constant by the addition of sodium perchlorate. The rates increased with the increase in hydrogen ion concentration. The plots between log k against pH is linear in each case (Fig. 3).

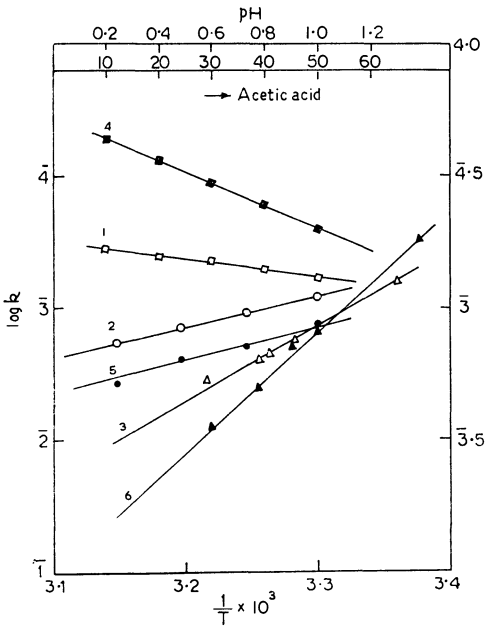

Fig. 3. Effect of solvent, temperature and pH on the rate constants.

1. [Cr(VI)]=3.33×10^{-3} M, [Glycollic acid]=2.50×10^{-2} M, pH=1.30, μ=0.06, Temp. 35°C
2. [Cr(VI)]=4.15×10^{-3} M, [Glycollic acid]=2.50×10^{-2} M, pH=0.22, μ=0.61
3. [Cr(VI)]=4.15×10^{-3} M, [Glycollic acid]=2.50×10^{-2} M
4. [Cr(VI)]=1.66×10^{-3} M, [Benzilic acid]=1.00×10^{-2} M, pH=1.0, μ=0.115, Temp. 35°C
5. [Cr(VI)]=1.38×10^{-3} M, [Benzilic acid]=8.3×10^{-2} M, pH=0.90, μ=0.14
6. [Cr(VI)]=1.38×10^{-3} M, [Benzilic acid]=8.3×10^{-2} M

The rates were also studied at different solvent composition of the reaction mixture. The solvent composition was varied by the addition of acetic acid. Figure 3 shows that the rate constant increases with increase in the proportion of acetic acid in the mixture. This is in agreement with previous observation.[5]

The results of the effect of pyridine on the rates of oxidations have been presented in Table 2. The base catalysis has been studied at constant [H$^+$] with varying [free base]. Since pyridine removes hydrogen ions, the effective hydrogen ion concentration in the presence of pyridine would correspond to {[H$^+$]–[Py]}. If pyridine catalyzes oxidation,[1] the value of $k/\{[H^+]-[Py]\}$ increases with increase in the concentration of pyridine. The value would decrease if pyridine inhibits the reaction and would be constant if pyridine has no effect on the rate of oxidation. Westheimer[3] has shown that the addition of a base like pyridine catalyzes the oxidation of isopropyl alcohol by chromic acid, but this was later shown to be incorrect.[6] At present there is no evidence[6] for the involvement of an external base in the rate controlling steps nor is there good evidence against such a process. We have also observed catalyzing behaviour of pyridine in the case of glycollic acid oxidation and slight retarding effect in the case of benzilic acid.

The influence of temperature was studied under identical conditions of [α-hydroxy acid]$_0$ and [Cr(VI)]$_0$. The Arrhenius plots of log k against $1/T$ gave straight lines (Fig. 3). The energies of activation were calculated to be 11.9 and 11.6 kcal/mol for glycollic and benzilic acids, respectively. The values of $-\Delta S^{\neq}$ were found to be 34.9 (e.u.) in each case. It is interesting that the values of energy and entropy of activation were found to be 12.86 kcal/mol and 34.6 (e.u.), respectively, in

Table 2. Effect of pyridine on the rate of oxidation

(a) [Glycollic Acid]=2.5×10^{-2} M, [Cr(VI)]=2.77×10^{-3} M, [H$^+$]=0.085 M, μ=0.1
(b) [Benzilic Acid]=8.3×10^{-3} M, [Cr(VI)]=1.38×10^{-3} M, [H$^+$]=0.166 M, μ=0.18

No.	[Pyridine]×10^2 M	k_a×10^4(sec^{-1})	k_b×10^3(sec^{-1})	$100k/\{[H^+]-[Py]\}$ (a)	(b)
1	0.00	2.34	1.88	2.75	1.13
2	1.66	1.92	1.34	2.81	0.90
3	3.32	1.53	1.16	2.97	0.87
4	4.98	—	1.00	—	0.86

6) K. B. Wiberg, "Oxidation in Organic Chemistry," Academic Press, New York (1965), Part A, p. 162.

Table 3. Influence of ionic strength on the rate of oxidation
[α-Hydroxy compound]$=8.33\times10^{-3}$ M, [Cr(VI)]$=1.38\times10^{-3}$ M, pH$=0.77$

No.	μ	$k_{\text{glycollic}}\times10^{4}(\text{sec}^{-1})$	μ	$k_{\text{benzilic}}\times10^{3}(\text{sec}^{-1})$
1	0.254	7.88	0.254	1.15
2	0.337	7.80	0.337	0.90
3	0.420	6.95	0.420	0.85

the chromic acid oxidation of isopropyl alcohol.[7] Such close values suggest that the same mechanism may be operative for the rate controlling step of the reactions of α-hydroxy acids with chromic acid.

The effect of changing ionic strength was also examined (Table 3). The ionic strength was varied by the addition of sodium perchlorate. The changes in ionic strength of the medium had a definite retarding influence. This is in agreement with the observations made by Wiberg and Mill.[8] The results in Table 1 show that the rate of reaction is not directly proportional to chromium(VI) concentration because of the following monomer-dimer equilibrium which is a function of ionic strength,

$$2HCrO_4^- \rightleftharpoons Cr_2O_7^{2-} + H_2O$$

Wiberg and Mill[8] have shown that increase in ionic strength will favour the formation of a divalent ion, which have a higher ion pair association constants than a univalent ion. This will shift the equilibrium towards dichromate ion as the ionic strength is increased, and the rate of reaction would correspondingly decrease.

The rate constants of the reactions of some α-hydroxy acids by chromium(VI) were also studied under comparable conditions of $[\alpha\text{-hydroxy acids}]_0$, $[\text{chromium(VI)}]_0$, pH and ionic strength. The concentrations of α-hydroxy acids and chromium (VI) used were 2.5×10^{-2} M and 2.70×10^{-3} M, respectively. Ionic strength and pH of each solution were maintained constant at 0.17 and 0.78, respectively. The rates increased with the increase in the substitution of hydrogen atom of the glycollic acid successively by phenyl nucleus. The values of 'k' in the cases of glycollic, mandelic and benzilic acids were found to be 0.767×10^{-3}, 0.921×10^{-3} and 4.07×10^{-3} (sec^{-1}), respectively. A comparison of the dissociation constants of glycollic, mandelic and benzilic acids show that the rates increased with the increase of dissociation constants which are 1.5×10^{-4}, 4.3×10^{-4} and 9.2×10^{-4}, respectively at 25°C. It will be difficult to interpret these data with rate constants, since the course of the reaction is mainly governed by two factors: (1) tendency of complex formation, (2) disproportionation of the complex to give products of the reaction. In the case of benzilic acid, the molecule appears to be sterically hindered due to the presence of two phenyl nucleus and the rate of the reaction with benzilic acid is expected to be the slowest. However, it seems very likely that benzilic acid molecule possibly violates the principle of steric hindrance, since due to the presence of two phenyl groups both hydroxyl and carboxyl groups are brought nearer, thereby facilitating the formation of the complex with chromic acid. Since hydroxyl and carboxyl groups are under strain, the benzilate chromate complex is expected to be most unstable in the series and hence its decomposition is fastest. In a similar way, glycollate chromate complex is more stable than benzilate chromate complex. This is possibly the reason why the rates follow the order $k_{\text{benzilate}}>k_{\text{mandelate}}>k_{\text{glycollate}}$.

Discussion

Kinetics and spectrophotometric results indicate that both glycollic and benzilic acids react with chromic acid to form an intermediate compound. They finally decompose slowly to give reaction products. Glycollic acid initially produces glyoxylic acid which subsequently is oxidized to formic acid. The other alternative would have been the oxidation of glyoxylic acid to oxalic acid, which on the way, might get oxidized to carbon dioxide. Since formic acid is one of the products of oxidation, it seems very unlikely that the reaction involves oxidation of glyoxylic acid to oxalic acid. Determination of stoichiometry also supports the above argument. Therefore, decarboxylation probably occurs as a part of the oxidation step. However, it has been shown recently during the oxidation of glyoxylic acid[9] by chromic acid, that decarboxylation of the molecule takes place followed by the oxidation of the hydrated formaldehyde molecule to afford formic acid. A few experiments were carried out using both glyoxylic acid with chromic acid and glycollic acid with chromic acid under comparable conditions. The rate constants were found to be 1.345×10^{-2} (sec^{-1}) and 1.072×10^{-3} (sec^{-1}), indicating the reaction is faster for glyoxylic acid. Again the activation energy in the case of the oxidation of glyoxylic acid by chromic acid

7) N. Venkatsubramanian, *Proc. Indian Acad. Sci.*, **50**, 156 (1960).

8) K. B. Wiberg and T. Mill, *J. Amer. Chem. Soc.*, **80**, 3022 (1958).

9) K. K. Sen Gupta and S. D. Bhattacharya, *Z. Phys. Chem.* (Leipzig), **240**, 279 (1969).

was found to be 5.5 kcal/mol as against 12.8 kcal/mol in the case of glycollic acid. This also supports that $k_{\text{glyoxylic}} > k_{\text{glycollic}}$.

On the basis of the above evidences, the reaction between glycollic acid and chromic acid may be explained in the following manner:

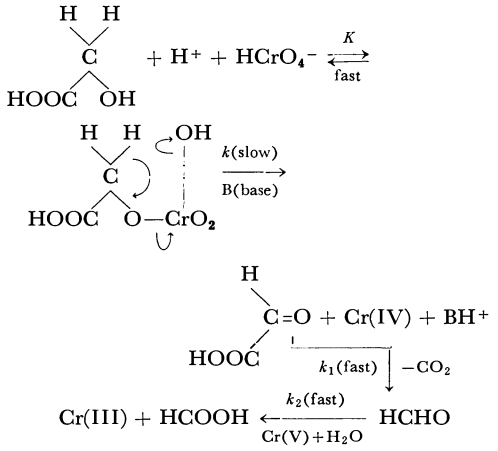

Scheme 1

The absence of C–H bond in benzilic acid suggests that the Westheimer type of mechanism is applicable in the other case. Moreover, the Kwart-Francis scheme in which proton is removed intramolecularly may also not be operative. In the case of benzilic acid, catalysis by pyridine has not been observed. Therefore, it may be proposed that the oxidation leads directly to the formation of a ketone and carbon dioxide by way of a chromate ester:

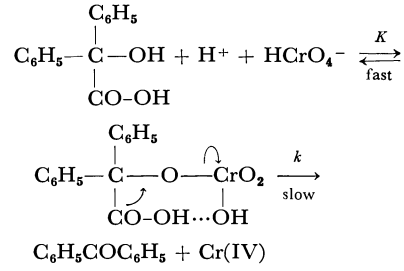

Scheme 2

In connection with the oxidation of pinacol by chromic acid, Chang and Westheimer have shown that an energy of 18.0 kcal/mol is needed during the rupture of a C–C bond. But in our case the value has been calculated to be 12.8 kcal/mol. This suggests that chromic acid possibly forms a more stable complex with symmetrical pinacol molecule than with benzilic acid.

It is clear that the first stage of the reaction involves a two electron transfer leading to chromium(IV), which is converted to chromium(V), either by reacting rapidly with chromium(VI) or chromium(IV) rapidly undergoing disproportionation to give chromium(V). The decreased rate of reaction on addition of Mn^{2+} ions suggests that intermediate valence states of chromium were formed.

Thanks are due to the Head of the Physical Chemistry Section for laboratory facilities.

BULLETIN OF THE CHEMICAL SOCIETY OF JAPAN VOL. 43 3846—3849 (1970)

Kinetic Studies of the Triethylenediamine-catalyzed Hydrolysis of 1,3-Diphenylurea in Dioxane

Yoshiaki Furuya,* Kazuo Itoho** and Sakiko Fukutaka**

* *Department of Industrial Chemistry, Faculty of Engineering, Kumamoto University, Kumamoto*

** *Daiichi College of Pharmaceutical Sciences, Fukuoka*

(Received March 26, 1970)

The rate of the hydrolysis of 1,3-diphenylurea (abbreviated as DPU) in dioxane in the presence of triethylenediamine (TED) was followed by ultraviolet spectrophotometry. The rate of the reaction satisfied the following equation:

$$v = \{k_2 - k_{3h}[H_2O]\}[DPU][H_2O] + \{k_{4uh}[H_2O] - k_{3u}\}[DPU]^2[H_2O] + \{k_{3c} - k_{4ch}[H_2O]\}[TED][DPU][H_2O] + \{k_{5cuh}[H_2O] - k_{4cu}\} \times [TED][DPU]^2[H_2O].$$

A probable mechanism which involves a nucleophilic attack of the lone pair of the O-atom of water and of the N-atom of TED on the carbonyl C-atom of DPU, passing through an ion pair of quaternary ammonium salt, is discussed.

In the kinetic studies of the TED-catalyzed transamidation of 1,3-diphenylurea with *n*-butylamine in dioxane which have been previously reported,[1] both non- and the TED-catalyzed hydrolyses were found. In the present paper, a probable mechanism of the hydrolysis, passing through an ion pair of quaternary ammonium salt, will be discussed.

Experimental

Materials. The 1,3-diphenylurea, the triethylenediamine, and the dioxane used as the reaction solvent were purified in a mannr similar to that described previously.[1]

Ultraviolet Spectrophotometry and Chemical Analyses. The absorption maxima of DPU and aniline were 255 and 234 mμ, while the minima were 227 and 214 mμ respectively. The absorption of TED is negligible at these wavelengths. Mixtures of DPU, aniline, and TED in known concentrations (corresponding to 0, 20, 40, 60, 80, and 100% conversion) were prepared at 90°C; plots of the extinction difference, $(E_{255}-E_{230})$ *vs.* $(E_{255}-E_{277})$, gave a straight line, and the cnoversions calculated from the values of $(E_{255}-E_{230})$ at 0 and 100% conversion agreed well with the conversions calculated from the mixtures within a 1% error.

Reaction-product Criterion. Aniline liberated from DPU in a reaction mixture was detected by paper chromatography in the manner described in a previous paper.[2]

A Typical Run for the Rate Measurements. A solution of 0.07 m*l* of 0.5M water in dioxane was added to a solution of 27.93 m*l* of 0.0143M DPU in dioxane; a solution of 12.00 m*l* of 0.05M TED in dioxane was poured into the solution of DPU in order to start the reaction after the three solutions had attained temperature equibrium at 90°C. Aliquots (0.2 m*l*, each) were pipetted out at appropriate intervals of time, and each one was diluted with methanol to a 2×10^{-5}M initial concentration of the reactant. The conversion was calculated graphically from the values of $(E_{255}-E_{230})$, and the value of the second-order rate constant, k_{2obs}, was calculated.

Determination of the Water. The water concentration in the reaction medium was determined by the Karl Fischer method.

Measurement of the Order of Self-association of DPU by the Cryoscopic Method. The order of the self-association of DPU in dioxane was measured by the cryoscopic method on solutions containing water ranging in concentration from 2×10^{-2} to 5×10^{-2}M.[3]

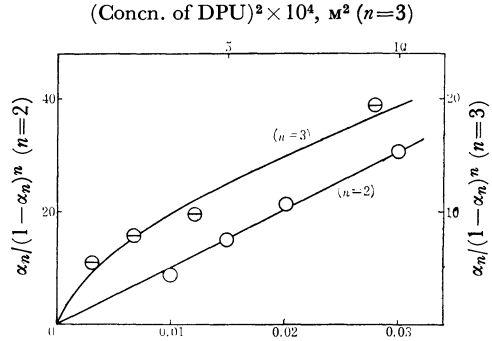

Fig. 1. Determination of the order of the self-association of DPU in dioxane.
Concn. of water: 0.02—0.05M

1) Y. Furuya, K. Itoho and H. Miyagi, This Bulletin, **42**, 2348 (1969).

2) Y. Furuya and K. Itoho, *Chem. & Ind.* (London), **1967**, 359.

It became evident that DPU existed in the dimer form, as is shown in Fig. 1.

However, DPU exists in the monomer form when the dioxane solution contains *n*-butylamine in the range from 1×10^{-2} to 5×10^{-2}M. Thus, the molecular weight of DPU gave the values of the monomer form, as is shown in Table 1.

Table 1. The values of the molecular weight of DPU in dioxane containing *n*-butylamine

Concn. of *n*-butylamine (M)	Molecular weight of DPU	
	Obsd*	Calcd
0.01	223.95	212.25
0.015	209.95	212.25
0.02	213.29	212.25
0.03	216.73	212.25

* They were obtained by cryoscopic method.

Results and Discussion

The reaction followed the second-order kinetics with DPU and H_2O. The plots of the observed second-order rate constant *vs.* the concentration of TED gave a straight line which does not pass through the point of origin, as is shown in Fig. 2.

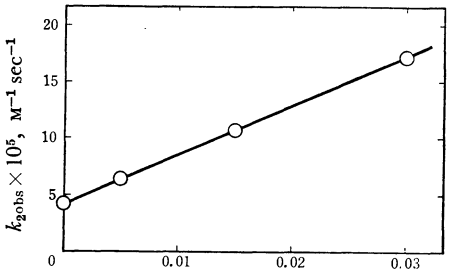

Initial concn. of TED, M

Fig. 2. The plots of k_{2obs} *vs.* the concentration of TED for the TED-catalyzed hydrolysis of DPU in dioxane at 90°C.
Initial concn. of DPU: 0.01M
Initial concn. of water: 0.02M

Therefore, the observed second-order rate constant is given by the following equation:

$$k_{2obs} = k_2'' + k_{3c}''[TED]. \quad (1)$$

The plots of k_2'' and k_{3c}'' *vs.* the concentration of DPU gave straight lines which have minus signs, as is shown in Figs. 3 and 4.

Thus, the rate constants, k_2'' and k_{3c}'', can be expressed by the following equations:

$$k_2'' = k_2' - k_{3u}'[DPU] \quad (2)$$

and

$$k_{3c}'' = k_{3c}' - k_{4cu}'[DPU]. \quad (3)$$

Moreover, k_2', k_{3u}', k_{3c}', and k_{4cu}' are variables for the concentration of water, as is illustrated in Figs. 5, 6, 7, and 8. Therefore, the following relationships are given:

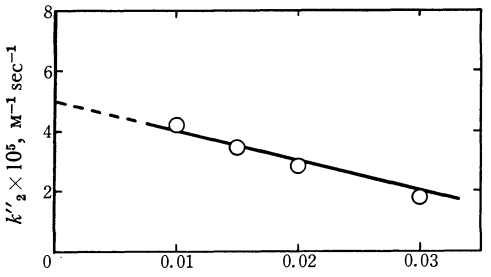

Initial concn. of DPU, M

Fig. 3. The plots of k_2'' *vs.* the concentration of DPU for the TED-catalyzed hydrolysis of DPU in dioxane at 90°C.
Initial Concn. of water: 0.02M

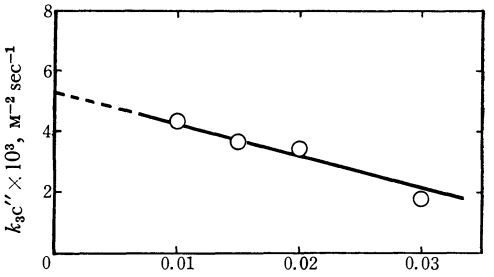

Initial concn. of DPU, M

Fig. 4. The plots of k_{3c}'' *vs.* the concentration of DPU for the TED-catalyzed hydrolysis of DPU in dioxane at 90°C.
Initial concn. of water: 0.02M

$$k_{2z}' = k_2 - k_{3h}[H_2O]$$
$$-k_{3u}' = -k_{3u} + k_{4uh}[H_2O]$$

and

$$k_{3c}' = k_{3c} - k_{4ch}[H_2O]$$
$$-k_{4cu}' = -k_{4cu} + k_{5cuh}[H_2O].$$

Consequently, the total kinetics may be given by the following equation:

$$v = \{k_2-k_{3h}[H_2O]\}[DPU][H_2O] + \{k_{4uh}[H_2O]-k_{3u}\}[DPU]^2[H_2O] + \{k_{3c}-k_{4ch}[H_2O]\}[TED][DPU][H_2O] + \{k_{5cuh}[H_2O]-k_{4cu}\}[TED][DPU]^2[H_2O] \quad (4)$$

The values of $k_2\times10^5M^{-1}$ sec^{-1}, $-k_{3h}\times10^3M^{-2}$ sec^{-1}, $k_{4uh}\times10^2M^{-3}$ sec^{-1}, $-k_{3u}\times10^3M^{-2}$ sec^{-1}, $k_{3c}\times10^3M^{-2}$

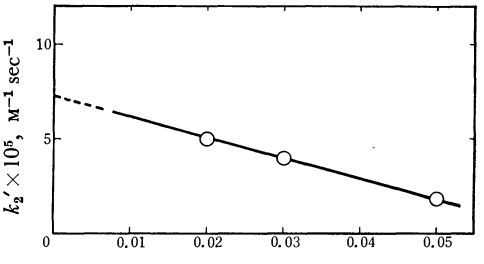

Concn. of H_2O, M

Fig. 5. The plots of k_2' *vs.* the concentration of water for the TED-catalyzed hydrolysis of DPU in dioxane at 90°C.

3) Cf. T. Tonomura, K. Okamoto, T. Fujishima and H. Yamamura, *Nippon Kagaku Zasshi*, **88**, 707 (1967).

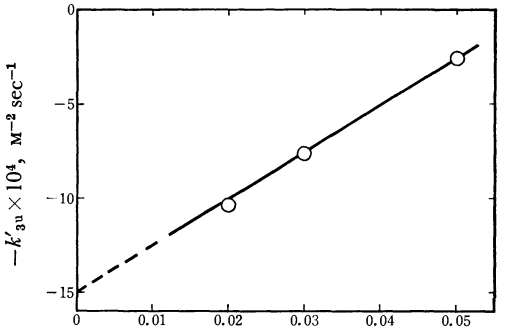

Fig. 6. The plots of $-k'_{3u}$ *vs.* the concentration of water for the TED-catalyzed hydrolysis of DPU in dioxane at 90°C.

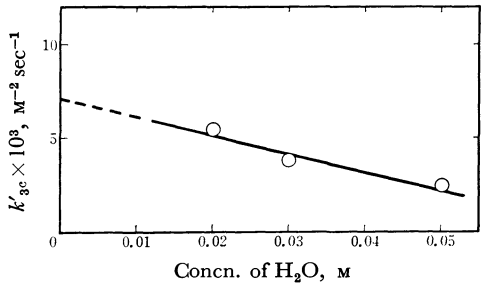

Fig. 7. The plots of k'_{3c} *vs.* the concentration of water for the TED-catalyzed hydrolysis of DPU in dioxane at 90°C.

sec^{-1}, $-k_{4ch} \times 10^2$M^{-3} sec^{-1}, k_{5cuh}M^{-4} sec^{-1}, and $-k_{4cu} \times 10^{-3}$ sec^{-1} were 7.28, −1.12, 2.49, −1.50, 7.10, −9.82, 2.39, and −1.54 respectively. The values of the rates of steps (5a) and (9) in non-catalyzed reactions and/or of steps (8c) and (10) in the TED-catalyzed hydrolyses are both comparable under these concentration conditions.

Here, four terms of both the non- and the TED-

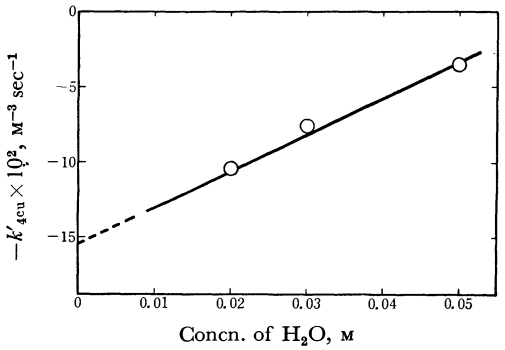

Fig. 8. The plots of $-k'_{4cu}$ *vs.* the concentration of water for the TED-catalyzed hydrolysis of DPU in dioxane at 90°C.

catalyzed hydrolyses of DPU contain the second-order terms with the concentration of DPU, though each term in the non- and the TED-catalyzed hydrolyses in the presence of *n*-butylamine contains only the first-order term with the concentration of DPU, as has been described in a previous paper.[1] The reasons for this are evident in view of the measurements of the order of the self-association of DPU in dioxanes containing water only and/or containing also *n*-butylamine, as has been described above.

As has been described in a previous paper,[1] the conductivity of the couple (DPU+TED) (10.87×10^{-6} Ω^{-1} cm^{-1}) is larger than the sum of the conductivities of the components (8.20×10^{-6} Ω^{-1} cm^{-1}); in that couple, the existence of quaternary ammonium salt was detected by Wagner's and Dragendorff's reagents.

From these findings, the following probable mechanism, one which involves a nucleophilic attack by the lone pairs of the N-atom of TED and the O-atom of water on the carbonyl C-atom of DPU, may be suggested:

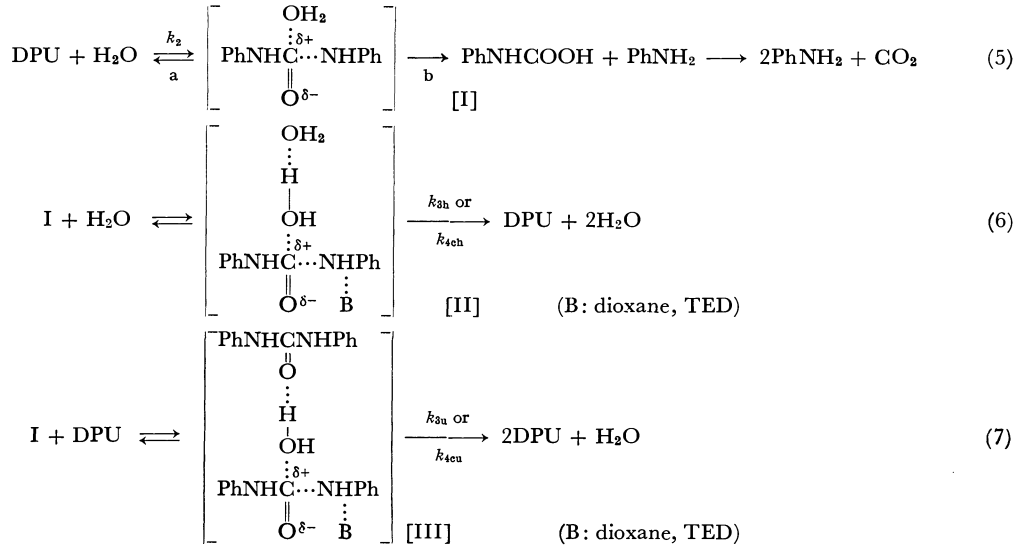

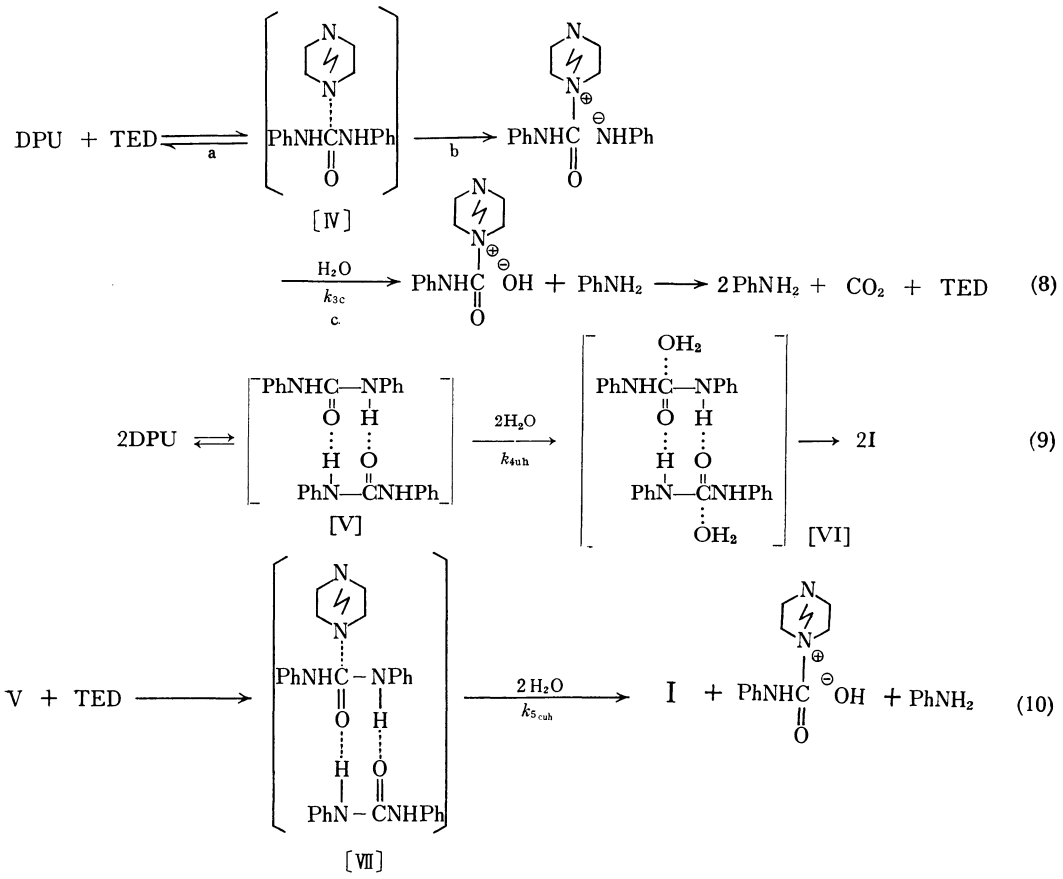

The authors are greateful to Meisei & Co., Ltd. for his gift of the material.

BULLETIN OF THE CHEMICAL SOCIETY OF JAPAN VOL. 43 3849—3852 (1970)

The Chemical Modification of Biopolymers. III. The Introduction of SH Groups into Taka-amylase A

Shuichi SUZUKI, Yutaka HACHIMORI and Ryuichi MATOBA

Research Laboratory of Resources Utilization, Tokyo Institute of Technology, Meguro-ku, Tokyo

(Received May 2, 1970)

The enzymic activity of Taka-amylase A on amylose, as measured by the blue-value method, increased to 180% of the original when one mole of mercaptosuccinyl group was introduced into one mole of the enzyme. Similar results were obtained for the activity measured by the Semogyi-Nelson method; the introduction of one or two mercaptosuccinyl groups raised the activity to 130—140% of that of the native enzyme. Even after the attachment of six mercaptosuccinyl groups per mole, the activity was 120% of the original. However, the enzymic activity was not elevated, but was lowered, by succinylation. When the sulfhydryl groups of the mercaptosuccinyl groups were blocked with *p*-chloromercurybenzoate or iodoacetamide, the enzyme was inhibited. These results suggest that the sulfhydryl groups of mercaptosuccinyl residues play an important role in increasing the enzymic activity.

Recently, Hartman and Wold[1] reported that the activity of bovine pancreatic Ribonuclease A (EC 2.7.7.16) treated with dimethyladipimidate was elevate to 160% of that of the natural material.

1) F. C. Hartman and F. Wold, *Biochemistry*, **6**, 2439 (1967).

Ikenaka[2] reported that phenylazobenzoyl-Taka-amylase had an activity on α-phenylmaltoside 2.5 times higher than that of the natural material, while its activity on amylose was diminished.

The introduction of sulfhydryl groups into proteins has been attempted by many investigators. Klotz[3] found that *S*-acetylmercaptosuccinic anhydride reacted selectively with free amino groups under mild conditions.

This paper will report on the preparation of mercaptosuccinyl Taka-amylase A (EC 3.2.1.1.) and their properties.

Experimental

Materials. The Taka-amylase A was prepared from Taka-diastase of the Sankyo Co., Ltd., by the method of Akabori *et al.*[4] The protein concentration was estimated by spectrophotometry, with an extinction coefficient, $E^{1\%}_{1cm}$, of 22.1 at 278.5 mμ,[5] or by the method of Lowry.[6] The *S*-acetylmercaptosuccinic anhydride was synthesized by adding thioacetic acid to maleic anhydride according to the method of Holmberg and Schjånberg,[7] it was recrystallized from benzene (melting point 76—77°C). The amylose was purchased from the Nagase Sangyo Co.

Preparation of the Modified Taka-amylase A. Mercaptosuccinyl and succinyl Taka-amylase were prepared as follows. One m*l* of a protein solution (3.6×10^{-4}M) was added to 6 m*l* of a 0.2M phosphate buffer, pH 8.0. One m*l* of *S*-acetylmercaptosuccinic anhydride or succinic anhydride (3.6×10^{-3}M to 1.8×10^{-1}M) in dioxane was then added to the buffered protein solution. After 30 min, 3 m*l* of a 0.33M hydroxylamine solution in a 0.2M phosphate buffer (pH 7.5) was added in order to remove the acetyl groups which blocked the sulfhydryl groups. The mixture was left to stand for 10 min at 20°C, and then dialyzed against distilled water for 24 hr at 20°C. The extent of mercaptosuccinylation was estimated by determining the sulfhydryl groups spectrophotometrically at 255 mμ by mercaptide formation using *p*-CMB, according to the method of Boyer.[8] The extent of succinylation was estimated by the decrease in the amino groups, using the method of Matsushima *et al.*[9]

Activity Measurement. The hydrolytic activity of the natural and modified Taka-amylase A was measured by the decrease in the absorbance at 700 mμ due to iodine-amylose complex formation (the blue-value method[10]) and by the increase in reducing groups (the Somogyi-Nelson method[11,12]). The digestion was conducted at 37°C for 30 min at pH 5.5.

Results and Discussion

Determination of mercaptosuccinyl Groups. *p*-Chloromercuribenzoate reacted with mercaptosuccinic acid stoichiometrically, the molar extinction coefficient of the product at 255 mμ was 5.8×10^3 at pH 4.6 in a 0.2M acetate buffer. The mercaptosuccinyl groups in protein were estimated by means of this coefficient after the *p*-chloromercuribenzoate had been reacted at 25°C for 24 hr.

The number of mercaptosuccinyl groups introduced per mole of the enzyme reached a constant value after 20 to 60 minutes' incubation (Fig. 1).

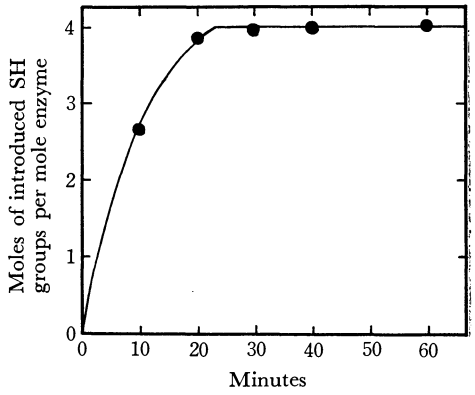

Fig. 1. The time course of mercaptosuccinylation reaction of Taka-amylase A at 2°C, in 0.15M phosphate buffer at pH 8.0.

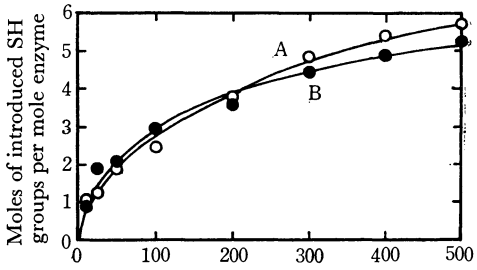

Fig. 2. The effect of concentration of *S*-acetylmercaptosuccinic anhydride on the extent of mercaptosuccinylation at 2°C (Curve B, closed circle) and 25°C (Curve A, open circle).

Figure 2 shows the effect of the concentration of *S*-acetylmercaptosuccinic anhydride on mercaptosuccinylation at 25°C and 2°C. The number of mercaptosuccinyl groups introduced into the enzyme increased in accordance with the increase in the

2) T. Ikenaka, *J. Biochem.*, **46**, 297 (1959).
3) I. M. Klotz and R. E. Heiney, *Arch. Biochem. Biophys.*, **96**, 605 (1962).
4) S. Akabori, R. Ikenaka and B. Hagihara, *J. Biochem.*, **41**, 577 (1954).
5) T. Takagi and H. Toda, *ibid.*, **52**, 16 (1962).
6) O. H. Lowry, N. J. Rosebrough, A. L. Farr and R. J. Randall, *J. Biol. Chem.*, **193**, 265 (1951).
7) B. Holmberg and E. Schjånberg, *Arkiv. Kemi. Mineral. Geol.*, **14A**, No. 7, 1 (1940).
8) P. D. Boyer, *J. Amer. Chem. Soc.*, **76**, 4331 (1954).
9) A. Matsushima, Y. Hachimori, Y. Inada and K. Shibata, *J. Biochem.*, **61**, 328 (1967).
10) H. Fuwa, *ibid.*, **41**, 583 (1954).
11) M. Somogyi, *J. Biol. Chem.*, **195**, 19 (1952).
12) N. Nelson, *ibid.*, **153**, 375 (1944).

Table 1. Folin test for *O*-succinylation of protein tyrosine[13]

The results are given in the ratio of optical densities (O.D.) at 750 mμ measured at pH 8.0 and at pH 11.0.

Moles introduced SH per mole enzyme	O.D. pH 8.0/O.D. pH 11.0		
	After 3h	24h	48h
8	0.98	0.95	0.95
4	0.98	0.96	0.99

concentration of *S*-acetylmercaptosuccinic anhydride, it was six when a 500-fold excess mole was applied.

O-Mercaptosuccinylation of Tyrosyl Residues. The extent of the acylation of tyrosyl residues in this enzyme was estimated by the Folin phenol reagent test.[13]

The buffered solutions of the modified enzyme with four and eight moles of mercaptosuccinyl groups per mole were adjusted to pH 8 and 11 respectively. After 3, 24, and 48 hrs incubation at 25°C, the Folin phenol reagent was added to the solutions and they measured for absorbancy at 750 mμ. The results are summarized in Table 1. It may be concluded that the *O*-esterification of the tyrosyl residues occurred to only a slight extent, if at all, during the mercaptosuccinylation reaction.

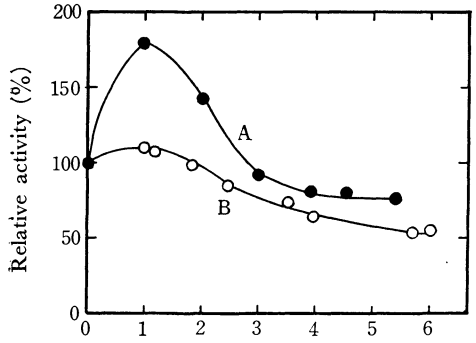

Fig. 3. The activities of native and modified Taka-amylase A on amylose measured by the blue value method. The modified enzymes mercaptosuccinylated at 2°C (Curve A, closed circle), and at 25°C (Curve B, open circle) were used.

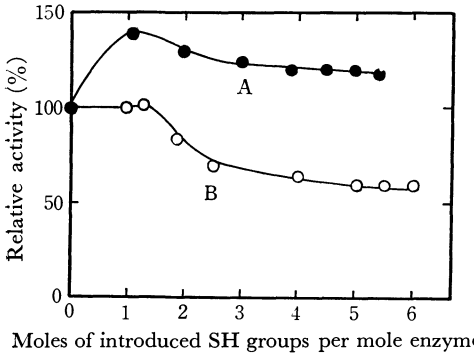

Fig. 4. The activities of native and modified Taka-amylase A on amylose measured by the Somogyi-Nelson method. The modified enzymes mercaptosuccinylated at 2°C (Curve A, closed circle) and at 25°C (Curve B, open circle) were used.

13) G. L. Miller, *ibid.*, **146**, 339 (1942).

Enzymic Activities of Mercaptosuccinyl Takaamylase A. The pH optimum of either the natural or the modified enzyme was around pH 5.5. The following experiments were, therefore, performed at this pH value. The results are shown in Figs. 3 and 4. When one mole of the mercaptosuccinyl group was introduced per mole of the enzyme at 2°C, the activity on amylose, measured by the blue-value method (Curve A in Fig. 3), increased to 180% of that of the natural material. The activities of the modified enzymes with more than three mercaptosuccinyl groups were, however, lower than that of the natural material. Similar results were obtained for the activity measured by the Somogyi-Nelson method (Curve A in Fig. 4); when one mercaptosuccinyl group was attached to the enzyme at 2°C, the activity was 140% of that of the natural

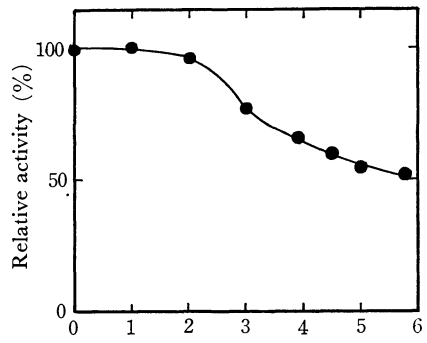

Fig. 5. The activities of native and succinyl Taka-amylase A on amylose measured by the Somogyi-Nelson method.

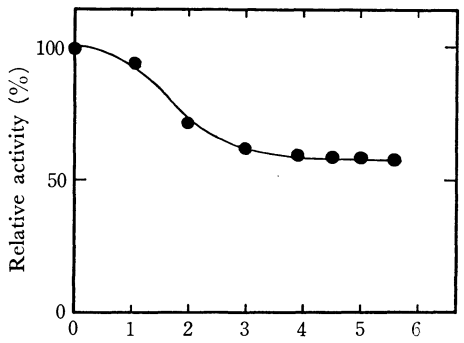

Fig. 6. The activities of native and succinyl Taka-amylase A on amylose measured by the blue value method.

material and 120% of the original activity was retained even after the attachement of six mercaptosuccinyl groups per mole of the enzyme. However, when the modification was made at 25°C, both activities of the modified enzymes decreased in proportion to the number of the mercaptosuccinyl residues introduced into the enzyme (Curves B in Figs. 3 and 4).

The difference between the activities of the modified enzymes prepared at 2°C and 25°C may be due to the difference in the mercaptosuccinylated sites.

Role of the Sulfhydyl Introduced into the Enzyme. The Activity of Succinyl Taka-amylase A. Succinyl Taka-amylase A was prepared has been described in the "Experimental" section, and its activity was compared with that of mercaptosuccinyl Taka-amylase A.

The optimum pH of the succinyl Taka-amylase A was the same as that of the natural enzyme. The activities of the modified enzymes prepared at 2°C were measured by the Somogyi-Nelson method and the blue-value method, and were then plotted against the numbers of succinyl groups introduced into the enzyme. These results are shown in Figs. 5 and 6. No enhancement of the activity was observed on succinylation by either method, in contrast to the case of mercaptosuccinylation.

Effect of the SH Reagents on the Activity of the Mercaptosuccinyl Taka-amylase A. One m*l* of iodoacetamide or *p*-CMB (1.44×10^{-7}M to 3.6×10^{-6}M) solution in a 0.2M phosphate buffer at pH 8.0 was added to 1m*l* of a natural or mercaptosuccinilated enzyme solution (7.2×10^{-9}M). After 4 hr, treatment at 25°C, the mixture was diluted and tested for the enzyme activity by the blue-value method at pH 5.5. The results are shown in Figs. 7 and 8.

The activity of the native enzyme on amylose was not affected by the addition of iodoacetamide (Curve B in Fig. 7), but that of the modified enzyme, which was elevated 1.8 times as compared with

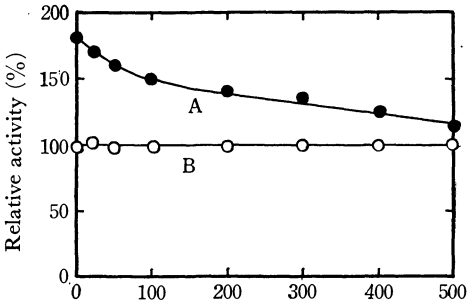

Fig. 7. The inhibition of native (Curve B, open circle) and modified Taka-amylase A (Curve A, closed circle) by iodoacetamide.

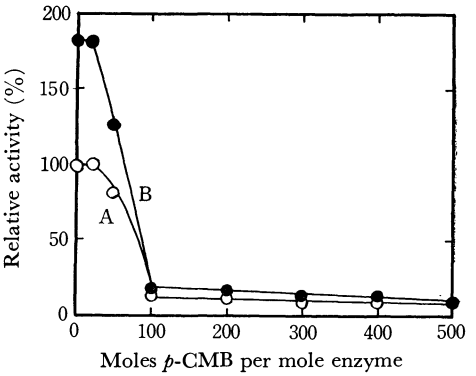

Fig. 8. The inhibition of native (Curve B, open circle) and modified Taka-amylaseA (Curve A, closed circle) by *p*-CMB.

that of the natural enzyme, was appreciably inhibited and approached that of the natural enzyme A in Fig. 7). On the contrary, *p*-CMB inhibited both modified and natural enzymes, as is shown in Fig. 8.

These results suggested that the sulfhydryl group of the mercaptosuccinyl residue plays an important role in the enhancement of the enzymic activity.

BULLETIN OF THE CHEMICAL SOCIETY OF JAPAN VOL. 43 3853—3857 (1970)

The Behaviour of the Copolymer of L-Proline and *O*-Benzyl-L-Tyrosine in a *n*-Propanol and Water System

Takayoshi Iio and Sho Takahashi*[1]

Department of Physics, Faculty of Science, Nagoya University, Chikusa-ku, Nagoya

and Shoyu Kobayashi

Institute of Molecular Biology, Faculty of Science, Nagoya University, Chikusa-ku, Nagoya

(Received May 4, 1970)

A copolymer consisting 95.8% of L-proline and 4.2% of *O*-benzyl-L-tyrosine was transformed in conformation from Form I to Form II as the propanol content changed from 100% to 74%. In Form I, the copolymer took a rod-like structure like that of poly-L-proline Form I, and the *O*-benzyl -L-tyrosyl residue moved independently of the molecular motion of the copolymer. On the other hand, the copolymer became flexible in Form II and the components associated with each other, forming an amorphous aggregation, when the propanol content decreased further, below the transition point. The hydrophobic interaction between the *O*-benzyl-L-tyrosyl side chain and the prolyl residue was the main factor which made the components of the copolymer associate with each other and form an amorphous aggregation. This was verified by a fluorescence study of the *O*-benzyl-L-tyrosyl residue.

Poly-L-proline exists in two forms, Form I and Form II, the structure of which have been elucidated by X-ray crystallography.[1-3] Form I forms, in the solid state, a right-handed helix with a translation of 1.90 Å and a rotation around the helix axis of 108° per proline residue, which the relationship between two successive C_α atoms around an amide bond is *cis*.[3] It has been shown by various investigators that Form I in solution maintains this structure and that its molecular shape is rod-like as a whole.[4] Form II possesses, in the solid state, a left-handed helical conformation with a translation of 3.12 Å and a rotation around the helix axis of 120° per proline residue, and the relationship between two successive C_α atoms around an amide bond is *trans*.[1,2] In solution, however, it has been shown that the polymer in Form II possesses a certain degree of flexibility.[4,5] The interconversion from Form I to Form II is induced by changing the solvent composition from unsubstituted aliphatic alcohol to aliphatic acid or water; this transformation is reversible.[5] The two conformations are very stable even when the temperature is changed.[5] On the other hand, *O*-benzyl-L-tyrosine is an amino acid forming α-helical polypeptide.[6]

We were interested in obtaining information about the states of fluorescent amino - acid side chains in polypeptides and proteins, and also about their secondary or higher structure, by a fluorescence study. One of the available methods was the method of fluorescence polarization measurements which was developed by Weber[7] and which has been applied to many proteins and polypeptides. For instance, Gill *et al.*[8] studied the helix-coil transition of polypeptide using this method. We planned to apply this method to the copolymer containing L-proline and *O*-benzyl-L-tyrosine. To avoid energy transfer between an excited chromophore and a non-excited one, which would complicate the analysis of fluorescence polarization, we used a sample with only a small amount of *O*-benzyl-L-tyrosine (4.2%). Since L-proline and *O*-benzyl-L-tyrosine were amino acids forming different polypeptide conformations, we first investigated the overall shape of the copolymer. In the course of our investigation we found a new fact, that the

*1 Present address: Institute for Chemical Research, Kyoto University, Uji-shi, Kyoto.

1) P. M. Cowan and S. McGavin, *Nature*, **176**, 1062 (1955).
2) V. Sasisekharan, *Acta Crystallogr.*, **12**, 897 (1959).
3) W. Traub and U. Shmueli, *Nature*, **198**, 1165 (1963).
4) E. Katchalski, A. Berger and J. Kurtz, "Aspects of Protein Structure," Academic Press, New York (1963), p. 205.
5) I. Z. Steinberg, W. F. Harrington, A. Berger, M. Sela and E. Katchalski, *J. Amer. Chem. Soc.*, **82**, 5263 (1960).
6) E. R. Blout, "Polyamino acids, Polypeptides, and Proteins," M. A. Stahmann Ed., Univ. Wisconsin Press (1962), p. 275.
7) G. Weber, *Biochem. J.*, **51**, 145 (1952).
8) T. J. Gill, III, and G. S. Omenn, *J. Amer. Chem. Soc.*, **87**, 4188 (1965).

components of the copolymer in Form II associated with each other and formed an amorphous aggregation. The hydrophobic interaction between the *O*-benzyl-L-tyrosyl side chain and the L-prolyl residue was the main factor which made the copolymer components associate with each other. This was verified by a fluorescence study of the *O*-benzyl-L-tyrosyl residue of the copolymer.

Experimental

The random copolymer of L-proline and *O*-benzyl-L-tyrosine was obtained by copolymerizing L-prolyl-*N*-carboxyanhydride (L-prolyl-NCA)[9] and *O*-benzyl-L-tyrosyl-NCA[9] in pyridine,[10] the molar ratio of L-prolyl-NCA to *O*-benzyl-L-tyrosyl-NCA being 21 : 1. The insoluble parts which appeared in the course of the polymerization were removed, and from the soluble parts the desired polymer was obtained by precipitation with ether. The precipitant was dissolved in acetic acid, and any insoluble parts which contained the *O*-benzyl-L-tyrosine rich polymer were removed. Then the polymer was reprecipitated with ether and dried under a vacuum. The molar ratio of the L-prolyl residue to the *O*-benzyl-L-tyrosyl residue of the copolymer was 22.6 : 1 (the molar content of *O*-benzyl-L-tyrosine was 4.2%). The average degree of polymerization, n, was determined as $n=72$ by the titration of the free carboxyl group with sodium methoxide in *n*-propanol, using a thymol blue indicator.

The vacuum-dried polymer was dissolved in *n*-propanol. The solution was then left overnight, and a portion was diluted by *n*-propanol and water to give a solution of the required solvent ratio. The final concentration was adjusted to 0.395 g/100 cc for solutions of various solvent ratios. These solutions were then used for measurements of the optical rotatory dispersion (ORD), the viscosity, the ultraviolet (UV) absorption, and the electric birefringence. The concentration of the solutions for the fluorescence measurements was 0.0152 g/100 cc.

The ORD was measured with a JASCO ORD/UV 5 apparatus made by the Japan Spectroscopic Co., Ltd., using a 1-cm cell; the UV absorption spectra with a Carl Zeiss spectrophotometer PMQ II, using a 1-cm cell, and the fluorescence spectra, with a Hitachi Fluorescence Spectrophotometer MPF-2A. The values of polarization,[11] p, were calculated at the 305-mμ emission peak of the *O*-benzyl-L-tyrosine fluorescence spectra with an excitation light of 282 mμ. The relative viscosities were measured in an Ostwald-type viscometer. The flowtime of the water at 25°C was 60 sec. The electric birefringence was measured using the optical method of O'Konski and Zimm[12] according to the usual procedure[13] at 20—23°C.

Results

Two weeks were necessary to obtain a constant value of specific rotation at 300 mμ and at room temperature. The equilibrium values thus obtained are shown in Fig. 1(a). After the equilibrium was

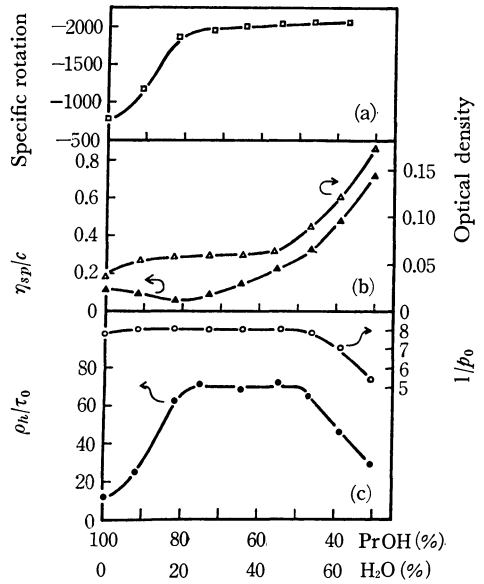

Fig. 1. Variations of specific rotation at 300 mμ (□), optical density at 500 mμ (△), η_{sp}/c (▲), $1/p_0$ (○) and ρ_h/τ_0 for $T/\eta_0=30000$ (●) with solvent composition.

attained, the specific rotation did not change even when the temperature was raised to 56°C. As may be seen in Fig. 1(a), a rapid change in the specific rotation from −615 to −1952 was observed in the range of the propanol content from 100 to 74%, and the rotation was almost unchanged below 74%. This behaviour shows that the copolymer is transformed in conformation from one to another as the solvent composition changes from 100% propanol to 74%. We here call the conformation in 100% propanol "Form I", and that in 74% or less propanol content, "Form II", following the studies of poly-L-proline.[4]

A positive electric birefringence was observed in the range from 100 to 83% of propanol, but it disappeared below 74%. In 100% propanol, a rotational relaxation time of 0.20 μsec was obtained at 20°C. It was suggested from the decay of the birefringence that the distribution of the molecular size was fairly narrow (see Fig. 2).[14]

On the other hand, the reduced viscosity, η_{sp}/c

9) J. Noguchi, "Polycondensation and Polyaddition Reaction" (in Japanese), Kyoritsu Shuppan, Tokyo (1952), p. 301.

10) R. Sakai, S. Ikeda and T. Isemura, This Bulletin, **39** 2308 (1966).

11) R. F. Chen, H. Edelhoch and R. T. Steiner, "Physical Principles and Techniques of Protein Chemistry," Part A, ed. by S. J. Leach, Academic Press, New York (1969), p. 171.

12) C. T. O'Konski and B. H. Zimm, *Science*, **111**, 113 (1950).

13) M. Taniguchi, S. Kobayashi and A. Yamaguchi, *Biochim. Biophys. Acta*, **188**, 140 (1969).

14) S. Kobayashi, *Biopolymers*, **6**, 1491 (1968).

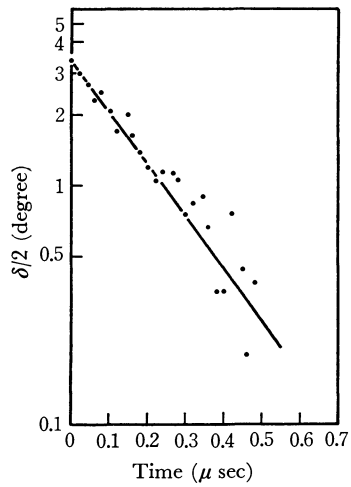

Fig. 2. Decay of electric birefringence of the copolymer in 100% propanol at 20°C.

(c=0.395 g/100 cc), in the same solvent system had its minimum at 83% propanol and rapidly increased below 50% propanol. The optical density at 500 mμ rapidly increased when the propanol content became less than 55% (Fig. 1(b)). Although we observed a small amount of precipitation in 30% propanol, we did not observe any precipitation above that.

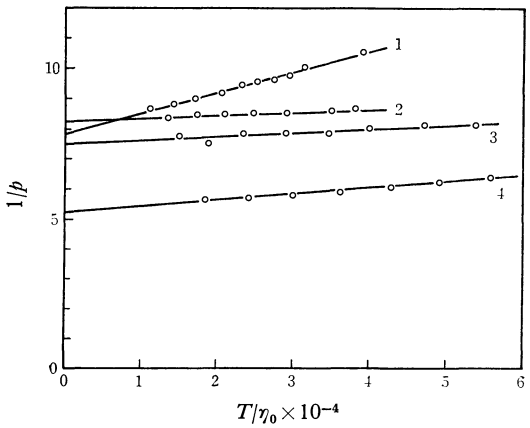

Fig. 3. Plots of reciprocal of polarization, $1/p$, against T/η_0 (degrees Kelvin per centipoise) for the copolymer in 100% propanol (1), 74% propanol (2), 38% propanol (3) and 30% propanol (4).

As may be seen in Fig. 3, linear plots of the reciprocal polarization, $1/p$, against T/η_0 were obtained, where p is the degree of the polarization of light emitted at a right angle to the direction of the excitation and where η_0 is the viscosity of the solvent. Therefore, we can calculate the value of ρ_h/τ_0 according to the Perrin equation:[15]

$$\left(\frac{1}{p}-\frac{1}{3}\right)=\left(\frac{1}{p_0}-\frac{1}{3}\right)\left(1+\frac{3\tau_0}{\rho_h}\right), \quad (1)$$

where τ_0 is the life time of the excited state of O-benzyl-L-tyrosine and where ρ_h is the harmonic mean of the two principal relaxation times of the rotation of the ellipsoidal molecule. The value of ρ_h/τ_0 increased at first as the propanol content decreased from 100% to 83%, stayed constant until 50%, and then decreased below a 50% propanol content (see Fig. 1(c)). The $1/p_0$ values stayed constant in the range from 100 to 50% of propanol, and then decreased below 50%.

Discussion

Assuming that the copolymer takes a rod-like structure in 100% propanol, we can obtain information about the molecular dimensions. We calculated the axial ratio, P, from the viscosity data alone, using the equation of Simha:[16]

$$[\eta]=\frac{\bar{v}\nu}{100} \quad (2)$$

where $\bar{v}$ is the partial specific volume and where ν is the well-known shape factor. We adopted the value of $\bar{v}$=0.758 cm³/g which was found for poly-L-proline.[17] An axial ratio of 8.5 was found for $[\eta]$=0.0868. The expected value of P, as calculated for the rod-like particle possessing the Traub and Shmueli configuration,[3] is 7.6 for n=72. The inconsistency of these two figures is reasonable, because the former assumes an ellipsoidal shape, and the latter, a rod-like one; therefore the value calculated by Eq. (2) may be expected to be larger than the latter.

On the other hand, we can calculate P from the rotational relaxation time, τ_{rot}, if the polymer length is known, by using the equation of Broersma:[18]

$$\frac{1}{6\tau_{rot}}=\frac{3kT}{8\pi\eta_0 a^3}\left[\ln 2P-1.57+7\left(\frac{1}{\ln 2P}-0.28\right)^2\right], \quad (3)$$

where η_0 is the viscosity of the solvent and where $2a$ is the polymer length. If we assume, based on n=72, a rod-like molecule with a length of 137 Å, Eq. (3) leads to P=7.8, which agrees well with the expected value of P=7.6. Therefore, it is confirmed that the copolymer in 100% propanol takes the same rod-like shape as poly-L-proline in Form I. This fact shows that the incorporation of a small amount of O-benzyl-L-tyrosine (4.2%) into poly-L-proline does not destroy the structure of Form I.

On the other hand, when the copolymer was transformed to Form II the electric birefringence disappeared. If the copolymer took a rod-like

15) F. Perrin, *J. Phys. Radium*, **7**, 390 (1926).

16) R. Simha, *J. Phys. Chem.*, **44**, 25 (1940).

17) P. M. Cowan and S. McGavin, *Nature*, **176**, 501 (1955).

18) S. Broersma, *J. Chem. Phys.*, **32**, 1626 (1960).

shape possessing the Cowan-McGavin configuration[1] (Form II), the electric birefringence should be observed beyond the transition point between Form I and II. Therefore, judging from the absence of the electric birefringence below 74% of propanol, the copolymer should be very flexible in this range. The reduced viscosity had a minimum value at 83% propanol, and increased rapidly below 50%. Even if the copolymer took the structure, Form II, of poly-L-proline, we could not expect a value of reduced viscosity larger than 0.24, judging from Simha's equation[16] and assuming a value of $P=14.4$. The value of the reduced viscosity should actually be smaller than this, since the copolymer chain is flexible rather than stiff and rod-like. Nevertheless, the observed values were larger than this value in the range of low propanol content. The optical density at 500 mμ, where the copolymer should not show any optical absorption, increased below 55%. All these observations suggest that, when the copolymer was transformed from Form I to Form II, the rod-like structure collapsed and the polymer chain became flexible, and that when the propanol content decreased further beyond the transition point between Form I and Form II, the flexible components of the polymer associated with each other, forming an amorphous aggregation which did not contribute to the electric birefringence.

Although poly-L-proline in Form II had a certain degree of flexibility,[4,19] its components have not been reported to associate with each other or to form an aggregation in water at room temperature. In higher temperatures (above 55°C), poly-L-proline in water takes a crystalline phase,[20] but in this discussion we can ignore this phase separation because all our experiments except for the fluorescence study were performed at room temperature, while the fluorescence study was performed using dilute solutions. Therefore, it is very interesting that the copolymer with only a small amount of *O*-benzyl-L-tyrosine (4.2%) became flexible and formed an amorphous aggregation which made solutions very viscous without causing any precipitation when transformed from Form I to Form II in these solvent systems.

It has been shown that the hydrophobic bond is one of the main factors which maintain the secondary or higher structure of polypeptides and proteins.[21] A hydrophobic interaction should exist between the benzyl or tyrosyl group and the prolyl residue. Although this interaction may be absent in 100% propanol, it may be a main factor in making the copolymer components associate with each other and form an amorphous aggregation in the range of low propanol content. This inference was verified by the following fluorescence study of the *O*-benzyl-L-tyrosyl residue.

From the value of ρ_h/τ_0, we can study the motion of the *O*-benzyl-L-tyrosyl residue.[22] For this purpose, it is necessary to know the value of τ_0, which is proportional to the quantum yield of the fluorescent molecule.[23] Since there were insufficient data about the lifetime of the *O*-benzyl-L-tyrosine, we adopted L-tyrosine as a reference. Therefore, it should be noted that the following calculation gives merely a rough estimation of the lifetime of the *O*-benzyl-L-tyrosyl residue in the copolymer. The ratio of the relative quantum yield of the *O*-benzyl-L-tyrosine of the copolymer in 100% propanol to that of L-tyrosine in water (pH 7.0) was obtained as 0.05. The lifetime of the excited state of L-tyrosine in water (pH 7.0) was 2.6 nsec.[24] From these values, $\tau_0=1.3\times10^{-10}$ sec was obtained for the *O*-benzyl-L-tyrosyl residue of the copolymer in 100% propanol, giving a value of $\rho_h=3.0\times10^{-9}$ sec at 20°C. On the other hand, the mean harmonic of the principal relaxation times of the ellipsoidal copolymer, whose volume and axial ratio were 3.48×10^{-20} cm^3 and 8.5 respectively, was 1.3×10^{-7} sec at 20°C in 100% propanol. This value is larger than ρ_h, so it may be concluded that the *O*-benzyl-L-tyrosyl residue moves independently of the molecular motion of the copolymer in Form I.

This fact showed that the hydrophobic interaction between *O*-benzyl-L-tyrosyl residue and prolyl residue did not exist in 100% propanol. It has been reported that alcohols break the hydrophobic bond.[25] In this case also, *n*-propanol might break the hydrophobic interaction between the *O*-benzyl-L-tyrosine side chain and the prolyl residue by covering the side chain with *n*-propanol; the aliphatic groups of *n*-propanol came in contact with the *O*-benzyl-L-tyrosine side chain, and the OH groups were arranged outside. Therefore, it was understandable why the intermolecular association was not observed and the *O*-benzyl-L-tyrosyl residue moved independently of the molecular motion of the copolymer in 100% propanol.

When the propanol content changed from 100% to 80%, the copolymer was transformed in conformation from Form I to Form II, and the ρ_h/τ_0 value increased according to the conformational change. The value was then almost unchanged

19) W. L. Mattice and L. Mandelkern, *Biochemistry*, **9**, 1049 (1970).
20) A. Ciferri and T. A. Orofino, *J. Phys. Chem.*, **70**, 3277 (1966).
21) G. Nemethy and H. A. Scheraga, *ibid.*, **66**, 1773 (1962).
22) G. Weber, *Advan. Protein Chem.*, **VIII**, 415 (1953).
23) J. R. Laurence, "Physical Methods in Macromolecular Chemistry," ed. by B. Carroll, Marcel Dekker, New York (1969), p. 275.
24) R. F. Chen, G. G. Vurek and N. Alexander, *Science*, **156**, 949 (1967).
25) a) R. F. Epand and H. A. Scheraga, *Biopolymers*, **6**, 1383 (1968). b) R. F. Epand and H. A. Scheraga, *ibid.*, **6**, 1551 (1968).

over the range from 80% to 50% propanol. We can calculate the ρ_h value by the same procedure as has been described above. In 80% propanol, $\tau_0=0.98\times10^{-10}$ sec and $\rho_h=1.4\times10^{-8}$ sec at 20°C. On the other hand, we have no equation for determining the rotational relaxation time, ρ, of a flexible polymer, so we here calculate the ρ value for a sphere with the same volume as the rod-like poly-L-proline Form II (Cowan-McGavin's configuration), with $n=72$, by means of this equation:

$$\rho = \frac{3\eta_0 v}{kT}$$

where v is the volume of the sphere. We obtain $\rho=8.4\times10^{-8}$ sec for the sphere in 80% propanol at 20°C.

This value is not very different from the ρ_h value. Therefore, it is sure that the hydrophobic interaction between the O-benzyl-L-tyrosine side chain and the prolyl residue begins to occur when the propanol content decreases beyond the transition point between Form I and Form II, and that then the motion of the O-benzyl-L-tyrosyl residue is suppressed. Although this hydrophobic interaction may exist between intramolecular residues, it may also exist between intermolecular residues. Judging from the behaviour of the reduced viscosity and the value of ρ_h/τ_0 beyond the transition point from Form I to Form II, it is reasonable to conclude that intermolecular hydrophobic interaction between the O-benzyl-L-tyrosine side chain and the prolyl residue is a main factor in making the components of the copolymer associate with each other and form an amorphous aggregation.

The suppression of the motion of the O-benzyl-L-tyrosine side chain by the hydrophobic interaction was observed more clearly in 100% water. The value of p in 100% water was much larger than that in the mixed solvents, and it increased as the temperature was raised to 45°C, as may be seen in Fig. 4. This increment can be explained

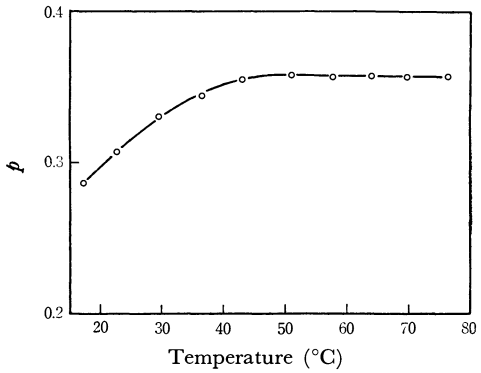

Fig. 4. Plot of polarization, p, against temperature for the copolymer in 100% water.

in terms of the general nature of the hydrophobic interaction.[21] Because of the positive ΔH value and the negative ΔF value, the hydrophobic interaction is more strengthened as the temperature is raised. The value of p decreased slowly above 45°C. This decrease may reveal a thermal rotational Brownian motion by a part of the polymer chain in which the side chain of the O-benzyl-L-tyrosine is fixed by the hydrophobic interaction.

In the propanol-content range from 50% to 30%, where the intermolecular associations became dominant and an amorphous aggregation is formed, the apparent decrease in ρ_h/τ_0 and $1/p_0$ was obvious. One possible interpretation was that the distance between the O-benzyl-L-tyrosyl residues was decreased because of the large amount of intermolecular associations and because energy transfer between the chromophores began to occur; this energy transfer might obviously decrease the value of ρ_h/τ_0.

The authors wish to thank Professor F. Oosawa and the members of his laboratory for their helpful advice and discussions in the course of this investigation. We also wish to thank Mr. M. Yura for his help in synthesizing the sample.

BULLETIN OF THE CHEMICAL SOCIETY OF JAPAN VOL. 43 3858—3861 (1970)

Hydrolysis of Dipeptides with Metal Oxides

Shinnichiro Suzuki and Ken-ichi Watanabe

Department of Chemistry, Faculty of Science, Tokyo Metropolitan University, Setagaya-ku, Tokyo

(Received May 14, 1970)

The hydrolysis of three dipeptides, Gly-Gly, Gly-L-Leu, and Gly-L-Phe, with metal oxide catalysts was studied. In most cases, the hydrolysis occurred in the pH range 5—6 accompanied by the formation of metal complexes of amino acids and dipeptides. Copper oxide, nickel oxide, cobalt oxide (III), and alumina have more catalytic activity than copper powder, cuprous oxide, commercial nickel oxide (II), and silica gel. Alumina and silica gel gave no metal complex. It is assumed that the hydrolysis proceeds by means of the formation of an active metal complex of dipeptide or by means of activation on the surface of the catalyst. The order of reactivity of the dipeptides was: Gly-Gly>Gly-L-Leu, Gly-L-Phe.

It has previously been reported[1] that 2-cyanopyridine and pyridine-2-carboxamide are easily hydrolyzed with nickel or copper oxide as a catalyst and that they afford chelate compounds of the acid with nickel or copper. This hydrolysis proceeds when they are refluxed in water without acid or alkali. On the other hand, 3 or 4-cyanopyridine is not hydrolyzed under the same reaction conditions. It is interesting to note that metal catalysts such as nickel or copper have no catalytic activity in this hydrolysis.

To develop this idea, thereupon, we attempted the hydrolysis of some dipeptides with metal oxides in the same manner. It has thus been found that the hydrolysis of dipeptides affords metal chelates of amino acids, along with metal complexes of the dipeptides. It is of interest that the hydrolysis of peptides thus takes place without acid or alkali. It has already been established that specific chelate catalysts,[2,3] an ion-exchange resin[4] or a copper (II) ion[5] can be effectively used for the hydrolysis. The reaction mechanism, especially in relation with metal ion catalyzed hydrolysis, will be discussed.

Results

Hydrolysis of Dipeptides with Metal Oxides. The dipeptides used were glycylglycine (Gly-Gly), glycyl-L-leucine (Gly-L-Leu), and glycyl-L-phenylalanine (Gly-L-Phe). The catalysts used were copper oxide, cuprous oxide, copper powder, nickel oxide-(A) (black), nickel oxide(B) (olive green, II), cobalt oxide (III), aluminum oxide (alumina), and silica gel. Copper powder, cuprous oxide, nickel oxide-(B), and silica gel showed very low activity for the hydrolysis of dipeptides. In general, hydrolysis started in the pH range 5—6. Soon after the reactions with copper oxide, nickel oxide(A), and cobalt oxide catalysts started, the reaction mixture colored, and the coloration was thereafter enhanced gradually. When copper powder, cuprous oxide, and nickel oxide(B) were used, the coloration was very slow. It is obvious that the dipeptides draw out the metal ions from the metal oxides and afford the water soluble metal complexes. The UV spectra of the reaction mixture after thirty minutes refluxing are shown in Table 1. As for the complex of Gly-Gly with copper, it is accordance with the data by Nakahara[6] (λ_{max} 643 mμ, logε=1.92).

Table 1. UV spectra of dipeptide complexes (after 30 min refluxing)

Dipeptide	Catalyst	Color	λ_{max} (mμ)
Gly-Gly	copper oxide	blue	643
Gly-Gly	nickel oxide(A)	light blue	376, 626, 1023
Gly-Gly	cobalt oxide	red violet	398, 519
Gly-Gly	alumina	no	—
Gly-Gly	silica gel	no	—
Gly-L-Leu	copper oxide	blue	638
Gly-L-Leu	nickel oxide(A)	light blue	380, 630, 1036
Gly-L-Leu	cobalt oxide	red violet	524
Gly-L-Phe	copper oxide	blue	641
Gly-L-Phe	nickel oxide(A)	light blue	377, 629, 1017

Spectrophotometer: Hitachi Recording Spectrophotometer EPS-3T

1) K. Sakai, T. Ito and K. Watanabe, This Bulletin, **40**, 1660 (1967).

2) A. Nakahara, K. Hamada, Y. Nakao and T. Higashiyama, *Coordin. Chem. Rev.*, **3**, 207 (1968).

3) D. A. Buckingham, J. P. Collman, D. A. R. Happer and L. G. Marzilli, *J. Amer. Chem. Soc.*, **89**, 1082 (1967).

4) J. R. Whitaker and F. E. Deatherage, *ibid.*, **77**, 3360 (1955).

5) I. J. Grant and R. W. Hay, *Aust. J. Chem.*, **18**, 1189 (1965).

6) A. Nakahara, This Bulletin, **32**, 1195 (1959); O. Yamaguchi, Y. Hirano, Y. Nakao and A. Nakahara, *Can. J. Chem.*, **47**, 3441 (1969).

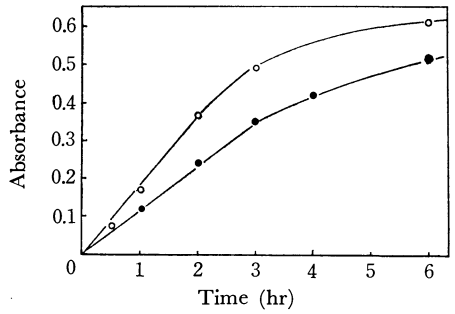

Fig. 1. Formation of dipeptide complexes: dipeptide 0.0023 mol, copper oxide 1.01 g, water 40 m*l*; ○ Gly-Gly, ● Gly-L-Leu. After the sample was diluted to five times with water, the absorbance was measured at 643 mμ for Gly-Gly and at 638 mμ for Gly-L-Leu.

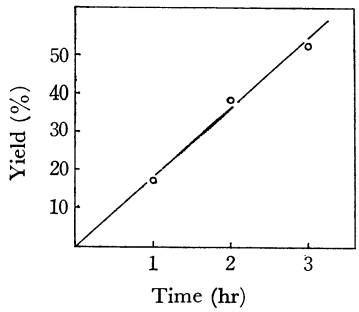

Fig. 2. The yield of Gly-Gly-Cu complex. The yield was calculated on the basis of UV spectrum of Gly-Gly-Cu complex prepared. The amount of glycine hydrolyzed at 3 hr was regarded as negligible.

In an earlier step of the reaction, the reaction solution was treated with ion-exchange resin (Dowex 50×2H type), in order to remove the metal ion, and was then analyzed by paper chromatography. The formation of complexes in the reaction with copper oxide is shown in Fig. 1 and Fig. 2. It is assumed that the formation of the Gly-Gly-Cu complex is *ca.* 50% after 3 hr reaction.

When the refluxing was continued longer than 3 hr, hydrolysis proceeded further in most cases. However, amino acids also formed complexes with metal ions, and usually no free acids were found in the reaction mixtures. The general profiles of the hydrolysis of three dipeptides with various catalysts are shown in Table 2. The pH values in the reactions are also shown in the table. On the whole, the hydrolysis proceeded in the pH range

Table 2. Hydrolysis of dipeptides with metal oxides
dipeptide, 0.0023 mol; water, 40 m*l*; catalyst, 1.0 g; temp, 100°C

Dipeptide	Catalyst	pH[a]		Gly, time (hr)[b]			
		S	E	1	3	9	21
Gly-Gly	copper powder	5.7	6.1	···	tr.	+	++
Gly-Gly	cuprous oxide	5.7	6.0	···	···	+	++
Gly-Gly	copper oxide	5.9	5.9	tr.	+	++	+++
Gly-Gly	nickel oxide(A)	6.0	7.9	+	++	+++	+++
Gly-Gly	nickel oxide(B)	5.9	6.9	···	···	tr.	+
Gly-Gly	silica gel	6.2	7.0	···	tr.	+	++
Gly-Gly	alumina	6.1	7.5	+	++	+++	+++
Gly-Gly	cobalt oxide	6.0	7.3	tr.	+	++	+++

Dipeptide	Catalyst	pH[a]		Gly, time (hr)				Leu, time (hr)			
		S	E	1	3	9	21	1	3	9	21
Gly-L-Leu	copper oxide	5.9	6.0	···	tr.	+	++	···	···	+	++
Gly-L-Leu	nickel oxide(A)	5.9	7.9	tr.	+	++	++	···	+	++	++
Gly-L-Leu	cobalt oxide	5.9	7.6	···	tr.	+	++	···	···	+	++
Gly-L-Leu	alumina	6.2	6.8	tr.	tr.	++	+++	···	···	++	+++

Dipeptide	Catalyst	pH[a]		Gly, time (hr)				Phe, time (hr)			
		S	E	1	3	9	21	1	3	9	21
Gly-L-Phe	copper oxide	5.7	5.8	···	tr.	+	++	···	···	···	+
Gly-L-Phe	nickel oxide(A)	6.0	7.9	···	+	++	++	···	···	+	++

a) pH: S=starting point, E=end point (21 hr refluxing)
b) The relative intensities of the spots on the chromatograms are represented thus: ···=no spot; tr.= trace, just visible; + to +++, increasing intensity of visible spots.
+: The amount of glycine was examined as 2—5% of the glycylglycine.

5—6 and the pH values increased more or less in the 21 hr reaction.

Since the hydrolysis of dipeptides hardly ever occurs without catalysts in this pH range,[5] it is evident that these metal oxides have a catalytic effect on the hydrolysis. It has been observed that the reactivity of the hydrolysis is dependent upon both the kinds of dipeptides and the kinds of catalysts, and that nickel oxide(A) turns a greenish gray and copper oxide turns brown in part, while the other metal oxides do not change color. Among the metal oxides, alumina is an especially active catalysts. In this case, free amino acid was obtained by the hydrolysis, but no aluminum complex of dipeptide was detected in the reaction mixture. The test was carried out with Gly-Gly (0.3 g) and alumina (1 g) in water (pH 6.3). After refluxing for 6 hr, the catalyst was filtered out and the filtrate was analyzed by the xylenol orange method.[7]

Hydrolysis of Dipeptide Complex. As has been mentioned above, it is apparent that both the formation of dipeptide complexes and the hydrolysis of dipeptides occur during the refluxing with the transition metal oxides. If the hydrolysis could proceed through the complex formation, it may be assumed that the sole dipeptide complex formed is hydrolyzed without catalysts and that it then affords the complexes of amino acids.

In order to examine this assumption, Gly-Gly was refluxed with copper oxide for 45 min, after which the catalyst was filtered out. It was then found by paper chromatography that no free glycine or glycine-Cu complex was present in the blue filtrate. On the other hand, the filtrate (pH 5.7, λ_{max} 643 mμ) was further refluxed and a few samples of it were taken out to be analyzed by paper chromatography. As is shown in Table 3, the hydrolysis of the Gly-Gly-Cu complex took place to give the glycine complex, and free glycine was detected in the solution refluxed for 21 hr. On the other hand, when the Gly-Gly-Cu complex[6] prepared beforehand was refluxed with water under about the same reaction conditions.*1 It gave about the same results (Table 3).

TABLE 3. HYDROLYSIS OF DIPEPTIDE CHELATE

	pH[a]		Gly, time (hr)			
	S	E	1	3	9	21
(1) filtrate	5.7	6.3	···	+	++	++
(2) Gly-Gly-Cu and Gly-Gly	5.6	5.6	···	+	++	—[b]

a) S=starting point, E=end point: (1) 21 hr, (2) 9 hr refluxing
b) not measured

7) J. Dvorak and E. Nyvltova, *Mikrochim. Acta*, **1966**, 1082.

*1 Gly-Gly-Cu, 0.0042 g; Gly-Gly, 0.20 g; H_2O, 40 m*l*.

Discussion

As was expected, copper oxide, nickel oxide(A)*2, and cobalt oxide are effective for the hydrolysis of the peptide bond as well as for the specific hydrolysis of 2-cyanopyridine. These transition metal oxides form metal complexes with dipeptides. As a result of our studies, two routes might be proposed for this hydrolysis:

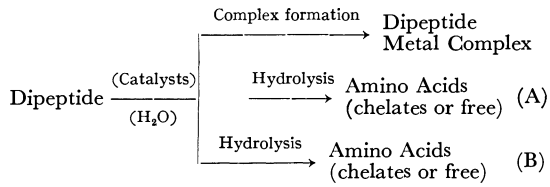

Route A is a mechanism in which metal complexes participate in the hydrolysis of peptides as the ligands; it is supported by the results of the experiment without heterogeneous catalysts (Table 3). In this mechanism, the metal oxides serve only as donors of metal ions to form complexes with dipeptides. As for the hydrolysis shown in Table 3, the concentration of the Gly-Gly-Cu complex is very low; therefore, the reaction velocity may be very slow in comparison with the hydrolysis in the presence of metal oxides. Grant[5] reported the hydrolysis of Gly-Gly with the Cu^{2+} ion in the pH range 3.5—6.0, in which Cu-Gly-Gly^+ type of active complex was assumed to participate in the reaction. In the case of our studies, it is also presumed that an analogous type of species might participate in the hydrolysis of Route A.

Route B is a mechanism which is regarded as a heterogeneous catalytic reaction on the solid surface. It is assumed that the amide bond of dipeptide is activated by the adsorption on the catalysts and that the nucleophilic attack of water may occur. Amino acids, the hydrolysis products, then may draw out the metal ions from the catalysts to form the chelates. When alumina or silica gel was used as the catalyst, free amino acids were obtained without forming any chelate. This is also evidence of direct catalytic hydrolysis. When copper powder, cuprous oxide, or nickel oxide(B) was used as the catalyst, the formation of metal complexes with dipeptides was extremely slow, and the hydrolysis proceeded very slowly, too. Route B might also be possible in the case of hydrolysis with transition metal oxides. It can be inferred, however, that the main route is A rather than B in the reactions with copper oxide, nickel oxide(A), and cobalt oxide.

As is shown in Table 2, the reactivity of dipeptide is in the order: Gly-Gly>Gly-L-Leu, Gly-L-Phe.

*2 In our previous paper,[1] NiO in Tables 1 and 2 should be corrected to nickel oxide (black), which is mentioned as nickel oxide(A) in the present paper.

The relatively low reactivity of Gly-L-Leu and Gly-L-Phe may be due to the steric effect of bulky groups in the α-position of the carboxyl group. This effect has also been pointed out in the case of hydrolysis with acid[8] or ion-exchange resin.[4]

Experimental

Materials. The glycylglycine, glycyl-L-leucine, and glycyl-L-phenylalanine were obtained from the Institute for Protein Research, Osaka University. They were examined by paper chromatography and were proved to be free from extraneous ninhydrin-reacting materials. Commercial copper powder, copper oxide (II), nickel oxide (II) (olive green, called nickel oxide(B) in this paper), cobalt oxide (III), alumina (Aluminum Oxide Woelm Neutral, Germany), and silica gel (300 mesh) were washed with distilled water and were then used as catalysts. The nickel oxide(A) (black) was prepared by the careful decomposition of nickel carbonate at 250—300°C and was then washed with ditstilled water. The cuprous oxide was prepared by the controlled reduction of a complex of copper sulfate and Rochelle salt with glucose.

The Hydrolysis of Dipeptides. 0.0023 mol of dipeptide and 1.0 g of a catalyst were refluxed in 40 m*l* of water. During the refluxing, 0.8 m*l* samples of the reaction mixture were taken out after 1, 3, 9 and 21 hr. Each fraction was filtered to remove a small amount of suspended catalysts, after which filtrate was treated with ion-exchange resin (Dowex 50×2H type) in a column (1 cm in diameter). Then, 1.4% ammonia solution as the eluent was passed through the column. Thus, metal ions were removed from the complexes and a solution containing free amino acid and dipeptide was obtained as the eluent. This was then evaporated *in vacuo* to *ca.* 0.3 m*l* for the analysis. In some cases, the cobalt ions of the complexes were precipitated as sulfide with hydrogen sulfide; the filtrate was then also treated as has been described above. In these processes, no hydrolysis of dipeptides took place.

Analysis of Amino Acids and Dipeptides. The analyses of hydrolyzed amino acids and of unchanged dipeptides were carried out by paper chromatography. Toyo filter paper No. 51 and *n*-butanol - ethanol - water (5 : 5 : 3) as the eluent were used. About a 5-μ*l* portion of the sample solution was spotted, and the chromatograms were run for from 12 to 24 hr. Amino acids and dipeptides were developed with a ninhydrin solution and by warming in an air oven at 95°C for 5 min. The results of the analysis (R_f value and coloration) are shown below.

	Gly-Gly	Gly	Gly-L-Leu	Leu	Gly-L-Phe	Phe
R_f	0.07	0.14	0.33	0.54	0.34	0.48
Color	Yellow	Violet	Yellow	Pink	Yellow	Pink

The authors wish to express their thanks to Professor Kazuo Hata and Professor Michio Kobayashi for their kind advice.

8) L. Lawrence and W. J. Moore, *J. Amer. Chem. Soc.*, **73**, 3973 (1951).

BULLETIN OF THE CHEMICAL SOCIETY OF JAPAN VOL. 43 3861—3865 (1970)

Polyamino-Zucker. V.[1,2] Modellreaktionen zur Aminierung cyclischer Nitrodiole

Toshio NAKAGAWA,*† Tohru SAKAKIBARA* und Frieder W. LICHTENTHALER**

* *Department of Chemistry, Tokyo Institute of Technology, Ō-okayama, Meguro-ku, Tokyo*

** *Institut für Organische Chemie, Technische Hochschule Darmstadt, 61 Darmstadt, B.R.D.*

(Eingegangen am 13. Mai, 1970)

On treatment of 1r,3c-diacetoxy-2t-nitrocyclohexane (**3**) or its 1,3-dimesyloxy analogue **4** with primary amines or ammonia, nitrodiamines (**5**—**11**) are obtained *via* an elimination-addition mechanism. Similar aminations of 1r-methyl-1-nitrocyclohexane-2c,6c-diol (**15**) or its di-*O*-acetate **16** give *C*-methyl branched nitrodiamines (**12**—**14**), which are also formed by reaction of glutaraldehyde with nitromethane and amines. Structures and conformations of the products obtained were deduced from IR and NMR data.

Glutardialdehyd und *cis*-1,3-Dioxolan-2,4-dialdehyd lassen sich mit Nitromethan und Benzylamin in 60 bzw. 53% Ausbeute zu Nitro-bisbenzylamino-Verbindungen cyclisieren, deren Hydrierung auf einfache Weise vicinale Triamine wie 1,2,3-Triaminocyclohexan und 2,3,4-Triaminoidosan zugäng-

*† Dem Andenken von Prof. Dr. Tetsuo Sato gewidmet.

lich macht[3–5]). Die Dialdehyd-Komponente dieser im Sinne einer Bisaminoalkylierung von Nitromethan verlaufenden Cyclisierungsreaktion ist jedoch nicht beliebig variierbar. *o*-Phthaldialdehyd, sowie die aus α- bzw. β-Methyl-D-glucosid und Uridin bzw. Glucosyl-theophyllin durch Perjodoxidation entstehenden Dialdehyde liefern bei analogen Umsetzungen komplexe Gemische, in denen sich dünnschicht chromatographisch bis zu acht Produkte nachweisen lassen. Ähnliche Schwierigkeiten werden bei stufenweiser Durchführung dieser Reaktion, d.h. bei Umsetzung der diesen Dialdehyden entsprechenden Nitromethan-Cyclisierungs produkte[6]) mit Benzylamin oder Ammoniak beobachtet.

Nur im Falle des 2t-Nitrocyclohexan-1r, 3c-diols (**1**)[7]) läßt sich bislang eine zweifache Aminierung glatt vollziehen; mit stark basischen primären oder sekundären Aminen entstehen Nitrodiamine des Types **2** in Ausbeuten über 70%.[3]) Mechanistisch läßt sich der Übergang **1**→**2** einerseits durch basenkatalysierte Ringöffnung im Sinne einer "Retro-Nitromethan-Addition" und anschließender Recyclisierung der aus Aldehyd und Amin gebildete Aminale interpretieren. Da jedoch das Nitromethin-Proton gegenüber dem der OH-Gruppe acider ist, erscheint ein Eliminierungs-Additions-Mechanismus, der hier zweimal, d.h. nach beiden Seiten hin, durchlaufen wird, wahrscheinlicher,[8]) in dem der geschwindigkeitsbestimmende Schritt die Eliminierung der OH-Gruppen sein dürfte. Ihre Überführung in bessere Abgangsgruppen, durch Acylierung oder Sulfonierung erreichbar, sollte unter schonenderen Bedingungen und möglicherweise einheitlicher zu den im Hinblick auf die Synthese von Polyamino-zuckern und -cycliten erwünschten Nitrodiaminen führen—im Hinblick auf die glatt verlaufenden Aminierungen von β-Acetoxy-nitro-Verbindungen mit aromatischen Aminen[11,12]) und mit Ammoniak[11,13–17]) nicht ohne Analogie.

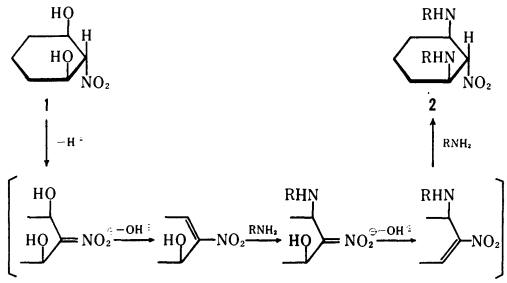

Aus diesen Überlegungen heraus wurden Modellversuche zur Diaminierung von 1r, 3c-Diacetoxy-2t-nitrocyclohexan (**3**) und des 1,3-Dimesyloxy-Derivates (**4**) unternommen, über die wir im folgenden berichten. Sie bildeten die Grundlage zu den inzwischen bereits durchgeführten Synthesen von Triaminoinositen[18,19]), Triaminozuckern[19–21]) und Triaminozucker-Nucleosiden.[22])

Ergebnisse und Diskussion

1. Darstellung cyclischer Nitrodiamine. Während die Umsetzung des Nitrodiols (**1**) mit Anilin nur durch Zusatz von Alkali erreicht werden kann und zu einem Gemisch führt, aus dem das *all-trans*-Isomere(**5**) in mäßiger Ausbeute (16%)

1) Als Mitteilung I—III werden Lit. 3—5 betrachtet;

2) IV. Mitteilung: T. Nakagawa, T. Sakakibara und S. Kumazawa, *Tetrahedron Lett.*, **1970**, 1645.

3) F. W. Lichtenthaler, T. Nakagawa und A. El-Scherbiney, *Angew. Chem.*, **79**, 530 (1967); *Angew. Chem., Int. Ed. Engl.*, **6**, 568 (1967).

4) F. W. Lichtenthaler, T. Nakagawa und A. El-Scherbiney, *Chem. Ber.*, **101**, 1837 (1968).

5) F. W. Lichtenthaler und T. Nakagawa, *ibid.*, **101**, 1846 (1968).

6) F. W. Lichtenthaler, *Angew. Chem.*, **76**, 84 (1964); *Angew. Chem. Int. Ed. Engl.*, **3**, 211 (1964); "Newer Methods of Preparative Organic Chemistry," **4**, 155 (1968); H. H. Baer, *Advan. Carbohyd. Chem.*, **24**, 67 (1969).

7) Zur r.c.t-Notation *vgl.* Rules for IUPAC Notation for Organic Compounds, S. 75, London 1961, sowie Beilsteins Handbuch der Organischen Chemie, Bd. V, 1 (3. Erg.-Werk), S. XXXV und L—LII.

8) Nach einem ähnlichen Eliminierungs-Additions-Mechanismus verlaufen die durch Alkali ausgelösten Epimerisierungen von Nitroinositen[9]) und Nitrozuckern.[10])

9) F. W. Lichtenthaler, *Chem. Ber.*, **94**, 3071 (1961); F. W. Lichtenthaler und H. O. L. Fischer, *J. Amer. Chem. Soc.*, **83**, 2005 (1961).

10) H. H. Baer und F. Kienzle, *Ann. Chem.*, **659**, 192 (1966).

11) F. D. Chattaway, *J. Chem. Soc.*, **1936**, 355.

12) R. L. Heath und J. D. Rose, *ibid.*, **1947**, 1486.

13) H. Irving, *ibid.*, **1936**, 797; H. Irving und H. I. Fuller, *ibid.*, **1948**, 1989.

14) C. A. Grob und W. v. Tscharner, *Helv. Chim. Acta*, **33**, 1070 (1950); C. A. Grob und F. Reber, *ibid.*, **33**, 1776 (1950); C. A. Grob und F. v. Sprecher, *ibid.*, **35**, 885, 902 (1952); C. A. Grob, C. Wagner und P. Zoller, *ibid.*, **38**, 1689 (1955).

15) C. A. Grob und K. Camenisch, *ibid.*, **36**, 37 (1953).

16) C. Satoh und A. Kiyomoto, *Chem. Pharm. Bull.* (Tokyo), **12**, 615 (1964); *Carbohyd. Res.*, **7**, 138 (1968).

17) H. H. Baer und T. Neilson, *J. Org. Chem.*, **32**, 1068 (1967).

18) F. W. Lichtenthaler und P. Voss, *Tetrahedron Lett.*, **1969**, 2297.

19) F. W. Lichtenthaler, P. Voss und N. Majer, *Angew. Chem.*, **81**, 221 (1969); *Angew. Chem. Int. Ed. Engl.*, **8**, 211 (1969).

20) T. Nakagawa, Y. Sato, T. Takamoto, F. W. Lichtenthaler und N. Majer, Dieses Bulletin, **43**, 3866 (1970).

21) H. H. Baer und F. Rajabalee, *Carbohyd. Res.*, **12**, 231 (1970).

22) F. W. Lichtenthaler, G. Trummlitz und H. Zinke, *Tetrahedron Lett.*, **1969**, 1213.

abtrennbar ist,[3] reicht zur Diaminierung des Nitrodiacetates(**3**) die Basizität des Anilins aus. Im entstehenden Isomerengemisch ist **5** jedoch nur in Spuren nachweisbar;[23] es besteht zu etwa gleichen Teilen aus dem *chiro*- (**10**) bzw. *cis*-Isomeren (**11**), die durch fraktionierte Kristallisation getrennt werden können. Damit sind nunmehr alle der theoretisch möglichen Isomere zugänglich.

Unter sehr milden Bedingungen (2 Stdn., 25°C in Chloroform) verlaufen auch die Umsetzungen von **3** oder **4** mit Benzylamin bzw. Cyclohexylamin. Die entsprechenden Nitrodiamine, **6** bzw. **7** entstehen, wie die Ausbeuten(<70%) zeigen, mit hoher Stereoselektivität.

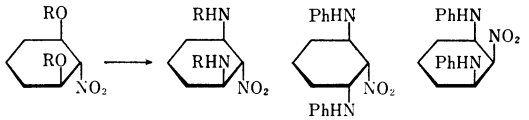

3 R=Ac
4 R=Ms

5 R=Ph
6 R=$PhCH_2$
7 R=C_6H_{11}
8 R=H
9 R=Ac

10 **11**

Auch Ammoniak läßt sich als Amin-Komponente einsetzen. So wird **3** sowohl durch Behandeln mit flüssigem Ammoniak, oder unter Bedingungen, wie sie bereits zur Aminierung von β-Acetoxy-nitro-Verbindungen herangezogen wurden—NH_3 in Dioxan,[14,15] Methanol[16] oder Tetrahydrofuran[17]—glatt in das entsprechende Nitrodiamin (**8**) übergeführt, das auf Grund seiner Instabilität[24] zweckmäßigerweise *N*-acetyliert wird. Die Ausbeuten an 1r, 3c-Diacetamino-2t-nitrocyclohexan (**9**) liegen am günstigsten bei Verwendung von Tetrahydrofuran (70%)[25] und wäßrigem Dioxan(74%).

2. Konfigurationsermittlung. Die *all-trans*-Konfiguration (1r,2t,3c)[7] der Verbindungen **5**—**9** geht in eindeutiger Weise aus dem Aufspalutungsmodus des für H^2(CH–NO_2) in $CDCl_3$ erhaltenen Signals hervor. Es wird allen Fällen als ein 1 : 2 : 1-Triplett erhalten—dies beweist bereits die sterische Identität der beiden benachbarten Protonen—mit einer Kopplungskonstante von $J_{1,2}=J_{2,3}\sim 10$ Hz, was die jeweils axiale Orientierung der Ringprotonen an C-1 bis C-3 indiziert.

Entsprechend lassen sich die Konformationen für **10** und **11** bestimmen. Das *cis*-Isomere (**11**) zeigt bei 4.58 τ ein 1.5 Hz-Triplett, das gegenüber dem für **5** erhaltenen (*vgl.* Tabelle) um 1.1 ppm nach niedrigerem Feld verschoben ist, und folglich[26] auf das Vorliegen eines äquatorialen H^2, bzw. einer axialen Nitrogruppe in **11** hinweist. Die für das Nitromethin-Proton in **10** beobachtete Aufspaltung von 2 und 6 Hz ließe sich auf Grund der für eine *Jaa*-Kopplung in Konformation **10a** zu kleinen Werte (z.B. 10 Hz in **5**) mit einer *a,e,e*-Anordnung der Ringwasserstoffe H^1–H^3(**10b**) in Einklang bringen; die chemische Verschiebung des Signals (5.08 τ), die in der Mitte zwischen den für **5** und **11** erhaltenen liegt (*vgl.* Tabelle) weist jedoch eher auf einen schnellen Übergang der beiden Alternativ-Konformationen **10a**⇌**10b** hin.

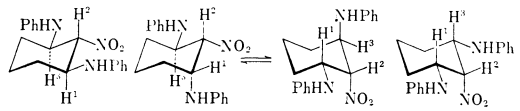

5 **10a** **10b** **11**

Bemerkenswert sind die Unterschiede, die diese Nitrodiamine in der Lage der NH-Valenzschwingung im Kristall(KBr) aufweisen. Sie wird bei den *trans*-Verbindungen **5**—**7** um 3340 cm^{-1} erhalten, ist bei dem *cis*-Isomeren (**11**) nach höheren Frequenzen (3400 cm^{-1}) verschoben, während bei chiraler Anordung der Substituenten (**10**) beide Banden (*vgl.* Tabelle) auftreten. Diese Abhängigkeit der NH-Streckfrequenz im Kristall von der molekularen Geometrie ist auf intermolekulare Wasserstoffbrückenbindungen zurückzuführen, da diese Unterschiede in Lösung (0.013—0.06 molar, in Chloroform, *vgl.* Tabelle) nicht beobachtet werden. Inwieweit diese Befunde generell zur Konfigurationsermittlung cyclischer Nitrodiamine herangezogen werden können, muß weiteren Untersuchungen vorbehalten bleiben.

Tabelle 1. NMR ($CDCl_3$)- und IR-Daten der isomeren 1,3-Dianilino-2-nitrocyclohexane

Verbindungen (Konfig.)	Lage (τ) und Aufsplatung für H^2(Hz)	NH-Absorptionsbande(cm^{-1})		
		KBr	in $CHCl_3$ 20 mg/ccm	in $CHCl_3$ 4 mg/ccm
5 (*all-trans*)	5.68 *t*(10)	3340	3410	3405
10 (*chiro*)	5.08 *q*(2 und 6)	3340 3410	3430	3420
11 (*all-cis*)	4.58 *t*(1.5)	3400	3425	3420

3. *C*-Methyl-verzweigte Nitrodiamine. Analog zur cyclisierenden Bisaminoalkylierung von Nitromethan[3] lassen sich bei Verwendung von Nitroäthan als Methylenkomponente *C*-Methyl-

23) Dünnschichtchromatographie auf Wako-Gel B5 (*Wako Pure Chemical Industries, Ltd., Japan*), mit Tetrachlorkohlenstoff-Äthylacetat (5 : 1) als Laufmittel; Sichtbarmachung durch Joddampf.

24) Zur Deutung der Instabilitat freien Nitramine und ihrer Salz *vgl.* Lt. 25.

25) H. H. Baer und M. C. T. Wang, *Can. J. Chem.*, **46**, 2793 (1968).

26) L. M. Jackman und S. Sternhell, "Applications of NMR-Spectroscopy in Organic Chemistry," 2. Auflg., S. 238 ff., Pergamon Press, London, 1969.

verzweigte Nitrodiamine darstellen. So liefert die Umsetzung von Glutardialdehyd mit Nitroäthan und Benzylamin im Molverhältnis 1 : 2 : 4 1r-Methyl-1-nitro-2c,6c-bisbenzylaminocyclohexan(**12**) in 56% Ausbeute, mit sekundären Aminen wie Piperidin und Morpholin entsprechend die Nitrodiamine **13** und **14**.

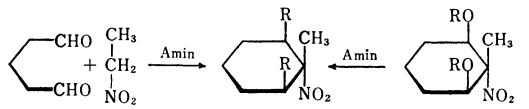

12 R = $PhCH_2NH$ **15** R = H

13 R = 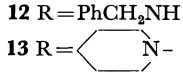 **16** R = Ac

14 R = 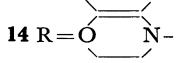

Dieselben Produkte lassen sich aber auch—und in besseren Ausbeuten—durch Umsetzung des Glutardialdehyd-Nitroäthan-Cyclisierungsproduktes **15** oder dessen Di-*O*-acetats (**16**) mit den entsprechenden Aminen gewinnen. Dieser Verlauf überrascht insofern, als diese Reaktionen nicht über einen Eliminierungs-Additions-Mechanismus, wie er für die Diaminierungen von **1**, **3** und **4** formuliert wurde, ablaufen können. In Ermangelung eines Nitromethin-Protons im Nitrodiol **15**—**16** wird unter den Reaktionsbedingungen primär ent-*O*-acetyliert dürfte hier durch die Base ein OH-Proton abstrahiert weden, wodurch Ringöffnung im Sinne einer "Retro-Nitroäthan-Cyclisierung" eintreten kann mit nachfolgender Recyclisierung der aus Aldehyd und Amin gebildeten Zwischenprodukte.

Beschreibung der Versuche

Die Schmelzpunkte wurden in Kapillarröhrchen bestimmt und sind nicht korrigiert. Die IR-Spektren wurden mit einem Hitachi-Perkin-Elmer 225 Gerät, die NMR-Spektren mit dem Jeolco 100 MHz-Gerät aufgenommen (in ppm, τ-Skala).

1r,3c-Dimesyloxy-2t-nitrocyclohexan (**4**). Zu 4.2 g (26 mMol) 2t-Nitrocyclohexandiol-(1r,3c) (**1**)[3,27] in 50 m*l* Toluol wurde unter Eiskühlung und Rühren ein Gemisch von 6.5 g (57 mMol) Methansulfochlorid und 4.5 m*l* Pyridin in 20 m*l* Benzol zugetropft und danach 5 Stdn. gerührt. Nach Abdampfen des Lösungsmittels i. Vak. und Versetzen des Rückstandes mit Wasser wurde der gebildete Niederschlag abgesaugt und aus Methanol umkristallisiert: 650 mg (8%) farblose Nadeln vom Schmp. 166—167°C. IR (KBr): 1565 (NO_2); 1345, 1180 cm^{-1} (SO_2); NMR ($CDCl_3$): τ 5.35 (1H-*t* mit $J_{1,2}=J_{2,3}=9.5$ Hz, $CHNO_2$); 7.01 (6H-*s*, $2CH_3SO_2$).

Gef.: C, 30.22; H, 4.58; N, 4.53; S, 20.20%. Ber. für $C_8H_{15}NO_8S_2$: C, 30.28; H, 4.76; N, 4.41; S, 20.21.%

1r,3c-Bis benzylamino-2t-nitrocyclohexan (**6**). *a) Aus 1r,3c-Diacetyloxy-2t-nitrocyclohexan* (**3**). Zu 2.45 g (10 mMol) **3**[27] in 10 m*l* alkohol-freiem Chloroform wurden 5.5 m*l* (5 Moläquiv.) Benzylamin gegeben und 2 Stdn. bei Raumtemperatur stehengelassen, wobei sich ein Niederschlag (Benzylamin-Hydroacetat) absetzte. Das Reaktionsgemisch wurde i. Vak. eingedampft, der Rückstand mit 5 m*l* Methanol versetzt und Wasser bis zur beginnenden Trübung zugegeben. Nach Stehenlassen über Nacht im Kühlschrank wurde der Niederschlag abgesaugt, zweimal mit wäßrigem Methanol (1 : 1) und dann gut mit Wasser gewaschen. Nach Umkristallisation aus Methanol: 2.7 g (79%) farblose Nadeln; Schmp. 90—91°C (Lit.[2,3] 90—91°C). IR- und NMR-Spektren waren mit dem aus **1** mit Benzylamin dargestellten Produkt[3] identisch.

b) Aus 1r,3c-Dimesyloxy-2t-nitrocyclohexan (**4**). Eine Lösung von 0.32 g (1 mMol) **4** in 10 m*l* alkohol-freiem Chloroform wurde mit 0.6 m*l* (5 mMol) Benzylamin versetzt, nach Stehenlassen über Nacht bei Raumtemperatur zweimal mit Wasser gewaschen, die organische phase über Na_2SO_4 getrocknet und i. Vak. eingedampft. Umkristallisation aus Methanol ergab 0.24 g (70%) **6**.

1r,3c-Bis-cyclohexylamino-2t-nitrocyclohexan (**7**). 2.45 g (10 mMol) **3** in 10 m*l* Chloroform wurden mit 5.5 m*l* (5 Moläquiv.) Cyclohexylamin versetzt und 2 Stdn. bei Raumtemperatur stehengelassen. Die Aufarbeitung erfolgte analog der Umsetzung von **2** mit Benzylamin (*s. oben*): 2.3 g (71%); Schmp. 118—120°C (Lit.[3]: 119—120°C). Das IR-Spektrum war mit dem aus **1** dargestellten Produkt[4] identisch.

1r,3c-Diacetamino-2t-nitrocyclohexan (**9**). In eine Lösung von 2.45 g (10 mMol) **3**[27] in 100 m*l* Dioxan wurde bei 40°C 5 Stdn. trockenes Ammoniak-Gas eingeleitet, sodann zur Entfernung noch gelösten Ammoniaks i. Vak. auf *ca.* 50 m*l* konzentriert,[28] unter Eiskühlung mit Acetanhydrid (8 m*l*) versetzt und über Nacht bei Raumtemperatur stehengelassen. Der entstandenne Niederschlag wurde abgesaugt und zusammen mit der aus der Mutterlauge durch Eindampfen zur Trockene und Behandeln mit Wasser gewonnenen zweiten Fraktion umkristallisiert (Methanol/Wasser): 1.81 g (74%) feiner Nadeln; Schmp. 294—296°C (Zers.) nach Sublimation um 245°C. NMR (DMSO-d_6): τ 1.91 (2H-*d* mit J= 9 Hz, NH); 5.58 (1H-*t* mit $J_{12}=J_{23}=9.5$ Hz, H^2); 5.86 (2H-*m* H^1 und H^3), 8.26 (6H-*s*, *N*Ac).

Gef.: C, 49.29; H, 7.13; N, 17.24%. Ber. für $C_{10}H_{17}N_3O_4$: C, 49.37; H, 7.04; N, 17.28%.

Umsetzungen von **3** in NH_3/Methanol (3 Stdn., 25°C), in flüssigem NH_3 (2 Stdn., −40°C) lieferte nach analoger Aufarbeitung **9** in 40—50% Ausbeute.

DL-*1r,3c-Dianilino-2c-nitrocyclohexan* (**11**) und *1r,3t-Dianilino-2c-nitrocyclohexan* (**10**). 9.8 g (40 mMol) **3**, in 18 m*l* (0.2 Mol) frisch dest. Anilin gelöst, wurden mit 50 m*l* absol. Methanol versetzt und 5 Tage bei Raumtemperatur stehengelassen. Nach Absaugen des gebildeten Niederschlags, der neben Spuren **5** (R_f=0.22[23]) etwa gleich Mengen an **10** und **11** (R_f=0.54 bzw. 0.64[23]) enthielt, wurde fraktioniert. Umkristallisation aus 500 m*l* Methanol lieferte eine Kristallfraktion (**11**), Eindampfen der Mutterlauge zur Hälfte und Stehenlassen über Nacht eine zweite, aus Nadelbüscheln (**11**) und Prismen (**10**) bestehend, die beim Absaugen bleicht manuell getrennt werden konnten.

Die **10** bzw. **11** enthaltenden Fraktionen wurden jeweils zweimal aus Methanol umkristallisiert: 2.5 g

27) F. W. Lichtenthaler, *Chem. Ber.*, **96**, 845 (1963).

28) Vollstandiges Abziehen des Dioxans i. Vak. hinterläßt eine weiße, kristalline Masse, die neben Ammoniumacetat das freie Nitrodiamin enthält. An der Luft tritt jedoch rasch Verfärbung ein.

(20%) **11** als gelbliche Nadeln vom Schmp. 187°C bzw. 3.7 g (30%) **10**, schwach-gelbe Blättchen vom Schmp. 127°C. IR- und NMR-Daten *vgl.* Tabelle.

Gef. (**10**): C, 69.69; H, 6.93; N, 13.49%. Gef. (**11**): C, 69.67; H, 6.61; N, 13.16%. Ber. für $C_{18}H_{21}N_3O_2$: C, 69.43; H, 6.80; N, 13.50%.

1r-Methyl-1-nitro-2c,6c-bis-benzylamino-cyclohexan **(12).** *a) Aus Glutardialdehyd, Nitroäthan und Benzylamin.* Zu einem Gemisch von 38 m*l* 25-proz. wäßr. Glutardialdehyd-Lösung (0.1 Mol) und 11 m*l* (0.15 Mol) Nitroäthan wurden 44 m*l* (0.4 Mol) Benzylamin unter Eiskühlung und Rühren tropfenweise zugegeben. Nach 12 Stdn. bei Raumtemperatur wurde mit Wasser versetzt, der gebildete Niederschlag abfiltriert und aus Methanol umkristallisiert: 20.1 g (56%) farblose Prismen; Schmp. 101—102°C. IR (KBr): 3320 (NH), 1545, 1360 cm^{-1} (NO_2); NMR ($CDCl_3$): τ 8.52 (3H-*s*, *C*-CH_3).

Gef: C, 71.43; H, 7.70; N, 11.94%. Ber. für $C_{21}H_{27}N_3O_2$: C, 71.36; H, 7.70; N, 11.89%.

b) Aus 1r-Methyl-1-nitrocyclohexandiol-(2c,6c) **(15)** *und Benzylamin*: 2.5 g (15 mMol) (**15**),[29] in 30 m*l* Äthanol wurden mit einem Gemisch von 6.5 m*l* (4 Moläquiv.) Benzylamin und 6 m*l* Wasser versetzt und 10 Stdn. bei Raumtemperatur gerührt. Der gebildete Niederschlag wurde abgesaugt und aus Methanol umkristallisiert: 4.2g (83%) **12**, identisch mit dem unter a) beschriebenen.

c) Aus 1r-Methyl-1-nitro-2c,6c-diacetoxy-cyclohexan **(16)** *und Benzylamin*: 2.6 g (10 mMol) **16**[29] in 10 m*l* Chloroform wurden mit 5.5 m*l* (5 Moläquiv.) Benzylamin versetzt, das Gemisch über Nacht bei Raumtemperatur stehengelassen und i. Vak. eingedampft. Der Rückstand wurde in Methanol aufgenommen und Wasser bis zur beginnenden Trübung zugesetzt. Nach Absaugen und Umkristallisation aus Methanol: 2.6 g (75%) **12**, identisch in allen Daten mit dem unter a) und b) beschriebenen Produkt.

1r-Methyl-1-nitro-2c,6c-bispiperidino-cyclohexan **(13)**: 2.0 g (11 mMol) **15**[29] in 20 m*l* Äthanol wurden mit 6 m*l* Piperidin versetzt. Nach kurzer Zeit bildete sich ein Niederschlag, der nach 4 Stdn. abgesaugt und aus Methanol umkristallisiert wurde: 1.8 g (51%) farblose Blättchen; Schmp. 143—144°C. NMR ($CDCl_3$): τ 6.90 (2H-*q* mit J=5 und 11 Hz, H^2 und H^6).

Gef.: C, 66.11; H, 10.06; N, 13.50%. Ber. für $C_{17}H_{31}N_3O_2$: C, 65.98; H, 10.10; N, 13.58%.

Umsetzung von Glutardialdehyd, Nitroäthan und Piperidin im Molverhältnis 1 : 1.5 : 4 in Wasser lieferte **13** in 8-proz. Ausbeute.

1r-Methyl-1-nitro-2c,6c-bismorpholino-cyclohexan **(14)**: Zu einem Gemisch von 38 m*l* (0.1 Mol) 25-proz. wäßr. Glutardialdehyd-Lösung, 8.5 m*l* (0.12 Mol) Nitroäthan wurden unter Eiskühlung und Rühren 26 m*l* (0.25 Mol) Morpholin tropfenweise zugegeben. Nach 4 Stdn. saugte man den gebildeten Niederschlag ab und kristallisierte aus Äthanol um: 10.1 g (35%) farblose Rhomben; Schmp. 176—177°C. NMR ($CDCl_3$): τ 6.42 (8H-*t* mit J=9 Hz, 4 *O*-CH_2); 6.90 (2H-*q* mit J=5 und 11 Hz, H^2 und H^6); um 7.4 (8H-*m*, 4*N*-CH_2); 8.50 (3H-*s*, CH_3).

Gef.: C, 57.47; H, 8.63; N, 13.39%. Ber. für $C_{15}H_{27}N_3O_4$: C, 57.48; H, 8.68; N, 13.41%.

Umsetzung von **15** mit Morpholin, durchgeführt analog zur Reaktion mit Piperidin (*s. oben*), lieferte **14** in 48% Ausbeute.

29) F. W. Lichtenthaler, H. Leinert und U. Scheidegger, *Chem. Ber.*, **101**, 1819 (1968).

Herrn Dr. M. Masaki (Ube Kosan, Ltd., Chiba, Japan) sind wir für die Aufnahme der IR-Spektren Herrn K. Fukukawa (Laboratory of Natural Products, Tokyo Institute of Technology) für die Aufnahme der NMR-Spektren zu Dank verpflichtet.

BULLETIN OF THE CHEMICAL SOCIETY OF JAPAN VOL. 43 3866—3869 (1970)

Polyamino-Zucker. VI.[1] Synthese von Derivaten der 2,3,4-Triamino-2,3,4-tridesoxy-β-D-glucose

Toshio NAKAGAWA,*† Yoshikuni SATO,* Tetsuyoshi TAKAMOTO,* Frieder W. LICHTENTHALER** und Norbert MAJER**

* *Department of Chemistry, Tokyo Institute of Technology, Ō-okayama, Meguro-ku, Tokyo*

** *Institut für Organische Chemie, Technische Hochschule Darmstadt, 61 Darmstadt, BRD*

(Eingegangen am 13. Mai, 1970)

A facile synthesis of methyl and phenyl glycoside derivatives of 2,3,4-triamino-2,3,4-trideoxy-β-D-glucopyranose is described, involving as the integral part the diamination with benzylamine or ammonia of 2,4,6-tri-*O*-acetyl-3-deoxy-3-nitro-hexosides of *gluco*- and *galacto*-configuration.

Obwohl bislang keine Kohlenhydrate mit mehr als zwei Aminofunktionen in der Natur aufgefunden wurden, hat sich der Chemie von Polyamino-zuckern und -cycliten in den letzten Jahren beachtliches Interesse zugewandt[2-8] Die vorwiegend benutzte Methode zur Einführung der Amino-Gruppen war hierbei die bei der Synthese von Mono- und Diamino-zuckern bewährte Solvolyse von Sulfonester-Gruppierungen durch Natriumazid mit anschließender Reduktion der Azido-Verbindungen.[2-5] Andere Verfahren[6-8] kamen dagegen nur sporadisch zur Anwendung; sie waren entweder präparativ zu aufwendig, oder konnten nur Synthese speziller Verbindungen, wie, z.B. *cis*-Inosatriamin-1,3,5 durch Hydrierung von Triaminophloroglucin[6] herangezogen werden.

Aus der Fortführung unserer Arbeiten zur cyclisierenden Bisaminoalkylierug von Nitromethan[7,9] sowie zur Diaminierung cyclischer Nitrodiole[9] hatte sich ergeben, daß bei Verwendung von Nitrodi-*O*-acetaten (**1**) auch mit Ammoniak als Amin-Komponente eine glatte Diaminierung zu Verbindung des Typs **2** (R=H bzw. Ac) erreicht werden kann,[1] deren Hydrierung vicinale Triamine (**3**) liefert. Durch Übertragung dieses Syntheseprinzips (**1**→**2**→**3**) auf Polyacetate von Nitrozuckern, durch Nitromethan-Cyclisierung von Zuckerdialdehyden leicht zugänglich,[10] eröffnete sich ein einfacher, generell gangbarer Syntheseweg in die Reihe der Triaminozucker und Inosatriamine, worüber wir im folgenden—zunächst an Hand der Synthese von 2,3,4-Triamino-2,3,4-tridesoxy-glucosiden[11]—berichten.

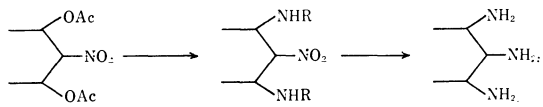

1 **2** **3**

Ergebnisse und Diskussion

Bei Diaminierung von Methyl-2,4,6-tri-*O*-acetyl-3-desoxy-3-nitro-β-D-glucopyranosid (**4**) oder dem entsprechenden Derivat mit galacto-Konfiguration (**5**) können theoretisch acht Isomere gebildet werden. Da diese Reaktion jedoch über einen Eliminierungs-Addition-Mechanismus verlaufen dürfte,[1] ist zu erwarten, daß die Isomeren-Verteilung im entste-

*† Dem Andenken von Prof. Dr. Tetsuo Sato gewidmet.

1) V. Mitteilung: T. Nakagawa, T. Sakakibara und F. W. Lichtenthaler, Dieses Bulletin, **43**, 3861 (1970).

2) W. Meyer zu Reckendorf, *Chem. Ber.*, **97**, 1275 (1964); *Chimia*, **24**, 16 (1970); *Tetrahedron Lett.*, **1970**, 287.

3) T. Suami, F. W. Lichtenthaler und S. Ogawa, Dieses Bulletin, **40**, 1488 (1967); S. Ogawa, T. Abe, H. Sano, K. Kotera und T. Suami, *ibid.*, **40**, 2405 (1967)

4) Y. Ali und A. C. Richardson, *J. Chem. Soc.*, **1969**, 320, 1764.

5) J. Hildesheim, J. Cléophax, A. M. Sépulchre und S. D. Géro, *Carbohyd. Res.*, **9**, 315 (1969); J. Cléophax, S. D. Géro, J. Hildesheim, R. D. Guthrie und C. W. Smith, *Chem. Ind.* (London), **1969**, 784.

6) F. W. Lichtenthaler und H. Leinert, *Chem. Ber.*, **99**, 903 (1966).

7) F. W. Lichtenthaler und T. Nakagawa, *ibid.*, **101**, 1846 (1968).

8) A. Hasegawa und H. Z. Sable, *Tetrahedron*, **25**, 3567 (1969).

9) F. W. Lichtenthaler, T. Nakagawa und A. El-Scherbiney, *Chem. Ber.*, **101**, 1819 (1968).

10) F. W. Lichtenthaler, *Angew. Chem.*, **76**, 84 (1964); *Angew. Chem. Int. Ed. Engl.*, **3**, 211 (1964); "Newer Methods of Preparative Organic Chemistry," Vol. IV, 156, Verlag Chemie, Weinheim, (1968); H. H. Baer, *Advan. Carbohyd. Chem.*, **24**, 67 (1969).

11) Vorläufige Mitteilung über Teile dieser Arbeit: F. W. Lichtenthaler, P. Voss und N. Majer, *Angew. Chem.*, **81**, 221 (1969); *Angew. Chem. Int. Ed. Engl.*, **8**, 211 (1969).

henden Nitrodiamin-Gemisch nur vom sterischen Verlauf der Ammoniak-Addition an die intermediär gebildeten Nitroolefine bestimmt wird, nicht dagegen von der sterischen Anordnung der funktionellen Gruppen im Nitro-diacetat-Vorläufer. Des weiteren sollte diese Umsetzung im Hinblick auf die bevorzugte äquatoriale Addition von Nucleophilen an Methyl-4,6-*O*-benzyliden-2,3-didesoxy-β-D-erythro-hex-2-enosid[12] mit hoher Stereoselektivität verlaufen, und zwar zugunsten der Bildung des Isomeren mit all-äquatorialer Orientierung der Substituenten.

Die experimentelle Befunde bestätigen diese Folgerungen. Bei Umsetzungen von Methyl-2,4,6-tri-*O*-acetyl-3-desoxy-3-nitro-β-D-glucopyranosid (**4**) oder der entsprechenden *galacto*-Verbindung (**5**) mit Ammoniak in Methanol und anschließender *N*-Acetylierung läßt sich Methyl-2,4-diacetamino-2,3,4-tridesoxy-β-D-glucopyranosid (**6**) in 53 bzw. 47% Ausbeute isolieren. Analoge Umsetzungen von **4** und **5** in flüssigem Ammoniak liefern dagegen niedrigere Ausbeuten (25—30%) an **6**. Bei Verwendung von Benzylamin als Amin-Komponente läßt sich die Diaminierung von **4** oder **5** unter Bedingungen durchführen (3 Stdn. in Chloroform bei 25°C), die keine gleichzeitige Ent-*O*-acetylierung der *C*-6-Acetoxy-Gruppe bewirken. Man erhält Methyl-6-*O*-acetyl-2,4-bisbenzylamino-2,3,4-tridesoxy-3-nitro-β-D-glucopyranosid (**7**) in Ausbeuten bis zu 35%.

Die Hydrierung der Nitro-Gruppen in **6** und **7** bereitet keine Schwierigkeiten. Mit 5—10% Palladium/Tierkohle/Wasserstoff entstehen aus **6** das Di-*N*-acetat **8**, als Hydroacetat charakterisiert, aus **7** infolge gleichzeitiger Hydrogenolyse der Benzyl-Reste ein Triamin, aus dem durch Acetylierung—ebenso wie aus **8**—das Tetraacetat des Methyl-2,3,4-triamino-2,3,4-tridesoxy-β-D-glucosids (**10**) erhalten wird.

In analoger Weise lassen sich 1-Phenyl-Derivate (**14**—**16**) darstellen, die aufgrund ihrer Überführbarkeit in 1,6-Anhydrozucker[13] Interesse besitzen. Ausgehend von Phenyl-β-D-glucopyranosid (**11**) wurde hierbei durch Perjodat-Oxidation und anschließenden Nitromethan-Cyclisierung primär Phenyl-3-desoxy-3-nitro-β-D-glucopyranosid (**12**) dar-

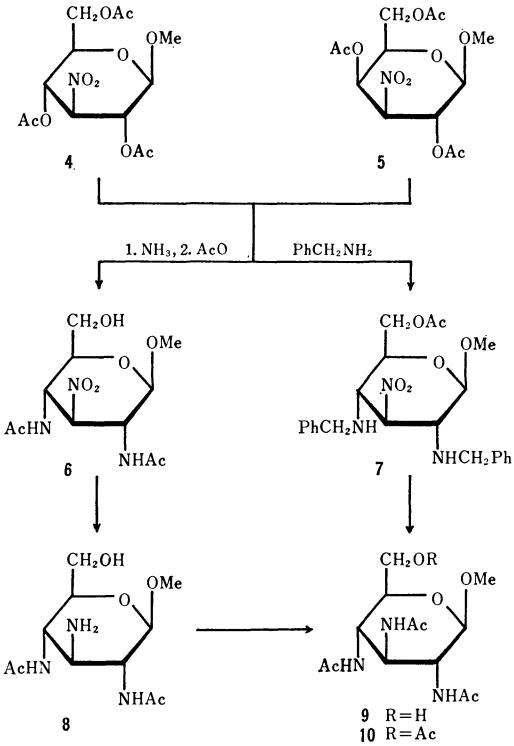

gestellt und dann mit Acetanhydrid/BF_3 in das Tri-*O*-acetat (**13**) übergeführt. Die Diaminierung von **13** mit Benzylamin lieferte in 59% Ausbeute die entsprechende Nitro-bisbenzylamino-Verbindung (**15**), während Umsetzung mit Ammoniak/Methanol und anschließende *N*-Acetylierung das Nitro-di-*N*-acetat **14** (44%) ergab. Beide konnten durch Hydrierung und Acetylierung in Phenyl-2,3,4-triacetamino-2,3,4-tridesoxy-β-D-glucopyranosid (**16**) übergeführt werden.

Die *gluco*-Konfiguration der Verbindungen **7**—**10** und **12**—**16** ließ sich eindeutig aus NMR-spektroskopischen Daten (*vgl.* Tabelle) ableiten. Für das anomere Proton (H^1) wird jeweils ein Dublett mit $J_{1,2}$=8—9 Hz erhalten, für das Nitro-methin-Proton (H^3) 1 : 2 : 1-Triplett mit $J_{2,3}=J_{3,4}$=10—11 Hz, was das Vorliegen axialer Ring-CH, bzw. äqua-

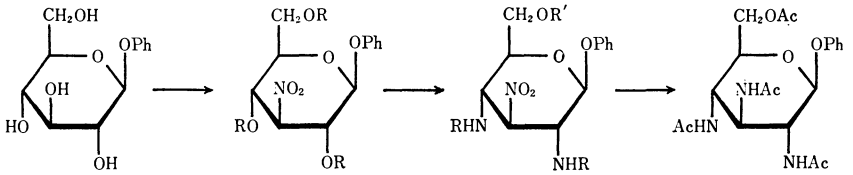

12) H. H. Baer, F. Kienzle und T. Neilson, *Can. J. Chem.*, **43**, 1829 (1965); H. H. Baer, T. Neilson und W. Rank, *ibid.*, **45**, 992 (1967); H. H. Baer und T. Neilson, *J. Org. Chem.*, **32**, 1068 (1967); H. H. Baer und K. S. Ong, *Can. J. Chem.*, **46**, 2511 (1968).

13) C. E. Ballou, *Advan. Carbohyd. Chem.*, **9**, 66 (1954); R. U. Lemieux, *ibid.*, **9**, 13 (1954).

TABELLE 1. NMR-DATEN DER DARGESTELLTEN VERBINDUNGEN

Verb.	Lösungsmittel	H^1-Dublett ($J_{1,2}$ in Hz)	H^3-Triplett ($J_{2,3}=J_{3,4}$ in Hz)	*O*Ac (Intens.)	*N*Ac (Intens.) [in τ]
6	DMSO-d_6	?*	4.88 (10)	—	8.22 (6H)
7	$CDCl_3$	5.82 (8)	5.49 (10)	7.96 (3H)	—
9	DMSO-d_6	?*	?*	—	8.23 (6H) 8.27 (3H)
10	DMSO-d_6	5.61 (9)	?*	8.00 (3H)	8.26 (6H) 8.28 (3H)
12	DMSO-d_6	4.88 (8)	5.30 (10)	—	—
13	$CDCl_3$	4.92 (8)	5.15 (10)	7.93 (9H)	—
14	DMSO-d_6	4.76 (8)	4.75 (11)	—	8.19 (3H) 8.21 (3H)
15	$CDCl_3$	5.16 (8)	5.45 (10)	7.98 (3H)	—
16	DMSO-d_6	4.87 (8)	?*	8.03 (3H)	8.26 (9H)

* Gibt zusammen mit den anderen Ring-CH ein komplexes Multiplett.

torialer Substituenten an C-1 bis C-4 beweist.[14] Die Lage der Acetyl-Resonanzen in DMSO-d_6—jeweils äquatoriale Orientierung der Acetamino-Gruppen in **6**, **9**, **10**, **14** und **16** auf Grund der Acetyl-Resonanzen-Regel[15]—bestätigen diese Zuordnungen.

Beschreibung der Versuche

Die Schmelzpunkte wurden in Kapillarröhrchen bestimmt und nicht korrigiert. Die IR-Spektren wurden mit dem Perkin-Elmer-125 Gerät, die NMR-Spektren mit Varian-A60- bzw. Jeolco JNM-4H-100-Geräten (in ppm, τ-Skala) aufgenommen. Zur Dünnschichtchromatographie diente Kieselgel PF_{254} der *Fa. E. Merck AG, Darmstadt*; Schichtdicke 0.2 mm; Laufmittel: Essigester-Äthanol-Wasser 15 : 2 : 1.

Methyl-2,4-diacetamino-2,3,4-tridesoxy-3-nitro-β-D-glucopyranosid (**6**). In eine Lösung von 4.2 g (14 mMol) **4**[16] in 500 m*l* Methanol wurde unter Eiskühlung und Rühren 2 Stdn. ein schwacher Ammoniakstrom eingeleitet und danach noch 1 Stde. stehengelassen. Der nach Abziehen des Lösungsmittels i. Vak. und Nachdampfen mit Methanol (100 m*l*) verbleibende Sirup wurde in 250 m*l* Methanol aufgenommen, mit 20 m*l* Acetanhydrid versetzt und über Nacht bei Raumtemperatur stehengelassen. Nach Eindampfen i. Vak. und mehrmaligen Nachdampfen mit Äthanol ließ man aus Äthanol kristallisieren. Umkristallisation aus Äthanol ergab 2.2 g (53%) farbloser Kristalle vom Schmp. 285°C (Zers.) und $[\alpha]_D^{22}$ −9.3° (*c* 0.4, Methanol); IR (KBr): 3545 (OH), 3270 (NH), 1660 (Amid I), 1555—1545 (Amid II, NO_2), 1375 cm^{-1}(NO_2).

Gef.: C, 43.48; H, 6.24; N, 13.48%. Ber. für $C_{11}H_{19}N_3O_7$: C, 43.27; H, 6.27; N, 13.76%.

Umsetzung von **5** mit Ammoniak unter gleichen Bedingungen lieferte **6** in 47% Ausbeute. Bei Aminierung von **4** bzw. **5** mit flussigem Ammoniak (8 Stdn., −40°C) und anschließender *N*-Acetylierung liegen die Ausbeuten an **6** tiefer (25—30%).

Methyl-6-O-acetyl-2,4-bisbenzylamino-2,3,4-tridesoxy-3-nitro-β-D-glucopyranosid (**7**). 3.5 g (10 mMol) **4** in 20 m*l* Chloroform wurden unter Rühren mit 7 m*l* Benzylamin versetzt und 3 Stdn. bei Raumtemperatur stehengelassen. Nach Abziehen des Chloroforms i. Vak. wurde in 5 m*l* Methanol aufgenommen, mit Wasser bis zur beginnenden Trübung versetzt und der ausgeschiedene Niederschlag nach 12-stdgm. Stehen im Kühlschrank abgesaugt. Waschen mit Methanol/Wasser (1 : 1) und Wasser lieferte nach Umkristallisation aus Äthanol/Petroläther 1.5 g (35%) farbloser Nadeln; Schmp. 138—139°C (Zers.), $[\alpha]_D^{20}$ +18° (*c* 1.5, Chloroform); IR (KBr): 3300 (NH), 1735 (OAc), 1560 und 1370 cm^{-1} (NO_2). NMR ($CDCl_3$): τ 5.49 (1H-*t*, J=10 Hz, H^3), 5.82 (1H-*d*, J=8 Hz, H^1), 7.96 (3H-*s*, *O*Ac).

Gef.: C, 62.53; H, 6.51; N, 9.40%. Ber. für $C_{23}H_{29}N_3O_6$: C, 62.29; H, 6.59; N, 9.48%.

Die analoge Umsetzung von **5** mit Benzylamin ergab **7** in 20% Ausbeute.

Methyl-2,4-diacetamino-3-amino-2,3,4-tridesoxy-β-D-glucopyranosid Hydroacetat (**8**-HOAc). 850 mg (2.8 mMol) **6** in 50 m*l* Methanol wurden zu einer vorhydrierten Suspension von 600 mg 10% Palladium/Tierkohle in 50 m*l* Methanol gegeben und die stöchiometrische Menge Eisessig zugesetzt. Nach *ca.* 1 Stde. fiel ein weißer Niederschlag aus, der durch Zusatz von 60 m*l* Wasser wieder in Lösung gebracht wurde. Nach 24 Stdn. war der berechnete Wasserstoff aufgenommen. Die Lösung wurde filtriert, und das Lösungsmittel abgezogen. Dabei schieden sich 830 mg des Hydroacetats als weiße Kristalle ab, Zers.-P.: ab 240°C, $[\alpha]_D^{22}$ −14.2° (*c* 1, Wasser).

Gef.: C, 46.10; H, 7.35; N, 12.31%. Ber. für $C_{13}H_{25}N_3O_7$: C, 46.56; H, 7.51; N, 12.53%.

Methyl-2,3,4-triacetamino-2,3,4-tridesoxy-β-D-glucopyranosid (**9**). 950 mg (3.1 mMol) **8**-Hydroacetat wurden in 25 m*l* Methanol unter Rühren und Eiskühlung mit 1.2 m*l* Acetanhydrid versetzt. Nach 30 Min. bildete sich eine klare Lösung, aus der beim Stehen im Kühlschrank (4°C) Kristalle ausfielen. Das Lösungsmittel wurde abgezogen, mehrmals mit Äthanol nachgedampft und aus Äthanol mit wenig Wasser umkristallisiert: 825 mg (87%) weiße Kristalle, Zers.-P. 315°C,

14) L. D. Hall, *Advan. Carbohyd. Chem.*, **19**, 65 (1965).

15) F. W. Lichtenthaler und P. Emig, *Carbohyd. Res.*, **7**, 121 (1968); F. W. Lichtenthaler, G. Bambach und P. Emig, *Chem. Ber.*, **100**, 2389 (1967).

16) H. H. Baer, F. Kienzle und F. Rajabalee, *Can. J. Chem.*, **46**, 80 (1968).

$[\alpha]_D^{22}$ −11.8° (*c* 0.5, Methanol); IR (KBr): 3280 (NH), 1650 (Amid I), 1545 cm^{-1} (Amid II).

Gef.: C, 46.57; H, 7.50; N, 11.81%. Ber. für $C_{13}H_{23}N_3O_6 \cdot H_2O$: C, 46.56; H, 7.51; N, 12.53%.

Methyl-2,3,4-triacetamino-6-O-acetyl-2,3,4-tridesoxy-β-D-glucopyranosid **(10).** *a) Durch Acetylierung von* **9**: 500 mg (1.5 mMol) **9** wurden unter Rühren und Eiskühlung in 8 m*l* Pyridin und 4 m*l* Acetanhydrid gelöst und 15 Stdn. bei Raumtemperatur stehengelassen. Danach wurden unter Eiskühlung 15 m*l* Wasser zugegeben, die Lösungsmittel abgezogen und mehrmals mit Wasser nachgedampft, bis die Masse kristallin wurde und der Geruch nach Pyridin verschwunden war. Nach dreimaliger Umkristallisation aus Äthanol erhielt man 330 mg (61%) weiße Kristalle, Zers.-P. 324—326°C, $[\alpha]_D^{22}$ −13.5° (*c* 0.3, Wasser); IR (KBr): 3200 (NH), 1737 (*O*Ac), 1648 (Amid I), 1540 cm^{-1} (Amid II).

Gef.: C, 49.86; H, 7.02; N, 11.47%. Ber. für $C_{15}H_{25}N_3O_7$: C, 50.13; H, 7.01; N, 11.69%.

b) Durch Hydrierung und Acetylierung von **7**. 2.2 g (5 mMol) **7** wurden in 50 m*l* Methanol und 3 m*l* Eisessig gelöst, und zu einer vorhydrierten Suspension von 500 mg Palladium/Tierkohle gegeben und die Hydrierung fortgesetzt, bis die berechnete Menge Wasserstoff aufgenommen war (2 Tage). Die Lösung wurde filtriert, mit Ammoniak neutralisiert, das Lösungsmittel abgezogen und mit 10 m*l* Äthanol nachgedampft. Der Rückstand wurde unter Eiskühlung und Rühren mit 6 m*l* Pyridin und 4 m*l* Acetanhydrid versetzt, über Nacht bei Raumtemperatur stehengelassen, die Lösungsmittel abgezogen, dreimal mit Äthanol/Toluol (1 : 1) nachgedampft und aus Äthanol umkristallisiert; 1.1 g (61%) farblose Nadeln, die mit der nach a) gewonnenen Substanz völlig übereinstimmten.

Phenyl-3-desoxy-3-nitro-β-D-glucopyranosid **(12).** Zu einer Lösung von 42.8 g (0.2 Mol) Natriummetaperjodat in 500 m*l* Wasser wurde innerhalb 10 Min. unter Eiskühlung und Rühren ein Gemisch von 29.2 g (0.1 Mol) Phenyl-β-D-glucopyranosid-dihydrat (**11**)[17] und 8.4 g Natriumhydrogencarbonat in mehreren Anteilen zugegeben. Nach 6 Stdn. wurde mit 400 m*l* Methanol versetzt, ein gebildeter Niederschlag abfiltriert und das Filtrat bei 40°C i. Vak. zur Trockne eingedampft. Der Rückstand wurde mit 60 m*l* Äthanol und 30 m*l* Äther versetzt, wieder filtriert und erneut eingedampft. Nach nochmaliger Wiederholung dieser Operation erhielt man einen klaren Sirup, der in 60 m*l* Methanol gelöst und mit 8 m*l* Nitromethan und dann tropfenweise mit 10 m*l* 2N Natriummethylat unter Eiskühlung und Rühren versetzt wurde. Nach Stehen über Nacht bei Raumtemperatur wurde das kristalline Produkt (10.4 g) abgesaugt. Aus der Mutterlauge wurde nach Neutralisierung mit Kationenaustauscher (H^+-Form) und Eindampfen auf ein Viertel des Volumens weitere 3.3 g erhalten. Das gesamte Rohprodukt wurde aus Äthanol/Petroläther umkristallisiert: 12.8 g (45%) farblose Kristalle, Zers.-P. 215—216°C, $[\alpha]_D^{20}$ −27.8° (*c* 0.85, Dioxan); IR (KBr): 3200, 3350, 3470 (OH), 1560, 1370 cm^{-1} (NO_2); NMR (DMSO-d_6): 4.88 (1H-*d*, J=8 Hz, H^1), 5.30 τ (1H-*t*, J=10 Hz, H^3).

Gef.: C, 50.67; H, 5.32; N, 5.06%. Ber. für $C_{12}H_{15}NO_7$: C, 50.52; H, 5.30; N, 4.91.%

Phenyl-2,4,6-tri-O-acetyl-3-desoxy-3-nitro-β-D-glucopyranosid **(13).** Zu 8.6 g (30 mMol) **12** in 100 m*l* Acetanhydrid wurden einige Tropfen Bortrifluorid-Ätherat unter Eiskühlung und Rühren zugegeben. Nach 5 Stdn. wurde mit Eiswasser versetzt, der Niederschlag abgesaugt und aus Äthanol umkristallisiert: 11.7 g (94%) farblose Nadeln, Zers.-P. 163—164°C, $[\alpha]_D^{20}$ −24.0° (*c* 1.0, Chloroform). IR (KBr): 1750, 1720 (*O*Ac), 1560 cm^{-1} (NO_2).

Gef.: C, 52.67; H, 5.28; N, 3.50%. Ber. für $C_{18}H_{21}NO_{10}$: C, 52.55; H, 5.15; N, 3.41%.

Phenyl-2,4-acetamino-2,3,4-tridesoxy-3-nitro-β-D-glucopyranosid **(14).** Umsetzung von 2.06 g (10 mMol) **13** in 120 m*l* Methanol mit Ammoniak und Aufarbeitung analog zur Darstellung von **6** ergab nach Umkristallisation aus Äthanol 1.6 g (44%) farbloser Kristalle; Zers.-P. 252°C, $[\alpha]_D^{20}$ −1.5° (*c* 0.25, Dioxan); IR (KBr): 3280 (NH), 1665 (Amid I), 1560 cm^{-1} (Amid II und NO_2).

Gef.: C, 52.54; H, 5.49; N, 11.29%. Ber. für $C_{16}H_{21}N_3O_7$: C, 52.31; H, 5.76; N, 11.44%.

Phenyl-6-O-acetyl-2,4-bisbenzylamino-2,3,4-tridesoxy-3-nitro-β-D-glucopyranosid **(15).** 3.0 g (7.3 mMol) **13** in 20 m*l* Chloroform wurden unter Rühren mit 5 m*l* Benzylamin versetzt, 3 Stdn. bei Raumtemperatur stehengelassen und sodann analog der Darstellung von **7** aufgearbeitet. Nach Umkristallisation aus Äthanol/Petroläther: 2.3 g (59%) farbloser Nadeln; Zers.-P. 130°C, $[\alpha]_D^{20}$ 0° (*c* 0.4, Chloroform); IR (KBr): 3300 (NH), 1740 (*O*Ac), 1560 cm^{-1} (NO_2).

Gef.: C, 66.38; H, 6.08; N, 8.50%. Ber. für $C_{28}H_{31}N_3O_6$: C, 66.52; H, 6.18; N, 8.31%.

Phenyl-2,3,4-triacetamino-6-O-acetyl-2,3,4-tridesoxy-β-D-glucopyranosid **(16).** *a) Aus* **14**: 730 mg (2 mMol) **14** wurden in 20 m*l* Dioxan und 5 m*l* 2N Essigsäure gelöst und mit 0.3 g vorhydriertem Katalysator (5% Palladium/Tierkohle) über Nacht hydriert. Nach Aufnahme der berechneten Menge Wasserstoff wurde filtriert, mit Ammoniak neutralisiert, das Lösungsmittel i. Vak. abgezogen und mehrmals mit Äthanol nachgedampft. Der Rückstand wurde mit 3 m*l* Pyridin und 2 m*l* Acetanhydrid versetzt, über Nacht bei Raumtemperatur stehengelassen, das Lösungsmittel abgezogen, dreimal mit Äthanol/Toluol (1 : 1) nachgedampft und aus Äthanol umkristallisiert: 650 mg (74%) farblose Nädelchen, Zers.-P. 280°C, $[\alpha]_D^{20}$ −12.5° (*c* 0.2, Dimethylsulfoxid); IR (KBr): 3270 (NH), 1738 (*O*Ac), 1650 (Amid I), 1550 cm^{-1} (Amid II).

Gef.: C, 57.09; H, 6.32; N, 10.01%. Ber. für $C_{20}H_{27}N_3O_7$: C, 57.00; H, 6.46; N, 9.97%.

b) Aus **15.** 2.0 g (4 mMol) **15** wurden mit 0.5 g vorhydriertem 5% Palladium/Tierkohle in einer Lösung von 40 m*l* Dioxan und 10 m*l* 2N Essigsäure hydriert, bis die berechnete Menge Wasserstoff aufgenommen war (3 Tage). Danach wurde das Reaktionsgemisch wie oben aufgearbeitet und mit 5 m*l* Acetanhydrid in 10 m*l* Pyridin acetyliert: 1.0 g (60%) an **16**, Zers.-P. und IR-Spektrum waren mit dem unter a) erhaltenen Produkt identisch.

17) E. Fischer und L. v. Mechel, *Ber.*, **49**, 2813 (1916); E. M. Montgomery, N. K. Richtmyer und C. S. Hudson, *J. Amer. Chem. Soc.*, **64**, 690 (1942).

BULLETIN OF THE CHEMICAL SOCIETY OF JAPAN VOL. 43 3870—3872 (1970)

Ester-Urethane Interchange Reaction

Hajime SUZUKI

Katata Research Institute, Toyobo Co., Ltd., Honkatata, Otsu

(Received June 1, 1970)

The ester-urethane interchange reaction has been studied by means of gas chromatography and NMR. The interchange reaction between low-molecular-weight ester and urethane was confirmed by the gas chromatography. Alternating copolyester-urethane was prepared by reacting bis-(hydroxyethyl)terephthalate with hexamethylene diisocyanate in anisole. When the polymer is melted at 190°C in the presence of sulfuric acid as a catalyst, the ester-urethane interchange reaction in alternating copolyester-urethane proceeds and causes a more random arrangement of the segments. This was proved by high-resolution nuclear magnetic resonance spectroscopy. An ethylene glycol residue adjacent to terephthalate on both sides, to diisocyanate on both sides, and to terephthalate and diiosyanate could be identified at 4.93, 4.48, and 4.71 ppm respectively in trifluoroacetic acid.

It is well known that condensation copolymers can be obtained by the following three general methods. One method is polycondensation with different kinds of monomer mixtures. The second is a so-called step-by-step polymerization with several kinds of monomer mixtures. Polyurethane elastomers are usually prepared by this method.[1] The third is an interchange reaction with different kinds of homopolymer mixtures. Copolyesters[2] and copolyamides[3] are easily prepared by this method. Usually, copolyester-urethane can be synthesized by the first and second methods. Recently, polyurethane was obtained by the urethane interchange reaction of dimethyl butane-1,4-dicarbamate with glycol;[4] however, no report has appeared describing the synthesis of copolyester-urethane by the interchange reaction. Therefore, this paper will describe the possibility of the synthesis of random copolyester-urethane from alternating copolyester-urethane by the ester-urethane interchange reaction.

The interchange reaction between low-molecular-weight urethane and an ester was studied as a model for the polymer by the aid of gas chromatography. The interchange reaction in polymer may be investigated by the following two methods; (1) an ester-urethane interchange reaction between the homopolyester and homopolyurethane and (2) an ester-urethane interchange reaction in the alternating copolyester-urethane. The melting points of polyethylene terephthalate, polyethylene hexamethylenecarbamate, and alternating copolyester-urethane prepared from hexamethylene diisocyanate and bis(hydroxyethyl)terephthalate are 256, 178, and 179°C respectively. Therefore, the transesterification reaction can be carried out at a lower temperature by using the alternating copolyester-urethane. In this work, the interchange reaction between ester groups and urethane groups in the polymer was studied through a transesterification reaction in the alternating copolyester-urethane, and was confirmed by NMR spectroscopy.

Experimental

Materials. Ethyl benzoate, *n*-butyl benzoate, *n*-butyl *n*-butyrate, and ethyl *n*-butyrate were fractionally distilled twice. *n*-Butyl phenylcarbamate, ethyl phenylcarbamate, ethyl *n*-propylcarbamate, and *n*-butyl propylcarbamate were prepared by reacting the corresponding isocyanates with alcohols. These structures were confirmed by elementary analysis and by a study of their NMR spectra; the gas chromatographs of these compounds showed them to be pure substances.

Interchange Reaction between Low-molecular-weight Urethane and Ester. Interchange reactions were carried out in sealed ampoules at 190°C for 43 hr. The products obtained by the interchange reaction were confirmed by comparing their retention times on gas chromatography with those of authentic samples. The gas chromatography was performed with a Yanagimoto gas chromatograph, model G8, with 15 ml/min of helium, using a 1.5-m column containing silicon DC-550 at 200°C.

Interchange Reaction in Molten Copolyester-urethane. Copolyester-urethane was prepared by reacting bis(hydroxyethyl)terephthalate with hexamethylene diisocyanate in anisole. The ester-urethane interchange reaction in the copolyester-urethane was carried out at 190°C in a stream of nitrogen, and new sequence units in the copolyester-urethane were confirmed by a

1) For example, H. Suzuki and H. Ono, This Bulletin, **43**, 687 (1970).

2) W. H. Charch and J. C. Shivers, *Text. Res. J.*, **29**, 538 (1959).

3) C. W. Ayers, *J. Appl. Chem.*, **4**, 444 (1954).

4) Y. Miyake, S. Ozaki and Y. Hirata, *J. Polym. Sci., Part A-1*, **7**, 899 (1969).

study of the NMR spectra. The NMR spectra were obtained with a Varian A-60 spectrometer operating at 60 MHz. The solutions containing 15% (w/v) polymers and tetramethylsilane as an external reference in trifluoroacetic acid were run at room temperature.

The viscosity measurements of polymers obtained by interchange reactions were carried out in an Ubbelohde viscometer at 30±0.03°C.

Results and Discussion

Confirmation of Interchange Reaction between Low-molecular-weight Urethane and an Ester. The interchange reaction was carried out in a sealed ampoule at 190°C for 43 hr in the presence of 0.05% sulfuric acid as the catalyst. Figure 1. (A)—(F) shows the results of the gas-

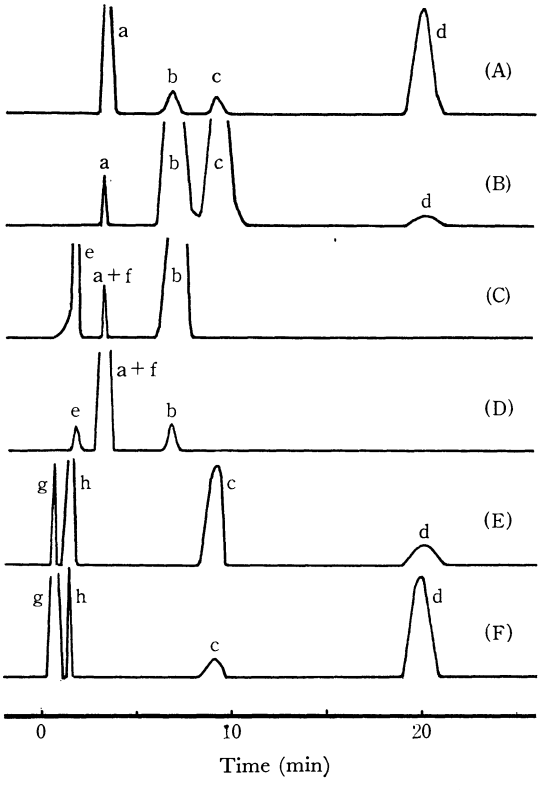

Fig. 1. Gas chromatograms of reaction mixtures. a, Ethyl benzoate; b, *n*-Butyl benzoate; c, Ethyl phenylcarbamate, d, *n*-Butyl phenylcarbamate; e, Ethyl *n*-propylcarbamate; f, *n*-Butyl *n*-propylcarbamate; g, Ethyl *n*-butyrate h, *n*-Butyl *n*-butyrate

chromatographic analysis of reaction mixtures of low-molecular-weight urethane and an ester. The peaks were identified by means of the retention data of pure substances. When the interchange reactions were carried out without sulfuric acid as the catalyst but otherwise under the same conditions as above, no new peak could be observed.

There have been a number of reports concerning the thermal dissociation of urethane.[5-7] These reactions can be shown by the following equations:

$$RNCO + R'NHCOOR'' \longrightarrow RNHCOOR'' + R'NCO \quad (1)$$

$$ROH + R'NHCOOR'' \longrightarrow R'NHCOOR + R''OH \quad (2)$$

$$RCOOH + R'NHCOOR'' \longrightarrow R'NHCOR + CO_2 + R''OH \quad (3)$$

It has been reported that ester interchange and interchange reaction between as ester and alcohol proceed easily. Judging from these reports, the first step in an interchange reaction between urethane and ester groups is probably the thermal dissociation of a urethane group, as is shown in Eq. (4). Therefore, the following reaction scheme may hold in the reaction between ester and urethane groups:

$$R_1COOR_2 + R_3NHCOOR_4 \rightleftarrows R_1COOR_2 + R_3NCO + R_4OH \quad (4)$$

$$R_1COOR_2 + R_3NCO + R_4OH \rightleftarrows \begin{pmatrix} R_1COOR_2 \\ \vdots \\ O-H \\ | \\ R_4 \end{pmatrix} + R_3NCO \quad (5)$$

$$\begin{pmatrix} R_1COOR_2 \\ \vdots \\ O-H \\ | \\ R_4 \end{pmatrix} + R_3NCO \rightleftarrows R_1COOR_4 + R_3NCO + R_2OH \quad (6)$$

$$R_1COOR_4 + R_3NCO + R_2OH \rightleftarrows R_1COOR_4 + R_3NHCOOR_2 \quad (7)$$

Confirmation of Interchange Reaction in Molten Copolyester-urethane. Recently, Miyake[4] synthesized polyurethane by the carbamate exchange reaction shown in the following scheme:

$$CH_3OCONH(CH_2)_4NHCOOCH_3 \xrightarrow[-CH_3OH]{+HO(CH_2)_nOH} [(CH_2)_nOCONH(CH_2)_4NHCOO]_m \quad (8)$$

The first step in the reaction may be assumed to proceed as is shown in Eq. (4). If the ester-urethane interchange reaction in copolyester-urethane proceeds, random copolyester-urethane may be prepared from the homopolyester and homopolyurethane as is shown in Eq. (9) or from alternating copolyester-urethane as is shown in Eq. (10):

$$(-T-G-)_n + (-I-G-)_m \longrightarrow [\{T-G\}_p\{I-G\}_q]_l \quad (9)$$

$$[\{T-G\}\{I-G\}]_l \longrightarrow [\{T-G\}_p\{I-G\}_q]_l \quad (10)$$

5) G. Muller, *Chem. Ber.*, **98**, 1097 (1965).
6) S. Murahashi and N. Nakanishi, *Gosei Sen-i Kenkyu*, **1**, 333 (1944).
7) T. Hoshino, T. Mukaiyama and H. Hoshino, This Bulletin, **25**, 396 (1952).

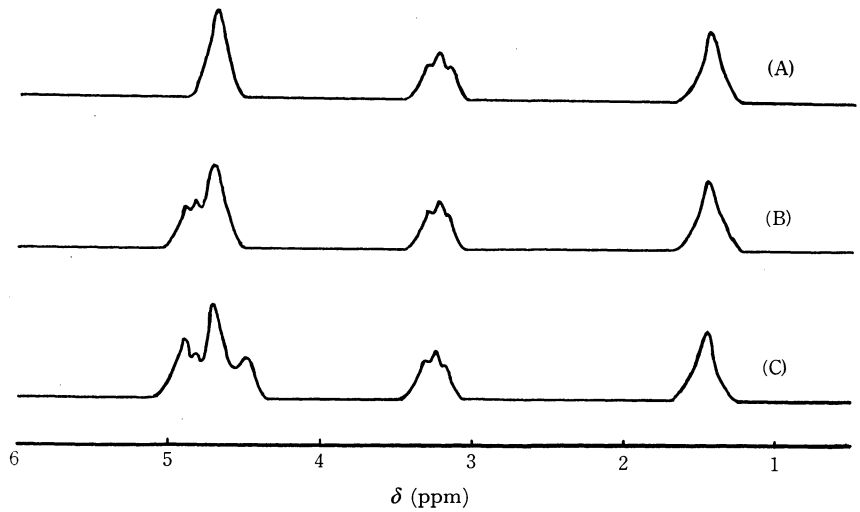

Fig. 2. NMR spectra of copolyester-urethane after interchange reaction. (A): 0 hr, (B): 4 hr, (C): 20 hr

where T=OC CO, G=OCH_2CH_2O, and I=CO-$NH(CH_2)_6NHCO$

The present work has been concerned with the application of nuclear magnetic resonance spectroscopy to the analysis of alternating copolyester-urethane that has been heated for various lengths of time.

In the first step of the reaction, the polymer has the T-G-I unit only. The ethylene glycol residue in the T-G-I unit was confirmed at 4.71 ppm. When the interchange reaction proceeds, new two kinds of ethylene glycol residues (–G–), one of which is adjacent to terephthalate (T) an both sides, T-G-T, and the other of which is adjacent to diisocyanate (I) an both sides, I-G-I, may be produced. The glycol residues could be confirmed at 4.93 and 4.48 ppm respectively by comparing the proton signal of the ethylene groups in polyethylene terephthalate and polyurethane prepared from ethylene glycol and hexamethylene diisocyanate. These assignments of the proton signals were reported in a previous paper.[8] If these three signals are confirmed in molten copolyester-urethane, the thermal interchange reaction between an ester and urethane in the polymer can be confirmed.

The interchange reaction was carried out at 190°C without a catalyst or in the presence of 0.2% sulfuric acid as the catalyst, and the intrinsic viscosities and NMR spectra of the polymers were measured. Figure 2 shows the results of the NMR spectra. When there was no catalyst in the copolymer, the T-G-T and I-G-I signals at 4.93 and 4.48 ppm could not be confirmed after 43 hrs reaction. On the other hand, when there was sulfuric acid as a catalyst in the copolymer, the T-G-T and I-G-I signals could be confirmed. The signal at 4.85 ppm is due to the hydroxyethyl end group produced by molecular scission due to the catalyst. Table 1 shows the proportions of the intensities of the four signals due to T-G-T, I-G-I, T-G-I and hydroxyethyl group, and the intrinsic viscosity.

Table 1. Molar fraction of the four structural units and intrinsic viscosity after the interchange reaction

Reaction time (hr)	T-G-T	I-G-I	T-G-I	Hydroxyethyl group	[η]
0	0.00	0.00	1.00	0.00	0.618
2	0.02	0.00	0.94	0.04	0.379
4	0.08	0.00	0.86	0.06	0.331
6	0.14	0.05	0.75	0.06	0.419
10	0.21	0.10	0.62	0.07	0.466
20	0.27	0.10	0.56	0.07	0.504

The molar fraction of the hydroxyethyl end group is related to the number-average molecular weight. Therefore, the decrease in intrinsic viscosity for the first 4 hours may correspond to the decrease in the number-average molecular weight. Although the molar fraction of the hydroxyethyl group is kept approximately constant after heating for 6 hrs, the intrinsic viscosity gradually increases. Since the number-average molecular weight remains constant, the increase in intrinsic viscosity after 6 hrs may be assumed to correspond to the change in sequence distribution.

8) H. Suzuki, H. Ono and T. Hongo, *Makromol. Chem.*, **132**, 309 (1970).

BULLETIN OF THE CHEMICAL SOCIETY OF JAPAN VOL. 43 3873—3882 (1970)

Synthesis of Corticotropin Peptides. XII. The Effect of Amino-terminal Substitution in the Corticotropin 1-18 Peptide

Ken INOUYE, Kunio WATANABE, Keiko NAMBA and Hideo OTSUKA

Biochemistry Division, Shionogi Research Laboratory, Shionogi & Co., Ltd., Fukushima-ku, Osaka

(Received June 11,1970)

The synthesis and biological properties are described of an octadecapeptide amide, α-aminoisobutyryl-tyrosyl-seryl-methionyl-glutamyl-histidyl-phenylalanyl-arginyl-tryptophyl-glycyl-lysyl-prolyl-valyl-glycyl-lysyl-lysyl-arginyl-arginine amide, corresponding to the first eighteen amino acid residues of corticotropin (ACTH) except for the amino terminal residue. The amino-terminal decapeptide as intermediate is built up from a tripeptide (positions 1—3) and a heptapeptide (4—10), where a benzyloxycarbonyl and a benzyl ester groups are used for protection of the terminal α-amino group and the γ-carboxyl group of 5-glutamic acid, respectively. These protecting groups are removed in the final step with hydrogen fluoride. The new method is successfully applied to the corresponding 1-β-alanine octadecapeptide amide, which has been synthesized previously by a different procedure. Adrenal-stimulating properties of the 1-α-aminoisobutyric acid peptide are compared with those of the 1-β-alanine peptide to show that the former peptide is more active than the latter when assayed by the adrenal-ascorbic acid depletion and the *in vivo* steroidogenesis methods. The lipotropic activity of the new peptide is also shown to be more prolonged than that of the 1-β-alanine peptide.

In 1965 we reported the synthesis of octadecapeptides, ACTH(1-18)-OH(Ia) and ACTH(1-18)-NH_2 (Ib), corresponding to the first eighteen amino acid residues of corticotropin (ACTH).[1] The amide analog (Ib) was also described by Ramachandran *et al.*[2] and Bajusz and Medzihradszky,[3] independently. Later the synthesis of the 1-glycine analog of Ib, [1-glycine]-ACTH(1-18)-NH_2 (Ic) was reported from this laboratory.[4] From synthetic and biological data on corticotropin peptides, including those of our own work, which have been compiled over the past decade[5] we have learned that the aminoterminal eighteen residues fulfill the minimal requirements for eliciting hig hadrenal-stimulating activity. The corresponding peptides Ia, Ib and Ic were, however, still found to be much less active than the native hormone, especially when they were administered for assays by subcutaneous or intramuscular routes.[1,6] This is probably associated with the fact that these peptides are inactivated very rapidly in the tissues, compared with the native hormone. In an effort to find out the mechanism of inactivation we have tried to improve the biological properties of octadecapeptide Ib by partially modifying its structure.

We synthesized [1-β-alanine]-ACTH(1-18)-NH_2 (Id) and found that the amino-terminal substitution by β-alanine caused not only remarkable enhancement but also prolonged duration of action of the adrenal-stimulating and the lipotropic activities over the corresponding 1-serine and 1-glycine peptides.[6,7] This finding offered evidence to support the view that the marked increase in biological

1) H. Otsuka, K. Inouye, F. Shinozaki and M. Kanayama, *J. Biochem.* (Tokyo), **58**, 512 (1965).

2) J. Ramachandran, D. Chung and C. H. Li, *J. Amer. Chem. Soc.*, **87**, 2696 (1965).

3) S. Bajusz and K. Medzihradszky, "Peptides," Proceedings of the 8th European Peptide Symposium, ed. by H. C. Beyerman, A. van de Linde and W. Maassen van den Brink, North-Holland Publishing Co., Amsterdam (1967), p. 209.

4) H. Otsuka, M. Shin, Y. Kinomura and K. Inouye, This Bulletin, **43**, 196 (1970).

5) a) E. Schröder and K. Lübke, "The Peptides," Vol. 2, Academic Press, New York and London (1966), p. 194; b) J. Ramachandran and C. H. Li, *Advan. Enzymol.*, **29**, 391 (1967).

6) K. Inouye, A. Tanaka and H. Otsuka, This Bulletin, **43**, 1163 (1970).

7) [Gly^1]-ACTH(1-18)-NH_2, (Ic) and [β-Ala^1]-ACTH(1-18)-NH_2 (Id) were found to possess 6.7×10^8 MSH units/g and 9.6×10^9 MSH units/g, respectively, as assayed by the *in vitro* frog skin method;[8] ACTH-(1-24)-OH (Synacthen, Ciba) possessed 2.1×10^8 MSH units/g in a narallel determination. H. Otsuka, K. Kondo and K. Inouye, unpublished.

8) K. Shizume, A. B. Lerner and T. B. Fitzpatrick, *Endocrinol.*, **54**, 553 (1954); A. B. Lerner and M. R. Wright, Method of Biochemical Analysis, **8**, 295 (1960).

activities, which was reported by Boissonnas *et al.*[9] and by Kappeler *et al.*[10] to occur when the amino-terminal L-serine of corticotropin peptides was replaced by D-amino acids, is a consequence of the decreased susceptibility of peptides toward the action of intracellular aminopeptidase. Geiger *et al.*[11] have also reported that [1-β-alanine]-ACTH(1-23)-NH_2 possesses a high potency over the 1-L-serine analog. The present communication will describe the synthesis of an octadecapeptide amide, α-aminoisobutyryl-tyrosyl-seryl-methionyl-glutamyl-histidyl-phenylalanyl-arginyl-tryptophyl-glycyl-lysyl-prolyl-valyl-glycyl-lysyl-lysyl-arginyl-arginine amide, [Ibu[1]]-ACTH(1-18)-NH_2 (Ie),[12] corresponding to the first eighteen amino acid residues of corticotropin except that the amino terminal serine in the native hormone has been replaced by α-aminoisobutyric acid.

$$\underset{1}{R_1}\text{-Tyr-}\underset{2}{\text{Ser}}\text{-}\underset{3}{\text{Met}}\text{-}\underset{4}{\text{Glu}}\text{-}\underset{5}{\text{His}}\text{-}\underset{6}{\text{Phe}}\text{-}\underset{7}{\text{Arg}}\text{-}\underset{8}{\text{Trp}}\text{-}\underset{9}{\text{Gly}}\text{-}\underset{10}{\text{Lys}}\text{-}\underset{11}{\text{Pro}}\text{-}\underset{12}{\text{Val}}\text{-}\underset{13}{\text{Gly}}\text{-}\underset{14}{\text{Lys}}\text{-}\underset{15}{\text{Lys}}\text{-}\underset{16}{\text{Arg}}\text{-}\underset{17}{\text{Arg}}\text{-}\underset{18}{R_2}$$

ACTH(1—18)-OH (Ia)[1]:

$$R_1=NH_2\text{-}\underset{\displaystyle CH_2OH}{\underset{|}{CH}}\text{-CO},\quad R_2=OH$$

ACTH(1—18)-NH_2 (Ib)[1]:

$$R_1=NH_2\text{-}\underset{\displaystyle CH_2OH}{\underset{|}{CH}}\text{-CO},\quad R_2=NH_2$$

[Gly[1]]-ACTH(1—18)-NH_2 (Ic)[4]:

$$R_1=NH_2\text{-}CH_2\text{-CO},\quad R_2=NH_2$$

[β-Ala[1]]-ACTH(1—18)-NH_2 (Id)[6]:

$$R_1=NH_2\text{-}CH_2\text{-}CH_2\text{-CO},\quad R_2=NH_2$$

[Ibu[1]]-ACTH(1—18)-NH_2 (Ie):

$$R_1=NH_2\text{-}\underset{\displaystyle CH_3}{\underset{|}{C}}\text{-CO},\quad R_2=NH_2$$

α-Aminoisobutyric acid (α-methylalanine) has no hydrogen atom on the α-carbon and therefore belongs to the type of amino acids which forms peptide bonds resisting the action of aminopeptidase. If the current view is right, the amino-terminal substitution by α-aminoisobutyric acid in a corticotropin peptide should result in a remarkable improvement in its biological activities, to the same extent as that produced by D-amino acids[9,10] or β-alanine.[6,11] The present synthesis was undertaken to examine this point and to provide more evidence for the view.

In the present work a new procedure was applied to the synthesis of the decapeptide intermediate corresponding to positions 1—10 of Ie. The procedure is outlined in Fig. 1. A benzyloxycarbonyl group and a benzyl ester group were used to protect the amino group of position 1 and the γ-carboxyl group of glutamic acid residue at position 5, respectively. Formation of the decapeptide was performed by coupling of the tripeptide azide (positions 1—3) with the heptapeptide (4—10) which was synthesized stepwise from the glycine at position 10 *via* a free pentapeptide H-His-Phe-Arg-Trp-Gly-OH (VI)[13] as an intermediate. This procedure eliminates the possibility of partial oxidation by nitrous acid of methionine that may occur when the hydrazide of a methionine containing peptide is subjected to azide formation prior to coupling reaction. Because of the presence of benzyloxycarbonyl and benzyl ester groups the final step to generate the free octadecapeptide amide (Ie) was hydrogen fluoride treatment,[14] by which all the protecting groups were removed very smoothly. The procedure was also applied to the synthesis of 1-β-alanine peptide (Id), which has been prepared before by a different procedure,[6] in order to provide a proof of its utility.

Synthesis of [Ibu[1]]-Octadecapeptide Amide (Ie). The acylation of α-aminoisobutyric acid with benzyl chloroformate proceeded smoothly under the ordinary conditions to give Z-Ibu-OH (II) in moderate yield, whereas acylation with *t*-butyl azidoformate gave the desired Boc-Ibu-OH in a yield of only 9%, even when the reaction was continued for over a week in the presence of excess azidoformate. This is probably due to the presence of the additional α-methyl group, which will reduce the reactivity of α-amino group sterically. Attempts to prepare the Ibu-Tyr-Ser sequence were made by two different procedures. There was no difficulty in coupling compound II with tyrosine methyl ester by the DCC method. The resulting dipeptide ester was readily converted into the hydrazide Z-Ibu-Tyr-$NHNH_2$. In the subsequent steps, however, the products could not be characterized as the

9) a) R. A. Boissonnas, St. Guttmann and J. Pless, *Experientia*, **22**, 526 (1966); b) W. Doepfner, *ibid.*, **22**, 527 (1966); c) M. Jenny, A. F. Muller and R. S. Mach, *ibid.*, **22**, 528 (1966).

10) H. Kappeler, B. Riniker, W. Rittel, P. Desaulles, R. Maier, B. Schär and M. Staehelin, "Peptides," Proceedings of the 8th European Peptide Symposium, ed. by H. C. Beyerman, A. van de Linde and W. Maassen van den Brink, North-Holland Publishing Co., Amsterdam (1967), p. 214.

11) R. Geiger, H.-G. Schröder and W. Siedel, *Ann. Chem.*, **726**, 177 (1969).

12) All amino acid residues are of the L-configuration, unless otherwise indicated. The abbreviated designation of amino acids, peptides and their derivatives accords with the proposal of the IUPAC-IUB Commission of Biochemical Nomenclature, which appeared in *Biochemistry*, **5**, 2485 (1966); *ibid.*, **6**, 362 (1967). Ibu: α-aminoisobutyric acid.

13) See Ref. 6. An alternative synthesis of VI with the use of N^G-tosyl-arginine will be described elsewhere.

14) S. Sakakibara and Y. Shimonishi, This Bulletin, **38**, 1412 (1965); S. Sakakibara, Y. Shimonishi, M. Okada and Y. Kishida, "Peptides," Proceedings of the 8th European Peptide Symposium, ed. by H. C. Beyerman, A. van de Linde and W. Maassen van den Brink, North-Holland Publishing Co., Amsterdam (1967), p. 44.

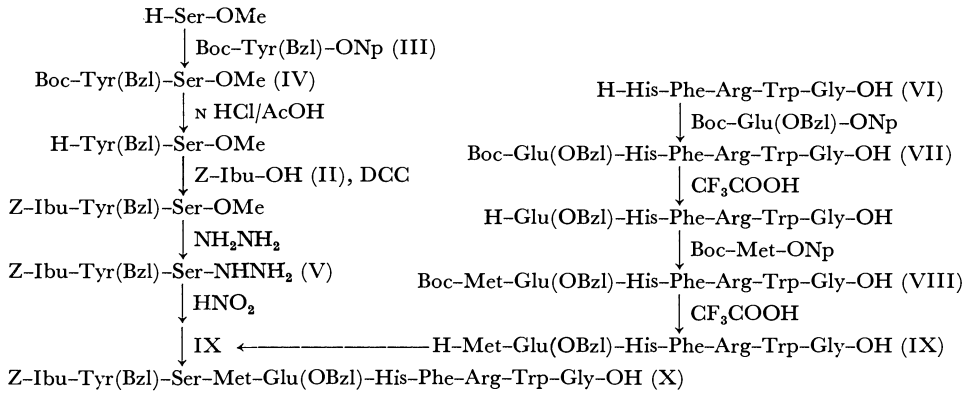

Fig. 1. Synthetic procedure of decapeptide intermediate X[12]

desired compounds, Z-Ibu-Tyr-Ser-OMe and its hydrazide. There must have been some complication in the azide coupling reaction. On the other hand, Boc-Tyr(Bzl)-ONp (III) was allowed to react with serine methyl ester to yield Boc-Tyr(Bzl)-Ser-OMe (IV). Compound II was then coupled by the DCC method with a crystalline dipeptide ester, derived from IV with N hydrogen chloride in acetic acid, to give a tripeptide Z-Ibu-Tyr(Bzl)-Ser-OMe, which was converted into the corresponding hydrazide (V).

A pentapeptide H-His-Phe-Arg-Trp-Gly-OH (VI), which was derived from Z-His-Phe-Arg-(NO_2)-Trp-Gly-OH[6] or from Z-His-Phe-Arg(Tos)-Trp-Gly-OH[13] by hydrogen fluoride treatment,[14] was acylated with Boc-Glu(OBzl)-ONp in the absence of added amine. The reaction was fairly complete in 24 hr. The product VII, isolated in 80% yield, was treated with trifluoroacetic acid and the resulting amino-free hexapeptide trifluoroacetate was then coupled with Boc-Met-ONp in the presence of triethylamine to obtain a heptapeptide Boc-Met-Glu(OBzl)-His-Phe-Arg-Trp-Gly-OH (VIII). Removal of the Boc group from VIII yielded the N^{α}-free heptapeptide (IX) as the key intermediate in the present synthesis of both Ie and Id. Coupling of IX with the azide derived from V gave the decapeptide derivative Z-Ibu-Tyr(Bzl)-Ser-Met-Glu(OBzl)-His-Phe-Arg-Trp-Gly-OH (X). Compound X was then converted into the dihydrochloride by lyophilization from acetic acid containing a small excess of hydrogen chloride, followed by esterification with *N*-hydroxysuccinimide by the carbodiimide method.[15] The active ester of X, which was isolated, was allowed to react with a partially protected octapeptide, H-Lys(Boc)-Pro-Val-Gly-Lys(Boc)-Lys(Boc)-Arg-Arg-NH_2,[16] in the presence of triethylamine to yield a protected octadecapeptide Z-Ibu-Tyr(Bzl)-Ser-Met-Glu(OBzl)-His-Phe-Arg-Trp-Gly-Lys(Boc)-Pro-Val-Gly-Lys(Boc)-Lys(Boc)-Arg-Arg-NH_2 (XI). The crude XI was, without purification, subjected to treatment with hydrogen fluoride[14] in the presence of anisole and methionine as radical scavengers. The crude deblocked octadecapeptide (Ie), obtained in the form of hydrofluoride, was treated with an anion exchange resin (acetate) to be converted into the acetate form, which was then chromatographed, for purification, on a column of carboxymethyl cellulose using an ammonium acetate buffer with a linear concentration gradient. After repeated chromatography, peptide Ie was obtained in pure form. The over-all yield of Ie for the final coupling, deblocking and purification steps was 50%. The product behaved as a single component in thin-layer chromatography and in paper electrophoresis. Quantitative amino acid analysis[17] showed that an acid hydrolysate of the product contained the individual amino acids in the ratios expected by theory with the exception of tryptophan. The tryptophan-tyrosine ratio of intact Ie was determined spectrophotometrically to be unity.

Synthesis of [β-Ala[1]]-Octadecapeptide Amide (Id). A synthesis of this octadecapeptide amide has been reported already in the preceding paper,[6] in which the terminal amino group was protected with a *t*-butyloxycarbonyl group and the γ-carboxyl group of the glutamic acid residue at position 5 by the formation of the *t*-butyl ester and the first decapeptide sequence was made up of tetrapeptide (positions 1—4) and hexapeptide (5—10). An alternative synthesis developed in the present work is summarized in Fig. 2. The amino-terminal tripeptide sequence was synthesized in the form of Z-β-Ala-Tyr-Ser-OMe (XIV) *via* Z-β-Ala-Tyr-$NHNH_2$ (XIII) as an intermediate. The tripeptide azide, derived from XV, was allowed to react with heptapeptide (IX) to give a decapeptide Z-

15) G. W. Anderson, J. E. Zimmerman and F. M. Callahan, *J. Amer. Chem. Soc.*, **86**, 1839 (1964); *ibid.*, **85**, 3039 (1963).

16) H. Otsuka, K. Inouye, M. Kanayama and F. Shinozaki, This Bulletin, **39**, 882 (1966).

17) D. H. Spackman, W. H. Stein and S. Moore, *Anal. Chem.*, **30**, 1190 (1958).

Z-β-Ala-OH
↓ H-Tyr-OMe, DCC
Z-β-Ala-Tyr-OMe (XII)
↓ NH_2NH_2
Z-β-Ala-Tyr-$NHNH_2$ (XIII)
↓ HNO_2
↓ H-Ser-OMe
Z-β-Ala-Tyr-Ser-OMe (XIV)
↓ NH_2NH_2
Z-β-Ala-Tyr-Ser-$NHNH_2$ (XV)
↓ HNO_2
↓ IX
Z-β-Ala-Tyr-Ser-Met-Glu(OBzl)-His-Phe-
-Arg-Trp-Gly-OH (XVI)

Fig. 2. Synthetic procedure of decapeptide intermediate XVI[12]

β-Ala-Tyr-Ser-Met-Glu(OBzl)-His-Phe-Arg-Trp-Gly-OH (XVI) in pure form in 62% yield. Compound XVI was then esterified with *N*-hydroxysuccinimide in the usual manner and the active ester was made react with the octapeptide H-Lys(Boc)-Pro-Val-Gly-Lys(Boc)-Lys(Boc)-Arg-Arg-NH_2.[16] The resulting crude preparation of protected octadecapeptide Z-β-Ala-Tyr-Ser-Met-Glu(OBzl)-His-Phe-Arg-Trp-Gly-Lys(Boc)-Pro-Val-Gly-Lys(Boc)-Lys(Boc)-Arg-Arg-NH_2 (XVII) was, without purification, deblocked with hydrogen fluoride to liberate peptide Id. The crude Id was then purified by chromatography on a column of carboxymethyl cellulose. These procedures, the final coupling, deblocking and purification steps, were carried out in a manner almost the same as that used in the synthesis of Ie. The over-all yield of Id thus obtained was 45%. The product was found to be homogeneous in thin-layer chromatography and in paper electrophoresis. The quantitative amino acid analysis[17] showed that an acid hydrolysate of the product contained the individual amino acids in the ratios expected by theory with the exception of tryptophan. The tryptophan-tyrosine ratio of intact Id was determined spectrophotometrically to be unity.[18] Optical rotation and chromatographic behaviors of the present preparation of Id were identical with those of a previous preparation obtained by a different synthetic procedure.[6]

Biological Properties of the Octadecapeptide Amides. Adrenal-stimulating activities of Ibu[1]-octadecapeptide amide (Ie) were compared with those of the present and previous preparations of β-Ala[1]-analog (Id) by six different assay procedures: 1) adrenal-ascorbic acid depletion,[19] 2) *in vitro* steroidogenesis,[20] 3) *in vivo* steroidogenesis in adrenal cannulation,[21] 4) *in vivo* steroidogenesis in dexamethasone-pentobarbital-blocked mouse,[22] 5) *in vivo* steroidogenesis in peripheral blood (intravenous administration), and 6) *in vivo* steroidogenesis in peripheral blood (intramuscular administration). The results are summarized in Table 1, in which the data on Gly[1]-analog (Ic)[4,6] are included for comparison. As is seen in Table 1, there is no significant difference in potency between the present preparation and the previous preparation of Id, proving their identity. This also proves the usefulness and safety of the new synthetic procedure, by which both peptides Id and Ie were prepared. The data in Table 1 clearly demonstrate that Ibu[1]-peptide (Ie) is endowed with a very high adrenal-stimulating activity and its potency appears to be more than twice that of β-Ala[1]-peptide (Id), when assayed by the adrenal-ascorbic acid depletion method and by the *in vivo* steroidogenesis methods. In addition, it is to be noted that the activity of Ie, estimated by the 11-hydroxycorticosteroid (11-OHCS) level in rat peripheral blood, is unchanged regardless of whether the peptide is administered intravenously or intramuscularly. In Ic and Id, however, the potency ratio of intramuscular *vs.* intravenous administration is 1/5 and 1/2, respectively. Tanaka has estimated the half-lives of a native corticotropin and the synthetic peptides Ic, Id, and Ie with the *in vitro* lipotropic activity[23] as a parameter. The results are shown in Table 2.[24] When the synthetic peptides are incubated in plasma, their half-lives are all the same, indicating that the inactivation of peptides in plasma is little associated with the action of aminopeptidase. On the other hand, when incubated with muscle fragments, the inactivation rate largely depends on the nature of the amino-terminal residue of peptides; Ibu[1]-peptide (Ie) can remain active rather longer than β-Ala[1]-peptide (Id). This may be correlated with the above observation that the intramuscular *vs.* intravenous potency ratio of Ie is larger than that of Id. In the preceding paper we described that β-Ala[1]-peptide (Id) was remarkably more potent, with a longer action in adrenal-stimulating activity than the corresponding Ser[1]-peptide (Ib) or Gly[1]-

18) G. H. Beaven and E. R. Holiday, *Advan. Protein Chem.*, **7**, 319 (1952); T. W. Goodwin and R. A. Morton, *Biochem. J.*, **40**, 628 (1946).

19) The United States Pharmacopeia, XVII, 147 (1965).

20) M. Saffran and A. V. Schally, *Endocrinol.*, **56**, 523 (1955).

21) H. S. Lipscomb and D. H. Nelson, *ibid.*, **71**, 13 (1962).

22) A. Tanaka and M. Nakamura, "Integrative Mechanism of Neuroendocrine System," Hokkaido University Medical Library Series, Vol. 1 (1968), p. 49.

23) A. Tanaka, B. T. Pickering and C. H. Li, *Arch. Biochem. Biophys.*, **99**, 294 (1962).

24) We thank Dr. A. Tanaka for of this Laboratory permission to include these data in the present communication.

Table 1. Adrenal-stimulating activities of synthetic octadecapeptide amides[a)]

Method	Administration route	Peptide[b)] Ic	Id	Ie
Adrenal-ascorbic acid depletion[19)]	subcutaneous	25.6	— (135)	140—286
In vitro steroidogenesis[20)]		27.2	— (237)	82.7
In vivo steroidogenesis in:				
adrenal cannulation[21)]	intravenous	151	220 (285)	480
dexamethasone-Nembutal-blocked mouse[22)]	intravenous	170	250 (259)	757
peripheral blood	intravenous	177	286 (—)	590
peripheral blood	intramuscular	50.5	115 (124)	495

a) The activities are expressed in USP units/mg, relative to the Third USP Corticotropin Reference Standard. The figures in parentheses are the data on the previous preparation.[6)]
b) Ic: [Gly^1]-ACTH(1-18)-NH_2, Id: [β-Ala^1]-ACTH(1-18)-NH_2, and Ie: [Ibu^1]-ACTH(1-18)-NH_2.

Table 2. Half-lives of corticotropin and related synthetic peptides as *in vitro* lipotropic agents[24)]

Peptide[a)]	*In vivo*[b)] (Intravenous injection)	*In vitro*,[c)] incubation with Plasma	Muscle
	min	min	min
Ic	2.0	30.0	42.6
Id	3.1	35.4	88.2
Ie	3.5	32.4	122.9
ACTH	4.4	59.2	250.9

a) Ic: [Gly^1]-ACTH (1-18)-NH_2, Id: [β-Ala^1]-ACTH (1-18)-NH_2, Ie: [Ibu^1]-ACTH (1-18)-NH_2, ACTH: native sheep corticotropin.
b) A peptide sample was injected intravenously into vena cava inferior and blood samples, collected from abdominal aorta in appropriate time intervals and acidified, were assayed for the *in vitro* lipotropic activity.[23)]
c) A sample was dissolved in the fresh plasma from anesthetized rat or in the Krebs-Ringer bicarbonate buffer containing thigh muscle slices of rat, bovine serum albumin and glucose. These mixtures were then incubated at 37°C and the aliquots taken from the mixtures in appropriate time intervals were assayed for the *in vitro* lipotropic activity.[23)]

peptide (Ic).[6)] The present results show that Ibu^1-peptide (Ie) also exceeds Ic greatly in the biological activity, exhibiting a similarity to Id. Since α-aminoisobutyric acid amide and β-alanine amide are equally known not to be cleaved by hog kidney leucine aminopeptidase,[25)] this similarity is not surprising, and it provides additional support for the view that the marked increase in biological activities as a main effect of the amino-terminal substitution is a consequence of the decreased susceptibility of peptide toward aminopeptidase action. However, peptide Ie still differs from peptide Id as seen in Tables 1 and 2, indicating that α-aminoisobutyric acid is preferred to β-alanine as the amino-terminal residue of corticotropin peptide, probably because of some favorable effects of the α-amino group in the former amino acid. Geiger *et al.*[26)] reported that removal of 1-glycine residue from [Gly^1]-ACTH(1-23)-tricosapeptide amide caused a 50% loss of activity. This finding would suggest a significant importance for activity of the distance separating the terminal amino group and the center of active site of the peptide. In Ibu^1-peptide (Ie) the amino-terminal amino group occupies the place where it sits in a native corticotropin, whereas the corresponding group in β-Ala^1-peptide (Id) is located one methylene unit away from the regular position. In addition, it is to be noted that the amino group of α-aminoisobutyric acid will have a pK value close to those of ordinary α-amino acids (*e. g.* serine 9.15) rather than that of β-alanine (10.19).[27)] These properties would affect a specific binding of the peptide to its receptor site and the tighter binding may, in turn, serve to further stabilize the peptide; peptide Ie thus could be more potent and have a longer action than Id. One of other possibilities which explain the difference between Id and Ie is the participation of an enzyme which can act on β-alanine peptides specifically. Because of the occurrence of β-alanine peptides, such as carnosine and anserine, in animal tissues, it is not unreasonable to assume the presence of such enzyme.

It has been shown that the amino-terminal substitution by unusual amino acids, such as β-alanine and α-aminoisobutyric acid, in a corticotropin pep-

25) E. L. Smith and D. H. Spackman, *J. Biol. Chem.*, **212**, 271 (1955).

26) R. Geiger, K. Sturm, G. Vogel and W. Siedel, *Z. Naturforsch.*, **19b**, 858 (1964).

27) J. P. Greenstein and M. Winitz, "Chemistry of Amino Acids," Vol. 1, John Wiley & Sons, Inc., New York (1961), p. 486.

tide improves its biological properties greatly in both enhancement of potency and prolongation of action. As is apparent in Table 2, however, the amino-terminal substitution improves the stability of peptide in tissues, but not the stability in blood, indicating that the inactivation of peptide in blood may be associated with the action of some endopeptidase, but not with an aminopeptidase action. The presence of such an endopeptidase is known.[28] A further improvement in allowing the short-chain peptide to come closer to a native corticotropin should be achieved by reducing the susceptibility of peptide toward the endopeptidase action without a considerable loss of activity. The synthesis of [β-Ala^1, Orn^{15}]-ACTH(1-18)-NH_2 may be one solution.[29] This new peptide possesses a moderate adrenal-stimulating activity and shows an excellent prolongation of action; the half-life in plasma is longer than that of the native hormone (76 min, see Table 2 for comparison).

Experimental

All melting points were uncorrected.

Benzyloxycarbonyl-α-aminoisobutyric Acid (II). To a solution of α-aminoisobutyric acid (5.16 g, 0.05 mol) and anhydrous sodium carbonate (5.30 g, 0.05 mol) in N sodium hydroxide (50 m*l*) was added benzyl chloroformate (9.39 g, 0.055 mol) at 0°C and the mixture was stirred for 3 hr. The reaction mixture was washed with ether to remove the excess reagent and acidified with 6N hydrochloric acid, followed by extraction with ethyl acetate. The organic extracts were combined, dried over sodium sulfate and evaporated *in vacuo* to give a crystalline residue, which was recrystallized from ethyl acetate - petroleum ether; yield 8.75 g (73%), mp 69—70°C. Lit,[30] mp 78°C.

Found: C, 61.04; H, 6.36; N, 6.07%. Calcd for $C_{12}H_{15}NO_4$: C, 60.75; H, 6.37; N, 5.90%.

***t*-Butyloxycarbonyl-α-aminoisobutyric Acid.** To a solution of α-aminoisobutyric acid (4.75 g, 0.046 mol) and sodium bicarbonate (4.25 g, 0.05 mol) in N sodium hydroxide (46 m*l*) and dioxane (30 m*l*) was added dropwise a dioxane solution of *t*-butyl azidoformate (7.25 g, 0.05 mol) and the mixture was stirred at 45—50°C for 5 days. An additional quantity of *t*-butyl azidoformate (6.6 g, 0.046 mol) and N sodium hydroxide (46 m*l*) was introduced and the mixture was stirred for 2 days at the same temperature and then concentrated *in vacuo* to remove most of the organic solvent. The concentrate was chilled and acidified with ice-cold 4N hydrochloric acid to pH 3, followed by extraction with ethyl acetate. The organic solution was dried over sodium sulfate and evaporated. The resulting crystals were recrystallized from ether; yield 0.81 g (8.7%), mp 119—120°C.

Found: C, 53.64; H, 8.39; N, 7.19%. Calcd for $C_9H_{17}NO_4$: C, 53.19; H, 8.43; N, 6.89%.

Benzyloxycarbonyl-α-aminoisobutyryl-tyrosine Hydrazide. Compound II (1.54 g, 6.5 mmol) and tyrosine methyl ester (free base, 1.27 g, 6.5 mmol) were dissolved in acetonitrile and to this solution was added *N,N'*-dicyclohexylcarbodiimide (DCC, 1.34 g, 6.5 mmol) at 0°C with acetonitrile as solvent. The mixture was kept at 4°C overnight. *N,N'*-dicyclohexylurea (DCU) which formed was filtered off and the filtrate was evaporated *in vacuo*. The residue was dissolved in ethyl acetate and the solution was washed with N hydrochloric acid and 5% sodium bicarbonate, dried over sodium sulfate and evaporated *in vacuo* to give the dipeptide ester as a sirupy residue. The residue was dissolved in ethanol (15 m*l*) and hydrazine hydrate (0.8 m*l*) was added. After the reaction mixture had been kept at room temperature for 2 days, water was added to separate the desired dipeptide hydrazide as crystals; yield 2.35 g (87%), mp 160—162°C. Recrystallization from aqueous ethanol yielded the pure material in a recovery of 92%; mp 164—165°C, $[\alpha]_D^{27}$ $-31.4\pm0.7°$ (*c* 1.078, methanol).

Found: C, 60.95; H, 6.41; N, 13.31%. Calcd for $C_{21}H_{26}N_4O_5$: C, 60.86; H, 6.32; N, 13.52%.

***t*-Butyloxycarbonyl-*O*-benzyl-tyrosine *p*-Nitrophenyl Ester (III).** To a solution of *t*-butyloxycarbonyl-*O*-benzyl-tyrosine (2.97 g, 8 mmol)[31] and *p*-nitrophenol (1.12 g, 8 mmol) in ethyl acetate was added an ethyl acetate solution of DCC (1.65 g, 8 mmol) at 0°C and the mixture was kept at 4°C for 3 hr. The DCU which formed was removed by filtration and the filtrate was evaporated *in vacuo*. The resulting solid residue was suspended in hot ethanol and the crystals were filtered off after refrigeration, washed with cold ethanol and dried *in vacuo* to give the desired active ester; yield 3.39 g (86%), mp 140—141°C, $[\alpha]_D^{22}$ $-0.3\pm0.4°$ (*c* 0.983, ethyl acetate).

Found: C, 65.93; H, 5.73; N, 5.67%. Calcd for $C_{27}H_{28}N_2O_7$: C, 65.84; H, 5.73; N, 5.69%'

***t*-Butyloxycarbonyl-*O*-benzyl-tyrosyl-serine Methyl Ester (IV).** To an ice-cold solution of serine methyl ester hydrochloride (1.03 g, 6.6 mmol) in dimethylformamide (DMF, 8 m*l*) was added triethylamine (0.92 m*l*, 6.6 mmol) and the amine hydrochloride which formed was filtered off. ADMF solution of III (2.96 g, 6.0 mmol) was added to the filtrate and the mixture was kept at 4°C for 2 days. After the solvent had been removed by evaporation *in vacuo* at a bath temperature of 45—50°C, the residue was dissolved in ethyl acetate and the solution was washed successively with ice-cold N hydrochloric acid, water, 2N aqueous ammonia and water, dried over sodium sulfate and evaporated *in vacuo*. The resulting gelatinous mass was precipitated from ethyl acetate - petroleum ether. Reprecipitation from methanol-water afforded the pure dipeptide; yield 2.75 g (97%), mp 73—77°C, $[\alpha]_D^{22}$ $+7.7\pm0.5°$ (*c* 1.046, methanol).

Found: C, 63.36; H, 6.97; N, 5.71.% Calcd for $C_{25}H_{32}N_2O_7$: C, 63.54; H, 6.83; N, 5.93%.

Benzyloxycarbonyl-α-aminoisobutyryl-*O*-benzyl-tyrosyl-serine Hydrazide (V). Compound IV (2.08 g,

28) W. F. White and A. M. Gross, *J. Amer. Chem. Soc.*, **79**, 1141 (1957).

29) K. Inouye, K. Watanabe, K. Namba and H. Otsuka, in preparation.

30) M. Bergmann, L. Zervas, J. S. Fruton, F. Schneider and H. Schleich, *J. Biol. Chem.*, **109**, 325 (1935).

31) R. Schwyzer, P. Sieber and H. Kappeler, *Helv. Chim. Acta*, **42**, 2622 (1959).

4.4 mmol) was dissolved in N hydrogen chloride in acetic acid (20 ml) and the mixture was allowed to stand at room temperature for 30 min. Evaporation of the solvent left an oily residue which solidified upon treatment with ether. The solid which was filtered off was dissolved in a mixture of water (6 ml) and dichloromethane (20 ml), and to this was added ice-cold 50% potassium carbonate (6 ml). The mixture was shaken well and the organic phase was separated, dried over sodium sulfate and evaporated *in vacuo*. The crystalline *O*-benzyl-tyrosyl-serine methyl ester (free base) thus obtained was dissolved in acetonitrile along with compound II (1.04 g, 4.4 mmol) and to this solution was introduced an acetonitrile solution of DCC (0.91 g, 4.4 mmol) at 0°C. The mixture was kept at 4°C overnight. The DCU which formed was filtered off and the filtrate was evaporated *in vacuo*. The residue was dissolved in ethyl acetate and the solution was washed successively with N hydrochloric acid, water and 5% sodium bicarbonate, dried over sodium sulfate and evaporated *in vacuo*, yielding the crude tripeptide ester which showed on a thin-layer chromatogram (in ethyl acetate) the presence of a smaller amount of an additional component. The crude ester was then dissolved in ethanol (20 ml) and hydrazine hydrate (1.0 ml, 20 mmol) was added. The reaction mixture was allowed to stand at room temperature for 2 days, followed by evaporation *in vacuo*. The residue was dissolved in ethyl acetate and the solution was washed with water and dried quickly over sodium sulfate. The precipitates which separated on standing were filtered off, washed with cold ethyl acetate and ether and dried *in vacuo* to give the desired hydrazide; yield 1.91 g (72%). Reprecipitation from ethanol gave the pure material in a recovery of 80%, mp 151—153°C, $[\alpha]_D^{22}$ $-2.2\pm0.4°$ (*c* 1.062, glacial acetic acid).

Found: C, 62.98; H, 6.31; N, 11.81%. Calcd for $C_{31}H_{37}N_5O_7$: C, 62.93; H, 6.30; N, 11.84%.

Benzyloxycarbonyl-β-alanyl-tyrosine Methyl Ester (XII). To a solution of benzyloxycarbonyl-β-alanine (8.9 g, 0.04 mol)[32] and tyrosine methyl ester (free base, 7.8 g, 0.04 mol) in acetonitrile was added a dichloromethane solution of DCC (8.3 g, 0.04 mol) at 0°C and the mixture was kept at 4°C overnight. After removal of DCU by filtration the filtrate was evaporated *in vacuo*. The resulting residue was dissolved in ethyl acetate and the solution was washed with N hydrochloric acid and 5% sodium bicarbonate, dried over sodium sulfate and evaporated *in vacuo* to yield a sirupy residue which crystallized from ethyl acetate - ether. After recrystallization from the same solvent the product amounted to 13.2 g (83%); mp 114—116°C, $[\alpha]_D^{27}$ $+6.2\pm0.4°$ (*c* 1.040, methanol).

Found: C, 62.94; H, 6.06; N, 6.85%. Calcd for $C_{21}H_{24}N_2O_6$: C, 62.99; H, 6.04; N, 6.93%.

Benzyloxycarbonyl-β-alanyl-tyrosine Hydrazide (XIII). Compound XII (4.81 g, 0.012 mol) was dissolved in ethanol (50 ml) and hydrazine hydrate (2.9 ml, 0.06 mol) was added. The mixture was allowed to stand at room temperature for a few hours and kept at 4°C overnight. The crystalline hydrazide which separated was filtered off, washed with cold ethanol and dried *in vacuo*; yield 4.72 g (98%). After treatment with hot ethanol the mp was 225—228°C; $[\alpha]_D^{26}$ $+3.9\pm0.4°$ (*c* 1.032, 50% acetic acid).

Found: C, 60.09; H, 6.16; N, 13.97%. Calcd for $C_{20}H_{24}N_4O_5$: C, 59.99; H, 6.04; N, 13.99%.

Benzyloxycarbonyl-β-alanyl-tyrosyl-serine Methyl Ester (XIV). Compound XIII (2.40 g, 6 mmol) was dissolved in DMF (7 ml) and N hydrochloric acid (15 ml) was added. The solution was chilled in ice and to this was added ice-cold 2M sodium nitrite (3. 6ml). After the mixture had been kept at 0°C for 4 min, the azide which separated was extracted with ice-cold ethyl acetate (25 ml×2). The organic extracts were combined, washed with ice-cold 5% sodium bicarbonate, dried over sodium sulfate. The resulting solution was added to a mixture of serine methyl ester hydrochloride (0.93 g, 6 mmol) and triethylamine (0.84 ml, 6 mmol) in 90% tetrahydrofuran (20 ml) and the mixture was stirred at 4°C for 48 hr. The gelationous precipitates which had separated were filtered off, washed with cold ethyl acetate and with water and dried *in vacuo*; yield 1.58 g (54%). After treatment with hot methanol the mp was 195—196°C; $[\alpha]_D^{26}$ $+2.1\pm0.4°$ (*c* 1.091, methanol).

Found: C, 59.29; H, 6.08; N, 8.63%. Calcd for $C_{24}H_{29}N_3O_8$: C, 59.13; H, 6.00; N, 8.62%.

Benzyloxycarbonyl-β-alanyl-tyrosyl-serine Hydrazide (XV). To a solution of compound XIV (1.46 g, 3 mmol) in DMF (5 ml) was added hydrazine hydrate (0.73 ml, 15 mmol) and the mixture was kept at 4°C for 24 hr. The hydrazide had separated as crystals. After addition of ethanol (10 ml) the crystals were filtered off, washed with ethanol and dried *in vacuo* (1.40 g). Treatment with hot ethanol gave the pure hydrazide; yield 1.32 g (90%), mp 220—224°C decomp, $[\alpha]_D^{25}$ $+15.7\pm0.5°$ (*c* 1.042, glacial acetic acid).

Found: C, 56.35; H, 6.04; N, 14.57%. Calcd for $C_{23}H_{29}N_5O_7$: C, 56.66; H, 6.00; N, 14.37%.

***t*-Butyloxycarbonyl-γ-benzyl-glutamic Acid Dicyclohexylamine Salt.** Glutamic acid γ-benzyl ester (9.5 g, 0.04 mol)[33] and sodium bicarbonate (12.5 g) were suspended in water (100 ml) and dioxane (80 ml) and to this was added *t*-butyl azidoformate (8.6 g, 0.06 mol) with dioxane (20 ml). The mixture was stirred at 45—50°C for 2 days, followed by concentration *in vacuo* to remove most of the dioxane. The concentrated solution was then acidified to pH 3—4 with ice-cold 4N hydrochloric acid at 0°C and the product was extracted with ice-cold ethyl acetate. The organic solution was washed with ice-cold N hydrochloric acid and water, dried over sodium sulfate and evaporated *in vacuo* to give an oily residue. The residue was dissolved in ether (50 ml) and dicyclohexylamine (7.3 g, 0.04 mol) was added. Crystalline precipitates which had separated upon standing at 4°C overnight were filtered off, washed with ether and dried *in vacuo*; yield 16.7 g (81%). After recrystallization from ethyl acetate the product showed mp 140—142°C, $[\alpha]_D^{27}$ $+13.3\pm0.5°$ (*c* 1.024, methanol). Lit,[34] mp 138—139°C, $[\alpha]_D^{25}$ $+11.9°$ (*c* 1, methanol).

Found: C, 67.03; H, 9.02; N, 5.68%. Calcd for $C_{17}H_{23}NO_6 \cdot C_{12}H_{23}N$: C, 67.15; H, 8.94; N, 5.40%.

32) R. H. Sifferd and V. du Vigneaud, *J. Biol. Chem.*, **108**, 753 (1935).

33) a) H. Yuki, *Nippon Kagaku Zasshi*, **77**, 44 (1956); b) W. E. Hanby, S. G. Waley and J. Watson, *J. Chem. Soc.*, **1950**, 3239; c) E. R. Blout and R. H. Karlson, *J. Amer. Chem. Soc.*, **78**, 941 (1956).

34) E. Schröder and E. Klieger, *Ann. Chem.*, **673**, 196 (1964).

***t*-Butyloxycarbonyl-γ-benzyl-glutamic Acid *p*-Nitrophenyl Ester.** *t*-Butyloxycarbonyl-γ-benzyl-glutamic acid dicyclohexylamine salt (9.0 g, 17.4 mmol) was shaken with Dowex 50W×8 (H^+ form, wet vol 18 cc) in 60% ethanol for 30 min. After the resin had been removed by filtration the filtrate was evaporated *in vacuo*. The residue was dissolved in ether and the solution was dried over sodium sulfate and evaporated *in vacuo* to afford the free acid quantitatively. This was dissolved in ethyl acetate together with *p*-nitrophenol (2.4 g, 17.4 mmol) and to this solution was added DCC (3.6 g, 17.4 mmol) at 0°C. The reaction mixture was kept at 4°C overnight. After removal of DCU by filtration the filtrate was evaporated *in vacuo* to give a residue which crystallized from ethanol. Recrystallization from the same solvent gave the active ester in a pure form; yield 7.0 g (88%), mp 118—119°C, $[\alpha]_D^{28}$ −33.1±0.7° (*c* 1.082, methanol). Lit,[35] mp 120—121°C, $[\alpha]_D^{25}$ −32.7° (*c* 1, methanol).

Found: C, 60.38; H, 5.80; N, 6.29%. Calcd for $C_{23}H_{26}N_2O_8$: C, 60.26; H, 5.72; N, 6.11%.

***t*-Butyloxycarbonyl-methionine Dicyclohexylamine Salt.** To a mixture of methionine (3.0 g, 0.02 mol) and sodium bicarbonate (3.8 g) in water-dioxane (1 : 1 by vol, 60 m*l*) was added *t*-butyl azidoformate (4.3 g, 0.03 mol) and the mixture was stirred at 45°C for 48 hr. The reaction mixture was worked up in the usual manner. The resulting acyl-methionine (oil, 4.3 g) was dissolved in ether and dicyclohexylamine (3.1 g, 0.017 mol) was added. The crystals were collected by filtration, washed with ether and dried *in vacuo*; yield 6.7 g (78%). A sample was recrystallized from ethyl acetate in a recovery of 92%; mp 141°C, $[\alpha]_D^{20}$ −18.2±0.9° (*c* 0.648, methanol).

Found: C, 61.56; H, 9.99; N, 6.68%. Calcd for $C_{10}H_{19}NO_4S \cdot C_{12}H_{23}N$: C, 61.36; H, 9.83; N, 6.51%.

***t*-Butyloxycarbonyl-methionine *p*-Nitrophenyl Ester.** *t*-Butyloxycarbonyl-methionine dicyclohexylamine salt (10.8 g, 0.025 mol) was treated with Dowex 50W×8 (H^+ form) in the same manner as above. The resulting oily acid and *p*-nitrophenol (3.5 g, 0.025 mol) were dissolved in ethyl acetate and to this was added an ethyl acetate solution of DCC (5.2 g, 0.025 mol) at 0°C. The mixture was allowed to stand at 4°C overnight. The DCU was filtered off and the filtrate was evaporated *in vacuo* to give a residue, which crystallized from ethanol. After recrystallization from ethanol the active ester was obtained in 84% yield; wt 7.8 g, mp 96—97°C, $[\alpha]_D^{27}$ −48.3±0.9° (*c* 1.020, methanol).

Found: C, 52.05; H, 5.97; N, 7.68%. Calcd for $C_{16}H_{22}N_2O_6S$: C, 51.88; H, 5.99; N, 7.56%.

***t*-Butyloxycarbonyl-γ-benzyl-glutamyl-histidyl-phenylalanyl-arginyl-tryptophyl-glycine (VII).** To a solution of histidyl-phenylalanyl-arginyl-tryptophyl-glycine monoacetate (VI, 1.20 g, 1.5 mmol)[36] in 50% DMF (10 m*l*) were added *t*-butyloxycarbonyl-γ-benzyl-glutamic acid *p*-nitrophenyl ester (1.03 g, 2.25 mmol) and DMF (25 m*l*), and the mixture was kept at 4°C for 3 days. The resulting solution was added dropwise into a mixture of ethyl acetate - ether (1 : 1 by volume, 200 m*l*) and the precipitates which formed were filtered off, washed with ethyl acetate and ether and dried *in vacuo* (1.86 g). These precipitates were redissolved in 50% acetic acid (*ca.* 10 m*l*) and ethanol (*ca.* 100 m*l*) was added. The resulting precipitates were collected and lyophilized from acetic acid; yield 1.37 g (89%), $[\alpha]_D^{22}$ −23.9±0.6° (*c* 1.020, 50% acetic acid).

Found: C, 56.40; H, 6.22; N, 15.40; CH_3CO; 3.25%. Calcd for $C_{51}H_{64}N_{12}O_{11} \cdot CH_3COOH \cdot 3H_2O$: C, 56.07; H, 6.57; N, 14.81; CH_3CO, 3.79%.

***t*-Butyloxycarbonyl-methionyl-γ-benzyl-glutamyl-histidyl-phenylalanyl-arginyl-tryptophyl-glycine (VIII).** Compound VII (1.26 g, 1.1 mmol) was dissolved in trifluoroacetic acid (6 m*l*) and the mixture was kept at room temperature for 30 min and then chilled in an ice bath. Addition of ether afforded the partially deblocked hexapeptide as precipitates (1.34 g). These precipitates were dissolved in DMF (10 m*l*) and to this solution were added triethylamine (0.46 m*l*, 3.3 mmol) and *t*-butyloxycarbonyl-methionine *p*-nitrophenyl ester (0.74 g, 2 mmol). The mixture was allowed to stand at 4°C for 24 hr and then introduced into an ice-cold mixture of ethyl acetate - ether (1:4 by volume, 250 m*l*). The resulting precipitates were filtered off, washed with ether and dried *in vacuo* (1.56 g). To this product was added ethanol (15 m*l*) and the suspension was heated to boiling point and then chilled. The precipitates were collected, washed with cold ethanol and ether and lyophilized from acetic acid; yield 1.16 g (88%), $[\alpha]_D^{22}$ −18.5±0.5° (*c* 1.072, DMF).

Found: C, 54.51; H, 6.16; N, 13.94%. Calcd for $C_{56}H_{73}N_{13}O_{12}S \cdot CH_3COOH \cdot 2H_2O$: C, 54.23; H, 6.67; N, 14.18%.

Benzyloxycarbonyl-α-aminoisobutyryl-*O*-benzyl-tyrosyl-seryl-methionyl-γ-benzyl-glutamyl-histidyl-phenylalanyl-arginyl-tryptophyl-glycine (X). Compound VIII (0.50 g, 0.4 mmol) was dissolved in trifluoroacetic acid (3 m*l*) containing one drop of water and the mixture was allowed to stand at room temperature for 30 min. The resulting heptapeptide trifluoroacetate (IX) was precipitated by the addition of ether. The precipitates collected by filtration were washed thoroughly with ether and dried *in vacuo*.

A mixture of V (0.47 g, 0.8 mmol), N hydrochloric acid (2 m*l*) and DMF (2 m*l*) was chilled in an ice bath and to this was added dropwise ice-cold 2M sodium nitrite (0.44 m*l*). The mixture was stirred at 0°C for 4 min and then extracted with ice-cold ethyl acetate. The organic extracts were combined, washed with ice-cold sodium bicarbonate and dried over sodium sulfate. The resulting solution was mixed with a solution of IX, obtained above, and triethylamine (0.25 m*l*, 1.6 mmol) in DMF (10 m*l*). The mixture was concentrated *in vacuo* at a bath temperature of 20°C until it became almost clear, and then kept at 4°C for 24 hr. Most of the solvent was removed by evaporation *in vacuo* at a bath temperature of 45°C. The precipitates which formed upon addition of ether were reprecipitated from methanol - ethanol (1 : 1 by vol); yield 0.96 g (82%), $[\alpha]_D^{24}$ −30.1±1.4° (*c* 0.515, DMF). Thin-layer chromatography:[38] R_f=0.44 (BAW), 0.68 (BAPW) and

35) C. H. Li, B. Gorup, D. Chung and J. Ramachandran, *J. Org. Chem.*, **28**, 178 (1963).

36) See Ref. 6. In the present work, this pentapeptide (VI) was purified before use in the manner described previously.[37]

37) K. Inouye, This Bulletin, **38**, 1148 (1965).

38) Solvent systems of chromatography are: BAW, *n*-butanol - acetic acid-water (4 : 1 : 2 by vol); BAPW, *n*-butanol - acetic acid - pyridine - water (30 : 6 : 20 : 24 by vol).

0.50 (ethyl acetate - acetic acid-water=8 : 3 : 2 by vol).

Found: C, 57.31; H, 5.82; N, 12.33%. Calcd for $C_{82}H_{98}N_{16}O_{17}S \cdot 2CH_3COOH \cdot 4H_2O$: C, 57.26; H, 6.37; N, 12.42%.

Benzyloxycarbonyl-β-alanyl-tyrosyl-seryl-methionyl-γ-benzyl-glutamyl-histidyl-phenylalanyl-arginyl-tryptophyl-glycine (XVI). A mixture of XV (0.86 g, 1.75 mmol), N hydrochloric acid (4 ml) and DMF (5 ml) was chilled in an ice bath and to this was added dropwise ice-cold 2M sodium nitrite (0.96 ml). The mixture was stirred at 0°C for 4 min, after which ice-cold DMF (10 ml) was introduced to dissolve the azide, which had separated, followed by addition of triethylamine (0.56 ml, 4.0 mmol). The resulting solution was added to an ice-cold solution of IX (derived from 1.09 g, 0.88 mmol, of VIII by treatment with trifluoroacetic acid) and triethylamine (0.49 ml, 3.5 mmol) in DMF (20 ml) and the mixture was allowed to stand at 0°C for 24 hr. After addition of acetic acid (1 ml) the solvent was removed by evaporation *in vacuo* at a bath temperature of 45°C to afford a sirupy residue. To this was then added ethanol (20 ml) and gelatinous precipitates were filtered off, washed thoroughly with ethanol, ethyl acetate and with ether and dried *in vacuo* (0.88 g). The filtrate and washes were combined and evaporated *in vacuo*. The residue was dissolved in ethyl acetate and insoluble precipitates were filtered off. These precipitates were heated with ethanol to boiling point and filtered off after refrigeration (0.27 g). The total yield amounted to 1.15 g (78%). The precipitates combined were boiled in ethanol for several minutes and collected by filtration in 80% recovery; $[\alpha]_D^{22}$ $-18.5 \pm 0.5°$ (*c* 1.067, DMF). Thin-layer chromatography: R_f=0.75 (BAPW). Paper chromatography: R_f=0.8 (BAW).

Found: C, 55.71; H, 6.06; N, 13.34%. Calcd for $C_{74}H_{90}N_{16}O_{17}S \cdot 2CH_3COOH \cdot 3H_2O$: C, 55.70; H, 6.23; N, 13.33%.

α-Aminoisobutyryl-tyrosyl-seryl-methionyl-glutamyl-histidyl-phenylalanyl-arginyl-tryptophyl-glycyl-lysyl-prolyl-valyl-glycyl-lysyl-lysyl-arginyl-arginine Amide, [Ibu¹]-ACTH(1-18)-NH₂ (Ie). To a solution of X (0.32 g, 0.18 mmol) in acetic acid was added N hydrogen chloride in acetic acid (0.4 ml) and the mixture was immediately lyophilized and dried over sodium hydroxide pellets *in vacuo*. The decapeptide hydrochloride thus obtained was dissolved in DMF (3ml) together with *N*-hydroxysuccinimide (0.083 g, 0.72 mmol) and to this was added a solution of DCC (0.15 g, 0.72 mmol) in DMF (2 ml). The mixture was allowed to stand at 4°C overnight. The DCU which had separated was filtered off and the filtrate was introduced into ice-cold ethyl acetate - ether (1 : 1 by vol, 100 ml) The resulting precipitates were filtered off, washed with ethyl acetate and ether and dried *in vacuo* to yield the decapeptide active ester (0.36 g).

The triacetate of N^{ε}-*t*-butyloxycarbonyl-lysyl-prolyl-valyl-glycyl-N^{ε}-*t*-butyloxycarbonyl-lysyl-N^{ε}-*t*-butyloxycarbonyl-lysyl-arginyl-arginine amide (derived from 0.12 mmol of the corresponding N^{α}-benzyloxycarbonyl derivative by catalytic hydrogenolysis)[16] was dissolved in DMF (2 ml) and triethylamine (0.18 ml) was added. This solution was mixed with a DMF solution of the active ester obtained above and the mixture (total volume, 4 ml) was kept at 4°C for 48 hr. The reaction mixture was then introduced into ice-cold ethyl acetate (100 ml) and the precipitates which separated were filtered off, washed with ethyl acetate and ether, lyophilized from acetic acid and dried over sodium hydroxide pellets *in vacuo*, affording the crude protected octadecapeptide (0.56 g).

The protected peptide obtained above was put into a reaction vessel (made of fluorinated polyethylene) with methionine (0.1 g) and anisole (0.5 ml), and hydrogen fluoride was introduced into the vessel placed in a dry ice-acetone bath. The mixture (*ca.* 10 ml) was stirred at 0°C for 90 min, followed by evaporation *in vacuo* to give a sirupy residue, which was dissolved in ice-cold water. The solution was washed with ethyl acetate and then passed through a column (1.7×12 cm) of Amberlite CG-400 (acetate form); the column was washed with portions of water. The aqueous solutions combined were concentrated to *ca.* 20 ml *in vacuo* and lyophilized. The crude deblocked peptide thus obtained (0.65 g) was subjected, for purification, to chromatography on a column (2.7×27 cm) of carboxymethyl (CM) celullose (Serva, 0.56 meq/g) using an ammonium acetate buffer (pH 6.8, 2000 ml) with a linear concentration gradient from 0.02 to 0.6M. Ten-ml fractions were collected and their absorptivity at 280 mμ was recorded. The fractions corresponding to a main peak (tubes 156—180) and its shoulder (tubes 181—200) were collected separately and the bulk of the solvent was removed by evaporation *in vacuo* at a bath temperature of 50—55°C. The residues were lyophilized to constant weights to give 189 mg (F-I) and 76 mg (F-II) of colorless powder from the former fractions and from the latter, respectively. F-I (189 mg) was rechromatographed on a CM cellulose column (2.2×25 cm) in the same manner as above and the pure peptide (137 mg, F-I-1) was obtained from a single peak. A small shoulder of the peak afforded F-I-2 (37 mg). F-II (76 mg) and F-I-2 (37 mg) were combined and the chromatography was repeated twice to obtain 29 mg of the pure peptide. Total yield of the octadecapeptide amide (Ie) thus obtained amounted to 166 mg (50%, as calculated on the basis of the amount of octapeptide used in the final coupling step); $[\alpha]_D^{23}$ $-58.4 \pm 1.9°$ (*c* 0.514, 0.1N acetic acid). $\lambda_{max}^{0.1N\ HCl}$=279 mμ ($E_{1cm}^{1\%}$=25.1), $\lambda_{shoulder}^{0.1N\ HCl}$=288 mμ ($E_{1cm}^{1\%}$=19.7); $\lambda_{max}^{0.1N\ NaOH}$= 281 mμ ($E_{1cm}^{1\%}$=25.2), 288 mμ ($E_{1cm}^{1\%}$=24.4). The peptide behaved as a single component to ninhydrin, Pauly, Ehrlich, Sakaguchi and methionine (PtI_6'') reagents in thin-layer chromatography (BAPW as solvent) and in paper electrophoresis (600 V/36 cm, in 2N acetic acid). Amino acid ratios in acid hydrolysate (6N HCl, 105°C, 40 hr):[17] Ser 0.83, Glu 1.00, Pro 1.07, Gly 2.10, Ibu 0.99, Val 1.00, Met 1.02, Tyr 0.97, Phe 1.04, Lys 3.17, His 0.92, Arg 2.90. The Trp/Tyr ratio in intact Ie was determined spectrophotometrically to be 1.12.[18]

β-Alanyl-tyrosyl-seryl-methionyl-glutamyl-histidyl-phenylalanyl-arginyl-tryptophyl-glycyl-lysyl-prolyl-valyl-glycyl-lysyl-lysyl-arginyl-arginine Amide, [β-Ala¹]-ACTH(1-18)-NH₂ (Id). Compound XVI (0.32 g, 0.18 mmol) was converted into the corresponding active ester hydrochloride by the same procedure as that described above in the preparation of Ibu¹-decapeptide active ester. A solution of the active ester in DMF (3 ml) was mixed with a solution of N^{ε}-*t*-butyloxycarbonyl-lysyl-prolyl-valyl-glycyl-N^{ε}-*t*-butyloxycarbonyl-lysyl-N^{ε}-*t*-butyloxycarbonyl-lysyl-arginyl-arginine amide triacetate (derived from 0.15 mmol of the corresponding N^{α}-benzyloxycarbonyl derivative)[16] and triethylamine (0.2 ml) in DMF (2 ml) and the mixture

was allowed to stand at 4°C for 4 days. The reaction mixture was then introduced into ice-cold ethyl acetate (100 m*l*) and the precipitates which formed were collected by filtration, washed with ethyl acetate and ether, lyophilized and dried over sodium hydroxide pellets *in vacuo*. The crude product (0.59 g) was dissolved in liquid hydrogen fluoride together with methionine (0.1 g) and anisole (0.5 m*l*) and the mixture (*ca.* 10 m*l*) was stirred at 0°C for 60 min, followed by evaporation *in vacuo*. A sirupy residue was dissolved in water and the solution was washed with ethyl acetate, treated with Amberlite CG-400 (acetate) and lyophilized, as described above, to yield the crude deblocked octadecapeptide amide (0.65 g). The crude product was subjected to chromatography on a column (2.6×23 cm) of CM cellulose (Serva, 0.56 meq/g) using an ammonium acetate buffer (pH 6.8, 2100 m*l*) with a linear concentration gradient of 0.02—0.6M. The fractions (10 m*l*/tube) corresponding to the main peak (tubes 151—190) and its shoulder (tubes 191—210) were collected separately. Removal of the bulk of the solvent, followed by lyophilization, yielded F-I (168 mg) and F-II (80 mg) from the peak and from its shoulder, respectively. F-I was rechromatographed on a CM cellulose column (2.2× 22 cm) in the same manner as above to give pure peptide (122 mg, F-I-1) and a less purified fraction (25 mg, F-I-2). F-II (80 mg) and F-I-2 (25 mg) were combined and rechromatographed to obtain an additional quantity of pure peptide (65 mg). Total yield of the octadecapeptide amide (Id) thus obtained amounted to 187 mg (45%, as calculated on the basis of the amount of octapeptide used in the final coupling step); $[\alpha]_D^{28}$ $-58.3\pm1.9°$ (*c* 0.527, 0.1N acetic acid). Lit,[6] $[\alpha]_D^{27}$ $-54.0\pm1.8°$ (*c* 0.515, 0.1N acetic acid). $\lambda_{max}^{0.1N\ HCl}$= 279 m$\mu$ ($E_{1\%}^{1cm}$=23.9), $\lambda_{shoulder}^{0.1N\ HCl}$=288 m$\mu$ ($E_{1cm}^{1\%}$=17.6), $\lambda_{max}^{0.1N\ NaOH}$=281 m$\mu$ ($E_{1cm}^{1\%}$=24.3), 288 mμ ($E_{1cm}^{1\%}$=23.8). The peptide behaved as a single component to ninhydrin, Pauly, Ehrlich, Sakaguchi and methionine (PtI_6'') reagents in thin-layer chromatography (BAPW as solvent) and in paper electrophoresis (600 V/36 cm, in 2N acetic acid). Amino acid ratios in acid hydrolysate (6N HCl, 105°C, 40 hr):[17] Ser 0.89, Glu 1.03, Pro 1.09, Gly 2.11, Val 1.00, Met 1.02, Tyr 1.09, Phe 1.07, β-Ala 1.08, Lys 2.91, His 0.92, Arg 2.71. The Trp/Tyr ratio in intact Id was 1.03 as determined spectrophotometrically.[18]

Grateful acknowledgement is made to Dr. Akira Tanaka and staff for performing biological assays, Dr. Mitsuo Ebata and staff for amino acid analysis, Dr. Kaoru Kuriyama and staff for optical rotation measurements, and members of our microanalysis laboratory for elemental microanalysis.

BULLETIN OF THE CHEMICAL SOCIETY OF JAPAN VOL. 43 3882—3886 (1970)

Tri(hetero) substituted Carbonium Ions. VI. An Anomalous Reaction of 2-Methylthio-1,3-dithiolanylium Ion with *N,N*-Dimethyldithiocarbamate Anion*1

Takeshi NAKAI and Makoto OKAWARA

Research Laboratory of Resources Utilization, Tokyo Institute of Technology, Ookayama, Meguro, Tokyo

(Received June 15, 1970)

The reaction of 2-methylthio-1,3-dithiolanylium ion (III) with *N,N*-dimethyldithiocarbamate anion ($^-$SN) has been studied with a view toward demonstrating the ambident character of the cation III. It was found that (i) the reaction afforded *S*-β-(*N,N*-dimethyldithiocarbamyl)ethyl-S′-methyltrithiocarbonate (IV; normal) together with ethylene bis(*N,N*-dimethyldithiocarbamate) (V; abnormal); (ii) methylthioxanthate anion ($^-$SS) was formed in the reaction; (iii) the formation of the abnormal product (V) was more favorable and this could not be ascribed to the attack of $^-$SN on the normal product (IV). The ambident reactivity of cation III has been compared with that of closely related cations, tris(methylthio)carbonium ion and 2-methylamino-1,3-dithiolanylium ion (Ia). It was also found that the reaction of Ia with ethylthioxanthate anion ($^-$SS′) afforded the *S*′-ethyl analog of IV (normal) together with a small amount of abnormal V. The mechanism for the formation of the abnormal product (V) both from III and $^-$SN and from Ia and $^-$SS′ has been suggested.

In previous papers[1-5] we reported that various dithiocarbamidium ions including 2-dialkylamino-

*1 Presented at the 21st Annual Meeting of the Chemical Society of Japan, Osaka, April, 1968.

1) T. Nakai, Y. Ueno and M. Okawara, *Tetrahedron Lett.*, **1967**, 3831; This Bulletin, **43**, 156 (1970).

2) T. Nakai and M. Okawara, *Tetrahedron Lett.*, **1967**, 3835; This Bulletin, **43**, 1864 (1970).

3) T. Nakai, Y. Ueno and M. Okawara, This Bulletin, **43**, 3175 (1970).

4) T. Nakai and M. Okawara, the 20th Annual Meeting of the Chemical Society of Japan, Tokyo. April, 1967; This Bulletin, **43**, 3528 (1970).

5) T. Nakai, K. Hiratani and M. Okawara, This Bulletin, **43**, 3016 (1970).

1,3-dithiolanylium ions (I) are ambident electrophiles capable of undergoing reactions with nucleophiles at two sites *a* and *b* in formula (I). Recently Tucker and Roof reported a similar behavior of tris(methylthio)carbonium ion (II).[6] However, little information on the ambident behavior of a cyclic analog of II, 2-methylthio-1,3-dithiolanylium ion (III), has can be found in literature, although reactions at the central carbon atom (site *a*) of III have been reported.[7]

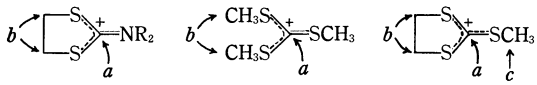

I II III

The purpose of this work is to demonstrate that cation III is also capable of undergoing electrophilic reactions at sites *b* or *c*. It has been established with some exceptions that cation I directs the attack of polarizable or bulky nucleophiles to site *b* and the attack of basic nucleophiles to site *a*.[2] Thus the reaction of III with *N,N*-dimethyldithiocarbamate anion, ranked as one of the most polarizable nucleophiles,[8] has been studied in detail.

In this paper anomalous results on the reaction of III with the dithiocarbamate anion are presented and the electrophilic reactivity of III is compared with that of closely related carbonium ions I and II.

Results

Isolation of Cation III as Perchlorate. Recently Gompper and Kutter[7] reported the formation of the methyl sulfate salt of III from the reaction of ethylene trithiocarbonate with dimethyl sulfate. However, the salt was not isolated. In this study, cation III was isolated as perchlorate (IIIa) in 72% yield by treatment of the methyl sulfate salt with an aqueous solution of sodium perchlorate. Recrystallization of the perchlorate from acetone gave colorless needles melting at 101—102°C. The NMR spectrum of IIIa showed two singlet signals at δ 3.21(CH_3S) and 4.37 ppm (CH_2S).

Reactions of 2-Methylthio-1,3-dithiolanylium Ion with *N,N*-Dimethyldithiocarbamate Anion. If we assume that III reacts with the dithiocarbamate anion in the same manner as cation I,[1,2] the reaction can be expected to yield *S*-β-(*N,N*-dimethyldithiocarbamyl)ethyl-*S'*-methyltrithiocarbonate(IV) as the sole product (Eq. (1)). There is another possibility that III and the dithiocarbamate anion would afford ethylene trithiocarbonate and methyl dithiocarbamate (Eq. (2)), if III behaves in the same manner as 2-methylthio-3-methyl-4,5-dihydrothiazolium ion.[9]

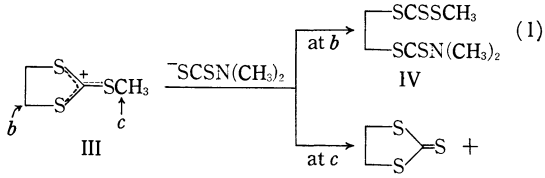

(1)

(2)

Thus the reaction of IIIa with sodium *N,N*-dimethyldithiocarbamate (abbreviated as NaSN) was carried out under various conditions. It was found that the reaction of III with NaSN gave ethylene bis(*N,N*-dimethyldithiocarbamate) (V) as a major product together with a very small amount of expected product IV. Bis(dithiocarbamate) V was identified by comparison of the IR and UV spectra with those of the authentic sample. Identification of product IV will be described below.

Table 1 shows yields of the unexpected product (V) under various conditions indicating that the yield of V increases either with reaction time or with an increase in the amount of NaSN employed. As a matter of course the formation of unexpected V must be accompanied by the elimination of thioxanthate moiety ($SCSSCH_3$) (abbreviated as SS) from cation III.

Table 1. Reaction of IIIa with NaSN

Run	IIIa mmol	NaSN mmol	DMF ml	Temp. °C	Time hr	Bis (dithiocarbamate) (V), Yield,[a] %
1	10	10	20	55	4	26
2	20	20	25	60	7	52
3	10	20	25	60	6	69
4	10	28	25	40	6	71

a) Based on IIIa

In order to prove occurrence of the elimination of the thioxanthate moiety, the UV spectrum of an aqueous solution of the resulting mixture was measured (Fig. 1). Comparison of this spectrum with that of NaSN and sodium ethylthioxanthate (NaSS') suggested that the aqueous solution contained both methylthioxanthate and unreacted dithiocarbamate anions.

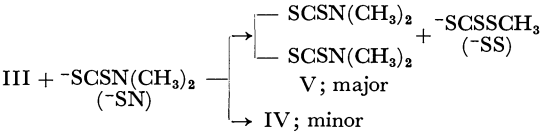

6) W. P. Tucker and G. L. Roof, *Tetrahedron Lett.*, **1967**, 2747; *J. Org. Chem.*, **33**, 3333 (1968).

7) R. Gompper and E. Kutter, *Angew. Chem. Int. Ed. Engl.*, **2**, 687 (1963); *Chem. Ber.*, **98**, 1365, 1374 (1965).

8) R. E. Davis, "Survey of Progerss in Chemistry," Vol. 2, ed. by A. Scott, Academic Press Inc., New York, N. Y. (1964), p. 189; R. E. Davis, H. Nakshbendi and A. Ohno, *J. Org. Chem.*, **31**, 2702 (1966).

9) T. Nakai, K. Hiratani and M. Okawara, the 19th Symposium on Organic Reaction Mechanisms, Yamagata, October, 1968; This Bulletin, to be published.

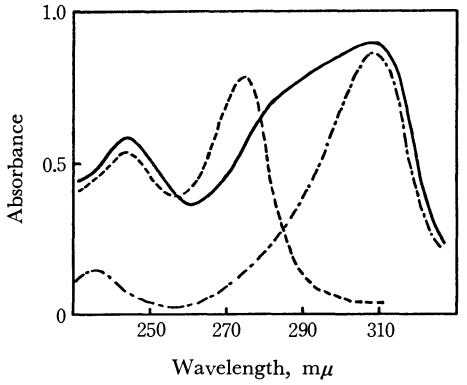

Fig. 1. UV spectra of the resulting aqueous solution (———), sodium *N,N*-dimethyldithiocarbamate (--------; ε_{max} (281 mμ) 12200) and sodium ethylthioxanthate (-·-·-·-; ε_{max} (335 mμ) 9300) in water.

The molar ratio of $^-$SS to $^-$SN remaining in the aqueous solution was calculated from absorbances at 281 and 335 mμ on the assumption that the molar extinction coefficient (ε) of $^-$SS is the same as that of $^-$SS′. It was found in the case of Run 3 that the molar ratio was 0.90 and, hence, 7.5 mmol of $^-$SN remained unreacted since the molar amount of $^-$SS eliminated should be the same as that of bis(dithiocarbamate) (V) formed (Table 2). The finding indicates that most of reacted $^-$SN is distributed in the unexpected product (V).

Table 2. The Distribution of SN Moiety (Run 3)

Before the reaction $^-$SN (mmol)	After the reaction (mmol)		
	V	Unreacted $^-$SN	($^-$SS)
20.0	13.8±2.0	7.5±1.0	(6.9±1.0)

Reaction of 2-Dimethylamino-1,3-dithiolanylium Ion with Ethylthioxanthate Anion. As has been shown,[1,2] 2-dimethylamino-1,3-dithiolanylium ion (Ia) reacts with sulfur nucleophiles to give the open-chain products (VI).

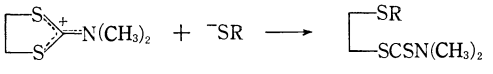

Ia VI

R=Et, Ar, CNR_2' (S)

In view of the separate preparation of the *S′*-ethyl analog (IV′) of the minor product (IV) obtained above, the reaction of the cation Ia with sodium ethylthioxanthate (NaSS′) was carried out. However, contrany to our expectation, it was found that Ia and $^-$SS′ gave an abnormal product, bis(dithiocarbamate) (V), in low yields along with the normal product (IV′) as the main product.

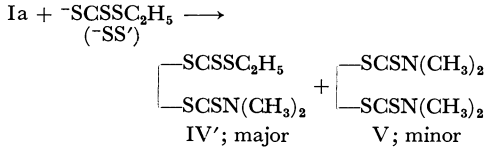

Table 3. Reactions of Ia with NaSS′

Ia mmol	NaSS′ mmol	DMF ml	Temp. °C	Time hr	Yields[a] (%) of products	
					IV′	V
20.0	30.0	25	70	6	37.0	5.5
50.0	50.0	40	60	6	22.0	0.7

a) Based on Ia

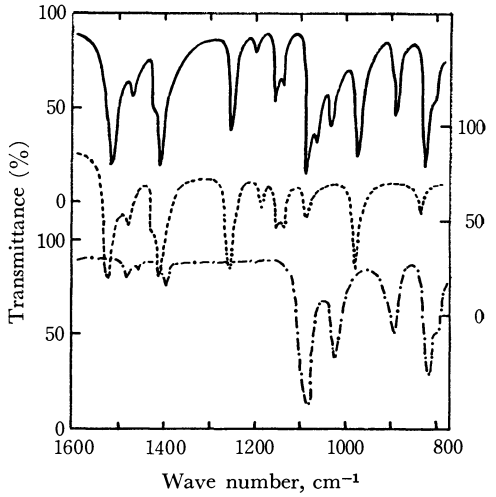

Fig. 2. IR spectra of product IV′ (neat; ———), bis(dithiocarbamate) V (KBr disk; --------) and *S,S′*-diethyltrithiocarbonate (neat; -·-·-·-).

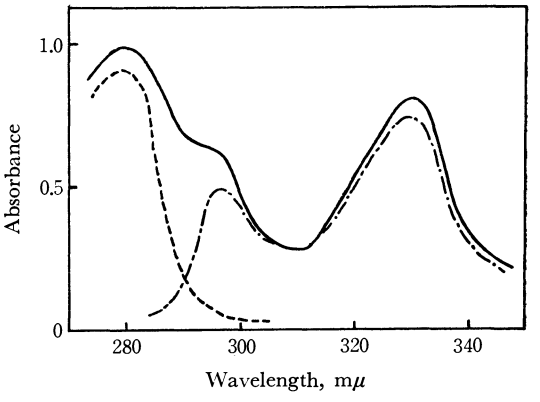

Fig. 3. UV spectra of product IV′ (———), *S*-ethyl *N,N*-dimethyldithiocarbamate (--------) and *S,S′*-diethyltrithiocarbonate (-·-·-·-) in ethanol.

Product IV′ (a yellowish liquid) was purified by means of column chromatography on alumina and

identified by IR and UV spectra, which are shown in Figs. 2 and 3 together with those of related compounds. It is apparent from these spectra that the product IV′ has both –S–CS–N< and –S–CS–S– moieties. The IR and UV spectra of the minor product (IV) obtained from III and $^{-}$SN were essentially identical with those of IV′.

Discussion

The Ambident Character of Cation III. The above results are summarized in the following scheme.

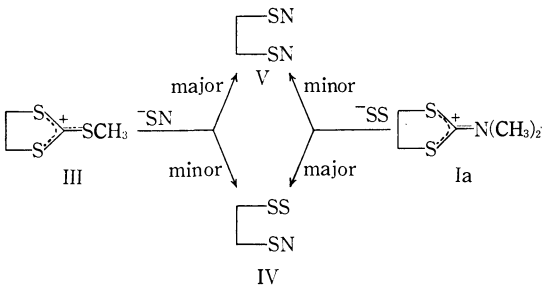

[SN=SCSN(CH$_3$)$_2$; SS=SCSSR′ (R′=CH$_3$ or C$_2$H$_5$)]

The normal product (IV) from III and $^{-}$SN is best explained as the result of the attack of $^{-}$SN on the *S*-methylene carbon atom (site *b*) of III presumably through the S_N2-like mechanism which has been accepted for the reactions of Ia with sulfur nucleophiles.[1,3] The combined results of the present work and that by Gompper and Kutter[7] reveal that cation III is an ambident electrophile with reactive sites at the central carbon (sp^2) and the *S*-methylene carbon (sp^3) atoms, although the mechanism of the formation of V remains unsettled.

The following evidence indicates that the *S*-methylene carbon atom of III is less reactive than that of Ia. Ia reacts with *p*-tolylmercaptide ion at 60°C giving VI (R=*p*-CH$_3$C$_6$H$_4$) in 77% yield,[2] while III does not react with the mercaptide ion under the same conditions. The smaller reactivity of III seems surprising because it would be more destabilized than Ia since the 2-SMe group in III is less electron-donating than the 2-NMe group in Ia.

Let us compare the electrophilic reactivities of cation III and its open-chain analog, tris(methylthio)carbonium ion (II). It has been established that the five membered cation Ia is more stabilized than its open-chain analog of Ia.[3,4] By analogy, it is believed that III is more stabilized (less electrophilic) than open-chain II. The following evidence indicates smaller reactivity of III; as decribed above, III does not react with $^{-}$SC$_6$H$_4$CH$_3$ at any sites under given conditions, whereas II is capable of undergoing reaction with a less nucleophilic mercaptide ion ($^{-}$SCH$_3$) at the central carbon atom (site *a*) to afford tetrakis(methylthio)methane.[6]

On the Mechanism of Formation of the Abnormal Product (V). Let us consider the mechanism of the formation of the abnormal product from III and $^{-}$SN. Another formation of V from Ia and $^{-}$SS′ would take place by the subsequent reaction of $^{-}$SN eliminated from Ia with another molecule of Ia.

Controlled experiments demonstrated that neither *S,S*′-dimethyltrithiocarbonate nor trithiocarbonate IV′ reacted with $^{-}$SN at all. The result undoubtedly eliminated the possibility that the formation of the abnormal product (V) took place by the attack $^{-}$SN on the normal product (IV). This also indicates that the formation of V is competition with the formation of IV in both cases.

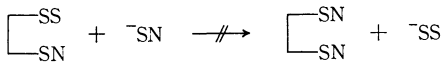

Thus, in order to explain the results, we have assumed the following scheme involving a direct interconversion between III and Ia.

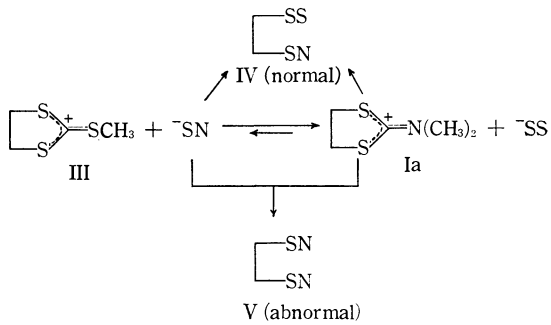

In the above scheme it has been established that (i) the *S*-methylene carbon atom of Ia is more electrophilic than that of III; (ii) $^{-}$SN is much more nucleophilic than $^{-}$SS;[9] (iii) Ia reacts preferentially with $^{-}$SN to afford bis(dithiocarbamate) V. From the scheme, the abnormal product (V) from III and $^{-}$SN is best explained as the result of an initial transformation of III with $^{-}$SN into Ia which then preferentially reacts with another molecule of $^{-}$SN, finally yielding V. Similarly V from Ia and $^{-}$SS′ is explained as the result of capturing $^{-}$SN formed *via* the interconversion process with another molecule of Ia.

The scheme may also account for both favorable formation of abnormal V from III and $^{-}$SN and favorable formation of normal IV′ from Ia and $^{-}$SS′; the more reactive cation Ia directs the attack of $^{-}$SS preferentially to the formation of IV, whereas the less reactive cation III reacts with $^{-}$SN preferentially to give cation Ia, finally yielding V.

As a result, in the absence of data to the contrary, it seems reasonable to assume the above scheme

for the formation of V and for the elimination of $^{-}$SS from III with $^{-}$SN.

Finally, the problem concerning the mechanism of the interconversion: III+$^{-}$SN⇆Ia+$^{-}$SS, still remains. Although the accurate mechanism of the interconversion process is not elucidated as yet, the following two-centered substitution might be assumed as a possible mechanism. However, its confirmation needs further studies.

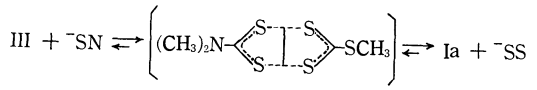

Experimental

Melting points are uncorrected. The IR and UV spectra were recorded with Hitachi EPI-S2 and EPS-2 spectrometers, respectively. The NMR spectrum of perchlorate IIIa was obtained on a Varian Associate A-60 spectrometer in a $(CD_3)_2SO$ solution using tetramethylsilane as an internal standard.

Materials. *Sodium N,N-dimethyldithiocarbamate.* A commercial product was washed with chloroform before use.

Sodium ethylthioxanthate was prepared, from sodium ethylmercaptide and carbon disulfide according to Barltrop *et al.*[10]

2-Dimethylamino-1,3-dithiolanylium perchlorate (Ia) was prepared by the method[2] given previously. mp 179—180°C (acetone).

Ethylene trithiocarbonate. A commercial product was purified by recrystallization before use.

Preparation of 2-Methylthio-1,3-dithiolanylium Perchlorate (IIIa). Ethylene trithiocarbonate (27.2 g, 0.02 mol) was dissolved in 25.2 g (0.02 mol) of dimethyl sulfate. When the mixture was heated to 50°C a vigorous exothermic reaction occurred. The reaction temperature was kept below 90°C. After the exothermic reaction ceased, the mixture was further stirred at 95°C for 30 min. On cooling the mixture was poured into 200 m*l* of a saturated aqueous solution of sodium perchlorate giving 35.8 g (72%) of pale yellowish precipitates. The precipitates were washed with ether and recrystallized from acetone giving colorless needles: mp 101—102°C.

Found: C, 18.84; H, 2.93%. Calcd for $C_4H_7ClO_4S_3$: C, 19.16; H, 2.82%.

Reactions of 2-Methylthio-1,3-dithiolanylium Perchlorate (IIIa) with Sodium *N,N*-Dimethyldithiocarbamate (NaSN). A typical run is as follows. Carbonium salt IIIa (2.50 g, 0.02 mol) and NaSN (3.60 g, 0.02 mol) were dissolved in 20 m*l* of DMF. The mixture was stirred at 60°C for 6 hr, then poured into 150 m*l* of cold water giving precipitates of ethylene bis(*N,N*-dimethyldithiocarbamate) (V). The precipitates were filtered and washed with ether: mp 188—189°C (DMF) (188—190°C[11]).

The IR spectrum of the product was in agreement with that of the authentic sample.

The filtrate was extracted with ether. The ethereal layer was dried over anhydrous sodium sulfate and the solvent evaporated under reduced pressure giving a small amount of a yellowish oil of *S*-β-(*N,N*-dimethyldithiocarbamyl)ethyl-*S'*-methyltrithiocarbonate (IV). The IR and UV spectra of the oily residue were essentially identical with those of *S*-β-(*N,N*-dimethyldithiocarbamyl)ethyl-*S'*-ethyltrithiocarbonate (IV') described below.

The UV spectrum of the aqueous layer was measured (Fig. 1) indicating that the aqueous solution contained both thioxanthate and dithiocarbamate anions.

Reactions of 2-Dimethylamino-1,3-dithiolanylium Perchlorate(Ia) with Sodium Ethylthioxanthate (NaSS'). A typical run is as follows. Carbonium salt Ia (12.5 g, 0.05 mol) and NaSS' (8.0 g, 0.05 mol) were dissolved in 40 m*l* of DMF. The reaction mixture was stirred at 60°C for 6 hr. The mixture was poured into 300 m*l* of cold water giving 0.31 g of precipitates of V: mp 188—189°C (DMF) (188—190°C[11]). The IR spectrum of the product was identical with that of the authentic sample.

The filtrate was extracted with ether. Work-up gave 5.8 g of yellowish oil of *S*-β-(*N,N*-dimethyldithiocarbamyl)ethyl-*S'*-ethyltrithiocarbonate (IV'). Distillation of the oil *in vacuo* was unsuccessful. Thus the oil was purified by means of column chromatography on alumina: n_D (25°C) 1.6605.

Found: N, 4.79%. Calcd for $C_8H_{15}NS_5$: N, 4.91%.

The IR and UV spectra of the oily product are shown in Figs. 2 and 3, respectively.

The authors are greateful to Sanshin Chem. Ind. Co., Ltd., for the gift of ethylene trithiocarbonate and to Sankyo Co., Ltd., for measurement of the NMR spectrum.

10) J. A. Barltrop, P. M. Hayes and M. Calvin, *J. Amer. Chem. Soc.*, **76**, 4348 (1954).

11) A. W. Campbell and R. F. Tryan, *Ind. Eng. Chem.*, **45**, 125 (1953).

BULLETIN OF THE CHEMICAL SOCIETY OF JAPAN VOL. 43 3887—3891 (1970)

The Reaction of β-Nitroalcohols and Reactive Aldehydes*1

Juji YOSHIMURA, Takao IIDA and Masuo FUNABASHI

Laboratory of Chemistry for Natural Products, Faculty of Science, Tokyo Institute of Technology, Meguro-ku, Tokyo

(Received June 23, 1970)

Condensation of acyclic or cyclic β-nitroalcohols with aldehydes was examined. In the case of non-protected 1-deoxy-1-*C*-nitro-D-glycitols and benzaldehyde, products caused by aldehyde-exchange reaction were obtained. However, the reaction of 2-methoxy-1-nitropentane or non-protected 2-nitrocyclohexanol and reactive aldehydes (formaldehyde, acetaldehyde and *n*-butyl glyoxylate) in the presence of sodium hydrogencarbonate gave the corresponding condensation products.

It is well known that nitromethane undergoes condensation with equimolar amount of aldehydes or dialdehydes in the presence of an alkaline catalyst to give acyclic β-nitroalcohols or cyclic β,β′-dihydroxynitro derivatives.[1,2] However, the possibility of further condensation of the products with a second aldehyde has not been clarified. Successful condensation of nitroethanol with aldehydes[3,4] or dialdehyde[5] seems to be attributed to the high reactivity of formaldehyde, because nitroethanol is an equimolar condensation product of nitromethane and formaldehyde, and three moles of the latter can be condensed with the former as an exception.[6]

Another important factor in such a condensation is the relative stability of *aci*-nitro salts of a starting material, the expected product, nitromethane, and the condensation product between nitromethane and a second aldehyde, because nitromethane condensation is a kind of reversible reaction. Moreover, the condensation product between a cyclic β-nitroalcohol and a second aldehyde is a tertiary nitro derivative which cannot form an *aci*-nitro salt. Thus the use of a strong alkali as a catalyst is undesirable.

In this paper, the reactions of acyclic or cyclic β-nitroalcohols with aldehydes are described.

Results and Discussion

At first 1-deoxy-1-*C*-nitroglycitol was used as an acyclic β-nitroalcohol without protection of the hydroxyl group. The reaction of 2,3-*O*-isopropylidene-D-glycerinaldehyde[7] and nitromethane in the presence of triethylamine at room temperature gave a mixture of 1-deoxy-3,4-*O*-isopropylidene-1-*C*-nitro-D-*threo*- and -*erythro*-tetritol (**1**) in 60% yield as a distilled sirup. Only when the reaction period was shorter than 12 hr, the isomer which was deduced from the rotational value to have *threo* configuration[8,9] was obtained as crystals. Moreover, 1-deoxy-3,4;5,6-di-*O*-isopropylidene-1-*C*-nitro-D-glucitol (**2**) and -D-mannitol (**3**) were newly synthesized by acetonation of the corresponding glycitols.[10] 1-Acetamido-1-deoxy-D-glucitol (**4**) and D-mannitol (**5**) were also derived from the same compounds by hydrogenation and *N*-acetylation. The position of isopropylidene groups in **2** and **3** was proved by the fact that both compounds and their mixture obtained by the condensation of 2,3 ; 4,5-di-*O*-isopropylidene-*aldehydo*-D-arabinose[11] with nitromethane were converted into the same α,β-unsaturated-nitro compound by acetylation and elimination.[12]

Treatment of **1** with benzaldehyde in the presence of sodium methoxide gave an intractable sirup,

*1 Part of this work was presented at the Autumn Meeting of the Chemical Society of Japan in October, 1969, in Nagoya.

1) Fr. W. Lichtenthaler, "Newer Method of Preparative Organic Chemistry," Vol. 4, Academic Press Inc., New York (1968), p. 115.

2) J. C. Sowden, "Advances in Carbohydrate Chemistry," Vol. 6, Academic Press Inc., New York (1951), p. 291.

3) J. Controulis, M. C. Rebstock and H. M. Crooks, *J. Amer. Chem. Soc.*, **71**, 2463 (1949).

4) J. C. Sowden, *ibid.*, **72**, 3325 (1950).

5) Fr. W. Lichtenthaler and H. Leinert, *Chem. Ber.*, **101**, 1815 (1968).

6) I. Gorsky and S. P. Makarov, *Chem. Ber.*, **67**, 996 (1934).

7) H. H. Baer and H. O. L. Fischer, *J. Biol. Chem.*, **128**, 463 (1939).

8) Y. Ohgo, J. Yoshimura, M. Kono and T. Sato, This Bulletin, **42**, 2957 (1969).

9) W. A. Bonner, *J. Amer. Chem. Soc.*, **73**, 3126 (1951).

10) J. C. Sowden and H. O. L. Fischer, *ibid.*, **69**, 1048 (1947).

11) L. F. Wiggins, *J. Chem. Soc.*, **1946**, 388.

12) E. Schmitt and G. Rutz, *Chem. Ber.*, **61**, 2142 (1928).

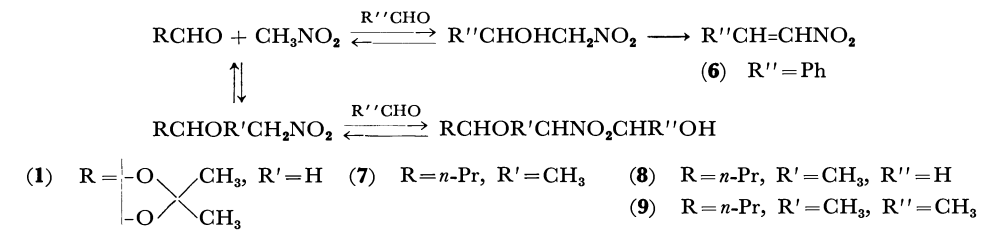

Scheme 1

from which only β-nitrostyrene (**6**) was isolated as crystals. A similar condensation of **3** with benzaldehyde also gave a sirup. In order to identify the products, the sirup was hydrogenated, hydrolyzed, *N*-acetylated and then examined by paper chromatography. The chromatogram showed three main spots, two of which were identified by comparison with authentic samples to be **5** and β-acetamido-α-phenylethanol.[13] An attempted separation of the third compound by a magnesol-celite column was unsuccessful. However, the presence of D-arabinitol was ascertained. This indicates that an aldehyde-exchange reaction occurred as shown in Scheme 1.

In order to prevent such a reverse nitromethane condensation, it was deduced that the protection of the hydroxyl group of an acyclic β-nitroalcohol is necessary, and as mild an alkaline condition as possible should be used. For instance, Magerlein[14] reported recently the successful condensation of methyl 6-deoxy-6-nitro-1-thio-α-D-galactopyranoside with acetaldehyde in a total synthesis of lincomycin, in which the hydroxyl group is protected by the pyranoside ring formation. As a simple model compound to prove the above deduction, 2-methoxy-1-nitropentane (**7**) was prepared by the reaction of 1-nitro-1-pentene[12] and sodium methoxide in absolute methanol at 0—7°C. As expected, condensation of **7** with formaldehyde or acetaldehyde in the presence of sodium hydrogencarbonate at room temperature for a week gave the corresponding product (**8** and **9**) in 26 and 38% yield, respectively. When sodium hydroxide was used as a catalyst in the case of formaldehyde, a small amount of olefinic byproducts were detected in the NMR spectrum of distilled **8**, in which two doublets (τ 3.52 and 4.24, J=1.3 Hz) and one triplet (τ 2.86, J=3.7 Hz) indicated the presence of the corresponding 1-olefin and 2-olefin, respectively. Because the absorption of a conjugated nitro group (ν_{max} 1520 cm^{-1}) was observed in the IR spectrum of undistilled **8**, it is concluded that a strong alkaline condition induced the elimination of water or methanol. The condensation product between **7** and *n*-butyl glyoxylate could not be purely isolated. However, it was isolated as methyl

(**10**) $CH_3(CH_2)_2CH(OCH_3)CH(NH_2\cdot HCl)$-$CHOHCOOCH_3$

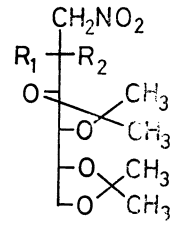

(**2**) R_1=H, R_2=OH
(**3**) R_1=OH, R_2=H

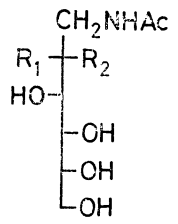

(**4**) R_1=H, R_2=OH
(**5**) R_1=OH, R_2=H

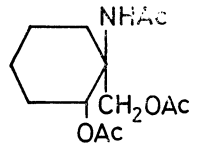

(**11a**)

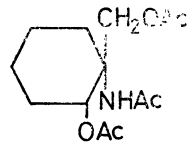

(**11b**)

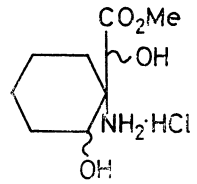

(**12**)

3-amino-2-hydroxy-4-methoxyheptanoate hydrochloride (**10**) by hydrogenation, esterification, and column-chromatography in 6% yield.

On cyclic β-nitroalcohols, Lichtenthaler and Leinert[5] reported that the condensation of glutardialdehyde and nitroethanol afforded 2-hydroxymethyl-*r*-2-nitrocyclohexan-*t*-1,*t*-3-diol. However, it decomposes to *r*-2-nitrocyclohexan-*t*-1,*t*-3-diol with liberation of formaldehyde in higher pH regions, and the reverse reaction did not take place. Instead of nitroethanol, ethyl nitroacetate was reported as an reactive nitro compound in a similar cyclisation.[15] Recently, Sakai described that the condensation of glutardialdehyde and α-methoxy-β-nitropropionic acid in the presence of sodium hydroxide gave a lactone of the aimed compound (7%) and the corresponding unsaturated

13) A. Pictet and A. Gams, *Chem. Ber.*, **43**, 2389 (1915).
14) B. J. Magerlein, *Tetrahedron Lett.*, **1970**, 33.
15) S. Zen, Y. Takeda, A. Yasuda and S. Umezawa, This Bulletin, **40**, 431 (1967).

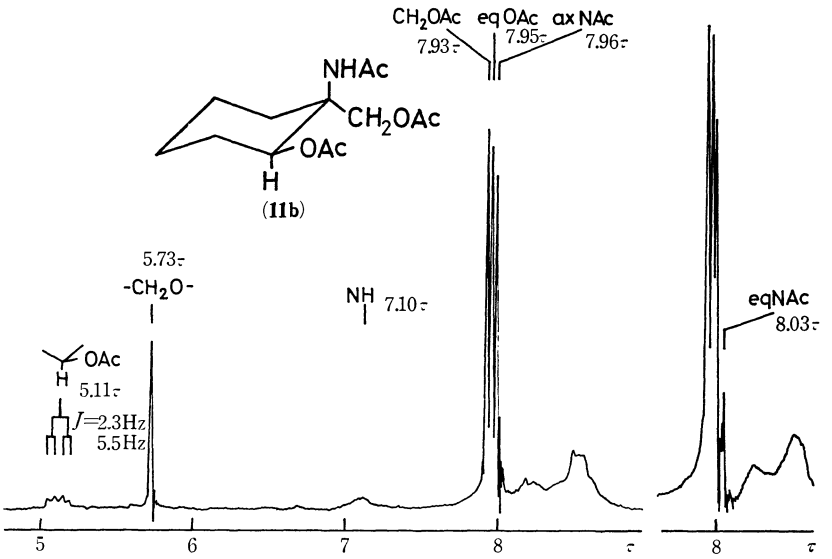

Fig. 1. NMR spectrum of **11b** and a mixture of **11a** and **11b** ($CDCl_3$, 100 MHz).

lactone (13%) in which the nitro group was eliminated.[16] In our experiments, 2-nitrocyclohexanol[17] and formaldehyde were treated under the same conditions as mentioned before, and the sirupy product was directly hydrogenated, acetylated and distilled to give the corresponding triacetate (**11**) in a total yield of 65%. The NMR spectrum of **11** indicated the presence of acetoxymethyl group (τ 7.93), equatorial-acetoxy group (τ 7.95), axial-acetamido group (τ 7.96) and equatorial-acetamido group (τ 8.03) as characteristic signals.[18] Because of the low intensity of the latter, it was deduced that **11** is a mixture of *r*-1-acetamido-*t*-2-acetoxy-1-acetoxymethylcyclohexane (**11a**) and its *c*-2-isomer (**11b**), and the latter is the main product. In fact, crystalline **11b** was obtained by standing for two months as shown in Fig. 1. Similarly, the condensation product of 2-nitrocyclohexanol with *n*-butyl glyoxylate was isolated as methyl α-(1-amino-2-hydroxycyclohexyl)glycolate hydrochloride (**12**) in a total yield of 12%, by hydrogenation, esterification and column-chromatography. However, the configuration of isomers in **12** could not be analyzed.

From these results, it is concluded that acyclic β-nitroalcohols in which the hydroxyl group is protected by ether-linkage and cyclic β-nitroalcohols without protection are successfully condensed with reactive aldehydes such as formaldehyde, acetaldehyde and glyoxylic acid in a weak alkaline condition.

16) K. Sakai, S. Oida and E. Ohki, *Chem. Pharm. Bull.* Tokyo, **16**, 1048 (1968).

17) H. Baldock, N. Levy and C. W. Fcaife, *J. Chem. Soc.*, **1949**, 2627.

18) Fr. W. Lichtenthaler and P. Emig, *Tetrahedron Lett.*, **1967**, 577.

Experimental

The solutions were evaporated under diminished pressure at a bath temperature not exceeding 45°C. All melting points are uncorrected. Optical rotations were measured in a 0.5-dm tube with a Carl Zeiss Photoelectric Precision Polarimeter. The NMR spectra were taken in deuteriochloroform with a JNM-4H-100 MHz Spectrometer, using tetramethylsilane as an internal standard.

1-Deoxy-3,4-*O*-isopropylidene-1-*C*-nitro-D-*threo*-and-*erythro*-tetritol (1). A solution of 2,3-*O*-isopropylidene-D-glycerinaldehyde[7] (14 g, 110 mmol), nitromethane (20 m*l*, 370 mmol) and triethylamine (10 m*l*, 73 mmol) in ethanol (40 m*l*) was allowed to stand for two days at room temperature, and then concentrated to give a sirup (21 g) which was distilled at 103—104°C/0.05 mmHg. Yield, 60% (12 g); $[\alpha]_D^{23}$ +9.5° (*c* 0.16, ethanol); IR (cm^{-1}) : 3430 (OH), 1540 and 1370 (NO_2).

Found: C, 43.22; H, 7.20; N, 7.25%. Calcd for $C_7H_{13}NO_5$: C, 43.97; H, 6.85; N, 7.33%.

When the reaction period was shorter than 12 hr, a part of the distilled product crystallized gradually. After recrystallisation from ether-petroleum ether it showed mp 58–59°C, $[\alpha]_D^{23}$ +17.6° (*c* 1.0, ethanol), and the analytical values consisted with the theoretical. The configuration of this isomer was deduced to be *threo* from the rotational value.[8,9]

1-Deoxy-3,4 ; 5,6-di-*O*-isopropylidene-1-*C*-nitro-D-glucitol (2). A solution of 1-deoxy-1-*C*-nitro-D-glucitol[10] (4 g, 19 mmol) and concentrated sulfuric acid (1.44 g) in acetone (90 m*l*) was allowed to stand overnight at room temperature, poured into aqueous sodium hydrogencarbonate (3 g), and extracted with chloroform. The extract was washed with water, dried over anhydrous sodium sulfate, and evaporated to give a sirup which was distilled at bp 131—133°C/0.03—0.04 mmHg. Yield, 3.2 g (60%), $[\alpha]_D^{23}$ +2.7°

(*c* 2.58, ethanol).

Found: C, 49.62; H, 7.31; N, 4.87%. Calcd for $C_{12}H_{21}NO_7$: C, 49.47; H, 7.27; N, 4.81%.

1-Deoxy-3,4;5,6-di-*O*-isopropylidene-1-*C*-nitro-D-mannitol (3). Treatment of 1-deoxy-1-*C*-nitro-D-mannitol[10] in just the same manner as above gave the corresponding product in 65% yield. Bp 126—128°C/0.02—0.03 mmHg, $[\alpha]_D^{23}$ +15.3° (*c* 1.13, ethanol).

Found: C, 49.73; H, 7.64; N, 5.02%. Calcd for $C_{12}H_{21}NO_7$: C, 49.47; H, 7.27; N, 4.81%.

Treatment of 2,3;4,5-di-*O*-isopropylidene-*aldehydo*-D-arabinose with nitromethane in the same manner as in the case of **1** gave a mixture of **2** and **3** in 65% yield (Found: C, 49.25; H, 7.24; N, 4.63%). Bp 130—132°C/0.03—0.04 mmHg, $[\alpha]_D^{23}$ +11.8° (*c* 1.10, ethanol). Conversion of this sirup, **2** and **3** to the corresponding same nitroolefine by the usual method[12] gave a sirup which could not be distilled. However, the consumption of bromine in chloroform by these sirups indicated that **2** and **3** have a free hydroxyl group at C-2 position.

1-Acetamido-1-deoxy-D-glucitol (4). A solution of 1-deoxy-1-*C*-nitro-D-glucitol[10] (3 g, 14.2 mmol) in absolute ethanol (60 m*l*) was shaken with hydrogen in the presence of 10% of palladium-charcoal (2 g) until the hydrogen uptake ceased, and then filtered. Acetic anhydride (3 g, 30 mmol) was added to the filtrate, which was concentrated after the reaction mixture had been allowed to stand for several hr at room temperature. The residue was crystallized from ethanol to give the product in 82% (2.8 g) yield. Mp 124—125°C, $[\alpha]_D^{23}$ −19.4° (*c* 1.03, methanol).

Found: C, 43.05; H, 7.80; N, 6.31%. Calcd for $C_8H_{17}NO_6$: C, 43.04; H, 7.68; N, 6.28%.

1-Acetamido-1-deoxy-D-mannitol (5). 1-Deoxy-1-*C*-nitro-D-mannitol was treated in just the same manner as above to give **5** in 75% yield. Mp 149—150°C, $[\alpha]_D^{23}$ −15.5° (*c* 1.10, methanol).

Found: C, 42.98; H, 7.62; N, 6.30%. Calcd for $C_8H_{17}NO_6$: C, 43.04; H, 7.68; N, 6.28%.

Reaction of 1 or 3 with benzaldehyde. To an ice-cooled solution of **1** (10.3 g, 51.8 mmol), benzaldehyde (6 g, 56.5 mmol) in methanol (20 m*l*) was added a solution of metal sodium (1.19 g), in methanol (20 m*l*), and allowed to stand overnight at room temperature. The reaction mixture was neutralized with 2 N hydrochloric acid (26 m*l*) and concentrated. The resulting sirup was redissolved in ethanol, filtered, and evaporated. Distillation of a part of the sirup was unsuccessful. An attempt to fractionate the sirup from ethanol-petroleum ether gave 0.8 g of β-nitrostyrene as crystals (mp 56—57°C, lit,[19] 57—58°C), but other products could not be identified even by paper chromatography.

A solution of **3** (6 g, 20.6 mmol), benzaldehyde (3 g, 28 mmol) and triethylamine (0.8 m*l*) in methanol (10 m*l*) was allowed to stand at room temperature until the mutarotation ceased (about 12 hr), and concentrated to dryness. The sirup obtained was hydrogenated in absolute ethanol in the presence of palladium-charcoal, hydrolyzed with 2N-hydrochloric acid, and then *N*-acetylated. The sirupy product showed three main spots; R_f=0.21, 0.62 and 0.84, on paper chromatography, using ethyl acetate-pyridine-water (12 : 5 : 4 in volume) as a developer and potassium permanganate as a detecting reagent. Of the spots, the first and the third were identified by comparison with authentic samples to be **5** and β-acetamido-α-phenylethanol,[13] respectively. An attempted column-chromatographic separation of the other compound, using magnesol-celite (1 : 1 in weight) as a carrier and petroleum ether-benzene, ethanol-benzene, ethanol-methanol in turn as effluents, resulted in the compounds eluating in the order of larger R_f value, though the pure compound could not be isolated. Rechromatography of an enriched part of the desired compound showed a similar result, except that D-arabinitol (R_f= 0.40) was ascertained.

2-Methoxy-1-nitropentane (7). To a solution of metal sodium (4.8 g, 208 mmol) in absolute methanol (100 m*l*) was added 1-nitro-1-pentene[12] (23 g, 200 mmol) slowly at 0—7°C, because of exothermic reaction. After being stirred for one hr at 10°C, the reaction mixture was poured into 50% acetic acid under cooling, and extracted with chloroform. The extract was dried over anhydrous sodium sulfate, and evaporated. Distillation of the residual sirup gave the main fraction which boils at 83—85°C/13 mmHg, as colorless liquid in 75% yield. IR (cm^{-1}): 1548 and 1380 (NO_2), 1099 (C–O–C).

Found: C, 48.99; H, 9.12; N, 9.35%. Calcd for $C_6H_{13}NO_3$: C, 48.69; H, 8.90; N, 9.52%.

3-Methoxy-2-nitrohexan-1-ol (8). A solution of **7** (3.0 g, 20 mmol), formaldehyde (1.6 g of 37% aqueous solution, 20 mmol) and sodium hydrogencarbonate (1.6 g, 20 mmol) in 50% methanol was allowed to stand at room temperature for a week, neutralized with IR-120 ion-exchanger, and evaporated. Distillation of the residual sirup at 98—99°C/2 mmHg gave 1.4 g (38%) of colorless liquid. IR (cm^{-1}): 3410 (OH), 1541 and 1375 (NO_2), 1090 (C–O–C).

Found: C, 47.70; H, 8.54; N, 7.69%. Calcd for $C_7H_{15}NO_4$: C, 47.44; H, 8.53; N, 7.91%.

4-Methoxy-3-nitroheptan-2-ol (9). Acetaldehyde (3.3 g, of 80% aqueous solution, 60 mmol) and **7** (3.0 g, 20 mmol) was treated by the same procedure as mentioned above, and a fraction which boils at 118—121°C/11 mmHg was obtained in 26.2% yield. IR (cm^{-1}): 1545 and 1379 (NO_2).

Found: C, 50.41; H, 8.80; N, 7.33%. Calcd for $C_8H_{17}NO_4$: C, 50.25; H, 8.95; N, 7.33%.

Methyl 3-Amino-2-hydroxy-4-methoxyheptanoate Hydrochloride (10). Treatment of **7** (3.0 g, 20 mmol), *n*-butyl glyoxylate (2.6 g, 20 mmol) and sodium hydrogen carbonate (2.5 g, 30 mmol) in 50% methanol (30 m*l*) by the same method as above gave crude 2-hydroxy-4-methoxy-3-nitroheptanoic acid in 70% yield. For the sake of identification, the sirup was hydrogenated in methanol in the presence of Raney nickel at 40°C under 90 kg/cm², and the filtrate was concentrated after removal of the catalyst. The remaining sirup in 2N sodium hydroxide (10 m*l*) was extracted with ether, acidified with hydrochloric acid, and concentrated. The residual sirup in methanol was filtered, and concentrated. The operation was repeated twice. The sirup was then chromatographed on a silicagel column (1.6 × 35 cm) using benzene-methanol (8 : 2 v/v) solution as an eluent. Fractions No. 3—4 in each 20 m*l* fractionation contained the

19) D. E. Worrall, "Organic Syntheses," Coll. Vol. I, p. 413 (1934).

methyl ester hydrochloride in the total yield of 6%. IR (cm^{-1}): 1740 (CO), 1625 (NH).

Found: C, 44.84; H, 6.98; N, 5.59%. Calcd for $C_9H_{19}NO_4Cl$: C, 44.73; H, 8.34; N, 5.80%.

Condensation of 2-Nitrocyclohexanol with Formaldehyde. A solution of 2-nitrocyclohexanol[17] (3.0 g, 20 mmol), formaldehyde (5.0 g of 37% aqueous solution, 60 mmol) and sodium hydrogencarbonate (4.0 g, 50 mmol) in 50% methanol (60 ml) was allowed to stand for a week at room temperature, neutralized with 2N hydrochloric acid, and concentrated. The resulting sirup in methanol was filtered, and the filtrate was evaporated. The operation was repeated twice. The sirup (3.9 g) obtained was hydrogenated in the presence of Raney nickel at 40°C under 110 kg/cm^2, and then the aminodialcohol obtained (3.2 g) was acetylated by the usual manner. The resulting triacetate was distilled at 149°C/0.1 mmHg. Yield, 3.5 g (65%). IR (cm^{-1}): 1740 and 1650 (CO), 1540 (NH), 1244 (C-O-C).

Found: C, 57.46; H, 7.95; N, 5.33%. Calcd for $C_{13}H_{21}NO_5$: C, 57.55; H, 7.80; N, 5.16%.

The main component of the triacetate; *r*-1-acetamido-*c*-2-acetoxy-1-acetoxymethylcyclohexane **(11b)**, crystallized on standing for two months showed mp 91—92°C, and the analytical values were consistent with the theoretical.

Condensation of 2-Nitrocyclohexanol with *n*-Butyl Glyoxylate. A solution of 2-nitrocyclohexanol (4.1 g, 28 mmol), *n*-butyl glyoxylate (5.2 g, 40 mmol) and sodium hydrogencarbonate (4.2 g, 50 mmol) in 50% methanol (50 m*l*) was allowed to stand for a week at room temperature, neutralized with 2N hydrochloric acid, and then extracted with chloroform. The extract was dried over anhydrous sodium sulfate and concentrated to give a sirup (5.3 g). The sirup was hydrogenated in methanol in the presence of Raney nickel at 40°C under 120 kg/cm^2 for 5 hr. The reaction mixture was filtered, and the filtrate was evaporated. The sirup obtained was dissolved in 20 m*l* of alkaline water (0.8 g of sodium hydroxide), and extracted with ether. The water layer was acidified with hydrochloric acid, and concentrated. Extraction of the residue with methanol gave the hydrochloride in 60% (3.0 g) overall yields. The paper chromatogram of the hydrochloride, using *n*-butanol - acetic acid - water (4 : 1 : 5 in volume) as a developer and ninhydrine as a detecting reagent, showed two violet spots; R_f=0.48 and 0.43. Fractionation on silicagel column (1.6×35 cm) using benzene-methanol (8 : 2 v/v) gave pure methyl α-(1-amino-2-hydroxycyclohexyl)glycolate hydrochlride (**12**) in 12% yield as a sirup. IR (cm^{-1}) : 1749 (CO), 1630 (NH).

Found: C, 45.10; H, 8.77; N, 5.97%. Calcd for $C_9H_{18}NO_4Cl$: C, 45.85; H, 7.69; N, 5.94%.

The authors wish to express their thanks to Mr. Sadao Ishige for his help in experiments, to Mr. Kiyofumi Fukukawa for measurements of NMR spectra, and to members of the Laboratory of Organic Analysis for elemental analyses.

BULLETIN OF THE CHEMICAL SOCIETY OF JAPAN VOL. 43 3891—3894 (1970)

Steric Effects of Alkyl Substituents upon the Opening of the Lactone Ring of Coumaran-2,3-diones

Teruo MATSUURA, Masao KAWAI and Yasuo BUTSUGAN*1

Department of Synthetic Chemistry, Faculty of Engineering, Kyoto University, Sakyo-ku, Kyoto

(Received June 24, 1970)

The stability of the lactone rings of alkyl substituted coumaran-2,3-diones against hydrolysis and alcoholysis is greatly affected by the positions of alkyl substituents. From UV spectral studies it was suggested that methyl substitutions at positions adjacent to the lactone ring contribute to stability for steric reasons.

Physalin A, the bitter principle of *Physalis Alkekengi var. Francheti*, was hydrogenated affording tetrahydrophysalin A,[1] which gave a yellow crystalline compound Ia ($C_{12}H_{12}O_3$) as a pyrolysis product. From the IR (KBr: 1820, 1730, 1635 and 1595 cm^{-1}) and the NMR ($CDCl_3$): 1.25 (t, J=8 Hz, 3H) 2.23 (s, 3H), 2.25 (s, 3H), 2.72 (q, J=8 Hz, 2H) and 6.89 (s, 1H)) spectra of Ia its structure was assumed to be 6-ethyl-4,7-dimethylcoumaran-2,3-dione, synthesized according to the scheme shown in Fig. 1.

The UV spectra of Ia in aprotic solvents as well as in acetic acid and in *t*-butyl alcohol (Fig. 2a) showed an absorption maximum at about 310 mμ (in dioxane 307, chloroform 317, carbon tetrachloride 308, acetic acid 314, *t*-butyl alcohol 314 mμ; ε 10000—11000) with a weak shoulder at about 370 mμ (ε *ca.* 2000). The UV absorption of Ia in dioxane-water (1 : 1) as well as in ethanol-

*1 Present address: Nagoya Institute of Technology, Showa-ku, Nagoya.

1) T. Matsuura, M. Kawai, R. Nakashima and Y. Butsugan, *Tetrahedron Lett.*, **1969**, 1083.

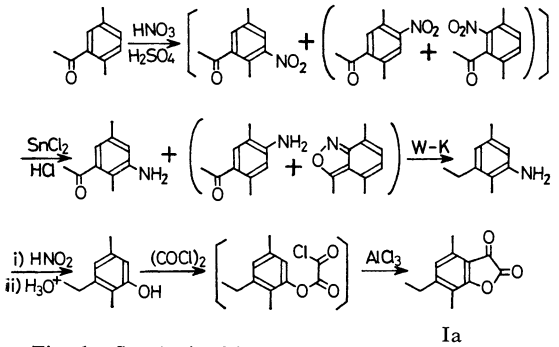

Fig. 1. Synthesis of 6-ethyl-4,7-dimethylcoumaran-2,3-dione (Ia).

water (1 : 1) (Fig. 2b) showed two maxima at 278 mμ (ε 14000) and 340 mμ (ε 3500) and the spectrum was similar to that of *o*-hydroxyphenylglyoxylic acid (IIb) (λ_{max}^{EtOH} 258 mμ, ε 14000; 330 mμ, ε 4000), suggesting that the lactone ring of Ia is opened in such media. The UV spectrum of Ia in ethanol (λ_{max} 280 mμ, ε 11000; λ_{sh} 320 mμ, ε 4200; λ_{sh} 360 mμ, ε 2400) (Fig. 2c) differs from the above spectra and does not resemble any of the spectra of III, IV and V, which were prepared in order to estimate the absorptions of the possible species formed from Ia in ethanol, VI, VII and VIII, respectively. The spectrum of Ia in ethanol can be explained as due to the absorption of the mixture of the open and the closed ring species (IIa + Ia) in the ratio 5 : 2, as shown by dotted and broken lines in Fig. 2c. Attempts to isolate 4-ethyl-2-hydroxy-3,6-dimethylglyoxylic acid (IIa) or its ester were unsuccessful.

Although it has been reported that 4,6- and 4,7-dimethylcoumaran-2,3-diones (If and Ie) are recovered on acidification from their alkaline solution and the corresponding open ring species (IIf and IIe) are not obtained,[2] unsubstituted coumaran-2,3-dione (Ib) and its 5,6- and 5,7-dimethyl derivatives (Id and Ic) were unstable against moisture to give *o*-hydroxyphenylglyoxylic acid derivatives, IIb, IId and IIc, respectively. This suggests that the stability of the lactone rings of alkyl substituted coumaran-2,3-diones against hydrolysis or alcoholysis is greatly affected by the positions of the alkyl substituents.

The UV spectra of five dimethyl and two trimethyl derivatives of Ib were measured in various solvents and the extents of the opening of the lactone rings were estimated from the spectra, as

Table 1. Extents of ring opening of coumaran-2,3-diones (I) estimated from UV spectra

Solvent	Id	Ic	If	Ig	Ie	Ih	Ia	Ii
t-Amyl alcohol	C	B	A	A	A	A	A	A
s-Butyl alcohol	E	E	D	D	D	C	C	B
Isopropyl alcohol	F	F	F	E	D	D	D	C
98% Ethanol aq.	F	F	F	F	E	D	D	D

I+ROH ⇌ II

	I(%)	II(%)
A	95—100	0— 5
B	85— 95	5— 15
C	50— 85	15— 50
D	15— 50	50— 85
E	5— 15	85— 95
F	0— 5	95—100

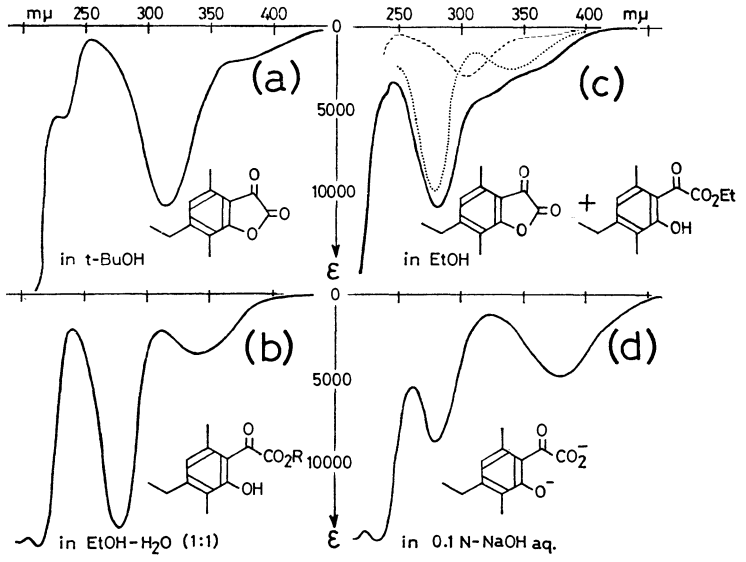

Fig. 2. UV spectra of 6-ethyl-4,7-dimethylcoumaran-2,3-dione (Ia). The broken line shows the absorption (×2/7) in dioxane and the dotted line the absorption (×5/7) in ethanol-water (1 : 1).

2) R. Stollé and E. Knebei, *Ber.*, **54B**, 1213 (1921).

summarized in Table 1. The lactone ring of each compound is more stable in the order *t*-amyl alcohol>*s*-butyl alcohol>*i*-propyl alcohol>98% ethanol. The extent of alcoholysis is smaller in the more sterically hindered alcohol.

The stability of the lactone ring against hydrolysis and alcoholysis are in the order; Id<Ic<If<Ig<Ie<Ih (≒ Ia)<Ii. The order can be explained in terms of steric effects of alkyl substituents of the benzene ring of I upon the stability of the lactone ring in the equilibrium (I + ROH⇌II). Methyl groups adjacent to the lactone ring (R_1 and R_4) make the lactone ring

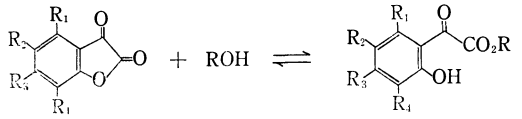

I (R=H, alkyl) II

	R_1	R_2	R_3	R_4
a	Me	H	Et	Me
b	H	H	H	H
c	H	Me	H	Me
d	H	Me	Me	H
e	Me	H	H	Me
f	Me	H	Me	H
g	Me	Me	H	H
h	Me	H	Me	Me
i	Me	Me	H	Me

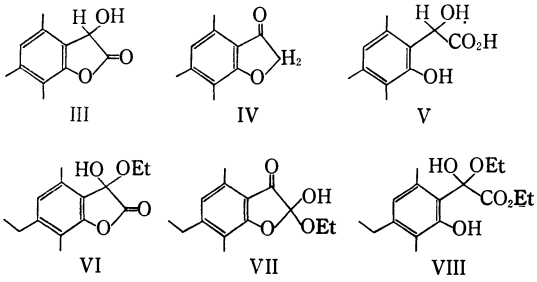

III IV V

VI VII VIII

Table 2. UV spectra of coumaran-2,3-diones (I) in $CHCl_3$ and in EtOH aq. containing Et_3N as the standard absorptions of I in closed and open states, respectively

λ_{max} in mμ (ε); (sh···shoulder)

	in $CHCl_3$	in 98% EtOH aq. containing Et_3N (0.5 mg/ml)
Ic	303(7600), 384(1400)	270(11700), 358(3200)
Id	303(10400), 377(1900)	269(11500), 340(3800)
Ie	308(7550), 378(1700)	270(8500), 342(2700)
If	309(10100), 360sh(1900)	273(11800), 329(3700)
Ig	301(8200), 380(1600)	267(5700), 338(2400)
Ih	320(10000), 375sh(1800)	279(13300), 342(3600)
Ii	310(7850), 390(1600)	284(7550), 352(2400)

stable and the effect is in the order $R_1>R_4$. The buttressing effects of R_2 and R_3 were observed; *i.e.* the stability of the lactone ring is in the order Ig>If, and also Ih and Ii>Ie.

Experimental

Melting points were uncorrected. IR spectra were measured for KBr discs.

Synthesis of 6-Ethyl-4,7-dimethylcoumaran-2,3-dione (Ia). According to the procedure of Buu-Hoï *et al.*[3] 2,5-dimethylacetophenone (63 g) was nitrated and then reduced with $SnCl_2$–HCl. After the usual treatment, the crude product (35 g) was shown by gas chromatography (Apiezone) to be a mixture of 3-amino-2,5-dimethylacetophenone, 4-amino-2,5-dimethylacetophenone and 3,4,7-trimethylanthranil in the ratio 8 : 7 : 3. The mixture was vacuum-fractionated and then purified by fractional crystallization (methanol). 3-Amino-2,5-dimethylacetophenone—colorless oil (3 g), bp 158°C/12 mmHg (lit,[3] 158°C/12 mmHg). 4-Amino-2,5-dimethylacetophenone—colorless prisms (1 g), mp 159—160°C (lit,[3] 157°C). 3,4,7-Trimethylanthranil—colorless prisms (4 g), mp 55—56°C, bp 140°C/12mm Hg. IR: 1630, 1580, 1555, 1230, 1085, 895, 840 cm^{-1}. NMR ($CDCl_3$) : δ 2.47(s, 6H), 2.87(s, 3H), 6.52(d, J= 7Hz, 1H), 6.83(d, J=7Hz, 1H) (Found: C, 74.3; H, 6.8; N, 8.6%).

3-Ethyl-2,5-dimethylaniline. 3-Amino-2,5-dimethylacetophenone (2.7 g) was reduced according to the Huang-Minlon method to give 3-ethyl-2,5-dimethylaniline (1.5 g) as a colorless oil. *N*-Acetyl derivative—colorless needles, mp 129—130°C (from aqueous methanol) (Found: C, 75.1; H, 9.0; N, 7.2%).

3-Ethyl-2,5-dimethylphenol. 3-Ethyl-2,5-dimethylaniline (1.15 g) in aqueous HCl was diazotized with $NaNO_2$ (555 mg) and the diazonium salt was decomposed in hot 70% H_2SO_4 (120°C). After the usual treatment, sublimation of the product gave 3-ethyl-2,5-dimethylphenol (350 mg) as colorless needles, mp 70—72°C (lit,[4] 71—72°C).

6-Ethyl-4,7-dimethylcoumaran-2,3-dione (Ia). The solution of 3-ethyl-2,5-dimethylphenol (200 mg) in ether (5 ml) was added to the mixture of oxalyl chloride (1 g) and ether (5 ml). After 48 hr the mixture was evaporated and the resulting oil (3-ethyl-2,5-dimethylphenyloxalyl chloride) was dissolved in CS_2 (5 ml). The solution was added to the suspension of $AlCl_3$ (1.9 g) in CS_2 (15 ml). After 24 hr water (50 ml) was added and the reaction mixture was extracted with ether. Sublimation of the extract (140°C/12 mmHg) gave 6-ethyl-4,7-dimethylcoumaran-2,3-dione (170 mg) as yellow needles, the IR spectrum of which was identical with that of Ia obtained from natural product.[1] Mp 154°C (from ether-light petroleum) and mixed mp 153—154°C.

Found: C, 70.5; H, 6.0%. Calcd for $C_{12}H_{12}O_3$: C, 70.6; H, 5.9%.

2-Hydroxy-3,4,6-trimethylphenylglycolic Acid (V). 4,6,7-Trimethylcoumaran-2,3-dione (Ih) (300 mg) in ethanol (40 ml) was hydrogenated at room

3) Ng. Ph. Buu-Hoï, B. Eckert and R. Royer, *J. Org. Chem.*, **17**, 1000 (1952).

4) E. C. Horning, K. E. Kirk, L. Schwenk, N. Taylor and M. Wilson, *ibid.*, **9**, 552 (1944).

temperature and atmospheric pressure over 10% Pd-charcoal for 18 hr. The reaction mixture was treated as usual and the resulting colorless solid was dissolved in hot aq. solution of NaOH (90°C). On acidification with aq. HCl 2-hydroxy-3,4,6-trimethylphenylglycolic acid (V) (140 mg) was obtained as colorless needles, mp 148—151°C (from acetone-benzene). IR: 3350, 1745, 1210, 1095 cm^{-1}. UV (ethanol): λ_{max} 283 mμ (ε 2400). NMR (DMSO-d_6): δ 2.00 (s, 3H), 2.12 (s, 3H), 2.23 (s, 3H), 5.38 (s, 1H), 4.48 (s, 1H).

Found: 62.7; H, 6.8%. Calcd for $C_{11}H_{14}O_4$: C, 62.6; H, 6.7%.

3-Hydroxy-4,6,7-trimethylcoumaran-2-one (III). Sublimation of V gave 3-hydroxy-4,6,7-trimethylcoumaran-2-one as colorless needles, mp 121—126°C (from benzene-light petroleum). IR: 3320, 1815, 1640, 1600 cm^{-1}. UV (dioxane): λ_{max} 282 mμ (ε 1600). NMR ($CDCl_3$): δ 2.19 (s, 3H), 2.30 (s, 3H), 2.38 (s, 3H), 5.36 (s, 1H), 6.82 (s, 1H).

4,6,7-Trimethylcoumaran-3-one (IV). This compound was prepared according to Smith and Boyack[5], mp 89—91°C. UV (ethanol): λ_{max} 266 mμ (ε 13000), 330 mμ (ε 4600).

Synthesis of Alkyl Substituted Coumaran-2,3-diones (I). Dimethyl- and trimethyl-coumaran-2,3-diones were prepared from the corresponding dimethyl- and trimethyl-phenols according to the general procedure based on the method of Stollé and Knebei[2].

General procedure. The solution of alkyl phenol (1.0 g) in ether (10 m*l*) was added to the solution of oxalyl chloride (1.3 g) in ether (10 m*l*). After standing for 48 hr the solvent and the excess oxalyl chloride were distilled off and the residual oil was dissolved in CS_2 (25 m*l*). $AlCl_3$ (3.0 g) was added to the solution and after a week ice-water (30 g) was added. The reaction mixture was extracted with ether or chloroform to give alkyl substituted coumaran-2,3-dione (I), which was purified by sublimation and/or recrystallization.

5,7-*Dimethylcoumaran*-2,3-*dione (Ic)*. From 2,4-dimethylphenol (1 g) Ic (1.15 g) was obtained, mp 147—148°C (sublimation). IR: 1825, 1735, 1615, 1490 cm^{-1}. On standing in an open container Ic was gradually hydrolyzed to give IIc, mp 91—96°C (from water). IR: 1730, 1630, 1600 cm^{-1}. (Found: C, 59.3; H, 5.5%. Calcd for $C_{10}H_{10}O_4 \cdot 1/2H_2O$: C, 59.1; H, 5.5%).

4,7-*Dimethylcoumaran*-2,3-*dione (Ie)*. Mp 136—137°C (lit,[2] 136°C).

4,6-*Dimethylcoumaran*-2,3-*dione (If)*. Mp 144—145°C (lit,[2] 144°C).

4,5-*Dimethylcoumaran*-2,3-*dione (Ig)*. From 3,4-dimethylphenol (1 g) a mixture (0.95 g) of Id and Ig was obtained. After standing in an open container the mixture was recrystallized from benzene to give IId (0.64 g) and Ig (0.19 g). Ig; mp 168—169°C (from methanol). IR: 1820, 1730, 1615, 1600, 1480 cm^{-1} (Found: C, 68.0; H, 4.8%).

5,6-*Dimethylcoumaran*-2,3-*dione (Id)*. Sublimation of IId, obtained from 3,4-dimethylphenol, gave Id, mp 176—177°C. IR: 1830, 1740, 1620 cm^{-1}. On standing Id was readily converted into IId, mp 148—150°C (from benzene). IR: 1765, 1640, 1570, 1500 cm^{-1} (Found: C, 62.1; H, 5.4%).

4,6,7-*Trimethylcoumaran*-2,3-*dione (Ih)*. Mp 151—152°C (lit,[6] 149—151°C).

4,5,7-*Trimethylcoumaran*-2,3-*dione (Ii)*. From 2,4,5-trimethylphenol (1 g) Ii (1.36 g) was obtained, mp 192—193°C (from ether-light petroleum). IR: 1815, 1730, 1630, 1595, 1490 cm^{-1} (Found: C, 69.7; H, 5.3%).

UV Spectra of Coumaran-2,3-diones (I). The extents of ring opening of I, summarized in Table 1, were estimated from the UV spectra assuming that the spectra of I measured in 98% aq. ethanol containing triethylamine (0.5 mg/m*l*) and in $CHCl_3$ (Table 2) give the standard absorptions of the open and the closed ring species (II and I), respectively.

5) L. I. Smith and G. A. Boyack, *J. Amer. Chem. Soc.*, **70**, 2687 (1948).

6) L. I. Smith and R. R. Holmes, *ibid.*, **73**, 4294 (1951).

BULLETIN OF THE CHEMICAL SOCIETY OF JAPAN VOL. 43 3895—3898 (1970)

The Polymerization of Vinyl Monomers in the Presence of Surface Active Agents. I. The Polymerization of Methyl Methacrylate

Teruzo ASAHARA, Manabu SENŌ, Shinsaku SHIRAISHI and Yoshikazu ARITA

Institute of Industrial Science, The University of Tokyo, Roppongi, Minato-ku, Tokyo

(Received July 2, 1970)

Methyl methacrylate polymerized in the presence of a surface active agent in an aqueous system without any ordinary initiators. Anionic surface active agents, such as sodium tetrapropylenebenzenesulfonate and sodium 2-dodecylbenzenesulfonate, markedly effected the polymerization of methyl methacrylate in the presence of water. The polymerization was inhibited by adding hydroquinone to the reaction system and was also affected adversely by oxygen. Water as a reaction medium was found to be indispensable. The polymerization in organic solvents afforded hardly any polymeric products.

The polymerization of methyl methacrylate (MMA) has been extensively investigated by many workers. Imoto and Takemoto[1] have reported the homo and graft polymerization of MMA onto fibers with hydroxylic pendant groups, especially onto cellulose. They proposed that the initiation step of the polymerization is mainly connected with the formation of a ternary complex of the hydroxyl group, water, and MMA, and also reported that the use of a surface active agent in the polymerization had a slight effect on the reaction. Matsumoto *et al.*[2] reported the polymerization of MMA in an aqueous medium in the presence of poly(methacrylic acid) and proposed that initiation is due to the peroxide of the MMA monomer.

We ourselves have previously reported the polymerization of MMA in the presence of an inorganic substance with a hydroxylic surface, such as clay or silica.[3] During the investigation, we have found that MMA polymerizes readily in the presence of an anionic surface active agent in water, without either hydroxylic surfaces or any ordinary radical initiators, to give poly(methyl methacrylate) with an unusually high molecular weight in a good yield. In this paper, the polymerization of MMA with various surface active substances will be described, and some consideration will be given to the reaction mechanism.

Experimental

Materials. *Monomer.* Methyl methacrylate was purified by the usual method and was stored in a refrigerator until use.

Anionic Surfactants. Sodium tetrapropylenebenzenesulfonate (ABS) was purified by the recrystallization of the methanol-soluble part of a commercial substance (from Lion Fat & Oil Co.) from ether. Sodium 2-dodecylbenzenesulfonate (LAS) was recrystallized from 2-propanol. Sodium lauryl sulfate (SLS) was purified by the procedure used for ABS. Sodium oleate (SO) was recrystallized from ethanol. These purified surfactants were all dried under a vacuum.

Nonionic Surfactants. Octaoxyethylene nonylphenyl ether and polyoxyethylene dodecyl ether were supplied by Kao Soap and Chem. Co. and were used without further purification.

Cationic Surfactant. Cetylpyridinium chloride (CPC) was purified by recrystallization from benzene.

Polymerization. *Method 1.* Into a four-necked, 100-m*l*, round-bottomed flask equipped with a condenser, a dropping funnel, a nitrogen inlet tube, and a thermometer, 0.15 g of a surfactant and 60 m*l* of deionized water were placed; the mixture was then preheated at the desired reaction temperature for 40 min, during which period a slow stream of nitrogen was introduced into the mixture. MMA was then added through the dropping funnel, after which the mixture was heated and stirred continuously under a nitrogen atmosphere for the desired reaction period. At the end of the period, the resultant mixture was poured into 300 m*l* of methanol in order to precipitate the polymer formed, which was filtered, washed with methanol, and dried at 60°C under a vacuum.

Method 2. In a 100-m*l*, round-bottomed flask were placed MMA, a surfactant, and water. The mixture was shaken well and subsequently frozen in an acetone-dry ice bath. It was then subjected to a vacuum below 10^{-3} mmHg in order to degas it, and then allowed to melt. The procedure described above was repeated three times to get a complete degassing. The degassed mixture was then heated at the desired reaction temperature in order to carry out the polymerization reaction. The subsequent procedure to polymerization was the same as that described above.

Determination of Molecular Weight. The molecular weight, $\overline{M}$, of the polymer thus obtained was

1) M. Imoto and K. Takemoto, *Kogyo Kagaku Zasshi*, **70**, 1851 (1967).

2) T. Matsumoto, I. So and A. Izutsu, *Kobunshi Kagaku*, **26**, 234 (1969).

3) M. Seno and T. Asahara, Proceedings of the Vth International Congress on Surface Active Substances, p. 983 (1969).

determined from the intrinsic viscosity, $[\eta]$, by using this equation:

$$[\eta] = 5.2\times10^{-5}\ \overline{M}^{0.76}$$ [4]

The viscosity of the polymer was measured in benzene at 30°C.

Analysis of Peroxide. The amount of peroxide in the materials used was determined by Wagner's method.[5]

Results and Discussion

The polymerization of MMA in the presence of various types of surfactants in an aqueous system was investigated. Among the surfactants used, all the anionic surfactants except sodium oleate were markedly effective in the polymerization, as is shown in Fig. 1. When either ABS or SLS was used, the polymer yield had a tendency to increase with the reaction time over a period of 6 hours. Sodium oleate, polyoxyethylene nonylphenyl ether, and cetylpyridinium chloride had little effect on the polymerization of MMA compared with the case in which no surfactant was used (Table 1).

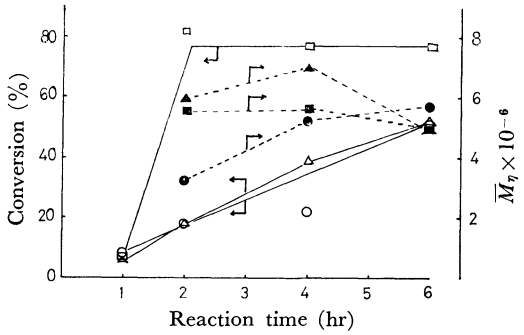

Fig. 1. Effect of Surfactants on polymer yield and molecular weight of Poly(methyl methacrylate) formed.
MMA, 5 g; surfactant, 0.15 g; water 60 m*l*; at 80°C under N_2.

	Conv.	$\overline{M}_\eta$
ABS	—△—	···▲···
SLS	—○—	···●···
LAS	—□—	···■···

TABLE 1. EFFECT OF SURFACTANTS ON POLYMER YIELD

Surfactant used	Reaction time (hr) 2	6
Octaoxyethylene nonylphenyl ether	1.6	0.2
SO	0.2	0.2
CPC	0.0	0.0
None (control)	0.0	0.2

MMA, 5g; surfactant, 0.15 g; water, 60 m*l*; at 80°C; under N_2.

The effects of the polymerization temperature and also of the reaction atmosphere were investigated. In the reaction temperature range from 60 to 100°C, a maximum in the polymer yield was observed at 80°C in every case, as may be seen in Fig. 2. The figure also shows that LAS had a higher efficiency in polymer yield throughout the reaction temperature range investigated than did the other surfactants.

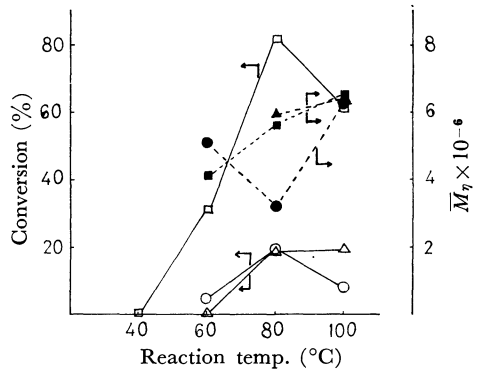

Fig. 2. Effect of surfactants on polymer yield and molecular weight of polymethyl(methacrylate) formed at various reaction temperature.
MMA, 5.0 g; surfactant, 0.15 g; water 60 m*l*; for 2 hr under N_2.

	Conv.	$\overline{M}_\eta$
LAS	—□—	···■···
ABS	—△—	···▲···
SLS	—○—	···●···

The polymerization was conducted under different reaction atmospheres; the results are summarized in Table 2. The polymerization *in vacuo* gave the highest yield and the highest molecular weight polymer. Under nitrogen or carbon dioxide, a high molecular weight polymer was obtained, but in a smaller yield. When air was passed through into the reaction mixture, however, no polymerization was observed. The addition

TABLE 2. EFFECT OF REACTION ATMOSPHERE ON THE POLYMERIZATION OF MMA

Reaction atmosphere	Polymer yield (%)	Molecular weight $\overline{M}$
N_2	18.4	5.94×10^6
CO_2	22.0	6.03×10^6
Air	0	—
in vacuo (1×10^{-3} mmHg)	24.0	7.24×10^6

MMA, 5.0 g; ABS, 0.15g ; water, 60 m*l* ; at 80°C for 2 hr.

4) "Analytical Chemistry of Polymers", Interscience Publishers, New York (1962), Part II, p. 17.
5) C. D. Wagner and R. H. Smith, *Ind. Eng. Chem. Anal. Ed.*, **19**, 976 (1947).

Table 3. Polymerization in various organic mediums

Solvent	Reaction temp. (°C)	Polymer yield (%)	Molecular weight $\overline{M}$
Water	80	18.4	5.94×10^6
Methanol	65 (reflux)	—*	—
Ethanol	78 (reflux)	—	—
THF	65 (reflux)	—	—
Benzene	80	—	—

MMA, 5.0 g; ABS, 0.15 g; solvent, 60 m*l*; for 2 hr.
* No detectable solid product was obtained.

of hydroquinone or diphenylpicrylhydrazyl to the reaction mixture also inhibited the polymerization. In each polymerization under a vacuum or a nitrogen or carbon dioxide atmosphere, the polymer formed was recovered as a fine powder by pouring the resultant mixture, which was a rather stable emulsion, into methanol.

The polymerization was also carried out in a non-aqueous medium, such as methanol, ethanol, tetrahydrofuran or benzene, but no polymerization was observed (Table 3). From these results, it is conceivable that water is inevitable for the polymerization under the present conditions, and also that the formation of a micelle may be an essential part of the polymerization reaction. The polymerization undoubtedly proceeds *via* a radical mechanism, in view of the experimental facts presented above.

In order to clarify the initiation step of the polymerization, the peroxide values of the surfactants used and of MMA were determined by Wagner's method. The results are summarized in Table 4. LAS, which afforded the highest efficiency in the polymerization, had the highest peroxide value. The approximate total amount of free radicals appearing in the reaction system is 10^{-6}—10^{-7} mol, as calculated from the molecular weight and the yield of the polymer formed, presuming only a radical coupling for the termination reaction of the polymerization. This value is roughly consistent with the peroxide value of the surfactant. It has not been, however, clear that the peroxides of the surfactants used participate in the initiation step, because no polymerization occurred in organic reaction media. At any rate, the presence of a charged interface in the reaction system may be very important for the propagation and/or initiation step. The most likely effect of anionic surfactants was also observed in the emulsion polymerization of MMA, with di-*t*-butyl peroxide used as a radical initiator, as may be seen in Fig. 3. However, the sulfonate anion itself is not very effective in the polymerization, judging from the results of the polymerization, of MMA with sodium *p*-toluenesulfonate and a nonionic surfactant, shown in Fig. 4.

Table 4. Analysis of peroxide in the surfactants used and in MMA

Material	Peroxide (mol/100 g)
LAS	2.7×10^{-3}
ABS	3.9×10^{-4}
SLS	3.6×10^{-5}
MMA	1.7×10^{-5}

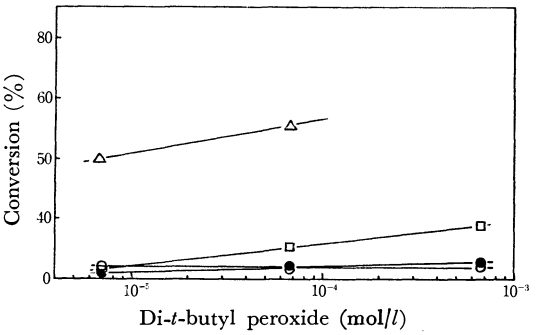

Fig. 3. Effect of surfactants on the polymerization of MMA with di-*t*-butyl peroxide in aqueous system.
MMA, 5.0 g; surfactant, 0.15 g; water, 60 m*l*; at 80°C for 2 hr under nitrogen atmosphere.
△ ABS, □ CPC, ○ octaoxyethylene nonylphenyl ether, ● none.

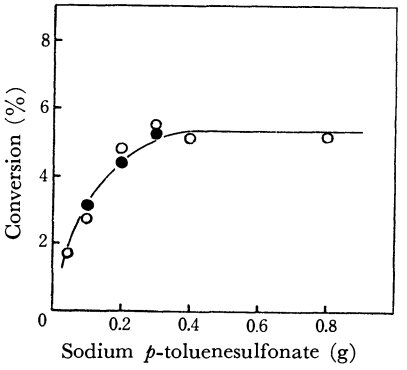

Fig. 4. Effect of sodium *p*-toluenesulfonate on the polymerization of MMA without any ordinary initiators.
MMA, 5.0 g; water, 60 m*l*; at 80°C for 2 hr under nitrogen atmosphere.
○ Sodium *p*-toluenesulfonate only.
● With 3 g of polyoxyethylene dodecyl ether.

The effort to detect free radicals in the reaction system by the ESR technique has not been successful. This might be because of the concentration of radicals was too low for them to be detected in such an aqueous emulsion system. The poly(methyl methacrylate) obtained had the same structure as that obtained by a conventional free radical polymerization, judging from the results

of the IR and NMR measurements.

A further mechanistic study of the polymerization and also of the variation of monomers is now in progress and its results will be presented in the near future.

The authors are indebted to Messrs. Tomoyoshi Yokoyama and Shigeki Shiozawa for their helpful technical assistance, and also to Lion Fat & Oil Co. and Kao Soap & Chem. Co. for supplying the surfactants.

BULLETIN OF THE CHEMICAL SOCIETY OF JAPAN VOL. 43 3898—3900 (1970)

Oxidation by Transition Metal Complexes. II. Oxidation of Styrenes Catalyzed by Rhodium Compounds

Kiyotomi TAKAO, Masami WAYAKU, Yuzo FUJIWARA, Toshinobu IMANAKA and Shiichiro TERANISHI

Department of Chemical Engineering, Faculty of Engineering Science, Osaka University, Machikaneyama, Toyonaka, Osaka

(Received July 9, 1970)

Catalytic activities of chlorotris(triphenylphosphine)rhodium(I) and rhodium(III) chloride for the oxidation of olefins have been studied. It has been found that the complex and $RhCl_3$ can cause catalytically the oxidation of aliphatic olefins such as styrene, α-methylstyrene or β-methylstyrene to produce carbonyl compounds under oxygen atmosphere. A remarkable solvent effect was observed in the reaction.

We have reported the catalytic oxidation of styrene and triphenylphosphine by means of some organoiridium complexes under oxygen stream.[1] In connection with this work, the catalytic function of oxidation by some rhodium compounds which form O_2-complexes, were investigated.

It was found that the complex ($RhX(PPh_3)_3$), especially chlorotris(triphenylphosphine)rhodium (I) can oxidize styrenes in the presence of oxygen to produce carbonyl compounds.[2] Styrene gave similar products to those reported in the case of organoiridium complex catalysts,[1] α-methylstyrene gave acetophenone, α-phenylpropionaldehyde and formaldehyde, and β-methylstyrene gave benzaldehyde and acetaldehyde in good yields.

In the present paper catalytic oxidation with the rhodium complex, $RhCl(PPh_3)_3$ and $RhCl_3$ will be presented.

Results and Discussion

As the general method of oxidation catalyzed by rhodium compounds, mixtures of the reactant styrene and the rhodium complex in toluene, ethanol or other solvents were heated for 8 hr under a constant bubbling of oxygen.

It was found that styrene can be easily oxidized with the use of $RhCl(PPh_3)_3$ or $RhCl_3$ to give similar oxidation products as those obtained with the use of iridium complexes.[1a] The results are summarized in Table 1. This is the first example of oxidation of aliphatic olefins with the use of rhodium complexes. It is remarkable that the oxidation differing from cases with iridium complexes,[1a] is affected by the solvent polarity. Thus, in dioxane (polar solvent) the oxidation resulted in the cleavage of the C=C double bond of styrene to give benzaldehyde as a main product in 611% yield based on the Rh-complex used.[5]

In contrast to this, in ethanol (protic solvent) acetophenone was obtained in excellent yield with a small amount of the double bond-cleavage product, and in toluene (non-polar solvent) the main products were both acetophenone (348%) and benzaldehyde (148%). This is different from results for dioxane and ethanol. In acetic acid and pyridine only a small amount of oxidation products was detected.

Table 1 shows a similar solvent effect in the

1) a) K. Takao, Y. Fujiwara, T. Imanaka and S. Teranishi, This Bulletin, **43**, 1153 (1970). b) K. Takao, Y. Fujiwara, T. Imanaka, M. Yamamoto, K. Hirota and S. Teranishi, *ibid.*, **43**, 2249 (1970).

2) Although the complex ($RhX(PPh_3)_3$) was used only in the oxidation of ethylbenzene[3] and cyclohexene[4], no application of the complex to any other olefins has been reported.

3) J. Blum, *Tetrahedron Lett.*, **1967**, 3665.

4) J. P. Collman, M. Kubota and J. W. Hosking, *J. Amer. Chem. Soc.*, **89**, 4809 (1967).

5) Formaldehyde was also obtained from the outlet gas.

Table 1. Oxidation of styrene with rhodium compounds

Catalyst	Reaction		Solvent	Product and yield,[a] %		
	Temp. °C	Time, hr		Benzaldehyde	Styrene oxide	Acetophenone
$RhCl(PPh_3)_3$	110	8	Toluene	148	trace	348
$RhCl(PPh_3)_3$	80	8	Toluene	213	trace	13
$RhCl(PPh_3)_3$	80	8	Dioxane	611	161	55
$RhCl(PPh_3)_3$	80	8	Tetrahydrofuran	225	106	103
$RhCl(PPh_3)_3$	80	8	Ethanol	17	trace	752
$RhCl(PPh_3)_3$	80	8	Pyridine	trace	trace	trace
$RhCl(PPh_3)_3$	110	8	Acetic acid	trace	trace	trace
$RhCl_3$	110	8	Toluene	867	1232	trace
$RhCl_3$	80	8	Ethanol	48	10	158
$IrCl_3$[1a]	110	8	Toluene	566	418	10
$IrCl_3$	80	8	Ethanol	trace	trace	45

a) Yields are based on the catalyst utilized.

case of the $RhCl_3$ catalyst, but the product distribution differs from that of $RhCl(PPh_3)_3$. The yields of styrene oxide and benzaldehyde increased in toluene, and the total yields decreased in ethanol. A similar result was obtained in the case of $IrCl_3$. The question of catalytic oxidation of styrene with rhodium complexes undergoing a remarkable solvent effect is now being investigated. It seems that the species $RhCl(PPh_3)_2$ (II) which is derived from the dissociation of $RhCl(PPh_3)_3$ has an important role in the reaction.[6]

$$RhCl(PPh_3)_3 \underset{PPh_3}{\overset{Solvent}{\rightleftharpoons}} RhCl(PPh_3)_2 + PPh_3$$

(I) (II)

Species II has a vacant site which may be essential to catalytic activity and will be coordinated easily with oxygen molecule under oxygen atmosphere.[6] We have postulated that oxidation might proceed *via* the coordination of both oxygen and styrene to Rh(I) metal as shown below.

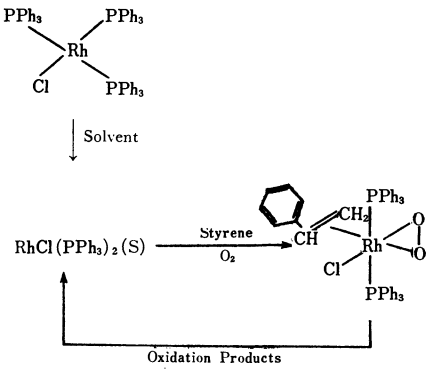

S: Solvent

Oxidation of α-Methylstyrene. The catalytic oxidation of α-methylstyrene with the Rh-complex was also investigated. The results are summarized in Table 2. Oxidation of α-methylstyrene gave acetophenone, formaldehyde, and α-phenylpropionaldehyde in considerable yields. Formations of acetophenone and formaldehyde are derived from the C=C double-bond cleavage of methylstyrene, and the formation of α-phenylpropionaldehyde corresponds to that of acetophenone in styrene. However, no epoxide type product such as styrene oxide could be obtained. The results differ from those of the Wacker process. In the Wacker process, in which $PdCl_2$ is used as an essential catalyst, α-methylstyrene gave only acetophenone and α-phenylpropionaldehyde.[7]

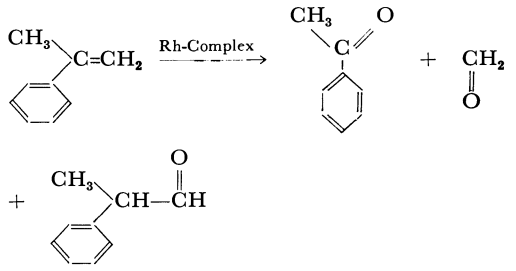

When iridium trichloride was used in the oxidation of α-methylstyrene a similar oxidation mixture (acetophenone and α-phenylpropionaldehyde) was obtained but the yields decreased in comparison with $RhCl_3$.

Oxidation of β-Methylstyrene. β-Methylstyrene was oxidized to benzaldehyde and acetaldehyde. The formation of acetaldehyde was confirmed by converting it to 2,4-dinitrophenylhydrozone. The results are shown in Table 3. We also tried the oxidation of *trans*-stilbene using the Rh-complex in toluene, but no oxidation product was obtained. From the results, it is clear that the reactivities to oxidation of styrenes

6) J. A. Osborn, F. H. Jardine, J. F. Young and G. Wilkinson, *J. Chem. Soc., A.*, **1966**, 1711.

7) R. Hüttel, J. Kratzer and M. Bechter, *Chem. Ber.*, **94**, 766 (1961).

Table 2. Oxidation of α-methylstyrene with rhodium compounds and iridium compound

Catalyst	Reaction		Solvent	Product and yield,[a] %	
	Temp. °C	Time, hr		Acetophenone	α-Phenylpropionaldehyde
$RhCl(PPh_3)_3$	110	8	Toluene	67	23
$RhCl(PPh_3)_3$	80	8	Ethanol	0	0
$RhCl_3$	110	8	Toluene	466	227
$RhCl_3$	80	8	Ethanol	96	trace
$IrCl_3$	110	8	Toluene	177	107

a) Yields are based on the catalyst utilized.

Table 3. Oxidation of β-methylstyrene with rhodium compounds

Catalyst	Reaction		Solvent	Benzaldehyde yield,[a] %
	Time hr	Temp. °C		
$RhCl(PPh_3)_3$	110	8	Toluene	134
$RhCl(PPh_3)_3$	80	8	Ethanol	trace
$RhCl_3$	110	8	Toluene	19
$RhCl_3$	80	8	Ethanol	9

a) Yields are based on the catalyst utilized.

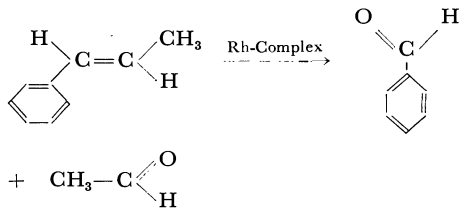

decrease as follows: styrene > α-methylstyrene > β-methylstyrene ≫ *trans*-stilbene. This suggests that a more sterically hindered olefin is difficult to coordinate with rhodium(I) and hence is less reactive to oxidation.

In conclusion, it has been found that the rhodium complex and rhodium trichloride have a catalytic function for the oxidation of styrene and methylstyrenes under oxygen atmosphere and that the product distribution undergoes a solvent effect.

Experimental

Materials and Analysis. All temperatures were uncorrected. VPC analysis was made by a Yanagimoto G-8 gas chromatograph usingan Apiezon L column. Rhodium trichloride trihydrate and iridium trichloride were of commercial grade. Toluene and acetic acid were purified as described previously.[1a] Ethanol was refluxed with calcium oxide and distilled. Pyridine was dried over barium oxide and distilled. Tetrahydrofuran was refluxed with sodium metal and distilled. Dioxane was purified by the method of Hess and Frahm.[8] Styrene, α-methylstyrene and β-methylstyrene were dried over anhydrous magnesium sulfate and distilled.

8) K. Hess and H. Frahm, *Ber.*, **71**, 2627 (1938).

Preparation of Chlorotris(triphenylphosphine)-rhodium. $RhCl(PPh_3)_3$ was prepared by the method of Osborn *et al.*[6] Mp 160—161°C (lit,[6] 157—158°C).

Oxidation of Styrene by Rhodium Complex. In a flask similar to that mentioned previously[1a], was placed a mixture containing 2.65 g (2.87 mmol) of $RhCl(PPh_3)_3$, 15 g (0.146 mol) of styrene, and 150 m*l* of toluene. The reaction was carried out at 110°C with continuous bubbling of oxygen for 8 hr. After evaporation of the solvent under reduced pressure, the residual material was chromatographed on alumina (80 g). Elution with 600 m*l* of ether and recrystallization gave 0.82 g of triphenylphosphine oxide. Further elution with methanol gave 0.24 g of an unidentified green complex.

From the solvent evaporated, we obtained styrene, 1.20 g of acetophenone, 0.45 g of benzaldehyde and a trace of styrene oxide.

Oxidation of α-Methylstyrene by Rhodium Complex. The apparatus was similar to that described above, except that the outlet gas from a condenser was bubbled into 2,4-dinitrophenylhydrazine solution. In a flask was placed a mixture containing 2.65 g (2.87 mmol) of $RhCl(PPh_3)_3$, 17 g (0.146 mol) of α-methylstyrene and 150 m*l* of toluene. The solution was refluxed with continuous bubbling of oxygen for 8 hr. Resulting reaction mixture was treated as usual, and the liquid phase was analysed and separated by VPC to give Ia (0.23 g) and Ib (0.09 g). Ia was assigned as acetophenone by comparison of NMR spectrum and retention time with those of an authentic sample. Ib was assigned as α-phenylpropionaldehyde by comparison of NMR spectrum and retention time with those of an authentic sample.

The solid phase was chromatographed on alumina (80 g). Elution with 2 *l* of ether and recrystallization gave 0.90 g of triphenylphosphine oxide. From 2,4-dinitrophenylhydrazine solution, 2,4-dinitrophenylhydrazone of formaldehyde was obtained as yellow crystals.

Oxidation of β-Methylstyrene by Rhodium Complex. The apparatus was similar to that described for α-methylstyrene. In a flask was placed mixture containing 0.55 g (0.60 mmol) of $RhCl(PPh_3)_3$, 2.27 g (19.2 mmol) of β-methylstyrene, and 45 m*l* of toluene. The solution was refluxed with continuous bubbling of oxygen for 8 hr. Resulting reaction mixture was treated as usual, and the liquid phase was separated by VPC to give 0.063 g of benzaldehyde. From 2,4-dinitrophenylhydrazine solution, 2,4-dinitrophenylhydrazone of acetaldehyde was obtained as yellow crystals.

BULLETIN OF THE CHEMICAL SOCIETY OF JAPAN VOL. 43 3901—3908 (1970)

ν_{O-H} Absorptions and Conformations of Epimeric 1-Tetralols and Chroman-4-ols

Hiizu IWAMURA and Kaoru HANAYA

Department of Chemistry, Faculty of Science, The University of Tokyo, Bunkyo-ku, Tokyo
and
Department of Chemistry, Faculty of Science, Yamagata University, Koshirakawa, Yamagata

(Received August 4, 1970)

The O–H stretching IR absorptions of epimeric 1-tetralols and chroman-4-ols were examined in dilute carbon tetrachloride solutions. The absorption pattern was found to be related to the conformation of the hydroxyl group; the epimers with the quasi-axial OH group showed a singlet ν_{O-H} at 3618 cm^{-1}, while those with the quasi-equatorial hydroxyl had doublet absorption at 3622 and 3600 cm^{-1}. Based on these findings 1-tetralol itself was shown to exist preferentially in the OH axial conformation. The bands at 3618 and 3600 cm^{-1} were assigned severally to the hydroxyl groups bonding to the π-electrons on the benzene ring. When an additional aryl group is present β to the hydroxyl, another O–H$\cdots\pi$ bonding to the aryl group becomes possible in addition to that between the OH group and the benzene ring of the tetralin and the chroman skeletons. The conformation of the aryl substituents was deduced by applying the empirical correlation relating the geometry of the molecule to the bonded ν_{O-H} frequency in a wide variety of aromatic alcohols which incorporate β-arylethanol moiety.

In connection with the stereochemical study of the reduction of α-tetralones, one of the present authors proposed previously a tentative configurational assignment of the resulting 1-tetralol epimers based on their different intramolecular O–H$\cdots\pi$ bonding as revealed by the O–H stretching (ν_{O-H}) absorption spectra.[1,2] A part of the conclusion was, however, found later to be contradictory to that derived from the NMR study and the mechanistic reasoning of their formation by the reductive reactions.[3] Thus the epimers of **1** (mp 96—98°C) and **2** (mp 113—115°C) which were established to be *trans* by the latter studies had been assigned to the contrary because they did not show the apparent O–H$\cdots\pi$ bonding absorption which was expected to be stronger for the *trans* epimer with the axial hydroxyl group.

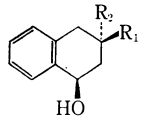

1a R_1=Ph, R_2=H
1b R_1=H, R_2=Ph
2a R_1=CH_3, R_2=H
2b R_1=H, R_2=CH_3

In view of the recent successful application of the intramolecular O–H$\cdots\pi$ bonding to the structural elucidation,[4,5] the consideration of the above controversy is intriguing. It is the purpose of the present paper to develop a more careful discussion relating the ν_{O-H} data to the conformation of tetralols and chroman-4-ols.

Results

In Table 1 are listed ν_{O-H} maxima of the 1-tetralols and chroman-4-ols, whose configurations have been established on the basis of both the dependence of the vicinal proton coupling constant on the dihedral angle due to the Karplus type equation and the mechanism of their formation.[3] Some of the typical IR absorption traces are reproduced in Figs. 1 and 2. From the data in Table 1 the following conclusions can be derived directly. (1) In a series of the alcohols with the substituent γ to the hydroxyl (**1**, **2**, **5** and **6**), the *cis* epimer has the doublet ν_{O-H} at 3622 and 3600 cm^{-1}, while the *trans* epimer has a skew singlet at 3618 cm^{-1}. (2) In a pair of **4**'s the above correlation between the ν_{O-H} pattern and the configuration is reversed: it is the *cis* isomer which shows a singlet ν_{O-H}. (3) 1-Tetralol itself has a doublet ν_{O-H} more like those with *cis*- γ- or *trans*-β-methyl substituent. The relative intensity of the two bands are, however, reversed. (4) When there is an aryl substituent β to the hydroxyl (**3**, **7**, **8** and **9**), the *trans* epimer gives the doublet absorption at 3614 and 3600 cm^{-1}, while the *cis* at 3616 and 3582 cm^{-1}.

1) K. Hanaya, *Nippon Kagaku Zasshi*, **87**, 745 (1966).
2) K. Hanaya, *ibid.*, **87**, 995 (1966).
3) S. Mitsui, A. Kasahara and K. Hanaya, This Bulletin, **41**, 2526 (1968).
4) M. Tichý, "Advances in Organic Chemistry: Methods and Results", Vol. 5, R. A. Raphael, E. C. Taylor and H. Wynberg, Ed., John Wiley & Sons, Inc., New York, N. Y. (1965), p. 115.
5) M. Ōki, H. Iwamura, T. Onoda and M. Iwamura, *Tetrahedron*, **24**, 1905 (1968).

Table 1. ν_{O-H} absorption of 1-tetralols and chroman-4-ols

Compound	ν_{max}	$\Delta\nu^{a}_{1/2}$	ε
1-Tetralol	3618	18	63
	3601	11	36
1a	3622	23	37
	3600	10	66
1b	3617	12	88
2a	3625	24	30
	3602	7	65
2b	3618	15	88
3a	3615	17	45
	3585	24	34
3b	3615	16	30
	3600	17	71
4a	3620	18	69
4b	3617	22	37
	3598	11	59
5a	3623	23	34
	3596	14	75
5b	3616	16	89
6a	3621	23	38
	3596	12	65
6b	3618	14	86
7a	3616	19	51
	3582	30	34
7b	3614	16	59
	3600	19	64
8a	3615	18	60
	3582	31	42
8b	3613	15	57
	3600	18	53
9a	3617	18	55
	3575	25	43
9b	3615	14	61
	3598	20	63

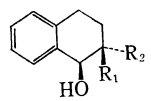

3a R_1=Ph, R_2=H
3b R_1=H, R_2=Ph
4a R_1=CH_3, R_2=H
4b R_1=H, R_2=CH_3

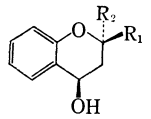

5a R_1=Ph, R_2=H
5b R_1=H, R_2=Ph
6a R_1=CH_3, R_2=H
6b R_1=H, R_2=CH_3

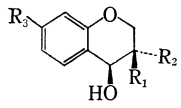

7a R_1=Ph, R_2=R_3=H
7b R_1=R_3=H, R_2=Ph
8a R_1=Ph, R_2=H, R_3=OCH_3
8b R_1=H, R_2=Ph, R_3=OCH_3
9a R_1=*p*-$CH_3OC_6H_4$, R_2=H, R_3=OCH_3
9b R_1=H, R_2=*p*-$CH_3OC_6H_4$, R_3=OCH_3

Discussion

There is enough rationalization in regarding the conformation of the cyclohexene moiety of 1-tetralols as a half-chair.[6] As for the chroman skeleton, no direct evidence seems to have been presented for the half-chair conformation of the dihydropyran. Although the sofa conformation in which all the atoms of the ring except $C_{(2)}$ are coplanar has once been proposed,[7] the half-chair model seems to be more consistent with the NMR data.[8] The observed difference in the ν_{O-H} pattern between the epimers means that the benzylic hydroxyl groups should never be equally inclined to the plane of the benzene ring in both cases, and the striking similarity in the IR absorptions with the corresponding 1-tetralol epimers as shown in Table 1 may be considered as another support for the half-chair conformation of

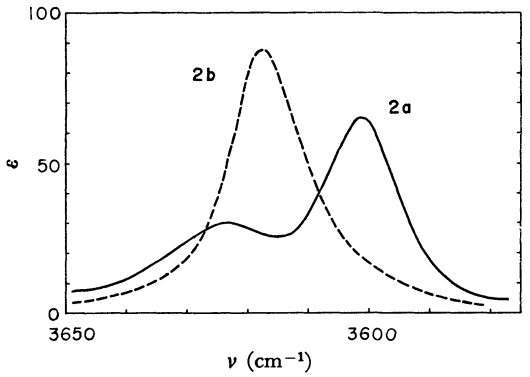

Fig. 1. ν_{O-H} Absorptions of *cis*- and *trans*-3-methyl-1-tetralols.

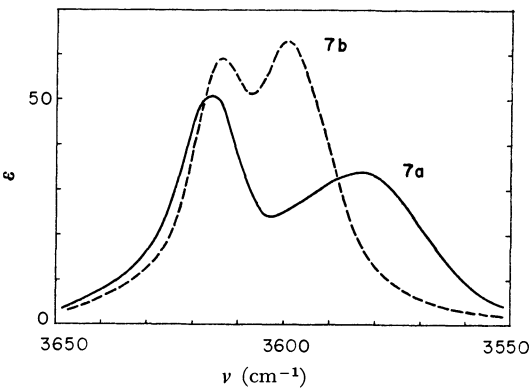

Fig. 2. ν_{O-H} Absorptions of 3-phenylchroman-4-ols.

6) E. J. Corey and R. A. Sneen, *J. Amer. Chem. Soc.*, **77**, 2505 (1955); E. L. Eliel, N. L. Allinger and G. A. Morrison, "Conformational Analysis", Interscience Publishers, New York, (1965); N. L. Allinger, J. A. Hirsch, M. A. Miller and I. J. Tyminski, *J. Amer. Chem. Soc.*, **90**, 5773 (1968); J. F. Chiang and S. H. Bauer, *ibid.*, **91**, 1898 (1969).

7) E. M. Philbin and T. S. Wheeler, *Proc. Chem. Soc.*, **1959**, 167.

8) J. W. Clark-Lewis, *Rev. Pure and Appl. Chem.*, **12**, 96 (1962); J. W. Clark-Lewis, L. M. Jackman and T. M. Spotwood, *Aust. J. Chem.*, **17**, 632 (1964).

the chroman nucleus.

Due to the conformational preference of the phenyl and the methyl groups over the hydroxyl,[9] the former groups may well be considered to assume preferentially the equatorial disposition on the 1-tetralol and chroman-4-ol skeletons. The conformation of the hydroxyl group should consequently be determined by its configuration with respect to the other substituents. Thus the *cis*- and *trans*-γ-substituted alcohols are expected to have the equatorial and axial hydroxyl groups, respectively. The 1-tetralols and chroman-4-ols with the *cis*- and *trans*-β-substituents are considered to have the axial and equatorial OH groups, respectively. Then the rules (1) and (2) derived in the preceding section can be restated as follows. It is the epimer with the quasi-equatorial benzylic hydroxyl group that shows the doublet absorption at 3622 and 3600 cm^{-1}. The OH quasi-axial epimer, to the contrary, displays only a 3618 cm^{-1} singlet.[11]

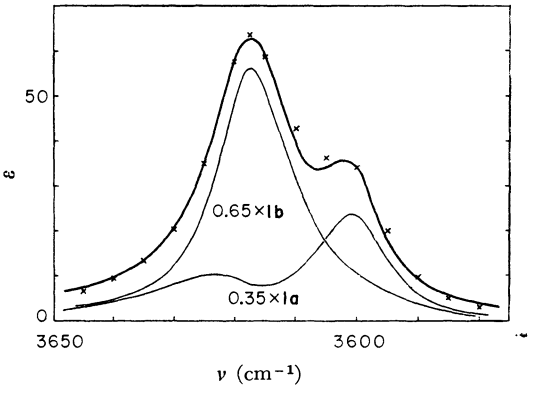

Fig. 3. ν_{O-H} Absorptions of 1-tetralol, **1a** and **1b**.
——— 1-tetralol (observed)
×× 0.35×**1a**+0.65×**1b**

It is instructive to note that graphical superposition of the spectra of **1a** and **1b**, or **2a** and **2b**, reproduces the apparent ν_{O-H} curve of 1-tetralol itself (Fig. 3) when the ratio of mixing is 0.54 to 1.[11a] Thus it is concluded that in 1-tetralol the OH quasi-axial conformation predominates and the apparent conformational energy ($-\Delta G_{25°}$) of the benzylic OH group is calculated to be −0.37 kcal/mol. This is not necessarily due to the O–H⋯π bonding energy because the steric hindrance between the equatorially oriented OH group and the parallelly disposed aromatic hydrogen atom is expected to be more serious than one 1,3-diaxial H–OH interaction in the cyclohexene ring. An analogous situation may be found in the allylic $A^{(1,2)}$ strain proposed by Johnson and Malhotra[12] for the 2,3-disubstituted cyclohexenes in which the substituent at the allylic 3 position often prefers the axial conformation.

Turning now to the interpretation of the ν_{O-H} frequencies, we could assign the bands at 3622 and 3618 cm^{-1} to the free OH group and only the low-frequency band at 3600 cm^{-1} to the one which is O–H⋯π bonded, by applying the naive concept of the effect of the hydrogen bonding on ν_{O-H} frequency. The assignment would be, however, rather confusing because it is at first glance the epimer with quasi-axial hydroxyl group which looks more advantageous for internal O–H⋯π bonding due to the perpendicular approach of the hydroxyl hydrogen to the π-electron cloud on the benzene ring. The interaction of the quasi-equatorial hydroxyl group with the benzene ring might be more horizontal. This is the reason why the opposite configurational assignment was made previously.[1,2] Therefore the truth must be either that the 3622 and/or 3618 cm^{-1} bands are not due to the free ν_{O-H} or that the quasi-axial hydroxyl group is not so favorably disposed for the internal O–H⋯π bonding as the quasi-equatorial epimer.

According to the conformational theory of the multiplicity of the ν_{O-H} absorptions,[13] the free ν_{O-H} frequencies of a pair of the epimeric alcohols under consideration may be expected to be as listed in the first column of Table 2 depending on the conformation of the OH group with respect to the C–O bond. The contribution of the type **a** conformation in which the OH bond is directed towards the center of the cyclohexene and dihydropyran ring may be smaller in the OH quasi-axial epimer because of the 1,3-diaxial interaction.[14] Therefore the singlet absorption at

9) The conformational energies ($-\Delta G_{25°}$) in the cyclohexyl derivatives are 3.1, 1.7 and 0.6 kcal/mol for the phenyl, methyl and hydroxyl groups, respectively.[10]

10) E. L. Eliel, *Angew. Chem.*, **77**, 784 (1965).

11) The same phenomenon has been observed in the epimeric pairs of conformationally fixed cyclohexen-3-ols in which nothing is different from the present system but the benzene ring is replaced by the ethylenic double bond.[5] This apparent reversal in the ν_{O-H} absorption patterns may in general be termed as the anomaly in the benzylic and allylic O–H⋯π bonding.

11a) G. F. Katekar and A. G. Moritz, *Aust. J. Chem.*, **22**, 2337 (1969).

12) F. Johnson and S. K. Malhotra, *J. Amer. Chem. Soc.*, **87**, 5492 (1965); S. K. Malhotra and F. Johnson *ibid.*, **87**, 5493 (1965).

13) a) M. Ōki and H. Iwamura, This Bulletin, **32**, 950 (1959); b) R. Piccolini and S. Winstein, *Tetrahedron Lett.*, **1959**, 4; c) F. Dalton, G. D. Meakins, J. H. Robinson and W. Zaharia, *J. Chem. Soc.*, **1962**, 1566; d) P. J. Krueger and M. D. Mettee, *Can. J. Chem.*, **42**, 347 (1964); e) J. Weinman, *Bull. Soc. Chim. Fr.*, **1967**, 4259; f) L. Joris, P. von R. Schleyer and E. Osawa, *Tetrahedron*, **24**, 4759 (1968).

14) H. S. Aaron and C. P. Rader, *J. Amer. Chem. Soc.*, **85**, 3046 (1963); H. S. Aaron, C. P. Ferguson and C. P. Rader, *ibid.*, **89**, 1431 (1967).

Table 2. Assignment of the ν_{O-H} absorptions in 1-tetralols and chroman-4-ols

Conformation of the OH group	Type	O-H bond staggered between	Free ν_{O-H}[13] expected	Bonded ν_{O-H} observed	$\Delta\nu_{O-H}$
Quasi-axial	**a**	C-C and C-C	3618	—	—
	b	C-C and C-H	3627	3618	9
	c[a]	C-C and C-H	3627	—	—
Quasi-equatorial	**a**	C-C and C-C	3618	3600	18
	b[a]	C-C and C-H	3627	—	—
	c	C-C and C-H	3627	3622	5

a) OH Group is not directed towards the π-electrons in these conformations.

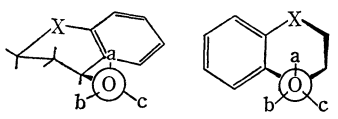

X=CH_2 or O

3618 cm^{-1} of the axial epimers is too low in frequency to be assigned to the free ν_{O-H}. Actually it corresponds well to the reported bonding ν_{O-H} of benzyl alcohols[15] in which the C–O bond has been estimated to be "axial" with respect to the plane of the benzene ring.[16] Thus it is more reasonable to regard this singlet absorption as the O–H···π bonded ν_{O-H}. The shift of ν_{O-H} as the result of the interaction ($\Delta\nu_{O-H}$) will be estimated to be 9 cm^{-1} (=3627−3618). In the quasi-equatorial alcohols, it is the type **a** conformation with the O–H bond staggered between the two C–C bonds which is expected to give relatively large ν_{O-H} shift. The OH hydrogen atom in this conformation is shown by molecular models to be favorably situated to overlap with the π-electrons on the benzene ring, while the hydroxyl group stays free in the **b** and lies close to the nodal plane of the π-orbitals on the benzene ring in the **c** conformations, respectively. Therefore the band at 3600 cm^{-1} should be regarded as the bonding ν_{O-H} in the **a** conformation. The second band at 3622 cm^{-1} may be an unresolved overlap of the free and weakly-bonded bands in the conformation **b** and **c**, respectively.[17]

Since the proposal by Badger and Bauer[18] it has been well-documented that $\Delta\nu_{O-H}$ provides a good measure of the strength of the hydrogen bonding especially when the closely related proton donors on the one hand and the acceptors on the other are compared.[19] In the previous papers[5,20] it has been shown that the strength of the O–H···π bonding is governed by the amount of overlap between the orbitals of the π-electrons and the hydroxyl group when a series of compounds with nearly equivalent basicity of the π-electrons and the acidity of the OH groups are compared. As one of the possible measures indicating the overlap between the interacting groups, the overlap integral S between the Slater's hydrogen 1s and the carbon 2p atomic orbitals has been shown to be appropriate.[5,20] In Table 3 are compared these parameters in each interacting conformation based on the geometry which was scaled on a Dreiding model. Although correlation with the observed $\Delta\nu_{OH}$ data is far from quantitative linearity, it is still the type **a** conformation of the quasi-equatorial hydroxyl which has the largest S as expected from the largest $\Delta\nu_{O-H}$. In this conformation, the O–H dipole is disposed anti-parallel to that of the 2$p\pi$ lobe on the adjacent carbon atoms in the benzene ring. The electrostatic force between the dipoles might also be contributing to effecting the largest $\Delta\nu_{O-H}$ shift in addition to the effect of the electron delocalization roughly estimated from S.

In the alcohols with β-aryl substituent (**3, 7, 8**

Table 3. Overlap between the hydroxyl group and the π-electrons on the benzene ring

Conformation of the OH group	Type	$\sum S$[a]	$\Delta\nu_{O-H}$ observed
Quasi-axial	**b**	0.099	9
Quasi-equatorial	**a**	0.110	18
	c	0.050	5

a) R. S. Mulliken, C. A. Rieke, D. Orloff and H. Orloff, *J. Chem. Phys.*, **17**, 1248 (1949).

15) M. Ōki and H. Iwamura, This Bulletin, **32**, 955 (1969).

16) J. C. Evans, *Spectrochim. Acta*, **17**, 129 (1961).

17) 13-Epiophiocarpin (**10**) is reported to give ν_{O-H}'s at 3625(shoulder) and 3597 cm^{-1} (M. Ohta, H. Tani and S. Morozumi, *Tetrahedron Lett.*, **1963**, 859. Contrary to the original interpretation, the latter band may be due to the bonded ν_{O-H} characteristic of the equatorial benzylic alcohols.

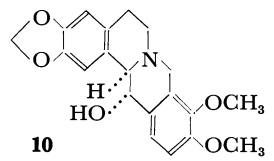

10

18) R. M. Badger and S. H. Bauer, *J. Chem. Phys.*, **5**, 839 (1937).

19) G. C. Pimentel and A. L. McClellan, "Hydrogen Bond", W. H. Freeman & Co., San Francisco (1960), p. 82.

20) M. Ōki and H. Iwamura, *J. Amer. Chem. Soc.*, **89**, 576 (1967).

and **9**), the internal bonding of the hydroxyl group with the π-electrons of the aryl group has to be taken into account in addition to the benzylic interaction discussed above. As the result of the preferentially equatorial disposition of the aryl group on the cyclohexene and the dihydropyran nuclei, the hydroxyl group should be quasi-axial in the *cis* epimers. The doublet absorptions at 3616 and 3582 cm^{-1} must have arisen from the O–H$\cdots\pi$ bonding to the benzo-ring and the aryl group (see **11**), respectively. This assignment may be confirmed by the observation that the *p*-methoxyl substitution in the aryl group shifts the latter absorption to the still lower frequency (*ca.* 3582 cm^{-1} in **3a, 7a** and **8a** to 3575 cm^{-1} in **9a**) by enhancing the basicity of the aryl π-electrons.[15,21] In the *trans*-β-aryl substituted series, **3b, 7b, 8b** and **9b,** the quasi-equatorial OH group can interact either with the benzo-benzene ring to exhibit 3600 cm^{-1} band as in the γ-substituted cases or with the β-aryl group to produce the new absorption at 3614 cm^{-1} in the type **b** conformation of the hydroxyl group (see **12**). Alternatively the band at 3600 cm^{-1} might be considered to be an overlap between the two kinds of the bonded bands. The relative intensity of the 3614 cm^{-1} bands is, however, almost unity and too high to be assigned to the hydroxyl group in the **c** type conformation which should be populated one third at best.

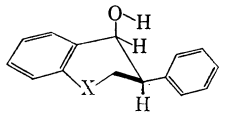

11 3582 cm^{-1}

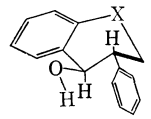

12 3614 cm^{-1}

In an attempt to delineate the spatial configuration of the plane of the aryl group relative to the rest of the molecule in **11** and **12,** it seemed intriguing to examine the ν_{O-H} absorptions in a wide variety of conformationally-fixed β-phenethyl alcohols. As summarized in Table 4, the bonded ν_{O-H} frequencies range from 3616 cm^{-1} down to 3560 cm^{-1}. It is rather apparent from molecular models that the larger ν_{O-H} shift in compounds **17** to **22** may be derived from the geometry which permits closer approach of the hydroxyl group to the π-electrons on the aromatic ring. In compounds **13** and **14,** on the contrary, the hydroxyl hydrogen lies close to the nodal plane of the carbon $2p\pi$ orbitals of the benzene ring with result of the smallest shift in the ν_{O-H} frequency.[22] When alcohols with the same framework are compared, their ν_{O-H}'s fall within the experimetal errors and support the idea that the geometrical factors are playing the major role in determining the absorption frequency.[23] As in the previous treatment,[5,20] one could compute the Slater overlap integral between the hydrogen 1*s* and the carbon 2*p* orbitals to represent the extent of overlap between the two interacting groups in each alcohol, but the dihedral angle θ made by the plane of the aromatic ring and the plane defined by the three carbon atoms, C_α,C_β and C_1 of the benzene ring has now been employed as a convenient measure expressing the geometrical relationship between the OH and the aromatic π-electrons. It is shown in Fig. 4 that it is by definition the quadrant described by θ and not the supplementary angle of θ which should contain the OH group. For each alcohol the angle θ was measured on a Dreiding model and/or estimated on the basis of the geometry of the partial structure when this is known. Thus the exact dimension of cyclopentene[24] was assumed for **15** and **24.** The consistent value of $\theta=144°$ was also obtained for **17** and **22** from the structure of norbornane and norbornadiene determined by the electron diffraction study.[25] The results are included in Table 4. It is not always proper to regard the apparent difference in frequencies of the doublet absorption peaks as the ν_{O-H} shift, because the conformational environment of the hydroxyl group which is well-documented[13] with its influence on the ν_{O-H} frequency does not necessarily coincide in the free and the bonded forms. To avoid ambiguity in

21) M. Ōki and H. Iwamura, This Bulletin, **32**, 1135 (1959).

22) To the authors knowledge, only one attempt has so far been presented which is partly successful in correlating ν_{O-H} data with the distance *r* between the hydroxyl hydrogen and the carbon atom carrying the π-electrons pertaining to the interaction (Y. Matsui, M. Takasuka and T. Kubota, *Shionogi Kenkyusho Nempo* (*Ann. Rept. Shionogi Res. Lab.*), **15** 125 (1965); T. Kubota, M. Takasuka and Y. Matsui, *ibid.*, **16**, 63 (1966)). This approach is, however, too approximate to be applied to conformational analysis.

23) It is noted by comparing pairs of **13a** and **13b**, **13c** and **13d**, and **8a** and **9a** that the methoxyl group produces further low frequency shift by 0, 3 and 7 cm^{-1} at 3616, 3600 and 3582 cm^{-1}, respectively, of the ν_{O-H} frequencies of the unsubstituted alcohols. The lowest frequency of 3560 cm^{-1} observed for epihaemanthamine **21** must be partly due to this electronic effect produced by the methylenedioxy group on the aromatic ring which is known to increase the basicity of the π-electron system just as the methoxyl group does. For the purpose of conformational discussion, it is necessary to eliminate from the observed ν_{O-H} value contribution of the electronic effect. By considering approximately twice as much shift as one methoxyl group, the corrected frequency for the unsubstituted homolog of **21** would be about 3574 $(=3560+2\times7)$ cm^{-1}.

24) G. W. Rathjens, *J. Chem. Phys.*, **36**, 2401 (1962); S. S. Butcher and C. C. Costain, *J. Mol. Spectroscopy*, **15**, 40 (1965); J. Laane and R. C. Lord, *J. Chem. Phys.*, **47**, 4941 (1967).

25) Y. Morino, K. Kuchitsu and A. Yokozeki, This Bulletin, **40**, 1552 (1967).

Table 4. ν_{O-H} Absorptions and geometries of conformationally-fixed β-phenylethanols

Compound	Free ν_{O-H}	Bonded ν_{O-H}	θ °	Ref.
Demethoxyepidihydrobuphanamine **13a**		3616	15	26
Epidihydrobuphanamine **13b**		3616	15	26
Epibuphanamine **14a**		3614	20	26
Indane-1-methanol **15**	3638	3605	65	27
β-Phenylethanol	3636	3606		21
cis-2-Phenylcyclohexanol **16a**	3627	3600		This work
trans-2-Phenylcyclohexanol **16b**	(3622)	3599		This work, 28, 29
1,2,5,7,7,8-Hexamethyl-3,4-benzotricyclo-[3.3.0.$0^{2,8}$] oct-3-en-6(*syn*)-ol **18**		3580	110	30
1,2,3,4-Tetrahydro-1,4-methanonaphthalen-2(*syn*)-ol **17**	3624	3576	115	This work, 22
Epihaemanthamine **21**		3560	115	31
1,2,3,4-Tetrahydro-1,4-ethanonaphthalen-2(*syn*)-ol **19**	3618	3586	120	This work, 32
1,4-Dihydro-1,2,3,4,10,10-hexamethyl-1,4-ethanonaphthalen-9(*syn*)-ol **20**	3635	3580	120	33
1,2,3,4-Tetrahydro-1, 4-methanonaphthalen-9(*syn*)-ol **22a**	3619	3575	145	34, 22
9(*anti*)-Methyl-1,2,3,4-tetrahydro-1,4-methanonaphthalen-9(*syn*)-ol **22b**	3625	3576	145	22
β-2,5-Dimethyl-9-hydroxy-2'-methoxy-6,7-benzomorphan **23a**	3634	3591	155	35
β-9-Hydroxy-2'-methoxy-2,5,9-trimethyl-6,7-benzomorphan **23b**	3622	3586	155	36
β-5-Ethyl-9-hydroxy-2'-methoxy-2-methyl-6,7-benzomorphan **23c**	3625	3595	155	37
β-2,9-Dimethyl-5-ethyl-9-hydroxy-2'-methoxy-6,7-benzomorphan **23d**	3610	3591	155	37
Buphanamine **14b**	3613	3584	160	26
Indan-2-ol **24**	3620	3592	165	38
Demethoxydihydrobuphanamine **13c**	(3620)	3602	165	26
Dihydrobuphanamine **13d**	(3620)	3599	165	26

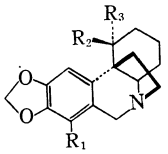

13a R_1=H, R_2=OH, R_3=H
13b R_1=OCH_3, R_2=OH, R_3=H
13c R_1=H, R_2=H, R_3=OH
13d R_1=OCH_3, R_2=H, R_3=OH

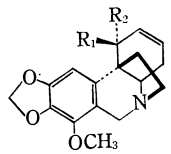

14a R_1=OH, R_2=H
14b R_1=H, R_2=OH

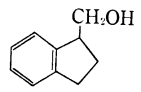

15

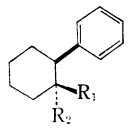

16a R_1=OH, R_2=H
16b R_1=H, R_2=OH

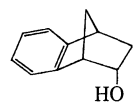

17

26) H. M. Fales and W. C. Wildman, *J. Amer. Chem. Soc.*, **85**, 784 (1963).
27) J. H. Brewster and J. G. Buta, *ibid.*, **88**, 2233 (1966).
28) P. von R. Schleyer, C. Wintner, S. S. Trifan and R. Backai, *Tetrahedron Lett.*, No. 14, 1 (1959).
29) C. R. Eddy, J. S. Showell and T. E. Zell, *J. Amer. Oil Chemists Soc.*, **40**, 92 (1963).
30) H. Hart and R. K. Murray, Jr., *J. Amer. Chem. Soc.*, **91**, 2183 (1969).
31) H. M. Fales and W. C. Wildman, *ibid.*, **82**, 197 (1960).
32) K. Kitahonoki and Y. Takano, *Tetrahedron Lett.*, **1963**, 1597.
33) A. C. G. Gray and H. Hart, *J. Amer. Chem. Soc.*, **90**, 2569 (1968).
34) H. Tanida, T. Tsuji and H. Ishitobi, *ibid.*, **86**, 4904 (1964).
35) H. Kugita and E. L. May, *J. Org. Chem.*, **26**, 1954 (1961).
36) E. L. May and H. Kigita, *ibid.*, **26**, 188 (1961).
37) S. Saito and E. L. May, *ibid.*, **26**, 4536 (1961).
38) W. R. Jackson and C. H. McMullen, *J. Chem. Soc.*, **1965**, 1170.

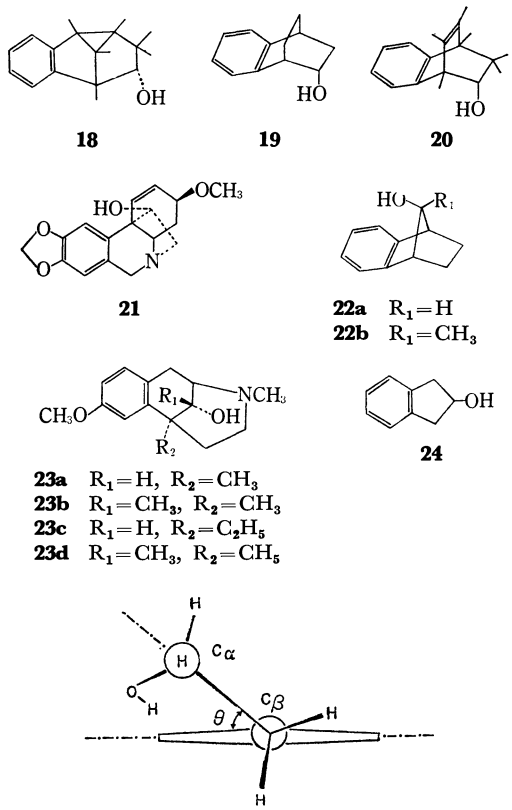

Fig. 4. Definition of the dihedral angle θ in β-phenylethanols.

evaluating the free ν_{O-H} which would be expected for the bonded conformer when it has not O–H···π bonding, the bonded frequency itself is tentatively to be compared without reference to the free ν_{O-H}. It is apparent that the lower the bonded O–H frequency the stronger the O–H···π bonding. Graphic presentation gives reasonably smooth bonded ν_{O-H} *versus* θ curve as shown in Fig. 5. The correlation may well be rationalized by inspection of molecular models (see Fig. 4) in such a way that when $\theta=120°$ the OH hydrogen is situated right above the π-cloud of the C_1 atom on the benzene ring and the overlap between the hydroxyl and the π-electrons is expected to be maximal. At $\theta=30°$ the hydroxyl hydrogen lies on the plane of the benzene ring, pointing the node of the π-electrons with result of no effective bonding at all. Correspondingly ν_{O-H}'s appear at the normal free ν_{O-H} region of 3620—3627 cm^{-1}. The argument is based on the assumption that in most of the bonded conformations of β-phenylethanols the C_α–O bond is staggered with the C_β–C_1 bond; the dihedral angle between the plane of O–C_α–C_β and that of C_α–C_β–C_1 is approximately 60°.

The curve in Fig. 5 could be approximated by Eq. (1) and will be of great use in conformational

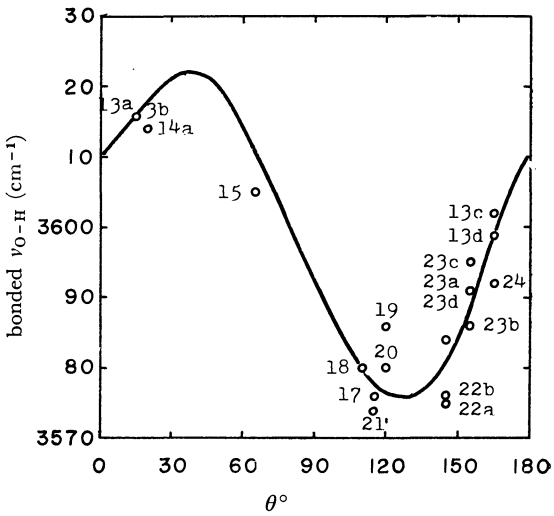

Fig. 5. Angular dependence of the observed ν_{O-H}.

study of β-phenylethanols. Thus it is possible

$$\nu_{O-H}^{bonded}\,(cm^{-1}) = 3625 - 50\cos 2(\theta - 30°) \qquad (1)$$

to estimate that in the bonded conformation of **11** θ must be about 120°. In **12** θ is estimated to be *ca.* 60°. Geometrically these conditions are satisfied in either epimer by fixing the plane of the benzene ring so that the $C_{(2)}$–$C_{(3)}$ bond of the chroman skeleton (bold lined in **11** and **12**) eclipses the plane. Analogously for 2-phenylcyclohexanols (**16a** and **16b**) $\theta=90°$; the $C_{(1)}$–$C_{(2)}$ bond in the cyclohexyl moiety is projected perpendicular to the plane of the benzene ring. This is not consistent with that proposed for phenylcyclohexane itself. The benzene ring has been estimated to be perpendicular to the plane defined by the $C_{(1)}$–$C_{(2)}$–$C_{(3)}$ atoms of the cyclohexane ring.[39] If the latter conformation were kept in **16,** markedly different ν_{O-H} frequencies should at least have been observed for **16a** and **16b,** because the spatial relation between the OH and the aromatic ring is quite different in both epimers. The θ defined as above amounts to 60° and 120° for the *cis* and the *trans* epimers, and the bonded ν_{O-H} of *ca.* 3615 and 3580 cm^{-1} should have been observed, respectively.

As another example on this line, mention should be made of the reported conformation of (+)-catechin teramethyl ether. Birch colaborated with Cole[40] concluded the 2-aryl-3-OH-diaxial

39) E. W. Garbisch and D. B. Patterson, *J. Amer. Chem. Soc.*, **85**, 3228 (1963); N. L. Allinger, J. Allinger, M. A. DaRooge and S. Greenberg, *J. Org. Chem.*, **27**, 4603 (1962).

40) A. J. Birch, J. W. Clark-Lewis and A. V. Robertson, *J. Chem. Soc.*, **1957**, 3586.

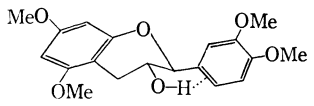

25

conformation on the assumption that the observed ν_{O-H} at 3594 cm^{-1} might be due to the internal hydrogen bonding to the ring oxygen of the chroman skeleton. The conclusion is, however, incompatible with the conformational energy of the axial aryl group.[9,10] Even stabilization of the OH axial conformation by the O-H···O hydrogen bonding does not seem to be enough to allow predominantly axial hydroxyl, because in the case of tetrahydropyran-3-ol the conformer with the equatorial OH group is still present in an appreciable concentration.[41] Therefore the preferred conformation of (+)-catechin tetramethyl ether would better be considered as 2,3-diequatorial with the hydroxyl group bonded to the π-electrons on the aryl group (**25**). The observed frequency of 3594 cm^{-1} is reasonably understood when the electron-donating effect of the two methoxyl substituents on the aryl ring is taken into account[23] in reference to 3599 cm^{-1} observed for the structurally analogous *trans*-2-phenylcyclohexanol (**16b**).[42]

41) S. A. Barker, J. S. Brimacombe, A. B. Foster, D. H. Whiffen and G. Zweifel, *Tetrahedron*, **7**, 10 (1959).

42) The corresponding hydroxyl groups in *cis*- and *trans*-flavan-3,4-diols are reported (E. M. Philbin, T. S. Wheeler, F. V. Brutcher, Jr., and W. Bauer, Jr., *J. Org. Chem.*, **27**, 4114 (1962)) to absorb at 3606 and 3608 cm^{-1}, respectively. Shift to higher frequency by several cm^{-1} when compared with those of **25** and **16b** might somehow be ascribed to the effect of the second 4-OH group which is bonding to the 3-OH consecutively.

Experimental

The infrared absorptions were measured either on a Perkin-Elmer 125 double beam or a 112G single beam grating high resolution IR spectrometer, the spectral slit width being 1.0 cm^{-1} in the region concerned. A quartz cell of 20 mm and a KCl cell of 30 mm in optical length were used. The concentration of the solutions was *ca.* 5 mmol/*l* in carbon tetrachloride distilled over phosphorus pentoxide at which dilution the band due to intermolecular hydrogen bonding was not observed. Sometimes ν_{O-H} absorptions were accompanied by a weak shoulder at 3630 cm^{-1} which was found later to be due to poor cancellation of the absorptions of water vapor in the optical path especially with a double beam spectrometer.

1-Tetralols and chroman-4-ols were prepared by reduction of the corresponding α-tetralones and γ-chromanones according to the literature.[2,43] We are indebted to Prof. N. Inoue who kindly supplied samples of 3-phenylchroman-4-ols.

As to the ν_{O-H} data quoted from the literature, reliable ones were carefully picked up which have been explicitly mentioned to have been measured in dilute carbon tetrachloride solutions on the IR spectrometer equipped with a grating or a fluoride prism.

43) S. Mitsui and A. Kasahara, *Nippon Kagaku Zasshi* **79**, 1382 (1958); K. Hanaya and K. Kose, *ibid.*, **89**, 1002 (1968).

BULLETIN OF THE CHEMICAL SOCIETY OF JAPAN VOL. 43 3909—3913 (1970)

Study on Oxazolopyrimidines. V. Preparation of 9-Substituted Hypoxanthines *via* 7-Aminooxazolo[5,4-*d*]pyrimidines

Yozo Ohtsuka

Sagami Chemical Research Center, Onuma, Sagamihara, Kanagawa

(Received August 8, 1970)

Reaction of 4-cyano-5-ethoxymethylenaminooxazoles with aliphatic amines gave 7-alkylaminooxazolo[5,4-*d*]pyrimidines. The structure of these compounds was discussed on the basis of spectroscopic properties. These oxazolopyrimidines were converted to 9-alkylhypoxanthines by treatment with aqueous alkali (Method A) or by heating in formamide (Method B). Reaction of the ethoxymethylenamino compounds with aromatic amines gave 9-arylhypoxanthines directly (Method C).

Conversion reaction of 7-aminooxazolo[5,4-*d*]pyrimidines into hypoxanthine derivatives has been reported in a previous paper.[1] The present work is concerned with the extension of this reaction to the preparation of 9-substituted hypoxanthines.

The procedure for the synthesis of fused pyrimidines by reaction of amines and heteroaromatic compounds which have a cyano and an ethoxymethylenamino group at adjacent positions has been applied to several systems.[2-5] The application of this method is convenient for preparing variously substituted fused pyrimidines which may be useful to biochemical studies.

Treatment of 4-cyano-5-ethoxymethylenaminooxazoles (I) with ammonia has been shown to afford 7-aminooxazolopyrimidines.[6] Analogous treatment of I with aliphatic amines gave the corresponding products II, most of which were led to 9-alkylhypoxanthines (III) under suitable conditions. The reaction of I with aromatic amines, however, required rather severe conditions, under which the conversion reaction of 7-arylamino intermediates (II) into 9-arylhypoxanthines (III) took place.

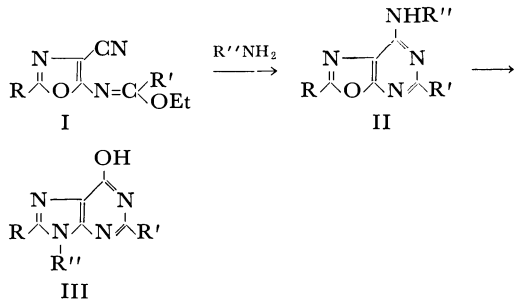

I II III

Synthesis and Structure of 7-Aminooxazolo[5,4-*d*]pyrimidines (II). Treatment of Ia (R=R′=H) with a cold aqueous solution of methylamine gave colorless crystals immediately. Its structure was supposed to be an amidine intermediate (IV) on the ground of its spectra (the presence of nitrile band in IR spectrum and the absence of ethoxyl group in NMR spectrum), considering the analogous reaction path with pyrazole derivatives.[2] The compound IV was easily converted into a second product, 7-methylaminooxazolpyrimidine (IIa), on standing in a basic medium. The structure of the latter compound was distinguished from that of 6-methyl-7(6*H*)iminooxazolopyrimidine (V) by the following reasons; *i*) From the study on 7-aminooxazolopyrimidines, a relatively low electron density on the pyrimidine moiety has been suggested,[6,7] and the rate of the Dimroth rearrangement has been known to be greatly enhanced with the pyrimidine derivatives having electron-withdraw-

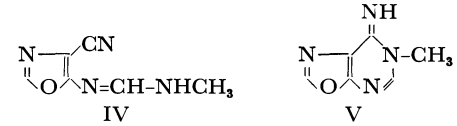

IV V

1) Y. Ohtsuka, This Bulletin, **43**, 954 (1970).

2) E. C. Taylor and K. S. Hartke, *J. Amer. Chem. Soc.*, **81**, 2456 (1959); E. C. Taylor and P. K. Loeffler, *ibid.*, **82**, 3147 (1960).

3) R. N. Prasad and R. K. Robins, *ibid.*, **79**, 6401 (1957).

4) K. Suzuki, T. Meguro, I. Kumashiro and T. Takenishi, Abstract of Papers, 21st Annual Meeting of Chemical Society of Japan, Osaka, March 1968, No. 3, p. 1775; K. Suzuki and I. Kumashiro, Brit. 1134974 (1968).

5) E. C. Taylor and E. E. Garcia, *J. Org. Chem.*, **29**, 2116 (1964); P. Rajagopalan and C. N. Talaty, *Tetrahedron*, **23**, 3541 (1967).

6) Y. Ohtsuka, This Bulletin, **43**, 187 (1970).

7) Y. Ohtsuka and K. Sugimoto, *ibid.*, **43**, 2281 (1970).

ing substituents.[8] Thus, the compound V was expected to be easily converted into IIa under such conditions as used in this experiment. Moreover, the previously isolated iminopyrimidines have been reported to be somewhat unstable on standing in moist air or on being treated in a polar solvent.[2,9] These properties are completely different from that of the product obtained here. *ii*) The UV spectrum of this compound was investigated at pH 1 and pH 10, and the difference of λ_{max} in acidic and in basic solution were compared with the values of 6-methylaminopurine ($\Delta\lambda=5$ mμ)[10] and of 1-methyl-6-(1*H*)iminopurine ($\Delta\lambda=11$ mμ).[11] While a relatively large value of $\Delta\lambda$ was expected for imino structure (V), the experimental value ($\Delta\lambda=3$ mμ) indicates that the structure of the product is IIa. Little pH-dependence has been observed also with the UV spectrum of 7-aminooxazolopyrimidine.[6] *iii*) Other spectroscopic properties of the compound seem to support the above conclusion. Its IR spectrum shows a band due to a secondary amine. In the mass spectrum, it preferentially expels 28 mass units from the molecular ion. Such a process has been observed previously with 6-methylaminopurine,[12] in which the initial fragmentation was attributed to loss of a methylamino group with concomitant transfer of one or two hydrogen atoms to the purine nucleus.

Table 1. 7-Alkylaminooxazolo[5,4-*d*]pyrimidine derivatives

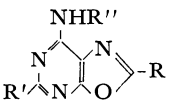

Compd	Substituent			Yield (%)	Mp (°C)
	R	R′	R″		
IIa	H	H	CH_3	80	182—184
IIb	H	CH_3	CH_3	62	170—171
IIc	H	C_2H_5	CH_3	82	140—142
IId	CH_3	H	CH_3	27	194—195
IIe	CH_3	CH_3	CH_3	67	184—185
IIf	H	H	C_2H_5	49	144—145
IIg	H	H	*n*-Pr	31	104—105
IIh	H	H	*i*-Pr	24	121—122
IIi	H	H	*n*-Bu	26	81— 82
IIj	H	H	*t*-Bu	—	—

By the reaction of I with various aliphatic amines, a number of oxazolopyrimidines were obtained. The IR, NMR and mass spectra of these products exhibit the characteristic patterns closely related with those of IIa, indicating that these products have 7-alkylamino structures (II). As shown in Table 1, both the yields and the mp's of these oxazolopyrimidines are dependent mainly upon the substituent R″. The bulkiness of R″ seems to be unfavorable to the reaction. The cyclized product was not obtained from the reaction of Ia with *t*-butylamine. The effect of other substituents, R and R′, seems to be small but the introduction of 2-substituent (R=CH_3) causes the oxazole ring to be somewhat unstable to alkali.

Preparation of 9-Substituted Hypoxanthine (III). 7-Alkylaminooxazolopyrimidines (IIa and IIb) were treated with aqueous alkali under the conditions similar to those with 7-amino compounds,[1] and the corresponding hypoxanthines (IIIa and IIIb) were obtained as shown in Table 2 (Method A). This treatment, however, has a limitation since the isolation of water-soluble products is tedious and hydrolysis with strong alkali is accompanied by the conversion reaction. In these cases, the conversion was carried out by heating II in formamide at around 200°C (Table 2, Method B). As for the reaction of I with aromatic amines, prolonged heating at higher temperatures was needed in contrast to the case of aliphatic amines, and the corresponding hypoxanthines were obtained directly (Table 2, Method C). Method C gave a better result than Method B in reaction of Ia with *n*-butylamine.

Table 2. Total yields of hypoxanthines derivatives

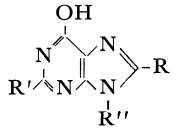

Compd	Substituent			Method[a]	Total yield from I (%)
	R	R′	R″		
IIIa	H	H	CH_3	A, B	69
IIIb	H	CH_3	CH_3	A	31
IIIe	CH_3	CH_3	CH_3	B	20
IIIf	H	H	C_2H_5	B	43
IIIg	H	H	*n*-Pr	B	27
IIIi	H	H	*n*-Bu	B	26
				C	48
IIIk	H	H	Ph	C	42
IIIl	H	H	*β*-Naph	C	17

a) A: Isolation of oxazolopyrimidine followed by treatment with aqueous NaOH.
B: Isolation of oxazolopyrimidine followed by heating in formamide.
C: One-step method.

8) D. J. Brown and J. S. Harper, *J. Chem. Soc.*, **1963**, 1276.
9) D. J. Brown, E. Hoerger and S. F. Mason, *ibid.*, **1955**, 4035.
10) G. B. Elion, E. Burgi and G. H. Hitchings, *J. Amer. Chem. Soc.*, **74**, 411 (1952).
11) N. J. Leonard and J. A. Deyrup, *ibid.*, **84**, 2148 (1962).
12) J. M. Rice and G. O. Dudek, *ibid.*, **89**, 2719 (1967).

The decreased yield of hypoxanthines having a bulky substituent at 9-position may be related partly with the formation of isomeric products. Thus, the treatment of IIh by Method B yielded an isomeric product, but the rearrangement accompanying this reaction will be reported in a subsequent paper.

This new route from oxazole derivatives to hypoxanthines may be applied best for the preparation of hypoxanthines having an *n*-alkyl substituent at 9-position.

Experimental

Melting points were measured on a hot-stage apparatus and uncorrected. The IR, NMR and UV spectra were determined with a Perkin-Elmer 337, a Varian HA-100 and a Carry-14 spectrometer, respectively. Mass spectra were recorded at ionization voltage of 70 eV, and samples were introduced directly into the ion source of a Hitachi RMU-6E mass spectrometer. Preparations of starting materials (I) from 5-amino-4-cyanooxazole derivatives and ortho-esters have been described in a previous paper.[6]

7-Methylaminooxazolo[5,4-*d*]pyrimidine (IIa). To an ice-cooled aqueous solution of methylamine (30%, 1 m*l*), 4-cyano-5-ethoxymethylenaminooxazole (Ia, 1.65 g) was added in one portion. A solid started to precipitate immediately from solution,[13] but on continued stirring it rapidly dissolved. After 10 min, a second solid precipitated. Filtration and washing with a small quantity of water gave a crystalline (1.20 g). For analytical purpose, recrystallization from water or ethanol gave colorless needles, mp 182—184°C. λ_{max}^{MeOH} mμ (log ε): 207 (4.20), 258 (4.20), 283 sh (3.71). $\lambda_{max}^{pH\ 1}$: 255 (4.03). $\lambda_{max}^{pH\ 10}$: 258 (3.84). λ_{max}^{KBr} cm^{-1}: 3295 (NH), 3071 (CH), 1630, 1604, 1535, 1492, 1142, 1062, 795. NMR (DMSO-d_6) δ: 3.03 (broad s, 3H, *N*-methyl protons), 8.12 (broad s, 1H, =*N*-proton), 8.33 (s, 1H, C_2-proton), 8.61 (s, 1H, C_5-proton). Mass spectrum (assignment, relative intensity, metastable peak) *m/e*: 150 (M^+, 100), 122 (M^+-28, 42, 99.0), 94 ([121]$^+$—HCN, 23, 73.0), 67 ([94]$^+$—HCN, 31, 48.7).

Found: C, 47.66; H, 4.09; N, 37.45%. Calcd for $C_6H_6N_4O$: C, 48.00; H, 4.03; N, 37.32%.

9-Methylhypoxanthine (IIIa). Method A. A mixture of IIa (1 g) and a 4N aqueous NaOH (5 m*l*) was stirred at room temperature for 30 min and then warmed gradually to dissolve the solid into the solution. After cooling, the solution was neutralized with HCl and resulting precipitate (0.8 g) was collected by filtration.

Method B. The compound IIa (1 g) was heated in formamide (5 m*l*) to a vicinity of 200°C for 40 min and then evaporated to nearly dryness under reduced pressure. Recrystallization from water gave 0.8 g of colorless crystals.

These products were identified as 9-methylhypoxanthine.[14]

13) A crude material was rapidly isolated from the reaction mixture. Its IR spectrum showed a nitrile band and its NMR spectrum showed no ethoxyl group. Furhter purification of the material gave IIa.

5-Methyl-7-methylaminooxazolo[5,4-*d*]pyrimidine (IIb). This compound was prepared from 4-cyano-5-ethoxyethylenaminooxazole (Ib) and methylamine by the procedure described above with 69% yield. Recrystallization from ethanol gave colorless needles, mp 170—171°C. ν_{max}^{KBr} cm^{-1}: 3249 (NH), 3118 (CH), 1677, 1600, 1555, 1519, 1160, 1040, 771. NMR (DMSO-d_6) δ: 3.54 (broad s, 3H, *N*-methyl protons), 7.21 (s, 1H, =N-proton), 8.35 (s, 1H, C_2-proton), 2.50 (s, 3H, C_5-methyl protons). Mass spectrum, *m/e*: 164 (M^+, 100), 149 (M^+-15, 16, 135.4), 136 (M^+-28, 16, 112.8), 96 ([136]$^+-C_2H_2N$, 19, -), 69 ([96]$^+$ -HCN, 47, 49.6).

Found: C, 51.08; H, 4.62; N, 34.61%. Calcd for $C_7H_8N_4O$: C, 51.21; H, 4.91; N, 34.13%.

2,9-Dimethylhypoxanthine (IIIb). This compound was prepared from IIb by Method A with 74% yield. Recrystallization from water gave colorless crystals, mp>320°C. The IR spectrum of the compound exhibited a broad band in the 2800—2600 cm^{-1} region which is characteristic of all the hypoxanthines studied here and a band due to a secondary amine was absent. Mass spectrum, *m/e*: 164 (M^+, 100), 123 (M^+-CH_3CN, 98, 92.3), 95 ([123]$^+$—28, 97, 73.4), 68 ([95]$^+$—HCN, 116, 48.7), 53 ([68]$^+-CH_3$, 50, 41.3), 41 ([68]$^+$—HCN, 84, 25.8).

Found: C, 51.36; H, 4.94; N, 34.29%. Calcd for $C_7H_8N_4O$: C, 51.21; H, 4.91; N, 34.13%.

5-Ethyl-7-methylaminooxazolo[5,4-*d*]pyrimidine (IIc). This compound was prepared from 4-cyano-5-ethoxypropylenaminooxazole (Ic) and methylamine with 82% yield. Recrystallization from ethanol gave colorless needles, mp 140—142°C. ν_{max}^{KBr} cm^{-1}: 3218 (NH), 3085 (CH), 1663, 1600, 1540, 1509, 1147, 1049, 810, 797. NMR (DMSO-d_6) δ: 3.56 (s, 3H, *N*-methyl protons), 8.40 (s, 1H, C_2-proton), 1.22 and 2.84 (5H, ethyl protons). Mass spectrum, *m/e*: 178 (M^+, 100), 177 (M^+–H, 47, 176.0), 163 (M^+-CH_3, 46, 149.3), 150 (M^+-28, 22, 126.4), 149 ([150]$^+$—H, 15, 148.0), 123 ([150]$^+$—HCN, 8, 100.9), 96 ([124]$^+$—28, 11, 74.3), 69 ([96]$^+$—HCN, 33, 49.6), 42 ([69]$^+$—HCN, 53, 25.6).

Found: C, 53.64; H, 5.30; N, 31.75%. Calcd for $C_8H_{10}N_4O$: C, 53.92; H, 5.66; N, 31.45%.

2-Methyl-7-methylaminooxazolo[5,4-*d*]pyrimidine (IId). This compound was prepared from 4-cyano-5-ethoxymethylenamino-2-methyloxazole (Id) and methylamine with 62% yield. Recrystallization from water gave colorless needles, mp 194—195°C. ν_{max}^{KBr} cm^{-1}: 3240 (NH), 3048 (CH), 1665, 1630, 1585, 1502, 1134, 911, 791. NMR (DMSO-d_6) δ: 2.99 (d, 3H, *N*-methyl protons), 7.90 (broad s, 1H, =N-proton), 8.22 (s, 1*H*, C_5-proton), 2.58 (s, 3*H*, C-methyl protons). Mass spectrum, *m/e*: 164 (M^+, 100), 136 (M^+-28, 77, 112.8), 108 ([135]$^+$—HCN, 27, 86.4).

Found: C, 51.18; H, 5.01; N, 33.66%. Calcd for $C_7H_8N_4O$: C, 51.21; H, 4.91; N, 34.12%.

2,5-Dimethyl-7-methylaminooxazolo[5,4-*d*]pyrimidine (IIe). An aqueous solution of methylamine (30%, 3.8 m*l*) was cooled with ice-salt mixture. To this, cooled and powdered 4-cyano-5-ethoxyethylenamino-2-methyloxazole (Ie, 5.4 g) was added in one

14) R. K. Robins and H. H. Lin, *J. Amer. Chem. Soc.*, **79**, 490 (1957).

portion. The mixture was stirred at room temperature for 30 min. The resulting semi-solid was dissolved in chloroform and the aqueous layer was separated. The colorform solution was poured into a large volume of ether. On cooling the mixture, white crystalline material separated gradually and filtration gave an amorphous solid (3.5 g). The solid was dissolved in water (10 ml) and the solution was heated under reflux for 1.5 hr. Filtration after cooling gave light-yellow needles (2.2 g), mp 181—182°C. For analytical purpose, recrystallization from water-ethanol gave colorless needles, mp 184—185°C. ν_{max}^{KBr} cm^{-1}: 3245 (NH), 3045 (CH), 1630, 1580, 1520, 1505, 1141, 1036, 791. NMR (DMSO-d_6) δ: 2.97(d, 3H, *N*-methyl protons), 7.70 (broad s, 1H, =N-proton), 2.53 s, 3H, C_2-methyl protons), 2.42 (s, 3H, C_5-methyl protons). Mass spectrum, *m/e*: 178 (M^+, 100), 150 (M^+-28, 48, 126.4), 137 (M^+-CH_3CN, 21, 105.4), 109 ([137]$^+-28$, 29, 86.7), 108 ([150]$^+-CH_3CNH$, 49, 77.8).

Found: C, 53.85; H, 5.79; N, 31.24%. Calcd for $C_8H_{10}N_4O$: C, 53.92; H, 5.66; N, 31.45%.

2,8,9-Trimethylhypoxanthine (IIIe). This compound was prepared from IIe by Method B with 74% yield. Recrystallization from acetonitrile gave colorless crystals, mp>330°C. The IR spectrum of the compound exhibited a broad band at around 2900 cm^{-1} and a band due to a secondary amine was absent. NMR (D_2O) δ: 2.01 (s, 6H, *C*-methyl protons), 3.88 (s, 3H, *N*-methyl protons). Mass spectrum, *m/e*: 178 (M^+, 100), 164 (M^+-CH_2, 14, —), 137 (M^+-CH_3CN, 28, 105.4), 95 ([137]$^+-CH_3CNH$, 18, 65.9).

Found: C, 53.88; H, 5.76; N, 31.54%. Calcd for $C_8H_{10}N_4O$: C, 53.92; H, 5.66; N, 31.45%.

7-Ethylaminooxazolo[5,4-*d*]pyrimidne (IIf). The compound Ia (1.65 g) was added into an ice-cooled aqueous solution of ethylamine (35%, 2 ml) and stirred for 10 min. Filtration gave a solid (1.24 g), which was quickly dried *in vacuo* for 30 min and then heated under reflux in ethanol (15 ml) for 4 hr. After cooling, the mixture was filtered and the filtrate was concentrated under reduced pressure. Crystals (0.75 g) were obtained from the residue on cooling. Recrystallization from water gave colorless needles, mp 144—145°C. ν_{max}^{KBr} cm^{-1}: 3230 (NH), 3090 (CH), 1630, 1591, 1560, 1516, 1135, 1060, 796. NMR (DMSO-d_6) δ: 8.22 (broad s, 1H, =N-proton), 8.34 (s, 1H, C_2-proton), 8.63 (s, 1H, C_5-proton), 1.22 and 3.62 (5H, *N*-ethyl protons). Mass spectrum, *m/e*: 164 (M^+, 64), 149 (M^+-CH_3, 100, 135.4), 136 (M^+-28. 58, 112.8), 122 ([149]$^+$—HCN, 16, 99.9), 109 ([136]$^+$—HCN, 19, 87.4), 94 ([121]$^+$—HCN, 12, 73.0), 81 ([109]$^+$—CO, 10, 60.2), 67 ([94]$^+$—HCN, 28, 47.7).

Found: 51.37; H, 5.19; N, 33.87%. Calcd for $C_7H_8N_4O$: C, 51.21; H, 4.91; N, 34.13%.

9-Ethylhypoxanthine (IIIf). The above compound (IIf) was treated by Method B and the reaction product (a brown oil) was crystallized from acetone (83%). Recrystallization from water gave colorless crystals, mp 264—266°C. This product was identified as 9-ethylhypoxanthine.[15]

7-*n*-Propylaminooxazolo[5,4-*d*]pyrimidine (IIg). This compound was prepared by the method analogous to that of IIf from Ia and *n*-propylamine in water with 31% yield. Recrystallization from water gave colorless needles, mp 104—105°C. ν_{max}^{KBr} cm^{-1}: 3230 (NH), 3060 (CH), 1629, 1589, 1561, 1518, 1142, 1052, 1044, 794. NMR (DMSO-d_6) δ: 8.23 (broad s, 1H, =N-proton), 8.33 (s, 1H, C_2-proton), 8.63 (s, 1H, C_5-proton), 1.43, 1.65 and 3.53 (7H, *N*-*n*-propyl protons).

Found: C, 53.93; H, 5.85; N, 31.20%. Calcd for $C_8H_{10}N_4O$: C, 53.92; H, 5.66; N, 31.45%.

9-*n*-Propylhypoxanthine (IIIg). Avove compound (IIg) was treated by Method B and the product was recrystallized from *i*-PrOH. Yield 87%. This compound was identified as 9-*n*-propylhypoxanthine.[16]

7-*i*-Propylaminooxazolo[5,4-*d*]pyrimidine (IIh). This compound was prepared in a similar way to the preparation of IIf from Ia and *i*-propylamine with 24% yield. Recrystallization from water gave colorless crystals, mp 121—122°C. ν_{max}^{KBr} cm^{-1}: 3230 (NH). 3075 (CH), 1636, 1590, 1562, 1520, 1113, 1071, 794, NMR (DMSO-d_6) δ: 8.03 (d, 1H, =N-proton), 8.30 (s, 1H, C_2-proton), 8.61 (s, 1H, C_5-proton), 4.5 and 1.26 (7H, *i*-propyl protons).

Found: C, 53.95; H, 5.73; N, 31.42%. Calcd for $C_8H_{10}N_4O$: C, 53.92; H, 5.66; N, 31.45%.

7-*n*-Butylaminooxazolo[5,4-*d*]pyrimidine (IIi). This compound was prepared in a similar way to the preparation of IIf from Ia and *n*-butylamine with 26% yield. Recrystallization from water-ethanol gave colorless crystals, mp 81—82°C. ν_{max}^{KBr} cm^{-1}: 3250 (NH), 3060 (CH), 1660, 1630, 1596, 1521, 1144, 1050, 798. NMR (DMSO-d_6) δ: 7.68 (s, 1H, =N-proton), 8.30 (s, 1H, C_2-proton), 8.59 (s, 1H, C_5-proton), 0.9, 1.5 and 3.5 (9H, *N*-*n*-butyl protons).

Found: C, 56.23; H, 6.50; N, 29.10%. Calcd for $C_9H_{12}N_4O$: C, 56.22; H, 6.29; N, 29.15%.

9-*n*-Butylhypoxanthine (IIIi). By Method B. Above compound IIi was treated by Method B and the product was recrystallized from water. The yield was nearly quantitative.

By Method C. To a solution of *n*-butylamine (1.5 g) in dry pyridine (25 ml), Ia (1.65 g) was added portionwise. The mixture was stirred for 15 min at room temperature and then heated under reflux for 2 hr. After concentration of the solution nearly to dryness under reduced pressure, the residual sirup was kept overnight in a refrigerator. The resulting precipitate was filtered off and washed with benzene. The product (0.8 g) was recrystallized from water and identified as 9-*n*-butylhypoxanthine.[17]

9-Phenylhypoxanthine (IIIk). Aniline (2.0 g) and Ia (3.3 g) were chilled with ice-water separately and mixed in one portion. On stirring at room temperature, the mixture changed into an amorphous solid. This was digested with 50 ml of water and the mixture was heated gradually to 70—80°C in the course of 2 hr. Light brown needles separated from the brown oil. Filtration after cooling and washing of the needles with acetone gave a product (2.0 g), which on recrystallization from 50% ethanol gave colorless needles identified

15) J. A. Montogomery and C. Temple, Jr., *J. Amer. Chem. Soc.*, **79**, 5238 (1957).

16) C. Temple, Jr., C. L. Kussner and J. A. Montogomery, *J. Med. Pharm. Chem.*, **5**, 866 (1962).

17) J. A. Montogomery and C. Temple, Jr., *J. Amer. Chem. Soc.*, **80**, 409 (1958).

as 9-phenylhypoxanthine.[18]

9-β-Naphthylhypoxanthine (IIII). Cooled and pulverized Ia (1.65 g) was mixed with β-naphthylamine (1.43 g). On stirring at room temperature, the mixture melted and crystals separated again. After 30 min, this was digested with water (50 ml) and the mixture was heated under reflux for 1 hr. The resulting solid was collected and washed with a small quantity of acetone. Reprecipitation from DMF-ether followed by recrystallization from 50% ethanol gave colorless crystals (0.45 g), mp 320°C. Its IR spectrum showed a broad band at around 2850 cm^{-1} and an intense band at 1700 cm^{-1}. NMR (NaOD-D_2O) δ: 8.58 (s, 1H, C_2-proton), 8.17 (s, 1H, C_8-proton). 8.3 (m, 7H, β-naphthyl protons). Mass spectrum, *m/e*: 262 (M^+, 100), 261 (M^+-H, 21, 260.0), 234 ($[261]^+-HCN$, 6, 209.8), 207 ($[234]^+-HCN$, 5, 183.1), 180 ($[207]^+$-HCN, 4, 156.5).

Found: C, 68.16; H, 3.86; N, 21.09%. Calcd for $C_{15}H_{10}N_4O$: C, 68.69; H, 3.84; N, 21.37%.

This compound was shown to be identical with the product prepared by the method of Robins *et al.*[18] from 5-amino-4,6-dichloropyrimidine and β-naphthylamine.

The author wishes to thank Dr. Shizuo Nakamura for his encouragement throughout this work, and Mr. Kikuo Sugimoto and Mr. Shigeru Kiuchi for their technical assistance.

18) S. M. Greenberg, L. O. Ross and R. K. Robins, *J. Org. Chem.*, **24**, 1314 (1959).

BULLETIN OF THE CHEMICAL SOCIETY OF JAPAN VOL. 43 3913—3916 (1970)

The Properties of Aqueous Solutions of Sodium 2-Sulfoethyl Alkanoates and Sodium Alkyl β-Sulfopropionates

Takeshi HIKOTA, Kiyoshi MOROHARA and Kenjiro MEGURO

Department of Chemistry, Faculty of Science, Science University of Tokyo, Kagurazaka, Shinjuku-ku, Tokyo

(Received May 8, 1970)

A series of sodium 2-sulfoethyl alkanoates $RCOO(CH_2)_2SO_3Na$ was prepared from sodium isethionate and fatty acids containing 9, 11, 13, and 15 carbon atoms. The Krafft point, the critical micelle concentration (CMC), the surface tension, the emulsifying power, the wetting time, the resistance to acid hydrolysis, and the calcium-ion stability of this series of surfactants were examined, and the results were compared with those of the corresponding sodium alkyl β-sulfopropionates $ROCO(CH_2)_2SO_3Na$, which have another structure of ester-linkage. The CMC values of sodium 2-sulfoethyl alkanoates almost coincide with those value of the sodium alkyl β-sulfopropionates with the same number of carbon atoms. However, the Krafft point and surface tension at the CMC of sodium 2-sulfoethyl alkanoates were lower than those of the sodium alkyl β-sulfopropionates with the same number of carbon atoms. Sodium 2-sulfoethyl alkanoates are more stable than sodium alkyl β-sulfopropionates in their resistance to hydrolysis and to the calcium-ion.

In the last few years, several authors have studied the relation between the molecular structure and the properties of surfactants containing an ester group.[1-3] However, ester linkage may be classified into two fundamental types: (a) those in which the hydrophobic group is derived from the higher fatty acid, and (b) those in which the hydrophobic group is derived from the higher alcohol. The object of this report is to clarify how this difference in ester linkage affects the surface and colloidal properties, such as the Krafft point, the CMC value, the surface tension, the emulsifying power, the wetting property, the resistance to acid hydrolysis, and the calcium-ion stability. The surfactants of the first type used for this experiment were sodium 2-sulfoethyl alkanotes, while the surfactants of later type were sodium alkyl β-sulfopropionates.

Experimental

Material. The preparation of sodium 2-sulfoethyl alkanoate and sodium alkyl β-sulfopropionate may be represented by the following equation:

(a) $RCOOH + HO(CH_2)_2SO_3Na \rightarrow RCOO(CH_2)_2SO_3Na + H_2O$

(b) $ROH + Br(CH_2)_2COOH \rightarrow ROCO(CH_2)_2Br + H_2O$

1) T. Hikota and K. Meguro, *J. Am. Oil Chemists' Soc.*, **46**, 579 (1969).
2) T. Hikota and K. Meguro, *ibid.*, **47**, 158 (1970).
3) T. Hikota, This Bulletin, **43**, 2236 (1970).

Table 1. Elementary analysis of the surfactants

Derivative	Abbreviation	C		H	
		Found	Calcd	Found	Calcd
$C_8H_{17}COO(CH_2)_2SO_3Na$	SEA-8	45.34	45.82	7.00	7.34
$C_{10}H_{21}COO(CH_2)_2SO_3Na$	SEA-10	49.05	49.35	7.73	7.96
$C_{12}H_{25}COO(CH_2)_2SO_3Na$	SEA-12	52.20	52.31	8.28	8.49
$C_{14}H_{29}COO(CH_2)_2SO_3Na$	SEA-14	54.64	54.82	8.63	8.93
$C_8H_{17}OCO(CH_2)_2SO_3Na$	SAP-8	46.01	45.82	7.15	7.34
$C_{10}H_{21}OCO(CH_2)_2SO_3Na$	SAP-10	49.76	49.35	7.73	7.96
$C_{12}H_{25}OCO(CH_2)_2SO_3Na$	SAP-12	52.32	52.31	8.61	8.49
$C_{14}H_{29}OCO(CH_2)_2SO_3Na$	SAP-14	55.00	54.82	8.78	8.93

$$ROCO(CH_2)_2Br + Na_2SO_3 \rightarrow ROCO(CH_2)_2SO_3Na + NaBr$$

Preparation of Odd-chain Fatty Acid. The odd-chain fatty acid used in the preparation of the (a)-type surfactant was synthesized from the even fatty alcohol with one less carbon atom.[4] The odd-chain fatty acid thus obtained was washed several times with water, dried, and then distilled under reduced pressure. The purity of the odd-chain fatty acids was confirmed by elementary analysis and by a study of the melting points (pelargonic acid, 11.7—12.5°C; undecylic acid, 28.3—29.2°C; tridecylic acid, 39.6—40.8°C; and pentadecylic acid, 50.8—51.9°C). The results of the chemical analyses of the carbon and hydrogen of the compounds gave the calculated values for their composition within ±0.3%. The octyl, decyl, dodecyl, and myristyl alcohols used as starting materials were purified by vaccum distillation from good commercial-grade alcohols, and were confirmed to be more than 98% pure by gas chromatographic analysis.

Preparation of Sodium 2-sulfoethyl Alkanoate. Sodium 2-sulfoethyl alkanoate was prepared by the following reaction. A solution of 0.32 mol of odd-chain fatty acid and 0.3 mol of sodium isethionate in 100 m*l* of toluene was stirred and then heated at the reflux temperature for 10 hr. The water of esterification was removed by azeotropic distillation using a Barrett trap. The reaction mixture was then cooled, and the precipitate, sodium 2-sulfoethyl alkanoate, were separated by filtration. The crude material was recrystallized three times from methanol, and then extracted with petroleum ether for 120 hr. The residue was dried at room temperature under reduced pressure to give the purified sodium 2-sulfoethyl alkanoate as a white flaky powder.

Preparation of Sodium Alkyl β-Sulfopropionate. The sodium alkyl β-sulfopropionates were prepared from β-bromopropionic acid, sodium sulfite, and higher alcohol containing from 8 to 14 even carbon atoms by a previously described method.[2] The crude material was recrystallized three times from ethanol, and then extracted with petroleum ether for 120 hr.

The results of the elementary analysis of these surfactants for carbon and hydrogen are summarized in Table 1.

Measurements. The Krafft point was taken as the temperature at which there was a rapid increase of the solubility of the surfactant in water upon gradual heating. The rapid increase in solubility at the Krafft point accompanied the rapid increase in electrical conductivity.[5] Therefore, the measurement of the rapid increase in the conductivity of the surfactant solution with the temperature in the presence of the solid surfactant made it possible to estimate the Krafft point. The values of conductivity were measured by means of a Towa Denpa Co. electro-conductivity bridge.

The CMC value of the surfactant was estimated by means of the electro-conductivity method[6] at 40°C. These CMC values were determined from the break point in the diagram of equivalent conductivity *vs.* the root of the concentration.

The surface-tension of an aqueous solution of the surfactant was measured by the Wilhelmy plate method at 30°C.

The emulsion was prepared from 5 m*l* of toluene and 10 m*l* of a 20-mmol aqueous solution of the surfactant by hand shaking at 40°C. The duration of the emulsion time was measured by the time elapsed from the moment of the cessation of the shaking to the separation of 9 m*l* of an aqueous volume from the emulsion layer.

The wetting power of the surfactant was measured by the disk-sinking method,[7] in which the wetting time of a felt disk in the surfactant solution become the scale for the wetting. The practical procedure was as follows: 75 m*l* of the 20-mmol surfactant solution to be tested was placed in a 150-m*l* beaker; then the disk (20 mm in diameter and 1 mm thick) was immersed in horizontal position. The time (in seconds) required for the disk to sink was recorded as the wetting time.

The experiment to measure the stability to hydrolysis was carried out by heating a 10-mmol equivalent of the surfactant solution in 20 m*l* of 2N sulfuric acid at 40°C.

The calcium-ion stability of the surfactant solution (10 mmol, 10 m*l*) was measured by a modified Hart method,[8] using 0.1N calcium chloride.

4) R. A. Smiley and C. Arnold, *J. Org. Chem.*, **25**, 257 (1960).

5) T. Ino, *Nippon Kagaku Zasshi*, **80**, 456 (1959).

6) O. Yoda, K. Meguro, T. Kondo and T. Ino, *ibid.*, **77**, 905 (1956).

7) W. Yano, T. Isaji and W. Kimura, *Yukagaku*, **11**, 183 (1962).

8) B. G. Wilkes and J. N. Wickert, *Ind. Eng. Chem.*, **29**, 1234 (1937).

Table 2. Surface active properties of surfactants

Derivative	Krafft point °C	CMC mmol/l		Surface tension (30°C)			Emulsifying power min : sec	Wetting time sec	Stability to hydrolysis min : sec	Calcium stability ppm
		Conductivity 40°C	Surface tension 30°C	γ at CMC dyn/cm	$\Gamma \times 10^{10}$ mol/cm^2	Å area/molec.				
SEA-8	0	47.5	46.0	39.0	3.18	52.3	: 53	8.8	47 : 33	4,500
SEA-10	8.1	13.2	10.5	38.7	3.21	51.8	6 : 07	3.6	39 : 43	1,790
SEA-12	24.2	3.4	2.2	38.5	2.86	58.1	6 : 43	3.5	24 : 06	210
SEA-14	36.2	0.9	—	—	—	—	3 : 20	4.3	10 : 32	55
SAP-8	0	48.7	48.0	41.4	2.90	57.4	1 : 06	7.5	49 : 16	4,500
SAP-10	12.5	13.1	11.0	40.7	2.81	59.2	5 : 25	3.3	32 : 40	650
SAP-12	26.5	3.0	2.2	40.0	2.56	65.0	5 : 40	3.8	15 : 36	160
SAP-14	39.0	0.9	—	—	—	—	3 : 48	3.3	4 : 52	40

Results and Discussion

Krafft Point. It has been stated that the ionic surfactant can be as soluble as the micelle only above the Krafft point. Therefore, the value of the Krafft point must be determined before the measurement of the CMC by means of electroconductivity and other surface active properties. The Krafft points of the sodium 2-sulfoethyl alkanoates and sodium alkyl β-sulfopropionates series are given in Table 2, and they are plotted against the alkyl chain length in Fig. 1. These plots become two nearly parallel straight lines for each series of surfactants. The Krafft points of the sodium 2-sulfoethyl alkanoates are lower than those of the corresponding sodium alkyl β-sulfopropionates.

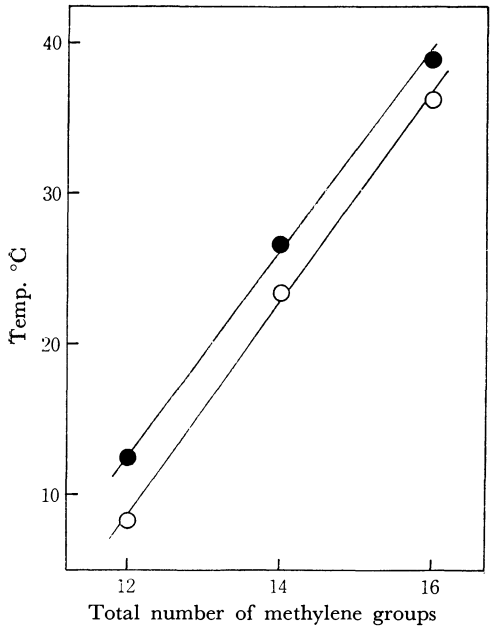

Fig. 1. Relation between Krafft point and total number of methylene groups in the chain. $RCOO(CH_2)_2SO_3Na$ (●), $ROCO(CH_2)_2SO_3Na$ (○).

Critical Micelle Concentration. The CMC values of two series of sodium 2-sulfoethyl alkanoates and sodium alkyl β-sulfopropionates, as estimated by conductivity method, are given in Table 2. The CMC value decreased with the increase in the length of the hydrocarbon chain, and the relation between the logarithm CMC and the alkyl chain length in the each surfactant series can be shown by the following equation:

$$\log \mathrm{CMC} = 1.6 - 0.29N$$

where N is the number of the methylene group in the alkyl chain.

As is shown in Fig. 2, the CMC values of sodium 2-sulfoethyl alkanoates fell on the same line as the CMC values of the sodium alkyl β-sulfopro-

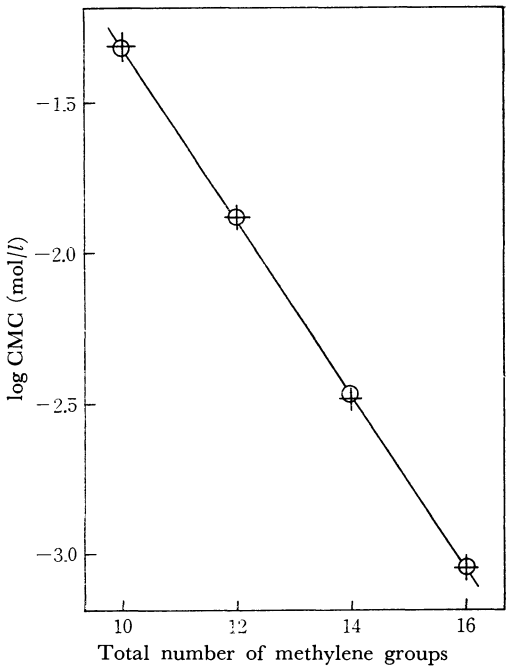

Fig. 2. Relation between log CMC and total number of methylene groups in the chain. $RCOO(CH_2)_2SO_3Na$ (○), $ROCO(CH_2)_2SO_3Na$ (+).

pionates. This indicates that the effect of the ester group on the CMC value is almost independent of the two different types of ester linkage (RCOO– and ROCO–), in sulfonate.[9]

Surface Tension. The values of the surface tension of aqueous solutions of the six surfactants (sodium 2-sulfoethyl pentadecanoate and sodium tetradecyl β-sulfopropionate are not shown) at 30°C are shown in Fig. 3.

The break point in the surface tension diagram coincides with the CMC values obtained by the electroconductivity method. The CMC values thus obtained from Fig. 3 are given in Table 2. As is shown in Fig. 4, the surface tension values at

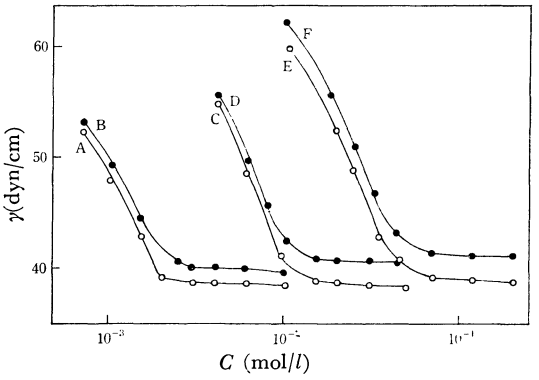

Fig. 3. Surface tension *vs.* concentration curves. SEA-12 (A), SAP-12 (B), SEA-10 (C), SAP-10 (D), SEA-8 (E), and SAP-8 (F).

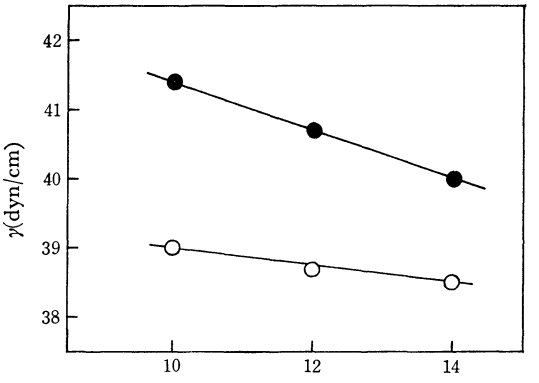

Fig. 4. Surface tension at CMC *vs.* total number of methylene groups. $RCOO(CH_2)SO_3Na$ (○), $ROCO(CH_2)_2SO_3Na$ (●).

9) T. Hikota and K. Meguro, *J. Am. Oil Chemists' Soc.*, **47**, 197 (1970).

CMC lower with an increase in the alkyl chain length. The sodium 2-sulfoethyl alkanoates have a lower surface tension than the sodium alkyl β-sulfopropionates with the same carbon chain.

According to the Gibbs adsorption isotherm equation, the inclination of the curves of the surface tension *vs.* the concentration gives the amount of surfactant adsorbed, Γ:

$$\Gamma = -\frac{1}{2RT} \times \frac{d\gamma}{d \ln C}$$

where γ is the surface tension and where C is the molar concentration. The area, A, occupied per surfactant molecule is calculated by the equation: $A = 1/N\Gamma$ from the amount of surfactant adsorbed; here, N is the Avogadro number. The values of the adsorption, the surface area, and the surface tension at the CMC of sodium 2-sulfoethyl alkanoates are compared with those of sodium alkyl β-sulfopropionates in Table 2.

Emulsion Stability. It is of interest to invesigate the effect of the difference in the ester linkage on the emulsifyng power of the surfactant. The emulsion stabilities of the surfactants are given in Table 2. The emulsions of all these surfactants with the exceptions of sodium 2-sulfoethyl pelargonate and sodium octyl β-sulfopropionate were more stable than that of sodium dodecyl sulfate. A comparison of sodium alkyl β-sulfopropionate and sodium 2-sulfoethyl alkanoate shows the later to be somewhat the better emulsifying agent.

Wetting Power. The wetting properties of the two different types of surfactants of the homologous series are shown in Table 2. It was difficult to find a certain relationship between the wetting properties and the alkyl chain length in the two series, sodium 2-sulfoethyl alkanoates and sodium alkyl β-sulfopropionates.

Stability to Hydrolysis and Calcium-ion Stability. The data obtained for stability to hydrolysis and the calcium-ion stability are shown in Table 2. The stability to hydrolysis of the sodium 2-sulfoethyl alkanoates is more stable than that of the corresponding sodium alkyl β-sulfopropionates, except for sodium 2-sulfoethyl pelargonate and sodium octyl β-sulfopropionate.

The calcium-ion stability of the surfactant decreases with an increase in the number of carbon atoms. This also shows that the calcium-ion stability of the sodium 2-sulfoethyl alkanoates is better than that of the sodium alkyl β-sulfopropionates.

NOTES

BULLETIN OF THE CHEMICAL SOCIETY OF JAPAN VOL. 43 3917—3919 (1970)

Viccosity of Water Vapor in the Temperature Range from 6°C to 29°C

Isao YASUMOTO

Department of Chemistry, Yonago Technical College, Hikona-cho, Yonago

(Received November 27, 1969)

The viscosities of gases[1,2] have already been measured over a wide range of temperatures and pressures. The viscosity of water vapor[3,4] at room temperature has, however, scarcely been measured because of the technical difficulties involved. This paper will present the results of our viscosity measurement of water vapor in the temperature range from 6 to 29°C by means of a new tandem capillary-flow viscometer.

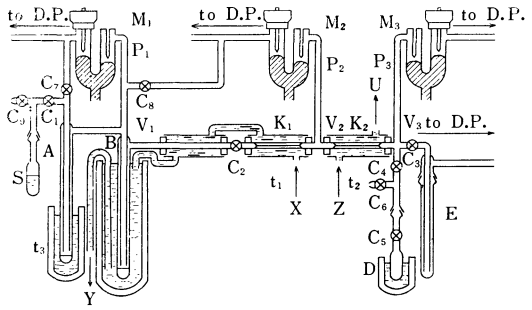

Fig. 1. Schematic diagram of the apparatus used for viscosity measurement of water vapor. The main part of the apparatus is constructed of borosilicate glass.

The apparatus used (Fig. 1) consists of a vapor-supply system, S; two traps, A and B; two capillaries, K_1 and K_2, in tandem; three vacuum gauges, M's; and a water-vapor collector, D. The main capillary, K_1, is 1.207 mm in diameter and 493.5 mm in length, while the auxiliary capillary, K_2, is about 1.2 mm in diameter and about 1.2 meter in length. The vacuum gauges are essentially the same as the mercury U-tube manometer devised by Meyer and Wade.[5] The details of the manometer as modified by the present author have already been published in his other report.[6]

The whole apparatus was evacuated until a pressure below 1×10^{-5} mmHg was attained. In carrying out a run, water was first freed from the dissolved gases by vacuum sublimation from the water reservoir, S, to the trap B, immersed in a dry ice-acetone mixture. The amount of water trapped there was about 10 cc. Then, by circulating water of a constant temperature from X to Y and from Z to U, the temperature of B and K_1 was held constant at t_1, and that of K_2, at t_2. The trap A was immersed in water of a constant temperature, t_3, approximately 0.5°C lower than t_1, in order to prevent the water vapor in the space V_1 from saturating and eventually condensing in the capillary tube K_1.

As the water vapor in the space V_1 flowed through the capillaries, K_1 and K_2, the pressure difference, P_1—P_2, was slowly developed across the capillary K_1 to become stationary after about 20 minutes. As a consequence of attaching K_2 in tandem, a laminar flow was attained throughout the capillary K_1. When the cock C_5 was turned on and C_3 closed, the water vapor in the space V_3 began to be condensed in the collector, D, cooled by liquid nitrogen, the pressures of P_1, P_2, and P_3 remaining practically unaltered. After condensation had proceeded for a certain length of time, C_5 was closed. The weight increase in the collector, D, was then determined.

The weight increase due to mercury and grease vapors condensed in D during a run was ascertained to be negligible. The influence of the total vacuum leak of this apparatus was also negligible, since it was less than 1×10^{-5} mmHg·l/hr. No correction for the thermal expansion of the capillary tube K_1 was made, since the temperature range covered was narrow.

The results of all the experiments performed

1) G. P. Flynn, R. V. Hanks, N. A. Lemaire and J. Ross, *J. Chem. Phys.*, **38**, 154 (1963).

2) A. K. Barua, M. Afzal, G. P. Flynn and J. Ross, *ibid.*, **41**, 374 (1964).

3) H. Braune and R. Linke, *Z. Phys. Chem.*, **A148**, 195 (1930).

4) J. Kestin and W. Leidenfrost, *Physica*, **25**, 1033 (1959).

5) D. E. Meyer and W. H. Wade, *Rev. Sci. Instr.*, **33**, 1283 (1962).

6) I. Yasumoto, *J. Vac. Soc. Japan*, **13**, 232 (1970).

Table 1. Results of all the experiments and viscosities calculated by the various equations

t_1*1 °C	P_1*2 mmHg at 0°C	P_2*2 mmHg at 0°C	Flow rate g/sec ($\times 10^5$)	η_1*3 poise ($\times 10^7$)	η_2*4 poise ($\times 10^7$)	η_3*5 poise ($\times 10^7$)	η_4*6 poise ($\times 10^7$)	η_5*7 poise ($\times 10^7$)
6.73	6.51	5.31	1.1646	887	913	901.9	907.6	843.7
7.18	6.97	5.61	1.4104	881	905	903.6	909.4	845.4
10.20	8.58	6.92	2.0476	907	927	915.0	921.1	857.1
13.10	10.48	8.45	2.9629	923	940	925.9	932.4	868.2
15.45	12.84	10.42	4.2595	932	946	934.8	941.5	877.3
17.11	13.47	10.93	4.6504	932	946	941.1	948.0	883.7
17.74	14.56	11.81	5.4267	935	948	943.4	950.4	886.1
19.90	15.20	12.31	5.8713	940	952	951.6	958.8	894.5
20.53	16.32	13.19	6.7866	942	954	954.0	961.3	896.9
22.27	17.61	14.22	7.8114	951	962	960.6	968.1	903.6
23.38	19.29	15.64	9.2427	947	958	964.8	972.4	907.9
24.03	19.52	15.84	9.3358	953	963	967.3	974.9	910.4
27.13	22.60	18.37	12.173	964	973	979.1	987.0	922.5
27.17	21.29	17.16	11.156	966	976	979.2	987.1	922.6
29.00	21.99	17.68	11.835	972	982	986.2	994.3	929.7
100.0					1270*8	1261	1269	1208
151.2					1450*8	1465	1466	1410
207.1					1680*8	1693	1678	1632
261.3					1900*8	1918	1880	1847
20.0					937.3*9	952.2	959.4	895.0
92.4					1178*10	1231	1240	1178
107.3					1242*10	1290	1298	1237
210.1					1638*10	1705	1689	1644
312.9					2049*10	2136	2069	2050
366.2					2261*10	2364	2260	2258
406.4					2422*10	2539	2401	2414
20.00					967.42*11			
24.91					969.40*11			

*1 t_1 is an average of temperatures measured at two minute intervals through out a run. The fluctuation of t_1 was ± 0.08°C.

*2 P_1 and P_2 are averages of pressures measured at two minute intervals through out a run.

*3 Calculated by the Hagen-Poiseuille equation from the present author's data given in column 1, 2, 3 and 4.

*4 Corrected for slip.

*5 Calculated by the new viscosity formula proposed by the present author:
$$\eta_3 = KT^{7/6} = 126\times 10^{-9}\times T^{7/6}.$$

*6 Calculated by the Sutherland's formula:
$$\eta_4 = KT^{3/2}/(T+C),$$
where C is 650 as is given by Smith. Using the Smith's data, K was calculated by the present author to be 180.25×10^{-7}.

*7 Calculated by the Sutherland's formula given by Braune and Linke:
$$\eta_5 = 223.6\times 10^{-7}\times T^{3/2}/(T+961).$$

*8 Smith's experimental values.

*9 Braune and Linke's (saturated water vapor).

*10 Braune and Linke's.

*11 Kestin and Leidenfrost's.

are tabulated in Table 1. The viscosity, η_1, of the water vapor, as calculated by the Hagen-Poiseuille equation, is shown in column 5. The viscosity, η_2, corrected for slip is shown in column 6, together with the values obtained by other authors. The correction was made by multiplying η_1 by the factor of $(1+4\zeta/r)$, where r is the radius of the capillary tube K_1 and where ζ is $0.85\,\lambda$. λ is an average of the mean free path inside K_1 expressed by $\lambda = \boldsymbol{k}T/(2^{1/2}\pi\sigma^2 P)$, where σ is the molecular diameter, as will be discussed below, and where P is equal to $(P_1 + P_2)/2$, as was shown by Smith.[7] The precision of the viscosity, η_2, obtained was estimated to be less than 0.5%.

A plot of the author's viscosities, η_2's, against

7) C. J. Smith, *Proc. Roy. Soc.*, **A106**, 83 (1924).

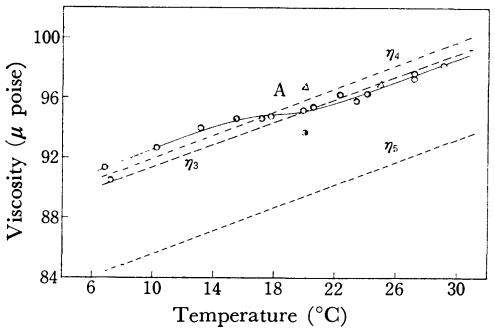

Fig. 2. ○; author's experimental values, ◑; Braune and Linke's (saturated water vapor), △; Kestin and Leidenfeost's. Broken lines represent η_3, η_4 and η_5, respectively.

the temperature shows the inflection shown in Fig. 2. A curve similar in form to the part A of this curve was also observed by Rankine[8] at room temperature in his experiment using bromine vapor. One of the two values obtained by Kestin and Leidenfrost by the oscillating-disk method is in good agreement with the present author's.

In Table 1, η_3 is calculated by the one-constant formula derived by the author, which will be discussed later. Taken in connection with Fig. 2, this formula can represent remarkably well (within 1%) not only one half of the author's experimental results (one half above 17°C because of the inflection), but also Smith's, extending from 100 to 261°C. Sutherland's two-constant formula, with the C value given by Smith and with the K value given by the present author, can also represent excellently (within approximately 1%) the present author's and Smith's results as a whole. The former formula gives a curve slightly concave upward, while the latter gives a curve slightly concave downward, so the latter curve in the highest temperature region gradually deviates from the former to approach the plot of Braune and Linke's experimental values, (Fig. 3). This plot is a nearly straight line extending from 90 to 406°C, and it is nearly perfectly represented by Sutherland's formula, with the C and K values given by Braune and Linke. It is parallel to, and situated lower than, the plot of Smith's data by the amount of *ca.* 50×10^{-7} poise.

The derivation of the author's formula used for the calculation of η_3 is as follows: The potential function, ϕ, for water-molecule interaction is

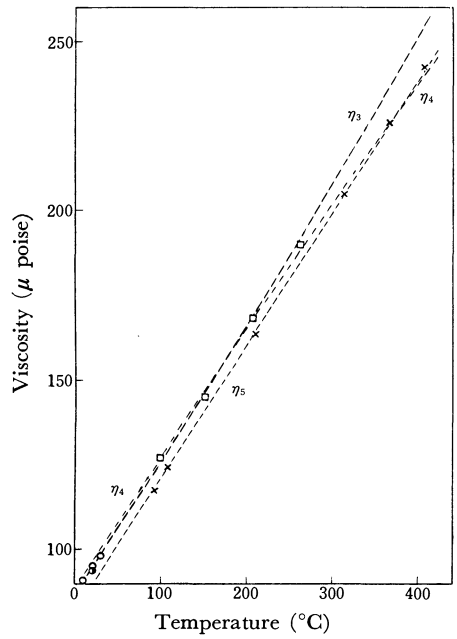

Fig. 3. ○: author's experimental values, ◑: Braune and Linke's (saturated water vapor), ×: Braune and Linke's, □; Smith's. Broken lines represent η_3, η_4 and η_5, respectively.

represented by[9]:

$$\phi = Aa^{-12} - Ba^{-6} - Ca^{-3},$$

where a is the distance between molecules and where A, B, and C are constants. Neglecting the first two terms, the approximate distance, a, in collision is deduced[10] to be:

$$a = (3C/2\boldsymbol{k}T)^{1/3},$$

which we may refer to as the diameter of capture, and which we may identify with σ, the molecular diameter. Denoting the mass of a molecule by m, the expression for the viscosity becomes:

$$\begin{aligned}\eta &= 1/\pi\sigma^2(m\boldsymbol{k}T/\pi)^{1/2} \\ &= 1/\pi(m\boldsymbol{k}/\pi)^{1/2}(2\boldsymbol{k}/3C)^{2/3}T^{1/2+2/3} \\ &= KT^{7/6}.\end{aligned}$$

Plotting η_2 against $T^{7/6}$, K was found to be 126×10^{-9}, from which C was calculated to be 2.55×10^{-36} erg·cm^3.

The author wishes to thank Professor Emeritus N. Sasaki and Professor K. Kodera, Kyoto University, for their interest and encouragement during this work.

8) A. O. Rankine, *ibid.*, **A88**, 575 (1913).

9) E. A. Moelwyn-Hughes, "Physical Chemistry," 2nd Revised Edition, Pergamon Press Limited, London (1961), p. 338.

10) *Ibid.*, p. 611.

BULLETIN OF THE CHEMICAL SOCIETY OF JAPAN VOL. 43 3920—3921 (1970)

The Effect of Solvents on the Optical Rotation of Propylene Oxide

Yoshiyuki KUMATA, Junji FURUKAWA and Takayuki FUENO*1

Department of Synthetic Chemistry, Kyoto University, Kyoto

(Received March 28, 1970)

It is known that the rotation of an optically active substance is varied according to the nature of the solvents. The so-called "rotivity", Ω, which is the rotation corrected for the refractive index of the solvent used, has been defined by the equation:[1]

$$3\Omega = \frac{3}{n^2+2}[\alpha]$$

where n, $[\alpha]$ and $3/(n^2+2)$ are the refractive index, the specific rotation and the Lorentz factor, respectively. This paper deals with the effect of solvents on the rotivity of propylene oxide.

Experimental

The solvents were selected widely from a stand point of chemical structure, dipole moment, dielectric constant and refractive index. Each solvent was purified by a conventional method. The optical rotation was measured by using a JASCO polarimeter Model ORD, UV-5 and a Yanagimoto polarimeter (OR-10) at ambient temperature. The concentration of propylene oxide in various solvents was fixed at 5.00 g/100 m*l*.

Propylene oxide was synthesized according to a fermentation method.[2] The specific rotation of the propylene oxide was +12.53° (neat, at 16°C).

Results and Discussion

The specific rotation, $[\alpha]_D$, and the rotivity multiplied by three, 3Ω, of propylene oxide observed in various solvents are listed in Table 1. Although the rotivity is said to be the specific rotation corrected for the refractive index of the solvents used, it still depends on solvent, as may be seen in Table 1. The tendency of this variation of rotivity with solvent is the same as that of the rotational strength of a steroidal compound.[3]

The rotivity data listed in Table 1 appear to show that the 3Ω value of propylene oxide tends to decrease with the increasing polarity of solvent. In Fig. 1 the 3Ω values are plotted against the solvent Z-values,[4] wherever available. Although the plotted points are somewhat scattered, there does seem to be a correlation between the two quantities.

Figures 2 and 3 are the plots of the 3Ω value of

TABLE 1. SPECIFIC ROTATION OF (R)-PROPYLENE OXIDE IN VARIOUS SOLVENTS

	Solvent	$[\alpha]_D$	$\frac{3[\alpha]_D}{n_D^2+2}$
A	Benzene	30.6	21.6
B	*N*,*N*-Dimethylaniline	29.0	19.6
C	Anisole	26.4	18.4
D	Tetrachloroethylene	20.1	14.1
E	Carbon disulfide	19.4	12.5
F	Chlorobenzene	19.4	13.5
G	Carbon tetrachloride	18.7	13.6
H	Hexamethylphosphoric triamide	18.4	13.4
I	Pyridine	18.1	12.7
J	*p*-Dioxane	18.0	13.4
K	*o*-Nitroanisole	17.7	12.0
L	Diethyl ether	17.0	13.3
M	Triethylamine	17.0	12.9
N	Nitrobenzene	16.4	11.2
O	Methylene iodide	15.6	9.3
P	*n*-Pentane	14.3	11.2
Q	*N*-Methylacetamide	14.1	10.5
R	Tetrahydrofuran	13.7	10.3
S	Ethyl acetate	13.1	10.1
T	*N*,*N*-Dimethylformamide	12.9	9.6
U	Dimethylsulfoxide	12.8	9.2
V	Cyclohexane	11.9	8.8
W	Aniline	11.9	7.9
X	Benzonitrile	9.4	6.5
Y	Chloroform	8.5	6.2
Z	Acetone	8.2	6.4
a	Ethanol	7.9	6.2
b	Cyclohexanone	7.9	5.8
d	Methanol	7.2	5.7
e	Acetonitrile	6.0	4.7
f	1,2-Dichloroethane	5.8	4.3
g	Methylene chloride	5.5	4.1
h	Nitromethane	5.0	3.8
i	Acetic acid	2.0	1.5
j	Water	−4.3	−3.4

*1 Present address: Faculty of Engineering Science, Osaka University, Toyonaka, Osaka.

1) R. Gans, *Zeits. f. physik.*, **27**, 164 (1924); *Ann. d. Physik.*, **79**, 547 (1926).

2) C. C. Price and M. Osgan, *J. Amer. Chem. Soc.*, **78**, 4787 (1956).

3) K. Kuriyama, T. Iwata, M. Moriyama and K. Yoshida, Preprints for the 19th Annual Meeting of the Chemical Society of Japan (1966), III, p. 26.

4) E. M. Kosower, *J. Amer. Chem. Soc.*, **80**, 3253 (1958).

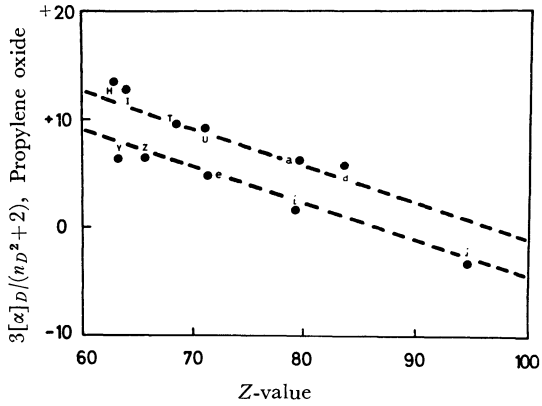

Fig. 1. Z-value *vs.* three times of rotivity.

propylene oxide against other polarity parameters of solvent, $(\varepsilon-1)/(\varepsilon+2)$ and E_T-value,[5] respectively. Addmittedly, these correlations of the rotivity with the various polarity parameters of solvent are poor, they will suffice to indicate a general trend. Thus, with increasing polarity of solvents, the rotivity may be continuously decreased until it may take on a value minus in sign. By this token, therefore, a change in the direction of optical rotation in differing solvents may well be something not abnormal, although it may certainly be an affair encountered only in limited cases.

In any discussion of solvent effects, it seem to be very important to consider the shape of cavity,[6,7] the anisotropy of the polarizability of solute[8,9]

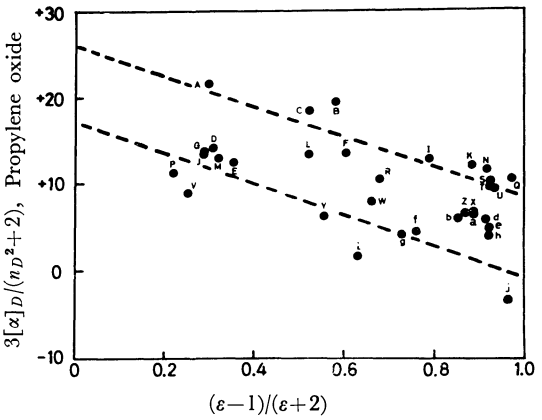

Fig. 2. $(\varepsilon-1)/(\varepsilon+2)$ *vs.* three times of rotivity.

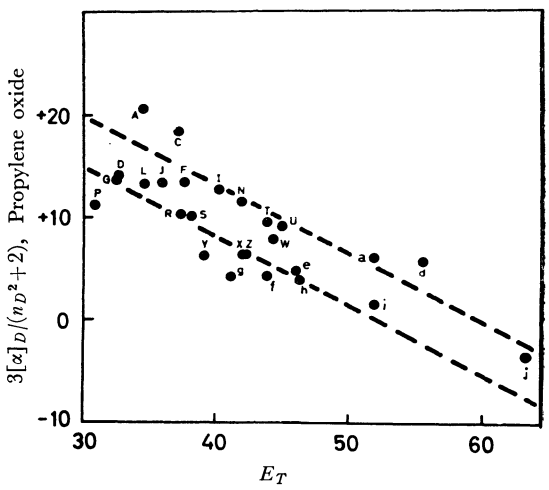

Fig. 3. E_T-values *vs.* three times of rotivity.

and the orientation of solvents to solute.[10,11] However, because the solvent effect on the optical rotation reflects a dynamical electromagnetic interaction between the dielectric groups of solute and solvents which have polarizability tensors, it will in general be extremely difficult to represent the effect with any simple parameter of solvents.

In Fig. 4, the effect of solvents on the optical rotatory dispersion of propylene oxide is shown. It should be noted that even a substance like propylene oxide, which has a rigid three-membered-ring and hence is incapable of changing its conformation in different solvents, shows an anomalous dispersion curve.

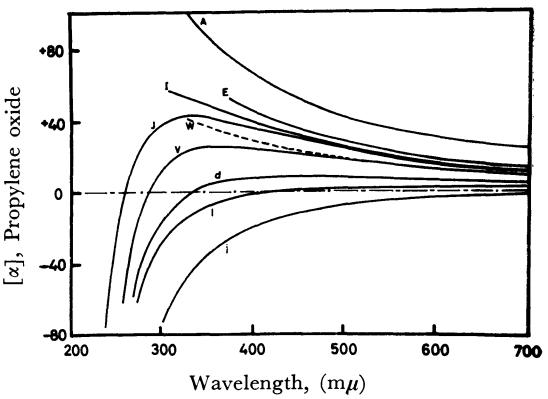

Fig. 4. Optical rotatory dispersion curve of (R)-propylene oxide in several solvents.

All the results described above would combine to give a serious warning against interpreting the optical behaviors of active substances in different solvents directly from their conformational change. Such interpretations might not be valid in general cases and would often be merely illusory.

5) K. Dimroth, C. Reichardt, T. Siepmann and F. Bohlmann, *Ann.*, **661**, 1 (1963); C. Reichardt, *Angew. Chem.*, **77**, 30 (1966).

6) K. Higasi, *Bull. Inst. Phys. Chem. Res.* (Tokyo), **14**, 146 (1935).

7) F. Buckley and A. A. Maryott, *J. Res. nat'l. Bur. Stand.*, **53**, 229 (1954).

8) C. G. LeFèvre and R. J. W. LeFèvre, *J. Chem. Soc.*, **1936**, 1747.

9) T. H. Scholte, *Physica*, **15**, 437; 450 (1949).

10) J. G. Kirkwood, *J. Chem. Phys.*, **7**, 911 (1939).

11) H. Fröhlich, *Trans. Faraday Soc.*, **44**, 238 (1948).

BULLETIN OF THE CHEMICAL SOCIETY OF JAPAN VOL. 43 3922—3924 (1970)

The Preparation of Halo-nucleosides

Kazuko HAGA, Masaharu YOSHIKAWA and Tetsuya KATO

Central Research Laboratories, Ajinomoto Co., Inc., Kawasaki

(Received April 6, 1970)

Attempts at the synthesis of halo-nucleosides have been made by the reaction of *p*-toluenesulfonyl nucleosides with an alkali-metal halide.[1,2] The present authors have also reported that 5′-chloro-5′-deoxy-2′,3′-*O*-isopropylidene nucleosides can be prepared *via* 5′-dichlorophosphoryl derivatives by the direct treatment of 2′,3′-*O*-isopropylidene nucleosides with phosphoryl chloride.[3] Recently, it has been reported that the reaction of suitably-protected nucleosides with methyltriphenoxy-phosphonium iodide affords iodo-nucleosides.[4,5] On the other hand, the conversion of some alcohols into chlorides with triphenylphosphine and carbon tetrachloride has been investigated.[6]

We have studied the preparation of a halo-nucleoside with triphenylphosphine and a suitable halogen source, such as carbon tetrachloride, bromine, cyanogen bromide, or iodine. For example, when 2′,3′-*O*-isopropylideneinosine(I) was treated in triethyl phosphate with three equiv. of triphenylphosphine in an excessive amount of carbon tetrachloride while being heated, 5′-chloro-5′-deoxy-2′,3′-*O*-isopropylideneinosine (IIa) was formed in a quantitative yield. The other halogen derivatives (IIb and IIc) were obtained in good yields by treatment with bromine, cyanogen bromide, or iodine and an equimolar amount of triphenylphosphine. The reactivity was extremely dependent on the kind of halogen source; the reaction with cyanogen bromide proceeded very rapidly at room temperature, while that with iodine required large excess of the reagent and an elevated reaction temperature. When dimethyl-formamide was used as a solvent in place of triethyl phosphate, the reactions did not proceed.

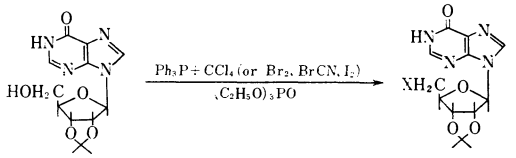

I II

a : X=Cl
b : X=Br
c : X=I

When 5′-*O*-acetylinosine(III) was treated similarly with triphenylphosphine and carbon tetrachloride, only the 3′-chloro derivative(IV) was obtained. The lack of the formation of the 2′-isomer may be due to the steric hindrance of the neighbouring purine base, which does not allow a rear-side attack by bulky phosphonium chloride at the *C*-2′ position. The hydrolysis of the reaction product with methanolic ammonium hydroxide afforded 3′-chloro-3′-deoxy-*β*-D-xylofuranosyl-hypoxanthine (V), together with a small amount of 2′,3′-anhydro-*β*-D-ribofuranosylhypoxanthine (VII).

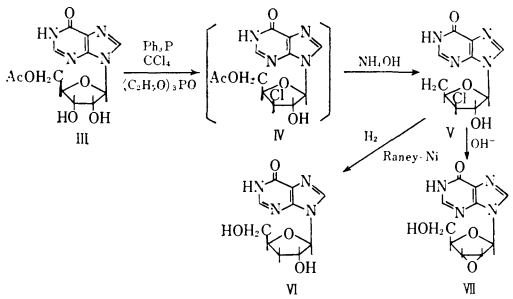

The NMR spectrum of V indicates that the substitution may have occurred at the *C*-3′ atom. The signals of the 2′-, 3′-, and 4′-protons shifted considerably downfields with respect to those of inosine (Table 1), while the chemical shift of the 1′-proton remained almost constant. Additional proof for the 3′-substitution was obtained from the fact that V afforded the 3′-deoxy compound (VI), the structure of which was characterized by the NMR spectrum (Table 1), on catalytic hydrogenation with Raney-nickel. The substituted chlorine atom was established to have the *β* configuration and so to be easily convertible to the epoxy compound (VII) under the basic conditions.[7] The structure of VII was proved to be that of the 2′,3′-anhydro compound of ribofuranosylhypo-

1) P. A. Levene and R. S. Tipson, *J. Biol. Chem.*, **109**, 623 (1935).
2) W. Jahn, *Chem. Ber.*, **98**, 1705 (1965).
3) K. Kusashio and M. Yoshikawa, This Bulletin, **41**, 142 (1968).
4) J. P. H. Verheyden and J. G. Moffatt, U. S. 3282921 (1966).
5) G. A. R. Johnston, *Aust. J. Chem.*, **21**, 513 (1968).
6) J. B. Lee and J. J. Nalan, *Can. J. Chem.*, **44**, 1331 (1966).
7) H. Ohle and C. A. Schultz, *Ber.*, **71b**, 2302 (1938).

Table 1. Chemical shifts and coupling constants[g)]

Proton	Inosine(I)[2)] (multiplicity[d)], J_{Hz})	3′-Chloro deriv. (VI)[a)]	3′-Deoxy inosine (VII)[b)]	2′,3′-Anhydro deriv. (VIII)[c)]
1′	5.92[e)] (d; 5.6)	5.89 (d; 3.7)	5.87 (d; 2.0)	6.28 (s)
2′	4.52 (d, d, d; 4.4, 4.4, 6.0)	4.74 (d, d; 3.7, 3.7)	4.2—4.6 (m)	4.65 (d; 2.4)
3′	4.18 (d, d, d; 3.6, 4.4, 5.0)	—4.5 (not resolved)	—2.0 (m)	4.42 (d; 2.4)
4′	3.99 (d, t; 3.6, 3.7)		4.2—4.6 (m)	4.49 (t; 5.4)
5′	3.65 (m)[f)]	3.75 (d; 4.5)	3.61 (m)	3.71 (d; 5.4)
2′-OH	5.47 (d; 6.0)	5.0 (broad)	5.65 (d; 4.0)	—
3′-OH	5.18 (d; 5.0)	—	—	—
5′-OH	5.07 (t; 5.3)	5.0 (broad)	5.00 (t; 5.4)	—

a) DMSO-d_6-$CDCl_3$, 100 MHz.
b) DMSO-d_6, 100 MHz.
c) D_2O, 60 MHz.
d) d, t indicates doublet of triplets and so on.
e) Chemical shifts are shown from internal TMS and DSS (D_2O solution).
f) This signal is appeared as AB part of ABX system on 5′-OH decoupling; $J_{5'a5'b}=12.0$, $J_{4'a5'b}=4.0$ Hz.
g) All parameters were obtained by the first order approximation. The assignments were established on the basis of the decoupling experiments.

xanthine (inosine) by the disappearance of $J_{1',2'}$ and $J_{3',4'}$.

Experimental

5′-Chloro-2′,3′-*O*-isopropylideneinosine (IIa). Triphenylphosphine (7.86 g, 0.03 mol) in carbon tetrachloride (80 m*l*) was added to a solution of 2′,3′-*O*-isopropylideneinosine (3.08 g, 0.01 mol) in anhydrous triethyl phosphate (40 m*l*). The mixture was heated at 100°C with stirring for 5 min. After cooling, the reaction mixture was poured into carbon tetrachloride (100 m*l*). A precipitate was collected on a filter, washed with cold water until the filtrate became neutral, and dissolved in chloroform (20—30 m*l*). After the solution had stood for about 30 min, the resulting precipitate was separated and recrystallized from methanol to give 2.8 g (85.8%) of IIa as colorless needles. Their IR spectrum and the melting point of the crystals were identical with those of the authentic sample.

5′-Bromo-5′-deoxy-2′,3′-*O*-isopropylideneinosine (IIb). *Method I.* To a solution of triphenylphosphine (7.8 g, 0.03 mol) in anhydrous triethyl phosphate (40m *l*), 2′,3′-*O*-isopropylideneinosine (3.08g, 0.01 mol) was added. Bromine was then added until the excessive addition of two drops gave the solution with an orange tint. The mixture was then heated at 80°C for 15 min. After cooling, the reaction mixture was poured into carbon tetrachloride (100 m*l*), and the resulting precipitate was collected on a filter. The precipitate was washed with cold water until the washings became neutral, and then with ethanol; then it was recrystallized from methanol to give 1.8 g (48.8%) of IIb, as colorless needles; mp 194°C (dec).

Found: C, 42.36; H, 4.19; N, 14.91; Br, 21.28%. Calcd for $C_{13}H_{15}N_3O_4Br$: C, 42.06; H, 4.07; N, 15.09; Br, 21.53%.

Method II. Cyanogen bromide (3.18 g, 0.03 mol) was used instead of bromine. The reaction proceeded exothermally. After the reaction mixture had been allowed to stand for about 5 min without heating, the solution was worked up in the manner described above (Method I) to give 2.2 g (59.6%) of IIb.

5′-Iodo-5′-deoxy-2′,3′-*O*-isopropylideneinosine (IIc). In a way similar to that used in the case of the 5′-chloro derivative (IIa), 2′,3′-*O*-isopropylideneinosine (3.08 g, 0.01 mol) in anhydrous triethyl phosphate (40 m*l*) was treated with triphenylphosphine (26.23 g) and iodine (25.38 g) for 30 min. After cooling, the solution was poured into ether (200 m*l*). The ether-insoluble materials were dissolved in chloroform (50 m*l*), and the solution was washed repeatedly with cold water until the washings became neutral. The chloroform layer was evaporated to dryness under reduced pressure at 40°C. The dark-reddish residue was redissolved in methanol (10 m*l*) and chromatographed on a column of neutral alumina in benzene. After the column had then been eluted successively with benzene and ether, 10% methanol-ether was passed through the column to elute IIc, the methanolic eluate was evaporated to dryness under reduced pressure, and the residue was crystallized from methanol to give 2.5 g (59.8%) of IIc as colorless plates; mp 195°C. (dec.).

Found: C, 37.38; H, 3.75; N, 13.15%. Calcd for $C_{13}H_{15}N_4O_4I$: C, 37.34; H, 3.62; N, 13.40%.

3′-Chloro-3′-deoxy-β-D-xylofuranosylhypoxanthine (V). To a solution of triphenylphosphine

(23.5 g, 0.09 mol) and carbon tetrachloride (66 m*l*) in triethyl phosphate (160 m*l*) was added 5′-*O*-acetylinosine (9.33 g, 0.03 mol). The mixture was refluxed at 110°C with stirring for 6 hr. After cooling, the solution was poured into ether (1 *l*). The ether-insoluble materials were dissolved in chloroform (300 m*l*), and the solution was extracted five times with an equivolume of cold water. The extractions were collected and evaporated to dryness under reduced pressure at 40°C. The residue was treated with 25 m*l* of concentrated ammonium hydroxide in 100 m*l* of methanol for 4 hr with ice-cooling and stirring. The solution was then evaporated under reduced pressure at 30°C, and the residue was dissolved in water (100 m*l*). A water-insoluble material was filtered off, and the filtrate was evaporated to dryness under reduced pressure. The dark-reddish residue was dissolved again in methanol (30 m*l*) and chromatographed similarly as in the case of the 5′-iodo derivative (IIc); 1.6 g (18.7%) of V was then obtained by recrystallization from aqueous methanol; colorless needles; mp 220°C (dec.).

Found: C, 41.88; H, 4.09; N, 19.77; Cl, 12.24%. Calcd for $C_{10}H_{11}N_4O_4Cl$: C, 41.90; H, 3.87; N, 19.55; Cl, 12.37%.

3′-Deoxyinosine (VI). To a solution of V (1.51 g, 0.006 mol) in a mixture of triethylamine (2.52 m*l*, 0.006 mol) and aqueous 50% methanol (120 m*l*) was added Raney-nickel; hydrogen was then allowed to pass through the suspension with shaking under atmospheric pressure at room temperature for 8 hr. The catalyst was filtered off, and the filtrate was evaporated to dryness under reduced pressure. The residue was washed with ethanol, and subsequently recrystallized from ethanol-water (8 : 1) to give 0.79 g (59.9%) of VI; colorless needles; mp 200°C.

Found: C, 47.38; H, 4.85; N, 22.02%. Calcd for $C_{10}H_{12}O_4N_4$: C, 47.62; H, 4.80; N, 22.22%.

2′,3′-Anhydro-β-D-ribofuranosylhypoxanthine (VII). The compound V (1 g) was dissolved in concentrated ammonium hydroxide and the solution was kept at room temperature for a week. The solvent was then removed under reduced pressure, and the residue was crystallized from water to give 0.6 g (68.9%) of VII; columns; mp 210°C (dec).

Found: C, 47.93; H, 4.31; N, 22.26%. Calcd for $C_{10}H_{10}O_4N_4$: C, 48.00; H, 4.03; N, 22.39%.

The authors wish to thank Mr. Masatsune Kainosho for his measurement of the NMR spectra and for his valuable discussions.

BULLETIN OF THE CHEMICAL SOCIETY OF JAPAN VOL. 43 3924—3925 (1970)

The Preparation of Ethyl 18-Nonadecenoate by a Mixed Coupling Reaction

Yasuo SUHARA and Shoji MIYAZAKI

Government Chemical Industrial Research Institute, Tokyo, Shibuya-ku, Tokyo

(Received April 13, 1970)

Long-chain terminal olefinic fatty esters are useful intermediates for the syntheses of various long-chain compounds. However, no paper reporting a simple preparation of the esters has been appeared. Concerning the electrolysis of terminal alkenoic acid, the preparation of 1,19-eicosadiene from 10-undecenoic acid by electrolysis with platinum electrodes has been attempted by Weedon *et al.*,[1] but the diene was contaminated by its positional isomers of the double bond. On the other hand, a 1,19-eicosadiene-rich-product was obtained when a platinum anode and a mercury cathode were used.[2]

In the present study, mixtures of 10-undecenoic acid (I) and ethyl hydrogen sebacate (II) were electrolyzed with platinum anode and a mercury cathode (procedures A and B) or with platinum electrodes (procedure C). The molar ratios of I to II employed were from 2 : 1 to 1 : 5. The coupling products were successfully separated by elution chromatography on silica gel.

Typical conditions of electrolysis, together with the products, are shown in Table 1. By procedure A, the desired ester, III, was obtained. The 45% yield of III was given by a 1 : 5 mixture of I and II. On the other hand, the largest weight percentage of III was given by an equimolar mixture of I and II. In procedure B, ester-exchange reaction of III and V proceeded. In procedure C, difficulty in obtaining unsaturated coupling compounds was experienced. The X, XI, and XII fractions comprised some positional isomers of the double bond. The key reaction may be illustrated as follows:

$$\underset{\text{(I)}}{CH_2{=}CH(CH_2)_8COOH} + \underset{\text{(II)}}{HOOC(CH_2)_8COOC_2H_5} \rightarrow$$

$$\underset{\text{(III)}}{CH_2{=}CH(CH_2)_{16}COOC_2H_5} + \underset{\text{(IV)}}{CH_2{=}CH(CH_2)_{16}CH{=}CH_2}$$

$$+ \underset{\text{(V)}}{H_5C_2OOC(CH_2)_{16}COOC_2H_5}$$

1) D. G. Bounds, R. P. Linsteasd and B. C. L. Weedon, *J. Chem. Soc.*, **1953**, 2393.

2) R. F. Gardwood, C. J. Scott and B. C. L. Weedon, *Chem. Commun.*, **1965**, No. 1, 14.

Table 1. Reaction procedures and products

Procedure		A	B	C
Substrate (mol)	I	0.05	0.05	0.05
	II	0.05	0.05	0.05
MeOH (ml)		207	207	207
Sodium (atom)		0.10	0.10	0.01
Current (A)		1	1	1
Current density (A/cm^2)		0.15	0.15	0.11
Terminal voltage (V)		30—100	30—100	30—100
Reaction time (hrs)		5.5	5.5	5.5
Reaction temp. (°C)		30—35	45—50	40—45
Products (%)	III*	24	—	—
	IV*	22	21	—
	V*	25	—	27
	VI*	—	23	—
	VII*	—	24	—
	VIII*	—	—	27
	IX*	—	—	23
	X*	—	—	2
	XI*	—	—	0.6
	XII*	—	—	0.9

* III, Ethyl 18-nonadecenoate; IV, 1,19-eicosadiene; V, diethyl 1,18-octadecanedioate; VI, methyl 18-nonadecenoate; VII, dimethyl 1,18-octadecanedioate; VIII, ethyl nonadecanoate; IX, eicosane; X, ethyl nonadecenoates; XI, eicosenes; XII, eicosadienes.

Experimental

The GLC was carried out by means of a Hitachi Gas Chromatograph K-23 on a column packed with 20% poly(diethylene glycol succinate) on Chromosorb WAW. The IR spectra were recorded with a Hitachi EPI-S2 Infrared Spectrophotometer in a KBr disk or in a liquid film. The IR spectra of III, IV, and VI showed bands assigned to terminal double bond at 3064—3053, 1825—1820, 1645—1640, 1420—1416, 1302—1298, 990—988, and 908—904 cm^{-1}. The spectra of III, V, VI, VII, and VIII showed a band assigned to the ester carbonyl group at 1740—1738 cm^{-1}. The NMR spectra were recorded with a JEOL JNM C-60HA NMR Spectrometer for a 10% carbon tetrachloride solution. The NMR spectra of III, VI, and VIII showed peaks at τ 5.07 (a, triplet). 4.3 (b, multiplet), 7.94—7.96 (c, doublet), 8.73 (d, singlet), 7.75—7.80 (e, unsymm. triplet), 5.96 (f, quartet), 8.74 (g, unsymm. triplet), 6.39 (h, singlet), and 9.11 (i, unsymm. triplet).

$\underset{\bar{a}}{CH_2}=\underset{\bar{b}}{CH}\underset{\bar{c}}{CH_2}(CH_2)_{14}\underset{\bar{d}}{CH_2}\underset{\bar{e}}{COO}\underset{\bar{f}}{CH_2}\underset{\bar{g}}{CH_3}$ (III),

$\underset{\bar{a}}{CH_2}=\underset{\bar{b}}{CH}\underset{\bar{c}}{CH_2}(CH_2)_{14}\underset{\bar{d}}{CH_2}\underset{\bar{e}}{COO}\underset{\bar{h}}{CH_3}$ (VI),

$\underset{\bar{i}}{CH_3}(CH_2)_{16}\underset{\bar{d}}{CH_2}\underset{\bar{e}}{COO}\underset{\bar{f}}{CH_2}\underset{\bar{g}}{CH_3}$ (VIII)

Oxidative ozonolysis was carried out according to the procedure of Ackman *et al.*[3] The cleavage products were elucidated by GLC.

Materials. Commercially-available Compound I was rectified by vacuum distillation; bp 121°C/1 mmHg. Compound II was prepared according to the procedure used in our previous experiments;[4] bp 150—154°C/1 mmHg; mp 35.5—36.5°C.

Procedures. Cells fitted with a platinum anode and a mercury cathode[5] (procedures A and B) and with platinum electrodes[4] (procedure C) were surrounded with water in order to maintain the electrolyte at the required temperature.

In procedure C, the current direction was changed every 3 sec. The products were treated as in our previous experiments,[4] and the coupling products were separated into three fractions by elution chromatography on silica gel with ligroin (bp 85—115°C) and then with methanol.

Products from Procedure A. The first fraction, mp 20—20.5°C (19.5—20°C[1]), was shown to be IV by elemental analysis and by its iodine value, along with the results obtained from its GLC, ozonolysis, and IR and NMR spectra. The second fraction, white crystals; mp 30—30.5°C (from ethanol), was shown to be III by its iodine and saponification values and also by a study of its GLC and ozonolysis, together with a study of its IR and NMR spectral data.

Found: C, 77.58; H, 12.39%. Calcd for $C_{21}H_{40}O_2$: C, 77.72; H, 12.42%.

The third fraction was shown to be V by comparing it with the specimen obtained by the procedure used in our previous experiments.[4]

Products from Procedure B. The first fraction was composed of IV; this was established by comparing it with the authentic compound obtained in the above paragraph. The second fraction, white crystals; mp 32—32.5°C (from ethanol), was shown to be VI by its iodine and saponification values and by a study of its GLC and ozonolysis, together with a study of its IR and NMR spectral data.

Found: C, 77.51; H, 12.30%. Calcd for $C_{20}H_{38}O_2$: C, 77.36; H, 12.34%.

The third fraction, white crystals; mp 59—59.5°C (57—58°C[6]) (from ethanol), was shown to be VII by elemental analysis and also by a study of its GLC, together with a study of its IR and NMR spectral data.

Products from Procedure C. The first fraction was shown to be a mixture of IX, XI, and XII by means of GLC, together with a study of its IR and NMR spectral data. The ozonolysis of XI gave a mixture of 1-, 2-, and 3-eicosenes, while XII gave a mixture of 1,19-, 1,18-, 1,17-. 2,18-, 2,17-, and 3,17-eicosadienes. The second fraction was shown to be a mixture of VIII and X, by GLC and by a study of its IR and NMR spectral data. The ozonolysis of X gave a mixture of ethyl 18-, 17-, 16-, 15-, and 14-nonadecenoates. The third fraction was successfully identified as V.

We are grateful to Mr. Masanori Yamamoto for his assistance in our experimental work.

3) R. G. Ackman, M. E. Retson, L. R. Gallay and F. A. Vandenheuvel, *Can. J. Chem.*, **39**, 1956 (1961).
4) Y. Suhara and S. Miyazaki, This Bulletin, **42**, 3022 (1969).
5) N. Dihn-Nguyen, *Acta Chem. Scand.*, **12**, 585 (1958).
6) S. Swann, Jr., and W. E. Garrison, Jr., "Organic Syntheses," Vol. 41, p. 33 (1961).

BULLETIN OF THE CHEMICAL SOCIETY OF JAPAN VOL. 43 3926—3927 (1970)

Studies of Diels-Alder-type Additions of Cyclic α-Carbonyl-Azo-Compounds*[1]

Shin-ichiro TAKASE and Tadayuki MOTOYAMA

Institute of Chemistry, College of General Education, Osaka University, Toyonaka, Osaka

(Received May 25, 1970)

The unstable cyclic diacyl diimides[1-3] and dioxotriazoline,[4] which were generated from the corresponding dihydro-compounds by oxidation with lead tetraacetate or *t*-butyl hypochlorite, gave the Diels-Alder adducts in the presence of the conjugated dienes. In recent papers, it has been shown that 4,4-diethyl-3,5-dioxo-1-pyrazoline[5,6] prepared from diethylmalonic acid hydrazide was reactive as a dienophile.

Several cyclic diacyl hydrazides were slowly oxidized with nickel peroxide[7] to prepare dicarbonyl-azo-compounds, they then gave the adducts by means of an *in situ* reaction with dienes. As the process was carried out in heterogeneous system, it was not so troublesome as with the above treatments to isolate the adducts from the degraded oxidants. Thus, the method provided a more convenient one-step synthesis of pyridazine derivatives. The proposed structure of the products is based on the molecular weights, the results of elemental analyses, and the IR and NMR spectra.

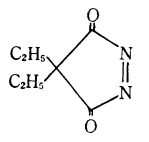

1c

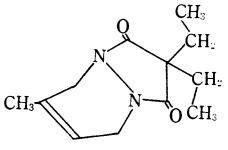

2c

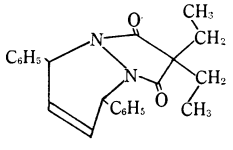

3c

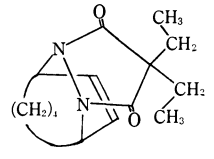

4c

When maleic hydrazide and nickel peroxide were suspended in methylene chloride and stirred at room temperature, 3,6-dioxopyridazine (**1a**) was produced, and a small amount of nitrogen has evolved because of the partial decomposition of hydrazide. A reaction *in situ* with isoprene gave 1,4-dihydro-2-methyl-6,9-dioxopyridazino-[1,2-*a*]pyridazine (**2a**) *via* the process shown by Equations (1) and (2). The IR (KBr) spectrum of **2a** showed a carbonyl absorption at 1638 cm^{-1}, but no imino absorption. The NMR ($CDCl_3$) spectrum exhibited signals at τ 8.10 (s, 3H, 2-CH_3), 5.56 (s, 2H, 1-CH_2), 5.75—5.35 (m, 2H, 4-CH_2), 4.24 (m, 1H, 3-olefinic H), and 3.05 (s, 2H, 7,8-olefinic H). The reactions with *trans,trans*-1,4-diphenyl-1,3-butadiene and 1,3-cyclooctadiene gave 1,4-dihydro-6,9-dioxo-1,4-diphenylpyridazino[1,2-*a*]pyridazine (**3a**) and 1,4-butano-1,4-dihydro-6,9-dioxopyridazino[1,2-*a*]pyridazine (**4a**) respectively.

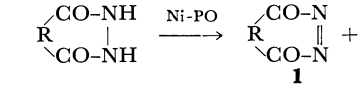

(1)

1 + diene ⟶ adduct (2)

Ni-PO = nickel peroxide

R = a: -CH=CH-, b: *o*-C_6H_4〈, c: $(C_2H_5)_2C$〈

diene = 2: isoprene, 3: diphenylbutadiene, 4: cyclooctadiene

Adducts:

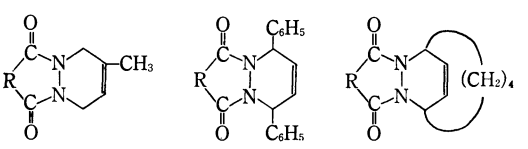

*1 Presented at the 22nd Annual Meeting of the Chemical Society of Japan, Tokyo, April, 1969.

1) R. A. Clement, *J. Org. Chem.*, **25**, 1724 (1960); **27**, 1115 (1962).

2) T. J. Kealy, *J. Amer. Chem. Soc.*, **84**, 966 (1962).

3) O. L. Chapman and S. Dominianni, *J. Org. Chem.*, **31**, 3862 (1966).

4) a) A. J. Solo, H. S. Sachdev and S. S. H. Gilani, *J. Org. Chem.*, **30**, 769 (1965); b) S. S. H. Gilani and D. J. Triggle, *ibid.*, **31**, 2397 (1966); c) B. T. Gillis and J. D. Hagarty, *ibid.*, **32**, 330 (1967); d) R. C. Cookson, S. S. H. Gilani and I. D. R. Stevens, *J. Chem. Soc., C*, **1967**, 1905; e) J. Sauer and B. Schröder, *Chem. Ber.*, **100**, 678 (1967); f) T. L. Popper, F. E. Carlon, H. M. Marigliano and M. D. Yudis, *Chem. Commun.*, **1968**, 1434; g) D. R. Arnold, A. B. Evnin and P. H. Kasai, *J. Amer. Chem. Soc.*, **91**, 784 (1969).

5) B. T. Gillis and R. A. Izydore, *J. Org. Chem.*, **34**, 3181 (1969).

6) A. B. Evnin, A. Y. Lam, J. J. Maher and J. J. Blyskal, *Tetrahedron Lett.*, **1969**, 4497.

7) a) K. Nakagawa, R. Konaka and T. Nakata, *J. Org. Chem.*, **27**, 1597 (1962); b) R. Konaka, S. Terabe and K. Kuruma, *ibid.*, **34**, 1334 (1969).

Table 1. Diels-Alder adducts

Adduct	Yield %	Mp[d] °C, (S)[e]	Formula	Mw[j]	Calcd. %			Found %		
					C	H	N	C	H	N
2a	33.7	117—118 (A)	$C_9H_{10}N_2O_2$	178	60.66	5.66	15.72	60.41	5.48	15.54
3a[a]	62.5	225—226 (B)	$C_{20}H_{16}N_2O_2$	316	75.93	5.10	8.86	75.85	5.00	8.67
4a	22.5	171—172 (A)	$C_{12}H_{14}N_2O_2$	218	66.03	6.47	12.84	66.08	6.50	12.76
2b	23.7	151—154.5 (A)	$C_{13}H_{12}N_2O_2$	228	68.41	5.30	12.27	68.51	5.26	12.22
3b[b]	79.2	217.5—218.5 (B)	$C_{24}H_{18}N_2O_2$	366	78.67	4.95	7.65	78.86	4.79	7.60
4b	89.5	200.5—201.0[f] (C)	$C_{16}H_{16}N_2O_2$	268	71.62	6.01	10.44	71.85	6.08	10.38
2c[c]	83.3	53—55[g] (A)	$C_{12}H_{18}N_2O_2$	222	64.84	8.16	12.60	64.62	8.37	12.37
3c[c]	55.6	154—156[h] (A)	$C_{23}H_{24}N_2O_2$	360	76.64	6.71	7.77	76.89	6.64	7.85
4c	7.8	137—138[i] (D)	$C_{15}H_{22}N_2O_2$		68.67	8.45	10.68	68.05	8.44	10.53

a) The reagents were refluxed in benzene.
b) The reaction was continued for 88 hr.
c) Lead tetraacetate was used as the oxidant of cyclic hydrazide.
d) Melting points are uncorrected.
e) Recrystallization from the following solvent: A, alcohol; B, benzene - alcohol; C, petroleum ether - *n*-hexane - ethanol; D, water.
f) Lit,[3] mp 208—210°C.
g) Lit,[5] mp 58.5—60°C.
h) Lit,[5] mp 147—148°C.
i) Lit,[5] mp 134—136°C.
j) Molecular weight determinations were made by analysis of the mass spectra.

The same process, when applied to 1,4-dioxophthalazine (**1b**) generated from phthalic acid hydrazide by nickel peroxide oxidation and isoprene, gave 1,4-dihydro-2-methyl-6,11-dioxopyridazino[1,2-*b*]phthalazine (**2b**). In the reaction of *trans*,*trans*-1,4-diphenyl-1,3-butadiene or 1,3-cyclooctadiene with **1b**, 1,4-dihydro-6,11-dioxo - 1,4 - diphenylpyridazino [1,2 - *b*] phthalazine (**3b**) or 1,4-butano-1,4-dihydro-6,11-dioxopyridazino[1,2-*b*]phthalazine (**4b**) respectively was isolated.

The procedure in which nickel peroxide was used as the oxidant of diethylmalonic acid hydrazide gave a small of the reaction product, or no yield at all, with diene. On the other hand, 4,4-diethyl-3,5-dioxo-1-pyrazoline (**1c**) prepared by oxidation with lead tetraacetate gave the 1,4-adducts in a high yield. They were 2,2-diethyl-2,3,5,8-tetrahydro-7-methyl-1,3 - dioxo - 1*H* - pyrazolo[1,2-*a*]pyridazine (**2c**), 2,2-diethyl-2,3,5,8-tetrahydro - 1,3 - dioxo - 5,8-diphenyl - 1*H*-pyrazolo-[1,2-*a*]pyridazine (**3c**), and 5,8-butano-2,2-diethyl-2,3,5,8-tetrahydro - 1,3 - dioxo - 1*H* - pyrazolo [1,2-*a*]-pyridazine (**4c**).

Experimental

General Procedure for the Reaction of Cyclic Diacyl Diimide with Dienes. The reagents, cyclic hydrazide (0.01 mol) and diene (0.01—0.03 mol), were slurried in methylene chloride (50 m*l*) at room temperature. A large excess of diene should be avoided. Fine powder of nickel peroxide (1.2—2.0 times the theoretical amount, as determined on available oxygen[7a]) was added, little by little, with magnetic stirring. Stirring was continued for *ca.* 20—40 hr at room temperature after the addition of the nickel peroxide. The loss of the methylene chloride was compensated for according to circumstances. The reaction mixture was then filtered, and the filtrate was evaporated on a rotary evaporator at <40°C to yield a crude adduct. The residue was purified by crystallization or by distillation under reduced pressure to give an analytical sample.

The Diels-Alder adducts thus prepared, along with their physical properties, yields and analyses, are listed in Table 1. The yields, based on the cyclic hydrazide, were determined from the weight of the raw crystals from the first recrystallization.

IR and NMR Spectra of Adducts. 3a: 1632 cm^{-1} (C=O); τ 3.67 (s, 4H, 2,3,7,8-olefinic H), 3.02 (s, 2H, methyne), 2.82 (s, 10H, phenyl). **4a**: 1637 cm^{-1}; τ 8.90—7.40 (m, 8H, methylene), 4.45 (m, 2H, methyne), 3.85 (m, 2H, 2,3-olefinic H), 3.10 (s, 2H, 7,8-olefinic H). **2b**: 1630 cm^{-1}; τ 8.08 (s, 3H, CH_3), 5.46 (s, 2H, 1-CH_2), 5.60—5.25 (m, 2H, 4-CH_2), 4.24 (m, 1H, 3-CH), 2.21 (m, 2H, 8,9-aromatic H), 1.70 (m, 2H, 7,10-aromatic H). **3b**: 1640 cm^{-1}; τ 3.61 (m, 2H, methyne or olefinic H), 3.50 (m, 2H, methyne or olefinic H), 2.81 (s, 10H, phenyl), 2.17 (m, 2H, 8,9-aromatic H), 1.68 (m, 2H, 7,10-aromatic H). **4b**: 1630 cm^{-1}; τ 8.70—7.30 (m, 8H, methylene), 4.20 (m, 2H, methyne), 3.80 (m, 2H, olefinic H), 2.23 (m, 2H, 8,9-aromatic H), 1.70 (m, 2H, 7,10-aromatic H). **2c**: 1725 and 1685 cm^{-1}; τ 9.16 (t, 6H, $C\underline{H}_3CH_2$), 8.20 (quar, 4H, $CH_3C\underline{H}_2$), 8.12 (s, 3H, 7-CH_3), 5.97 (s, 2H, 8-CH_2), 6.10—5.76 (m, 2H, 5-CH_2), 4.43 (m, 1H, 6-CH). **3c**: 1689 cm^{-1}; τ 9.71 (t, 3H, $C\underline{H}_3CH_2$), 9.15 (t, 3H, $C\underline{H}_3CH_2$), 8.65—8.00 (quin, 4H, $2CH_3C\underline{H}_2$), 4.40 (m, 2H, 2CH), 4.08 (m, 2H, olefinic H), 2.80—2.30 (m, 10H, phenyl). **4c**: 1717 and 1666 cm^{-1}; τ 9.45—8.85 (m, 6H, $2C\underline{H}_3CH_2$), 8.60—7.60 (m, 12H, methylene), 5.15—4.75 (m, 2H, 2CH), 4.00—3.80 (m, 2H, olefinic H).

BULLETIN OF THE CHEMICAL SOCIETY OF JAPAN VOL. 43 3928—3929 (1970)

The Reaction of Aliphatic Amines with *p*-Benzoquinone. The Effect of the Alkyl Group of Amines on the Reaction

Aizo HIKOSAKA

Engineering Research Institute, Faculty of Engineering, The University of Tokyo, Hongo, Bunkyo-ku, Tokyo

(Received May 25, 1970)

The most general reaction between quinones and amines has been established for both primary and secondary, aliphatic and aromatic.[1-5] *p*-Benzoquinone undergoes two nuclear substitutions, but single substitutions are frequently observed with secondary amines under selected conditions.

The ease with which an amine enters the quinone nucleus depends to a large extent on the nature of the amine.[6] Under the present conditions (see General Procedure), *p*-benzoquinone gave bis-(alkylamino)-*p*-benzoquinones with primary amines, but with secondary amines it gave monoamino derivatives only.

p-Benzoquinone forms substitution products with 1 or 2 mol of amine, accompanied by the reduction of 1 or 2 mol of the benzoquinone respectively. These substitution products undergo a reversible oxidation or reduction on the dropping-Hg electrode, like the system quinone-hydroquinone itself. To follow the chemical change, polarography has been used.

In the present work, the effects of the alkyl group of the amine on the pattern and the rate of the reaction of *p*-benzoquinone with amines were determined.

Experimental and Results

General Procedure of the Reaction of *p*-Benzoquinone with Amines. *p*-Benzoquinone (3×10^{-4} mol) was dissolved in 10 m*l* of isopropanol or ethanol, and into the resulting solution we added amine (2×10^{-4} mol) with constant stirring at 25°C. At regular time intervals, 0.1 m*l* aliquots of the reaction mixture were taken out and diluted to 10 m*l* with a polarographic base solution (isopropanol: phosphate buffer = 1 : 1). This dilution practically quenched the reaction. Any oxygen was removed from the solution by bubbling it with nitrogen, and the oxygen-free solution was subsequently polarographed by an ordinary method.

Materials and Apparatus. *p*-Benzoquinone (mp 116°C) was purified by the sublimation of commercially available chemicals. The amines used were commercially available and were identified by means of gas chromatography. The buffers used were prepared by the method of Sörensen in our laboratory.

The gas-chromatographic determinations were made with a Yanagimoto Gas Chromatograph, GCG-5DH, while the polarographic determinations were made with a Yanagimoto Pen Recording Polarograph, PA-102.

The Reaction of Primary Amines with *p*-Benzoquinone. In the reaction of *p*-benzoquinone with alkylamines in alcohols at ordinary temperatures, *p*-benzoquinone undergoes two nuclear substitutions, as is shown in Eq. (1).

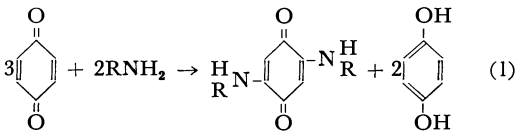

(1)

In this study, the effect of branching on the position

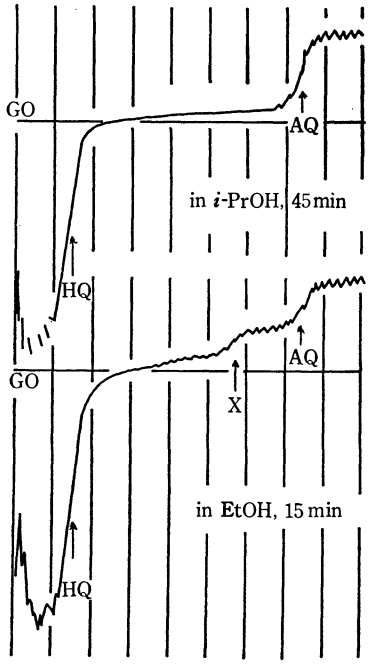

Fig. 1. Polarograms for the reaction of *p*-benzoquinone with *s*-butylamine. (1) in isopropanol after 45 min; (2) in ethanol after 15 min.
HQ; Hydroquinone
X; Unknown product
GO; Galvano. Zero Line

1) R. N. Harger, *J. Amer. Chem. Soc.*, **46**, 2540 (1946).
2) F. Mylius, *Ber.*, **18**, 468 (1885).
3) A. W. Hofman, *Proc. Roy. Soc.*, **13**, 4 (1863).
4) M. Martynoff and G. Tsatsas, *Bull. soc. chim.*, **14**, 52 (1947).
5) O. Suchanek, *J. prakt. Chem.*, **90**, 467 (1914).
6) H. Suida and W. Suida, *Ann.*, **426**, 116 (1918).

of the carbon atom adjacent to the nitrogen atom of the amine upon the rate of the reaction between alkylamine and *p*-benzoquinone was determined. Furthermore, the effect of the solvents, ethanol and isopropanol, upon the reaction was studied.

According to the procedure described above, methylamine, ethylamine, *n*-propylamine, and *n*-butylamine reacted with *p*-benzoquinone to form 2,5-bis(alkylamino)-*p*-benzoquinone in isopropanol or ethanol at 25°C within 5 min. In the case of isopropylamine and *s*-butylamine, the completion of the reaction in isopropanol required 45 min, the reaction in ethanol required only 15 min, but this was produced an unknown by-product which showed a cathodic wave (see Fig. 1). In the case of the *t*-butylamine-*p*-benzoquinone reaction in isopropanol, the rate of the reaction was still slower; even after 120 min the reaction had not been completed and a part of the quinone remained. In ethanol, *t*-butylamine did not give 2,5-bis(*t*-butylamino)-*p*-benzoquinone under the present conditions, though the quinone used decreased and hydroquinone was produced.

The Reaction of Secondary Amines with *p*-Benzoquinone. With alkylamines, *p*-benzoquinone gives bis(alkylamino)-*p*-benzoquinones; with dialkylamines, *p*-benzoquinone gives monoamino derivatives only.

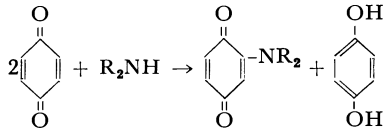

(2)

In the present work, a study of the condensations of *p*-benzoquinone with dialkylamines was made; the experimental conditions were the same as in the general procedure except for the use of isopropanol only as a solvent.

In these reactions, their rates depended upon the kind of alkyl group in the amine used. In this report, dimethylamine, diethylamine, di-*n*-propylamine, and di-*n*-butylamine were used.

The quinone used disappeared within one minute in the case of dimethylamine, within 90 min in the case of diethylamine, and within 180 min in the cases of di-*n*-propylamine and di-*n*-butylamine. The rate of the reaction of *p*-benzoquinone with dialkylamines depends to a large extent on the size of the alkyl group of the amine in the case of the lower dialkylamine members.

BULLETIN OF THE CHEMICAL SOCIETY OF JAPAN VOL. 43 3929—3932 (1970)

The Electronic Structures and Chemical Properties of O, S Containing Six-membered Heterocycles and Their Benzo-derivatives

Mamoru KAMIYA

Shizuoka College of Pharmacy, Oshika, Shizuoka-shi

(Received May 28, 1970)

It is known that compounds such as 1,4-dithiadiene, -oxathiadiene and -dioxadiene and their benzo-derivatives exhibit several characteristic chemical properties related to the electronic effects of the sulfur and oxygen atoms. That is, 1,4-dithiadiene exhibits a somewhat unusual thermal stability, as was first found by Levi,[1] who reported that the molecule underwent a Friedel-Crafts reaction; later Parham *et al.* reported that the hetero-ring in benzo-1,4-dithiadiene and/or -oxathiadiene exhibited electrophilic substitutions usually associated with an aromatic character. It is also well known that dibenzo-1,4-dithiadiene has a high thermal stability and undergoes a reaction typical of an aromatic system. Such an aromaticity of these molecules, atypical of aliphatic ethers, was correlated, by Parham *et al.*, with the ability of sulfur to expand its valence shell and with the electron-releasing property of oxygen. However, the theoretical support for the observed electronic effects of the sulfur and oxygen atoms seems insufficient, though there have been a few molecular orbital studies of the electronic structure and chemical properties of these molecules, such as simple LCAO calculations neglecting σ-π interaction and the participation of sulfur *d*-orbitals on 1,4-dithiadiene[6] and dibenzo-1,4-dithiadiene,[7] and Pariser-Parr-Pople SCF calculations of 1,4-dithiadiene,[8] benzo-1,4-dioxadiene, and dibenzo-1,4-dioxadiene.[9]

1) L. Levi, *Chem. News*, **62**, 216 (1890).
2) W. E. Parham, T. M. Roder and W. R. Hasek, *J. Amer. Chem. Soc.*, **75**, 1647 (1953).
3) W. E. Parham and J. D. Jones, *ibid.*, **76**, 1068 (1954).
4) W. E. Parham, H. Wynberg and F. L. Ramp, *ibid.*, **75**, 2065 (1953).
5) W. E. Parham and G. L. Willette, *J. Org. Chem.*, **25**, 53 (1960).
6) M. M. Kreevoy, *J. Amer. Chem. Soc.*, **80**, 5543 (1958).
7) A. K. Chandra, *Tetrahedron*, **19**, 471 (1963).
8) D. S. Sappenfield and M. Kreevoy, *Tetrahedron*, **19**, Suppl. 2, 157 (1963).
9) R. J. Wratten and M. A. Ali, *Mol. Phys.*, **13**, 233 (1967).

This paper will report semiempirical SCF-MO-CI calculations on all the related molecules and will then consider generally the relative electronic effects of the sulfur and oxygen atoms.

Calculation Method

The P-P-P method,[10] with the CI procedure including all the singly-excited configurations, is used since recent SCF calculations[8,9] on the UV spectra of the related molecules indicate that if the molecule is non-planar, a treatment assuming the separability of σ and π electrons can be allowed for in the proper choice of parameters. The values of the valence-state ionization potentials (I) and the electron affinities (A) of the π-orbitals of several atoms are taken as follows, with reference to the paper of Hinze and Jaffe[11]:

I(=C-) 11.16 eV, I(-O-) 32.90 eV,
I(-S-) 23.59 eV
A(=C-) 0.03 eV, A(-O-) 11.37 eV,
A(-S-) 10.54 eV

The sulfur *d*-orbitals are not explicitly included because it has been pointed out by Johnstone and Ward that the observed π-π^* transitions of sulfur heterocycles are generally reproduced by a small variation in the core integrals.[12] The one-center repulsion integral is obtained by the I-A approximation, while the two-center repulsion integral is evaluated by the Nishimoto-Mataga formula.[13] The core resonance integral is evaluated by adopting the variable β-core approximation,[14] because the effect of the non-planarity of the molecules upon the β_{C-O} and β_{C-S} may be properly included by adjusting the parameters. At present the following equations are tentatively used for all the molecules;

$$\beta_{C-C} = -0.51\ P_{C-C} - 1.84,$$
$$\beta_{C-O} = -0.56\ P_{C-O} - 2.20,$$
$$\beta_{C-S} = -0.33\ P_{C-S} - 1.80$$

Here, P_{rs} corresponds to the usual π-bond order. The bond lengths of all the molecules are taken as 1.395 Å.

Results and Discussion

Electronic Spectra. The theoretical findings on the singlet π-π^* transition energy and oscillator strength are given in table 1, together with the available experimental data. The relative ordering of the intensities of the first allowed transitions of 1,4-dioxadiene and -dithiadiene is predicted correctly, and it is found that the introduction of the oxygen atom causes increase in the first allowed transition energy. As regards benzo-1,4-dithiadiene the assignment of the three observed bands is straight foward because of the agreement between the predicted and observed orderings of the absorption intensity. The effect of the hetero-ring structure upon the oscillator strength of the first allowed transition is quite decreased from the monocyclic molecule to the monobenzo-derivatives. In the case of benzo-1,4-oxathiadiene, the polarization direction of the second allowed transition (5.08 eV) is varied to such an extent that the transition moment makes an angle of 68° to the *x*-axis. This is interesting because it suggests that a shortly polarized structure, such as , contributes to the excited state, just as is to be expected from the relative electron-releasing order of the sulfur and oxygen atoms.

In the case of the dibenzo-derivatives also, the calculated spectra well reflect the effect of hetero-atom replacement. In dibenzo-1,4-oxathiadiene, the first two forbidden bands are little enhanced through the lowering of the molecular symmetry. In dibenzo-1,4-dioxadiene, the observed band at 4.29 eV was assigned by Wratten and Ali[9] to the second forbidden band, which becomes allowed through a slight folding about the line joining the heteroatoms. It is of interest to note that the second and third allowed transitions, with very different intensities, tend to degenerate in all the calculated spectra and to change their mutual order from dibenzo-1,4-dioxadiene to the other two molecules.

Ionization Potentials. The negatives of the ho and lv orbital energies are given in table 2, together with the available experimental data on ionization potentials. It is usually accepted that the ionization potentials calculated by Koopman's Theorem are 1—2 eV too large in comparison with the experimental values; such is also true for the present results. Interestingly, the effect of the hetero-ring structure upon the calculated ionization potentials and electron affinities is almost independent of the introduction of a benzene-ring. The calculated ionization potentials of the dibenzo-derivatives exhibit an ordering identical to that of the experimental values determined by the electron-impact method.

Electron Distributions. The calculated findings on the π-electron densities and π-bond orders are shown in Fig. 1. First, it is established that the sulfur atom in monocyclic molecules more

10) R. Pariser and R. G. Parr, *J. Chem. Phys.*, **21**, 466,767 (1953); J. A. Pople, *Trans. Faraday Soc.*, **49**, 1375 (1953).
11) J. Hinze and H. H. Jaffe, *J. Amer. Chem. Soc.*, **84**, 540 (1962).
12) R. A. W. Johnstone and S. D. Ward, *Tetrahedron*, **25**, 5484 (1969).
13) K. Nishimoto and N. Mataga, *Z. Physik. Chem.*, **12**, 335 (1957).
14) K. Nishinoto and L. S. Forster, *Theoret. Chim. Acta*, **4**, 155 (1966).

TABLE 1. CALCULATED AND EXPERIMENTAL DATA OF ELECTRONIC SPECTRA

	Calculated			Experimental	
	ΔE_s	Sym.	f	ΔE_s	$\log \varepsilon_{max}$
1,4-Dioxadiene [1]	2.72	(B_{1g})	—		
	5.13	(B_{2u})	0.13	~4.96	~3.0[a]
	7.54	(B_{2u})	1.38		
1,4-Oxathiadiene [2]	2.92	(B_2)	0.00		
	5.00	(A_1)	0.15		
	7.41	(A_1)	1.22		
1,4-Dithiadiene [3]	3.07	(B_{1g})	—		
	4.87	(B_{2u})	0.18	4.59[b]	3.65[c]
	7.12	(B_{3u})	0.24	5.748	—
Benzo-1,4-dioxadiene [4]	3.15	(B_2)	0.00		
	3.75	(A_1)	0.08		
	5.19	(B_2)	0.14		
	5.27	(A_1)	0.53		
	5.83	(B_2)	0.04		
Benzo-1,4-oxathiadiene [5]	3.27	(A)	0.00		
	3.77	(A)	0.08		
	5.08	(A)	0.18		
	5.21	(A)	0.44		
	5.81	(A)	0.05		
Benzo-1,4-dithiadiene [6]	3.37	(B_2)	0.00		
	3.78	(A_1)	0.08	4.12	2.91[d]
	4.97	(B_2)	0.18	4.73	3.81
	5.14	(A_1)	0.40	4.90	4.23
	5.80	(B_2)	0.05		
Dibenzo-1,4-dioxadiene [7]	3.51	(B_{1g})	—		
	3.75	(B_{3u})	0.19	4.13	[e]
	4.08	(A_g)	—	4.29	3.87
	5.07	(B_{3u})	1.50	5.44	4.73
	5.11	(B_{2u})	0.14	5.58	4.64
	5.63	(B_{1g})	—		
	5.75	(A_g)	—		
	5.85	(B_{2u})	0.78	6.11	
Dibenzo-1,4-oxathiadiene [8]	3.59	(B_2)	0.00		
	3.79	(B_2)	0.17	4.20	3.60[e]
	4.06	(A_1)	0.00		
	5.00	(A_1)	0.14	5.14	4.50
	5.04	(B_2)	1.37	5.21	4.50
	5.54	(A_1)	0.03	5.64	
	5.73	(B_2)	0.02		
Dibenzo-1,4-dithiadiene [9]	3.66	(B_{1g})	—		
	3.81	(B_{3u})	0.16	~4.13	~2.9[f]
	4.05	(A_g)	—		
	4.90	(B_{2u})	0.16	4.81	4.60[e]
	5.01	(B_{3u})	1.27	5.10	
	5.45	(B_{1g})	—		
	5.70	(A_g)	—		
	5.81	(B_{2u})	0.12	5.93	

ΔE_s=transition energy (eV).

f=oscillator strength, where the basic transition moment of $i \rightarrow j$ singly excited transition is calculated by the equations: $m_x = \sum_r \sqrt{2} c_r^i c_r^j \bar{x}_{rr}$, $m_y = \sum_r \sqrt{2} c_r^i c_r^j \bar{y}_{rr}$, $m_z = 0$.

sym.=transition symmetry denoted from planar structure.

a) L. W. Pickett and E. Sheffield, *J. Org. Chem.*, **68**, 216 (1946).

b) Reference 8. c) Reference 4. d) Reference 2.

e) B. Lamatte and G. Berthier, *J. Chim. Phys.*, **63**, 369 (1966).

f) L. Lang, "Absorption Spectra in the Ultraviolet and Visible Region," Part II, Akadémiai Kiadó, Budapest (1961).

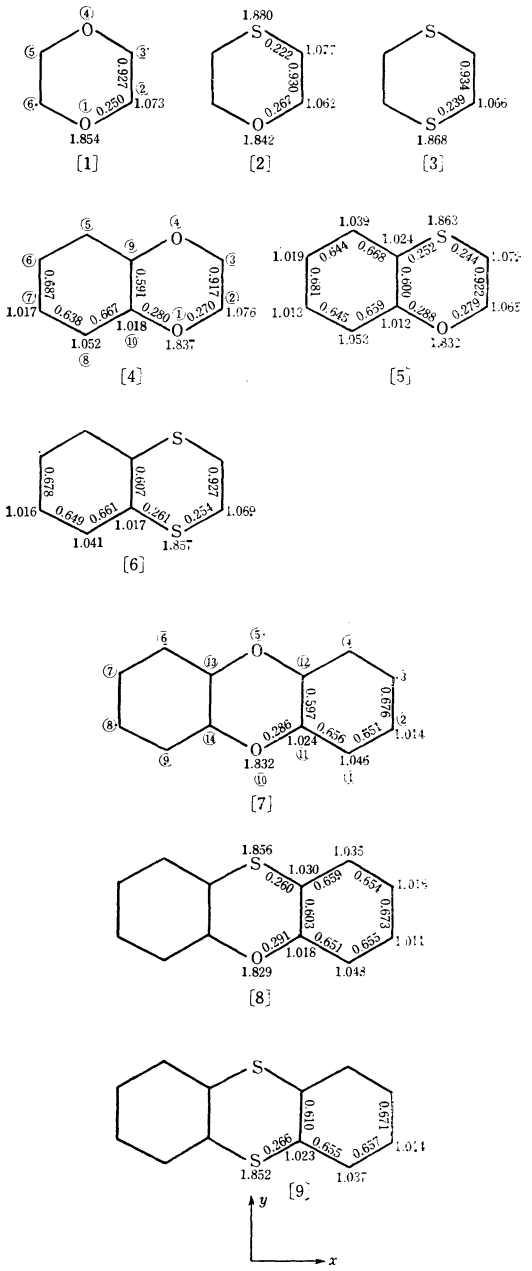

Fig. 1. π-Electron density and π-bond order.

Table 2. Theoretical and experimental data on ionization potential (I_p) and electron affinity (E_A)

Compound	Calcd. I_p (eV)	Calcd. E_A (eV)	Obsd. I_p (eV)
[1]	7.71	0.75	
[2]	7.74	0.68	
[3]	7.74	0.58	
[4]	8.11	1.13	
[5]	8.09	1.06	
[6]	8.07	0.98	
[7]	8.43	1.33	8.10*
[8]	8.39	1.26	7.98
[9]	8.35	1.17	7.80

* Evaluated from electron-impact method. B. Lamatte and G. Berthier, *J. Chim. Phys.*, **63**, 369 (1966).

favours the fixation of the diene-structure. It is of interest to note that such a difference between the sulfur and oxygen atoms is more enlarged in the hetero-ring containing both hetero-atoms. The same thing is true for the benzo-derivatives. In the case of benzo-1,4-dithiadiene, the predicted site for electrophilic attack, C-2(3) in the hetero-ring, is in agreement with that observed by Parham *et al.*[2-5] A further prediction from the electron distributions is that the electrophilic substitutions of benzo-1,4-oxathiadiene and/or -dioxadiene should also occur at the hetero-ring. As regards the dibenzo-derivatives, it is found that a characteristic relation, $P^{\pi}{}_{\beta-\beta} > P^{\pi}{}_{\alpha-\beta}$, previously noted as a result of a simple LCAO calculation of Chandra[7] is also valid for all the molecules, and that this tendency is slightly promoted by the presence of an oxygen atom.

The present calculations were carried out with an HITAC 5020-E computer at the Computation Center of the University of Tokyo. The author wishes to thank Professor Y. Akahori for his interest and valuable discussions.

BULLETIN OF THE CHEMICAL SOCIETY OF JAPAN VOL. 43 3933—3935 (1970)

The Far-infrared Torsional Frequencies of Monohalogenoethanes

The (late) Susumu KINUMAKI and Muneteru KOZUKA

Chemical Research Institute of Non-Aqueous Solution, Tohoku University, Sendai

(Received June 12, 1970)

In the case of the "one-top problem", it is known that intramolecular vibrations other than the torsion contribute quite little to the fine structure of the microwave spectrum.[1] Thus, we can obtain some information about the extent of interaction between the torsion and the other intramolecular vibrations by comparing the torsional frequencies observed in the infrared spectra with those obtained from the microwave splitting through the calculation by using the P.A.M.[2] (principal-axes method) or the I.A.M.[2] (internal-axis method).

The far-infrared spectra were recorded on a Hitachi FIS-1 vacuum, grating, double-beam spectrophotometer. All the monohalogenoethanes used were obtained from commercial sources; they were purified by vapor-phase chromatography and then dried with phosphorus pentoxide. Considerable precautions were taken to remove the residual water. The vapor of monohalogenoethane was introduced into a gas-cell which had been especially built for the instrument. Its path length is veriable in increment of 1.2 m up to 6 m. In order to avoid interference, wedged polyethylene sheets were used as the cell windows.

The observed torsional frequencies are given in Table 1, together with those values calculated from the microwave splitting data.[2,3] The torsional frequencies for ethyl fluoride and ethyl chloride have been reported by Sage and Klemperer[4] and Fateley and Miller[5] respectively. We observed not only those frequencies, but also the 3E→4E transition bands for these molecules (see Fig. 1). It is of some interest to note the splitting of the A and E levels for higher vibrational states, as is expected from the theory.[2,3] Such splitting has not previously been observed.[4-6] Although the reason for this is not clear, it may be remembered that the previous data were obtained

TABLE 1. CALCULATED (FROM MICROWAVE DATA) AND OBSERVED INFRARED TORSIONAL FREQUENCIES FOR MONOHALOGENOETHANES

v-v'	C_2H_5F MW[a]	C_2H_5F IR (cm^{-1})	C_2H_5Cl MW[b]	C_2H_5Cl IR (cm^{-1})	C_2H_5Br MW[c]	C_2H_5Br IR (cm^{-1})	C_2H_5I MW[d]	C_2H_5I IR (cm^{-1})
0—1 A	244	243.5	250.8	250.8	247.2	247.8	228	237.0
0—1 B	244		250.8		247.2		228	
1—2 E	227	226.5	235.0	235.0	231.8	232.8	213	221.0
1—2 A	227		235.0		231.8		213	
2—3 A	208	209.0	217.3	218.0	214.7	216.4	196	
2—3 E	207		216.9		214.4		195	
3—4 E	186	189.6	197.0	199.5	195.2	194.0	176	
3—4 A	176	178.4	192.8	196.1	191.8	(191.2)	170	
V_3(cal/mol)	3330±100[a]		3685±12[b]		3684±10[c]		3220±100[d]	
S	80.0[a]		94.43[b]		97.4[c]		87.1[d]	

a) D. R. Herschbach, *J. Chem. Phys.*, **25**, 358 (1956).
b) R. H. Schwendeman, *ibid.*, **36**, 1245 (1962).
c) C. Flanagan and L. Pierce, *ibid.*, **38**, 2963 (1962).
d) T. Kasuya, *J. Phys. Soc. Jap.* **15**, 1273 (1960).

1) D. Kivelson, *J. Chem. Phys.*, **22**, 1733 (1954); **23**, 2230, 2236 (1955); P. R. Swan and M. W. P. Strandberg, *J. Mol. Spectrosc.*, **1**, 333 (1957); K. T. Hecht and D. M. Dennison, *J. Chem. Phys.*, **26**, 31 (1957); T. Nishikawa, *J. Phys. Soc. Jap.*, **11**, 781 (1956); B. Kirtman, *J. Chem. Phys.*, **37**, 2516 (1962).

2) C. C. Lin and J. D. Swalen, *Rev. Mod. Phys.*, **31**, 841 (1959).

3) D. R. Herschbach, *J. Chem. Phys.*, **31**, 91 (1959).

4) G. Sage and W. Klemperer, *ibid.*, **39**, 371 (1963).

5) W. C. Fateley and F. A. Miller, *Spectrochim. Acta*, **19**, 611 (1963).

6) K. D. Möller, A. R. De Meo, D. R. Smith, and L. H. London, *J. Chem. Phys.*, **47**, 2609 (1967).

with a single-beam spectrometer. The infrared torsional frequencies for gaseous ethyl bromide and ethyl iodide are observed for the first time in the present study (Fig. 2). In the case of ethyl iodide, the agreement between the infrared frequencies and those obtained from the microwave splitting data is not so good. This is probably due to experimental error in the microwave measurements; Kasuya[7] has reported that his microwave datum for ethyl iodide will be refined in the future.

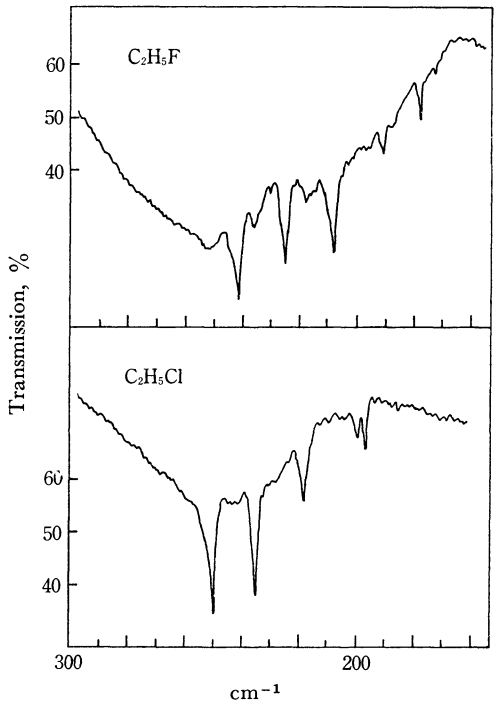

Fig. 1. Far-infrared spectra of ethyl fluoride and ethyl chloride.
(Path length: 4.8 m,
Pressure: Saturated vapor pressure at room temperature)

The 201 cm^{-1} band of the gaseous ethyl iodide in Fig. 2 was identified as the difference band between two fundamentals, 947 cm^{-1} (A') and 741 cm^{-1} (A''), despite the fact that it was stronger than the torsion bands. This assignment is based on the following reasons: (1) In the liquid spectrum, the corresponding band was observed at 204 cm^{-1}, and its envelope was rather sharper than that in the gas (Fig. 3). However, a torsion band is usually weaker and broader in the liquid than in the gas phase. (2) If the torsional frequencies were 201 cm^{-1}, the barrier height, V_3, would be calculated to 2590 cal/mol. This is curiously low, since the value in ethane is 3000

7) T. Kasuya, *J. Phys. Soc. Jap.*, **15**, 1273 (1960).

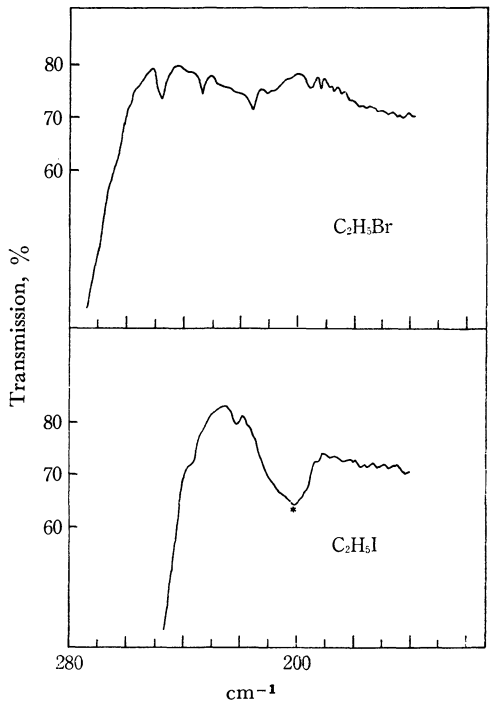

Fig. 2. Far-infrared spectra of ethyl bromide and ethyl iodide.
(Path length: 1.0 m for ethyl bromide, 3.6 m for ethyl iodide.
Pressure: Saturated vapor pressure at room temperature, for the both)
* This band was identified as a difference band.

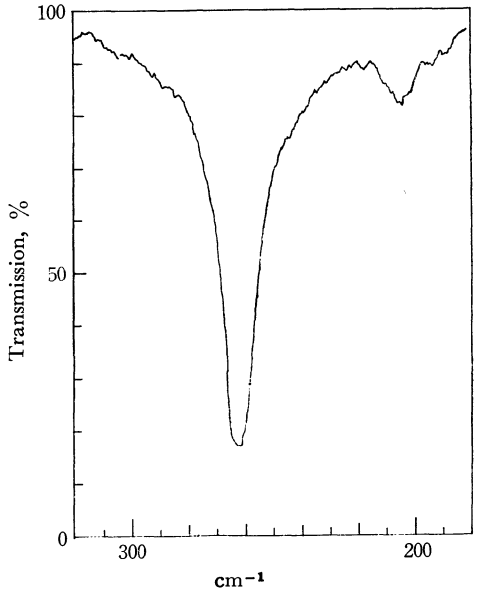

Fig. 3. Far-infrared spectra of liquid ethyl iodide.
Path length: 0.3 mm; The 262 cm^{-1} band is an A' fundamental, associated with CCI bending.

cal/mol.[8] (3) The band remained constant in intensity and frequency in the course of time. No rotation bands of hydrogen iodide were observed, either. Therefore, the band is not due to any decomposition product. (4) The combination band of the fundamentals appeared at 1709 cm^{-1}. The difference between the calculated and observed frequencies, 21 cm^{-1}, seems to be a little large. This is because the 1709 cm^{-1} band is very broad (the half band-width, 120 cm^{-1}) and consists of two combination bands, corresponding to 1712 (1210 A′ + 502 A″) and 1688 cm^{-1} (947 A′ + 741 A″).[9]

Except for the case of ethyl iodide, the agreement between the infrared frequencies and those obtained from the microwave splitting data is excellent. This suggests that the coupling of the CH_3 torsional vibration with the other intramolecular vibrations is quite small. This, in turn, justifies the treatment for obtaining the potential barrier to internal rotation from the infrared torsional frequency.[4-6] This is further supported by the fact that the potential energy distributions for the tosional vibration in the trans configuration of 1,2-dichloro-[10,11] and 1,2-dibromoethane[12] are 90 and 80% respectively.

8) K. S. Pitzer, *Discuss. Faraday Soc.*, **10**, 66 (1951); D. R. Lide, Jr., *J. Chem. Phys.*, **29**, 1426 (1958); S. Weiss and G. E. Leroi, *ibid.*, **48**, 962 (1968).

9) M. Kozuka, unpublished work.

10) T. Miyazawa and K. Fukushima, Preprint for the 16th Annual Meeting of the Chemical Society of Japan (April, 1963), **1S14**.

11) T. Miyazawa and K. Fukushima, *J. Mol. Spectroscs*, **15**, 308 (1965).

12) S. Sugano and T. Miyazawa, Preprint for the 17th Annual Meeting of the Chemical Society of Japan (April, 1964), **1XO2**.

BULLETIN OF THE CHEMICAL SOCIETY OF JAPAN VOL. 43 3935—3937 (1970)

The Preparation and Properties of Metal Complexes in Non-aqueous Solution. II. Diiodotetrakisdimethylsulfoxidecobalt Iodide*[1]

Masayuki MUTO, Masaaki YAMAGUCHI and Hayami YONEDA

Department of Chemistry, Wakayama University, Masagocho, Wakayama

(Received June 16, 1970)

The object of this investigation was, in its early stage, to obtain diiodotetraamine-type cobalt(III) complexes. With this object in mind, the replacement of Cl^- in $[CoCl_2en_2]^+$, $[CoCl_2pn_2]^+$, *etc.* by I^- in the presence of a small amount of iodine was attempted, using dimethylsulfoxide (DMSO) as the solvent. The product thus obtained was, however, not the expected diiodotetraamine-type complex, but instead, $CoI_3 \cdot 4$(DMSO) in all cases. This means that the substitution of I^- for Cl^- caused a purge of the coordinated amine ligands from the coordination sphere. Here it is surprising that even a tetradentate ligand, triethylenetetramine, is expelled by DMSO molecules. This suggests that DMSO has a strong coordinating ability with cobalt in the presence of I^-. Thus, the direct synthesis of $CoI_3 \cdot 4$(DMSO) was also attempted from CoI_2, I_2, and DMSO in absolute ethanol, the same product was obtained. The present paper will describe the method of preparation and the properties of this complex.

*[1] Presented at the 19th Symposium of Coordination Chemistry held at Tohoku University, Sendai, September 27, 1969.

Experimental

Preparation. *1) From trans-*$[CoCl_2en_2]NO_3$. One half gram of *trans-*$[CoCl_2en_2]NO_3$, 0.2 g of I_2, and 0.8 g of NaI were dissolved in 5 m*l* of warm DMSO. The mixture became a complete solution after one hour's gentle heating under constant stirring. This solution was added to 50 m*l* of ethanol and then placed in a refrigerator overnight. The precipitated sodium chloride was then filtered off, and the filtrate was stirred. A reddish-brown crystalline precipitate came out. The precipitate was filtered, washed with a small amount of ethanol and then with ether, and dried in a vacuum desiccator. Yield, 0.2 g.

Found: C, 12.49; H, 3.34; I. 50.57%. Calcd for $CoI_3 \cdot 4(C_2H_6SO)$: C, 12.77; H, 3.21; I, 50.61%.

From $[CoCl_2pn_2]NO_3$, $[CoCl_2tn_2]NO_3$, and $[CoCl_2$ trien$]NO_3$, the same product was obtained.

2) Direct Synthesis. One half gram of CoI_2 and 0.5 g of DMSO were dessolved in 10 m*l* of warm ethanol. The pink precipitate which appeared at first soon disappeared, and the solution became dark blue. Then, 0.15 g of I_2 in a small amount of ethanol was added slowly. Reddish-brown crystals came out. Crystals were filtered out, washed with ethanol and ether, and dried in a vacuum desicator. Yield, 2 g, In this preparation, the addition of iodine solution should be stopped before the blue color disappeared in

the solution.

Physical Measurements. The IR spectra were recorded with a Hitachi EPI-S2 spectrophotometer equipped with NaCl optics. The KBr disk method was adopted for the complex, but for the ordinary and deuterated DMSO samples sandwiched with NaCl plates were used for the measurements.

The UV absorption spectra of the solutions were obtained with a Hitachi Spectrophotometer 124, using 1-cm quartz cells. The magnetic moment was determined by the Gouy method at 12°C.

Results and Discussion

IR Spectra. Figure 1 shows the IR spectrum of the new complex, $CoI_3 \cdot 4(DMSO)$, together with those of the know complex, $[Co(DMSO)_6]I_2$[1], and the free ligand, DMSO. These spectra consist of a relatively few bands, among which consist of a relatively few bands, among which the two appearing at about 950 cm^{-1} and at 1000–1100 cm^{-1} are significant in discussing the coordinated state of the lignad. There has been confusion concerning the assignment of these two bands.

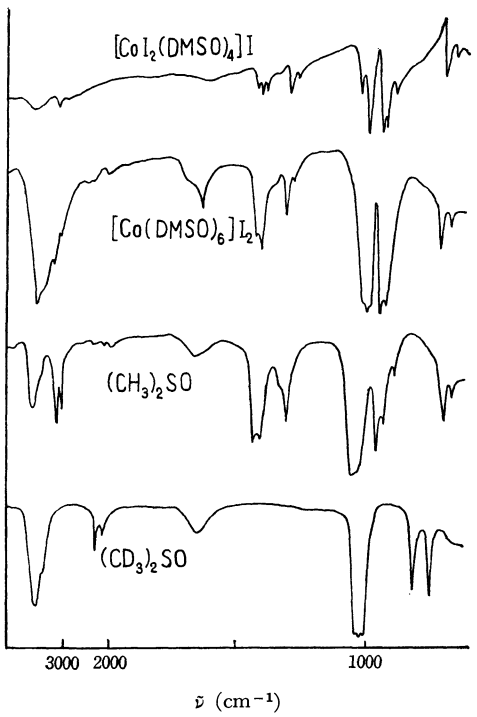

Fig. 1. IR absorption spectra of the free and coordinated states of dimethylsulfoxide.

Cotton and his collaborator[1] studies the IR spectra of sulfoxide complexes and concluded that coordination occurred through oxygen in $[Co(DMSO)_6]I_2$, since the SO stretching frequencies of the complex were lower than those of the free ligand, which absorbed at 1100–1055 cm^{-1}. Their assignment seems unnatural, however, of the two bands, the one at the lower frequencies was taken as the SO stretching band in the case of the complex, while the one at the higher frequencies was taken as the SO stretching band in the case of the free ligand. Thus, Drago and Meek[2] rejected Cotton's assignment and asserted that the band at lower frequencies was due to the methyl rocking mode, and that at higher frequencies, to the SO stretching mode, both in the complex and in the free ligand. If this is valid, the SO stretching frequency is not very sensitive to the nature of the metal.

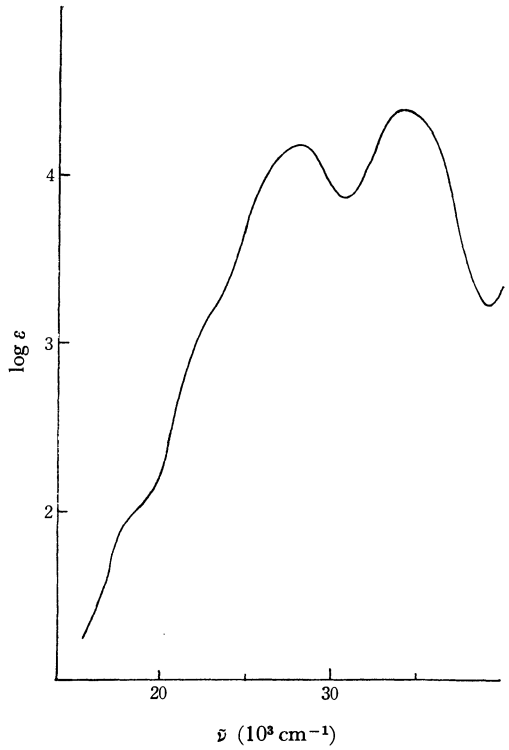

Fig. 2. Visible and UV absorption spectrum of $CoI_3 \cdot 4(DMSO)$ in 0.01 M NaI ethanol solution.

To confirm their assignments, the spectrum of deuterated DMSO was measured and compared with that of the ordinary DMSO. As may be been in Fig. 1, the band at lower frequencies completely disappears, while that at higher frequencies remains almost unchanged. This means that the lower one is due to the methyl rocking mode, which should be shifted further to lower frequencies upon the deuteration of the methyl group. Thus, the validity of Drago's assignment was confirmed. Since the SO stretching band of the free ligand is

1) F. A. Cotton, R. Francis and W. D. Horrocks, *J. Phys. Chem.*, **64**, 1534 (1960).

2) R. S. Drago and D. W. Meek, *ibid.*, **65**, 1446 (1961).

shifted slightly to lower frequencies upon coordination to Co(II) (from 1100–1050 cm^{-1} to 1050–1000 cm^{-1}), coordination through oxygen was also confirmed. In the new complex, $CoI_3 \cdot 4(DMSO)$, the frequency of each band is quite similar to that of $[Co(DMSO)_6]I_2$. Thus, the coordination through oxygen may be presumed. Although the new complex can be formulated as $[CoI_2(DMSO)_4]I$, in which the central cobalt ion is assumed to be tervalent, there is no indication in the IR spectra which positively supports the existence of the tervalent cobalt ion.

Visible and UV Absorption Spectra. Figure 2 show the visible and UV absorption spectra of $CoI_3 \cdot 4(DMSO)$ in an ethanol solution. The large absorption peaks at 28000 and 34200 cm^{-1} are assigned to charge-transfer band due to the coordinated I^-, because the spectrum of $[CoI(NH_3)_5]^{2+}$ has two bands at almost the same frequencies. The spectra have, in addition, two shoulders at about 17000 and 21200 cm^{-1} which are regarded as ligand-field bands.

Magnetic Moment. The magnetic moment of $CoI_3 \cdot 4(DMSO)$ was determined to be 4.45 B.M..

Structure of Complexes. From the above-mentioned data, we can formulate the complex as $[CoI_2(DMSO)_4]I$. The electronic structure of the complex may be represented by a resonance hybrid of the following structures;

$$[Co^{3+}(I^-)_2(DMSO)_4]^+ \leftrightarrow [Co^{2+}(I^-)(I^0)(DMSO)_4]^+$$

BULLETIN OF THE CHEMICAL SOCIETY OF JAPAN VOL. 43 3937—3938 (1970)

The Reactions of Dihydropyridones (II)

Noboru SUGIYAMA, Makoto YAMAMOTO and Choji KASHIMA

Department of Chemistry, Tokyo Kyoiku University, Otsuka, Tokyo

(Received June 17, 1970)

As dihydropyridones are typical β-amino-enones which are sterically fixed to a *cis*-s-*trans* structure,[1] it is interesting to examine the difference in its reactivity from β-amino-enones of other types. Recently, we reported on the protonation, oxidation, reduction,[2] photoisomerization,[3] and the relation between the structure and the spectral properties of dihydropyridone.

The present paper will describe the aldol condensation of dihydropyridone and related reactions.

6-Methyl-1,2-diphenyl-2,3-dihydro-4-pyridone (**1**) was treated with benzaldehyde in an alkaline ethanol solution. The expected condensation product at C-3 methylene was not detected, but an unexpected product, 1,2-diphenyl-6-styryl-2,3-dihydro-4-pyridone (**2**) was obtained in a 33% yield. From the spectral data and elemental analyses, the structure of **2** was determined.

The mechanism of the formation of **2** can be explained as follows: C-6 methyl is more active than C-3 methylene, and benzaldehyde condenses at C-6 methyl to give 6-(β-hydroxyphenethyl)-1,2-diphenyl-2,3-dihydro-4-pyridone (**3**), which then produces **2** by the elimination of water.

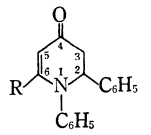

1: R=-CH_3
2: R=-CH=CH-C_6H_5
3: R=-$CH_2CHC_6H_5$ (OH)
4: R=-$CH_2CH_2C_6H_5$

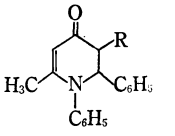

5: R=-$CH_2C_6H_5$
7: R=-CH·C_6H_5 (OH)

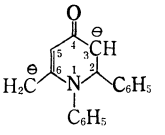

6

Fig. 1.

For the purpose of confirming this, the alkylation reaction of **1** with benzyl bromide was carried out in the presence of an equimolar sodium amide in liquid ammonia.[4] If C-6 methyl is more reactive than C-3 methylene, the alkylation product at C-6 methyl, 6-phenethyl-1,2-diphenyl-2,3-dihydro-4-pyridone (**4**), may be expected to be produced. In fact, dihydropyridone **4** was obtained, and a trace of the alkylation product at C-3 methylene,

1) C. Kashima, M. Yamamoto and N. Sugiyama, *J. Chem. Soc., C*, **1970**, 111.

2) C. Kashima, M. Yamamoto and N. Sugiyama, This Bulletin, **42**, 2690 (1969).

3) C. Kashima, M. Yamamoto, Y. Sato and N. Sugiyama, *ibid.*, **42**, 3596 (1969).

4) N. Sugiyama, M. Yamamoto and C. Kashima, *ibid.*, **42**, 1357 (1969).

3-benzyl-6-methyl-1,2-diphenyl-2,3-dihydro-4-pyridone (**5**), was detected.

The formation of **5** shows that C-3 methylene has a reactivity. In order to confirm this, **1** was treated with benzaldehyde in the presence of two molar equivalents of sodium amide in liquid ammonia. When two molar equivalents of a base are used in liquid ammonia, the dianione (**6**) of **1** will be produced, and it is expected that the C-3 methylene position will be more reactive than that of C-6 methyl, much as is the case with the dipotassium salt of acetylacetone in liquid ammonia.[5]

From the reaction mixture, 3-(α-hydroxybenzyl)-6-methyl-1,2-diphenyl-2,3-dihydro-4-pyridone (**7**) was obtained in a 25.5% yield. No condensation product at C-6 methyl was detected. The structure of **7** was proved by the spectral data and by the results of elemental analyses.

The C-6 methyl of dihydropyridone **1** is the most reactive in the molecule, and aldol condensation occurred at this position. This is a novel type of aldol condensation. C-3 methylene has some reactivity in liquid ammonia, but this position is less reactive than C-6 methyl.

Experimental

6-Methyl-1,2-diphenyl-2,3-dihydro-4-pyridone (1). Compound **1** was prepared from acetylacetone and benzylidenaniline in the presence of three moles of potassium amide in liquid ammonia.[4] NMR (in $CDCl_3$): τ 8.13 (singlet, 3H, C-6 methyl protons), 7.09 (double quartet, 2H, C-3 methylene protons), 5.08 (quartet, 1H, C-2 methine proton), 4.81 (singlet, 1H, C-5 olefin proton), and 2.6—3.2 (multiplet, 10H, aromatic protons).

1,2-Diphenyl-6-styryl-2,3-dihydro-4-pyridone (2). To a solution containing 0.5 g of **1** and 0.3 g of benzaldehyde in 20 m*l* of ethanol, a 5% sodium hydroxide solution (10 m*l*) was added. The reaction vessel was closed with a rubber stopper to prevent oxidation, and, after shaking for 10 min, the mixture was left to stand at room temperature for 12 hr. The mixture was then poured into 50 g of crushed ice and 200 m*l* of water, and acidified with dilute hydrachloric acid. The aqueous solution was extracted with chloroform. The organic layer was washed with water two times, and then dried over calcium chloride. After the removal of the solvent, the residue was chromatographed on a silica-gel (Merck 7729) column with a benzene - ethyl acetate (4 : 1 *v/v*) mixture. A fraction which showed R_f 0.35 upon silica-gel (Wako gel B-5) thin-layer chromatography with a benzene - ethyl acetate (4 : 1 v/v) mixture was collected to give 220 mg (33%) of **2**, as yellow plates; mp 164—165°C.

Found: C, 85.06; H, 6.11; N, 3.97%. Calcd for $C_{25}H_{21}NO$: C, 85.44; H, 6.02; N, 3.99%.
IR (KBr): 1630, 1535, 755 and 690 cm^{-1}.
UV: λ_{max}^{EtOH} 236 (ε 14200), 314 mμ (ε 20600).
$\lambda_{max}^{HCl/EtOH}$ 235 (ε 11900), 353 mμ (ε 28900).
NMR (in $CDCl_3$) (τ): 7.25, 6.69 (double quartet, 2H, C-3 methylene protons), 4.86 (quartet, 1H, C-2 methine proton), 4.80 (singlet, 1H, C-5 olefin proton), 3.58 (doublet, 1H, α-olefin proton of the C-6 styryl group, $J_{\alpha\beta}=16.5$ Hz) and 2.56—2.90 (multiplet, 16H, β-olefin proton of the C-6 styryl group and aromatic protons).

The Condensation of 1 with Benzyl Bromide. In a 200-m*l*, three-necked flask, about 150 m*l* liquid was placed; 0.20 g of metalic sodium was then added to produce sodium amide. To this solution 2.0 g of **1** was added, and it was stirred for an hour; then equimolar benzyl bromide (1.23 g) in 10 m*l* of anhydrous ether was added. After stirring for one hour, the mixture was neutralized with excess solid ammonium chloride. The liquid ammonia was rapidly evaporated on a water bath, and to the residue there was added about 100 m*l* of water. The aqueous layer was extracted with ether, and the ethereal layer was washed with water and dried over anhydrous sodium sulfate. The formation of **4** and **5** was confirmed by thin-layer chromatography by a comparison of their R_f values with those of authentic specimens.[4]

3-(α-hydroxybenzyl)-6-methyl-1,2-diphenyl-2,3-dihydro-4-pyridone (7). In the presence of two molar equivalents of sodium amide, 1.32 g of **1** were allowed to react with equimolar benzaldehyde. The crude reaction product was purified by silciag-el (Merck 7729) column chromatography. The eluting solvent: benzene - ethyl acetate (2 : 1 v/v). Yield, 0.47 g of **7** (25.5%); colorless prisms; mp 122—123°C.

Found: C, 81.12; H, 6.30; N, 3.63%. Calcd for $C_{25}H_{23}NO_2$: C, 81.26; H, 6.28; N, 3.79%.
IR (KBr): 3380, 1625, 1550, 710 and 695 cm^{-1}.
UV: λ_{max}^{EtOH} 338 mμ (ε 16900).
NMR (in $CDCl_3$) (τ): 8.00 (singlet, 3H, methyl protons), 7.20 doublet, 1H, methine proton), 5.63 (singlet, 1H, methine proton), 5.01 (doublet, 1H, methine proton), 4.69 (singlet, olefin proton), 2.72—3.24 (multiplet, 15H, aromatic protons) and 6.25—7.20 (broad, 1H, hydroxy proton, disappeared by D_2O).

The Treatment of 7 with Concentrated Sulfuric Acid. To 200 mg of **7**, 10 m*l* of concentrated sulfuric acid were added; the mixture was then allowed to stand at room temperature for two hours. To the reaction mixture were added about 50 g of crushed ice, and the resulting suspension was extracted with chloroform. The chloroform layer was washed with water and then dried over calcium chloride. However, the expected product, **8** or **9**, was not detected by thin-layer chromatagraphy.[6]

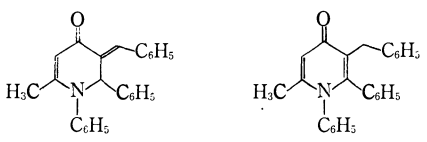

8 **9**

Fig. 2.

5) C. R. Hauser and T. M. Harris, *J. Amer. Chem. Soc.*, **80**, 6360 (1958).

6) G. R. Clemo and H. J. Johnson, *J. Chem. Soc.*, **1930**, 2136.

BULLETIN OF THE CHEMICAL SOCIETY OF JAPAN VOL. 43 3939—3940 (1970)

The Conformation of Acid Form γ-Polyglutamic Acid

Takehiko WATANABE, Takafumi INA, Kozo OGAWA,* Takeshi MATSUMOTO, Sumihiko SAWA** and Sôzaburo ONO

*Laboratory of Biophysical Chemistry and** Laboratory of Fermentational Chemistry, College of Agriculture, University of Osaka Prefecture, Sakai*
** Radiation Center of Osaka Prefecture, Shinke-cho, Sakai*

(Received June 22, 1970)

In the previous paper,[1] the dissolved state of γ-polyglutamic acid solution at different pH's was studied by means of rotatory dispersion, flow birefringence and intrinsic viscosity. And it was reported that the polymer molecule in neutral and alkaline media will be in the form of a highly expanded chain while that in acid medium in a contracted form having a some ordered chain conformation. Edelhoch and Lippoldt[2] reported that γ-poly-D-glutamate obtained from the capsule of *Bacillus anthracis* exists in a hydrogen-bonded hyper coiled form in water at low degrees of ionization. Later Rydon[3] suggested that the unionized acid form polymer possesses a helical structure from the optical rotatory dispersion measurement from 250 to 600 mμ.

In the present paper, the conformation of γ-polyglutamic acid in acid form was studied by rotatory dispersion and infrared spectra.

Experimental

Materials. γ-polyglutamic acid, or γ-PGA is a polymer of glutamic acid linked through the γ-carboxyl and α-amino group and is produced by the *Bacillus subtilis* No. 5E[4] from glucose and urea. γ-PGA is isolated by the NaCl-alcohol precipitation method[5] from the culture. The extracted γ-PGA was dissolved in 3% NaCl and 30—35% alcohol aqueous solution and centrifuged for the removal of cells, and then precipitated by pouring the centrifuged solution in alcohol. This procedure was repeated and the centrifuged solution was dialyzed against distilled water until free of chloride and the dialyzed solution was lyophilized. Thus obtained sample is the sodium salt of γ-PGA (Naγ-PGA) and its intrinsic viscosity obtained in 10% NaCl solution at 25°C is 4.71 dl/g and sedimentation constant at infinite dilution (in 10% NaCl solution) is 6.80×10^{-13}. The molecular weight calculated by Mandelkern and Flory equation[6] is 1×10^{6}. To obtain the acid form γ-PGA (Hγ-PGA), the Naγ-PGA was successively treated with ion exchange resin Dowex-50, Amberlite IRA-400 and Dowex-50 as the 0.2% aqueous solution and the treated solution was lyophilized. Both Naγ-PGA and Hγ-PGA were hydrolyzed with 6N HCl at 105—110°C for 15—24 hr. Degree of optical rotation of both hydrolyzed samples was coincided with that of the mixture of 75% D-glutamic acid and 25% L-anomer.

Measurements. Optical rotatory dispersion measurement was carried out with a Yanagimoto ORD-185. Mean residual rotation [R] was calculated as the correction factor $3\overline{M}/100\ (n_\lambda^2+2)\fallingdotseq1$, where $\overline{M}$ is mean residual weight of glutamic acid and n_λ is the refractive index of solvent.

Infrared spectra was measured using a Perkin-Elmer Spectrophotometer Model 221.

Results and Discussion

The optical rotatory dispersion curves of Hγ-PGA at pH=9.0, 4.7 and 2.5 are shown in Fig. 1. The curves show a negative Cotton effect with a trough at 230 mμ*1 and the depth of the trough becomes deeper with decreasing in pH. According to Sarkar and Doty[7] and Iizuka and Yang[8], the appearance of the trough at 230 mμ on optical rotatory dispersion curve suggests that the polymer dissolved in acid medium is in a β-form, not the helical structure which was proposed by Rydon[3] under the deficiency of the data obtained from the optical rotatory measurement at lower wavelength below 250 mμ, where the Cotton effect is

1) T. Mineshita, S. Matsumura, H. Ono, T. Watanabe and S. Ono, This Bulletin, **42**, 594 (1969).
2) H. Edelhoch and R. E. Lippoldt, *Biochem. Biophys. Acta*, **45**, 205 (1960).
3) H. N. Rydon, *J. Chem. Soc.*, **1964**, 1328.
4) S. Murao, T. Murakawa, S. Sawa, S. Okumura and S. Omata, *Nippon Nogei Kagaku Kaishi*, **43**, 595 (1969).
5) S. Sawa, S. Murao, T. Murakawa and S. Omata, will be published in *Nippon Nogei Kagaku Kaishi*.
6) L. Mandelkern and P. J. Flory, *J. Chem. Phys.*, **20**, 212 (1952).

*1 In the previous paper (Ref. 1, Fig. 6), a deep trough due to Cotton effect was observed at 225 mμ and a shallow trough was observed on curves at the wavelength of 260—270 mμ. The discrepancies of the results from that of the present one may be brought about by the coexistence of unknown substance (in small amounts) which has a absorption peak at 260—270 mμ. The substance was almost perfectly eliminated from the γ-PGA in the course of the treatment with the ion exchange resins.

7) P. K. Sarkar and P. Doty, *Pro. Nat. Acad. Sci. U.S.*, **55**, 981 (1966).
8) E. Iizuka and J. T. Yang, *ibid.*, **55**, 1175 (1966).

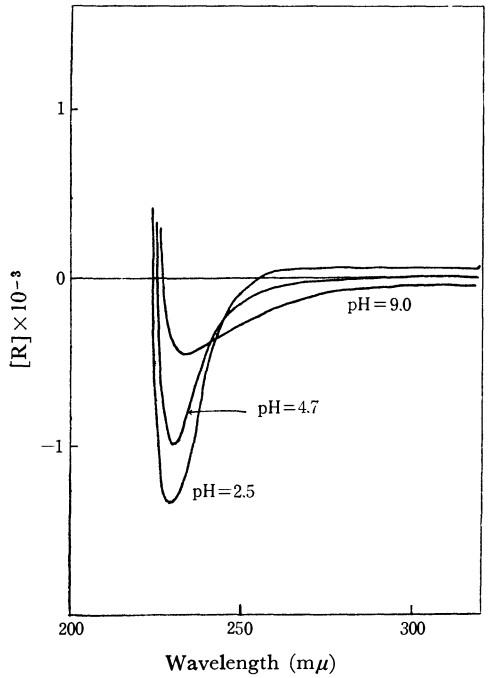

Fig. 1. Optical rotatory dispersion curves of Hγ-PGA at different pH's.

observed. With the value of [R], the negative value is obtained at 230 mμ and this result corresponds to the one reported in literature for α-linked L-polymer,[7,8] in spite of the presence of large excess amounts of D-polymer. The magnitude of the value of [R] expected for pure D-polymer at pH=2.5, is $-1350 \times 2 = -2700$, if we assume a compensative effect on the value of [R] between D- and L-polymer based on the composition ratio of D : L=3 : 1. However, this value of −2700 is far different from the value of $[R] = -6 \times 10^3$ reported for α-linked L-polymer.[7,8]

The infrared spectra of Naγ-PGA and Hγ-PGA obtained with KBr disc method are shown in Fig. 2. With Hγ-PGA, the amide I bands were observed at 1630 cm^{-1} (strong) and 1650 cm^{-1} (weak) and the amide II bands were observed at 1530 cm^{-1}

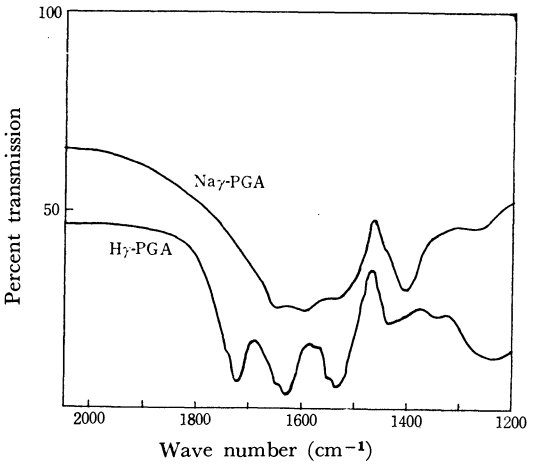

Fig. 2. Infrared spectra of Hγ-PGA and Naγ-PGA.

(strong) and 1550 cm^{-1} (weak), indicating that the Hγ-PGA is in the β-form, according to the results obtained with α-linked polymers by Miyazawa and Blout[9] and Masuda *et al.*[10] With Naγ-PGA, the amide I and II bands in disordered form (random coil)[9,10] were observed at 1655 and 1535 cm^{-1}, respectively, however these bands are quite diffuse due to the overlapping by the band due to the COO^- groups around 1600 cm^{-1}. The above result was obtained with the lyophilized polymer, however, the same conformation may be taken in solution, because the infrared spectrum obtained with acid form α-poly-D-glutamic acid (product of Miles-Yeda Ltd.) by KBr disc method shows the characteristic spectrum of α-helix.

From the above result, γ-PGA molecule will be mostly in a β-form in acid medium and will take a contracted form with folding of the sheet of β-form molecule, as stated in the previous paper.[1]

9) T. Miyazawa and E. R. Blout, *J. Amer. Chem. Soc.*, **83**, 712 (1961).

10) Y. Masuda, K. Fukushima, T. Fujii and T. Miyazawa, *Biopolymers*, **8**, 91 (1969).

BULLETIN OF THE CHEMICAL SOCIETY OF JAPAN VOL. 43 3941—3942 (1970)

The Reaction of 3-Methyl-5-methylmercapto-2,4-diphenylthiazolium Iodide with Bases. Preparation of Mesoionic Imidazoles

Toshie SHIBA and Hiroshi KATO*1

Department of Chemistry, Faculty of Science, Shinshu University, Asahi, Matsumoto

(Received June 23, 1970)

In connection with our interest in photolyses and pyrolyses of mesoionic compounds in general,[1] we needed a convenient synthetic approach for various mesoionic ring systems. For this purpose, mesoionic oxazol-5-one derivatives, first prepared by Huisgen and his collaborators[2], are ideal starting materials. The preparation of several mesoionic compounds by the reaction of 3-methyl-2,4-diphenyloxazol-5-one (I) and a few hetero-cumulenes has previously been described.[3] Further, the phenyl isothiocyanate adduct, mesoionic 1-methyl-2,3,5-triphenylimidazole-4-thione (II, R=Ph), has been reported to isomerize to mesoionic *N*-phenyl-3-methyl-2,4-diphenyl-thiazol-5-imine (III, R=Ph) by hydrogen chloride.[3] Since we were unable to reproduce this rearrangement under various conditions, we attempted to prepare this compound *via* methylmercaptothiazolium salt.

The treatment with methyl iodide of mesoionic 3-methyl-2,4-diphenylthiazole-5-thione (IV), prepared by the reaction of I and carbon disulfide,[3] gave the corresponding *S*-methyl salt, 3-methyl-5-methylmercapto-2,4-diphenylthiazolium iodide (V). It was anticipated that the methylmercaptothiazolium salt V would give the corresponding imines, III, by the reaction with amines.[4]

The treatment of V with methylamine gave a product with a composition in agreement with the expected mesoionic imine (III. R=Me), but the NMR methyl signals (τ 6.33 and 6.55) suggested that the two methyl groups are substituted on aromatic-ring nitrogen atoms. Further, its infrared spectrum showed no absorption in the region expected for an imine group, but, instead, absorptions at 1310 and 1071 cm^{-1}, regions earlier assigned to an azole-thione structure.[5] These spectral data strongly suggest that the product is 1,3-dimethyl-2,5-diphenylimidazole-4-thione (II, R=Me). To support further this structural assignment, it was treated with methyl iodide to give methiodide VI (R=Me), the NMR spectrum of which, showing a new methyl signal at τ 7.55 (*S*-Me), is thus wholly consistent with the proposed structure. This is the first example of a mesoionic imidazole-4-thione with an aliphatic substituent on the 3-position; thus, this reaction sequence may be regarded as an attractive synthetic route for this type of compounds.[6]

The reaction of V and aniline took a different course, and gave another quaternary salt, the NMR spectrum of which exhibits the presence of two types of methyl groups by signals at τ 6.33 and 7.85. This suggests that the product is 1-methyl-4-methylmercapto-2,5-diphenylimidazolium iodide (VI, R=Ph); it was identified as such by comparison with a specimen prepared by the methylation of II (R=Ph)[3] by methyl iodide. The two iodides VI (R=Me and Ph) were no longer reactive to aniline or methylamine, even under forcing conditions.

The reaction of imidazolium iodides, VI, with alkali may be expected to give mesoionic imidazol-4-ones, VII, but this reaction only gave resinous products. The expected imidazolone (VII, R=Ph), however, could be prepared by the cycloaddition reaction of I with phenyl isocyanate. In this case, in contrast to the reactions with other hetero-cumulenes, the corresponding cycloadduct, VIIIa or VIIIb, was isolated; this was converted to the imidazolone VII by the elimination of carbon dioxide only after heating in xylene. To date, this compound is the only example of a non-fused

*1 To whom inquires should be addressed.

1) For a review of mesoionic compounds, see, M. Ohta and H. Kato, "Nonbenzonoid Aromatics," ed. by J. P. Snyder, Academic Press, New York (1970), p. 117.

2) R. Huisgen, H. Gotthardt, H. O. Bayer and F. C. Schaefer, *Angew. Chem.*, **76**, 185 (1964).

3) R. Huisgen, E. Funke, F. C. Schaeffer, H. Gotthardt and E. Brunn, *Tetrahedron Lett.*, **1967**, 1809.

4) For a similar type of reactions, see, K. Ichimura and M. Ohta, This Bulletin, **38**, 707 (1965).

5) M. Ohta, H. Kato and T. Kaneko, *ibid.*, **40**, 579 (1967), and references cited therein. See also, S. Sato and M. Ohta, *ibid.*, **42**, 2054 (1969); F. Kröhnke and H. H. Steuernagel, *Chem. Ber.*, **97**, 1118 (1964); L. B. Kier and M. K. Scott, *J. Heterocycl. Chem.*, **5**, 277 (1968); T. G. Stewart and L. B. Kier, *J. Pharm. Sci.*, **54**, 731 (1965).

6) The preparation of compounds of this type by the reaction of I and aliphatic isothiocyanate was unsuccessful: T. Shiba and H. Kato, unpublished results.

mesoionic imidazol-4-one with no acyl substituents.[7]

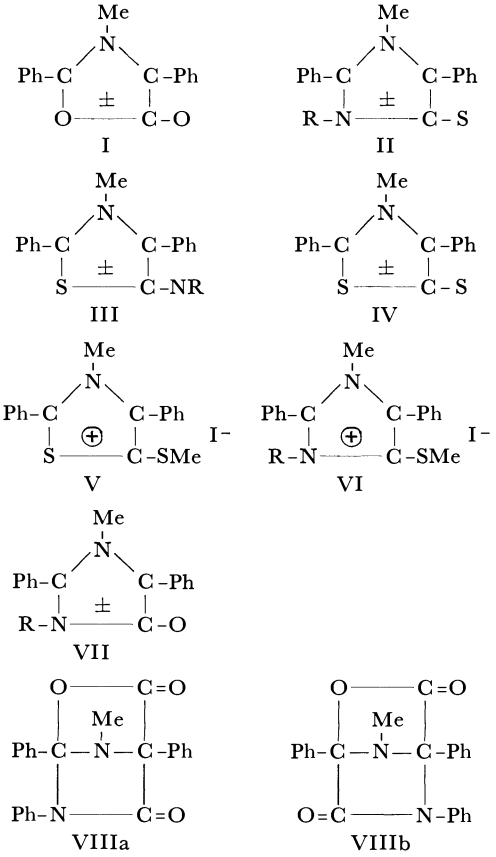

Experimental[8]

3-Methyl-5-methylmercapto-2,4-diphenylthiazolium Iodide (V). A mixture of 1 g of IV[3] and 0.6 g of methyl iodide in 10 m*l* of ethanol was stirred at room temperature for two hours. Ether was then added to the mixture, and the precipitate was recrystallized from ethanol to give 1.06 g (70% yield) of pale yellow prisms melting at 133—134°C. NMR: 1.84—2.50 (m, 10H, Ph), 6.12 (s, 3H, *N*-Me), 7.46 τ (s, 3H, *S*-Me).

Found: C, 48.26; H, 3.80; N, 3.19%. Calcd for $C_{17}H_{16}NS_2I$: C, 48.00; H, 3.76; N, 3.29%.

Mesoionic 1,3-Dimethyl-2,5-diphenylimidazole-4-thione (II, R=Me). A mixture of 1 g of V, 3 m*l* of 30% aqueous methylamine, and 10 m*l* of ethanol was stirred at room temperature for ten hours. The mixture was then concentrated, and the crystals which seperated out were recrystallized from ethanol to give 0.6 g (90% yield) of pale yellow needles melting at 191—192°C. IR (cm^{-1}): 1310, 1071. NMR: 2.20—2.72 (m, 10H, Ph), 6.33 τ (s, 3H, Me), 6.55 τ (s, 3H, Me).

Found: C, 72.36; H, 5.70; N, 9.67%. Calcd for $C_{17}H_{15}N_2S$: C, 72.83; H, 5.75; N, 9.99%.

1,3-Dimethyl-4-methylmercapto-2,5-diphenylimidazolium Iodide (VI. R=Me). A mixture of 0.5 g of II (R=Me) and 0.3 g of methyl iodide in 3 m*l* of ethanol was stirred at room temperature for two hours; the crystals which separated out were recrystallized from ethanol to give 0.6 g (80% yield) of colorless prisms melting at 175.8—176.7°C. NMR: 1.90—2.45 (m, 10H, Ph), 6.20 (s, 3H, *N*-Me), 6.50 (s, 3H, *N*-Me), 7.55 τ (s, 3H, *S*-Me).

Found: C, 51.20; H, 4.54; N, 6.60%. Calcd for $C_{18}H_{19}N_2SI$: C, 51.16; H, 4.50; N, 6.63%.

1-Methyl-4-methylmercapto-2,3,5-triphenylimidazolium Iodide (VI, R=Ph). a) A mixture of 0.7 g of V, 0.5 g of aniline, and 10 m*l* of *n*-butanol was refluxed for ten hours. Ether was added to the concentrated mixture, and the precipitate was crystallized from ethanol to give 0.5 g (60% yield) of colorless prisms melting at 236—237°C. NMR: 1.41—2.20 (m, 5H, Ph), 2.40—2.70 (m, 10H, Ph), 6.33 (s, 3H, *N*-Me), 7.85 τ (3H, *S*-Me).

Found: C, 56.66; H, 4.33; N, 5.24%. Calcd for $C_{23}H_{21}N_2SI$: C, 57.03; H, 4.37; N, 5.78%.

b) A solution of 1 g of II (R=Ph)[3] and 0.53 g of methyl iodide in 10 m*l* of acetone was stirred for two hours at room temperature. The solution was then concentrated, and the precipitate was recrystallized from ethanol to give 1.0 g (70% yield) of colorless prisms melting at 236—237°C, identical with the specimen prepared by Procedure **a**.

Phenyl Isocyanate Adduct of I (VIII). A solution of 5 g of I and 4.5 g of phenyl isocyanate in 100 m*l* of xylene was stirred at 70°C for four hours. The mixture was then concentrated, and ether was added; the precipitate was recrystallized from benzene to give 5.5 g (90% yield) of colorless prisms melting at 160—161°C. IR (cm^{-1}): 1735 (lactone C=O), 1640 (lactam C=O). NMR: 2.08—2.29 (m, 5H, Ph), 2.40—2.80 (m, 10H, Ph), 7.28 τ (s, 3H, Me).

Found: C, 74.50; H, 4.70; N, 7.50%. Calcd for $C_{23}H_{18}N_2O_3$: C, 74.59; H, 4.86; N, 7.46%.

Mesoionic 1-Methyl-2,3,5-triphenylimidazol-4-one (VII, R=Ph). A solution of 1 g of the adduct VIII in 30 m*l* of xylene was heated under reflux for thirty minutes. The solution was concentrated and then petroleum ether was added; the precipitate which separated out was recrystallized from acetone to give 0.2 g (23% yield) of pale yellow prisms melting at 190—192°C. IR (cm^{-1}): 1650 (C=O). NMR: 2.50—3.05 (m, 15H, Ph), 6.97 τ (s, 3H, Me).

Found: C, 81.75; H, 5.87; N, 9.14%. Calcd for $C_{22}H_{18}N_2O$: C, 82.21; H, 5.52; N, 8.59%.

We are indebted to Professor Masaki Ohta of Tokyo Institute of Technology and to Professor Kameji Yamane of this Department for discussion and encouragement.

7) The preparation of mesoionic 5-acylimidazol-4-ones by way of a different route has been reported: A. Lawson and D. H. Miles, *J. Chem. Soc.*, **1959**, 2865. After the completion of this work, a report on the preparation of a mesoionic imidazol-4-one which also has an acetyl substituent on the 5-position has appeared: E. B. Roche and D. W. Stansloski, *J. Heterocycl. Chem.*, **7**, 139 (1970).

8) All melting points were determined on a micro hot stage, and are uncorrected. The infrared spectra were recorded as KBr disks on a Hitachi model EPI-SII Spectrophotometer. The NMR spectra were measured using a JEOLCO JNM-4H-100 (100 MHz) Spectrometer in deuteriochloroform solutions containing tetramethylsilane as internal standard, and the chemical shifts are given in τ values.

BULLETIN OF THE CHEMICAL SOCIETY OF JAPAN VOL. 43 3943—3945 (1970)

Triplet-State Zero-Field Splittings. III.[1] Effect of the Two-Center Coulomb Repulsion Integrals

Yasuhiko GONDO and Yoshiya KANDA

Department of Chemistry, Faculty of Science, Kyushu University, Hakozaki, Fukuoka

(Received June 29, 1970)

We here report that a Pariser-Parr-type approximation[2] for the two-center Coulomb repulsion integrals yields much better triplet-state zero-field splitting (ZFS) parameters for aromatic hydrocarbons and nitrogen heterocycles than the Nishimoto-Mataga-type approximation.[3] Compounds studied are shwon in Fig. 1 with a coordinate system adopted.

In our previous paper,[1] it was shown that the SCF-AO's expanded by Löwdin are useful for the calculation of the electron spin dipolar interactions in the triplet-state ZFS's of aromatic molecules, and particularly for the ZFS calculation the SCF-AO's have formally replaced the Slater AO's used in the wavefunction calculation. In other words, the SCF-AO's have been used for the evaluation of the electron spin dipolar interactions in combination with a set of approximations consisting of (1) the π-electron approximation (Pariser-Parr-Pople method),[2,4] (2) the use of configurations which are only singly excited with respect to the lowest-energy singlet configuration for the triplet-state wavefunctions, and (3) the two-center integral approximation for the electron spin dipolar interactions.

Thus, in Part I[1] we have obtained excellent agreement with experiments for benzene and naphthalene, and also some promising results for aromatic nitrogen heterocycles such as quinoline and isoquinoline, as shown in Table 1 under the heading of Eq. (1), employing the following Nishimoto-Mataga-type formula of the two-center Coublomb repulsion integrals for all interatomic distances R_{pq},

$$(pp|qq) = 6.588/(Z_p^{-1}+Z_q^{-1}+0.457529\,R_{pq})\ \text{eV}, \quad (1)$$

where R_{pq} is given in angstroms, and Z_p stands for the effective nuclear charge of the p-th $2p\pi$AO and was given 3.25 and 3.90 for carbon and nitrogen, respectively. Eq. (1) was obtained by combining the approximations proposed by Paoloni[5]

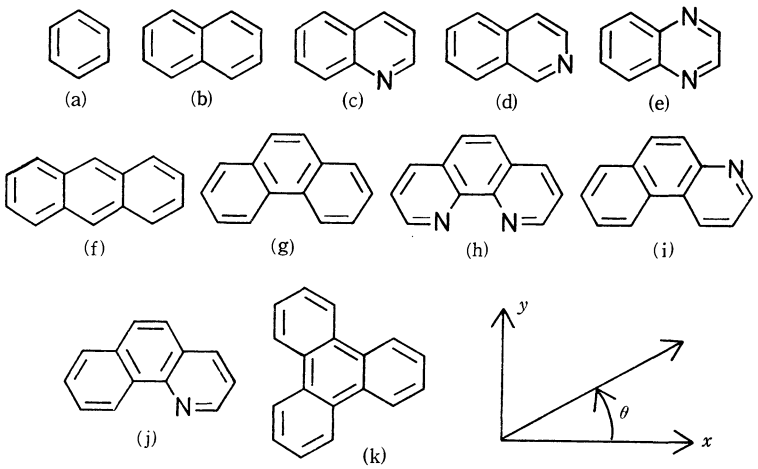

Fig. 1 Compounds studied in this work, with coordinate axes: (a) benzene, (b) naphthalene, (c) quinoline, (d) isoquinoline, (e) quinoxaline, (f) anthracene, (g) phenanthrene, (h) 1,10-phenanthroline, (i) 5,6-benzoquinoline, (j) 7,8-benzoquinoline, (k) triphenylene.

1) Y. Gondo and A. H. Maki, *J. Chem. Phys.*, **50**, 3270, 3638 (1969), called Parts I and II of this series, respectively.

2) R. Pariser and R. G. Parr, *ibid.*, **21**, 466, 767 (1953).

3) K. Nishimoto and N. Mataga, *Z. Phys. Chem.* (Frankfurt), **12**, 335 (1957).

4) J. A. Pople, *Trans. Faraday Soc.*, **49**, 1375 (1953),

5) L. Paoloni, *Nuovo Cimento*, **4**, 410 (1956).

Table 1. Calculated and observed ZFS parameters for the lowest excited triplet states of some aromatic hydrocarbons and nitrogen heterocycles[a] (cm^{-1})

Compound	Calculated						Observed			
	Formulas for $(pp\|qq)$ integrals									
	Eq. (1)[b]			Eq. (2)[c]						
	D	E	θ[d]	D	E	θ[d]	D	E	θ[d]	Ref.
Benzene	0.1598			0.1565			0.1581	0.0064		8
Naphthalene	0.1142	−0.0281		0.1027	−0.0243		0.10119	−0.01411		9
Quinoline	0.1180	−0.0352	5.1°	0.1054	−0.0293	3.8°	±0.1030	∓0.0162	±13°	10
Isoquinoline	0.1191	−0.0301	14.8°	0.1033	−0.0249	14.7°	±0.1004	∓0.0117	±25°	10
Quinoxaline	0.1225	−0.0406		0.1101	−0.0347		±0.1007	∓0.0182		10
Anthracene	0.0836	−0.0161		0.0747	−0.0117		0.072	−0.007		11
Phenanthrene	0.1197	−0.0475		0.1102	−0.0537		0.10044	−0.04658		9
1,10-Phenanthroline	0.1277	−0.0493		0.1158	−0.0564		±0.1038	∓0.0485		12
5,6-Benzoquinoline	0.1219	−0.0461	−5.0°	0.1105	−0.0544	−17.6°	±0.1023	∓0.0477		12
7,8-Benzoquinoline	0.1233	−0.0495	−3.2°	0.1113	−0.0565	−12.0°	±0.1011	∓0.0468		12
Triphenylene	0.1374			0.1316			±0.134			13

a) For the coordinate axes, see Fig. 1.
b) Ref. 1 and this work.
c) For $R_{pq}>2.8$ Å, the multipole expansion formula has been used. See text.
d) Principal axis direction of the ZFS tensor as defined in Fig. 1.

and by Nishimoto and Mataga.[3]

In this note the following quadratic Pariser-Parr-type expression,[6]

$$(pp|qq) = 3.294Z + (3.836-1.993Z)R_{pq} - (0.7661-0.3004Z)R_{pq}^2 \text{ eV}, \quad (2)$$

where $Z=1/2(Z_p+Z_q)$, is employed for $R_{pq}\leq 2.8$ Å, and for $R_{pq}>2.8$ Å a multipole expansion formula.[7] Eq. (2) is derived through the Paoloni approximation[5] and the application of the multipole expansion formula for $R_{pq}=2.8$ and 3.7 Å.[2] The ZFS parameters calculated with this approximation are shown in the columns under the heading Eq. (2), of Table 1. The whole computational scheme is the same as Method 1 of Part I, namely the SCF-AO's are used for all interatomic distances in evaluating the electron spin dipolar interactions.

Comapring the data calculated with the observed ZFS parameters given in Table 1, it can be concluded that the Pariser-Parr-type formula is much better than the Nishimoto-Mataga-type formula at least for the triplet-state ZFS calculation. For quinoxaline, phenanthrene and azaphenanthrenes, agreement with experiments is not so good as that for the other compounds listed in Table 1, although considerably improved. The reason for this is not clear at present.

We are grateful to the Kyushu University Computer Center for the use of its facilities.

6) Y. Gondo and Y. Kanda, to be submitted to this Bulletin.

7) R. G. Parr, *J. Chem. Phys.*, **33**, 375 (1960).

8) M. S. de Groot, I. A. M. Hesselmann and J. H. van der Waals, *Mol. Phys.*, **16**, 45 (1969).

9) R. W. Brandon, R. E. Gerkin and C. A. Hutchison, Jr., *J. Chem. Phys.*, **37**, 447 (1962).

10) J. S. Vincent and A. H. Maki, *ibid.*, **39**, 3088 (1963); **42**, 865 (1965).

11) J. H. van der Waals and G. ter Maten, *Mol. Phys.*, **8**, 301 (1964).

12) Y. Gondo and A. H. Maki, *J. Phys. Chem.*, **72**, 3215 (1968).

13) M. S. de Groot and J. H. van der Waals, *Mol. Phys.*, **3**, 190 (1960); J. B. Farmer, C. L. Gardner and C. A. McDowell, *J. Phys. Chem.*, **69**, 953 (1965).

BULLETIN OF THE CHEMICAL SOCIETY OF JAPAN VOL. 43 3945—3947 (1970)

Drynap Reduction. IV. The Reduction of Cyclic Styrene Derivatives with a Commercial Sodium-Lead Alloy

Katsumi TABEI and Kouichi TAKAZAWA

Tokyo College of Pharmacy, Kitashinjuku, Shinjuku-ku, Tokyo

(Received July 2, 1970)

In a previous paper of this series, one of the present authors reported that a commercial sodium-lead alloy, "Drynap", can be used as a reducing agent in the reduction of α,β-unsaturated carbonyl compounds in place of a sodium amalgam.[1]

In the present experiment, the alloy was used in the reduction of four cyclic styrene derivatives: coumarin, isocoumarin, *N*-methylcarbostyril, and isocarbostyril. A little of the information thus obtained will be reported here.

The reduction of coumarin with Drynap in an aqueous sodium hydroxide solution was attempted using the method of Erlenmeyer[2]; 3,4-dihydrocoumarin was thus obtained in about a 70% yield, as was expected. Isocoumarin, *N*-methylcarbostyril, and isocarbostyril were not reduced with the alloy in an aqueous solvent; isocoumarin was, thereby polymerized in an alkaline solution, even in the cold, and a yellowish brown tar was obtained. *N*-methylcarbostyril and isocarbostyril were recovered almost quantitatively.

In an ethanolic solution, coumarin was reduced with Drynap to 3,4-dihydrocoumarin in a 20% yield, but the main products were two isomers of 3,3′,4,4′-tetrahydro-4,4′-bicoumarin (the total yield of the mixture was about 50%). The mixture was separated by the method of Asahina and Fujita *via* the fractional crystallization of the corresponding carboxylic acid.[3] and two compounds which were difficult to separate were thus obtained: a less soluble isomer, mp 278—280°C (decomp.), and a more soluble one, mp 246—248°C (decomp.). Harle and Lyons have already assigned the above two isomers to the meso and

1) K. Tabei, H. Hiranuma and N. Amemiya, This Bulletin, **39**, 1085 (1966).

2) A. Erlenmeyer, *Ann. Chem.*, **121**, 375 (1862); **137**, 334 (1866).

3) Y. Asahina and Y. Hujita, *Yakugaku Zasshi*, **444**, 97 (1915).

4) A. J. Harle and L. W. Lyons, *J. Chem. Soc.*, **1950** 1575.

racemic forms respectively.[4] The IR and NMR spectra of the compound can not be discussed in detail in the present report.

The NMR spectra of the latter compound, the more soluble isomer, revealed doublet signals of methylene protons attached to the carbonyl group at 6.92 τ (4H), and triplet signals of the methine proton attached to the phenyl group at 7.00 τ (2H), in the deuteriochloroform solution, so it is certain that the dihydrocoumarin rings are united at the 4-position.

N-Methylcarbostyril was reduced with Drynap in the manner which has been described for use with coumarin; a new dimeric reduction product, $C_{20}H_{20}N_2O_2$, (mp 284—286°C) was thus obtained in about a 60% yield. The mass spectra of the dimer gave a characteristic peak of the monomer ion at *m/e* 160 as well as the molecular ion peak at *m/e* 320. The out-of-plane deformation vibration of olefinic hydrogen of *N*-methylcarbostyril disappeared in the IR spectra of the dimer, and the carbonyl stretching mode of the dimer absorbed in a wavelength region shorter by 12 cm^{-1} at 1673 cm^{-1}. The NMR spectra of the dimer exhibit the doublet signals of methylene protons adjacent to carbonyl group at 7.37 τ (4H). and triplet signals of the methine proton adjacent to the phenyl ring at 7.17 τ (2H), in the deuteriochloroform solution. The product can thus be identified as 3,3′,4,4′-tetrahydro-1,1′-dimethyl-4,4′-bicarbostyril.

Isocoumarin and isocarbostyril were also not reduced with Drynap in an ethanolic solution; isocoumarin gave a yellow tar, and isocarbostyril was recovered from the reaction mixture.

The above results were not improved by several alterations of the reduction conditions. We can thus conclude that the α,β-unsaturated carbonyl group is necessary for the Drynap reduction or reductive dimerization of cyclic styrene derivatives, even in a limited experiment.

Experimental

Materials. Commercial coumarin of a GR grade was purified by distillation under reduced pressure before use. The isocoumarin was synthesized from homophthalic acid *via* the decarboxylation of 4-carboxyisocoumarin, following the method of Johnston *et al.*[5] The product was purified by distillation at 155°C/20 mmHg; mp 45°C.

The *N*-methylcarbostyril was derived from quinoline methiodide following the method of Decker.[6] The product was purified by recrystallization from ligroin; mp 72—73°C.

The isocarbostyril was also derived from isoquinoline by the method of Brown and White.[7] The product was purified by recrystallization from methanol; mp 213—214°C.

Measurement of the Spectra. The IR spectra of the compounds were measured by using a JASCO DS-301 infrared spectrophotometer and using tablets of potassium bromide or in a chloroform solution.

The NMR spectra of the compounds were measured by using a JNM 4H-100 NMR spectrometer in a deuteriochloroform solution.

The mass spectra of the reduced dimers were measured by using a Hitachi RMU-7L apparatus.

Drynap Reduction of Coumarin in a Sodium Hydroxide Solution. Three grams of coumarin (0.02 mol) dissolved in 50 m*l* of a 5% NaOH solution were reduced with 30 g of Drynap (0.13 mol of sodium metal): the reaction procedure was the same as has been described in a previous report. The yield of 3,4-dihydrocoumarin was 2.2 g (73%); bp 142—144°C/7 mmHg, mp 24°C. Dihydrocoumarin was identified by a mixed-melting-point determination with an authentic derivative; 3,5-dibromo-2-hydroxyphenylpropionic acid, mp 117—118°C, and by IR and NMR spectral studies of dihydrocoumarin. From the distillation residue, 0.2 g of the starting material, 2-hydroxycinnamic acid, was recovered; mp 207—208°C.

Drynap Reduction of Coumarin in an Ethanolic Solution. To a solution of 3.0 g of coumarin in 50 m*l* of ethanol, 30 g of Drynap and 7.5 g of acetic acid (0.12 mol) were added alternately in small portions at 60—70°C. After 1.5—2.0 hr, the mixture was decanted from the sludge, which was then washed with a new ethanol. The ethanol was evaporated from the combined ethanol solution, and the resultant residue was extracted with ether.

Some of the insoluble material remained after the above extraction. The ether solution was washed with a 5% sodium hydrogencarbonate solution and then with water, and dried over sodium sulfate. After the evaporation of the ether, the residual oil was distilled under reduced pressure; 0.6 g of 3,4-dihydrocoumarin was thus obtained (yield 20%); bp 142—144°C/7 mmHg.

From the distillation residue and the above-cited insoluble material, 1.5 g of a mixture of the two isomeric dimeric reduction products were obtained (total yield, 50%).

Separation of Isomeric Dimers. The isomeric mixture was dissolved in a 10% sodium hydroxide solution and hydrolyzed by boiling. After the acidification of the alkaline solution with concentrated hydrochloric acid, the water-soluble 3,4-bis-(2-hydroxyphenyl)adipic acid thus obtained was extracted with ether and then subjected to fractional crystallization from ether.

A less soluble acid (0.1 g, mp 200—220°C (decomp.)) and a more soluble isomer (0.7 g, mp 153—155°C (decomp.)) were thus obtained.

The acids were re-lactonized, by boiling in a mixture of acetic acid and a few drops of conc. hydrochloric acid, to the corresponding tetrahydro-bicoumarin. After several recrystallizations from glacial acetic acid, 300 mg of the less soluble lactone was obtained from the less soluble acid; mp 278—280°C (decomp.); Found: C, 73.65; H, 4.88%, mol wt (mass) *m/e* 294.

The other acid gave 0.5 g of the more soluble lactone; mp 246—248°C (decomp.); Found: C, 73.46; H,

5) H. W. Johnston, C. E. Kaslow, A. Langsjeon and R. I. Shriner, *J. Org. Chem.*, **13**, 477 (1948).

6) H. Decker, *Ber.*, **25**, 443 (1892).

7) R. B. Brown and D. White, *J. Chem. Soc.*, **1957**, 1589.

4.80%, mol wt (mass) *m/e* 294. $\nu_{C=O}$ 1764 cm^{-1}, H-3; 6.92 τ (4H) doublet (J=4 Hz), H-4; 7.00 τ (2H) triplet.

Drynap Reduction of *N*-Methylcarbostyril in an Ethanolic Solution. A mixture of 3.5 g of *N*-methylcarbostyril (0.02 mol) and 50 m*l* of ethanol was reduced with 30 g of Drynap and 7.5 g of acetic acid following the method described in the case of coumarin. The crude product was extracted with ethyl acetate, and the extracted product was recrystallized from ethanol. Rhombic crystalls were thus obtained (1.7 g); mp 284—286°C; Found: C, 75.19; H, 6.50; N, 8.86%; mol wt (mass), *m/e* 320. Calcd. for $C_{20}H_{20}N_2O_2$; C, 74.97; H, 6.29; N, 8.74%. $\nu_{C=O}$ 1673 cm^{-1}, N–CH_3 7.67 τ (6H) singlet, H-3; 7.37 τ (4H) doublet (J=4 Hz), H-4; 7.17 τ (2H) triplet.

The authors wish to express their deep thanks to the members of the Center of Instrumental Measurement of the Tokyo College of Pharmacy for their measurement of the IR, NMR, and mass spectra.

BULLETIN OF THE CHEMICAL SOCIETY OF JAPAN VOL. 43 3947—3948 (1970)

The Occurrence of (−)-(2R : 5R)-*trans*-2,5-Diethyltetrahydrofuran in "Hōyō" Mint Oil

Yasuaki ITAHARA, Hajime WATANABE and Jun KATSUHARA

Sun Star Dentifrice Company, Research Laboratory, Takatsuki, Osaka

(Received July 2, 1970)

To data, more than fourteen kinds of low-boiling, oxygenated non-terpenoidal compounds have been isolated from the essential oil of *Mentha* genus.

We have recently isolated (−)-*trans*-2,5-diethyltetrahydrofuran (I) as a novel component of the *Mentha* essential oil. To our knowledge, this is the first example of the occurrence of (−)-I in the vegetable kingdom. We wish, at this time, to report on the isolation, structure elucidation, assignment of absolute configuration, and confirmation of this substance by means of the synthesis of enantiomeric (+)-I.

The low-boiling fraction of a "Hōyō" dementholized mint oil was rectified on a helix-packed column to give several fractions, from among which the cut distilling over the range from 131.5 through 152.0°C was further purified by means of preparative vpc to afford a liquid, boiling at 143—144°C, in an over-all yield of 0.009% (based on the crude oil used). The purity of this sample was demonstrated by the sharp single peak in the vapor-phase chromatogram. The molecular ion peak at *m/e* 128 in the mass spectrum, coupled with the results of the elemental analysis, showed the molecular formula of this compound to be $C_8H_{16}O$. The absence of hydroxyl, carbonyl, isopropyl, and geminal dimethyl groups and a double bond were indicated by the IR analysis, the results of which suggested a saturated cyclic ether structure. Similarly, the NMR spectrum showed a methin proton signal centered at τ 6.2 (2H; $\underline{\text{C}}\underline{\text{H}}$–O–$\underline{\text{C}}\underline{\text{H}}$), methylene proton signals at τ 7.9—8.9 (8H), and methyl proton signals at τ 9.1 (6H triplet, J= 6 Hz). The oxiran structure was precluded by the complete inertness of (−)-I toward lithium aluminum hydride. The NMR spectral data, when combined with the intense fragment ion peaks at *m/e* 99 (M-29) and *m/e* 29 (C_2H_5), led us to the convincing deduction of the structure as 2,5-diethyltetrahydrofuran. Moreover, in *a priori* symmetry considerations, the optical activity as manifested in the levorotation found for I, $[\alpha]_D^{24}$ −9.9°, logically necessitates the point group C_2 for this molecule, thus enabling us reasonably to assign the *trans*-geometry.

In order to confirm this deduction, to establish the absolute configuration, and also to ascertain whether or not (+)-(3S)-octanol (II), a constituent of very frequent occurrence in mint oil, is a biogenetic precursor of (−)-I, the oxidative cyclization of (+)-II with silver oxide and bromine was carried out according to the Mihailovic procedure[1] in the following manner (Scheme 1). The structure of the resulting (+)-I was fully substantiated by a comparison of its physical properties, and IR and mass spectra with those of the authentic specimen described in the literature.[2] The IR and mass spectral comparisons gave unambiguous evidence that the naturally-derived (−)-I is the enantiomer of the synthetic (+)-I. The conversion of the (+)-II with the well-defined S-configuration into (+)-I *via* the present process, which does not jeopardize the chiral carbon, permits us to identify the (2S : 5S)-configuration as

1) M. Lj. Mihailovic, Z. Cekovic and J. Stankovic, *Chem. Commun.*, **1969**, 981.

2) M. Lj. Mihailovic, R. I. Mamuzic, Lj. Zigic-Mamuzic, J. Bosnjak and Z. Cekovic, *Tetrahedron*, **23**, 215 (1967).

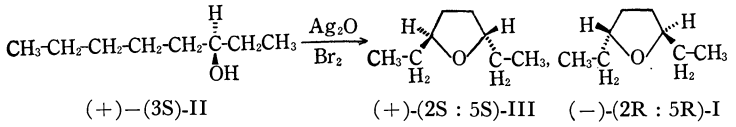

(+)−(3S)-II (+)-(2S : 5S)-III (−)-(2R : 5R)-I

Scheme 1

the synthetic (+)-I and, consequently, the (2R : 5R)-configuration as the naturally-derived enantiomer, (−)-I. This implies also that, in contrast to expectation, the naturally-occurring (−)-(2R : 5R)-I can not find its genetic origin in (+)-(3S)-II in the biosynthesis of *Mentha* plants.

Experimental

Isolation of (−)-*trans*-2,5-Diethyltetrahydrofuran (−)-(I). A forerun (5 kg) obtained by the steam-distillation of "Hōyō" dementholized mint oil (300 kg) was redistilled under reduced pressure to yield a low-boiling fraction (420 g). A part of this fraction (300 g) was rectified on a Helipack-type precision still to give a fraction distilling over the range from 131.5 through 150.0°C (23.5 g); this fraction was further purified by means of preparative vpc to yield I; bp 143—144°C; n_D^{24} 1.4201, $[\alpha]_D^{24}$ −9.9° ± 0.1° (c 2.0, ethanol). Fragment ion peaks in the mass spectrum: *m/e* 128 (molecular ion; 3.5%), 99 (24), 81 (100), 59 (21), 57 (45), 55 (100), 43 (63), 42 (53), 41 (45), 39 (27), 31 (11), 29 (68), 28 (15), 27 (39).

Found: C, 74.94; H, 12.65%. Calcd for $C_8H_{16}O$: C, 75.00; H, 12.50%. IR Spectrum: 2980 s, 2950 sh, 2890 sh, 1470 s, 1380 m, 1110 s, 1090 s, 1020 s, 990 sh, 930 m, 875 m cm^{-1}.

Synthesis of (+)-(2S : 5S)-*trans*-2,5-Diethyltetrahydrofuran (+)-(I). Bromine (7.5 g) was stirred, drop by drop, into a mixture of (+)-3-octanol (II) ($[\alpha]_D^{24}$ + 9.0 ± 0.2° (*c* 1.2, ethanol), 96.5% optical purity (3.0 g)) and silver oxide (5.7 g) in 80 m*l* of *n*-pentane in a nitrogen atmosphere over a 3-hr period. The reaction mixture was kept at 18—20°C during the addition, and then the stirring was continued for a further 2 hr. After this period, the reaction mixture was filtered to remove the silver bromide, the filtrate was washed successively with a 10% sodium thiosulfate solution, a 10% sodium hydrogencarbonate solution and water, dried over anhydrous sodium sulfate, and concentrated until a *n*-pentane-free residue was obtained (2.6 g). This residue was further purified by means of vpc to give (+)-I; bp 142—144°C, n_D^{24} 1.4188, $[\alpha]_D^{24}$ + 4.4±0.3° (c 1.2, ethanol). The IR and mass spectra of (+)-I were identical in every respect with those of the authentic specimen described in the literature[2] and also with those of the naturally-derived (−)-I.

The authors wish to thank Professor Yūzō Inouye of Kyoto University for many helpful discussions during the course of this work and Dr. Hideo Urushido of Hokuren for his generous gift of a sample. Thanks are also due to Dr. Shigeru Muraki of the Takasago Perfumery Co., for his measurements of the NMR and mass spectra, and to Dr. Tsutomu Sakai and his staff of the Institute of Food Chemistry for their measurement of the optical rotation.

BULLETIN OF THE CHEMICAL SOCIETY OF JAPAN VOL. 43 3949—3951 (1970)

Relation between the Size of the Electrode and Rotation Velocity at Rotating Ring Disk Electrode

Akira FUJISHIMA, Hideo IKETANI and Kenichi HONDA

Institute of Industrial Science, The University of Tokyo, Roppongi, Minato-ku, Tokyo

(Received July 9, 1970)

In electrolysis it is very difficult to detect and determine quantitatively intermediates produced at the electrode surface, especially in the cases of unstable materials. The rotating-ring-disk electrode method, developed by Frumkin and Nekrasov[1], has been recently regarded as one of the most useful means for the investigation of the intermediates of electrode reactions. Intermediates produced at the disk electrode would be transported by convective-diffusion to the ring electrode, where the electrochemical properties of the intermediates can be identified. When the rotation velocity is changed between 100 and 8000 rpm, a wide range of first-order rate constants of the intermediate reactions can be studied from 4×10^{-2} to 10^{3} sec^{-1}.[2] The higher the rotation velocity becomes, the faster the chemical intermediate reaction that can be measured.

When the species produced electrochemically on the disk electrode are stable, the ratio of the ring-limiting current to the disk-electrode current has been defined as the collection efficiency, N,[3] which is a function of the radii of the disk and ring electrodes. It has been shown that the collection efficiency, N, which is a very important factor in quantitative investigations, is independent of the angular velocity of rotation, the kinematic viscosity of the solution, the diffusion coefficient, and the concentrations of the species involved. The collection efficiency, N, can be calculated from the table which Albery and Bruckenstein[3] reported only when the flow in the vicinity of the electrode surface is laminar. On the contraty, at a high rotation velocity, which is often required in order to investigate fast intermediate chemical reactions, the Reynolds number increases and the flow in the vicinity of the electrode surface may become turbulent. Therefore, it is considered that each ring-disk electrode has a limit of maximum rotation rates, the limit depending on the total radius of the electrode involving the shroud part.

In this paper, as a basic study for the rotating-ring-disk electrode, the collection efficiency, N, was measured with various rotation velocities using an electrode in which the sizes of the disk and ring electrodes were constant, but in which the total radius of the electrode involving the shroud part was changed by setting arbitrary covers. It is shown that there is a maximum value of rotation velocity for each total radius of ring-disk electrodes. Moreover when the rates of the fast intermediate chemical reactions are to be measured, it may be pointed out that both the rotation velocity and the size of the electrode should be taken into consideration.

Experimental

Electrodes. The structure of the rotating-ring-disk electrode is shown in Fig. 1. A platinum disk electrode and a platinum ring electrode with platinum lead wires were fixed into a Teflon rod treated with a lathe. The disk radius was 5.00 mm, while the inner ring radius and outer ring radius were 5.50 and 6.50 mm respectively. The radius of the Teflon rod was

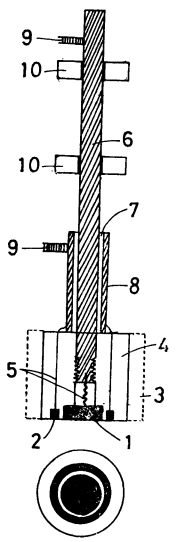

Fig. 1. Ring disk electrode.
1: Pt disk electrode, 2: Pt ring electrode, 3: Tube of acrylic resin, 4: Teflon, 5: Pt lead wire, 6: Shaft of steel, 7: Tube of acrylic resin, 8: Tube of brass, 9: Brushes of silver-carbon, 10: Bearings.

1) A. N. Frumkin and L. N. Nekrasov, *Dokl. Akad. Nauk SSSR*, **126**, 115 (1959).

2) W. J. Albery and S. Bruckenstein, *Trans. Faraday Soc.*, **62**, 1946 (1966).

3) W. J. Albery and S. Bruckenstein, *ibid.*, **62**, 1920 (1966).

8.00 mm, and by covering the tubes made with acrylic resin, the total radius of the electrode could be change to 12.5, 15.0, 20.0, or 30.0 mm. The Teflon and the steel shaft were connected by screwing down the shaft into the Teflon; the rotation showed little eccentricity. The shaft was supported by bearings at two points and was rotated by means of the rotation system. The external electrical contact of the shaft was made with silver-carbon brushes. As pretreatment, the electrode was polished to a mirror finish with sandpaper and and alumina powder and then electrolyzed both anodically and cathodically. Such electrode had a satisfactory reproducibility. The immersion depth of the electrode into the electrolyte solution was about 5 mm.

Electrolysis Vessel. The electrolysis vessel, the inner radius of which was 40.0 mm, has an upward capillary in the center and two platinum counter electrodes at the bottom of the vessel. Using a vessel the inner radius of which was 70.0 mm, the effect of the size of the vessel on the relation between the collection efficiency and the rotation velocity was tested.

Reagents, Solutions and Atmosphere. The water was distilled once, after it was treated with an ion-exchange resin. All the chemicals were of reagent-grade quality. The electrolyte solution was a $CuCl_2$ (10^{-3} mol/l) aqueous solution, with KCl (0.2 mol/l) used as a supporting electrolyte. The electrode rotation assembly was set in a large, dry box made of acrylic resin and vekulite sheets. In this box liquid nitrogen was placed in a jar in order to introduce a nitrogen atmosphere; furthermore, by passing purified nitrogen gas through during all the experiments, the electrolyte solution was deoxygenated. The temperature of the electrolyte solution was 17°C.

Measurements. Two potentiostats, Hokuto Denko PS-1000 A, were used to control the potentials of the ring and disk electrodes independently. The reference electrode was a saturated calomel electrode. The ring current was measured with a Toa Recorder, EPR-2T, and the disk current, with a Keithley Electrometer, 610B. The electrode rotation assembly was made so that its rotation velocity could be changed from zero to 7000 rpm, and the rotation velocity was measured by a revolution-indicator.

Results and Discussion

In this investigation, the oxidation-reduction reaction;

$$Cu^{2+} + e^- \rightleftarrows Cu^+ \qquad (1)$$

was taken as a model reaction. The potential of the disk electrode was set to form Cu^+ at -0.15 V, which is the cathodic limiting-current region of Reaction (1), and the ring electrode, at 0.60 V, the anodic limiting-current region. The collection efficiency of the electrode used here was 0.309 (on the base of the table of Albery and Bruckenstein's paper)[3]. The whole outer radii involving the shroud of the ring-disk electrode were changed in the manner described before. The collection efficiencies were measured and plotted against the rotation velocities, as is shown in Fig. 2. The collection efficiencies obtained agreed with the

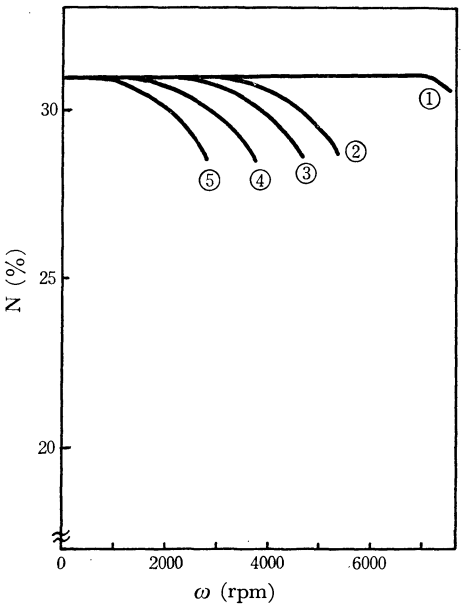

Fig. 2. Relation between rotation velocity and collection efficiency. Total radius of rotating ring disk electrode (cm), ①: 0.80, ②: 1.25, ③: 1.50, ④: 2.00, ⑤: 3.00.

value of 30.9% when the rotation velocity was not so high. As is illustrated in Fig. 2. the value of N began to decrease with the increase in the rotation velocity. Moreover, this decrease appeared at a lower rotation velocity when the electrode radius was larger. When the rotation velocity was higher than a certain critical value, which was related to the radius of the electrode, the collection efficiency, N, came to decrease; at the same time, it was recognized that the electrolyte solution bacame turbulent and that the bubbles were engulfed at the electrode surface. This reason has also been studied at the rotating-disk elecctrode[4,5], as a result of the increase in the Reynolds number N_{Re}, the laminar flow becomes a turbulent flow as the rotation velocity increases. The Reynolds number is related to the kinematic viscosity ν (cm²/sec), the radius of the electrode r (cm), and the rotation angular velocity ω(rad/sec):

$$N_{Re} = \frac{r^2\omega}{\nu} \qquad (2)$$

When the electrode surfaces are smooth enough and there is no eccentricity of rotation, the critical point of the Reynolds number where the flow of the solution changes from laminar to turbulent may be unchanged with the same electrolyte solution even if the radii of the electrodes are different. From Eq. (2) it can be understood that the larger

4) V. G. Levich, "Physicochemical Hydrodynamics," Prentice-Hall (1962).

5) Z. Gaus and R. N. Adams, *J. Phys. Chem.*, **67**, 866 (1963).

the radius of the electrode, the lower is rotation velocity which is the critical point for the change from laminar flow to turbulent.

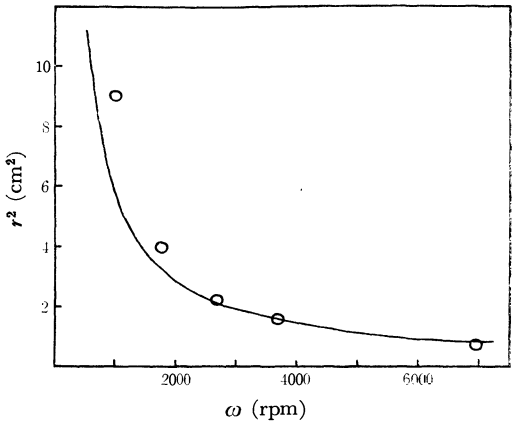

Fig. 3. Relation between r^2 and critical rotation velocity.
Solid line: $N_{Re}=6\times10^4$.

Figure 3 shows the $r^2-\omega$ relation. The solid line indicates the value calculated when $N_{Re}=6\times10^4$. In this case, the kinematic viscosity $\nu=0.01$ (cm^2/sec) is used. The measured points agreed quite well with the solid line. When the radius of the electrode is large, the critical points deviate slightly from the solid line. This may be explained by considering that, though, at the outer side of the shroud, the flow is turbulent, at the inner region, where the ring and disk electrode are locates, the flow may be laminar. In the study of the rotating-disk electrode, it was reported that the critical point is reached when N_{Re} is $10^4\sim10^5$. Therefore, $N_{Re}=6\times10^4$ is a reasonable value. Further, the same results were obtained when the electrolysis vessel with a radius of 70 mm was used instead of one with a 40 mm radius.

It may be concluded that there are limited regions of rotation velocity, depending on the electrode size. In cases where high rates of mass transport are desired, the total radius of the electrodes must be as small as possible for the rotating ring-disk electrode method. For example, when we study the intermediates with a rate constant of 10^3 sec^{-1}, the rotation velocity must be higher than 8000 rpm, but at the same time the total radius of the electrode must be smaller than 0.7 cm because of the laminar flow (probably also dependent on the eccentricity of the rotation). However, in such a high rotation velocity, special regard should be paid to the so-called edge effect, the mixing effect, etc.[6]

On the other hand, a turbulent flow is generally required for effective mixing and shorter reaction times in heterogeneous chemical reactions. Therefore, this method is interesting in connection with a quantitative investigation of the turbulent flow. As the critical point from laminar flow to turbulent can be simply and briefly measured by means of the rotating ring-disk electrode technique, using the relation between the collection efficiency and the rotation velocity, this method is considered to be a good tool for liquid turbulence studies.

The authors wish to thank Dr. M. Sukigara for his useful discussions.

6) R. N. Adams, "Electrochemistry at Solid Electrodes," Marcel Dekker, New York (1969).

BULLETIN OF THE CHEMICAL SOCIETY OF JAPAN VOL. 43 3952—3954 (1970)

The Conformation of *trans*-4-Acetoxyisoflavans and Related Compounds*[1]

Shozo YAMAGUCHI, Kuninobu KABUTO, Yoriko NINOMIYA and Naoto INOUE

College of General Education, Tohoku University, Kawauchi, Sendai

(Received July 10, 1970)

As a part of the investigation of the stereochemistry of isoflavan-4-ols,[1] our interest in conformational preference effects in the chroman ring led us to investigate *trans*-4-acetoxyisoflavans and related compounds.

In the NMR spectra (Table 1) of *trans*-4-acetoxy- (I), *trans*-4-acetoxy-7-methoxy- (II), and *trans*-4-acetoxy-4′,7-dimethoxyisoflavan (III), the signals of the C-2 and C-3 protons show a simple pattern; the AB portion (the C-2 proton) appears as a 1 : 1 doublet, the X region (the C-3 proton) shows a 1 : 2 : 1 triplet ($J_{2,3}=J_{3,4}=5.0$ Hz), and none of the diaxial couplings expected for the conformations (Ie), (IIe), and (IIIe) appear in them. Upon irradiation at the C-4 proton of II, the quartet due to the C-3 proton changes to a triplet ($J_{2,3}=5.0$ Hz). These results strongly suggest that I, II, and III exist largely as conformations (Ia), (IIa), and (IIIa), in which the acetoxyl group at C-4 is in a *quasi*-axial environment. The present results can be explained by the pseudo-allylic effect,[2] which has been termed the $A^{(1,3)}$ strain, inherent in the conformations (Ie), (IIe), and (IIIe).

On the other hand, 2-methyl-4,7-diacetoxyisoflavan (2/3 *trans*, 3/4 *trans*) (IV)[3] seems to exist mainly as the conformation (IVe) ($J_{2,3}=J_{3,4}=10.2$ Hz), for there is a severe 1,3-diaxial repulsion in IVa (methyl-acetoxyl, around 1.9—2.4 kcal/mol)[4] which is considerably larger than the $A^{(1,3)}$ strain in IVe.

In the *trans*-4-hydroxyisoflavans, (I′), (II′), and (III′), the preferred conformations seem to be I′e, II′e, and III′e ($J_{3,4}=7.4$—8.5 Hz).*[2] In I′, II′, and III′, the unfavourable $A^{(1,3)}$ strain is considered to be partly overcome by the intramolecular hydrogen bonding[5] between the C-3 phenyl and C-4 hydroxyl groups.

The ABX protons (decoupled at the methyl signal at 100 MHz) of *trans*-3-methyl-4-benzoyloxychroman (V) show no diaxial coupling*[2] ($J_{2,3}=$ 2.4, 4.3: $J_{3,4}=4.1$ Hz); thus, the conformation Va is favoured. This result is substantiated by the existence of the long-range coupling ($J_{2,4}=$

TABLE 1. COUPLING CONSTANTS IN ISOFLAVANS AND CHROMANS

	Compounds	$J_{2,3}$ (Hz)	$J_{3,4}$ (Hz)	Preferred conformation
I	*trans*-4-AcO-IF	5.0	5.0	Ia
II	*trans*-4-AcO-7-MeO-IF	5.0	5.0	IIa
III	*trans*-4-AcO-4′,7-$(MeO)_2$-IF	5.0	5.0	IIIa
IV	*trans*-2-Me-4,7-$(AcO)_2$-IF	10.2	10.2	IVe
I′	*trans*-4-OH-IF	8.5, 5.6	8.5	I′e
II′	*trans*-4-OH-7-MeO-IF	7.4, 5.3	7.4	II′e
III′	*trans*-4-OH-4′,7-$(MeO)_2$-IF	7.9, 5.3	7.4	III′e
V	*trans*-3-Me-4-BzO-CR	2.4, 4.3	4.1	Va
V′	*trans*-3-Me-4-OH-CR	3.1, 6.1	5.5	V′a
IX	4-AcO-CR		3.8	IXa
X	1-AcO-Tetralin		4.0	Xa

IF: Isoflavan, CR: Chroman

*1 A part of this study was presented at the 22th Annual Meeting of the Chemical Society of Japan. Tokyo, April, 1969, Proceedings III, p. 1382.

1) S. Yamaguchi, S. Ito, A. Nakamura and N. Inoue, This Bulletin, **38**, 2187 (1965). A. S. R. Anjaneyulu, M. G. Rao, L. R. Row and C. S. Krishna, *Tetrahedron Lett.*, **1966**, 3199.

2) S. K. Malhotra and F. Johnson, *J. Amer. Chem. Soc.*, **87**, 5493 (1965). F. Johnson, *Chem. Rev.*, **68**, 375 (1968).

3) N. Inoue and S. Ito, *Chem. Ind.* (London), **84**, 1382 (1965).

4) E. L. Eliel, N. J. Allinger, S. J. Angyal and G. A. Morrison, "Conformational Analysis," John Wiley and Sons, Inc., New York, (1965), pp. 44, 114, 356.

*2 The ABX portion of these spectra were analysed by the method of Pople. J. A. Pople, W. G. Schneider and H. J. Bernstein, *Can. J. Chem.*, **35**, 63 (1957).

5) K. Hanaya, private communication.

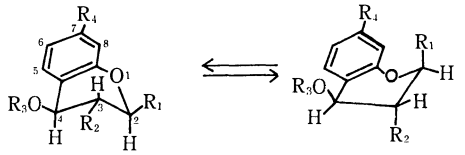

(Ie)	$R_1=R_4=H$, $R_2=Ph$, $R_3=Ac$	(Ia)
(I'e)	$R_1=R_3=R_4=H$, $R_2=Ph$	(I'a)
(IIe)	$R_1=H$, $R_2=Ph$, $R_3=Ac$, $R_4=OMe$	(IIa)
(II'e)	$R_1=R_3=H$, $R_2=Ph$, $R_4=OMe$	(II'a)
(IIIe)	$R_1=H$, $R_2=p$-MeO-C_6H_4, $R_3=Ac$, $R_4=OMe$	(IIIa)
(III'e)	$R_1=R_3=H$, $R_2=p$-MeO-C_6H_4, $R_4=OMe$	(III'a)
(IVe)	$R_1=Me$, $R_2=Ph$, $R_3=Ac$, $R_4=OAc$	(IVa)
(Ve)	$R_1=R_4=H$, $R_2=Me$, $R_3=Bz$	(Va)
(V'e)	$R_1=R_3=R_4=H$, $R_2=Me$	(V'a)
(IXe)	$R_1=R_2=R_4=H$, $R_3=Ac$	(IXa)

Fig. 1

1.0 Hz) expected from the W letter rule. Unlike as in the spectra of I', II', and III', the $J_{3,4}$ values of *trans*-3-methyl-4-hydroxychroman (V'), in which the stabilization by the intramolecular hydrogen bonding can not be expected, is similar (5.5 Hz) to that of I—III; the preferred conformation is probably V'a, as in the case of V.

For the estimation[6] of the conformational equilibrium of II, standard $J_{3,4}$ valuse are selected as follows; $J_{3a,4a'}$: $J_{3a,4a'}$ (10.2 Hz) in IV[3]; $J_{3e,4e'}$: $J_{3e,4e'}$ (3.2 Hz) in *cis*-4-acetoxy-7-methoxyisoflavan (VI).[1] This assumption seems to be correct on the basis of the following points: (1) as has been described above, the conformation of IV is considered to be almost fixed to IVe; this is also supported by the equal value of $J_{3a,4a'}$ (10.2 Hz) in *cis*-4-benzoyloxyflavan (VII),[7] in which the conformation should be homogeneous. (2) Since the value of $J_{2a,3a}$ (11.9 Hz) in VI[1] is as large as that of *trans*-4-benzoyloxyflavan (VIII),[7] the conformation of VI is almost fixed; the assumption ($J_{3a,4e'}\approx J_{3e,4e'}$) is supported by the experimental data ($J_{3e,4e'}=J_{3e,4e'}=3.0$ Hz in VIII[7] and 3.2 Hz in *trans*-2-alkyl-4-acetoxychromans).*3 The calculation using the above standard $J_{3,4}$ values shows that IIa exists mainly (~75%) in the conformational equilibrium. A consideration of the 1,3-diaxial interaction (acetoxyl-hydrogen, ~0.35 kcal/mol)[4] associated with IIa and the free energy difference of 0.65 kcal/mol between the conformers in favor of IIa implies that the $A^{(1,3)}$ interaction (acetoxyl-hydrogen) in IIe is ~1.0 kcal/mol.*4

In 4-acetoxychroman (IX) and 1-acetoxytetralin (X), the preferred conformations are IXa and Xa, since the signals of the C-4 proton show a pattern [4-H(t), $J_{3,4}=3.8$ and 4.0 Hz respectively] similar to that of VIII [4-H(t), $J_{3,4}=3.0$ Hz][7] and since the conformational equilibrium of IX can be calculated[8] from the distance (4-acetoxychroman; 8.0 Hz) between the two outside peaks of the C-4 proton resonance based on the distances of *cis*- and *trans*-2-methyl-4-acetoxychromans*3 ($J_A=16.5$ Hz and $J_B=6.0$ Hz), selected as model compounds.*5 This calculation affords the results that IXa (~81%) is predominant and that the allylic strain is 1.1—1.2 kcal/mol, as large as that of II.

Experimental

Measurement. The NMR spectra were determined in $CDCl_3$ at 37°C (60 MHz) and 30°C (100 MHz), using a Varian A-60 and H-100 spectrometer with TMS as the internal standard.

Materials. The *trans*-4-acetoxyisoflavan (I),[9] *trans*-4-acetoxy-7-methoxyisoflavan (II)[9], *trans*-4-acetoxy-4',7-dimethoxyisoflavan (III),[9] *trans*-2-methyl-4,7-diacetoxyisoflavan (IV),[3] *trans*-4-hydroxyisoflavan (I'),[9] *trans*-4-hydroxy-7-methoxyisoflavan (II'),[9] and *trans*-4-hydroxy-4',7-dimethoxyisoflavan (III')[9] were prepared by methods previously reported. The 4-acetoxychroman (IX) and 1-acetoxytetralin (X) were obtained by the acetylation of chroman-4-ol and tetralin-1-ol respectively with acetyl chloride in pyridine.

trans-3-*Methyl*-4-*hydroxychroman (V')*. To a solution of 11.0 g of sodium borohydride in 220 m*l* of ethanol, 11.3 g of 3-methylchromone[10] was added. The mixture was refluxed for 4 hrs and then left to stand overnight at room temperature. After the ethanol had been removed under reduced pressure, 200 m*l* of water and 100 m*l* of 50% acetic acid were added to the residue. The solution was then extracted with ether. The extract was washed with 5% sodium hydroxide and with water, and was dried on anhydrous sodium sulfate. The mixture of *cis*- and *trans*-3-methyl-4-hydroxychromans remaining after the removal of the ether was partly crystallized. One of the isomers was obtained by repeated recrystallization from *n*-hexane - benzene; 2.2 g; mp 97.5—98.0°C.

Found: C, 73.31; H. 7.52%. Calcd for $C_{10}H_{12}O_3$: C, 73.14; H, 7.37%.

This isomer was identical with the *trans*-3-methyl-4-hydroxychroman (V') prepared by the hydroboration of the 3-methylchromene obtained by the dehydration

6) N. C. Franklin and H. Feltkamp, *Angew. Chem. In. Ed.*, Engl. **4**, 774 (1956).

7) B. J. Bolger, A. Hirwe, K. G. Marathe, E. M. Philibin and M. A. Vickars, *Tetrahedron*, **22**, 621 (1966).

*3 Unpublished results. Synthesis and stereochemistry of these compounds will be reported elsewhere.

*4 Johnson and Malhotra have shown that the magnitude of $A^{(1,3)}$ strain (methyl-hydrogen) is approximately 1.4 kcal/mol. S. K. Malhotra and F. Johnson, *Chem. Commun.*, **1968**, 1149.

8) G. O. Pierson and O. A. Runquist, *J. Org. Chem.*, **33**, 2572 (1968).

*5 The coupling constants observed for other 2-alkyl-4-acetoxychromans are consistent with the values chosen for J_A and J_B.

9) S. Yamaguchi, S. Ito, I. Suzuki and N. Inoue, This Bulletin, **41**, 2073 (1968).

10) A. Schönberg and A. Sina, *J. Chem. Soc.*, **1950**, 3344.

of a mixture of 3-methyl-4-hydroxychromans with acetic acid - hydrochloric acid (4 : 1).

trans-3-Methyl-4-benzoyloxychroman (V). By the usual method, the benzoate (V) was prepared by reaction with acetyl chloride - pyridine; mp 84.5—85.0°C.

Found: C, 76.26; H, 6.17%. Calcd for $C_{17}H_{16}O_3$: C, 76.10; H, 6.01%.

BULLETIN OF THE CHEMICAL SOCIETY OF JAPAN VOL. 43 3954—3956 (1970)

The Solid-phase Synthesis of Ile^5-Angiotensin II to Demonstrate the Use of N^{im}-Tosyl-histidine*[1a,b]

Toshiyuki FUJII*[2] and Shumpei SAKAKIBARA*[3]

Peptide Center, Institute for Protein Research, Osaka University, Kita-ku, Osaka

(Received July 23, 1970)

There are still several problems about the protection of imidazole groups during the incorporation of histidyl residues into peptides by the solid-phase method.[1] Recently, we proposed a new method for protecting the imidazole residue of histidine with a Tos-group, and several N^{α}-protected N^{im}-Tos-histidine derivatives (I) were synthesized.[2] The present study is concerned with the application of I in the solid-phase method.

There are several advantages in the use of the Aoc-, Boc-, Z(OMe)-, or Nps-derivatives of I in the solid-phase method. That is, these derivatives are easily synthesized by conventional methods, and they are soluble in CH_2Cl_2, which is known to be the most suitable solvent for coupling reactions with dicyclohexylcarbodiimide (DCC) in the solid-phase synthesis. Further, as was mentioned in the preceeding paper,[2] the Tos-group can be removed simultaneously with other protective groups in the final stage of the synthesis, when the free peptide is isolated from the peptide-resin with HF.[3] Therefore, many difficulties which are encountered during the incorporation of histidyl residues into peptide chains by the solid-phase procedure can be overcome by the use of I. Among these N^{α}-protected derivatives, Aoc-His(Tos)-OH (II)[2] seemed to be the most suitable for solid-phase synthesis because it is highly soluble in CH_2Cl_2. Some of the Tos-groups are known to be cleaved when the N^{α}-Aoc-groups are removed with anhydrous acids,[2] but partial cleavage is probably not a serious problem in solid-phase synthesis. In this connection, it may be recalled that Gutte and Merrifield tried to synthesize ribonuclease A with unprotected Boc-histidine.[4]

The synthesis of human angiotension II was attempted with Compound II. The standard procedures of Marshall and Merrifield were followed for the synthesis;[5] the Aoc group was used for the N^{α}-protection of the amino acids, and all the coupling procedures were carried out in CH_2Cl_2 with DCC. The tyrosyl and the arginyl residues were incorporated as Aoc-Tyr(Bzl)-OH[6] and Aoc-Arg(Tos)-OH (III) respectively. The final aspartyl residue was coupled with Z-Asp(OBzl)-OH.[7] All the coupling reactions proceeded smoothly in CH_2Cl_2; this was in contrast with reports that Boc-His(Bzl)-OH[5] and Boc-Arg(Tos)-OH[8] had to be coupled in DMF or in a mixture of DMF and CH_2Cl_2 (1 : 9) at the risk of acyl-urea formation.[9] The high solubility and reactivity of Aoc-Arg(Tos)-OH in CH_2Cl_2 should also be counted as favorable properties due to the Aoc-group.

Finally, the free peptide was taken out from the

*[1a] This work was presented at the 7th Symposium of Peptide Chemistry, Tokyo, November 21, 1969.

*[1b] The abbreviations used conform with those tentatively proposed by the IUPAC-IBC: *J. Biol. Chem.*, **241**, 2491 (1966). DMF–dimethylformamide. Aoc=*t*-amyloxycarbonyl. The amino-acid symbols denote the L-configuration.

*[2] Present address: Tanabe Seiyaku Co., Ltd., Higashiyodogawa-ku, Osaka.

*[3] To whom requests for reprints should be addressed.

1) J. M. Stewart and J. D. Young, "Solid-phase Peptide Synthesis," Freeman, San Francisco (1969), p. 20.

2) S. Sakakibara and T. Fujii, This Bulletin, **42**, 1466 (1969).

3) S. Sakakibara, Y. Kishida, R. Nishizawa and Y. Shimonishi, This Bulletin, **41**, 438 (1968); J. Lenard and A. B. Robinson, *J. Amer. Chem. Soc.*, **89**, 181 (1967).

4) B. Gutte and R. B. Merrifield, *ibid.*, **91**, 501 (1967).

5) G. R. Marshall and R. B. Merrifield, *Biochemistry*, **4**, 2394 (1965).

6) I. Honda, Y. Shimonishi and S. Sakakibara, This Bulletin, **40**, 2415 (1967).

7) A. Berger and E. Katchalski, *J. Amer. Chem. Soc.*, **73**, 4084 (1951).

8) J. Blake and C. H. Li, *ibid.*, **90**, 5882 (1968).

9) J. C. Sheehan, M. Goodman and G. P. Hess, *ibid.*, **78**, 1367 (1956); *cf.* Ref. 5.

peptide-resin by the HF-procedure,[3] and the bound HF was removed by passing the crude product through a column of Dowex-1; this procedure was also effective in removing almost all side products. Thus, practically pure angiotensin II was obtained without the use of any other specific procedure.

Experimental

Materials. Chloromethylated polystyrene (divinylbenzene 2%; 100—200 mesh; Cl-content, 1 mmol/g) was obtained from the Protein Research Foundation; it was converted to an Aoc-L-phenylalanyl-resin (0.29 mmol/g) by the procedure of Marshall and Merrifield.[5] The Aoc-amino acids were synthesized as has been reported previously.[6,10]

Aoc-Arg(Tos)-OH (III). Arg(Tos)[11] (9.9 g, 0.03 mol) was allowed to react with Aoc-azide[6] (5 g, 0.032 mol) at 35.0°C for 48 hrs in a mixture of dioxane (30 ml), 1N NaOH (30 ml), and triethylamine (4.2 ml, 0.03 mol). The reaction mixture was treated as described previously,[6] and the crude product was extracted into AcOEt. The AcOEt solution was concentrated under reduced pressure at room temperature. The crystalline residue was recrystallized from AcOEt, and dried over P_2O_5 *in vacuo*; wt, 11.8 g (88.7%); mp 79.5—83°C, $[\alpha]_D^{25}$ −13° (*c* 1.9, pyridine).

Found: C, 50.74; H, 6.85; N, 11.96%. Calcd for $C_{19}H_{30}N_4O_6S \cdot 1/2\,H_2O$: C, 50.54; H, 6.92; N, 12.41%.

Z-Aps(OBzl)-Arg(Tos)-Val-Tyr(Bzl)-Ile-His(Tos)-Pro-Phe-resin (IV). Aoc-L-phenylalanyl-resin (2 g, 0.58 mmol) was placed in a manual solid-phase apparatus, and synthesis was started as has been described in the literature.[1,4] The cleavage of the Aoc-groups was carried out with 50% trifluoroacetic acid in CH_2Cl_2,[4] and the amino groups generated were neutralized with triethylamine in DMF. Each Aoc-amino acid (3 eq) was coupled with DCC (3 eq) in CH_2Cl_2 for 3 hrs at room temperature. The couplings of Aoc-Ile-OH and Compound III were ensured by repeating the coupling procedure twice for each compound.

Finally, the protected peptide-resin (IV) (2.7 g) was obtained and dried over P_2O_5 *in vacuo* at 50°C. The overall yield (about 90%) was estimated at this stage from the weight-increase.

Ile^5-Angiotensin II. The peptide resin (IV) (700 mg) was placed in an HF-reaction vessel and mixed with anisole (0.5 ml). Anhydrous HF (10 ml) was then introduced into the vessel, and the mixture was allowed to react at 0°C for an hour. After the excess HF had then been evaporated off *in vacuo* at 0°C, the generated free peptide was extracted with 1% acetic acid. The extract was washed with ether and lyophilized; wt, 131.4 mg (90%, calcd from the amount of phenylalanyl-resin).

Then, the crude product (100 mg) was applied to a column of Dowex-1 × 2 (AcO^- form, 0.85 × 50 cm). This was eluted with water, and the UV absorption of each fraction was measured at 280 mμ (see Fig. 1).

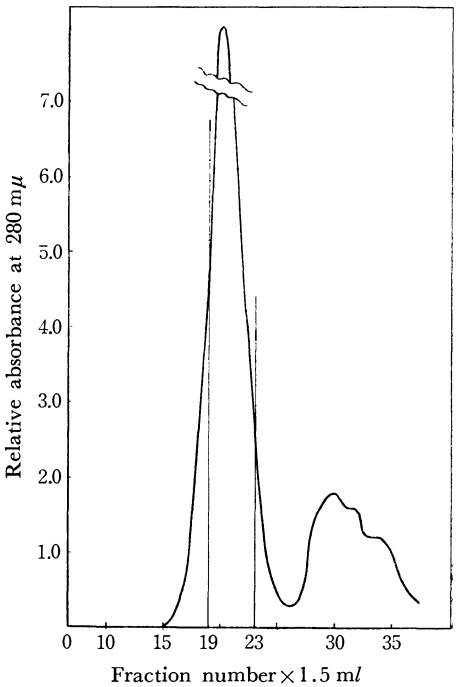

Fig. 1. Purification of synthetic angiotensin II by column chromatography.
Material was eluted from a column (0.85 × 50 cm) of Dowex 1 × 2 (Acetate form, 100—200 mesh) with water. 1.5 ml fractions were collected and their UV-absorption at 280 mμ was measured.

The major fractions (19—23) were combined and lyophilized to obtain the final product; wt, 45 mg (45% calcd from the crude product); $[\alpha]_D^{15}$ −67.8° (c 0.3, N HCl): reported $[\alpha]_D^{20}$ −66.98° (c, 0.4, N HCl),[12] $[\alpha]_D^{23}$ −67.3° (c 1.13, N AcOH),[13] $[\alpha]_D^{25}$ −66° (c 0.8, N HCl).[5]

Found: C, 54.40; H, 6.75; N, 15.35%. Calcd for $C_{50}H_{71}N_{13}O_{12} \cdot C_2H_4O_2 \cdot 3H_2O$: C, 53.83; H, 7.04; N, 15.69%.

This material showed a single spot (R_f 0.26) on paper chromatography with a solvent system *n*-butanol-acetic acid-water (4 : 1 : 1); reported R_f 0.29,[12] R_f 0.28.[5] Ratios of amino acids: Acid hydrolysate; $Asp_{1.02}Arg_{1.02}Val_{0.98}Tyr_{1.00}Ile_{0.93}His_{0.93}Pro_{1.05}Phe_{1.07}$. Amino-peptidase M digest;*4 $Asp_{1.00}Arg_{0.97}Val_{1.02}Tyr_{1.00}Ile_{1.09}His_{0.00}Pro_{0.00}Phe_{1.12}$.

This material showed full hypertensive activity when

10) S. Sakakibara, I. Honda, K. Takada, M. Miyoshi, T. Ohnishi and K. Okumura, This Bulletin, **42**, 809 (1969).

11) J. Ramachandran and C. H. Li, *J. Org. Chem.*, **27**, 4006 (1962).

12) K. Arakawa and F. M. Bumpus, *J. Amer. Chem. Soc.*, **83**, 728 (1961).

13) R. Schwyzer and H. Turrian, *Vitamins and Hormones*, **18**, 237 (1960).

*4 The disappearance of proline and its adjacent amino acid during digestion with AP-M has also been reported in the following articles: E. C. Jorgensen, G. C. Windredge, W. Patton and T. C. Lee, *J. Med. Chem.*, **12**, 733 (1969); N. Yanaihara, T. Hashimoto, C. Yanaihara and N. Sakura, *Chem. Pharm. Bull.* (Tokyo), **18**, 417 (1970).

assayed on a rat carotid artery, using Hypertensin-Ciba as the standard.

The authors are grateful to Dr. H. Akutsu of Osaka University for his determination of the biological activity, and to Miss S. Yoshimura for her expert technical assistance.

BULLETIN OF THE CHEMICAL SOCIETY OF JAPAN VOL. 43 3956—3958 (1970)

ESR ^{13}C Hyperfine Structures of the Meta-substituted *t*-Butyl Biphenyl Anion Radical*[1]

Kazuhiko ISHIZU*, Yasuo INUI*, Kazuo MUKAI*, Hideo SHIKATA* and Hideo HASEGAWA**

* *Department of Chemistry, Faculty of Science, Ehime University, Matsuyama*
** *Japan Electron Optics Laboratory, Akishima*

(Received August 13, 1970)

The ESR observation of the ^{13}C hyperfine structure has never been established for biphenyl anion radicals, because the weaker ^{13}C hyperfine structures were incidentally smeared out by superimposed ring proton hyperfine splittings, particularly those due to the meta-protons.

In the present studies, all of the meta positions were substituted by *t*-butyl groups and we attempted to reduce the superposition of the proton hyperfine structures; that is, the 3,3′,5,5′-tetra-*t*-butyl biphenyl was synthesized and the ESR ^{13}C hyperfine splittings were tentatively studies for the anion radical of this alkylated biphenyl.

Experimental

The synthesis of the 3,3′,5,5′-tetra-*t*-butyl biphenyl has not been described in the literature, however, the material was obtained from the Grignard reagent of the 3,5-di-*t*-butyl bromobenzene[1] prepared in an anhydrous tetrahydrofuran (THF) by following the process of Kharasch and Fields.[2] A pure material recrystallized from ethyl alcohol melted at 172.8—173.3°C. Found: C, 88.62; H, 11.17%. Calcd: C, 88.82; H, 11.18%. IR absorption in KBr. γ (=CH); 837 cm^{-1}, δ' (ring); 720 cm^{-1}. UV absorption in *n*-hexane. λ_{max}; 253 mμ ; ε ; 17300 M^{-1} cm^{-1}.

The anion radicals were prepared in a solution of THF by reduction with lithium. The ESR spectra were recorded at room temperature.

Results and Discussion

The proton hyperfine structures shown in Fig. 1, consist of only nine lines, and a_2^H and a_4^H were determined to be $a_2^H=-2.59$ and $a_4^H=-5.14$ gauss respectively, which are closed to those for the biphenyl anion radical. Both $\rho_2^\pi=0.100$ and $\rho_4^\pi=0.218$ were calculated using Colpa-Bolton's equation: for an anion radical, $a_i^H=Q^H_{CH}(0)\rho_i^\pi-K^H_{CH}[\rho_i^\pi]^2$, $Q^H_{CH}(0)=-27$, and $K^H_{CH}=-12$ gauss.[3] As is designated by the figures (1)—(4) in the lower part of Fig. 2, ^{13}C hyperfine splittings are observed as the doublet lines of (1) 0.90, (2) 1.98, (3) 4.34, and (4) 8.20 gauss, and the intensity ratios are (1) : (2) : (3) : (4) = 1 : 2 : 2 : 1. These intensity ratios distinguished either a_1^C or a_4^C from a_2^C and a_3^C. The a_4^C is assumed to be (4) 8.20 gauss, since the contribution of the spin-polarization is negligible as a result of the small value of ρ_3^π, thus, its magnitude depends substantially on the large spin density of ρ_4^π.

Following the method of Karplus-Fraenkel,[4] the a_i^C values have been calculated by the following equation:

$$a_i^C = (S^C + \sum_{i=1}^{3} Q^C_{C_iX_k})\rho_i^\pi + \sum_{i=1}^{3} Q^C_{X_kC_i}\rho_k^\pi$$

where $S^C=-12.7$ is the contribution from the 1s electron of C_i, $Q^C_{C_iX_k}$ ($Q^C_{C_iH}=19.5$, $Q^C_{C_iC_k}=14.4$), the $\sigma-\pi$ interaction parameter produced by ρ_i^π on the C_i atom, and where $Q^C_{C_kC_i}=-13.9$ represents a polarization from the neighboring atom, C_k. By substituting the values of a_4^C and ρ_4^π into the equation, $\rho_3^\pi=-0.016$ was primarily determined. In the same manner, $\rho_1^\pi=0.113$ can be derived from $\rho_2^\pi=0.100$ and $a_1^C=-0.90$. Here, the negative value is assigned for for a_1^C, for the normalization of the spin density,

*1 This work was presented at 8th ESR Symposium of the Chemical Society of Japan, Hiroshima, November 15th, 1969.

1) P. D. Bartlett, M. Roha and R. M. Stiles, *J. Amer. Chem. Soc.*, **76**, 2349 (1954).

2) M. S. Kharasch and E. K. Fields, *ibid.*, **63**, 2316 (1941).

3) J. P. Colpa and J. R. Bolton, *Mol. Phys.*, **6**, 273 (1963).

4) M. Karplus and G. K. Fraenkel, *J. Chem. Phys.*, **35**, 1312 (1961).

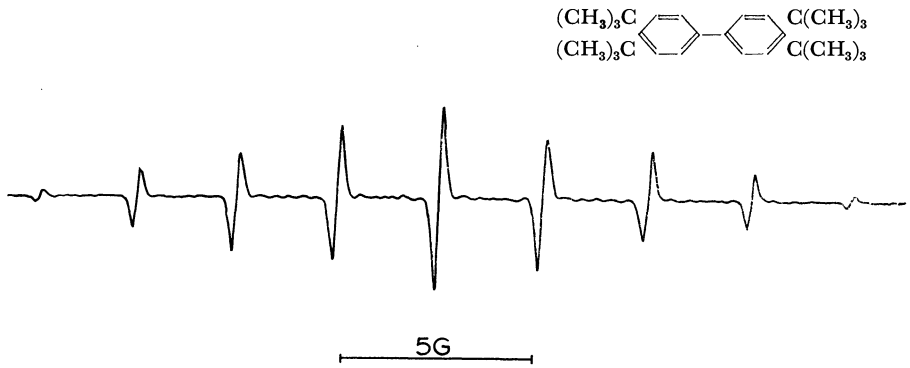

Fig. 1. Proton hyperfine structures of 3,3′,5,5′-tetra-*t*-butyl biphenyl anion radical.

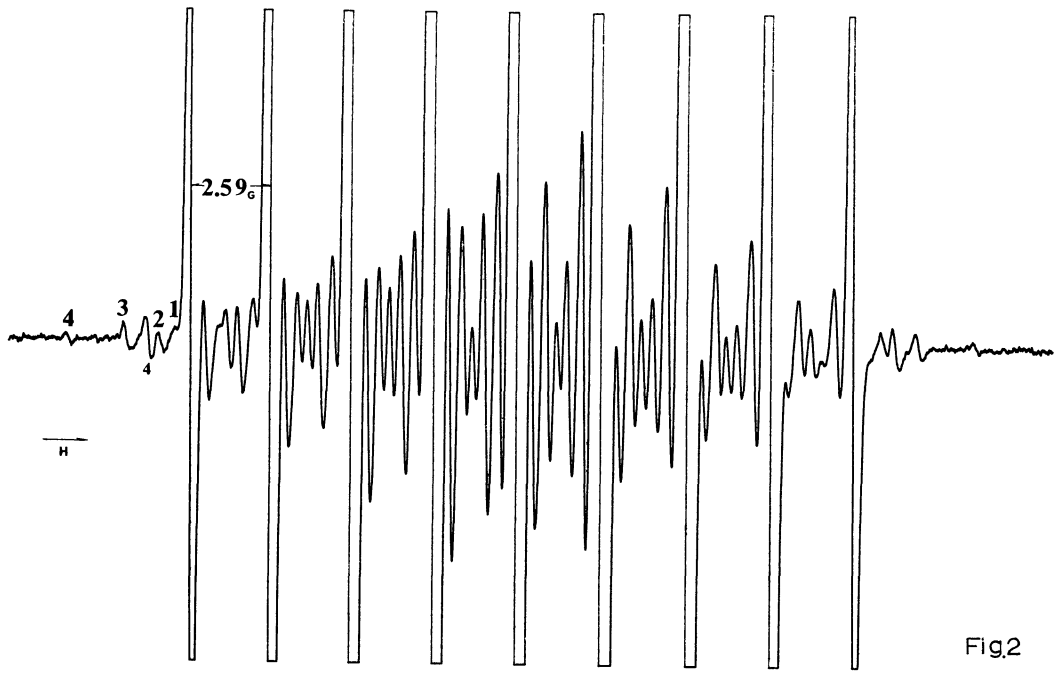

Fig. 2. ^{13}C hyperfine structures of 3,3′,5,5′-tetra-*t*-butyl biphenyl anion radical.

TABLE 1. EXPERIMENTAL AND THEORETICAL VALUES OF THE ^{13}C COUPLING CONSTANT AND THE SPIN DENSITY

Position		1	2	3	4
a_i^C (gauss)	(Exp)	−0.90	1.98	−4.34	8.20
	(Calcd)[a)]	−0.95	2.53	−4.83	7.02
ρ_i^π	(Exp)	0.113	0.100	−0.016	0.218
	(Calcd)	0.134	0.114	−0.020	0.182

a) Theoretical values of a_i^C were calculated based on the McLachlan's spin density.

$\sum\rho_i^\pi = 1$, cannot be held if the positive value is assumed. Finally, we proved that the observed values of both a_2^C and a_3^C are consistently explainable with the present ρ_i^π value and that a_3^C also has a negative value; that is, a_2^C: Obsd 1.98, Calcd 2.21 gauss, a_3^C: Obs. −4.34, Calcd. *2 −4.98 gauss.

*2 $a_3^C = (S^C + 2Q_{C-C(CH_3)_3}{}^C)\rho_3^\pi + Q_{CiC_3}{}^C(\rho_2^\pi + \rho_3^\pi)$
The spin density on the *t*-butyl group was neglected and $Q_{C-C(CH_3)_3}{}^C \fallingdotseq Q_{C-CH_3}{}^C = 16.3$ gauss[5)] was assumed.

5) R. W. Fessenden, *J. Phys. Chem.*, **71**, 74 (1967).

McLachlan's MO calculation was carried out taking the Coulomb integral of the meta-position to be $\alpha_3=\alpha-0.15\beta$; the results are summarized in Table 1. A good agreement can be obtained between the observed ^{13}C hyperfine coupling constant and their theoretical values. The ^{13}C coupling constants for the biphenyl anion radical would also be similar to those established by the present work, since it has been shown that an alkyl substitution always causes only a minor perturbation in the spin density.[6]

6) K. Ishizu, K. Mukai, H. Hasegawa, K. Kubo, H. Nishiguchi and Y. Deguchi, This Bulletin, **42**, 2808 (1969).

BULLETIN OF THE CHEMICAL SOCIETY OF JAPAN VOL. 43 3958—3960 (1970)

ESR Study of Spin-Spin Interactions in Verdazyl Biradicals. II

Kazuo MUKAI, Nagao AZUMA*[1], Hideo SHIKATA and Kazuhiko ISHIZU

Department of Chemistry, Faculty of Science, Ehime University, Matsuyama

(Received August 25, 1970)

The verdazyls, a series of very stable free radicals containing four nitrogen nuclei, were recently studied by Kuhn, Neugebauer and Trischmann[1,2]. Preliminary susceptibility measurements showed the presence of one unpaired electron per molecule. The combination of two 3-verdazylyl residues by a 1,3- or 1,4-phenylene bridge gives fully-conjugated, nearly planar, green biradicals with properties which correspond to those of the simple verdazyls. The results of the paramagnetic susceptibility measurements revealed that the two unpaired electrons in the π-electron system of each biradical are practically free from coupling down to 77°K, in contrast to the case with the other stable biradicals.[3-5]

However, all of the bi- and tri-radicals of this series shows less well resolved ESR spectra than those of the monoradicals. Fischer[6] proposed that, judging from the results of HMO theory, each biradical has a node in the odd electron orbitals at the aryl system connecting the radical parts and should, consequently, exhibit little intramolecular spin exchange, and that, further, through step-by-step polarographic oxidation, the broadening of lines in the ESR spectra can be attributed mainly to dipole-dipole interaction, and not to electron exchange and or slow molecular tumbling motion as a consequence of the large molecular size.

The purpose of this note is to present new ESR spectra which not only yield the quantitative values of dipole-dipole interaction in these verdazyl biradicals, but also show existence of a triplet state in these radicals due to electron-exchange in-

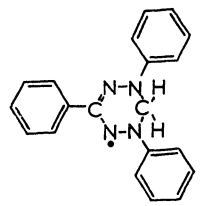

I

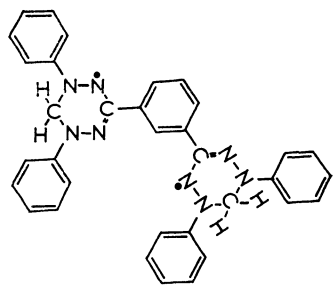

II

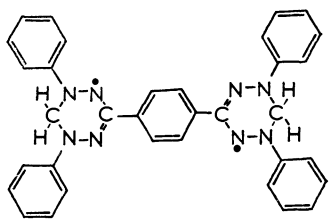

III

*[1] Present address: Department of Chemistry, Faculty of Science, Kyoto University, Sakyo-ku, Kyoto.

1) R. Kuhn and H. Trischmann, *Angew. Chem.*, **75**, 294 (1963); *Mh. Chem.*, **94**, 457 (1964).

2) R. Kuhn, F. A. Neugebauer and H. Trischmann, *Angew. Chem.*, **76**, 691 (1964); *Mh. Chem.*, **97**, 525 (1966).

3) R. Kuhn and H. Katz, *Angew. Chem.*, **46**, 478 (1933); E. Muller and I. Müller-Rodloff, *Ann.*, **521**, 81 (1936).

4) R. Kuhn and W. Blau, *Ann.*, **615**, 99 (1958).

5) K. Mukai, K. Ishizu and Y. Deguchi, *J. Phys. Soc. Jap.*, **27**, 783 (1969).

6) P. H. H. Fischer, *Tetrahedron*, **23**, 1939 (1967).

teraction. This has been accomplished through the observation of the dipolar splitting of two verdazyl biradicals in 2-MeTHF at 77°K.

Experimental

1,3,5-triphenyl-verdazyl (I), mp 142.0—142.1°C (lit, 140—141°C), 1,3-bis-(1,5-diphenyl-verdazyl-3-yl) benzene (II), mp 182.2—183.3°C (lit, 184—185°C), and 1,4-bis-(1,5-diphenyl-verdazyl-3-yl) benzene (III), mp 197.5—198.0°C (lit, 195—196°C) were prepared from the corrsponding formazans according to the method of Kuhn, Neugebauer and Trischhmann.[1,2] After the formation of the s-tetrazyl ring with formaldehyde for I and II and with paraformaldehyde for III, the reaction I and II and with paraformaldehyde for III, the reaction mixture was neutralized with sodium hydroxide. A dark green crystalline compound was isolated from the DMF-solution, it was recrystallized three times from acetone-methanol for the I radical and from dioxane-methanol for the II radical, but in the case of the III radical it was washed two times with hot acetone.

All the ESR measurements were carried out using a JES-3BX spectrometer equipped with 100 kc/sec field modulation.

Results and Discussion

We followed the ESR spectrum of a 2-MeTHF solution of the verdazyl biradical (II) in a sealed, degassed system. A nine-line, considerably-overlapped ($a_N=6.0$ gauss) spectrum, as noted by Kuhn *et al.*[2] in a benzene solution, was observed. When this solution was frozen to a rigid glass at 77°K, the broad ESR spectrum clearly showed that it was a triplet species, as is shown in Fig. 1(a).

On the other hand, the spectrum of the verdazyl biradical III in 2-MeTHF at room temperature presents 17 overlapped lines ($a_N=2.8$ gauss), unlike the one observed by Kuhn *et al.* Fig. 2 shows such a spectrum. The existence of the triplet state in the III biradical was also confirmed by ESR measurement in a rigid solution at 77°K, as is shown in Fig. 1(b).

These spectra at 77°K can be interpreted on the basis of a randomly-oriented set of triplets with axial symmetry*[2]; thus the values of the dipolar splitting, D, are 52.7 gauss for the II biradical and 43.1 gauss for the III biradical, as one half of the outer two lines splitting. The observed increase in the splitting constants, $D(\mathrm{II})>D(\mathrm{III})$. is consistent with the structure. Using a model of two-point dipoles, that is the relation $D=(3/2)g\mu_B r^{-3}$, the average interelectronic distances in the II and III biradicals are calculated as 8.1 Å and 8.7 Å respectively. The relative intensity of central singlet varied with the samples, that is, with the radical concentration of the samples. Since the, monoradical I in 2-MeTHF solution at 77°K gives a singlet ESR spectrum of a line width of about 10 gauss, the central singlet spectra of the biradicals of $\Delta H_{msl}=5-10$ gauss in Fig. 1(a) and (b) may be due to unknown species of monoradicals produced as by-products of the synthesis.

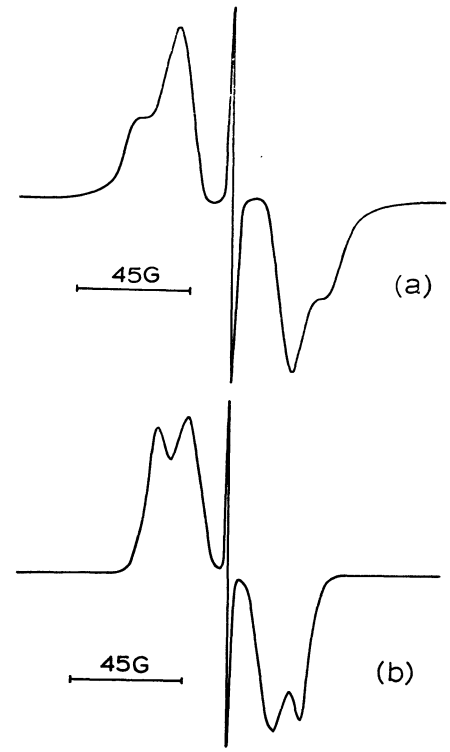

Fig. 1. ESR spectra of the two verdazyl biradicals in 2-MeTHF at 7°K.
(a) Biradical(II) (b) Biradical(III)

The ESR spectrum of a 2-MeTHF solution of the (I) monoradical at room temperature consists of a nine-line, well-resolved ($a_N=5.8$ gauss) spec-

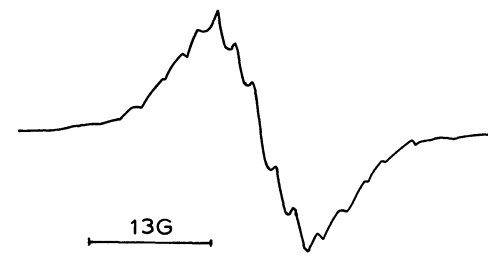

Fig. 2. ESR spectra of the verdazyl biradical (III) in 2-MeTHF at room temperature.

*[2] We have tentatively calculated the zerofield splittings, D and E, for the biradical III, assuming the distribution of the 1/4 unpaired electron on each nitrogen atom, and, further, using a model of a one-point dipole.[7] These values are $D=47.1$ gauss and $E=1.0$ gauss respectively. Therefore, in this note, we shall assume $E=0$ in interpreting the spectra.

7) D. A. Wiersma and J. Kommandeur, *Mol. Phys.*, **13**, 241 (1967).

trum. On the other hand, the ESR measurements of two verdazyl biradicals in a rigid solution at 77°K indicate that a triplet state exists in these radicals. If there is strong scalar exchange interaction, J, between the two electrons such that $J \gg a_N$, the spectrum will consist of 17 lines separated by $a_N/2$, corresponding to an interaction with 8 nearly-equivalent nitrogen nuclei[8]. In fact, the ESR spectrum of the III verdazyl biradical in 2-MeTHF shows 17 lines of $a_N = 2.8$ gauss. However, in the ESR spectrum of the II biradical, a hyperfine interaction with only four nearly equivalent nitrogen nuclei seems indicated, although the distance between the two verdazyl rings is smaller in the II biradical than in the II biradical and thus a larger exchange interaction in the former may be expected. This is probably because of the poorer resolution due to a larger dipolar broadening in the II biradical than in the III biradical.

Spin concentrations for the three species of verdazyl radicals were obtained from the results of the paramagnetic susceptibility measurements[9] at room temperature, after correcting for the diamagnetic contribution calculated by the Pascal method. The values were 97% for the I radical, 110% for II, and 104% for III, assuming the Curie law. The magnetic susceptibilities of usual organic radical solids, including several verdazyl radicals,[10] follow the Curie-Weiss law, and the values of the Curie-Weiss constant, θ, are negative, showing a inter-molecular negative exchange interaction. These facts show the possibility of intra-molecular positive spin coupling for such molecules as the II and III biradicals which have no C_3 or greater symmetry. We are now planning to measure the magnetic susceptibility over the temperature range of 1.8°K—300°K in order to clarify the above experimental results.

The authors wish to express their gratitude to Professors Hideo Takaki and Yasuo Deguchi for making the ESR spectrometer available for this study and for their encouragement throughout the course of this work.

8) C. P. Slichter, *Phys. Rev.*, **99**, 479 (1955).
9) M. Mekata, *J. Phys. Soc. Jap.*, **17**, 796 (1962).
10) K. Mukai, N. Azuma and K. Ishizu, This Bulletin, **43**, 3618 (1970).

BULLETIN OF THE CHEMICAL SOCIETY OF JAPAN VOL. 43 3960—3962 (1970)

ESR Studies of Radicals Generated by the PbO_2 Oxidation of Some Mono- and Bis-formazans

Nagao AZUMA,*[1] Kazuo MUKAI and Kazuhiko ISHIZU

Department of Chemistry, Faculty of Science, Ehime University, Matsuyama

(Received August 25, 1970)

Several investigators[1-3] have reported that the air oxidation of formazans or the reduction of tetrazolium salts gives rise to a paramagnetic product whose ESR spectrum generally shows 9 lines easily explained by two pairs of equivalent nitrogens, and have proposed two structures for the radical, that is, (a) the openchain formazyl radical and (b) the cyclic tetrazolinyl radical.

Neugebauer and Russel[4] obtained much better resolved spectra due to four nitrogens and further phenyl ring protons in a benzene solution by the

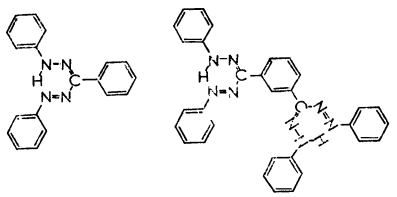

I II

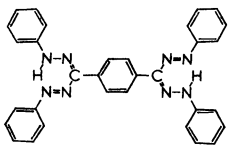

III

*1 Present address: Department of Chemistry, Faculty of Science, Kyoto University, Sakyo-ku, Kyoto.

1) R. T. Lofbert, *Nature*, **206**, 503 (1965).

2) O. W. Maender and G. A. Russell, *J. Org. Chem.*, **31**, 442 (1966).

3) Y. Deguchi and Y. Takagi, *Tetrahedron Lett.*, 3179 (1967).

4) F. A. Neugebauer and G. A. Russell, *J. Org. Chem.*, **33**, 2744 (1968).

abstraction of a hydrogen atom formazans by di(*p*-tolyl)nitrogen. They attributed these spectra to a cyclic structure, based on McLachlan molecular orbital calculations performed for the above two structures. Moreover, from the fact that the ESR spectrum of the radical derived from *N,N'* diphenyl-C-benzeneazoformazan shows 9 groups easily interpreted by only four nitrogen atoms, Neugebauer[5] concluded that the radical has the cyclic structure.

We with to report here the ESR spectra observed when the mono- or bis-formazans I-III are oxidized with lead dioxide in 2-methyltetrahydrofuran (2-MeTHF) under a vacuum.

Experimental

The formazans I—III (I, mp 177.2—178.0°C, II, mp 204.6—205.0°C, III, mp 222.5—222.8°C), were prepared following the method of Kuhn, Neugebauer and Trischmann[6] and were recrystallized, from alcohol for I, from aceton for II, and from DMF for III, as dark red crystals. All the ESR measurements were carried out using a JES-3BX spectrometer equipped with 100 Kc/sec field modulation.

Results and Discussion

Powder samples of the I-III formazans do not show any ESR spectra in 2-MeTHF at room temperature. An initial slight oxidation of the I-III formazans with PbO_2 gives the ESR spectra shown in Fig. 1(a), indicating an interaction with four equivalent nitrogens. We assign the spectra to the corresponding tetrazolinyl monoradicals (I(M), a_N=6.2 G; II(M), a_N=6.1 G; III(M), a_N=6.2 G), which have tetrazolinyl ring. There is no apparent interaction with the protons in the conjugated phynyl rings. Further oxidation of the monoformazan solution causes a marked decrease in the intensity of the ESR spectrum. However, in the case of the II and III bisformazans, as the oxidation proceeds the nine-line spectra of the monoradicals begin to overlap with each other and, finally, are completely altered to the spectra shown in Fig. 1(b). These spectra, which consist of nine considerably overlapped lines, were unchanged at the lowest concentration at which they could be detected; thus they are thought to be due to tetrazolinyl biradicals (II(B), a_N=6.3 G; III(B), a_N=6.5 G). These facts show that the broadening of lines in the ESR spectra of the tetrazolinyl biradicals can be attributed mainly to electron-electron interaction, and not to slow molecular tumbling motion as a consequence of the large molecular size. These circumstances are very similar to those of verdazyl radicals, which have a π-electron system closely related to that of tetrazolinyl radicals.[6-8]

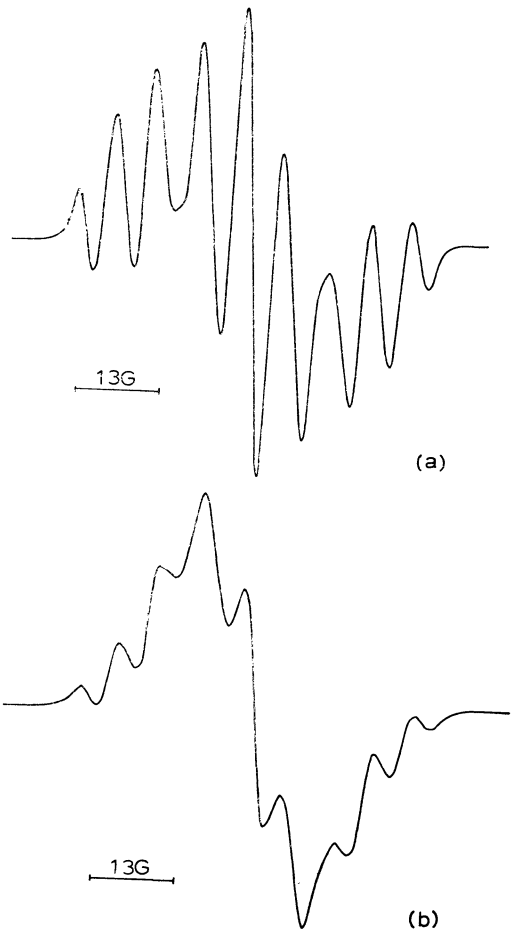

Fig. 1(a). First-derivative ESR spectrum observed for the II(M) monoradical, produced by the PbO_2 oxidation of formazan II in 2-MeTHF. (b). ESR spectrum observed for the II(B) biradical, produced by the further oxidation of the II(M) monoradical in 2-MeTHF.

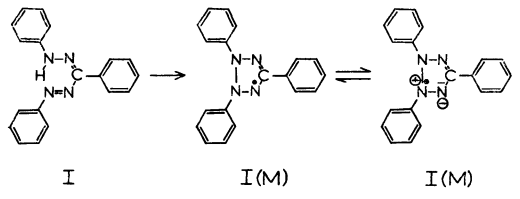

When the reddish-purple solution containing the II(B) biradical is frozen into a rigid glass (77°K),

5) F. A. Neugebauer, *Tetrahedron Lett.*, 2129 (1968).
6) R. Kuhn, F. A. Neugebauer and H. Trischmann, *Mh. Chem.*, **97**, 525 (1966).
7) P. H. H. Fischer, *Tetrahedron*, **23**, 1939 (1967).
8) K. Mukai, N, Azuma, H. Shikata and K. Ishizu, This Bulletin, **43**, 3958 (1970).

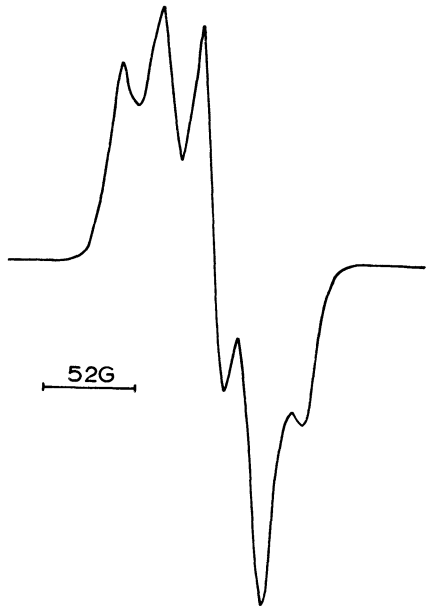

Fig. 2. ESR spectrum of the II(B) biradical in 2-MeTHF at 77°K.

one can observe dipolar splitting, as is shown in Fig. 2. The spectrum remained unchanged after a period of a few hours at 77°K. Upon annealing at room temperature, however, the reddish-purple color disappeared along with the ESR spectrum. The III (B) biradical gave similar, less resolved spectrum. No triplet signal could be observed from I(M) at 77°K.

The assignment of the observed peaks to the usual triplet-state spin Hamiltonian gave the zero-field splitting parameters, $D=51.2$ G for II(B) and $D=37.9$ G for III(B). These small splittings may be explained by the large separtion between the two tetrazolinyl rings and the small unpaired spin density on the centered phynylene ring and two carbon atoms bonded to the ring.[4,7] The dipolar splittings, $D=51.2$ G and 37.9 G, obtained using a model of two-point dipoles, indicate that the average interelectronic distances in II(B) and III(B) are about 8.2 and 9.0 Å respectively. The observed increase in splitting constants, $D(\text{II}) > D(\text{III})$, is consistent with the structure.

BULLETIN OF THE CHEMICAL SOCIETY OF JAPAN VOL. 43 3962—3963 (1970)

Two Modifications of Bi-Nuclear Copper(II) Chloride Complexes with *N*-Methylsalicylideneimine

Yoneichiro MUTO, Michinobu KATO*, Tadashi TOKII, Kyoko IMAI* and Hans B. JONASSEN**

Department of Chemistry, Saga University, Saga, Aichi Prefectural University, Mizuho-ku, Nagoya*
*** Department of Chemistry, Tulane University, New Orleans, Louisiana, U.S.A.*

(Received February 16, 1970)

We reported previously[1,2] that two modifications of a compound of composition Cu($\overset{2}{O}\cdot C_6H_1\cdot \overset{1}{C}H{=}N{-}CH_3$)Cl (1) were obtained in the reaction of bis-*N*-methylsalicylideneiminatocopper(II) and cupric chloride in ethanol. The brown form (1.5 Bohr magnetons) was prepared by refluxing the alcoholic mixture, whereas the orange one (0.9 B.M.) was obtained at lower temperatures. In order to obtain further information about the polymeric nature of these complexes, we have determined their temperature dependence of magnetic susceptibilities. The observed χ-T data fitted the Bleaney-Bowers equation well,[3] confirming an essentially dimeric structure for both forms (*cf.* Fig. 1) with $J=242$ cm^{-1} and $g=2.10$ for the brown form, and $J=580$ cm^{-1} and $g=2.20$ for the orange form. The d-d bands of these two modifications are markedly different; the brown form showed three bands at 815, 667 and 457 mμ suggesting tetrahedral nature of the stereochemistry around the copper(II) ion,[2] whereas the orange form gave rise to a broad band at 1055 mμ with a shoulder at 855 mμ. In order to investigate some factors which lead to the formation of these two modifications, complexes with a substituent (R) at the 5-position of the benzene ring in (1) have been prepared. The complex

1) Y. Muto, M. Kato, H. B. Jonassen, H. N. Ramaswamy and K. Imai, the paper presented at the 10th International Conference on Coordination Chemistry, Nikko, September, 1967, Proceedings, p. 337.

2) M. Kato, Y. Muto, H. B. Jonassen, K. Iami, K. Katsuki and S. Ikegami, This Bulletin, **42**, 2555 (1969).

3) B. Bleaney and K. D. Bowers, *Proc. Roy. Soc.*, **A 214**, 451 (1952).

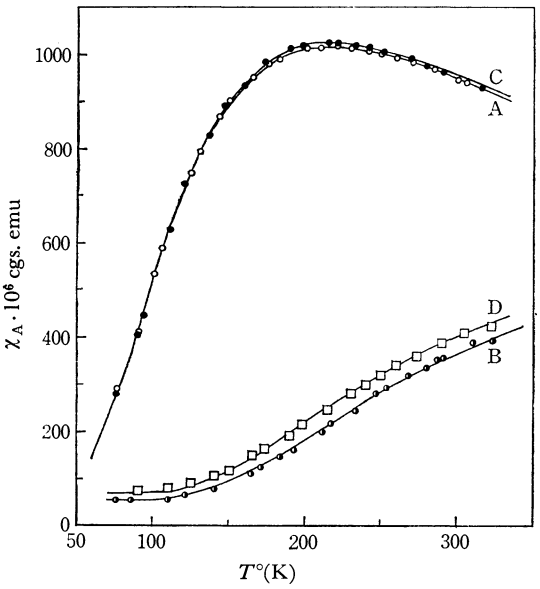

Fig. 1. Variation of magnetic susceptibilities with temperature.
A: R=H* brown form ○, B: R=H* orange form ◑, C: R=CH_3* ●, D: R=Cl* □.
The temperature independent paramagnetism (N_α)[3] is 60(A), 50(B), 60(C) and 60(D) in 10^{-6} cgs, emu respectively.
* *cf.* the text

with R=CH_3 was obtained only in a brown form at lower or higher temperatures (J=243 cm^{-1} and g=2.11), whereas the complex with R=Cl was obtained in an orange form (J=553 cm^{-1} and g=2.17). The complex with R=NO_2 was obtained only as an orange form; the shape of its χ-T curve at low temperatures indicated that it contained a small amount of a paramagnetic impurity. The appropriate values of J (574 cm^{-1}) and g (2.17) for this compound were derived from the χ-T data corrected for the impurity contribution. The details of such variations will be reported shortly. This seems to indicate that electron attracting groups (Cl, NO_2) lead preferably to the formation of the orange form, whereas electron donating group (CH_3) forms the brown complex preferably. The medium polarity of H might explain why the unsubstituted (R=H) complex forms both forms depending upon reaction conditions.

The complexes in the present study all exhibit a bridging phenolic C-O band at *ca.* 1550 cm^{-1}.[4] This indicates that the two copper(II) ions in a dimeric molecule are bridged by phenolic oxygen atoms.

4) C. M. Harris and E. Sinn, *J. Inorg. Nucl. Chem.*, **30**, 2723 (1968).

SHORT COMMUNICATIONS

A Betaine Intermediate in the Copper Chelate Catalyzed Decomposition of *o*-Methoxycarbonyl-α-diazoacetophenone

Matsuji TAKEBAYASHI, Toshikazu IBATA, Kozaburo UEDA and Takeshi OHASHI

Department of Chemistry, College of General Education, Osaka University, Toyonaka, Osaka

(Received July 27, 1970)

In a previous paper,[1] we showed that the copper chelate catalyzed reaction of α-diazoacetophenone with aromatic compounds such as benzaldehyde and acetophenone gave the corresponding tetrahydrofurans and dioxolanes, and that the mechanism of the reaction could be explained by assuming betaine intermediate, produced by the reaction of a ketocarbene-copper chelate complex with carbonyl compounds. This paper deals with a new type of betaine intermediate.

The copper chelate catalyzed decomposition of *o*-methoxycarbonyl-α-diazoacetophenone[2] (I, 0.0098 mol) was carried out in benzene at 80°C in the presence of conjugated dienes (0.367 mol). In the presence of isoprene, the reaction gave two stereoisomeric products (IVa and IVb) in yields of 43 and 34%, respectively. IR of IVa: 2900, 1700, 1635, 1290, 1050 and 765 cm^{-1}. NMR of IVa (in $CDCl_3$): 1.9—2.8(m, 4H), 4.7—5.8 (m, 3H), 6.55(s, 3H), 6.6—9.2(m, 5H) and 8.13 τ (s, 1H). IR of IVb: The same as above. NMR of IVb (in $CDCl_3$): 1.9—2.8(m, 4H), 4.7—5.8 (m, 3H), 6.55(s, 3H), 6.6—9.2(m, 5H) and 8.27 τ(s, 1H). The Ha of IVa is deshielded by 0.14 ppm in comparison with that of IVb, owing to π-electrons of the ethylenic linkage (Scheme 1). The results indicate that the isoprene employed reacts with a new type of betaine intermediate (III),

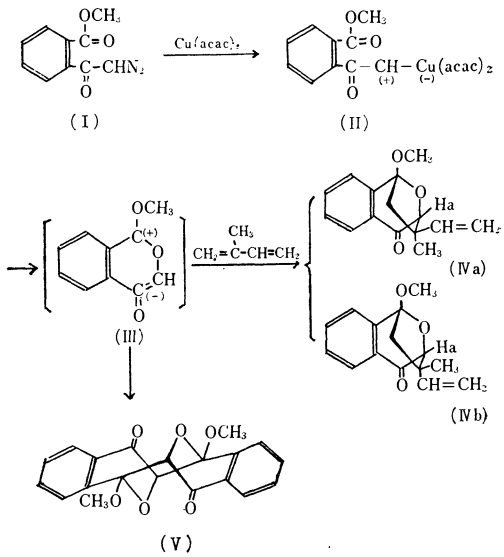

Scheme 1

produced from a ketocarbene-copper chelate complex (II), by 1,2-addition to give IVa and IVb. 1,3-Cyclooctadiene also reacted with III to give 1,2-addition products.

When the reaction was carried out without conjugated dienes, a dimer (V), mp 233—235°C, of III was obtained in 30% yield. NMR of V (in $CDCl_3$): 1.8—2.7(m, 8H), 5.08(s, 1H), 5.62 (s, 1H), 6.30(s, 3H) and 6.54 τ(s, 3H).

1) M. Takebayashi, T. Ibata and K. Ueda, This Bulletin, **43**, 1500 (1970).

2) M. S. Newman and P. F. Beal, *J. Amer. Chem. Soc.*, **71**, 1506 (1949).

Solvent Effect on the Reduction of Butenyl Chlorides by Pentacyanocobaltate(II)

Takuzo FUNABIKI and Kimio TARAMA

Faculty of Engineering, Kyoto University, Sakyo-ku, Kyoto

(Received August 6, 1970)

We studied the reaction of the two butenyl chlorides with pentacyanocobaltate(II) in several solvents in the absence of hydrogen.

The reaction was carried out in a similar manner to that reported previously,[1] except that chlorides were added by an injection-syringe through a gum-stopper. Composition of the products was generally constant, although the reaction was rapid in water solution and slow in other solutions. Some of these results are shown in Tables 1 (CN/Co=6.0) and 2 (CN/Co=5.0). The data in the tables are those of after 3 hr from the start of the reaction. We obtain the following results; 1) At CN/Co=5.0, *trans*-2-butene is the main product in all solvents. 2) At CN/Co=6.0, mole fraction of 1-butene decreases and that of 2-butene increases in the solvents in which *cis*-2-butene is produced selectively in the butadiene hydrogenation. 3) Two chlorides bring the same results in each solvent. From this result we should consider a common intermediate for the reaction of the two chlorides. 4) Yield of butadiene is generally very low and does not vary in the course of the reaction. This result is differs largely from that by Kwiatek and Seyler. 5) Yield of butenes is larger in H_2O than in other solvents at CN/Co=6.0, and *vice versa* at CN/Co=5.0.

We consider these results are important in the study on pentacyanocobaltate(II). The detailed mechanism of this reaction and the role of the solvent will be discussed later.

TABLE 1. EFFECT OF SOLVENT ON PRODUCTS OF THE REDUCTION OF BUTENYL CHLORIDES AT CN/Co=6.0 ($CoCl_2$=10 mmol) (20°C)

Solvent	*trans*-1-Chloro-2-butene, product (mol %)			butd.[b]	3-Chloro-1-butene, product (mol %)			butd.[b]
	1-b	*t*-2-b	c-2-b		1-b	*t*-2-b	c-2-b	
H_2O (50 m*l*)	89 (41.6)[c]	9 (4.2)	2 (0.7)	0.6 (0.3)	92 (34.3)	7 (2.7)	1 (0.5)	2.0 (0.8)
glycerol (35 m*l*) +MeOH (15 m*l*)	60 (13.1)	27 (5.9)	13 (0.3)	0.9 (0.2)	63 (12.3)	22 (4.3)	15 (3.0)	0.4 (0.1)
Ethylene glycol (40 m*l*) +H_2O (10 m*l*)	61 (16.3)	28 (7.4)	11 (2.7)	0.1 (0.02)	67 (18.1)	22 (5.9)	11 (2.8)	0.2 (0.1)
H_2O[a]	87	10	3	89	90	8	2	86

a) By Kwiatek and Seyler[2]; CN/Co=7.0, 200 m*l* H_2O, 0.15 M cobalt, 0.15 M KOH
b) Butadiene assuming that total yield of butenes is 100.
c) The data in parentheses are relative yields of butenes and butadiene.

TABLE 2. EFFECT OF SOLVENT ON PRODUCTS OF THE REDUCTION OF BUTENYL CHLORIDES AT CN/Co=5.0 ($CoCl_2$=10 mmol) (20°C)

Solvent	*trans*-1-Chloro-2-butene, product (mol %)			butd.[b]	3-Chloro-1-butene, product (mol %)			butd.[b]
	1-b	*t*-2-b	c-2-b		1-b	*t*-2-b	c-2-b	
H_2O (50 m*l*)	15 (1.8)[c]	83 (9.8)	2 (0.2)	9.8 (1.2)	14 (1.9)	84 (11.7)	2 (0.3)	6.6 (0.9)
Glycerol (35 m*l*) +MeOH (15 m*l*)	10 (3.3)	87 (27.1)	3 (0.9)	0.5 (0.2)	11 (3.5)	86 (27.5)	3 (1.0)	0.4 (0.1)
H_2O[a]	16	82	2	114	17	81	2	112

a) By Kwiatek and Seyler[2]; CN/Co=5.1, 200 m*l* H_2O, 0.15 M cobalt, 0.15 M KOH
b), c) See footnotes b) and c) in Table 1

1) K. Tarama and T. Funabiki, This Bulletin, **41**, 1744 (1968).

2) J. Kwiatek and J. K. Seyler, *Advan. Chem. Ser.*, **70**, 207 (1968).

Aromatic Substitution of Olefins. XIV. Reaction of σ-Bonded Olefin-Palladium(II) Complexes with Benzene: Evidence for the Mechanism of the Aromatic Substitution of Olefins

Sadao DANNO

Polymer Research Laboratory, Ube Industries Ltd., Ichihara, Goi, Chiba

and Ichiro MORITANI, Yuzo FUJIWARA and Shiichiro TERANISHI

Faculty of Engineering Science, Osaka University, Machikaneyama, Toyonaka, Osaka

(Received August 18, 1970)

The substitution reaction of olefins is as follows:[1]

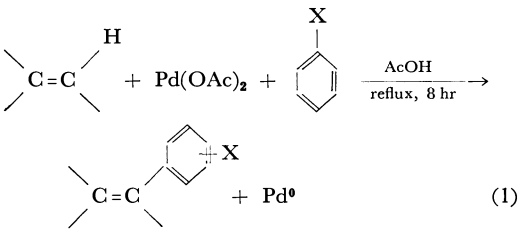

(1)

We have demonstrated that this is the general reaction occurring between common olefins and aromatics to produce aromatic-substituted olefins and that the reaction proceeds through a different mechanism from that of the Wacker process.[2]

The mechanism proposed involves σ-bonded olefin-palladium(II) intermediate.[3] In order to prove this mechanism, we have performed the reaction of a σ-bonded 2,2-dichlorovinyl-palladium(II) complex (I) with benzene. If the proposed mechanism is reasonable, the σ-bonded complex bearing a C=C double bond would react with benzene to produce an aryl-substituted olefin. The starting complex (I) was prepared by Fitton,[4] and the reaction was carried out using complex(I), benzene, acetic acid, and silver acetate under reflux for 8 hr. The silver acetate was introduced to abstract a chloride ligand from (I) to enable benzene to coordinate to palladium(II) metal.*1 From the reaction mixture, β,β-dichlorostyrene was obtained in a 7.4% yield based on complex(I) (equation 2).*2*3

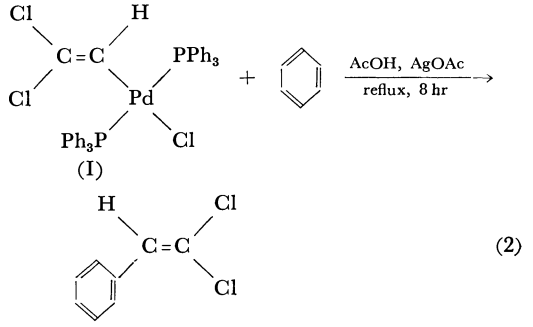

(2)

Moreover, σ-bonded *cis*- and *trans*-2-chlorovinyl-palladium(II) complexes reacted with benzene to produce corresponding β-chlorostyrenes.

These results clearly show that the aromatic substitution of olefins proceeds *via* formation of a σ-bond between olefin and palladium(II) metal, and support the proposed mechanism.[3]

1) Y. Fujiwara, I. Moritani, S. Danno and S. Teranishi, *J. Amer. Chem. Soc.*, **91**, 7166 (1969).

2) S. Danno, I. Moritani and Y. Fujiwara, *Chem. Commun.*, **1970**, 610; S. Danno, I. Moritani, Y. Fujiwara and S. Teranishi, *J. Chem. Soc., B*, in press.

3) S. Danno, I. Moritani and Y. Fujiwara, *Tetrahedron*, **25**, 4819 (1969).

4) P. Fitton and J. E. McKeon, *Chem. Commun.*, **1968**, 4.

*1 As silver acetate alone cannot bring about the reaction, it is apparent that the reaction takes place by the action of palladium(II) of complex (I).

*2 That the σ-complex(I) is stable under the reaction condition without benzene was confirmed by a separate experiment.

*3 Note added in Proof. When the reaction time was 1.5 hr to present the polymerization of the styrene formed, the yield increased up to 80%.

Photochemical Interconversion between Norfriedelin and 5α-Vinyl-10β-formylmethyl-des-A-friedelane

Reiko AOYAGI, Takahiko TSUYUKI and Takeyoshi TAKAHASHI

Department of Chemistry, Faculty of Science, The University of Tokyo, Hongo, Bunkyo-ku, Tokyo

(Received August 24, 1970)

The photochemical reaction of aldehyde in the presence of olefin to saturated ketone has already been reported.[1,2] We now wish to describe a photochemical reaction of 5α-vinyl-10β-formylmethyl-des-A-friedelane (I) in *n*-hexane to yield norfriedelin (II)[3] (path A). This would be the first instance of the intramolecular ketone formation reaction of an olefinic aldehyde. As I was formed on irradiation of II in the same solvent (path C), it is noteworthy that the photochemical interconversion between I and II took place.

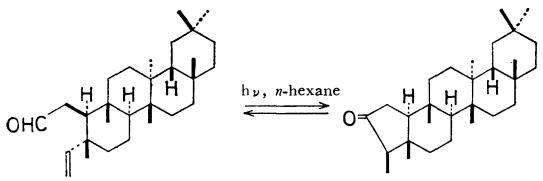

Fig. 1

Norfriedelin (II, 1.00 g) in *n*-hexane (700 m*l*) was irradiated with a high pressure mercury lamp for 50 hr. Dry column chromatography and recrystallization afforded I [223 mg, mp 162.5—163.5°C, IR (Nujol) 3075, 1625, 907 ($CH=CH_2$), 2700, 1715 cm^{-1} (CHO), NMR (in $CDCl_3$, δ; an internal standard: TMS) 9.70 ($-CH_2\underline{C}HO$, t, J=2—3 Hz), MW(mass) M^+ 412].

A solution of I, (35 mg) was heated under reflux with bubbling of argon for 1 hr. The solution was then irradiated with a high pressure mercury lamp at room temperature for 30 hr.

The solvent was distilled off and the reaction products were separated with silica gel dry column chromatography. Elution with petroleum ether–benzene (10 : 1) gave hydrocarbon mixture (~6 mg), and the starting material (13 mg) was then recovered.

Norfriedelin (II) was eluted with benzene and weighed about 2 mg. The IR spectrum ($\nu_{C=O}$ 1750 cm^{-1}), mass spectrum (M^+ 412) and R_f value on TLC were identical with those of the authentic sample. In gas chromatographic examination, however, two peaks appeared at t_R= 31.5 and 28.9 min in the case of Diasolid H-523 at 250°C and t_R=12.0 and 11.0 min in the case of OV-17 at 290°C. The peak with longer t_R was predominant and was shown to be due to norfriedelin (II) and the other due to 4-epinorfriedelin (II′). However, no isolation of II′ has yet been achieved.

Formation of norfriedelin (II) from the olefinic aldehyde (I) could be interpreted by the following mechanism (path A). Intermediate radical (III) may attack either C_4 or C_{23} carbon atom of the double bond, giving rise to IV or V, respectively. Radical (IV) is converted immediately to tertiary radical (VI) by migration of hydrogen atom at C_4 to C_{23}. As hydrogen must attack the resulting radical (VI) from both sides, norfriedelin (II) is accompanied with its 4α-methyl epimer (II′). A part of II′ could be also formed from photochemical isomerization of II. As no cyclohexane derivative was formed, the process leading to radical (V) (path B, or *via* IV) is considered unfavourable under the above conditions. These findings are in accord with the observation that cyclopentane formation is a kinetically favoured process for free radical cyclization.[4]

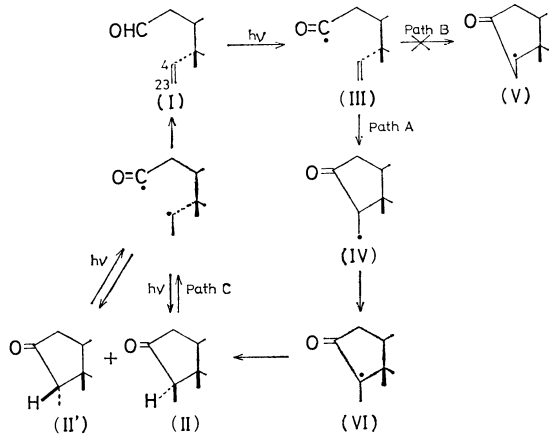

Fig. 2

1) M. S. Kharash, W. H. Urry and B. M. Kuderna, *J. Org. Chem.*, **14**, 248 (1949).

2) C. H. Krauch, S. Farid and G. O. Schenck, *Chem. Ber.*, **98**, 3102 (1965).

3) L. Ruzicka, O. Jeger and P. Ringnes, *Helv. Chim. Acta*, **27**, 972 (1944).

4) M. Julia, *Pure and Appl. Chem.*, **15**, 167 (1967); M. Julia and M. Maumy, *Bull. Soc. Chim. Fr.*, **1968**, 1603; D. L. Struble, A. L. J. Beckwith and G. E. Gream, *Tetrahedron Lett.*, **1968**, 3701.

Photolyses of Aliphatic Ketones Adsorbed on Porous Vycor Glass

Yutaka KUBOKAWA, Masanori KUBO and Gohei NANJO

Department of Applied Chemistry, University of Osaka Prefecture, Sakai, Osaka

(Received August 26, 1970)

In contrast to extensive photochemical studies in gas phase and solution, few studies have been made on the photochemical reactions in the adsorbed layer. In the present work, photolyses of aliphatic ketones (acetone, methyl ethyl ketone and 2-pentanone) adsorbed on porous Vycor glass (Corning, No. 7930) have been investigated. After a certain amount of the vapor of ketone was allowed to be adsorbed, photolysis in the adsorbed layer was carried out at room temperature in the absence of ketone vapor. An ultra high pressure mercury lamp was used. After the photolysis, products which can be desorbed up to 100°C were analysed by gas chromatography. Prior to the experiments, the glass was oxidized in air at 600°C followed by outgassing at 500°C for 7 hr.

Photochemical reactivity of the ketones in the adsorbed layer was as follows: acetone, $R(CH_4) + R(C_2H_6)$, 0.05; methyl ethyl ketone, $R(C_2H_6)$, 1.00; 2-pentanone, $R(C_2H_4) + R(C_3H_8)$, 12.18. R(hydrocarbons)=[(Rate of formation of hydrocarbon, cc. S.T.P./hr)/(Amount of ketone adsorbed, cc. S.T.P.)] × 100. A marked difference can be seen in the reactivity of the three ketones. In contrast to the photolysis in gas phase the appearance of CO in the gas phase was negligible.[1] The results together with those in Table 1 show that in the adsorbed layer 2-pentanone undergoes the Norrish type I process ($CH_3COC_3H_7 \rightarrow CH_3CO + C_3H_7$) as well as the Norrish type II process ($CH_3COC_3H_7 \rightarrow CH_3COCH_3 + C_2H_4$). It is well-known that in gas phase and solution aliphatic ketones with γ hydrogen such as 2-pentanone undergo type II process predominantly at room temperature.[2] The results in Table 1 also show that with increasing outgassing temperature and after removal of acidic sites by nitric acid treatment,[3] $R(C_3H_8)$ decreases, while $R(C_2H_4)$ decreases little or remains unchanged. It can be concluded that the occurrence of type I process (formation of radicals) in the adsorbed layer becomes much easier on the surface with surface hydroxyl groups in a high concentration and also with acidic sites. The effect of the amount of 2-pentanone adsorbed on its photolysis was examined. As seen in Fig. 1, with the decrease of the amount adsorbed, values of $R(C_3H_8)/R(C_2H_4)$ as well as the rate of photolysis increased. Although the nature of such behavior is not clear at present, the results in Fig. 1 might be explained by assuming a heterogeneity of the glass surface.

Table 1. Photolysis of 2-pentanone adsorbed

Temp of outgassing, °C		500	800	800[a]
$R(C_3H_8)$	Type I	5.13	2.66	1.45
$R(C_2H_4)$	Type II	7.05	7.14	7.68

a) The glass was treated by nitric acid before outgassing at 800°C.

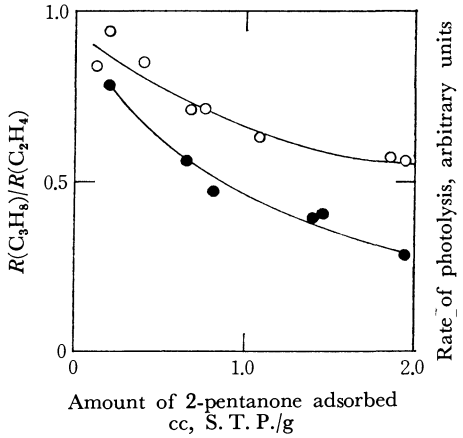

Fig. 1. Photolysis of 2-pentanone adsorbed, -○-, $R(C_3H_8)/R(C_2H_4)$; -●-, rate of photolysis.

1) In the case of 2-pentanone, both R(CO) and $R(CH_4)$ were below 0.2.

2) In the gas phase photolysis of 2-pentanone, no formation of C_3H_8 occurred at 23°C and 7.3 mmHg of 2-pentanone.

3) L. H. Little, H. E. Klauser and C. H. Amberg, *Can. J. Chem.*, **39**, 42 (1961).

Conformational Analysis of Poly-γ-benzyl-glutamates by Monolayer Method

Takuya YAMASHITA and Shinsuke YAMASHITA

Department of Chemistry and Department of Polymer Science, Faculty of Science, Osaka University, Toyonaka, Osaka

(Received September 7, 1970)

It has been found that esters of polyglutamic acid and synthetic polypeptides with long hydrocarbon side-chains yield well defined transition points in force-area curves.[1-3] In the present communication, we wish to report the relation between the temperature coefficient of the monolayer transition pressure and the conformation of synthetic polypeptide in the solid state.

The polymers examined were L, DL-copolymers of γ-benzyl-glutamate (L/(D+L)=0.5—1.0). They consist of regular helix, perturbed helix and random coil, and were analyzed by means of infrared spectroscopy.[4,5] No β-components were detected. The polymers were dissolved in purified chloroform, and spread on the surface of twice-distilled water filled in a Teflon trough. The initial spreading area was 55 Å²/residue, and compressed at the rate of 0.2 Å²/residue/min. The surface pressure was measured by the Wilhelmy method at temperatures 10—20°C, where a linear relationship was obtained between the film transition pressure and temperature.

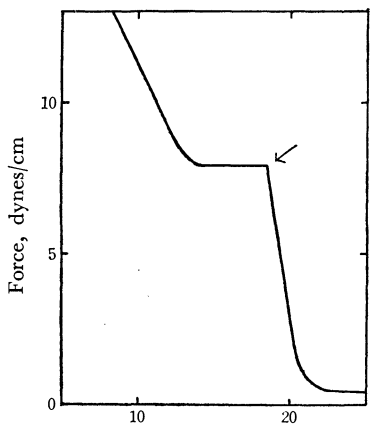

Fig. 1. Force-area curve for poly-γ-benzyl-DL-glutamate.
20°C; $[H_R]=38.5\%$

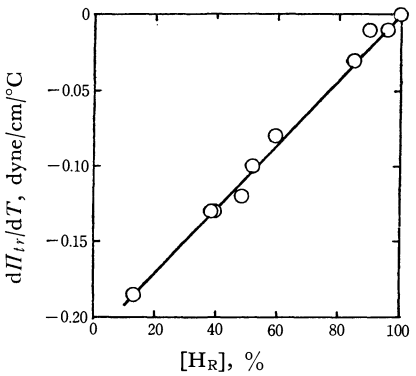

Fig. 2. Plot of $d\Pi_{tr}/dT$ *versus* $[H_R]$.

Figure 1 shows a typical force-area curve for poly-γ-benzyl-DL-glutamate, where a transition point can be seen. In Fig. 2 is shown the plot of temperature coefficient of the transition pressure $d\Pi_{tr}/dT$ *versus* percentage of regular helix $[H_R]$ for poly-γ-benzyl-glutamate monolayers. The value of $d\Pi_{tr}/dT$ is negative, and increases linearly with the increase in $[H_R]$. At 100% regular helix, $d\Pi_{tr}/dT$ is zero. The relation between $d\Pi_{tr}/dT$ and $[H_R]$ can be expressed in the form

$$\frac{d\Pi_{tr}}{dT} = -2.125 \times 10^{-1} + 2.125 \times 10^{-3}[H_R]$$

From this equation, we can estimate the content of regular helix in poly-γ-benzyl-glutamate by means of the monolayer method. Usually, the amount of polymer required to determine a transition pressure is small (less than 50 μg).

As regards the percent total helix (percent regular helix + percent perturbed helix), no simple linear relationship was found between the temperature coefficient and the percent total helix.

The present results appear to indicate that the regular helix is stable even in the monolayer state. Conformation of poly-γ-benzyl-glutamates at the interface will be discussed elsewhere.

1) T. Isemura and K. Hamaguchi, This Bulletin, **25**, 40 (1952).
2) T. Isemura and K. Hamaguchi, *ibid.*, **26**, 425 (1953).
3) B. R. Malcolm, *Proc. Roy. Soc.*, **A 305**, 363 (1968).
4) M. Tsuboi, Y. Mitsui, A. Wada, T. Miyazawa and N. Nagashima, *Biopolymers*, **1**, 297 (1963).
5) Y. Masuda, *Kobunshi Kagaku*, **20**, 161, 166, 171, 206, 210 (1963).

Tetracyano-Bis(triphenylphosphine) and -Bis(triphenylarsine)-Cobaltate(III) Complexes

Nobufumi MAKI and Kanji OHSHIMA

Department of Chemistry, Faculty of Engineering, Shizuoka University, Johoku, Hamamatsu

(Received September 8, 1970)

Previously, we concluded that the disulfito- and diaquo-tetracyanocobaltate(III) complexes take a *trans*-configuration on the evidence of their polarographic behavior and absorption spectra.[1]

The present communication is concerned with the method of preparing and confirming two kinds of tetracyanocobaltate(III) complexes involving triphenylphosphine or triphenylarsine, $Na[Co(CN)_4(P{\equiv}\phi_3)_2]\cdot 3H_2O$ and $Na[Co(CN)_4(As{\equiv}\phi_3)_2]\cdot 3H_2O$ (a new complex),*1 from the *trans*-disulfito complex. The former was ascertained to be quite identical with that prepared by the method of Watanabe *et al.*[2]

The disulfito complex, $Na_5[Co(SO_3)_2(CN)_4]\cdot 3H_2O$[3] (9.38 g), was suspended in 300 m*l* of glacial acetic acid containing 10.0 g of triphenylphosphine and refluxed at 75—80°C for six hours with stirring. The disulfito complex gradually dissolved into acetic acid.

The slurry residue, which was insoluble in acetic acid, was filtered off if it was yielded in the final stage of the reaction. The yellow filtrate was then diluted to 1200 m*l* by adding water and allowed to stand overnight under ice-cooling. The desired complex crystallized from the solution; it was filtered and washed with water, benzene, and ether to eliminate any excess ligands. Recrystallizations were made from an ethanolic solution by adding water. Found: Co, 7.67; C, 62.94; N, 7.38; H, 4.83%. Calcd for $Na[Co(CN)_4(P{\equiv}\phi_3)_2]\cdot 3H_2O$: Co, 7.71; C, 62.83; N, 7.33; H, 4.75%.

Analogously, the $Na[Co(CN)_4(As{\equiv}\phi_3)_2]\cdot 3HO_2$ complex was prepared as orange-yellow crystals by treating 11.66 g of $Na_5[Co(SO_3)_2(CN)_4]\cdot 3H_2O$ with 14.52 g of triphenylarsine in 600 m*l* of acetic acid (100%) at 75°C for ten hours. Found: Co, 6.88; C, 56.42; N, 6.61; H, 4.30%. Calcd for $Na[Co(CN)_4(As{\equiv}\phi_3)_2]\cdot 3H_2O$: Co, 6.91; C, 56.36; N, 6.57; H, 4.26%.

Figure 1 shows the absorption spectra of tetracyanocobaltate(III) complexes in the visible and ultraviolet regions.

All the aspects of the polarographic behavior of the tetracyano complexes derived from the disulfito complex are very similar to each other; this suggests that their configurations are all *trans*-form. Table 1 summarizes the electrode processes and their half-wave potentials.

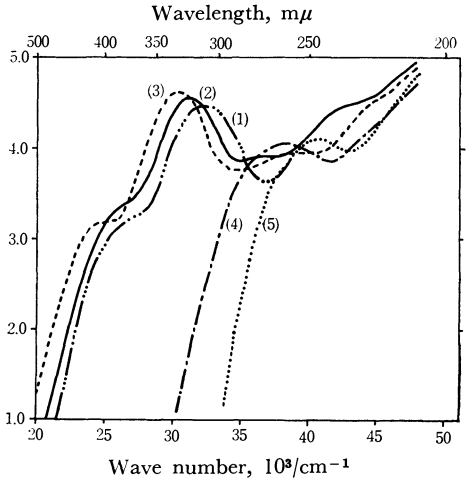

Fig. 1. The absorption spectra of the cobaltate-(III) complexes in methanol solutions (25°C). (1) ----- *trans*-$Na_5[Co(SO_3)_2(CN)_4]\cdot 3H_2O$; (2) —— $Na[Co(CN)_4(P{\equiv}\phi_3)_2]\cdot 3H_2O$; (3) ---- $Na[Co(CN)_4(As{\equiv}\phi_3)_2]\cdot 3H_2O$; —·—· (4) $P{\equiv}\phi_3$ in ethanol; (5) ····· $As{\equiv}\phi_3$ in ethanol.

TABLE 1. HALF-WAVE POTENTIALS OF THE WAVES FOR TETRACYANOCOBALTATE(III) COMPLEXES (25°C)

Compound	1st wave	2nd wave	3rd wave
$Na[Co(CN)_4(P{\equiv}\phi_3)_2]\cdot 3H_2O$	−0.98 ($Co^{III} \rightarrow Co^{I}$)	−2.06 ($Na^{I} \rightarrow Na^{0}$)	
$Na[Co(CN)_4(As{\equiv}\phi_3)_2]\cdot 3H_2O$	−0.58 ($Co^{III} \rightarrow Co^{II}$)	−1.06 ($Co^{II} \rightarrow Co^{I}$)	−2.06 ($Na^{I} \rightarrow Na^{0}$)

DMSO solution containing 0.1 M $[(C_2H_5)_4N]ClO_4$ V *vs.* SCE

1) N. Maki and K. Yamamoto, This Bulletin, **43**, 2450 (1970).

2) K. Watanabe, H. Nishikawa and M. Shibata, *ibid.*, **42**, 1150 (1969).

*1 ϕ=phenyl radical: C_6H_5-.

3) H. H. Chen, M-S. Tsao, R. W. Gaver, P. H. Tewari and W. K. Wilmarth, *Inorg. Chem.*, **5**, 1913 (1966).

The Stereochemistry of Binuclear Complexes of Chromium(III)

Akio URUSHIYAMA, Teruo NOMURA and Masayoshi NAKAHARA

Department of Chemistry, Faculty of Science, Rikkyo University, Nishi-ikebukuro, Toshima-ku, Tokyo

(Received September 19, 1970)

The normal rhodo chromic complex ion, $[(NH_3)_5Cr(OH)Cr(NH_3)_5]^{5+}$, and the basic rhodo complex ion, $[(NH_3)_5Cr(O)Cr(NH_3)_5]^{4+}$, have both been characterized in terms of their magnetic[1] and spectroscopic[2,3] behaviour, which is at least in part, to be ascribed to the Cr–O–Cr angles in the complex ions. In the present work, in order to establish the stereochemistry of binuclear Cr(III) complexes, the crystals of the rhodo compounds have been subjected to three-dimensional X-ray analysis.

Their crystal data are as follows: normal rhodo chromic chloride, $[(NH_3)_5Cr(OH)Cr(NH_3)_5]Cl_5 \cdot H_2O$-tetragonal, space group $P4_12_12$ (or $P4_32_12$), $a=16.26$, $c=14.80$ Å, $Z=8$, $D_m=1.65$, $D_x=1.65$ g·cm^{-3}; basic rhodo chromic chloride, $[(NH_3)_5Cr(O)Cr(NH_3)_5]Cl_4 \cdot H_2O$-orthorhombic, space group *Pbca*, $a=11.94$, $b=11.71$, $c=13.40$ Å, $Z=4$, $D_m=1.58$, $D_x=1.59$ g·cm^{-3}. Their structures have been solved by the heavy-atom method and refined to $R=0.16$ for the acid rhodo salt, and to $R=0.11$ for the basic rhodo salt, by least-squares analysis based on 1169 and 811 three-dimensional data respectively.

The structures of the complexes are shown in

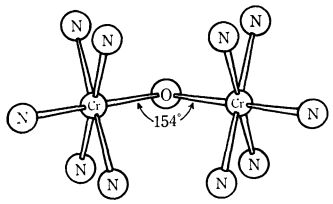

Fig. 1. Perspective drawing of the acid rhodo chromic complex ion, $[(NH_3)_5Cr(OH)Cr(NH_3)_5]^{5+}$.

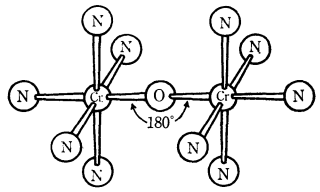

Fig. 2. Perspective drawing of the basic rhodo chromic complex ion, $[(NH_3)_5Cr(O)Cr(NH_3)_5]^{4+}$.

Figs. 1 and 2. In the normal rhodo chromic complex, a bridging oxygen atom is located on the two-fold rotation axis. Approximately, there are two mirror planes, perpendicular to one another, in the complex. Thus, the acid rhodo complex has a quasi-C_{2v} symmetry. The Cr–O–Cr bond angle is 154°. The coordination around the chromium atoms is approximately octahedral, with bond distances of Cr–O 2.00 Å and Cr–N 2.07 Å (average). In the basic rhodo chromic complex, a bridging oxygen atom is situated on the inversion center. Therefore, the complex exactly has a center of symmetry and, accordingly, a linear Cr–O–Cr system. As the complex has approximately a four-fold rotation axis passing through a sequence of the N–Cr–O–Cr–N atoms, it seems reasonable to say that the basic rhodo chromic complex has D_{4h} symmetry. The eight N–Cr–O angles are nearly 90°, and the Cr–N bond distance is 2.11 Å(average). The Cr–O distance is 1.80 Å, which is quite short compared with that in the acid rhodo chromic complex. The linear Cr–O–Cr system and its short bond distance suggest the presence of an extensive π-bonding in this system like that in similar oxo-bridged binuclear complexes, $K_4[Cl_5Ru–O–RuCl_5]$ (Ru–O= 1.86 Å)[4] and $K_4[Cl_5Re–O–ReCl_5]$ (Re–O= 1.80 Å)[5], both of which have been confirmed to be of D_{4h} symmetry by the X-ray method.

1) A. Earnshaw and J. Lewis, *J. Chem. Soc.*, **1961**, 396.

2) C. E. Schäffer, *J. Inorg. Nucl. Chem.*, **8**, 149 (1958).

3) L. Dubicki and R. L. Martin, *Aust. J. Chem.*, **23**, 215 (1970).

4) A. G. Mathieson, D. P. Mellor and N. C. Stephenson, *Acta Crystallogr.*, **5**, 185 (1952).

5) J. C. Morrow, *ibid.*, **15**, 851 (1962).

Schiff Base Oxovanadium(IV) Complexes with Subnormal Magnetic Moments

Yoshio KUGE* and Shoichiro YAMADA**

* *Public Health Institute, Morimachi, Higashi-ku, Osaka*

** *Institute of Chemistry, College of General Education, Osaka University, Toyonaka, Osaka*

(Received October 16, 1970)

It was reported previously that *N*-(hydroxyalkyl)-salicylideneimines (Formula I, abbreviated as X-SAL. Y-OH) formed magnetically subnormal copper(II) complexes, which were concluded to have a binuclear structure with exchange coupling between the two copper(II) ions.[1,2] Through the hole-formalism, the oxovanadium(IV) ion with a d^1 configuration is known to be somewhat similar to the copper(II) ion with a d^9 configuration. However, no report is available on the corresponding oxovanadium(IV) complexes. The present communication deals with preparation of new Schiff base complexes with oxovanadium(IV) having subnormal magnetic moments.

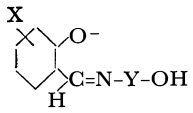

I

Oxovanadium(IV) complexes of the type VO (X-SAL. Y-O) were obtained as crystals by the following method. To an ethanolic solution of $VOCl_2$ (0.01 mol) was added the preformed Schiff base, *N*-(hydroxyalkyl)salicylideneimine (0.015 mol), and the resulting solution was stirred at room temperature for a few hours. Microcrystals, which deposited in the solution, were filtered off, and washed with ethanol several times.

Analytical data, which are shown in Table 1, agree with the formula given above. The magnetic moments for these complexes, as shown in Table 1, are much smaller than the spin-only moment for the d^1 system. The subnormal magnetic moments are considered to be due to an exchange interaction between vanadium(IV) ions. It is most likely that these oxovanadium(IV) complexes have a binuclear structure similar to that of the corresponding copper(II) complexes.[1-3] A similar binuclear structure was proposed previously for oxovanadium(IV) complexes with 5-substituted *N*-(2-hydroxyphenol)salicylideneimines, which were also reported to nave subnormal magnetic moments.[4,5] The electronic spectra of these complexes differ significantly from those of the complexes of the type VO(X-SAL. alkyl)$_2$, which involve no interaction between vanadium(IV) ions.

TABLE 1. ANALYTICAL DATA OF COMPLEXES OF THE TYPE VO(X-SAL. Y-O)

		Calcd, %			Found, %			
X	Y	C	H	N	C	H	N	μ
H	$(CH_2)_2$	46.98	3.94	6.09	46.45	4.33	6.01	1.06
H	$(CH_2)_3$	48.99	4.94	5.71	49.14	4.95	5.74	1.36
3-CH_3O	$(CH_2)_3$	48.19	4.78	5.11	48.01	4.78	4.82	0.87

μ: magnetic moment at room temperature in B. M.

1) S. Yamada, Y. Kuge and K. Yamanouchi, *Inorg. Chim. Acta*, **1**, 139 (1967); S. Yamada, H. Nishikawa, Y. Kuge and K. Yamanouchi, *Sci. Repts.* (Coll. Gen. Educ. Osaka Univ.), **16**, 11 (1967).

2) M. Kato, Y. Muto, H. B. Jonassen, K. Imai and A. Harano, This Bulletin, **41**, 1864 (1968).

3) J. A. Bertrand, J. A. Kelley and J. L. Breece, *Inorg. Chim. Acta*, **4**, 247 (1970).

4) V. V. Zelentsov, *Russ. J. Inorg. Chem.*, **7**, 670 (1962).

5) A. P. Ginsberg, E. Koubek and H. J. Williams, *Inorg. Chem.*, **5**, 1656 (1966).

Syntheses and Stereochemistry of Optical Isomers of tris(2,4-Pentanediamine)cobalt(III) Complex

Fujio MIZUKAMI, Haruko ITO, Junnosuke FUJITA and Kazuo SAITO

Department of Chemistry, Faculty of Science, Tohoku University, Sendai

(Received October 20, 1970)

Tris(trimethylenediamine)-cobalt(III) ion has been found to have chair form chelates in its bromide crystal.[1] The conformation of 2,4-pentanediamine (ptn) metal chelate was studied by PMR spectra.

We have synthesized a diastereomeric pair of $[Co(R,R\text{-ptn})_3]^{3+}$ and an opticaly active $[Co(R,S\text{-ptn})_3]^{3+}$. Racemic and meso-ptn were prepared by the known method.[2,3] The $(-)_D$-ptn was assigned to R,R (D,D)-configuration.[3]

Perchlorate and chloride of *trans*-$[CoCl_2(ptn)_2]^+$ were synthesized with R,R- and R,S-ptn, respectively.[4] The former was warmed with R,R-ptn and activated charcoal to give orange diastereomeric mixture of $[Co(R,R\text{-ptn})_3](ClO_4)_3$. The filtered solution was cooled together with 60% perchloric acid, and the orange prismatic crystals were recrystallized from water. $(-)_{546}$-$[Co(R,R\text{-ptn})_3]\cdot(ClO_4)_3\cdot H_2O$: Found: C, 26.35; H, 6.51; N, 12.07%. Calcd for $CoC_{15}H_{44}N_6Cl_3O_{13}$: C, 26.42; H, 6.50; N, 12.33%.

trans-$[CoCl_2(R,R\text{-ptn})_2]ClO_4$ was converted into chloride, and warmed with R,R-ptn in 50% aqueous ethanol. The orange needles were recrystallized in a similar way. $(+)_{546}$-$[Co(R,R\text{-ptn})_3]Cl_3\cdot 2H_2O$: Found: C, 36.08; H, 9.09; N, 16.12%. Calcd for $CoC_{15}H_{46}N_6Cl_3O_2$: C, 35.47; H, 9.13; N, 16.55%.

trans-$[CoCl_2(R,S\text{-ptn})_2]Cl$ was warmed with R,S-ptn and activated charcoal. The filtered solution was treated with perchloric acid. The reddish orange product was recrystallized from water, resolved with silver *d*-tartrate and converted into needle-like perchlorate. $(-)_{546}$-$[Co(R,S\text{-ptn})_3](ClO_4)_3\cdot 3H_2O$: Found: C, 25.31; H, 6.30; N, 11.72%. Calcd for $CoC_{15}H_{48}N_6Cl_3O_{15}$: C, 25.10; H, 6.74; N, 11.71%. Both isomers of $[Co(R,R\text{-ptn})_3]^{3+}$ give a sharp doublet of methyl signal in its 60 MHz PMR spectrum in D_2O. This suggests that the complex has D_3 symmetry with twist-form six-membered chelate rings and the two methyls have equatorial orientation. On the other hand, the PMR spectrum of $[Co(R,S\text{-ptn})_3]^{3+}$ gives a broader methyl signal, which seems to be due to overlapped two signals. This complex can have two geometrical isomers with respect to the mer and fac coordination of the amino groups near R- and S-α-carbon. Study of molecular models disclosed that the stable chair form has the two methyls equatorial and only the fac isomer is formed without large steric hindrance. The apparent two kinds of methyl signal seem to be due to C_3 symmetry of this fac complex. From the CD sign in the first *d-d* transition region, the prismatic and the needlelike $[Co(R,R\text{-ptn})_3]^{3+}$ are tentatively assigned to absolute configurations *Λ* and *Δ*, respectively. $(-)_{546}$-$[Co(R,S\text{-ptn})_3]^{5+}$ seems to have absolute configuration *Λ*.

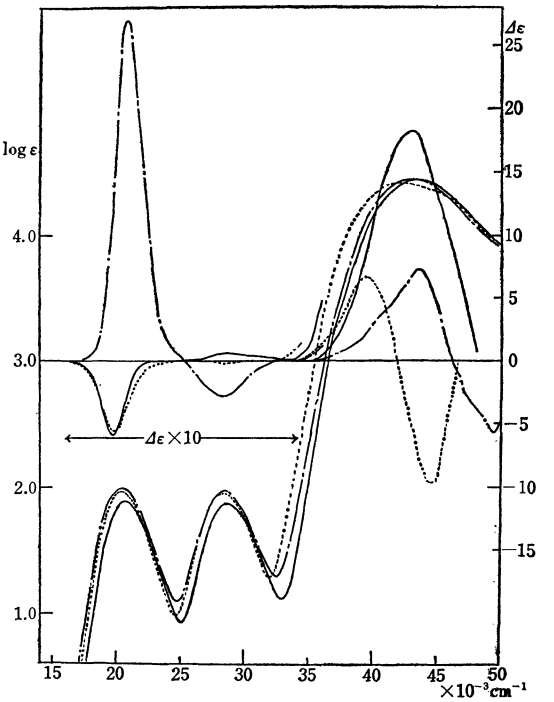

Fig. 1. Absorption and circular dichroism (CD) spectra of
Λ-$[Co(R,R\text{-ptn})_3]Cl_3\cdot 2H_2O$ (——),
Λ-$[Co(R,R\text{-ptn})_3](ClO_4)_3\cdot H_2O$ (——) and
Λ-$[Co(R,S\text{-ptn})_3](ClO_4)_3\cdot 3H_2O$ (- - - - -) in water.

1) Y. Saito, T. Nomura and F. Marumo, This Bulletin, **41**, 530 (1968).

2) T. G. Appleton, and J. R. Hall, *Inorg. Chem.*, **9**, 1800 (1970).

3) F. Mizukami, H. Ito, J. Fujita and K. Saito, This Bulletin, **43**, 3633 (1970).

4) C. J. Dippel and F. M. Jaeger, *Rec. Trav. Chim. Pays-Bas*, **50**, 547 (1931).